BULLETIN OF THE CHEMICAL SOCIETY OF JAPAN VOL. 41 1—7 (1968)

Studies on the Liquid-Liquid Partition Systems. VI. Solvent Extraction Study of the Dissociation of Sulfurous, Selenious and Tellurous Acids in Acid Perchlorate Media*1

Tatsuya SEKINE, Hidehiko IWAKI, Mitsuo SAKAIRI and Fumitake SHIMADA

Department of Chemistry, Science University of Tokyo, Kagurazaka, Shinjuku-ku, Tokyo

and Mariko INARIDA

Laboratory of Nuclear Chemistry, Institute of Physical and Chemical Research, Yamatomachi, Kitaadachi-gun, Saitama

(Received May, 4, 1967)

Liquid-liquid distribution behavior of sulfur(IV), selenium(IV) and tellurium(IV) in acid perchlorate media was studied at 25°C. The distribution of sulfur(IV) into carbon tetrachloride was determined by iodometry and that of selenium(IV) into methylisobutyl carbinol or of tellurium(IV) into hexane containing trioctylphosphine oxide was determined by radiometry. The changes in the distribution ratio caused by the changes in the hydrogen ion concentration were explained in terms of the distribution of sulfurous, selenious or tellurous acid as the noncharged form into the organic phase and the dissociation of these acids in the aqueous phase. The distribution constants as well as the dissociation constants of these acids were determined by a graphical method. In acid perchlorate media, sulfurous and selenious acids exist as neutral and mononegative species while tellurous acid exists as monopositive, neutral and mononegative species, and the neutral species exists only in a narrow hydrogen ion concentration range.

Although the dissociation constants of sulfurous and selenious acids have been reported by many authors,[1] very few has been known about the dissociation of tellurous acid in acid aqueous solutions.[1,2] This may be due to the insoluble nature of tellurous acid in weakly acid aqueous solutions.

In the present paper, the authors have studied the liquid-liquid distribution behavior of sulfur(IV) at low concentration and that of selenium(IV) and tellurium(IV) at tracer concentration in acid perchlorate media at 25°C. From the distribution data given as a function of the hydrogen ion concentration, the acid dissociation constants of sulfurous, selenious and tellurous acids in 0.1 and 3 M perchlorate media were determined by a graphical method.

Statistical Treatment

The dioxide of sulfur, selenium and tellurium in an aqueous solution may be hydrated with unknown number of water molecules. Accordingly the noncharged acids should be described as the general form, $QO_2(H_2O)_m$. Here, m represents zero or any positive integer, while Q represents one of these elements. In the present study, however, they will be always denoted by H_2QO_3. Further it is assumed that only this neutral species can be extracted into the organic phase in a liquid-liquid distribution system.

The stepwise dissociation constants of these acids are described as;

$$K_{a_n}=[H_{2-n}QO_3^{-n}][H^+]/[H_{3-n}QO_3^{-(n-1)}] \quad (1)$$

The distribution constant of the neutral species is described as;

$$K_D=[H_2QO_3]_{org}/[H_2QO_3] \quad (2)$$

The net distribution ratio, D, may be described as;

$$D=[Q]_{org,total}/[Q]_{total}$$
$$=[H_2QO_3]_{org}/\sum[H_nQO_3^{n-2}] \quad (3)$$

In a system where only H_2QO_3 and HQO_3^- species exist, Eq. (3) can be written

$$D = K_D/(1 + Ka_1[H^+]^{-1}) \quad (4)$$

On the other hand, in a system where the three species $H_3QO_3^+$, H_2QO_3 and HQO_3^- are found, Eq. (3) is transformed into;

$$D = K_D/(Ka_0^{-1}[H^+] + 1 + Ka_1[H^+]^{-1}) \quad (5)$$

The equilibrium constants in Eq. (4) or (5) can be determined graphically by a curve-fitting

*1 A part of this work was presented to the International Conference on Solvent Extraction Chemistry, Göteborg, Sweden (1966), "Solvent Extraction Chemistry", p. 32, North-Holland (1967).

1) L. G. Sillén and A. E. Martell, "Stability Constants," The Chemical Society, London, spec. pub. 17 (1964).

2) W. A. Dutton and W. C. Copper, *Chem. Revs.*, **66**, 657 (1966).

method. As the details of the graphical treatments were given in the previous work,[3] only the final equations are given in this paper.

When the distribution ratio can be represented by Eq. (4), the log$D$ *vs.* $-\log[H^+]$ plot is fitted with the standard curve;

$$Y = \log(1 + v), \quad X = \log v \tag{6}$$

and when it is represented by Eq. (5), the log D *vs.* $-\log[H^+]$ plot is found to fit one of the following family of standard curves,

$$Y = \log(v^{-1} + p + v), \quad X = \log v \tag{7}$$

Experimental

Tracers. Selenium-75 was obtained from the Oak Ridge National Laboratory, U. S. A. as a hydrochloric acid solution. It was diluted in 0.1 M perchloric acid or a mixture of 0.1 M perchloric acid and 2.9 M sodium perchlorate and used as the stock tracer solution. Tellurium tracer (a mixture of various radioactive tellurium isotopes) was prepared as follows; tellurium powder (four nine grade) was irradiated with thermal neutrons in JRR-2 reactor at Japan Atomic Energy Research Institute, Tokai, Ibaragi. This was let stand about two weeks and dissolved in a hot 1 : 1 nitric acid. The solution was then shaken five times with 100% tributylphosphate in order to remove radioactive iodine[4] and washed with hexane. This aqueous solution was evaporated to dryness on a water bath and the residue was dissolved in 0.1 M perchloric acid or a mixture of 0.1 M perchloric acid and 2.9 M sodium perchlorate and stored as the stock tracer solution.

Reagents. All of the reagents were of analytical grade. Sodium perchlorate prepared from perchloric acid and sodium carbonate was recrystallized two times from water. Methylisobutyl carbinol was obtained from Tokyo Kasei Co. Trioctylphosphine oxide (TOPO) was obtained from Dijindo & Co. The methylisobutyl carbinol or 0.2 M TOPO hexane solution was washed with 0.1 M perchloric acid, water, 0.1 M sodium hydroxide solution and then several times with water respectively.

Procedures. All of the procedures were carried out in a thermostated room at 25 ± 0.5°C. Two liquid phases were equilibrated in a glass stoppered tube (volume 20 m*l*).

The Experiments for Sulfur(IV). Ten to twenty milligrams of sodium sulfite, various amounts of perchloric acid, sodium perchlorate solution and carbon tetrachloride were placed in the tubes. The two phases in the tubes were agitated vigorously with a mechanical shaker for 5 min and centrifuged. Two milliliter portion was pipetted from each phase and transferred into 120 m*l* Erlenmeyer flasks and the sulfur(IV) content was determined by iodometry.

The Experiments for Selenium(IV) and Tellurium(IV). One tenth milliliter portion of the tracer stock solution, various amounts of perchloric acid and sodium perchlorate solution and then the organic solution were placed in the tubes. The initial concentration of selenium in the aqueous phase was less than 10^{-6} M and that of tellurium was 1.0×10^{-4} M. In some experiments with tellurium(IV), a small amount of sodium sulfanilate or sodium acetate (initial concentration in the aqueous phase was 0.01 M) was added in order to buffer the aqueous phase. No buffer was added to the system containing selenium(IV). The two phases in the tubes containing selenium(IV) were agitated on a mechanical rotating framework usually for one week. The two phases containing tellurium(IV) were shaken 15 min by a mechanical shaker and were then centrifuged for 3 min at 2000 rpm. Two milliliter portion was pipetted from each phase and transferred into small test tubes. The γ-radioactivity of these samples was measured with a well-type (NaI) scintillation counter. Another small portion was also pipetted from the aqueous phase and the hydrogen ion concentration was determined potentiometrically by using a standard solution, 0.0100 M $HClO_4$ + 0.09 M $NaClO_4$ or 0.0100 M $HClO_4$ + 2.99 M $NaClO_4$ as the standard of $-\log[H^+] = 2.000$. A correction was made for the emf data by using a series of standard solutions when the aqueous phase contained more than 0.01 M hydrogen ion. The ionic media was 0.1 M (H, Na)ClO_4 or 3 M (H, Na)ClO_4 in all experiments. The initial volume of the aqueous phase was always 5.0 m*l* and that of the organic phase was 5.0, 5.0 and 3.0 m*l* respectively for the experiments with sulfur(IV), selenium(IV) and tellurium(IV). In some experiments with tellurium(IV), the tracer was first extracted into the organic phase by similar procedures as described above and then it was back extracted from this organic phase to a fresh aqueous solution and the distribution ratio was determined.

Results

Dependence of D on $-\log[H^+]$. Figures 1a and 2a give the distribution of sulfur(IV) between carbon tetrachloride and the aqueous phase whereas Figs. 1b and 2b give that of selenium(IV) between methylisobutyl carbinol and the aqueous phase as a function of the hydrogen ion concentration. In both cases it is seen that the plot has two asymptotes with a slope zero and minus one. The dependence of D on the $-\log[H^+]$ is explained by Eq. (4), that is, both of sulfurous and selenious acids exist as H_2QO_3 and HQO_3^- species in the aqueous phase of this $-\log[H^+]$ range. By the curve fitting with the standard curve given by Eq. (6), the distribution constant of the acids in the neutral form, K_D, and the dissociation constant, K_{a_1}, were determined as they are listed in Table 1.

Figures 1c and 2c give the distribution ratio of tellurium(IV) between hexane containing 0.2 M TOPO and the aqueous phase as a function of $-\log[H^+]$. No difference was observed between the results when the tracer initially added to the aqueous phase and those when the tracer was initially added to the organic phase. Figures 1c and 2c contain both kind of the results obtained by the extraction or by the back extraction. Except for the lowest $-\log[H^+]$ region in 0.1 M

3) D. Dyrssen and T. Sekine, *J. Inorg. Nucl. Chem.*, **26**, 981 (1964).

4) M. Inarida, *Nippon Kagaku Zasshi (J. Chem. Soc. Japan, Pure Chem. Sect.)*, **79**, 721 (1958).

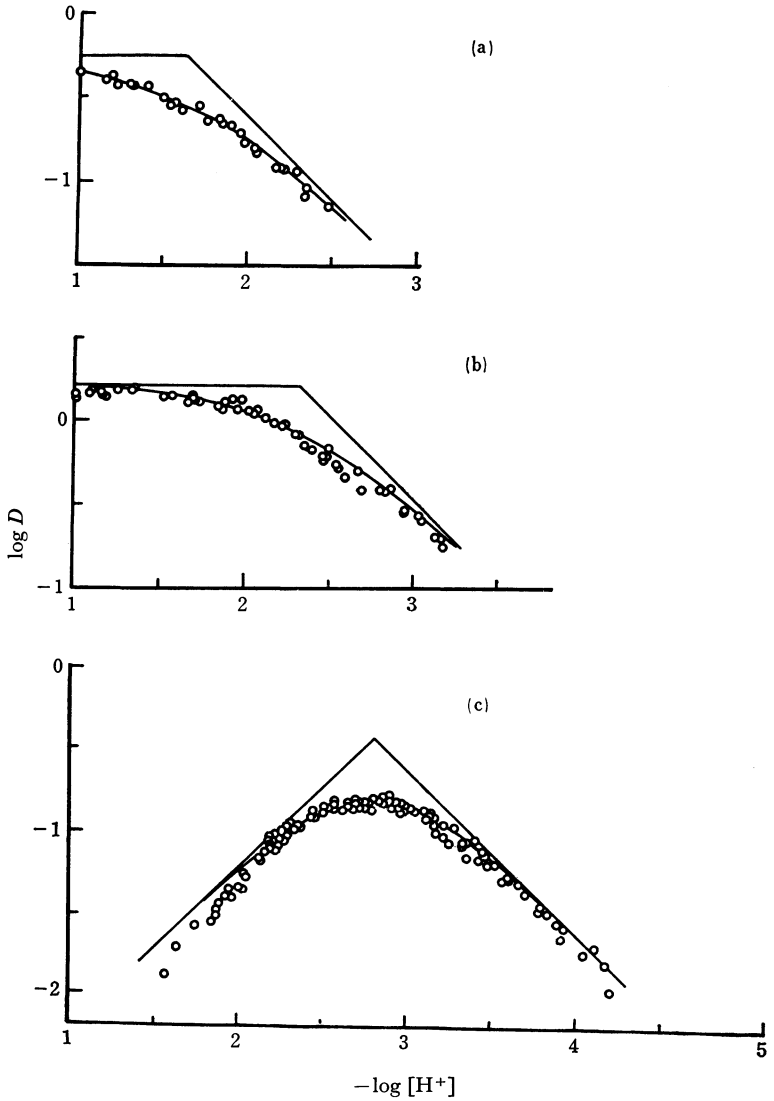

Fig. 1. Distribution of (a) sulfur(IV), (b) selenium(IV) and (c) tellurium(IV) in 0.1 M perchlorate media. The organic phases are described in Table 1. The two asymptotes and the distribution curve were obtained from the constants in Table 1.

TABLE 1. DISTRIBUTION AND DISSOCIATION CONSTANTS OF THE ACIDS AT 25°C (*cf.* Eqs. (1) and (2))

	Ionic media M, (H, Na)ClO_4	$\log K_D$	$-\log K_{a_0}$	$-\log K_{a_1}$
Sulfurous acid	0.1	−0.25	—	1.62
	3.0	−0.23	—	2.03
Selenious acid	0.1	0.21	—	2.33
	3.0	0.56	—	2.24
Tellurous acid	0.1	−0.08	3.16	2.46
	3.0	0.39	4.17	3.07

Organic phase sulfurous acid: carbon tetrachloride
Selenious acid: methylisobutyl carbinol
Tellurous acid: hexane containing 0.2 M trioctylphosphine oxide

perchlorate media, the plot has two asymptotes with a slope plus one and minus one and has a pronounced maximum between them and this indicates that the monopositive species, $H_3TeO_3^+$, is predominant in the lower $-\log[H^+]$ region while the mononegative species, $HTeO_3^-$, is predominant in the higher $-\log[H^+]$ region. Thus it is anticipated that the proportion of the neutral species, H_2TeO_3, is low all over the $-\log[H^+]$ region because if there were a region where the neutral species is predominant, an asymptote of a slope zero should be seen. The plot was fitted with one of the family of standard curves in Eq. (7) and the distribution constants and the dissociation constants for tellurous acid were determined from the parameters of the best-fit standard

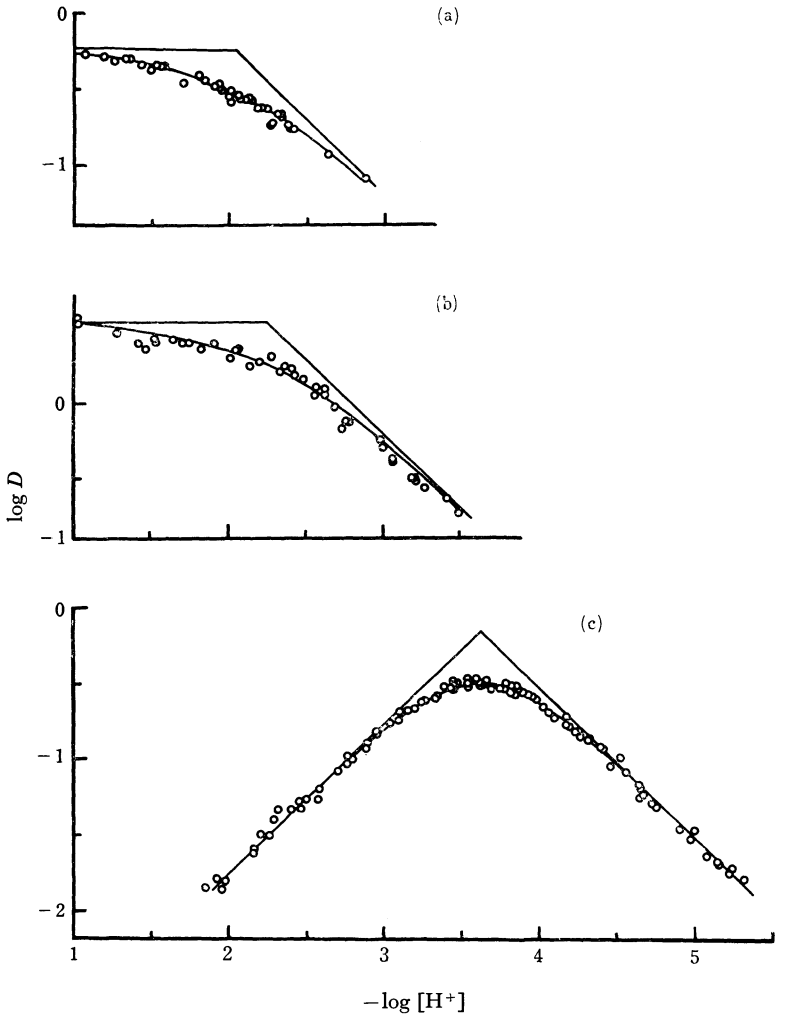

Fig. 2. Distribution of (a) sulfur(IV), (b) selenium(IV) and (c) tellurium(IV) in 3.0 M perchlorate media. The organic phases are described in Table 1. The two asymptotes and the distribution curve were obtained from the constants in Table 1.

curve as they are listed in Table 1.

Rate of the Extraction. The extraction of selenium(IV) in aqueous solutions into the methylisobutyl carbinol phase was a slow reaction. Figure 3 gives the increasing D with time when the tracer was initially added to the aqueous phase. The figure shows that the extraction rate is larger in the higher $-\log[H^+]$ range. It was observed that the rate of the back extraction of selenium-(IV) from the organic phase to the aqueous phase was very small. No appreciable amount was back extracted into the aqueous phase even after an agitation over one week. On the other hand, the rate of the extraction or the rate of the back extraction of sulfur(IV) and tellurium(IV) was much larger than that of selenium(IV) all over the $-\log[H^+]$ range studied. The distribution equilibrium of these species was attained by an agitation for five minutes.

Effect of the Concentration of the Acids. No change in the distribution ratio or the rate of the extraction of sulfur(IV) was observed when the amount of sodium sulfite initially added was changed from 5 to 20 mg. The distribution ratio of selenium(IV) decreased very much by adding 10^{-4} to 10^{-3} M selenium(IV) carrier to the aqueous phase. It was also observed that an organic solution of selenious acid at macro concentration was not stable. Namely, red precipitates which looked like elementary selenium were formed in methylisobutyl carbinol solutions containing macro amounts of selenious acid. Thus it was concluded that the distribution equilibrium of selenium(IV) is established only when the concentration is

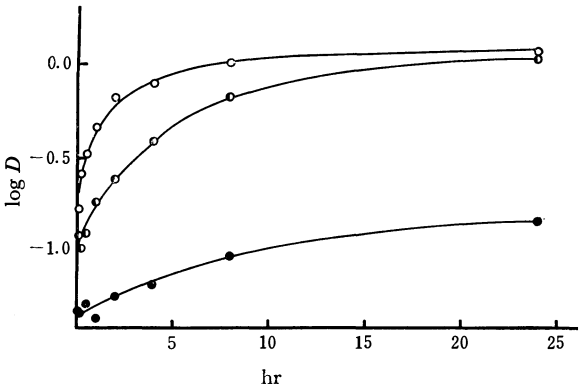

Fig. 3. Increase in the distribution ratio of selenium(IV) in 0.1 M perchlorate media at $-\log[H^+]$ 1.00 (open circles), 1.96 (half-closed circles) and 2.84 (closed cirles) into methylisobutylcarbinol as a function of time.

low and when the tracer is initially added to the aqueous phase. Practically no difference of the distribution ratio of tellurium(IV) was observed when the initial concentration in the aqueous phase was 5×10^{-5}, 1×10^{-4}, 2×10^{-4}, 3×10^{-4} and 4×10^{-4} M in 3 M perchlorate media at $-\log[H^+]$ 3.7 and 4.6. This seems to indicate that no polynuclear tellurium(IV) species are formed in the aqueous phase within the experimental accuracy.

Extraction by Using Other Solvents. The extraction of sulfur(IV) seems to be the lowest when non-polar solvents such as hexane or carbon tetrachloride are used. The distribution of sulfur(IV) increases with increasing the polarity of the solvent. The distribution of selenium(IV) between various organic solvents and an aqueous solution containing 0.1 M perchloric acid and 2.9 M sodium perchlorate was also studied. Most of the solvents like benzene, chloroform, carbon tetrachloride or hexane extracted selenium(IV) only poorly; the D value was 10^{-2} or less. Some polar solvents extracted selenium(IV) to some extent. For example, tributylphosphate or methyl isobutyl ketone extracted selenium(IV) with the D of arround 10^{-1}. Thus it was concluded that the extraction of selenium(IV) with methylisobutyl carbinol is exceptionally large among the solvents studied.

No organic solvent was found to extract tellurium(IV) to any appreciable amount without TOPO. Some experiments were carried out using different organic solvents as the diluent of TOPO. When the TOPO concentration was the same, the extraction of tellurium(IV) from an aqueous solution at a certain $-\log[H^+]$ into benzene or carbon tetrachloride was one third or one tenth of that into hexane and the extraction was negligibly small when chloroform was used as the diluent of TOPO.

Dependence of Tellurium(IV) Extraction on the TOPO Concentration. The dependence

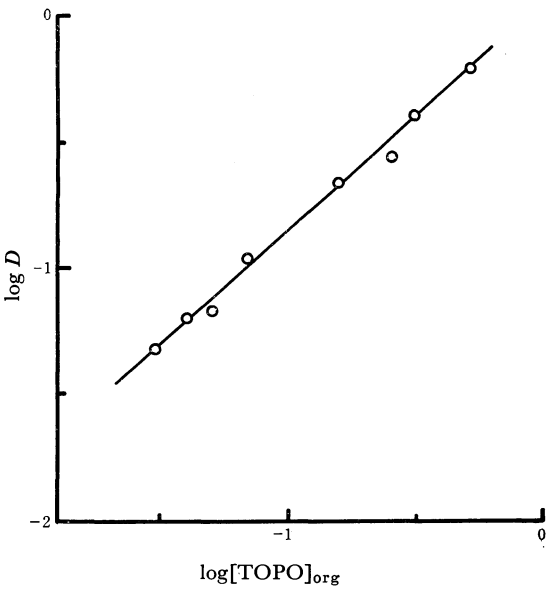

Fig. 4. Distribution of tellurium between hexane containing various amounts of TOPO and 3 M perchlorate media at $-\log[H^+]$ 3.9 as a function of TOPO concentration in the organic phase.

of tellurium(IV) extraction on the TOPO concentration in hexane has been studied. Figure 4 gives the plot log$D$ *vs.* $\log[TOPO]_{org}$ when the aqueous phase was 3 M perchlorate solution at $-\log[H^+]$ 3.9. The plot falls on a straight line with a slope plus one. This indicates that one molecule of TOPO combines with one molecule of H_2TeO_3 species in the organic phase. This can be described as follows;

$$H_2TeO_3+TOPO(org) \rightleftharpoons H_2TeO_3\cdot TOPO(org)$$

Reproducibility of the Results. The recovery of sulfur(IV) from the two phases was almost quantitative. The loss of sulfur(IV) from the two phases as sulfur dioxide after the phase separation was negligible. The recovery of selenium(IV) or tellurium(IV) from the both phases was also quantitative.

An addition of buffering agent such as sulfanilate or acetate to the aqueous phase increased the distribution ratio of selenium(IV) systematically. No effect of the buffer was, however, observed in the extraction of tellurium(IV) when the buffer concentration was less than 0.01 M.

It was necessary to purify the tellurium tracer by a preliminary extraction cycle in order to obtain reproducible results. No purification of the selenium tracer by the extraction method was carried out because the rate of the back extraction was very small. The results of selenium(IV) or of tellurium(IV) extraction seem to be affected by various factors such as the presence of dusts

more than many other solvent extraction experiments.

Discussion

It is difficult to compare the dissociation constants of these acids in the present study directly with the previous data which have been determined in ionic media at different concentration. Further, the dissociation constants were calculated by using the stoichiometric concentration ($-\log[H^+]$) in the present study while those have been calculated by using the activity of the hydrogen ion (pH) in most of the previous work.

The first dissociation constant of sulfurous acid, pK_{a_1}, in the previous papers are in the range 1.76 to 1.92[1] when the ionic concentration is low and the present pK_{a_1} values in 0.1 and 3 M perchlorate media is a little smaller and a little larger than those previous values.

The first dissociation constant of selenious acid, pK_{a_1}, in dilute ionic media in the previous papers[1] are in the range 2.46 to 2.62 which are a little higher than the present results in 0.1 and 3 M perchlorate media.

It was observed that the rate of the extraction of selenium(IV) is very small especially when some amounts of carrier was added, that the back extraction was not possible and that the quadrivalent state of selenium in methylisobutyl carbinol at macro concentrations was unstable. Still the distribution ratios of selenium(IV) at tracer concentration in Figs. 1b and 2b are well explained by Eq. (4) and the dissociation constants obtained look reasonable. Thus it may be concluded that selenium(IV) in such a distribution system is enough stable and the rate of the extraction is large enough to achieve the distribution equilibrium by an agitation for one week.

There were not many reports on the first dissociation constant of tellurous acid. This may be due to the insoluble nature of tellurous acid in aqueous solutions. The dissociation constants in the previous work were obtained from the analysis of the acid dependence of the solubility of tellurous acid.[1] The existence of the positive charged species of tellurous acid in acid aqueous solutions has been pointed out by some authors from the solubility data,[5-7] cation-exchange data[8] or by the dithizone extraction data.[9] However, none of them have determined the dissociation constant for the first proton in this positive charged species, $H_3TeO_3^+$ or $TeOOH^+$. Dutton and Cooper[2] recommended 3×10^{-3} as K_{a_1} ($=[HTeO_3^-]\,[H^+]/[H_2TeO_3]$) of tellurous acid in the recent review but they did not discuss the dissociation constant of this positive charged species. As is seen in Fig. 5, contribution of the non charged species to the whole tellurium concentration is small over all hydrogen ion concentration region (this corresponds to the fact that there is no region in Figs. 1c and 2c where the slope $d\log D/d\log[H^+]^{-1}$ is zero). It is indispensable to take the dissociation of the positive charged species into the account for the calculation of the K_{a_1} of tellurous acid. Thus although the value given by Blanc,[10] $K_{a_1}=2.7\times10^{-3}$, agrees with the present value in 0.1 M perchlorate media, $K_{a_1}=3.5\times10^{-3}$, still it is necessary to reexamine this previous value.

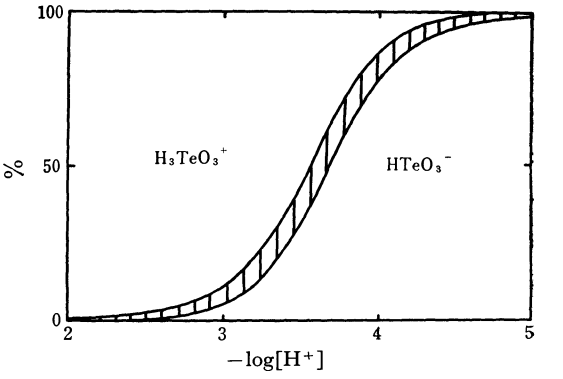

Fig. 5. Distribution of hydrolyzed species as a function of $-\log[H^+]$. The virtically liniated part represents the H_2TeO_3 species.

Figure 1c shows the plot deviates from the asymptote with a slope plus one. The same kind of deviation was also observed in the distribution of vanadium(V), HVO_3, between methylisobutyl carbinol and 0.5 M (H, Na)ClO_4[3] and Dyressen and Sekine explained this deviation as the change in K_D when sodium ions are replaced by hydrogen ions. The deviation in Fig. 1c seems to be also explained by this explanation, the fact that the deviation does not appear in the experiments in 3 M (H, Na)ClO_4 in Fig. 2c where the change in the cation is not large even in the lower $-\log[H^+]$ region may support the explanation.

Table 1 elucidates that the K_D value in 3 M perchlorate media is larger than that in 0.1 M media. This increase in the distribution constant, the salting-out effect, increases in the sequence sulfurous, selenious and tellurous acids. This sequence also agree with that of the basicity of the necessary extractant for these acid in aqueous solution.

The authors are grateful to Professor Nobufusa Saito, the head of the laboratory of Nuclear Chemistry, Institute of Physical and Chemical

5) J. Kasarnowsky, *Z. Phys. Chem.*, **109**, 287 (1924).
6) R. Shuhmann, *J. Am. Chem. Soc.*, **47**, 356 (1925).
7) E. Deltombe, N de Zoubor and M. Pourbaix, Cebelcor Rapp Tech., No 33 (1956).
8) Y. Sasaki, *Japan Analyst*, **4**, 637 (1955).
9) H. Mabuchi and I. Okada, This Bulletin, **38**, 1478 (1965).
10) E. Blanc, *J. Chim. Phys.*, **18**, 28 (1920).

Research where some part of this work was carried out. The authors are also grateful to Professor David Dyrssen of Göteborg University, Sweden and to Dr. Akira Yamasaki of the University of Tokyo for the helpful discussion and Messrs. Takeshi Hamada, Hiroyuki Okamoto and Ichiro Kobayashi of Science University of Tokyo for their experimental aids.

BULLETIN OF THE CHEMICAL SOCIETY OF JAPAN VOL. 41 7—17 (1968)

Condensation of Methylolmelamine

Kenji SATO*[1]

Tokyo Research Laboratory, Nippon Carbide Ind., Co., Inc., Ota-ku, Tokyo

(Received October 17, 1966)

The condensation of methylolmelamine in the range of *ca.* pH 8—1 was investigated. An aqueous-dimethylsulfoxide (DMSO) solution (*ca.* 1 : 2, vol. ratio) was mainly used as the solvent, because it was revealed that the condensate in the latter stage of the condensation is soluble in DMSO solvent, and also that in this solvent methylolmelamine scarcely decomposes into a lower methylolmelamine liberating formaldehyde; then, the condensation mechanism of that methylolmelamine whose composition corresponds approximately to di-, tri-, and hexa-methylolmelamine, was investigated, not only in the early stage but also in the latter stage. It was found that the condensation rates of di- and tri-methylolmelamines (low methylolmelamines) in the early stage show maxima at *ca.* [HCl]/[methylolmelamine]=0.5 (molar ratio), *i. e.*, at *ca.* pH=log$K$, where K is the equilibrium constant between the molecular form of the methylolmelamine and its conjugate acid, and that in hexa-methylolmelamine (high methylolmelamine) the above maximum appears at *ca.* [HCl]/[methylolmelamine]=0.5—1.0 (molar ratio). Also, the above maxima were found to shift toward smaller [HCl]/[methylolmelamine] (molar ratio) values as the condensation proceeded (the latter stage). From these results, a condensation mechanism was proposed for the early stage of the condensation.

Moldings and laminates are prepared by curing methylolmelamine with a composition corresponding approximately to di- or tri-methylolmelamine; an acid catalyst is usually added just prior to the cure because the condensation rate increases remarkably upon the addition of a small amount of an acid[1] (near the neutral range). However, there have been no reports on the condensation of methylolmelamines in a more strong acidic range. For this reason, the condensation of methylolmelamine in the range of *ca.* pH 8—1 was investigated in detail.

It has recently been revealed by the present author[2,3] that dimethylsulfoxide (DMSO) is a good solvent for melamine, methylolmelamine, and the condensate, and that neither the iodometric nor the sulfite method is affected by the presence of a small amount of DMSO.

Moreover, methylolmelamine was found by this study to decompose scarcely into a lower methylolmelamine liberating formaldehyde, in DMSO or even in an aqueous-DMSO solution (*ca.* 1 : 2, vol ratio); consequently, the condensation mechanism of a methylolmelamine with a different number of methylol groups can be investigated by the use of an aqueous-DMSO solution, even in the latter stage of the condensation.

There was another purpose of this study: In the reaction of melamine with formaldehyde, the hydroxymethylation and the condensation proceed almost simultaneously; also, the hydroxymethylation rate shows quite different values with the change in pH values.[4,5] Hence, a hydroxymethylation product prepared in the neutral range (see "Preparation of Methylolmelamine"), *i. e.*, methylolmelamine (monomer), was used as the starting substance for the study of the condensation mechanims.

The present report will summarize in detail our findings on the condensation rate *vs.* the acidity, some properties of the condensate, the rate of

*1 Present address: No. 3824, Uchiya Kasukabe, Saitamaken.

1) J. F. Blais, "Amino Resins," Reinhold Publishing Corporation, New York, Champan & Hall Ltd., London (1959), p. 20; K. Koeda, *Kogyo Kagaku Zassi (J. Chem. Soc. Japan, Ind. Chem. Sect.)*, **60**, 1567 (1957).

2) K. Sato, This Bulletin, **40**, 724 (1967).

3) K. Sato, *ibid.*, **40**, 1547 (1967).

4) M. Okano and Y. Ogata, *J. Am. Chem. Soc.*, **74**, 5728 (1952).

5) K. Sato, presented at the 16th Annual Meeting of the Chemical Society of Japan, Tokyo, April, 1963.

decrease in the methylol group *vs.* the acidity, and the change in pH value during the reactions: samples with compositions approximating di-, tri-, and hexa-methylolmelamine were used (for they have different numbers of methylol groups); among these items, we will emphasize the condensation rate *vs.* the acidity. These studies may imply a probable mechanism for the early stage of the condensation. In addition, methylolmelamine was investigated by differential thermal analysis and by thermobalance measurements.

Experimental

Materials. Pure commercial melamine was recrystallized from water. The formaldehyde was the best grade formaline (*ca.* 37 wt%). Pure commercial DMSO was purified by a known method[6]; bp 47°C/3 mmHg.

Preparation[7] of Methylolmelamine. Formaline was added to 126 g (1 mol) of melamine in the formaldehyde/melamine molar ratios of 2, 3, and 8, and the pH was adjusted to 8.0 with 0.1 N sodium hydroxide. This mixture was dissolved by heating it at 70°C, and then heated for an additional 5 min after dissolution; the solution thus formed was quickly poured into a large amount of an ice-cooled methanol and left standing overnight. The precipitate thus formed (methylolmelamine) was collected on a Büchner funnel, washed with methanol, and then dried *in vacuo* (50°C). These products were analyzed by the conventional method[7,8]; the results obtained show that the molar ratios of the combined formaldehyde to melamine are 1.98, 2.68, and 5.65, and that scarcely any condensation takes place in any case, *i. e.*, only the monomer of methylolmelamine is formed since the reaction time is short.

Thus, samples with compositions approximating di-, tri-, and hexa-methylolmelamine were prepared. Henceforth, these will be represented as M1.98F, M2.68F, and M5.65F respectively.

Reaction and Measurement. A definite amount of an aqueous-DMSO solution containing an appropriate amount of M1.98F was prepared. Next, definit amounts of an aqueous solution containing various amounts of hydrochloric acid were prepared. Each solution was then introduced into a thermostat regulated to the operating temperature, and the above solutions were mixed to react them. The initial pH values were controled by [HCl]/[M1.98F] (molar ratio). Aliquots were taken out at appropriate intervals of time and were analyzed by the iodometric and sulfite methods after neutralization, the pH values being measured by means of a glass electrode pH meter; the iodometry was carried out after adding DMSO[3] to the aliquot. The condensation rate, *i. e.*, the rate of the formation of the methylene linkage, was directly computed iodometrically. The results are shown graphically in Fig. 1(1), where the "methylene linkage"/"melamine rest (remainning) in methylolmelamine" molar ratio *vs.* the pH is indicated in connection with the reaction times. The rate of decrease in the methylol group was computed from the difference between the two values obtained by the iodometric and sulfite methods. The results are shown in Fig. 1(2), where the "methylol group"/"melamine rest in methylolmelamine" molar ratio *vs.* the pH is indicated in connection with the reaction times.

Experiments concerning M2.68F and M5.65F were carried out similarly; these results are shown in Figs. 2(1), (2)—4(1), (2).

For comparison, an investigation was also carried out with regard to M1.98F in an aqueous solution instead of an aqueous-DMSO solution. The results are shown in Figs. 5(1) and (2).

Differential Thermal Analysis and Thermobalance Measurement. The investigations were carried out using a 100 mg portions of M2.68F and M5.65F. The temperature was raised at the rate of 5°C/min for the differential thermal analysis, and at the rate of 3°C/min for the thermobalance measurement. For comparison, a 100 mg portion of melamine was also used in these investigations. The results of the differential thermal analysis are shown in Fig. 6, and those of the thermobalance measurement, in Fig. 7.

Results and Discussion

Solvent. Penta- or hexa-methylolmelamine (high methylolmelamine) is almost insoluble in water; therefore, water cannot be used as a solvent in this case. With regard to di- or tri-methylolmelamine (low methylolmelamines) also, water is not suitable as a solvent, because, although these substances are slightly soluble in water, they easily decompose, liberating formaldehyde to become lower methylolmelamines.

However, it became clear from this study that the decomposition of methylolmelamine is almost suppressed in DMSO, even in an aqueous-DMSO solution (*ca.* 1 : 2 vol ratio). For example, an aqueous solution containing 0.040 mol/*l* of M1.98F and of M2.68F were prepared at 50°C, and the formaldehyde thus liberated was determined immediately by the sulfite method. These results indicate that the former decomposes into M1.51F, and the latter, into M1.83F. Then, DMSO solutions containing 0.040 mol/*l* of M1.98F, M2.68F, and M5.65F were similarly tested using the sulfite method. As a result, each of the methylolmelamines was revealed to decompose very little, even after 50 hr (50°C); the same was almost true in the case of aqueous-DMSO solutions (*ca.* 1 : 2, vol ratio) of M1.98F, M2.68F, and M5.65F. The above results suggest a facility of solvation between DMSO and methylolmelamine; such solvation must be associated with the fact that DMSO is a polar solvent and that it dissolves a large amount of methylolmelamine; *e. g.*, the solubilities of M1.98F in water and DMSO are *ca.* 0.9 wt% and 56 wt%[3] respectively at 30°C.

Moreover, when an aqueous-DMSO solution (*ca.* 1 : 2 vol ratio) of methylolmelamine is used,

6) C. A. Kingsbury, *J. Org. Chem.*, **29**, 3262 (1964).
7) T. Kitagawa, *Kogyo Kagaku Zassi (J. Chem. Soc. Japan, Ind. Chem. Sect.)*, **53**, 181 (1950).
8) J. J. Levenson, *Ind. Eng. Chem. Anal. Ed.*, **12**, 332 (1940).

no precipitate appears, even in the latter stage of the condensation shown in Figs. 1(1)—4(1), because DMSO is a good solvent for the condensate. However, when an aqueous solution is used instead of the above solution, it soon becomes turbid; then a precipitate is deposited as the condensation proceeds. Therefore, the aliquot was taken out in this case after the solution had been agitated vigorously with a glass rod. Thus, the value obtained using an aqueous solution is not as accurate as that obtained using an aqueous-DMSO solution; in particular, the values of (c) and (d), which correspond to a reaction time of 3.5 hr, shown in Fig. 5 could not be obtained, because the aliquot could not be taken out because the precipitate was deposited at the bottom of the vessel.

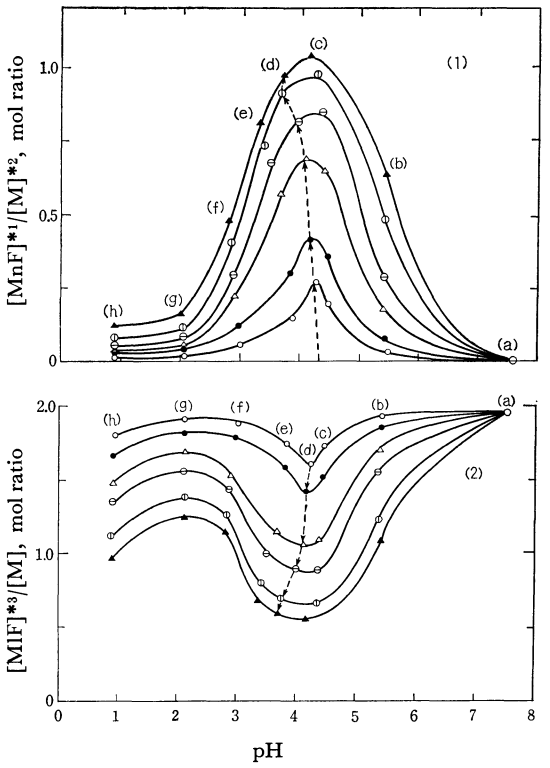

Fig. 1. The constituent change of di-methylolmelamine (Ml. 98F) *vs.* pH in DMSO-water mixed solution (*ca.* 2 : 1, vol ratio) at 50°C.
(1) Condensation rate *vs.* pH
(2) Decrease rate of methylol group concentration *vs.* pH
-○-: 0.25 -●-: 0.5 -△-: 1.0 -⊖-: 1.5
-◫-: 2.5 -▲-: 3.5 reaction time (hr)
(a): 0 (b): 0.10 (c): 0.40 (d): 0.50
(e): 0.70 (f): 1.00 (g): 1.80 (h): 11.00
[HCl]/[Ml. 98F] (mol ratio)
Initial concentration: [Ml. 98F]=0.0634 (mol/*l*)
*1 [MnF]: Methylene linkage
*2 [M]: Melamine rest in methylolmelamine
*3 [MlF]: Methylol group concentration

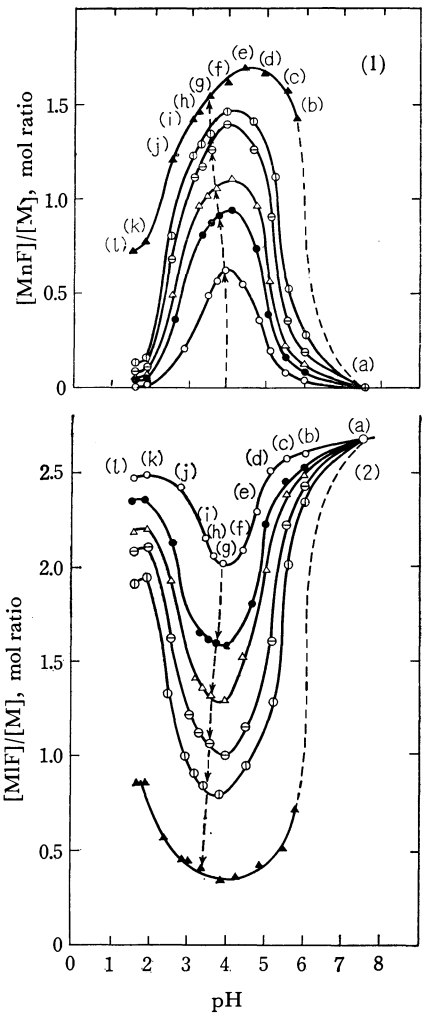

Fig. 2. The constituent change of tri-methylolmelamine (M2. 68F) *vs.* pH in DMSO-water mixed solution (*ca.* 2 : 1, vol ratio) at 45°C.
(1) Condensation rate *vs.* pH
(2) Decrease rate of methylol group concentration *vs.* pH
-○-: 0.5 -●-: 1.0 -△-: 1.5 -⊖-: 2.5
-◫-: 3.5 -▲-: 33.0 reaction time (hr)
(a): 0 (b): 0.03 (c): 0.05 (d): 0.10
(e): 0.20 (f): 0.40 (g): 0.50 (h): 0.60
(i): 0.70 (j): 1.00 (k): 2.00 (l): 3.00
[HCl]/[M2. 68F] (mol ratio)
Initial concentration: [M2. 68F]=0.0776 (mol/*l*)

Consequently, the advantage of using an aqueous-DMSO solution is that the condensation mechanism of methylolmelamine with different numbers of methylol groups can be investigated not only in the early stage but also in the latter stage.

Relation between the Condensation Rate and the Acidity. The results obtained are shown in Figs. 1(1), 2(1), 3(1), 4(1), and 5(1).

As is well known, the condensation rate of methylolmelamine increases as a solution becomes

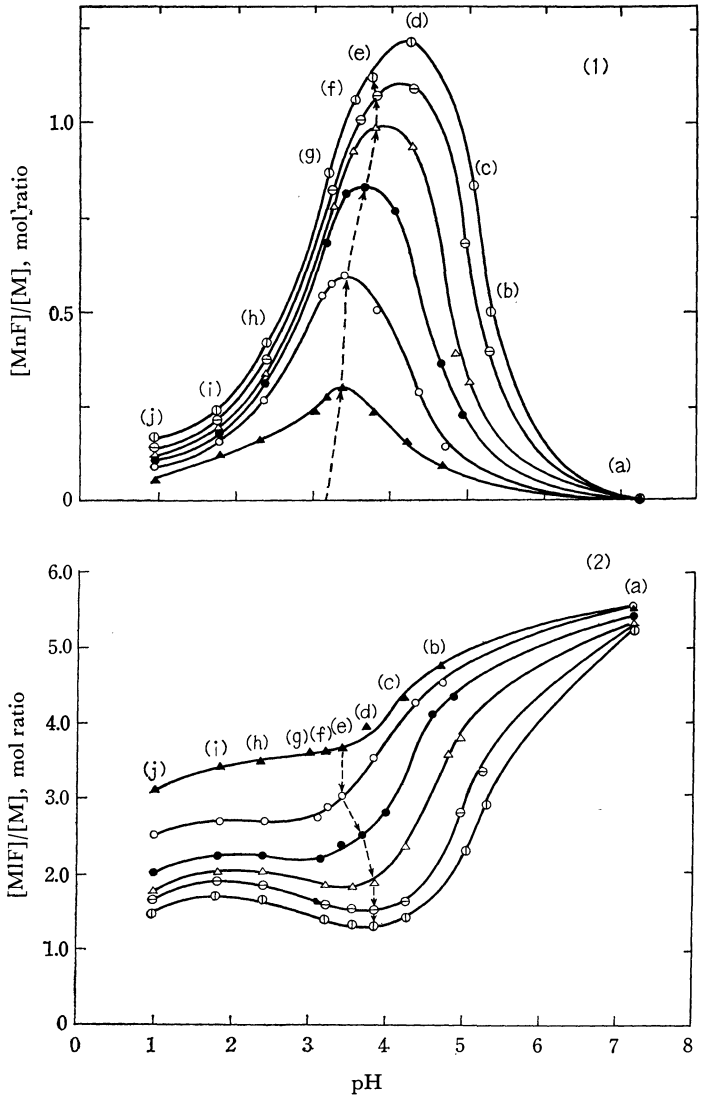

Fig. 3. The constituent change of hexa-methylolmelamine (M5.65F) *vs.* pH in DMSO-water mixed solution (*ca.* 3 : 1, vol ratio) at 65°C.
(1) Condensation rate *vs.* pH
(2) Decrease rate of methylol group concentration *vs.* pH
-▲-: 0.3 -○-: 0.5 -●-: 1.0 -△-: 1.5 -⊖-: 2.5 -◐-: 3.5 reaction time (hr)
(a): 0 (b): 0.05 (c): 0.10 (d): 0.35 (e): 0.50 (f): 0.70 (g): 1.00
(h): 3.00 (i): 10.00 (j): 50.00 [HCl]/[M5.65F] (mol ratio)
Initial concentration: [M5.65F]=0.0205 (mol/*l*)

more acidic (near the neutral range: *ca.* pH 8*[2]→ 7).[1] However, there have been no reports on the condensation in a range more acidic than this.

It may be found from the above figures that the condensation rates of Ml.98F, M2.68F, and M5.65F show a maximum value in each curve. For example, with regard to M1.98F and M2.68F, *i. e.*, low methylolmelamines, the maximum appears at *ca.* [HCl]/[M]=0.5 (molar ratio)*[3] in the early stage, where [M] represents the concentration of the melamine rest in the starting methylolmelamine, and [HCl], that of hydrochloric acid. When an aqueous solution was used

*[2] Since methylolmelamine is basic, the pH value of a solution containing methylolmelamine is somewhat larger than 7.0.

*[3] In an acidic region, DMSO may form its conjugate acid ($(CH_3)_2SO \rightarrow H^+$), but the additional proton would be remarkably small. In the presence of some hydrochloric acid, the pH value of an aqueous-DMSO solution is somewhat different from that of an aqueous solution. For this reason, the maximum has been discussed in terms of [HCl]/[M] (molar ratio).

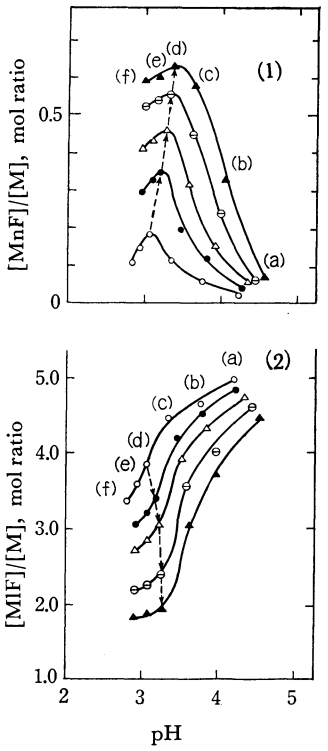

Fig. 4. The constituent change of hexa-methylolmelamine (M5. 65F) *vs.* pH in DMSO-water mixed solution (*ca.* 3 : 1, vol ratio) at 40°C.
(1) Condensation rate *vs.* pH
(2) Decrease rate of methylol group concentration *vs.* pH
-○-: 0.5 -●-: 1.0 -△-: 1.5 -⊖-: 2.5
-▲-: 3.5 reaction time (hr)
(a): 0.10 (b): 0.30 (c): 0.50 (d): 1.00
(e): 1.40 (f): 1.80 [HCl]/[M5. 65F] (mol ratio)
Initial concentration: [M5. 65F]=0.0205 (mol/*l*)

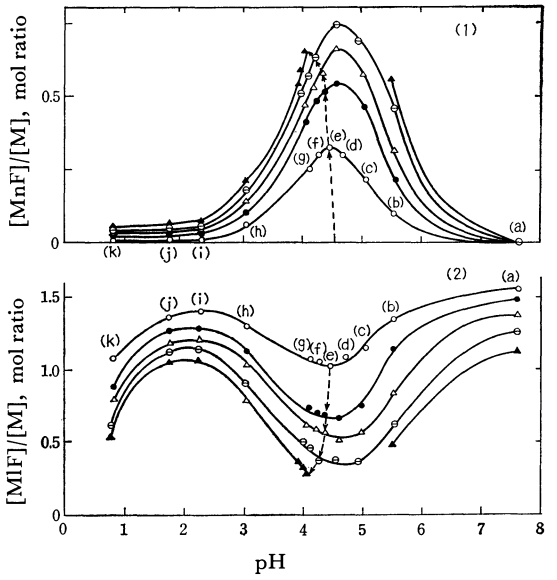

Fig. 5. The constituent change of di-methylolmelamine (Ml. 98F) *vs.* pH in aqueous solution at 50°C.
(1) Condensation rate *vs.* pH
(2) Decrease rate of methylol group concentration *vs.* pH
-○-: 0.5 -●-: 1.0 -△-: 1.5 -⊖-: 2.5
-▲-: 3.5 reaction time (hr)
(a): 0 (b): 0.10 (c): 0.30 (d): 0.40
(e): 0.50 (f): 0.60 (g): 0.70 (h): 1.00
(i): 1.50 (j): 2.50 (k): 25.00
[HCl]/[Ml. 98F] (mol ratio)
Initial concentration: [Ml. 98F]=0.0312 (mol/*l*)

instead of an aqueous-DMSO solution, as has been stated above, no such accurate data can be obtained as in the case of an aqueous-DMSO solution, but the maximum appears at *ca.* [HCl]/[M]=0.5 (molar ratio) (Fig. 5(1)).

Furthermore, the maximum was found to shift toward smaller [HCl]/[M] (molar ratio) values as the condensation proceeds (the latter stage); *e. g.*, as is clear in Fig. 2(1), the maximum shifts from 0.5 to 0.4, and then to 0.2 (molar ratio). The above fact may be explained from the consideration that the melamine rest in the condensate is less basic than that of the starting methylolmelamine (see "Change in pH Value during Reaction" and "Condensation Mechanism for the Early Stage").

Next, the effect of the concentration of methylolmelamine and that of the temperature upon the maximum were studied. Investigations were carried out by adjusting the concentrations of M2.68F to twice the starting concentration shwon in Fig. 2, and also by adjusting the reaction temperature to 60°C and 40°C from the 45°C shown in Fig. 2. These results show that maxima in the early stage appear at *ca.* [HCl]/[M]=0.5 (molar ratio) in all cases, regardless of the concentration of methylolmelamine and the reaction temperature.

High methylolmelamines differ from low methylolmelamines in the following behavior. In M5.65 F, a high methylolmelamine, maxima in the early stage appear at *ca.* [HCl]/[M]=0.5 and 1.0 (mol ratio) at 65°C and 45°C respectively, as Figs. 3(1) and 4(1) show. The maximum of a high methylolmelamine, thus, shifts toward smaller [HCl]/[M] (molar ratio) values, and it approaches that of a low methylolmelamine, *i.e.*, [HCl]/[M]=0.5 (molar ratio), with an elevation in temperature. These results will be discussed below in connection with the condensation mechanism (see "Condensation Mechanism for the Early Stage").

Some Properties of the Condensate. According to Eqs. (3) and (4) (*cf.* "Condensation Mechanism for the Early Stage"), the "methylene linkage"/"melamine rest in methylolmelamine" ratio of the dimer is 0.5 (molar ratio). Kohler

et al.[9] stated that the above value of the molded product of the methylolmelamine prepared under the usual molding conditions is *ca.* 1.2 (molar ratio) and that it does not dissolve in solvents. From Figs. 1 (1) and 2 (1), it was found that the value of the condensate in the latter stage is *ca.* 1.2—1.6 (molar ratio), and also that this condensate is easily soluble in an aqueous-DMSO solution.

Thus, the above value of the condensate in the latter stage is almost the same or somewhat larger than that of the molded product; also, melamine resin is one of the thermosetting resins.

Therefore, this condensate (in the latter stage) may be predicted to show a three-dimensional structure with a remarkably large molecular weight, and to be insoluble in any solvent. However, the molecular weight of this condensate has been estimated by this research to be not as large as had been predicted, since the above condensate is soluble in an aqueous-DMSO solution.

Relation between the Rate of Decrease in the Methylol Groups in Methylolmelamine and the Acidity. The results obtained are shown in Figs. 1(2), 2(2), 3(2), 4(2), and 5(2).

First, it may be inferred that the methylol group is decreased by the formation of the methylene linkage and by the liberation of formaldehyde through the decomposition, which is mainly due to an acid.

Concerning M1.98F and M2.68F, Figs. 1(1), (2) and 2(1), (2) show that the maximum in the rate of decrease in the methylol group, *i. e.*, the minimum in the methylol group (present) *vs.* the pH, almost coincides with the maximum in the condensation rate; that is to say, it appears at *ca.* [HCl]/[M]=0.5 (molar ratio) in the early stage and shifts toward smaller [HCl]/[M] values as the condensation proceeds. Furthermore, regarding the early stage, from the above figures, it can be seen that the decrease in the methylol group is roughly the same as the increase in the methylene linkage formed in the range of *ca.* pH 7—3; therefore, the methylol group has been confirmed to be consumed mainly by the condensation within this pH range; however, within *ca.* pH 1—2, the decrease in the methylol group is considerably larger than the increase in the methylene linkage; this confirms that the methylol group is decreased by the decomposition due to a large amount of acid in this pH range.

On the other hand, as for M5.65F, the above mentioned minimum can scarcely be observed, and the decrease in the methylol group in the early stage is remarkably larger than the increase in the methylene linkage, even in a weak acidic range (Figs. 3(1), (2) and 4(1), (2)); this fact suggests that high methylolmelamines are unstable and easily liberate formaldehyde, even in the presence of a small amount of an acid.

Change in pH Value during Reaction. With regard to M1.98F and M2.68F, the pH values of the solution gradually shift toward smaller pH values as the reactions proceed, as Figs. 1(1), 2 (1) and 5(1) show, particularly at [HCl]/[M]= 0.5 (molar ratio). Thus, the change in pH value is observed, in particular, when the condensation rate is large. The melamine rest in the condensate is surely less basic than that of methylolmelamine; this effect accounts for the above fact.

On the contrary, with regard to M5.65F, the pH values were found to shift toward larger pH values (Figs. 3(1) and 4(1)). This fact may be explained as follows: During the course of reactions, high methylolmelamines easily decompose into lower methylolmelamines, liberating formaldehyde, as has been described above. Hence, the basicity of the solution increases as the decomposition proceeds, because the basicity increases in the order of M1.98F>M2.68F≫M5.65F (based on their neutralization curves). The observed change in the pH value is mainly affected by the above effect, only slightly by the opposing effect of the decrease in the basicity as the result of the formation of the condensate.

Differential Thermal Analysis and Thermobalance Measurement. As is shown in Fig. 6 (differential thermal analysis), the endothermic peaks, somewhat flattened, were observed at *ca.* 150°C in M2.68F and M5.65F.

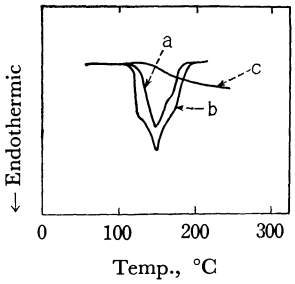

Fig. 6. Investigations by differential thermal analysis.
a: M2. 68F b: M5. 65F c: Melamine

General molding in methylolmelamine, irrespective of the type of molding, is carried out at *ca.* 150°C[10] in commercial practice; hence, the condensation must proceed considerably at this temperature. Since the temperature of endothermic peak closely coincides with that of the molding, this peak may be explicable from the considerations that the condensation proceeds upon

9) A. Gam, G. Widmer and W. Fisch, *Helv. Chem. Acta*, **24**, 302E (1941); R. Kohler, *Kolloid. Z.*, **103**, No. 2, 138 (1943); H. P. Wohnsiedler, *Ind. Eng. Chem.*, **45**, 2307 (1953).

10) J. F. Blais, "Amino Resins," Reinhold Publishing Corporation, New York, Champan & Hall Ltd., London (1959), p. 77.

the discharge of a large amount of water (according to Eqs. (3) and (4), 1 mol of water is discharged for 1 mol of each methylene linkage), and that the heat of vaporization of water is large.*4

Next, Fig. 7 (thermobalance) shows the reduction in the weight of methylolmelamine that was observed during the rise in the temperature. This reduction may result from the liberation of formaldehyde by the thermal decomposition of methylolmelamine, and that of water by the condensation of methylolmelamine. Also, a more striking reduction in weight was observed in M5.65F than in M2.68F. This result may be explained from the thermal unstability of M5.65F, which easily liberates formaldehyde.

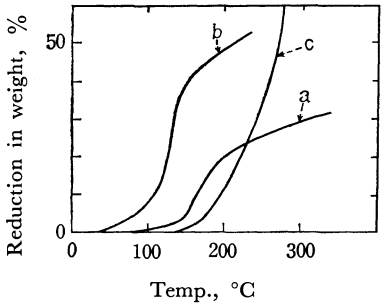

Fig. 7. Investigations by thermo-balance.
a: M2.68F b: M5.65F c: Melamine

Besides, melamine sublimes[12] easily. The observed endothermic behavior (Fig. 6(c)) and reduction in weight (Fig. 7(c)) may be due to this sublimation.

Condensation Mechanism for the Early Stage. Since the curve showing the condensation rate *vs.* the acidity for methylolmelamine resembles that of an acid-catalyzed semicarbazone formation,[13] and since a C–N linkage is formed in both reactions, a similarity in mechanism may be suggested.

Methylolmelamine and methylolurea are both amino resins. The condensation rate of methylolurea[14] increases with an increase in the acidity, but, contrarily, that of methylolmelamine passes through a maximum. This different behavior in the condensation rate *vs.* the acidity suggests a difference in their condensation mechanisms; it may be explained in brief in terms of the large difference in their basicities.

Let us discuss the condensation mechanisms of low and high methylolmelamines for the early stage.

(1) Di- and Tri-methylolmelamine. Although low methylolmelamines such as di- and trimethylolmelamine are slightly less basic[15,16] (mono-acidic)[17] than melamine, these low methylolmelamines, unlike methylolurea, have sufficient basicity to combine with an equivalent amount of hydrochloric acid to form the conjugate acid. The relation between the molecular form of methylolmelamine, MCH_2OH, and its conjugate acid, $\overset{+}{H}MCH_2OH$, is shown in Eq. (1):

$$MCH_2OH + H_3O^+ \overset{K}{\rightleftarrows} \overset{+}{H}MCH_2OH + H_2O \quad (1)$$

$$K = \frac{[\overset{+}{H}MCH_2OH]}{[MCH_2OH][H_3O^+]} \quad (1')$$

The structure of the conjugate acid has been demonstrated by Dixon *et al.*[15-18] on the basis of the ultraviolet absorption spectra (Eqs. (1a) and (1b)):

Di-methylolmelamine:

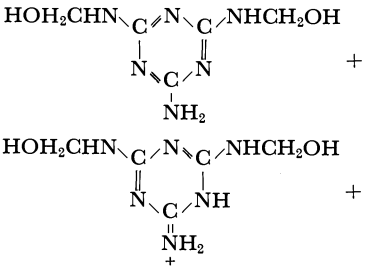

(1a)

Tri-methylolmelamine:

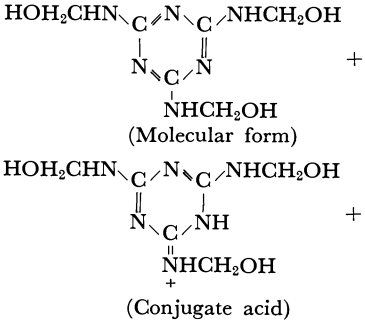

(1b)

(Conjugate acid)

Therefore, the condensation takes place between them, and Eq. (2) may be derived:

*4 In the case of hexa-methylolmelamine-hexamethylether,[11] scarcely no endothermic peak was observed at *ca.* 150°C (or even in the range of *ca.* 30—200°C). This result may be due to the fact that this condensation occurs with the liberation of methanol, as is well known, and that the heat of the vaporization of methanol is markedly small.

11) R. N. Housekeeper, U. S. Pat. 2998411 (1961).
12) "Beilstein Handbuch der Organishen Chemie," XXVI (1937), p. 246.
13) B. M. Anderson and W. P. Jenks, *J. Am. Chem. Soc.*, **82**, 1773 (1960); R. Wolfenden and W. P. Jenks, *ibid.*, **83**, 2763 (1961); I. D. Fiarman and J. D. Gettler, *ibid.*, **84**, 961 (1962).
14) S. Takahashi, *Kobunshi Kagaku (Chem. High Polymers Japan)*, **9**, 50 (1952) and others.
15) J. K. Dixon, N. T. Woodberry and G. W. Costa, *J. Am. Chem. Soc.*, **69**, 599 (1947).
16) G. W. Costa, R. C. Hirt and D. J. Salley, *J. Chem. Phys.*, **18**, 434 (1950).
17) R. C. Hirt and R. G. Schmitt, *Spectrochem. Acta*, **12**, 127 (1958).
18) E. N. Boitsov, *Opt. Spectry.*, **9**, 26 (1960); *ibid.*, **12**, 108 (1962); *ibid.*, **13**, 151 (1962).

	MCH_2OH	$\overset{+}{H}MCH_2OH$
MCH_2OH	k_1	k_2
$\overset{+}{H}MCH_2OH$	k_2	k_3

$$\text{Rate} = k_1[MCH_2OH]^2 \quad \text{(molecular form, molecular form)} \quad \text{1st term}$$
$$+ k_2[MCH_2OH][\overset{+}{H}MCH_2OH] \quad \text{(molecular form, conjugate acid)} \quad \text{2nd term} \qquad (2)$$
$$+ k_3[\overset{+}{H}MCH_2OH]^2 \quad \text{(conjugate acid, conjugate acid)} \quad \text{3rd term}$$

where k_1, k_2, and k_3 are the respective rate constants of the elementary reaction in Eq. (2).

The condensation without an acid is evidently a reaction between the molecular forms themselves, *i. e.*, the first term of Eq. (2). This reaction is markedly slow because the condensation without an acid does not proceed even after a long time has elapsed, as is clear from (a) of Figs. 1(1), 2(1) and 5(1).

The condensation may occur by an attack of the electrophilic carbon of the amino-methylol group on the nitrogen of the amino group or on that of the amino-methylol group of methylolmelamine. In view of this, the carbon of the amino-methylol group of the conjugate acid is markedly more electrophilic, that is to say, conspicuously more reactive, than that of the molecular form of methylolmelamine; also, the amount of the conjugate acid (reactive) increases with an increase in the acidity. The enhancement of the rate with an increase in the acidity in the range of [HCl]/[M]< 0.5 (molar ratio) can be explained by this mechanism. This is expressed in Eqs. (3) and (4):

$$\overset{+}{H}\text{-MNHCH}_2\text{OH} + H_2NM \rightarrow \overset{+}{H}\text{-MNHCH}_2\text{NHM} + H_2O \qquad (3)$$

(the formation of the *methylene bisamide linkage*)

$$\overset{+}{H}\text{-MNHCH}_2\text{OH} + \text{HN}\overset{\text{CH}_2\text{OH}}{\overset{|}{\text{M}}} \rightarrow \overset{+}{H}\text{-MNHCH}_2\text{N}\overset{\text{CH}_2\text{OH}}{\overset{|}{\text{M}}} + H_2O \qquad (4)$$

(the formation of the *methylol methylene bisamide linkage*)

However, this effect is counteracted by the increasing removal of the molecular forms of methylolmelamines by the formation of the conjugate acid in the range of [HCl]/[M]>0.5 (molar ratio). The result of these opposing factors obviously is that a maximum appears at *ca.* [HCl]/[M]=0.5 (molar ratio); this 0.5 (molar ratio) value corresponds to pH=log$K$*5 where K is an equilibrium constant between the molecular form of methylolmelamine and its conjugate acid (see Eq. (1')).

In other words, the maximum can be explained from Eq. (2) as follows: According to the above electronic theory, k_2 is markedly larger than k_1 or k_3. (k_1 shows the smallest value because the smallest condensation rate is observed without an acid, as is shown in Fig. 1(1), 2(1) and 5(1).) Thus, k_2 is larger than k_1, and k_3 is smaller than k_2, thus accounting for the increase in the rate in the range of [HCl]/[M]<0.5 (molar ratio), and the decrease in the rate in the range of [HCl]/[M]> 0.5 (molar ratio). Also, the $[MCH_2OH][\overset{+}{H}MCH_2OH]$ (concentration product) of the second term in Eq. (2) shows a maximum at $[MCH_2OH]=[\overset{+}{H}MCH_2OH]$, as is clear from Eq. (1').*6 Consequently, a maximum in the rate appears at this point. In view of this, it may be considered that the main reaction in the condensation among the three reactions of Eq. (2) in the range of 0< [HCl]/[M]<1.0 (molar ratio) is that between the molecular form of methylolmelamine and its conjugate acid (the second term).

In this case, methylolmelamine is converted into its conjugate acid by the addition of the proton in an acidic region, as has been stated above (*cf.* Eqs. (1), (1a) and (1b)); hence, the proton is scarcely added to methylolmelamine to form carbonium ion (Eq. (5)). Therefore, the carbonium ion, $\overset{+}{M}CH_2$, must play a minor part in the condensation, unlike methylolurea.*7 On the assumptions that the carbonium ion is rapidly formed, *i. e.*, that the

*5 As is well known, the K (or the base constant of methylolmelamine, K_b) is obtained from the pH value of the solution at [HCl]/[methylolmelamine]= 0.5 (molar ratio). The pK_b[15] values of M1.99 F and M3.00F are 9.5 and 10.1 (25°C) respectively; hence, the K is amount to $10^{4.5}$ and $10^{3.9}$ respectively. Therefore, the pH value of the observed maximum agreed fairly well with that computed from the pK_b of the literature.

*6 From Eq. (1'), the following relation can be derived between pH and $\overset{+}{H}MCH_2OH$ (or MCH_2OH):

$$\text{pH} = \log K - \log \frac{\alpha}{1-\alpha}$$

($[\overset{+}{H}MCH_2OH] = \alpha$, $[MCH_2OH]=1-\alpha$)

*7 For example, the condensation of mono-methylolurea in an acidic range[19] is as follows:

$$H_2NCONHCH_2OH + H_3O^+ \rightleftarrows H_2NCONHCH_2\overset{+}{O}H_2 + H_2O \rightleftarrows H_2NCONH\overset{+}{C}H_2 + 2H_2O$$
$$H_2NCONH\overset{+}{C}H_2 + H_2NCONHCH_2OH \rightarrow H_2NCONHCH_2NHCONHCH_2OH + H^+$$

19) G. Smeth, *J. Poly. Sci.*, **8**, 371 (1952); L. E. Smythe, *J. Am. Chem. Soc.*, **75**, 574 (1953) and others.

reaction of Eq. (5) is fast, and that the succeeding reaction of the carbonium ion with the molecular form of methylolmelamine (Eq. (6)) is the rate-determining step, the observed maximum may be explained on the basis of this mechanism because the carbonium ion is proportional to the conjugated acid formed (Eq. (1)) at the same pH values, as is clear from the relationship between Eqs. (1) and (5):

$$MCH_2OH + H_3O^+ \rightleftarrows MCH_2\overset{+}{O}H_2 + H_2O \rightleftarrows M\overset{+}{C}H_2 + 2H_2O \quad (5)$$

$$M\overset{+}{C}H_2 + MCH_2OH \rightarrow M\overset{+}{C}H_2MCH_2OH \quad (6)$$

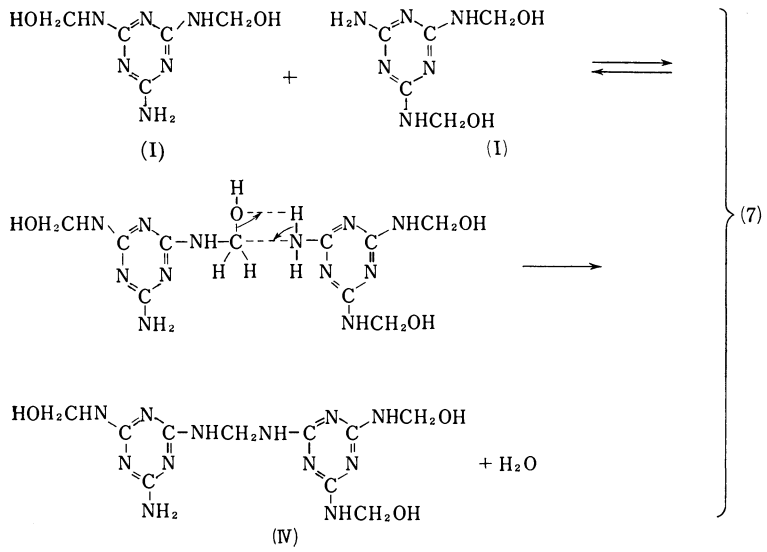

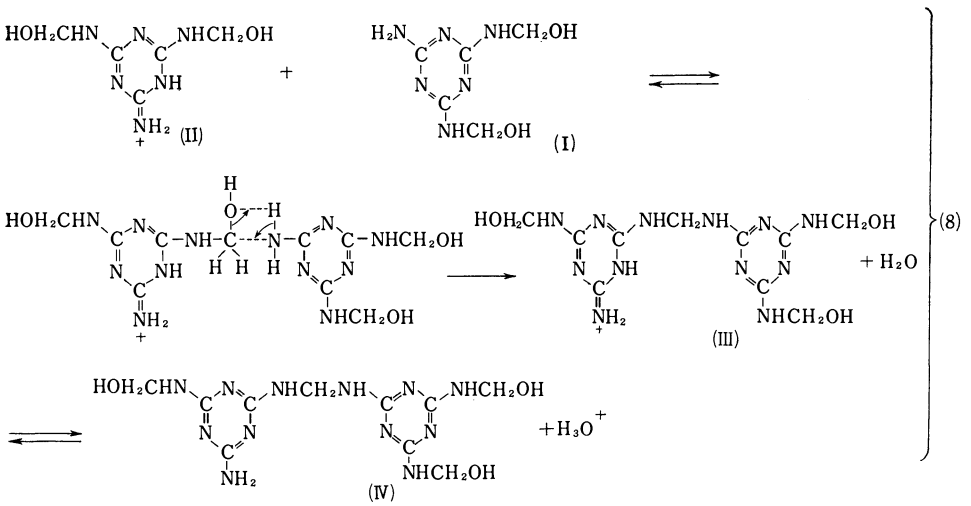

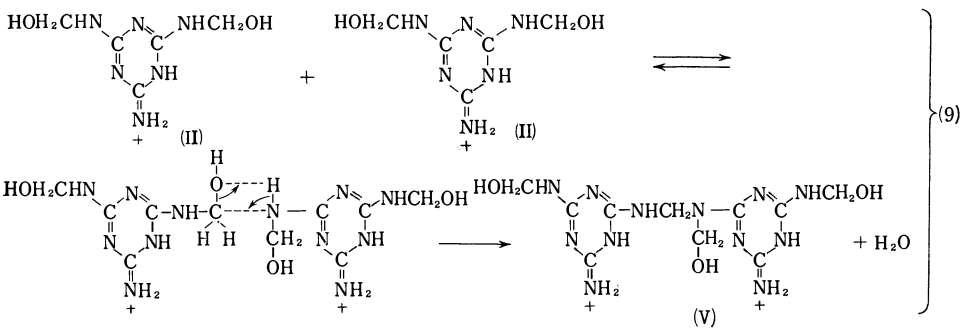

However, it is not clear whether or not these assumptions are reasonable. On the other hand, *if the conjugate acid itself reacts as an active species,* the observed maximum can readily be accounted for without any assumption, as has been indicated above.

Furthermore, the main reaction for the condensation among the three reactions of Eq. (2) in the range of [HCl]/[M]>1.0 (molar ratio) may be considered to be that between the conjugate acids of methylolmelamine themselves, *i. e.,* the third term of Eq. (2), because the concentration of the molecular form of methylolmelamine is markedly small (methylolmelamine turns almost completely into its conjugate acid) and the observed rate (Figs. 1(1), 2(1) and 5(1)) is considerably larger than that of a reaction between the molecular form of methylolmelamine and its conjugate acid, both concentrations being computed from the base constant[15] of methylolmelamine. (That is, if the main reaction in this range is the second term of Eq. (2), the rate must be considerably smaller than the observed one; the same is true for the first term of Eq. (2). Consequently, the main reaction in this range is neither the first term nor the second term of Eq. (2).)

Previously[20] it has been speculated that the condensation of methylolmelamine in such a strong acidic range takes place between the conjugate acids themselves; but there has been no experimental evidence for this. Nevertheless, the present findings may support this speculation. In a strongly acidic range, reactions between conjugate acids themselves have often been reported.[21]

Next, in view of the above, let us propose some structural mechanisms of the reaction between the molecular forms (I) themselves, the conjugate acid (II) and the molecular form, and the conjugate acids themselves to form the dimer in the early stage. Those mechanisms are illustrated in relation to di-methylolmelamine in Eqs. (7), (8), and (9) respectively.

In Eq. (8), with the formation of the dimer with the conjugate acid form (III), this dimer converts into its molecular form (IV: triazine with the conjugate double bond) with the release of the proton, because the melamine rest of the dimer is less basic than that of the starting methylolmelamine; this probably takes place to a major extent with the molecular form of methylolmelamine and its coexisting conjugate acid (0<[HCl]/[M]<1.0 (molar ratio)). Hence, the proton thus released combines with ane quvalent amount of the molecular form of methylolmelamine to form its conjugate acid (reactive). The fact that the maximum shifts toward smaller [HCl]/[M] values as the condensation proceeds is thus obviously accounted for. Also, in the case of methylolmelamine, small changes in the acidity have a greater effect on the condensation rate than in the case of methylolurea (near the neutral region)[22]; this fact, which is well known from experience, may be explained by this mechanism.

With the further growth of the condensate, additional protons are released as the basicity decreases, so that in the case of the trimer a smaller proportion would exist in the charged form, *i. e.,* in the conjugate acid form, than in that of the dimer. (In Eq. (7), the release of the proton does not take place.)

On the other hand, the reaction of Eq. (9) takes place to a major extent in the range of [HCl]/[M]>1.0 (molar ratio), as has been stated above; hence, more hydrochloric acid than methylolmelamine is present in this range. Therefore, the release of the proton in the dimer with the conjugate acid form (V) seems to be markedly smaller than that in the reaction of Eq. (8) in this range. However, since the melamine rest of the condensate in the latter stage is markedly less basic, this condensate may easily release the proton more than in the case of the dimer.

(2) Hexa-methylolmelamine. Hexa-methylolmelamine has the terminal group $-(CH_2OH)_2$. Hence, it is assumed that a dimethylene ether linkage, $-CH_2OCH_2-$, is formed with the liberation of water, and then this linkage, completely or partially or not all, is converted into a methylene linkage with the liberating formaldehyde during the course of the condensation. This is shown in Eq. (10):

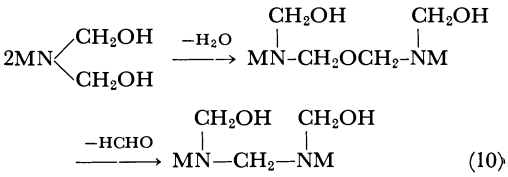

(10)

The reaction of Eq. (10) may play a minor part in the condensation under the conditions of Figs. (3) and (4), because no dimethylene ether linkage could be found by the conventional analytical method[23] during the course of the reactions; what is more, when the rate of the formation of the methylene linkage of M2.68F was compared with that of M5.65F under the same conditions (The investigation was carried out in the medium of an aqueous-DMSO solution without an acid.), the

20) H. P. Wohnsiedler, *Ind. Eng. Chem.,* **44**, 2679 (1952); J. F. Blais, "Amino Resins," Reinhold Publishing Corporation, New York, Champan & Hall Ltd., London (1959), p. 21.
21) E. S. Gould, "Mechanism and Structure in Organic Chemistry," Henry Hold and Company, Inc., New York (1959), p. 432 and others.
22) J. F. Blais, "Amino Resins," Reinhold Publishing Corporation, New York, Champan & Hall Ltd., London (1959), p. 20.
23) K. Tanimoto, M. Nemoto and T. Akita, *Kobunshi Kagaku (Chem. High Polymers Japan)*, **13**, 288 (1956).

rate of M5.65F was confirmed to be negligibly smaller than that of M2.68F.

Contrarily, in the polycondensation reaction of melamine-formaldehyde, Gam *et al.*[24] have attached particular importance to the dimethylene ether linkage and have assigned a minor role to the methylene linkage as a condensate—forming linkage. However, as has been demonstrated above, the reaction forming a dimethylene ether linkage is slow; this linkage would be formed if the temperature were higher and the solution more concentrated than in the present experiments.

From this evidence, the condensation mechanism of hexa-methylolmelamine may be considered to be that hexa-methylolmelamine first decomposes into a lower methylolmelamine such as tri- or tetra-methylolmelamine in the presence of an acid, and that then the condensation proceeds by the same mechanism as in the case of a low methylolmelamine. The observed results can be explained by this mechanism. The decomposition of hexa-methylolmelamine at a high temperature proceeds even in the presence of a small amount of an acid. Therefore, as the temperature is raised, the maximum shifts toward smaller [HCl]/[M] values and approaches to *ca.* [HCl]/[M]=0.5 (molar ratio), as has been stated above. On the other hand, with a lowering of the temperature, the maximum shifts toward larger [HCl]/[M] values, because the decomposition of hexa-methylolmelamine proceeds slowly and more acid is necessary for its decomposition with a lowering of the temperature.

24) A. Gam, G. Widmer and W. Fisch, *Brit. Plastics.*, **14**, 508 (1943).

BULLETIN OF THE CHEMICAL SOCIETY OF JAPAN VOL. 41 17—25 (1968)

Stability of Hydrosol of Arsenic Trisulphide in the Light of D. L. V. O. Theory

K. L. DALUJA and S. N. SRIVASTAVA

Department of Chemistry, Agra College, Agra, India

(Received May 1, 1967)

The stability of negative As_2S_3 sol of mean particle diameter 90 Å has been studied in presence of different valent cations *viz.* Na^+, Ba^{2+}, UO_2^{2+}, Al^{3+} and Th^{4+} using D. L. V. O. theory. The zeta potential (assumed to be equal to the surface potential) of the sol particles was calculated from the electrophoretic measurements as a function of ionic strength. The knowledge of zeta potential permitted the calculation of repulsive energy V_R, and the energy of attraction V_A was estimated from physico-chemical data. The stability ratio, W, was calculated from interaction profiles which were made from the combination of the two energies. Stability factor, F, was also estimated from the Derjaguin equation, but it was not satisfactory presumably owing to the exclusion of V_A. In general, the interaction between As_2S_3 particles could be interpreted in the light of D. L. V. O. theory. The flocculation powers of cations were in the order of $Al^{3+} > Th^{4+} > UO^{2+} > Ba^{2+} > Na^+$. The anomalous behaviour of thorium is perhaps due to its hydrolysis.

From the survey of literature it appears that sufficient data are available on As_2S_3 sol.[1-10] However, there is a lack of quantitative data especially in the light of some recent developments on the stability theory of lyophobic colloids. In the present work, therefore, an attempt has been made to apply the modern theory of the subsidence of lyophobic sols due to Derjaguin, Landau,[11,12]

1) S. S. Bhatnagar and D. L. Srivastava, *J. Phys. Chem.*, **28**, 730 (1924).
2) S. N. Mukherjee, *Kolloid. Z.*, **53**, 159 (1930).
3) B. N. Ghosh and N. R. Dhar, *J. Phys. Chem.*, **29**, 668 (1925).
4) B. N. Ghosh, *J. Chem. Soc.*, **1929**, 2693.
5) J. N. Mukherjee *et al.*, *J. Indian Chem. Soc.*, **2**, 296 (1925); **4**, 493 (1927); **5**, 735 (1928).
6) S. S. Joshi and A. J. Rao, *ibid.*, **10**, 237, 247 (1933).
7) B. P. Yadava and A. C. Chatterji, *ibid.*, **21**, 227 (1944).
8) J. N. Mukherjee, S. P. Roychowdhury and S. G. Rajkumar, *ibid.*, **10**, 27 (1933).
9) H. R. Kruyt *et al.*, *Z. Physikal. Chem.*, **130**, 170 (1927).
10) H. Freundlich, *Z. Physik. Chem.*, **44**, 129 (1903); **73**, 385 (1910).
11) B. Derjaguin, *Trans. Faraday Soc.*, **36**, 203, 730 (1940).
12) B. Derjaguin and L. D. Landau, *Acta Phys. Chim. USSR*, **14**, 633 (1941).

Verwey and Overbeek[13] (D. L. V. O. theory) to the flocculation results of the hydrosol of arsenic trisulphide. The use of the three important variables namely particle radius a, surface potential ϕ_0 and Debye-Hückel reciprocal length κ has been made while applying the D. L. V. O. theory in order to calculate interaction energies, stability factor and flocculating concentrations.

Theoretical

The Stability Theory and Its Application to the Present System. According to the well known theory of the stability of lyophobic colloids the stability depends upon the total energy of interaction between two colloidal particles consisting of a long range electrical repulsion and van der Waals attraction. If the resultant potential energy barrier is high enough, *viz.* $V \geqslant 15\,\boldsymbol{k}T$, the colloidal system is stable, otherwise a portion of colliding colloidal particles can surmount it, leading to flocculation. The potential energies of repulsion and attraction and the total attraction are given below.

Potential Energy of Repulsion V_R. The potential energy of repulsion between two spherical particles of radius a, electrical potential ϕ_0, interparticle distance H_0 is given by a simple approximate equation (*loc. cit.*),

$$V_R = \frac{\varepsilon a \phi_0^2}{u+2} e^{-\tau u} \tag{1}$$

which is valid only for the small value of τ, where ε is the dielectric constant of the medium, $u = H_0/a$ and $\tau = \kappa a$.

Potential Energy of Attraction V_A. The potential energy of attraction can be put into the simple form[14]

$$V_A = \frac{-A}{12u} \qquad \text{(Provided } u \ll 1\text{)} \tag{2}$$

Here A is the van der Waals or Hamaker constant.

Total Potential Energy of Interaction V and the Stability Ratio W. The total energy of interaction V, for the present system where other energies can be neglected, is simply the sum of the repulsive and attractive energies. For slow flocculation, the theory is developed by Fuchs[15] who found that the effective collisions were reduced by a factor W which is termed the stability ratio. This ratio is related to the potential energy of interaction V as follows,

$$W = 2\int_2^\infty \exp \frac{1}{\boldsymbol{k}T}\left(\frac{\varepsilon a \phi_0^2}{u+2} e^{-\tau u} - \frac{A}{12u}\right) \times \frac{du}{(u+2)^2} \tag{3}$$

Here the value of W has to be obtained by graphical integration using the plots of $\exp(V/\boldsymbol{k}T)/s^2$ against s.

An approximate equation[16] as given below may also be used for the value of stability ratio of lyophobic colloid.

$$W = \exp\left(V_{max}/\boldsymbol{k}T\right)/2\kappa a \tag{4}$$

where V_{max} is the maximum in the potential energy curves.

Derjaguin (*loc. cit.*) has also described a formula for the stability of lyophobic sols as given below,

$$F = \frac{\varepsilon a \phi_0^2}{2\boldsymbol{k}T} \tag{5}$$

in which attraction force has been neglected. Here F is the stability factor and other terms have the usual significance.

Theoretical Calculation of van der Waals Constant A. To calculate London-van der Waals attraction constant A, Hamaker (*loc. cit.*) has given an equation (*cf.* Srivastava[17])

$$A = \pi^2 q^2 L \tag{6}$$

where q is the number of atoms (molecules) in 1 m*l* of the substance composing the particles and L is the London constant which is calculated from the following equations.

(i) The Slater-Kirkwood[18] (S-K) equation.

$$L_{\text{S-K}} = 11.25 \times 10^{-24}\, \nu^{1/2} P^{3/2} \tag{7}$$

(ii) The Slater-Kirkwood equation modified by Moelwyn-Hughes[19] (S–K–M)

$$L_{\text{S-K-M}} = 7.8 \times 10^{-24}\, \nu P^{3/2} \tag{8}$$

(iii) Neugebauer[20] (N) equation

$$L_{\text{N}} = -1.62 \times 10^{-6}\, \kappa P \tag{9}$$

where ν is the number of valency electrons in the outer shell, P is the polarizability and κ is the diamagnetic susceptibility. Polarizability is calculated from the classical Clausius-Mosotti equation.

However, the value of A obtained from Eq. (6) is for the interaction between two As_2S_3 solid particles in vacuum. Therefore, to calculate the interaction between As_2S_3 solid particles in water a correction has been made and interaction was calculated from the expression (*loc. cit.*)

$$A = \left(A^{1/2}_{As_2S_3\text{-}AS_2S_3} - A^{1/2}_{H_2O\text{-}H_2O}\right)^2 \tag{10}$$

Experimental Procedure

Materials. All the chemicals were of B. D. H. Analar grade. All glassware was of Pyrex and was thoroughly cleaned before use. Ordinary distilled

13) E. J. W. Verwey and J. Th. G. Overbeek, "Theory of Stability of Lyophobic Colloids," Elsevier Publishing Co., Amsterdam (1948).
14) H. C. Hamaker, *Physica*, **4**, 1058 (1937).
15) N. Fuchs, *Z. Physik.*, **89**, 736 (1934).
16) H. R. Kruyt, "Colloid Science," Vol. I, Elsevier, Amsterdam (1952), p. 285.
17) S. N. Srivastava, *Indian J. Chem.*, **3**, 376 (1965).
18) J. C. Slater and J. G. Kirkwood, *Phys. Rev.*, **37**, 682 (1931).
19) E. A. Moelwyn-Hughes, "Physical Chemistry," Pergamon Press, London (1957), p. 383.
20) Th. Neugebauer, *Z. Physik.*, **107**, 785 (1937).

water redistilled from an all Pyrex apparatus and having the specific conductance $\approx 1\times10^{-6}$ ohm^{-1}cm^{-1} was used for all experimental work.

Preparation of the As_2S_3 Sol. To prepare the arsenic trisulphide sol a very slow stream of hydrogen sulphide gas was bubbled through 250 m*l* redistilled water in which 250 m*l* aqueous solution 0.4% arsenic trioxide was added dropwise. The speed of the drops and stream of hydrogen sulphide were adjusted in such a manner that the addition of each drop of aqueous solution of arsenic trioxide was followed by 3—4 bubbles of H_2S gas. The excess of H_2S gas was then removed by passing a current of purified hydrogen gas till the H_2S gas completely removed. The light yellow sol of As_2S_3 so obtained was then dialysed in a parchment paper bag against slow running distilled water for one and a half day. The conductance of the As_2S_3 sol thus obtained was 3.2×10^{-5} ohm^{-1} cm^{-1}.

Electrophoretic Mobility Measurements. The mobility measurements were made by moving boundary method. To measure the elcctrophoretic mobility of the sol, the experiments were carried out in a modified apparatus[21] of Burton tube fitted with two wide side tubes. Constant current was supplied to the platinum foil electrodes in wide tubes and the potential drop across the two Pt electrodes in U-tube was measured with a vacuum tube voltmeter. Measurements were made at sharp descending boundary between the colloidal solution and an equiconducting aqueous solution of acetic acid.

The zeta potential was calculated by the Overbeek[22,23] formulae for symmetrical and unsymmetrical electrolytes from the following equations (*cf.* Hückel[24])

$$U=\frac{\varepsilon\zeta}{6\pi\eta}\left[f_1(\kappa a)-v^2\left(\frac{e\zeta}{kT}\right)^2 f_3(\kappa a)-\frac{\rho_+ +\rho_-}{2e}\cdot\frac{\varepsilon kT}{6\pi\eta e}\left(\frac{e\zeta}{kT}\right)^2 f_4(\kappa a)\right] \quad (11)$$

$$U=\frac{\varepsilon\zeta}{6\pi\eta}\left[f_1(\kappa a)-(v_- - v_+)\left(\frac{e\zeta}{kT}\right)f_2(\kappa a)-\frac{\rho_+ v_+ -\rho_- v_-}{(v_+ +v_-)e}\cdot\frac{\varepsilon kT}{6\pi\eta e}\left(\frac{e\zeta}{kT}\right)^2 f_4(\kappa a)\right] \quad (12)$$

Here $f_1(\kappa a)$ is identical with the Henry function and the $f_2(\kappa a)$, $f_3(\kappa a)$ and $f_4(\kappa a)$ have been tabulated by Overbeek.[23] v_+ and v_- are the valencies of the cations and anions respectively. ρ_+ and ρ_- are the frictional constant of the cations and anions respectively of the used electrolyte. Other terms have their usual meaning.

Electron Microscopic Size of the Colloidal As_2S_3 Particles. A Sample of the colloidal solution under investigation was diluted 10 times. A specimen for electron microscopy was prepared by allowing a small drop of specimen in liquid suspension to dry on 200 mesh copper grid support which had earlier been covered with thin film of collodion. The electron photograph was taken on Siemens Elmiskop I electron microscope at 100kV (due to courtesy of Dr. K. Bahadur, Officer in-charge of electron microscopy Division, Defence Science Laboratory, Delhi).

21) P. D. Bhatnagar and A. K. Bhattacharya, *Koll. Zeit.*, **170**, 29 (1960).
22) J. Th. G. Overbeek, *Koll. Beheifte*, **54**, 287 (1943).
23) J. Th. G. Overbeek, "Advances in Colloid Science," Vol. III, Elsvier, London (1950), p. 115.
24) E. Hückel, *Physik. Z.*, **25**, 204 (1924).

Results and Discussion

Size of the Particles of As_2S_3 Sol. A typical electron micrograph of As_2S_3 sol particles is given in Fig. 1 and the particles size distribution curve obtained from this is given in Fig. 2. The mean particle radius was found to be 45 Å.

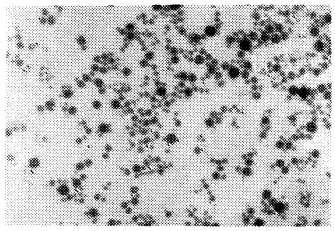

Fig. 1. Electron micrograph of negative As_2S_3 sol under the magnification of 1.2×10^5.

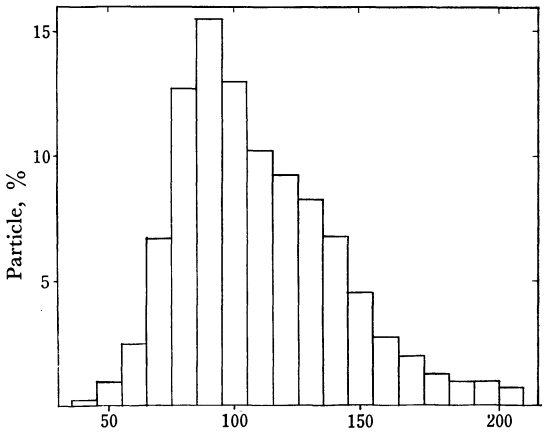

Fig. 2. Particle size distribution of negative arsenic trisulphide sol.
Number of particles counted=400
Mean diameter of the particles=90 Å

The Zeta Potentials. The concentration and pH of the 50% diluted sol were 1.2×10^{-3} g/m*l* and 4.0±0.05. The experimental value obtained for the mobility of the above arsenic trisulphide sol was 5.4 (μ/sec)/(V/cm) at 26°C. The zeta potential calculated from this value was 102.6 mV.

The mobility and zeta potential of As_2S_3 sol particles as a function of log molar concentration of different electrolytes are given in Figs. 3 and 4 respectively. In general, it is seen that the mobility and the zeta potential decrease as the concentration of electrolytes increases. With NaCl the fall of the zeta potential is almost linear throughout but with $BaCl_2$, $UO_2(NO_3)_2$, $AlCl_3$ and $Th(NO_3)_4$, it is comparatively slow in the initial stages and then becomes sharp. The minimum zeta potential that could be conveniently measured was about 60 mV below which there was visible flocculation of the sol particles.

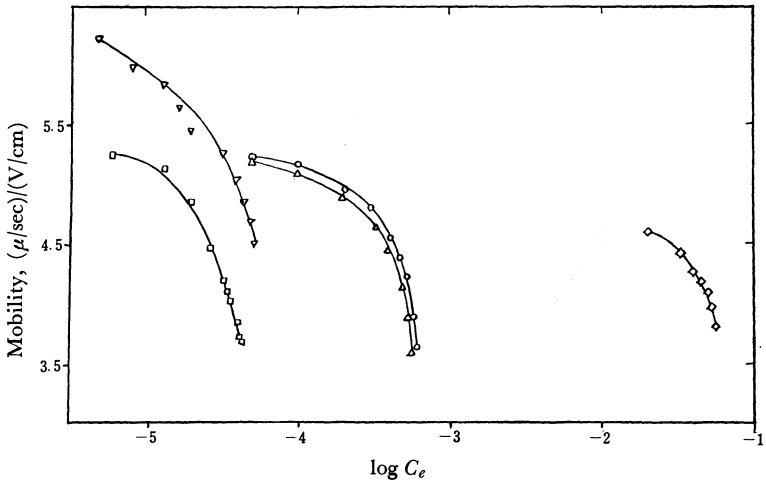

Fig. 3. Mobility *versus* log C_e (C_e=molar concentration of electrolyte) curves.
◇ NaCl; ○ $BaCl_2$; △ $UO_2(NO_3)_2$; □ $AlCl_3$; ▽ $Th(NO_3)_4$

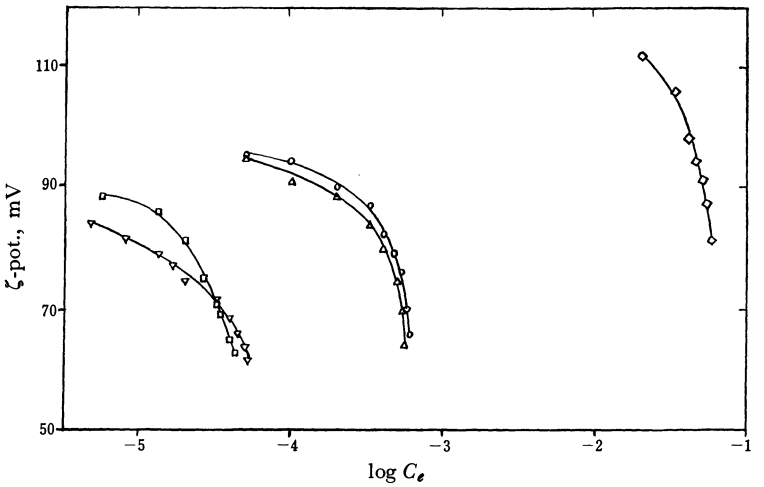

Fig. 4. Zeta potential against log C_e curves.
◇ NaCl; ○ $BaCl_2$; △ $UO_2(NO_3)_2$; □ $AlCl_3$; ▽ $Th(NO_3)_4$

Calculation of van der Waals Constant. The value of the London constant is required to calculate van der Waals constant which was calculated using the susceptibility of one gram formula wt.[25] $=-7.00\times10^{-5}$, $\nu=28$ and $P=2.16\times10^{-23}$ (calculated from Clausius-Mosotti equation using refractive index data of As_2S_3.[26] With the proper choice of units the London constant, calculated from Eqs. (7), (8) and (9) are as follows

$$L_{S\text{-}K}^{As_2S_3} = 6.0\times10^{-57}\ \text{erg cm}^6$$

$$L_{S\text{-}K\text{-}M}^{As_2S_3} = 22.02\times10^{-57}\ \text{erg cm}^6$$

and

$$L_N^{As_2S_3} = 4.08\times10^{-57}\ \text{erg cm}^6$$

Now the use of Eq. (6) permits the calculation of van der Waals constant for As_2S_3 from each of the three equations by finding $q(=8.4\times10^{21})$ and density (=3.43). Similarly, the corresponding constant for water is given by Verwey and Overbeek (*loc. cit.*) (see also Watillon[27]) and hence the net attraction constant of As_2S_3 particles in water can be estimated from Eq. (10). The results are summarized in Table 1.

It is found that the value of the van der Waals constant calculated from S-K-M formula yields comparatively high value. Therefore, in the

25) "Handbook of Chem. and Phys.," 43rd ed. Chemical Rubber Publishing Co. (1961—1962), p. 2683.
26) "International Critical Tables," Vol. I, p. 174.
27) A. Watillon and A. M. Joseph-Petit, "Proceedings, Third International Congress on Surface Activity," Butterworths Scientific Publication (London), **1**, 145 (1960).

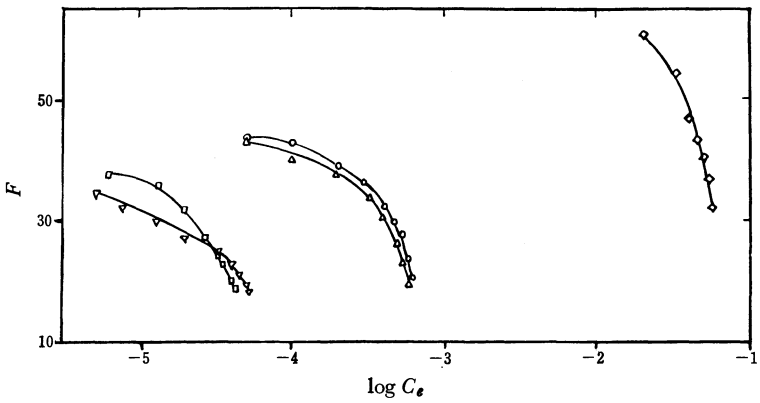

Fig. 5. *F versus* log C_e.
◇ NaCl; ○ $BaCl_2$; △ $UO_2(NO_3)_2$; □ $AlCl_3$; ▽ $Th(NO_3)_4$

TABLE 1. VALUE OF THE VAN DER WAALS CONSTANT CALCULATED FROM DIFFERENT EQUATIONS USING $M=246.1$, $P=2.16\times10^{-23}$ ml/mol, $q=8.4\times10^{21}$

Equation used	$A_{As_2S_3\text{-}As_2S_3}$ $\times10^{12}$ erg in vacuum	$A_{H_2O\text{-}H_2O}$ $\times10^{13}$ erg in vacuum	$A\times10^{12}$ erg As_2S_3 in water
S-K	4.18	5.95	1.62
S-K-M	15.32	7.70	9.23
N	2.84	5.61	0.87

present calculations, the value of $A_{S\text{-}K\text{-}M}$ has been neglected and for further calculations the mean value of the remaining two ($=1.25\times10^{-12}$ erg) formulae has been used.

An Estimate of the Stability Factor *F*, from the Derjaguin Equation. The stability of the colloid has been first estimated by Derjaguin's Eq. (5) and results have been depicted in Fig. 5. According to theoretical expectation F should be higher than 10 for a colloid to be stable. But for the present system the value of F is not less than 15 even for a reasonably flocculated sol examined within 45 min after preparation. This is inconsistent with the Derjaguin theory. In the application of Derjaguin's Eq. (5) only one approximation ($\psi_0\approx\zeta$) is used which is not expected to effect the results so much. Therefore, the reason for this discrepancy seems to be in the neglect of the van der Waals attraction forces and Debye-Hückel parameter which also play an important part in the stability as discussed before.

Potential Energy. In Fig. 6, Curves I, II and III show the repulsive energy V_R, attractive energy V_A and net potential energy of interaction $V(=V_R+V_A)$ of the As_2S_3 sol corresponding to zeta potential=102.6 mV. This has an energy maximum, $V_{max}=33.4\,\boldsymbol{k}T$ (using van der Waals constant $A=1.25\times10^{-12}$ erg) which is a sufficiently high value to show that the sol is stable.

Potential energy curves of colloidal particles as

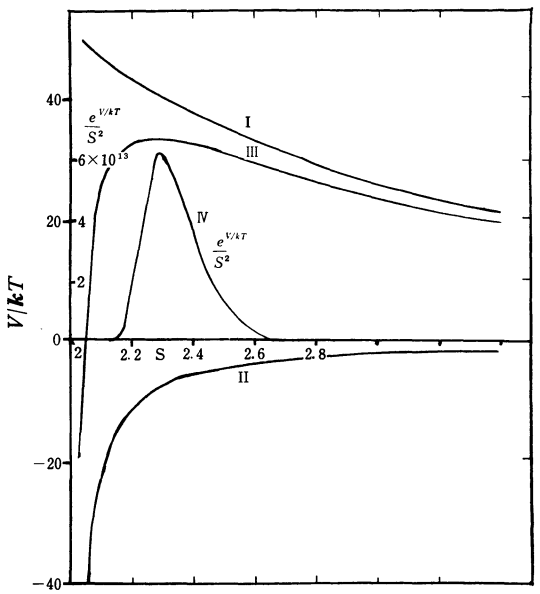

Fig. 6. Curves of potential energy of (I) repulsion, (II) attraction (III) interaction and (IV) of the quantity $\exp(V/\boldsymbol{k}T)/s^2$ *versus* s for the values of $a=45$ Å, $\kappa=4.52\times10^5$ cm^{-1}, $A=1.25\times10^{-12}$ erg and $\zeta=(\psi_0)=102.6$ mV of 50% diluted As_2S_3 sol.

a function of distances between their surfaces are shown in Figs. 7—10 respectively in the presence of NaCl, $UO_2(NO_3)_2$, $AlCl_3$ and $Th(NO_3)_4$ which are in good agreement with theoretical prediction. The value of V_{max} in each case shows the range of slow flocculation till V_{max} decreases to a sufficiently low value which is the threshold of rapid coagulation. In Fig. 8 a dotted curve without relaxation correction to zeta potential=98.8 mV (after correction zeta potential=95 mV) has also been given. This gives an idea of the magnitude of error likely to be introduced if relaxation is not taken into account.

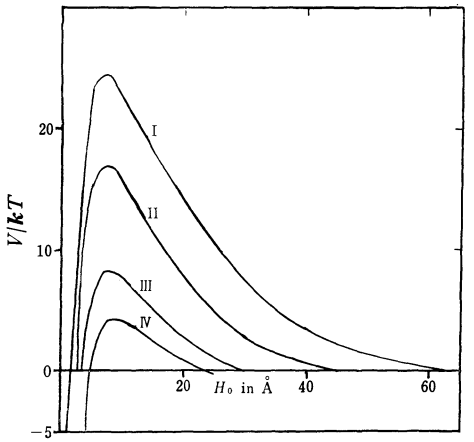

Fig. 7. Curves for potential energy of interaction (V), in the presence of NaCl against H_0.
Curve I for zeta pot.=112.0 mV
Curve II for zeta pot.=106.0 mV
Curve III for zeta pot.= 94.5 mV
Curve IV for zeta pot.= 87.4 mV

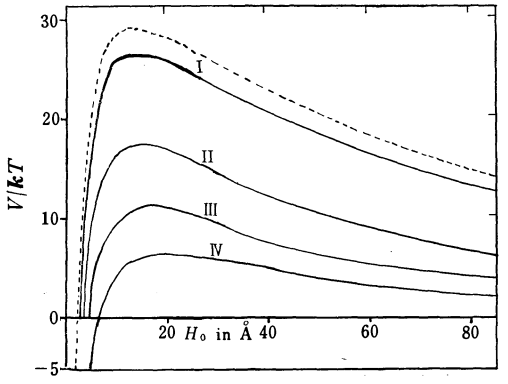

Fig. 8. Curves for potential energy of interaction (V), in the presence of $UO_2(NO_3)_2$ against H_0.
Curve I for zeta pot.=95.0 mV
Curve II for zeta pot.=84.3 mV
Curve III for zeta pot.=74.4 mV
Curve IV for zeta pot.=64.0 mV
Curve dotted for zeta pot.=98.8 mV

Stability Factor *W*. Stability factor was calculated by graphical integration of Eq. (3), as well as from an approximate Eq. (4) and the results are reported in Table 2. In Fig. 6 a typical Curve IV of $\exp(V/\boldsymbol{kT})/s^2$ *versus* s has been shown to calculate the stability ratio in the absence of electrolytes, where $W=2.63\times10^{13}$, while the value of W calculated from approximate Eq. (4) is 7.4×10^{14}. In Figs. 11 and 12, the curves for log W against log C_e are given for varying concentration of the electrolytes which are of the similar shapes and the slope in the lower part of the slow coagulation range is also almost in the same range. It is found that the values of W obtained from the method of approximate equation are higher than

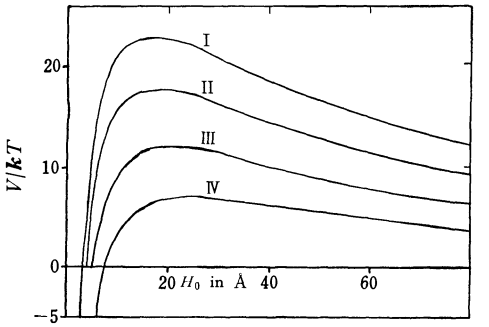

Fig. 9. Curves for potential energy of interaction (V), in the presence of $AlCl_3$ against H_0.
Curve I for zeta pot.=88.7 mV
Curve II for zeta pot.=81.5 mV
Curve III for zeta pot.=71.0 mV
Curve IV for zeta pot.=62.8 mV

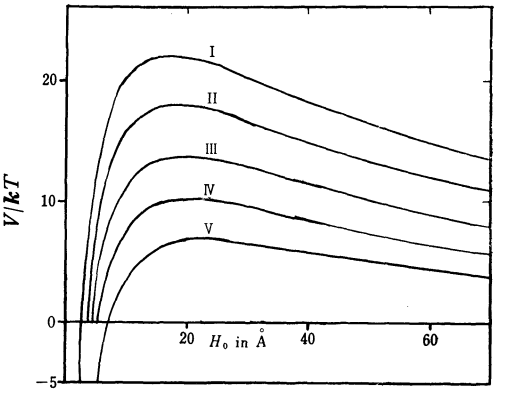

Fig. 10. Curves for potential energy of interaction (V), in the presence of $Th(NO_3)_4$ against H_0.
Curve I for zeta pot.=87.2 mV
Curve II for zeta pot.=81.5 mV
Curve III for zeta pot.=74.7 mV
Curve IV for zeta pot.=68.6 mV
Curve V for zeta pot.=61.3 mV

those calculated from graphical integration. The values of the stability ratio in the zone of slow coagulation are comparable with those obtained by Ottewill and co-workers[28,29] on AgI and arachidic acid systems. The general shape of the log W *versus* zeta potential curves given in Fig. 13 is in keeping with the theory. It is obvious from the curves that higher the value of τ higher is the zeta potential at which flocculation can occur.

To calculate the coagulation concentration of various salts which are used to coagulate As_2S_3 sol the extrapolation of the linear portion of log W against log C_e curve was made to log C_e axis (*loc.*

28) R. H. Ottewill and A. Watanabe, *Koll. Zeit.*, **170**, 38 (1960); **173**, 122 (1960).
29) R. H. Ottewill and D. J. Wilkins, *Trans. Faarday Soc.*, **170**, 132 (1960); **58**, 608 (1962); III Inter. Cong. Surf. Act. Cologne, **11**, 653 (1960).

TABLE 2. DATA OF STABILITY RATIO W FOR As_2S_3 SOL ($W=2.63\times10^{13}$)

Cation	Concentration mol/l	Zeta potential in mV	W from graphical integration	W from approximate Eq. (4)
Na^+	2.00×10^{-2}	112.0	1.38×10^{9}	9.84×10^{9}
	3.33×10^{-2}	106.0	1.61×10^{6}	4.45×10^{6}
	4.00×10^{-2}	98.4	3.22×10^{3}	1.36×10^{4}
	4.50×10^{-2}	94.5	1.63×10^{2}	5.64×10^{2}
	5.00×10^{-2}	91.5	3.04×10	1.00×10^{2}
	5.33×10^{-2}	87.4	3.80	1.13×10
	5.66×10^{-2}	81.3	0.46	1.01
Ba^{2+}	5.00×10^{-5}	95.4	3.50×10^{10}	7.20×10^{11}
	1.00×10^{-4}	94.5	—	—
	2.00×10^{-4}	90.3	5.65×10^{8}	3.18×10^{9}
	3.00×10^{-4}	87.3	1.80×10^{7}	2.23×10^{8}
	4.00×10^{-4}	82.3	6.96×10^{5}	6.59×10^{6}
	4.66×10^{-4}	79.2	9.60×10^{4}	8.31×10^{5}
	5.33×10^{-4}	76.2	1.56×10^{3}	1.30×10^{4}
	5.66×10^{-4}	70.0	8.80×10^{2}	6.28×10^{3}
	6.00×10^{-4}	65.8	1.61×10^{2}	9.15×10^{2}
UO_2^{2+}	5.00×10^{-5}	95.0	2.38×10^{10}	5.09×10^{11}
	1.00×10^{-4}	91.1	1.08×10^{9}	2.11×10^{10}
	2.00×10^{-4}	89.1	6.10×10^{7}	8.66×10^{8}
	3.33×10^{-4}	84.3	3.03×10^{6}	3.87×10^{7}
	4.00×10^{-4}	80.2	2.12×10^{5}	2.09×10^{6}
	5.00×10^{-4}	74.4	7.95×10^{3}	6.31×10^{4}
	5.50×10^{-4}	69.8	9.05×10^{2}	5.76×10^{3}
	5.70×10^{-4}	64.0	9.30×10	5.69×10^{2}
Al^{3+}	6.00×10^{-6}	88.7	8.50×10^{8}	1.98×10^{10}
	1.33×10^{-5}	86.3	1.33×10^{8}	2.85×10^{9}
	2.00×10^{-5}	81.5	6.25×10^{5}	1.14×10^{8}
	2.66×10^{-5}	75.1	1.57×10^{5}	2.52×10^{6}
	3.33×10^{-5}	71.0	1.92×10^{4}	2.65×10^{5}
	3.50×10^{-5}	69.2	7.65×10^{3}	1.00×10^{5}
	4.00×10^{-5}	65.0	1.18×10^{3}	1.32×10^{4}
	4.33×10^{-5}	62.8	1.92×10^{2}	1.93×10^{3}
Th^{4+}	1.00×10^{-6}	87.2	3.70×10^{8}	9.43×10^{9}
	8.33×10^{-6}	81.5	7.25×10^{6}	1.48×10^{7}
	1.33×10^{-5}	78.8	1.29×10^{6}	2.24×10^{7}
	2.00×10^{-5}	74.7	1.17×10^{5}	1.68×10^{6}
	3.33×10^{-5}	71.7	1.46×10^{4}	2.17×10^{5}
	4.00×10^{-5}	68.6	3.98×10^{3}	4.10×10^{4}
	4.50×10^{-5}	66.0	1.13×10^{3}	1.19×10^{4}
	5.00×10^{-5}	63.6	4.10×10^{2}	3.53×10^{3}
	5.20×10^{-5}	61.3	1.82×10^{2}	1.25×10^{3}

TABLE 3. COAGULATION DATA FOR As_2S_3 SOL

Electrolyte	Coagulation concentration, mol/l		$-\mathrm{d}\log W/\mathrm{d}\log C_e$	
	For W from Eq. (4)	For W from graphical integration	For W from Eq. (4)	For W from graphical integration
NaCl	5.8×10^{-2}	5.7×10^{-2}	15.1	21.9
$BaCl_2$	7.0×10^{-4}	7.0×10^{-4}	42.6	32.4
$UO_2(NO_3)_2$	6.6×10^{-4}	6.4×10^{-4}	38.8	35.5
$AlCl_3$	6.3×10^{-5}	5.7×10^{-5}	19.8	18.00
$Th(NO_3)_4$	8.5×10^{-5}	7.5×10^{-5}	11.5	14.1

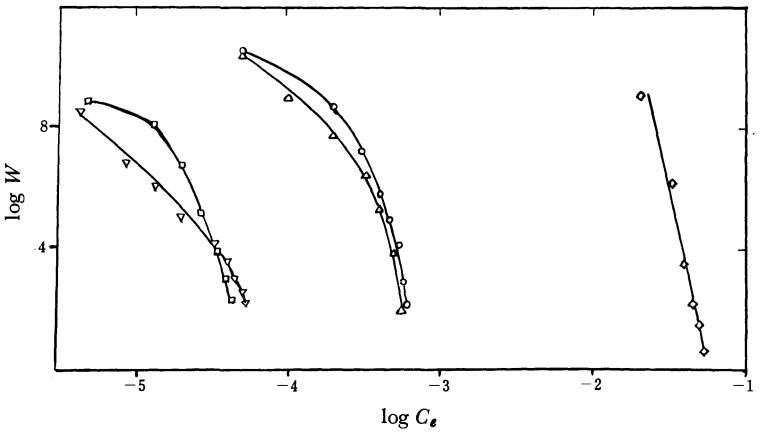

Fig. 11. log W *versus* log C_e curves (W from graphical integration).
◇ NaCl; ○ $BaCl_2$; △ $UO_2(NO_3)_2$; □ $AlCl_3$ ▽ $Th(NO_3)_4$

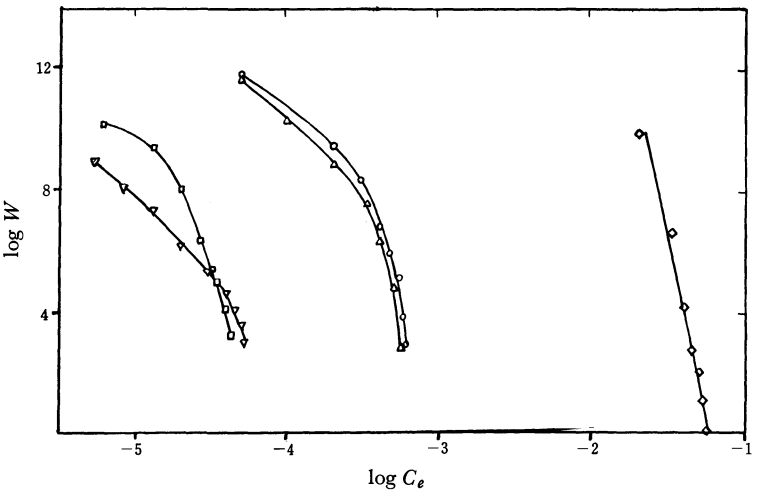

Fig. 12. log W *versus* log C_e curves (W from approximate equation).
◇ NaCl; ○ $BaCl_2$; △ $UO_2(NO_3)_2$; □ $AlCl_3$; ▽ $Th(NO_3)_4$

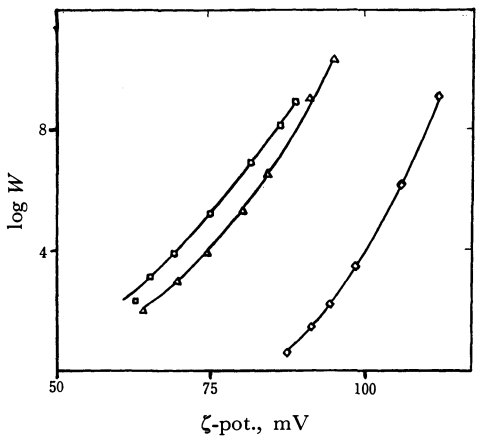

Fig. 13. log W against zeta potential (W from graphical integration).
◇ NaCl; △ $UO_2(NO_3)_2$; □ $AlCl_3$

cit.) where log $W=0$ assuming the validity of the equation[30,31]

$$\log W = K_1 - K_2 \log C_e$$

The values obtained in this manner are given in Table 3. Comparison of the coagulation data given in Table 3 shows that the coagulating concentration is slightly higher in the case when the results were calculated by approximate Eq. (4) than for the results calculated by graphical integration. To confirm the flocculating concentrations so obtained, the turbidity work was carried out.[32]

From the view point of the Schulze-Hardy rule the flocculating concentrations of mono, bi, tri and tetra valent ions would be expected to be

30) H. H. Paine, *Koll. Beheifte*, **4**, 24 (1912).
31) H. Reerink and J. Th. G. Overbeek, *Discussions Faraday Soc.*, **18**, 74 (1954).
32) K. L. Daluja and S. N. Srivastava, to be published.

in the ratio of 100 : 1.6 : 0.13 : 0.024 taking the monovalent ion as 100. Experimentally the ratio for Na^+, UO_2^{2+}, Ba^{2+}, Al^{3+} and Th^{4+} was found to be 100 : 1.12 : 1.23 : 0.100 : 0.311 taking Na^+ ions as 100. Thus a marked deviation from the Schulze-Hardy rule occurs particularly with thorium. It appears that the thorium ion present in the pH ranges about 4 was not a simple tetravalent species but contaminated with ions of different valencies as a result of hydrolysis.[33,34]

Reversal of charge with polyvalent ions as usually expected with colloids is absent in the present work. This is in conformity with the work of Troelstra[35,36] who showed that in acid solutions when pH is low the reversal of charge was absent or at least difficult. This was also pointed out by Matijevic and co-workers[37] who showed that the reversal of charge is obviated owing, in all probability, to the presence of the insoluble hydroxide of thorium formed as a result of hydrolysis.

It may be concluded that the D. L. V. O. theory seems to apply reasonably well to the present system for small spherical colloidal particles and high zeta potentials as it gives a satisfactory interpretation of the interactions between As_2S_3 sol particles.

The authors are extremely grateful to the Ministry of Education, Government of India for the award of research training scheme scholarship to one of them (K. L. D.)

33) E. Chauvenet and J. Tonnet, *Bull. Soc. Chim. France.*, [4], **47**, 701 (1930).
34) E. Chauvenet and Mme. Souteyrand-Franck, *ibid.*, [4], **47**, 1123 (1930).
35) S. A. Troelstra, Thesis Utrecht (1941), pp. 125, 132.
36) H. R. Kruyt and S. A. Troelstra, *Koll. Beihefte*, **54**, 284, 277 (1943).
37) E. Matijevic *et al.*, *J. Phys. Chem.*, **64**, 1157 (1960).

BULLETIN OF THE CHEMICAL SOCIETY OF JAPAN VOL. 41 25—33 (1968)

The Nephelauxetic Effect in Praseodymium(III) and Neodymium(III) Complexes

Seizo Misumi, Sigeo KIDA,*1 Toshiyuki ISOBE and Akio INAZUMI

Inorganic Chemistry Laboratory, Faculty of Science, Kyushu University Hakozaki, Fukuoka

(Received May 19, 1967)

The absorption spectra of praseodymium(III) and neodymium(III) complexes were measured in an aqueous alkaline solution with an excess of ligands. The experimental data being used, the Racah parameter, E^3, and the Landè parameter, ζ_{4f}, werc ealculated by the least-squares method on the assumption that the energy separation between J-levels of the $4f^n$-configuration is a function of E^3 and ζ_{4f}. The nephelauxetic effect in the Pr(III) and the Nd(III) complexes was then discussed by using the values of E^3 thus obtained.

It has been known that the radial integrals of the valence orbitals of a metal ion decrease when the free metal ion combines with ligands to form a metal complex.[1] This phenomenon is called the nephelauxetic effect, which means the expansion of electron clouds; it may be regarded as a measure of the covalency of coordination bands.[1] Although the nephelauxetic effect has been extensively investigated in d-transition metal complexes, the study of f-transition metal complexes has been rather limited because of the theoretical and experimental difficulties.

The absorption bands of lanthanide(III) ions, which are attributed to the electronic transitions within the $4f^n$-configuration ($n=2$—12), are shifted when the environment of the ion is changed. This is undoubtedly an indication of a change in the radical integrals.[2] However, in lanthanide(III) ions the spin-orbit interaction can not be neglected and the radial integrals should be treated by an intermediate coupling scheme.[3] The separation between J-levels of the $4f^n$-configuration may be expressed in terms of the radial integrals (f)[4] and the spin-orbit coupling parameter.

* Present address: Department of Chemistry, Wakayama University, Masago-cho, Wakayama.

1) C. K. Jørgensen, *Prog. Inorg. Chem.*, **4**, 73 (1962).

2) C. K. Jørgensen, "Absorption Spectra and Chemical Bonding in Complexes," Pergamon Press, New York (1962), p. 143.

3) B. G. Wybourne, "Spectroscopic Properties of Rare Earth," Interscience, New York (1965), pp. 42—49.

4) The radial integral of the $4f$-orbital is usually expressed in terms of Slater-Condon Parameters, F^k's ($k=0$, 2, 4, and 6) or Racah parameters, E^k's ($k=0$, 1, 2, and 3). In this paper we used E^k for convenience.

Jørgensen and others[5-9] took the value of $1-\beta=\Delta\tilde{\nu}/\tilde{\nu}_{aquo}=(\tilde{\nu}_{aquo}-\tilde{\nu}_{complex})/\nu_{aquo}$ (where ν stands for the wave number of an absorption band of a lanthanide(III) ion) as a measure of the nephelauxetic effect, assuming that each J-level of a $4f^n$-configuration is linearly dependent only on the radial integrals. On this assumption, the $\Delta\tilde{\nu}/\tilde{\nu}_{aquo}$ of all bands of the same lanthanide(III) complex should be identical; however, an inspection of the experimental data[9] has revealed that the $\Delta\nu/\nu_{aquo}$ values for different J-bands of a lanthanide complex differ from each other considerably. Therefore, it is necessary to obtain the radial integrals or Racah parameters, E^k's (interelectronic repulsion parameters), and the spin-orbit coupling constant or Landè parameter, ζ_{4f}, simultaneously on the assumption that the energy of the J-levels is a function of E^k's and ζ_{4f}.

Calculation

In the intermediate coupling scheme, the energy separations between J-levels of an f^n configuration ($n=2-12$) are expressed approximately in terms of radial integrals, F_2, F_4 and F_6 (Slater-Condon parameter), or E^1, E^2, and E^3 (Racah parameter), and the spin-orbit coupling parameter, ζ_{nf} (Lande parameter).*2

According to Wybourne, if a hydrogenic wave function is assumed,[6] the ratios of the radial integrals are given by:

$$E^1 : E^2 : E^3 = 14.6817 : 0.0768463 : 1.48447 \quad (1)$$

This relation being used, the energy of a J-level can be expressed as a function of the two variables, E^3 and ζ_{4f}.

Applying Taylor's theorem and neglecting the higher order terms, one may obtain:

$$g_i(E^3, \zeta) = g_i(E_0{}^3, \zeta_0) + \left(\frac{\partial g_i}{\partial E^3}\right)_{E^3=E_0{}^3}\chi + \left(\frac{\partial g_i}{\partial \zeta_0}\right)_{\zeta=\zeta_0} y \quad (2)$$

where $g_i(E^3, \zeta)$ denotes the energy of the ith J-level from the ground state, $E^3=E_0{}^3+\chi$, $\zeta=\zeta_0+y$, $E_0{}^3 \gg \chi$ and $\zeta_0 \gg y$. The numerical values of the parameters of the trivalent lanthanide compounds, $E_0{}^3$ and ζ_0, may be taken from the literature,[10] then $g_i(E_0{}^3, \zeta_0)$, $(\Delta g_i/\Delta E^3)_\zeta$ and $(\Delta g_i/\Delta\zeta)_{E^3}$ can be calculated by solving the secular equation derived from the spin-orbit matrix and the LS term energies. Accordingly, $g_i(E^3, \zeta)$ is simplified to a linear function of χ and y, assuming that

$$(\Delta g_i/\Delta E^3)_\zeta = \partial g_i/\partial E^3 = a_i:$$
$$(\Delta g_i/\Delta\zeta)_{E^3} = \partial g_i/\partial\zeta = b_i.$$
$$g_i(E^3, \zeta) = k_i + a_i\chi + b_i y \quad (2')$$

where $k_i = g_i(E_0{}^3, \zeta_0)$.

Based on Eq. (2'), χ and y are obtainable by the least-squares method using the experimental values.

Pr(III). The LS term energies and the spin-orbit matrices were obtained by Condon and Shortley[11] and by Satten and Margolis[12] respectively. The calculation was carried out by putting $E_0{}^3=451.36\ cm^{-1}$ and $\zeta=729.5\ cm^{-1}$. Four experimental values were used for the least-squares calculation for each praseodymium(III) complex (*Cf.* Table 2).

Nd(III). Instead of doing laborious calculations, we have made use of the results of the detailed calculation of Carlson and Crosswhite.[13] Putting $E_0{}^3=492.00\ cm^{-1}$ and $\zeta=861.72\ cm^{-1}$, we obtained the numerical values of $g_i(E_0{}^3, \zeta_0)$, $(\partial g_i/\partial E^3)_{E^3=E_0{}^3}$ and $(\partial g_i/\partial\zeta)_{\zeta=\zeta_0}$ for each J_i-level; then we carried out the least-squares cal-

Table 1. The ratios of metal to ligand and pH of the solutions used for the measurements

Ligand	Pr(III)		Nd(III)	
	metal/ligand	pH	metal/ligand	pH
Aquo	—	—	—	—
Glycine	1 : 10	10.45	1 : 10	10.05
Alanine	1 : 10	10.45	1 : 10	10.25
Malate	1 : 1.5	11.15	1 : 1.5	10.55
Tartarate	1 : 1.5	11.35	1 : 1.5	10.55
NTA	1 : 3	12.05	1 : 3	12.05
Serine	1 : 10	10.75	1 : 10	10.60
EDTA	1 : 1.5	12.85	1 : 1.5	12.85
TPHA	1 : 1.1	10.50	1 : 1	10.50
Citrate	1 : 3	13.50	1 : 3	13.35
Cysteine	1 : 10	10.80	1 : 10	10.55

NTA: nitorilotriacetic acid.
EDTA: ethylendiaminetetraacetic acid.
TPHA: tetraetylenepentaamineheptaacetic acid.

5) C. K. Jørgensen, *Mat. Fys. Medd. Dan. Selk.*, 30, (1956).
6) C. K. Jørgensen, R. Pappalardo and E. Ritterhaus, *Z. Naturforsch.*, **19a**, 424 (1964).
7) C. K. Jørgensen, *Acta Chem. Scand.*, **11**, 1981 (1957).
8) S. P. Sinha, *J. Inorg. Nucl. Chem.*, **27**, 115 (1965).
9) S. P. Sinha, *Spectrochim. Acta*, **22**, 57 (1966).
*2 According to Carnell and Wybourne, it has been a trandition of theoretical spectroscopy to treat the Slater radial integrals and a spin-orbit coupling integral, ζ_{4f}, as parameters to be determined from the available data, usually deriving their magnitudes by a least-squares adjustment to known energy levels. W. T. Carnell and B. G. Wybourne, *J. Chem. Phys.*, **40**, 3428 (1964); B. G. Wybourne, *ibid.*, **36**, 2295, 2301 (1962); E. Y. Wong, *ibid.*, **35**, 544 (1961).
10) C. K. Jørgensen, "Orbitals in Atoms and Molecules", Academic Press, New York (1962), p. 148; B. G. Wybourne, "Spectroscopic Properties of Rare Earth," Interscience, New York (1965), p. 191.
11) E. U. Condon and G. H. Shortley, "The Theory of Atomic Spectra," Cambridg University Press, Cambridg (1951), p. 207.
12) R. A. Satten and J. S. Margolis, *J. Chem. Phys.*, **32**, 573 (1960).
13) E. H. Carlson and H. M. Crosswhite, *Johns Hopkins Univ. Spectroscopic Report*," 19 (1960).

TABLE 2. THE OBSERVED WAVE NUMBERS OF *J*-BANDS AND AN EXAMPLE OF CALCULATED WAVE NUMBER OF *J*-LEVELS OBTAINED FROM THE RESULTS OF LEAST SQUARE METHOD (cm^{-1})

	J-Level	Cald for aquo ion	Aquo	Glycine	Alanine	Malate	Tartrate
Pr(III)	$^3P_2$	22473	22523	22351	22346	22386	22331
	$^3P_1$	21309	21413	21204	21155	21177	21209
	$^3P_0$	20729	20725	20572	20576	20619	20534
	$^1D_2$	17123	16935	16869	16846	16906	16835
Nd(III)	$^4D_{1/2}$	29134	28893	28662	28662	28629	28637
	$^4D_{3/2}$	28420	28257	28011	28003	28011	27980
	$^2P_{1/2}$	22793	23397	23256	23245	23245	23234
	$^4G_{11/2}$	21823	21650	21524	21505	21542	21505
	$^2G_{9/2}$	19578	19554	19444	19467	19482	19444
	$^4G_{7/2}$	19045	19171	19048	19004	19044	19019
	$^4G_{5/2}$	17259	17271	17241	17229	17241	17221
	$^4F_{9/2}$	14590	14663	14620	14599	14663	14620
	$^4F_{7/2}$	13570	13550	13495	13459	13477	13477
	$^4F_{5/2}$	12583	12563	12500	12484	12500	12484
	$^4F_{3/2}$	11458	11468	11468	11442	11468	11442

	J-Level	NTA*	Serine	EDTA*	TPHA*	Citrate	Cysteine
Pr(III)	$^3P_2$	22356	22326	22311	22262	22371	22277
	$^3P_1$	21268	21182	21186	21200	21254	21137
	$^3P_0$	20636	20568	20525	20462	20576	20492
	$^1D_2$	16943	16863	16807	16779	16892	16807
Nd(III)	$^4D_{1/2}$	28629	28637	28604	28571	28637	28547
	$^4D_{3/2}$	28027	27996	27988	27980	27956	27956
	$^2P_{1/2}$	23256	23234	23229	23229	23207	23202
	$^4G_{11/2}$	21552	21505	21551	21552	21529	21496
	$^2G_{9/2}$	19436	19451	19444	19444	19399	19417
	$^4G_{7/2}$	19011	18990	18997	19015	18997	18997
	$^4G_{5/2}$	17147	17182	17227	17200	17197	17173
	$^4F_{9/2}$	14641	14620	14641	14665	14577	14620
	$^4F_{7/2}$	13477	13441	13459	13441	13405	13441
	$^4F_{5/2}$	12469	12469	12484	12453	12453	12438
	$^4F_{3/2}$	11468	11429	11390	11442	11377	11390

* *Cf.* the footnote of Table 1.

culation using eleven experimental values for each neodymium(III) complex (*Cf.* Table 2).

Experimental

Measurements. The absorption spectra were measured at room temperature (about 20°C) with a Hitachi EPS-2 spectrophotometer, a 10 mm quartz cell being used.

The concentration of the solution was 0.1 mol/*l* for the lanthanide(III) perchlorate. Enough excess ligand was used as to cause complex formation. Since the absorption spectra may be affected by the pH of the solution under some conditions, ammonia was added to the solution until the increase in pH did not affect the absorption bands any more. The pH values and the ratio of metal to ligand in the solution are listed in Table 1.

Materials. The lanthanide(III) perchlorate solutions were prepared by dissolving pure lanthanide

TABLE 3. E^3 AND ζ (cm^{-1})

Ligand	Nd(III)		Pr(III)	
	E^3	ζ	E^3	ζ
Aquo	489.8	930.1	459.8	708.6
Glycine	486.5	928.3	455.9	707.9
Alanine	486.2	928.4	455.5	707.6
Malate	486.1	932.1	456.3	709.8
Tartarate	485.9	928.9	455.2	709.8
NTA*	485.8	931.1	457.4	703.3
Serine	485.8	927.8	455.9	703.0
EDTA*	485.4	932.5	455.0	706.4
TPHA*	485.3	932.8	454.3	705.8
Citrate	485.2	928.3	456.3	710.5
Cystein	484.7	930.2	454.0	708.1

* *Cf.* the footnote of Table 1.

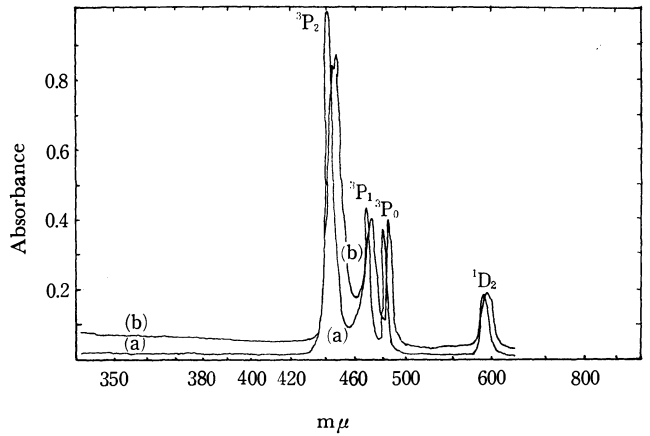

Fig. 1. Absorption spectra of glycinate and aquo complexes of Pr(III) in aqueous solutions. pH=10.45, 25°C.

(a) Pr^{3+} aquo (b) Pr^{3+} + glycine (1 : 10)

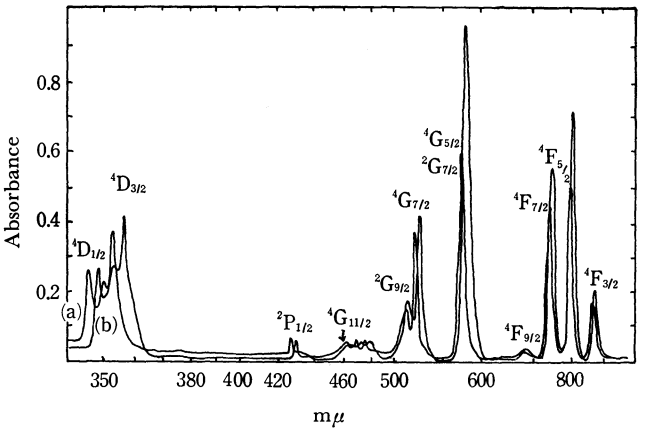

Fig. 2. Absorption spectra of glycinate and aquo complexes of Nd(III) in aqueous solutions. pH=10.05, 25°C.

(a) Nd^{3+} aquo (b) Nd^{3+} + glycine (1 : 10)

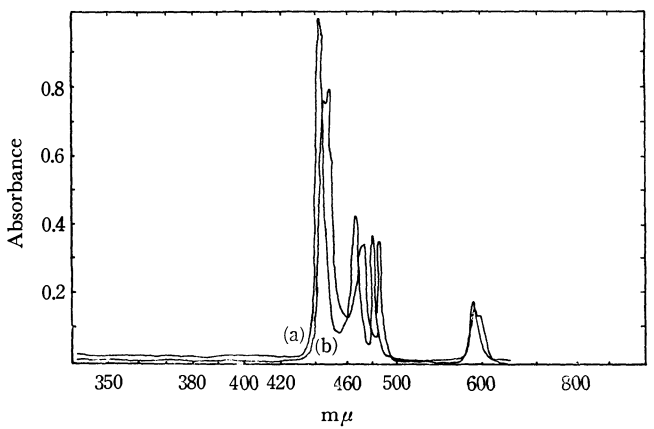

Fig. 3. Absorption spectra of alaninate and aquo complexes of Pr(III) in aqueous solutions. pH=10.45, 25°C.

(a) Pr^{3+} aquo (b) Pr^{3+} + alanine (1 : 10)

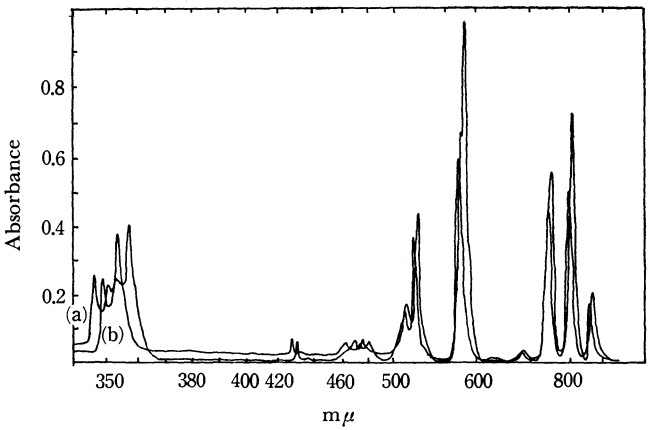

Fig. 4. Absorption spectra of alaninate and aquo complex of Nd(III) in aqueous solutions. pH=10.25, 25°C.

(a) Nd^{3+} aquo (b) Nd^{3+} + alanine (1 : 10)

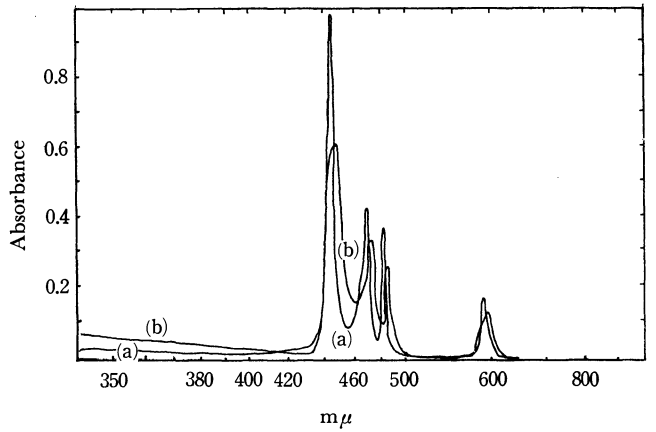

Fig. 5. Absorption spectra of malate and aquo complexes of Pr(III) in aqueous solutions. pH=11.15, 25°C.
(a) Pr^{3+} aquo (b) Pr^{3+} + malate (1 : 1.5)

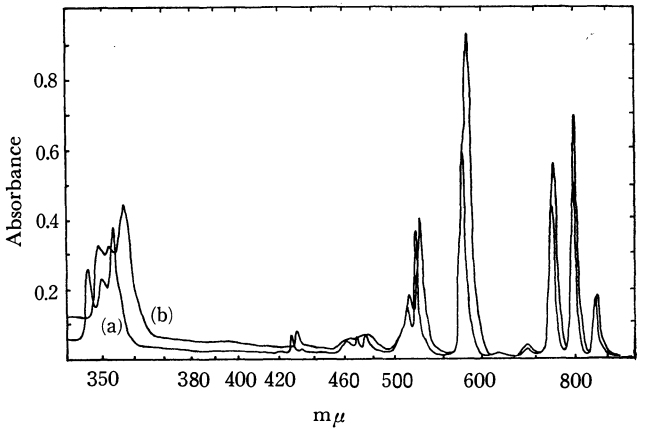

Fig. 6. Absorption spectra of malate and aquo complexes of Nd(III) in aqueous solutions. pH=10.55, 25°C.
(a) Nd^{3+} aquo (b) Nd^{3+} + malate (1 : 1.5)

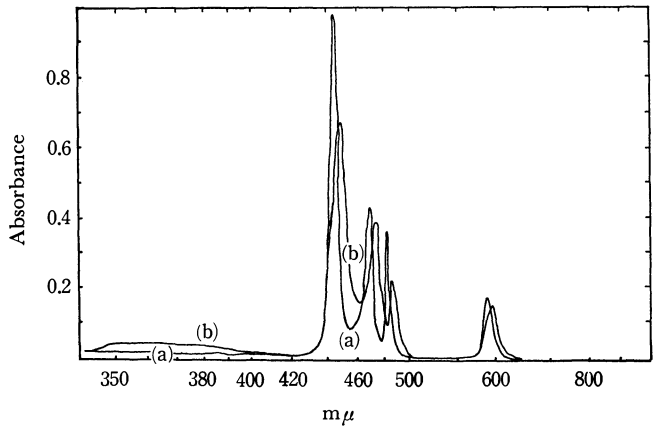

Fig. 7. Absorption spectra of tartarate and aquo complexes of Pr(III) in aqueous solution. pH=11.35, 25°C.
(a) Pr^{3+} aquo (b) Pr^{3+} + tertarate (1 : 1.5)

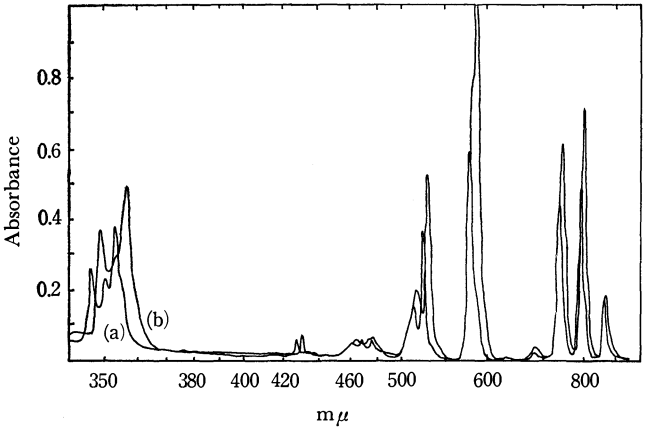

Fig. 8. Absorption spectra of tartarate and aquo complexes of Nd(III) in aqueous solutions. pH=10.55, 25°C.
(a) Nd^{3+} aquo (b) Nd^{3+} + tartarate (1 : 1.5)

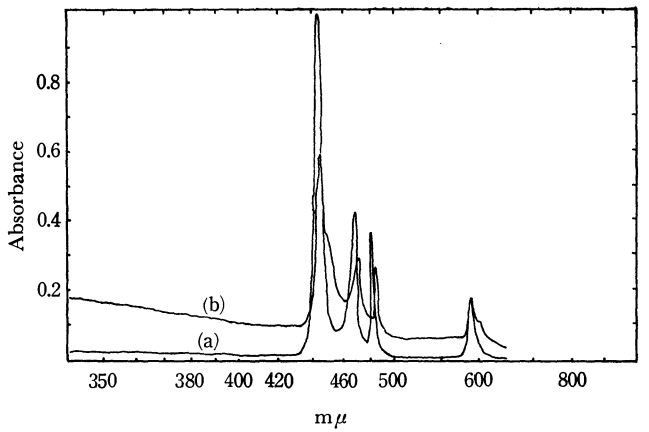

Fig. 9. Absorption spectra of NTA and aquo complexes of Pr(III) in aqueous solutions. pH=12.05, 25°C.
(a) Pr^{3+} aquo (b) Pr^{3+} + NTA (1 : 3)

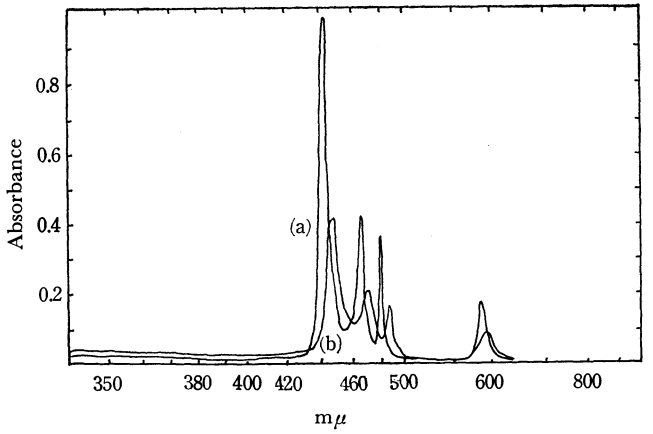

Fig. 11. Absorption spectra of serinate and aquo complexes of Pr(III) in aqueous solutions. pH=10.75, 25°C.
(a) Pr^{3+} aquo (b) Pr^{3+} + serine (1 : 10)

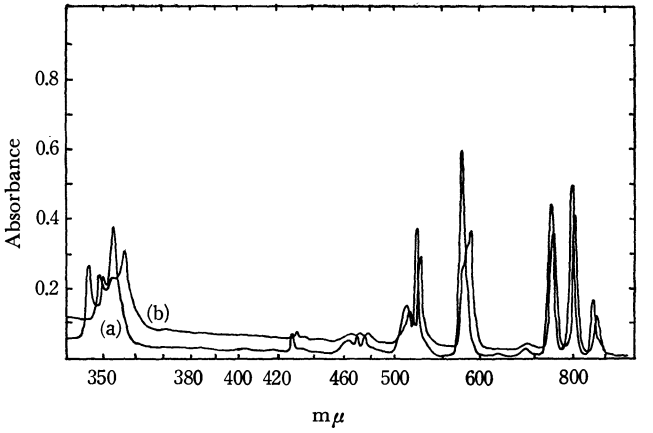

Fig. 10. Absorption spectra of NTA and aquo complexes of Nd(III) in aqueous solutions. pH=12.05, 25°C.
(a) Nd^{3+} aquo (b) Nd^{3+} + NTA (1 : 3)

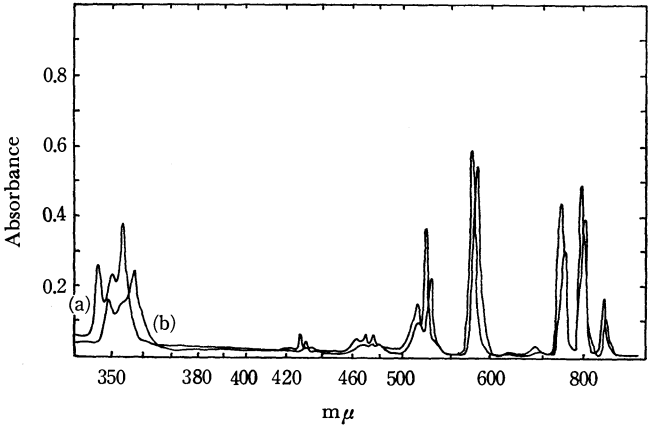

Fig. 12. Absorption spectra of serinate and aquo complexes of Nd(III) in aqueous solutions. pH=10.60, 25°C.
(a) Nd^{3+} aquo (b) Nd^{3+} + serine (1 : 10)

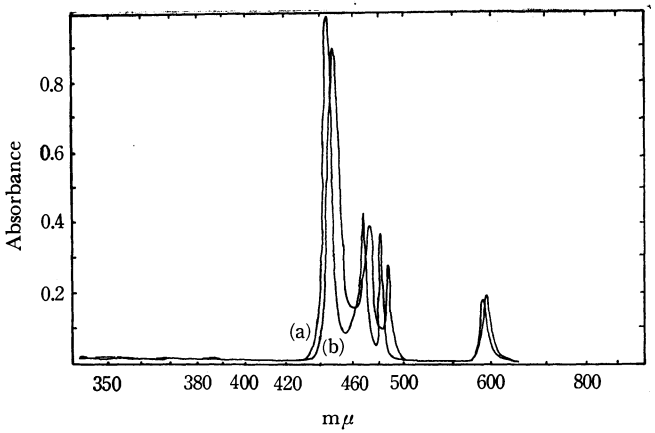

Fig. 13. Absorption spectra of EDTA and aquo complexes of Pr(III) in aqueous solutions. pH=12.85, 25°C.
(a) Pr^{3+} aquo (b) Pr^{3+} + EDTA (1 : 1.5)

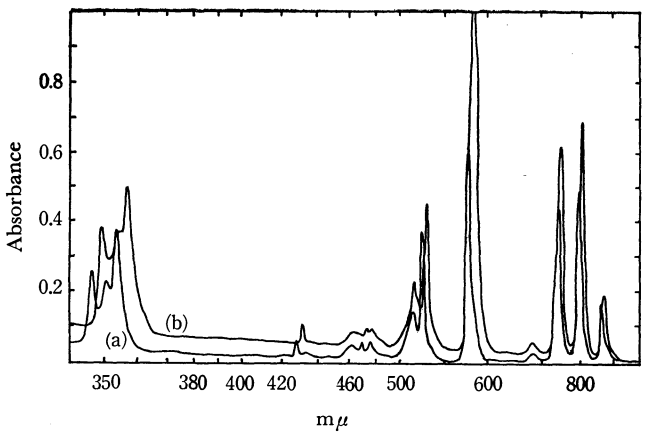

Fig. 14. Absorption spectra of EDTA and aquo complexes of Nd(III) in aqueous solutions. pH=12.85, 25°C.
(a) Nd^{3+} aquo (b) Nd^{3+} + EDTA (1 : 1.5)

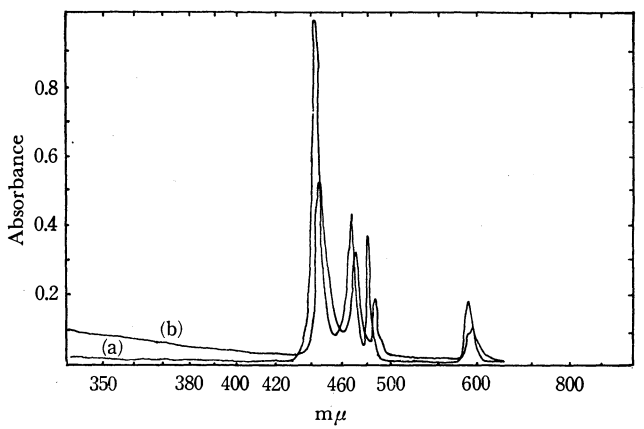

Fig. 15. Absorption spectra of TPHA and aquo complexes of Pr(III) in aqueous solutions. pH=10.50, 25°C.
(a) Pr^{3+} aquo (b) Pr^{3+} + TPHA (1 : 1.1)

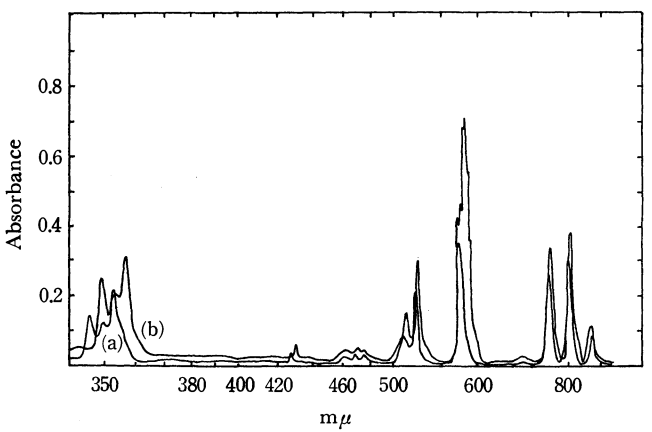

Fig. 16. Absorption spectra of TPHA and aquo complexes of Nd(III) in aqueous solutions. pH=10.50, 25°C.
(a) Nd^{3+} aquo (b) Nd^{3+} + TPHA (1 : 1)

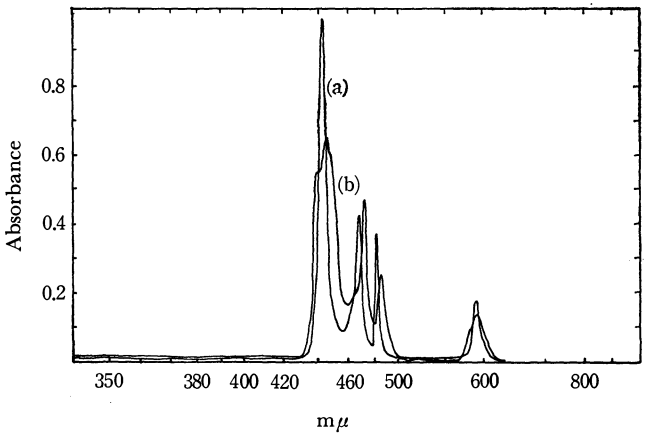

Fig. 17. Absorption spectra of citrate and aquo complexes of Pr(III) in aqueous solutions. pH=13.50, 25°C.
(a) Pr^{3+} aquo (b) Pr^{3+} + citrate (1 : 3)

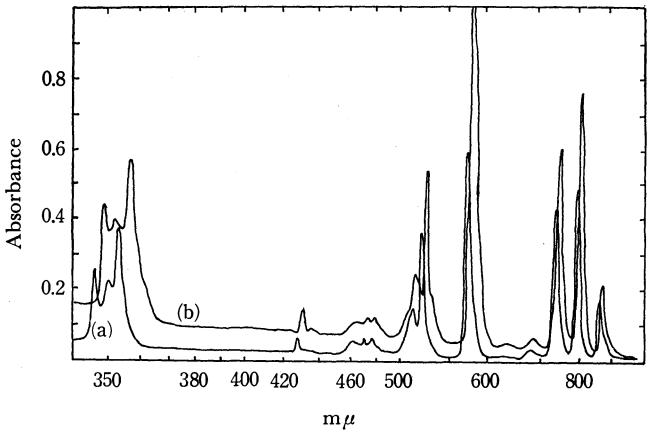

Fig. 18. Absorption spectra of citrate and aquo complexes of Nd(III) in aqueous solutions. pH=13.35, 25°C.
(a) Nd^{3+} aquo (b) Nd^{3+} + citrate (1 : 3)

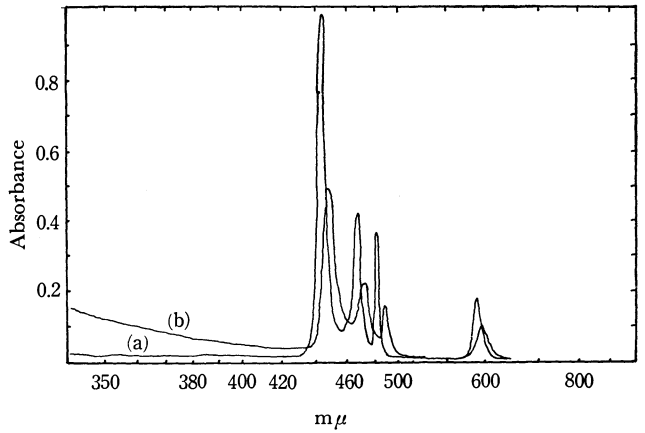

Fig. 19. Absorption spectra of cysteine and aquo complexes of Pr(III) in aqueous solutions. pH=10.80, 25°C.
(a) Pr^{3+} aquo (b) Pr^{3+} + cysteine (1 : 10)

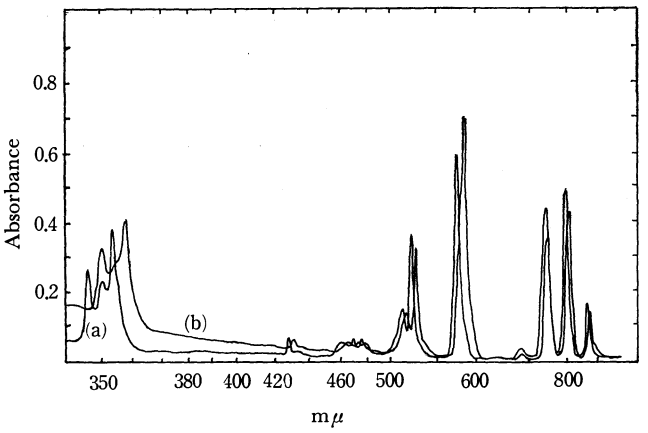

Fig. 20. Absorption spectra of cysteine and aquo complexes of Nd(III) in aqueous solutions. pH=10.55, 25°C.
(a) Nd^{3+} aquo (b) Nd^{3+} + cysteine (1 : 10)

TABLE 4. THE NAPHLAUXETIC EFFECT OF $4f$- AND $3d$-TRANSITION METAL COMPLEXES

Metal ion	Co(III)	Ni(II)	Mn(II)	Pr(III)	Nd(III)
Ligand	3(oxalate)	EDTA	EDTA	EDTA	EDTA
β'	0.88	0.91	0.96	0.990	0.991
$1-\beta'$	0.12	0.09	0.04	0.010	0.009

oxides (purity: more than 99.99%) in perchloric acid. Since the absorption spectra of the aqueous solutions were completely in accord with the literature,[14] they were not purified further.

Results and Discussion

Since it was difficult to obtain the barricenter of the J-band experimentally, we had to be satisfied with taking the center of the band (not the peak).

The energies of the J-levels of each lanthanide(III) complex were obtained using the results of the least-squares calculations.

The accordance of the calculated values with the observed values was satisfactory. The calculated values of the aquo complexes are shown as examples in the second column of Table 2.

The values of E^3 and ζ_{4f} obtained are listed in Table 3. By using these data, the degree of the nephelauxetic effect of $4f$-transition metal complexes can be compared with that of d-transition metal complexes in terms of $1-\beta'$ (where $\beta'=F_k(\text{complex})/F_k(\text{aquo})$), as illustrated in Table 4.

Jørgensen[5] has made a similar comparison by regarding $(\tilde{\nu}_{\text{aquo}}-\tilde{\nu}_{\text{comp}})/\tilde{\nu}_{\text{aquo}} \fallingdotseq 1-\beta'$, assuming that the separation between J-levels is linearly dependent only on E^3. He studied several lanthanide(III) complexes with tartarate, citrate, EDTA, *etc.* in solution and obtained $1-\beta'=0.8$—1.2×10^{-2} for Pr(III) and 0.4—0.7×10^{-2} for Nd(III). In the present study, the values of $1-\beta'$ were 0.8—1.0×10^{-2} for Pr(III) and 0.7—0.9×10^{-2} for Nd(III). Jørgensen's values agree with ours fairly well, considering his simple method and the small differences in materials and conditions.

In connection with the above discussion, it should be noted that the absorption spectrum of a lanthanide(III) complex in an aqueous solution depends not only on the species of the metal ion and the ligand, but also on the metal-ligand ratio and the pH of the solution. The experimental conditions for the nephelauxetic effect, $1-\beta'$, obtained in this study are shown in Table 1. In spite of this limitation, however, the results of the present study are still useful for estimating the covalent character of the $4f$ electrons of the lanthanide(III) ion.

Furthermore, in some cases, the present data may serve to give some information on the configuration of the complex. For example, as may be seen in Table 3, the cysteine complex shows the smallest E^3 and is located on the bottom of the nephelauxetic series in either a praseodymium(III) or a neodymium(III) complex; on the other hand, the other α-amino acids, such as glycine, alanine, and serine, are placed on the upper positions of the series in both praseodymium(III) and neodymium(III) complexes. This fact suggests that the sulfur atom of cysteine takes part in the formation of the cysteine complex in the solution. Jørgensen[15] has already shown that the nephelauxetic effect of sulfur-coordinated metal ions is much stronger in covalency than that of oxygen- or nitrogen-coordinated metal ions.

This study was partly supported by grants from the Ministry of Education and the Japan Society for the Promotion of Science, to both of which organizations the authors wish to express their thanks.

14) C. V. Banks and P. W. Klingman, *Anal. Chim. Acta*, **15**, 356 (1956).

15) C. K. Jørgensen, *J. Inorg. Nucl. Chem.*, **24**, 1571 (1962).

BULLETIN OF THE CHEMICAL SOCIETY OF JAPAN VOL. 41 34—41 (1968)

Electronic Absorption and Emission Spectra of 9, 10-Dichloroanthracene and 9, 10-Dibromoanthracene Crystals

Jiro TANAKA and Masao SHIBATA

Department of Chemistry, Nagoya University, Chikusa, Nagoya

(Received June 12, 1967)

The electronic absorption spectra of three crystalline modifications of anthracene derivatives have been measured; they are the α and β form of 9, 10-dichloroanthracene and 9, 10-dibromoanthracene. The assignment has been presented for each absorption band. The charge transfer absorption which is regarded to the transition between two stacked molecules has been observed in the α-form of 9, 10-dichloroanthracene; also a Rydberg type transition which has an out of plane polarization is found in this crystal starting at 290 mμ. It is unusually broad and is regarded as a band to band transition. The emission band has been measured at different temperature; it is found that excimer type emission is most prominent in the β-form of 9, 10-dichloroanthracene, in which intermolecular approach in the excited state will occur with less difficulty. A criterion for strong, medium, and weak interactions in the excited state is presented by comparing the shift, and the shape of the emission band with the intermolecular vibrational spacing. These results show that the charge transfer interaction and excimer formation are greatly dependent on the relative orientation of molecules, the π-electron overlap, and the difficulty of intermolecular approach in the excited state, particularly with its correlation to the steric repulsion of the bulky substituent groups.

Recently a number of investigations have been published on the problem of excimer and the charge transfer state of aromatic hydrocarbon crystals. The absorption spectra of anthracene crystals have been studied by many people,[1-3] but spectroscopic evidence of the charge transfer state has not been obtained as yet. On the other hand, recent experiments on the photoconductivity of anthracene crystal by Castro and Hornig,[4] Geacintov and Pope,[5] and by Chaiken and Kearns[6] have shown that a band to band transition may exist in pure anthracene crystal in the 280 mμ region. As regards the excimer of anthracene derivatives, Chandross and Ferguson[7] have succeeded in observing excimer emission and absorption spectra at lower temperature in solution. Kuwano and Kondo[8] have found a new crystalline form of 9, 10-dichloroanthracene, and have discussed the anomalous emission characteristics of the new form. Trotter[9,10] has already analysed the crystal structure of the other form of 9, 10-dichloroanthracene, and 9, 10-dibromoanthracene. The comparison of absorption and emission spectra of different types of crystals will clarify the mechanism of excimer formation in the crystalline state, the charge transfer absorption, and the band to band transition of anthracene type crystals.

Experimental

9, 10-dichloroanthracene was synthesized by the method of Ware and Borchert.[11] Actually, the reactants were purified before starting the synthesis and after reaction the product was purified by repeated recrystallization from hexane and several passages of column chromatography. 9, 10-Dibromoanthracene was a product of the Tokyo Kasei Co., and was recrystallized for five to six times from hexane solution. The crystal for emission measurement was grown from hexane solution and the new crystal form of 9, 10-dichloroanthracene was made by heating the crystal in a sealed glass tube at 180°C for twenty hours. This temperature is reported to be the transition point from the α to the β-form. The crystals for the absorption measurement were made by three different methods: first, by the usual

*1 Present address: Governmental Industrial Research Institute, Tosu, Saga.

1) D. P. Craig and J. R. Walsh, *J. Chem. Soc.*, **1958**, 1613.
2) M. S. Brodin and S. V. Marisova, *Opt. Spect.*, **10**, 242 (1961).
3) R. S. Berry, J. Jortner, J. C. Mackie, E. S. Pysh and S. A. Rice, *J. Chem. Phys.*, **42**, 1535 (1965).
4) G. Castro and J. F. Hornig, *ibid.*, **42**, 1459 (1965).
5) N. Geacintov and M. Pope, *ibid.*, **45**, 3884 (1966).
6) F. Chaiken and D. R. Kearns, *ibid.*, **45**, 3966 (1966).
7) E. A. Chandross and J. Ferguson, *ibid.*, **45**, 3546 (1966).
8) H. Kuwano and M. Kondo, This Bulletin, **39**, 2779 (1966).
9) J. Trotter, *Acta Cryst.*, **12**, 54 (1956).
10) J. Trotter, *ibid.*, **11**, 803 (1958).
11) C. Ware and E. E. Borchert, *J. Org. Chem.*, **26** 2263 (1961).

recrystallization method, second, by dropping a solution onto a quartz plate and growing the crystals on the plate and, third, by sublimation in a small beaker onto cotton wool. All crystals were examined with a polarization microscope in order to find the orientation, and the crystalline axis of some crystals was confirmed by taking X-ray photographs.

The absorption of the crystals was measured using an ultraviolet microspectrophotometer, consisting of a Carl Zeiss monochromator and light detection system, an Olympus microscope with Ultrafluar lenses of Carl Zeiss, and a Rochon type polarizer made of quartz. This instrument is capable of measuring crystals as small in area as $10\,\mu \times 10\,\mu$; the wavelength region is from 220 mμ to 2.0 μ. The emission spectra were observed using a Carl Zeiss spectrophotometer PMQ II combined with a mercury excitation lamp and suitable filters, and were also photographed using a Shimadzu Spectrograph GE-100 with Kodak 103a-F plates. The polarization of emission spectra was measured using a specially designed microscope of the Olympus Optical Co.

Results and Discussion

1. Absorption Spectra of Crystals. *a) α-Form of 9,10-Dichloroanthracene.* The electronic absorption and fluorescence spectra of 9,10-dichloroanthracene (hereafter called DCA) in hexane solution are shown in Fig. 1. They resemble that of anthracene, and the lower excited state at 27000 cm^{-1} is regarded as the $^1B_{3u}$ (^1L_a) excited state, with the polarization being along the short-axis, and the second excited state at 34900 cm^{-1} is assigned to the $^1B_{2u}$ (^1B_b) excited state, the polarization being along the long axis. The crystalline structure analysis made by Trotter[9] on the α-form of DCA showed that the molecules are nearly parallel to the bc plane (Fig. 3).

The crystals grown from solution and by sublimation show a habit of developing the ac plane. The a-axis is nearly perpendicular to the plane of the benzene ring, therefore, it does not involve the component of the π-π transition. If we take the isolated-molecule approximation (oriented-gas model) in the crystal then molecular π-π

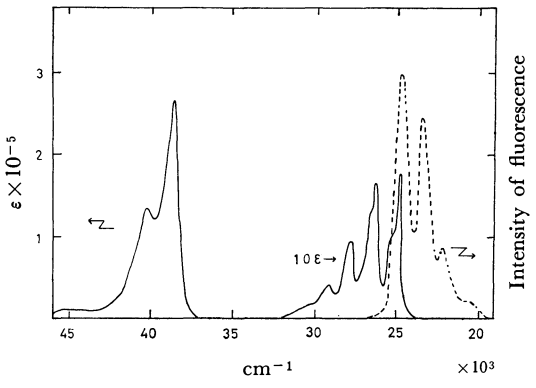

Fig. 1. Absorption and fluorescence spectra of 9,10-dichloroanthracene in hexane solution.

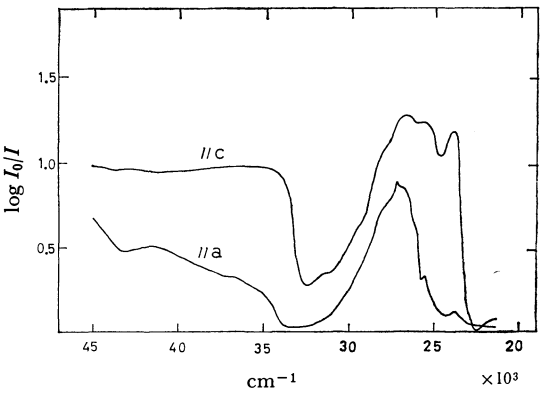

Fig. 2. Crystalline absorption spectra of α-form of 9,10-dichloroanthracene.

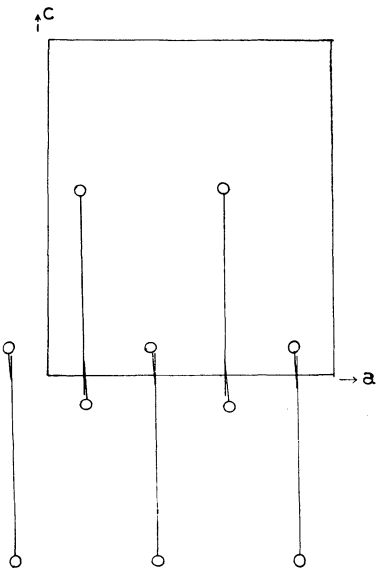

Fig. 3(a).

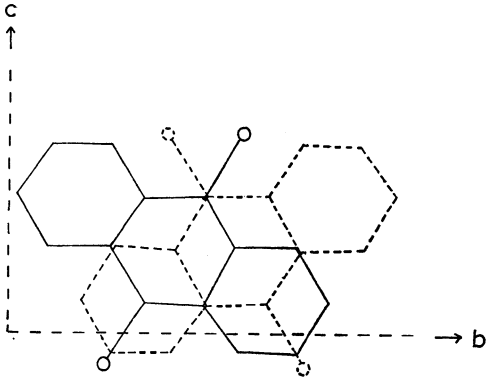

Fig. 3(b).

Fig. 3. Projection of 9,10-dichloroanthracene molecules onto ac and bc plane in α-form crystal (a) ac-projection (b) bc-projection.

transition to both the $^1B_{3u}$ and $^1B_{2u}$ excited states may occur only along the c axis in the ac plane. The crystalline spectrum is shown in Fig. 2.

The first absorption band at 23800 cm^{-1} is in good agreement with this prediction, since the first 0–0 transition is much stronger along the c axis than the a axis, and the second peak at 25500 cm^{-1} is also stronger along the c axis. The third peak around 26600 —27000 cm^{-1} shows a significant deviation from this character, therefore this band should be regarded as being mixed with a band different origin than that of the first and second peaks. The measured plane is an ac plane of a monoclinic crystal, therefore the possibility of Davydov type band splitting can be eliminated since there is no difference in the crystalline selection rule between the a-axis and the c-axis. The most reasonable explanation for the appearance of the out of plane absorption band in this region can be based on a charge transfer mechanism between the molecules in the crystal. The direction of the transition moment for the charge transfer absorption band should be along the line connecting the center of the donor and acceptor molecules. Therefore in the region around 26000—28000 cm^{-1}, there might be two bands with different polarization character which are overlapping each other. The first is the in-plane band, which is the third vibrational progression of the transition to the $^1B_{3u}$ state, and the second is the charge transfer transition, which has a polarization vertical to the plane of the benzene rings in this crystal. Rice and his coworkers[12] have estimated the charge transfer level for the anthracene crystal to be 3.5±0.5 eV, while the present result shows that it is 3.36 eV in this crystal.

The next absorption band around the 34000 to 40000 cm^{-1} region also shows peculiar characteristics. The absorption band along the c-axis might be the transition to the $^1B_{2u}$ state, the polarization being along the long axis of the molecule, but the structure is blurred. The a-axis component shows again an exceptional out-of-plane polarization, therefore it should be regarded as a Rydberg type transition of $2p\pi$ to 3s or to higher Rydberg states in an isolated molecule. However, the 3s and 4s or higher s orbitals have larger radii than the $2p\pi$ orbital, therefore the Rydberg levels of 3s or *n*s will form broader energy bands in the crystal. The ionization continuum level may be lowered in the crystal, thereby causing mixing of the ns band with the continuum level. The position of this band starts at 34000 cm^{-1}, which is in good agreement with the energy threshold for the anthracene[4-6] band to band transition. The band shape of this transition shows a gradual increase up to the higher energy region; this characteristic is certainly different from the usual band shape of molecular transitions. Anyway, the so-called band to band transition found by photoelectric conductivity measurement should be regarded as due to the $2p\pi$ band - *n*s Rydberg band transition.

The c-axis polarized absorption band shows unusually smooth features, although the absorption peak of the $^1B_{2u}$ molecular excited state transition should be located in this region. A drastic change in the molecular $^1B_{2u}$ excited state might be resulted through the interaction of the $2p\pi$ excited state with the Rydberg *n*s and continuum states.

The developed plane of the α-form of DCA crystal presents a fortunate case for observing a charge transfer absorption and the band to band transition of a 2p→*n*s type. It is confirmed that a charge transfer absorption takes place even between the same molecules, one acting as a donor and the other as an acceptor. It should also be emphasized that spectroscopic evidence of the Rydberg and continuum states is obtained for the present crystal in which the molecules are stacked parallel to each other, but which are actually in a skewed sandwich configuration in an infinitely linear array. The intensity of the charge transfer absorption band is extraordinarily enhanced in the present crystal, which may mean that the charge transfer transition is borrowing intensity from the continuum level of the band to band transition.

b) β-Form of 9, 10-Dichloroanthracene. By sublimation both the α-form and the β-form of DCA crystal could be obtained; it was possible to distinguish between the two forms with a polarization microscope. The crystalline absorption of the β- form of DCA is presented in Fig. 4, in which spectra are shown for light polarized along the c- and the a-axis. The crystalline structure analysis of the β- form is now being carried out by Kuwano and Kondo,[13] and we present their preliminary results in Fig. 5.

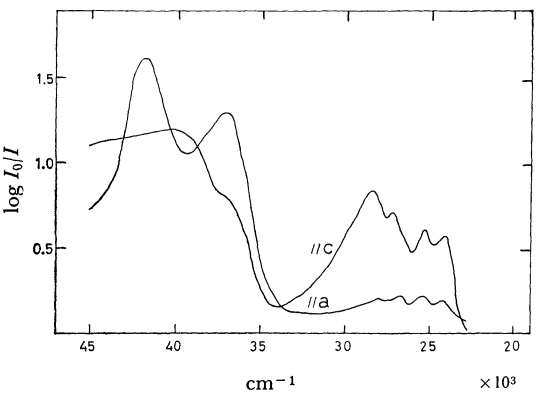

Fig. 4. Crystallin absorption spectra of β-form of 9, 10-dichloroanthracene crystal.

12) S. A. Rice, Private communication.

13) H. Kuwano and M. Kondo, private communication.

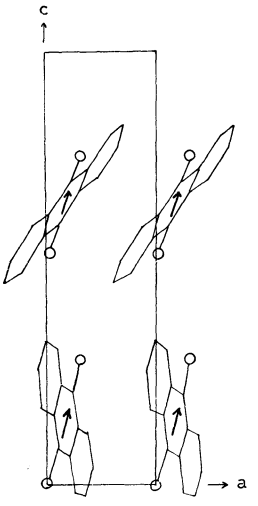

Fig. 5. Projection of 9,10-dichloroanthracene molecules onto ac plane in β-form crystal, where arrows means the direction of the short-axis polarized transition.

The first absorption band at 23800 cm^{-1} is assigned to the short axis polarized band of $^1B_{3u}$ character.

The molecular exciton state function for a triclinic crystal including two molecules in a unit cell is written as

$$\left.\begin{aligned}\Psi_+ &= \frac{1}{\sqrt{2N}}\left(\sum_{i=1}^{N}\phi_{1i}' + \sum_{j=1}^{N}\phi_{2j}'\right)\\ \Psi_- &= \frac{1}{\sqrt{2N}}\left(\sum_{i=1}^{N}\phi_{1i}' - \sum_{j=1}^{N}\phi_{2j}'\right)\end{aligned}\right\} \quad (1)$$

in which ϕ_{1i}' means that the molecule in the 1st site of the ith cell is excited and all other molecules are in the ground state. In the present case the (+) state of the $^1B_{3u}$ excited state has an additional contribution from the transition moments of both molecules, while in the (−) state two transition moments nearly cancel each other, with a slight residual moment along the c-axis.*2 The polarization ratio calculated for the (+) $^1B_{3u}$ excited state by using the assumption of the oriented-gas model is 12.6, while the observed value is 7.6.

The band splitting for each vibronic band is: the first peak is split by about 300 cm^{-1}, the c-axis is lower in energy, the splitting of the second peak is about 150 cm^{-1}. Around the third peak we found rather curious band shapes, and the c-axis band is much more separated from the 2nd peak and the splitting $(\nu_a - \nu_c)$ is −550 cm^{-1}. The splitting of the fourth peak is −450 cm^{-1}.

The next transition in the 37000—42000 cm^{-1} region is related to the $^1B_{2u}$ molecular excited state.

*2 Here the (+) state means in-phase combination of two transition moments shown in Fig. 5.

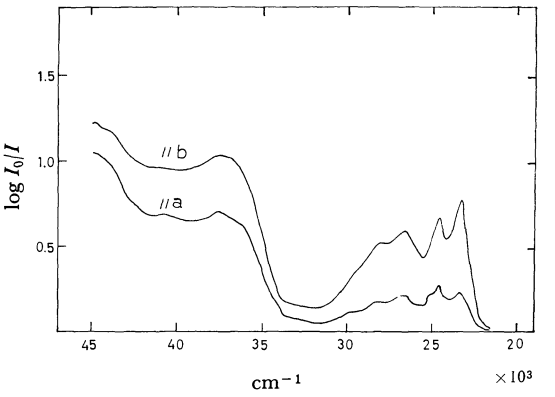

Fig. 6. Crystalline absorption spectra of 9,10-dibromoanthracene crystal.

The two peaks along the c-axis polarized band are separated by about 4800 cm^{-1}, and this might be correlated with the (+) and (−) states of Eq. (1) of the $^1B_{2u}$ molecular excited state.

The intensity ratio for (+) and (−) states is calculated to be 4 : 1, but the observed bands are overlapped, and it is difficult to separate into components and to discuss the intensity ratio for each transition. By combining those two transitions, the c-axis polarized band should have a much larger intensity than the a-axis polarized band, but it is actually smaller and broader. Following the result presented for the α-form of DCA, this could be the band to band transition in this region. It is expected that the mixing of the Rydberg or ionized continuum states with the molecular excited state will lead to such a complicated pattern of spectra.

c) 9,10-Dibromoanthracene. The crystalline absorption spectra of DBA are shown in Fig. 6, which is measured with the ab plane by the light polarized along the a- and b-axes. The projection of molecules onto the ab plane is shown in Fig. 7 following the result of Trotter.[10] The exciton state of the triclinic crystal is given by Eq. (1), and the band splitting and polarization ratio can be discussed in terms of these exciton state functions.

The first absorption band around the 32400 cm^{-1} region is regarded as the transition to the $^1B_{3u}$ excited state, but the vibrational progression is slightly distorted as compared with the solution spectra. By careful examination of the a- axis spectra, it is found that a little hump exists at 25300 cm^{-1} in the a-axis polarized spectrum. This small shoulder might be assigned to a transition of the charge transfer type between molecules in the same crystallographic position. The reason for the small intensity of this band might be due to the weak electron overlap between the molecules. The vibrational progressions of the apparent 0-0, 0-1 and 0-2 transitions are different from that in solution; this discrepancy may be attributed

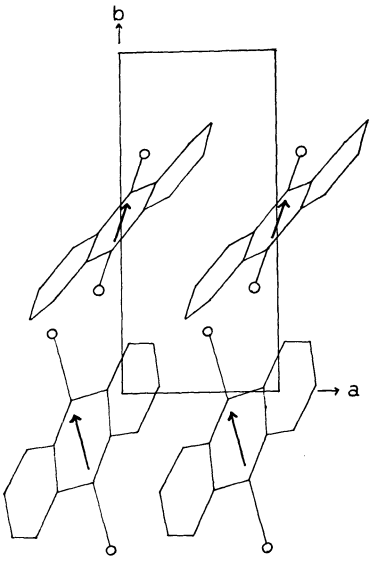

Fig. 7. Projection of 9, 10-dibromoanthracene molecules onto the ab plane, where arrows means the direction of the short-axis polarized transition.

to the interaction between the vibronic state and the charge transfer state.

The polarization ratio of the first 0-0 band (I_b/I_a) is 3.2, while the value calculated on the basis of the oriented gas model is 12.1. These values are not in good agreement, but this sort of discrepancy can be explained as due to crystal field mixing with higher excited states.

The second absorption band around the 37000 cm^{-1} region does not show any appreciable splitting. When we take the excition state function as given by Eq. (1) (see Fig. 7), transitions to the (+) state should occur both along the a- and b-axes, but transitions to the (−) state may cancel and will therefore not be seen in the crystal absorption.

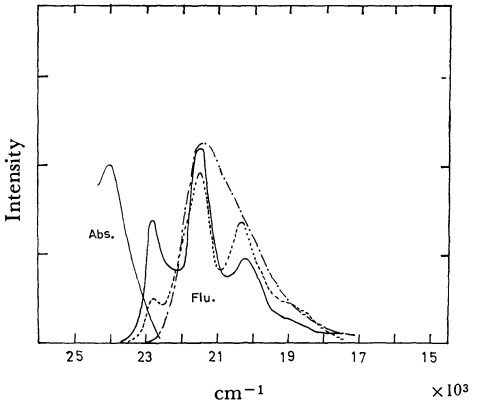

Fig. 8. Temperature dependence of crystalline flourescence spectrum of α-form of 9, 10-dichloroanthracene.
—— 4.2°K ····· 77°K ·—· 330°K

The polarization ratio (I_a/I_b) observed is 1.5 while the calculated value is 0.9. The third absorption band increases in intensity with increasing energy in the 45000 cm^{-1} region, and it may be related to the higher molecular excited states and the continuum state. Also a contribution from the band to band transition may occur in this region.

2. Fluorescence Spectra of Crystals. *a) α-Form of 9, 10-Dichloroanthracene.* The fluorescence spectra of the α-form of DCA is shown in Fig. 8 for different temperatures, the measurement being made with a Carl Zeiss monochromator with a slit width of less than 0.1 mm. The absorption edge at 300°K is also shown in order to illustrate the effect of reabsorption by the crystal. The absorption starts at 22500 cm^{-1} at 300°K, while emission begins at 23700 cm^{-1} at 4.2°K. The origin of the emission band is overlapped with the absorption at 300°K, therefore the effect of reabsorption will change the shape of the emission band at 300°K. At lower temperatures the absorption band edge moves to the shorter wavelength region, and therefore the first 0-0 emission band in the crystal can be clearly recognized. The fluorescence spectra of DCA thus far reported[7,14] are all different from the present result, and it may be that these spectra have been reported for crystals not as pure as the present one. The fluorescence spectra show a resolved vibrational progressions of about 1400 cm^{-1} at 4.2°K, while the solution value for emission is 1400 cm^{-1}.

The shift of the first 0-0 band from absorption to emission is about 860 cm^{-1} and it is almost certain that excimer formation does not take place in this crystal as judged from the shift and the shape of the emission band. This situation is illustrated in Fig. 9 together with cases of stronger interaction in the excited state. In this figure, the electronic energy level is correlated with the intermolecular distance R. The horizontal levels drawn in the potential curve denote the energy of the intramolecular vibrational mode, not the intermolecular vibration. The three potential

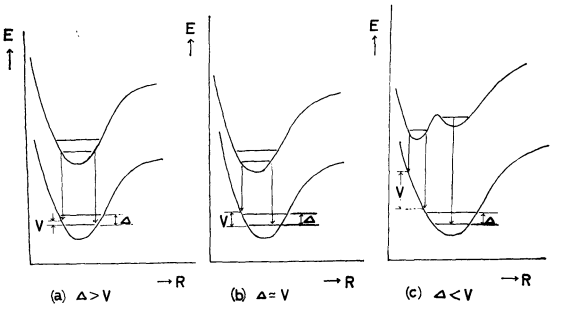

Fig. 9. Potential energy diagram of the excited and ground state of the dimer pair.

14) E. Bock, J. Ferguson and W. G. Schneider, *Can. J. Chem.*, **36**, 507 (1958).

curves illustrate the weak, medium and strong types of excited state interaction. It is thought that excimer formation will occur after excitation by the exciton and the charge transfer type interaction at a closer intermolecular distance than in the ground state. In this case the movement of molecules is considered to occur so as to avoid the steric repulsion between the bulky substituent groups. The magnitude of the stabilization will be dependent on the intermolecular distance and electron overlap between molecules.[15]

However, the energy of the emission band of the excimer is also dependent on the potential energy curve of the repulsive ground state, and this might be the reason why the excimer emission is always broad and structureless. In Fig. 9 the V-value shows the uncertainty in the ground state potential energy, and we assume that this value represents the width of the ground state potential energy. Therefore we will take this value as the uncertainty in the energy under the condition that emission is occurring at the bottom of the excited state potential curve. From this criterion, the α-form of DCA has a V-value smaller than the intramolecular vibrational spacing, Δ, implying that the center of the excited state potential function moves slightly to smaller intermolecular distances in the excited state.

This behavior may be explained on the basis of the steric repulsion between the two chlorine atoms, which have larger van der Waals radii than the carbon atoms. The present crystal has an unfavorable configuration to form the excimer, since intermolecular appoach in the excited state will be hindered by the overcrowding of the chlorine atoms.

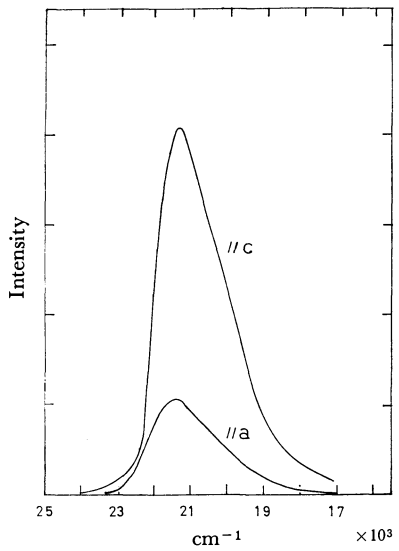

Fig. 10. Polarization of the fluorescence spectrum of α-form of 9,10-dichloroanthracene.

Further evidence for molecular characteristics in the emission of α-form type crystal is that the polarization ratio of the emission along the c-axis is much stronger than along the a-axis (*cf.* Fig. 10). The ratio is 4 : 1 ($I_c : I_a$), which is less than in the case of absorption (12 : 1), but still the high dichroic ratio indicates the molecular character of the $^1B_{3u}$ excited state in the emission.

b) β-Form of 9, 10-Dichloroanthracene. The emission spectra of the β-form of DCA at several different temperatures are shown in Fig. 11, and it is found that drastic change in emission spectra

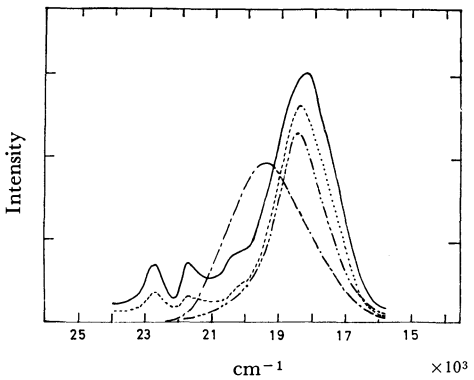

Fig. 11. Temperature dependence of the crystalline fluorescence spectra of β-form of 9,10-dichloroanthracene.
—— 4.2°K ····· 13°K —··— 77°K
—·— 300°K

occurs with the change of temperature. A broad emission band is observed at 19280 cm^{-1} at 300°K, which is 4700 cm^{-1} below the first crystalline absorption peak. This broad band moves to lower frequency at 77°K, the peak being at 18600 cm^{-1}, which is 5400 cm^{-1} below the crystal absorption. At liquid helium temperature the peak shifts to 18200 cm^{-1}, and in addition to this broad band, a monomer band with two or three vibrational bands has been observed starting at 22940 cm^{-1}. The appearance of two kinds of emissions, one, that of the excimer, and the other, that of the monomer, can be explained by assuming a hump in the potential energy curve in the excited state.*3 A similar situation has been recognized in the case of perylene excimer emission.[16] This mechanism will be explained by the energy diagram in

15) J. N. Murrell and J. Tanaka, *Mol. Phys.*, **7**, 363 (1964).

*3 The possibility of a phase transition from the β-form to the α-form at lower temperature is excluded since the change in the fluorescence spectra is reversibly observed with change of the temperature, in spite of the fact that a modification of the crystalline form was not observed. If the phase transition were taking place at lower temperature a significant change in the optical properties of the crystal should be detectable with a polarization microscope.

16) J. Tanaka, This Bulletin, **36**, 1237 (1963).

Fig. 9 (c) where the excited molecule will move to a shorter intermolecular distance to form the excimer, but the movement of the molecule will be hindered at lower temperatures due to the existence of the little hump in the potential curve and eventually will emit monomer type emission. The broader band character of the longer wavelength emission can be explained by assuming a V-value which is larger than the vibrational spacing. The relatively large temperature dependence of the longer wavelength band at higher temperature is typical of excimer emission. It is interesting that the so-called 6000 cm^{-1} rule[17] is nearly satisfied in the present crystal, the value at 4.2°K being 5800 cm^{-1}.

c) 9, 10-Dibromoanthracene. The fluorescence spectra of DBA have been measured at several different temperatures, and are shown in Fig. 12. They show relatively little temperature dependence, but the emission band as a whole shifts to lower frequency as compared with the α-form of DCA. The shift measured at the first 0-0 transition is 2150 cm^{-1}, which is larger than the α-form of DCA, but far less than the β-form of DCA. The potential energy levels based on these numbers are pictured in Fig. 9 (b), and it is estimated that the V-value is nearly the same order of magnitude as the Δ-value of the vibrational spacing. It is also interesting that the 0–0 emission band is clearly seen at 77°K rather than at 4.2K; this indicates that the equilibrium configuration of the excited state is shifted from the center of the ground state configuration, resulting in a small Franck-Condon overlap factor for the 0-0 transition at 4.2°K. Comparison with the cases of the α- and β-forms of DCA shows that both the shift of the emission band and the V-value are intermediate in the DBA crystal. The polarization ratio of the emission band measured along the b- and a-axes is 1.7,

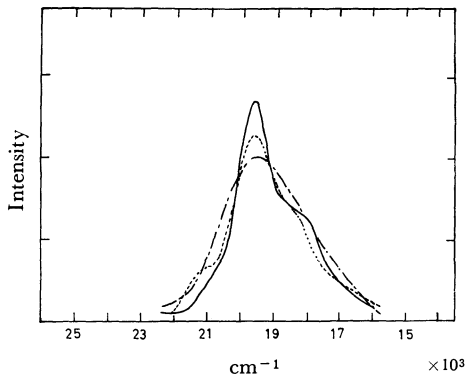

Fig. 12. Temperature dependence of the crystalline flourescence spectrum of 9, 10-dibromoanthracene.
—— 4.2°K ····· 77°K —·— 300°K

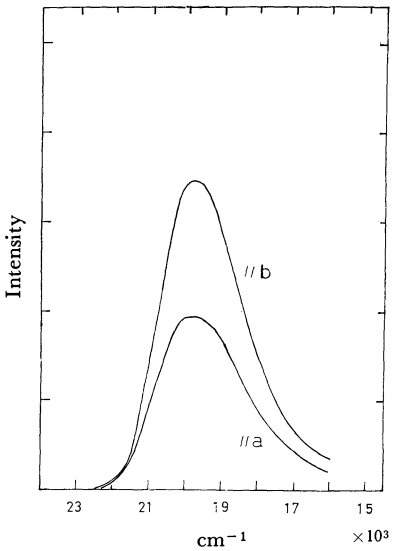

Fig. 13. Polarization of the fluorescence spectrum of 9, 10-dibromoanthracene.

while that of the absorption is 3.2 (*cf.* Fig. 13). The decrease in the dichroic ratio means that the charge transfer contribution to the emission component is increased in the DBA crystal.

The results obtained for the three different crystals indicate that excimer formation is most favorable when intermolecular approach in the excited state is not hindered by bulky substituent groups. The larger shift for β-DCA compared with DBA indicates that the π-electron overlap is more efficient for β-DCA than for DBA even in a similar crystallographic relationship, since the van der Waals radii are smaller for chlorine atoms than for bromine.

Conclusion

The electronic interaction of molecules in a crystal is primarily governed by the relative orientation and the interatomic distances between molecules. The charge transfer absorption band could be observed for the α-DCA crystal where the inter-molecular electron overlap in the ground state configuration is apparently larger than for other crystals. The excimer type emission is found most prominently in the β-DCA, and DBA crystals, where the molecules are stacked nearly parallel to each other but at relatively large distances. This configuration is most favorable for excimer formation, since the bulky substituent groups are located in such a way that the molecular movement to the shorter intermolecular distance in the excited state may be least hindered. The intermolecular electron overlap is essential for excimer formation, therefore it can be naturally concluded that the molecules will move to as short an intermolecular distance as possible in the excited state.

17) J. B. Birks, M. O. Lumb and I. H. Munro, *Proc. Roy. Soc., (London)*, **A280**, 289 (1964).

For the ground state configuration the intermolecular separation is larger for the β-DCA and DBA crystals than for the α-DCA crystal, therefore it is most probable that the excimer force should operate to bring the molecules into a closer position in the excitd state. The nature of the excimer force has not been fully discussed in the present text. It is conventionally divided into two parts: the exciton type and charge transfer type interactions will be most important; the former will be dominant at longer distances, and the latter is significant in the region of strong electron overlap. At the real excimer equilibrium distance, both forces will be strongly mixed and will be balanced by the potential of the exchange repulsion. The van der Waals radius of each atom in the ground state will be determined by this latter type of exchange repulsion between closed-shell atomic systems. For the excited state, however, an open-shell electron configuration will allow the molecules to approach each other, since the exchange repulsion between open-shell excited configuration and ground configuration will be smaller than that with closed shell ground electron configurations. It will mean that the van der Waals radius may be smaller for the excited state than the ground state configuration.

Finally, it should be emphasized again that the band to band transition of $2p\pi$ to ns type is found for the α-DCA crystal in the 34000 cm^{-1} region. This finding should throw some light on the mechanism of photoconductivity in organic crystals.

The authors wish to express their sincere thanks to Drs. H. Kuwano and M. Kondo of the Sankyo Pharmaceutical Co. for their kind communication of their X-ray crystal results prior to publication.

BULLETIN OF THE CHEMICAL SOCIETY OF JAPAN VOL. 41 41—44 (1968)

An NMR Study of Proton Exchange in Alcohols. II.*1 Proton Transfer in the Water-Isopropanol System

Toshio FUKUMI, Yuzuru FUJIWARA, Yoji ARATA and Shizuo FUJIWARA

Department of Chemistry, Faculty of Science, The University of Tokyo, Hongo, Tokyo

(Received June 16, 1967)

Proton exchange has been investigated in the system of water and isopropanol by means of high-resolution nuclear magnetic resonance. The rates of proton transfer have been obtained at different hydrogen ion concentrations and at different ratios of water and isopropanol. It has been shown that the exchange reaction is of higher order with respect to water and isopropanol concentrations. Possible mechanisms of proton transfer have been discussed, and values for their respective rate constants given.

Proton transfer in systems of water and simple aliphatic alcohols has been studied by several workers.[1-3] In these studies the exchange reaction has been assumed to be of first order with respect to water and alcohol concentrations. However, this assumption has not been verified in all the cases which have been reported so far. In this note, we attempted to check the validity of this assumption using a water-isopropanol system. Several types of exchange reaction will be proposed to explain the rate of proton transfer obtained experimentally, and values for their respective rate constants will be given. For this purpose, the water-isopropanol system has the following advantages: (i) spectral analysis can always be done to a good approximation using first-order perturbation theory, and (ii) since the proton exchange is much slower than in the cases of methanol-water and ethanol-water systems, the proton transfer can be studied over a wide range of molar ratios of water and isopropanol, thus making it possible to determine the order of the exchange reactions in some cases.

Experimental

Commercial reagent-grade isopropanol was dried by treatment with magnesium and a trace of iodine,[4] and was then distilled several times at ordinary pressure. Water was deionized by passing it through a

*1 Part I, S. Fujiwara, Y. Fujiwara and M. Nagai, This Bulletin, **39**, 2356 (1966).

1) E. Grunwald, C. F. Jumper and S. Meiboom, *J. Am. Chem. Soc.*, **84**, 4664 (1962).

2) Z. Luz, D. Gill and S. Meiboom, *J. Chem. Phys.*, **30**, 1540 (1959).

3) W. G. Paterson, *Can. J. Chem.*, **41**, 2472 (1963).

4) H. Lund and J. Bjerrum, *Ber.*, **64**, 210 (1931).

column packed with a cation exchange resin, and was boiled just before use. In the following, the readings of a Toa Dempa Model HM-5A pH meter with micro glass and calomel electrodes will be cited as h.

A Varian HA-100 high-resolution NMR spectrometer operating at 100 Mc/sec was employed at 28°C under the condition of slow passage and negligible saturation. Several examples of the spectra are shown in Fig. 1. Chemical shift data for the protons of water and isopropanol are summarized in Fig. 2.

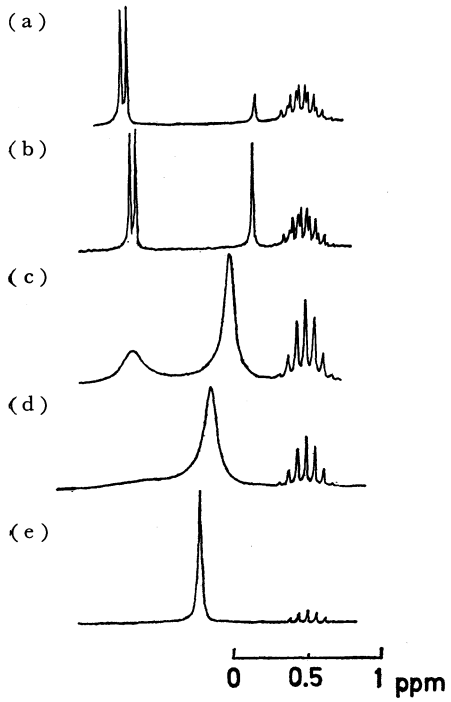

Fig. 1. NMR spectra of isopropanol containing water at various concentrations, $[H_2O]$ being (a) 2.78 M, (b) 5.56 M, (c) 11.1 M, (d) 22.2 M, and (e) 33.4 M.

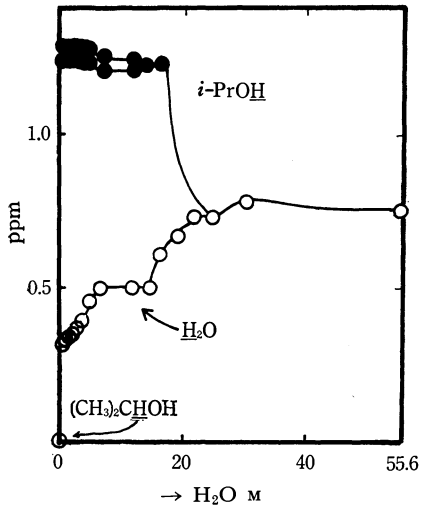

Fig. 2. The change in the chemical shifts of the OH protons of water and isopropanol in the water-isopropanol system. The CH proton signal of isopropanol is tentatively taken as a reference of the chemical shifts.

The average times a proton is bonded to a specific oxygen atom of isopropanol, and water are designated as τ_A, and τ_W, respectively. τ_A^{-1} may be expressed as:

$$\tau_A^{-1} = \tau_{AA}^{-1} + \tau_{AW}^{-1} \quad (1)$$

where τ_{AA}^{-1}, and τ_{AW}^{-1} refer to the proton transfer rate between isopropanol and isopropanol, and that between water and isopropanol, respectively. When the OH signals of water and isopropanol are observed separately, the full widths of the resonance line at half height (in cycles per second), Δ_A and Δ_W, are measured to obtain the specific rate of exchange. τ_A and τ_W are given by the relations:

$$\begin{aligned} \tau_W^{-1} &= \pi\Delta_W - \pi\Delta_W^0 \\ \tau_A^{-1} &= \pi\Delta_A - \pi\Delta_A^0 \end{aligned} \quad (2)$$

where Δ_W^0, and Δ_A^0 are full widths at half height for the OH protons of water, and isopropanol in the absence of exchange. When the two OH signals collapse into a singlet, the line-width, Δ, is given by[5]:

$$\Delta = p_A\Delta_A^0 + p_W\Delta_W^0 + \pi^{-1}p_A^2p_W^2(2\pi\delta)^2(\tau_{AW}+\tau_W) \quad (3)$$

where p_A, and p_W, are the fractional populations for the OH protons of isopropanol, and water, respectively, and δ is the chemical shift difference (in cycles per second) between the OH protons of water and isopropanol, which is dependent on the ratio of water and isopropanol. From Eq. (3), the sum $(\tau_{AW}+\tau_W)$ can be obtained, and using the relation

$$\frac{[i\text{-PrOH}]}{\tau_{AW}} = \frac{2[H_2O]}{\tau_W}, \quad (4)$$

which is valid for equilibrium, τ_{AW}, and τ_W can be obtained separately.

Results and Discussion

In Fig. 3, the line-widths for the OH protons of water and isopropanol at $h=6.5$ are plotted as a function of the molar concentration of water, $[H_2O]$. The line-widths, and therefore the exchange rates, are strongly dependent on h. For $[H_2O]=2.78$ M, the exchange is shown to be of first order with respect to h. In Figs. 4 and 5 $(\tau_W h)^{-1}$, $(\tau_{AW}h)^{-1}$, and $(\tau_{AA}h)^{-1}$ are plotted as a function of $[H_2O]$.

For the proton exchange between water and isopropanol, the following reaction schemes are assumed:

$$a\,i\text{-PrOH} + b\,H_2O + H_3O^+ \xrightarrow{k_1} \quad (I)$$

$$c\,i\text{-PrOH} + d\,H_2O + i\text{-PrOH}_2^+ \xrightarrow{k_2} \quad (II)$$

For these reactions, the following relation holds:

5) See *e. g.*, J. A. Pople, W. G. Schneider and H. J. Bernstein, "High-resolution Nuclear Magnetic Resonance," McGraw-Hill, New York (1959), p. 222.

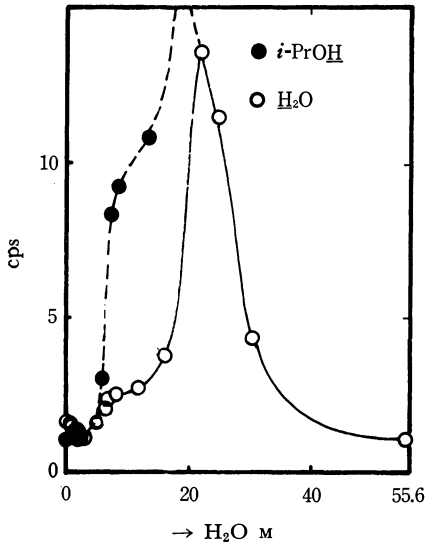

Fig. 3. The change in the line-widths of the OH protons of water and isopropanol in the water-isopropanol system.

$$-\frac{d}{dt}[H_2O] = \frac{2}{\tau_W}[H_2O] = k_1[i\text{-PrOH}]^a[H_2O]^b[H_3O^+] + k_2[i\text{-PrOH}]^c[H_2O]^d[i\text{-PrOH}_2^+] \quad (5)$$

It is assumed that the following equilibrium exists in the solution:

$$i\text{-PrOH} + H_3O^+ \overset{K}{\rightleftharpoons} i\text{-PrOH}_2^+ + H_2O$$

and that h is equal to $-\log([H_3O^+]+[i\text{-PrOH}_2^+])$.

$$(\tau_W h)^{-1} = \frac{1}{2}(k_1[i\text{-PrOH}]^a[H_2O]^{b-1} + k_2K[i\text{-PrOH}]^{c+1}[H_2O]^{d-2}) \times (1+K[i\text{-PrOH}][H_2O]^{-1})^{-1} \quad (6)$$

For $[H_2O] \lesssim 0.3$ M, $(\tau_W h)^{-1}$ decreases with increasing $[H_2O]$, as shown in Fig. 4. In this case, Eq. (6) can be approximated as:

$$(\tau_W h)^{-1} = \frac{1}{2}k_2K[i\text{-PrOH}]^{c+1}[H_2O]^{d-2} \times (1+K[i\text{-PrOH}][H_2O]^{-1})^{-1} \quad (7)$$

For $[H_2O] > 0.3$ M, $(\tau_W h)^{-1}$ increases with increasing $[H_2O]$. In this case, Eq. (6) can be approximated as:

$$(\tau_W h)^{-1} = \frac{1}{2}k_1[i\text{-PrOH}]^a[H_2O]^{b-1} \quad (8)$$

From Eqs. (7) and (8) and Fig. 4, it is found that $a=1$, $b=2$, and $d=1$. When $[H_2O]$ is small, $(\tau_W h)^{-1}$ changes greatly with a small change in $[H_2O]$. Since $[i\text{-PrOH}]$ changes only a little in this region of low concentration, c cannot be determined from this experiment. In the proton transfer reactions (I) and (II), the roles of water

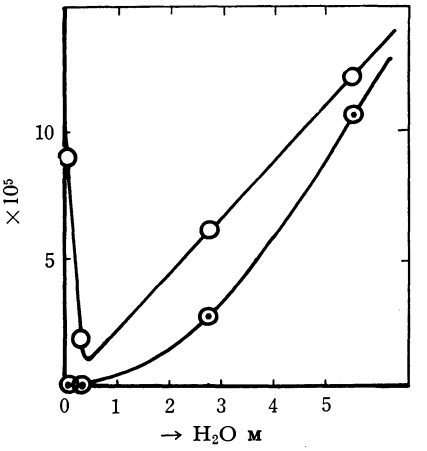

Fig. 4. The change in $(\tau_W h)^{-1}$ and $(\tau_{AW} h)^{-1}$ with the concentration of water in the water-isopropanol system. ○ and ⊙ refer to $(\tau_W h)^{-1}$ and $(\tau_{AW} h)^{-1}$, respectively.

and isopropanol molecules are interchanged, so that it is assumed that $c=2$. From these results, the constants k_1, k_2, and K can be determined. These constants can also be determined from the change in $(\tau_{AW}h)^{-1}$ in a similar way. The results are as follows:

$$k_1 = 2 \times 10^4 \quad l^3\,\text{mol}^{-3}\,\text{sec}^{-1}$$
$$k_2 = 5 \times 10^3 \quad l^3\,\text{mol}^{-3}\,\text{sec}^{-1}$$
$$K = 2 \times 10^{-4}$$

In order to explain the change in $(\tau_{AA}h)^{-1}$, the following reaction schemes are assumed:

$$e\,i\text{-PrOH} + f\,H_2O + H_3O^+ \xrightarrow{k_3} \quad \text{(III)}$$

$$g\,i\text{-PrOH} + i\text{-PrOH}_2^+ \xrightarrow{k_4} \quad \text{(IV)}$$

From Fig. 5, it is found that $f=1$. However, e and g cannot be determined for a reason similar

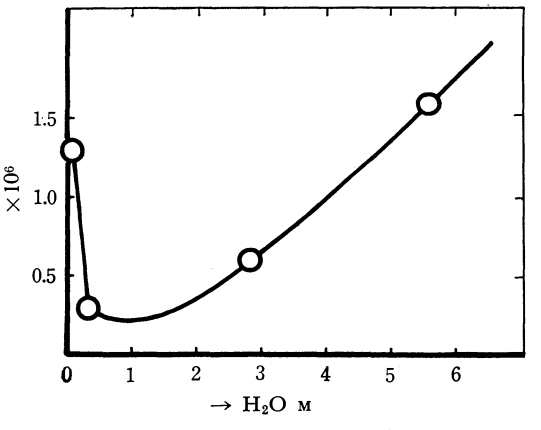

Fig. 5. The change in $(\tau_{AA} h)^{-1}$ with the concentration of water in the water-isopropanol system.

to that mentioned above for c in reaction (II). If both e and g are tentatively assumed to be unity, the constants k_3 and k_4 become:

$$k_3 = 2 \times 10^6 \quad l^2\,\mathrm{mol}^{-2}\,\mathrm{sec}^{-1}$$

$$k_4 = 3 \times 10^6 \quad l\,\mathrm{mol}^{-1}\,\mathrm{sec}^{-1}$$

Another possible reaction for proton exchange between water and isopropanol is the following one, which is not catalyzed by acid:

$$i\text{-PrOH} + H_2O \xrightarrow{k_5} \qquad \text{(V)}$$

From the values for τ_W^{-1} and τ_{AW}^{-1} obtained for the sample with no acid added externally, k_5 is found to be $2\,l\,\mathrm{mol}^{-1}\,\mathrm{sec}^{-1}$.

From the above results, it is clear that in the water-isopropanol system, proton exchange reactions are not of first order with respect to water and isopropanol concentrations, as has been assumed in previous works. Possible mechanisms for proton transfer will be discussed in the following.

Possible Mechanisms for Proton Transfer. At low water concentrations, the isopropyloxonium ion plays a majar role in proton transfer. Possible models for proton transfer are shown in the following:

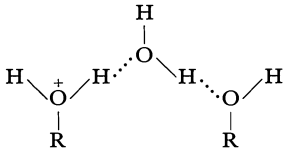

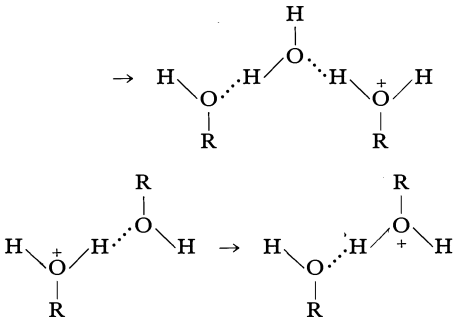

At higher water concentrations, a possible model for proton exchange is:

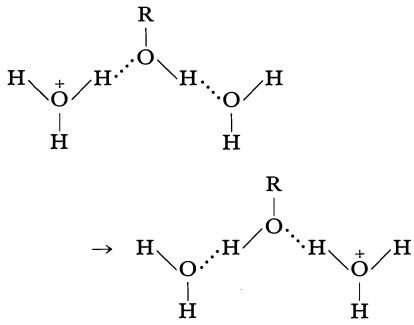

The above mechanisms can be responsible for the proton transfer between water and isopropanol, and for that between isopropanol and isopropanol.

BULLETIN OF THE CHEMICAL SOCIETY OF JAPAN VOL. 41 45—48 (1968)

The Dimerization of Propylene over a Nickel Oxide-Silica-Alumina Catalyst

Hisao IMAI, Touji HASEGAWA and Hiroshi UCHIDA*1

Government Chemical Industrial Research Institute, Tokyo, Shibuya-ku, Tokyo

(Received July 1, 1967)

The composition of hexene isomers produced by the dimerization of propylene over a nickel oxide-silica-alumina catalyst has been examined under the following experimental conditions: 10—300 kg/cm², 100 and 200°C. Under a typical set of experimental condition (50 kg/cm², 200°C), eight hexene isomers, *i. e.*, 4-methyl-*trans*-2-pentene, 4-methyl-*cis*-2-pentene, 2-methyl-1-pentene, *trans*-2-hexene, *cis*-2-hexene, 3-methyl-*trans*-2-pentene, 3-methyl-*cis*-2-pentene, and 3-methyl-1-pentene, have been found to be the primary products of the dimerization. Among these, more trans isomers are produced initially than the corresponding cis isomers for 4-methyl-2-pentenes and 2-hexenes, but the reverse is true for 3-methyl-2-pentenes. Under higher pressures, 2, 3-dimethylbutenes are also produced at 200°C. A reaction scheme assuming the intermediates of cyclobutane derivatives has been proposed to explain the above findings. The scheme may also explain the unique order of the activity of the present catalyst for a series of *n*-olefins.

The catalyst consisting of nickel oxide, silica, and alumina has been found to be an effective catalyst for the dimerization of olefins.[1-3] One of the remarkable features of this catalyst system is its activity in relation to a series of *n*-olefins. In contrast to usual acid-type catalysts, the nickel oxide-silica-alumina shows a higher activity for a lower olefin, *i. e.*, the highest activity for ethylene.[2,3] Although some efforts have previously been made to elucidate this feature of the catalyst,[2,4] the problem remains practically unsettled.

In the dimerization of ethylene over this catalyst system, the composition of butene isomers was examined in order to get an insight into the mechanism of the reaction.[5-7] It may be expected that more information on the mechanism can be obtained in the dimerization of propylene because of the more complex shape of a propylene molecule, and so the composition of the hexene isomers produced by the dimerization of propylene has been examined in order to determine the primary products of the reaction.*2 A reaction scheme assuming the intermediates of cyclobutane derivatives has been proposed; this scheme may also suffice to explain the above-mentioned feature of the nickel oxide-silica-alumina catalysts.

Experimental

Materials. A nickel oxide-silica-alumina catalyst composed of 3 atom% nickel, 3 atom% aluminum, and 94 atom% silicon was prepared by a co-precipitation method described elsewhere.[5] The structural characteristics of the catalyst are summarized in Table 1. The specific surface area (S) was obtained by applying the standard B. E. T. method to the adsorption isotherm of nitrogen at −196°C; the mean pore diameter (d) was estimated by the equation, $d=4V_g/S$, where the total pore volume (V_g) was obtained from the amount of nitrogen adsorbed at the relative pressure of 0.967 in the adsorption of nitrogen at −196°C; the acidity was measured by a quinoline chemisorption method at 300°C on the catalyst samples before and after the removal of nickel oxide, and the acidity after the removal was defined as the acidity due to alumina-silica, and the difference between the two, as the acidity due to nickel oxide-silica.[5]

Table 1. Structural characteristics of the catalyst

Composition (Ni : Al : Si)	3 : 3 : 94 by atom ratio
Specific surface area	342 m²/g
Mean pore diameter	48.1 Å
Acidity	
Acidity due to nickel oxide-silica	1.50×10^{-4} meq./m²
Acidity due to alumina-silica	1.73×10^{-4} meq./m²

*1 Present address: Faculty of Engineering, Nagoya University, Chikusa-ku, Nagoya.

1) K. Morikawa, N. R. Trenner and H. S. Taylor, *J. Am. Chem. Soc.*, **59**, 1103 (1937).
2) M. Koizumi, *J. Institute Polytechnics, Osaka City University*, **4**, 1 (1953).
3) J. P. Hogan, R. L. Banks, W. C. Lanning and A. Clark, *Ind. Eng. Chem.*, **47**, 752 (1955).
4) A. Ozaki, *Bull. Tokyo Inst. Tech., Series-B*, 109 (1960).
5) H. Uchida and H. Imai, This Bulletin, **35**, 989, 995 (1962).
6) H. Imai and H. Uchida, *ibid.*, **38**, 925 (1965).
7) T. Matsuda and T. Shiba, *Nippon Kagaku Zasshi (J. Chem. Soc. Japan, Pure Chem. Sect.)*, **88**, 308 (1967).

*2 Recently, Schultz *et al.* have studied the product distribution in the dimerization of propylene over cobalt-oxide-on-carbon catalysts; R. G. Schultz, J. M. Schuck and B. S. Wildi, *J. Catalysis*, **6**, 385 (1966).

Polymerization-grade propylene (purity>99.9%) was obtained from the Nippon Petrochemicals Co., Ltd., and was further purified by passing it successively through alkaline silica gel, sodium hydroxide, a supported copper catalyst, and alkaline silica gel. The standard samples of hexene isomers were obtained from the Tokyo Kagaku Seiki Co., Ltd.

Apparatus and Procedures. The dimerization of propylene was carried out by using a high-pressure flow system. The reactor body consisted of 25 mm-I. D. (50 mm-O. D.) stainless steel tubing, 50 cm long. A 5-m*l* portion of the catalyst was placed after the 10 cm preheating section at the entrance of the reactor. A thermocouple junction for measuring the reaction temperature was located at the center of the catalyst bed in a 2 mm-I. D. (4 mm-O. D.) stainless steel tube inserted through the bottom of the reactor. The temperature of the reactor was controlled by fluidizing heated iron powder around the reactor. The purified propylene was fed to the reactor by a high-pressure plunger pump, and the reactor effluent was cooled to −20°C in order to condense the dimerization products. A correction was made for uncondensed products by analyzing the uncondensed effluent gas.

The total dimers, trimers, and tetramers were determined by gas chromatographic analysis with a 3% silicon oil on a diasolid column (1 m) at 200°C, a hydrogen flame ion detector being used. All the hexene isomers, except for the *cis*-3-hexene from *trans*-3-hexene, were separated from one another and analyzed by gas chromatography using a 75-m silicon oil-coated capillary coulmn.

Prior to the reaction, the catalyst was treated *in situ* in a stream of dried air for 16 hr at 500°C, and then in a stream of purified nitrogen for 4 hr at the same temperature. After the temperature of the catalyst had been lowered to a reaction temperature in the nitrogen atomosphere, the feeding in of propylene was started.

Results

The conversion of propylene and the composition of the hexene isomers obtained under typical experimental conditions (200°C, 50 kg/cm²) are plotted against the contact time*3 in Fig. 1. Under these experimental conditions more than 80% of the products were dimers. The figure shows that the contents of eight isomers, *i. e.*, 4-methyl-*trans*-2-pentene, 4-methyl-*cis*-2-pentene, 2-methyl-1-pentene, *trans*-2-hexene, *cis*-2-hexene, 3-methyl-*trans*-2-pentene, 3-methyl-*cis*-2-pentene, and 3-methyl-1-pentene, decrease as the contact time is increased, while those of the other isomers increase with an increase in the contact time.

As only three types of chain structure were found in the hexenes produced, the contents of the hexene isomers with the same chain structure were summed up to give the total amounts of *n*-hexenes, 2-methylpentenes, and 3-methylpentenes.

*3 Contact time is defined by $1/SV$, where the space velocity (SV) is expressed in terms of m*l* of propylene (at NTP) per hr per m*l* of the catalyst.

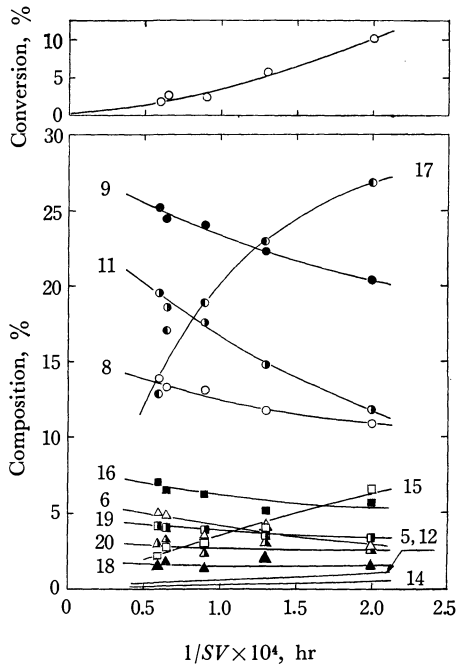

Fig. 1. Conversion of propylene as well as the composition of hexenes produced plotted against contact time.
Experimental condition: 200°C, 50 kg/cm²
5: 4-methyl-1-pentene, 6 △: 3-methyl-1-pentene, 8 ○: 4-methyl-*cis*-2-pentene, 9 ●: 4-methyl-*trans*-2-pentene, 11 ◑: 2-methyl-1-pentene, 12: 1-hexene, 14: 2-ethyl-1-butene, 15 □: *cis*- and *trans*-3-hexene, 16 ■: *trans*-2-hexene, 17 ◐: 2-methyl-2-pentene, 18 ▲: 3-methyl-*trans*-2-pentene, 19 ◨: *cis*-2-hexene, 20 ◭: 3-methyl-*cis*-2-pentene.

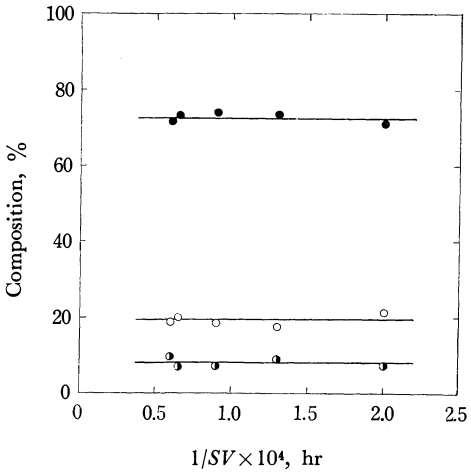

Fig. 2. Composition of hexenes expressed in terms of their chain structures as the function of contact time.
○: *n*-hexenes, ●: 2-methylpentenes, ◑: 3-methylpentenes

The composition of the product was classified in this way, and is plotted against the contact time in Fig. 2. The figure reveals that the content of the individual type remains constant with an increase in the contact time.

In Fig. 3, the ratios of trans- and cis-isomers are plotted against the contact time. The ratios of trans- and cis-isomers remain almost constant with an increase in the contact time; this is consistent with the results obtained in the dimerization of ethylene.[5] The figure also indicates the following fact; in the cases of 2-hexenes and 4-methyl-2-pentenes, more trans isomers are produced initially than the corresponding cis isomers, while in the case of 3-methyl-2-pentenes the reverse is true.

The composition of the products, expressed in terms of their chain structures, remained almost

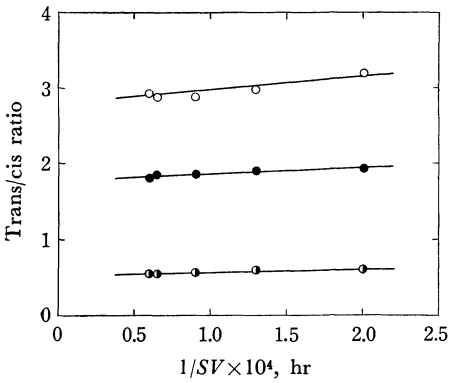

Fig. 3. Trans/cis ratios plotted against contact time.
○: 2-hexene, ●: 4-methyl-2-pentene,
◐: 3-methyl-2-pentene

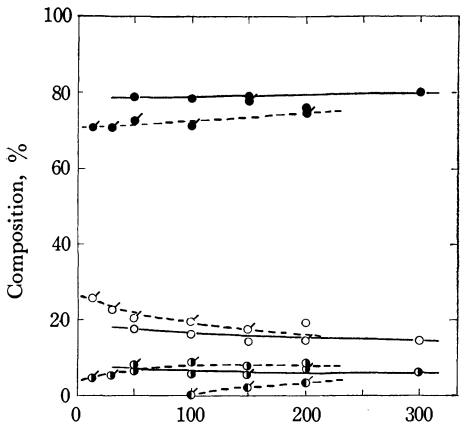

Fig. 4. Chain structures of hexenes produced at different experimental conditions.
n-hexenes at 100 (○) and 200°C (◌́)
2-methylpentenes at 100 (●) and 200°C (●́)
3-methylpentenes at 100 (◑) and 200°C (◑́)
2, 3-dimethylbutenes at 200°C (◐́)

constant with an increase in the contact time under all the experimental conditions studied; in Fig. 4 the average values are plotted against the reaction pressures for the reactions carried out at 100 and at 200°C. The figure shows that *n*-hexenes, 2-methylpentenes, and 3-methylpentenes are produced under all the experimental conditions studied, and that, at 200°C, 2, 3-dimethylbutenes are produced at higher pressures. The 2, 3-dimethylbutene content was too small for us to determine the primary product of the dimerization.

Discussion

Figure 1 shows that eight hexene isomers, *i. e.*, 4-methyl-*trans*-2-pentene, 4-methyl-*cis*-2-pentene, 2-methyl-1-pentene, *trans*-2-hexene, *cis*-2-hexene, 3-methyl-*trans*-2-pentene, 3-methyl-*cis*-2-pentene, and 3-methyl-1-pentene, are the primary products of the dimerization. It should be noticed that the 3-methyl-pentenes are primary dimerization products. The presence of 3-methylpentenes in the products of propylene dimerization was previously reported by Wachter,[8] who attributed them to the products of the secondary rearrangement. Indeed, the 3-methylpentenes cannot be explained as the primary products of the dimerization by a carbonium-ion mechanism[9] nor by any other mechanisms which assume an open-chain hydrocarbon as the activated intermediate, but they can be explained as being produced by secondary skeletal isomerization. Figure 2 shows that the composition of the hexene isomers, as expressed by their chain structures, does not change with the contact time, remaining at a constant value which is far from the equilibrium.[10] This fact indicates that no skeletal isomerization occurs under the experimental conditions studied, although double-bond-shift reactions are taking place. Thus, it may be concluded that the 3-methylpentenes are not produced by the secondary skeletal isomerizations of *n*-hexenes or 2-methylpentenes, but are produced directly by the dimerization of propylene.

The above conclusion, as well as the facts shown in Figs. 3 and 4, cannot be explained by the carbonium-ion mechanism nor by any other cation polymerization mechanisms which assume an open-chain hydrocarbon as the activated intermediate, although the catalyst activity is proportional to the number of nickel acid sites, as determined by the chemisorption of a basic molecule.[5]

Schoepfle and Ryan[11] proposed a mechanism

8) A. Wachter, *Ind. Eng. Chem.*, **30**, 822 (1938).
9) F. C. Whitmore, *ibid.*, **26**, 94 (1934).
10) Calculated from the thermodynamic data; F. C. Rossini *et al.*, "Selected Values of Physical and Thermodynamic Properties of Hydrocarbons and Related Compounds," Carnegie Press, Pa. (1953).
11) C. S. Schoepfle and J. D. Ryan, *J. Am. Chem. Soc.*, **52**, 4021 (1930).

of the dimerization of diphenylethylene which assumed an intermediate of a cyclobutane derivative. An examination of the present results has shown that the same mechanism may hold for the present reaction. A reaction scheme assuming the intermediates of cyclobutane derivatives can be described as follows:

$$C{=}C{-}C + S(Ni) \rightarrow C{=}C{-}C(ad) \quad (1)$$

(I)

$$I + C{=}C{-}C \rightarrow \underset{\text{(II)}}{\begin{array}{l} C_4\text{--}C_1 \\ \vert\ \ \vert \\ C_3\text{--}C_2 \end{array}}\!\!\begin{array}{l} \diagup C \\ \\ \diagdown C \end{array} + \underset{\text{(III)}}{\begin{array}{l} C_4\text{--}C_1 \\ \vert\ \ \vert \\ C_3\text{--}C_2 \end{array}}\!\!\begin{array}{l} \diagup C \\ \\ \diagdown C \end{array} \quad (2)$$

$$II \rightarrow C{-}C{=}C{-}C{-}C{-}C \quad (3)$$

$$II \rightarrow C{=}\overset{\overset{C}{\vert}}{C}{-}C{-}C + C{-}C{=}\overset{\overset{C}{\vert}}{C}{-}C{-}C \quad (4)$$

$$II \rightarrow C{=}\overset{\overset{C}{\vert}}{C}{-}\overset{\overset{C}{\vert}}{C}{-}C \quad (5)$$

$$III \rightarrow C{=}\overset{\overset{C}{\vert}}{C}{-}C{-}C{-}C + C{-}C{=}C{-}\overset{\overset{C}{\vert}}{C}{-}C \quad (6)$$

A propylene molecule is chemisorbed on a nickel acid site (Eq. (1)). The chemisorbed propylene molecule, I, then further reacts with a propylene molecule to form the intermediates of cyclobutane derivatives, II and III, on the nickel acid site (Eq. (2)). In the intermediate II, the breaking of the C_1-C_2, C_2-C_3, and C_3-C_4 bonds leads to the formation of 2-hexenes (Eq. (3)), 3-methylpentenes (Eq. (4)), and 2, 3-dimethylbutene (Eq. (5)) respectively. In the intermediate III, the same ring-opening processes lead to the formation of 2-methyl-1-pentene and 4-methyl-2-pentenes as the primary products (Eq. (6)). In this way, the reaction scheme can explain the presence of all the primary products found. Under the experimental conditions of 200°C and 50 kg/cm², no 2, 3-dimethylbutene was formed, and more *n*-hexenes than 3-methylpentenes were formed. This fact may be explained by assuming that the order of ease in the C–C bond breaking of the cyclobutane intermediate II is C_1-$C_2 > C_2$-C_3 $(= C_1$-$C_4) > C_3$-C_4. These cyclobutane intermediates, however, may not be the activated complexes which are at the top of the energy barrier, because the selectivity in the ring-opening reactions changes with the experimental conditions, as Fig. 4 shows.

Figure 3 shows that more of the trans isomers were produced initially than the corresponding cis isomers for 2-hexenes and 4-methyl-2-pentenes, and that the reverse was true for 3-methyl-2-pentenes. This fact can be explained on the reasonable assumptions that the two propylene molecules are chemisorbed on the catalyst surface so that the two methyl groups of the cyclobutane intermediate direct opposite to the catalyst surface (the cyclobutane ring lies horizontally on the catalyst surface), and that during the course of the ring-opening process on the catalyst surface the rotation of a C–C bond of the cyclobutane ring is retarded by the steric hindrance of the methyl groups.

Finally, we wish to refer to an interesting feature of the nickel oxide-silica-alumina catalysts. Unlike the usual acid-type catalysts over which the polymerization of olefins is considered to take place *via* a carbonium-ion mechanism, the nickel oxide-silica-alumina catalysts exhibit a higher activity for a lower olefin, *i. e.*, the highest activity for ethylene.[2,3] This fact cannot be explained by the carbonium-ion mechanism. The present mechanism may suffice to explain this fact, in view of the steric hindrance of the alkyl group in the formation of the intermediates of cyclobutane derivatives.

BULLETIN OF THE CHEMICAL SOCIETY OF JAPAN VOL. 41 49—52 (1968)

Mössbauer Effect of the ^{119}Sn in the Molecular Complexes of Tin Tetrachloride with Some Aliphatic Compounds

Sumio ICHIBA, Mitsuo MISHIMA, Hiroshi SAKAI and Hisao NEGITA

Department of Chemistry, Faculty of Science, Hiroshima University, Hiroshima

(Received July 1, 1967)

Molecular complexes of tin tetrachloride with some aliphatic compounds, such as alcohols and esters, were investigated by means of the Mössbauer effect due to ^{119}Sn, irradiation being made by 23.8 keV γ-rays from the ^{119m}Sn in tin dioxide. Most of these complexes show quadrupole splittings resulting from the addition of organic molecules to tin tetrachloride, although broad absorption curves are observed in some cases. The isomer shifts range from 0.30 to 0.45 mm/sec. They are much smaller than that of tin tetrachloride itself. The results are interpreted by taking account of the electronic structures of the complexes.

A number of molecular complexes of tin tetrachloride with oxygen-containing aliphatic compounds, *i. e.*, Lewis bases, have been examined by means of the Mössbauer effect due to ^{119}Sn. Previous structural studies of these complexes have been made mostly by means of the infrared spectra, though sometimes, rarely, by X-ray analysis.[1-3] When tin tetrachloride complexes with such monofunctional donors as alcohols, esters, and ketones, 1 : 2 complexes are generally formed, and the molecular shape changes from a tetrahedron to a octahedron which has either a cis- or a trans-form. On the basis of the infrared spectra of several 1 : 2 complexes, it has been suggested[1,4] that small ligands tend to give cis-complexes. In the course of this work, however, both cis- and trans-complexes were examined.

The purpose of the present study is to clarify the changes in the electron density and the bond character in the $SnCl_4$-complexes. Some of the results obtained are similar to those obtained by Stukan *et al.*,[5] but they are slightly different from those obtained by Khristrov *et al.*[6] The Mössbauer spectra of most of the complexes are doublets. These doublets are caused by quadrupole splitting, 2ε, and are regarded as a direct measure of the electric-field gradient at a tin nucleus or, in qualitative terms, as a measure for the deviation from spherical symmetry of the electron cloud around the tin nucleus.

The difference between the center of the splitting and the zero Doppler velocity, δ, is the isomer shift, which is a relative value with respect to the source. It gives a measure of the s-electron density at the tin nucleus. The source in the present work was radioactive tin dioxide, $^{119m}SnO_2$, and was used at room temperature. Although a small quadrupole splitting is observed in tin dioxide,[7,8] it is preferable as a source because it has a large recoilless fraction of 23.8 keV γ-rays, even at room temperature.

All the δ-values of the molecular complexes fall in the range from 0.3 to 0.45 mm/sec with respect to tin dioxide and are smaller than that of tin tetrachloride. This means that the s-electron density at the nucleus decreases when tin tetrachloride complexes with oxygen-containing organic compounds.

Experimental

Preparation of Molecular Complexes. The $SnCl_4$-complexes were prepared by mixing reactants in benzene or petroleum ether, or by adding tin tetrachloride to ice-cold bases in suitable proportions. Generally the complexes precipitated immediately. They were then filtered off in a dry air stream, washed with a pure solvent, and recrystallized or sublimed under reduced pressure. The complexes with alcohols were prepared by a method previously reported in the literature.[9,10]

The 1 : 2 complexes were obtained by adding the tetrachloride (1/10 mol) to an ice-cold benzene solution of an alcohols (2/10 mol) except ethyl alcohols. The complexes were then purified by sublimation under reduced pressure. The complex of tin tetrachloride

1) I. R. Beattie, R. Hulme and L. Rule, *J. Chem. Soc.*, **1965**, 1581.
2) C. E. Brauden, *Acta Chim. Scand.*, **17**, 759 (1963).
3) Y. Hermodsoon, *Acta Cryst.*, **13**, 656 (1960).
4) I. R. Beattie, G. P. McQuillan and M. Webster, *J. Chem. Soc.*, **1963**, 1514.
5) R. A. Stukan, T. N. Sumarokova, V. A. Trukhatanov and V. V. Khrapov, *Dokl. Acad. Nauk SSSR*, **156**, 400 (1964).
6) D. Khristrov, Tsv. Bonchev and Kl. Burin, *Compt. Rend. Acad. Bulgare Sci.*, **19**, 293 (1966).
7) K. P. Mitrofanov, M. V. Plotnikova and V. S. Shpinel, *Zh. Eksperim. i Teor. Fiz.*, **48**, 791 (1965); *Soviet Phys. JETP*, **21**, 524 (1965).
8) H. A. Stöckler, H. Sano and R. Herber, *J. Chem. Phys.*, **45**, 1182 (1966).
9) D. C. Bradley, E. V. Caldwell and W. Wardlaw, *J. Chem. Soc.*, **1957**, 3039.
10) A. W. Laubengayer and WM. C. Smith, *J. Am. Chem. Soc.*, **76**, 5985 (1955).

with ethyl alcohol was prepared by adding tin tetrachloride to ice-cold ethyl alcohol directly. The crystalline tin trichloride monoethoxide ethanolate was obtained when the tetrachloride and ethyl alcohol were mixed in benzene. It was recrystallized from a benzene solution.

The 1 : 4 complex of tin tetrachloride with isopropyl alcohol was prepared by refluxing tin tetrachloride (27 g) and isopropyl alcohol (40 g) for several hours; it was crystallized spontaneously on cooling. A crop of cubic crystals was obtained.

The complexes of tin tetrachloride with ester, tetrahydrofuran (THF), dioxane, acetone, cyclohexanone, and acetonitrile were prepared by adding tin tetrachloride to a petroleum ether solution of the bases in accordance with the usual method.[4,11] The complexes were then purified by sublimation under reduced pressure.

The compound was identified by measuring its melting point. The results are summarized in Table 1, along with the literature values. They are in good agreement with each other.

Table 1. Melting points of $SnCl_4$-complexes

Complexes	Melting point, °C[a] obs.	lit.
$SnCl_4 \cdot 2CH_3OH$	99—106	98—103[b]
$SnCl_4 \cdot 2C_2H_5OH$	51— 58	53—56[b]
$SnCl_4 \cdot 2n\text{-}C_3H_7OH$	106—108	95—98[b]
$SnCl_4 \cdot 2(CH_3)_2CHOH$	112—113	104—106[b]
$SnCl_4 \cdot 4(CH_3)_2CHOH$	61— 68	
$SnCl_4 \cdot 2(C_2H_5)_2O$	80.0—86.5	78—80,[b] 92,[c] 80.6[d]
$SnCl_4 \cdot 2(CH_2)_4O$	S : 155—	S : 165—175[b]
$SnCl_4 \cdot 2O(CH_2)_4O$	S : 175—	S : 175—195[b]
$SnCl_4 \cdot 2(CH_3)_2CO$	93—96	94—96[b]
$SnCl_4 \cdot 2(CH_2)_5CO$	75.5—76.5	74—76[b]
$SnCl_4 \cdot 2CH_3CN$	104—117	
$SnCl_3 \cdot OC_2H_5 \cdot C_2H_5OH$	190—197	191—193,[b] 187[d]

a) Sublimation temperature is designated by "S."
b) Ref. 11.
c) Ref. 10.
d) W. Hieber and E. Reindl, *Z. Electrochem. Angew. Phys. Chem.*, **46**, 559 (1940).

Measurements. The isomer shift and the quadrupole splittings were observed by changing the Doppler-velocity of the absorber. An apparatus of this type was supplied by the Nuclear Science Engineering Company (NSEC, Model B).

The detector was a single channel γ-ray spectrometer made by the Nippon Musen Irigaku Kenkyusho Company. It was equipped with an NaI (1 mm in thickness) scintillation detector. The γ-ray radiation source was tin dioxide containing 2mCi ^{119m}Sn. The source was used at room temperature, while the absorber was cooled with liquid nitrogen. The thickness of the absorber was about 15 mg/cm^2 for Sn. X-Rays were cut off by a Palladium foil attached to the absorber. The activity at a given velocity was accumulated until it reached about 10^5 counts in order to reduce the statistical errors. The accuracy of the apparatus was checked by observing the Mössbauer spectrum of barium stannate, $BaSnO_3$. The isomer shift obtained by this apparatus was in good agreement with the literature value ($\delta < 0.1$ mm/sec).[12] The resonant absorption of the sample was not examined at room temperature.

11) E. T. Hitchcock and P. J. Elving, *Anal. Chim. Acta*, **28**, 417 (1963).

Results and Discussion

The results of the Mössbauer effect measurement are summarized in Table 2. The isomer shift and quadrupole splitting in molecular complex are presented in the first and second columns of this table, while the third column gives the half-width of the absorption curve, $R_{1/2}$, which will be defined below. All the shifts are shown relative to that of tin dioxide; the positive values indicate the motion of the absorber toward the source. The quadrupole splittings were determined by a procedure to be described below. All the numerical values of δ and 2ε are given in mm/sec.

Table 2. Mössbauer parameters for $SnCl_4$-complexes

Complexes	δ mm/sec[a]	2ε mm/sec[b]	$R_{1/2}$ mm/sec[c]
$SnCl_4 \cdot 2CH_3OH$[d]	0.43	0.70	2.00
$SnCl_4 \cdot 2C_2H_5OH$[d]	0.33	0.70	2.00
$SnCl_4 \cdot 2n\text{-}C_3H_7OH$	0.43	0.50	1.80
$SnCl_4 \cdot 2(CH_3)_2CHOH$[d]	0.35	0.70	2.00
$SnCl_4 \cdot 4(CH_3)_2CHOH$	0.30	0	1.50
$SnCl_4 \cdot 2(C_2H_5)_2O$[d]	0.45	1.10	2.65
$SnCl_4 \cdot 2(CH_2)_4O$[e]	0.43	1.14	2.70
$SnCl_4 \cdot 2O(CH_2)_4O$	0.45	1.10	2.60
$SnCl_4 \cdot 2(CH_3)_2CO$[d]	0.40	small	1.70
$SnCl_4 \cdot 2(CH_2)_5CO$	0.35	0	1.50
$SnCl_4 \cdot 2CH_3CN$	0.43	0.70	2.00
$SnCl_3 \cdot OC_2H_5 \cdot C_2H_5OH$	0.33	small	1.65

a) δ is the isomer shift relative to the source of SnO_2 crystal. The accuracy in the measurement is $\pm 5\%$.
b) 2ε is the quadrupole splitting.
c) $R_{1/2}$ is the half-width.
d) D. Khristrov *et al.* (Ref. 6) obtained values of δ and 2ε different from those in this table.
e) δ-value obtained by Stukan *et al.* (Ref. 5) is 0.70 relative to SnO_2. They did not observe the quadrupole splitting.

Isomer Shift. The values for all the molecular complexes fall in a range from 0.30 to 0.45 mm/sec. It may be noted that these values are smaller than those of $SnCl_4$, 0.78 ± 0.07,[13] 0.9 ± 0.1,[14] $0.7 \pm$

12) V. A. Bryukhanov, N. N. Delyagin, A. A. Opalenko and V. S. Shpinel, *Zh. Eksperim. i Teor. Fiz.*, **43**, 432 (1962); *Soviet Phys. JETP*, **16**, 310 (1963).
13) A. Yu. Aleksandrov, N. N. Delyagin, N. P. Mitrofanov, L. S. Poluk and V. S. Shpinel, *Zh. Eksperim. i Teor. Fiz.*, **43**, 1242 (1962); *Soviet Phys. JETP*, **16**, 879 (1963).
14) M. Cordey-Hayes, *J. Inorg. Nucl. Chem.*, **26**, 915 (1963).

0.08,[5] and 0.8±0.05,[6] with respect to SnO_2. The isomer shift can be expressed as follows:

$$\delta = (4\pi Ze^2R^2c/5E_\gamma)[|\psi(0)_a|^2 - |\psi(0)_s|^2](\Delta R/R)$$

where $|\psi(0)_a|^2$, $|\psi(0)_s|^2$, Z, R and E_γ are the s-electron densities at the nucleus of the absorber and the source, the nuclear charge, the mean nuclear radius, and the energy of the γ-rays respectively. The value of $\Delta R/R$, which is the fractional change of the radius from the ground state to the excited state, was found to be 1.16×10^{-4} [15] (1.1×10^{-4} by Boyle *et al.*,[16] and 1.2×10^{-4} by Cordey-Hayes[14]). Thus, the fact that the complexes have a smaller isomer shift means that the s-electron density at the tin nucleus decreases when the complexes are formed.

The outer electron configuration of a tin atom in $SnCl_4$ is expressed by the tetrahedral sp^3 hybrid. If the Sn-Cl bond in $SnCl_4$ is completely covalent, its s-electron character is 0.25. The ionic character of the Sn-Cl bond in $SnCl_4$ was estimated to be 0.38 by the pure quadrupole resonance (PQR) resulting from chlorine atom,[17] while it was deduced to be 0.42 or 0.50 from the isomer shift of the Mōssbauer effect.[14,15] If the ionic character is approximated by 0.40, the 5s-electron character of the tin atom will amount of $0.25\times(1-0.40)=0.15$, since a quadrivalent tin ion has the $(4d)^{10}$ configuration outside the krypton core. Accordingly, the value of $|\psi(0)_a|^2$ is smaller for $SnCl_4$ than for β-Sn, in which tin networks are formed by sp^3 hybrid orbitals, and the isomer shift is diminished.

When tin tetrachloride forms molecular complexes with oxygen-containing organic compounds, atoms around the tin atom in the $SnCl_4\cdot2D$ complex (D : donor) occupy the corners of a distorted octahedron formed approximately by sp^3d^2 hybrid orbitals. The lone-pair electrons of oxygen atoms serve as the 5d-electrons, and one of the 5s-electron of the tin atom is promoted to the 5p-orbital, as in the complexes of $SnCl_4\cdot2(CH_2)_4S$[1] and $SnCl_4\cdot2SeOCl_2$.[3] If each of the bonds is formed by the sp^3d^2 hybrid, its s-character would be 0.17. From the PQR data in the $SnCl_4\cdot2(C_2H_5)_2O$ complex,[18] it may be seen that the ionic character of the Sn-Cl bond is about 10 percent larger than that for $SnCl_4$ itself. That is, the ionic character may be assumed to be 0.44. Therefore, the 5s-electron character of the tin atom may be estimated to be $0.17\times(1-0.44)=0.09$. However, it should be kept in mind that the pure sp^3d^2 hybrid bonds are not formed in the complexes with nonequivalent ligands, as listed in Table 2. Furthermore, the 5s-electron will be shielded, especially by the 5d-electron. When the results of tin tetrachloride are compared with those of its complexes with oxygen-containing organic compounds, it is expected that the $|\psi(0)_a|^2$ of the tin atom will decrease and that the isomer shift will be reduced in forming the complex. This is the case in the present work.

It is difficult to understand why the isomer shift for the $SnCl_4\cdot2C_2H_5OH$ complex is small in comparison with those of other alcohol complexes. For the 1 : 4 complex $SnCl_4\cdot4(CH_3)_2CHOH$, in which the quadrupole splitting has not been observed, it is not evident how four isopropyl alcohol molecules coordinate to a tin atom. Its structural analysis has not been performed as yet, but it seems plausible that two of them coordinate to a tin atom through oxygen atoms of the donors.

As for the isomer shift of $SnCl_4\cdot2(CH_2)_4O$, the present value (0.43 mm/sec) differs from that of Stukan *et al.* (0.70 mm/sec).[5] According to them, both $SnCl_4$ and $SnCl_4\cdot2(CH_2)_4O$ have the same isomer shift. This seems unreasonable in light of the s-electron density described above.

Quadrupole Splitting. The quadrupole splitting was observed for almost all the compounds. The observed values of the splitting are given in the second column of Table 2. The quadrupole

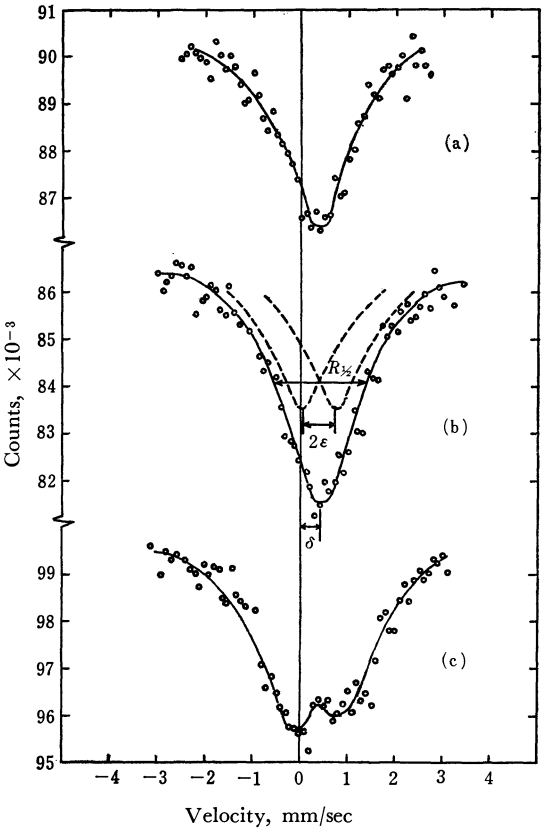

Fig. 1. Mōssbauer spectra of $SnCl_4$-complexes.
(a) $CnCl_4\cdot2(CH_2)_5CO$ (b) $SnCl_4\cdot2CH_3CN$
(c) $SnCl_4\cdot2(CH_2)_4O$

15) D. A. Shirley, *Rev. Mod. Phys.*, **36**, 339 (1964).
16) A. J. F. Boyle, D. St. P. Bunbury and C. Edwards, *Proc. Roy. Soc. (London)*, **A79**, 416 (1962).
17) A. L. Schalow, *J. Chem. Phys.*, **22**, 1211 (1954).
18) D. Biedenkapp and A. Weiss, *Z. Naturforsch.*, **119**, 1518 (1964).

splittings were clearly observed only in complexes with esters, while broad absorption curves were found in the other complexes. A few examples of the spectra are shown in Fig. 1. The minimum value of the observed width, 1.5 mm/sec, is almost equal to that of $BaSnO_3$, which shows no splitting. In the example of the $SnCl_4 \cdot 2CH_3CN$ complex shown in Fig. 1(b), the observed spectrum seems to have a single peak. However, the half-width, $R_{1/2}$, is larger than 1.5 mm/sec, so that there must be some quadrupole splitting. Here $R_{1/2}$ was used to distinguish it from the notation, $\Gamma_{1/2}$, usually used for natural half-widths.

Assuming that the observed curve is composed of Lorentzian curves with the half-width of 1.5 mm/sec, the magnitude of the quadrupole splitting can be deduced easily. The component curves obtained in this way reproduce the original when they are combined. If the components have a width other than 1.5 mm/sec, *e. g.*, 1.4 or 1.6 mm/sec, the combined curves deviate from the experimental curves at the tail part or at the peak. However, this procedure for the derivation of the quadrupole splitting cannot be free from some small errors, since various factors may affect the line width.

In general, the electric field gradient may be caused by two sources, *i. e.*, the charges of the distant ion and the nonspherically distributed electrons around the nucleus. In ionic crystals, the latter effect vanishes, and only the former appears. On the contrary, in covalent crystals the electric field gradient arises mostly from the latter.

In the $SnCl_4$-complexes, both cis- and trans-forms exist, as may be seen in Fig. 2. Among the complexes examined in the present study, both $SnCl_4 \cdot 2CH_3CN$ and $SnCl_4 \cdot 2(CH_3)_2CO$ are known to exist in the cis-form in a benzene solution,[4] but their crystal structures have not yet been determined. If each of these complexes preserves the cis-form in the solid, a twofold axis exists, as in the $SnCl_4 \cdot 2SeOCl_2$ complex shown in Fig. 2(a). Thus the field gradient will appear at tin nuclei, and the quadrupole splitting will be observed to some extent. This is confirmed in Table 2.

The quadrupole splitting of the $SnCl_4 \cdot 2(CH_2)_4O$ complex has been observed, contrary to the results reported by Stukan *et al.*,[5] though its crystal structure has not yet been determined. Beattie *et al.*[1] indicated that a similar molecular complex, $SnCl_4 \cdot 2(CH_2)_4S$, is a centrosymmetric molecule with a trans-form; they ascertained this by studying the X-ray diffraction as well as the Raman and infrared spectra (*cf.* Fig. 2(b)). The infrared investigations[19,20] of the $SnCl_4 \cdot 2(CH_2)_4O$ complex show that the two donor molecules coordinate to a tin atom to yield a trans-form. Thus, the shape of the $SnCl_4 \cdot 2(CH_2)_4O$ complex may be almost the same as that of the $SnCl_4 \cdot 2(CH_2)_4S$ complex, which has a twisted form. Consequently, the distribution of the electric charge around the tin nucleus in the $SnCl_4 \cdot 2(CH_2)_4O$ deviates from spherical symmetry, and the quadrupole coupling arises. An interesting fact is that the magnitude of the quadrupole splitting is larger for a trans-complex than for a cis-complex.

The complex compound $SnCl_3OC_2H_5 \cdot C_2H_5OH$ was investigated by means of measurements of the vapor pressure of a benzene solution and the infrared absorption of the solid by Laubengayer *et al.*,[10] as well as by means of the dipole moment in a benzene solution by Osipov *et al.*[21] From these results the dimer structure shown in Fig. 3 was proposed. According to the Mössbauer effect on this compound, the quadrupole splitting is very small, although the value was not determined. Therefore, it seems likely that the compound exists as a cis-form in the solid state.

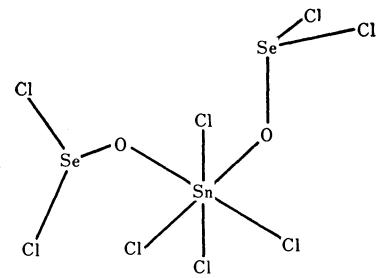

(a)

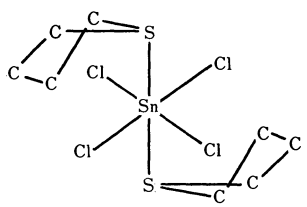

(b)

Fig. 2. Structures of tin(IV) chloride complexes.
(a) *cis*-Diseleninylchloride tin(IV) chloride
(b) *trans*-Bis(tetrahydrothyophen) tin(IV) chloride

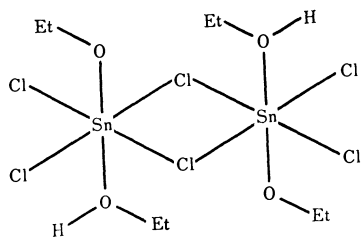

Fig. 3. Structure of tin trichloride monoethoxide ethanolate.

19) I. R. Beattie and L. Rule, *J. Chem. Soc.*, **1964**, 3267.
20) I. R. Beattie and L. Rule, *ibid.*, **1965**, 2995.
21) O. A. Osipov, B. M. Artemova and H. P. Bedarev, *Zh. Obshchei Khim.*, **29**, 975 (1959).

BULLETIN OF THE CHEMICAL SOCIETY OF JAPAN VOL. 41 53—60 (1968)

Thermal Decomposition of Ketene in Shock Waves

Morizo TSUDA*1 and Kenji KURATANI

Space and Aeronautical Research Institute, The University of Tokyo, Komaba, Meguro-ku, Tokyo

(Received July 12, 1967)

With the use of a single pulse shock tube of a magic hole type, the thermal decomposition of ketene was studied at temperatures from 1140 to 1530°K. The formation of carbon monoxide, that is, the disappearance of ketene, followed a kinetic order of 1.5 with respect to ketene and its rate constant was represented by

$$k = 10^{14.2} \exp[(-65600 \pm 1100)/\boldsymbol{R}T] l^{1/2} \text{ mol}^{-1/2} \text{ sec}^{-1}.$$

The thermal decomposition of mixtures of ketene and ethylene in argon was also studied, and the formation of methylene radicals during the pyrolysis of ketene is deduced from the presence of propylene and cyclo-propane in the products of these three component reactants. The rate of ketene disappearance was not affected by the addition of ethylene, or nitric oxide. A chain mechanism in which methylene radicals play a principal part, and a combined molecular mechanism of first, and second orders were proposed tentatively to explain the observed 1.5th order reaction rate.

Methylene is formed in the thermal decomposition of diazomethane, as well as in the photochemical decomposition of diazomethane and ketene.[1] However, there have been few studies of the thermal decomposition of ketene at high temperatures, and one cannot presume the formation of methylene radicals in the pyrolysis of ketene.

In the rather lower temperature range from 400 to 600°C, Young,[2] and Guenther and Walters[3] studied the thermal decomposition of ketene and found that the main products in the initial stages were allene and carbon dioxide. On the other hand, data available at higher temperatures are only those of Muller and Peytral,[4] and they found carbon monoxide and ethylene as the major products at 1150°C. According to these studies, it seems that there is clear difference between the results obtained at different temperatures.

To confirm the formation of methylene radicals in the thermal decomposition of ketene, we have studied the pyrolysis of ketene by the use of a single pulse shock tube. A shock-heating procedure is suitable to generate high temperature, and we were able to investigate the decomposition of ketene in the higher temperature range, and to know whether the mechanism of decomposition at high temperature is different from that at low temperature of not.

Experimental

Materials. Ketene was prepared according to a modification of Back's method.[5] Vapor of G. R. grade acetic anhydride in nitrogen carrier gas was heated at 510+5°C in a quartz tube. Unreacted anhydride was removed by passage through a dry ice-acetone trap, and the pyrolyzed products were collected at −196°C. Crude ketene was degassed at −196°C, and purified by repeated distillations at about −120°C (an *n*-propyl alcohol bath was used). Usually purified ketene contains 0.1—0.3% carbon dioxide.*2

One lot of ketene was introduced into a 7 cm long cell at 150 mmHg, and surveyed by an infrared spectrometer. No absorption band was observed except those belonging to ketene. Immediately after purification, ketene was diluted with a large excess of argon to a concentration of 4% or 5%, and the mixture was stored in a 5 *l* flask at room temperature. At a total pressure of less than 600 mmHg, there was no change in composition during the storage period.

High quality argon, supplied by Tomoe Co. (oxygen content less than 0.2 ppm), and 99.7% ethylene obtained from Takachiho Co. were used without further purification.

Apparatus and Procedure. A single pulse shock tube of a new design, developed at Cornell University,[6]

*1 Present address: Faculty of Hygienical Science, Kitasato University, Shiba-shirogane-sankocho, Minato-ku, Tokyo.

1) H. M. Frey, "Progress in Reaction Kinetics," Vol. 2, Pergamon Press., Oxford (1964), p. 131.

2) J. R. Young, *J. Chem. Soc.*, **1958**, 2909.

3) W. B. Guenther and W. D. Walters, *J. Am. Chem. Soc.*, **81**, 1310 (1959).

4) J. A. Muller and E. Peytral, *Compt. rend.*, **196**, 379 (1933).

5) M. H. Back, *Can. J. Chem.* **43**, 106 (1965).

*2 One lot of ketene which contained 1.3% carbon dioxide and a trace of ethylene was used to check the effect of impurities, but there was no appreciable effect of carbon dioxide on the reaction rate and product distribution.

6) J. E. Klepeis, Thesis, Graduate School of Aeronautical Eng., Cornell Univ. (1961); A. Lifshitz, S. H. Bauer and E. L. Restler, Jr., *J. Chem. Phys.*, **38**, 2056 (1963). We thank Professor Bauer for his kind advice to construct this tube.

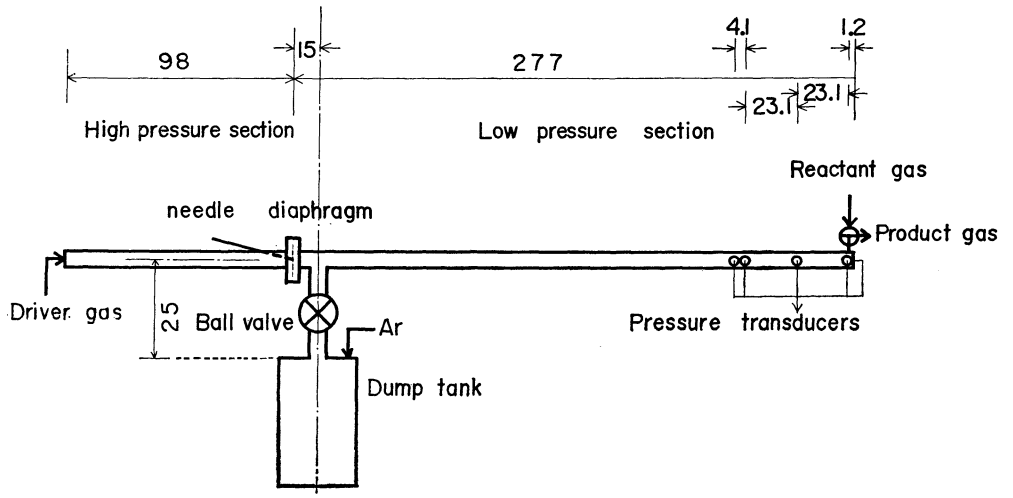

Fig. 1. Single pulse shock tube.

has a dump tank at the upstream end of a driven section. Using this device, it is not necessary to burst out two diaphragms at the preset time interval, and the whole system becomes very simple. We were greatly interested in this new design, and made a tube of this type as shown in Fig. 1. The inner diameter of our tube was 4 cm, and the length of the driver, and the driven sections were 98 and 277 cm, respectively. A dump tank of 19 *l* volume was attached to the driven section 15 cm downstream from the diaphragm through a branch tube and a ball valve of the same diameter. The main portion of the driven section was made of "Terex" glass, and the driver section of steel tubing, and was equipped with a needle to burst the diaphragms.

Four barium titanate-lead zirconate pressure transducers were mounted on the wall, flush with the inner surface, 51.5, 47.4, 24.3, and 1.2 cm from the end plate. The signals produced by the passage of an incident shock wave over these transducers were fed into amplifiers and converted into pulses by thyratrons. The pulsed output of the first transducer was used to trigger both a raster circuit, and an oscilloscope, to measure the shock velocity, and to show the pressure profile at the downstream end, respectively. Amplified pulses from the remaining three gauges were recorded on a raster synchroscope system having ten-microsecond marks. The incident shock wave velocity and its mean attenuation at the positions of these gauges were determined by measuring the time interval of the pulses shown on the pictures of the synchroscope display. The observed values of attenuation extended to nearly 0.4% when the incident shock wave travelled the distance of 23.1 cm, and they were taken into account to evaluate the incident shock wave velocity at the downstream end.

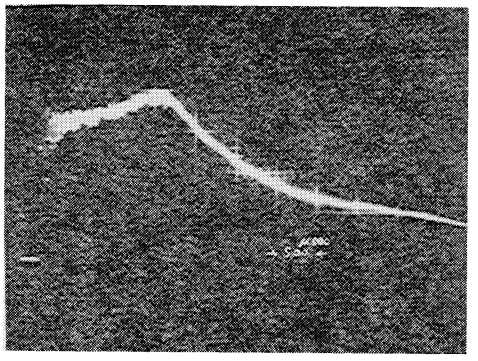

Fig. 2. A typical pressure profile at the end plate. In ordinary cases, pressure behind a reflected shock wave rises gradually, but the slope in Fig. 2 is too high. This disagreement may be derived from the narrowness of our shock tube.

One more piezo-electric pressure transducer was embedded in the end plate and was used to measure the pressure profile at the downstream end. The signal from this gauge was displayed on an oscilloscope, and the length of the plateau of the pressure profile was taken as the dwell time of the reaction.

A typical record of this pressure profile is illustrated in Fig. 2.

Prior to an experimental run, both the driver and the driven sections (including the dump tank) were evacuated, the latter especially, attaining a pressure of less than 0.2 μHg. Then the valve located between the dump tank and the main driven section was closed, and the former was filled with pure argon, and the latter with the sample gas highly diluted in argon. The pressure of both parts was kept at the same level, and just before pressurization of the driver section, the above valve was again opened.

The sample gas is heated only once by an incident and reflected shock wave in the shock tube. However, the former heating process is ignored, and the temperature behind the reflected shock wave, T_5, is taken to be the reaction temperature. The temperature T_5, and the density behind the reflected shock wave were calculated as functions of incident shock wave velocities at the downstream end, assuming that there was no chemical change behind the shock waves. The necessary enthalpy values for ketene at higher temperatures were taken from the table given by Moore and Pimentel,[7] or calculated using the same

7) C. B. Moore and G. C. Pimentel, *J. Chem. Phys.*, **38**, 2816 (1963).

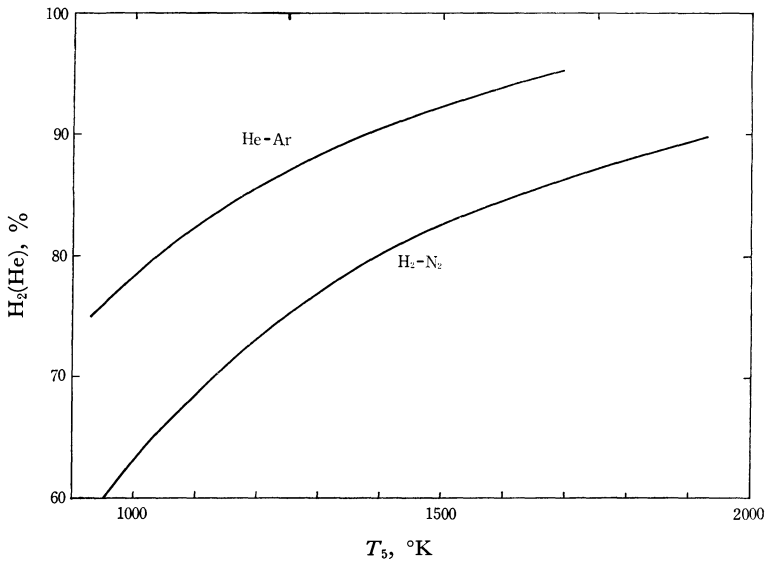

Fig. 3. Optimum composition of driver gas; T_1=290°K, 2.0% ketene in argon.

TABLE 1. GAS CHROMATOGRAPHIC ANALYSES

Gas analyzed	Column	Column length	Temp.	Carrier gas	Detecter
H_2, He	molecular shieve 5A	3 m	room temp.	Ar	catharometer
Ar, N_2, CH_4, CO	molecular shieve 5A	2 m	100°C	He	catharometer
CH_4, CO_2	charcoal	2 m	100°C	He	catharometer
CH_4, C_2H_2 C_2H_4, C_2H_6	charcoal	2 m	150°C	He	ionizn. flame
C_3-hydrocarbons	7% $\beta\beta'$-DPN + 93%DBM* in chromosorb + alumina	5 m	room temp.	He	ionizn. flame
		2 m	150°C		

* H. Miyake and M. Mitooka, *Nippon Kagaku Zasshi (J. Chem. Soc. Japan, Pure Chem. Sect.)*, **84**, 923 (1963).

molecular parameters adopted by them. To minimize the error in T_5, caused by neglecting the heat of reaction, most of the kinetic studies were carried out with mixtures of 0.5—2.0% ketene in argon.

"Lumirror" (trade name of poly-ethylene terephthalate, a product of Toyo Rayon Co.) sheets of various thickness were used as diaphragms to separate the higher and lower pressure section. When the pressure and composition of the driver gas were brought to previously determined values, diaphragms were pierced manually with a needle.

To achieve the highest cooling rate with a rarefaction wave, the tube should be tuned so that the head of the wave reflected from the end of the high pressure section, meets the reflected shock wave and the gas interface at approximately the same point. Since the length of the driver section of our tube is fixed at 98 cm, this adjustment was performed by the proper choice of the driver gas composition. A satisfactory composition was obtained according to the shock wave diagram calculation as shown in Fig. 3. Actually, it takes a finite time to rupture the diaphragms, and the calculated composition is regarded as an approximation. Fortunately, however, this estimate was proved to be accurate enough for our purpose, judging from the pressure profile at the end plate. A mixture of hydrogen and nitrogen was mainly used as the driver gas, and occasionally when it was planned to carry out a complete analysis of the products, a helium-argon mixture was used.

Analytical. The shock heated gas was rapidly cooled by a rarefaction wave, and immediately after the rupture of the diaphragms the reaction mixture was withdrawn to an evacuated vessel of 130 cc volume and analyzed by gas chromatography. A Yanagimoto G. C. G.-3DH gas chromatograph with a flame ionization attachment G. C. F.-103 was used for hydrocarbon analysis. Analyses of inorganic gaseous products were carried out with a usual thermal conductivity cell. In the latter case, in order to raise sensitivity, the output was recorded on a Sanei "Galvanograph", having a sensitivity of 0.25 mV full scale. For the determination of the small amount of hydrogen produced by pyrolysis, a helium-arogn mixture was used as the driver gas, since, even if we took extreme care to avoid migration of the driver gas into the sampling vessel, it was almost impossible to keep the reaction products completely free of the driver gas. Therefore, the

contents of the driver gas components were also analyzed for every run, and yields of product gases were corrected in accordance with the amount of driver gas migration.

For the separation of cyclopropane from propylene, a 5 m long column, at room temperature, packed with 7% $\beta\beta'$-oxy-dipropionitrile and 93% dibutylmaleate on chromosorb was connected in front of an alumina column 2 m in length at 150°C. With the use of this combined column, the relative retention volumes of propane, propylene, acetylene, cyclopropane, and allene to *n*-butane were found to be 0.32, 0.48, 0.56, 0.71, and 0.97, respectively.*3 Columns, and the experimental conditions used by us are shown in Table 1.

Results

On the Products. In several experimental runs we have measured the amount of unreacted ketene through absorption at 2163 and 2135 cm^{-1}, and confirmed that almost all oxygen atoms derived from pyrolyzed ketene are detected as carbon monoxide, and dioxide. This conclusion is consistent with the finding of Young,[2] and hereafter we assume that the amount of decomposed ketene is equal to the sum of $[CO]+2[CO_2]$ produced.

TABLE 2. YIELDS OF PRODUCTS IN TYPICAL RUNS

Run No.	Total concn. (ρ_5 in mol/l)	Ketene concn. in %	T_5	Dwell time in ms	Product distributions in %		
					CO	CO_2	H_2
577	1.96×10^{-2}	0.5	1530°K	1.40	0.299	0.0043	*
643	3.93×10^{-2}	2.0	1520	1.40	1.19	0.0006	0.170
640	4.01×10^{-2}	2.0	1500	1.40	1.10	0.006	0.156
625	4.11×10^{-2}	2.0	1495	1.30	1.13	0.0077	0.223
642	3.81×10^{-2}	2.0	1475	1.35	1.12	0.0047	0.118
644	3.62×10^{-2}	2.0	1360	1.55	0.619	0.004	0.0177
645	3.57×10^{-2}	2.0	1330	1.55	0.362	0.0011	0.0093
646	3.55×10^{-2}	2.0	1290	1.60	0.154	*	0.0036
674	3.64×10^{-2}	2.0	1260	1.55	0.065	*	0

Run No.	Product distributions in %					
	CH_4	C_2H_2	C_2H_4	C_2H_6	C_3H_6	C_3H_4
577	0.027	0.037	0.073	0.0072	*	*
643	0.18	0.17	0.12	0.0056	0.0014	0.0023
640	0.15	0.16	0.15	0.010	0.0019	*
625	0.185	0.14	0.13	0.0085	*	*
642	0.17	0.17	0.17	0.010	0.0027	0.0038
644	0.076	0.072	0.12	0.0097	0.0020	0.0038
645	0.041	0.039	0.063	0.0047	0.00097	0.0024
646	0.021	0.017	0.028	0.0017	0.00035	0.0015
674	0.0079	0.0083	0.018	0.00094	*	*

* No analysis was made.

TABLE 3. MASS BALANCES OF PRODUCTS

Run No.	ΣO	ΣC_2	ΣH_2	$\Sigma C_2/\Sigma O$	$\Sigma H_2/\Sigma O$
643	1.191	0.984	0.960	0.83	0.81
640	1.112	0.951	0.948	0.86	0.85
625	1.146	0.942	1.021	0.82	0.89
642	1.129	1.013	1.028	0.90	0.91
644	0.627	0.562	0.525	0.90	0.84
645	0.364	0.313	0.278	0.86	0.76
646	0.154	0.137	0.128	0.89	0.83
674	0.065	0.064	0.063	0.98	0.97

*3 These values shifted from 0.29, 0.51, 0.77, 0.67, and 1.04 to 0.33, 0.48, 0.50, 0.73, and 0.94 as the alumina column temperature was raised from 120°C to 170°C. 150°C was the best choice with respect to the separation of acetylene from the other components.

The product distributions of some typical runs are shown in Tables 2 and 3. In these tables, corrected values of $[CO_2]$, reducing the amounts contained in the original reactant mixtures from the values obtained by the product analyses, are listed, but since the amount of CO_2 in the reactant was comparable to that produced, the values of $[CO_2]$ shown in these tables are rather erroneous. However, as illustrated in Fig. 4, the ratio of

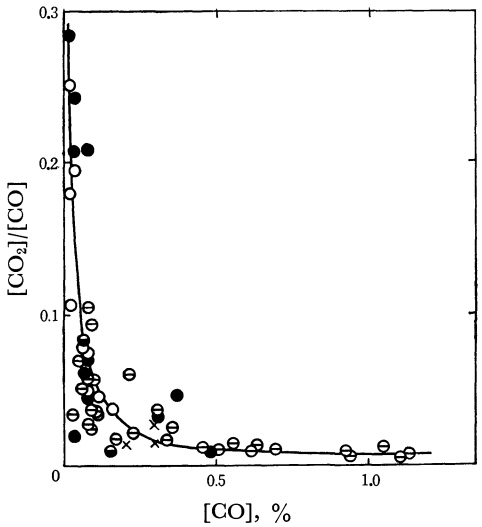

Fig. 4. Relationship between yields of carbon dioxide and carbon monoxide.
× 0.5% mixture ○ 1.0% mixture
⊖ 2.0% mixture ◒ 4.0% mixture
● 5.0% mixture

$[CO_2]/[CO]$ decreases rapidly with increase in the amount of CO produced. Furthermore, the yield of CO_2 itself is extremely small. Therefore, it seems a good approximation to take the rate of CO formation in place of the pyrolysis rate of ketene itself, especially in the higher temperature range studied by us.

The deficiencies of mass balances of carbon and hydrogen atoms compared with that of the oxygen atom, extend in some cases to 10—20%, and they may be attributable to the formation of a small amount of hydrocarbon polymers and carbon soot. However, when the yields of methane and acetylene are plotted against that of CO, as shown in Fig. 5, linear relationships among the yields of products are revealed, independent of the reaction temperatures and initial concentrations of ketene. That is, the ratios $[CH_4]/[CO]$, and $[C_2H_2]/[CO]$ are almost constant and equal to 0.15, and 0.13, respectively, throughout the experimental runs. As for ethylene, the ratio $[C_2H_4]/[CO]$ is held constant at 0.28 as long as the extent of reaction is less than 10%, but when the reaction proceeds further, this ratio decreases gradually.*4 Yields of hydrogen, ethane, and C_3-hydrocarbons are relatively small and considered to be minor products.

On the Rate Constant. According to the aforementioned assumption, the initial rate of the thermal decomposition of ketene is transformed to the following equation,

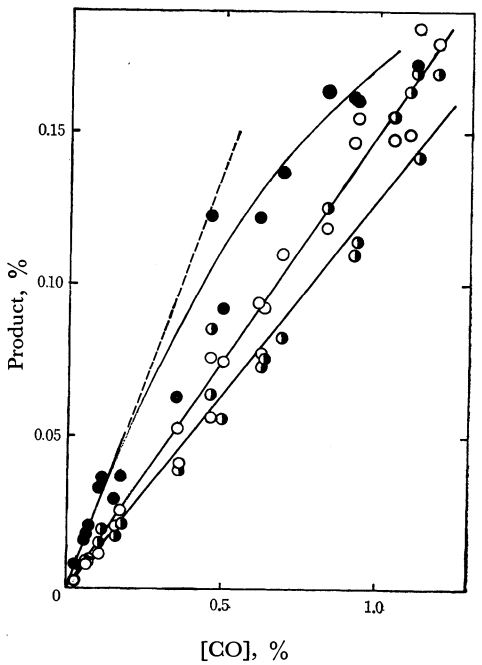

Fig. 5. Yields of methane, acetylene and ethylene.
○ methane ◑ acetylene ● ethylene

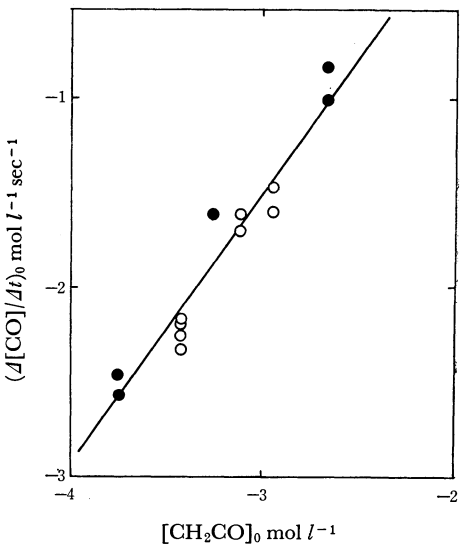

Fig. 6. Determination of reaction order at 1290°K.

*4 Contrary to the formation of ethylene, only small amounts of hydrogen are formed at the lower levels of reaction, but the ratio $[H_2]/[CO]$ increases rapidly at higher levels of reaction.

$$(-\mathrm{d[ketene]}/\mathrm{d}t)_0 = (\mathrm{d[CO]}/\mathrm{d}t)_0 = \Delta[\mathrm{CO}]/\Delta\tau \quad (1)$$

where $\Delta\tau$ represents the dwell time measured at the downstream end. Succeeding this, we assume that the reaction rate is expressed by the formula,

$$\Delta[\mathrm{CO}]/\Delta\tau = k[\mathrm{ketene}]^n[\mathrm{argon}]^m \quad (2)$$

where exponents n and m represent the order with respect to each reactant component.

However, to determine the reaction orders with respect to the initial concentrations of the reactants from Eq. (2), it is necessary to keep the extent of reaction less than 10%, and a reaction temperature of 1290°K was adopted for this reason. The observed rates at 1290°K with the various compositions of ketene and the total pressures are plotted in Fig. 6.

At first, assuming argon to be ineffective, Eq. (2) becomes

$$\Delta[\mathrm{CO}]/\Delta\tau = k'[\mathrm{ketene}]_0^n \quad (3)$$

According to formula (3), the exponent n was determined as the slope of Fig. 6 by a least squares method and found to be

$$n = 1.46 \pm 0.04.$$

In Fig. 6, open circles show the rates obtained with reaction mixtures of the same initial composition. Therefore, in these runs the following relations will hold,

$$[\mathrm{ketene}]_0 \propto [\mathrm{argon}]_0 \propto [\text{total concentration}]_0,$$

and

$$\text{rate} \propto [\text{total concentration}]_0^{n+m}.$$

When attention is paid to only these runs, the abscissa in Fig. 6 can be read as showing total concentrations in arbitrary units. That is, the slope obtained from these experimental points must show the exponent $n+m$. Thus, the total order of the reaction was calculated in a similar manner as

$$n + m = 1.64 \pm 0.08$$

Although the value of $n+m$ is slightly different from that of n, the total order of the reaction is regarded as the same as the order with respect to ketene, and a value of 1.5 was adopted. This conclusion derives the zeroth order with respect to argon, and the assumption made at the begining may be appreciated.

From the integral formula in the case of a three-halves order reaction, the rate constant is expressed as

$$k = 2\{(C_0/C)^{1/2} - 1\}/C_0^{1/2} \cdot \Delta\tau, \quad (4)$$

where $C_0 = [\mathrm{ketene}]_0$, and $C = [\mathrm{ketene}]_t = C_0 - \Delta[\mathrm{CO}]$. Rate constants at different temperatures from 1140° to 1530°K were calculated by means of Eq. (4) and plotted against the reciprocal of the reaction temperatures. From the Arrhenius plot

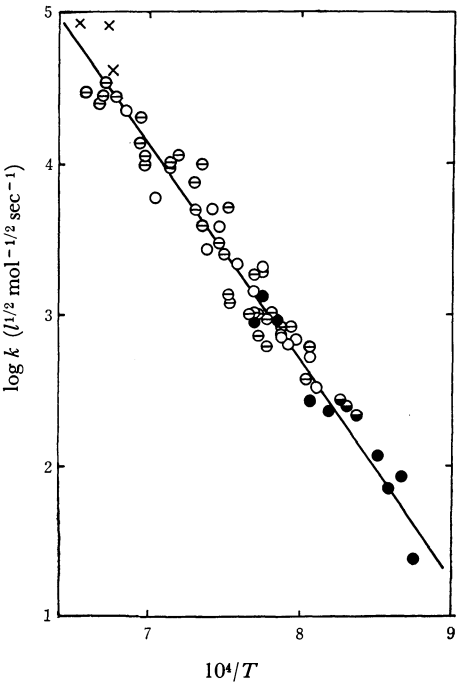

Fig. 7. Arrhenius plot of reaction rate.
× 0.5% ○ 1.0% ⊖ 2.0% ◒ 4.0% ● 5.0%

in Fig. 7, the apparent activation energy was evaluated as 65.6—1.1 kcal/mol, and finally the rate constant was given by

$$k = 10^{14.15} \exp\{(-65600 \pm 1100)/\boldsymbol{RT}\}$$

$$l^{1/2}\,\mathrm{mol}^{-1/2}\,\mathrm{sec}^{-1}$$

Discussion

In the thermal decomposition of ketene at higher temperatures above 1140°K, a small amount of carbon dioxide is found in the final products. For example, when 50% ketene was decomposed, the relative conversion of ketene into carbon dioxide, $2[CO_2]/([CO]+2[CO_2])$, is only about 1.6%. This fact is in remarkable contrast with the results obtained at temperatures below 900°K, where the relative conversion into carbon dioxide exceeds 50% at the corresponding extent of reaction. Accordingly, we might tentatively ignore the formation of carbon dioxide in the following discussion.

The product distributions of photo-decomposition of ketene at room temperature, which have been studied by Knox[8] and Chanmugan[9], are similar to our results. Since it has been established that methylene is an important radical in the photolysis of ketene, the similarity of the product

8) K. Knox, R. G. W. Norrish and G. Porter, *J. Chem. Soc.*, **1952**, 1477.
9) J. Chanmugan and M. Burton, *J. Am. Chem. Soc.*, **78**, 509 (1956).

Table 4. Yields of C_3-hydrocarbons

Run No.	Reaction mixture, in %			Total concn. (ρ_5 in mol/l)	T_5 °K	Dwell time msec	Product distributions in $\% \times 10^4$			
	ketene	ethylene	argon				C_3H_8	C_3H_6	cyclo-C_3H_6	C_3H_4
651	4.0	4.3	91.7	0.049	1299	1.25	0.6	120	0.7	39
648	4.0	4.3	91.7	0.048	1276	1.20	0.4	80	1.2	35
650	4.0	4.3	91.7	0.043	1132	1.55	0	3	1.0	3.3
652	0	4.0	96.0	0.044	1310	1.40	4	12	0	3
646	2.0	0	98.0	0.036	1290	1.60	0	3	0	15

distributions between the thermal- and photo-decomposition of ketene suggests a resemblance of both reaction schemes. These facts may be interpreted as circumstantial evidence of the formation of methylene radical by the pyrolysis of ketene.

To prove the existence of methylene radicals, the thermal decomposition of ketene containing considerable amounts of ethylene was studied, and a small but not ignorable amount of propylene and a trace of cyclopropane were detected as shown in Table 4. The existence of these molecules in pyrolyzed products supports our aforementioned interpretation, since cyclopropane and propylene may be produced by the reactions

$$CH_2 + C_2H_4 \rightarrow \text{cyclo-}C_3H_6 \rightarrow \text{propylene.}$$
(fast isomerization)

We found another important result from these experiments. That is, the addition of ethylene or NO to ketene scarcely alters the rate of carbon monoxide production.*5 The rate constants of these mixtures calculated with the 1.5th order rate equation are plotted in Fig. 8 and these rate constants coincide with those obtained from a ketene-argon mixture.*6 This result excludes a chain reaction mechanism in which a mono-radical plays a main role, and suggests the dominance of a molecular reaction scheme, or the contribution of a bi-radical to the ketene pyrolysis.

We assume further that the small amounts of hydrogen and higher hydrocarbons are obtained as secondary products, and propose the following reaction schemes for the early stage of the thermal decomposition of ketene.

The first of these schemes assumes the following chain reaction mechanism,

$$CH_2CO \rightarrow CH_2 + CO \quad (5)$$

$$CH_2 + CH_2CO \rightarrow C_2H_4 + CO \quad (6)$$

$$CH_2 + CH_2CO \rightarrow CH_3 + CHCO \quad (7)$$

$$CH_3 + CH_2CO \rightarrow CH_4 + CHCO \quad (8)$$

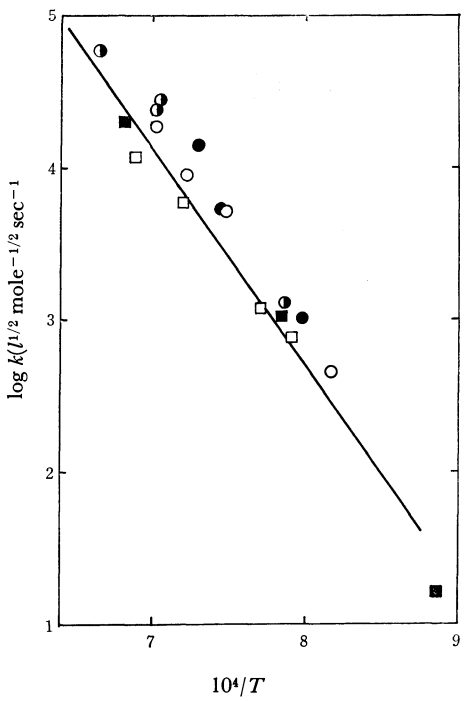

Fig. 8. Effect of ethylene and nitric oxide on the decomposition rate.
- □ 2% ethylene + 4% ketene
- ■ 4% ethylene + 4% ketene
- ○ 0.2% nitric oxide + 2.0% ketene
- ◑ 0.4% nitric oxide + 2.0% ketene
- ● 0.54% nitric oxide + 2.0% ketene

$$CHCO \rightarrow CH + CO \quad (9)$$

$$CH + CH_2CO \rightarrow CH_2 + CHCO \quad (10)$$

$$CHCO + CHCO \rightarrow C_2H_2 + 2CO \quad (11)$$

$$CH_2 + CH_2 \rightarrow C_2H_4 \quad (12)$$

In this scheme, we omit the reaction path to ethane,*7 since the yield of this substance is very small. Then, the rate of carbon monoxide formation or the thermal decomposition rate of ketene will be expressed as

$$\left.\begin{aligned} -R(\text{ketene}) &= R_5 + R_6 + R_7 + R_8 + R_{10} \\ &= R_5 + R_6 + R_9 + 2R_{11} \end{aligned}\right\} \quad (13)$$

*5 No inhibition of NO to ketene photolysis was already pointed out by Burton *et al.* M. Burton, T. W. Davis, A. Gordon and H. A. Taylor, *J. Am. Chem. Soc.*, **63**, 1956 (1941).

*6 In fact, the presence of NO rather accelerates the rate of ketene decomposition, as shown in Fig. 8.

*7 Ethane will be obtained by $CH_3 + CH_3 \rightarrow C_2H_6$.

where R denotes the rate of an individual step. If one assumes steady state concentrations of radicals, the following relations will be obtained:

$$R_9 = R_{10},$$
$$R_5 + R_{10} = R_6 + R_7 + 2R_{12},$$
$$R_7 = R_8,$$
$$R_7 + R_8 + R_{10} = R_9 + 2R_{11}$$

The second of these equations is rewritten as

$$[CH_2] = \{-(k_6+k_7-k_{10}) + [(k_6+k_7-k_{10})^2 + 8k_5k_{12}/[K]]^{1/2}[K]\}/4k_{12}$$

where [K] denotes the concentration of ketene, and if we assume $(k_6+k_7-k_{10})^2$ $[K]^2$ is very small compared with $8k_5k_{12}[K]$,*8 it follows that

$$[CH_2] = (k_5[K]/2k_{12})^{1/2} \quad (14)$$

and the reaction rate is represented by

$$-R(\text{ketene}) = R_5+2R_6+3R_7 = \{k_5+2k_6[K]^{1/2}+3k_7[K]^{1/2}\}[K]. \quad (15)$$

This expression is consistent with the observed order of the reaction if we ignore the first term. In a similar way, the ratios of methane, acetylene, and ethylene yields against that of CO are given by

$$[CH_4]/[CO] = R_7/(2R_6 + 3R_7),$$
$$[C_2H_2]/[CO] = R_7/(2R_6 + 3R_7),$$
$$[C_2H_4]/[CO] = R_6/(2R_6 + 3R_7).$$

Since the yield of ethylene at the lower extent of conversion was about twice as large as that of methane, as shown in Fig. 5, one might assume

$$R_6 = 2R_7,$$

and one can obtain numerical values for these ratios:

$$[CH_4]/[CO] = 0.14,$$
$$[C_2H_2]/[CO] = 0.14,$$

and

$$[C_2H_4]/[CO] = 0.28.$$

These results are also in excellent agreement with our observations.

The second proposal assumes the simultaneous decomposition of ketene by first and second order reactions, that is, the first order reactions

$$CH_2CO \rightarrow CH_2 + CO \quad (5)$$

and

$$CH_2 + CH_2CO \rightarrow C_2H_4 + CO \quad (6)$$

are combined with the second order reaction

$$2CH_2CO \rightarrow C_2H_4 + 2CO \quad (16)$$

With this tentative frame work, the rate of the carbon monoxide formation will be represented as

$$d[CO]/dt = k[\text{ketene}]^{1-2}.$$

The other products, such as methane and acetylene, will be derived through processes (7)—(11). This scheme is also in agreement with the observed relative yields of methane and acetylene, because

$$[CH_4]/[C_2H_2] = R_8/R_{11} = 2R_8/(R_7 + R_8) = 1.$$

Although experimental results concerning the yield of CO_2 are rather unreliable as already indicated in previous sections, the reaction rate of CO_2 formation in our experiment was found to be roughly proportional to the square of the initial ketene concentration. Moreover, a small amount of allene was detected in the products. These findings are in accord with the reaction path,

$$2CH_2CO \rightarrow CH_2{=}C{=}CH_2 + CO_2,$$

proposed by Young,[2] and Guenther and Walters.[3] Young suggested that allene splits into methylene and acetylene,

$$CH_2{=}C{=}CH_2 \rightarrow CH_2 + C_2H_2.$$

This step might be a secondary source of methylene radicals in addition to step (5).

At any rate, in our reaction scheme, methylene radicals may be formed, but it is not certain whether they play a leading role in the reaction sequence or not. The presence of methyl radicals is also demonstrated by the formation of a small amount of ethane as shown in Tables 2 and 3.

The authors wish to thank Messrs. Takuji Sakai and Shiro Hasumi for their assistance in construction of a single pulse shock tube.

*8 In order to derive an expression consistent with the observed order of our reaction rate, this assumption is very useful as shown in the text. But it seems rather artificial and the scheme proposed here should be regarded as a tentative one.

BULLETIN OF THE CHEMICAL SOCIETY OF JAPAN VOL. 41 61—64 (1968)

Structural Study of the Molecular Complex of Antimony Trichloride with Benzene by Means of the Pure Quadrupole Resonance

Tsutomu OKUDA, Akira NAKAO, Masaharu SHIROYAMA and Hisao NEGITA

Department of Chemistry, Faculty of Science, Hiroshima University, Hiroshima

(Received July 17, 1967)

The Zeeman effect of ^{35}Cl pure quadrupole resonance was studied on a single crystal of the $2SbCl_3 \cdot C_6H_6$ molecular complex at room temperature; it was found that the Cl-Sb-Cl bond angles of two nonequivalent $SbCl_3$ molecules are 96.2°, 94.7°, 92.2°; 94.5°, 92.8°, and 95.2°, with an uncertainty of 1°. The asymmetry parameters for the six chlorine atoms were found to be 0.085 ± 0.001, 0.055 ± 0.004, 0.117 ± 0.005, 0.119 ± 0.005, 0.112 ± 0.005, and 0.160 ± 0.007, listed in the order of decreasing resonance frequencies. The bond character of the Sb-Cl bond was also calculated from the quadrupole coupling constant. It was found that the Sb-Cl bond corresponding to the lowest resonance lines in each nonequivalent $SbCl_3$ molecule has a larger ionicity than the remainder. Moreover, the former has less of a temperature dependence than the latter. Finally, this complex may be assigned to the C_i or C_1 symmetry class from the patterns of zero-splitting and from the intensity ratios of the multiplet of the spectrum.

It is well known that antimony trichloride forms 2 : 1 or 1 : 1 molecular complexes with a number of aromatic compounds. These complexes have been studied by various methods, but their crystal structures are still unknown. Studies of the pure quadrupole resonance on these complexes have been performed by several authors.[1-3] All of them, however, used polycrystalline samples, and their information was limited to the bond nature of the component. The aim of the present work is to deduce the asymmetry parameters of the electric-field gradient at the relevant nuclei, the nature of the Sb-Cl bond, and the bond angles of Cl-Sb-Cl, as well as to assign the resonance lines and find the crystallographic symmetry. The 2 : 1 molecular complex of antimony trichloride with benzene was chosen as the sample for the basic research in order to see how the molecular shape and the bond character of antimony trichloride change in forming the complex.

The study of antimony trichloride itself was performed prior to that of the complex. Fortunately, its crystal structure had already been established by X-ray analysis[4,5] as well as by the pure quadrupole resonance.[4,6]

Experimental

The molecular complex was prepared in the following way.[7] One mole of pure benzene and two moles of pure antimony trichloride were dissolved in carbon disulfide individually, and then these solutions were mixed together. After the solution had been concentrated, the crystal was filtered and dried *in vacuo*. The complex was identified by determining the melting point and the chlorine content. The single crystal of the complex was obtained by a melting method described previously.[8] It was 10 mm in diameter and 25 mm long.

The spectrometer consisted of a super-regenerative oscillator, an amplifier, and a detector. The absorption lines were displayed on an oscilloscope. A Zeeman field of about 200 gauss was applied by a Helmholtz coil. The crystal could be rotated about a fixed axis of the crystal, and its angle Φ could be measured to within $\pm0.1°$. On the other hand, the magnetic field could be rotated on a horizontal plane, and its angle Θ could be measured to within $\pm1'$. The patterns of zero-splitting were observed at about 21°C.

Results and Discussion

The $2SbCl_3 \cdot C_6H_6$ molecular complex has six resonance lines of the same intensity, all due to ^{35}Cl, at room temperature as well as at the temperature of liquid nitrogen,[3] as is shown in Table 1. Let us now label the six resonance lines $\nu_1, \nu_2, \cdots, \nu_6$ from the lower to the higher, and the chlorine atoms contributing to $\nu_1, \nu_2, \cdots \nu_6$, $Cl_1, Cl_2 \cdots, Cl_6$.

The pattern of the zero-splitting was obtained by measuring the Zeeman effect on the resonance

1) V. S. Grechiskin and I. A. Kyuntsel, *Zh. Struct. Khim.*, **4**, 269 (1963).
2) V. S. Grechiskin, I. A. Kyuntsel and G. B. Soifer, *Zavodsk. Lab.*, **29**, 1310 (1963).
3) D. Biedenkapp and A. Weise, *Z. Naturforsch.*, **19a**, 1518 (1964).
4) G. E. Peterson, Thesis, Pittsburgh, 1962.
5) I. Lindqvist and A. Niggli, *J. Inorg. Nucl. Chem.*, **2**, 345 (1956).
6) T. C. Wang, *Phys. Rev.*, **99**, 566 (1955).
7) S. Shinomiya and T. Asahina, *Nippon Kwagaku Kwaishi (J. Chem. Soc. Japan)*, **59**, 1165 (1938).
8) H. Negita, T. Tanaka, T. Okuda and H. Shimada, *Inorg. Chem.*, **5**, 2126 (1966).

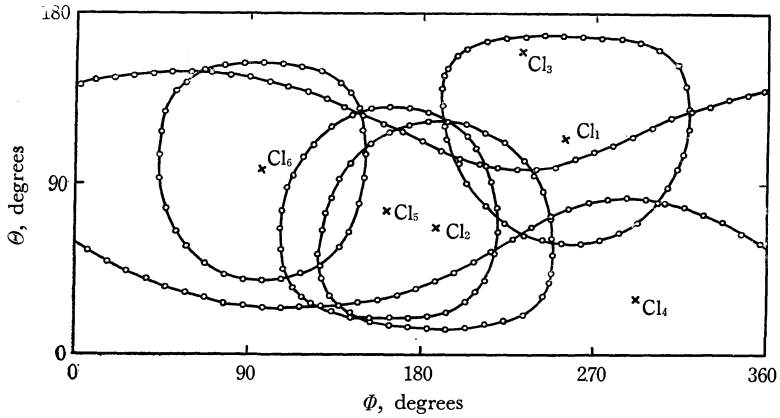

Fig. 1. Zero-splitting patterns of Zeeman lines of the complex $2SbCl_3 \cdot C_6H_6$. The axis of $\Theta=0$ is taken as the rotational axis of the sample tube. The plane of $\Phi=0$ is arbitrarily chosen.

TABLE 1. PURE QUADRUPOLE RESONANCE FREQUENCIES DUE TO ^{35}Cl IN ANTIMONY TRICHLORIDE AND ITS COMPLEX WITH BENZENE

Compound		Resonance frequency, Mc/sec		$\Delta\nu$[a] kc/sec
		21°C	−196°C	
$2SbCl_3 \cdot C_6H_6$	ν_1	18.543	18.655	112
	ν_2	18.647	18.749	102
	ν_3	19.606	20.068	462
	ν_4	19.973	20.349	376
	ν_5	20.047	20.459	412
	ν_6	20.077	20.509	437
$SbCl_3$	ν'_1	19.179	19.304	116
	ν'_2	20.419	20.912	480

a) $\Delta\nu$ is the difference between the resonance frequencies at 21 and −196°C.

line; it is reproduced in Fig. 1. Although the Zeeman patterns of six resonance lines are shown in Fig. 1, one of them was missing in the original sample because the principal z axis of the field gradient at the chlorine atom contributing to the missing line was nearly parallel to the rf coil axis, thus reducing its intensity considerably. In order to observe the pattern, we had to use another sample, a single crystal in which the crystal axes were oriented differently. For this sample, however, another resonance line was missing. Combining both results, the six patterns shown in Fig. 1 were obtained.

The direction of the principal z axis of the field gradient of the chlorine atom can be determined by the zero-splitting pattern.[9] Generally the z axis is parallel to the direction of the Sb-Cl bond in the complex. Consequently, the angle between any two Sb-Cl bonds can be deduced; these angles are listed in Table 2. It should be remarked here that the z axis may deviate slightly from the direction of the bond which is bound to the benzene ring. As has been stated above,

TABLE 2. THE ANGLES BETWEEN THE Sb-Cl BONDS[a]

Bond	$Sb-Cl_1$	$Sb-Cl_2$	$Sb-Cl_3$	$Sb-Cl_4$	$Sb-Cl_5$
$Sb-Cl_2$	69°28′				
$Sb-Cl_3$	128°46′	94°39′			
$Sb-Cl_4$	94°48′	93°46′	140°19′		
$Sb-Cl_5$	94°28′	25°17′	78°24′	95°9′	
$Sb-Cl_6$	139°15′	96°12′	92°9′	48°29′	78°8′

a) The experimental error is ±1°.

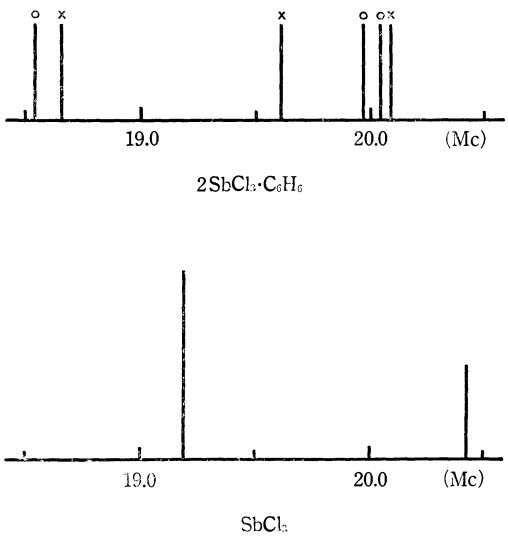

Fig. 2. Pure quadrupole resonance spectra of antimony trichloride and its complex with benzene. Resonance lines with the same mark, circle or cross come from the same antimony trichloride molecule.

9) K. Shimomura, *J. Phys. Soc. Japan*, **12**, 657 (1957).

six resonance lines of the same intensity are observed in a polycrystalline sample, but they can not be grouped into any sets. This problem can, however, be solved easily when the Zeeman effect on the resonance lines is examined. The results are shown in Fig. 2, in which those lines labeled by the same mark, a circle or a cross, come from the same molecule. The ν_1 and ν_2 resonance frequencies are considerably lower than the remainder. These lowering must be caused by some factors other than the crystal field. One possibility is that they correspond to the bonds which reside on the benzene ring.

The values of the asymmetry parameter are determined from the distortion of zero-splitting loci by the following equation:[10]

$$\eta = 3(\sin^2\theta_{max} - \sin^2\theta_{min})/(\sin^2\theta_{max} + \sin^2\theta_{min}) \quad (1)$$

where θ_{max} and θ_{min} are maximum and minimum zero-splitting angles, corresponding to $\phi=0°$ and 90° respectively. Consequently, the quadrupole coupling constants are calculated by this equation, substituing the value of η:

$$\nu = (eQq_{zz}/2h)(1 + \eta^2/3)^{1/2} \quad (2)$$

The values of η and eQq_{zz} derived in this way are listed in Table 3.

The bond character of the Sb-Cl bond can be determined from η and eQq_{zz}. The resonance structures are considered to be as shown in Fig. 3 in general. There is no doubt about the existence of covalent (1) and ionic (2) structures, but there must be a double-bond structure (3) as well.

Table 3. The nature of Sb-Cl bonds in $SbCl_3$ Molecule

Compound	Species	eQq_{zz} Mc/sec	U_p %	η %	i %
$2SbCl_3\cdot C_6H_6$	Cl_1	36.927	33.7	16.0±0.7	60.4
	Cl_2	37.216	33.9	11.2±0.5	60.1
	Cl_3	39.122	35.7	11.9±0.5	58.0
	Cl_4	39.854	36.3	11.7±0.5	57.3
	Cl_5	40.074	36.5	5.5±0.4	57.1
	Cl_6	40.106	36.6	8.5±0.1	56.9
$SbCl_3$	Cl'_1	38.205	34.8	15.3	59.0
	Cl'_2	40.794	37.2	5.7	56.1

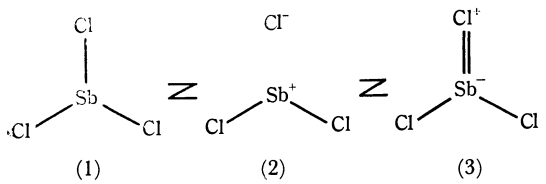

(1) (2) (3)

Fig. 3. Resonance structures of antimony trichloride.

10) C. Dean, *Phys. Rev.*, **96**, 1053 (1954).

Since the ground state of antimony is $5s^25p^3$, the sp^3 hybrid orbital seems to occur in $SbCl_3$ to some extent. Kimball[11] discussed the possibilities of double-bond formation by treating the problem of direct valence from the viewpoint of the group theory. According to him, the sp^3 hybrid orbital is capable of forming a strong π bond with d^2 and a weak π bond with d^3. However, Gordy[12] proposed that the tendency to form a double bond by using d orbitals falls off rapidly in descending rows in the periodic table, essentially vanishing for such fifth-row elements as Sn and Sb. The Sb-Cl bond length of $SbCl_3$, as claculated by the equation of Schomaker and Stevenson,[13] is in good agreement with the observed value if the Sb-Cl bond has a little double-bond character in $SbCl_3$. If the double-bond character of the Sb-Cl bond can be neglected, the bond character can be derived as follows.

The number of the unbalanced p-electron is given by:

$$U_p = (1 - i)(1 - s) \quad (3)$$

where i is the ionic character and s is the s electron character, which is assumed to be equal to 0.15.[14] On the other hand, the value of U_p is evaluated from the observed quadrupole coupling constant:

$$U_p = (eQq_{zz})_{obs}/(eQq_{zz})_{atom} \quad (4)$$

where $(eQq_{zz})_{atom}$ is 109.7 Mc/sec.[15] The ionic character, i, can be calculated from Eqs. (3) and (4). The results are listed in Table 3. It may be noted that the Sb-Cl_1 and Sb-Cl_2 bonds have a larger ionic character than do the other bonds, which have nearly the same ionic character as those of $SbCl_3$ in its pure state. Thus it seems likely that the π electron of the benzene is transferred to the chlorine atom through the Sb-Cl_1 or Sb-Cl_2 bond.

The molecular shape of the $SbCl_3$ in the complex and its pure crystal are shown in Fig. 4, the bond angles being taken from Table 2. Two nonequivalent $SbCl_3$ molecules in the complex crystal have almost the same shape, but show differently-spaced resonance frequencies. That is, in the $Sb-Cl_3$ molecule (A) the smallest angle is between $Sb-Cl_3$ and $Sb-Cl_6$, which correspond to the middle and the highest frequencies respectively, whereas in the other molecule, $SbCl_3$ (B), the smallest angle is between Sb-Cl_1 and Sb-Cl_4, the lowest and the middle frequencies. The shape

11) G. E. Kimball, *J. Chem. Phys.*, **8**, 188 (1940).
12) W. Gordy, W. V. Smith and R. F. Trambarulo, "Microwave Spectroscopy," John Wiley and Sons, Inc., New York (1953), p. 313.
13) V. Schomaker and D. P. Stevenson, *J. Am. Chem. Soc.*, **63**, 37 (1941).
14) C. H. Townes and B. P. Dailey, *J. Chem. Phys.*, **17**, 782 (1949).
15) V. Jaccarino and L. G. King, *Phys. Rev.*, **83**, 471 (1951).

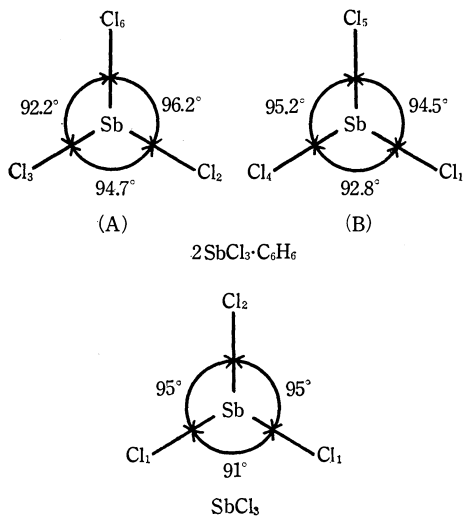

Fig. 4. Shapes of antimony trichloride molecule in the pure state[4] and its complex with benzene.

of $SbCl_3$ (B) is similar to that of $SbCl_3$ in its pure crystal; accordingly, the asymmetry parameter of Sb in the former should be equal to that in the latter. This is really the case; the findings on the ^{123}Sb resonance will be reported elsewhere. In this complex, benzene may combine with the chlorine atom to form the complex; that is, some charge may be transferred to the chlorine atom from benzene. Therefore, the bond angles of $SbCl_3$ in the complex may be expected to increase as a result of the stronger coulombic repulsion between chlorine atoms; however, only a little change may be seen, as is shown in Fig. 4.

We will now discuss the structure of $SbCl_3$ in the complex further. Daasch[16] assumed, from its infrared spectrum, that the $2SbCl_3 \cdot C_6H_6$ molecular complex has C_{2v} symmetry in the solid state and C_{3v} symmetry in the liquid state. Perkampus and Baumgarten[17] proposed, from the infrared spectrum, that the possible symmetry of the complex crystal was C_{2v}, C_s, or C. From the present Zeeman analysis it may be concluded that this complex has C_i or C_1 symmetry in the solid state; there is only one kind of pattern for each resonance line, as is shown in Fig. 1, and the intensities of all the resonance lines are equal.[18] If the structure of this complex has C_{2v} or C_s symmetry, at least one resonance line has two kinds of patterns. However, it is impossible to distinguish C_i from C_1 by the Zeeman analysis, because both positive and negative directions of the z axis of the field gradient give the same result.

Ashkanaji *et al.*[19] and Raskin[20] have reported on the Raman spectrum of a solution of antimony trichloride in benzene. The former authors observed two new lines which Raskin could not observe; they attributed these lines to the bending and stretching vibrations of the bond between antimony and benzene. On the contrary, it seems more probable, for the following reasons, that benzene combines with the chlorine atom. First, the lowest resonance frequency, ν_1, or ν_2, in each $SbCl_3$ molecule has the least temperature dependence, as may be seen in Table 1. This runs parallel to the more restricted motion of the chlorine atom bound to benzene. Second, the chlorine, Cl_1 or Cl_2, corresponding to the lowest line has the largest ionic character, which may be interpreted as having been brought about by the charge transfer from benzene. A somewhat similar situation arises in the molecular complex of carbon tetrabromide with *p*-xylene.[21] Two bromine atoms of the carbon tetrabromide in this complex are bound to benzene rings, while the other two bromine atoms are free from complexing. Hooper[22] tentatively assigned the lower frequency to the complexing bromine atoms. These results may support our conclusion, although the final decision should be made on the basis of X-ray analysis.

16) L. W. Daasch, *Spectrochim. Acta*, **9**, 726 (1959).
17) H. H. Perkampus and E. Baumgarten, *Z. Physik. Chem.*, **39**, 1 (1963).
18) K. Shimomura, *J. Phys. Soc. Japan*, **12**, 652 (1957).
19) M. S. Ashkanaji, P. U. Kurnosova and V. S. Finkelstein, *J. Phys. Chem. (U. S. S. R.)*, **8**, 438 (1936).
20) Sh. Sh. Raskin, *Opt. i Specktroskopiya*, **1**, 516 (1956).
21) F. J. Strieter and D. H. Templeton, *J. Chem. Phys.*, **37**, 161 (1962).
22) H. O. Hooper, *J. Chem. Phys.*, **41**, 599 (1964).

BULLETIN OF THE CHEMICAL SOCIETY OF JAPAN VOL. 41 65—70 (1968)

Reactivity of Solid Acids with Methylene Chloride

Isao MOCHIDA, Jun-ichiro TAKE, Yasukazu SAITO and Yukio YONEDA

Department of Synthetic Chemistry, Faculty of Engineering, The University of Tokyo, Hongo, Tokyo

(Received July 20, 1967)

In order to discriminate the natures of solid acids, the reactivity of methylene chloride with solid acids like alumina, silica-alumina and alumina-boria to give carbon monoxide and methyl chloride was studied with a pulse technique. The reactivities varied about ten thousandfold among these solid acids. The methyl chloride formation was predominant on alumina particularly at low reaction temperatures, with a distinctly small activation energy in comparison with that on silica-alumina or alumina-boria. The nature of the active sites for this reaction was discussed in connection with the effect of the calcination temperature as well as of the sodium ion-poisoning on activity. Furthermore, it was found that the feature of this reaction was in marked contrast with the typical solid acid catalysis such as the dealkylation reaction of alkylbenzenes. The reaction of methylene chloride with a set of the surface hydroxyl group and the oxidizing site is assumed to give methyl chloride through a radical mechanism.

It is well known that alumina and silica-alumina are in remarkable contrast with each other as solid acid catalysts. Silica-alumina has about one thousand times or even more higher catalytic activity than alumina has in such typical catalytic reactions as dealkylation of alkylbenzenes,[1] isomerization of xylene or cyclohexene[1] and oligomerization of propylene.[2] It is also to be noted that the ethylene/ether selectivities in dehydration of ethanol at 325°C on alumina and silica-alumina are quite different, although both give nearly the same activity.[3]

Alumina is known to exhibit exceedingly higher catalytic activities than silica-alumina does for the H-D exchange reaction between hydrogen and deuterium or between the surface hydroxyl groups and either deuterium or deuterated methane.[4] For example, the activation energy of the exchange reaction of the hydroxyl groups with deuterated methane was 5.7 kcal/mol for alumina, but 33.4 for silica-alumina.[4]

Many works have already been published concerning the triphenylcarbonium ion formation from triphenyl methane on solid acids.[5] Lately, Arai *et al.*[6] reported an interesting contrast between alumina and silica-alumina for the triphenyl methane chemisorption; a considerable amount of triphenyl methyl radical alone was formed on alumina, whereas both triphenylcarbonium ion and triphenyl methyl radical were formed on silica-alumina.

As well as silica-alumina, all of alumina-boria-(10% B_2O_3)[1] and aluminas treated with boron trifluoride, hydrogen fluoride or ammonium fluoride[1,7] gave higher catalytic activities for the dealkylation and other acid-catalyzed reactions.

The present authors have found that methylene chloride reacts with solid acids to give methyl chloride and carbon monoxide as the gaseous products and that the rate and the selectivity of methyl chloride/carbon monoxide varied extermely with the kind of the solid acid.[8] In other words, this reaction can characterize the specific nature of alumina as the solid acid in comparison with silica-alumina. The specific nature of alumina may be due to the cooperation of both the surface hydroxyl group and the oxidizing site for the radical reaction, as is previously concluded by the LFER (Linear Free Energy Relationships) approach with the aid of the simple molecular orbital theory.[8]

Experimental

Reagents. Methylene chloride and *n*-butylamine of G. R. grade (Tokyo Kasei Co.) were used without any purification. No impurities were detected by gas chromatography.

1) I. Mochida and Y. Yoneda, *J. Catalysis*, **7**, 386, 393 (1967).
2) M. Misono and Y. Yoneda, This Bulletin, **40**, 42 (1967).
3) J. Take and Y. Yoneda, to be published.
4) J. G. Larson and W. K. Hall, *J. Phys. Chem.*, **69**, 3080 (1965).
5) W. K. Hall and R. P. Porter, *J. Catalysis*, **5**, 366 (1966); A. E. Hirshler and J. O. Hudson, *ibid.*, **3**, 239 (1964).
6) H. Arai, Y. Saito and Y. Yoneda, This Bulletin, **40**, 312 (1967).
7) E. V. Ballor, R. T. Barth and R. A. Flinn, *J. Phys. Chem.*, **65**, 1639 (1961); H. R. Gerberich, F. E. Vutinsky and W. K. Hall, *J. Catalysis*, **6**, 209 (1966).
8) I. Mochida and Y. Yoneda, *ibid.*, **9**, 57 (1967).
9) R. J. Kokes, H. Tobin and P. H. Emmett, *J. Am. Chem. Soc.*, **77**, 5860 (1955); D. W. Bassett and H. W. Habgood, *J. Phys. Chem.*, **64**, 769 (1960).

TABLE 1. CATALYSTS

No.	Catalyst		Surface area m^2/g	Composition	Remarks
	Symbol	Name			
1	A-3-550[1]	alumina	170		(a)
2	A-3-700[1]	alumina	110		(a)
3	A-3-900[1]	alumina	45		(a)
4	A-3-Na[2]	alumina-NaOH	150		(b)
5	A-B[2]	alumina-boria	290	10% B_2O_3	(c)
6	Al-S[2]	aluminum sulfate		0.4 mmol/g-SiO_2	
7	SA-1[2]	silica-alumina	540	13% Al_2O_3	(d)
8	SA-2[2]	silica-alumina	310	27% Al_2O_3	(d)
9	SA-1-Na-1[2]	silica-alumina-NaOH	450	0.048 meq Na/g	(e)
10	SA-1-Na-2[2]	silica-alumina-NaOH	480	0.087 meq Na/g	(e)
11	SA-1-Na-3[2]	silica-alumina-NaOH	480	0.168 meq Na/g	(e)
12	SM-1[2]	silica-magnesia	560	16% MgO	(f)
13	S-1[2]	silica	600		(g)
14	S-F[2]	silica-NH_4F			(h)
15	H-10X[3]	H-Molecular Sieve 10X			(i)

1) The tail numerals designate the calcination temperature.
2) Calcined at 550°C.
3) Calcined at 450°C.
a) F-110, active alumina of Alcoa.
b) By impregnation of A-3 with aq. NaOH.
c) By coprecipitation of $Al(NO_3)_3$ and H_3BO_3 with NH_4OH.
d) Nippon Cat, a cracking catalyst of Shokubi Kasei Co.
e) By impregnation of SA-1 with aq. NaOH.
f) TY-13, a cracking catalyst of Nikki Kagaku Co.
g) Q-12, active silica gel for chromatograph of Wako Co.
h) By treatment of S-1 with aq. NH_4F.
i) By protonation of Molecular Sieve 10X with the NH_4Cl exchange method.

Solid Acids. Solid acids are listed in Table 1. They were calcined for 8 hr in air. All acids in Table 1 except for 13, 14, and 15 were used also in the previous work[1] as catalysts.

Apparatus and Procedure. An ordinary pulse technique was adopted.[9] Hydrogen as the carrier gas was purified by removing water and oxygen with a dry ice - ethanol cold trap and activated copper on kieselguhr, respectively. No difference in the reactivity or the selectivity was observed even if helium was used as the carrier gas. Tricresyl phosphate (Japan Chromato Co.) was used in the analytical column (4 m) at the room temperature. The identification of the products, *i. e.* carbon monoxide and methyl chloride was made by gas chromatography with an analytical column of silica gel and Molecular sieve 5A at the room temperature for the former and by mass spectrometry for the latter. By-products such as chloroform or formaldehyde were not detected at all by gas chromatography.

The reaction temperature was set between 250 and 420°C. After the solid acid was pretreated for 1 hr in a hydrogen gas flow at 450°C, 2 μl of methylene chloride was injected into the gas flow at the top of the reactor through a silicon serum cap with a microsyringe. The reaction was nearly first order under experimental conditions and the conversion was proportional to the reciprocal space velocity under low conversions, so that the initial rate constant, k (ml/g·min), was obtained directly from the slope.[9] This unit of the rate constant is converted into the usual one, mol/min·atm·g-cat, by the multiplication of a factor, 4.16×10^{-5}. The reactivity decreased remarkably pulse by pulse. Owing to the prevailing poisoning for the carbon monoxide formation, the ratio of CH_3Cl/CO increased pulse by pulse. Therefore, the rate constant was obtained from the conversion of the first pulse for a fresh catalyst. The rate and the selectivity of the first pulse were satisfactorily reproducible. The initial selectivities were constant under 30% conversion.

Results and Discussion

The reactivities of the fifteen solid acids were summerized in Fig. 1. The maximum reactivity was 8.2×10^{2} ml/g·min for H-10X and the minimum, 9.9×10^{-2} for S-1. All the solid acids have nearly equal surface areas (170—600 m^2/g) with a few exceptions. Therefore, the difference in the reactivity should be attributed to their surface nature.

The activation energies for methyl chloride and carbon monoxide formation were different from each others. On alumina, the former was smaller than the latter, with the reverse trend on alumina-boria, as shown in Table 2, It is unlikely that the trend in the adsorption strengths of the two

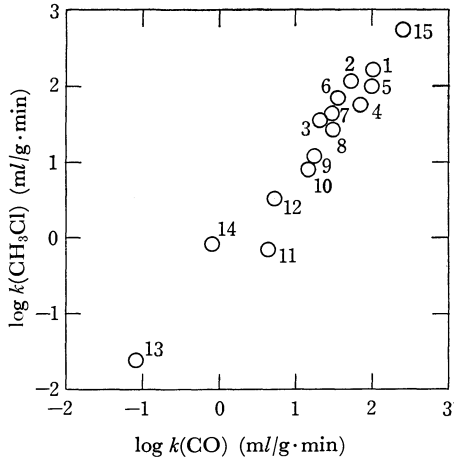

Fig. 1. Reactivities of various solid acids. (400°C)
Numbers refer to Table 1.

Table 2. Activation energy of the carbon monoxide and methyl chloride formation

Solid acid	Carbon monoxide kcal/mol	Methyl chloride kcal/mol
A-3-550	21	6.1
A-3-700	21	6.5
A-3-900	23	21
A-3-Na-550	24	23
A-B	21	27
SA-1	24	40
SA-2	(24)*	(40)*
SA-1-Na-3	(24)*	(70)*
H-10X	21	26

* Calculated from the rates at two reaction temperatures.

products on alumina is opposite to that on alumina-boria. The addition of *n*-butylamine before the reaction caused a severe posioning for both formations, especially for methyl chloride, as will be discussed later. Hence, different routes for each product should be postulated.

By the titration with silver nitrate in aqueous solution, nearly all chlorine atoms lost during the reaction were found to remain on alumina. This reaction may be analogous to that of alumina with carbon tetrachloride to synthesize anhydrous aluminum chloride.[10]

The Carbon Monoxide Formation. The temperature dependence of the rate constant of the carbon monoxide formation, together with the values of activation energies is shown in Fig. 2 and Table 2. The activation energy was nearly the same for all solid acids that contained alumina, although the rate constants themselves varied

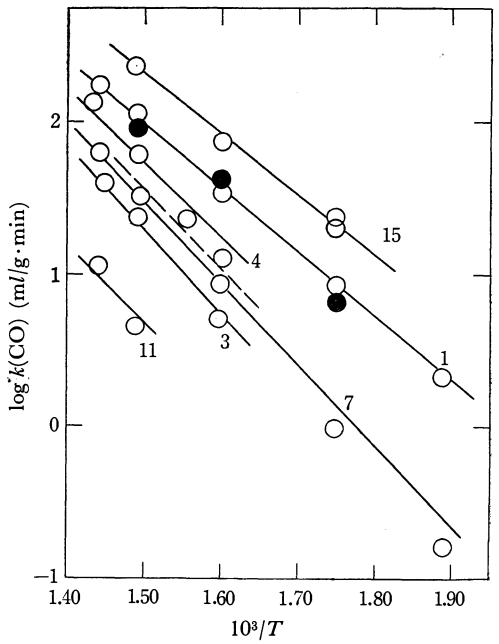

Fig. 2. Arrhenius plots of carbon monoxide formation on various solid acids containing alumina as a component.
Numbers refer to Table 1. The closed circles are for A-B and the dotted line is for SA-2.

greatly among them. The rate constant per unit surface area was large for the solid acid of high alumina content. At 400°C alumina had larger reactivity per unit surface area by five thousands times than silica had, as shown in Fig. 1. The correlation between the reactivity per unit weight of the component alumina and the surface area is

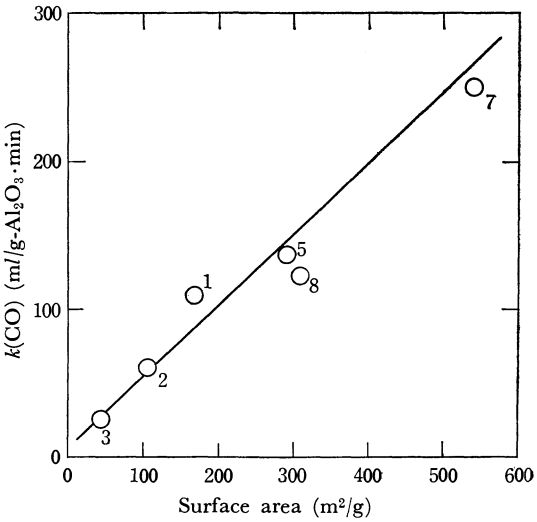

Fig. 3. Rate constants of carbon monoxide formation *vs.* the surface area of various solid acids containing alumina.
Numbers refer to Table 1.

10) K. Knox, R. D. Srivanstava, V. Norman, J. Y. Basserr and J. H. Hollowing, *J. Am. Chem. Soc.*, **79**, 3358 (1957).

shown in Fig. 3. Several solid acids, appearing in Fig. 3, were prepared by coprecipitation so that the aluminum atoms may be distributed throughout the surface and the bulk. The average rate constant of the carbon monoxide formation per unit surface area of the component alumina was 0.5 ml/min. From this close correlation, the "surface aluminate group," a group of a surface aluminum ion and its surrounding oxygen ions, which disperses on the surface as mentioned above, is proposed to participate in the carbon monoxide formation on these solid acids.

A series of the sodium ion-poisoned silica-alumina catalysts (SA-1, SA-1-Na-1, SA-1-Na-2, and SA-1-Na-3) gave the declining reactivities linearly with the increasing extent of sodium ion-poisoning, as shown in Fig. 4, with the activation energy uninfluenced (Table 2). These facts suggest the decrease in the amount of the active sites. Because the surface hydroxyl groups existing on silica-alumina are only silanols that are reportedly not influenced by this poisoning,[11] sodium ions

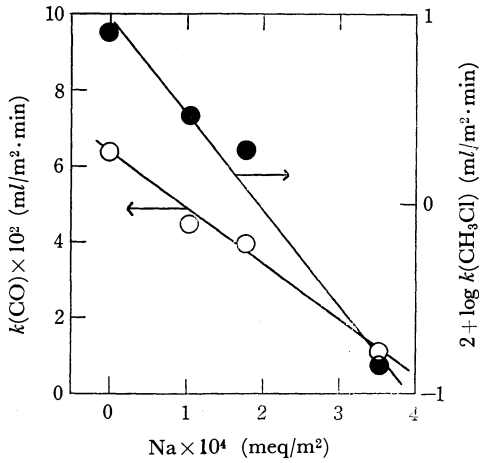

Fig. 4. Rate constants of carbon monoxide and methyl chloride formation *vs.* the amount of sodium ion. Catalyst, SA-1.

impregnated to SA-1 are possibly coordinated to the surface aluminate groups.

The Methyl Chloride Formation. The activation energy for the methyl chloride formation depends largely on the kind of the solid acids, which is in remarkable contrast to the case of the carbon monoxide formation. The temperature dependence and the activation energy are shown in Fig. 5 and Table 2, respectively. The alumina catalyst, A-3-550, had a markedly large activity of 1.2 ml/m^2·min at 400°C and a small activation energy of 6.1 kcal/mol whereas the silica-alumina catalyst, SA-1, had 7.8×10^{-2} ml/m^2·min and

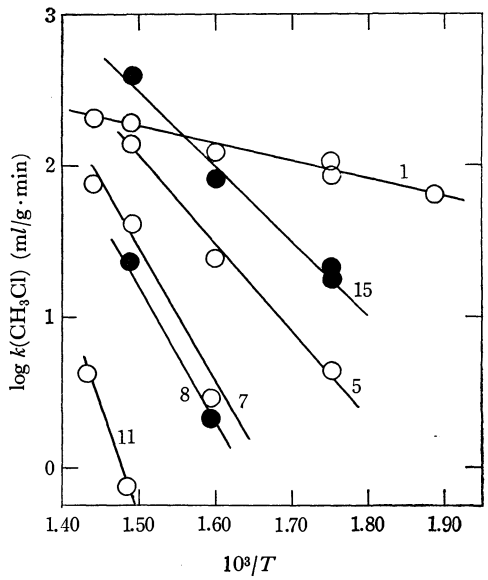

Fig. 5. Arrhenius plots of methyl chloride formation on various solid acids.
Numbers refer to Table 1.

40 kcal/mol, respectively. The difference of the activation energies for the methyl chloride formation between alumina and silica-alumina thus resembles the case of the H-D exchange reaction between deuterated methane and the surface hydroxyl groups on these solid acids.[4]

The surface hydroxyl groups, throughout these solid acids including alumina, should be concluded to participate in the methyl chloride formation from the following experimental results.

(1) This reaction resembles the H-D exchange reaction between deutereated methane and the surface hydroxyl groups of alumina or silica-alumina, as mentioned above.

(2) Each pulse of the reactant decreased largely and irreversively the reactivity of the solid acid.

(3) Any product of the disproportionation reaction, *e. g.* chloroform, was not detected.

(4) The reaction rate was not changed by the carrier gas of hydrogen or helium.

(5) The active hydroxyl groups on alumina surface with the highest wave number in the infrared spectroscopy were found to react with carbon tetrachloride at 200°C by Peri and Hannan.[12]

The reactivities of alumina calcined at various temperatures, as well as the sodium ion-poisoned alumina, are shown in Fig. 6 and Table 3. The impregnation of sodium ion and the calcination at high temperatures decreased the reactivity of alumina to a great extent. Analogus poisoning effects of sodium ion to alumina were reported for

11) M. R. Basila, *J. Phys. Chem.*, **66**, 2223 (1962) (IR); W. K. Hall, H. P. Leftin, F. J. Chersleke and D. E. O'Relly, *J. Catalysis*, **2**, 506 (1963) (NMR).

12) J. B. Peri and H. B. Hannan, *J. Phys. Chem.*, **64**, 1526 (1960); J. B. Peri, *ibid.*, **70**, 2937 (1966) (silica gel).

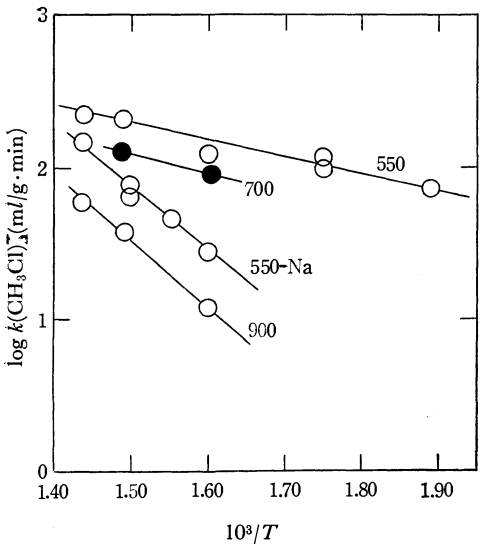

Fig. 6. Arrhenius plots of methyl chloride formation on alumina calcined at various temperatures.
Numerals represent the calcination temperatures.

Table 3. The calcination temperature effect on the methyl chloride formation activity of alumina

Alumina	Calcination temp. °C	Activity of the unit surface area at 400°C ml/m²·min
A-3-550	550	1.2
A-3-700	700	1.2
A-3-900	900	0.85
A-3-Na-550	550	0.48

the H_2-D_2 exchange reaction.[13] These deactivation may be due to the decrease in both the reactivity and the amounts of the hydroxyl groups and the oxidizing sites. Peri[14] reported by infrared spectroscopy the decrease of the surface hydroxyl groups of alumina by the calcination.

A linear relationship between the logarithms of the reaction rate constants and the amounts of sodium ion added was observed in the series of the sodium ion-posioned silica-alumina catalysts, as shown in Fig. 4. The activation energy also increased with sodium ion-poisoning, as shown in Table 2. These facts resemble the case of the typical solid acid catalysis. Sodium ion is coordinated to the surface aluminate group, as was discussed for the carbon monoxide formation. The hydroxyl groups on silica-alumina have been identified as the silanol groups and no Al-OH has been detected by either IR or NMR.[11] Silica-alumina had larger activity by about three thousands times than silica gel for the methyl chloride formation at 400°C, as shown in Fig. 1, in spite of the fact that the same amount of the hydroxyl groups was present on silica-alumina and silica gel both calcined at 550°C.[11] With sodium ions coordinated to the surface aluminate groups, the cooperation of the exposed aluminum ion with the neighboring silanol groups will be lost according to the decrease in the reactivity of the both sites. Therefore, the methyl chloride formation may be largely retarded by the sodium ion-poisoning, as is the case for the typical solid acid catalysis. It is also reasonable that the two silica-alumina catalysts of different alumina content (SA-1 and SA-2) exhibited nearly the same activation energy for the methyl chloride formation.

Alumina-boria (10% B_2O_3) has higher activity for the typical solid acid catalysis such as dealkylation,[1] but it was less reactive than alumina for the methyl chloride formation. The activation energy of alumina-boria for this reaction was about 20 kcal/mole larger than alumina (Table 2) and the reactivity per unit surface area at 400°C was 4.6×10^{-1} ml/m²·min for alumina-boria, whereas 1.2 for alumina. These results are understandable, if the hydroxyl groups are assumed not preferably to be bound to aluminum but rather to boron on the alumina-boria surface.

The Effect of the *n*-Butylamine Addition before the Reaction. The effect of the *n*-butylamine addition before the reaction is shown in Table 4. Both the reaction temperature and the addition temperature were 350°C. The addition of *n*-butylamine hindered strikingly both the methyl chloride and the carbon monoxide formations with alumina as well as alumina-boria, probably because of its strong coordination to the active sites. By exposing the amine-poisoned solid acids in the hydrogen gas flow at the reaction temperature for a certain period, the reactivity was gradually recovered presumably in accordance with the desorption of *n*-butylamine. The recovery from the *n*-butylamine poisoning of alumina was much faster than that of alumina-boria for the methyl chloride formation, as shown in Table 4. The reactivity was recovered up to 79% of the fresh alumina after 60 min, but only up to 11% for alumina-boria after 75 min. This slow recovery may be due to the stronger acidity of alumina-boria than alumina. The fresh alumina, however, was more active than alumina-boria for the methyl chloride formation, as described previously.

For the recovery of the reactivity for the carbon monoxide formation, it was also slower for alumina-boria than for alumina; the recovery of 71% for alumina after 60 min and of 13% for alumina-boria after 75 min. The active sites for the carbon monoxide formation on alumina-boria should be

13) H. Pines and J. Ravoire, *ibid.*, **65**, 1859 (1961).
14) J. B. Peri, *ibid.*, **69**, 211 (1965).

TABLE 4. THE EFFECT OF *n*-BUTYLAMINE ADDITION BEFORE THE REACTION

	Alumina (A-3-550)			Alumina-boria (A-B)		
Catalyst amount (mg)	40.5	40.8	38.7	90.8	79.6	86.0
n-Butylamine amount (μl)	0	0.4	0.4	0	0.4	0.4
Time of elution* (min)	—	3	60	—	2	75
CH_3Cl formation rate ($ml/g \cdot min$)	3.76×10^2	9.58	2.98×10^2	3.80×10	3.28	4.16
CO formation rate ($ml/g \cdot min$)	1.05×10^2	1.78×10	7.46×10	4.54×10	3.89	5.77
CH_3Cl/CO	3.46	0.54	4.0	0.84	0.84	0.72

* The period of keeping the solid acids in the hydrogen gas flow at 350°C between the *n*-butylamine addition and the reaction.

more acidic than on alumina, since *n*-butylamine interacts more strongly with the former than the latter. But the difference in their acidities may be unrelated to their oxidizing abilities.

Proposed Reaction Mechanism. In aspect to the reactivities of alumina, silica-alumina or alumina-boria, the methyl chloride formation is similar to the H-D exchange reaction between their surface hydroxyl groups and deuterated methane, that may proceed through the radical mechanism, but is different from the typical solid acid catalysts that have been confirmed to be caused by the Bronsted acid sites. This reaction was unrelated to the strength of *n*-butylamine adsorption on these solid acids. Furthermore, alumina was found to have a lot of triphenyl methyl radical-forming sites.[6] These facts strongly suggest a radical mechanism to form methyl chloride from methylene chloride with these solid acids, and also that alumina is more reactive in some radical reactions than silica-alumina or alumina-boria, which is more acidic. The radical mechanism of the methyl chloride formation is consistent with the previous conclusion deduced from the reactant effects with the utilization of the simple LCAO-MO reactivity indexes.[8]

Our thanks are due to Mr. Masao Maruyama of the Engineering Research Institute of our Faculty for his analysis by a mass spectrometer.

BULLETIN OF THE CHEMICAL SOCIETY OF JAPAN VOL. 41 71—75 (1968)

Solubility of Chlorine in Hydrochloric Acid*1

Fumio HINE and Shusei INUTA

Kyoto University, Uji, Kyoto

(Received July 20, 1967)

The solubility of chlorine in a concentrated HCl solution at various conditions of concentration, partial pressure, and temperature was determined. The concentration of chlorine in a solution as the sum of Cl_2 and Cl_3^- was found to be proportional to the partial pressure of chlorine in the gas phase, and its slope was a function of the HCl concentration and the temperature. Empirical equations representing these relations and the solubility of chlorine were obtained. It was confirmed that the results agreed with the experimental data in the 2—10 N HCl concentration range at partial pressures of chlorine lower than 1 atm and at 30—90°C. Such physicochemical properties as the Gibbs free-energy change were considered by using the data of solubility, and the behavior of the system consisting of Cl^-, Cl_2, and Cl_3^- was discussed.

The solubility of chlorine in water or in an aqueous solution of sodium chloride under various conditions has been studied by several authors previously,[1-3] but only a few results in an HCl solution at room temperature have been obtained.[4,5]

Today, many chlorine engineers are concerned with the recovery of chlorine from by-products or waste HCl, and they require more information and data on such properties of chlorine in an HCl solution as solubility.[6]

Experimental work was carried out at various conditions of temperature, concentrations and partial pressure, then some characteristic values, such as the Henry coefficient and the free energy, were evaluated from the solubility data thus obtained.

Experimental Procedure

The apparatus employed was essentially the same as that of Whitney and his collaborator,[2] who determined the solubility of chlorine in water with well-designed equipment, though we made some modifications for our own convenience.

The flow diagram is shown in Fig. 1. The absorption chamber and the gas pre-treatment system were set in a water bath so as to keep it at a constant temperature of ±0.1°C during the experiment.

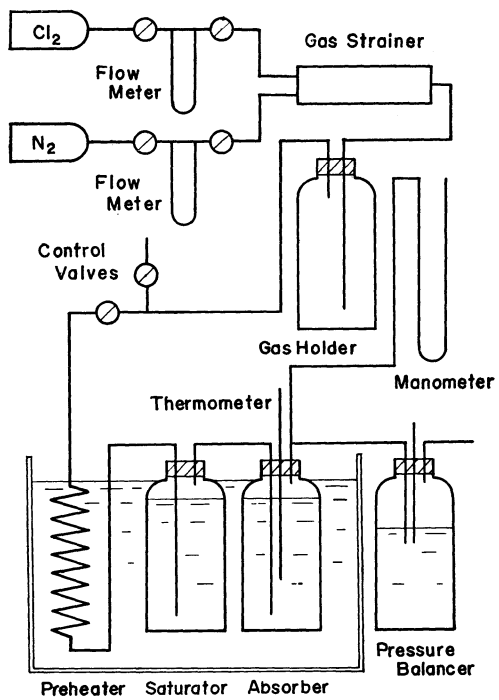

Fig. 1. Apparatus for experiment.

Chlorine and nitrogen from the cylinders were delivered to the gas strainer, which was packed with glass wool in order to mix the two gases thoroughly. The flow rate of chlorine and nitrogen was separately measured with a capillary-type flow meter.

The moisture and temperature of the gas were brought to equilibrium before it was introduced into the absorption chamber. The partial pressure of chlorine was maintained by mixing it with nitrogen, and was determined by chemical analysis. The total pressure of gas in the absorption chamber was assumed to be

*1 This paper was presented at the Spring Meeting of the Electrochemical Society of Japan, Tokyo, April, 1967.

1) F. W. Adams and R. G. Edmonds, *Ind. Eng. Chem.*, **29**, 447 (1937).
2) R. P. Whitney and J. E. Vivian, *ibid.*, **33**, 741 (1941).
3) N. Yokota, *Kagaku Kogaku (Chem. Eng., Japan)*, **22**, 476 (1958).
4) M. S. Sherrill and E. F. Izard, *J. Am. Chem. Soc.*, **50**, 1670 (1928).
5) M. S. Sherrill and E. F. Izard, *ibid.*, **53**, 1667 (1931).
6) F. Hine, S. Yoshizawa, K. Yamakawa and Y. Nakane, *Electrochem. Techn.*, **4**, 556 (1966).

the sum of the partial pressures of chlorine, nitrogen, hydrogen chloride, and water vapor, and was determined by means of a manometer. The partial pressure of water vapor was mostly obtained from Reference 7, though some data were confirmed empirically.

The sample gas was passed through the absorption chamber for an hour in order to gain an equilibrium state prior to measurement.

A certain amount of the solution at the equilibrium was pipetted out quickly, added to a 10% solution of potassium iodide, and diluted with water until its pH reached about 1. Its solution was then titrated by iodometry to measure the chlorine dissolved.

Results and Discussion

Sherrill and Izard[5] and Jokowkin[8] have studied the effects of HCl on the solubility of chlorine in water. They concluded that while the solubility of chlorine decreased upon the addition of a small amount of HCl, it increased in relatively concentrated HCl solutions because of the formation of tri-chloride ions by the combination of Cl_2 and Cl^- as follows:

$$Cl_2 + Cl^- = Cl_3^- \quad (1)$$

Furthermore, HClO may form in a weak acid solution when the pH of the solution is larger than 2. However, no such formation occurs in the present experiment because the concentration of hydrochloric acid is as high as 2—10 N. The results of titration show the sum of chlorine dissolved physically, or "free chlorine," and tri-chloride ions, it also shows the solubility of chlorine in a solution, that is:

$$S = (Cl_2) + (Cl_3^-) \quad (2)$$

where S is the solubility of chlorine, and where (Cl_2) and (Cl_3^-) are the concentrations of free chlorine and tri-chloride ions, respectively.

Experiment was carried out in a 2—12 N HCl solution at 30—90°C. The solubility obtained was plotted as a function of the partial pressure of chlorine under given conditions of HCl concentration and temperature, and the straight lines shown in Figs. 2—6 were thus obtained. The solubility of chlorine in HCl, then, follows Henry's Law; that is,

$$S = Hp \quad (3)$$

where p is the partial pressure of chlorine, and H is Henry's coefficient, which is a function of the temperature and HCl concentration.

Figure 7 shows the relationship between H and the HCl concentration at various temperatures.

Henry's coefficient is a function of the concentration as follows:

$$H = \alpha C + \beta \quad (4)$$

where C is the concentration of HCl, and where

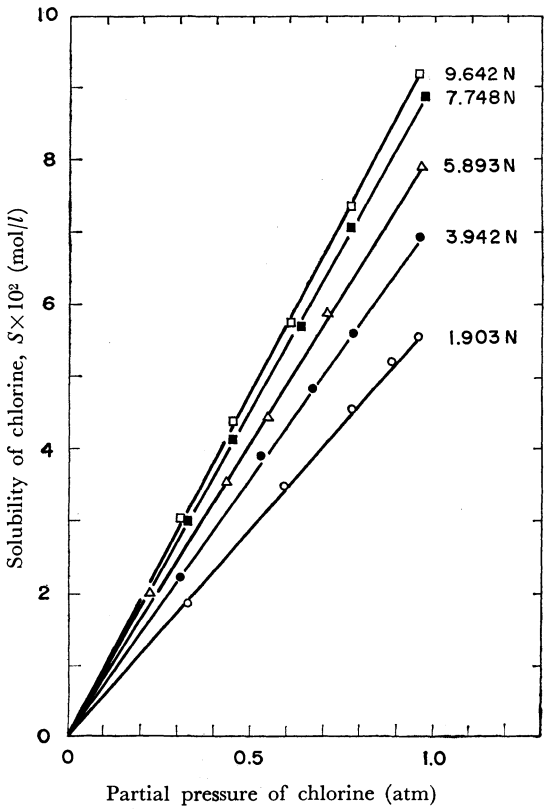

Fig. 2. Solubility of chlorine as a function of its partial pressure of chlorine at 30°C.

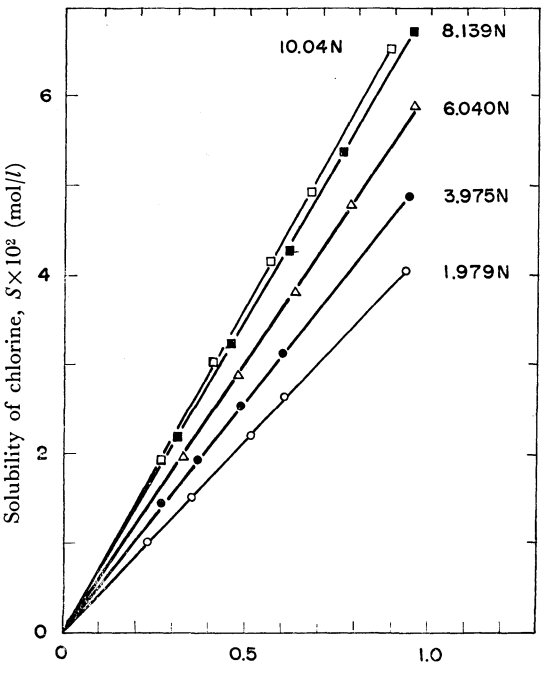

Fig. 3. Solubility of chlorine as a function of its partial pressure at 40°C.

7) J. H. Perry, "Chemical Engineers' Handbook," 4th Ed., 3-60 (1963).
8) A. A. Jakowkin, *Z. Physik. Chem.*, 29, 613 (1899).

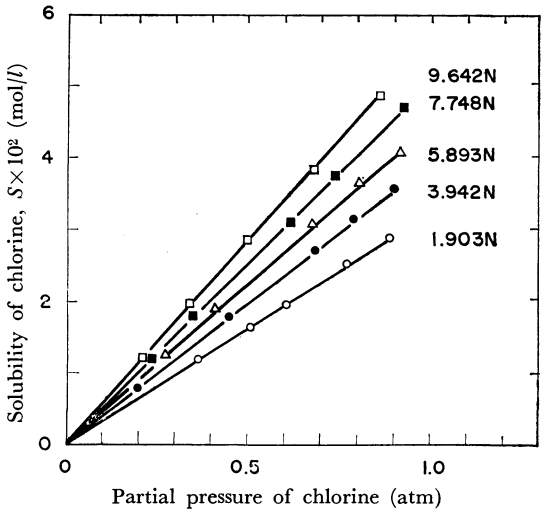

Fig. 4. Solubility of chlorine as a function of its partial pressure at 50°C.

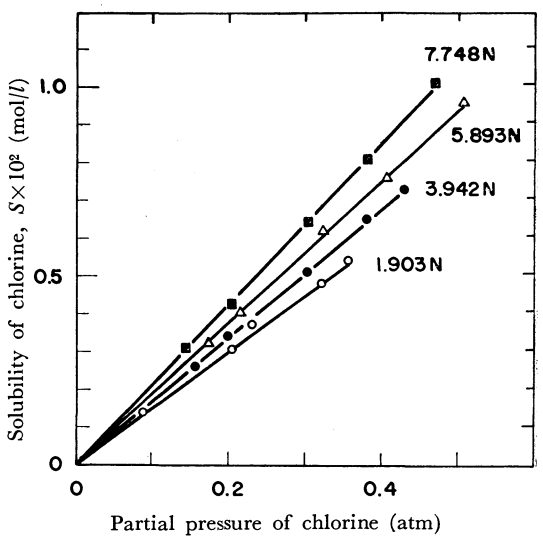

Fig. 6. Solubility of chlorine as a function of its partial pressure at 90°C.

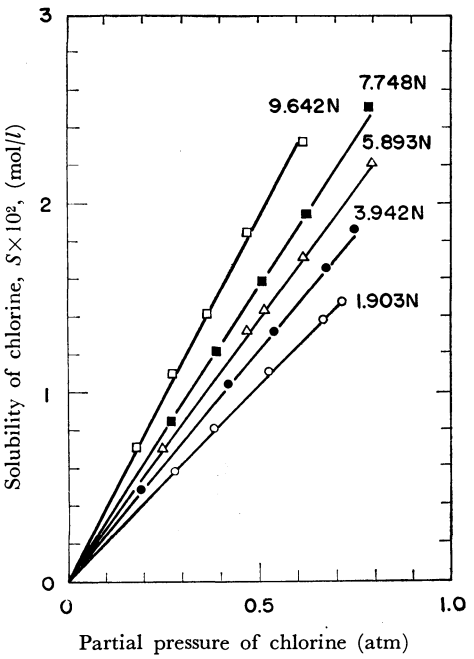

Fig. 5. Solubility of chlorine as a function of its partial pressure at 70°C.

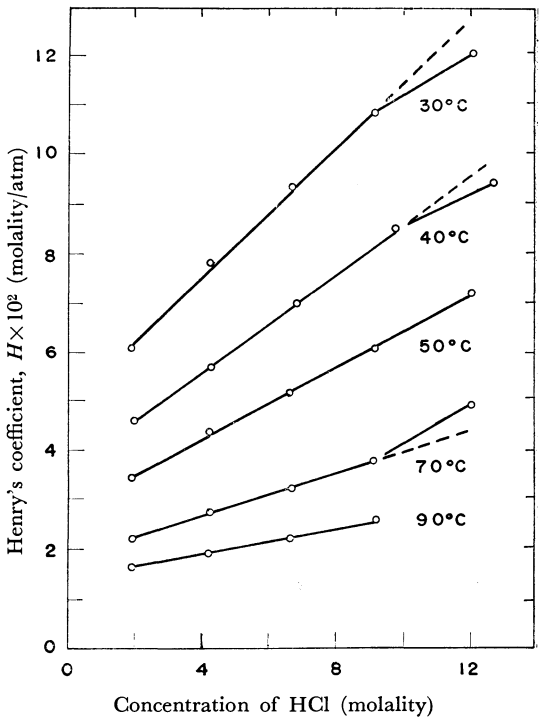

Fig. 7. Henry's coefficient at various temperatures as a function of HCl concentration.

α and β are constants. The substitution of H into Eq. (3) gives the following expression:

$$S = (\alpha C + \beta)p \qquad (5)$$

While the concentration of chlorine and HCl are represented in "molality" in these figures, relations similar to those above, also expressed in "grams per liter," were obtained.

As shown in Fig. 7, Henry's coefficient, and hence both α and β, could easily be derived as functions of the temperature. Figure 8 shows the relationship between α and the temperature: the logarithm of α is proportional to t°C. On the other hand, the logarithm of β *vs.* the logarithm of the temperature is linear, as shown in Fig. 9. Therefore, the empirical equations for α and β be written as follows:

$$\log \alpha = -1.21\times10^{-2}t - 1.603 \qquad (6)$$

and:

$$\beta = 2.14\times10^2 t^{-1.21} \qquad (7)$$

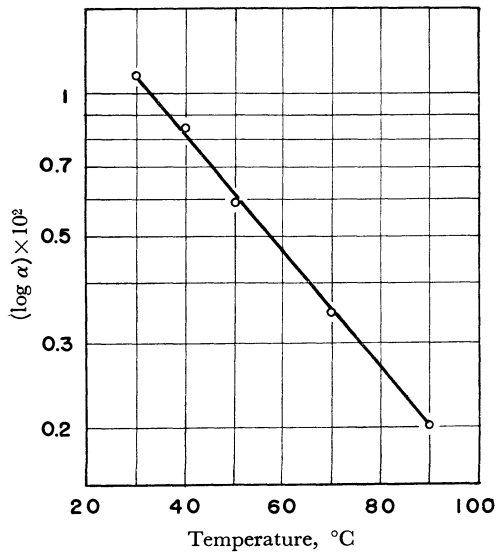

Fig. 8. Logarithm of α *vs.* temperature curve.

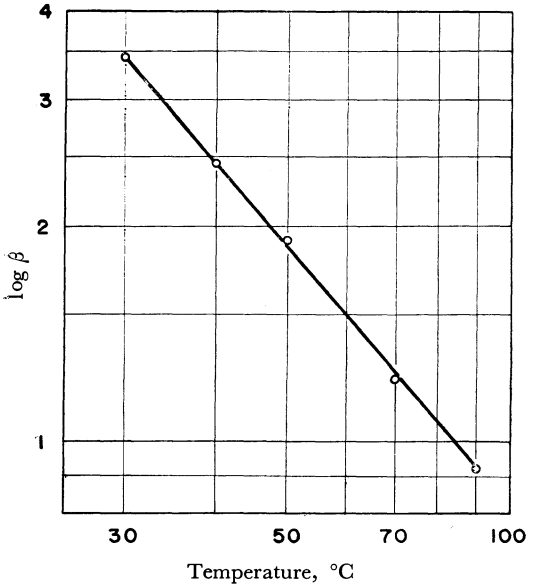

Fig. 9. Logarithm of β *vs.* logarithm of temperature.

where α and β are expressed in grams per liter-chlorine/grams per liter-HCl·atm and grams per liter-chlorine/atm respectively, and the temperature, in degrees centigrade.

Figure 10 shows the values calculated by Eqs. (5), (6), and (7) in comparison with the observed values. A good agreement was obtained between them at 30—90°C in HCl solutions of concentrations less than 10 N under partial pressures of chlorine lower than 1 atm.

It is well known that the equilibrium constant, K, for the reaction (1) may be represented as follows:

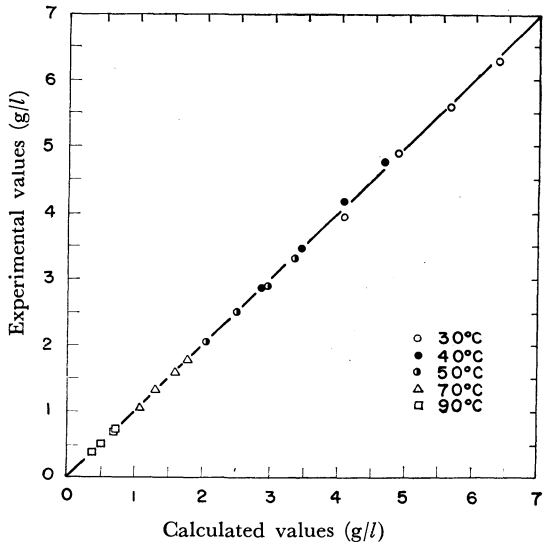

Fig. 10. Solubility of chlorine calculated by the empirical equation in comparison with the data determined.

$$K = \frac{a_{Cl_3^-}}{p \cdot a_{Cl^-}} = \frac{\gamma_{Cl_3^-} \cdot (Cl_3^-)}{p \cdot \gamma_{Cl^-} \cdot (Cl^-)} \tag{8}$$

where:

$a_{Cl_3^-}$	Activity of Cl_3^-	mol/l
a_{Cl^-}	Activity of Cl^-	mol/l
$\gamma_{Cl_3^-}$	Activity coefficient of Cl_3^-	
γ_{Cl^-}	Activity coefficient of Cl^-	

The unit of concentration of chlorine and trichloride ions, (Cl^-) and (Cl_3^-), is mol/l in this case.

Although the activity coefficient of Cl^- in aqueous solutions has been determined,[6] meagre data are available on the activity of Cl_3^-. Assuming that $\gamma_{Cl_3^-} = \gamma_{Cl^-}$, as Sherrill and Izard did,[5] the following equation was obtained:

$$K = \frac{(Cl_3^-)}{p \cdot (Cl^-)} = \frac{(Cl_3^-)}{p \cdot C} \tag{9}$$

where C is the concentration of Cl^- in mol/l.

On the other hand, we may assume that the concentration of chlorine dissolved, or "free chlorine," in a solution, is proportional to the partial pressure of chlorine in the gas phase, such as,

$$(Cl_2) = hp \tag{10}$$

where h is a constant.

By substituting Eqs. (9) and (10) into Eq. (3), we obtain the equation:

$$S = (KC + h)p \tag{11}$$

Therefore, it is evident that K and h should correspond to the two constants, α and β, in Eq. (4) or (5) respectively, if the same units of concentration, pressure, and temperature are used. Table 1 shows these values obtained at various temperatures: the values of α and β using conventional

TABLE 1. THE COEFFICIENTS, α and β, IN HENRY'S EQUATION (5)

Temperature		α		β	
°C	1/(°K)	mol/mol·atm	gpl/gpl·atm	mol/atm	gpl/atm
30	3.300×10^{-3}	6.57×10^{-3}	1.08×10^{-2}	4.85×10^{-2}	3.42
40	3.195	5.11	0.844	3.49	2.46
50	3.096	3.65	0.592	2.72	1.92
70	2.915	2.20	0.350	1.76	1.22
90	2.755	1.38	0.204	1.32	0.916

units are also listed in the table.

According to the van't Hoff Law, we may obtain the following equation:

$$\frac{d(\ln K)}{d(1/T)} = -\frac{\Delta H^\circ}{R} \qquad (12)$$

where T is the temperature in °K; R, the gas constant, and ΔH°, the standard enthalpy change for Reaction (1). The logarithm of K was plotted as a function of the reciprocal temperature, $1/T$, as shown in Fig. 11. That is, ΔH° is independent of the temperature. The enthalpy change, ΔH°, was calculated, from the slope of this curve, to be -5.77 kcal/mol.

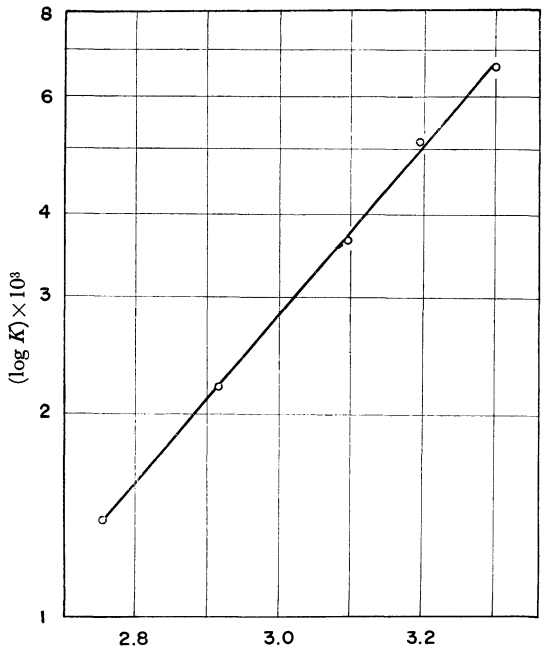

Fig. 11. Logarithm of K *vs.* reciprocal temperature curve.

The Gibbs free energy change, ΔG°, has the following relations with K:

$$\Delta G^\circ = -RT\ln K \qquad (13)$$

and:

$$\Delta G^\circ = \Delta H^\circ - T\Delta S^\circ \qquad (14)$$

where ΔS° is the entropy change. The free energy change, ΔG°, was plotted against the temperature; it was completely linear, as shown in Fig. 12. The empirical equation for ΔG° is as follows:

$$\Delta G^\circ = 2.147 + 0.0290t \quad \text{(kcal/mol)} \qquad (15)$$

The entropy change, ΔS°, was then evaluated to be 29.0 cal/mol·°K, which was independent of the temperature.

The equation for K is as follows:

$$\log K = \frac{1.26\times10^3}{T} - 6.34 \qquad (16)$$

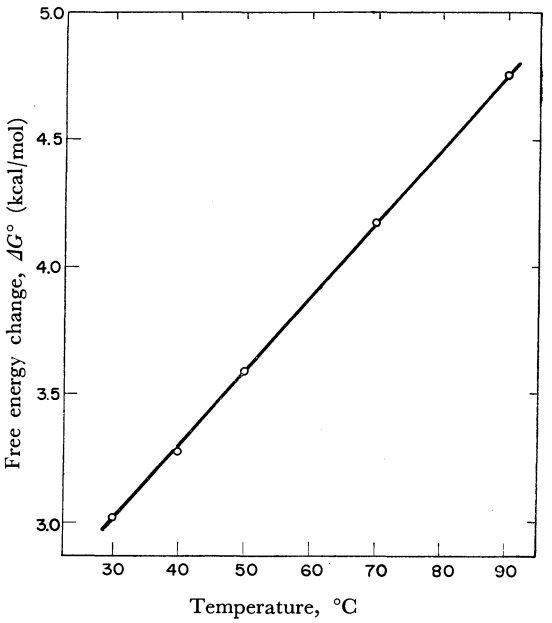

Fig. 12. Free energy change *vs.* temperature.

Summary

The solubility of chlorine in hydrochloric acid solutions of 2—12 N at partial pressures of chlorine lower than 1 atm and at 30—90°C was determined. Henry's Law was found to hold good in this range. Some thermodynamic characteristics of the system consisting of Cl_2, Cl^-, and Cl_3^- were also discussed.

BULLETIN OF THE CHEMICAL SOCIETY OF JAPAN VOL. 41 76—82 (1968)

Scission Probabilities of the Skeletal Bond of Aliphatic Ethers by Electron Impact*1

Kozo HIROTA and Jun'ichi TAKEZAKI*2

Department of Chemistry, Faculty of Science, Osaka University, Toyonaka, Osaka and Osaka Laboratory, Japanese Association for Radiation Research on Polymers (JARRP), Neyagawa, Osaka

(Received July 28, 1967)

Mass spectra of eight aliphatic mono- and di-ethers have been measured with apparatuses of both ordinary and high resolution type, and scission probability of their skeletal bonds has been determined. By application of the molecular orbital theory on bond-scission by electron impact, the scission probability of the skeletal bonds has been evaluated, using only a few constants peculiar to the C–O bond so as to determine the molecular orbital. Comparison between theory and experiment has been found satisfactory on such ethers, even though they have lone-pair electrons in the inner part of the molecules. Thereby, scission of the skeletal bond has been shown explainable quite well by the primary processes in most ethers, except highly symmetric or large ethers.

Mass spectra of alkyl ethers were extensively studied by McLafferty,[1] and several characteristic rules were recognized on the fragmentation by electron impact. Recently, the rules were investigated in more details by Gjerassi and Fenslau.[2] Their discussion on the fragmentation processes, however, seems to remain in qualitative explanation and to lack in its molecular-theoretical derivation.

In the present report, probabilities of the skeletal bond-scission of several aliphatic ethers are investigated by determining the ions produced by use of apparatuses of both ordinary and high resolution type, and the molecular orbital (MO) theory is applied to explain the results quantitatively, generalizing the theory if necessary. The ethers to be investigated are methyl ethyl ether (MEE), methyl propyl ether (MPE), methyl butyl ether (MBE), diethyl ether (DEE), di-isopropyl ether (DIPE), methylal, ethyleneglyccl dimethyl ether (EGDME), and ethyleneglycol diethyl ether (EGDEE). Their structures are shown in Table 1, where the numerals attached to the bonds will become necessary in the following paragraphs.

Theory

In the previous reports on chain compounds,[3] it was assumed that the scission probability of skeletal bonds of the parent ion produced by electron impact is proportional to the positive charge density of the highest occupied (HO) molecular orbital (MO) localized at the bonds. This assumption on the initial fragmentation, though imcompatible with the widely accepted scheme of competitive and successive fragmentation,[4] will be understood, if the parent ion is a kind of super-excited ion of a short life[5] which is less than the time of a molecular vibration, so that it dissociates immediately into ion and radical, being followed by secondary fragmentation. A part of the theoretical basis on the above scheme was proposed in details elsewhere, making cycloalkanes as examples. In the present report, theoretical investigation will not be carried out so far, regarding the MO theory just as a semiempirical "tool" of investigating mass spectra of complex organic molecules.

Calculation

In actual calculation, the charge density is assumed to be equal in amount of the electron density of the corresponding neutral molecule, and it will, therefore, be evaluated approximately by the following LCBO*-MO-method. The MO belonging to the skeletal bond, φ, is expressed by Eq. (1),[6]

$$\Phi = \sum_{i=1}^{n} c_i \varphi_i \qquad (1)$$

*1 The IXth report of the molecular orbital theory of mass spectra (VIII: K. Hirota, *J. Phys. Chem.*, **71** sec. (1967).

*2 Present address: Osaka Lab., Japan Atomic Energy Research Institute, Neyagawa, Osaka.

1) F. W. McLafferty, *Anal. Chem.*, **29**, 1782 (1957).

2) C. Gjerassi and C. Fenslau, *J. Am. Chem. Soc.*, **87**, 5747 (1965).

3) K. Fueki and K. Hirota, *Nippon Kagaku Zasshi (J. Chem. Soc. Japan, Pure Chem. Sect.)*, **81** 212 (1960).

4) H. M. Rosenstock, M. B. Wallenstein, A. L. Wahrhaftig and H. Eyring, *Proc. Natl. Acad. Sci. U. S.*, **38**, 667 (1952).

5) R. L. Platzman, *Radiation Res.*, **17**, 419 (1962).

*3 Linear Combination of Bond Orbital.

6) R. D. Brown, *J. Chem. Soc.*, **1953**, 2615.

TABLE 1. ETHERS TO BE STUDIED IN THE PRESENT RESEARCH

(1)	Methyl ethyl ether	MEE	$CH_3^{1}-O^{2}-CH_2^{3}-CH_3$
(2)	Methyl propyl ether	MPE	$CH_3^{1}-O^{2}-CH_2^{3}-CH_2^{4}-CH_3$
(3)	Methyl butyl ether	MBE	$CH_3^{1}-O^{2}-CH_2^{3}-CH_2^{4}-CH_2^{5}-CH_3$
(4)	Diethyl ether	DEE	$CH_3^{1}-CH_2^{2}-O^{3}-CH_2^{4}-CH_3$
(5)	Di-isopropyl ether	DIPE	$(CH_3^{1})(CH_3^{2})CH^{3}-O^{4}-CH^{5}(CH_3^{6})(CH_2)$
(6)	Methylal		$CH_3^{1}-O^{2}-CH_2^{3}-O^{4}-CH_3$
(7)	Ethyleneglycol dimethyl ether	EGDME	$CH_3^{1}-O^{2}-CH_2^{3}-CH_2^{4}-O^{5}-CH_3$
(8)	Ethyleneglycol diethyl ether	EGDEE	$CH_3^{1}-CH_2^{2}-O^{3}-CH_2^{4}-CH_2^{5}-O^{6}-CH_2^{7}-CH_3$

where, φ_i is the bond-orbital of the ith skeletal bond, and summation is carried out on all the bonds, adopting united atom approximation.[7] Hence, the electron density in problem may be given by square of the expansion coefficient C_i of the HO molecular orbital. By the calculus variation, the energy levels can be determined by the secular equation (2), as usually done in the LCAO-MO method.

$$|e_{ij} - \delta_{ij}E| = 0 \qquad (2)$$

In Eq. (2), e_{ij} denotes the matrix elements given by Eq. (3), and is to be called coulombic or exchange integral, according as $i=j$ or $i=j\pm1$.

$$e_{ij}=\int \varphi_i H \varphi_j d\tau \qquad (3)$$

where H denotes the hamiltonian for an electron in the field of bare nuclei and inner shells of electrons. Both integrals concerning hydrocarbons will be denoted by α and β, respectively, hereafter.

Since the so-called Hückel approximation is adopted, all the e_{ij} in Eq. (2) becomes coulombic integral α_i or exchange integral β_{ij}. However, coulombic integral at the terminal CH_3-C bond α_t is equated to $\alpha+2\beta$. As an exceptional case, $\alpha+1.5\beta$ is used for α_t of MEE, improvement ought to be understood as empirical, but not due to the inductive effect at the terminal methyl group of neutral molecules.[8]

The coulombic and exchange integrals of the C–O bond are equated preliminarily to $\alpha+2\beta$ and β, respectively, but coulombic integrals of the terminal CH_3–O bond are equated to $\alpha+3\beta$. Such a selection of constants for the C–O bond is qualitatively allowable if the effect of lone-pair electrons at the oxygen atom be considered.

Using the α_i and β_{ij} defined above, the energy values of the HO orbital E_h and expansion coefficients at the orbital were calculated. Thereby, it was found sufficient only to determine the value of $\lambda_h=(\alpha-E_h)/\beta$ instead of E_h itself. At the same time, it was found not necessary to know the absolute values of α_i and β_{ij}, but sufficient to know their relative values to α and β.

7) J. L. Franklin, *J. Chem. Phys.*, **32**, 1304 (1954). The accuracy of this method was discussed in Part VIII of the present series of research.

8) *Cf.* L. C. Lorquet, *Molec. Phys.*, **9**, 101 (1965).

Experimental

Since the mass spectra obtained with an ordinary apparatus are often difficult to assign each peak to a definite ion, mass spectra were measured on a high

TABLE 2. MASS SPECTAR OF METHYL ETHYL ETHER AND DIETHYL ETHER

A, Hitachi RMU-5; B, Hitachi RMU-7hr; C, API

m/e	MEE $CH_3OCH_2CH_3$			DEE $CH_3CH_2OCH_2CH_3$		
	A	B	C	A	B	C
15	8*	7.2	9	2.5		
16		0.2				
26	3.4	2.5		1.6	1.5	
27	7.9	7.0	7	7.4	2.0	5
28	3.0	4.1	3	2.5	2.0	1.5
29	18.9	15.1	18	15.4	17.3	12
30	1.3	0.9	1	0.6	0.8	0.6
31	7.7	7.3	7	24.3	33.7	30
32	0.8	0.4	1	0.5	0.4	
41	0.3	0.2		1.4	1.3	2
42	0.6	0.4	1	0.3	0.5	0.3
43	2.7	2.0	2	2.3	2.3	2
44	0.3	0.9		0.7	0.7	0.6
45	38.6	35.8	37	10.3	11.0	12
46	0.6	0.7				
59	4.2	3.9	4	15.4	12.0	16
60	10.0	10.8	10	0.5	0.4	
73	—			0.6	0.6	1
74	—			8.9	6.4	11

* Estimated value

resolution apparatus as well as on ordinary one. In order to check the discrimination due to apparatus, the mass spectra obtained on MEE and DEE are compared with those of literature (Table 2), making total sum of the peaks to be 100. Column A is the one run on an apparatus of ordinary type (Hitachi RUM-5A) installed at JARRP, and column B on an apparatus of high resolution type (Hitachi RMU-7hr) installed at Osaka University, its resolution being *ca.* 5000. Both are of a magnetic scanning type, but their normal operating conditions are different as follows:

	Ionizing voltage, V	Accelerating voltage	Electron current, μA
RMU-5A:	90	1500	80
RMU-7hr:	80	2000	100

Column C is the spectra recalculated from the API mass spectral catalog (CEC Model 21-103). In column B, multiplet peaks appearing practically at the same *m/e* are summed up. Discrepancies among these spectra are not large, in spite of the measurement of different apparatuses and operating conditions. Similar tendency was obtained on other six ethers, so that the present data are assumed sufficient to be utilized in discussion.

In order to meet the requirement to be explained, MEE-d_3, $CD_3OCH_2CH_3$ was synthesized and its spectrum was measured and used mainly in discussion.

Results

Assignment of Peaks and Allotment of Ions. By combining the results of ordinary and high resolution spectra, multiplet peaks were allotted to each composite ions; *e. g.*, in the case of MPE, ratio of $C_2H_5^+$ to CHO^+ ions was estimated to be 22.5%/77.5% from the doublet peaks at *m/e* 29. Thus, ratio of the doublet peaks was determined and the results are summarized in Table 3, which indicates that some major peaks consist of two ions. Taking this point into consideration, spectral peaks with their assigned ions are shown in Table 4, where sums of the total ions including parents ions are made 100%. Details of the assignment of each peak to corresponding ions are described in the next paragraph as well as number of the ruptured bond to produce the corresponding ions.

Table 3. Allotment of multiplet peaks to ions in MEE, MPE, DEE and methylal

	m/e	MEE	MPE	DEE	Methylal
28	C_2H_4	92	81.5	93	75
	CO	8	18.5	7	25
29	C_2H_5	53.5	22.5	86	
	CHO	46.5	77.5	14	
30	C_2H_6	15		50	
	CH_2O	85		50	
40	C_3H_4		91.5		66.5
	C_2O		8.5		34.5
41	C_3H_5	70		98	
	C_2HO	30		2	
42	C_3H_6		14.5	2.5	80
	C_2H_2O		85.5	97.5	20
43	C_3H_7		29.5	2	85
	C_2H_3O		70.5	98	15
44	C_3H_8	22	14	18.5	22
	C_2H_4O	78	86	81.5	20
	CO_2	—	—	—	58

Ruptured Bond. It is easy for most of the ions to estimate the ruptured bond, if their chemical formula is known, but it is still difficult for several ions. For instance, the *m/e* 15 peak can be assigned to be CH_3^+ ion without ambiguity by high resolution spectra, but the ruptured bond cannot be determined uniquely as shown by the following example:

$$CH_3\overset{1}{\underset{\alpha}{|}}O\overset{2}{|}CH_2\overset{3}{|}CH_2\overset{4}{\underset{\beta}{|}}CH_3 \longrightarrow \begin{cases} \overset{\alpha}{\rightarrow} CH_3^+ + \dot{O}CH_2CH_2CH_3 \\ \overset{\beta}{\rightarrow} CH_3OCH_2\dot{C}H_2 + CH_3^+ \end{cases} \quad (4)$$

However, both processes could be discriminated in the case of MEE by comparing the spectrum of $CD_3OCH_2CH_3$ with that of $CH_3OCH_2CH_3$, and ratio of α and β bond-scission could be determined, if the isotopic effect be neglected. Such procedure was not taken up in other ethers, because amount of the CH_3^+ ions was always so small that their origin is not important in order to discuss the degree of agreement between theory and experiment entirely.

There are several ions, however, whose ruptured bond is difficult to be determined. Among them, estimation of the origin of the $(CHO)^+$ ion is comparatively easy. In the case of MEE, this ion can be produced from the $(CH_3O)^+$ ion either by successive scission of the second bond with 2H detachment,

$$(CH_3O\overset{2}{|}CH_2CH_3)^+ \rightarrow (CH_3O)^+ + \dot{C}H_2CH_3$$
$$\xrightarrow{-2H} (CHO)^+ + \dot{C}H_2CH_3 + 2H \quad (5)$$

or by double scissions of the first and third bonds with H detachment.

$$(CH_3\overset{1}{|}O\overset{2}{|}CH_2\overset{3}{|}CH_3)^+ \rightarrow$$
$$(OCH_2)^+ + 2\dot{C}H_3 \rightarrow (OCH)^+ + 2\dot{C}H_3 + H \quad (6)$$

However, the process (5) was considered reasonable, because scission probability of the second bond is theoretically large, besides the simpleness of the process. This conclusion is supported by the mass spectrum of MEE-d_3, where CH_3O^+ and CH_2O^+ are shown negligible few in Table 4. In the cases of other ethers, (MPE, MBE and EGDME), the same allotment was adopted, because the situation may be the same.

Of all the ethers, DIPE includes the largest

number of ambiguous ions, *i. e.*, only 38% of the total ions could be allotted without ambiguity. Of the remaining ions, 51.9% requires at least two bond scissions, and it is difficult to estimate which scission is the first of the two, as explained on the orgin of the CH_3^+ ions. Therefore, determination of scission-probability of DIPE was more difficult than that of other ethers. DEE was also

Table 4. Assigned ions and their relating bond-scission

1) MEE-d_3

Ion	Peak height %		Ruptured bond
CD_3	9.8		
CD_2	1.9		
CD	1.7	16.5	1
C_2H_3O	0.6		
C_2H_2O	2.5		
C_2H_5	9.9		
C_2H_4	3.3		
C_2H_3	6.1		
C_2H_2	3.2		
C_2H	0.3	33.2	2
CDO	8.9		
CD_2O	1.4		
CD_3O	0.1		
CH_3	3.6		
CD_3OCH_3	30.9	35.1	3
CD_3OCH	0.6		
		84.8	
CD_2H	1.1		
CH_3O	0.1		
CD_2HO	3.9	5.7	u
C_2D_2, CD_4O	0.6		
M-1	2.9		
M[a)]	6.7	9.6	p
Total		100.1	

2) MPE

Ion	Peak height %		Ruptured bond
CH_3	4.9		
C_3H_7O	0.2	5.1	1 or 4
CHO	7.0		
CH_3O	1.0		
C_3H_7	0.6		
C_3H_6	0.2	15.7	2
C_3H_5	4.5		
C_3H_3	2.4		
C_2H_5	2.0		
C_2H_4	1.7		
C_2H_3	5.3		
C_2H_2	0.8		
C_2H_5O	64.2	77.5	3
C_2H_6O	1.2		
C_2H_3O	1.4		
C_2H_2O	0.9		
		98.3	
CO	0.5	0.5	u
M-1	0.4		
M[a)]	1.0	1.4	p
Total		100.2	

a) M denotes the parent ion.

3) MBE

Ion	Peak height %		Ruptured bond
CH_3	3.3	3.3	1 or 5
CH_3O	0.8		
CHO	1.1		
C_4H_9	0.8	13.2	2
C_4H_8	9.7		
C_4H_7	0.8		
C_3H_8	0.5		
C_3H_7	0.5		
C_3H_6	0.1		
C_3H_5	4.8		
C_3H_4	0.3		
C_3H_3	2.4	66.8	3
C_2H_6O	0.9		
C_2H_5O	56.0		
C_2H_4O	0.3		
C_2H_3O	0.5		
C_2H_2O	0.5		
C_2H_5	6.1		
C_2H_4	2.4		
C_2H_3	4.5	14.7	4
C_2H_2	0.6		
C_2H_7O	1.1		
		98.0	
CO	0.5	0.5	u
M	1.8	1.8	p
Total		100.3	

4) DEE

Ion	Peak height %		Ruptured bond
CH_3	2.5		
C_3H_8O	0.5	18.4	1 or 4
C_3H_7O	15.4		
C_2H_6	0.3		
C_2H_5	13.3		
C_2H_4	2.5		
C_2H_3	7.4		
C_2H_2	1.6	38.6	2 or 3
C_2H_5O	10.3		
C_2H_4O	0.6		
C_2H_3O	2.3		
C_2H_2O	0.3		
		57.0	
CHO	2.4		
CH_2O	0.3	32.2	
CH_3O	29.3		
CH_4O	0.5		
C_3H_8	0.1	1.5	u
C_3H_5	1.4		
M-1	0.6		
M	8.9	9.5	p
Total		100.2	

TABLE 4 (Continued)

5) DIPE

Ion	Peak height %		Ruptured bond
CH_3	2.3	11.1	1, 2, 5 or 6
$C_5H_{11}O$	8.8		
C_3H_3	0.3	26.8	3 or 4
C_3H_7	15.5		
C_3H_6	1.0		
C_3H_5	4.9		
C_3H_7O	4.1		
C_3H_6O	1.0		
		37.9	
C_2H_4	0.4	4.8	i_1 1+3 *etc.*
C_2H_3	4.2		
C_2H_2	0.2		
C_2H_5O	44.1	47.1	i_2 1+4 *etc.*
C_2H_4O	0.3		
C_2H_3O	2.7		
Unknown peaks		8.4	u
M	1.8	1.8	p
Total		100.0	

6) Methylal

Ion	Peak height %		Ruptured bond
CH_3	2.3	2.3	1 or 4
C_2H_6O	0.8	70.2	2 or 3
C_2H_5O	38.1		
C_2H_4O	0.7		
C_2H_3O	0.5		
CH_4O	0.3		
CH_3O	5.1		
CH_2O	2.2		
CHO	22.5		
		72.5	
CO	1.0	3.5	u
m/e 47	1.9		
CO_2	0.4		
C_2H_6	0.2		
M-1	23.3	31.1	p
M	0.8		
Total		100.1	

7) EGDME

Ions	Peak height %		Ruptured bond
CH_3	0.3	1.5	1 or 5
CH_2	1.2		
C_2H_6	0.1	32.5	2 or 4
C_2H_5	3.1		
C_2H_4	1.9		
C_2H_3	1.9		
C_2H_2	0.7		
CH_3O	3.2		
CH_2O	0.9		
CHO	9.9		
C_3H_8O	5.8		
C_3H_7O	1.5		
C_3H_6O	3.5		
C_2H_6O	1.2	59.1	3
C_2H_5O	53.6		
C_2H_4O	0.3		
C_2H_3O	3.2		
C_2H_2O	0.7		
		93.1	
CO	0.6	1.0	u
CO_2	0.4		
M	5.8	5.8	
Total		99.9	

8) EGDEE

Ions	Peak height %		Ruptured bond
CH_3	2.1	2.4	1 or 7
$C_5H_{10}O_2$	0.3		
C_2H_6	0.2	16.1	2 or 6
C_2H_5	7.8		
C_2H_4	2.0		
C_2H_3	5.2		
C_2H_2	0.9		
C_2H_6O	0.4	34.8	3 or 5
C_2H_5O	17.8		
C_2H_4O	1.5		
C_2H_3O	6.2		
C_2H_2O	0.6		
$C_4H_{11}O$	0.3		
$C_4H_{10}O$	6.4		
C_4H_9O	1.1		
C_4H_8O	0.5		
C_3H_9O	0.3	17.4	4
C_3H_8O	0.5		
C_3H_7O	16.6		
		70.7	
CH_4O	0.3	20.2	i
CH_3O	18.1		
CH_2O	0.2		
CHO	1.6		
Unknown peaks		7.7	u
M		0.6	p
Total		99.2	

difficult, though of lesser degree in allotment of ions, because 57% of the total ions would be allotted without ambiguity. Similar difficulty exists in the largest ethers (EGDEE). The reason of bringing about such results will be explained afterwards.

After the above procedure, scission probability of each bond can mostly be evaluated on all the ethers. For instance, the probability at the second bond of DEE is given by the sum of $C_2H_5^+$ and $(C_2H_5O)^+$ ions. Summarized result on eight ethers is shown in Table 4, where u and p in the column of the ruptured bonds denote undeterminable ions and parent ions (M and M-1), respectively, and i in the same column denotes the ions produced by multiple scissions.

TABLE 5. OBSERVED AND CALCULATED SCISSION PROBABILITY OF ETHERS

MEE			MPE			MBE			DEE		
Bond	Obs.	Calcd.	Bond	Obs.	Calcd.	Bond	Obs.	Calcd.	Bond	Obs.	Calcd.
1	19.4	7	1, 4	5.2	10	1, 5	3.4	4	1, 4	32.3	27.5
2	39.2	44	2	16.0	12	2	13.5	5		(38.9)	
3	41.2	48	3	78.8	77	3	68.2	48	2, 3	67.4	72.5
						4	15.0	45		(61.3)	
$C^1-O^2-C^3-C$			$C^1-O^2-C^3-C^4-C$			$C^1-O^2-C^3-C^4-C^5-C$			$C^1-C^2-O^3-C^4-C$		
$x=3\ 2\ 1.5$			$x=3\ 2\ 0\ 2$			$x=3\ 2\ 0\ 0\ 2$			$x=2\ 2\ 2\ 2$		
$\lambda_h=-0.54$			$\lambda_h=0.76$			$\lambda_h=1.32$			$\lambda_h=-0.38$		

DIPE			Methylal			EGDME			EGDEE		
Bond	Obs.[a]	Calcd.	Bond	Obs.	Calcd.	Bond	Obs.	Calcd.	Bond	Obs.	Calcd.
1+2	29	9	1, 4	3.2	16	1, 5	1.6	2	1, 7	3.4	1
5+6	(41)		2, 3	96.8	84	2, 4	34.9	24	2, 6	22.6	4
3, 4	71	91				3	63.5	75	3, 5	49.3	24
	(59)								4	24.6	71
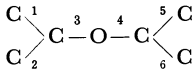			$C^1-O^2-C^3-O^4-C$			$C^1-O^2-C^3-C^4-O^5-C\cdots$			$C^1-C^2-O^3-C^4-C^5-O\cdots$		
$x=2\ 2\ 2\ 2$			$x=3\ 2\ 2\ 3$			$x=3\ 2\ 0$			$x=2\ 2\ 2\ 0$		
$\lambda_h=1.45$			$\lambda_h=-0.69$			$\lambda_h=0.79$			$\lambda_h=0.83$		

a) Values in parenthesis are calculated by allotting u peaks equally to both kinds of scissions.

Scission Probability. Scission probability thus determined from the data of Table 4 is summarized in Table 5. Thereby, only the ions whose ruptured bonds were determinable are considered and the probability is expressed in %. In Table 5, calculated probability is compared with the observed and the HO energy level in λ_h unit on each ether is shown, in addition to the $x_i=(\alpha-\alpha_i)/\beta$ used in the calculation.

Among the eight ethers, DIPE is the worst in coincidence between theory and experiment, because of the particular situation of this ether, whose determinable ions were less than 40% of the total. Similar tendency, though of less degree, is shown in the case of DEE. Other ethers especially, if MBE and EGDEE are excluded, show a good coincidence between theory and experiment.

Before entering into the paragraphs of discussion, it might be noted that the above probability obtained is the one at normal operating condition of the mass spectrometer.

Discussion

First, the peculiarity of ethers might be noted in comparison with the compounds hitherto investigated in the present series of study; *i. e.*, an atom containing lone-pair electrons exists in the inner skeletal bond of each ether. Considering this situation, such a degree of agreement of the theory with the experiment is quite good. Taking it into account, several points will be discussed.

TABLE 6. MAIN PEAKS IN THE SPECTRA OF DEE AND MBE *vs.* IONIZING POTENTIAL

A. DEE $C\overset{15}{\underset{59}{}}-C\overset{29}{\underset{45}{}}-O\overset{45}{\underset{29}{}}-C\overset{59}{\underset{15}{}}-C$

m/e		Ionizing pot. volt[a]				
		90	50	25	20	15
15	CH_3	0.4	0.3	—	—	—
29	C_2H_5	15	14	11	5	1
31	CH_3O	30	30	34	33	17
45	C_2H_5O	10	10	11	10	4
59	C_3H_7O	11	15	21	27	34
74	Parent ion	10	9	13	19	40
Sensitivity		5.5	1.0	0.41	0.34	0.13

B. MBE $C\overset{15}{\underset{}{}}-O\overset{31}{\underset{57}{}}-C\overset{45}{\underset{}{}}-C\overset{59}{\underset{29}{}}-C\overset{73}{\underset{15}{}}-C$

m/e		Ionizing pot. volt[a]				
		90	50	25	20	15
15	CH_3	2	3	—	-	—
29	C_2H_5	6	8	—	4	0.6
31	CH_3O	0.7	0.9	—	—	—
41	C_3H_5	5	5	4	3	2
45	C_2H_5O	56	53	65	68	67
56	C_4H_8	11	10	14	17	20
57	C_4H_9	1	1	1	1	1
59	C_3H_7O	1	1	2	1	2
Sensitivity		—	1.0	0.1	0.1	0.07

a) Absolute values are not so exact.

Secondary Scissions. Among the three unsymmetric ethers, MPE is the best in coincidence, followed by MEE-d_3 and MBE. Concerning MBE, the result may be partly due to improper selection of integral values. Another important cause would be occurrence of multiple scissions which ought to be expected. Even though this process cannot be recognized in the procedure of determining the ruptured bond, this possibility exists, as will be discussed again. Comparatively large disagreement in MEE-d_3 may be due to the same reason rather than the isotopic effect of bond scission.

Similar cause of disagreement may occur in the cases of symmetric ethers, and EGDEE is the typical example, because many ions (about 20%) cannot be explained without assuming multiple scissions, besides the unassignable ions reaching *ca.* 8%. Concerning other symmetric ethers, secondary scissions also seem to occur with high probability, as already mentioned, though the assignment to definite ions was easy.

For the sake of confirmation of the secondary scission, the effect of ionizing potential on bond-scission was investigated on several ethers. The result on DEE is shown in Table 6A.

Though the *m/e* 59 peaks may be produced from DEE by the primary scission of bond 1 or 4, the highest *m/e* 31 peaks can be ascribed to a secondary scission from the *m/e* 59 ion.

$$CH_3\overset{1}{-}CH_2\overset{2}{-}O\overset{3}{-}CH_2\overset{4}{-}CH_3$$

$$\rightarrow CH_3CH_2\text{-}O^+\text{-}CH_2 \quad (m/e\ 59)$$

$$\rightarrow CH_2{=}CH_2 + HO^+{=}CH_2 \quad (m/e\ 31) \qquad (7a)$$

$$\rightarrow CH_3\text{-}CH_2^+ + O{=}CH_2 \quad (m/e\ 29) \qquad (7b)$$

If the above mechanism be true, the *m/e* 31 ion will be smaller at lower ionizing voltage, because excess energy which is necessary for the secondary processes would decrease. At the same time, the *m/e* 59 ion would increase on the contrary. This expectation is supported by comparing the ratio of the *m/e* 31 ion to the *m/e* 59 ion in Table 6A. The effect of ionizing potential on the *m/e* 29 peak can be explained similarly. *Cf.* Eq. (7b).

Another example of the effect of ionizing potential on the bond-scission is shown on MBE. Table 6B indicates that the *m/e* 56 ion increases and *m/e* 29 ion decreases with the decrease of ionizing potential. This finding denotes apparently increase of scission at bond 4 and decrease of scission at bond 2, suggesting that the observed scission probability has to increase at bond 4 and to decrease at bond 2, as compared with the data in Table 5. Thus the agreement of the calculated result of MBE with the observed would be improved.

It was found also that the discrepancy in MEE-d_3 decreased markedly by lowering the ionizing potentil; *i. e.*, scission probability at bond 2 becomes apparently larger than the theoretical due to secondary scission. The worst result of DIPE may be explained similarly, if the effect of ionization potential be studied.

Lone-pair Electrons and Fragmentation. In connection to the above discussion, the behavior of the lone-pair electrons at oxygen atom against the electron bombardment will be discussed, taking DEE as an example. The HO level of this ether is calculated to be -14.43 V from $\lambda_h = -0.38$ (*cf.* Table 5), assuming α and β of C-C bond to be -13.75 V and -1.80 V, respectively. The value is lower by four volts than its ionization energy (10.2 V).[9] This result indicates that at lower ionizing potential the lone-pair electrons would be expelled out, producing parent ions. However, as the ionizing potential is increased, electrons at the skeletal bonds are also expelled out, because the difference of the energy level of both electrons is so small that the ionizing potential of normal operating condition of mass spectrometers is sufficiently large. This reasoning can be explained by the fact that relative amount of the parent ion decreases according to the increase of the ionizing potential, as Table 6 indicates.

Concerning the role of lone-pair electrons, the difference of the C-C bond and C-O bond might be mentioned. In the present treatment, the MO of the skeletal bond was constructed from both kinds of bond, putting aside the presence of lone-pair electrons. However, some interaction may exist between the positive hole at the C-O bond and lone-pair electrons. The effect would appear to decrease the positive hole formed at the C-O bond. The reason why proper coulombic integral at the C-O bond may be $\alpha+2\beta$ can be explained.

Conclusion

It has been shown possible to apply the MO method of mass spectra to alkyl ethers which include lone-pair electrons in the inner part of the molecules.

The authors wish to express their sincere thanks to Dr. Motoyoshi Hatada (JARRP) of his discussion.

9) J. D. Morrison and A. J. C. Nicholson, *J. Chem. Phys.*, **20**, 1021 (1952). Unpublished result measured by J. Takezaki.

BULLETIN OF THE CHEMICAL SOCIETY OF JAPAN VOL. 41 83—87 (1968)

The Polarized Absorption Spectra of Solid Molecular Compounds of Chloranil and Aromatic Amines

Takako AMANO, Haruo KURODA and Hideo AKAMATU

Department of Chemistry, Faculty of Science, The University of Tokyo, Hongo, Tokyo

(Received August 3, 1967)

The polarized absorption spectra of the single crystal were observed for six molecular compounds which involve chloranil as the electron acceptor and aromatic amines as the electron donor. The molecular compounds of *N*, *N*-dimethylaniline, 1-naphthylamine, and *N*, *N*-dimethyl-2-naphthylamine have a non-ionic ground state. In these cases, the locations of the charge-transfer bands in the crystal spectra are similar to those of the corresponding bands of the 1 : 1 molecular complexes formed in the solution. The solid molecular compounds of *p*-phenylenediamine, *N*, *N*, *N'*, *N'*-tetramethyl-*p*-phenylenediamine, and diaminodurene can be regarded as ionic crystals composed of the positive ion of the donor and the negative ion of the acceptor. In these cases, the absorption bands associated with the component ions are observed in the crystal spectra, but they are broadened and appreciably shifted to a higher energy as compared with the case of the solution spectra of the ions. The absorption band associated with the charge transfer between ions is observed in the near-infrared region of the crystal spectra of these molecular compounds.

In most solid molecular compounds, the charge transfer from the electron donor to the electron acceptor is quite small in their ground states. It has been suggested, however, that a molecular compound composed of a strong electron donor and a strong electron acceptor may have an ionic ground state. Such an example can actually be found among the solid molecular compounds which involve aromatic amines as the electron donor, and *p*-chloranil or another quinone derivative as the electron acceptor.[1-5] These molecular compounds are also interesting from the view point of organic semiconductors, since they often exhibit a relatively good electronic conduction.[6-8]

The optical absorption spectra of the solid molecular compounds formed between aromatic amines and chloranil have been studied by several workers in an attempt to elucidate the electronic structures of these molecular compounds.[3-7,9,10] In most cases, however, the spectra were measured on powder samples by means of the KBr-pellet method or by the diffuse reflection method. Consequently, the absorption bands were usually not well resolved in the observed spectra, and their assignments were often quite ambiguous. As is well known, it is of great significance to study the polarized absorption spectra of the single crystal in order to examine the nature of the transition associated with an absorption band. No single crystal spectrum has been reported on the aromatic amine-chloranil compounds except the specular reflection spectra of the compound composed of tetramethyl-*p*-phenylenediamine and chloranil, which spectra have been recently reported by Anex and Hill.[11] Therefore, we have studied the polarized absorption spectra of the single crystals of various aromatic amine-chloranil compounds, including the ones with non-ionic ground states as well as those with ionic ground states.

In the present paper, we shall report on the crystal spectra obtained for the six molecular compounds which involve *N*, *N*-dimethylaniline, 1-naphthylamine, *N*, *N*-dimethyl-2-naphthylamine, *N*, *N*, *N'*, *N'* - tetramethyl - *p* - phenylenediamine (TMPD), *p*-phenylenediamine, and diaminodurene as the electron donors.

Experimental

The polarized absorption spectra of the single crystals were measured with a microspectrophotometer. The

1) H. Kainer, D. Bijl and A. C. Rose-Innes, *Naturwissenschaften* **41**, 303 (1954).
2) D. Bijl, H. Kainer and A. C. Rose-Innes, *J. Chem. Phys.*, **30**, 675 (1959).
3) H. Kainer and A. Überle, *Chem. Ber.*, **88**, 1147 (1955).
4) R. Foster and T. J. Thomson, *Trans. Faraday Soc.*, **59** 296 (1963).
5) D. L. Kronick, H. Scott and M. M. Labes, *J. Chem. Phys.*, **40**, 890 (1964).
6) Y. Matsunaga, *Nature*, **211**, 183 (1966).
7) Y. Matsunaga, *ibid.*, **205**, 72 (1965).
8) D. D. Eley, H. Inokuchi and M. R. Willis, *Discussions Faraday Soc.*, **28**, 54 (1959).
9) M. M. Labes, R. Sehr and M. Bose, *J. Chem. Phys.*, **32**, 1570 (1960); *ibid.*, **33**, 868 (1960).
10) Y. Matsunaga, *ibid.*, **40**, 3453 (1964); *ibid.*, **42** 1982 (1965).
11) B. G. Anex and E. B. Hill, Jr., *J. Am. Chem. Soc.*, **88**, 3648 (1966).

details of the apparatus and the procedures of measurement have been described in a previous paper.[12] Minute crystals of the molecular compounds were prepared by crystallization from solutions containing an appropriate amount of each component. The crystals thus obtained were usually in the form of a needle or a lath elongated along one of the crystal axes. The absorption spectra were measured from the direction normal to the developed face of the crystal with the polarizations, both parallel and perpendicular, to the elongated axis. In the present paper, we shall denote the elongated axis as the "l-axis." In most cases, this is the direction along which donor and acceptor molecules are alternately stacked on each other. All the measurements were carried out at room temperature. The infrared absorption spectra of the solid molecular compounds were also examined in order to ascertain the ionic character of the ground state.

Results and Discussion

***N*, *N*-Dimethylaniline-Chloranil (1 : 1) Compound.** Deep blue needle crystals of this compound can be obtained from a dimethylaniline solution of chloranil. This compound has a non-ionic ground state. The crystal spectrum observed with the light polarized parallel to the l-axis, "the $//l$ spectrum", and that observed with the light polarized perpendicular to the l-axis, "the $\perp l$ spectrum", are shown in Fig. 1. There is a relatively strong absorption band with a maximum located at 15.3 kK in the $//l$ spectrum, but no corresponding band can be found in the $\perp l$ spectrum. Seemingly the 15.3kK band is exclusively polarized along the l-axis. The second absorption band, located at about 32.8 kK, is different from the first band as regards the direction of the transition moment: its intensity is stronger in the $\perp l$ spectrum that in the $//l$ spectrum.

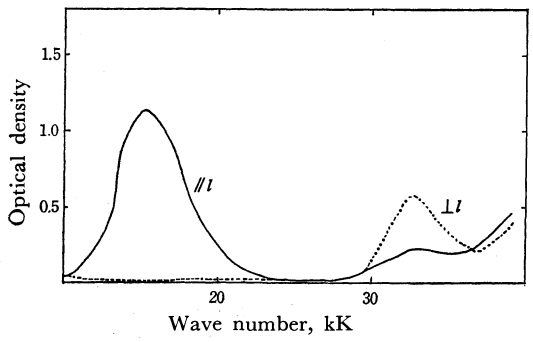

Fig. 1. Absorption spectra of *N*, *N*-dimethylaniline-chloranil compound.

Neither dimethylaniline nor chloranil exhibits any absorption in the 10—25 kK region. The lowest π–π^* transition of dimethylaniline is located at 33.9 kK ($\log \varepsilon = 3.2$), while that of chloranil is at 27 kK ($\log \varepsilon = 2.5$).[13] Therefore, the 15.3 kK band of the $//l$ spectrum can not be attributed to any intramolecular excitation of the component molecules. It must be a band associated with the intermolecular charge-transfer. In the spectrum of the 1 : 1 complex formed between dimethylaniline and chloranil in a carbon tetrachloride solution, the chrage-transfer band appears at 15.4 kK, a value which is associated with the charge transfer from the highest occupied molecular orbital of dimethylaniline to the lowest vacant molecular orbital of chloranil. Apparently the 15.3 kK band of the crystal spectrum corresponds to this charge-transfer band of the 1 : 1 complex. Therefore, we assign it to the charge transfer from the highest occupied orbital of a dimethylaniline molecule to the lowest vacant orbital of the nearest chloranil molecules in the crystal lattice. On the other hand, the polarization of the 32.8 kK band is that expected for a band associated with intramolecular transitions of the component molecules; also, the location of the band nearly corresponds to the lowest π–π^* transition of dimethylaniline or the 34.3 kK π–π^* transition of chloranil. We thus consider that this band of the molecular compound is a local excitation band associated with these transitions of the component molecules.

1 - Naphthylamine - Chloranil (1 : 1) Compound. This molecular compound is obtainable as green needles from a carbon tetrachloride solution. The ground state seems to be non-ionic. The $//l$ spectrum and the $\perp l$ spectrum are shown in Fig. 2. There are two absorption bands which appear more strongly in the $//l$ spectrum than in the $\perp l$ spectrum. Their maxima are located at 15 kK and at 24 kK. Evidently the 15 kK band can not be assigned to a local excitation, since neither component molecule has any transition in the corresponding region. The 1 : 1 complex of 1-naphthylamine and chloranil

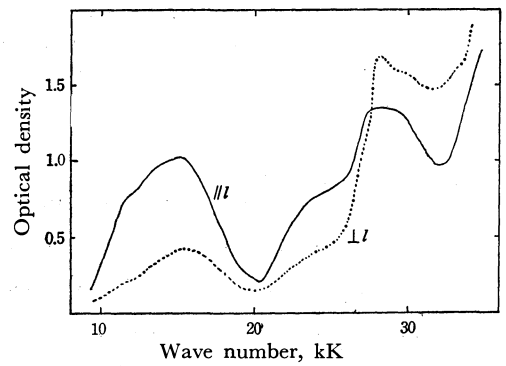

Fig. 2. Absorption spectra of 1-naphthylamine-chloranil compound.

12) H. Kuroda, T. Kunii, S. Hiroma and H. Akamatu, *J. Mol. Spectry.*, **22**, 60 (1967).

13) "Organic Electronic Spectral Data", Vols. I, II, III, IV, Interscience Publishers, New York.

formed in the carbon tetrachloride solution shows a charge-transfer band with a maximum at 15.9 kK. Therefore, we shall assign the 15 kK band of the crystal spectra to the lowest charge-transfer excitation.

The orbital energies of the highest and second-highest occupied molecular orbitals of 1-naphthylamine are, respectively, −8.37 and −9.88 eV according to the SCF MO calculations.*1 Therefore, we can expect that the band associated with the charge-transfer from the second-highest occupied orbital of a naphthylamine molecule to the lowest vacant orbital of the nearest chloranil molecules will be located, if it appears at all, at a wave number separated by about 12 kK from the first charge-transfer band. This means that the location of its absorption maximum will be at about 27 kK. Seemingly the 24 kK band observed with $//l$ polarization corresponds to this absorption band. The charge-transfer band corresponding to this band of the crystal spectra may also be expected to appear in the spectrum of the 1 : 1 complex formed in solution, but it should be hardly observed since it overlaps with the tail of the absorption band of naphthylamine. The π–π^* transitions of 1-naphthylamine are located at 29.9 kK ($\log \varepsilon = 3.8$), 31.3 kK ($\log \varepsilon = 3.9$), and 32.8 kK ($\log \varepsilon = 3.9$) according to the spectrum observed for the cyclohexane solution.[13] The absorption in the 28—35 kK region of the crystal spectra is probably associated with these transitions of naphthylamine or with the π–π^* transitions of chloranil.

N, N-Dimethyl-2-naphthylamine - Chloranil (1 : 1) Compound. The crystals of this compound were obtained from a carbon tetrachloride solution as blue-green needles. The $//l$ and $\perp l$ spectra are shown in Fig. 3. The 11.9 kK band is exclusively polarized along the l-axis. We assign it to the lowest charge-transfer excitation. In the spectrum of the 1 : 1 complex in the carbon tetrachloride solution, two charge-transfer bands are observed; their absorption maxima are located at 13 and at 21.8 kK. Apparently the 11.9 kK band in the $//l$ spectrum of the crystal corresponds to the first charge-transfer band of the 1 : 1 complex. The band corresponding to the second charge-transfer band of the 1 : 1 complex, however, is hardly observed in the crystal spectra. Probably the overlap between the second-highest occupied orbital of the donor and the lowest vacant orbital of the acceptor is quite small for the relative orientation of the donor and acceptor in the crystal of this compound.

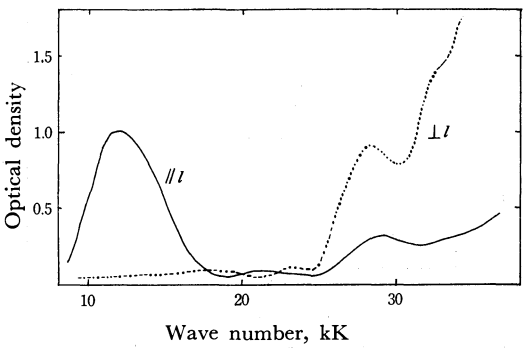

Fig. 3. Absorption spectra of *N*, *N*-dimethyl-2-naphthylamine-chloranil compound.

The absorption in the 25—35 kK region is stronger in the $\perp l$ spectrum than in the $//l$ spectrum. This indicates that the local excitations are responsible for the absorption in this region. In the ethanol-solution spectrum of the dimethyl-2-naphthylamine, the absorption maxima are found at 29 kK ($\log \varepsilon = 3.35$) and 35.5 kK ($\log \varepsilon = 3.86$).[13] It seems that the 28.3 kK band of the crystal spectra is associated with the 29 kK π–π^* transition of dimethyl-2-naphthylamine. The shoulder at about 32.4 kK could be a band associated with the 35.5 kK π–π^* transition of the amine or with the 34.3 kK π–π^* transition of chloranil.

N, N, N', N'-Tetramethyl-p-phenylenediamine-Chloranil (1 : 1) Compound. A reddish-brown crystalline powder of this molecular compound was prepared from a benzene solution. The crystal is either a needle or a thin plate elongated in one direction. This molecular compound

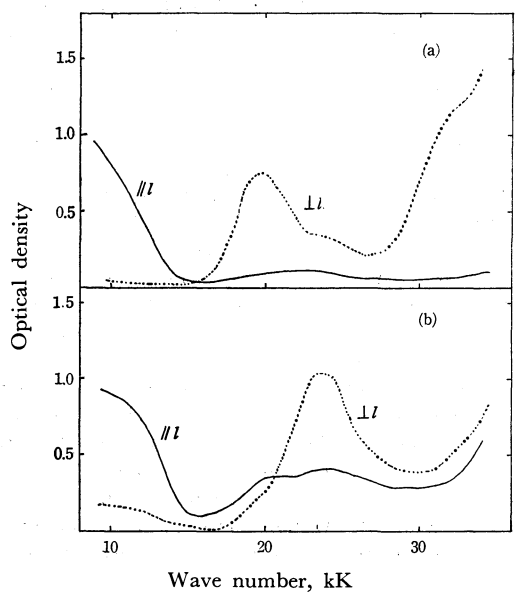

Fig. 4. Absorption spectra of *N*, *N*, *N'*, *N'*-tetramethyl-*p*-phenylenediamine-chloranil compound.
(a) needle crystal
(b) plate crystal

*1 The calculations were made by T. Kunii of our laboratory (Thesis, The University of Tokyo, 1967).

is known to have an ionic ground state.[7,14,15] The spectra observed for a needle crystal and those observed for a plate crystal are shown in Fig. 4a and Fig. 4b respectively. An appreciable difference is found between these two cases. This is probably due to the fact that the developed face of a needle crystal is crystallographically different from that of a plate crystal.

Both Fig. 4a and Fig. 4b indicate the presence of a strong absorption band in the near-infrared region. It is polarized along the *l*-axis, which is the direction of the alternate stacking of donors and acceptors. The band maximum seems to be located at a wave number appreciably lower than 10 kK, but we were not able to determine its location exactly since the spectral region measurable with our microspectrophotometer is limited to the area above 9 kK. This band seemingly corresponds to the 8 kK band found by Kainer and Überle[3] in the powder spectrum observed by means of the KBr-pellet method.

The absorption in the 20—35 kK region is different as regards the polarization from the near-infrared band described above. This can be most clearly seen in Fig. 4a. The absorption is stronger in the $\perp l$ spectrum than in the $//l$ spectrum. There seem to be three absorption bands, located at 19.4, 23.5, and 32 kK. In the $\perp l$ spectrum of Fig. 4a, a strong absorption maximum is found at 19.4 kK, accompanied by a weak shoulder located at about 24 kK. On the other hand, the 23.5 kK band is much stronger than the 19.4 kK band in the $\perp l$ spectrum of Fig. 4b. These facts clearly indicate that the direction of the transition moment is different in the 19.4 kK band and in the 23.5 kK band. From a comparison between Fig. 4a and Fig. 4b, we may also conclude that the polarization of the 32 kK band is the same as that of the 19.4 kK band. These conclusions are in good agreement with the observations reported by Anex and Hill.[11]

The absorption spectrum of the TMPD monopositive ion has been studied by Albrecht and Simpson,[16] who have shown that the π-π^* transitions located at 17.7 kK and at 30.8 kK are polarized along the long axis of TMPD, whereas the weak π-π^* transition at 25.3 kK is of the short-axis polarization. We consider that the 19.4 kK band and the 32 kK band of the molecular compound are associated, respectively, with the 17.7 kK band and the 30.8 kK band of the TMPD ion. There is a possibility that the 23.5 kK band of the molecular compound is due to the 25.3 kK band of the TMPD ion. However, the 23.5 kK band seems to be too strong for this assignment to be acceptable. An alternate assignement is to attribute it to the lowest π-π^* transition of the chloranil ion, located at about 22.2 kK, a transition which has been identified as a transition polarized perpendicular to the molecular axis that passes through the two oxygen atoms of chloranil.[17] It has been reported by Wallwork[18] that, in the crystal of the TMPD-chloranil compound, the component molecules are alternately stacked, face-to-face, on each other along a crystal axis, and that the molecular axis of chloranil mentioned above is parallel to the long axis of TMPD. Therefore, we can predict that the polarization of the local excitation band associated with the 22.2 kK band of the chloranil ion will be perpendicular to those of the bands assocaited with the long-axis polarized transitions of the TMPD ion. This is in agreement with the observed polarization of the 23.5 kK band of the molecular compound.

In conclusion, let us assign the near-infrared absorption band of the molecular compound to the charge transfer from the chloranil ion to the TMPD ion; the 19.4 and 32 kK bands, to the local excitation associated with the TMPD ion, and the 23.5 kK band, to the lowest π-π^* transition of the chloranil ion. It should be noticed, however, that the local excitation bands are considerably broadened and are shifted to a higher energy as compared with the corresponding bands observed in the solution spectrum of each component. These facts, as well as the high intensity of the charge-transfer band, suggest the presence of a relatively strong electronic interaction between the TMPD and chloranil ions.

***p*-Phenylenediamine - Chloranil (1 : 1) Compound.** A greenish-black crystalline powder of this compound was obtained from a benzene solution. This is also known as an ionic compound.[7,15] The observed crystal spectra, shown in Fig. 5, are very similar to the spectra observed

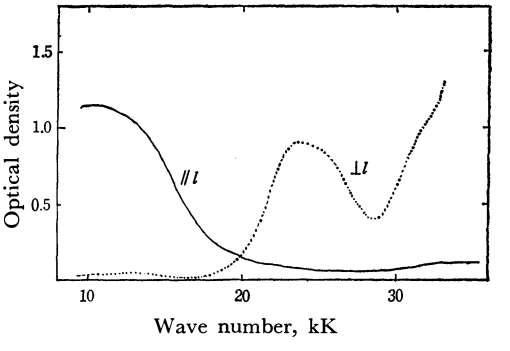

Fig. 5. Absorption spectra of *p*-phenylenediamine-chloranil compound.

14) H. Kainer and W. Otting, *Chem. Ber.*, **88**, 1921 (1955).
15) Y. Matsunaga, *J. Chem. Phys.*, **41**, 1609 (1964).
16) A. C. Albrecht and W. T. Simpson, *J. Am. Chem. Soc.*, **77**, 4454 (1955).
17) G. Giacometti, D. L. Nordio and G. Rogatti, *Nuovo Cimento*, **23**, 433 (1962).
18) S. C. Wallwork, *J. Chem. Soc.*, **1961**, 494.

for the TMPD-chloranil compound. There is a strong absorption band in the near-infrared region; this band is exclusively polarized along the *l*-axis. We assign this band to the charge transfer between the *p*-phenylenediamine mono-positive ion and the chloranil mono-negative ion. The absorption maximum of this band is located at about 10 kK.

The broad absorption band located at 23.5 kK and polarized perpendicular to the *l*-axis can be regarded as a local excitation band. The p-phenylenediamine ion has the lowest π-π^* transition at 21.6 kK, while the chloranil ion has its at 22.2 kK. The 23.5 kK band of the molecular compound seems to be due to either of these transitions of the ions. In the present study, we were not able to determine which of these two transitions is actually responsible for the 23.5 kK band. In any case, however, we should consider that the local excitation band in the crystal spectra is shifted to a considerably higher energy as compared with the corresponding absorption band of the free ions.

Diaminodurene-Chloranil (1 : 1) Compound. A black crystalline powder of this compound was prepared from a benzene solution. This compound has an ionic ground state.[7,15] The crystal spectra are shown in Fig. 6. The general features of the crystal spectra are again quite similar to those of the TMPD-chloranil compound. The strong absorption band in the near-infrared region is polarized along the *l*-axis. This band can be assigned to the charge transfer from the chloranil mono-negative ion to the diaminodurene mono-positive ion. The absorption maximum of this charge-transfer band is located at about 10 kK.

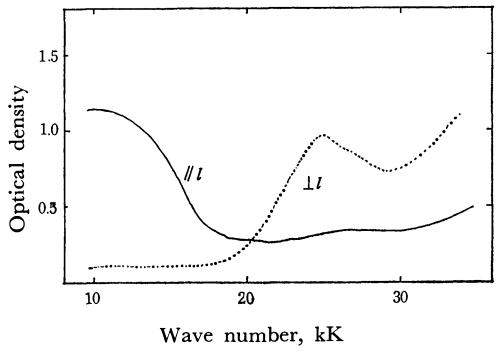

Fig. 6. Absorption spectra of diaminodurene-chloranil compound.

The 25 kK band in the $\perp l$ spectrum must be a local excitation band. The diaminodurene ion has its lowest π-π^* transition at 20.8 kK. We can not tell whether the 25 kK band is associated with this transition of the diaminodurene ion or with the 22.2 kK transition of the chloranil ion. At any rate, though, we can conclude that the local excitation band is shifted to a higher energy than the corresponding bands of the component ions.

Conclusion

We have studied the polarized absorption spectra of solid molecular compounds composed of aromatic amines and chloranil. The observed spectra can be classified into two types: the spectra of the non-ionic molecular compounds, and the spectra of the ionic molecular compounds. In the spectra of a non-ionic compound, the charge-transfer band appears at a wave number similar to that of the corresponding charge-transfer band of the (1 : 1) complex formed in the solution, and the locations of the local excitation bands also are not very different, or are shifted to an energy only a little lower, from those of the absorption bands in the solution spectrum of each component. In most cases the charge-transfer band is definitely polarized in the direction of the alternate stack of donors and acceptors. These general features of the crystal spectra are quite similar to those of the spectra of the molecular compounds formed between polycyclic aromatic hydrocarbons and tetracyanoethylene, which have been reported on in a previous paper.[12]

In the case of the ionic compounds, an absorption band associated with the charge transfer between ions is observed in the near-infrared region with a relatively high intensity. The band associated with the intra-molecular transitions of the component ions are appreciably broadened and are shifted to considerably higher energies compared with the corresponding bands in the solution spectra of the free ions. These phenomena suggest the presence of a relatively strong charge-transfer interaction between the radical ions in the solid molecular compounds.

BULLETIN OF THE CHEMICAL SOCIETY OF JAPAN VOL. 41 88—93 (1968)

The Mössbauer Spectra of Various Natural Minerals

Yoshimasa TAKASHIMA and Shigeru OHASHI

Department of Chemistry, Faculty of Science, Kyushu University, Hakozaki, Fukuoka

(Received February 16, 1967)

The Mössbauer spectra have been measured for sixteen samples of natural minerals, including siderite, vivianite, garnets, olivines, pyroxenes, and other silicate minerals, The spectra were analyzed for the isomer shifts and quadrupole splittings, and the information thus obtained was correlated with the oxidation states of irons and the crystal structure of minerals. The relative abundances of the various sites present in a given mineral were also estimated by measuring the relative intensities of the absorption peaks in the resolved spectrum of the mineral. All the basic Mössbauer spectral patterns observed for the natural minerals are presented in graphic form.

In recent years considerable attention has been paid to the chemical application of the Mössbauer effect. There are a number of papers that allow one to evaluate the usefulness of Mössbauer spectroscopy as a tool for studying chemical bonding. Although a number of works have dealt with synthetic chemical compounds, however, comparatively little work has been done in measuring the Mössbauer spectra of naturally-occurring substances. The suggestion that Mössbauer spectroscopy can be well applied to a study of natural minerals was first made by Pollak[1] (1962). More recently, a similar studies of different types of minerals have been done successfully by Herzenberg *et al.*[2] and Sprenkel-Segel *et al.*[3] The chief application of Mössbauer spectroscopy to minerals has thus far been associated with the mineral structure as well as the oxidation states of iron atoms. In practice, the characteristic features of the spectra are well related to the chemical environment around the Mössbauer nucleus.

The present work on natureal minerals was performed with emphasis on the mineral structure. However, the possibilities of identifying the oxidation states and of determining their ratios were also discussed. It seems that we may expect the Mössbauer spectroscopic technique to be applied to many other areas of mineralogy in the futrue.

Experimental

Apparatus and Procedure. The apparatus and procedure employed were essentially the same as those described in a previous paper.[4] A part of the instrument, however, was altered so that the measurements could be made more easily and accurately. Namely, γ rays were detected with a thin NaI(Tl) crystal coupled to a 400-channel pulse-height analyzer.

All measurements were made at room temperature. In general, runs were made with total counts in excess of 10^4 per Doppler velocity. Statistical error was taken into account in drawing the spectral lines. The isomer shifts are all expressed in mm/sec relative to stainless steel.

Mineral Samples. Most of the mineral samples used were bought from the Japan Earth Science Company, Kyoto. The vivianites, axinite, and biotite were obtained from our own collection. Some olivines and pyroxenes were provided by Mr. Kiyoshi Ishibashi of Kyushu University, Department of Geology. The sixteen minerals studied are summarized in Table 1.

The bulk of the mineral was first crushed into small pieces. Then the sample was carefully selected through a microscope so as to exclude any impurity. Finally, the sample was pulverized in an agate mortar. The powder (*ca.* 100 meshes) was mounted as uniformly

TABLE 1. MINERAL SAMPLES AND THEIR LOCALITIES

Sample	Locality
Siderite	Ogoya, Ishikawa Pref.
Vivianite	Himeshima, Ohita Pref.
Vivianite	Kobe, Hyogo Pref.
Lievrite	Unknown
Andradite	Kamaishi, Iwate Pref.
Almandite	Ishikawa, Ishikawa Pref.
Forsterite	Karasu, Saga Pref.
Fayalite	Kosei, Shiga Pref.
Augite	Nishigadake, Saga Pref.
Augite	Karatsu, Saga Pref.
Diopside	Karatsu, Saga Pref.
Hedenbergite	Kitahira, Yamaguchi Pref.
Axinite	Obira, Ohita Pref.
Biotite	Sugiyama, Saga Pref.
Tourmaline	Ishikawa, Ishikawa Pref.
Hornblende	Matsuyama, Ehime Pref.

1) H. Pollak, M. de Coster and S. Amelinckx, *Phys. Stat. Sol.*, **2**, 1653 (1962).
2) C. L. Herzenberg and D. Toms, *J. Geophys. Res.*, **71**, 2661 (1966).
3) E. L. Sprenkel-Segel and S. S. Hanna, *Geochim. Cosmochim. Acta*, **28**, 1913 (1964).
4) Y. Takashima and S. Ohashi, This Bulletin, **38**, 1684 (1965).

as possible on an absorber disk. The samples ranged in thickness from 10 to 24 mg Fe/cm², depending on the iron content in the minerals.

Chemical Analysis of Iron. The determination of the iron(II) and iron(III) in minerals was carried out by means of the permanganate titration technique. The pulverized mineral was brought into the solution by treating it with sulfuric acid and hydrofluoric acid, with special care taken to prevent the oxidation of iron(II) in the process. The solution in a platinum crucible was transferred without removing the cover to 80 ml of a cold, saturated boric acid solution. The sample solution thus obtained was titrated at once with a 0.1 N potassium permanganate standard solution. Then the total iron content was determined in the same way by using the same solution after the iron in the solution had been reduced to the bivalent state with a zinc-amalgam reductant. The iron(III) content can be found by deducting the iron(II) content from the total iron content. This method is sufficiently accurate to be useful.

Results and Discussion

It is well known that there are three basic Mössbauer spectral patterns, *i. e.*, a single absorption line, double absorption lines, and six-splitted absorption lines. The last one is produced by a Zeeman splitting resulting from the interaction of the nuclear magnetic dipole with the magnetic field produced at the nuclear site by the electrons. Such spectra were observed in the cases of iron oxides[5] and sulfides.[6,7] In our measurements, however, such samples were intentionally avoided because they have already been extensively studied and our instrument is not suited for the measurement of such a wide range of velocity. Most of the samples studied were of a silicate form, but some were of phosphate and carbonate forms.

The spectra were analyzed for the isomer shifts and quadrupole splittings, and the information thus obtained was correlated with the oxidation states of iron and the crystal structures of the minerals. In principle, however, numerous difficulties are inherent in any detailed analysis of the Mössbauer spectrum. The trial-and-error method is necessary to make possible a reasonable analysis of the spectrum. The absorption peak intensity was roughly evaluated in order to obtain an estimate of the iron content in any particular crystal site. To eliminate the saturation effect in the absorption, the absorbers were made thin ranging, from 10 mgFe/cm² to 15 mgFe/cm². In some cases, however, thicker absorbers were used because of the difficulty inherent in the preparation technique. The saturation was observed in samples with thicknesses of >15 mgFe/cm².

Siderite ($FeCO_3$). The siderite exhibits only a sharp doublet Mössbauer pattern similar to a typical ionic ferrous compound. The isomer shift (δ) and the quadrupole splitting (ε) observed were $\delta = 1.38$ mm/sec and $\varepsilon = 0.94$ mm/sec respectively. The former value is typical of the ferrous ion, while the latter is somewhat small for the ferrous ion in ferrous compounds. This means that the binding of iron atoms in the siderite is similar to that of a typical ionic ferrous salt, but that the iron is in a nonspherical environment.

Vivianite [$Fe_3(PO_4)_2 \cdot 8H_2O$]. The spectrum of vivianite shows three absorption lines. The authors have resolved the spectrum into two doublets. The spectra of two vivianites are reproduced in Fig. 1. The first two bands are due to trivalent-state iron, and the second two bands, to bivalent-state iron. The spectrum of Himeshima vivianite was compared with that of Kobe vivianite by measuring each absorber with the same areal iron density. A difference in the intensity of the trivalent iron peak between the two vivianites was observed. On the contrary, the general trends of the X-ray powder patterns of the two minerals

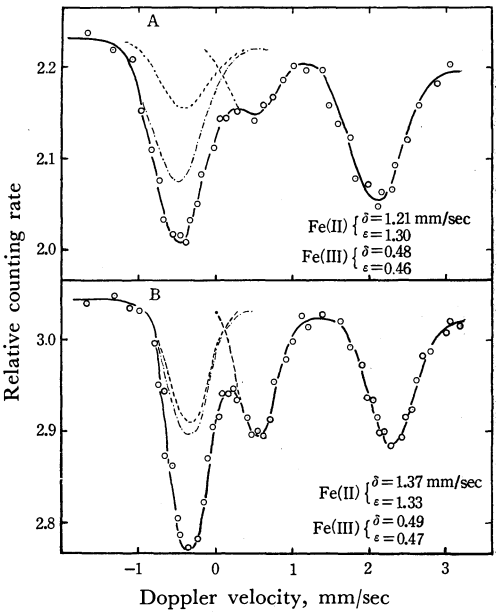

Fig. 1. Mössbauer spectra of vivianites.
Thickness=15 mg Fe/cm²
A: Himeshima vivianite, B: Kobe vivianite

are very similar. The above facts suggest that, *in some cases*, the Mössbauer absorption pattern can be used in the locality identification of minerals.

The presence of the trivalent iron in these minerals may be attributed to the erosive oxidation in the light of the δ and ε values, *i. e.*, the isomer shift and the quadrupole splitting of Fe_2O_3 are similar to those of the vivianites.

5) G. Shirane, D. E. Cox and L. Ruby, *Phys. Rev.*, **125**, 1158 (1962).
6) K. Ôno, A. Ito and E. Hirahara, *J. Phys. Soc. Japan*, **17** 1615 (1962).
7) I. Solomon, *C, R. Acad. Sci., Paris*, **250**, 3818 (1960).

Garnets. The garnet group is repersented by the general formula, $A_3B_2Si_3O_{12}$, where A=Fe, Ca, Mg, Mn, *etc.*, and where B=Al, Fe, Cr, *etc.* As is shown in Fig. 2, the silicon-oxygen tetrahedra exist as independent groups linked to the octahedra of the trivalent ions, while the bivalent metal ions are situated in the center of the oxygen dodecahedra. Of the many kinds of garnets, andradite and almandite were chosen as samples. The Mössbauer spectra of these two minerals are compared with each other in Fig. 3. In this case, the absorbers were so prepared that the areal iron density was approximately 10 mgFe/cm^2. The andradite spectrum can be resolved into a single line with a high intensity and a doublet with a weak intensity. The intense single line may be an unresolved doublet, for its half-width is a little larger than that of stainless steel. The values of both the isomer shifts lie in the range characteristic of the trivalent state iron. The intense line indicates a more covalent nature in bonding than the weak one. This supports the assumptions that there are two different iron sites in the crystal, and that most of the iron atoms are at the B site and only a few, at the A site.

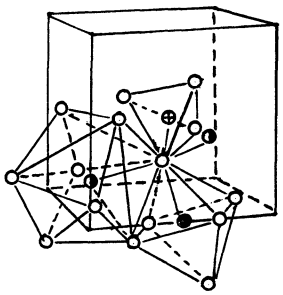

Fig. 2. Crystal structure of garnet ($A_3B_2Si_3O_{12}$).
○: O
●: Al, Fe, Cr,··· (B)
◑: Fe, Ca, Mg, Mn,··· (A)
⊕: Si

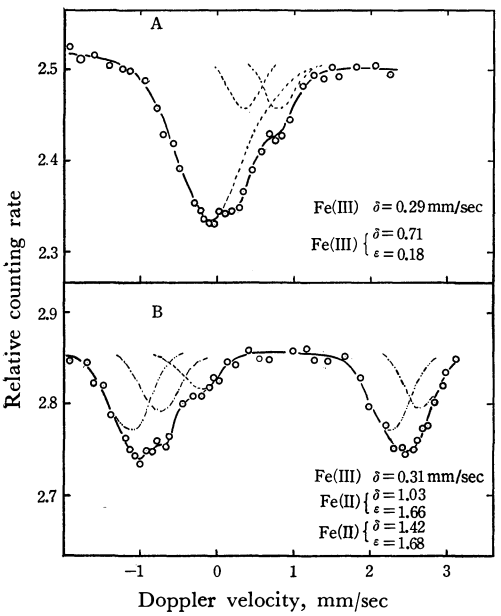

Fig. 3. Mössbauer spectra of garnets.
Thickness=10 mg Fe/cm^2.
A: Andradite, B: Almandite

The spectrum of almandite showed a relatively complex structure. It is resolved into two doublets characteristic of bivalent iron and a single line characteristic of trivalent iron. Since the isomer shift of the trivalent iron in the almandite is close to that of the covalently-bonded iron atoms, the trivalent iron must be located at the B site, together with a large amount of bivalent iron. Accordingly, the other bivalent iron, of about an equal amount, must be located at the A site.

Olivines. The Mössbauer spectra of two kinds of olivine, forsterite and fayalite, are shown in Fig. 4. The isomer shift and quadrupole splitting were of the same order as for almandite, showing the ionic nature of the iron bonding present.

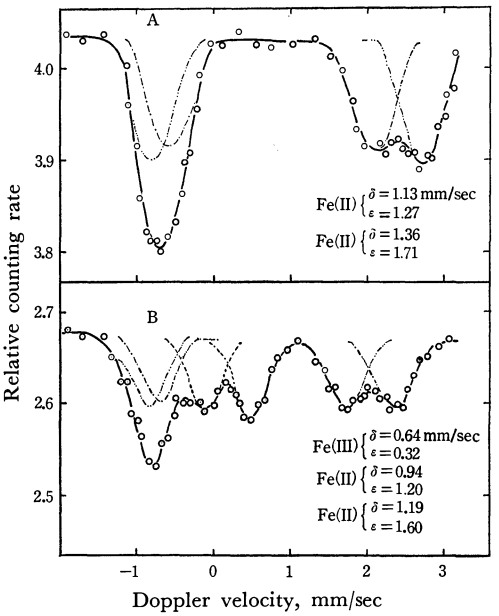

Fig. 4. Mössbauer spectra of olivines.
Thickness=24 mg Fe/cm^2.
A: Forsterite, B: Fayalite

The compositions of olivines vary from that of forsterite, Mg_2SiO_4, to that of fayalite, Fe_2SiO_4, there being a complete diadocky between manganese and iron atoms. The crystal structure parallel to the (100) plane is shown in Fig. 5. In Fig. 5, the silicon atoms at the center of the tetrahedra are not shown. Small open circles (Mg or Fe atoms) are at $x=0$, while small solid circles (Mg or Fe atoms) are at $x=1/2$. The fact that the Mössbauer spectrum has resolved into two

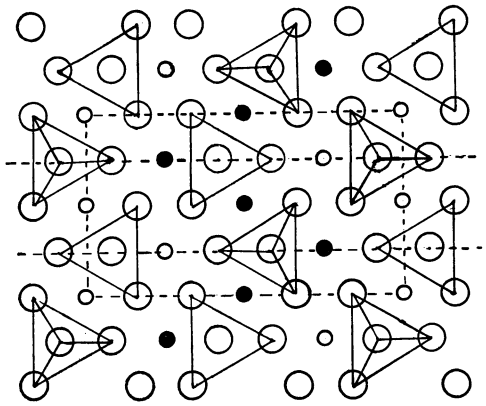

Fig. 5. Crystal structure of olivine.
○: O; ○ ●: Mg, Fe

doublets of equal intensities is consistent with the crystal structure. Namely, half of the metal (Mg or Fe) is located at the site having as nearest neighbors two oxygen atoms from two adjacent

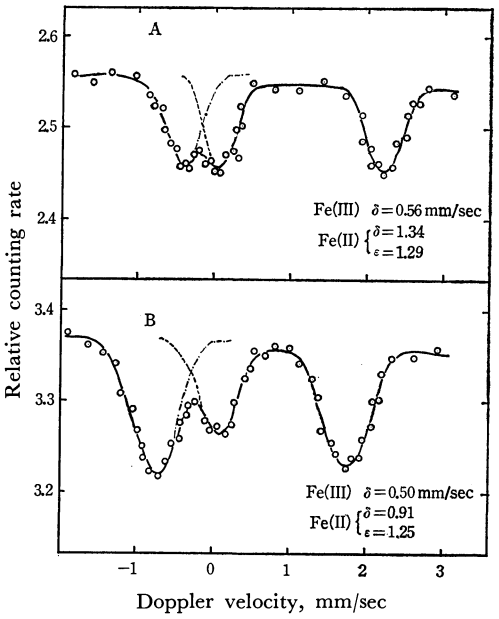

Fig. 6. Mössbauer spectra of pyroxenes.
Thickness=14 mg Fe/cm².
A: Nishigadake augite, B: Karatsu augite

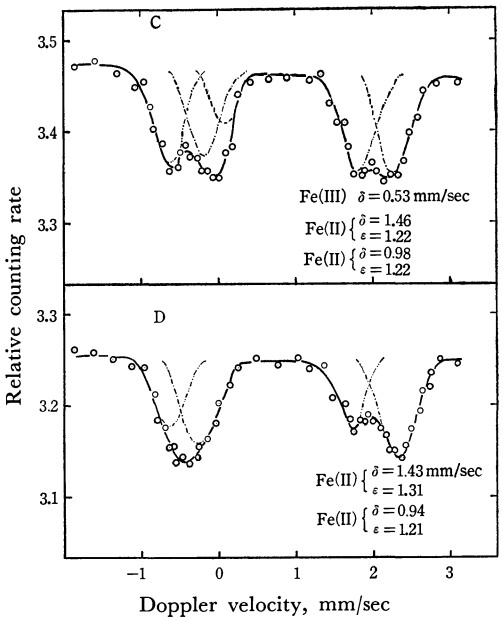

Fig. 7. Mössbauer spectra of pyroxenes.
Thickness=15 mg Fe/cm².
C: Diopside, D: Hedenbergite

tetrahedra, but the other half is located at the other site, having two oxygens from one adjacent trahedron. In these two Mössbauer spectra the predominant absorption patterns correspond to that of bivalent state iron. Only fayalite gave a weak absorption pattern corresponding to that of trivalent state iron.

Pyroxenes. The pyroxenes include varieties which have orthorhombic and monoclinic symmetries. The authors used four monoclinic samples, *i. e.*, two augites, a diopside, and a hedenbergite, for the measurement. The Mössbauer spectra obtained are shown in Figs. 6 and 7. The locality difference in the Mössbauer patterns was observed between the two augites as for the vivianites. The resolution of the spectra is shown by the dotted curves. The results indicate that the single site is available to the bivalent iron in the crystal structure of augite, while two sorts of sites are available in the cases of diopside and hedenbergite. No peak attributable to trivalent state iron was observed in the hedenbergite spectrum.

Table 2. Isomer shifts and quadrupole splittings of several silicate minerals

	Fe(II)		Fe(II)		Fe(III)	
	δ(mm/sec)	ε(mm/sec)	δ(mm/sec)	ε(mm/sec)	δ(mm/sec)	ε(mm/sec)
Axinite	1.39	1.2			0.60	0.14
Biotite	1.18	1.32	1.46	1.60	0.48	0
Tourmaline	1.06	0.98	1.42	1.34	0.89	0
Hornblende	0.98	1.13	1.38	1.62	0.66	0.20
Lievrite	1.30	1.37	1.25	0.89	0.54	0.32

Other Silicate Minerals. As has been discussed above, the Mössbauer spectrum measured for each mineral can be interpreted in terms of valency state, lattice sites, the covalency of bonding, and crystal distortion. Among the number of silicate minerals, axinite, biotite, tourmaline, hornblende, and lievrite were investigated by the present authors. Some of the same sort of minerals had already been measured by other people.[1,2] The silicate minerals generally give complicated Mössbauer spectra, the most complicated patterns being obtained in the cases of the hornblende and lievrite. They both consist of three doublets, our analysis shows. The values of the isomer shift and of the quadrupole splitting for these minerals are summarized in Table 2.

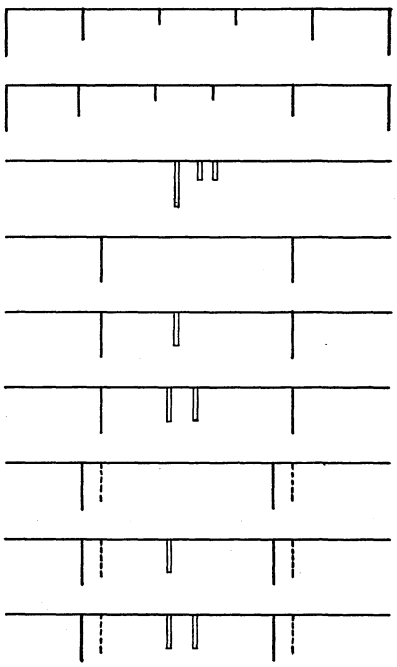

Fig. 8. Basic Mössbauer patterns observed in the natural minerals.
Solid and dotted lines represent bivalent iron.
Open lines represent tivalent iron.

Summary of the Mössbauer Spectra of Minerals. The absorption of resonant gamma rays produces various patterns characteristic of the various minerals. Nine basic patterns and their modifications have so far been observed for the natural minerals. Of these patterns, seven were observed in the wide variety of minerals examined here. The other two resulted from such ferromagnetic iron minerals as iron sulfides. The basic patterns are illustrated in Fig. 8, where the absorption peaks are abbreviated by the single lines, and where the intensity, peak position, and splitting scales are arbitrarily chosen.

Relationship between Peak Intensity and Iron Content. The amount of iron in a sample can be determined from the intensity of the Mössbauer spectrum if the nuclei are located in fairly identical environments. The correlation between the peak intensity (peak area) and the iron content was examined by using a stainless steel and a vivianite mineral of varying thicknesses. As the thickness was increased, the intensity increased, as is shown in Table 3.

TABLE 3. COMPARISON OF ABSORBER THICKNESS AND PEAK INTENSITY

Sample	Stainless steel	Vivianite
Ratio of iron content taken	1* : 4 : 12	1** : 2 : 3
Ratio of absorption peak area observed	1 : 2.1 : 4.5	1 : 1.6 : 1.9

* Thickness=6 mg Fe/cm^2
** Thickness=15 mg Fe/cm^2

The next point examined was the relation between the Fe(II)/Fe(III) ratios and their peak

TABLE 4. RELATION BETWEEN Fe(II)/Fe(III) RATIO AND RATIO OF ABSORPTION PEAK

Sample	Absorber thickness (mgFe/cm^2)	From chemical analysis data			From the Mössbauer spectrum
		Fe(II) %	Fe(III) %	Fe(II)/Fe(III)	Ratio of absorption peak area due to Fe(II) and Fe(III)
Vivianite (Himeshima)	15	22.7	9.1	2.49	2.49
Vivianite (Kobe)	15	13.2	12.6	1.05	1.12
Almandite	10	18.3	2.0	9.15	8.81
Fayalite	24	31.1	15.1	2.06	2.10
Augite (Nishigadake)	14	4.5	2.1	2.14	2.21
Augite (Karatsu)	14	5.4	2.0	2.70	2.96
Diopside	15	6.5	1.4	4.64	8.60
Axinite	10	4.4	1.5	2.93	2.96
Biotite	15	19.0	1.9	10.00	9.80
Tourmaline	10	5.2	1.4	3.64	5.11
Hornblende	12	7.1	4.2	1.69	1.73
Lievrite	20	27.4	12.2	2.28	2.15

intensity ratios. The results obtained are summarized in Table 4. It may be seen from Table 4 that there is in most cases a fairly good agreement between the ratios of the iron content determined by chemical analysis and the ratios of peak intensity obtained from the Mössbauer spectrum. The apparent discrepancies observed in several cases could result from several causes: 1) drift of the pulse-height analyzer, 2) nonidentical environment around the iron nuclei, 3) counting error, 4) effect of higher energy γ rays on 14.4 keV γ rays, and 5) saturation effect in the absorption. In view of the spectrometer employed, further discussion of the subject is premature. Experiments to elucidate this subject would need to be conducted with a better spectrometer.

The Mössbauer absorption peak does not appear when the iron content in the mineral is less than 1%. This would seem to be the limit of detection in this experiment.

The authors wish to thank Mr. Kiyoshi Ishibashi for contributing several mineral specimens, and Mr. Terumasa Nakamura for providing the X-ray powder pattern measurements. We also wish to extend our thanks to Mr. Toyoaki Kusaba who assisted in the experiments.

This study has been supported in part by a grant-in-aid for Scientific Research from the Ministry of Education.

BULLETIN OF THE CHEMICAL SOCIETY OF JAPAN VOL. 41 93—99 (1968)

On the Structures of Alkali Polyaluminates

Goro YAMAGUCHI

Department of Industrial Chemistry, Faculty of Engineering, The University of Tokyo, Hongo, Tokyo

and Kazutaka SUZUKI

Nagoya Institute of Technology, Syowa-ku, Nagoya

(Received March 27, 1967)

Besides the so-called β-Al_2O_3 ($R_2O\cdot 11Al_2O_3$; R=Na or K), there have been found two kindred compounds with approximate formulas, $R_2O\cdot 7Al_2O_3$ (β'-Al_2O_3) and $R_2O\cdot 5Al_2O_3$ (β''-Al_2O_3). The structure determination of the latter two compounds was undertaken; the results are compared with the structure of β-Al_2O_3 in the present paper. These three structures are composed of spinel layers of the same configuration. The structures of β and β' are very similar to each other, both equally bearing a layer-stacking according to a two-fold screw symmetry, while β'' differs from these two in exhibiting another way of layer-stacking, according to a three-fold screw symmetry.

It has been established that the so-called β-Al_2O_3 is in fact an alkali polyaluminate with the chemical formula of $Na_2O\cdot 11Al_2O_3$ or $K_2O\cdot 11Al_2O_3$. In 1943 one of the present authors (G. Y.)[1] studied its formation during a sintering reaction between Al_2O_3 and alkali carbonate; he thus found a new substance whose X-ray powder diffraction pattern displayed a close resemblance to that of β-Al_2O_3. However, a few lines in the pattern, such as the strong 1.954A and 1.382A lines, failed to be properly indexed unless the c-axis of the crystal was assumed to be 3/2 or 3 times as long as that of β-Al_2O_3. He also pointed out that the above two lines coincide in spacings with the 400 and 440 reflections, respectively, from the spinel structure.

About ten years later, Yamaguchi[2] reinvestigated the material by chemical as well as X-ray methods. and reported that two phases were revealed, one with the approximate composition, $Na_2O\cdot 8Al_2O_3$ or $K_2O\cdot 8Al_2O_3$, and the other, with $Na_2O\cdot 5A_2O_3$ or $K_2O\cdot 5Al_2O_3$. The former was designated β'-Al_2O_3 (β'_{Na}, β'_{K}), and the latter, β''-Al_2O_3 (β''_{Na}, β''_{K}). He then reported in another paper[3] that the experimental formulas were $Na_2O\cdot 8.1Al_2O_3$ for β'_{Na}, $Na_2O\cdot 5.8Al_2O_3$ for β''_{Na}, and $K_2O\cdot 5.6Al_2O_3$ for β'_{K}, and that the way of oxygen packing in the β' structure might be similar to that in β, both being reflection-symmetrical across planes perpendicular to the c-axis, while that in

1) G. Yamaguchi, *Elect. Chem. Soc. Japan*, **11**, 260 (1943).

2) G. Yamaguchi, Preprint for the 7th Annual Meeting of the Chemical Socity of Japan (April, 1954), p. 192.

3) G. Yamaguchi, Doctor Thesis, University of Tokyo (1954).

β'' was after the manner of cubic closest-packing, with some layers replaced by those bearing less oxygen and some alkali ions. He thus explained the fact that the two lines characteristic of β'' coincide in spacings with the 400 and 440 lines from spinel, and gave the lattice parameters reproduced in Table 1.

TABLE 1. LATTICE PARAMETERS (IN Å) OF β'-Al_2O_3 AND β-Al_2O_3[3]

	β'_{Na}	β''_{Na}	β''_{K}
a	5.594	5.595	5.596
c or 2c	22.56	67.86	68.01

Recently, Théry *et al.*[4] have published a report on substances which are probably the same as the alkali polyaluminates under consideration; one is $Na_2O{\cdot}5Al_2O$ with the lattice parameters of $a=5.61$ Å and $c=33.95$Å, and the other, $Na_2O{\cdot}7.02Al_2O_3$, with $a=5.595$Å and $c=34.02$Å.

In the present paper, the authors will describe the structures of these alkali polyaluminates.

TABLE 2. SYNTHETIC DATA AND PROPERTIES OF β'- AND β''-Al_2O_3

Species	Experimental formula	Ideal formula	Mixing ratio R_2CO_3 : $2Al(OH_3)$	Heating temp., °C	Heating period	Density
β'_{Na}	$Na_20.7.02Al_2O_3$	$Na_20.7.22Al_2O_3$	1 : 3	1400	20 min	3.22
β'_{K}	$K_20.6.8Al_2O_3$	$K_20.7.22Al_2O_3$	1 : 3	1400	20 min	3.35
β''_{K}	$K_20.5.1Al_2O_3$	$K_20.5.34Al_2O_3$	1 : 1	1380	8 hr	3.50—3.39

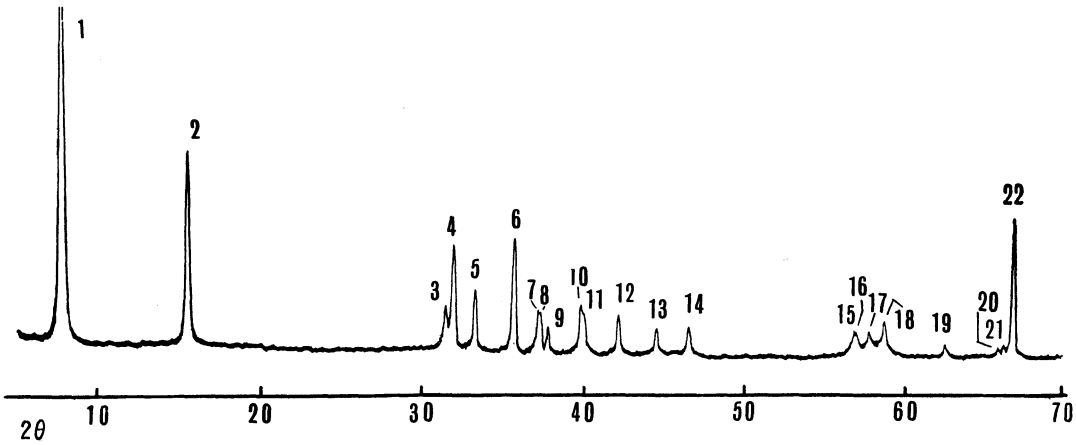

Fig. 1. X-Ray powder diffraction pattern of β'-Al_2O_3 (Cu$K\alpha$).

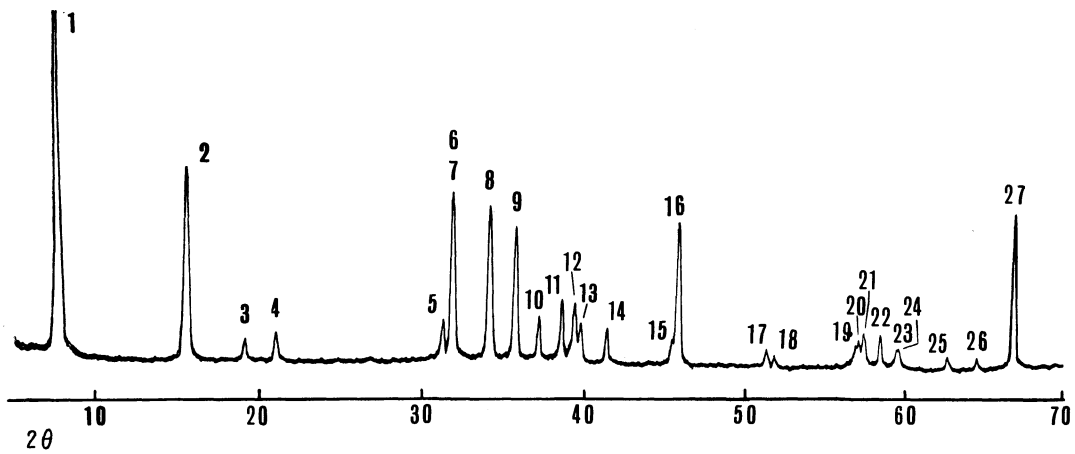

Fig. 2. X-Ray powder diffraction pattern of β''-Al_2O_3 (Cu$K\alpha$).

4) J. Théry *et al.*, *Compt. Rend. Acd. Sci. (Paris)*, **254**, 2782 (1962); *Rev. Temper. et Refract.*, 221 (1964).

Since no single crystal had yet been obtained for any of these materials, we were obliged to carry out this work using their powder data only. Therefore, we cannot claim that the results we deduce here are highly accurate, but we still believe them to be essentially correct.

Experimental

Mixtures of aluminum hydroxide and alkali carbonate in appropriate ratios were heated. The products were then washed with dilute HCl and water, and their chemical compositions and densities examined. The results, together with the suitable conditions for their preparations, are listed in Table 2. Though both sodium and potassium are capable of forming β' and β'', the former tends to favor the production of β', while the latter favors β''. The X-ray powder diffraction patterns shown in Figs. 1 and 2 were obtained with β'_{Na} and β''_{K} respectively. The observed lines were indexed with the aid of the lattice parameters given in Table 1, and their peak intensities were measured for a fixed exposure time. The results are tabulated in Tables 3 and 4, where the relative values of intensities have been put onto such a scale as to minimize the R-factors and where the calculated values for the strongest lines are taken to be 100. The lattice parameters newly derived from these two sets of data are given in Table 5.

Table 3. X-Ray powder diffraction data of β'_{Na}
$a=5.592$ Å, $c=22.711$ Å

Peak No.	$hk\,l$	Observed d (Å)	Observed I	Calculated d (Å)	Calculated I
1	00 2	11.3651	127	11.3631	100
2	00 4	5.6815	46	5.6815	33
3	00 8	2.8408	11	2.8408	7
4	11 0	2.8034	28	2.8034	20
5	01 7	2.6955	18	2.6955	30
6	11 4	2.5157	35	2.5140	38
7	02 0	2.4165	14	2.4278	—
8	02 1			2.4141	14
9	02 2	2.3840	6	2.3742	10
10	00,10	2.2631	15	2.2726	6
11	11 6	2.2533	14	2.2533	7
12	02 5	2.1441	15	2.1415	18
13	02 6	2.0342	8	2.0440	9
14	02 7	1.9513	10	1.9443	11
15	00,14	1.6233	6	1.6233	3
16	03 0	1.6195	3	1.6185	1
17	12 7	1.5924	7	1.5976	4
18	02,11	1.5722	11	1.5734	13
19	12 9	1.4890	3	1.4847	5
20	00,16	1.4204	1	1.4204	—
21	02,13	1.4193	1	1.4187	11
22	22 0	1.4012	41	1.4017	40

Table 4. X-Ray powder diffraction data of β''_{K}
$a=5.595$ Å, $c=34.226$ Å

Peak No.	$hk\,l$	Observed d (Å)	Observed I	Calculated d (Å)	Calculated I
1	00 3	11.4080	142	11.4088	100
2	00 6	5.7044	111	5.7044	69
3	01 2	4.5679	10	4.5681	2
4	01 4	4.2214	12	4.2162	1
5	00,12	2.8507	16	2.8522	14
6	11 0	2.7975	98	2.7974	66
7	01,10			2.7955	45
8	01,11	2.6184	60	2.6181	46
9	11 6	2.5114	56	2.5118	118
10	02 1	2.4164	20	2.4166	11
11	02 4	2.3304	32	2.3310	34
12	00,15	2.2800	22	2.2818	6
13	11 9	2.2635	12	2.2534	4
14	02 7	2.1753	12	2.1708	32
15	11,12	1.9897	8	1.9972	15
16	02,10	1.9781	84	1.9774	74
17	02,13	1.7829	4	1.7827	—
18	11,15	1.7692	8	1.7681	—
19	03 0	1.6132	12	1.6151	11
20	01,20			1.6136	1
21	02,16	1.6029	20	1.6035	30
22	12,11	1.5782	16	1.5787	—
23	03 6	1.5525	19	1.5540	13
24	02,17			1.5484	13
25	01,22	1.4836	5	1.4813	3
26	02,19	1.4465	6	1.4455	1
27	22 0	1.3987	97	1.3987	95

Table 5. Lattice parameters newly obtained in this experiment

	a (Å)	c (Å)
β'_{Na}	5.592	22.711
β'_{K}	5.594	22.728
β''_{K}	5.595	34.226

Structure Analysis

At the onset of the structure determination of these two crystals, the diffraction pattern of β-Al_2O_3 was produced for comparison; the results are given in Fig. 3 and Table 6. On the base of the structure of this material as worked out by Beevers and Ross[5] and reproduced here in Fig. 4 and Table 7, the calculated intensities were deduced and compared with the observed intensities, shown in Table 6. The R-factor was found to be 0.30. It may be noted in Fig. 4 that the structure is composed of layers of the spinel structure, and that each layer is flanked by a pair of planes perpendicular to the c-axis and containing alkali ions (R in

5) C. A. Beevers and M. A. S. Ross, *Z. Krist.*, **97**, 59 (1937).

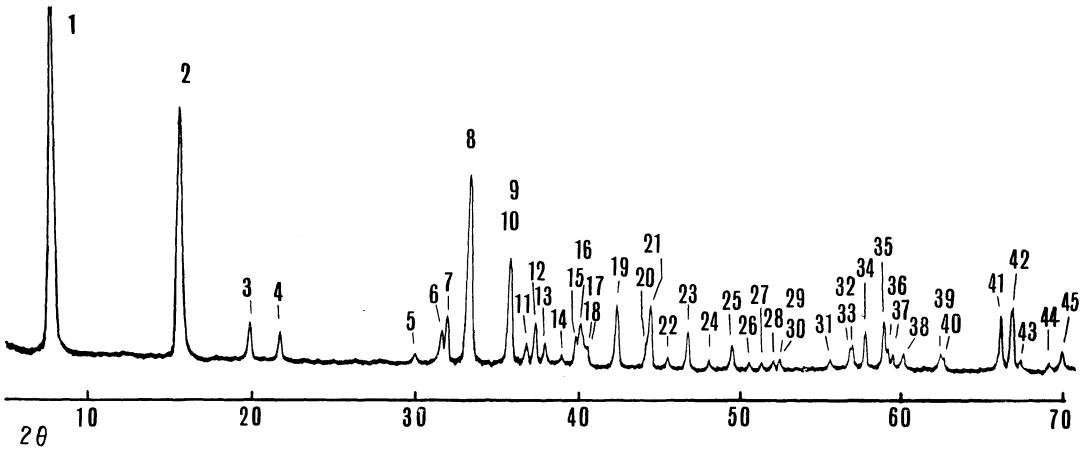

Fig. 3. X-Ray powder diffraction pattern of β-Al_2O_3 (Cu$K\alpha$).

TABLE 6. X-RAY POWDER DIFFRACTION DATA OF β_{Na} $a=5.593$ Å, $c=22.610$ Å

Peak No.	*hk l*	Observed		Calculated		Peak No.	*hk l*	Observed		Calculated	
		d (Å)	*I*	*d* (Å)	*I*			*d* (Å)	*I*	*d* (Å)	*I*
1	00 2	11.3136	120	11.2891	100	24	01, 11	1.8926	1	1.8902	—
2	00 4	5.6570	51	5.6446	24	25	02 8	1.8404	5	1.8391	4
3	01 2	4.4579	7	4.4556	11	26	11 2	1.8074	1	1.8088	1
4	01 3	4.0800	6	4.0764	3	27	12 3	1.7797	2	1.7805	—
5	01 6	2.9714	1	2.9729	—	28	01, 12	1.7539	1	1.7541	—
6	00 8	2.8228	6	2.8223	3	29	02 9	1.7439	2	1.7434	1
7	11 0	2.7991	8	2.7997	13	30	12 4			1.7429	—
8	01 7	2.6895	44	2.6856	28	31	02, 10	1.6533	2	1.6524	3
9	00 9	2.5089	23	2.5087	—	32	03 0	1.6159	6	1.6164	2
10	11 4			2.5087	29	33	00, 14	1.6121	6	1.6127	2
11	01 8	2.4345	4	2.4392	—	34	12 7	1.5933	10	1.5936	7
12	02 1	2.4101	10	2.4108	9	35	02, 11	1.5658	11	1.5666	12
13	02 2	2.3707	6	2.3706	4	36	11, 12	1.5622	4	1.5616	3
14	02 3	2.3084	1	2.3074	2	37	03 4	1.5526	1	1.5540	6
15	00, 10	2.2611	8	2.2578	1	38	12 8	1.5374	4	1.5372	—
16	11 6	2.2476	11	2.2462	11	39	03 6	1.4851	4	1.4853	3
17	01 9	2.2290	7	2.2282	—	40	12 9	1.4809	4	1.4800	—
18	02 4			2.2278	4	41	02, 13	1.4133	14	1.4119	14
19	02 5	2.1359	15	2.1362	14	42	22 0	1.4002	17	1.3999	30
20	00, 11	2.0491	6	2.0526	—	43	22 2	1.3897	1	1.3892	2
21	02 6	2.0380	15	2.0382	17	44	22 4	1.3592	1	1.3587	2
22	11 8	1.9918	2	1.9875	—	45	14 1	1.3428	6	1.3430	2
23	02 7	1.9392	10	1.9381	10						

the figure). These planes shall hereafter be called "alkali layers," and the part, within a unit cell, of a spinel layer, a "spinel block."

Structure of β'-Al_2O_3. The powder pattern of β'_{Na} was used for this purpose. As will be recognized upon comparisons of Fig. 4 with Fig. 3 and of Table 3 with Table 6, the powder pattern of β'-Al_2O_3 closely resembles that of β-Al_2O_3. This fact, together with the similarity in lattice parameters between these two substances, strongly suggests that both structures have the same principle. In fact, the pattern of β'-Al_2O_3 is completely in harmony with the space group of β-Al_2O_3, $P6_3/mmc$; namely, the $hh\bar{2}hl$ reflections are missing when l is odd. Therefore, it was assumed at the beginning of the analysis that the structure of β'-Al_2O_3 consists of spinel blocks which have the same configuration and mode of arrangement as in the structure of β-Al_2O_3.

Next, if we compare the experimental formula of the substance, shown in Table 2, with the composition of β-Al_2O_3, we shall find that the former

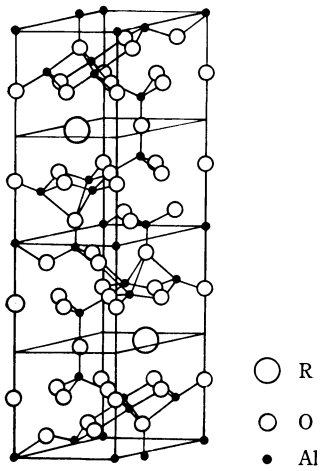

Fig. 4. Structure of β-Al_2O_3.

contains one and a half times as much alkali as the latter, both against a certain amount of oxygen. Therefore, $R_{1.50}Al_{10.83}O_{17}$ or $R_2O{\cdot}7.22Al_2O_3$ was tentatively adopted as the ideal formula for this phase. The theoretical values of density from this formula are 3.26 for β'_{Na} and 3.38 for β'_{K}, in good agreement with the observed values, 3.22 and 3.35 respectively.

Then, taking into account the fact that the spinel block is so densely constituted that no alkali ion is admitted into it, we could restrict the probable positions for excessive alkali ions in or near the alkali layers. Trial-and-error procedures carried out with the aid of an electronic computer then led us to the final structure, shown in Fig. 5.

In this structure, two sites for alkali ions per spinel block are statistically occupied by 1.5 ions, while the positions for Al ions (two per block) nearest the alkali layers are occupied by 1.83 such ions. The atomic coordinates are listed in Table 8, while the calculated intensities for the structure are given in Table 3. The *R*-factor for I deduced from this table is 0.26. It has also been confirmed that the intensities calculated for unobserved reflections are all less than 1 on the intensity scale of the table.

Structure of β''-Al_2O_3. Potassium-bearing β''-Al_2O_3 was chosen for this study; its powder data are given in Table 4. Since in every observed reflection there holds, between its indices, a $-h+k+l\equiv 0$ (mod 3) relation, no other condition being associated, the only conclusion deducible is that the crystal lattice is rhombohedral. However, there are five space groups altogether, each based upon the rhombohedral lattice and satisfying the above relation, so from the powder data alone it is impossible to identify the space group of the crystal further. Accordingly, we had to search for the structure on the base of the knowledge of the crystal lattice and by assuming the structure also to be built up of spinel blocks.

Next, a comparison of the experimental formula of this phase with the composition of β-Al_2O_3 suggests that a spinel block contains nearly two alkali ions in the present case. Therefore, $R_2Al_{10.67}O_{17}$ or $R_2O{\cdot}5.34Al_2O_3$ was considered as the ideal formula, for which the calculated density was 3.45.

The procedures described above were then employed for the derivation of the probable solution; the final result obtained is a structure based upon the $R\bar{3}m$ space group and illustrated in Fig. 6.

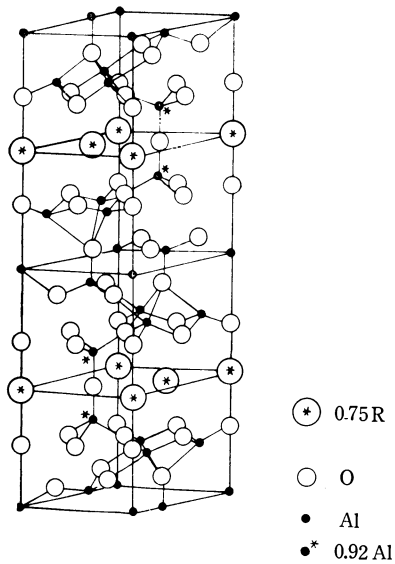

Fig. 5. Structure of β'-Al_2O_3.

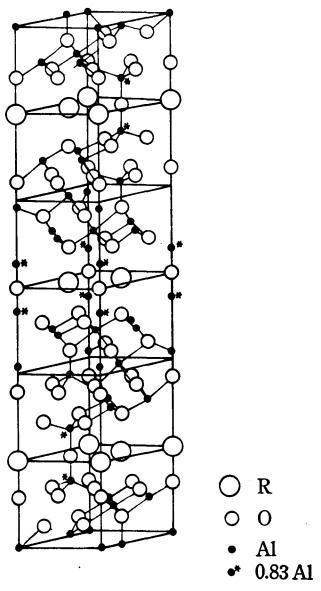

Fig. 6. Probable atomic arrangement in β''-Al_2O_3.

TABLE 7. ATOMIC PARAMETERS OF β_{Na} (SPACE GROUP, $P6_3/mmc$)

Atom	Number of atom	x	y	z
Na	2	0.667	0.333	0.250
Al_1	2	0	0	0
Al_2	4	0.333	0.667	0.022
Al_3	12	0.333	0.167	0.106
Al_4	4	0.333	0.667	0.178
O_1	12	0.167	0.333	0.050
O_2	4	0.667	0.333	0.050
O_3	4	0	0	0.144
O_4	12	0.500	0.500	0.144
O_5	2	0.333	0.667	0.250

TABLE 8. ATOMIC PARAMETERS OF β'_{Na} (SPACE GROUP, $P6/mmc$)

Atom	Number of atom	x	y	z
Na_1	2×0.75	0	0	0.250
Na_2	2×0.75	0.667	0.333	0.250
Al_1	4	0.333	0.667	0.170
Al_2	2	0	0	0
Al_3	4	0.333	0.667	0.030
Al_4	12	0.333	0.167	0.105
O_1	12	0.167	0.333	0.050
O_2	4	0.667	0.333	0.050
O_3	12	0.500	0	0.144
O_4	4	0	0	0.144
O_5	2	0.333	0.667	0.250

TABLE 9. ATOMIC PARAMETERS OF β''_K (SPACE GROUP, $R\bar{3}m$)

Atom	Number of atom	x	y	z
K	6	0	0	0.184
Al_1	3	0	0	0
Al_2	6	0	0	0.346
Al_3	18	0.333	0.167	0.073
Al_4	6×0.83	0	0	0.443
O_1	18	0.167	0.333	0.040
O_2	6	0	0	0.293
O_3	6	0	0	0.092
O_4	13	0.167	0.333	0.241
O_5	3	0	0	0.500

In this structure, a statistical distribution is observed only over the positions of the Al ions, two per block, nearest the alkali layers; they are occupied by 1.67 such ions. The coordinates are tabulated in Table 9, and the calculated intensities, in Table 4. The R-factor for **I** is 0.28; the statement given above concerning the unobserved reflections of β'-Al_2O_3 also applies in this case.

Discussion

According to the results of analysis so far described, some conclusions may now be reached. The three phases, β, β', and β'', are all composed of spinel layers of the same configuration. The former two are almost identical structurally, but are different in the amounts of alkali and aluminum present. On the other hand, the last one has its own way of layer-stacking. Thus, the former two structures may be looked upon as characterized by layer-stacking according to a two-fold screw symmetry, shown in Fig. 7, while the

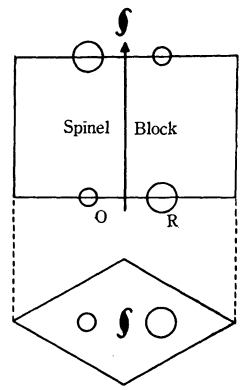

Fig. 7. Mode of stacking of spinel blocks in the β and β'-Al_2O_3 structures.

last, by that according to a three-fold screw symmetry, given in Fig. 8. These findings, together with the fact previously mentioned that sodium and potassium favor the formation of β' and β'' respectively, seem to suggest that the mode of layer-stacking in this series of structures depends upon the amount and kind of alkali.

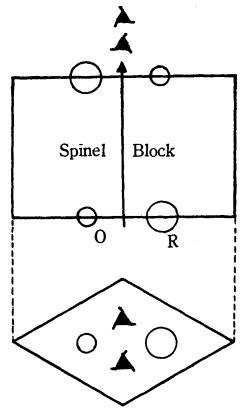

Fig. 8. Probable mode of stacking of spinel blocks in the β''-Al_2O_3 structure.

From the view-point of ionic distribution, β-Al_2O_3 may be considered an ordered phase, while β' and β'' are disordered phases, exhibiting a

statistical distribution of cations over sites in and near the alkali layers. An example of such a distribution has been found in an imperfect spinel, $RO \cdot nAl_2O_3$.[6]

Finally, it should be noted that, because of the restriction imposed upon the present work, namely, the difficulty of obtaining a single crystal for any of the substances under investigation, our results are liable to be some what inaccurate with regard to the atomic coordinates. For example, a position for excess alkali given above to β' or β'' in all probability indicates only the center of gravity of a more dispersed statistical distribution of the ion. However, the authors believe that, in spite of such minute uncertainties, the structural principles of this series of compounds have now been established satisfactorily.

6) G. Yamaguchi, *J. Ceram. Assoc. Japan*, **61**, 500 (1953).

BULLETIN OF THE CHEMICAL SOCIETY OF JAPAN VOL. 41 99—105 (1968)

The Extraction of Uranium(VI) from Sulphuric Acid Solutions by Di-*n*-octylamine

Taichi SATO

Department of Applied Chemistry, Faculty of Engineering, Shizuoka University, Hamamatsu, Shizuoka

(Received May 11, 1967)

The partition of uranium(VI) between sulphuric acid solutions and solutions of di-*n*-octylamine (DOA) in benzene has been investigated at different concentrations of sulphuric acid, solvent and aqueous uranium, and at different temperatures. The acidity and the water content of the organic phase, and the effect of the organic solvent on the extraction have also been examined. An infrared spectral study has been made of the organic solutions. The mechanism of the extraction of uranium from sulphuric acid solutions by DOA is discussed on the basis of the results obtained, and a composition is proposed for the complex formed in this extraction system.

The extraction of uranium(VI) from sulphuric acid solutions by high molecular-weight amines in organic solvents has been investigated by many researchers.[1] The present author has also studied these extraction systems,[2] and this paper constitutes the work extended to the extraction with di-*n*-octylamine (DOA).

Experimental

Reagents. The DOA (the Kao Soap Co., Ltd.) was of a high purity and was used without further purification. It was diluted with various organic solvents, but was not pre-equilibrated with sulphuric acid solutions. The other chemicals were of analytical reagent grade. The uranyl sulphate solution was prepared by dissolving the uranyl sulphate tri hydrate in sulphuric acid of selected concentration, and its concentration is generally indicated in g/*l* for UO_2SO_4.

Extraction and Analytical Procedures. Equal volumes (20 m*l*) of DOA solution and uranyl sulphate solution were shaken for 10 min in 50 m*l* stoppered conical flasks in a water bath thermostatted at the required temperature (preliminary experiments showed that equilibration is established in 10 min). After the separation of the aqueous and organic phases by centrifugation, uranium in the organic phase was back-extracted with 1 N hydrochloric acid, and then the partition coefficient (the ratio of the equilibrium concentration of uranium in the organic phase to that in the aqueous phase) was determined. Uranium was determined gravimetrically: precipitated as ammonium diuranate and ignited to U_3O_8. The water content of the organic solution was determined by the Karl Fischer titration method.

Infrared Spectral Measurement. The infrared spectra were measured by a Shimadzu Model IR-27C recording spectrophotometer equipped with sodium chloride prisms. The spectra of organic extracts were determined with benzene as reference liquid, in a matched pair cell of fixed path length 0.1 mm, with thallium halide window.

Results and Discussion

Dependence on Acid Concentration and Extraction in Presence of Sodium Sulphate. The extraction of uranyl sulphate solutions (5 g/*l*) containing sulphuric acid at various concentrations

1) *E. g.* C. F. Coleman, K. B. Brown, J. G. Moore and K. A. A. Allen, Proc. 2nd United Nationes Int. Conf. Peaceful Uses of Atomic Energe, Geneva, 1958, Vol. 28, p. 278, United Nations, New York (1958); C. F. Coleman, K. B. Brown, J. G. Moore and D. J. Crouse, *Ind. Eng. Chem.*, **50**, 1756, (1958); C. F. Coleman, *Atomic Energy Review*, **2**, (No. 2), 3 (1963); C. Deptuła and S. Minc, *J. Inorg. Nucl. Chem.*, **29**, 221 (1967).

2) T. Sato, a) *J. Appl. Chem.*, **12**, 130 (1962); b) *J. Inorg. Nucl. Chem.*, **24**, 1267 (1962); **25**, 441 (1963); c) *ibid.*, **26**, 171, 181 (1964).

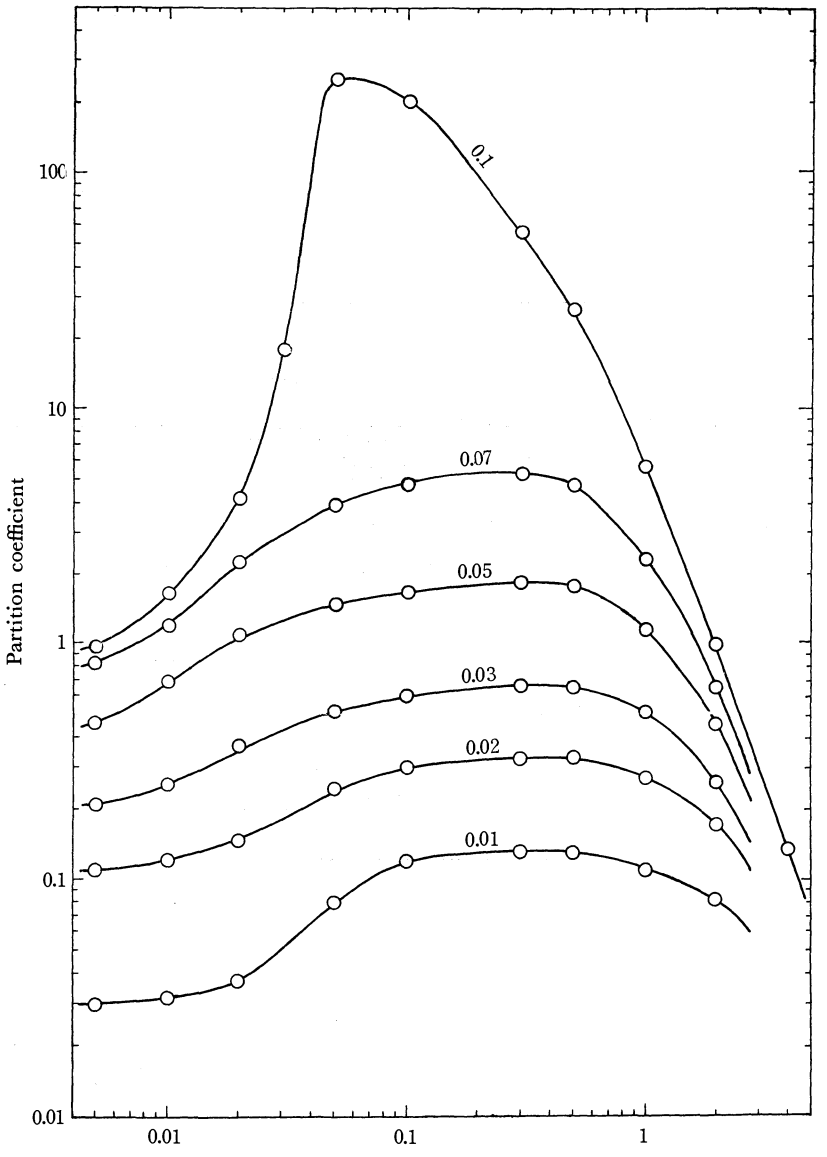

Fig. 1. Extraction of uranium(VI) from sulphuric acid solutions by solutions of DOA in benzene. numerals on curves are DOA concentrations, M.

with solutions of DOA in benzene at 20°C gave the results shown in Fig. 1.

The maximum partition coefficient appears at 0.05 M initial aqueous sulphuric acid concentration for the extraction with 0.1 M DOA and becomes indeterminate for the extraction below 0.07 M DOA, but the shape of the extraction curve resembles the forms of the curves with other amines.[2] It is thus postulated that at low aqueous acidities the increase in the partition coefficient arises from the formation of DOA-uranyl sulphate complex; at higher aqueous acidities the decrease in the partition coefficient is attributed either to competition between uranium and sulphuric acid for association with the amine or to the formation of less readily extractable complexes. This interpretation is confirmed with the result in Fig. 2, illustrating the data for the extraction of uranyl sulphate solutions (5 g/*l*) containing sulphuric acid and sodium sulphate with 0.1 M DOA in benzene at 20°C. This shows that when the sulphuric acid in the aqueous phase is partly replaced by sodium sulphate, the decrease in the partition coefficient is checked because of the removal of competition for uranium between sulphuric acid and the amine. The gradual decrease in the partition coefficient with

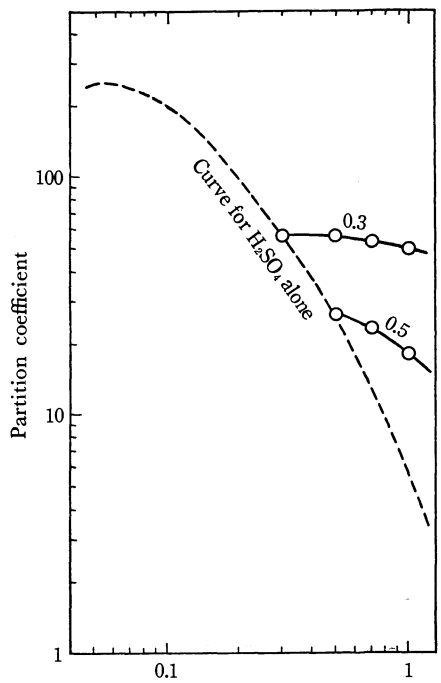

Fig. 2. Extraction of uranium(VI) from sulphuric acid solutions containing sodium sulphate by 0.1 M DOA in benzene.
(Numerals on curves are initial aqueous sulphuric acid concentrations, M).

increasing the sulphate concentration may be explained as being due to the formation of the inextractable species $UO_2(SO_4)_2^{2-}$, since the species UO_2SO_4 and $UO_2(SO_4)_2^{2-}$ exist in the aqueous uranyl sulphate solution containing sulphate ion.[3]

Dependence on Uranium and DOA Concentrations. The variation in the uranium concentration of organic phase with the initial aqueous uranium concentration at 0.05 M aqueous acidity was examined with 0.1 M DOA in benzene at 20°C. The result in Fig. 3 shows that the uranium concentration of organic phase approaches a limiting value (~0.025 M) with increasing the initial aqueous uranium concentration, indicating that four amine molecules are associated with each uranium ion. This is supported by the dependence of the partition coefficient on the DOA concentration at higher aqueous acidities. In the extraction of uranyl sulphate solutions (5 g/*l*) containing sulphuric acid with the solutions of DOA in benzene at 20°C, log-log plots of E_a° *vs.* (C_A-4C_U), in which E_a° is the partition coefficient, C_A the total DOA concentration and C_U the uranium concentration of organic phase, gave straight lines whose slopes are 2.0, 1.5 and 1.0 at 0.5, 1.0 and 2.1 M sulphuric acid concentrations respectively. At low aqueous acidities, on the other hand, it is considered that the value of the association number is apparently not always four, but approaches four in 0.05 M initial aqueous sulphuric acid as the aqueous acidity is increased.

Extraction of Sulphuric Acid. The acidity and water content of the organic phase from the extraction of uranyl sulphate solutions (5 g/*l*) containing sulphuric acid at various concentrations with 0.1 M DOA in benzene at 20°C are shown in Figs. 4 and 5, compared with the data for the similar extraction of sulphuric acid solutions alone. In the extraction of sulphuric acid from

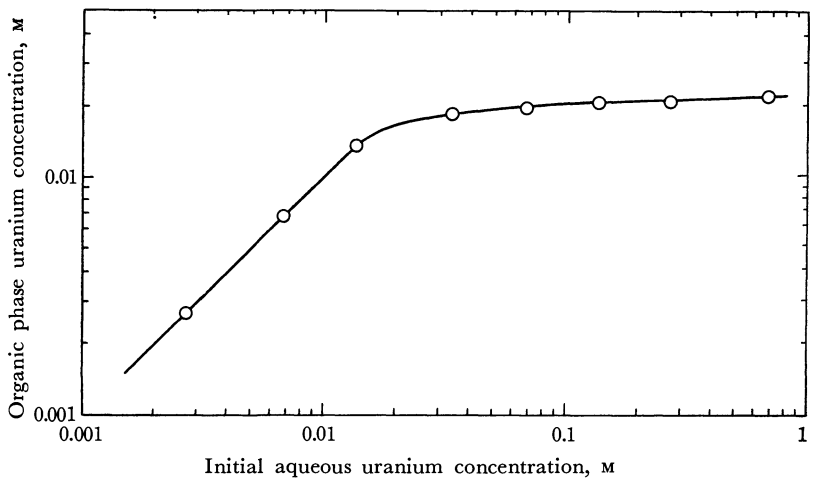

Fig. 3. Variation in uranium concentration of organic phase with initial aqueous uranium concentration in the extraction of uranium(VI) from 0.05 M sulphuric acid solution by 0.1 M DOA in benzene.

3) W. J. McDowell and C. F. Bases, *J. Phys. Chem.*, **62**, 777 (1958).

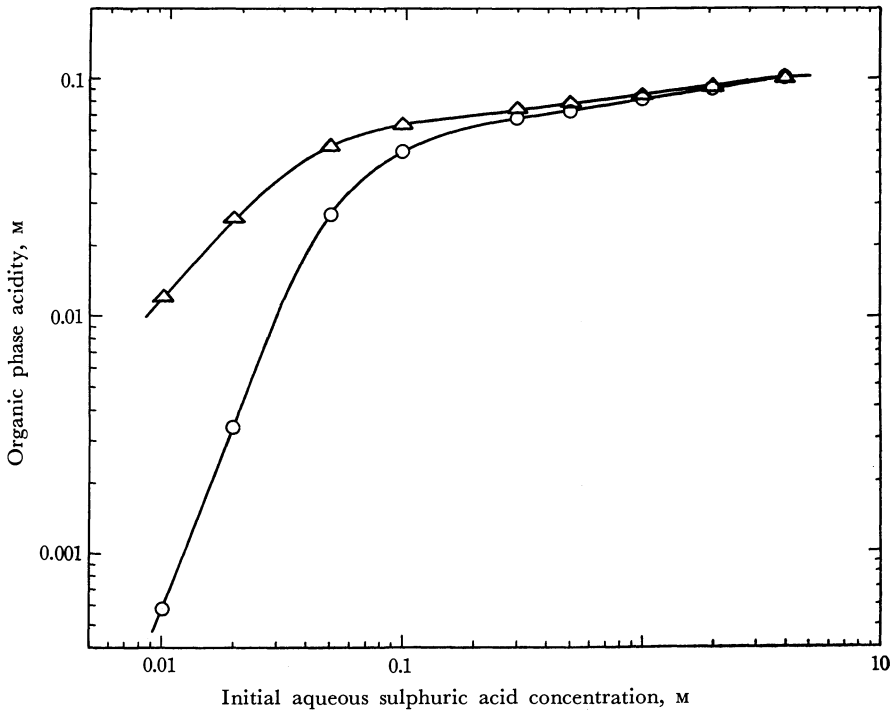

Fig. 4. Change in acidity of organic phase in the extraction of uranium(VI) from sulphuric acid solutions by 0.1 M DOA in benzene.
○ in the absence of uranium, △ in the presence of uranium).

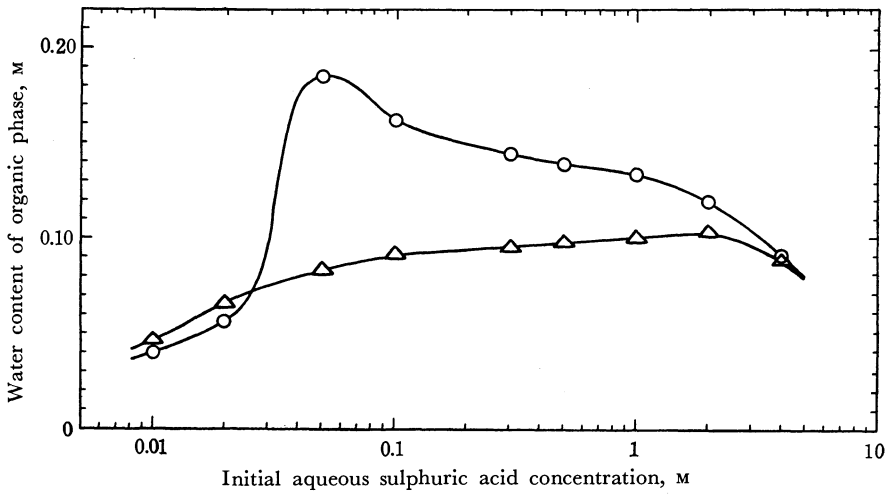

Fig. 5. Change in water content of organic phase in the extraction of uranium(VI) from sulphuric acid solutions by 0.1 M DOA in benzene
○ in the absence of uranium, △ in the presence of uranium.

aqueous solutions with solutions of DOA in benzene, the slope of log-log plots of the sulphuric acid distribution ratio *vs.* the initial DOA concentration was nearly two in 0.05 M H_2SO_4 and unity in 0.5 and 2.0 M H_2SO_4 respectively.

By analogy with the case of TOA (tri-*n*-octylamine),[4] it is considered that the equilibrium between DOA and sulphuric acid is expressed as follows: at low acidities

$$H_2SO_4(a) + 2R_2NH(o) \rightleftarrows (R_2NH_2)_2SO_4(o) \quad (1)$$

and at higher acidities

$$(R_2NH_2)_2SO_4(o) + H_2SO_4(a) \rightleftarrows 2(R_2NH_2)HSO_4(o) \quad (2)$$

4) T. Sato, *J. Appl. Chem.*, **15**, 10 (1965).

in which (a) and (o) denote aqueous and organic phases respectively, and R is C_8H_{17}.

The acidity of the organic phase in the presence of uranium is higher than that in the absence of uranium, but this difference is remarkably decreased above 0.1 M initial aqueous acidity. This probably implies that the reaction of the extraction at low acidities is different from that at higher acidities. From Fig. 5 it is deduced that the hydrated amine sulphate is gradually replaced by the unhydrated amine bisulphate as the aqueous acidity is further increased, and the water content of the organic phase is diminished by the formation of the DOA - uranyl sulphate complex. Further it is inferred that the DOA not associated with uranium is present in the bisulphate form at higher aqueous acidities, and is likely to be present as the free amine form at low aqueous acidities since the concentration of the amine sulphate present as the available amine is restricted by the aqueous acidity.

Infrared Spectral Study. The organic phases from the extraction of uranyl sulphate solutions (5 and 25 g/*l*) containing sulphuric acid of various concentrations by 0.1 M DOA in benzene at 20°C were examined by infrared spectroscopy. Similar measurements were also made of the organic solutions from the extraction of sulphuric acid solutions alone. The spectra are presented in Fig. 6.

In the extraction of sulphuric acid, the following results are observed as the aqueous acidity is increased: for 0.02 M sulphuric acid, the bands of

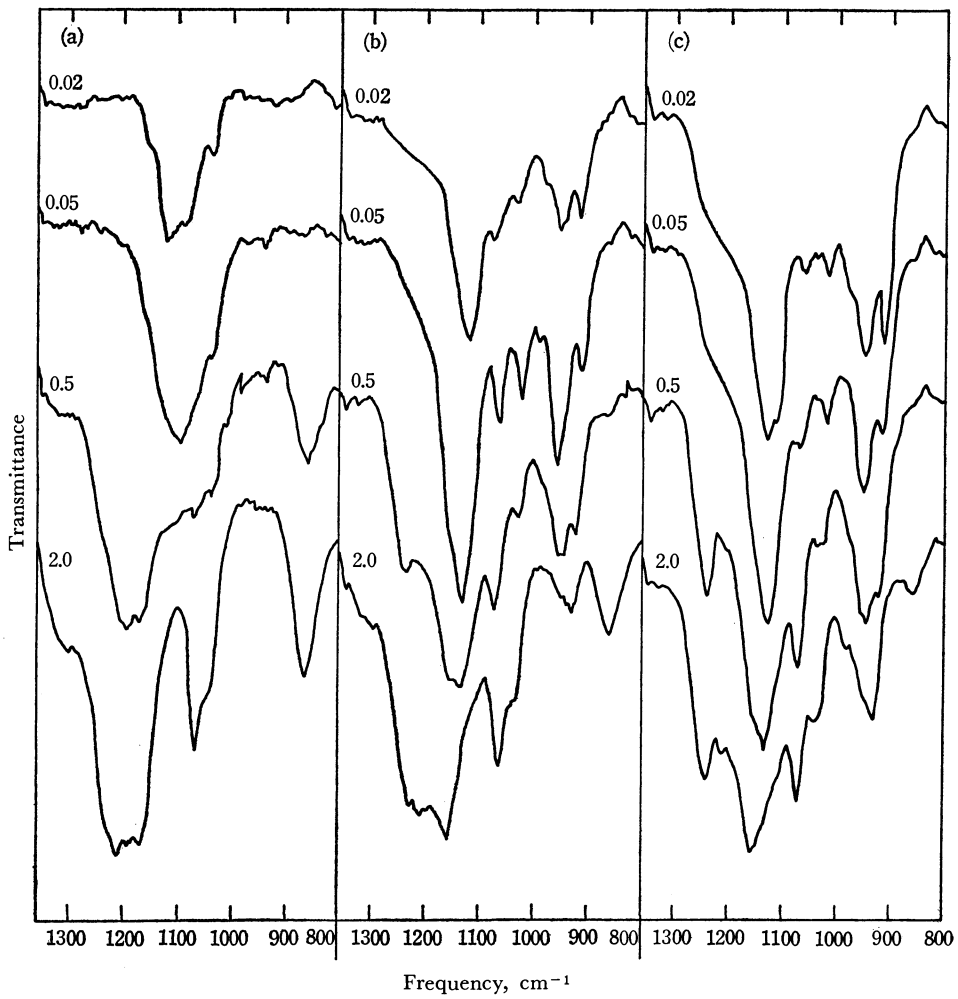

Fig. 6. Infrared spectra of the organic solutions from the extraction of uranium(VI) from sulphuric acid solutions at various concentrations by 0.1 M DOA in benzene.
Numerials on curves are sulphuric acid concentration, M.
(a) sulphuric acid solutions without uranium
(b) uranyl sulphate solutions at 5 g/*l*
(c) uranyl sulphate solutions at 25 g/*l*.

sulphate ion[5-7] appear at 1120—1080 and 1038 cm^{-1}, the NH_2^+ stretching vibration[8,9] which indicates the presence of hydrogen-bonding in the broad band centred at 3100 cm^{-1}, and the OH stretching and bending bands at 3560—3380 and 1635 cm^{-1} respectively; for 0.05 M sulphuric acid, the above absorption bands were more intense; for 0.5 M sulphuric acid, the absorptions due to the bisulphate ion[6,7] at 1210—1165, 1070, and 860 cm^{-1} were accompanied, whereas those of the sulphate ion become weaker; for 2.0 M sulphuric acid, the bands of the bisulphate ion show a progressive increase in intensity, and the intensities of the OH bands decrease, corresponding to the result in Fig. 5.

For the spectra in the presence of uranium, the band at 955 cm^{-1} is assigned to the asymmetric stretching frequency of the uranyl group,[10] and the bands at 1130, 1070, 1020 and 915 cm^{-1} to the vibrational frequencies of the sulphato group,[11] indicating a lower symmetry (point group C_{2v} symmetry) than the sulphate ion (point group T_d symmetry), due to covalent bonding to the uranyl ion. At the same time the absorption assigned to the NH_2^+ stretching vibration, which probably indicates the formation of the hydrogen bond in the complex, is observed at 2830 cm^{-1}. These are stronger in the extraction of uranyl sulphate solutions at 25 g/*l*, since the uranium concentration of organic phase is higher than those at 5 g/*l*. At low acidities the absorptions due to the amine-uranyl sulphate complex become stronger with increasing the aqueous acidity because of the increase in the concentration of amine sulphate formed by the extraction of acid, while at higher acidities the absorption bands due to the bisulphate ion appear in addition to the weaker bands of the amine - uranyl sulphate complex. These results closely resemble those for cyclohexyl- and benzyl-alkylamines,[2a,c] and is basically analogous to the cases of TOA and TDA (tri-*n*-dodecylamine).[2b]

Consequently the following mechanism is proposed for the extraction of uranium(VI) from sulphuric acid solutions by DOA:
at low acidities

$$UO_2SO_4(a) + 2(R_2NH_2)_2SO_4(o) \rightleftarrows [(R_2NH_2)_2SO_4]_2UO_2SO_4(o) \quad (3)$$

and at higher acidities

$$UO_2SO_4(a) + 4(R_2NH_2)HSO_4(o) \rightleftarrows [(R_2NH_2)_2SO_4]_2UO_2SO_4(o) + 2H_2SO_4\ (a)\ . \quad (4)$$

As reported previously,[12] the TOA or TDA-uranyl sulphate complex further shows the absorption assigned to the stretching vibration of the sulphate ion. For the spectrum of the DOA - uranyl sulphate complex, this point is not distinct since the strong band due to the vibration of the sulphato group, co-ordinated to the uranyl ion, at 1130 cm^{-1} overlaps to the absorption assigned to the sulphate ion. However, the organic solution from the extraction of aqueous solution containing 250 g/*l* of uranyl sulphate in 0.05 M sulphuric acid solution with 0.1 M DOA in benzene at 20°C was found to contain uranium: sulphate : amine : water in the mole ratio 1 : 3 : 4 : 3, indicating the stoichiometry to be $(R_2NH_2)_4UO_2(SO_4)_3(OH_2)_3$, *i. e.* $[(R_2NH_2)_2SO_4]_2UO_2SO_4(OH_2)_3$. As this composition resembles the cases of TOA or TDA, it is assumed that the structure similar to the TOA or TDA - uranyl sulphate complex[12] may be given for the DOA - uranyl sulphate complex:

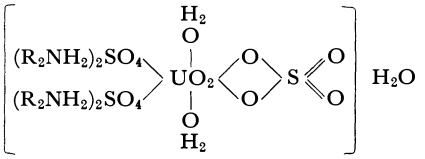

Dependence on Temperature. The extraction of uranyl sulphate solution (5 g/*l*) containing 0.02 and 1.0 M sulphuric acid with 0.1 M DOA in benzene at temperatures between 10 and 50°C gave the result shown in Fig. 7, where the logarithm of the partition coefficient is plotted against the reciprocal of the absolute temperature. This shows that the partition coefficient decreases with rising temperature, and accordingly the heat of reaction (change in enthalpy, kcal/mol) is 4.3 in 0.02 M H_2SO_4 and 4.5 in 1.0 M H_2SO_4.

Effect of Organic Solvent. Table 1 shows the results for various DOA - organic solvent systems in the extraction of uranyl sulphate solutions (5 g/*l*) containing 0.02 and 1.0 M sulphuric acid at 20°C, together with some properties of the solvent (dielectric constant and dipole moment).[13] It is

5) G. Herzberg, "Molecular Spectra and Molecular Structure. II. Infra-red and Raman Spectra of Polyatomic Molecules," D. Van Nostrand Co., Inc., New York (1945), p. 167.
6) F. A. Miller and C. H. Wilkins, *Analyt. Chem.*, **24**, 1253 (1952).
7) G. E. Walrafen and D. M. Dodd, *Trans. Faraday Soc.*, **57**, 1286 (1961).
8) E. A. V. Ebsworth and N. Sheppard, *Spectrochim. Acta*, **13**, 261 (1959); J. Bellanato, *ibid.*, **16**, 1344 (1960).
9) L. J. Bellamy, "Infra-red Spectra of Complex Molecules," 2nd Edn, John Wiley & Sons, Inc., New York (1958), p. 259.
10) B. M. Gatehouse and A. E. Comybes, *J. Chem. Soc.*, **1958**, 3965; G. L. Caldow, A. B. VanCleave and R. L. Eager, *Canad. J. Chem.*, **38**, 772 (1960).
11) K. Nakamoto, J. Fujita, S. Tanaka and M. Kobayashi, *J. Am. Chem. Soc.*, **79**, 4904 (1957).
12) T. Sato, *J. Inorg. Nucl. Chem.*, **26**, 2229 (1964); *Naturwissenschften*, **52**, 258 (1965).
13) A. Weissberger, E. S. Proskauer, J. A. Riddck and E. E. Toops, Jr., "Technique of Organic Chemistry," Vol. 7, Organic Solvents," 2nd Edn, Interscience, New York (1955).

TABLE 1. EXTRACTION OF URANIUM(VI) FROM 0.02 AND 1.0 M SULPHURIC ACID SOLUTIONS BY 0.1 M DOA IN VARIOUS ORGANIC SOLUVENTS

Diluent	Dielectric constant*	Dipole moment	Partition coefficient	
			0.02 M H_2SO_4	1.0 M H_2SO_4
Carbon tetrachloride	2.238	0.00	1.32	9.96
Benzene	2.284	0	4.93	4.90
Toluene	2.379	0.39	3.50	5.43
Chloroform	4.806	1.15	3.26	3.16
Chlorobenzene	5.621	1.56	6.84	5.78
o-Dichlorobenzene	9.93	2.26	6.66	5.74
1, 2-Dichloroethane	10.36	2.06	30.4	2.38
Nitrobenzene	34.8	3.99	46.2	1.03

* All values at 25°C except for carbon tetrachloride, benzene and chloroform at 20°C.

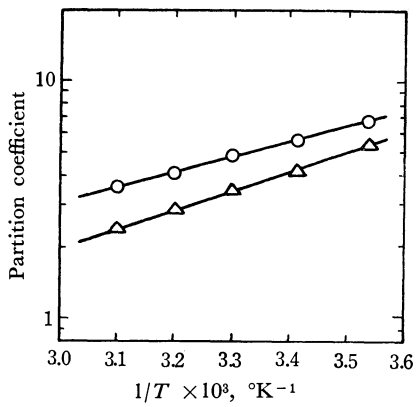

Fig. 7. Temperature-dependence of partition coefficient in the extraction of uranium(VI) from sulphuric acid solutions by 0.1 M DOA in benzene.
△ and ○ represent 0.02 and 1.0 M sulphuric acid concentration respectively.

seen that although the partition coefficient depends markedly on the nature of the diluent, no simple relationship holds between the extraction efficiency of DOA and the physical parameter of organic solvent in these systems. It is presumed, however, that at low aqueous acidity, the extraction efficiency of DOA is enhanced with the diluents which have relative a large dielectric constant such as nitrobenzene and 1, 2-dichloroethane, and contrarily, at high aqueous acidity, these solvents reduce the extraction; at high acidity, carbon tetrachloride gives high extraction efficiency, but chloroform which solvates the amine relatively strongly, presumably through hydrogen-bonding, is not always good extraction medium; halogen substituted aromatic hydrocarbon exhibits considerable good extraction. Similar effect is also observed in the extraction by TOA.[14]

The author wishes to thank Messrs. K. Horibe and M. Nishizaki for assistance with experimental work. He also thanks the Kao Soap Co., Ltd. for a gift of di-*n*-octylamine.

14) T. Sato, unpublished data.

BULLETIN OF THE CHEMICAL SOCIETY OF JAPAN VOL. 41 106—110 (1968)

Diphenyl Sulphoxide Complexes of Lanthanide and Yttrium Perchlorates

S. K. RAMALINGAM and S. SOUNDARARAJAN

Department of Inorganic and Physical Chemistry, Indian Institute of Science, Bangalore-12, India

(Received May 10, 1967)

Diphenyl sulphoxide complexes of nine lanthanide perchlorates of the general composition $[Ln(DPSO)_6](ClO_4)_3$ where Ln=La, Ce, Pr, Nd, Sm, Gd, Ho and Yb and Y have been synthesised and characterized. Infrared studies indicate coordination through the oxygen atom of the ligand and the retention of the Td symmetry of the perchlorate group. The molar conductance and cryoscopic studies suggest a coordination number of six for the metal ions. Cryoscopic studies in DMSO indicate that DMSO is a better donor than DPSO. DTA and UV data are also presented.

The number of complexes of diphenyl sulphoxide (DPSO) reported in the literature is meagre compared with that of its alkyl analogue *viz.*, dimethyl sulphoxide (DMSO). Apart from the hydrogen-bonding[1,2] and the charge-transfer[3,4] studies involving complexes of DPSO in solution, the solid isolable complexes reported include the Lewis adducts with CdI_2,[5] BCl_3, tin halides,[6] BF_3, antimony halides,[7] Re_3Cl_9[8] and UCl_4,[9] the oxyhalide adducts of Nb and Ta[10]; and some transition and non-transition metal compounds.[11] An attempt to prepare $Hg(ClO_4)_2$ complex failed.[12] We have previously reported the DMSO complexes of some lanthanides.[13,14] It was of interest to investigate the DPSO complexes for two reasons: (i) due to its greater bulk than DMSO, DPSO can restrict the coordination number of the metal ion and (ii) DPSO may present a crystal field different from DMSO on account of the conjugation of its phenyl rings with the sulphoxide group. The present paper describes the isolation and characterization of nine new complexes of DPSO with lanthanide and yttrium perchlorates and the structural studies on them. The perchlorate salts were chosen due to their low anionic contribution to complexation.

Experimental

Materials. DPSO was prepared by the reaction of $SOCl_2$ with dry benzene in presence of anhydrous $AlCl_3$, as described by Shriner, Struck and Jorison.[15] The product was recrystallized from petroleum ether. Mp 71°C.

The hydrated lanthanide perchlorates were prepared from the respective oxides (Lindsey Chemical Co., U. S. A.) by treatment with aqueous perchloric acid (E. Merck).

The solvents, dimethyl formamide (DMF), nitrobenzene, nitromethane and acetonitrile were purified by standard methods.[16] DMSO was dried over CaO and fractionated under reduced pressure.

Preparation of the Complexes. All the complexes were prepared by the following general method. A solution of about 2.3 g of DPSO in 5 m*l* of dry methanol was added dropwise with stirring, to a solution of 1 g of the hydrated metal perchlorate in about 5 m*l* of methanol. The complex precipitated as fine crystals. It was filtered, washed with 2 m*l* of ice-cold methanol and then repeatedly shaken with small amounts of dry CCl_4. The product was filtered and dried in vacuum over P_2O_5 at room temperature. In some cases the complexes were recrystallized from acetonitrile.

1) A. Wagner, H. J. Becher and K. G. Kottenhahn, *Chem. Ber.*, **89**, 1708 (1956).
2) P. Biscarini, G. Galloni and S. Ghersetti, *Boll. Sci. Fac. Chim. Ind. Bologna.*, **21**, 154 (1963). *Cf. Chem. Abstr.*, **60**, 2448g (1964).
3) E. Augdahl and P. Klaeboe, *Acta Chem. Scand.*, **18**, 18 (1964).
4) P. Klaeboe, *ibid.*, **18**, 999 (1964).
5) R. H. Pickard and J. Kenyon, *J. Chem. Soc.*, **91**, 896 (1907).
6) a) M. F. Lappert and J. K. Smith, *ibid.*, **1961**, 3224; **1965**, 7102. b) J. S. Morrison and H. M. Haendler, *J. Inorg. Nucl. Chem.*, **29**, 393 (1967).
7) I. Lindqvist, "Inorganic Adduct Molecules of OXO-compound," Springer-verlag, Berlin (1963). Also, I. Lindqvist and P. Einarsson, *Acta Chem. Scand.*, **13**, 420 (1959).
8) F. A. Cotton, S. J. Lippard and J. T. Mague, *Inorg. Chem.*, **4**, 508 (1965).
9) J. Selbin, N. Schober and J. D. Ortego, *J. Inorg. Nucl. Chem.*, **28**, 1385 (1966).
10) D. B. Copley, F. Fairbrother, K. H. Grundy and A. Thompson, *J. Less-Common Metals*, **6** (5), 407 (1964). *Cf. Chem. Abstr.*, **61**, 3904g (1965).
11) P. W. N. M. Van Leeuwen and W. L. Groeneveld, *Recueil*, **85**, 1173 (1966). Also P. W. N. M. van Leeuwen, *ibid.*, **86**, 201, (1967).
12) R. L. Carlin, J. Roitman, M. Dankleff and J. O. Edwards, *Inorg. Chem.*, **1**, 182 (1962).
13) S. K. Ramalingam and S. Soundararajan, *Curr. Sci. (India)*, **35** (9), 233 (1966).
14) S. K. Ramalingam and S. Soundararajan, *J. Inorg. Nucl. Chem.* **29**, 1763 (1967).
15) R. L. Shriner, H. C. Struck and W. J. Jorison, *J. Am. Chem. Soc.*, **52**, 2060 (1930).
16) A. Weissberger and R. S. Proskauer, "Organic Solvents, Technique of Organic Chemistry," Vol. VII, Interscinence, New York (1955).

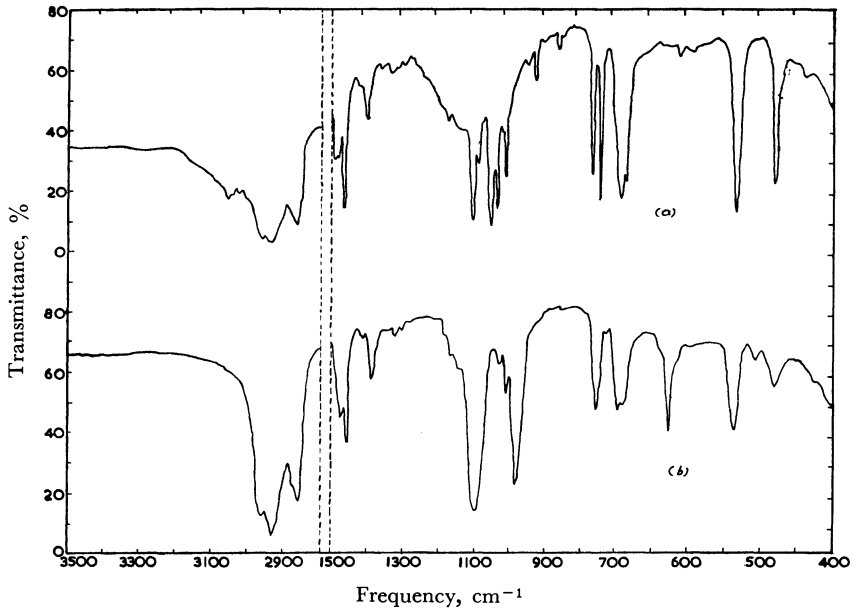

Fig. 1. Infrared spectra of (a) DPSO and (b) $Pr(DPSO)_6(ClO_4)_3$ in Nujol mull.

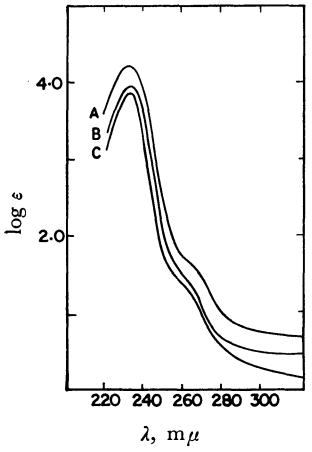

Fig. 2. UV spectra of DPSO (A) and its Pr (B) and Yb (C) complexes in CH_3CN.

Analyses. In the case of the lighter lanthanide complexes, the metal was estimated gravimetrically by the oxalate-oxide method. Y, Ho and Yb were estimated volumetrically by EDTA tritrations using xylenol orange as the indicator.[17] Perchlorate was estimated by the Kurz method.[18] Micro analyses of C, H and S were carried out for some representative complexes through the courtesy of the CIBA Research centre, Bombay. The analytical results along with some physical data are listed in Table 1.

Instrumentation. *Thermal Studies.* Owing to the explosive nature of the complexes, the differential thermal analysis (DTA) was carried out by diluting the complexes with alumina (~1 : 10 by weight). The apparatus employed was of a manual type provided with chromel-alumel thermocouples. The heating rate was 8°±1°C/min. The decomposition temperature is characterized by a sharp exotherm in the DTA profile. The DTA curves for three representative complexes are presented in Fig. 3.

Spectral Studies. The IR spectra of the complexes and of pure DPSO were measured in Nujol mulls in the region 4000—400 cm^{-1} employing Carl Zeiss UR-10 spectrophotometer. Spectral data for a typical case are presented in Table 2. The UV spectra were taken with a Beckman DB-10 recording spectrophotometer. Acetonitrile was used as the solvent and the concentration of the solutions was 10^{-5} M (*vide* Fig. 2).

Conductometric Measurements. The molar conductances of the complexes in various solvents were determined at 30°C in a Siemen's conductivity bridge with an immersion cell (Type LTA), previously calibrated with standard KCl solutions. It had a cell constant of 0.665. The data are given in Table 3.

Molecular Weight Data. These were obtained in nitrobenzene and DMSO using a crysocopic apparatus fitted with a Beckmann thermometer and a mercury-seal stirrer to exclude moistrure. The data are listed in Table 3.

Properties of the Complexes. In contrast to the high deliquescent nature of the lanthanide perchlorates, the complexes are non-hygroscopic. They are insoluble in solvents like CCl_4 and C_6H_6 but are appreciably soluble in acetone, acetonitrile, methanol, nitrobenzene, nitromethane, DMF and DMSO. In water they decompose to precipitate the insoluble ligand part. The colours of the complexes closely resemble those of their parent salts but are less in intensity. Some of the complexes under conditions of continuous evacuation over P_2O_5 develop a brown colour. Many of the physical and chemical data for all the complexes are very similar.

17) I. M. Kolthoff and P. J. Elving, "Treatise on Analytical Chemistry Part II," Vol. 8, Interscience, New York (1963), p. 57.
18) E. Kurz, G. Kober and M. Berl, *Anal. Chem.*, **30**, 1983 (1958).

TABLE 1. PHYSICAL AND

Sl. No.	Complex	Colour	Melting point °C	% Metal Found	% Metal Cald
1	$La(DPSO)_6(ClO_4)_3$	white	171	8.38	8.43
2	$Ce(DPSO)_6(ClO_4)_3$	white	172—175	8.41	8.49
3	$Pr(DPSO)_6(ClO_4)_3$	pale green	173—177	8.58	8.53
4	$Nd(DPSO)_6(ClO_4)_3$	pale pink	154—158	8.61	8.72
5	$Sm(DPSO)_6(ClO_4)_3$	pale yellow	196—201	8.92	9.05
6	$Gd(DPSO)_6(ClO_4)_3$	white	177	9.36	9.43
7	$Y(DPSO)_6(ClO_4)_3$	white	156—160	5.66	5.56
8	$Ho(DPSO)_6(ClO_4)_3$	pale yellow	140—145	9.92	9.85
9	$Yb(DPSO)_6(ClO_4)_3$	white	168	10.39	10.28

TABLE 2. INFRARED DATA FOR DPSO AND ITS LANTHANIDE COMPLEXES

DPSO cm^{-1}	Complex	Assignment
3058 kink	3058 kink	C-H stretch (A_1)
1589 w	1590 w	C-C stretch (A_1)
1472 m	1470 m	C-C stretch (A_1)
1450 s	1454 s	C-C stretch (B_1)
1320 w	1320 w	C-C stretch (B_1)
1162 w, sh	1170 w, sh	C-H def. (A_1)
1092 vs	1090—1105 vs, bd	Mass dependent (A_1) and ν_3 ClO_4
1078 sh	—	C-H def. (B_1)
1043 vs	982 vs	S-O stretch
1028 s	1028 m	C-H def. (A_1)
1000 m	1004 m	Ring def. (A_1)
920 w	925 w, bd	C-H def. (B_1)
760 s	762 m	C-H def. (B_2)
740 s	750 s	—
696 s	695 m	Ring def. (B_2)
684 s	688 m	C-S stretch
—	625 m	ν_4ClO_4
538 s	535 s	—
—	508 w	—
480 s	482 m	Out of plane ring def.
438 w, bd	425 w	—

Abbreviations: vs, very strong; s, strong; m, medium; w, weak; sh, shoulder and bd, broad
Note: The spectra of the different complexes (in Mulls) are quite similar (within $\pm 2\ cm^{-1}$). Except for the perchlorate bands the other assignments are based on the work of Lappert and Smith.[6]

Discussion

Single-crystal studies on diphenyl sulphoxide[19] have confirmed a pyramidal arrangement of the three bonds about the sulphur atom. With a semipolar S→O linkage and with unshared pairs of electrons on both S and O, it is possible that DPSO can form complexes with metal ions either through O or S atom. Hence it is of interest to determine the site of coordination.

Infrared studies of the complexes (Table 2 and Fig. 1) indicate that the DPSO molecules are bonded through their oxygen atom. This is evidenced by a considerable decrease in the S–O stretching frequency in the complexes ($\sim 60\ cm^{-1}$) compared to that in the free ligand. Such an inference stems from a consideration of the following structures for the complexes, where I represents O bonding and II, S bonding.

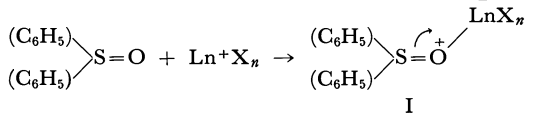

I

or

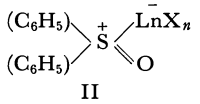

II

Ln is the lanthanide metal ion and X is the anion.

The S–O bond in the sulphoxide may be regarded as substantially, a double bond, with p_π-d_π $(\overset{-}{S}\text{-}\overset{+}{O})$ bonding from oxygen to sulphur, superimposed on the SO σ bond $(\overset{+}{S}\text{-}\overset{-}{O})$. Structure I implies a lengthening of the S–O bond accompanied by a decrease in the p_π-d_π back bonding in the complexes compared with the free ligand. Hence a decrease in S–O stretching frequency would be expected. On the other hand structure II requires an increase in the S–O stretching fundamental. Also the fact that the sulphoxide shift is nearly the same for all the lanthanide complexes studied, indicates that they all have nearly the same stability.

The unsplit IR band at 1096 (vs, bd) and the one at 625 (m) cm^{-1} suggest that the Td symmetry of the ionic perchlorate[20] is retained in the complexes. (Fig. 1)

Molar conductance data in solvents of different

19) S. C. Abrahams, *Acta Cryst.*, **10**, 417 (1957).

20) S. D. Ross, *Spectrochim. Acta*, **18**, 225 (1962).

ANALYTICAL DATA

% Perchlorate		% C		% H		% S	
Found	Cald	Found	Cald	Found	Cald	Found	Cald
18.21	18.09	52.21	52.44	3.97	3.64	11.51	11.64
18.17	18.08	—	—	—	—	—	—
18.18	18.07	—	—	—	—	—	—
18.14	18.03	—	—	—	—	—	—
17.86	17.97	—	—	—	—	—	—
17.84	17.88	51.62	51.84	3.91	3.60	11.34	11.51
18.82	18.66	—	—	—	—	—	—
17.95	17.81	—	—	—	—	—	—
17.87	17.73	51.06	51.39	3.76	3.57	11.26	11.41

TABLE 3. CONDUCTANCE AND CRYOSCOPIC DATA

Complex	Molar conductance Λ, $ohm^{-1} cm^2 mol^{-1}$			Molecular weight		Calcd. molecular weight	No. of species	
	NM	NB	DMSO	NB	DMSO		NB	DMSO
La	211.2	68.86	108.1	427.2	161.2	1649	3.86	10.23
Ce	213.7	—	107.2	441.2	160.5	1650	3.74	10.28
Pr	206.2	68.42	103.6	432.2	158.1	1651	3.82	10.44
Nd	—	72.10	103.1	446.1	162.5	1655	3.71	10.19
Sm	—	71.62	—	453.8	168.5	1661	3.66	9.86
Gd	214.7	70.59	—	—	163.2	1668	—	10.22
Y	213.2	69.85	104.6	412.2	155.2	1599	3.88	10.39
Ho	214.4	—	104.1	—	162.5	1675	—	10.31
Yb	217.6	70.24	103.7	439.3	166.0	1683	3.84	10.14

Note: 10^{-3} M solutions were used for conductance measurements. Λ for 1 : 1 electrolytes in nitromethane (NM),[21] nitrobenzene (NB)[21] and DMSO[22] lie in the range 70—100, 20—30 and ~40 mhos $cm^2 mol^{-1}$ respectively.

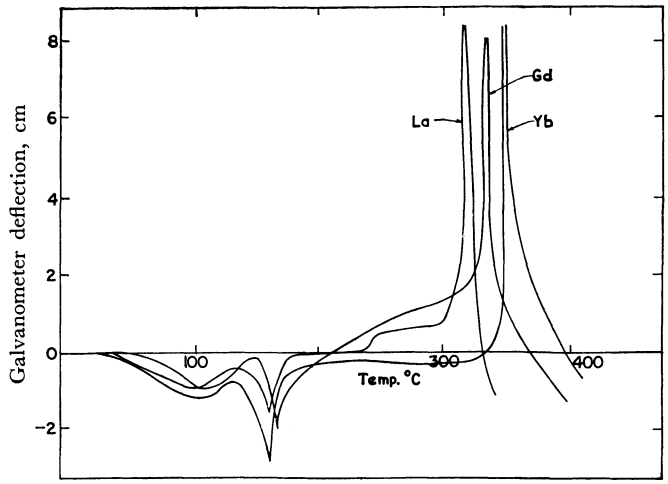

Fig. 3. DTA studies.

donor strengths such as nitromethane, nitrobenzene, acetonitrile and DMSO reveal a uni-trivalent structure for the complexes (see Table 3). Cryoscopic studies in nitrobenzene, a solvent of poor donor properties, show the presence of four species only, suggesting that the DPSO molecules bonded to the metal are not dissociated in solution. In accordance with these observations the complexes

21) M. Cox, J. Lewis and R. S. Nyholm, *J. Chem. Soc.*, **1962**, 2177.
22) P. G. Sears, G. R. Lester and L. R. Dawson, *J. Phys. Chem.*, **60**, 1433 (1956).

can be formulated as $[Ln(DPSO)_6]^{3+}$ $3(ClO_4)^-$, giving a coordination number six for the metal.

However, molecular weight studies of the complexes in DMSO show the presence of ten species, indicating that all the DPSO molecules are displaced from the coordination sphere by the solvent molecules. This implies that of the two ligands DMSO and DPSO, the former is a more powerful donor than the latter with respect to the lanthanide ions. This is probably a consequence of conjugation between the aromatic rings and the sulphoxide group. Hydrogen bonding[1,2] and charge-transfer[4] studies of some complexes of these ligands in solution, have also revealed a similar order of donor strengths for the two ligands.

The UV spectrum of DPSO in acetonitrile exhibits two maxima, one at 228mμ($\log \varepsilon = 4.2$) and the other at 265mμ(inflection) (see Fig. 2). Presumably, the former band is attributable to the absorption arising from the S–O group and the latter to the benzanoid chromophore. In the spectra of the complexes there is no significant shift in the position of either band. In the visible region the complexes were transparent throughout. The limited solubility of the complexes in suitable solvents restricted work on this line.

The DTA studies suggest that the complexes have nearly the same thermal stability. The decomposition temperatures for the different complexes, characterized by sharp exothermic peaks, lie in a close range (315—360°C) (Fig. 3). The small endothermic peak at ~100°C represents the exclusion of any absorbed moisture and the one at 160—190°C represents the melting point of the complexes. The Yb complex heated separately at 350°C, on infrared analysis showed the absence of any perchlorate ion or DPSO.

The physical data, thus suggest a coordination number of six for the lanthanides and yttrium. In many DMSO complexes of the lanthanides[13,14,23] the coordination number has been shown to be eight. Thisreduction in the coordination capacity of the metal ions in the DPSO complexes is presumably due to steric factors.

The authors thank Professor M. R. A. Rao for his keen interest in the work and Professor T. R. Govindachari, Director, CIBA Research Center for microanalytical data.

23) V. N. Krishnamurthy and S. Soundararajan, *J. Inorg. Nucl. Chem.*, **29**, 517 (1967).

BULLETIN OF THE CHEMICAL SOCIETY OF JAPAN VOL. 41 110—114 (1968)

Manganese(II) and Mercury(II) Complexes Containing a Thio Derivative of Acetylacetone*1

Akiko FURUHASHI, Kunihiko WATANUKI*2 and Akira OUCHI*2

Department of Chemistry, College of Engineering and Science, Aoyama Gakuin University, Megurisawa Setagaya, Tokyo

(Received June 12, 1967)

New compounds of the type $M(C_5H_7S_2)_2Cl_4$, where M is Mn(II) or Hg(II), were obtained by passing hydrogen chloride and hydrogen sulfide through ethanol solutions containing acetylacetone and metal chlorides. Such adducts seem to be isostructural to iron compounds, and are stable in the solid state. They seem to decompose when brought into contact with such solvents as water, methanol and dimethylformamide. Their magnetic susceptibilities show that these compounds are all bivalent. The infrared spectra and electronic spectra resemble those of the dithioacetylacetonato iron compound.

The dithio derivatives of acetylacetonato complexes are expected to have many interesting properties, but their syntheses were not successful until only recently.

Martin and Stewart[1] have succeeded in synthesizing dithioacetylacetonate of nickel(II), cobalt(II), palladium(II) and platinum(II).

The present authors have investigated the syntheses of the dithioacetylacetonato complex of various other metals, and have come to synthesize

*1 A part of this paper was presented at the 20th Annual Meeting of the Chemical Society of Japan, Tokyo, March, 1967.

*2 College of General Education, University of Tokyo, Komaba, Meguro-ku, Tokyo.

1) L. Martin and I. M. Stewart, *Nature*, **210**, 522 (1966).

a series of $M(C_5H_7S_2)_2Cl_4$ type complexes where M is manganese(II), mercury(II) or iron(II). These compounds are mutually very similar in properties as well as in IR spectra but are a little different from the group of $M(C_5H_7S_2)_2$ complexes where M is nickel(II) or cobalt(II).

Recently Knauer, Hemerich and Van Voorst have published[2] a note about the synthesis of $Fe(C_5H_7S_2)_2Cl_4$. Although we have accomplished our synthesis of the iron complex independently, the compound is exactly the same properties as the one reported by Knauer and others. In this paper, therefore, the syntheses and the properties of the manganese(II) and mercury(II) complexes are mainly reported.

Knauer and others reported in their paper[2] that iron complexes dissociated in aqueous solution into dithiolium ion, ferrous ion and chloride ion. In fact, it is only by assuming the presence of dithiolium unit ($C_5H_7S_2^+$), instead of the usual dithioacetylacetonato unit ($C_5H_7S_2^-$), that the bivalency of iron and the above formula can be reconciled. The merucry and manganese compounds reported in this paper are considered to have similar constitutions.

Experimental

Materials and Instruments. The starting materials were of GR grade and were used without further purification. IR spectra were obtained by the KBr disc procedure using a DS 403G infrared spectrophotometer of the Japan Spectroscopic Co., Ltd. Electronic spectra were obtained with an Hitachi EPS-2 type automatic spectrophotometer.

Syntheses of Dithioacetylacetonato Manganese(II). Three grams of manganese(II) dichloride tetrahydrate (0.015 mol) was dehydrized by direct heating. The anhydrous salt and 3.1 m*l* of acetylacetone (0.030 mol) were dissolved into 30.0 m*l* of absolute ethanol. Hydrogen chloride and then hydrogen sulfide were passed through it. The solution thus obtained was mixed with an equivolume of petroleum ether and kept overnight. Fine yellow crystals were obtained. Yield was about 30%.

The same method as for manganese(II) compounds was effective for the synthesis of the mercury(II) compound from mercury(II) chloride, and for the synthesis of the iron(II) compound from iron(III) chloride hexahydrate. Yields were about 25% and 45% respectively.

All these three compounds are only very slightly soluble in usual organic solvents such as benzene, chloroform and acetone. On the other hand, they are soluble in water, methanol dimethylformamide and dimethylsulfoxide, with probable decomposition. Because of this, their recrystallization has not yet been successful.

Results and Discussion

Analytical data of these compounds are summarized in Table 1. Significant features of the infrared spectra are shown in Table 2, and those of the visible reflection spectra in Fig. 1, both including the data on the iron compound for comparison.

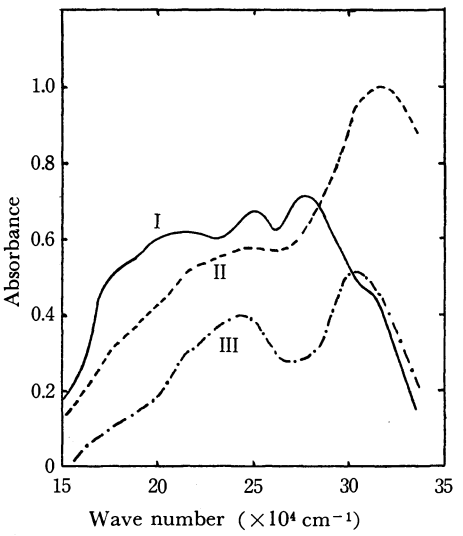

Fig. 1. Reflection spectra of the complexes.
Solid samples were diluted ten times with calcium carbonate (in weight). Reference was calcium carbonate.
I: $FeCl_4(L_{ss})_2$, II: $MnCl_4(L_{ss})_2$,
III: $HgCl_4(L_{ss})_2$

Table 1. Analytical results of the complexes
(Figures are shown in %)

		$FeCl_4(C_5H_7S_2)_2$	$MnCl_4(C_5H_7S_2)_2$	$HgCl_4(C_5H_7S_2)_2$
Metal	Calcd	12.14	11.97	33.15
	Found	12.10	12.11	33.30
C	Calcd	26.10	26.19	19.90
	Found	26.79	26.23	20.97
H	Calcd	3.05	3.05	2.32
	Found	3.13	3.34	2.36
S	Calcd	27.85	27.92	21.20
	Found	27.80	26.92	20.05
Cl	Calcd	30.90	31.00	23.50
	Found	30.40	31.40	23.66

* The oxydation of sulfur in this compound is very difficult and alway smaller values were obtained.

The magnetic moment of the manganese compound measured by Gouy's balance is 5.92 B. M. per one mole of metal indicating the existence of 5 unpaired electrons, while the mercury compound is diamagnetic, indicating the absence of any unpaired electron. The iron(II) compound seems to have 4 unpaired electrons, as it shows 4.99 B. M.

2) K. Knauer, P. Hemmerich and J. D. W. Van Voorst, *Angew. Chem. Intern. Ed. Engl.*, **6**, 262 (1967).

TABLE 2. INFRARED SPECTRA OF THE COMPLEXES
Figures are given in cm^{-1}. L_{ss} means $(C_5H_7S_2)$.

$FeCl_4(L_{ss})_2$	$MnCl_4(L_{ss})_2$	$HgCl_4(L_{ss})_2$	$Ni(L_{ss})_2$	$Ni(L_{oo})_2$	Tentative assignment
				1598	ν(C=O)
1470 s	1485 s	1480 s	1495 s	1514	ν(C=C)+δ
1420—1430	1432 m	1430 m	1433 w	1453	
1375 s	1378 w	1375 m		1398	$\delta(CH_3)$
1353 s	1357 m	1355 m	1353 m	1367	
			1314 m		ν(C-CH_3)+
			1290 m	1261	ν(C=C)
1230 m	1234 m	1230 m			$\rho(CH_3)$,
1200 s	1208 s	1205 s		1198	ν(C=S)
			1159 s		
1093 w	1095 w	1095 w			
1007 m	1022 w	1020 w	1013 m	1020	$\rho(CH_3)$
	1010 m	1008 m			
997 m	1000 w	1000 w			
982 w	985 w	982 w			ν(C-CH_3),
				929	ν(C=O)
860 s	865 s	862 s	841 s		ν(C=S)
			749 m	764	π(C-H)
710 w	717 w	715 w	705 w		
696 s	703 w	700 s			
				666	δRing+
					ν(M-O)
573 w	578 w	575 w		579	
557 s	559 s	557 s	558 s	563	π
523 w	527 w	525 w			
459 w	460 w	458 w			
436 s	439 s	438 s	422 w	427	π
422 w	422 w	420 w			

per iron atom. These facts show that these compounds have high spin octahedral or tetrahedral structures and not planar or distorted tetragonal ones. This supports the assumption proposed by Knauer and others.[2]

The infrared spectra data for the above compounds are summarized in Table 2 together with those of acetylacetonato-[3] and dithioacetylacetonatonickel(II)[4]. The general feature of the former resembles those of acetylacetonates except some additional special bands. The tentative assignments of many bands were given from the comparison with the acetylacetonates as shown in Table 2.

These compounds show no ν(C=O) band near 1570 cm^{-1} and this fact shows that they do not have any carbonyl oxygens. The ν(C=S) bands of these compounds, containing two dithioacetylacetonate ligand per one metal ion, appear near 1200 and 862 cm^{-1}, but on the other hand those of bisdithioacetylacetonate of nickel(II) and cobalt(II) appear near 1160 and 844 cm^{-1}. In other words, ν(C=S) has about 40—20cm^{-1} higher wave numbers in these tetrachloro compounds. This fact seems to indicate that the C–S bond in these tetrachloro compounds has a more covalent character and the metal-sulfur bond may not be as strong as in nickel or cobalt bisdithioacetylacetonate.

Reflection spectra of these compounds are shown in Fig. 1. Since usual Hg(II), Mn(II), as well as Fe(II) compounds have no marked d–d absorption in this region, the peaks in these spectra should be due to charge transfer, or to π-π transfer bands.

When these compounds are dissolved, they seem to be decomposed, and the spectra of the solutions are not the same as those in the solid state. But the solutions of these compounds, after staying about one hour at room temperature (20°C),

3) K. Nakamoto, P. J. McCarthy, A. Ruby and A. E. Martell, *J. Am. Chem. Soc.*, **83**, 1066, 1272 (1961).
4) A. Ouchi, M. Hyodo and Y. Takahashi, This Bulletin, **40**, 2819 (1967).

TABLE 3. ELECTRONIC SPECTRA OF THE COMPLEXES DISSOLVED IN SOME SOLVENTS*
(After 1 hr at 20°C, 10^{-3}—10^{-5} mol/l)
Figures are given in cm^{-1} for wave numbers and log ε for intensities (in palentheses).

Methanol solution					
$FeCl_4(L_{ss})_2$	37700	34500	27400	21720	16650
	(4.13)	(4.19)	(2.19)	(2.07)	(1.71)
$MnCl_4(L_{ss})_2$	38500	34650		22800	16660
	(3.86)	(3.85)		(2.49)	(0.70)
$HgCl_4(L_{ss})_2$	37000	34100		23600	17550
	(4.15)	(4.24)		(3.52)	(2.92)
Aqueous solution					
$FeCl_4(L_{ss})_2$	38300	34600		23200	
	(4.18)	(4.31)		(1.35)	
$MnCl_4(L_{ss})_2$	37600	34650	27800	23300	
	(3.96)	(4.09)	(1.37)	(1.12)	
$HgCl_4(L_{ss})_2$	37700	34500	30600	23710	18200
	(4.09)	(4.20)	(3.92)	(4.54)	(2.37)
Dimethyl formamide solution					
$FeCl_4(L_{ss})_2$	36400		30300	22800	17550
	(4.51)		(4.02)	(4.10)	(2.33)
$MnCl_4(L_{ss})_2$	35500		28200	23300	16700
	(3.38)		(3.74)	(3.48)	(2.30)
$HgCl_4(L_{ss})_2$	36750	33300	28200	21720	16700 sh
	(4.12)	(4.07)	(3.98)	(3.30)	(2.50)

* These spectra should be those of some reaction products of complexes with solvents and may not be the spectra of the complex itself.

show reproducible spectra; the ε in appearance almost follows Beer's law in the concentration region of 10^{-3}—10^{-4} mol/l in the case of visible spectra, and 10^{-4}—10^{-5} mol/l in the case of ultraviolet region. From this fact, decomposition seems to be almost complete in solutions. The maxima and ε's (in appearance) of the main peaks are shown in Table 3.

In aqueous solution these complexes seems to be decomposed into M^{2+}, $(C_5H_7S_2)^+$ and Cl^- (where $M^{2+}=Fe^{2+}$, Mn^{2+} or Hg^{2+}). The color of the aqueous solution is weaker than that of solid or dimethylformamide solution. In the case of the iron complex, the existence of Fe^{2+} was recognized by the formation of bipyridine complex by Knauer and others,[2] and by the formation of *O*-phenanthroline complex in our study. The existence of Cl^- was found by the immediate precipitation of silver chloride by the addition of silver nitrate in our research. The existence of $[C_5H_7S_2]^+$ was proved by Knauer *et al.*[2] by the formation of picrate $C_{11}H_9O_7N_3S_2$. They also assigned the 280 mμ and 265 mμ peaks in aqueous solution to the π-π transition in the dithiolium ring.

The existence of the free dithiolium ion in aqueous solutions of the complex is very interesting, although the dithiolium ions were already reported in many papers.[5-8] They are the planar, benzenoid, heterocyclic, monopositive ions. Such salts as perchlorate or chloride are colorless and stable.

The aqueous solution of Mn(II) and Hg(II) compounds also reacts with silver nitrate and precipitates silver chloride immediately. Moreover, the wave numbers and ε's of the absorption in maxima in the ultraviolet region are very similar to that of the Fe(II) compounds. This fact shows that the aqueous solution of Mn(II) and Hg(II) compounds also contains dithiolium ion.

A complicated solvation phenomenon was found when Mn(II), Hg(II) and Fe(II) complexes are dissolved in dimethylformamide; the solution was violet immediately after the dissolution, but in a few minutes, the color turned yellow at room temperature. If the fresh yellow solution is diluted by more dimethylformamide the color turns blue, but the blue color is very unstable, turning yellow after a while. The old yellow solution does not change its color upon dilution. The values given in Table 3 are those of the final yellow solution.

5) E. Klingsberg, *J. Am. Chem. Soc.*, **83**, 2934 (1961).
6) E. Klingsberg, *J. Org. Chem.*, **31**, 3489 (1966).
7) G. Barinkow and H. Kunzeh, *Z. Chem.*, **6**, 343 (1966).
8) D. Leaver and W. A. H. Robertson, *Proc. Chem. Soc.*, **1960**, 252.

The kinetic approach of the above change has not yet been successful. The mean molecular weight of the species in the dimethylformamide solution of the iron complex was 110 as found by vapor pressure depression measurement, and this fact shows that the iron complex should be split into four or more parts in the solution. By analogy, the Mn(II) and Hg(II) complexes should also be split into several pieces in the solution.

The ultraviolet spectra of all of these compounds in water, methanol and dimethylformamide show two characteristic peaks (Table 3), and they are assigned to the π-π transition of the dithiolium ion ring as in the case of dithiolium derivatives.[5-8]

In the case of the dimethylformamide solution, the maxima of the two peaks in the ultraviolet region shift to lower wave number; 36000, and 28000 cm^{-1}, respectively. This fact may show that in dimethylformamide solution a part of the metal-sulfur bonding structure is kept, although it is not the same as that in the solid state.

It should be noted that a dimer of dithioacetylacetone is also very easily produced when acetylacetone is treated with hydrogen sulfide. This dimer is very stable, not decomposing easily. However, the infrared spectra of the dimer is very different from those of the complexes mentioned above.

In the case of dithioacetylacetonato nickel(II), or cobalt(II), the complexes are easily soluble in a non-polar solvent, but not in water. On the other hand, the complexes of iron, manganese and mercury are hardly soluble in non-polar solvents, and soluble in water (though accompanied by some decomposition). Infrared spectra of complexes of these two types are also different from each other.

From these data it is concluded that the dithioacetylacetone in these complexes does not exist in dimer form, nor in the usual dithioacetylacetonato $[C_5H_7S_2]^-$ form (as found in the nickel complex). Knauer and other's assumption[2] of the existence of dithiolium ion in it thus seems to be the most reasonable one. They have suggested two hypothetical formulae; (a) $FeCl_2(C_5H_7S_2)^{2+}Cl_2^-$, (b) $FeCl_2[CH_3(Cl)CS\,CH\,CS\,CH_3(Cl)]_2^0$ to explain the intense color of the solid iron complex. However, there seems to be still several other possibilities. The X-ray study which is going on by the present authors is expected to clarify this point. The manganese, and mercury complexes probably have the same type of structure.

The authors wish to thank to the Analytical Division of the Department of Pharmacy, The University of Tokyo for their elemental analyses of these compounds as well as for the measurement of infrared spectra; we also acknowledge Professor Yukichi Yoshino and the colleagues of our laboratory for helpful discussions.

A part of this research was carried out with a Scientific Research Grant from the Ministry of Education to which the authors' thanks are due.

BULLETIN OF THE CHEMICAL SOCIETY OF JAPAN VOL. 41 115—119 (1968)

The Chemistry of Protactinium. VI. A Study of the Sulfato-Complex of Pa(IV) by Means of TTA-Benzene Extraction

Toshikazu MITSUJI

The Research Institute for Iron, Steel and Other Metals, Tohoku University, Katahira-cho, Sendai

(Received July 4, 1967)

The behavior of Pa(IV) during extraction with TTA was investigated in perchlorate, chloride, and sulfate solutions (pH 0.4—1.1). In perchlorate and chloride solutions, the extraction equilibrium may be written as:

$$Pa(OH)_2^{2+} + 4HT \rightleftharpoons PaT_4 + 2H_2O + 2H^+$$

On the other hand, the extraction by TTA from the sulfate solution may be described as:

$$Pa(SO_4)(OH)^+ + 4HT \rightleftharpoons PaT_4 + HSO_4^- + H_2O + 2H^+$$

Therefore, the formation of the sulfato-complex of Pa(IV) is considered to occur as follows:

$$Pa(OH)_2^{2+} + HSO_4^- \rightleftharpoons Pa(SO_4)(OH)^+ + H_2O$$

The equilibrium constant for the above reaction has been determined to be 320 at the ionic strength of 0.50 (temperature: 10±0.5°C).

Guillaumont investigated the distribution of Pa(IV) between the perchlorate solution with the ionic strength of 3 and the TTA-benzene solution, and reported that Pa^{4+} gradually hydrolyzed to $Pa(OH)_3^+$ over the pH range from −0.5 to 3.0.[1] The same author also studied chloro-, sulfato-, and fluoro-complexes in aqueous solutions and calculated their stability constants at the ionic strength of 3.[2] In these papers, however, the experimental data were not reported in detail.

Two points have chiefly prevented the investigators from studying the behavior of Pa(IV) by using the ^{233}Pa tracer. One is the difficult reduction of Pa(V) in microquantities, and the other is the lack of a method to identify Pa(IV) in microquantities. In the foregoing paper, however, the present author showed that the ^{233}Pa(V) tracer was readily reduced by means of a liquid zinc amalgam in the presence of more than 10^{-4} M of Cr(III) and proposed that the co-precipitation with thorium fluoride gave an excellent method identifing of Pa(IV) in microquantities.[3]

The present author has also investigated the absorption spectra of Pa(IV) and inferred that the sulfato-complexes of Pa(IV) exist even in a dilute sulfuric acid solution, but that Pa(IV) is then reluctant to form chloro-complexes.[4] In this study, the sulfato-complex of Pa(IV) was investigated in detail by means of TTA-benzene extraction, after confirming the valency state of protactinium by the thorium fluoride co-precipitation method.

Experimental

Reagents. ^{231}Pa and ^{233}Pa were prepared by the method reported by Suzuki and Inoue.[5] All the reagents used were of the highest purity. Water was purified by distillation, followed by ion exchange treatment. Benzene was purified by distillation.

Apparatus. A reduction apparatus described earlier[4] was used for both reduction and extraction. The solvent extraction was carried out on a Iwaki universal mechanical shaker, Model V-S. The radioactivity was measured by means of a Kobe Kogyo well-type scintillation counter.

Procedure. The experimental procedures were as follows, unless otherwise noted. Pa(V) was reduced by means of a liquid zinc amalgam in the presence of 10^{-2} M Cr(III), as has been described in a previous report.[4] After the liquid zinc amalgam has been removed from the cell, the solvent extraction was carried out on a mechanical shaker for 25 min. The initial volumes of both the organic and the aqueous phases were 5.0 *ml*. The organic phase was pre-equilibrated by contact with its opposite. After the two phases had completely separated, an aliquot of each phase was transferred into a polyethylene test tube and its γ-radioactivity counted. The distribution ratio (D) was calculated by the following equation:

$$D = \frac{\gamma\text{-activity per ml of the organic phase}}{\gamma\text{-activity per ml of the aqeous phase}}$$

The concentration of protactinium was 10^{-7} M, and the ionic strength was kept constant at 0.50 throughout this experiment. The hydrogen ion concentration of

1) R. Guillaumont, *Bull. Soc. Chim. France*, **1965**, 1416.
2) R. Guillaumont, *ibid.*, **1965**, 4739.
3) T. Mitsuji, This Bulletin, submitted.
4) T. Mitsuji. *ibid.*, in press.
5) S. Suzuki and Y. Inoue, *ibid.*, **39**, 490 (1966).

the aqueous phase in equilibrium was determined by titration with the standard sodium hydroxide solution.

Results

The Confirmation of the Valency State of Protactinium. The protactinium which had been extracted into the benzene phase was back-extracted into the aqueous phase and then subjected to the thorium fluoride method described in a foregoing paper.[3] More than 95% of protactinium was always co-precipitated with thorium fluoride. This means that protactinium remains tetravalent during solvent extraction.

Solvent Extraction from Perchlorate and Chloride Solutions. The TTA extraction of Pa(IV) was first carried out in a perchlorate solution as a non-complexing solvent. The relationship between the TTA concentration and the distribution ratio was examined in 0.37 M perchloric acid. As is shown in Fig. 1, the log-log plot of the distribution ratio and the TTA concentration shows a good linearity, with a slope of 4.

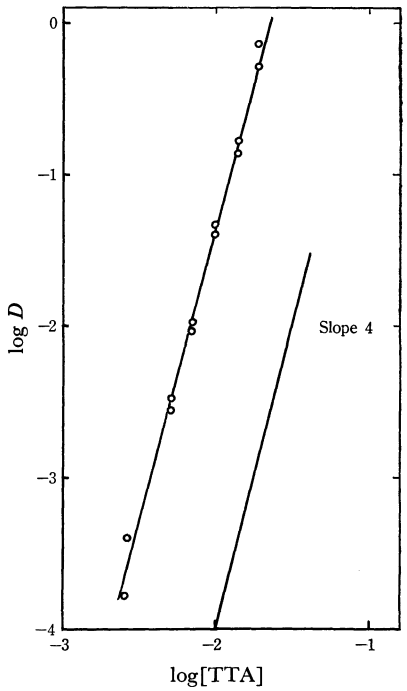

Fig. 1. Relationship between log D and log[TTA], 0.37 M $HClO_4$.

The effect of the hydrogen ion concentration on the extraction was examined by using a 10^{-2} M TTA-benzene solution. As Fig. 2 shows, the relationship between log D and $-\log[H^+]$ is linear, with a slope of 2, over the $-\log[H^+]$ range from 0.4 to 1.1.

The same experiments were also carried out in a chloride solution. The acid dependency of the distribution ratio was found to be second-power, as Fig. 3 shows.

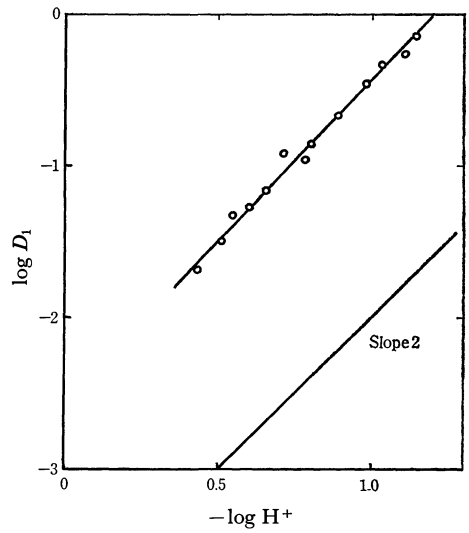

Fig. 2. Dependence of log D_1 on $-\log[H^+]$ in the extraction from perchlorate solution.

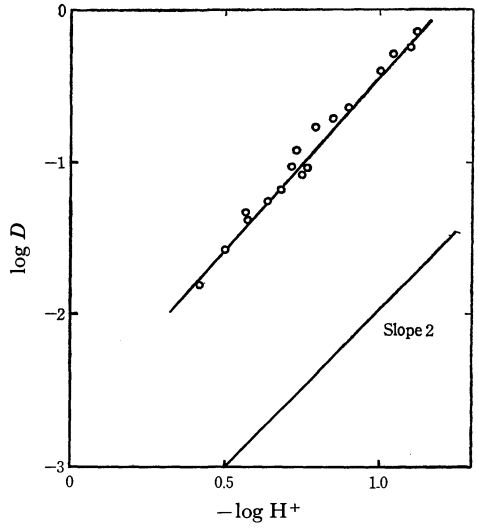

Fig. 3. Dependence of log D on $-\log[H^+]$ in the extraction from chloride solution.

Solvent Extraction from Sulfate Solution. To confirm the existence of sulfato-complexes of Pa(IV), solvent extraction was performed in a sulfate solution. The relationship between the TTA concentration and the distribution ratio was examined in 0.24 M sulfuric acid. The plot of the logarithm of the distribution ratio against the logarithm of the TTA concentration shows a linear relationship, with a slope of 4 (Fig. 4).

The relation of log D *versus* $-\log[H^+]$ was also investigated at a TTA concentration of 10^{-2} M. Figure 5 shows the linear relationship between them, with a slope of 2.

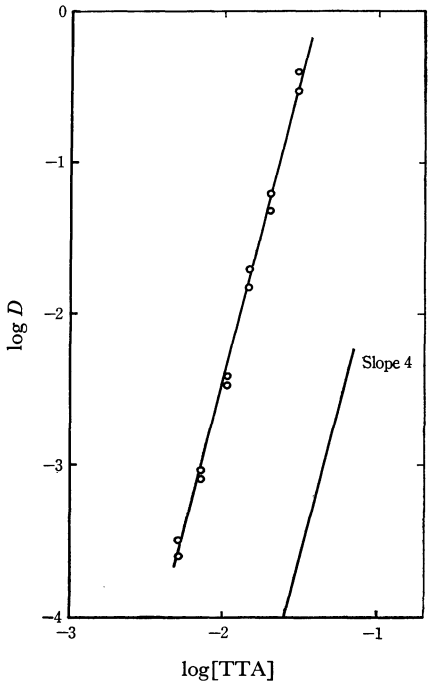

Fig. 4. Relationship between log D and log[TTA], 0.24 M H_2SO_4.

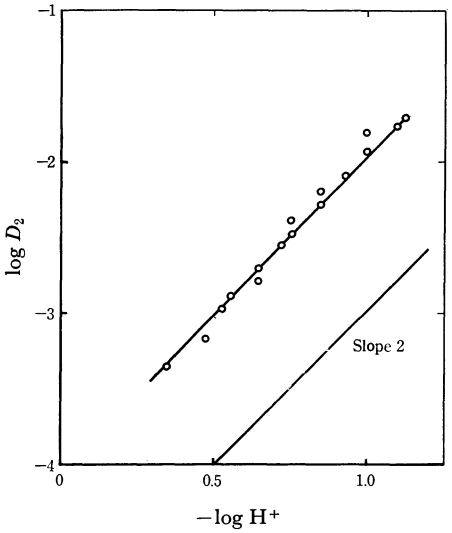

Fig. 5. Dependence of log D_2 on $-\log[H^+]$ in the extraction from sulfate solution.

Discussion

If the species extractable into the organic phase are considered to be non-charged, the general equation for the TTA extraction of Pa(IV) from the perchlorate solution can be written as follows:

$$Pa(OH)_m^{(4-m)+} + 4HT \rightleftharpoons PaT_4 + mH_2O + (4-m)H^+ \quad (1)$$

where HT represents the TTA molecule and T, the enolate ion of TTA.

If the activity coefficients of all the species are assumed to be constant, the equilibrium constant, k_1, can be defined as:

$$k_1 = \frac{[PaT_4][H_2O]^m[H^+]^{(4-m)}}{[Pa(OH)_m^{(4-m)+}][HT]^4} \quad (2)$$

where square brackets are used to represent the concentration of the relevant species.

Supposing only one kind of protactinium species exists in the aqueous solution, the distribution ratio can be defined as follows:

$$D_1 = \frac{[PaT_4]}{[Pa(OH)_m^{(4-m)+}]} \quad (3)$$

As the solvent extraction was performed at a constant temperature and with a constant TTA concentration, both k_1 and HT are constant. Under these conditions, the following equation is obtained by substituting Eq. (2) into Eq. (3) and taking the logarithm:

$$\log D_1 = -(4-m)\log[H^+] + \text{const.} \quad (4)$$

As may be seen in Fig. 2, the slope of the log-D_1—log $[H^+]$ plot is minus 2; that is, $(4-m)$ is equal to 2. Therefore, the protactinium species in the perchlorate solution may be in the form of $Pa(OH)_2^{2+}$ over the $-\log[H^+]$ range studied; one can then describe the extraction reaction as:

$$Pa(OH)_2^{2+} + 4HT \rightleftharpoons PaT_4 + 2H_2O + 2H^+ \quad (1')$$

This finding is in agreement with the finding of Guillaumont.[1]

On the other hand, the D-values in the extraction from the chloride solution were almost equal to the corresponding D-values in the extraction from the perchlorate solution. Therefore, Pa(IV) is probably reluctant to form chloro-complexes in dilute hydrochloric acid and may be predominantly in the form of $Pa(OH)_2^{2+}$ in the acidity range studied. This finding is in good agreement with the finding of the absorption spectroscopy undertaken by the present author.[3]

The general equation for the TTA extraction of Pa(IV) from a sulfate solution can be expressed as:

$$Pa(SO_4)_n(OH)_m^{(4-2n-m)+} + 4HT \rightleftharpoons PaT_4 + nHSO_4^- + mH_2O + (4-m-n)H^+ \quad (5)$$

The extraction constant k_2 equals:

$$\frac{[PaT_4][HSO_4^-]^n[H_2O]^m[H^+]^{(4-m-n)}}{[Pa(SO_4)_n(OH)_m^{(4-2n-m)+}][HT]^4} \quad (6)$$

On the assumption that only one kind of protactinium species is predominant in dilute sulfuric acid, the distribution ratio can be expressed as:

$$D_2 = \frac{[PaT_4]}{[Pa(SO_4)_n(OH)_m^{(4-2n-m)+}]} \quad (7)$$

By substituting Eq. (6) into Eq. (7), and by taking the logarithm, the following equation is obtained, provided both k_2 and HT are constant:

$$\log D_2 = -n\log [HSO_4^-] - (4-m-n)\log [H^+] + \text{cost.} \quad (8)$$

Let us now consider the dissociation of H_2SO_4. As H_2SO_4 is a strong acid, it is completely dissociated to HSO_4^- or SO_4^{2-} in a dilute aqueous solution.

$$HSO_4^- \rightleftharpoons SO_4^{2-} + H^+ \quad (9)$$

$$K = \frac{[SO_4^{2-}][H^+]}{[HSO_4^-]} \quad (10)$$

As pK is equal to 2.0,[6] Eq. (10) may be rewritten as follows:

$$\log \frac{[HSO_4^-]}{[SO_4^{2-}]} = 2 + \log [H^+] \quad (11)$$

When $-\log [H^+]$ is varied from 0.5 to 1.0, the ratio of $[HSO_4^-]$ to $[SO_4^{2-}]$ changes from about 32 to 10. Therefore, all the sulfuric acid is considered to be present as HSO_4^- over the entire $-\log [H^+]$ range studied. This, in turn, results in a constant concentration of HSO_4^-, regardless of the acidity. Hence, Eq. 8 may be rewritten as follows:

$$\log D_2 = -(4-m-n)\log [H^+] + \text{const.} \quad (8')$$

The coefficient of the first term of this equation, $-(4-m-n)$, should be 2, as is shown in Fig. 5; that is, $m+n=2$. Therefore, the possible protactinium species in a sulfuric acid solution are:

1) $m=0$, $n=2$, $Pa(SO_4)_2$
2) $m=1$, $n=1$, $Pa(SO_4)(OH)^+$
3) $m=2$, $n=0$, $Pa(OH)_2^{2+}$

It is unlikely that no change species such as $Pa(SO_4)_2$ is extracted into the benzene phase by TTA. It is also clear from Fig. 5 and Fig. 2 that the sulfato-complex of Pa(IV) exists. Therefore, the most probable ionic species may be considered to be $Pa(SO_4)(OH)^+$; Eq. (5) then becomes:

$$Pa(SO_4)(OH)^+ + 4HT \rightleftharpoons PaT_4 + HSO_4^- + H_2O + 2H^+ \quad (5')$$

The formation of the sulfato-complex of Pa(IV) can be expressed as:

$$Pa(OH)_2^{2+} + HSO_4^- \rightleftharpoons Pa(SO_4)(OH)^+ + H_2O \quad (12)$$

In the above equation, the equilibrium constant, k_3, may be defined as:

$$k_3 = \frac{[Pa(SO_4)(OH)^+][H_2O]}{[Pa(OH)_2^{2+}][HSO_4^-]} \quad (13)$$

6) G. Charlot, "L'analyse qualitative et les reactions en solution," Masson et Cie, Parris (1957).

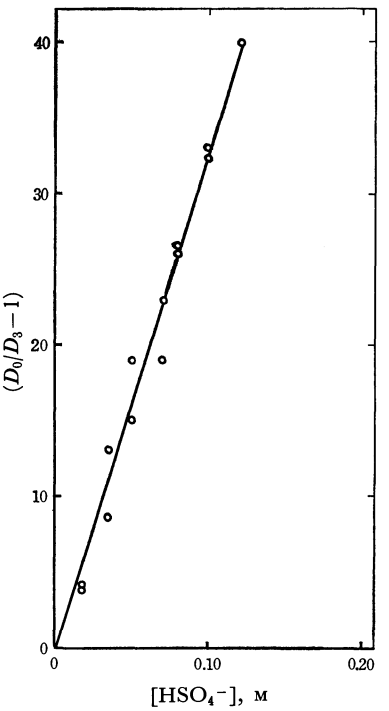

Fig. 6. Relationship between (D_0/D_3-1) and $[HSO_4^-]$ at pH of 0.50.

Since the extracted species from both the perchlorate solution and the sulfate solution is PaT_4, and since the protactinium species in the perchlorate solution and the sulfate solution are $Pa(OH)_2^{2+}$ and $Pa(SO_4)(OH)^+$ at a pH value of 0.5, the distribution ratio in various mixtures of perchlorate solutions and sulfate solutions at a constant pH can be defined as:

$$D_3 = \frac{[PaT_4]}{[Pa(OH)_2^{2+}] + [Pa(SO_4)(OH)^+]} \quad (14)$$

By substituting Eq. (13) into Eq. (14) and by rearranging, the following equation is introduced:

$$D_0/D_3 - 1 = k_3[HSO_4^-] \quad (15)$$

where D_0 represents the distribution ratio in the absence of the complexing anion, HSO_4^-. The relationship between (D_0/D_3-1) and $[HSO_4^-]$ was examined at the pH value of 0.50 and at 10°C. As is shown in Fig. 6, the plot of (D_0/D_3-1) *versus* the concentration of sulfate ions has a straight line, with a slope of 320. This supports finding that $Pa(SO_4)(OH)^+$ exists; the equilibrium constant, k_3, was determined to be 320 from the slope of the straight line.

Summary

1) The TTA extraction behavior of Pa(IV) was investigated in perchloric, hydrochloric, and sulfuric acid solutions (pH 0.4—1.1).

2) $Pa(OH)_2^{2+}$ was the most probable ionic species in the perchlorate solution, and the extraction reaction was considered tobe:

$$Pa(OH)_2^{2+} + 4HT \leftrightharpoons PaT_4 + 2H_2O + 2H^+$$

3) Pa(IV) was reluctant to form the chlorocomplexes and was considered to be in the form of $Pa(OH)_2^{2+}$ in the dilute hydrochloric acid solution.

4) $Pa(SO_4)(OH)^+$ was the most probable ionic species in the sulfuric acid solution. The extraction reaction into the benzene phase was considered to proceed as follows:

$$Pa(SO_4)(OH)^+ + 4HT \rightleftharpoons PaT_4 + HSO_4^- + H_2O + 2H^+$$

5) In the sulfuric acid solution used as a complexing agent, the following complexing reaction was considered to take place:

$$Pa(OH)_2^{2+} + HSO_4^- \rightleftharpoons Pa(SO_4)(OH)^+ + H_2O$$

and its equilibrium constant was determined to be 320 at the ionic strength of 0.50 (temperature 10 ± 0.5°C).

This author wishes to thank Professor Hidehiro Goto, Professor Shin Suzuki, and Dr. Yasushi Inoue for their kind and valuable advice throughout this study. A part of the expense has been defrayed by a grant-in-aid from the Ministry of Education.

BULLETIN OF THE CHEMICAL SOCIETY OF JAPAN VOL. 41 119—126 (1968)

Effect of the Counter-Electrode Material on the Emission Spectrochemical Determination of Silicon and Manganese in Steel

Takanori SUZUKI*1 and Tomihito KAMBARA

Department of Chemistry, Faculty of Science, Hokkaido University, Sapporo

(Received July 10, 1967)

The line intensities of Si and Mn appear much more strongly in the spectrochemical analysis of high-carbon low-alloy steels when a low-voltage spark is employed. Considering the change in the line intensity with the time under various excitation conditions with graphite and zinc counter-electrodes, the present authors have established an improved method for the spectrochemical determination of Si and Mn. The effect of the heat-treatment on the metallurgical structure has been investigated by means of an electron-probe microanalyzer, and the results compared with the spectrochemical data.

The accuracy of an emission spectrochemical determination is influenced by many factors, such as the fractional distillation, the excitation conditions, self-absorption, and third-element effects. These complicated factors are generally called the matrix effect, which has been discussed in many articles.[1-5] In the analysis of iron and steel, one must also take metallurgical hysteresis and the structure of the specimen into consideration. Several investigations dealing with the matrix effects in special steels[6-11] have been reported, and solution methods[12-13] and powder

*1 Present address: Muroran Plant, Japan Steel Works (Nihon Seikosho, Ltd.), Muroran.

1) L. H. Ahrens and S. R. Taylor, "Spectrochemical Analysis," 2nd Ed., Chapt. 9 and 10, Addison-Wesley Co., Massachusetts (1961).

2) B. F. Scribner and M. Margoshes, "Emission Spectroscopy," in "Treatise on Analytical Chemistry," Part 1, Vol. 6, ed. by I. M. Kolthoff and P. J. Elving, Interscience-Wiley, New York (1965), pp. 3347—3461.

3) V. A. Fassel, lecture translated into Japanese by H. Kamada, *Bunseki Kagaku (Japan Analyst)*, **12**, 73, 187 (1963).

4) T. Nakajima, "Emission Spectrochemical Analysis," (in Japanese), article in "Shin Bunseki Kagaku Koza," Vol. 3, Kyoritsu-Shuppan, Tokyo (1960), pp. 203—265.

5) E. Minami and R. Ishida, "Emission Spectrochemical Analysis," (in Japanese), article in "Bunseki Kagaku Koza," Vol. 8-C, Kyoritsu-Shuppan, Tokyo (1957), p. 91.

6) R. Ishida, T. Nakajima and T. Koizumi, *Bunko Kenkyu (J. Spectr. Soc. Japan)*, **6**, 15 (1957).

7) H. Iijima, *ibid.*, **4**, 3 (1956).

8) K. Yoshino, S. Sakai and M. Kaneko, *ibid.*, **10**, 45 (1961).

9) H. Nemoto and S. Kuramoto, *ibid.*, **12**, 236 (1964).

10) S. Maekawa and T. Suzuki, *Bunseki Kagaku (Japan Analyst)*, **14**, 424 (1965).

11) T. Hamaguchi and N. Nakao, *Bunko Kenkyu (J. Spectr. Soc. Japan)*, **6**, 13 (1957).

12) H. A Heller and R. W. Lewis, *Anal. Chem.*, **25**, 1038 (1953).

13) A. Bordocz and F. Varsanyi, *ibid.*, **28**, 989 (1956).

Table 1. Low and high voltage spark (LVS and HVS) excitation conditions

No.	Spectrograph	Primary voltage Volt	Secondary voltage Volt	Capacity μF	Inductance μH	Resistance Ω	Counter-electrode	Estimated temp. K°
LVS	GQ-220		870	10	50	1.25	Graphite	—
HVS 1	GQ-220	150	16500	0.007,0	0	0	Zinc	—
HVS 2	GQ-220	150	16500	0.007,0	100	0	Graphite and zinc	—
HVS 3	GE-340	70	10500	0.006,6	800	0	Graphite	5170—5430
HVS 4	GE-340	70	10500	0.006,6	80	0	Graphite	5540—5730
HVS 5	GE-340	70	10500	0.006,6	80	0	Zinc	6380—6610

methods[14-16] have both been proposed in order to overcome the above-mentioned difficulties.

The results of the spectrochemical determination of silicon and manganese in high-carbon low-alloy steel have now been found to depend remarkably on the metallurgical structure. In the present study the excitation conditions for a more accurate determination will be examined.

Experimental

Apparatus. A direct-reading Quantorecorder (GQ-220) and an Ebert-mounting grating spectrograph (GE-340), both made by Shimadzu, were employed. The spark was generated by means of a multisource Feussner equipment. In the photographic measurement of line intensities, a microphotometer was used. The electron-probe microanalyzer was a product of the Japan Electron Optics Laboratory (Nihon Denshi), type JXA-304.

Electrodes. The steel specimens were used as the plane self-electrodes. As the counter-electrodes we employed graphite rods, 6 mm in diameter and 120° in cone angle, and zinc rods, 5 mm in diameter and 80° in cone angle, prepared by casting metal 99.9% pure.

Excitation Conditions. Six conditions were chosen for the determination of silicon and manganese; they are listed in Table 1.

Analytical Lines. The characteristics of the spectral lines utilized for the quantitative analysis are listed in Table 2. All the manipulations were done according to the Japanese Industrial Standards.[17]

Table 2. Analytical lines

Wavelength of analytical line Å	Excitation voltage, eV	Spectrograph used
Fe II 2714.41	7.90	GQ-220
Si I 2516.12	8.12	GQ-220
Mn II 2933.06	12.83	GQ-220, GE-340
Fe II 2926.59	13.12	GE-340
Si I 2881.58	5.08	GE-340
Fe I 2874.17	4.31	GE-340
Fe 2880.76	13.19	GE-340

14) E. K. Jaycox, *ibid.*, **28**, 1544 (1956).
15) J. Y. Ellenburg, *ibid.*, **34**, 230 (1962).
16) I. Taira, *Bunko Kenkyu (J. Spectr. Soc. Japan)*, **6**, 23 (1957).
17) JIS K-0116 (1965) General Rules on the Emission Spectrochemical Analysis.

Results and Discussion

Results Obtained with the Direct-reading Quantorecorder. Quenched and annealed specimens of five steel samples were analyzed spectrochemically for several elements by means of the working curves prepared for routine analysis with a series of BCS standard steels. The results are tabulated in Table 3. The results of the standard chemical analysis are given in Table 4 for comparison.

It can be seen that the spectrochemical results for nickel, chromium, copper, and molybdenum agree well with the values obtained by the standard chemical analysis. However, remarkable positive deviations were found for silicon and manganese, especially with the quenched specimens. In the LVS excitation with a graphite counter-electrode it was found that the spark did not focus well. The change in the line intensities with the time was measured by changing the presparking time, as is shown in Fig. 1. Both silicon and manganese always showed stronger intensities than the theoretical values throughout the 360-sec presparking time. When a zinc rod was used as the counter-electrode, the intensities of not only silicon and

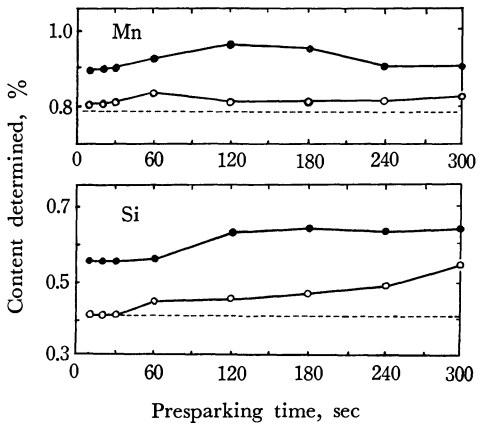

Fig. 1. Change of line intensity. Excitation condition LVS. Sample No. 2. ○ Annealed and ● quenched specimen. The horizontal dashed lines show the contents determined by the standard chemical analysis. Analytical lines: Fe 2714, Si 2516, Mn 2933 Å.

TABLE 3. ANALYTICAL RESULTS OBTAINED WITH LVS EXCITATION

Sample No.[a]	Si, %		Mn, %		Ni, %		Cr, %		Cu, %		Mo, %	
	Found	d[b]	Found	d	Found	d	Found	d	Found	d	Found	d
1Q	0.55	+0.15	1.30	+0.35	0.15	0	1.06	+0.01	0.18	−0.01	0.39	+0.01
1A	0.43	+0.03	1.10	+0.15	0.14	−0.01	1.04	−0.01	0.17	−0.02	0.37	−0.01
2Q	0.55	+0.14	0.90	+0.14	0.28	−0.01	1.08	−0.02	0.12	0	0.31	−0.01
2A	0.40	−0.01	0.85	+0.09	0.28	−0.01	1.07	−0.03	0.11	−0.01	0.30	−0.02
3Q	0.64	+0.09	1.10	+0.11	0.15	0	1.04	−0.01	0.13	−0.01	0.38	0
3A	0.53	−0.02	1.06	+0.07	0.15	0	1.03	−0.02	0.13	−0.01	0.36	−0.02
4Q	0.46	+0.10	0.95	+0.07	0.11	+0.01	1.00	0	0.13	−0.01	0.33	−0.01
4A	0.37	+0.01	0.89	+0.01	0.11	+0.01	0.98	−0.02	0.13	−0.01	0.33	−0.01
5Q	0.67	+0.13	1.16	+0.20	0.14	+0.01	0.98	+0.01	0.11	−0.01	0.34	+0.01
5A	0.52	−0.02	1.05	+0.09	0.12	−0.01	0.99	+0.02	0.12	0	0.32	−0.01

a) Q=quenched, A=annealed specimen.
b) d=difference of spectrochemical data from those obtained by standard chemical analysis.

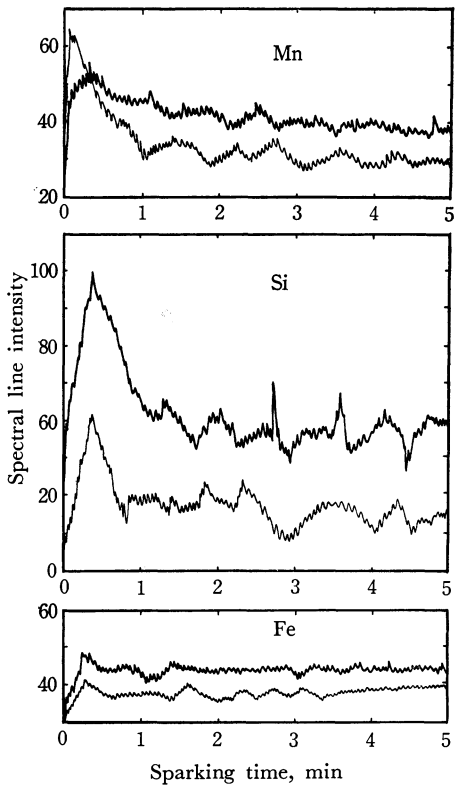

Fig. 2. Change of line intensity. Excitation condition HVS 1. Sample No. 2. Fine line indicates the annealed specimen and bold line the quenched. Analytical lines are the same as in Fig. 1.

manganese but also of iron decreased considerably.

Since the annealed specimen behaves differently from the quenched specimen, it may be supposed that the change in metallurgical structure has caused a matrix effect.

Figures 2, 3, and 4 show the changes in the spectral line intensities with the time under the excitation conditions of HVS 1 and 2, listed in Table 1. With HVS 1 the Fe 2714 Å line intensity is stable, but the lines of silicon and manganese fluctuate, as Fig. 2 shows. Figures 3 and 4 obviously show that the spectral lines of the three elements show stable intensities after 3 min. Thus, it may be safe to say that the interference by the metallurgical structure can well be eliminated under the HVS 2 excitation condition.

Results Obtained with the Ebert-mounting Spectrograph. The intensity ratios for iron-silicon and iron-manganese couples were measured, with varying presparking times, under the excitation conditions of HVS 3, 4, and 5. The results are illustrated in Figs. 5, 6, and 7 respectively. With a graphite counter-electrode, the stabilization of the line intensity ratio takes about 3 min, while with a zinc electrode the persistent and stable intensity ratio can be attained within 2 min.

Measurement of the Spark Temperature. Let us now discuss the ionization equilibrium in the gas phase on the basis of the famous Saha equation.[18] Provided that the light source is thermally equilibrated, one has for the radiation intensity, I, of a spectral line the following expression:[1-5]

$$I = A\boldsymbol{h}\nu N_0 \cdot \frac{g}{g_0} \cdot \exp\left(\frac{-E}{\boldsymbol{k}T}\right) \qquad (1)$$

Here, A is the transition probability; ν, the frequency of the spectral line; N_0, the number of atoms or ions in the ground state; g and g_0, the statistical weights for the activated and ground states respectively and E, the excitation potential, while $\boldsymbol{h}$, $\boldsymbol{k}$, and T have their usual significances. In the Gerlach internal standard method, therefore, the two line intensities, I_1 and I_2, of two elements are related by:

18) M. N. Saha, *Phil. Mag.*, (6) **40**, 472 (1920).

TABLE 4. RESULTS OBTAINED BY THE STANDARD CHEMICAL ANALYSES

Sample No.	Si, %	Mn, %	Ni, %	Cr, %	Cu, %	Mo, %	C, %
1	0.40	0.95	0.15	1.05	0.19	0.38	1.20
2	0.41	0.76	0.29	1.10	0.12	0.32	1.21
3	0.55	0.99	0.15	1.05	0.14	0.38	1.42
4	0.36	0.88	0.10	1.00	0.14	0.34	1.17
5	0.54	0.96	0.13	0.97	0.12	0.33	1.37

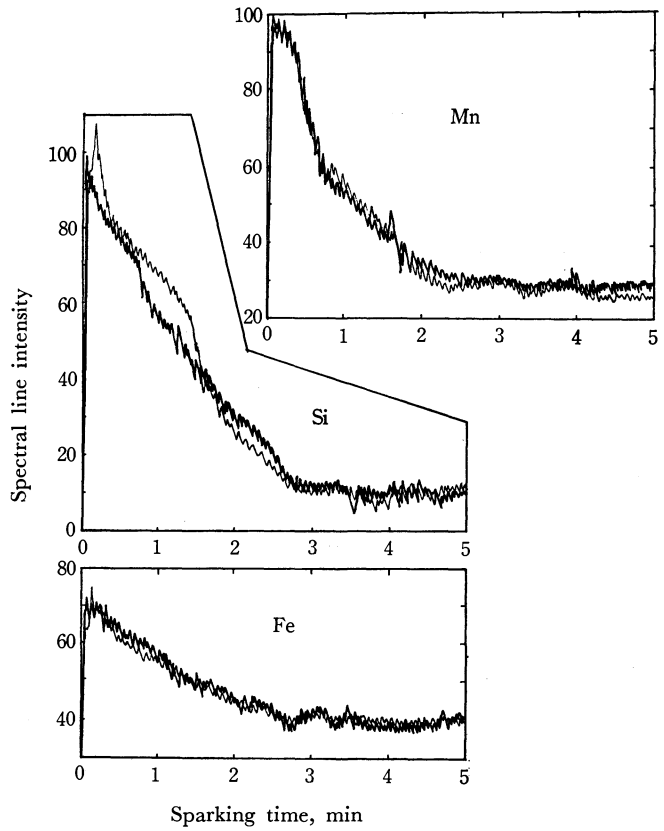

Fig. 3. Change of line intensity. Excitation condition HVS 2 with a graphite counter-electrode. Others are the same as in Fig. 2.

$$\frac{I_1}{I_2} = \text{const} \cdot \frac{N_1}{N_2} \cdot \exp\left\{\frac{-(E_1-E_2)}{kT}\right\} \qquad (2)$$

If the two excitation potentials, E_1 and E_2, differ a little, the ratio of line intensities should be proportional to the ratio of the amounts of the two elements.

Several authors[19-21] have reported on the spark temperature as measured by the intensity ratio method. As Ornstein[21] has shown, by taking the logarithm of Eq. (1), one derives:

TABLE 5. SPECTRAL LINES OF IRON EMPLOYED FOR THE TEMPERATURE MEASUREMENT

Wavelength Å	Excitation energy cm^{-1}	νgA[a]	log I HVS 3	log I HVS 4	log I HVS 5
2999.52	40527	309	0.6335	0.7076	0.3979
3024.03	33947	14.1	1.0828	1.1523	0.7993
3030.15	52613	3230	1.4014	1.3324	0.8325
3031.21	52769	2820	1.4914	1.3711	0.8808

a) From Shimazu.[19] See also "American Institute of Physics Handbook," 7-87, McGraw-Hill, New York (1957).

19) M. Shimazu, *Bunko Kenkyu (J. Spectr. Soc. Japan)*, **9**, 81 (1961).
20) Research Group Concerning Spectroscopic Light Sources, H. Kawaguchi *et al.*, *ibid.*, **13**, 1 (1964).
21) L. S. Ornstein, *Physik. Z.*, **32**, 517 (1931).

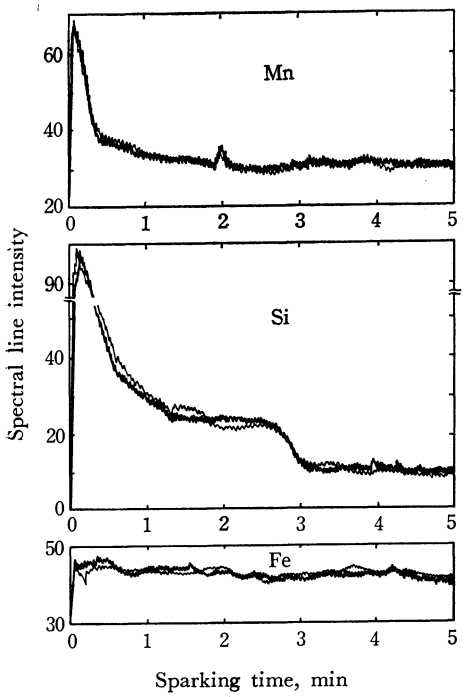

Fig. 4. Change of line intensity. Excitation condition HVS 2 with zinc counter-electrode. Others are the same as in Fig. 2.

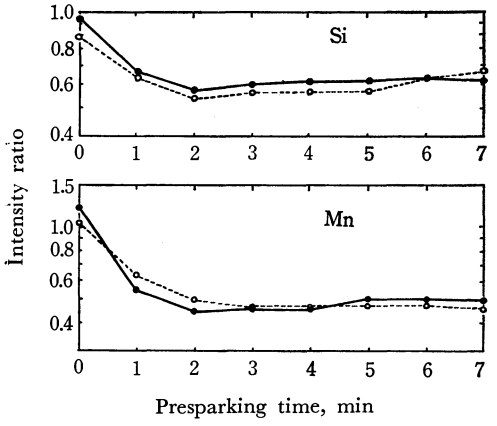

Fig. 5. Change of intensity ratio with time. ○ Annealed and ● quenched specimen. Excitation condition HVS 3. Line pairs are Fe 2880/Si 2881 and Fe 2926/Mn 2933.

$$\log \frac{I}{\nu g A} = \log \frac{N_0 h}{g_0} - \frac{0.625}{T} E' \qquad (3)$$

Here E' is the excitation energy expressed in cm^{-1}. From the slope of the plot of $\log (I/\nu g A)$ against E', we can estimate the light source temperature, as is shown in Fig. 8. The numerical values utilized are listed in Table 5.

A small deviation from linearity is seen in Fig. 8, but such a tendency has already been reported by Shimazu.[19] The estimated temperatures are listed in Table 1.

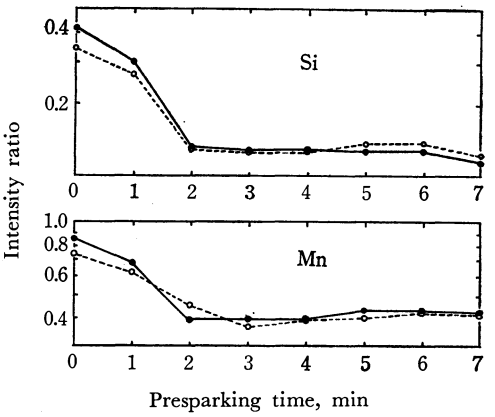

Fig. 6. Change of intensity ratio with time. Excitation condition HVS 4. Others are the same as in Fig. 5.

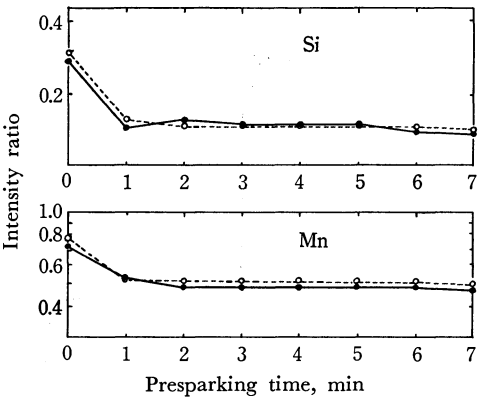

Fig. 7. Change of intensity ratio with time. Excitation condition HVS 5. Others are the same as in Fig. 5.

Metallurgical Structure. The structure of high-carbon low-alloy steel varies with different heat treatments. Figure 9 shows microscopic pictures of this. In many cases cementite appears in a net-structure at the boundaries of the austenite and surrounds the pearlite. Whether silicon and manganese are distributed uniformly or locally was investigated with the aid of an X-ray micro-analyzer. As Fig. 10 shows, it can be concluded that manganese is enriched a little in the cementite phase (from 0.95 to 1.06%) but is depleted in pearlite (from 0.95 to 0.71%). As to the other elements, such as silicon, nickel, chromium, and molybdenum, no appreciable segregation is observed.

Discharge Crater. The property of a spark may be judged by the discharge crater remaining on the iron plane electrode surface. The craters observed on the various counter-electrode materials are shown in Fig. 11. It was found that, with the

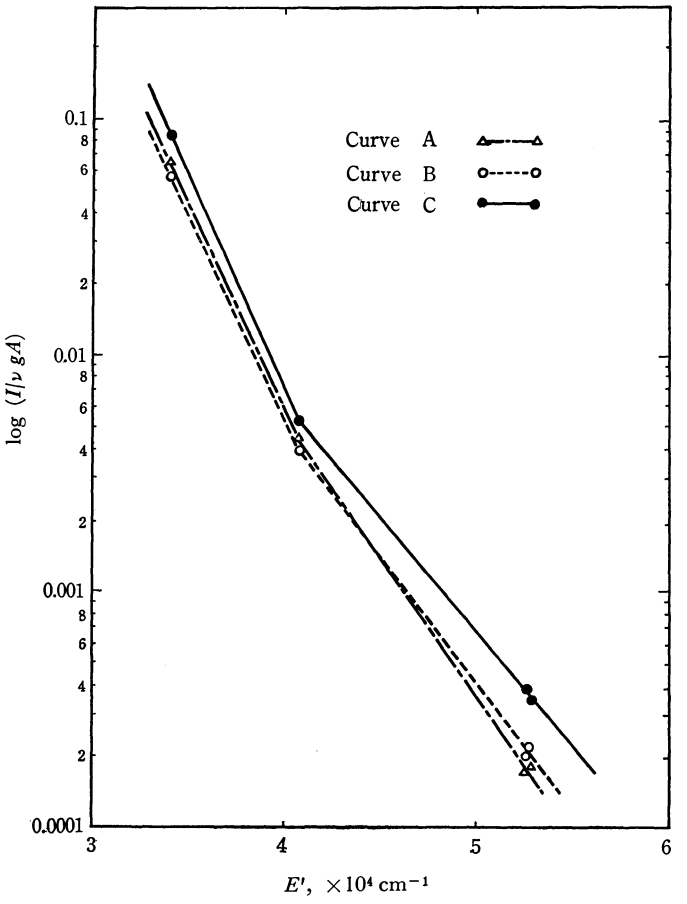

Fig. 8. log $(I/\nu gA)$ plotted against E'. Curve A HVS 3, B HVS 4 and C HVS 5.

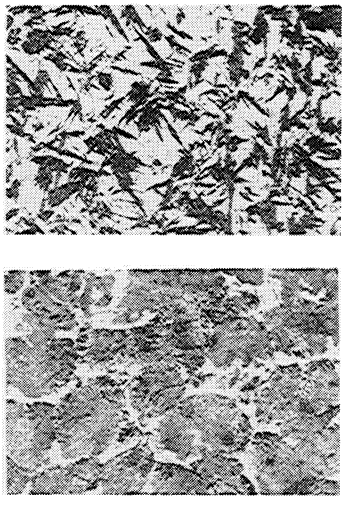

Fig. 9. Microscopic pictures. The sample steel was taken in a steel mould (30 mm diameter 50 mm length). Etched with 1% nitric acid in alcoholic picric acid solution. ×400. The specimens are sample No. 1, water-quenched (upper) and sample No. 2, air-quenched (lower).

zinc electrode, the spark plasma was stable and well-focused. With the graphite electrode, however, the spark tended to dance and to be diffuse. As Table 1 shows, with the zinc electrode the temperature became about 800°K higher than with graphite (HVS 4 and 5).

As for the other electrode materials, with silver the spark does not focus well in the atmospheric environment, while with magnesium, as Fig. 11 shows, although a well-focused and stable spark is attained, the strong lines of Mg 2802, 2928, 2936, and 3092 Å strongly interfere with the determination.

Improved Method of Determination. From the above experimental results, it can be expected that, under the excitation conditions of HVS 2 and 5, one may obtain better determination data than under the conditions of LVS, HVS 1, 3, and 4. Utilizing the series of BCS standard steels, the calibration curves for HVS 2 and 5 were prepared, with which the determination of silicon and manganese was then carried out. The results are tabulated in Tables 6 and 7.

The deviation of the results of the analysis by

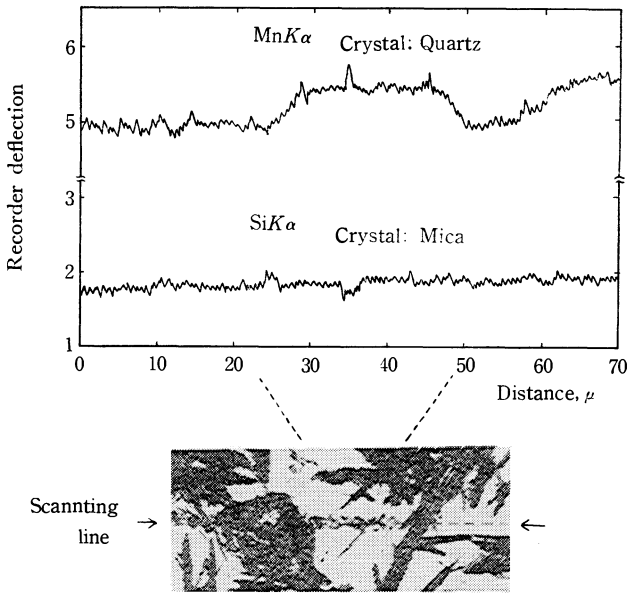

Fig. 10. Analysis by electron probe microanalyzer. The upper curves show the variations of characteristic X-ray intensities and the lower picture the corresponding electron microscopic photograph. The dashed line indicates the scanning line. Acceleration voltage 20 kV. Electron probe diameter 2 μ. Current absorbed by specimen 0.20 μA. Detector: Proportional gas flow counter.

Table 6. Analytical results obtained by HVS 2 excitation with zinc counter-electrode

Sample[1]	Si, %		Mn, %	
	Found	d[2]	Found	d[2]
1Q	0.39	−0.01	0.90	−0.05
	0.39	−0.01	0.92	−0.03
1A	0.42	+0.02	0.85	−0.10
	0.41	+0.01	0.89	−0.06
2Q	0.38	−0.03	0.69	−0.07
	0.37	−0.04	0.70	−0.06
2A	0.39	−0.02	0.74	−0.02
	0.39	−0.02	0.72	−0.04
3Q	0.60	+0.05	0.93	−0.06
	0.58	+0.03	0.96	−0.03
3A	0.55	0	0.94	−0.05
	0.55	0	0.95	−0.04
4Q	0.35	−0.01	0.91	+0.03
	0.35	−0.01	0.90	+0.02
4A	0.34	−0.02	0.88	0
	0.35	0	0.89	+0.01
5Q	0.59	+0.05	0.98	+0.02
	0.60	+0.06	0.97	+0.01
5A	0.52	−0.02	0.99	+0.03
	0.51	−0.03	0.97	+0.01

1) Q=quenched, A=annealed specimen
2) d=difference of spectrochemical data from those obtained by standard chemical analysis.

Table 7. Analytical results obtained by HVS 5 excitation

Sample[1]	Si, %		Mn, %	
	Found	d[2]	Found	d[2]
1Q	0.38	−0.02	0.94	−0.01
1A	0.39	−0.01	0.92	−0.03
2Q	0.40	−0.01	0.77	+0.01
2A	0.41	0	0.78	+0.02
3Q	0.53	−0.02	0.97	−0.02
3A	0.54	−0.01	0.97	−0.02
4Q	0.35	−0.01	0.89	+0.01
4A	0.34	−0.02	0.90	+0.02
5Q	0.52	−0.02	0.93	−0.03
5A	0.53	−0.01	0.92	−0.04

1) and 2) same as in Table 6.

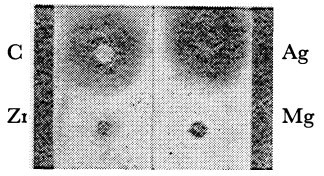

Fig. 11. Variation of the spark discharge craters produced on the iron plane electrode with varying counter-electrode materials. Excitation condition HVS 5.

the spectrochemical method from the results obtained by the standard chemical analysis is treated statistically. The familiar Student t test has already been applied to test the difference between the means obtained by the two methods in a number of analyses of specimens differing in their composition.[22]

The results of the t tests are tabulated in Table 8. The distinct deviations of the silicon and manganese determinations by LVS from the data obtained by the standard chemical analyses are obviously much improved by applying HVS 5, only the silicon determination still showing a significant difference. Under the strong excitation conditions with HVS 2, the observed t_0-value being less than the t-value in the table, no difference between the means can be seen at the significant level of 5%.

TABLE 8. THE t TESTS

Excitation condition	t from table ($\alpha=0.05$)	Degree of freedom	Heat treatment	t_0 for Si	t_0 for Mn
LVS	2.776	4	Q	*10.517*	*4.000*
			A	0.208	*3.644*
HVS 2 (Zn)	2.262	9	Q	0.701	1.964
			A	1.489	2.080
HVS 5	2.776	4	Q	*6.530*	1.025
			A	2.577	0.793

Note. Italic figures indicate $t_0>t$, *i. e.* there is a significant difference between two means.

22) V. V. Nalimov, "The Application of Mathematical Statistics to Chemical Analysis," translated from Russian by P. Basu and edited by M. Williams, Pergamon, Oxford (1963), p. 103.

Conclusion

The remarkable positive deviation in the determination data of silicon and manganese in high-carbon low-alloy steel when analyses are carried out under low-voltage excitation conditions is due to the matrix effect caused by the differences in the volatilization rate and the degree of ionization or excitation in the spark plasma, *etc.* The metallurgical structure of the sample steel clearly affects the analytical results. The application of the high-voltage spark with a zinc counter-electrode results in a much stronger excitation and permits an accurate determination to be made, that is not interferred with by the metallurgical structure.

The authors wish to express their heartfelt thanks to Drs. Shimoda and Maekawa of the Japan Steel Works, Muroran, Dr. Matsumae of the Government Industrial Development Laboratory-Hokkaido, and Professors Niwa and Matsubara and Dr. Kasamatsu of Hokkaido University for their kind help and support throughout this study.

BULLETIN OF THE CHEMICAL SOCIETY OF JAPAN VOL. 41 127—130 (1968)

Spectrophotometric Study of Metal Chelates of Eriochrom Black T (BT). II. Solution Equilibria between BT and Lead(II)-Nitrilotriacetate (NTA) or Cadmium(II)-*N'*-(Hydroxyethyl)-ethylenediamine-*N*, *N*, *N'*-triacetate (EDTA-OH)

Mutsuo KODAMA and Chifumi SASAKI

Department of Chemistry, Ibaraki University, Mito, Ibaraki

(Received July 12, 1967)

The solution equilibria between BT and lead(II)-NTA or cadmium(II)-EDTA-OH chelates were studied spectrophotometrically, and the composition and the stability constants of the BT chelates of these metal ions were determined. In the presence of an excess amount of NTA or EDTA-OH, lead(II) and cadmium(II) ions join with BT to form a chelate with a 1-to-1 composition. The magnitude of the stability constants ($10^{13.19}$ and $10^{12.74}$ respectively, $\mu=0.30$) can explain satisfactorily the well-known experimental fact that BT can be used as a metallochromic indicator in Pb(II)- and Cd(II)-EDTA titrations.

In a previous paper,[1] the stability constants of the zinc(II)- and copper(II)-BT chelates with a 1-to-1 composition were determined by measuring spectrophotometrically the concentration of uncomplexed and complexed BT, which are in equilibrium with the chelon (NTA or EDTA-OH) and its metal chelates in the solution.

In this paper, the results of a spectrophotometric study of the solution equilibria between BT and the lead(II)-nitrilotriacetate or cadmium(II)-EDTA-OH chelate and of a determination of the compositions and the stability constants of the BT chelates of these metal ions will be presented.

From the viewpoint of the chemical equilibrium, a theoretical consideration of the use of BT as a metallochromic indicator in the EDTA titrations of lead(II)[2] and cadmium(II)[3] will also be presented.

Lead(II) and cadmium(II) ions were found to form exclusively chelates with a 1-to-1 composition with BT in the presence of an excess of NTA or EDTA-OH, the magnitude of their stability constants can successfully explain the well-known fact that BT dye is a useful indicator in the EDTA titrations of lead(II) and cadmium(II) and fulfills the titrimetric requirements theoretically expected.

Experimental

Apparatus and Procedure. The apparatus (spectrophotometer and pH meter) and the experimental procedure employed were the same as have been described previously.[1]

Reagents. Commercial Eriochrom Black T (BT) was purified by the procedure proposed by Diehl and Lindstrom.[4] The way of preparing the standard solution of cadmium(II) perchlorate was described in the previous paper.[1] The concentration of the cadmium(II) solution was determined by EDTA titration, using BT as an indicator.[3] A standard solution of lead(II) was prepared by dissolving a known amount of pure lead(II) nitrate (analytical-reagent grade) into redistilled water. The concentration was standardized against a standard CyDTA solution.[5] The preparation and the standardization of nitrilotriacetic acid (NTA) have been described previously.[1] Reagent grade *N'*-(hydroxyethyl)ethylenediamine-*N*, *N*, *N'*-triacetic acid (EDTA-OH) recrystallized from water was used. The concentration of its solution was standardized against a standard copper(II) solution by titration using murexide as an indicator.

All the other chemicals used were of an analytical-reagent grade, and all the absorption and pH measurements were conducted on solution with an ionic strength of 0.30 with sodium perchlorate.

Results and Discussion

Determination of Stability Constants of Lead(II)- and Cadmium(II) Chelates of BT. The solution equilibria between BT and the lead(II)-NTA or cadmium(II)-EDTA-OH chelate were studied over the pH range from 8.50 to 10.50. In this pH range, the solution containing free NTA or EDTA-OH is considered to have a buffer capacity sufficient to keep the pH value

1) M. Kodama and H. Ebine, This Bulletin, **40**, 1857 (1967).
2) H. Flaschka and F. Huditz, *Z. anal. Chem.*, **137**, 172 (1952).
3) W. Biedermann and G. Schwarzenbach, *Chimia (Switz.)*, **2**, 56 (1948).
4) H. Diehl and F. Lindstrom, *Anal. Chem.*, **31**, 414 (1959).
5) C. A. Geotz and F. J. Debbrecht, *ibid.*, **27**, 1972 (1955).

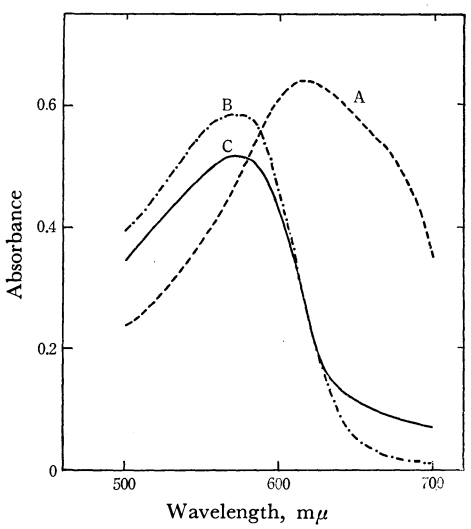

Fig. 1. Absorption curves.
A) 2.00×10^{-5} M BT, 10.0 mM EDTA, $\mu=0.30$ pH=9.50
B)**2.00×10^{-5} M BT, 30 mM NTA, 30 mM Cd(II), $\mu=0.30$, pH=10.0
C) 2.00×10^{-5} M BT, 30 mM NTA, 25 mM Pb(II), $\mu=0.30$, pH=9.65
** The complete displacement of NTA from its chelate by BT and the formation of CdD^- were confirmed by the present authors.

of the solution constant. For this reason, no other buffer reagent was used in this study.

The absorption spectra of uncomplexed and complexed BT were given in Fig. 1. These absorption spectra clearly suggest that the concentrations of BT and its chelates can be determined successfully by measuring the absorbancy at the wavelength of either 630 or 640 mμ.

Lead(II) ion has been reported to form only a 1-to-1 chelate, PbZ^-, with NTA under usual experimental conditions.[6] The cadmium(II) ion also forms exclusively chelate with a 1-to-1 composition with EDTA-OH.[7] Therefore, under the present pH conditions, the chemical equilibrium between BT and lead(II)-NTA or cadmium(II)-EDTA-OH can be written as follows:

$$HD^{2-} + MZ^{2-n} = MD^- + Z^{n-} + H^+ \quad (1)$$

where Z^{n-} refers to completely-dissociated chelon species.

For this equilibrium, thermodynamically Eq. (2) can be derived as in the case of the Cu(II)-CyDTA-BT system.[1]

$$\log\frac{A_D - A}{A - A_{MD}} = \log\frac{K_{MD}\cdot(\alpha_H)_z}{K_{MZ}\cdot(\alpha_H)_{BT}} + \log\frac{[MZ]_t}{[Z]_f} \quad (2)$$

The symbols used in Eq. (2) have the same meanings as those used in the previous paper.[1]

When the following equilibrium becomes important;

$$HD^{2-} + MZ^{2-n} = MDZ^{2-(n+3)} + H^+ \quad (3)$$

the (4) relation can be assumed in place of (2).

$$\log\frac{A_D - A}{A - A_{MD}} = \log\frac{K^{MZ}_{MDZ}}{(\alpha_H)_{BT}} + \log[MZ]_t \quad (4)$$

The above relations indicate that when MD^- is formed, only the plot of $\log(A_D-A)/(A-A_{MD})$ against $\log([MZ]_t/[Z]_f)$ can give a straight line with a slope of unity, but when the chemical equilibrium (3) becomes important, the plot of $\log(A_D-A)/(A-A_{MD})$ *vs.* $\log[MZ]_t$ yields a straight line with a slope of unity.

The experimental data obtained for lead(II)-NTA and cadmium(II)-EDTA-OH systems under the conditions where uncomplexed and complexed chelons are present in a large excess over BT were analyzed with the aid of Eqs. (2) and (4). Typical examples are shown in Figs. 2 and 3. In both systems, under the experimental conditions employed, only the plot of $\log(A_D-A)/(A-A_{MD})$ against $\log([MZ]_t/[Z]_f)$ gave a straight line with a slope of unity, indicating the formation of the normal chelate, MD^-.

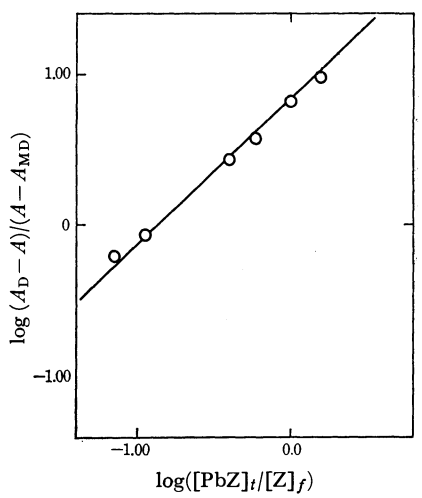

Fig. 2. The plot of $\log(A_D-A)/(A-A_{MD})$ *vs.* $\log([PbZ]_t/[Z]_f)$ for determining the equilibrium constant.
$\lambda=640$ mμ, pH=9.65, $\mu=0.30$
Total concentration of NTA=30.0 mM
Total concentration of BT=2.5×10^{-5} M
Concentration of Pb(II) ranges from 2.0 mM to 20.0 mM

The stability constants for lead(II)- and cadmium-(II)-BT chelates were calculated from the $\log(A_D-A)/(A-A_{MD})$ value obtained when $\log([MZ]_t/$

6) G. Schwarzenbach and R. Gut, *Helv. Chim. Acta*, **39**, 1589 (1956).
7) S. Chaberek, Jr., and A. E. Martell, *J. Am. Chem. Soc.*, **77**, 1477 (1955).

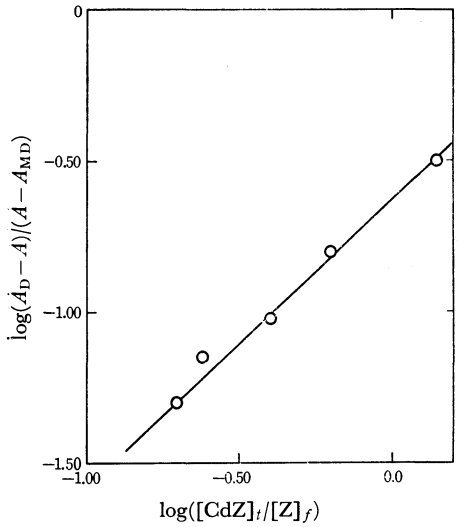

Fig. 3. The plot of $\log(A_D-A)/(A-A_{MD})$ *vs.* $\log([CdZ]_t/[Z]_f)$ for determining the equilibrium constant.
$\lambda=630$ mμ, pH=10.50, $\mu=0.30$
Total concentration of Cd(II)=2.32 mM
Total concentration of BT=2.50×10^{-5} M
Concentration of EDTA-OH ranges from 4.0 mM to 14.0 mM

TABLE 1

i) Dissociation constants of EDTA-OH and BT (mixed constants, $\mu=0.30$)
a) EDTA-OH[8] $pK_1=1.98$, $pK_2=5.14$, $pK_3=9.53$
b) BT $pK_1=6.80$, $pK_2=11.31$
ii) Formation constants of chelates ($\mu=0.30$)
K[6]$_{Pb\text{-}NTA}=10^{10.94}$ K[7]$_{Cd\text{-}EDTA\text{-}OH}=10^{12.55}$
$K^*_{PbD}=10^{13.19}$ $K^*_{CdD}=10^{12.74}$
* Obtained by the present authors

$[Z]_f$) is zero. The numerical values for EDTA-OH,[8] its cadmium(II) chelate,[7] and the lead(II)-NTA chelate[6] used in the calclations are listed in Table 1, along with the dissociation constants of BT.[9] These values were calculated in ways which have been described previously.[1] The dissociation constants of NTA used in the calculation have also been given previously.[1]

Theoretical Considerations of the Use of BT as an Indicator in the Lead(II)- and Cadmium(II)-EDTA Titrations. Reilley and Schmid[10] have proposed a simple but quantitative method for the rapid prediction of the optimum titration conditions. Provided that the concentration of the indicator is negligibly small and the degree of contrast between the colors of the indicator before and after the end point is large enough, the sharpness of an end point can be characterized simply by two numbers, Δ_1 and Δ_2, defined as follows.

$$\Delta_1 = \log K_{MD} - \log(\alpha_H)_{BT} + \log C_M - \log \beta_{MX} \quad (5)$$

$$\Delta_2 = \log K_{MY} + \log(\alpha_H)_{BT} - \log K_{MD} - \log(\alpha_H)_Y \quad (6)$$

Here, Δ_1 is a measure of the tightness of the metal-indicator complex and Δ_2, of the extent to which the chelon displaces the indicator fromithe metal-indicator complex.

To obtain the end point exactly, it is necessary that both Δ_1 and Δ_2 are greater than 3.0. Here, however, Δ values larger than 4.0 gives no practical improvement.

BT has been reported to have been used successfully as an indicator in the EDTA titrations of lead(II) ion in solutions of tartrate[2] and of cadmium(II) ions in an ammonia buffer[3] at pH values from 8.0 to 10.0. In the EDTA titration of lead(II), when the initial concentration of lead(II) is 1.00×10^{-2} M, the Δ_1 and Δ_2 values defined by Eqs. (5) and (6) were calculated to be 7.07 and 5.28 respectively, using the K_{PbD} value, the dissociation constants of BT[4] and tartaric acid,[11] and the stability constants of lead(II)-tartrate[12] and of the lead(II)-EDTA chelate.[13] Although the

TABLE 2

i) Dissociation constants
a) Tartaric acid[11]
$pK_1=2.88$, $pK_2=3.94$
b) Alanine[14]
$pK_1=2.34$, $pK_2=9.87$
c) Ammonia[15]
$pK=9.27$
ii) Stability constants of metal complexes
a) Pb(II)-tartarate complex[12]
$K_1=10^{3.78}$
b) Pb(II)-alanine complexes[14]
$K_1=10^{5.00}$, $K_2=10^{3.24}$
c) Cd(II)-NH_3 complexes[15]
$K_1=10^{2.74}$, $K_2=10^{2.21}$, $K_3=10^{1.37}$
$K_4=10^{1.13}$
d) Pb(II)-EDTA chelate[13] ($\mu=0.30$)
$K_{PbY}=10^{17.44}$
e) Cd(II)-EDTA chelate[13] ($\mu=0.30$)
$K_{CdY}=10^{15.86}$

8) H. Kroll, AEC Contract (30-1)-2096 Annual Report, 1959.
9) G. Schwarzenbach and W. Biedermann, *Helv. Chim. Acta*, **31**, 678 (1948).
10) C. N. Reilley and R. W. Schmid, *Anal. Chem.*, **31**, 887 (1959).
11) R. K. Cannan and A. Kibrik, *J. Am. Chem. Soc.*, **60**, 2314 (1938).
12) V. E. Panova, *Zhur. neorg. Khim.*, **1**, 422 (1956).
13) G. Schwarzenbach, R. Gut and G. Anderegg, *Helv. Chim. Acta*, **37**, 937 (1954).
14) C. B. Monk, *Trans. Faraday Soc.*, **47**, 292 (1951).
15) C. G. Spike, Thesis, Univ. of Michigan, Univ. Microfilms 5098 (1953).

Table 3. The titration of Pb(II) ion in the alanine solution of pH 8.50 with EDTA

The concentration of alanine is 0.10 M.

i) The concentrations of EDTA and Pb(II) are 10.0 mM.

V_{Pb}, m*l*	V_{EDTA} added, m*l*
5.00	5.02
10.00	10.00

ii) The concentrations of EDTA and Pb(II) are 1.00 mM.

V_{Pb}, m*l*	V_{EDTA} added, m*l*
5.00	4.96
10.00	9.90

stability and dissociation constants under varying titration conditions differ by several tenths of the pK unit from the literature values, the above results of the calculations can satisfactorily explain the well-known observations reported by Flaschka *et al.*[2]

For 1.00×10^{-2} M Pb(II) ions in a 0.10 M alanine solution of pH 8.50, the Δ_1 and Δ_2 values can be calculated as 4.82 and 5.55 respectively, using the numerical values for alanine and its complexes[14] given in Table 2. This clearly suggests that Pb(II) ions in a 0.10 M alanine solution of pH 8.50 can be successfully titrated with EDTA, using BT as a metallochromic indicator. The demonstrative results of the titrations shown in Table 3 can be regarded as satisfactory.

In the case of Cd(II)-EDTA titration, the Δ_1 and Δ_2 values (5.87 and 4.15 respectively) calculated for 1.00×10^{-2} M cadmium(II) and 0.10 M ammonia by using the above-determined K_{CdD} value and the numerical values[13,16] given in Table 2 can be considered to have a magnitude which can explain well the facts given by Schwarzenbach *et al.*[13]

From the facts obtained and the theoretical discussion given above, it can be safely concluded that reasonable K_{PbD} and K_{CdD} values have been determined.

The present authors wish to thank the Ministry of Education for the financial support given to this research.

16) H. Lunden, *J. Chim. Phys.*, **5**, 574 (1907).

BULLETIN OF THE CHEMICAL SOCIETY OF JAPAN VOL. 41 130—135 (1968)

The Partial Resolution of Racemic α-Alanine through the Cobalt(III) Complexes of Optically Active Aspartic or Glutamic Acid*1

Muraji SHIBATA, Hiroaki NISHIKAWA and Kinya HOSAKA

Department of Chemistry, Faculty of Science, Kanazawa University, Kanazawa

(Received July 20, 1967)

When a hundred per cent excess of racemic α-alanine was reacted, in the presence of activated charcoal, with a reaction mixture of tricarbonatocobaltate(III) and L-asparate, water-insoluble β-tris(alaninato)cobalt(III) was precipitated. The recovery of alanine from this triscomplex showed a partial resolution; the D form of alanine was preferentially complexed, and the optical purity of the alanine recovered was about 38%. Spectroscopic measurements (absorption, ORD and CD) showed that the predominantly-existing species in the above reaction mixture was the (−)-$[Co\ CO_3(L\text{-asp})_2]^{3-}$ anion, and that the reaction of this complex anion with racemic alanine led to the predominant formation of β(−)-$[Co(D\text{-ala})_2(L\text{-ala})]$ (the (−) sign refers to the sign of the Cotton effect in the first absorption band region). Similar experiments were carried out with D-aspartate and L-glutamate in place of L-aspartate. Through all the experiments, we have found that the complexes which are effective for the resolution of racemic alanine and the product or tris(alaninato)cobalt(III) have the same sign of the Cotton effect in their first-band regions.

Gott and Bailar[1] first reported that when the carbonatobis(levo-propylenediamine)cobalt(III) cation was treated with a racemic organic acid, the dextro form of the acid entered the coordination sphere of the complex more readily than the levo form. By means of this preferential coordina-

*1 Presented at the 20th Annual Meeting of the Chemical Society of Japan, Tokyo, April, 1967.

1) A. D. Gott and J. C. Bailar, Jr., *J. Am. Chem. Soc.*, **74**, 4820 (1952).

tion of one of the active forms, Sarma and Bailar[2] resolved propylenedimaine, tartaric acid, and α-alanine; the resolutions of racemic alanine attained through the L-tartratocopper(II) complex and copper(II) L-glutamate were 3.8 and 3.3% respectively.

Later, we reported in a short paper[3] that the same amino acid was more effectively resolved by the use of a cobalt(III) complex with L-aspartate (about 30%). Incidentally, the resolution of DL-aspartic acid by the utilization of copper(II) chelates of D- or L-alanine, *etc.*, has been reported by Harada.[4] The present paper is an augmentation of the previous one;[3] it will report further investigations of the partial resolution of α-alanine. In addition to the cobalt(III) complexes of L- or D-aspartic acid, those of L-glutamic acid were also used as a material that effects the resolution. We found a correlation between the active form of alanine preferentially coordinated and the configuration of the cobalt(III) complexes.

Experimental

Resolution through the Complexes of L(or D)-Aspartic Acid. *Procedure 1.* Throughout the procedures described below, "the green solution" of tricarbonatocobaltate(III) was first prepared as a stock for the preparation of aspartato or glutamato complexes. A cold mixture of an aqueous solution (about 20 m*l*) containing cobalt chloride hexahydrate (6.0 g, 0.025 mol) and 30% hydrogen peroxide (10 m*l*, excess) was added, drop by drop, to an ice-cooled slurry of potassium bicarbonate (17.5 g, 0.175 mol) in water (18 m*l*); the resulting green solution was then stirred for a few minutes further in the cold.

Monopotassium L(or D)-aspartate (8.6 g, 0.050 mol) was added to the green solution, and the mixture was stirred at 60°C for 5 hr, whereupon the color of the solution became red-violet. A hundred per sent excess of racemic α-alanine (13.5 g, 0.150 mol) was added to the above solution, and the mixture was adjusted to pH 9.5—10 with an aqueous solution of potassium hydroxide. After the addition of activated charcoal (2 g), the solution was stirred at about 50°C for 2 hr, whereby the β(cis-cis)-complex of tris(alaninato)-cobalt(III) was precipitated. The complex was collected with the charcoal and washed thoroughly with hot water and ethanol, and then ether. After dyring, this material was suspended in hot dilute aqueous ammonia and treated with hydrogen sulfide to decompose the complex. After the removal of the cobalt sulfide by filtration, the filtrate was concentrated to a small volume under reduced pressure. When the concentrate became turbid, it was clarified by filtering it with a small amount of activated charcoal. Acetone was added in the cold to the final clear concentrate to recover alanine. A 5% solution of this alanine in 1 N hydrochloric acid was used for the measurement of the optical rotation at the sodium-D line. The percentage of the resolution or the "optical purity" was represented by the quotient of the observed specific rotation divided by the value for pure L-alanine ($[\alpha]_D=14.47$).

Alanine recovered in the case of the L-aspartato complex, 3.0 g, 3.0 g; $[\alpha]_D=-5.62$, -5.52; optical purity, 38.8%, 38.1%.

Alanine recovered in the case of the D-aspartato complex, 2.8 g; $[\alpha]_D=5.60$; optical purity, 38.7%.

In order to isolate the complex existing in the reaction mixture of tricarbonatocobaltate(III) and L-aspartate, we prepared the same solution, neutralized it with dilute acetic acid, and then added a large amount of methanol. A red-violet material precipitated, but it was very hygroscopic (it probably was potassium salt). Therefore, it was treated with an aqueous solution of silver nitrate to produce a less soluble silver salt.

Found: C, 13.65; H, 1.94; N, 3.65%. Calcd for $Ag_3[CoCO_3(C_4H_5NO_4)_2]\cdot 4H_2O$; C, 13.91; H, 2.33; N, 3.60%.

Thus, it was assumed that the predominant complex in the reaction mixture was the carbonatobis(L-aspartato)cobaltate(III) anion.

Procedure 2. The reaction mixture mentioned above was prepared with L-aspartate, and the mixture was once acidified with dilute acetic acid in order to decompose all of its carbonate ions. The resulting solution was then adjusted to pH 10 with dilute potassium hydroxide. This was treated with racemic alanine under the same conditions as have been described in Procedure 1.

Alanine recovered, 2.6 g; $[\alpha]_D=-5.91$; optical purity, 40.8%.

Procedure 3. A little higher resolution was attained by a slight alteration of Procedure 1, *i. e.*, the amount of L-aspartate was increased (12.1 g, 0.075 mol). Tricarbonatocobaltate(III) was reacted with aspartate in the presence of activated charcoal (0.5 g) at room temperature for 2 hr. Thereafter, the process was the same as has been described in Procedure 1.

Alanine recovered, 1.9 g, 1.8 g; $[\alpha]_D=-6.45$, -6.34; optical purity, 44.5%, 43.8%.

Procedure 4. Recently, we reported the isolation of the four isomers of trihydrogen tris(L-aspartato)-cobaltate(III).[5] By the use of solubility differences depending on the pH values, the α(+)-, α(−)-, β(+)- and β(−)-isomers were obtained from a reaction mixture of tricarbonatocobaltate(III) and L-aspartate. The fourth procedure concerns these isomers.

A certain amount (0.025 mol) of each isomer was dissolved in a very diluted aqueous solution of potassium hydroxide. Racemic alanine was then added to this solution, and the mixture was adjusted to pH 9.5—10. In the presence of activated charcoal (2 g), the mixture was stirred at 50°C for 2 hr. It was found that only one isomer of the four, α(−), produced a precipitate of water-insoluble β-tris(alaninato)cobalt(III).

Alanine recovered, 4.3 g; $[\alpha]_D=-4.47$; optical purity, 30.0%.

Resolution through the Cobalt(III) Complexes of L-Glutamic Acid. Except for the use of L-glutamate in place of L (or D)-aspartate, the same procedure was followed. Monopotassium L-glutamate (9.3 g,

2) D. Sarma and J. C. Bailar, Jr., *ibid.*, **78**, 895 (1956).
3) M. Shibata, Y. Fujita, N. Naito and K. Hori, This Bulletin, **36**, 485 (1963).
4) K. Harada, *Nature*, **205**, 590 (1965).
5) M. Shibata, H. Nishikawa and K. Hosaka, This Bulletin, **40**, 236 (1967).

0.05 mol) was added to a tricarbonatocobaltate(III) solution, and the mixture was stirred at 60°C for 5 hr. The resulting red-violet solution was treated with racemic alanine.

Alanine recovered, 4.3 g, 4.3 g; $[\alpha]_D = -2.60$, -2.75; optical purity, 18.0%, 19.0%.

In the manner of Procedure 1, a carbonato complex was isolated as a silver salt.

Found: C, 15.97; H, 2.48; N, 3.83%. Calcd for $Ag_3[CoCO_3(C_5H_7NO_4)_2]\cdot 4H_2O$: C, 16.42; H, 2.73; N, 3.48%.

A higher percentage of resolution was obtained by a procedure similar to Procedure 2.

Alanine recovered, 3.6 g, 3.0 g; $[\alpha]_D = -4.33$, -4.38; optical purity, 29.9%, 30.3%.

Instrumental Measurements. Optical rotations at the Na-D line were measured with a Yanagimoto Model OR-20 photo-magnetic direct-reading polarimeter at room temperature. The absorption, optical rotatory dispersion (ORD), and circular dichroism (CD) spectra were all measured on a Jasco Model UV-5 optical rotatory dispersion recorder with a CD attachment. X-Ray powder patterns were taken with a Rigaku-denki Geigerflex, using a Co-target.

Results and Discussion

On the Reaction. A distinctive feature of the reactions which we adopted for the partial resolution of alanine is that the water-insoluble β-tris(alaninato)cobalt(III) precipitates from the reaction mixture of the asparatato (or glutamato) complex and racemic alanine. For this precipitation reaction, the presence of activated charcoal is an indispensable condition. The amount of charcoal influenced the yield and the optical purity of the recovered alanine. A series of experiments were carried out according to the previously-described procedure;[3] when the amounts of the charcoal were 0.4, 2.0, 4.0 and 6.0 g, the yields of alanine were 2.3, 3.4, 2.9 and 2.4 g, and the optical purities were 13.8, 33.5, 38.0 and 34.1%, respectively. Consequently, it may be assumed that activated charcoal is necessary for both the reactions of ligand exchange and preferential coordination. In the present experiments, 2.0 g of charcoal were used for easier handling and for a higher recovery of alanine. In our previous paper,[3] we reported that the co-existence of cellulose powder with activated charcoal increases the percentage of resolution. We now believe that not only the cellulose, but also the charcoal plays an effective role in the preferential coordination of one active form of racemic alanine.

On the Mechanism. Although the mechanism of the present reaction has not yet been clarified, there seems to be a certain correlation between the active form of alanine preferentially complexed and the configuration of the cobalt(III) complex that effects this resolution. Recently, several workers reported the isolation of the possible geometrical-optical isomers of tris(L- or D-alaninato)-cobalt(III).[6-8] They stated that one of the four isomers of [Co(L or D-ala)$_3$], the β(+)- or the β(−)-isomer, was completely insoluble in water (the (+) and (−) signs refer to the sign of the Cotton effect in the first absorption band region). If this solubility property holds in our reaction product, it must be a non-equimolar mixture of the β(−) and β(+) isomers. In this respect, the CD spectrum of the product obtained by Procedure 1 is compared with that of β(+)-[Co(L-ala)$_3$] under the same conditions (in 50% H_2SO_4) (Fig. 1). The two spectra differ considerably in the intensity of the first CD peaks, $\Delta\varepsilon = -1.27$ (or $+1.27$) for the product and $\Delta\varepsilon = -1.00$ for the [Co(L-ala)$_3$]. This fact suggests that the product concerned is not a mixture of the β(−) and β(+) isomers, and that the formation

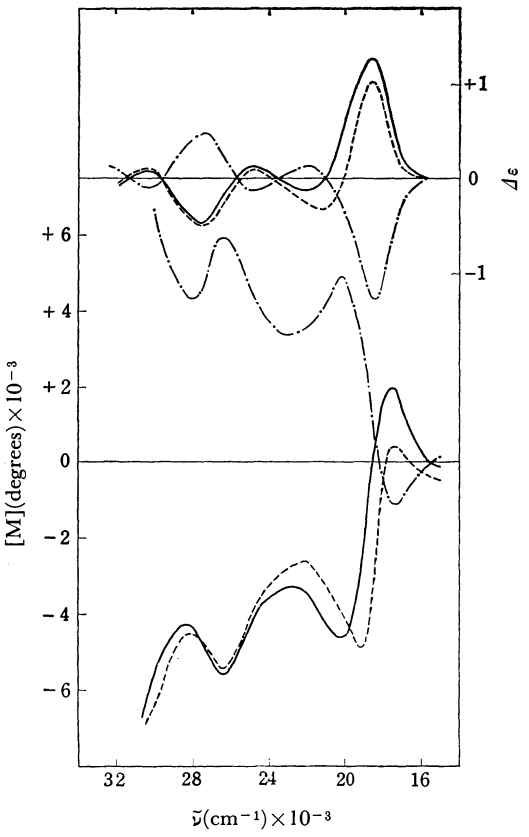

Fig. 1. ORD and CD curves for:
(·—·) Reaction product of L-aspartato complex with racemic alanine in 50% H_2SO_4,
(——) Reaction product of D-aspartato complex with racemic alanine in 50% H_2SO_4,
(·····) β(+)-[Co(L-ala)$_3$] in 50% H_2SO_4.

6) B. E. Douglas and S. Yamada, *Inorg. Chem.*, **4**, 1561 (1965).
7) J. H. Dunlop and R. D. Gillard, *J. Chem. Soc.*, **1963**, 6531.
8) R. G. Denning and T. S. Piper, *Inorg. Chem.*, **5**, 1056 (1966).

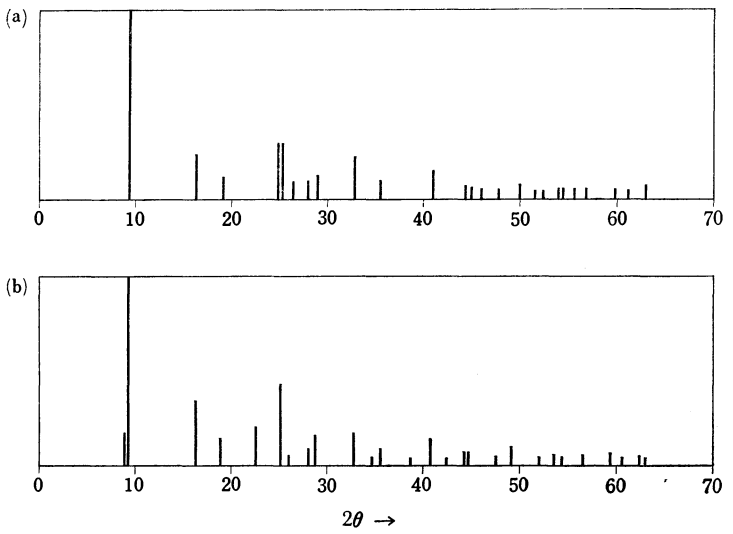

Fig. 2. X-Ray powder diffraction patterns of:
(a) Reaction product of L-aspartato complex with racemic alanine,
(b) β(+)-[Co(L-ala)$_3$].

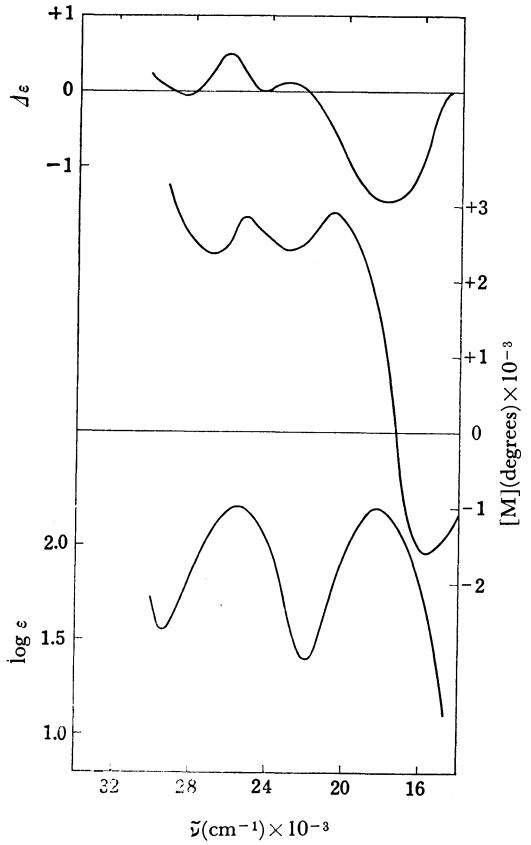

Fig. 3. Absorption, ORD and CD curves for $[CoCO_3(L\text{-asp})_2]^{3-}$ in N NaCl.

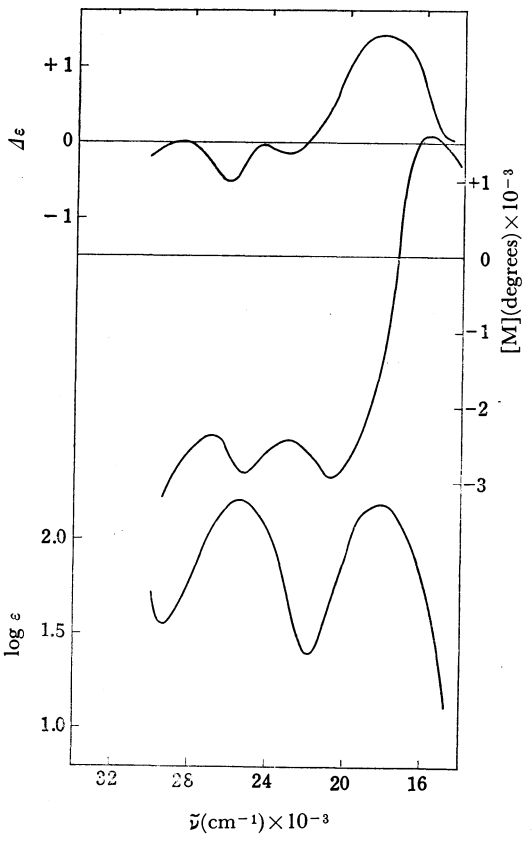

Fig. 4. Absorption, ORD and CD curves for $[CoCO_3(D\text{-asp})_2]^{3-}$ in N NaCl.

of such a mixed-ligand isomer as β(− or +)-[Co(D- or L-ala)$_2$(L- or D-ala)] must be considered. In order to ascertain whether or not the product is such a mixture, the X-ray powder patterns of the reaction product and of β(+)-[Co(L-ala)$_3$] were compared (Fig. 2). The two patterns are

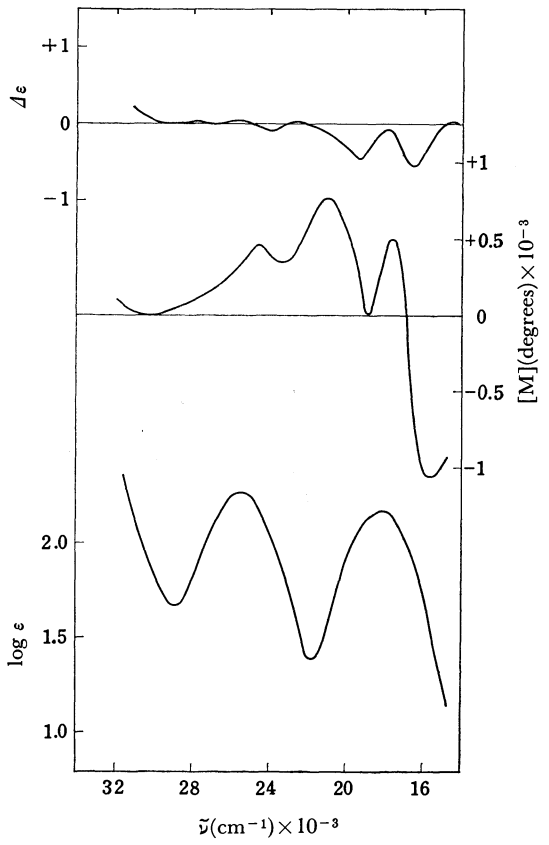

Fig. 5. Absorption, ORD and CD curves for $[CoCO_3(L\text{-glu})_2]^{3-}$ in N NaCl.

similar, but are not identical with each other. By the way, the pattern for the reaction product obtained by the use of D-asparatate was identical with that for the product obtained by the use of L-aspartate (Fig. 2(a)). Very recently, we[9] have prepared $\beta(+)$-$[Co(L\text{-ala})_2(D\text{-ala})]$ by the reaction of $[Co(L\text{-ala})_2CO_3]^-$ with D-alanine; the $\Delta\varepsilon$ value was found to be 1.33.

Next, let us discuss the configuration of the complexes containing optically active aspartate or glutamate anions. The absorption, ORD, and CD spectra for carbonatobis(L- or D-aspartato)-cobaltate(III) are given in Figs. 3 and 4, while Fig. 5 gives the data for the corresponding glutamato complex. For these complexes, three geometrical isomers are possible, *i. e.*, (a) *cis(N)-cis(O)*, (b) *cis(N)-trans(O)* and (c) *trans(N)-cis(O)*. Among these, the possibility of (c) may be excluded because of the non-splitting of the first absorption band. Matsuoka *et al.*[10] have recently reported that the *trans(N)* isomer of the oxalatobis(glycinato) cobaltate(III) complex shows a splitting of the first band.

The carbonato complex with L-aspartate anions shows a distinctive negative Cotton effect in the region of the first band. The complex with D-aspartate anions shows a distinctive positive Cotton effect. These facts indicate the predominance of the (−)- or (+)-isomer in the reaction mixture of tricarbonatocobaltate(III) and L- or D-aspartate. On the other hand, the corresponding carbonato complex with L-glutamate ions has a somewhat complicated ORD and CD spectra, although the sign of the CD is unchanged (negative).

Figure 6 shows the absorption, ORD, and CD spectra of $\alpha(-)$-$[Co(L\text{-asp})_3]^{3-}$ in water. The ORD and CD spectra show a distinctive negative Cotton effect in the region of the first band. Thus, we may generalize that the complexes which are effective for the resolution of racemic alanine and the reaction product have the same sign of the Cotton effect in the first band region. An X-ray study[11] has shown that the absolute configuration of $\alpha(+)$-$[Co(L\text{-ala})_3]$ is

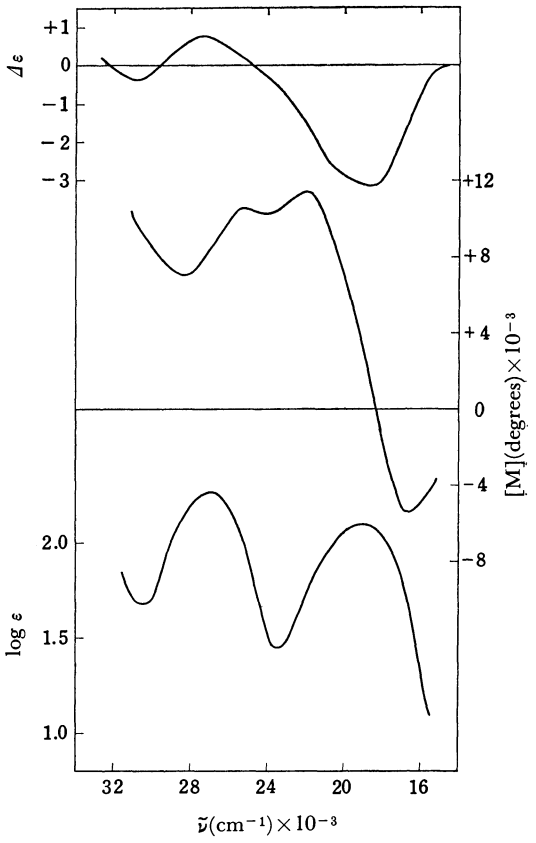

Fig. 6. Absorption, ORD and CD curves for $\alpha(-)$-$[Co(L\text{-asp})_3]^{3-}$ in water.

9) M. Shibata, H. Nishikawa and Y. Nishida, *Inorg. Chem.*, in contribution.

10) N. Matsuoka, J. Hidaka and Y. Shimura, presented at the 16th Symposium on Coordination Chemistry, Tokyo, Dec., 1966.

11) M. G. B. Drew, J. H. Dunlop, R. D. Gillard and D. Rogers, *Chem. Commun.*, 42 (1966).

$\Delta(C_2)$; hence, that of the corresponding $\alpha(-)$-isomer is $\Lambda(C_2)$. From this the present $\alpha(-)$-$[Co(L\text{-asp})_3]^{3-}$ may be identified as $\Lambda(C_2)$. The configuration of the carbonato complex of L or D-aspartic acid would also be Λ or $\Delta(C_2)$. Thus, it may be concluded that the Λ(or Δ) (C_2)-complex reacts with racemic alanine to produce the predominant formation of the β-Λ (or Δ)-isomer of DDL(or LLD)-tris(alaninato)cobalt(III). The fact that the $\alpha(+)$-isomer of tris(L-aspartato)cobaltate-(III) does not participate in the formation of the insoluble product may be due to the inertness of the isomer for a ligand-exchange reaction.

BULLETIN OF THE CHEMICAL SOCIETY OF JAPAN VOL. 41 135—139 (1968)

Glass Transition Temperature and Isothermal Volume Change of Selenium

Shuichi HAMADA, Tadao SATO and Toshiaki SHIRAI

Department of Chemistry, Faculty of Science, Science University of Tokyo, Kagurazaka, Shinjuku-ku, Tokyo

(Received July 14, 1967)

The viscoelastic behavior of selenium and of partially-chlorinated selenium was studied by the dilatometric method. The glass transition temperature, T_g, of selenium was determined to be 32.0°C at a cooling rate of 0.2°C/min. The glass transition temperature decreased linearly with the reciprocal of the average chain length of selenium. The chain length was calculated using the degree of chlorination. An abrupt increase in T_g was observed at a chlorine content of about 0.013%. The volume-time curves obtained by the determination of the volume of selenium in the neighborhood of T_g were superposed on each other by sliding them along the abscissa. The values of the shift factor and of T_g fit well in Williams, Landel and Ferry's equation. The parameters in the WLF equation, C_1^g and C_2^g, of selenium were calculated to be 6.86 and 28.6 respectively. Both the parameters increased with an increase in the chlorine content up to 0.0125%, and reached the values of usual polymers above 0.0125%. The WLF f_g value of selenium was calculated to be 6.33×10^{-2}. This value decreased with an increase in the chlorine content, and reached the universal value of usual polymers (2.5×10^{-2}) when the chlorine content was more than 0.0125%. The chlorine content corresponds to 0.0125% when all the radicals at both ends of the linear chain molecules of selenium have been used in forming bonds with chlorine atoms. Therefore, it may be concluded that the existence of radicals at the molecular ends of selenium chains brings about an augmentation of the fraction of the free volume at T_g.

Amorphous selenium is considered to be a mixture of Se_8 ring molecules and long chains.[1] The properties of amorphous selenium should be governed by those of the long-chain molecules, since the content of the ring molecules in amorphous selenium has been estimated to be only 0.22 wt% at 230°C.[2] The number of selenium atoms in a chain of average length was calculated to be 7200 at 230°C by the thermodynamic theory developed by Eisenberg and Tobolsky.[1] This result agreed with that obtained by Shirai and Hamada by means of measurements of the viscosity of molten selenium.[3] The linear chains may be considered to be diradical molecules with an unpaired electron at each end of the chains. The presence of radicals in amorphous selenium was reported by Abdullaev *et al.*[4] and by Sampath *et al.*[5] on the basis of their ESR studies. Sampath[6] reported that the results obtained by Eisenberg and Tobolsky, and by Shirai and Hamada were supported by the value of the spin concentration in amorphous selenium.

In our work, the viscoelastic behavior of amorphous selenium was investigated by the method of isothermal volume contraction, similar to Kovacs' measurments of organic polymers.[7] Moreover,

1) A. Eisenberg and A. V. Tobolsky, *J. Polymer Sci.*, **46**, 19 (1960).
2) G. Briegleb, *Z. Phys. Chem.*, **A144**, 321 (1929).
3) T. Shirai and S. Hamada, *Nippon Kagaku Zasshi (J. Chem. Soc. Japan, Pure Chem. Sect.)*, **84**, 968 (1963).
4) G. Abdullaev, W. I. Ibragimov, Sh. V. Mamedov, T. Ch. Dzhuvarly and G. H. Aliev, *Dokl. Akad. Nauk Azerb. SSR*, **20**, 13 (1964).
5) P. I. Sampath and R. C. Keezer, *Bull. Am. Phys. Soc.*, **10**, 613 (1965).
6) P. I. Sampath, *J. Chem. Phys.*, **45**, 3519 (1966).
7) A. J. Kovacs, *J. Polymer Sci.*, **30**, 131 (1958).

the effect of radicals on the viscoelastic behavior of amorphous selenium was studied.

Experimental

Materials. The selenium was obtained from the Yokozawa Chemical Company; the guaranteed purity was more than 99.999%. The sample of amorphous selenium was prepared by quenching the molten selenium; the selenium was heated in an electric furnace at 230°C for 1 hr, then dropped in cold water and dried in a cooled vacuum dessicator. Chlorinated selenium was prepared by the method described in a previous paper.[8] The sample of chlorinated selenium was prepared by the same method which was used in preparing the amorphous selenium. The chlorine content in the chlorinated selenium was determined by the colorimetric method described in the previous paper.

Procedure. The glass transition temperatures, T_g, of the selenium and of the chlorinated selenium were estimated by the dilatometric method. A specimen of about 7 g of the amorphous selenium was sealed in a dilatometer containing about 62 g of mercury. The capillary was 0.726 mm in diameter and about 250 mm long. The height of the meniscus of mercury in the capillary was measured, using a measuring microscope, to the accuracy of 1/100 mm. The dilatometer was kept at 50°C for 30 min to establish the thermal equilibrium; then it was allowed to cool slowly at a cooling rate of 0.2°C/min. The glass transition temperature of the amorphous selenium was estimated graphically from the specific volume-temperature relationship.

The isothermal volume contraction phenomena of the amorphous selenium were also studied by the dilatometric method. The dilatometer was first kept at 50°C for 30 min; then it was quickly immersed into a water bath kept at a specified temperature in the neighborhood of T_g. The accuracy of the temperature was about ±0.1°C. The change in the height of the mercury column in the capillary was followed against the time in which the dilatometer had been immersed in the water bath.

Results

The Glass Transition Temperature of the Selenium. Figure 1 shows the specific volume-temperature relationship of the selenium when the specimen was cooled at a rate of 0.2°C/min. This relation was similar to those of usual organic polymers. The glass transition temperature of the selenium was estimated graphically to be 32.0°C at the cooling rate studied. This value was nearly equal to that obtained by Tammann and Kohlhaas (31°C).[9] The value of T_g was reproducible. It is well known that T_g depends on the rate of cooling. The glass transition temperature of selenium was also governed by the time scale of the measurement.[10,11] In the present work, therefore, the cooling rate of the specimen was kept at 0.2°C/min.

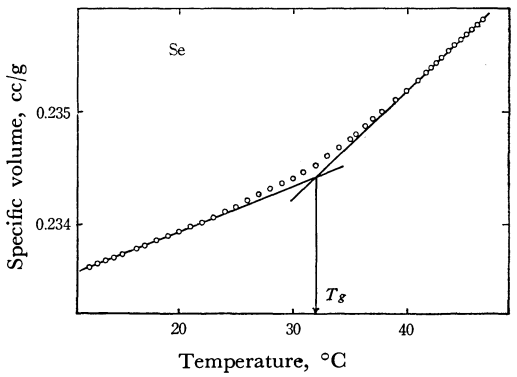

Fig. 1. Plot of specific volume against temperature.

The Glass Transition Temperature of the Chlorinated Selenium. The specific volume-temperature relationships of the chlorinated selenium specimens were similar to that of the selenium. Figure 2 shows the relationship between the T_g of the chlorinated selenium and the chlorine content. The glass transition temperature of selenium decreased as the chlorine content increased up to about 0.013%, while an abrupt increase in T_g was observed at about 0.013%.

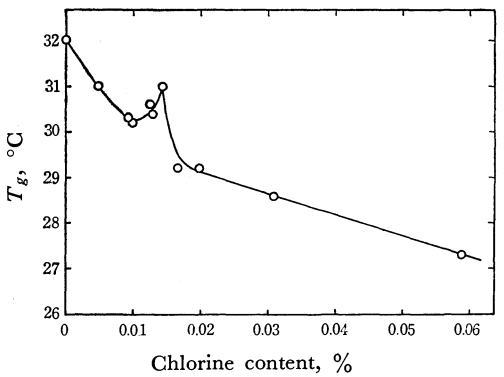

Fig. 2. Plot of T_g against chlorine content.

It is well known that an elevation of the T_g of organic polymer is observed when the polar group is introduced into the chain molecules. The abrupt increase in the T_g of the chlorinated selenium at a chlorine content of about 0.013% probably arose because of the large electronegative character of the introduced chlorine atoms, which terminated the radicals at the chain ends of the selenium molecules. The glass transition temperature of the chlorinated selenium with a chlorine

8) S. Hamada, T. Sato and T. Shirai, This Bulletin, **40**, 864 (1967).
9) G. Tammann and A. Kohlhaas, *Z. anorg. Chem.*, **182**, 49 (1929).
10) E. Jenckel, *Z. Elektrochem.*, **43**, 796 (1947).
11) T. Sekiguchi, *Sci. Papers I. P. C. R.*, **54**, 281 (1960).

content above 0.013% decreased linearly with an increase in the chlorine content. Fox and Flory[12] reported that the T_g of polystyrene decreased linearly with the reciprocal of the molecular weight when the molecular weight was not very large. The relation between the number of selnium atoms in an average-length chain of chlorinated selenium, Z_n, and the chlorine content, p, is shown as follows, after the chain ends have been terminated by chlorine atoms:

$$Z_n = 2\times 35.5(100-p)/78.96p$$

If the chlorine content is very small, Z_n is expressed as follows:

$$Z_n = 89.92/p$$

That is, the chlorine content is proportional to the reciprocal of the number of selenium atoms in an average-length chain of chlorinated selenium. The glass transition temperature of the chlorinated selenium decreased linearly with an increase in the chlorine content, as is shown in Fig. 2. This result agrees with that obtained by Fox and Flory.

The Isothermal Volume Change of the Selenium. A retardation of the volume change of the selenium was observed as in the case of organic polymers. Figure 3 shows the relation between the volume change of the selenium and the time, when the specimen kept at 50°C for 30 min was quickly immersed into a water bath kept at a specified temperature in the neighborhood of T_g. The volume changes, which were the differences between the equilibrium volume, $V_{T(\infty)}$, and the volume at the time $(t-a)$, $V_{T(t-a)}$, at several temperatures, are shown as the readings of the mercury meniscus in the capillary. The time which the dilatometer had been immersed in the water bath was expressed as $t-a$. The corrective factor, a, is a half of the time needed to attain the thermal equilibrium from 50°C to a specified temperature. The value of a was estimated to be 25 sec by a measurement made when the dilatometer containing mercury alone was quickly cooled in the same manner.

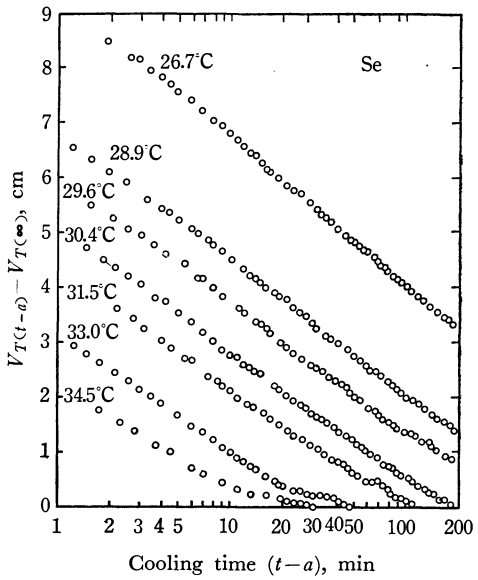

Fig. 3. Relationship between volume change and cooling time.

In order to study the volume relaxation phenomena of the selenium, the time-temperature superposition principle was applied.[7,13] The values of the shift factor, a_T, were estimated, since the volume-time curves could superpose upon each other by sliding along the abscissa. From

Table 1. Parameters of the WLF equation of selenium and of chlorinated selenium

Chlorine content %	T_g °C	C_1^g	C_2^g	f_g (WLF) $\times 10^{-2}$	f_g (Kovacs) $\times 10^{-2}$	α_f $\times 10^{-4}$	$\Delta\alpha$ $\times 10^{-4}$	$\Delta\alpha T_g$ $\times 10^{-2}$
Se	32.0	6.86	28.6	6.33	4.80	22.1	2.80	8.54
0.00488	31.0	7.74	22.1	5.60	5.03	25.5	2.43	7.39
0.00928	30.3	8.56	27.8	5.07	4.56	18.2	2.25	6.90
0.0100	30.2						2.28	6.93
0.0125	30.6	15.5	68.6	2.80	2.23	4.08	2.16	6.54
0.0128	30.4	16.7	63.5	2.62	2.20	4.09	2.18	6.60
0.0137	31.0	16.4	54.5	2.65	2.43	4.85	2.27	6.89
0.0166	29.2						2.24	6.77
0.0198	29.2	14.5	55.8	2.94	2.69	5.27	2.20	6.65
0.0310	28.6	14.7	55.0	2.96	2.34	5.39	2.22	6.69
0.0588	27.3						2.24	6.72
Usual polymers		17.4	51.6	2.5±0.3		(4.8)		11.3

12) T. G. Fox and P. J. Flory, *J. Polymer Sci.*, **14**, 315 (1954).

13) T. Sekiguchi, *Sci. Papers I. P. C. R.*, **55**, 148 (1961).

the estimated a_T and T_g values, the parameters, C_1^g and C_2^g, in the WLF equation,[14] $\log a_T = -C_1^g(T-T_g)/(C_2^g+T-T_g)$, were calculated to be 6.86 and 28.6 respectively. These values were small compared with those of usual organic polymers (17.4 and 51.6 respectively).

The Isothermal Volume Change of the Chlorinated Selenium. The volume relaxation phenomena of the chlorinated selenium were similar to that of the selenium. The volume-time curves of the chlorinated selenium could superpose upon each other as in the case of the selenium. The values of the C_1^g and C_2^g of the chlorinated selenium were estimated from a_T and T_g.

The glass transition temperatures and the values of C_1^g and C_2^g are listed in Table 1.

Though both the values of C_1^g and C_2^g were small and increased only with an increase in the chlorine content, they were nearly equal to those of usual polymers (17.4 and 51.6 respectively) at chlorine contents above 0.0125%.

Discussion

The retardation phenomena of the volume contractions of the selenium and of the chlorinated selenium were observed as viscoelastic behavior. As the relation between T_g and a_T was shown as the WLF equation, the fraction of the free volume at T_g, f_g, of the selenium can be discussed using the values of the WLF parameters, C_1^g and C_2^g.

Williams, Landel, and Ferry[14] expressed f_g and the expansion coefficient of the free volume, α_f, on the basis of their empirical equation and Doolittle's free space equation for viscosity[15] as follows:

$$f_g = B/2.303C_1^g \qquad \alpha_f = B/2.303C_1^gC_2^g$$

where B is the constant in Doolittle's equation. Therefore, α_f corresponds to the difference, $\Delta\alpha$, between the expansion coefficient of the supercooled liquid state of the polymer, α_l, in the temperature range above T_g and the expansion coefficient of the glassy state, α_g, in the temperature range below T_g. The constant, B, can be ragarded as unity.[15] Bueche[16] supported this assumption by his theoretical treatment. Therefore, f_g and α_f are represented as $1/2.303C_1^g$ and $1/2.303C_1^gC_2^g$ respectively.

The calculated values of f_g and α_f and the empirical values of $\Delta\alpha$ are listed in Table 1.

Kovacs[7] expressed f_g on the basis of the WLF equation as follows:

$$f_g = (\alpha_f[\beta]_g/2.303\Delta\alpha v_g)^{1/2}$$

where $[\beta]_g$ is the slope of the volume-time curve at T_g in Fig. 2, and where v_g is the specific volume at T_g.

The calculated values of f_g, as defined by Kovacs, are listed in Table 1. Because both the values of f_g, that defined by WLF and that defined by Kovacs, were in good agreement with each other, they are likely to be reasonable values. Figure 4 shows the relationship between f_g and the chlorine content. The fraction of the free volume decreased with an increase in the chlorine content, and then reached about a constant value at chlorine contents above 0.0125%, as in the case of usual polymers (2.5×10^{-2}).

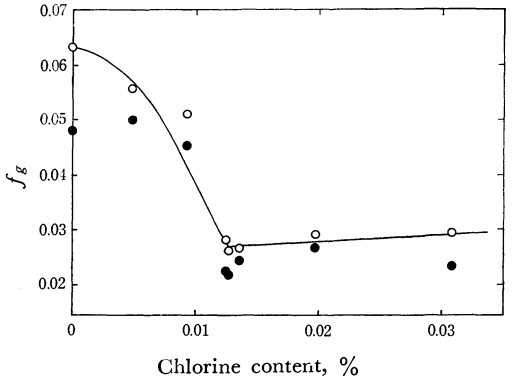

Fig. 4. Plot of f_g against chlorine content.
○: WLF's f_g ●: Kovacs' f_g

The calculated values of α_f, however, were about ten times larger than the empirical $\Delta\alpha$ values of the selenium and of the chlorinated selenium with chlorine contents of less than about 0.0125%, while the order of α_f values were the same as those of $\Delta\alpha$ at chlorine contents above 0.0125%. This notable disagreement of the values of α_f and $\Delta\alpha$ under these conditions may be caused by an abnormal value of B in Doolittle's equation. This has often been observed in usual polymers.[17] Therefore, the values of f_g defined by WLF and by Kovacs under these conditions can not be readily appraised as to their reasonableness.

Simha and Boyer[18] defined the fraction of the free volume at T_g to be $\Delta\alpha T_g$. The calculated values of $\Delta\alpha T_g$ are listed in Table 1. Though the value of $\Delta\alpha T_g$ increased with a decrease in the chlorine content at chlorine contents of less than about 0.0125%, nearly constant values of $\Delta\alpha T_g$ were observed above 0.0125%, as is shown in Fig. 5. The values of $\Delta\alpha T_g$, defined as the fraction of the free volume by Simha and Boyer, gave a curve with the same appearance as that

14) M. L. Williams, R. F. Landel and J. D. Ferry, *J. Am. Chem. Soc.*, **77**, 3701 (1955).
15) A. K. Doolittle, *J. Appl. Phys.*, **22**, 1471 (1951).
16) F. Bueche, *J. Chem. Phys.*, **24**, 418 (1956).
17) J. D. Ferry, "Viscoelastic Properties of Polymers," John Wiley & Sons, New York (1961), p. 226.
18) R. Simha and R. F. Boyer, *J. Chem. Phys.*, **37**, 1003 (1962).

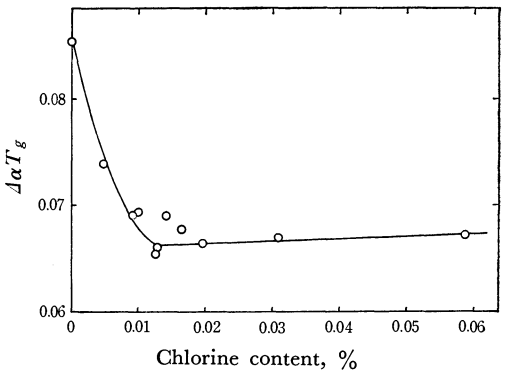

Fig. 5. Plot of $\Delta\alpha T_g$ against chlorine content.

obtained by WLF. This suggests that the f_g values of the selenium and of the chlorinated selenium with chlorine contents of less than 0.125% are larger than that of usual polymers (2.5×10^{-2}) in spite of an uncertainty regarding the values of the WLF f_g under these conditions.

As the number of selenium atoms in an average-length chain of the selenium at 230°C is 7200, the chlorine content corresponds to 0.0125% when all the radicals at both ends of linear chain molecules of the selenium have been dispensed in forming bonds with chlorine atoms. Thus, it may be concluded that the existence of radicals at the molecular ends of selenium chains brings about an augmentation of the fraction of the free volume at T_g. Though the mechanism of the augmentation of the fraction of the free volume at T_g by the existence of radicals has not been established, it may be considered to be due to bond interchange between neighboring selenium chains,[19] or to repulsion between radicals.

19) A. Eisenberg and A. V. Tobolsky, *J. Polymer Sci.*, **61**, 483 (1962).

BULLETIN OF THE CHEMICAL SOCIETY OF JAPAN VOL. 41 139—141 (1968)

The Viscosities of Aqueous Solutions Containing Metal Complexes. I. Luteo-type Co(II) and Co(III) Complexes and Ethylenediaminetetraacetato Complexes*[1]

Motoo YASUDA

Department of General Education, Nagoya University, Chikusa-ku, Nagoya

(Received July 21, 1967)

The viscosities of aqueous solutions containing cobalt complexes formed with ammonia, ethylenediamine (en), propylenediamine (pn), 2, 2'-bipyridine (bip), 1, 10-phenanthroline (phen), and ethylenediaminetetraacetic acid (H_4edta) were determined with a Cannon-Fenske capillary viscometer. Measurements were made in a Shibata viscosity bath maintained at 25± 0.01°C. The Jones-Dole viscosity *B*-coefficients of Co(III) complex cations formed with NH_3, en, pn, bip, and phen increase in that order. There is no significant difference between the *B*-coefficients of $[Cobip_3]^{3+}$ and $[Cobip_3]^{2+}$, or $[Cophen_3]^{3+}$ and $[Cophen_3]^{2+}$. On the other hand, a pronounced difference is found between the *B*-coefficients of $[Coedta]^-$ and $[Coedta]^{2-}$. This might suggest that there is a marked difference in the structure of $[Coedta]^-$ and $[Coedta]^{2-}$ anions.

The viscosities of aqueous electrolyte solutions have been accurately measured by many authors, but very few data are available for the metal complexes. Charles,[1] who measured the viscosities of the ethylenediaminetetraacetic acid and Schiff base chelates, showed that significant information concerning the configuration and the degree of solvation of the metal chelates could be obtained by viscosity measurements. It was felt that a thorough study on the viscosity of the metal complexes might supply useful information regarding the structure of the complexes. A study was therefore made of the viscosities of aqueous solutions containing cobalt complexes.

*1 Presented at the Symposium on Coordination Chemistry of the Chemical Society of Japan, Tokyo, Dec., 1966.

1) R. G. Charles, *J. Am. Chem. Soc.*, **78**, 3946 (1956); **81**, 1793 (1959).

Experimental

Complexes. Co(III) complexes such as $[Co(NH_3)_6]Cl_3$,[2] $[Coen_3]Cl_3 \cdot 3H_2O$,[3] $[Copn_3]Cl_3$,[4] $K[Coedta] \cdot 2H_2O$,[5] and $[Cophen_3]Cl_3 \cdot 7H_2O$,[6] were prepared following the literature method. The first four complexes were obtained by oxidizing a solution of a mixture of cobalt(II) chloride and ligand with hydrogen peroxide; the last one, by oxidizing with chlorine. An analogous procedure (*i. e.* oxidization with chlorine) was used for the preparation of $[Cobip_3]Cl_3 \cdot 3H_2O$, which was originally obtained from cobalt(III) sulfate and bipyridine.[7] All these well-known complexes were checked by analysis of chloride ion and/or water contents. But Co(II) complexes such as $[Cobip_3]Cl_2$, $[Cophen_3]Cl_2$ and $Na_2[Coedta]$, were not isolated as crystals. Instead, solutions of these chelates were made up with the standard $CoCl_2$ solution, the weighed amount of ligand and distilled water. The concentration of the $CoCl_2$ stock solution was determined by the chelatometric titration.

Measurements. Viscosities were determined with a Cannon-Fenske capillary viscometer having efflex time *ca.* 240 sec for distilled water. Measurements were made in a Shibata viscosity bath maintained at 25± 0.01°. Efflex times, measured with a stopwatch to the 0.1 sec, were easily reproducible to 0.2 sec. Densities of the solutions were also determined in the same constant temperature bath used for the viscosities.

Calculations. According to Jones and Dole,[8] the viscosities of aqueous electrolyte solutions have the following relation with the solute molarity, C:

$$\frac{\eta}{\eta_0} = 1 + A\sqrt{C} + BC$$

where η and η_0 are viscosities of solution and water, respectively; A and B are constants characterestic of the solute. The square-root term was attributed to the interionic electrostatic forces and the experimental values of A were found to be positive in every case studied. The coefficient B of the electrolytes is composed additively of contributions from each of the solute species present in the solution. And Gurney[9] divided the B-coefficient of -0.014 for KCl equally between K^+ and Cl^- ions (thus $B_{K^+} = B_{Cl^-} = -0.007$). Although his division of the B-coefficient of KCl into individual ionic values is a rather arbitrary process, it is regarded as a good approximation. The contributions depend on the size of the ions and on the interaction between the ions and the surrounding solvent.

When $((\eta/\eta_0)-1)/\sqrt{C}$ was plotted against $\sqrt{C}$, a straight line was obtained for each of the complexes studied. The slope of the resulting straight line gives the value of B-coefficient and the intercept gives the value of A-coefficient. The B-value of the complex ions is obtained by subtracting a relatively small correction for the ions present in the solution.

Results and Discussion

A part of the viscosity and density data for $[Coen_3]Cl_3$ and $CoCl_2$ are listed in Tables 1 and 2. Table 3 contains the B-values of the complex ions at 25°C obtained in this study, together with those reported by Kaminsky[10] and by Charles[1]. The trivalent $[Co(NH_3)_6]^{3+}$ ion, having a much smaller radius than that of any of the other complex ions studied, is expected to form an ion pair much more easily with the anion, chloride ion. Accordingly, the B-value of this complex ion is the least accurate.

Table 1. Viscosity and density data for $[Coen_3]Cl_3$

C	d	η/η_0
0.01500	0.99924	1.01009
0.03981	1.00317	1.02484
0.07606	1.00798	1.04427
0.1305	1.01630	1.07536
0.1858	1.02426	1.10700

Table 2. Viscosity and density data for $CoCl_2$

C	d	η/η_0
0.02302	0.99953	1.01216
0.06906	1.00526	1.03146
0.1381	1.01312	1.05885
0.2302	1.02374	1.09683

Table 3. The B-values of cobalt complexes (25°C)

Complex	B	Complex	B
$[Co(NH_3)_6]^{3+}$	0.17	$[Co(H_2O)_6]^{2+}$	0.38 (0.36*)
$[Coen_3]^{3+}$	0.56	$[Cobip_3]^{2+}$	1.37
$[Copn_3]^{3+}$	0.88	$[Cophen_3]^{2+}$	1.61
$[Cobip_3]^{3+}$	1.31	$[Coedta]^{2-}$	0.85 (0.88**)
$[Cophen_3]^{3+}$	1.53	$[Coedta]^-$	0.41

* Ref. 10 (at 35°C)
** Ref. 1 (at 30°C)

According to Kaminsky, the temperature coefficient of B is negative for the strongly hydrated ions such as Li^+, Be^{2+}, Mg^{2+}, Fe^{2+}, and Ce^{3+}, as seen from Table 4. Therefore, the B-value of 0.38 obtained for $[Co(H_2O)_6]^{2+}$ ion at 25° is very reasonable, compared with the Kaminsky's value of 0.36 at 35°.

The B-value for $[Co(NH_3)_6]^{3+}$ ion is much smaller than that for $[Co(H_2O)_6]^{2+}$ ion, as seen

2) "Inorganic Syntheses," Vol. 2, p. 216 (1946).
3) "Inorganic Syntheses," Vol. 2, p. 221 (1946).
4) I. L. Jenkins and C. B. Monk, *J. Chem. Soc.*, **1951**, 68.
5) F. P. Dwyer, E. C. Gyarfas and D. P. Mellor, *J. Phys. Chem.*, **59**, 296 (1955).
6) P. Pfeiffer and B. Werdelmann, *Z. anorg. Chem.*, **263**, 31 (1950).
7) F. Blau, *Monath.*, **10**, 372 (1889).
8) G. Jones and M. Dole, *J. Am. Chem. Soc.*, **51**, 2950 (1929).
9) R. W. Gurney, "Ionic Processes in Solution," McGraw-Hill Book Company, Inc., New York (1953).
10) M. Kaminsky, *Discussions Faraday Soc.*, **24**, 171 (1957).

from Table 3. This might suggest that the water molecules coordinated to the metal ion have a greater interaction with the surrounding molecules of solvent than the ammonia molecules, much more tightly bound to the metal ion, have.

The *B*-values of Co(III) complex cations formed with NH_3, en, pn, bip, and phen, all of which might be called as the luteo-Co(III) ions, increase considerably in that order, as may be expected. The *B*-value of Co(II) chelate of bip (or phen) is almost the same to that of corresponding Co(III) chelate. Moreover, the chelate derived from the bulky ligand, such as bip or phen has a rather large ionic radius, so it may be assumed that such a chelate ion has no large interaction with the solvent molecules. Accordingly, it might be considered that the Co(II) and Co(III) chelates of bip or phen have the similar structure one another.

TABLE 4. *B*-VALUES AND DEPENDENCE ON TEMPERATURE[10]

t°C	Be^{2+}	Mg^{2+}	Fe^{2+}	Co^{2+}	Ce^{3+}
15	0.4345	0.4091	—	—	0.5841
25	0.3923	0.3852	0.4160	—	0.5765
35	0.3444	0.3625	0.3955	0.360	0.5573
42.5	0.3105	0.3472	—	—	0.5427

On the other hand, as seen from Table 3, the *B*-value of the $[Coedta]^-$ chelate is only 0.41, much smaller than the *B*-value of 0.85 of $[Coedta]^{2-}$. In this connection, it is especially interesting to compare these *B*-values with those of EDTA-complexes reported by Charles (Table 5). The *B*-value of the $[Coedta]^-$ is much smaller than that of any other divalent metal chelates given in Table 5. Further, it is easily seen from Table 5, which contains also the values of stability constants reported by Schwarzenbach *et al.*,[11] that metals with a greater affinity for the ligand generally form chelates with smaller *B*-values. These facts might suggest that Co(III) chelate has a stable hexa-coordinated structure, but that divalent metal chelates, having not so stable hexa-coordinated structure as the Co(III) chelate, are present as a penta-coordinated structure or as a mixture of the penta- and hexa-coordinated structures.

TABLE 5. *B*-VALUES AND STABILITY CONSTANTS (k) OF ETHYLENEDIAMINETETRAACETATO COMPLEXES

Metal	*B*	log k
Cu^{2+}	0.82	18.80
Ni^{2+}	0.86	18.62
Co^{2+}	0.88	16.31
Zn^{2+}	0.88	16.50
Mn^{2+}	0.91	14.04
Cd^{2+}	0.98	16.46
Pb^{2+}	0.83	18.04
Mg^{2+}	0.88	8.69
Ca^{2+}	1.07	10.70
Sr^{2+}	1.13	8.63
Ba^{2+}	1.17	7.76

11) G. Schwarzenbach, R. Gut and G. Anderegg, *Helv. Chim. Acta*, **37**, 937 (1954).

BULLETIN OF THE CHEMICAL SOCIETY OF JAPAN VOL. 41 142—149 (1968)

Studies of Phosphorylation. II. Reaction of 2′, 3′-*O*-Isopropylideneinosine and -guanosine with Phosphoryl Chloride[1]

Koji KUSASHIO and Masaharu YOSHIKAWA

Central Research Laboratories, Ajinomoto Co., Inc., Kawasaki

(Received March 20, 1967)

Several reactions accompanied by the phosphorylation of 2′, 3′-*O*-isopropylidene nucleosides with phosphoryl chloride in the absence of an organic solvent were investigated. When the reaction temperature exceeded 30°C, 2′, 3′-*O*-isopropylideneinosine gave 5′-chloro-5′-deoxy-2′, 3′-*O*-isopropylideneinosine and 5′-deoxy-2′, 3′-*O*-isopropylidene-3, 5′-cycloinosine. This cycloinosine, was then further subjected to rapid cleavage in a pyrimidine ring to give 5-amino-4-carbamoyl-N^5, 5′-cyclo-1-β-D-(5′-deoxy-2′, 3′ - *O* - isopropylideneribofuranosyl) - imidazole, 5-amino-4-cyano-N^5, 5′-cyclo-1-β-D-(5′-deoxy-2′, 3′-*O*-isopropylideneribofuranosyl)-imidazole, and the N^5-formyl derivative of the latter. Similar sequences of the chlorination at the 5′-position and the cyclization between 3 and 5′-positions were observed in the case of 2′, 3′-*O*-isopropylideneguanosine, but the resulting 5′-deoxy-2′, 3′-*O*-isopropylidene-3, 5′-cycloguanosine was not susceptible to ring cleavage under the conditions used. The factors affecting these reactions were described, and possible mechanisms were proposed.

A previous paper[2] reported a successful method for the preparation of 5′-nucleotides by a simple procedure. This method, involving the reaction of 2′, 3′-*O*-isopropylidene nucleosides with a large excess of phosphoryl chloride in the absence of any organic solvent, has given the maximum yields of the corresponding 5′-nucleotides at 0—15°C. A slight elevation of the reaction temperature or a prolongation of the reaction time, however, resulted in a gradual decrease in the yield as a result of several side reactions and the glycosidic cleavage. The present paper deals with the identification of all of the side products obtained by the reactions of 2′, 3′-*O*-isopropylideneinosine and -guanosine with phosphoryl chloride, and discuss possible mechanisms.

Results and Discussion

Identification of the Products. The reaction mixtures were treated with ether to precipitate the products, which were then hydrolyzed under mild acidic conditions. The two-dimensional paper chromatographies of the hydrolyzates using solvent 1 and then solvent 2 are shown in Figs. 1 and 2. The products, named H-1, H-2,··· and H-6, and G-1, G-2,··· and G-4, are represented in the figures. The R_f values of the products with three kinds of solvents are summarized in Table 1.

The spots of H-1 and G-1 were positive to the Hanes-Isherwood reagent[3] and negative to the periodate-benzidine test.[4] These properties indicate that both products are nucleotides substituted at one or both hydroxyl groups at 2′ and 3′-positions. Their R_f values and electrophoretic mobilities were in good agreement with those of authentic 2′(or 3′), 5′-diphosphoric esters of inosine and guanosine.

All spots of the other side-products were negative to the Hanes-Isherwood reagent.

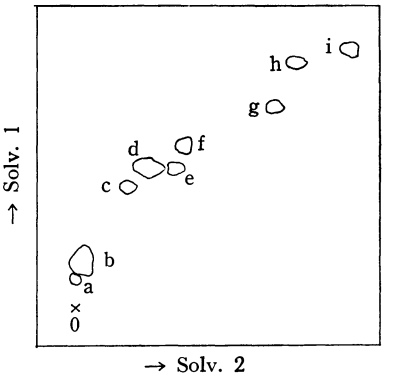

Fig. 1. Two-dimensional paper chromatography of reaction mixture of Ia.
0: original point
a: H-1, b: 5′-IMP, c: H-2, d: inosine
e: hypoxanthine, f: H-3, g: H-4
h: H-5, i: H-6

1) Presented at the Hokkaido Meeting of the Chemical Society of Japan, Sapporo, July 19, 1965.
2) M. Yoshikawa and T. Kato, This Bulletin, **40**, 2849 (1967).
3) C. S. Hanes and F. A. Isherwood, *Nature*, **164**, 1107 (1949).
4) M. Viscontini, D. Hoch and P. Karrer, *Helv. Chim. Acta*, **38**, 642 (1955).

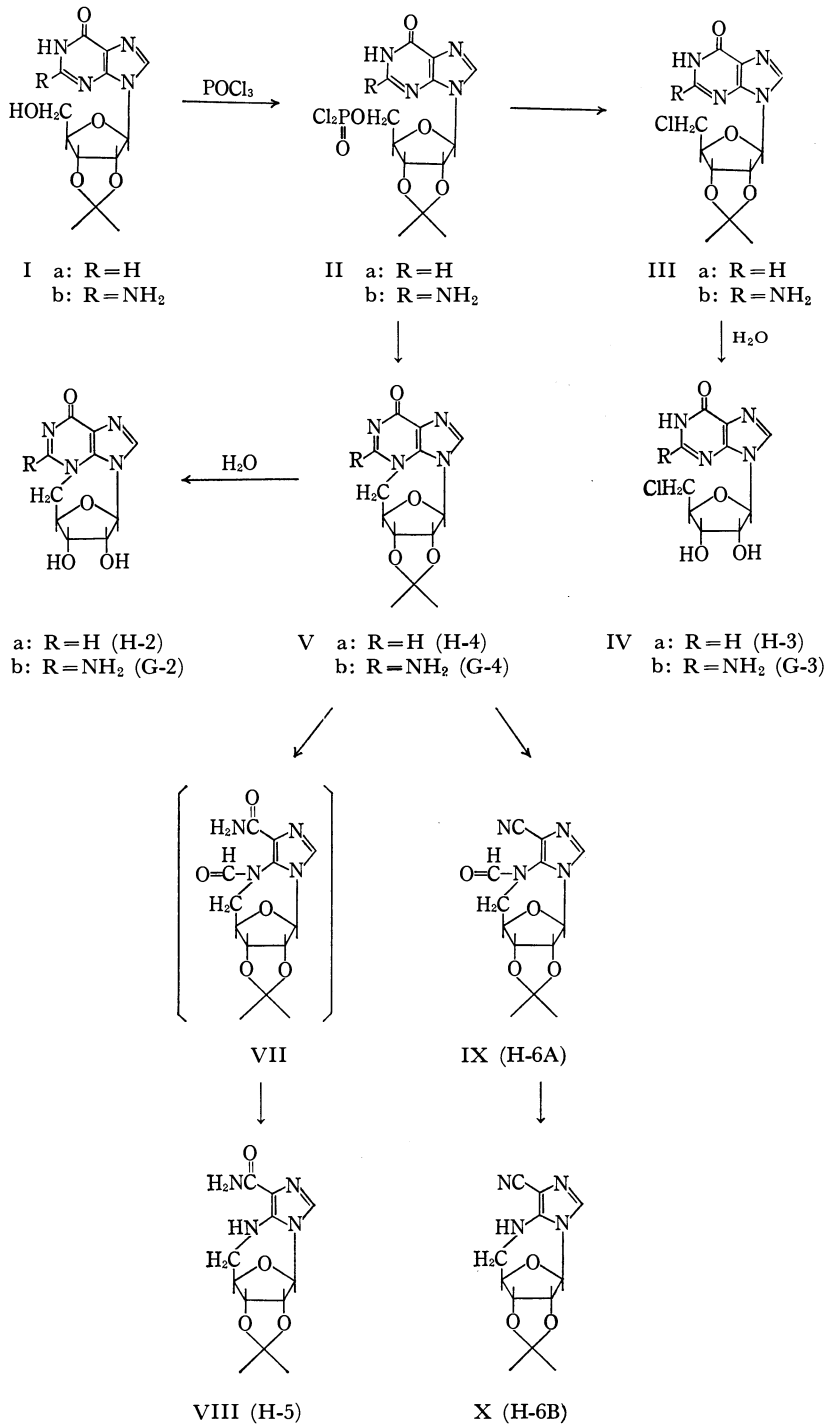

The spot of H-3 gave a positive periodate-benzidine test, and the ultraviolet absorption spectra proved to be similar to those of inosine. These results show the absence of the isopropylidene group and the presence of the unchanged base. The treatment of H-3 in 0.1 N sodium hydroxide under reflux afforded inosine. 5′-Chloro-5′-deoxy-2′, 3′-*O*-isopropylideneinosine (IIIa) was isolated from the chloroform extract of the reaction products and was entirely identical with the compound synthesized by the nucleophilic replacement of 2′, 3′-*O*-isopropylidene-5′-methane-sulfonylinosine with lithium chloride. The R_f values of its acid hydrolyzate were in good agreement with those

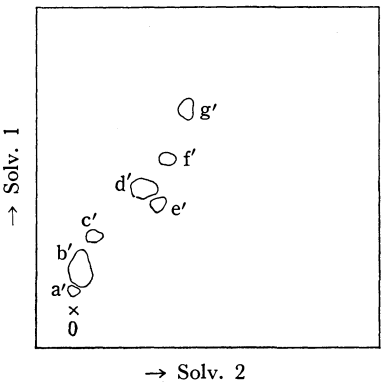

Fig. 2. Two-dimensional paper chromatography of reaction mixture of Ib.

0: original point
a′: G-1, b′: 5′-GMP, c′: G-2
d′: guanosine, e′: guanine, f′: G-3
g′: G-4

TABLE 1. R_f VALUES OF PRODUCTS

Compound	Solv. 1	Solv. 2	Solv. 3
H-1	0.10	0.00	0.68
5′-IMP*	0.15	0.02	0.06
H-2	0.40	0.17	—
Inosine	0.46	0.24	0.48
Hypoxanthine	0.46	0.32	0.30
H-3	0.53	0.35	0.32
H-4	0.76	0.65	0.22
H-5	0.81	0.72	0.14
H-6A	0.85	0.90	0.29
H-6B	0.85	0.90	0.21
G-1	0.06	0.00	0.58
5′-GMP*	0.14	0.02	0.49
G-2	0.24	0.06	—
Guanosine	0.40	0.22	0.36
Guanine	0.35	0.27	0.20
G-3	0.50	0.30	0.18
G-4	0.66	0.37	0.22

* 5′-IMP and 5′-GMP represent inosine 5′-phosphate and guanosine 5′-phosphate respectively in tables and figures.

of H-3. In view of the above facts, it may be concluded that H-3 is 5′-chloro-5′-deoxyinosine (IVa).

The isopropylidene derivative of G-3 was readily separated from the aqueous solution of the reaction products. The acidic removal of the protective group gave G-3. The composition of G-3 satisfied $C_{10}H_{12}O_4N_5Cl$, corresponding to formula IVa. G-3 gave a positive periodate-benzidine test and the same ultraviolet absorption spectra as those of guanosine. After refluxing in 0.1 N sodium hydroxide, G-3 afforded guanosine. From these observations, G-3 was identified as 5′-chloro-5′-deoxyguanosine (IVb).

The infrared and ultraviolet spectra, melting point, and R_f values of H-4 proved to be the same as those[5] of the 5′-deoxy-2,′ 3′-*O*-isopropylidene-3, 5′-cycloinosine (Va) prepared *via* 2′, 3′-*O*-isopropylidene-5′-*O*-(*p*-toluenesulfonyl)-inosine according to the Robins method.[6] The structure was characterized by a single peak at 3.64 τ assigned to a proton at the 1′-position in the NMR spectrum.[7]

Such a characteristic peak of a proton at the 1′-position was also observed in the other 3, 5′-cyclonucleoside derivatives described below, which are summarized in Table 2.

The yield of G-4 was increased nearly 50% by elevating the reaction temperature to 40°C. The ultraviolet absorption spectra were very similar to those of 5′-deoxy-2′, 3′-*O*-isopropylidene-3, 5′-cycloguanosine reported by Chambers *et al.*[8] 3, 5′-(5′-Deoxy-D-ribofuranosyl)-guanine and 5′-deoxy-2′, 3′-*O*-isopropylidene-3, 5′-cycloxanthosine were formed when G-4 was refluxed in 1 N hydrochloric acid and in 1 N sodium hydroxide respectively. These compounds were confirmed by the ultraviolet spectra measurement of the spots on a paper chromatogram according to the Robins method.[6] Also, the NMR spectrum of G-4 supported the 2′, 3′-*O*-isopropylidene cyclonucleoside structure. On the basis of these results, G-4 was concluded to be 5′-deoxy-2′, 3′-*O*-isopropylidene-3, 5′-cycloguanosine (Vb).

The compound Vb could also be prepared directly by the reaction of Ib with methanesulfonyl chloride in pyridine.

The minor products, H-2 and G-2, gave positive periodate-benzidine tests. Their respective ultraviolet spectra were identical with those of Va and Vb, convincing evidence that they were 5′-deoxy-3, 5′-cycloinosine (VIa) and -guanosine (VIb). In fact, the R_f values of the acid hydrolyzates of Va and Vb were in complete agreement with those of H-2 and G-2 respectively.

The ultraviolet absorption spectra of H-5 were very different from those of the starting nucleoside. The NMR spectrum showed a single peak at 3.65 τ due to –NH–, in addition to the peaks indicating a 2′, 3′-*O*-isopropylidene cyclonucleoside structure, and the infrared spectrum exhibited an amide band at 1647 cm^{-1}. These spectral results and the composition supported the theory that H-5 was 5-amino-4-carbamoyl-N^5, 5′-cyclo-1-β-D-(5′-deoxy-2′, 3′-*O*-isopropylideneribofuranosyl)-imidazole (VIII).

5) The absorption maximum at pH 1 was in disagreement with their description.

6) R. E. Holmers and R. K. Robins, *J. Org. Chem.*, **28**, 3483 (1963).

7) The dihedral angle between the $H_1'C_1'C_2'$ plane and the $H_2'C_2'C_1'$ plane becomes nearly 90° upon the 3, 5′-cyclization in purine nucleoside.

8) R. W. Chambers, J. G. Moffatt and H. G. Khorana, *J. Am. Chem. Soc.*, **79**, 3747 (1957).

Table 2. Properties of the products

Compound	max (mμ) pH 1	max (mμ) pH 11	Solvent	NMR (τ) $H_{1'}$	$J_{1'2'}$ (cps)	Isopropylidene group		Characteristic group
IIIa	252	254	DMSO	3.78	2.5	8.48	8.65	
Va	258—263	271	C_5H_5N	3.64	0	8.50	8.76	
IIIb	258	258—267	DMSO	3.93	2.5	8.46	8.65	
Vb	251—257	218, 267	D_2O	3.51	0	8.42	8.68	
VIII	255—264	273	$CDCl_3$	4.24	0	8.49	8.69	3.65(-NH-)
IX	251	252	$CDCl_3$	4.11	0	8.49	8.70	1.52(-CHO)
X	251	252	DMSO	3.90	0	8.57	8.72	3.24(-NH-)

The compound H-6 was too small to isolate, but it was increased in the reaction with a mixture of phosphoryl chloride and pyrophosphoryl tetrachloride. Two compounds (named H-6A and H-6B, as is shown in Table 1) were separated by the careful treatment of the crude H-6 precipitates on an alumina column. From the assignment of the NMR spectra, both H-6A and H-6B were found to be isopropylidene cyclonucleosides.

H-6B had a sharp band due to a conjugated cyano group at 2225 cm^{-1} in the infrared spectrum and a broad peak due to –NH– at 3.24 τ in the NMR spectrum. These spectral observations and the composition led us to conclude that H-6B was 5-amino-4-cyano-N^5, 5′-cyclo-1-β-D-(5′-deoxy-2′,3′-*O*-isopropylideneribofuranosyl)-imidazole (X).

The infrared spectrum of H-6A showed a new band due to a formyl group at 1705 cm^{-1} in addition to a cyano group at 2230 cm^{-1}. The NMR spectrum showed the presence of a formyl proton at 1.52 τ and the absence of the –NH– group. These results indicate that H-6A is the N^5-formyl derivative of X (IX).

Discussion of the Mechanism. One possible mechanism for the formation of the nucleoside 2′(or 3′), 5′-diphosphoric ester from 2′,3′-*O*- isopropylidene nucleoside is illustrated by the reaction of the intermediate, 2′,3′-*O*-isopropylidenenucleoside 5′-phosphorodichloridate (II), with dichlorophosphoric acid according to the following equation:

Table 3. Influence of water for preparation of IVa

Molar ratio H_2O/Ia	Time hr	Yield of product (mol%) IVa	5′-IMP
0	2	7	75
0	16	22	42
0.5	2	2	76
0.5	16	10	53
1.0	2	trace	77
1.0	16	4	67
2.0	2	nothing	52
2.0	16	nothing	46

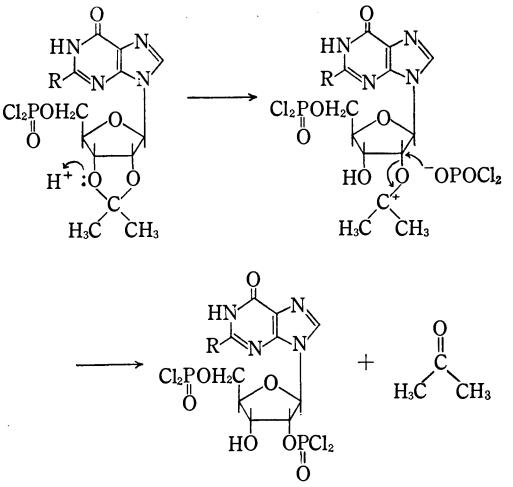

The 5′-chloro derivative IVa, which was a major side product from Ia, decreased with an increase in the amount of water added to the reaction mixture, as is shown in Table 3. This fact indicates that the formation of 5′-chloro-5′-deoxy-2′,3′-*O*-isopropylideneinosine (IIIa) is not due to the reaction of 2′,3′-*O*-isopropylideneinosine (Ia) with the hydrogen chloride produced. In the reaction without the addition of water, the amount of IVa increased with a decrease in 2′,3′-*O*-isopropylideneinosine 5′-phosphorodichloridate (IIa) (analyzed as inosine 5′-phosphate) even after the starting nucleoside Ia (analyzed as inosine) had phosphorylated, as is shown in Fig. 3. From these results, it seems reasonable to assume that the compound III is formed by the intramolecular rearrangement of the compound II.

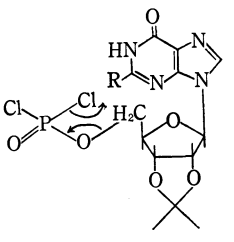

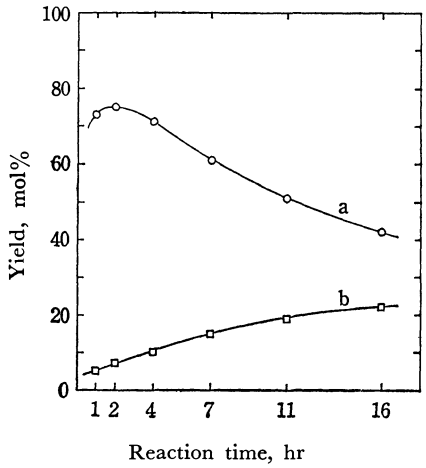

Fig. 3. Influence of reaction time for preparation of IVa.

Experimental condition; Ia: 10 mmol, $POCl_3$: 170 mmol, 20°C
a: 5'-IMP, b: IVa

The formation of the 3, 5'-cyclonucleoside derivative V is considered to be caused by the elimination of the dichlorophosphoryl group from the compound II. The possibility of this mechanism is supported by the increase in the cycloguanosine derivative Vb and the concurrent decrease in the compound IIb with the prolongation of the reaction period, as is shown in Fig. 4.

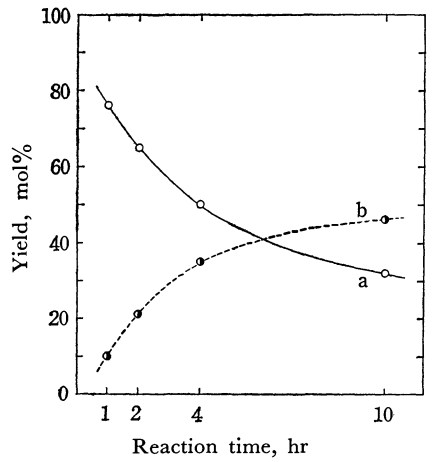

Fig. 4. Influence of reaction time for the preparation of Vb.

Experimental condition; Ib: 10 mmol, $POCl_3$: 170 mmol, H_2O: 5 mmol, 40°C
a: 5'-GMP, b: Vb

3, 5'-Cyclonucleoside has been synthesized *via* 2', 3'-*O*-isopropylidene-5'-*O*-(*p*-toluenesulfonyl)-nucleoside.[6,9] It can be considered that the reaction is dependent on the inductive effect of the tosyl group, and a similar effect can also be expected for the dichlorophosphoryl group. The 3, 5'-cyclization of 2', 3'-*O*-isopropylidene-5'-*O*-(*p*-toluenesulfonyl)-inosine has been more difficult than that of the same guanosine derivative, and the ease of the formation of such cyclonucleosides has been reported to be a function of the basicity of their purine bases.[9] A similar tendency was observed in the present studies. The cycloderivative Vb was more easily produced than the chloroderivative IIIb in the reaction of Ib, in contrast to the case of Ia. The ease of the cyclization of the compound IIb seems to be due to an increase in the electron density of the nitrogen atom at the 3-position because of the electromeric effect of the 2-amino group in the guanine base in addition to the decrease in the electron density of the carbon atom at the 5'-position because of the inductive effect of the dichlorophosphoryl group.

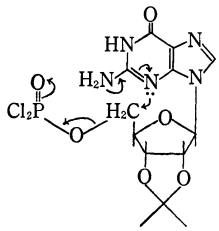

The isopropylidene group of Vb resisted mild acidic hydrolysis, as is shown in Fig. 5, which also exhibits the difference in the elimination rate from those of Ib and Vb. The increase in the stability of the dioxolane ring in cyclonucleoside seems to be due to a decrease in the strain as a result of the cyclization between the ribose and the purine base.

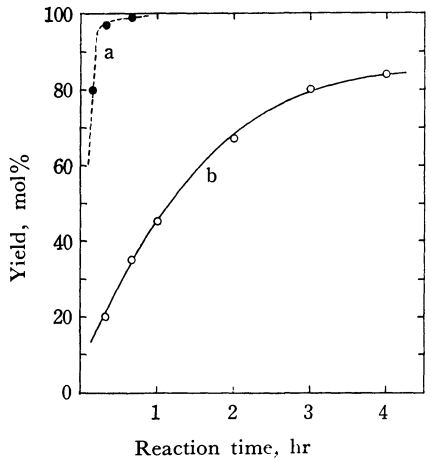

Fig. 5. Elimination rate of isopropylidene groups of Ib and Vb.

Experimental condition; pH 1.5, 70°C
a: guanosine produced, b: VIb produced

9) V. M. Clark, A. R. Todd and J. Zussman, *J. Chem. Soc.*, **1951**, 2952.

The degradation of 3, 5′-cyclopurinenucleoside involving ring cleavage has been studied by Baker[10] and by Todd.[11] It has been illustrated that the degradation is due to the attack of the hydroxyl anion on the carbon atom at the 2-position of the original cyclonucleoside. A similar explanation is acceptable in the present case, since the cleaved compounds, VIII and IX, were given when the cycloinosine derivative Va was heated with phosphoryl chloride hydrolized partially by a small amount of water. The ring cleavage of Va to VIII during the phosphorylation can be attributable to the nucleophilic attack of the dichlorophosphate anion on the 2-position, as is illustrated in following equation:

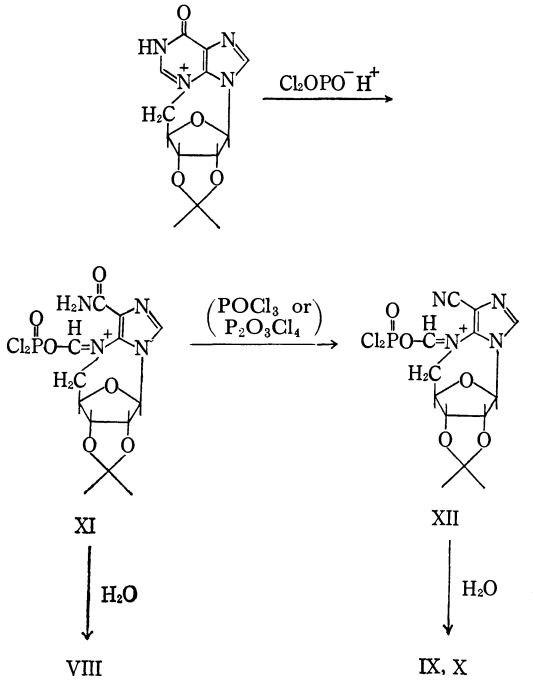

The labile intermediate XI is subjected to the rapid hydrolysis to give VIII.

The dehydration of the intermediate XI by phosphoryl chloride seems to form the compound IX. The addition of a more powerful dehydrating agent, pyrophosphoryl tetrachloride, promoted the formation of IX, as had been expected.

The corresponding ring-opening products of 5′-deoxy-2′, 3′-*O*-isopropylidene-3, 5′-cycloguanosine are not found in the reaction mixture under similar conditions. This may be attributable to the decrease in the positivity of the carbon atom at the 2-position because of the electromeric effect of the amino group. The formyl groups of the compounds VII and IX must be eliminated during the mild acidic hydrolysis.

10) B. R. Baker and J. P. Joseph, *J. Am. Chem. Soc.*, **77**, 15 (1955).

11) A. M. Michelson "The Chemistry of Nucleoside and Nucleotide," Academic Press, London(1963), p. 20.

Experimental

The melting points were determined on a Mitamura Riken hot stage and are uncorrected. The ultraviolet spectra were recorded on Hitachi EPS-2U spectrophotometer, and the infrared spectra on Hitachi EPI-2 and Perkin-Elmer 221 spectrophotometers. The NMR spectra were run on Varian A60 spectrometer, using tetramethylsilane as the internal standard. The paper chromatographies were carried out by the ascending technique on Toyo Roshi No. 51 (40×40 cm), using the following solvent system: Solv. 1, *n*-propyl alcohol - concentrated ammonium hydroxide - water, 20 : 12 : 3; Solv. 2, *n*-butyl alcohol - acetic acid - water, 4 : 1 : 1; Solv. 3, isopropyl alcohol - saturated ammonium sulfate - water, 2 : 79 : 19.

The Isolation of 5′-Chloro-5′-deoxy-2′, 3′-*O*-isopropylideneinosine (IIIa). To phosphoryl chloride (100 m*l*) 2.0 g of 2′, 3′-*O*-isopropylideneinosine (Ia) were added, after which the solution was warmed while being stirred for 5 hr at 40°C. After cooling, the reaction mixture was poured into 500 m*l* of petroleum ether in order to precipitate a syrupy product. The precipitate was centrifuged, washed with petroleum ether, and suspended in 50 m*l* of chloroform, and the solution was poured into an aqueous sodium hydrogen carbonate. After the separated aqueous layer had been extracted with four 50 m*l* portions of chloroform, all the chloroform solutions were collected, dried over anhydrous sodium sulfate, and evaporated to dryness under reduced pressure. The residue was recrystallized from methyl alcohol to give 1.0 g (47%) of IIIa, mp 195—196°C.

Found: C, 47.40; H, 4.79; N, 17.17; Cl, 10.70%. Calcd for $C_{13}H_{15}O_4N_4Cl$: C, 47.78; H, 4.59; N, 17.45; Cl, 10.87%.

The ultraviolet spectrum was similar to that of 2′, 3′-*O*-isopropylideneinosine. R_f values: 0.81 (Solv. 1), 0.94 (Solv. 2).

The Preparation of 2′, 3′-*O*-Isopropylidene-5′-*O*-methanesulfonylinosine. To a solution of Ia (3.08 g) in 50 m*l* of anhydrous pyridine, 1.25 g of methanesulfonyl chloride were added, after which the solution was stirred for 3 hr at 40°C. After it had stood overnight at room temperature, the reaction mixture was poured into 200 m*l* of water and the aqueous solution was extracted with 150 m*l* of chloroform. The chloroform layer was dried over anhydrous sodium sulfate and evaporated to dryness under reduced pressure. The recrystallization of the residue from ethyl alcohol gave 2.0 g of a pure product, mp 172—173°C.

Found: C, 43.67; H, 4.91; N, 14.70%. Calcd for $C_{14}H_{18}O_7N_4S$: C, 43.52; H, 4.66; N, 14.51%.

The Preparation of 5′-Chloro-5′-deoxy-2′, 3′-*O*-isopropylideneinosine (IIIa). 2′, 3′-*O*-Isopropylidene-5′-*O*-methanesulfonylinosine (10 g) and lithium chloride (2.2 g) were added to a mixture of 20 m*l* of acetone and 30 m*l* of ethyl alcohol, and the mixture was heated in a sealed tube for 5 hr at 100°C. The reaction mixture was then concentrated under reduced pressure and poured into ice water to precipitate a colloidal material. After being centrifuged, the product was dried under reduced pressure and recrystallized

from methyl alcohol to yield 1.5 g of an amorphous solid, mp 195—196°C.

Found: C, 47.53; H, 4.85; N, 17.80; Cl, 10.70%. Calcd for $C_{13}H_{15}O_4N_4Cl$: C, 47.78; H, 4.59; N, 17.45; Cl, 10.87%.

The melting point was not depressed on admixture with the IIIa isolated from the phosphorylation mixture; the infrared spectrum was also in complete agreement with that of the isolated IIIa.

The Preparation of 5'-Chloro-5'-deoxyinosine from IIIa. 5'-Chloro-5'-deoxy-2', 3'-*O*-isopropylideneinosine (IIIa) was dissolved in water and hydrolyzed for 1 hr at 70°C after the pH of the solution had been adjusted to 1.5. The hydrolyzed product did not crystallize after concentration owing to its strongly hygroscopic nature, but the product showed the same R_f values (Solv. 1, 0.53; Solv. 2, 0.35) as that of H-3 on paper chromatography. The concentrated residue obtained from the hydrolyzed solution after neutralization afforded hypoxanthine when refluxed in a 0.1 N hydrochloric acid solution and a small amount of inosine when refluxed in a 0.1 N sodium hydroxide solution.

The Preparation of 5'-Deoxy-2', 3'-*O*-isopropylidene-3,5'-cycloinosine (Va). 5'-Deoxy-2',3'-*O*-isopropylidene-3, 5'-cycloinosine was prepared *via* 2', 3'-isopropylidene-5'-*O*-(*p*-toluenesulfonyl)-inosine according to the directions of Holmers and Robins.[6] The melting point, 260—262°C, was slightly lower than their decription, 266—269°C.

The Isolation of 5'-Deoxy-2', 3'-*O*-isopropylidene-3, 5'-cycloinosine (Va). 2' 3'-*O*-Isopropylideneinosine (10 g) was added to a mixture of 46 m*l* of phosphoryl chloride and 0.3 m*l* of water, after which the solution was stirred for 18 hr at 40°C. The reaction mixture was then poured into ether to precipitate the reaction products. After the precipitate had been dissolved in water, the aqueous solution was adjusted to pH 1.5 with a sodium hydroxide solution, heated for 40 min at 70°C, and adjusted again to pH 3. The solution was passed through a Dowex 1-X8 (Cl^- form) (100—200 mesh) column with a bed volume of approximately 500 m*l*, and the ultraviolet absorbing effluent was divided into fraction I and fraction II, each 2 *l* in volume.

The fraction I was neutralized and concentrated to about 50 m*l* under reduced pressure to give a white precipitate. This precipitate was recrystallized twice from water to afford 327 mg (3.3%) of Va, mp 260—262°C, the melting point of which was not depressed by the addition of the authentic sample obtained in the preceding experiment.

Found: C, 50.60; H, 5.44; N, 18.10%. Calcd for $C_{13}H_{14}O_4N_4 \cdot H_2O$: C, 50.64; H, 5.23; N, 18.18%.

The ultraviolet and infrared spectra were entirely superimposable upon those of the corresponding spectra of Va synthesized above.

When this product was heated in an acidic solution of pH 1 for 3 hr at 70°C, the paper chromatography showed the same spot as those of H-2.

The Isolation of 5-Amino-4-carbamoyl-N^5, 5'-cyclo-1-β-D-(5'-deoxy-2', 3'-*O*-isopropylideneribofuranosyl)-imidazole (VIII). The fraction II obtained by the treatment with Dowex 1 in the preceding experiment was evaporated to dryness under reduced pressure, and the residue was extracted with chloroform. Paper chromatography revealed that the chloroform layer contained VIII, plus small amounts of Va, IX, and X. The chloroform layer was dried over anhydrous sodium sulfate and passed through a column (2×60 cm) of alumina (treated with concd. hydrochloric acid, washed with water, and dried at 100°C). The column was eluted with chloroform, and 50 m*l* fractions were collected. Fractions 12—22 were concentrated to give 550 mg (6%) of VIII as a colorless solid, mp 120—125°C (decomp.).

Found: C, 51.56; H, 5.87; N, 19.98%. Calcd for $C_{12}H_{16}O_4N_4$: C, 51.42; H, 5.75; N, 19.99%.

IR (KBr): ν_{max} 1647 ($-CONH_2$), 1598 (C=C) cm^{-1}.

The compounds IX and X were too small to be isolated in this experiment.

The Isolation of 5-Amino-4-cyano-N^5, 5'-cyclo-1-β-D-(5'-deoxy-2', 3'-*O*-isopropylideneribofuranosyl)-imidazole (X) and Its N^5-Formyl Derivative (IX). To a mixture of 27.6 m*l* of phosphoryl chloride and 10.9 m*l* of pyrophosphoryl tetrachloride, 10 g of Ia were added, after which the solution was worked up according to the method used in the case of the isolation of Va. The fraction II obtained by treatment with Dowex 1 was adjusted to pH 7, concentrated to 100 m*l* under reduced pressure, and extracted with chloroform. The chloroform solution was dried over anhydrous sodium sulfate and evaporated to dryness to give 400 mg of a white solid. Paper chromatography showed that the solid consisted almost entirely of IX (H-6A) and X(H-6B). The solid was dissolved in chloroform and passed through a column (1.5×20 cm) of alumina (treated by the preceding method). The column was then eluted with chloroform, and the eluate was fractionated into 50 m*l* portions. Fractions 3—4 were combined and evaporated to dryness under reduced pressure. The recrystallization of the residue from water gave 50 mg of IX, mp 211°C (decomp.).

Found: C, 54.14; H, 5.17; N, 19.20%. Calcd for $C_{13}H_{14}O_4N_4$: C, 53.79; H, 4.86; N, 19.31%.

IR (KBr): ν_{max} 2230 ($-C\equiv N$), 1705 (-CHO), 1596 (C=C) cm^{-1}.

When fractions 7—8 were also combined and evaporated to dryness under reduced pressure, 150 mg of a white powder were obtained. The powder was recrystallized from methyl alcohol to give white needles, mp 270—271.5°C.

Found: C, 54.80; H, 5.58; N, 20.89%. Calcd for $C_{12}H_{14}O_3N_4$: C, 54.96; H, 5.38; N, 21.36%.

IR (KBr): ν_{max} 2225 ($-C\equiv N$), 1614 (C=C) cm^{-1}.

The Isolation of 5'-Chloro-5'-deoxy-2', 3'-*O*-isopropylideneguanosine (IIIb). A solution of 2.0 g of Ib suspended in 150 m*l* of phosphoryl chloride was warmed for 3 hr at 50—55°C and then poured into ether after cooling. The precipitated product was slowly dissolved in 100 m*l* of water so that the pH of the aqueous solution was maintained at about 7 by the gradual addition of a sodium hydroxide solution, after which the insoluble material was collected on a filter. The insoluble material was then washed with hot water and dissolved in a dilute sodium hydroxide solution. The solution was treated with charcoal and neutralized with hydrochloric acid to precipitate 183 mg (8.7%) of IIIb, mp 275—280°C (decomp.).

Found: C, 45.07; H, 4.80; N, 19.76%. Calcd for $C_{13}H_{16}O_4N_5Cl \cdot \frac{1}{4}H_2O$: C, 45.16; H, 4.81; N, 20.26%.

R_f values: 0.80 (Solv. 1), 0.58 (Solv. 2). The

ultraviolet spectra were similar to those of Ib.

The Preparation of 5-′Chloro-5′-deoxyguanosine (IVb) from IIIb. A solution of 200 mg of IIIb suspended in 50 m*l* of water was adjusted to pH 1.5 and heated for 2 hr at 70°C. The solution was then neutralized with concentrated ammonium hydroxide, concentrated to 7 m*l* under reduced pressure, and cooled to afford a syrupy product. Recrystallization from water gave 120 mg of a white solid, mp 240°C, with a gradual decomposition.

Found: C, 39.18; H, 4.10; N, 22.85; Cl, 11.86%. Calcd for $C_{10}H_{12}O_4N_5Cl\cdot\frac{1}{4}H_2O$: C, 39.23; H, 4.11; N, 22.87; Cl, 11.58%.

This product consumed one equivalent mole of periodic acid per mole of the nucleoside as formula IVb upon oxidation by the Fleury-Lange method.[12] When refluxed in 0.1 N hydrochloric acid and 0.1 N sodium hydroxide solutions, this product gave guanine and a small amount of guanosine respectively. The treatment of this solid with acetone according to the method of Mori *et al.*[13] afforded 5′-chloro-5′-deoxy-2′,3′-*O*-isopropylideneguanosine (IIIb).

The Isolation of 5′-Deoxy-2′,3′-*O*-isopropylidene-3,5′-cycloguanosine (Vb). To a mixture of 27.6 m*l* of phosphoryl chloride and 10.9 m*l* of pyrophosphoryl tetrachloride, 10 g of Ib were added, after which the mixture was stirred for 7 hr at 40°C. Ether was added to the reaction mixture, and the precipitated product was collected on a filter and dissolved in 300 m*l* of ice water. The solution was adjusted to pH 5, and passed through a Dowex 1-X2 (Cl^- form) (100—200 mesh) column (200 m*l* bed volume), and the column was washed with water. The ultraviolet absorbing effluent was then collected, adjusted to pH 7, and concentrated under reduced pressure until the product began to precipitate, after which it was kept at room temperature. The precipitate was collected on a filter, washed with 10% ethyl alcohol, and dried to give 5.2 g of white crystals. Recrystallization from water afforded 4.25 g of white needles, mp 250—255°C (decomp., with a gradual coloring from 240°C).

Found: C, 50.70; H, 5.02; N, 22.55%. Calcd for $C_{13}H_{15}O_4N_5$: C, 51.14; H, 4.95; N, 22.94%.

When a part of the crystals were refluxed in 1N hydrochloric acid for 1 hr and the solution was developed on paper chromatography, a new spot was found at the R_f value of 0.09 by Solv. 1 and at 0.08 by Solv. 2. This spot was identified as 3,5′-(5′-deoxy-D-ribofuranosyl)-guanine by comparing its ultraviolet absorption maxima with the values of the literature.[6] When refluxed in a 1 N sodium hydroxide solution, Vb gave a new spot which showed R_f values of 0.68 (Solv. 1) and 0.58 (Solv. 2). This product was similarly identified as 5′-deoxy-2′,3′-*O*-isopropylidene-3,5′-cycloxanthosine.

The Preparation of 5′-Deoxy-2′,3′-*O*-isopropylidene-3,5′-cycloguanosine (Vb). A solution containing 3.4 g of Ib and 1.25 g of methanesulfonyl chloride in 50 m*l* of anhydrous pyridine was heated for 2 hr at 80°C. The resulting solution was then poured into 200 m*l* of water and evaporated to dryness under reduced pressure. After the residue had been dissolved in water, the pH of the solution was adjusted to 7 and ethyl alcohol was added to the solution. The precipitate was collected on a filter and recrystallized three times from water to give 1.3 g (40%) of white needles.

The crystal was indistinguishable spectrally (infrared and ultraviolet) from a sample of the Vb isolated in the preceding experiment.

The Preparation of 5′-Deoxy-3,5′-cycloguanosine (VIb). A solution of 2.0 g of Vb in 50 m*l* of water was adjusted to pH 1.5 with hydrochloric acid and then heated for 6 hr at 70°C. The resulting solution was neutralized with concentrated ammonium hydroxide, concentrated, and cooled to give a gelationous product. This product was changed to a powdery white precipitate with slight warming in ethyl alcohol. The precipitate was filtered, quickly dried, and reprecipitated from water-ethyl alcohol to give 0.2 g of a product. Although an attempt at elemental analysis failed due to its hygroscopic nature, it was confirmed by the ultraviolet spectra and R_f values that the product was G-2 itself.

The authors wish to express their deep gratitude to Dr. Tetsuya Kato of the Ajinomoto Co., Inc., for his unfailing guidance throughout the course of this work, and Dr. Akihiro Yamazaki for his help with the identification of some of the products.

12) P. F. Fleury and J. Lange, *J. Pharm. Chim.*, **17**, 107, 196 (1933).

13) H. Mori et al., Presented at the Annual Meeting of the Agricultural Chemical Society of Japan, Sapporo, July 21, 1964, p. 269; Ajinomoto Co., U. S. Pat. 3201388 (1965).

BULLETIN OF THE CHEMICAL SOCIETY OF JAPAN VOL. 41 150—155 (1968)

Reaction of Butadiene with Ethylene. IV.*1 Synthesis of 1, 4-Hexadiene by a Cobaltous Chloride-Ditertiary Phosphine Complex and an Organoaluminum Compound Catalyst

Masao IWAMOTO and Sadao YUGUCHI*2

Central Research Laboratories, Toyo Rayon Company, Ltd., Sonoyama, Otsu

(Received May 5, 1967)

A new catalyst consisting of a cobaltous chloride-ditertiary phosphine complex and an organoaluminum compound was found to be effective for the selective preparation of 1, 4-hexadiene by the reaction of butadiene with ethylene. The effects of the reaction variables on the activity and on the selectivity in 1, 4-hexadiene formation were studied. It is considered that a coordination of the ditertiary phosphine on the catalytically activated intermediate is essential for the selective catalysis. A reaction mechanism is proposed which involves an activated hydrido-cobalt complex as intermediate.

This investigation has been undertaken in order to find catalysts suitable for the highly-selective synthesis of 1, 4-hexadiene from butadiene and ethylene. The catalytic preparation of the diene has been reported by Hata[1] and by Alderson *et al.*[2] In Hata's process, the maximum selectivity[3] in 1, 4-hexadiene formation was, at most, 50%, and a fairly large amount of the charged butadiene was consumed in forming higher oligomers and polymeric substances. Binary catalysts containing various iron compounds gave similar results. In a previous paper,[4] however, we reported that a new catalyst consisting of an iron halide, an organoaluminum compound, and a ditertiary phosphine exerted an excellent selectivity (more than 80%) is the formation of the diene.

Since Wilke has opened a new field of cyclic butadiene oligomer formation, involving such substances as cyclododecatriene and cyclooctadiene, numerous patents and reports have been published in this field.[5] The formation of 1, 4-hexadiene is formally a 1, 4-addition of ethylene to butadiene; this type of oligomerization is found in the linear dimerization of butadiene catalyzed by cobalt-containing compounds.[6-9] A transfer of one hydrogen atom is involved in these reactions.

Table 1 summarizes the characteristic catalytic activities of iron, cobalt, and nickel compounds in the addition reactions of butadiene and butadiene-ethylene. It seems likely that the cobalt complex is one of the most suitable catalysts for the oligomerization of butadiene involving hydrogen transfer. The reaction of butadiene with ethylene catalyzed by a cobalt compound metal alkyl catalyst gave 1, 3-hexadiene as a 1 : 1 addition product.[9] A ternary iron catalyst consisting of ferric chloride, triphenylphosphine, and triethylaluminum acted similarly to the cobalt catalyst in the reaction of butadiene, while a different behavior was observed in the reaction of butadiene with ethylene.[10] By adding triphenylphosphine to a binary cobalt catalyst, *e.g.*, a cobalt tris-(acetylacetonate) and triethylaluminum catalyst, the activity with regard to the dimerization of butadiene disappeared.[8] In the reaction of butadiene with ethylene, however, no ternary cobalt catalyst containing a phosphorus compound has been investigated.

In this paper the results of our studies of the addition reaction of butadiene with ethylene catalyzed by a cobaltous halide-ditertiary phosphine complex and an organoaluminum compound will be described.

*1 Part III: M. Iwamoto and S. Yuguchi, *Kogyo Kagaku Zasshi (J. Chem. Soc. Japan, Ind. Chem. Sect.)*, **70**, 1221 (1967).

*2 Present address: Basic Research Laboratories, Toyo Rayon Company, Kamakura, Kanagawa.

1) G. Hata, *J. Am. Chem. Soc.*, **86**, 3903 (1964).

2) T. Alderson, E. L. Jenner and R. V. Lindsey, Jr., *ibid.*, **87**, 5638 (1964).

3) Defined as moles of 1, 4-hexadiene obtained divided by moles of butadiene converted $\times 100$.

4) M. Iwamoto and S. Yuguchi, *J. Org. Chem.*, **31**, 4290 (1966).

5) H. Müller, D. Wittenberg, H. Seibt and E. Scharf, *Angew. Chem.*, **77**, 318 (1965).

6) S. Otsuka, T. Kikuchi and T. Taketomi, *J. Am. Chem. Soc.*, **85**, 3709 (1963).

7) T. Saito, T. Ohno, Y. Uchida and A. Misono, *Kogyo Kagaku Zasshi (J. Chem. Soc. Japan, Ind. Chem. Sect.)*, **66**, 1099 (1963).

8) S. Tanaka, K. Mabuchi and N. Shimazaki, *J. Org. Chem.*, **29**, 1926 (1964).

9) D. Wittenberg, *Angew. Chem.*, **75**, 1124 (1963).

10) M. Iwamoto and S. Yuguchi, This Bulletin, **39**, 2001 (1966).

TABLE 1. CATALYTIC ACTIVITIES OF IRON, COBALT, AND NICKEL COMPLEXES

System[a]	Reactant	Iron	Cobalt	Nickel
$M(acac)_n$-R_3Al	Butadiene	Linear trimer[b]	Linear dimers[c]	Cyclic trimer[d]
$M(acac)_n$-$P(C_6H_5)_3$-R_3Al	Butadiene	Linear dimers[e]	No reaction[c]	Cyclic dimer[d]
$M(acac)_n$-R_3Al	Butadiene and Ethylene	1,4-Hexadiene[f]	1,3-Hexadiene[g]	Cyclic C_{10}-diene[d]
MCl_n-$P(C_6H_5)_3$-R_3Al	Butadiene and Ethylene	C_6-Dienes[h]		Cyclic C_{10}-diene[d]

a) M=Iron, cobalt, or nickel, acac=acetylacetonate, $n=2$ or 3.
b) M. Hidai, Y. Uchida and A. Misono, This Bulletin, **38**, 1243 (1965).
c) Ref. 7. d) Ref. 5. e) H. Takahashi, S. Tai and M. Yamaguchi, *J. Org. Chem.*, **30**, 166 (1965).
f) Ref. 1. g) Ref. 9. h) Ref. 10.

Results

As shown in Table 2, the dienylation reaction to yield 1, 3-hexadiene and linear dimers of butadiene was predominant, although the formation of 1, 4-hexadiene was slightly promoted by the cobaltous halide-triphenylphosphine complex catalyst. The results also suggest the possibility of modifying the catalytic properties of the cobalt compound by the addition of a proper ligand. It has been reported before that a ditertiary phosphine had an excellent effect in making the ternary iron catalyst highly selective for the preparation of 1, 4-hexadiene.[4]

The cobaltous chloride-1, 2-bis(diphenylphosphino)ethane complex, in which the ditertiary phosphine was coordinated as a chelate ligand to the cobaltous ion, was used as one component of the catalyst. The results are summarized in Table 3. At a relatively high concentration of the catalyst, a rapid exothermic reaction proceeded and the absorption of ethylene stopped in a short time. An almost exclusive formation of one product was found by gas chromatographic analysis; this product was identified by its boiling point, its retention volume in a gas chromatogram, the results of a mass analysis, and its infrared absorption spectrum, as 1, *cis*-4-hexadiene.

TABLE 2. CATALYTIC ACTION OF $CoX_2(P(C_6H_5)_3)_2$-$(C_2H_5)_3Al$ SYSTEM IN THE REACTION OF BUTADIENE WITH ETHYLENE

(Toluene 20 m*l*, Butadiene 33.5 g (0.62 mol), Cobalt complex, 2 mmol, $(C_2H_5)_3Al$ 7.3 mmol, Ethylene 40 kg/cm², 80°C, 16 hr)

Cobalt Complex	Product (g)
$CoCl_2$	1,3-Hexadiene (2.5)
	Butadiene dimers (4.5)
	Tacky soild polymer
$CoCl_2(P(C_6H_5)_3)_2$	1,4-Hexadiene (2.2)
	1,3-Hexadiene (a small quantity)
	Butadiene dimers (4.6)
$CoBr_2(P(C_6H_5)_3)_2$	1,4-Hexadiene (2.1)
	1,3-Hexadiene (9.6)
	Butadiene dimers (8.1)

TABLE 3. SYNTHESIS OF 1,4-HEXADIENE: $CoCl_2[(C_6H_5)_2PCH_2$-$CH_2P(C_6H_5)_2]_2$-$(C_6H_5)_3Al$ SYSTEM

No.	1	2	3	4
Co Complex, g	0.167	0.09	0.09	0.09
Al, g	0.92	0.47	0.92	0.5
Solvent,[a] m*l*	CB 50	T20	T20	T20
Butadiene, g	33.5	53.6	80.4	80.4
Ethylene, kg/cm²	20	25	50	50
Temp., °C	70—80	80	90	80
Time, hr	1.25	2	5	17.3
Product, g				
1,4-Hexadiene	45.4	48.1	48.3	66.5
Others	6	1.3	5.3	3.2
Conversion,[b] %	100	61.6	44.5	57
Selectivity,[c] %	89.6	97	90.5	97

a) CB=Monochlorobenzene, T=Toluene
b) Based on the charged butadiene
c) 1,4-Hexadiene (mol)/Butadiene reacted (mol) ×100

The effects of reaction temperatures ranging from 30 to 140°C are shown in Fig. 1. It seems likely that the optimum reaction temperature is

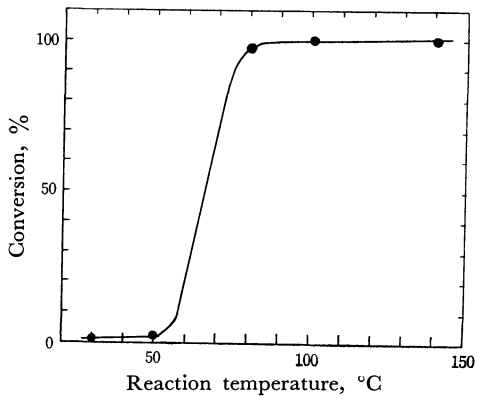

Fig. 1. Reaction temperature *vs.* conversion of the butadiene charged.

in the range from 80 to 100°C. At temperatures higher than 100°C, a considerable isomerization of 1, 4-hexadiene to conjugated dienes, mainly to 2, 4-hexadiene, was observed. The product obtained at 140°C contained 71.6% of the 2, 4-isomer in the C_6-fraction. When the reaction was carried out at 150°C or above, only the 2, 4-isomer appeared. The effect of the molar ratio of Al/Co on the reaction was also studied; the results are shown in Tables 4 and 5. The selectivity of 1, 4-hexadiene was not influenced by the molar ratio. In using this catalyst, a large amount of triethylaluminum was required for the activation, in particular at a low concentration of the cobalt complex, it is considered that the purity of the reactions and solvents also affects the molar ratio of Al/Co.

Table 4. Effect of Al/Co molar ratio (I)
(Toluene 50 m*l*, $(C_2H_5)_3Al$ 0.46 g (4 mmol), Butadiene 33.5 g, Ethylene 50 kg/cm², 90—100°C, 2 hr)

Al/Co Molar ratio	Product, g			Conversion %
	1, 4-Hexadiene	2, 4-Hexadiene	Residue	
8	46.3	3.3	0.4	96.2
16	49.7	3.8	0.4	100
25	45.7	3.2	1.0	100

Table 5. Effect of Al/Co molar ratio (II)
(Toluene 50 m*l*, Cobalt complex 0.09 g (0.097 mmol), Butadiene 33.5 g, Ethylene 55 kg/cm², 80—90°C, 2 hr)

Al/Co Molar ratio	Product, g			Conversion %
	1, 4-Hexadiene	2, 4-Hexadiene	Residue	
10.5	2.5	0.2	0.34	6.9
29.9	6.5	0.2	0.27	14.8
49.5	35.3	2.0	0.6	77.4
71.9	45.6	4.4	0.4	99.4

Although the cobalt complex is insoluble in common organic solvents, a homogeneous catalyst solution can be obtained by mixing the two components of the catalyst. The solution can be stored at room temperature without a decline in catalytic activity (Table 6). The cobalt complex is soluble in 1, 2-dichloroethane to give a dark green solution. A more rapid reaction occurred in the initial stage when 1, 2-dichloroethane was used as the solvent. In this case the control of the reaction temperature was impossible and side reactions occurred to a considerable extent to give the 2, 4-isomer and C_8-dienes. In Table 7 the results obtained by using a variety of solvents are shown. Although the reaction could be carried out smoothly without any solvent, a higher conversion was attained when a proper solvent was used. 1, 4-Hexadiene itself can also be used as a solvent.

In all the reactions described above, triethylaluminum was used as a reducing component. In addition, some other organometallic compounds were also used as reducing agents; the results are summarized in Table 8. It was found that triisobutylaluminum, diisobutylaluminum hydride, and diethylzinc were highly effective in making

Table 6. Activity of the catalyst solution after storage

Period of ftorage, day	Butadiene g	Product, g			Conversion %
		1, 4-Hexadiene	2, 4-Hexadiene	Residue	
2	33.5	36.4	1.05	0.3	75.7
12	36.5	38.3	0.9	0.4	74.8

Table 7. Effect of solvent

Solvent m*l*	None	$C_6H_5CH_3$ 50	C_6H_5Cl 50	*n*-C_7H_{16} 50	$Cl_2C{=}CCl_2$ 50	$(CH_2Cl)_2$ 4	$(CH_2Cl)_2+C_6H_5CH_3$ 4+50
Co complex, g	0.09	0.09	0.169	0.169	0.09	0.09	0.09
$(C_2H_5)_3Al$, g	0.46	0.92	0.92	0.46	0.83	0.83	0.83
Butadiene, g	67	68.4	67	33.5	33.5	67	33.5
Ethylene, kg/cm²	40	20	20	40	40	50	50
Temp., °C	80	70	70	80	95	90	90
Time, hr	2	1	2	2	2	2	2
Product, g							
1, 4-HD	53.4	80	74.6	39.8	57.3	59.6	38.6
2, 4-HD	1.4	1.8	11	9.1	3.1	16.5	2.2
Others	1.1	0.2	1.8	1.0	1.2	18.9[a)]	1.2
Conversion, %	56.2	80	86.5	100	100	90.1	85

a) C_3-dienes were contained.

Table 8. Effect of various organometallics[a]

Organo-metallics	g	Time hr	Product, g			Conversion %
			1,4-Hexadiene	2,4-Hexadiene	Residue	
$(i\text{-}C_4H_9)_3Al$	1.5	2	15.3	0.5	0.4	32.6
$(i\text{-}C_4H_9)_2AlH$	1.5	3	15.8	1.1	0.6	35.3
$(C_2H_5)_2AlCl$	1.0	2	19.7		10.6	73.5
$(C_2H_5)_3Al_2Cl_3$	1.0	2	0	0	22	65.6
$(C_2H_5)_2Al(OC_2H_5)$	1.3	16	0	0	0	0
$(C_2H_5)_2Zn$	1.18	16	11.4	1.02	0.77	26.8
$(C_2H_5)_2Mg$	0.65	16	trace			

a) $CoCl_2[(C_6H_5)_2PCH_2CH_2P(C_6H_5)_2]_2$ 0.08 g, Toluene, 20 ml, Butadiene, 33.5 g, 40 kg/cm^2, 80°C.

the cobalt catalysts selective for 1, 4-hexadiene formation. Although the activity of the catalyst containing diethylaluminum chloride or ethylaluminum sesquichloride was fairly high, the selectivity of 1, 4-hexadiene was low and a considerable amount of polymeric substance was formed. Diethylaluminum ethoxide reacted with the cobalt complex to give a dark brown solution, but no catalytic activity was observed.

It was confirmed that butadiene did not react with isobutene and *n*-butene under the reaction conditions. Therefore, it is possible to use the B-B fraction as a source of butadiene instead of pure butadiene.

Discussion

In a previous paper,[4] the effect of the ditertiary phosphine in the iron ternary catalyst on the selective formation of 1, 4-hexadiene was discussed. It is expected that the ditertiary phosphine will occupy one or more coordination sites around the catalytically active metal atom and that, hence, the coordination of reactants will be suppressed. The ditertiary phosphine, having an apt structure for chelate coordination, was effective. In the preparation of a catalyst for the linear oligomerization of butadiene, the catalyst components should be mixed in the presence of butadiene in order to obtain a highly-active catalyst; otherwise, a black precipitate is separated and no active catalyst is obtained. On the other hand, the cobaltous chloride-ditertiary phosphine complex catalyst can be prepared in the absence of the reactants and kept without a decline in catalytic activity. This fact indicates that low-valent cobalt, formed by a reaction of the cobalt complex with triethylaluminum, is stabilized by the coordination of the ditertiary phosphine. The function of the phosphine in stabilizing a low-valent state of a metal atom is generally accepted.[11] It is known that a reaction of cobaltous chloride-1, 2-bis(diphenylphosphino)-ethane complex with lithium aluminum hydride or sodium borohydride gives a hydride-cobalt complex, $CoH((C_6H_5)_2PCH_2CH_2P(C_6H_5)_2)_2$.[12] A reaction of cobalt tris(acetylacetonate) with diethylaluminum ethoxide in the presence of the ditertiary phosphine also gives the hydride-cobalt complex.[13] However, these combinations of the cobalt complex with lithium aluminum hydride and diethylaluminum ethoxide are catalytically inactive; these facts suggest that the hydrido-cobalt complex itself is not an active species, because the hydrido-cobalt complex is coordinately saturated. It is considered that an organoaluminum compound in the catalyst acts in two ways, that is, as a reducing agent to form the hydrido-cobalt complex, and as an activating agent to place the hydrido-cobalt complex in a coordinately-unsaturated state.

It was found that 1, 2-bis(diphenylphosphino)-ethane formed a 2 : 1 complex with cobaltous chloride, whereas 1, 3-bis(diphenylphosphino)propane formed a 1 : 1 complex. The 1 : 1 complex combined with triethylaluminum revealed a selective activity for the preparation of 1, 4-dienes.[14] On the basis of these findings, it seems that a complete inhibition of the dienylation reaction can be realized by blocking one or two coordination sites around the catalytically active cobalt atom. The coordination of nitrogen-containing ligands to cobalt chloride was, however, ineffective in preparing the diene selectively (Table 9).

From these experimental results, the following mechanism may be proposed; first, the hydrido-cobalt complex is formed as a transient intermediate by the reaction of the cobaltous chloride-1, 2-bis(diphenylphosphino)ethane complex with triethylaluminum, and then the hydrido-cobalt complex is activated to a coordinately unsaturated state by the action of the organoaluminum compound. Butadiene reacts with the activated complex to

11) J. Chatt, *J. Inorg. Nucl. Chem.*, **8**, 515(1958).

12) F. Zingales, F. Canziani and A. Chiesa, *Inorg. Chem.*, **2**, 1303 (1963).

13) Toyo Rayon, Japanese Patent Publication No. 42-2426 (Feb. 2, 1967).

14) M. Iwamoto, Unpublished work.

Table 9. Effect of nitrogen containing chelate ligands[a]

Cobalt Complex[b] mmol	$(Co(Dipy)_3)Cl_2 \cdot 6H_2O$ 1	$(Co(en)_2Cl_2)Cl$ 0.5	$(Co(en)_3)Cl$ 1
$(C_2H_5)_3Al$, mmol	16	8	8
Temperature, °C	80	80	70
Product, g	36.9	31	25.2
Composition, wt%			
1,4-Hexadiene	2.4	1.1	0.6
2,4-Hexadiene	1.9	1.0	0
1,3-Hexadiene	16.0	17.8	15.9
MHT[c]	34.2	48.7	54.5
n-OT[d]	7.8	10.3	7.9
High Boilers	37.6	21.0	21.1
Conversion, %	86.5	68.0	56.7

a) Butadiene 33.5 g, Toluene 50 m*l*, Ethylene pressure 50 kg/cm^2, Reaction time 2 hr.
b) Dipy=α,α'-Dipyridyl, en=Ethylenediamine.
c) MHT=3-Methyl-1,4,6-heptatriene.
d) *n*-OT=*n*-1,3,6-Octatriene.

give a π-butenyl complex such as that derived from butadiene and cobalt hydrocarbonyl.[15] An ethylene molecule coordinated to the activated cobalt complex attacks the π-allyl part of the butenyl group to give a 4-hexenyl complex. This intermediate finally yields 1, *cis*-4-hexadiene, which is set free, while, at the same time, the hydrido-complex is regenerated for further reaction. The exclusive formation of the *cis*-isomer and the facile and selective reaction of butadiene with ethylene constitute strong evidence for the coordination mechanism.

Experimental

Reagents. The solvents were purified by conventional methods. The butadiene (Japan Synthetic Rubber Co.) was dried by passing it through columns of a sodium glycolate-ethylene glycol solution, potassium hydroxide, activated alumina, and a molecular sieve, and then condensed in a measuring vessel kept in a dry ice-acetone bath. The ethylene (Nihon Petrochemical Co.) was used without further purification. The organoaluminum compounds (Ethyl Corp.) were obtained commercially. The triphenylphosphine (Techno Chemie G. m. b. H.) was used without purification. The ditertiary phosphines were prepared according to the method described by Hewertson and Watson.[16] Commercially available ethylenediamine and α,α'-dipyridyl were used. The cobalt halide-triphenylphosphine complex was prepared according to the method of Venanzi.[17]

The cobalt halide-ditertiary phosphine complex was obtained by the reaction of anhydrous cobaltous halide with the ditertiary phosphine in ethanol. The hydrido-cobalt complex was prepared according to the method of Zingales.[12] The cobalt complexes with chelate ligands containing nitrogen atoms were prepared according to the method described in the literature.[18,19]

Reaction Procedure. The reaction was usually carried out in a 200-m*l* pressure vessel equipped with a magnetic stirrer. Under a nitrogen atmosphere, calculated amounts of the solvent, the cobalt complex, liquified butadiene, and the organoaluminum compound were charged in this order into the vessel. After the vessel had then been tightly closed, ethylene was injected directly from the cylinder until a given pressure was reached at a reaction temperature. The mixture was heated with agitation for a given time, cooled to room temperature, and vented to remove any unreacted ethylene. The catalyst was then deactivated by the addition of a small amount of methanol containing dilute hydrochloric acid. The reaction mixture was repeatedly washed with water, after which the organic layer was separated and dried with anhydrous sodium sulfate overnight. A distillate obtained at atmospheric pressure was analyzed by gas chromatography using a copper tube (3 mm in diameter and 3 m long) packed with Apiezon Grease L at 100°C. The yield was calculated by comparing the peak area with that of a substance added as an internal standard. The validity was confirmed by the analysis of a known mixture.

Effect of the Storage of the Catalyst Solution on the Activity. The catalyst solution was prepared by mixing 0.74 g (0.8 mmol) of the cobalt-ditertiary phosphine complex and 3.65 g (32 mmol) of triethylaluminum in 100 m*l* of toluene. The solution was then stored in a 300-m*l* Erlenmeyer flask equipped with a glass stopper under a nitrogen atmosphere at room temperature. After 2 days and 12 days, 20-m*l* portions of the solution were used as catalysts for the reaction of butadiene with ethylene, carried out at 80°C for 2 hr; the results are shown in Table 6.

B-B Fraction as a Source of Butadiene. A B-B fraction purchased from the Mitsubishi Petrochemical Co. was vaporized from a cylinder and condensed in a glass pressure vessel. The B-B fraction was purified by

15) H. B. Jonassen, R. I. Stearns, J. Kenttamaa, D. W. Moore and A. G. Whittaker, *J. Am. Chem. Soc.*, **80**, 2586 (1958).
16) W. Hewertson and H. R. Watson, *J. Chem. Soc.*, **1962**, 1490.
17) L. M. Venanzi, *ibid.*, **1958**, 719.
18) J. B. Work, "Inorganic Syntheses," Vol. II, p. 221 (1946).
19) J. C. Bailar, Jr., *ibid.*, Vol. II, p. 222.

passing it through the column system for butadiene purification described above. It was then again condensed in a measuring vessel. The content of butadiene in the purified B-B fraction was 42.4% while the remainder consisted of C_4-olefins and lower homologues. A 200-m*l* pressure vessle was charged with 10 m*l* of 1, 2-dichloroethane, 100 m*l* of the liquefied B-B fraction, 0.09 g of the cobalt complex, and 0.944 g of triethylaluminum. Under an ethylene pressure of 50 kg/cm^2, the reaction was then carried out for 2 hr at 100°C. Gas chromatographic analysis of the reaction mixture showed that 58.5 g of 1, 4-hexadiene and 2.2 g of 2, 4-hexadiene were produced.

The authors wish to express their appreciation to Mr. M. Taguchi and Mr. T. Aziki for their assistance in the experimental work, and to Toyo Rayon Company for permission to publish this work.

BULLETIN OF THE CHEMICAL SOCIETY OF JAPAN VOL. 41 155—158 (1968)

The Preparation of Optically Active Trimethylcyclododecatriene by the Resolution of Racemic Oligomers and the Asymmetric Oligomerization

Junji FURUKAWA

Department of Synthetic Chemistry, Kyoto University, Sakyo-ku, Kyoto

and Tsuneo KAKUZEN, Hiroyuki MORIKAWA, Ryuzo YAMAMOTO and Osamu OKUNO

Institute for Chemical Research, Kyoto University, Takatsuki

(Received May 17, 1967)

Trimethylcyclododecatriene was prepared by the oligomerization of pentadiene, using the diethylaluminum chloride - titanium tetrabutoxide system as a catalyst. The resulting oligomer was fractionated by vapor-phase chromatography into geometrical (cis and trans) and structural (head-to-tail and head-to-head) isomers with respect to the pentadiene units involved. The structures of these isomers were proposed on the basis of infrared and NMR spectra of the oligomers and their hydrogenated products. The results of the oxidative degradation of the oligomers were compatible with the proposed structures. Further, the existence of stereoisomers was shown by resolution and asymmetric oligomerization. The resolution of *d*- and *l*-enantiomers was carried out through the asymmetric hydroboration of the oligomers, while the asymmetric oligomerization was achieved using the titanium menthoxide - diethylaluminum chloride system as a catalyst.

The cyclotrimers of butadiene[1] and pentadiene[2] have been known to be prepared by means of a transition metal catalyst. The geometrical isomers of the cyclotrimer of butadiene seem to be interesting in relation to the stereochemistry of oligomerization. Among possible isomers, *ttt*-, *ttc*-, and *tcc*-trimers have been reported by Wilke,[1] but little is known of the cyclotrimers of pentadiene-1, 3. In the latter there should exist stereoisomers as well as cis-trans and head-to-tail isomers, but no research has ever been undertaken on stereoisomers of this sort.[2] This paper will describe the separation of the geometrical isomers of the cyclotrimers of pentadiene-1, 3 by means of vapor-phase chromatography with a Gorey column, and the resolution of *d*- and *l*-enantiomers through asymmetric hydroboration. The asymmetric synthesis of optically active oligomers has also been successfully completed by using a titanium catalyst containing asymmetric component. The oligomers thus obtained are low in optical rotation and may, therefore, not be high in optical purity, but this report may have same value as the first one concerning the resolution of such oligomers and asymmetric oligomerization.

Trimethylcyclododecatriene was synthesized using titanium tetrabutoxide and diethylaluminum chloride as catalysts. The reaction was accompanied by the formation of a large amount of polymer of a low molecular weight, and the vacuum distillation afforded trimethylcyclododecatriene as a fraction with a boiling point of 80—100°C at 2 mmHg (whose yield was, however, as low as 15.7%). This compound showed the infrared absorptions for trans and cis unsaturations at 955 cm^{-1} and 735 cm^{-1} respectively. Its ultraviolet

1) G. Wilke, *J. Polymer Sci.*, **38**, 45 (1959); *Angew. Chem.*, **75**, 10 (1963); *Makromol. Chem.*, **69**, 18 (1963).
2) G. Wilke, Japanese Pat. 263197; Brit. Pat. 860377.

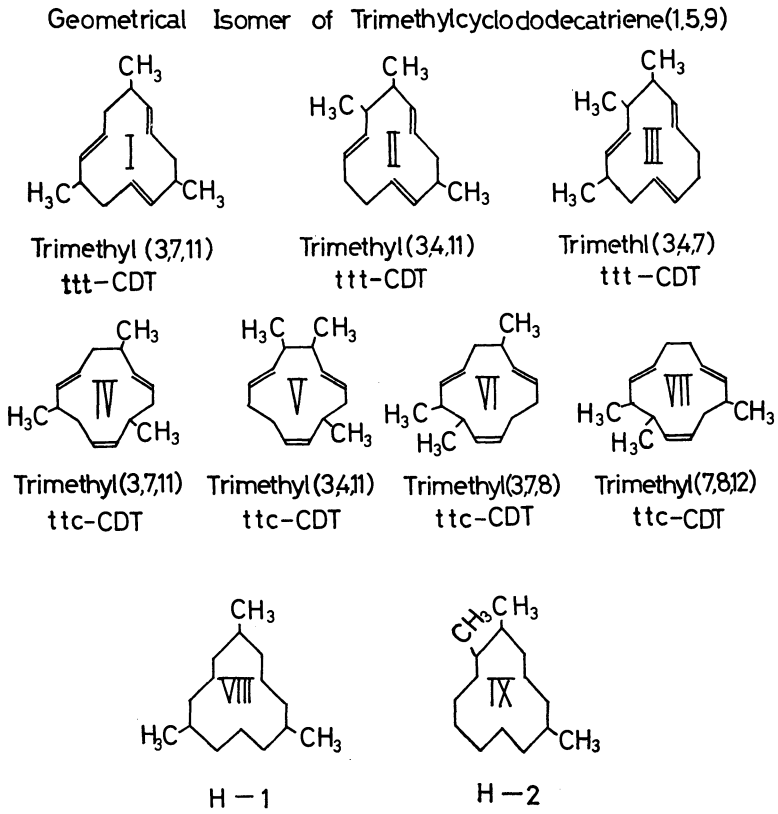

Fig. 1.

spectrum showed no absorption peak corresponding to the conjugated diene structure (at 230 mμ). Its NMR spectrum contained an olefinic proton absorption at $\tau=4.7$—5.2, methine- and methylene-absorptions at $\tau=7.7$—8.2, and a methyl absorption at $\tau=8.8-9.3$, the intensity ratio being 6 : 9 : 9. In the hydrogenated product the ratio of methyl to methine and methylene was 9 : 21. These results accord with any of the cyclic structures, I—VII, in Fig. 1.

Of these, I and IV have all head-to-tail structures, while II, III, V, VI, and VII involve head-to-head and head-to-tail structures. Therefore, there should be two types of hydrogenated products. Hydrogenation with palladium black in ether yielded two products, which were then fractionated into two fractions (named H-1 and H-2) by vapor-phase chromatography using an Apiezone L column at 200°C. NMR study indicated that both H-1 and H-2 contained methyl and other protons in a ratio of 9 : 21, and that H-1 involved methyl absorption at 9.1 and 9.2, whereas H-2 involved such absorption at 9.15 and 9.25, together with that at 9.1 and 9.2. This fact may be accounted for by assuming that the H-1 fraction consists entirely of head-to-tail structures and involves three methyl groups located symmetrically to each other (structure VIII), while the H-2 fraction contains two types of methyl groups, resulting from both head-to-head and head-to-tail structures (structure IX).

Further fractionation by means of Gorey-column vapor-phase chromatography (Hitachi F6D-Q-45) at 180°C indicated that H-1 and H-2 consisted of two and three fractions respectively. This fact may be associated with the presence of cis and trans isomers of methyl groups.

The original trimethylcyclododecatriene was fractionated into five fractions, 1 through 5, forming 7, 13, 21, 15, and 44% of the total respectively. Their infrared spectra indicate that the fractions 1 and 2 correspond to the *ttt*-structure (I, II, or III), while the fractions 3, 4, and 5 correspond to the *ttc*-structure (IV, V, VI, or VII).

The hydrogenation of the fractions 1 and 3 gave H-1, whereas the fractions 2, 4, and 5 gave H-2. Furthermore, methylsuccinic acid was yielded exclusively from the fraction 1 by oxidative degradation with potassium permanganate, while the unfractionated oligomer gave a mixture of succinic, methylsuccinic, and α, α'-dimethylsuccinic acids. Thus, the fractions 1 and 3 must be symmetric in structure.

From these results we may conclude that the fractions 1, 2, and 3 correspond to the structures I, II (or III), and IV respectively. However, it

still remains uncertain to which structure (V, VI, or VII) the fractions 4 and 5 correspond.

The original trimethylcyclododecatriene was resolved by asymmetric hydroboration with diisopinocampheyl borane,[3] which had itself been prepared from BF_3 etherate, sodium borohydride and α-pinene $[\alpha]_D^{20}=+43.8°$, followed by hydroxylation with hydrogen peroxide. From the reaction product, the *ttt*- and *ttc*-oligomers remaining unreacted were fractionated by vapor-phase chromatography, these oligomers showed optical rotations of $-8.0°$ and $-15.7°$ respectively. The other products were hydroxylated products of the oligomer, $[\alpha]_D^{20}=-11.4°$, and isopinocampheol, $[\alpha]_D^{20}=-28.3°$. The optical rotations of unreacted and reacted oligomers are not high, but the resolution may take place to a significant extent.

Finally, we tried to synthesize the optically active oligomer by means of asymmetric oligomerization, using titanium tetramenthoxide or tetraamyloxide and diethylaluminum monochloride as catalysts. The fractions with boiling points of 80—100°C/2 mmHg (yield 10%) and of 100—120°C/2 mmHg (yield 4%) distilled from the reaction product were treated with triethylaluminum and phenylisocyanate in order to remove the menthol. The two fractions thus obtained, which were confirmed by vapor-phase chromatography and IR to contain no menthol, had optical rotations, $[\alpha]_D^{15}$, of $-8.6°$ and $-4.4°$. The distillation residue had $[\alpha]_D^{15}=-2.0°$.

In the case of the titanium tetraamyloxide-diethylaluminum chloride catalyst also, the optically active oligomer was obtained by the same method. The optical rotations were as follows: fraction 80—100°C/2 mmHg, $[\alpha]_D^{15}=-0.9°$ (yield 12%), and the distillation residue, $[\alpha]_D^{15}=-0.5°$.

In conclusion, we have succeeded in the resolution and asymmetric synthesis of trimethylcyclododecatriene.

Our success in the fractionation of geometrical isomers and in the resolution of the enantiomer shows the existence of such isomers. The success in asymmetric oligomerization suggests the possibility that the asymmetric ligand, if present, in titanium catalyst has an asymmetric steric effect on the formation of trimethylcyclododecatriene.

Experimental

Preparation of Trimethylcyclododecatriene. In a 50 m*l* test tube there were placed 10 m*l* (0.1 mol) of purified pentadiene-1, 3, 10 m*l* of purified benzene, and 1 mmol of purified titanium tetra-*n*-butoxide under a nitrogen atmosphere. After 6 mmol of diethylaluminum monochloride had then been added, the test tube was sealed and subjected to a reaction. After the reaction had continued for 48 hr at 40°C, the reaction product was treated with 2 m*l* of methanol and washed with diluted sulfuric acid. After drying with calcium chloride, fractional distillation under a vacuum yielded 1.2 g (15.7%) of trimethylcyclododecatriene (80—100°C/2 mmHg), together with a liquid polymer. The trimethylcyclododecatriene had a boiling point of 256—261°C/760 mmHg and a refractive index, n_D^{20}, of 1.4918.

Found: C, 87.97; H, 11.69%; mol wt (cryoscopic method), 204. Calcd for $C_{15}H_{24}$; C, 88.16; H, 11.84%; mol wt, 204.

The infrared spectrum showed trans- and cis-unsaturations at 955 cm^{-1} and 735 cm^{-1} respectively, but no vinyl unsaturation. The ultraviolet spectrum showed no peak at 230 mμ corresponding to that of the conjugated double bond. NMR study confirmed the presence of methine, methylene, and methyl groups in a 6 : 9 : 9 ratio.

Hydrogenation of Trimethylcyclododecatriene. Two hundred milligrams of purified trimethylcyclododecatriene were hydrogenated in 2 m*l* of ether with 200 mg of a Pd-black catalyst at 25°C under H_2-pressure (300 mmH_2O). The product was trimethylcyclododecane, which was a mixture of H-1 and H-2.

Oxidative Degradation of Trimethylcyclododecatriene. Trimethylcyclododecatriene was oxidized by the drop-by-drop addition of a potassium permanganate solution for 4 hr at 5°C. After the oxidation, sulfur dioxide was passed through until the solution became clear. After the product had then been extracted with ether, the ether was evaporated off and the residue esterified in a mixture of benzene and ethanol by the azeotropic method. The distillates (bp 104—110°C/18 mmHg) were identified as the ethyl esters of succinic, methylsuccinic, and α, α'-dimethylsuccinic acid by vapor-phase chromatography.

Resolution of Trimethylcyclododecatriene. 0.90 g of sodium borohydride was dissolved in 25 m*l* of the diethylene glycol dimethylester (diglyme) and then admixed with 9.8 g of α-pinene $[\alpha]_D^{20}=+43.8°$.

A solution of boron trifluoride-etherate (3.9 g in 5 m*l* of diglyme) was added, drop by drop, over a 15 min period at 0—5°C, after which the mixture was stirred for 4 hr. Furthermore, 4.2 g of trimethylcyclododecatriene were added, drop by drop, over a 15 min period, after which the reaction mixture was subjected to the reaction for 4 hr while being stirred under cooling with ice. One milliliter of water was added to decompose the residual hydride. The reaction mixture was then separated into two layers; the lower layer involved diglyme and water, while the upper layer contained organo-borane, coming from trimethylcyclododecatriene, and unreacted trimethylcyclododecatriene. The upper layer was treated with 30 m*l* of a 3 N sodium hydroxide solution and 30 m*l* of 30% hydrogen peroxide at room temperature and with stirring for one hour. The vacuum distillation of the reaction product yielded 7.2 g of the fraction of 80—100°C/2 mmHg, together with a solid residue. The former fraction contained trimethylcyclododecatriene (optically active), isopinocampheol, and a trace of α-pinene; the latter solid was a mixture of hydroxylated trimethylcyclododecatriene, a solid residue, and a trace of isopinocampheol. They were further fractionated by fractional vapor-phase

3) H. C. Brown, N. R. Ayyangar, G. Zweifel and T. Munekata, *J. Am. Chem. Soc.*, **86**, 397, 1071, 1076 (1964).

chromatography. Their optical rotations were as follows: *ttt*-trimethylcyclododecatriene, $[\alpha]_D^{20} = -8.0°$, *ttc*-trimethylcyclododecatriene, $[\alpha]_D^{20} = -15.7°$, isopinocampheol, $[\alpha]_D^{20} = -28.3°$ (literature[3] $-32.4°$), and hydroxylated trimethylcyclododecatriene, $[\alpha]_D^{20} = -11.4°$.

Asymmetric Synthesis of Optically Active Trimethylcyclododecatriene. Optically active trimethylcyclododecatriene was synthesized in a manner similar to that adopted for the optically inactive one, except for the use of an asymmetric titanium alkoxide catalyst, which was prepared in a way to be described later. In order to remove the menthol, 5 m*l* of the product oligomer was treated with 1.5 m*l* of triethylaluminum and 1.5 m*l* of phenyl isocyanate. In the oligomer thus treated, no trace of menthol was found by vapor-phase chromatography or by IR.

Preparation of Titanium Tetraamyloxide. One mol of titanium tetrachloride, purified by refluxing it in the presence of copper powder under nitrogen, was reacted with 5 mol of purified amylalcohol ($[\alpha]_D^{15} = -4.9°$) in *n*-hexane solution at room temperature for 4 hr under dehydrated ammonia vapor. The reaction product was then filtered and subjected to distillation; boiling point 150—152°C/1 mmHg (literature 154°C/0.5 mmHg[4]). The vapor-phase chromatography of the decomposition product obtained with methanol-water showed the presence of tetraamylalcoxide.

Preparation of Titanium Tetramenthoxide. Titanium tetramenthoxide (white powder, melting point over 200°C) was prepared from titanium tetrachloride and menthol ($[\alpha]_D^{15} = -48°$) by the same method.

4) D. C. Bradley, R. C. Mehrotra and W. Wardlew, *J. Chem. Soc.*, **1952**, 2027.

BULLETIN OF THE CHEMICAL SOCIETY OF JAPAN VOL. 41 158—161 (1968)

Studies of the Organic Reactions of Metal Carbonyls. XIII.*1 The Reduction of Olefin Oxides with Potassium Iron Carbonylates

Yoshinobu TAKEGAMI, Yoshihisa WATANABE, Takeaki MITSUDO, Isao KANAYA and Hiromitsu MASADA

Department of Hydrocarbon Chemistry, Faculty of Engineering, Kyoto University, Sakyo-ku, Kyoto

(Received May 27, 1967)

The reaction between potassium iron carbonylates ($KHFe(CO)_4$, $K_2Fe(CO)_4$, and $K_2Fe_2(CO)_8$) and olefin oxides has been studied. Styrene oxide reacts readily with these carbonylates and with carbon monoxide under an atmospheric pressure and at 30°C. As the reaction products, styrene, ethylbenzene, and α- and β-phenylethyl alcohol are obtained. The major product is styrene or β-phenylethyl alcohol for the reaction of $K_2Fe(CO)_4$ or $KHFe(CO)_4$ and $K_2Fe_2(CO)_8$ respectively. The effects of solvents and additives are examined. Further, propylene oxide and epichlorohydrin are found to react with $K_2Fe(CO)_4$ and carbon monoxide to give not only carbonylated products, but also propylene. The results indicate that olefin oxides are generally reduced with $K_2Fe(CO)_4$ and carbon monoxide to give the corresponding olefins and carbon dioxide.

$$R\text{-}CH\text{-}CH_2 + CO \xrightarrow{K_2Fe(CO)_4} R\text{-}CH{=}CH_2 + CO_2$$
(O)

Previous work in this laboratory has shown that propylene oxide and ethylene oxide react with potassium iron carbonylates ($KHFe(CO)_4$, $K_2Fe(CO)_4$ and $K_2Fe_2(CO)_8$) and carbon monoxide[1]; carbon monoxide is readily absorbed, and, as the carbonylated products, β-hydroxy esters*2 are obtained by the treatment of the reaction mixture with iodine and alcohol, indicating that the corresponding β-hydroxyacyliron carbonyls are formed. However, the yield of the esters is very low. This suggests that some reaction other than the carbonylation also occurs.

In the present investigation, the reaction of styrene oxide and epichlorohydrin with the iron carbonylates has been mainly studied in detail in examining for a reaction other than the carbonylation.

Experimental

The Preparation of Potassium Iron Carbonylates, $KHFe(CO)_4$, $K_2Fe(CO)_4$ and $K_2Fe_2(CO)_8$. These salt solutions in alcohols were prepared according to the method described in a previous paper[1]: A

*1 Part XII: Y. Takegami, Y. Watanabe and H. Masada, This Bulletin, **40**, 1459 (1967).

1) Y. Takegami, Y. Watanabe, H. Masada and I. Kanaya, This Bulletin, **40**, 1456 (1967).

*2 β-hydroxybutyrate and β-hydroxypropionate.

50-m*l* portion of 0.22 M $KHFe(CO)_4$, $K_2Fe(CO)_4$, or a 0.11 M $K_2Fe_2(CO)_8$ solution was used in each run.

When $K_2Fe(CO)_4$ is prepared, two equivalent moles of water are formed:[2]

$$Fe(CO)_5 + 4KOH \xrightarrow{\text{in alcohol}} K_2Fe(CO)_4 + K_2CO_3 + 2H_2O \quad (a)$$

Therefore, when a dry solution of $K_2Fe(CO)_4$ was required, the solvent of $K_2Fe(CO)_4$ was once distilled off under a vacuum and then 50-m*l* of a new dry solvent was added.

Materials. The styrene oxide, propylene oxide, epichlorohydrin, iron pentacarbonyl, and other compounds employed in this study were all commercial products.

Reaction Procedures. *Styrene Oxide.* To the solution of the potassium iron carbonylate described above, 3.2 g of styrene oxide were added; the mixture was then agitated vigorously for 3 to 8.5 hr at 30 to 50°C, under an atmosphere of carbon monoxide or nitrogen. The amount of carbon monoxide absorbed was determined by following the change in the readings of a buret. After a certain reaction time, the reaction mixture was poured into a separatory funnel, in which 100-m*l* of water had been placed, and extracted with two 100-m*l* portions of *n*-hexane. The *n*-hexane solution was concentrated to about 10-m*l*, and then submitted to analysis.

Propylene Oxide or Epichlorohydrin. The reaction of $K_2Fe(CO)_4$ with propylene oxide or epichlorohydrin was similarly carried out, and the gas over the reaction mixture was analyzed.

Analytical Procedures. The reaction products were analyzed by gas chromatography and by means of their infrared spectra, which had been taken on a Shimadzu model IR-27 infrared spectrophotometer. Further, styrene was confirmed by being converted to ethylbenzene; after hydrogenation with Raney nickel, the peak of styrene in the gas chromatogram vanished and a new peak of ethylbenzene appeared.

Results

The Reaction of $K_2Fe(CO)_4$ with Styrene Oxide. *The Relation between the Amount of Carbon Monoxide Absorbed and the Yield of the Products.* The results of the reactions are summarized in Table 1 and Fig. 1. All of the reactions were carried out at 30°C under an atmosphere of carbon monoxide, except for Exp. 4, which was carried out under nitrogen.

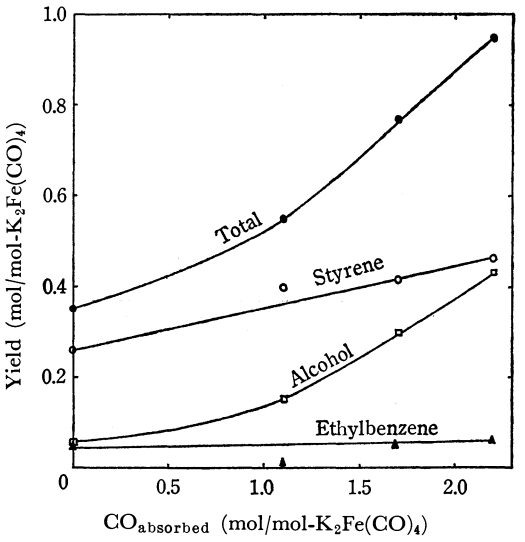

Fig. 1. The reaction of $K_2Fe(CO)_4$ with styrene oxide.

As Table 1 shows, styrene oxide readily reacts with $K_2Fe(CO)_4$ and carbon monoxide, while the reaction solution turns from light brown to dark red. As the reaction products, styrene, which is the major product, ethylbenzene, and α- and β-phenylethyl alcohol are obtained. However, no carbonylated product is obtained.*3 The gas absorption amounts to more than two moles,*4 therefore, the total yield of the products is almost equivalent to the $K_2Fe(CO)_4$ used (see Exp. 3). The plots of the yield of the products against the amount of carbon monoxide absorbed are illustrated in Fig. 1. As Fig. 1 shows, the yields of all products except ethylbenzene increase with the amount of carbon monoxide absorbed.

Table 1. The reaction of $K_2Fe(CO)_4$ with styrene oxide

Exp. No.	Reaction condition*1		CO absorbed	Products			
	Atmosphere	hr		Styrene	Ethylbenzene	Alcohols*2	Total
				mol/mol-$K_2Fe(CO)_4$			
1	CO	3	1.1	0.40	~0	0.15	0.55
2	CO	4	1.7	0.41	0.05	0.31	0.77
3	CO	8.5	2.7	0.46	0.06	0.43	0.95
4	N_2	4	—	0.26	0.05	0.05	0.36

*1 At 30°C, under one atmosphere

*2 α- and β-Phenylethyl alcohol. About 2/3 of the alcohols is β.

2) P. Krumholz and H. M. A. Stettiner, *J. Am. Chem. Soc.*, **71**, 3035 (1949).

*3 No carbonylated product, such as β-hydroxy-β-phenylpropionate, was detected by gas chromatography, even when the reaction mixture was treated with iodine and alcohol.

*4 "Mole" means mole per g atom of Fe, which exists as an iron carbonylate.

TABLE 2. THE REACTION OF $K_2Fe(CO)_4$ WITH STYRENE OXIDE
— Effects of solvents and additives —

Exp. No.	Reaction condition*1			CO absorbed	Product			
	Solvent	Additive*3	hr		Styrene	Ethylbenzene	Alcohol*4	Total
					mol/mol-$Fe(CO)_4$			
5	dry EtOH	—	4	1.6	0.59	~0	0.22	0.81
6*2	dry EtOH	—	4	2.2	0.65	0.05	0.33	1.03
7	dry tetrahydrofuran	—	4	0.06	0.11	~0	0.05	0.16
8	EtOH + H_2O	10	4	1.8	0.23	0.07	0.35	0.65
9	EtOH*5 + Pyridine	10	8	1.4	0.47	~0	~0	0.47

*1 At 30°C except Exp. 6. Under one atmosphere of carbon monoxide.
*2 At 50°C.
*3 mol/mol-$K_2Fe(CO)_4$.
*4 α- and β-Phenylethyl alcohol. About 2/3 of the alcohols is β.
*5 2 mol/mol-$K_2Fe(CO)_4$ of water is included.

TABLE 3. THE REACTION OF $KHFe(CO)_4$ OR $K_2Fe_2(CO)_8$ WITH STYRENE OXIDE

Exp. No.	Reaction condition*1		CO absorbed	Product			
	Iron carbonylate	Atmosphere		Styrene	Ethylbenzene	Alcohol*2	Total
				mol/g·atom·Fe*3			
10	$KHFe(CO)_4$	CO	1.6	0.16	0.04	0.52	0.72
11	$KHFe(CO)_4$	N_2	—	0.14	0.06	0.13	0.33
12	$K_2Fe_2(CO)_8$	CO	1.2	0.13	0.03	0.33	0.49

*1 At 30°C under one atmosphere. Reaction time: 4 hr. Solvent: EtOH.
*2 α- and β-Phenylethyl alcohol. About 2/3 of the alcohols is β.
*3 Fe exists as iron carbonylates.

Effects of Solvents and Additives. The effects of solvents and additives on reactions analogous to Exp. 2 were examined. The results are summarized in Table 2.

In the reaction in dry ethyl alcohol at 30 and 50°C (Exps. 5 and 6), the yield of styrene is better and that of phenylethyl alcohols is worse than those in Exp. 2, in which some of the water formed during the preparation of the iron carbonylate is present in the solvent. This fact indicates that a dry solvent is favorable to the production of styrene and that a relatively small amount of water has an effect on the distribution of the reduction products. In dry tetrahydrofuran solution, scarcely no reaction occurs (Exp. 7).

As additives, water and pyridine were used (Exps. 8 and 9). When 10 mol of water are added, the yield of styrene decreases to about half that in Exp. 2, but the yields of the alcohols increase slightly. When 10 mol of pyridine are added, scarcely no reduction product other than styrene is formed. These results show that the water added has an inhibitory effect on the formation of styrene, but that the pyridine added retards the production of phenylethyl alcohols completely.

The Reaction of $KHFe(CO)_4$ or $K_2Fe_2(CO)_8$ with Styrene Oxide. The results are summarized in Table 3. $KHFe(CO)_4$ and $K_2Fe_2(CO)_8$ also readily react with styrene oxide and carbon monoxide to give styrene and phenylethyl alcohols. As for the reaction of $KHFe(CO)_4$, the major product is not styrene, but β-phenylethyl alcohol (Exp. 10), the yield of which is about 1.7 times as much as that in the reaction of $K_2Fe(CO)_4$ (Exp. 2), indicating that $KHFe(CO)_4$ is very favorable for the production of the alcohol. As Exp. 12 shows, $K_2Fe_2(CO)_8$ is also more favorable for the production of the alcohol than for that of styrene.

The Reaction of $K_2Fe(CO)_4$ with Propylene Oxide or Epichlorohydrin. Propylene oxide and epichlorohydrin also readily react with $K_2Fe(CO)_4$ and carbon monoxide,*5 the reaction solution thus turning from light brown to red brown. Propylene was detected in the gas over both reaction mixtures, the amount being at least 0.2 mol in both cases.

Discussion

The results obtained here show that olefin oxides generally react with $K_2Fe(CO)_4$ and carbon monoxide to give the corresponding olefins. In the course of the reaction, carbon dioxide is definitely

*5 At 20°C, about 2 mol of carbon monoxide were absorbed in both cases.
*6 Analyzed by gas chromatography and by means of a mass spectrum taken on a JMS=OISG mass spectrometer (Japan Electron Optics Laboratory Co.).

produced.*7 Thus, the following reaction appears to occur:

$$R\text{-}\underset{\diagdown\,\diagup}{\underset{O}{CH}}\text{-}CH_2 + CO \xrightarrow{K_2Fe(CO)_4} R\text{-}CH{=}CH_2 + CO_2 \qquad (b)$$

This reaction is not considered to proceed *via* α- and β-phenylethyl alcohol, because they do not react with the iron carbonylate and carbon monoxide. The reaction mechanism, however, is not yet completely clear.

The yield of styrene is best when $K_2Fe(CO)_4$ and a dry ethanol solvent are used at 50°C. On the other hand, the reaction of $KHFe(CO)_4$ gives phenylethyl alcohols in the best yield. The addition of water to the $K_2Fe(CO)_4$ reaction system causes a significant decrease in the yield of styrene and a slight increase in the yield of the alcohols. This fact may be explained by assuming that an equilibrium between $K_2Fe(CO)_4$ and $KHFe(CO)_4$ exists in the reaction solution; the reaction of $K_2Fe(CO)_4$ gives styrene, and that of $KHFe(CO)_4$ gives phenylethyl alcohols.

$$K_2Fe(CO)_4 + H_2O \rightleftharpoons KHFe(CO)_4 + KOH \qquad (c)$$

The fact that pyridine used as an additive remarkably inhibits the formation of the alcohols suggests that the pyridine disturbs the reaction of $KHFe(CO)_4$ and styrene oxide by forming a kind of salt between $KHFe(CO)_4$ and the pyridine.

$K_2Fe_2(CO)_8$ shows a rather reduced reactivity in comparison with $K_2Fe(CO)_4$ and $KHFe(CO)_4$.

The reaction of epichlorohydrin with $K_2Fe(CO)_4$ involves another problem; in this reaction, allyl chloride, the corresponding olefin, was not detected by gas chromatography, but propylene was obtained. On the other hand, allyl chloride was found to react readily with $K_2Fe(CO)_4$ under the same conditions as in Exp. 2, with an evolution of propylene.*8 This suggests that the active halogen atom of allyl chloride is readily replaced by a hydrogen atom under these conditions. Therefore, epichlorohydrin may be reduced to allyl chloride in the first step, and then the allyl chloride is converted to propylene as follows:

$$H_2C\text{-}\underset{\diagdown\,\diagup}{\underset{O}{CH}}\text{-}CH_2Cl \rightleftharpoons H_2C{=}CH\text{-}CH_2\text{-}Cl \rightleftharpoons H_2C\text{-}\underset{\diagdown\,\diagup}{\underset{O}{CH}}\text{-}CH_3 \longrightarrow H_2C{=}CH\text{-}CH_3 \qquad (d)$$

This work was supported in part by The Kawakami Foundation, to which our thanks are due.

*7 Carbon dioxide was evolved when the reaction mixture was treated with concentrated hydrochloric acid. The amount of carbon dioxide evolved was almost equal to the sum of the carbon dioxide formed according to Eqs. (a) and (b).

*8 The absorption of carbon monoxide did not occur.

BULLETIN OF THE CHEMICAL SOCIETY OF JAPAN VOL. 41 161—165 (1968)

A New Synthesis of Pyridoxal-5-phosphate

Masaru IWANAMI, Toshiko NUMATA and Masuo MURAKAMI

Central Research Laboratory, Yamanouchi Pharmaceutical Co., Ltd., Azusawa-cho, Itabashi-ku, Tokyo

(Received June 5, 1967)

By the hydrolysis of pyridoxal-5-phosphate Schiff bases, pyridoxal-5-phosphate was prepared in a crystalline form without any further purification. Pyridoxal-5-phosphate Schiff bases were prepared in good yields by the phosphorylation of pyridoxal Schiff bases and were easily purified by alkali-acid reprecipitation. The pyridoxal-5-phosphate thus obtained was demonstrated to be identical with an authentic sample by a study of its UV, IR, and NMR spectra.

It is generally accepted that the biological activity of vitamin B_6 is due to the participation of a phosphorylated derivative, pyridoxal-5-phosphate[1,2] (I). The synthesis of I has been reported by many investigators. Peterson and Sober first obtained I in a crystalline form by the oxidation of pyridoxamine phosphate and by purification through chromatography on cation-exchange resin.[3] The Hoffman La Rosche Co. improved this method and obtained I by the transamination of pyridoxamine phosphate with pyruvic acid in the presence of a metal ion and by purification

1) W. W. Umbreit and I. C. Gunsalus, *J. Biol. Chem.*, **179**, 279 (1949).

2) D. Heyl, E. Jus, S. A. Harris and K. Folkers, *J. Am. Chem. Soc.*, **73**, 3430 (1951).

3) E. A. Peterson and H. A. Sober, *ibid.*, **76**, 169 (1949).

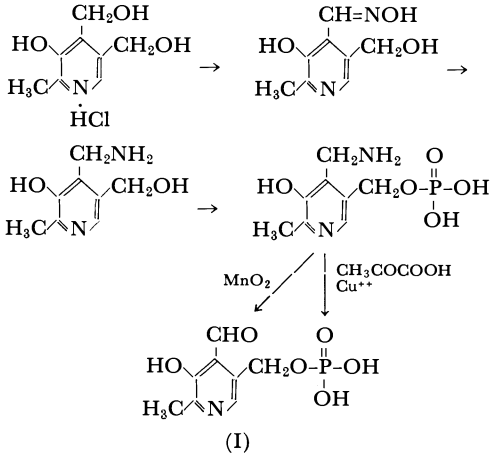

Fig. 1. Synthesis of pyridoxal-5-phosphate from pyridoxamine.

through chromatography on cation-exchange resin,[4] as shown in Fig. 1. In the present study it was established that I can be successfully prepared by the phosphorylation of pyridoxal Schiff bases followed by the hydrolysis of the phosphorylated products.[5]

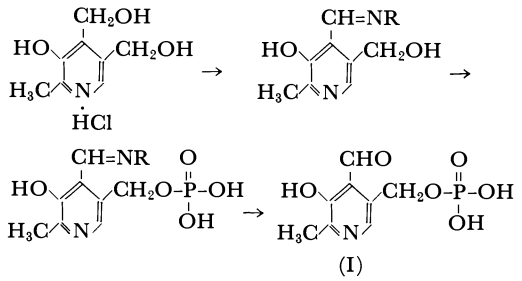

Fig. 2. A new synthesis of pyridoxal-5-phosphate from pyridoxal Schiff bases.

There have been few investigations concerning the synthesis of pyridoxal Schiff bases,[6] which were prepared in this paper from the three different substances described below. Pyridoxal (II) was used at first as the starting substance.[6] Pyridoxal Schiff bases were prepared from II by reaction with amines in methanol. Secondly, a pyridoxal sodium bisulfite addition compound (III), which could be obtained more easily than II from pyridoxine hydrochloride (IV), was used. Various pyridoxal Schiff bases were synthesized from III in yields varying from 30 to 95%, as Fig. 3 shows. Further, a more convenient method for the preparation of pyridoxal Schiff bases was established by the manganese dioxide oxidation of IV, followed by subsequent condensation with amines.

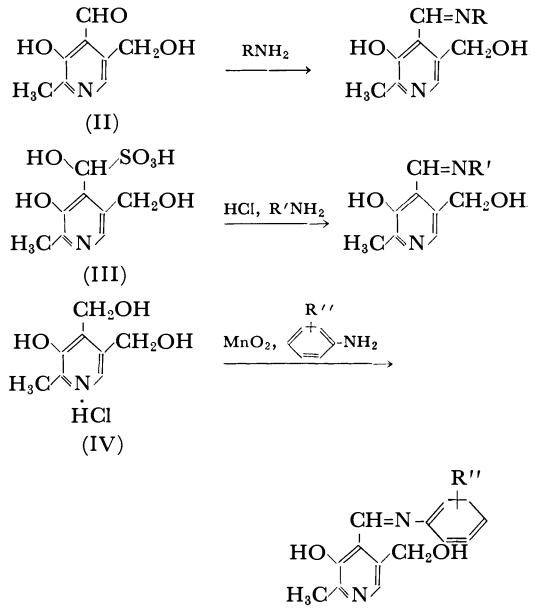

Fig. 3. Synthesis of pyridoxal Schiff bases.

This procedure is best suited to the synthesis of aromatic Schiff bases, since they are insoluble in water and therefore can be isolated as precipitates from the reaction mixture. For example, pyridoxal *p*-toluidine and pyridoxal *o*-phenetidine Schiff bases were obtained in good yields (80—85%) by this procedure.

Because of their instability, especially under acidic conditions, the Schiff bases have generally been considered to be unsuitable for the protection of the aldehyde group. Aromatic pyridoxal Schiff bases are unstable compared with pyridoxamine, which has been used for the starting material of I in a previous method.[3,4] On the other hand, it was found that pyridoxal Schiff bases were stable in a nonaqueous solution, and a mixture of 85% phosphoric acid and phosphorus pentoxide (1.1 : 1) was used for the phosphorylation of pyridoxal Schiff bases. In the case of pyridoxamine, the phosphorylation could be carried out at 60°C without decomposition, but aromatic pyridoxal Schiff bases decomposed almost completely at the same temperature and the yields of I were very low. However, aromatic pyridoxal Schiff bases gave I in good yields when the temperature for phosphorylation was fixed at 40—50°C, while the phosphorylation of aliphatic pyridoxal Schiff bases was effected at higher temperatures, such as at 60°C for 18 hr. The yields of I from various pyridoxal Schiff bases are shown in Table 1.

It can be noticed that aromatic pyridoxal Schiff bases react more rapidly than aliphatic Schiff bases with the phosphorylating agent, and that the presence of such an electron-repulsive substituent as a methoxy, ethoxy, or methyl group in the benzene rings of aromatic pyridoxal Schiff bases

4) R. F. Long, U. S. Pat. 2755284 (1956).
5) M. Murakami, M. Iwanami and T. Numata, Belgium Pat. 651001.
6) D. H. Ellen Luz and S. A. Harris, *J. Am. Chem. Soc.*, **70**, 3669 (1948).

TABLE 1. THE YIELD OF PLP* FROM PL** SCHIFF BASES (ISOLATION THROUGH CATION-EXCHANGE RESIN)

PL aromatic Schiff bases[a] 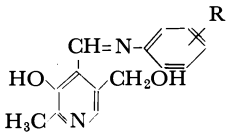		PL aliphatic Schiff bases[b] 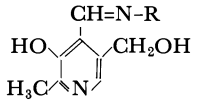	
R	Yield of PLP(%)	R	Yield of PLP(%)
p-Cl	40.3	CH_3	68.2
H	60.5	*n*-C_4H_9	67.0
o-CH_3	75.0	*t*-C_4H_9	61.5
p-CH_3	90.0	*n*-C_6H_{13}	65.6
m-CH_3	85.3	$-CH_2-C_6H_5$	72.5
o-OCH_3	87.9		
p-OCH_3	87.9	$-CH_2-CH_2-C_6H_5$	43.4
o-OC_2H_5	85.0		
p-OC_2H_5	92.0		

* Pyridoxal-5-phosphate ** Pyridoxal
a) Reaction condition: 45°C, 6 hr
b) Reaction condition: 60°C, 18 hr

increases the yields of the phosphorylated products.

Pyridoxal-5-phosphate was isolated in a crystalline form from pyridoxal phosphate Schiff bases obtained by the above-mentioned procedure by a simple treatment. Pyridoxal phosphate Schiff bases were precipitated from the reaction mixture by adjusting the pH to 3—4 and were purified by alkali-acid reprecipitation. Purified pyridoxal phosphate Schiff bases were converted to pure I and amines simply by making the solution strongly alkaline by the addition of sodium hydroxide at room temperature. After the amines had been extracted with organic solvents, I remained as its sodium salt in the water layer, I was isolated in a crystalline form by the adjusting pH to 3—4 by the addition of hydrochloric acid. All of the earlier methods for preparation of I required chromatography on cation-exchange resin and the condensation of the dilute eluate up to the crystalline form, the present method is unique in that it does not involve such a complicated procedure. In the case of *p*-toluidine and *p*-phenetidine Schiff bases, phosphorylated products were obtained in more than 90% yields.

Experimental

Pyridoxal Methylamine Schiff Base. To an aqueous solution of 1.5 g of II, 3 m*l* of 30% methylamine were added. The reaction mixture was then neutralized to pH 7 with a sodium carbonate solution, and extracted twice with 30 m*l* portions of chloroform. The evaporation of the solvent gave a crude pyridoxal methylamine Schiff base, which was then recrystallized from *n*-hexane, mp 148—150°C. Pyridoxal *n*-hexylamine and *n*-butylamine Schiff base were prepared similarly. (Table 2).

Pyridoxal *t*-Butylamine Schiff Base. To a mixture of 1.0 g of II and 0.36 g of *t*-butylamine in 3 m*l* of absolute ethanol, alcoholic potassium hydroxide was added and the solution was heated to reflux for 2 hr. After cooling, the evaporation of the solvent gave an oily residue which was taken up in ether. The evaporation of the ether gave a crude *t*-butylamine Schiff base which was recrystallized from benzene, mp 56—57°C.

Pyridoxal Schiff Base from III (General Procedure). A solution of 3.0 g of III in 10 m*l* of 25% hydrochloric acid was heated at 60°C for 10 min under a nitrogen atmosphere. After cooling, amine was added to the solution. The pyridoxal Schiff base was precipitated from the solution by neutralization with a potassium carbonate solution.

Pyridoxal' *p*-Toluidine Schiff Base from Pyridoxine Hydrochloride. To an aqueous solution of 10.0 g of pyridoxine hydrochloride, manganese dioxide which had been prepared from 8.0 g of potassium permanganate, 9.5 g of sodium bisulfite, and 10.0 g of 50% sulfuric acid were added. After the solution had then been stirred for 4—5 hr, 7.8 g of *p*-toluidine were added. The pyridoxal *p*-toluidine Schiff base was precipitated from the solution, mp 274—275°C. Yield 10.2 g (82%)

The pyridoxal *o*-phenetidine Schiff base, the pyridoxal

TABLE 2. PYRIDOXAL SCHIFF BASES

PL* aromatic Schiff bases 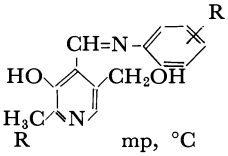

R	mp, °C	Analysis N% Found	Calcd
p-Cl	231	10.20	10.12
o-CH_3	191—192	10.60	10.90
p-CH_3	191—192	11.20	10.90
m-CH_3	188—189	10.69	10.90
H**	178—179	11.47	11.58
o-OCH_3	194—195	10.25	10.30
p-OCH_3	215—216	10.49	10.30
o-OC_2H_5	209—210	10.00	9.78
p-OC_2H_5	200—201	9.48	9.78

PL* aliphatic Schiff bases 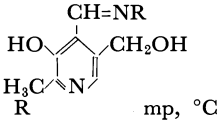

R	mp, °C	Analysis N% Found	Calcd
n-C_4H_9	72— 74	12.77	12.60
t-C_4H_9	56— 57	12.31	12.60
n-C_6H_{13}	83— 84	11.29	11.18
$-CH_2-C_6H_5$**	113—114	10.85	10.94
$-C_2H_4-C_6H_5$**	103—104	10.70	10.36

* Pyridoxal.
** Lit. *J. Am. Chem. Soc.*, **70**, 3669 (1948).

TABLE 3. PYRIDOXAL PHOSPHATE SCHIFF BASES

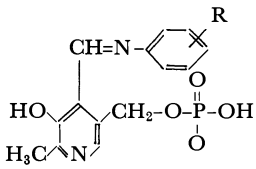

R	Formula	Analysis, % Calcd C	Calcd H	Calcd N	Found C	Found H	Found N	Yield %
p-Cl	$C_{14}H_{14}N_2O_4P\,Cl$	47.10	3.96	7.85	46.91	4.01	7.65	35.0
H	$C_{14}H_{15}N_2O_4P$	52.17	4.65	8.70	51.90	4.82	8.43	68.0
p-CH_3	$C_{15}H_{17}N_2O_4P$	53.57	5.06	8.34	53.23	5.29	8.19	82.0
o-OCH_3	$C_{15}H_{17}N_2O_5P$	51.20	4.86	7.94	50.17	4.94	7.62	78.5
p-OC_2H_5	$C_{16}H_{19}N_2O_5P$	52.46	5.19	7.65	52.02	5.19	7.38	92.0
o-OC_2H_5	$C_{16}H_{19}N_2O_5P$	52.46	5.19	7.65	52.30	5.29	7.75	77.0

p-anisidine Schiff base, *etc.*, were prepared similarly (Table 2).

Pyridoxal Phosphate Schiff Base (General Procedure). To a mixture of 5.0 g of phosphorus pentoxide and 6.5 g of 85% phosphoric acid, 1.0 g of the pyridoxal Schiff base was added. The reaction mixture was then heated at 45°C for 6 hr. After cooling, 5 m*l* of 0.1 N hydrochloric acid was added and the solution was heated at 60°C for 10 min. The reaction mixture was then neutralized with a 50% sodium hydroxide solution. The pyridoxal phosphate Schiff base was precipitated from the solution. The pyridoxal phosphate Schiff bases thus obtained are summarized in Table 3.

Isolation of Pyridoxal-5-phosphate through Chromatography on Cation-exchange Resin (General Procedure) in the Case of Aliphatic Pyridoxal Schiff Bases. To a mixture of 5.0 g of phosphorus pentoxide and 6.5 g of 85% phosphoric acid, 1.0 g of pyridoxal Schiff base was dissolved. The mixture was then heated at 60°C for 18 hr. The resulting solution, after the addition of 5 m*l* of 0.1 N hydrochloric acid, was again heated at 60°C for 10 min and then carefully applied to a 70 m*l* Amberlite IR-120 (acid form) column and eluted with water. The eluate was collected in 10—20 m*l* fractions. As the ultraviolet absorption spectra of pyridoxal-5-phosphate have a maximum at 390 mμ in a neutral or alkaline solution, the absorption spectra of each fraction were measured at 320 and 390 mμ, and those in which $E390\,m\mu/E320\,m\mu = 2.4 \pm 0.1$ were mixed. The first fraction, containing inorganic acid, was subjected to the column again. All the fractions containing pure pyridoxal-5-phosphate were combined and evaporated under reduced pressure below 40°C. A representative elution curve is presented in Fig. 4.

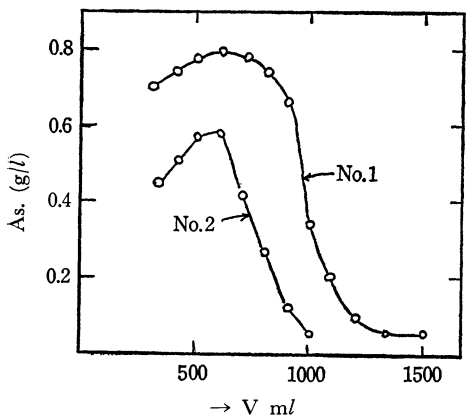

Fig. 4. A elution curve of pyridoxal-5-phosphate.

The curve No. 1 shows the elution pattern of pyridoxal-5-phosphate, while the curve No. 2 shows the elution pattern recovered from the acid part. The yields of pyridoxal-5-phosphate have been summarized in Table 1.

In the Case of Aromatic Pyridoxal Schiff Bases. In a mixture of 5.0 g of phosphorus pentoxide and 6.5 g of 85% phosphoric acid, 1.0 g of the pyridoxal Schiff base was dissolved. The solution was heated at 45°C for 4 hr, and to this 0.1 N hydrochloric acid was added after cooling. The resulting solution was heated again at 60°C for 10 min, carefully subjected to the column after cooling, and eluted with water. Pyridoxal-5-phosphate was obtained from the eluate by the method described above. The yields of pyridoxal-5-phosphate have been summarized in Table 1.

Isolation of Pyridoxal-5-phosphate from Pyridoxal Phosphate Schiff Base (General Procedure). To a suspension of 2.0 g of the pyridoxal phosphate

TABLE 4. THE YIELD OF PLP* FROM PLP* SCHIFF BASES

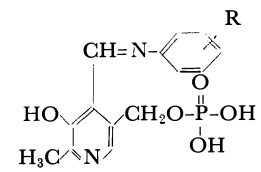

R	Yield of PLP %
p-Cl	63.0
H	70.2
o-CH_3	61.0
p-CH_3	74.7
m-CH_3	61.0
o-OC_2H_5	76.0
p-OC_2H_5	71.0

* Pyridoxal-5-phosphate

TABLE 5. UV SPECTRA DATA OF PLP

Solvent	Max. mμ	E_M	E_M (Lit.)
0.1 N HCl	295	6750	6700
pH 6.9 Buffer soln.	330 388	2500 4920	2500 4900
0.1 N NaOH	305 388	1100 6700	1100 6600

Schiff base in 5 m*l* of water, 10 m*l* of a 2 N sodium hydroxide solution was added. The reaction mixture was extracted twice with 20 m*l* portions of ether. To the water layer, 10 m*l* of 2 N hydrochloric acid was added. The solution was then cooled at 0—5°C overnight. Pure pyridoxal-5-phosphate was thus obtained in a crystalline form from the solution.

The yields of pyridoxal-5-phosphate are summarized in Table 4.

The pyridoxal-5-phosphate thus obtained was demonstrated to be identical with an authentic sample by a study of its UV, IR, and NMR spectra. The ultraviolet spectra data are summarized in Table 5.

The authors wish to express their gratitude to the staff of the analysis laboratory for their elementary analysis and infrared and ultraviolet spectra measurements

BULLETIN OF THE CHEMICAL SOCIETY OF JAPAN VOL. 41 165—167 (1968)

The Cyclization of Ethyl Acetoacetate and Ketones by Ammonium Acetate

Akio SAKURAI and Hiroshi MIDORIKAWA

The Institute of Physical and Chemical Research, Komagome, Bunkyo-ku, Tokyo

(Received June 16, 1967)

The reactions of ethyl acetoacetate with cyclic ketones and aromatic methyl ketones by using excessive ammonium acetate gave some heterocyclic compounds, such as 2-hydroxy-4-methyl-5, 6, 7, 8-tetrahydroquinoline (III), 2-hydroxy-4-methyl-6, 7-dihydro-5*H*-1-pyrindine (IV), and 2-hydroxy-4-methyl-6-alkyl-pyridines (VI). The structures of these compounds were investigated by means of their infrared and NMR spectra.

In a previous paper,[1] the synthesis of pyridone derivatives and related heterocyclic compounds by the condensation of ethyl cyanoacetate with various ketones in the presence of excessive ammonium acetate was reported.

The present paper will deal with the synthesis of hydroxyquinoline and hydroxypyridine derivatives by the reactions of ethyl acetoacetate and aromatic ketones or cyclic ketones with ammonium acetate. The cyclizations between ethyl acetoacetate and the ketones were quite limited compared with the case of ethyl cyanoacetate previously reported.

The cyclization reactions with a number of ketones were attempted; cyclic ketones, such as cyclohexanone and cyclopentanone, and aromatic methyl ketones, such as acetophenone and methyl α-naphthyl ketone, could be involved in this reaction, the hydroxyquinoline derivative (III) and the hydroxypyridine derivatives (IV) and (VI) being products. However, attempts to prepare the hydroxypyridine derivatives by reaction with aliphatic methyl ketones, such as acetone and methyl ethyl ketone, were unsuccessful under similar conditions. The infrared spectra of the dihydro-2-pyridone derivatives (I) described in the previous paper showed sharp bands at 3200 cm^{-1} and 1660 cm^{-1} attributed to the imino group and the carbonyl group of pyridone ring respectively. The NMR spectra of these compounds revealed a signal at 7.8—8.6 ppm due to the imino proton of the pyridone ring.

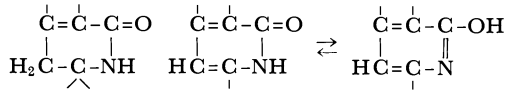

I II

On the other hand, 2-pyridone derivatives (II) gave no signal at 7.8—8.6 ppm and no infrared absorption band at 3200 cm^{-1}. The carbonyl band always appeared in the 1640—1660 cm^{-1} region. None of the infrared spectra of the compounds, III, IV and VI, in the present study exhibited a band at 3200 cm^{-1}, only a broad and weak band at 3370—3440 cm^{-1} and a strong band at 1640—1650 $cm.^{-1}$ Furthermore, the NMR

1) A. Sakurai and H. Midorikawa, This Bulletin, **40**, 1680 (1967).

spectra of these compounds showed no signal in the 7.8—8.6 ppm region, but they did show a signal at 10—12.5 ppm corresponding to one proton. Presumably, the infrared absorption at 3370—3440 cm^{-1} and the NMR signal at 10—12.5 ppm are due to the hydroxy group; dihydro-2-pyridone derivatives are predominantly in the -NH-CO- form, but the 2-quinolone derivatives (III) and the 2-pyridone derivatives (IV and VI) in both the -NH-CO- and -N=C(OH)- forms, as in the structure II. However, the NMR spectra seem to indicate that the -N-C(OH)- form rather than the -NH-CO- form is predominant.

The condensation between ethyl acetoacetate and cyclic ketones in a 1 : 1 molar ratio took place. The corresponding tetrahydroquinoline derivative (III) or dihydropyrindine derivative (IV) were obtained with the elimination of water and alcohol. The scheme of these reactions is

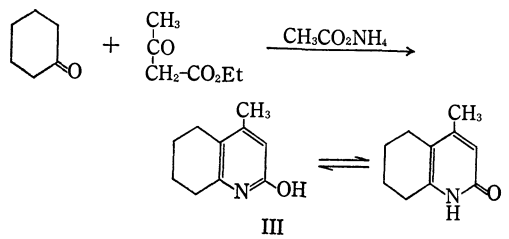

III

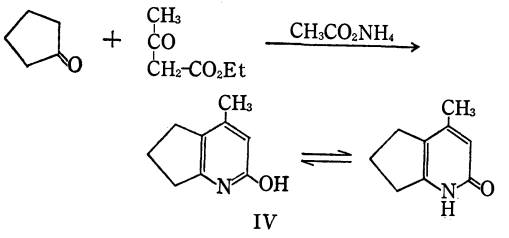

IV

indicated as follows. The dehydration takes place between the carbonyl group of ethyl acetoacetate and the methylene group adjacent to the carbonyl group of ketones.

The condensation of ethyl cyanoacetate with ethylidenecyclohexanone[1] proceeds through a Michael reaction; 2-hydroxy-3-cyano-4-methyl-5, 6, 7, 8-tetrahydroquinoline (V) is thus obtained. On hydrolysis, the cyano group of V gave 2-hydroxy-4-methyl-5,6,7,8-tetrahydroquinoline (mp 251—252°C), as is illustrated below:

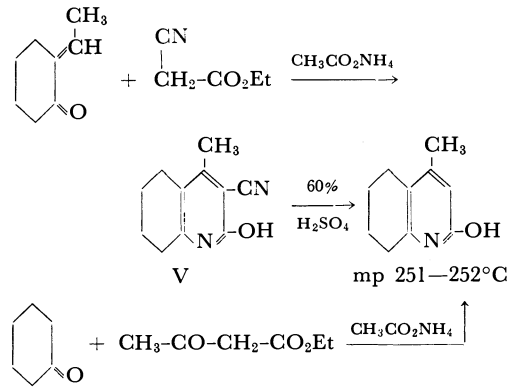

V mp 251—252°C

The compound III was identical with this tetrahydroquinoline (mp 251—252°C) in its melting point, infrared spectrum, and NMR spectrum. Therefore, the condensation products obtained from ethyl acetoacetate and cyclic ketones can be relied upon to have the structures indicated in the scheme A.

The condensations of aromatic methyl ketones with ethyl acetoacetate are considered to proceed similarly to those of cyclic ketones (molar ratio 1 : 1). The dehydration between the carbonyl group of ethyl acetoacetate and the methyl group of the ketones and the elimination of alcohol took place to form hydroxypyridine derivatives. The

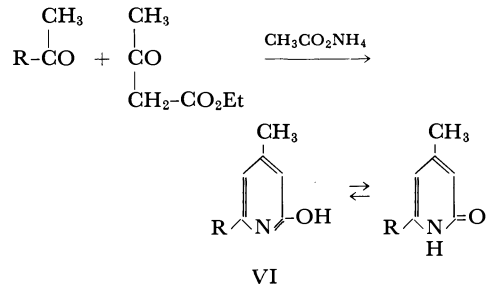

VI

a R=C_6H_5
b R=$C_{10}H_7$

compound VIa was identical with the known 6-phenyl-4-methyl-2-pyridone[2] in its melting point.

All the compounds (III, IV, VIa, and VIb) were colored a reddish orange by alcoholic ferric chloride.

Experimental

All the melting points are uncorrected.

The infrared spectra were determined by means of pressed potassium bromide disks.

The NMR spectra were determined in deuteriochloroform or trifluoroacetic acid at a frequency of 60 Mc, using tetramethylsilane as the internal standard. The chemical shifts are given as ppm downfield from tetramethylsilane.

2-Hydroxy-4-methyl-5, 6, 7, 8-tetrahydroquinoline (III). A mixture of ethyl acetoacetate (13 g, 0.1 mol), cyclohexanone (9.8 g, 0.1 mol), and ammonium acetate (7.7 g, 0.1 mol) was refluxed for 12 hr. After cooling, and after water had been added the reaction mixture was allowed to stand overnight; a crystalline matter was thus precipitated. Recrystallization from alcohol gave colorless needles, mp 252—253°C (lit[3] mp 217—218°C and lit[4] mp 240—241°C); yield 1.9 g (12%).

2) J. C. Bardhan, *J. Chem. Soc.*, **1929**, 2223.
3) A. Dornow and E. Neuse, *Arch. Pharm.*, **287**, 361 (1954).
4) A. I. Meyers and G. Garcia-Munonz, *J. Org. Chem.*, **29**, 1435 (1964).

Found: C, 73.64; H, 7.66; N, 8.60%. Calcd for $C_{10}H_{13}ON$: C, 73.59; H, 8.03; N, 8.58%.

IR: 3370 (broad, ν OH), 1645 (ν C=O), 1620 (ν C=C).

NMR: 2.5 (CH_3, singlet), 2.0, 2.8 (ring CH_2, broad), 7.04 (=CH–, singlet), 11.7—12 (OH, broad).

2-Hydroxy-4-methyl-6, 7-dihydro-5*H*-1-pyrindine (IV). A mixture of ethyl acetoacetate (13 g, 0.1 mol), cyclopentanone (8.4 g, 0.1 mol), and ammonium acetate (7.7 g, 0.1 mol) was refluxed for 8 hr. After the reaction mixture had then stood overnight, a crystalline matter was precipitated. Recrystallization from glacial acetic acid afforded colorless needles, mp 243—244°C; yield 3.5 g (23.5%).

Found: C, 72.47; H, 7.27; N, 9.36%. Calcd for $C_9H_{11}ON$: C, 72.45; H, 7.43; N, 9.39%.

IR: 3440 (broad, ν OH), 1650 (ν C=O), 1620, 1580 (ν C=C), 1450, 1375 (δ CH_3).

NMR: 2.5 (CH_3, singlet), 2—2.8 (ring CH_2, multiplet), 2.85—3.5 (ring CH_2, multiplet), 7.0 (=CH–, singlet), 12—12.5 (OH, broad).

2-Hydroxy-4-methyl-6-phenylpyridine (VIa). A mixture of ethyl acetoacetate (26 g, 0.2 mol), acetophenone (24 g, 0.2 mol), and ammonium acetate (15.4 g, 0.2 mol) was refluxed for 15 hr. After the reaction mixture had then stood several days, a crystalline compound separated. Recrystallization from alcohol gave colorless needles, mp 181—182°C;[2] yield 2.3 g (6%).

Found: C, 77.87; H, 5.84; N, 7.64%. Calcd for $C_{12}H_{11}ON$: C, 77.81; H, 5.99; N, 7.56%.

IR: 3420 (broad and weak, ν OH), 1645 (ν C=O), 1600 (ν C=C).

NMR: 2.26 (CH_3, singlet), 6.36 (=CH–, singlet), 7.55 (C_6H_5, multiplet), 10—10.5 (OH, broad).

2-Hydroxy-4-methyl-6-(α-naphthyl)pyridine (VIb). A mixture of ethyl acetoacetate (13 g, 0.1 mol), methyl α-naphthyl ketone (17g, 0.1mol), and ammonium acetate (7.7 g, 0.1 mol) was refluxed for 12 hr. After the reaction mixture had then been cooled, it was washed with water and extracted with benzene. After the solvent had been removed, the residue was allowed to stand more than three days. A pale yellow powder was thus obtained. Recrystallization from methanol and benzene gave colorless crystals, mp 204—206°C; yield 2 g (8.5%).

Found: C, 81.93; H, 6.11; N, 5.78%. Calcd for $C_{16}H_{13}NO$: C, 81.68; H, 5.57; N, 5.95%.

IR: 1640 (ν C=O), 1600, 1580, 1550, 1510 (ν C=C).

NMR: 2.2 (CH_3, singlet), 6.2 (=CH–, singlet), 7.3—8.0 ($C_{10}H_7$, multiplet), 11.3—11.8 (OH, broad).

The authors wish to express their hearty thanks to Dr. Taro Hayashi and Dr. Tatsuo Takeshima for their kind advice. Thanks are also to Dr. Haruo Homma and his staff for their microanalyses.

BULLETIN OF THE CHEMICAL SOCIETY OF JAPAN VOL. 41 167—171 (1968)

Dehydrocyclization of 3-Methyl Heptatriene-1, 4, 6

Youji KOMATSU

Research Center, Chiba Office, Maruzen Oil Co., Ltd., 824, Konakadaicho, Chiba

(Received June 26, 1967)

Xylenes, mainly consisting of *p*-xylene and *o*-xylene, were selectively synthesized by the dehydrocyclization of 3-methyl heptatriene-1, 4, 6 (MHT) using a chromia-alumina catalyst. MHT was easily converted to xylenes in a good yield; this reaction proceeded even under mild conditions, as at 200°C. The effects of the catalyst composition, and the influence of the reaction temperature on the conversion of MHT, the xylene yield, the by-products, *etc.*, were studied.

The dehydrocyclization of 3-methyl heptatriene-1, 4, 6 (MHT), obtained by butadiene oligomerization,[1-4] was carried out using chromia-alumina, molybdena-alumina, and platforming catalysts.

Though many reports[5-13] have been presented regarding the dehydrocyclization of paraffins

1) G. Wilke, *Angew. Chem.*, **75**, 10 (1963).
2) T. Saito, T. Ohno, Y. Uchida and A. Misono, *Kogyo Kagaku Zasshi (J. Chem. Soc. Japan, Ind. Chem. Sect.)*, **66**, 1094 (1963).
3) S. Ohtsuka, *J. Japan Pet. Inst.*, **9**, 129 (1966).
4) D. Wittenberg, *Angew. Chem.*, **77**, 318 (1965).
5) H. Steiner, "Catalyst," Vol. 4, ed. by P. H. Emett, Reinhold Publishing Corp., New York, N. Y. (1960), p. 529.
6) V. Haensel, "The Chemistry of Petroleum Hydrocarbons," Vol. 2, ed. by B. T. Brooks, Reinhold Publishing Corp., New York, N. Y. (1955), p. 189.
7) K. Ziegler, Brit. Pat. 766876 (1957); *Chem. Abstr.* **51**, 12971 (1957).
8) H. Suzumura H. Yoshida, Y. Tomita and H. Fujiwara, *J. Japan Pet. Inst.*, **8**, 249 (1965).
9) H. Pines and C. T. Goetschel, *J. Org. Chem.*, **30**, 3548 (1965).
10) S. Akiyoshi, A. Matsuda, G. Yamashita and M. Fujii, *Kogyo Kagaku Zasshi (J. Chem. Soc. Japan, Ind. Chem. Sect.)*, **59**, 446 (1956).
11) H. S. Taylor and H. Fehrer, *J. Am. Chem. Soc.*, **63**, 1387 (1941).
12) F. J. Zuiderweg, H. Hoog and J. Verheus, *Trans. Faraday Soc.*, **35**, 997 (1939).
13) E. F. G. Herington and E. K. Rideal, *Proc. Roy. Soc.*, **184**, 434 (1945).

and olefins, and investigating the catalyst, the mechanism of dehydrocyclization, *etc.*, the dehydrocyclization of trienes such as MHT has not yet been examined. It was found that MHT was converted to xylenes (including ethylbenzene) in a good yield with a trace of *m*-xylene.

Experimental

MHT. MHT was obtained through the oligomerization[2] of butadiene by a cobalt(III) acetylacetonate-triethyl aluminum catalyst. Bp 57—58°C/100 mmHg; purity, 98.6%.

Catalyst. All the catalysts except the platforming catalyst were prepared by the impregnation method; active alumina (8—14 mesh) was used as the support, and an aqueous solution of metal nitrates was used as the catalyst-metal source. Each catalyst was pretreated with oxygen at 500—550°C for 2 hr. The platforming R-7 catalyst was used as the platinum alumina catalyst.

Apparatus and Procedure. A conventional flow-type reactor was used as the experimental apparatus. After 50 cc of catalyst had been placed in it, the reactor (d. 15 mm, l. 100 cm) was kept at 500°C for 2 hr in a hydrogen stream; the reaction of MHT (LHSV 1.0—1.3 v/v/hr) was carried out at the reaction temperature and at a normal pressure of the hydrogene stream (H_2/MHT mol ratio 1.0—1.3). Beginning 5 min after the first drop of the product appeared, liquid and gas were collected during a 1-hr period as the reaction products. The liquid product was analyzed by gas chromatography (PEG column; d. 0.15 mm, l. 90 m, 90°C) and the gas was analyzed both by gas chromatography and using a mass spectrometer (Hitachi RMU-5). A typical gas chromatogram of the reaction product is shown in Fig. 4.

Results

Catalyst. Several kinds of catalysts were examined in order to compare the catalyst activity and the selectivity in the dehydrocyclization of MHT. The results are shown in Table 1. It was found that, except for the platforming catalyst, the catalysts used produced a xylene fraction which contained only a trace of *m*-xylene, and that the total aromatics yield decreased in the following order: chromia-alumina, molybdena-alumina, and the platforming catalyst. Under these experimental conditions, the K_2O-Ce_2O_3-Cr_2O_3-Al_2O_3 catalyst showed the best xylene yield, but even in the other catalysts, xylenes were obtained in 52—82 wt% yields per pass. It is very interesting that *m*-xylene were not formed when the chromia-alumina or molybdena-alumina catalysts were used, but when the platforming catalyst was used, *m*-xylene was formed at nearly the same level of equilibrium content.

Influence of Temperature. In the case of the chromia-alumina catalyst, the reaction conditions, the xylene yield, the by-products, *etc.* were investigated.

1) MHT Conversion and Xylene Yield. In the experimental reaction temperature range (150—540°C), the conversion of MHT reached 99—100 mol% (Fig. 1). In the case of the dehydrocyclization of *n*-heptane[8] and 3-methyl heptane[9], the conversion was 41.7% (*n*-heptane) under the same conditions as those used for MHT, and 31—41% (3-methyl heptane) at the temperature of 527°C and the contact time of 3 sec using a chromina-alumina catalyst. When these data were compared with those of MHT, it was considered that the conversion rate of MHT was faster than that of paraffins and olefins. At reaction temperatures higher than 200°C, the higher the temperature, the better the yield of xylenes. At 400—450°C the xylene yield reached maximum; at temperatures higher than 450°C much decomposition and coking began to occure, causing a decrease in the yield of xylenes. The maximum yield of xylenes was attained at the reaction temperature of 450°C, and the total yield of xylenes and *p*-xylene were 82.0 wt% and 48.4 wt% respectively. Akiyoshi and his co-workers[10] obtained a maximum aromatics yield of 53.0% in the dehydrocyclization of 3-methyl heptane with the chromia-alumina catalyst at 450—570°C, and Pines[9] reported that the xylene yield was 10—20 wt% in the aromatization of 3-methyl heptane with the chromia-alumina catalyst.

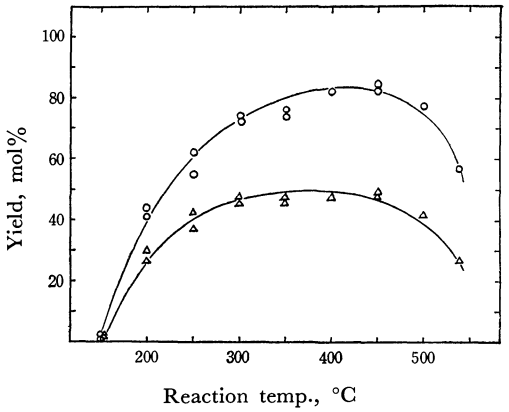

Fig. 1. Relation between xylenes yield and reaction temperature with K_2O-Ce_2O_3-Cr_2O_3-Al_2O_3 catalyst.
—○— Total xylenes —△— *p*-Xylene

In comparing these results, it should be noted that MHT has a higher reactivity than paraffinic hydrocarbons with the same carbon skeltone.

2) Xylene Composition. As shown in Fig. 2, the *p*-xylene content in the xylenes decreased slowly, while the *o*-xylene and ethylbenzene contents gradually increased with the temperature increase. It is remarkable that no *m*-xylene was found below 400°C, while at 400°C a trace of *m*-xylene appeared and at higher temperatures, *m*-xylene was formed in small amounts.

3) By-products. Many kinds of by-products, but in small amounts found in the products. Benzene

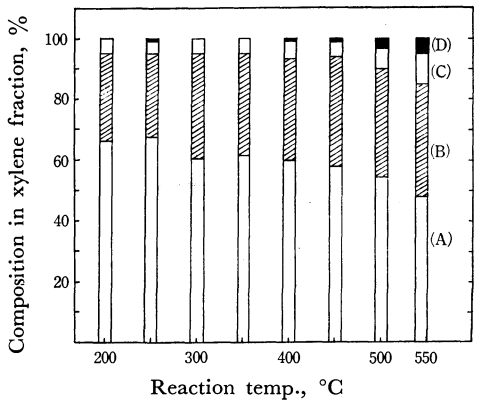

Fig. 2. Xylene composition at various reaction temperature.
(A) *p*-Xylene (B) *o*-Xylene
(C) Ethylbenzene (D) *m*-Xylene

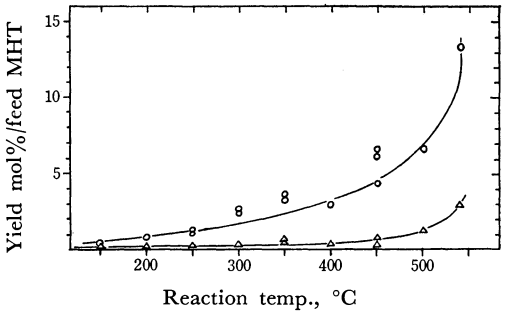

Fig. 3. Benzene and toluene yield.
—○— Toluene —△— Benzene

and toluene were produced in small amounts, but their yields showed a rapid increase above 500°C (Fig. 3)

In our discussion, the other by-products were classified into 2 groups, unknown group 1 (UK-1) and unknown group 2 (UK-2). The UK-1 group has a shorter retention time than toluene in the gas chromatogram (PEG Golay type column, 90°C), while the other has a longer one, as shown in Fig. 4. The boiling points of these unknown substances were determined by means of squalane column gas chromatography (Golay type, 90°C), caliburated by standard hydrocarbon smaples. UK-1 consisted of 9 main compounds; the boiling range assumed to be 85—111°C. UK-2 had 5 major compounds and a boiling range assumed to be 111—135°C. The relationship between the unknown-substance yields and the reaction temperature is shown in Fig. 5. A distinct difference in temperature dependency appeared between the amounts of UK-1 and of UK-2. The UK-1 yield almost does not change at all over the experimental-reaction temperature range. On the con-

Table 1. Dehydrocyclization of MHT with various catalysts

Exp. No.	X-2	X-4	X-7	X-8	X-151
Catalyst					
Components	K_2O	Cr_2O_3	MoO_3	MoO_3	Pt
	Ce_2O_3	Al_2O_3	Al_2O_3	Al_2O_3	
	Cr_2O_3				
	Al_2O_3				Al_2O_3
Composition (wt%)	1.7	12.1	12.1	12.1	0.36
	1.5	87.9	87.9	87.9	
	12.1				
	84.7				98.9
Reaction temp. (°C)	450	450	450	400	450
MHT conversion (mol%)	99.9	99.9	99.9	99.9	99.5
Yield of					
Liq. products (wt%)	94.3	95.5	95.3	95.2	81.2
Aromatics (mol%)	84.1	86.1	80.8	68.3	57.2
Xylenes (mol%)	83.8	82.6	75.7	64.1	52.7
Comosition of liq. product (wt%)					
Benzene	0.7	0.3	0.5	0.6	0.5
Toluene	7.4	6.1	7.4	6.5	4.1
Ethylbenzene	4.4	6.6	7.5	6.0	3.8
m-Xylene	0.4	0.3	0.9	0.9	21.4
p-Xylene	49.2	46.4	40.5	34.9	25.1
o-Xylene	29.4	28.9	26.4	22.1	13.4
MHT	0.1	0.1	0.1	0.2	0.6
UK-1	7.5	10.7	16.2	27.6	20.5
UK-2	0.7	0.6	0.2	1.0	3.2
C_8 up	tr	tr	0.3	0.2	7.4

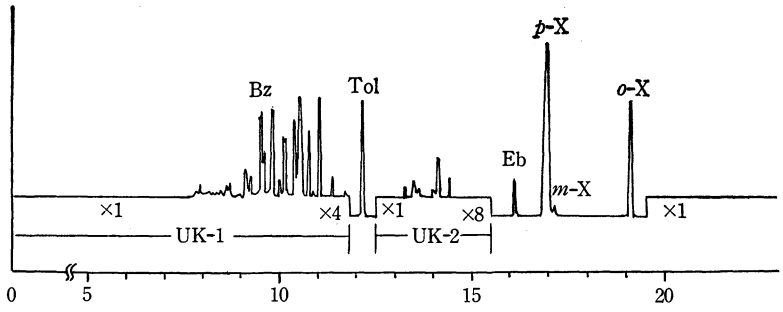

Fig. 4. Reaction product gas chromatogram.

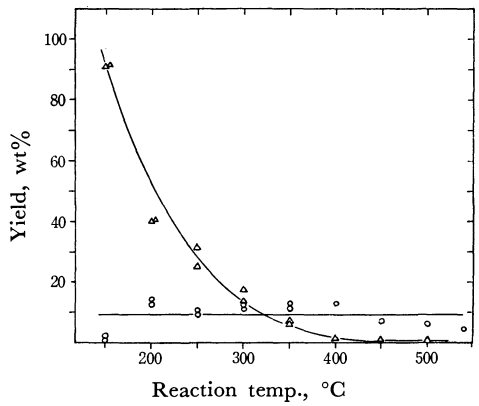

Fig. 5. UK-1 and UK-2 Yield.
—○— UK-1 —△— UK-2

trary, UK-2 was not detected above 400°C, and the UK-2 yield decreased along with the temperature increase, until at 150°C the yield reached about 90%. This reaction product, containing about 90% UK-2, was used instead of MHT as a reaction feed stock for the dehydrocyclization in order to ascertain the character of UK-2. The reaction of this feed stock, diluted with benzene, was carried out at 450°C using a K_2O-Ce_2O_3-Cr_2O_3-Al_2O_3 catalyst. The products of this reaction were analyzed, and the xylene yield calculated. It was found that, the xylene composition and yield were about the same as when MHT was used as the feed stock (Table 2).

4) Deposit on the Catalyst. The yields of the substances on the catalyst at 150—540°C are shown in Fig. 6. It is very interesting to see that deposit-material yield showed a minimum at 300°C. At 500°C, after the reaction, the catalyst surface was covered with a black material which looked like carbonaceous matter, but at 150°C and 200°C, the appearance of the catalyst did not change after the reaction. The reason for the different appearances between 150°C and 540°C was clarified by carbon and hydrogen analyses of these spent catalyst. At 150°C, 200°C, and 540°C the C/H ratios were 6.4, 6.5, and 19.2 respectively (8.0 in MHT). These results shown that, at higher

TABLE 2. DEHYDROCYCLIZATION OF UK-2

Exp. No.	X-141
Catalyst	K_2O-Ce_2O_3-Cr_2O_3-Al_2O_3*1
Reaction temp. (°C)	450
Feed composition (wt%)	
UK-1	1.6
UK-2	58.5
Benzene	39.9
Yield of (mol%)	
Benzene	−2.0*2
Toluene	2.4
Ethylbenzene	4.0
p-Xylene	39.0
m-Xylene	0.0
o-Xylene	19.5
UK-1	18.6
UK-2	2.1
C_8 up	0.3
Xylenes	62.6
Aromatics	62.9

*1 Composition was same as exp. No. X-2 (Table 1).
*2 Charged benzene (for diluent) was not completly recovered, and so the yield showed minus value.

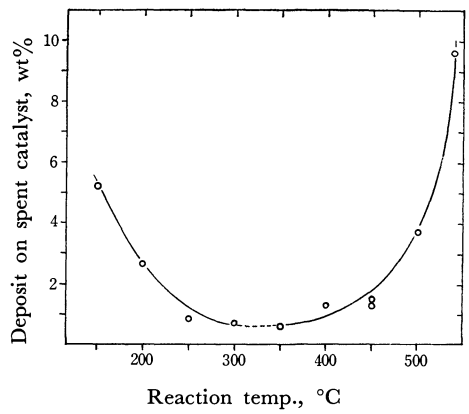

Fig. 6. Deposit on spent catalyst at various reaction temperatures.

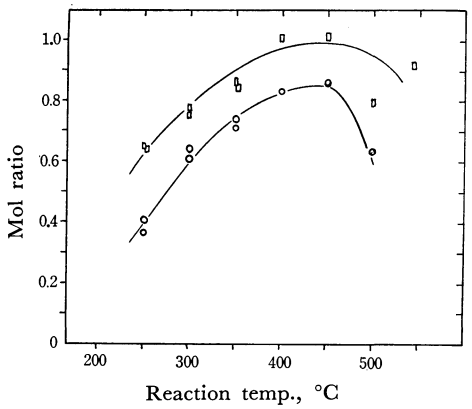

Fig. 7. Evolved hydrogen yield.
—□— H_2/Formed xylenes
—○— H_2/Consmed MHT

temperatures, the deposits on the catalyst were mainly coke, whereas at lower temperatures they seemed to be polymerization products of MHT.

5) Exit Gas. All the exit gas except that at 540°C consisted of 99—90% hydrogen. The mole ratios of evolved hydrogen/consumed MHT and evolved hydrogen/formed xylenes at 200—540°C are shown in Fig. 7. At the reaction temperature between 300—450°C, hydrogen was evolved about stoichiometrically to the xylenes formed, and the evolved hydrogen/consumed MHT mole ratio was about 0.8, which was helpful in estimating the reaction mechanism.

Discussion

Without a catalyst, only 2.5% and 8% of the MHT was converted, the rest was recovered as MHT at 300°C and 450°C respectively. This shows that thermal reaction can be neglected, and that the xylene-formation reaction is undoubtedly accelerated by these catalysts.

On the basis of the above results, let us suggest an alternative assumption regarding the route by which MHT is converted to aromatics:

(1) At first the cyclization of MHT takes place, followed by dehydrogenation.

(2) On the contrary, the dehydrogenation of MHT took place first, and then cyclization took place.

It was presumed, except in the case of the platforming catalyst, that this reaction was carried out *via* the route of assumption (1); this presumption is based on the fact that the amount of hydrogen evolved was about stoichimetrical to the xylenes. Though many dehydrocyclization mechanisms have been presented and discussed,[9-13] *m*-xylene was not formed from MHT; therefore, it seemed in the case of MHT that neither isomerization in its carbon skelton[13] nor the formation of a severn-membered ring took place[9] during this reaction.

Table 3. Reaction of xylenes on chromia-alumina and platforming catalyst

Exp. No.	X-111	X-112
Catalyst	Plat. R-7*	K_2O-Ce_2O_3-Cr_2O_3-Al_2O_3**
Reaction temp. (°C)	450	450
LHSV (v/v/hr)	1.24	1.19
H_2/Feed mole ratio	0.963	0.963
Feed composition		
p-Xylene	62.3	62.0
o-Xylene	36.0	36.8
m-Xylene	0.7	0.0
Ethylbenzene	0.2	0.3
Product composition		
p-Xylene	61.3	62.0
o-Xylene	36.3	36.8
m-Xylene	1.5	0.0
Ethylbenzene	0.3	0.2
Benzene	0.1	tr
Toluene	0.4	0.1

* Composition was same as exp. No. X-151 (Table 1).
** Composition was same as exp. No. X-2 (Table 1).

In our experiments we could not ascertain what kind of intermediate was formed, but xylenes were formed from UK-2 as they were from MHT, and the fact that the catalyst deposit was about the same C-H ratio as that of MHT is very helpful in finding the intermediate.

In the case of the platforming catalyst, the products contained a lot of *m*-xylene. A mixture of *o*- and *p*-xylene was treated at 450°C with the platforming and K_2O-Ce_2O_3-Cr_2O_3-Al_2O_3 catalysts in order to ascertain the difference in these catalysts effects (Table 3). The resulting product composition was the same within the limit of experimental error; this showed that the platforming catalyst did not isomerize *o*- and *p*-xylene. Therefore, it could be understood that the *m*-xylene in the product was not the isomerization product of the *o*- and *p*-xylene which came from the dehydrocyclization of MHT. According to this finding, it could be estimated that, on the platforming catalyst, the dehydrocyclization mechanism of MHT was different from the cases of the chromia and molybdena catalyst.

The author wishes to thank Professor Ryozo Goto, Kyoto University, and Dr. H. Hasegawa for their many helpful discussions and suggestions during this work, and also the manager of the Maruzen Oil Co. Ltd., for permission to publish this work. Thanks are also due to Messrs. T. Tamura, M. Iriuchijima, H. Taniguchi and H. Okamoto for these experimental work and I. Koyabu for gas chromatographic analysis.

BULLETIN OF THE CHEMICAL SOCIETY OF JAPAN VOL. 41 172—176 (1968)

Copolymerization of *N*-Phenylethylenimine and β-Propiolactone

Tsutomu KAGIYA, Tomizo KONDO, Shizuo NARISAWA and Kenichi FUKUI

Faculty of Engineering, Kyoto University, Sakyo-ku, Kyoto

(Received June 30, 1967)

The copolymerization of *N*-phenylethylenimine and β-propiolactone was carried out at 0°C in an acetonitrile solution. *N*-Phenylethylenimine and β-propiolactone copolymerized without any catalyst to give a powdery or a resinous polymer. From the results of a study of the infrared spectrum, X-ray diffraction, differential thermal analysis, and hydrolyses of the copolymer, it was concluded that the homopolymerization of neither monomer took place, and that the copolymer contained the ester structure of —(–N(C$_6$H$_5$)–CH$_2$CH$_2$OC(=O)–CH$_2$CH$_2$–)$_n$– in the main chain. The monomer reactivity ratios of *N*-phenylethylenimine (r_1) and β-propiolactone (r_2) were estimated to be $r_1=7.5$ and $r_2=0.15$.

It is well known that aziridines polymerize to polyimines[1] with various cationic catalysts, and that β-propiolactone to the crystalline polyester with pyridine or other amines.[2,3] It has already been reported by the present authors[4] that ethylenimine and β-propiolactone serve as mutual polymerization catalysts, and that, when these two substances are mixed in bulk, the copolymerization takes place explosively and gives a polymer mainly with a branching structure of β-propiolactone to the polyethylenimine.

As a part of the investigation of the copolymerization of aziridines and cyclic ester, the copolymerization of *N*-phenylethylenimine and β-propiolactone was studied. It was found that the copolymerization took place without any catalyst and gave a white crystalline copolymer. The purpose of the present paper is to determine the structure and composition of the copolymer by means of a study of the infrared spectrum, X-ray diffraction, the differential thermal analysis, and an analytical study of the hydrolysis products of the copolymer.

Experimental

Copolymerization Procedure. Commercial β-propiolactone was distilled over calcium hydride under reduced pressure at 59°C/20 mmHg. The *N*-phenylethylenimine was prepared according to the literature[5] from β-bromoethylaniline hydrobromide. It was dried over sodium sulfate and fractionated twice before use; bp 70—70.5°C/13 mmHg. The acetonitrile was purified by the usual method.[6]

Measured amounts of β-propiolactone and a solvent were placed into a glass ampule under a nitrogen atmosphere, and then *N*-phenylethylenimine was added to this system at −78°C. After the ampule had been sealed and maintained at 0—1°C for a definite period of time, the products were washed with chloroform and diethyl ether, separated by a centrifuge, and dried *in vacuo*.

Physical Analyses of the Copolymer. The melting point of the copolymer was measured visually in a nitrogen atmosphere in a capillary on an electric heater. The reduced viscosity of a 0.25% solution of 90% formic acid was measured at 35°C with an Ostwald viscometer. The infrared spectrum was obtained with the use of the potassium bromide-pellet technique on a Shimadzu infrared spectrophotometer, Model IR-27. The X-ray diffraction diagram was recorded with a powder camera on a Shimadzu X-ray diffractometer, Model GX-3B. The differential thermogram was obtained with the use of a Rigaku Denki differential thermal apparatus, Model VIP-32.

Determination of the Composition of the Copolymer. The absorption peak of the infrared spectrum at 1740 cm^{-1} assigned to the ester group of β-propiolactone, and that at 1600 cm^{-1} assigned to the phenyl group of *N*-phenylethylenimine were used in order to determine the composition of the copolymer.

1) G. D. Jones, in P. H. Plesch, ed., "The Chemistry of Cationic Polymerization," Pergamon, Oxford (1963), Chapter 14.
2) T. Kagiya, T. Sano and K. Fukui, *Kogyo Kagaku Zasshi (J. Chem. Soc. Japan, Ind. Chem. Sect.)*, **67**, 951 (1964).
3) Y. Etienne and R. Sonlas, *J. Polymer Sci.*, **C4**, 1061 (1964).
4) T. Kagiya S. Narisawa, K. Manabe, and K. Fukui, *Kogyo Kagaku Zasshi (J. Chem. Soc. Japan, Ind. Chem. Sect.)*, **68**, 1741 (1965); T. Kagiya, S. Narisawa, K. Manabe and K. Fukui, *J. Polymer Sci.*, **B3**, 617 (1965).
5) H. W. Heine, B. L. Kapur and C. S. Mitch, *J. Am. Chem. Soc.*, **76**, 1173 (1954).
6) A. Weissberger *et al.*, "Technique of Organic Chemistry, Vol VII, Organci Solvents," Interscience Publishers, Inc., New York (1955).

Table 1. Correlation between composition of the copolymer and the optical density ratio, D_{1740}/D_{1600}

Sample No.	Elementary analyses			Composition of copolymer (mol%)		Optical density ratio
	C	H	N	Imine	Lactone	D_{1740}/D_{1600}
1	77.81	7.59	11.17	97.0	3.0	0.215
2	77.21	7.78	10.99	94.0	6.0	0.289
3	69.73	6.94	9.69	88.4	11.6	0.369
4	75.47	7.19	9.86	76.1	23.9	0.688
5	70.11	7.07	9.11	75.5	24.5	0.517
6	66.06	6.57	8.35	71.0	29.0	0.690
7	65.81	6.49	8.23	69.4	30.6	0.883
8	73.20	7.13	9.17	68.2	32.8	1.04
9	73.80	6.81	9.05	66.9	33.1	0.906

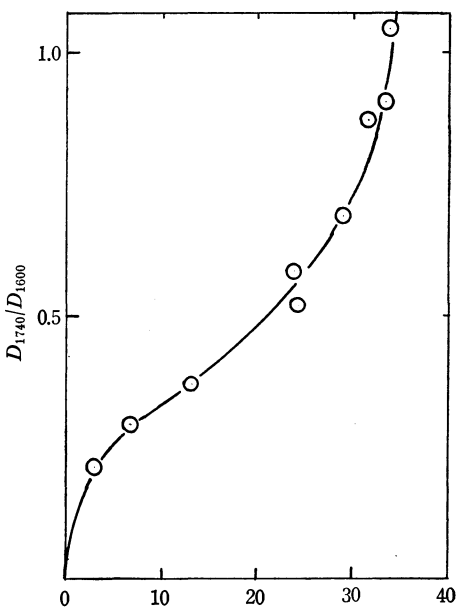

Fig. 1. Calibration curve of the copolymer of *N*-phenylethylenimine and β-propiolactone.

The calibration curve was obtained by plotting the optical density ratio, D_{1740}/D_{1600}, against the mole fraction of β-propiolactone, which was itself determined from the carbon and nitrogen contents by elementary analyses (Fig. 1 and Table 1).

Polymers of *N*-Phenylethylenimine and β-Propiolactone. A white crystalline polymer (mp 287—292°C) of *N*-phenylethylenimine was obtained by polymerization in water at 0°C without a catalyst, while the polymerization of β-propiolactone was carried out in acetonitrile at 0°C with a pyridine catalyst.

Hydrolysis of the Copolymer. In 5 m*l* of 1/10 N sodium hydroxide-ethanol, about 70 mg of the copolymer were hydrolyzed under reflux for 20 hr and then back-titrated with 1/20 N hydrochloric acid, using a 5% alcoholic solution of phenolphthalein as an indicator.

Reaction of Poly-*N*-phenylethylenimine with β-Propiolactone. A mixture of 0.293 g of poly-*N*-phenylethylenimine, 0.571 g of β-propiolactone, and 5 m*l* of acetonitrile was heated in a sealed tube at 35°C for 20 hr without a catalyst, the reaction product was then washed in chloroform and dried *in vacuo*. The amounts of carboxylic acid in these polymers were determined as follows. About a 70-mg portion of the polymer was added to 5 m*l* of 1/10 N sodium hydroxide-ethanol, and the solution was back-titrated with 1/20 N hydrochloric acid.

Results and Disscusion

The results of the copolymerization without a catalyst in acetonitrile at 0°C are summarized in Table 2. The copolymer obtained was a white powdery or a yellowish resinous solid polymer which was soluble in formic acid, but insoluble in chloroform, ethanol, dimethylformamide, and other organic solvents. The melting points of the copolymers were 245°C to 279°C, between those of poly-β-propiolactone (75°C) and poly-*N*-phenylethylenimine (287—292°C).

The infrared spectra of the resulting polymer showed the characteristic absorptions at 1740 cm^{-1} and 1600 cm^{-1} based on the ester linkage (β-propiolactone unit) and the benzene nucleus (*N*-phenylethylenimine unit) respectively (see Fig. 2). In order to determine whether the polymer obtained here was the copolymer or a mixture of the corresponding homopolymers, the resulting polymer was fractionated in chloroform, which is a solvent for only poly-β-propiolactone. The infrared spectrum of the fraction insoluble in chloroform is shown in Fig. 2. This infrared spectrum proves that the insoluble fraction of the resulting copolymer contained the β-propiolactone units. On the other hand, the infrared spectrum of the insoluble fraction of the mixture of the homopolymers does not show the peak of the ester linkage. These results indicate that the copolymer of *N*-phenylethylenimine with β-propiolactone was produced.

TABLE 2. COPOLYMERIZATION OF *N*-PHENYLETHYLENIMINE AND β-PROPIOLACTONE WITHOUT CATALYST IN ACETONITRILE AT 0°C

Exp. No.	Monomer (mol)		Time hr	Yield %	$\eta_{sp/c}$ dl/g	Melting point °C	Copolymer, mol%	
	N-Phenyl-ethylenimine	β-Propio-lactone					*N*-Phenyl-ethylenimine	β-Propio-lactone
1	0.002	0.018	6.5	8.43	1.26	245—260	67.1	32.9
2	0.004	0.016	2.0	3.43	0.954	259—260	76.2	23.8
3	0.006	0.014	2.0	3.76	1.17	260—263	80.0	20.0
4	0.008	0.012	2.0	3.62	0.980	269—272	85.0	15.0
5	0.010	0.010	2.0	3.71	0.744	275—276	93.2	6.8
6	0.012	0.008	2.0	3.34	0.674	286—287	95.0	5.0
7	0.014	0.006	3.0	3.98	0.523	276—278	95.2	4.8
8	0.016	0.004	6.5	6.85	0.824	275—279	96.6	3.4

Solvent: 10 ml

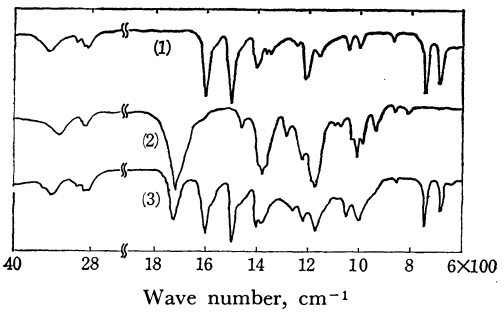

Fig. 2. Infrared spectra of the poly-*N*-phenylethylenimine, poly-β-propiolactone and the copolymer of *N*-phenylethylenimine and β-propiolactone.
(1) Poly-*N*-phenylethylenimine (2) Poly-β-propiolactone (3) Copolymer of *N*-phenylethylenimine and β-propiolactone.

Structure of the Copolymer. X-Ray diffraction diagrams of the copolymer (β-propiolactone 31.8 mol%), the poly-β-propiolactone, and poly-*N*-phenylethylenimine are shown in Fig. 3. The characteristic peaks (2θ) of these polymers are listed in Table 3.

The peaks of the copolymer were similar to characteristic peaks of poly-*N*-phenylethylenimine, but not to those of poly-β-propiolactone. Although no attempt was made to determine the ratio of the crystallinity, it may be considered in view of the relative half-value widths, that the crystallinity of the copolymer is smaller than that of poly-*N*-phenylethylenimine. Figure 4 shows the differential thermogram of the copolymer (β-propiolactone 31.8 mol%) in comparison with those of both homopolymers. We observed the endothermic peak corresponding to the melting point of neither homopolymer, but a new peak of the copolymer was observed, as Fig. 4 shows.

From these results, it may be concluded that neither poly-β-propiolactone nor poly-*N*-phenylethylenimine is present in the copolymer.

It is well known that β-propiolactone polymerizes by opening the ring between acyl-oxygen or alkyl carbon-oxygen bonds. In the copolymerization of *N*-phenylethylenimine with β-propiolactone,

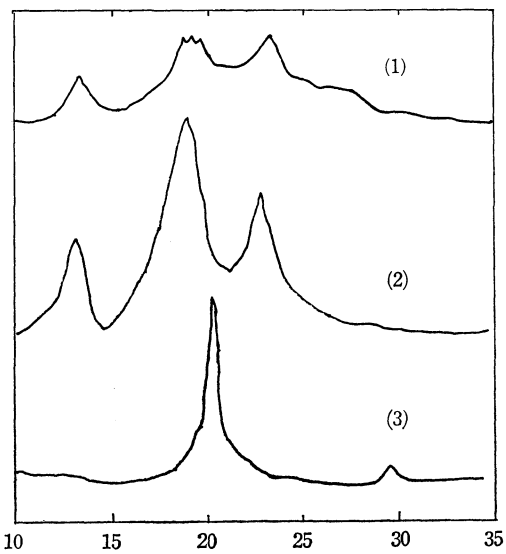

Fig. 3. X-Ray diffraction diagrams of the copolymer of *N*-phenylethylenimine and β-propiolactone, poly-*N*-phenylethylenimine, and poly-β-propiolactone.
(1) Copolymer of *N*-phenylethylenimine and β-propiolactone (β-propiolactone 31.8 mol%) (2) Poly-*N*-phenylethylenimine (3) Poly-β-propiolactone.

TABLE 3. CHARACTERISTIC PEAKS OF X-RAY DIFFRACTION DIAGRAMS OF THE POLYMERS

	2θ (°)				
Poly-*N*-phenyl-ethylenimine	13.6	19.4	23.5		
Poly-β-propio-lactone	21.2	29.2			
Copolymer	13.6	18.8	19.3	19.9	23.3

TABLE 4. QUANTITY OF CARBOXYLIC ACID AND REDUCED VISCOSITY OF COPOLYMERS

		Copolymer	Graft copolymer
	Composition of copolymer (β-propiolactone mol%)	14.0	10.5
Before hydrolysis of copolymer	Quantity of carboxylic acid (g equivalent/g copolymer)	0.0	5.90×10^{-4}
	Reduced viscosity (dl/g)	0.828	0.173
After hydrolysis of copolymer	Quantity of carboxylic acid (g equivalent/g copolymer)	16.9×10^{-4}	17.0×10^{-4}
	Reduced viscosity (dl/g)	0.0943	0.127

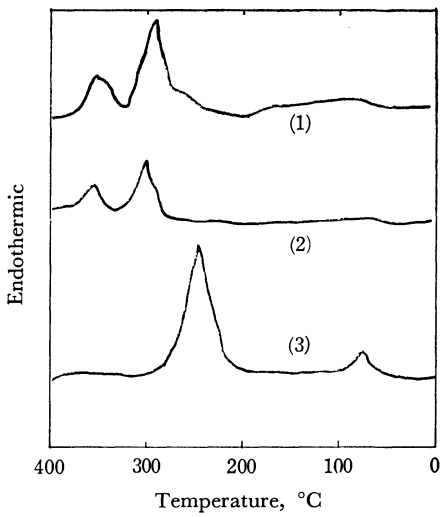

Fig. 4. Differential thermal analysis diagrams of the copolymer of *N*-phenylethylenimine and β-propiolactone, poly-*N*-phenylethylenimine, and poly-β-propiolactone.
(1) Copolymer of *N*-phenylethylenimine and β-propiolactone (β-propiolactone 31.8 mol%)
(2) Poly-*N*-phenylethylenimine
(3) Poly-β-propiolactone

it is possible that the copolymer contains the following structures, according to the different modes of lactone-ring cleavage:

Cleavage of the acyl-oxygen bond:

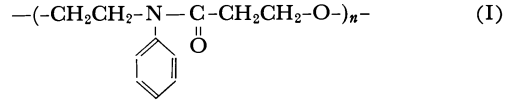

(I)

Cleavage of the alkyl carbon-oxygen bond:

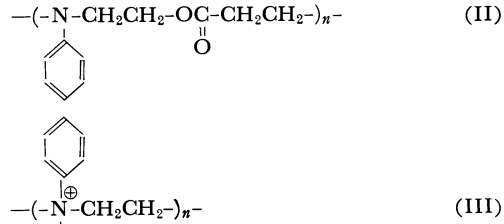

(II)

(III)

The absence of the characteristic peak of tertiary amide at 1650 cm^{-1} indicates that the copolymer does not contain the polyamide ether structure (I). Poly-*N*-phenylethylenimine and β-propiolactone could be reacted at 35°C to produce a branched polymer (III), but not at 0°C. The intrinsic viscosity and the carboxylic-group contents of the copolymer and the branched polymer are shown in Table 4.

The amount of the carboxyl group of the branched product was 5.90×10^{-4} g equivalent/g polymer, but no carboxylic group was present in the copolymer. This result indicates that the copolymer has not carboxyl group. It was observed that the amount of the carboxylic acid was equivalent to that of lactone present in the hydrolyzed product of the copolymer. The infrared spectrum of the hydrolyzed product displayed its peak at 1700 cm^{-1}, which was assigned to carboxyl bond, and the peak of the ester bond (1740 cm^{-1}) disappeared. The viscosity of the copolymer was depressed by the hydrolysis, whereas that of the branched copolymer was not changed. From these facts, it may be concluded that the copolymer contains the ester structure (II) in the main chain.

Monomer Reactivity Ratio. The relation

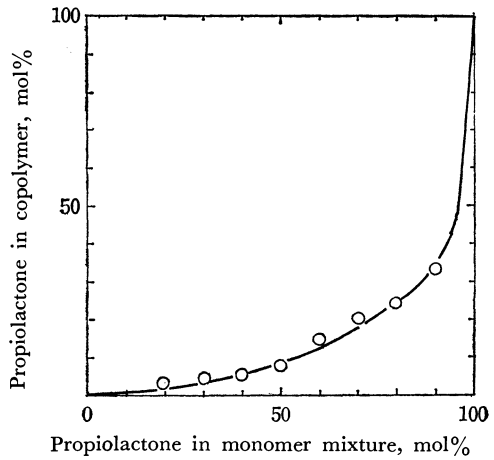

Fig. 5. Copolymerization of *N*-phenylethylenimine and β-propiolactone. Copolymer composition curve.

between the mole percentage of β-propiolactone in the copolymer and that in the monomer feed is shown in Fig. 5. From the curve, the monomer reactivity ratio of *N*-phenylethylenimine (r_1) and that of β-propiolactone (r_2) were estimated to be $r_1=7.5$ and $r_2=0.15$ respectively by the usual method.

The results show that *N*-phenylethylenimine reacted about 50 times as fast as β-propiolactone in this copolymerization, which gave a copolymer containing a small amount of the β-propiolactone. Further work on the mechanism of the initiation and propagation of this copolymerization will be reported in a subsequent paper.

BULLETIN OF THE CHEMICAL SOCIETY OF JAPAN VOL. 41 176—182 (1968)

Intramolecular Interaction between Hydroxyl Group and Carbonyl Moiety in Keto-alcohols[1)]

Michinori Ōki, Hiizu Iwamura, Jun-ichi Aihara and Hiroshi Iida

Department of Chemistry, Faculty of Science, The University of Tokyo, Hongo, Tokyo

(Received July 3, 1967)

The O–H stretching absorption (ν_{O-H}) spectra of some keto-alcohols have been examined. The ν_{O-H} shift to the lower frequency due to the intramolecular O–H···O bonding can roughly be correlated to the geometry of the hydroxyl group relative to the *n*-electrons on the carbonyl oxygen. When the bonding is forbidden because of the conformational restriction, a weaker interaction between the hydroxyl group and the π-electrons on the carbonyl group is observable as the lower shift of the ν_{O-H} by 10—30 cm^{-1} as far as the conformation is favorable for the interaction.

It has been well established by physico-chemical methods that the π-electrons on the olefinic and aromatic hydrocarbons function as a proton acceptor in the interaction with the hydroxyl group.[1,2)] As a nautral extension of the survey for a new type of the hydrogen bond acceptor, the π-electrons on the carbonyl double bond, a typical example of the multiple bonds carrying a hetero-atom, have now been taken into account. In addition to a pair of π-electrons, the carbonyl group has two lone-pairs of electrons, one of which can be regarded approximately of 2s character while the other of 2p character (n-electrons).[3)] The basicity or the donor ability of the carbonyl compounds in forming metallic and hydrogen bonded complexes has been ascribed entirely to the latter electrons, because these are more easily donated to an electron acceptor owing to the lower ionization potential (*ca.* 10 eV) and to the open nature to the attacking electrophile.[4)] The donor character of the carbonyl π-electrons which are assumed to have the ionization potential of *ca.* 12 eV, to the contrary, seems to have been less recognized.[5)] In order to observe the interaction of the carbonyl π-electrons with the hydroxyl group, some geometrical devices are necessary which exclude the preferential interaction involving the carbonyl n-electrons. In the present paper, the intramolecular interaction between the hydroxyl and the carbonyl groups in keto-alcohols has been investigated through the O–H stretching absorption (ν_{O-H}) spectra. In fulfilment of the above requirement, special emphasis has been laid on some conformationally-fixed keto-alcohols in which the hydroxyl group is so oriented as to approach the carbonyl group only from the upper side of the π-electrons clouds and perpendicularly to the n-electrons.

1) Part XXIII of "Intramolecular Interaction between Hydroxyl Group and π-Electrons." For part XXII see M. Ōki, H. Iwamura, T. Onoda and M. Iwamura, *Tetrahedron*, in press.

2) a) M. Tichý, "Advances in Organic Chemistry, Methods and Results," Vol. 5, ed, by R. A. Raphael, E. C. Taylor and H. Wynberg, Interscience Publishers, (1965) p. 115; b) Z. Yoshida and E. Osawa, *Nippon Kagaku Zasshi (J. Chem. Soc. Japan, Pure Chem. Sect.)*, **87**, 509 (1966); c) M. Ōki, *Kagaku no Ryōiki*, **13**, 839 (1959); d) H. Iwamura, *Kagaku to Kōgyō*, **17**, 617 (1964).

3) G. Berthier and J. Serre, "The Chemistry of the Carbonyl Group," ed. by S. Patai, Interscience Publishers, London (1966), Chapter 1.

4) a) H. McConnell, *J. Chem. Phys.*, **20**, 700 (1952); b) G. J. Brealey and M. Kasha, *J. Am. Chem. Soc.*, **77**, 4462 (1955); c) D. Cook, *ibid.*, **80**, 49 (1958); d) G. P. Rossetti and B. P. Susz, *Helv. Chim. Acta*, **47**, 289, 299 (1964).

Results and Discussion

Typical ν_{O-H} absorption curves are shown in Figs. 1 to 3. In Tables 1 and 2 are summarized the spectral parameters of all the keto-alcohols

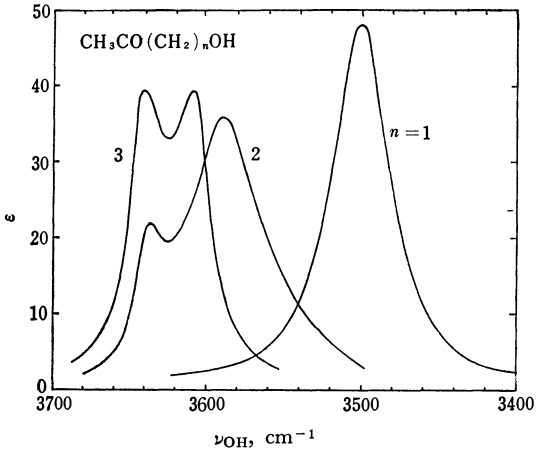

Fig. 1. ν_{O-H} absorptions of ω-hydroxy-2-alkanones.

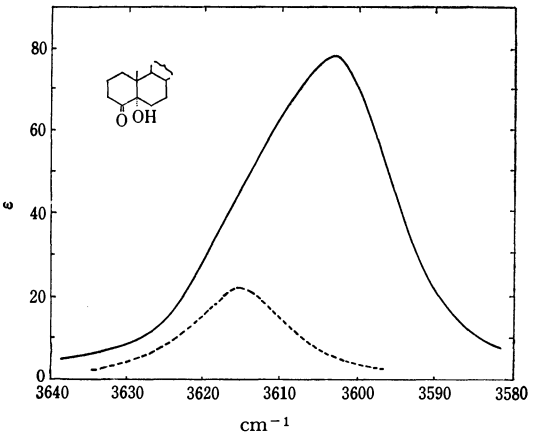

Fig. 2. ν_{O-H} absorption of 5α-cholestan-5α-ol-4-one (I).

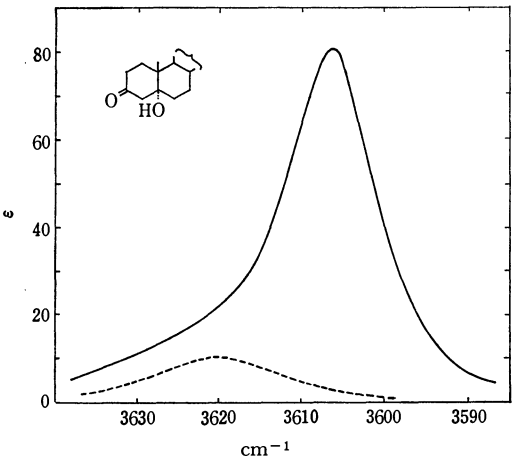

Fig. 3. ν_{O-H} absorption of 5α-cholestan-5α-ol-3-one (II).

5) In this connection the following papers deserve mention. It had once been considered that the band at 3427 cm^{-1} of 4-hydroxycyclohexanone might be due to the hydroxyl group intramolecularly bonded (i) (W. von E. Doering and A. A.-R. Sayigh, *J. Org. Chem.*, **26**, 1365 (1961)). The possibility was, however, eliminated by observing the survival of the band when the OH group was transformed into an OD group by deuterium exchange, and thus the 3427 cm^{-1} absorption was reassigned to the first overtone of the carbonyl stretching vibration at 1725.5 cm^{-1} (R. D. Stolow, *J. Am. Chem. Soc.*, **84**, 686 (1962)). Dalton and coworkers[6] have reported the anomalously low O-H stretching maxima in 5α-cholestan-5α-ol-3-one, 5β-cholestan-5β-3-one and the decalone analogs, but did

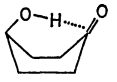

i

not notice the role of the π-electrons of the carbonyl group. The shape of the broad band due to the O-H stretching vibration of the hydrogen bond complexes of phenol with ketonic proton acceptors has been studied (H. Fritzsche, *Z. phys. Chem.*, **43**, 154 (1964); *Spectrochim. Acta*, **21**, 799 (1965)). It deviates from the normal symmetric type. The phenomenon was interpreted by assuming the superposition of two symmetrical bands and ascribed to the presence of two types of the hydrogen bond, the model for the second band requiring the participation of the π-electrons. Lately, the O-H stretching maximum at 3588 cm^{-1} of 2-hydroxy-4, 6-di-*t*-butylbenzophenone has been assigned to the hydroxyl group interacting with the π-electrons of the carbonyl group (A. T. Shulgin and H. O. Kerlinger, *Chem. Commun.*, **1966**, 249). However, the possibility of the interaction with the π-electrons of the phenyl group may not be ruled out, since the phenomenon is observed also in the structurally analogous 2-benzylphenol, the ν_{O-H} being at 3560 cm^{-1} (M. Ōki and H. Iwamura, This Bulletin, **33**, 681 (1960)).

6) F. Dalton, J. I. McDougall and G. D. Meakins, *J. Chem. Soc.*, **1963**, 4068.

examined together with some of those reported in the literature.

O–H···O Hydrogen Bond. As has been pointed out,[7,8] α-, β- and γ-keto-alcohols whose molecules are not fixed have ν_{O-H} maxima shifted to the lower frequency, and it is clear that the ordinary O–H···O hydrogen bond to form five, six and seven membered rings is taking place to a certain extent. The apparent ν_{O-H} shifts ($\Delta\nu_{O-H}$) are 135, 48 and 31 cm^{-1} for 1-hydroxy-2-propanone, 4-hydroxy-2-butanone and 5-hydroxy-2-pentanone, respectively. The trend is in sharp contrast with that of the inetrnal O–H···O bonding in α, ω-alkanediols and ω-methoxyalkanols, in which the value of $\Delta\nu_{O-H}$ increases on going from

7) V. S. Korobkov, *Doklady Mezhvuz. Nauch. Konf. po Spektroskopii i Spektr. Analizu, Tomsk. Univ.*, **1960**, 97; *Chem. Abstr.*, **56**, 115i (1962).

8) Tables on pp. 210—214 and papers cited therein, of Ref. 2.

Table 1. ν_{O-H} data for keto-alcohols
(O-H···O Hydrogen bond)

Compound	ν_{max} cm^{-1}	$\Delta\nu^{a}_{1/2}$ cm^{-1}	$A\times10^{-3}$ $mol^{-1}\,l\,cm^{-2}$	$\Delta\nu_{O-H}$[a] cm^{-1}
CH_3COCH_2OH	3501	44	9.8	135
2-Hydroxycyclohexanone	3500	46	—	127
5β-Cholestan-5β-ol-4-one	3480	42	11.7	138
5β-Cholestan-5β-ol-6-one	3481	45	13.3	137
2-Hydroxycyclododecanone	3497	45	9.0	130
$CH_3COCH_2CH_2OH$	3637	16	0.70	48
	3589	63	8.2	
$CH_3COCH_2CHMeOH$[9]	3600			
	3557	90	9.3	70
$CH_3COCH_2CMe_2OH$[9]	3612	25	0.68	
	3532	56	10.9	80
2-(Hydroxymethyl)cyclohexanone	3642	16	0.46	
	3584	40	8.0	58
(+)-10-Nor-8-oxoneomenthol (ii)[10]	3625	20	0.53	
	3537	87	14.4	88
(−)-10-Nor-8-oxomenthol[10]	3625	14	1.0	
	3598	60	7.7	27
Methyl icterogenin	3635[11]		(25)[b]	
	3518		(35)	117
$CH_3COCH_2CH_2CH_2OH$	3639	14	3.5	
	3608	14	3.5	31
11α-Hydroxy-25D-5β-spirostan-2-one	3534[12]			93
12β-Hydroxy-12α-methyl-5α-pregnane-3,20-dione	3463[13]			155
3β,14β-Dihydroxy-12β-benzoyloxypregn-5-en-20-one	3437[12]			181
3β-Acetoxy-14β,15α-dihydroxypregn-5-en-20-one	3434[12]			184
3β-Acetoxy-5α-hydroxy-9α-ergostan-11-one	3418[14]		(170)[b]	200

a) When the free ν_{O-H} is not observable, it is assumed to be 3636, 3627 and 3618 cm^{-1} for primary, secondary and tertiary alcohols, respectively.
b) ε

vicinal to 1, 4-difunctional derivatives, where it attains its maximum.[16] The difference between the two series may be due mainly to the different geometry around the proton accepting functions.

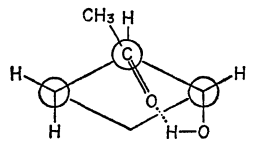

ii

Thus the carbonyl carbon atom is sp^2-hybridized and the α-carbon atom lies always on the same plane with the n-orbital of the oxygen atom. In 2-(hydroxymethyl)cyclohexanone and the derivatives, molecular models indicate even the hydroxylic oxygen atom is placed nearly on the very plane. The planar cyclic hydrogen bond is formed resulting in the ν_{O-H} shift of *ca.* 130 cm^{-1} which does not change materially over a whole range of examples.[8,9,11,17] Judging from the nearly equivalent $\Delta\nu_{O-H}$, the conformation of 1-hydroxy-2-propanone and other unfixed α-keto-alcohols may also be planar. Under the circumstances, the hydroxylic hydrogen atom participating in the hydrogen bond will be situated just on the extension line of the n-orbital of the carbonyl oxygen, as shown in

9) M. St. C. Flett, *Spectrochim. Acta*, **10**, 21 (1957).
10) Samples were provided through the courtesy of Dr. T. Suga by whom the conformation of the acetyl group is assigned as ii (T. Suga, Y. Shishibori and T. Matsuura, 20th Annual Meeting of the Chemical Society of Japan, Tokyo, April, 1967. Abstract 3Y-020).
11) A. R. H. Cole and G. T. A. Müller, *J. Chem. Soc.*, **1959**, 1224.
12) T. Kubota, M. Takasuka and Y. Matsui, *Ann. Rep. Shionogi Research Lab.*, No. 16, 63 (1966).
13) Y. Matsui, M. Takasuka and T. Kubota, *ibid.*, No. 15, 125 (1965).
14) C. J. W. Brooks, G. Eglinton and L. Hanaineh, *Spectrochim. Acta*, **22**, 131 (1966).
15) J. Rigaudy and P. Courtot, *Compt. rend.*, **248**, 3016 (1959).
16) $\Delta\nu_{O-H}$'s of butane-1, 4-diol and 4-methoxybutan-1-ol are 156 and 184 cm^{-1}, respectively.
17) A number of examples are available for α-keto-alcohols in the following literatures and their ν_{O-H}'s fall always in the region of 3480—3500 cm^{-1}; R. N. Jones, P. Humphries, R. F. Herling and K. Dobriner, *J. Am. Chem. Soc.*, **74**, 2820 (1952); C. Duculot, *Compt. rend.*, **241**, 1738, 1925 (1955); J. Elks, G. H. Phillips, T. Walker and L. J. Wyman, *J. Chem. Soc.*, **1956**, 4330; G. DeStevens, *J. Org. Chem.*, **23**, 1752 (1958).

TABLE 2. ν_{O-H} DATA FOR KETO-ALCOHOLS
(O-H···π Hydrogen bond)

Compound	ν_{max} cm^{-1}	$\Delta\nu^{a)}_{1/2}$ cm^{-1}	$A\times10^{-3}$ $mol^{-1}\,l\,cm^{-2}$	$\Delta\nu_{O-H}$[a)] cm^{-1}
5α-Cholestan-5α-ol-4-one	3614	15	1.2	
	3603	17	4.4	11
5α-Cholestan-5α-ol-6-one	3614	13	1.1	
	3602	16	4.4	12
(−)-2-Hydroxyisopinocamphone	3586	18	5.4	32
α-Digiprogenin 3β-acetate	—[12)]			
	3603			15
5α-Cholestan-5α-ol-3-one	3620	20	0.63	
	3606	12	3.5	14
5β-Cholestan-5β-ol-3-one	3620	18	0.40	
	3609	13	3.8	11
10β-Hydroxy-9β-methyl-3-decalone	3610[6)]	19	(60)[b)]	8
5α-Hydroxyergosta-7,22-dien-3-one	3608[6)]	21	(55)[b)]	10
	3594	25	(50)	24
Methyl hederagonate	3630[11)]		very weak	
	3602		(40)	34
	3540		(20)	96
4-Hydroxycycloheptanone[15)]	3624	10	3.3	
	3601	10	3.3	23

a), b) See footnotes of Table 1.

Fig. 4, effecting strong hydrogen bond formation.[18)] In contrast with the α-keto-alcohols, the conformation about the ethylene glycol and 2-methoxyethanol has been shown not to be eclipsed but staggered and not only the distance between the bonding groups but also the angle are not most favorable for the intramolecular hydrogen bond.[19)]

In β-keto-alcohols, the values of $\Delta\nu_{O-H}$ range from 30 to 120 cm^{-1}. The variety may be due to the difference in the conformation of the bonding species which has been considered to be unaltered in α-keto-alcohols. It may be argued that the bonding form of 4-hydroxy-2-butanone is planar because stabilization by hydrogen bond formation overwhelms the conformational energy. If it were the case, however, the distance between the hydroxylic hydrogen and the carbonyl oxygen would amount to 1.2 Å, and the stronger interaction which is reflected by greater shift to the lower frequency than those of α-keto-alcohols would have been observed. Therefore, in the bonding form of 2-(hydroxymethyl)cyclohexanone, the hydroxymethyl group is assumed to be equatorial with the hydroxyl group staggered between the axial hydrogen and the carbonyl carbon atoms. If the hydroxyl hydrogen is staggered between a methylene hydrogen and the ring carbon to which the hydroxymethyl group is attached, the distance between the hydroxyl hydrogen and the carbonyl oxygen atoms in this model becomes

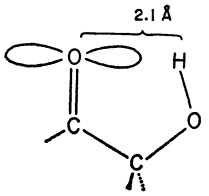

Fig. 4. Geometry of intramolecular hydrogen bond in α-keto-alcohols.

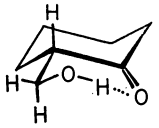

Fig. 5. Bonding conformation of 2-(hydroxymethyl)cyclohexanone.

18) When methanol and acetone are mixed in carbon tetrachloride to make a solution of 0.012 and 0.45 mol/l with respect to each component, a broad band due to the intermolecular hydrogen bond formation appears at 3534 cm^{-1}. Since there seems to be no geometrical restriction in the intermolecular association, the interacting groups are mutually so disposed that the greatest enthalpy of the interaction is attained. The fact that $\Delta\nu_{O-H}$ as a measure of the enthalpy of the interaction in α-keto-alcohols is greater even than those intermolecular bonding may suggest a factor which is advantageous to the intramolecular bonding. A possible electronic interaction through hyperconjugation of the intervening methylene group is excluded because α, α-disubstituted derivatives have similarly intensified hydrogen bond. It may be an explanation that the electrostatic field effect on the hydrogen bond is playing a great role, since the dipolar O–H and C=O groups are, as shown in Fig. 4, placed nearly anti-parallel with the result of some additional stabilization.

19) P. J. Krueger and H. D. Mettee, *J. Mol. Spectrys.*, **18**, 131 (1965); H. Matsuura and T. Miyazawa, This Bulletin, **40**, 85 (1967); P. Buckley and P. A. Giguere, *Can. J. Chem.*, **45**, 397 (1967).

nearly 2.1 Å coincident with those of α-keto-alcohols, but the angle made by the direction of the carbonyl n-orbital and the line connecting the hydroxyl hydrogen with the carbonyl oxygen atoms amounts to as high as 40° (see Fig. 5). It follows, therefore, that $\Delta\nu_{O-H}$ is reduced nearly to half of that in α-keto-alcohols.[20]

In an attempt to find correlation between the conformation and $\Delta\nu_{O-H}$ due to hydrogen bonding,

Table 3. The geometrical relation between hydroxyl and carbonyl groups in keto-alcohols as defined by Fig. 6

Compound	R, Å	θ
α-Keto-alcohols (1—3)	2.1	8
4-Hydroxy-2-butanones (4—6)	2.1	40
2-(Hydroxymethyl)cyclohexanone (7)	2.3	35
(+)-10-Nor-8-oxoneomenthol (8)	2.0	30[10]
(−)-10-Nor-8-oxomenthol (9)	2.3	55[10]
Methyl icterogenin (10)	1.9	25[21]
11α-Hydroxy-25D-5β-spirostan-2-one (11)	1.9	40
12β-Hydroxy-12α-methyl-5α-pregnane-3, 20-dione (12)	1.8	20
3β, 14β-Dihydroxy-12β-benzoyloxy-pregn-5-en-20-one (13)	1.6	20
3β-Acetoxy-14β, 15α-dihydroxypregn-5-en-20-one (14)	1.6	20
3β-Acetoxy-5α-hydroxy-9α-ergostan-11-one (15)	1.4	35

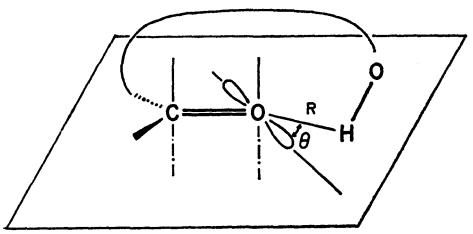

Fig. 6. Parameters representing the geometrical relation between hydroxyl and carbonyl groups.

the latter values have been plotted against $\cos\theta/R$, in which R and θ are defined as shown in Fig. 6, and estimated by examination of a Dreiding model (Table 3). The parameters were tentatively employed because it is easily expected that the enthalpy of the hydrogen bond increases as the distance between the interacting groups is shortened and the overlap between them becomes heavilier.

It is rather surprising that a smooth relationship has been obtained as shown in Fig. 7, when one considers that, to the hydrogen bond, several mechanisms such as electrostatic interaction, delocalization energy, repulsive force and dispersion force[22] are contributing which should be expressed in terms of a complex function of R and θ. It is beyond the purpose of the present authors to discuss the relative contribution of the above mechanisms from the relationship now obtained, but the atuhors would like to point out that $\Delta\nu_{O-H}$ due to the intramolecular hydrogen bond in keto-alcohols is dependent on the distance between the two groups and the direction of approach of the hydroxyl group to the head of the n-orbital on the carbonyl oxygen.[23] A few examples of γ-keto-alcohols and the higher homologs also conform to the same relationship and are included in Fig. 7.

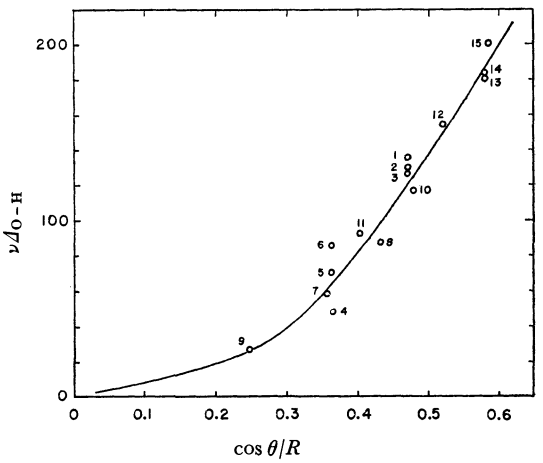

Fig. 7. Relation between the conformation and $\Delta\nu_{O-H}$ due to hydrogen bonding in keto-alcohols (numbers in Table 3).

O–H···π Interaction. In Table 2 are collected ν_{O-H} data of keto-alcohols in which R is not shorter than 3 Å, $\cos\theta/R$ parameter smaller than 0.9, and consequently the contribution to the hydrogen bond by n-electrons can be regarded geometrically

20) There seems to be a controversy as to the hybridization of the proton accepting n-orbital of the carbonyl group. W. G. Schneider (*J. Chem. Phys.*, **23**, 27 (1955)) regarded the hybridization of the carbonyl oxygen to be sp^2 in his electrostatic interpretation of the hydrogen bond, while a self-consistent field calculation of formaldehyde (P. L. Goodfriend, F. W. Birss and A. B. F. Duncan, *Rev. Mod. Phys.*, **32**, 307 (1960)) shows a clearly defined 2p-lone pair on the oxygen atom. Since trigonal sp^2 lone pair would have been more favorable geometrically for the hydrogen bond formation in β-keto-alcohols than for α-homologs, the above observations may provide another support for the 2p-character of the oxygen lone pair.

21) Contrary to the original authors,[11] the ring A of methyl icterogenin and methyl hederagonate was assumed to be a boat which has frequently been encountered in the lanostan-3-one derivatives (E. L. Eliel, N. L. Allinger, S. J. Angyal and G. A. Morrison, "Conformational Analysis," Interscience Publishers, New York (1965), p. 469).

22) C. A. Coulson, "Hydrogen Bonding," ed. by D. Hadzi and W. H. Thompson, Pergamon Press, London (1959), p. 339.

23) Kubota and co-workers[12] found an empirical relation, $\Delta\nu_{O-H}=-143R+412$ (cm^{-1}).

forbidden. According to the relationship found in Fig. 7, any low-frequency band may not be expected ($\Delta\nu_{O-H}<10\ cm^{-1}$). In these examples, however, the apparent ν_{O-H} maxima are always shifted to the lower frequency and a shoulder band is usually observed at the higher frequency side which is located at the normal position of the free ν_{O-H} (Figs. 2 and 3). Instead of the *n*-electrons, π-electrons on the carbonyl group are now situated favorably for accepting the hydroxyl hydrogen as depicted in Fig. 8, and it is postulated that the lower frequency bands are assigned to the ν_{O-H} due to the O-H···π interaction. The ν_{O-H} shifts range from 8 to 34 cm^{-1} and are roughly in accord with the degree of overlap between the orbitals of the hydroxyl group and π-electrons as estimated by the Dreiding model.[21,24] $\Delta\nu_{O-H}$ of 11, 14 and 34cm^{-1} in 5α-cholestan-5α-ol-4-one (I), 5α-cholestan-5α-ol-3-one (II) and methyl hederagonate (III), respectively, may be compared with those of structurally analogous 5-*trans*-*t*-butyl-2-methylenecyclohexanol ($\Delta\nu_{O-H}=9\ cm^{-1}$), epicholesterol (34 cm^{-1}) and 3β-acetoxychlolest-5-en-19-ol (52 cm^{-1}).[1] In these latter examples, the ethylenic π-electrons are playing the role of the proton acceptor. Near parallelism in the order of $\Delta\nu_{O-H}$'s between the keto-alcohols and the olefinic alcohols can be noted and, when structurally related alcohols in which only the C=O group is replaced by C=C are compared, $\Delta\nu_{O-H}$ in the former series is about half of the latter series. The trend is interpretable in terms of the reduced basicity of the carbonyl π-electrons compared to that of the ethylenic π-electrons as indicated by the higher ionization potential of the former.[3,4,25] Best illustration of the competition between the basicity of the carbonyl group and the ethylenic linkage is afforded by 5α-hydroxyergosta-7, 22-dien-3-one (V),[6] in which, under the nearly equivalent geometrical environment, $\Delta\nu_{O-H}$ is 10 and 24cm^{-1}, respectively. α-Axial keto-alcohols,[26] 5α-cholestan-5α-ol-4-one, -6-one and α-digiprogenin 3β-acetate, are rather exceptional in that $\Delta\nu_{O-H}$'s are even larger than those of the corresponding α-axial olefinic alcohols. This may be due to the strengthened interaction as a result of the enhanced acidity of the hydroxyl group which is located α

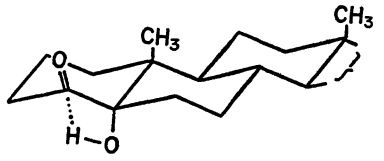

I

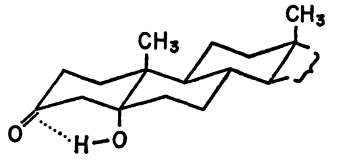

II

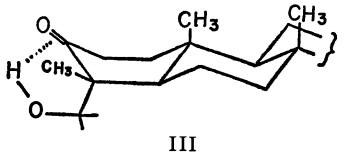

III

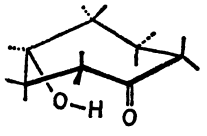

IV

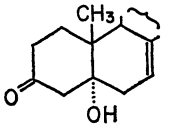

V

Table 4. $\nu_{C=O}$ data for keto-alcohols

Compound	ν_{max}	ε
CH_3COCH_2OH	1727	(406)
2-Hydroxycyclohexanone	1718	(—)
5β-Cholestan-5β-ol-4-one	1703	(650)
5β-Cholestan-5β-ol-6-one	1704	(598)
$CH_3COCH_2CH_2OH$	1716	(303)
$CH_3COCH_2CMe_2OH$	1712[30]	
2-(Hydroxymethyl)cyclohexanone	1705	(442)
$CH_3COCH_2CH_2CH_2OH$	1720	(293)
5α-Cholestan-5α-ol-4-one	1718	(597)
5α-Cholestan-5α-ol-6-one	1718	(528)
(−)-2-Hydroxyisopinocamphone	1721	(505)
5α-Cholestan-5α-ol-3-one	1721	(448)
5β-Cholestan-5β-ol-3-one	1720	(430)
5α-Hydroxyergosta-7, 22-dien-3-one	1722	(430)[6]

24) The similarity of the ν_{O-H} absorption spectra between 5α-cholestan-5α-ol-4-one (I) and 5α-cholestan-5α-ol-6-one, and 5α-cholestan-5α-ol-3-one and 5β-cholestan-5β-ol-3-one provides a support for the normal chair conformation of the ring-A cyclohexanone in I and 5β-3-keto-steroid (N. L. Allinger and C. L. Neumann, *Tetrahedron*, **23**, 1279 (1967)). The 3540 cm^{-1} absorption of methyl hederagonate (III) may be due to the O-H···O bonding in a ring-A chair conformation which is in equilibrium with the boat form.[21] The conformation of 4-hydroxycycloheptanone was regarded to be chair (IV) (N. L. Allinger, *J. Am. Chem. Soc.*, **81**, 5727 (1959)). For 2-hydroxyisopinocamphone see, R. L. Erskine and S. A. Knight, *Chem. & Ind.*, **1960**, 1160.

25) Polarization of the carbonyl π-electrons in the sense $C\overset{\delta+}{=}O\overset{\delta-}{}$ will also be contributing, because in the pertinent examples the hydroxyl group is interacting with the π-electrons on the carbon atom rather than that on the oxygen atom geometrically.

26) Recently an intramolecular O-H···O bonding has been reported for iii, but no interaction is noticed in the OH-epimer (A. G. Yurchenko, *Zh. Organokhim.*, **2**, 1604 (1966); *Chem. Abstr.*, **66**, 64933b (1967)).

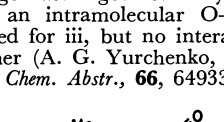

iii

to the electron-attracting carbonyl function. A support for this inductive effect may be obtained by the relatively low free ν_{O-H}'s at 3614 cm^{-1} of these α-keto-alcohols which should otherwise be expected to occur at 3618—3620 cm^{-1}.

Experimental

All the samples were of analytical purity and the physical constants agreed well with those in the literature.[27]

Spectral measurement was carried out as described in the previous papers.[1,28] Special care was taken to employ a little more dilute solution ($c \leq 10^{-3}$ mol/l) in carbon tetrachloride than usual, because it has often been mentioned[6,29] that in keto-alcohols the association through intermolecular hydrogen bond survives rather tenaciously even in *ca.* 5×10^{-3} mol/l solution.

The C=O stretching bands were measured in a sodium chloride cell of 0.55 cm optical length, and the data are summarized in Table 4. As has been pointed out,[30] the effect of the hydroxyl group in shifting the $\nu_{C=O}$ is not clear especially in the O–H$\cdots\pi$ interaction.

27) 2-Hydroxycyclohexanone is notorious for its spontaneous formation of a dimer with the hemiacetal structure (J. C. Sheehan, R. C. O'Neill and M. A. White, *J. Am. Chem. Soc.*, **72**, 3376 (1950)), and so the freshly distilled (bp, 87°C/18 mmHg) sample was used within five minutes after distillation.

28) M. Ōki and H. Iwamura, This Bulletin, **32**, 567 (1959).

29) H. M. Fales and W. C. Wildman, *J. Am. Chem. Soc.*, **85**, 784 (1963).

30) H. Minato, This Bulletin, **36**, 1020 (1963).

BULLETIN OF THE CHEMICAL SOCIETY OF JAPAN VOL. 41 182—186 (1968)

The Peptide Synthesis. II. Use of the Phenol Resin for the Peptide Synthesis*1

Noriyoshi INUKAI, Kohzi NAKANO and Masuo MURAKAMI

Central Research Laboratory, Yamanouchi Pharmaceutical Co., Ltd., Azusawa-cho, Itabashi-ku, Tokyo

(Received July 4, 1967)

The phenol resin is useful as support of the solid phase peptide synthesis. Its use is particularly advantageous for the synthesis of the *N*-protected peptide fragments, and those which have the intramolecular disulfide bond, such as oxytocin. In the latter case, the application of *S*-ethylmercapto group as the protector of thiol group of cysteine residue was combined successfully. Oxytocin and physalaemin derivatives were thus synthesized.

Recently, the solid phase peptide synthesis introduced by Merrifield[1,2] has provoked keenest interest. The essential feature of this method is protection of the carboxyl group of an amino acid by esterification with polymeric derivatives of benzyl alcohol; the products being insoluble in the usual solvents, they can be isolated and purified simply by washing with a series of appropriate solvents. Many active peptides, such as bradykinin,[3,4] angiotensin,[5] insulin[6] and others were thus synthesized simply, rapidly and automatically. Long chain peptides which were difficult to synthesize to date are further expected to be synthesized by this method. However, many problems still remain; (1) The introduction of the starting acyl amino acid to polymer requires rather drastic condition, which may give rise to racemization and other side reactions. It is difficult to introduce the acyl peptide direct to the polymer. (2) *C*-Terminal of many important active peptides is often amide, as in oxytocin, vasopressin, eledoisin, physalaemin and gastrin. Synthesis of these peptide amides as described by Bodanszky *et al.*[7] are troublesome and peptide hydrazide is also hard to prepare. (3) To obtain the acyl peptide fragments is impossible, for the removal of peptide from polymer is performed by hydrogen bromide in trifluoroacetic acid, or liquid hydrogen fluoride,[8] *etc.*

We found that the polyphenol resin is an useful

*1 This study was presented at the 20th Annual Meeting of the Chemical Society of Japan, Tokyo, April, 1967.

1) R. B. Merrifield, *J. Am. Chem. Soc.*, **85**, 2149 (1963).
2) R. B. Merrifield, *Science*, **150**, 178 (1965).
3) R. B. Merrifield, *J. Am. Chem. Soc.*, **86**, 304 (1964).
4) R. B. Merrifield, *Biochemistry*, **3**, 1385 (1964).
5) G. R. Marshall and R. B. Merrifield, *ibid.*, **4**, 2394 (1965).
6) A. Marglin and R. B. Merrifield, *J. Am. Chem. Soc.*, **88**, 5011 (1966).
7) M. Bodanoszky and J. T. Sheehan, *Chem. & Ind. (London)*, **1964**, 1423; *ibid.*, **1966**, 1597.
8) J. Lenard and A. B. Robinson, *J. Am. Chem. Soc.*, **89**, 181 (1967).

support. Conditions of its synthesis will be described in the present investigation. The phenol resin as support of the solid phase peptide synthesis has not only all the merits of Merrifield's method, but also it can solve some of the problems of Merrifield's method as described above.

The phenol resin was synthesized by reacting phenol and equimolar amount of *S*-trioxane in bis-(2-ethoxyethyl)-ether containing catalytic amount of *p*-toluenesulfonic acid at 150°C in a sealed tube for 24 hr. This phenol resin is insoluble in the usual solvents employed for the peptide synthesis but it swells in them.

The introduction of the first acyl amino acid, such as *N*-*t*-amyloxycarbonyl-,[9] *N*-*t*-butyloxycarbonyl-[10] or *N*-carbobenzoxy[11]-amino acid, to the phenol resin is carried out with *N*, *N'*-dicyclohexylcarbodiimide[12] in dimethylformamide. The resulting resinous derivative of acyl amino acid phenyl ester was isolated and purified simply by washing with a series of appropriate solvents. The acyl group was removed by hydrogen halide in suitable solvent. The resulting hydrogen halide salt was converted to the free base with triethylamine in dimethylformamide, and it was coupled with the next acyl amino acid or acyl peptide by active ester method,[13-17] or *N*, *N'*-dicyclohexylcarbodiimide method in dimethylformamide. Excess reagents and by-products were removed from the insoluble product by filtration and through washing with suitable solvents. Further elongation of peptide bond was carried out in the same way by alternate deprotecting and coupling with the appropriate acyl amino acid or acyl peptide.

Choice of solvent was important for the coupling reaction. Of the several solvents examined, dimethylformamide was the best one which had high dielectric constant and also swelled the resin. Pyridine was also satisfactory, whereas chloroform, benzene, ethyl acetate and dioxane were unfit not swelling the resin or having low dielectric constant.

Selection of the coupling methods for the formation of the peptide bond was also important. The several methods were examined, and the order of the coupling efficiency was as follows;

N, *N'*-Dicyclohexylcarbodiimide, *p*-Nitrophenyl ester[13] > 2, 4-Dinitrophenyl ester,[14] *N*-Hydroxysuccinimide ester,[15] > 2, 4, 5-Trichlorophenyl ester[16] > Pentachlorophenyl ester[17] ≫ Azide,[18] mixed anhydride.[19]

The yield was excellent, when the coupling was performed by *p*-nitrophenyl ester method and *N*, *N'*-dicyclohexylcarbodiimide method. In the active ester methods, the coupling potency depended on the bulkiness of the esters, *i. e.* the steric effect.

When the coupling was completed, the protected peptide was cleft from the resin by treatment with aqueous N sodium hydroxide in methanol, 25% ammonia in methanol or hydrazine hydrate in dimethylformamide as the corresponding acyl peptide, acyl peptide amide or acyl peptide hydrazide. The crude acyl peptide derivatives are easily purified by one or two recrystallizations, and column chromatography for the purposes of purification was not necessary. But this method was unfit to synthesize the acyl peptides which were unstable under the basic condition.*2

Some examples of acyl peptide derivatives synthesized are listed in the table.

Optical rotation of these acyl peptide derivatives nearly agreed with that of the standard samples synthesized by the usual method and racemization was scarcely observed.*3

The latter five peptides in the table are the active fragments of physalaemin and its analogues. The activities of these free peptides deprotected were compared with that of a synthetic bradykinin[20] by the hypotensive effect in rabbit.

Oxytocin was synthesized for two reasons. First, it was of interest as a further test of the applicability of the phenol resin, since oxytocin is an active peptide rather hard to prepare containing the comparatively unstable amino acids; cystine, asparagine and glutamine. Secondly, it may be expected that the two deprotected free thiol groups of cysteine residues are converted to an intramolecular disulfide bond on the phenol resin instead of forming an intermolecular disulfide bond which often occurs in usual synthetic method of oxytocin.

9) S. Sakakibara, M. Shin, M. Fujino, Y. Shimonishi, S. Inoue and N. Inukai, This Bulletin, **38**, 1522 (1965).
10) L. A. Carpino, *J. Am. Chem. Soc.*, **79**, 98 (1957); G. W. Anderson and A. C. McGregor, *ibid.*, **79**, 6180 (1957).
11) M. Bergmann and L. Zervas, *Ber.*, **65B.**, 1192 (1932).
12) J. C. Sheehan and G. P. Hess, *J. Am. Chem. Soc.*, **77**, 1067 (1955).
13) M. Bodanszky, *Nature*, **175**, 685 (1955).
14) M. Bodanszky and M. A. Ondetti, *Chem. & Ind. (London)*, **1966**, 26.
15) G. W. Anderson, J. E. Zimmerman and F. M. Callahan, *J. Am. Chem. Soc.*, **86**, 1839 (1964).
16) J. Pless and R. A. Boissonnas, *Helv. Chim. Acta*, **46**, 1609 (1963).
17) G. Kupryszewski and M. Formela, *Roczniki Chem.*, **35**, 1533 (1961); *Chem. Abstr.*, **57**, 7373 (1962).
18) T. Curtius, *Ber.*, **35**, 3226 (1902).
19) J. R. Vaughan, Jr., *J. Am. Chem. Soc.*, **73**, 3547 (1951).

*2 For example, the cleavages of prolyl-proline-, seryl-proline- and arginyl-proline-bonds were often observed under the basic conditions.

*3 Racemization was about 3% in the following tests; (1) Many isoleucine derivatives were synthesized on the resin using L-isoleucine, and the ratio of L-isoleucine to allo-isoleucine was determined by amino acid analyzer. (2). *N*-Carbobenzoxy-glycyl-phenylalanyl-glycine which was synthesized stepwise on the resin using L-phenylalanine, was converted to ethyl ester and it was subjected to the Anderson's racemization test.

20) S. Sakakibara and N. Inukai, This Bulletin, **39**, 1567 (1966).

TABLE 1. THE SYNTHESIS OF PEPTIDES BY THE PHENOL RESIN

Peptide[a]	Mp °C	$[\alpha]_D^{23}$ c 0.4, in DMF Found/Cited[b]	Anal. % Found/Calcd C	H	N	Activity.[c] Synthetic Bradykinin =1
Z-Glu-OH └Cys(Bz)-Gly-OH	110—120	−36.8 (c=1, EtOH)	56.36 56.49	5.71 5.50	7.79 7.91	
AOC-Phe-Phe-Phe-Gly-NHNH$_2$ 1/2 H$_2$O	208—210	−33.0 −32.4	64.29 64.31	6.86 6.94	12.64 12.86	
AOC-Phe-Tyr-Gly- Leu-Met-NH$_2$	200—202 211—212[b]	−31.5 −30.9	60.05 59.82	7.29 7.33	11.18 11.31	0.5
(AOC)$_2$-Lys-Phe-Tyr- Gly-Leu-Met-NH$_2$	140—145	−31.2 −33.5	59.33 59.73	7.65 7.78	11.53 11.37	100
(AOC)$_2$-Lys-Phe-Tyr(Me)- Gly-Leu-Met-NH$_2$	210—215	−32.0 −32.3	59.78 60.10	7.96 7.87	11.06 11.21	100
AOC-Phe-Phe-Tyr(Me)- Gly-Leu-Met-NH$_2$	214—215	−36.9 −38.4	62.41 62.44	7.13 7.24	10.65 10.84	10
AOC-Phe-Phe-Phe- Gly-Leu-Met-NH$_2$	230—232	−43.9 −43.3	63.12 63.21	7.29 7.26	11.28 11.22	1

a) The all amino acids are L-form.
b) The standard samples were prepared by the usual synthetic methods.
c) The activity of the deprotected free peptide was compared with that of a synthetic Bradykinin.[20] Z=carbobenzoxy; AOC=t-amyloxycarbonyl; Bz=Benzyl; Tyr(Me)=p-methoxytyrosine residue; DMF=dimethylformamide.

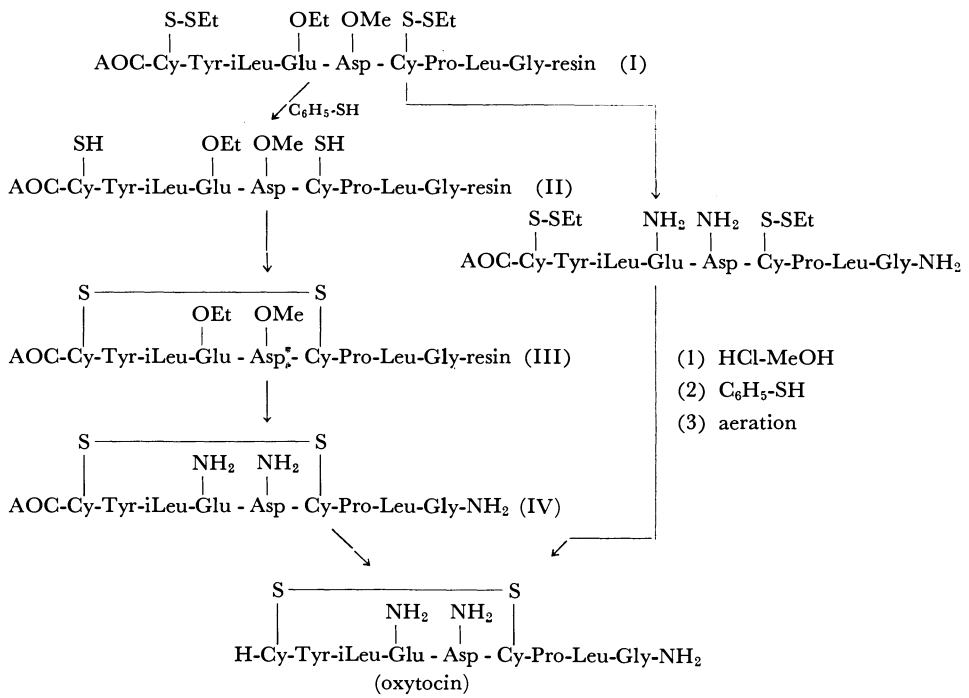

Fig. 1. The synthetic scheme of oxytocin.
AOC=t-amyloxycarbonyl; resin=polyphenol resin

The synthetic scheme of oxytocin was shown in the figure.

Peptide bonds were lengthened stepwise with the N-t-amyloxycarbonyl amino acids on the phenol resin. S-Ethylmercapto-L-cysteine which was reported in the proceeding paper[21] was used for this purpose, because the S-ethylmercapto group is

21) N. Inukai, K. Nakano and M. Murakami, This Bulletin, **40**, 2913 (1967).

easily removed by thiophenol.

From the completed *N-t*-amyloxycarbonyl-*S*-ethylmercapto-L-cysteinyl-L-tyrosyl-L-isoleucyl-γ-ethyl-L-glutamyl-β-methyl-L-aspartyl-*S*-ethylmercapto-L-cysteinyl-L-prolyl-L-leucylglycine phenol resin, *S*-ethylmercapto groups were removed by treating with thiophenol, the free two thiol groups of cysteine residues were converted to the intramolecular disulfide bond by aeration, and finally the peptides were cleft from the resin by treatment with 25% ammonia in methanol. By removing of the protecting group from the *N-t*-amyloxycarbonyl oxytocin thus obtained, the oxytocin could be synthesized. Its biological activity was found to be about two-thirds of that of a standard sample,[21] as determined by rat-uterine contractive activity. This result indicated that the stepwise synthesis of peptide bonds, the removal of *S*-ethylmercapto groups of cysteine residues and the formation of the intramolecular disulfide bond of cystine occured simply, rapidly and automatically on the resin without any complications.

In conclusion, the phenol resin as support of the solid phase peptide synthesis is very useful, especially so for the synthesis of the acyl peptide fragments which are stable under the basic condition. It could be employed successfully for the synthesis of the peptide derivatives which have the intramolecular disulfide bond, by the concomitant application of *S*-ethylmercapto group as protector of the thiol group of cysteine residue.

Experimental

Polyphenol Resin. The solution of phenol (18.8 g, 0.2 mol), *S*-trioxan (6.12 g, 0.068 mol) and *p*-toluenesulfonic acid (0.4 g) in bis-(2-ethoxyethyl)-ether (10 m*l*) was allowed to react at 150°C for 24 hr in the sealed tube in an oil bath. The tube is then permitted to cool to room temperature and is opened cautiously often wrapping in a towel. The amorphous solid product was repeatedly washed with acetone, dimethylformamide and ethanol and dried over phosphorus pentoxide *in vacuo*. Yield 13.8 g.

The Esterification Step. A solution of *t*-amyloxycarbonyl (AOC) amino acid or carbobenzoxyl (Z) amino acid (0.02 mol) and *N, N'*-dicyclohexylcarbodiimide (DCCD) (0.02 mol) in dimethylformamide (DMF) (20—30 m*l*) were added to the phenol resin (1 g) and the suspension was stirred at room temperature overnight. The resinous derivative was filtered and washed several times with DMF, ethanol and acetic acid to remove excess reagents and by-products, especially dicyclohexylurea was throughly removed by washing with acetic acid. 30—40% of phenolic hydroxyl group was esterified.*4 The phenolic hydroxyl group which remained was esterified with acetic anhydride.

The Deprotection Step. a) AOC-Amino acid phenol resin (containing 0.01 mol of AOC-amino aicd) was treated with 10% HCl in methanol or dioxane (20 m*l*) for 2 hr at room temperature. The suspension was filtered and washed with methanol, DMF and ethyl acetate. The resulting hydrogen chloride salt was then neutralized by shaking for 20 min in DMF (20 m*l*) containing triethylamine (0.04 mol). The solvent was removed by filtration and the resin was washed with methanol and DMF. The free base thus obtained was used to the coupling with the next acylamino acid or peptide.

b) Z-Amino acid phenol resin (containing 0.01 mol of Z-amino acid) was treated with 33% HBr in acetic acid (20 m*l*) shaking for 2 hr at room temperature. The suspension was diluted with 30 m*l* acetic acid, and filtered and washed with acetic acid, methanol and DMF. The resulting hydrogen bromide salt was neutralized with triethylamine in DMF as described above.

The Peptide-forming Step. *a) The DCCD Method.* AOC- or Z-Amino acid phenol resin (containing 0.01 mol of acylamino acid) was deprotected and neutralized as described above. The free base was suspended in DMF (20 m*l*) and the next AOC- or Z-amino acid or peptide (0.02 mol) was added and then a solution of DCCD (0.02 mol) in DMF (5 m*l*) was added. The suspension was shaken overnight. The resinous derivative was filtered and washed several times with DMF, acetic acid and methanol until dicyclohexylurea, excess reagents and byproducts are completely removed.

b) The p-Nitrophenyl Ester Method. AOC- or Z-Amino acid phenol resin (containing 0.01 mol of acylamino acid) was deprotected and neutralized as described above. The free base was suspended in DMF (20 m*l*) and the next AOC- or Z-amino acid or peptide *p*-nitrophenyl ester (0.02 mol) was added and then the suspension was shaken overnight. The resinous derivative was filtered and washed several times wiih DMF and methanol to remove excess reagents and by-products.

The Peptide Liberation Step. *a) AOC- or Z-Peptide.* The completed AOC- or Z-peptide resin (containing 0.001 mol of peptide) was saponified by shaking in a solution of 30 m*l* of ethanol-DMF (1 : 1) and 5 m*l* of aqueous N NaOH for 2 hr at room temperature. The phenol resin was removed by filtration and the filtrate was concentrated to a syrup. water (3 m*l*) was added to the syrup obtained and the solution was acidified with dilute aqueous HCl; the separated product was extracted with the suitable solvent and washed with water. The solvent was evaporated off and the crystal residue was recrystallized once or twice from the suitable solvents.

b) AOC- or Z-Peptide Amide. The completed AOC- or Z-peptide resin was treated with large excess of 25% ammonia in methanol for 2 days at room temperature in a sealed tube. The phenol resin was filtered off, the filtrate was concentrated, and the crystal residue was washed with dilute aqueous HCl, dilute aqueous sodium bicarbonate and water, and recrystallized once or twice from the suitable solvents.*5

*4 A fixed quantity of AOC- or Z-amino acid resin was saponified with aqueous N-NaOH in DMF and a ratio of the esterfication was calculated from the quantity of AOC- or Z-amino acid recovered.

*5 The rearrangement from the α-linkages of asparagine- and glutamine-residues to the β- and γ-linkages was 0—40%; it was checked by the methods of A. C. Chibnall *et al.* (*Biochem. J.*, **68**, 114 (1958)) and P. T. Lansbury (*J. Am. Chem. Soc.*, **83**, 429 (1961)).

c) AOC- or Z-Peptide Hydrazide. The completed AOC- or Z-peptide resin was treated with large excess of hydrazine hydrate in DMF overnight. The phenol resin was filtered off. Water was added to the filtrate and the precipitated crystal was collected by filtration and recrystallized from the suitable solvents.

***N-t*-AOC-*S*-Ethylmercapto-L-cysteinyl-L-tyrosyl-L-isoleucyl-γ-ethyl-L-glutamyl-β-methyl-L-aspartyl-*S*-ethylmercapto-L-cysteinyl-L-prol-yl-L-leucyl-glycine Resin (I).** Each peptide bonds were lengthened stepwise from the *C*-terminal with the AOC-amino acids by the DCCD method. These procedures were all carried out by the general method as described above.

***N-t*-AOC-L-Cysteinyl-L-tyrosyl-L-isoleucyl-γ-ethyl-L-glutamyl-β-methyl-L-asparatyl-L-cysteinyl-L-prolyl-L-leucyl-glycine resin (II) and Its Oxydated Derivative (III).** The compound I (0.5 g) was suspended in dioxane (10 m*l*) and thiophenol (0.1 m*l*) was added. The suspension was shaken for 10 hr at 45°C, and filtered and then washed with dioxane. II obtained was suspended in dioxane (5 m*l*) and methanol (5 m*l*) and CO_2 free air was bubbled for 4 hr. The oxidized derivative (III) was collected by filtration and washed with dioxane and methanol.

AOC-Oxytocin (IV). The compound III (0.4 g) was left for 2 days in 25% ammonia in methanol (20 m*l*) in a sealed tube. The phenol resin was removed by filtration and the filtrate was concentrated. The solid residue was dissolved in ethyl acetate and washed with 0.2 N aqueous HCl and water and dried over anhydrous sodium sulfate and then solvent was evaporated off. The crude amorphous solid (0.2 g) obtained was purified on a 2×30 cm Merck's silica gel G column by elution with chloroform - methanol - acetic acid (95 : 5 : 3 v/v); yield 0.1 g, mp 100—120°C, $[\alpha]_D^{23}$ −48.8 (*c* 0.5, DMF).

Found: C, 52.95; H, 6.94; N, 15.39%. Calcd for $C_{49}H_{76}N_{12}O_{14}S_2$: C, 52.48; H, 6.83; N, 14.99%.

Oxytocin. A fixed quantity of the AOC-oxytocin IV was treated with 7% aqueous HCl for 30 min, then the insoluble material was filtered off and pH of the filtrate was adjusted to 4 with dilute aqueous ammonia. The oxytocic activity of this final solution was found to be about two-thirds of that of a standard sample,[21] as determined by rat-uterine contractive activity.

The authors wish to express their thanks to Dr. Yuji Kawashima for his encouragement and valuable advice.

BULLETIN OF THE CHEMICAL SOCIETY OF JAPAN VOL. 41 186—191 (1968)

Reactive Monomers Derived from *p*-Vinylbenzoic Acid

Yoshio IWAKURA,* Keikichi UNO,* Nobuo NAKABAYASHI** and Takakazu KOJIMA*

**Department of Synthetic Chemistry, Faculty of Engineering, The University of Tokyo, Hongo, Bunkyo-ku, Tokyo*
***Institute for Medical and Dental Engineering, Tokyo Medical and Dental University, Chiyoda-ku, Tokyo*

(Received July 5, 1967)

Reactive monomers derived from *p*-vinylbenzoic acid have been prepared which have both a vinyl group and another functional group for addition reaction or condensation reaction. The radical polymerization of these monomers gives high polymers. Monomer reactivity ratios in relation to styrene were obtained for three of these monomers. Plots of Alfrey-Price's *e* value *vs.* Hammett's σ value show a linear relationship in the case of substituted styrenes. σ values are then estimated by this relation, using *e* values based on the monomer reactivity ratios. The σ constants assumed for the COCl, $COOCH_2CHCH_2$ (O), and NCO substituents are 0.71, 0.64, and 0.27 respectively. These σ values are confirmed by other supporting facts.

Wide investigations of reactive polymers have been carried out in our laboratory.[1-3] Generally speaking, there are two ways to introduce reactive functional groups into macromolecules. One way is the reaction of a polymer with some compound which has functional groups. The other is the polymerization of vinyl monomers which have functional groups for a polymer reaction. Such a vinyl monomer has been called a reactive monomer.[4] The latter way is rather more favorable than the former because of the uniform composition of the polymer obtained.

The present paper will describe the preparation of reactive monomers derived from *p*-vinylbenzoic acid. The reactive groups introduced are those for addition reaction or condensation reaction: epoxide, aziridine, isocyanate, acid chloride, and

1) Y. Iwakura, T. Kurosaki and N. Nakabayashi, *Makromol. Chem.*, **44/46**, 570 (1961).
2) N. Nakabayashi and Y. Iwakura, *ibid.*, **81**, 180 (1965).
3) Y. Iwakura, T. Kurosaki, N. Ariga and T. Ito, *ibid.*, **97**, 128 (1966).
4) Y. Iwakura, K. Uno, N. Nakabayashi and T. Kojima, This Bulletin, **38**, 1223 (1965).

β-chloroethylsulfonamide. All of these monomers belong to *p*-substituted styrenes. The monomer reactivity ratios of these monomers in relation to styrene showed some correlation with the polar effect of the group.

Results and Discussion

Preparation of *p*-Substituted Styrenes. In the present study, *p*-substituted styrenes (II—VIII) were synthesized from *p*-vinylbenzoic acid[5-7] according to the following equations:

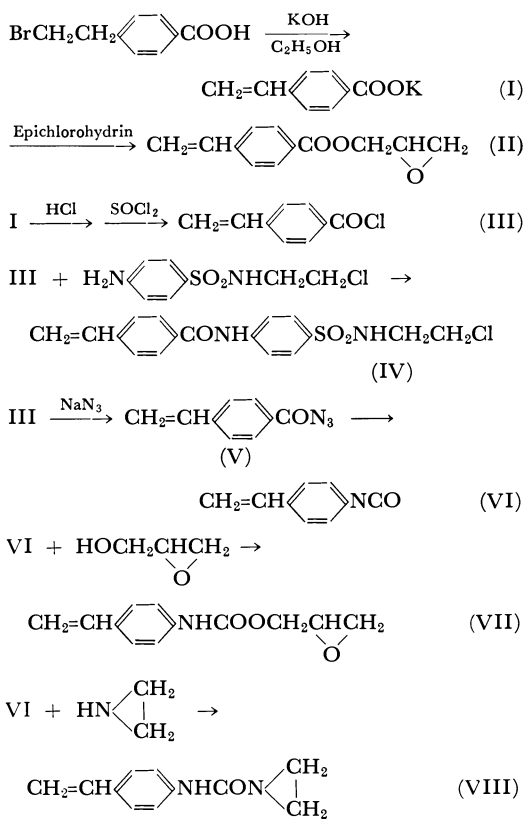

Potassium *p*-vinylbenzoate (I) was obtained according to Jäger's method. The glycidyl ester (II) was obtained in a good yield by the reaction of compound I with an excess amount of epichlorohydrin in the presence of quaternary ammonium salts serving as catalysts.

p-Vinylbenzoyl chloride (III) was prepared by Adrova.[8] In this reaction, the amount of thionyl chloride used must be carefully measured. Using an excess amount of thionyl chloride gives *p*-(α-chlorovinyl)benzoyl chloride, accompanied by a resinous polymer. The reaction of compound III with *N*-β-chloroethyl sulfanilamide[2] and sodium azide gave compound IV and compound V respectively.

A mixture of *o*- and *p*-isomers of vinylphenyl isocyanate is known to have been synthesized from *o*- and *p*-vinylaniline by phosgenation.[9] In the present study, *p*-vinylphenyl isocyanate (VI) was obtained by the Curtius rearrangement of the acid azide V. Furthermore, glycidyl urethane (VII) and *N*, *N*-ethylene urea (VIII) were derived through the reaction of VI with glycidol and aziridine respectively. The physical and infrared absorption data of these monomers are summarized in Table 1.

Polymerization of *p*-Substituted Styrenes. The radical polymerization of these monomers was carried out in a solution, using azo-bis-isobutyronitrile (AIBN) as an initiator. All of the monomers gave white powders soluble in such organic solvents as dioxane and dimethylformamide (DMF). The infrared spectra of these polymers give absorptions characteristic of the functional groups. The polymers from III and VI were very sensitive to moisture, and they became insoluble in an instant. The results of the homopolymerization of these reactive monomers are summarized in Table 2.

The isocyanates are known to undergo anionic polymerization easily even when sodium cyanide is used as an initiator.[10] On the other hand, styrene does not give any polymer in the presence of sodium cyanide. The compound VI has both vinyl and isocyanate groups; an anionic polymerization of it in DMF with sodium cyanide as an initiator was undertaken. The polymer thus obtained was soluble in DMF, and gave IR absorptions at 1630, 985, and 910 cm^{-1}, which are characteristic absorptions of vinyl group, and no absorptions around 2300 and 2900 cm^{-1}. These results indicate that the polymerization of VI proceeded exclusively through the isocyanate group. The further polymerization of the residual functional group in the polymer obtained from VI was then examined in order to get a ladder polymer. However, the radical polymerization of the pendant vinyl group in the isocyanate polymer failed, since the isocyanate polymer was readily degraded in DMF at room temperature. The anionic polymerization of the isocyanate group in the vinyl polymer could not be carried out either because of insolubility of the vinyl polymer.

Copolymerization. Compounds II, III, and VI were submitted to copolymerization with styrene. The monomer reactivity ratios of these compounds were obtained by the intersecting

5) C. S. Marvel and C. G. Overberger, *J. Am. Chem. Soc.*, **67**, 2250 (1945).
6) S. H. Merrill, *J. Org. Chem.*, **26**, 1301 (1961).
7) P. Jäger and E. S. Waight, *J. Chem. Soc.*, **1963**, 1339.
8) N. A. Adrova and K. K. Khomenkova, *Zh. Obshch. Khim.*, **32**, 2267 (1962).
9) E. L. Kropa and A. S. Nyquist, U. S. Pat. 2468713 (1949).
10) V. E. Shashoua, W. Sweeny and R. F. Tietz, *J. Am. Chem. Soc.*, **82**, 866 (1960).

TABLE 1. PHYSICAL PROPERTY AND IR SPECTRA

Compound	mp, °C (bp, °C)	IR Spectra cm^{-1}
II	(115.5—116.5/0.1 mmHg)	1718, 1629, 1608, 1402, 1342, 1275, 1176, 1102, 1011, 987, 907 856, 839, 779, 708
III	(69.5—70.0/0.1 mmHg)	1770, 1730, 1632, 1604, 1405, 1210, 1180, 988, 922, 873, 850, 768
IV	186.0—186.5	3300, 1653, 1590, 1513, 1498, 1323, 1150, 1098, 1087, 975, 910 835, 813, 770, 685
V	54.0—54.5	2180, 1681, 1630, 1605, 1401, 1250, 1188, 1113, 989, 930, 912, 855, 778, 768, 691
VI	(40.5—41.5/0.1 mmHg)	2290, 1630, 1605, 1522, 1108, 988, 910, 893
VII	95.5—97.0	3330, 1698, 1611, 1585, 1525, 1403, 1308, 1228, 1060, 984, 904 858, 833, 782, 761
VIII	108.0—108.5	3320, 1673, 1636, 1615, 1590, 1535, 1403, 1335, 1250, 1150, 997, 988, 900, 872, 831

TABLE 2. RADICAL POLYMERIZATION

Monomer g	Solvent ml		Time hr	Temperature °C	Yield g	η*
II 1.5	Dioxane	0.3	2	51	1.0	1.00**
III 0.8	Dioxane	0.5	4	75	0.7	—
IV 0.5	Acetone	3.0	11	70	0.35	0.16
	DMF	2.0				
VI 0.5	Toluene	2.0	0.5	60	0.3	—
VII 0.5	Dioxane	1.0	3	60	0.05	0.39
VIII 0.55	Dioxane	1.0	0.5	55	0.05	0.10***

* η_{inh} in DMF (C=0.2 g/dl) at 30.0°C.
** $[\eta]$ in DMF at 30.0°C
*** accompained with gel formation

TABLE 3. REACTIVITY RATIO AND Q, e VALUE

M_2	r_1	r_2	Q_2	e_2	Temp., °C
II	0.40±0.02	0.95±0.10	1.14	0.18	70.0
III	0.17±0.03	1.80±0.20	2.46	0.28	60.0
VI	0.75±0.10	1.10±0.10	0.94	−0.36	60.0

M_1=Styrene

method[11] from the compositions of the monomer feeds and copolymers obtained. The compositions of the copolymers were determined by analysis of the epoxy group for the copolymer from II, by analysis of chlorine for the copolymer of III, and by elemental analysis of nitrogen for VI. The monomer reactivity ratios and Alfrey-Price's Q and e values are shown in Table 3. The copolymer composition curves of styrene (M_1) with compounds II, III, and VI are shown in Fig. 1, where the mol% of m_1 in the copolymers is plotted against the mol% of M_1 in the monomer feeds.

The compounds II, III, and VI have electron-withdrawing groups, that is, $COOCH_2\underset{\diagdown O \diagup}{CH}CH_2$, COCl, and NCO. It has been reported that, on the copolymerization of styrene (M_1) with p-substituted styrenes, there is a good linear relation between $\log(1/r_1)$ and σ^-,[12] or between $\log(1/r_1)$ and σ, using a modification of Hammett's equation.[13] e values have also been said to show polarity, and to have some correlation with σ in substituted ethylenes.[14] When the e values of p-substituted styrenes were plotted against the σ values for substituents, a good linear correlation was observed, as is shown in Fig. 2. The e and σ values are taken from Perrin's and Young's

11) G. E. Ham, "Copolymerization," ed. by G. H. Ham, Interscience Publishers, New York (1964), p. 29.

12) C. Walling, E. R. Briggs, K. B. Walfstein and F. Mayo, *J. Am. Chem. Soc.*, **70**, 1537 (1948).
13) M. Imoto, M. Kinoshita and M. Nishigaki, *Makromol. Chem.*, **94**, 238 (1966).
14) J. Furukawa and T. Tsuruta, *J. Polymer Sci.*, **36**, 275 (1959).

Table 4. Spectra data

Compound	UV λ_{max} (ε) mμ	NMR τ(ppm) phenyl	NMR τ(ppm) vinyl	Substituent	σ
VI	259 (1.6×10^4)	2.81 2.93 3.10 3.23	3.14 3.32 3.41 3.58 4.17* 4.46* 4.64* 4.83*	NCO	0.27
II	268 (1.9×10^4)	1.94 2.08 2.54 2.68	3.03 3.21 3.32 3.50 4.02* 4.32* 4.57* 4.75*	$COOCH_2CHCH_2$ (O)	0.64
III	280 (1.5×10^4)	2.18 2.30 2.70 2.82	3.11 3.27 3.38 3.55 3.98* 4.26* 4.45* 4.63*	COCl	0.71

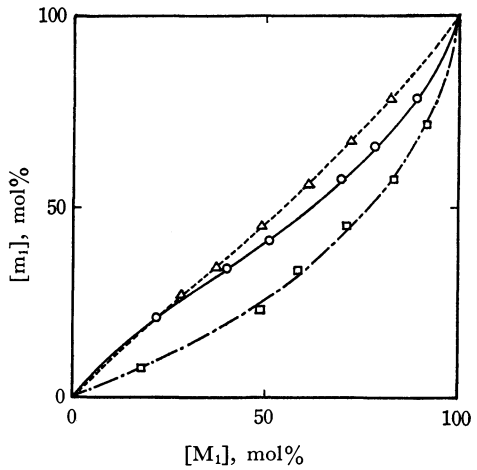

Fig. 1. Copolymer composition curves.
○ styrene (M_1)−II (M_2)
□ styrene (M_1)−III (M_2)
△ styrene (M_1)−VI (M_2)
Lines are calculated from the monomer reactivity ratios and spots are from experimental data.

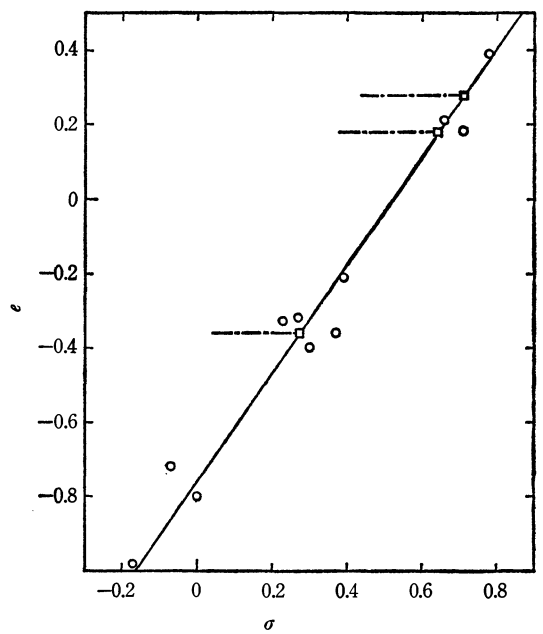

Fig. 2. Correlation between e and σ.
○ announced value[15,16]
□ this experiment

tables[15,16] respectively.

When the σ values for the substituents of compounds II, III, and VI were estimated from the e-σ map (Fig. 2). The following values were obtained for $-COOCH_2CHCH_2$, -COCl, and -NCO:

0.64, 0.71, and 0.27.

The σ value for *p*-NCO has been reported to be 0.24,[17] which is close to the estimated value of 0.27. The σ value for *p*-COCl can be estimated by Charton's method.[18] If X denotes a substituent with a known σ constant and Y an intervening group, the σ constant for the XY group can be estimated by the equation: $\sigma_{XY}=\alpha+\beta\sigma_X$. In this case, X=CO and Y=H, OCH_3, NH_2, and OH. The σ value given for *p*-COCl is 0.70, which is almost the same value as the estimated

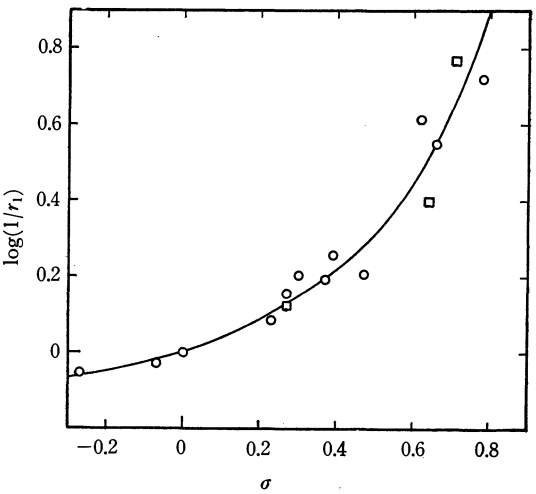

Fig. 3. Relationship between $\log(1/r_1)$ and Hammett's σ.
○ announced value[15,16]
□ this experiment

15) J. Clark and D. D. Perrin, *Quart. Reviews*, **18**, 295 (1964).
16) L. J. Young, *J. Polymer Sci.*, **54**, 411 (1961).
17) J. H. Saunders and K. C. Frisch, "Polyurethanes," Interscience Publishers, New York (1962), p. 144.
18) M. Charton, *J. Org. Chem.*, **28**, 3121 (1963).

value, 0.71. If the α and β values calculated by Charton are used, the σ value may be 0.60, but the Y groups used by him include substituent of a different type (COO^-), which deviates from the equation given above, and so the error must be much greater. The σ value for the glycidyl ester has not yet been obtained. The value obtained here is a little higher than the value for $-COOC_2H_5$, 0.45.[15] This can be attributed to the inductive effect of oxygen in a three-membered ring. The λ_{max} in UV and τ values in NMR for CH_2= (asterisked value) of these three monomers show an orderly correlation with the σ value assumed here (Table 4). The values of $\log(1/r_1)$ are plotted against σ in Fig. 3. This figure also shows that the σ values obtained here are reasonable, because the cubic points (our results) are almost on the plotted curve.

Experimental

Monomers. *Glycidyl p-Vinylbenzoate (II).* *p*-(β-Bromoethyl)benzoic acid was prepared from *p*-(β-bromoethyl)acetophenone by the procedure of Foreman,[19] using sodium hypochlorite (antiformine). Potassium *p*-vinylbenzoate (I) was obtained by heating *p*-(β-bromoethyl)benzoic acid with potassium hydroxide and hydroquinone in ethanol. Finely-powdered crude I (15.0 g), epichlorohydrin (120 m*l*), triethylbenzylammonium chloride (150 mg), and hydroquinone (80 mg) were heated while being stirred under reflux for 30 min. The resulting potassium chloride was filtered, and the excess epichlorohydrin was removed under reduced pressure. The fractional distillation of the residue gave 7.2 g (67%) of a colorless product; bp 115.5—116.5°C/0.1 mmHg. The epoxide content was over 99.0% (HCl-dioxane method[20]). $n_D^{20}=1.5622$.

Found: C, 70.63; H, 6.01%. Calcd for $C_{12}H_{12}O_2$: C, 70.57; H, 5.92%.

p-Vinylbenzoyl Chloride (III). To a mixture of *p*-vinylbenzoic acid (10.0 g) and *p-t*-butylpyrocathecol (10 mg), a 20 m*l* portion of thionyl chloride was added under cooling. The reaction mixture was kept below 10°C for 5 hr, and then gradually warmed to 40°C and maintained there for 1 hr. After the removal of the thionyl chloride, distillation gave 8.8 g (78%) of colorless liquid; bp 69.5—70.0°C/0.1 mmHg. $n_D^{20}=1.6020$.

The reaction of *p*-vinylbenzoic acid (10.0 g) with a large excess of thionyl chloride (60 m*l*) gave a product (bp 90—100°C/1 mmHg) which solidified on standing; recrystallization from *n*-hexane gave white needles which melted at 86.0—86.5°C.

IR: 1760, 1601, 1410, 1208, 1170, 933, 885, 847, 808 cm^{-1}

NMR: 2.04, 2.17, 2.62, 2.74 (quartet) and 3.15 (singlet)

Found: C, 53.65; H, 3.24; Cl, 34.57%. Calcd for $C_9H_6OCl_2$: C, 53.50; H, 3.00; Cl, 35.09%.

From these data, the product was identified as *p*-(α-chlorovinyl)benzyol chloride.[21]

p'-β-Chloroethylaminosulfonyl-p-vinylbenzanilide (IV). *N*-β-Chloroethylsulfoanilamide (2.6 g) and triethylamine (1.2 g) were dissolved in a mixture of acetone (3 m*l*) and ether (10 m*l*). To this solution acid chloride III (1.9 g) was added, drop by drop, on cooling in an ice-salt bath. In an hour of stirring a white precipitate appeared. The product was filtered, washed with water, and dried. It weighed 3.0 g (75%). Recrystallization from benzene-ethanol gave white crystals; mp 186.0—186.5°C.

Found: C, 56.14; H, 4.70; N, 7.62%. Calcd for $C_{17}H_{17}N_2O_3ClS$: C, 55.98; H, 4.70; N, 7.68%.

p-Vinylphenyl Isocyanate (VI). To a solution of sodium azide (10.0 g) in distilled water (26 m*l*), there was added, drop by drop, a solution of III (8.3 g) in ether (7 m*l*) at a temperature around 0°C. The mixture was then agitated for 30 hr at 0°C. The *p*-vinylbenzazide V thus deposited was filtered, washed thoroughly with water and then with a small amount of *n*-hexane, and dried. It weighed 8.0 g (93%); mp 54.0—54.5°C (recrystallized from *n*-hexane).

A solution of V (8.0 g) in toluene was gradually heated; gas evolved about 80°C. The solution was then refluxed for 30 min. After the removal of the toluene, the distillation of the residual liquid gave a colorless liquid, 4.4 g (66%); bp 40.5—41.5°C/0.1 mmHg. $n_D^{20}=1.5785$. This product gave methyl *p*-vinylcarbanilate by a reaction with methanol; mp 85.5—86.5°C (recrystallized from ether-petroleum ether).

Found: N, 7.68%. Calcd for $C_{10}H_{11}NO_2$: N, 7.91%.

Glycidyl p-Vinylcarbanilate (VII). This compound was obtained by the reaction of VI with glycidol in ether. The yield was 96%; mp 95.5—97.0°C (recrystallized from benzene-*n*-hexane).

Found: C, 65.42; H, 5.92; N, 6.32%. Calcd for $C_{12}H_{13}NO_3$: C, 65.74; H, 5.98; N, 6.39%.

N-p-Vinylphenyl-N', N'-ethyleneurea (VIII). This compound was obtained by the reaction of VI with aziridine in cooled ether. The yield was 70%; mp 108.0—108.5°C (recrystallized from aqueous methanol).

Found: C, 69.83; H, 6.17; N, 14.74%. Calcd for $C_{11}H_{12}N_2O$: C, 70.18; H, 6.43; N, 14.88%.

Polymerization. *Radical Polymerization.* The radical polymerization was carried out with an appropriate solvent in a sealed ampule using AIBN as the initiator. The polymer was obtained by pouring the reaction mixture into methanol (for II, IV, VII, and VIII) or into anhydrous *n*-hexane (for III and VI). The viscosities were measured in a DMF solution at 30.0°C.

Anionic Polymerization. The procedure for the anionic polymerization of VI was the same as that described by Shashoua.[10] The yield of the polymer was 32%. If the polymer obtained was dissolved in DMF at room temperature, it was degraded to a cyclic trimer and symmetrical urea. Therefore, the viscosity of the isocyanate polymer could not be obtained. Radical polymerization by the high dilution of this polymer in DMF failed for the same reason.

Copolymerization. Two grams of a pair of monomers and 10 mg of AIBN were mixed in a sealed tube under nitrogen. The polymerization was then carried out at a fixed temperature. The conversion of the copolymer was less than 8%. The resulting polymer was

19) E. L. Foreman and S. M. McElvain, *J. Am. Chem. Soc.*, **62**, 1435 (1940).
20) G. King, *Nature*, **164**, 1106 (1949).
21) W. K. Detweiler and E. D. Amstutz, *J. Am. Chem. Soc.*, **72**, 2882 (1950).

precipitated with *n*-hexane, dried under a vacuum, and submitted to the analysis of the epoxy group[20] or to elemental analysis.

Spectra Analyses. The infrared spectra were obtained with a Hitachi Model EPI-2 double-beam spectrometer. The NMR spectra were measured at room temperature with a Japan Electron Optics Laboratory C-60 spectrometer. The UV spectra were measured in an *n*-hexane solution with a JASCO ORD/UV-5 spectrometer.

The authors wish to express their thanks to the Nissō Kakō Co., Ltd., for kindly supplying the starting materials.

BULLETIN OF THE CHEMICAL SOCIETY OF JAPAN VOL. 41 191—197 (1968)

Proton Magnetic Resonance Studies of 2, 2'-Anhydro-2-*C*-hydroxymethyl-1, 3 : 4, 6-di-*O*-isopropylidene-L-sorbitol[1]

Takashi MAEDA, Kazuo TORI, Masako OHTSURU and Kanji TOKUYAMA

Shionogi Research Laboratorry, Shionogi & Co., Ltd., Fukushima-ku, Osaka

(Received July 8, 1967)

The PMR spectra of 2,2'-anhydro-2-*C*-hydroxymethyl-1, 3:4, 6-di-*O*-isopropylidene-L-sorbitol were examined in several solvents to confirm its structure. The conformation of this molecule is also discussed.

In a recent paper,[2] we have reported that the treatment of 1, 3 : 4, 6-di-*O*-isopropylidene-β-L-sorbofuranose (I) with diazomethane in ether-methanol afforded a mixture of 2, 2'-anhydro-2-*C*-hydroxymethyl-1, 3 : 4, 6-di-*O*-isopropylidene-L-xylohexitol (II) and 2, 5-anhydro-2-*C*-hydroxymethyl-1, 3 : 4, 6-di-*O*-isopropylidene-L-iditol (III) accompanied with trace of methyl 1, 3 : 4, 6-di-*O*-isopropylidene-β-L-sorbofuranoside (IV), and that II was easily transformed to III even in the absence of an acid. Ring opening of an epoxide proceeds with inversion at that carbon atom which is attacked.[3,4] Therefore, it can be anticipated that the structure of II should be 2, 2'-anhydro-2-*C*-hydroxymethyl-1, 3 : 4, 6-di-*O*-isopropylidene-L-sorbitol but not 2, 2'-anhydro-2-*C*-hydroxymethyl-1, 3 : 4, 6-di-*O*-isopropylidene-L-iditol (V). This paper deals with the confirmation of the structure of II by means of PMR spectroscopy. Further the conformations of II in several solvents are discussed.

The 100 Mc PMR spectra of II were measured in carbon tetrachloride, chloroform-d, acetone-d_6, pyridine-d_5, and dimethylsulfoxide-d_6 in order to apply the solvent effects to the assignment of proton signals. The data obtained by the first-order approximation are shown in Table 1.

The spectrum of II in carbon tetrachloride shows the signal of epoxidic protons as an AB-type quartet at τ 7.06 and 7.45 ($J_{2'A,2'B}$=4.4 cps), as shown in Fig. 1a. The upfield-half of the quartet shows extra splittings of 0.8_5 cps. Double irradiation on this proton causes the collapse of the downfield-half of the quartet into a singlet and the change of a broad doublet due to H_3 at τ 5.90 ($J_{3,4}$= 3.0 cps) into a sharper doublet, but did not cause any changes to an AB-type quartet due to H_1 and $H_{1'}$ at τ 6.13 and 6.47 ($J_{1,1'}=(-)12.5$ cps) (Fig. 1b). Conversely, double irradiation at the resonance position of H_3 causes sharpning of the upfield-half of the quartet due to the epoxidic protons as well as the collapse of the multiplet arising from H_4 at τ 6.33 into a doublet ($J_{4,5}$= 2.0 cps) (Fig. 1c). Thus, the presence of a long-range spin coupling between only one of the epoxidic and C-3 protons was revealed. A doublet signal at τ 6.99 (J=7.0 cps) is thought to be due to the OH proton coupled to H_5. Decoupling of this proton by double irradiation (Fig. 1d) and by deuterium exchange by an addition of a small amount of deuterium oxide to the solution examined (Fig. 1f) made a broad multiplet at τ 6.58 narrower. Thus this multiplet was assignable to H_5 signal. The remaining AB-type quartet further split into doublets at τ 6.18 ($J=(-)12.2$ and 2.4 cps) and 6.38 ($J=(-)12.2$ and 2.5 cps) arises obviously from C-6 protons. Figures 1e and 1g show other examples of spin-decoupling experiments on II.

Similar decoupling experiments on II in chloroform-d (see Fig. 2) and acetone-d_6 (see Fig. 3) gave similar results. In these solutions the OH proton signals appear at positions so close to those

1) Sorboses. X. For Part IX, see Ref. 2.
2) T. Maeda, This Bulletin, **40**, 2122 (1967).
3) S. Peat, *Advan. Carbohydrate Chem.*, **2**, 37 (1946).
4) J. G. Buchanan and E. M. Oakes, *Tetrahedron Letters*, **1964**, 2013.

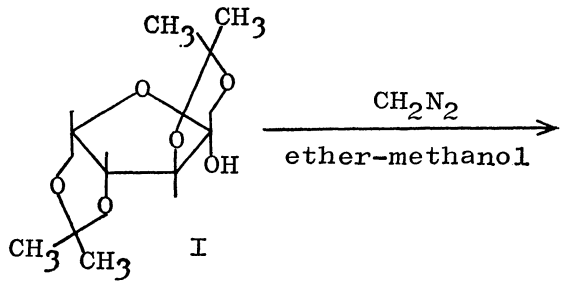

I

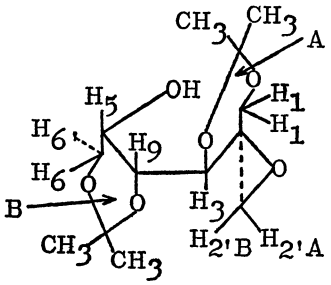

II

+

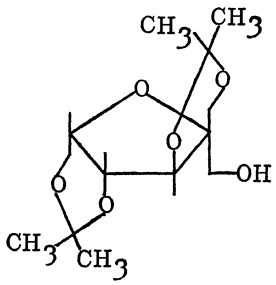

III

+

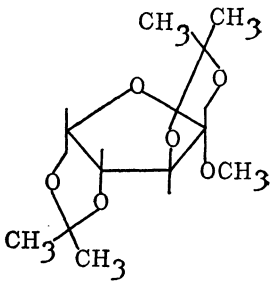

IV

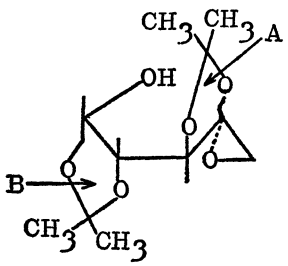

V

of H_5 signals that their patterns are much complicated, but the additions of deuterium oxide to the solutions examined make the signal patterns very clear with disappearing of the OH-signals. It is very interesting to note that decoupling of the OH proton in these solvents, particularly in chloroform-d, changes one of the C-6 methylene proton signals (at the lower field) into a sharp quartet. This observation implies the presence of long-range spin coupling between the OH- and the C-6 protons.

The infrared spectrum of II in a dilute solution of carbon tetrachloride shows two OH bands at 3539 and 3578 cm^{-1}; the former indicates the presence of a strong intramolecular hydrogen-bonding (the distance between OH–O is claculated about 1.76 Å) and the latter (shoulder) does a weak hydrogen-bonding (the distance is about 2.18 Å).[5]

The values for $J_{3,4}$ (2.7—3.6 cps) led us to determination of the dihedral anagle between H_3 and H_4 according to the well known Karplus correlation;[6] the angle is about 60° in a very rough estimation.[7] The values for $J_{4,5}$, $J_{5,6}$, and $J_{5,6'}$ (2—2.5 cps) are essentially unchanged with the change of solvents. Applying the Karplus equation to these values likewise in a rather qualitative

5) The distances were calculated according to Y. Matsui, M. Takasuka and T. Kubota, *Ann. Rept. Shionogi Res. Lab.*, **15**, 125 (1965), and T. Kubota, M. Takasuka and Y. Matsui, *ibid.*, **16**, 63 (1966), provided that the absorption band of an ordinary secondary OH group appears at 3630 cm^{-1}.

6) M. Karplus, *J. Chem. Phys.*, **30**, 11 (1959); *J. Am. Chem. Soc.*, **85**, 2870 (1963).

7) It is a well known fact that much caution should be exercised when deriving the dihedral angle between a set of protons from the Karplus equation. For example, see N. S. Bhacca and D. H. Williams, "Applications of NMR Spectroscopy in Organic Chemistry," Holden-Day, Inc., San Francisco (1964).

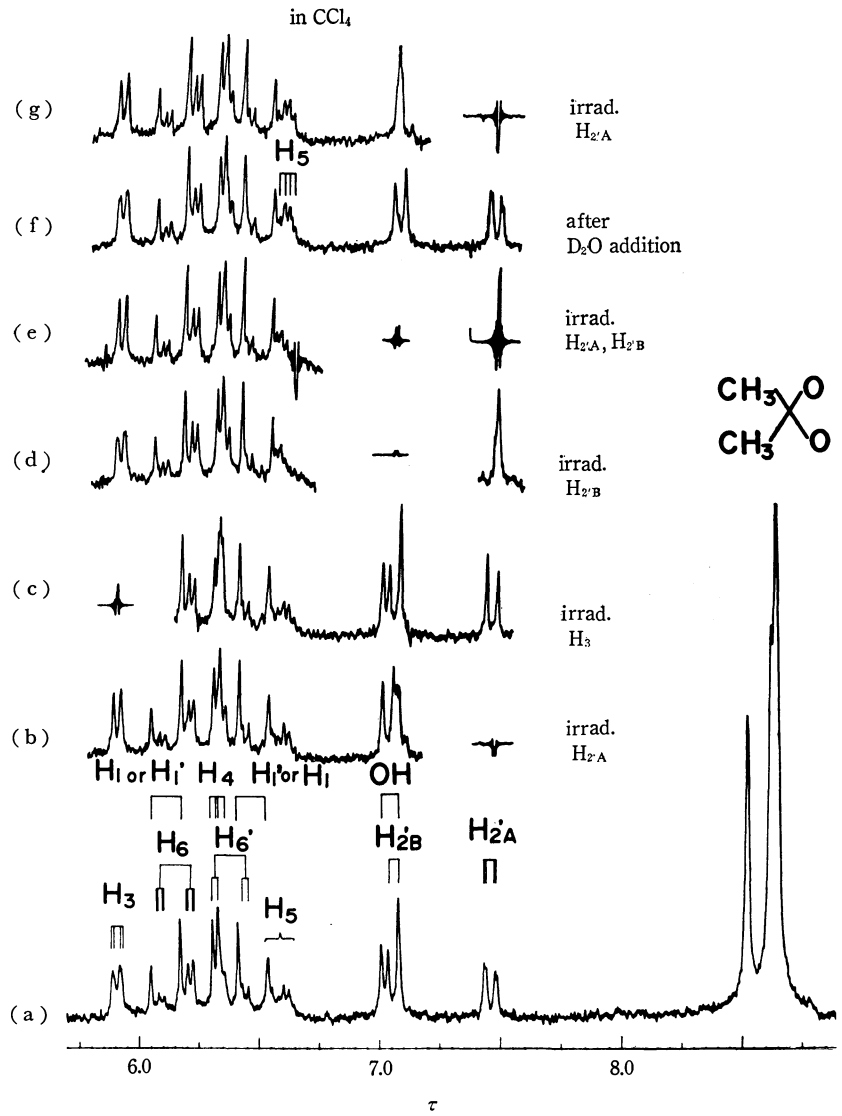

Fig. 1. PMR spectra of II in carbon tetrachloride at 100 Mc.
(a) Normal spectrum, (b)—(e) double and triple resonance spectra, (f) normal spectrum measured after adding a small amount of D_2O to the solution, and (g) double resonance spectrum.

sense, we can conclude that the 4, 6-*O*-isopropylidene ring (ring B) has a chair form; the C-5 OH group has an axial conformation. Examination of Dreiding models shows that it is difficult to form the molecular conformation so as to enable the intramolecular hydrogen-bonding of this OH group toward the epoxide ring owing to strong steric hindrance. Therefore, the OH group should possibly, and perhaps dominantly, be hydrogen-bonded to the oxygen atom at C-3; but partly, as the infrared spectrum indicates, a weak hydrogen-bonding between the OH group and either of oxygen atoms in ring B is thought to be formed. The presence of the long-range spin couplings between one epoxidic and C-3 protons and between the OH- and one C-6 protons is useful for inferring the stereochemistry of II. The stereochemical relationship between these protons should obey the "W-letter" rule for the long-range spin coupling across four single bonds.[8] The "W-letter" arrangement between the OH- and the axial C-6 protons also explains the coupling constant between the OH- and C-5 protons in carbon tetrachloride; the dihedral angle between these two protons is

8) For example, see S. Sternhell, *Rev. Pure and Appl. Chem.*, **14**, 15 (1964); K. Tori, K. Aono, Y. Hata, R. Muneyuki, T. Tsuji and H. Tanida, *Tetrahedron Letters*, **1966**, 9, and references therein.

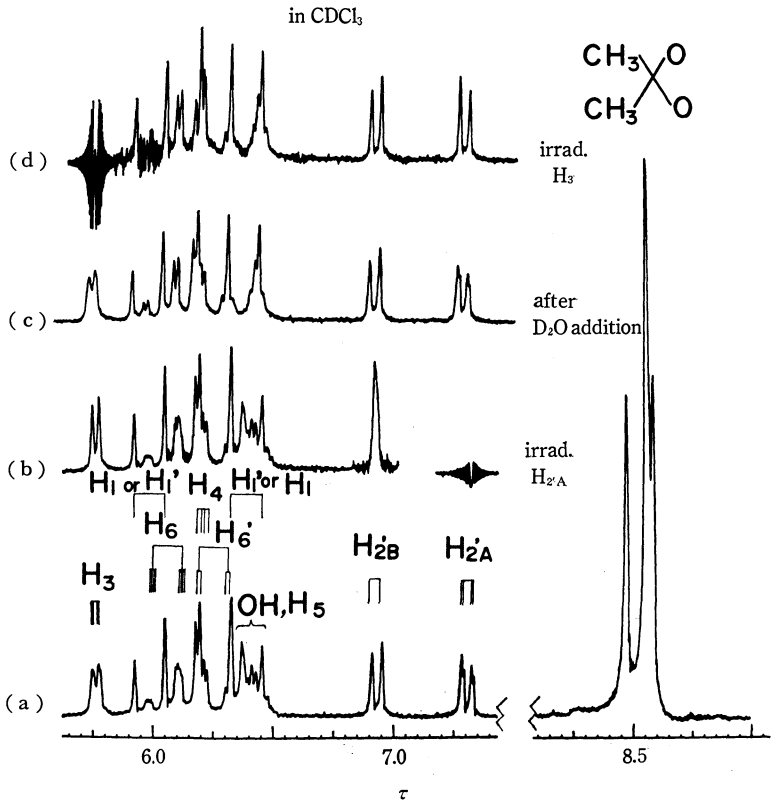

Fig. 2. PMR spectra of II in chloroform-d at 100 Mc.
(a) Normal spectrum, (b) double resonance spectrum, (c) normal spectrum measured after adding a small amount of D_2O, and (d) double resonance spectrum.

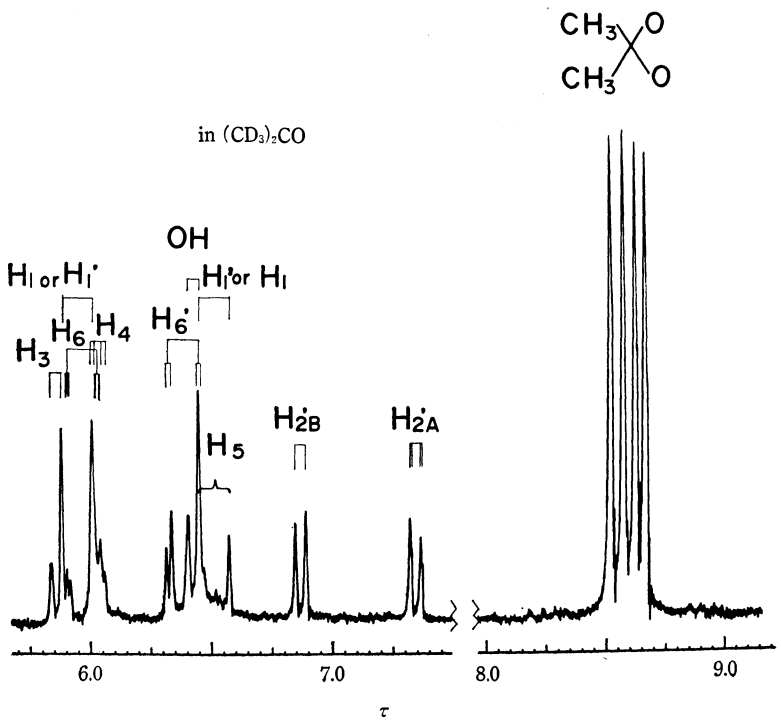

Fig. 3. PMR spectrum of II in acetone-d_6 at 100 Mc.

TABLE 1. CHEMICAL SHIFTS (τ) AND COUPLING CONSTANTS (J, cps) OF 2, 2'-ANHYDRO-2-*C*-HYDROXYMETHYL-1, 3 : 4, 6-DI-*O*-ISOPROPYLIDENE-L-SORBITOL (II) IN VARIOUS SOLVENTS

	Solvent				
	Carbon tetrachloride	Chloroform-d	Acetone-d_6	Pyridine-d_5	Dimethyl-sulfoxide-d_6
Chemical shift					
H_1 and $H_{1'}$	6.13 6.47	5.98 6.36	5.93 6.49	5.78 6.25	5.95 6.57
$H_{2'A}$	7.45	7.28	7.31	7.20	7.31
$H_{2'B}$	7.06	6.90	6.85	6.56	6.90
H_3	5.90	5.76	5.84	5.42	6.06
H_4	6.33	6.13	6.00	5.75	5.96
H_5	6.58	6.37	6.45	6.30	6.65
H_6	6.18	6.03	5.95	5.93	6.04
$H_{6'}$	6.37	6.20	6.37	6.03	6.47
OH	6.99	~6.37	6.43	4.17	5.69
C-CH_3	8.51 8.61 8.63(6H)	8.46 8.55(6H) 8.57	8.51 8.56 8.62 8.66	8.41 8.53 8.54 8.55	8.58 8.62 8.63 8.69
Coupling constant					
$J_{1,1'}$	(−)12.5	(−)12.8	(−)12.5	(−)12.5	(−)12.5
$J_{2'A,2'B}$	4.4	4.0	4.3	4.5	4.5
$\|J_{2'A,3}\|$	0.8_5	1.0	0.7	—	—
$J_{3,4}$	3.0	2.7	3.6	5.5	6.4
$J_{4,5}$	2.0	1.5	2.0	1.8	1.8
$J_{5,6}$	2.5	2.0	2.0	2.2	2.0
$J_{5,6'}$	2.4	1.8	1.8	2.0	2.0
$J_{6,6'}$	(−)12.2	(−)12.5	~(−)12.5	(−)12.4	(−)12.4
$J_{5,OH}$	7.0	a)	a)	—	5.4
$\|J_{6,OH}\|$	0.7	0.7	0.7	—	—

a) Obscured.

about 30—40°. The fact that in contrast to the general rule, the axial C-6 proton signal appears at a lower field than the equatorial C-6 proton is accounted for by the long-range shielding effects of the OH group in *trans*-diaxial relation to the axial C-6 proton and of the isopropylidene methyl group 1, 3-diaxial to this proton.[9] Provided that the OH group is strongly hydrogen-bonded to C-3 oxygen, only one skew-boat conformation of 1, 3-*O*-isopropylidene ring (ring A) in II can satisfy the "W-letter" relationship between $H_{2'A}$ and H_3, as Dreiding models indicate. However, any conformations of ring A in the structure V cannot explain the presence of the long-range spin coupling only between one epoxidic proton and H_3. Thus, we reached in the conclusion that the product II was confirmed to be 2, 2'-anhydro-2-*C*-hydroxymethyl-1, 3 : 4, 6-di-*O*-isopropylidene-L-sorbitol which has the molecular conformation shown in Fig. 4 in carbon tetrachloride, chloroform-d, and acetone-d_6. This conformation also well explains the appearance of the $H_{2'B}$ signal at a lower field than the $H_{2'A}$ signal because $H_{2'B}$

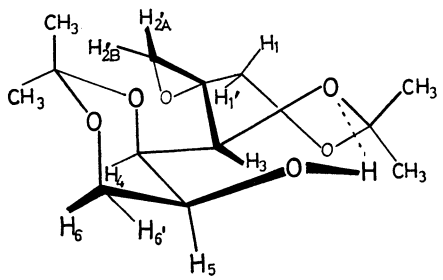

Fig. 4. The conformation of II.

is closely situated to one of the oxygen atom in ring B, which can exert deshielding effects on $H_{2'B}$.

This conclusion was further evidenced by the measurements of the spectra of II in pyridine-d_5 and dimethylsulfoxide-d_6; these solvents can be expected to remove the hydrogen-bonding owing to their strong basicity.[10-12] Seemingly, acetone

9) K. Tori and T. Komeno, *Tetrahedron*, **21**, 309 (1965).

10) O. L. Chapman and R. W. King, *J. Am. Chem. Soc.*, **86**, 1256 (1964).

11) D. Barnard, J. Fabian and H. Koch, *J. Chem. Soc.*, **1949**, 2442.

12) A. Allerhand and P. von R. Schleyer, *J. Am. Chem. Soc.*, **85**, 1715 (1963).

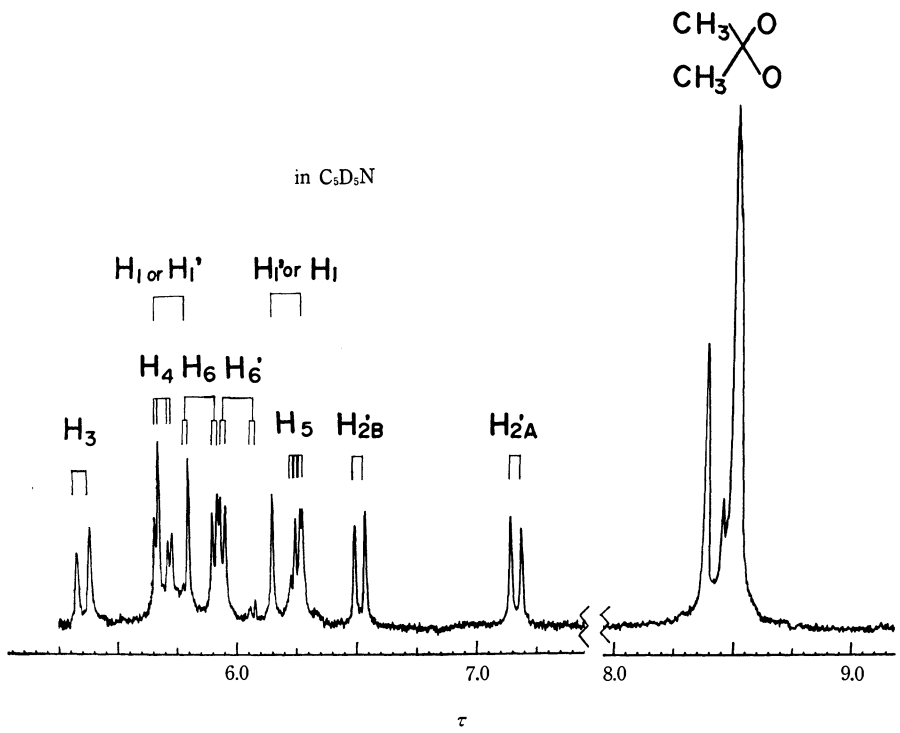

Fig. 5. PMR spectrum of II in pyridine-d_5 at 100 Mc.

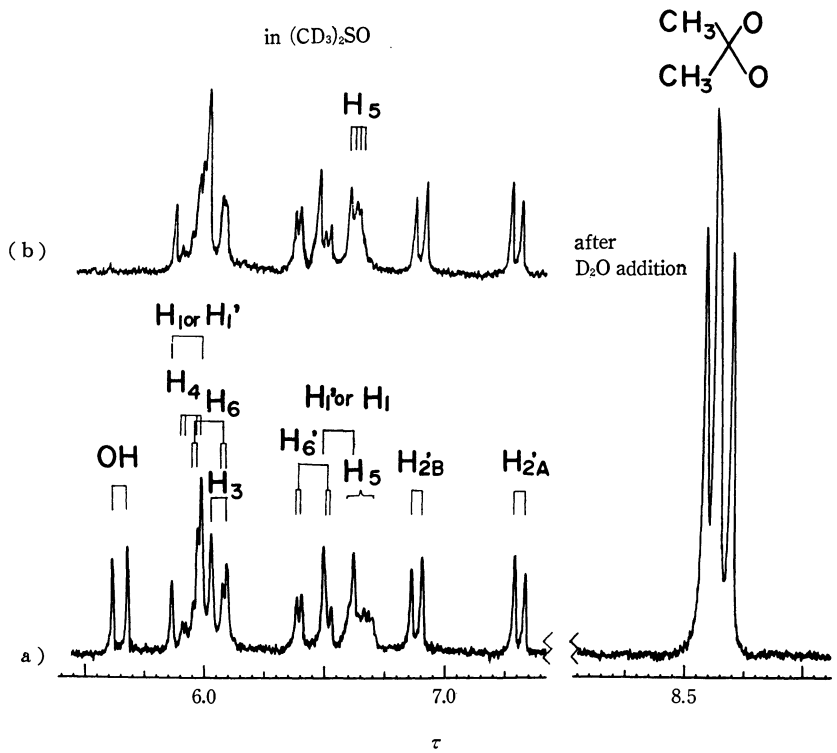

Fig. 6. PMR spectra of II in dimethylsulfoxide-d_6 at 100 Mc.
(a) Normal spectrum and (b) spectrum measured after adding a small amount of D_2O.

does not have sufficient basicity to remove such a strong intramolecular hydrogen-bonding between the C-5 OH and C-3 oxygen.

The spectrum of II in pyridine-d_5 shown in Fig. 5 exhibits well-separated signals, which were easily assigned. In the spectrum in dimethylsulfoxide-d_6 (Fig. 6a), the signals seemed somewhat complicated; but by an addition of deuterium oxide to the solution examined the lowest-field doublet ($J=5.4$ cps) disappears with the change of the H_5 signals (little changes in the chemical shift were caused as shown in Fig. 6b). This doublet is due to the C-5 OH proton. The signal assignment was made as indicated in Fig. 6. In these cases, the signals of $H_{2'A}$ appear as a clear doublet showing no further splittings. The larger values for $J_{3,4}$ obtained (5.5 and 6.4 cps) imply the increasing of population of the *trans*-conformation between H_3 and H_4 in these solvents. These observations can be due to the disappearance of the intramolecular hydrogen-bonding; instead, the intermolecular hydrogen-bondings between the OH group and the solvents were formed strongly. Thus, the above conclusion was amply justified by these facts also.

Experimental

The PMR spectra were taken with a Varian HA-100 spectrometer operating at 100 Mc by using about 5% solutions of the sample in carbon tetrachloride, chloroform-d, acetone-d_6, pyridine-d_5, and dimethylsulfoxide-d_6 in the frequency-swept and tetramethylsilane (TMS)-locked mode. Calibration of the spectrometer was checked by a Hewlett-Packard 5212A electronic counter. Spin-decoupling experiments were carried out by using two Hewlett-Packard 200ABR audiooscillators. Chemical shifts are expressed in τ unit (± 0.02) and coupling constants in cps (± 0.2 cps).

The infrared spectrum of II was measured with a Nippon Bunkō DS402G infrared spectrometer by using a 3.5 mg/8 cc (in 20 mm cell) solution in carbon tetrachloride.

We thank Dr. Ken'ichi Takeda, Director of this Laboratory, for his interest, and dedicate this paper to him in celebration of his sixtieth birthday.

BULLETIN OF THE CHEMICAL SOCIETY OF JAPAN VOL. 41 197—203 (1968)

Anionic Polymerization of *trans*-β-Methylstyrene

Yoshio OKAMOTO and Heimei YUKI

Department of Chemistry, Faculty of Engineering Science, Osaka University, Toyonaka, Osaka

and Shunsuke MURAHASHI

Department of Polymer Science, Faculty of Science, Osaka University, Toyonaka, Osaka

(Received July 17, 1967)

The anionic polymerization of *trans*-β-methylstyrene by *n*-butyllithium was carried out in hydrocarbon solvents and in tetrahydrofuran. In hydrocarbon solvents the monomer was consumed by *n*-butyllithium, but gave no polymer insoluble in methanol. In tetrahydrofuran the polymerization proceeded rapidly, giving a polymer insoluble in methanol. This polymer was produced by the normal addition polymerization of a C=C double bond. The relatively lower degree of polymerization of poly-β-methylstyrene indicated a chain transfer in the reaction. The chain transfer reaction due to the active hydrogen of a methyl group in this monomer was also observed by means of the electronic spectra of the reaction mixtures. The polymer anion was converted to inactive anions at high temperatures.

Staudinger[1] proposed that β-methylstyrene may be polymerized by a cationic initiator to give the so-called 1, 3-polymer by means of a hydrogen shift mechanism:

$$CH_3\text{-}CH{=}CH\text{-}C_6H_5 \rightarrow \left(\text{-}CH_2\text{-}CH_2\text{-}\underset{\displaystyle C_6H_5}{\underset{|}{CH}}\text{-}\right)_n$$

Recently, however, the reexamination of this cationic polymerization has proved that β-methylstyrene polymerizes only by means of the usual mechanism through the opening of a C=C double bond.[2,3]

On the other hand, regarding the anionic

1) H. Staudinger and E. Dreher, *Ann.*, **517**, 73 (1935).

2) J. P. Kennedy, *J. Polymer Sci.*, **A2**, 5171 (1964).

3) S. Murahashi, S. Nozakura, K. Tsuboshima and Y. Kotake, This Bulletin, **38**, 156 (1965).

polymerization of β-methylstyrene only a little information is available in the literature.[4,5] The present authors investigated the anionic polymerization of this monomer using *n*-butyllithium as a catalyst. It was found that in tetrahydrofuran the polymerization of this monomer took place by the normal addition of a C=C double bond, accompanied by the chain transfer to the monomer. The electronic spectra of the reaction mixtures were also investigated in order to correlate them with the reaction mechanism.

Experimental

***trans*-β-Methylstyrene (β-MeSt).** According to the method of Park,[6] β-methylstyrene was prepared by the dehydration of ethylphenylcarbinol with alumina at 300±10°C. The *trans*-isomer was collected by fractional distillation and was purified by redistillation under nitrogen from a flask containing lithium aluminum hydride. The purity was checked by gas chromatography. Bp 76—77°C/28 mmHg, n_D^{20} 1.5504: lit.,[7] n_D^{20} 1.5507.

Tetrahydrofuran (THF). Tetrahydrofuran which had been dried over sodium was refluxed over lithium aluminum hydride and then transferred by a vacuum system to a glass ampule before use.

Benzene and *n*-Hexane. Each solvent was purified by the usual method[8] and before use was transferred by the vacuum line from a flask containing a small amount of *n*-butyllithium to an ampule.

***n*-Butyllithium (*n*-BuLi).** *n*-Butyllithium was prepared in *n*-heptane according to the method of Ziegler.[9] The concentration was determined by the double-titration method of Gilman.[10]

Sodium Naphthalene (Na-Naph). Sodium naphthalene was prepared in tetrahydrofuran;[11] its concentration was determined by titration with 0.1 N hydrochloric acid, using phenolphthalein as an indicator.

Sodium-dispersion (Na-disp.). Sodium-dispersion in *n*-octane was used; the concentration was 30%.

Polymerization. The polymerization was carried out in a glass ampule which had been cleaned and dried completely. The solvent was first transferred into a glass ampule by means of a vacuum line, and then the monomer and initiator were added by syringes under an atomosphere of dried nitrogen. The solution was then allowed to stand in a constant temperature bath. The reaction was terminated by the addition of a trace of methanol. The concentration of unchanged *trans*-β-methylstyrene was determined spectrophotometrically by using a part of the solution. The optical density was measured at 293.5 mμ (ε_{max} 790), where it obeyed Beer's law. On the other hand, the residual solution was poured into a large amount of methanol and the precipitated polymer was separated by filtration, dried, and weighed.

In the following, the monomer consumption obtained by the spectrophotometric measurements and the yield of the methanol-insoluble polymer will be defined as "conversion" and "yield" respectively, while "polymer" will refer to the methanol-insoluble part otherwise stated.

Measurement. The molecular weight of the polymer was determined cryoscopically in a benzene solution. The infrared spectrum was measured on a Nihon Bunko DS-21 Spectrometer. The NMR spectrum was obtained in a carbon tetrachloride solution using a JNM-4H-100 Spectrometer (Japan Electron Optics Laboratory Co., Ltd.) at 100 Mc/sec, by using tetramethylsilane as an internal standard. The electronic spectrum was obtained with a Hitachi Perkin-Elmer 139 Spectrophotometer or a Hitachi EPS-2 Spectrophotometer. The spectrum of the living anion was measured in tetrahydrofuran according to the technique of Waack.[12]

Results

Polymerization in Hydrocarbon. Polymerizations were carried out in hydrocarbon solvents using *n*-BuLi, sodium-dispersion, and sodium naphthalene as initiators. The results are summarized in Table 1. A yellow color appeared two or three hours after the addition of an initiator, and its intensity gradually increased. When the reaction was performed for a prolonged time, it was observed that a considerable amount of the monomer was consumed, but no methanol-insoluble polymer was obtained. However, a small amount of the polymer was obtained in the polymerization where sodium naphthalene was used as an initiator and where a trace of tetrahydrofuran was present as the solvent of the initiator solution.

Polymerization in Tetrahydrofuran. The polymerization of *trans*-β-methylstyrene with *n*-BuLi was carried out in tetrahydrofuran. As soon as *n*-BuLi was added to the monomer solution, a red color appeared; the density of this color did not change during the reaction at room temperature.

The time dependencies of the conversion (obtained from the UV spectrum) and the yield (wt% of the methanol-insoluble polymer against the monomer charged) at 0 and 30°C are shown in Fig. 1. The monomer consumption was quantitative after 24 hr, but the yield of the methanolinsoluble polymer was much less than that. The molecular weights of the polymers obtained at 0 and 30°C were

4) H. F. Herbranderson and D. S. Mooney, *J. Am. Chem. Soc.*, **79**, 5809 (1957).
5) D. N. Bhattacharyya, C. L. Lee, J. Smid and M. Szwarc, *ibid.*, **85**, 553 (1963).
6) W. R. R. Park and G. F. Wright, *J. Org. Chem.*, **19**, 1435 (1954).
7) C. G. Overberger, D. Tanner and E. M. Pearce, *J. Am. Chem. Soc.*, **80**, 4566 (1958).
8) A. Weissberger, E. S. Proskauer, J. A. Riddick and E. E. Toops, Jr., "Organic Solvents," 2nd Ed., Interscience Publishers, New York (1955).
9) K. Ziegler and A. Colonius, *Ann.*, **479**, 135 (1930).
10) H. Gilman and A. H. Haubein, *J. Am. Chem. Soc.*, **66**, 1515 (1944).
11) M. Morton and R. Milkovich, *J. Polymer Sci.*, **A1**, 443 (1963).
12) R. Waack and M. A. Doran, *J. Am. Chem. Soc.*, **85**, 1651 (1963).

TABLE 1. POLYMERIZATION OF *trans*-β-METHYLSTYRENE IN HYDROCARBON SOLVENT
Monomer, 10 mmol; solvent, 20 ml

Solvent	Initiator	Monomer / Initiator (mol/mol)	Temp. °C	Time day	Conv.[a] %	Yield[b] %
Benzene	*n*-BuLi	30	30	88	14.3	0
Benzene	Na-disp.	44	30	44	—	0
Benzene	*n*-BuLi	90	60	90	9.0	0
Hexane	Na-disp.	2	60	90	51.3	0
None	Na-Naph	90	30	90	—	6.6

a) Obtained from UV spectrum. b) Methanol-insoluble polymer.

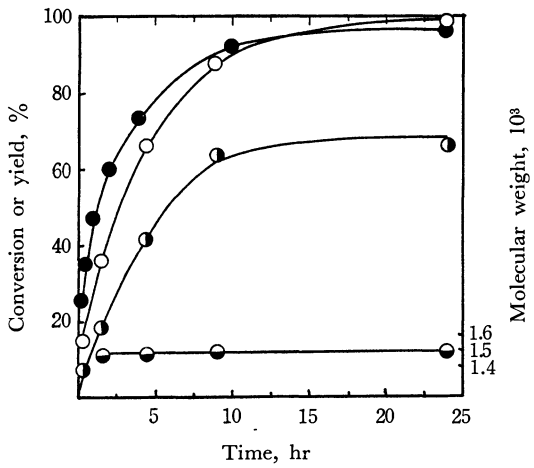

Fig. 1. Anionic polymerization of *trans*-β-methylstyrene by *n*-BuLi in THF.—Time *vs.* conversion.
○: Conversion at 0°C
●: Conversion at 30°C
◑: Yield of methanol insoluble polymer at 0°C
◒: Molecular weight of methanol-insoluble polymer obtained at 0°C, $[M]_0$ 0.41 mol/*l*, [*n*-BuLi] 4.5×10^{-3} mol/*l* at 0°C, 4.0×10^{-3} mol/*l* at 30°C.

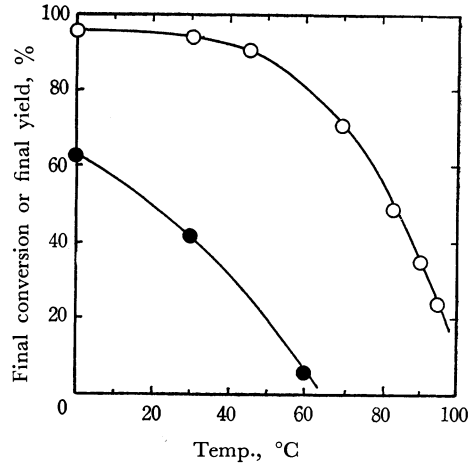

Fig. 2. Anionic polymerization of *trans*-β-methylstyrene by *n*-BuLi in THF.—Effect of temperature.
○: Final conversion
●: Final yield
$[M]_0$ 0.43 mol/*l*
[*n*-BuLi] $0.43—0.49\times10^{-2}$ mol/*l* Time 48 hr

about 1500 and 1300 respectively and were independent of the yield.

It was found that when the reaction ceased the monomer remained unchanged at high reaction temperatures. In order to investigate the effects of the temperature on the final conversion and the final yield, prolonged reactions were carried out at various temperatures between 0 and 100°C, using *n*-BuLi as an initiator. The results are shown in Fig. 2. The curves show that both the final conversion and the final yield gradually decreased at elevated temperatures. The color of the reaction mixture was red at 0 and 30°C, but turned purple above 60°C. A similar tendency was also observed in the polymerization initiated by sodium naphthalene.

The polymerization was carried out for 48 hr at 30°C, while varying the concentration of *n*-BuLi. As shown in Fig. 3, the final conversion, the final yield, and the molecular weight of the polymer were all independent of the concentration of *n*-BuLi.

The relationships between the final yield of the methanol-insoluble polymer and the initial monomer concentration are shown in Fig. 4. The yield increased with an increase in the initial monomer concentration independently of the reaction temperature. However, the yield at 30°C was less than that at 0°C with each initial monomer concentration. In this case the molecular weight of the polymer was also independent of the reaction conditions.

The data shown in Fig. 1 are plotted in Fig. 5 as if the reaction were first-order with respect to the monomer concentration. The reaction rates decreased with the reaction time and deviated from the first-order plots at the initial stage of the reaction, but later the relation between $\ln([M]_0/[M])$ and the reaction time became straight lines with the same slope at 0 and at 30°C.

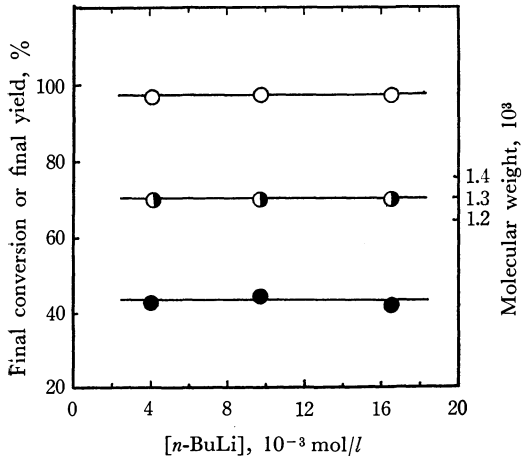

Fig. 3. Anionic polymerization of *trans*-β-methylstyrene by *n*-BuLi in THF.—Effect of initiator concentration
○: Final conversion
●: Final yield
◑: Molecular weight of methanol-insoluble polymer
$[M]_0$ 0.41 mol/*l*, Temp. 30°C, Time 48 hr

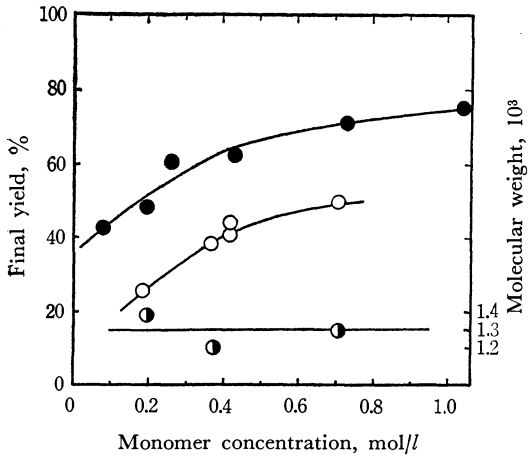

Fig. 4. Anionic polymerization of *trans*-β-methylstyrene by *n*-BuLi in THF.—Effect of monomer concentration.
●: Final yield at 0°C
○: Final yield at 30°C
◑: Molecular weight of polymer obtained at 30°C
[*n*-BuLi] 0.40×10^{-2} mol/*l*, Time 48 hr

The existence of an equilibrium in the polymerization of *trans*-β-methylstyrene at 60°C was checked. The monomer was polymerized at 60°C; after the reaction had ceased, (1) a fresh monomer was added to the reaction mixture, or (2) the reaction mixture was cooled to 0°C and left to stand 48 hr at this temperature. As shown in Table 2, the conversion did not change from that in the original reaction mixture, indicating that there is no equilibrium in the reaction at 60°C.

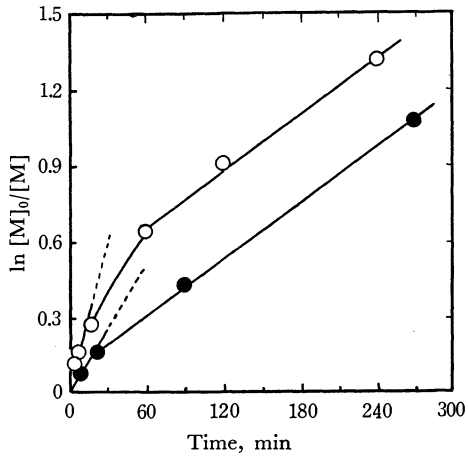

Fig. 5. Anionic polymerization of *trans*-β-methylstyrene by *n*-BuLi in THF.—First order plot of reaction rate.
●: At 0°C,
○: At 30°C,
$[M]_0$ 0.41 mol/*l*,
[*n*-BuLi] 4.5×10^{-3} mol/*l* at 0°C; 4.0×10^{-3} mol/*l* at 30°C

Table 2. Testing of equilibrium in the polymerization of *trans*-β-methylstyrene in tetrahydrofuran

Solvent: THF, 20 ml; initiator: *n*-BuLi, 0.1 mmol

Monomer g	Temp. °C	Time hr	Conversion %
1.12	60	48	72
1.12+1.15[a]	60	96	34[b]
1.12	60 0	48 then 48	72

a) Added after 48 hr.
b) Against total monomer.

Electronic Spectra of Reaction Mixtures. The electronic spectra of the solutions are shown in Fig. 6. The reactions were carried out between *trans*-β-methylstyrene and *n*-BuLi, and between allylbenzene and *n*-BuLi, in tetrahydrofuran. Curve A, with an absorption maximum at 340 mμ in Fig. 6, is the spectrum of the reaction product of *trans*-β-methylstyrene with an excess of *n*-BuLi at room temperature. Curve B shows the spectrum of the reaction product after 48 hr in the polymerization of *trans*-β-methylstyrene with *n*-BuLi at 0°C. It has an absorption maximum at 398 mμ. A very similar spectrum (Curve B′) was obtained from the reaction product between allylbenzene and an equimolar amount of *n*-BuLi at room temperature. At 60°C this spectrum shifted to Curve D, which has an absorption maximum at 570 mμ. When *trans*-β-methylstyrene was polymerized with *n*-BuLi at 60°C, after 48 hr the reaction mixture

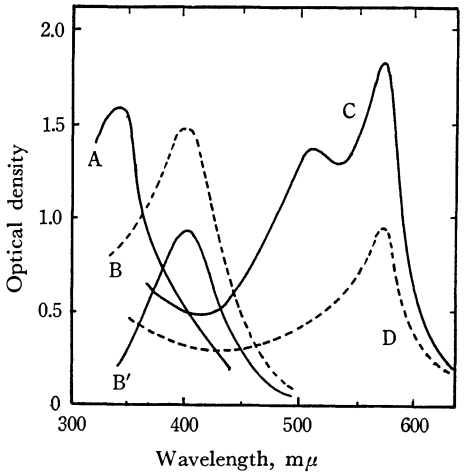

Fig. 6. Electronic spectra of anions in THF.

A: β-MeSt+excess *n*-BuLi, at room temp., after 5 min
B: Excess β-MeSt+*n*-BuLi, at 0°C, after 48 hr
B': Allylbenzene+*n*-BuLi, at room temp., after 5 min
C: Excess β-MeSt+*n*-BuLi, at 60°C, after 48 hr
D: Allylbenzene+*n*-BuLi, at 60°C, after 48 hr

gave the spectrum shown as Curve C in Fig. 6. This spectrum contains two absorption maxima, at 510 and 570 mμ.

Structure of Polymer. The infrared spectrum of the methanol-insoluble polymer obtained at 30°C is shown in Fig. 7. As a whole the spectrum was very similar to that of polystyrene, except for the strong absorption bands at 2960, 2875, and 1377 cm^{-1} due to methyl groups and the extremely weakened band at 2925 cm^{-1} due to methylene groups. The IR-spectrum of the methanol-soluble fraction, which has an average molecular weight of 360, was just the same as that of the methanol-insoluble fraction, but it showed a strong absorption at 2925 cm^{-1}

The ultraviolet spectrum of the methanol-soluble and insoluble fractions showed no C_6H_5–CH=CH– structure, which may be expected to have a strong absorption at about 292 mμ due to the conjugation between a phenyl group and a C=C double bond.

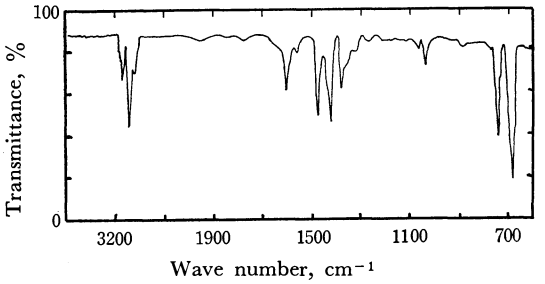

Fig. 7. Infrared spectrum of poly-β-methylstyrene (KBr).

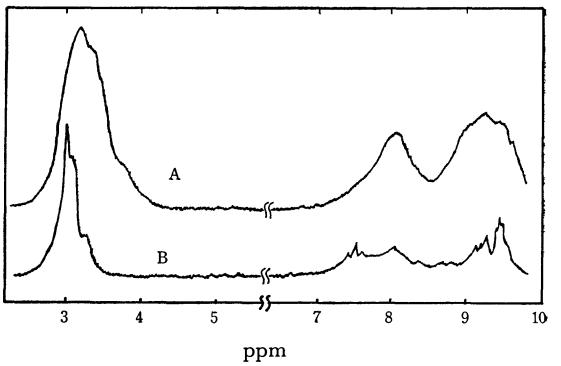

Fig. 8. NMR spectra of poly-β-methylstyrene.

A: Methanol-insoluble fraction
B: Methanol-soluble fraction

In Fig. 8 the NMR spectra of the methanol-insoluble and soluble polymers are shown. In neither the spectra was there any absorption at 3.5—5 ppm, where the signal of a proton attached to a C=C double bond appears. The spectrum of the methanol-insoluble polymer showed that the ratios of methyl to methylene protons and of phenyl to other protons were 3 : 2 and 5 : 5 respectively.

These results indicate that the polymer was formed by the usual addition polymerization at the C=C double bond, and that there is no essential difference between the structures of the methanol-soluble and -insoluble polymers.

Discussion

In spite of the long reaction time, the anionic polymerization of *trans*-β-methylstyrene in hydrocarbon solvents gave no polymer with a molecular weight high enough to be insoluble in methanol. However, the spectroscopic measurements showed that, compared with the amount of the initiator used, much of the monomer was consumed by the reaction, suggesting conversion to low-molecular-weight products.

Morton *et al.*[13] investigated the reaction between β-methylstyrene and *n*-amylsodium in *n*-pentane at room temperature. They reported that the carbonation of anions produced in the reaction gave mostly the I and II acids, but very small amounts of products with higher molecular weights.

C_6H_5–CH=CH–CH_2–COOH (I) C_6H_5–CH(COOH)–CH=CH_2 (II)

Pines *et al.*[14] also reported that the main product of the reaction between β-methylstyrene and metallic

13) A. A. Morton and E. Grovenstein, Jr., *J. Am. Chem. Soc.*, **74**, 5437 (1952).
14) H. Pines and J. Shabtai, *J. Org. Chem.*, **29**, 2408 (1964).

sodium in cyclohexane at 100°C was the following compound, III:

$$R^- + C_6H_5\text{-}CH{=}CH\text{-}CH_3 \longrightarrow RH + C_6H_5\text{-}CH{=}CH\text{-}CH_2^-$$

$$C_6H_5\text{-}CH{=}CH\text{-}CH_2^- + C_6H_5\text{-}CH{=}CH\text{-}CH_3 \xrightarrow{H^+} C_6H_5\text{-}CH{=}CH\text{-}CH_2\text{-}\underset{\displaystyle CH_3}{\underset{|}{CH}}\text{-}CH_2\text{-}C_6H_5$$

III

These results indicate that, in hydrocarbon solvents, carbanion does not attack the C=C double bond, but abstracts a proton from the methyl group of the monomer.

In tetrahydrofuran, *trans*-β-methylstyrene polymerizes to give a methanol-insoluble polymer as well as a soluble one; even in a non-polar solvent it gave the same polymers, though the amounts were small, in the presence of a small quantity of tetrahydrofuran (Table 1). The two polymers, methanol-soluble and -insoluble, were the same in their structure (*i. e.*, the polymers were formed by the usual addition polymerization at the C=C double bond), but they were different in molecular weight.

The structure of the polymer shows that the propagation reaction in the polymerization of *trans*-β-methylstyrene proceeds through the addition of a benzyl-type anion, IV, to the monomer. It has been known that benzyl-type anions have their absorption maxima at around 340 mμ.[12,15] Therefore, the absorption band at 340 mμ (Fig. 6, A) shown by the fresh reaction mixture between *n*-BuLi and *trans*-β-methylstyrene must be due to the benzyl-type anion. Herbranderson *et al.*[4] obtained Compounds V and VI, plus a small amount of high-molecular-weight materials, as the main products of the reaction between equimolar amounts of β-methylstyrene and *n*-BuLi in diethyl ether. These results indicate that, in a polar solvent, carbanion adds to the C=C double bond of β-methylstyrene rather than abstracts a proton of a methyl group in this monomer. The polymerization of *trans*-β-methylstyrene is an extreme example of solvent effects on the polymerizability of a monomer by an anionic mechanism.

$$\sim\!\!\sim CH(CH_3)\text{-}CH(C_6H_5)^-$$

IV

$$n\text{-}C_4H_9\text{-}CH(CH_3)\text{-}CH_2\text{-}CH(C_6H_5)^-$$

V

$$n\text{-}C_4H_9\text{-}CH(CH_3)\text{-}CH(C_6H_5)\text{-}CH(CH_3)\text{-}CH_2\text{-}CH(C_6H_5)^-$$

VI

In the anionic polymerization of *trans*-β-methylstyrene in tetrahydrofuran, the monomer can be completely consumed during a long reaction period at 0—30°C, although the rate is very slow compared with the polymerization of styrene. Szwarc *et al.*[5,17] found that the rate constant of the addition of living sodium polystyrene to β-methylstyrene was *ca.* 20 *l* mol^{-1} sec^{-1} at 25°C in tetrahydrofuran, and that of the same anion to styrene, *ca.* 500 *l* mol^{-1}. sec^{-1}, suggesting a smaller reactivity of β-methylstyrene.

The molecular weight of the polymer was independent of the yield, and of the concentrations of the monomer and the initiator, indicating a controlled chain growth by chain transfer to the monomer.

The absorption at 398 mμ (Fig. 6, B) observed in the reaction mixture at the later stage was that of the allyl anion, VII, which was also obtained by Waack *et al.*[12] in the reaction between allylbenzene and *n*-BuLi in tetrahydrofuran:

$$R^- + C_6H_5\text{-}CH{=}CH\text{-}CH_3 \longrightarrow C_6H_5\text{-}CH{=}CH\text{-}CH_2^- + RH$$

VII

The VII anion was produced by chain transfer to the monomer in the anionic polymerization of *trans*-β-methylstyrene in tetrahydrofruan, as is shown above. It is fairly stable and can exist at a concentration sufficient to be observed in the solution. Szwarc *et al.*[5] also observed the abstraction of a proton of the methyl group of β-methylstyrene by a polystyryl anion. Figure 6 shows that the anion, IV, produced at the initial stage of the reaction diminished, while the VII anion gradually appeared with time.

The average degree of polymerization of the methanol-insoluble polymer obtained at 0°C was about 15. Therefore, the chain-transfer constant ($=k_p/k_{tr}$) may be smaller than 15 at this temperature because of the presence of lower-molecular-weight products soluble in methanol. The decrease in the methanol-insoluble polymer at elevated reaction temperatures shows that the rate of the chain transfer increases with the elevation of the temperature more than that of the propagation does. The re-initiation by the allyl anion produced by the chain transfer reaction is considered to be rather slow because of the stability of the allyl anion. This slow re-initiation may be the cause of the retardation of the polymerization observed after the initial stage of the reaction.

The polymerization of *trans*-β-methylstyrene at 60°C gave only a low final conversion and no polymer insoluble in methanol, in spite of the presence of living anions, recognized by means of

15) S. Bywater, A. F. Johnson and D. J. Worsfold, *Can. J. Chem.*, **42**, 1225 (1964).

16) R. Asami, M. Levy and M. Szwarc, *J. Chem. Soc.*, **1962**, 361.

17) D. N. Bhattacharyya, C. L. Lee, J. Smid and M. Szwarc, *J. Phys. Chem.*, **69**, 612 (1965).

the color. As the cause of the lower final conversion at an elevated temperature two mechanisms are possible: the equilibrium polymerization due to a low ceiling temperature, and the conversion of an active chain end to an inactive carbanion. The possibility of equilibrium polymerization can, however, be eliminated in view of the results shown in Table 2.

On the other hand, the production of unreactive carbanions was supported by spectroscopic measurements. The absorption at 510 mμ observed in the reaction at 60°C in tetrahydrofuran may be considered to be due to the VIII anion as follows:

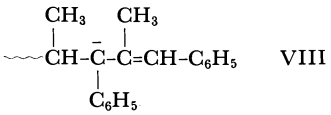

VIII

Szwarc *et al.*[16] have reported that the stable anion IX, with an absorption maximum at 535 mμ was produced in the polymerization of styrene by sodium in tetrahydrofuran:

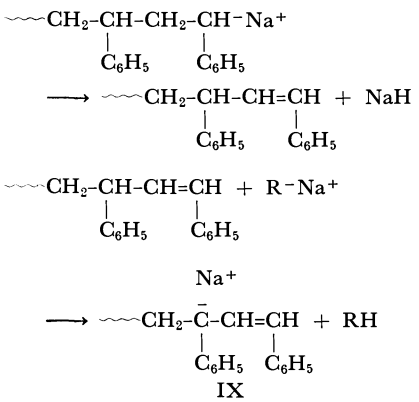

IX

The anion VIII will be formed from poly-β-methylstyrene if a reaction similar to the above takes place. The anion will show then an absorption band at rather a lower wavelength than that of the anion IX. This may be caused by the lower conjugation between the C=C double bond and the benzene nuclei due to the steric hindrance of the methyl group. It is also known that a lithium counter ion lowers the λ_{max} of carbanion.[18] The structure of the other anion produced at 60°C and with a λ_{max} at 570 mμ is not certain at the present time, but it may be produced by the further change of the anion of allylbenzene VII. Both the anions with absorptions at 510 and 570 mμ are quite stable, as evidence by the fact that they could not initiate the polymerization of *trans*-β-methylstyrene. They could, however, cause the polymerizations of styrene and methyl methacrylate. The production of the anions is accelerated at higher temperatures.

The infrared and NMR spectra of the polymer showed that the monomer polymerizes by the normal addition polymerization mechanism. The chain transfer to the monomer produces the allyl anion VII, and so it may be expected that the polymer initiated by this anion will have a C=C double bond at the chain end. However, IR, UV, and NMR spectroscopies indicate that there is no aliphatic unsaturation, even in the low-molecular-weight polymer. The one possibility of the elimination of the double bond in the polymer is the following reaction:

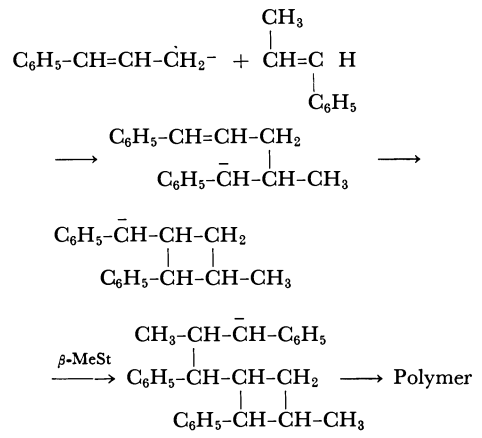

18) J. E. Hogen-Esch and J. Smid, *J. Am. Chem. Soc.*, **88**, 307 (1966).

BULLETIN OF THE CHEMICAL SOCIETY OF JAPAN VOL. 41 204—207 (1968)

The Reactivities of Nuclear-Substituted Phenyl Methacrylates in Radical Copolymerization with Styrene

Takayuki Otsu, Toshio Ito, Yoshihiro Fujii and Minoru Imoto

Department of Applied Chemistry, Faculty of Engineering, Osaka City University, Sugimotocho, Sumiyoshi-ku, Osaka

(Received July 18, 1967)

In order to clarify the effects of the alkyl substituents on the reactivities of methacrylate monomers toward the attack of a radical, the copolymerizations of a series of nuclear-substituted phenyl methacrylates with styrene were investigated. From the results, the monomer reactivity ratios and the Alfrey-Price Q and e values were determined. It was found that the relative reactivities toward the polystyryl radical were not correlated with the ordinary Hammett equation, but a linear relationship was obtained with a modified Hammett equation which contained a term of the resonance contribution by the substituents. Accordingly, it was considered that the reactivities of substituted phenyl methacrylates depend on both polar and resonance effects caused by the substituents.

In previous papers,[1-3] we have found that the relative reactivities ($1/r_1$) of alkyl methacrylates and acrylates (M_2) toward a polystyryl radical are dependent on the polar substituent constants (σ^*) of the alkyl groups, but not on their steric substituent constants (E_s) in the modified Taft equation (1):

$$\log (1/r_1) = \rho^*\sigma^* + \delta E_s$$

where ρ^* and δ are the constants which give the susceptibility of a given reaction series caused by polar and steric effects of the substituents respectively. In these cases, the findings indicate that the reactivities are subsject to the polar effect of the alkyl substituents, but not to their steric effects.

In order to evaluate the substituent effect, the correlation between the relative reactivities of nuclear-substituted phenyl methacrylates toward the polystyryl radical and Hammett's σ constants of the substituents were investigated in the present study. In the case of nuclear-substituted phenyl methacrylates, the steric effects by the substituents should be similar, because all of the substituents lie across the benzene ring.

The nuclear-substituted phenyl methacrylates used in this study have the following substituents (X): p-OCH_3, p-CH_3, H, p-Cl, m-Cl, p-$COCH_3$, m-NO_2, and p-NO_2.

Experimental

Preparation of Substituted Phenyl Methacrylates (X-PhMA). The Schotten-Baumann reaction of methacrylyl chloride with the corresponding phenols was used to prepare X-PhMA. Then the resulting monomers were purified by fractional distillation under reduced pressure (for PhMA, p-CH_3-PhMA,

Table 1. Physical constants for X-PhMA monomers*

X in X-PhMA	Bp °C/mmHg	Mp °C	n_D^{20}
p-OCH_3		61.0—62.0 (63)	
p-CH_3	81.0—82.0/2		1.5108**
H	73.5—74.0/3 (83—84/4)		1.5152 (1.5156)
p-Cl	93.0—94.0/2 (113—114/6)		1.5299 (1.5292)
m-Cl	91.0—92.0/2		1.5301
p-$COCH_3$		90.5—92.0	
m-NO_2		59.0—60.0	
p-NO_2		95.5—96.0 (95)	

* Values in parentheses indicate the reference values of Kumanodani.[4]
** Date at 25°C.

1) T. Otsu, T. Ito and M. Imoto, *J. Polymer Sci.*, **B3**, 113 (1965).
2) T. Otsu, T. Ito and M. Imoto, *ibid.*, **C** (16), 2121 (1967).
3) T. Otsu, T. Ito, T. Fukumizu and M. Imoto, This Bulletin, **39**, 2257 (1966).

TABLE 2. RESULTS OF COPOLYMERIZATIONS OF X-PhMA (M_2) WITH STYRENE (M_1) AT 60°C

X in X-PhMA	$[M_2]$ in Comonomer, mole fraction	Time min	Conversion %	C(%) in Copolymer	$[m_2]$ in Copolymer, mole fraction
H	0.076	60	2.5	86.92	0.212
	0.242	60	3.4	83.41	0.379
	0.582	60	5.2	79.78	0.584
	0.748	60	9.0	77.96	0.703
p-CH_3	0.095	60	2.8	86.25	0.241
	0.191	60	3.7	83.90	0.358
	0.337	60	4.5	81.64	0.487
	0.482	60	5.9	81.20	0.514
	0.739	45	7.7	78.52	0.698
p-OCH_3	0.119	60	3.3	82.69	0.263
	0.301	40	3.3	78.35	0.423
	0.399	40	4.3	76.41	0.505
	0.500	40	2.8	75.05	0.571
	0.602	20	3.6	74.55	0.597
	0.705	15	3.8	73.27	0.662
	0.800	60	10.4	72.64	0.731
p-Cl	0.100	60	3.4	6.65[b]	0.235
	0.195	60	4.3	9.13[b]	0.352
	0.344	60	5.6	10.84[b]	0.443
	0.490	45	5.6	12.27[b]	0.529
	0.744	45	9.3	13.89[b]	0.638
m-Cl	0.099	60	1.4	7.18[b]	0.260
	0.251	100	1.2	10.12[b]	0.403
	0.400	100	1.4	11.75[b]	0.498
	0.502	100	1.3	12.32[b]	0.533
	0.650	65	1.6	13.45[b]	0.608
	0.802	100	1.9	14.64[b]	0.696
p-$COCH_3$[a]	0.121	90	5.6	82.23	0.295
	0.276	90	7.6	78.17	0.456
	0.467	70	8.0	76.66	0.543
	0.693	60	10.6	74.67	0.654
	0.835	60	13.5	72.82	0.775
m-NO_2[a]	0.125	240	2.2	3.76[c]	0.325
	0.270	240	1.3	3.94[c]	0.422
	0.457	240	1.4	4.57[c]	0.523
	0.690	240	5.3	5.35[c]	0.672
	0.834	240	9.6	5.60[c]	0.741
p-NO_2[a]	0.123	100	1.1	3.16[c]	0.307
	0.276	100	2.4	3.93[c]	0.411
	0.456	100	3.1	4.51[c]	0.502
	0.690	90	2.6	5.05[c]	0.597
	0.833	70	3.6	5.32[c]	0.650

a) Copolymerized in 50 vol% benzene solution.
b) Chlorine % in the copolymers.
c) Nitrogen % in the copolymers.

p-Cl-PhMA, and *m*-Cl-PhMA), or by recrystallization from ethanol (for *p*-OCH_3-PhMA, *p*-$COCH_3$-PhMA, *p*-NO_2-PhMA, and *m*-NO_2-PhMA). These purifications were repeated until the absorptions of the unreacted phenols disappeared in the IR spectra.

Table 1 shows the physical constants of these methacrylate monomers. The boiling points, melting points, and refractive indices of PhMA, *p*-OCH_3-PhMA, *p*-Cl-PhMA, and *p*-NO_2-PhMA were all in good agreement with the reported values.[4] The results of the

4) T. Kumanodani, *Kobunshi*, **11**, 917 (1962).

elementary analyses of the other methacrylate monomers were as follows:

p-CH_3-PhMA: Found: C, 75.02; H 7.14%. Calcd for $C_{11}H_{12}O_2$: C, 74.97; H, 6.86%.

p-$COCH_3$-PhMA: Found: C, 70.28; H, 6.23%. Calcd for $C_{12}H_{12}O_3$: C, 70.58; H 5.98%.

m-Cl-PhMA: Found: C, 61.07; H, 4.82%. Calcd for $C_{10}H_9O_2Cl$: C, 61.08; H, 4.61%.

m-NO_2-PhMA: Found: N, 6.78%. Calcd for $C_{10}H_9O_4N$: N, 6.76%.

Other Materials. The styrene used as a reference monomer was purified by a usual method. The α, α'-azobisisobutyronitrile (AIBN) used as the radical initiator was purified by recrystallization from ethanol. The benzene, methanol, and other solvents were also purified by ordinary methods.

Table 3. Monomer reactivity ratios for styrene (M_1) - X-PhMA (M_2) copolymerizations, and Q_2, e_2 values for X-PhMA

X in X-PhMA	σ-Values of X	E_R-Values of X	r_1	r_2	$1/r_1$	Q_2*	e_2*
p-OCH_3	−0.268	0.11	0.28	0.60	3.57	1.23	0.53
p-CH_3	−0.170	0.03	0.30	0.70	3.33	1.23	0.45
H	0.000	0.00	0.30	0.60	3.33	1.17	0.51
p-Cl	0.226	0.10	0.22	0.45	4.55	1.35	0.72
m-Cl	0.373	0.08	0.21	0.40	4.76	1.36	0.77
p-$COCH_3$	0.516	0.21	0.15	0.49	6.67	1.82	0.82
m-NO_2	0.710	0.35	0.18	0.36	5.56	1.47	0.86
p-NO_2	0.778	0.41	0.19	0.22	5.26	1.27	0.98

* Calculated by assuming that $Q_1=1.0$ and $e_1=-0.8$ for styrene (M_1).

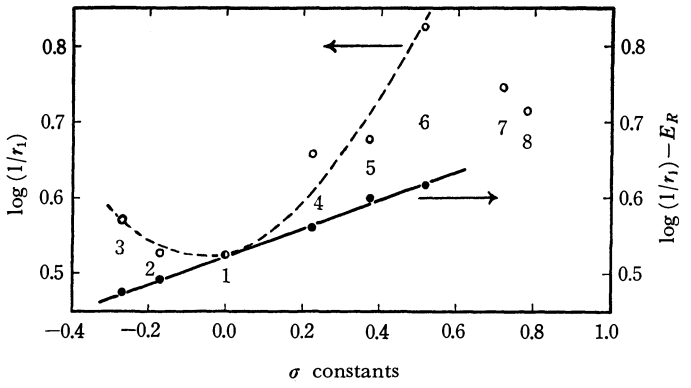

Fig. 1. Correlation between relative reactivities of X-PhMA and Hammett σ constants: 1 PhMA, 2 *p*-CH_3-PhMA, 3 *p*-OCH_3-PhMA, 4 *p*-Cl-PhMA, 5 *m*-Cl-PhMA, 6 *p*-$COCH_3$-PhMA, 7 *m*-NO_2-PhMA, 8 *p*-NO_2-PhMA.

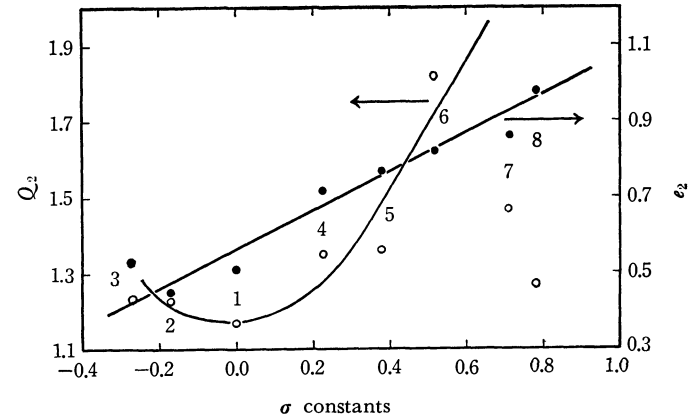

Fig. 2. Correlation between Q_2, e_2 values of X-PhMA and Hammett σ constants: the numbers are the same as those indicated in Fig. 1.

Copolymerization Procedure. The copolymerizations of X-PhMA (M_2) with styrene (M_1) were carried out in a glass tube with AIBN (6.1×10^{-3} mol/*l*) in bulk or in a benzene solution at 60°C. The resulting copolymers were precipitated in a large amount of methanol, and then reprecipitated from benzene and methanol. Most of the copolymerizations were continued up to 10% conversion. The composition of the copolymers was determined by nitrogen analysis for the copolymers of *p*- and *m*-NO_2-PhMA, by chlorine analysis for the copolymers of *p*- and *m*-Cl-PhMA, and by carbon analysis for the other copolymers. The monomer reactivity ratios were calculated by the method described by Fineman and Ross.[5]

Results and Discussion

The results of the copolymerization of X-PhMA (M_2) with styrene (M_1) at 60°C are shown in Table 2. From the results of this table, the monomer reactivity ratios (r_1 and r_2) and the Q_2 and e_2 values for X-PhMA were calculated to be as given in Table 3.

As can be seen from Table 3, the relative reactivities ($1/r_1$) of X-PhMA toward the attack of the polystyryl radical increase with the introduction of the substituents (X) in PhMA. The relation obtained is shown in Fig. 1, which the log ($1/r_1$) of X-PhMA is plotted *vs.* the σ-constants of the ordinary Hammett equation (2):

$$\log(1/r_1) = \rho\sigma \qquad (2)$$

where σ is the Hammett substituent constant and ρ is a reaction constant. As may be understood from this figure, no linear relationship between the log ($1/r_1$) and the σ constants is observed. Since the nitro group has been known to inhibit the radical polymerization, the values for NO_2-PhMA may include a rather large error. If these values are eliminated, the concave curve indicated by the dotted line is obtained. The value for *p*-OCH_3-PhMA was reconfirmed from a duplicate experiment.

It is well known that the resonance effect as well as the polar effect caused by the substituent is impotat in many radical reactions, as has already been pointed out by Alfrey and Price,[6] and Bamford and his co-workers.[7] Recently, one of the present authors proposed the following modified Hammett equation (3) for radical reactions:[8,9]

$$\log(1/r_1) = \rho\sigma + \gamma E_R \qquad (3)$$

where E_R is the resonance substituent constant (see Table 3) and γ is a reaction constant.

When Eq. (3) was applied in this case, a good linear relationship with $\rho=0.21$ and $\gamma=1.0$, except for the values for NO_2-PhMA, was obtained, as is also shown in Fig. 1. Accordingly, it may be expected that both polar and resonance effects of the substituents are important in considering the radical reactivities of X-PhMA.

Figure 2 shows the correlation of the Q_2 and e_2 values of X-PhMA with the σ-constants of their substituents. The Q_2 values are not linearly correlated with the σ-constants as well as in Fig. 1, but they are correlated with the resonance substituent constants (E_R), as Fig. 3 shows. Although the spectroscopic data of X-PhMA have been described in a previous paper,[10] no exact explanation of such a resonance effect is possible at the present time. From Fig. 2 it may be observed that the e_2 values show a straight-line relationship.

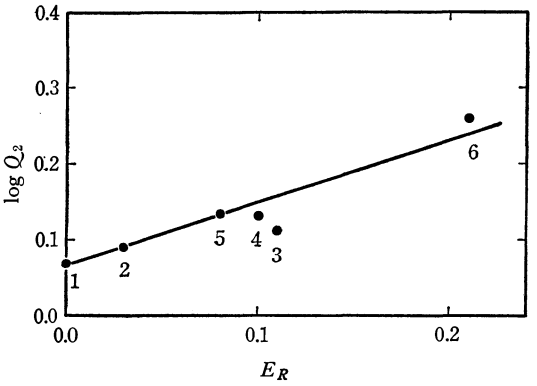

Fig. 3. Correlation between Q_2 values of X-PhMA and E_R constants: the numbers are the same as those indicated in Fig. 1.

5) M. Fineman and S. D. Ross, *J. Polymer Sci.*, **5**, 269 (1950).
6) T. Alfrey, Jr., and C. C. Price, *ibid.*, **2**, 101 (1947).
7) C. H. Bamford, A. D. Jenkins and R. Johnston, *Trans. Faraday Soc.*, **55**, 418 (1959); **59**, 530 (1963).
8) T. Yamamoto and T. Otsu, *Chem. & Ind.*, **1967**, 787.
9) T. Otsu and T. Yamamoto, *J. Soc. Org. Synth. Chem., Japan*, **23**, 643 (1965).
10) T. Otsu, T. Ito and M. Imoto, *J. Polymer Sci.*, **A1(4)**, 733 (1966).

BULLETIN OF THE CHEMICAL SOCIETY OF JAPAN VOL. 41 208—211 (1968)

Structure and Properties of the Condensation Product of 2-Amino-3-ethoxycarbonyl-1-azaazulene and Formamide[1]

Tetsuo Nozoe, Shuichi Seto[2] and Takashi Toda

Department of Chemistry, Faculty of Science, Tohoku University, Katahira-cho, Sendai

(Received July 18, 1967)

The structure of the condensation product of 2-amino-3-ethoxycarbonyl-1-azaazulene and formamide is proved not to be the expected cyclohepta[2, 3]pyrrolo[5, 4-*d*]pyrimidine derivative, but 5, 6-pentamethylene-7*H*-pyrrolo[2, 3-*d*]pyrimidin-4(3*H*)-one. The chemical properties of the obtained pyrrolo-pyrimidine are investigated, and then the tautomerism of the above compound is discussed.

Many heterocyclic compounds containing pyrimidines and purines are physiologically very important substances. Therefore, it is interesting to synthesize unsaturated seven-membered ring systems (such as tropolones and azulenes) which condensed with such heterocyclic nuclei, and to investigate the chemical and physiological properties of the resulting new heterocyclic compounds.

For this purpose, we attempted the condensation reaction of 2-amino-3-ethoxycarbonyl-1-azaazulene (I) with formamide, expecting to obtain a cyclohepta[2, 3]pyrrolo[5, 4-*d*]pyrimidine derivative such as (A). The condensation reaction was carried out in excess formamide by means of a modification of the method of Robins *et al.*[3,4]; this gave an almost colorless substance (II) in a

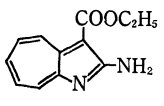

(I)

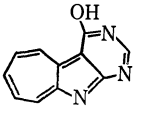

(A)

35—40% yield. II is hard to purify because of its insolubility in most organic solvents, and it can not be analyzed well. However, by a consideration of the results of the analysis of the its monoacetate (III)and monomethyl derivative (IV), the molecular formula of II is found to be not the expected $C_{11}H_7ON_3$, but $C_{11}H_{13}ON_3$. Neither the results of elemental analysis nor the ultraviolet spectra of II and IV show any absorption band longer than 320 mμ, as is shown in Fig. 1, even though the spectra of azaazulenes and their 2-hydroxy derivatives show strong absorption bands in the visible region.[5] The shape of the spectrum of II is analogous to those of 7-azaindole,[6] pyrrolo-[2, 3-*d*]pyrimidine,[7] and purines.[8] The IR spectrum of II (Fig. 2) shows strong bands at 2838

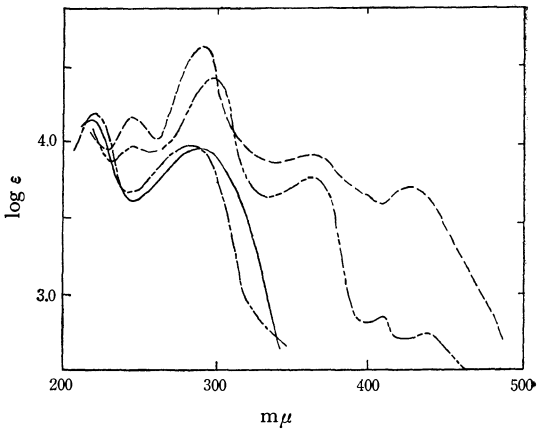

Fig. 1

I ——— II ———
IV —·—· VIII —··—··

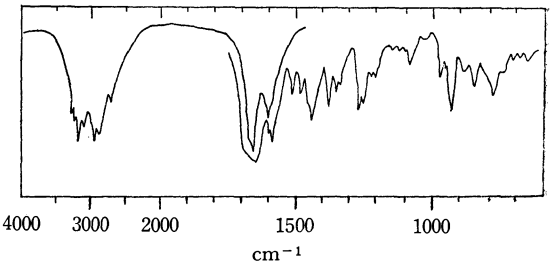

Fig. 2. KBr pellet.

1) Part of the D. Sc. thesis of Takashi Toda, March, 1958, Tohoku University.
2) Present address: the Chemical Research Institute of Non-aqueous Solutions, Tohoku University.
3) R. K. Robins, K. J. Dille, C. H. Willits and B. E. Christensen, *J. Am. Chem. Soc.*, **75**, 263 (1953).
4) C. C. Cheng and R. K. Robins, *J. Org. Chem.*, **21**, 1240 (1956).
5) T. Nozoe, S. Seto, S. Matsumura and T. Terasawa, *Chem. & Ind.*, **1954**, 1357, 1358.
6) M. M. Robison, F. P. Butler and B. L. Robison, *J. Am. Chem. Soc.*, **79**, 2573 (1957).
7) J. Davoll, *J. Chem. Soc.*, **1960**, 131.
8) J. F. Cavalierie, A. Bendich, J. F. Tinker and G. B. Brown, *J. Am. Chem. Soc.*, **70**, 3875 (1948).

and 2920 cm^{-1} due to methylene CH stretching,[9] and at 1650 cm^{-1} a broad, strong bands correspond to the carbonyl band of pyrimidin-4-ones,[10] while the three bands at 1478, 1511 and 1588 cm^{-1} are assigned to the skeltal vibration of such heterocyclic compounds as pyrimidines.[11] It is known that 1-azaazulenes are sensitive to reducing reagents and that the reduction of the seven-membered ring of those compounds takes place easily to give perhydro-compounds.[12] The consideration of the above facts and of the properties of formamide as a reducing reagent leads to the conclusion that the seven-membered ring of I is reduced by formamide during the reaction; therefore, the structure of II is 5, 6-pentamethylene-7*H*-pyrrolo[2, 3-*d*]pyrimidin-4(3*H*)-one.

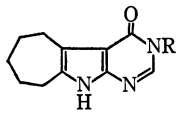

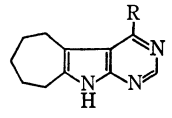

II: R=H
IV: Me

V: R=Cl
VI: OMe
VII: $NHNH_2$

Under milder conditions, however, the condensation reaction does not take place and I is recovered. The reason for the low yield of II is the formation of some intractable powder which is not soluble in most organic solvents. Although the molecular weight of the powder could not be measured because of its insolubility, this powder is presumably a mixture of the dimers or polymers formed by self-condensation during the reaction.

The treatment of II with phosphorous oxychloride afforded 4-chloro-5, 6-pentamethylene-7*H*-pyrrolo[2, 3-*d*]pyrimidine (V). 4-Methoxy (VI) and 4-hydrazino derivatives (VII) were derived when V was treated with sodium methoxide in methanol and with hydrazine respectively. VI was also obtained when V was treated with hydrazine in methanol, but VII was not obtained.

In order to obtain 5, 6-pentamethylene-7*H*-pyrrolo[2, 3-*d*]pyrimidine, a modified Stevenes-McFadyen decomposition reaction[13] was applied to VII, but the attempt was unsuccessful. The dehydrogenation of II by means of chloranil afforded a dark yellow, gummy substance (VIII) in a poor yield. Although it was hard to obtain in an analytically pure state, the ultraviolet and visible spectra of VIII are analogous to those of I, as is shown in Fig. 1; VIII is thus probably the expected cyclohepta[2, 3]pyrrolo[5, 4-*d*]pyrimidine derivative. However, VIII could not be investigated further because of the low yield of VIII and the lack of the starting material.

It is possible that II exists in such tautomeric forms as IIA, IIB and IIC. However, the ultraviolet spectra of II and IV differ from those of V and VI as Figs. 1 and 3 show, and the following investigation of their IR spectra leads to the conclusion that II is favorable to the IIA form.

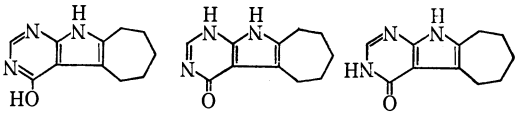

IIA IIB IIC

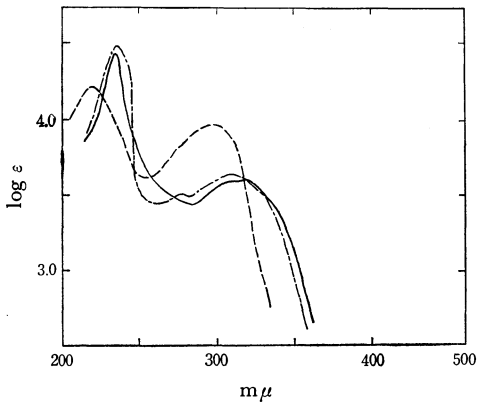

Fig. 3
V ——— VI —·—· VII ———

The strong band at 1650 cm^{-1} and several bands between 3100 and 3300 cm^{-1} of II in its IR spectrum can be reasonably explained on the basis of the IIA form which possess carbonyl and NH groups. α- or γ-Pyridone makes several different kinds of inter- and intramolecular hydrogen bonds between carbonyl and NH groups in the solid state; this is the reason why II shows a strong broad carbonyl band and several different kinds of NH stretching bands. IV shows a strong carbonyl band at 1655 cm^{-1} in its IR spectrum and so differs from VI, which does not show a carbonyl band. The problem of the α- or γ-pyrimidone form can be solved from the analogy with 4-hydroxypyrimidines; a consideration of their ultraviolet spectra and chemical properties shows the tautomeric form of those compounds to favor α-pyrimidones.[14] Thus the structures of II and IV are 5, 6-pentamethylene-7*H*-pyrrolo[2, 3-*d*]pyrimidin-4(3*H*)-one and 3*N*-methyl-5, 6-pentamethylene-7*H*-pyrrolo-[2, 3-*d*]pyrimidin-4(3*H*)-one respectively.

9) L. J. Bellamy, "The Infrared Spectra of Complex Molecules," 2nd ed., Methurn, London (1958).
10) L. N. Short and H. W. Thompson, *J. Chem. Soc.*, **1952**, 168.
11) H. Tsubomura, *Nippon Kagaku Zasshi (J. Chem. Soc. Japan, Pure Chem. Sect.)*, **78**, 1528 (1957).
12) Unpublished observation made in the authors' laboratory.
13) S. Seto, *Sci. Repts. Tohoku Univ., Ser. I*, **37**, 286, 295 (1953).
14) D. J. Brown and L. N. Short *J. Chem. Soc.*, **1953**, 331.

The ultraviolet spectrum of VII is rather analogous to that of II, but not to those of V and VI. VII presumably exists in its tautomeric (hydrazone) form. The IR spectrum of VII is not very helpful in determining its tautomeric form. Other evidence to support the tautomeric form of VII is as follows: the ultraviolet spectrum of VII is analogous to that of 4-pyrimidones, but not to that of 4-chloropyrimidines.[4] This relation is parallel with the relation of II, V, and VII, described above.

Experimental[15]

2-Amino-3-ethoxycarbonyl-1-azaazulene (I). In an autoclave, a solution of 5.0 g of 2-chloro-3-ethoxycarbonyl-1-azaazulene[5] in 50 m*l* of alcohol, which had been saturated with ammonia, was heated for 5 hr at 120°C. After cooling, the alcohol was removed and the residue was washed with water, dried, and chromatographed on alumina. From the benzene eluate, 4.5 g of yellow needles were obtained, while recrystallization from cyclohexane afforded yellow scales of I, mp 150—151°C.

Found: C, 66.89; H, 5.31; N, 13.27%. Calcd for $C_{12}H_{12}O_2N_2$: C, 66.65; H, 5.59; N, 12.96%.

5, 6-Pentamethylene-7*H*-pyrrolo[2, 3-*d*]pyrimidin-4(3*H*)-one (II). A solution of 3.20 g of I and 10.0 m*l* of formamide was heated for one and a half hours at 200°C. After the reaction, the solution was poured into 100 m*l* of cold water, and the precipitate thus formd was separated by filtration, washed with water and a small amount of ethyl acetate, and dried *in vacuo*. A pale brown powder, 2.40 g, was thus obtained. This powder decomposed near 280°C when heated. The powder is hardly soluble at all in benzene, ether, chloroform, ethyl acetate, acetone, and ethanol, but soluble in acetic acid and dioxane. It does not dissolve in aqueous sodium bicarbonate, but it does dissolve in dilute alkali. However, if the pH of the solution goes below 9, the precipitate forms immediately.

Finally, the reaction product (3.20 g) was dissolved in a large amount of methanol and chromatographed on alumina. The first eluate was recrystallized from methanol to give 1.20 g of micro prisms of II, mp 326—328°C (colored about 260°C, Koffler block).

Found: C, 62.92; 63.24; H, 6.14; 6.05; N, 20.16; 20.20%. Calcd for $C_{11}H_{13}ON_3$: C, 65.00: H, 6.45; N, 20.68%.

The methanol-water eluate of the chromatograph could not be obtained in a pure state and did not show any clear melting point but it gradually blackened between 250—300°C.

Acetylation of II (III). A solution of 0.10 g of II in 1.0 m*l* of acetic anhydrided was heated to reflux for 4 hr, and then the excess acetic anhydride was removed under reduced pressure to give pale yellow micro needles of III, mp 234—236°C. The recrystallization of this crude product from ethyl acetate and decolorizing charcoal afforded 0.08 g of pale yellow micro needles of III, mp 237—239°C.

Found: C, 63.24; H, 5.81; N, 17.26%. Calcd for $C_{13}H_{15}O_2N_3$: C, 63.66; H, 6.16; N, 17.13%.

λ_{max}^{MeOH} mμ (log ε); 237 (4.10), 265 (3.86) and 308 (3.82).

Methylation of II with Dimethyl Sulfate (IV). To a solution of 0.10 g of II and 0.04 g of sodium hydroxide in 1.0 m*l* of water, 0.07 g of dimethyl sulfate was added, and then the solution was shaken continuously for 5 hr. The pH of the solution was adjusted to about 6 with N hydrochloric acid to form resinous precipitate. This precipitate was separated by filtration, washed with water, extracted with ethyl acetate, and dried over sodium sulfate. After the sodium sulfate had been filtered off, the ethyl acetate was removed under reduced pressure to give a crystalline substance. The crude IV thus obtained was recrystallized from ethyl acetate with active charcoal to give 0.05 g of colorless scales of IV, mp 318—320°C (colored about 280°C, Koffler block).

Found: N, 18.91%. Calcd for $C_{12}H_{15}ON_3$: N, 19.34%.

λ_{max}^{MeOH} mμ (log ε); 220 (4.19) and 285 (4.00).

4-Chloro-5, 6-pentamethylene-7*H*-pyrrolo[2,3-*d*]pyrimidine (V). A solution of 0.30 g of II in 2.0 m*l* of phosphorous oxychloride in a sealed tube was heated for 3 hr at 100°C, and the excess phosphorous oxychloride was removed under reduced pressure. The pH of the residue was adjusted to about 8.5 with diluted aqueous ammonia, extracted with ethyl acetate, and dried over sodium sulfate. The sodium sulfate was then separated by filtration, and the residue was sublimed under reduced pressure (0.5 mmHg at 150°C). The sublimate was recrystallized from benzene to give 0.14 g of pale yellow prisms of V, mp 228°C.

Found: C, 59.63; H, 5.00; N, 19.00%. Calcd for $C_{11}H_{12}N_3Cl$: C, 59.59; H, 5.46; N, 18.96%.

λ_{max}^{MeOH} mμ (log ε); 234 (4.40) and 316 (3.60).

4-Methoxy-5, 6-pentamethylene-7*H*-pyrrolo[2, 3-*d*]pyrimidine (VI). A suspension of 0.20 g of V and 1.20 g of hydrazine hydrate (80%) in 5.0 m*l* of methanol was refluxed for 4 hr, after which the excess methanol was removed under reduced pressure. The residue was sublimed under reduced pressure (0.1 mmHg at 150°C), and the sublimate was recerystallized from acetone to give colorless scales of VI, mp 246—247°C; yield, 0.14 g.

Found: N, 19.16%. Calcd for $C_{12}H_{15}ON_3$: N, 19.34%.

λ_{max}^{MeOH} mμ (log ε); 234 (4.14), 275 (3.40) and 310 (3.53).

A mixed-melting-point determination of VI with IV clearly showed a depression. When sodium methoxide was used instead of hydrazine, VI was obtained in a quantitative yield.

4-Hydrazino-5, 6-pentamethylene-7*H*-pyrrolo-[2, 3-*d*]pyrimidine (VII). A mixture of 0.1 g of V and 1.0 m*l* of hydrazine hydrate (80%) was refluxed for 5 hr, thus the precipitate was formed. The formed precipitate was then recrystallized from methanol to give 0.07 g of colorless scales of VII, mp 233—235°C (decomp.).

Found: C, 60.86; H, 6.43; N, 31.81%. Calcd for $C_{11}H_{15}N_5$: C, 60.80; H, 6.96; N, 32.24%.

λ_{max}^{MeOH} mμ (log ε); 216 (4.22) and 294 (3.98).

The Decomposition of VII. A solution of 0.05 g of VII in 1 m*l* of acetic acid was poured into a boiling solution of 0.50 g of cupric sulfate in 1 m*l* of water.

15) All melting points are uncorrected.

The solution turned black with the evolution of gas; after it had cooled, 10 m*l* of water were added. The pH of the solution was then adjusted to about 8 by means of aqueous bicarbonate and extracted with ethyl acetate. The organic layer was dried over sodium sulfate, separated by filtration, and concentrated to give an intractable, gummy substance.

Dehydrogenation of II. To a solution of 0.50 g of II in 10 m*l* of refluxing isoamyl alcohol, 1.50 g of chloranil were added in five portions over a period of 2 hr; refluxing was then continued for 4 hr. The amyl alcohol was removed under reduced pressure, and the residue was dissolved in ethyl acetate. The ethyl acetate solution was then chromatographed on silica gel; a small amount of amorphous powder was thus obtained.

λ_{max}^{MeOH} mμ; 245, 300, 368 and 399.

The powder dissolved in benzene, ethyl acetate, and acetone, but it formed a gelly substance when concentrated. Further purification by means of recrystallization and other methods failed to produce a pure substance.

This research was supported in part by a grant from the Up John Co., for which grant the authors' thanks are due.

BULLETIN OF THE CHEMICAL SOCIETY OF JAPAN VOL. 41 211—217 (1968)

Ring-opening Polymerization of Norbornene and Its Derivatives by $MoCl_5$, WCl_6 and $ReCl_5$ Catalysts

Takao OSHIKA and Hiroyoshi TABUCHI

The Central Research Laboratory, Toa Nenryo Kogyo Co., Ohi-machi, Iruma-gun, Saitama

(Received July 21, 1967)

Norbornene and such of its derivatives as *exo*-5, 6-trimethylene norbornene (*exo*-TMN) and *endo*-dicyclopentadiene (*endo*-DCPD) have been polymerized ***via*** ring cleavage to high-molecular-weight polymers, soluble in aromatics, by the use of $MoCl_5$, WCl_6, and $ReCl_5$ catalysts in a carbon tetrachloride solvent. The ring-opening polymers obtained by $MoCl_5$ have a trans-structure almost exclusively, on the other hand the polymers obtained by $ReCl_5$ are rich in cis structures and those obtained by WCl_6 are mixtures of the two. The reactivities of the monomers on those catalysts have been found to have the order of decreasing reactivity: *exo*-TMN>NE> *endo*-DCPD. In the ring-opening polymerization of norbornene by $MoCl_5$, carbon disulfide and carbon tetrachloride have been found to be effective solvents. The yield increases with the rise in temperature and also upon the addition of a catalytic amount of tertiary amines in the midst of the polymerization procedure, while the structures of the polymers obtained do not change. The Co-catalyst H_2O is not necessary. Chlorine atoms are found in the polymers. Those results suggest that the ring-opening polymerization of norbornene over $MoCl_5$ occurs through a specific coordinated mechanism.

Three modes of reaction have been established for the polymerization of norbornene: a vinyl polymerization and two types of ring-opening polymerization, giving polymers with trans and cis double bonds. Ring-opening-type polymers have been obtained by Truett,[1] Sartori,[2] and Furukawa[3] using Ziegler-Natta catalysts, and by Michelotti[4] and Rinehart[5] using Ir^{3+}, Ru^{3+} and Os^{3+} in polar media. It has been concluded that the ring-opening polymerization proceeds through the coordinated anionic mechanism.[1,4] On the other hand, the vinyl-type polymer has been obtained using such cationic catalysts as $AlCl_3$, $TiCl_4$, and BF_3.[3] In a previous work in this series[6] it has been shown that the ring-opening polymer of norbornene can be obtained by the use of uni-component catalyst, $MoCl_5$, in carbon tetrachloride.

In this paper we wish to report on the ring-opening polymerization of norbornene, *exo*-TMN, and *endo*-DCPD by $MoCl_5$, WCl_6 and $ReCl_5$ catalysts and to discuss the polymerization mechanism from the point of view of the effects of the temperature, the solvents, and the co-catalysts.

1) W. L. Truett, D. R. Johnson, I. M. Robinson and B. A. Montage, *J. Am. Chem. Soc.*, **82**, 2337 (1960).
2) G. Sartori, F. Ciampelli and W. Gameli, *Chim. e. ind. (Milano)*, **45**, 1473 (1963).
3) T. Tsujino, T. Saegusa, S. Kobayashi and J. Furukawa, *Kogyo Kagaku Zasshi (J. Chem. Soc. Japan, Ind. Chem. Sect.)*, **67**, 1961 (1964).
4) F. W. Michelotti and W. P. Keaveney, *J. Polymer Sci.*, **A3**, 895 (1965).
5) R. E. Rinehart and H. P. Smith, *ibid.*, **B3**, 1049 (1965).
6) T. Oshika, S. Murai and Y. Koga, *Chem. High Polymers, Japan*, **22**, 633 (1965).

Experimental

Materials. The Diels-Alder reaction of ethylene and dicyclopentadiene gave norbornene, bp 96.0—97.0°C (lit.[7] 94—97°C/740 mmHg). *exo*-5, 6-Trimethylene norbornene was prepared from dicyclopentadiene by hydration, hydrogenation, and esterification reactions, followed by pyrolysis; bp 54—56°C/8 mmHg, $n_D^{25}=1.4948$ (lit.[8] $n_{25}^{D}=1.4943$). An *endo*-dicyclopentadiene received from the Eastman Kodak Company was distilled prior to use; $n_D^{25}=1.5120$ (lit.[9] $n_D^{25}=1.5121$). The solvents were purified by conventional methods.

$NbCl_5$ and $SeCl_4$ were prepared from their respective metals by chlorination.[10] $MnCl_2$[11] was prepared from $MnCl_2 \cdot 2H_2O$; UCl_4[12] was prepared by refluxing UO_3 in disulfo dichloride. $MoCl_4$ was prepared according to the method of Larson.[13] Found: Cl, 55.1; Mo, 40.6%. Calcd for $MoCl_4$: Cl, 59.7; Mo, 40.4%. The other metal chlorides were commercially available in anhydrous pure grades and so were used without further purification.

Polymerization. Polymerization was carried out in a sealed glass tube under an argon atmosphere. The following is a typical example of the procedure employed. Into a 50 m*l* glass tube there was placed 0.682 g of $MoCl_5$; then were added 10 m*l* of CCl_4. After it had thus stood for ten minutes, the tube was immersed and chilled in a dry ice - methanol bath, after which a solution of 4.70 g of norbornene in CCl_4 (10 m*l*) was introduced into the tube; then the tube was sealed off. Polymerization was carried out with agitation in a water bath controlled thermostatically at 50°C. After 4 hr, the contents were poured into a large excess of methanol containing phenyl β-naphthyl amine as a stabilizer. The dark, crude polymer thus obtained was separated and dried at 40°C under vacuum; yield 2.40 g.

In 200 m*l* of hot benzene, 1.0 g of the crude polymer was dissolved and reprecipitated with methanol. There was thus obtained 0.59 g of a white, fibrous polymer, which was soluble in benzene, and 0.01 g of a black, insoluble polymer. Found (for the benzene soluble polymer): C, 88.98; H, 10.63%. Calcd for $(C_7H_{10})_n$: C, 89.29; H, 10.71%. The yields stated in this paper are the totals of the benzene-soluble and -insoluble polymers. The intrinsic viscosity was determined for *p*-xylene solutions at 100°C. The infrared spectrum was recorded using a Japan Spectroscopic Co. apparatus, Model DS 402G.

Results

Polymerization of Norbornene. Polymerization was carried out at 50°C using various metal chlorides in carbon tetrachloride. Table 1 shows that the low-molecular-weight vinyl-type polymers were obtained using such catalysts as $AlCl_3$, $ZrCl_4$, VCl_4, $NbCl_5$, and $TaCl_5$; of these $AlCl_3$ showed the highest activity.

The initially homogeneous system of norbornene polymerized by $MoCl_5$, WCl_6, or $ReCl_5$ becomes heterogeneous as the reaction progresses due to the insolubility of the polymer. The produced polymers are soluble in hot benzene and structurally similar to the products previously reported,[1,2] in which a major portion of the polymer chain consists of cyclopentane rings linked in a *cis*-1, 3 configuration with either trans- or cis double bonds.

In Table 1, $D_{965}/D_{740}/D_{1445}$ are the ratios of the optical densities at 965, 740, and 1445 cm^{-1} in the infrared spectra; these densities are assigned to the deformation of *trans* C=C, *cis* C=C, and CH_2 respectively. Furukawa[3] has found a linear correlation between the D_{965}/D_{1445} ratio and the amounts of trans double bonds in polymers. By the use of this correlation, the trans units can be calculated; then the cis units may be estimated from the difference between the total double bonds as determined by the Wijs method and the trans units as calculated above. By that calculation, it is found that the polynorbornene catalyzed by $MoCl_5$ is of trans units 80—95% and cis units 4—5%; the polymer catalyzed by WCl_6, of trans 50% and cis 39%, and the polymer catalyzed by $ReCl_5$, of trans 23% and cis 75%.

Under the same conditions described in Table 1, no polymer was found when those catalysts were used: $CdCl_2$, BF_3OEt_2, $TiCl_4$, $SnCl_4$, $AsCl_3$, $SbCl_5$, $CrCl_3$, $SeCl_4$, $MoCl_4$, UCl_4, $MnCl_2$, $FeCl_3$, $CoCl_3$, and $RuCl_3$.

Polymerization of *exo*-5, 6-Trimethylene Norbornene (TMN). A number of catalysts like Mo(V), W(VI), and Re(V) which were active in the polymerization of norbornene were found to be also active in the polymerization of TMN, giving benzene-soluble and high-molecular-weight polymers in a maximum total conversion of 75% as shown in Table 2. The polymer obtained by $MoCl_5$ had a strong absorption at 965 cm^{-1}, indicating substantial amounts of trans unsaturation along the polymer chain. On the other hand, the polymer obtained by $ReCl_5$ had strong absorptions at 2980, 1408, and 740 cm^{-1}, absorptions which were attributed to cis double bonds. Since the infrared absorptions of the polymers were similar to those of polynorbornenes obtained by the same catalysts, the structures of poly-TMN must be of a ring-opening trans- or cis-type similar to those of polynorbornenes.

The films or powders of poly-TMN prepared with $MOCl_5$, Ziegler, or $AlCl_3$ catalysts were all found by X-ray diffraction to be amorphous.

Polymerization of *endo*-Dicyclopentadiene (DCPD). Many examples have been known of the

7) "Organic Syntheses," Vol. 37, p. 65.
8) S. J. Cristol, W. K. Seifert and S. B. Soloway, *J. Am. Chem. Soc.*, **82**, 2351 (1960).
9) H. E. Simmons, E. P. Blanchard and R. D. Smith, *ibid.*, **86**, 1347 (1964).
10) "Inorganic Synthesis," Vol. 5, p. 125.
11) B. B. Bose and M. H. Khundkar, *J. Indian Chem. Soc., Ind. & News Ed.*, **14**, 39, 45 (1951).
12) E. Uhleman and W. Fishbach, *Z. Chem.*, **3** (11) 431 (1963); *Chem. Abstr.*, **60**, 3708 (1964).
13) M. L. Larson and F. W. Moore, *Inorg. Chem.*, **3**, 285 (1964).

Table 1. Polymerization of norbornene

Catalyst	Yield %	Soluble/Insoluble in boiling benzene	Characteristics of the soluble fraction		
			$D_{965}/D_{740}/D_{1445}$	$[\eta]$	Softening range, °C
$MoCl_5$	32.6	93/7	3.4/0.5/1.0	0.25	108—128
WCl_6	22.4	100/0	2.1/0.8/1.0	0.70	95—103
$ReCl_5$	83.8	88/12	0.8/1.7/1.0	0.34	94—108
$AlCl_3$	32.0	100/0	0.1/0.0/1.0	0.03	84— 92
$AlBr_3$	11.3	100/0	0.0/0.0/1.0	0.01	45— 60
$ZrCl_4$	1.5	100/0	0.0/0.0/1.0	—	—
VCl_4	3.6	100/0	0.0/0.0/1.0	—	65—120
$NbCl_5$	21.9	100/0	0.1/0.0/1.0	—	vis. liquid
$TaCl_5$	8.1	100/0	0.1/0.0/1.0	—	vis. liquid

Monomer: 4.70 g; concentration: 2 mol/*l*; cat.: 5 mol% of monomer; solvent: CCl_4; polymn. time: 4 hr; temp.: 50°C

Table 2. Polymerization of *exo*-5, 6-trimethylene norbornene

Catalyst	Yield %	Soluble/Insoluble in boiling benzene	Characteristics of the soluble fraction		
			$D_{965}/D_{740}/D_{1445}$	$[\eta]$	Softening range, °C
$MoCl_5$	71.7	83/17	2.3/0.2/1.0	1.62	142—145
WCl_6	74.8	85/15	1.3/0.5/1.0	2.47	139—146
$ReCl_5$	71.5	100/0	0.1/0.8/1.0	1.61	106—115
$AlCl_3$	9.8	100/0	0.1/0.0/1.0	0.04	126—142
$AlEt_3$-$TiCl_4$[a]	49.0	10/90	1.7/0.1/1.0	0.83	160—175

Polymerization conditions are the same as in Table 1.
a) $AlEt_3$: 8 mol%; Al/Ti: 4; *n*-heptane solvent

polymerization[14] of DCPD as a third component in the ethylene-propylene-terpolymer. Recently Imoto[15] reported the homopolymerization of DCPD using Ziegler-type catalysts.

Independently, we also obtained the poly *endo*-DCPD by two kinds of catalysts: metal halides and Ziegler-type catalysts. The results of the polymerization are summarized in Table 3. The polymers had absorptions of a double bond on a cyclopentane ring at 1617 and 940 cm^{-1}, but had no absorption of the double bond on a bicyclic ring at 1575 cm^{-1}, as is shown in Fig. 1. These facts suggest that the latter double bond reacted in the polymerization, while the former one did not react. This is in accordance with the results of the addition reaction of H_2O, HX, ROH, and RCOOH to DCPD, in which only the double bond on the bicyclic ring can be attacked.[16] Since the poly-DCPD catalyzed by $MoCl_5$ had a strong absorption at 973 cm^{-1} (*trans* C=C), its structure must be of a ring-opening trans type (II):

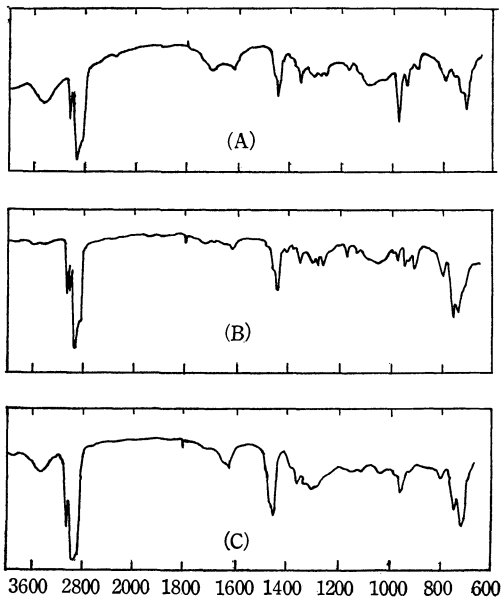

Fig. 1. IR spectra of *endo*-DCPD, (A): $MoCl_5$-catalyzed; (B): $ReCl_5$-catalyzed; (C): $AlCl_3$-catalyzed.

14) For example a) E. K. Gladding, B. S. Fisher and J. W. Collette, *I & EC*, **1**, No. 2, 65 (1962). b) G. Sartori, A. Valvassori and S. Faina, *Rubber Chem. Tec.*, 620 (1965). c) R. E. Cunningham, *J. Polymer Sci.*, **A3**, 3157 (1965).
15) S. Takada, T. Otsu and M. Imoto, *Kogyo Kagaku Zasshi (J. Chem. Soc. Japan, Ind. Chem. Sect.)*, **69**, 711, 715 (1966).
16) a) H. A. Bruson and T. W. Riener, *J. Am. Chem. Soc.*, **67**, 723, 1178 (1945); *ibid.*, **68**, 8 (1946). b) F. Bergmann and H. Japhe, *ibid.*, **69**, 1826 (1947).

Table 3. Polymerization of *endo*-dicyclopentadiene

Catalyst	Temp. °C	Time hr	Yield %	Soluble/Insoluble in boiling benzene	Characteristics of the soluble fraction $D_{973}/D_{755}/D_{1445}$	Characteristics of the soluble fraction $[\eta]$
$MoCl_5$	50	4	23.3	3/97	3.8/0 /1.0[a]	—
WCl_6	50	4	23.6	55/45	0.3/0.5/1.0	0.14
$ReCl_5$	50	4	45.2	86/14	0.4/1.7/1.0	0.45
$AlCl_3$	50	4	25.4	80/20	0.0/0.0/1.0	—
$AlCl_3$	−15	120	19.5	73/27	0.1/0.0/1.0	—
$TiCl_4$	50	10	0.3	—	0.0/0.0/1.0	—
$AlEt_3$-$TiCl_4$[b]	50	10	6.0	0/100	2.6/0.1/1.0[a]	—
$AlEt_3$-$MoCl_5$[b]	−15	10	3.5	0/100	0.3/1.7/1.0[a]	—

Polymerization conditions are the same as in Table 1.
a) Insoluble fraction
b) $AlEt_3$: 8 mol%; Al/Ti (or Al/Mo): 4; *n*-heptane solvent

Table 4. Polymerization of olefins

Monomer	Temp. °C	Time hr	Yield %	Molecular weight	Micro-structure of polymer	Ref.
Isobutylene	−20	2	37	4990	Polyisobutylene	
Styrene	30	1	90	8240	Amorphous	
α-Methylstyrene	30	4	7	2500		
Trioxane	30	4	50	$[\eta]=0.61$	Polyether	
Isoprene	50	4	95	1820	Bicyclic structure	17
Butadiene	50	4	10	—	Cyclization	
4-Vinylcyclohexene	50	4	4	—	Cyclization	18
Cyclopentene	50	4	3	—	Double bond opening	19

Cat.: $MoCl_5$; 2—5 mol% of monomer; solvent: CCl_4

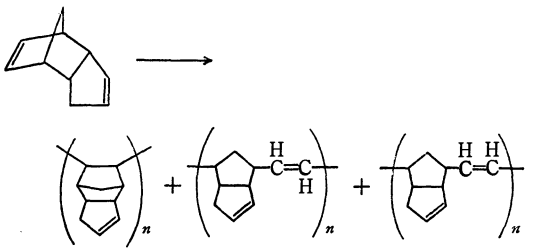

(I) (II) (III)

On the other hand, the polymer catalyzed by $ReCl_5$ was soluble in boiling benzene, and its IR spectrum showed sharp absorptions at 3000, 1408 and 755 cm^{-1}, absorptions which can be assigned to the cis double bond along the main chain. Thus, the structure is mainly of a ring-opening cis type (III).

The poly-DCPDs produced by Ziegler-type catalysts, $AlEt_3$-$TiCl_4$ or $AlEt_3$-$MoCl_5$, consisted mostly of ring-opening trans- or cis-type structures respectively. It was also possible to get the polymer with a vinyl-type structure (I) by using such Lewis acid catalysts as $AlCl_3$ and $TiCl_4$. Therefore, the effect of catalyst on the micro-structure of poly-DCPD was the same as that on the structures of polynorbornene and poly-TMN.

The polymerization rates of DCPD on various catalysts were smaller than those of norbornene and TMN, and none of the resultant poly-DCPD showed clear softening points, while they decomposed gradually at 150—400°C.

Polymerization of Olefins by $MoCl_5$. The microstructure of polynorbornene obtained by means of $MoCl_5$ was different from those obtained by usual cationic polymerization catalysts, *e.g.*, $AlCl_3$ and $TiCl_4$. To study this point further, it seemed of interest to carry out the polymerization of the other olefins over $MoCl_5$.

As is shown in Table 4, polyisobutylene, mol wt 4990, was obtained at −20°C, and the molecular weight increased with a decrease in the temperature. In the polymerization of isoprene, a low-molecular-weight polymer was obtained in a high yield, and the structure was not linear but of a bicyclic type, as has been reported by Golub.[17] Chloroprene was found poor in polymerizability. Cyclopentene, 4-vinylcyclohexene, and cyclohexadiene were somewhat polymerizable.

For these olefins, it was concluded that $MoCl_5$ catalyzes a normal cationic polymerization as well as typical Lewis acid catalysts.

17) M. A. Golub and J. Heller, *Can. J. Chem.*, **41**, 937 (1963).

Table 5. Effect of solvent

Solvent	Yield %	Soluble/Insoluble in boiling benzene	Characteristics of the soluble fraction	
			$D_{965}/D_{740}/D_{1445}$	$[\eta]$
CS_2	69.6	61/39	3.1/0.5/1.0	0.39
CCl_4	32.6	93/7	3.5/0.5/1.0	0.25
$CHCl_3$	31.2	24/76	1.4/0.6/1.0	0.19
CH_2Cl_2	20.8	10/90	1.3/0.3/1.0	—
$C_2H_4Cl_2$	52.8	12/88	1.1/0.3/1.0	0.10
	17.6	76/24	2.5/0.5/1.0	0.42
	38.0	—	2.5/0.5/1.0	—

Monomer: norbornene; cat.: $MoCl_5$, 5 mol% of monomer; 50°C; 4 hr

The copolymerization of norbornene with styrene was attempted in carbon disulfide using a $MoCl_5$ catalyst. The polymer thus obtained was only a mixture of two homopolymers. This suggests that the polymerization mechanism of norbornene is different from that of styrene.

The results of the copolymerization of norbornene with trioxane were complicated. When $MoCl_5$ was added to a carbon disulfide solution of norbornene and trioxane, no polymer was formed. There was the same result when trioxane was added to the brown-colored norbornene-$MoCl_5$ complex. However, when the norbornene was added to the light blue trioxane-$MoCl_5$ complex, only the homopolymer of trioxane was formed. In no case, did we found any evidence of the formation of a copolymer.

Mechanism of Ring-opening Polymerization of Norbornene by $MoCl_5$. *Solvent Effect.* Solvents greatly influenced the yield and the microstructure of the polymer. According to Table 5, the most effective solvents for the polymerization were halogenated hydrocarbons and carbon disulfide. Polymers were not formed in hydrocarbon solvents such as *n*-heptane. When such non-polar solvents as CCl_4 and CS_2 were used, the polymerization rates were large and the structures were predominantly of ring-opening types. In CH_2Cl_2 and $C_2H_4Cl_2$, which are more polar than the solvents mentioned above, the formation of ring-opening polymers decreased. In a very polar solvent such as CH_3NO_2, no polymer was formed.

It has been said that $MoCl_5$ is reduced to $MoCl_4$ in CCl_4 as follows.[20]

$$2\ MoCl_5 \xrightarrow{\text{in } CCl_4} 2\ MoCl_4 + Cl_2$$

Furthermore, it is known that the reaction of $MoCl_5$ with refluxing benzene gives $MoCl_4$ and chlorobenzene.[13] We found that $MoCl_4$ could not polymerize norbornene. From these results, it may be concluded that the true catalyst for polymerization is $MoCl_5$ and not the low valence molybdenum species ($Mo \leqq 4$), although $MoCl_5$ has a tendency to liberate its chlorine atom as an anion in CCl_4 and benzene.

Effect of Cocatalyst. It is well known that cationic polymerization by a Lewis acid generally needs a cocatalyst such as H_2O. If the polymerization over $MoCl_5$ proceeds through a cationic intermediate, therefore, it seems small amounts of water will be necessary, because the solvent, CCl_4, can not work as a cocatalyst.

The effect of the water on the polymerization was examined for dehydrated CCl_4 (water content 18 ppm) and water-saturated CCl_4 (water content 69 ppm). It is clear from Table 6 that the yield decreased with an increase in the water content. A detailed discussion is impossible at the present time, because a completely anhydrous solvent could not be prepared. Roughly, however, water may not be necessary for the polymerization. It is interesting that the structures of the polymers obtained were not influenced by the water content in the polymerization system.

Effect of Temperature. The rate of polymerization increased greatly with an increase in the polymerization temperature. For example, the yield

Table 6. Effect of co-catalyst

No.	$MoCl_5/H_2O$	Yield %	$D_{965}/D_{740}/D_{1445}$
1	1.0/0.60	2.7	3.9/0.5/1.0
2	1.0/0.26	5.7	3.8/0.5/1.0
3	1.0/0.17	17.5	4.2/0.5/1.0
4	1.0/0.034	19.6	3.2/0.5/1.0
5	1.0/0.013	17.0	3.5/0.5/1.0

Monomer: norbornene; solvent: CCl_4; cat.: $MoCl_5$, 2 mol% of monomer; 50°C; 4 hr for No. 1—3 and 0.5 hr for Nos. 4 and 5.

18) G. B. Butler and M. L. Miles, *J. Polymer Sci.*, **A3**, 1609 (1965).
19) G. Natta, G. Dall'asta and G. Mazzanti, *Angew. Chem.*, **76**, 765 (1964).
20) I. M. Pearson and C. S. Garner, *J. Phys. Chem.*, **65**, 690 (1961).

Table 7. Addition of tertiary amines

Monomer	Amine	Yield %	Characteristics of the soluble fraction	
			$D_{965}/D_{740}/D_{1445}$	$[\eta]$
Norbornene	none	9.2	3.6/0.6/1.0	0.25
Norbornene	Et_3N	59.5	3.4/0.6/1.0	0.50
Norbornene	n-Bu_3N	26.6	3.8/0.6/1.0	0.76
DCPD	none	4.4	1.2/0.0/1.0[a]	—
DCPD	Et_3N	15.1	1.6/0.0/1.0[a]	—

Cat.: $MoCl_5$; solvent: CCl_4
Amount of amine: equal mole to cat. was added 30 min after the reaction had started.
For norbornene: 30°C, 4 hr
For DCPD: 50°C, 2 hr
a) $D_{973}/D_{755}/D_{1445}$

of polymers varied with the rise of temperatures in such a manner as: 1.9% (−15°C, 24 hr), 3.6% (0°C, 12 hr), 8.5% (30°C, 2 hr), and 19.6% (50°C, 0.5 hr). The microstructures and intrinsic viscosities of the polymers changed little within the range of polymerization temperature of −15°C—+50°C.

Elementary Analysis of Polymer. The results of carbon and hydrogen analysis of the polynorbornene have been shown in the Experimental section. The polymer produced by $MoCl_5$ in benzene was found to be 0.13% chlorine. Since the molecular weight of this polymer was 20900, one polymer should contain about one chlorine atom. The polymers prepared in carbon tetrachloride or carbon disulfide contained more chlorine atoms than those prepared in benzene.

Addition of t-Amines. The reaction between tertiary amines and $MoCl_5$ in a CCl_4 solution gives an insoluble black complex, R_3N-$MoCl_5$[21] This complex was inactive in the polymerization of norbornene. However, the tertiary amines were apparently active promoters of the polymerization only when the amines were added to a polymerization system in which an active growing chain of the polymer was present. Thus, norbornene was polymerized by $MoCl_5$ in a glass tube sealed with a stopper. Thirty minutes after the reaction had started, a mole of Et_3N equal to the catalyst was added; the contents then suddenly became viscous. As Table 7 and Fig. 2 show, the yield and the molecular weight increased remarkably upon the addition of Et_3N, but the microstructures remained unchanged. These results suggest that the addition of tertiary amine strongly increases the rate of propagation.

On the other hand, such primary amines as $EtNH_2$ and n-$BuNH_2$, and such secondary amines as n-Bu_2NH, pyridine, and α-picoline were all effective chain stoppers. There was no increase

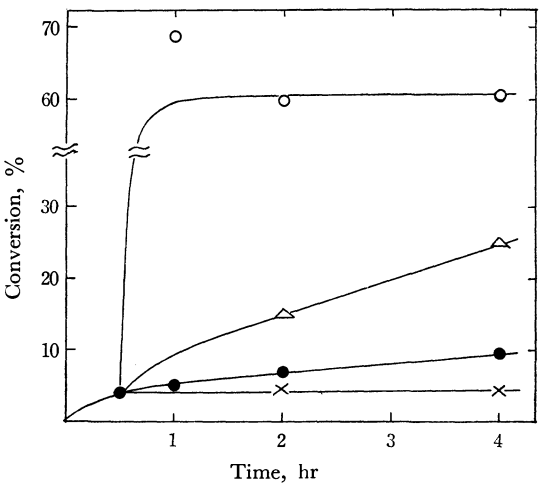

Fig. 2. Addition of amines to norbornene polymerization. Amine was added 30 min after reaction had started.
(○): Et_3N, (△): n-Bu_3N, (×): pyridine, (●): without amine. Polymerization conditions are the same as in Table 7.

in the yield upon the addition of such electron donors as triphenylphosphine, dioxane, trioxane, and tetrahydrofuran.

Discussion

Ring-opening-type polymers of norbornene, *exo*-TMN, and *endo*-DCPD can be prepared with unicomponent catalysts, $MoCl_5$, WCl_6, and $ReCl_5$. The microstructures of the polymers are influenced by the type of transition metals in the catalysts. The order of increase in the trans units is $MoCl_5 > WCl_6 > ReCl_5$. The reverse order is that of the increase of cis-type polymers. The polymerization activities of the monomers on these catalysts are; *exo*-TMN > norbornene > *endo*-DCPD.

It has been reported that Ziegler-type catalysts modified by the addition of several amines increase

21) D. A. Edward and G. W. A. Fowles, *J. Chem. Soc.*, **1961**, 24.

the activity in ring cleavage in the polymerization of norbornene.[3,22] In our study, it was found that the addition of a tertiary amine to the polymerization system remarkably increased the polymerization rate and the molecular weight, without making any change in the microstructures. In addition, several new facts were found in the polymerization of norbornene catalyzed by $MoCl_5$. Ring-opening polymers were produced by using such nonpolar solvents as CCl_4 and CS_2; on the other hand, vinyl-type polymers were predominant when a more polar solvents, like CH_2Cl_2 and $C_2H_4Cl_2$, were used. Water was not effective as a cocatalyst. The polymerization rate increased with the rise in the temperature. The polymers contained chlorine atoms which had been liberated from the catalyst. Molybdenum tetrachloride did not work as a catalyst. Copolymers with styrene or trioxane could not be formed.

There are two types of polynorbornene: a vinyl type and a ring-opening type. The former is prepared with typical Lewis acid catalysts, such as $AlCl_3$, $AlBr_3$, BF_3, and $TiCl_4$, through a usual cationic mechanism.[3] The latter is obtained only by those catalysts which act through an anionic coordination mechanism. Included in the latter group are LiAl $(C_7H_{15})_4$-$TiCl_4$ $(Al/Ti \geqq 2)$,[1] $AlEt_3$-$TiCl_4$ $(Al/Ti \geqq 2)$,[3] Al*iso*$(C_4H_9)_3$-$MoCl_5$ $(Al/Mo=2)$,[2] and $RuCl_3$ in alcohol.[4]

Judging from the general view that vinyl-type polymers are derived through cationic polymerization, and ring-opening-type polymers, through coordinated anionic polymerization, it may be concluded that the formation of ring-opening polynorbornene with $MoCl_5$ is through the coordinated anionic mechanism. Experimental findings on the effects of solvents, the temperature, and the addition of amines and water supported this mechanism.

At first sight it seems contradictory that $MoCl_5$ is an effective catalyst for Friedel-Crafts alkylation and acylation and also a cationic catalyst for α-olefins and dienes, while at the same time it acts as a coordinated catalyst for norbornene and its derivatives. However, this abnormal polymerization of norbornene by $MoCl_5$ may be due to the specific characteristics of both the monomer and the catalyst. Because of the great ring strain,[4,15] a bicyclic olefin like norbornene is attacked easily at the 1 and 2 carbon atoms by nucleophilic agents. Another important cause is that $MoCl_5$ is unstable enough to liberate its chlorine as an anion.[13]

The above evidence suggests the following mechanism, which is similar in nature to the ring-opening mechanism by Ziegler-type catalysts.[1]

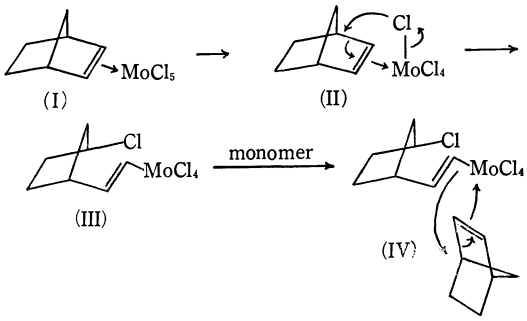

The monomer is initially activated through π-complex formation (I), followed by a simultaneous, concerted, ring-opening displacement reaction on the bridgehead carbon by the Cl^- derived from the catalyst (II); this regenerates the active metal center (III) in a reduced oxidation state. The intermediate (III) may further activate another monomer. The repetition of this process leads to the propagation.

The chlorine atom introduced in the initiation step is found in the polymer. As soon as the same moles of norbornene as that of the catalyst are added to the carbon tetrachloride solution of $MoCl_5$, the red color due to Mo(V) disappears and a pale-colored precipitate is produced. This phenomenon suggests a complex formation between the monomer and the catalyst. Since molybdenum tetrachloride is catalytically inactive, it is considered that molybdenum is not reduced below Mo(IV).

22) T. Saegusa, T. Tsujino and J. Furukawa, *Makromol. Chem.*, **78**, 32 (1964); **85**, 71 (1965).

BULLETIN OF THE CHEMICAL SOCIETY OF JAPAN VOL. 41 218—221 (1968)

Medium-Sized Cyclophanes. VI. High-Temperature NMR Spectra of [2. 2]Metacyclophane and Optical Resolution of 4, 14-Disubstituted Derivatives[1]

Takeo SATO,* Sadatoshi AKABORI,* Masatsune KAINOSHO** and Kazuo HATA*

* *Department of Chemistry, Faculty of Science, Tokyo Metropolitan University, Setagaya-ku, Tokyo*
** *Ajinomoto Co., Inc., Kawasaki*

(Received July 25, 1967)

The NMR spectra of [2.2]metacyclophane have been shown to be held unchanged over a wide range of temperature, *ca.* −80 to 190°C, indicating that the ten-membered ring system undergoes no inversion and is frozen in a chair conformation. It may, then, be expected that suitably substituted derivatives of [2.2]metacyclophane would become disymmetric due to restricted inversion; such was proved to be the case by carrying out the optical resolution of the 4, 14-di-substituted derivatives. The 4, 14-dimethyl derivative was resolved by means of a complex formation with Newman's reagent, $[\alpha]_{578}^{26}=-3.4$ and $+4.2°$. 4, 14-Dicarboxylic acid was also resolved by converting it to the quinine salt, $[\alpha]_{D}^{22}=+5.0°$.

Among the medium-sized ring compounds [2.2]metacyclophane (I) is one of the few examples whose molecular geometry has been completely elucidated using the X-ray technique.[2] The compound has been shown to exist as a step-like molecule with two slightly distorted benzene rings, which are arranged on two parallel planes. As a consequence, the distance between C_8 and C_{16} has been found to be as short as 2.689 Å in spite of deformation in both the aryl and aliphatic bonds to relieve steric overcrowding. These structural features have been shown to be well reflected in the absorption spectra of I.[3] By comparing the UV spectrum of I with that of 3, 3'-dimethylbibenzyl, a corresponding open-chain compound, it has been noticed[4] that the absorption maximum of I at 270 mμ, devoid of any fine structure, shifts to a longer wavelength and a lower intensity, thus indicating an appreciable distortion in the aryl moiety. The absorption minimum of 3, 3'-dimethyl bibenzyl occurs at 236 mμ with a low intensity ($\varepsilon=75$,) whereas I has a higher extinction (log $\varepsilon=3.67$) at the same wavelength and the absorption minimum shifts to 260 mμ. The fact is explainable by assuming the presence of bands due to transannular interaction between the two benzene rings in this region.[4] Further, the examination of the NMR spectra of I has revealed the unusual nature of the 8, 16-protons and conformational details of the ten-membered ring. In addition to an AB_2-type absorption of the peripheral aryl protons at $C_{5,13}$ and $C_{4,6,12,14}$ at δ 7.18 and 6.97 respectively, a triplet assignable to intraannular aryl protons at $C_{8,16}$ appeared at δ 4.23 ($J=1.8$ cps). The up-field shift of almost 3 ppm is due to the diamagnetic ring current effect of the diametrical benzene rings, over which the intraannular protons are extended. Methylene protons appeared as A_2B_2-type absorptions, which were analyzed as $\delta_A=2.04$ and $\delta_B=3.05$, indicating the presence of nonequivalent protons. Since the ten-membered ring in I exists in a chair conformation, it is quite natural to assign these as arising from axial (H_A) and equatorial (H_B) protons, as is shown in structure II.

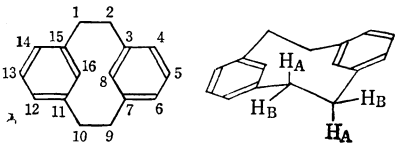

I II

The temperature dependence of NMR spectra has been proved to be a powerful tool for the detection of possible inversion in cyclic systems and has found wide application. Our interest in the conformational equilibrium of the ten-membered ring system in I led us to study the high-temperature NMR spectra of I.[5] The spectra were determined at *ca.* −80, 27, 67, 126, and 190°C; they are shown in Fig. 1. The assignments of the

1) Part V: T. Sato, Y. Goto and K. Hata, This Bulletin, **40**, 1994 (1967).
2) C. J. Brown, *J. Chem. Soc.*, **1953**, 3278.
3) B. H. Smith, "Bridged Aromatic Compounds," Academic Press Inc., New York, N. Y. (1964), pp. 359, 407.
4) N. L. Allinger, M. A. DaRooge and R. B. Hermann, *J. Am. Chem. Soc.*, **83**, 1974 (1961).
5) The results appeared in a preliminary form, see T. Sato, S. Akabori, M. Kainosho and K. Hata, This Bulletin, **39**, 856 (1966).

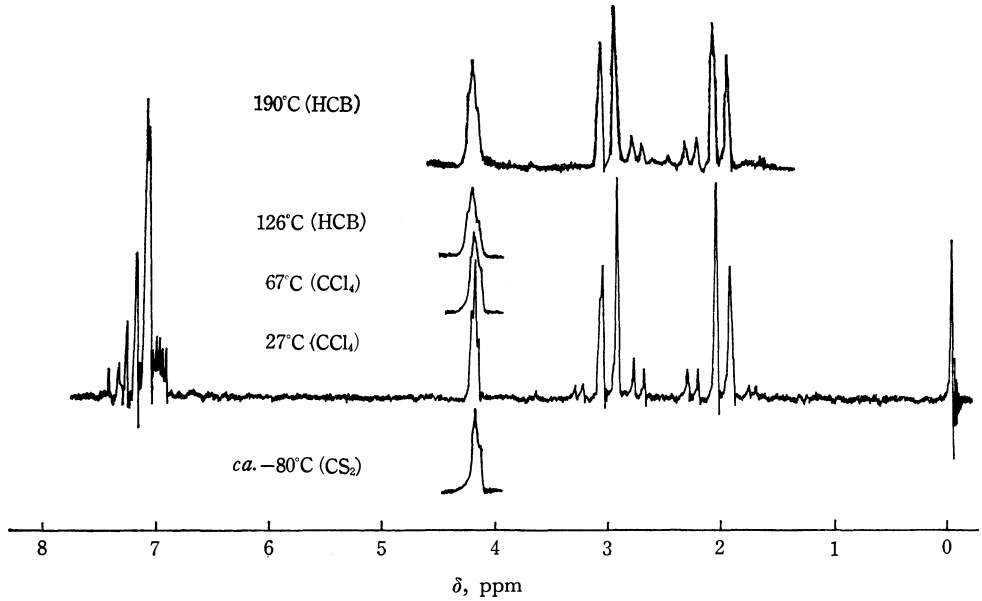

Fig. 1. NMR spectra of [2.2]metacyclophane (I) at various temperatures.

TABLE 1. NMR SPECTRA DATA OF [2.2]METACYCLOPHANE AT VARIOUS TEMPERATURES[a]

Temp., °C	Solvent	AB_2		Triplet[b]	A_2B_2,[c] 1, 2, 9, 10-H	
		5, 13-H	4, 6, 12, 14-H	8, 16-H	Equatorial	Axial
190	HCB[d]	431.6	418.6	270.9	193.7	135.3
126	HCB	430.4	417.4	256.6	182.2	122.6
67	CCl_4	430.2	417.1	254.5	181.7	122.7
27	CCl_4	430.8	416.0	253.8	183.3	122.7
27	HCB	431.8	418.6	254.2	182.2	122.8
27	CS_2	429.8	416.3	251.6	181·6	120.6
ca. −80	CS_2	428.4	415.2	247.4	181.2	120.0

a) The spectra were recorded on a Varian A-60 spectrometer with variable-temperature probe and expressed in cps relative to internal TMS as 0.
b) $J=1.8$ cps.
c) Analyzed by AB type approximation.
d) Hexachlorobutadiene.

proton signals are summarized in Table 1. Except for a small shift due to solvent effect, no significant changes in the spectral pattern were observable. It was of special note that the A_2B_2 absorption was kept surprisingly unchanged even at 190°C, indicating that the molecule is frozen in the chair conformation II, thus eliminating the possibility of interconversion between the inverted isomers. It is also noteworthy, however, that 8, 16-protons experience a small yet definite down-field shift upon going to higher temperatures. At 190°C the signal occurred at 270.9 cps down-field from TMS, whereas at room temperature it appeared at 254.2 cps, both values being determined in a hexachlorobutadiene solution. An increase in the thermal motion at higher temperatures brings about distortions of bond angle and bond length, so that the distance of 8,16-protons from the center of the opposite benzene ring increases. This molecular deformation might be responsible for the slight down-field shift of the proton signal. Recently, Griffin and his co-worker[6] have demonstrated that the higher homolog, 2, 2-dicarbethoxy-[3.2]metacyclophane, experiences a ring inversion evidenced by the coalescence of the AB and A_2B_2 systems to two singlets above 125°C.

It is, then, to be expected that those [2.2]metacyclophane derivatives in which substituents are introduced unsymmetrically in relation to a plane of symmetry which bisects both of the benzene rings may become optically resolvable. As the

6) R. W. Griffin, Jr., and R. A. Coburn, *Tetrahedron Letters*, **1964**, 2571.

possible disymmetric molecules, two 4, 14-disubstituted derivatives III and IV, the optical antipodes of which are represented by Va and Vb, were prepared. The Wurtz dimerization reaction of 2, 4-bis(chloromethyl)toluene under high-dilution conditions using disodium tetraphenylethane as a condensing agent has been shown[5] to proceed stereospecifically to afford only the cis compound III, and not the possible trans isomer, the 4, 12-dimethyl derivative. The structural determination was achieved by the NMR spectral measurements. Dicarboxylic acid IV was obtained by the oxidation of [2.2]metacyclophane-4, 14-dicarbaldehyde, which had itself been prepared from III by bisbromination reaction with NBS, followed by the Sommelet reaction. Full accounts of the syntheses and a structural consideration based on the spectral data will be presented elsewhere.

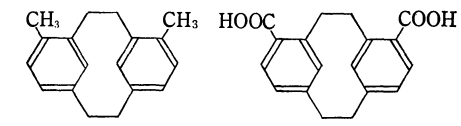

III IV

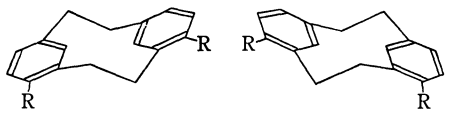

Va Vb

The optical resolution of compound III, which is devoid of suitable functional grouping, was achieved by using (−)-α-(2, 4, 5, 7-tetranitro-9-fluorenylideneaminooxy)propionic acid[7] as a complex-forming reagent. When kept in a refrigerator, a benzene solution of the reagent and III deposited a crystalline complex, which, by column chromatography on alumina using benzene as an eluent, was found to decompose to afford (−)-III as colorless needles, mp 54—64°C, $[\alpha]_{578}^{26}=-3.4°$. By the chromatography of the material contained in the filtrate of the complex formation, a dextrorotatory isomer, mp 58—61°C, $[\alpha]_{578}^{26}=+4.2°$, was obtained. These two isomers showed negative and positive plain ORD curves respectively, and had infrared spectra identical with those of the racemic compound. Dicarboxylic acid IV was resolved by the aid of quinine. A solution of IV and quinine in ethanol was left to stand, thus producing a crystalline salt; on recrystallization from ethanol this salt melted at 150—160°C. A benzene solution of the optically active acid, after liberation by dilute hydrochloric acid, was evaporated to give a colorless powder, mp >300°C, $[\alpha]_{D}^{22}=+5.0°$.

Obviously these are the first examples which demonstrate that suitably substituted [2.2]metacyclophane derivatives become disymmetric due to the restricted inversion of the ten-membered ring system. After the completion of the present studies, two papers along similar lines have appeared. Lüttringhaus and his co-worker[8] have achieved a partial resolution of a cyclotriveratrylene derivative, the molecular disymmetry of which is due to a restricted inversion of the 9-membered ring, by passing its benzene solution through a column of cellulose-2 1/2-acetate, thus obtaining optical isomers with $[\alpha]_{405}^{22}=+7.5$ and $-5°$ As a new optically resolvable [mn]paracyclophane due to the restricted rotation of the aromatic rings, disymmetric tetramethyl[2.2]paracyclophane has been resolved into optical antipodes, $[\alpha]_{D}^{27}=-3.2$ and $+4.2°$, with the aid of Newman's reagent.[9]

Experimental

Physical Measurements. The measurements of NMR spectra at various temperatures were carried out using a Varian A-60 spectrometer equipped with a V-6040 variable temperature controller. Calibrations at high and low temperatures were performed by using ethylene glycol and methanol respectively; this method permitted an accuracy of ±1°C at higher temperatures. ORD curves were recorded with a Nihon Bunko ORD/UV-5 spectrometer. The optical rotations were measured by using a Carl Zeiss LEP A-2 or an Applied Electric Lab. Model MP-1T polarimeter.

Materials. 4, 14-Dimethyl[2.2]metacyclophane (III) was prepared[5] as colorless needles, mp 68—69°C, by the dimerization reaction of 2, 4-bis(chloromethyl)-toluene under high-dilution conditions realized by the slow addition (68 hr) of the latter compound to disodium tetraphenylethane in THF at −60 to −70°C. [2.2]-Metacyclophane-4, 14-dicarboxylic acid (IV), mp >300°C, was obtained either by the direct oxidation of III with potassium permanganate or *via* [2.2]metacyclophane-4, 14-dicarbaldehyde, which had itself been prepared from III by dibromination with NBS, followed by treatment with 2-nitropropane and sodium ethoxide in DMSO.[10]

Optical Resolution. a) A solution of 300 mg (1.0 mmol) of III and 300 mg (0.67 mmol) of (−)-α-(2, 4, 5, 7-tetranitro-9-fluorenylideneaminooxy)propionic acid in 2 m*l* of benzene was kept in a refrigerator for 4 days. Orange-red crystals of the complex were collected by filtration; a benzene solution of these was then submitted to column chromatography on alumina, using benzene as an eluent. There were thus obtained 49 mg of colorless needles which had a mp of 54—64°C and an $[\alpha]_{578}^{26}$ value of −3.4°(*c* 1.8, ethanol).

Similar treatment of the filtrate from the complex formation furnished 80 mg of colorless needles, mp 58—61°C, which showed $[\alpha]_{578}^{26}=+4.2°$ (*c* 3.3, ethanol).

The two compounds showed negative and positive

7) M. S. Newman and W. B. Lutz, *J. Am. Chem. Soc.*, **78**, 2469 (1956).

8) A. Luttringhaus and K. C. Peters, *Angew. Chem. internat. Edit.*, **5**, 593 (1966).

9) D. T. Longone and M. T. Reetz, *Chem. Commn.*, **1967**, 46.

10) B. H. Klanderman, *J. Org. Chem.*, **31**, 2618 (1966).

plain ORD curves respectively and had IR spectra identical with those of the racemic compound.

b) A solution of 330 mg (1.1 mmol) of IV and 730 mg (2.3 mmol) of quinine, which had been liberated from the hydrochloride, in 9 m*l* of hot ethanol was left to stand at room temperature for one day. Filtration then afforded 280 mg of a crystalline salt, which was recrystallized from ethanol, mp 150—160°C. Dicarboxylic acid was freed from the salt by shaking it with 20 m*l* of benzene and 10 m*l* of dilute hydrochloric acid. By the evaporation of the benzene solution, there were obtained 45 mg of a colorless powder, mp >300°C, with $[\alpha]_D^{22}=+5°$ (*c* 1.8, ethanol). It had IR spectra identical with those of the racemic compound.

The authors wish to express their hearty thanks to the Ministry of Education for a grant-in-aid for fundamental scientific research.

BULLETIN OF THE CHEMICAL SOCIETY OF JAPAN VOL. 41 221—225 (1968)

The Reaction of Benzylic Alcohols with Dimethyl Sulfoxide-Polyphosphoric Acid

Takeo SATO, Akihiko TAKATSU, Yoshitaka SAITO, Takafumi TOHYAMA and Kazuo HATA

Department of Chemistry, Faculty of Science, Tokyo Metropolitan University, Setagaya-ku, Tokyo

(Received July 25, 1967)

The reaction of dimethyl sulfoxide-polyphosphoric acid mixture with benzylic alcohols has been shown to afford a complex mixture of the products; this is in contrast to the case of aliphatic alcohols, which yield the corresponding acetal as the major product. By carrying out reactions using several benzylic alcohols and a series of benzyl alcohols, it was found that, in addition to the acetal formation reaction, dehydration and oxidation reactions, as well as a methyl thioether-formation reaction, were occurring. Possible pathways for the formation of these products are presented.

In continuing our work[1] aimed at the development of a new use of dimethyl sulfoxide (DMSO) in organic reactions, this paper will record the reactions of benzylic alcohols with DMSO, polyphosphoric acid (PPA), or a DMSO-PPA mixture.

In another study, a facile dehydration reaction of α-(bromomesityl)benzyl alcohol to give the corresponding ether has been achieved[2] by treatment with PPA. Current interest in DMSO as an efficient dehydrating agent[3] has led us to investigate the ether formation reaction of benzylic alcohols in DMSO.[2] By heating benzhydrol (IIId) in a DMSO solution, bis(diphenylmethyl) ether (IVd) was isolated in a 88% yield. Likewise, α-(bromomesityl)benzyl alcohol afforded an ether. Similar results have concurrently been reported by Traynelis and his co-worker.[4] In contrast, 9-hydroxyfluorene produced only a 14% yield of bis(9-fluorenyl) ether under similar conditions, the major product being 9-fluorenone, which was obtained in a yield of up to 56%. An attempted dehydration reaction of benzyl alcohol with either DMSO or PPA, however, resulted in the formation of only a small amount of benzaldehyde or of a polymeric material respectively.

Recently considerable interest has arisen in the reaction in which DMSO is used as a reactant as well as a solvent in acidic media. A novel oxidation method developed by Moffatt and his co-workers[5] utilizes DMSO-dicyclohexylcarbodiimide (DCC)-orthophosphoric acid for the selective oxidation of primary alcohols to aldehydes. It has also been reported from our laboratories[6] that a new reagent, a DMSO-PPA mixture, reacts even with aliphatic primary alcohols to form the corresponding acetal I in a 50—90% yield. These alcohols, which are inert toward DMSO, are known to produce only polymeric hydrocarbons on reaction with PPA.[6,7]

1) For the previous paper of this series, see T. Sato, H. Inoue and K. Hata, This Bulletin, **40**, 1502 (1967).
2) T. Sato, A. Takatsu and K. Hata, *ibid.*, **37**, 902 (1964).
3) T. Sato, *Yuki Gosei Kagaku Kyokaishi (J. Soc. Org. Synth. Chem. Japan)*, **23**, 768, 867 (1965).
4) V. J. Traynelis, W. L. Hergenrother, H. T. Hanson and J. A. Valicenti, *J. Org. Chem.*, **29**, 123 (1964); V. J. Traynelis and W. L. Hergenrother, *J. Am. Chem. Soc.*, **86**, 298 (1964).
5) A. H. Fenselau and J. G. Moffatt, *ibid.*, **88**, 1762 (1966) and earlier papers in this series.
6) T. Sato, Y. Saito, M. Kainosho and K. Hata, This Bulletin, **40**, 391 (1967).
7) H. R. Snyder and J. X. Werber, *J. Am. Chem. Soc.*, **72**, 2965 (1950); J. W. Jean, U. S. Pat. 2373475 (1945).

TABLE 1. THE REACTION OF BENZYLIC ALCOHOLS III WITH DMSO-PPA

Benzylic alcohol	Product, %				
	IV	V	VI	VII	others
IIIa	10	16	8.5	13[a]	
IIIb, X=NO_2	—	46	20	4.9	
IIIc	27	—	0.5	—	styrene, 19
IIId	53	—	13	20	

a) Determined by gas chromatography using Carbowax-1500 on celite-408 column at 199°C.

TABLE 2. NMR AND IR SPECTRA DATA

Compound	NMR,[a] δ(ppm)				IR, cm^{-1}
	OCH_2O	OCH_2S	ArCH(or CH_2)	SCH_3	
II, R=cyclohexyl		4.58(2)		2.08(3)	1323, 1065
II, R=(−)-menthyl		4.62(2)		2.08(3)	1320, 1060, 1050
IVa			4.50(4)		1200, 1095
IVc			4.37(2)		1085
IVd			5.35(2)		1050
Va	4.68(2)		4.53(4)		1163, 1101, 1045, 1023
Vb, X=NO_2	4.94(2)		4.78(4)		1170, 1125, 1105, 1060, 1010
VIIa			3.58(2)	1.87(3)	1325, 675
VIIb, X=NO_2			3.75(2)	1.96(3)	1325, 675
VIId			4.97(1)	1.91(3)	1325, 675

a) Determined on Varian A-60 spectrometer as a carbon tetrachloride solution except for Vb and VIIb (X=NO_2) which were dissolved in deuteriochloroform. All the signals, relative to TMS (δ=0.0 ppm), appeared as a singlet except for IVc, which were consisted of a pair of quartets. Numerals in parentheses denote the number of protons.

The treatment of benzylic alcohols with this DMSO-PPA mixture at a water-bath temperature for 2—5 hr produced a complex mixture of the ether IV, the acetal V, the carbonyl compound VI, and the methylthio compound VII. In contrast to the aliphatic series, acetal was no longer the main product, and no methylthiomethyl ether corresponding to II was detectable. Among the benzylic alcohols studied, 1-phenylethanol (IIIc) behaved differently and afforded only dehydration products, styrene and bis(1-phenylethyl) ether (IVc).[8] The results of representative examples are shown in Table 1. The reaction products were analyzed either by column chromatography on alumina or by gas chromatography. The carbonyl compounds were determined as 2, 4-dinitrophenylhydrazones. The pertinent NMR and IR data used for the identification of the materials are compiled in Table 2.

$$ROH \xrightarrow{\text{DMSO-PPA}} \underset{\text{I}}{ROCH_2OR} + \underset{\text{II}}{ROCH_2SCH_3}$$

$$\underset{\text{III}}{ArCHOH} \xrightarrow{\text{DMSO-PPA}} \underset{\text{IV}}{ArCHOCHAr} + \underset{\text{V}}{ArCHOCH_2OCHAr}$$

$$\underset{\text{VI}}{ArCOR} + \underset{\text{VII}}{ArCHSCH_3}$$

	Ar	R
a	C_6H_5	H
b	p-X-C_6H_4	H
c	C_6H_5	CH_3
d	C_6H_5	C_6H_5

As a typical example, the reaction products from benzyl alcohol (IIIa) were analyzed in the following manner. By gas chromatographical analyses using Carbowax-1500 on celite column, benzaldehyde (VIa), benzyl methyl sulfide (VIIa), unreacted alcohol (IIIa), dibenzyl ether (IVa), and dibenzyloxymethane (Va) (listed in the order of the retention time) were identified. Column chromatography on alumina using *n*-hexane containing an increasing amount of ether as an eluent furnished VIIa, IVa, Va, and IIIa, in that order. The treatment of IIIa with DMSO-85% orthophosphoric acid resulted in the recovery of the starting material, while the mixture made from DMSO and phosphorus pentoxide decomposed

8) Dehydration of 1-phenylethanol to styrene required much drastic conditions when carried out in DMSO alone, see V. J. Traynelis, W. L. Hergenrother and J. A. Valicenti, *J. Org. Chem.*, **27**, 2377 (1962).

vigorously before it could be brought into the reaction.[9]

The formation of the ether IV, which is absent in the aliphatic series[6] but is formed in as high as a yield as 53% with IIId, is favored in benzylic alcohols, since the reaction proceeds through a carbonium ion mechanism. This may also explain the formation of VII, by assuming the reaction of benzylic carbonium ion either with methyl mercaptan, one of the possible decomposition products of DMSO in acidic media, or with any species capable of generating it.[10]

The yields of benzaldehydes derived from a series of *p*-substituted benzyl alcohols (IIIb) are shown in Table 4 (see the Experimental section). It is apparent that the presence of an electron-withdrawing group favors the formation of the oxidation products. The fact that aliphatic alcohols do not produce any oxidation product, but instead afford the methylthiomethyl ether II, which is absent in the benzyl series, suggests that the formation of VI from benzylic alcohols and that of II from aliphatic alcohols share a common intermediate X. The reaction of DMSO with PPA produces VIII, which, upon an attack from the back by an alcohol, is converted to the alkoxysulfonium compound IX. Further reactions of the ylide X derived from IX are dependent on the nature of the alkyl residues. In the case of aliphatic compounds, carbanion preferentially attacks oxygen to produce methylthiomethyl ether, while in the benzyl series the ylide decomposes into a carbonyl compound and dimethyl sulfide. The benzyl alcohol bearing an electron-withdrawing group is more easily oxidized, since the benzyl hydrogen becomes more acidic, thus facilitating the attack by the carbanion. The intermediacy of X in a number of reactions in which DMSO serves as an oxident has been well established.[5] Further, relevant examples found in recent papers include the formation of II by the reaction of alcohol with DMSO containing DCC,[11,12] or acid anhydride.[13,14]

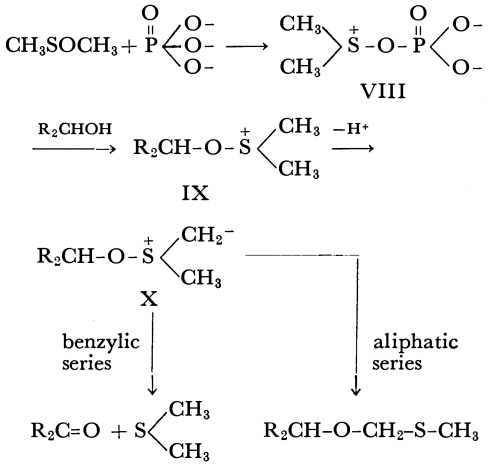

Experimental

α-(Bromomesityl)benzyl Alcohol. Benzoylbromomesitylene[15] was reduced with lithium aluminum hydride in the usual manner. Colorless prisms, mp 65—67°C, were then obtained in a 95% yield by recrystallization from benzene - petroleum ether.

Found: C, 62.77; H, 5.51%. Calcd for $C_{16}H_{17}OBr$: C, 62.96; H, 5.61%.

IR (KBr): 3450 and 1150 cm^{-1}.

Acetylation with acetic anhydride containing pyridine afforded an acetate as colorless prisms, mp 99—100°C.

Found: C, 62.07; H, 5.21%. Cacld for $C_{18}H_{19}O_2Br$: C, 62.25; H, 5.51%.

Bis[α-(Bromomesityl)benzyl] Ether. To 32 g of PPA, 2.0 g (6.6 mmol) of the above alcohol was added, after which the mixture was heated on a water bath for 15 min. The reaction mixture was then diluted with water, and the crystalline material was recrystallized from benzene - ethanol to give 1.5 g (77% yield) of colorless prisms, mp 147—149°C. After five successive recrystallizations, the melting point was raised to 176—177°C.

Found: C, 64.51; H, 5.51%. Calcd for $C_{32}H_{32}OBr_2$: C, 64.87; H, 5.45%.

The combined mother liquors were evaporated, and the residue was passed through an alumina column, using petroleum ether as an eluent; thereby we obtained another compound, mp 152—154°C which was assumed to be a structural isomer.

The Reaction with DMSO. *a) Bis(diphenylmethyl) Ether (IVd).* A mixture of IIId in DMSO was heated at 165—170°C under various conditions, summarized in Table 3. After the reaction was over, the mixture was diluted with water and the resulting IVd was recrystallized from ethanol; mp 108—109°C (lit. 108°C).

9) Recently, however, DMSO-P_2O_5 was used for the oxidation of carbohydrates, see K. Onodera, S. Hirano and N. Kashimura, *J. Am. Chem. Soc.*, **87**, 4651 (1965).

10) Compound B which arose *via* A may be responsible for the origin of methylthio group as well as formaldehyde.

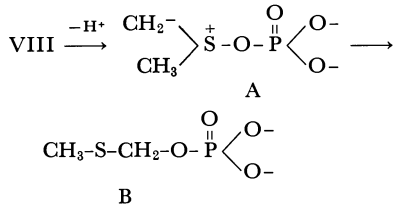

11) J. B. Jones and R. C. Wigfield, *Tetrahedron Letters*, **1965**, 4103.

12) K. E. Pfitzner and J. G. Moffatt, *J. Am. Chem. Soc.*, **87**, 5670 (1965).

13) J. D. Albright and L. Goldman, *ibid.*, **87**, 4214 (1965).

14) An alternative mechanism[12,13] which postulates the intermediacy of $CH_3\overset{+}{S}=CH_2$ has also been advanced, see also K. E. Pfitzner and J. G. Moffatt, *J. Am. Chem. Soc.*, **87**, 5661 (1965).

15) J. F. Hyde and R. Adams, *ibid.*, **50**, 2503 (1928).

Table 3. Bis(diphenylmethyl) ether (IVd) formation reaction at 165—170°C

IIId mol	DMSO mol	Time hr	Yield of IVd, %
0.03	0.6	4	63
0.03	0.6	8	88
0.02	0.02	8	68
0.08	0.4	8	66
0.03	0.6	24	82

No ether formation was observed when IIId itself or a diethylene glycol solution was heated at 165—170°C for 11—18 hr.

b) Bis[α-(bromomesityl)benzyl] Ether. A mixture of 3.0 g (0.01 mol) of α-(bromomesityl)benzyl alcohol and 15.6 g (0.2 mol) of DMSO was heated at 165—170°C for 16 hr. Colorless prisms, mp 156.5—158°C, were thus obtained (0.6 g). The IR spectra agreed with the product obtained by the PPA dehydration reaction described above.

c) Bis(9-fluorenyl) Ether. A mixture of 3.6 g (0.02 mol) of 9-hydroxyfluorene and 31.2 g (0.4 mol) of DMSO was heated at 165—170°C for 24 hr. The recrystallization of the product from ethanol afforded 0.2 g of bis(9-fluorenyl) ether, mp 223—225°C (lit. 228°C). The rest of the material was analyzed by column chromatography on alumina, using benzene - chloroform - ethanol as an eluent; this afforded 0.2 g of an unidentified yellow solid, mp 232—237°C, 0.3 g of bis(9-fluorenyl) ether (total yield 14.3%), and 1.2 g (33.4%) of 9-fluorenone, mp 73—76°C, together with the starting material (14.3% recovery).

The same experiment carried out at 165—185°C for 25 hr afforded a 56% yield of 9-fluorenone.

d) Attempted Reaction of Benzyl Alcohol. A mixture of 5.4 g (0.05 mol) of benzyl alcohol and 78 g (1.0 mol) of DMSO was heated at 160—170°C for 20 hr. A part of the reaction mixture was then treated with a 2, 4-dinitrophenylhydrazine solution to give a 15.7% yield of the benzaldehyde hydrazone, mp 231.5—234°C. About 60% of the starting alcohol was recovered by simple distillation.

Methylthiomethyl Ether (II). *a) Cyclohexyl Methylthiomethyl Ether (II, R=Cyclohexyl).* The treatment of cyclohexanol with DMSO-PPA afforded,[6] in addition to a 44% yield of dicyclohexyloxymethane (I, R=cyclohexyl), a fraction which boiled at 97—99°C/15 mmHg. From its IR and NMR spectra it was identified as II (R=cyclohexyl), it was obtained in a 8.6% yield.

NMR (CCl_4): δ 4.58 (2H), 3.60 (1H), 2.08 (3H) and 1.1—1.8 (10H).

Found: C, 60.85; H, 10.10%. Calcd for $C_8H_{16}OS$: C, 59.98; H, 10.07%.

b) (−)-Menthyl Methylthiomethyl Ether (II, R=Menthyl). The same reaction as above but using (−)-menthol furnished a 28.9% yield of dimenthyloxymethane (I, R=menthyl), bp 207°C/23 mmHg, mp 58°C and a 4.5% yield of II (R=menthyl), bp 138—140°C/17 mmHg.

NMR (CCl_4): δ 4.62 (2H), 3.45 (1H), 2.08 (3H) and 0.7—2.3 (18H).

Found: C, 67.15; H, 11.26%. Calcd for $C_{12}H_{24}OS$: C, 66.63; H, 11.18%.

The Reaction with DMSO-PPA. *a) Benzyl Alcohol (IIIa).* To a mixture which had been prepared under cooling by adding 78 g (1.0 mol) of DMSO to 54 g of 80% PPA, 21.6 g (0.2 mol) of IIIa was added. After the reaction mixture had then been heated on a water bath for 5 hr, it was diluted with water and extracted with diisopropyl ether. A part of the extract was treated with a 2, 4-dinitrophenylhydrazine solution to give the benzaldehyde hydrazone in a 9.5% yield. The rest of the material was chromatographed through an alumina column, using *n*-hexane containing an increasing amount of ether; this eluted VIIa, IVa (10% yield), Va (16% yield), and unreacted IIIa successively. All the compounds had satisfactory NMR and IR spectra compared with the authentic specimens (Table 2). By gas chromatography using Carbowax-1500 on celite-408 column, VIa, VIIa, IIIa, IVa, and Va (in the order of the retention time) were identified. As VIIa tended to co-distill with *n*-hexane, the yield for this material (13% yield) was obtained from the gas chromatographical measurements.

b) p-Nitrobenzyl Alcohol (IIIb, X=NO_2). A mixture of 7.6 g (0.05 mol) of IIIb (X=NO_2), 19.5 g (0.25 mol) of DMSO, and 13.5 g of PPA was heated at water-bath temperature for 5 hr. A 20% yield of aldehyde VIb (X=NO_2) was then attained by converting it to 2, 4-dinitrophenylhydrazone.

Column chromatography on alumina using benzene as an eluent furnished sulfide VIIb (X=NO_2) in a yield of 4.9%.

Found: C, 52.51; H, 4.85; N, 7.28%. Calcd for $C_8H_9O_2NS$: C, 52.46; H, 4.95; N, 7.65%.

No ether formation was observed, and the next fraction contained acetal Vb (X=NO_2) as colorless needles mp 98—99°C; it was isolated in a 46% yield.

Found: N, 8.70%. Calcd for $C_{15}H_{14}O_6N_2$: N, 8.80%.

In one experiment, benzaldehyde bis(*p*-nitrobenzyloxy) acetal was isolated from the reaction mixture as a colorless, amorphous material, mp 202—206°C.

Found: N, 9.52%. Calcd for $C_{21}H_{17}O_8N_3$: N, 9.56%.

c) p-Substituted Benzyl Alcohols (IIIb). The same reaction was applied to a series of IIIb. The yields of the benzaldehydes formed are tabulated in Table 4.

Table 4. The formation of benzaldehydes (VIb) from *p*-substituted benzyl alcohols (IIIb)

IIIb	Yield of VIb, %
X: CH_3O	11
CH_3	9.4
H	8.5
Cl	39[a]
NO_2	20

a) Including *p*-chlorobenzoic acid.

d) 1-Phenylethanol (IIIc). A mixture of 24 g (0.2 mol) of IIIc, 120 g (1.5 mol) of DMSO, and 50 g of PPA was heated on a water bath for 5 hr. The diisopropyl ether extract was then distilled to give a 19% yield of styrene, bp 63—70°C/70 mmHg, and a 27% yield of the ether IVc, bp 158—162°C/70 mmHg,

n_D^{21} 1.5375. From the intermediate fraction, acetophenone (VIc) was isolated as 2, 4-dinitrophenylhydrazone (0.5% yield).

e) Benzhydrol (IIId). A mixture of 4.8 g (0.025 mol) of IIId, 9.8 g (0.125 mol) of DMSO, and 6.8 g of PPA was brought into the reaction as above. When water was then added to the reaction mixture, IVb was isolated as colorless plates, mp 102—104°C. From the filtrate, benzophenone was isolated as 2, 4-dinitrophenylhydrazone in a 13% yield. The diisopropyl ether extract of the filtrate was analyzed by alumina-column chromatography.

n-Hexane eluted VIId, mp 33—33.5°C, in a yield of 20%. The sulfide VIId was also isolated, together with benzophenone, by the direct distillation of the reaction mixture.

Found: C, 78.59; H, 6.34; S, 14.82%. Calcd for $C_{14}H_{14}S$: C, 78.48; H, 6.59; S, 15.00%.

BULLETIN OF THE CHEMICAL SOCIETY OF JAPAN VOL. 41 225—229 (1968)

The Use of Carbon Monoxide in Low-temperature Sintering of High-density UO_2 Pellets*1

Kazuhide MIYAZAKI

Central Research Laboratories, Mitsui Mining & Smelting Co., Mitaka-shi, Tokyo

(Received May 27, 1967)

The fundamental effects of carbon monoxide on UO_2-pellet densification are described. A high density of more than 95% of the theoretical level is attained using carbon monoxide as the sintering atmosphere at a low sintering temperature of 1400°C for laboratory-processed UO_2 powders. An approximate prediction of the density for any given UO_2 powder may be made from the following two experimental criteria: (a) The experimental activation energy for the rate of dissolution of the material into nitric acid may be taken as a measure for the low-temperature sinterability. The density of sintered oxides rises to a maximum at a point where the value of the activation energy for dissolution is about 20 kcal/mol, which is actually very close to the value for the diffusion of oxygen in uranium oxides. (b) The relative intensity of the (220) peak of the X-ray diffraction pattern furnishes another foundation for judging the densification behavior of the UO_2 sample.

The present investigation is primarily concerned with basic data aimed at uncovering the role of carbon monoxide, which has seldom been used in uranium dioxide industries, in obtaining high-density UO_2 pellets at a low sintering temperature. The sinterabilities are, therefore, examined in the neighborhood of 1400°C instead of in the conventional 1600—1800°C range.

Various approaches have long been taken by many workers to lower the sintering temperature of uranium dioxide. For instance, non-stoichiometric uranium oxide containing an excess of oxygen[1] increases the degree of sintering. Small amounts of such additives as TiO_2 and CaO have been proposed[2,3] as binding materials between grains of sintered uranium dioxide. In some cases, uranium dioxide has been blended with U_3O_8 to prepare a non-stoichiometric uranium oxide mixture and the sintering temperature has been reduced to as low as 1300°C; however, the sintered product here was actually $UO_{2.30}$.[4] Moreover, an irradiation test elsewhere has indicated that the O/U ratio of the fuel should be less than 2.15 if we are to minimize cracking and fission gas release.[5]

In the present work, experimentation is carried out to examine the possibility of lowering the sintering temperature by using carbon monoxide to participate in a reduction-sintering schedule for a high-density pellet of more than 95% of the theoretical level. Also, we propose to describe the densification behavior in terms of the activation energy for the rate of dissolution in nitric acid and a specific X-ray diffraction peak of UO_2 powder as practical criteria for judging the feasibility of the material for use in low-temperature sintering.

Experimental

Materials. The materials were prepared at an elevated temperature by the simultaneous thermal decomposition and reduction of the ammonium diuranate

*1 A part of this work was presented to The 15th Annual Meeting of The Chemical Society of Japan, Kyoto, 1962.

1) P. Murray *et al.*, *TID-7546*, 432 (1957).
2) C. Y. Ang and E. W. Burkhammer, *J. Nucl. Mat.*, **2**, No. 2, 176 (1960).
3) H. G. Sowman and G. L. Ploetz, *KAPL-1556*, 1956.
4) K. Langrod, *Ceram. Bull.*, **39**, No. 7, 366 (1960).
5) O. J. C. Runnalls, *Nucleonics*, **17**, 104 (1959).

precipitate obtained from a purified nitrate solution. Commercially-available tank hydrogen and/or carbon monoxide were used as the reducing gas; the purities of these gases were graded as 99.9% H_2 and 99.5% CO respectively. Reducing gas was introduced into the inlet of the laboratory tube furnace with a static charge for several hours at an elevated temperature. The O/U ratio determinations were performed by the oxidation method, which involved igniting the original uranium dioxides to U_3O_8 in air and establishing the weight gain,[6,7] the composition of the starting materials was in the range of $UO_{2.07-2.11}$. The thermobalance technique was employed to simultaneously observe the thermogravimetric characteristics of the starting uranium dioxides in the course of the O/U ratio determinations. The UO_2 powders were stored in N_2-filled polyethylene containers.

Sintering Tests. The straight cold-press-and-sinter powder metallurgical technique was used. The granulations were performed by a method similar to that described by Langrod.[4] A high-chromium stainless steel-lined mold was designed to obtain an optimum lubrication of compact UO_2 under pressing as well as to eliminate the need for costly carbide dies. No additives were used to flux the grain boundaries of UO_2 at a low sintering temperature, the granulated powder was compacted into pellets 1.0 cm in diameter at a pressure of 3 tons/cm^2. The rather low compacting pressure of 3 tons/cm^2 was employed to insure a amooth release from the die and to minimize the cracking frequently incurred on green products under higher compacting pressures. The pellets were then sintered at 1400°C with an experimental furnace, either in an atmosphere of carbon monoxide or in hydrogen gas flowing through the furnace, and the densities were measured with the lapse of the sintering time. The density of the sintered UO_2 pellet was determined from the weight and geometrical dimensions of the pellet.[7] A dial-depth gauge was used to read the mean values of the diameter and length of the sintered UO_2 body.[8]

Characterization of UO_2 Powder in Relation to the Sintering Behavior. Two tests were performed in an attempt to devise a measure to characterize the sinterability of UO_2 powder. The various UO_2 powders used were prepared either by the pyrolysis of various precipitates of ammonium diuranate or by the partial air-oxidization of the reduced UO_2 samples. Oxide samples with O/U ratios in the range of 2.05—2.16 were thus obtained. In this paper a new experimental criterion will be proposed for judging the low-temperature sinterability of UO_2 in terms of another physico-chemical property rather than the well-known O/U ratio of the material.

(a) Determination of the Activation Energy for Nitric Acid Dissolution. One gram of the oxide was immersed in 100 m*l* of 1 N nitric acid. A test tube-type glass container was used as the dissolution cell, and the dissolution temperature was controlled to ±1°C throughout the run by means of a water-bath. After a given time has elapsed the cell was incorporated into a centrifugal machine and a 1-m*l* aliquot of the supernatant liquid was pipetted out, thus the dissolved amount of UO_2 milligrams could be determined over several time-intervals as measured in minutes. The total liquid volume consumed for the analysis of the dissolved UO_2 was not more than 5 m*l* per 100 m*l*. Arrhenius plots of the dissolution rate constant for the nitric acid solution were made at 15, 30, 40, and 60°C.

(b) Intensities of X-ray Diffraction Peaks. The deviation in relative intensities of the X-ray diffraction peaks of a given UO_2 powder was examined in terms of the density of the pellet when sintered. As a standard of the intensities, the ASTM Card listing the Swanson and Fuyat data[9] for $UO_{2.03}$ was used. An X-ray instrument was operated with the following set of conditions: Target, Cu; filter, Ni; voltage, 30 kV; current, 10 mA; divergency, 1°, and G. M. counting self-rocorder.

Results and Discussion

Figure 1 shows that, when a hydrogen atmosphere is used for sintering, the use of carbon monoxide in part or wholly as the reducing gas replacing the conventional H_2 reduction will be effective in obtaining more densified products in the relatively shorter period of sintering time of less than about 9 hr at 1400°C. However, the conventional hydrogen-reduced UO_2 powder gradually exceeds the pellet's density with the lapse of sintering time. The maximum density shown in Fig. 1 was still less than 95% as a fraction of the theoretical density, 10.97 g/cc, obtained by the use of carbon monoxide as the reducing gas.

On the other hand, the use of carbon monoxide as the sintering atmosphere densificates significantly higher when hydrogen-reduced UO_2 powder is provided for sintering, as is shown in Fig. 2. It is interesting to note that the combination of hydrogen reduction and carbon monoxide sintering is particularly beneficial for a low-temperature operation. In this case a density of more than 10.6 g/cc (*i. e.*, 96.6% of the theoretical level) is achieved in a firing time of 10 hr. Otherwise, however, the participation of carbon monoxide in the reduction gas will not appreciably contribute to the densification. It may be seen that carbon monoxide can more advantageously be employed as a sintering atmosphere than as a reducing gas.

A further comparison of carbon monoxide and hydrogen as a sintering atmosphere was made by two-stage sintering tests through the medium of nitrogen gas. At the firing temperature of 1400°C green compacts pressed with a hydrogen-reduced UO_2 sample were first sintered in an atmosphere of nitrogen, and then the atmosphere was successively switched over either to hydrogen or carbon monoxide. Figure 3 illustrates the surprising result that the successive introduction of hydrogen

6) W. T. Bourns and L. C. Watson, *A. E. C. L.-757, CRCE-716*, 3 (1958).
7) N. Fuhrman, L. D. However, Jr., and R. B. Holden, *J. Am. Ceram. Soc.*, **46**, 114 (1963).
8) H. K. Lonsdale, *Nucl. Sci. Abstr.*, **16** (17); Abstr. No. 22590 (1962).
9) H. E. Swnson and R. K. Fuyat, *Natl. Bur. Standards (U. S.) Circ.*, No. 539, Vol. II, 33 (1953).

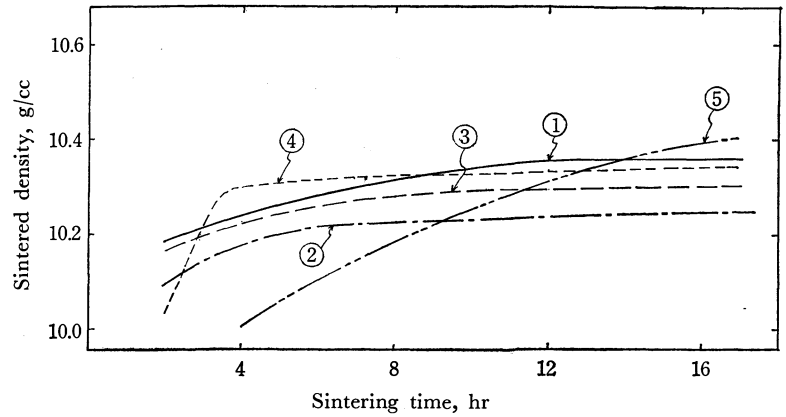

Fig. 1. Sintered density of carbon monoxide-reduced UO_2 pellets sintered in atmospheres of carbon monoxide in part or overall. (1): Sintered in CO, (2): in H_2+2CO, (3): in H_2+CO, (4): in $2H_2+CO$, and (5): in H_2, at 1400°C.

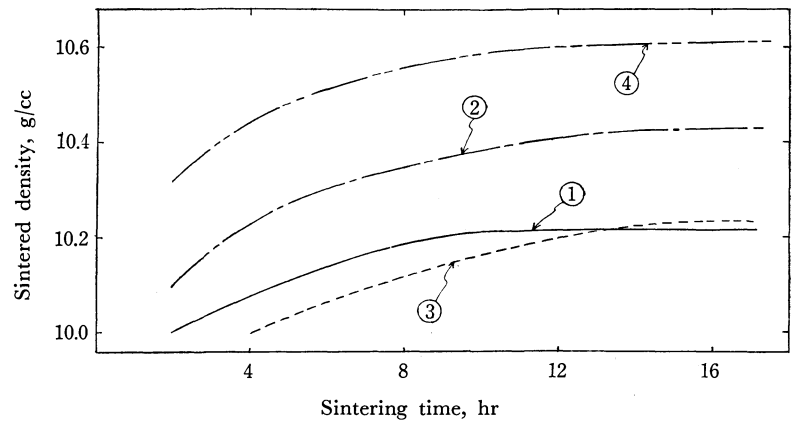

Fig 2. Sintered density of hydrogen-reduced UO_2 pellets sintered in atmospheres of carbon monoxide in part or overall. (1): Sintered in CO, (2): in H_2+2CO, (3): in $2H_2+CO$, and (4): in H_2, at 1400°C.

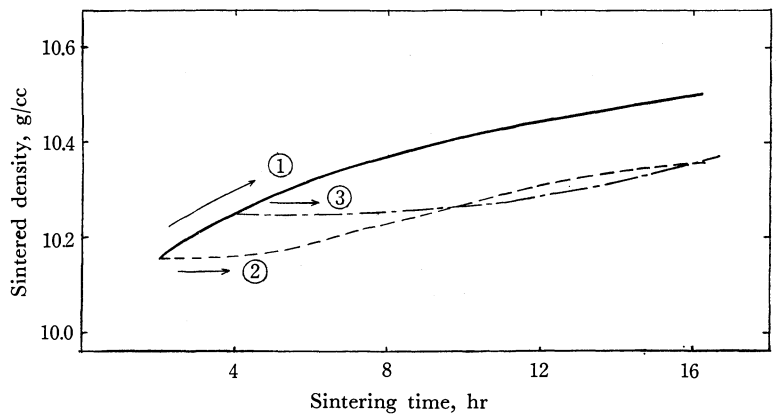

Fig. 3. Two-stage sintering in nitrogen followed by hydrogen atmosphere *versus* sintering time at 1400°C, with the use of hydrogen-reduced UO_2 pellets. (1): Sintered in N_2 only, (2): Sintering in H_2 after 2 hr sintering in N_2, and (3): Sintering in H_2 after 4 hr sintering in N_2.

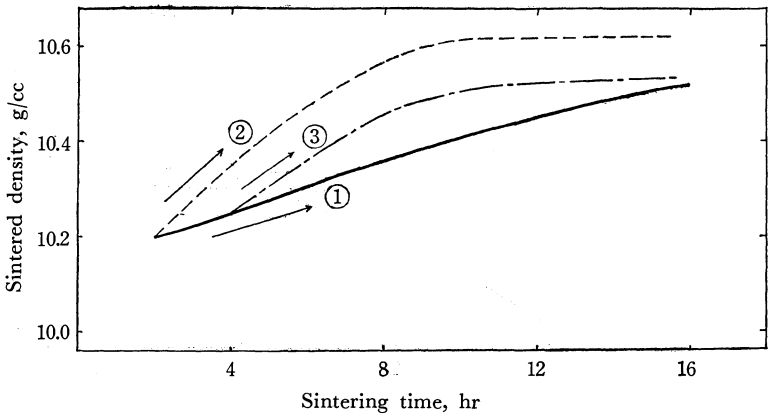

Fig. 4. Two-stage sintering in nitrogen followed by carbon monoxide atmosphere *versus* sintering time at 1400°C, with the use of hydrogen-reduced UO_2 pellets. (1): Sintered in N_2 only, (2): Sintering in CO after 2 hr sintering in N_2, and (3): Sintering in CO after 4 hr sintering in N_2.

hindered the densification of the pellets; *i. e.*, the density of the product, which would otherwise be increased along with the initial sintering atmosphere, was considerably decreased by admitting the hydrogen gas.

It is worth noting, on the other hand, that the nitrogen firing, followed by carbon monoxide-introduction, was remarkably effective in the densification of the product, as is shown in Fig. 4, where a density of 10.6 g/cc is obtained by a 2-hr nitrogen sintering plus a 7-hr carbon monoxide sintering. It is also interesting to observe in this case that the pellet which is treated longer with nitrogen (*e. g.*, 4 hr) emerges with a lower sintered density than that described above in spite of the successive carbon monoxide treatment.

The dissolution process into nitric acid as regards sintered pellets was undertaken by Taylor *et al.*[10] in an attempt to provide data for the design of a plant for the continuous dissolution of uranium oxide fuel in nitric acid; the sintered pellets exhibited activation energies of about 15 kcal/mol for much higher nitric acid concentrations.

However, the raw-material UO_2 has not yet been dissolved as a measure for describing the densification behavior. An examination of the Arrhenius plots for the nitric acid dissolution rates of the raw-material UO_2 powders has shown that the values of the activation energy vary from sample to sample, ranging from 12 to 24 kcal/mol; typical examples are illustrated in Fig. 5. Accordingly, it is clear from Fig. 6 that, with an increase in the activation energy up to about 20 kcal/mol, the pellet density sintered in carbon monoxide also increases up to a maximum of about 10.6 g/cc, while that with the higher activation energies, beyond 20 kcal/mol, shows an inferior densification

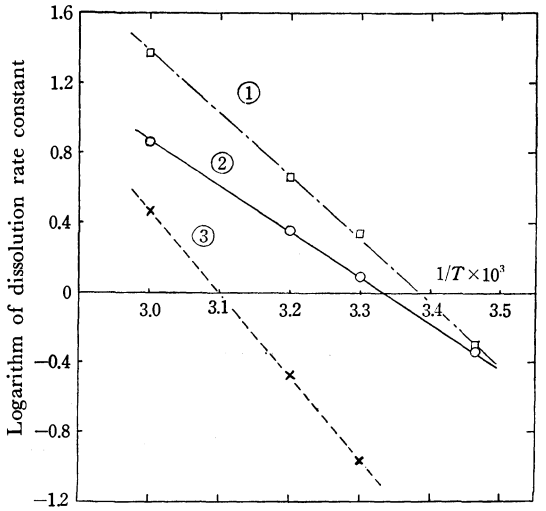

Fig. 5. Arrhenius plot of dissolution rates for typical UO_2 samples. (1): 10 g U/*l*, no-washed ADU, simultaneous decomposition and reduction by H_2; $E=16$ kcal/mol, (2): 100 g U/*l*, washed ADU, decomposition before reduction by H_2, $E=12$ kcal/mol, (3) 100 g U/*l*, no-washed ADU, with decomposition before reduction by H_2, $E=22$ kcal/mol.

behavior.

It is also of interest to survey several values of the activation energies for the diffusion of oxygen in uranium oxides investigated elsewhere and to compare these values with the value of 20 kcal/mol obtained for the maximum sinterability in terms of nitric acid dissolution. Ristic and Kostic[11] obtained 20.2 kcal/mol for the sintering of UO_2. Stamenkovic and Ristic[12] obtained 24.5

10) R. F. Taylor, E. W. Sharratt, L. E. M. de Chazal and D. H. Logsdail, *J. Appl. Chem.*, **13**, 32 (1963).

11) M. M. Ristic and E. Kostic, *Nucl. Sci. Abstr.*, **17** (19), Abstr. No. 32658 (1963).

12) I. Stamenkovic and M. M. Ristic, *Keram. Z.*, **16** (9), 561 (1964).

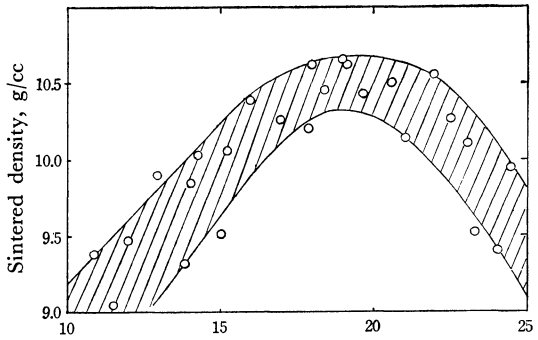

Fig. 6. Nitric acid dissolution activation energies of UO_2 powders *versus* sintered densities of the UO_2 pellets at 1400°C with carbon monoxide.

kcal/mol for the oxidation of UO_2 powders at 172—220°C. Walder[13] determined the value of activation energies for the oxidation of UO_2 at 120—360°C to be 20—27 kcal/mol. Therefore, it appears possible to say that the activation energies exhibited by the two independent phenomena, the dissolution of UO_2 into nitric acid and the self-diffusion of oxygen in solid UO_2, come very close to each other in magnitude, suggesting that the mechanism of the self-diffusion of oxygen which takes place in oxidation and the sintering of UO_2 powders can possibly be described by analogy with the behavior in the nitric acid dissolution of the material. At this early stage of investigation, however, it is impossible to extend say anything further about this problem.

Most importantly, however, it may be pointed out that the value of the activation energy for nitric acid dissolution will provide an approximate measure for judging the sinterability of a given UO_2 powder, being one of the outstanding characteristics inherited from the foregoing powder production process.

In parallel with this, the X-ray diffraction patterns of the prepared UO_2 samples were examined in order to obtain another convenient characteristic measure for dealing with their low-temperature sinterability. Figure 7 plots the deviations of the relative intensities of the (220) peak against the sintered densities at 1400°C obtained in an atmosphere of carbon monoxide. As a standard reference of the relative intensity of the (220) peak, the ASTM Card gives the value of 49 as the fraction of the intensity of (111), which is taken as 100.

The plots in Fig. 7 have been distributed around a well-defined convexity to the above; it may be seen that the sintered density rises to a maximum at the point where the relative intensity of (220) is slightly stronger than the standard value of 49, and then decreases. It can not yet be decided

13) D. B. Y. Walker, *J. Appl. Chem.*, **15**, 128 (1965).

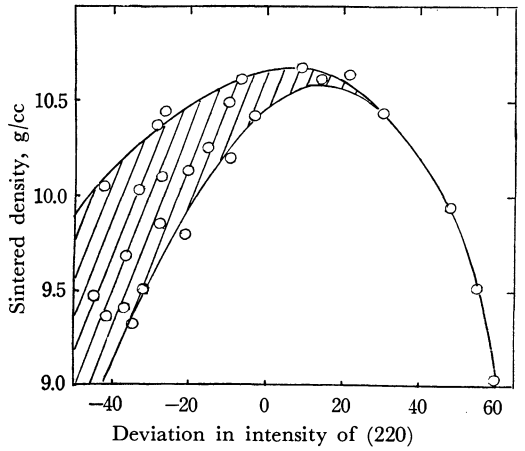

Fig. 7. Deviations in relative intensity of (220) X-ray diffraction peak of UO_2 powders *versus* the sintered densities at 1400°C with carbon monoxide.

whether this slight shift from neutral is substantially significant or whether it is a mere experimental discrepancy. Figure 7 implies, however, that a lattice disorder, if any, present in the UO_2 crystalline phase will possibly act as a resistance to the sound composition of UO_2 grains when sintered at a minimum sintering temperature such as 1400°C. At the same time, it is of interest to note that a UO_2 sample with a stronger intensity for the (220) peak was much less frequently encountered among the laboratory-produced UO_2 powders in comparison with one with a weaker intensity of the peak.

It should be noted that the examination of the relative intensity for a specific X-ray peak of UO_2 powder seems, particularly with an industrial point of view, to be a quite feasible criterion for making a quick estimation regarding the low-temperature sinterability.

Summary

The effect of carbon monoxide on the densification of UO_2 pellets was examined at around 1400°C instead of in the conventional 1600—1800°C range. A high density (above 95% of the theoretical level) was obtained using carbon monoxide as the sintering atmosphere.

The densities of the sintered UO_2 pellets were related to the activation energy of the dissolution rate for a nitric acid solution and a specific X-ray diffraction peak of UO_2 powder. The density showed a maximum for the UO_2 samples with an activation energy of about 20 kcal/mol. The densification behavior was inferior in a UO_2 powder with much deviations from the standard relative intensity of the (220) peak. The above two characteristics furnish experimental criteria for judging the low-temperature sinterability of UO_2 samples.

NOTES

Studies of Seven-membered Heterocyclic Compounds Containing Nitrogen. IX. The Synthesis of 5-Ethoxycarbonyl-1-azacycloheptan-4-one and Its Derivatives

Tamon MORIYA, Toichi OKI, Seiki YAMAGUCHI, Shiro MOROSAWA and Akira YOKOO

Department of Chemistry, Faculty of Science, Okayama University, Tsushima, Okayama

(Received February 22, 1967)

As an extension of our previous study[1] of the synthesis of the seven-membered ring ketone containing nitrogen through the reaction of 1-benzyl-1-azacyclohexan-4-one (I) with nitrosomethylurethane, the ring expansion of I and 1-ethoxycarbonyl-1-azacyclohexan-4-one (II) has been carried out using ethyl diazoacetate.

The ring expansion of I was examined first, using zinc chloride as a catalyst, according to the method of Eistert *et al.*,[2] the product, 1-benzyl-5-ethoxycarbonyl-1-azacycloheptan-4-one (III), was isolated as a hydrochloride. The yield of the reaction was 20%. This was improved to 34% by the use of boron trifluoride etherate as a catalyst, according to the method developed by Tal and Warnhoff.[3] In neither case, however, was it possible to isolate the free base (III) by the direct distillation of the reaction mixture, but III liberated from its hydrochloride was safely distilled. The decarboxylation of III by refluxing it with hydrochloric acid yielded the hydrochloride of 1-benzyl-1-azacycloheptan-4-one (V), which was found, by a mixed-melting-point determination and by a comparison of IR spectra, to be identical with an authentic sample.[1] The ring expansion of II, using boron trifluoride etherate, furnished 1, 5-diethoxycarbonyl-1-azacycloheptan-4-one (IV). IV was also derived from III by hydrogenolysis and subsequent ethoxycarbonylation.

III and IV gave the corresponding derivatives (VII—X) of a type of pyrazole or pyrazolone when treated with hydrazine or phenylhydrazine, while they gave normal 2, 4-dinitrophenylhydrazones. Debenzylation by the hydrogenolysis of VII in the presence of hydrochloric acid gave a hydrochloride of compound XI. A similar compound (XII) was obtained by the hydrogenolysis of VIII. XII was also derived from VI.

The methylation of III afforded 1-benzyl-5-ethoxycarbonyl-5-methyl-1-azacycloheptan-4-one (XIII). XIII was converted into 1-ethoxycarbonyl-5-methyl-1-azacycloheptan-4-one (XIV) by decarboxylation and debenzylation, followed by ethoxycarbonylation.

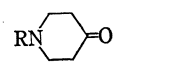

(I) R=$PhCH_2$
(II) R=COOEt

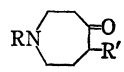

(III) R=$PhCH_2$, R'=COOEt
(IV) R=R'=COOEt
(V) R=$PhCH_2$, R'=H
(VI) R=H, R'=COOEt
(XIV) R=COOEt, R'=CH_3

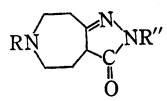

(VII) R=$PhCH_2$, R''=H
(VIII) R=$PhCH_2$, R''=Ph
(IX) R=COOEt, R''=H
(X) R=COOEt, R''=Ph
(XI) R=R''=H
(XII) R=H, R''=Ph

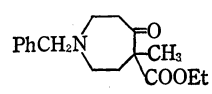

(XIII)

Experimental

Procedure for Ring Expansion of I and II. Into a solution of 0.28 mol of I or II in dry ether, maintained at −50——60°C, these were vigorously stirred, drop by drop, a solution of 0.26 mol of a freshly-distilled boron trifluoride etherate in 50 cc of dry ether and a solution of 0.85 mol of ethyl diazoacetate in 100 cc of dry ether were added. The addition of the two solutions was started simultaneously; it took 30 min for the addition of the former solution, and 100 min for the latter. After the reaction mixture had been stirred for an additional 30 min at the same temperature, the stirring was continued until the temperature of the mixture reached room temperature. The mixture was then shaken with a 20% aqueous potassium carbonate solution, and the ether layer was separated. The water layer was extracted with ether. The organic layer

1) S. Morosawa, This Bulletin, **31**, 418 (1958).
2) B. Eistert, F. Haupter and K. Schank, *Ann.*, **665**, 55 (1963).
3) W. T. Tal and E. W. Warnhoff, *Can. J. Chem.*, **42**, 1333 (1964).

was dried over anhydrous potassium carbonate, and then treated in either of the ways shown below. (I): Dry hydrogen chloride was passed through to the organic layer, thus depositing a hydrochloride of III. This was recrystallized from ethanol. (II): After the solvent had been removed from the organic layer, IV was distilled under reduced pressure. The following results were obtained: III·HCl, yield, 34%, mp 164.5°C (dec.). Found: C, 61.68; H, 7.13; N, 4.55%. Calcd for $C_{16}H_{21}O_3N$·HCl: C, 61.63; H, 7.11; N, 4.49%; III, bp 160—162°C/0.4 mmHg. Found: C, 69.65; H, 7.50; N, 5.02%. Calcd for $C_{16}H_{21}O_3N$: C, 69.78; H, 7.68; N, 5.08%; Hydrochloride of 2, 4-dinitrophenylhydrazone, mp 179°C (dec.); IV, yield, 30.5%, bp 133—135°C/0.15 mmHg. Found: C, 56.33; H, 7.87; N, 5.45%. Calcd for $C_{12}H_{19}O_5N$: C, 56.02; H, 7.44; N, 5.42%; 2, 4-dinitrophenylhydrazone, mp 119.5°C.

The hydrochloride of VI was obtained by the hydrogenolysis of the hydrochloride of III in ethanol, using palladium as a catalyst. Yield, 81%, mp 133—134°C. Found: C, 49.03; H, 7.42; N, 6.44%. Calcd for $C_9H_{15}O_3N$·HCl: C, 48.75; H, 7.28; N, 6.32%; VI, bp 112—114°C/0.6 mmHg. Found: C, 58.01; H, 8.37; N, 7.39%. Calcd for $C_9H_{15}O_3N$: C, 58.36; H, 8.16; N, 7.55%.

The Preparation of VII—X. A mixture of III (1 equiv.), hydrazine hydrate (2 equiv.), and ether was warmed on a water bath for 15 min. In a similar method, each of the following mixtures was warmed for 1—3 hr; III·CHl (1 equiv.), hydrochloride of phenylhydrazine (1 equiv.), sodium acetate (2 equiv.), and water; IV (1 equiv.) and hydrazine hydrate (1 equiv.); IV (1 equiv.) and phenylhydrazine (1 equiv.). The following results were obtained: VII, yield, 95%, mp 220°C (dec.). Found: C, 69.61; H, 7.63; N, 17.03%. Calcd for $C_{14}H_{17}ON_3$: C, 69.20; H, 7.05; N, 17.29%; VIII, yield, 92%, mp 198°C (dec.). Found: C, 75.22; H, 6.61; N, 12.84%. Calcd for $C_{20}H_{21}ON_3$: C, 75.21; H, 6.63; N, 13.13%; IX, yield, 35%, mp 242—243°C (dec.). Found: C, 53.24; H, 6.65; N, 18.87%. Calcd for $C_{10}H_{15}O_3N_3$: C, 53.35; H, 6.72; N, 18.66%; X, yield, 76%, mp 144.5°C. Found: C, 63.93; H, 5.96; N, 13.58%. Calcd for $C_{16}H_{19}O_3N_3$: C, 63.77; H, 6.32; N, 13.95%.

XI and XII were prepared by the hydrogenolysis of VII and VIII in ethanol, (in the case of VII, the ethanol contained hydrochloric acid) by using palladium as a catalyst: XI·HCl, yield, 46%, mp 270°C (dec.). Found: C, 38.02; H, 6.54; N, 18.92%. Calcd for $C_7H_{11}ON_3$·2HCl: C, 37.71; H, 6.24; N, 18.58%. XII, yield, 41%, mp 203—204°C (dec.). Found: C, 63.34; H, 6.84; N, 16.70%. Calcd for $C_{13}H_{15}ON_3$·H_2O: C, 63.14; H, 6.93; N, 16.99%.

Preparation of XIII. To a solution of 1.2 g of metallic sodium in 20 cc of absolute ethanol, there was added a solution of 8 g of the hydrochloride of III in a small amount of absolute ethanol with stirring and ice-salt cooling. After 30 min of stirring, 3.7 g of methyl iodide was added, drop by drop, over a 10 min period, and then the stirring was continued for 2 more hours. After a large amount of water had been added to the reaction mixture, it was extracted with benzene. XIII was distilled under reduced pressure from the benzene layer; (yield 33%), colorless oil, bp 171—173°C/0.2 mmHg. Found: C, 70.69; H, 7.78; N, 4.48%. Calcd for $C_{17}H_{23}O_3N$: C, 70.95; H, 7.95; N, 4.83%.

Preparation of XIV. A mixture of 2.4 g of XIII and 70 cc of 4 N hydrochloric acid was refluxed for 2.5 hr, concentrated under reduced pressure, and made alkaline by adding solid potassium carbonate. The liberated oil was separated and hydrogenolized in 30 cc of water containing 0.1 cc of concentrated hydrochloric acid, in the presence of palladium chloride as a catalyst. After the removal of the catalyst, the solution was concentrated under reduced pressure. To the residue were added 7 cc of a 5% potassium hydroxide solution and 1.5 g of anhydrous potassium carbonate under ice-water cooling. Into the mixture was added 1.5 g of ethyl chloroformate under stirring. After 1 hr of stirring, XIV was extracted with ether. Colorless oil, bp 93—95°C/0.1 mmHg. Found: C, 60.17; H, 8.23; N, 6.51%. Calcd for $C_{10}H_{17}O_3N$: C, 60.35; H, 8.54; N, 7.03%. 2, 4-Dinitrophenylhydrazone, yellow plates (from ethanol), mp 145—146°C, Found: C, 50.54; H, 5.72; N, 18.46%. Calcd for $C_{16}H_{21}O_6N_5$: C, 50.65; H, 5.42; N, 18.46%.

Nuclear Magnetic Resonance Spectra of Carbanions. I. 1, 1-Diphenylethylene Dimer Dianion

Kensuke TAKAHASHI and Ryuzo ASAMI

Department of Industrial Chemistry, Nagoya Institute of Technology, Gokiso-cho, Showa-ku, Nagoya

(Received April 25, 1967)

Carbanions are of particular interest from the standpoint of their charge distribution, since the excess charges are substantially larger than in neutral molecules. Only a few NMR studies have been carried out on carbanions, particularly some organolithium compounds[1] and the cyclopentadienyl anion.[2] 1, 1-Diphenylethylene dissolved in

1) V. R. Sandel and H. H. Freedman, *J. Am. Chem. Soc.*, **85**, 2328 (1963); R. Waack, M. A. Doran, E. B. Baker and G. A. Olah, *ibid.*, **88**, 1272 (1966).

2) G. Fraenkel, R. E. Carter, A. McLachlan and J. H. Richards, *ibid.*, **82**, 5846 (1960).

THF gives colored solutions in contact with excess alkali metals at room temperature for about twenty-four hours. These colored solutions served as samples for the NMR measurements. The evolved reaction in THF might be expressed as follows:[3]

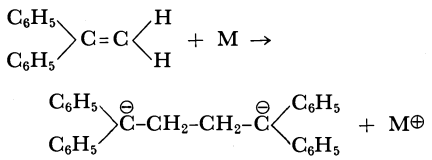

Typical spectra are shown in Fig. 1, representing a solution produced from 1, 1-diphenylethylene in contact with potassium sodium alloy in THF.[4] The peaks in the region of aromatic protons are clearly divided into three, appearing as a doublet, a triplet, and a triplet respectively from the lower to the higher field. Since their intensity ratios are 2 : 2 : 1, it seems that they can be assigned to the peaks of ortho-, meta-, and para-protons respectively, similar to those of triphenylmethyllithium in THF as assigned by Sandel and Freedman.[1] The chemical shifts are given in Table 1, in which the solvent peak serves as an internal reference (the higher-field peak of THF is taken to be at 1.79 ppm from TMS). The chemical shifts

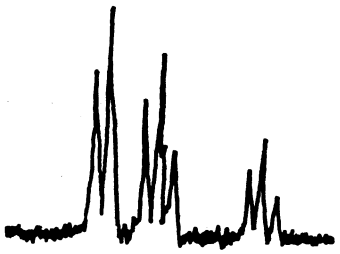

Fig. 1. The spectrum in the region of aromatic protons of the carbanion produced from 1, 1-diphenylethylene in contact with excess potassium sodium alloy in THF. Applied magnetic field increases from left to right, at 60 Mcps.

Table 1. The chemical shifts of aromatic protons of carbanions produced from 1, 1-diphenylethylene in contact with excess alkali metals in THF, in ppm at 60 Mcps

Metal used	Assignment		
	Ortho	Meta	Para
Potassium	7.01	6.55	5.67
Sodium	7.18	6.61	5.75
Lithium	7.03	6.49	5.66

between the ortho- and para-protons amount to about 1.4 ppm, but they are not sensitive to the kind of alkali metal. The chemical shift values shown in Table 1 exhibit shifts to a higher field as compared with that of benzene, which shows an absorption at 7.32 ppm in THF. Since the shift of about 10 ppm is assumed to be the contribution of one excess electron,[2] more than fifty per cent of the negative charge of the 1, 1-diphenylethylene dimer dianion might be located on the phenyl rings,[1] but this is only a rough estimate because we lack information on carbons with no protons and on methylene groups. In the solutions of these carbanions, a single peak is observed near 2.5 ppm, just between two large solvent peaks. The 1, 1, 4, 4-tetraphenylbutane which was prepared by treating these carbanions with water shows PMR signals at 2.00, 3.88, and 7.14 ppm in a carbon tetrachloride solution; these signals are identified as coming from the methylene, methine, and phenyl protons in this compound respectively. From this knowledge, the peak at 2.5 ppm mentioned above might be assigned as coming from the methylene protons in the carbanion. If this assignment is correct, one interesting point is the shift towards a lower field of the methylene protons of the carbanion as compared to those of the corresponding hydrocarbon; this shift can not be attributed to the charge, but it may be due to the change in the hybridization of the carbon atom from the hydrocarbon to the carbanion.

The carbanions produced from α-methylstyrene and cumyl methyl ether also showed large higher-field shifts in the aromatic regions of the spectra. These will be described later elsewhere.

3) W. Schlenk, J. Appernodt, A. Michael and A. Thal, *Ber.*, **47**, 473 (1914); M. Szwarc, *J. Polymer Sci.*, **C1**, 339 (1963).

4) Only potassium reacts with 1, 1-diphenylethylene.

The Reaction of Disulfides with Dinitrogen Tetroxide

Norio KUNIEDA and Shigeru OAE

Department of Applied Chemistry, Faculty of Engineering, Osaka City University, Sumiyoshi-ku, Osaka

(Received May 4, 1967)

Dinitrogen tetroxide displays a unique feature in various oxidation processes. It can restrict a reaction to a single oxidation stage, when further oxidation still appears to be possible. Several workers have, therefore, used this reagent for the oxidation of alkyl,[1] aryl,[2] and alicyclic[3] sulfides to the corresponding sulfoxides.

In this note, we would like to report the oxidation of several disulfides with this reagent; this oxidation was carried out in a manner similar to the oxidation of sulfides.[2] We expected that the oxidation of disulfides with this reagent would proceed to yield, successively, thiolsulfinates (RSO·SR), thiolsulfonates (RSO_2SR), and disulfones (RSO_2SO_2R), since such a step-by-step oxidation is known to take place in the oxidation reaction of disulfides with hydrogen peroxide[4] or peroxy acids.[5] However, when alkyl or aryl disulfides were allowed to react with an excess of dinitrogen tetroxide in carbon tetrachloride, only the corresponding sulfonic anhydrides were obtained in good yields; neither thiolsulfinates nor thiolsulfonates were obtained. The yields and melting or boiling points of the products are listed in Table 1.

These products were allowed to react with aniline to afford the corresponding sulfonanilides quantitatively. In an attempt to isolate a possible intermediate of this reaction, diethyl disulfide (7.0 g, 0.057 mol) was treated with an equimolar amount of dinitrogen tetroxide (5.2 g, 0.057 mol), but only ethanesulfonic anhydride (4.7 g) was thus obtained, together with the recovered disulfide (2.8 g); no other intermediary products could be detected.

We have also found that *p*-toluenesulfonic anhydride was obtained in a 94% yield when *p*-toluenethiolsulfinate was treated with an excess of this reagent in a manner similar to that used for the disulfides, but *p*-tolyl *p*-toluenethiolsulfonate and *p*-tolyl disulfone did not react with this reagent, even without a solvent.

In view of these results, it is not probable that the oxidation of disulfides with this reagent proceeds through a step-by-step oxidation involving the successive formation of thiolsulfonate, sulfinylsulfone, and disulfone, such as is the case with peroxy acids; rather, it appears to proceed in a fashion similar to that which Barnard has postulated for the ozonolysis of disulfides.[6] However, further investigation is necessary before we can obtain any clear understanding of the dinitrogen tetroxide oxidation.

Experimental

Materials. *Disulfides* were prepared by the oxidation of the corresponding mercaptans with iodine by the method described by McAllan.[10]

TABLE 1. YIELDS OF SULFONIC ANHYDRIDES (RSO_2OSO_2R)

R	Yield, %	Mp or bp (°C) (lit)	Elemental analysis			
			Found, %		Calcd, %	
			C	H	C	H
CH_3	85	69.5—70.5 (69.5—70)[7]				
C_2H_5	78	110—110.5/3 mmHg (94/0.5 mmHg)[7]	23.91	5.05	23.76	4.98
n-C_3H_7	74	131.5—132/4 mmHg ($85/10^{-3}$ mmHg)[6]				
C_6H_5	81	88—90.5 (88—91)[8]				
p-CH_3-C_6H_4	92	129.5—131 (129.5—131.5)[8]	51.17	4.47	51.50	4.32
p-Cl-C_6H_4	90	149—151 (150)[9]				

1) L. Horner and F. Hübenett, *Ann.*, **579**, 193 (1953); C. C. Addison and J. C. Sheldon, *J. Chem. Soc.*, **1956**, 2705.
2) S. Oae, N. Kunieda and W. Tagaki, *Chem. & Ind.*, **1965**, 1790.
3) C. R. Johnson, *J. Am. Chem. Soc.*, **86**, 2935 (1964); R. D. Whitaker and H. H. Sisler, *J. Org. Chem.*, **25**, 1038 (1965).
4) W. G. Christiansen and M. A. Dolliver, U. S. Pat. 2242236 (1941); B. Weibull, *Arkiv Kemi*, **3**, 171 (1951).
5) H. J. Backer, *Rec. Trav. Chim.*, **67**, 894 (1948); C. J. Cavallito and La. V. D. Small, U. S. Pat. 2508745 (1950).
6) D. Barnard, *J. Chem. Soc.*, **1957**, 4547.
7) L. Field and P. H. Setlage, *J. Am. Chem. Soc.*, **76**, 1222 (1954).
8) L. Field, *ibid.*, **74**, 394 (1952).
9) V. O. Lukaskenich, *Dokl. Akad. Nauk, S.S.S.R.*, **114**, 1025 (1957).
10) D. T. McAllan, T. V. Cullum, R. A. Dean and F. A. Fidler, *J. Am. Chem. Soc.*, **73**, 3629 (1951).

p-Tolyl p-Toluenethiolsulfinate was prepared by the reaction of *p*-tolyl mercaptan with *p*-toluenesulfinyl chloride. Mp 94—94.5°C, yield 92%.

p-Tolyl p-Toluenethiolsulfonate was prepared by the oxidation of di-*p*-tolyl disulfide with hydrogen peroxide. Mp 77—78°C, yield 86%.

p-Tolyl Disulfone was prepared by the reaction of sodium *p*-toluenesulfinate with *p*-toluenesulfonyl chloride. Mp 206—206.5°C, yield 83%.

Dinitrogen Tetroxide was prepared by the pyrolysis of dinitrogen pentoxide.[11]

Reaction of Disulfides with Dinitrogen Tetroxide. The carbon tetrachloride solution of dinitrogen tetraoxide was cooled under 0°C, then a solution of disulfides, in which the mole ratio of the disulfide to the dinitrogen tetroxide was 1 : 3—5, was added slowly. The mixture was kept standing for 2 hr under 0°C, and then warmed at 30—50°C for 2 hr. Finally the mixture was distilled under reduced pressure to remove the excess reagent and solvent. The residual crude products were distilled or recrystallized. Methane-, benzene-, *p*-toluene-, and *p*-chlorobenzenesulfonic anhydrides were recrystallized from ether-benzene.

Sulfonanilides. The sulfonic anhydrides were dissolved or suspended in dry ether into which two molar equivalent of aniline had been added, then the anilinium sulfonate thus formed was filtered off. In this manner the sulfonanilides were obtained from the filtrate in good yields. ($C_6H_5NHSO_2R$); (R, mp(°C) (Lit)); (CH_3, 99(96)[12]), (C_2H_5, 59—60(55)[12]), (C_6H_5, 108.5 (112)[13]), (*p*-CH_3-C_6H_4, 101—102(101—102.5)[14]), (*p*-Cl-C_6H_4, 104.5 (105.5)[15]).

The Reaction of *p*-Tolyl *p*-Toluenethiolsulfinate with Dinitrogen Tetroxide. *p*-Tolyl *p*-toluenethiolsulfinate was reacted with 4.6 times the molar quantity of dinitrogen tetroxide in the same treatment as that used for disulfides. The anhydride was thus obtained in a 94% yield; mp 130—130.5°C.

11) A. Pedler and F. H. Pollard, "Inorganic Syntheses," Vol. V, ed. by T. Moeller, McGraw-Hill Book Company, Inc., N. Y. (1957), pp. 87—90.

12) A. G. Kastova, *Zh. Obshch. Khim.*, **22**, 1433 (1952).

13) E. Yu. Tsekhanovich, I. Ya. Pastovskiĭ and V. F. Degtyrev, *ibid.*, **25**, 1162 (1955).

14) D. Klamann and H. Bertsh, *Chem. Ber.*, **92**, 2610 (1959).

15) V. O. Lukashevich, *Dokl. Akad. Nauk, S.S.S.R.*, **99**, 995 (1954).

Sesquiterpene Hydrocarbons of the Essential Oil of the Kusunoki (*Cinnamomum Camphora Sieb.*)

Shûichi HAYASHI, Nanao HAYASHI, Katsumi YANO, Masayoshi OKANO and Tamon MATSUURA

Department of Chemistry, Faculty of Science, Hiroshima University, Hiroshima

(Received May 9, 1967)

The investigation concerning sesquiterpene constituents of camphor oil was first undertaken by workers at Schimmel & Co., who detected bisabolene[1] and cadinene;[2] it was then continued by many workers. In this way, caryophyllene was identified by Simonsen,[3] α-santalene by Kato,[4] and α-humulene and nerolidol by Hirota,[5] while recently cadina-9, 11(12)-diene has been detected by Araki.[6] Further, Ono,[7] Komatsu[8] and Kafuku[9] have pointed out the presence of new sesquiterpene constituents characteristic of camphor oil.

The present study was made of a high-boiling fraction of camphor oil commercially obtained. Nine newly-found constituents, α-ylangene, β-elemene, β-santalene, δ-guaiene, δ-cadinene, calamenene, calacorene, 1, 6-dimethyl-4-isopropyl-7, 8-dihydronaphthalene, and γ-patchoulene, and four formerly-detected constituents, caryophyllene, α-santalene, α-humulene, cadina 9, 11(12)-diene, were identified. α-Santalene, α-ylangene, β-santalene, and δ-cadinene are the main constituents, each amounting to more than ten per cent, while cadina-9, 11(12)-diene, which was detected as a main constituent by Araki,[6] was very little in quantity. It was the first case of the detection of 1,6-dimethyl-4-isopropyl-7,8-dihydronaphthalene in a natural product. The bisabolene previously reported and the constituents whose structures were

1) Ber. Schimmel & Co., April, **1889**, 9.
2) *Ibid.*, October, **1909**, 24.
3) J. L. Simonsen and T. P. Ghose, *J. Soc. Chem. Ind.*, **39**, 296 T (1920).
4) T. Katô, T. Mukai and T. Nozoe, 3rd Symposium on the Chemistry of Terpenes, Essential Oils and Aromatics, Tokyo, 1959.
5) N. Hirota and M. Hiroi, *The Kôryô*, No. 70, 23 (1962).
6) M. Araki, T. Ôhara, T. Yamada and R. Gotô, *Nippon Kagaku Zasshi (J. Chem. Soc. Japan, Pure Chem. Sect.)* **87**, 63 (1966).
7) K. Ono, *Mem. Coll. Science Imp. Univ. Kyoto*, **8**, 1 (1925).
8) S. Komatsu, H. Fuzimoto and S. Tanaka, *Nippon Kwagaku Kwaishi (J. Chem. Soc. Japan)*, **51**, 489 (1930).
9) K. Kafuku, T. Ikeda and M. Kato, *ibid.*, **54**, 311 (1933).

assumed by Ono,[7] Komatsu[8] and Kafuku[9] could not be detected.

Experimental

The high-boiling fraction (bp above 215°C, 6135 g) of camphor oil, after being treated with 3% aqueous solutions of sodium carbonate and of sodium hydroxide successively, was distilled under reduced pressure; the sesquiterpene hydrocarbon fraction (bp 85—145°C/2 mmHg) was thus obtained. By repeating the precise fractionation with a packed-type distillation column, and the adsorption chromatography on an alumina or silica gel column using *n*-hexane, the hydrocarbon fraction was separated into individual hydrocarbons; these hydrocarbons were identified as will be described below.

α-Ylangene (17.7%).*1 Found: C, 88.39; H, 11.61%. Calcd for $C_{15}H_{24}$: C, 88.16; H, 11.84%. The constituent consumed one equivalent of hydrogen in catalytic hydrogenation with platinum oxide in glacial acetic acid. The IR[10] and NMR[11] spectra of the original hydrocarbon coincided with those of α-ylangene; this spectrometric result was also supported by a gas chromatographic comparison with authentic α-ylangene.

β-Elemene (5.0%). The constituent ($[\alpha]_D^{25}$ −21.0°) showed IR[12] and NMR[13] spectra, and the gas chromatogram agreed with those of β-elemene.

α-Santalene (34.8%). Found: C, 87.85; H, 11.71%. Calcd for $C_{15}H_{24}$: C, 88.16; H, 11.84%. This hydrocarbon ($[\alpha]_D^{25}$ +11.1°) had a molecular weight of 204 (mass spectrometry, Fig. 1-A), and its IR[14] and NMR[15] spectra agreed with those of α-santalene. Besides, a nitrosochloride of colorless needles melted at 115—115.5°C, thus corresponding to α-santalene nitrosochloride.[16]

β-Santalene (12.0%). Found: C, 88.30; H, 11.70%. Calcd for $C_{15}H_{24}$: C, 88.16; H, 11.84%. The molecular weight of this hydrocarbon was 204 (mass spectrometry, Fig. 1-B). Its IR[14] and NMR[15] spectra showed a good agreement with those of β-santalene.

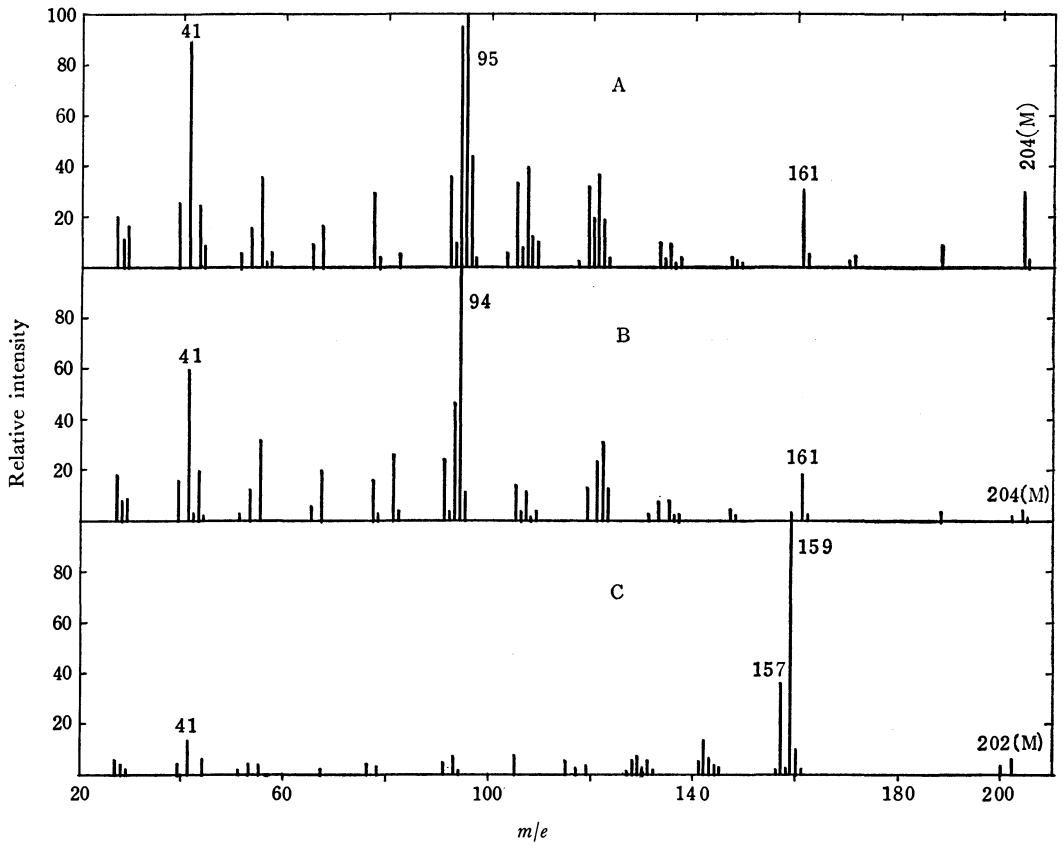

Fig. 1. Mass spectra of α-santalene (A), β-santalene (B) and calamenene (C).

*1 The content (%) of each constituent was calculated from the relative peak area of the gas chromatogram, which was obtained by use of a Golay Apiezon-L column at 150°C, and which showed 21 peaks, including 8 unidentified ones.

10) G. L. K. Hunter, Chemist, Fruit and Vegetable Products Laboratory, Fla., private communication.

11) O. Motl, V. G. Bucharov, V. Herout and F. Šorm, *Chem. & Ind.*, **1963**, 1759.

12) C. Asselineau and J. Asselineau, *Bull. Soc. Chim. France*, **1957**, 1361.

13) M. Takahashi, K. Isoi, Y. Kimura and M. Yosikura, *J. Pharm. Soc. Japan*, **84**, 752 (1964).

14) V. Herout, V. Jarolím and J. Plíva, *Coll. Czech. Chem. Commn.*, **22**, 775 (1957).

15) E. J. Corey, R. Hartmann and P. A. Vatakencherry, *J. Am. Chem. Soc.*, **84**, 2611 (1962).

16) M. Guerbet, *Compt. Rend.*, **130**, 417, 1324 (1900).

α-Humulene (2.5%). The constituent had the same IR spectrum as that of α-humulene,[17] and the gas chromatograms of the constituent and α-humulene were identical.

δ-Guaiene (0.2%). The constituent was dehydrogenated by heating with sulfur and produced s-guaiazulene in a good yield. The IR spectrum and the gas chromatogram of the constituent agreed with those of δ-guaiene,[18] and the NMR spectrum, which has two broad singlets at 5.36—5.62 τ (2H, exocyclic methylene) and two near-singlets at 8.37 τ (6H, two methyl groups attached to double bonds,) supported the structure of δ-guaiene well.

δ-Cadinene (11.2%). Found: C, 88.35; H, 11.58%. Calcd for $C_{15}H_{24}$: C, 88.16; H, 11.84%. $[\alpha]_D^{25}$ +24.54°, molecular weight 204 (mass spectrometry). The IR,[19] NMR,[20] and mass spectra[21] agreed with those of δ-cadiene. This hydrocarbon produced cadinene dihydrochloride; 116—116.5°C, confirmed admixing.

Calamenene (2.5%). When the residue of the precise fractional distillation was chromatographed on a silica-gel adsorption column using petroleum ether as the solvent, calamenene, calacorene, and 1, 6-dimethyl-4-isopropyl-7, 8-dihydronaphthalene were eluted in this order. The first-eluted constituent ($[\alpha]_D^{25}$ −44.0°) had a molecular weight of 202 (mass spectrometry, Fig. 1-C). The IR[22] and NMR[23] spectra and the gas chromatogram were the same as calamenene.

Calacorene (0.4%). $[\alpha]_D^{25}$ +15.40°. The IR[19] and UV[19] spectra agreed with those of calacorene, and the NMR spectrum, which has a singlet at 7.74 τ (3H, a methyl group on a double bond conjugated with a benzene ring) and a doublet at 8.05 τ (3H, methyl group), fit the structure of calacorene well.

1, 6-Dimethyl-4-isopropyl-7, 8-dihydronaphthalene (0.3%). The IR and UV spectra of this constituent agreed with those of 1, 6-dimethyl-4-isopropyl-7, 8-dihydronaphthalene.[24]

Caryophyllene (3.0%), **γ-Patchoulene** (0.6%), **and Cadina-9, 11(12)-diene** (2.3%) were identified only by depending upon a gas chromatographic comparison with authentic specimens using a Golay Apiezon-L column.

The authors are indebted to Professor Shô Ito of Tohoku University for his measurement of the NMR spectra and Mr. Hiroshi Sato of the Hitachi Co., Ltd., for his measurement of the mass spectra.

17) V. Benesova, V. Herout, B. Schneider and F. Šorm, *Coll. Czech. Chem. Commn.*, **26**, 1834 (1961).
18) J. Plíva, M. Horâk, V. Herout and F. Šorm, "Die Terpen Sammlung der Spektren und physikalischen Konstanten," Teil I, Berlin (1960), p. 138.
19) J. Plíva, V. Herout, B. Schneider and F. Šorm, *Coll. Czech. Chem. Commn.*, **18**, 500 (1953).
20) P. de Mayo, R. E. Williams, G. Büchi and S. H. Feairheller, *Tetrahedron*, **21**, 619 (1965).
21) G. L. K. Hunter and W. B. Brogden, *Anal. Chem.*, **36**, 1122 (1964).
22) S. Hayashi, K. Yano and T. Matsuura, This Bulletin, **37**, 474 (1964).
23) B. N. Joshi, R. Seshadri, K. K. Charavarti and S. C. Bhattacharyya, *Tetrahedron*, **20**, 2911 (1964).
24) Ref. 18, p. 72.

Synthesis of Adamantane Derivatives. I. Application of the Ritter Reaction to 1-Bromoadamantane

Tadashi SASAKI, Shoji EGUCHI and Takeshi TORU

Institute of Applied Organic Chemistry, Faculty of Engineering, Nagoya University, Chikusa-ku, Nagoya

(Received May 15, 1967)

The Ritter reaction is known to be an excellent method for the preparation of amides from tertiary alcohols, tertiary halides, or olefins.[1] Recently adamantane derivatives have attracted much attention, for the practical purpose of their pharmacological activity[2] and for their theoretical interest for organic chemists.[3] Stetter *et al.* have used the Ritter reaction to prepare *N*-1-adamantylacetamide from 1-bromoadamantane and acetonitrile[4]; more recently Haaf has reported a modified procedure, in which adamantane has been directly amidated in the presence of tertiary carbonium ions with hydrogen cyanide.[5] From our repetition of the above two methods, we found that Haaf's method always gave many by-products, which caused a lowering of the yield of the main product, and that, furthermore, the procedure of Haaf's method was more complicated than that of Stetter's. From these reasons we chose 1-bromoadamantane, easily obtainable from adamantane,[6] as the starting material.

1) a) J. Ritter and P. Minieri, *J. Am. Chem. Soc.*, **70**, 4045 (1948); b) J. Ritter and J. Kalish, *ibid.*, **70**, 4048 (1948); c) F. Benson and J. Ritter, *ibid.*, **71**, 4128 (1949); d) L. Hartzel and J. Ritter, *ibid.*, **71**, 4130 (1949); e) R. Lusskin and J. Ritter, *ibid.*, **72**, 5577 (1950).

2) For example, K. Gerson, E. Krumkalns, R. Brindle, F. Marshall and M. Root, *J. Med. Chem.*, **6**, 760 (1963).

3) For a recent review, see R. Fort, Jr., and P. von R. Schleyer, *Chem. Revs.*, **64**, 277 (1964).

4) H. Stetter, J. Mayer, M. Schwarz and K. Wulff, *Chem. Ber.*, **93**, 226 (1960).

5) W. Haaf, *ibid.*, **97**, 3234 (1964).

6) H. Stetter, M. Schwarz and A. Hirschhorn, *ibid.*, **92**, 1629 (1959).

Results and Discussion

The formation of amides by the Ritter reaction of 1-bromoadamantane can be explained by the following reaction scheme:

$$\underset{\text{I}}{\text{Ad-Br}} + H_2SO_4 \rightleftarrows \underset{\text{II}}{\text{Ad}^{\oplus}HSO_4^{\ominus}} + HBr \quad \text{(a)}$$

$$\underset{\text{II}}{\text{Ad}^{\oplus}HSO_4^{\ominus}} + RCN \rightleftarrows \underset{\text{III}}{\text{Ad-N=C}^{\oplus}\text{-R}\cdot HSO_4^{\ominus}} \quad \text{(b)}$$

$$\underset{\text{III}}{\text{Ad-N=C}^{\oplus}\text{-R}\cdot HSO_4^{\ominus}} + H_2O \rightarrow \underset{\text{IV}}{\text{AdNHCOR}} \quad \text{(c)}$$

Consequently, it might be expected that the formation of an intermediate adamantyl immonium ion complex, III, is a key factor in carrying

Table 1. *N*-1-Adamantylamides from the reaction of 1-bromoadamantane with various nitriles[a]

Run No.	Nitrile	Molar ratio of RCN to AdBr	Solvent	React. time	Product	Yield[c] %
1	CH_3CN	30	None	12 hr	$AdNHCOCH_3$[d]	90
2	$(CH_3)_2CHCN$	10	None	17	$AdNHCOCH(CH_3)_2$	78
3	$CH_3(CH_2)_2CN$	10	None	42	$AdNHCO(CH_2)_2CH_3$	56
4	$CH_2=CHCN$[b]	1	AcOH	48	$AdNHCOCH=CH_2$	84
5	C_6H_5CN	30	None	6	$AdNHCOC_6H_5$	66.5
6	$NCCH_2CO_2C_2H_5$	10	*n*-Bu_2O	48	$AdNHCOCH_2CO_2C_2H_5$	53
7	$NCCH_2CN$	10	*n*-Bu_2O & AcOH (1 : 2)	20	$AdNHCOCH_2CN$	64
8	$NC(CH_2)_2CN$	10	*n*-Bu_2O & AcOH (1 : 2)	48	$AdNHCO(CH_2)_2CN$	20
9	H_2NCH_2CN	5	*n*-Bu_2O & AcOH (1 : 1)	62	Not isolated	
10	NH=CNHCN NH_2	10	*n*-Bu_2O & AcOH (4 : 1)	62	Not isolated	
11	$NCCH_2CONH_2$	5	*n*-Bu_2O & AcOH (2 : 3)	11 days	Not isolated	

a) Reactions were carried out at room temperature (about 20°C) in the presence of 6 mol of conc. H_2SO_4 except where otherwise noted.
b) The reaction was carried out at 40°C in the presence of 1 mol of conc. H_2SO_4 and 1 mol of BF_3-Et_2O.
c) The yields were calculated on the products recrystallized once.
d) See Ref. 4.

Table 2. Properties of *N*-1-adamantylamides

Amide (mp, °C)	IR(KBr), cm^{-1}			Formula		Anal. %		
	ν_{NH}	Amide-I & II				C	H	N
$AdNHCOCH(CH_3)_2$	3250	1640		$C_{14}H_{23}ON$	Found	75.76	10.82	6.37
(147)		1550			Calcd	75.97	10.47	6.33
$AdNHCO(CH_2)_2CH_3$	3300	1650		$C_{14}H_{23}ON$	Found	75.62	10.84	6.51
(119—120)		1550			Calcd	75.97	10.47	6.33
$AdNHCOCH=CH_2$	3440	1670	1630[a]	$C_{13}H_{19}ON$	Found	75.12	9.41	6.84
(155—156)		1520			Calcd	76.05	9.33	6.82
$AdNHCOC_6H_5$	3440	1655	1580[b]	$C_{17}H_{21}ON$	Found	80.13	8.38	5.33
(149—150)		1515			Calcd	79.96	8.29	5.49
$AdNHCOCH_2CO_2C_2H_5$	3360	1670	1720[c]	$C_{15}H_{23}O_3N$	Found	67.93	8.79	5.26
(103—104)		1550			Calcd	67.89	8.74	5.28
$AdNHCOCH_2CN$	3440	1690	2280[d]	$C_{13}H_{18}ON_2$	Found	71.29	8.52	12.84
(147—148)		1530			Calcd	71.52	8.31	12.83
$AdNHCO(CH_2)_2CN$	3260	1650	2240[e]	$C_{14}H_{20}ON_2$	Found	72.45	8.01	12.60
(194—195)		1560			Calcd	72.38	8.68	12.06

a) $\nu_{C=C}$ b) Phenyl $\nu_{C=C}$ c) Ester $\nu_{C=O}$ d, e) $\nu_{C\equiv N}$

out the Ritter reaction successfully. However, it is known that 1-bromoadamantane is less reactive than other nonbridged tertiary halides because of the difficulty of forming the carbonium ion, II.[7] Since both reactions, (a) and (b), are thought to be reversible, the use of excess concentrated sulfuric acid and nitrile seems to favor the formation of II and, therefore, of III. In order to carry out the reaction homogeneously, liquid nitriles such as *n*-butyronitrile, isobutyronitrile, and benzonitrile were used as the solvents, but when nitriles could not be used as the solvents because of the solid state or low solubility of 1-bromoadamantane, *n*-butyl ether, glacial acetic acid or their mixture was used as the solvent. All of the results, including the products, are summarized in Table 1. From this table it may be seen that most amides were prepared in good yields, but the reactions with some nitriles which have strong electron-withdrawing groups, such as dicyandiamide, cyanoacetamide, and acetaminonitrile, were not successful. This fact can be explained by the lowered electron density of the nitrile group and, thus, the smaller affinity with the adamantyl carbonium ions. When 1-bromoadamantane was treated with acrylonitrile in concentrated sulfuric acid, many side reactions were observed involving polymerizations, from which none of the expected acrylamide derivatives could be separated. However, when the reaction was carried out in acetic acid by using a mixture of concentrated sulfuric acid and boron trifluoride etherate as a catalyst at 40°C, the desired *N*-1-adamantylacrylamide was obtained in a yield of 84%.

7) P. von R. Schleyer and R. Nicholas, *J. Am. Chem. Soc.*, **83**, 2700 (1961).

Experimental

The microanalyses were performed on a Yanagimoto C. H. N. Corder, Model MT-1, while the IR spectra were obtained on a JASCO Model IR-S infrared spectrophotometer. All the melting points were measured on a Yanagimoto micromelting-point apparatus and are uncorrected.

General Procedure of the Ritter Reaction. The reaction was carried out at room temperature by using an excess of nitrile and of concentrated sulfuric acid to 1-bromoadamantane. After making sure by the thin-layer chromatography that no more 1-bromoadamantane existed in the reaction mixture, the mixture was poured onto cracked ice-water and the product was extracted with ether. The ether layer was dried over anhydrous sodium sulfate and evaporated to dryness to give a crude amide. Crude amide was usually purified by recrystallization from aqueous methanol, and in some cases by chromatography on a silica-gel column. The results are summarized in Table 1. Table 2 shows the analytical and some physical properties of these products.

Synthesis of Adamantane Derivatives. II.[1] Preparation of Some Derivatives from Adamantylacetic Acid

Tadashi SASAKI, Shoji EGUCHI and Takeshi TORU

Institute of Applied Organic Chemistry, Faculty of Engineering, Nagoya University, Chikusa-ku, Nagoya

(Received July 31, 1967)

Adamantylacetic acid (I) was prepared in 1959 for the first time by Stetter and his co-workers[2] through the Arndt-Eistert rearrangement of the corresponding diazoketone; recently Bott and Hellmann[3] have prepared it in good yields directly from vinylidene chloride and 1-bromoadamantane, which is now commercially available.*1 The present paper will deal with the syntheses of some derivatives starting from adamantylacetic acid (I). Acid chloride II was obtained by stirring a mixture of I and thionyl chloride diluted with petroleum ether at room temperature for two days, since heating I with thionyl chloride without a solvent lowered the yield of II and some decomposition products were observed. II was an oily material exhibiting an infrared band at 1810 cm^{-1} (ν_{CO}) and was used for the following reactions directly, without any further purification.

The treatment of this crude II with an excess amount of ethereal diazomethane gave adamantyl acetyl diazomethane III as an oil (ν_{N_2} at 2160 cm^{-1} and ν_{CO} at 1630 cm^{-1}), which was identified by the formation of adamantylpropionyl anilide IV, mp 154—155°C, after irradiation in the presence of aniline. The reaction of II with such amines as ammonia and aniline gave the corresponding amides, in those cases Va and Vb respectively, in good yields.

The Hofmann reaction of Va with bromine and alkali afforded crystalline solids with mps of

1) Part I: T. Sasaki, S. Eguchi and T. Toru, This Bulletin, **41**, 236 (1968).
2) H. Stetter, M. Schwarz and A. Hirschhorn, *Chem. Ber.*, **92**, 1629 (1959).
3) K. Bott and H. Hellmann, *Angew. Chem.*, **78**, 932 (1966).
*1 Aldrich Cat. No. 967 (1967).

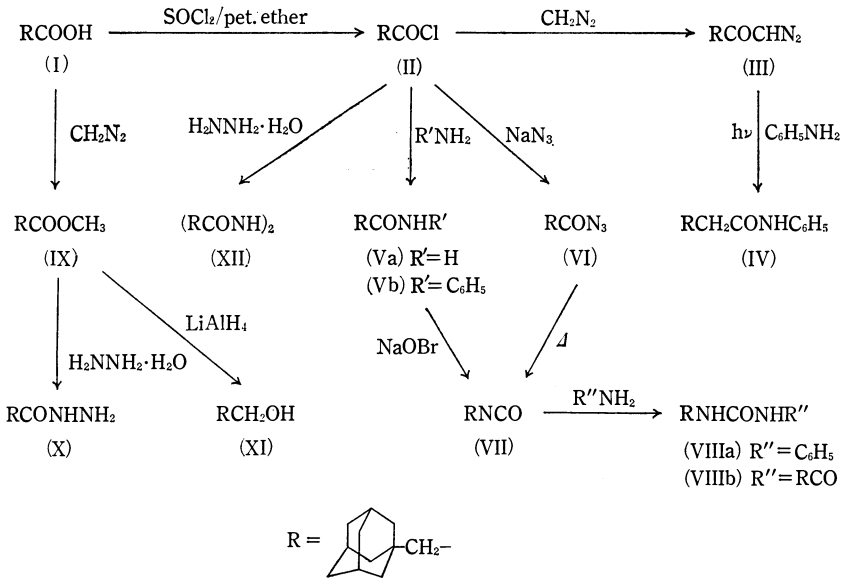

Scheme 1. Reactions of adamantylacetic acid.

254—255°C (dec.) in 76.5% yield based on I. The structure of this compound was identified as VIIIb on the basis of the results of the microanalysis and the infrared spectrum. The formation of the isocyanate (VII) as an intermediate was confirmed by the appearance in the course of the reaction of a band at 2280 cm^{-1} (ν_{NCO}) in the infrared spectrum of the reaction mixture, but it could not be isolated.

On the contrary, this isocyanate (VII) could be separated as an oil (ν_{NCO} at 2280 cm^{-1}) in a good yield by the Curtius rearrangement of acid azide VI, which was easily obtainable as an oil (ν_{N_3} at 2150 cm^{-1} and ν_{CO} at 1715 cm^{-1}) from II and sodium azide. The isocyanate structure of VII was confirmed by its conversion to the corresponding urea derivative, VIIIa, with aniline.

Acid chloride II and hydrazine hydrate afforded the corresponding bishydrazide XII, while methyl adamantylacetate IX and hydrazine hydrate gave monohydrazide X. The lithium aluminum hydride reduction of IX gave adamantylethanol XI with a mp of 73.5—75.0°C.

All of these results are summarized in Scheme 1.

Experimental

Microanalyses were performed on a Yanagimoto C. H. N. Corder Model MT-1, while the IR spectra were obtained on a JASCO Model IR-S infrared spectrophotometer. All the melting points were measured on a Yanagimoto micromelting-point apparatus and have not been corrected.

Adamantyl-1-acetamide (Va). Concentrated aqueous ammonia (11.0 m*l*) was, over a period of 30 min, stirred, drop by drop, into a stirred solution of II, prepared from 1.0 g of I, in 4.0 m*l* of dry tetrahydrofuran under cooling with ice-water. The stirring was continued for 6 hr, and then crystalline precipitates were filtered out. The addition of water to the filtrate gave the second crop. The combined precipitates were washed with water and dried to give 740 mg (74%*2) of Va. Repeated recrystallizations from aqueous methanol gave an analytical sample with a mp of 180°C.

ν_{max}^{KBr} 3360 (NH), 3200 (NH), 1660 (amide-I) and 1628 (amide-II) cm^{-1}.

Found: C, 72.00; H, 9.82; N, 6.85%. Calcd for $C_{12}H_{19}ON \cdot \frac{1}{2}H_2O$: C, 71.24; H, 9.97; N, 6.92%.

Hofmann Reaction of Va. Into an ice-cooled bromine-alkali reagent, freshly prepared from 1.0 g of bromine, 1.0 g of sodium hydroxide, and 10 m*l* of water, 0.5 g of Va was stirred. The temperature was then slowly raised to 80°C over a 3.5-hr period and kept there for 10 min. After cooling, the separated solids were filtered and washed with water. Recrystallization from chloroform-petroleum ether (bp 38—65°C) gave pure VIIIb, 380 mg (76.5%*2), mp 254—255°C.

ν_{max}^{KBr} 3300 (NH), 3240 (NH), 3120 (NH), 1685 (amide-I) and 1565 (amide-II) cm^{-1}.

Found: C, 74.82; H, 9.56; N, 7.34%. Calcd for $C_{24}H_{36}O_2N_2$: C, 74.96; H, 9.44; N, 7.29%.

Adamantyl-1-acetanilide (Vb). A mixture of II, prepared from 0.5 g of I, 0.5 g of aniline, and 20 m*l* of dry benzene, was refluxed for 15 min. The cooled reaction mixture was washed with 5% hydrochloric acid and then with water, and dried over anhydrous sodium sulfate. After the removal of the solvent, the residue was recrystallized from methanol to give 0.4 g (71%*2) of Vb, mp 195—196°C.

ν_{max}^{KBr} 3280 (NH), 3050 (phenyl CH), 1660 (amide-I), 1605 (phenyl C=C) and 1548 (amide-II) cm^{-1}.

Found; C, 79.90; H, 8.22; N, 4.98%. Calcd for $C_{18}H_{23}ON$: C, 80.25; H, 8.61; N, 5.20%.

*2 All yields are based on I.

***N, N'* - Bisadamantyl - 1 - acetohydrazide (XII).** Into an ice-cooled solution of 1.6 g of 80% hydrazine hydrate in 1.0 m*l* of tetrahydrofuran was stirred and stirring was continued for 7 hr at room temperature, and then the mixture was allowed to stand in a refrigerator overnight. The deposited solids were then filtered and recrystallized from methanol to give pure XII, 380 mg (71%*[2]), mp 268—269°C.

ν_{max}^{KBr} 3200 (NH), 1680 (shoulder, CO), 1640 (shoulder, CO), 1610 (CO) and 1520 (NH) cm^{-1}.

Found: C, 74.51; H, 9.36; N, 7.20%. Calcd for $C_{24}H_{36}O_2N_2$: C, 74.96; H, 9.44; N, 7.29%.

Acid Azide VI and Its Curtius Rearrangement. Into a solution of II, prepared from 0.5 g of I, in 2 m*l* of acetone, a solution of 2.0 g of sodium azide in 5 m*l* of water was stirred. Stirring was continued for 2 hr at room temperature. The reaction mixture was then diluted with 15 m*l* of water and extracted with ether (30 m*l*×2). The combined ether extracts were washed with water, dried over anhydrous sodium sulfate, and evaporated to give an oil which had an infrared band at 2290 cm^{-1} (weak, ν_{NCO}) as well as one at 2160 cm^{-1} (strong, ν_{N_3}); the appearance of the former band shows that the rearrangement had already occurred during the procedure. To complete the rearrangement, this crude azide was heated in dry benzene for 1 hr. The infrared spectrum of the oil after the removal of the solvent had a very strong band at 2290 cm^{-1} (ν_{NCO}), while the band at 2160 cm^{-1} (ν_{N_3}) had almost completely disappeared.

A half amount of this oil was treated with 0.15 m*l* of aniline in *n*-hexane at room temperature for 13 hr. The precipitates were then filtered to give 200 mg (55%*[2]) of crude VIIIa. Recrystallization from methanol gave an analytical sample, mp 172—173°C.

ν_{max}^{KBr} 3340 (NH), 3050 (phenyl CH), 1645 (amide-I) and 1570 (amide-II) cm^{-1}.

Found: C, 75.91; H, 8.78; N, 10.01%. Calcd for $C_{18}H_{24}ON_2$: C, 76.02; H, 8.51; N, 9.85%.

Adamantyl-1-propionanilide (IV). A solution of II, prepared from 0.5 g of I, in 10 m*l* of ether was added to a solution of diazomethane in 100 m*l* of ether under ice-water cooling, after which the reaction mixture was allowed to stand for two days at room temperature. The solvent was stripped off *in vacuo*, and the residual oil, III, was characterized as having a diazoketone structure on the basis of the infrared absorptions at 2100 (ν_{N_2}) and 1625 (ν_{CO}) cm^{-1}. III and 0.7 g of aniline were dissolved in 100 m*l* of anhydrous benzene, and the mixture was irradiated with a 100-W high-pressure mercury lamp (Ushio, UM-102) through a quartz cooler in a nitrogen stream at room temperature. After 9 hrs' irradiation, the solution was washed successively with 10% hydrochloric acid, 5% sodium hydroxide, and then water. The solution was dried over anhydrous sodium sulfate, and the benzene was distilled off *in vacuo*. The residual brown oil was triturated with 10 m*l* of *n*-hexane to give white crystals. The isolated solids were dissolved in 50 m*l* of ethanol, and the solution was treated with active charcoal. The solvent was distilled off *in vacuo*, and the residue was recrystallized from methanol to afford colorless needles, 100 mg (14%*[2]), mp 154—155°C.

ν_{max}^{KBr} 3240 (NH), 3029 (phenyl CH), 1655 (amide-I), 1600 (phenyl C–C) and 1555 (amide-II) cm^{-1}.

Found: C, 80.32; H, 8.74; N, 5.06%. Calcd for $C_{19}H_{25}ON$: C, 80.52; H, 8.89; N, 4.94%.

Adamantyl-1-ethanol (XI) from I *via* IX. To an ethereal solution of diazomethane, a solution of 0.5 g of I in 20 m*l* of ether was gradually added. The solution was allowed to stand overnight at room temperature, and then the ether was removed *in vacuo* to give a colorless oil, which was characterized as IX on the basis of the infrared band at 1730 (ν_{CO}) cm^{-1}. All of this oil was dissolved in 50 m*l* of dry ether, and then 1.1 g of lithium aluminum hydride was added to the solution. The reaction mixture was then stirred overnight at room temperature and diluted with 50 m*l* of water. The aqueous solution was acidified with concentrated hydrochloric acid and extracted with ether. The ether extract was washed with water and dried over anhydrous sodium sulfate. The ether was removed to give colorless crystals, 340 mg (73.2%*[2]). Recrystallization from *n*-hexane gave an analytical sample, mp 73.5—75.0°C.

ν_{max}^{KBr} 3300 (OH), and 1047 (CO) cm^{-1}.

Found: C, 79.91; H, 11.11%. Calcd for $C_{12}H_{20}O$: C, 79.94; H, 11.18%.

Adamantyl-1-acetohydrazide (X). A mixture of the crude methyl ester, prepared from 0.5 g of I, 0.2 m*l* of 80% hydrazine hydrate and 0.2 m*l* of water, was heated at 95—100°C for 9 hr and then at 110—120°C for 1 day in a sealed tube. After cooling, a 50 m*l* portion of water was added to the reaction mixture and the separared crystals were filtered and recrystallized from methanol to give white granular crystals of X, 390 mg (73%*[2]), mp 113—118°C.

ν_{max}^{KBr} 3280 (NH), 1640 (amide-I) and 1520 (amide-II) cm^{-1}.

Found: C, 68.85; H, 10.11; N, 13.04%. Calcd for $C_{12}H_{20}ON_2$: C, 69.19; H, 9.68; N, 13.45%.

Synthesis of 4-Amino-5-imidazolecarbonitrile and 4-Amino-5-imidazolecarboxamide from 4, 5-Dicyanoimidazole[1]

Yoshitaka YAMADA, Izumi KUMASHIRO and Tadao TAKENISHI

Central Research Laboratories, Ajinomoto Co., Inc., Kawasaki

(Received June 5, 1967)

In a previous communication,[2] we have reported that adenine and 4, 5-dicyanoimidazole were formed by heating anhydrous hydrogen cyanide, or an equivalent mixture of sodium cyanide and ammonium chloride, in excess liquid ammonia. In the present paper, the synthesis of 4-amino-5-imidazolecarbonitrile and 4-amino-5-imidazolecarboxamide (AICA) from 4, 5-dicyanoimidazole will be reported. AICA is a useful synthetic intermediate of purine derivatives. It has been prepared by various methods, from, for example, 4-nitro-5-imidazolecarboxylic acid[3] or ethyl aminocyanoacetate[4], however, these methods are complicated and the overall yields are unsatisfactory. It has now been found that 4-amino-5-imidazolecarbonitrile and AICA can be readily prepared from 4, 5-dicyanoimidazole by the use of Hofmann's rearrangement reaction:

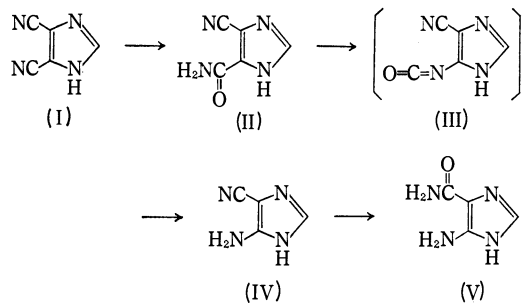

(I) (II) (III) (IV) (V)

Since 4, 5-dicyanoimidazole were found to be resistant to a boiling dilute aqueous solution of ammonia or hydrogen chloride, the partial hydrolysis of I to 4-cyano-5-imidazolecarboxamide (II) has been accomplished with a 1 N sodium hydroxide solution. II was treated with a 0.1 N solution containing 1.25 equivalents of sodium hypochlorite at 0°C for 30 min. A concentrated sodium hydroxide solution was then added so as to make 4 equivalents based on II, after which the reaction mixture was warmed at 80°C for 3 hr. The infrared absorption spectra of 4-amino-5-imidazolecarbonitrile (IV), which was isolated by the ion-exchange resin treatment, agreed well with those of an authentic sample.[5,6] By hydrolysis in a strongly basic medium at a higher temperature, IV was converted to AICA (V). When the intermediate (III), probably isocyanate, was hydrolyzed directly under drastic conditions, AICA could not be obtained successfully, but a tarry substance was found to be formed.

Experimental[7]

4-Cyano-5-imidazolecarboxamide (II). After a solution of 4, 5-dicyanoimidazole (30 g) in 600 m*l* of 1 N sodium hydroxide had been kept at 40°C for 6 hr, it was neutralyzed to pH 6 with concentrated hydrochloric acid. The solid precipitates, which were formed immediately, were filtered, washed with ice water, and recrystallized from hot water to give colorless needles. Yield: 31 g (90%); mp 272—273°C; infrared (CN) 2240, (amide CO) 1695 cm^{-1}; ultraviolet $\lambda_{max}^{pH\ 1}$ 253 mμ (ε 8.32×10^3); $\lambda_{max}^{pH\ 13}$ 274 mμ (ε 10.10×10^3).

Found: C, 44.25; H, 3.05; N, 41.25%. Calcd for $C_5H_4N_4O$: C, 44.12; H, 2.96; N, 41.17%.

4-Amino-5-imidazolecarbonitrile (IV). To a solution of 600 m*l* of 0.22 N sodium hydroxide, chlorine gas (1.28 *l*) was dissolved at 0°C. To this solution, II (6 g) was added at 0°C; the resulting solution was stirred at the same temperature for 30 min, and then 1.5 N sodium hydroxide (120 m*l*) was added to the reaction mixture. After being heated at 80—85°C for further 3 hr, the reaction mixture was passed through a column of Amberlite IR-120 (H^+ form). Then the column was washed with water and eluted with 3 N ammonium hydroxide. The eluate was decolorized and evaporated under reduced pressure to give the crude IV. This crude substance was recrystallized twice from hot water. Yield: 3.2 g (67%); mp 129—129.5°C; ultraviolet $\lambda_{max}^{pH\ 1}$ 237 mμ (ε 9.57×10^3) and 252 mμ (ε 8.27×10^3); $\lambda_{max}^{pH\ 13}$ 255 mμ (ε 1.08×10^4).

Found: C, 44.57; H, 3.98; N, 52.15%. Calcd for $C_4H_4N_4$: C, 44.44; H, 3.73; N, 51.83%.

The ultraviolet and infrared absorption spectra were

1) Presented at the 19th Annual Meeting of the Chemical Society of Japan, Yokohama, April, 1966.
2) H. Wakamatsu, Y. Yamada, T. Saito, I. Kumashiro and T. Takenishi, *J. Org. Chem.*, **31**, 2035 (1966).
3) A. Windaus and W. Langenbeck, *Ber.*, **56**, 683 (1923).
4) A. H. Cook, Sir. I. Heilbron and W. Smith, *J. Chem. Soc.*, **1949**, 1440.
5) K. Suzuki (of our Laboratories), private communication. He prepared the compound by the dehydration of AICA with phosphoryl chloride.
6) J. P. Ferris and L. E. Orgel, *J. Am. Chem. Soc.*, **88**, 3829 (1966).
7) All the melting points are uncorrected. The ultraviolet and infrared absorption spectra were measured with Hitachi EPS-2 and JASCO model IR-S recording spectrophotometers.

identical with those of an authentic sample.

4-Amino-5-imidazolecarboxamide (V). An alkaline reaction mixture of IV was heated at 125—130°C for 6 hr in a sealed vessel and then passed through a column of Amberlite IR-120 (H^+ form). By treating the eluate as in the case of IV, 5.0 g (70%) of crude V were obtained. By recrystallization from dilute hydrochloric acid, the hydrochloride of V was obtained as colorless crystals, mp 254.5—255°C. Ultraviolet $\lambda_{max}^{pH\ 1}$ 242 mμ (ε 6.30×10^3) and 269 mμ (ε 8.66×10^3); $\lambda_{max}^{pH\ 13}$ 278 mμ (ε 1.06×10^4).

Found: C, 29.58; H, 4.42; N, 34.68%. Calcd for $C_4H_6N_4O\cdot HCl$: C, 29.55; H, 4.34; N, 34.46%.

The product was identified with those of an authentic sample by a study of the spectral data, the paper chromatographic behavior, and the mixed melting point.

The authors wish to express their deep thanks to Mr. Shinichi Motozaki, Director of the Central Research Laboratories, for his kind encouragement. The assistance of Mr. Takashi Zama throughout this work is also gratefully acknowledged.

Oxidative Decarboxylation of Phenylacetic Acid[1)]

Takao WATANABE, Naomichi FURUKAWA and Shigeru OAE

Department of Applied Chemistry Faculty of Engineering, Osaka City University, Sumiyoshi-ku, Osaka

(Received June 12, 1967)

The cuprous ion catalyzed oxidative decarboxylation of benzoic acid to phenol is not only useful but also an interesting reaction which recently has been shown to proceed through a cyclic 6-membered transition state by use of ^{14}C and ^{18}O tracer techniques.[2,3)] Meanwhile this procedure has been used to prepare various aromatic phenolic compounds from the corresponding carboxylic acids; such as substituted benzoic, naphthoic, and heteroaromatic carboxylic acids.[4)] Recently Bigot and his co-workers[5)] have shown the oxidative decarboxylation reaction of cyclohexanecarboxylic acid. Phenylacetic acid has been known to undergo a facile decarboxylation to give toluene[6)] and hence an interesting compound to study the nature of this intriguing oxidative decarboxylation. We have carried out the oxidative decarboxylation of phenylacetic acid catalyzed by cuprous oxide, expecting to obtain either *o*-cresol, benzyl alcohol or diphenylethane. However we found that the reaction is more complicated and gives a variety of products. This paper will describe the detailed accounts of our investigation.

Results and Discussion

The apparatus used for the decarboxylation reaction was the same as the one described previously.[3)] The reaction was found to begin at around 180°C. The products isolated were characterized by comparing the IR and NMR spectra with those of the authentic samples. The products initially came out from the reaction vessel were benzaldehyde and carbon dioxide, both of which were trapped as the bisulfite adduct and barium carbonate, respectively. From the residue were isolated the following three neutral products I, II, III, the structures of which were characterized by IR and NMR spectra. The compounds I and II were actually synthesized by the procedures as was found to be identical,[7,8)] while the structure of the compound III was suggested based on the NMR spectrum and other evidences. However neither cresol nor other hydroxy compound could be isolated among the products. The products and yields are tabulated in Table 1.

The reaction is undoubtedly catalyzed by copper metal since most phenylacetic acid were recovered without copper catalyst. (Run 9). The presence of oxygen is also important because no products isolated when the reaction was carried out under nitrogen stream. (Run 7). Although benzaldehyde was isolated, diphenylethane and toluene were not found among the products, apparently suggesting that benzyl radical is not the intermediate in this reaction and that the reaction proceeds through ionic mechanism. Recently, Cohen *et al.*,[9)] have isolated I and II by the treatment of phenylacetic acid with pyridine-*N*-oxide

1) Phenols and Phenolic Esters. XIII.
2) W. Shoo, V. J. Veenland, J. A. Bigot and F. L. J. Sixma, *Rec. Trav. Chim.*, **80**, 134 (1961).
3) S. Oae, T. Watanabe and N. Furukawa, This Bulletin, **39**, 1329 (1966).
4) W. W. Kaeding, *J. Org. Chem.*, **26**, 3144 (1961); W. W. Kaeding, R. O. Lindblom and R. G. Temple, *Ind. Eng. Chem.*, **53**, 805 (1961).
5) J. A. Bigot and P. L. Kerkhoffs, *Rec. Trav. Chim.*, **82**, 677 (1964).
6) V. N. Ipatief, J. E. Germain and H. Pines, *Bull. Soc. Chim. France*, **1951**, 259.
7) R. B. Davis and J. A. Ward, Jr., "Organic Syntheses," Coll. Vol. IV, p. 392 (1963).
8) S. Gabriel and G. Cohn, *Ber.*, **24**, 3229 (1891).
9) T. Cohen and L. H. Fragger, *J. Am. Chem. Soc.*, **87**, 5701 (1965).

TABLE 1. PRODUCTS FROM THE OXIDATIVE DECARBOXYLATION OF PHENYLACETIC ACID CATALYZED BY Cu_2O

Run	Reaction time hr	Weight of reactant g	Recovered $C_6H_5CH_2CO_2H$	C_6H_5CHO	Neutral[a] product	I	II	III	$BaCO_3$ g
1	5	2.24	0.65	0.21	0.50	—	0.05	0.05	—
2	4	2.47	—	0.20	0.54	0.03	—	0.05	1.43
3	6.5	8.98	3.54	0.12	1.67	0.03	0.15	0.78	3.37
4	7.3	8.98	—	0.26	1.51	—	—	0.94	3.12
5	7	2.24	4.64	—	—	0.06	—	1.00	2.90
6	6.5	2.24	0.67	0.02	0.80	—	0.02	0.26	—
7[b]	6.5	2.24	1.18	trace	0.11	0	0	0.02	trace
8[c]	6.4	2.24	0.43	0.13	0.78	0.10	—	0	1.76
9[d]	6.5	2.24	1.77	trace	0.14	trace	0	0	0.47

a) Containing I, II, III.
b) Under nitrogen stream.
c) Catalyst, Cu_2O alone without MgO.
d) Catalyst, MgO alone without Cu_2O.

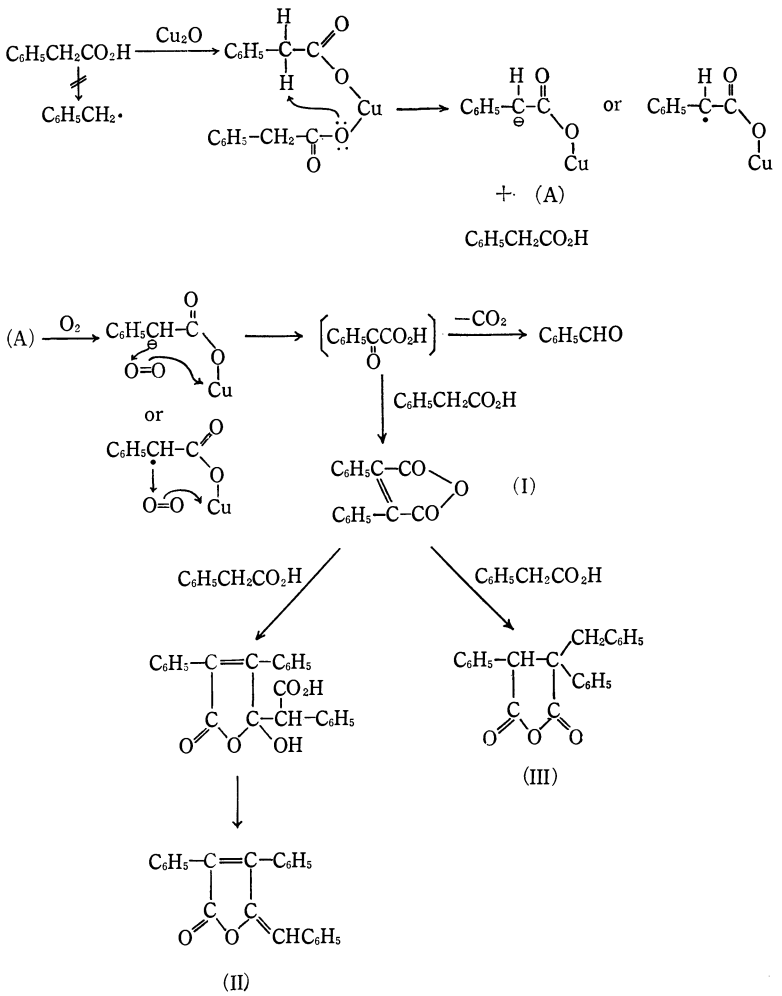

Fig. 1. Mechanism.

in addition to a few other products such as benzoylformic acid and benzaldehyde and suggested that benzoylformic acid might be the key intermediate, while, in this, the copper ion catalyzed decarboxylation, benzoylformic acid might be postulated as the key intermediate, the formation of which is

illustrated by either radical or ionic mechanism. The whole reaction may be schematically shown as below. (Fig. 1)

Experimental

The Decarboxylation. A typical example of the reaction is as follows.

Phenylacetic acid (8.98 g) was mixed with 0.16 g of cuprous oxide and 0.37 g of magnesium oxide and then the whole mixture was placed into the reactor and heated with an electric muffle heater with slowly introducing air while keeping the temperature at 195—205°C for 6.5 hr. Benzaldehyde and carbon dioxide eluted were trapped with sodium bisulfite and barium hydroxide, respectively. After the reaction, the residue remaining in the vessel was extracted with ether and washed with water. Ether extract was washed with dilute hydrochloric acid, and then with water and sodium carbonate solution. The ether layer was dried over magnesium sulfate. When ether was removed, red brownish oil (1.67 g) was obtained. Keeping the oil in cold, the crystals appeared. To this crystals ether was added and collected the crystals on a filter paper. Then the ether was removed from the mother liquor and the second crop of the crystals was obtained. Thus, by repeating this operation, three different products were isolated.

The weight and melting point of I, II, III, were, I, 0.03 g, mp 159—160°C (from benzene - *n*-hexane); II, 0.15 g mp 178—179°C (from benzene - *n*-hexane); III, 0.78 g, mp 211.5—212.5°C (from benzene or ethanol). The product I was identified from its mp and IR of that of the authentic 1, 2-diphenylmaleic anhydride which was prepared from benzaldehyde and phenylacetonitrile and sodium cyanide.[7] The product II, having slightly yellow color, IR absorption at 1765 cm^{-1} was identified as 5-oxo-3, 4-diphenyl-2-benzaldihydrofuran II which was prepared authentically from heating a mixture of I and phenylacetic acid with sodium acetate at 230°C for 2 hr.[8]

The product III, IR spectrum 1775, 1813 (doublet; lactone carbonyl) and 1150 cm^{-1} (anhydride); molecular weight determination. Calcd 342, Found, 336—343. Elemental analysis: Found: C, 81.04, H, 4.98%. Calcd: C, 80.68, H; 5.30%. The NMR spectrum of III has methylene quartet centered at 5.70 ppm and complex multiplet centered at 2.75 ppm in which benzene protons and highly deshielded methine proton are involved.

The pyrolysis of II led to 1, 2-diphenylmaleic anhydride which upon the treatment with phenylacetic acid in the presence of the catalyst at 200°C regenerating III. These experimental evidences showed that the products had a five membered lactone ring and three benzene ring involving methylene, thus III was suggested to have the structure of benzylsuccinic anhydride.

Studies of Poly-2-vinylpyridine. IV. Crystalline Bands in the Infrared Absorption Spectrum of Stereospecific Poly-2-vinylpyridine

Shizuo ARICHI

Department of Chemistry, Faculty of Science, Kumamoto University, Kurokami-machi, Kumamoto

(Received June 12, 1967)

In 1960, Natta and others[1,2] reported systematic studies of the method and mechanism of the stereospecific polymerization of 2-vinylpyridine, and also of some properties of the polymer. They made use of the diffraction of X-rays as a direct method for the characterization of the crystals of poly-2-vinylpyridine. They also confirmed that the crystallized polymers are insoluble in hot acetone. However so far as this polymer is concerned, no method in which the infrared absorption spectrum is used for the characterization of the crystals has yet been reported. The present author has recognized that there are distinct absorption bands in the infrared spectrum at the wave numbers of 928 and 1180 cm^{-1}, which are characteristic of crystallized poly-2-vinylpyridine.

The stereospecific polymerization of 2-vinylpyridine and the purification of the polymer were carried out according to the method of Natta and others.[2] In the polymerization, phenylmagnesium bromide was used for the catalyst, and toluene for the diluent. A series of isotactic poly-2-vinylpyridines was then obtained by the same procedure, but by varying the concentrations of the catalyst and the polymerization temperatures. The crystallization of the polymer was effected by first maintaining the amorphous polymer for seven hours at 155—157°C under a nitrogen atmosphere, and by then treating the whole polymer in hot acetone. The polymerization conditions and some properties of the polymer, S-3, which was mainly used in this study are summarized in Table 1. As for the atactic, noncrystallizable poly-2-vinylpyridine, which was used for comparison, the G-2 fraction, described in the preceding paper,[3] was used.

1) G. Natta, G. Mazzanti, G. Dall'Asta and P. Longi, *Makromol. Chem.*, **37**, 160 (1960).

2) G. Natta, G. Mazzanti, P. Longi, G. Dall'Asta and F. Bernardini, *J. Polymer Sci.*, **51**, 487 (1961).

3) S. Arichi, This Bulletin, **39**, 439 (1966).

TABLE 1. THE POLYMERIZATION CONDITION AND THE PROPERTIES OF ACETONE INSOLUBLE FRACTION OF STEREOSPECIFIC POLY-2-VINYLPYRIDINE (SAMPLE No. S-3)

Monomer	C_6H_5MgBr	Toluene	Temp.	Time	Polymer	Yield	Acetone insoluble polymer				
							g/g of whole polymer %	Melting point °C	$[\eta]^{25°}_{benzene}$ dl/g	$[\eta]^{25°}_{methanol}$ dl/g	M_w by light scattering meas.
50 g	7.29 g	500 g	45°C	4 hr	45 g	90%	96.1	190—195	0.182	0.293	12.3×10^4

The Geiger-counter registration of the X-ray diffraction spectrum for the acetone-insoluble fraction of S-3 is shown in Fig. 1, and the photograph of the Debye-Scherrer ring for the same fraction, in Fig. 2. The crystal structure of S-3, characterized by an identity period of about 6.7 Å, which was estimated from Fig. 1, is essentially in accordance with the one reported by Natta and others.[2] When the same X-ray examination was carried out of the atactic poly-2-vinylpyridine, G-2, neither peak nor ring such as is seen in Fig. 1 and Fig. 2 was observed.

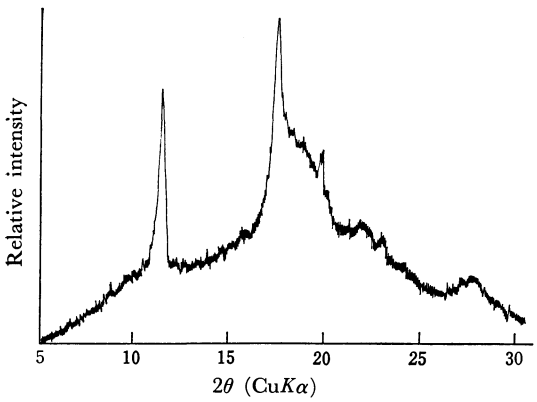

Fig. 1. Geiger counter registration of X-ray diffraction spectrum of the crystalline poly-2-vinylpyridine.

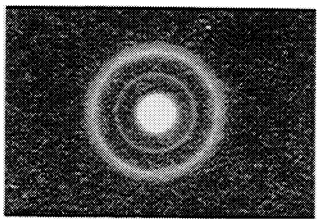

Fig. 2. Photograph of Debye-Scherrer ring for the crystalline poly-2-vinylpyridine.

The infrared absorption spectra of the crystallized poly-2-vinylpyridine, S-3, and the atactic poly-2-vinylpyridine, G-2, measured in the form of KBr pellets, are shown in Fig. 3. The characteristic absorption bands, shown in this figure, are observed in the spectrum of crystallized poly-2-vinylpyridine, S-3, at the wave numbers of 928 and 1180 cm^{-1}. These bands had been observed in the S-3 sample, neither before it was treated for crystallization nor when the acetone-soluble films which were prepared from a methanol or benzene solution of the S-3, sample, were examined without treatment for crystallization. The bands were, nevertheless, observed when the films had been treated in decalin at 120—130°C and proved to be acetone-insoluble.

The experimental results may allow us to conclude, at least qualitatively, that the characteristic absorption bands, especially the one at 928 cm^{-1},

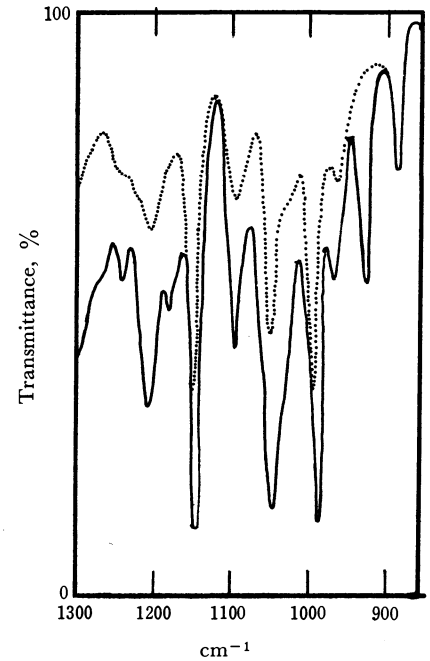

Fig. 3. Infrared absorption spectra of the crystalline (——), and atactic, (·····), poly-2-vinylpyridine.

can be used as an indicator of the degree of the crystallization of isotactic poly-2-vinylpyridine. The bands may even be useful in confirming the tacticity of poly-2-vinylpyridine.

In spite of various attempts, we have not yet been successful in detecting any dichroism in the infrared absorption spectrum of the stereospecific poly-2-vinylpyridine. Further investigations of the quantitative relationship between the degree of crystallization and the intensity of the bands at 928 cm^{-1} in the absorption spectrum are in progress.

An Analysis of Long-term Observations of ^{90}Sr Deposition*1

Takeshi SOTOBAYASHI, Toshio SUZUKI and Yukio KANDA

Department of Chemistry, Faculty of Science, Niigata University, Niigata

(Received June 19, 1967)

Measurements of the monthly deposition rate of ^{90}Sr and its time variation[1] have been made on a long-term scale of several years in our laboratory in order to estimate the cumulative deposition of ^{90}Sr per unit area and obtain more detailed information on its geochemical behavior in the atmosphere. We have recently discussed the ^{90}Sr fallout from surface and underground nuclear tests,[2] and, even more recently, the geochemical behavior of fresh nuclear debris of a known origin,[3] on the basis of radiochemical data for ^{89}Sr and ^{90}Sr. In the present paper we will make a brief analysis of our long-term observations of ^{90}Sr, a representative long-lived and hazardous fission product; further, we will estimate the cumulative deposition of ^{90}Sr per unit of area per unit of the activity produced by a series of atmospheric nuclear fission events.

Results and Discussion

More than 4 years after the termination of the atmospheric nuclear tests of 1961—62, measurable amounts of ^{90}Sr activity have been still detected in rain and ground-air samples at Niigata, although the yearly fall-rate had by 1966 lowered to one-eighth that of 1963. Table 1 shows the monthly deposition of ^{90}Sr per unit of area (mCi/km^2) and the monthly mean specific activity in precipitation (pCi/mm) during 1965—66. As can be seen in Table 1, a peak in the monthly deposition rate was observed in March for both years, while the peaks of the specific activity were in March for 1965 and in April for 1966; in 1966 the maximum values of the deposition rate and the specific activity decreased by 40 and 45 per cent respectively compared to those in 1965. The minimum deposition rates for both 1965 and 1966 were obviously found in August, but the 1966 rate dropped to 50 percent of that of 1965; the minimum specific activity in 1965 was clearly found in September, but in 1966 the specific activity ranged from 0.5 to 0.7 pCi/mm, with no definite trend observable during the period from July to December; it was difficult to determine which month of the year had a minimum value. Such a unique pattern of the specific activity remaining rather constant during the 4th quarter of a year was here observed for the first time since the beginning of our measurement of fallout activities.*2

Table 1. Monthly deposition of ^{90}Sr and its specific activity at Niigata during 1965—1966

Month of collection	1965		1966	
	Monthly deposition mCi/km^2	Specific activity pCi/mm	Monthly deposition mCi/km^2	Specific activity pCi/mm
Jan.	0.81	3.9	0.21	2.4
Feb.	0.60	5.9	0.27	2.5
Mar.	0.86	11.6	0.35	3.3
Apr.	0.21	3.9	0.33	5.2
May	0.74	6.0	0.29	2.5
June	0.38	2.4	0.26	2.4
July	0.43	1.2	0.19	0.5
Aug.	0.06	1.5	0.03	0.6
Sept.	0.11	0.8	0.11	0.5
Oct.	0.19	1.4	0.14	0.5
Nov.	0.24	1.2	0.15	0.7
Dec.	0.37	1.2	0.12	0.5

Table 2 shows the yearly total of ^{90}Sr deposition per unit of area and the ratio between the two yearly totals of two consecutive years, namely, the yearly decrease rate, during the periods of 1960—61 and 1964—66, together with the yearly amount of rainfall. The decrease rate for 1960—61, 2 to 3 years after the termination of the 1957—58 test series, showed almost the same value as those for 1964—1965 and 1965—1966, 2 to 4 years after the 1961—62 test series. This finding would suggest that the decrease rate seems to have shown a nearly constant value of 0.5 more than one year after the end of each test series in spite of a number of differences in the actual test conditions, *e. g.*, the total energy yields and the altitude at which the nuclear explosions took place. Meanwhile, during the 1964—66 period there were 6 instances of radioactive air contamination at Niigata, resulting from 5 Chinese nuclear tests and an

*1 Presented at the 20th Annual Meeting of the Chemical Society of Japan, Tokyo, April, 1967.

1) T. Sotobayashi and S. Koyama, *J. Fac. Sci. Niigata Univ., I*, **3**, 111 (1962).
2) T. Sotobayashi and S. Koyama, *Science*, **152**, 1059 (1966).
3) T. Sotobayashi, S. Koyama and T. Suzuki, This Bulletin, **40**, 1269 (1967).

*2 According to our long-term ivnestigation of detailed seasonal variation in the monthly ^{90}Sr deposition at Niigata, the monthly value usually showed an increasing trend from October to December of any given year. *Nippon Kagaku Zassi (J. Chem. Soc. Japan, Pure Chem. Sect.)*, **89**, 206 (1968).

accidental release of nuclear debris due to a Russian underground test,[4] but the contribution to the total by the ^{90}Sr originating from these tests was small; the percentages of contributions by the ^{90}Sr fraction newly arising from each nuclear detonation to the yearly total were estimated to be 0.7, 3.0, and 2.4 per cent for 1964, 1965, and 1966 respectively. (In this estimation the two respective ^{90}Sr fractions resulting from the May 14, 1965, and the December 28, 1966, tests have not been taken into account, because data for the former were unavailable and the latter made no significant contribution to the yearly total of ^{90}Sr in 1966.)

TABLE 2. THE YEARLY TOTAL OF ^{90}Sr DEPOSITION AND THE YEARLY DECREASE RATE

Year of collection	Yearly total of ^{90}Sr mCi/km^2	Rain fall mm	Decrease rate %
1960	1.67	1780	53
1961	0.88*	2030	
1964	9.35	1880	54
1965	5.00	1880	50
1966	2.48	1950	

* This figure represents a value corrected for the contribution from the ^{90}Sr fraction originating from the 1961—1962 test series.

Table 3 gives two 10 year total depositions of ^{90}Sr per unit of area after the end of each test series; they were evaluated on the assumption that the yearly deposition of ^{90}Sr originating separately from the 1957—58 and the 1961—62 tests would independently continue to decrease at a decrease rate of 0.5 for 1962—68 and 1967—72 respectively.

4) S. Koyama, T. Sotobayashi and T. Suzuki, *Nature*, **209**, 239 (1966).

TABLE 3. ESTIMATED TEN-YEAR TOTAL OF ^{90}Sr DEPOSITION AND ITS RATIO TO TOTAL ^{90}Sr ACTIVITY PRODUCED

Test series	Estimated 10-year total of ^{90}Sr per unit area, mCi/km^2	Total ^{90}Sr activity produced* MCi	Total ^{90}Sr deposition/ ^{90}Sr produced mCi/km^2/MCi
1957—1958	26	4.0	6.5
1961—1962	55	9.6	5.7

* U.S. Federal Radiation Council Data (Ref. 5)

The values obtained are approximately equal to the expected total deposition at Niigata of ^{90}Sr which would be derived separately from each of the two test series. Thus, from these figures, the ratio of a 10 year total of ^{90}Sr deposition per unit of area to an estimated total of ^{90}Sr activity[5] produced by each of the two test series (Table 3) was estimated to be 6.5 and 5.7 mCi/km^2 per megacurie for the test series of 1957—58 and 1961—62 respectively. The fact that these ratios nearly equalled each other leads to the possible conclusion that a total deposition of ^{90}Sr per unit of area obtained at an observation site as a result of considerably long-term measurements would be proportional to the total ^{90}Sr activity produced, so long as nuclear tests have been performed in the atmosphere, in spite of the actual different test conditions. However, it should be noticed that this is not true for the case of a land-surface burst, such as the October 16, 1964, test by the Chinese; the corresponding ratio for the Chinese test[2] was estimated to be 32 mCi/km^2 per megacurie, about 5 times greater than those obtained above.

The authors wish to thank Professor Seitaro Koyama for his interest and encouragement.

5) Value taken from data in the Fourth Report of the U. S. Federal Radiation Council (July, 1963).

The Solid Complex Formation of Benzoic Acid with Piperidine

Setsuo KASHINO

Department of Chemistry, Faculty of Science, Okayama University, Tsushima, Okayama

(Received June 20, 1967)

A study of the carboxylic acids - amines system in benzene led Bruckenstein and Saito[1] to identify the 1 : 1, 2 : 1, and 3 : 1 acid-base adducts in solutions. Moreover, with regard to benzoic acid and piperidine, they identified the 1 : 1 and 2 : 1 acid-base adducts in benzene by infrared study.

The present study will deal with the formation and identification of solid complexes of benzoic acid (HA) with piperidine (B). It was found that the 1 : 1 and 2 : 1 benzoic acid - piperidine complexes exist in the solid state. The 1 : 1 complex (B·HA) was formed from a cyclohexane solution containing equimolar amounts of benzoic acid and piperidine. The complex is highly hygroscopic. When the complex is exposed to the atmosphere, it forms a complex ($B \cdot HA \cdot H_2O$) with a benzoic acid - piperidine - water ratio of 1 : 1 : 1. The infrared spectra in the KBr disks of the 1 : 1 and 1 : 1 : 1 complexes were very similar. As is shown in Table 1, however, their X-ray diffractions are apparently different.

The melting-point diagram for the benzoic acid-piperidine system is shown in Fig. 1. This shows the existence of a molecular compound with an acid-base ratio of 2 : 1. The complex (B·HA·HA) was isolated from a cyclohexane solution containing benzoic acid and piperidine in a mole ratio of 2 : 1. The X-ray diffraction data of the complex are given in Table 1.

The infrared data of these solid state complexes are given in Table 2, along with the data of

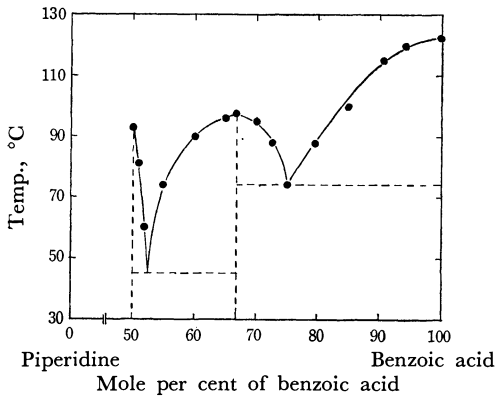

Fig. 1. The melting point diagram for the system benzoic acid - piperidine.

1) S. Bruckenstein and A. Saito, *J. Am. Chem. Soc.*, **87**, 698 (1965).

TABLE 1. X-RAY DIFFRACTION DATA OF THE SOLID COMPLEXES BETWEEN BENZOIC ACID (HA) AND PIPERIDINE (B)

B·HA		$B \cdot HA \cdot H_2O$		B·HA·HA	
2θ(°)	$H/H°$	2θ(°)	$H/H°$	2θ(°)	$H/H°$
11.56	7	13.52	20	9.85	26
13.92	7	14.25	18	10.60	21
15.05	46	15.20	10	14.40	12
16.72	19	17.20	29	16.06	16
18.35	21	18.40	100	17.50	34
19.40	39	19.30	34	19.34	100
20.70	100	20.65	22	21.35	13
21.90	18	21.90	14	22.80	19
22.60	47	22.85	16	24.10	30
23.95	7	23.40	58	25.45	5
24.90	8	24.60	58	26.70	11
25.70	15	25.40	19	27.55	10
26.80	47	27.10	27	28.75	14

θ=Bragg angles.
$H/H°$=relative height of diffraction peak.

Bruckenstein and Saito[1] for a benzene solution. As may be seen in Table 2, the infrared absorptions of the 1 : 1 complex in the solid state are almost identical with the absorptions in a benzene solution, though the ν-CO_2^- absorptions in the solid state shift to slightly higher frequencies. The 1 : 1 complex shows ν-CO_2^- absorptions, but no absorptions of ν-C=O. This indicates that the 1 : 1 complex has an ionic structure in the solid state as well as in a solution.

The infrared data of the 2 : 1 complex suggest that the complex has both C=O and CO_2^- groups. The main absorptions of the 2 : 1 complex in the solid state are also observed in a solution, though some absorptions observed in a solution disappear in the solid state.

The facts presented above give clear evidence of the existence of solid complexes between benzoic acid and piperidine.

Experimental

Materials. The piperidine (E. P.-grade reagent) was used without further purification. The benzoic acid was recrystallized from cyclohexane and dried at 100°C for one hour. The cyclohexane was dried over metallic sodium and distilled.

The Complex Formation. The 1 : 1 complex was prepared as follows: To a warm (*ca.* 60°C),

TABLE 2. INFRARED DATA OF THE COMPLEXES BETWEEN BENZOIC ACID (HA) AND PIPERIDINE (B)

Frequency, cm^{-1} (observed absorbance)				Assignment
B·HA		B·HA·HA		
a	b	a	b	
—	—	1720 (0.10)	1730 (0.10)	ν-C=O
—	—	—	1690 (0.12)	ν-C=O
1630 (0.15)	1620 (0.13)	—	1620 (0.13)	—
1600 (0.25)	1590 (0.09)	1595 (0.10)	1590 (0.13)	ν-CO_2^-
1550 (0.30)	1540 (0.10)	—	1540 (0·14)	ν-CO_2^-
—	—	1455 (0.10)	—	ν-CO+δ-OH
1385 (0.50)	1368 (0.31)	1385 (0.10)	1368 (0.35)	ν-CO_2^-

a : Data of the solid complexes in KBr disk, present studies.
b : Data of the complexes in benzene solution, Bruckenstein and Saito.[1]
ν : Streching. δ: Bending.

saturated solution of 2.9 g of benzoic acid in cyclohexane, an equimolar amount (2.0 g) of piperidine in the same solvent was added. After the solution had stood at room temperature for about one hour, colorless needles of the complex separated out. These needles were recrystallized repeatedly from cyclohexane, and then dried *in vacuo* over $CaCl_2$; mp 93—94°C. The complex was not subjected to elemental analysis, since it was highly hygroscopic. The complex was then exposed to the atmosphere overnight to form the 1 : 1 : 1 benzoic acid - piperidine - water complex; mp 51—52°C.

Found: C, 64.60; H, 8.61; N, 6.21%. Calcd for $C_{12}H_{17}NO_2(H_2O)$: C, 63.96; H, 8.50; N, 6.22%.

The 2 : 1 complex was prepared by a method virtually identical with that described for the 1 : 1 complex, but here the mole ratio of benzoic acid to piperidine was 2 : 1. Colorless needles, mp 97—98°C.

Found: C, 69.42; H, 7.31; N, 4.22%. Calcd for $C_{19}H_{23}NO_4$: C, 69.28; H, 7.08; N, 4.25%.

Identification. In all the experiments the 1 : 1 complex was treated in a dry box. The IR spectrum was obtained according to the usual KBr disk method. The X-ray powder-diffractometry was made with a Rigaku Denki diffractometer, Geigerflex, by the use of Cu$K\alpha$ radiation. For the melting-point diagram, a mixture of the 1 : 1 complex and benzoic acid in appropriate proportions was ground in a mortar and then sealed into capillaries. The melting point was obtained by the usual method.

The author wishes to express his thanks to Professor Shigeo Hasegawa and Dr. Norio Nishimura for their helpful discussions, and to Miss Sachiko Kusunoki for her experimental aid.

The Decomposition of *t*-Butylperoxy *o*-Phenylbenzoate

Hiroshi MINATO, Hisako MATSUZAKI and Kikuyo MIWA

Department of Chemistry, International Christian University, Mitaka, Tokyo

(Received July 1, 1967)

Bentrude and Martin[1] reported that the first-order thermal decompositions of some *o*-substituted *t*-butyl perbenzoates were very fast. Relative rates in chlorobenzene at 60°C varied with the *o*-substituents in the order:

$$PhS > MeS \gg I \gg (CH_3)_3C > H.$$

The tremendous rate enhancements observed with the first two of these peresters and the lesser effect accompanying the decomposition of the *o*-iodo perbenzoate were ascribed to the neighboring-group participation in a homolytic bond cleavage, the O-O bond cleavage being accompanied by simultaneous O-S (or O-I) bond formation.

It seems to be of great interest to investigate the decomposition of *t*-butylperoxy *o*-phenylbenzoate as to the possibility of the phenyl participation at the transition state of the decomposition, and this paper describes the results of the investigation of this perester.

Table 1 summarizes the kinetic data on *t*-butylperoxy *o*-phenylbenzoate together with those of *t*-butyl perbenzoate for comparison.

These very small acceleration of the decomposition (the ratio of the rate constants is 2.74 at 110°C and 2.56 at 130°C) seems to exclude the possibility of the *o*-phenyl participation at the transition state.

1) W. G. Bentrude and J. C. Martin, *J. Am. Chem. Soc.*, **84**, 1561 (1962).

TABLE 1. DECOMPOSITION RATES OF PERESTERS $RCO_3C(CH_3)_3$

R	Solvent	First-order const. (sec^{-1})				$\Delta H^{\neq}$	$\Delta S^{\neq}$
		110°C	119.4°C	124°C	130°C	kcal/mol,	cal/deg
o-$C_6H_5C_6H_4$	Cumene	9.40×10^{-5}		2.71×10^{-4}	8.60×10^{-4}	35.8	15.6
C_6H_5	p-Chlorotoluene	3.42×10^{-5}	1.01×10^{-4}		3.36×10^{-4}	34.5	14.1[a]

a) A. T. Blomquist and A. F. Ferris, *J. Am. Chem. Soc.*, **73**, 3408 (1951).

TABLE 2. PRODUCTS OF DECOMPOSITION OF t-BUTYL-PEROXY o-PHENYLBENZOATE IN CUMENE AT 125°C

	moles/mole of perester
Carbon dioxide	0.27
Acetone	0.23
t-Butyl alcohol	0.51
Fluorenone	0.11
o-Phenylbenzoic acid	0.22
3, 4-Benzcoumarin	0.32
Biphenyl	0.16
Bicumyl	0.20

The products of the decomposition of the perester in cumene at 125°C are listed in Table 2. It is interesting that about 32% of the perester was converted to 3, 4-benzcoumarin. This finding indicates that, even though the cleavage of the peroxide bond is not helped by the ortho phenyl π-system, the odd electron of the o-phenylbenzoyloxy radical formed reacts with the ortho phenyl π-system. The formation of fluorenone is rather difficult to explain. One speculation is that the perester decomposes to form fluorenone and t-butyl hydroperoxide, the latter being further decomposed to acetone and t-butyl alcohol.

The products of the decomposition of the perester indicate that the o-phenylbenzoyloxy radicals formed are converted into three products, namely, 3, 4-benzcoumarin, o-phenylbenzoic acid or biphenyl.

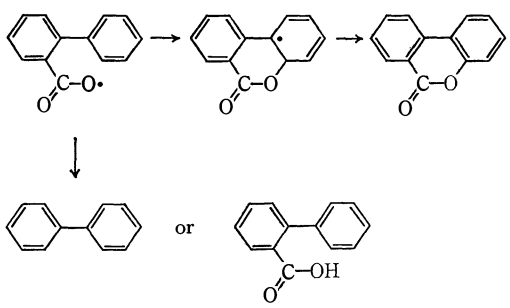

It is interesting to compare these findings with the studies on some of the peresters, the structures of which suggest the possibility of phenyl ring participation with the decomposition.

Greene *et al.*[2] studied the decomposition of o-phenylbenzoyl peroxide, and found that o-phenyl ring did not participate at the transition state but reacted with the carboxy radical to form 3, 4-benzcoumarin.

It seems worth commenting on the facile cyclization of o-phenylbenzoyl chloride to form fluorenone, the phenomenon observed when the acid was being converted into the acid chloride. Since a general method for preparation of an acid chloride is to reflux an acid with thionyl chloride, o-phenylbenzoic acid was refluxed with excess thionyl chloride for one hour. The product was fluorenone, not o-phenylbenzoyl chloride. Therefore, this reaction was further investigated at 30°C. Since the use of unpurified thionyl chloride resulted in the faster cyclization, hydrogen chloride was suspected to be the catalyst for this Friedel-Crafts reaction. When 0.02 g of water was carefully added into the mixture of 0.091 g of the acid and 0.331 m*l* of thionyl chloride in order to increase the content of hydrogen chloride in the mixture, the cyclization was faster. The reaction was followed by the changes of carbonyl absorptions in the infrared, and the results were shown in Fig. 1. Hydrogen chloride, though not reported as a catalyst for Friedel-Crafts reaction in literatures, could function as the catalyst.

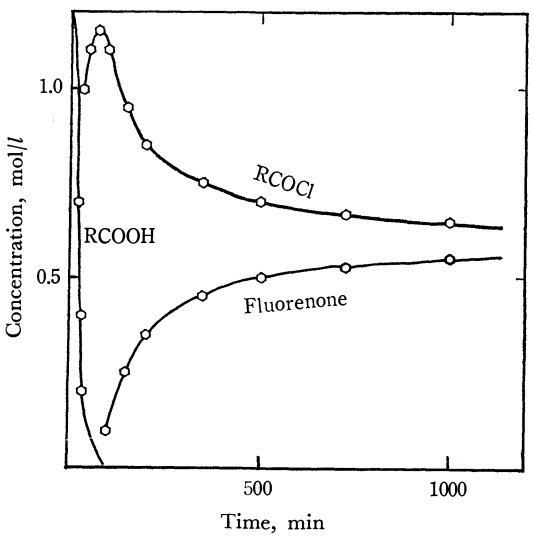

Fig. 1. Conversion of acid chloride to fluorenone. RCOOH=0.091 g, $SOCl_2$=0.331 m*l*, H_2O=0.02 g, 30.0°C

2) F. D. Greene, G. R. Van Norman, J. C. Cantrill and R. D. Gilliom, *J. Org. Chem.*, **25**, 1790 (1960).

The suppression of this Friedel-Crafts cyclization was investigated, and it was found that the addition of weak proton acceptor such as diethyl ether or diphenyl ether resulted in the almost complete suppression of the cyclization and the formation of the acid chloride in a good yield.

Experimental

o-Phenylbenzoic Acid. *o*-Phenylbenzoic acid was prepared from fluorenone by the method of Huntress and Seikel.[3]

Mp 114°C (lit[4] 114°C).

o-Phenylbenzoyl Chloride. Usually acid chlorides are prepared by heating acids with thionyl chloride. Greene *et al.*[2] reported that *o*-phenylbenzoyl chloride was prepared by the action of thionyl chloride on the acid and the distillation at 99.5—101°C/0.3 mmHg. They observed that some closure to fluorenone occurred during distillation (weak carbonyl absorption in the infrared at 1728 cm^{-1}).

However, when the acid was refluxed in thionyl chloride at 80°C for one hour almost all the acid was converted into fluorenone. After various attempts, the following method was found to be the best. A mixture of 1 g of the acid, 1 g of diethyl ether and 2.60 m*l* of thionyl chloride was let to react in an oil bath at 30°C for 120 min. Then the excess thionyl chloride was evaporated by aspirator. The residual oil was the acid chloride with a very small amount of fluorenone. The distillation at 99.5—101°C/0.3 mmHg yielded the pure acid chloride.

t-Butylperoxy o-Phenylbenzoate. A solution of 3.163 g (35.14 mmol) of *t*-butyl hydroperoxide in 10 m*l* of petroleum ether was added to a solution of 1 g (5.02 mmol) of the acid chloride in 10 m*l* of petroleum ether. 3.033 g (38.4 mmol) of pyridine in 10 m*l* of petroleum ether was then added slowly to this ice-cooled mixture. The solution was stirred at 0°C by a magnetic stirrer until the precipitation of pyridinium chloride was complete. The mixture was washed with a cold 10% sulfuric acid solution, a 5% sodium carbonate solution and water. The perester solution was then dried with anhydrous sodium sulfate. The evaporation of petroleum ether and other low-boiling impurities under vacuum yielded 1.13 g (83.4%) of the perester as a yellow oil. The infrared spectrum of this oil showed the strong absorption of the perester at 1765 cm^{-1}. When this oil in petroleum ether was passed down through a short chromatographic column packed with alumina, the decomposition of the perester occurred on the column. However, since the perester freed from low-boiling impurities was found to be of fair purity, this perester was used for kinetic and product studies. (Found: C, 76.03, H, 6.50%. Calcd for $C_{17}H_{18}O_3$, C, 75.53, H, 6.71%.).

Kinetic Procedure. A weighed quantity of perester was dissolved in cumene. The concentration of the solution was calculated to bring the concentration of the perester within the range of about 20 to 80% transmission as to the carbonyl absorption at the infrared.

The solution was transferred to about ten small test tubes. The tubes were then sealed at atmospheric pressure without degassing and placed in the thermostated oil bath at each decomposition temperature. The initial solution was taken as the zero time sample. At suitable intervals one of the tubes was subsequently withdrawn and cooled rapidly in ice. The infinity sample was left in the bath for about ten half lives. Each sample was stored at −5°C until the infrared analysis was carried out.

A Hitachi Infrared Spectrophotometer was used with cells of 0.1 mm thickness for the determination of the amount of the perester remaining.

The relative concentration at time t was calculated from the equation:

$$P/P_0 = \frac{\log T_\infty - \log T_t}{\log T_\infty - \log T_0}$$

Where T_∞ is the percentage transmission of the sample at infinite time against pure solvent, and T_0 is the percentage transmission of the initial sample.

Product Studies. 1.285 g (4.76 mmol) of the perester was dissolved in 10 m*l* of cumene in a decomposition flask and was attached onto a vacuum system. The solution was degassed three times by alternately freezing with dry ice - methanol mixture and evacuating the flask. The flask was sealed under vacuum and immersed in an oil bath at 125°C for about ten half lives until the perester decomposition was complete. The flask was again attached to the vacuum system. The amount of the gas not condensible with liquid nitrogen, which was presumably methane, was not determined. After the non-condensible gas was evacuated, the pressure of carbon dioxide released from the flask to the vacuum system was read on the manometer. The vacuum distillation of the solution yielded the liquid products and the non-distillable residue.

From the pressure of the gas and the known volume of the vacuum system, the number of moles of carbon dioxide formed was determined.

The volatile products in the solvent were identified to be acetone and *t*-butyl alcohol by the gas chromatography, and their amounts were quantitatively determined by a Shimadzu Gas Chromatograph Type GC-2B.

The infrared spectrum of the non-distillable residue indicated the presence of 3, 4-benzcoumarin (1747 cm^{-1}), *o*-phenylbenzoic acid (1690 cm^{-1}) and fluorenone (1717 cm^{-1}). The residue was chromatographed on alumina. The fractions were identified by the comparison of their infrared spectra and melting points with those of the authentic samples. The products found were biphenyl, bicumyl, fluorenone, 3, 4-benzcoumarin and *o*-phenylbenzoic acid.

Grateful acknowledgement is made to the donors of The Petroleum Research Fund, administered by the American Chemical Society, for support of this research.

3) E. H. Huntress and M. K. Seikel, *J. Am. Chem. Soc.*, **61**, 816 (1939).

4) "Kagaku Daijiten," Vol. VII, Kyoritsu, Tokyo (1961), p. 497.

A Simple Modification of Vilsmeier Method for the Preparation of Formylferrocene

Masaru SATO, Hiromichi KONO, Mikio SHIGA, Izumi MOTOYAMA and Kazuo HATA

Department of Chemistry, Faculty of Science, Tokyo Metropolitan University, Setagaya, Tokyo

(Received July 25, 1967)

Various routes to obtain formylferrocene (III), which serves as an important starting material for the synthesis of many ferrocene derivatives, have been reported.[1-6] The Vilsmeier reaction of ferrocene with *N*-methylformanilide and phosphoryl chloride was most conveniently utilized for the preparation of the aldehyde.[1-5] Graham and his coworkers[3] reported that the aldehyde could be prepared also with dimethylformamide and phosphoryl chloride as formylating reagent, but their method gave only 23% yield. In the course of synthetic investigation of ferrocene derivatives, the present authors found a modified Vilsmeier method using dimethylformamide instead of *N*-methylformanilide, in which the yield of the aldehyde was much improved and the separation of the product from the reaction mixture was much easier than the original method,[3] a troublesome chromatographic separation being unnecessary. In this modification, phosphoryl chloride was introduced into a chloroform solution of the mixture of ferrocene and dimethylformamide to form a Vilsmeier complex (II), which on careful neutralization by sodium carbonate afforded the aldehyde (III). The addition of ferrocene to the mixture of dimethylformamide and phosphoryl chloride also gave no unfavorable effect on the reaction. However, direct addition of phosphoryl chloride to ferrocene at the primary stage of the reaction decreased the yield of the product. This is probably due to the decomposition of ferrocene which is expected to occur to a certain extent by the action of phosphoryl chloride.

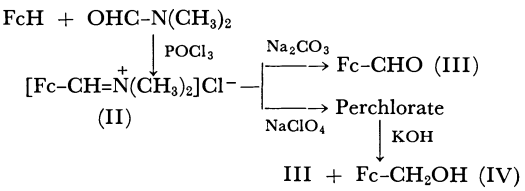

Fc = Ferrocenyl

When an aqueous solution of sodium perchlorate was added to the initial reaction mixture, followed by decomposition by water at the end of the reaction, violet crystals separated from the solution. Their IR spectrum showed the existence of $-C=\overset{+}{N}-$ group by the characteristic absorption band at 1668 cm^{-1}. Therefore, this substance is considered to be a perchlorate of the Vilsmeier complex (II) corresponding to that previously suggested by Jutz.[7] The perchlorate gave formylferrocene and hydroxymethylferrocene by treatment with 10% aqueous potassium hydroxide solution. Neither the Vilsmeier complex itself nor formylferrocene gave hydroxymethylferrocene by the action of aqueous alkali.

Experimental

A typical procedure for the modified Vilsmeier method was carried out as follows:

14.6 g (0.2 mol) of dimethylformamide was added to the solution of 18.6 g (0.1 mol) of ferrocene in 75 m*l* of dry chloroform and the resulting mixture was stirred in an ice-bath under nitrogen atmosphere for 10 min. Then, 30.6 g (0.2 mol) of phosphoryl chloride was added dropwise to the mixture over about half an hour. After the addition had been completed, the reaction mixture was kept stirring for 20 hr under heating at 55—60°C on a water-bath taking care that the temperature did not exceed 60°C. At the end of the reaction, chloroform was evaporated off under reduced pressure below 60°C,* and the residue was poured into the mixture of ice and water. Solid precipitates, most of which should be unreacted ferrocene, was filtered off. The filtrate, aqueous solution of the Vilsmeier complex, was neutralized carefully with sodium carbonate powder and then was extracted repeatedly with ether. All the extracts were combined together and dried over anhydrous magnesium sulfate after washing with water. The crude product obtained by evaporation of the solvent was pure enough for most synthetic purpose. Recrystallization from a mixed solvent (dichloromethane 3 : *n*-hexane 1) gave pure formylferrocene as reddish-brown crystals, mp 124.5°C. The yield was 15.2—15.7 g (71—74%).

1) G. D. Broadhead, J. M. Osgerby and P. L. Pauson, *Chem. Ind. (London)*, **1957**, 209.
2) G. D. Broadhead, J. M. Osgerby and P. L. Pauson, *J. Chem. Soc.*, **1958**, 650.
3) P. J. Graham, R. V. Lindsey, G. W. Parshall, M. L. Peterson and G. M. Whitman, *J. Am. Chem. Soc.*, **79**, 3416 (1957).
4) M. Rosenblum, *Chem. Ind. (London)*, **1957**, 72.
5) K. Schlögl, *Monatsh. Chem.*, **88**, 601 (1957).
6) K. Schlögl and A. Mohar, *ibid.*, **92**, 219 (1961).
7) C. Jutz, *Tetrahedron Letters*, **1959**, 1.

* The evaporation of solvent above 60°C will be hazardous because of accidental explosion.

A Correction Factor for Electrostatic Free Energy in Micelle Formation

Fumikatsu TOKIWA and Kenji OHKI

Research Laboratories, Kao Soap Company, Minato-Yakushubata, Wakayama-shi

(Received July 28, 1967)

It is well known that the critical micelle concentration (CMC) of a surfactant changes markedly with the concentration of counter-ions, c_i. There is in general a linear relation between log CMC and log c_i.[1-5] However, the log-log relation which we have obtained for straight-chain sodium decylbenzene sulfonate (SDBS) over a wide range of counter-ion concentrations is discrepant from the linear relation.*1 The present paper will discuss a correction factor for electrostatic free energy in micelle formation based on the dependence of CMC on the concentration of counter-ions.

Figure 1 shows the relation between log CMC and log c_i for SDBS.*2 The curves I and II are, respectively, the best-fitting straight and quadratic lines for the observed values in the sense of least squares. These two curves are written in the following forms:

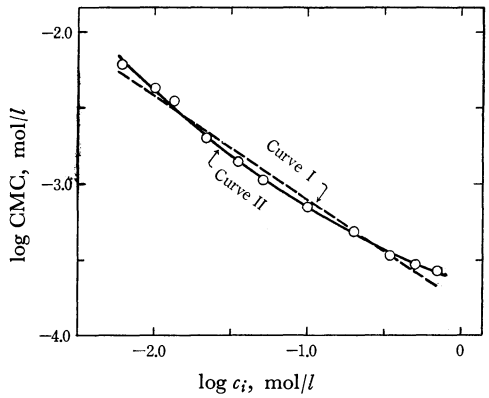

Fig. 1. The relation between log CMC and log c_i for SDBS at 25°C. The CMC values were taken from the sharp breaks in the solubilization curves for an oil-soluble dye, Yellow-OB, the method being described in previous papers.[7,8]

For the curve I,

$$\log \mathrm{CMC} = A + B \log c_i \qquad (1)$$

$$A = -3.77, \text{ and } B = -0.67$$

For the curve II,

$$\log \mathrm{CMC} = A' + B' \log c_i + C' (\log c_i)^2 \qquad (2)$$

$$A' = -3.66,\ B' = -0.40, \text{ and } C' = 0.12$$

Comparing the curves I and II, we may take the latter curve as the log CMC *vs.* log c_i relation for SDBS, since the curve II may be seen to be more fitting to the values experimentally determined than the curve I.

The micelle formation of ionic surfactants is generally governed by two energies: the cohesive energy among the hydrocarbon chains and the repulsive energy among the charged groups.[5,9,10] Thus, the CMC is expressed as:

$$\boldsymbol{k}T \ln \mathrm{CMC} = \Delta G_{\mathrm{HC}} + \lambda \varepsilon \phi_0 + K \qquad (3)$$

or:

$$\log \mathrm{CMC} = (0.434/\boldsymbol{k}T)(\Delta G_{\mathrm{HC}} + \lambda \varepsilon \phi_0 + K) \qquad (4)$$

where ΔG_{HC} is the free energy change in the hydrocarbon part by micelle formation; ϕ_0, the surface potential of the micelle; $\boldsymbol{k}$, the Boltzmann constant; T, the absolute temperature; ε, the elementary charge, and K, the constant which appears when the CMC value is expressed in moles per liter. The λ in Eq. (3) is the correction factor for the electrostatic free energy; that is, $\lambda \varepsilon \phi_0$ is the effective electrical energy.[7] If we assume a charged flat surface for the micelle, the surface potential of the micelle and the concentration of counter-ions are related by the Gouy-Chapman equation[11]:

$$\varepsilon \phi_0 / 2\boldsymbol{k}T = \sinh^{-1} \Theta c_i^{-1/2} = \ln\{\Theta c_i^{-1/2} + [1 + (\Theta c_i^{-1/2})^2]^{1/2}\} \qquad (5)$$

$$\Theta = (1000 \pi \sigma^2 / 2 \boldsymbol{N}_{\mathrm{A}} D \boldsymbol{k} T)^{1/2} \qquad (6)$$

where σ is the charge density; $\boldsymbol{N}_{\mathrm{A}}$, the Avogadro number, and D, the dielectric constant. The

*1 Such a deviation from the linear log-log relation has also been reported by Mysels.[6]

*2 The SDBS was prepared by the sulfonation of pure decylbenzene; it was neutralized with sodium hydroxide. The sample was purified by removing the unreacted material and inorganic salt.

1) M. E. Hobbs, *J. Phys. Chem.*, **55**, 675 (1951).
2) H. Lange, *Kolloid-Z.*, **121**, 66 (1951).
3) K. Shinoda, *J. Phys. Chem.*, **59**, 432 (1955).
4) M. J. Schick and F. M. Fowkes, *ibid.*, **61**, 1062 (1957).
5) K. Shinoda *et al.*, "Colloidal Surfactants," Academic Press, New York, N. Y. (1963).
6) E. K. Mysels and K. J. Mysels, *J. Colloid Sci.*, **20**, 315 (1965).
7) F. Tokiwa and K. Ohki, *J. Colloid Interface Sci.*, **23**, 456 (1967).
8) F. Tokiwa, This Bulletin, **36**, 222 (1963).
9) M. F. Emerson and A. Holtzer, *J. Phys. Chem.*, **69**, 3718 (1965).
10) K. Shinoda, This Bulletin, **26**, 101 (1953).
11) E. J. W. Verwey and J. Th. G. Overbeek, "Theory of the Stability of Lyophobic Colloids," Elsevier Publishing Co., New York, N. Y. (1948).

quantity of $(\Theta c_i^{-1/2})^2$ is much greater than unity, as will be shown later; therefore, Eq. (5) may be reduced to:

$$\varepsilon\psi_0/2\boldsymbol{k}T \simeq \ln 2\Theta c_i^{-1/2} = 2.30(\log 2\Theta - \tfrac{1}{2}\log c_i) \quad (7)$$

or:

$$\log c_i \simeq 2\log 2\Theta - (0.434/\boldsymbol{k}T)\varepsilon\psi_0 \quad (8)$$

By inserting Eq. (8) into Eq. (2) and comparing Eq. (2) with Eq. (4), we obtain the relation:

$$\lambda = C'(0.434/\boldsymbol{k}T)\varepsilon\psi_0 - (B' + 4C'\log 2\Theta) \quad (9)$$

The λ in Eq. (3) or (4) is thus a linear function of ψ_0, as may be seen in Eq. (9). The value of λ can be calculated in terms of Eq. (9) when B', C', and Θ are known. The B' and C' constants have already been given in Eq. (2). The value of Θ is estimated to be 2.26 $(\mathrm{mol}/l)^{1/2}$ from Eq. (6) by assuming a reasonable value of 8.0×10^4 esu/cm^2 for σ. The area of the micellar surface in cm^2/molecule, S, is assumed to be approximately 6.0×10^{-15},[12] which gives the above σ value, since $\sigma=\varepsilon/S$.

Figure 2 shows the λ *vs.* ψ_0 plots, ψ_0 being calculated in terms of Eq. (7). The value of λ is not constant, but increases with an increasing ψ_0 value. A similar result has been obtained for a nonionic-cationic surfactant, dimethyldodecylamide oxide (DDAO), which is also shown in Fig. 2.[7] Figure 2 suggests that the extent of interaction among the charged heads changes with the surface potential of the micelle. The difference in the λ *vs.* ψ_0 plots between SDBS and DDAO may be attributed to different ways of interaction among the charged heads. Further, the molecular structure of these surfactants probably has some relation with the interaction.

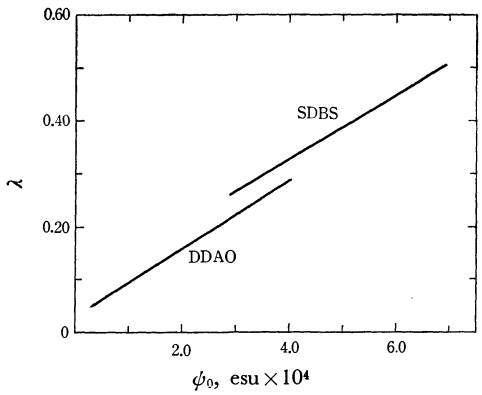

Fig. 2. The values of λ plotted against ψ_0. The plots for dimethyldodecylamine oxide is also shown for comparison.[7]

12) F. van Voorst Vader, *Trans. Faraday Soc.*, **56**, 1067 (1960).

The Dimerization of Butadiene in Methanol by a Palladium Complex Catalyst

Shigetoshi TAKAHASHI, Hiroshi YAMAZAKI and Nobue HAGIHARA

The Institute of Scientific and Industrial Research, Osaka University, Sakai, Osaka

(Received July 29, 1967)

In a previous work[1] we have reported how palladium complexes catalyzed a dimerization of butadiene to form a linear dimer. The dimerization of butadiene in benzene, tetrahydrofuran, or acetone gave octatriene-1.3.7, while the reactions in alcohols proceeded more smoothly to give 1-alkoxyoctadiene-2.7 and/or octatriene-1.3.7, depending on the nature of the alcohols employed. We now wish to report in detail on studies of the products derived from the dimerization reaction in methanol. It was found that the dimerization of butadiene in methanol at 70°C in the presence of bis(triphenylphosphine)(maleic anhydride)palladium gave 1-methoxyoctadiene-2.7 (85%), plus small amounts of octatriene-1.3.7 (3%) and an isomer (I) (5%) of methoxyoctadiene. When tetrakis(triphenylphosphine)platinum was used as the catalyst, the reaction proceeded slowly, but the proportion of the isomer I in the products was relatively greater. The pure isomer I was isolated from this reaction mixture by preparative gas chromatography. The isomer I is a colorless liquid with a bp of 145—146°C, n_D^{20} 1.4321. (Found: C, 77.17; H, 11.51%. Calcd for $C_9H_{16}O$: C, 77.09; H, 11.50%.) The infrared spectrum of the compound I showed the presence of terminal double bonds (994, 923, 910 cm^{-1}) and an ether group (1101 cm^{-1}). The NMR spectrum showed the presence of a methoxy group (6.88 τ), two $=CH_2$ and two =CH– groups, and a partial structure, $=CH-CH(OCH_3)-CH_2-$. These spectra indicate that the compound I is 3-methoxyoctadiene-1.7, $H_2C=CH-CH(OCH_3)-CH_2-CH_2-$

1) S. Takahashi, T. Shibano and N. Hagihara, *Tetrahedron Letters*, **1967**, 2451.

CH_2–CH=CH_2.*1

It is obvious that the formation of octatriene-1.3.7 in this catalytic dimerization in aprotic solvents involves hydrogen migration. Accordingly, the increasing rate of the reaction in protic solvents suggests the participation of the proton of the solvent. Because of our interest in the mechanism, therefore, the dimerization was carried out in CH_3OD. The main product, II (bp 164°C, n_D^{20} 1.4416), was recognized as monodeuterio-1-methoxyoctadiene-2.7 on the basis of its infrared (ν_{C-D} 2145 cm^{-1}) and NMR spectra. The position of the deuterium in the compound II could not be determined simply because the signals of the protons on C^4 and C^6 completely overlapped in its NMR spectrum. In order to distinguish them, the terminal double bond in the compound II was hydrogenated with $Ru(Ph_3P)_3Cl_2$ catalyst[2] in benzene-ethanol. It was confirmed that the compound II was 1-methoxy-6-deuteriooctadiene-2.7 because the hydrogenated product, III (bp 85—86°C/37 mmHg, n_D^{20} 1.4298), was found to be 1-methoxy-6-deuteriooctene-2 on the basis of a comparison of its NMR spectrum with that of 1-methoxyoctene-2 (bp 82—83°C/33 mmHg, n_D^{20} 1.4307).

$$2H_2C{=}CH{-}CH{=}CH_2 + CH_3OD \rightarrow CH_3{-}O{-}CH_2{-}CH{=}CH{-}CH_2{-}CH_2{-}CHD{-}CH{=}CH_2$$

(II)

$$\xrightarrow{H_2} CH_3{-}O{-}CH_2{-}CH{=}CH{-}CH_2{-}CH_2{-}CHD{-}CH_2{-}CH_3$$

(III)

These results suggest the presence of a π-allyl intermediate (IV) similar to that proposed by Wilke *et al.*,[3] although attempts to isolate the intermediate have thus far been unsuccessful. Thus, octatriene-1.3.7 may be produced through a reaction course which involves the $C^4 \rightarrow C^6$ migration of hydrogen, and two isomers of the methanol adduct, through the two different modes of the addition of methanol to the intermediate (1, 6 addition and 3, 6 addition).

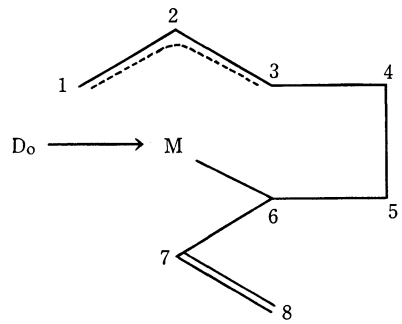

(IV) M=Pt or Pd

*1 The isomer of the acetic acid adduct, which was characterized as 4-acetoxyoctadiene-2.7 in our previous paper,[1] may really have the 3-acetoxyoctadiene-1.7 structure, similar to that of the isomer of the methanol adduct.

2) P. S. Hallman, D. Evans, J. A. Osborn and G. Wilkinson, *Chem. Commn.*, **1967**, 305.

3) G. Wilke, B. Bogdanović, P. Hardt, P. Heimbach, W. Kiem, M. Kröner, W. Oberkirch, K. Tanaka, E. Steinrücke, D. Walter and H. Zimmermann, *Angew. Chem.*, **78**, 157 (1966).

The Proton Magnetic Resonance Spectrum of the Palladium(II) Schiff Base Complex Derived from Glycine and Pyruvic Acid

Hayami YONEDA,* Yukiyoshi MORIMOTO,** Yasuo NAKAO*** and Akitsugu NAKAHARA***

*Chemistry Department, Wakayama University, Masagocho, Wakayama
**Research Laboratories, Fujisawa Pharmaceutical Company, Kashimacho, Higashiyodogawa-ku, Osaka
***Institute of Chemistry, College of General Education, Osaka University, Toyonaka, Osaka

(Received August 4, 1967)

Nakao, Sakurai, and Nakahara[1] prepared a pair of copper(II) complexes of Schiff bases derived from pyruvic acid and glycine, and from glyoxylic acid and α-alanine. Although they had been belived to have different structures, A and B, in the light of many results obtained by similar preparations earlier, it was disclosed that they were

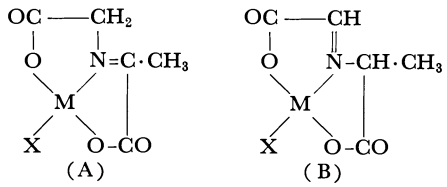

(A) (B)

M: Cu, Pd
X: H_2O in the case of Cu
Cl in the case of Pd

1) Y. Nakao, K. Sakurai and A. Nakahara, This Bulletin, **38**, 687 (1965); **39**, 1471 (1966).

identical, both having the same structure, A. Since the A and B structures are different only in the relative positions of the double bond and the hydrogen atoms, the finding suggests that transamination reactions proceed *via* proton transfer. Therefore, in order to obtain deeper insight into the mechanism of transamination reactions, it is necessary to determine the behavior of the hydrogen atoms in the Schiff base complexes by some physicochemical means.

Proton magnetic resonance spectroscopy would seem to be a powerful tool for this purpose. As the copper(II) complexes were not suitable for PMR measurements, we prepared the corresponding palladium(II) complexes of Schiff bases derived from pyruvic acid and glycine, and from glyoxylic acid and α-alanine. Like the copper(II) complexes, the palladium(II) complexes proved to be identical with each other. Figure 1 shows the spectrum run in a D_2O solution. It exhibits only the signal due to the CH_3 group. This suggests that the CH_2 protons were completely exchanged for deuterium immediately after dissolution. Thus the lability of the CH_2 protons in the Schiff base complex was revealed. This kind of lability reminds us of the active methylene of the malonato chelate. Previously[2] we found that the signal due to the CH_2 protons in the malonato complexes dissolved in D_2O decreased in intensity with time. We interpreted the lability of the CH_2 protons as a result of the electron-withdrawing effect of the two adjacent carbonyl groups. In the Schiff base complex, the electron density of the CH_2 group may be expected to be reduced by the two unsaturated groups, $-C=O$ and $-N=C\langle$, and also through the coordination of the N atom to the metal ion. Therefore, the CH_2 protons may be expected to be highly active. Thus, it is not surprising to see the CH_2 protons more active than those in the malonato complex.

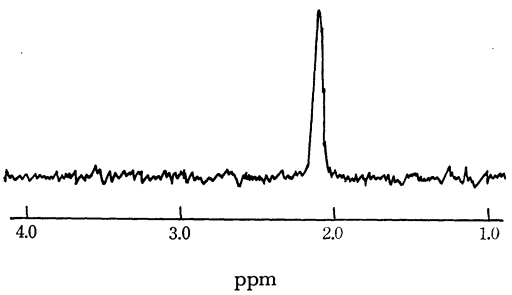

Fig. 1. The PMR spectrum of Na[Pd(pyv=gly)Cl] in D_2O.

The experimental details will be presented below.

Preparation of the Complex. Into 9 m*l* of a water : ethanol mixture (2 : 1 by volume) were stirred 0.62 g of sodium pyruvate and 0.42 g of glycine, and then 1 g of palladium chloride. After the solution had been kept at about 40°C for 2.5 hr under constant stirring, it was placed in an ice-bath. Yellow crystals thus came out. The crude product was recrystallized from a water : ethanol mixture (1 : 1 by volume). Found: C, 17.85; H, 2.53; N, 4.22%. Calcd for Na[Pd(CH_3·C(COO)=N·CH_2·COO)Cl]2H_2O: C, 17.45; H, 2.61; N, 4.08%. The same complex was obtained from glyoxylic acid and α-alanine.

NMR Measurements. The spectrum was recorded on a Varian A60 spectrometer. The chemical shift was measured relative to the sodium salt of trimethylsilyl propane sulfonic acid, taken as an internal standard.

2) H. Yoneda and Y. Morimoto, *ibid.*, **40**, 1737 (1967).

Polycondensation of β-Amino Acid Derivatives

Kohei SANUI, Mitsuo ISHIDA and Naoya OGATA

Chemistry Department, Sophia University, Chiyoda-ku, Tokyo

(Received August 4, 1967)

It was previously shown[1-3] that acrylate adds to amino alcohol and then, polycondensation follows at room temperature in the presence of an alkoxide to form polyamide as described below:

$$CH_2{=}CHCOOR + NH_2R'OH \rightarrow$$

$$HOR'NHCH_2CH_2COOR \rightarrow$$

$$\left[\begin{array}{l} \quad R'OH \\ -[-\overset{|}{N}CH_2CH_2CO-]- \\ -[-NHR'OCH_2CH_2CO-]- \end{array}\right] + ROH$$

The reaction medium has an influence on the course of the polycondensation and *N*-(hydroxyalkyl) poly-β-alanine is mainly formed in alcohol solution and polyamide ether is obtained in other polar solvent such as tetrahydrofuran. However,

1) N. Ogata and T. Asahara, This Bulletin, **39**, 1486 (1966).
2) N. Ogata and T. Asahara, *J. Polymer Sci.*, **B-4**, 273 (1966).
3) N. Ogata and K. Sanui, This Bulletin, in press.

when diamines were used in place of amino alcohol, polycondensation did not occur at room temperature in tetrahydrofuran solution and only a low molecular weight polymer was obtained in methanol solution.

In this paper, several *N*-(amino alkyl) β-alanine esters were synthesized from diamines and ethyl acrylate and their thermal polycondensation has been carried out in the presence of various catalysts. Following diamines were used for the synthesis:

$$NH_2R'NH_2 + CH_2{=}CHCOOR \rightarrow$$
$$NH_2R'NHCH_2CH_2COOR \rightarrow$$
$$-[-NHR'NHCH_2CH_2CO-]- + ROH$$

R': $-(CH_2)_2-$, $-(CH_2)_4-$, $-(CH_2)_6-$, $-(CH_2)_8-$, $-(CH_2)_{10}-$, $-CH_2-C_6H_4-CH_2-$

Commercially available ethylenediamine and hexamethylenediamine were used and, tetramethylenediamine and octamethylenediamine were synthesized from adipamide and sebacamide through the Hoffmann's reaction. Decamethylenediamine and *p*-xylylenediamine were synthesized from dehydration of sebacamide and terephthalamide followed by hydrogenation of the nitriles.

When equal moles of diamine and acrylate were mixed together in a solvent, an addition reaction took place immediately at the vinyl group of acrylate at room temperature. Infrared spectrum of the product showed absorptions owing to amino and ester carbonyl groups as can be seen in Fig. 1. The acid titration curve exhibited two inflection points which corresponded with one amino and one imino groups. Color reactions of primary and secondary amine groups were also observed. Therefore, it is presumed that the addition product has a structure of *N*-(amino alkyl) β-alanine ester.

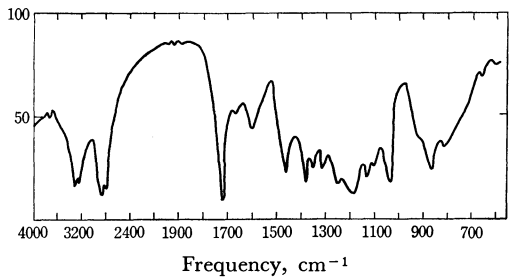

Fig. 1. Infrared spectrum of the reaction product of ethylene diamine and ethyl acrylate.

Table 1. Thermal polycondensation of $NH_2(CH_2)_nNHCH_2CH_2COOC_2H_5$*

n	Catalyst 1 mol%	Yield %	η_{inh}**	M.W.	Degree of crosslinking	Character
2	—	100	0.05[a]	500	—	yellow grease
	K	95	0.05[a]		—	yellow grease
	$SnCl_2$	67	0.09[a]		—	yellow solid
	$SnCl_4$	98	0.09[a]		—	yellow solid
	$TiCl_4$	93	0.13[a]	1000	—	yellow solid
	$AlCl_3$	93	0.11[a]		—	yellow solid
	$ZnCl_2$	90	0.07[a]		—	yellow solid
	BF_3OEt_2	96	0.08[a]		—	yellow solid
4	—	100	0.11[a]		—	white solid
	$SnCl_4$	100	0.21[a]	1800	—	white solid
	$TiCl_4$	100	0.14[a]	1400	—	white solid
6	—	100	0.04[b]	460	—	white grease
	$SnCl_2$	98	—	—	30%	white elastic
	$SnCl_4$	100	—	—	15%	white elastic
	$TiCl_4$	100	—	—	22%	white elastic
	$AlCl_3$	98	0.27[b]	—	—	white solid
	$ZnCl_2$	95	0.08[b]		—	white grease
	BF_3OEt_2	100	—	—	28%	white elastic
8	$SnCl_4$	100	—	—	48%	white solid
10	—	100	—	—	19%	white elastic
	Na	100	—	—	51%	white elastic
	$SnCl_4$	100	—	—	67%	white solid
	$TiCl_4$	100	—	—	52%	white solid
	$AlCl_3$	100	—	—	27%	white elastic
	$ZnCl_2$	100	—	—	18%	white elastic

* Polymerization temperature, 153°C; time, 5 hr; vacuum, 2 mmHg.
** Measured a) in water, b) in methanol, at 30°C.

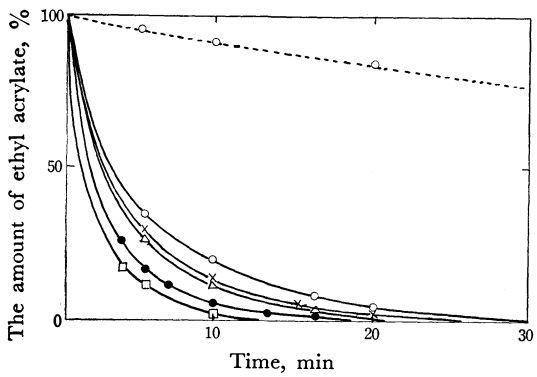

Fig. 2. The rate of reaction of diamines and ethyl acrylate (Concn., 1 mol/*l*, at 20°C).
----: in THF, ——: in methanol
○: $-(CH_2)_2-$, ×: $-(CH_2)_4-$, ●: $-(CH_2)_6-$
□: $-(CH_2)_8-$, $-(CH_2)_{10}-$,
△: $-CH_2-C_6H_4-CH_2-$

These esters were purified by a fractional distillation or recrystallization from alcohol and water.

The rates of the addition of several diamines to acrylate were determined in tetrahydrofuran or methanol solutions at 25°C by gas chromatographic analysis. The results in Fig. 2 show that the rate becomes faster with increasing carbon numbers of diamine and the rate in methanol solution is about 100 times as fast as in tetrahydrofuran solution. The accerelating effect of alcohol on the Michael reaction of acrylate was previously reported.[4]

The boiling or melting points of the esters is as follows; $NH_2(CH_2)_2NHCH_2CH_2COOC_2H_5$: bp 97°C/2 mmHg, $NH_2(CH_2)_4NHCH_2CH_2COOC_2H_5$: bp 140°C/7 mmHg, $NH_2(CH_2)_6NHCH_2CH_2COOC_2H_5$: bp 135°C/3 mmHg, $NH_2(CH_2)_{10}NHCH_2CH_2COOCH_3$: mp 92°C. *N*-(4-Aminomethyl benzyl) β-alanine ethyl ester polycondensated easily during distillation and it was used for polycondensation without distillation.

The thermal polycondensation of the esters was carried out by heating in vacuum in the presence of 1 mol% of basic or acidic catalysts. Results are shown in Tables 1 and 2. It is seen that acidic catalysts such as $SnCl_4$ or $TiCl_4$ are effective for the thermal polycondensation of *N*-(amino alkyl) β-alanine esters and the degree of crosslinking of polymers increases with increasing number of *N*-alkyl group.

Table 2. Thermal polycondensation of $NH_2CH_2-C_6H_4-CH_2NHCH_2CH_2COOC_2H_5$*

Catalyst 1 mol%	Yield %	η_{inh}**	M.W.	Character
—	85	0.03	670	yellow solid
K	88	0.03	—	yellow solid
$SnCl_4$	73	0.07	1800	yellow solid
$TiCl_4$	75	0.06	—	yellow solid
$AlCl_3$	82	0.04	—	yellow solid
BF_3OEt_2	80	0.05	—	yellow solid

* Polymerization temperature, 153°C; time, 5 hr; vacuum, 2 mmHg.
** Measured in methanol at 30°C.

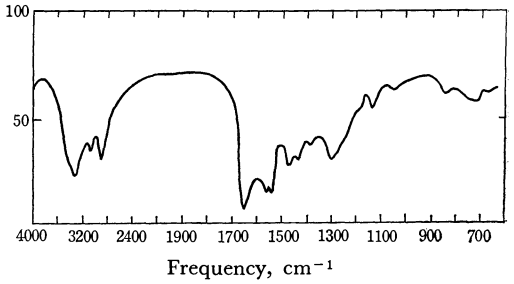

Fig. 3. Infrared spectrum of the polymer of $NH_2(CH_2)_2NHCH_2CH_2COOC_2H_5$.

Infrared spectrum of the polymers showed absorptions owing to secondary amide group as can be seen in Fig. 3 and it is presumed that the polycondensation takes place between primary amino and ester groups since no amide II band should be appeared at 1550 cm^{-1} if polycondensation takes place between imino and ester groups.

Solubility of the polymers in various solvents is summarized in Table 3. Solubility decreases in

Table 3. Solubility of polyamide imine $-[-NHRNHCH_2CH_2CO-]-$* in various solvents

Solvent	$-(CH_2)_2-$	$-(CH_2)_4-$	$-(CH_2)_6-$	R $-(CH_2)_8-$	$-(CH_2)_{10}-$	$-CH_2-C_6H_4-CH_2-$
H_2O	○	○	△	△	×	×
CH_3OH	○	○	△	△	△	○
H_2SO_4	○	△	△	—	—	○
HCOOH	○	○	△	—	—	○
DMF	×	×	×	△	△	○
DMSO	○	△	△	—	—	○
$[(CH_3)_2N]_3PO$	×	△	△	—	—	○

○: Soluble ×: Insoluble △: Swelling * Catalyst: $SnCl_4$, 153°C, 5 hr, 2 mmHg

4) N. Ogata and K. Sanui, *Kogyo Kagaku Zasshi (J. Chem. Soc. Japan, Ind. Chem. Sect.)*, to be submitted.

the following order owing to crosslinking: *N*-amino alkyl group, $-CH_2-\langle\bigcirc\rangle-CH_2-$, $-(CH_2)_2-$ $>-(CH_2)_4->-(CH_2)_6->-(CH_2)_8-$, $-(CH_2)_{10}-$.

N-(2-Aminoethyl) β-alanine ethyl ester gave a polymer with a molecular weight of 1000, which had a greenish yellow fluorescence and was water-soluble, and *N*-(4-aminobutyl) β-alanine ethyl ester yielded a white solid with a molecular weight of 1800 which was also water-soluble. *N*-(4-Aminomethyl benzyl) β-alanine ethyl ester gave a water-insoluble but alcohol-soluble polymer. It is assumed from their solubility that linear polyamide imines were obtained in these cases. However, thermal polycondensation of higher *N*-alkyl esters resulted in a white, elastic and infusible polymer which had a crosslinked structure. It is assumed that the reactivity of imino group increases with increasing carbon number of *N*-alkyl group, resulting in a crosslinked polymer. The degree of crosslinking, which was determined by acid titration, was about 15 to 30%. The film from *N*-(6-aminohexyl) β-alanine ester could be elongated almost 300%.

In the case of thermal polycondensation of *N*-(6-aminohexyl) β-alanine ester, two-steps polycondensation is possible to obtain an elastic polymer film, that is, pre-polycondensation followed by secondary polycondensation in the presence of acidic catalyst. This method leads to the processing or the film casting. It might be possible to use these polymers as an anion exchange resin since basic imino group is placed in the polymer.

Asymmetric Synthesis with Sugar Derivatives. IV. Catalytic Hydrogenations of Phenylglyoxylic Esters of Sugar Derivatives

Masajiro KAWANA and Sakae EMOTO

Rikagaku Kenkyusho (The Institute of Physical and Chemical Research), Yamato-machi, Kita-Adachi-gun, Saitama

(Received August 9, 1967)

In connection with the studies[1] of asymmetric synthesis with sugar derivatives, the present work was undertaken to examine the effects of the sugars on the stereochemical course of the hydrogenations of phenylglyoxylic sugar-esters over the metal catalysts. The following sugar esters were employed: 1, 2; 5, 6-di-*O*-cyclohexylidene-3-*O*-phenylglyoxyl-α-D-glucofuranose (I), its isopropylidene derivative (II), 5-*O*-ethyl-1, 2-*O*-isopropylidene-3-*O*-phenylglyoxyl-α-D-xylofuranose (III), and its 5-deoxy derivative (IV). These esters were hydrogenated over Raney nickel or palladium in ethanol to the diastereomeric sugar mandelates, which were rapidly hydrolyzed under alkaline conditions[2] at room temperature to produce mandelic acid in 44.6% (maximum) optical yield (Table 1).

The easy removal of the sugar parts is of great advantage to asymmetric synthesis of optically unstable substances.

Mitsui *et al.*[3a] reported that (−)-menthyl phenylglyoxylate (V) was hydrogenated in the presence of various catalysts to diastereomeric (−)-menthyl mandelates, which gave either enatiomer of mandelic acid in excess after partial hydrolysis[4] with acid (Table 1). The direction of the asymmetric induction dependend on the natures of the catalysts used: 5% palladium on charcoal (Pd-C) prepared by the reduction of palladium chloride with hydrogen, or with formaldehyde in an alkaline solution contains extremely small quantities of acid (A) or base (B), respectively, and Raney nickel (Ni) has also trace amounts of alkali. They found that the acid or the base in the catalysts exerted influence on an equilibrium between (−)-menthyl ester (V) and its hemiketal in ethanol, and explained the steric course of the asymmetric hydrogenation according to Prelog's rule[5] as described below.[3a-d]

In the presence of Pd-C-A, *s*-cis (-COCO-) conformer of (−)-menthyl ester (V) will exist predominantly over *s*-trans one since the hemiketal of the former is more stabilized than that of the latter by the formation of intramolecular hydrogen bonding between the hydroxyl and the ester

1) Part III: M. Kawana and S. Emoto, This Bulletin, **40**, 2168 (1967).

2) A. McKenzie, *J. Chem. Soc.*, **85**, 1249 (1904); M. Kawana and S. Emoto, This Bulletin, **40**, 618 (1967).

3) a) S. Mitsui, T. Kamaishi, M. Imaizumi and K. Takamura, *Nippon Kagaku Zasshi (J. Chem. Soc. Japan, Pure Chem. Sect.)*, **83**, 1115 (1962); *Chem. Abstr.*, **59**, 11569 (1963); b) T. Kamaishi and S. Mitsui, *Nippon Kagaku Zasshi (J. Chem. Soc. Japan, Pure Chem. Sect.)*, **86**, 623 (1965); *Chem. Abstr.*, **65**, 2326 (1966); c) S. Mitsui and A. Kanai, *Nippon Kagaku Zasshi (J. Chem. Soc. Japan, Pure Chem. Sect.)*, **87**, 179 (1966); *Chem. Abstr.*, **65**, 17006 (1966); d) S. Mitsui and Y. Imai, *Nippon Kagaku Zasshi (J. Chem. Soc. Japan, Pure Chem. Sect.)*, **88**, 86 (1967).

4) It was verified that (−)-menthyl (±)-mandelate was hydrolyzed with acid at equal rate.

5) V. Prelog, *Helv. Chim. Acta*, **36**, 308 (1953); V. Prelog and H. Scherrer, *ibid.*, **42**, 2227 (1959).

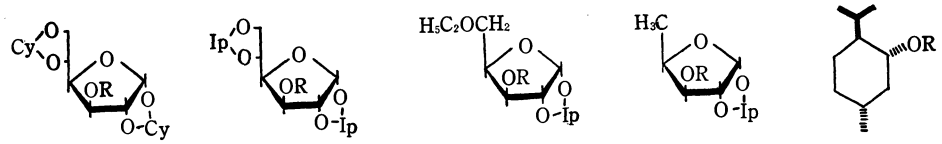

I II III IV V

R=-COCOC$_6$H$_5$, Cy=Cyclohexylidene, Ip=Isopropylidene

TABLE 1. ASYMMETRIC SYNTHESIS OF MANDELIC ACID

Ester[a]	Catalyst,[b]	mg	Reduction time, hr	Yield %	$[\alpha]_D$ (c, H_2O), °C	Optical[c] yield, %
I	Raney Ni	300 (wet)	2.5	72.4	−70.5° (0.44) 25	44.6
	5% Pd-C-B	50	8.0	71.1	−36.1° (0.44) 21	22.8
	5% Pd-C-A	50	2.0	70.4	+38.1° (0.42) 20	24.1
II	Raney Ni	500 (wet)	1.0	76.3	−58.0° (0.46) 25	36.7
	5% Pd-C-B	50	4.5	80.3	−24.4° (0.45) 26	15.4
	5% Pd-C-A	50	1.5	83.6	+32.0° (0.41) 20	20.3
III	Raney Ni	250 (wet)	1.5	72.3	−31.4° (0.43) 25	19.9
	5% Pd-C-B	33	3.0	82.2	+ 2.3° (0.44) 26	1.5
	5% Pd-C-A	33	4.0	89.1	+14.9° (0.41) 26	9.4
IV	Raney Ni	350 (wet)	2.0	72.4	−22.1° (0.48) 26	14.0
	5% Pd-C-B	50	5.3	78.9	−20.0° (0.40) 21	12.7
	5% Pd-C-A	50	1.5	77.0	+20.2° (0.45) 25	12.8
V[d]	Raney Ni	1000 (wet)	1	—	−25.4° (4.6) 4	16.1
	5% Pd-C-B	500	10	—	−15.8° (3.2) 28	10.0
	5% Pd-C-A	100	5	—	+21.2° (5.1) 12	13.4

a) One mmol of the ester was hydrogenated except III and V, which were 0.67 and 10 mmol, respectively.
b) 5% Pd-C-B or -A means 5% palladium on charcoal contained base or acid, respectively; see Ref. 6. The catalysts from the same batch were used throughout the present experiments.
c) Calculated on the base of $[\alpha]_D$ 158° for optically pure mandelic acid.
d) Mitsui's data, see Ref. 3a.

carbonyl group. As a result of the reduction of the dominant *s*-cis conformer, L(+)-mandelic acid was produced in excess after the hydrolysis. In the presence of Pd-C-B or Ni, however, the *s*-trans conformer will be dominant since the formation of the hydrogen bonding of the hemiketal is prevented by the base contained in the catalyst. Therefore, preponderance of D(−)-mandelic acid was brougt about.

The data for the sign of rotation of mandelic acid from the sugar esters were in agreement with Mitsui's results except for 5-*O*-ethyl derivative (III), which afforded L(+)-acid in slightly excess by the reduction over Pd-C-B; such a specific property of Pd-C-B was observed in the asymmetric hydrogenation of (−)-menthyl α-naphtylglyoxylate.[3d] It seemed likely that the exposure of oxygen of the ethoxyl group in 5-*O*-ethyl derivative (III) played an important role for III being absorbed on Pd-C-B.

Regarding to the optical yields of mandelic acid, nickel gave better results than palladium did, and this trend appeared in the hydrogenation of (−)-menthyl ester (V). In the case of 5-deoxy derivative (IV), however, the difference of the optical yield between Ni and Pd was very small.

From these experiments it is concluded that in the asymmetric hydrogenation as well as the asymmetric Grignard addition[1] the sugar derivatives in the esters behaved like (−)-menthol in regard to determining the stereochemical course, one exception being included.

Experimental

Optical rotations were measured with a Perkin-Elmer Model 141 photoelectric polarimeter in a 1 dm tube.

Starting materials were prepared according to the procedure described earlier.[1]

Asymmetric Synthesis of Mandelic Acid. A solution of the sugar ester (1.0 mmol) in absolute ethanol (15 m*l*) was hydrogenated over 5% palladium on

charcoal[6] or Raney nickel (W-7)[7] catalyst at room temperature and ordinary pressure. Hydrogen absorption stopped or nearly stopped after the consumption of 1.0—1.2 mmol of hydrogen. The catalyst was removed by filtration and washed with ethanol. Evaporation of ethanol at 25°C and reduced pressure gave the crude sugar mandelate whose infrared spectrum did not showed the absorption of the keto carbonyl group. The reduction products were hydrolyzed without purification with a mixture of sodium hydroxide (80 mg) in water (3 m*l*) and methanol (10 m*l*) at room temperature for 30 min. After water (7 m*l*) had been added under cooling, the mixture was concentrated to about 10 m*l* at 25°C and reduced pressure, diluted with water (5 m*l*) and extracted several times with chloroform (70—140 m*l*, total volume) until the sugar in the last extract could not be detected by thin-layer chromatography of silica gel G (E. Merck, Darmstadt, Germaney) with ether-petroleum ether (3 : 7, v/v) solvent system.[8]

From the extract the crude sugar derivative was recovered in 84—99% yield. The complete hydrolysis of the reduction products was ascertained by the measurement of infrared spectrum of the extract.

The water layer was acidified with 6 N hydrochloric acid (1 m*l*) and extracted with ether (100 m*l*). The extract was washed twice with a small quantities of water and dried over sodium sulfate. Evaporation of ether afforded the crude acid, which, on treatment with charcoal (20 mg) in water (5 m*l*), gave mandelic acid. The infrared spectrum of the acid was identical with that of the commercially available one.

The results and other experimental conditions are summarized in Table 1.

6) R. Mozingo, "Organic Syntheses," Coll. Vol. III, ed. by E. C. Horning, p. 685 (1955); 5% Pd-C-B and Pd-C-A were prepared by the procedures B and C, respectively. Pd-C-A was used for the hydrogenation without washing with ethanol.

7) H. R. Billica and H. Adkins, "Organic Syntheses," Coll. Vol. III, ed. by E. C. Horning, p. 176 (1955); The catalyst was sufficiently washed with water.

8) The developed layer was visualized by spraying with a mixture of methanol, sulfuric acid, and *p*-anisaldehyde (17 : 2 : 1, v/v) and then heating.

The Structure of the Oxazolidine-2-thione Derivative of D-Glucose*[1]

Juji YOSHIMURA and Hironobu HASHIMOTO

The Department of Chemistry, Tokyo Institute of Technology, Ookayama, Meguro-ku, Tokyo

(Received August 22, 1967)

Some reducing sugars[1-3] have been reported to give crystalline condensation products having an oxazolidine-2-thione ring by reaction with thiocyanic acid. The structural studies on the mode of condensation between oxazolidine-2-thione ring and sugar ring in these compounds have been mainly performed for the corresponding glucose derivative (I).

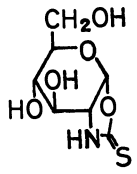

A

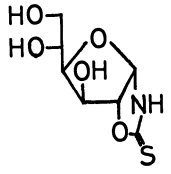

B

Zemplen *et al.*[1] gave the formula A for I, however, the formula B has generally been accepted from the following facts. Edward and Martlew[4] showed by paper chromatography the presence of 1-aminoglucose and diglucosylamine in the hydrolysate of I, but no glucosamine was demonstrated which was expected from the formula A. Wickström and Wold[5] also supported the formula B by comparison of the pK_a value of I with those of simple oxazolidine-2-thiones. As for the ring size of the sugar moiety in I, Schwarz[6] concluded the presence of a furanose ring from the facts that one mole of formaldehyde was liberated by periodate oxidation and orthoformate was formed by treatment with ethyl orthoformate.

Recently Jochims *et al.*[7] reported on the synthesis and the structure of I and its homologues in which I was proved to be D-glucofurano[1′, 2′: 4, 5]-oxazolidine-2-thione (formula B) from the NMR data in dimethylsulfoxide-d_6. H_1 (the proton attached to the C-1 of the sugar moiety) was found to be weakly coupled to NH and H_4 not to any hydroxyl protons. The authors have also obtained the same results by NMR studies of some derivatives of I.

It will be rationally expected that the *N*-acetylation of I should affect most strongly the chemical

*1 This paper was presented at the 20th Annual Meeting of The Chemical Society of Japan, April, 1967.

1) G. Zemplen, A. Gerecs and M. Rados, *Ber.*, **69**, 748 (1936).
2) G. Zemplen, A. Gerecs and E. Illes, *ibid.*, **71**, 590 (1938).
3) N. H. Bromund and R. M. Herbst, *J. Org. Chem.*, **10**, 2267 (1945).
4) J. T. Edward and E. F. Martlew, *Chem. Ind. (London)*, **1952**, 1034.
5) A. Wickström and J. K. Wold, *Acta. Chem. Scand.*, **13**, 1129 (1959).
6) J. P. C. Schwarz, *J. Chem. Soc.*, **1954**, 2644.
7) J. C. Jochims, A. Seeliger and G. Taigel, *Chem. Ber.*, **100**, 845 (1967).

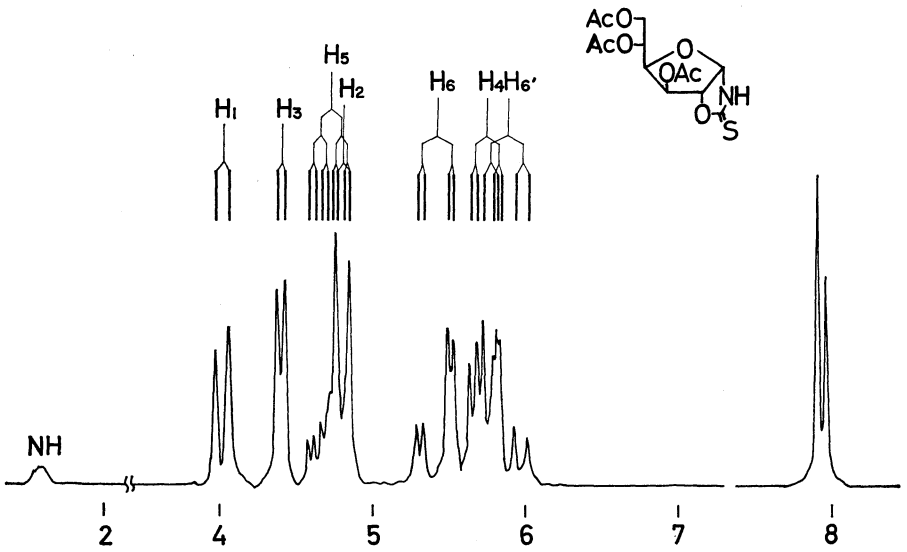

Fig. 1. NMR spectrum of II in $CDCl_3$ at 60 Mc.

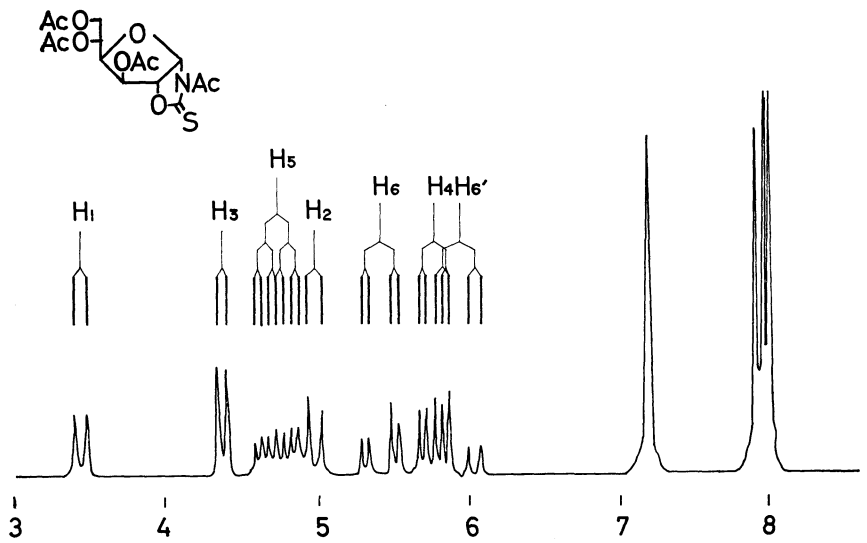

Fig. 2. NMR spectrum of III in $CDCl_3$ at 60Mc.

shift of the proton on the carbon attached to the nitrogen atom. In comparison of the NMR spectra of the tri-*O*-acetate (II) and tetra-*N*, *O*-acetate (III) of I[1] (Figs. 1 and 2), it was observed that the chemical shift of H_1 was shifted far to the lower field, but that of H_2 was slightly to the higher field although those of other ring protons were almost identical (Table 1). This fact indicates that the nitrogen is attached to C-1 of the sugar ring. The unexpected shift of H_2 will be explained by the prevention of the contribution from the en-thiol structure in the *N*-acetyl derivative.

The dihedral angles in compounds II and III calculated from observed coupling constants by the modified Karplus equation of Abraham and coworkers[8] were 40° and 42° between H_1 and H_2, 80° and 80° between H_2 and H_3, and 53° and 53° between H_3 and H_4 respectively. These values imply that the furanose ring in these compounds has a "twist" conformation in which C-2 and C-3 are out of the plane containing the other ring members as shown in the case of 1, 2-*O*-isopropylidene-D-glucofuranose and its derivatives.[8]

The presence of the furanose ring in I was also ascertained by chemical methods. It is known

8) R. J. Abraham, L. D. Hall, L. Hough and K. A. McLauchlan, *J. Chem. Soc.*, **1962**, 3699.

TABLE 1. THE NMR SPECTRAL DATA OF D-GLUCOFURANO[1′,2′:4,5]OXAZOLIDINE-2-THIONE DERIVATIVES

Chemical shifts (τ values)

Compound	H_1	H_2	H_3	H_4	H_5	H_6	$H_{6'}$	OH
II	4.03 d	4.82 d	4.41 d	5.75 q	4.73 m	5.42 q	5.89 q	—
III	3.50 d	5.02 d	4.43 d	5.81 q	4.78 m	5.46 q	5.98 q	—
IV	4.12 d	4.92 d	5.80 d	6.37 q	5.68 m	6.10 q	6.18 q	4.28 d
V	4.00 d	4.75 d	5.18 d	...	...	...	...	4.84 t
VI	4.05 d	4.90 d	5.65 b	6.12 q	5.60 m	5.90 q	6.05 q	4.20 d

Coupling constants (cps)

Compound	$J_{1,2}$	$J_{2,3}$	$J_{3,4}$	$J_{4,5}$	$J_{5,6}$	$J_{5,6'}$	$J_{6,6'}$	$J_{H,OH}$
II	5.1	<0.5	3.0	9.0	2.6	5.4	12.3	—
III	4.8	<0.5	3.0	9.0	2.7	5.7	12.3	—
IV	5.4	<0.5	2.5	6.0	6.0	6.0	6.5	5.0
V	6.0	<0.5	2.0	...	...	...	...	*ca.* 5.0
VI	5.4	<0.5	2.5	5.0	6.0	6.0	6.0	*ca.* 5.0

d: doublet, t: triplet, q: quartet, m: multiplet, b: broad.
--- These peaks were not resolved.

that the glucopyranose ring can not be isopropylidenated,[9] however, I gave a mono-isopropylidene derivative (IV), whose NMR spectrum measured in dimethyl sulfoxide-d_6 showed the hydroxyl signal at 4.28 (τ value) in doublet, indicating the presence of the secondary hydroxyl group. Therefore, IV should be 5′, 6′-*O*-isopropylidene-D-glucofurano[1′, 2′:4, 5]oxazolidine-2-thione, but not the corresponding 3′, 5′-*O*-isopropylidene derivative.

When I was benzylidenated with benzaldehyde and zinc chloride, two isomers which showed mp 232—233°C (V) and 186—188°C (VI) respectively were obtained. In the NMR spectra of these compounds also measured in dimethyl sulfoxide-d_6, each hydroxyl proton appears at 4.83 in triplet and at 4.20 in doublet, indicating the presence of a primary and a secondary hydroxyl group respectively. So V and VI were proved to be 3′, 5′-*O*-benzylidene- and 5′, 6′-*O*-benzylidene-D-glucofurano[1′, 2′: 4, 5]oxazolidine-2-thione respectively.

Experimental

NMR spectra were measured on JNM-3H-60 spectrometer at 60 Mc in deuterochloroform for II and III, and in dimethyl sulfoxide-d_6 for IV, V and VI respectively. Tetramethylsilane was used as an internal reference in each case.

5′, 6′-*O*-Isopropylidene-D-glucofurano[1′,2′ : 4,5]-oxazolidine-2-thione (IV). To a suspension of I (2.4 g) in dry acetone (60 m*l*) concentrated sulfuric acid (0.8 m*l*) was added dropwise with stirring in an ice-water bath, and the stirring was continued for a few hours. The reaction mixture was poured into ice-water containing sodium bicarbonate (5 g), and extracted with methylene chloride (100 m*l*). Methylene chloride layer was washed with water and dried over anhydrous sodium sulfate. Evaporation of methylene chloride gave white residue, which was recrystallized from ethanol, mp 220—221°C, $[\alpha]_D^{22}$ +33.0° (*c* 1.8, pyridine), yield 1.7 g.

Found: C, 46.05; H, 5.74; N, 5.48%. Calcd for $C_{10}H_{15}O_5NS$: C, 45.97; H, 5.79; N, 5.36%.

3′, 5′-*O*-Benzylidene- and 5′, 6′-*O*-Benzylidene-D-glucofurano[1′, 2′ : 4, 5]oxazolidine-2-thione (V and VI). A suspension of I (2.5 g) and anhydrous zinc chloride (3.0 g) in benzaldehyde (20 m*l*) was shaken for 1 hr to give a clear solution. The reaction mixture was poured into ice-water, stirred with petroleum ether, and the petroleum ether layer was decanted. It was repeated twice more to give a mixture of crystals and hard sirup. When this mixture was dissolved in hot ethanol (*ca.* 30 m*l*), a small amount of crystals was remained undissolved, which was filtered and recrystallized from a little larger amount of ethanol to give V as white crystals, mp 232—233°C, $[\alpha]_D^{22}$ +66.5° (*c* 1.0, pyridine), yield 0.2 g.

Found: C, 54.27; H, 4.84; N, 4.57%. Calcd for $C_{14}H_{15}O_5NS$: C, 54.36; H, 4.89; N, 4.53%.

From the filtrate, another crystals were separated and recrystallized from ethanol to give VI, mp 186—188°C, $[\alpha]_D^{22}$ +68.1° (*c* 1.0, pyridine), yield 0.6 g.

Found: C, 54.43; H, 4.92; N, 4.68%. Calcd for $C_{14}H_{15}O_5NS$: C, 54.36; H, 4.89; N, 4.53%.

The authors thank Mr. T. Tanaka of Science University of Tokyo for the oxazolidine-2-thione derivative of D-glucose.

9) J. A. Mills, "Advances in Carbohydrate Chemistry," Vol. 10, ed. by C. S. Hudson and S. M. Cantor, Academic Press Inc., Publishers, New York, N. Y. (1955), p. 1.

SHORT COMMUNICATIONS

Studies of 2-Azabicyclo[3, 2, 2]nonanone-3. I. A New Synthesis of 2-Azabicyclo[3, 2, 2]nonanone-3

Masaaki TAKAHASHI and Shigeyuki SUZUKI

Tokyo Research Laboratory, Kureha Chemical Co., Ltd., Hyakunin-cho, Shinjuku-ku, Tokyo

(Received September 25, 1967)

Although 2-azabicyclo[3, 2, 2]nonanone-3 (I)[1-3] seems to be an interesting modifier for the polyamide obtained from ε-caprolactam, no detailed report has yet been published on the copolymerization of I with ε-caprolactam.

In the course of our studies of the copolymerization, we have achieved a new synthesis of I, starting from bicyclo[2, 2, 2]octene-2 (II). II has been obtained by the reaction of 1, 3-cyclohexadiene (III) with excess ethylene under pressure in an pressure vessel at 200°C.[4]

The addition of nitrosyl chloride to II in the presence of hydrogen chloride at 0—5°C in triclene

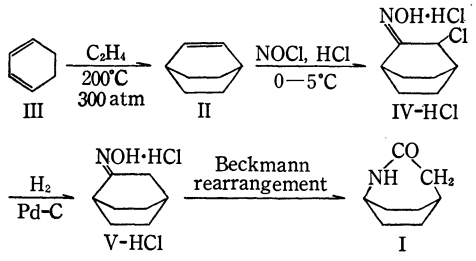

afforded 3-chlorobicyclo[2, 2, 2]octanone-2-oxime hydrochloride (IV-HCl), mp 127.5—130°C (dec.), in a 80% yield.

The treatment of IV-HCl with dilute NH_4OH gave the free chloroxime (IV), mp 106—106.5°C. The structures of IV-HCl and IV have been confirmed by elemental analysis, and by a study of their NMR and IR spectra.

The chlorine in the chloroxime was replaced with hydrogen under an atmospheric pressure, using Pd-C as the catalyst. Surprisingly enough, both IV and IV-HCl were smoothly hydrogenated at room temperature in ethanol. Bicyclo[2, 2, 2]octanone-2-oxime-hydrochloride (V-HCl) was obtained in an excellent yield, upon neutralization, this afforded the free oxime (V).

The Beckmann rearrangements of both V and V-HCl were carried out with benzenesulfonyl chloride in an alkaline solution. The product had a melting point identical with that of the lactam obtained from bicyclo[2, 2, 2]octanone-2 and hydroxylamine.[1]

The structure of the lactam was further confirmed by a study of the NMR spectrum and by the reduction of the carbonyl group with $LiAlH_4$.

Interesting polyamides have been obtained by the copolymerization of I with ε-caprolactam in various molar ratios. More detailed studies, including that of the copolymerization of I, will be published in the near future.

1) H. K. Hall, Jr., *J. Am. Chem. Soc.*, **82**, 1209 (1960).
2) Swiss Pat. 276924 (1949).
3) G. Reinisch, H. Bara and H. Klare, *Chem. Ber.*, **99**, 856 (1966).
4) H. M. Walborsky and D. F. Loncrini, *J. Am. Chem. Soc.*, **76**, 5396 (1954).

A New Route to Mellophanic Dianhydride

Masaaki TAKAHASHI

Tokyo Research Laboratory, Kureha Chemical Co., Ltd., Hyakunin-cho, Shinjuku-ku, Tokyo

(Received September 25, 1967)

Mellophanic dianhydride (I), the dianhydride of benzene 1, 2, 3, 4-tetracarboxylic acid (II), is thought to be an interesting raw material for high-temperature-resistant polyimide. Until the present time, however, there has been no satisfactory method for preparing I of a high purity in a large quantity, although convenient methods have been developed for the preparation of pyromellitic dianhydride.[1]

The present author wishes to report a new method of synthesizing I, starting from 1, 3-cyclohexadiene (III) and maleic anhydride.

The reaction sequence is shown below:

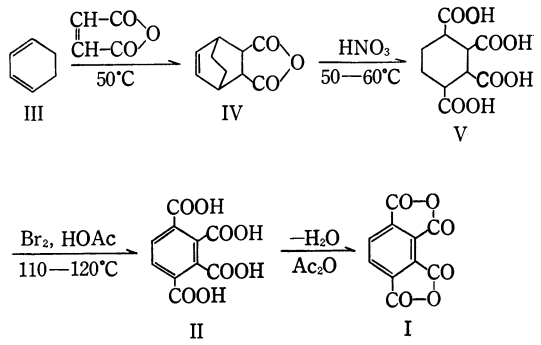

Bicyclo[2, 2, 2]-5-octene-2, 3-dicarboxylic anhydride (IV) was easily obtained by the Diels-Alder reaction of III with maleic anhydride.[2] The liquid-phase nitric acid oxidation of IV at 50—60°C, catalyzed by vanadium, afforded cyclohexane-1, 2, 3, 4-tetracarboxylic acid (V), mp 167°C (monohydrate), in a 70—80% yield.

The configurational relationship between the four carboxyl groups has been identified as 1, *cis*-2, *cis*-3, *cis*-4, by the fact that bicyclo[2, 2, 2]-octene-2 gave *cis*-1, 4-dicarboxycyclohexane in the nitric acid oxidation, and by examining the NMR spectrum of the V-tetramethyl ester. The dianhydride, mp 199—199.4°C, was obtained by treating V with excess acetic anhydride. The catalytic dehydrogenation of V using a Pd catalyst has been unsuccessful because of tar formation. II has been smoothly prepared by the oxidative dehydrogenation of V using bromine. The treatment of V with a three-fold equivalent of bromine in acetic acid at 110—120°C afforded II in an excellent yield.

The subsequent dehydration was carried out by treating II with excess acetic anhydride under reflux. The purification of the resultant dianhydride by sublimation, followed by recrystallization from benzene, afforded pure I mp 196—197°C (lit[3] 193—196°C). The structure was further confirmed by elemental analysis and by a study of the IR spectrum.

An interesting high-temperature-resistant polyimide has been obtained by the polycondensation of I with aromatic diamine. The thermal stability of polymellophanimide is similar to that of the corresponding polypyromellitimide.

A detailed discussion will be presented elswhere.

1) L. I. Smith and G. D. Byrkit, *J. Am. Chem. Soc.*, **55**, 4305 (1933); J. Braun and G. Lemke, *Ber.*, **57**, 681 (1924); French Pat. 1409396 (Aug. 27, 1965).
2) O. Diels and K. Alder, *Ann.*, **460**, 98 (1928).
3) H. Bamford and J. L. Simonson, *J. Chem. Soc.*, **97**, 1904 (1910).

Copper Complexes of Heptan-2, 4, 6-triones*

Fumio SAGARA, Hiroshi KOBAYASHI and Keihei UENO

Department of Organic Synthesis, Faculty of Engineering, Kyushu University, Fukuoka

(Received October 14, 1967)

Heptan-2, 4, 6-trione [H_2A] (I),[1] which was for the first characterized by Feist,[2] behaves as a bidentate or a terdentate ligand, depending upon the degree of enolization, to give a mononuclear 1 : 2 (metal : ligand) complex as well as a dinuclear 2 : 2 complex with a metal ion forming a square planer coordination. The degree of enolization of I seems to increase at a higher temperature in a less polar solvent.

Here we present some interesting behaviors of I upon complex formation with cupric ion. A blue mononuclear copper complex [$Cu(HA)_2 \cdot 2H_2O$] (II) precipitates when an aqueous cupric acetate is added into a methanolic solution of I at about 0°C. Found: C, 43.75; H, 6.09; Cu, 16.4%. Calcd: C, 43.80; H, 5.81; Cu, 16.6%. When the preparation is carried out at about 30°C, a green dinuclear complex [Cu_2A_2] (III) is obtained. Found: C, 41.41; H, 3.89; Cu, 31.0%; mol wt (Vapor Pressure Osmometer), 411.7. Calcd: C, 41.27; H, 3.96; Cu, 31.2%; mol wt, 407.4.

The complex III shows a multiplet absorption between 1500 and 1600 cm^{-1} ascribable to ethylenic bonds and coordinated carbonyl groups. In addition to those, in the case of II, a free carbonyl band at 1715 cm^{-1}, an enolic hydroxy band at 3530 cm^{-1} and a sharp absorption at 795 cm^{-1} of coordinated water are observed together with a broad band extending from 3200 to 3500 cm^{-1}.

The complex II dissolves in methanol, acetone and chloroform to some extent as long as the solution being kept at low temperature, while III dissolves only in pyridine, affording a pyridine adduct; two pyridine molecules bound to III [$Cu_2A_2 \cdot 2Py$].

The solid complex II transforms into III at about 80°C under reduced pressure, liberating an excess of the ligand. The same is observed when the methanolic solution of II is heated at its boiling point. On the other hand, the complex III in pyridine changes into II in the presence of a large excess of the ligand, when the solvent is removed at 0°C under reduced pressure. The observed transformations seem to indicate that III is stable at an elevated temperature, while II prefers a lowered temperature, and that the conversion from one to the other is reversible.

Alkylation of 3- and 5-carbon atoms of I affords the ligands which have the similar chelating tendencies for copper ion. Alkylation are carried out by treating a disodium salt of I with a little more than two moles of alkyl iodide in ethanol, to give a monomethyl- (IV) and a dimethyl triketone (V), mp 82.5—83.5°C (Found: C, 63.23; H, 8.54%. Calcd for $C_9H_{14}O_3$: C, 63.51; H, 8.29%), with methyl iodide, and with *n*-propyl iodide only a mono-*n*-propyl derivative (VI). The triketones IV and VI were characterized as copper complexes, which are best fractionated by column chromatography on silica gel. The copper complexes of the alkylated triketones are again 2 : 2 dinuclear as well as 1 : 2 mononuclear, and the latter structure seems to be enough stable even at room temperature; it gives usually a mononuclear complex alone at room temperature and, in order to obtain a dinuclear complex of V, the mononuclear complex once formed has to be heated at 60°C for a long time.

It is interesting to note that the mononuclear complexes of the alkylated ligands do not carry any coordinated water and that the uncoordinated carbonyl group takes a keto form and not an enol at all.

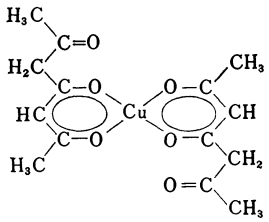

II

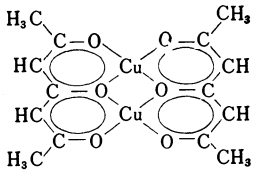

III

* Contribution No. 124. from the Department of Organic Synthesis, Kyushu University.

1) J. R. Bethell and P. Maitland, *J. Chem. Soc.*, **1962**, 3755.

2) F. Feist, *Ann.*, **257**, 276 (1890).

Syntheses of Some Substituted Heterocyclic Compounds from Propargyl Cyanide and Methylpropargyl Cyanide*[1]

Eiichi HARUKI, Yasuo HIRAI and Eiji IMOTO

Department of Applied Chemistry, College of Engineering, University of Osaka Prefecture, Sakai, Osaka

(Received October 25, 1967)

It has been well established that α, β-unsaturated nitriles condense with the nucleophilic reagents such as hydrazine derivatives and hydroxylamine to give heterocyclic compounds substituted by an amino group.[1] The first step of this cyclization reaction is the Michael addition of the nucleophiles to the α, β-unsaturated nitriles.

We wish to report that the reactions of β, γ-unsaturated nitriles such as propargyl cyanide with nucleophiles, *i. e.*, hydroxylamine and phenylhydrazine led also to heterocyclic compounds substituted by an amino group. However, it was found that the different type of heterocyclic compounds were produced from propargyl cyanide (I) and methylpropargyl cyanide (V). A typical example of the reaction was carried out as follows: a mixture of 2.0 g of I, 2.2 g of hydroxylamine hydrochloride and 0.7 g of sodium in 20 m*l* of methanol was refluxed for 10 hr. After reaction the solvent was removed. Distillation of the residue under reduced pressure gave a pale yellow liquid, bp 120—140°C/1 mmHg which was solidified by cooling and after recrystallization from ligroin afforded the pure methylisoxazole (III), mp 80—81°C. Compound III thus obtained was identified with the authentic sample synthesized from β-iminobutyronitrile and hydroxylamine by the mixed melting point and infrared spectrum. Similar treatment of I with phenylhydrazine afforded 5-amino-3-methyl-1-phenylpyrazole (IV), mp 110—111°C (from carbon tetrachloride) in 50% yield. These cyclization reactions would be rationalized in terms of the reaction scheme outlined in Chart 1.

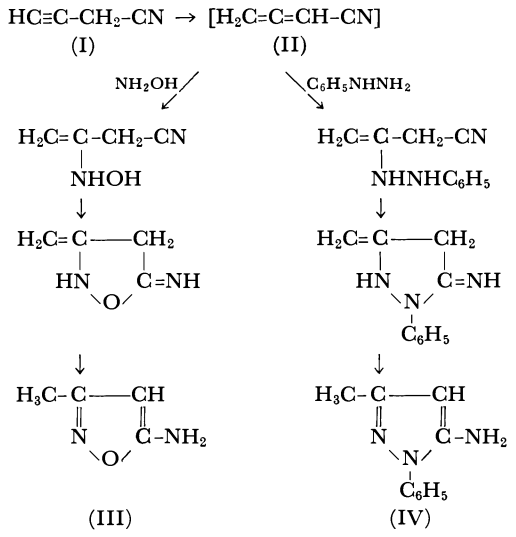

Chart 1

In the first step, I was converted to the allen type compound II, then, the nucleophiles attacked to form the heterocyclic compounds.

However, when methylpropargyl cyanide (V)*[2] was treated hydroxylamine by a similar way, 3-amino-5-ethylisoxazole (VI), mp 70—72°C, was obtained in 50% yield. By comparison of the melting points and the infrared spectra, VI was identified with the authentic sample.[2] This cyclization reaction of V may be interpreted as outlined in chart II. The reaction seems to proceed through the first attack of hydroxylamine toward the nitrile group.

The difference of the chemical behaviors of I and V for the nucleophilic attack can not be explained at present.

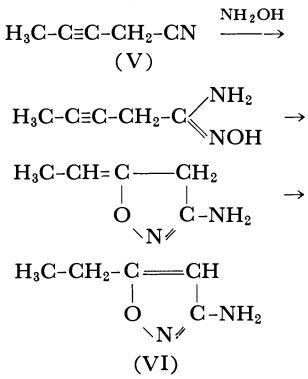

Chart II

The scope and mechanisms of the reported reactions are under investigation.

*1 This constitutes Part V of a series entitled "Studies on the Syntheses of Heterocyclic Compounds."

*2 Methylpropargyl cyanide was prepared by the reaction of methylpropargyl bromide[3] with cuprous cyanide in 75% yield.

1) C. Moureu and I. Lazennec, *Bull. Soc. Chim. France*, [4] **1**, 1079 (1907); P. Schmidt and J. Drucy, *Helv. Chim. Acta*, **41**, 306 (1958); I. Iwai and N. Nakamura, *Chem. Pharm. Bull. (Tokyo)*, **14**, 1277 (1966).

2) Shionogi and Co., Ltd., Brit. Pat. 875458 Sept. 21 (1964); *Chem. Abstr.*, **56**, 8720 (1962).

3) K. E. Schulte and K. P. Reiss, *Chem. Ber.*, **87**, 964 (1954).

Reduction of Cupric Ion to Zero Valent Metal by Benzophenone Ketyl Radical

Kenji TAKEDA and Yoshio IWAKURA

Department of Synthetic Chemistry, Faculty of Engineering, The University of Tokyo, Hongo, Tokyo

(Received October 30, 1967)

While photoreduction of benzophenone in hydrogen-donating solvent has been extensively studied,[1-3] not many works[1,3] have been carried out on the reactivity of benzophenone ketyl radical ($C_6H_5\dot{C}OH$–C_6H_5), the intermediate of photoreduction of benzophenone. The present communication deals with the reduction of metallic ions such as Cu^{2+} to zero valent metal by benzophenone ketyl radical.

Irradiation of 0.5 M benzophenone and 0.5 M cupric acetate in isopropyl alcohol by near ultraviolet rays from a high or low pressure mercury vapor lamp for a few minutes, led to form a metallic mirror of copper on the inner wall of the reaction vessel. The copper mirror was retained unchanged in the absence of oxygen, but it was oxidized into cupric oxide followed by the conversion to cupric acetate by the introduction of air.

Other metallic salts such as $Co(OCOCH_3)_2$, $Ni(OCOCH_3)_2$, $Pb(OCOCH_3)_2$, $Cd(OCOCH_3)_2$, $Hg(OCOCH_3)_2$, $PdCl_2$, Bi_2O_3 were also reduced to the metallic state in the same reaction system.

We have concluded that cupric ion was reduced to zero valent metal by the reaction with benzophenone ketyl radical *via* the following sequence of reactions.

$$(C_6H_5)_2C{=}O + (CH_3)_2CHOH \xrightarrow{h\nu}$$
$$(C_6H_5)_2\dot{C}{-}OH + (CH_3)_2\dot{C}{-}OH$$
$$(CH_3)_2\dot{C}{-}OH + (C_6H_5)_2C{=}O \rightarrow$$
$$(CH_3)_2C{=}O + (C_6H_5)_2\dot{C}{-}OH$$
$$2(C_6H_5)_2\dot{C}{-}OH \longrightarrow$$
$$(C_6H_5)_2C(OH)C(C_6H_5)_2OH$$
$$2(C_6H_5)_2\dot{C}{-}OH + Cu^{2+}(OCOCH_3)_2 \rightarrow$$
$$2(C_6H_5)_2C{=}O + Cu^0 + 2CH_3COOH$$

Benzophenone ketyl radical was reconverted to benzophenone by cupric acetate, while cupric acetate was converted to copper metal and acetic acid. Acetic acid was detected by gas chromatography. Acetylacetone was also detected by the same method when bisacetylacetonatocopper(II) was used in place of cupric acetate.

Support for the mechanism is based on the following experimental observations: (1) Both benzophenone and isopropyl alcohol were necessary for reduction of cupric ion to the metallic state by ultraviolet rays irradiation. Cupric ion was also reduced in the reaction system consisting of carbonyl compounds such as benzophenone, 4-methylbenzophenone, 4-methoxybenzophenone, acetophenone, propiophenone, *etc.* and of hydrogen-donating solvents such as methyl, ethyl, propyl, and butyl alcohols, ethanolamine and dicyclohexylamine, *etc.* On the other hand, carbonyl compounds such as 4-hydroxybenzophenone, 4-nitrobenzophenone, 4-phenylbenzophenone and benzoin, *etc.* which are not reduced to pinacol and solvents with no labile hydrogen such as benzene and carbon tetrachloride were ineffective reagents. For example, cupric ion in a reaction mixture consisting of 2-hydroxybenzophenone, cupric acetate and isopropyl alcohol was not reduced to the metallic state. In another reaction mixture consisting of benzophenone, 2-hydroxybenzophenonecopper chelate and isopropyl alcohol, cupric ion was reduced to zero valence. Other chelate compounds such as bisglycinatobisethylenediaminecopper(II) and bissalcilaldehydatocopper (II) were also reduced to metallic copper.

(2) Reduction to zero valence occurred in the reaction system involving only one intermediate radical, $(C_6H_5)_2\dot{C}$–OH, *i. e.*, benzophenone-benzhydrol system. Reduction of cupric ion by the radical $(CH_3)_2\dot{C}$–OH is still under investigation.

(3) Reduction of benzophenone to benzopinacol was retarded or inhibited by cupric ion. Irradiation of 0.5 M benzophenone in isopropyl alcohol for 12 hr led to 84.8% isolation of benzopinacol, however, 10^{-2} M of cupric acetate retarded the reduction of benzophenone and trace amount of benzopinacol were obtained.

(4) Studies by polarography supported the possibily of the reduction of cupric ion by benzophenone ketyl radical. The halfwave potentials of benzophenone and cupric acetate in isopropyl alcohol were -1.54 and -0.32 V (*vs.* Hg pool) respectively using 0.1 M LiCl as the supporting electrolyte.

Further investigations are desirable to elucidate the mechanism of the reaction between bezophenone ketyl radical and metallic ions.

1) J. N. Pitts, Jr., and R. L. Letsinger, *J. Am. Chem. Soc.*, **81**, 1068 (1959).
2) W. M. Moore, G. S. Hammond and R. P. Foss, *ibid.*, **83**, 2789 (1961).
3) S. G. Cohen, S. Orman and D. A. Laufer, *ibid.*, **84**, 3905 (1962).

Paramagnetic Susceptibilities of Para-substituted Hydrazyl Free Radicals

Noriko OHIGASHI and Hiroo INOKUCHI

The Institute for Solid State Physics, The University of Tokyo, Roppongi, Tokyo

(Received November 6, 1967)

The static magnetic susceptibilities of the stable free radicals, 2,2-diphenyl-1-picrylhydrazyl(DPPH) and 2,2-bis(*p*-chlorophenyl(*p*-bromophenyl, or *p*-methoxyphenyl))-1-picrylhydrazyl(abbreviated to DCl_2(DBr_2 or $D(CH_3O)_2$)*1, were measured in the temperature range from 10°K to 300°K. The measurements were made by the Faraday method. About 10 mg of the polycrystalline samples were placed in a cylindrical quartz cell (diameter 7mm, height 8mm) suspended by a quartz string from the arm of a vacuum balance. All the measurements were carried out in an oxygen-free helium atmosphere of 30 mmHg.

The paramagnetic susceptibility, χ_p, of DPPH followed the Curie-Weiss law, $\chi_p = Ng^2\beta^2S(S+1)/3k(T-\theta)$, with a Weiss constant, θ, of -24°K between 70°K and room temperature. DPPH is known to have several crystal modifications. Our sample is the one recrystallized from CS_2 and may belong to the DPPH (III) crystal modification, according to Weil *et al.*[1] The observed Curie constant corresponded to a spin concentration of 74%.

The susceptibility, χ_p, of DCl_2, recrystallized from benzene, followed the Curie law over the entire temperature range, and no co-operative phenomenon was observed. The spin concentration was estimated from the Curie constant to be 82%.

DBr_2, which was recrystallized from benzene, was found to have a susceptibility maximum at 15°K, while at higher temperatures it followed the Curie law, with a spin concentration of 82%. The magnetic susceptibility of $D(CH_3O)_2$ had its maximum at 21°K (Fig. 1). The numerical results were analyzed on the basis of the singlet-triplet model;

$$\chi_p = \frac{N/2g^2\beta^2S(S+1)}{3kT} \cdot \frac{3}{3+\exp(J/kT)} + \frac{C}{T} \qquad (1)$$

where J is the singlet-triplet energy separation and where the second term represents the contribution of an assumed isolated paramagnetic "impurity." If we take $J/k = 33.8$°K and assume the impurity concentration to be 8.7%, Eq. (1) reproduces fairly well the experimental results shown in Fig. 1. The electron spin resonance measurements were made on this sample between 77°K and room temperature. The absorption spectrum was very sharp, the ΔH_{msl} value being smaller than 1 gauss. As the absorption shape did not change with the temperature, the peak heights of the first derivative curves are thought to be proportional to the absorption intensity. These values are in good agreement with the static susceptibility data, as may be seen in Fig. 1. Of the four compounds, $D(CH_3O)_2$ has the smallest hyperfine coupling constants of the nitrogens,[2] showing that the unpaired electron in this compound delocalizes most extensively over the phenyl rings. The large intermolecular interaction observed in $D(CH_3O)_2$ can be attributed to this delocalization of the unpaired electron.

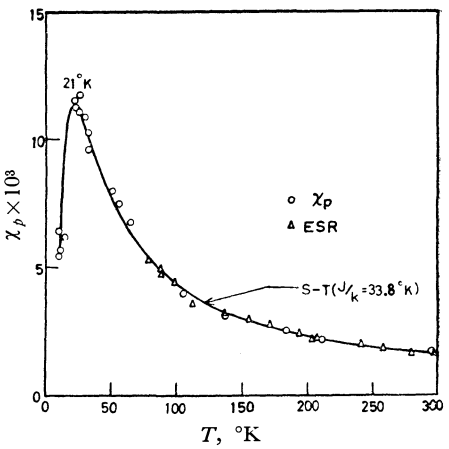

Fig. 1. Paramagnetic molar susceptibility of $D(CH_3O)_2$. The data have been corrected for an assumed impurity paramagnetism. The solid-line curve is the theoretical fit with $J/k = 33.8$°K. The ESR data (arbitrarily normalized at 300°K) are also plotted.

*1 These three compounds were kindly provided by Professor R. I. Walter, Haverford College.

1) J. A. Weil and J. K. Anderson, *J. Chem. Soc.*, **1965**, 5567.

2) M. M. Chen, K. V. Sane, R. I. Walter and J. A. Weil, *J. Phys. Chem.*, **65**, 713 (1961).

New Hydrido- and Oxygen-complexes of Rhodium

Masahiko TAKESADA, Hiroshi YAMAZAKI and Nobue HAGIHARA

The Institute of Scientific and Industrial Research, Osaka University, Sakai, Osaka

(Received November 18, 1967)

Hydrido- and oxygen-complexes of transition metals have found attention in connection with their catalytic behavior.[1] We now wish to report the preparations of new hydrido- and oxygen-complexes of rhodium which were obtained during studies on the hydrogenation of olefins, and the oxidation of triarylphosphines catalyzed by phenyl-(1, 5-cyclooctadiene)-(triphenylphosphine)-rhodium (I)*1.

During the treatment of a solution of I and triphenylphosphine (five molar equivalent to I) in toluene with hydrogen (1 atm) at room temperature for 30 min, approximately one mole of hydrogen was absorbed and yellow crystals were deposited. The reaction mixture was filtered and washed with toluene to give yellow crystals of hydrido-tetrakis-(triphenylphosphine)-rhodium, $HRh(PPh_3)_4$, (II) (Yield, 89%; mp 162—163°C (decomp). Found: C, 75.17; H, 5.31; P, 10.96%. Calcd for $RhC_{72}H_{61}P_4$: C, 75.00; H, 5.33; P, 10.74%.). II was unstable in air, especially in solution, and sparingly soluble in acetone, tetrahydrofuran, dichloromethane and benzene. II was diamagnetic and its infrared spectrum showed a sharp absorption at 2152 cm^{-1} (in Nujol mull; at 2140 cm^{-1} in KBr disk), which was assigned to the stretching vibration of the rhodium-hydrogen bond. The yellow deuterium analog was synthesized by a similar procedure with molecular deuterium, and its infrared spectrum showed an absorption at 1548 cm^{-1} (Nujol mull). Confirmation of the presence of a Rh-H bond in II by NMR was unsuccessful due to the low solubility. Yellow crystals of hydrido-(triphenylphosphine) - tris(triphenylarsine)-rhodium, $HRh(PPh_3)(AsPh_3)_3$,(III), were also obtained by a similar procedure (Yield, 20%; mp 168—169°C (decomp). Found: C, 67.18; H, 4.88%. Calcd for $RhC_{72}H_{61}As_3P$: C, 67.30; H, 4.79%. IR (Nujol mull): 2118 cm^{-1} with a shoulder at 2140 cm^{-1}). Hydrido-di(1, 2-bisdiphenylphosphinoethane)-rhodium[2] was also prepared by a similar treatment, obtaining a 67% yield.

Yellow crystals were obtained by a virtually similar method to that described for II except that molecular hydrogen was replaced with oxygen or air. Elemental analysis conformed to a composition, $Rh(PPh_3)_3O_2$, (IV) (Yield, 65%; mp 135—137°C (decomp). Found: C, 70.44; H, 4.96; P, 9.52%. Calcd for $RhC_{54}H_{45}O_2P_3$: C, 70.36; H, 4.92; P, 10.09%.). IV was explosive and sparingly soluble in common organic solvents. Its infrared spectrum showed an absorption at 815 cm^{-1} (KBr disk), assignable to the stretching vibration of the peroxy group. The diamagnetism of IV seems to suggest that the complex has a dimeric structure, but X-ray analysis should be carried out to determine the exact structure. By a similar procedure, $Rh(PPh_3)(AsPh_3)_2O_2$ was also prepared (Yield, 3%; mp 137—139°C. Found: C, 64.45; H, 4.51%. Calcd for $RhC_{54}H_{45}As_2O_2P$: C, 64.24; H, 4.49%. IR (KBr disk): 810 cm^{-1}.).

Detailed studies of these complexes will be published in the near future.

*1 This compound was prepared by the treatment of chloro-(1, 5-cyclooctadiene) - (triphenylphosphine)-rhodium with phenylmagnesium bromide.

1) a) J. A. Osborn, F. H. Jardine, J. F. Young and G. Wilkinson, *J. Chem. Soc. (A)*, **1966**, 1711; and the literatures therein; b) S. Takahashi, K. Sonogashira and N. Hagihara, *Nippon Kagaku Zasshi (J. Chem. Soc. Japan, Pure Chem. Sect.)*, **87**, 610 (1966); c) G. Wilke, H. Schott and P. Heinbach, *Angew. Chem.*, **79**, 62 (1967); d) S. Otsuka, A. Nakamura and Y. Tatsuno, *Chem. Commn.*, **1967**, 836.

2) A. Sacco and R. Ugo, *J. Chem. Soc.*, **1964**, 3274.

BULLETIN OF THE CHEMICAL SOCIETY OF JAPAN VOL. 41 271—274 (1968)

A Study of the Charge-Transfer Complexes. V. The Complexes of Tetracyanoethylene with *trans*-Stilbene and Related Compounds*1,*2

Taku MATSUO*3 and Hiroshi AIGA*4

Department of Organic Synthesis, Faculty of Engineering, Kyushu University, Hakozaki, Fukuoka

(Received August 11, 1967)

The charge-transfer (CT) absorptions of complexes of tetracyanoethylene with *trans*-stilbene and related compounds were measured both in solution and in solid media. The first and the second CT bands were found to be affected differently by the substituents on the donor molecule; thereupon they were assigned to the transitions of an electron from, respectively, the highest occupied and the second highest occupied orbitals of the donor to the lowest unoccupied orbital of the acceptor. Both the location and the intensity of the first CT band were found to be extremely sensitive to variation in media and temperature. The explanation was arrived at by the use of a model where an acceptor molecule was assumed to associate independently with several different sites of a donor molecule.

In contrast to the presence of abundant information on the charge-transfer (abbreviated to CT hereafter) complexes of condensed aromatic hydrocarbons, no paper has been devoted to the study of the donor properties of linear polyenes and their analogues. In this connection, it is very interesting to investigate the CT complexes of stilbene, the smallest α,ω-diphenylpolyene. In one of the preceding papers of this series, the CT complexes between methyl-substituted *trans*-stilbenes and chloranil or pyromellitic dianhydride have been reported on.[1] The donor strength of stilbene has been found, there, to be strongly dependent on the distortion of the molecular plane. In this paper, a study will be made of the interactions between stilbene derivatives and tetracyanoethylene (TCNE). In order to elucidate the nature of the second CT band, the donor properties of biphenyl, diphenyl ether, and other related compounds will also be investigated.

Experimental

Materials. The diphenyl ether, biphenyl, *p*-terphenyl, and naphthalene were reagent-grade chemicals supplied by the Tokyo Kasei Organic Chemicals Co., and were used after repeated purifications. The cyclohexane and methylene chloride were purchased from the Wako Pure Chemical Co., and were purified by the standard procedure for each solvent. All the other compounds were synthesized in the authors' laboratory by authentic processes, and were repeatedly and carefully purified. The melting points, results of CH analysis, IR and NMR spectra were used to identify the prepared compounds. The purity was checked by gas chromatography, if that was possible.

Spectroscopic Measurements. The solutions of CT complexes were prepared by mixing the respective components to suitable concentrations (donor, 0.01—0.1 mol/*l*; acceptor, 0.005—0.015 mol/*l*). The spectra were measured by a conventional method, using either a Hitachi model EPS-2U or a Shimazu-Bausch & Lomb model SP 505 recording spectrometer. The solid complexes were obtained from the cyclohexane solutions as sharp needles. The crystals were dispersed in starch, and their relative diffuse reflectance measured by a method described before.[2]

Results and Discussion

The wave numbers for the CT absorption bands of the complexes between TCNE and stilbene derivatives in methylene chloride are summarized in Table 1. As may be seen in the table, the two CT absorption bands behave differently upon the introduction of substituents. In the cases of the compounds II, III, and VII, the molecular planes are considered to be distorted due to the presence of steric hindrance. As to the complexes of the compounds in this group, the first CT bands are found at larger wave numbers than that for *trans*-stilbene, while the second bands are found at almost the same positions. The effect of methyl substitution on the benzene ring also gives very important information (compounds IV, V, VI,

*1 Presented in part at the 20th Annual Meeting of the Chemical Society of Japan, Tokyo, April, 1967.

*2 Contribution No. 137 from the Department of Organic Synthesis, Faculty of Engineering, Kyushu University.

*3 The person whom any correspondence should be addressed to.

*4 Present address: Research Division, Mitsui Chemical Industry Co., Ltd., Oomuta-shi.

1) H. Shosenji and T. Matsuo, *Nippon Kagaku Zasshi (J. Chem. Soc. Japan, Pure Chem. Sect.)*, **87**, 802 (1966).

2) Y. Nakayama, Y. Ichikawa and T. Matsuo, This Bulletin, **38**, 1674 (1965).

Table 1. The charge-transfer absorption bands of TCNE complexes with *trans*-stilbene and the related compounds in methylene chloride

Donor	The first band (kK)	The second band (kK)
trans-Stilbene (I)	16.6±0.1	25.3±0.2
cis-Stilbene (II)	18.7±0.1	24.8±0.2
trans-α-Methylstilbene (III)	17.3±0.1	25.2±0.2
trans-2-Methylstilbene (IV)	16.7±0.1	23.9±0.2
trans-3-Methylstilbene (V)	16.5±0.1	24.5±0.2
trans-4-Methylstilbene (VI)	15.7±0.1	25.0±0.2
trans-α, α'-Dimethylstilbene (VII)	18.5±0.2	24.8±0.2
trans-4, 4'-Dimethylstilbene (VIII)	14.8±0.1	25.0±0.2
trans-4-Methoxystilbene (IX)	14.3±0.1	23.8±0.3
trans-4, 4'-Dimethoxystilbene (X)	12.8±0.1	21.9±0.2
trans-4, 4'-Dibromostilbene (XI)	16.9±0.1	25.4±0.2
trans-4, 4'-Diacetoxystilbene (XII)	16.8±0.1	25.9±0.3
Styrene (XIII)	20.6±0.1	25.1±0.2
trans-α, ω-Diphenylbutadiene (XIV)	14.9±0.1	24.2±0.3

and VIII). The second CT band shows an appreciable red shift if a methyl group is at 2- or 3-position. The first CT band, on the other hand, is affected by the methyl group at the 4-position. The effects of methyl substitutions, as has been described above, are well correlated to the first-order perturbation effects on the highest occupied and the second highest occupied π-orbitals, as calculated by simple LCAO MO theory. The highest occupied orbital mainly consists of the p-orbitals of the carbon atoms at the 1-, 4-, and α-positions. The second highest occupied orbital, on the other hand, does not involve the carbon atoms of the central double bond. In other words, the second highest occupied orbital is localized at the benzene rings. The methyl substitution at the 4-position and the decrease in conjugation in the C_1-C_α bond are, therefore, expected to have a much larger effect on the energy level of the highest occupied orbital than on that of the second highest occupied orbital. An exactly opposite situation is expected if the substituent is at either the 2- or 3-position. On the basis of the above facts, the first and the second CT bands may be assigned to the electronic transition originating from the highest occupied orbital and that from the second highest occupied orbital of stilbene respectively. By the use of the results of Beveridge and Jaffes' LCAO-SCF-CI computation,[3] the second highest occupied orbital of *trans*-stilbene is estimated to be 1.4 eV below the highest occupied orbital.*[5] In good agreement with this value, the separation between the first and the second CT bands in Table 1 is found to be 1.1 eV.

In the cases of methoxystilbenes, the second CT band, like the first band, is appreciably affected by the substituent at the 4-position. It may be suggested, then, that the effect of the methoxyl group is somewhat larger than a simple perturbation of the donor orbital. The minor effects of the bromine and acetoxyl groups may be due to the slightly electron-withdrawing natures of these substituents.

The effect of extended conjugation may be seen by examining the absorption bands of the complexes of TCNE with styrene, *trans*-stilbene, and *trans*-α, ω-diphenylbutadiene. The wave number for the first CT band rapidly decreases in the above order of donors. The second CT band, on the other hand, is affected to a much smaller extent.

In order to investigate the nature of these second

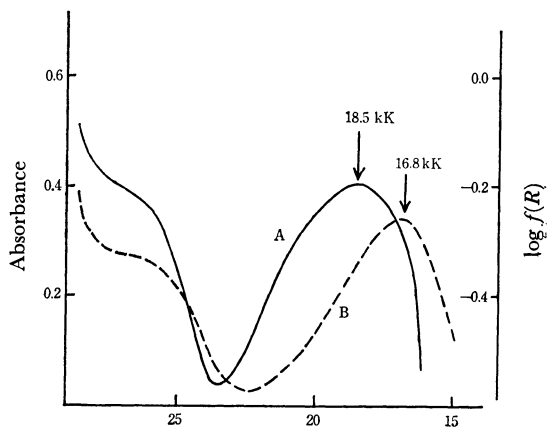

Fig. 1. The CT absorption spectra of TCNE complex with *trans*-stilbene.
A: The diffuse reflectance spectra (the complex, 6 mg; starch, 300 mg). The function $f(R)$ is the Kubelka-Munk function as defined as

$$f(R)=(R-1)^2/2R$$

where R is the relative diffuse reflectance (see Ref. 2 for further detail).
B: The absorption spectra in cyclohexane (the acceptor, 0.03 mol/*l*; the donor, 0.05 mol/*l*).

3) D. L. Beveridge and H. H. Jaffe, *J. Am. Chem. Soc.*, **87**, 5340 (1965).

*5 The energy for the ^1G state, which corresponds to the excitation of an electron from the second highest occupied orbital to the lowest unoccupied orbital of *trans*-stilbene, was estimated by taking an arithmetic mean of those for the $^1G^-$ and $^1G^+$ states given in Ref. 3.

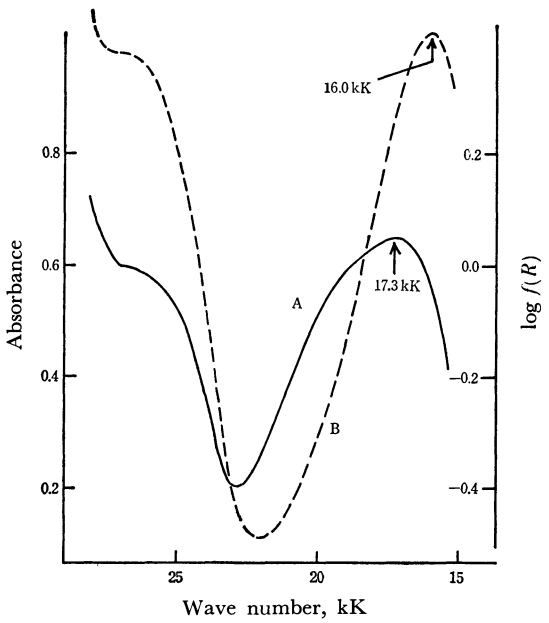

Fig. 2. The CT absorption spectra of TCNE complex with *trans*-4-methylstilbene.
A: The diffuse reflectance spectra (the complex, 9 mg; starch, 300 mg).
B: The absorption spectra in cyclohexane (the acceptor, 0.002 mol/*l*; the donor, 0.05 mol/*l*).

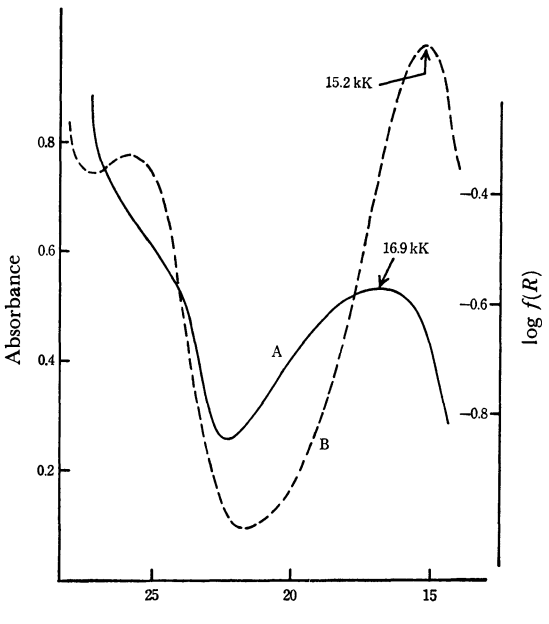

Fig. 3. The CT absorption spectra of TCNE complex with *trans*-4,4'-dimethylstilbene.
A: The diffuse reflectance spectra (the complex, 20 mg; starch, 400 mg).
B: The absorption spectra in cyclohexane (the acceptor, 0.002 mol/*l*; the donor, 0.05 mol/*l*).

CT bands further, the diffuse reflectance spectra of solid complexes have been measured (Figs. 1—3). In comparison with the absorptions in the solutions, the second CT bands of the solid complex appear in slightly lower wave-number regions. The first bands, on the other hand, shifts to considerably higher wave numbers. This blue shift of the CT band is extraordinary, since the frequencies of the absorption bands of crystals of TCNE complexes with polycyclic aromatic hydrocarbons are always lower than those observed with the solutions.[4] Even in the case of solid complexes, the CT absorption bands are almost entirely determined by the interactions between donor and acceptor molecules in contact each other. This suggests that the configuration of TCNE complexes of *trans*-stilbene in solid media may be quite different from that in solution.

Analogously to the case of stilbene, many donor molecules with two benzene rings connected by essential single bonds are expected to have second highest occupied orbitals which are localized on

Table 2. The charge-transfer absorption bands of TCNE complexes with biphenyl and the related compounds in methylene chloride

Donor	The first band (kK)	The second band (kK)
Biphenyl	19.9±0.1	25.2±0.2
p-Terphenyl	18.0±0.1	25.5±0.2
Diphenyl ether	20.1±0.1	26.4±0.2
Diphenyl sulfide	17.0±0.1	26.0±0.2
Diphenylamine	13.0±0.1	26.3±0.2

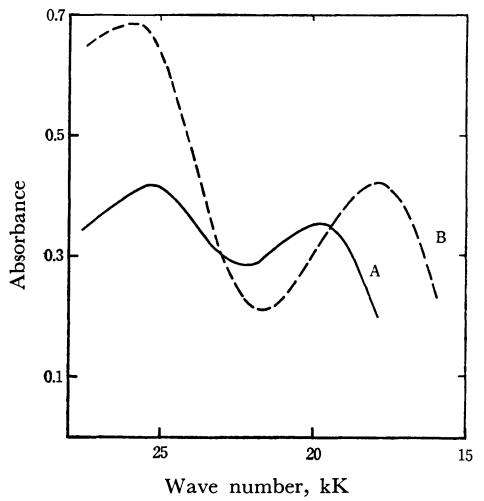

Fig. 4. The CT absorption spectra of TCNE complexes with biphenyl (A) and *p*-terphenyl (B) in methylene chloride.

4) H. Kuroda, M. Kobayashi, M. Kinoshita and S. Takemoto, *J. Chem. Phys.*, **36**, 457 (1962).

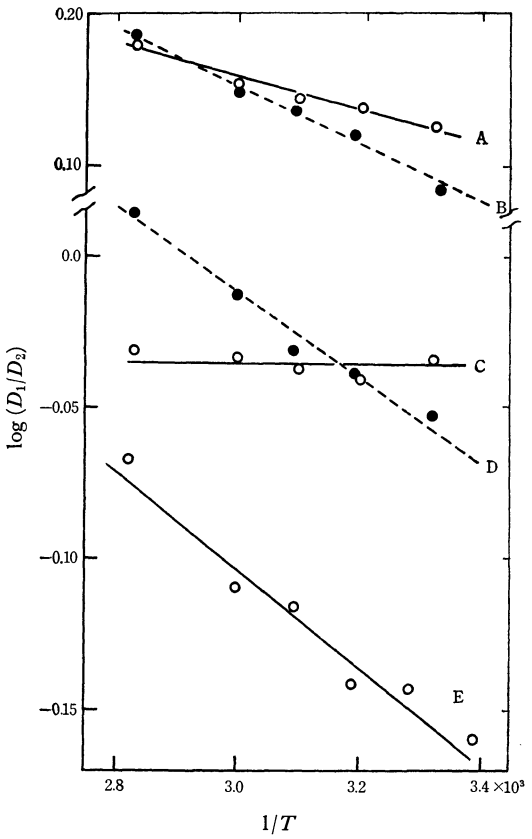

Fig. 5. The temperature dependences of the intensity ratios between the first and the second CT bands.
A: *p*-Terphenyl-TCNE complex
B: *trans*-α-Methylstilbene-TCNE complex
C: Naph-thalene-TCNE complex
D: *trans*-Stilbene-TCNE complex
E: Diphenylamine-TCNE complex
The absorbances at the absorption maxima of the first and the second CT bands are given by D_1 and D_2 respectively.

each benzene ring. The CT bands of TCNE complexes with such donors are summarized in Table 2. In contrast to the large variation in the first CT bands, the second CT bands remain relatively consistent throughout the complexes. In the case of the TCNE-*p*-terphenyl complex, it is also noticed that the intensity ratio between the first and the second CT bands is more than twice that in the TCNE-biphenyl complex (Fig. 4). Furthermore, the intensities of the two CT bands are found to show different temperature dependences, as Fig. 5 shows. The intensity ratio for the naphthalene complex, on the other hand, is independent of the temperature. Therefore, it is obvious that the CT complexes studied here can not be represented by the same single complex for each system and at various states. Briegleb, Czekalla, and Reuss have reported similar observations on the CT complexes of some condensed polycyclic aromatic hydrocarbons, and have suggested that the variation is due to the statistical fluctuation of the conformations.[5]

Here the authors would like to suggest a model for the CT complexes. In the case of a donor molecule with a long, conjugated π-electron system, as has been studied here, there are several sites which may be used for association with an acceptor molecule. The donor-acceptor pairs associated at the different sites will give different CT spectra. As the first CT band of the TCNE-stilbene complex shows a large blue shift in solid media, the conformation of the complex in crystal form seems to be less suited to the CT interaction than that in solution. In other words, intermolecular interaction other than CT force are very important in determining the conformations of the complex in solid media. This type of intermolecular interaction is naturally expected to be present even in the case of complex in solution. As a consequence, the relative importance of the sites for the complex formation is expected to be strongly dependent on the nature of the media and on the temperature. The CT spectra of the system may, then, be affected by the same factors.

5) G. Briegleb, J. Czekalla and G. Reuss, *Z. Phys. Chem. N. F.*, **30**, 316 (1961).

BULLETIN OF THE CHEMICAL SOCIETY OF JAPAN VOL. 41 275—284 (1968)

Electron Spin Resonance of X-Irradiated Single Crystals of Zinc Acetate Dihydrate: Hindered Rotation of Methylene Group in a Free Radical CH_2COO^-*1

Hiroji OHIGASHI and Yukio KURITA

Basic Research Laboratories, Toyo Rayon Co., Ltd., Tebiro, Kamakura

(Received August 17, 1967)

Electron spin resonance spectra of X-irradiated single crystals of zinc acetate dihydrate have been studied at 9.2 Gc in the temperature range from 77°K to 380°K. The radicals trapped at 77°K are CH_3 and CH_2COO^-. The former disappears above 150°K. The latter is stable and persists up to 370°K. The principal values of hyperfine coupling constants for two indetical hydrogens of the radical CH_2COO^- have been found to be 10.5, 20.6 and 33.4G. The CH_2 group in the radical undergoes restricted rotation about the C–C bond. Analysis of the ESR spectra at different temperatures with a modified Bloch equation shows the activation energy and the frequency factor for the restricted rotation to be 5.8 ± 0.2 kcal/mol and $(4.4\pm2.7)\times10^{12}$ sec^{-1}, respectively.

Electron spin resonance (ESR) studies of free radicals have given valuable information on the structure of the radicals as well as their restricted motion. Changes in ESR spectra with temperature due to motion of free radicals have been found and analyzed in some irradiated organic substances. Methyl groups undergo restricted reorientation about a C–C bond in such radicals as CH_3-$CHCOOH$ trapped in alanine[1,2] and CH_3C-$(COOH)CH_2COOH$ trapped in itaconic acid[3]. Their rotation is nearly quenched below 100°K, but the methyl group of a radical $CH_3C(COOH)_2$ in irradiated malonic acid executes nearly free rotation even at 4.2°K.[4] Restricted torsional motion of a methylene group about a C–C bond has also been found in radicals trapped in an irradiated crystal of hexamethylenediammonium adipate,[5] in an irradiated mixed crystal of urea-fumaric acid[6] and in irradiated ethylmalonic acid and *n*-propylmalonic acid.[7] Reorientation of a terminal methylene group, however, has not been found in a radical of the type CH_2R within the knowledge of the present authors, except insufficient evidence for the reorientation motion in a radical CH_2COO^- trapped in an irradiated crystal of glycine.[8]

In this paper, the ESR studies of X-irradiated single crystals of zinc acetate dihydrate $Zn(CH_3COO)_2\cdot2H_2O$ are presented. The trapped radicals have been identified as CH_3 and CH_2COO^-. A marked temperature dependence has been found in the absorption spectra of the radical CH_2COO^-, from which it is concluded that the motion of the CH_2 group is quenched at low temperatures but undergoes rapid reorientation around the C–C bond above room temperatures. A quantitative analysis of the temperature dependence of the ESR spectra has been undertaken to give the activation energy and the frequency factor for the internal rotation of the radical in the crystal.

Experimental Procedures and Outline of the ESR Spectra

Single crystals of zinc acetate dihydrate were grown from the aqueous solution by slow evaporation. The crystal structure has been determined by Niekerk *et al.*[9]; the lattice is monoclinic with space group $C2/c$-C_{2h}^6, $a=14.5$, $b=5.32$, $c=11.02$ Å and $\beta=100.0°$ with four molecules per unit cell. The crystal axes were determined by comparing interfacial angles calculated from the lattice constants with those observed with an optical goniometer available from the Stoe Co. An orthogonal

*1 Presented at the 5th Symposium on Electron Spin Resonance, Sendai, Sept., 1966.

1) I. Miyagawa and K. Itoh, *J. Chem. Phys.*, **36**, 2157 (1962).

2) A. Horsfield, J. R. Morton and D. H. Whiffen, *Mol. Phys.*, **5**, 115 (1962).

3) M. Fujimoto, *J. Chem. Phys.*, **39**, 846 (1963).

4) C. Heller, *ibid.*, **36**, 175 (1962).

5) M. Kashiwagi and Y. Kurita, *ibid.*, **39**, 3165 (1963).

6) C. Corvaja, *ibid.*, **44**, 1958 (1966).

7) N. Tamura, M. A. Collins and D. H. Whiffen, *Trans. Faraday Soc.*, **62**, 1037 (1966); *ibid.*, **62**, 2434 (1966).

8) R. F. Weiner and W. S. Koski, *J. Am. Chem. Soc.*, **85**, 873 (1963); J. R. Morton, *ibid.*, **86**, 2325 (1964).

9) J. N. van Niekerk, F. R. L. Schoening and J. H. Talbot, *Acta Cryst.*, **6**, 720 (1953).

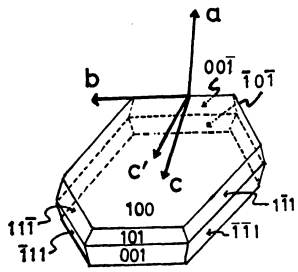

Fig. 1. The crystal form and the crystal axes of zinc acetate dihydrate. The orthogonal set of the *a*, *b* and *c'* axes are chosen for analysis of the ESR spectra.

set of the axes *a*, *b* and *c'* was chosen for the analysis of the spectra as shown in Fig. 1.

The crystals were exposed to X-rays (180 kV, 23 mA) to the extent of approximately 1 Mrad at 77°K. Second derivative ESR spectra were recorded with a Varian 4501 Spectrometer with 100 kc and 40 cps double field modulation. The spectra at 77°K were obtained for the irradiated crystal mounted in a quartz Dewar filled with liquid nitrogen for various orientations of the crystal. The spectra at various temperatures in the range from 77°K to 380°K were taken at two fixed field directions, parallel to the *c* axis and parallel to the direction which made an angle of +23° with the *a* axis in the *ac'* plane. The temperature control was achieved using a Varian V-4547 variable temperature equipment by passing heated or cooled nitrogen gas around the crystal. The temperature was measured with a copper-constantan thermocouple located near the crystal, with probable error of 3°C. ESR spectra of zinc acetate dihydrate powder irradiated at room temperature were also measured at various temperatures.

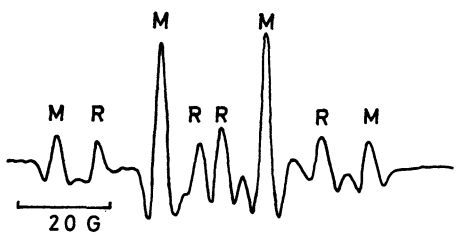

Fig. 2. Second derivative ESR spectra of a single crystal of zinc acetate dihydrate irradiated at 77°K. The spectra were obtained at 77°K for external magnetic field parallel to the *a* axis.

Figure 2 shows an ESR spectrum of the crystal irradiated at 77°K, which is measured immediately after the end of the irradiation, at the same temperature with magnetic field parallel to the *a* axis. The spectrum is composed of a quartet of peaks with equal spacings and with the intensity ratio of 1 : 3 : 3 : 1 (hereafter referred to as M for the sake of convenience), and a quartet (a doublet-doublet) of peaks with equal intensity (referred to as R). The integrated intensity of M is about twice as large as that of R. Above 150°K, the spectrum M disappears, while R persists up to 370°K where water of hydration is taken off. The pattern of R changes reversibly when the crystal is cooled or warmed in the temperature range from 77°K to 350°K. For the crystal irradiated at room temperature, only the spectrum R was observed at any temperature. The substitution of water of hydration by D_2O had no effect on the spectra except narrowing of the line width.

The spectrum M is essentially isotropic and its splitting is 23±1G. A paramagnetic species responsible for M is identified with no doubt as a methyl radical CH_3 which reorients rapidly. The same radical with coupling constants 21.8, 22.5, 22.5G was found in an X-irradiated sodium acetate trihydrate by Rogers and Kispert.[10] The spectrum R is highly anisotropic and its doublet splittings vary from 9 to 33G with the crystal orientation. It will be shown in the following section that the quartet R is attributable to a radical CH_2COO^-.

Analysis of ESR Spectra at Low Temperature and Structure of a Free Radical CH_2COO^-

Typical absorption spectra at 77°K are shown in Fig. 3 for the crystal irradiated at room temperature. In general, the spectra consist of two sets of quartets (doublet-doublet) with equal intensity, which coalesce into a quartet when the magnetic field

TABLE 1. PRINCIPAL ELEMENTS OF *g* FACTORS AND HYPERFINE SPLITTING CONSTANTS A^1 AND A^2 a)

Principal value		Direction consines with regard to the *a*, *b* and *c'* axis		
g_1	2.0013	0.726	∓0.639	0.252
g_2	2.0024	0.247	±0.585	0.773
g_3	2.0031	0.641	±0.499	−0.583
A_1^1	11.8 G	0.431	±0.730	0.530
A_2^1	20.6 G	0.781	∓0.596	0.185
A_3^1	33.3 G	0.451	±0.334	−0.827
A_1^2	9.1 G	0.176	∓0.040	−0.984
A_2^2	21.0 G	0.758	∓0.632	0.162
A_3^2	33.4 G	0.628	±0.774	0.082

a) The standard deviations are 0.0002 and 4° for the principal values and the principal axes of the *g* factors, respectively. For A^1 and A^2, they are 0.2G and 1°, respectively.

10) M. T. Rogers and L. D. Kispert, *J. Chem. Phys.*, **46**, 221 (1967).

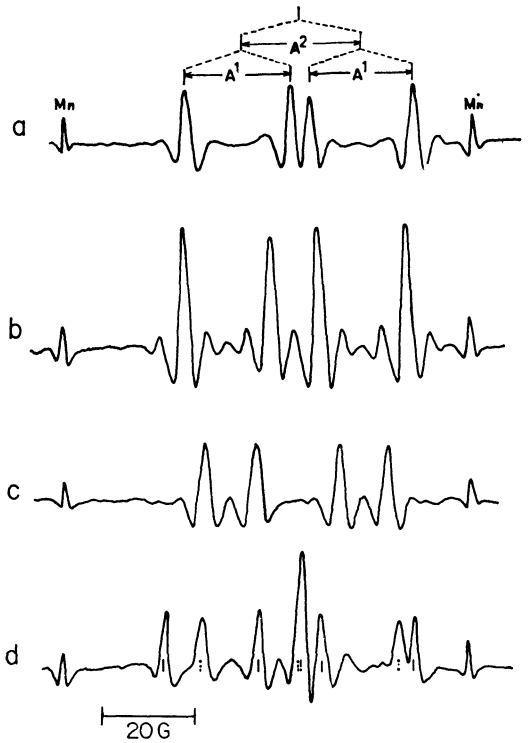

Fig. 3. Second derivative spectra of the crystal irradiated at room temperature and measured at 77°K with the magnetic field (a) parallel to the *a* axis, (b) parallel to the *b* axis, (c) parallel to the *c* axis and (d) at an angle of 30° from the *a* axis toward the *b* axis in the *ab* plane. The outermost lines are of Mn^{2+} in MgO powder which is used as field marker (spacing; 87.5 G).

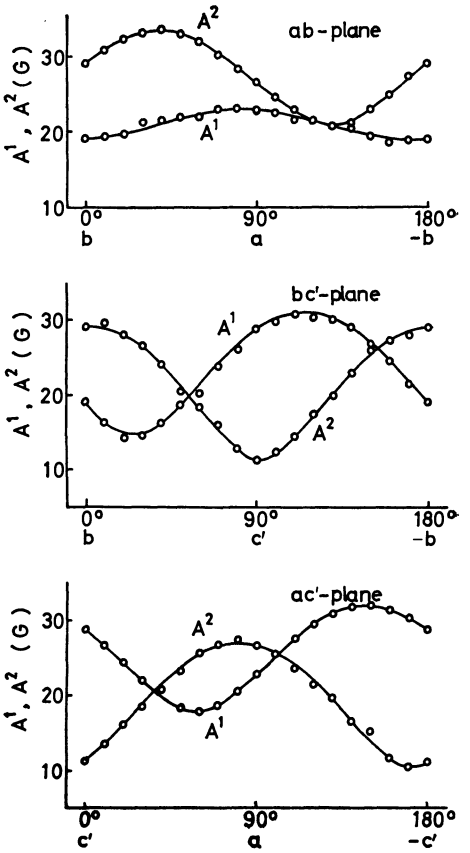

Fig. 4. Calculated (solid lines) and observed (circles) hyperfine splittings at low temperature with the magnetic field in the *ab*, *bc'* and *ac'* planes in a single crystal of zinc acetate dihydrate irradiated at room temperature. The angular dependences of A^1 and A^2 are illustrated for one of the two quartets observed with the magnetic field in the *ab* and *bc'* planes. A 180° rotation of the curves illustrated in the figure about the *b* axis gives the curves omitted.

is parallel to the *b* axis or in the *ac'* plane. The same spectra were obtained when the direction of the field is (l, m, n) or $(l, -m, n)$, where l, m and n are the direction cosines of the magnetic field with respect to the *abc'* system. These facts are compatible with the expectation that the two chemically equivalent but magnetically different radicals are trapped in the crystal with monoclinic symmetry.

It is evident that each quartet arises from two protons with different nuclear hyperfine coupling constants which are referred to as A^1 and A^2 as shown in Fig. 3. Figure 4 shows angular dependences of A^1 and A^2 observed when the magnetic field is in the *ab*, *bc'* or *ac'* planes. The observed data were analyzed by means of least mean square method with the aid of the second-order equations. The calculation was performed by an electronic computer. Table 1 shows the values determined for the principal elements of the tensors $\boldsymbol{A}^1$ and $\boldsymbol{A}^2$, and those of the spectroscopic splitting tensor $\boldsymbol{g}$. The angular dependences of A^1 and A^2 calculated from the results given in Table 1 are shown graphically in Fig. 4. The principal values of $\boldsymbol{A}^1$ and $\boldsymbol{A}^2$ are identical within the limit of experimental error. Therefore, the radical responsible for the spectrum R must contain CH_2 and is most likely

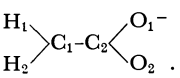

Further analysis confirms this identification. An unpaired electron is in the p_π orbital of the sp^2 configuration of C_1. In such a radical, it has been shown both theoretically and experimentally that the smallest g value ($\boldsymbol{g}_1$) should occur along the direction parallel to the symmetry axis of the p_π orbital (perpendicular to the radical plane) and the directions corresponding to the minimum, medium and maximum value of the principal elements of the hfs tensor are parallel to the C-H bond, parallel

TABLE 2. THE ORIENTATION OF THE RADICAL CH_2COO^- AND THE PARENT MOLECULE CH_3COO^- IN A CRYSTAL OF ZINC ACETATE DIHYDRATE[a)]

Direction	Vector[b)]	Direction cosine with respect to the *abc'* system[c,d)]			
C_1-C_2 (radical)	$(\boldsymbol{A}_1^1+\boldsymbol{A}_2^1)$	0.592	0.675	−0.443	$(\boldsymbol{n}_{r1})$
	$\boldsymbol{g}_3$	0.641	0.449	−0.583	$(\boldsymbol{n}'_{r1})$
C_1-C_2 (molecule)	From crystal structure[9)]	0.662	0.534	−0.531	$(\boldsymbol{n}_{m1})$
Normal to the plane of $H_1H_2O_1O_2$ (radical)	$(\boldsymbol{A}_1^1\times\boldsymbol{A}_1^2)$	0.792	−0.588	0.165	$(\boldsymbol{n}_{r2})$
	$\boldsymbol{g}_1$	0.726	−0.639	0.252	$(\boldsymbol{n}'_{r2})$
Normal to the plane of $O_1O_2C_1C_2$ (molecule)	From crystal structure[9)]	0.892	−0.446	0.115	$(\boldsymbol{n}_{m2})$

The angle between C_1-C_2 (radical) and C_1-C_2 (molecule) is 9° ($\angle\boldsymbol{n}_{m1}$, $\boldsymbol{n}_{r1}$) or 13° ($\angle\boldsymbol{n}_{m1}$, $\boldsymbol{n}'_{r1}$). The angle between the normal to the plane of $H_1H_2O_1O_2$ (radical) and that of $O_1O_2C_1C_2$ (molecule) is 9° ($\angle\boldsymbol{n}_{m2}$, $\boldsymbol{n}_{r2}$) or 16° ($\angle\boldsymbol{n}_{m2}$, $\boldsymbol{n}'_{r2}$).

a) The atoms in the radical and the parent molecule are designated as;

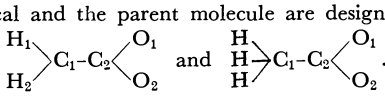

b) $\boldsymbol{A}_1^1$, $\boldsymbol{A}_1^2$, $\boldsymbol{g}_3$ and $\boldsymbol{g}_1$ represent the principal vectors shown in Table 1.

c) Of the two crystallographically unequivalent species, direction cosines are tabulated for one species.

d) Unit vectors having these direction cosines are designated as $\boldsymbol{n}_{r1}$, $\boldsymbol{n}'_{r1}$, *etc.*

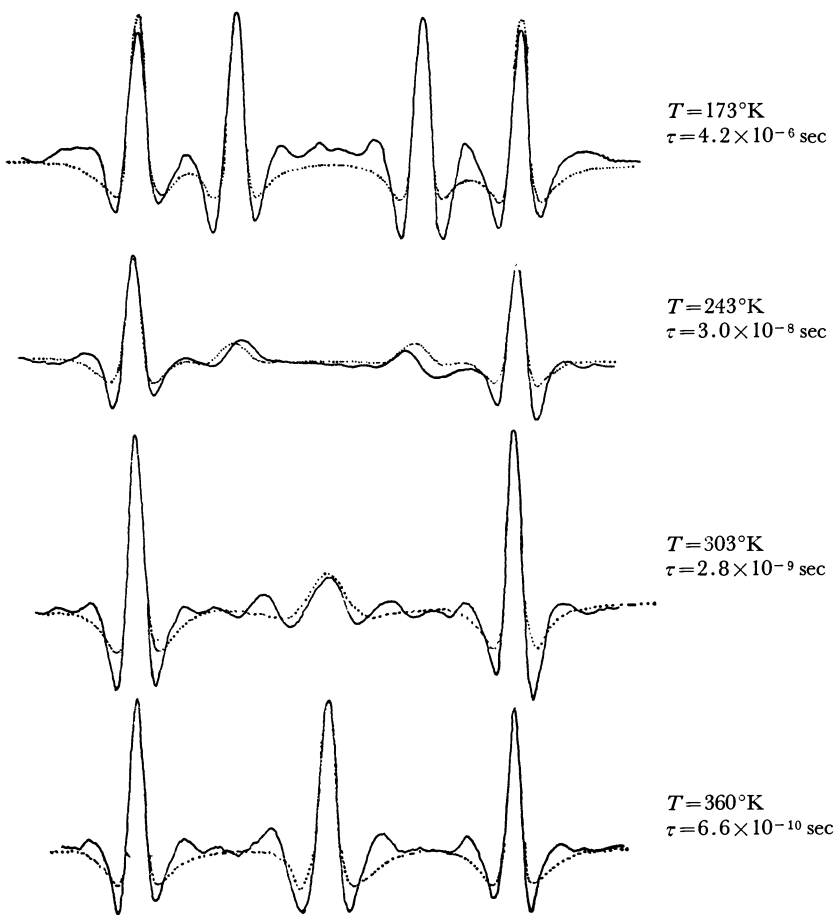

Fig. 5. Observed (solid lines) and calculated (dotted lines) second derivative ESR spectra of CH_2COO^- in the crystal for the magnetic field parallel to the *c* axis at different temperature *T*. The calculated spectra are obtained according to Eq. (2) together with Eq. (3) and the values of $\boldsymbol{E}$ and f_0 indicated in (4).

Fig. 6. Second derivative absorption curves of CH_2COO^- similar to Fig. 5, except that the applied magnetic field is in the ac' plane and makes an angle of 23° with the a axis toward the c' axis.

to the symmetry axis of the p_π orbital and perpendicular to these two directions, respectively.[11-13]

In addition, a symmetry consideration on the radical predicts that the direction of the C_1-C_2 bond is parallel to a bisector of the directions of the minimum principal values of $\boldsymbol{A}^1$ and $\boldsymbol{A}^2$ or is parallel to $\boldsymbol{g}_2$ or $\boldsymbol{g}_3$, where $\boldsymbol{g}_2$ and $\boldsymbol{g}_3$ are the medium and maximum principal elements of g tensor, respectively.

The direction of the C_1-C_2 bond and the normal to the plane $H_1C_1C_2H_2$ of the radical are determined from the values given in Table 1 and compared with the orientation of the parent molecule in the crystal which is determined by X-ray analysis.[9] The direction normal to the plane $H_1C_1C_2H_2$ (perpendicular to $\boldsymbol{A}_1^1$ and $\boldsymbol{A}_1^2$) agrees within 8° with the direction along the symmetry axis of p_π orbital (parallel to $\boldsymbol{g}_1$). The angle $\angle H_1C_1H_2$ (angle between $\boldsymbol{A}_1^1$ and $\boldsymbol{A}_1^2$) is obtained as 118°±3°. As shown in Table 2, the direction of the C_1-C_2 bond of the radical agrees with that of the parent molecule. Moreover, the plane $H_1C_1C_2H_2$ of the radical is parallel to the plane $O_1O_2C_1C_2$ of the parent molecule. These facts indicate that the free radical is formed from the parent molecule CH_3COO^- by loss of a hydrogen atom followed by a reorientation of the CH_2 group to make a planar radical. The orientation of $O_1O_2C_2$ is unchanged when the loss of hydrogen occurs. The principal values of the hfs tensor of the radical CH_2COO^- trapped in a zinc acetate dihydrate crystal (10.4, 20.8, 33.4G) are nearly equal to those of the radical CH_2COO^- produced in glycine (10.3, 21.8, 32.5G),[14] and to those of CH_2COOH produced in malonic acid (11.9, 20.5, 32.6G).[15] It is concluded that the spin density on the α-carbon atom in these radicals is

11) H. M. McConnell, C. Heller, T. Cole and R. W. Fessenden, *J. Am. Chem. Soc.*, **82**, 766 (1960).
12) H. M. McConnell and R. E. Robertson, *J. Phys. Chem.*, **61**, 108 (1957).
13) H. M. McConnell and J. Strathdee, *Mol. Phys.*, **2**, 129 (1959).
14) H. C. Box, H. G. Freund and E. E. Budinski, *J. Am. Chem. Soc.*, **88**, 658 (1966).
15) A. Horsfield, J. R. Morton and D. H. Whiffen, *Nature*, **189**, 481 (1961).

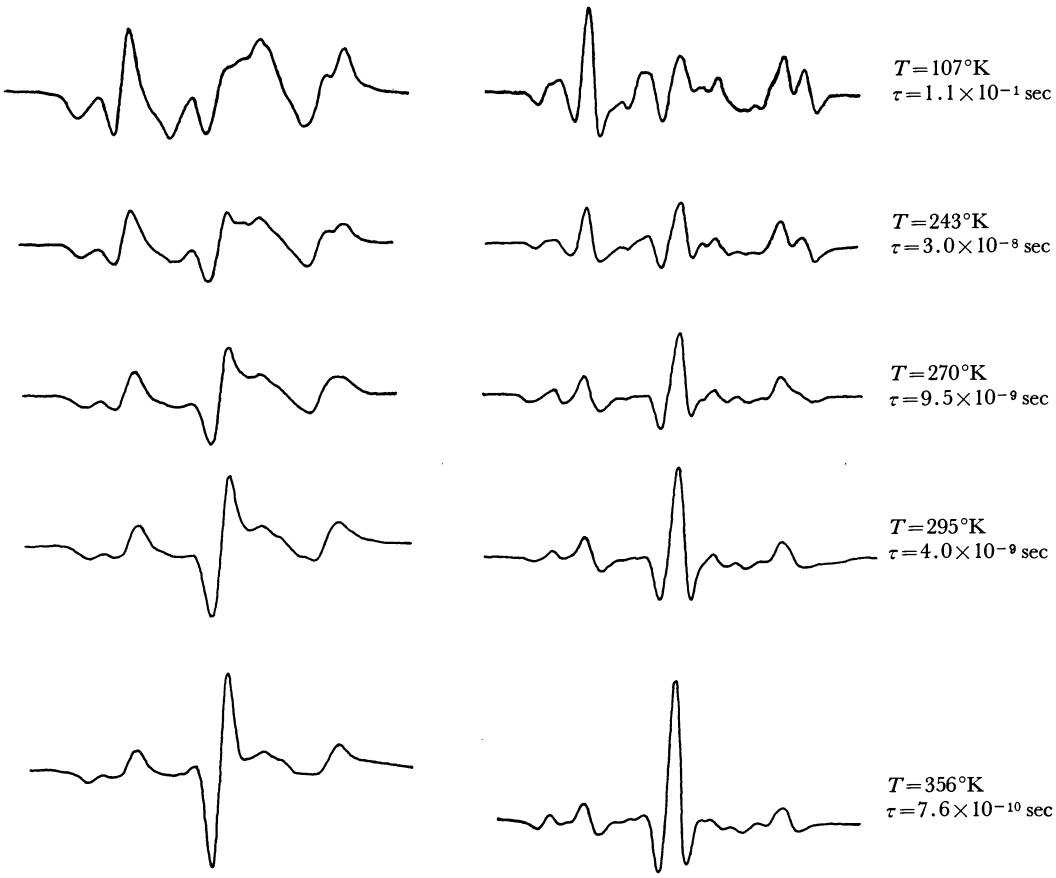

Fig. 7. Temperature dependences of the first (left side) and second (right side) derivative ESR spectra of CH_2COO^- trapped in X-irradiated zinc acetate dihydrate powder. The value of τ given in each spectrum is calculated from Eq. (3) with E and f_0 indicated in (4).

unaffected whether the COO group is linked with neighboring molecules by hydrogen bonds or makes ionic bonds with Zn^{2+}.

Temperature Dependence of ESR Spectra; The Hindered Rotation of CH_2 Group of CH_2COO^-

Figures 5 and 6 show the ESR spectra of CH_2COO^- recorded at various temperatures with the magnetic field in the *ac'* plane. In the temperature range from 77°K to 170°K the spectrum is composed of a quartet with equal intensity. At higher temperatures, the outer lines of the quartet are unchanged, whereas the inner lines become broadened, their peak heights decrease, and their separation also decreases. Near 270°K the inner lines practically disappear. At higher temperature a line appears at the center of outer lines and its intensity increases with increase of temperature and approaches twice the intensity of the outer lines. First and second derivative ESR spectra of CH_2COO^- trapped in zinc acetate dihydrate powder obtained at different temperatures are illustrated in Fig. 7 for comparison with the crystal ESR spectra.

The temperature dependence mentioned above is characteristic of the system in which the two hydrogen atoms exchange their sites with each other through a rotation of the CH_2 group about the C-C bond, the rate of the exchange increasing with increasing temperature. This is easily recognized qualitatively as illustrated in Fig. 8. If the reorientation rate, τ^{-1}, is much smaller than $|A^\alpha - A^\beta|$, the spectrum will be a quartet, where A^α and A^β are the hyperfine coupling constants in frequency unit of the protons located at equilibrium positions "α" and "β", respectively. The resonant frequencies of the quartet are $\nu_0 \pm |A^\alpha + A^\beta|/2$ (outer lines), corresponding to the nuclear spin states $(++)$ and $(--)$ of the two protons H_1 and H_2, and $\nu_0 \pm |A^\alpha - A^\beta|/2$ (inner lines), corresponding to $(+-)$ and $(-+)$, where ν_0 is the resonant frequency of the unpaired electron with no hfs and $(+-)$, for example, designates the state in which H_1 and H_2 have nuclear spin components of $+1/2$ and $-1/2$, respectively.

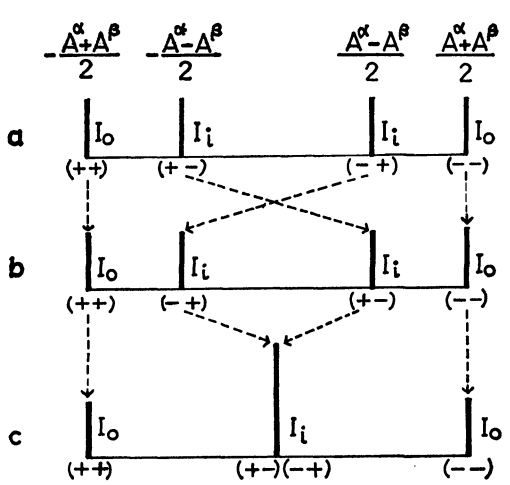

Fig. 8. Patterns of absorption spectra of CH_1H_2R.

(a) H_1 and H_2 are in the equilibrium positions "α" and "β", respectively.
(b) H_1 and H_2 exchanges their positions through rotation around the C-C bond. H_1 and H_2 are in "β" and "α", respectively.
(c) The methylene group undergoes rapid reorientation.

The relation $A^\alpha > A^\beta > 0$ is assumed.

When $\tau^{-1} \gg |A^\alpha - A^\beta|$, the spectrum is a triplet with the intensity ratio of 1 : 2 : 1, the resonant frequencies of which are $\nu_0 \pm |A^\alpha + A^\beta|/2$, corresponding to (++) and (−−), and ν_0 which corresponds to (+−) and (−+). If τ^{-1} is comparable to $|A^\alpha - A^\beta|$, the positions and intensities of the outer lines are the same as those in the two cases mentioned above but inner lines become broadened and its separation becomes smaller than $|A^\alpha - A^\beta|$. These changes of the spectra with change of τ^{-1} is caused by the fact that the nuclear spin state of the protons is unchanged during the reorientation and, then, the inner lines exchange their positions with each other but the outer lines do not through the reorientation. The exchange or reorientation effects of protons on NMR spectra have been analyzed by Gutowsky and Holm[16] with modified Bloch equations. The effects of rotation of methyl group in a radical CH_3CHR on ESR spectra have been investigated with a similar procedure by Miyagawa and Itoh.[1] After their procedure, we analyzed numerically the second derivative ESR spectra of a radical with two protons which transfer between two sites.

If the splitting of the inner lines H_{spl}($|A^\alpha - A^\beta|$ in gauss) and the maximum slope line width

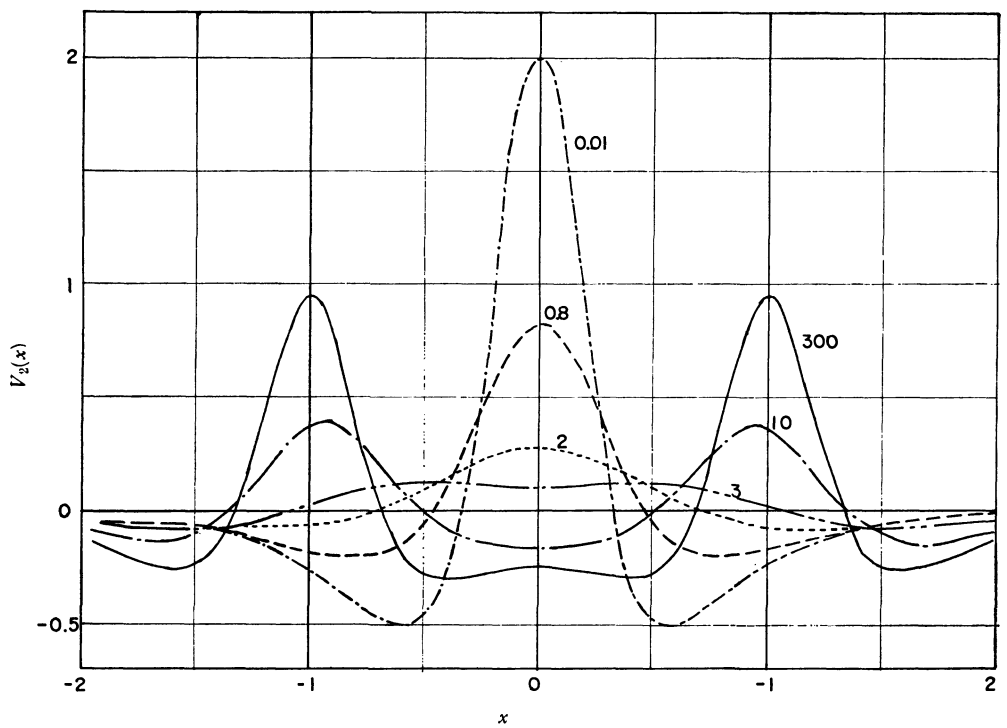

Fig. 9. Second derivative curves $V_2(x)$ for $r=0.33$ with different reduced exchange rates t. The values of t are given on each curves.

16) H. S. Gutowsky and C. H. Holm, *J. Chem. Phys.*, **25**, 1228 (1956); see also, J. A. Pople, W. G. Schneider and H. J. Bernstein, "High-Resolution Nuclear Magnetic Resonance," McGraw-Hill Book Company, Inc., New York (1959), Chapt. 10.

ΔH_{msl}, both in the absence of the reorientation, are known, the spectra of the inner lines can be calculated for any given life time of the reorientation, τ. The absorption curve, V_0, is given as a function of reduced magnetic field x by the expression

$$V_0(x) = \frac{\sqrt{3}}{2} rt \,\mathrm{Real}\left\{\frac{f_\alpha + f_\beta}{1 - f_\alpha - f_\beta}\right\}, \qquad (1)$$

and the second derivative of the absorption curves by

$$V_2(x) = \frac{3\sqrt{3}}{8} (rt)^3 \times \mathrm{Real}\left\{\frac{(f_\alpha - f_\beta)^2(f_\alpha + f_\beta - f_\alpha f_\beta) + f_\alpha f_\beta (f_\alpha + f_\beta)}{(1 - f_\alpha - f_\beta)^3}\right\} \qquad (2)$$

where f_α and f_β are complex functions expressed as

$$\left.\begin{aligned} f_\alpha &= \left\{\frac{\sqrt{3}}{2} rt + 2 - i\frac{t}{2}(1 - x)\right\}^{-1} \\ f_\beta &= \left\{\frac{\sqrt{3}}{2} rt + 2 + i\frac{t}{2}(1 + x)\right\}^{-1} \\ &\qquad (i = \sqrt{-1}) \end{aligned}\right\} \qquad (3)$$

where

$$x = \frac{2}{H_{spl}} (H - H_0),$$

$$r = \Delta H_{msl}/H_{spl},$$

and

$$t = \tau\gamma H_{spl}.$$

In the above expressions, H is applied magnetic field, H_0 is magnetic field at the center of the inner doublet and γ is electronic gyromagnetic ratio.

Line shape of each absorption line has been assumed to be Lorentzian and, therefore, $\Delta H_{msl} = 2/(\sqrt{3}\,\gamma T_2)$, where T_2 is spin-spin relaxation time. Equations (1) and (2) are normalized so as $V_0(\pm 1) = V_2(\pm 1) = 1$ when $\tau = \infty$. The maximum value of $V_2(x)$ is the ratio of the peak intensity of the inner line, I_i, to that of the outer line, I_o, which can be calculated from Eq. (2) as a function of τ for given r and H_{spl}.

At 77°K, τ is large enough to assume that the rotation of the CH_2 group of the radical CH_2COO^- does not take place practically and hence the linewidth and the separation between inner lines observed at this temperature can be taken as ΔH_{msl} and H_{spl}, respectively. The values of H_{spl} and ΔH_{msl} have been observed to be 20.1G and 2.52G (r=0.125), respectively, for H parallel to the c axis, and to be 8.1G and 2.67G (r=0.33), respectively, for the magnetic field parallel to a line which makes an angle of +23° with the a axis in the ac' plane. Figure 9 shows the calculated spectra of the inner lines for several values of t

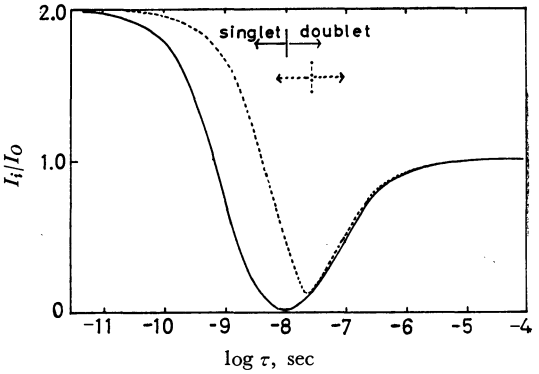

Fig. 10. Relation between τ and I_i/I_O for H_{spl}= 20.1 G and ΔH_{msl}=2.59 G (r=0.125) (solid line) and for H_{spl}=8.1 G and ΔH_{msl}=2.67 G (r=0.33) (dotted line).

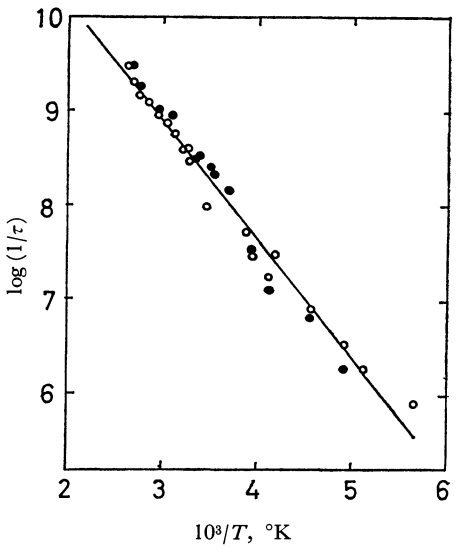

Fig. 11. Arrhenius plot of $1/\tau$ *versus* $1/T$. The straight line illustrates Eq. (3) with E=5.8 kcal/mol and $f_0 = 4.4 \times 10^{12}$ sec^{-1}. (○: H_{spl}=20.1 G, ΔH_{msl}=2.59 G, ●: H_{spl}= 8.1 G, ΔH_{msl}=2.67 G)

for the case of r=0.33. The ratios I_i/I_o calculated for r=0.125 and r=0.33 are shown in Fig. 10 as functions of τ. Comparing the quantities I_i/I_o observed at various temperatures with the calculated values, τ has been determined for the temperatures at which the spectra were obtained. The plots of $\log(1/\tau)$ *versus* $1/T$ are shown in Fig. 11. The linear relation between $\log(1/\tau)$ and $1/T$ indicates that τ follows the equation;

$$\frac{1}{\tau} = f_0 \exp(-E/RT), \qquad (3)$$

where f_0 and E are interpreted as the frequency factor and activation energy for the rotation of the CH_2 group about the C_1-C_2 bond, respectively.

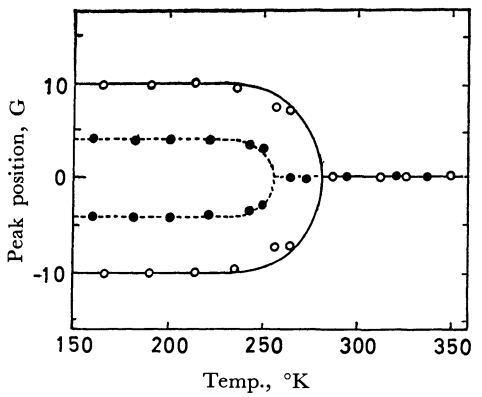

Fig. 12. Observed (dots) and calculated (lines) positions of the inner line peaks of the absorption spectra of CH_2COO^- in a zinc acetate dihydrate single crystal with varying temperature. The peak positions from the center of the spectra are measured in Gauss.
(○, ——: for $H_{spl}=20.1$ G and $\Delta H_{msl}=2.59$ G,
●, ----: for $H_{spl}=8.1$ G and $\Delta H_{msl}=2.67$ G)

The values for E and f_0 are found from Arrhenius plots in Fig. 11 as:

$$\left.\begin{aligned} E &= 5.8 \pm 0.2 \text{ kcal/mol} \\ f_0 &= (4.4 \pm 2.7) \times 10^{12} \text{ sec}^{-1}. \end{aligned}\right\} \quad (4)$$

In Figs. 5 and 6 the spectra calculated by Eqs. (2), (3) and (4) are illustrated with dotted lines for given temperatures. These figures show that the calculated spectra are in good agreement with the observed ones except tail parts of the absorption lines. The position of the inner line peaks has been calculated by the similar procedure as before and compared with the observation (Fig. 12). It is found in Fig. 12 that the observation is in good agreement with the calculation. The value of the frequency factor f_0 given in (4) is also in good agreement with 5.2×10^{12} sec^{-1} which is evaluated by the equation $f_0=kT/h$ based on the absolute rate theory,[17] where T is assumed to be 250°K. Lefebvre and Maruani[18] have calculated the absorption and first derivative spectra of randomly oriented CH_2COOH in which the methylene group rotate freely or is completely quenched arround the C-C bond (see Fig. 13 of their paper). It can be seen that Fig. 13 of their paper also reporduces the first derivative curves of the irradiated zinc acetate dihydrate powder (Fig. 7) in fair detail.

Disagreement of the calculated curves with the observed ones in the tail region (Figs. 5 and 6) arises from the following two reasons. Firstly, the calculation was carried out with an assumption that the shape function of each absorption line is Lorentzian but the real absorption line was nearly Gaussian. Secondly, the second-order effect or the "forbidden" transition was not taken into account, which was caused by a simultaneous transition of electronic and nuclear spins, though it was really observed in both sides of the absorption lines, as seen in Figs. 5 and 6.

For such radicals as $CH_2NHCONH_2$ (from methylurea),[19] CF_2CONH_2 (from trifluoroacetamide)[20] and CH_2COOH (from malonic acid),[15] the rotation of the CH_2 or CF_2 group does not occur even at room temperature. Activation energy of these groups is estimated to be higher than 9 kcal/mol. If it is assumed that $f_0=5\times10^{12}$ sec^{-1} and $H_{spl}=10$G, the lower energy than 9 kcal/mol would reveal the effect of the rotation on their ESR spectra. Therefore, it is of interest to examine, using a simple model, the cause of the fairly low activation energy for the CH_2 rotation in the case of CH_2COO^- in a crystal of zinc acetate dihydrate.

Now, we define θ as the angle between the plane $H_1C_1H_2$ and the plane $O_1O_2C_2$, and consider only an internal energy $V(\theta)$ of the radical which is a function of θ. $V(\theta)$ is a sum of the energies of five π-electrons $V_\pi(\theta)$ plus a repulsive energy $V_r(\theta)$ between the CH_2 and COO^- groups;

$$V(\theta) = V_\pi(\theta) + V_r(\theta). \quad (5)$$

$V_\pi(\theta)$ will be minimum at $\theta=0$ and π, and maximum at $\theta=\pi/2$ and $3\pi/2$, whereas $V_r(\theta)$ is maximum at $\theta=0$ and π, and minimum at $\theta=\pi/2$ and $3\pi/2$. The activation energy E for the rotation may be approximately $V(\pi/2)-V(0)$. With the simple Hückel MO method $V_\pi(\pi/2)-V_\pi(0)$ was calculated as follows.[21] Taking Coulomb energy for C_1, C_2, O_1 and O_2 to be α, $\alpha+0.2\beta$ $\alpha+2\beta$, and $\alpha+2\beta$, respectively, and taking the resonance energy for the C_1-C_2, C_2-O_1 and C_2-O_2 bonds to be $\beta\cos\theta$, $\sqrt{2\beta}$ and $\sqrt{2\beta}$, respectively, it is found that $V_\pi(\pi/2)-V_\pi(0)=-0.562\beta$. If β is taken as -18 kcal/mole,[21] which have been evaluated from the resonance energy for benzene, $V_\pi(\pi/2)-V_\pi(0)$ is 10.1 kcal/mol.

$V_r(\theta)$ is not known experimentally, but $V_r(0)-V_r(\pi/2)$ can be roughly evaluated as follows. Assuming the repulsive energy between a hydrogen atom and an oxygen atom is the same in CH_2COO^- and CH_3COOH, the activation energy for the hindered rotation of CH_2COO^- may be larger than that of the methyl group in CH_3COOH, which has been known to be 2.5 ± 0.7 kcal/mol.[22]

17) S. Glasstone, K. J. Leidler and H. Eyring, "The Theory of Rate Processes" McGraw-Hill Book Company, Inc., New York (1941), Chapt. 4.
18) R. Lefebvre and J. Maruani, *J. Chem. Phys.*, **42**, 1480 (1965).
19) T. S. Jaseja and R. S. Anderson, *ibid.*, **35**, 2192 (1961).
20) R. J. Rontz and W. Gordy, *ibid.*, **37**, 1357 (1962).
21) A. Streitwieser, Jr., "A Molecular Orbital Theory for Organic Chemists," John Wiley & Sons, Inc., New York (1961), Chapts. 4 and 9.
22) W. Weltner, Jr., *J. Am. Chem. Soc.*, **77**, 3941 (1955).

This is because the height of two fold potential barrier (in the case of CH_2COO^-) is larger than that of three fold potential barrier (in the case of CH_3COOH). Thus, $V_r(0)-V_r(\pi/2)$ may be estimated without serious error as twice the activation energy for CH_3COOH, *i. e.*, 5.0 ± 1.4 kcal/mol. Therefore, the activation energy for the rotation of CH_2 in CH_2COO^- is $V(\pi/2)-V(0)=10.1-(5.0\pm1.4)$kcal/mol$=5.1\pm1.4$ kcal/mol, which is in good agreement with the observed value 5.6 ± 0.2 kcal/mol.

The agreement of the calculated activation energy with the observation for CH_2COO^- in a crystal of zinc actetate dihydrate suggests that the contribution of the surrounding molecules to the hindered rotation of the CH_2 group is negligibly small and that the activation energy is essentially determined by the internal energy of the radical. For the radicals of the type CH_2R having a high activation energy, however, the rotation of the CH_2 group may be hindered by the force acting on the radicals from the surrounding molecules in the crystals.

The authors' thanks are due to Mr. H. Iguchi for his help in the experiment.

BULLETIN OF THE CHEMICAL SOCIETY OF JAPAN VOL. 41 284—290 (1968)

Reactions of *cis*- and *trans*-2-Butenes Photosensitized by $Hg(^3P_1)$ and $Cd(^3P_1)$

Shigeru TSUNASHIMA and Shin SATO

Department of Applied Physics, Tokyo Institute of Technology, Ookayama, Meguro-ku, Tokyo

(Received August 31, 1967)

A comparative study has been made of the reactions of *cis*- and *trans*-2-butenes photosensitized by mercury($^3P_1$) at room temperature and by cadmium($^3P_1$) at temperatures ranging from 275 to 350°C. In both cases, the main reaction was cis-trans isomerization. The initial quantum yield of isomerization was the same for the two butenes. The rate of decomposition was about 10^{-2} and 10^{-3} times less than that of isomerization in the Hg- and Cd-photosensitizations, respectively. The ratio of *trans*- to *cis*-2-butene after prolonged irradiation was unity and did not vary with pressure in the Cd-photosensitization, while in the Hg-photosensitization it increased with decreasing initial pressure. This is probably due to the difference in the rates of decomposition of *trans*- and *cis*-2-butenes. It was found that the pressure dependence of Hg-photosensitized *cis-trans* isomerization could not be explained in terms of the simple mechanism proposed before. A possible mechanism is discussed.

The rate of photosensitized isomerization of an olefin depends upon three factors; (1) the electronic state of the excited sensitizer molecule and its lifetime, (2) the mechanism of energy transfer from sensitizer to olefin, and (3) the reactivity of the excited olefin molecules. Recent studies have uncovered many interesting features of photosensitized isomerizations and have indicated the importance of the above factors in determining the rate of isomerization.

Photosensitized isomerization of 2-butenes in the gas phase has been investigated with mercury,[1,2] benzene[3] and several organic compounds[4] as sensitizers, but no report has appeared yet with cadmium. LeRoy and Steacie reported only on the decomposition of 2-butene in Cd-photosensitization.[5]

This paper presents a detailed study of the reactions of 2-butenes photosensitized by $Hg(^3P_1)$ and $Cd(^3P_1)$. Some of the results are obviously at variance with the data reported previously.

Experimental

cis- and *trans*-2-Butenes supplied by Takachiho-Shoji Co. were used after degassing at liquid nitrogen

1) R. J. Cvetanović, H. E. Gunning and E. W. R. Steacie, *J. Chem. Phys.*, **31**, 573 (1959).
2) R. B. Cundall, F. J. Fletcher and D. G. Milne, *Trans. Faraday Soc.*, **57**, 1692 (1961).
3) S. Sato, K. Kikuchi and M. Tanaka, *J. Chem. Phys.*, **39**, 239 (1963); M. Tanaka, T. Terao and S. Sato, This Bulletin, **38**, 1645 (1965); M. Tanaka, K. Kato and S. Sato, *ibid.*, **39**, 1423 (1966); R. B. Cundall, F. J. Fletcher and D. G. Milne, *Trans. Faraday Soc.*, **61**, 1146 (1965).
4) R. B. Cundall, "Progress in Reaction Kinetics," Vol. 2, ed. by G. Porter, Pergamon Press, Oxford (1964); D. Phillips, *J. Phys. Chem.*, **71**, 1839 (1967).
5) D. J. LeRoy and E. W. R. Steacie, *J. Chem. Phys.*, **10**, 683 (1942).

temperature. Major impurities observed by gas-chromatography were *trans-cis* isomers, the amounts being at most below 0.5%. *trans*-2-Butene-d_8 was synthesized from butadiene-d_6[6] and was purified by gas-chromatography. The isotopic purity of *trans*-2-butene-d_8 was determined to be at least above 98%. Special grade nitrogen, nitrous oxide and sulfur hexafluoride supplied by Takachiho-Shoji Co. were used without further purification. Six 9's pure cadmium stick was used as supplied by Soekawa Chemical Co.

Quartz reaction cells were cylindrical (5 cm in diameter, 8, 5 and 3 cm long) and contained a drop of mercury or a few small pieces of cadmium.

Light sources were spiral low pressure mercury discharge lamps (filled with 4 mm Ne) and a cadmium discharge lamp of the same type (filled with 2 mm Ar).

To eliminate the $^1S_0$-$^1P_1$ resonance line, a Toshiba UV-25 filter which cuts off below 2000 Å or a Toshiba UV-29 filter which cuts off below 2500 Å, was inserted between the light source and the reaction cell.

For cadmium-photosensitization, the light source and the reaction cell were placed separately in two electric furnaces controlled by Toshiba Thermister Temperature Controllers to within ± 2°C and ± 1°C, respectively.

After each run, materials were transferred to a trap at liquid nitrogen temperature. The non-condensables were analyzed and measured with a combination of Toepler pump, gas buret and furnace (*ca.* 260°C) packed with cuprous oxide. The condensables were analyzed by gas-chromatography. The columns used were packed with a celite-dimethylsulpholane mixture (30 m long, supplied by Shimadzu Co.) and with activated alumina containing tailing reducer (7 m long, supplied by Nishio Kogyo Co.).

The isotopic distribution of hydrogen was determined by mass-spectroscopy.

In the experiments using mercury-photosensitization, the light intensity of the 2537 Å resonance line was determined by the amount of hydrogen produced from 13 mmHg of ethylene, assuming the quantum yield of hydrogen to be 0.35.[7]

Results

Cadmium-photosensitization. For cadmium photosensitization, it is necessary to elevate the temperature of the reaction cell in order to obtain a sufficiently high vapor pressure of cadmium. To check for the possibility of thermal isomerization of 2-butene, 10 mmHg of *cis*-2-butene was kept in the reaction cell at 350°C for two hours. However, after this period of time, neither isomerization nor decomposition products could be detected. After one hour irradiation of 9.8 mmHg of *cis*-2-butene at room temperature with a cadmium lamp, likewise no reaction product was found. These results show that isomerization of 2-butene is not effected by radiation of the 3261 Å resonance line since the 2288 Å line is filtered out and that the light source used is not contaminated by mercury lines.

In the presence of cadmium vapor, *cis*- or *trans*-2-butene were isomerized to *trans*- or *cis*-2-butene by the radiation from the cadmium lamp. The initial rates of isomerization were constant over the pressure range 2 to 100 mmHg. There was no

Table 1. Products from the cadmium-photosensitization
(Reaction cell, 166 ml; Initial pressure, 10 mmHg)

Temperature °C	Time min	Products μmol				
		H_2	CH_4	C_3H_6	*trans*-2-C_4H_8	*cis*-2-C_4H_8
cis-2-Butene						
275	5	—	—	—	1.9	37.0
	180	0.09	0.1	0.2	23.1	23.1
300	5	—	—	—	4.1	33.1
	180	0.13	0.5	1.0	20.6	19.7
325	3	—	—	—	3.45	34.5
	120	0.19	0.65	1.5	19.7	18.1
350	3	—	—	—	4.4	32.0
	120	0.17	1.1	1.7	18.1	16.5
trans-2-Butene						
275	5	—	—	—	37.1	2.0
	180	0.09	0.11	0.3	23.2	20.8
300	5	—	—	—	34.1	4.0
	180	0.13	0.5	0.9	20.4	19.5
325	3	—	—	—	34.8	3.5
	180	0.16	1.0	1.8	19.5	18.1
350	3	—	—	—	32.6	4.1
	120	0.17	1.0	1.8	16.7	15.9

6) H. Hatano and S. Shida, *J. Chem. Phys.*, **46**, 4784 (1967).

7) B. DeB. Darwent, *ibid.*, **19**, 258 (1951).

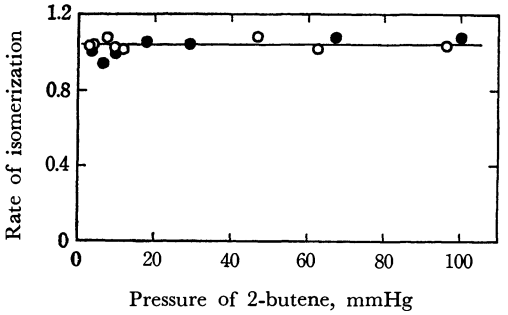

Fig. 1. Rate of isomerization at various pressures in the cadmium-photosensitization at 275°C. (○, cis → trans; ●, trans → cis)

difference in rate between two isomers (Fig. 1).

After prolonged irradiation, hydrogen, methane and propylene were observed. Their rates of formation were very small, *ca.* 10^{-3} of that of isomerization (Table 1).

After prolonged irradiation, the concentration ratio of *trans*- to *cis*-2-butene approached a value (unity) which was independent of the temperature (Table 2). The reduction in the total amount of 2-butene during an irradiation was negligibly small.

TABLE 2. THE RATIO OF *trans* TO *cis* AFTER PROLONGED IRRADIATION AT VARIOUS TEMPERATURES IN THE CADMIUM-PHOTOSENSITIZATION

Temperature, °C	Ratio of *trans* to *cis*
275	1.0_6
300	1.0_4
325	1.0_8
350	1.0_9

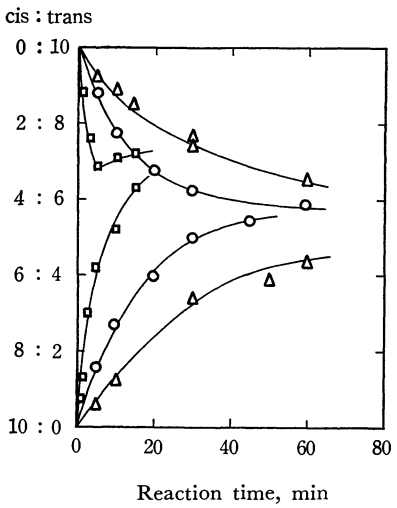

Fig. 2. Ratio of *trans*- to *cis*-2-butene in the mercury-photosensitization at room temperature. (Initial pressure: □, 1 mmHg; ○, 5 mmHg; △, 20 mmHg)

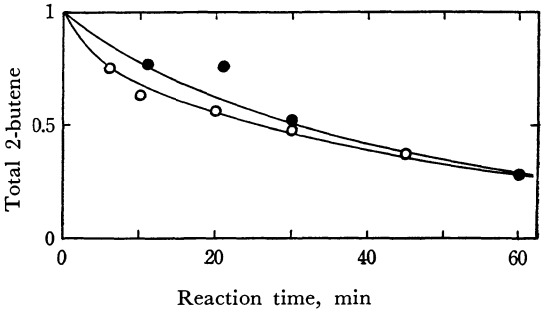

Fig. 3. Reduction of total amount of 2-butene in the mercury-photosensitization. (Initial pressure: 5.1 mmHg; ○: *cis*; ●: *trans*)

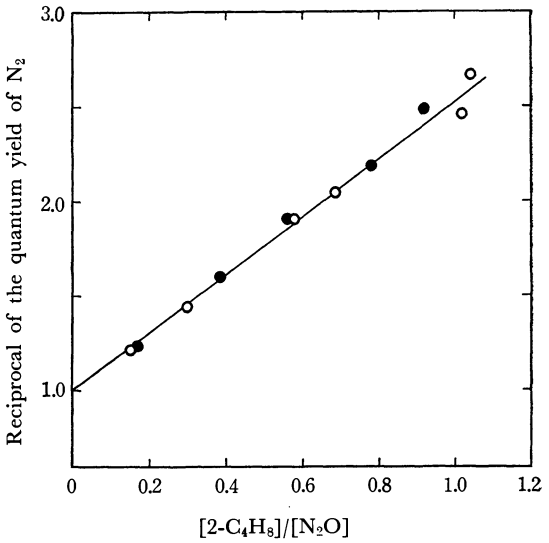

Fig. 4. Plots of the reciprocal of the quantum yield of nitrogen as a function of the ratio of the pressure of 2-butene to that of nitrous oxide. (○: *cis* → *trans*; ●: *trans* → *cis*)

Mercury-photosensitization. The products of the reaction of 2-butene photosensitized by $Hg(^3P_1)$ at room temperature were cis-trans isomer and small amounts of hydrogen, methane, propylene, *n*-butane and 1-butene. The rate of decomposition was *ca.* 10^{-2} of that of isomerization (Table 3).

The total amount of 2-butenes decreased with increasing reaction period and with decreasing initial pressure. After prolonged irradiation, the concentration ratio of *trans*- to *cis*-2-butene approached a constant value which was larger than unity and increased with decreasing pressure (Figs. 2 and 3).

Figure 4 shows the reciprocal of the quantum yield of nitrogen formation plotted against the ratio of the pressure of 2-butene to that of nitrous oxide, which is kept at 100 mmHg. The slope of the straight line in Fig. 4 obtained by the method of least squares was 1.6 ± 0.1 for both butenes.

TABLE 3. PRODUCTS FROM THE MERCURY-PHOTOSENSITIZATION AT ROOM TEMPERATURE
(Reaction cell, 166 ml)

Initial pressure mmHg	Reaction time min	Products μmol					
		H_2	CH_4	C_3H_6	n-C_4H_{10}	1-C_4H_8	*trans-cis* isomer
cis-2-Butene							
5.1	5	0.73	0.10	0.28	0.21	0.39	34.6
5.1	45	0.59	0.99	1.01	1.20	1.01	54.4
19.0	5	0.65	0.32	0.07	0.21	0.17	49.6
19.6	60	0.76	0.88	1.24	2.09	1.70	286
trans-2-Butene							
5.1	10	0.91	0.16	0.32	0.53	0.55	52.0
5.0	30	0.77	0.55	0.87	0.92	1.08	56.4
19.0	5	0.12	—	—	0.64	0.30	20.6
20.4	30	0.97	0.21	0.37	1.04	0.60	161

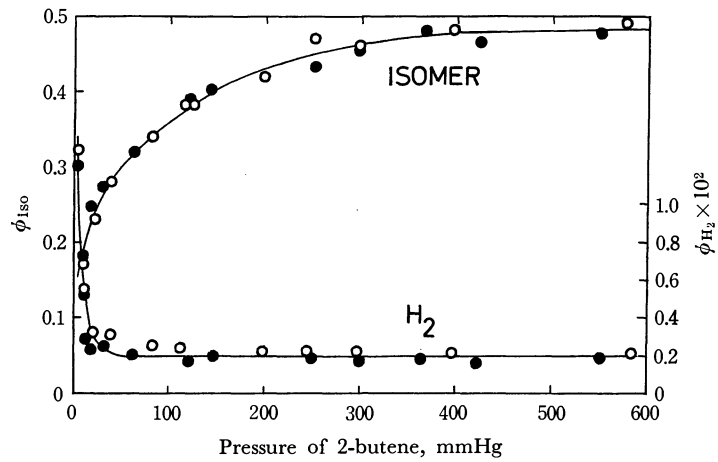

Fig. 5. Pressure dependence of the quantum yields of isomer and hydrogen formed in the mercury-photosensitization. (○, *cis*; ●, *trans*)

Assuming 17 Å² for the quenching cross section of nitrous oxide,[8] the quenching cross section of 2-butenes was estimated to be 30±2 Å².

The quantum yield of isomerization was identical for the two reactant isomers and increased with increasing initial pressure, approaching a value of about 0.5 above 300 mmHg (Fig. 5). The quantum

TABLE 4. QUANTUM YIELDS OF ISOMER WITH VARIOUS LIGHT SOURCES AND INTENSITIES IN THE MERCURY-PHOTOSENSITIZATION
(Initial pressure: 20 mmHg)

Light source	Intensity Einstein/min	Reactant isomer	Quantum yield
A	3.55	*cis*	0.236
A	3.49	*trans*	0.224
A	3.94	*cis*	0.243
A	5.21	*cis*	0.214
B	11.6	*cis*	0.221
B	11.6	*trans*	0.221

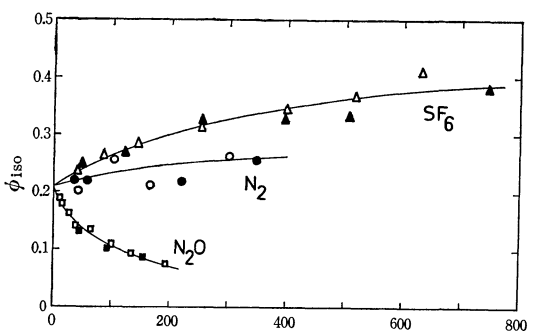

Fig. 6. Effects of foreign gases on the quantum yield of isomer formed in the mercury-photosensitization. (Initial pressure of 2-butene is 20 mmHg; △ ○ □, *cis*; ▲ ● ■, *trans*.)

8) A. J. Yarwood, O. P. Strausz and H. E. Gunning, *J. Chem. Phys.*, **41**, 1705 (1964).

yield of hydrogen decreased with increasing pressure and leveled off at 0.002 above 50 mmHg.

Table 4 shows the quantum yields of isomerization at 20 mmHg with various light intensities and lamps.

Figure 6 shows the effect of added gas; sulfur hexafluoride, nitrogen and nitrous oxide upon the quantum yield of isomerization at 20 mmHg of 2-butene. The quantum yield increased with sulfur hexafluoride, decreased with nitrous oxide and increased a little with nitrogen.

Discussion

Cadmium - photosensitization. *Decomposition Products.* The observed small amounts of decomposition products, hydrogen, methane and propylene, may be produced in the following mechanism;

$$Cd^* + C_4H_8 \rightarrow CdH + C_4H_7$$
$$CdH \rightarrow Cd + H$$
$$H + C_4H_8 \rightarrow \begin{cases} H_2 + C_4H_7 \\ CH_3 + C_3H_6 \\ C_4H_9 \end{cases}$$
$$CH_3 + C_4H_8 \rightarrow CH_4 + C_4H_7$$

Here, Cd* stands for $Cd(^3P_1)$. C_4H_7 and C_4H_9 radicals may produce stable molecules by disproportionation or recombination. The total amount of these decomposition products is about 10^{-3} of that of isomerization which is one order of magnitude less than that in the case of mercury-photosensitization. This result may be due to the smaller energy available for decomposition in the case of Cd-photosensitization.

Mechanism of Isomerization. Neglecting the small amount of decomposition, the following mechanism may be considered for cis-trans isomerization of 2-butene;

$$Cd + h\nu \rightarrow Cd^* \quad (I)$$
$$Cd^* \rightarrow Cd + h\nu \quad (0)$$
$$Cd^* + T \rightarrow Cd + B^* \quad (1t)$$
$$Cd^* + C \rightarrow Cd + B^* \quad (1c)$$
$$B^* + M \rightarrow \alpha T + (1-\alpha)C + M \quad (2)$$

Here, T and C are *trans-* and *cis*-2-butenes, respectively. B* is the triplet state of 2-butene. α is the fraction of trans isomer formed from B*. The steady-state treatment gives the following relations;

$$\left.\begin{aligned} d[C]/dt &= I((1-\alpha)k_{1t}[T] - \alpha k_{1c}[C])/ \\ &\quad (k_0 + k_{1t}[T] + k_{1c}[C]) \\ d[T]/dt &= I(\alpha k_{1c}[C] - (1-\alpha)k_{1t}[T])/ \\ &\quad (k_0 + k_{1t}[T] + k_{1c}[C]) \end{aligned}\right\} \quad (I)$$

Table 5. Isotopic distribution of hydrogen formed in the mercury-photosensitization of 1 : 1 mixture of *trans*-2-butene-d_0 and -d_8

Initial pressure mmHg	H_2	HD %	D_2	$[HD]^2/[H_2][D_2]$
6.5	46.6	30.7	22.7	0.89
32.0	65.8	25.7	8.5	1.2

When reaction starts from pure isomers, the initial rates of isomerization should be expressed as follows;

$$\left.\begin{aligned} R_{T\rightarrow C} &= (1-\alpha)Ik_{1t}[T]/(k_0 + k_{1t}[T]) \\ R_{C\rightarrow T} &= \alpha Ik_{1c}[C]/(k_0 + k_{1c}[C]) \end{aligned}\right\} \quad (II)$$

The relations, $k_0 \ll k_{1t}[T]$ or $k_{1c}[C]$ and $\alpha = 1-\alpha$, hold because, as Fig. 1 shows, $R_{T\rightarrow C} = R_{C\rightarrow T}$ and the rates of isomerization were not affected by the pressure change. Using the lifetime of $Cd(^3P_1)$ atom (2.4×10^{-6} sec[9]), k_0 and $k_{1t}(=k_{1c})$ were calculated to be 4.2×10^5 sec^{-1} and 9.4×10^6 $mm^{-1}sec^{-1}$, respectively, *i. e.*, $k_0 \ll k_{1t}[T]$ or $k_{1c}[C]$ at the pressure over 1 mmHg. This is consistent with the present result.

The ratio of *trans-* to *cis*-2-butene obtained after prolonged irradiation ($[T]_\infty/[C]_\infty$) can be derived by setting $(d[C]/dt)_\infty = (d[T]/dt)_\infty = 0$ as follows,

$$[T]_\infty/[C]_\infty = \alpha k_{1c}/(1-\alpha)k_{1t} \quad (III)$$

Because $[T]_\infty/[C]_\infty$ is unity for all temperature ranges (Table 1), k_{1t} should be equal to k_{1c}, *i. e.*, the quenching cross section of *cis*-2-butene for $Cd(^3P_1)$ is equal to that of *trans*-2-butene.

Mercury - photosensitization. *Mechanism of Hydrogen Formation.* Hydrogen formation from an olefin molecule in Hg-photosensitization has been ascribed to the C–H bond cleavage of an excited olefin molecule.[11] Accordingly, the quantum yield of hydrogen should approach zero at high pressures because of collisional deactivation. Figure 5, however, shows that the quantum yield of hydrogen does not approach zero even at 500 mmHg. This leads us to speculate that the following process plays a part in the mechanism;

$$Hg(^3P_1) + C_4H_8 \rightarrow (Hg\cdots H\cdots C_4H_7)^* \rightarrow Hg + H + C_4H_7 \quad (3)$$

This kind of quenching process was proposed by Gunning *et al.*[12] to account for the results of a study of the Hg-photosensitized decomposition of cyclohexene. Using the quantum yield of

9) F. W. Byron, Jr., M. N. McDermott and R. Novick, *Phys. Rev.*, **134**, A 615 (1964).
10) E. W. R. Steacie and D. J. LeRoy, *J. Chem. Phys.*, **11**, 164 (1943).
11) R. J. Cvetanović, "Progress in Reaction Kinetics," Vol. 2, ed. by G. Porter, Pergamon Press, Oxford (1964).
12) G. R. DeMare, O. P. Strausz and H. E. Gunning, *Can. J. Chem.*, **43**, 1329 (1965).

hydrogen at the pressure higher than 50 mmHg and the ratio of the rate of abstraction to that of addition (0.023 and 0.076 for *cis*- and *trans*-2-butene,[13] respectively), the quantum yields of the complex formation were estimated to be 0.09 and 0.025 for *cis*- and *trans*-2-butenes, respectively.

The quantum yield of hydrogen decreased with increasing initial pressure (Fig. 5). This behavior may be explained in terms of C-H bond cleavage of excited 2-butene molecules. Mixtures of *trans*-2-butene-d_0 and -d_8 were decomposed by Hg-photosensitization, in order to investigate the mechanism of hydrogen formation. The results are listed in Table 5. Obviously, the molecular elimination reaction occurred. Although the result seems to show the decrease of the molecular elimination with increasing pressure, further discussions can not be made because of the small rate of hydrogen formation.

The Ratio of trans- to cis-2-Butene. As is shown in Figs. 2 and 3, the ratio $[T]_\infty/[C]_\infty$ increased with decreasing initial pressure and at the same time, some disappearance of total 2-butene was observed. Possible explanations for this observation are as follows; (1) *trans*- and *cis*-2-butenes have different quenching cross sections for $Hg(^3P_1)$, (2) the ratio of *trans*- to *cis*-2-butene formed from the excited olefin molecule is not unity, (3) the ratio is affected by the disproportionation reaction of butyl and butenyl radicals and (4) the ratio is affected by the reduction of total 2-butene, *i. e.*, the rates of decomposition of cis and trans are different. The possibility (1) may be eliminated in view of the identical quenching cross sections found for the two isomers (Fig. 4). The possibility (2) can be omitted because the quantum yields of isomer do not differ for the two reactant isomers (Fig. 5). (3) may be ruled out because the amounts of the products of the disproportionation reaction such as 1-butene and *n*-butane are too small to explain the change of the ratio with pressure. The most probable explanation is the possibility (4), because the rate of decomposition of *cis*-2-butene is faster than that of *trans*-isomer (Fig. 3).

The Pressure Dependence of Quantum Yield of Isomer. Cundall *et al.*[2] assumed only one precursor for the isomerization of 2-butene photosensitized by $Hg(^3P_1)$ and derived the following relation.

$$P/R_{iso} \propto P \qquad \text{(IV)}$$

Here, P and R_{iso} mean the initial pressure of 2-butene and the rate of isomerization, respectively. Equation (IV), however, explains the present results only approximately. We have attempted to establish a relationship which accounts for the pressure dependence of the quantum yield of isomerization. The following equation gives the relationship. The reaction mechanism which predicts the relationship will be discussed later.

$$\phi_{iso} = \frac{b+c[P]}{1+a[P]} \frac{d[P]}{1+d[P]} \qquad \text{(V)}$$

Here, [P] is the initial pressure of 2-butene in mmHg and ϕ_{iso} is the quantum yield of isomerization. The letters a, b, c and d are experimental parameters which are calculated to be 3×10^{-2} $mmHg^{-1}$, 0.1, 1.5×10^{-2} $mmHg^{-1}$ and 1.3 $mmHg^{-1}$, respectively.

As seen in Fig. 5, the sum of the quantum yield of precursor for isomerization which is equal to $2\phi_{iso}$ and that of C-H bond cleavage is almost unity above 300 mmHg. The quantum yield of C-H bond cleavage was estimated from that of hydrogen formed, using the ratio of the rate of abstraction to that of addition of a hydrogen atom.[13] In this estimation, the fraction of molecular elimination reaction was neglected, since it does not affect the present discussion. If the *cis-trans* isomerization and the cleavage of C-H bond are the only reactions induced by Hg-photosensitization, part of the absorbed light energy is lost at pressures below 300 mmHg of olefin. Incomplete quenching which can be estimated from the lifetime of $Hg(^3P_1)$ atoms (1.08×10^{-7} sec[14]) and from the quenching cross section of 2-butene (30 Å^2), is negligibly small above a pressure of 10 mmHg. A careful search was made for products other than *cis-trans* isomer, such as methyl cyclopropane (observed in the reaction of 1-butene photosensitized by $Hg(^3P_1)$[15]), cyclobutane, isobutene, 1-butene and C_8-compounds; but they were very small or not found at all. The disappearance of incident photons, therefore, remains unexplained.

The quantum yield of isomerization was unaffected by the light intensity. This suggests that the triplet-triplet anihilation of excited mercury atoms and of excited 2-butene, stepwise excitation processes and self reversal of the resonance line are negligible.

Cundall *et al.*[2] examined the effect of foreign gas on the isomerization and found that some compounds reduced the rate of isomerization with a competitive quenching for excited mercury atoms and some gave no effect because of the small quenching cross section of the foreign gas.

The effect of nitrous oxide, as is shown in Fig. 6, may be due to the competition for excited mercury atoms with 2-butene. The slight increase of the quantum yield of isomerization by adding nitrogen may be explained as the result of Lorentz

13) K. R. Jennings and R. J. Cvetanović, *J. Chem. Phys.*, **35**, 1233 (1961).

14) A. C. G. Mitchell and M. W. Zemansky, "Resonance Radiation and Excited Atoms," Cambridge University Press, London (1961).

15) R. J. Cvetanović and L. C. Doyle, *J. Chem. Phys.*, **37**, 543 (1962).

broadening. The apparent increase of the quantum yield can be estimated by using Kang Yang's data[16] under the assumption that collision broadening of 2-butene is the same as that of ethylene. The estimated values are consistent with the experimental values within experimental error. Although nitrogen is known to be a quencher for the process, $Hg(^3P_1 \rightarrow {}^3P_0)$, the pressure used is still not high enough to induce the participation of $Hg(^3P_0)$ in this system.[11] The effect of sulfur hexafluoride appears to be complex. The quantum yield of isomerization increases with increasing pressure of added sulfur hexafluoride. Clearly, this effect cannot be associated with the removal of vibrational energy from the precursor since sulfur hexafluoride is known to be an effective quencher of vibrational energy.

With these data in mind, the following reaction mechanism is tentatively considered to explain the pressure dependence of the isomerization.

$$Hg + h\nu \rightarrow Hg^* \quad (4)$$

$$Hg^* \rightarrow Hg + h\nu \quad (5)$$

$$Hg^* + C \text{ (or T)} \rightarrow HgC^* \text{ (or } HgT^*) \quad (6)$$

$$HgC^* \text{ (or } HgT^*) \rightarrow Hg + B^* \quad (7)$$

$$HgC^* \text{ (or } HgT^*) \rightarrow Hg + C^\dagger \text{ (or } T^\dagger) \quad (8)$$

$$HgC^* \text{ (or } HgT^*) + M \rightarrow Hg + B^* + M \quad (9)$$

$$B^* \rightarrow (1/2)C + (1/2)T \quad (10)$$

$$C^\dagger \text{ (or } T^\dagger) \rightarrow C \text{ (or T)} \quad (11)$$

Here, Hg*, C and T mean $Hg(^3P_1)$, *cis*- and *trans*-2-butene, respectively. B* may be the triplet state of 2-butene. HgC* or HgT* is a transient complex of *cis*- or *trans*-2-butene and excited mercury atom. $C^\dagger$ and $T^\dagger$ mean the vibrationally excited ground state of *cis*- and *trans*-2-butene which do not isomerize. The steady state treatment of the mechanism gives a relation of the type (V).

In this mechanism, the pressure dependence of the quantum yield of isomerization is explained by the competitive reactions, (7), (8) and (9). The effects of sulfur hexafluoride, nitrogen and nitrous oxide may be explained as follows; HgC* or HgT* is quenched efficiently by sulfur hexafluoride, but not by nitrogen and nitrous oxide. The reasoning of the mechanism, especially the reaction (8), must await further investigation.

The authors are indebted to Dr. K. F. Preston (National Research Council, Canada) for his assistance in correcting the manuscript.

16) Kang Yang, *J. Am. Chem. Soc.*, **86**, 3941 (1964).

BULLETIN OF THE CHEMICAL SOCIETY OF JAPAN VOL. 41 291—296 (1968)

Phase Transitions in Crystalline Divalent Metal Dicalcium Propionates. II. Proton Magnetic Resonance Investigation*[1]

Nobuo NAKAMURA, Hiroshi SUGA, Hideaki CHIHARA and Syûzô SEKI

Department of Chemistry, Faculty of Science, Osaka University, Toyonaka, Osaka

(Received September 6, 1967)

The motions of the propionate anions in strontium-, lead-, and barium-dicalcium propionates were examined with the proton magnetic resonance method at low temperatures. It was found that the methyl groups rotate about the C_3-axes even at 20°K in the Sr-, and the Ba-salts. In the Sr-salt the gradual decrease of the second moment below the ferroelectric transition point was observed and this phenomenon was related to the large angle torsional oscillations of the ethyl groups about the C_3'-axes as introduced in Part I: Near the ferroelectric transition point the observed second moment shows the possibility of excitation of the C_3'-rotation which would make the crystal to be paraelectric above the transition point. It was expected that the C_3'-torsion is to some extent excited in the Pb-salt at liquid nitrogen temperature, a slight discrete change being observed at the lower transition point. A sharp line width transition was also observed in the Ba-salt and this fact resulted in the finding of a new λ-type phase transition with the peak at about 204°K by the differential thermal analysis. A slight decrease of the second moment was observed at the upper transition point and the C_3'-rotation was assumed to be fully excited above that point.

In 1955 calorimetric and dilatometric studies were carried out on $BaCa_2(C_2H_5CO_2)_6$ in the authors' laboratory, and a phase transition was found to occur at −8.5°C.[1] Calorimetric study was also performed on the mixed crystals between the Ba-salt and $PbCa_2(C_2H_5CO_2)_6$ and it was suggested that ordering effect of the orientations of the methyl groups in the propionate anions is responsible to the phase transition of the Ba-salt.

On the other hand, Matthias and Remeika have found in 1957 that $SrCa_2(C_2H_5CO_2)_6$ undergoes a ferroelectric phase transition at 8.5°C.[2]

In the previous paper[3] the present authors reported the results of the calorimetric study on the Sr-salt and suggested, on the basis of the crystal symmetry consideration and of the fact that the anomaly in the heat capacity is of typical λ-type, that the ferroelectric phase transition is closely related to an orientational ordering of the methyl groups in the propionate anions. An attempt was made to correlate the torsional oscillation of the ethyl group around the $C_{carboxyl}$-C_α axis to the temperature dependence of the spontaneous polarization near the Curie point. The X-ray analysis was performed later by Tomiie and others on the room temperature phase of this substance.[4] There was shown the possibility of the rotational motion of the ethyl groups about the $C_{carboxyl}$-C_α axes from extremely large temperature factors of C_α-carbons and also from the undeterminable positions of the methyl-carbon atoms. In addition, it was found a new phase transition takes place at 104.2°K by the calorimetric study and the features of this transition were already described in Part I.

In the case of $PbCa_2(C_2H_5CO_2)_6$ two phase transitions were found at 191.5°K and 333°K, respectively, and no existence of the ferroelectric phase was confirmed by a hysteresis bridge method as reported in Part I.

It has been suggested there that the proton magnetic resonance is a powerful method of obtaining further informations about the motions of the propionate anions in the Ba-, Sr-, and Pb-salts. In this paper, the results of the second moment measurement are reported. It will be shown that for the Sr-salt, the result of NMR experiment supports the assumptions on the motions of the propionate anions proposed in Part I: In the Pb-salt, the full account of the nature of the phase transitions remains still in difficulty even applying the NMR method. The line width transition observed in the proton resonance study of the

*1 This paper was read before the 17th Annual Meeting of the Chemical Society of Japan, Tokyo, April, 1964. (See abstract of the Meeting, p. 461)

1) S. Seki, M. Momotani, K. Nakatsu and T. Ôshima, *J. Chem. Phys.*, **19**, 1061 (1951); This Bulletin, **28**, 411 (1955).

2) B. T. Matthias and J. P. Remeika, *Phys. Rev.*, **107**, 1727 (1957).

3) N. Nakamura, H. Suga, H. Chihara and S. Seki, This Bulletin, **38**, 1779 (1965), afterwards referred to as Part I.

4) Y. Tomiie, private communication.

Ba-salt will be discussed based on the new transition phenomenon at 204°K found by the differential thermal analysis.

Experimental

The procedure of the sample preparation was already described in the previous papers.[1,3] Proton second moments were measured on the powdered specimens by a Robinson-type spectrometer at 20 MHz; the absence of the saturation effect was confirmed by changing the rf-levels especially at low temperatures; the correction of the modulation width was made after Andrew.[5] The temperature was left to increase very slowly and the resonance signals were recorded with measuring the temperatures by a chromel-constantan thermocouple; the temperature increase in each sweep is within 1°C above the liquid nitrogen temperature and at most 1.5°C near liquid hydrogen temperature.

Experimental Results and Discussion

Figures 1, 2 and 3 show the results of the second moment measurements on the Sr-, Pb- and Ba-salts, respectively, the heat capacity curves being illustrated for reference.

Calculation of the Second Moment. For a propionate anion the intra-ionic contribution to the second moment was calculated by the usual method[6] by using the values, $r_{CC}=1.54$ Å, $r_{CH}=1.10$ Å, $\angle HCH=\angle HCC=\angle CCC=109°28'$. The second moments were calculated for the typical four cases: 1) the rigid lattice (the *trans*-conformation was assumed); 2) the lattice in which only the rotation of the methyl group about the axis connecting α- and β-carbon atoms is excited (C_3-rotation); 3) both the C_3-rotation and the torsional oscillation of the methyl and ethyl groups about the $C_{carboxyl}$-C_α axis (C'-torsion) are excited; 4) both the C_3-rotation and the rotation of the methyl and ethyl groups about the $C_{carboxyl}$-C_α axis are

TABLE 1. CALCULATED VALUE OF THE SECOND MOMENT FOR THE PROPIONATE ANION

	Second moment (gauss²)
Intra-ionic contribution	
Rigid lattice	20.02
C_3-rotation	11.62
C_3-rotation + C_3'-torsion	$2.38+1.10\cdot J_0^2(\theta_1)+8.14\cdot J_0^2(2\theta_1)$
C_3-rotation + C_3'-rotation	2.38
Inter-ionic contribution	
C_3-rotation + C_3'-rotation (for the Ba-salt)	~1.8

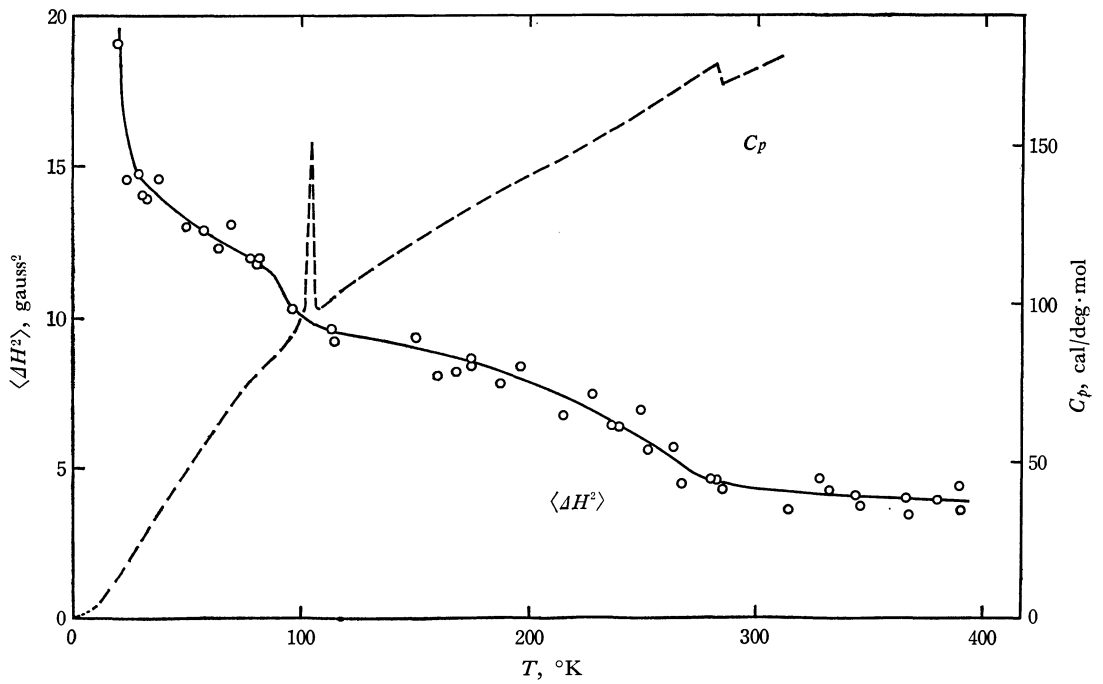

Fig. 1. Temperature dependence of the second moment (—○—) and of the heat capacity (——) of $SrCa_2(C_2H_5CO_2)_6$.

5) E. R. Andrew, *Phys. Rev.*, **91**, 425 (1953).
6) J. H. Van Vleck, *ibid.*, **74**, 1168 (1948); J. G. Powles and H. S. Gutowsky, *J. Chem. Phys.*, **21**, 1704 (1953); E. R. Andrew and R. A. Newing, *Proc. Phys. Soc.*, **72**, 959 (1958).

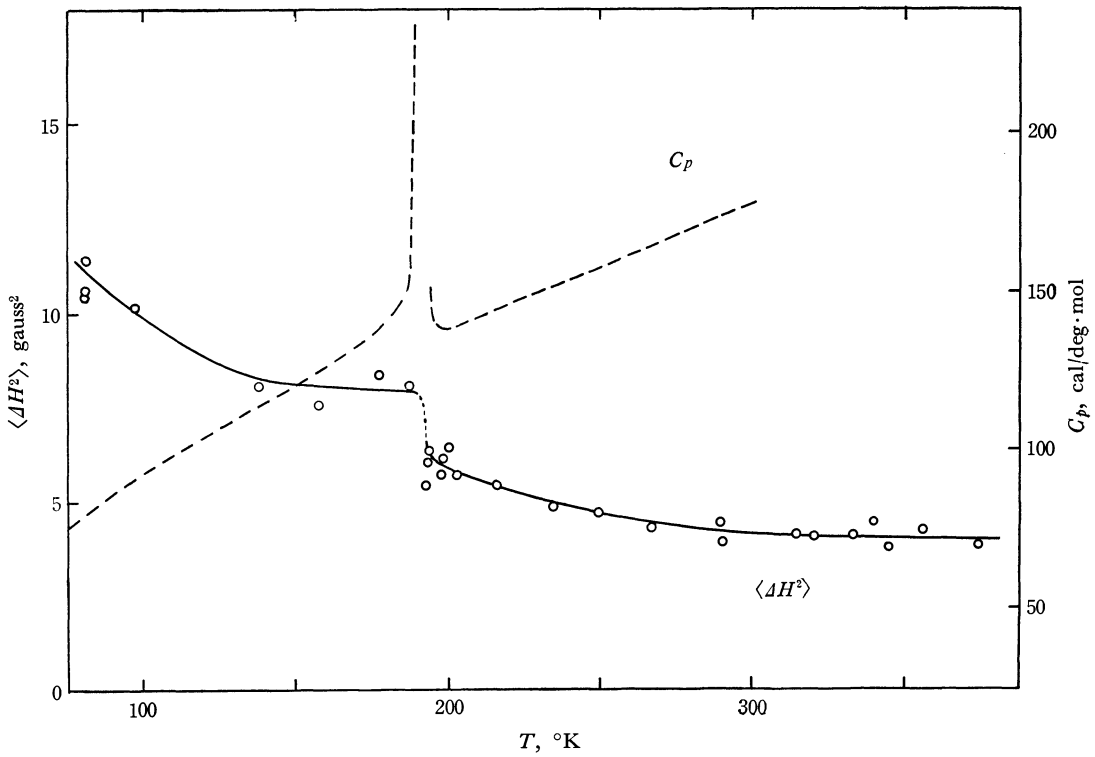

Fig. 2. Temperature dependence of the second moment (-○-) and of the heat capacity (----) of $PbCa_2(C_2H_5CO_2)_6$.

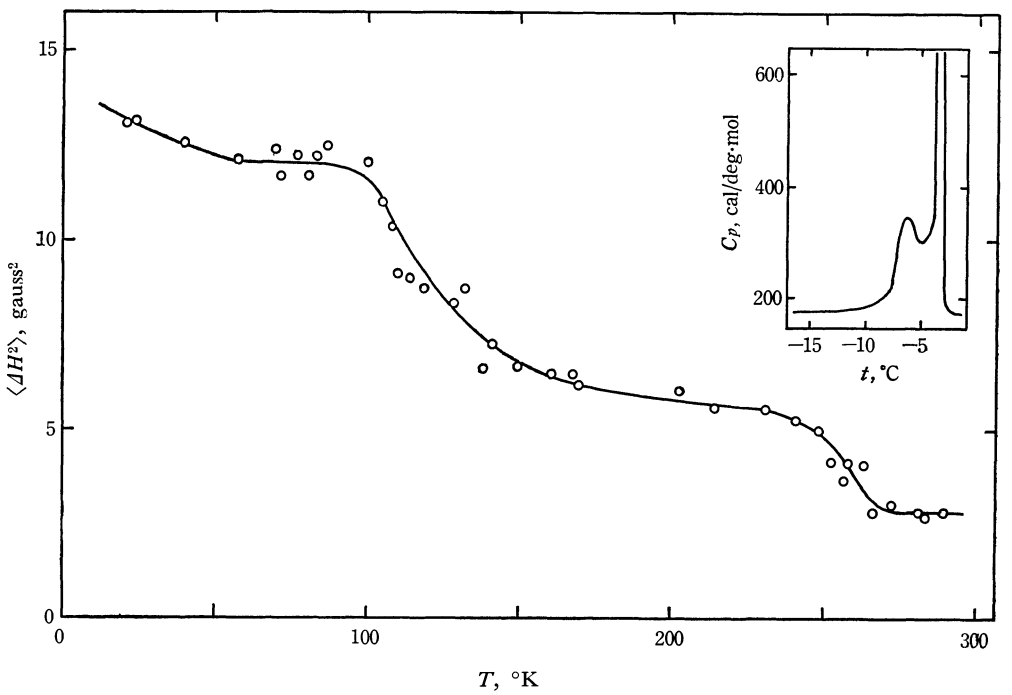

Fig. 3. Temperature dependence of the second moment of $BaCa_2(C_2H_5CO_2)_6$. The inset figure shows the heat capacity near the upper transition point.

excited (C_3'-rotation). The results of the calculation are given in Table 1, where J_0's are the Bessel's functions of zeroth order, and θ_1 the mean amplitude of the C_3'-torsional oscillation.

The inter-ionic contribution was only estimated for the Ba-salt, by using the crystal structure data for the room temperature phase, and by assuming both the C_3- and the C_3'-rotations. The result of the calculation is also given in Table 1. In the case of the lower temperature phase of the Ba-salt, as well as of each phase of the Sr- and Pb-salts, no crystallographic data is available for the calculation of the inter-ionic contribution. In the following we proceed to the discussion of the temperature variation of the molecular motion in each salt, separately.

$SrCa_2(C_2H_5CO_2)_6$. The second moment at the liquid hydrogen temperature, *i. e.*, 19.1 gauss^2, as shown in Fig. 1, is smaller than the rigid lattice value which should somewhat be larger than 20.02 gauss^2 (See Table 1) if we add the inter-ionic contribution to this value. The C_3-rotation, therefore, may be excited to some extent already at this temperature. Above the liquid hydrogen temperature the second moment decreases down rapidly to the value 11.9 gauss^2 at 85°K. This value is only 0.3 gauss^2 larger than the value for the C_3-rotation. Accordingly it is reasonable to consider that the C_3-rotation is completely excited at 85°K. For the calculation of the contribution from the C_3-rotation, the following equation presented by Powles and Gutowsky may be applied:[7]

$$\ln\{(\langle\Delta H^2\rangle_r/\langle\Delta H^2\rangle)^{1/2}\tan(\pi/6\cdot\langle\Delta H^2\rangle/\langle\Delta H^2\rangle_r-1)\} = E_a/\boldsymbol{R}T + C,$$

$$C = \ln\{4\pi\mu\tau_0(\langle\Delta H^2\rangle_r)^{1/2}/\boldsymbol{h}\},$$

where $\langle\Delta H^2\rangle$ is the second moment at temperature T and $\langle\Delta H^2\rangle_r$ corresponding to the complete free rotation, E_a the activation energy for the C_3-rotation, and τ_0 the mean life-time at one of the three possible equilibrium positions for the methyl group. The experimental data were analysed with the aid of this equation, and the plot of $\ln\{\cdots\}$ against $1/T$ is shown in Fig. 4, where $\langle\Delta H^2\rangle_r$ was set to be 11.9 gauss^2 (at 85 °K): From the slope of this straight line, $E_a=1.5$ kcal/mol and $\tau_0=9.4\cdot10^{-8}$s were obtained, respectively.

A small but significant decrease in the second moment was found between 90°K and 100°K. This abrupt change of the second moment may be due to the change in the crystal structure accompanied with the phase transition found in Part I.

A gradual decrease of the value from 10.0 gauss^2 at 100°K to 7.8 gauss^2 at about 200°K may be attributed to the partial averaging out of the dipolar interactions caused by the gradual excitation of the large angle torsional oscillation of each ethyl group about the C_3'-axis: Such an assumption on the motion of the ethyl group was already introduced in Part I in order to explain the temperature dependence of the spontaneous polarization in the ferroelectric phase. In the case of the C_3'-torsion which is simultaneously accompanied with the C_3-rotation the following expression for the intra-ionic contribution to the second moment may be written by making a small modification of the Andrew's theory;[8] $\langle\Delta H^2\rangle=2.38+1.10\cdot J_0^2(\theta_1)+8.14\cdot J_0^2(2\theta_1)$, (in gauss^2), where θ_1 is the mean amplitude of the C_3'-torsion and $J_0(x)$ the Bessel function of zeroth order. If one assumes that the inter-ionic contributions to the second moment remain constant from 100°K to above the ferroelectric transition point, one can estimate the force constant for the C_3'-torsion by using the classical relationship: $\kappa\theta_1^2=\boldsymbol{k}T$, and by fitting the experimental data to the above relation. The analysis gives $\kappa=5\cdot10^{-3}$mdyn/Å and this value corresponds to the mean amplitude of torsional oscillation of $\pi/5$ at 150°K. This result does not agree exactly with the value of $\kappa=1.1$—$1.6\cdot10^{-3}$ mdyn/Å obtained in Part I from the P_s *vs.* T curve, but it seems to be reasonable to consider that the ethyl groups in the propionate anions librate with considerably large amplitudes below the ferroelectric transition point.

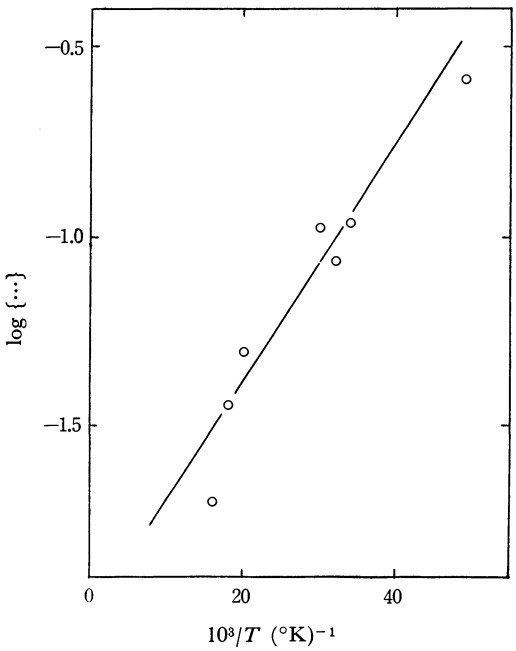

Fig. 4. The term $\ln\{\cdots\}$ plotted against $1/T$ for the experimental second moment of $SrCa_2(C_2H_5CO_2)_6$ between 20°K and 85°K.

7) J. G. Powles and H. S. Gutowsky, *J. Chem. Phys.*, **23**, 1692 (1955).

8) E. R. Andrew, *J. Chem. Phys.*, **18**, 607 (1950).

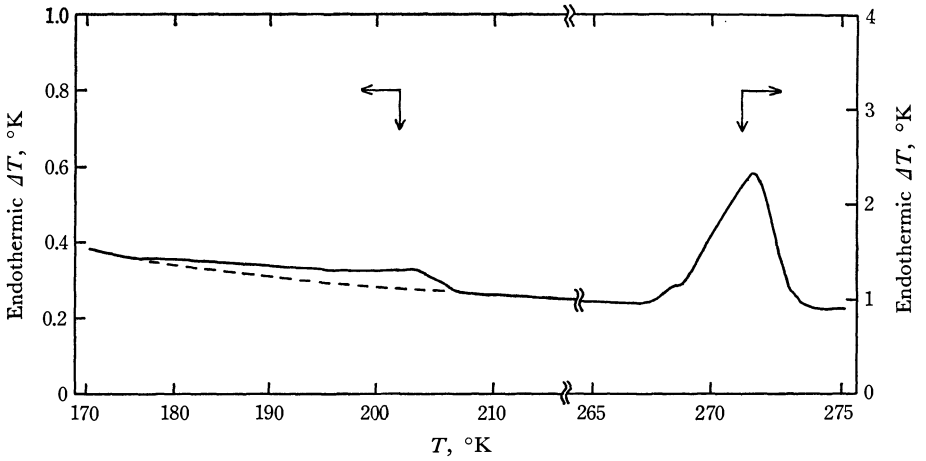

Fig. 5. Differential thermal analysis curve of $BaCa_2(C_2H_5CO_2)_6$. The plausible base line for the lower transition region is indicated by the broken line.

Further decrease of the second moment near the ferroelectric transition point may reflect the onset of the C_3'-rotation. In this case, some modification of Powles and Gutowsky's equation[7] gives the following expression:

$$\ln\{(\langle\Delta H^2\rangle_r/\langle\Delta H^2\rangle)^{1/2}\cdot\tan 0.128\pi\cdot(\langle\Delta H^2\rangle/\langle\Delta H^2\rangle_r-1)\} = E_a/\boldsymbol{R}T + C,$$

$$C = \ln 4\pi\mu\tau_0(\langle\Delta H^2\rangle_r)^{1/2}/\boldsymbol{h}$$

The meaning of the notations in this equation is the same as before. The analysis of the experimental data gives $E_a=630$ cal/mol and $\tau_0=1.2\cdot10^{-6}$s, and the latter seems to be somewhat unreasonable. Anyhow, it is possible to consider that the C_3'-rotation removes the polarization due to propionate anions which were originally aligned parallel to the crystalline c-axis and as the result the paraelectric phase appears. The continuous change from C_3'-torsion to C_3'-rotation may explain that the transition is of order-disorder type as assumed in Part I.

Above the transition point no distinct change was observed in the second moment, and 4.3 gauss^2 at room temperature may be the sum of the intra-ionic contributions of 2.38 gauss^2 and inter-ionic contribution of about 1.9 gauss^2.

$PbCa_2(C_2H_5CO_2)_6$. The second moment of 10.9 gauss^2 at liquid nitrogen temperature may be explained by the partial excitation of the C_3'-torsion in addition to the C_3-rotation. Near the transition temperature, 191.5°K, a slight discrete change was observed as shown in Fig. 2. This discontinuity in the second moment as well as the discontinuity in the dielectric constant described in Part I may be due to the change in the crystal structure accompanied with the phase transition.

Above the transition temperature the second moment decreases gradually and settled down to 4.0 gauss^2 above room temperature. The value of 4.0 gauss^2 is comparable to 4.3 gauss^2 for the room temperature phase of the Sr-salt. Therefore, it may be concluded that the C_3- and C_3'-rotations are completely excited in the Pb-salt above the room temperature.

No remarkable change in the second moment was observed through the transition at 333°K where the dielectric constant shows a large anomaly.

$BaCa_2(C_2H_5CO_2)_6$. The second moment decreases slightly from the liquid hydrogen temperature to about 100°K, and 12.0 gauss^2 at this temperature suggests the complete excitation of the C_3-rotation. The second moment falls further remarkably from 12.0 gauss^2 to about 6 gauss^2 at 160°K. This line width transition can be treated by the following theoretical expressions developed by Gutowsky and Pake;[9]

$$(\delta\nu)^2 = B^2 + C^2(2/\pi)\tan^{-1}(\alpha\cdot\delta\nu/\nu_c) \text{ and}$$

$$\nu_c = \nu_0\cdot\exp(-E_a/\boldsymbol{R}T),$$

where $A=(B^2+C^2)^{1/2}$ is the line width in the rigid lattice, B the narrowed line width characteristic to a motion, ν_c the correlation frequency, ν_0 the frequency factor and α a numerical factor characterized by the line shape. Form the activation plot the activation energy, $E_a=1.5$ kcal/mol, and the frequency factor $\nu_0=1.5\cdot10^7$ s^{-1} were obtained by assuming $\alpha=1$. Such a decrease of the second moment may be explained by assuming the C_3'-rotation of only four among six propionate anions in the unit cell, if we want to fit the magnitude of the second moment at 160°K (6.2 gauss^2) with the crystal model. The preliminary differential thermal analysis study shows the existence of a small λ-type anomaly with the

9) H. S. Gutowsky and G. E. Pake, *J. Chem. Phys.*, **18**, 162 (1950).

peak at about 204°K which is the evidence of a kind of phase transition (See Fig. 5). It is, therefore, considered that the phase transition may be related to some anisotropic motion of the propionate anions mentioned above.

Further remarkable decrease of the second moment occurs at 267°K which corresponds to the first order phase transition reported previously.[1]

Note Added in Proof

After the completion of this work, we noticed that the second moment of $BaCa_2(C_2H_5CO_2)_6$ has been measured by Chezeau, Dufourcq and Lemanceau in the temperature region from 100 to *ca.* 320°K:[10] Their second moment values are slightly larger than ours just below the upper transition point, but their model assumed for the motion of the ethyl group is essentially the same as that proposed by us.

As to the second moment of $SrCa_2(C_2H_5CO_2)_6$ Nakamura, Hikichi and Furuichi have reported also their data obtained between −190°C and +100°C;[11] their experimental second moments are quite consistent with our results.

Although we referred to the structural data on $SrCa_2(C_2H_5CO_2)_6$ as a private communication from Tomiie (Ref. 4), the short communications on the crystal structures of the para- and ferroelectric phases of $SrCa_2(C_2H_5CO_2)_6$ were published after this paper was submitted.[12]

The authors would like to express their thanks to Mr. Takuji Nakamura for his help in the measurements.

10) Jean-Michel Chezeau, J. Dufourcq and B. Lemanceau, *J. Chim. Phys.*, **64**, 412 (1967).

11) E. Nakamura, K. Hikichi and J. Furuichi, *J. Phys. Soc. Japan*, **23**, 471 (1967).

12) H. Maruyama, Y. Tomiie, I. Mizutani, Y. Yamazaki, Y. Uesu, N. Yamada and J. Kobayashi, *ibid.*, **23**, 899 (1967); I. Mizutani, Y. Yamazaki, Y. Uesu, N. Yamada, J. Kobayashi, H. Maruyama and Y. Tomiie, *ibid.*, **23**, 900 (1967).

BULLETIN OF THE CHEMICAL SOCIETY OF JAPAN VOL. 41 296—303 (1968)

Addition of Some Simple Molecules to Transition Metal-Phosphine Complex and the Crystal and Molecular Structure of $Pd\{(C_6H_5)_3P\}_2(CS_2)$

Toshihide KASHIWAGI, Noritake YASUOKA, Tatzuo UEKI, Nobutami KASAI and Masao KAKUDO

Department of Applied Chemistry, Osaka University, Higashinoda Miyakojima, Osaka

and Shigetoshi TAKAHASHI and Nobue HAGIHARA

Institute of Scientific and Industrial Research, Osaka University, Sakai, Osaka

(Received September 18, 1967)

From the reaction of $M\{(C_6H_5)_3P\}_4$ (M=Pd or Pt) with CS_2, $M\{(C_6H_5)_3P\}_2(CS_2)$ has been isolated. It has been found that $M\{(C_6H_5)_3P\}_2$ also reacts with sulfur dioxide to form a novel complex, $[M\{(C_6H_5)_3P\}_4(SO_2)_n]$. The structure of one of these compounds, $Pd\{(C_6H_5)_3P\}_2(CS_2)$, was determined by means of X-rays. $Pd\{(C_6H_5)_3P\}_2(CS_2)$ crystallizes in the monoclinic system, space group $P2_1/c$, with four molecules in a unit cell of dimensions: $a=11.55$, $b=19.52$, $c=18.38$ Å and $\beta=128°53'$. The most remarkable feature of the whole structure is the coordination of CS_2 to the Pd: only one of the S atoms, S(2), coordinates to the Pd, while the CS_2 ligand is bent at an angle of 140°. The Pd, two P's, S(2) and C(1) in CS_2 lie approximately on the same plane. The Pd-C(1) distance of 2.00 Å is slightly shorter than the sum of the covalent radii, 2.06 Å. But the S(2)-Pd-C(1) angle of 44° is very small.

Recently, the relationship between the catalytic activities of transition metal complexes and their structure has been widely discussed. Vaska and Diluzio[1] treated the catalyst, $IrCl(CO)\{(C_6H_5)_3P\}_2$, with molecular oxygen, or hydrogen, and obtained a complex in which O_2, or H_2 coordinates to the iridium atom. They considered those complexes to be intermediates in the oxygenation or hydrogenation, and discussed the relation between the catalytic mechanism and the structure of $IrCl(CO)\{(C_6H_5)_3P\}_2$. Successively, the structural studies of

1) L. Vaska and J. W. Diluzio, *J. Am. Chem. Soc.*, **84**, 679 (1962).

the complexes with simple molecules have been made by X-ray diffraction. LaPlaca and Ibers determined the structures of $IrO_2Cl(CO)\{(C_6H_5)_3P\}_2$[2a] and $IrSO_2Cl(CO)\{(C_6H_5)_3P\}_2$,[2b] and they gave some information about the catalytic activities of $IrCl(CO)\{(C_6H_5)_3P\}_2$.

Hagihara and his co-workers[3] recognized that the $M\{(C_6H_5)_3P\}_4$ (M=Pd or Pt) molecule catalyzes the following reactions.

$$2(C_6H_5)_3P + O_2 = 2(C_6H_5)_3PO$$

$$2(n\text{-}C_4H_9)_3P + O_2 = 2(n\text{-}C_4H_9)_3PO$$

$$2C_6H_{11}NC + O_2 = 2C_6H_{11}NCO$$

They obtained $M\{C_6H_5)_3P\}_nO_2$ as a reaction product of $M\{(C_6H_5)_3P\}_4$ and molecular oxygen.[4,5] $M\{(C_6H_5)_3P\}_nO_2$ is considered to be an active intermediate in the oxygenation.

The addition of the simple molecules, carbon disulfide or sulfur dioxide, to triphenylphosphine-palladium or -platinum complex is described in this paper.

The crystal and molecular structure of one of these compounds, $Pd\{(C_6H_5)_3P\}_2(CS_2)$, was determined to examine the coordination of CS_2 to $Pd\{(C_6H_5)_3P\}_2$ and to get some information about the catalytic mechanism.

Experimental

Materials. Tetrakis(triphenylphosphine)palladium, $Pd\{(C_6H_5)_3P\}_4$, and -piatinum, $Pt\{(C_6H_5)_3P\}_4$, were prepared according to a modified method of Malatesta.[3,6,7]

All the procedures mentioned below were performed under a nitrogen atmosphere.

Reaction of $M\{(C_6H_5)_3P\}_4$ with Carbon Disulfide. At room temperature 578 mg of $Pd\{(C_6H_5)_3P\}_4$ was dissolved in 20 m*l* of carbon disulfide. A small amount of orange crystalline -solid separated. After 30 min carbon disulfide was gradually removed under reduced pressure and the orange residue was recrystallized from hot carbon disulfide to give 220 mg (62% yield) of $Pd\{(C_6H_5)_3P\}_2(CS_2)$ (Ia): mp 130—133°C (decomp.).

Found: C, 63.00; H, 4.26; S, 9.33%. Calcd for $C_{37}H_{30}P_2S_2Pd$: C, 62.84; H, 4.28; S, 9.07%.

The platinum - carbon disulfide complex was prepared in a similar manner. In 15 m*l* carbon disulfide 622 mg of $Pt\{(C_6H_5)_3P\}_4$ was dissolved with stirring. After a few minutes the crystals of platinum - carbon disulfide complex began to separate. The crystals were filtered, washed with carbon disulfide, and dried. Pink crystals (350 mg, 88% yield) of $Pt\{(C_6H_5)_3P\}_2\cdot(CS_2)$ (Ib) were isolated, but further purification could not be attained because of its insolubility. Mp 151—154°C (decomp.)

Found: C, 55.65; H, 3.82; S, 8.15%. Calcd for $C_{37}H_{30}P_2S_2Pt$: C, 55.84; H, 3.80; S, 8.06%.

Preparation of $Pd\{(C_6H_5)_2PCH_2CH_2P(C_6H_5)_2\}(CS_2)$. A solution of 200 mg (0.5 mmol) of 1, 2-bis-(diphenylphosphino)-ethane in 10 m*l* carbon disulfide was added dropwise with stirring to a suspension of $Pd\{(C_6H_5)_3P\}_2(CS_2)$ in 20 m*l* carbon disulfide prepared from 578 mg of $Pd\{(C_6H_5)_3P\}_4$ and carbon disulfide. The crystals of $Pd\{(C_6H_5)_3P\}_2(CS_2)$ then dissolved, and the solution gradually became orange red. After 1 hr the solvent was removed and the residue, on recrystallization from hot carbon disulfide (15 m*l*), afforded 190 mg (67% yield) of red brown crystals, $Pd\{(C_6H_5)_2PCH_2CH_2P(C_6H_5)_2\}(CS_2)$ (II): mp 115—124°C (decomp.) in a sealed capillary filled with nitrogen.

Found: C, 55.80; H, 4.23; S, 11.28%; mol wt (cryoscopic in nitrobenzene), 596. Calcd for $C_{27}H_{24}P_2S_2Pd$: C, 55.82; H, 4.16; S, 11.04%; mol wt, 580.9.

Reaction of $M\{(C_6H_5)_3P\}_4$ with Sulfur Dioxide.[*1] Sulfur dioxide was bubbled through a solution of 578 mg (0.5 mmol) of $Pd\{(C_6H_5)_3P\}_4$ in 30 m*l* benzene at room temperature. The reaction mixture became dark red. After 1.5 hr the solvent was gradually removed in a water-aspirator vacuum, leaving a red purple solid. Recrystallization from hot benzene gave 285 mg (48% yield) of analytically pure red purple needles, $[Pd\{(C_6H_5)_3P\}_4(SO_2)]_n$ (IIIa). It decomposed at 84—85.5°C without melting in a sealed capillary filled with nitrogen.

Found: C, 70.76; H, 4.08; O, 2.88; S, 2.54; P, 10.07%. Calcd for $C_{72}H_{60}O_2P_4SPd$: C, 70.90; H, 4.96; O, 2.62; S, 2.63; P, 10.16%.

According to a similar procedure the reaction between 622 mg (0.5 mmol) of $Pd\{(C_6H_5)_3P\}_4$ and sulfur dioxide in 20 m*l* benzene gave 360 mg (55% yield) of red purple needles $[Pt\{(C_6H_5)_3P\}_4(SO_2)]_n$ (IIIb). They decomposed at 124—125°C without melting in a sealed capillary filled with nitrogen.

Found: C, 65.98; H, 4.74; O, 2.79; S, 2.69; P, 9.28%. Calcd for $C_{72}H_{60}O_2P_4SPt$: C, 66.10; H, 4.62; O, 2.45; S, 2.45; P, 9.47%.

Density Measurement of $Pd\{(C_6H_5)_3P\}_2(CS_2)$. The density, 1.457 g·cm^{-3}, was measured by the flotation method in carbon tetrachloride - dioxane solution at room temperature.

X-Ray Diffraction. $Pd\{(C_6H_5)_3P\}_2(CS_2)$ gives light orange needle-like (along the *c* axis) crystals, which were very stable in air during the X-ray work. The crystals belong to the monoclinic system and the unit cell dimensions are:

$a=11.55\pm0.03$, $b=19.52\pm0.02$, $c=18.38\pm0.03$ Å. and $\beta=128°53'\pm10'$. From the systematic absence of $0k0$ reflections for k odd and $h0l$ for l odd, the space

2a) S. J. LaPlaca and J. A. Ibers, *ibid.*, **87**, 2581 (1965). b) S. J. LaPlaca and J. A. Ibers, *Inorg. Chem.*, **5**, 405 (1966).

3) S. Takahashi, K. Sonogashira and N. Hagihara, *Nippon Kagaku Zasshi (J. Chem. Soc. Japan, Pure Chem. Sect.)*, **87**, 610 (1966).

4) G. Wilke, H. Schott and P. Heimbach, *Angew. Chem. Int. Ed. Engl.*, **6(1)**, 92 (1967).

5) C. D. Cook and G. S. Jauhal, *Inorg. Nucl. Chem. Letters*, **3**, 31 (1967).

6) L. Malatesta and C. Cariello, *J. Chem. Soc.*, **1958**, 2323.

7) L. Malatesta and M. Angoletta, *ibid.*, **1957**, 1186.

*1 It was reported that Levison and Robinson obtained $Pt\{(C_6H_5)_3P\}_3(SO_2)\cdot xC_6H_6$ ($x\cong1.5$) and $Pd\{(C_6H_5)_3P\}_3(SO_2)$ by the reaction of $M\{(C_6H_5)_3P\}_4$ (M=Pd or Pt) with sulfur dioxide (*Chem. Commn.*, **1967**, 198).

TABLE 1.

(a) The final atomic coordinates and their standard deviations, $\sigma(10^{-2}\text{Å})$ and the isotropic thermal parameters, B (Å^2)

Atom	x	$\sigma(x)$	y	$\sigma(y)$	z	$\sigma(z)$	B
Pd	0.0866	0.2	0.1042	0.1	0.2757	0.2	*
S(1)	−0.2125	0.8	0.1108	0.7	0.2743	1.1	*
S(2)	0.0363	0.8	0.2051	0.6	0.3163	1.1	*
P(1)	−0.0114	0.7	−0.0025	0.5	0.2101	0.8	*
P(2)	0.3202	0.7	0.1172	0.5	0.3046	0.8	*
C(1)	−0.068	3	0.137	2	0.285	3	*
C(11)	0.094	2	−0.060	2	0.190	3	2.9
C(12)	0.135	3	−0.126	2	0.231	3	4.2
C(13)	0.215	3	−0.165	2	0.206	3	4.5
C(14)	0.245	3	−0.141	3	0.150	4	5.3
C(15)	0.201	3	−0.074	3	0.112	4	5.2
C(16)	0.127	3	−0.033	2	0.132	3	4.3
C(21)	−0.196	3	−0.000	2	0.091	3	3.6
C(22)	−0.247	3	−0.060	2	0.031	3	4.5
C(23)	−0.384	3	−0.058	2	−0.053	3	4.8
C(24)	−0.470	3	0.004	3	−0.089	4	4.9
C(25)	−0.410	3	0.062	2	−0.032	3	4.3
C(26)	−0.271	2	0.061	2	0.063	3	3.2
C(31)	−0.035	2	−0.052	2	0.286	3	3.1
C(32)	−0.140	3	−0.106	3	0.248	4	5.6
C(33)	−0.147	3	−0.143	2	0.313	3	4.5
C(34)	−0.063	4	−0.124	3	0.402	4	6.3
C(35)	0.043	4	−0.069	3	0.439	4	6.3
C(36)	0.055	3	−0.034	2	0.378	3	4.5
C(41)	0.456	2	0.170	2	0.407	2	1.9
C(42)	0.408	3	0.230	2	0.423	3	4.6
C(43)	0.507	3	0.270	2	0.505	4	4.9
C(44)	0.659	3	0.253	3	0.570	4	5.9
C(45)	0.708	3	0.197	3	0.546	4	5.8
C(46)	0.606	3	0.155	2	0.468	3	4.3
C(51)	0.431	2	0.043	2	0.331	3	2.3
C(52)	0.429	3	−0.009	2	0.383	3	3.8
C(53)	0.531	3	−0.064	3	0.415	4	5.1
C(54)	0.619	3	−0.071	3	0.386	4	5.5
C(55)	0.617	3	−0.020	2	0.332	3	4.4
C(56)	0.522	3	0.038	2	0.306	3	3.8
C(61)	0.298	3	0.166	2	0.212	3	3.6
C(62)	0.424	3	0.202	2	0.230	3	3.7
C(63)	0.399	3	0.237	2	0.157	3	4.1
C(64)	0.267	3	0.237	2	0.067	4	4.9
C(65)	0.145	3	0.199	2	0.051	3	4.2
C(66)	0.166	3	0.162	2	0.125	3	3.9

* Refinement was undertaken with anisotropic thermal parameters. These parameters are listed in (b).

(b) The anisotropic thermal parameters for Pd, S, P and C(1). The thermal parameters are of the form: $\exp\{-(\beta_{11}h^2+\beta_{22}k^2+\beta_{33}l^2+\beta_{12}hk+\beta_{13}hl+\beta_{23}kl)\}$

Atom	β_{11}	β_{22}	β_{33}	β_{12}	β_{13}	β_{23}
Pd	0.0080	0.0017	0.0045	−0.0002	0.0084	−0.0002
S(1)	0.0119	0.0040	0.0082	−0.0009	0.0152	−0.0013
S(2)	0.0122	0.0027	0.0107	−0.0033	0.0163	−0.0043
P(1)	0.0096	0.0016	0.0045	−0.0016	0.0099	−0.0011
P(2)	0.0093	0.0016	0.0035	−0.0000	0.0070	0.0001
C(1)	0.0139	0.0037	0.0049	0.0013	0.0153	−0.0009

group was determined to be $P2_1/c$. The observed density, 1.457 g·cm^{-3}, suggested four molecules in a unit cell, the calculated density being 1.456 g·cm^{-3}.

A set of three-dimensional intensity data was collected on multifilm equi-inclination Weissenberg photographs with nickel-filtered Cu$K\alpha$ radiation. Layers 0 to 11 were recorded around the c axis. Intensities of 4079 independent reflections were measured.

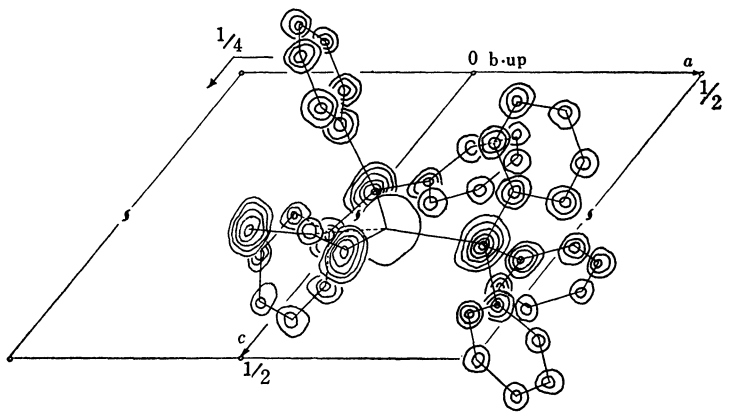

Fig. 1. A composite drawing of the final electron density map, viewed along the b axis. Contours are drawn at 3, 4 e.Å^{-3}... for carbon, and at 5, 8 e.Å^{-3}... for phosphorus and sulfur.

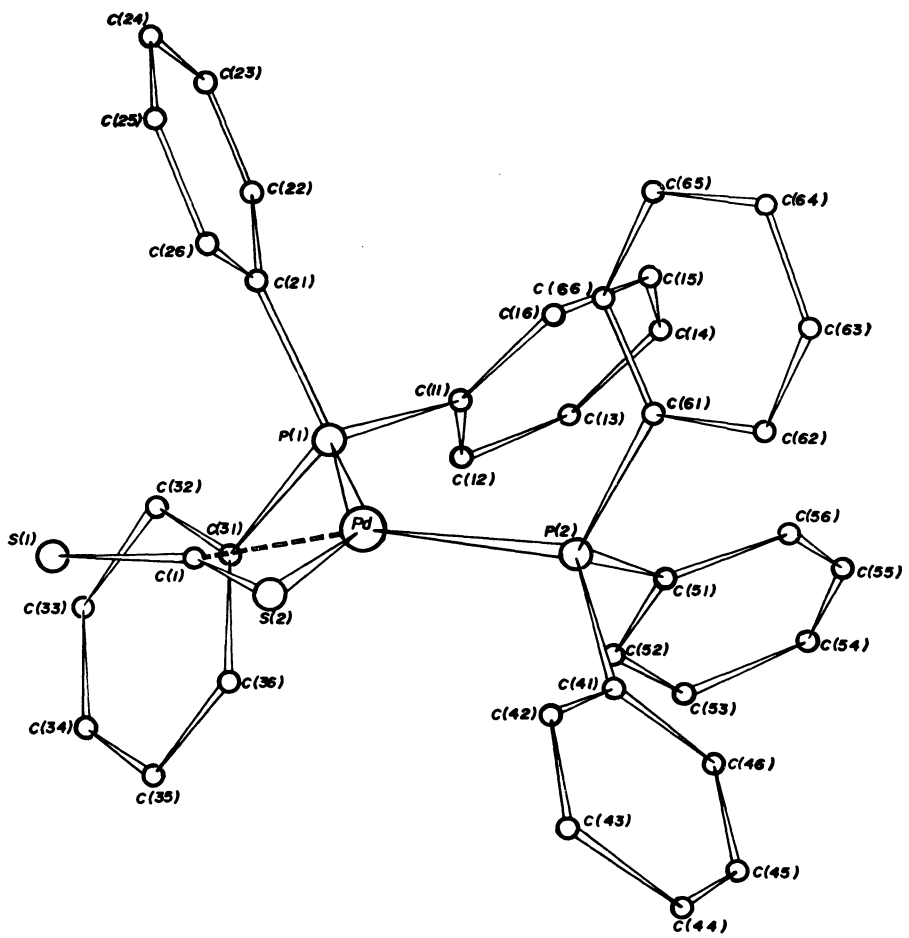

Fig. 2. View of molecule along the b axis.

visually. These intensities cover approximately 56% of possible reflections for Cu$K\alpha$. In order to get interlayer scale-factors, intensities around the a axis were also recorded. These intensities were corrected for the usual Lorentz and polarization factors, and spot-shape effects were also taken into account. As the dimensions of the crystal used in the experiment were about $0.09\times0.10\times0.27$ mm, the absorption correction was ignored in spite of the large absorption coefficient for Cu$K\alpha$, $\mu=70.81$ cm^{-1}.

Structure Determination and Refinement

The approximate position of Pd was deduced from the Patterson projections: P(U, V) and P(U,W). The Pd, S, P and twenty-seven C atoms were then obtained by inspection of the three-dimensional minimum function superposed by four equivalent positions of the Pd. The remaining ten C atoms were easily found in an electron density map based on the phases from the atoms which had already been determined. At this stage, the calculation of structure factors with a B of 3.0 Å^2 for all atoms gave a discrepancy factor, $R=\sum||F_o|-|F_c||/\sum|F_o|$, of 0.34.

The least-squares refinement was done on a HITAC 5020-E computer at the University of Tokyo with the program written by T. Ashida. The refinement of overall and interlayer scale-factors, and positional and thermal parameters was undertaken by the block-diagonal least-squares method. Because of the limited capacity of the computer memories, the number of reflections used for the refinement was reduced to 3432 ($\sin\theta/\lambda=0.56$), in which 461 non-observed reflections were included. In the refinement, the minimized function used was $\sum w(\Delta F)^2$, and the weight w was taken as unity for all reflections. The atomic scattering factors used were taken from those of Hanson *et al.*[8] After three cycles of the refinement, the R factor reduced to 0.176 for non-zero reflections. Another five cycles with anisotropic thermal parameters for Pd, S, P, and C(1) gave $R=0.133$ for non-zero reflections ($R=0.146$ for all reflections).

The final atomic coordinates with their standard deviations and thermal parameters are listed in Table 1. Tables of the observed and calculated structure factors are deposited by the Chemical Society of Japan.*2 The final electron density map, and molecular structure viewed along the b axis are shown in Figs. 1 and 2, respectively.

8) H. P. Hanson, F. Herman, J. D. Lea and S. S. Skillman, *Acta Cryst.*, **17**, 1040 (1964).

*2 The complete data of the F_o-F_c table are kept as Document No. 6801 at the office of the Bulletin of the Chemical Society of Japan. A copy may be secured by citing the document number and remitting, in advance, ¥200 for photoprints. Pay by check or money order payable to: Chemical Society of Japan.

Discussion

Synthetic Aspect. It has been found that $M\{(C_6H_5)_3P\}_4$ reacts readily with carbon disulfide to form novel complexes Ia and Ib (Eq. (1)).

$$M\{(C_6H_5)_3P\}_4 + CS_2 \longrightarrow M\{(C_6H_5)_3P\}_2(CS_2) \quad (1)$$
(Ia: M=Pd; Ib: M=Pt)

Independently, Baird and Wilkinson[9] also obtained complex I in a manner similar to that indicated by Eq. (1). These complexes are air-stable in the solid state. Complex I was treated with triphenylstibine in benzene to form the substituted product with the simultaneous liberation of carbon disulfide.

$$M\{(C_6H_5)_3P\}_2(CS_2) + 2(C_6H_5)_3Sb \longrightarrow \{M(C_6H_5)_3P\}_2\{(C_6H_5)_3Sb\}_2^{3)} + CS_2 \quad (2)$$

The quantitative determination of the carbon disulfide liberated in the above reaction by gas chromatographic analysis indicated that about one mole of carbon disulfide per one mole of complex was generated. This fact suggests that the complex I involves carbon disulfide attached directly to metal atom. Attempts to prepare the diphosphine-metal-carbon disulfide complexes by the direct reaction of $M\{(C_6H_5)_2PCH_2CH_2P(C_6H_5)_2\}_2$ with carbon disulfide were not successful. However, complex II was prepared from the reaction of the phosphine complex Ia with equivalent diphosphine in carbon disulfide solution as shown in Eq. (3).

$$Pd\{(C_6H_5)_3P\}_2(CS_2) + (C_6H_5)_2PCH_2CH_2P(C_6H_5)_2 \longrightarrow Pd\{(C_6H_5)_2PCH_2CH_2P(C_6H_5)_2\}(CS_2) + 2(C_6H_5)_3P \quad (3)$$

The infrared spectra of the complexes exhibit characteristic CS_2 bands as shown in Table 2. The bands appearing at $1200-1100$ cm^{-1} are probably to be assigned to the carbon-sulfur stretching vibration of the multiple bond of carbon disulfide. These absorption bands are shifted (*ca.* 300 cm^{-1}) toward lower frequencies by coordination to the metal atom in comparison with that of uncoordinated carbon disulfide.

Table 2. INFRARED FREQUENCIES (in cm^{-1}) OF COORDINATED CS_2 AND FREE CS_2 (in Nujol mulls)

Ia	$Pd(Ph_3P)_2(CS_2)$	1190	1177	1152	636
Ib	$Pt(Ph_3P)_2(CS_2)$	1179	1163	1145	653
II	$Pd(Ph_2PCH_2CH_2PPh_2)(CS_2)$	1178	1167	1152	632
	CS_2*,[10]		1510		656

* Liquid state

9) M. C. Baird and G. Wilkinson, *Chem. Commn.*, **1966**, 514.

10) T. Wentink, Jr., *J. Chem. Phys.*, **29**, 188 (1958).

TABLE 3. BOND LENGTHS AND ANGLES IN THE MOLECULE WITH THEIR ESTIMATED STANDARD DEVIATIONS (σ)

Bond		σ	Bond		σ
Pd-S(2)	2.305Å	0.011Å	Pd-P(1)	2.316Å	0.008Å
Pd-P(2)	2.415	0.008	Pd-C(1)	2.00	0.03
S(1)-C(1)	1.63	0.03	S(2)-C(1)	1.65	0.03
P(1)-C(11)	1.85	0.03	P(1)-C(21)	1.86	0.03
P(1)-C(31)	1.86	0.03	P(2)-C(41)	1.83	0.03
P(2)-C(51)	1.80	0.03	P(2)-C(61)	1.83	0.03
C-C(av.)[a]	1.41	0.05			

Angle		σ	Angle		σ
S(2)-Pd-P(2)	108.3°	0.4°	P(1)-Pd-P(2)	108.8°	0.3°
S(2)-Pd-C(1)	44	1	P(1)-Pd-C(1)	99	1
Pd-S(2)-C(1)	58	1	Pd-C(1)-S(2)	78	1
Pd-C(1)-S(1)	142	2	S(1)-C(1)-S(2)	140	2
Pd-P(1)-C(11)	119	1	Pd-P(1)-C(21)	114	1
Pd-P(1)-C(31)	110	1	Pd-P(2)-C(41)	114	1
Pd-P(2)-C(51)	119	1	Pd-P(2)-C(61)	112	1
C(11)-P(1)-C(21)	101	1	C(11)-P(1)-C(31)	105	1
C(21)-P(1)-C(31)	107	1	C(41)-P(2)-C(51)	100	1
C(41)-P(2)-C(61)	101	1	C(51)-P(2)-C(61)	109	1
C-C-C(av.)[a]	120	3			

a) The average value in benzene rings.

The complex $Pd\{(C_6H_5)_2PCH_2CH_2P(C_6H_5)_2\}(CS_2)$ II was recognized to be mononuclear in nitrobenzene solution by means of molecular weight measurement. The similarity in the infrared absorption bands may imply that $M\{(C_6H_5)_3P\}_2(CS_2)$ has a structure analogous to that of II.

The sulfur dioxide complexes, IIIa and IIIb, are unstable in air, particulary in solution. When $[Pd\{(C_6H_5)_3P\}_4(SO_2)]_n$, IIIb was treated with triphenylstibine in benzene solution, bis(triphenylphosphine)bis(triphenylstibine)palladium, $Pd\{(C_6H_5)_3P\}_2\{(C_6H_5)_3Sb\}_2$, was quantitatively obtained and the simultaneous liberation of sulfur dioxide was verified by gas chromatographic analysis. Therefore it is evident that the complex (III) contains sulfur dioxide as a ligand (Eqs. (4) and (5)).

$$M\{(C_6H_5)_3P\}_4 + SO_2 \longrightarrow [M\{(C_6H_5)_3P\}_4(SO_2)]_n \quad (4)$$
(IIIa: M=Pd, IIIb: M=Pt)

$$[Pd\{(C_6H_5)_3P\}_4(SO_2)]_n + (C_6H_5)_3Sb \longrightarrow Pd\{(C_6H_5)_3P\}_2\{(C_6H_5)_3Sb\}_2 \quad (5)$$

The infrared spectra of the complex $[M\{(C_6H_5)_3P\}_4(SO_2)]_n$ exhibit characteristic strong bands near 1200 cm^{-1} and 1050 cm^{-1} (IIIa: 1206, 1051 cm^{-1}; IIIb: 1198, 1047 cm^{-1}; in Nujol mull) ascribed to the asymmetric, and symmetric stretching modes of the $-SO_2-$ group attached to the metal. Unfortunately, further detailed information about the structure was not obtained, because the molecular weight of the complex could not been measured owing to its low solubility. We have not, as yet, been able to comfirm whether complex III has a monomeric structure such as $IrCl(SO_2)(CO)\{(C_6H_5)_3P\}_2$,[11,2b] or a dimeric structure with a sulfur dioxide bridge such as the iron carbonyl-sulfur dioxide complex.[12]

Crystal and Molecular Structure of $Pd\{(C_6H_5)_3P\}_2(CS_2)$. Intramolecular distances and angles with their standard deviations are listed in Table 3.

The most remarkable feature of the whole structure is the coordination of CS_2 to the Pd atom. Figure 3 shows the geometry around the

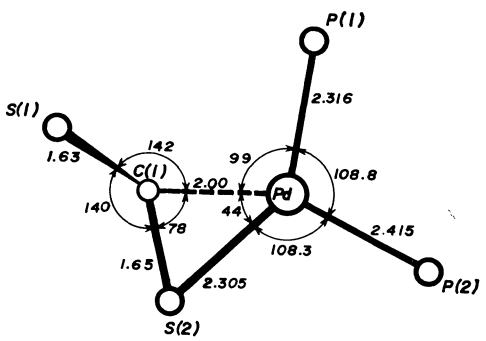

Fig. 3 Neighbors of the palladium atom in $Pd(Ph_3P)_2(CS_2)$, interatomic distances (Å) and bond angles (degree).

11) L. Vaska and S. S. Bath, *J. Am. Chem. Soc.*, **88**, 1333 (1966).
12) E. H. Braye and W. Hübel, *Angew. Chem.*, **75**, 345 (1963).

Pd atom. With only one of the S atoms, S(2), coordinated to the Pd, the CS_2 ligand, which is linear in a free molecule, is bent, the ∠S–C–S being 140°. The Pd atom and its neighboring atoms, P(1), P(2), S(2), and C(1) lie approximately on the same plane. The following is the equation of the least-squares plane;

$$0.11X + 0.73Y - 0.92Z + 3.12 = 0.0$$

where $X = ax + cx \cdot \sin\beta$, $Y = by$, and $Z = cz \cdot \sin\beta$.

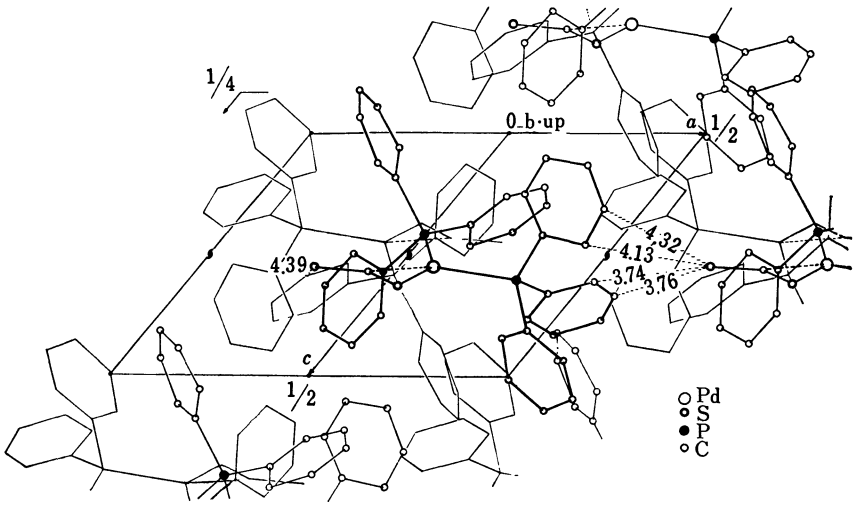

Fig. 4. The crystal structure viewed along the *b* axis.

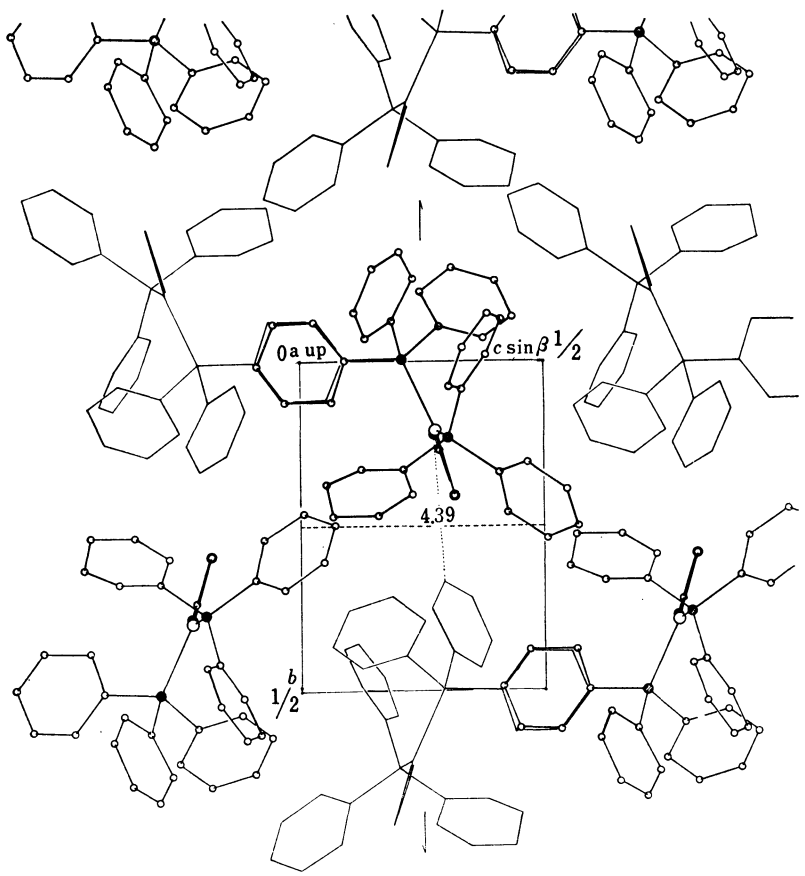

Fig. 5. The crystal structure viewed along the *a* axis.

Table 4. Deviations from the least-squares plane

Atom	Deviation
Pd	0.00Å
S(2)	0.08
P(1)	0.05
P(2)	−0.03
C(1)	−0.10
S(1)	−0.31

The angle between the S(1)–C(1) vector and this plane is 7°. The deviations of above-mentioned atoms from the best plane are listed in Table 4.

The Pd-S(2) distance is 2.305 Å, while Pd-S(1) is 3.441 Å (sum of the covalent radii, 2.36 Å). The S(1) atom is located far from any atoms of the surrounding molecules by over 3.74 Å as Figs. 4 and 5 show (sum of the van der Waals radii for S and benzenic C, 3.55 Å). The Pd-C(1) distance of 2.00 Å is slightly shorter than the sum of the covalent radii for Pd and trigonal hydridized C, 2.06 Å. But the ∠S(2)–Pd-C(1) of 44° is very small. One of the possible explanations for the C(1)-Pd bond is the bent-bond configuration. The two C-S distances in the CS_2 ligand are 1.63 Å and 1.65 Å (E. S. D., 0.034 Å), and they show no significant difference. However, these distances are longer than the ordinary C-S distance of 1.55 Å in a free molecule.[13] Recently, in Pt-$\{(C_6H_5)_3P\}_2(CS_2)$ a similar coordination of CS_2 to Pt (instead of Pd) as described above was found by Baird *et al.*[14] They also mentioned that $Pd\{(C_6H_5)_3P\}_2(CS_2)$ and $Pt\{(C_6H_5)_3P\}_2(CS_2)$ are isostructural. In this case, though, they reported preliminary results which indicated a big difference between the two C–S distances in the CS_2 ligand.

The Pd–P(1), and Pd–P(2) distances are 2.316, and 2.415 Å, respectively, and they differ significantly from each other. The longer Pd–P(2) distance may be interpreted as due to the trans-lengthening effect found in $(PdCl_2C_2H_4)_2$[15] and $(PdCl_2CH_2CHC_6H_5)_2$.[16] The Pd–P(1) distance of 2.316 Å is considerably shorter than the sum of the covalent radii (2.42 Å). This value corresponds to Pd–P=2.31 Å in $(C_4H_7)PdP(C_6H_5)_3$,[17] and also to Ir-P (av.)=2.34 Å in $IrO_2Cl(CO)\{(C_6H_5)_3P\}_2$.[2a] Such a shortening of the Pd–P distance may be a result of the partial double bond character acquired through back donation[18] of electrons from the Pd atom into the two P's.

Since the average angles of ∠C–P–C's, and ∠Pd–P–C's are 104°, and 115°, respectively, the geometry around the P atom is a distorted tetrahedral arrangement.

In benzene rings of $P(C_6H_5)_3$ groups the average bond distance, and angle are normal, 1.41 Å, and 120°C, respectively. Like a three-bladed propeller, the three planes of the benzene rings bonded to the P(1) rotate in the same direction, the average dihedral angle between these planes being 108°. However, this is not so in the case of benzene rings bonded to P(2), because these are in contact with the S(1) of the next molecule. An ordinary contact, 3.54 Å, is found as the shortest intermolecular benzene-benzene distance.

The present study was supported partly by a Scientific Research Grant from the Ministry of Education.

13) A. H. Guenther, *J. Chem. Phys.*, **31**, 1095 (1959).
14) M. Baird, G. Hartwell, Jr., R. Mason, A. I. M. Rae and G. Wilkinson, *Chem. Commn.*, **1967**, 92.
15) J. N. Dempsy and N. C. Baenziger, *J. Am. Chem. Soc.*, **77**, 4984 (1955).
16) J. N. Dempsy and N. C. Baenziger, *ibid.*, **77**, 4987 (1955).
17) M. Mason and D. R. Russel, *Chem. Commn.*, **1966**, 26.
18) A. A. Hock and O. S. Mills, *Acta Cryst.*, **14**, 139 (1961).

BULLETIN OF THE CHEMICAL SOCIETY OF JAPAN VOL. 41 304—306 (1968)

Ionic Species in the Radiolysis of Cyclohexane

Shin SATO

Department of Applied Physics, Tokyo Institute of Technology, Ookayama, Meguro-ku, Tokyo

(Received September 23, 1967)

A diffusion model proposed in the previous paper (*Bull. Chem. Soc. Japan*, **40**, 1818 (1967)) has been applied to explain the ionic reactions occurring in the γ-radiolysis of cyclohexane. The effects of an electron scavenger (N_2O) and a positive ion detector (CH_3OD) were consistently interpreted. The ratio of the diffusion coefficient of electrons to that of parent positive ions has been estimated from the calculation to be in the range of 4 to 5. The calculating method has been compared with that recently published by Freeman (*J. Chem. Phys.*, **46**, 2822 (1967)).

γ-Radiolysis of liquid occurs through two processes; one, ionic, the other, non-ionic. The ratio probably depends upon the molecular structure of the liquid. In cyclohexane, roughly 1 to 1 has been estimated for the ratio of the two processes which contribute to the formation of hydrogen.[1]

Ionic species produced in cyclohexane by γ-ray irradiation are electrons and the parent positive ions. Their excess energies are dissipated in a short time, probably of the order of 10^{-13} sec, through many collisions with solvent molecules. Thus thermalized electrons and the parent positive ions are distributed in the solvent, but not homogeneously; each pair being attracted by the Coulombic interaction which depends on the dielectric property of the solvent. In the previous paper,[2] the function proportional to $r^2 \exp(-\alpha r^2)$ was proposed for the initial distribution of the pair and 50 Å was estimated for the average separation in cyclohexane. Thus ion pairs drift towards each other and neutralize. The heat of neutralization leads to the decomposition of a cyclohexane molecule, as follows.

$$c\text{-}C_6H_{12}^+ + e \rightarrow H \text{ or } H_2 + \text{residue} \quad (1)$$

$$H + c\text{-}C_6H_{12} \rightarrow H_2 + c\text{-}C_6H_{11} \quad (2)$$

One neutralization reaction corresponds to the formation of a hydrogen molecule.[1]

Since the average time interval for the neutralization is estimated to be 10^{-9} sec,[2] electrons can react with electron scavengers in the solution, if present. When nitrous oxide is used as the scavenger, the following reactions seem to occur.[1]

$$e + N_2O \rightarrow N_2 + O^- \quad (3)$$

$$O^- + N_2O \rightarrow N_2 + O_2^- \quad (4)$$

Neutralization reaction between O^- or O_2^- and $c\text{-}C_6H_{12}^+$ does not lead to the formation of hydrogen. The reactions may be as follows, but have not been studied thoroughly.

$$c\text{-}C_6H_{12}^+ + O^- \text{ or } O_2^- \rightarrow c\text{-}C_6H_{11} + OH \text{ or } HO_2 \quad (5)$$

Anyway, the yield of nitrogen can be used as an indicator for the reaction of electrons ejected from cyclohexane molecules.

If a positive ion detector such as CH_3OD is present in the system,*1 the following reaction occurs and produces a constant fraction of deuterated hydrogen.

$$c\text{-}C_6H_{12}^+ + CH_3OD \rightarrow c\text{-}C_6H_{11} + CH_3ODH^+ \quad (6)$$

The yield of deuterated hydrogen can be used as an indicator for the reaction of parent positive ions.[3]

Data is now available for the reactions described above. This paper reports that the diffusion model proposed in the previous paper can explain these data consistently.

Calculation

In the previous paper,[2] only electrons were treated as a diffusing species. Obviously, parent positive ions can also diffuse in the system. Therefore, a modification is needed in the formulation. When electrons and the parent positive ions diffuse in the system, the number of jumps which both entities make in the diffusion before the neutralization may be approximated as follows,[2]

$$n_{\pm} = \gamma_{\pm}(2r^3/\sigma^2 r_c)$$

Here, the subscripts + and − correspond to positive

1) S. Sato, R. Yugeta, K. Shinsaka and T. Terao, This Bulletin, **39**, 156 (1966).
2) S. Sato, T. Terao, M. Kono and S. Shida, *ibid.*, **40**, 1818 (1967).

*1 Deuterated ammonia, ND_3, was also used by Williams.[4] This compound is about 3 times less efficient as a scavenger than CH_3OD. The reaction, therefore, may not be diffusion controlled.

3) J. W. Buchanan and F. Williams, *J. Chem. Phys.*, **44**, 4377 (1966).
4) F. Williams, *J. Am. Chem. Soc.*, **86**, 3954 (1964).

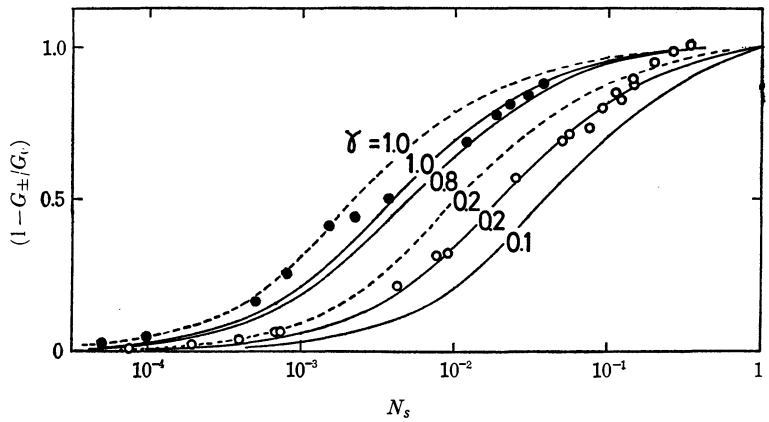

Fig. 1. Comparison of the calculated curves with the experimental data. ○: the fraction of positive ions scavenged by CH_3OD. ●: the fraction of electrons scavenged by N_2O. Full lines for $r_{av}=50$Å. Dashed lines for $r_{av}=60$Å.

ion and electron. r is an initial distance between the two entities. σ is the diameter of the solvent molecule. r_c is defined by the relation, $r_c=e^2/\varepsilon kT$. $\gamma_\pm$ is the fraction of the sum of two diffusion coefficients, D_+ and D_-.

Other formulations are the same as those in the previous paper,[2] except that the fraction $(1-N_s)^{zn\pm}$ is used in place of $(1-zN_s)^{n\pm}$, since, as Freeman stated,[5] the former expression is more exact than the latter. Thus, the G-values of positive ions (G_+) and electrons (G_-) which escape from scavenging are expressed by the relation,

$$G_\pm = G_0\frac{1}{N}\int_0^\infty \phi(r)(1-N_s)^{zn\pm}\mathrm{d}r$$

G_0 is the G-value of the initial ion pairs. z is the coordination number. N_s is the mole fraction of the scavenger. N is the normalization factor. $\phi(r)$ is the distribution function, for which we proposed the function, $r^2\exp(-\alpha r^2)$, in the previous paper.[2] As stated in the previous paper, G-value of electrons which escape geminate recombination in a non-polar solvent such as cyclohexane, is negligibly small compared with the total G-value of ejected electrons. In the case of a polar solvent, however, G-value of such electrons may be much larger. The function $\phi(r)$ should be modified as follows,

$$\phi(r) = r^2\exp(-\alpha r^2)(1-\exp(-r_c/r))$$

where, the fraction $\exp(-r_c/r)$ shows the probability of electrons which escape from the field of the parent positive ion.[6]

Figure 1 shows a typical result of the calculation, where $\gamma_\pm$ is used as a parameter. A pair of curves obtained for $\gamma_+ + \gamma_- = 1$ should be compared with the experimental data. Filled circles in Fig. 1 show the ratios, $G(N_2)/G_0(N_2)$. Here, $G_0(N_2)=6$ is assumed because the G-value of electrons has been estimated to be 3.[2] The data shown at the concentrations lower than 10^{-2} mol/l of nitrous oxide is newly obtained for this paper. Open circles are quoted from the data reported by Buchanan and Williams.[3],*2 Obviously, a pair of curves for $\gamma_+=0.8$ and $\gamma_-=0.2$ coincides best with the experimental results.

In Fig. 1, 50 and 60 Å are used as the average initial distances between a positive ion and the electron. Different distances can also be used for the calculation but the coincidence with the experimental results is never obtained unless r_{av} is in the range of 50 to 60 Å and the ratio of γ_-/γ_+ in the range of 4 to 5.

Discussion

The basic idea of the calculation presented here is the same as that proposed by Freeman.[5] The difference is in the assumption of the initial distribution of ion pairs produced in the system. Figure 2 compares the two distributions. Although the distribution used in the present calculation appears to be more plausible than that of Freeman, further examinations are needed to determine which is a better approximation.

Recently, Mozumder and Magee showed that,[7,8] in addition to isolated spurs, more densely charged spurs, namely, short tracks and blobs play important roles even in the γ-radiolysis of liquids. If this is taken into account in the calculation, the present formulation has to be modified, because, in this formulation, each ion pair is assumed to be independent from other pairs The modification

5) G. R. Freeman, *J. Chem. Phys.*, **46**, 2822 (1967).
6) L. Onsager, *Phys. Rev.*, **54**, 554 (1938).

*2 Plotted values are the ratios of corrected G-values for deuterated hydrogen to the maximum value, 1.55.
7) A. Mozumder and J. L. Magee, *Radiation Res.*, **28**, 203 (1966).
8) A. Mozumder and J. L. Magee, *J. Chem. Phys.*, **45**, 3332 (1966).

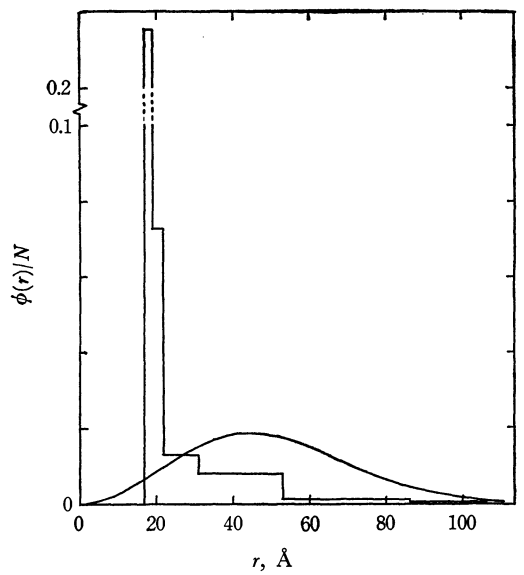

Fig. 2. Comparison of the initial distribution of ion pairs assumed in the present calculation (r_{av}=50Å) with that estimated by Freeman.

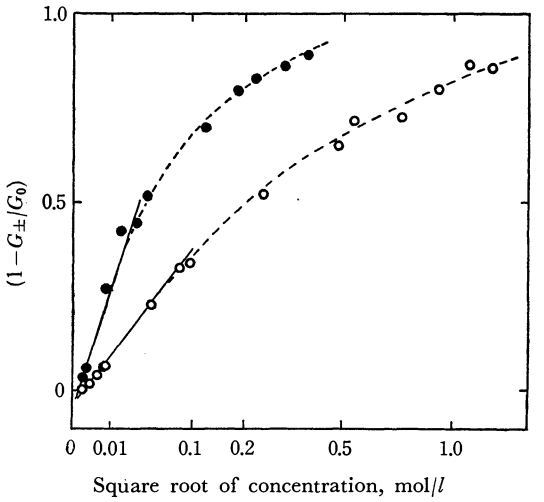

Fig. 3. Concentration-dependence of the effect of scavengers.
○: for CH_3OD. ●: for N_2O.

may be very much intricate.

In the present calculation, adjustable parameters are the distribution constant, α (or r_{av}) and the fraction, $\gamma_{\pm}$ from which the diffusion coefficient of electrons can be estimated if the diffusion coefficient for positive ions is known. This value is not known but may be equal to that of cyclohexane molecule itself, which is reported to be 1.38×10^{-5} cm^2 sec^{-1} at 25°C. According to the result calculated in the previous section, the diffusion coefficient of electrons in cyclohexane should be 4 or 5 times larger than that of the positive ions. This is very much smaller than that expected if the electron is not solvated and diffuses freely in the solution. Freeman assumed that $D_-/D_+\approx 5$ in his calculation.[5]

Using a photoelectronic technique to produce electrons in *n*-hexane, LeBlanc has measured the mobility of electrons at room temperature.[9] The value obtained was 1.4×10^{-3} cm^{2}V^{-1}sec^{-1}, which corresponds to a diffusion coefficient of 3.5×10^{-5} cm^2 sec^{-1}. Such a small value has led LeBlanc to conclude that electrons in *n*-hexane must be partially solvated by the solvent molecules. This is consistent with our present findings. Quantitatively, however, the ratio of $D_-/D_+=2.5$ $(=3.5\times 10^{-5}/1.38\times 10^{-5})$ calculated from LeBlanc's results, assuming that the diffusion coefficient for electrons in cyclohexane is equal to that in *n*-hexane, is about one half of that estimated in the present calculation. The discrepancy might arise from the speculations involved in the present treatment, but it is also possible that it may arise from the experimental error on D_-, although the recent measurement of conductivity of *n*-hexane irradiated by X-rays gave the value[10] consistent with that of LeBlanc.

In homogeneous systems, the rate of a reaction is proportional to the product of reactant concentrations, but this does not always hold in heterogeneous systems. Noyes has shown that the effect of a scavenger on a geminate recombination reaction is almost proportional to the square root of the scavenger concentration.[11] In the reaction of ND_3 with cyclohexane positive ion, Williams showed that this was the case.[4] However, when CH_3OD is used as a scavenger, Noyes' prediction does not fit well, probably because the range of the CH_3OD concentration is too wide to apply his approximation. This is shown in Fig. 3 along with the similar test for electron scavenging by nitrous oxide. Obviously, the proportionality to the square root of concentration holds only in a narrow range (from 0.002 to 0.02 mol/l for electrons and from 0.01 to 0.1 mol/l for positive ions) and a small negative intercept exists.

Even in a heterogeneous reaction, we are apt to assume that the rate of reaction with a scavenger is proportional to the concentration if it is very low. This was found to be correct even in the present case, but the maximum concentration used was quite low $\sim 10^{-3}$ mol/l. Therefore, we must be careful when we apply homogeneous kinetics to the radiolysis of a solution such as a liquid scintillator, where ionic species play an important role.[12]

9) O. H. LeBlanc, *ibid.*, **30**, 1443 (1959).

10) A. Hummel and A. O. Allen, *ibid.*, **44**, 3421 (1966).

11) R. M. Noyes, "Progress in Reaction Kinetics," Vol. 1, G. Porter Ed., Pergamon Press, Oxford (1961), p. 129.

12) T. Yoshida and S. Sato, This Bulletin, **40**, 2216 (1967).

BULLETIN OF THE CHEMICAL SOCIETY OF JAPAN VOL. 41 307—311 (1968)

Infrared and Raman Spectra of 2, 3-Dichloro-2, 3-dimethylbutane*1

Tsutomu KOIDE and Tsutomu ODA

Laboratory of Physical Chemistry, The Kyoiku Daigaku of Osaka, Tennoji, Osaka

and Kiyoshi EZUMI, Koji IWATANI and Tanekazu KUBOTA

Shionogi Research Laboratory, Shionogi and Co., Ltd., Fukushima-ku, Osaka

(Received September 27, 1967)

Infrared spectra of $Cl(CH_3)_2C$–$C(CH_3)_2Cl$ were obtained over the region from 400 cm^{-1} to 4000 cm^{-1} at room temperature in the gas phase, dilute solutions, and KBr-disk. In the KBr-disk case, spectra were also obtained at lower temperatures. In the gas phase, and in the disk at lower temperatures, spectral simplifications were obtained. Raman spectra at room temperature were photographed for the crystalline sample, and also for 17—25% solutions in several solvents. The coexistence of trans-gauche isomers in the high-temperature solid phase of this compound was verified by spectral comparison between trans- and gauche-isomers. The energy difference between two isomers was estimated to be about 1.5 kcal/mol from temperature changes in the infrared intensities.

The existence of an equilibrium mixture of two rotational isomers*2 for 1, 2-disubstituted-ethanes such as ClH_2C–CH_2Cl has been well established by spectroscopic studies.[1] For the case of 2, 3-dichloro-2, 3-dimethylbutane, $Cl(CH_3)_2C$–$C(CH_3)_2Cl$, and 2, 3-dibromo-2, 3-dimethylbutane, $Br(CH_3)_2C$–$C(CH_3)_2Br$, which have molecular structures analogous to ClH_2C–CH_2Cl, Morino *et al.* have reported the existence of trans-gauche equilibrium mixtures for the molecular system in carbon tetrachloride, heptane, and benzene solutions by dipole moment measurements.[2] Park *et al.*[3] observed the infrared and Raman spectra of $Br(CH_3)_2C$–$C(CH_3)_2Br$, and they reported that there is no evidence for the existence of an equilibrium mixture of trans- and gauche-rotational isomers in the solid state, while in the liquid, and in dilute solution the gauche form was found to exist. For $Cl(CH_3)_2C$–$C(CH_3)_2Cl$, our previous paper[4] revealed that in the high-temperature solid phase above −112°C, the molecule has some degree of rotational or reorientational freedom in the crystalline lattice. The analysis of the transition entropy of this compound has suggested the possibility of the existence of the rotational isomers in the high-temperature phase.[5]

Experimental

Sample. Pinacon was treated with an aqueous solution of hydrochloric acid saturated at about −20°C, and the mixture was allowed to stand for two weeks before filtration. The precipitate was purified by recrystallization from ethyl alcohol three times, and by fractional sublimation under a vacuum of about 10^{-5} mmHg. The melting point was found to be 158°C in a sealed tube.

Equipment. Infrared spectra were recorded with an infrared recording spectrometer Model DS-402 G of the Japan Spectroscopic Co., Ltd. The spectral region investigated was from 400 cm^{-1} to 4000 cm^{-1}. For the lower temperature measurements, the low-temperature cell of the Japan Spectroscopic Co., Ltd. was used. As the cooling material, a dry-ice - acetone solution was used for measurements at −80°C, and liquid nitrogen was used for measurement at −170°C.

Raman spectra were photographed with a model RL-II Raman Spectrograph (Yuki-Gosei-Yakuhin Co., Ltd.), which was modified for measurement of the crystalline sample, as reported in another paper.[6] The exciting light from a mercury lamp (4358 Å) was filtered through a layer of saturated aqueous solution of potassium nitrite. The mercury lamp was used with an electric current of 24—25 A. The slit width was 3—5×10^{-2} mm, and exposure time 3—5 hr. Neopan SSS

*1 A part of this work was presented at the Symposium on Molecular Structure, Sapporo, 7th Oct., 1967.

*2 There are actually three isomers, two of them are spectroscopically identical.

1) For instance a) S. Mizushima, "Structure of Molecule and Internal Rotation," Academic Press, New York (1954); b) N. Sheppard, *Adv. Spectroscopy*, **1**, 288 (1959); c) W. F. Edgell and G. J. Glocker, *J. Chem. Phys.*, **9**, 375 (1941); d) J. T. Neu and W. D. Gwinn, *ibid.*, **18**, 1642 (1950); e) G. J. Szasz, N. Sheppard and D. H. Rank, *ibid.*, **16**, 704 (1948); **17**, 86 (1947); f) W. E. Fitzgerald and G. J. Janz, *J. Mol. Spectry.*, **1**, 49 (1957).

2) Y. Morino, I. Miyagawa, T. Haga and S. Mizushima, This Bulletin, **28**, 165 (1955).

3) P. J. D. Park and E. Wyu-Jones, *Chem. Commn.*, **1966**, 557.

4) T. Koide and T. Oda, This Bulletin, **29**, 208 (1956).

5) T. Koide, *Nippon Kagaku Zasshi (J. Chem. Soc. Japan, Pure Chem. Sect.)*, **88**, 152 (1967).

6) Y. Matsui, T. Kubota, H. Tadokoro and T. Yoshimura, *J. Polymer Sci.*, **A3**, 2275 (1965).

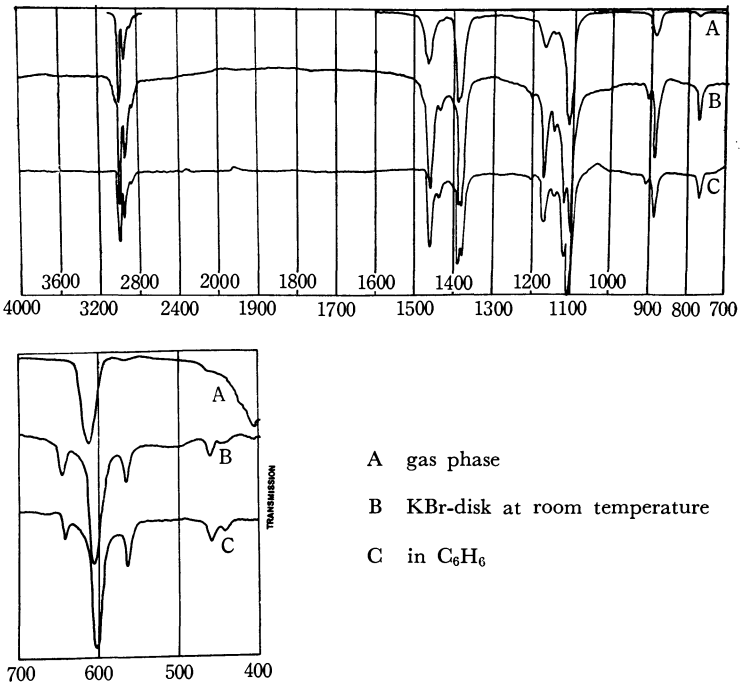

Fig. 1. Infrared spectrum for $Cl(CH_3)_2C\text{-}C(CH_3)_2Cl$.

film of the Fuji Film Co., Ltd. was used. The usual Raman tube was not suitable for the present measurements because of the high volatility of the sample. For this reason, the sample was put into a flat-bottomed test tube. After evacuating the tube for two or three minutes, it was filled with nitrogen gas, and sealed-off 10 cm from the bottom.

Results

The infrared spectra at room temperature were observed for the gas phase, KBr-disk, Nujol, and dilute solutions with the solvents carbon tetrachloride, benzene, carbon disulfide, *N*, *N*-dimethylformamide, and acetonitrile. In the case of the KBr-disk, spectra were also obtained at temperatures of about −80°C and −170°C. Raman spectra were obtained for the crystalline state, and 17—25% solutions in carbon tetrachloride, *n*-heptane, and acetonitrile.

The results of the infrared measurements in the gas phase, KBr-disk, and the dilute benzene solution are collected in Fig. 1 and Table 1. In Table 1, the results of the Raman measurements are also summarized together with the previous results of Kahovec.[7] The present Raman spectra may be seen to be in accord with those of Kahovec *et al.*[7]

In Fig. 2, infrared spectra taken under various conditions are shown for the frequency range from

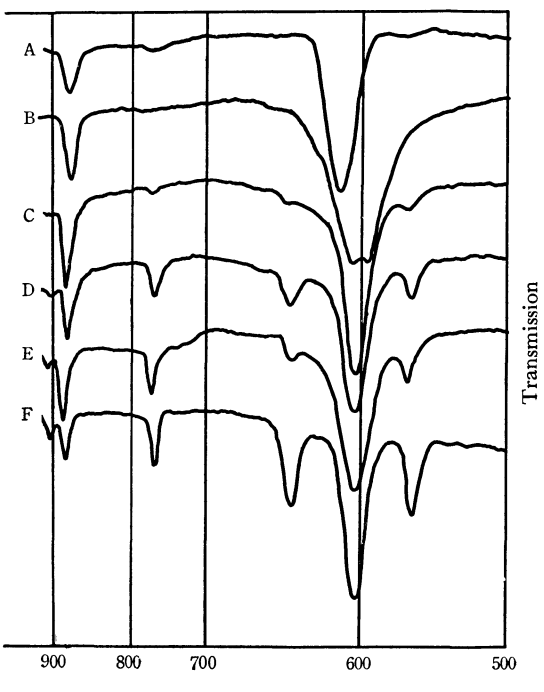

Fig. 2. The infrared spectrum of $Cl(CH_3)_2C\text{-}C(CH_3)_2Cl$ under various conditions.
A, gas phase; B, KBr-disk at −170°C; C, KBr-disk at −80°C; D, KBr-disk at room temperature; E, C_6H_6 solution; F, CH_3CN solution.

7) L. Kahovec and J. Wagner, *Z. phys. Chem.*, **48**, 1347 (1940).

TABLE 1. THE INFRARED AND THE RAMAN SPECTRA OF $Cl(CH_3)_2C\text{-}C(CH_3)_2Cl$ (Unit in cm^{-1})

Infrared					Raman					
Gas at 50—60°C	Solution		Solid		Solid				Solution	
	in C_6H_6	in CH_3CN	at 25°C	at −80°C	Present		Kahovec*		in CCl_4	in CH_3CN
					216	1/3				
					370	1/2			372 2	373 1
	444 vw	442 w	443 vw							
	460 w	459 w	462 w	462 vw						
	564 w	562 m	565 w	564 vw	568	1/3			569 1/2	566 1/2
					596	2	595	2	596 2	596 1
613 s	604 vs	604 vs	604 vs	607 vs						
	644 w	646 m	648 w	650 vw						
					757	1	754	2		755 1
768 vw	765 w	762 m	766 w	766 vw						
880 m	880 m	880 m	879 m	880 s						
	900 vw	901 w	902 vw							
	925 vw									
	942 vw	946 vw								
							954	1/4		
			1000 vw							
1100 vs	1095 vs	1095 vs	1095 vs	1094 vs						
1105 vs	1111 w	1111 s	1110 m	1110 w						
					1133	1/2	1130	1/2	1134 0	1138 1
1139 w	1139 w	1140 w	1139 w	1140 w						
1163 m	1164 m	1163 m	1164 m	1164 m						
	1201 vw	1202 w								
							1231	0		
1379 s	1375 s		1373 s	1373 s						
1385 s	1383 s		1380 s	1380 m			1387	100		
1390 m	1432 w		1431 m	1431 w						
							1448	1/2		
1458 m	1456 s		1456 s	1456 s						
1464 m			1462 m	1462 m						
1470 m										
							2762	0		
			2873 w							
			2943 w		2940	1	2935	3		
			2990 s		2990	1/2	2988	3		
					3003	1/2				

* L. Kahovec and J. Wagner, *Z. phys. Chem.*, **48**, 1347 (1940).

900 to 400 cm^{-1}. In Fig. 3, infrared spectra of the KBr-disk at lower temperatures are shown, for the frequency region 700—400 cm^{-1}. In this figure, the temperatures indicated for each curve are the averaged temperatures for the run of each measurement except for 25, −80, and −170°C; the apparatus used for the low temperature measurements was not temperature controlled during the interval of the measurement except for the above three temperatures. The temperature was maintained to within ±0.5°C at 25, −80, and −170°C, and at other temperatures, the change in temperature was about ten degrees for each interval of measurement.

The general pattern of the infrared spectra for each sample at room temperature was very close to each other except for those of the gas phase, in which spectral simplifications are observed, as shown in curve A of Fig. 1, and Fig. 2. Namely, the absorption bands at 443, 462, 565, and 648 cm^{-1} of the KBr-disk (Fig. 1 B) disappeared in the gas phase. The same simplifications stated above are also observed in the KBr-disk at lower-temperatures. (See Fig. 2B, and Table 1)

The spectral simplifications suggest the coexistence of rotationally isotropic forms in the molecular system of the KBr-disk sample, as compared with the case of 1, 2-disubstituted ethanes.[1] The problem of rotational isomerism in the present substance will be discussed in the next section.

Discussion

Rotational Isomerism. If we confine the problem to whether rotational isomers exist or not, it is sufficient to focus our attention on the C–Cl stretching band.

In general, the C–Cl stretching bands are said to appear in the region of 600—800 cm^{-1}. Actually, for the case of ClH_2C-CH_2Cl, the C–Cl stretching frequencies are observed at 665 (A), 675 (B), and 709 (Bu) cm^{-1}.[8] However, Mizushima *et al.*[9] have shown that the C–Cl stretching frequencies of the tertiary carbon atom such as $Cl(CH_3)_2C$– appeared in the regions of 610—640 cm^{-1} and 550—580 cm^{-1}. For instance, in the case of $Cl(CH_3)_2C$-CH_2Cl,[9] the C–Cl stretching appeared at 621 cm^{-1} (T_x*3) and 572 cm^{-1} (T_H*3), and in the case of $Cl(CH_3)_2C$-$CH_2(CH_3)$[9] at 613 cm^{-1} (T_x) and 558 cm^{-1} (T_H).

At room temperature, the KBr-disk of $Cl(CH_3)_2C$-$C(CH_3)_2Cl$ shows three frequency bands in this region, at 565, 604, and 648 cm^{-1}. Therefore, these bands seem to be the C–Cl stretching frequencies. This supposition may be ensured from the comparison of the Raman spectra with the infrared spectra.

The point groups of the molecular configurations and the types of vibrations expected for trans- and gauche-isomers of this compound are summarized in Table 2.[10] In the case of the gauche isomer, all the fundamental modes are active for both Raman and infrared spectra, while in the case of the trans-form the fundamental modes are mutually exclusive.

Inspection of Table 1 shows that the rule of mutual exclusion holds at 596 and 757 cm^{-1} for Raman spectra, and also at 604 cm^{-1} for infrared for the solid sample. Nevertheless, the band at 565 cm^{-1} is active for both Raman and infrared spectra. From the above considerations, the infrared band at 604 cm^{-1} be attributed to a may Bu-type vibration of C–Cl stretching, and that at 565 cm^{-1} is considered due to the gauche-form vibration.

TABLE 2. TYPES OF VIBRATION

Trans form (C_{2h}) Activity			Gauche form (C_2) Activity		
Type	Raman	IR	Type	Raman	IR
A_g	+	–	A	+	+
A_g	–	+			
B_g	+	–	B	+	+
B_u	–	+			

Furthermore, to confirm these assignments, the comparison of the intensity of these bands obtained under various conditions is also available. From Fig. 2, for the KBr-disk, and the benzene solution at room temperature, the bands (565, 604, 648, and 766 cm^{-1}) show patterns almost simillar to each other, and further their relative intensities show a similarity (see curves D and E in Fig. 2). On the other hand, for the dilute solutions of this compound with polar solvents of $HCON(CH_3)_2$*4 and CH_3CN,*4 the intensities at 565, 648 and 766 cm^{-1} increased more than that at 604 cm^{-1} as shown in curve F of Fig. 2.

The same increase in intensities in polar solvent is also observed in the Raman spectra; *i. e.*, as seen in Table 1, the relative intensity of the Raman bands at 568, 596, and 757 cm^{-1} is 1/6 : 1 : 1/2 for the KBr-disk, and 1/2 : 1 : 1 for the CH_3CN solution.

Concerning the effect of the polar solvents, Mizushima *et al.* have reported that the "gauche" molecule should be more stable in a continuous polar medium than in the gaseous state.[14] The increases in intensities observed in the polar solvent

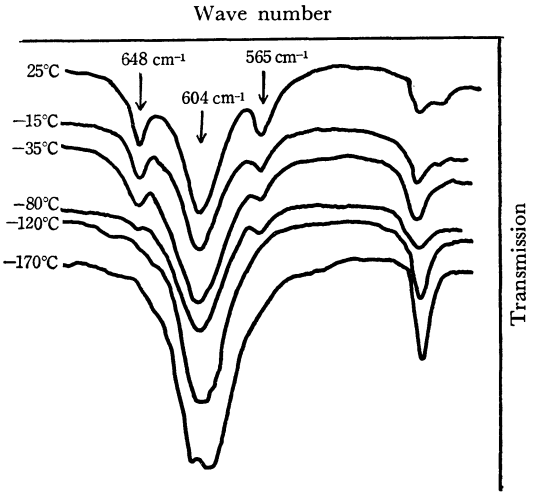

Fig. 3. The temperature change of the infrared spectrum for KBr-disk sample of $Cl(CH_3)_2C$-$C(CH_3)_2Cl$.

8) I. Nakagawa and S. Mizushima, *J. Chem. Phys.*, **21**, 2195 (1953).

9) S. Mizushima, T. Shimanouchi, K. Nakamura, M. Hayashi and S. Tsuchiya, *J. Chem. Phys.*, **24**, 970 (1957).

*3 T_X and T_H are the notations used by Mizushima *et al.* in Ref. 9. The configuration with C or Cl atom in the trans-position with respect to the Cl atom is referred as T_X, and the configuration with the H atom in the trans-position is referred as T_H.

10) For instance G. Herzberg, "Molecular Spectra and Molecular Structure I. Infrared and Raman Spectra of Polyatomic Molecules," van Nostrand (1945).

*4 The values of the dipole moment and the dielectric constant of $HCON(CH_3)_2$ and CH_3CN are respectively 3.8 D,[11] 36.71[12] and 3.4 D,[11] 37.5.[13]

11) A. L. McClellan, "Tables of Experimental Dipole Moments," W. H. Freeman and Co., San Francisco (1963).

12) G. R. Leader and J. F. Gormley, *J. Am. Chem. Soc.*, **73**, 5731 (1951).

13) G. R. Leader, *ibid.*, **73**, 856 (1951).

14) S. Mizushima and H. Okazaki, *ibid.*, **71**, 3411 (1949).

for the 565, 648, and 766 cm^{-1} bands of the infrared, and for 596, and 755 cm^{-1} of the Raman indicate that these bands belong to vibrations of the "gauche" form. The Raman bands corresponding to 648 and 766 cm^{-1} of the infrared spectra are not observed even in the polar solvents; the reason is not known.

Turning to the solid state, the temperature dependence of the infrared spectra of the KBr-disk is shown in Fig. 3. Although the indicated temperatures in Fig. 3 are not equilibrium temperatures, except 25, −80, and −170°C, as described earlier, it is clearly shown that the bands at 565, 648, and 766 cm^{-1} show a decrease in their intensities with a lowering of the temperature. These bands disappeared below −120°C, and almost in the gas phase.

Contrary to this, the intensity of the 604 cm^{-1} band of the trans-form is not so dependent upon the experimental conditions. Therefore, these changes in intensity, along with the comparison of Raman and infrared spectra, indicate that the 604 cm^{-1} band belongs to the trans-form (C_{2h}), whereas the band at 565, 648, and 766 cm^{-1} are attributed to the gauche-form (C_2).

From the considerations of the Raman, and infrared spectra mentioned above, it is clearly seen that there is a coexistence of trans- and gauche-rotational isomers in the molecular system of the high-temperature solid phase as well as in the dilute solutions of $Cl(CH_3)_2C$-$C(CH_3)_2Cl$. For the dilute solution, the present conclusion is coincident with that of Morino *et al.*[2] In the gas phase, the majority of the molecular configurations will be trans-, together with a small number of the gauche-form.

Some comments are added here with regard to the infrared bands below −120°C for the KBr-disk sample. The band at 604 cm^{-1} for the KBr-disk observed at room temperature increases in width with decreasing temperature below −120°C, and split into two bands at 609, and 599 cm^{-1} at about −170°C. The splitting of the band may be due to a change in the crystal at the transition point (−112°C), as shown in the case of an other compound.[15]

The Energy Difference between Trans- and Gauche-form. From the temperature dependence of the infrared intensities, the energy difference, ΔE, between the trans- and gauche-positions may be calculated. The intensities of the trans-, and gauche-bands are approximately related to ΔE by the formula,[1a,1f,16]

$$I_{(g)}/I_{(t)} = A \exp(\Delta E/RT)$$

where $I_{(g)}/I_{(t)}$ is the ratio of the integrated intensities for the gauche- and trans-bands; A is a constant. Taking the 604 cm^{-1} band to be trans-, and the 565, and 648 cm^{-1} to be gauche-, we obtained

$$I_{565}/I_{604} = 0.10 \text{ at } 300°K$$
$$= 0.03 \text{ at } 190°K,$$

and

$$I_{648}/I_{604} = 0.13 \text{ at } 300°K$$
$$= 0.03 \text{ at } 190°K.$$

Then we have

$$\Delta E = 1.3 \text{ kcal/mol from } I_{565}/I_{604}$$
$$= 1.7 \text{ kcal/mol from } I_{648}/I_{604}.$$

The values of ΔE are of the same order as the results of Morino *et al.*, who have estimated ΔE= 1.6 kcal/mol for dilute solutions of this compound from dipole moment measurements.[2]

The values of ΔE indicate that in the high-temperature solid phase the trans-form has a lower energy than the gauche-form. In connection with the values given above, we should like to refer to the values of ΔE for 1, 2-disubstituted-ethanes. In the gas phase for ClH_2C–CH_2Cl and BrH_2C–CH_2Br, it was reported that the trans-form is the lower energy configuration.[1a] In contrast, for 1, 2-dicyanoethane (succinonitrile),[17] the gauche-form is the lower energy structure in the solid and liquid states, although the trans-form is the lower energy configuration in the gas phase. According to the discussion of Mizushima *et al.*,[14] the greater stability of the gauche-form in the solid and liquid phases of succinonitrile should be attributed to the high dielectric constant[18] and to the much greater dipole moment (5—6 D) of this structure compared with those of the dihaloethanes (2.23 D for dichloro-[19], and 2.62 D for Dibromo-[19] ethane). In the case of $Cl(CH_3)_2C$-$C(CH_3)_2Cl$, the dipole moment for the gauche-form is 3.1 D,[2] and further the dielectric constant for the high-temperature phase is not a high-value.[20] Therefore, the relation between the values of ΔE and the molecular configuration for the present compound seems to be similar to the case of the dihaloethanes.

The authors express their hearty thanks to Professor Hiroyuki Tadokoro of Osaka University for his interest during this study, and for his discussions. They also wish to express their thanks to Professor Tatsuo Miyazawa of Osaka University for his useful suggestions and discussions.

15) For instance M. P. Marzocchi, V. Schettrino and S. Califano, *J. Chem. Phys.*, **45**, 1400 (1966).
16) For instance C. Komaki, I. Ichishima, K. Kuratani, T. Miyazawa, T. Shimanouchi and S. Mizushima, This Bulletin, **28**, 330 (1955).
17) W. E. Fitzgerald and G. J. Janz, *J. Mol. Specty.* **1**, 49 (1957).
18) A. H. White and S. O. Morgan, *J. Chem. Phys.*, **5**, 655 (1937).
19) I. Miyagawa, *Nippon Kagaku Zasshi (J. Chem. Soc. Japan, Pure Chem. Sect.)*, **75**, 1057 (1954).
20) A. H. White and W. S. Bishop, *J. Am. Chem. Soc.*, **62**, 8 (1937).

BULLETIN OF THE CHEMICAL SOCIETY OF JAPAN VOL. 41 312—321 (1968)

Thermal Properties of Alkali Halide Crystals with the CsCl-type Structure. I.*[1] Construction of a Calorimeter for the Temperature Region 1—20°K and Heat Capacities of Caesium Bromide and Caesium Iodide between 1.5 and 300°K

Michio SORAI, Hiroshi SUGA and Syûzô SEKI

Department of Chemistry, Faculty of Science, Osaka University, Toyonaka, Osaka

(Received October 14, 1967)

An adiabatic low-temperature calorimeter, capable of measuring the heat capacities of solid or liquid between 1.4 and 21.0°K, was constructed. A mechanical thermal switch is used for cooling the sample cell, the temperature of which is measured with a doped germanium thermometer. The resistance-temperature calibration data for the resistor was fitted to a function of the form $\log_{10}R=A/T+B+CT+DT^2$. By using this formula the thermodynamic temperature scale is represented to within ±0.02°K and by combining the correction curves the final deviations of the calibration data from the thermodynamic temperature scale were within ±0.003°K in the whole temperature range investigated. The heat capacity measurements of CsBr and CsI crystals were made with two kinds of adiabatic calorimeter assemblies, one for the temperature range 1.4 to 21°K and the other for the range 12 to 300°K. Values of the heat capacity $C_p°$, entropy $S°$, enthalpy function $(H°-H_0°)/T$, and Gibbs energy function $-(G°-H_0°)/T$, at 298.15°K are: 12.441, 26.785, 10.415, and 16.370 for CsBr and 12.571, 29.127, 10.788, and 18.339 for CsI, respectively, in cal·mol^{-1}·°K^{-1}.

It is of some interest to note the fact that the alkali halides crystallize at standard temperature and pressure in the NaCl-type structure, with the exception of CsCl, CsBr, and CsI which crystallize in the CsCl-type structure, although polymorphic transitions between the NaCl and CsCl structure have been observed to occur for some of these crystals with increasing temperature or pressure. Although a great deal of work has been done on the alkali halides with the NaCl structure, theoretical and experimental studies of the alkali halide crystals with the CsCl structure seem to have received little attention in the past. Some theoretical investigations have been made to interpret which structure will be more stable under a given set of conditions. Among them Mayer[1] showed that van der Waals potential contributes to the stability of the CsCl-type lattice for CsCl, CsBr, and CsI at absolute zero. Tosi and Fumi[2] succeeded in establishing which phase has the lower free energy and is thus thermodynamically more stable under a given set of conditions. From the standpoint of lattice dynamics Hardy and Karo[3] accounted for the instability of the NaCl-type lattice under the condition just below the pressure-induced phase transition. Some experimental results[4-7] have been also reported in which the difference in the crystal structures seems to be reflected.

The purpose of the present investigation is to obtain detailed thermal data on CsBr and CsI crystals in the temperature range from 1.5 to 300°K, and, in particular, to study how the difference in structure is reflected in their thermal properties. An adiabatic calorimeter for the heat capacity measurements below 20°K is also described.

Experimental

Calorimeter and Cryostat. The main parts of the adiabatic calorimeter consist of calorimeter cell, cryostat, thermometer and electrical circuit. Figure 1 shows diagrammatically the cryostat assembly and its essential features are depicted in Fig. 2. There are two refrigerant compartments; an outer one (for the liquid nitrogen) consisting of a stainless-steel Dewar vessel and an inner one (for the liquid helium or liquid

*1 The first half was read before the 18th Annual Meeting of the Chemical Society of Japan (1965), Osaka and the latter half before the 1st Japanese Calorimetry Conference (1965), Osaka.

1) J. E. Mayer, *J. Chem. Phys.*, **1**, 270 (1933).

2) M. P. Tosi and G. F. Fumi, *J. Phys. Chem. Solids*, **23**, 359 (1962).

3) J. R. Hardy and A. M. Karo, "Lattice Dynamics," Pergamon Press, Oxford (1964), p. 195.

4) E. E. Havinga and A. J. Bosman, *Phys. Rev.*, **140**, A292 (1965).

5) S. P. Nikanorov and A. V. Stepanov, *Fizika Tverdogo Tela*, **6**, 1987 (1964) (English translation; *Soviet Phys.—Solid State*, **6**, 1569 (1965)).

6) S. P. Nikanorov, A. A. Nran'yan and A. V. Stepanov, *Fizika Tverdogo Tela*, **6**, 1996 (1964) (English translation; *Soviet Phys.—Solid State*, **6**, 1576 (1965)).

7) G. K. White, *Proc. Roy. Soc.*, **A286**, 204 (1965).

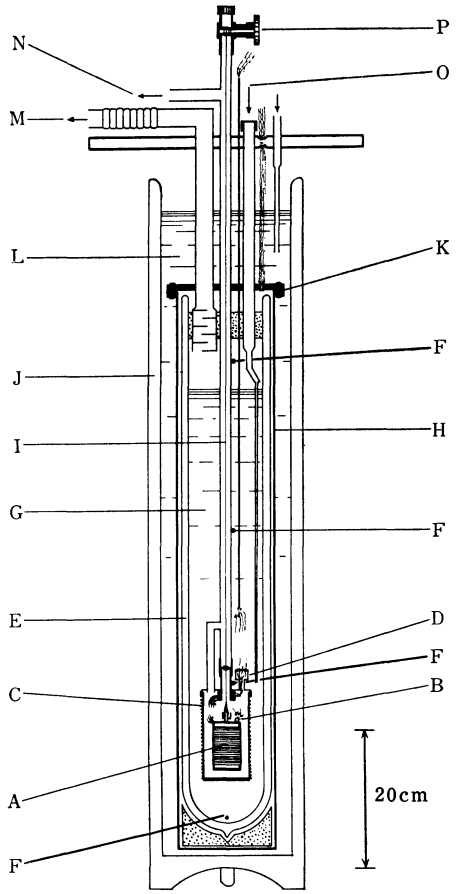

Fig. 1. Calorimeter and liquid helium cryostat assembly: (A) calorimeter cell; (B) germanium resistance thermometer; (C) vacuum jacket; (D) hermetic seals for lead outlets; (E) glass Dewar; (F) carbon resistors for level indicator; (G) liquid He or H_2; (H) brass jacket; (I) nylon thread; (J) metal Dewar vessel; (K) compression seal with a lead O-ring; (L) liquid N_2; (M) liquid He pumping line; (N) to high vacuum pump; (O) liquid He transfer tube; (P) winch.

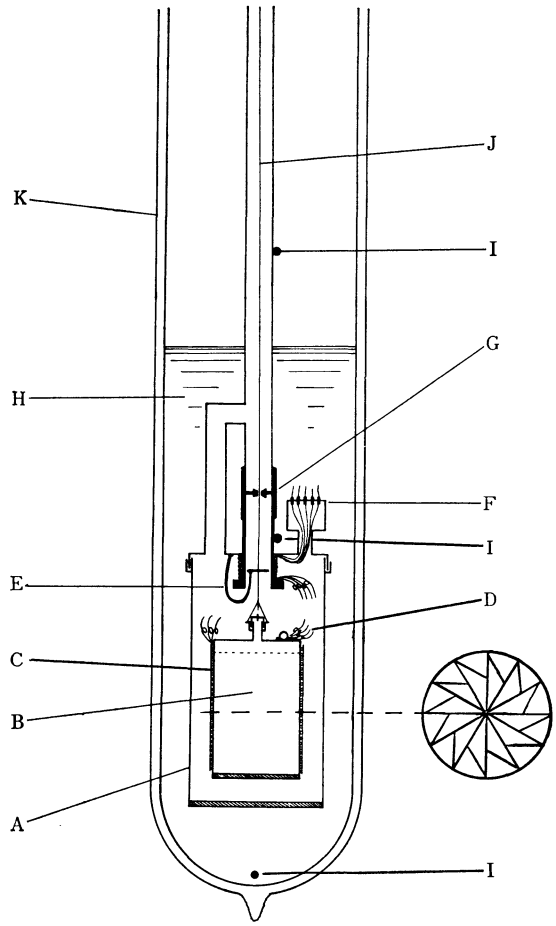

Fig. 2. Schematic diagram of low-temperature calorimeter (1.4–21.0°K): (A) vacuum jacket; (B) calorimeter cell; (C) heating element; (D) germanium resistance thermometer; (E) radiation shield; (F) hermetic seals for lead outlets; (G) radiation shield; (H) liquid He or H_2; (I) carbon resistors for level indicator; (J) nylon thread; (K) glass Dewar.

hydrogen) consisting of a large glass Dewar of approximately 7 *l* capacity. Carbon resistors (Allen-Bradley, 47 Ω nominal resistance) positioned conveniently on the stainless-steel tube serve as useful refrigerant-level indicators. The third innermost compartment, which houses the high vacuum for the calorimeter cell, consists of a brass can apart from its bottom made of thick copper plate. All conduits are made of stainless-steel. To prevent that large amount of energy is imparted to a sample from room temperature radiation, two radiation traps are placed at the bottom of the central tube (E and G in Fig. 2). Styro-form plate located at the entrant of the glass Dewar also serves as a radiation shield from liquid nitrogen temperature.

The body of the calorimeter cell consists of a cylinder of copper. Thin copper fins project radially from a small tube which is centrally located along the vertical axis of the calorimeter (see Fig. 2). These fins are soldered with the tube and the calorimeter wall. The filling tube of the calorimeter cell is fitted with a small brass cap to the center of which is brazed a short piece of tubulation that permits evacuation of the sample in the calorimeter and filling helium gas for heat exchange. The diameter of the calorimeter cell is about 4.5 cm, the overall length (including cap) being approximately 9 cm and the volume about 110 cm^3.

A Minneapolis-Honeywell germanium resistor (Honeywell Series II) was used as a working thermometer. It was firmly embedded in a small copper pipe brazed to the top of the calorimeter. To further insure the good thermal contact it was varnished (GE adhesive # 7031). The current used for the measurements of resistance of the germanium resistor was selected as to render maximum accuracy; *i. e.* in the liquid helium region varied from 2.0 to 10.0 μA and in the liquid hydrogen region from 10 to 30 μA. The details of the calibrations of the thermometer will be described in the next section.

The heating element of the calorimeter is formed of about 1000 ohms of a strain-free constantan wire (Driver-Harris Co., #36). The wire was wound non-inductively around the calorimeter cell and varnished to insure good thermal contact. To minimize any exchange of energy between the calorimeter and the environment (refrigerant bath) the lead wires from the heating element and the thermometer were made thermal contact with the periphery of the calorimeter and coiled helically in the vacuum space. These wires entered the refrigerant compartments by means of hermetic seals (New Nippon Electric Co., Ltd., #A241). The electrical circuits for energy supply are the same as those for the calorimeter[8] previously described, which is operative in the temperature range 12 to 300°K. Determinations of the heat input and the resistances of the thermometer were all made on a Wenner-type potentiometer (Leeds & Northrup Co.). The heating time was read on a timer placed in the energy circuit.

The mechanical thermal switch consists of a "make and break" contact between the smoothly polished surface of the bottom of the calorimeter cell and the bottom of the vacuum jacket. The vertical movement of the cell is controlled by a winch mechanism located at the top of the cryostat. The connection between the winch and the calorimeter is accomplished by a fine nylon thread. The "making and breaking" of the contact is detected through a micro-ammeter by the "on and off" of the current controlled by the thermal switch. By means of this device the calorimeter cell may be cooled conveniently from room temperature down to about 1.4°K (lowest pumping temperature) in a vacuum better than 10^{-6} Torr without the use of any heat exchange gas.

Temperature Scales. The germanium resistance thermometer was calibrated in the temperature range from 1.4 to 4.4°K against the vapor pressure temperature scale (the T_{58} scale) compiled by Brickwedde *et al.*[9] In the temperature range between 11.8 and 21.0°K, on the other hand, the thermometer was calibrated against a Leeds & Northrup platinum resistance thermometer certified by the National Bureau of Standards (the NBS scale). These calibrations were performed by separate experiments before the germanium thermometer being fixed to the calorimeter. To complete the calibration of a germanium thermometer, some adequate functional relationships between resistance, R, and temperature, T, should be needed. Such attempts to find an empirical formula were made by, for examples, Lindenfeld,[10] Ahlers,[11] and Cataland and Plumb.[12] In the present case, however, a rather simple formula[13] of the form,

$$\log_{10} R = A/T + B + CT + DT^2, \qquad (1)$$

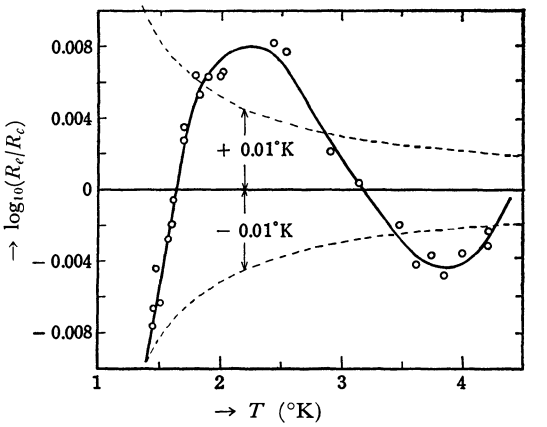

Fig. 3. Correction curve for the calibration of the germanium thermometer in the range 1.4 to 4.4°K.

was fitted to the experimental R_e and T_e calibration data of the germanium resistor by the method of least squares, where A, B, C, and D are numerical constants. A comparison between the R_e and the R_c (calculated value from formula (1)) is illustrated in Fig. 3 in the case of liquid helium temperature region. It is clear in the figure that formula (1) may reproduce the R_e and T_e relationship within ± 0.02°K. The same held well in the liquid hydrogen temperature region where the last term of the right-hand side of formula (1) was

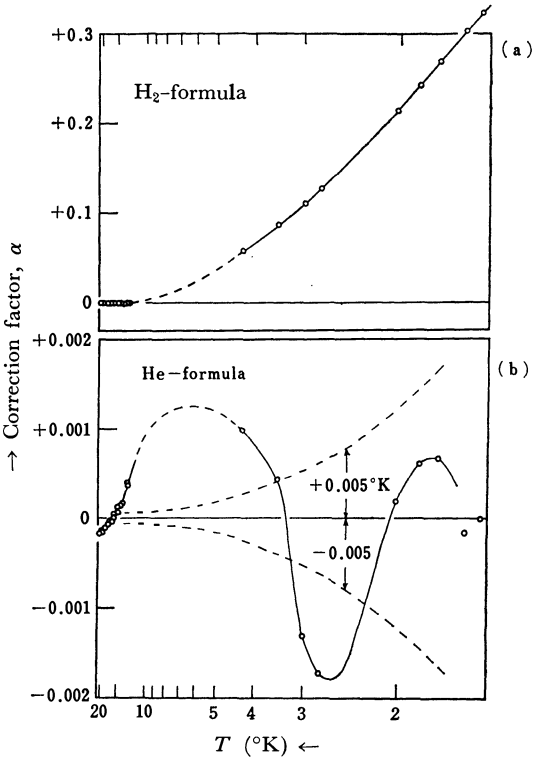

Fig. 4. Determination of the correction factor, α, for the carbon resistor in the range 4.4 to 11.8°K.

8) H. Suga and S. Seki, This Bulletin, **38**, 1000 (1965).
9) F. G. Brickwedde, H. van Dijk, M. Durieux, J. R. Clement and J. K. Logan, *J. Res. Nat. Bur. Stand.*, **64A**, 1 (1960).
10) P. Lindenfeld, *Rev. sci. Instrum.*, **32**, 9 (1961).
11) G. Ahlers, *J. Chem. Phys.*, **41**, 86 (1964); *Phys. Rev.*, **135**, A10 (1964).
12) G. Cataland and H. H. Plumb, *J. Res. Nat. Bur. Stand.*, **70A**, 243 (1966).
13) M. Sorai, H. Suga and S. Seki, Preprints for the 18th Annual Meeting of the Chemical Society of Japan (April, 1965), 32311.

omitted. To improve the effectiveness of formula (1), it is necessary to define a correction term as

$$\Delta = \log_{10} R_e - \log_{10} R_c. \quad (2)$$

Finally the smoothed values of resistance of the germanium resistor, R_s, were calculated by the following formula,

$$\log_{10} R_s = A/T + B + CT + DT^2 + \Delta, \quad (3)$$

and the tables of R_s *versus* T were made every interval of 0.01°K in the region 1.40 to 4.40°K and of 0.1°K in the region 11.8 to 21.0°K by the NEAC 2203 computer. Deviations of the calibration points, T_e, from formula (3) are shown in Fig. 6. In order to check the stability of thermometer after temperature cycling the calibrations were repeated six times and no significant changes were observed. This fact is consistent with the results by Kunzler *et al.*,[14] and Plumb *et al.*[15] The final deviations of the calculated curve by using formula (3) from the T_{58} scale and the NBS scale, respectively, are within ±0.003°K.

In general a commercially available germanium resistance thermometer had disadvantages such as that the resistance-temperature relation is complicated and should be established by calibration at many temperatures. Thus, without the use of a gas thermometer there is no method for evolving a "working" temperature scale between the liquid helium and the liquid hydrogen temperature region, *i. e.* 4.4—11.8°K, as far as a germanium resistor is used. For these reasons there is always an uncertainty in evaluating the thermodynamic temperature scale in this region, so the high-precision calorimetric investigations in this temperature region are rather scarce. An attempt has been made by DeSorbo and Nichols[16] to circumvent

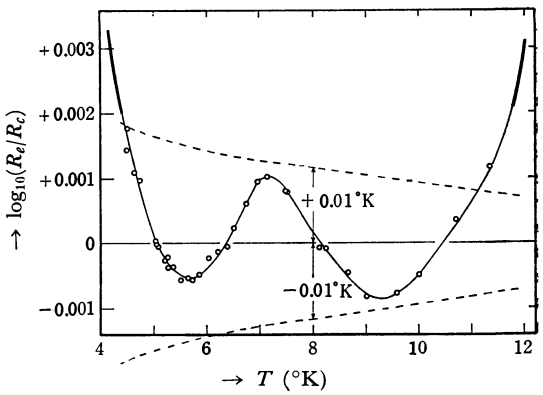

Fig. 5. Correction curve for the germanium thermometer in the temperature range 4.4 to 11.8°K.

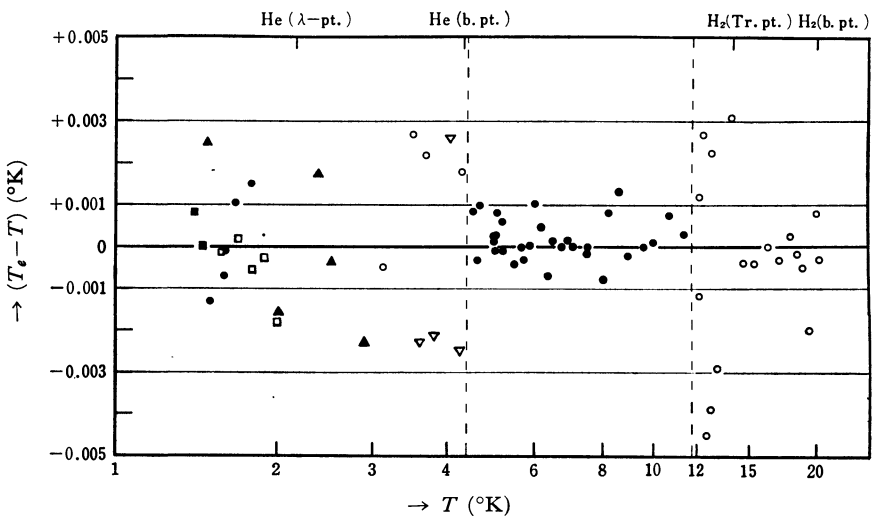

Fig. 6. Deviations of the calibration points for the germanium thermometer from the T_{58} scale (1.4—4.4°K), from "the Carbon scale" (4.4—11.8°K), and from the NBS scale (11.8—21.0°K). Various marks in the liquid helium region mean different runs of the calibration.

Table 1. Spectrographic analysis of the salts

Compound	Impurity, percent					
	K	Na	Rb	Ca	Mg	Al
CsBr	<0.01	<0.01	<0.01	0.06	<0.01	<0.01
CsI	<0.01	<0.01	<0.01	0.06	<0.01	<0.01

14) J. E. Kunzler, T. M. Geballe and G. W. Hull, Jr., "Temperature. Its Measurement and Control in Science and Industry," Vol. 3, Part 1, Reinhold Pub. Corp., New York (1962), p. 391.

15) M. H. Edlow and H. H. Plumb, *ibid.*, Vol. 3, Part 1 (1962), p. 407.

16) W. DeSorbo and G. E. Nichols, *J. Phys. Chem. Solids*, **6**, 352 (1958).

this problem, at least approximately, with a careful analysis of the carbon resistor data obtained both in the liquid helium and liquid hydrogen temperature regions. The working temperature scale adopted here between 4.4 and 11.8°K is based on this convenient method, that is to say "the Carbon scale". The procedure adopted is to evaluate the correction factor, α, for the region 1.4—4.4°K and 11.8—21.0°K, first by using the constants A and B evaluated from the R-T data for the liquid hydrogen region (see Fig. 4(a)) and secondly by using constants A and B determined for the liquid helium region (Fig. 4(b)). Here A and B are constants appeared in the formula, $\sqrt{(\log R)/T}=A\log R+B$, for the R-T relation of carbon resistor proposed by Clement and Quinnell.[17] By a method of successive approximation, the two interpolated segments of the curves shown in Figs. 4(a) and 4(b) by broken lines were determined to give a minimum discrepancy in $\Delta T(T(H_2\text{-formula})\text{-}T(\text{He-formula}))$. Uncertain deviations of "the Carbon scale" from the thermodynamic temperature scale will probably be introduced in the process of drawing the interpolated segments. An ambiguity in this procedure, however, does not seem to exceed ±0.02°K (see Figs. 4(a) and 4(b)). The working temperature scale for the germanium resistance thermometer was, thus, established by using both "the Carbon scale" and the formula (3).

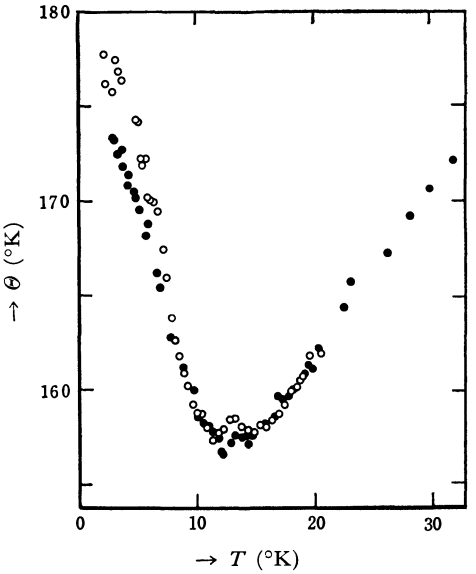

Fig. 7. Comparison of the heat capacity of KBr in terms of the Debye characteristic temperature below 21°K: ○, present work; ●, Berg and Morrison.[18]

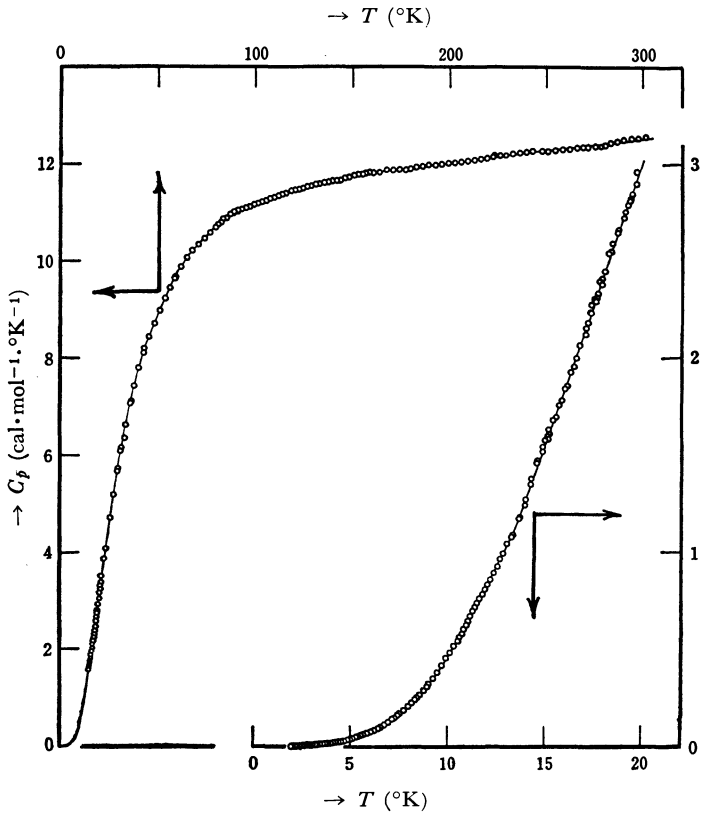

Fig. 8. Heat capacity of CsBr in the temperature region from 1.5 to 300°K.

17) J. R. Clement and E. H. Quinnell, *Rev. sci. Instrum.*, **23**, 213 (1952).

18) W. T. Berg and J. A. Morrison, *Proc. Roy. Soc.*, **A242**, 467 (1957).

The correction curve in this region is illustrated in Fig. 5. Two thick solid lines in the vicinity of 4 and 12°K mean the T_{58} scale and the NBS scale, respectively. Final deviation plots of all the calibration points for the germanium resistor from "the Carbon scale" are shown in Fig. 6.

Materials. Powder crystals of CsBr and CsI of high purity optical grade were obtained from Mitsuwa's Pure Chemicals. The salts were recrystallized twice from distilled water and then dried at temperatures between 100 and 120°C in a vacuum for 15 hr. The results of spectrographic analysis of this purified samples are given in Table 1. Potassium bromide crystal of high purity optical grade was obtained from E. Merck AG. Procedure of purification was the same as mentioned above.

For the heat capacity measurements in the temperature range 1.5 to 21.0°K the calorimeter contained 104.743 g (0.49219 mol) of CsBr, 184.462 g (0.70999 mol) of CsI, and 150.582 g (1.2653 mol) of KBr, respectively, as well as a small amount of helium exchange gas. For the measurements at higher temperatures, on the other hand, the calorimeter contained 43.8972 g (0.20627 mol) of CsBr and 46.2041 g (0.17784 mol) of CsI, respectively, and helium gas as heat exchanger.

Heat Capacities of CsBr and CsI. The heat capacity measurements were made with the low-temperature adiabatic calorimeter (denoted as calorimeter-A hereafter) described above in the temperature region 1.5 to 21.0°K and with the automatic adiabatic calorimeter[8] (calorimeter-B) described previously in the range 15 to 300°K. Approximately 230 heat capacity data were determined for CsBr and CsI with various small temperature rise (0.05—0.5°K below 20°K and 1—3°K above 15°K).

The Precision and Accuracy of the Measurements. The scatter of the results obtained with the calorimeter-A is at worst ±3% at the lowest temperatures and ±1% for $T>4$°K. The precision of the calorimeter-B appears to be ±2% for $T<20$°K, ±1% for 20°K$<T<$50°K, and ±0.3% for $T>50$°K. The accuracy is more difficult to assess. It is likely that the most serious error arises from the uncertainty in temperature scales. The accuracy has therefore to be judged by comparison of results obtained from independent assemblies. A comparison of the two sets of results between 15 and 21°K provides a measure of accuracy in this range. For each of two salts the average deviation of one set from the other was within the experimental errors. The accuracy of the calorimeter-B had been checked previously[8] by using it to measure the heat capacity of the Calorimetry Conference sample of benzoic acid in the temperature range 13 to 300°K. Another comparison may also be made with the measurements of other workers. In order to check the accuracy of the calorimeter-A heat capacity of potassium bromide was also measured between 1.5 to 21°K. The results are compared with the data by Berg and Morrison[18] in Fig. 7 in terms of the Debye characteristic temperature. Agreement between them seems to be very satisfactory if the experimental errors are taken into account. For caesium iodide heat

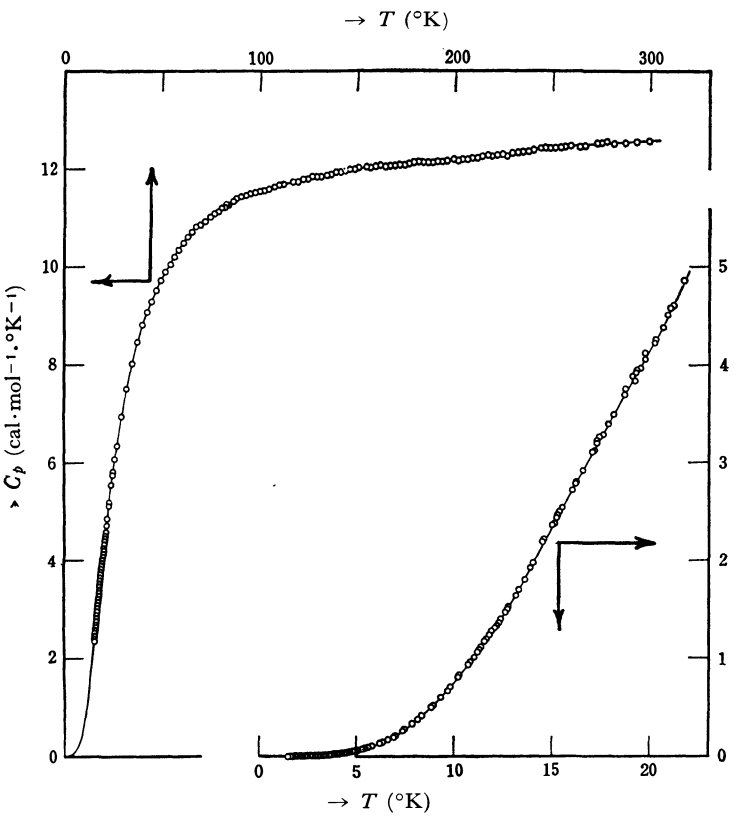

Fig. 9. Heat capacity of CsI in the temperature region from 1.5 to 300°K.

TABLE 2. HEAT CAPACITY OF CsBr
(Molecular weight 212.809)

T (°K)	C_p (cal/mol·°K)	T (°K)	C_p (cal/mol·°K)	T (°K)	C_p (cal/mol·°K)	T (°K)	C_p (cal/mol·°K)
	Calorimeter-A				Calorimeter-B		
2.810	0.00596	11.962	0.8083	15.100	1.579	122.935	11.507
3.242	0.00955	11.993	0.8252	17.233	2.183	125.088	11.523
3.358	0.01046	12.160	0.8568	19.260	2.794	127.231	11.556
3.493	0.01192	12.280	0.8804	19.373	2.814	129.365	11.563
3.757	0.01473	12.439	0.9164	21.701	3.509	131.490	11.597
3.877	0.01624	12.663	0.9739	22.830	3.884	133.651	11.607
4.282	0.02224	12.849	0.9967	23.538	4.097	135.848	11.631
4.688	0.02942	12.981	1.049	26.014	4.722	138.037	11.652
4.699	0.02998	13.607	1.186	27.777	5.206	140.219	11.673
4.913	0.03540	13.924	1.270	29.869	5.744	142.394	11.690
5.101	0.03972	14.200	1.329	31.726	6.161	144.564	11.688
5.258	0.04423	14.243	1.355	33.899	6.637	146.727	11.736
5.270	0.04458	14.510	1.415	36.103	7.082	148.884	11.758
5.476	0.05049	14.571	1.428	38.164	7.440	151.083	11.785
5.711	0.05784	14.822	1.484	40.392	7.795	153.324	11.807
5.920	0.06606	14.869	1.511	42.985	8.106	155.560	11.803
6.107	0.07366	15.108	1.563	45.659	8.441	158.599	11.843
6.323	0.08319	15.402	1.670	48.566	8.734	161.082	11.848
6.562	0.09477	15.561	1.687	51.336	8.981	164.449	11.837
6.774	0.1067	15.714	1.752	53.995	9.227	171.132	11.904
6.950	0.1180	15.864	1.781	56.563	9.443	174.506	11.899
6.968	0.1190	15.997	1.844	59.396	9.691	179.759	11.929
7.183	0.1348	16.171	1.854	62.062	9.880	183.056	11.945
7.254	0.1404	16.295	1.926	64.980	10.071	186.345	11.965
7.417	0.1529	16.481	1.960	68.140	10.223	189.527	11.986
7.519	0.1622	16.601	2.000	71.207	10.340	192.899	12.009
7.753	0.1824	16.798	2.071	74.250	10.462	196.214	12.015
7.966	0.2030	17.099	2.128	77.215	10.584	199.570	12.041
8.177	0.2240	17.110	2.161	80.127	10.696	202.918	12.049
8.388	0.2466	17.374	2.238	81.534	10.753	206.259	12.061
8.601	0.2694	17.644	2.302	82.992	10.798	209.612	12.076
8.815	0.2937	17.753	2.317	83.496	10.893	212.980	12.098
9.029	0.3218	17.913	2.382	85.516	10.901	216.340	12.127
9.265	0.3523	17.966	2.407	87.559	10.983	219.523	12.141
9.494	0.3835	18.119	2.451	89.586	11.025	222.865	12.173
9.705	0.4156	18.439	2.560	91.594	11.053	226.300	12.185
10.158	0.4842	18.760	2.661	93.647	11.081	229.626	12.203
10.404	0.5240	19.053	2.736	95.747	11.106	232.944	12.229
10.548	0.5464	19.091	2.764	97.832	11.143	236.252	12.253
10.610	0.5613	19.357	2.836	99.903	11.183	239.583	12.273
10.659	0.5685	19.426	2.852	101.963	11.210	247.602	12.252
10.786	0.5984	19.747	2.889	104.011	11.244	251.128	12.271
10.913	0.6134	20.318	3.055	106.047	11.274	254.645	12.275
11.031	0.6341	20.346	3.144	108.113	11.314	258.323	12.293
11.086	0.6492	20.645	3.226	110.207	11.339	262.142	12.309
11.170	0.6620	20.663	3.217	112.290	11.374	265.933	12.326
11.429	0.7190			114.363	11.403	269.715	12.339
				116.427	11.422	270.987	12.345
				118.771	11.475	278.834	12.363
				120.832	11.485	280.605	12.393

TABLE 3. HEAT CAPACITY OF CsI
(Molecular weight 259.809)

T (°K)	C_p (cal/mol·°K)	T (°K)	C_p (cal/mol·°K)	T (°K)	C_p (cal/mol·°K)	T (°K)	C_p (cal/mol·°K)
	Calorimeter-A			29.433	6.959	148.358	12.008
1.501	0.00149	6.910	0.2016	32.083	7.534	150.704	12.043
1.760	0.00254	6.956	0.2062	34.817	8.035	154.228	12.071
1.931	0.00335	7.366	0.2574	37.465	8.479	156.730	12.043
2.091	0.00424	7.480	0.2714	39.974	8.816	159.219	12.063
2.175	0.00460	7.857	0.3279	42.342	9.086	161.703	12.081
2.249	0.00518	8.150	0.3764	44.615	9.309	164.183	12.050
2.309	0.00547	8.358	0.4117	46.999	9.527	166.652	12.069
2.440	0.00655	8.835	0.5016	49.465	9.730	169.120	12.059
2.557	0.00761	8.901	0.5137	51.847	9.899	171.584	12.097
2.568	0.00764	9.330	0.6019	54.154	10.062	174.041	12.083
2.694	0.00885	9.643	0.6735	56.399	10.197	176.492	12.118
2.709	0.00930	9.806	0.7119	58.589	10.351	178.939	12.152
2.817	0.01026	10.255	0.8231	60.731	10.496	181.382	12.152
2.860	0.01082	10.725	0.9427	62.892	10.617	183.823	12.142
2.947	0.01174	10.793	0.9667	65.077	10.721	186.086	12.153
3.016	0.01287	11.025	1.032	67.166	10.820	188.516	12.137
3.090	0.01352	11.182	1.074	69.502	10.860	190.938	12.174
3.186	0.01503	11.281	1.110	71.803	10.923	193.357	12.147
3.239	0.01561	11.307	1.124	74.159	11.031	195.772	12.168
3.244	0.01579	11.580	1.204	76.573	11.104	199.057	12.233
3.361	0.01784	11.646	1.216	78.953	11.127	201.488	12.183
3.408	0.01858	11.807	1.270	80.265	11.234	203.920	12.196
3.546	0.02112	11.933	1.288	81.396	11.201	206.355	12.199
3.604	0.02225	12.136	1.352	83.903	11.271	208.783	12.227
3.737	0.02515	12.322	1.394	86.380	11.349	211.250	12.231
3.805	0.02658	12.752	1.527	90.226	11.444	213.755	12.273
3.931	0.02922	13.266	1.702	92.733	11.469	218.758	12.259
3.983	0.03092	13.862	1.915	95.220	11.495	221.420	12.289
4.136	0.03369	14.473	2.140	97.670	11.536	224.082	12.302
4.364	0.04020	15.361	2.477	100.119	11.561	232.026	12.339
4.546	0.04677	15.514	2.527	102.574	11.566	234.666	12.355
4.594	0.04794	16.203	2.790	104.999	11.608	237.311	12.347
4.830	0.05744	16.572	2.924	107.396	11.651	239.951	12.392
5.074	0.06793	17.057	3.112	109.776	11.676	245.927	12.418
5.373	0.08350	17.108	3.124	112.143	11.696	248.553	12.430
5.430	0.08670	17.901	3.409	116.913	11.764	251.183	12.400
5.816	0.1105	18.708	3.705	119.414	11.759	253.813	12.396
6.207	0.1377	19.492	3.964	121.895	11.800	256.438	12.450
6.321	0.1472	20.272	4.247	124.363	11.809	264.190	12.450
6.578	0.1681	20.703	4.431	126.815	11.855	266.805	12.478
				129.252	11.847	272.474	12.547
	Calorimeter-B			131.677	11.852	275.074	12.551
15.269	2.254	21.271	4.581	134.089	11.874	277.674	12.561
17.282	3.208	22.816	5.158	136.490	11.915	281.569	12.513
19.286	3.940	24.755	5.757	138.883	11.960	287.186	12.524
19.335	3.948	24.954	5.821	141.267	11.942	293.218	12.547
20.954	4.538	25.903	6.088	143.639	11.968	299.212	12.569
21.098	4.576	27.027	6.357	146.003	11.995		

capacity data have been reported by Taylor *et al.*[19] in the range 13 to 300°K. They agree with the present results to within ±1% above 60°K, but the systematic deviation appears with decreasing temperature to amount to +5% below 20°K. Heat capacities of CsBr and CsI above room temperature have been reported by Brönsted.[20] His value is 0.6% higher at 300°K for CsBr and 1.4% higher for CsI.

Table 4. Thermodynamic properties of CsBr crystal (in cal/mol·°K)

T (°K)	$C_p°$	$S°$	$\frac{H°-H_0°}{T}$	$\frac{-(G°-H_0°)}{T}$
2	0.00216	0.00108	0.00067	0.00041
4	0.01798	0.00662	0.00471	0.00191
6	0.06923	0.02239	0.01657	0.00582
8	0.2059	0.05905	0.04496	0.01409
10	0.4588	0.1308	0.1011	0.0297
15	1.549	0.5043	0.3863	0.1180
20	3.008	1.147	0.8567	0.2902
25	4.467	1.977	1.434	0.5423
30	5.766	2.910	2.052	0.8582
35	6.859	3.884	2.663	1.221
40	7.704	4.857	3.242	1.615
45	8.377	5.804	3.777	2.027
50	8.923	6.716	4.265	2.451
60	9.728	8.418	5.112	3.306
70	10.315	9.965	5.816	4.149
80	10.700	11.369	6.404	4.965
90	10.993	12.647	6.898	5.749
100	11.184	13.815	7.318	6.497
110	11.339	14.889	7.677	7.212
120	11.473	15.881	7.987	7.894
130	11.583	16.804	8.260	8.544
140	11.675	17.666	8.501	9.165
150	11.767	18.475	8.715	9.760
160	11.835	19.237	8.909	10.328
170	11.885	19.956	9.082	10.874
180	11.932	20.636	9.239	11.397
190	11.990	21.283	9.382	11.901
200	12.040	21.899	9.514	12.385
210	12.085	22.488	9.635	12.853
220	12.128	23.051	9.748	13.303
230	12.175	23.591	9.852	13.739
240	12.220	24.110	9.950	14.160
250	12.262	24.610	10.042	14.568
260	12.305	25.092	10.128	14.964
270	12.345	25.557	10.209	15.348
280	12.381	26.006	10.286	15.720
290	12.416	26.441	10.359	16.082
300	12.447	26.863	10.428	16.435
273.15	12.356	25.700	10.234	15.466
298.15	12.441	26.785	10.415	16.370

Table 5. Thermodynamic properties of CsI crystal (in cal/mol·°K)

T (°K)	$C_p°$	$S°$	$\frac{H°-H_0°}{T}$	$\frac{-(G°-H_0°)}{T}$
2	0.00358	0.00178	0.00111	0.00067
4	0.03089	0.01115	0.00796	0.00319
6	0.1226	0.03867	0.02877	0.00990
8	0.3511	0.1019	0.0777	0.0242
10	0.7563	0.2217	0.1707	0.0510
15	2.363	0.8147	0.6190	0.1957
20	4.168	1.743	1.281	0.4615
25	5.791	2.852	2.026	0.8268
30	7.084	4.027	2.765	1.262
35	8.080	5.198	3.457	1.741
40	8.815	6.327	4.083	2.244
45	9.352	7.398	4.640	2.758
50	9.793	8.406	5.133	3.273
60	10.422	10.252	5.967	4.285
70	10.896	11.898	6.641	5.257
80	11.192	13.374	7.192	6.182
90	11.422	14.706	7.650	7.056
100	11.570	15.917	8.035	7.882
110	11.681	17.025	8.362	8.663
120	11.778	18.046	8.642	9.404
130	11.864	18.992	8.887	10.105
140	11.938	19.874	9.102	10.772
150	12.008	20.700	9.294	11.406
160	12.059	21.477	9.465	12.012
170	12.090	22.209	9.619	12.590
180	12.121	22.901	9.757	13.144
190	12.156	23.557	9.882	13.675
200	12.194	24.182	9.997	14.185
210	12.237	24.778	10.102	14.676
220	12.279	25.348	10.200	15.148
230	12.327	25.895	10.292	15.603
240	12.374	26.420	10.378	16.042
250	12.414	26.926	10.458	16.468
260	12.452	27.414	10.534	16.880
270	12.487	27.884	10.606	17.278
280	12.521	28.339	10.674	17.665
290	12.549	28.779	10.738	18.041
300	12.576	29.205	10.799	18.406
273.15	12.497	28.029	10.628	17.401
298.15	12.571	29.127	10.788	18.339

Experimental Results

The results of the heat capacity of CsBr and CsI in the region 1.5 to 300°K are plotted in Figs. 8 and 9, respectively. Tables 2 and 3 list their numerical values. The calorie defined as equal to 4.1840 absolute joules was used. The ice-point was taken as 273.15°K. The molecular weights are based on the 1966 IUPAC report on atomic weights.

Smoothed values of the heat capacity, entropy,

19) A. R. Taylor, Jr., T. E. Gardner and D. F. Smith, *U. S. Bur. Mines Rept. Invest.*, No. 6157 (1963).
20) J. N. Brönsted, *Z. Elektrochem.*, **20**, 554 (1914).

enthalpy function, and Gibbs energy function, and also of the standard thermodynamic values at 298.15°K, are listed in Tables 4 and 5, for CsBr and CsI, respectively. The differential heat capacity, $C_p°$, listed in the tables, which is obtained from the observed values of $\Delta H/\Delta T$, was not corrected for curvature because of the small rise in temperature, ΔT.

Other thermal properties of these crystals and significant differences between the alkali halide crystals with the NaCl-type structure and the CsCl-type one are fully described in part II.[21]

The authors wish to express their sincere thanks to Mr. Nobukatsu Fujino of Sumitomo Metal Industries, Ltd. for spectrographic analysis of the specimen for metal impurities. They are also indebted to Messrs. Takasuke Matsuo and Masayasu Sugisaki for their help in part of the measurements.

21) M. Sorai, *J. Phys. Soc. Japan*, **24** (1968) (in press).

BULLETIN OF THE CHEMICAL SOCIETY OF JAPAN VOL. 41 321—325 (1968)

Studies on the Sol-Gel Transformation of Aluminium Hydroxide in the Presence of Dyes

Wahid U. MALIK and Iqbal A. KHAN

Chemical Laboratories, University of Roorkee, Roorkee, India

(Received April 9, 1966)

The influence of dyes on the gelation of aluminium hydroxide sol has been studied with the help of viscometric and pH metric methods. From these studies it is inferred that the behaviour of acid dyes towards alumina is different from that of basic dyes. The results have been interpreted in terms of various structural changes taking place in the dye molecule. Adsorption studies reveal that the data do not fit well into the Langmuir or Freundlich adsorption isotherm equation in the case of alizarin sulphoric acid, while in the cases of methyl orange, methylene blue, and malachite green, the data are found to fit well into the Langmuir adsorption equation.

A large amount of work has been done on the adsorption of dyes, especially of the alizarin class, on hydrous oxide sols. Mokuskin and Esin,[1] White and Gorden,[2] and Porter[3] have studied the association of several dyes with hydrous oxides. Weiser[4] has also made several studies in this direction. Other problems, however, for instance, the nature of the binding between sol and dye, the determination of the miceller size of hydrous oxide sols by dye interaction, and the influence of dyes on the gelation of sols, have not yet been comprehensively studied. In the present paper the results of the gelation of aluminium hydroxide in the presence of acid (alizarin sulfonic acid and methyl orange) and basic (methylene blue and malachite green) dyes are reported.

Experimental

Reagents. *(a) Aluminium Hydroxide Sol.* Positively-charged aluminum hydroxide sol was prepared by the method described by Weiser.[5] 10 g of aluminium chloride (E. Merck) was dissolved in 500 cc of doubly-distilled water, and the resulting solution was heated to boiling. Aluminium hydroxide was precipitated with a slight excess of ammonia, and the suspension was boiled for five minutes. The precipitate was then placed in a centrifuge tube and suspended in doubly-distilled water, after which the suspension was centrifuged for 15 min. The supernatant liquid was poured off, doubly-distilled water was again added, and the precipitate was washed. The process of washing was repeated many times. The precipitate was then transferred to a 500 cc Pyrex beaker and suspended with doubly-distilled water. The suspension was then heated to boiling. The precipitate of $Al_2O_3 \cdot xH_2O$ was peptized to alumina sol by gradually adding 0.2 N HCl in 1 cc portions and boiling the solution for ten minutes after each addition. The pH of the solution containing the alumina sol was lowered to the required value by the addition of the requisite amount of a 0.1 N HCl solution. The concentration of alumina in the colloidal solution was determined gravimetrically[6] by precipitating it

1) G. W. Mokuskin and G. L. Esin; *J. Russ. Phys. Chem. Soc.*, **58**, 882 (1926); *Kolloid-Z.*, **41**, 104 (1927).
2) P. L. Marker and G. Gorden, *Ind. Eng. Chem.*, **16**, 1188 (1924); C, E. White and G. Gorden, *J. Phys. Chem.*, **31**, 1764 (1927).
3) J. L. Porter *J. Phys. Chem.*, **31**, 1704 (1927).
4) H. B. Weiser, *ibid.*, **26**, 401 (1922).
5) H. B. Weiser, *ibid.*, **26**, 525 (1926).
6) A. I. Vogel, "A Text Book of Quantitative Inorganic Analysis," 2nd edition, Longman's Green and Co., London, p. 410; and W. W. Scott, "Standard Method of Chemical Analysis" Vol. 1, ed. by H. Furman, D. Van Nostrand Company, Inc., New York (1945), p. 9.

as $Al_2O_3 \cdot xH_2O$ in the pH range 7—7.5 and by then igniting the precipitate to Al_2O_3.

b) The dyes, alizarin sulphonic acid (sod. salt), methyl orange (sod. salt), methylene blue (chloride), and malachite green (chloride) were either B. D. H. or Merck products.

Apparatus and Technique. The viscosity measurements were carried out using a modification of Scarpa's method.[7] The pH measurements were made with a Cambridge bench pH-meter. Adsorption experiments were carried using the Bausch and Lomb "Spectronic 20."

Procedure. 2.0×10^{-2} M stock solutions of the dyes (alizarin sulphonic acid, methyl orange, methylene blue and malachite green) were prepared in doubly distilled water and kept in all-Pyrex glass vesseles. The following sets of mixtures were used for gelation measurements. (i) 20 cc sol + a varying amount of the dye (0, 0.5, 1.0, and 1.5 cc of 2.0×10^{-2} M methyl orange); (ii) 20 cc of sol + a varying amount of the dye (0.5, 1.0, and 1.5 cc of 2.0×10^{-2} M alizarin sulphonic acid); (iii) 20 cc sol + a varying amount of the dye (0.5, 1.0, and 1.5 cc of 2.0×10^{-2} M methylene blue); (iv) 20 cc sol + a varying amount of the dye (0.5, 1.0, and 1.5 cc of 2.0×10^{-2} M malachite green). In each case the total volume was made up to 30 cc with doubly-distilled water.

The viscometric and pH metric studies were carried out at 30±0.1°C during the dialysis of the above sets (i, ii, iii and iv in) different dialysing bags of the same size.

Dye Adsorption Measurements. The alumina gel (the adsorbent) was prepared by the continuous dialysis of the sol, and then dried between 50 and 80°C. The finely powdered gel was weighed and presoaked in a small quantity of doubly-distilled water prior to the addition of a dye solution. The following sets of mixtures were prepared: (i) 100 mg of alumina gel + a varying amount of the dye (1.0, 2.0, 3.0, 4.0, and 5.0 cc of 1.5×10^{-4} M alizarin sulphonic acid); (ii) 100 mg of alumina gel + a varying amount of the dye (1.0, 2.0, 3.0, 4.0, and 5.0 cc of 4.51×10^{-5} M methyl orange); (iii) 100 mg of alumina gel + a varying amount of the dye (1.0, 2.0, 3.0, 4.0, and 5.0 cc of 3.14×10^{-5} M methylene blue); (iv) 100 mg of alumina gel + a varying amount of the dye (1.0, 2.0, 3.0, 4.0, and 5.0 cc of 1.96×10^{-5} M malachite green). In each case the total volume was made up to 10 cc with doubly-distilled water.

Adsorption isotherms were run by making successive additions of 1.0, 2.0, 3.0, 4.0, and 5.0 cc of the dye solution to 100 mg of alumina gel. The adsorbent and the dye solution were agitated to equilibrium after each addition of dye prior to a colorimetric measurement of the dye solute. The volume of the solutions was 10 cc. The readings were made after a sufficient time of mixing, when the solution had attained equilibrium. The equilibrium solutions were then centrifuged for transmittance measurements.

Discussion

Before discussing the experimental findings on the sol-gel transformation of aluminium hydroxide in the presence of dyes, it is worthwhile considering the behaviour of the pure sol when converted into a gel by prolonged dialysis. A plot of the time of dialysis against the viscosity (Fig. 1) reveals that, after a certain stage of dialysis, there is an abrupt increase in the viscosity. This means that with a progressive dialysis the optimum conditions necessary to bring about gelation are realized, and that the time after which an abrupt increase in viscosity takes place may conveniently be termed the "gelation time"[8,9] (it is quite distinct from the time of the setting of a gel-forming mixture).

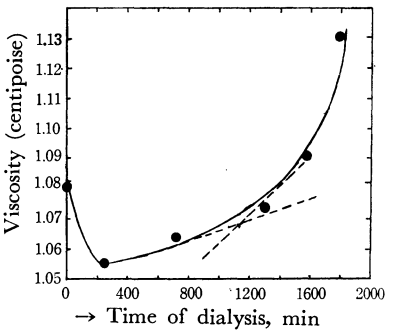

Fig. 1

The data (Table 1) show that, although the time of setting is different for samples subjected to dialysis for different time intervals (the minimum time being 4.5 hr), when samples are dialysed for 30 hr, the time required for all the samples of one mixture to attain the optimum conditions for gelation had the same value, ranging between 1040 and 1300 min.

Although an abrupt rise in viscosity in colloidal systems may be explained in the light of several factors, the solvation, the electroviscous effect, and adhesion of particles, *etc.*, in the case of pure sol, a forthright explanation is difficult in complex systems comprising mixtures of a sol and a foreign substance, or of two different sols. In such cases due consideration has to be given to structural changes accompanying the interaction of the different chemical entities involved besides the factors enumerated above.

Gelation of an Alumina Sol - Dye Mixture. With (acid or) anionic dyes the viscosity of the mixtures first decreases, and then increases near the gelation time, while with (basic or) cationic dyes the behaviour is quite different: the viscosity shows an initial decrease, followed by a gradual increase. These data may be discussed from the following two angles. (i) the variation in the viscosity with a progressive dialysis in the presence of a fixed amount of dye, and (ii) a change in the

7) O. Scarpa, *Gaz. Chim.*, **40**, 271 (1910).

8) W. U. Malik and F. A. Siddiqui, *J. Phys. Chem.*, **66**, 357 (1962).

9) W. U. Malik and F. A. Siddiqui, *Kolloid-Z.* (U. Z. polymer), **184**, 41 (1962).

TABLE 1. TIME OF SETTING AND GELATION TIME FOR DIALYSED ALUMINA SOL AT pH=3.7

Time of dialysis	Time of setting by Fleming's method	Viscosity (centipoise)	Gelation time as determined from the abrupt rise in viscosity
0	—	1.081	1040 to 1300 min
4.25 hr (255 min)	—	1.060	
12.25 hr (735 min)	—	1.063	
22.5 hr (1300 min)	24 hr	1.074	
26.2 hr (1575 min)	20 hr	1.091	
30.0 hr (1800 min)	4.5 hr	1.13	

TABLE 2. VARIATIONS IN VISCOSITY WITH DIALYSIS OF ALUMINA SOL - DYE MIXTURE CONTAINING 1.0 mmol/*l* OF DYE

Time of dialysis min	Viscosity				
	Pure sol (centipoise)	Sol + methyl orange (centipoise)	Sol + aliz. s. acid (centipoise)	Sol + methylene blue (centipoise)	Sol + malachite green (centipoise)
0	1.08	2.12	2.30	1.08	1.09
255	1.06	1.55	1.64	1.08	1.07
735	1.06	1.32	1.56	1.07	1.06
1300	1.07	1.26	1.47	1.06	1.07
1575	1.09	1.18	1.47	1.08	1.13
1800	1.13	1.20	1.50	1.08	1.13

TABLE 3. VARIATIONS IN VISCOSITY AND pH OF A DIALYSED ALUMINA SOL CONTAINING VARYING AMOUNTS OF DYES

Concn. of dye mmol/*l*	Sol + methyl orange mixture		Sol + aliz. s. acid mixture		Sol + methylene blue mixture		Sol + malachite green mixture	
	Viscosity (centipoise)	pH	Viscosity (centipoise)	pH	Viscosity (centipoise)	pH	Viscosity (centipoise)	pH
0	1.09	5.40	1.09	5.40	1.09	5.40	1.09	5.40
0.33	1.12	4.47	1.05	4.69	1.04	4.72	1.05	4.76
0.66	1.17	4.52	1.09	4.55	1.10	4.71	1.07	4.74
1.0	1.18	4.57	1.47	4.37	1.08	4.60	1.13	4.84

viscosity with gradually increasing amounts of the dye in a sol dialysed for a fixed period of time. In (i) a continuous decrease in viscosity with dialysis is observed with acid dyes, the extent to which this change takes place being dependent on the nature of the dye employed. In the presence of a fixed concentration of the dye, 1.0 mmol/*l*, the following variations are observed.

On considering the viscosity data for samples dialysed for a period greater than the gelation time of the pure sol (say, 30 hr), it will be seen that there is considerable decrease in viscosity, 42.5% and 36.0% in the cases of methyl orange and alizarin sulphonic acid respectively, although there is an overall increase of 0.92% in the case of pure sol. With the basic dyes the results are different; the viscosity changes are very small, and only slight increases in viscosity are observed (0.18% for methylene blue and 3.4% for malachite green).

The decrease in viscosity on prolonged dialysis may be explained in terms of peptization. The

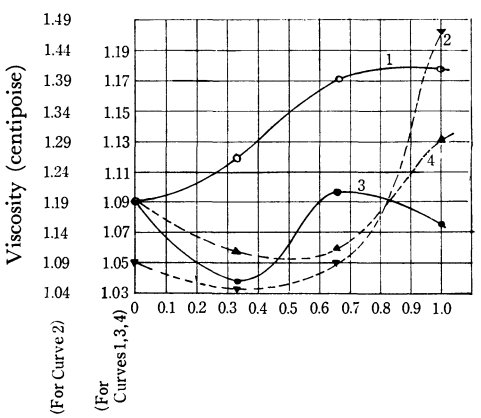

Concn. of dye, mmol/*l*

Fig. 2

○ 1. Al_2O_3sol + methyl orange mixture
▼ 2. Al_2O_3sol + aliz. S. acid mixture
● 3. Al_2O_3sol + methylene blue mixture
▲ 4. Al_2O_3sol + mal. green mixture

dye used may prevent agglomeration by the adsorption of the anionic part of the dye on the sol particles, which may keep the sol in the stable state and not allow it to undergo gelation. These data are supported by the work of Ghosh and his coworkers,[10] who observed that hydrous oxides, especially of the amphoteric type, develop a large adsorption capacity for anions. The findings on the changes in viscosity and pH with a variation in the concentrations of dyes after a fixed period of dialysis are worth considering.

Figure 2, indicates that the final viscosity increases with an increase in the concentration of the dye, in the cases, of both methyl orange (Curve 1) and alizarin sulphonic acid (Curve 2), although the natures of the two curves are different; in the case of alizarin sulphonic acid viscosity slightly decreases in the initial state (Table 3, Column 4), while in the case of methyl orange there is a continuous increase in viscosity. With basic dyes the behaviour is quite different; that is, the concentration-viscosity curve shows a decrease over a wide concentration range, followed by an abrupt increase in the case of malachite green (Curve 4), while there is an initial decrease, followed by an increase and then a slight decrease again, in the case of methylene blue (Curve 3). The difference in the nature of the products obtained with basic and acid dyes is also evident from the stability curves (a plot of the stability against C_e, where C_e is the concentration of the dye). That is, the stability of the sol increases slightly and then dedecreases rapidly with an increase in the concentration of the dye in the case of basic dyes, but in the case of acid dyes no such decrease is marked (Fig. 3, Curves 1 and 2).

Another factor worth taking into account in explaining the gelation tendency of alumina in the presence of dyes in the structure of the dyes and the molecular rearrangements in the different pH ranges. Since the alumina sol has a fairly low pH, the dye molecule may either undergo protonation or reorientation to give the quinoidal structure.

Preliminary experiments have shown that methylene blue does not change its colour in either an acidic or a basic medium. The addition of sol, however, brings about a slight fading of the coluor, indicating the possibisity of adsorption. The change in the pH of the sol upon addition of methylene blue supports this view (Fig. 4, Curve 3). The behaviour with malachite green can be explained on similar lines, except for the fact that there is nothing inherent in the structure of the molecule which may point towards some sort of interaction between the dye and the sol.

With acid dyes a lake formation takes place. The alizarin lakes of the hydrous oxides are ordinarily formed by an exchange adsorption process

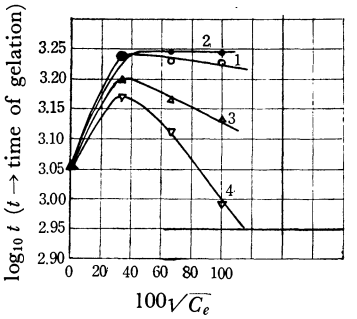

Fig. 3.

Stability curves

○ 1. Al_2O_3 sol + methyl orange
● 2. Al_2O_3 sol + aliz. s. acid
△ 3. Al_2O_3 sol + methylene blue
▽ 4. Al_2O_3 sol + mal. green

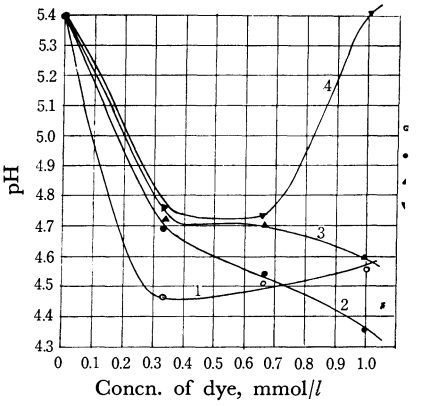

Fig. 4

○ 1. Al_2O_3 sol + methyl orange
● 2. Al_2O_3 sol + aliz. s. acid
▲ 3. Al_2O_3 sol + methylene blue
▼ 4. Al_2O_3 sol + mal. green

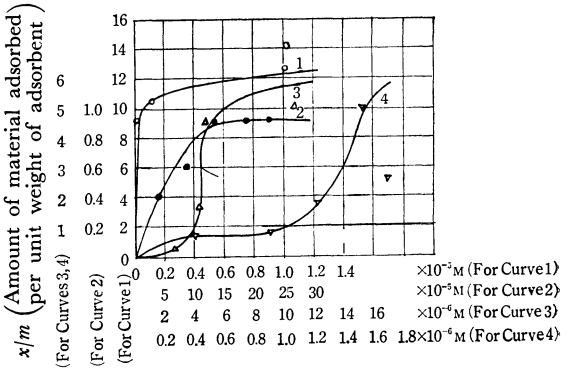

Fig. 5

○ 1. Al_2O_3 gel + aliz. s. acid
● 2. Al_2O_3 gel + methyl orange
△ 3. Al_2O_3 gel + methylene blue
▽ 4. Al_2O_3 gel + mal. green

10) S. Ghosh *et at.*, *Z. anorg. u. allgem. Chem.*, **271**, 150 (1952).

in which the relatively strongly-adsorbed alizarate ions displace such more weakly desorbed ions as chloride from the hydrous oxide. According to the view of Morgan,[11] the alizarin lakes are definite metal chelate compounds.

The various changes taking place can be represented by the following scheme:

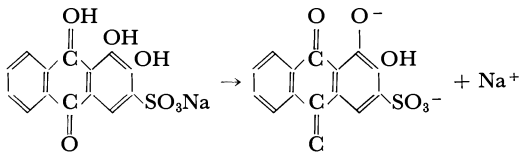

alizarin sulphonic acid (sod. salt)

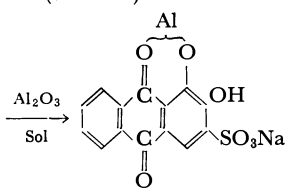

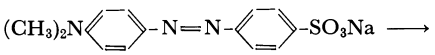

methyl orange

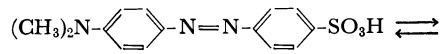

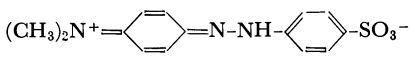

11) G. T. Morgan and J. D. Wain-Smith, *J. Chem. Soc.*, **119**, 704 (1921); **121**, 160, 1956, 2857, 2866 (1922).

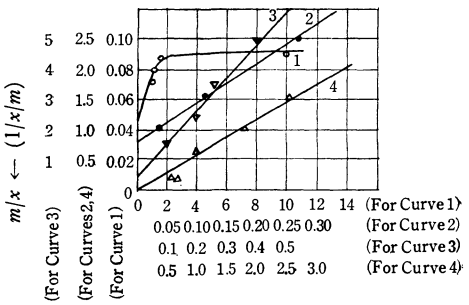

C_s (Equilibrium concn. of dye)

Fig. 6

○ 1. Al_2O_3 gel + ariz. S. acid
● 2. Al_2O_3 gel + methyl orange
▽ 3. Al_2O_3 gel + methylene blue
△ 4. Al_2O_3 gel + mal. green

In the case of alizarin sulphonic acid, the data on adsorption do not fit well into either the Langmuir or the Freundlich adsorption equation (Figs. 5 and 6, Curve 1). The extent of adsorption in this case is probably more closely related to the chemical nature of the substances than to their molecular size or molecular weight. In the case of methyl orange, methylene blue, and malachite green, the data are found to fit the Langmuir adsorption equation well (Figs. 5 and 6, Curves 2, 3, and 4 respectively).

BULLETIN OF THE CHEMICAL SOCIETY OF JAPAN VOL. 41 325—328 (1968)

Effect of the Dielectric Constant on the Reaction between the Iodide Ion and Hexacyanoferrate(III) in Acid Media

B. KRISHNA and H. S. SINGH

Department of Chemistry, University of Allahabad, Allahabad, India

(Received May 19, 1966)

In the reaction between the iodide ion and hexacyanoferrate(III), the order is unity with respect to the iodide ion and two with respect to the ferricyanide ion. It has been observed that the rate of the reaction increases with the increase in the dielectric constant of the medium. It has also been observed that the reaction occurred between trivalent and univalent negative ions.

The effect of the dielectric constant on the reaction between the iodide ion and ferricyanide in acid media has not yet been studied. The kinetic data show that the order with respect to ferricyanide is two, while that with respect to iodide is unity. By increasing the dielectric constant of the medium, the rate of the reaction is increased; this effect will be discussed in this paper, using the Brönsted-Christiansen-Scatchard[1] equation. The product of the ionic charges of the two reacting species will be calculated, and lastly we will come to the

1) E. S. Amis, "Kinetics of Chemical Change in Solution" (1949), 99.

conclusion that the reaction occurs between trivalent and univalent negative ions.

Experimental

Materials Employed. The solution of potassium ferricyanide was prepared by dissolving an ANALAR (B. D. H.)-grade reagent in distilled water.

The solution of potassium iodide was prepared by dissolving an approximate quantity of a G. R. (E. Merck)-grade reagent in water. The solution was then standardized by titrating it with a standard solution of silver nitrate, employing eosin[2] as an indicator.

ANALAR (B. D. H.)-grade hydrochloric acid was used throughout the experiments.

Absolute ethyl alcohol was redistilled in a quick-fit apparatus; the fraction boiling at 78.2°C was used.

Measurement of the Dielectric Constants. The dielectric constants were measured by a dielectrometer (Dielektrometer Type TRK No. 53015), working on the principle of the heterodyne-beat method. The null point was obtained with the help of a magic eye (Bridge Type). The values for the dielectric constant of absolute alcohol-water mixtures were obtained with a cell 1.68$\mu\mu$F in capacity. This cell had been previously brated with standard liquids of known dielectric constants.

A Study of the Progress of the Reaction. An excess of the potassium ferricyanide solution was placed in a conical flask and kept in a thermostat. The requisite quantities of potassium iodide, an alcohol-water mixture, and a hydrochloric acid solution were placed in a separate conical flask and kept in the same thermostat. When the solutions had attained the temperature of the bath, the requisite quantity of potassium ferricyanide was sucked in a pipette and poured into the solution containing potassium iodide and hydrochloric acid. The progress of the reaction was followed by sucking out an aliquot (10 m*l*) and pouring it into ice cold water in order to quench the reaction. The liberated iodine was then titrated with a standard solution of sodium thiosulphate, using starch as an indicator.

The following tables show the results at different concentrations of potassium ferricyanide and at a constant concentration of the other reactant.

A perusal of Tables 1 and 2 will show that the values of the second-order constant are fairly constant throughout the course of reaction. This proves that the order of reaction with respect to ferricyanide is two. The increase in the k_s value with the decrease in the concentration of ferricyanide is not clear at present, but the value of Z_AZ_B has been determined at a fixed concentration of ferricyanide. Therfore, the variation in ferricyanide will not affect the study of the dielectric constant. Similarly, Table 3 contains the results at different concentrations of potassium iodide.

TABLE 1

Temperature 30°C
$[K_3Fe(CN)_6] = 4.44\times10^{-3}$ N
[KI] $= 5.00\times10^{-2}$ N
[HCl] $= 10.00\times10^{-2}$ N

Time min	Sodium thiosulphate 5.00×10^{-3} N m*l*	$k_2\times10^3$
0	0.00	—
5	0.46	1.23
10	0.94	1.33
20	1.84	1.47
30	2.56	1.54
40	3.08	1.49
50	3.62	1.55
60	4.06	1.58
80	4.74	1.61
100	5.26	1.63
120	5.50	1.53
∞	8.88	—

Average value $=1.50\times10^{-3}$
$k_s=2.89\ l\cdot g\cdot equiv^{-1}\cdot min^{-1}$

TABLE 2

Temperature 30°C
$[K_3Fe(CN)_6] = 5.00\times10^{-3}$ N
[KI] $= 5.00\times10^{-2}$ N
[HCl] $= 10.00\times10^{-2}$ N

Time min	Sodium thiosulphate 5.00×10^{-3} N m*l*	$k_2\times10^3$
0	0.00	—
5	0.60	1.27
10	1.10	1.23
15	1.40	1.08
20	1.80	1.07
30	2.56	1.14
40	3.16	1.12
50	3.70	1.17
60	4.14	1.18
70	4.54	1.15
80	4.80	1.15
100	5.36	1.15
120	5.50	1.02
∞	10.00	—

Average value $=1.15\times10^{-3}$
$k_s=2.29\ l\cdot g\cdot equiv^{-1}\cdot min^{-1}$

TABLE 3

Temperature 30°C
$[K_3Fe(CN)_6] = 5.00\times10^{-3}$ N
[HCl] $= 0.10$ N

Concentration of potassium iodide 10^{-2}	k_s $l\cdot g\cdot equiv^{-1}\cdot min^{-1}$	k_s/[KI]
5.00 N	2.29	45.80
4.00 N	1.84	46.00
3.33 N	1.37	45.21
2.00 N	0.95	47.50
1.80 N	0.82	45.10

2) I. Vogel, "A Text-Book of Quantitative Inorganic Analysis," Longmans, Green & Co., London (1962), p. 262.

The values in the last column are practically constant; this shows that the rate of the reaction is directly proportional to the concentration of potassium iodide.

In the following table the results are summarized for various concentrations of alcohol at 30°C, 35°C, and 40°C.

A perusal of Table 4 shows that the rate of the reaction increases with an increase in the dielectric constant of the medium.

TABLE 4

$[K_3Fe(CN)_6] = 0.005$ N
[KI] $= 0.050$ N $\mu = 0.18$
[HCl] $= 0.10$ N

Temperature °C	% Alcohol	Dielectric constant D	Standard second-order constant k_s
30	0	77.25	2.295
30	5	75.15	2.061
30	10	72.83	1.909
30	15	70.95	1.666
30	20	68.44	1.489
35	0	76.03	3.334
35	5	74.15	2.660
35	10	71.67	2.560
35	15	69.36	2.283
35	20	67.32	2.168
40	0	73.38	4.300
40	5	72.06	4.022
40	10	69.53	3.728
40	15	67.16	3.458

Results and Discussion

In order to study the nature of the charge of the reacting ions, the above data were studied in the light of the Brönsted-Christiansen-Scatchard equation:

$$\ln k_s = \ln \underset{\substack{\chi=0 \\ D=\infty}}{k} - \frac{Z_A Z_B \varepsilon^2 N}{DRTr} + \frac{Z_A Z_B \varepsilon^2 N}{DRT}\chi \qquad (1)$$

This equation has been extensively employed by Amis[3-5] in his study of isodielectric and isocomposition activation energies. Here k_s is the observed velocity constant, while $\underset{\substack{\chi=0 \\ D=\infty}}{k}$ is the velocity at zero ionic strength and at an infinite dielectric constant. N is the Avogadro number, D is the dielectric constant of the medium, and r is the minimum distance of approach. χ is the constant which occurs in the Debye-Hückel theory of strong electrolytes; it can be calculated by the following equation:

$$\chi = \sqrt{\frac{8\pi\varepsilon^2 N^2 \mu}{1000DRT}} \qquad (2)$$

By substituting the value of χ into Eq. (1):

$$\log k_s = \log \underset{\substack{\chi=0 \\ D=\infty}}{k} - \frac{Z_A Z_B \varepsilon^2 N}{2.303RTr}\left[\frac{1}{D} - \frac{2\varepsilon Nr}{D^{3/2}}\sqrt{\frac{2\pi\mu}{1000RT}}\right] \qquad (3)$$

If in the above equation the quantity in square brackets is plotted against log k_s, a straight line is obtained the slope of which is equal to:

$$-\frac{Z_A Z_B \varepsilon^2 N}{2.303RTr}$$

TABLE 5

Temperature °C	Dielectric constant D	$k_s \times 10^3$ $l \cdot$ g equiv^{-1} min^{-1} sec^{-1}	$3 + \log k_s$	$\left[\frac{D^{1/2}-x}{D^{3/2}}\right] \times 10^3$
30	77.25	38.24	1.5826	8.162
30	75.15	34.35	1.5359	8.343
30	72.83	31.82	1.5027	8.509
30	70.95	27.68	1.4422	8.662
30	68.44	24.81	1.3947	8.874
35	76.03	55.56	1.7448	8.296
35	74.15	44.34	1.6468	8.441
35	71.67	42.66	1.6301	8.644
35	69.36	38.05	1.5804	8.843
35	67.32	36.14	1.5568	9.024
40	73.38	71.66	1.8553	8.547
40	72.06	67.01	1.8262	8.648
40	69.53	62.13	1.7862	8.874
40	67.16	57.63	1.7606	9.086

3) E. S. Amis and F. C. Holmes, *J. Am. Chem. Soc.*, **61**, 2231 (1941).
4) E. S. Amis and S. E. Cook, *ibid.*, **63**, 2621 (1941).
5) E. S. Amis and J. E. Potts, *ibid.*, **63**, 2883 (1941).

The value of the velocity constant, k_s has been calculated in seconds.

The value of r taken here is quite in accordance with the value of r taken in the reaction between potassium persulphate[5] and the iodide ion. The reaction between persulphate and the iodide ion takes place between bivalent and univalent negative ions; the value of r which Amis and Pottes have taken is 1.76×10^{-8} cm. Therefore, the value of r which we have taken is quite reasonable. By substituting the values;

$\varepsilon=4.8025\times10^{-10}$ e. s. u.; $\boldsymbol{R}=8.31436\times10^{7}$ ergs/deg;

$\boldsymbol{N}=6.023\times10^{23}$ $r=2.65\times10^{-8}$ cm

$\mu=0.18$ $\pi=3.1416$

and $T=(273+30)$, $(273+35)$, and $(273+40)$ into Eq. (3), we obtain for three different temperatures the following equations:

$$\log k_s = \log k - \frac{Z_A Z_B \varepsilon^2 \boldsymbol{N}}{2.303\boldsymbol{R}Tr}\left[\frac{D^{1/2}-x}{D^{3/2}}\right] \qquad (4)$$

$(\chi=0,\ D=\infty)$

where the values of x at three different temperatures (*viz.* 303, 308 and 313) are 3.247, 3.221, and 3.194 respectively.

Table 5 has been reproduced in graphic form (Fig. 1) by employing Eq. (4). The measured slope of the curve and the value of $Z_A Z_B$ obtained therefrom are given in Table 6. From a perusal of Table 6 it is obvious that the product of Z_A and Z_B does not deviate very much from 3. Hence, we may conclude that the rate-determining step occurs between a univalent negative ion and a trivalent negative ion.

TABLE 6

Temperature t°C	Slope	$\frac{\varepsilon^2\boldsymbol{N}}{2.303\boldsymbol{R}Tr}$	$Z_A Z_B$
30	274.4	90.35	3.03
35	256.0	88.86	2.88
40	254.5	87.46	2.91

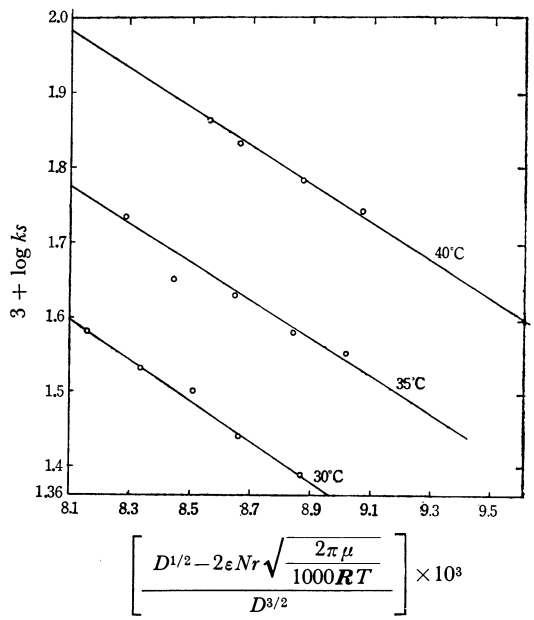

Fig. 1.

One of the present authors (Dr. H. S. Singh) is indebted to the Council of Scientific and Industrial Research, Government of India, for financing the project.

BULLETIN OF THE CHEMICAL SOCIETY OF JAPAN VOL. 41 329—333 (1968)

An Internal-Monitor Method for the Activation Analysis of Silver in Palladium with Thermal Neutrons

Yoshinaga OKA, Toyoaki KATO, Hui-Tuh TSAI and Koichi NOMURA

Department of Chemistry, Faculty of Science, Tohoku University, Katahira-cho, Sendai

(Received May 10, 1967)

An internal-monitor method has been developed to eliminate many of the errors probable with activation analysis. This method involves the measurement of the composed radioactivity of the species to be analyzed and of an appropriate internal-monitor, and the estimation of the ratio of the induced activity of both the species. The present report will describe the principles and the applicability of the method to the determination of a trace amount of silver in palladium by means of thermal neutron irradiation. After the silver activity is chemically separated from the irradiated sample, the γ-ray spectrum corresponding to the mixture of ^{110m}Ag and ^{111}Ag formed by the β^- decay of ^{111}Pd is measured. Synthetic mixtures of silver and palladium with known weight ratios have been prepared to check the accuracy of the method. A good proportionality has been obtained between the ratios of the ^{110m}Ag to ^{111}Ag activities and the ratios of the concentrations. By using this relationship, silver analysis can easily be achieved. Contents of silver in a palladium sample down to about 1 ppm can be determined with a relative error of within $\pm 2\%$. By this method the errors which arise from neutron flux irregularities and self-shielding effects can be avoided, and no correction for chemical yield is necessary.

Although radioactivation analysis has been widely employed as one of the most sensitive analytical methods for the determination of many elements, the errors accompanying this method are usually significant. A comparative technique is used more frequently than the absolute determination method. An important source of errors can be due to a difference in neutron flux between the sample and the reference. Such differences are to be attributed to neutron flux irregularities and to different self-shielding effects in the substances. To correct for these differences, Leliaert *et al.*[1] have developed a method of activation analysis using an internal standard. This method involves the standard addition of the desired element to a portion of the sample. Both spiked and unspiked samples are irradiated, and the specific activity of the desired element is estimated by means of the activity difference. In activation analysis by charged particles or by high-energy photons, errors from the flux inhomogenuities become serious. When the comparative technique is used, therefore, it is difficult to get a good accuracy even when extreme care and effort are taken. To overcome these errors, Oka *et al.*[2] have developed a method using a matrix species as an internal-monitor in non-destructive activation analysis with bremsstrahlung γ-rays.

A second source of error which is likely to be important is the effect of competing reactions. Interferences may proceed either directly or through second-order nuclear reactions.[3] In addition to these nuclear factors, several additional factors can be expected to lead to serious inaccuracies. These are mainly connected with radiochemical and counting processes. The stage of yield correction can give rise to errors, and in the final stage of radioactivity measurement errors due to poor counting statistics can also be considerable. In ordinary activation analysis, thus, errors effected by these sources are accumulated to a significant extent, so that, in most cases, it is difficult to get an accuracy better than $\pm 5\%$. The use of an internal-monitor method can, however, eliminate many of the errors probable with activation analysis. This can be illustrated by the determination of trace silver in palladium by means of thermal neutron activation, with radiochemical separation and subsequent γ-ray spectrometry.

Illustration of the Method

The counting rate of the photopeak, A, due to any induced γ-ray emitter is given by:

1) G. Leliaert, J. Hoste and Z. Eeckhaut, *Nature*, **182**, 600 (1958); *Anal. Chim. Acta*, **19**, 100 (1958); *Talanta*, **2**, 115 (1959).

2) Y. Oka, T. Kato and M. Sasaki, *Nippon Kagaku Zasshi (J. Chem. Soc. Japan, Pure Chem. Sect.)*, **84**, 588 (1963); *ibid.*, **86**, 612 (1965); Y. Oka and T. Kato, *ibid.*, **86**, 835 (1965); *ibid.*, **87**, 1057 (1966); Y. Oka, T. Kato and K. Nomura, *ibid.*, **87**, 147 (1966); Y. Oka, T. Kato and T. Saito, *ibid.*, **87**, 154 (1966); *ibid.*, **88**, 866 (1967); Y. Oka, T. Kato and I. Nagai, *ibid.*, **88**, 871 (1967).

3) R. C. Koch, "Activation Analysis Handbook," Academic Press, New York (1960), p. 10.

$$A = \varepsilon N \phi \sigma S \quad (1)$$

where N=the number of target nuclei, ϕ=flux of the bombarding particle, σ=a reaction cross section, ε=the photopeak efficiency of counting process, and S=the saturation factor.

For two species, I and II, in a homogeneous sample:

$$\frac{A_{\mathrm{I}}}{A_{\mathrm{II}}} = \frac{(\varepsilon N \phi \sigma S)_{\mathrm{I}}}{(\varepsilon' N' \phi \sigma' S')_{\mathrm{II}}} \quad (2)$$

Accordingly,

$$\frac{W_{\mathrm{I}}}{W_{\mathrm{II}}} = K \frac{A_{\mathrm{I}}}{A_{\mathrm{II}}} \quad (3)$$

where the W's are the weights of the target elements and K is a constant.

The ratio of the photopeak activities attributed to these two species is a linear function of the ratio of the concentrations. Hence, the combination of an unknown (I) with a properly chosen internal-monitor (II) allows an accurate determination.

In the case of silver in palladium matrix, it can be assayed by γ-ray spectrometry through the induced ^{110m}Ag in an irradiated sample. Palladium, on the other hand, gives seven radionuclides as (n, γ) reaction products: ^{103}Pd, ^{107m}Pd, ^{107}Pd, ^{109m}Pd, ^{109}Pd, ^{111m}Pd, and ^{111}Pd. However, the major radionuclides are represented by the following sequences:

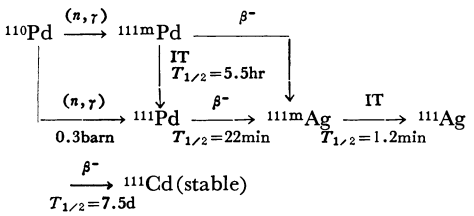

When the silver activity is separated from the irradiated sample, therefore, a composite γ-ray spectrum which corresponds to both the 253-day ^{110m}Ag and the 7.5-day ^{111}Ag as the β^--decay product of ^{111}Pd is measured. By detecting the photopeak activities of both nuclides at an identical time after each irradiation,[4] the following relationship can be obtained:

$$\frac{W_{\mathrm{Ag}}}{W_{\mathrm{Pd}}} = K' \frac{A_{\mathrm{Ag\text{-}110m}}}{A_{\mathrm{Ag\text{-}111}}} \quad (4)$$

Now if R_W is the ratio of concentrations and R_{A_0} is the ratio of the measured photopeak areas related at the end of the irradiation, Eq. (4) becomes:

$$R_W = K' R_{A_0} \quad (5)$$

The constant, K', can be determined by irradiating synthetic mixtures of silver and palladium with known compositions. By using this relationship, it is possible to determine the content of silver in a palladium sample provided that the irradiation period and the counting process are identical to those of the standard mixtures. It is obvious that this internal-monitor method offers several advantages with regard to accuracy and precision over ordinary activation analysis: i) Since results can be calculated on the basis of the activity ratios, the effects of flux irregularities and self-shielding are cancelled out. ii) Since the correction for yield is not necessarily taken into account, the errors arising in this stage can be avoided completely. iii) The effects of the (n, p) and the (n, α) reactions induced by fast neutrons give no trouble.

Experimental

Materials and Irradiation. A series of synthetic palladium-silver mixtures was prepared in the following manner. Fifty milligrams of palladium powder was weighed into a quartz tube with an internal diameter of 6 mm, and then known amounts of an aqueous silver nitrate solution were added. After evaporation to dryness, the tube was sealed. The palladium powder was processed from 99.99% palladium metal as follows. The metal was dissolved in aqua regia, evaporated nearly to dryness, repeatedly evaporated with additional conc. hydrochloric acid, and then subjected to anion exchange purification.[5] Palladium was eluted from a Dowex 1×8 column with an aqueous ammonium chloride-ammonia mixture. The metallic powder was precipitated from this eluate by reduction with formic acid, repeatedly washed with water, and dried in a vacuum. The aqueous silver nitrate solution was prepared by dissolving a reagent purified by repeated recrystallizations. Proper dilution with water was made from this just before use. The hydrochloric acid, nitric acid, and water were all redistilled. All the other chemicals were of a guaranteed grade.

Two kinds of electrolytic palladium plates were tested for their silver contents. From these samples, small pieces of approximately 30 mg were cut out and analyzed. The samples, a series of the synthetic mixtures, and 50 mg of the original palladium powder were put together in an aluminum capsule for pile irradiation. The irirradiation was performed for 72.8hr in the JRR-2 reactor of the Japan Atomic Energy Research Institute. The reactor was operated at 10 MW, providing a thermal neutron flux of 2.5×10^{13} $n/\mathrm{cm}^2/\mathrm{sec}$ at the irradiation site. After the irradiation, the samples were subjected to the radiochemical procedure for the isolation of the silver activities.

Radiochemical Procedure. The radiochemical procedure for the isolation of the silver activities is diagrammed in Table 1.

Separations were performed for each sample after ^{111}Pd had been allowed to decay to ^{111}Ag completely. The final aqueous layer was drained into a polyethylene tube for γ-ray spectrometric measurements.

γ-Ray Measurements. For the γ-ray spectrometric measurements, a $1^1/_2'' \phi \times 1^1/_2''$ NaI(Tl) crystal

4) For comparison, these activities were corrected for decay to the end of the irradiation, as will be described later.

5) W. M. MacNevin and W. B. Crummett, *Anal. Chem.*, **25**, 1628 (1953).

TABLE 1. SEPARATION SCHEME FOR RADIOSILVER FROM IRRADIATED PALLADIUM

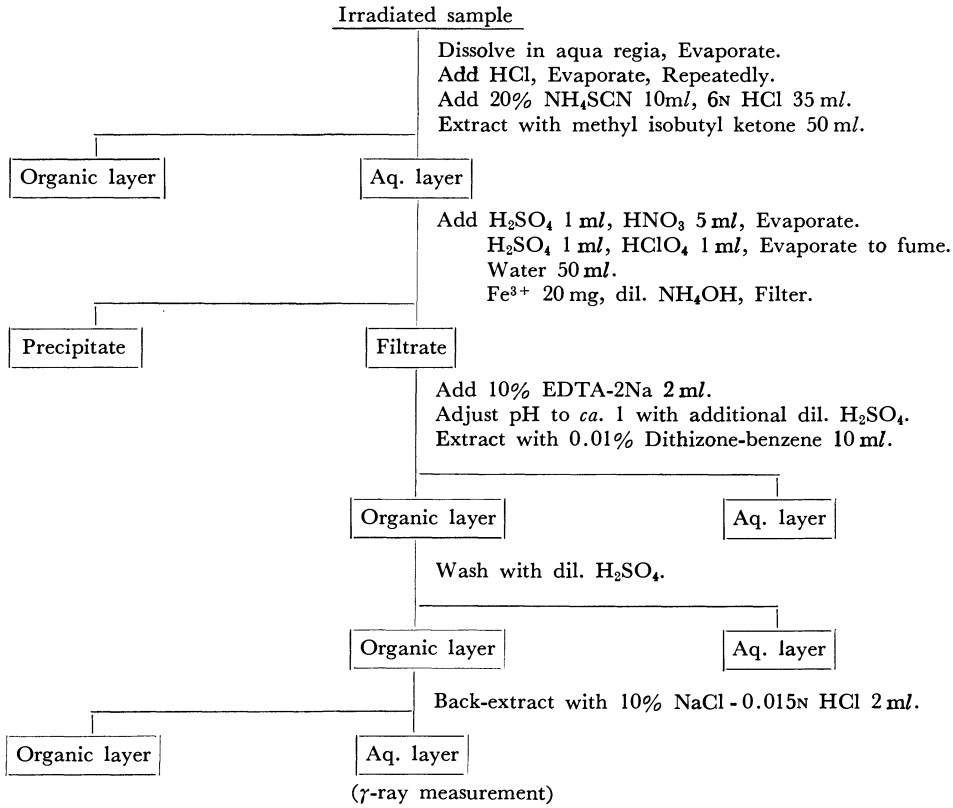

coupled with a 800-channel pulse-height analyzer made by the Tokyo Shibaura Electric Co., Ltd., Japan, was used. The peeling-off method[6] was employed to determine the accurate photopeak areas from the γ-ray spectra obtained.

Results and Discussion

Radiochemical Process. The recovery of radiosilver in each step in Table 1 was studied using ^{110m}Ag as a tracer. The results are shown in Table 2. Although about 27.5% of the radiosilver was coprecipitated with ferric hydroxide, this scavenging technique made possible a successful decontamination from other radionuclides.[7]

TABLE 2. RECOVERY OF SILVER ACTIVITY IN SEPARATION STEP OF TABLE 1

Chemical step	^{110m}Ag recovery, %			
				Mean
Filtrate in ferric hydroxide scavenging	70.3	75.6	71.6	72.5
Dithizone extraction	98.8	99.7	99.4	99.7
Back extraction with chloride solution	97.5	97.3	96.8	97.2

6) W. S. Lyon, Jr., ed., "Guide to Activation Analysis," D. Van Nostrand Co., Princeton, N. J. (1964), p. 104.

The final recovery was about 70%. In the final chloride solution, a composite γ-ray spectrum which corresponded to the mixture of ^{110m}Ag and ^{111}Ag, as shown in Fig. 1-(1), was obtained. The decay curve followed on the 0.342 MeV photopeak area showed a half-life of 7.5 days, corresponding to the literature value of ^{111}Ag.[8]

R_W *vs.* R_{A_0}. The marked difference in the energy of γ-rays emitted from ^{110m}Ag and ^{111}Ag permits a γ-ray spectrometric determination of silver in palladium. From the composite spectra obtained from silver-palladium mixtures, photopeak areas were measured on the 0.342 MeV γ-rays for ^{111}Ag, and on the 0.656 and 0.885 MeV γ-rays for ^{110m}Ag.

These values were corrected for decay to the end of the irradiation,[9] and the R_{A_0}'s were computed on the basis of the illustration given earlier in this paper. At that time, the correction coefficient for silver in the original palladium, α,[10]

7) This technique was especially effective for the removal of ^{192}Ir .

8) Nuclear Data Sheets, Natl. Academy of Science-Natl. Research Council, Washington, D. C. (1961).

9) For convenience, the ^{111}Ag activities were determined by interpolating the counting rates to the end of the irradiation using a half-life of 7.5 days.

10) The α values obtained under the present conditions were 9.49×10^{-5} from the 0.656 MeV peak and 4.77×10^{-5} from the 0.885 MeV peak.

TABLE 3. R_W *vs.* R_{A_0} FOR SILVER-PALLADIUM MIXTURES

R_W	R_{A_0}		R_W/R_{A_0}	
	From 0.656 MeV peak	From 0.885 MeV Peak	From 0.656 MeV peak	From 0.885 MeV peak
1.73×10^{-4}	2.03×10^{-3}	9.54×10^{-4}	8.53×10^{-2}	1.81×10^{-1}
2.73×10^{-5}	3.24×10^{-4}	1.46×10^{-4}	8.42×10^{-2}	1.87×10^{-1}
1.30×10^{-5}	1.49×10^{-4}	7.02×10^{-5}	8.72×10^{-2}	1.85×10^{-1}
4.02×10^{-6}	4.68×10^{-5}	2.18×10^{-5}	8.60×10^{-2}	1.87×10^{-1}
2.51×10^{-6}	2.87×10^{-5}	1.33×10^{-5}	8.74×10^{-2}	1.89×10^{-1}
		Mean:	8.60×10^{-2}	1.86×10^{-1}
		Std. dev.:	$\pm0.12\times10^{-2}$	$\pm0.03\times10^{-1}$
			($\pm1.4\%$)	($\pm1.6\%$)

TABLE 4. RESULTS OF SILVER ANALYSES

Sample	R_{A_0}		Silver content, ppm			
	From 0.656 MeV peak	From 0.885 MeV peak	From 0.656 MeV peak	From 0.885 MeV peak	Mean	Average
A	8.83×10^{-5}	3.96×10^{-5}	7.5_9	7.3_7	7.4_8	$7.4_5\pm0.0_3$
	8.78×10^{-5}	3.91×10^{-5}	7.5_5	7.2_7	7.4_1	
	8.76×10^{-5}	3.97×10^{-5}	7.5_3	7.3_8	7.4_6	
	8.74×10^{-5}	3.91×10^{-5}	7.5_2	7.2_7	7.4_0	
	8.78×10^{-5}	3.97×10^{-5}	7.5_5	7.3_8	7.4_7	
B	1.54×10^{-4}	6.99×10^{-5}	13.3	13.0	13.2	13.2
	1.55×10^{-4}	7.04×10^{-5}	13.3	13.1	13.2	
	1.56×10^{-4}	6.99×10^{-5}	13.4	13.0	13.2	

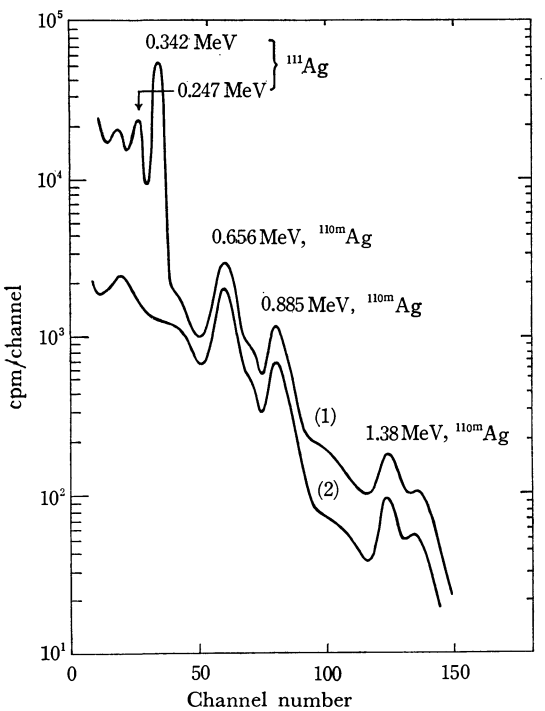

Fig. 1. γ-Ray spectra of radiosilver; (1) separated from irradiated silver-palladium mixture (Ag/Pd = 1.73×10^{-4}), 37 days after irradiation, and (2) standard ^{110m}Ag spectrum.

was introduced in Eq, (4); thus we obtained:

$$\frac{W_{Ag}}{W_{Pd}} = K'\left(\frac{A'_{Ag\text{-}110m}}{A_{Ag\text{-}111}} - \alpha\right)_{t=0} \qquad (6)$$

where:

$$\alpha = \left(\frac{A_{Ag\text{-}110m}}{A_{Ag\text{-}111}}\right)_{original}$$

On the standard series, the relation between the weight ratios and the corrected photopeak activity ratios was calculated. Table 3 shows these experimental results. In each case, a good proportionality was obtained between R_W and R_{A_0}. Relative standard deviations of $\pm1.4\%$ for the 0.656 MeV peak and $\pm1.6\%$ for the 0.885 MeV peak were obtained under the present conditions. The present results show that an accurate determination can be expected when using these relationships.

The separation procedure diagrammed in Table 1 can isolate the silver activity without any contamination of undesired activities; hence, the individual silver photopeak areas were measured with minimum relative errors. When a minimum photopeak area of 50 cpm is selected as the limit of detection, silver contents in palladium down to about 0.8 ppm (0.04 μg in a 50-mg sample) from the 0.656 MeV peak and down to about 2 ppm (0.1 μg in a 50-mg sample) from the 0.885 MeV

peak can be determined with relative errors of within $\pm 2\%$.

Silver Analysis. This method of silver analysis was tested on electrolytic palladium plates. After irradiation, samples were cooled for about 10 days, and then subjected to radiochemical procedure. As Table 4 shows, a good agreement in the silver contents was obtained, indicating satisfactory precision in the method.

Applicability of the Method. In general cases, where the atomic number of the element to be analyzed is higher by one unit than that of the matrix element, and where the nuclear characteristics of the (n, γ) reaction product of the former and the secondary β^--decay product from the latter are favorable for subsequent γ-ray spectrometric measurements, it is possible to use the present method in the determination. For example, the determinations of gold in platinum and of antimony in tin by the thermal neutron activation technique can be performed. Moreover, the technique of combining an unknown with an additional internal-monitor offers a general applicability.

Further application of this method would be found in the activation with high-energy photons by which the neutron defficient radionuclide is formed by the (γ, n) process. This primary product undergoes in the main β^+ and/or EC decay to produce a secondary nuclide. When this secondary activity is combined with the (γ, n) reaction product from the element to be analyzed, it is possible to determine the element in question with an atomic number smaller by one unit than that of the species chosen as the internal-monitor.

BULLETIN OF THE CHEMICAL SOCIETY OF JAPAN VOL. 41 333—342 (1968)

Synthetic Inorganic Ion-exchange Materials. X. Preparation and Properties of So-called Antimonic(V) Acid

Mitsuo ABE and Takuji ITO

Department of Chemistry, Tokyo Institute of Technology, Ookayama, Meguro-ku, Tokyo

(Received June 2, 1967)

The preparation of so-called antimonic acid under various experimental conditions has been investigated in order to establish its usefulness as a chemically-stable cation-exchange material. In this experiment, the antimonic acid was mainly obtained by the hydrolysis of antimony pentachloride, and was rarely obtained from metallic antimony or potassium pyroantimonate. The hydrolyzed precipitate was amorphous at first, but it was gradually transformed into crystalline powder by keeping it in the mother liquor for a long time. The crystallization of the amorphous precipitate was facilitated by raising the temperature within a range of 0—80°C, and by increasing the concentration of strong mineral acid on aging, regardless of the kinds of starting antimony substances. The water-content of the air-dried samples is decreased by increasing the period of aging; the composition of the sample approximates $Sb_2O_5 \cdot 4H_2O$. The crystal of the antimonic acid is cubic and belong to the space group $O_h^7(Fd3m)$, with a lattice constant of 10.38_2 Å. The measurement of solubilities for the air-dried antimonic acid showed that both the amorphous and the glassy acids are soluble forms and that the crystalline is an insoluble form. The uptakes of potassium ions on these antimonic acids were little changed on the kinds of form; the uptake of lithium ions on the crystalline acid was very small as compared those on the amorphous and the glassy acids. This behavior may be attributed to the existence of different types of so-called antimonic acid, with different selectivities of their lithium ion adsorption, rather than to any difference in the size of the particle.

As was first shown in a previous paper,[1] the hydrous oxides of pentavalent metals, such as niobium, tantalum and antiomony, have useful cation adsorptive properties, including a high uptake of potassium ions. The so-called antimonic(V) acid has an especially large adsorption capacity, larger than that of any other metal hydrous oxides, which show a reasonable rate for adsorption and desorption when used in column operations. The adsorption and desorption of potassium ions on the antimonic acid have been found to be attributable to the exchange between the hydrogen ions in the acid and the potassium

1) M. Abe and T. Ito, *Nippon Kagaku Zasshi (J. Chem. Soc. Japan, Pure Chem. Sect.)*, **86**, 1259 (1965).

ions in the external solution in contact with the acid.[2] Furthermore, the mutual separation of alkali metal ions has been completely achieved with a relatively small antimonic acid column ($0.8\phi \times 6.0$ cm).[3]

However, the antimonic acid obtained by the hydrolysis of antimony pentachloride is gradually peptized or dissolved by contact with pure water or with an alkaline solution for a long time.

In this experiment, the preparation of antimonic acid under various conditions is studied in order to obtain a chemically-stable material.

Much pertinent information regarding the antimonic acid or hydrous antimony pentoxide is to be found in the literature pertaining to inorganic chemistry. This information is well summarized in the standard works of Mellor[4] (1929) and Gmelin[5] (1949). Even here, however, some confusion is apparent, and contradictory statements are not hard to find. No comprehensive investigations of the so-called antimonic acid have yet been made. Fremy[6] and Senderens[7] showed that the water-content in the antimonic acid varies according to the kind of starting antimony salt. However, Conrad,[8] Daubrawa[9] and others showed opposite results, according to which a definite hydrate is obtained under the same drying conditions in spite of the different kinds of starting salt. In previous works, much attention had been devoted to determining whether or not several hydrates, such as ortho-($Sb_2O_3 \cdot 3H_2O$), pyro-($Sb_2O_5 \cdot 2H_2O$) and meta-($Sb_2O_5 \cdot H_2O$), well known in the case of hydrated P_2O_5, exist in so-called antimonic acid. Analysis made by Conrad[8], Fremy[6] and others of the air-dried product have given results ranging from 15.77 to 20.02 per cent of water, a figure corresponding with that of the tetrahydrate. The results of the analysis made by Conrad,[8] Daubrawa[9] and Senderens[7] of the product dried over concentrated sulfuric acid show 12.87—14.53 per cent of water, figures in agreement with that of the trihydrate, $Sb_2O_5 \cdot 3\,H_2O$. According to Daubrawa and others, products dried at 100°C and at 175—200°C possess water contents corresponding with dihydrate as pyro-antimonic acid and with monohydrate as meta-antimonic acid. Senderens[7] regarded the trihydrate as ortho-antimonic acid. However, the dehydration curves of the hydrate obtained by the hydrolysis of the pentachloride were found by Simon and Thaler[10] to be of the continuous type, with the characteristics of hydrated metal oxides of the hydrogel type. Therefore, they question the existence of the above-mentioned stoichiometrical composition shown by Daubrawa[9] and others. Fremy[6] found that the tetrahydrate obtained by the hydrolysis of antimony pentachloride, and that obtained by the action of mineral acid on a solution of the alkali antimonate, have different properties. The former was said to be dissolved in a large amount of water, and to be precipitated by acid from an aqueous solution. Its precipitate was dissolved in concentrated ammonia, whereas that obtained from the latter acid was not so dissolved. Conrad, Beilstein, and Bläse showed, however, that there is no real difference between the two products.[4] Senderens and Delacroix agreed that a soluble and an insoluble form of antimonic acid existed, and they called them ortho-antimonic acid and pyro-antimonic acid; however they differed as to which was which.[4] Simon and Thaler proved that hydrated antimony pentoxide crystallized when heated with water under pressure.[10] The product gave a definite indication of the existence of $3Sb_2O_5 \cdot 5H_2O$, which had a point of inflection.

It appears that such confusion as is indicated in the above information regarding the hydrous antimony pentoxides is mainly due to uncertainty concernig the preparation and the resulting properties of the oxides.

In the present experiment, much attention was given to the temperature of the hydrolysis, the effect of aging, and the concentration of acids.

Preparation

Hydrolysis of Antimony Pentachloride. When liquid antimony pentachloride is added to a large amount of water, an irregular precipitate is easily obtainable by means of a violent hydrolysis and a simultaneous exothermic reaction. Hence, a concentrated antimony pentachloride solution was prepared, liquid antimony pentachloride being dropped into the same volume of cold distilled water; the mixture was then hydrolyzed in a large amount of water at the prescribed temperature. The precipitate was aged by being kept in the mother liquor for some time at the said temperature. When 30 m*l* of the concentrated solution was hydrolyzed in 1 *l* of distilled water, the acid concentration of the supernatant liquid became a 0.5 N hydrochloric acid solution as a result of a by-product formed by the hydrolysis. The adjustment of the hydrochloric acid concentration to 0.25 or to 1.0 N was carried out, respectively, by dilution with water or by the addition of concentrated hydrochloric acid to the hydrolyzed solution. The precipitated antimonic acid was filtered under suction. When the hydrochloric acid in the

2) M. Abe and T. Ito, *ibid.*, **87**, 1174 (1966).
3) M. Abe and T. Ito, This Bulletin, **40**, 1013 (1967).
4) J. W. Mellor, "Comprehensive Treatise on Inorganic and Theoretical Chemistry," Vol. IX, Longmans, Green and Co., Ltd., London (1929).
5) L. Gmelin, "Handbuch der anorganischen Chemie," 8th ed. Vol. 18 (1949).
6) E. Fremy, *Ann. chim. phys.*, **23**, 304 (1848).
7) J. B. Senderens, *Bull. Soc. Chim.*, **21**, 48 (1899).
8) C. P. Conrad, *Chem. news*, **40**, 189 (1879).
9) H. Daubrawa, *Ann. Chem. Liebigs*, **186**, 118 (1877).
10) A. Simon and E. Thaler, *Z. anorg. Chem.*, **161**, 116 (1927).

precipitate has almost all been washed away, the antimonic acid passed through fine filter-paper (such as Toyo filter paper 5C) by the peptization. Therefore, it was impossible to wash the antimonic acid until free from chloride ions by the filtration process. Very pure antimonic acid was obtained by washing the precipitate with cold water with the aid of a centrifuger operated at about 10000 rpm; as a result of this treatment, the metamorphosis of the precipitates was avoided. These products were dried at room temperature by the aid of a fan, then they were transformed into granular materials which were suitable for column operation.

Other Preparations. 1) S_{K-1}. A solution of 1.5 *l* of potassium pyroantimonate (32 g/*l*) was vigorously stirred, drop by drop, the same volume of 6 N nitric acid at 25—30°C. The precipitate was then kept in the mother liquor for 3 days at the same temperature. The potassium ions in the liquor were thus tenaciously adsorbed in the precipitate, they could not be removed only by washing with distilled water, though they could be remove by repeated washings with 2 N nitric acid. The precipitate was then washed with distilled water until it was free from nitric acid by means of a centrifuger, and dried in air using a fan.

2) S_{K-2}. A normal nitric acid was vigorously stirred into the above-mentioned potassium pyroantimonate solution at 25—30°C, and then the pH of the mother liquor was adjusted to 1 by dilution. The precipitate was kept in the mother liquor for 4 hr at 25—30°C, and then washed and dried in the same manner as S_{K-1}.

3) Sb-1 and Sb-2. The antimony metal (99.999%) (30 g) was dissolved in 150 m*l* of a mixed solution of $HCl+HNO_3$ (4 : 1). The solution was hydrolyzed and aged in 2 *l* of water at 20°C (Sb-1) or 60°C (Sb-2).

4) S_G. It has been known that freshly-prepared antimonic acid in a wet state can be dissolved in a large amount of water; the solution gradually becomes turbid when kept for a long time. To avoid such turbidity, the following treatment must be completed in a relatively short time; the amorphous precipitate in a wet state is rapidly dissolved in 300 m*l* of hot water. A glassly material was obtained by evaporating the moisture in the solution after cooling.

5) S_{200} *and* S_{300}. The above-mentioned fresh precipitate (10 g) was suspended in 100 m*l* of distilled water and then heated at 200 or 300°C for 4 hr under presure. The S_{200} sample was obtained as a fine crystalline powder, while the S_{300} sample was obtained as a thin hexagonal crystal.

Uptake of Lithium and Potassium Ions. Our previous report showed that when the antimonic acid was added to a neutral solution, hydrogen ions in the material were equivalently liberated as a result of exchange with the cation in the external solution. The measurement of the uptakes of lithium and potassium ions were made by both batch and column techniques, neutral solution of the corresponding salts being used. Each solution containing the liberated hydrogen ions was titrated with a standard 0.1 N sodium hydroxide solution.

Solubilities of Antimonic Acid. The solubilities of the antimonic acids were determined in various reagents. The procedure for determining the solubilities was as follows; the sample (0.4 g) of 100—200 mesh size was put into a 200-m*l* bottle equipped with a glass stopper, and then 100 m*l* of the reagent was added. The bottle was kept in a thermostated bath set at 25±0.05°C for a period of 1 to 10 days and shaken from time to time. The dissolved amount of the antimonic acid was measured by the polarographical method in 3 N hydrochloric acid, after the Sb^{5+} in the suppernatant liquor had been reduced to Sb^{3+} with a sodium sulfite solution.

X-Ray Examinations. The X-ray diffraction patterns of all the sample were measured with a Rigaku Denki Geiger Flex X-ray Diffractometer, filtered Cu$K\alpha$ being used.

Result and Discussion

Composition of So-called Antimonic Acid. The precipitates of the antimonic acid obtained by various preparations were dried in air with the aid of slow-moving electric fan. The time-composition curves of the antimonic acid samples are given in Fig. 1. The very rapid initial dehydration may be due to the evaporation of the adherent water in the precipitates, slow dehydration immediately follows, as in the case of the hydrous oxide gel of tin(IV), Zr and Ti. On the amorphous and glassy acid, the slow dehydration continued for a long time. These samples did not show a constant composition even if they were dried for a

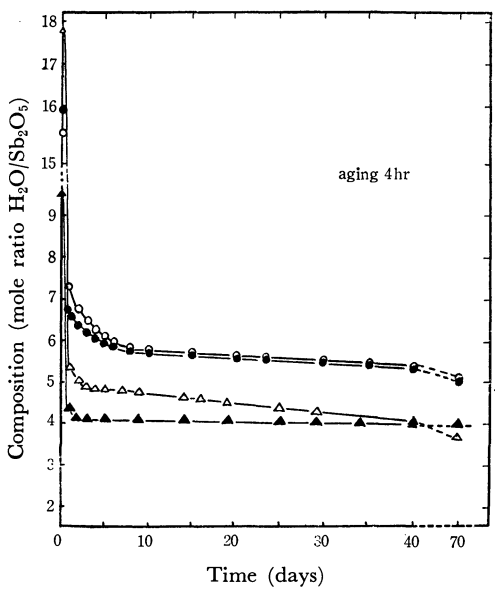

Fig. 1-1. Time-composition curves of precipitated antimonic acid (effect of hydrolyzed temperature).
Hydrolyzed temp. and initial composition of sample:
—○—, 0°C and 13.8 H_2O
—●—, 20°C and 15.4 H_2O
—▲—, 60°C and 7.1 H_2O
—△—, 90—98°C and 29.3 H_2O
All sample aged for 4 hr.

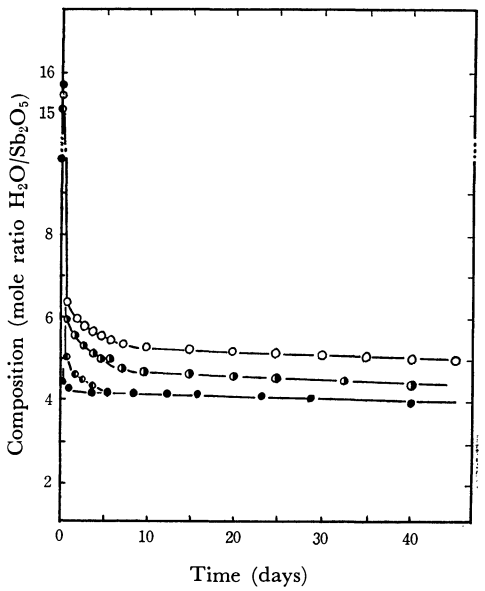

Fig. 1-2. Time-composition curves of precipitated antimonic acids (effect of aging).
Aging: —○—, 1 day —◑—, 3 days
—◐—, 5 days —●—, 7—30 days
Hydrolysis: 25°C

period of about 6 months. In contrast, the samples aged over 7 days at 25—30°C showed an almost constant weight for a relatively short time of about 3 weeks.

The water-composition of the antimonic acids was determined gravimetrically on the assumption that Sb_2O_4 was formed by ignition at 900°C for 2—3 hr. As Table 1 shows, the water-composition (mole ratio of H_2O/Sb_2O_5) obtained by the various preparations was decreased by raising the temperature of hydrolysis and by lengthening the period of aging. The decrease in the H_2O/Sb_2O_5 ratio in antimonic acid was slightly facilitated by increasing the concentration of hydrochloric acid, even under the same aging conditions. These values of the water-compositions agree with those reported by Simon and Thaler. When the sample was obtained by hydrolysis at 20°C and then aged at 70°C for 4 hr, the water-composition was almost the same as that of the sample which was hydrolyzed at 70°C and aged for 4 hr at the same temperature.

The samples aged for a long period of more than 7 days had a definite composition of $Sb_2O_5 \cdot 4H_2O$. The results of other preparations, such as S_{K-1}, S_{K-2}, Sb-1 and Sb-2, showed phenomena similar to that of hydrolysis of antimony pentachloride.

In the hydrothermic treatment of the freshly-prepared antimonic acid at 300°C, Simon and Thaler showed the formation of a definite hydrate, $3Sb_2O_5 \cdot 5H_2O$.[10] In the present experiment, however, it was shown that a thin hexagonal crystal had a relatively small water-composition, that is, $Sb_2O_5 \cdot 0.49H_2O$. The composition of S_{200}

Table 1. Compositions of antimonic acids by various preparations
(mole ratio H_2O/Sb_2O_5)

1) Effect of hydrolyzed temperature

Hydrolyzed temperature °C	0	20	40	60	90—98
Aging (same temp.)					
1 hr	5.14[A]	5.05[A]	—	4.46[A]	4.50[G]
4	5.05[A]	5.00[A]	5.05[A]	3.76++++	3.65[G]
24	4.91[A]	5.00[A]	4.91+	—	—

2) Effect of aging and concentration of acid (HCl) (hydrolysis and aging at 25—30°C)

Aging (day)	1	3	5	7	10	15—30
Concn. of acid						
0.25 N	5.02[A]	4.75+	4.10++	4.08+++	4.04++++	—
0.50	4.96[A]	4.45+	4.00++	4.09++++	4.07++++	4.07++++
1.0	5.00[A]	4.35++	4.08+++	4.09++++	—	—

3) Other preparations

Treatment	Hydrothermal		$K[Sb(OH)_6] + HNO_3$		Metallic Sb + Aqua regia		Dissolving and drying
Sample No.	S_{200}	S_{300}	S_{K-1}	S_{K-2}	Sb-1	Sb-2	S_G
H_2O/Sb_2O_5	2.57	0.49[H]	4.00++++	4.70[A]	5.15[A]	3.70++++	4.16[G]

A: Amorphous, G: Glassy material, H: Thin hexagonal crystal
Crystallization to cubic system increases in the following order: +, ++, +++ and ++++.
All the samples were dried for a period of 6 months at room temperature.

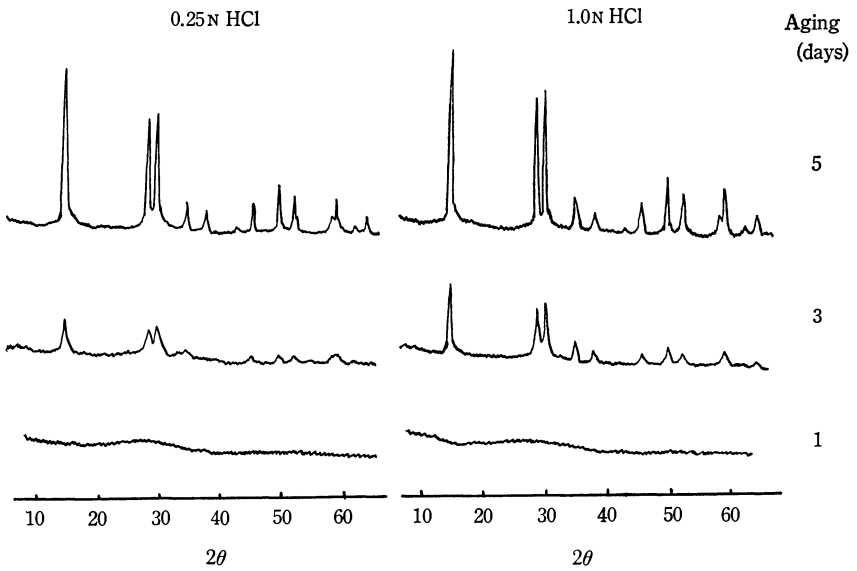

Fig. 2. Comparison between crystallization in 0.25 N and 1.0 N acid solution.

Table 2. Comparison of the crystalline antimonic acid with corresponding hydrated antimony pentoxides in the cards of the A.S.T.M. file of X-ray diffraction data

	(1) $Sb_2O_5 \cdot 4H_2O$		(2) $Sb_2O_5 \cdot 3H_2O$		(3) $Sb_2O_5 \cdot H_2O$		(4) Sb_2O_5		(5) Sb_2O_5		(6) Sb_2O_5	
h k l	*d*(Å)	I/I_0	*d*(Å)	I/I_0	*d*(Å)	I/I_0	*d*(Å)	I/I_0	*d*(Å)	I/I_0	*d*(Å)	I/I_0
1 1 1	5.985	100			5.90	40	5.91	20	6.0	100	5.952	27
3 1 1	3.128	70	3.09	40	3.08	40			3.10	80	3.108	22
2 2 2	2.995	75	2.96	60	2.95	60	2.96	60	2.97	80	2.976	100
4 4 0	1.836	31	1.81	80	1.81	80	1.81	80	1.82	50	1.821	24
6 2 2	1.565	24	1.55	100	1.54	100	1.54	100	1.55	36	1.553	29
8 4 0	1.161	7	1.14	70	1.14	80	1.14	70	1.15	4	1.152	8
$\bar{a}$(Å)	10.38_2		10.2		10.2		10.2		10.3		10.305	
A.S.T.M. No.			2-1383		2-1386		2-1385		1-0154		11-690	

$\bar{a}$: lattice constant
(1): Present experiment, with Cu, 1.5405 Å at 25°C
(2) to (4): Natta and Baccaredda, with Mo, 0.7107 Å[12]
(5): Hanawalt and Rinn, with Mo, 0.709 Å[11]
(6): National Bureau of Standards, with Cu, 1.5405 Å at 26°C[13]

showed an intermediate value between those of S_{300} and the other dried samples.

X-Ray Examinations of Antimonic Acid. The X-ray diffraction paterns of the antimonic acids obtained by the hydrolysis of antimony pentachloride ranged from completely amorphous patterns to those containing a number of distinct reflections, as Figs. 2 and 3 show. The antimonic acids obtained by hydrolysis at 25°C began to crystallized after having been aged for a relatively long time at 25—30°C; the identical diffraction intensity was also shown after aging for a period of more than 10 days. The extent of the crystallization corresponded well with the change in the water-composition of the antimonic acid. Therefore, the results showed that the H_2O/Sb_2O_5 ratio of these acids decreased in proportion to the extent of crystallization.

The crystallization of the antimonic acids was facilitated by raising the temperature when the hydrolysis and the aging were carried out below 80°C. The extent of the crystallization of the sample obtained by hydrolysis at 60°C, followed by aging for 4 hr at the same temperature, was shown to be similar to that of another sample obtained by

11) J. D. Hanawalt and H. W. Rinn, *Ind. Eng. Chem., Anal. Ed.*, **18**, 310 (1946).
12) G. Natta and M. Baccaredda, *Gazz. chim. ital.*, **66**, 308 (1936).
13) H. E. Swanson, M. I. Cook, E. H. Evans and J. H. deGoot, *N. B. S (U.S.A) circ.*, **539**, Vol. 10, 8 (1960).

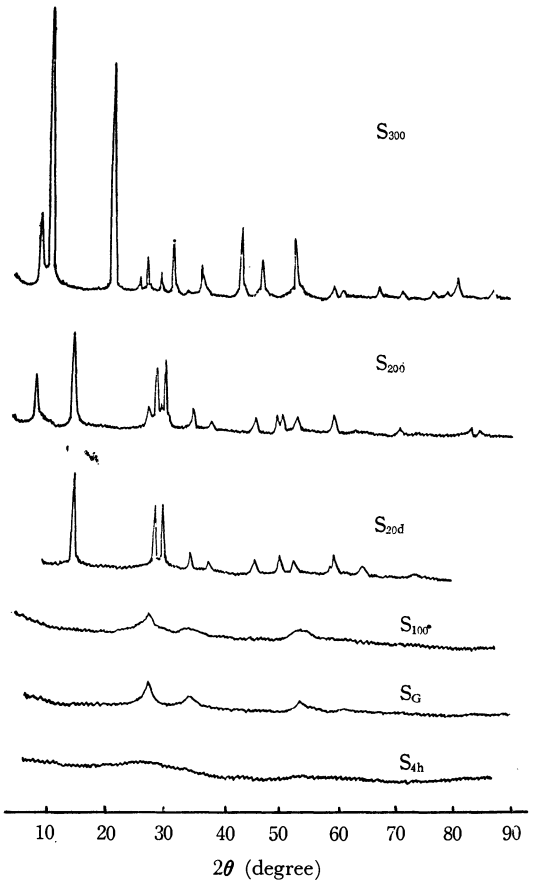

Fig. 3. X-Ray diffraction patterns of precipitated samples by various preparations.

hydrolysis at 25°C and by aging for 7 days at 30°C. Therefore, it seems that the crystallization of antimonic acid is facilitated by raising the temperature of the aging rather than that of the hydrolysis. The sample with a higher crystallization was shown to be a definite hydrate, $Sb_2O_5 \cdot 4\,H_2O$ (crystalline antimonic acid).

The comparison between 0.25 and 1.0 N portions of hydrochloric acid solutions on aging showed that the crystallization was facilitated by increasing the concentration of the acid. Similar results were observed in the samples obtained by other methods of preparation at temperature below 80°C.

The glassy sample produced by hydrolysis at 90—98°C was largely amorphous, except for the presence of five weak reflections (d: 3.28, 2.63, 1.72, 1.64 and 1.38 Å), indicating the presence of a new compound in a form different from the above-mentioned crystalline antimonic acid (Fig. 3).

The X-ray diffraction pattern of the S_G sample, which was made by treating prepared antimonic acid with hot water, was analogous to that of the glassy sample. The sample treated under a given pressure at 200°C showed a mixed pattern, composed of reflections indicating the crystalline antimonic acid and of reflections indicating an unknown material. The S_{300} sample showed a pattern different from that of any other prepared samples.

The X-ray diffraction data of the crystalline antimonic acid are compared in Table 2 with those of a number of antimony compounds indexed on the relevant cards published by the American Society for Testing Materials (A.S.T.M.). All of these substances belong to the same space group O_h^7 ($Fd3m$). The data relative to the crystalline antimonic acid are essentially similar to those of the Sb_2O_5 reported by Hanawalt and Rinn.[11] However, it seems that the conditions of

Table 3. X-ray powder diffraction data for crystalline antimonic acid
(Cu$K\alpha$ 1.5405 Å, at 25°C intensity estimated by diffractometer)

$h\ k\ l$	d(Å)	I/I_0	a^*(Å)
1 1 1	5.985	100	10.366
3 1 1	3.128	70	10.374
2 2 2	2.995	75	10.375
4 0 0	2.594	15	10.376
3 3 1	2.381	11	10.379_5
4 2 2	2.119	2	10.380_9
5 1 1	1.998_4	17	10.382_9
4 4 0	1.835_8	31	10.384_8
5 3 1	1.754_8	22	10.381_5
5 3 3	1.583	11	10.380_4
6 2 2	1.565_2	24	10.382_4
4 4 4	1.498_3	6	10.380_5
7 1 1	1.453_8	12	10.382_2
7 3 1	1.351_6	12	10.381_8
8 0 0	1.298	3	10.384
7 3 3	1.268_4	1	10.382_3
8 2 2	1.223_3	1	10.380
7 5 1	1.198_7	4	10.381
6 6 2	1.190_7	8	10.380_3
8 4 0	1.160_8	7	10.382_5
9 1 1	1.139_5	5	10.381_3
9 3 1	1.088_3	4	10.381_7
8 4 4	1.059_7	4	10.382_8
9 3 3	1.043_4	3	10.381_7
9 5 1	1.003_5	4	10.380_3
10 2 2	0.9989	6	10.381
9 5 3	0.9677	2	10.377_4
11 1 1	0.9362	1	10.383_0
8 8 0	0.9174	1	10.379_2
11 3 1	0.9070	5	10.381_1
11 3 3	0.8807	4	10.383_3
10 6 2	0.8776	8	10.383_9
12 0 0	0.8652	5	10.382_4
11 5 1	0.8566_5	2	10.386_2
11 5 3	0.8337_8	3	10.380_5
12 4 0	0.8209	4	10.383_6

$\bar{a} = 10.38_2$ Å

a^*; lattice constant

preparing its antimony pentoxide were uncertain. According to Natta and Baccaredda,[12] hydrated antimony pentoxide prepared by the decomposition of potassium pyroantimonate with nitric acid was at first amorphous, but after 5 years it became a crystalline substance, $Sb_2O_5 \cdot 3H_2O$ and then after 10 years changed to another crystalline substance, $Sb_2O_5 \cdot H_2O$. The elementary cells of the hydrated Sb_2O_5 had lattice constants of 10.21—10.25 Å and belonged to the cubic system with the space group O_h^7, like cubic Sb_2O_3 (senarmontite).

The accurate lattice constant of the crystalline antimonic acid was determined by means of a Phillip X-ray diffractometer (Table 3). All the data were calibrated by standardized metallic silicon; they showed a lattice constant of 10.38_2 Å, which is larger than any other data listed in Table 2. The X-ray diffraction data of the crystalline antimonic acid were essentially identical in molecular crystal forms with the modification of Sb_2O_3 expressed by the mineral" senarmontite". The symmetry of the antimony trioxide is cubic, with a unit containing 16 molecules, and the structure consists of Sb_4O_6 molecules packed together in a unit cell in the same manner as the carbon atoms in a diamond.[14] The structure of the crystalline antimonic acid is probably similar to that of cubic antimony trioxide. The X-ray diffraction patterns of other crystalline powdered samples, such as S_{60}, $S_{K\text{-}1}$ and Sb-1, showed that in spite of different kinds of starting salt they were identical with that of the crystalline antimonic acid obtained by aging for a long time.

The freshly-prepared antimonic acid can be dissolved in pure water, but the solution becomes turbid and then a white precipitate appears. The X-ray investigation of the precipitate revealed the same compound as the crystalline antimonic acid.

Solubilities of Various Antimonic Acids in Water. As has been previously explained, there is contradictory information and confusion regarding the solubility of antimonic acid. The wet precipitate of pure antimonic acid is easily dissolved or peptized, but it becomes difficult to dissolve the acid dried for a long period. Such a phenomenon is similar to that observed in a number of hydrous oxide gels, such as stannic and zirconium hydrous oxide gel.

The physicochemical solubility must, in general, be determined in an equilibrium state. However, it is difficult to establish the conditions for determining the solubilities of the hydrous oxide because of the depolymerization or hydration which occurs in the oxides. In the present experiment, the solubilities of various antimonic acid sample were measured in order to examine the chemical stabilities with a view to their use as exchangers.

Three dried samples—a crystalline sample, S_{20d} aged for 20 days, an amorphous sample, S_{4h} aged for 4 hr at 25—30°C, and a dry sample, S_{4h}', dried S_{4h} in an air bath at 60°C for 24 hr—were studied in order to determine their time-solubility relationship. The S_{20d} and S_{4h} were dried more than 6 months in air at room temperature, just as in the case of the X-ray examinations. The sample S_{4h} was gradually dissolved in water; it took about 2 weeks to be completely dissolved. Such a slow dissolution of the amorphous samples in water may be due to depolymerization involving the hydration from a higher polymer of hydrous antimony pentoxide to a lower one (Fig. 4). The rate of the dissolution of S_{4h}' was slightly slower than that of S_{4h}, but S_{4h}' was completly dissolved after a long period. This is probably due to the fact that S_{4h} was changed to a higher polymer, S_{4h}', by drying at 60°C.

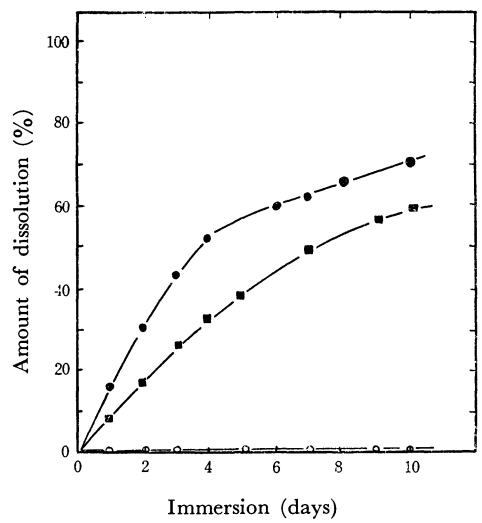

Fig. 4. Time-solubility curves for air-dried samples.
—●—; S_{4h} (amorphous)
—■—; S_{4h}' (amorphous) dried S_{4h} at 60°C for 24 hr
—○—; S_{20d} (crystalline)
Condition; 0.40 g of 100—200 mesh in 100 ml of pure water at 25°C.

The extent of the solubility of the crystalline antimonic acid, S_{20d}, was extremely small as compared with those of amorphous substances; the amount dissolved increased little even when S_{20d} was immersed for a long time. On the semi-crystalline sample aged for 3 days, for example, dissolution and peptization were simultaneously observed. The solubilities of the sample obtained by other methods of preparation (except for that obtained by the hydrothermal teratment) were measured under the same condition. From these results, it is fairly conclusive that the other crystalline

14) R. M. Bozorth, *J. Am. Chem. Soc.*, **45**, 1621 (1923).

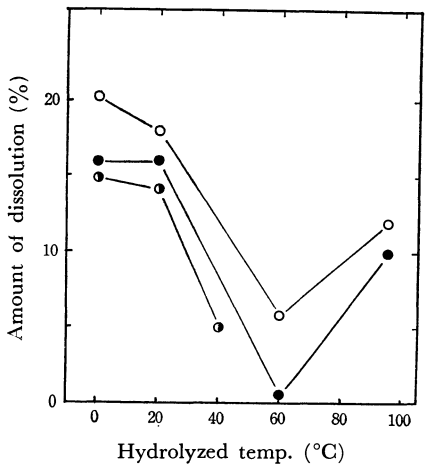

Fig. 5-1. Water-solubilities of the antimonic acids prepared by hydrolysis at various temperature.
Sample: 0.40 g 100—200 mesh of air-dried for 6 mounths.
Immersion: 25°C, 24 hr in 100 m*l* of water
—○—, aging for 1 hr at the same temp.
—●—, aging for 4 hr at the same temp.
—◑—, aging for 24 hr at the same temp.

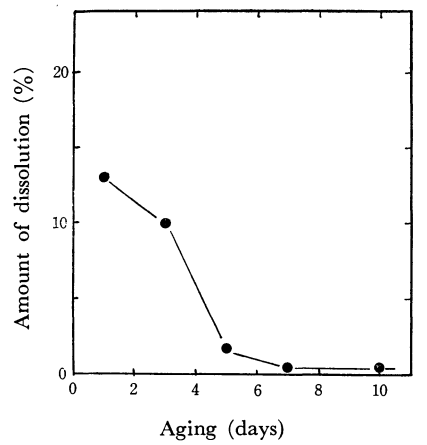

Fig. 5-2. Water-solubilities of the antimonic acids (effect of aging).
Sample: 0.40 g 100—200 mesh of air-dried for 6 mounths.
Immersion: 25°C, 24 hr in 100 m*l* of water.

sample, for example those aged for 4 hr at 60°C, have much smaller solubilities than an amorphous and glassy samples. The solubility of the glassy sample S_G was almost idential with that of the $S_{90°C}$ produced by hydrolysis at 90—98°C.

Consequently, it is evident that amorphous or glassy antimonic acid is a soluble form, while crystalline antimonic acid is an insoluble form. Such soluble and insoluble forms of antimonic acid can be formed by merely establishing suitable conditions for their preparation, regardless of the starting antimony substances.

It seems that the previous confusion regarding antimonic acid is due to the complex conditions of its preparation, such as temperature and the period of aging, the concentration of acid in the solution, and the temperature of the hydrolysis.

Chemical Stabilities. The chemical stabilities of the crystalline acid in common reagent are compared with those of amorphous substances in Table 4; the results are favorable. The soluble samples, both amorphous and glassy antimonic acid, are more stable in a dilute hydrochloric acid or in a neutral salt solution than in pure water or in an alkaline solution. Therefore, it is possible to use them as cation exchangers in these solutions. The crystalline antimonic acid is extremely stable against most reagents, and it is very difficult to dissolve it, even by heating it with concentrated hydrochloric acid; it is dissolved by the presence of potassium iodide. This high degree of stability of the crystalline antimonic acid is one of the important characteristics as an ion-exchange material.

Adsorptions of Lithium and Potassium Ions. Adsorptive properties of a number of hydrous oxides, as is well known, vary with the conditions of preparation, such as aging and hydrolysis.

Simon showed that the adsorptive amount of lithium ions on hydrated antimony pentoxide decreases with a rise in the temperature during the hydrolysis.[15] Our previous report showed that the uptake of potassium ions does not vary in spite of the changes in the temperature on hydrolysis.[2] To explain the difference between Simon's conclusion and ours, the uptake of lithium and potassium ions on various samples was determined by both column and batch techniques.

Table 4. Comparison of chemical stabilities between amorphous and crystalline antimonic acid
Concn. of antimony (mol/*l*) in immersed solution

Reagent	H_2O	1 N HCl	1 N KCl	1 N KOH
Amorphous antimonic acid*1	3.2×10^{-3}	1.8×10^{-3}	4×10^{-4}	4.0×10^{-3}
Crystalline antimonic acid*2	8.0×10^{-5}	4×10^{-5}	$<4\times10^{-5}$	2.5×10^{-4}

Sample taken: 0.4 g; total vol.: 100 m*l*; immersion: 24 hr at 25±0.05°C
*1: S_{4h}, *2: S_{20d} (Both samples were air-dried for 6 months and then sieved through 100—200 mesh.)

15) G. Jander and A. Simon, *Z. anorg. u. allgem. Chem.*, **127**, 68 (1923).

TABLE 5. UPTAKES OF LITHIUM IONS AND POTASSIUM IONS ON VARIOUS SAMPLES (BY BATCH EQUILIBRATION)

Sample No.	S_{1d}	S_{20d}	S_{K-1}	S_{K-2}	Sb-1	Sb-2	S_G	S_{200}	S_{300}
Form*	A	C	C	A	A	C	G	—	H
Li^+ uptake (meq./g)	0.93	0.33	0.34	0.72	0.95	0.30	0.69	<0.02	<0.02
K^+ uptake (meq./g)	1.25	1.29	1.28	1.25	1.23	1.30	1.18	0.80	0.52

Form*: A, amorpous; C, crystalline; G, glassy; H, hexagonal.
Sample taken: 1.00 g of 100—200 mesh size; immersion: 25°C, 48 hr; Alkali metals solution: 0.1 M, 100 ml.

The uptake of lithium ions on the antimonic acid obtained by the hydrolysis of antimony pentachloride was related to the extent of the crystallization of its acid as well as to the solubility. The uptake decreased with the growth of the crystal, as illustrated in Figs. 6-1 and 6-2. In contrast, the uptake of potassium ions was little changed by the difference in the extent of the crystallization. Of the samples obtained by other methods of preparation, the adsorptive properties were similar to those of the hydrolyzed sample. The results are summarized in Table 5. In batch equilibration made by the addition of a neutral salt solution, the uptakes of lithium ions are 0.72—0.92 meq./g on the amorphous antimonic acids and 0.30—0.34 meq./g on the crystalline antimonic acids, while those of potassium ions are 1.23—1.25 meq./g on the former and 1.28—1.30 meq./g on the latter.

The previous investigators regarded a number of freshly-precipitated oxide gels as hydrates of orthohydroxides and thought that the aging process consisted of either a polymerization or a condensation involving the isolation of water from one or more molecules of orthohydroxide, thus producing polyhydroxide of a gradually increasing complexity. They showed that no definite hydrates were actually formed out of the several products composed of the corresponding oxides of various particle sizes with various amounts of adsorbed water, and that the larger particles obtained by aging frequently showed a lower adsorption capacity for ions, a lower capacity responding to the decrease in specific surface. It is very difficult to explain the differences in adsorptive properties between amorphous and crystalline antimonic aicd as being due simply to the variety of particle sizes in these materials. These differences suggest the presence of two types of antimonic acid, with different selectivities of the adsorption for lithium ions.

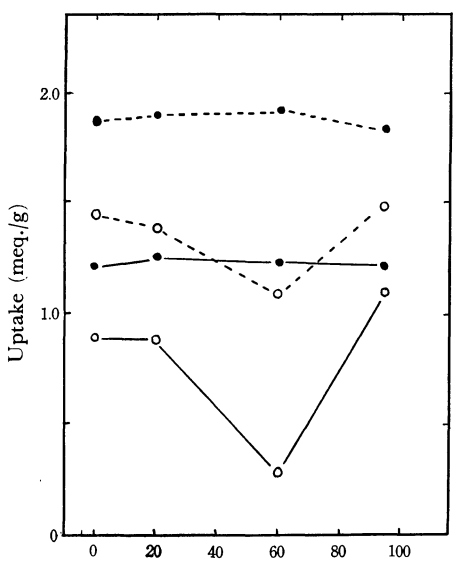

Fig. 6-1. Adsorption of lithium and potassium on the prepared sample by hydrolysis at various temperature.
—●—, K^+ uptake (Batch)
—○—, Li^+ uptake (Batch)
--●--, K^+ uptake (Column)
--○--, Li^+ uptake (Column)

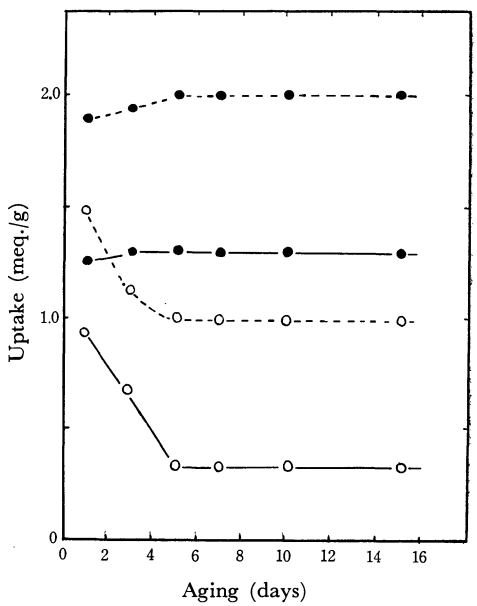

Fig. 6-2. Adsorption of lithium and potassium on the prepared samples by aging.
—●—, K^+ uptake (Batch)
—○—, Li^+ uptake (Batch)
--●--, K^+ uptake (Column)
--○--, Li^+ uptake (Column)

The samples, S_{200} and S_{300}, obtained by hydrothermal treatment, have limited use as cation exchangers, as they show a very small uptake of lithium and potassium ions.

Summary

1) The very pure products obtained by the hydrolysis of antimony pentachloride exist as three different types, amorphous, glassy, and crystalline antimonic acids, according to the different experimental conditions prevailing at temperatures below 100°C.

2) The freshly-prepared precipitate is an amorphous mass at first; it is transformed to a crystalline powder upon aging in contact with the mother liquid for a long period at 25—30°C. The crystallization of the antimonic acid can be facilitated by raising the temperature and by increasing the concentration of the acid in the solution used for aging. The glassy material is obtained by hydrolysis at 80—100°C and by washing and drying.

3) The preparation of this crystalline antimonic acid is accomplished under suitable conditions of temperature, aging, and concentration of acid, regardless of the starting antimony substances.

4) The experiment on the solubilities of the samples in various reagents revealed the presence of two soluble forms and one insoluble form of antimonic acid. The soluble forms are the amorphous and glassy forms, whereas the insoluble form is crystalline.

5) The crystal of the antimonic acid, $Sb_2O_5 \cdot 4H_2O$, has a cubic lattice (space group; $O_h^7 = Fd3m$) with a unit-cell dimension (lattice constant) of 10.38_2 Å, a value which can be deduced from the data for all the diffractions at 25°C.

6) The uptake of potassium ions on the crystalline antimonic acid is scarcely different from those of amorphous and glassy acid, whereas the uptake of lithium ions in the former is very small as compared with those of the latter two acids. Therefore, these results show the presence of more than two types of antimonic acids with different selectivities for lithium adsorption.

7) It has been shown that the sample produced by hydrothermal treatment at 300°C has a smaller water content than the definite hydrate, $3\,Sb_2O_5 \cdot 5H_2O$, reported by Simon and Thaler.[10] A sample with an intermediate water content is easily obtainable at 200°C.

BULLETIN OF THE CHEMICAL SOCIETY OF JAPAN VOL. 41 342—347 (1968)

$Ca_3(PO_4)_2$ - $CaNaPO_4$ System

Jumpei ANDO and Seiichi MATSUNO

Department of Industrial Chemistry, Faculty of Science and Engineering, Chuo University, Bunkyo-ku, Tokyo

(Received June 30, 1967)

As a fundamental research of a calcined defluorinated phosphate containing a small amount of sodium, the system $Ca_3(PO_4)_2$(tricalcium phosphate, T) - $CaNaPO_4$(Rhenanite, R) was studied by high temperature X-ray diffraction, differential thermal analysis, *etc.*, and the phase diagram determined. During heating, T inverted from β to α at 1180°C, and then possibly from α to α' at 1280°C. R inverted from β to α at 690°C. In the composition range containing R from about 10 to 98% by weight, (βT+βR), the stable phase at room temperature, inverted to (βT+αR) at 650°C. The (βT+αR) changed at 980°C to form a compound "A" $Ca_5Na_2(PO_4)_4$ for the sample containing 50.5% R, and ("A"+βT) for samples containing a smaller amount of R. The ("A" +βT) then changed to "A" solid solution at elevated temperatures. The crystals of "A" consisted of a superlattice of αR. "A" and the solid solution changed to αR solid solution at higher temperature. By quenching the samples containing 35 to 50.5% R from 1400°C, a single phase "A" or "A" solid solution was obtained at room temperature. The "A" solid solution was the major phase of the calcined defluorinated phosphate. During heating of samples containing more than 50.5% R, (βT+αR) changed to αR solid solution at or below 980°C; during cooling of the solid solution ("A" + βR) formed at 650°C.

Recently in Japan, and in the United States of America, a large amount of defluorinated phosphate for fertilizer, as well as for animal food, has been produced by the calcination of phosphate ore blended with small amounts of phosphoric acid and sodium carbonate at 1350°C to 1400°C.

Ando[1,2] identified the principal mineral of the phosphate to be a solid solution of a new compound "A" $Ca_5Na_2(PO_4)_4$, and suggested that the crystals of "A" might consist of a superlattice of hexagonal α-$CaNaPO_4$.

The compound "A" is highly soulble in both 2% citric acid, and ammonium citrate. The products of the calcined defluorinated phosphate, however, contained not only "A", but also considerable amounts of β-$Ca_3(PO_4)_2$, which was less soluble.[3]

In the present study, the system $Ca_3(PO_4)_2$-$CaNaPO_4$ was investigated to determine the phase diagram, and to find the optimum condition to increase the "A" content of the calcined defluorinated phosphate.

Experimental

The samples of tricalcium phosphate and Rhenanite were prepared with refined calcium oxide, phosphoric acid, and sodium carbonate by blending and calcination at 1100°C. The samples, and their mixtures in various ratios, were submitted for differential thermal and high temperature X-ray diffraction analyses up to 1450°C. Some fusion tests were carried out in an effort to make a complete phase diagram; however, these tests, were not successful because of the high melting points of the samples (above 1700°C), and the volatilization of sodium at the high temperature.

In another series of tests, the mixtures were heated to 1400°C, cooled at different rates to room temperature, and tested by quantitative X-ray analysis to determine the amounts of the compounds in the products. The lattice constants of "A" and its solid solutions were also determined by X-ray diffraction.

Results and Discussion

Phase Changes. Differential thermal analysis curves taken during heating at a rate of 5°C/min are shown in Fig. 1. The temperatures at which thermal reactions started are plotted in Fig. 2. High temperature X-ray diffraction tests were made during heating and cooling for many compositions including all of those shown in Figs. 1 and 2. Some of the diffraction patterns are shown in Figs. 3 to 6.

Differential thermal analysis was also carried out during cooling. Four examples of the curves taken during cooling at a rate of 5°C/min are shown in Fig. 7, in which phases identified by X-ray tests are indicated. The phase diagram obtained from the above tests is shown in Fig. 8.

During heating, pure tricalcium phosphate (T) inverted from βT to αT at 1180°C, and then showed

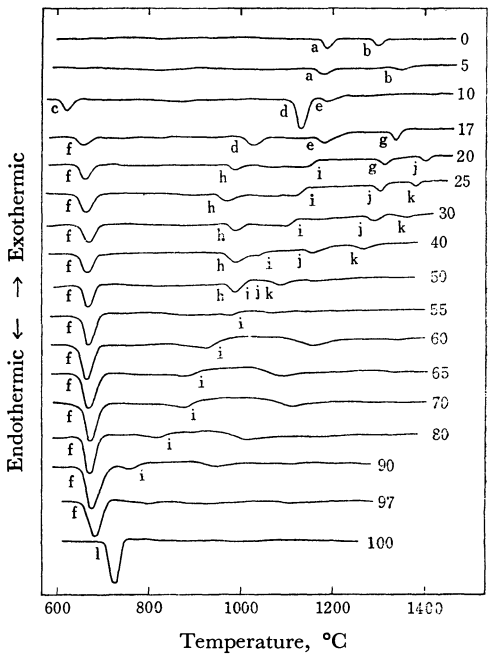

Fig. 1. DTA curves during heating (5°C/min). (Numbers in the figure indicate R content.)

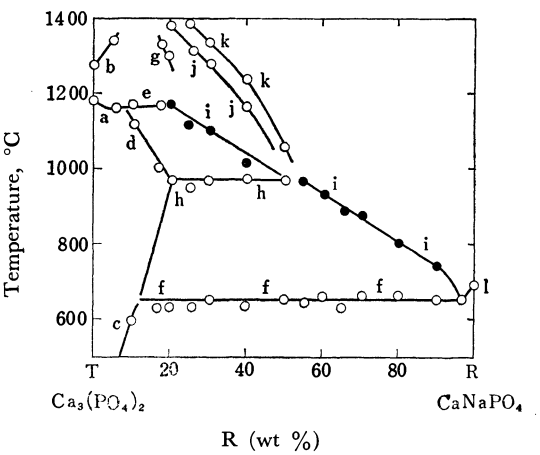

Fig. 2. Temperatures at which thermal reactions started during heating (5°C/min.).
○ endothermic reactions
● slow exothermic reactions

another thermal change around 1280°C. Nurse[4] recently reported the stable presence of α'T at above 1430°C. The present tests, however, did not show any appreciable change around 1430°C. In other tests with tricalcium phosphate produced from phosphate ore containing about 3% R_2O_3, a change occurred around 1430°C. For pure tricalcium phosphate, the inversion between αT and α'T might occur around 1280°C. Pure

1) J. Ando, K. Sumi and Y. Shikatani, *Kogyo Kagaku Zasshi (J. Chem. Soc. Japan, Ind. Chem. Sect.)*, **63**, 1971 (1960).
2) J. Ando, *Reports of Faculty of Engineering, Chuo University*, D-20, No. 74 (1961).
3) J. Ando, Studies on Chemical Fertilizers, Nissin Shuppan K. K., Tokyo (1965), p. 215.
4) R. W. Nurse, J. H. Welch and W. Gutt, *Nature*, **182**, 1230 (1958).

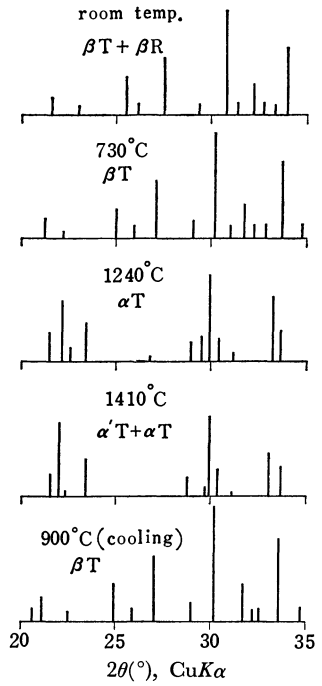

Fig. 3. High temperature X-ray diffraction patterns of the sample containing 10% R.

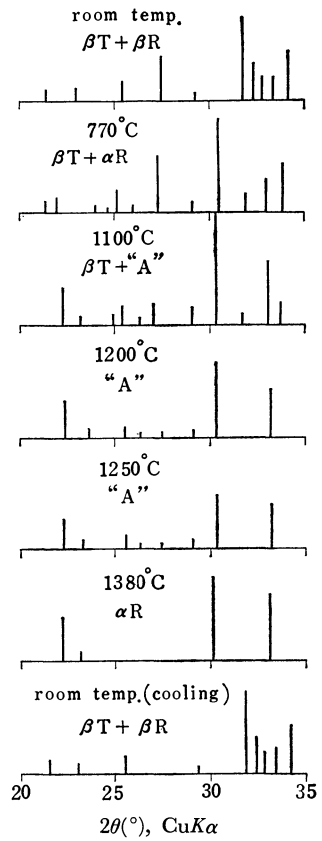

Fig. 4. High temperature X-ray diffraction patterns of the sample containing 30%.

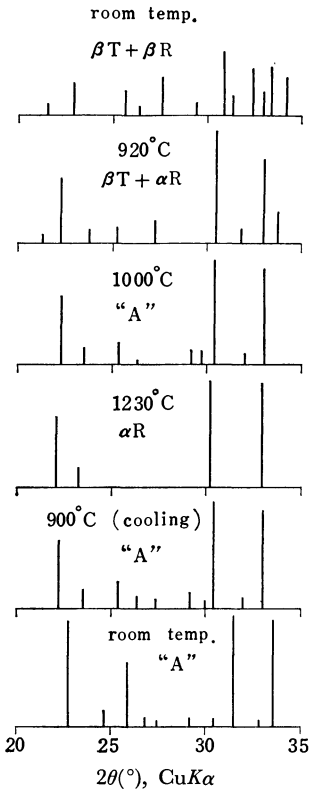

Fig. 5. High temperature X-ray diffraction patterns of the sample containing 50% R.

Rhenanite (R) inverted at 690°C from βR to αR during heating.

Complicated changes occurred for samples blended with T and R. When the R content was less than about 10% by weight, R dissolved during heating into βT to form βT solid solution which then inverted to αT a little below 1180°C. For samples containing 10 to 97% R, βR changed to αR at 650°C to give mixtures of βT and αR.

In the samples containing 20 to 50.5% R, mixtures of "A" and βT formed at 980°C. Larger amounts of "A" with smaller amounts of βT formed as the R content approched 50.5%, where single phase "A" with a stoichiometric composition of $Ca_5Na_2(PO_4)_4$ formed. At elevated temperatures, the βT dissolved into "A" to form "A" solid solution. At yet higher temperature, "A" and the solid solution inverted to αR solid solution.

When the αR solid solution was cooled, "A" solid solution formed again, βT separated during further cooling, and then "A" diminished at 980°C to form αR and βT. The decomposition of "A" occurred more slowly for solid solutions containing a larger amount of R. "A" with the stoichiometric composition, $Ca_5Na_2(PO_4)_4$, decomposed very slowly as will be described later in detail.

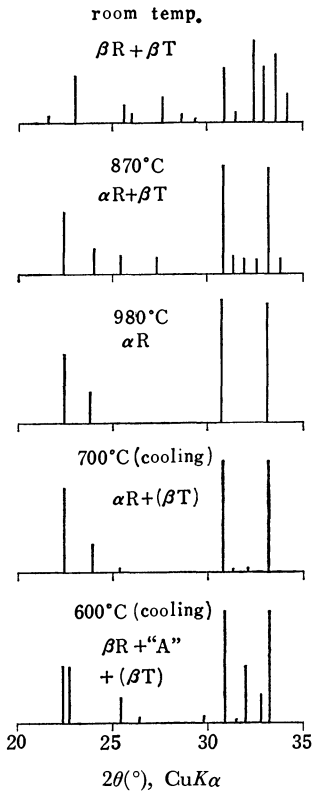

Fig. 6. High temperature X-ray diffraction patterns of the sample containing 70% R. (βT in the parentheses means very minor.)

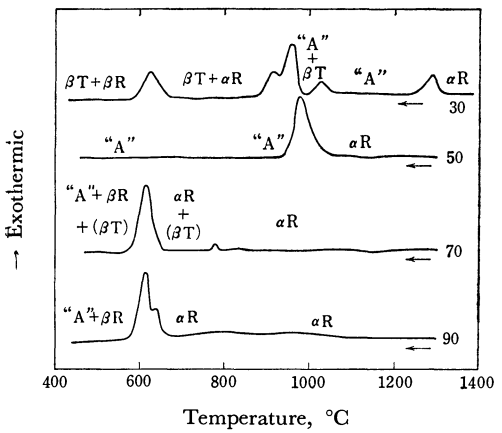

Fig. 7. DTA curves during cooling (5°C/min). (Numbers in the figure indicate R content. βT in the parentheses means very minor.)

In samples containing R from 50.5 to 97%, βT disappeared during heating between 650°C and 980°C to form αR solid solution. The formation of "A" was not detected by high temperature X-ray diffraction during heating.

The phase diagram shows that when the αR solid solution containing 55 to 97% R was cooled,

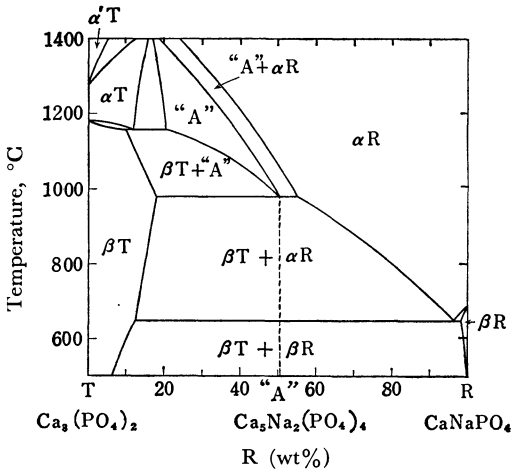

Fig. 8. Phase diagram of the system $Ca_3(PO_4)_2$-$CaNaPO_4$. (In the range containing 50.5 to 97% R, αR solid solution is easily supercooled to 650°C without forming βT, thereby "A" and βR form.)

βT should first form from the solid solution. The rate of formation of βT, however, was so small that appreciable amounts of βT did not form at the cooling rate of 5°C/min. The αR solid solution was thus supercooled down to 650°C, where βR and "A" formed simultaneously and rapidly as shown in Fig. 7.

Mineral Content of the Cooled Products. The mineral content of the samples cooled from 1400°C to room temperature at a rate of 10°C/min is given in Fig. 9.

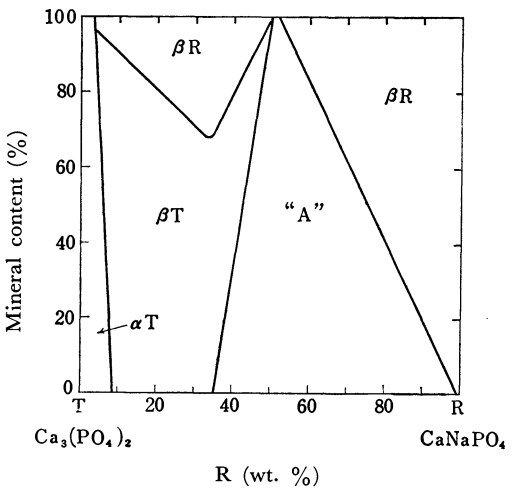

Fig. 9. Mineral content of the products cooled at a rate of 10°C/min.

For a pure sample of T, an α modification was obtained at room temperature because the inversion from α to β was very slow. When a small amount of R was present, the inversion was promoted and mixtures of βT and βR were obtained.

"A" was present in samples containing more than 35% R. The amount of "A" increased to 100% as the R content increased to 50.5%, indicating that the decomposition rate of "A" during cooling was decreased as the R content approached the stoichiometric amount. Samples containing more than 50.5% R consisted of "A" and βR.

Although "A" with the stoichiometric composition was fairly stable, decomposition occurred slowly below 980°C. When "A" was maintained at 850°C, decomposition occurred to the extent of 20% in 20 hr, and to the extent of 80% in 120 hr. The "A" solid solutions containing 35 to 40% R decomposed nearly completely at this temperature in 20 min, but the decomposition was very slow at 500°C.

In an other series of tests, the samples were quenched by air from 1400°C to 500°C in about 30 sec, and to room temperature in an additional 1 min. The mineral content of the quenched products is shown in Fig. 10.

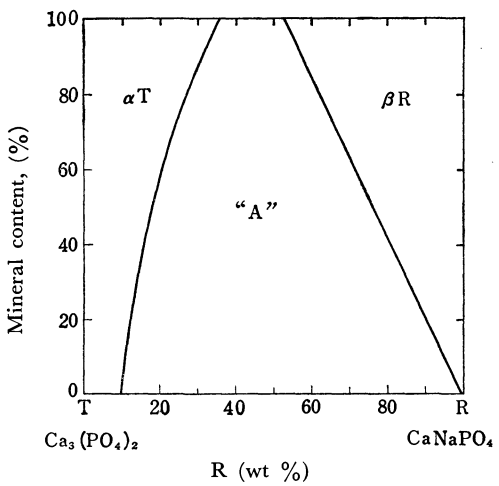

Fig. 10. Mineral content of the quenched products.

Single phase αT was obtained when the R content was less than 10%. Mixtures of αT and "A" were obtained in the range from 10 to 35% R although the phase diagram shows that αT should not form when the R content exceeds 20%. Presumably, the formation of αT in the samples containing 20 to 35% R was peculiar, and due to the rapid cooling from the high temperature at which the αR solid solution was present. Other tests showed that when samples containing 20 to 35% R were cooled rapidly after being kept for a while between 1200 and 1250°C, where "A" was stable, essentially no αT was present in the products while the main mineral "A" was accompanied by small amounts of βT which seemed to have formed from the "A" solid solution during cooling.

Single phase "A" was obtained in the 35 to 50.5% R range. Mixtures of "A" and βR were obtained when the R content exceeded 50.5% in the same manner as shown in Fig. 9.

These results show that to maximize the amount of "A" in the calcined defluorinated phosphate, the raw materials should be blended to maintain an R content of between 35 and 50.5%, and the calcined phosphate should be quenched to below 500°C from the temperature range in which single phase "A" is stable, or from a higher temperature.

Composition and Structure of "A". The X-ray diffraction data of "A" which has the stoichiometric composition, $Ca_5Na_2(PO_4)_4$, are shown in Table 1, and compared with those of pure α-$CaNaPO_4$.[5] The principal diffractions of "A" agree with those of αR, indicating that the structure of "A" is related to that of αR. "A" shows other minor diffractions which are not shown by αR.

The compound "A" contains a smaller number of cations in comparison with αR, $Ca_4Na_4(PO_4)_4$. Apparently "A" has lattice vacancies due to the lack of cations, and the vacant lattice points are arranged to form a superlattice of αR which is fourfold in *a* direction and threefold in *c* direction (Table 1).

At high temperature, the lattice vacancies are disordered by an endothermic reaction resulting in the formation of a lattice which is similar to that of αR except for the presence of the lattice vacancies which are distributed at random, and therefore do not give the typical diffraction lines of "A". When the αR solid solution was cooled, the lattice vacancies were again arranged to form "A" by an exothermic reaction.

It is also quite likely that Nagelschmidtite, $Ca_7Si_2P_2O_{16}$, which is isomorphic with "A", consists of a superlattice of α-Ca_2SiO_4 which is isomorphic with αR.[1,2]

Although the formation of "A" was not detected by X-ray during heating of samples containing more than 50.5% R, as was already mentioned, differential thermal analysis showed that considerable exothermic reactions occurred slowly after βT disappeared to form αR solid solution. For example, exothermic reactions occurred slowly between 930 and 1180°C for a sample with 60% R, and between 750 and 950°C for another sample with 90% R (Fig. 1).

The exothermic reactions may indicate the formation of "A" which has considerable disorder and do not give clearly the typical X-ray diffraction lines of "A". In those samples, the number of lattice vacancies is less than that required to form "A" because of the presence of an excessive R component. The formation of well-arranged "A" thus may not be easy.

During cooling, the imperfect "A", which is similar to the αR solid solution, was easily supercooled down to 650°C. The separation of βR

5) R. Bredig, *J. Phys. Chem.*, **46**, 754 (1942).

TABLE 1. X-RAY POWDER DIFFRACTION DATA OF "A" AND α-$CaNaPO_4$

"A" (Hexagonal $a_0=21.33$, $c_0=21.69$)				α-$CaNaPO_4$ (Hexagonal $a_0=5.23$, $c_0=7.04$)		
I	d(exp.)	d(calc.)	(hkl)	(hkl)	d(exp.)	I
10	8.52	8.50	201			
10	7.05	7.03	202			
10	5.71	5.70	203			
10	4.79	4.79	222			
70	3.892	3.892	403	101	3.82	60
10	3.618	3.614	006	002	3.51	40
40	3.445	3.447	421			
20	3.323	3.325	422			
10	3.152	3.145	423			
10	2.993	2.992	226			
20	2.938	2.935	424			
100	2.845	2.846	406	102	2.78	100
10	2.720	2.711	008			
80	2.666	2.666	440	110	2.62	100
10	2.414	2.414	623			
10	2.330	2.338	408			
10	2.309	2.310	800			
20	2.199	2.199	803	201	2.17	40
10	2.032	2.031	643			
10	1.974	1.975	644			
40	1.946	1.946	806	202	1.91	80
10	1.806	1.807	0012	004	1.77	40

from the solid solution at this temperature resulted in an increase in the number of lattice vacancies in the remaining component which resulted in the formation of "A". Presumably, if the αR solid solution was cooled so slowly that a sufficient amount of βT could first separate from the solid solution, the formation of "A" at 650°C would be depressed.

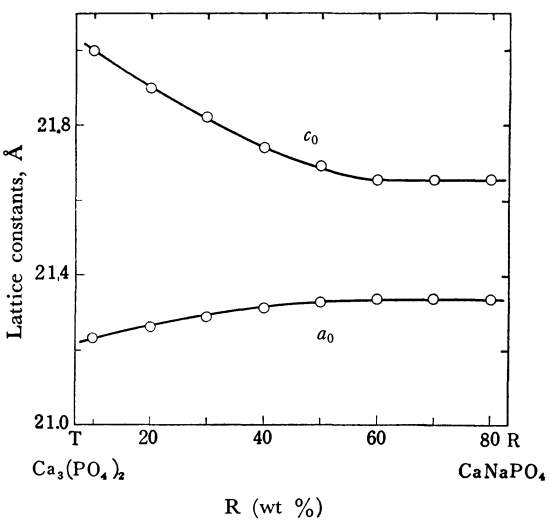

Fig. 11. Relation between R content and lattice constants of "A" and the solid solution present in the quenched products.

The relation between the R content and the lattice constants of "A" and "A" solid solution present in the products quenched from 1400°C is shown in Fig. 11.

The lattice constant a_0 increased slightly, and c_0 decreased remarkably as the R content increased from 10 to 50.5%. Essentially no change was observed when the R content exceeded 50.5%, indicating that the composition of "A" formed in the samples was close to the stoichiometric composition, $Ca_5Na_2(PO_4)_4$, due to the separation of the excessive R component at 650°C.

The "A" solid solution formed in samples containing less than 50.5% R includes more lattice vacancies than required to form "A", because tricalcium phosphate $Ca_6(PO_4)_4$ contains less cations than does $Ca_5Na_2(PO_4)_4$. The rate of the decomposition of the solid solution during the cooling thus increased with decrease in R content, due to the increase in the number of vacancies.

BULLETIN OF THE CHEMICAL SOCIETY OF JAPAN VOL. 41 348—353 (1968)

The Hydration and Crystallization of ρ-Alumina and Alumina-gel in Aqueous Solutions of Various Basic Reagents

Goro YAMAGUCHI and Wen-Chau CHIU

Department of Industrial Chemistry, Faculty of Engineering, The University of Tokyo, Hongo, Tokyo

(Received July 10, 1967)

Alumina gel, boehmite gel, ρ-alumina, η-alumina, and γ-alumina were treated with aqueous solutions of various inorganic and organic reagents at temperatures below 100°C. Boehmite gel, η-alumina and γ-alumina were found to show no change upon this treatment, while alumina gel and ρ-alumina either remained unchanged or changed into fairly well-crystallized boehmite, boehmite gel, gibbsite, bayerite, or nordstrandite, according to the treating conditions. It has been newly established that water-containing pyridine and aniline, the aqueous solution of hydrazine hydrate, and the aqueous solution of *o*, *m*-phenylenediamine are effective in forming fairly well-crystallized boehmite, nordstrandite, and gibbsite respectively.

A precipitate obtained from an aluminum salt aqueous solution by neutralization with ammonia and dried at a low temperature is found to be amorphous by X-ray analysis. The present authors have designated it as "alumina gel." Willstätter[1] had designated such an amorphous gel as C_α-gel; he also designated the precipitate which showed diffused boehmite-like X-ray diffractions as C_β-gel, and the one which showed X-ray diffractions of bayerite as C_γ-gel. He had described the occurrence of these gels as being dependent on the neutralization conditions and said that C_α-gel had a tendency to change into C_β-gel, and then gradually into C_γ-gel. These experimental results have been confirmed by several succeeding investigators. In this paper, C_β-gel will be called "boehmite gel."

Nordstrand[2] found a new aluminum trihydroxide, "nordstrandite," which was different from gibbsite and bayerite in the stacking sequence of its layer structure.[3] Afterward nordstrandite was found to occur in nature[4] and was also synthesized by treating alumina gel with an aqueous solution of ethylenediamine.[5]

Funaki *et al.*[6] studied the aging process of alumina gel and presented a mechanism whereby three crystalline hydrates and one gelatinous hydrate were formed independently. However, they did not describe the favorable conditions for each process.

alumina gel → gibbsite
alumina gel → bayerite
alumina gel → nordstrandite
alumina gel → boehmite gel

As for the aging of ρ-alumina, Tertian[7] reported that ρ-alumina had a tendency to change into bayerite upon rehydration.

In this experiment the present authors aged ρ-alumina and alumina gel with aqueous solutions of organic and inorganic basic reagents at temperatures below 100°C. Boehmite gel, η-alumina, and γ-alumina were also treated under the same conditions, but no reaction was observed with them.

Specimen

Alumina Gel. An $AlCl_3$ aqueous solution of 0.5 mol/*l* was treated with a 14% aqueous solution of ammonia in order to adjust the pH to 8.0. The alumina gel thus obtained was then thoroughly washed and used in the wet state. This gel is amorphous to X-rays and contains about 5 mol of adhered and combined water per mole of Al_2O_3.

ρ-Alumina. Gibbsite was heated at 600°C in a vacuum (below 3 mmHg). The dehydrated

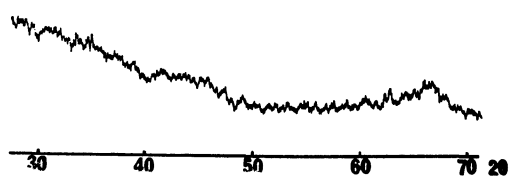

Fig. 1. X-Ray diffraction diagram of ρ-alumina.

1) R. Willstätter, H. Kraut and O. Erbacher, *Ber.*, **58B**, 2449 (1925).
2) R. A. Nordstrand, *Nature*, **177**, 713 (1956).
3) B. C. Lippens, "Structure and Texture of Aluminas," Proetschrift Delft, Netherlands (1961), p. 40.
4) J. C. Hathaway and S. O. Schlanger, *Am. Mineralogist*, **50**, 1029 (1965).
5) U. Hauschild, *Z. Anorg. Allg. Chem.*, **B24**, 15 (1963).
6) Y. Funaki and Y. Shimizu, Preprint for the 12th Annual Meeting of the Chemical Society of Japan (April, 1959).
7) R. Tertian and D. Papee, *J. Chem. Phys.*, **55**, 341 (1958).

alumina thus obtained gives the X-ray diffraction pattern shown in Fig. 1, a pattern which shows only one peak, at $d=1.40$ Å.

Experimental

Hydration. Alumina gel and ρ-alumina were treated with water, an NaOH aqueous solution, an NH_3 aqueous solution, various organic amines, and their aqueous solutions.

Identification. The identification was made by referring to the characteristic equistructural diffraction peaks of gibbsite and bayerite, shown in Fig. 2, and to the superstructural diffraction peaks of nordstrandite, shown in Fig. 3. Boehmite gel was identified from its three broad diffraction peaks, shown in Fig. 4.

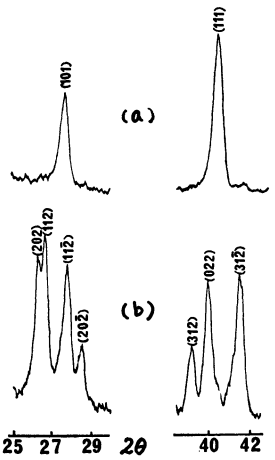

Fig. 2. X-Ray diffraction diagrams of bayerite (a) and gibbsite (b).

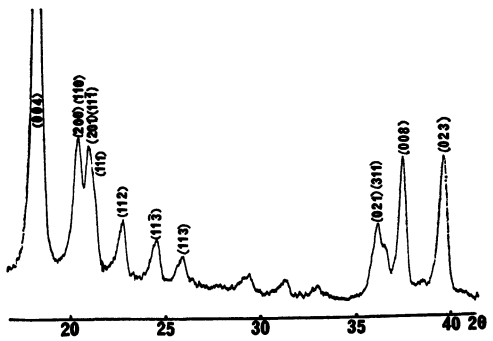

Fig. 3. X-Ray diffraction diagram of nordstrandite.

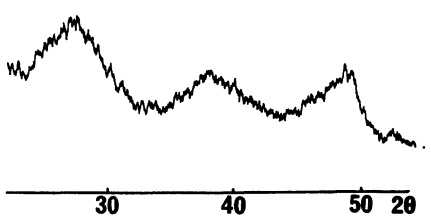

Fig. 4. X-Ray diffraction diagram of boehmite gel.

Results

The conditions of the hydration and the results of identification are shown in Table 1. The X-ray diffraction patterns of some typical specimens are shown in Fig. 5, Fig. 6, Fig. 7, and Fig. 8.

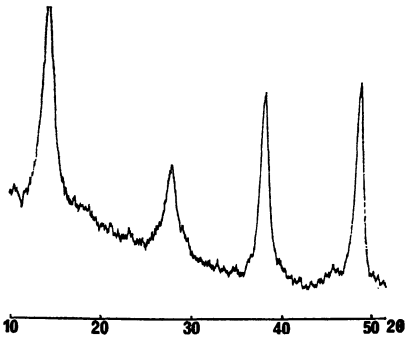

Fig. 5. X-Ray diffraction diagram of boehmite. (Condition: 95% Pyridine aq. soln., ρ-alumina, 70°C, 3 day. No. 39)

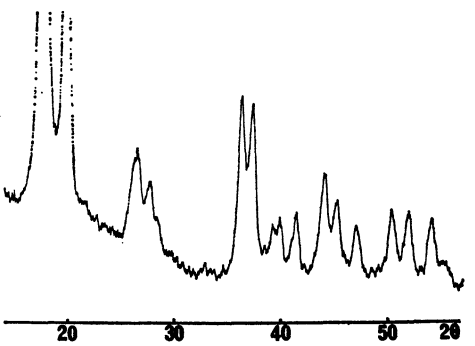

Fig. 6. X-Ray diffraction diagram of gibbsite. (Condition: *m*-Phenylenediamine sat soln., gel, 40°C, 15 day. No. 64)

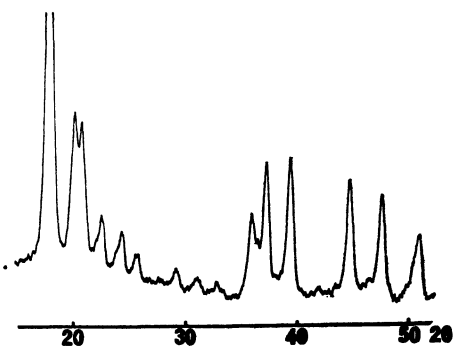

Fig. 7. X-Ray diffraction diagram of nordstrandite. (Condition: 5% Ethylenediamine aq. soln., gel, 40°C, 2 day. No. 69)

TABLE 1

Aging solution		Starting material	Temp. °C	Period day	Result	No.
H_2O	pH≒7	ρ	70, 50, 40 30	3	bo gel + bay	1
				15	bay + sq bo gel	2
			15	15	bay + bo gel	3
		gel	70, 50, 30	3	bo gel	4
			15	10	bo gel	5
	pH≒6		15	60	gel	6
6 N NaOH		gel	70	3	gib + bo gel	7
2 N NaOH					bo gel + vsq gib	8
0.1 N NaOH					bo gel	9
		gel, ρ	50, 30, 15	3	bay	10
NaOH aq. Soln.	pH > 10	gel	room temp.	60	bay	11
	pH = 10—8				bay + nor	12
	pH = 8—7				bay + bo gel	13
14% NH_4OH, 1 N Na_2CO_3		gel	50, 30, 15	3	bay	14
NH_4OH or Na_2CO_3 aq. soln.	pH > 10.5	gel	room temp.	60	bay	15
	pH = 10.5—8.5				bay + nor	16
	pH = 8—7				bo gel + bay	17
$(C_2H_5)_2NH$		gel	70, 60	30	bo	18
			50, 40, 30	3	bay > nor	19
			15	15	bay + sq bo gel	20
50% $(C_2H_5)_2NH$ soln.		ρ	50, 30, 15	3	bay	21
		gel	60	20	bo gel + vsq bay	22
			50, 40, 30	3	bay + bo gel	23
			15	15	bay + bo gel	24
10% $(C_2H_5)_2NH$ soln.		ρ	50, 40, 30	3	bay	25
			15	3	bay + bo gel	26
				15	bay + sq bo gel	27
		gel	50, 40, 30	3	nor + bay	28
5—10% $(C_2H_4OH)_2NH$ soln.		ρ	60, 40, 30	10	ρ + bo gel + sq gib	29
				30	gib + sq bo gel	30
		gel	60, 40, 30	30	bo gel	31
			15	3	gel + bo gel	32
				20	bo gel + bay	33

TABLE 1 (Continued)

Aging solution	Starting material	Temp. °C	Period day	Result	No.
	ρ	70, 50, 30 15	20	ρ	34
	gel	70, 60	30	bo gel	35
		40, 30	3	gel + sq gib	36
			30	gib + bo gel	37
		15	30	bo gel + bay	38
85—95% soln.	ρ	70, 60, 50	3	bo	39
		40, 30	3	bo + ρ	40
			20	bo	41
		15	20	bo gel	42
50% soln.		70, 60, 50	3	bo + sq bay	43
		40, 30	5	bay + bo	44
		15	10	bo gel + sq bay	45
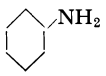		70, 50, 40 15	20	ρ	46
96—97% 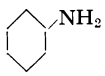 soln.	gel, ρ	70, 60, 50	3	bo + sq bay	47
		40, 30	10	bo gel + sq bay	48
		15	20		
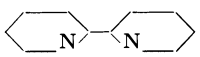 sat soln.	gel	40, 30, 15	20	gel	49
	ρ			bay	50
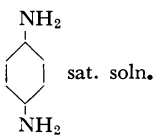 sat. soln.	gel	60	30	gel + sq (bay + gib)	51
		50, 40, 30	3	gel + sq (bay + gib)	52
			15	gib + sq bay	53
		15	3	bay + sq gel	54
			15	bay	55
	ρ	60, 40, 30	3	bay	56
		15	3	bay + ρ	57
			20	bay	58
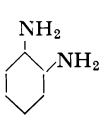 and 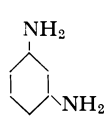 sat. soln.		60, 40, 30	3	bay	59
		15	3	bay + ρ	60
			20	bay	61
	gel	60	30	bo gel	62
		50, 40, 30	3	gel + sq gib	63
			15	gib	64

TABLE 1 (Continued)

Aging solution	Starting material	Temp. °C	Period day	Result	No.
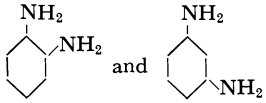 sat. soln.	gel	15	3	bay + sq gib	65
			15	bay	66
$H_2NC_2H_4NH_2$	ρ	70, 50, 30 10	30	ρ	67
1—20% $H_2NC_2H_4NH_2$ soln.	gel, ρ	60	30	nor + bo gel	68
		50, 40, 30	2	nor	69
		15	5	nor (20 days for ρ)	70
0.1% $H_2NC_2H_4NH_2$ soln.	gel	50, 40, 30	30	gel + sq nor	71
5% $H_2NC_2H_4NH_2$ soln. 50 28% NH_4OH soln. 1	gel	40	3	nor	72
$H_2NC_2H_4NH_2$ 1 28% NH_4OH soln. 19				nor > bay	73
$H_2NC_2H_4NH_2$ 1 14% NH_4OH soln. 19				nor ≒ bay	74
$H_2NC_2H_4NH_2$ 1 14% NH_4OH soln. 99				bay + vsq nor	75
30—80% $H_2NNH_2H_2O$ soln.	gel, ρ	60	30	bo + gel + sq nor	76
		50, 40, 30	2	nor	77
		15	10	nor (20 days for ρ)	78
20% $CO(NH_2)_2$ soln.		60	30	bo + sq bay	79
		50, 30, 15	20	bo gel + bay	80
10% $(C_2H_4)(NH)_2(C_2H_4NH_2)_2$ and $NH(C_2H_4NH_2)_2$ soln.	gel	60	7	bo gel + nor + bay	81
		50, 40, 30	2	bay + sq nor	82
		15	2	bay	83
		60	7	bo gel + nor + bay	84
		50, 40, 30	2	nor + bay	85
		15	2	bay + vsq nor	86

gel: wet-alumina gel, ρ: ρ-alumina, gib: gibbsite, bay: bayerite, nor: nordstrandite, bo: boehmite, bo gel: boehmite gel, sq: small quantity, vsq: very small quantity

Discussion and Conclusion

1) Boehmite gel, η-alumina, and γ-alumina did not change under any conditions, so it is clear that they are stable enough under treatment with basic reagents at temperatures below 100°C.

2) Alumina gel and ρ-alumina behaved almost the same under all conditions, but when treated with unhydrous reagents, the different water contents of alumina gel and ρ-alumina were found to cause some differences in their crystallization processes.

3) As for alumina gel and ρ-alumina, the observed phenomena can be classified into the following 6 types:

a. Starting material remains unchanged.
b. Starting material changes into fairly well-crystallized boehmite.
c. Starting material changes into boehmite gel.
d. Starting material changes into bayerite.
e. Starting material changes into gibbsite.

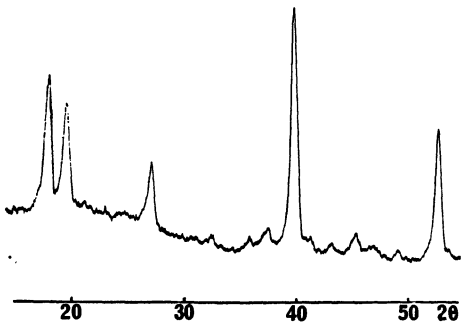

Fig. 8. X-Ray diffraction diagram of bayerite. (Condition: 10% Triethylenetetramine aq. soln., ρ-alumina, 15°C, 2 day. No. 83)

f. Starting material changes into nordstrandite.

4) ρ-Alumina remained unchanged when treated with unhydrous reagents, as in No. 34, No. 46, and No. 67; no similar phenomenon was observed in alumina gel, however since it contains a considerable amount of water. Alumina gel remained unchanged in No. 6 and No. 49. No. 6 shows that the crystallization of alumina gel does not proceed in such a sligtly acidic aqueous solution. The reason for No. 49 is not clear.

5) The "b" phenomena are caused by treating ρ-alumina at rather high temperatures with pyridine and aniline which contain a small amount of water, as in cases of No. 39, No. 40, No. 41, No. 43, and No. 47, and by treating alumina gel with a α, α'-diphenylamine aqueous solution and with aniline which are pure or which contain some water, as in cases of No. 18, No. 22, and No. 47.

From these results, the most favorable conditions for fairly well-crystallized boehmite formation seem to be a rather large solubility of the alumina and a low activity of the water.

6) The "c" phenomena are caused by treating alumina gel with pure water at any temperature and with slightly basic reagents at rather high temperatures, as in cases of No. 4, No. 5, No. 9, No. 31, and No. 35. However, the pure boehmite gel can not be obtained from ρ-alumina under the same treatment except in the cases of No. 1, No. 42, and No. 45.

These results can be attributed to the different solubilities of alumina gel and ρ-alumina. The solubility of ρ-alumina is larger than that of alumina gel. A favorable condition for forming boehmite gel is a rather small solubility. The solubility of ρ-alumina is too large and the temperature conditions of No. 42 and No. 45 are too low for forming fairly well-crystallized boehmite, so boehmite gel has been formed under these conditions.

7) The "d" phenomena are caused by conditions of large alumina solubility, high water activity, and comparatively low temperatures, as in the cases of No. 10, No. 11, No. 14, No. 15, No. 20, No. 21, No. 25, No. 50, No. 55, No. 56, No. 58, No. 59, No. 61, No. 66, No. 83, and No. 86.

The effect of low temperatures on bayerite formation can be sufficiently observed in the cases of No. 10, No. 20, No. 55, No. 66, No. 83, and No. 86. This effect is also observed in the Bayer process, in which gibbsite is formed at higher temperatures and bayerite, at lower temperatures.

The effect of solubility is confirmed from the fact that ρ-alumina changes more easily into bayerite than does alumina gel under the same conditions.

8) The "e" phenomena are found in the cases of No. 7, No. 30, No. 37, No. 53, and No. 64, but only in No. 64 are conditions sufficient for forming pure gibbsite. The conditions of No. 7 somewhat resemble those of the Bayer process; these conditions are a rather larger solubility and a high temperature. The conditions of No. 64, treating alumina gel with an *o, m*-phenylenediamine aqueous solution, constitute a new method for gibbsite formation.

9) The "f" phenomena are found in the cases of No. 69, No. 70, No. 72, and No. 78. The effect of an ethylenediamine aqueous solution had already been established,[5] but that of a hydrazine hydrate aqueous solution is first established by our experiment.

10) The reason why bayerite, gibbsite, or nordstrandite is formed selectively under treatment with a certain basic reagent is very interesting, but it can not be well explained now, remaining as a problem for furture study. This effect is possibly related to the molecular structures of the basic reagents.

BULLETIN OF THE CHEMICAL SOCIETY OF JAPAN VOL. 41 354—358 (1968)

D. C. and A. C. Polarographic Behavior of Thallium(I) Ions in Diethylenetriaminepentaacetate Solutions

Mutsuo KODAMA, Tomohiko NODA and Mitsuko MURATA

Department of Chemistry, Ibaraki University, Mito, Ibaraki

(Received July 12, 1967)

The reduction reaction of Tl(I) ions in DTPA solutions was studied d.c.- and a.c.-polarographically, and the composition and the stability constants of normal and hydrogen chelates of Tl(I) ions with DTPA, TlZ^{4-}, and $TlHZ^{3-}$ were determined. The reduction of Tl(I)-DTPA chelates at the DME proceeds reversibly in the polarographic sense according to this scheme:

$$\begin{array}{ccccc} TlZ^{4-} & + e^- + Hg & \rightleftharpoons & Tl(Hg) & + Z^{5-} \\ {\scriptstyle H^+}\downarrow\uparrow & & & & {\scriptstyle nH^+}\downarrow\uparrow \\ TlHZ^{3-} & & & & H_nZ^{n-5} \end{array}$$

The stability constants of TlZ^{4-} and $TlHZ^{3-}$ were found to be $10^{5.45}$ and $10^{4.24}$ ($\mu=0.40$). The determination of the a.c. summit-potentials, E_p, and the introduction of E_p into the Kolthoff and Lingane equation of polarographic waves of metal complexes were also discussed.

Trace quantities of surface-active substances can often exert a strong effect on the electrode process. In most cases, it has been shown that even minute amounts of surface-active substances present in the background solutions of analytical-grade-reagents are sufficient to change the measured rate of the electrode processes by a factor of 50 and to decrease the height of a. c. polarographic waves quite markedly.[1,2]

For this reason, an electrode reaction which proceeds reversibly in the d. c. polarographic sense cannot always be expected to be reversible under the influence of an alternating voltage.

Gupta and Chatterjee[3] have introduced a. c. polarographic summit-potentials in place of d. c. polarographic half-wave potentials into the Kolthoff-Lingane equation[4] for the reduction of a metal complex ion and have tried to determine the ligand number and the stability constants of the cadmium ammonia complex. However, the introduction they attempted can be safely undertaken only when the electrode reaction is reversible in both d. c. and a. c. polarography.

The theory of the a. c. polarography predicts that the plot of the d. c. potential, E, against $\log[(I_p/I)^{1/2}-((I_p-I)/I)^{1/2}]$ will give a straight line with a $\pm 0.118/n$ V slope for reversible electrode processes. Consequently, the reversibility of the electrode process can be tested by this log-plot, and the summit-potential can be determined to be the potential where the two linear portions intersect; *i. e.*, the $\log[(I_p/I)^{1/2}-((I_p-I)/I)^{1/2}]$ is equal to zero.

The a. c. polarographic behavior of a thallium-(I) ion and its complexes has been known to be apparently reversible, and exceptionally unaffected by the addition of such surface-active substances as gelatin.[5] In view of the fact that the rate constant of the reduction reaction of thallium(I) is markedly decreased by the addition of a surface-active substance, this may indicate that, even in the presence of surface-active substances, the rate constant of the reduction process remains so large that the process behaves reversibly. At the dropping mercury electrode, thallium(I)-DTPA chelate ions also give a single well-defined reversible wave both d. c. and a. c. polarographically. In this study, the electrode reaction of thallium(I)-DTPA chelates was investigated by d. c. and a. c. polarographic methods, and the stability constant of thallium(I)-DTPA chelate and the protolytic stability constant of its hydrogen chelate, $TlHZ^{3-}$, were determined.

Experimental

Reagents. The standard solution of thallium(I) perchlorate was prepared by dissolving a known amount of pure thallium metal in a reagent-grade perchloric acid.

Commercial reagent-grade diethylenetriaminepentaacetic acid (DTPA) was recrystallized from an aqueous

1) B. Breyer and H. H. Bauer, "Alternating Current Polarography and Tensammetry," Interscience, New York (1963), p. 268.
2) N. Tanaka, R. Tamamushi and M. Kodama, *Anal. Chim. Acta*, **20**, 573 (1959).
3) S. L. Gupta and M. K. Chatterjee, *J. Electroanal. Chem.*, **8**, 245 (1964).
4) I. M. Kolthoff and J. J. Lingane, "Polargoraphy," Vol. 1, Interscience, New York (1952).
5) J. E. B. Randles, *Discussions Faraday Soc.*, **1**, 11 (1947).

solution by adding hydrochloric acid, and then dissolved into a sodium hydroxide solution. The concentration of a DTPA solution was standardized against pure metallic zinc.

Apparatus. All d.c. current-voltage curves were measured by using a manual polarograph similar to that of Kolthoff and Lingane[4] and were corrected for the residual current and the *i-R* drop. The a.c. polarograms were recorded with a Yanagimoto PA-102 pen-recording polarograph operated manually. The d.c. potentials applied were accurately determined by using a Shimadzu K-2 potentiometer.

The rate of the flow of mercury, m, and the drop time, t_d, of the dropping mercury electrode (DME) were 1.24_8 mg/sec and 6.30 sec respectively, as measured in an air-free 0.1 M acetate buffer solution of pH 4.80 with an open circuit and at 60 cm of a mercury column at 25°C. A saturate calomel electrode (SCE) with a large area was used as the reference electrode; it was connected to the cell solution through a Hume and Harris-type salt bridge.[6] In the a.c. polarographic measurements, a 200 μF condenser was used to minimize the effect of the cell resistance.[7] The pH value of the solution was measured with a glass electrode pH meter (Hitachi-Horiba Model M4).

The dissolved oxygen in the solution was removed by bubbling pure nitrogen gas through the solution, and all the measurements were conducted on solutions with a constant ionic strength of 0.4 ($NaClO_4$).

Results and Discussion

Reversibility of the Electrode Reaction of Thallium(I) - Diethylenetriaminepentaacetate at the DME. The electrode reaction of thallium(I) ions in solutions containing an excess of DTPA was studied over the pH range from 7.30 to 10.20. In the present study, no other buffer reagent was used because in the pH range studied the system containing an excess of DTPA is considered to have enough buffer capacity to maintain the pH value of the solution constant.

A Tl(I)-DTPA chelate gives a single well-defined d. c. polarogram (Fig. 1); its limiting current was found to be proportional to the square root of the effective pressure of mercury applied to the DME (Table 1) and to the concentration of thallium(I) ions (Fig. 2). The relation between $\log[i/(i_l-i)]$ and E, where i, i_l and E have their usual meanings, gave exclusively a straight line with a slope of 60 mV, corresponding to a one-electron reduction (Fig. 3).

In a. c. polarography, also, typical polarograms were obtained; their summit potentials coincided with the half-wave potential of the d. c. polarogram (Fig. 1). This may mean that the electrode reaction of a Tl(I)-DTPA chelate proceeds reversibly in the a. c. polarographic sense. This conclusion can also be confirmed by the facts that the peak

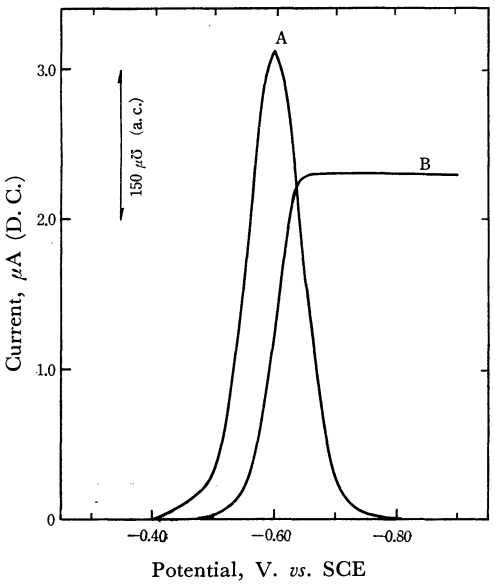

Fig. 1. Polarograms of Tl(I)-DTPA chelate.
pH=8.8, μ=0.40, C_{Tl^+}=1.09 mM
C_{DTPA}=25.0 mM
A: D. c. polarogram, B: A. c. polarogram,
senstivity=6.0 μA/mm

Table 1. The relation between the limiting current, i_l, and the effective pressure, h_c, on the DME
pH=9.88, C_{DTPA}=40 mM, C_{Tl^+}=1.09 mM

h_0, cm	$h_c^{1/2}$	i_l, μA	$i_l/h_c^{1/2}$
50	6.97	2.04_0	0.293
60	7.66	2.24_1	0.293
70	8.28	2.45_0	0.296
80	8.86	2.65_5	0.299

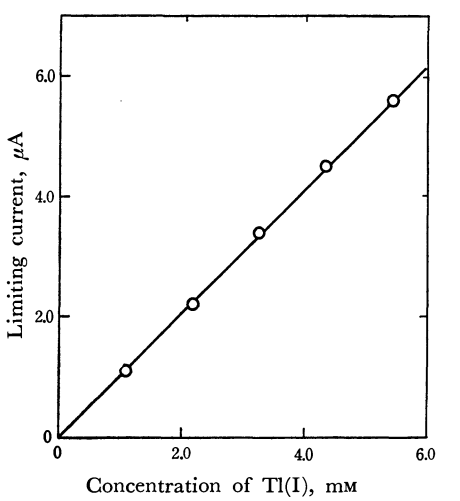

Fig. 2. The relation between the concentration of thallium ion and the limiting current.
pH=9.90, μ=0.40, C_{DTPA}=40.0 mM

6) D. N. Hume and W. E. Harris, *Ind. Eng. Chem., Analyt. Ed.*, **15**, 465 (1943).
7) B. Breyer, F. Gutamann and S. Hacobian, *Australian J. Sci. Res., Ser. A*, **4**, 595 (1951).

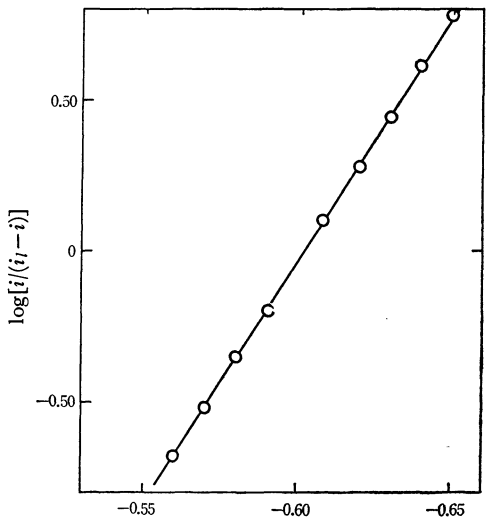

Fig. 3. The d. c. log-plot analysis of the cathodic wave of Tl(I)-DTPA chelate.
pH=8.80, μ=0.40, C_{Tl^+}=1.09 mM
C_{DTPA}=25.0 mM

height of the a. c. polarogram is exactly proportional to the concentration of the Tl(I)-DTPA chelate that the ratio of the peak height of a Tl(I)-DTPA chelate to that of a Tl(I) ion is nearly equal to the ratio of their limiting currents.

To be more exact, the reversibility of the electrode reaction at the electrode, which is polarized under the influence of an a. c. voltage of a small amplitude, should be tested by the a. c. log-plot method, *i. e.*, the plot of $\log[(I_p/I)^{1/2}-((I_p-I)/I)^{1/2}]$ against E, where I_p and I are the peak height and the height of a. c. polarogram at a given value of E, respectively.

The well-known relation (2) of the a. c. polarographic current derived for the following electrode reaction[8,9];

$$O + ne^- = R \qquad (1)$$

holds only when the reaction (1) proceeds reversibly in the polarographic sense:

$$I = (n^2F^2 \cdot A/4RT) \cdot D_0^{1/2} \cdot \omega^{1/2} \cdot C_0 \cdot \Delta E \times \mathrm{sech}^2[(nF/2RT)(E - E_{1/2})] \cdot \sin(\omega t + \pi/4) \qquad (2)$$

The notation definitions are as follows:

n=number of electrons involved in the electrode reaction
F=Faraday's constant, A=electrode area
R=ideal gas constant,
T=absolute temperature
D_0=diffusion coefficient of the species 0
C_0=bulk concentration of the species 0,
ω=frequency,
ΔE=amplitude of the applied alternating potential,
$E_{1/2}$=reversible polarographic half-wave potential for the electrode reaction (1)

Similarly, in the reduction of a metal complex,

$$MX_m^{n-mb} + ne^- + Hg = M(Hg) + mX^{b-} \qquad (3)$$

when the boundary condition (4), which shows conclusively that the electrode reaction (3) is reversible, is satisfied by the system under the a. c. polarographic conditions, the relation (5) can be obtained by the mathematical treatment employed by Matsuda,[8] Delmastro and Smith,[9] and Underkofler and Shain[10] to derive the relation (2):

$$(C_{MX_m}/C_{M(Hg)})_{x=0} = \theta \cdot \exp[-\nu \sin \omega t] \qquad (4)$$

where $\theta = \exp[nF/RT(E-(E_{1/2})_c)]$,

$\nu = nF \cdot \Delta E/RT$,

$(E_{1/2})_c = E^\circ_{M(Hg)} + RT/nF[\ln k_{M(Hg)} \cdot f_c/k_c - \ln K_c - m \cdot \ln C_x \cdot f_x]$[4],

E=d. c. potential applied,
$E^\circ_{M(Hg)}$=standard potential,
k's=diffusion current constants,
f's=activity constants,
C_x=the concentration of X^{b-} at the electrode surface, and

$K_c=[MX_m^{n-mb}]/[M^{n+}]\cdot[X^{b-}]^m$.

$$I = (n^2F^2 \cdot A/4RT) \cdot D^{1/2}{}_{MX_m} \cdot \omega^{1/2} \cdot C_{MX_m} \cdot \Delta E \times \mathrm{sech}^2[(nF/2RT)(E-(E_{1/2})_c)] \cdot \sin(\omega t + \pi/4) \qquad (5)$$

By casting the relation (5) into logarithmic form and by rearranging the resulting equation, one can obtain the following equation at 25°C;

$$E = (E_{1/2})_c + 2 \times 0.0591/n \log[(I_p/I)^{1/2}-(I_p-I/I)^{1/2}] \qquad (6)$$

Here I_p represents the peak height of the a. c. polarogram of MX_m^{n-mb}.

This relation, (6), clearly indicates that the summit potential in a. c. polarography can be safely equated with the half-wave potential in d. c. polarography when the electrode reaction is reversible, even under a. c. polarographic conditions, that the plot of E against $\log[(I_p/I)^{1/2}-((I_p-I)/I)^{1/2}]$ gives a straight line with a slop of $\pm$0.118/nV, and that the summit potential can be determined as the potential where the $\log[(I_p/I)^{1/2}-((I_p-I)/I)^{1/2}]$ is zero.

A typical example of an a. c. log-plot is shown in Fig. 4. The slopes found were +134 mV and −132 mV respectively, and the summit potential determined by the method described above agreed well with the half-wave potential (Table 2). Considering the effects of spherical diffusion,[10] of

8) H. Matsuda, *Z. Elektrochem.*, **61**, 489 (1957).
9) J. R. Delmastro and D. E. Smith, *Anal. Chem.*, **38**, 169 (1966).
10) W. L. Underkofler and I. Shain, *Anal. Chem.*, **37**, 218 (1965).

Table 2. The effect of pH on the half-wave potential and on the summit potential

$C_{DTPA}=25.0$ mM, $C_{Tl^+}=1.09$ mM

pH	$E_{1/2}$ V *vs.* SCE	E_p V *vs.* SCE
7.30	-0.521_0	-0.523_1
7.60	-0.536_0	-0.539_0
8.27	-0.576_5	-0.577_0
8.80	-0.602_0	-0.598_0
9.18	-0.616_1	-0.613_0
9.80	-0.617_2	-0.619_0

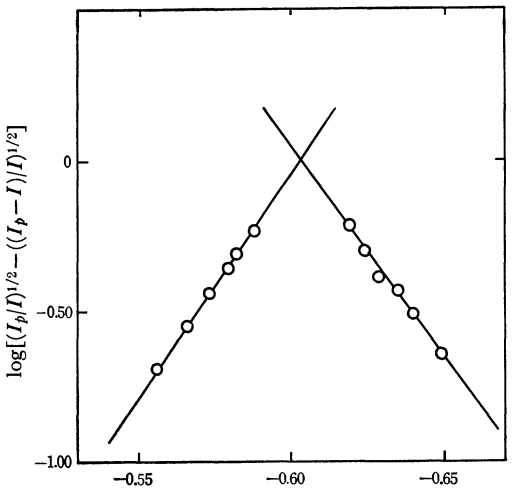

Fig. 4. The a. c. log-plot analysis of the cathodic wave of Tl(I)-DTPA chelate.
pH=8.80, $\mu=0.40$, $C_{Tl^+}=1.09$ mM
$C_{DTPA}=25.0$ mM

Table 3.

a) The relation between the concentration of Tl(I) ion and the half-wave potential or the summit potential (E_p).

$C_{DTPA}=40$ mM, pH=10.00

C_{Tl^+} mM	$E_{1/2}$ V *vs.* SCE	E_p V *vs.* SCE
1.09	-0.635_0	-0.638_0
2.18	-0.634_0	-0.640_0

b) The effect of the concentration of DTPA on $E_{1/2}$ or E_p.

$C_{Tl^+}=1.09$ mM, pH=9.20

C_{DTPA} mM	$E_{1/2}$ V *vs.* SCE	$\Delta E_{1/2}$ mV	E_p V *vs.* SCE	ΔE_p mV	$\Delta E_{calcd.}$ mV
15	−0.598	0	−0.593	0	0
25	−0.617	16	−0.613	20	15
40	−0.633	35	−0.624	31	33

the charging current[10] and of the incomplete compensation for the ohmic resistance of the cell circuit,[11] the above facts may be taken as conclusively indicating the reversible process.

The Mechanism of the Electrode Reduction of Tl(I)-DTPA Chelate at the DME. In view of the experimental facts that the half-wave potential or the summit potential is independent of the concentration of Tl(I) ions added (Tables 3a, 3b), but shifts with a change in the concentration of DTPA, C_{DTPA}, according to the relation;

$$\Delta E_{1/2}/\Delta \log C_{DTPA}$$
$$\text{or} \quad \Delta E_s/\Delta \log C_{DTPA} = -0.0591 \text{ V}$$

the following mechanism can be assumed for the reduction of the Tl(I)-DTPA chelate when the presence of a hydrogen chelate of Tl(I)-DTPA is taken into consideration, as in the case of other metal chelates of DTPA:[12]

$$\begin{array}{ccccc} TlZ^{4-} & + e^- + Hg = & Tl(Hg) & + Z^{5-} \\ \downarrow\uparrow H^+ & & & {}^{n}H^+ \downarrow\uparrow \\ TlHZ^{3-} & & & H_n\cdot Z^{n-5} \end{array} \qquad (7)$$

where Z^{5-} refers to the completely-dissociated DTPA.

Assuming that $a_{Hg}=1$ and $f_{Tl(Hg)}=1$, the relation (8) can be derived for the mechanism (7):

$$(E_{1/2})_{TlZ} = E^\circ_{Tl(Hg)} + 0.0591\left[\log\frac{f_{Tl^+}\cdot k_{Tl(Hg)}}{k_{TlZ}} - \log C_{DTPA} + \log\frac{\alpha_H}{K_{TlZ}\cdot(1+K^H_{TlHZ}[H^+])}\right] \qquad (8)$$

where $K_{TlZ} = [TlZ^{4-}]/[Tl^+]\cdot[Z^{5-}]$,
$K^H_{TlZ} = [TlHZ^{3-}]/[TlZ^{4-}]\cdot[H^+]$,
and $\alpha_H = [H^+]/k_5 + [H^+]^2/k_4\cdot k_5 + \cdots + [H^+]^5/k_1\cdot k_2\cdot k_3\cdot k_4\cdot k_5$.

Remembering the relation theoretically predicted for the half-wave potential of the reduction of a Tl(I) ion at the DME,[4,13] the shift of the half-wave potential of a Tl(I) ion, $\Delta E_{1/2}$, by the chelate formation with DTPA can be derived as:

$$\Delta E_{1/2} = 0.0591\left[\log\frac{k_{TlZ}}{k_{Tl^+}} + \log C_{DTPA} + \log\frac{K_{TlZ}(1+K^H_{TlHZ}[H^+])}{\alpha_H}\right] \qquad (9)$$

From the above theoretical consideration, it can be concluded that, for the reaction mechanism (7), the plot of antilog$[\Delta E_{1/2}/0.0591+\log\alpha_H+\log k_{Tl^+}/k_{TlZ}-\log C_{DTPA}]$ against $[H^+]$ can give a linear relation with a slope of $K^H_{TlHZ}\cdot K_{TlZ}$, and that the antilog value at $[H^+]=0$ corresponds to K_{TlZ}. Here, the shift of the summit-potential, ΔE_p,

11) E. R. Brown, T. G. McCord, D. E. Smith and D. D. Deford, *Anal. Chem.*, **38**, 1119 (1966).
12) M. Kodama and A. Kimura, This Bulletin **40**, 1639 (1967).
13) M. Kodama, S. Naito and M. Ebine, *Nippon Kagaku Zasshi (J. Chem. Soc. Japan, Pure Chem. Sect.)*, **84**, 576 (1963).

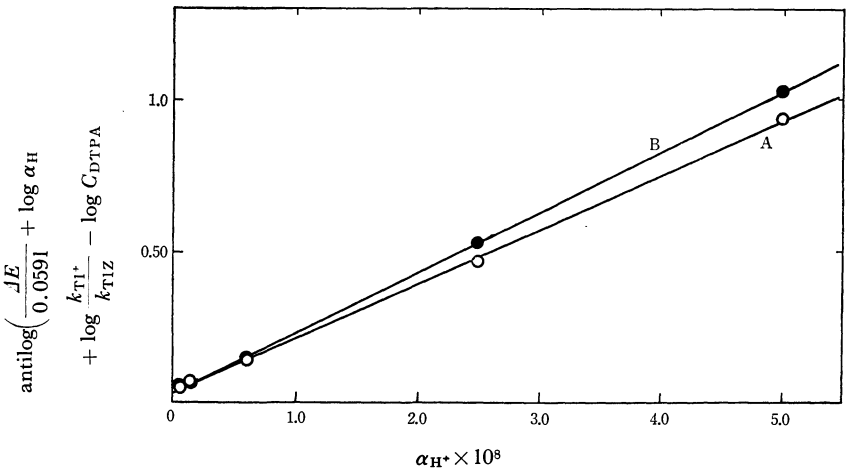

Fig. 5. The plot of antilog [ΔE/0.0591 + log α_H + log k_{Tl^+}/k_{TlZ} −log C_{DTPA}] against [H^+].
μ=0.40, C_{Tl^+}=1.09 mM, C_{DTPA}=25.0 mM
A: d. c., B: a. c.

by the chelate formation can be used in place of $\Delta E_{1/2}$.

The theoretical conclusion thus obtained was tested by using some of the typical data. The results are shown in Fig. 5. From the tangents of the linear relations and the antilog value at [H^+]=0 in Fig. 5, the K_{TlZ} and K^H_{TlHZ} values were determined; they are listed in Table 4, together with dissociation constants and diffusion current constants used in the calculations. The dissociation constants listed were calculated by using the value reported by Vandegaer *et al.*[14]; calculation was done in a manner similar to that described previously.[12]

TABLE 4

i) Dissociation constant of DTPA[13] (mixed constants, μ=0.40)
pK_1=1.75, pK_2=2.43, pK_3=4.20, pK_4=8.45, pK_5=10.02

ii) Formation constants of chelates* (μ=0.40)

	D. C.	A. C.
K_{TlZ}	$10^{5.45}$	$10^{5.53}$
K^H_{TlHZ}** $\left(=\frac{[TlHZ^{3-}]}{[TlZ^{4-}][H^+]}\right)$	$10^{8.81}$	$10^{8.78}$

iii) Diffusion current constants, k's
k_{Tl^+}=4.44 (μA/mM)
k_{TlZ}=2.12 (μA/mM) at pH 9.90

iv) The ratio of peak height between Tl(I) ion and Tl(I)-DTPA chelate.
Ratio = $\frac{(I_p)_{Tl^+}}{(I_p)_{TlZ}}$ = 2.39

* Obtained by the present authors
** Mixed constant

It is very interesting that the K^H_{TlHZ} value found is much greater than the K_{TlZ} value, making a marked contrast with that of the DTPA chelates of divalent or tervalent metal ions.

The complex formation reaction has been known to provide many useful polarographic methods for the analysis of metal ions. For instance, in a mixture of lead(II) and thallium(I) ions not containing a complex-forming reagent, it is very difficult to determine simultaneously those metal ions by the polarographic method, because the two metal ions are reduced at potentials so close togehter. However, in the solution containing a chelating reagent such as EDTA, the reduction wave of the lead(II) ion shifts to the negative potential, and so the resolutive determination of lead(II) and thallium(I) can be effected successfully. The resolution of the polarographic waves has generally been treated in an experimental manner, and few theoretical and quantitative discussions on it have appeared. In a. c. polarography, it has been reported[15] that, when the difference in the summit potential, ΔE_p, of a. c. polarograms is greater than 40 mV, the peak height of each polarogram can be determined accurately. However, this conclusion is somewhat experimental. From the foregoing discussion, it is very clear that the magnitude of the resolution of a. c. polarograms can be estimated quantitatively with the aid of Eq. (6). In the most favorable cases, a ΔE_p value greater than 117/n mV is theoretically required to determine the a. c. peak height within a 3.0% limit of error.

14) J. Vandegaer, S. Chaberek and A. E. Frost, *J. Inorg. Nucl. Chem.*, **11**, 210 (1959).

15) T. Fujinaga and M. Maruyama, "Polarography," Vol. 1, Nankodo, Tokyo (1962), p. 97.

BULLETIN OF THE CHEMICAL SOCIETY OF JAPAN VOL. 41 359—364 (1968)

Spectroscopic Studies of Mixed Amine Carbonyl Complexes of d^6 Structure. I. Visible and Ultraviolet Absorption Spectra of Diamine-tetracarbonyl Complexes of Chromium(0), Molybdenum(0) and Tungsten(0)

Hide SAITO, Junnosuke FUJITA and KAZUO SAITO

Department of Chemistry, Faculty of Science, Tohoku University, Katahira-cho, Sendai

(Received July 17, 1967)

Chromium(0), molybdenum(0) and tungsten(0) complexes of $[M\cdot(CO)_4AA]^0$ type (AA= ethylenediamine (en), *l*-propylenediamine (*l*-pn), trimethylenediamine (tn), bipyridyl (bp), and phenanthroline (phen); *l*-pn and tn derivatives are new compounds) have been synthesized and their absorption spectra, rotatory dispersion (RD) and circular dichroism (CD) measured in methanol at room temperature. The nature of the absorption bands has been discussed by comparing them with one another and with those of hexacarbonyl- and piperidinepentacarbonyl complexes of these elements. The peaks in the region 23000 to 25000 cm^{-1} seem to be due to spin-allowed d–d transition. The bands at 30000 to 33000 cm^{-1} appears to correspond to the metal to carbonyl charge transfer band of hexacarbonyls at *ca.* 36000 cm^{-1}. Besides them, complexes of aromatic amines (bp and phen) show broad and strong bands at 21000 to 22000 cm^{-1} which seem to owe to metal to amine charge transfer.

Although many carbonyl compounds of VIB group elements of the periodic table have been studied,[1] little[2-5] is known of their optical properties except the infrared absorption spectra. Gray and Beach[2] measured the ultraviolet absorption spectra of hexacarbonyls of VIB group elements in the vapor state, and assigned the bands on a molecular orbital model. They gave thus several remarkable features of metal-carbonyl bonds. Strohmeier and Gerlach[4] measured the visible and ultraviolet absorption spectra of some mono- and diamine derivatives of metal carbonyls of group VIB elements and found that the patterns of spectra are all similar to one another. However, the character of each band was not made clear.

The bond between metal and carbon monoxide ligand has a significant π-character, whereas that between metal and amines is of almost pure σ-character. Hence studies of mixed complexes containing both kinds of ligand seem quite worthwhile. We have measured the absorption spectra of 15 kinds of mixed diamine carbonyls of the type $[M(CO)_4AA]$ ($M=Cr^0$, Mo^0, W^0; AA=ethylenediamine [en], *l*-propylenediamine [*l*-pn], trimethylenediamine [tn], bipyridyl [bp], phenanthroline [phen]) as well as their circular dichroism (CD) and rotatory dispersion (RD) and discussed the results in conjunction with those of hexacarbonyl complexes.

Experimental

Material. New compounds $[M(CO)_4$*l*-pn] and $[M(CO)_4$tn] were prepared by a similar method to Krainhanzel's,[6] which was useful for the preparation of $[M(CO)_4$en]. Bipyridyl and phenanthroline complexes, $[M(CO)_4$bp] and $[M(CO)_4$phen] were synthesized by Abel's method.[7] Each compound was identified by infrared spectra in the CO-stretching region and chemical analysis of carbon, hydrogen and nitrogen. The results of chemical analysis of the new compounds are shown in Table 1. Optically active *l*-pn was obtained by resolving commercial propylenediamine according to Dwyer.[8] The aqueous solution of *l*-isomer was acidified with hydrochloric acid and evaporated to dryness. Water was completely eliminated by adding ethanol and evaporating off ethanol together with water, twice. Anhydrous *l*-pn dihydrochloride was dissolved in absolute methanol containing an equivalent amount of sodium methylate, the sodium chloride decanted and the free *l*-pn distilled twice in the presence of metallic sodium. (yield after resolution, 26%) $[\alpha]_D^{25}$° −34.3° (2% in benzene, by Dwyer's method.[8]) The solvent methanol was purified by the usual method in nitrogen atmosphere.

1) G. R. Dobson, I. W. Stoltz and R. K. Sheline, *Advances in Inorg. Chem. and Radiochem.*, **8**, 1 (1966).
2) H. B. Gray and N. A. Beach, *J. Am. Chem. Soc.*, **85**, 2922 (1963).
3) D. S. Alderdice, *J. Mol. Spectry.*, **15**, 509 (1965).
4) W. Strohmeier and Kl. Gerlach, *Z. Phys. Chem., N. F.*, **27**, 439 (1961).
5) S. Yamada, H. Yamazaki, H. Nishikawa and R. Tsuchida, This Bulletin, **33**, 481 (1960).
6) C. S. Krainhanzel and F. A. Cotton, *Inorg. Chem.*, **2**, 533 (1963).
7) E. W. Abel, M. A. Bennett and G. Wilkinson, *J. Chem. Soc.*, **1959**, 2323.
8) F. P. Dwyer, F. L. Garvan and A. Shulman, *J. Am. Chem. Soc.*, **81**, 292 (1959).

Table 1. Chemical analysis of the complexes

	C, %		H, %		N, %	
	Calcd	Obs	Calcd	Obs	Calcd	Obs
[M(CO)$_4$*l*-pn]						
$CrC_7H_{10}O_4N_2$	35.54	35.30	4.03	4.23	11.83	11.76
$MoC_7H_{10}O_4N_2$	29.63	29.81	3.38	3.57	10.00	9.93
$WC_7H_{10}O_4N_2$	23.01	22.72	2.54	2.72	7.77	7.57
[M(CO)$_4$tn]						
$CrC_7H_{10}O_4N_2$	36.19	35.30	4.40	4.23	11.14	11.76
$MoC_7H_{10}O_4N_2$	30.93	29.81	4.02	3.57	9.46	9.93
$WC_7H_{10}O_4N_2$	23.72	22.72	2.86	2.72	7.27	7.57

Measurements. Visible and ultraviolet absorption spectra were measured with Hitachi EPS-3 Automatic Recording Spectrophotometer in the region where log ε is greater than 2. RD and CD were recorded with JASCO ORD/CD-5 Recorder in the wave number region below 35000 cm^{-1}. The measurements were all made in freshly prepared absolute methanol solution at room temperature. The mixed complexes tend to decompose in this solution, especially in the presence of dissolved oxygen.

Results and Discussion

Absorption curves of the diamine complexes are shown in Figs. 1 to 5, and the numerical data summarized in Tables 2 and 3. From these figures it is seen that the spectra depend on the ligand more remarkably than on the central metal atom. Especially, as seen from Fig. 5, bipyridyl and phenanthroline complexes give quite a different feature from those of aliphatic diamine complexes including ethylenediamine and trimethylenediamine derivatives. Such a difference can be expected from the aromaticity of ligand.

Bands at 23000 to 25000 cm^{-1}. All the complexes give bands in this wave number region, although bipyridyl and phenanthroline complexes give only shoulders. The wave numbers of the

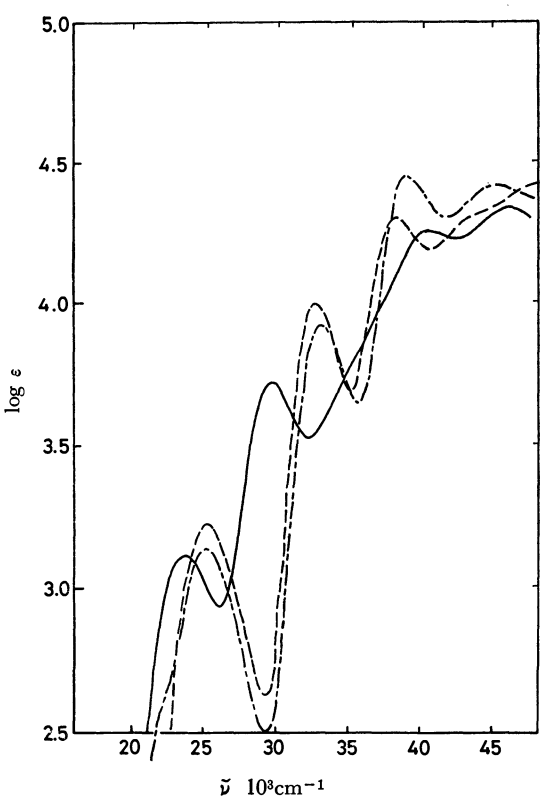

Fig. 1. Absorption spectra of [Cr(CO)$_4$en] (——), [Mo(CO)$_4$en] (----) and [W(CO)$_4$en] (-·-·) in methanol.

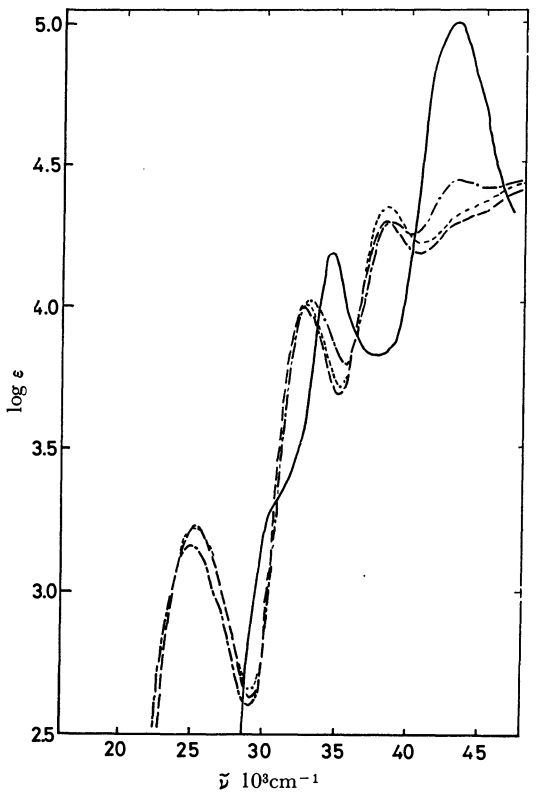

Fig. 2. Absorption spectra of [Mo(CO)$_6$] (——), [Mo(CO)$_4$en] (----), [Mo(CO)$_4$ *l*-pn] (····) and [Mo(CO)$_4$tn] (-·-·) in methanol.

TABLE 2. ABSORPTION MAXIMA OF THE COMPLEXES [M(CO)$_4$AA] (AA=en, *l*-pn, tn) IN METHANOL

Complex	Tentative assignment[2]					
	d-d		M → π_{CO}*(1)	uncertain	M → π_{CO}*(2)	uncertain
[Cr(CO)$_4$en]	——	23.6(3.12)	29.7(7.73)	35.5(sh 3.8)	40.3(4.26)	46.2(4.34)
[Mo(CO)$_4$en]	——	25.3(3.23)	32.7(4.00)	——	38.4(4.30)	43.4(sh 4.3)
[W(CO)$_4$en]	22.2(sh 2.6)	25.2(3.15)	33.2(3.92)	——	39.2(4.45)	45.0(4.42)
[Cr(CO)$_4$*l*-pn]	——	23.6(3.13)	29.7(3.74)	35.0(sh 3.8)	40.3(4.28)	45.9(4.32)
[Mo(CO)$_4$*l*-pn]	——	25.3(3.22)	32.8(4.02)	——	38.5(4.35)	43.4(sh 4.3)
[W(CO)$_4$*l*-pn]	22.2(sh 2.6)	25.2(3.14)	33.2(3.84)	——	39.2(4.38)	45.8(4.38)
[Cr(CO)$_4$tn]	——	<23.6	29.7	——	40.6	<46.2
[Mo(CO)$_4$tn]	——	25.0(3.18)	33.1(4.05)	——	38.7(4.33)	43.5(4.48)
[W(CO)$_4$tn]	22.2(sh 2.7)	24.7(3.14)	33.6(4.02)	——	39.5(4.48)	45.5(4.48)

The frequencies are given in $10^3 cm^{-1}$, and the intensity by log ε in parentheses.
sh: shoulder

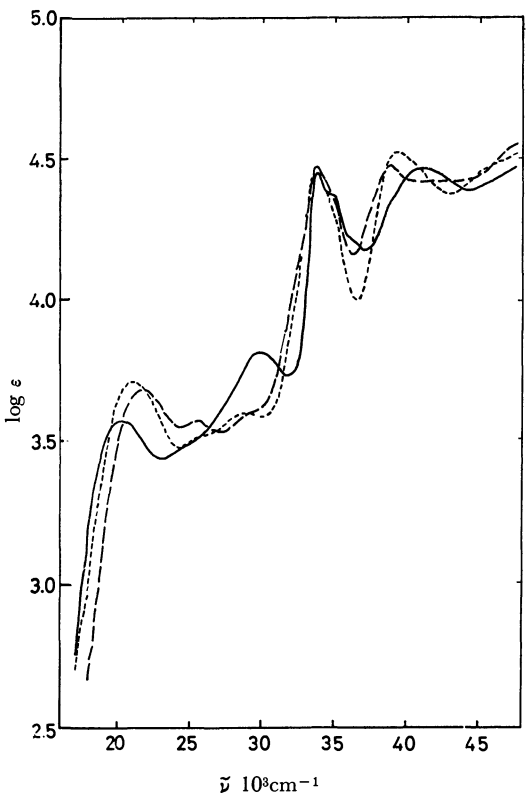

Fig. 3. Absorption spectra of [Cr(CO)$_4$bp] (——), [Mo(CO)$_4$bp] (----) and [W(CO)$_4$bp] (····) in methanol.

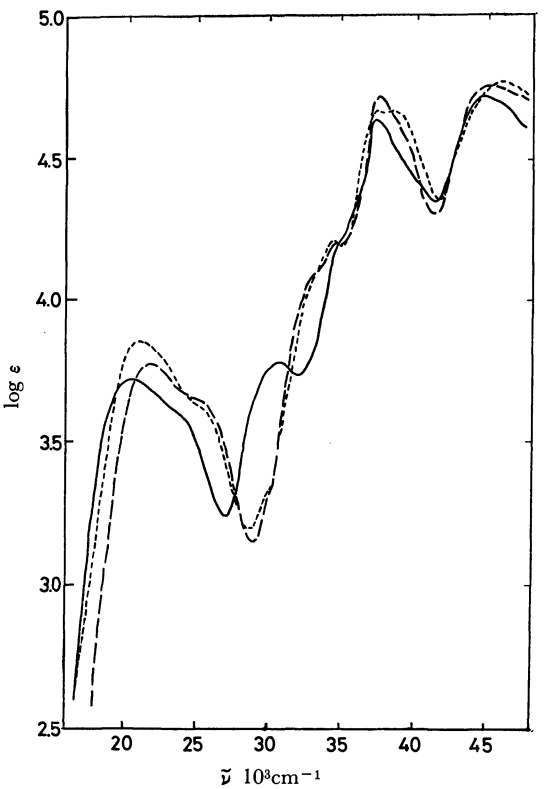

Fig. 4. Absorption spectra of [Cr(CO)$_4$phen] (——), [Mo(CO)$_4$phen] (----) and [W(CO)$_4$phen] (····) in methanol.

peak of molybdenum and tungsten complexes are similar to each other and significantly greater than those of the chromium complex. The molar extinction coefficient ε increases slightly in the sequence chromium, tungsten and molybdenum. The absorption spectra of ethylenediamine and *l*-propylenediamine complexes are almost identical and their absorption maxima are at a higher wave number than those of trimethylenediamine complexes by *ca.* 500 cm^{-1}. Such a tendency is seen only for the bands in this region, and coincides with that expected from the spectrochemical series. Hence these bands are regarded to be mainly due to the spin-allowed d–d transition. The d–d transition of the cobalt(III) complexes, $[Co(CN)_4en)]^-$, and $[Co(CN)_4tn]^-$, which are isoelectronic with the mixed diamine carbonyls of chromium(0), shows the same trend.

Table 3. Absorption maxima of the complexes [M(CO)$_4$AA] (AA=bp, phen) in methanol

Complex											
[Cr(CO)$_4$bp]	20.11 (3.57)	24.75 (sh 3.5)	—	—	30.00 (3.84)	—	33.78 (4.44)	34.72 (sh 4.4)	40.88 (4.46)	—	—
[Mo(CO)$_4$bp]	21.60 (3.68)	25.45 (3.57)	29.07 (sh 3.6)	—	32.6 (sh ca. 4)	—	33.85 (4.46)	34.97 (sh 4.4)	38.91 (4.46)	40.65 (4.41)	42.37 (4.41)
[W(CO)$_4$bp]	20.98 (3.71)	25.84 (sh 3.5)	28.94 (3.60)	—	32.5 (sh ca. 4)	—	33.68 (4.44)	34.72 (sh 4.4)	39.31 (4.52)	40.62 (sh 4.5)	45.87 (sh 4.5)
[Cr(CO)$_4$phen]	20.37 (3.72)	23.53 (sh 3.6)	—	29.67 (sh 3.7)	30.75 (3.78)	34.72 (sh 4.2) / 35.71 (sh 4.3)	37.37 (4.67)	—	44.72 (4.74)	—	—
[Mo(CO)$_4$phen]	21.68 (3.77)	25.25 (3.64)	—	29.94 (sh 3.3)	32.68 (sh 4.1)	34.51 (4.20)	37.47 (4.72)	—	45.15 (4.75)	—	—
[W(CO)$_4$phen]	21.01 (3.85)	25.25 (sh 3.6)	—	29.90 (sh 3.3)	32.68 (sh 4.1)	34.39 (4.23)	37.38 (4.69) / 38.46 (4.69)	—	45.87 (4.79)	—	—

The frequencies are given in $10^3 cm^{-1}$, and the intensity by log ε in parentheses.
sh: shoulder

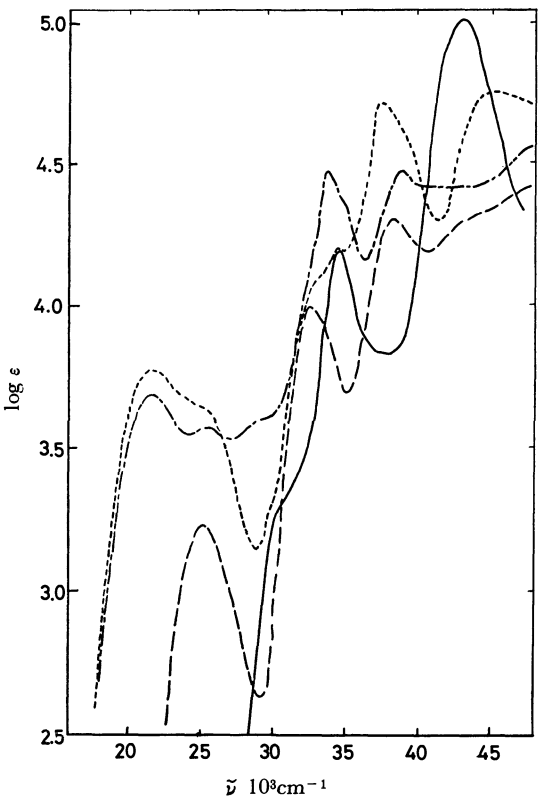

Fig. 5. Absorption spectra of [Mo(CO)$_6$] (——), [Mo(CO)$_4$en] (----), [Mo(CO)$_4$bp] (-·-·) and [Mo(CO)$_4$phen] (····) in methanol.

This conclusion is further supported by the fact that the location and extinction coefficient seem to be compared to those of the d–d transition ($^1A_{1g} \rightarrow {}^1T_{1g}$) of hexacarbonyls at 31000 to 33000 cm^{-1}, which are regarded to be spin-allowed.[2] The apparent differences in transition energy between diamine-tetracarbonyl and hexacarbonyl complexes (in cyclohexane) are estimated to be 7800, 6100 and 7400 cm^{-1} for the chromium, the molybdenum and the tungsten complex, respectively. These bands are subject to significant solvent effect. The estimation should be modified to be 9000 and 6900 cm^{-1} for the chromium and the molydbenum complexes in cyclohexane, respectively, when McRae's theoretical equation is applied.[9] Contribution of the solvent effect cannot be appropriately estimated for the tungsten complex. The difference is only 3800 cm^{-1} for the corresponding hexa- and tetracyano cobalt(III) complexes. Such a remarkable difference between the carbonyl and the cyano complexes can be regarded as due to the greater destabilization of d_π levels on replacement of two carbonyls by diamine, as compared in case of the cyano cobalt(III) complexes. Such a view is also supported by infrared studies.[6,10]

Strohmeier[4] measured the absorption spectra of piperidinepentacarbonyl complexes of chromium(0), molybdenum(0) and tungsten(0) in cyclohexane and found that they also have absorption bands at 23000 to 26000 cm^{-1}. Their characteristics are very similar to those of the diamine-tetracarbonyl complexes given above, except for intensity. These bands are also considered to be mainly due to spin-allowed d–d transition.

Since these bands are considered to be a split component of d–d transitions which are triply degenerate in the hexacarbonyl complexes, it seems worthwhile, to examine whether their

9) H. Saito, J. Fujita and K. Saito, This Bulletin, **41**, No. 4 (1968).
10) H. Sugi, Thesis, Tohoku Univ. (1964).

TABLE 4. SHIFT OF THE FIRST BAND DUE TO REPLACEMENT OF LIGANDS BY YAMATERA'S THEORY

Electronic transition	$[MA_6]$	$[MA_5B]$	*cis*-$[MA_4B_2]$
$d_{xy} \rightarrow d_{x^2-y^2}$	0 } T_{1g}	0 A_2	$1/2\,\delta$ B_1
$d_{yz} \rightarrow d_{y^2-z^2}$	0	$1/4\,\delta$ } E	$1/4\,\delta$ } A_1 and B_2
$d_{zx} \rightarrow d_{z^2-x^2}$	0	$1/4\,\delta$	$1/4\,\delta$
mean	0	$1/6\,\delta$	$1/3\,\delta$

δ, $(=\delta_\pi+\delta_\sigma)$ energy difference of the first band between $[MA_6]$ and $[MB_6]$.
The maximum frequency of the first band of $[Cr(CO)_6]$ is taken as zero.

locations are in accord with Yamatera's theory.[11] A similar trial was successful for the corresponding cyano complexes.[12] Ethylenediamine-tetracarbonylchromium(0) is insoluble in cyclohexane, but the location of maximum of d-d transition in cyclohexane is estimated to be at about 22170 cm^{-1} from the solvent effect.[9] The transition of piperidinepentacarbonylchromium(0) is observed at 23800 cm^{-1} in cyclohexane. We can estimate the wave numbers of the spin-allowed d-d transition of $[Cr(CO)_6]^0$, $[Cr(CO)_5pip]^0$ and $[Cr(CO)_4en]^0$ to be 31300, 23800, and 22170 cm^{-1}, respectively in cyclohexane. The ratio (31300—23800)/(31300—22170) is 3.3/4. According to Yamatera's theory, the expected shift of split componenets of the first bands of two mixed carbonyl complexes, $[MA_5B]$ and *cis*-$[MA_4B_2]$ type, are shown in Table 4. If the observed first bands of the two mixed carbonyl complexes were regarded as due to the three components averaged simply, the expected ratio mentioned above should be $(1/6\delta)/(1/3\delta)=1/2$, which is much smaller than the observed value. However, it would be possible to assign the observed band of $[Cr(CO)_5pip]$ as the E component of the first band, since the magnitude of shift seems to be extraordinarily remarkable, and further the theoretically forbidden A_2 component would have weaker intensity than the allowed E component has. The observed band of $[Cr(CO)_4en]$ shows no indication of splitting, on the other hand, and might consist of the three components mixed one another. Thus the magnitude of shift is $1/4\ \delta$ for $[Cr(CO)_5pip]$ and $1/3\delta$ for $[Cr(CO)_4en]$ and the ratio is 3/4. This value equals nearly to the observed value. However, the present case will be the first example, where Yamatera's theory applied to the band shifts of mixed carbonyl complexes involving low oxidation state metal and π-character ligand. More detailed study would be needed to elucidate the applicability of this theory to such complexes.

Bands at 21000 to 22000 cm^{-1}. Broad and strong bands are observed in this region only in the spectra of aromatic diamine tetracarbonyl complexes. Their characteristics are different from those of the spin-allowed d-d bands mentioned above. The wave number of the absorption maximum increases with almost equal differences (700 cm^{-1}) in the order chromium, molybdenum and tungsten, and the extinction co-efficient in the same order for a given diamine. Two low-spin d^6 type complexes $[Fe(bp)_3]^{2+}$ and $[Fe(phen)_3]^{2+}$, have metal to ligand charge transfer bands at about 20000 cm^{-1} [13] and these seem to correspond to those of diamine-tetracarbonyl complexes in question.

Bands in Other Regions. The bands of diamine-tetracarbonylchromium(0) at 30000 and those of molybdenum and tungsten complex at 33000 cm^{-1} (shoulders for aromatic diamine complexes) would be metal to carbonyl charge transfer bands, because their extinction coefficients are very great and they would possibly correspond to the bands of hexacarbonyl complexes at 35000 cm^{-1} ($^1A_{1g}$ to $^1T_{1u}$[1]) charge transfer).[2] The remaining bands of aliphatic diamine complexes at 40000 cm^{-1} appear to correspond to those of hexacarbonyl complexes at 44000 cm^{-1}, which are assigned to metal to carbonyl transition band in molecular orbital sense[2] (see Fig. 6).

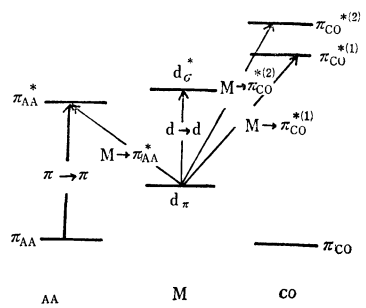

Fig. 6. Schematic energy level diagram for mixed carbonyls.

The sharp bands of bipyridyl-tetracarbonyl complexes at *ca.* 34000 cm^{-1} are little affected by the central metal and accompanied by shoulders

11) H. Yamatera, This Bulletin, **31**, 95 (1958).
12) K. Ohkawa, J. Fujita and Y. Shimura, *ibid.*, **38**, 66 (1965).
13) S. F. Mason, A. J. McCaffery and B. J. Norman, *Proc. Chem. Soc.*, **1964**, 259.

at a higher wave number by about 1000 cm^{-1}. They are likely due to intra-ligand transition ($\pi-\pi^*$), as exemplified by many bipyridyl complexes. The bands of phenanthroline-tetracarbonyl complexes at 37000 cm^{-1} seem also to be mainly due to the intra-ligand transition.

d_π-Levels. As seen from Figs. 3 and 4, the intra-ligand $\pi-\pi^*$ transition energy of the bipyridyl and the phenanthroline complexes is rather constant regardless of the kind of central metal. Hence the energy level of π_{AA}^* does not change significantly by complex formation with different metal atoms. Thus the shift of metal-to-diamine charge transfer bands would reflect the energy of metal d_π levels. This level is destabilized by 700 cm^{-1} each in going from molybdenum to tungsten and from tungsten to chromium.

On the other hand, the location of d-d band is rather independent of the kind of diamine for complexes of a given metal. The differences in d-d transition energies are estimated from the absorption spectra of ethylenediaminetetracarbonyl complexes of these metals: *i. e.* 1700 cm^{-1} between chromium and molybdenum, and 1600 cm^{-1} between chromium and tungsten complex. From these values and the d_π levels mentioned above, it is seen that the d_σ^* levels are destabilized in the order, chromium, molybdenum and tungsten, and the difference is 300 cm^{-1} between chromium and molybdenum, and 900 cm^{-1} between chromium and tungsten.

The difference of energy of π_{CO}^*[2] levels can be also calculated from the data in Table 3 and the relative height of the d_π levels. They are destabilized in the order, molybdenum, tungsten and chromium, and the difference is 100 cm^{-1} between molybdenum and tungsten, and 500 cm^{-1} between molybdenum and chromium. The order is the same as that for the d_π levels, to indicate that the antibonding levels of carbon monoxide in these complexes are stabilized as the d_π levels of the central metals are stabilized.

Rotatory Dispersion and Circular Dichroism of *l*-Propylenediaminetetracarbonyl Complexes. The curves are shown in Fig. 7. For the spin-allowed d-d transition of [$Cr(CO)_4$*l*-pn], negative and positive Cotton effect are observed from the lower wave number region. The RD curve has two inflection points, whose wave number coincides with the peaks of CD curve. *l*-Propylenediamine-tetracyanocobaltate(III) [$Co(CN)_4$*l*-pn]$^-$, isoelectronic to the chromium complex, also has such a CD pattern on the first d-d transition.[14] Although cyanide ions have weaker π-bonding character than carbonyl ligands has, the common pattern seems to support the assignment.

The splitting of d-d transition peak is not very great. The CD and the RD of molybdenum and tungsten complexes are very similar. They give only positive Cotton effect with large $\Delta\varepsilon$ values at the absorption maxima, and this feature is obviously different from that of the chromium complex. However, the reason cannot be appropriately accounted for at the present stage. Another positive Cotton effect seems to be in the $M\rightarrow\pi^*_{CO}$[1] C. T. region, but its detailed discussion cannot be made because of the difficulty in accurate measurement.

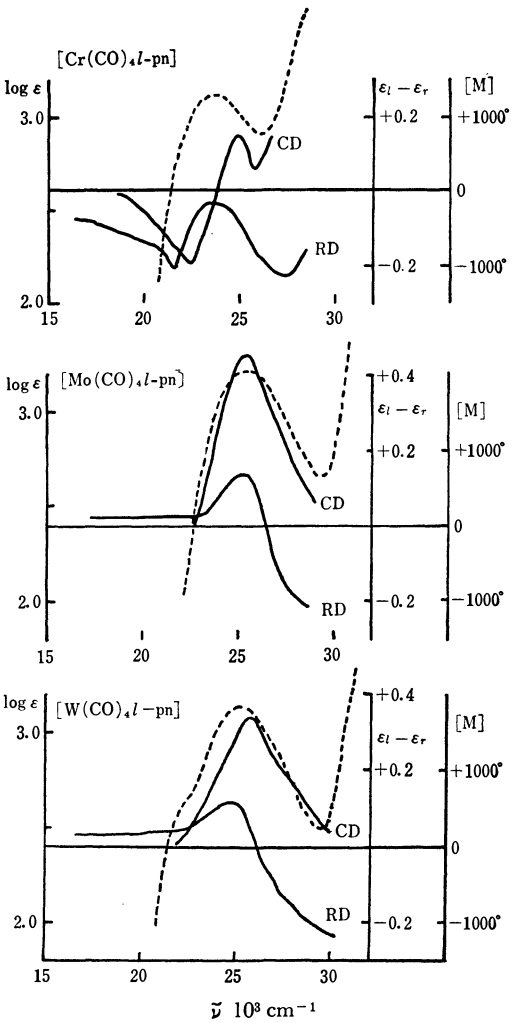

Fig. 7. Absorption spectra (····), CD and RD of the complexes [$Mo(CO)_4$ *l*-pn] (M=Cr, Mo, W) in methanol.

The authors thank Professor Muraji Shibata, Dr. Hiroaki Nishikawa and other members of Chemistry Department, Kanazawa University for their co-operation in measuring RD and CD of the complexes.

14) J. Fujita, to be published

BULLETIN OF THE CHEMICAL SOCIETY OF JAPAN VOL. 41 365—373 (1968)

Electronic Structure of Tris(α-diimine)iron(II) Complexes

Tasuku Ito and Nobuyuki Tanaka

Department of Chemistry, Faculty of Science, Tohoku University, Katahira-cho, Sendai

and Ichiro Hanazaki and Saburo Nagakura

The Institute of Physical and Chemical Research, Honkomagome, Bunkyo-ku, Tokyo and The Institute for Solid State Physics, The University of Tokyo, Azabu, Tokyo

(Received July 17, 1967)

The electronic structures of tris(α-diimine)iron(II) complexes have been investigated. The theoretical consideration has revealed that a considerable π-back donation takes place in the ground state and as a result unusually stable complexes of iron(II) are formed. The intense band which appears in the visible region has been proved to be due to the charge transfer transition from 3dπ AO (atomic orbital) of iron to the lowest vacant π MO (molecular orbital) of the ligand α-diimine. It was found both theoretically and experimentally that the π→π* transition with the lowest energy in α-diimine is polarized parallel to the nitrogen-nitrogen direction of the molecule, and that transition dipoles in the three ligands of tris(α-diimine)iron(II) ion interact to give resultant $A_1 \rightarrow A_2$ and $A_1 \rightarrow E$ transitions in the metal complex with D_3 symmetry. Details of the electronic structures, including the splitting energy and the intensity of the local excitation in α-diimine molecule and the nature of the charge transfer band, have been discussed.

It is well known that α-diimine, 2, 2'-bipyridine and 1, 10-phenanthroline form intensely colored stable complexes with iron(II) ions. The chromophoric nature and the unusual stability of such complexes have received a considerable attention and a number of experimental studies have been carried out.[1,2] Some researchers emphasized the importance of the π-bond formation between the ligands and the central metal ion.[3,4]

The aim of the present work is to extend the theoretical treatment previously developed for the acetylacetonato complexes[5] to tris(α-diimine)iron(II) ions and to study the electronic structures of the latter complexes as quantitatively as possible.*1 The absorption spectra, not only visible but also ultraviolet, of three kinds of tris(α-diimine)iron(II) complexes, namely tris(glyoxal-bis-*N*-methylimine)-, tris(biacetyl-bis-*N*-methylimine)- and tris(biacetyl-bis-*N*-butylimine)iron(II) ions, were measured to obtain the information on the electronic energy levels of the complexes.

Experimental

Materials. Tris(glyoxal-bis-*N*-methylimine)iron(II) iodide,[1] tris(biacetyl-bis-*N*-methylimine)iron(II) iodide[1] and tris(biacetyl-bis-*N*-butylimine)iron(II) tetrafluoroborate[6] were prepared by the methods described in the literatures. For the measurements of ultraviolet absorption spectra, the above iodides were converted to tetrafluoroborates. Among these three ligands, only biacetyl-bis-*N*-butylimine was able to be isolated by the method of Barany *et al.*[7]

Measurements. A Hitachi recording spectrophotometer Model EPS-3 was used for the measurements of the visible and the ultraviolet absorption spectra. The measurements in the vacuum ultarviolet region were made down to 182 mμ in aqueous solutions with 0.1 mm quartz cells using a vacuum ultraviolet spectrophotometer[8] at the Institute for Solid State Physics, the University of Tokyo.

Experimental Results

The absorption spectra of three kinds of tris(α-diimine)iron(II) complex were measured in aqueous solutions. As may be seen in Fig. 1, very similar spectra were obtained not only in the visible but also in the ultraviolet region, though a slight frequency shift was observed. A band

1) P. Krumholz, *J. Am. Chem. Soc.*, **75**, 2163 (1953).
2) E. Bayer, *Angew. Chem.*, **76**, 76 (1964).
3) D. H. Busch and J. C. Bailar, Jr., *J. Am. Chem. Soc.*, **78**, 1137 (1956).
4) K. Nakamoto, "Advances in the Chemistry of the Coordination Compounds," ed. by S. Kirschner, Macmillan, New York (1961), p. 437.
5) I. Hanazaki, F. Hanazaki and S. Nagakura, *J. Chem. Phys.*, to be published.
*1 Similar studies on the electronic structure of 2, 2'-bipyridine and 1, 10-phenanthroline complexes of iron(II) ion will be described elsewhere.
6) S. Otsuka, T. Yoshida and A. Nakamura, *Inorg. Chem. (Washington)*, **6**, 20 (1967).
7) H. C. Barany, E. A. Braude and M. Pianka, *J. Chem. Soc.*, **1949**, 1898.
8) H. Tsubomura, K. Kimura, K. Kaya, J. Tanaka and S. Nagakura, This Bulletin, **37**, 417 (1964).

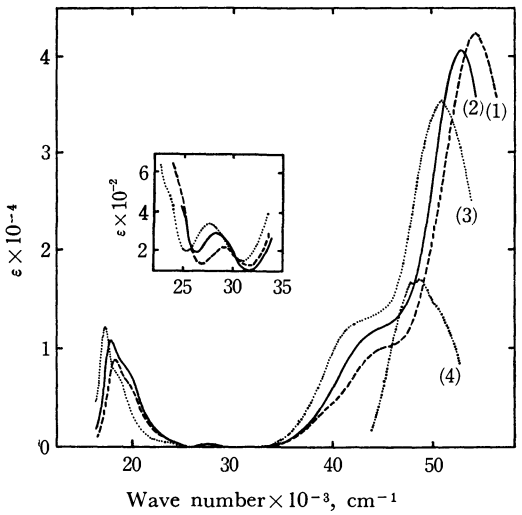

Fig. 1. The absorption spectra of (1) tris(glyoxal-bis-*N*-methylimine)iron(II) tetrafluoroborate, (2) tris(biacetyl-bis-*N*-methylimine)iron(II) tetrafluoroborate, (3) tris(biacetyl-bis-*N*-butylimine)iron-(II) tetrafluoroborate in an aqueous solution and (4) biacetyl-bis-*N*-butylimine in an ethanol solution.

appearing near 18000 cm^{-1}, which is the origin of the intense color, has received much attention. On the other hand, an intense band near 50000 cm^{-1} with a moderately intense shoulder has not attracted any attention, and nothing has been reported of it, probably because of the difficulty of the measurement. It should be noted that there are two shoulder bands which are difficult to observe. One appears in all cases near 25000 cm^{-1} with molar extinction coefficient of ~400, whereas the other is observed only with tris(glyoxal-bis-*N*-methylimine)iron(II) ion at ~38000 cm^{-1}.

The observed spectrum of the ligand, biacetyl-bis-*N*-butylimine, is also shown in Fig. 1. The spectrum of the free ligand was measured in an ethanol solution, which well accorded with the result of Barany *et al.*[7]

Theoretical Consideration and Calculation of Electronic Structure

The structures of an α-diimine molecule and a tris(α-diimine)iron(II) complex are shown in Figs. 2 and 3 together with the coordinate systems used. Since no experimental data of their geometrical structures were reported, it was assumed that the C–N and the C–C bond distance in the conjugated system were 1.37 and 1.46 Å, respectively, and also the angle between the C–N and the C–C bond was 120°.

The method of theoretical treatment was already described for the acetylacetonato complexes of transition metals.[5] The outline of the calculation will be given below. The integral values characteristic for the present complex ions, however, will be discussed in detail.*3

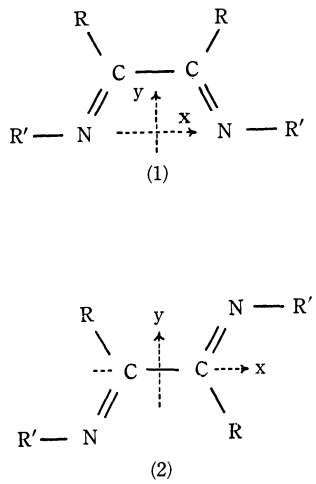

Fig. 2. Structure of α-diimine in cis form (1) and trans form (2). R=H, R′=CH_3, glyoxal-bis-*N*-methylimine; R=CH_3, R′=CH_3, biacetyl-bis-*N*-methylimine; R=CH_3, R′=C_4H_9, biacetyl-bis-*N*-butylimine.*2

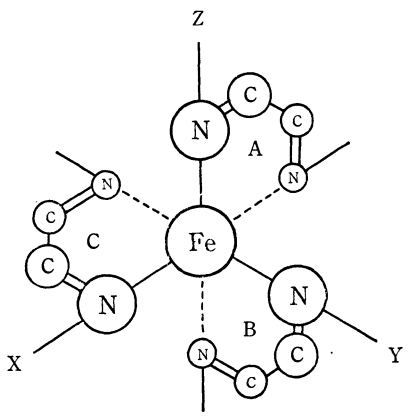

Fig. 3. The geometrical structure of tris(α-diimine)iron(II) complex and the coordinate system adopted. The Fe–N bond distance was assumed to be 2.00 Å. Only metal ion and chelate rings are shown.

SCF MO and the Lower Excited States of α-Diimine. α-Diimine molecule has four electrons in its π electron system which is made of two

*2 The IUPAC nomenclatures of glyoxal-bis-*N*-methylimine, biacetyl-bis-*N*-methylimine and biacetyl-bis-*N*-butylimine are *N*, *N*′-dimethyl-1, 2-ethanediimine, *N*, *N*′-dimethyl-2, 3-butanediimine and *N*, *N*′-dibutyl-2, 3-butanediimine, respectively.

*3 The numerical calculation was carried out by means of an OKITAC 5090H electronic computer at the Institute of Physical and Chemical Research, a NEAC 2230 at Tohoku University and a HITAC 5020E at the University of Tokyo.

TABLE 1. SCF MO AND ITS ORBITAL ENERGY (ε) OF α-DIIMINE IN CIS AND TRANS CONFORMATION

	Sym.	ε, eV	Coefficients of AO's			
			N	C	C′	N′
Cis conformation (C_{2v})						
φ_1	b_2	−14.034	0.4611	0.5361	0.5361	0.4611
φ_2	a_2	−12.010	−0.6170	−0.3454	0.3454	0.6170
φ_3	b_2	−2.428	−0.5361	0.4611	0.4611	−0.5361
φ_4	a_2	0.575	0.3454	−0.6170	0.6170	−0.3454
Trans conformation (C_{2h})						
φ_1	a_u	−14.212	0.4757	0.5231	0.5231	0.4757
φ_2	b_g	−12.068	−0.6163	−0.3466	0.3466	0.6163
φ_3	a_u	−2.637	−0.5231	0.4757	0.4757	−0.5231
φ_4	b_g	0.513	0.3466	−0.6163	0.6163	−0.3466

carbon 2pπ AO's and two nitrogen 2pπ AO's. The nitrogen atom may be in an sp^2 hybrid valence state so that the lone-pair electrons in sp^2 hybrid AO's make a coordinate bond with a metal ion.

Following Pariser-Parr-Pople's treatment,[9,10] self-consistent field molecular orbitals (SCF MO's) were calculated. Then, the energies and the wave functions of lower excited states were determined by taking into consideration the configuration interaction (CI) between all singly-excited configurations. The valence state ionization potentials (I) and the electron affinities (A) were obtained from the table given by Pilcher and Skinner[11] as follows:

$I=11.22$ eV and $A=0.62$ eV for carbon, and

$I=14.51$ eV and $A=1.20$ eV for nitrogen.

On the zero-differential overlap approximation, the core resonance integrals between adjacent AO's were calculated with the relation,

$$\beta_{ij} = \frac{S_{ij}}{S_0}\beta_0 \qquad (1)$$

where S_0 (0.248) and β_0 (−2.39 eV) are the overlap integral and the core resonance integral for benzene molecule, respectively. Evaluating the overlap integral, S_{ij}, from the table of Mulliken *et al.*,[12] the core resonance integrals were determined to be

$$\beta_{CC} = -2.130 \text{ eV} \quad \text{and} \quad \beta_{CN} = -1.947 \text{ eV}.$$

α-Diimine molecule is considered to exist in preferred trans conformation in a free state, but in cis conformation when chelated in the metal complex. To examine the geometrical effect, the calculation of SCF-CI was carried out for both cis and trans conformations.

The calculated SCF MO's are shown in Table 1. The results of the calculation of the configuration interaction are summarized in Tables 2 and 3.

Barany *et al.*[7] reported that biacetyl-bis-*N*-butylimine showed the $\pi\rightarrow\pi^*$ absorption spectrum, at 207 mμ (5.99 eV) with the molar extinction coefficient of 17000. From the observed spectrum the oscillator strength of the band was determined to be ~0.5.

As can be seen from Tables 2 and 3, the excitation energy and the intensity calculated for the first excited state, especially, those of the trans conformation, are both in reasonable agreement with those of the observed band.*4 The lowest excited state is mainly composed of the $\varphi_2\rightarrow\varphi_3$ configuration in both conformation. The lowest transition is antisymmetric in cis conformation with respect to the symmetry plane perpendicular to the plane of the α-diimine molecule (x-polarization, see Fig. 2).*5

SCF Calculation of the Ligand in the Complex. The MO's of α-diimine obtained above are self-consistent with respect to the field of the free molecule. For the ligands in the complex ion, however, the effects of the electrostatic potential fields caused by the other ligands and the metal ion are considerably strong and must be taken into account in the SCF calculation, so that the MO's used for the calculation of the electronic

9) R. Pariser and R. G. Parr, *J. Chem. Phys.*, **21**, 466, 767 (1953).
10) J. A. Pople, *Proc. Phys. Soc. (London)*, **A68**, 81 (1955).
11) G. Pilcher and H. A. Skinner, *J. Inorg. Nucl. Chem.*, **24**, 937 (1962).
12) R. S. Mulliken, C. A. Ricke, D. Orloff and H. Orloff, *J. Chem. Phys.*, **17**, 1248 (1949).

*4 Using the β_{CN} value larger than that evaluated by Eq. (1), the better agreement between the calculated and the observed results was obtained for the free ligand molecule but not for the ligand in the metal complex. It may be due to either the inaccuracy of the assumed interatomic distances or the essential difference of C–N bond character between in a free state and in a chelated state (see the discussions given in Refs. 4 and 13).
13) T. Ito, N. Tanaka, I. Hanazaki and S. Nagakura, *Sci. Repts. Tohoku Univ., First Ser.*, **50**, 168 (1967).
*5 Moreover, the absorption intensity and excitation energy of cis conformation were calculated to be lower than those of trans conformation, in accord with the original inference of Mulliken for *cis-* and *trans-*butadienes.[14]
14) R. S. Mulliken, *J. Chem. Phys.*, **7**, 21 (1939).

Table 2. Calculated and observed values of transition energy (E) and oscillator strength (f) for α-diimine

State	Calculated						Observed*	
	Cis conformation			Trans conformation				
	Sym.	E, eV	f	Sym.	E, eV	f	E, eV	f
W_1	B_1	4.58	0.38	B_u	5.02	0.96	5.99	~0.5
W_2	A_1	6.05	0.21	A_g	5.90	0		
W_3	A_1	6.82	0.47	A_g	6.72	0		
W_4	B_1	8.18	0.03	B_u	8.45	0.14		

* Observed value for biacetyl-bis-*N*-butylimine

Table 3. Wave functions of the lower excited states of α-diimine*

State	Cis conformation	Trans conformation
W_1	$0.1567\Phi(1^{-1}4) + 0.9877\Phi(2^{-1}3)$	$0.1213\Phi(1^{-1}4) + 0.9926\Phi(2^{-1}3)$
W_2	$0.9706\Phi(1^{-1}3) - 0.2406\Phi(2^{-1}4)$	$0.9754\Phi(1^{-1}3) + 0.2205\Phi(2^{-1}4)$
W_3	$0.2406\Phi(1^{-1}3) + 0.9706\Phi(2^{-1}4)$	$-0.2205\Phi(1^{-1}3) + 0.9754\Phi(2^{-1}4)$
W_4	$0.9877\Phi(1^{-1}4) - 0.1567\Phi(2^{-1}3)$	$0.9926\Phi(1^{-1}4) - 0.1213\Phi(2^{-1}3)$

* $\Phi(i^{-1}j)$ means the one-electron excited configuration from the ith MO to the jth one.

Table 4. SCF MO and its orbital energy (ε) of chelated α-diimine in iron complex*

	Sym.	ε, eV	Coefficients of AO's			
			N	C	C′	N′
φ_1	b_2	−23.675	0.5106	0.4892	0.4892	0.5106
φ_2	a_2	−22.067	0.6388	0.3033	−0.3033	−0.6388
φ_3	b_2	−12.246	−0.4892	0.5106	0.5106	−0.4892
φ_4	a_2	−8.925	0.3033	−0.6388	0.6388	−0.3033

* Obtained for the case when the formal charge of iron is zero.

Table 5. Lower four energy levels and their wave functions of chelated α-diimine in iron complex*

State	Sym.	Energy, eV	f	Wave function
W_1	B_1	4.67	0.34	$-0.1696\Phi(1^{-1}4) + 0.9855\Phi(2^{-1}3)$
W_2	A_1	5.92	0.34	$0.9991\Phi(1^{-1}3) + 0.0423\Phi(2^{-1}4)$
W_3	A_1	7.15	0.29	$-0.0423\Phi(1^{-1}3) + 0.9991\Phi(2^{-1}4)$
W_4	B_1	8.28	0.02	$0.9855\Phi(1^{-1}4) + 0.1696\Phi(2^{-1}3)$

* Obtained for the case when the formal charge of iron is zero.

structure of the metal complex are self-consistent with the distribution of π-electrons in the other ligand, the electrostatic potential field of the central metal ion being taken into account.[5] Since the degree of σ-donation caused by the coordination was uncertain, the calculations were carried out for three cases in which the number of the formal charge of iron was assumed to be 0, +1 and +2. When the charge of the central metal ion is neutralized or partly neutralized, the σ-hole appears at the coordinated nitrogen atoms. The potential due to the σ-hole was also included in the core part of the Hartree-Fock operator. Its energy was calculated from Roothaan's table,[15] using Slater 2s and 2p AO of nitrogen and 2pπ AO of carbon. The parameters in the improved SCF calculation were determined similarly, but varied according to the degree of σ-donation.

Tables 4 and 5 show the results of the SCF-CI calculation obtained for the case when the formal charge of iron is zero. These results were used in the following calculation because of the reason discussed later.*6

15) C. C. J. Roothaan, "Tables of Two-Center Coulomb Integrals Between 1s, 2s and 2p Orbitals," Special Technical Report of the University Chicago (1955).

*6 The results for the other cases are reported elsewhere.[13] The parameters for nitrogen atom used in the calculation of the results given in Tables 4 and 5 are: I=18.68, A=4.52 and β_{CN}=−1.866 eV.

The Symmetries of the Electronic Configurations of Tirs(α-diimine)iron(II) Complex. It was found by the measurement of magnetic susceptibility that the electronic spin of tris(biacetyl-bis-*N*-methylimine)iron(II) iodide is singlet in its ground state.[3] Therefore, six electrons of iron(II) may be in $3d\pi$ AO, d_{xy}, d_{yz} and d_{zx} with antiparallel spins.

As we consider explicitly only π-electron systems, tris(α-diimine)iron(II) complexes can be divided into four components, namely, a π-electron system of metal ion and those of the three ligands. By placing π-electrons in the appropriate orbitals, the wave function for the ground configuration can be represented by the equation,

$$G = |(1\bar{1}2\bar{2})^{A}(1\bar{1}2\bar{2})^{B}(1\bar{1}2\bar{2})^{C}d_{xy}\overline{d_{xy}}d_{yz}\overline{d_{yz}}d_{zx}\overline{d_{zx}}|$$

where superscripts A, B and C denote the three coordinated α-diimine molecules shown in Fig. 3.

In addition to the ground configuration, eighteen charge transfer (CT) configurations and twelve locally excited (LE) configurations were taken into account, which are given in Table 6.

The CT configuration is constructed by transferring an electron from one of the $3d\pi$ AO's to the vacant MO φ_3 or φ_4 of one of the three ligands. The LE configuration is constructed by exciting an electron in an occupied MO of one of the three ligands to a vacant MO of the same ligand.

Table 6. Singly-excited configurations taken into account for the configuration interaction calculation

Configuration	Orbitals from	Orbitals to
CT	$\left\{\begin{matrix} d_{xy} \\ d_{yz} \\ d_{zx} \end{matrix}\right\}$	$\left\{\begin{matrix} \varphi_3^{A}, & \varphi_4^{A} \\ \varphi_3^{B}, & \varphi_4^{B} \\ \varphi_3^{C}, & \varphi_4^{C} \end{matrix}\right\}$
LE	φ_1^{A}	φ_3^{A} and φ_4^{A}
	φ_2^{A}	φ_3^{A} and φ_4^{A}
	Similar eight transitions in ligand B and C	

In a way similar to the ground configuration, the wave function for a CT configuration in which one electron is transferred from d_{xy} to φ_3^{A} is expressed as,

$$CT(d_{xy}\rightarrow\varphi_3^{A}) = \frac{1}{\sqrt{2}}\{|(1\bar{1}2\bar{2})^{A}(1\bar{1}2\bar{2})^{B}(1\bar{1}2\bar{2})^{C}\varphi_3^{A}\overline{d_{xy}}d_{yz}\overline{d_{yz}}d_{zx}\overline{d_{zx}}| + |(1\bar{1}2\bar{2})^{A}(1\bar{1}2\bar{2})^{B}(1\bar{1}2\bar{2})^{C}d_{xy}\overline{\varphi_3}^{A}d_{yz}\overline{d_{yz}}d_{zx}\overline{d_{zx}}|\}$$

Similarly, the wave function for a LE configuration in which one electron in φ_2^{A} is excited to φ_3^{A} is expressed as,

$$LE(\varphi_2^{A}\rightarrow\varphi_3^{A}) = \frac{1}{\sqrt{2}}\{|(1\bar{1}3\bar{2})^{A}(1\bar{1}2\bar{2})^{B}(1\bar{1}2\bar{2})^{C}d_{xy}\overline{d_{xy}}d_{yz}\overline{d_{yz}}d_{zx}\overline{d_{zx}}| + |(1\bar{1}2\bar{3})^{A}(1\bar{1}2\bar{2})^{B}(1\bar{1}2\bar{2})^{C}d_{xy}\overline{d_{xy}}d_{yz}\overline{d_{yz}}d_{zx}\overline{d_{zx}}|\}$$

Other CT and LE configurations are expressed in a similar way. By taking the linear combination of the above-mentioned wave functions, the ground, the CT and the LE configurations are classified into the irreducible representations of D_3 symmetry, which are given below.

A_1:

$$G = G$$

$$CT_1^{A_1} = \frac{1}{\sqrt{6}}\{CT(d_{xy}\rightarrow\varphi_3^{A}) - CT(d_{yz}\rightarrow\varphi_3^{A}) - CT(d_{xy}\rightarrow\varphi_3^{B}) + CT(d_{zx}\rightarrow\varphi_3^{B}) + CT(d_{yz}\rightarrow\varphi_3^{C}) - CT(d_{zx}\rightarrow\varphi_3^{C})\}$$

$$CT_2^{A_1} = \frac{1}{\sqrt{6}}\{CT(d_{xy}\rightarrow\varphi_4^{A}) + CT(d_{yz}\rightarrow\varphi_4^{A}) + CT(d_{xy}\rightarrow\varphi_4^{B}) + CT(d_{zx}\rightarrow\varphi_4^{B}) + CT(d_{yz}\rightarrow\varphi_4^{C}) + CT(d_{zx}\rightarrow\varphi_4^{C})\}$$

$$CT_3^{A_1} = \frac{1}{\sqrt{3}}\{CT(d_{zx}\rightarrow\varphi_4^{A}) + CT(d_{yz}\rightarrow\varphi_4^{B}) + CT(d_{xy}\rightarrow\varphi_4^{C})\}$$

$$LE_1^{A_1} = \frac{1}{\sqrt{3}}\{LE(\varphi_1^{A}\rightarrow\varphi_3^{A}) + LE(\varphi_1^{B}\rightarrow\varphi_3^{B}) + LE(\varphi_1^{C}\rightarrow\varphi_3^{C})\}$$

$$LE_2^{A_1} = \frac{1}{\sqrt{3}}\{LE(\varphi_2^{A}\rightarrow\varphi_4^{A}) + LE(\varphi_2^{B}\rightarrow\varphi_4^{B}) + LE(\varphi_2^{C}\rightarrow\varphi_4^{C})\}$$

A_2:

$$CT_1^{A_2} = \frac{1}{\sqrt{6}}\{CT(d_{xy}\rightarrow\varphi_3^{A}) + CT(d_{yz}\rightarrow\varphi_3^{A}) + CT(d_{xy}\rightarrow\varphi_3^{B}) + CT(d_{zx}\rightarrow\varphi_3^{B}) + CT(d_{yz}\rightarrow\varphi_3^{C}) + CT(d_{zx}\rightarrow\varphi_3^{C})\}$$

$$CT_2^{A_2} = \frac{1}{\sqrt{3}}\{CT(d_{zx}\rightarrow\varphi_3^{A}) + CT(d_{yz}\rightarrow\varphi_3^{B}) + CT(d_{xy}\rightarrow\varphi_3^{C})\}$$

$$CT_3^{A_2} = \frac{1}{\sqrt{6}}\{CT(d_{xy}\rightarrow\varphi_4^A) - CT(d_{yz}\rightarrow\varphi_4^A) - CT(d_{xy}\rightarrow\varphi_4^B) + CT(d_{zx}\rightarrow\varphi_4^B) + CT(d_{yz}\rightarrow\varphi_4^C) - CT(d_{zx}\rightarrow\varphi_4^C)\}$$

$$LE_1^{A_2} = \frac{1}{\sqrt{3}}\{LE(\varphi_2^A\rightarrow\varphi_3^A) + LE(\varphi_2^B\rightarrow\varphi_3^B) + LE(\varphi_2^C\rightarrow\varphi_3^C)\}$$

$$LE_2^{A_2} = \frac{1}{\sqrt{3}}\{LE(\varphi_1^A\rightarrow\varphi_4^A) + LE(\varphi_1^B\rightarrow\varphi_4^B) + LE(\varphi_1^C\rightarrow\varphi_4^C)\}$$

E:

$$CT_1^E = \frac{1}{2}\{CT(d_{xy}\rightarrow\varphi_3^B) + CT(d_{zx}\rightarrow\varphi_3^B) - CT(d_{yz}\rightarrow\varphi_3^C) - CT(d_{zx}\rightarrow\varphi_3^C)\}$$

$$CT_2^E = \frac{1}{\sqrt{12}}\{2CT(d_{xy}\rightarrow\varphi_3^A) - 2CT(d_{yz}\rightarrow\varphi_3^A) - CT(d_{zx}\rightarrow\varphi_3^B) + CT(d_{xy}\rightarrow\varphi_3^B) - CT(d_{yz}\rightarrow\varphi_3^C) + CT(d_{zx}\rightarrow\varphi_3^C)\}$$

$$CT_3^E = \frac{1}{\sqrt{2}}\{CT(d_{yz}\rightarrow\varphi_3^B) - CT(d_{xy}\rightarrow\varphi_3^C)\}$$

$$CT_4^E = \frac{1}{\sqrt{12}}\{2CT(d_{xy}\rightarrow\varphi_4^A) + 2CT(d_{yz}\rightarrow\varphi_4^A) - CT(d_{xy}\rightarrow\varphi_4^B) - CT(d_{zx}\rightarrow\varphi_4^B) - CT(d_{yz}\rightarrow\varphi_4^C) - CT(d_{zx}\rightarrow\varphi_4^C)\}$$

$$CT_5^E = \frac{1}{2}\{CT(d_{zx}\rightarrow\varphi_4^B) - CT(d_{xy}\rightarrow\varphi_4^B) - CT(d_{yz}\rightarrow\varphi_4^C) + CT(d_{zx}\rightarrow\varphi_4^C)\}$$

$$CT_6^E = \frac{1}{\sqrt{6}}\{2CT(d_{zx}\rightarrow\varphi_4^A) - CT(d_{yz}\rightarrow\varphi_4^B) - CT(d_{xy}\rightarrow\varphi_4^C)\}$$

$$LE_1^E = \frac{1}{\sqrt{6}}\{2LE(\varphi_1^A\rightarrow\varphi_3^A) - LE(\varphi_1^B\rightarrow\varphi_3^B) - LE(\varphi_1^C\rightarrow\varphi_3^C)\}$$

$$LE_2^E = \frac{1}{\sqrt{6}}\{2LE(\varphi_2^A\rightarrow\varphi_4^A) - LE(\varphi_2^B\rightarrow\varphi_4^B) - LE(\varphi_2^C\rightarrow\varphi_4^C)\}$$

$$LE_3^E = \frac{1}{\sqrt{2}}\{LE(\varphi_2^B\rightarrow\varphi_3^B) - LE(\varphi_2^C\rightarrow\varphi_3^C)\}$$

$$LE_4^E = \frac{1}{\sqrt{2}}\{LE(\varphi_1^B\rightarrow\varphi_4^B) - LE(\varphi_1^C\rightarrow\varphi_4^C)\}$$

There is another similar set of ten wave functions with E representation which are orthogonal to the above wave functions.

Configuration Interaction. The matrix elements of the total electronic Hamiltonian between the configurations were calculated in a way similar to the case of the acetylacetonato complex.*7 The diagonal element of the CT configuration, $E_{CT(i)}$, is represented by means of the equation,

$$E_{CT(i)} = I(\text{metal}) - A_{(i)}(\text{ligand}) + \Delta_{(i)} \qquad (2)$$

where, I(metal) is the valence state ionization potential of 3dπ AO of iron, $A_{(i)}$(ligand), the electron affinity to put an electron into the ith vacant MO of the ligand and $\Delta_{(i)}$, the electrostatic interaction energy between the electron donor and acceptor. $A_{(i)}$(ligand) may be equal to the orbital energy with sign reversed of the MO to which an electron is transferred. There remains difficulty in the actual evaluation of E_{CT}, because it is very sensitive to the σ-electron distribution and, also, because $A_{(i)}$(ligand) cannot be determined accurately (see the discussion given in Ref. 5).

Figure 4 shows the relation between $E_{CT(1)}$ and the formal charge of iron, which was roughly evaluated by the calculation of an appropriate two-center repulsion integral with the point charge approximation. Considering the fact that the CT band appears at about 2.2 eV ($\sim$18000 cm^{-1}), the formal charge of iron seems to be close to zero though there is some uncertainty in the estimated value of E_{CT}. Therefore, the MO's of the ligands used in the following calculation are those constructed with the condition that the formal charge of iron is zero.

As is evident from the above discussion, the accurate evaluation of E_{CT} is quite difficult. Therefore, in the present calculation, $E_{CT(1)}$, the diagonal element of CT configurations corresponding to d$\rightarrow\varphi_3$ transition, was treated as a parameter and set to be 1.0 eV. The value of $E_{CT(2)}$ corresponding to d$\rightarrow\varphi_4$ transition was determined to be $E_{CT(2)} = E_{CT(1)} + 3.87$ eV, considering the difference of $A_{(i)}$ and $\Delta_{(i)}$ between φ_3 and φ_4.

*7 The details of the matrix elements are shown in Ref. 13.

TABLE 7. WAVE FUNCTIONS AND ENERGIES OF THE LOWER ELECTRONIC STATES OF TRIS(α-DIIMINE)IRON(II) ION

	E, eV*	Sym.	Wave function**
W_0	−1.391	A_1	$-0.8015\,G-0.5797\,CT_1^{A_1}+0.1353\,CT_2^{A_1}$
W_1	0.784	E	$-0.9720\,CT_1^{E}-0.2342\,LE_3^{E}$
W_2	0.816	A_2	$-0.9794\,CT_1^{A_2}-0.2014\,LE_1^{A_2}$
W_3	0.896	E	$0.9896\,CT_2^{E}+0.1441\,LE_1^{E}$
W_4	4.553	E	$-0.9423\,CT_4^{E}-0.3345\,LE_2^{E}$
W_5	4.579	E	$0.1855\,CT_1^{E}+0.5972\,CT_5^{E}-0.7412\,LE_3^{E}+0.2441\,LE_4^{E}$
W_6	4.701	A_2	$0.9551\,CT_3^{A_2}-0.1854\,LE_1^{A_2}+0.2268\,LE_2^{A_2}$
W_7	4.819	E	$-0.1430\,CT_1^{E}+0.7777\,CT_5^{E}+0.6095\,LE_3^{E}$
W_8	5.318	A_2	$-0.1958\,CT_1^{A_2}+0.2258\,CT_3^{A_2}+0.9438\,LE_1^{A_2}-0.1410\,LE_2^{A_2}$
W_9	5.917	E	$0.1440\,CT_2^{E}-0.9890\,LE_1^{E}$

* The energy of the ground configuration is taken to be zero.
** Only main configurations are written.

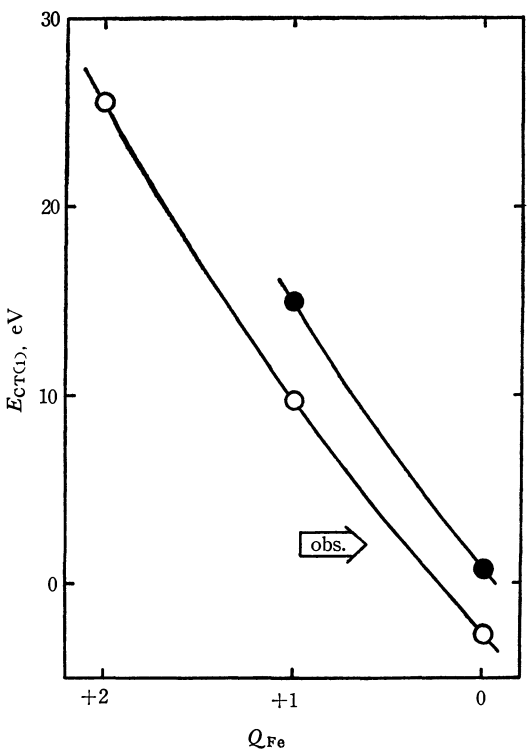

Fig. 4. The relation between $E_{CT(1)}$ and the formal charge of iron, Q_{Fe}, where $E_{CT(1)}$ is the diagonal element of the CT configuration with the lowest energy. ○ and ● correspond to d^n and $d^{n-1}s$ configuration, respectively.

The diagonal elements of LE configurations are expressed as the sum of the excitation energy of the chelated ligand molecule, $E_{LE}(\varphi_i\rightarrow\varphi_j)$, and the additional term including the integral K'_{ij}. The latter is the repulsion integral defined by

$$K'_{ij}=\int\varphi_i^{A}(1)\varphi_j^{A}(1)\frac{e^2}{r_{12}}\varphi_i^{B}(2)\varphi_j^{B}(2)d\tau_{12} \quad (3)$$

The K'_{ij}'s were calculated with the zero-differential overlap and the point charge approximation.*8

The off-diagonal matrix elements between G and CT and between CT and LE were accounted for only by means of β, the core resonance integral between the appropriate $3d\pi$ AO of iron and $2p\pi$ AO of nitrogen. It was evaluated with the relation,[16]

$$\beta=-S\frac{I_{Fe}+I_N}{2} \quad (4)$$

TABLE 8. COMPARISON OF OBSERVED VALUES WITH CALCULATED ELECTRONIC STRUCTURES OF TRIS(α-DIIMINE)IRON(II) ION

Transition from W_0 to	Calculated E eV**	Calculated f	Observed* E, eV**	Observed* f
W_1	2.18	0.002	2.19 ~2.4 (shoulder)	0.17
W_2	2.21	0.002		
W_3	2.29	0.357		
W_4	5.94	~0		
W_5	5.97	0.076	~5.3 (shoulder)	1.5
W_6	6.09	0.024		
W_7	6.21	0.266	6.56	
W_8	6.71	0.675		
W_9	7.31	0.655		

* Observed values for tris(biacetyl-bis-*N*-methylimine)iron(II) tetrafluoroborate in aqueous solutions.
** Transition energy.

*8 In contrast with the treatment reported previoulsy,[5] the LE configuration is constructed with only one kind of singly-excited configuration. Therefore, $E_{LE}(\varphi_i\rightarrow\varphi_j)$'s appearing in the diagonal elements of the LE configurations correspond to the transition energies without CI. The interactions among the LE configurations were taken into account in the calculation of the CI for the whole complex.

16) R. S. Mulliken, *J. Phys. Chem.*, **56**, 295 (1952).

where S is the overlap integral, and I_{Fe} and I_N are the valence state ionization potentials of iron and nitrogen, respectively. The estimation of the overlap integral was made with the aid of the Slater AO of nitrogen and the two-term expanded AO of iron determined by Richardson *et al.*[17] It was calculated to be 0.084, using the table given by Jaffé.[18] I_{Fe} and I_N are 5.07 eV and 18.68 eV respectively and β amounts to -0.99 eV.

The results obtained by the configuration interaction calculation are shown in Table 7, and the calculated transition energy and oscillator strength are compared with the observed ones in Table 8.

Stabilization caused by the Charge Transfer. According to the present theoretical investigation, the energy of the ground state is lower than that of the ground configuration by 1.39 eV (32.0 kcal/mol). This stabilization is caused by the interaction between the ground and the CT configurations; the contribution of the CT configuration to the ground state amounts to about 30%. This means that the so-called π-back donation from the metal to the ligands is considerably large. This phenomenon may be responsible for the one of the origins of the unusual stability of tris(α-diimine)iron(II) complexes.

Interpretation of the Electronic Spectra

The spectra given in Fig. 1 exhibit a weak absorption band near 28000 cm^{-1} in all tris(α-diimine)iron(II) complexes investigated. The careful measurement also revealed a shoulder band with almost the same intensity near 25000 cm^{-1}. The shoulder and the peak may be assigned to the d→d transitions which correspond to the $^1A_{1g}\rightarrow {}^1T_{1g}$ and the $^1A_{1g}\rightarrow {}^1T_{2g}$ transition of the octahedral case, in view of their low intensities and also on the basis of the study reported by Shimura *et al.*[19] They found that the absorption frequencies of the iron(II) complex are smaller by 7×10^{13} sec^{-1} than those of the corresponding cobalt(III) complex independent of the kind of ligand, as far as the same kind of absorption bands are compared and both complexes assume the diamagnetic $(3d)^6$ configuration. Any further discussion on these bands is not given, because the authors were concerned with a parity-allowed transition of the π-electron system in the present study.

From the results given in Table 7, it can be concluded that the observed intense band at the visible region is reasonably assigned to the almost pure CT absorption accompanying the π-electron migration from $3d\pi$ AO of iron to the lowest vacant π MO, φ_3, of the ligands.

Since the α-diimine ligands has C_{2v} symmetry in the cis form, the $\pi\rightarrow\pi^*$ transition in the ligand has a transition moment either parallel (x) or perpendicular (y) to the nitrogen-nitrogen direction in the plane of the molecule (see Fig. 2). As has been disucssed by Larsen *et al.*,[20] the x-polarized transition in three ligands in the metal complex of D_3 symmetry gives rise to the $A_1\rightarrow A_2$ and the $A_1\rightarrow E$ transition, while y-polarized transition, the $A_1\rightarrow A_1$ and the $A_1\rightarrow E$ one, the $A_1\rightarrow A_1$ transition being symmetrically forbidden. Consequently, if the transition is y-polarized, there should appear a single band with its intensity three times as large as that of single α-diimine ligand. On the other hand, if the transition is x-polarized, the intensity ratio of the LE bands corresponding to the $A_1\rightarrow E$ and the $A_1\rightarrow A_2$ ought to be 1 : 2. Furthermore, the energy separation between these bands is $6K'_{ij}$ for $\varphi_i\rightarrow\varphi_j$ transition.

The observed spectrum in the ultraviolet region was composed of an intense peak and a moderately intense shoulder at the side of longer wavelengths. In view of their large intensities and energies and also in comparison with the absorption spectrum of the free ligand (see Fig. 1), both of them should be assigned to the lowest LE transitions. In fact, the calculated result predicts that the LE transitions corresponding to the x-polarized excitation $\varphi_2\rightarrow\varphi_3$ in the ligand appear in this region with splitting by 0.67 eV into the A_2 and E components. The observed spectra really show the splitting, which supports, at least qualitatively, the theoretical prediction. Quantitatively, however, the splitting was found to be nearly twice as large as the calculated value. This discrepancy seems to be explained by considering the mixing of the second CT transition d→φ_4 into the loewst LE transitions. The calculation has revealed that this second CT configuration appears in almost the same energy as the lowest LE configuration and that its mixing especially with the E component of the LE band is significant.*9

Therefore, it seems reasonable to conclude that the main peak results from the LE transition with $A_1\rightarrow A_2$ symmetry whereas the shoulder is due to the overlap of the d→φ_4 transition and the LE transition with $A_1\rightarrow E$ symmetry or their mixed states.

The replacement of the alkyl groups (R or R') attached to the conjugated system of the ligand with a larger alkyl group gives rise to a shift of absorption maxima of both the visible and the

17) J. W. Richardson, W. C. Nieuwpoort, R. R. Powell and W. F. Edgell, *J. Chem. Phys.*, **36**, 1057 (1962).
18) H. H. Jaffé, *ibid.*, **21**, 258 (1953).
19) Y. Shimura, N. Matsuoka and T. Yasui, *Nippon Kagaku Zasshi (J. Chem. Soc. Japan, Pure Chem. Sect.)*, **85**, 635 (1964).
20) E. Larsen, S. F. Mason and G. H. Searle, *Acta Chem. Scand.*, **20**, 191 (1966).
*9 Another shoulder band is observed near 38000 cm^{-1} in the spectrum of tris(glyoxal-bis-*N*-methylimine)-iron(II) complex, which may be due to the interaction of CT(d→φ_4) and the E component of LE band.

ultraviolet bands toward longer wavelengths, as shown in Fig. 1. Such a frequency shift was also observed for alkyl derivatives of butadiene.[21] Although the sensitivity to the alkyl substitution is different between the visible and the ultraviolet band, the origin of the frequency shift may be the same. It is also said that the larger the substituent is, the lower the energy of the lowest vacant orbital may be.

The authors wish to express their hearty thanks to Dr. Koji Kaya of the Institute of Physical and Chemical Research, Tokyo, for measuring the vacuum ultraviolet spectra. They also thank the Ministry of Education for the financial support granted for this research.

21) A. I. Scott, "Interpretation of the Ultraviolet Spectra of Natural Products," International Series of Monographs on Organic Chemistry ed. by D. H. R. Barton and W. Doering, Vol. 7, Pergamon Press, Oxford (1964), p. 21.

BULLETIN OF THE CHEMICAL SOCIETY OF JAPAN VOL. 41 373—377 (1968)

Complexes of Copper Chlorides with Benzophenoneimine

Akira MISONO, Tetsuo OSA and Seiichiro KODA

Department of Industrial Chemistry, Faculty of Engineering, The University of Tokyo, Hongo, Bunkyo-ku, Tokyo

(Received August 1, 1967)

We tried to prepare complexes of copper chlorides with benzophenoneimine. The complex $CuCl_2 \cdot 2Ph_2C{=}NH$ and the complex $CuCl \cdot Ph_2C{=}NH$ were newly prepared, and some of their properties were investigated by physico-chemical techniques. Besides these, two other complexes were obtained, but they were not completely stoichiometric compounds.

It is well known that aldimines and ketimines which can act as multi-dentate ligands form stable complexes with copper ions.[1] Several investigations have been published on the complexes of amines with copper halides.[2] However, there seems not yet to have been any report on the complex formation of benzophenoneimine with copper halides. The present authors have been interested in the cleavage of the bond between nitrogen and hydrogen[3] and have tried to prepare complexes of copper chlorides with benzophenoneimine in order to clarify the effect of complex formation on the oxidation of benzophenoneimine. In this paper, the authors wish to report on the preparation of such complexes.

Results and Discussion

It was observed that when benzophenoneimine was added to the acetonitrile solution of copper(II) chloride, some precipitates began to appear immediately. They were found to be complexes of copper(II) chloride with benzophenoneimine. From the precipitates, the complex, $CuCl_2 \cdot 2Ph_2C{=}NH$ (I) was isolated as a grey-purple powder. It became a green solution in chloroform. The curve of the absorption spectrum (Fig. 1, full line: ν_{max} ~13.7 kK, $\log \varepsilon = 2.3$) was similar to that of copper(II) dipyridine dichloride ($CuCl_2py_2$), though the absorption maximum of $CuCl_2py_2$ due to the d-d transition is at about 13.2 kK (in

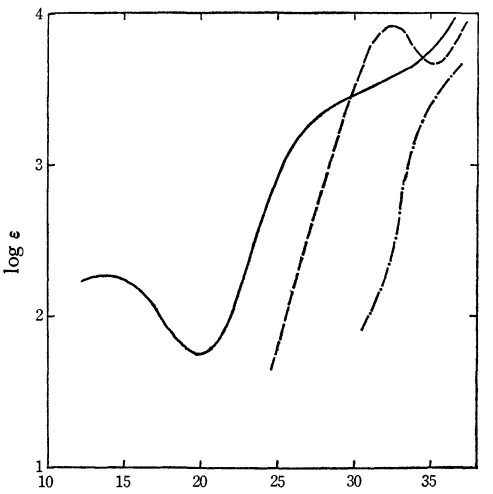

Fig. 1. The absorption spectra in chloroform.
——: $CuCl_2 \cdot 2Ph_2C{=}NH$
— —: $CuCl \cdot Ph_2C{=}NH$
·—·: $Ph_2C{=}NH$

1) D. F. Martin, *Preparative Inorg. Reactions*, **1**, 59 (1964).
2) a) J. F. Weiss, G. Tollin and J. T. Yoke, III, *Inorg. Chem.*, **3**, 1344 (1964). b) J. R. Clifton and J. T. Yoke, III, *ibid.*, **5**, 1630 (1966). c) A. R. Burkin, *J. Chem. Soc.*, **1950**, 122; R. G. Wilkins and A. R. Burkin, *ibid.*, **1950**, 127.
3) A. Misono, T. Osa and S. Koda, This Bulletin, **40**, 912 (1967).

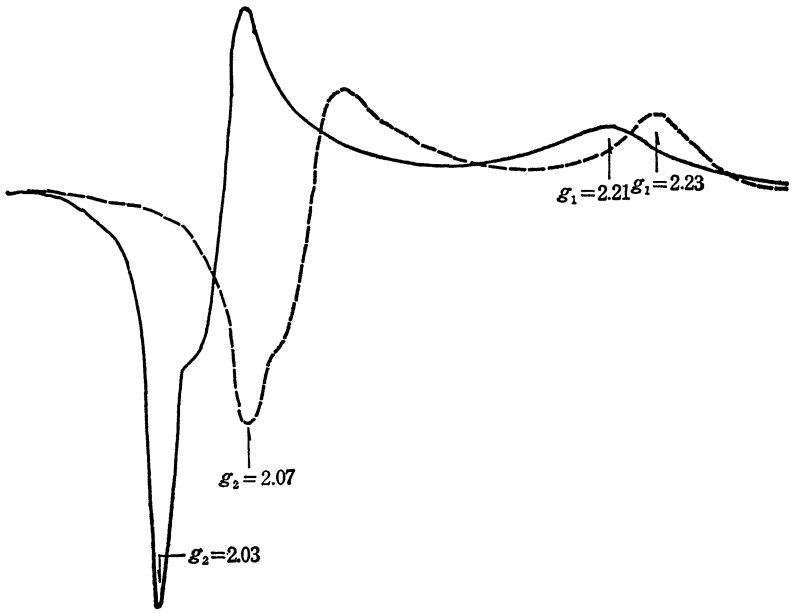

Fig. 2. The e. p. r. signal in the powder state at room temperature.
——: $CuCl_2 \cdot 2Ph_2C{=}NH$ ——: $CuCl_2py_2$

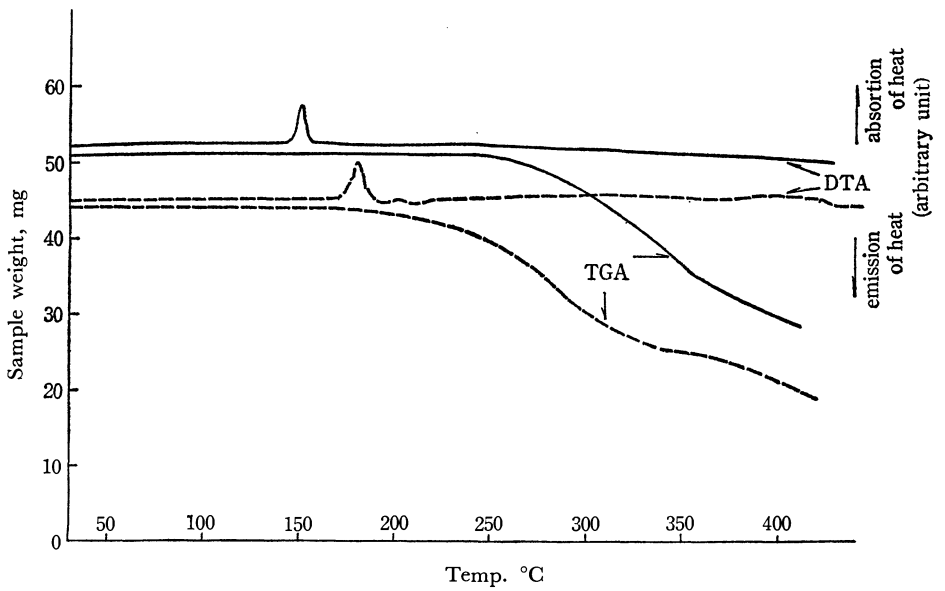

Fig. 3. The differential thermal analyses (DTA) and the thermogravimetric analyses (TGA).
——: $CuCl_2 \cdot 2Ph_2C{=}NH$ (44 mg) ——: $CuCl \cdot Ph_2C{=}NH$ (51 mg)
The elevating speed of the temperature, 2.5°C/min
In the atmosphere of nitrogen
The reference for DTA, α-alumina

pyridine).[4] This complex was slightly soluble in benzene and acetonitrile. The e. p. r. signal of this complex showed a typical resolution of the d^9 Cu(II) resonance according to the anisotropy in the g values (g_1=2.21, g_2=2.03), as shown in Fig. 2. The g values can be estimated approximately from the e. p. r. spectra of the complex in the

4) E. Ochiai, *Tetrahedron*, **20**, 1831 (1964); V. S. Sergeeva and S. V. Plyushcheva, *Zh. Neorgan. Khim.*, **7**, 2357 (1962).

powder state.[5] For a comparative study, the e. p. r. spectrum of $CuCl_2py_2$ in the powder state was observed under similar conditions (Fig. 2, dashed line). The observed g values ($g_1=2.23$, $g_2=2.07$) approximated the g values obtained in the vitreous state ($g_{\parallel}=2.241$, $g_{\perp}=2.079$).[6] The g values of the complex I were smaller than those of the triethylamine complex of copper(II) chloride, $CuCl_2\cdot 2Et_3N$ ($g_1=2.27$, $g_2=2.06$).[2a] Generally speaking, the g values decrease with an increase in the "covalency" between ligands and the central metal ion.[7] Therefore, smaller g values of the complex I in comparison with the complex $CuCl_2\cdot 2Et_3N$ may indicate a greater "covalency", which can be expected from the existence of a C=N double bond and the phenyl groups adjacent to it in the ligand, benzophenoneimine. The complex I was stable at room temperature in the solid state, as can be seen from the invariable results of the two elementary analyses, one of which was performed soon after the preparation, and the other, after 12 days. However, it was gradually decomposed at higher temperatures to yield a dark complicated mass, while the e. p. r. signal due to the divalent copper disappeared. This complex or its mixture with its decomposition products melted at about 180°C (Fig. 3, dashed line), at which time, the e. p. r. signal decreased rapidly (Fig. 4). The decomposition products seemed to be composed of various components, from which $CuCl\cdot Ph_2C{=}NH$ (*cf.* the next section) was isolated. The decomposition of the complex I may be a thermal-induced oxidation-reduction, similar to that of the triethylamine complex of copper(II) chloride, $CuCl_2\cdot 2Et_3N$.[2a] However, it is interesting to note that this complex, I, was considerably more stable than $CuCl_2\cdot 2Et_3N$, which has been reported to decompose completely at 20°C.[2a]

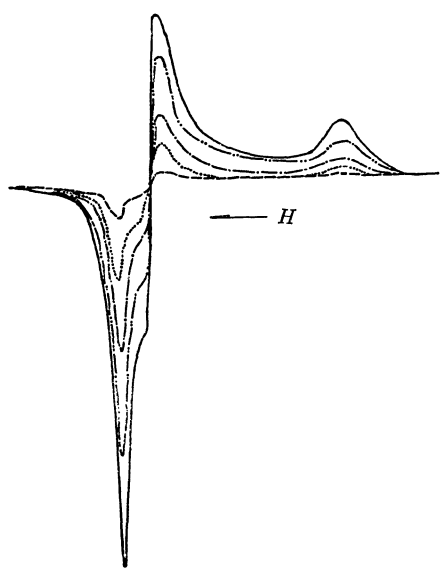

Fig. 4. The decrease of the e. p. r. signal according to the thermal decomposition.
———: Before heating and/or after 30 min (100°C)+10 min (130°C)
—··—: After additional 15 min (150°C)+20 min (160°C)+5 min (165°C)+5 min (170°C)
—·—·: After additional 5 min (177°C)
·····: After additional 5 min (180°C)
———: After additional 20 min (180°C)

Besides the complex I, another complex, II, was produced. It did not seem to be a simple species, but was perhaps mainly a 1 : 1 complex. This complex was produced as a yellow precipitate and as a by-product when the complex I was recrystallized from a hot chloroform solution. Besides, a similar yellow precipitate was formed when copper(II) chloride was stirred into a chloroform solution of the complex I. This complex, II, was insoluble in chloroform or in other ordinary solvents. It seemed probable that this complex was a binuclear (or sometimes polynuclear) complex bridged by chloride ions. The relation between the complex I and the complex II may correspond to that between the copper(II) chloride complexes of acetonitrile ($CuCl_2\cdot 2CH_3CN$ and $Cu_2Cl_4(CH_3CN)_2$, $Cu_3Cl_6(CH_3CN)_2$).[8]

The complex I was also produced in chloroform by mixing copper(II) chloride with benzophenoneimine.

A pale yellow complex, $CuCl\cdot Ph_2C{=}NH$ (III), and a red complex, $CuCl\cdot nPh_2C{=}NH$ (IV) (n is about two), were obtained by mixing benzophenoneimine with copper(I) chloride in benzene. The molecular weight of the complex III in benzene, obtainable from the vapor pressure osmometry at about 30°C, corresponded to 1.35 times the formula weight. Considering the facts[9] that the copper(I) halide complexes with phosphine derivatives were tetrameric in crystalline state and were in equilibrium with tetrameric and monomeric forms in solutions, this value seems not to be unreasonable. This complex was mostly transparent in the visible region (Fig. 1, dashed line). The complex III was quite stable against oxygen in the solid state, but the benzene solution of this complex absorbed oxygen rather easily and turned gradually greenish-brown. This complex melted at about 135°C. Correspondingly, the absorption of heat was observed to begin at about

5) *Jikken Kagaku Koza, zoku* 13 *(Lectures on Experimental Chemistry,* the second series, Volume 13), p. 195, ed. by Chemical Society of Japan, Maruzen Co., Ltd., Tokyo (1967).
6) H. R. Gersmann and J. D. Swalen. *J. Chem. Phys.*, **36**, 3221 (1962).
7) D. Kivelson and R. Neiman, *ibid.*, **35**, 149 (1961).
8) R. D. Willett and R. E. Rundle, *ibid.*, **40**, 838 (1964).
9) F. G. Mann, D. Purdie and A. F. Wells, *J. Chem. Soc.*, **1936**, 1503.

140°C (Fig. 3, full line). The discrepancy in the temperatures may be caused by the faster elevating speed of the temperature in the differential thermal analysis.

The complex IV was unstable, judging from the fact that the *n* value often easily changed. For example,[2b] the complex $CuCl\cdot(C_2H_5)_2NH$ is known to be more stable than the complex, $CuCl\cdot 2(C_2H_5)_2NH$.

The coordinated benzophenoneimine showed, at different positions, absorption peaks corresponding to those at 3252 (N-H stretching), 1363, 1197, and 892 cm^{-1} in the free benzophenoneimine. The other peaks in the region from 4000 to 500 cm^{-1} shifted slightly in the coordinated benzophenoneimine (Fig. 5).

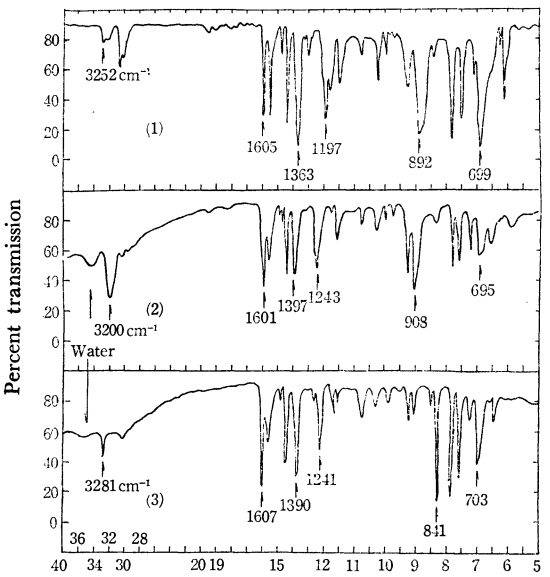

Fig. 5. The infrared spectra.
(1) Free $Ph_2C{=}NH$ (capillary)
(2) $CuCl\cdot Ph_2C{=}NH$ (KBr)
(3) $CuCl_2\cdot 2Ph_2C{=}NH$ (KBr)

Experimental

Reagents. *Copper(II) Chloride.* Anhydrous copper(II) chloride was prepared through the dehydration by thionyl chloride from commercial copper(II) chloride dihydrate.[10]

Copper(I) Chloride. Commercial copper(I) chloride was treated by dilute sulfurous acid.[11]

Benzophenoneimine. Benzophenoneimine was prepared from phenyl magnesium bromide and benzonitrile[12] and was then distilled and stored under dried nitrogen (bp 146.5—148°C/7.5 mmHg). It contained a small amount of benzophenone as an impurity, judging from its infrared spectrum.

Benzene and n-Hexane. Commercial solvents were dried with sodium, distilled, and stored under dried nitrogen.

Acetonitrile. Commercial acetonitrile was dried with phosphorus pentoxide, distilled, and stored under dried nitrogen.

Chloroform. Commercial chloroform was passed through an alumina column, distilled, and stored under dried nitrogen.

Copper(II) Dipyridine Dichloride ($CuCl_2py_2$). This complex was precipitated by adding pyridine to a methanol solution of copper(II) chloride.

Found: C, 40.66; H, 3.36; N, 9.52%. Calcd. for $CuCl_2\cdot 2C_5H_5N$: C, 41.03; H, 3.45; N, 9.57%.

Procedure. All parts of the preparation of the complexes were carried out under dried nitrogen.

The e. p. r. spectra were observed with a Japan Electron Optics Laboratory Co., Ltd., e. p. r. spectrometer, Model JS-3BS-X. The value of field strength was calculated from the observed signal of the manganese marker. The estimation of the *g* values were based on accurate measurements of the changes in field strength from the point of approximate calibration.

The infrared spectra were measured with two Japan Spectroscopic Co., Ltd., infrared spectrometers, Model DS-402G and Model DS-301. The spectra of the complexes were measured in the KBr disk (sample 1 mg/KBr 150 mg).

The absorption spectra were observed with a Hitachi Co., Ltd., Hitachi spectrometer, Model ESP-2.

The thermal analyses were carried out with a Rigaku-Denki Co., Ltd., differential thermal and thermogravimetric analyzer.

The melting points were observed with a Yanagimoto Seisakusho Co., Ltd., micro-melting-point apparatus.

Copper(II) Chloride Complexes. a) To 150 m*l* of acetonitrile there were added 0.618 g (4.59 mmol) of copper(II) chloride and 1.701 g (9.40 mmol) of benzophenoneimine. The mixture was then stirred for 1 hr at room temperature, and the precipitates thus formed were separated (1.990 g). These precipitates were recrystallized from a chloroform solution. A grey-purple powder was thus obtained.

Found: C, 61.59; H, 4.30; N, 5.69%. Calcd for $CuCl_2\cdot 2Ph_2C{=}NH$: C, 62.85; H, 4.47; N, 5.64%.

After it had been stored for 12 days under nitrogen at room temperature, the powder was again analyzed.

Found: C, 61.54; H, 4.30; N, 5.67%.

A yellow-brown powder was also obtained as a by-product in the course of recrystallization. This was washed with sufficient amounts of acetonitrile and chloroform.

Found: C, 47.51; H, 3.43; N, 4.52%. Calcd for $CuCl_2\cdot Ph_2C{=}NH$: C, 49.46; H, 3.52; N, 4.44%.

b) In 90 m*l* of chloroform, 4.031 g (30.0 mmol) of copper(II) chloride and 3.567 g (19.7 mmol) of benzophenoneimine were stirred for 45 min at room temperature. The resulting mixture was then filtered. To the green filtrate 90 m*l* of acetonitrile were added, and the resulting precipitate was separated. A grey-purple powder was thus obtained; 0.820 g.

Found: C, 61.23; H, 4.43; N, 5.81; Cl, 15.11%. Calcd for $CuCl_2\cdot 2Ph_2C{=}NH$: C, 62.85; H, 4.47; N, 5.64; Cl, 14.27%.

10) A. R. Pray, *Inorg. Syn.*, **5**, 153 (1957).
11) R. N. Keller and H. D. Wycoff, *ibid.*, **2**, 1 (1946).
12) P. L. Pickard and T. L. Tolbert, *Org. Syn.*, **44**, 51 (1964).

Thermal Decomposition of the Copper(II) Chloride Complex, I, $CuCl_2 \cdot 2Ph_2C{=}NH$. The complex I was introduced into an e. p. r. sample tube under reduced pressure. This tube was heated in a thermostat at a certain temperature for a desired period. Then the e. p. r. spectrum was observed at room temperature. This procedure was repeated until the signal due to divalent copper disappeared (100°C, 30 min; 130°C, 10 min; 150°C, 15 min; 160°C, 20 min; 165°C, 5 min; 170°C, 5 min; 175°C, 5 min; 177°C, 5 min; 180°C, 5 min; 180°C, 20 min).

The complex I, in a sealed tube under dried nitrogen, was heated at 175°C for 30 min. A dark mass (viscous around 175°C) remained. This was washed with *n*-hexane, and then with hot benzene. From the benzene washing, a yellow powder was obtained after evaporating the benzene. This powder was again dissolved in benzene. By adding *n*-hexane to this benzene solution, a yellow powder was precipitated. The infrared spectrum of this powder was almost identical with that of the complex III.

Found: C, 55.84; H, 4.00; N, 5.53; Cl, 13.69%. Calcd for $CuCl \cdot Ph_2C{=}NH$: C, 55.71; H, 3.91; N, 5.00; Cl, 12.65%.

Copper(I) Chloride Complexes. In 25 m*l* of benzene, 1.064 g (10.7 mmol) of copper(I) chloride and 5.874 g (32.4 mmol) of benzophenoneimine were mixed and then stirred for 140 min at room temperature; this resulted in a red solution. To this solution were added 50 m*l* of *n*-hexane. A red viscous liquid was then separated. This liquid was dried under reduced pressure (about 20 mmHg) for 90 min. To the residue there were then added 25 m*l* of benzene. Some insoluble pale yellow needles were obtained after filtration; 2.160 g.

Found: C, 56.02; H, 4.23; N, 4.98; Cl, 12.58%. Calcd for $CuCl \cdot Ph_2C{=}NH$: C, 55.71; H, 3.96; N, 5.00; Cl, 12.65%.

From the benzene solution, there remained a red viscous mass after the benzene had been stripped off. This mass gradually crystallized to yield a red, needle-like powder. The powder was then washed with a small amount of *n*-hexane, and analyzed.

Found: C, 68.77; H, 4.93; N, 6.03%. Calcd for $CuCl \cdot 2Ph_2C{=}NH$: C, 67.66; H, 4.81; N, 6.07; Cl, 7.68%.

In another case, however, the powder was washed with a larger amount of *n*-hexane and then analyzed.

Found: C, 61.42; H, 4.36; N, 5.81; Cl, 10.23%.

BULLETIN OF THE CHEMICAL SOCIETY OF JAPAN VOL. 41 377—380 (1968)

Electrometric Studies on the Reaction between Pb(II) and Alkali Meta-Vanadate

R. S. SAXENA and C. P. SHARMA

Department of Chemistry, Malaviya Regional Engineering College, Jaipur, India

The reaction between Pb^{2+} and VO_3^- was investigated by means of electrometric techniques involving potentiometric, pH-metric and conductometric titrations between $Pb(NO_3)_2$ and $NaVO_3$ at several concentrations, with each of the reagents alternately used as titrant. The sharp breaks and inflections obtained in titration curves evidenced the formation of lead meta-vanadate having the molecular composition $PbO \cdot V_2O_5$ at pH range 4.25—5.25. The precipitation of the compound has been found to be almost quantitative and the titration results are very accurate and reproducible.

Meagre references are available in the literature on the study of lead vanadates and most of the workers have based their conclusions on the analytical studies of the products formed by double decomposition. Berzelius, Roscoe and Carnot[1] obtained lead meta-vanadate by treating ammonium or alkali meta-vanadate with lead salts. Zolotavin[2] made a study of sparingly soluble vanadates of some metals including lead from the point of law of series by analysis and reported that precipitation of lead meta-vanadate was complete and instantaneous. The lowest pH at which such precipitation took place was determined. Henriguiter[3] reported the formation of lead meta-vanadate as a function of the pH and obtained $PbO \cdot V_2O_5$ by double decomposition and recommended it as a gravimetric method for determination of lead. In view of the insufficient details of the reports of earlier workers on analytical studies and in the absence of any available electrometric data on the subject it was considered desirable and necessary to investigate precisely the reaction between lead salts and alkali meta-vanadate, employing recent electrometric techniques which

1) J. J. Berzelius, H. E. Roscoe and A. Carnot, *Proc. Roy. Soc.*, **16**, 220 (1868); *Phil. Trans.*, **158**, 1 (1868).

2) V. L. Zolotavin, *Zhur. Annal. Khim.*, **2**, 364 (1947).

3) Henri Guiter, *Ann. Chim.*, **15**, 5 (1941).

TABLE 1. SUMMARY OF THE RESULTS OF E. M. F., pH AND CONDUCTOMETRIC TITRATIONS

Clarity of solutions $Pb(NO_3)_2$: $Na_2O \cdot V_2O_5$		Calcd	Equivalence points, m*l* Obs. E. M. F.	pH	Condc.	Formula suggested
Direct titrations: Figs. 1, 2 and 3; Curves I and II						
M/10	M/60	3.33	3.25	3.25	3.20	
M/30	M/150	4.00	3.95	3.95	3.80	$PbO \cdot V_2O_5$
M/60	M/350	3.42	3.35	3.35	3.30	
Reverse titrations: Figs. 1, 2 and 3; Curves III and IV						
M/30	M/5	3.33	3.45	3.35	3.30	
M/200	M/25	2.50	2.55	2.55	2.50	$PbO \cdot V_2O_5$
M/400	M/60	3.00	3.00	3.00	2.95	

have provided more conclusive information on the formation and composition of such compounds.[4-8]

Experimental

Merck's guaranteed extra pure reagents, V_2O_5, NaOH and lead nitrate were used and their solutions prepared in air free conductivity water. The standard solution of sodium meta-vanadate was prepared by adding four moles of HNO_3 to a solution containing one mole of ortho-vanadate at 100°C. The latter was prepared by dissolving one mole of V_2O_5 in boiling solution of NaOH containing six moles of it.

E. M. F., pH and Conductometric Titrations. The pH and E. M. F. of the solutions were measured on a Cambridge (null-deflection type) pH-meter by means of a glass electrode and a bright platinum foil as an indicator electrode respectively, in conjunction with saturated calomel electrode. The observed values of e.m.f. and pH during the course of titrations were plotted as a function of milliliter of titrant added. The end points were located graphically and checked further by calculating maximum values of dE/dV and dpH/dV. Twenty m*l* of the titre was taken in the cell each time thermostated at 25±0.1°C. Conductance measurements were carried out by a LBR type conductometer (W. T. W. Germany) taking 20 m*l* of solution in the cell.

Using different concentrations of the reactants, a series of direct and reverse e.m.f., glass electrode and conductometric titrations were performed in aqueous and aqueous-alcoholic media. Similar strengths of solutions were employed in these titrations for the sake of comparison of results. Only three diagrams illustrating direct and reverse e.m.f. (Fig. 1), pH (Fig. 2) and conductometric (Fig. 3) titrations have been given. The results have been summarised in Table 1.

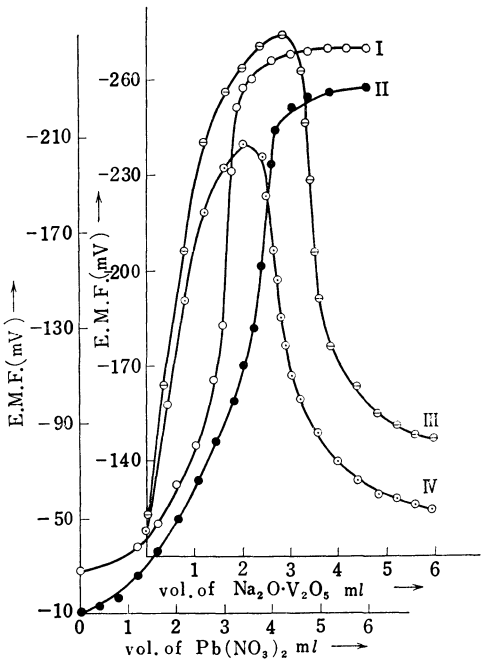

Fig. 1. Direct (I and II) and reverse (III and IV) potentiometric titrations between $Pb(NO_3)_2$ and $Na_2O \cdot V_2O_5$.
Curve I: m*l* of M/10 $Pb(NO_3)_2$ added to 20 m*l* of M/60 $Na_2O \cdot V_2O_5$
Curve II: m*l* of M/30 $Pb(NO_3)_2$ added to 20 m*l* of M/150 $Na_2O \cdot V_2O_5$
Curve III: m*l* of M/5 $Na_2O \cdot V_2O_5$ added to 20 m*l* of M/30 $Pb(NO_3)_2$
Curve IV: m*l* of M/25 $Na_2O \cdot V_2O_5$ added to 20 m*l* of M/200 $Pb(NO_3)_2$

Discussion

The vanadate anion (VO_4^{3-}) in acid medium shows anomalous behaviour and forms different isopoly anions of varying compositions through a series of intermediate steps. The systematic electrometric investigations carried out by the authors[9-11] on such systems have shown the formation of three different poly anions *viz.* pyro$(V_2O_7)^{4-}$,

4) R. S. Saxena, C. P. Sharma and M. L. Mittal, *J. Praktische. Chem.* (1967), in press.
5) R. S. Saxena and O. P. Sharma, *Z. anorg. u. allgem. Chem.*, **333**, 1 (1964).
6) R. S. Saxena and M. L. Mittal, *J. Nucl. & Inorg. Chem.*, **27**, 2553 (1965).
7) R. S. Saxena and M. L. Mittal, *Z. anorg. u. allegem. Chem.*, **324**, 208 (1963).
8) R. S. Saxena and O. P. Sharma, *Talanta*, **2**, 863 (1964).
9) R. S. Saxena and O. P. Sharma, *J. Inorg. Nucl. Chem.*, **28**, 1881 (1966).
10) R. S. Saxena and M. L. Mittal, *Acta Chim. Acad. Sci. Hung.*, **40**, 109 (1964).
11) R. S. Saxena and M. L. Mittal, *Naturwissenschaften*, **51**, 1 (1964).

meta (VO_3^-) and $(V_{10}O_{27})^{4-}$ in the vicinity of pH 10, 7 and 4.5 respectively. With a view to ascertaining whether these polyanions form the corresponding heavy metal derivatives, the reaction between VO_3^- and Pb(II) has been investigated electrometrically.

Figure 1 illustrates the direct and reverse e.m.f. titrations between $Pb(NO_3)_2$ and $Na_2O{\cdot}V_2O_5$ using a bright platinum foil as an indicator electrode. In direct titrations (Fig. 1, curves I—II) when $Pb(NO_3)_2$ solution was added from a micro-burette to sodium meta-vanadate solution, a gradual rise in e.m.f. was observed from the start of the reaction with a sharp jump in potential obtained at the end point corresponding to the formation and precipitation of lead meta-vanadate $PbO{\cdot}V_2O_5$. Beyond the stoichiometric end-point the e.m.f. attains almost a constant value. In the case of reverse titration (Fig. 1, curves III and IV), when sodium meta-vanadate was used as titrant, the first addition of the latter causes a sharp rise in e.m.f. which continues upto the addition of about 0.5 mol of $Na_2O{\cdot}V_2O_5$ per mole of $Pb(NO_3)_2$ but on further addition, the e.m.f. value starts decreasing, resulting in the occurrence of sharp inflection or maxima in dE/dV at the endpoint indicating the precipitation of the same compound $PbO{\cdot}V_2O_5$. The inverse titration curves are peculiar in form but provide accurate and reproducible results.

The pH of the $Pb(NO_3)_2$ and $Na_2O{\cdot}V_2O_5$ was measured by means of glass electrode and found to be about 4.60 and 7.40 respectively. The titration curves (Fig. 2, curves I and II) represent the changes occurring in H^+ ion concentrations when $Pb(NO_3)_2$ solution was treated with alkali-vanadate solution.

The direct glass electrode titration curves are regular in form and yield one break corresponding to the formation of lead meta-vanadate. Reverse titrations, however, are found to yield sharp upward jump at the same stoichiometric endpoint but are peculiar in form. Although the pH of the sodium meta-vanadate is about three units higher than that of $Pb(NO_3)_2$, but the first addition of the former causes an appreciable fall in pH and this decrease continues even upto the addition of about half the amount of alkali vanadate per mole of lead nitrate. Beyond this position pH begins to increase and a sharp upward jump is

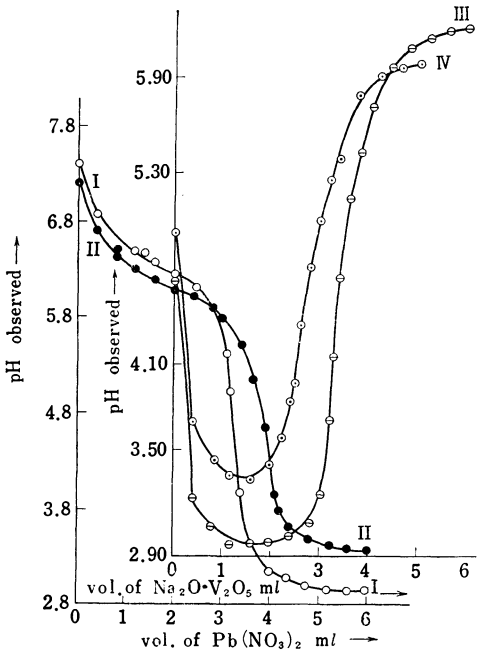

Fig. 2. Direct (I and II) and reverse (III and IV) pH titrations between $Pb(NO_3)_2$ and $Na_2O{\cdot}V_2O_5$.
Curve I: m*l* of M/10 $Pb(NO_3)_2$ added to 20 m*l* of M/60 $Na_2O{\cdot}V_2O_5$
Curve II: m*l* of M/30 $Pb(NO_3)_2$ added to 20 m*l* of M/150 $Na_2O{\cdot}V_2O_5$
Curve III: m*l* of M/5 $Na_2O{\cdot}V_2O_5$ added to 20 m*l* of M/30 $Pb(NO_3)_2$
Curve IV: m*l* of M/25 $Na_2O{\cdot}V_2O_5$ added to 20 m*l* of M/200 $Pb(NO_3)_2$

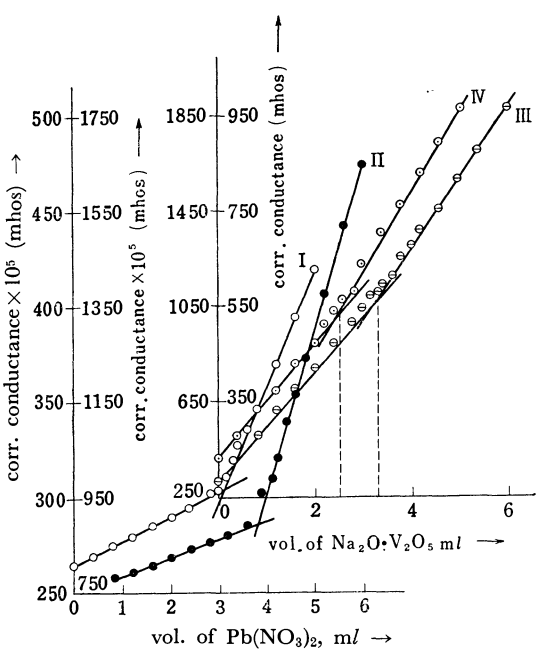

Fig. 3. Direct (I and II) and reverse (III and IV) conductometric titrations between $Pb(NO_3)_2$ and $Na_2O{\cdot}V_2O_5$.
Curve I: m*l* of M/10 $Pb(NO_3)_2$ added to 20 ml of M/60 $Na_2O{\cdot}V_2O_5$
Curve II: m*l* of M/30 $Pb(NO_3)_2$ added to 20 m*l* of M/150 $Na_2O{\cdot}V_2O_5$
Curve III: m*l* of M/5 $Na_2O{\cdot}V_2O_5$ added to 20 m*l* of M/30 $Pb(NO_3)_2$
Curve IV: m*l* of M/25 $Na_2O{\cdot}V_2O_5$ added to 20 m*l* of M/200 $Pb(NO_3)_2$

obtained at stoichiometric end-point (Fig. 2, curves III and IV).

This initial fall in pH, which continues upto the addition of half mole of alkali meta-vanadate per mole of lead nitrate (Fig. 2, curves III—IV) indicate the liberation of free acid during the course of reaction due to hydrolysis and the formation of basic lead-vanadate which on further addition of alkali vanadate gradually changes into lead meta-vanadate, simultaneously liberating equivalent amount of NaOH, which consequently results in the increase of pH. Finally a sharp upward jump was obtained at the molecular ratio of PbO: V_2O_5 as 1 : 1 confirming the formation of lead meta-vanadate ($PbO \cdot V_2O_5$). These observations are clearly borne out by the shape of pH-titration curves. The probable mechanism of the reaction can be stated as follows:

$$Pb(NO_3)_2 + 0.5(Na_2O \cdot V_2O_5) + H_2O \rightarrow Pb(VO_3)OH + HNO_3 + NaNO_3 \quad (1)$$

$$Pb(VO_3)OH + 0.5(Na_2O \cdot V_2O_5) \rightarrow Pb(VO_3)_2 + NaOH \quad (2)$$

The course of this reaction was also followed by means of conductometric titrations between the reactants at different concentrations. The end-points indicate the formation of lead meta-vanadate, $PbO \cdot V_2O_5$. The feeble breaks obtained in reverse titration curves as a consequence of appreciable increase in conductance values in initial stages of titration, indicates clearly the liberation of highly mobile H^+ ions and provide strong support to the observation noted in reverse pH titrations.

It was noticed that after each addition of the reagent, it takes a little time for the e.m.f., pH and conductance values to become steady. The presence of ethanol slightly improves the end-point as it decreases the dielectric constant of the medium and consequently the solubility of the precipitated compound. The accuracy and reproducibility of these electrometric titrations have been found to be excellent.

BULLETIN OF THE CHEMICAL SOCIETY OF JAPAN VOL. 41 380—384 (1968)

A Study on the Yield of (γ, p) Reactions with 20 MeV Bremsstrahlung

Yoshinaga OKA, Toyoaki KATO, Koichi NOMURA, Tatsuya SAITO and Hui-Tuh TSAI

Department of Chemistry, Faculty of Science, Tohoku University, Katahira-cho, Sendai

(Received August 16, 1967)

The yields of the (γ, p) reactions on 13 elements up to an atomic number of 80, irradiated with 20 MeV bremsstrahlung, have been given through the γ-ray spectrometric measurements of the resultant activities. The yield values, as measured in absolute disintegration rates at the end of irradiation per mole per roentgen, have been plotted against atomic number of the target nuclides. The shape of the yield curve thus obtained is similar to that of the curve for the photoproton yield as a function of atomic number. The yield values are 10^5 order of magnitude in the lower-Z region, and drop rapidly with increasing atomic number up to a Z of 50. For barium and mercury targets, a yield value of 2.2×10^4 was obtained. Neutron excess nuclides were found to be restrictive to the (γ, p) processes. The present results permit a study of general behavior of the (γ, p) reaction yields as well as of the applicabilities of the resultant activities to photoactivation analyses for many elements distributed throughout the periodic table.

A general feature of the photon absorption cross section for a nucleus is characterized by a peak 5—6 MeV wide at an energy located between the photodisintegration threshold and about 30 MeV.[1] For most nuclei, an excitation energy of 20 MeV is sufficient to cause the emission of one neutron, or one proton, and occasionally two particles. When bremsstahlung, with a maximum energy of 20 MeV, is attenuated by various target elements, the resultant nuclides are mainly attributed to those arising from (γ, n), and (γ, p) reactions. In a previous paper,[2] the yields of radioactivities resulting from (γ, n) reactions on many elements from lithium up to bismuth have been determined by utilizing a 20 MeV linear electron accelerator and by applying the residual activity method based on the γ-ray spectrometry. The applicabilities of these photoactivation products to activation analyses have also been discussed from the data thus obtained.[3] Although the proton

1) R. Montalbetti, L. Katz and J. Goldenberg, *Phys. Rev.*, **91**, 659 (1953).

2) Y. Oka, T. Kato, K. Nomura and T. Saito, This Bulletin, **40**, 575 (1967).

3) Y. Oka, T. Kato, K. Nomura and T. Saito, *J. Nucl. Sci. Technol.*, **4**, 346 (1967).

yields from many elements irradiated with bremsstrahlung radiation of moderate energy have been determined by several workers through the direct detection of the emitted protons,[4-9] this only represents the sum of the yields of the (γ, p), (γ, pn), and other proton emitting reactions on the relevant element. These yield data will sometimes be ambiguous when applied to a more general consideration convering photoactivation analyses of many elements using particular residual nuclides generated from each of the (γ, p) reactions.

In the present work, consequently, a study has been carried out to obtain the yields of (γ, p) reactions of some 13 elements irradiated with 20 MeV bremsstrahlung γ-rays through γ-ray spectrometric measurements of the resultant activities. In addition, the yields of some (γ, pn) reactions which occurred in this energy region have been determined separately.

Experimental

Samples and Irradiation. Samples of the target materials with high chemical purity,[10] either in the form of the element or some simple compound, were irradiated for 1 hr with bremsstrahlung γ-rays of 20 MeV maximum energy produced by the linear electron accelerator of the Japan Atomic Energy Research Institute. Each sample had a weight of 100 mg and was contained in a small quartz tube having an internal diameter of 4 mm. It was located in a target holder immediately behind the converter platinum plate. To monitor the bremsstrahlung flux to which the sample was exposed, a gold foil[11] was wrapped around each sample tube, and after irradiation, the 6.18 d ^{196}Au activity produced by the ^{197}Au(γ, n) reaction was measured from its characteristic 0.354 MeV γ-ray photopeak. The dose rate of bremsstrahlung γ-rays to which the sample was exposed has been estimated to be 9.4×10^{6} R/min.

The above experimental method is essentially the same as that described in detail in previous papers.[2,3,12]

Chemical Separation. For many elements chosen for this experiment, non-destructive γ-ray spectrometric measurements could be performed after having been cooled for a time. It was possible to let the activities of the desired (γ, p) reaction products be much larger than those from the (γ, n) and other reaction products without any chemical separation. This is not the case, however, for zinc, germanium, strontium, and barium targets. After irradiation, chemical separation was performed for these targets by the following procedures.

Copper from Zinc. After the addition of copper carrier (25 mg), the zinc target was dissolved with 8 N hydrochloric acid, and then subjected to an anion exchange procedure.[13] Copper was eluted from a Dowex 1×8 column with 3.5 N hydrochloric acid, and precipitated from this eluate by the addition of aqueous sodium hydroxide solution at pH 7. After separation by centrifuge, the precipitate was ignited to obtain copper(II) oxide. The chemical yield was 67.3%. The final oxide was packed in a small glass tube having an internal diameter of 4 mm for γ-ray counting.

Gallium from Germanium. An irradiated germanium dioxide target was transferred to a 50 m*l* distilling flask, and was brought into solution by adding 7 N hydrochloric acid along with gallium (269 mg) and zinc carriers. Almost all germanium activities were removed by distillation. From the resultant solution, gallium was extracted with isopropyl ether. The organic layer was evaporated to dryness, and the residue was dissolved in dilute hydrochloric acid. Gallium hydroxide was separated from this solution by the addition of aqueous ammonia, and then ignited to obtain gallium(III) oxide. The chemical yield was 90.9%.

Rubidium from Strontium. A strontium carbonate target was dissolved in dilute hydrochloric acid with the addition of 40 mg of rubidium carrier, and evaporated to dryness. The residue was extracted with water. Sodium tetraphenyl borate was added to precipitate rubidium.

The precipitate was separated by centrifuge, washed with water containing a small amount of acetic acid, and dried at 110°C. The chemical yield was 72.1%.

Cesium from Barium. The chemical procedure for the isolation of cesium activity from a barium carbonate target was similar to that used for rubidium from strontium. Cesium tetraphenyl borate was used to determine the chemical yield, and γ-ray activity. The chemical yield was 91.6%.

Measurement of radioactivity was carried out with a 3″ dia. × 3″ NaI(Tl) detector coupled to a TMC 400-channel pulse-height analyzer.

Yield Determination. The yield value was obtained for each (γ, p) reaction through the absolute measurement of the resultant activity. To obtain the disintegration rate from the counting rate of the characteristic γ-ray photopeak, appropriate corrections were made for the variation of photopeak efficiency with γ-ray energy.[14] The decay schemes used were those listed in the Nuclear Data Sheets.[15] The tables of internal conversion coefficients were also used.[16] Decay curve analyses have been performed to separate the undesired activities. From the data thus obtained, the yield ($Y_{(E)}$) was calculated by the following equation.

4) D. C. Diven and G. M. Almy, *Phys. Rev.*, **80**, 407 (1950).
5) A. K. Mann and J. Halpern, *ibid.*, **82**, 733 (1951).
6) M. E. Toms and W. E. Stephens, *ibid.*, **82**, 709 (1951).
7) M. E. Toms and W. E. Stephens, *ibid.*, **92**, 362 (1953).
8) W. A. Butler and G. M. Almy, *ibid.*, **91**, 58 (1953).
9) E. V. Weinstock and J. Halpern, *ibid.*, **94**, 1651 (1954).
10) 99.99% or over.
11) 10 μ thick, 3 mm × 15 mm.
12) Y. Oka, T. Kato and I. Nagai, *J. Nucl. Sci. Technol.*, **4**, 300 (1967).
13) K. A. Kraus and G. E. Moore, *J. Am. Chem. Soc.*, **75**, 1460 (1953).
14) S. Flügge Ed., "Handbuch der Physik, Bd. XLV. Instrumentelle Hilfsmittel der Kernphysik II," Springer-Verlag, Berlin (1958), p. 113.
15) Nuclear Data Sheets, Natl. Academy of Science-Natl. Research Council, Washington, D. C. (1961).
16) M. E. Rose, "Internal Conversion Coefficient," North-Holland Publ. Co., Amsterdam (1958).

$$Y_{(E)} = \frac{D_0}{IM(1-e^{-\lambda t})}$$

where D_0 is the disintegration rate at the end of irradiation; I is the radiation dose rate; M is the amount of target nucleus expressed in moles; λ is the decay constant.

Effect of Photoneutrons. During irradiation in this experiment, there was a considerable neutron flux at the site of the target sample which was due to photoneutrons ejected from the platinum converter. These photoneutrons induce extraneous neutron reactions such as (n, p), (n, α), and (n, 2n) reactions. For a number of elements the resultant nuclide formed by the (n, p) reaction is the same as that from the (γ, p) reaction on the corresponding element. In such cases, it was necessary to correct the observed activity for the contribution of the (n, p) reaction. To investigate such contributions, the neutron flux to which the sample was exposed has been determined. For this purpose, ^{27}Al(n, α)^{24}Na reaction was chosen as a monitor reaction.[17] The energy distribution curve of photoneutrons emitted from a bismuth target irradiated with 20 MeV bremsstrahlung which had been given by Mutsuro *et al.*[19] was also used.[20]

When a piece of aluminum metal of 4 mm×4 mm (126 mg) was irradiated for 1 hr with 20 MeV bremsstrahlung, as pecific activity of 3.2×10^{-3} μCi ^{24}Na/mg Al was found at the end of irradiation. By using this value, the intensity of the energy distribution curve was normalized to the neutron flux at the various neutron energies. The resultant curve is shown in Fig. 1-(1).[21]

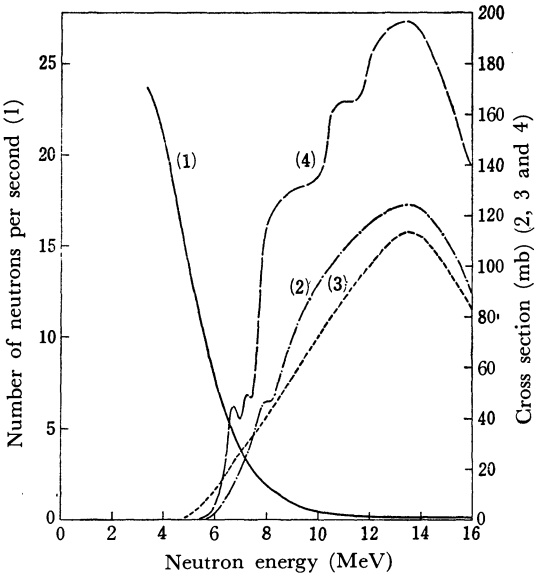

Fig. 1. Neutron flux at the target position as a function of neutron energy (1); The excitation curves for (2) the ^{27}Al(n, α)^{24}Na[18], (3) the ^{56}Fe(n, p)^{56}Mn[23] and (4) the ^{24}Mg(n, p)^{24}Na[18] reaction.

By using this curve and the excitation function for the particular (n, p) reaction, the reaction rate can be calculated in the form of $NS\int_{E_{th}}^{\infty}\sigma(E)\phi(E)dE$, where N is the number of target nuclides; S is the saturation factor; $\sigma(E)$ is the cross section at a neutron energy (E); $\phi(E)$ is the neutron flux at energy (E); and E_{th} is the threshold energy of the reaction.

In the irradiation of an iron target, ^{56}Mn activity is produced both by the ^{57}Fe(γ, p)^{56}Mn, and by the ^{56}Fe(n, p)^{56}Mn reactions. The production rate of the latter was estimated by the proposed method[22] to be 2.3×10^{-3} μCi ^{56}Mn/mg Fe. This corresponds to 2.8% of the total ^{56}Mn activity. Next, ^{24}Na activity from a magnesium target formed by the ^{24}Mg(n, p)^{24}Na reaction[24] was calculated to be 5% of the total ^{24}Na activity. Mostly, the excitation curve for the (n, p) reaction exhibits a threshold energy of 2—5 MeV, and is characterized by a maximum value of ~100 mb.[23] Because of this, it can be concluded that the (n, p) reactions contribute only a small fraction in the total resultant activity, which can thereby be attributed, in major part, to the decay of the (γ, p) reaction products.

Results and Discussion

The (γ, p) Reaction Yield. Table 1 lists the particulars and the data obtained on 16 γ-ray emitting products of the (γ, p) reactions from the elements studied. Column three in Table 1 gives the proton separation energy (S_p), the energy required to separate one proton from a parent nucleus, presented by Yamada and Matsumoto,[25] for most of the nuclei by the use of mass formulas and nuclear systematics. The last two columns show the experimental results. The yield value was expressed as the disintegration rate at the end of irradiation per mole of target nuclide per roentgen. This can be taken as the number of the (γ, p) processes which occurred during irradiation. The yield values were also plotted against atomic number of the parent nuclides in Fig. 2 in which the symbol noted near each plot indicates the parent nuclide. The shape of the yield curve is similar to that of the curve for the photoproton yield as a function of atomic number presented by Weinstock and Halpern.[9]

17) The cross section values for this reaction were taken from the data of Butler *et al.*,[18] which is shown in Fig. 1-(2).
18) J. P. Butler and D. C. Santry, *Can. J. Phys.*, **41**, 372 (1963).
19) N. Mutsuro *et al.*, To be published.
20) It can be said that this energy distribution curve is practically the same as that for photoneutrons from the converter platinum taking account of the characteristics of the photonuclear process.
21) From the result, the neutron flux necessary to produce the ^{24}Na activity was estimated to be 5.3×10^5 n/sec at the target position.
22) The excitation function for the ^{56}Fe(n, p)^{56}Mn reaction, shown in Fig. 1-(3), was taken from the data compiled by Hughes *et al.*[23]
23) D. N. Hughes and J. A. Harvey, "Neutron Cross Sections," BNL-325 (1955).
24) The excitation function presented by Butler *et al.*,[18] shown in Fig. 1-(4), was used.
25) M. Yamada and Z. Matsumoto, *J. Phys. Soc. Japan*, **16**, 1497 (1961).

TABLE 1. SUMMARY OF DATA ON (γ, p) REACTIONS WITH 20 MeV BREMSSTRAHLUNG

Nuclide: Parent (Natural abundance, %)	Nuclide: Residual (Half-life)	S_p (MeV)	Observed γ-ray: Energy (MeV)	Observed γ-ray: Branching ratio (%)	Observed γ-ray: Type of multipole transition	Yield determined: μCi/mg[a]	Yield determined: Yield/mol·R
^{25}Mg (10.11)	^{24}Na (15 hr)	12.06	1.37	100	$E2$	1.48×10^{-1}	1.7×10^{5}
^{29}Si (4.71)	^{28}Al (2.27 min)	12.33	1.78	100	$E2$	1.91	2.8×10^{5}
^{30}Si (3.12)	^{29}Al (6.56 min)	13.59	1.28	93.8	$E2+M1$	6.51×10^{-1}	1.5×10^{5}
^{44}Ca (2.06)	^{43}K (22.4 hr)	12.17	0.374	85	$E2+M1$	7.86×10^{-3}	1.3×10^{5}
^{47}Ti (7.32)	^{46}Sc (84.1 d)	10.47	0.887	100	$E2$	7.11×10^{-4}	3.1×10^{5}
^{48}Ti (73.99)	^{47}Sc (3.4 d)	11.44	0.160	100	$E2+M1$	6.83×10^{-2}	1.2×10^{5}
^{49}Ti (5.46)	^{48}Sc (1.8 d)	11.35	1.31	100	$E2$	4.40×10^{-3}	5.8×10^{4}
^{53}Cr (9.55)	^{52}V (3.8 min)	11.15	1.43	100	$E2$	5.01×10^{-1}	6.6×10^{4}
^{57}Fe (2.17)	^{56}Mn (2.58 hr)	10.57	1.81	23.5	$E2+M1$	8.10×10^{-2}	2.1×10^{5}
^{74}Ge (36.74)	^{73}Ga (4.8 hr)	10.92	0.295	97	($E2$)	3.70×10^{-1}	1.3×10^{5}
^{77}Se (7.58)	^{76}As (26.5 hr)	9.61	0.559	41	$E2$	1.48×10^{-2}	1.3×10^{5}
^{87}Sr (7.02)	^{86}Rb (19 d)	9.41	1.08	9	$E2$	5.15×10^{-4}	9.9×10^{4}
^{113}Cd (12.26)	^{112}Ag (3.2 hr)	9.74	1.39	35	$E2$	1.91×10^{-2}	2.1×10^{4}
^{117}Sn (7.57)	^{116m}In (54 min)	9.58	1.27	84	$E2$	9.80×10^{-3}	6.9×10^{3}
^{137}Ba (11.32)	^{136}Cs (13 d)	8.67	0.830	100	$E2$	1.68×10^{-4}	2.2×10^{4}
^{199}Hg (16.84)	^{198}Au (2.7 d)	7.27	0.412	100	$E2$	8.43×10^{-4}	2.2×10^{4}

a) The value corrected at the end of 1 hr irradiation (9.4×10^{6} R/min).

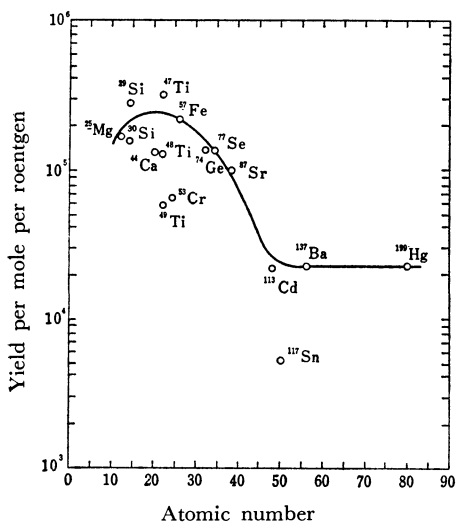

Fig. 2. The yield curve for the (γ, p) reaction with 20 MeV bremsstrahlung.

It has been pointed out that the photon absorption cross section for a nucleus is an increasing function of Z, and this fact has been well explained in a study on the relation between the (γ, n) reaction yield and the atomic number of the target nuclide.[1,2] The yield of radioactive nuclide increases regularly with atomic number from 10^3 to 10^7 orders of magnitude.[2] On the other hand, photoproton emission from a nucleus is a decreasing function of Z because of the restrictive effect of the Coulomb barrier. Accordingly, the yield curve for the photoproton emission will exhibit a peak.

According to the results of Weinstock and Halpern,[9] this peak occurs at nickel (Z=28). They have also shown that between a Z of 28 and 50 the experimental photoproton yields are in excellent agreement in absolute magnitude with those calculated from the evaporation model.

Although the initial rise of the yield curve, shown in Fig. 2, is not markedly observed in the lower-Z region, a typical decrease in the yield value with Z can be seen from iron (Z=26) up to tin (Z=50). On the barium and mercury targets, however, the yield values are much higher than those expected from a rapid drop until a Z of 50. These discrepancies can be attributed to the direct photoelectric emission mechanism. It has often been pointed out that the evaporation model as usually formulated is inadequate to explain the photoproton yields for elements of high atomic number.[9,26] In such cases, a considerable portion of the photoproton yield can be accounted for by the direct photoelectric emission of a proton without the formation of a compound nucleus.

As for titanium isotopes, including ^{47}Ti, ^{48}Ti, and ^{49}Ti, the yield values decrease in order. This fact shows that the cross section for photoproton emission from a neutron excess nuclide is expected to be small. Similarly, the yield for the ^{29}Si(γ, p)^{28}Al reaction is higher than that for the ^{30}Si(γ, p)^{29}Al reaction.

Of the target nuclides under study, ^{44}Ca (Z=20) and ^{117}Sn (Z=50) are proton magic. The yield values for these nuclides are fairly low as compared with those for the neighboring nuclides in the yield curve.

26) V. G. Shevchenko and B. A. Yuryev, *Nucl. Phys.*, **37**, 495 (1962).

In the comparison of the results in Table 1 with the yield values of the (γ, n) reactions, the (γ, p) reactions can be produced by same order of magnitude as the latter in elements with lower-Z. With higher-Z elements, however, they contribute only a small fraction to the observed activity. The yield values are less than 0.1% of those for the (γ, n) reaction in elements with Z greater than 50.

It would appear that the use of the resultant activities in Table 1 for photoactivation analysis of lighter elements should enhance the efficacy. Silicon, calcium, and titanium can be specifically detected by γ-ray counting. They are elements from which either very short-lived nuclides, or only low γ-activities, are produced by activation with thermal neutrons.

In conclusion, the authors believe that the present results permit a study of the general considerations covering photoactivation analyses of many elements utilizing (γ, p) reaction products.

The (γ, pn) Reaction. It is expected that the (γ, pn) reactions take place to an appreciable extent, apart from the (γ, n) and (γ, p) reactions, in various elements in the energy region covered in this experiments. The resultant activities from (γ, pn) reaction in iron, zinc,[27] and palladium targets could be measured. The yield values obtained are given in Table 2. This is a preliminary survey to indicate the yield values from the (γ, pn) reaction in various elements. It is obvious that more points at higher atomic number are required. It is planned to investigate these problems in the near future.

TABLE 2. THE YIELDS OF SOME (γ, pn) REACTIONS WITH 20 MeV BREMSSTRAHLUNG

Reaction	Half-life of product	Specific activity[a] (μCi/mg)	Yield ($mol^{-1} \cdot R^{-1}$)
$^{56}Fe(\gamma, pn)^{54}Mn$	314 d	2.5×10^{-6}	3.6×10^{2}
$^{66}Zn(\gamma, pn)^{64}Cu$	13 hr	7.2×10^{-3}	7.5×10^{3}
$^{104}Pd(\gamma, pn)^{102}Rh$	210 d	1.1×10^{-6}	1.7×10^{3}

a) The value corrected at the end of 1 hr irradiation (9.4×10^{6} R/min).

27) Apart from ^{64}Cu, ^{67}Cu from ^{68}Zn by the (γ, p) process was measured by its characteristic 0.093, 0.184, 0.296, and 0.388 MeV γ-rays. The yield calculation for this reaction was excluded in this experiment since the decay scheme for ^{67}Cu has not been well-established.

BULLETIN OF THE CHEMICAL SOCIETY OF JAPAN VOL. 41 384—389 (1968)

Kinetics of Isotopic Exchange between Acetylacetone-^{14}C and Tris-acetylacetonatoaluminum in Tetrahydrofuran

Kazuo SAITO and Kazuyo MASUDA

Chemistry Department, Faculty of Science, Tohoku University, Katahira-cho, Sendai

(Received September 11, 1967)

Tris-acetylacetonatoaluminum [Al(acac)$_3$] is precipitated crystalline from tetrahydrofuran (THF) solution containing an excess of acetylacetone (acacH) by adding chilled petroleum ether. This fact enables a kinetic study of isotopic exchange of acac$^-$ between [Al(acac)$_3$] and acacH with the aid of acetylacetone-^{14}C. The exchange rate is independent of the concentration of acacH and dependent on that of water. The rate formula at 25°C is as follows:

$$R = [\mathrm{Al(acac)_3}](6\times 10^{-5} + 2.0\times 10^{-2}[\mathrm{H_2O}])\ \mathrm{mol}\ l^{-1}\ \mathrm{min}^{-1}$$

This exchange reaction is catalysed by acids; the stronger the acid, the greater the catalytic effect. One of the acetylacetonate ligands would be present with one end free, and break of the remaining bond of unidentate acetylacetonate seems to be the rate determining step. Water can occupy the vacant coordination site of aluminum ion to retard recombination of the unidentate ligand. The donation of proton to the free end of acetylacetonate appears to impede the recombination, too, and facilitate the exchange. Hydronium ion seems to be the unique proton carrier.

Little information is available concerning the isotopic exchange of organic ligands of non-electrolytic complexes in organic solvents. Such kinetic studies with complexes of typical elements seem very interesting, because no influence is expected from charge, ligand field stabilization energy, hydrolytic decomposition, and ionic strength. One of the present authors measured the exchange rate of radioactive indium between its tris-acetylacetonato- and tris - 8 - quinolinolato (oxinato) complex in chloroform and found that it is measurable at room temperature (*e. g.* half period

11 min at 25°C).[1] He also found that the exchange between the corresponding zinc complexes is very fast.[2] These experiments exemplified that complexes of tervalent typical elements can undergo slow isotopic exchange under certain conditions, but failed to give further information concerning the mechanism.

The difficulties involved in carrying out such studies are to separate one of the participants in the exchange reaction free from the other, and to measure the specific activity (or specific counting rate) with reasonable accuracies. The present authors have examined the solubility of acetylacetone (acacH) and tris-acetylacetonatoaluminum [$Al(acac)_3$] in a variety of organic solvents, and found that the latter is precipitated crystalline free from the former in tetrahydrofuran solution (THF) on addition of petroleum ether at a low temperature. By use of acetylacetone labelled with ^{14}C, they have succeeded in studying the isotopic exchange kinetics at room temperature, and have posturated a reasonable reaction mechanism.

Experimental

Materials. Acetylacetone-^{14}C was synthesized by the method given in Ref. 3, slightly modified to suit for a small scale synthesis. Metallic sodium powder (4.6 g) was refluxed with ethanol (12 m*l*) for 7 hr in ethylether, the ether evaporated off, the product treated with ethylacetate (80 m*l*), acetone-1, 3-^{14}C (0.5 mCi, 0.11 mg) and acetone (15 m*l*) for 1 hr with reflux, and set aside for 20 hr at room temperature. The product was treated with water (170 m*l*), the ether layer discarded, and the aqueous solution made acid with dilute sulfuric acid. The liberated acetylacetone-1, 3, 5-^{14}C was extracted with ethylether, dried with anhydrous sodium sulfate for 24 hr, and distilled to collect a fraction boiling at 120 to 134°C. The distillate was further dried with potassium carbonate, diluted with inactive acetylacetone to adjust the specific activity to the order of 0.02 μCi/mg, and distilled (boiling point 134 to 136°C). The water content of the product was estimated to be 0.31 and 0.71 M (two batches) as mentioned below.

Tris-acetylacetonatoaluminum was synthesized by the ordinary method,[4] from commercial aluminum sulfate made free from iron and inactive acetylacetone, and sublimed at 5 mmHg at 165°C, to give colorless crystals. Water content of the sublimate was *ca.* 0.06 M. Commercial extra pure THF was refluxed with sodium for 1 hr, distilled and the distillate further dehydrated with lithium aluminum hydride, and distilled. The product contained less than 0.005 M water, and preserved in a desiccator as long as two weeks without being contaminated by atmospheric moisture. *m*-Toluic acid, trichloroacetic acid and phenol were sublimed at 5 mmHg at 105, 50 and 35°C respectively and dissolved in THF without being in contact with air. The concentration and the water content were determined by alkalimetric and Karl Fischer titration, respectively.

Commercial anisole was shaken with sodium hydroxide solution, dried with calcium chloride, refluxed with sodium and distilled. *p*-Terphenyl was recrystallized from xylene. *p*-Di-(5-phenyl-2-oxazolyl)-benzene (POPOP) was of scintillation grade and used without further purification. Other chemicals were of chemically pure grade.

Experimental Procedure. A given amount of tris-acetylacetonatoaluminum (0.2 to 0.7 g) was dissolved in anhydrous THF (10.0 m*l*) and the acetylacetone-^{14}C (0.02 to 0.2 g) was added, the amounts being known from the weight difference. Other reagents such as acids and water were added to the THF in advance, whenever necessary, and their amounts known from the weight difference. The water content thus determined coincided well with those measured by Karl Fischer titration within an erorr less than 0.003 M in the reaction mixture.

The reaction mixture was kept in a thermostat at 25 or 35°C, and an aliquot (*e. g.* 1 m*l*) was added to chilled petroleum ether (−20°C) at appropriate intervals. Crystalline [$Al(acac)_3$] separated out on standing at −20°C for 4 hr. The standing time did not affect the results, and there was no appreciable zero-time exchange. The supernatant was decanted, the precipitate washed with petroleum ether and dried at 80°C. Its weighed portion (4 to 15 mg) was dissolved in anisole (15.0 m*l*), mixed with POPOP (0.02%) and *p*-terphenyl (0.8%) in anisole (15.0 m*l*) and the counting rate measured by the scintillation technique. Five to six aliquots were taken during one kinetic run and about 70 runs were carrierd out under various conditions as mentioned below.

The absorption spectra of reaction mixtures coincide with the sum of those of tris-acetylacetonatoaluminum and acetylacetone. Hence the reaction mixture does not undergo any reaction other than isotopic exchange, regardless of the presence of other ingredients such as water and organic acid.

Since water accelerates the exchange and the reaction mixture absorbs water slightly, the water content was carefully determined during the course of exchange reaction, to find that the change in content of water is less than 0.1 mg per m*l*, *i. e.* less than 0.005 M. In extreme cases, the mean value before and after the exchange reaction was used for calculation.

Measurement of Radioactivity. A coincidence liquid scintillation counter, made by Institute for Nuclear Study, the University of Tokyo was used for the β-ray counting. The quenching effect was examined with standard ^{14}C-benzoic acid and inactive acetylacetone and tris-acetylacetonatoaluminum, to find that it is negligible in the presence of less than 20 mg per 30 m*l* anisole under the given conditions. The counting rate was proportional to the amount of carbon-14 in the range from 10^{-3} to 10^{-2} μCi of either acetylacetone or tris-acetylacetonatoaluminum. The counting rate at the end of exchange reaction (infinite time) was calculated from that of the acetylacetone-^{14}C and the used amounts of the respective compounds.

Other Measurements. The NMR spectra were recorded with Varian A 60 Spectrometer (60 mega

1) K. Saito and M. Tamura, *J. Inorg. Nucl. Chem.*, **13**, 334 (1960).
2) K. Saito and M. Tamura, This Bulletin, **32**, 532 (1959).
3) "Organic Synthesis," **20**, 7 (1940).
4) "Inorganic Synthesis," **2**, 25 (1946).

cycle) at room temperature. The absorption spectra in the visible and ultraviolet region were measured with Hitachi EPU-2A Spectrometer. Karl Fischer titration apparatus of Mitsubishi Kasei type with electric end-point indicator was used for the analysis of water; propyleneglycol containing 25% (v/v) pyridine was the useful titration medium.

Results

The experimental data were treated in accordance with McKay's formula,[5]

$$R = -2.303 \cdot \frac{3ab}{3a+b} \cdot \frac{\log(1-F)}{t} \qquad (1)$$

where a and b are the molar concentrations of tris-acetylacetonatoaluminum (containing three moles of exchangable acetylacetonate per mole) and acetylacetone, respectively, F is the fraction of reaction and t the lapse of time in minutes.

Influence of the Concentration of Complex, Free Ligand and Water. The influence of a upon R is illustrated in Fig. 1, which clearly shows that R is proportional to a in the given concentration range. More dilute solutions did not yield the precipitate on addition of chilled petroleum ether.

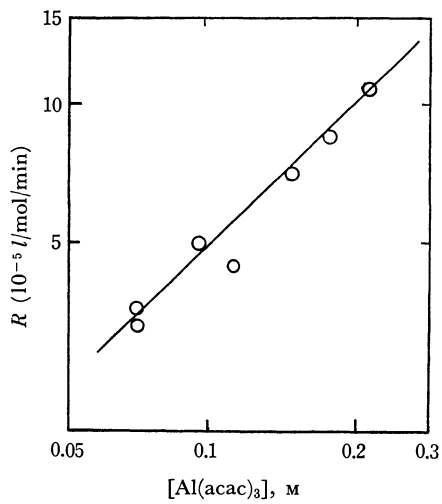

Fig. 1. Influence of the concentration of tris-acetylacetonatoaluminum on the exchange rate. [acacH], 0.070 M; [H_2O], 0.027 M; 25°C

Water in the reaction mixture accelerates the exchange reaction. So far as its concentration was kept constant, however, the rate was independent of b, as seen from Table 1. Hence R is expressed as

$$R = k_0 a \qquad (2)$$

Since the acetylacetone-^{14}C contained a small amount of water, which cannot be removed by accessible dehydrating agents, change in b also brought about change in concentration of water in the reaction mixture. However, such a contribution is negligible, when the amount of added water in THF is large. The difference in water content coming from varying amounts of the complex *etc.* is even smaller and can be ignored.

Table 1. Influence of concentration of acetylacetone-^{14}C on the exchange rate

[H_2O], M	[acacH], M	k_0, min^{-1}
0.0046	0.067	1.3×10^{-4}
0.0047	0.144	1.4×10^{-4}
0.045	0.031	1.1×10^{-3}
0.046	0.051	1.1×10^{-3}
0.046	0.066	1.1×10^{-3}
0.047	0.095	1.2×10^{-3}

[$Al(acac)_3$], 0.070 M; 25°C

When R was measured in THF solutions containing varying amounts of water at given a and b values, the R *vs.* [H_2O] diagram was almost a straight line on log-log scale (Fig. 2). On the other hand, when R was measured with varying b values in the absence of added water in THF containing a given amount of the complex, the diagram really indicates the influence of water concentration. Both the diagrams coincide with each other, to reconfirm that R is independent of b. By extrapolating the anti-logarithmic diagram corresponding to Fig. 2 to zero concentration, the k_0 value in the absence of water, k_1, is known. The accuracy of the concentration of water is low especially in less than 0.01 M solution, and only an approximate amount of k_1 is known by extrapolation, to be less than 6×10^{-5} min^{-1} or less. When this value is subtracted from the measured k_0 values and the difference plotted against [H_2O], a straight line of a gradient 45° is obtained on log-

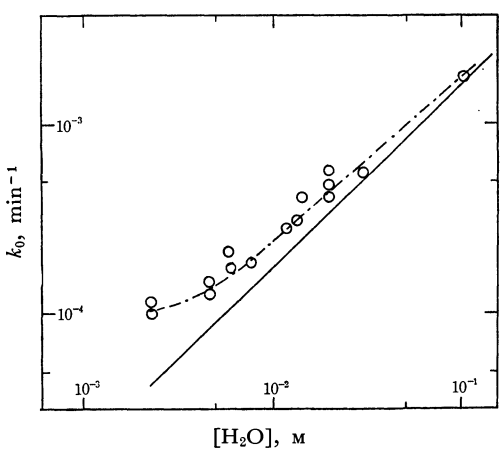

Fig. 2. Influence of the concentration of water on the exchange rate constant. [$Al(acac)_3$], 0.070 M; [acacH], 0.070 M; 25°C

5) H. A. McKay, *Nature*, **142**, 997 (1939).

Table 2. The influence of various acids on the exchange rate

No.	Acid (pK)	Concn. of acid (10^{-2} M)	Concn. of water (10^{-2} M)	k_0 10^{-4} min^{-1}	k_2'' l^2 mol^{-2} min^{-1}
1	Trichloroacetic (pK=0.635)	2.5	2.5	13.3	12
2		2.5	1.9	10.0	11
3		2.5	1.4	7.9	12
4	*m*-Toluic (pK=4.272)	1.5	3.0	12.3	1.3
5		1.5	1.6	9.0	2.1
6		1.5	1.0	6.8	2.8
7		0.27	1.6	5.8	2.2
8	Phenol (pK=9.998)	0.36	3.5	10.6	2.5
9		1.1	3.5	16.5	2.2
10		1.6	3.5	21.1	2.5
11		0.45	2.3	7.7	2.5
12		1.2	2.3	14.0	3.2

[Al(acac)$_3$], 0.070 M; [acacH], 0.070 M; 25°C

log scale, as seen in Fig. 2. Hence Eq. (2) is written as Eq. (3).

$$R = k_0 a = a(k_1 + k_2[H_2O]) \quad (3)$$

At 25° Eq. (3) is numerically expressed as Eq. (4).

$$R = [\text{complex}](6\times10^{-5} + 2.0\times10^{-2}[H_2O]) \quad (\text{mol } l^{-1} \text{ min}^{-1}) \quad (4)$$

Acid catalysis. The exchange is accelerated by acids, although the variety of useful acids is very much limited because of their solubility in THF. The influence of acid concentration in the presence of a given amount of water is shown in Fig. 3.*1 It is seen that the rate increases with increase in concentration of a particular acid. Figure 4 illustrates the influence of the concentration of water in the presence of a given amount of particular acids. Since water is contained more or less in the reagents and solvent, experiments in the absence of water could not be substantiated. However, when the diagrams are exptraporated to zero concentration, the intercept would indicate the rate in the absence of water.

The reaction kinetics is expressed by Eq. (5).

$$R = a\{k_1 + k_1'[\text{acid}] + [H_2O](k_2' + k_2''[\text{acid}])\} \quad (5)$$

The accuracy of the extrapolated values is low and

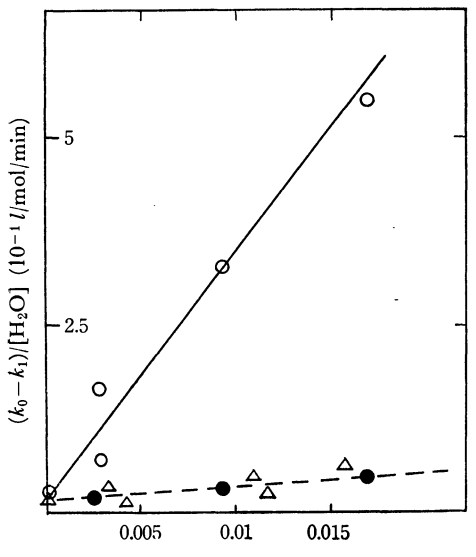

Fig. 3. Influence of the concentration of acids on the reaction rate.
[Al(acac)$_3$], 0.070 M; [acacH], 0.070 M; 25°C
—○— Trichloroacetic acid
--△-- *m*-Toluic acid
--●-- Phenol

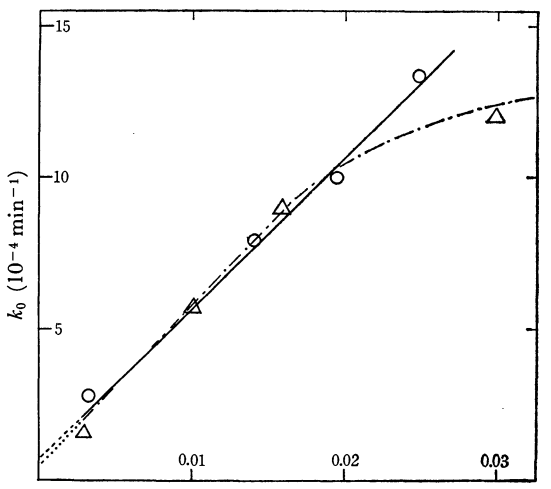

Fig. 4. Influence of the concentration of water on the rate constant in the presence of acids.
[Al(acac)$_3$], 0.070 M; [acacH], 0.070 M; 25°C
—○— Trichloroacetic acid 2.5×10^{-3} M
·—·△·—· *m*-Toluic acid 1.5×10^{-2} M

*1 The absolute water content is known only within an error *ca.* 0.003 M, but experience showed that the relative error for one sets of reaction mixtures simultaneously prepared was much less than that.

it remains uncertain whether the difference between the intercept of Fig. 4 (the second term of Eq. (5)) and k_1 in the absence of acid catalysis is really significant or not. Nevertheless it is quite clear that its contribution is of far less importance as compared with that of the last term of Eq. (5), when the mechanism of acid catalysis is discussed. The k_2'' values are listed in Table 2 together with the acid dissociation constants.

Temperature Dependence. The R values were measured at 0, 25 and 35°C to find the Arrhenius activation energy to be 22 kcal per mole in the presence of 0.020 M water. Since the contribution of k_1 is very small, this value is regarded as corresponding to that of water catalyzed exchange.

Discussion

Dissociation Mechanism. The experimental results indicate that the exchange mechanism is of dissociative nature and the rate determining step is the liberation of coordinated acetylacetonate from the complex. The second term of Eq. (3) corresponds to the catalytic action of water in THF. Since simultaneous break of two metal-oxygen bonds of one ligand is not probable, a possible reaction mechanism can be presented as shown in Fig. 5.

One of the three ligands can be present as unidentate and the break of its remaining bond will bring about the exchange of ligand. Thus the constant k_1 is expressed by $k_b^+ \cdot k_u^+ / k_b^-$, where k_b^+, k_u^+ and k_b^- are the rates of bond break of bidente and unidentate acetylacetonate and of bond formation to give bidentate acetylacetonate, respectively. The small value of k_1 reflects the ease with which the free end of unidentate ligand recombines with aluminum rather than the remaining bond is broken to result in isotopic exchange, in the absence of catalyst.

Function of Water. In the presence of water, it can occupy the vacant coordination site of aluminum formed by break of one of the Al-O bonds to retard the recombination and to facilitate the exchange (Fig. 5).

The k_1 is rather small as compared with $k_2[H_2O]$; especially when the water concentration is higher than 0.01 M as in most cases in experiments in atmosphere, the contribution of the former is negligible. In other words, the second term is really of great importance, unless the exchange reaction takes place under extraordinally dehydrated media. When tris-acetylacetonatoaluminum was to be precipitated on addition of petroleum ether to the THF solution containing a large amount of water (*e. g.* more than 0.1 M) gelatinous precipitate of aluminum was formed, which appeared to be hydrated aluminum oxide. This suggests that the water is present rather coordinated in the reaction intermediate. The same fact makes a kinetic run under such a condition impossible. Experiments with tris-acetylacetonatogallium and -indium under similar conditions could not be substanciated because gelatinous precipitate of the metal ions were formed. These findings could be also related with the ease with which water is substituted for acetylacetonate ligand even in such a medium as THF.

Acid Catalysis. As mentioned in "Results", the contribution of the second term of Eq. (5) would be very small, even if it were significant. The k_2'' values calculated by Eq. (5) without considering the contribution of the second term are practically constant for each of the three acids, (Table 2) to indicate that such a simplification is quite reasonable. The last term of Eq. (5) reflects the establishment of the following equilibrium,

$$HX + H_2O \rightleftarrows X^- + H_3O^+ \qquad (6)$$

where X^- stands for the acid anion. Rapid establishment of this equilibrium is also demonstrated by proton nuclear magnetic resonance (NMR) spectra of the acids in 1 M water solution in THF. They all give one sharp or broad band due to acid proton. The fact that the apparent k_2'' values calculated in No. 4—6 experiments in Table 2 decreases with increase in water concentration would indicate that an equilibrium as Eq. (6) should be attained for such a weak acid as *m*-toluic, when the concentrations of acid and water are comparable.

As illustrated in Fig. 5, hydronium ions give up proton to the free end of unidentate ligand to facili-

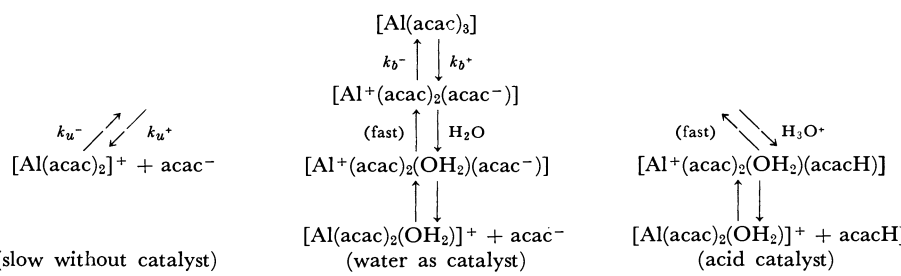

Fig. 5. A possible reaction mechanism of isotopic exchange reaction between tris-acetylacetonatoaluminum and acetylacetone-^{14}C in THF.

tate its liberation to a greater extent than water does. The difficulty of direct transfer of protons from the acid molecule, *i. e.*, the rather specific proton transportion by hydronium ions, could be understood by considering that the free end of unidentate acetylacetonate would remain in the neighborhood of the metal ion owing to electrostatic attraction, and that only a small particle like H_3O^+ can approach the end and hand over the proton to the negatively charged oxygen. Examination with molecular structure models discloses such a circumstance clearly.

Table 2 indicates that a strong acid accelerates the reaction more than a weak acid does. However, the Brønsted plot does not give a straight line. Some other factors, *e. g.* structural, could be operating. Further, free acetylacetone, being an acid with an acid dissociation constant 1.5×10^{-6}, could have acted as an acid catalyst. As carefully examined in Table 1 and Fig. 2, however, its concentration does not affect the rate of exchange at all, and this fact should be related to a structural factor, too.

Proton magnetic resonance spectrum of acetylacetone in THF has a sharp peak at 5.45 ppm and a very broad band at 14.5 ppm to indicate that this compound is present mainly in enol form and hydrogen bonded. The NMR spectrum of water has a sharp peak at 2.75 ppm to suggest a rapid exchange of protons with THF. An equimolar mixture of acetylacetone and water gives a broad band at 6.00 ppm and the peaks of water at 2.75 and of acetylacetone at 14.5 ppm disappear. The peak of vinyl proton remains at 5.35 ppm almost unchanged.

These spectra indicate that there could really be an interaction between acetylacetone and water in THF. However, the effective acid strength of acetylacetone in THF containing water to give H_3O^+ must be much weaker than that expected from its dissociation constant measured in water. Thus its failure to behave as an acid catalyst under the experimental condition would be ascribed to the difficulty with which proton is transferred from acetylacetone to water molecule. This "difficulty" certainly reasons rather thermodynamic sense than kinetic, because the proton exchange seems to occur at a rate of the order of 10^7 per sec as indicated by NMR studies at 60 Mc. The rather poor correlation between the acid dissociation constant and the k_2'' values is similarly accounted for by considering the different ease with which proton is transferred from the acid to water in THF. This ease is qualitatively parallel to the acid dissociation constant for the acids used, but would not be quantitatively.

An entirely different reaction mechanism could be encountered by considering direct attack by water, or proton transfer from hydronium ion upon the oxygen atom coordinated to aluminum ion. However, the fact that a spontaneous liberation of coordinated acetylacetonate is possible without catalytic action, although the rate is quite small, would be more reasonably understood by considering an intermediate, in which one of the ligands is unidentated. The catalytic actions are thus interpreted more consistently.

The authors wish to express their sincere thanks for financial support given by Nishina Memorial Foundation.

BULLETIN OF THE CHEMICAL SOCIETY OF JAPAN VOL. 41 390—396 (1968)

The Synthesis of Methacrylic Esters by the Carboxylation Reaction of Methylacetylene. II. Catalytic Synthesis of Methyl Methacrylate using Nickel Carbonyl as the Catalyst

Sango KUNICHIKA, Yasumasa SAKAKIBARA*1 and Tadao NAKAMURA*2

Institute for Chemical Research, Kyoto University, Daigaku-cho, Takatsuki, Osaka

(Received June 1, 1967)

The catalytic synthesis of methyl methacrylate by the carboxylation reaction of methylacetylene using nickel carbonyl as a catalyst was studied under various conditions. The experimental results concerning the effects of the reaction conditions on the reaction rate, the stability (regeneration) of nickel carbonyl, and the product yields suggested the most desirable conditions for the synthesis. It was ascertained that, in the catalytic process, the pressure of carbon monoxide played a very important roles; a high pressure gave a good regeneration of nickel carbonyl, *i. e.*, a high value of 95% in the so-called catalytic level, but the initial reaction rate decreased remarkably with an increase in the pressure, probably in reverse proportion to its second power, or more. A semicontinuous process was much better for the synthesis than a batch process. A good yield of 85% (based on the methylacetylene used) of the total of methyl methacrylate and methacrylic acid and a high catalytic level of 95% were obtained when the reaction was carried out semicontinuously in the presence of methacrylic acid and water at a total pressure of 13 atm (initial charge of carbon monoxide at room temp.: 4 atm) at 130°C. A mechanism for the catalytic reaction was proposed to account for the experimental results.

In a previous paper,[1] it has been reported that methylacetylene was more difficult to carboxylate than acetylene and that methyl methacrylate was obtained in unsatisfactory yields under the carboxylation conditions studied. It was also observed that, in the catalytic process using nickel carbonyl as a catalyst, the pressure of carbon monoxide appeared to play a very important role and that water acted as an accelerator of the reaction, as do mineral acids as well known.

The present paper will describe a further investigation of the catalytic synthesis of methyl methacrylate from methylacetylene and carbon monoxide, using nickel carbonyl as a catalyst. The effects of the reaction conditions on the reaction rate, the stability of nickel carbonyl, and the product yields will be examined in order to determine the most suitable conditions for this synthesis and in order to obtain useful information about the carboxylation reaction. Special attention will be paid to the stability (regeneration) of the nickel carbonyl catalyst. A mechanism for the carboxylation reaction will be proposed to account for the experimental results.

Experimental

Materials. Commercial methylacetylene was purified by fractional distillation through a Podbielniak-type low-temperature column (80 cm × 1.5 cm); bp −23—−22°C. The purity was higher than 98.5 mol% on gas chromatographic analysis. Commercial carbon monoxide (99.7 mol% pure) was used. Nickel carbonyl was prepared by the usual method[2]; bp 42—43°C (lit. 43°C).

Apparatus and Procedures. Two reaction processes were employed.

1) Batch Process. This process was favored over the semicontinuous process for collecting the kinetic data of the reaction. The general procedure was as follows. A 350 m*l* shaking-type stainless-steel autoclave (shaking speed: 240 times per min) was charged with methanol, additives such as water and/or acids, hydroquinone, and a catalytic amount of nickel carbonyl under nitrogen. The vessel was then cooled to about −50°C and evacuated, and the air was completely replaced by nitrogen. Carbon monoxide was introduced to give the specified pressures. Then the vessel was heated to the reaction temperature, at which temperature all the methylacetylene was injected at once through a pipe-line from an injection pump.*3 After the lapse of an introduction period, the absorption of carbon monoxide was observed; in most cases, the reaction was continued until the absorption had practically ceased. During the reaction period, the total reaction pressure was

*1 Present address: Chemical Laboratory of Textile Fibers, Kyoto University of Industrial Arts and Textile Fibers, Kyoto.

*2 Present address: The Research Laboratory, Asahi Glass Co., Ltd., Yokohama.

1) Y. Sakakibara, This Bulletin, **37**, 1601 (1964).

*3 By means of an injection pump manufactured by the Tokyo Koatsu Co., liquefied methylacetylene was n ject ed all at once through a handling operation or ntrod uced at a constant rate of 0.5—17 m*l*/hr mechanically.

kept constant by introducing carbon monoxide continuously from a 120 ml carbon monoxide-pressure storage tank. The amount of carbon monoxide introduced was calculated from the pressure drop in the pressure storage. After the reaction had been completed, the autoclave was cooled and the reaction mixture was analyzed.

2) Semicontinuous Process. A 200 ml rotational-stirring-type stainless-steel autoclave (used at about 900 rpm) was used as the reaction vessel. This process was the same as the above batch process except that methylacetylene was added continuously at the reaction temperature using the injection pump. The addition of methylacetylene was made by first introducing a small portion (0.5—0.8 g of it) quickly; after the reaction had started, the residual portion was added continuously at a moderate rate.

Analytical Procedures. The decomposed and, in several cases, undecomposed nickel carbonyl was analyzed to determine the catalytic level of nickel carbonyl; the catalytic level is expressed as the ratio of the product (ester, carbonic acid) carbonyl coming from gaseous carbon monoxide to the total available carbon monoxide, including that from the nickel carbonyl decomposed. The undecomposed nickel carbonyl was thoroughly removed from the reaction mixture after the gas remaining in the autoclave had been vented off, first by passing nitrogen through the vessel under a slight heating or under stirring, and then by bubbling nitrogen into the reaction mixture in a flask at about 50°C. All of these gases were passed through a mixture consisting of carbon tetrachloride, bromine, and water to decompose the nickel carbonyl, and the nickel was analyzed by the dimethylglyoxime method.[3] The decomposed nickel carbonyl was determined by analyzing the nickel in the aqueous layer coming from the extraction procedure described below.

The reaction products, esters and acetone, were determined by gas chromatography using a 2.5 m column of 25% polyethylene glycol 1000 and a 2.4 m column of 25% squalane at 70°C. Toluene was used as the internal standard substance. Carboxylic acids in the reaction mixture were titrated with a sodium hydroxide solution and were regarded as methacrylic acid because gas chromatographic analysis showed that the acids mainly consisted of methacrylic acid.[1] Furthermore, the yield of methacrylic acid given assumes that all the nickel resulting from the decomposed nickel carbonyl exists as nickel methacrylate. The remaining reaction mixture was poured into dilute sulfuric acid and extracted with methylene chloride. The aqueous layer was thus provided for the determination of the decomposed nickel carbonyl. The extract was condensed and flash-distilled under reduced pressure.

Results and Discussion

The experimental results for the batch and the semicontinuous process are shown in Tables 1 and 2.

The Effect of Reaction Conditions on the Reaction Rate. In order to examine the effect of reaction conditions on the reaction rate, the experiments were carried out by the batch process at a temperature regulated to about ±2°C (Table 1, Exps. 1—11). Concerning the reaction conditions, such conditions as that the catalytic level was over 90% were examined in order to obtain kinetic data about the catalytic reaction. Under the specified conditions, the reaction began after a short induction period and then proceeded smoothly and catalytically. In these cases, the resulting reaction mixture was a transparent yellow-green liquid without any precipitate. The absorption curves of carbon monoxide under various conditions, listed in Exps. 1—11 of Table 1, are shown in Figs. 1—5. In these figures, the absorption amount has been roughly corrected by taking into account the facts that the partial pressure of methylacetylene in the gas phase of the autoclave decreases with the progress of the reaction and that, as a result, carbon monoxide enters into the autoclave to compensate for the decrease. On the assumption that the partial pressure of methylacetylene is proportional to the total methylacetylene and that the partial pressure is zero at the 90% absorption of the theoretical amount of carbon monoxide, the following correction factor, f, was introduced:

The corrected absorption amount = The apparent absorption amount $\times f$

$$f = V_t \times 0.9/(V_t \times 0.9 + V_v \cdot P)$$

where V_t is the theoretical absorption amount of carbon monoxide; V_v, the volume of the vacant part of the autoclave; and P, the partial pressure of methylacetylene at the start of the reaction, being about 9 atm at 170°C and 10.5 atm at 180°C. The relative initial reaction rates were calculated roughly from the absorption curve of carbon monoxide.

The Effect of the Temperature. The reaction rate is quite sensitive to the temperature, as is shown in Fig. 1. Increasing the temperature from 170

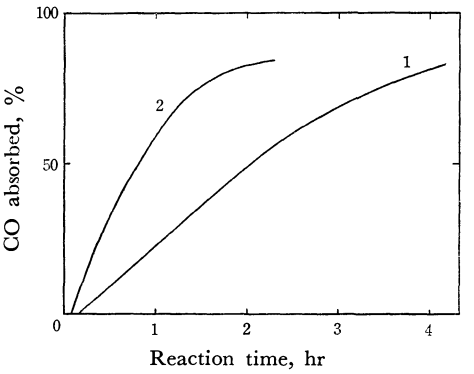

Fig. 1. CO absorption *vs.* time plots for the reaction—Effect of reaction temperature.
Curve number corresponds with Exp. No. in Table 1. Curve 1: 170°C, Curve 2: 180°C

2) W. Reppe *et al.*, *Ann.*, **582**, 116 (1953).
3) E. R. H. Jones, T. Y. Shen and M. C. Whiting, *J. Chem. Soc.*, **1951**, 766.

TABLE 1. EXPERIMENTAL AND ANALYTICAL DATA FOR BATCH PROCESS
Hydroquinone, 0.1 g

Exp. No.	C_3H_4 g	CH_3OH ml	$Ni(CO)_4$ g	Additive		CO		Reaction temp. °C	Reaction time hr	Product[c]				Decomposed $Ni(CO)_4$ %	Catalytic level %
				H_2O ml	Acid g	Pressure[a] atm	Absorption amount[b] %			MMA %	MAA %	MC %	Rd g		
1	8.1	70	2.0	10	None	10(45)	83	169—171	4.2	57.7	15.3	6.4	1.3	43	89
2	8.1	70	2.0	10	None	10(53)	84	180—181	2.3	62.3	12.1	7.3	0.8	21	94
3	8.1	70	2.0	10	None	12(55)	83	180—181	2.7	56.5	11.6	6.5	1.1	20	95
4	8.1	70	2.0	10	None	14(58)	70	178—184	3.8	52.6	9.5	5.8	1.4	26	92
5	8.1	70	1.3	10	None	10(53)	73	179—181	2.8	56.5	11.5	6.3	1.0	30	94
6	8.1	70	1.0	10	None	10(53)	66	179—181	4.5	53.0	13.9	5.7	0.5	46	93
7	4.0	70	2.0	10	None	10(45)	75	169—172	3.5	52.7	11.6	5.9	1.0	11	94
8	8.1	63	2.0	18	None	10(45)	83	169—172	2.7	51.2	20.8	5.4	1.2	34	91
9	8.1	70	2.0	10	MAA 0.5	10(45)	77	170—172	2.0	60.7	10.9	5.4	1.0	39	90
10	8.1	70	2.0	10	MAA 1.0	10(44)	77	169—171	1.5	45.0	10.0	4.5	1.3	18	95
11	8.1	70	2.0	10	IBA[d] 1.0	10(45)	61	169—171	1.7	48.8	—	5.9	—	28	91
12	8.7	140	2.0	10	None	5.5(31—26)	82	158—161	3.0	62.7	11.9	7.4	1.5	26(70)[e]	94
13	8.6	120	2.0	35	MAA 5.0	4.5(18—16)	81	125—135	7.0	61.4	17.3	3.9	0.8	35(60)	92

a) The initial pressure of carbon monoxide at room temperature is shown. The values in parentheses show the total pressure at reaction temperature.
b) Expressed as percentage of the theoretical amount based on the methylacetylene used.
c) MMA=methyl methacrylate, MAA=methacrylic acid, MC=methyl crotonate (*trans*), Rd=residue (high boiling materials of bp 60—100°C/50 mmHg, consisting of methacrylic acid mainly, were distilled off.) The yields were calculated on the basis of the methylacetylene used. In Exps. 9, 10, and 13, the yields were given in taking account of the methacrylic acid added.
d) IBA=isobutyric acid e) The values in parentheses show the percentage of the undecomposed nickel carbonyl.

TABLE 2. EXPERIMENTAL AND ANALYTICAL DATA FOR SEMICONTINUOUS PROCESS*
Methanol, 50 ml; nickel carbonyl, 2.0 g; hydroquinone, 0.1 g

Exp. No.	C_3H_4 g	Additive		CO		Reaction temp. °C	Reaction time[a] hr	Product				Decomposed $Ni(CO)_4$ %	Catalytic level %
		H_2O ml	MAA g	Pressure atm	Absorption amount %			MMA %	MAA %	MC %	Rd g		
14	15.7	7	2.0	9(25)	86	158—162	2.2(1.8)	67.6	14.3	8.7	1.5	31(53)	96
15	9.9	0	5.0	4(13)	87	129—130	2.8(1.8)	80.2	0	8.1	0.7	24(65)	95
16	9.8	2	5.0	4(13)	88	128—130	3.0(1.9)	80.5	4.2	7.4	0.6	23(66)	95
17	10.0	7	2.0	4(13)	85	130—133	2.4(1.6)	70.1	13.6	6.8	0.6	25(66)	95
18	9.9	12	3.0	4(12)	86	128—130	2.5(1.8)	63.2	19.5	5.7	0.8	26(56)	95

* Refer to Footnote a—e in Table 1. a) The values in parentheses show the time of injection of methylacetylene.

to 180°C raised the initial rate by a factor of 3.0. With 160°C, a long induction period of about 1.5 hr was required for the reaction and the rate was very slow.

The Effect of the Pressure of Carbon Monoxide. Increasing the pressure reduces the reaction rate remarkably (Fig. 2). The relative initial rates at 10, 12, and 14 atm pressures (at room temperature) of carbon monoxide were 1.0, 0.6, and 0.3 respectively. From these values, it can roughly be estimated that the initial rate is reversely proportional to the second power of the pressure, or more.

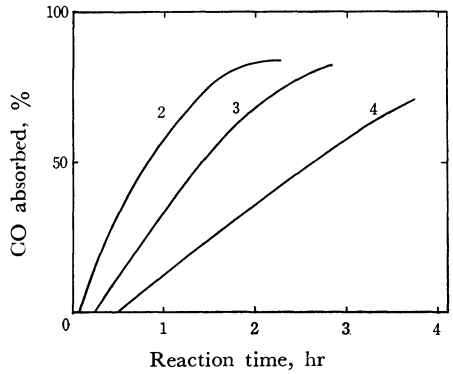

Fig. 2. CO absorption *vs.* time plots for the reaction—Effect of pressure of carbon monoxide.
Curve No.: Exp. No.
Curve 2: 10 atm, Curve 3: 12 atm, Curve 4: 14 atm

In addition, the induction period of the reaction was reduced with a decrease in the pressure, being about 5 min at the 10 atm pressure (Exp. 2).

The Effect of the Amounts of Nickel Carbonyl and Methylacetylene. A decrease in the amount of nickel carbonyl reduces the reaction rate (Fig. 3). The relative initial rates with 2.0, 1.3, and 1.0 g of nickel carbonyl were 1.0, 0.6, and 0.3 respectively.

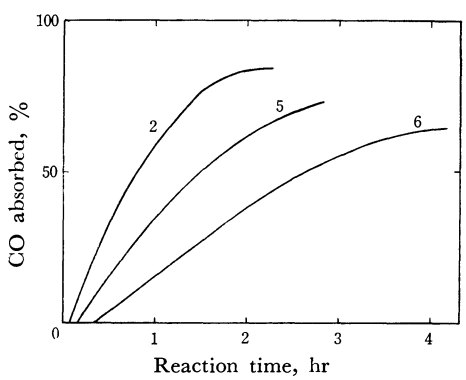

Fig. 3. CO absorption *vs.* time plots for the reaction—Effect of amount of nickel carbonyl.
Curve No.: Exp. No.
Curve 2: 2.0 g, Curve 5: 1.3 g, Curve 6: 1.0 g

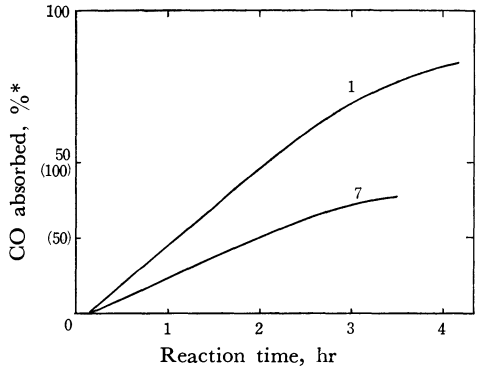

Fig. 4. CO Absorption *vs.* time plots for the reaction—Effect of amount of methylacetylene.
Curve 1: 8.1 g, Curve 7: 4.0 g
* The percentage in parentheses is for Curve 7 in consideration of the absolute amount of carbon monoxide absorbed.

The results suggest that the initial rate might be first-order with respect to the concentration of nickel carbonyl.

Increasing the amount of methylacetylene raises the reaction rate (Fig. 4). The initial rate of Exp. 1, conducted with 8.1 g of methylacetylene, was just twice as fast as that of Exp. 7, with 4.0 g. These results suggest that the initial rate may be first-order also with respect to the concentration of methylacetylene, though the experimental data are yet incomplete.

The Effects of Additives. The reaction did not proceed easily without the addition of certain accelerators; substances with an active hydrogen as inorganic and organic acids and water are known to be effective. Figure 5 and Table 3 show the effects of additives on the reaction rate. Of water, methacrylic acid, isobutyric acid, and hydrogen chloride, hydrogen chloride is the most effective (Exp. 20 in Table 3); the decreasing order of the effect of these additives per mole is

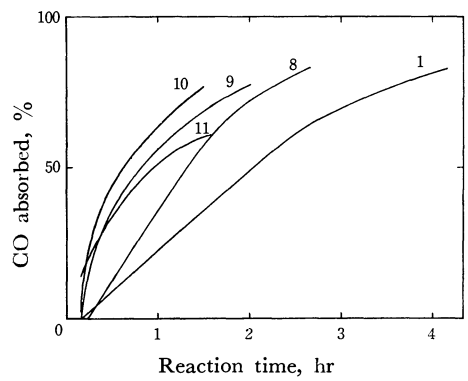

Fig. 5. CO absorption *vs.* time plots for the reaction—Effect of additives.
Curve No.: Exp. No.
See Table 3 concerning the kinds and amounts of additives.

TABLE 3. EFFECT OF ADDITIVES ON REACTION RATE

Exp. No.[a]	Additive		Relative initial rate (Exp. 1=1.0)
	Water		
1	10		1.0
8	18		1.9
	Water + Methacrylic acid		
9	10	0.0	5.9
10	10	1.0	10.2
	Water + Isobutyric acid		
11	10	1.0	(5.0)
	Water + Methacrylic acid		
19[b]	7.0	2.0	1.0[c]
	Water + Hydrogen chloride		
20[b]	7.0	0.9	(7)[c]

a) The Exp. No. corresponds with Exp. No. in Table 1 and Curve No. in Fig. 5.
b) Exps. 19 and 20 were made at 28 atm total pressure (initial charge of carbon monoxide at room temp.: 10 atm) at 130°C with 8.0 g C_3H_4, 50 m*l* CH_3OH, 2.0 g $Ni(CO)_4$, and 0.1 g hydroquinone using the rotational stirring-type autoclave descrived above.
c) These two values were expressed as Exp. 19=1.0.

as follows: hydrogen chloride > methacrylic acid ≒ isobutyric acid ≫ water. In the use of hydrogen chloride under the conditions studied, however, the reaction rate decreased quite rapidly, probably as a result of the loss of hydrogen chloride by the $CH_3OH + HCl \rightarrow CH_3Cl + H_2O$ reaction. In the case of both water and methacrylic acid, the reaction rate increased with an increase in their amounts. The initial rates were roughly twice as fast when their amounts were doubled (Exps. 1 and 8; Exps. 9 and 10).

A systematic examination of the effect of mixing was not made, though it appeared to be the most important physical variable. Recently,[4] in the catalytic reaction of acetylene under low pressure (total pressure 1.5 atm, usually under atmospheric pressure), it has been reported that the liquid diffusion of carbon monoxide is an important rate step and that it is necessary to keep the liquid diffusion of carbon monoxide rate-controlling in order to maintain the reaction. For obtaining most of the kinetic data, however, it is best to keep the chemical variables rate-controlling. Judging from the above results concerning the effects of certain variables on the reaction rate, the chemical reaction rate appeared to be rate-controlling under the conditions studied.

The Regeneration of Nickel Carbonyl (Catalytic Level). Concerning the catalytic level of nickel carbonyl in the catalytic carboxylation reaction, very little has been known except for the information on the low-pressure catalytic reaction of acetylene.[5] Recently, with acetylene, it has been reported by Ehrreich *et al.*[4] that a catalytic level of 85% at the maximum, and usually 70—80%, was obtained in the low-pressure process by controlling the material-feed rates accurately under certain conditions. Furthermore, they have pointed out that the maximum catalytic levels for the reaction of substituted acetylenes were much less than that for unsubstituted acetylene, though no details were given.

A high pressure of carbon monoxide was necessary for obtaining a high catalytic level, though the high pressure reduced the reaction rate: in practice, a pressure of about 10 atm (at room temperature) was used at 170°C and one of about 4 atm, at 130°C. Consequently, even in the batch method, catalytic levels higher than 90% were obtained easily (Table 1). In the semicontinuous method, the catalytic levels were all above 95% (Table 2). The carbon monoxide pressure in these experiments might be high enough to produce such catalytic levels, though the critical limits of carbon monoxide pressure have not been clarified. On the other hand, even if the apparent pressure of carbon monoxide was high, the catalytic levels were low in cases of either an insufficient mixing of the reactants or the occurrence of a temporary violent reaction. In the batch method especially it was necessary to choose the reaction conditions so that no violent reaction occurred in the early stage of the reaction.

By-products. Methyl crotonate, methyl isobutyrate, and acetone were found as the main by-products, besides the polymerization products of methylacetylene and/or methyl methacrylate formed.[1] Of these by-products, methyl crotonate was measured in largest quantities, especially at higher reaction temperatures. This amount

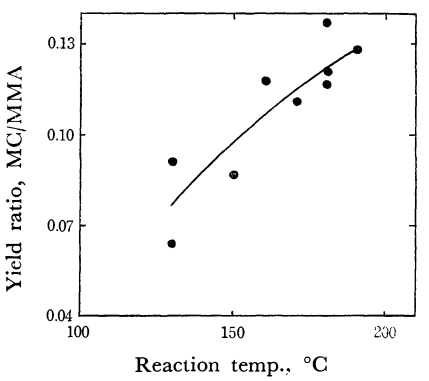

Fig. 6. Yield ratio of methyl crotonate to methyl methacrylate against reaction temp.

4) J. E. Ehrreich, R. G. Nickerson and C. E. Ziegler, *Ind. Eng. Chem. Process Design Develop.*, **4**, 77 (1965).

5) M. Salkind, E. H. Riddle and R. W. Keefer, *Ind. Eng. Chem.*, **51**, 1328 (1959); Numerous patents.

decreased, however, with a decrease in the reaction temperature and the yield ratio of methyl crotonate to methyl methacrylate dropped from about 0.13 at 190°C to about 0.08 at 130°C, as Fig. 6 shows. The amount of methyl isobutyrate was very small (below 0.2%), in most cases being only a trace, in the catalytic reactions conducted at high catalytic levels, as was to be expected from the very small decomposition of nickel carbonyl. Acetone also was found in only a trace under those conditions.

Although the loss of methylacetylene due to its polymerization appeared to be a main cause of the poor yield of the carboxylation products in the batch method, as has been described in the previous paper,[1] the polymerization was markedly decreased by adding methylacetylene continuously and by carrying out the reaction at a low temperature (Table 2).

Optimum Conditions for the Synthesis of Methyl Methacrylate. The above results concerning the reaction rate, the catalytic level, and the by-products in the catalytic reaction give some hints for a search after the optimum conditions for this synthesis, though their determination is difficult. As expected, it would be advantageous to carry out this reaction under the following conditions: at as low and constant a pressure as possible, in order to make the reaction rate fast, within the critical limits for maintaining high catalytic levels; at as low and constant a temperature as possible, to suppress the formation of methyl crotonate, taking account of the reaction rate; in the presence of such effective additives as acids and water; under a mixing sufficient to keep the liquid diffusion of carbon monoxide good; and by a continuous process, to suppress the polymerization of methylacetylene and methyl methacrylate and to avoid a temporary violent reaction.

Therefore, the synthesis was attempted semi-continuously using a laboratory apparatus by which at least methylacetylene and carbon monoxide were each introduced continuously, though it would be better to feed all the raw materials continuously under accurate control. Several results are shown in Table 2. Under the present conditions, the catalytic reaction began a short time after the addition of a small amount (0.5—0.8 g) of methylacetylene, and thence proceeded smoothly at a high catalytic level, over 95%. The total yield of methyl methacrylate and methacrylic acid was 82—85%. The best yield, 85%, was obtained when the reaction was carried out in the presence of methacrylic acid and a small amount of water at a total pressure of 13 atm (initial charge of carbon monoxide at room temperature: 4 atm), a reaction temperature of 130°C, and a feed rate of 4.8 g/hr (Exp. 16). The use of a lower carbon monoxide pressure is promising and would possibly be more advantageous. With a lower pressure, however, it was difficult to control and maintain the catalytic reaction using our apparatus, because the effect of the fluctuation of the carbon monoxide pressure on the reaction rate and the catalytic level becomes remarkably large with a decrease in the pressure. Recently, Happel *et al.*[6] have reported the synthesis of methyl methacrylate by a low pressure catalytic carbon monoxide-nickel carbonyl-methylacetylene process, as used with acetylene itself. The catalytic level, however, seems to be lower than 70%.

Reaction Mechanism. The mechanism of the catalytic carboxylation reaction has not yet been well clarified though it has been discussed by several workers.[7] On the basis of our experimental results, the following mechanism, similar to one of the possible mechanisms presented by Heck,[7a] may be proposed:

$$Ni(CO)_4 + HX \underset{k_2}{\overset{k_1}{\rightleftharpoons}} HNi(CO)_{4-n}X + nCO \quad (1)$$

$$CH{\equiv}CR + HNi(CO)_{4-n}X \xrightarrow{k_3} CH_2{=}\overset{R}{\overset{|}{C}}Ni(CO)_{4-n}X\ (+\ RCH{=}CHNi(CO)_{4-n}X) \quad (2)$$

$$CH_2{=}\overset{R}{\overset{|}{C}}Ni(CO)_{4-n}X + CO \xrightarrow{k_4} CH_2{=}\overset{R}{\overset{|}{C}}CONi(CO)_{4-n}X \quad (3)$$

$$CH_2{=}\overset{R}{\overset{|}{C}}CONi(CO)_{4-n}X + R'OH \xrightarrow{k_5} CH_2{=}\overset{R}{\overset{|}{C}}CO_2R' + HNi(CO)_{4-n}X \quad (4)$$

HX = water, organic or inorganic acids
R′ = H or alkyls

Assuming that reaction (1) is a rapid reversible reaction and that reaction (2) is the rate-determining step, which is followed by the two rapid reactions, (3) and (4), the initial rate of the overall reaction can be given by the following equation:

$$\text{Initial rate} = (k_1k_3/k_2)[Ni(CO)_4][HX][RC{\equiv}CH]/(P_{CO})^n$$

The experimental results concerning the initial reaction rate seem to confirm the above relation ship, though they are rough.

Reaction (1) forms a hydronickel carbonyl hydroxide ($HNi(CO)_{4-n}X$, X=OH), which is the true catalyst. This reaction (1) is supported by the experimental finding that the reaction rate was accelerated by the presence of such additives as water and acids, and markedly decreased with an increase in the carbon monoxide pressure.

6) J. Happel and C. J. Marsel, Belg. Pat. 639260 (1964) (*Chem. Abstr.*, **62**, 9019 (1965)).
7) a) R. F. Heck, *J. Am. Chem. Soc.*, **85**, 2013 (1963); b) C. W. Bird, *Chem. Revs.*, **62**, 283 (1962); c) P. L. Pauson, *Proc. Chem. Soc.*, **1960**, 297.

Furthermore, effective additives may be supposed to form a highly reactive $HNi(CO)_{4-n}X$. The n value in $HNi(CO)_{4-n}X$ would probably be 2 or higher, in view of the fact that the initial rate is reversely proportional to over the second power of the carbon monoxide pressure. The subsequent steps, reactions (2)—(4), are similar to those proposed to explain the hydroformylation reaction,[8] except for replacing hydrogen reduction with hydrolysis or alcoholysis. In addition, judging from the distribution of the reaction products, it may be concluded that, under the conditions studied, reaction (2) proceeds predominantly to give an addition product, alkenylnickel carbonyl hydroxide (X=OH), with a branched chain.

8) R. F. Heck and D. S. Breslow, *J. Am. Chem. Soc.*, **83**, 4023 (1961); J. A. Bertrand, C. L. Aldridge, S. Husebye and H. B. Jonassen, *J. Org. Chem.*, **29**, 790 (1964).

BULLETIN OF THE CHEMICAL SOCIETY OF JAPAN VOL. 41 396—401 (1968)

Dimerization of Acrylonitrile by Ruthenium Chloride

Akira MISONO, Yasuzo UCHIDA and Masanobu HIDAI

Department of Industrial Chemistry, The University of Tokyo, Hongo, Tokyo

and Hiroyuki SHINOHARA and Yoshihisa WATANABE

Mizonokuchi Research Laboratory, Mitsubishi Petrochemical Company Ltd., Kawasaki

(Received July 17, 1967)

The end-to-end dimerization of acrylonitrile was effected with a ruthenium trichloride trihydrate catalyst under a hydrogen atmosphere, thus obtaining a mixture of *cis*- and *trans*-1, 4-dicyano-1-butene as the main products. Under nitrogen, however, only very small amounts of these products were formed. The reaction occurred at temperatures of 120—200°C under moderate hydrogen pressures in alcoholic media such as ethanol. The effects of various salts or electron-donating compounds on the catalysis were examined.

Previously we reported[1] that acrylonitrile was, though not catalytically, converted at an elevated temperature to a mixture of propionitrile, 2-methylglutaronitrile, and adiponitrile with several systems involving hydride complexes of cobalt or iron. The end-to-end dimerization of methyl acrylate by a rhodium or ruthenium chloride catalyst has been found by Alderson *et al.*[2] However, acrylonitrile does not dimerize successfully in the same reaction. In this paper, we wish to report the successful catalytic dimerization of acrylonitrile, which primarily gives end-to-end coupling products. The reaction was effected with ruthenium trichloride trihydrate under a hydrogen atmosphere; it was not, however, catalytic under a nitrogen atmosphere. The variation in the reaction temperature and the hydrogen pressure was examined, and the effects of the addition of various salts or electron-donating compounds were also studied.

Results and Discussion

The reaction of acrylonitrile by the use of various second- and third-row transition metal compounds, especially chlorides, was investigated in order to obtain the dimers of acrylonitrile. A part of the results are shown in Table 1. The reaction of acrylonitrile by ruthenium chloride under a nitrogen atmosphere yielded only a small percentage of propionitrile and acrylonitrile dimers. The replacement of the nitrogen atmosphere with ethylene improved the yield of the dimers to 10%. When acrylonitrile was treated with an ethanol solution of ruthenium chloride under a hydrogen atmosphere, acrylonitrile was catalytically converted to a mixture of propionitrile and acrylonitrile dimers. Gas chromatographic analysis showed that the dimers were a mixture of three components. The three components were isolated by the fractional distillation of the mixture. The fraction with a bp of 107°C/2 mmHg was identified as adiponitrile by a comparison of the retention time and the infrared spectrum with those of an authentic sample. Both the fraction with a bp of 95°C/2 mmHg, A, and the fraction with a bp of 175—180°C/2 mmHg, B, were hydrogenated over palladium black at room temperature to

1) A. Misono, Y. Uchida, K. Tamai and M. Hidai, This Bulletin, **40**, 931 (1967).

2) T. Alderson, E. L. Jenner and R. V. Lindsey, Jr., *J. Am. Chem. Soc.*, **87**, 5638 (1965).

Table 1. The reaction of acrylonitrile in the presence of transition metal chlorides[a]

Chlorides	mmoles	Reaction atmosphere	Reaction temp., °C	Reaction time, hr	Conv. %	PN[b] %,	Dimers yield[c]
$RuCl_3 \cdot 3H_2O$	0.77	N_2, 1 atm	170	4	33	2	5
$RuCl_3 \cdot 3H_2O$	0.77	C_2H_4, 10 atm	170	5	15	3	10
$RuCl_3 \cdot 3H_2O$	0.77	H_2, 30 atm	150	0.5	94	51	44
$RhCl_3 \cdot 3H_2O$	0.76	H_2, 30 atm	140	1.3	60	60	
$MoCl_5$	2.2	H_2, 30 atm	120	3	18	11	
$MoCl_5$	1.3	H_2, 30 atm	170	3	85	15	
WCl_6	1.8	H_2, 30 atm	120	3	10	7	
$IrCl_4$	0.59	H_2, 30 atm	170	3	55	45	
$PdCl_2$	0.77	H_2, 30 atm	140	0.5	79	74	

a) All reactions used 10 m*l* of acrylonitrile and 20 m*l* of ethanol or methanol. b) Propionitrile.
c) % based on the acrylonitrile originally fed in.

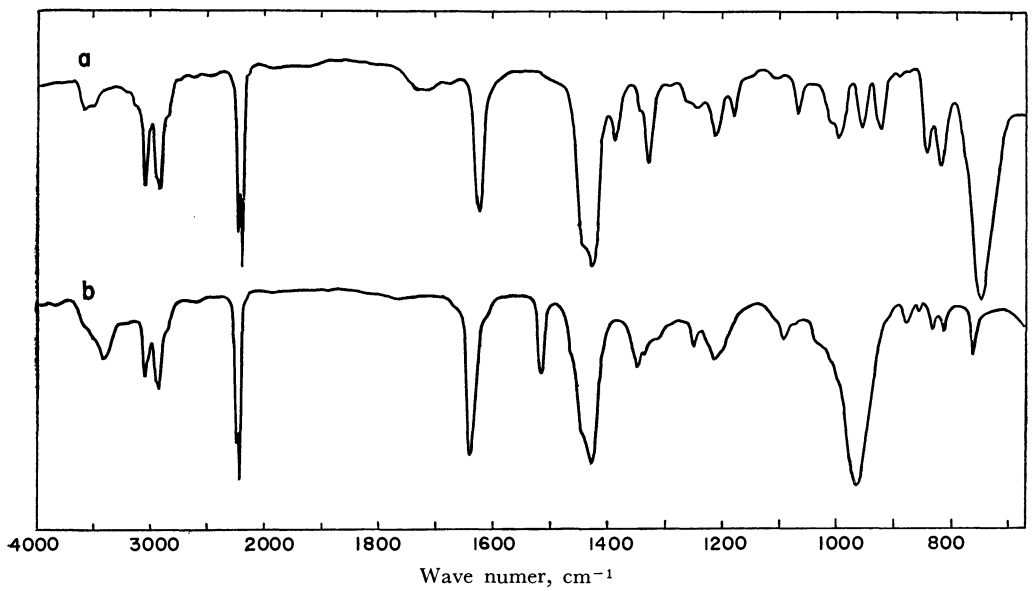

Fig. 1. Infrared spectra of (a) *cis*-1,4-dicyano-1-butene and (b) *trans*-1,4-dicyano-1-butene.

give adiponitrile. The amount of hydrogen gas absorbed indicated that both A and B were dimers of acrylonitrile carrying a double bond. The infrared spectrum of A (Fig. 1) showed the presence of two different nitrile groups (*ca.* 2230 and 2210 cm^{-1}) and a cis double bond (1630 and 750 cm^{-1}). The NMR spectrum of A (Fig. 2) showed the complex bands at $\tau=7.9$, a doublet at $\tau=4.9$, and the complex band at $\tau=4.1$ in an intensity ratio of 4 : 1 : 1. The bands at $\tau=7.9$ were assignable to the four methylene protons of $-CH_2CN$ and $-CH_2-CH=CH-$. The doublet at $\tau=4.9$ with a spin-spin coupling constant of 10 cps was assigned to the cis olefinic proton, H_a, in

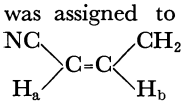

, while the band at $\tau=4.1$ was assigned to the other olefinic proton, H_b. On the other hand, the infrared spectrum of B (Fig. 1) showed the presence of two different nitrile groups (*ca.* 2240 and 2220 cm^{-1}) and a trans double bond (1640 and 965 cm^{-1}). The NMR spectrum of B (Fig. 2) showed a doublet at $\tau=5.1$ with a large spin-spin coupling constant of 16 cps; it was assigned to the trans olefinic proton, H_a, in

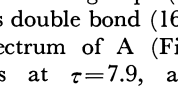

. From these results, A and B were identified as *cis*- and *trans*-1,4-dicyano-1-butene respectively.

$$CH_2{=}CHCN \xrightarrow[\text{under } H_2]{RuCl_3 \cdot 3H_2O} \begin{cases} CH_3CH_2CN \\ NCCH{=}CHCH_2CH_2CN \text{ (cis and trans)} \\ NC(CH_2)_4CN \end{cases}$$

Other transition metal chlorides, such as rhodium, palladium, tungsten, molybdenum, or iridium chlorides, gave only propionitrile in reactions

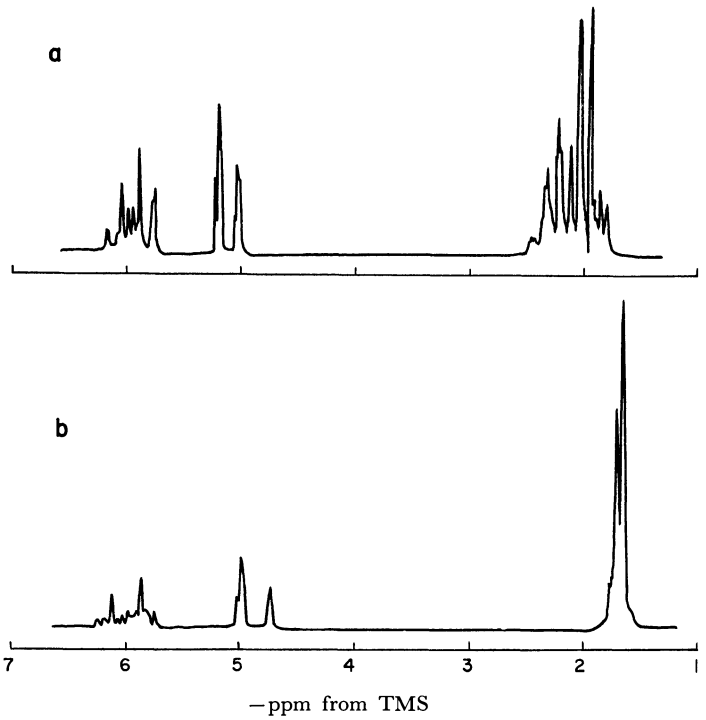

Fig. 2. NMR spectra of (a) *cis*-1,4-dicyano-1-butene and (b) *trans*-1,4-dicyano-1-butene in benzene.

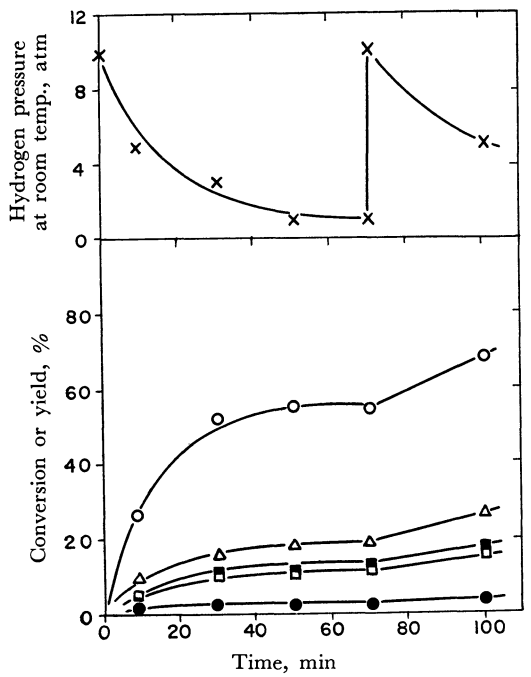

Fig. 3. Relationship between reaction time and hydrogen pressure or yields of products at 150°C: ○, conversion of acrylonitrile; △, yield of propionitrile; □, yield of *cis*-1,4-dicyano-1-butene; ●, yield of adiponitrile; ■, yield of *trans*-1,4-dicyano-1-butene.

under a hydrogen atmosphere.

In this catalytic conversion of acrylonitrile to a mixture of *cis*- and *trans*-1,4-dicyano-1-butene, adiponitrile, and propionitrile by the use of ruthenium chloride, hydrogen appears to play an important role in the reaction mechanism, as the reaction did not proceed catalytically in the absence of hydrogen. Figure 3 shows the relationship between the reaction time or the hydrogen pressure and the yields of the products. When 10 atm of hydrogen (the pressure at room temperature) was charged into the reaction vessel at 150°C, a rapid uptake of hydrogen occurred, and propionitrile and the dimers were formed. When the hydrogen pressure (converted to the value at room temperature) went below 1 or 2 atm after *ca.* 30 min, the reaction of acrylonitrile nearly stopped. However, when another 9 atm of hydrogen was charged into the reaction vessel after 70 min, the absorption of hydrogen again started, and propionitrile and the dimers were obtained. This would suggest that the reaction proceeds through a ruthenium hydride complex, which is regenerated by a large amount of hydrogen. We have already reported[3] that two yellow complexes, which catalyzed the dimerization of acrylonitrile, were obtained by the reaction of acrylonitrile and ruthenium trichloride under a nitrogen or hydrogen

3) A. Misono, Y. Uchida, M. Hidai and H. Kanai, *Chem. Commun.*, 357 (1967).

atmosphere. The first complex, $(CH_2=CHCN)_3RuCl_2$, was obtained by refluxing a solution of ruthenium trichloride in ethanol with a large excess of acrylonitrile under nitrogen. In the complex, acrylonitrile was bonded to the metal through the nitrogen lone pair. The other complex obtained by the reaction under hydrogen at 150°C had a cyanoethyl group attached to the metal. The following reaction mechanism may be assumed on the basis of these results. An intermediate complex may be formed in the reaction in which a hydride ion and at least two molecules of acrylonitrile are coordinated to ruthenium. When a cyanoethyl group formed by the insertion reaction of acrylonitrile into the ruthenium-hydride bond reacts with hydrogen, propionitrile will be formed, while a dicyanobutyl complex will be formed by the insertion of an acrylonitrile molecule into the ruthenium-cyanoethyl bond. This dicyanobutyl complex may decompose to give 1, 4-dicyano-1-butene or may react with hydrogen to yield adiponitrile.

Figure 4 shows the effect of the initial hydrogen pressure on the reaction. The yields of propionitrile and adiponitrile increased with an increase in the initial hydrogen pressure, while the yield of 1, 4-dicyano-1-butene decreased. This would imply that, under a high hydrogen pressure, a cyanoethyl complex and a dicyanobutyl complex easily react with hydrogen to give propionitrile and adiponitrile respectively.

The formation of the dimers and propionitrile is strongly dependent on the reaction temperature, as Fig. 5 shows. Below 120°C, the reaction was slow. The conversion of acrylonitrile varied with the reaction temperature, although the composition of the products was almost unchanged at temperatures of 140—180°C. Above *ca.* 180°C, the yield of propionitrile gradually decreased, while the yield of the dimers greatly decreased with an increase in the reaction temperature. These may be explained by the thermal instability of such reaction intermediates as a hydride complex and a cyanoethyl complex.

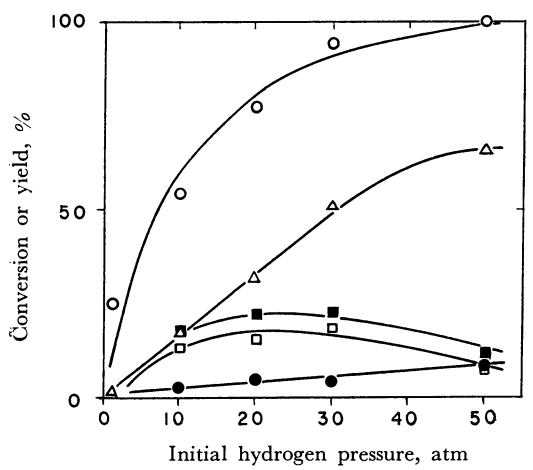

Fig. 4. The effect of initial hydrogen pressure on the formation of products: reaction temp., 150°C; about 0.5 hr was used for heating up, and the mixture was kept at 150°C for 0.5 hr; ○, conversion of acrylonitrile; △, yield of propionitrile; □, yield of *cis*-1, 4-dicyano-1-butene; ●, yield of adiponitrile; ■, yield of *trans*-1, 4-dicyano-1-butene.

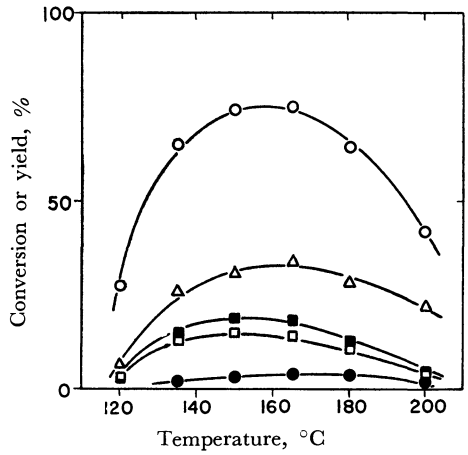

Fig. 5. The effect of reaction temperature on the formation of products: initial hydrogen pressure, 20 atm; reaction time, 40 min; ○, conversion of acrylonitrile; △, yield of propionitrile; □, yield of *cis*-1, 4-dicyano-1-butene; ●, yield of adiponitrile; ■, yield of *trans*-1, 4-dicyano-1-butene.

Various salts or electron-donating compounds were added to the reaction solution in order to change the valency state of ruthenium or to replace the ligands of ruthenium trichloride with other ligands. The results of the addition of those compounds are given in Table 2. Propionitrile was mainly formed when acrylonitrile was treated under a hydrogen atmosphere with a dark-blue ethanol solution of ruthenium(II) chloride prepared by the reduction of ruthenium trichloride with titanium trichloride. This ruthenium(II) chloride has been known to catalyze the homogeneous hydrogenation of olefinic bonds in compounds, such as maleic, fumaric, and acrylic acids, in which the double bond is activated by the presence of an adjacent carboxyl group.[4] Wilkinson has reported[5] that, on heating solutions of ruthenium trichloride trihydrate with tin dichloride in ethanol, dark-blue solutions which appear to contain ruthenium(II) are obtained. The addition of tin dichloride to the reaction solution also gave propionitrile as the main product.

4) J. Halpern, J. F. Harrod and B. R. James, *J. Am. Chem. Soc.*, **83**, 753 (1961); *ibid.*, **88**, 5150 (1966).
5) J. F. Young, R. D. Gillard and G. Wilkinson, *J. Chem. Soc.*, **1964**, 5176.

Table 2. Effects of additives on the formation of products[a]

Additives	Add./Ru[b]	Reaction temp., °C	Conv. %	PN	ADN %, yield	cis	trans[c]
none		150	94	51	4	18	22
none		170	94	54	6	13	17
$TiCl_3$	10	170	72	43	t[d]	t	t
$SnCl_2 \cdot 2H_2O$	5	170	42	26	1	2	2
LiCl	10	170	100	54	9	16	21
KCl	5	170	98	53	6	14	14
LiBr	6	150	93	49	4	15	20
NaI	2	150	91	39	5	15	18
C_5H_5N	1	150	65	32	2	12	16
C_5H_5N	2	150	10	6		t	t
	11	170	92	52	6	16	24

a) Reaction conditions: 10m*l* of acrylonitrile; 20m*l* of ethanol; 0.200 g of $RuCl_3 \cdot 3H_2O$; 30 atm of initial hydrogen pressure. About 0.5 hr was used for heating up, and the mixture was kept at the designated temperature for 0.5 hr. b) Molar ratio of an additive to $RuCl_3 \cdot 3H_2O$. c) Abbreviations: PN, propionitrile; ADN, adiponitrile; cis, *cis*-1,4-dicyano-1-butene; trans, *trans*-1,4-dicyano-1-butene. d) Trace.

On the other hand, the reaction was hardly affected at all when potassium chloride, lithium chloride, lithium bromide, or sodium iodide was added to the reaction solution in order to vary the concentration of chloride ions or in order to replace the chloride ions of ruthenium trichloride with bromide or iodide ions.[6] The reaction was, however, strongly inhibited by the addition of two moles of pyridine per mole of ruthenium trichloride to the reaction solution. This may be explained by the coordination of pyridine to ruthenium, which prevents the coordination of the acrylonitrile molecules or the activation of the hydrogen molecule. The reaction was, however, hardly affected at all by the addition of large amounts of quinoline, which is a weaker coordinating agent than pyridine. In the dimerization of acrylonitrile, three coordination sites around the ruthenium atom may be required for a hydride ion and two molecules of acrylonitrile, as in the case of the dimerization of ethylene using a rhodium trichloride catalyst.[7] The reaction may be strongly affected when other ligands such as pyridine occupy those coordination sites.

Experimental

Reagents. Acrylonitrile was distilled under nitrogen, and 0.1% of hydroquinone was added to the acrylonitrile distilled. Methanol and ethanol were dried with Drierite and distilled under nitrogen. All transition-metal chlorides were commercially obtained.

The Reaction of Acrylonitrile by the Use of Ruthenium Trichloride Trihydrate. *A. The Reaction under a Nitrogen Atmosphere.* A 100-m*l* stainless-steel autoclave was charged with 20 m*l* of ethanol, 10 m*l* of acrylonitrile, and 0.200 g of ruthenium trichloride trihydrate under nitrogen. The mixture was then heated to 170°C and kept at that temperature for 4 hr. The reaction products, when quantitatively analyzed by means of gas chromatography, were found to be propionitrile (2% of the acrylonitrile originally fed in) and *cis*- and *trans*-1,4-dicyano-1-butene (5%).

B. The Reaction under a Hydrogen Atmosphere. A reaction solution was prepared as above. The atmosphere was replaced with 30 atm of hydrogen, and the mixture was heated to 150°C. About 0.5 hr was used for the heating-up, after which the mixture was kept at 150°C for 0.5 hr. Gas chromatographic analysis showed that the products were propionitrile (51%), adiponitrile (4%), *cis*-1,4-dicyano-1-butene (18%), and *trans*-1,4-dicyano-1-butene (22%). The conversion of acrylonitrile was 94%.

In order to examine the effects of the reaction temperature and the reaction time on the formation of the products, the reaction mixture prepared under a nitrogen atmosphere was heated up to a reaction temperature, and hydrogen gas of a definite pressure was charged into the reactor at that temperature. A rapid uptake of hydrogen occurred, and propionitrile, *cis*- and *trans*-1,4-dicyano-1-butene, and adiponitrile were formed.

C. Addition of Salts or Electron-donating Compounds. A reaction solution was prepared as above except that a calculated amount of an additive was added. The atmosphere was replaced with 30 atm of hydrogen, and then the mixture was heated to 150 or 170°C and kept at that temperature for 0.5 hr. The products were analyzed by gas chromatography.

The Reaction of Acrylonitrile by the Use of Other Transition-metal Chlorides. The reaction solution was prepared in a way similar to that used in the case of ruthenium chloride. The atmosphere was

6) F. A. Cotton and G. Wilkinson, "Advanced Inorganic Chemistry," Interscience, New York (1962), p. 818; T. A. Stephenson and G. Wilkinson, *J. Inorg. Nucl. Chem.*, **28**, 945 (1966).

7) R. Cramer, *J. Am. Chem. Soc.*, **87**, 4717 (1965).

replaced with 30 atm of hydrogen, and the mixture was heated to a reaction temperature. The products were analyzed by gas chromatography.

Isolation and Identification of the Products. The reaction products were isolated by the fractional distillation of the reaction solution. Propionitrile and adiponitrile were identified by a comparison of their retention times and infrared spectra with those of authentic samples. The *cis*- and *trans*-1, 4-dicyano-1-butene isolated by the fractional distillation were characterized by their infrared and NMR spectra. They were hydrogenated over palladium black at room temperature to give adiponitrile.

Gas Chromatographic Analysis of the Products. For the analysis of acrylonitrile and propionitrile, a 2.5-m tricresyl phosphate column was used. The conditions were: column temperature, 100°C; flash evaporator temperature, 150°C; helium gas speed, 40 m*l*/min. For the analysis of *cis*- and *trans*-1, 4-dicyano-1-butene and adiponitrile, a 2-m polyoxyethylene sorbitan monooleate column was used, and the conditions were: column temperature, 200°C; inlet temperature, 250°C; helium gas speed, 50 m*l*/min.

BULLETIN OF THE CHEMICAL SOCIETY OF JAPAN VOL. 41 401—407 (1968)

Studies on Separation of Amino Acids and Related Compounds. III. Separation of Diastereomers of Leucyl Dipeptides by Ion-Exchange Chromatography

Kosaku NODA, Hideo OKAI, Tetsuo KATO and Nobuo IZUMIYA

Laboratory of Biochemistry, Faculty of Science, Kyushu University, Hakozaki, Fukuoka

(Received July 21, 1967)

A series of experiments on a column chromatography of Dowex 50 with ammonium acetate solvent systems as eluent was carried out in order to find optimal conditions for the separation of the diastereomers of leucylalanine, leucylvaline, leucylleucine and leucyltyrosine. The effects of pH concentration of the salt and alcohols in the solvent systems for the separation of the diastereomers were studied. Among many conditions tested, the change of pH in the solvent system afforded most remarkable influence for the separation; the order of elution of the diastereomers of the dipeptide was found to be inverted at near pH 5.0. On a preparative scale L-leucyl-DL-valine was successfully separated into the two diastereomers by using a fairly large column. Attempt to separate benzyloxycarbonyl-L-leucyl-DL-valine benzyl ester with a column of Sephadex LH-20 was described, also.

Previous papers from this laboratory have dealt with the analytical and preparative separation of hydroxyproline diastereomers on columns of the ion-exchange resin.[1] In the present paper, we describe the manipulation of the variables in the ion-exchange technique and the preparative separation of leucyl dipeptide diastereomers.

Several investigators have reported the separation of the diastereomers of dipeptide on paper[2] and thin-layer chromatography.[3] On an ion-exchange column chromatography of Dowex 50, Blackburn and Tetley reported the separation of L-leucyl-L-tyrosine and L-leucyl-D-tyrosine with citrate buffer of pH 4.8,[4] and Neuhaus separated alanylalanine diastereomers.[5] Yanari *et al.* separated a mixture of leucyltyrosine diastereomers by the use of DEAE-cellulose column.[6] Although these investigators cited above carried out the chromatographies in analytical manner using several mg or less of dipeptide diastereomers, Wieland and Bende reported recently the separation of several dipeptide diastereomers on a preparative scale; for example, they separated 200 mg of DL-alanyl-L-tyrosine into each pure diastereomer with a Sephadex G-50 column (1.5 × 100 cm) using a solvent of aqueous pyridine.[3]

In this investigation, each diastereomer of leucylalanine, leucylvaline, leucylleucine and leucyltyrosine were prepared in the conventional manner as the first step of the experiment. For

1) H. Aoyagi, H. Okai, M. Ohno and N. Izumiya, *Nippon Kagaku Zasshi (J. Chem. Soc. Japan, Pure Chem. Sect.)*, **85**, 656 (1964); H. Aoyagi, M. Ohno, N. Izumiya and B. Witkop, *J. Org. Chem.*, **29**, 1382 (1964).

2) For example, T. Sokolowska and J. F. Biernat, *J. Chromatogr.*, **13**, 269 (1964).

3) T. Wieland and H. Bende, *Chem. Ber.*, **98**, 504 (1965).

4) S. Blackburn and P. Tetley, *Biochim. Biophys. Acta*, **20**, 423 (1956).

5) F. C. Neuhaus, *J. Biol. Chem.*, **237**, 778 (1962).

6) S. Yanari, M. Volini and M. A. Mitz, *Biochim. Biophys. Acta*, **45**, 595 (1960).

example, L-leucyl-L-alanine was synthesized as follows:

$$\text{Z-Leu-OH} + \text{H-Ala-OBzl} \xrightarrow{\text{mixed anhydride method}}$$

$$\text{Z-Leu-Ala-OBzl} \xrightarrow{H_2/Pd} \text{H-Leu-Ala-OH}$$

(Z, benzyloxycarbonyl; OBzl, benzyl ester)

It was observed that a diastereomeric mixture of any peptide was separated appreciably enough by paper chromatography (Table 1).

As a preliminary experiment of a column chromatography, ion-exchange (strong acid type) paper chromatography was carried out with leucylleucine and leucyltyrosine in order to find the effect of pH and alcohols in an ammonium acetate solvent system (Tables 2 and 3). However, it was observed that anticipation to find the optimal condition for a separation of the diastereomers on a column through the study of ion-exchange paper chromatography appeared to be difficult. Then, the effects of variations of pH, alcohol, and concentration of ammonium acetate in the solvent system were studied by using a small column (0.9 $\times$ 50 cm) with Dowex 50X8.

In the course of the column chromatographic experiment, we observed the interesting phenomena; each L-L diastereomer of leucylalanine, leucylvaline or leucylleucine with a solvent of higher pH than 5.0 was eluted more rapidly than the corresponding L-D isomer, whereas each L-L isomer was eluted slower at pH 4.5 (Figs. 4—6). To elucidate these inversions, the titration experiments of the L-L and L-D isomer of each peptide were carried out by using a pH-stat, and it was found that the titration curves for the diastereomers of each peptide crossed each other around pH 5 (Figs. 10—12). Then, the inversion in the chromatographic pattern may be explained by the interpretation that the main interaction between the resin and the dipeptide is due to ionic forces and the ionic conditions of the diastereomers of the dipeptide are inverted each other at a definite pH near 5.

As an experiment on a preparative scale, a L-leucyl-DL-valine preparation was tried to separate with a large column (1.8 $\times$ 110 cm) of Dowex 50 under the good condition which was found previously by using smaller column. For the synthesis of L-leucyl-DL-valine, the mixed anhydride of benzyloxycar-L-leucinebonyl was coupled with DL-valine benzyl ester and the benzyloxycarbonyl-dipeptide ester obtained as syrup was hydrogenated to crude dipeptide, L-Leu-DL-Val, which was subjected to the separation experiment without further purification.[7] With the large column using 0.2 M ammonium acetate of pH 7.0, we could separate 1 g of the crude peptide into 0.40 g of pure L-leucyl-L-valine and 0.48 g of L-leucyl-D-valine.

Separation of the oily Z-L-Leu-DL-Val-OBzl preparation with a column (0.9 $\times$ 50 cm) of Sephadex LH-20 using dioxane or methanol as solvent was attempted; it was found that the separation was occurred partially (Fig. 13). Reviewing the literature on the separation of acyldipeptide ester, Weygand *et al.* reported the separation of the diastereomeric mixture of trifluoroacetyl-phenylalanylvalyl methyl ester by gas chromatographic technique.[8] As the studies using a Sephadex LH-20 or methylated Sephadex column, Waki and Izumiya applied it successfully for the separation of benzyloxycarbonyl-substituted gramicidin S and cyclosemigramicidin S,[9] and Mutt *et al.* reported the separation of Z-L-Leu-L-Leu-OMe and *p*-nitrophenol during a peptide synthesis by the active ester method.[10]

Experimental

The melting points were uncorrected. Optical rotations were determined with a Yanagimoto Photometric Polarimeter, OR-20 type.

D-Valine Benzyl Ester *p*-Toluenesulfonate (I). A mixture of D-valine, benzyl alcohol, *p*-toluenesulfonic acid monohydrate, and benzene was heated as has been described for the preparation of the corresponding L-isomer.[11] Yield, 78%; mp 157—158°C; $[\alpha]_D^{25}$ +4.8° (*c* 2, ethanol) (Found: C, 60.05; H, 6.74; N, 3.68%).

DL-Valine Benzyl Ester *p*-Toluenesulfonate (II). The crude crystals obtained by the usual way were recrystallized from ethanol-ether; yield, 94%, mp 138—140°C (Found: C, 59.88; H, 6.88; N, 3.75%).

D-Leucine Benzyl Ester *p*-Toluenesulfonate (III). This compound was obtained according to the procedure for the L-isomer.[11] Yield, 75%; mp 155—156°C; $[\alpha]_D^{25}$ −0.5° (*c* 2, ethanol) (Found: C, 60.96; H, 7.05; N, 3.67%).

Benzyloxycarbonyl-L-leucyl-L-alanine Benzyl Ester (IV)[12] To a chilled solution of benzyloxycarbonyl-L-leucine[13] (2.65 g) and triethylamine (1.4 ml) in tetrahydrofuran (20 ml), isobutyl chloroformate (1.32 ml) was added at −5°C. After 15 min, a mixture of L-alanine benzyl ester *p*-toluenesulfonate[11] (3.51 g) and triethylamine (1.4 ml) in chloroform (20 ml) was added. The mixture was left to stand overnight at room temperature, and then evaporated *in vacuo*. The residue was dissolved in ethyl acetate (30 ml), then the solution was successively washed with 4% sodium bicarbonate, 2% hydrochloric acid and water, and dried

7) It was found that the ratio of the L-L and L-D isomer in the crude dipeptide was 82 : 100 by an amino acid analyzer.

8) F. Weygand, A. Prox and W. König, *Chem. Ber.*, **99**, 1451 (1966).

9) M. Waki and N. Izumiya, *J. Am. Chem. Soc.*, **89**, 1278 (1967); This Bulletin, **40**, 1687 (1967).

10) V. Mutt, E. Nyström and J. Sjövall, *J. Chromatogr.*, **24**, 205 (1966).

11) N. Izumiya and S. Makisumi, *Nippon Kagaku Zassi (J. Chem. Soc. Japan, Pure Chem. Sect.)*, **78**, 662, 1768 (1957).

12) We are indebted to Mr. M. Waki in this laboratory who performed the syntheses of the L-L and L-D isomer of leucylalanine.

13) M. Bergmann, L. Zervas and W. F. Ross, *J. Biol. Chem.*, **111**, 245 (1935).

over sodium sulfate. The filtrate was evaporated *in vacuo*, and the oily residue was solidified by the addition of petroleum ether. The product was recrystallized from ethyl acetate - ether - petroleum ether; yield, 2.78 g (65%), mp 111°C; $[\alpha]_D^{25}$ −45.5° (*c* 2, ethanol).

Found: C, 67.55; H, 7.25; N, 6.69%. Calcd for $C_{24}H_{30}O_5N_2$: C, 67.58; H, 7.09; N, 6.57%.

Benzyloxycarbonyl-L-leucyl-D-alanine Benzyl Ester (V). The mixed anhydride of benzyloxycarbonyl-L-leucine was coupled with a mixture of D-alanine benzyl ester *p*-toluenesulfonate[14] and triethylamine in chloroform as described above; yield, 67%; mp 120—121°C; $[\alpha]_D^{25}$ +1.2 °(*c* 2, ethanol).

Found: C, 67.80; H, 7.14; N, 6.54%.

Benzyloxycarbonyl-L-leucyl-DL-valine Benzyl Ester (VI). Benzyloxycarbonyl-L-leucine (2.65 g, 10 mmol) was coupled with II (10 mmol) by the mixed anhydride, and the compound (VI) was obtained as syrup; yield, 4.01 g (88%).

Benzyloxycarbonyl-L-leucyl-D-leucine Benzyl Ester (VII). This compound was obtained from benzyloxycarbonyl-leucine and III; yield, 68%; mp 110—112°C; $[\alpha]_D^{25}$ +2.3° (*c* 2, ethanol).

Found: C, 68.96; H, 7.68; N, 5.99. Calcd for $C_{27}H_{36}O_5N_2$: C, 69.20; H, 7.74; N, 5.98%.

L-Leucyl-L-alanine. A solution of IV (2.13 g) in a mixture of acetic acid (30 m*l*), methanol (15 m*l*), and water (5 m*l*) was treated with hydrogen in the presence of palladium black. The filtrate from the catalyst was evaporated *in vacuo* to dryness. The residual crystals were recrystallized from methanol-acetone-ether; yield of L-Leu-L-Ala monohydrate, 0.96 g (87%); $[\alpha]_D^{25}$ +27.6° (*c* 1, H_2O), +21.8°C (*c* 1, methanol) (Found: C, 49.52; H, 9.15; N, 12.96%). Polglase and Smith reported the synthesis of L-Leu-L-Ala by the hydrogenolysis of Z-Leu-Ala-OH which was obtained by saponification of Z-Leu-Ala-OMe; $[\alpha]_D^{24}$ +22.9° (methanol).[15]

L-Leucyl-D-alanine. V (2.13 g) was hydrogenolyzed as described above; yield of L-Leu-D-Ala monohydrate, 0.93 g (85%); $[\alpha]_D^{25}$ +77.8° (*c* 1, H_2O) (Found: C, 45.67; H, 9.21; N, 12.02%). Reported value, $[\alpha]_D^{24}$ +76° (H_2O).[15]

L-Leucyl-L-valine. Benzyloxycarbonyl-leucine (1.32 g, 5 mmol) was coupled with L-valine benzyl ester as described for the preparation of IV. The oily Z-Leu-Val-OBzl thus obtained was hydrogenolyzed, and the residue was recrystallized from methanol-ether. Yield of L-Leu-L-Val monohydrate, 1.05 g (85%); $[\alpha]_D^{20}$ +18.0° (*c* 1, N HCl) (Found: C, 53.25; H, 9.46; N, 11.17%). Reported value, $[\alpha]_D^{23}$ +18.2° (N HCl).[16]

L-Leucyl-D-valine. Benzyloxycarbonyl-leucine (1.23 g) was coupled with I, and the oily Z-Leu-Val-OBzl obtained was hydrogenolyzed; yield of L-Leu-D-Val monohydrate, 90%; $[\alpha]_D^{20}$ +55.0° (*c* 1, H_2O) (Found: C, 53.41; H, 9.71; N, 11.32%). Reported value, $[\alpha]_D^{24}$ +55.3° (H_2O).[16]

L-Leucyl-DL-valine (VIII). The oily VII (2.27 g, 15 mmol) was hydrogenated in the usual manner, and the filtrate from the catalyst was evaporated to dryness; the yield of the residual powder was 1.18 g (95%, calcd as monohydrate). This powder was used for the experiment of separation without recrystallization. The weight ratio between the L-L and L-D diastereomer in the powder was determined as 82 : 100 by the use of an amino acid analyzer.

L-Leucyl-L-leucine. Benzyloxycarbonyl-leucine (1.32 g) was coupled with leucine benzyl ester, and the oily Z-Leu-Leu-OBzl obtained was hydrogenolyzed. Recrystallization from hot water yielded 0.79 g (63%) of L-Leu-L-Leu hemihydrate; $[\alpha]_D^{20}$ −13.4° (*c* 1, N NaOH) (Found: C, 56.67; H, 9.84; N, 10.89%). Reported value, $[\alpha]_D^{23}$ −13.4° (N NaOH).[16]

L-Leucyl-D-leucine. This compound was obtained from VII by the hydrogenolysis; yield of L-Leu-D-Leu dihydrate, 72%; $[\alpha]_D^{20}$ +68.0° (*c* 1, N HCl) (Found: C, 51.47; H, 9.63; N, 9.80). Reported value, $[\alpha]_D^{24}$ +68.5° (N HCl).[16]

L-Leucyl-L-tyrosine and L-Leucyl-D-tyrosine. These dipeptides were prepared as has been described in the literatures.[17]

Separation Studies on Paper Chromatographies. *a) Paper Chromatography.* A paper chromatography was carried out with ascending technique using Toyo Roshi No. 52 paper, and a peptide on the paper was revealed with ninhydrin. As shown in Table 1, it was observed that the diastereomers of each peptide were clearly separated on a chromatogram.

Table 1. R_f values of dipeptides on paper chromatography

Dipeptide	R_f	
	L-L	L-D
Leu-Ala[a]	0.73	0.52
Leu-Ala[b]	0.66	0.64
Leu-Val[b]	0.83	0.75
Leu-Leu[b]	0.90	0.81
Leu-Tyr[b]	0.78	0.66

a) Solvent system: pyridine-water (4 : 1, v/v)
b) Solvent system: *n*-butanol - acetic acid - pyridine - water (4 : 1 : 1 : 2, v/v).

b) Ion-exchange Paper Chromatography. As the preliminary experiment for a column chromatography, a paper of Amberlite SA-II, NH_4^+ form, was applied for a dipeptide or a mixture of the two diastereomers using 0.2 M ammonium acetate solvent at a chosen pH. As shown in Tables 2 and 3, a mixture of the diastereomers was successfully separated at the different pH. Since a diastereomeric mixture of 4-hydroxyproline or 3-hydroxy-2-aminobutyric acid had been separated more effectively by the addition of alcohol such as methanol in the ammonium acetate solvent system,[1] the effect of alcohol to the solvent was studied; the addition of various alcohol afforded little effect on the separation pattern (Table 3).

14) M. Winitz, L. Bloch-Frankenthal, N. Izumiya, S. M. Birnbaum, C. G. Baker and J. P. Greenstein, *J. Am. Chem. Soc.*, **78**, 2423 (1956).
15) W. J. Polglase and E. L. Smith, *ibid.*, **71**, 3081 (1949).
16) E. L. Smith, D. H. Spackman and W. J. Polglase, *J. Biol. Chem.*, **199**, 801 (1952).
17) N. Izumiya, H. Uchio and T. Yamashita, *Nippon Kagaku Zassi (J. Chem. Soc. Japan, Pure Chem. Sect.)*, **79**, 420 (1958); B. F. Erlanger, W. V. Curran and N. Kokowsky, *J. Am. Chem. Soc.*, **80**, 1128 (1958).

TABLE 2. R_f VALUES OF DIPEPTIDES ON ION-EXCHANGE PAPER CHROMATOGRAPHY (EFFECT OF pH)

pH	R_f			
	Leu-Leu		Leu-Tyr	
	L-L	L-D	L-L	L-D
6.0	0.44	0.52	0.28	0.39
4.0	0.14	0.20	0.08	0.14

TABLE 3. R_f VALUES OF DIPEPTIDES ON ION-EXCHANGE PAPER CHROMATOGRAPHY (EFFECT OF ALCOHOL)

Alcohol (20%)	R_f			
	Leu-Val[a]		Leu-Leu[b]	
	L-L	L-D	L-L	L-D
—	0.73	0.68	0.34	0.28
Methanol	0.74	0.70	0.31	0.27
Ethanol	0.76	0.71	0.30	0.26
n-Propanol	0.73	0.67	0.32	0.28
Isopropanol	0.70	0.64	0.30	0.25
t-Butanol	0.75	0.70	0.31	0.26

a) pH of buffer: 7.0
b) pH of buffer: 4.5

Separation Studies on Column Chromatography. *a) Column and Solvent System.* A column (0.9×50 cm) was filled with Dowex 50WX8 (200—400 mesh), NH_4^+ form, and equilibrated by washing with an appropriate solvent system. A solvent of 0.2 M ammonium acetate, which was used in most cases, was prepared in the following manner. Ammonium acetate (15.4 g, 0.2 mol) was dissolved in water (500 m*l*), and acetic acid was added until the solution reached the desired pH. The solution was made up to 1 *l* with water, and adjusted again to the desired pH by the addition of acetic acid or ammonia.

b) Chromatography of Model Mixture. A mixture of each 0.05 mmol of a L-L form and L-D form of each dipeptide was dissolved in water (1 m*l*), and the solution was applied to the column and eluted with the appropriate solvent system at room temperature and a flow rate of about 10 m*l*/hr. Two-milliliter fractions were collected, and 0.01 m*l* of the eluate in each test tube was spotted on a strip of filter paper. The strip was dried up, immersed in a 0.2% ninhydrin-acetone solution, and heated at 100°C to find the presence of the peptide (Fig. 1A). Then, 0.01 m*l* of the eluate in the tubes which contain the peptide was applied on the paper chromatography (Fig. 1B). The amounts of color developed were determined by Atago AG-4 densitometer with slit 1×8 mm and 610 mμ (Fig. 1C) and

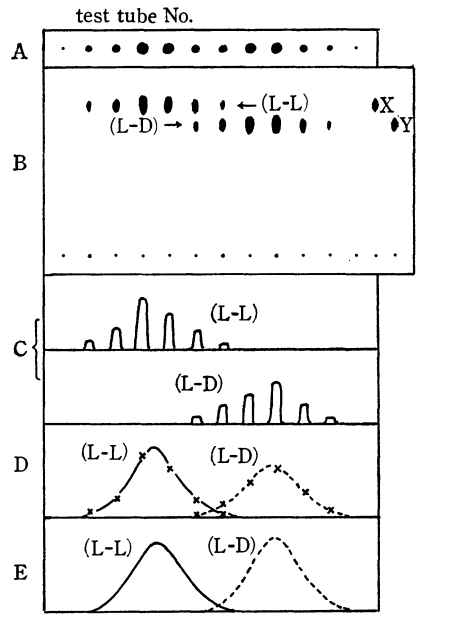

Fig. 1. Separation and assay of a mixture of dipeptide diastereomers on Dowex 50WX8.
Markers: X, spot by a L-L diastereomer of dipeptide; Y, spot by a L-D diastereomer

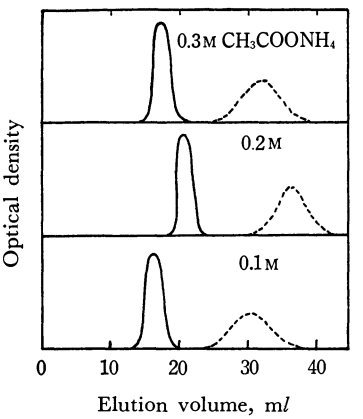

Fig. 2. Effect of concentration of ammonium acetate in buffer system (pH 7.0) on separation of Leu-Val.
Solid line, L-Leu-L-Val; dotted line, L-Leu-D-Val

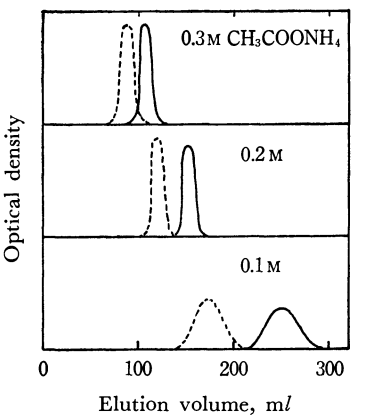

Fig. 3. Effect of concentration of ammonium acetate in buffer system (pH 4.5) on separation of Leu-Leu.
Solid line, L-Leu-L-Leu; dotted line, L-Leu-D-Leu

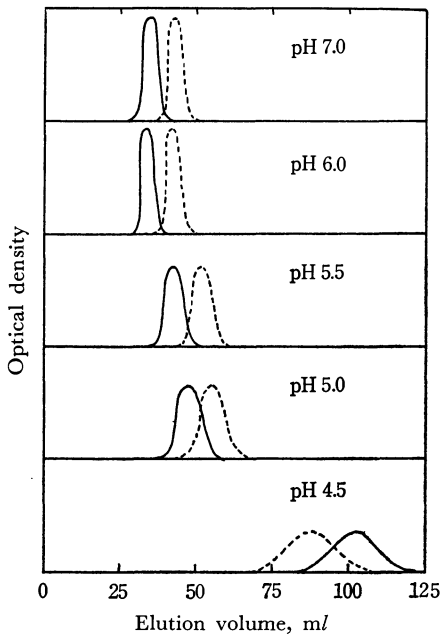

Fig. 4. Effect of pH in buffer system on separation of Leu-Ala.
Solid line, L-Leu-L-Ala; dotted line, L-Leu-D-Ala

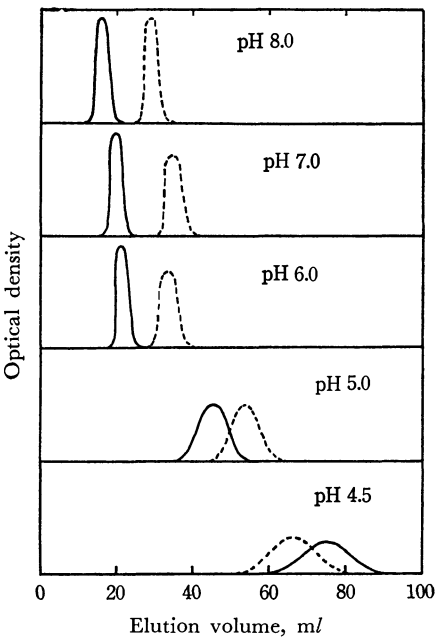

Fig. 5. Effect of pH in buffer system on separation of Leu-Val.
Solid line, L-Leu-L-Val; dotted line, L-Leu-D-Val

the integrated areas were plotted on a graph (Fig. 1D). It was observed that the color intensity of a L-D isomer was about 70% compared with that of the corresponding L-L isomer. In many figures (*e. g.*, Figs. 2—8) the area of the L-D isomer was corrected as of the value of the L-L isomer (Fig. 1E).

c) Effect of Concentration of Salt in Solvent System. Effect of variation in concentration (0.1—0.3 M) of ammonium acetate in a solvent was examined, and the patterns obtained were shown in Fig. 2 for Leu-Val and Fig. 3 for Leu-Leu. Since the 0.2 M ammonium acetate solvent gave best results for the separation, this solvent system was used in most cases in a series of experiments.

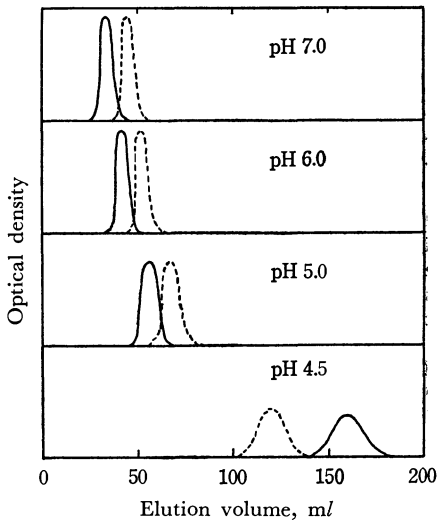

Fig. 6. Effect of pH in buffer system on separation of Leu-Leu.
Solid line, L-Leu-L-Leu; dotted line, L-Leu-D-Leu

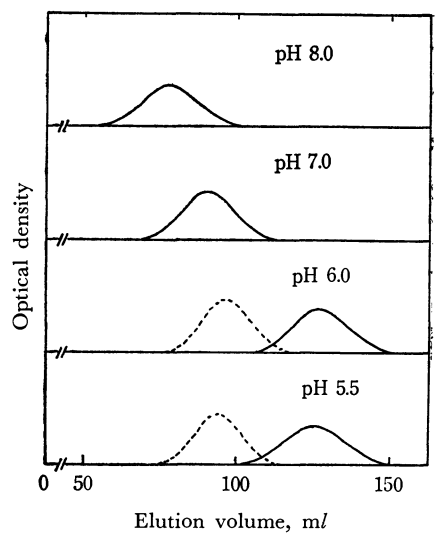

Fig. 7. Effect of pH in buffer system on separation of Leu-Tyr.
Solid line, L-Leu-L-Tyr; dotted line, L-Leu-D-Tyr
In the case of pH 7.0 or 8.0 buffer, the curve by the L-L isomer coincided with that by the L-D isomer.

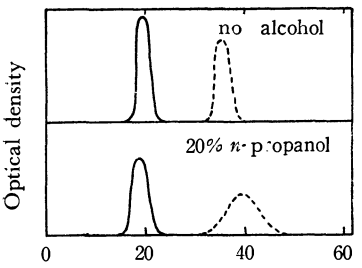

Fig. 8. Effect of alcohol in buffer system (pH 7.0) on separation of Leu-Val.
Solid line, L-Leu-L-Val; dotted line, L-Leu-D-Val

d) Effects of pH and Alcohol in Solvent System. Change of pH in the solvent was examined. As noted in Figs. 4—6, each L-L diastereomer of Leu-Ala, Leu-Val or Leu-Leu dipeptide with a solvent at higher pH than 5.0 was eluted more rapidly than the corresponding L-D isomer, on the contrary each L-L isomer was eluted slower at pH 4.5. In the case of Leu-Tyr, the observation of such an inversion of the order of elution was of difficult since the elution of this dipeptide was retarded and broadend remarkably at lower pH than 5. An optimum pH for best separation appeared to differ toward a diasteremeric mixture of each peptide; that pH are about 7.0 for Leu-Ala and Leu-Val, and 4.5 for Leu-Leu. Although it had been observed in the experiment with the ion-exchange paper that the addition of an alcohol in a solvent system hardly affected on separation, the effect of *n*-propanol in a column chromatography was examined (Fig. 8). The result showed again that the addition of the alcohol did not improve the separation.

e) Separation with Amino Acid Analyzer. A mixture of each 0.2 μmol of the L-L form and L-D form of Leu-Val was analyzed with Hitachi amino acid analyzer, model KLA-3, under these conditions: length of the column with spherical resin, 0.9×50 cm; solvent, citrate buffer at pH 4.25; flow rate, 60 ml/hr; jacket temperature, 55°C. The chromatogram obtained was shown in Fig. 9. The ratio of color intensities between L-Leu-L-Val and L-Leu-D-Val, which was calculated from the integrated areas on the chromatogram, was found to be 100 : 63.[18]

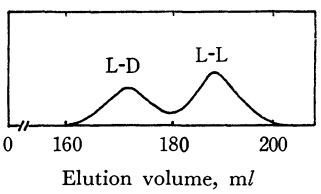

Fig. 9. Chromatogram of a diastereomeric mixture of Leu-Val by an amino acid analyzer.

18) In this connection, it would be noteworthy that the ratio of color intensities between L-Alloile-L-Tyr and D-Alloile-L-Tyr was 100 : 45; see, T. Yamashita, H. Uchio and N. Izumiya, *Nippon Kagaku Zasshi (J. Chem. Soc. Japan, Pure Chem. Sect.)*, **80**, 767 (1959).

pH Titration Curve. Each diastereomer (0.05 mmol) of Leu-Ala, Leu-Val and Leu-Leu was dissolved in 1/30 N sodium hydroxide (3 ml), and automatic titration was carried out with 0.5 N hydrochloric acid with Radiometer pH-Stat, model TTT-1, at room temperature (Figs. 10—12). As noted from the figures, it was

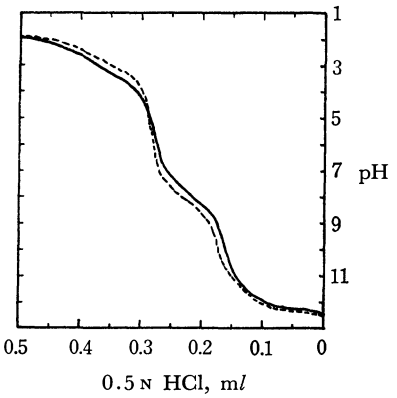

Fig. 10. pH titration curves of Leu-Ala.
Solid line, L-Leu-L-Ala; dotted line, L-Leu-D-Ala

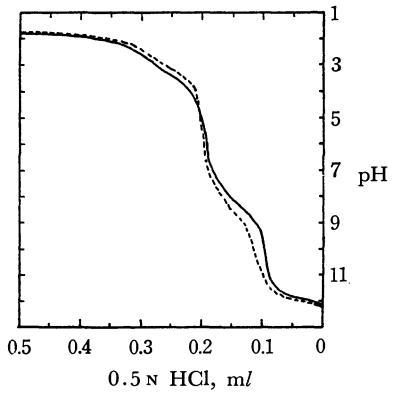

Fig. 11. pH titration curves of Leu-Val.
Solid line, L-Leu-L-Val; dotted line, L-Leu-D-Val

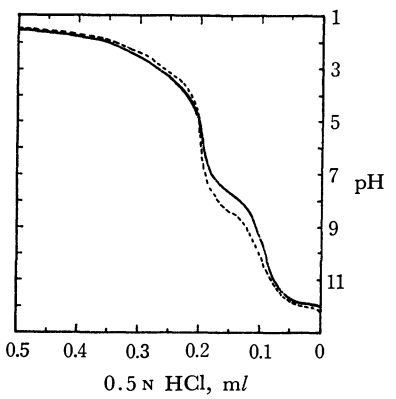

Fig. 12. pH titration curves of Leu-Leu.
Solid line, L-Leu-L-Leu; dotted line, L-Leu-D-Leu

observed that the titration curves of the diastereomers crossed each other around pH 5 in which the inversions of the elution patterns of the diastereomers were observed as shown in Figs. 6—8.

Preparative Separation of L-Leu-DL-Val (VIII). A solution of VIII (1 g, 5 mmol) in a 0.2 M ammonium acetate solvent (40 m*l*) of pH 7.0 was put on a column (1.8×110 cm) of the Dowex 50, and eluted with the same solvent at a flow rate of 20 m*l*/hr. Each fraction (5 m*l*) was tested on a paper strip with ninhydrin, and the strip demonstrated that a mixture of the diastereomers was separated into two portions with the column. The faster eluting fractions from tube number 22 to 33 were evaporated *in vacuo* to dryness. Most of the ammonium acetate was removed by sublimation *in vacuo* for about 1 hr at 100°C. To remove completely the ammonium acetate still contaminated, a solution of the residue in water was put on a column of Dowex 50 (0.9×10 cm), H^+ form, and the column was eluted with 2 N ammonium hydroxide. The eluate was evaporated, and the residual crystals were recrystallized from methanol-ether; yield of L-Leu-L-Val monohydrate, 0.396 g (40%); $[\alpha]_D^{20}$ +17.5° (*c* 1, N HCl).

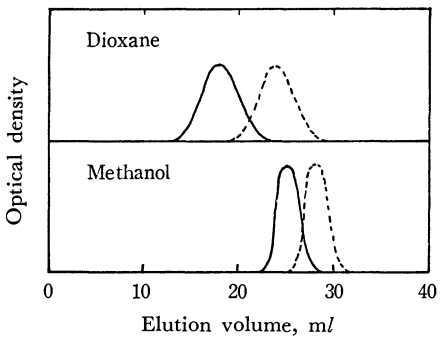

Fig. 13. Chromatogram of Z-L-Leu-DL-Val-OBzl on Sephadex LH-20 column.
Solid line, Z-L-Leu-L-Val-OBzl; dotted line, Z-L-Leu-D-Val-OBzl

Found: C, 53.13; H, 9.49; N, 11.15%. Calcd for $C_{11}H_{22}O_3N_2 \cdot H_2O$: C, 53.20; H, 9.74; N, 11.28%. The slower eluting fractions from tube number 34 to 47 were treated in the same manner as described above. Yield of L-Leu-D-Val monohydrate, 0.476 g (48%); $[\alpha]_D^{20}$ +55.0° (*c* 1, H_2O).

Found: C, 53.56; H, 9.53; N, 11.24%.

The weight ratio between the L-L and L-D isomer was calculated as 84 : 100 which agreed with the ratio of 82 : 100 observed for the crude L-Leu-DL-Val (VIII) by the amino acid analyzer.

Separation Studies of Z-L-Leu-DL-Val-OBzl (VII). Sample of the syrup (VII) (23 mg, 0.05 mmol) was applied to a column (0.9×50 cm) of Sephadex LH-20, and the column was eluted with dioxane or methanol at room temperature and a flow rate of about 5 m*l*/hr. One-m*l* fractions were collected, and small amount of each test tube was spotted on a thin-layer plate. The compound on the plate was detected by spraying 47% hydrobromic acid and then ninhydrin. Then, 0.05 m*l* of the elute in the test tubes which contain benzyloxycarbonyl-dipeptide ester was hydrogenated, and the filtrate from the catalyst was applied on paper chromatography, and Fig. 13 was prepared in the same manner as described for the preparation of Fig. 1B-1E.

The authors wish to thank Mr. Yoichi Kashihara for his valuable technical assistance.

BULLETIN OF THE CHEMICAL SOCIETY OF JAPAN VOL. 41 408—418 (1968)

Asymmetric Hydrogenating Activity of Modified Raney Nickel Catalyst

Susumu TATSUMI*1

Division of Organic Chemistry, Institute for Protein Research, Osaka University, Kita-ku, Osaka

(Received July 22, 1967)

In the asymmetric hydrogenation of methyl acetoacetate to methyl 3-hydroxybutyrate using Raney nickel catalysts modified with optically active hydroxy dicarboxylic acids and related compounds (for example, Y. Izumi, S. Tatsumi and M. Imaida, *Bull. Chem. Soc. Japan*, **39**, 2223 (1966)), the relationship between the asymmetric activities of the catalysts and the chemical or stereochemical structures of modifying reagents was discussed on the basis of data obtained previously. The effects of the conditions used for modification upon the asymmetric activity were also discussed inclusively. Moreover, the stability of asymmetric activity in the modified catalysts has been found to be very excellent.

Only a few attempts to obtain asymmetric hydrogenation using asymmetric catalysts have been recorded during the past ten years. In 1956, Akabori *et al.*[1-3] first reported on the asymmetric hydrogenation observed in experiments using silk-palladium catalysts. Subsequently, Isoda *et al.*[4] also reported the occurrence of asymmetric hydrogenation using an amino acid-palladium catalyst following a similar principle. The efficiencies of these catalysts, however, were rather low and the results were inconsistent because of the complexity of the conditions used.

Recently, Izumi and coworkers[5-6] obtained an excellent asymmetric hydrogenation catalyst. They reported that a Raney nickel catalyst treated with aqueous solutions of optically active amino acids has an asymmetric activity in the hydrogenation of carbonyl compounds to the corresponding alcohols. The author[7] also reported that in the hydrogenation of methyl acetoacetate to methyl 3-hydroxybutyrate similar asymmetric activities are observed on the modifications*2 of a Raney nickel catalyst with optically active hydroxy acids, and that the hydroxy acids derived from the corresponding amino acids retaining their absolute configurations have reverse asymmetric effects in the direction of their optical rotation upon a Raney nickel catalyst to the parent amino acids. Subsequently, several reports on the asymmetric hydrogenation of methyl acetoacetate by catalysts modified with various optically active amino acids, hydroxy acids and their derivatives have appeared from our laboratory.[8-12]

$$CH_3COCH_2COOCH_3 \xrightarrow[\text{Modified Raney nickel catalyst}]{+2H} CH_3\underset{\displaystyle OH}{\underset{|}{C}}HCH_2COOCH_3$$

Thus, high asymmetric activities were obtained by modifications with optically active hydroxy dicarboxylic acids, such as D- or L-tartaric acid, L-malic acid and their *C*-alkyl or *C, C'*-dialkyl derivatives. An especially high asymmetric effect was observed on modification with optically active 2-methyltartaric acid,[10,13] the configuration of which has recently been assigned the threo form by the author.[14] However, there are no reports on the relationship between the chemical or stereochemical structures of modifying reagents and the

*1 Present address: Central Research Laboratories, Ajinomoto Co., Inc., Suzuki-cho, Kawasaki.

*2 Modification refers to the altering of the behavior of the catalyst by treatment with certain reagents. The reagent used for the modification is called the modifying reagent in this paper.

1) S. Akabori, Y. Izumi, S. Sakurai and Y. Fujii, *Nature*, **178**, 323 (1956).
2) S. Akabori, Y. Izumi, Y. Fujii and S. Sakurai, *Nippon Kagaku Zassi (J. Chem. Soc. Japan, Pure Chem. Sect.)*, **77**, 1374 (1956).
3) S. Akabori, Y. Izumi and Y. Fujii, *ibid.*, **78**, 886 (1957).
4) T. Isoda, A. Ichikawa and T. Shimamoto, *Riken Hokoku (J. Sci. Res. Inst.)*, **34**, 134 (1958).
5) Y. Izumi, M. Imaida, H. Fukawa and S. Akabori, This Bulletin, **36**, 21 (1963).
6) Y. Izumi, M. Imaida, H. Fukawa and S. Akabori, *ibid.*, **36**, 155 (1963).
7) S. Tatsumi, M. Imaida, Y. Fukuda, Y. Izumi and S. Akabori, *ibid.*, **37**, 846 (1964).
8) Y. Izumi, S. Akabori, H. Fukawa, S. Tatsumi, M. Imaida, Y. Fukuda and S. Komatsu, "Proceedings of the 3rd International Congress on Catalysis," North-Holland Publishing Co., Amsterdam (1964), p. 1364.
9) Y. Izumi, S. Tatsumi, M. Imaida, Y. Fukuda and S. Akabori, This Bulletin, **38**, 1206 (1965).
10) Y. Izumi, S. Tatsumi, M. Imaida, Y. Fukuda and S. Akabori, *ibid.*, **39**, 361 (1966).
11) Y. Izumi, S. Tatsumi and M. Imaida, *ibid.*, **39**, 1087 (1966).
12) Y. Izumi, S. Tatsumi and M. Imaida, *ibid.*, **39**, 2223 (1966).
13) S. Tatsumi, Y. Izumi, M. Imaida, Y. Fukuda and S. Akabori, *ibid.*, **39**, 602 (1966).
14) S. Tatsumi, *ibid.*, **39**, 2202 (1966).

asymmetric activities of the catalysts. It is very important to find this relationship in order to obtain an effective asymmetric catalyst and elucidate the mechanism of this asymmetric hydrogenation.

In this paper, the relationship between the asymmetric activities of the catalysts in the hydrogenation of methyl acetoacetate to optically active methyl 3-hydroxybutyrate and the chemical or stereochemical structures of modifying reagents, such as optically active hydroxy dicarboxylic acids and related compounds, is discussed on the basis of the data obtained previously. The relation between the asymmetric activities and the conditions used for the modification of Raney nickel catalyst is also discussed. Moreover, the stability of asymmetric activity in the catalyst is studied.

The Occurrence of Asymmetric Activity*3

When a Raney nickel catalyst was modified with aqueous solutions of D- or L-tartaric acid[12] adjusted to pH 3—11, it had a high asymmetric hydrogenating activity, as shown in Fig. 1. On the contrary, under the same conditions the catalyst modified with optically inactive meso or racemic tartaric acid[12] did not.

Similar differences were observed on modifications with DL- and L-malic acid[12] and with DL- and L-citramalic acid (α-*C*-methylmalic acid),[12] as shown in Fig. 2.

These results clearly show that the presence or absence of asymmetric activity in the modified catalyst depends on the optical purity of the reagent used for the modification. Moreover, on modification with a reagent of the L-configuration, the catalyst produces the L-hydrogenation product, methyl L-3-hydroxybutyrate; while with a reagent of the D-configuration, the D-hydrogenation product is formed. The asymmetric activities of the catalysts in both cases were the same except for their direction of optical rotation. From these results, it is clear that on modification with a racemic form, two kinds of catalyst are produced in

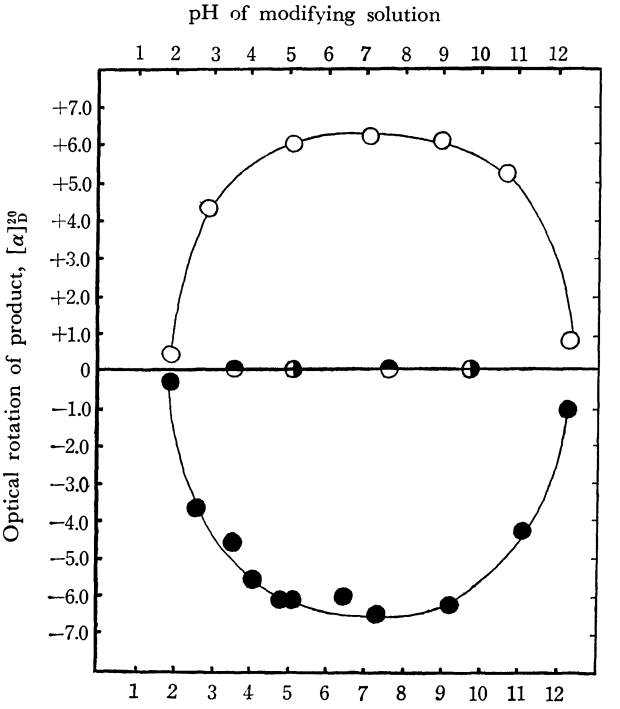

Fig. 1. Modifications with optically active and inactive tartaric acids. (Modified at 0°C)
● D-Tartaric acid ◑ DL-Tartaric acid
○ L-Tartaric acid ◓ *meso* Tartaric acid

*3 The asymmetric activity is provided by the observed specific rotation value of the hydrogenation product, methyl 3-hydroxybutyrate. According to Levene and Haller (Ref. 15), optically pure methyl 3-hydroxybutyrate has the value, $[\alpha]_D^{20}$ ±20.9° (without a solvent) and the levorotatory and dextrorotatory compounds correspond to the D- and L-series, respectively, in absolute configuration. The symbols, D and L, for the configurations used in this paper are based on the D_S- and L_S-series.

15) P. A. Levene and H. L. Haller, *J. Biol. Chem.*, **65**, 49 (1925).

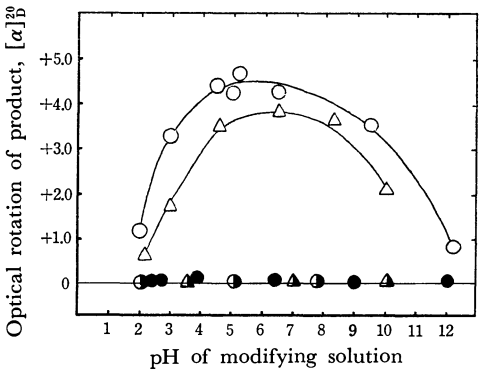

Fig. 2. Modifications with DL- or L-malic acid, DL- or L-citramalic acid and L-methylsuccinic acid. (Modified at 0°C)
○ L-Malic acid ▲ DL-Citramalic acid
△ L-Citramalic acid ● L-Methylsuccinic acid
◑ DL-Malic acid

the same ratio; one has the asymmetric activity to hydrogenate the substrate predominantly to the L-product and the other has the opposite asymmetric activity. As a result of the two activities the product is thus optically inactive and no asymmetric effect of the catalyst on the hydrogenation is observed.

On the other hand, when the modifying reagents loose their ability to be adsorbed on Raney nickel due to acylation of their hydroxyl groups and esterification of their carboxyl groups, the resulting catalysts have only very low asymmetric activities. In spite of the high asymmetric effect with D-tartaric acid, diethyl D-tartrate and *O*, *O'*-diacetyl D-tartaric acid had only very low or no asymmetric effects upon a Raney nickel catalyst.[6-7] These results show that the free hydroxyl and carboxyl groups of the modifying reagent play important roles in the asymmetric modification.

A similar result was observed on modification with an optically active dicarboxylic acid which has no hydroxyl groups in the molecule, such as L-methylsuccinic acid.[12] Although, like L-malic acid, L-methylsuccinic acid has one asymmetric center on the α-carbon atom, it has little or no asymmetric effect upon a Raney nickel catalyst. This is in marked contrast to the high asymmetric effect obtained on modification with L-malic acid, as shown in Fig. 2.

The difference in the asymmetric effects of these two optically active acids is clearly due to the fact that L-methylsuccinic acid does not contain a hydroxyl group which can be adsorbed or chelated to the nickel metal.

Thus it is concluded that to obtain an effective asymmetric catalyst the modifying reagent must possess at least two functional groups such as a hydroxyl group and a carboxyl group, and the reagent must have a strong ability to be adsorbed or chelated to a Raney nickel catalyst.

The Direction of Optical Rotation of the Asymmetric Activity

Catalysts modified with D-tartaric acid gave methyl D-3-hydroxybutyrate as a hydrogenation product, while those modified with L-tartaric acid gave methyl L-3-hydroxybutyrate, as shown in Fig. 1. Moreover, on modifications with compounds of the D-configuration, such as monomethyl D-tartrate,[12] *O*-monobenzoyl D-tartaric acid,[7] and D-*threo*-2, 3-dihydroxybutyric acid,[12] D-hydrogenation products were obtained. On the contrary, with compounds of the L-configuration, such as L-malic acid,[12] and several L-hydroxy monocarboxylic acids,[7,12] L-products were obtained. The same tendency was also observed on modification with an optically active α-*C*-alkyl-substituted hydroxy carboxylic acid such as L-citramalic acid.[12]

This relationship between the direction of optical rotation of asymmetric activity of the catalyst and the absolute configuration of the modifying reagent was also clearly recognized on modifications with solutions containing various proportions of D- and L-tartaric acid. As shown in Fig. 3, there was a linear relationship between the optical activity of the hydrogenation product and the ratio of modifying reagents in the mixture. An optically inactive product was obtained by catalyst modified with a solution containing equal proportions of D-tartaric acid and L-tartaric acid. These results offer additional evidence in support of the consideration on the occurrence of asymmetric activity mentioned in the preceding chapter.

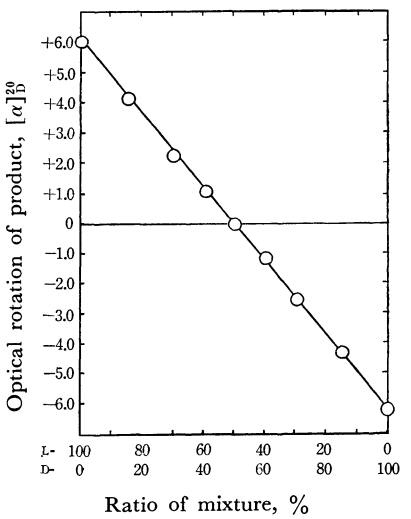

Fig. 3. Effect of ratio of mixture of D- and L-tartaric acid.
(Modified at 0°C and at pH 5.0)

Thus, on modifications with hydroxy carboxylic acids containing one asymmetric center or containing two asymmetric centers of identical absolute

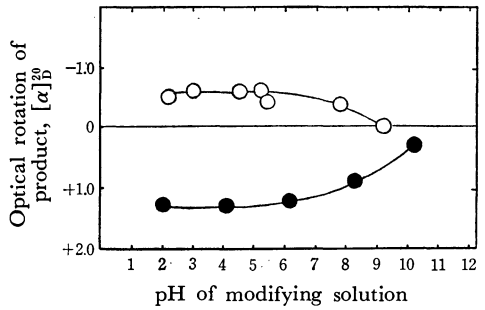

Fig. 4. Modifications with L-*erythro*- and D-*threo*-2, 3-dihydroxybutyric acid.
(Modified at 0°C)
○ D-*threo*-2, 3-Dihydroxybutyric acid
● L-*erythro*-2, 3-Dihydroxybutyric acid

configuration, it is concluded that catalysts modified with D-hydroxy carboxylic acids produce methyl D-3-hydroxybutyrate in the hydrogenation of methyl acetoacetate, while those modified with L-hydroxy carboxylic acids give methyl L-3-hydroxybutyrate.

Modifications with L-*erythro*- and D-*threo*-2, 3-dihydroxybutyric acid were also studied.[12] Since both the α- and β-asymmetric centers of L-*erythro*-2, 3-dihydroxybutyric acid are assigned the L-configuration,[16] the catalyst modified with this compound evidently gave the product of the L-configuration, as shown in Fig. 4.

With D-*threo*-2, 3-dihydroxybutyric acid, however, although the α- and β-asymmetric centers are opposite in configuration and belong to the D- and L-series respectively,[16] the product was predominantly of the D-configuration. This shows that, when a hydroxy monocarboxylic acid used for modification has two asymmetric centers of opposite configuration in its α- and β-carbon atoms, the direction of optical rotation of the asymmetric activity of the catalyst is decided by the configuration of the α-asymmetric center carrying the functional groups which have the highest affinity for the Raney nickel catalyst.

This conclusion will hold good for catalysts modified with optically active polyhydroxy monocarboxylic acids which have asymmetric centers of different configuration.

The Effect of the Modifying Conditions on the Asymmetric Activity

The Effect of the pH of the Modifying Solution. The asymmetric activities of catalysts modified with hydroxy dicarboxylic acids were influenced more by the pH of the modifying solution than those of catalysts obtained on modifications with hydroxy monocarboxylic acids.[7,10-12] Maximal asymmetric activities were observed at pH 5—9 on modifications with hydroxy dicarboxylic acids and there was considerable diminution in activity at both higher and lower pH values, as shown in Figs. 1 and 2. This optimum pH range approximately corresponded to the pH-jumping region of the neutralization curves of these acids.[10] However on modifications with hydroxy monocarboxylic acids,[7] a similar decrease in activity was observed only when the pH value was increased, as shown in Fig. 5.

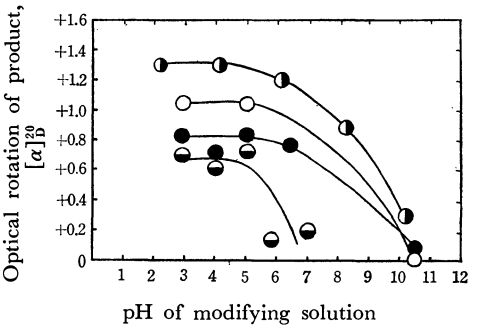

Fig. 5. Modifications with L-hydroxy monocarboxylic acids.
(Modified at 0°C)
◑ L-*erythro*-2, 3-Dihydroxybutyric acid
○ L-2-Hydroxyisovaleric acid
● L-2-Hydroxyisocaproic acid
◒ L-2-Hydroxy-3-phenylpropionic acid

Izumi *et al.*[5] reported that optically active α-amino acids have very small asymmetric effects on a Raney nickel catalyst under alkaline conditions. These workers determined the amount of amino acid adsorbed on the catalyst and concluded that the weak asymmetric effects of amino acids under alkaline conditions are caused by desorption of amino acids from the catalyst. On the other hand, it was reported from the Accumulatoren-Fabrik[17] that a Raney nickel catalyst maintains its original properties for a long time under strongly alkaline conditions, even if it is treated with solutions containing substances with which it can form complexes, such as tartaric acid and amino aliphatic compounds. This indicates that under strongly alkaline conditions a Raney nickel catalyst can hardly be affected by these substances.

In connection with these observations, the amount of hydroxy carboxylic acid adsorbed on the catalyst in the asymmetric modification was determined. The results[18-19] obtained with D-tartaric acid are

16) J. P. Greenstein and M. Winitz, "Chemistry of the Amino Acids," Vol. 1, John Wiley & Sons, Inc., New York (1961), p. 178.

17) Accumulatoren-Fabrik A. G., Berg. Pat. 613541 (1962).

18) The preparation and modification of Raney nickel catalyst were performed as described in a previous paper.[7]

19) D-Tartaric acid adsorbed on the catalyst was eluted by treatment with N sodium hydroxide at 90—95°C for one hour. The acid eluted was determined by the method of Sharma with a slight modification. N. N. Sharma and R. C. Mehrotra, *Anal. Chim. Acta*, **11**, 414 (1954).

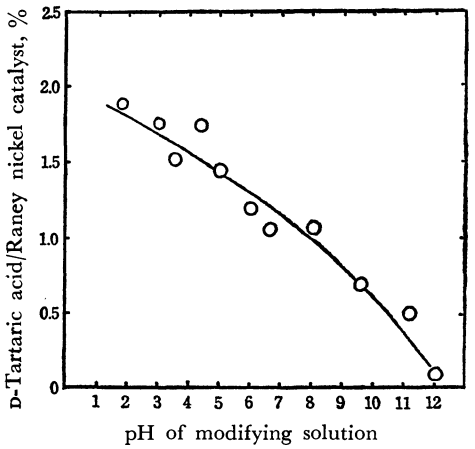

Fig. 6. Adsorption of D-tartaric acid on Raney nickel catalyst.
Raney nickel (0.62 g) was modified with 100 m*l* of a 2% D-tartaric acid solution at 0°C for 1.5 hr.

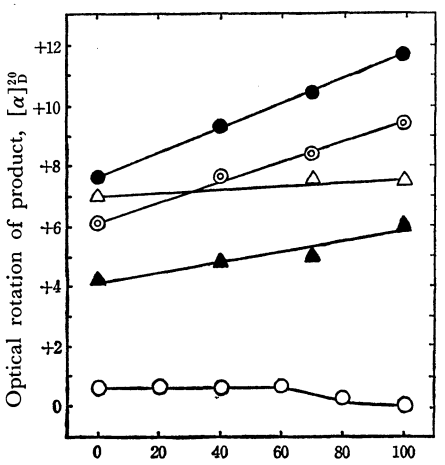

Fig. 7. Effect of temperature on modifications with hydroxy dicarboxylic acids.
(Modified at pH 5.0—5.2)
● (+)-*threo*-2-Methyltartaric acid
○ (−)-*erythro*-2-Methyltartaric acid
△ (+)-2,3-Dimethyltartaric acid
◎ L-Tartaric acid ▲ L-Malic acid

shown in Fig. 6.

The amount of D-tartaric acid adsorbed on the catalyst was much influenced by the pH of the modifying solution and decreased considerably with increase in the pH value. Under strongly alkaline conditions the reagent is adsorbed very little onto the catalyst. The acid must loose its ability to be adsorbed onto the nickel metal under these conditions because of the conversion to its alkali salt, and so it is desorbed. The weak asymmetric activity observed at high pH values, thus, is evidently caused by desorption of the reagent from the catalyst.

On the other hand, under acidic conditions there is a characteristic difference between the asymmetric activities of catalysts modified with hydroxy dicarboxylic acids and those of catalysts modified with hydroxy monocarboxylic acids. As pointed out at the beginning of this section, on modifications with hydroxy dicarboxylic acids the asymmetric activities decreased remarkably with increase of acidity, while with hydroxy monocarboxylic acids there was no similar decrease. However, as can be seen in Fig. 6, the amount of the hydroxy dicarboxylic acid adsorbed on the nickel metal does not decrease with increase of acidity, but in fact it increases considerably. The above difference in activity, therefore, cannot be explained by the amount of the reagent adsorbed on the catalyst. It is probably related to the presence or absence of the β-carboxyl group in the modifying reagent.[20]

The Effect of the Temperature of the Modifying Solution. On modifications with hydroxy dicarboxylic acids,[10-12] the asymmetric activities of catalysts increased with elevation of the modifying temperature except in the case of (−)-*erythro*-2-methyltartaric acid,[10] as shown in Fig. 7. A similar tendency was observed with several hydroxy monocarboxylic acids.[7]

As reported in a previous paper,[7] however, in contrast to the asymmetric activities of the modified catalysts their catalytic hydrogenation activities decreased considerably with elevation of the modifying temperature. It is likely that when a Raney nickel catalyst is modified at a certain pH value, the interaction between the modifying reagent and the nickel metal is intensified by elevation of the temperature, and the reagent spreads itself over the surface of the metal. Consequently a catalyst with many compactly adsorbed asymmetric centers is produced, which thus has a high asymmetric activity in spite of its decreased catalytic hydrogenation activity.

The Effect of the Time of Immersion. To study the effect of the time of immersion of a Raney nickel catalyst upon the asymmetric activity, modifications with a 2% aqueous solution of D-tartaric acid adjusted to pH 5.0 were carried out at 0°C.[18] The asymmetric activities of the resulting catalysts were compared and the results are shown in Fig. 8.

Maximal asymmetric activity was attained when a Raney nickel catalyst was immersed in the solution for 10 min. Immersion for more than 10 min resulted in no further increase in asymmetric activity. It is likely that the adsorption of the modifying reagent on the nickel metal reaches an equilibrium within 10 min at 0°C.

20) The role of the β-carboxyl group will be discussed in the subsequent chapter.

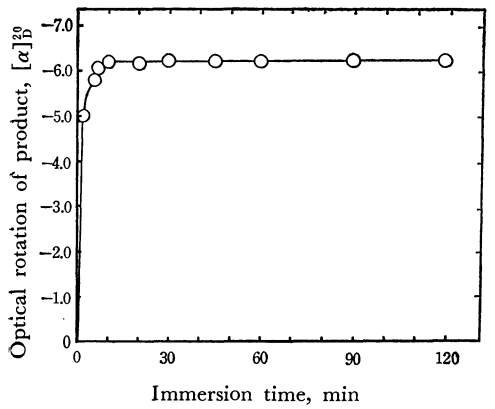

Fig. 8. Effect of time of immersion on modification with D-tartaric acid.
(Modified at pH 5.0 and at 0°C)

Even immersion for 2 or 5 min, however, gives a rather high asymmetric activity to a Raney nickel catalyst. It seems that as soon as Raney nickel is added to the modifying solution, it is strongly adsorbed by the reagent, and the adsorption quickly reaches almost the state of equilibrium.

The Effect of the Concentration of the Modifying Reagent. The effect of the amount of modifying reagent upon the asymmetric activity of the catalyst was studied using aqueous solutions of D-tartaric acid.[18] The results are shown in Fig. 9.

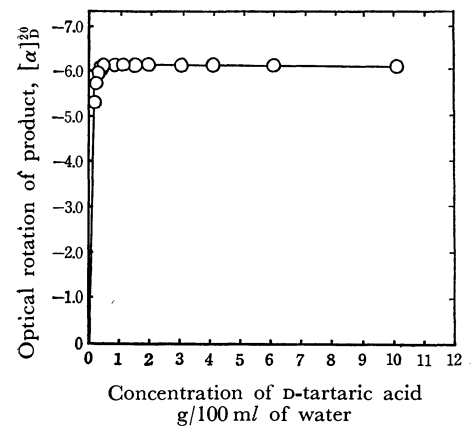

Fig. 9. Effect of concentration of modifying reagent.
(Modified at pH 5.0 and at 0°C)

The asymmetric activity of the catalyst was independent of the concentration of D-tartaric acid in the range of 0.4 to 10%.

Izumi *et al.*[5] observed a similar tendency on modification of a Raney nickel catalyst with an aqueous solution of L-glutamic acid. They reported that the asymmetric activity was not affected by the concentration of the acid in a range of 0.0625 to 6%.

These results clearly show that the adsorption of modifying reagent on Raney nickel readily reaches saturation at a lower concentration.

The Stability of the Asymmetric Activity

To study the stability of the asymmetric activity, a Raney nickel catalyst modified at 0°C with a 2% aqueous solution of D-tartaric acid adjusted to pH 5.0[18] was employed repeatedly in the hydrogenation reaction at 60°C.[21] The results of the stability test are shown in Table 1.

Table 1. Stability test of asymmetric activity

Catalyst sample	Optical rotation of product, $[\alpha]_D^{20}$
Original modified catalyst	−6.22°
After 1st recovery	−6.30°
After 2nd recovery	−6.09°
After 3rd recovery	−6.01°
After 4th recovery	−6.25°
After 5th recovery	−6.19°

As can be seen in Table 1, the asymmetric activity in the catalyst was very stable. The original asymmetric activity persisted to at least the sixth run. This shows that the modifying reagent is firmly adsorbed on the catalyst and hence the asymmetric centers formed on the surface of the metal are not destroyed during recovery or under the conditions used in the hydrogenation reaction.

The Effect of the Structure of the Modifying Reagent on the Asymmetric Activity

The Effect of the *α*-*C*-Substituted Alkyl Group of the Modifying Reagent. The asymmetric activity of catalyst modified with L-citramalic acid (L-*α*-*C*-methylmalic acid) was lower than that of catalyst modified with L-malic acid, as shown in Fig. 2. This difference is obviously caused by the methyl group on the asymmetric *α*-carbon atom of L-citramalic acid. Similar differences were observed between modifications with glutamic acid and those with *α*-*C*-substituted glutamic acids, such as (+)-2-*C*-methylglutamic acid and (+)-2-*C*-benzylglutamic acid.[9]

These results clearly show that the *α*-*C*-substituted groups play important roles in the formation of an asymmetrically active site of the catalyst, and that to obtain an effective asymmetric catalyst the asymmetric *α*-carbon atom of the modifying reagent should not possess a bulky substituted group in addition to the hydroxyl group, carboxyl

21) The hydrogenation reaction and the measurement of the asymmetric activity of the catalyst were performed as described in a previous paper.[7]

group and β-carbon chain. A small group, such as the hydrogen atom in L-malic acid or in L-glutamic acid, seems to be effective for the α-*C*-substituted group. Probably, four groups on the asymmetric α-carbon atom which are rather unbalanced in bulk favor asymmetric hydrogenation.

The Role of the β-Substituted Group of the Modifying Reagent and the Effect of Its Configuration. D-Tartaric acid was more effective for asymmetric activity of a Raney nickel catalyst than L-malic acid, as shown in Figs. 1 and 2. This clearly shows that the β (or α')-hydroxyl group of tartaric acid and its configuration have a great influence on the formation of an asymmetric catalyst. On the other hand, on modifications with isomeric optically active 3-methylmalic acids, both the (−)-*threo*- and (+)-*erythro*-compounds[12,22] were less effective for asymmetric activity than D-tartaric acid. However, the former was more effective than L-malic acid, while the latter was less effective.[12] The difference in the asymmetric effects of (−)-*threo*-3-methylmalic acid and D-tartaric acid is due entirely to their β-substituted groups, that is, the methyl group of (−)-*threo*-3-methylmalic acid and the hydroxyl group of D-tartaric acid, because *threo*-3-methylmalic acid has the same structure as tartaric acid except that one hydroxyl group is replaced by a methyl group. Moreover, the difference in the asymmetric effects of (+)-*erythro*- and (−)-*threo*-3-methylmalic acid and L-malic acid is also caused by the methyl group attached to the β-carbon atom of malic acid and by its configuration. Thus, like the β-hydroxyl group, the β-methyl group has a great influence on the formation of an asymmetric catalyst though less than the β-hydroxyl group.

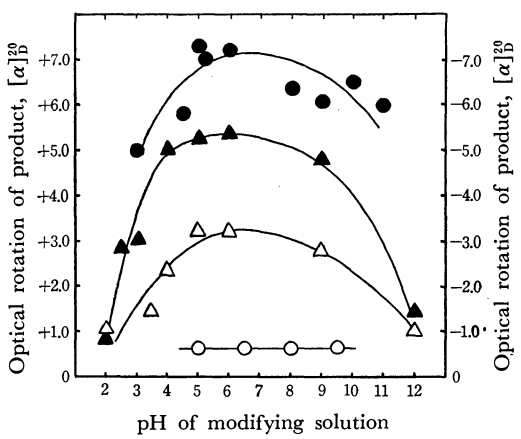

Fig. 10. Modifications with isomeric 3-methylmalic acids and 2-methyltartaric acids. (Modified at 0°C)
● (+)-*threo*-2-Methyltartaric acid
○ (−)-*erythro*-2-Methyltartaric acid
▲ (−)-*threo*-3-Methylmalic acid
△ (+)-*erythro*-3-Methylmalic acid
The left scale represents (+)-*threo*- and (−)-*erythro*-2-methyltartaric acid, and the right scale represents (−)-*threo*- and (+)-*erythro*-3-methylmalic acid.

To study the effect of the erythro-threo configuration of a modifying reagent on the asymmetric activity, comparisons were made of the asymmetric activities of catalysts modified with optically active α, β-diasymmetric hydroxy dicarboxylic acids, such as (−)-*threo*- and (+)-*erythro*-3-methylmalic acid[12,22] and (+)-*threo*- and (−)-*erythro*-2-methyltartaric acid.[10,13] The results are shown in Fig. 10.

As can be seen in Fig. 10, optically active *threo*-3-methylmalic acid and *threo*-2-methyltartaric acid were more effective for asymmetric activity than the corresponding optically active erythro forms. These results clearly show that the asymmetric activities of catalysts are much influenced by the erythro-threo configuration of the modifying reagents.

The same absolute configuration is assigned to the α- and β-asymmetric centers of optically active *threo*-3-methylmalic acid,[23] and the β-methyl group is situated in the same position relative to the α-hydroxyl group as one hydroxyl group of optically active tartaric acid is to the other. However, the β-methyl group of optically active *erythro*-3-methylmalic acid is situated in the same position relative to the α-hydroxyl group as the one hydroxyl group of meso tartaric acid is to the other, since the α- and β-asymmetric centers of this compound have the opposite absolute configuration to each other.[23]

Moreover, in these two acids the functional groups to be adsorbed predominantly upon the nickel metal are similar; these are the α-hydroxyl group and the α-carboxyl group which have higher affinities for the metal than the other groups. Therefore, it is clearly conceivable that the difference in the asymmetric activities of catalysts modified with these two acids is caused by this difference in configuration of the asymmetric centers.

A similar difference can be seen between modifications with (−)-*erythro*-2-methyltartaric acid and

22) S. Tatsumi, M. Imaida and Y. Izumi, This Bulletin, **39**, 1818 (1966).

23) The threo isomer of 3-methylmalic acid was identified by deamination of *threo*-3-methylaspartic acid with nitrous acid. Since this deamination of an α-amino acid does not affect the configuration, the resulting α-hydroxy acid is identical in configuration with the parent amino acid. On the other hand, from the investigation of Baker *et al.* (H. A. Baker, R. D. Smyth, E. J. Wawszkiewicz, M. N. Lee and R. M. Wilson, *Arch. Biochem. Biophys.*, **78**, 468 (1958).) the α- and β-asymmetric centers of optically active *threo*-3-methylaspartic acid are assigned the same absolute configuration, while those of optically active *erythro*-3-methylaspartic acid are opposite in absolute configuration to each other. Therefore the configurations of *erythro*- and *threo*-3-methylmalic acid can easily be correlated.

(+)-*threo*-2-methyltartaric acid. The catalyst modified with the erythro form has only a very low asymmetric activity, while that modified with the threo form has a very high one. This difference in asymmetric activity can best be explained in a similar way to the difference between modifications with the optically active 3-methylmalic acids described above. As previously reported by the author,[14] the two hydroxyl groups of *threo*-2-methyltartaric acid are situated in the same position relative to each other as those of tartaric acid; while in *erythro*-2-methyltartaric acid the situation of the two hydroxyl groups corresponds to that of the two hydroxyl groups of meso tartaric acid. It thus appears that the α- and β-asymmetric centers of the threo form have the same absolute configuration and those of the erythro form have the opposite configuration to each other.

However, the difference between the asymmetric effects of these two reagents was greater than that between the effects of isomeric 3-methylmalic acids. This result is probably related to the fact that each of the two asymmetric carbon atoms of 2-methyltartaric acid, unlike those of 3-methylmalic acid, has a hydroxyl group. As has been pointed out above, the asymmetric activity of the catalyst is much influenced by a hydroxyl group located on an asymmetric carbon atom, this influence being greater than that of the corresponding methyl group, and also two hydroxyl groups which are identical in configuration cause an increase in the asymmetric activity, while two with the opposite configuration to each other decrease the activity. Therefore, the low asymmetric effect of (−)-*erythro*-2-methyltartaric acid and the high effect of (+)-*threo*-2-methyltartaric acid must be related to the roles of their hydroxyl groups and to their configurations.[24]

The Effect of the *C*, *C'*-Dialkyl Groups of Tartaric Acids. To study the effects of two alkyl groups attached to the asymmetric carbon atoms of tartaric acid upon the asymmetric activity, measurements were made of the asymmetric activities of catalysts modified with (+)-2, 3-dimethyltartaric acid[10,13] and (+)-1, 2-dihydroxycyclohexane-1, 2-dicarboxylic acid.[11,25] The results are shown in Fig. 11.

On modification with (+)-2, 3-dimethyltartaric acid the asymmetric activity shows a tendency similar to that obtained on modification with D-tartaric acid, except for the direction of optical rotation.

(+)-2, 3-Dimethyltartaric acid has the same chemical or stereochemical structure as optically active tartaric acid except that both hydrogens on the asymmetric carbon atoms are replaced by

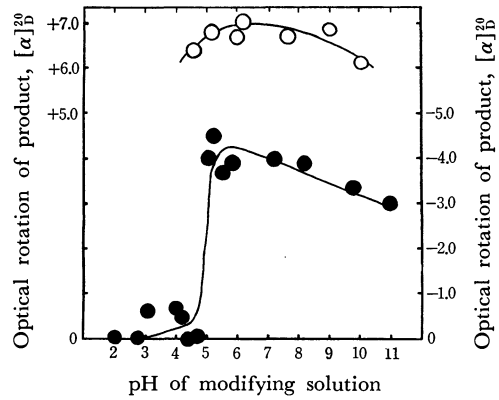

Fig. 11. Modifications with (+)-2, 3-dimethyltartaric acid and (+)-1, 2-dihydroxycyclohexane-1, 2-dicarboxylic acid. (Modified at 0°C)
○ (+)-2, 3-Dimethyltartaric acid
● (+)-1, 2-Dihydroxycyclohexane-1, 2-dicarboxylic acid
The left scale represents (+)-2, 3-dimethyltartaric acid and the right scale represents (+)-1, 2-dihydroxycyclohexane-1, 2-dicarboxylic acid.

methyl groups. The two methyl groups, therefore, are situated in the same threo position relative to each other as the two hydroxyl groups.[14] The two asymmetric centers of this compound are assigned the same absolute configuration and contribute equally to the optical direction of the asymmetric activity of the catalyst. The resemblance in the asymmetric effects of (+)-2, 3-dimethyltartaric acid and D-tartaric acid is due entirely to the above similarity in configuration. In this respect, these reagents are quite different from (−)-*erythro*-2-methyltartaric acid and (+)-*erythro*-3-methylmalic acid.

On the other hand, it seems probable that, like meso tartaric acid, 2, 3-dimethyltartaric acid which is assigned the meso form, has no asymmetric effect upon a Raney nickel catalyst.

As shown in Fig. 7, (+)-2, 3-dimethyltartaric acid is less effective for asymmetric activity, particularly at high modifying temperatures, than (+)-*threo*-2-methyltartaric acid. This difference is considered to be due to the presence or absence of an α-*C*-methyl group in the modifying reagents. As can be seen from the difference in the asymmetric effects of L-malic acid and L-citramalic acid, the α-*C*-methyl group is unfavorable for asymmetric activity. In (+)-2, 3-dimethyltartaric acid the group is present, while in (+)-*threo*-2-methyltartaric acid it is not because this compound is preferentially adsorbed with its 3-hydroxyl group and 3-carboxyl group (C_4-carboxyl group) upon the nickel metal[26] and hence its C_2-asymmetric carbon atom, on which the methyl group is located, acts as a

24) Further discussion of this will be given in the subsequent section.
25) S. Tatsumi, M. Imaida and Y. Izumi, This Bulletin, **39**, 2543 (1966).
26) The form of adsorption of this compound on the nickel metal will be discussed in the next section.

β-carbon atom in the asymmetric modification. However, (+)-2, 3-dimethyltartaric acid is more effective for asymmetric activity than (−)-*erythro*-2-methyltartaric acid. This indicates that the asymmetric activities of catalysts are influenced far more by the configuration of the modifying reagents and orientation of methyl groups and hydroxyl groups in space, than by the hindrance due to the α-*C*-methyl group.

Thus, the asymmetric effects of tartaric acid and its *C*-methyl and *C*, *C'*-dimethyl derivatives assigned the threo form are greater than those of malic acid and its *C*-methyl derivatives. To obtain an especially high asymmetric activity, two hydroxyl groups situated in the threo position relative to each other are indispensable for a modifying reagent.

When a Raney nickel catalyst was modified with (+)-1, 2-dihydroxycyclohexane-1, 2-dicarboxylic acid, its asymmetric activity was greatly influenced by the pH of the modifying solution, as shown in Fig. 11, the influence being quite different from those of catalysts obtained on modifications with optically active tartaric acid, malic acid and their *C*-methyl and *C*, *C'*-dimethyl derivatives. Maximal asymmetric activities were observed at pH 5—7; this pH range approximately corresponds to the pH-jumping region of the neutralization curve of this acid.[11] However there was a very great diminution in activity at pH values below pH 5. Under acidic conditions both carboxyl groups of the acid are adsorbed upon the nickel metal and hence the alicyclic ring forms a bulky steric hindrance over the surface of the metal. Therefore it seems that the hydrogenation substrate can hardly be affected by the stereoselectivity of asymmetric centers of the acid.

The Role of the β-Carboxyl Group and the Form of the Modifying Reagent Adsorbed on the Catalyst. To study the role of the β (or α')-carboxyl group of the modifying reagent, the asymmetric activities of catalysts modified with D-tartaric acid, monomethyl D-tartrate and D-*threo*-2, 3-dihydroxybutyric acid were compared.[12]

Monomethyl D-tartrate and D-*threo*-2, 3-dihydroxybutyric acid are characterized by the lack of an acidic property of one of the two carboxyl groups of D-tartaric acid. In the former compound it is lost by esterification and in the latter the carboxyl group is replaced by a methyl group.

As shown in Fig. 12, on modifications with these two reagents, a maximal asymmetric activity is observed under acidic conditions and there is a decrease in activity under alkaline conditions. These curves of asymmetric activity are quite different in character from that obtained on modification with D-tartaric acid but similar to those obtained with several hydroxy monocarboxylic acids. These results evidently show that the considerable decrease of asymmetric activity observed

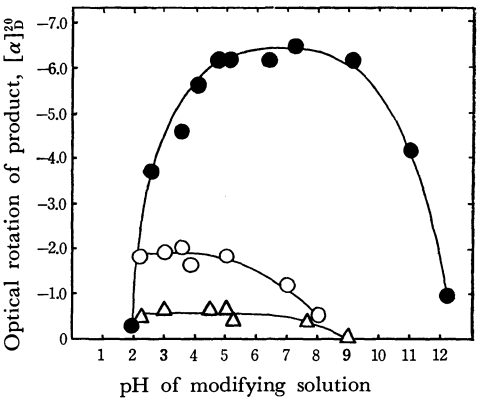

Fig. 12. Modifications with D-tartaric acid, monomethyl D-tartrate and D-*threo*-2, 3-dihydroxybutyric acid. (Modified at 0°C)
● D-Tartaric acid
○ Monomethyl D-tartrate
△ D-*threo*-2, 3-Dihydroxybutyric acid

under acidic conditions on modifications with hydroxy dicarboxylic acids depends on the presence of a functional β (or α')-carboxyl group. It is likely that both carboxyl groups of hydroxy dicarboxylic acids are readily adsorbed on the surface of nickel metal in the absence of alkali. When the acidity of the modifying solution decreases, one carboxyl group is detached from the surface of the metal and the resulting group, carrying a high polarity, produces a massive hindrance, which effectively regulates the form of approach of the hydrogenation substrate to the catalyst and causes an increase in asymmetric activity.

On the contrary, since on modifications with monomethyl D-tartrate and D-*threo*-2, 3-dihydroxybutyric acid the ester and methyl groups are less affected by the modifying conditions,[27] the form in which they are adsorbed on the surface of the metal is similar under all acidic conditions. Consequently, under acidic conditions catalysts modified with these two reagents do not show such a great decrease in asymmetric activity as the catalyst modified with D-tartaric acid.

This also holds good for modifications with other hydroxy monocarboxylic acids.

In dihydroxy dicarboxylic acids such as optically active tartaric acid, 2, 3-dimethyltartaric acid and 1, 2-dihydroxycyclohexane-1, 2-dicarboxylic acid, the two asymmetric centers are similar in configuration or in the orientation of their groups in space, and hence whether the reagent is adsorbed preferentially by its α-hydroxyl and α-carboxyl groups upon the nickel metal or by its β (or α')-hydroxyl and β (or α')-carboxyl groups, the asymmetric

27) According to Welch, ester and methyl groups are poorly adsorbed upon Raney nickel irrespective of the conditions of treatment. C. M. Welch, H. A. Smith and J. B. Cole, *J. Phys. Chem.*, **65**, 705 (1961).

activity of the resulting catalyst is the same in capacity and in direction of optical rotation.

On the other hand, since the two asymmetric centers of optically active 2-methyltartaric acid are dissimilar, whether the adsorption with the 2-hydroxyl group and the 1-carboxyl group predominates or that with the 3-hydroxyl group and the 4-carboxyl group does, has a great influence on the asymmetric activity of the catalyst.

As can be seen from Figs. 1 and 10, (+)-*threo*-2-methyltartaric acid is more effective for asymmetric activity than D-tartaric acid. This result seems to indicate that this compound is not preferentially adsorbed by its 2-hydroxyl group and 1-carboxyl group on the catalyst, but by its 3-hydroxyl group and 4-carboxyl group. If the adsorption by the 2-hydroxyl group and the 1-carboxyl group were predominant, the 2-methyl group would serve as the α-methyl group in the asymmetric modification and would cause a decrease in the asymmetric effect. Consequently, the asymmetric activity of catalyst modified with this compound would be smaller than that of catalyst modified with D-tartaric acid. However, no such difference in asymmetric activity is observed. Moreover, this compound is more effective for asymmetric activity than (+)-2, 3-dimethyltartaric acid, as shown in Figs. 10 and 11. The difference in the asymmetric effects of these reagents is obviously caused by the α-methyl group of (+)-2, 3-dimethyltartaric acid and then it is nearly equal to the difference in the asymmetric effects of L-malic acid and L-citramalic acid. These results evidently support the above conclusion.

Considering the great influences of hydroxyl groups and their configurations upon the asymmetric effect, it seems reasonable that (−)-*erythro*-2-methyltartaric acid has only a very weak asymmetric effect on a Raney nickel catalyst.

Conclusion

The presence or absence of asymmetric activity in the modified Raney nickel catalyst depends on the optical purity of the reagent used for the modification. A racemate and a meso compound have no asymmetric effects upon Raney nickel. Moreover, there is a linear relationship between the capacity of asymmetric activity of the catalyst and the optical purity of the modifying reagent. When a modifying reagent loses its ability to be adsorbed on Raney nickel, the resulting catalyst has little or no asymmetric activity. To obtain an asymmetric catalyst an α-carbon atom of the modifying reagent must have at least two kinds of functional groups such as a hydroxyl group and a carboxyl group which can be adsorbed strongly or chelated to Raney nickel.

On modification with a hydroxy carboxylic acid containing one asymmetric center or containing two asymmetric centers of identical absolute configuration, the catalyst modified with a D-hydroxy acid has an asymmetric activity to produce predominantly the hydrogenation product of the D-configuration; while that modified with an L-hydroxy acid gives a product of the L-configuration. When enantiomeric compounds are used as the modifying reagents, the asymmetric activities of the resulting catalysts are the same except for the direction of optical rotation. On modification with a racemic compound, therefore, two kinds of catalyst are produced in the same ratio; one has the asymmetric activity to hydrogenate the substrate predominantly to the product of the L-configuration and the other has the opposite asymmetric activity. On modification with a hydroxy monocarboxylic acid containing two asymmetric centers of opposite absolute configuration in its α- and β-carbon atoms, the rotatory direction of the asymmetric activity is decided by the configuration of the α-asymmetric center.

The asymmetric activity of catalyst is much influenced by the pH of the modifying solution. On modification with a hydroxy dicarboxylic acid, the maximal asymmetric activity is obtained at pH 5—9 and there is a considerable diminution in activity at both higher and lower pH values; while with a hydroxy monocarboxylic acid a similar decrease is obtained only under alkaline conditions. In both cases, the weak asymmetric activity observed at high pH values is caused by desorption of the reagent from the catalyst. On the other hand, the weak asymmetric effect of a hydroxy dicarboxylic acid observed at low pH values is not related to desorption of the reagent, but to the presence of the β-carboxyl group.

The asymmetric activity of catalyst, in general, increases with elevation of the temperature of the modifying solution.

A maximal asymmetric activity is attained in 10 min when a Raney nickel catalyst is immersed in a modifying solution at 0°C. Immersion for more than 10 min results in no further increase in the activity. It is likely that the adsorption of the reagent on the catalyst reaches an equilibrium within 10 min. Moreover, the asymmetric activity of catalyst is independent of the concentration of reagent in the range of 0.4—10%. It seems that the adsorption of a reagent on Raney nickel readily reaches saturation at a low concentration.

The asymmetric activity in the modified catalyst is very stable. The original activity persisted for at least six runs of the hydrogenation reaction.

An α-*C*-substituted alkyl group in the modifying reagent, such as the methyl group of citramalic acid, reduces the asymmetric activity of the catalyst.

To obtain an effective asymmetric catalyst, an asymmetric α-carbon atom of α-hydroxy carboxylic acid used for the modification should not possess a bulky substituted group in addition to the carboxyl

group, hydroxyl group and β-carbon chain.

On modifications with tartaric acid and its derivatives, like their α-hydroxyl groups, the β (or α')-hydroxyl groups play an important role in the formation of an asymmetric catalyst. The methyl group of 3-methylmalic acid also has a great influence on the asymmetric activity of the catalyst though less than the β (or α')-hydroxyl groups of tartaric acid and its derivatives. On modifications with 2-methyltartaric acid and 3-methylmalic acid, the asymmetric activities of the catalysts are greatly influenced by the configurations of the α- and β-asymmetric centers of the reagents. To obtain an effective asymmetric catalyst, the same configuration should be assigned to the α- and β- asymmetric centers. Moreover, the asymmetric activities of catalysts are far more influenced by the configurations of the modifying reagents than by hindrances due to the substituted groups themselves. 2,3-Dimethyltartaric acid has a high asymmetric effect upon the catalyst similar to that of tartaric acid. However, 1,2-dihydroxycyclohexane-1,2-dicarboxylic acid, which is a sort of 2,3-dialkyl tartaric acid, has a quite different asymmetric effect from tartaric acid, malic acid and their *C*-alkyl derivatives. This difference is due to the alicyclic ring of 1,2-dihydroxycyclohexane-1,2-dicarboxylic acid.

The asymmetric effects of tartaric acid and its *C*-methyl and *C*, *C'*-dimethyl derivatives assigned the threo form are greater than those of malic acid and its *C*-methyl derivatives. To obtain an especially high asymmetric activity, two hydroxyl groups situated in the threo position relative to each other are indispensable for a modifying reagent.

On modification with a hydroxy dicarboxylic acid, both the β (or α')-carboxyl group of the reagent and the α-carboxyl group play important roles in the formation of an asymmetric catalyst. It is likely that both carboxyl groups are readily adsorbed on the surface of the catalyst in the absence of alkali. When the acidity of the modifying solution decreases, the β (or α')-carboxyl group is detached from the catalyst and the resulting group, carrying a high polarity, effectively regulates the form of approach of the hydrogenation substrate to the catalyst. On the contrary, on modification with a hydroxy monocarboxylic acid the form of adsorption of the reagent on the surface of the catalyst is similar under all acidic conditions used.

On modification with 2-methyltartaric acid, the 2-methyl group and 1-carboxyl group of this compound serve as a β-methyl group and a β-carboxyl group, respectively, in the formation of an asymmetric catalyst. It is likely that adsorption with the 3-hydroxyl group and 4-carboxyl group is predominant in the asymmetric modification.

The author wishes to express his sincere thanks to Professor Shiro Akabori and Professor Yoshiharu Izumi for their valuable advice and encouragement throughout this work.

This work was made possible by support from the Ajinomoto Co., Inc., Tokyo and the Kawaken Fine Chemicals Co., Ltd., Tokyo.

BULLETIN OF THE CHEMICAL SOCIETY OF JAPAN VOL. 41 419—423 (1968)

Studies of Organic Catalytic Reactions. VI.[1] The Function of Pyridine and Copper in the Rosenmund-von Braun Reaction

Takehiko Ito and Ken-ichi Watanabe

Department of Chemistry, Faculty of Science, Tokyo Metropolitan University, Setagaya-ku, Tokyo

(Received July 28, 1967)

The Rosenmund-von Braun reaction with aryl halide, with its Ar-X+CuCN-Base→Ar-CN+CuX-Base, has been studied in nitrobenzene in place of an organic base at 160—180°C. The free nitriles formed during the reaction were determined exactly by gas chromatography. In the use of bases with suitable coordination forces to CuCN, the reactivity of the base for the substitution was found to be in the order: prim.>sec.>tert. A steric hindrance of the base was observed, and the reactivity of the pyridine homologue followed the order: pyridine>quinoline >α-picoline>2, 6-lutidine. Ortho-substituted groups in the halobenzene seem to manifest no steric hindrance on the reaction. From the results of the kinetic study, it can be said that CuCN participates in the reaction essentially in the form of a Base(1 mol)-CuCN complex. The overall reaction is second-order, $dc/dt=k$[Complex][Ar-X]. The rate-determining step may be in the halogen exchange stage in the intervening complex, Base-CuCN-Ar-X, where the plane including CN-Cu-X and that of the benzene ring may be nearly perpendicular to each other. When an excess of CuCN over the base is used, the base is liberated from the Base-CuX complex, after the displacement, and then coordinates to the unreacted CuCN again.

It has previously been reported[2] that the Rosenmund-von Braun reaction in which nitriles are obtained from aryl bromides and cuprous cyanide is generally useful for the preparation of aromatic nitriles. In that study, the aryl halides were converted to the nitriles in a good yield by refluxing them in pyridine. The succeeding study with four sorts of halobenzene established that the ease of the displacement of halogen is in the order: I>Br>Cl≫F. Representative examples are shown in Table 1.

Improvements of this reaction have been reported by Newman and his co-workers,[3,4] who used *N*-methylpyridone or dimethylformamide as the solvent. Bacon and his co-workers[5] studied the reaction, Ar-hal+Cu-X→Ar-X+Cu-hal (X=Cl, Br, CN, SCN), in various polar solvents and explained that the reaction proceeds as a bimolecular type between Ar-hal and Cu-X. In the studies mentioned above, however, the reactions were carried out through the dissolution of the complex (solvent-CuCN) in the same solvent (organic base); therefore, the quantity of the base that participated in the reaction could not be elucidated. Further, in the experimental procedure, the separation of the nitrile from the reaction mixture was very troublesome because the reaction mixture containing the nitrile was obtained as a solid complex at room temperature; it then had to be decomposed with ammonia or concentrated hydrochloric acid to get the free nitrile.

This paper will deal with studies of the Rosenmund-von Braun reaction in a nitrobenzene solution attempting to overcome the disadvantages mentioned above. In this way, the ratio of the organic base to CuCN can be calculated, and the nitrile formed during the reaction is liberated as a free form in a nitrobenzene solution. Therefore, the behavior of the organic base, aryl halide, and cuprous cyanide can be examined, and the formation of the nitrile can be determined exactly. The mechanism of this reaction is presented here.

In this study, bromobenzene and pyridine were mainly used; they were heated with cuprous cyanide at 180°C in nitrobenzene. It did not matter whether the reaction was carried out in the air or in an oxygen-free nitrogen atmosphere. Cuprous cyanide and cuprous chloride were hardly ever soluble in nitrobenzene and did not react with bromobenzene without the addition of pyridine or other organic bases. When the organic base was added to the copper salt in nitrobenzene, both of them were dissolved by the mild heating forming the complex. As far as our tests were concerned, nitrobenzene was the best solvent for this reaction.

1) Paper V: K. Sakai, T. Ito and K. Watanabe, This Bulletin, **40**, 1660 (1967).
2) N. Akanuma, H. Amemiya, T. Hayashi, K. Watanabe and K. Hata, *Nippon Kagaku Zasshi (J. Chem. Soc. Japan, Pure Chem. Sect.)*, **81**, 333 (1960); *Chem. Abstr.*, **56**, 406 (1962).
3) L. Friedman and H. Shechter, *J. Org. Chem.*, **26**, 2522 (1961).
4) M. S. Newman and H. Boden, *ibid.*, **26**, 2535 (1961).
5) R. G. R. Bacon and H. O. Hill, *J. Chem. Soc.*, **1964**, 1097.

Table 1. Rosenmund-von Braun reaction in pyridine[1]

Exp. No.	Aryl halide	g	CuCN g	Pyridine g	Reaction temp. °C	Reaction time hr	Yield of nitrile %
1	Iodobenzene	20	10.8	15	170—190	6	80
2	Bromobenzene	20	12.0	15	140—155	9	85
3	*o*-Bromonitrobenzene	10	5.0	10	140—155	2	91
4	*p*-Bromonitrobenzene	20	9.9	20	140—155	9	80
5	Bromomesitylene	20	9.9	10	165—175	8	80
6	*o*-Bromoacetophenone	25	12.5	75	120	1.5	70
7	β-Bromonaphthalene	5	6	10[2]	260—280	3	78
8[3]	Chlorobenzene	22.6	20	15	140—150	14	trace
9	*o*-Chloronitrobenzene	10	12.5	15	160—180	3	80
10	Fluorobenzene	5.8	14.4	10	140—160	3	—

1) The reaction method by Newman was employed; M. S. Newman, "Organic Syntheses," Coll. Vol. III, p. 631 (1955).
2) Quinoline was used as solvent instead of pyridine.
3) By the reaction in an autocreave at 250°C for 9 hr, the yield of the nitrile was 34%.

Decalin, benzyl alcohol, or cyclohexanone was unfavorable, and the reaction proceeded under heterogeneous conditions.

After the reaction was started, the heterogeneous reaction mixture turned into a brownish homogeneous solution at *ca.* 120°C. When the reaction was completed, the reaction mixture was cooled to room temperature; a brownish mass was then obtained by filtration. When the mass was extracted enough with ether, very small quantities of nitrile and unreacted bromobenzene were obtained. Both the ether fraction and the nitrobenzene solution were analyzed by gas chromatography; the ratios of nitrile to bromobenzene were almost the same in both fractions. By the IR spectrum analysis of the crystals after the ether extraction, only the pyridine used for the reaction was detected. Thus, the tests revealed that the quantities of halide and nitrile can be determined by the gas chromatographic analysis of the reaction mixture in the course of the reaction*1 (Fig. 1).

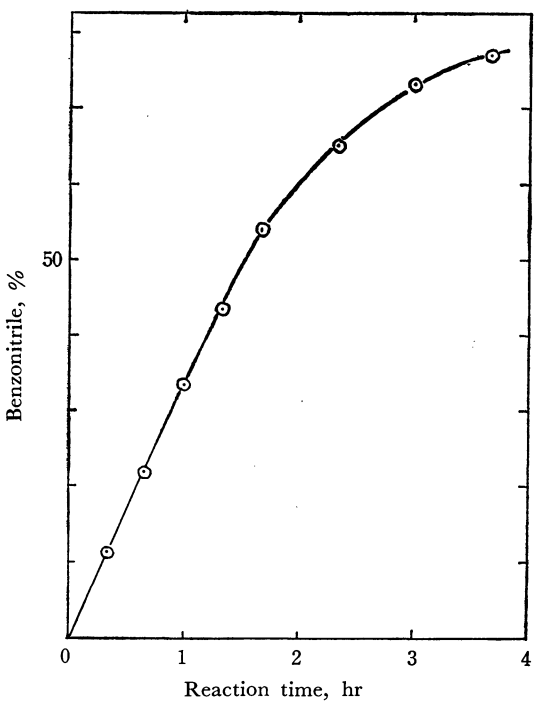

Fig. 1. The formation of benzonitrile.
Bromobenzene 1.0 m*l*, cuprous cyanide 1.0 g, pyridine 1.0 m*l*, nitrobenzene 20 m*l*, reaction temp. 177°C.

Table 2.*3 The reaction of bromobenzene with cuprous cyanide in nitrobenzene

Bromobenzene 4 m*l*, CuCN 3 g, Nitrobenzene 20 m*l*, React. temp. 180°C

Exp. No.	Base	m*l*	Reaction time hr	Benzonitrile %
1	Pyridine	0.2	6	49
2	Pyridine	0.5	6	86
3	Pyridine	1.0	6	79
4	Pyridine	5.0	6	82
5	Pyridine[2]	1.0	3	73
6	γ-Picoline	1.0	3	83
7	Quinoline	1.0	3	59
8	α-Picoline	1.0	3	28
9	2,6-Lutidine	1.2	3	26
10	Aniline	4.0	5	68
11	Diethylamine	1.0	3	24
12	Dimethylaniline	1.0	3	—
13	Ethylenediamine	3.0	6	25[3]
14	Picolinic acid	1.0	3	22

1) The yield was calculated by gas chromatographic analysis based on the amount of bromobenzene.
2) The yield of the product rised to 78% when 0.5 g of hydroquinone was added.
3) Unknown 35%.

*1 In the results of the gas chromatographic analysis, no other product was detected.

When a complex of CuCN with pyridine was prepared*2 beforehand and was used for the reaction with bromobenzene, the reaction proceeded as well as in the case of the ordinary method. In order to examine whether the free nitrile formed would participate in the reaction or not, benzonitrile was used in place of pyridine, but no change in bromobenzene was observed.

The results of the reactions with various kinds of bases in nitrobenzene are shown in Table 2.*3 The reactions were carried out at 180°C; no reaction occurred below 130°C. The organic bases used in the reaction should coordinate moderately to the copper atom of the cuprous cyanide.*4 In the use of bases with suitable coordination forces, the reactivity of the substitution depended on their basicity: prim.>sec.>tert. No reaction occurred with dimethylaniline. The steric hindrance of the substituents of bases had an influence upon the reactivity of the complexes of the pyridine homologues; the reactivity was found to be in the order: pyridine > quinoline > α-picoline > 2, 6-lutidine. Bacon[5] pointed out this problem as a solvent effect. The methyl group of the γ-picoline seemed to enhance the coordination ability of the base by means of its 1-effect (Exp. 6, Table 2). It is assumed that the activity of the complex is dependent upon both the character and the molecular structure of the base.

In order to investigate the mechanism of this reaction, simple kinetic studies were done. Some were carried out in a bromobenzene solution, the mole ratio of Py/CuCN was set up as 1, 2, or 3.

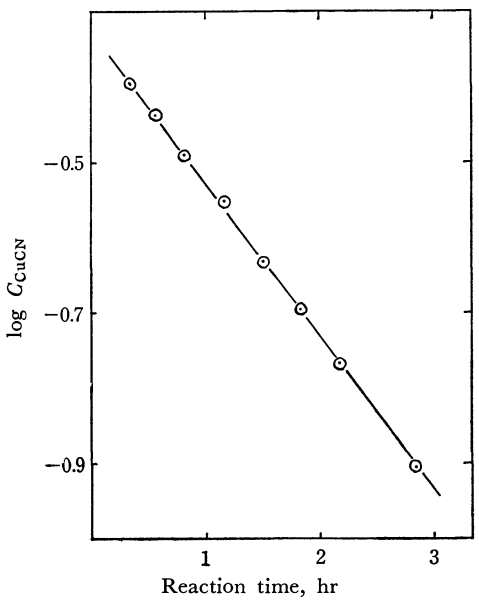

Fig. 2. The correlation of C_{CuCN} *vs.* reaction time.
Bromobenzene 25 m*l*, cuprous cyanide 4.0 g, pyridine 2.0 m*l*, reaction temp. 152°C.

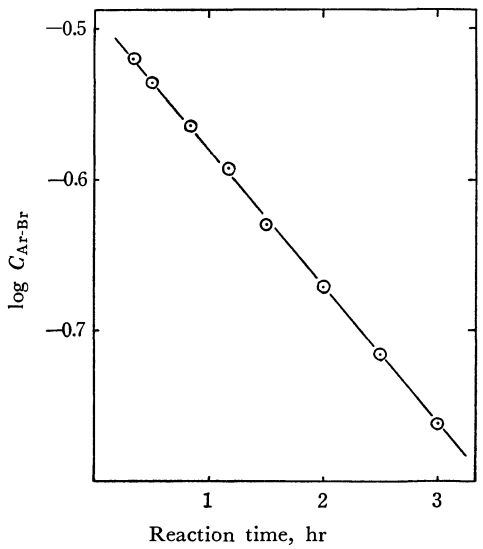

Fig. 3. The correlation of C_{Ar-Br} *vs.* reaction time.
Bromobenzene 1.0 m*l*, cuprous cyanide 4.0 g, pyridine 2.0 m*l*, nitrobenzene 30 m*l*, reaction temp. 159°C

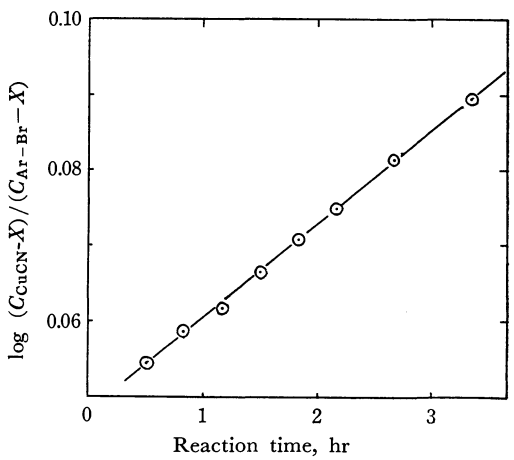

Fig. 4. Ar-Br (1.0 m*l*) + CuCN(1.0 g) + pyridine (1.0 m*l*) in nitrobenzene (20 m*l*) at 160°C.

*2 Pyridine and cuprous cyanide were heated at 120°C for about 30 min and then cooled. The yellow material thus obtained was used directly in the reaction.

*3 All the reactions except Exp. 4 proceeded heterogeneously, for the amount of the bases used was less than that of the cuprous cyanide, so a part of the cyanide remained insoluble in the solvent. On the other hand, the amount of the cyanide used was less than that of the bromobenzene; therefore, the conversion of the bromobenzene into benzonitrile could not reach 100% even if all of the cyanide did react with the bromobenzene.

*4 Ethylenediamine afforded a stable copper complex, the process being accompanied by a side reaction, and the yield of the nitrile was very low (Exp. 13, Table 2). No reaction occurred when dimethylglyoxime or acetyl acetone was used as the base. When 8-oxyquinoline or picolinic acid was used, the reaction proceeded extremely slowly.

Table 3.

A. Cyanization

Bromobenzene 1.0 m*l*, Nitrobenzene 20.0 m*l*, React. temp. 159±0.5°C

Base	m*l*	CuCN g	Base/CuCN	Initial rate mol/min×10³	Reaction rate ratio
Pyridine	1.0	2.0	0.62	3.06	0.59
Pyridine	1.0	1.0	1.24	5.18	1.0
Pyridine	2.0	1.0	2.48	5.17	1.0

B. Chlorination

Bromobenzene 1.0 m*l*, CuCl 1.0 g, Nitrobenzene 40 m*l*, React. temp. 180±0.5°C, in an oxygen free nitrogen

Base	m*l*	Base/CuCl	Initial rate mol/ min×10³	Reaction rate ratio
α-Picoline	0.5	0.5	9.0×10^{-1}	0.5
α-Picoline	1.0	1.0	1.77	1.0
α-Picoline	2.0	2.0	1.75	1.0
α-Picoline	4.0	4.0	1.7	1.0
2,6-Lutidine*	1.0	0.85	1.6	0.86
2,6-Lutidine*	2.0	1.7	1.87	1.0

* 1.0 m*l* of *o*-bromotoluene was used instead of bromobenzene.

Table 4. Effect of methyl group in bromobenzene

CuCl 1.0 g, Base/CuCl 1.8—2.2, Nitrobenzene 40 m*l* (solvent), React. temp. 181±0.5°C, in an atomosphere of oxygen-free nitrogen

Aryl halide (1.0 m*l*)	Base (2.0 m*l*)	Rate const. *l* mol⁻ min⁻¹	k_{ortho}/k_{para}
Bromobenzene	2,6-Lutidine	1.78×10^{-2}	
o-Bromotoluene	2,6-Lutidine	4.27×10^{-2}	2.07
p-Bromotoluene	2,6-Lutidine	2.05×10^{-2}	
o-Bromotoluene	Pyridine	3.82×10^{-1}	2.08
p-Bromotoluene	Pyridine	1.84×10^{-1}	
Bromobenzene	α-Picoline	3.29×10^{-2}	

Some representative results of the reactions are shown in Fig. 2, in which the reactions are first-order with regard to the CuCN. When an excess of CuCN over pyridine was used, the relation between the quantity of nitrile formed and the reaction time was linear. These facts indicate that the CuCN participates in the form of the CuCN-pyridine complex and that the concentration of the complex is approximately constant during the initial period of the reaction. On the other hand, other reactions were carried out in a nitrobenzene solution with an excess of CuCN over pyridine, these reactions were found to be first-order with regard to the bromobenzene (Fig. 3). As a result, the overall reaction is shown as a second-order reaction, $dc/dt=k$[Complex][Ar-Br], in Fig. 4.

To elucidate the correlation of the reaction rate with the number of base molecules coordinated to the copper atom, some kinetic studies were done in a nitrobenzene solution with bromobenzene. Pyridine, α-picoline, and 2, 6-lutidine were used as the bases, while CuCN and CuCl were used as the copper salt. The results of the experiments are shown in Table 3. The reaction rate was set at 1 when the mole ratio of the base to the Cu-salt was equal to 1 (Base/Cu-salt=1). When Base/Cu-salt>1, the ratio of the reaction rate was also equal to 1. On the other hand, when Base/Cu-salt<1, the ratio was equal to that of Base/Cu-salt. Accordingly, it could be inferred that the reaction may occur by the coordination of bromobenzene to the complex of one mole of the base with one mole of the Cu-salt. This is independent of the kinds of base and Cu-salt present. Even though more than one mole of the base coordinate to the copper, it still may not be capable of affecting the reaction essentially.

In order to study the steric hindrance of the halide coordinated to the copper salt, reactions

with bromobenzene, *o*-, and *p*-bromotoluene were examined. Pyridine, α-picoline, and 2, 6-lutidine were used as the bases, while nitrobenzene was used as the solvent. The rate constant is presented in Table 4. It is apparent that the methyl group in the ortho position of the halobenzene does not exert any steric hindrance on the reaction, but that, rather, the reaction is accelerated.*5 The ratio of the reaction rate of *o*- to *p*-bromotoluene is approximately equal to 2, independent of the kind of base. The promoting effect of the *o*-substituted group in the halobenzene might be explained by the effect of expelling the halogen from the ortho position (Table 4 and Table 1). On the other hand, the steric effect of the methyl group in the pyridine nucleus can be accurately observed (Table 4). It seems most reasonable to say that, in the coordination of base-CuCN-halide, the plane including CN-Cu-X and that of the benzene ring are nearly perpendicular to each other (Fig. 5).

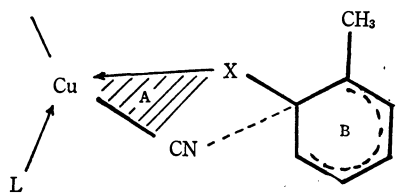

Fig. 5. The model of intervened complex Base-CuCN-Ar·X, L=Base, A⊥B.

From these discussions, it seems that the Rosenmund-von Braun reaction proceeds as follows:

$$\mathrm{CuCN} + \mathrm{L} \xrightarrow{\text{fast}} \underset{\mathrm{I}}{\mathrm{CN}\\ |\\ \mathrm{Cu\cdots L}} \quad (1)$$

$$\mathrm{Ar{-}X} + \mathrm{I} \rightleftarrows \underset{\mathrm{II}}{\mathrm{Ar\cdots CN}\\ |\quad |\\ \mathrm{X\cdots Cu\cdots L}} \quad (2)$$

$$\mathrm{II} \longrightarrow \mathrm{Ar{-}CN} + \underset{\mathrm{III}}{\mathrm{X{-}Cu\cdots L}} \quad (3)$$

$$\mathrm{III} \longrightarrow \mathrm{Cu{-}X} + \mathrm{L} \quad (4)$$

L: Ligand (Base) X: Halogen

When I which had been prepared beforehand was used in the reaction (2), no difference was observed in the kinetic study. Thus, it is conceivable that the rate-determining step is not in the reaction (1) but in the halogen-CN exchange stage in the intervening complex II, the reaction (3). The order of the reactivity, I>Br>Cl≫F, supports this assumption. When an excess of the CuCN over the base is used, a ligand is liberated from III (4); it coordinates to the unreacted CuCN to form I again (1).*6 That is, the base may act as a catalyst.

*5 No steric hindrance of the aryl halides in the reaction with CuCN is observed either as is roughly shown in Table 1.

Experimental

Materials. The cuprous chloride and cupric chloride, obtained from the Wako Pure Chemical Industry Co., Ltd., Tokyo, were used without further treatment. The cyanide was prepared from copper sulfate and sodium cyanide.[6] Commercial pyridine, picoline, 2, 6-lutidine, and nitrobenzene were diried and distilled under reduced pressure. All of the liquid reagents used in the studies was checked by gas chromatographic analysis.

Reaction Procedure in Table 2 (Exp. 4). In a 100-m*l*, three-necked, round flask fitted with a sealed stirrer, a thermometer, and a reflux condenser, were placed 4.0 m*l* of bromobenzene, 3.0 g of cuprous cyanide, 5.0 m*l* of pyridine (in the case of Exp. 4), and 20 m*l* of nitrobenzene. The contents were then heated to 180°C in 15 min while being stirred well; then the contents were maintained for 6 hr at 180°C. After the required time, the contents were cooled to room temperature, and a brownish complex of the CuBr-Base was precipitated from the solution. A part of the solution containing benzonitrile and bromobenzene was analyzed by gas chromatography; benzonitrile 82%; bromobenzene 18%. The other experiments in Table 2 were carried out using the same procedure.

Kinetic Measurements (Fig. 4). In a 100-m*l*, three-necked, round flask fitted with a sealed stirrer, a thermometer, and a reflux condenser, were placed 20.0 m*l* of nitrobenzene, 1.0 g of cuprous cyanide, and 1.0 m*l* of pyridine. The contents were then heated to 160°C on an oil bath. When the temperature became constant (160±0.5°C), 1.0 m*l* of bromobenzene was added to the mixture. A tiny quantity of the reaction mixture (nitrobenzene solution) was extracted every 20 min and analyzed by gas chromatography. From these measurements the reaction rate was calculated.

Gas Chromatography. Apparatus: Yanagimoto-GCG 220 Type. Yanagimoto Mfg. Co., Ltd., Kyoto, Japan. Column, 10% Cyanosilicone XF-1150 on Chromosorb 60—80 mesh; length, 2 m; temp., 160°C; flow rate, 35—40 m*l*/min; carrier gas, H_2. Relative retention time, ArBr : ArCN : $ArNO_2$=1 : 3 : 5.2. Column, 5% Carbowax 1500 on Chromosorb 60—80 mesh; length, 2 m; temp., 130°C; flow rate, 40 m*l*/min; carrier gas, H_2. Relative retention time, ArCl : ArBr : $ArNO_2$=1 : 1.4 : 5.7.

The authors wish to express their hearty thanks to Professor Kazuo Hata for his kind advice. Thanks are also due to Mr. Yoshiyuki Funakoshi and Miss Kimiko Horiuchi for their assistance in the first part of the experimental work.

*6 See Exps. 1—4, Table 2.

6) H. J. Barben, *J. Chem. Soc.*, **1943**, 79.

BULLETIN OF THE CHEMICAL SOCIETY OF JAPAN VOL. 41 424—429 (1968)

The Reaction of Tropolones with Phosphorus Oxychloride. The Rearrangement Reaction of 5-Arylazo-2-chlorotropones to 2-Aryl-4, 5-dichloroindazoles

Katsuo KIKUCHI, Masaki YAGI*1 and Kunio TAKADA*2

Department of Chemistry, Faculty of Liberal Arts and Science, Yamagata University, Koshirakawa-cho, Yamagata

(Received July 31, 1967)

The reaction of tropolone and phosphorus oxychloride gave 2-chlorotropone. Similarly, 5-cyano-, 5-nitro, and 5-chlorotropolones afforded the corresponding 2-chlorotropone derivatives in moderate yields. 3-Cyanotropolone gave 2-chloro-7-cyanotropone, while 3-phenyltropolone afforded only 2-chloro-3-phenylbenzaldehyde. When 3-bromotropolone and 5-bromotropolone were treated similarly, 2, 7-dichloro- and 2, 5-dichlorotropones were obtained respectively, with a facile halogen exchange. The further treatment of 2, 5-dichlorotropone with phosphorus oxychloride afforded 2, 5-dichloro- and 3, 4-dichlorobenzaldehydes. The reaction of 5-*p*-tolylazo-, 5-phenylazo-, and 5-*p*-nitrophenylazotropolones with phosphorus oxychloride gave the corresponding 5-arylazo-2-chlorotropones, which, on further treatment with an excess of the reagent, gave 2-aryl-4, 5-dichloroindazoles.

2-Chlorotropone derivatives, important intermediates for the preparation of many kinds of 2- (or 7-) substituted tropones, azulenes and seven-membered aromatic compounds fused with several kinds of heterocyclic rings, have generally been prepared (a) by the copper sulfate-catalyzed decomposition of 2-hydrazinotropones with concentrated hydrochloric acid,[1-3] and (b) by the reaction of thionyl chloride on appropriate tropolones.[2,4-6]

We have found that the reaction of tropolone derivatives with phosphorus oxychloride also gave 2-chlorotropones with moderate yields, and that the 5-arylazo-2-chlorotropones thus obtained were, by an excess of the reagent, rearranged to 2-aryl-4, 5-dichloroindazoles; these results will be described in this paper.

When tropolone in dimethylformamide was treated with phosphorus oxychloride at room temperature for about 4 hr, 2-chlorotropone (Ia) was obtained in about a 40% yield. When the reaction was carried out in benzene or chloroform under reflux, however, no detectable amount of Ia was isolated; only a colorless crystalline powder (II) was obtained. The compound (II), because of its sparing solubility in usual organic solvents, could not be purified. II was decomposed gradually with hot water to regenerate tropolone, and reacted with alcoholic methylamine to give 2-methylaminotropone and tropolone.

A similar reaction carried out with 5-cyanotropolone and 5-nitrotropolone gave 2-chloro-5-cyanotropone (Ib) in a 73% yield and 2-chloro-5-nitrotropone (Ic) in a 90% yield respectively. The reaction of 5-chlorotropolone with an equimolar amount of the reagent gave 2, 5-dichlorotropone (Id) in about a 50% yield. However, when an excess of the reagent was applied to 5-chlorotropolone or to Id, 2, 5-dichlorobenzaldehyde (III) and 3, 4-dichlorobenzaldehyde (IV) were isolated. Such a type of rearrangement had already been observed in the reaction of tropolone with thionyl chloride to give 2-chlorobenzaldehyde.[4] In the present reaction, these dichlorobenzaldehydes are thought to be formed through a tetrachloro compound. The attack of water on the intermediate, followed by rearrangement, will give the final products depicted below, though such an intermediate has not actually been isolated.

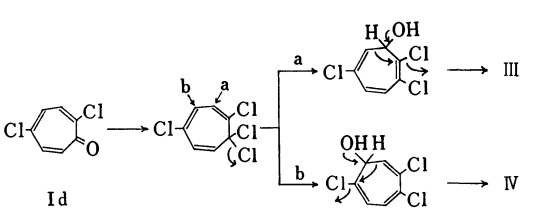

*1 Present address: Adeka Argus Chemical Co., Ltd., Higashiogu, Arakawa-ku, Tokyo.

*2 Present address: The Research Institute for Iron, Steel and Other Metals, Tohoku University, Katahira-cho, Sendai.

1) S. Seto, *Sci. Repts. Tohoku Univ., Ser. I*, **37**, 275, 286, 297 (1953).

2) T. Sato, *Nippon Kagaku Zasshi (J. Chem. Soc. Japan, Pure Chem. Sect.)*, **80**, 1167, 1171, 1342 (1959).

3) T. Nozoe, Y. Kitahara, K. Takase and I. Murata, This Bulletin, **37**, 1292 (1964).

4) B. J. Abadir, J. W. Cook, J. D. Loudon and D. K. V. Steel, *J. Chem. Soc.*, **1952**, 2350.

5) W. von E. Doering and L. H. Knox, *J. Am. Chem. Soc.*, **74**, 5683 (1952).

6) T. Mukai, This Bulletin, **32**, 272 (1959).

The reaction of 5-bromotropolone and phosphorus oxychloride also afforded Id, with a facile halogen exchange.

The reaction of 3-substituted tropolones with phosphorus oxychloride should give two isomeric products, *i. e.*, 2-chloro-3-substituted and 2-chloro-7-substituted tropones; actually, however, only one of the two was isolated. Thus, the reaction of 3-cyanotropolone and 3-bromotropolone with phosphorus oxychloride gave 2-chloro-7-cyanotropone (Ie)[3] in a 70% yield and 2, 7-dichlorotropone (If) in a 45% yield respectively. Contrary to the above two cases, the reaction of 3-phenyltropolone afforded colorless crystals (V), $C_{13}H_9OCl$, instead of the expected 2-chloro-phenyltropone, even when some of the reactant was recovered unchanged. The infrared spectrum of V exhibited an absorption band at 1683 cm^{-1}, and the oxidation of V with potassium permanganate afforded a monocarboxylic acid (VI), $C_{13}H_9O_2Cl$. The treatment of the acid with concentrated sulfuric acid did not afford a fluorenone derivative, suggesting that the carboxyl group is not adjacent to the phenyl group. V is thought to be 2-chloro-3-phenylbenzaldehyde formed in a manner similar to that in the formation of III from 5-chlorotropolone. In accordance with the postulated formula, the NMR spectrum[7] of V exhibited, besides the signals characteristic of an aldehyde proton (−0.40, singlet) and aromatic protons (2.35—2.8, multiplet, phenyl, C_4 and C_5 protons), an additional low-field quartet at 2.06 τ (J=6.7 and 2.8 cps, intensity one proton). The chemical shift and splitting indicate that this signal is generated by the C_6 proton coupled with the C_5 and C_4 protons. The ultraviolet spectrum of V in alcohol [λ_{max}, 241 and 307 mμ (log ε, 4.29 and 3.18)] is similar to that of 3-phenylbenzaldehyde,[8] and quite different from that of 4-phenylbenzaldehyde.[9]

We then turned our attention to the preparation of 5-arylazo-2-chlorotropones. When 5-*p*-tolylazotropolone in dimethylformamide was treated with an equimolar quantity of phosphorus oxychloride under ice-cooling, brownish-orange crystals (VIIa) and colorless crystals (VIIIa) were obtained in 78 and 6% yields respectively. VIIIa was also obtained in about a 50% yield when VIIa was treated with an excess of the reagent. The reaction of 5-*p*-tolylazotropolone with thionyl chloride in benzene also gave VIIa. The ultraviolet spectrum of VIIa exhibits absorption maxima at 300—315 and 385 mμ (log ε, 3.96 and 4.44), and the infrared spectrum shows a carbonyl band in the region below 1650 cm^{-1}, a spectral feature agreeing with that of troponoid compounds.[10] These data and the analytical values show that VIIa is 2-chloro-5-*p*-tolylazotropone.

The compound (VIIIa), $C_{14}H_{10}N_2Cl_2$, is stable toward dilute alkali and acids, and is not oxidized by potassium permanganate in acetone at room temperature. The ultraviolet spectrum of VIIIa is shown in Fig. 1. The NMR spectrum of VIIIa exhibits signals at 7.62 (3H, singlet), 2.15—2.85 (6H, multiplet) and 1.66 τ (1H, singlet), suggesting that VIIIa is an aromatic compound with a pyrazole or a similar heteroaromatic ring system.

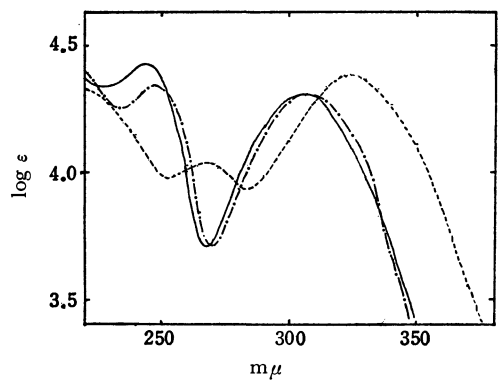

Fig. 1. Ultraviolet spectra of VIIIa (—·—·—) VIIIb (——) and VIIIc (----) in ethanol.

VIIIa was oxidized with chromic acid to give an acid (IX), $C_{14}H_{10}O_2N_2Cl_2$, and with nitric acid to give the same acid (IX), plus two mononitro compounds (XI and XII). The ultraviolet spectrum of the methyl ester (X) of IX exhibits maxima at 342 and 430—440 mμ, resembling those of azobenzene derivatives. The catalytic reduction of IX gave *p*-toluidine and 2-amino-5, 6-dichlorobenzoic acid (XIII), which decomposed above its melting point (175°C) to give 3, 4-dichloroaniline (XIV). The acid (IX) is, therefore, 3, 4-dichloro-4'-methylazobenzene-2-carboxylic acid. It is known that 2-phenylindazole, on oxidation with chromic acid, gives azobenzene-2-carboxylic acid;[11] the results obtained above can be explained on the assumption that VIIIa is 4, 5-dichloro-2-*p*-tolylindazole. This structure was confirmed by the following results. The catalytic reduction of VIIIa gave 2-*p*-tolyl-4, 5, 6, 7-tetrahydroindazole (XV). The NMR spectrum of XV exhibits signals at 8.25 (C_5- and C_6-methylene protons, multiplet), 7.68 (methyl protons, singlet), 7.40 (C_4- and C_7-methylene protons, multiplet) and 2.5-3.0 τ

7) The NMR spectra were measured in deuteriochloroform, using tetramethylsilane as an internal standard, on a Varian A-60 spectrometer.
8) J. J. Godfroid, *Compt. rend.*, **257**, 2296 (1963).
9) H. Suzuki, This Bulletin, **33**, 613 (1960).
10) For the spectra of troponoid compounds, see M. Tsuboi, This Bulletin, **25**, 369 (1952); S. Kinumaki, K. Aida and Y. Ikegami, *Sci. Repts, Res. Inst. Tohoku Univ.*, **A-8**, 263 (1956); E. Kloster-Jensen, N. Tarkoy, A. Eschenmoser and E. Heilbronner, *Helv. Chim. Acta*, **39**, 780 (1956).
11) J. D. Loudon, "Chemistry of Carbon Compounds, A Modern Comprehensive Treatise," Vol. IV, Part A, ed. by E. H. Rodd. Elsevier Publishing Co., Amsterdam (1957), p. 278.

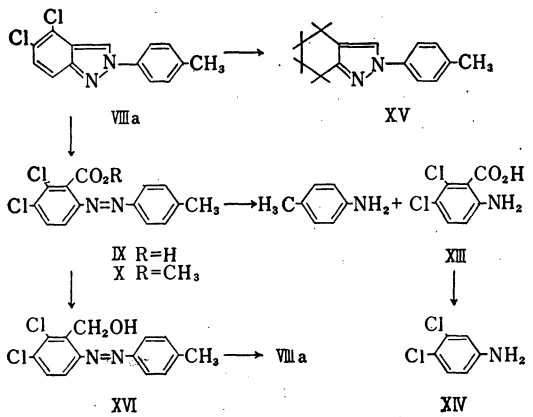

benzene-ring protons and C_3-proton, multiplet). The reduction of the ester (X) with lithium aluminum hydride gave a 2-hydroxymethylazobenzene derivative (XVI) and a 2-hydroxymethylhydrazobenzene derivative (XVII). The oxidation of XVII with bromine afforded XVI. The heating of XVI with 75% sulfuric acid afforded the original indazole (VIIIa), as expected.[11]

The bromination of VIIIa afforded 3-bromo-4, 5-dichloro-2-*p*-tolylindazole (XVIII); the position of the bromine atom was confirmed by the nitric acid oxidation aimed at giving IX. The position of the nitro group in XI and XII is not clear.

The reaction of 2-methoxy-5-*p*-tolylazotropone[12] and phosphorus oxychloride gave the same indazole (VIIIa) in about a 57% yield. The mechanism of the formation of VIIIa from VIIa is assumed to be as follows:

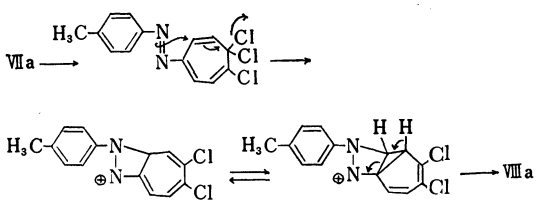

The reaction of 5-phenylazotropolone and phosphorus oxychloride gave 2-chloro-5-phenylazotropone (VIIb) and 4, 5-dichloro-2-phenylindazole (VIIIb). Similarly, 5-*p*-nitrophenylazotropolone afforded 2-chloro-5-*p*-nitrophenylazotropone (VIIc) and 4, 5-dichloro-2-*p*-nitrophenylindazole (VIIIc). The ultraviolet spectra of VIIIb and VIIIc are shown in Fig. 1.

It is known that 5-arylazotropolone with isopropyl, ethyl and acetamidoethyl groups on the 4-position undergo cyclization to give a cyclohepta[*c*]pyrazole-5, 6-dione derivative (A)[13] and a 5-hydroxycyclohepta[*c*]pyrazole-6-one derivative (B),[14,15] and that 7-bromo-3, 4-benzotropolone, upon an azo-coupling reaction, directly affords a benz[*g*]indazole-4, 5-dione derivative (C).[16] The formation of VIIIa-VIIIc is another interesting example of the rearrangement reaction of 5-arylazotropone derivatives.

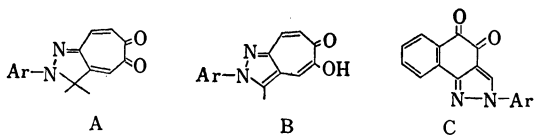

Experimental

The Reaction of Tropolone and Phosphorus Oxychloride. a) To a solution of 2.0 g of tropolone in 8 m*l* of dimethylformamide, 3.0 g of phosphorus oxychloride was added; the mixture was then left to stand for about 4 hr. The mixture was diluted with water and extracted with chloroform. The chloroform solution was washed with water, and the solvent was evaporated under reduced pressure. The crystalline residue was recrystallized from cyclohexane to give 920 mg of colorless crystals, mp 59—62°C, not depressed on admixture with an authentic sample of 2-chlorotropone (Ia).

b) To a solution of 3.00 g of tropolone in 20 m*l* of dry benzene, 4.50 g of phosphorus oxychloride was added, after which the mixture was refluxed on a water bath for 5 hr. The crystalline solid that separated was filtered and washed successively with benzene and ether to give 4.57 g of white powder (II). It is insoluble in usual organic solvent, such as chloroform, benzene, acetonitrile, and dimethylformamide, and has no distinct melting point. The filtrate from II afforded 35 mg of a dark oil which could not be crystallized.

The Reaction of II and Methylamine. A 1.00-g sample of the II obtained above was suspended in 3.0 m*l* of ethanol, and then 2.0 m*l* of ethanol saturated with methylamine was added under ice cooling and stirring. After 30 min, the solvent was evaporated under reduced pressure. A dilute sodium carbonate solution was then added to the residue, and the mixture was extracted with chloroform. The chloroform solution was washed with water, and the solvent was evaporated to give reddish-orange crystals, mp 65—75°C. Chromatographic separation on an alumina column, followed by recrystallization from cyclohexane, afforded 310 mg of yellow crystals, mp 75—79°C, not depressed on admixture with an authentic sample of 2-methylaminotropone.[17] The alkaline solution was acidified with dilute hydrochloric acid and extracted with chloroform. The chloroform solution afforded 220 mg of tropolone, mp 46—50°C.

12) T. Nozoe, K. Takase and H. Matsumura, "Dai Yuki Kagaku," Vol. 13, Asakura Shoten, Tokyo (1960), p. 287.
13) T. Nozoe, T. Ikemi and T. Ozeki, *Proc. Japan Acad.*, **31**, 455 (1955), and the references cited therein.
14) T. Nozoe, K. Takase and K. Umino, This Bulletin, **38**, 358 (1965).
15) T. Nozoe, K. Takase and K. Suzuki, *ibid.*, **38**, 362 (1965).
16) S. Ebine, *ibid.*, **38**, 2029 (1965).
17) T. Nozoe, S. Seto, H. Takeda, S. Morosawa and K. Matsumoto, *Sci. Repts. Tohoku Univ., Ser. I*, **36**, 126 (1952).

The Reaction of II and Water. A 1.00-g sample of II was suspended in 20 m*l* of water and then left at room temperature for about 5 hr, but no appreciable change was observed. When the mixture was heated at about 70°C, it gradually dissolved to give a pale brown solution. After it had stood overnight, the solution was extracted with chloroform to give 400 mg of tropolone.

2-Chloro-5-cyanotropone (Ib). To a solution of 100 mg of 5-cyanotropolone in 1.0 m*l* of dimethylformamide, 200 mg of phosphorus oxychloride was added under ice cooling. After it had stood for 1.5 hr, the mixture was poured into 10 m*l* of water. The crystals that separated were collected and washed with water to give 82 mg (73%) of pale brown crystals, mp 140—144°C, not depressed on admixture with an authentic sample of Ib.[18]

2-Chloro-5-nitrotropone (Ic). a) The similar treatment of a mixture of 200 mg of 5-nitrotropolone and 300 mg of phosphorus oxychloride in 1.0 m*l* of dimethylformamide gave 202 mg of Ic as pale yellow needles, mp 135—140°C. Recrystallization from a mixture of benzene and cyclohexane raised the melting point to 138—140°C. IR (KBr): 1632, 1602 cm^{-1} (C=C and C=O).

Found: C, 45.60; H, 2.28; N, 7.65%. Calcd for $C_7H_4O_3NCl$; C, 45.31; H, 2.17; N, 7.55%.

b) A mixture of 300 mg of 5-nitrotropolone and 900 mg of thionyl chloride in 10 m*l* of dry benzene was refluxed for 6 hr and then left to stand overnight. The evaporation of the solvent and an excess of thionyl chloride under reduced pressure afforded 330 mg of yellowish-orange crystals, mp 120—134°C. Recrystallization from benzene gave 245 mg of Ic, mp 133—138°C, not depressed on admixture with the sample obtained above.

2, 5-Dichlorotropone (Id) and Its Rearranged Products. *a) The Reaction of 5-Chlorotropolone and Phosphorus Oxychloride.* A mixture of 400 mg of 5-chlorotropolone and 400 mg of phosphorus oxychloride in 3.0 m*l* of dimethylformamide was left to stand at room temperature for 2.5 hr, and then diluted with 50 m*l* of water to give 246 mg of crystals, mp 90—98°C. Recrystallization from ethanol afforded 2, 5-dichlorotropone (Id), mg 95—97°C, not depressed on admixture with an authentic sample of Id.[2]

b) The Reaction of 5-Bromotropolone and Phosphorus Oxychloride. The similar treatment of 500 mg of 5-bromotropolone and 400 mg of phosphorus oxychloride in 4.0 m*l* of dimethylformamide gave 280 mg of crystals, mp 60—75°C. Recrystallization from ethanol afforded 143 mg of crystals, mp 91—95°C. Further recrystallization afforded Id as colorless crystals, mp 95—97°C, not depressed on admixture with the sample obtained above.

c) The Reaction of 5-Chlorotropolone with an Excess of Phosphorus Oxychloride. A solution of 400 mg of 5-chlorotropolone and 1.00 g of phosphorus oxychloride in 2.0 m*l* of dimethylformamide was left to stand overnight. The subsequent dilution of the mixture with water separated a viscous oil which gradually solidified. It was collected, washed with water, dissolved in cyclohexane, and passed through a silica gel column. The fraction eluted with cyclohexane afforded 158 mg (35%) of pale yellow crystals, mp 54—56°C. Recrystallization from aqueous ethanol afforded 2, 5-dichlorobenzaldehyde (III) as colorless needles, mp 55—56°C (Found: C, 47.59; H, 2.72%), which were identified by converting them to 2, 5-dichlorobenzoic acid; mp and mixed mp 152—154°C.

The fraction eluted with a mixture of benzene and cyclohexane (1 : 1) gave 58 mg of pale yellow crystals, mp 39—42°C. Recrystallization from aqueous ethanol afforded colorless crystals, mp 43—44°C, not depressed on admixture with an authentic sample of 3, 4-dichlorobenzaldehyde (IV).

d) The Reaction of 2, 5-Dichlorotropone and Phosphorus Oxychloride. The similar treatment of 350 mg of Id with 930 mg of phosphorus oxychloride gave 153 mg of III and 50 mg of IV.

2-Chloro-7-cyanotropone (Ie). The similar treatment of a mixture of 600 mg of 3-cyanotropolone and 960 mg of phosphorus oxychloride in 3.0 m*l* of dimethylformamide gave 532 mg of colorless crystals, mp 155—160°C. Recrystallization from benzene afforded Ie as colorless crystals, mp 159—161°C, not depressed on admixture with an authentic sample.[3]

2, 7-Dichlorotropone (If) from 3-Bromotropolone. The similar treatment of 3-bromotropolone with phosphorus oxychloride afforded If, mp 128—130°C, in about a 40% yield; no other pure substance was isolated.

The Reaction of 3-Phenyltropolone and Phosphorus Oxychloride. A solution of 600 mg of 3-phenyltropolone and 1.40 g of phosphorus oxychloride in 6 m*l* of dimethylformamide was left to stand for 6 hr and then diluted with water. The crystals, which separated at first as an oil, were collected, dissolved in benzene, and washed with dilute sodium hydroxide and water. The alkaline solution, on acidification with hydrochloric acid, gave 145 mg of 3-phenyltropolone. The benzene solution, after the evaporation of the solvent, left a crystalline residue which was dissolved in a mixture of benzene and petroleum ether (1 : 1) and passed through a silica gel column. The fraction eluted with the same solvent mixture gave 320 mg of 2-chloro-3-phenylbenzaldehyde (V) as colorless prisms, mp 104—106°C. Recrystallization from ethanol raised the melting point to 106—107°C.

Found: C, 72.24; H, 4.16%. Calcd for $C_{13}H_9OCl$: C, 72.40; H, 4.21%.

When an equimolar quantity of the reagent was used (6 hr, at room temperature), only 3-phenyltropolone was isolated unchanged.

The oxidation of V with potassium permanganate in acetone afforded 2-chloro-3-phenylbenzoic acid (VI) as colorless plates, mp 156—158°C (after recrystallization from ethanol).

Found: C, 67.13; H, 3.63%. Calcd for $C_{13}H_9O_2Cl$: C, 67.11; H, 3.90%.

2-Chloro-5-*p*-tolylazotropone (VIIa) and 4, 5-Dichloro-2-*p*-tolylindazole (VIIIa). a) To a suspension of 240 mg of 5-*p*-tolylazotropolone in 1.2 m*l* of dimethylformamide, 170 mg of phosphorus oxychloride was added under ice cooling. After the crystals were dissolved, 2-chloro-5-*p*-tolylazotropone (VIIa) gradually separated out. After the mixture had stood for 4.5 hr, these crystals were collected and washed with water. Recrystallization from benzene gave 155 mg of VIIa as brownish-orange plates, mp 161—163°C.

18) K. Kikuchi, This Bulletin, **40**, 355 (1967).

The filtrate was diluted with water, and the yellow crystals that separated out were collected and washed with water. These crystals, combined with the residue obtained by the evaporation of the mother liquor from the above recrystallization, were dissolved in a mixture of benzene and cyclohexane (1 : 1) and chromatographed on 1.5 g of silica gel. The fraction eluted with the same solvent mixture gave 16 mg of 4, 5-dichloro-2-*p*-tolylindazole (VIIIa), mp 130—134°C. The fraction eluted with benzene gave 48 mg of VIIa, mp 160—162°C.

An analytical sample of VIIa was recrystallized from ethanol to give brownish-orange plates, mp 162—163°C. IR (KBr): 1624, 1593 cm^{-1} (C=C and C=O).

Found: C, 65.15; H, 4.38; N, 10.56%. Calcd for $C_{14}H_{11}ON_2Cl$: C, 65.00; H, 4.25; N, 10.87%.

An analytical sample of VIIIa was recrystallized from ethanol to give colorless microcrystals, mp 136.5—137°C.

Found: C, 60.43; H, 3.55; N, 10.34%. Calcd for $C_{14}H_{10}N_2Cl_2$: C, 60.67; H, 3.64; N, 10.11%.

VIIIa was stable toward alkali and acids, and did not give a picrate.

b) To a solution of 240 mg of 5-*p*-tolylazotropolone in 2.5 m*l* of benzene, 130 mg of thionyl chloride was added; the solution was then refluxed for 2.5 hr. The evaporation of the solvent and an excess of the reagent left a dark brown crystalline residue, which was dissolved in benzene and passed through an alumina column. The fractions eluted with benzene and a mixture of benzene and chloroform (1 : 1) afforded 105 mg of VIIa, mp 157—159°C, undepressed on admixture with the sample obtained above.

The Reaction of 5-Phenylazotropolone (and 5-*p*-Nitrophenylazotropolone) with Phosphorus Oxychloride. a) A solution of 300 mg of 5-phenylazotropolone and 240 mg of phosphorus oxychloride in 1.2 m*l* of dimethylformamide was treated in the manner described above to give 200 mg of 2-chloro-5-phenylazotropone (VIIb), mp 127—129°C, and 32 mg of 4, 5-dichloro-2-phenylindazole (VIIIb), mp 90—92°C.

The recrystallization of VIIb from a mixture of benzene and cyclohexane gave reddish-orange plates, mp 128—129°C. IR (KBr): 1630, 1597 cm^{-1} (C=C and C=O).

Found: C, 64.69; H, 3.86; N, 11.11%. Calcd for $C_{13}H_9ON_2Cl$: C, 63.77; H, 3.70; N, 11.49%.

The recrystallization of VIIIb from methanol gave colorless needles, mp 93—94°C.

Found: C, 59.23; H, 3.18; N, 10.48%. Calcd for $C_{13}H_8N_2Cl_2$: C, 59.37; H, 3.06; N, 10.65%.

b) The similar treatment of 200 mg of 5-*p*-nitrophenylazotropolone and 120 mg of phosphorus oxychloride in 1.0 m*l* of dimethylformamide gave 118 mg of 2-chloro-5-*p*-nitrophenylazotropone (VIIc), mp 200—205°C (decomp.), and several milligrams of 4, 5-dichloro-2-*p*-nitrophenylindazole (VIIIc), mp 207—212°C.

The recrystallization of VIIc from dioxane afforded deep reddish-brown prisms, mp 205°C (decomp.). IR (KBr): 1630, 1598 cm^{-1} (C=C and C=O).

Found: C, 53.88; H, 2.87; N, 14.52%. Calcd for $C_{13}H_8O_3N_3Cl$: C, 53.90; H, 2.79; N, 14.51%.

The recrystallization of VIIIc from dioxane afforded yellow microcrystals, mp 212—213°C.

Found: C, 50.72; H, 2.91%. Calcd for $C_{13}H_7O_2N_3Cl_2$: C, 50.67; H, 2.29%.

The Formation of VIIIa from VIIa or 2-Methoxy-5-*p*-tolylazotropone. a) To a solution of 1.22 g of VIIa in 10 m*l* of dimethylformamide, 1.10 g of phosphorus oxychloride was added, after which the mixture was allowed to stand at room temperature overnight. The solution was then diluted with water, and the crystals were collected. The chromatographic separation of these crystals on an alumina column, followed by recrystallization from a mixture of benzene and cyclohexane, gave 615 mg of VIIIa, mp 135—137°C.

b) The addition of 300 mg of phosphorus oxychloride to a suspension of 200 mg of 2-methoxy-5-*p*-tolylazotropone in 3.0 m*l* of dimethylformamide gave a clear, deep red solution. After standing for 4 hr, the mixture was treated similarly to give 125 mg of VIIIa, mp 134—136°C.

The Formation of VIIIb (and VIIIc) from VIIb (and VIIc). a) The similar treatment of 1.00 g of VIIb gave pale brown crystals, mp 85—105°C. Distillation under reduced pressure (2 mmHg; bath temperature 100—125°C), followed by recrystallization from methanol, afforded 250 mg of VIIIb, mp 92—95°C.

b) The similar treatment of 200 mg of VIIc gave 90 mg of VIIIc as pale yellow crystals, mp 207—209°C.

Oxidation of 4, 5-Dichloro-2-*p*-tolylindazole (VIIIa). *a) Chromic Acid Oxidation.* To a solution of 133 mg of chromic anhydride in 0.2 m*l* of water and 2.0 m*l* of acetic acid, 140 mg of VIIIa was added; the mixture was then heated on a water bath for 4 hr. The mixture was diluted with water, and the crystals that separated out were collected and washed with water to give 110 mg of brownish-orange crystals, mp 210—225°C (decomp.). The separation of the acidic part with a dilute sodium hydroxide solution gave 44 mg of 3, 4-dichloro-4'-methylazobenzene-2-carboxylic acid (IX), mp 229—233°C (decomp.). An analytical sample was recrystallized from acetic acid to give reddish-orange prisms, mp 236—238°C (decomp.).

Found: C, 54.10; H, 3.03; N, 9.21%. Calcd for $C_{14}H_{10}O_2N_2Cl_2$: C, 54.39; H, 3.26; N, 9.06%.

Methyl Ester (X). Obtained by the addition of ethereal diazomethane to IX. Recrystallization from methanol gave X as orange plates, mp 95—96°C.

Found: C, 55.63; H, 3.80; N, 8.45%. Calcd for $C_{15}H_{12}O_2N_2Cl_2$: C, 55.74; H, 3.74; N, 8.67%.

b) Nitric Acid Oxidation. To a solution of 300 mg of VIIIa in a mixture of 3.0 m*l* of acetic acid and 0.3 m*l* of acetic anhydride, 300 mg of nitric acid (sp. gr., 1.50) was added; the mixture was then warmed at 85°C for 1 hr. The crystals that separated out were collected and washed with water to give 100 mg of IX, mp 228—235°C (decomp.). The filtrate was diluted with water, and extracted with chloroform, and the chloroform solution was treated with a dilute sodium hydroxide solution. The alkaline solution was acidified to give 60 mg of the second crop of IX, mp 232—236°C (decomp.).

The chloroform solution was washed with water, and dried, and the solvent was evaporated to give yellow crystals. These crystals were dissolved in a mixture of benzene and cyclohexane (1 : 1) and chromatographed on 1.5 g of silica gel. The first fraction, eluted with the same solvent mixture, gave 30 mg of 4, 5-dichloro-

x-nitro-2-*p*-tolylindazole (XI), mp 168—172°C. The third and fourth fractions, eluted with the same solvent mixture and with benzene, gave 27 mg of 4, 5-dichloro-*x'*-nitro-2-*p*-tolylindazole (XII), mp 189—192°C.

The recrystallization of XI from acetic acid gave fine yellow needles, mp 173—174°C.

Found: C, 52.36; H, 2.92; N, 12.72%. Calcd for $C_{14}H_9O_2N_3Cl_2$: C, 52.19; H, 2.82; N, 13.04%.

The recrystallization of XII from acetic acid gave yellow needles, mp 193—194°C.

Found: C, 52.19; H, 3.06; N, 12.31%. Calcd for $C_{14}H_9O_2N_3Cl_2$: C, 52.19; H, 2.82; N, 13.04%.

Catalytic Reduction of the Acid (IX). A 300 mg sample of IX in 60 m*l* of ethanol was catalytically hydrogenated in the presence of Adam's catalyst. The uptake of hydrogen was about 80 m*l* at an ordinary pressure and temperature. The removal of the solvent under reduced pressure afforded a brown oil. The benzene solution of this oil was shaken with a dilute sodium hydroxide solution, and the alkaline solution was acidified with acetic acid. The extraction of the solution with ether and the evaporation of the solvent gave 95 mg of colorless crystals, mp 160—168°C (decomp.). Several recrystallizations from aqueous ethanol afforded 2-amino-5, 6-dichlorobenzoic acid (XIII) as colorless needles, mp 173—175°C (decomp.) (Found: C, 41.08; H, 2.53; N, 6.75%).

The acid (XIII) was heated above its melting point for 5 min, and the product was recrystallized from cyclohexane to give colorless crystals, mp 69—71°C, not depressed on admixture with an authentic sample of 3, 4-dichloroaniline (XIV).

The benzene solution was washed with water, and the solvent was evaporated to give a dark red oil. Acetylation of this oil with acetic anhydride afforded 25 mg of acet-*p*-toluidide, mp 143—145°C.

Catalytic Reduction of 4, 5-Dichloro-2-*p*-tolylindazole (VIIIa). A solution of 400 mg of VIIIa and 250 mg of sodium acetate in 50 m*l* of ethanol was catalytically hydrogenated in the presence of 100 mg of Adam's catalyst. The removal of the catalyst and the evaporation of the solvent gave colorless crystals. Recrystallization from petroleum ether gave 125 mg of colorless crystals, mp 65—70°C. Purification through its picrate, followed by the recrystallization of the regenerated product from aqueous ethanol, gave 2-*p*-tolyl-4, 5, 6, 7-tetrahydroindazole (XV) as colorless prisms, mp 71—72.5°C.

Found: C, 79.64; H, 8.03; N, 13.00%. Calcd for $C_{14}H_{16}N_2$: C, 79.21; H, 7.60; N, 13.20%.

Reduction of the Ester (X) with Lithium Aluminum Hydride. To a solution of 380 mg of X in 5 m*l* of absolute ether, a solution of 45 mg of lithium aluminum hydride in 3 m*l* of absolute ether was added; the solution was then refluxed for 3.5 hr. The excess of the reagent was decomposed with water, the precipitate was filtered off, and the filtrate was washed with water. The solvent was removed, and the residue was dissolved in a mixture of benzene and cyclohexane (1 : 1) and passed through an alumina column (5 g). A fraction eluted with the same solvent mixture gave 130 mg of the unchanged ester (X), while a fraction eluted with a mixture of benzene and chloroform (1 : 1) gave 52 mg of reddish-orange crystals, mp 100—107°C. Recrystallization from ethanol afforded 3, 4-dichloro-2-hydroxymethyl-4'-methylazobenzene (XVI) as organge needles, mp 103—105°C (sintered at about 100°C).

Found: C, 56.94; H, 3.96; N, 9.24%. Calcd for $C_{14}H_{12}ON_2Cl_2$: C, 56.96; H, 4.10; N, 9.49%.

The fraction eluted with a mixture of chloroform and methanol gave 15 mg of pale brown crystals, mp 145—150°C. Recrystallization from benzene afforded 3, 4-dichloro-2-hydroxymethyl-4'-methylhydrazobenzene (XVII) as colorless crystals, mp 159—160°C.

Found: C, 56.78; H, 4.63; N, 9.12%. Calcd for $C_{14}H_{14}ON_2Cl_2$: C, 56.58; H, 4.75; N, 9.43%.

When about two molecular equivalents of lithium aluminum hydride were applied, XVII was isolated in about a 75% yield.

The Formation of XVI from XVII. To a solution of 240 mg of XVII in 6.0 m*l* of ethanol, a solution of 200 mg of bromine in 1.0 m*l* of ethanol was added. After the mixture had then stood for 30 min, the solvent was evaporated under reduced pressure and the residue was diluted with water. The crystals thereby obtained were dissolved in benzene and passed through an alumina column. The fraction eluted with a mixture of benzene and chloroform gave orange crystals, mp 92—105°C; yield, 130 mg. Recrystallization from ethanol gave XVI as orange needles, mp 95—105°C.

The Formation of VIIIa from XVI. A 30 mg sample of XVI in 0.4 m*l* of 75% sulfuric acid was heated at 90°C for 20 hr; the crystals thereby separated were then filtered and washed several times with water to give 15 mg of pale brown crystals, mp 134—136°C. These crystals showed no depression of the melting point on admixture with a sample of VIIIa, and the infrared spectrum was also identical with that of VIIIa.

Bromination of VIIIa. To a solution of 50 mg of VIIIa in 1.0 m*l* of acetic acid, 35 mg of bromine was added. After the mixture had been heated for about 15 min at 85°C, the crystals that separated out were filtered and washed with water to give 52 mg of crystals, mp 183—184.5°C. Recrystallization from acetic acid gave 3-bromo-4, 5-dichloro-2-*p*-tolylindazole (XVIII) as fine, colorless needles, mp 184.5—185.5°C.

Found: C, 47.06; H, 2.28; N, 7.61%. Calcd for $C_{14}H_9N_2BrCl_2$: C, 47.22; H, 2.55; N, 7.87%.

Oxidation of XVIII with Nitric Acid. A 80 mg sample of XVIII was treated with 100 mg of nitric acid (sp. gr., 1.50), as in the case of the oxidation of VIIIa, to give 9 mg of orange crystals, mp 236—238°C (decomp.). The infrared spectrum of these crystals was identical with that of IX.

BULLETIN OF THE CHEMICAL SOCIETY OF JAPAN VOL. 41 430—432 (1968)

The Cyclization of Malononitrile and Ketones by Ammonium Acetate

Akio SAKURAI and Hiroshi MIDORIKAWA

The Institute of Physical and Chemical Research, Komagome, Bunkyo-ku, Tokyo

(Received August 4, 1967)

Hitherto various heterocyclic compounds have been synthesized by the reaction of ketones with ethyl cyanoacetate or ethyl acetoacetate in the presence of excessive ammonium acetate. On the basis of these facts, the reaction of malononitrile with ketones by ammonium acetate was carried out; aminopyridine derivatives, such as 2, 4-diamino-3, 5-dicyano-6-alkylpyridines (I) and 2-amino-3-cyano-4, 6-dialkylpyridines (II), were thus obtained.

Some active methylene compounds give heterocyclic compounds containing one nitrogen atom by condensation with ketones in the presence of ammonium acetate. Thus, ethyl cyanoacetate gives hydroxypyridines,[1] and ethyl acetoacetate gives hydroxyquinoline derivatives.[2]

The present paper will deal with the synthesis of aminopyridine derivatives by the condensation of malononitrile and various ketones (methyl ketones and α, β-unsaturated ketones) in the presence of ammonium acetate.

Condensations between aliphatic methyl ketones and malononitrile were carried out in a 1 : 2 molar ratio; 2, 4-diamino-3, 5-dicyano-6-alkylpyridines were thus obtained, with the elimination of one mole each of methane and water, as is indicated in the following scheme:

$$CH_3\text{-}CO\text{-}R + 2CH_2(CN)_2 \xrightarrow{CH_3CO_2NH_4}$$

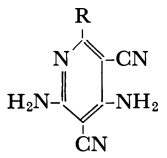

I

a $R=CH_3$ b $R=C_2H_5$ c $R=n\text{-}C_3H_7$
d $R=n\text{-}C_5H_{11}$ e $R=n\text{-}C_6H_{13}$ f $R=n\text{-}C_9H_{19}$
g $R=i\text{-}C_4H_9$

The structure of I was proved from the infrared spectra and NMR spectra, as is shown in Tables 2 and 3. Furthermore, Ic was also obtained by the condensation of 1-methylbutylidenemalononitrile with malononitrile in the presence of ammonium acetate. The two products were established as identical by the results of elemental analyses, their infrared spectra, and by the fact these a mixed-melting-point determination showed no depression.

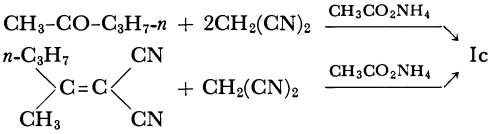

In the reaction with acetone, a compound (mp 340—342°C, $C_{14}H_{17}O_2N_5$) was obtained along with Ia. This compound was formed by the elimination of 1 mol each of methane, water, and hydrogen from 3 mol of acetone, 2 mol of malononitrile, and 1 mol of ammonia; it was also obtained by the use of mesityl oxide instead of acetone. Its structure could not be confirmed in this study.

α, β-Unsaturated ketones and malononitrile reacted in a 1 : 1 molar ratio to give 2-amino-3-cyano-4, 6-dialkylpyridines (II) through Michael reaction, with the elimination of 1 mol each of water and hydrogen.

$$R\text{-}CH{=}CH\text{-}CO\text{-}R' + CH_2(CN)_2 \xrightarrow{CH_3CO_2NH_4}$$

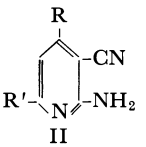

II

a $\begin{cases} R=C_6H_5 \\ R'=CH_3 \end{cases}$ b $\begin{cases} R=C_6H_5 \\ R'=C_2H_5 \end{cases}$
c $\begin{cases} R=C_6H_5 \\ R'=n\text{-}C_3H_7 \end{cases}$ d $\begin{cases} R=C_6H_5 \\ R'=C_6H_5 \end{cases}$

The hydrolysis of the cyano group of IId by heating with potassium hydroxide in alcohol gave an amide melting at 210—211°C; this amide was hydrolyzed to a carboxylic acid (III) by heating it with potassium hydroxide in glycerol. Compound III showed a mp of 233—234°C with decomposition. On the other hand, the reaction of ethyl cyanoacetate with benzalacetophenone in the presence of ammonium acetate[1] gave ethyl 2-amino-4, 6-diphenylnicotinate (IV). The carboxylic acid III was proved to be identical with the compound obtained by the hydrolysis of IV by the results of elemental analyses and by their infrared spectra.

1) A. Sakurai and H. Midorikawa, This Bulletin, **40**, 1680 (1967).
2) A. Sakurai and H. Midorikawa, to be published.

Table 1. Aminopyridine derivatives obtained by the reaction of malononitrile with ketones

Ketone	Product	Reaction time, hr	Mp °C	Crystn. solv.	Yield %	Formula	Calcd, %			Found, %		
							C	H	N	C	H	N
Acetone	Ia	3	336—338	Acetic acid	24	$C_8H_7N_5$	55.48	4.07	40.44	55.32	3.98	40.42
Methyl ethyl	Ib	5	304—306	Acetic acid	32	$C_9H_9N_5$	57.74	4.85	37.41	57.54	4.74	37.37
Methyl *n*-propyl	Ic	5	234—236	Acetic acid	34	$C_{10}H_{11}N_5$	59.68	5.51	34.81	59.44	5.29	34.82
Methyl *n*-amyl	Id	6	212—213	Acetic acid +methanol	21	$C_{12}H_{15}N_5$	62.86	6.60	30.55	62.92	6.17	29.96
Methyl *n*-hexyl	Ie	6	207—208	Methanol	25	$C_{13}H_{17}N_5$	64.17	7.04	28.79	64.47	6.72	28.46
Methyl *n*-nonyl	If	4	204—205	Alcohol +water	19	$C_{16}H_{23}N_5$	67.33	8.12	24.54	67.65	7.85	24.68
Methyl isobutyl	Ig	7	254—255	Methanol	4	$C_{11}H_{13}N_5$	61.37	6.09	32.54	61.56	5.61	32.36
Methyl styryl	IIa	5	235—236	Acetic acid +methanol	24	$C_{13}H_{11}N_3$	74.62	5.30	20.08	74.68	5.01	20.14
Ethyl styryl	IIb	3	197—199	Alcohol	34	$C_{14}H_{13}N_3$	75.31	5.87	18.82	74.94	5.56	19.24
Propyl styryl	IIc	7	150—151	Benzene	15	$C_{15}H_{15}N_3$	75.92	6.37	17.71	75.54	6.02	17.94
Phenyl styryl	IId	7	186—187	Alcohol	33	$C_{18}H_{13}N_3$	79.68	4.83	15.49	79.79	4.63	15.50

Table 2. IR spectra of aminopyridine derivatives (KBr: cm^{-1})

Compound	ν NH_2	ν C≡N (conj)	δ NH_2	ν C=C (conj)
Ia	3480, 3365, 3250, 3130 3340	2220 2200	1665 s, 1635 s	1560 s, 1490m
Ib	3480, 3380, 3240, 3110 3330	2220	1665 s, 1645 s	1565 s, 1490m
Ic	3470, 3380, 3240, 3120 3340	2210	1655 s, 1645 s	1560 s, 1490m
Id	3430, 3340, 3240, 3100	2225 2210	1665 s, 1640 s	1560 s, 1490m
Ie	3430, 3340, 3240, 3110 3320	2225 2205	1665 s, 1640 s	1565 s, 1490m
If	3420, 3320, 3230, 3090	2220 2200	1665 s, 1635 s	1560 s, 1490m
IIa	3400, 3320, 3160	2220	1650 s	1580 s, 1555 s, 1500m
IIb	3390, 3305, 3170	2210	1640 s	1580 s, 1555 s, 1500m
IIc	3400, 3305, 3130	2205	1650 s	1575 s, 1555 s, 1500m
IId	3470, 3310, 3180	2220	1640 s	1600w, 1590m, 1575 s 1550m, 1500m

s: strong m: medium w: weak

Table 3. NMR spectra of aminopyridine derivatives in CF_3CO_2H (ppm from TMS)

Compound	CH_3	CH_2	=CH	NH_2	C_6H_5
Ia	2.82 s			7.33 s, 7.50 s	
Ib	1.53 t	3.15 q		7.37 s, 7.55 s	
Ie	0.95 t	1.20—2.20m 3.10 t		7.35 s, 7.52 s	
IIa	2.80 s		7.15 s	7.25—7.55 br	7.72 s
IIb	1.50 t	3.05 q	7.12 s	7.25—7.50 br	7.70 s
IIc[a)]	1.00 t	1.50—2.10m 2.70 t	6.67 s	5.55 s	7.50 s

a) in $CDCl_3$ s: singlet t: triplet q: quartet m: multiplet br: broad

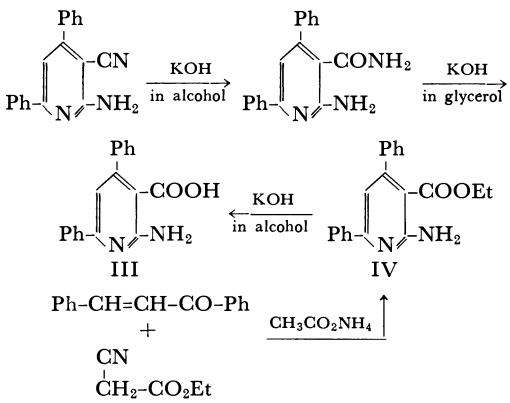

The structure of II was supported by the infrared and NMR spectra, shown in Tables 2 and 3. The reaction with mesityl oxide did not give the expected product, but it was the same compound as that obtained by the reaction with acetone.

The reactions of malononitrile with acetophenone and cyclohexanone were abnormal, giving 3-cyano-5, 6-dihydro-4, 6-diphenyl-2-pyridone and 4-cyano-1, 5, 6, 7, 8, 8a-hexahydroisocarbostyryl-1-spiro-1'-cyclohexane respectively. The identities of these compounds with the substances obtained by the reactions of ethyl cyanoacetate with acetophenone and cyclohexanone respectively were supported by their melting points, and infrared spectra, and by the results of elemental analyses.

Experimental

All melting points are uncorrected.

The infrared spectra were determined by means of pressed potassium bromide disks.

The NMR spectra were determined in trifluoroacetic acid at a frequency of 60 Mc, using tetramethylsilane as an internal standard. The chemical shifts are given as ppm downfield from tetramethylsilane.

The Reaction of Malononitrile with Aliphatic Methyl Ketones. A mixture of malononitrile (0.1 mol), ketone (0.05 mol), and ammonium acetate (0.08 mol) was refluxed for 3—7 hr. From the solution a pale yellow, crystalline matter was then separated. The results are summarized in Table 1.

The Reaction of Malononitrile with 1-Methylbutylidenemalononitrile. A mixture of malononitrile (4.6 g, 0.07 mol), 1-methylbutylidenemalononitrile (9.4 g, 0.07 mol), and ammonium acetate (3.9 g, 0.05 mol) in 5 m*l* of alcohol was refluxed for 1.5 hr. After cooling, a crystalline matter separated; this was filtered and recrystallized from glacial acetic acid to give colorless crystals, mp 232—233°C. This compound was proved to be identical with Ic by a mixed-melting-point determination and by a study of its infrared spectrum.

Found: C, 59.42; H, 5.04; N, 35.00%. Calcd for $C_{10}H_{11}N_5$: C, 59.68; H, 5.51; N, 34.81%.

The Reaction with α, β-Unsaturated Ketones. A mixture of malononitrile (0.1 mol), ketones (0.1 mol), and ammonium acetate (0.8 mol) was refluxed in alcohol (15 m*l*) or without a solvent for 2—5 hr. After cooling, a crystalline matter precipitated; this was then worked up as usual. The results are summarized in Table 1.

Hydrolysis of 2-Amino-3-cyano-4, 6-diphenylpyridine (IId). Compound IId (2 g) was heated with 20% alcoholic potassium hydroxide (30 m*l*) for 5 hr. After the addition of water (20 m*l*) to the reaction mixture, it was left to stand overnight. The pale yellow crystals which precipitated were then recrystallized from alcohol to give 2-amino-3-carbamoyl-4, 6-diphenyl-pyridine, mp 210—211°C.

Found: C, 74.42; H, 5.00; N, 14.34%. Calcd for $C_{18}H_{15}ON_3$: C, 74.72; H, 5.23; N, 14.53%.

To a solution of potasium hydroxide (4 g) in glycerol (20 m*l*), 2-amino-3-carbamoyl-4, 6-diphenylpyridine (1 g) was added, and the mixture was boiled at 200°C for 5 hr. After cooling, the solution was neutralized with dilute hydrochloric acid; a crystalline solid separated, which was then recrystallized from methanol to afford 2-amino-3-carboxy-4, 6-diphenylpyridine, mp 232—234°C with decomposition. The results of elemental analyses and its infrared spectrum proved this substance to be identical with the compound obtained by the hydrolysis of ethyl 2-amino-4, 6-diphenylnicotinate.[1]

Found: C, 74.06; H, 4.55; N, 9.29%. Calcd for $C_{18}H_{14}O_2N_2$: C, 74.48; H, 4.83; N, 9.66%.

The Reaction with Acetophenone. A mixture of malononitrile (3.3 g, 0.05 mol), acetophenone (6 g, 0.05 mol), and ammonium acetate (3.85 g, 0.05 mol) was heated for 7 hr. After standing overnight, the crystalline matter which was precipitated was recrystallized from alcohol to give 3-cyano-5, 6-dihydro-4, 6-diphenyl-6-methyl-2-pyridone, mp 213—214°C (lit.[3] mp 213—214°C). This compound was identified with the compound obtained by the condensation of ethyl cyanoacetate and acetophenone by ammonium acetate.[1]

Found: C, 79.11; H, 5.33; N, 9.85%. Calcd for $C_{19}H_{16}ON_2$: C, 79.14; H, 5.59; N, 9.72%.

The Reaction with Cyclohexanone. A mixture of malononitrile (4.6 g, 0.07 mol), cyclohexanone (6.9 g, 0.07 mol), and ammonium acetate (5.4 g, 0.07 mol) was heated for 7 hr. After cooling, a crystalline matter separated; this was recrystallized from glacial acetic acid to afford 4-cyano-1, 5, 6, 7, 8, 8a-hexahydroisocarbostyryl-1-spiro-1'-cyclohexane, mp 244—246°C. By ts infrared spectrum and the results of elemental analyses, this compound was identified with the substance obtained by the reaction of ethyl cyanoacetate with cyclohexanone.[1]

Found: C, 73.69; H, 8.05; N, 11.38%. Calcd for $C_{15}H_{20}ON_2$: C, 73.77; H, 8.20; N, 11.47%.

The authors wish to express their grateful thanks to Dr. Taro Hayashi and Dr. Tatsuo Takeshima for their kind advice. Thanks are also due to Dr. Haruo Homma and his staff for their microanalyses, to Mr. Jun Uzawa for his measurements of the NMR spectra, and to Mr. Teruo Kurihara for his measurements of the IR spectra.

3) S. M. McElvain and D. H. Clemens, *J. Am. Chem. Soc.*, **80**, 3915 (1958).

BULLETIN OF THE CHEMICAL SOCIETY OF JAPAN VOL. 41 433—437 (1968)

Synthesis of Natural Human Angiotensin I[1)]

Haruhiko AOYAGI,* Kikuo ARAKAWA** and Nobuo IZUMIYA*

* *Laboratory of Biochemistry, Faculty of Science, Kyushu University, Hakozaki, Fukuoka*

** *Research Institute of Angiocardiology, Faculty of Medicine, Kyushu University, Katakasu, Fukuoka*

(Received August 14, 1967)

The synthesis of a decapeptide, H-L-Asp-L-Arg-L-Val-L-Tyr-L-Ile-L-His-L-Pro-L-Phe-L-His-L-Leu-OH, which has an amino acid sequence assumed by Arakawa *et al.* for natural human angiotensin I, has been performed. The chemical and biological properties of the synthetic product have shown to be in agreement with those of the natural material, thus the structure of human angiotensin I has been confirmed by the present synthesis.

Angiotensin was found in 1939 during experiment with animals as a causal substance responsible for the experimental renal hypertension in animals.[2)] Angiotensin I, decapeptides, have been isolated from horse[3)] and bovine[4)] materials; these peptides have been liberated from precursor molecule angiotensinogen contained in plasma protein by the proteolytic action of renin which derived from kidney. The decapeptides are then converted to angiotensin II, octapeptides, by the removal of a dipeptide, H-His-Leu-OH, from its carboxy terminal by the action of a specific enzyme, called converting enzyme,[5)] which exists abundantly in plasma. The resulting angiotensin II are the most potent pressor substances ever known. The species difference resides in the fifth position which is occupied by isoleucine in horse[6)] and valine in bovine.[7)]

The menchanism of liberation of angiotensin, thus clarified only in animals except human, has been a working hypothesis in the pathogenesis of human hypertension. The fact that it had never been isolated nor elucidated in chemical terms in human has been the weekest point of the hypothesis in understanding the pathogenetic role of angiotensin in human hypertension. However, Arakawa *et al.* recently isolated pure human angiotensin from an incubation mixture of human serum protein and renin.[8)] They reported that amino acid analysis of the natural peptide from human revealed the same composition as that known for horse angiotensin in which the structure has been established to be [Ile^5]-angiotensin I, *i. e.*, H-L-Asp-L-Arg-L-Val-L-Tyr-L-Ile-L-His-L-Pro-L-Phe-L-His-L-Leu-OH.[9)]

Therefore, the amino acid sequence of human angiotensin has been plausibly anticipated to be same as that for [Ile^5]-angiotensin I. Since [Ile^5]-angiotensin I decapeptide had never been synthesized before, the present authors attempted to prepare the decapeptide (XVIII) mentioned above and to compare the identity of XVIII with the human angiotensin.

The sequence of reactions employed for the synthesis of the decapeptide (XVIII) is shown in Fig. 1. To obtain the final protected decapeptide *p*-nitrobenzyl ester (XVII), we selected a route involving the coupling of a mixed anhydride derived from benzyloxycarbonyl-β-benzylaspartic acid with the nonapeptide ester (XVI) which was derived from the benzyloxycarbonyl-nonapeptide ester (XV) by the action of hydrogen bromide in acetic acid. Similarly, the protected nonapeptide ester (XV) was prepared by coupling a mixed anhydride of benzyloxycarbonyl-nitroarginine with the octapeptide ester (XIV) which was obtained from the benzyloxycarbonyl-octapeptide ester (XIII). The acyl-octapeptide ester (XIII) was prepared by coupling the benzyloxycarbonyl-tripeptide azide derived from the hydrazide (XII) with the pentapeptide ester (VIII) which had been prepared from the benzyloxycarbonyl-pentapeptide ester (VII). Similarly, the acylpentapeptide ester (VII) was obtained by coupling the acyl-tripeptide azide from the corresponding hydrazide (VI)

1) A part of this work has been briefly communicated: H. Aoyagi, K. Arakawa and N. Izumiya, *J. Am. Chem. Soc.*, **89**, 4239 (1967).

2) I. H. Page and O. M. Helmer, *Proc. Central Soc. Clin. Invest.*, **12**, 17 (1939); E. Braun-Menéndez, J. C. Fasciolo, L. F. Leloir and J. M. Muñoz, *Rev. Soc. Argent. Biol.*, **15**, 420 (1939).

3) L. T. Skeggs, Jr., W. H. Marsh, J. R. Kahn and N. P. Shumway, *J. Exptl. Med.*, **102**, 435 (1955).

4) W. S. Peart, *Biochem. J.*, **62**, 520 (1956).

5) L. T. Skeggs, Jr., J. R. Kahn and N. P. Shumway, *J. Exptl. Med.*, **103**, 295 (1956).

6) L. T. Skeggs, Jr., K. E. Lentz, N. P. Shumway and K. R. Woods, *ibid.*, **104**, 193 (1956).

7) D. F. Elliott and W. S. Peart, *Biochem. J.*, **65**, 246 (1957).

8) K. Arakawa, M. Nakatani and M. Nakamura, *Nature*, **214**, 278 (1967).

9) K. Arakawa, M. Nakatani, A. Minohara and M. Nakamura, *Biochem. J.*, in press (1967).

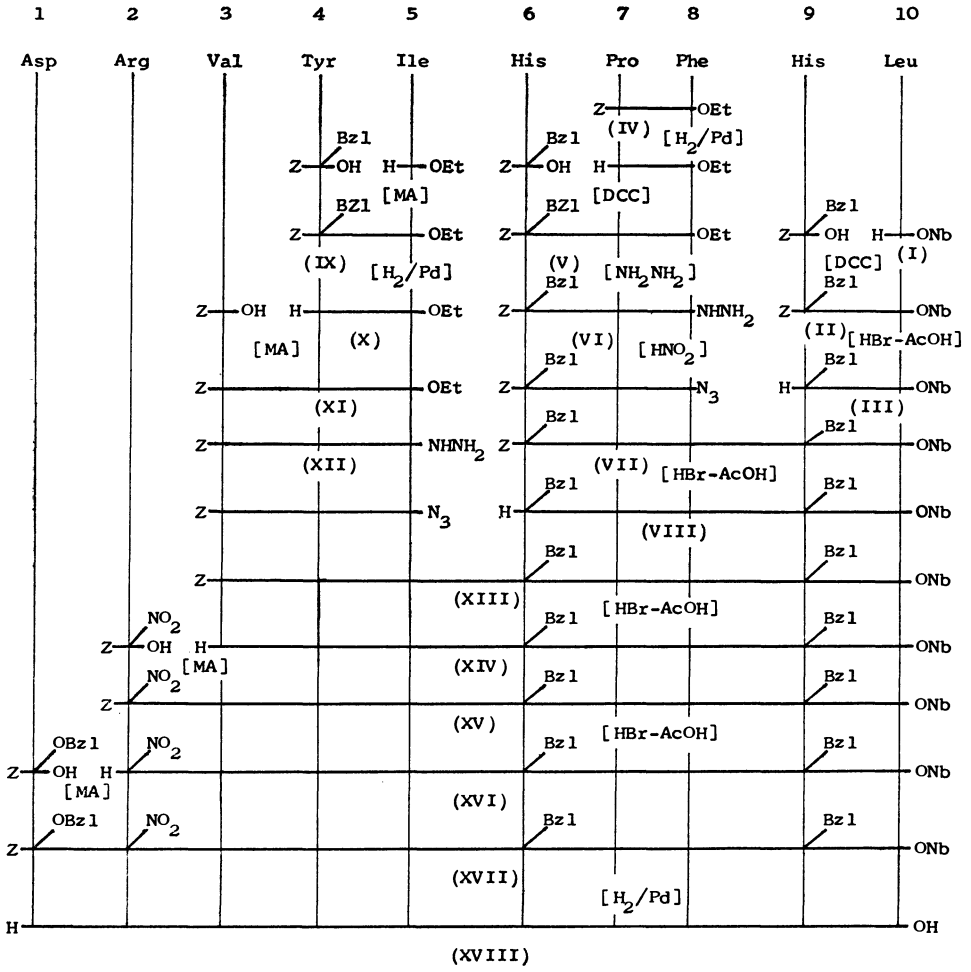

Fig. 1. Schematic diagram of synthesis of the decapeptide.
Z, benzyloxycarbonyl; Bzl, benzyl; $NHNH_2$, hydrazide; ONb, *p*-nitrobenzyl ester

with the dipeptide ester (III). The derivative (II, V or XI) of either the dipeptide or tripeptide was built up by stepwise elongation of the peptide chain from the carboxyl toward the amino end. Coupling of a benzyloxycarbonyl-amino acid with an amino component was mainly accomplished by carboxy activation through use of dicyclohexylcarbodiimide[10] or method of the mixed anhydride.[11]

The *p*-nitrobenzyl group was used for the protection of the carboxylic acid function of the *C*-terminal amino acid residue, and the benzyl group for the imidazoyl function of the histidine residue. It has been recognized that the action of hydrogen bromide in acetic acid removes the benzyloxycarbonyl group[12] without cleavage of the *p*-nitrobenzyl ester bond,[13] the imidazoyl-benzyl[14] or the nitro group;[13] many intermediate peptide ester hydrobromides (*e.g.*, XVI) were obtained in this manner.

The protected decapeptide *p*-nitrobenzyl ester (XVII) was hydrogenated with palladium black in a solvent of methanol - acetic acid - water at room temperature. The proceeding of the hydrogenolysis was followed at various times with the assay of paper chromatographic technique and with the bioassay of the pressor activity, and the highest activity was observed after some 48 hr though small part of the imidazoyl-benzyl groups was still remained untouched. The crude material after the hydrogenation was purified by a set of the column chromatographies which have proved to be very effective in isolating natural human

10) J. C. Sheehan and G. P. Hess. *J. Am. Chem. Soc.*, **77**, 1067 (1955).
11) J. R. Vanghan, Jr., and R. L. Osato, *ibid.*, **74**, 676 (1952).
12) D. Ben-Ishai and A. Berger, *J. Org. Chem.*, **17**, 1564 (1952).
13) K. Arakawa and F. M. Bumpus, *J. Am. Chem. Soc.*, **83**, 728 (1961).
14) K. O. Kopple and D. E. Nitecki, *ibid.*, **84**, 4457 (1962).

angiotensin.[8,9] The active fractions from the column were finally lyophilized leaving a white powder (acetate of XVIII, presumably); the homogeneity and stereospecific purity of the powder were ascertained by many chromatographic assays, the amino acid analysis and the digestion with the proteolytic enzymes.

The synthetic decapeptide obtained as the powder was then compared with natural human angiotensin I. In addition to having the same R_f values in paper and thin-layer chromatographies and affording a single peak in cochromatography of Bio-Gel column with the natural preparation, the synthetic and natural preparations were indicated to have the same specific activity on the bioassay of the rat pressor activity test. These results show that the synthetic product is identical to natural product, and the structure of human angiotensin I anticipated by Arakawa *et al.*[9] has been decided by the present synthesis.

Experimental

All the melting points are uncorrected. The optical rotations were measured on a Yanagimoto Photometric Polarimeter, OR-20 type.

L-Leucine *p*-Nitrobenzyl Ester *p*-Toluenesulfonate (I·TsOH). A solution of L-leucine (5.24 g, 40 mmol), *p*-nitrobenzyl alcohol (7.36 g, 48 mmol) and toluenesulfonic acid monohydrate (8.36 g, 44 mmol) in benzene (500 m*l*) was stirred under heating, and the water liberated was removed as an azeotropic mixture. The reaction mixture was concentrated *in vacuo*, and the residual oil was solidified by adding ether. The product was recrystallized from 80% methanol. Yield, 11.65 g (67%); mp 202°C; $[\alpha]_D^{22}$ +10.2° (*c* 1, ethanol); R_f 0.78.[15]

Found: C, 54.42; H, 5.98; N, 6.41%. Calcd for $C_{20}H_{26}O_7N_2S$: C, 54.78; H, 5.98; N, 6.39%.

Z-His(*im*-Bzl)-Leu-ONb (II). Into a solution of benzyloxycarbonyl-(*im*)benzyl-L-histidine[16] (3.80 g, 10 mmol) and I (4.36 g, 10 mmol) in dimethylformamide (30 m*l*) there were added triethylamine (1.40 m*l*) and dicyclohexylcarbodiimide[10] (2.08 g) at 0°C. After it had been stirred overnight at room temperature, the mixture was evaporated *in vacuo* and the residue was diluted with ethyl acetate; then the dicyclohexylurea thus precipitated was filtered off. The filtrate was washed successively with 3% hydrochloric acid, 4% sodium bicarbonate and water, and dried over sodium sulfate. The filtered solution was evaporated *in vacuo*. The product was obtained as an oil. Yield, 5.56 g (89%); R_f 0.76.[15]

H-His(*im*-Bzl)-Leu-ONb Dihydrobromide (III·2HBr). To a solution of II (5.00 g, 8 mmol) in acetic acid (8 m*l*), 3 N dry hydrogen bromide - acetic acid (16 m*l*) was added. After it had been stood for one hour, the solution was evaporated to dryness *in vacuo*. The residue was triturated with ether and washed repeatedly with ether by decantation. The product was collected by filtration with the aid of ether. Yield, 4.97 g (95%); mp 122—124°C; $[\alpha]_D^{22}$ +13.2° (*c* 1, ethanol); R_f 0.76.[15]

Found: C, 45.97; H, 5.23; N, 10.43%. Calcd for $C_{26}H_{35}O_5N_5Br_2 \cdot H_2O$: C, 46.37; H, 5.24; N, 10.40%.

Z-Pro-Phe-OEt (IV). *a) DCC Method.* Into a solution of benzyloxycarbonyl-L-proline (2.49 g, 10 mmol) and L-phenylalanine ethyl ester hydrochloride (1.93 g, 10 mmol) in chloroform (30 m*l*) there were added triethylamine (1.40 m*l*) and dicyclohexylcarbodiimide (2.06 g) at 0°C. After it had been stood overnight at 0°C, the desired product was obtained by the procedure described in the case of II. The residue obtained was solidified by adding ether and petroleum ether. The product was recrystallized from ethyl acetate - ether - petroleum ether. Yield, 3.30 g (78%); mp 65—68°C; $[\alpha]_D^{22}$ −33.8° (*c* 1, ethanol); R_f 0.87.[15] This compound was obtained previously as an oily product.[17]

Found: C, 67.72; H, 6.64; N, 6.61%. Calcd for $C_{24}H_{28}O_5N_2$: C, 67.90; H, 6.65; N, 6.60%.

b) MA Method. To a mixed anhydride prepared at −5°C from benzyloxycarbonyl-L-proline (2.4 g), isobutyl chloroformate (1.31 m*l*) and triethylamine (1.40 m*l*) in tetrahydrofuran (20 m*l*), a chilled solution of L-phenylalanine ethyl ester hydrochloride (1.93 g) dissolved in a mixture of triethylamine (1.40 m*l*) and chloroform (20 m*l*) was added. The reaction mixture was then allowed to stand overnight and then evaporated *in vacuo*. The oily residue was treated as described in the case of II. Yield, 3.00 g (71%); mp 65—68°C; R_f 0.87.[15]

Z-His(*im*-Bzl)-Pro-Phe-OEt (V). This compound was prepared by the same procedure as has been described for the preparation of II. One and ninety hundredths grams (5 mmol) of benzyloxycarbonyl(*im*)-benzyl-L-histidine and H-Pro-Phe-OEt·HCl[17] (1.64 g, 5 mmol), which was prepared from IV, gave 2.44 g (75%) of V as an oily product; R_f 0.73.[15]

Z-His(*im*-Bzl)-Pro-Phe-NHNH$_2$ (VI). A solution of V (3.00 g, 4.6 mmol) and hydrazine hydrate (4.6 m*l*, 92 mmol) in methanol (10 m*l*) was allowed to stand at room temperature for 2 days. The solution was then evaporated *in vacuo*. The oily residue was dissolved in ethyl acetate, washed with water and the organic layer was dried over sodium sulfate and then evaporated *in vacuo*. The semi-solid residue weighed 2.50 g (85%); R_f 0.77.[15]

Z - His(*im* - Bzl) - Pro - Phe - His(*im* -Bzl)-Leu-ONb (VII). To a solution of VI (2.16 g, 3.4 mmol) dissolved in dimethylformamide (10 m*l*) cooled at 0°C, 3.8 N hydrogen chloride (1.80 m*l*, 6.8 mmol) in dioxane was added, followed by isoamyl nitrite (0.46 m*l*, 3.4 mmol).[18] After it had been allowed to stand for 6 min with occasional stirring, triethylamine (0.95 m*l*, 6.8 mmol) was added to the solution. To this, a chilled solution of III·2HBr (2.28 g, 3.4 mmol) dissolved in

15) The R_f value refers to the thin-layer chromatography with Merck silica gel G and to the *n*-butanol - acetic acid - pyridine - water (4 : 1 : 1 : 2, v/v) system. Compounds possessing a free amino group were detected by spraying them with ninhydrin, and those with a blocked amino group, by spraying them with 47% hydrobromic acid, and then with nihnhydrin.

16) B. G. Overell and V. Petrow, *J. Chem. Soc.*, **1955**, 232.

17) N. Izumiya and J. S. Fruton, *J. Biol. Chem.*, **218**, 59 (1956).

18) J. Honzl and J. Rudinger, *Collection Czech. Chem. Commun.*, **26**, 2333 (1961).

a mixture of triethylamine (1.14 ml, 8.2 mmol) and dimethylformamide (7 ml) was added. The solution was stirred for 2 days at 0°C and then evaporated *in vacuo*. The oily residue was dissolved in ethyl acetate, and the solution was washed successively with 3% hydrochloric acid, 4% sodium bicarbonate and water, dried over sodium sulfate, and then evaporated *in vacuo*. The residual oil weighed 1.72 g (46%); R_f 0.84.[15] All attempts to crystallize this oil failed.

H-His(*im*-Bzl)-Pro-Phe-His(*im*-Bzl)-Leu-ONb Trihydrobromide (VIII·3HBr). To a solution of VII (3.85 g, 3.5 mmol) in acetic acid (10 ml), 3 N hydrogen bromide-acetic acid (20 ml) was added. After it has been allowed to stand for 1 hr, the solution was evaporated to dryness *in vacuo*. The oily residue was then treated as has been described in connection with the preparation of III. Yield, 4.02 g (95%); R_f 0.76.[15]

Z-Tyr(*O*-Bzl)-Ile-OEt (IX). Nine and ten hundredths grams (20 mmol) of benzyloxycarbonyl-*O*-benzyl-L-tyrosine[19] was coupled with L-isoleucine ethyl ester *p*-toluenesulfonate[20] (6.62 g, 20 mmol) by the mixed anhydride method, following the procedure described for the preparation of IV. Recrystallization from ethyl acetate-petroleum ether gave 8.58 g (82%); mp 128°C; $[\alpha]_D^{25}$ +10.7° (*c* 1, acetic acid); R_f 0.97.[15]

Found: C, 70.43; H, 7.03; N, 5.18%. Calcd for $C_{32}H_{38}O_6N_2$: C, 70.31; H, 7.01; N, 5.13%.

H-Tyr-Ile-OEt Hydrochloride (X·HCl). Three and forty hundredths grams (6.5 mmol) of IX dissolved in 0.5 N methanolic hydrogen chloride (14.3 ml) was hydrogenated in the presence of palladium black. The filtrate from the catalyst was evaporated to dryness *in vacuo*. Yield of an oily product, 2.40 g (94%); R_f 0.77.[15]

Z-Val-Tyr-Ile-OEt (XI). This compound was prepared by the mixed anhydride method as has been described for the preparation of IV. Two and fifty-one hundredths grams (9 mmol) of benzyloxycarbonyl-L-valine and X·HCl (3.53 g, 9 mmol) gave 4.40 g of the crude product. It was recrystallized from methanol-ether. Yield, 4.00 g (80%); mp 191°C; $[\alpha]_D^{22}$ −20.2° (*c* 1, acetic acid); R_f 0.97.[15]

Found: C, 64.68; H, 7.30; N, 7.75%. Cacld for $C_{30}H_{41}O_7N_3$: C, 64.84; H, 7.44; N, 7.56%.

Z-Val-Tyr-Ile-NHNH$_2$ (XII). To a solution of XI (5.56 g, 10 mmol) in dimethylformamide (30 ml), hydrazine hydrate (10 ml) was added; the solution was allowed to stand for 2 days at 30°C. The reaction mixture was evaporated *in vacuo*. The hydrazide which precipitated upon the addition of water was filtered, washed with water and dried. The product was recrystallized from dimethylformamide-ethyl acetate. Yield, 5.35 g (97%); mp 279—280°C.

Found: C, 60.98; H, 7.26; N, 12.59%. Calcd for $C_{28}H_{39}O_6N_5\cdot\frac{1}{2}H_2O$: C, 61.07; H, 7.32; N, 12.71%.

Z-Val-Tyr-Ile-His(*im*-Bzl)-Pro-Phe-His(*im*-Bzl)-Leu-ONb (XIII). To a solution of XII (0.54 g, 1 mmol) dissolved in a mixture of acetic acid (160 ml) and water (10 ml), N hydrochloric acid (3 ml) was added, followed by N sodium nitrite (1.1 ml). After it had stood for 5 min at 0°C, the solution was diluted with cold water (200 ml). The azide which precipitated was collected by filtration, washed with 4% sodium bicarbonate and water, and then dried in a desiccator *in vacuo* at 0°C. The dried azide was added to a chilled solution of VIII·3HBr (1.176 g, 1 mmol) dissolved in a mixture of triethylamine (0.50 ml, 3.6 mmol) and dimethylformamide (12 ml); the solution was stirred for 3 days at 0°C, and then evaporated *in vacuo*, The residual oil was dissolved in ethyl acetate, and the solution was washed successively with 3% hydrochloric acid, 4% sodium bicarbonate and water. Oily residue was solidified by adding ether and pertroleum ether. The product was recrystallized from ethanol-ether-petroleum ether. Yield, 0.506 g (34%); mp 125—134°C; $[\alpha]_D^{18}$ −41.0° (*c* 0.38, acetic acid); R_f 0.78.[15]

Found: C, 65.06; H, 7.15; N, 12.05%. Calcd for $C_{81}H_{95}O_{14}N_{13}\cdot H_2O$: C, 65.17; H, 6.55; N, 12.20%.

H-Val-Tyr-Ile-His(*im*-Bzl)-Pro-Phe-His(*im*-Bzl)-Leu-ONb Trihydrobromide (XIV·3HBr). XIII (472 mg, 0.3 mmol) was treated with 3 N hydrogen bromide-acetic acid (3 ml) as has been described in connection with the preparation of III. Yield of an oily product, 494 mg (97%); R_f 0.60.[15]

Z-Arg(NO$_2$)-Val-Try-Ile-His(*im*-Bzl)-Pro-Phe-His(*im*-Bzl)-Leu-ONb (XV). To a mixed anhydride prepared from of benzyloxycarbonyl-nitro-L-arginine[21] (170 mg, 0.48 mmol), isobutyl chloroformate (0.062 ml, 0.48 mmol) and triethylamine (0.068 ml, 0.48 mmol) in tetrahydrofuran (2 ml), a chilled solution of XIV·3HBr (508 mg, 0.32 mmol) dissolved in a mixture of triethylamine (0.162 ml, 1.15 mmol) and dimethylformamide (2 ml) was added. The reaction mixture was then allowed to stand overnight. The precipitate which formed upon the addition of 3% hydrochloric acid to the solution was collected, washed with 3% hydrochloric acid, 4% sodium bicarbonate and water, and dried. It was recrystallized from ethanol-ether. Yield, 448 mg (78%); mp 135—142°C; $[\alpha]_D^{18}$ −32.5° (*c* 0.4, acetic acid); R_f 0.75.[15]

Found: C, 58.19; H, 6.57; N, 14.54%. Calcd for $C_{87}H_{106}O_{17}N_{18}\cdot 6H_2O$: C, 58.57; H, 6.67; 14.13%.

H-Arg(NO$_2$)-Val-Tyr-Ile-His(*im*-Bzl)-Pro-Phe-His(*im*-Bzl)-Leu-ONb Trihydrobromide (XVI·3HBr). XV (428 mg, 0.24 mmol) in 3 N hydrogen bromide-acetic acid (3 ml) was treated as has been described in connection with the preparation of III. Yield of a hygroscopic powder, 412 mg (96%); R_f 0.68.[15]

Z-Asp(OBzl)-Arg(NO$_2$)-Val-Tyr-Ile-His(*im*-Bzl)-Pro-Phe-His(*im*-Bzl)-Leu-ONb (XVII). This compound was prepared by the mixed anhydride method as has been described for the preparation of XV. One hundred and twenty two milligrams (0.35 mmol) of benzyloxycarbonyl-β-benzyl-L-aspartic acid[22] and XVI·3HBr (410 mg, 0.23 mmol) gave 362 mg (79%) of XVII; mp 138—144°C; $[\alpha]_D^{18}$ −30.0° (*c* 0.3, acetic acid); R_f 0.90.[15]

Found: C, 58.82; H, 6.34; N, 13.38%. Calcd for $C_{93}H_{117}O_{20}N_{19}\cdot 6H_2O$: C, 59.17; H, 6.54; N, 13.39%.

H-Asp-Arg-Val-Tyr-Ile-His-Pro-Phe-His-Leu-OH (XVIII). Two hundred milligrams (0.1 mmol) of

19) E. Wünsch, G. Fries and A. Zwick, *Chem. Ber.*, **91**, 5421 (1958).
20) T. Kato, S. Makisumi, M. Ohno and N. Izumiya, *Nippon Kagaku Zasshi (J. Chem. Soc. Japan, Pure Chem. Sect.)*, **83**, 1151 (1962).
21) M. Bergmann, L. Zervas and H. Rinke, *Z. Physiol. Chem.*, **224**, 40 (1934).
22) N. Izumiya, H. Uchio and T. Yamashita, *Nippon Kagaku Zassi (J. Chem. Soc. Japan, Pure Chem. Sect.)*, **78**, 420 (1958).

XVII dissolved in a mixture (30 ml) of methanol : acetic acid : water (60 : 20 : 15, v/v) was subjected to hydrogenolysis in the presence of palladium black with vigorous stirring for 48 hr.[23] After removal of the catalyst by filtration the solvent was removed *in vacuo*. Evaporation was repeated with the addition of dioxane. The crude residue, 130 mg, was collected with the aid of a mixture of dioxane and ether. The paper chromatography of the residue indicated the presence of a major spot, R_f 0.53,[24] positive with ninhydrin, Sakaguchi and Pauly reaction, besides several weak spots positive with ninhydrin. A material in the major spot revealed strong pressor activity when it was extracted with dilute acetic acid. The crude residue (120 mg) was divided to six portions, and each portion was purified by subsequent column chromatography using carboxymethyl cellulose (2.5×50 cm; solvent, ammonium acetate with a gradient from 0.05 to 0.4 M), DEAE-Sephadex A-25 (1.5×50 cm; solvent, pyridine-collidine-acetate buffer with a gradient from pH 8.1 to 7.0), and Bio-Gel P-2 (0.8×100 cm; solvent, 0.1 N acetic acid) which have proved to be most effective in isolating natural human angiotensin I.[8,9] The six active fractions from the Bio-Gel column were pooled and lyophilized, leaving a white powder (acetate of XVIII, presumably), 8.6 mg; $[\alpha]_D^{26}$ $-63\pm3°$ (*c* 0.08, 0.05 N acetic acid;[25] amino acid ratios in acid hydrolysate, aspartic acid 0.98, arginine 1.03, valine 1.12, tyrosine 0.88, isoleucine 0.92, histidine 1.98, proline 1.10, phenylalanine 1.03, leucine 1.06. The homogeneity of the powder was ascertained by paper, thin-layer and column chromatography as described later. Furthermore, the stereospecific purity of each amino acid residue of the powder was confirmed by the enzymic method; with leucine aminopeptidase[7] the sample was degraded completely to nine amino acid residues leaving no decapeptide, while incubation of the sample with carboxypeptid ase A[26] caused the liberation of leucine, histidine and phenylalanine leaving H-Asp-Arg-Val-Try-Ile-His-Pro-OH as an unhydrolyzable core.

Comparison of Synthetic XVIII and Natural Human Angiotensin I. The powder (acetate of XVIII) obtained above was chromatographed on Toyo Roshi No. 51 paper affording R_f 0.53[24] and 0.51,[27] and on Serva TLC thin-layer affording R_f 0.71;[28] these values were exactly identical with those of natural human angiotensin I. The chemical identy was confirmed further by the cochromatography of a mixture of the preparations from the synthesis and the human origin with the Bio-Gel column (0.8×100 cm; solvent, 0.1 N acetic acid). Bioassay with the rat pressor activity was performed as has been described in the paper;[9] the specific pressor activity of the synthetic decapeptide was identical with that of the natural material within the limit of the experimental error. Oxytocic activity of the synthetic material was nil, also as has been observed in natural material.[9]

We wish to thank Mr. Kosaku Noda for amino acid analysis and Miss Junko Yamada for skillful technical assistance.

23) The reaction was followed at various times with a paper chromatography, and the bioassay of the pressor activity; the highest activity observed after the hydrogenation of some 48 hr. However, the chromatography indicated that a small part of the imidazoyl-benzyl groups was remained untouched; this fact might be one of the reasons that the yield (8.6 mg) of pure product was poor. Treatment of the hydrogenated material of XVII with sodium-liquid ammonia did not give a product bearing stronger pressor activity.

24) The R_f value refers to the paper chromatography with the solvent system of *n*-butanol - acetic acid - pyridine - water (4 : 1 : 1 : 2 v/v).

25) We could not determine the specific rotation of natural human angiotensin I because of the scantity of material. Neither Skeggs *et al.* nor Peart *et al.*, also, did not determine the specific rotation of natural horse and bovine angiotensin I.[3,4] It would be of noteworthy that the specific rotations of synthetic [Val^5]-angiotensin I are reported as value of close resemblance with that of the powder (acetate of XVIII); $[\alpha]_D$ $-67.5\pm2°$ (*c* 1.69, H_2O) (R. Schwyzer *et al.*, *Helv. Chim. Acta*, **41**, 1273 (1958)) and $[\alpha]_D^{22}$ $-74\pm3°$ (*c* 1.6, 0.05 N acetic acid) (St. Guttmann, *ibid.*, **44**, 721 (1961)) for the synthetic [Val^5]-angiotensin I as an acetate salt.

26) F. Sanger and E. O. P. Thompson, *Biochem. J.*, **53**, 366 (1953).

27) Solvent, *n*-butanol - acetic acid - water (7 : 1 : 2, v/v).

28) Solvent, *s*-butanol - 3% ammonium hydroxide (100 : 44; v/v).

BULLETIN OF THE CHEMICAL SOCIETY OF JAPAN VOL. 41 438—441 (1968)

Use of Anhydrous Hydrogen Fluoride in Peptide Synthesis. II. Procedures for the Syntheses of Simple Peptides

Shumpei SAKAKIBARA, Yasuo KISHIDA, Rinzo NISHIZAWA*1 and Yasutsugu SHIMONISHI

Peptide Center, Institute for Protein Research, Osaka University, Kita-ku, Osaka

(Received August 10, 1967)

Detailed conditions for handling simple peptide-derivatives with anhydrous hydrogen fluoride (HF) were presented. Since HF has a strong affinity for peptides, the removal of excess HF from the reaction products is rather difficult, but is essential to obtain the product as good crystals. Syntheses of the following peptides were carried out successfully as examples of the HF procedure: tosyl-L-phenylalanyl-L-phenylalanine, L-leucylglycine, L-arginylglycine, carbobenzoxy-L-prolyl-L-leucylglycine ethyl ester, L-aspartyl-L-phenylalanine amide, and BOC-β-alanyl-L-tryptophyl-L-methionyl-L-aspartyl-L-phenylalanine amide.

The possibility of removing the S-benzyl group by acidolysis was the first indication of the usefulness of anhydrous hydrogen fluoride (HF) for peptide synthesis;[1] this was confirmed by the formation of oxytocin from the fully-protected nonapeptide. The general properties of HF as a reagent for the removal of various protective groups have been discussed in our preceding papers.[2,3] In this study, detailed conditions for the synthesis of simple peptides were investigated to demonstrate how the HF-procedure can be applied in general peptide synthesis. The HF reaction was carried out in the apparatuses described in the preceding papers.[2,3] Although completely dry HF is desirable for accelerating the cleaving reaction, a further drying procedure was unnecessary for the synthesis of simple peptides when HF of more than 99% purity was used under mild conditions. Generally, the HF molecule has a strong affinity for peptides through the hydrogen bonds, and it takes a very long time to remove the excess HF from peptides, even *in vacuo*. The results shown in Fig. 1 demonstrate that 0.19, 1.57, and 1.81 equivalents of HF were still attached to acetyl-L-leucine, L-leucylglycine and L-leucylglycylglycine respectively, even when their HF-solution had been kept under a vacuum (2—3 mmHg) for 20 hr at room temperature. These results indicate that about 1.4 equivalents of HF are bound to an amino group and that about 0.2 equivalent of HF is attached to one peptide-bond under these conditions. Therefore, the difficulty in removing HF from peptides increases with the number of the peptide-bonds. Nevertheless, the complete removal of the bound HF in some way is essential if we are to obtain the product as good crystals.

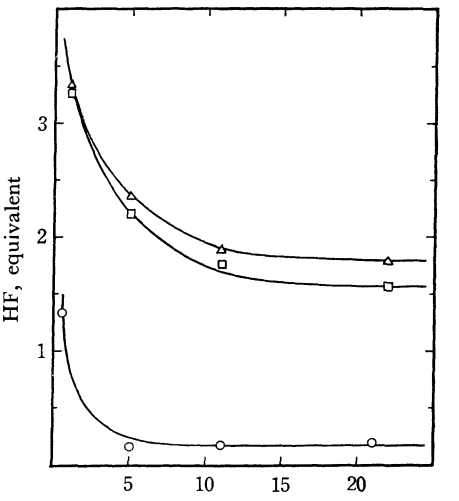

Evacuation time at 2—3 mmHg, hr

Fig. 1. Amount of absorbed HF in acetyl-amino acid or free peptides. Each material (0.1 g) was dissolved in HF (1 m*l*), and excess HF was removed using a plastic water pump (20—30 mmHg) for 30 min. Then, the residue was kept *in vacuo* (2—3 mmHg) at room temperature. Remaining HF was determined by titration with 0.1 N sodium hydroxide.
○ Acetyl-L-leucine
□ L-Leucylglycine
△ L-Leucylglycylglycine

First, we attempted to remove the isopropyl ester group from the tosyl-L-phenylalanyl-L-phenylalanine isopropyl ester. The reaction was carried out at 20°C for one hour in the presence of an equimolar amount of anisole. The excess HF was then removed by distillation *in vacuo*. In this case, the product is water-insoluble, and there is no free amino group in the molecule. Therefore,

*1 Present address: Ohji Pharmaceutical Factory, Nippon Kayaku Co., Ltd., Shimo-cho, Kita-ku, Tokyo.

1) S. Sakakibara and T. Shimonishi, This Bulletin, **38**, 1412 (1965).
2) The 8th European Peptide Symposium, Sept. 18—23, Holland (1966).
3) S. Sakakibara, Y. Shimonishi, Y. Kishida, M. Okada and H. Sugihara, This Bulletin, **40**, 2164 (1967).

the small amount of HF remaining was easily removed by washing the product with water. When carbobenzoxy-L-leucylglycine was treated with HF, the product was absorbed once on a Dowex-50 column (H^+ form), and the excess HF was washed out thoroughly with water. Then the desired free peptide was recovered quantitatively by elution with ammonia. In another example, the bound HF was removed by passing the aqueous solution through a column of IR-45 (acetate form); the product, free L-leucylglycine, was thus obtained in about a 70% yield. This lower yield may be attributed to the partial absorption of the small peptide on the resin.

N^{α}-Carbobenzoxy-N^{G}-nitro-L-arginylglycine was treated with HF at 0°C for 30 min in the presence of two equivalents of anisole. Since the product is strongly basic, it was treated with IRA-400 (OH^- form) and then crystallized as acetate in a satisfactory yield. This procedure should be useful for the general synthesis of arginine-peptides.

In the case of the carbobenzoxypeptide ethyl ester, only the carbobenzoxy group is susceptible to HF; the ethyl ester group should stay intact during the reaction.[2,3] Thus, the carbobenzoxy-L-leucylglycine ethyl ester was treated with HF, and the product was directly combined with the carbobenzoxy-L-proline *p*-nitrophenyl ester to transform the product into a crystallizable compound. The excess HF was neutralized with triethylamine for the coupling reaction; carbobenzoxy-L-prolyl-L-leucylglycine ethyl ester was thus obtained in more than a 90% yield.

Next, carbobenzoxy-β-isopropyl-L-aspartyl-L-phenylalanine amide was treated with HF in the presence of three equivalents of anisole, after which the product was treated with IR-45 (acetate form) to eliminate the remaining HF. During the treatment, this material was also found to be absorbed onto the resin; the yield of L-aspartyl-L-phenylalanine amide was 67%. Paper electrophoresis of the reaction mixture showed no evidence of the formation of β-aspartyl peptide during the treatment, and the analytical data on the final product were identical with those reported by Davey *et al.*[4] Generally, aspartyl peptides are sensitive to acid; Dowex-50 treatment to remove the HF, followed by elution with ammonia, resulted in the partial decomposition of the product.

Finally, *t*-amyloxycarbonyl-L-tryptophyl-L-methionyl-L-aspartyl-L-phenylalanine amide was treated with HF. The product was then coupled with the *t*-butoxycarbonyl-β-alanine *p*-nitrophenyl ester to convert the product into *t*-butoxycarbonyl-β-alanyl-L-tryptophyl-L-methionyl-L-aspartyl-L-phenylalanine amide, which has been reported to be a biologically-active and crystallizable compound.[4] The yield and purity of the reaction product were satisfactory, as will be shown in the Experimental section; these results also indicate that aromatic amino acid and methionine residues suffered no serious side-reactions with HF during the procedure.

The application of the HF procedure to more complicated peptide derivatives is now in progress in our laboratory.

Experimental

HF-Reactions. Anhydrous hydrogen fluoride with a purity of 99.5% was obtained from the Matheson Chemical Co., U. S. A. It was used for the reactions without further drying. The HF reactions were carried out in the apparatus shown in Figs. 1 and 2 of the preceding paper,[3] and the reported procedure[3] was generally followed in handling HF. Although the minimum amount of HF which is required for completion of the reaction has not yet been determined, 5 to 10 m*l* of HF were sufficient for one gram of peptide. When a protective group which is slow to be removed is applied to the HF reaction, the use of more HF is recommended. After each reaction, the excess HF was removed using a plastic water-pump at 0°C and then the residue was kept under a vacuum (2—3 mmHg) for more than 5 hr, as has been described before.[3] Stirring was continued as long as possible during the evacuation procedure. Then, the residue was extracted with water, and some water-insoluble material was removed by extraction with chloroform or by passing the mixture through Hyflo Super-cel before the succeeding treatment. Used reaction cylinders were washed successively with water, methanol, and acetone, and then further cleaned with a mixture of conc. hydrochloric acid and conc. nitric acid (3 : 1 v/v). The outer diameters of the reaction vessels, which are made of Daiflon, gradually increase during repeated dryings at temperatures above 50°C. Therefore, they should be dried in a desiccator at room temperature after washing.

***p*-Toluenesulfonyl-L-phenylalanyl-L-phenylalanine Isopropyl Ester.** A solution of tosyl-L-phenylalanyl chloride[5] (4.63 g, 0.0137 mol) in tetrahydrofuran (30 m*l*) was slowly added to a suspension of L-phenylalanine isopropyl ester tosylate[3] (5.20 g, 0.0137 mol) and triethylamine (2 m*l*, 0.0143 mol) in tetrahydrofuran (40 m*l*) at −10°C. One more equivalent of triethylamine was then slowly stirred into the reaction mixture at the same temperature. After 2 hrs' stirring, the precipitate which had formed was filtered off, and then the filtrate was concentrated to a syrup, which was dissolved in ethyl acetate. The solution was washed with N hydrochloric acid, 5% sodium bicarbonate, and water, and dried over magnesium sulfate. The concentration of the dried solution gave crystals which were recrystallized from ethyl acetate and petroleum ether; yield, 5.20 g (75%); mp 125.5—126.5°C; $[\alpha]_D^{23}$ +15.7° (*c* 2, dimethylformamide). Found: C, 65.81; H, 6.25; N, 5.41%. Calcd for $C_{28}H_{32}O_5N_2S$: C, 66.13; H, 6.34; N, 5.51%.

***p*-Toluenesulfonyl-L-phenylalanyl-L-phenylalanine.** The tosyl-L-phenylalanyl-L-phenylalanine isopropyl ester (1.13 g, 2.2 mmol) and anisole (0.24 g, 2.2 mmol) were placed in a reaction cylinder together

4) J. M. Davey, A. H. Laird and J. S. Morley, *J. Chem. Soc.* (C), **1966**, 555.

5) E. A. Popenoe and V. du Vigneand, *J. Am. Chem. Soc.*, **76**, 6202 (1954).

with a Teflon-coated stirring bar. HF (10 ml) was added to it by distillation, and then the mixture was allowed to react at 20°C for one hr while being stirred. The excess HF was removed by distillation with a plastic water pump, and then the residue was kept under a vacuum for about 5 hr at room temperature. The residue was dissolved in ethyl acetate, and the desired product was extracted with a 5% sodium bicarbonate aqueous solution. The bicarbonate solution was acidified to pH 2 with 6 N hydrochloric acid, and the oily material which appeared was taken up in ethyl acetate. The ethyl acetate extract was dried over sodium sulfate, and then concentrated to a syrup which was crystallized by adding petroleum ether; yield, 0.88 g (85%); mp 197°C; $[\alpha]_D^{21}$ +22.8° (*c* 2, dimethylformamide). Found: C, 64.57; H, 5.84; N, 5.84%. Calcd for $C_{25}H_{26}O_5N_2S$: C, 64.37; H, 5.62; N, 6.01%.

L-Leucylglycine. Carbobenzoxy-L-leucylglycine[6] (1.0 g, 3.1 mmol) and anisole (0.33 ml, 3.1 mmol) were placed in a reaction cylinder[3] together with a Teflon-coated stirring bar. HF (about 10 ml) was added, and the mixture was stirred for 30 min at 0°C. The excess HF was removed under reduced pressure, and the residue was dried thoroughly for 10 hr *in vacuo* (3 mmHg), as has been described before. The dried residue was then dissolved in water, some insoluble material was removed with Hyflo Super-cel, and the solution was passed through a column of IR-45 (acetate form; about 7 ml of the resin were required). After washing the column with 5% acetic acid, the combined effluent was concentrated under reduced pressure, and the residue was dissolved in a minimum amount of water and crystallized by adding ethanol and ether. The crystals were dried *in vacuo* at 80°C for 24 hr; yield, 0.42 g (72%); $[\alpha]_D^{29}$ +85.0° (*c* 2, water). Value reported in the literature[6]: $[\alpha]_D$ +85.8° (*c* 2, water).

The dried reaction product of another run on the same scale was dissolved in water, and the solution was passed through a column of Dowex 50, X-8 (100—200 mesh; H^+ form; about 4 ml of the resin were used). The column was washed thoroughly with water until the washings became neutral, and then the product was eluted with 6 N ammonia. The concentration of the eluate under reduced pressure gave crystals which were recrystallized as has been described before. Yield of the dried crystals, 0.53 g (91%); $[\alpha]_D^{27}$ +85.6° (*c* 2, water).

L-Arginylglycine Acetate, Acetic Acid Solvate. N^{α}-Carbobenzoxy-N^{G}-nitro-L-arginylglycine[7] (1.5 g, 3.7 mmol) and anisole (0.8 ml, 7.4 mmol) were placed in an HF-reaction cylinder,[3] together with a Teflon-coated stirring bar, and HF (10 ml) was added to the mixture. The HF reaction was carried out at 0°C for 30 min with stirring, and then the excess HF was removed by distillation. The residue was dissolved in water, an insoluble material was extracted with chloroform, and the water solution was passed through a column of IRA-400 (OH^- form; 15 ml of resin were used). After adding 0.5 ml of acetic acid, the effluent was concentrated to a residue which was crystallized from glacial acetic acid and ethyl acetate. The crystals (mono-acetate, acetic acid solvate) were dried over phosphrous pentoxide at 80°C for 20 hr; yield, 1.14 g (89%); mp 167—170°C; $[\alpha]_D^{28}$ +38.3° (*c* 1, water). Value reported in the literature: mp 167—169°C;[7] $[\alpha]_D^{28}$ +38.9° (*c* 5.75, water);[7] $[\alpha]_D^{24-25}$ +37.6° (*c* 1, water).[8]

Found: C, 41.01; H, 7.28; N, 19.69%. Calcd for $C_{12}H_{15}O_7N_5$: C, 41.01; H, 7.19; N, 19.93%.

Carbobenzoxy-L-prolyl-L-leucylglycine Ethyl Ester. The carbobenzoxy-L-leucylglycine ethyl ester[6] (1.75 g, 5.0 mmol) and anisole (0.5 ml) were treated with HF (10 ml) as has been described previously. The excess HF was removed by distillation *in vacuo*. The dried product was dissolved in chloroform (30 ml), and the carbobenzoxy-L-proline *p*-nitrophenyl ester (1.85 g, 5.0 mmol) was added to the solution. The mixture was then neutralized with triethylamine (1 ml, 7 mmol) and with the *N*, *N*-diethylglycine ethyl ester[9] (2 ml), and allowed to react for 2 days at room temperature. The solution was then washed with N ammonia to remove the *p*-nitrophenol, and dried over magnesium sulfate. The concentration of the dried solution left crystals which were recrystallized from ethanol-water; yield, 2.1 g (94%); mp 150—151.5°C; $[\alpha]_D^{26.5}$ −80° (*c* 2.5, ethanol). Ressler and du Vigneaud reported a mp of 148—149°C and $[\alpha]_D$ −79.8° (*c* 2, ethanol).[10]

Bis-(Carbobenzoxy-L-aspartic Acid β-Isopropyl Ester) Piperazine Salt. β-Isopropyl-L-aspartate (29 g, 0.165 mol)[3] was treated with carbobenzoxy chloride (30 g, 0.17 mol) at room temperature by the Schotten-Baumann reaction using sodium bicarbonate (34 g, 0.4 mol). The reaction mixture was washed 3 times with ether, and then acidified to pH 2 with 6 N hydrochloric acid. The oil which separated was extracted with ether, and the ether extract was dried over sodium sulfate. Then the dried solution was concentrated to a syrup under reduced pressure. The residue was dissolved in methanol, and piperazine hexahydrate (16.1 g, 0.083 mol) was added to the solution. The mixture was concentrated to a residue under reduced pressure; this residue was flushed twice with toluene, and then recrystallized from 300 ml of methanol; yield 41.2 g (71%); mp 149—151°C: $[\alpha]_D^{26}$ −3.6° (*c* 2, dimethylformamide).

Found: C, 57.93; H, 6.89; N, 7.92%. Calcd for $C_{34}H_{48}O_{12}N_4$: C, 57.94; H, 6.86; N, 7.95%.

Carbobenzoxy-β-isopropyl-L-aspartyl-L-phenylalanine Amide. The carbobenzoxy-L-aspartic acid β-isopropyl ester (0.05 mol), which had been prepared from the piperazine salt (17.6 g) by shaking it with excess 2 N hydrochloric acid, and L-phenylalanine amide hydrochloride (10.0 g, 0.05 mol) were dissolved in dimethylformamide (50 ml), after which triethylamine (7 ml, 0.05 mol) was added to the mixture. Dicyclohexylcarbodiimide (10.3 g, 0.05 mol) was then stirred into the mixture at −10°C. These reagents were allowed to react for 30 min at the same temperature, and then for an additional 5 hr at room temperature. The urea formed was filtered off, and water (250 ml) was added to the filtrate to precipitate the product as crystals, which were collected by filtration and then recrystallized from hot ethanol (300 ml) and water

6) M. Bergmann, L. Zervas and J. Fruton, *J. Biol. Chem.*, **111**, 225 (1935).
7) K. Hofmann, W. D. Peckham and A. Rheiner, *J. Am. Chem. Soc.*, **78**, 238 (1956).
8) L. Zervas, T. T. Otani, M. Winitz and J. P. Greenstein, *ibid.*, **81**, 2878 (1959).
9) S. Sakakibara and M. Itoh, This Bulletin, **40**, 656 (1967).
10) C. Ressler and V. du Vigneaud, *J. Am. Chem. Soc.*, **76**, 3107 (1954).

(200 ml); yield, 17 g (74.6%); mp 171—174°C; $[\alpha]_D^{26}$ −27.5° (*c* 2.9, dimethylformamide).

Found: C, 63.11; H, 6.42; N, 9.22%. Calcd for $C_{24}H_{29}O_6N_3$: C, 63.28; H, 6.42; N, 9.23%.

L-Aspartyl-L-phenylalanine Amide. Carbobenzoxy-β-isopropyl-L-aspartyl-L-phenylalanine amide (1 g, 2.2 mmol) and anisole (0.71 ml, 6.6 mmol) were treated with HF (20 ml) at 0°C for 100 min. The excess HF was removed under reduced pressure, and the residue was dried thoroughly under a vacuum for more than 5 hr. The dried product was dissolved in water, and the solution was passed through a column of IR-45 (acetate form). The effluent was lyophilized, and the residue was crystallized from acetone and water and then dried over phosphorus pentoxide at room temperature; yield, 430 mg (66.6%); mp 189—190°C (decomp.); $[\alpha]_D^{23}$ +20.5° (*c* 1, dimethylformamide containing 1 eq. of N HCl).*2 Davey *et al.* reported mp 188—189°C (decomp.) and $[\alpha]_D$ +20.6° (*c* 1, dimethylformamide containing 1 eq. of N HCl).[4]

Found: C, 52.06; H, 6.62; N, 13.81%. Calcd for $C_{13}H_{17}O_4N_3 \cdot H_2O$: C, 52.51; H, 6.44; N, 14.13%.

***t*-Amyloxycarbonyl-L-tryptophyl-L-methionine Hydrazide.** Dicyclohexylcarbodiimide (2.1 g, 0.01 mol) was added to a solution of *t*-amyloxycarbonyl-L-tryptophan[11] (3.18 g, 0.01 mol) in tetrahydrofuran (60 ml) at −10°C. After about 10 min, a solution of L-methionine methyl ester hydrochloride (2.2 g, 0.011 mol) and triethylamine (1.54 ml, 0.011 mol) in chloroform (30 ml) was added to the reaction mixture. The whole mixture was kept 1 hr at 0°C, and then overnight at room temperature. The solvent was removed under reduced pressure, and the residue was dissolved in ethyl acetate (100 ml). Some insoluble materials were filtered off, and the filtrate was washed with 0.5 N hydrochloric acid, 5% sodium bicarbonate, and water, and dried over anhydrous sodium sulfate. The dried solution was concentrated to a syrup, which was then dissolved in ethanol (50 ml), and 90% hydrazine hydrate (5.56 g, 0.1 mol) was added to the solution. After 2 days at room temperature, the mixture was concentrated to a residue; this residue was flushed 3 times with toluene and then crystallized from ethanol by the addition of water. Yield of crude material, 3.50 g. This material was recrystallized from ethanol-water, and dried over phosphorus pentoxide *in vacuo* at 80°C for 10 hr; yield, 2.92 g (63.1%); mp 158—163°C; $[\alpha]_D^{24}$ −22.4° (*c* 1.08, dimethylformamide).

Found: C, 56.68; H, 7.30; N, 14.94%. Calcd for $C_{22}H_{33}O_4N_5S$: C, 57.00; H, 7.18; N, 15.11%.

***t*-Amyloxycarbonyl-L-tryptophyl-L-methionyl-L-aspartyl-L-phenylalanine Amide.** To a solution of *t*-amyloxycarbonyl-L-tryptophyl-L-methionine hydrazide (13.9 g, 0.03 mol) in dimethylformamide (30 ml), a 2.0 N hydrogen chloride-dioxane solution (30 ml, 0.06 mol) was added at −10°C, and then isoamyl nitrite (3.68 g, 0.0315 mol) was added slowly to the mixture at −20°C. After 30 min, a cold mixture of L-aspartyl-L-phenylalanine amide monohydrate (9.80 g, 0.033 mol) and triethylamine (15.6 ml, 0.11 mol) in dimethylformamide (75 ml) was added to the previous mixture, and the mixture was stirred at 0—3°C for 3 days. Then, cold water (300 ml) was added, and the pH of the mixture was adjusted to 2—3 with N hydrochlorci acid in order to precipitate the product. The precipitate was collected by filtration, and was washed with water and then ether. The crude product (19.4 g) obtained was recrystallized from ethanol; yield, 16.2 g (76.0%); mp 229—230°C (decomp.); $[\alpha]_D^{14}$ −31.3° (*c* 1, dimethylformamide).

Found: C, 59.04; H, 6.53; N, 11.67%. Calcd for $C_{35}H_{46}O_8N_6S$: C, 59.14; H, 6.52; N, 11.82%.

***t*-Butoxycarbonyl-β-alanine *p*-Nitrophenyl Ester.** Dicyclohexylcarbodiimide (2.50 g, 0.012 mol) was added to a solution of *t*-butoxycarbonyl-β-alanine (1.89 g, 0.01 mol)[12] and *p*-nitrophenol (1.67 g, 0.012 mol) in ethyl acetate (16 ml) at 0°C. The mixture was stirred for 1 hr at the same temperature, and then for an additional 24 hr at room temperature. The urea formed was removed by filtration, and the filtrate was concentrated to a residue under reduced pressure and crystallized by tritration with petroleum ether. The crude crystals were recrystallized from ethyl acetate-petroleum ether; yield, 1.53 g (49.3%); mp 59—61°C.

Found: C, 53.91; H, 5.82; N, 9.08%. Calcd for $C_{14}H_{18}O_6N_2$: C, 54.19; H, 5.85; N, 9.03%. The yield of the second crop of crystals was 0.36 g (11.6%).

***t*-Butoxycarbonyl-β-alanyl-L-tryptophyl-L-methionyl-L-aspartyl-L-phenylalanine Amide.** *t*-Amyloxycarbonyl-L-tryptophyl-L-methionyl-L-aspartyl-L-phenylalanine amide (294 mg, 0.41 mmol) and anisole (0.46 ml) were placed in a HF reaction cylinder, and then HF (about 5 ml) was distilled into the cylinder under a vacuum using a dry ice-methanol bath. The mixture was stirred for 30 min at 0°C, and then the excess HF was removed by distillation. After drying *in vacuo* for more than 10 hr at room temperature, the residue was extracted with water and some water-insoluble materials were removed with the aid of Hyflo Super-cel. The filtrate was lyophilized, the residue was suspended in dimethyl formamide (8 ml), and the *t*-butoxycarbonyl-β-alanine *p*-nitrophenyl ester (155 mg, 0.5 mmol) was added to the suspension together with triethylamine (0.2 ml, 1.50 mmol). The mixture was stirred at room temperature for 2 days, by which time the presence of free amino groups could no longer be recognized by thin-layer chromatography. Then, water was added to the mixture, and the pH was adjusted to 2 with 0.5 N hydrochloric acid. The mixture was kept for a while in a refrigerator, and then the crystalline product was collected by filtration. The crystals were washed with cold water and ether, and dried over phosphorus pentoxide *in vacuo*. The dried material was recrystallized from dimethylformamide-water, collected by filtration, washed with 50% aqueous dimethylformamide, water, and ether, and dried. After successive recrystallizations, the product was obtained as fine colorless crystals which were dried over phosphorus pentoxide *in vacuo* at room temperature for 24 hr; yield, 0.21 g (67%); mp 227—228°C (decomp.); $[\alpha]_D^{20}$ −28.8° (*c* 1, dimethylformamide). Values reported in the literature: mp 229—230°C (decomp.) and $[\alpha]_D^{20}$ −28.8° (*c* 1, dimethylformamide).[4]

Found: C, 57.80; H, 6.56; N, 12.51%. Calcd for $C_{37}H_{49}O_9N_7S$: C, 57.87; H, 6.43; N, 12.76%.

*2 This value was calculated from the dry weight.

11) S. Sakakibara, M. Shin, M. Fujino, Y. Shimonishi, S. Inouye and N. Inukai, This Bulletin, **38**, 1522 (1965); I. Honda, Y. Shimonishi and S. Sakakibara, *ibid.*, **40**, 2415 (1967).

12) P. H. Bentley, H. Gregory, A. H. Laird and J. S. Morley, *J. Chem. Soc.*, **1964**, 6130.

BULLETIN OF THE CHEMICAL SOCIETY OF JAPAN VOL. 41 442—444 (1968)

Synthesis of Trimethylhydroquinone from *p*-Xylene*[1]

Kikumasa SATO, Yoshito FUJIMA and Arihiro YAMADA

Department of Applied Chemistry, Faculty of Engineering, Yokohama National University, Minami-ku, Yokohama

(Received August 31, 1967)

The synthesis of trimethylhydroquinone from *p*-xylene was carried out *via* two routes; one includes the formylation of *p*-xylene, followed by nitration, and the other, the chloromethylation of nitro-*p*-xylene. The oxidation of the trimethylanilines, VI and IX, prepared from 2, 5-dimethyl-6-nitrobenzaldehyde and 2, 5-dimethyl-3-chloromethylnitrobenzene and their subsequent reduction gave trimethylhydroquinone (TMH) in appreciable yields.

α-Tocopherol (vitamin E) may be obtained by the condensation of TMH with phytol[1] or its derivatives.[2] Earlier papers in this series have described how TMH has been synthesized from 2-methylhydroquinone, 3, 5-dimethylhydroquinone,[3] and pseudocumene.[4]

In this study the synthesis of TMH was carried out from *p*-xylene. No report could be found concerning such a synthesis of TMH from *p*-xylene. *p*-Xylene is now obtained readily through the petroleum chemical industry, so the synthesis of TMH from *p*-xylene may well prove of great interest. Two routes of synthesis are shown below.

The reaction of aromatic hydrocarbons with dichloromethyl methyl ether in the presence of a Lewis acid has been reported to give aromatic aldehydes.[5] The treatment of *p*-xylene with dichloromethyl methyl ether gave 2, 5-dimethylbenzaldehyde (II) in a 63% yield. The catalytic reduction of the 2, 5-dimethyl-6-nitrobenzaldehyde (III) prepared by the nitration[6] of II gave the methylolaniline IV, which was not reduced further even at a higher temperature. The attempted Clemmensen reduction of III or IV was also unsuccessful. The fact that the catalytic reduction of III can not provide VI is probably attributable

Route (1)

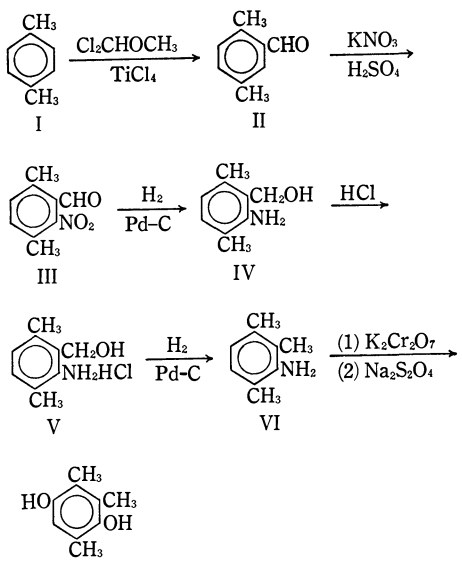

Route (2)

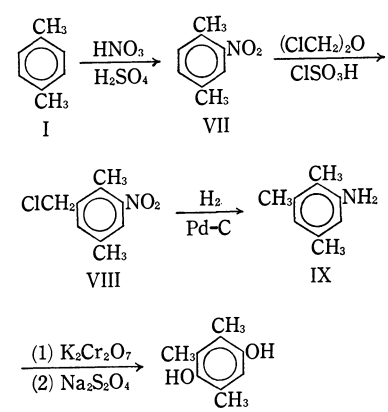

*1 Paper V of Studies of the Synthesis of Vitamin E.

1) P. Karrer, H. Salmon and H. Fritzshe, *Helv. Chim. Acta*, **21**, 309 (1938); Hoffmann-La Roche and Co., Swiss Pat. 212353 (1941); P. Karrer and O. Isler, U. S. Pat. 2411968 (1946); O. Ehrman, German Pat. 1015446 (1958).

2) Hoffman-La Roche and Co., Swiss Pat. 208446 (1940); P. Karrer and O. Isler, U. S. Pat. 2411969 (1946); P. Karrer, R. Esher, H. Fritzsche, K. Keller, B. Ringier and H. Salmon, *Helv. Chim. Acta*, **21**, 939 (1938); P. Karrer and H. Keller, *ibid.*, **21**, 1161 (1938); J. D. Surmatis and J. Weber, U. S. Pat. 2723278 (1955); J. D. Surmatis and J. Weber, Canadian Pat. 530254 (1956); L. I. Smith and H. E. Ungnale, U. S. Pat. 2421811 (1947); J. Weicht, *Chem. Listy*, **52**, 722 (1958); L. Blaha, J. Hodosova and J. Weicht, *Collection Czech Chem. Commun.*, **24**, 2023 (1959); L. Blaha and J. Weicht, Czech Pat. 88904 (1959).

3) K. Sato and S. Abe, *J. Org. Chem.*, **28**, 1928 (1963).

4) K. Sato and Y. Fujima, *Yukigoseikagaku Kyokaishi (J. Synth. Org. Chem. Japan)*, **25**, 252 (1960).

5) A. Rieche, H. Gross and E. Höft, *Chem. Ber.*, **93**, 88 (1960); H. Gross, A. Rieche and G. Mattley, *ibid.*, **96**, 308 (1963).

6) L. Gattermann, *Ann.*, **393**, 221 (1912).

to the poisonous effect of the resulting amino-group on the catalyst.[7] The methylolaniline IV was converted into the hydrochloride V. The catalytic reduction of V gave 2, 3, 6-trimethylaniline (VI) in a 33% yield. TMH was obtained in a 67% yield by the oxidation of VI, followed by reduction. Each step in Route (1) gives a comparatively good yield except the reduction. If the method for the conversion of III to VI can be improved, therefore, Route (1) may be useful for the synthesis of TMH. The reduction of aldehyde involving the nitro-group was hard in Route (1), so chloromethylation was carried out *via* Route (2).

The chloromethylation of nitrotoluenes with bis-(chloromethyl) ether in chlorosulfonic acid has been reported by Berezovskii[8] and other workers.[9,10] The chloromethylation of VII with bis(chloromethyl) ether afforded 2, 5-dimethyl-3-chloromethylnitrobenzene (VIII) in a 67% yield, along with a considerable amount of a by-product. As Table 1 shows, when the reaction temperature was 5—10°C and the reaction time was 64 hr, the chloromethyl compound, VIII, was obtained in a maximum yield. The material VII was recovered at a lower temperature in spite of the long reaction time. The chloromethylation of VII at a higher temperature yielded more of the by-product.

Table 1. The chloromethylation of nitro-*p*-xylene with bis(chloromethyl) ether in various conditions

No.	Reaction		Yield of product, %	
	Temp. °C	Time hr	A[1]	B[1]
1	0— 5	36	32.4[2]	—[3]
2	0— 5	72	50.0[2]	—[3]
3	5—10	64	67.0	—[3]
4	7—10	12	21.6[2]	—[3]
5	10—15	24	44.5	12
6	10—15	64	25.2	32
7	15—20	24	41.6	15
8	20—25	16	27.6	24

1) A=2,5-dimethyl-3-chloromethylnitrobenzene (VIII); B=2,5-bis(chloromethyl)-3,6-dimethylnitrobenzene.
2) The material VII was recovered.
3) The yield was not measured.

The structure of VIII was identified on the basis of the infrared spectrum and confirmed by the retention time[11] of trimethylaniline, IX, in gas chromatography. The by-product was regarded as 2, 5-di(chloromethyl)-3, 6-dimethylnitrobenzene on the basis of the results of the elementary analysis and infrared spectroscopy, and by the fact that 2, 3, 5, 6-tetramethylaniline was obtained by the catalytic reduction.

The catalytic reduction of VIII gave 2, 3, 5-trimethylaniline (IX), which was then converted into TMH in a 44% yield.

Route (2) does not have the same difficulty in reduction as Route (1), as has fewer steps as well. TMH is obtained in a better yield from VI than from IX. Route (2), however, gives higher yields than Route (1) on the whole.

Experimental[12]

Materials. Dichloromethyl methyl ether was prepared from methyl formate by the procedure of Rieche.[5] The preparation of 2, 5-dimethyl-6-nitrobenzaldehyde-(III) followed the method of Gattermann.[6] Nitro-*p*-xylene was obtained by the nitration of *p*-xylene with mixed acid.[13] Bis(chloromethyl) ether was prepared by the procedure of Berezovskii.[8]

2, 5-Dimethylbenzaldehyde (II). Into a cold mixture of 106 g of *p*-xylene and 190 g of titanium tetrachloride, 57.5 g of dichloromethyl methyl ether was added, drop by drop, at 5—10°C, then the mixture was stirred for about 1 hr, poured into ice water, and extracted with benzene. After drying, the benzene was removed and the residue was distilled under reduced pressure. II was obtained in a yield of 42.2 g (63%), bp 99—100°C/16 mmHg; ν_{max}^{film} 1680 cm^{-1} (CHO). Its semicarbazone showed a melting point of 215°C.

Found: C, 62.80; H, 6.85%. Calcd for $C_{10}H_{13}N_3O_3$ of the semicarbazone: C, 62.81; 6.72%.

2, 3, 6-Trimethylaniline (VI). In the presence of 5%-palladium-carbon, 10 g of III in methanol was reduced under a pressure of about 100 atm of hydrogen at room temperature in an autoclave. After opening the bomb, the catalyst was removed by filtration and the solvent distilled off. Recrystallization from benzene gave 7.3 g (98%) of IV, mp 106°C. IV in methanol was converted into its hydrochloride V, mp 251°C (dec.), by dry hydrogen chloride. The methanol was then removed, and the V was dried over sodium hydroxide. The hydrochloride, V, in methanol was reduced in the presence of 5%-palladium-carbon under a pressure of about 110 atm of hydrogen in an autoclave at 60°C. After opening the bomb, the catalyst was removed and the solvent distilled off. The residue was

7) E. B. Maxted, "The Poisoning of Metallic Catalysts" in "Advances in Catalysis and Related Subjects," Vol. III, Academic Press Inc., N. Y. (1951), p. 129; M. H. Dilike, D. D. Eley and E. B. Maxted, *Nature*, **161**, 804 (1948); E. B. Maxted, *J. Chem. Soc.*, **1949**, 1987.
8) V. M. Berezovskii, V. A. Kurdyukova and N. A. Preobrazhenskii, *Zhur. Obshchei. Khim.*, **21**, 1163 (1951); *ibid.*, **21**, 1269 (1951); *Chem. Abstr.*, **46**, 5006 (1952).
9) W. Polaczkowa and N. Porowska, *Roczniki Chem.*, **31**, 1207 (1957).
10) U. S. Pat. 2758137.
11) J. H. Jones, C. D. Ritchie and K. S. Heine, Jr., *J. Assoc. Offic. Agr. Chemists*, **41**, 749 (1958).
12) All melting points and boiling points are uncorrected. Infrared spectra were recorded on a Hitachi Model EPI-S2 spectrophotometer and gas chromatographic analyses were carried out on Shimadzu Model GC-IC chromatograph.
13) M. Ya. Kraft and A. M. Tsyganova, *Med. Prom. S. S. S. R.*, **14**, No. 10, 27—30 (1960).

treated with a 30% aqueous solution of potassium hydroxide, and extracted with ether. After drying, the ether was removed, distillation under a reduced pressure then gave 2.8 g (33%) of VI, bp 98—99°C/8 mmHg. The melting point of its acetyl derivative was 188—189°C (Lit.[14] mp 186°C).

Trimethylhydroquinone from VI. A solution of 36 g of sulfuric acid in 160 g of water was cooled to 5°C, and then 2 g of VI was added. The subsequent addition of 1.8 g of potassium bichromate to the solution took about 1 hr, after which the solution was stirred for 11 hr at 3—5°C. To the solution, 2.6 g of potassium bichromate was added again over a 1-hr period. After stirring for thirty minutes, the solution was extracted with ether and treated with a saturated solution of sodium hydrosulfite in water. After drying, the ether was removed. Recrystallization from water gave 1.5 g (67%) of TMH, mp 168—169°C.

2, 5-Dimethyl-3-chloromethylnitrobenzene (VIII). Into a mixture of 20 g of VII and 16 g of bis-(chloromethyl) ether, 24 g of chlorosulfonic acid were added, drop by drop, the temperature being 5—10°C. After having been stirred for 64 hr, the mixture was poured into ice water and extracted with ether, and the ethereal extract was dried over sodium sulfate. The ether was removed, and the distillation of the residue under reduced pressure gave 16.7 g (67%) of VIII, bp 112—113°C/2 mmHg, ν_{max}^{film} 1525, 1370 (NO_2), 840 (C–H) and 720 cm^{-1} (C–Cl).

Found: C, 54.40; H, 4.98%. Calcd for $C_9H_{10}ClNO_2$: C, 54.15; H, 5.05%.

2, 3, 5-Trimethylaniline (X). In the presence of 4 g of 5%-palladium-carbon and 25 g of triethylamine, VIII (39.2 g) in ethanol was reduced under a pressure of about 80 atm of hydrogen at room temperature. After opening the bomb, the catalyst was removed by filtration and the ethanol was distilled off. The residue was dissolved into water and extracted with ether. After drying with potassium hydroxide, the ether was removed. The distillation of the residue under a reduced pressure gave 21.4 g (84%) of IX, bp 110°C/9 mmHg, mp 35—37°C (Lit.[15] mp 36°C).

Trimethylhydroquinone from IX. The trimethylaniline, IX (2 g), was added into a mixture of concentrated sulfuric acid (16 g) and water (60 ml). The mixture was then cooled to 10—15°C, and potassium bichromate (2 g) was added to the mixture over a 1-hr period. After the mixture had been stirred for about 10 hr, potassium bichromate (3.3 g) was further added. Then the mixture was extracted with ether, and the extract was treated with a saturated solution of sodium hydrosulfite in water. After drying, the ether was removed. Recrystallization from water gave 1 g (44%) of TMH, mp 168—170°C.

14) F. Mayer, *Ber.*, **20**, 972 (1887).

15) F. M. Beringer and I. Ugelow, *J. Am. Chem. Soc.*, **75**, 2635 (1953).

BULLETIN OF THE CHEMICAL SOCIETY OF JAPAN VOL. 41 444—450 (1968)

Correlation between the Chemical Reactivity and the Unpaired Electron Distribution of Anion Radicals

Kazuhiro MARUYAMA and Tetsuo OTSUKI

Department of Chemistry, Faculty of Science, Kyoto University, Sakyo-ku, Kyoto

(Received September 5, 1967)

Anion radicals of mono-, di-nitrobenzophenones, dinitrobenzil, and nitrophenanthraquinone generated by reduction with alkali metal were studied by means of electron-spin resonance. The hyperfine coupling constant and the effect of the metal species on it were investigated. The correlation between the localization of the unpaired electron and the chemically reducible position was also discussed.

A large number of studies of anion radicals generated by the reduction of aromatic carbonyl compounds and aromatic nitro compounds, as made by means of ESR, have been reported.[1] The facility with which those compounds accept an electron and the rather great stability of the resultant anion radicals have attracted the attention of many investigators. Anion radicals can be generated by electrolytic reduction,[2] by reduction with alkali metal in a suitable solvent,[1,3] or by reduction with alkaline sodium dithionite in an aqueous solution.[4]

1) a) N. M. Atherton and S. I. Weissman, *J. Am. Chem. Soc.*, **88**, 1330 (1961); b) R. L. Ward, *J. Chem. Phys.*, **32**, 410 (1960); *J. Am. Chem. Soc.*, **83**, 1296 (1961); c) K. Maruyama, R. Tanikaga and R. Goto, This Bulletin, **35**, 1746 (1962); d) D. H. Geske, J. A. Ragle, M. A. Bambenek and A. L. Balch, *J. Am. Chem. Soc.*, **86**, 987 (1964); *etc.*

2) A. H. Maki and D. H. Geske, *J. Am. Chem. Soc.*, **83**, 1852 (1961).

3) R. L. Ward, *J. Chem. Phys.*, **30**, 852 (1959).

4) P. L. Kolker and W. A. Waters, *J. Chem. Soc.*, **1964**, 1136.

The investigation of anion radicals resulting from the compounds with both nitro and carbonyl groups in a molecule is of much interest from the viewpoint of their free-spin localization and their chemical reactivity. In this study, all the anion radicals were generated by reduction with alkali metal in order to get information about the ion-pair between the anion radical and the metal cation.

Experimental

All the compounds used were synthesized in our laboratory. Their physical constants and the methods of synthesis are shown in Table 1. For the ESR measurement, the compound to be reduced was dissolved in *ca.* 10 m*l* of dry dimethoxyethane to give about a 10^{-3} M solution *in vacuo*, and then the anion radical was generated by bringing the solution in contact with the fresh surface of an alkali metal. A 3BX-type ESR spectrometer with a 100 kc modulation manufactured by the Japan Electron Optics Lab. was used in these measurements. The spectra obtained were calibrated by reference to the hyperfine coupling constant of peroxylamine disulfonate.

Results and Discussion

Unpaired Electron Delocalization of Anion Radicals. Mono- and Di-nitrobenzophenone Anion Radicals. The results shown in Table 2 indicate that the unpaired electron of anion radicals generated from nitrobenzophenones is localized only on a nitro-substituted phenyl group, although the compounds have two reducible functional groups.[5] This was definitely confirmed by the observation of the ESR spectrum of the anion radical of d_5-phenyl *p*-nitrophenyl ketone. The spectrum observed was just the same as that of the anion radical generated from *p*-nitrobenzophenone. This conclusion can also be substantiated by other observations. The anion radicals generated from 4-methyl-4'-nitrobenzophenone and from 4-methoxy-4'-nitrobenzophenone showed spectra similar to that of the *p*-nitrobenzophenone anion radical. Furthermore, each of the observed hyperfine structures of nitrobenzophenone anion radicals was very similar to each of those of the corresponding monohalogeno nitrobenzene anion radicals.[6,7] The anion radicals of nitrobenzophenones, therefore, can be considered to be anion radicals of benzoyl-substituted nitrobenzenes.

There have been a large number of experiments and calculations on the free-spin delocalization of the substituted nitrobenzene anion radicals.[2-7] For example, Geske and his co-workers[8] investigated the substituted nitrobenzene anion radicals by ESR. Their calculation on the nitrobenzene anion radical consisting with their experimental

Table 1. Preparation and physical constants of nitro compounds

Compound	Method of Synthesis	Mp, °C
Benzophenone		
p-Nitro-	Friedel-Crafts reaction[1]	138
m-Nitro-	Friedel-Crafts reaction[2]	95
o-Nitro-	Oxidation of *o*-nitrodiphenylmethane[3]	105
4-Methyl-4'-nitro-	Friedel-Crafts reaction[4]	122
4-Methoxy-4'-nitro-	Friedel-Crafts reaction[5]	121
4, 4'-Dinitro-	Oxidation of 4, 4'-dinitrodiphenylmethane[6]	189
3, 3'-Dinitro-	Nitration of benzophenone[7]	154.5—155.3
2, 2'-Dinitro-	Nitration of benzophenone[7]	194.8—195.0
Benzil		
4, 4'-Dinitro-	Nitration of dihydrobenzoin[8]	211.0—211.5
Phenanthraquinone		
2-Nitro-	Nitration of phenanthraquinone[9]	257
2, 7-Dinitro-	Nitration of phenanthraquinone[9]	302—303

1) G. Schroeter, *Ber.*, **42**, 3360 (1909).
2) R. Geigy and W. Koenigs, *ibid.*, **18**, 2401 (1885).
3) R. Geigy and W. Koenigs, *ibid.*, **18**, 2403 (1885).
4) H. Limpricht and E. Samietz, *Ann.*, **286**, 321 (1895).
5) K. Auwers, *Ber.*, **36**, 3898 (1903).
6) W. Staedel, *Ann.*, **194**, 347, 369 (1878).
7) W. Staedel, *ibid.*, **194**, 349 (1878), **283**, 164 (1894).
8) F. D. Chatterway and E. A. Coulson, *J. Chem. Soc.*, **1928**, 1363.
9) A. Werner, *Ann.*, **321**, 336 (1902).

5) For the analytic details of the ESR spectra, see K. Maruyama and R. Goto, *Rev. Phys. Chem. Japan*, **34**, 30 (1964).
6) P. H. Lieger and G. K. Fraenkel, *J. Chem. Phys.*, **39**, 609 (1963).
7) T. Fujinaga, Y. Deguchi and K. Umemoto, This Bulletin, **37**, 822 (1964).
8) D. H. Geske, J. A. Ragle, M. A. Bambenek and A. L. Balch, *J. Am. Chem. Soc.*, **86**, 987 (1964).

TABLE 2. HYPERFINE COUPLING CONSTANTS OF ANION RADICALS*4

Substance	Alkali metal	a_N	a_{H_1}*5	a_{H_2}*5	a_{H_3}*5	a_{H_4}*5	a_M*6
p-Nitrobenzophenone	Li	8.41	3.10	3.10	0.68	0.68	0.00
	Na	8.14	3.10	3.10	0.62	0.62	0.30
	K	7.41	2.91	2.91	0.68	0.68	0.20
m-Nitrobenzophenone	Li	8.14	2.81	2.62	2.45	0.90	0.00
	Na	8.07	3.02	2.72	2.44	0.81	0.30
	K	7.37	3.28	2.88	2.49	0.87	0.20
o-Nitrobenzophenone	Li*2	—	—	—	—	—	—
	Na	7.80	3.03	2.60	0.82	0.82	0.10
	K	7.29	2.96	2.57	0.79	0.79	0.00
4, 4'-Dinitrobenzophenone	Li	7.96	3.05	3.05	0.77	0.77	0.00
	Na	7.14	2.83	2.83	0.63	0.63	0.27
	K	6.37	2.79	2.79	0.65	0.65	0.17
4-Methoxy-4'-nitrobenzophenone	Li	8.45	3.02	3.02	1.00	1.00	0.00
	Na	7.90	3.11	3.11	0.76	0.76	0.30
	K	7.24	3.02	3.02	0.75	0.75	0.15
4-Methyl-4'-nitrobenzophenone	Li	8.50	3.02	3.02	0.94	0.94	0.00
	Na	8.03	3.02	3.02	0.72	0.72	0.25
	K	7.10	2.92	2.92	0.66	0.66	0.10
3, 3'-Dinitrobenzophenone	Li	10.60	4.17	3.78	3.47	1.11	0.00
	Na	10.45	4.27	3.80	3.30	1.07	0.37
	K	9.28	4.33	3.79	3.22	1.16	0.17
2, 2'-Dinitrobenzophenone	Li*1	—	—	—	—	—	—
	Na	9.40	4.36	3.25	1.20	1.20	0.00
	K	9.33	4.28	3.25	1.20	1.20	0.00
4, 4'-Dinitrobenzil*2	Li*1	—	—				
	Na	0.00	0.85				
	K	0.00	0.84				
	Rb	0.00	0.84				
4, 4'-Dinitrobenzil*3	Li	5.17	—	2.58			
	Na	4.90	—	2.10			
	K	4.82	—	2.18			
	Rb	4.00	—	2.10			
2-Nitrophenanthraquinone	K	0.00	1.94	0.97	0.44		
2, 7-Dinitrophenanthraquinone	K	0.00	1.94	0.97	0.44		

*1 Anion radical could not be obtained.
*2 Anion radical which shows the smaller overall splitting.
*3 Anion radical which shows the larger overall splitting.
*4 Measurements are all conducted at 18—20°C, Solvent: Dimethoxyethane.
*5 Positions of protons are listed below.
*6 Coupling constant due to alkali metal.

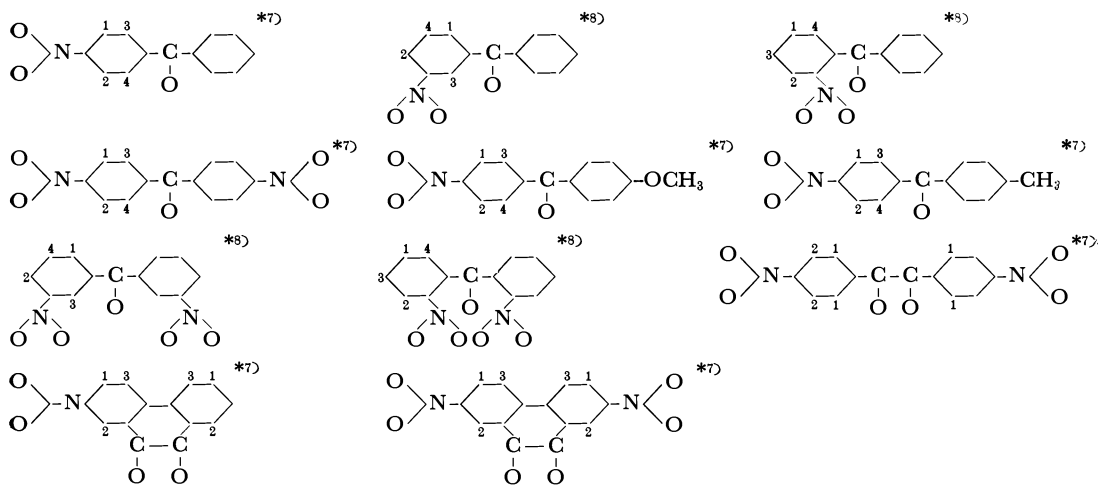

*7) Assignment of splittings to positions was done on the basis of the experiments.
*8) Assignment of splittings to positions was done tentatively from a comparison with a result of SHMO calculation.

result showed that ~65% of the free spin was localized on the nitro group. Since such a substituent as a halogen atom or a carbonyl group can not induce an drastic change in the free-spin delocalization—— as can be deduced from a comparison with the coupling constant due to the nitrogen atom of the nitro group, the position of the highest free-spin density is on the nitro group.

Anion radicals of dinitrobenzophenone generated from 2, 2'-, 3, 3'- and 4, 4'-dinitrobenzophenone showed spectra indicating that the unpaired electron was delocalized only on one phenyl group; their ESR spectra quite resemble that of the anion radical generated from the corresponding mononitrobenzophenone.[5] Therefore, the position of the highest free-spin density is on one of two nitro groups for the same reason as has been given above.

Another outstanding phenomenon of these mono- and dinitrobenzophenone anion radicals was that the hyperfine coupling constant due to the nitrogen atom varied systematically with the species of alkali metal. This may be unambigously attributable to the ion-pair formation between the anion radical and the cation. It was found that the ^{13}C hyperfine coupling constant of benzophenone carbonyl carbon also varied with the species of alkali metal[9]; it was ascribed to the existence of the ion-pair.

Dinitrobenzil Anion Radicals. The anion radicals of dinitrobenzil obtained by reduction with alkali metals showed some unusual phenomena. Typical observed ESR spectra are shown in Fig. 1. By the usual procedure an unsymmetrical spectrum with a larger overall splitting was observed, regardless of the species of alkali metals. However, a symmetrical spectrum with a smaller overall splitting could be observed if it was very much diluted. This change from the unsymmetrical to the symmetrical was dependent on the temperature and on the ionic size of the cation with which anion radical was forming the ion-pair. In general, we could observe the unsymmetrical spectrum at lower temperatures, even if it was diluted. Moreover, if metallic lithium was used for the reduction, only the unsymmetrical spectrum could be observed, while if metallic rubidium was used, then the symmetrical spectrum with the smaller overall splitting was easily observed. From the results described above, it may

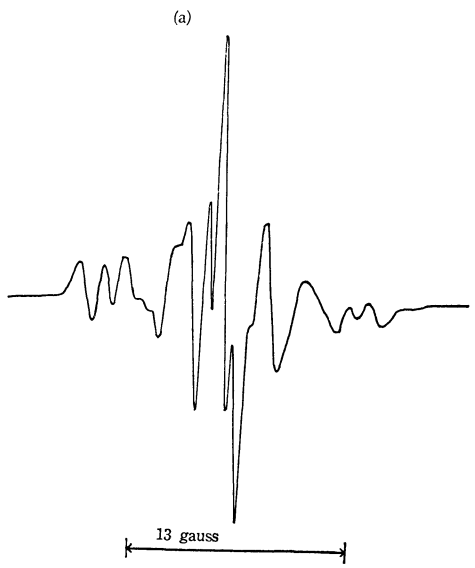

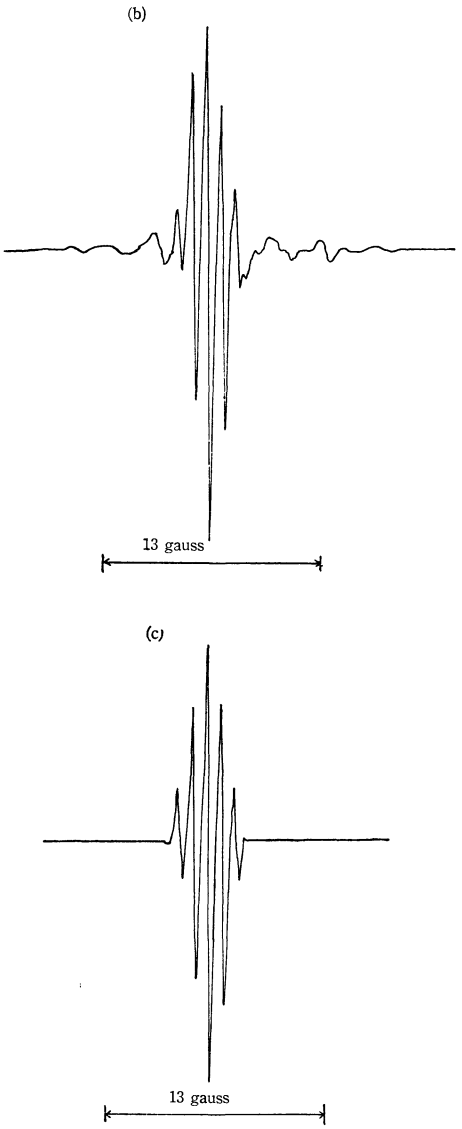

Fig. 1. ESR spectra of sodium dinitrobenzil anion radical.
(a) in a higher concentration
(b) in a medium concentration
(c) in a extremely diluted concentration

9) N. Hirota, *ibid.*, **89**, 32 (1967).

be concluded that there is an equilibrium between the ion-pair monomer, which shows a symmetrical spectrum, and the ion-pair dimer, which shows a spectrum with a larger overall splitting. Therefore, the spectrum actually observed in usual concentrations is a superposition of the two.

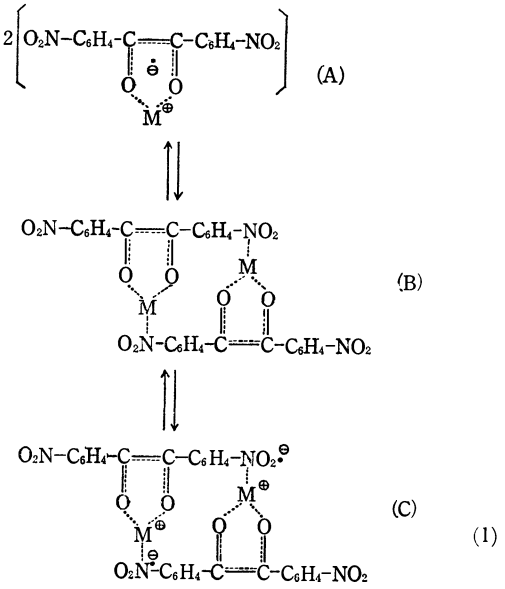

M⊕: metal cation
M: atomic metal

There must be a rapid equilibrium among the ion-pair monomer (A) and ion-pair dimers (B and C), for the observed spectrum is unusually broad. The symmetrical five line spectrum (intensity ratio; 1 : 4 : 6 : 4 : 1) with the smaller overall splitting (4.1 gauss) will correspond to the A structure, while the spectrum with the larger overall splitting (19.9 gauss) will correspond to the C structure. The B structure seems to be a transient stage for the electron-transfer reaction. This may be explained by the fact that the overall splitting of the spectrum of α-diketone ketyls is, in general, about 5 gauss, while that of anion radicals of nitro compounds is larger than 10 gauss, consisting of three equivalent lines due to the nitrogen atom accompanying with the other hyperfine structure.[1-8,10] For example, the overall splitting of potassium benzil ketyl is 4.5 gauss and the hyperfine coupling constant due to the four hydrogen atoms occupying the position α to α-dicarbonyl group is 0.96 gauss. Estimating from the hyperfine coupling constant (0.85 gauss), $\sim$75% of the free-spin is localized on the α-dicarbonyl group in A.

Mono- and Di-nitrophenanthraquinone. The anion radicals of 2-nitro- and 2, 7-dinitrophenanthraquinone, both generated by reduction with alkali metal, showed quite similar symmetrical ESR spectra, with an overall splitting of about 7 gauss. The solution of anion radicals was pink, but it turned into a green diamagnetic solution if it was present in a high concentration. Analogous phenomena have been found in the case of phenanthraquinone ketyls.[11] The hyperfine structure of 2, 7-dinitrophenanthraquinone can be analysed as a spectrum consisting of three sets of two equivalent hydrogen atoms (the coupling constants are 1.94 gauss, 0.97 gauss, and 0.44 gauss respectively). Estimating from the coupling constants obtained, more than 70% of the free spin is localized on the α-dicarbonyl group in the anion radical of 2-nitro- or 2, 7-dinitrophenanthraquinone. Thus, the unpaired electron delocalizes only on the aromatic ring, is highly concentrated on the α-dicarbonyl group, and does not delocalize on the nitro group.

The hyperfine coupling constants obtained are summarized in Table 2.

Correlation between Chemical Reactivity and Unpaired-electron Distribution. In the compounds which have two or three functional groups in a molecule, the problem of which group is the most reactive for a reagent is of great interest to the organic chemist. Nitrobenzophenones, nitrobenzil, and nitrophenanthraquinone have two or three functional groups for the reduction. From the results of the ESR study we can determine the position which has the highest free-spin density in a molecule. The positions to be reduced and the positions of the highest free-spin density in the compounds which have two or more functional groups are tabulated in Table 3. As can be seen in Table 3, there is a definite correlation between the most reactive position of a compound for the chemical reduction and the highest free-spin density of the anion radical generated from the corresponding compound. In nitrobenzophenone anion radicals, the position of the highest free-spin density is on the nitro group, and nitrobenzophenone can be reduced at the nitro group to the corresponding reduced compound, regardless of the species of the reducing reagent.

By the reduction of dinitrobenzil, both α-dicarbonyl and nitro groups can be reduced at the same time; the results obtained by ESR study show the existence of an equilibrium between the anion radical monomer and the anion radical dimer in the system because the concentration of the substrate is high enough to form the dimer. As has been described above, the unpaired electron delocalizes mainly on the α-dicarbonyl group in the monomer anion radical, whereas the unpaired electron delocalizes mainly on the nitro group in the anion radical dimer. The experimental results, therefore, completely support the idea that

10) R. Dehl and G. K. Fraenkel, *J. Chem. Phys.*, **39**, 1793 (1963).

11) K. Maruyama, This Bulletin, **37**, 553 (1964).

TABLE 3. THE REDUCED GROUP AND GROUP HAVING THE HIGHEST FREE SPIN DENSITY

Substance	Group having highest free spin density	Reducing reagent	Product
Benzophenone			
p-Nitro-	$-NO_2$	Sn+HCl	*p*-Aminobenzophenone[1]
		Zn+NaOH	4, 4'-Dibenzoylazo- and 4, 4'-dibenzoylazoxybenzene[2]
m-Nitro-	$-NO_2$	Sn+HCl	*m*-Aminobenzophenone[3]
		Zn+NaOH	3, 3'-Dibenzoylazo- and 3, 3'-dibenzoylazoxybenzene[2]
		Electroly. (alkaline)	3, 3'-Dibenzoylazo- and 3, 3'-dibenzoylazoxybenzene[4]
		Electroly. (acidic)	*m*-Aminobenzophenone[4]
o-Nitro-	$-NO_2$	Sn+HCl	*o*-Aminobenzophenone[3]
		Zn+NaOH	*o*-Aminobenzophenone[5]
4, 4'-Dinitro-	$-NO_2$	Sn+HCl	4, 4'-Diaminobenzophenone[6]
3, 3'-Dinitro-	$-NO_2$	$SnCl_2$	3, 3'-Diaminobenzophenone[7]
		Na-Hg	3, 3'-Diaminobenzhydrol[8]
2, 2'-Dinitro-	$-NO_2$	Sn+HCl	2, 2'-Diaminobenzophenone[9]
Benzil			
Non-substituted	$-\overset{O}{\overset{\|\|}{C}}-\overset{O}{\overset{\|\|}{C}}-$	$SnCl_2$	Benzoin[10]
4, 4'-Dinitro-	$-\overset{O}{\overset{\|\|}{C}}-\overset{O}{\overset{\|\|}{C}}-$	Sn+HCl	4, 4'-Diaminodesoxybenzoin[11]
p-Nitrobenzaldehyde	$-NO_2$[14]	$SnCl_2$	*p*-Aminobenzaldehyde[12]
		$Zn+NH_4Cl$	*p*-Hydroxyaminobenzaldehyde[13]
p-Nitroacetophenone	$-NO_2$[14]	Zn+HCl	*p*-Aminoacetophenone[15]
m-Nitroacetophenone	$-NO_2$[14]	Zn+HCl	*m*-Aminoacetophenone[16]
		Electroly. (acidic)	*m*-Aminoacetophenone[4]
Phenanthraquinone			
2-Nitro-	$-\overset{O}{\overset{\|\|}{C}}-\overset{O}{\overset{\|\|}{C}}-$	$C_6H_5NHNH_2$ CH_3COOH	2-Nitro-9, 10-dihydroxyphenanthrene[17]
		$H_2S+C_2H_5OH$	2-Nitro-9, 10-dihydroxyphenanthrene[17]
		Sn+HCl	2-Amino-9, 10-dihydroxyphenanthrene[18]
2, 7-Dinitro-	$-\overset{O}{\overset{\|\|}{C}}-\overset{O}{\overset{\|\|}{C}}-$	$C_6H_5NHNH_2$ $+CH_3COOH$	2, 7-Dinitro-9, 10-dihydroxyphenanthrene[17]
		$H_2S+C_2H_5OH$	2, 7-Dinitro-9, 10-dihydroxyphenanthrene[17]
		Sn+HCl	2, 7-Diamino-9, 10-dihydroxyphenanthrene[18]
m-Dinitrobenzene		Na_2S_2	*m*-Nitroaniline[19]
		Sn+HCl	*m*-Nitroaniline[19]
		Electroly.	*m*-Nitroaniline[17]
Naphthalene[20]		$Na+C_2H_5OH$	1, 4-Dihydronaphthalene[21] 1, 4, 5, 8-Tetrahydronaphthalene

1) A. Baeyer and V. Villiger, *Ber.*, **37**, 605 (1904). 2) P. Carré, *Compt. rend.*, **144**, 34 (1907). 3) R. Geigy and W. König, *Ber.*, **18**, 2403 (1885). E. Bamberger and S. Lindberg, *ibid.*, **42**, 1723 (1909). 4) K. Elbs and A. Wogrinz, *Z. Elektrochem.*, **9**, 428 (1903). 5) P. Carré, *Compt. rend.*, **148**, 492 (1909). 6) W. Staedel, *Ann.*, **218**, 344 (1883). 7) A. Baeyer, *ibid.*, **354**, 192 (1907). 8) P. J. Montagne, *Ber.*, **48**, 1036 (1915). 9) W. Staedel, *Ann.*, **283**, 171 (1894). 10) H. Apitzsch, *Ber.*, **40**, 1803 (1907). 11) H. Golubeff, *ibid.*, **6**, 1252 (1873). 12) B. Flurscheim and T. Simon, *J. Chem. Soc.*, **93**, 1482 (1908). 13) F. J. Alway and M. D. Welsh, *J. Am. Chem. Soc.*, **24**, 1056 (1902). 14) P. H. Lieger and G. K. Fraenkel, *J. Chem. Phys.*, **37**, 2811 (1962). 15) V. B. Drewsen, *Ann.*, **212**, 160 (1882). 16) H. Hunnius, *Ber.*, **10**, 2009 (1877). 17) J. Schmidt and A. Kampf, *ibid.*, **35**, 3117, 3126 (1902). 18) R. Anschütz and P. Mayer, *ibid.*, **18**, 1943 1885). 19) K. Brand, *ibid.*, **38**, 4009, 4014 (1906). 20) D. Lipkin, D. E. Paul, D. E. Townsend and S. I. Weissman, *Science*, **117**, 534 (1953). 21) E. Bamberger and W. Lodter, *Ber.*, **20**, 1705, 3075 (1887); *Ann.*, **288**, 75 (1895).

the more reactive position is the position of the highest free-spin density. Thus, if the chemical reduction is performed under extremely diluted conditions, it can be supposed that dinitrobenzoin will be the reduction product.

Much as in the case of dinitrobenzil, the reduction products of mono- and dinitrophenanthraquinone are mono- and dinitro-9, 10-dihydrophenanthrene if reduction is performed under mild conditions using such reducing reagents as hydrogen disulfide and phenylhydrazine.[12] However, both nitro and α-dicarbonyl group can be reduced if one uses such a strong reducing reagent as tin and hydrochloric acid. The free-spin density of nitrobenzaldehyde anion radicals has been investigated by Rieger and Fraenkel[13]; the position of the highest free-spin density is on the nitro groups for all isomers. By the chemical reduction they are all reduced at the nitro group to give amino- or azobenzaldehydes according to the species of reducing reagent. Such a general rule can be applied even to the aromatic hydrocarbon. For example, the position of the highest free-spin density is the α-position in the naphthalene anion radical, and 1, 4-dihydro- or 1, 4, 5, 8-tetrahydronaphthalene is the first reduction product of naphthalene with metallic sodium and ethanol. Although it is generally accepted that the first stage of the reduction is the formation of the anion radical, the successive steps remain ambiguous. From the above discussion, however, it seems plausible that the successive reduction step is the formation of the dinegative ion which is in a state of contact ion-pair with the counter cation. The counter cation might be a cation from heavy metal, a cation from alkali metal, an ammonium cation, and or even a proton. In support of this discussion, it is instructive to consider the reduction of *m*-dinitrobenzene. The anion radical of the compound has been studied in detail by several investigators. If one reduces *m*-dinitrobenzene with alkali metal,[1b,3]: one of the two nitro groups has a higher free-spin density as a result of ion-pair formation, whereas if one reduces it electrolytically,[14] then the two nitro groups have an equivalent free-spin density. By the chemical reduction of *m*-dinitrobenzene with the usual mild reducing reagents, one of the two nitro groups can be reduced to amino, hydroxyamino, or azo groups, *etc.*[15] Even if the compound is reduced electrolytically, one of the two nitro groups can be reduced predominantly.[16] These experimental results suggest that there is a contribution of the ion-pair even in the course of the electrolytic reduction. Although the stable anion radical of *m*-dinitrobenzene has two equivalent nitro groups in such a aprotic solvent as acetonitrile, a proton might be a counter cation of the ion-pair in an electrolysis conducted in a protic solvent which is a usual solvent in electrolytic reduction, and the accession of a proton to the anion radical may cause the localization of an electron on one of the two nitro groups. Thus, for example, the reduction of nitro group may proceed as in Eq. (2);

$$\mathrm{R\text{-}NO_2} \xrightarrow{e} \mathrm{R\text{-}\dot{N}O_2^{\ominus}M^{\oplus}} \xrightarrow{e} \mathrm{R\text{-}\ddot{N}O_2^{\ominus\ominus}2M^{\oplus\oplus}}$$

$$\xrightarrow{H^{\oplus}} \mathrm{R\text{-}N(O)(OH)} \xrightarrow{H^{\oplus}} \mathrm{R\text{-}NO + H_2O}$$

$$\xrightarrow{2e,\ 2H^{\oplus}} \mathrm{R\text{-}NHOH} \xrightarrow{H^{\oplus}} \mathrm{R\text{-}NH^{\oplus}} \xrightarrow{2e} \mathrm{R\text{-}NH_2}$$

$M^{\oplus}$: metal cation (2)

Therefore, it may be concluded that the chemical reduction proceeds with an ion-pair formation in every case.

12) J. Schmidt and A. Kampf, *Ber.*, **35**, 3117, 3126 (1902).
13) P. H. Rieger and G. K. Fraenkel, *J. Chem. Phys.*, **37**, 2811 (1962).
14) P. H. Rieger and G. K. Fraenkel, *ibid.*, **39**, 609 (1963).
15) K. Brand, *Ber.*, **38**, 4011 (1906).
16) K. Brand, *ibid.*, **38**, 4009, 4014 (1906).

BULLETIN OF THE CHEMICAL SOCIETY OF JAPAN VOL. 41 451—454 (1968)

Coumarins. IV. The Acid-catalyzed Reaction of Phenols with Allyl Cyanide[1]

Takeshi AMAKASU[2]

Chemical Laboratory, Seimi Chemical Co., Ltd., Chigasaki, Chigasaki-shi, Kanagawa

(Received September 11, 1967)

A new route to the syntheses of 4-methyldihydrocoumarins has been developed by means of the aluminum chloride-catalyzed reaction of phenols with allyl cyanide. The reaction of excess phenol with allyl cyanide in the presence of 2 equivalents of anhydrous aluminum chloride and an excess of hydrogen chloride yielded β-(*p*-hydroxyphenyl)-butyronitrile in a 16% yield. In contrast, the corresponding 4-methyldihydrocoumarins were obtained, together with β-arylbutyronitriles, from *o*- and *m*-cresols. *p*-Cresol gave rise to 4, 6-dimethyldihydrocoumarin as the sole product in a 8% yield. In diisopropyl ether, resorcinol underwent a similar reaction with allyl cyanide and afforded 4-methyldihydroumbelliferone in a 50% yield.

In the first paper of this series[3] dealing with the direct synthesis of dihydrocoumarins, it was established that anhydrous aluminum chloride, accompanied by dry hydrogen chloride, was an effective catalyst for the reaction of phenols with α, β-unsaturated nitriles. These studies have now been extended to 3-butenenitrile, *i. e.*, allyl cyanide. Although the aluminum chloride-catalyzed addition reaction of benzene to allyl cyanide has previously been shown[4] to give an excellent yield of β-phenylbutyronitrile, the present author could find no report concerning the acid-catalyzed reaction of phenols with allyl cyanide.

In the present study the author has examined the acid-catalyzed reaction of phenols with allyl cyanide, using anhydrous aluminum chloride and dry hydrogen chloride (Scheme 1).

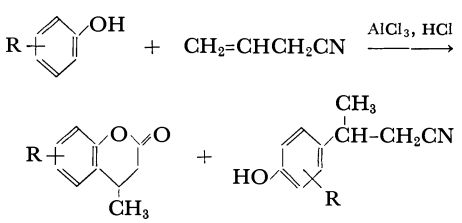

Ia, R=6-CH_3 IIa, R=H
b, R=7-CH_3 b, R=2-CH_3
c, R=8-CH_3 c, R=3-CH_3
d, R=7-OH

Scheme 1

When 5 equivalents of *m*-cresol were treated with allyl cyanide in the presence of 2 equivalents of anhydrous aluminum chloride and an excess of hydrogen chloride, the corresponding dihydrocoumarin, Ib, and white crystals (mp 100—100.5°C) were obtained in 13 and 14% yields respectively. The structure of the former follows from the infrared spectrum (Table 2), which clearly shows a lactone C=O band at 1770 cm^{-1}. The analytical data of the latter agreed with the formula $C_{11}H_{13}NO$, which is in accord with the structures of the addition products, IIb, III, and IV. The infrared spectrum exhibited hydroxyl and cyano absorptions respectively at 3370 and 2230 cm^{-1}, in addition to an out-of-plane deformation of aromatic C–H at 810 cm^{-1}. This eliminates the possibility of such a structure as carbon-oxygen addition products, but not such as III and IV.

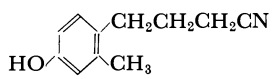

III

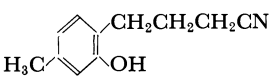

IV

Finally, a NMR spectrum was obtained which was in complete accord with the β-aryl-butyronitrile structure. The characteristic doublets at 8.62 (J= 7 cps) and 7.51 (J=7 cps) τ were assigned to the terminal methyl and the methylene protons, while the two singlets at 7.73 and 5.25 τ were due to ortho-methyl and hydroxyl protons respectively. The aromatic multiplet appeared between 2.77—3.82 τ, along with that of the methine proton at

1) This investigation was presented at the 20th Annual Meeting of the Chemical Society of Japan, Tokyo, April, 1967; and was supported mainly by Asahi Glass Co., for which the author is grateful. Part III of this series: T. Amakasu and K. Sato, This Bulletin, **40**, 1428 (1967).

2) Present address: Department of Applied Chemistry, Faculty of Engineering, Yokohama National University, Ohka-machi, Minami-ku, Yokohama.

3) K. Sato, T. Amakasu and S. Abe, *J. Org. Chem.*, **29**, 2971 (1964).

4) I. P. Tsukervanik and A. D. Grebenyuk, *Dokl. Akad. Nauk SSSR*, **76**, 223 (1951).

TABLE 1. THE ACID-CATALYZED REACTION OF PHENOLS WITH ALLYL CYANIDE

Phenol R	Procedure[a]	Reaction Temp. °C	Reaction hr	Product yield, % I	Product yield, % II
H	A	100—105	3	—	16
2-CH_3	A	105—110	5	8	16
3-CH_3	A	100—105	5	13	14
4-CH_3	A	105—110	5	8	—
3-OH	B	50— 55	4	50	—

a) See experimental section.

6.68 τ. Thus, it may be concluded that the β-substituted butyronitrile structure, II, must be assigned to the latter product from *m*-cresol.

o-Cresol behaved analogously when treated with allyl cyanide, giving the corresponding dihydrocoumarin, IC, as well as the butyronitrile, IIc. In contrast, only 4, 6-dimethyldihydrocoumarin (Ia) was obtained from *p*-cresol, while phenol, upon similar treatment with allyl cyanide, underwent nuclear-addition reaction leading to β-(*p*-hydroxyphenyl)butyronitrile (IIa). The results, summarized in Table 1, indicate that phenols predominantly undergo the nuclear addition reaction to allyl cyanide, while the resulting *o*-addition

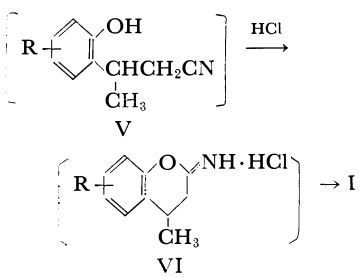

Scheme 2

intermediates V, β-(*o*-hydroxyphenyl)butyronitriles, afford the corresponding dihydrocoumarins, I, through subsequent intramolecular cyclization, followed by acid hydrolysis (see Scheme 2).

Neither V nor VI could be isolated in any case, whereas the acid-catalyzed reaction of phenols with benzoylacetonitrile has been demonstrated[5] to furnsih 4-phenyl-2-iminocoumarins, VII, corresponding to VI, and 3-cyano-4-methyliminocoumarin (VIII) may be obtained by the base-catalyzed condensation of 2-hydroxyacetophenone with malononitrile.[6] This is presumably due to the difference in resonance stability between the intermediates VI and either VII or VIII.

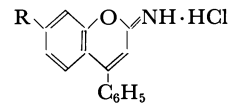

VII

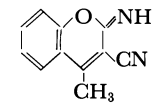

VIII

R=OH, OCH_3, CH_3

On the other hand, 4-methyldihydroumbelliferone (Id) was obtained, in a 50% yield, on a similar treatment of resorcinol with allyl cyanide in a diisopropyl ether solution at 50—55°C for 4 hr. Under the same conditions, however, no reaction occurred between the less reactive phenols, such as crescls, and allyl cyanide. Moreover, the use of such other inert solvents as tetrachloroethane for the reaction of the monohydride phenols resulted in the recovery of the starting phenols.

Tables 2 and 3 summarize the analytical characteristics of compounds I and II respectively. The most significant feature in Table 3 is the definite difference between the physical properties of IIb and those of either IIa or IIc. This might be related, to a certain degree, to the steric strain and the conformational rigidity involved only in IIb.

It is interesting to note whether the Friedel-Crafts reaction of phenols, particularly *o*- and *m*-cresols,

TABLE 2. ANALYTICAL CHARACTERISTICS OF 4-METHYLDIHYDROCOUMARINS (I)

Compd	Bp, °C/mmHg	n_D^{20}	Retention times, min[e]	IR, cm^{-1} C=O	C, % Found	C, % Calcd	H, % Found	H, % Calcd
Ia	74—77/1.5[a]	1.5061	6.0	1765				
Ib	109—114/0.5[b]	1.5395[b]	20.6	1770	74.98	74.97	6.67	6.86
Ic	85—90/1[c]	1.5061[c]	5.0	1765	75.25	74.97	7.06	6.86
Id	164—169/1[d]	d)		1740				

a) Ref. 3 (lit.[3] bp 100—105°C/5 mmHg).
b) K. Fries and G. Fickewirth [*Ann.*, **362**, 44 (1908)] have not reported the boiling point for Ib (lit. n_D^{20} 1.5321).
c) This is a new compound.
d) Mp 110—110.5°C (lit.[12] mp 109—110°C): (lit.[12] bp 190—193°C/7 mmHg).
e) Their retention times were determined under the conditions for gas chromatography described as follows; a 150 cm column packed with PEG (10%) on Diasolid; column temperature, 173°C, carrier gas, helium, 30 ml/min.

5) T. Amakasu and K. Sato, to be published; presented at the 19th Annual Meeting of the Chemical Society of Japan, Yokohama, April, 1966.
6) H. Junek, *Monatsh.*, **95**, 234 (1964).

TABLE 3. IDENTIFICATION OF β-ARYLBUTYRONITRILES (I)[a]

Compd	Bp, °C/mmHg	n_D^{20}	Retention times min[c]	IR, cm^{-1}			C, %		H, %	
				O-H	CN	C-H (aromatic)	Found	Calcd	Found	Calcd
IIa	135—141/1	1.5398	26.7	3400	2250	830	74.35	74.51	7.19	6.88
IIb	168—171/0.5	b)	22.3	3370	2230	810	75.20	75.40	7.60	7.48
IIc	115—118/1	1.5398	26.5	3400	2250	820	75.59	75.40	7.75	7.48

a) They are the hitherto unknown compounds.
b) Mp 100—100.5°C; recrystallized from benzene.
c) Their retention times were taken under the conditions for vapor phase chromatography shown as follows; a 150 cm column packed with PEG (10%) on Diasolid; column temperature, 200°C; carrier gas, helium, 60 ml/min.

takes place at the position ortho or para to the hydroxyl group. The results presented in Table 1 appear to contrast with those of a number of previous studies on the acid-catalyzed C-alkylation of them, indicating that attacks by electrophiles, in general, occur at both positions,[7] ortho and para to the hydroxyl group, except in some cases which lead to the predominant formation of an *o*-[8] or *p*-substituted product.[9] In addition, it is noteworthy that 4-methyldihydrocoumarin (I, R=H) can not be obtained from the reaction of phenol with allyl cyanide, while the reaction with crotononitrile may favor its formation.[3]

Experimental[10]

Materials. The allyl cyanide was prepared from allyl chloride and cuprous cyanide.[11] The other materials were obtained from commercial sources.

The Acid-catalyzed Reaction of Phenols with Allyl Cyanide. *General Procedure A.* Finely-powdered anhydrous aluminum chloride (0.4 mol) was added slowly to a mixture of allyl cyanide (0.2 mol) and the phenol (1 mol), after which stirring was vigorously continued at 30—40°C. Dry hydrogen chloride was passed into a viscous slurry; then the mixture, into which dry gas had been continuously passed, was gradually heated in an oil bath and kept under the conditions shown in Table 1. Thereafter the resulting mixture was chilled and poured over water containing crushed ice and concentrated hydrochloric acid. The organic layer was separated from the aqueous layer, which was then shaken with ether. The extract was combined with the separated organic material, and then washed with water. After the extract had been dried over anhydrous magnesium sulfate and the solvent had been removed, the residue was distilled under reduced pressure to give the crude products, I and/or II (containing phenol and unidentified by-products as contaminants). The analytical sample was prepared by vapor-phase chromatographic fractionation. The results with individual compounds are shown in Table 1. The infrared spectrum of 4, 6-dimethyldihydrocoumarin (Ia) was identical with that reported previously.[3] The analytical data for Compounds I and II are presented in Tables 2 and 3 respectively.

4-Methyldihydroumbelliferone (Id). *Procedure B.* To a stirred solution of resorcinol (22 g, 0.2 mol) and

7) D. R. Stevens and R. S. Bowman, U. S. Pat. 2560666 (1951); Ng. Ph. Buu-Hoi, H. Le Bihan and F. Binon, *J. Org. Chem.*, **17**, 243 (1952); J. F. Miquel, Ng. Ph. Buu-Hoi and R. Royer, *J. Chem. Soc.*, **1955**, 3417; V. L. Vaĭser and A. M. Polikarpova, *Dokl. Akad. Nauk SSSR*, 108, 469 (1956); E. A. Viktorova, N. I. Shuĭkin and G. V. Popova, *Vestn. Mosk. Univ., Ser. II, Khim.*, **15**, No. 6, 62 (1960); E. A. Viktorova, N. I. Shuĭkin and P. N. Komarov, *ibid.*, **16**, No. 2, 53 (1961); N. I. Suĭkin, E. A. Viktorova and I. E. Pokrovskaya, *Izv. Akad. Nauk SSSR, Otd. Khim. Nauk*, **1961**, 1094, 2192; E. A. Viktorova, N. I. Shuĭkin and E. A. Karakhanov, *ibid.*, **1962**, 1080; N. I. Shuĭkin and E. A. Viktorova, *Novye Metody Ratsional. Ispol'z Mestnykh. Topliv, Trudy Soveshchaniya Riga*, **1958**, 265; E. A. Viktorova, N. I. Shuĭkin, I. E. Pokrovskaya and S. L. Aleksandrova, *Neftekhimiya*, **1**, 648 (1961); V. I. Isagulyants and V. P. Evstaf'ev, *Dokl. Akad. Nauk Arm. SSSR*, **38**, 235 (1964); *Mosk. Inst. Neftekhim. i Gaz. Prom.* No. **51**, 105 (1964); D. E. Mishiev, M. M. Guseinov and A. A. Mekhraliev, *Azerb. Khim. Zh.*, **1964**, 23; R. A. Babakhanov, D. E. Mishiev, E. E. Gaidarova and T. Samedova, *ibid*, **1965**, 42; A. I. Kakhniashvili and D. Ya. Bugianishvili, *Zh. Organ. Khim.*, **1**, 1043 (1965).

8) V. M. Dixit and A. M. Kanakudati, *J. Indian Chem. Soc.*, **28**, 323 (1951); I. Miyagawa, K. Sakurayama and K. Sawai, *Research Rept. Nagoya Ind. Sci. Research Inst.*, No. 8, 31 (1955); N. I. Shuĭkin, E. A. Viktorova and V. P. Litvinov, *Vestn. Mosk. Univ., Ser. Mat., Astron., Fiz. i Khim.*, **12**, No. 5, 121 (1957); B. Arventiev, H. Wexler and M. Strul, *Acad. rep. Polulalare Romîne Filiala Iasi, Studic cercetări stünt., Chim.*, **11**, 63 (1960); E. A. Viktorova, N. I. Shuĭkin and G. S. Korostelera, *Vestn. Mosk. Univ., Ser. II, Khim.*, **16**, No. 2, 56 (1961); L. S. Kharchenko and S. V. Zavgorodnii, *Ukr. Khim. Zh.*, **30**, 261 (1964).

9) J. E. Driver and J. B. Sousa, *J. Chem. Soc.*, **1954**, 985; R. Maki, Y. Ishida, K. Satake and R. Oda, *Nippon Kagaku Zasshi (J. Chem. Soc. Japan, Ind. Chem. Sect.)*, **57**, 42 (1954); I. Romadane and R. Slitke, *Uch. Zap. Rizksk. Politekhn. Inst. Khim. Fak.*, **6**, 123 (1962); L. S. Kharchenko and S. V. Zavgorodnii, *Zh. Prikl. Khim.*, **37**, 165 (1964); I. Romadane and E. A. Kochetkova, *Latvijas PSR Zinatnu Akad. Vestis. Khim. Ser.*, **1964**. 77: A. I. Kakhniaskvili and D. Ya. Bugianishvili, *Soobshch. Akad. Nauk Gruz. SSSR*, **37**, 53 (1965); A. I. Topchiev, B. M. Tumerman and E. M. Buslova, Tr., *Mosk. Inst. Neftekhim. i Gaz. Prom.*, No. **51**, 9 (1964).

10) All melting points and boiling points are uncorrected. Infrared spectra were recorded on a Hitachi Model EPI-S2, and gas chromatographic analyses were carried out on a Shimadzu Model GC-1b chromatograph. NMR spectra were taken in D-chloroform on a JEOL Model INM 4H-100 instrument with tetramethylsilane as an internal standard.

11) E. Rietz, "Organic Syntheses," Coll. Vol. III, p. 852 (1955).

allyl cyanide (13.4 g, 0.2 mol) in 200 m*l* of a solvent such as diisopropyl ether, anhydrous aluminum chloride (53.4 g, 0.4 mol) was added, portion by portion. The mixture, into which dry hydrogen chloride had been passed, was heated on a steam bath and kept for 4 hr at 50—55°C. The subsequent procedure followed Procedure A, already described. After the removal of the solvents, the residual oil was fractionated to give 17.6 g (50%) of a viscous oil: bp 164—169°C/1 mmHg (Lit.[12] bp 190—193°C/7 mmHg): ν_{max}^{film} 3280 (O-H), 1740 (lactone C=O), and 850, 810 cm^{-1} (aromatic C-H). It solidified after standing for a long time and melted at 108—110°C.

The recrystallization from benzene afforded Id; mp 110—110.5°C (lit.[12] mp 109—110°C). Compound Id showed a positive ferric chloride test.

On the other hand, the alternative procedure of adding a solution of resorcinol and allyl cyanide in ether to a stirred suspension of aluminum chloride in ether provided the same results as have been presented above.

The author wishes to thank Professor Kikumasa Sato of Yokohama National University for his valuable advice, and Mr. Katsuhiko Takeda for his great help in carrying out the study described in this report. The author is also indebted to the Central Research Laboratories of the Meiji Seika Kaisha, Ltd., for the determination of the NMR spectra reported in this work.

12) T. Kawai, T. Shimizu and M. Suzuki, *Yakugaku Zasshi*, **72**, 553 (1952).

BULLETIN OF THE CHEMICAL SOCIETY OF JAPAN VOL. 41 454—460 (1968)

The Dimerization of Butadiene by Palladium Complex Catalysts

Shigetoshi TAKAHASHI, Toshiki SHIBANO and Nobue HAGIHARA

The Institute of Scientific and Industrial Research, Osaka University, Sakai, Osaka

(Received September 16, 1967)

It has been found that palladium-phosphine complexes coordinated by dienophile and tetrakis-(triphenylphosphine)palladium catalyzed the linear dimerization of butadiene. The dimerization of butadiene with bis(triphenylphosphine)(maleic anhydride)palladium in aprotic solvents, such as benzene, tetrahydrofuran, and acetone, gave octatriene-1,3,7 selectively in good yields. In such alcohols as methanol, ethanol, and isopropanol, butadiene was converted to 1-alkoxyocta-diene-2, 7 and/or octatriene-1, 3, 7, depending on the nature of the alcohols employed. The dimerization in secondary amines, such as morpholine, piperidine, and diisopropylamine, gave butadiene dimer-amine adducts of the $R_2N(C_8H_{13})$ type, while that in primary amines, such as aniline and *n*-butylamine, gave a mixture of $RNH(C_8H_{13})$ and $RN(C_8H_{13})_2$. Phenoxy- and acetoxyoctadiene were also obtained from the reactions in phenol and acetic acid respectively.

It is well-known that butadiene is converted selectively to cyclic oligomers with various catalysts, for example, Ziegler-type catalysts.[1] Recently, it has been reported that linear dimerizations of butadiene can be carried out with cobalt[2]-, iron[3]- or rhodium[4]-containing catalysts to form methyl-heptatriene and/or *n*-octatriene. The dimerization with a nickel catalyst usually gives cyclic dimers; however, there is a linear dimerization in alcoholic media with low-valent nickel complexes.[5] A large number of reports on the oligomerization of butadiene with nickel catalysts have been presented, but there have been only a few reports[6] on the catalytic behavior of the palladium complex in response to butadiene.

In the course of an examination of the reactions

1) See, for example, G, Wilke, *Angew. Chem.*, **75**, 10 (1963).

2) S. Otsuka, T. Taketomi and T. Kikuchi, *Kogyo Kagaku Zasshi (J. Chem. Soc. Japan, Ind. Chem. Sect.)*, **66**, 1094 (1963); T. Saito, T. Ono, Y. Uchida and A. Misono, *ibid.*, **66**, 1099 (1963); S. Otsuka and T. Taketomi, *European Polymer J.*, **2**, 289 (1966); D. Wittenberg, *Angew. Chem.*, **75**, 1124 (1963); S. Tanaka, K. Mabuchi and N. Shimazaki, *J. Org. Chem.*, **29**, 1626 (1964).

3) H. Takahashi, S. Tai and M. Yamaguchi, *J. Org. Chem.*, **30**, 1661 (1965).

4) T. Alderson, E. L. Jenner and R. V. Lindsey, Jr., *J. Am. Chem. Soc.*, **87**, 5638 (1964).

5) a) T. Yoshida and S. Yuguchi, 19th Annual Meeting of the Chemical Society of Japan, Osaka, April, 1965; b) H. Müller, D. Wittenberg, H. Seibt and E. Scharf, *Angew. Chem.*, **77**, 318 (1965); J. Feldman, B. A. Saffer and O. D. Frampton, U. S. Pat. 3284529 (1966) (*Chem. Abstr.*, **66**, 28373 (1967)).

6) a) G. Wilke, B. Bogdanović, P. Hardt, P. Heimbach, W. Kiem, M. Kröner, W. Oberkirch, K. Tanaka, E. Steinrücke, D. Walter and H. Zimmermann, *Angew. Chem.*, **78**, 157 (1966); b) Neth. Appl. Pat. 6606567 (1966) (*Chem. Abstr.*, **67**, 11427 (1967)).

of dienophile-coordinated palladium-phosphine complexes[7] with butadiene, we have found that bis(triphenylphosphine) (maleic anhydride) palladium catalyzed a dimerization of butadiene, thus forming a linear butadiene dimer in a good yield. The preliminary results have been described in previous papers.[8,9] We have also studied the dimerization of butadiene by palladium complexes in alcohols or amines in considerable detail and have found that the dimerization in these solvents gave butadiene dimer-alcohol or -amine adducts in good yields.

Results and Discussion

The Dimerization Reaction in an Aprotic Solvent. When butadiene was heated at 100—120°C in benzene in the presence of bis(triphenylphosphine) (maleic anhydride) palladium,[7] Pd-$(Ph_3P)_2(C_4H_2O_3)$, it was converted to octatriene-1, 3, 7; there were no other butadiene dimers except a small amount of a thermal reaction product, 4-vinylcyclohexene-1.[8]

$$2\ H_2C{=}CH{-}CH{=}CH_2 \rightarrow H_2C{=}CH{-}CH{=}CH{-}CH_2{-}CH_2{-}CH{=}CH_2 \quad (1)$$

The dependence of the yield on the reaction temperature was investigated between 80—120°C; the results obtained are summarized in Table 1.

Although the yield of octatriene was good at an elevated temperature, the reaction at 120°C caused the decomposition of the catalyst and the products contained butadiene trimer (ca. 5%) and vinylcyclohexene as by-products. For the preparation of octatriene-1, 3, 7 in benzene, therefore, the reaction might better be carried out at a temperature between 110—115°C.

The reactions in tetrahydrofuran and acetone also gave octatriene-1, 3, 7; the experimental results are shown in Table 1.

Table 1. The dimerization in aprotic solvents

Solvent	Reaction temp., °C	Reaction time, hr	Yield[a] of octatriene-1, 3, 7, %
Benzene	80	7	trace
Benzene	100	7	23
Benzene	110	7	46
Benzene	120	7	64
T.H.F.	115	7	82
Acetone	115	7	86

a) Gas chromatographic analysis.
Catalyst $Pd(Ph_3P)_2(C_4H_2O_3)$ 219 mg (0.3 mmol); Solvent 20 ml; Butadiene 13 g.

The Dimerization Reaction in Alcohol. The dimerization of butadiene was also carried out in alcohols. In contrast to the reactions in such aprotic solvents as benzene or acetone, the dimerization in alcohols proceeded smoothly even at lower temperatures (40—100°C) to give 1-alkoxyoctadiene-2, 7 and/or octatriene-1, 3, 7, depending on the nature of the alcohols employed. There have been a few reports on the oligomerization of butadiene, which affords a butadiene dimer-alcohol adduct.[5a,6b,10]

In methanol butadiene easily dimerized, at a low temperature and a short reaction time, with the bis(triphenylphosphine)(maleic anhydride)-palladium catalyst to give 1-methoxyoctadiene-2, 7 and its isomer, 3-methoxyoctadiene-1, 7, along with a small amount of octatriene-1, 3, 7 (Eq. (2), $R=CH_3$).

$$2\ H_2C{=}CH{-}CH{=}CH_2 + ROH \rightarrow R{-}O{-}CH_2{-}CH{=}CH{-}CH_2{-}CH_2{-}CH_2{-}CH{=}CH_2 + H_2C{=}CH{-}CH(OR){-}CH_2{-}CH_2{-}CH_2{-}CH{=}CH_2 \quad (2)$$

It is obvious that methoxyoctadiene is not derived from the reaction of octatriene with methanol, for octatriene was found not to react with alcohol under the same reaction conditions as these employed in the dimerization reaction of butadiene. The trans-configuration of 1-methoxyoctadiene-2, 7 obtained from the above reactions was suggested by the fact that its infrared spectrum showed a strong band at 970 cm^{-1} which is attributable to the CH out-of-plane deformation of trans -CH=CH-.

Bis (triphenylphosphine) (dimethylfumarate) palladium, bis(triphenylphosphine)(*p*-benzoquinone)-palladium, tetrakis(triphenylphosphine)palladium, and -platinum could also be employed as catalysts, although these complexes were found to be almost ineffective in aprotic solvents. The dependence of the distribution of the products on the catalyst and reaction conditions is shown in Table 2.

The platinum complex was less effective than palladium complexes.

In abs. ethanol the dimerization of butadiene with the bis(triphenylphosphine)(maleic anhydride)-palladium catalyst gave octatriene-1, 3, 7 and 1-ethoxyoctadiene-2, 7, plus a small amount of an isomer of ethoxyoctadiene, whereas in isopropanol octatriene-1, 3, 7 was obtained as the main product. The ratio of ethoxyoctadiene to octatriene was independent of the reaction time, and the use of a large amount of ethanol as the solvent resulted in a higher ratio, as Table 3 shows.

Although bis(triphenylphosphine)(*p*-benzoquinone)palladium was found to exhibit similar catalytic behavior, tetrakis(triphenylphosphine)palla-

7) S. Takahashi and N. Hagihara, *Nippon Kagaku Zasshi (J. Chem. Soc. Japan, Pure Chem. Sect.)*, **88**, 1306 (1967).
8) S. Takahashi, T. Shibano and N. Hagihara, *Tetrahedron Letters*, **1967**, 2451.
9) S. Takahashi, H. Yamazaki and N. Hagihara, This Bulletin, **41**, 254 (1968).
10) K. C. DeWhirst, *J. Org. Chem.*, **32**, 1297 (1967).

TABLE 2. THE DIMERIZATION IN METHANOL

Catalyst	Reaction temp., °C	Reaction time, hr	Yield, % 1-RO-OD	3-RO-OD*	OT*
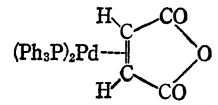	40	2	62	1	0
	70	1	85	5	3
	90	1	73	6	4
	40	2	87	7	1
$(Ph_3P)_4Pd$	70	1	90	8	1
	90	1	86	9	2
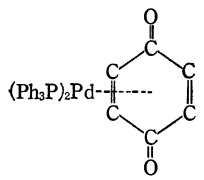	70	1	85	2	1
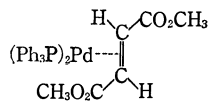	70	1	86	4	1
$(Ph_3P)_4Pt$	90	3	26	4	0

* 1-RO-OD: 1-methoxyoctadiene-2,7; 3-RO-OD: 3-methoxyoctadiene-1,7; OT: octatriene-1,3,7
Catalyst 0.1 mmol; Methanol 20 m*l*; Butadiene 13 g

TABLE 3. THE DIMERIZATION IN ETHANOL OR ISOPROPANOL

Catalyst	Solvent	Reaction temp., °C	Reaction time, hr	Yield, % OT[a]	RO-OD[a]	RO-OD/OT[b]
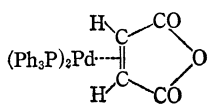	C_2H_5OH	110—115	1	50	33	0.66
	C_2H_5OH	110—115	6	49	35	0.71
	C_2H_5OH[c]	100	3	25	68	2.7
	i-C_3H_7OH[d]	100	4	75		
$(Ph_3P)_4Pd$	C_2H_5OH	110—115	6	27	62	
	i-C_3H_7OH[d]	112—116	7.5	11		
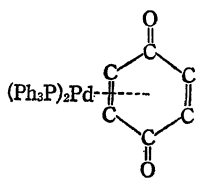	C_2H_5OH	110	1.5	48	39	
	i-C_3H_7OH[d]	110—114	4.5	77		

a) OT: octatriene-1,3,7; RO-OD: 1-ethoxyoctadiene-2,7.
b) Molar ratio of 1-ethoxyoctadiene-2,7 to octatriene-1,3,7.
c) Butadiene 6.5 g; ethanol 50 m*l*.
d) A small amount of a butadiene dimer-isopropanol adduct was detected by gas chromatography.

dium was less effective in ethanol and was almost entirely inactive in isopropanol. The dependence of the reaction products on the nature of the alcohols employed is of considerable interest in respect to the mechanism of the catalysis.

The Dimerization Reaction in Phenol or Acetic Acid. The dimerization of butadiene in more acidic solvents, such as phenol or acetic acid, was attempted; it was found to give a butadiene dimer-phenol or -acetic acid adduct. The reaction of butadiene and phenol in a benzene solution at 80°C with the $Pd(Ph_3P)_2(C_4H_2O_3)$ catalyst proceeded smoothly, giving the phenol adduct in a 57% yield and lower-boiling butadiene dimers

Table 4. The dimerization in amines

Amine, mmol		Solvent[a]	Reaction temp., °C	Reaction time, hr	Yield, % OT[b]	$R_2N(C_8H_{13})$	$RN(C_8H_{13})_2$
Morpholine	230	None[c]	80	1	0	90	
Piperidine	200	None[c]	110	5	0	60	
Diisopropylamine	140	None[c]	100—110	5	34	51	
Morpholine	160	Acetone	80—90	1	0	97	
Diisopropylamine	160	Acetone	100—104	3	trace	69	
Carbazole	120	Acetone	120—125	5	trace	57	
2-Pyrrolidone	210	None[c]	110—115	6	64	0	
Acetoamide	160	Acetone	114—116	5	64	0	
Aniline	160	Acetone	100—104	0.5	0	60	25
Aniline[d]	160	Acetone	113—115	2	8	44	23
n-Butylamine	200	None[c]	90—98	8	trace	29	42

a) 20 m*l*. b) OT: octatriene-1, 3, 7. Gas chromatographic analysis. c) Catalyst 0.3 mmol.
d) $Pd(Ph_3P)_4$ catalyst. Catalyst $Pd(Ph_3P)_2(C_4H_2O_3)$ 0.2 mmol; Butadiene 13 g (240 mmol).

Table 5. The dimerization in aniline derivatives

Amine	pK_a[11]	Reaction temp., °C	Reaction time, hr	Yield, % $RNH(C_8H_{13})$	$RN(C_8H_{13})_2$
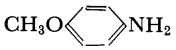	5.29	90	0.5	54	33
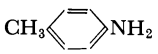	5.07	90—95	0.5	48	36
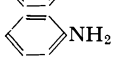	4.58	90—95	0.5	46	24
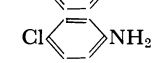	3.81	90—95	0.5	58	0
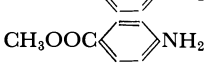	2.47	102—104	2.0	48	0

Catalyst $Pd(Ph_3P)_2(C_4H_2O_3)$ 0.2 mmol; Solvent acetone 20 m*l*;
Butadiene 13 g (240 mmol); Amine 160 mmol.

which were not completely characterized.

The gas chromatograph and the NMR spectrum indicated that the phenol adduct consisted of 78% 1-phenoxyoctadiene-2, 7 and 22% of its isomer, probably 3-phenoxyoctadiene-1, 7 (Eq. (2), R=C_6H_5), which could not been separated by fractional distillation. Recently, it has been reported[6b] that the reaction between butadiene and phenol with palladium chloride gives 1-phenoxyoctadiene-2, 7.

The dimerization of butadiene in acetic acid with $Pd(Ph_3P)_2(C_4H_2O_3)$ or $Pd(Ph_3P)_4$ at 120°C gave a low conversion to a mixture (*ca.* 30% yield) of esters, containing 1-acetoxyoctadiene-2, 7 and its isomer, probably 3-acetoxyoctadiene-1, 7 (Eq. (2), R=CH_3COO), and lower-boiling butadiene dimers.

The reaction at a higher temperature gave a somewhat higher conversion, but the yield of acetic acid adduct was almost unchanged.

The Dimerization Reaction in Amine. Attempts to synthesize butadiene dimer-amine adducts were also carried out. The reactions of butadiene with secondary amines, such as morpholine, piperidine and diisopropylamine, in the presence or absence of the solvent afforded butadiene dimer-amine adducts of the $R_2N(C_8H_{13})$ type, while reactions with primary amines, such as aniline and *n*-butylamine, afforded a mixture of $RNH(C_8H_{13})$ and $RN(C_8H_{13})_2$, as shown in Eqs. (3) and (4). The experimental results are summarized in Table 4.

$$2\ H_2C{=}CH{-}CH{=}CH_2 + R_2NH \rightarrow R_2N{-}CH_2{-}CH{=}CH{-}CH_2{-}CH_2{-}CH_2{-}CH{=}CH_2$$
$$2\ H_2C{=}CH{-}CH{=}CH_2 + RNH_2 \rightarrow RNH{-}CH_2{-}CH{=}CH{-}CH_2{-}CH_2{-}CH_2{-}CH{=}CH_2 \quad (3)$$
$$+$$
$$CH_2{-}CH{=}CH{-}CH_2{-}CH_2{-}CH_2{-}CH{=}CH_2$$

$$\begin{array}{l} \\ N{-}R \\ \\ \end{array} \qquad \begin{array}{l} CH_2{-}CH{=}CH{-}CH_2{-}CH_2{-}CH_2{-}CH{=}CH_2 \\ \\ CH_2{-}CH{=}CH{-}CH_2{-}CH_2{-}CH_2{-}CH{=}CH_2 \end{array} \quad (4)$$

11) "Constants of Organic Compounds", in Series of Comprehensive Organic Chemistry, ed. by M. Kotake, Asakura, Tokyo (1963), p. 652.

The amine adducts produced from the above reactions were easily isolated by fractional distillation and were found to be somewhat unstable in air. Trans-configurations of octa-2, 7-dienylamine and diocta-2, 7-dienylamine derivatives were suggested by their infrared spectra, which showed a strong band near 970 cm^{-1}, as did 1-alkoxyoctadiene-2, 7. Although the products were thought to include a small amount of an isomer of the amine adduct as well as alcohol adducts, they could not be separated by fractional distillation.

The use of amines, such as morpholine and aniline, gave high conversions to amine adducts under mild reaction conditions, whereas a weak base such as carbazole gave a low rate of conversion to an amine adduct even under more vigorous conditions. When such amines as 2-pyrrolidone and acetoamide were employed, no amine derivatives were formed and octatriene-1, 3, 7 was obtained. The reactivities of aniline derivatives in terms of the dimerization rate of butadiene were investigated (Table 5) and found to increase in the order:

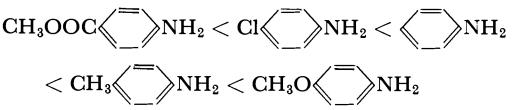

These facts suggest that there is a relationship between the reactivity and the basicity of amine in the dimerization reaction of butadiene.

The tetrakis(triphenylphosphine)palladium catalyst was less effective than the bis(triphenylphosphine)(maleic anhydride)palladium catalyst in amines. Under more vigorous conditions, the reaction in aniline with $Pd(Ph_3P)_4$ gave aniline adducts, as Table 4 shows.

Investigations of the mechanism of catalysis will be reported in a forthcoming publication.

Experimental

Reagents. Butadiene was dried over a molecular sieve. Tetrakis(triphenylphosphine)palladium, $Pd(Ph_3P)_4$, and -platinum, $Pt(Ph_3P)_4$, were prepared by a modification[12] of the method of Malatesta.[13,14] Bis(triphenylphosphine)(maleic anhydride)palladium and other dienophile-coordinated palladium complexes were prepared by the reaction of $Pd(Ph_3P)_4$ and dienophile by a method described in an earlier report.[7]

Analysis. The infrared spectra of the products were taken with a Jasco Model DS-402G grating spectrometer, while the ultraviolet spectra were taken with a Beckman DK-2 spectrophotometer. The NMR spectra were recorded on a Varian Model A-60 instrument, using tetramethylsilane as an internal standard in carbon tetrachloride. The molecular weights were measured in a benzene solution using a Knauer Vapor-pressure Osmometer.

Gas Chromatography. Octatriene-1, 3, 7 and alkoxyoctadiene were analyzed, using a 3 m silicon-grease 550 column, with a Shimadzu Gas Chromatograph, Model GC-2B. The conditions were as follows: octatriene-1, 3, 7: column temperature, 120°C; carrier gas (nitrogen) speed, 38 m*l*/min; internal standard, benzene; methoxyoctadiene: column temperature, 170°C; carrier gas (nitrogen) speed, 28 m*l*/min; internal standard, acetophenone; ethoxyoctadiene: column temperature, 175°C; carrier gas (nitrogen) speed, 27 m*l*/min; internal standard, nitrobenzene.

The Dimerization Reactions of Butadiene. The boiling points and refractive indices of the products obtained in this work are listed in Tables 6 and 7. The results of the elemental analysis and molecular-weight measurement of the compounds are summarized in Table 8. Typical procedures of the dimerization reactions of butadiene are as follows:

A) In an Aprotic Solvent. A 100 m*l*, stainless-steel autoclave was charged with 30 m*l* of acetone and 219 mg (0.3 mmol) of bis(triphenylphosphine)(maleic anhydride)palladium. Butadiene (20 g) was then condensed into the autoclave. The reaction mixture was heated to 115°C and held there for 8 hr while being stirred. In order to separate the reaction product from the catalyst, the yellow reaction mixture was distilled into a cold trap at ~60°C under reduced pressure. The distillate gave 14 g (70 % yield) of octatriene-1, 3, 7 (bp 124—125°C) by fractional distillation under a nitrogen atmosphere. It also contained a small amount of 4-vinylcyclohexene-1 (*ca.* 5%). The octatriene-1, 3, 7 was characterized[8] by its infrared, ultraviolet, and NMR spectra, and by hydrogenation to *n*-octane. The ultraviolet spectrum (C_2H_5OH solution) showed a band at 225 mμ (ε_{max} 22000). The infrared spectrum showed bands at 1638 (C=C), 1600

Table 6. Octatriene and its derivatives

	Compound	bp, °C/mmHg	n_D^{20}
I	CH_2=CH-CH=CH-CH_2-CH_2-CH=CH_2	124—125	1.4682
IIA$_1$	CH_3-O-CH_2-CH=CH-CH_2-CH_2-CH_2-CH=CH_2	163—164	1.4417
IIA$_2$	CH_2=CH-CH(OCH_3)-CH_2-CH_2-CH_2-CH=CH_2	145—146	1.4321
IIB*	C_2H_5-O-CH_2-CH=CH-CH_2-CH_2-CH_2-CH=CH_2	105—107/70	1.4422
IIC*	C_6H_5-O-CH_2-CH=CH-CH_2-CH_2-CH_2-CH=CH_2	171—174/33	1.5178
III*	CH_3COO-CH_2-CH=CH-CH_2-CH_2-CH_2-CH=CH_2	72—82/6	1.4486

* Contains an isomer.

12) S. Takahashi, K. Sonogashira and N. Hagihara, *Nippon Kagaku Zasshi (J. Chem. Soc. Japan, Pure Chem. Sect.)*, **87**, 610 (1966).

13) L. Malatesta and M. Angoletta, *J. Chem. Soc.*, **1957**, 1186.

14) L. Malatesta and C. Cariello, *ibid.*, **1958**, 2323.

Table 7. Amine adducts

R_2N-CH_2-CH=CH-CH_2-CH_2-CH_2-CH=CH_2 or RNH-CH_2-CH=CH-CH_2-CH_2-CH_2-CH=CH_2

	R_2N- or RNH-	bp, °C/mmHg	n_D^{20}
IVA	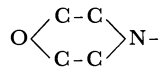	141—142/23	1.4778
IVB	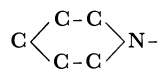	139—140/25	1.4790
IVC	(i-C_3H_7)$_2$N-	132—133/27	1.4568
IVD	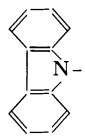	217—218/5	1.6193
IVE_1	n-C_4H_9NH-	133—134/35	1.4576
IVF_1		184—186/25	1.5436
IVG_1	CH_3O 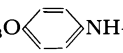	148—151/2	1.5444
IVH_1	CH_3 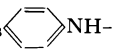	166—167/8	1.5388
IVI_1	Cl	186—188/8	1.5552
IVJ_1	CH_3OOC	190—192/1	(mp 35—38°C)

RN(-CH_2-CH=CH-CH_2-CH_2-CH_2-CH=CH_2)$_2$

	RN<	bp, °C/mmHg	n_D^{20}
IVE_2	n-C_4H_9N<	167—170/6	1.4774
IVF_2		209—210/5	1.5387
IVG_2	CH_3O 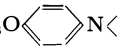	148—151/2	1.5350
IVH_2	CH_3 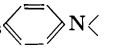	215—216/6	1.5338

(conjugated C=C) and 1002, 912, and 898 cm^{-1} (-CH=CH_2). The NMR spectrum showed complex bands at 3.5—4.8 (=CH-), 4.8—5.4 (=CH_2) and centered at 8.0 τ (-CH_2-).

Other experiments on the dimerization of butadiene in aprotic solvents are summarized in Table 1.

B) In Methanol. The autoclave described above was charged with 30 m*l* of methanol, 73 mg (0.1 mmol) of bis(triphenylphosphine)(maleic anhydride)palladium, and 20 g of butadiene. The reaction mixture was heated to 70°C and held there for 2 hr while being stirred. The yellow reaction mixture was distilled into a cold trap at ~70°C under reduced pressure. The distillate gave 20 g (77% yield) of 1-methoxyoctadiene-2, 7 (bp 103—105°C/83 mmHg) by fractional distillation, which contains a small amount (*ca.* 3%) of 3-methoxyoctadiene-1, 7 (bp 145—146°C). The methoxyoctadiene was characterized[8,9] by its infrared and NMR spectra. The infrared spectrum of 1-methoxyoctadiene-2,7 showed bands at 1670 (internal C=C), 1638 (terminal C=C), 1115 (CH_3-O-), 970 (trans -CH=CH-) and 991, and 910 cm^{-1} (-CH=CH_2). Its NMR spectrum showed bands at 4.0—4.7 (multiplet, =CH-), 4.7—5.2 (multiplet, =CH_2), 6.22 (doublet, J=4 cps, O-CH_2-C=), 6.78 (singlet, O-CH_3), 7.7—8.2 (multiplet, =C-CH_2-C-CH_2-C=), and 8.2—8.7 τ (multiplet, -C-CH_2-C-).

Gas chromatography was employed to isolate 3-methoxyoctadiene-1, 7. Its infrared spectrum showed bands at 1643 (C-C), 1101 (CH_3-O-) and 994, 923, and 910 cm^{-1} (-CH=CH_2). The NMR spectrum showed bands at 3.9—4.7 (multiplet, =CH-), 4.7—5.3 (multiplet, =CH_2), 6.3—6.8 (multiplet, -C-CH-C), 6.88 (singlet, O-CH_3), 7.7—8.3 (multiplet, =C-CH_2-C-CH_2-C=), and 8.3—8.8 τ (multiplet, -C-CH_2-C-).

1-Methoxyoctadiene-2, 7 was hydrogenated over a platinum catalyst in n-hexane to give 1-methoxyoctane (bp 161—162°C, n_D^{20} 1.4137), and with a $Ru(Ph_3P)_3Cl_2$ catalyst[15] in ethanol-benzene to give 1-methoxyoctene-2[9] (bp 82—83°C/33 mHg, n_D^{20} 1.4307).

The results of other experiments on dimerization in methanol and other alcohols are summarized in Tables 2 and 3.

C) In Aniline. The autoclave described above was charged with 20 m*l* of acetone, 15 g (160 mmol) of

15) P. S. Hallman, D. Evans, J. A. Osborn and G. Wilkinson, *Chem. Commn.*, **1967**, 305.

TABLE 8. ELEMENTAL ANALYSIS

Compound		Found				Calcd			
		C%	H%	N%	Mol wt	C%	H%	N%	Mol wt
I	C_8H_{12}	88.75	11.66		111*	88.82	11.18		108.2
IIA_1	$C_9H_{16}O$	76.63	11.46		140*	77.09	11.50		140.2
IIA_2	$C_9H_{16}O$	77.17	11.51			77.09	11.50		
IIB	$C_{10}H_{18}O$	77.74	11.66		153*	77.87	11.76		154.2
IIC	$C_{14}H_{18}O$	83.12	8.97		205	82.95	8.91		202.3
III	$C_{10}H_{16}O_2$	71.16	9.52		171	71.39	9.59		168.2
IVA	$C_{12}H_{21}NO$	73.50	10.78	7.05	193	73.80	10.84	7.17	195.3
IVB	$C_{13}H_{23}N$	80.95	12.03	7.01	197	80.77	11.99	7.24	193.3
IVC	$C_{14}H_{27}N$	80.21	12.88	6.27	214	80.31	13.00	6.69	209.4
IVD	$C_{20}H_{21}N$	87.57	7.61	5.07	275	87.23	7.69	5.09	281.2
IVE_1	$C_{12}H_{23}N$	79.76	12.76	7.47	190	79.49	12.79	7.73	181.3
IVE_2	$C_{20}H_{35}N$	82.80	11.94	4.67	274	82.97	12.19	4.84	289.5
IVF_1	$C_{14}H_{19}N$	83.27	9.59	6.57	205	83.53	9.51	6.96	201.3
IVF_2	$C_{22}H_{31}N$	85.05	10.16	4.74	313	85.38	10.10	4.53	309.5
IVG_1	$C_{15}H_{21}NO$	77.96	9.03	6.10	232	77.88	9.15	6.05	231.3
IVG_2	$C_{23}H_{33}NO$	71.48	9.86	4.33	337	81.36	9.80	4.13	339.5
IVH_1	$C_{15}H_{21}N$	83.60	9.85	6.46	222	83.66	9.83	6.51	215.3
IVH_2	$C_{23}H_{33}N$	85.28	10.44	4.09	336	85.39	10.28	4.33	323.5
IVI	$C_{14}H_{18}NCl$	71.59	7.85	5.99	246	71.32	7.69	5.94	235.1
IVJ	$C_{16}H_{21}NO_2$	74.38	8.26	5.45	263	74.10	8.16	5.40	259.3

* Cryoscopic method in benzene.

aniline, 146 mg (0.2 mmol) of bis(triphenylphosphine)-(maleic anhydride)palladium, and 13 g (240 mmol) of butadiene. The reaction mixture was then heated to 100°C and held there for 0.5 hr while being stirred. The yellow reaction mixture was distilled to give 14.4 g (60% yield) of phenylocta-2, 7-dienylamine (bp 184—186°C/25 mmHg) and 4.8 g (25% yield) of phenyldiocta-2, 7-dienylamine (bp 209—210°C/5 mmHg).

The infrared spectrum of Phenylocta-2,7-dienylamine showed bands at 3420 (N-H), 1640 (C=C), 1605 (conjugated C=C), 971 (trans -CH=CH-), 993, 913 (-CH=CH_2) and 750, and 695 cm^{-1} (-C_6H_5). The NMR spectrum showed bands at 2.6—3.7 (multiplet, C_6H_5-), 4.2—4.7 (multiplet, =CH-), 4.7—5.3 (multiplet, CH_2), 6.36 (doublet, J=4 cps, N-CH_2-C=), 6.54 (singlet, N-H), 7.7—8.2 (multiplet, =C-CH_2-C-CH_2-C) and 8.2—8.8τ (multiplet, -C-CH_2-C-).

The infrared spectrum of phenyldiocta-2, 7-dienylamine showed bands at 1642 (C=C), 1602 (conjugated C=C), 971 (trans -CH=CH-), 993, 913 (-CH=CH_2) and 750, and 695 cm^{-1} (-C_6H_5). The NMR spectrum showed bands at 2.6—3.7 (multiplet, C_6H_5-), 4.0—4.7 (multiplet, =CH-), 4.7—5.4 (multiplet, =CH_2), 6.20 doublet, J=4 cps, N-CH_2-C=), 7.5—8.2 (multiplet, =C-CH_2-C-CH_2-C=), and 8.2—8.9 τ (multiplet, -C-CH_2-C-). Other experiments on dimerization in amines are summarized in Tables 4 and 5.

BULLETIN OF THE CHEMICAL SOCIETY OF JAPAN VOL. 41 461—464 (1968)

Oxidation of Phosphites by Means of *p*-Quinones and Benzyl Alcohol

Oyo MITSUNOBU*1, Kyoko KODERA and Teruaki MUKAIYAMA

Laboratory of Organic Chemistry, Tokyo Institute of Technology, Ookayama, Meguro-ku, Tokyo

(Received September 19, 1967)

Triethyl phosphite and tri-*n*-butyl phosphite were oxidized to the corresponding trialkyl phosphates by means of *p*-quinones and benzyl alcohol. On the other hand, when diethyl (*N*-diethyl)phosphoroamidite was treated with *p*-benzoquinone and benzyl alcohol, 4-ethoxyphenyl ethyl (*N*-diethyl)phosphoroamidate was obtained in a 69% yield and no diethyl (*N*-diethyl)-phosphoroamidate was isolated. The reaction of 2, 3, 5, 6-tetrachloroquinone with diethyl benzyl phosphite in the presence of ethanol resulted in the formation of triethyl phosphate and 4-benzyloxy-2, 3, 5, 6-tetrachlorophenyl diethyl phosphate in 16% and 68% yields respectively.

Preceding paper[1] describes the oxidation of phosphites or phosphines to the corresponding phosphates or phosphine oxides by means of diethyl azodicarboxylate and benzyl alcohol. The reaction proceeds through the proposed intermediates of an imidoyl phosphonium salt (I) and benzyloxy phosphonium salt (II) from which the corresponding pentavalent phosphorus compound and diethyl *N*-benzylhydrazodicarboxylate were formed (Eq. (1)).

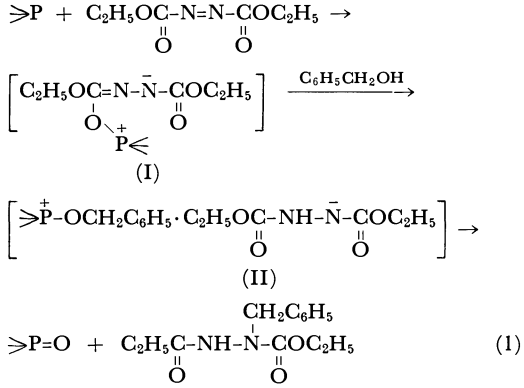

(1)

In the course of work aimed at the synthesis o esters of phosphoric acid, first objective of the present study was the oxidation of phosphites by the use of *p*-quinones and benzyl alcohol.

The reactions of quinones with trivalent phosphorus compounds have been investigated in considerable detail.[2] For example, Ramirez[3] demonstrated that the reaction of *p*-quinones with trialkyl phosphites resulted in the formation of the corresponding dialkyl 4-alkoxyaryl phosphates *via* quaternary phosphonium salt (III) (Eq. (2)).

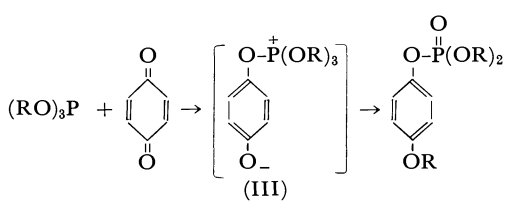

(2)

Since the intermediate (III) is analogous in structure to I, III may be expected to react with benzyl alcohol to give benzyloxy phosphonium salt (IV). On the basis of the results reported earlier,[1,4] the phosphonium salt (IV) would decompose with the formation of trialkyl phosphate and 4-benzyloxyphenol (Eq. (3)).

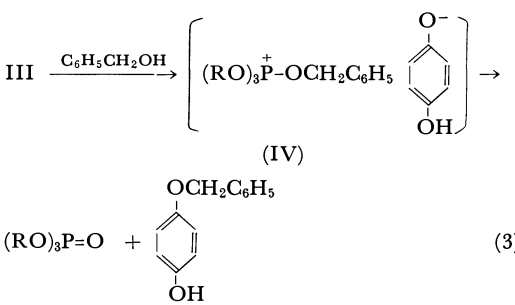

(3)

When triethyl phosphite was treated with equimolar amounts of *p*-benzoquinone and benzyl alcohol in benzene at room temperature, triethyl phosphate, hydroquinone and hydroquinone dibenzyl ether were obtained in 80%, 71% and 44%

*1 Present address: Department of Chemistry, College of Science and Engineering, Aoyamagakuin University, Megurisawa-cho, Setagaya-ku, Tokyo

1) O. Mitsunobu, M. Yamada and T. Mukaiyama, This Bulletin, **40**, 935 (1967).

2) R. G. Harvey and R. DeSombre, "Topics in Phosphorus Chemistry (Edited by M. Grayson and E. J. Griffith), Vol. 1," Interscience Publishers, New York (1964), p. 96.

3) F. Ramirez and S. Dershowitz, *J. Am. Chem. Soc.*, **81**, 587 (1959); F. Ramirez, E. H. Chen and S. Dershowitz, *ibid.*, **81**, 4338 (1959).

4) T. Mukaiyama, O. Mitsunobu and T. Obata, *J. Org. Chem.*, **30**, 101 (1965).

TABLE 1. THE OXIDATION OF TRIALKYL PHOSPHITES BY THE USE OF *p*-QUINONES AND BENZYL ALCOHOL

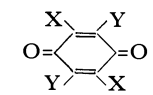 X	Y	$(RO)_3P$	Product: $(RO)_3P=O$	Product: 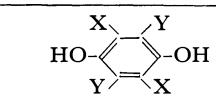	Product: 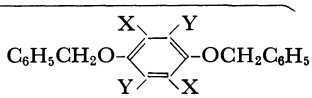
		R	Yield, %	Yield, %	Yield, %
H	H	C_2H_5	80	71	44
H	H	*n*-C_4H_9	88		46
CH_3	H	C_2H_5	66	55	26
CH_3	H	*n*-C_4H_9	53		
Cl	Cl	C_2H_5	72	50	44
Cl	Cl	*n*-C_4H_9	47	53	54

yields, respectively. No benzyloxyphenol, an expected product, could be isolated. The result suggests that an initially formed intermediate of benzyloxy phosphonium salt (IV) converts into a second quaternary phosphonium salt (V) and hydroquinone. The quaternary phosphonium salt (V) then in turn decomposes into the phosphate and the hydroquinone dibenzyl ether (Eq. (4)).

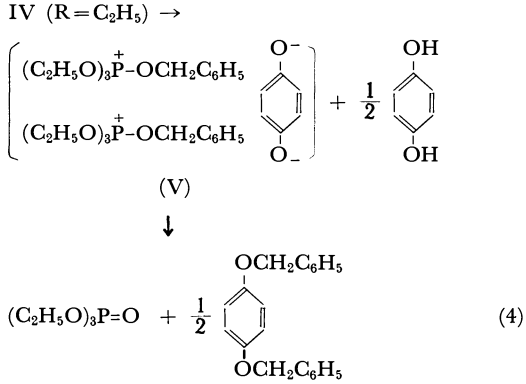

(4)

Similarly, triethyl phosphite and tri-*n*-butyl phosphite were oxidized to triethyl phosphate and tri-*n*-butyl phosphate by means of either 2, 3, 5, 6-tetrachloroquinone or 2, 5-dimethylquinone in the presence of benzyl alcohol. The results are summarized in Table 1.

Contrary to the successful oxidation of trialkyl phosphites by the use of *p*-quinones and benzyl alcohol, diethyl (*N*-diethyl)phosphoroamidate could not be obtained by the oxidation of diethyl (*N*-diethyl)phosphoroamidite by the present method. When diethyl (*N*-diethyl)phosphoroamidite was treated with equimilar amounts of *p*-benzoquinone and benzyl alcohol in refluxed benzene, 4-ethoxyphenyl ethyl (*N*-diethyl)phosphoroamidate was obtained in a 69% yield and benzyl alcohol(89%) was recovered. This result may be explained as follows. The positive charge of the initially formed phosphonium salt (VI) is not located on the phosphorus atom, but also resides partially on the nitrogen atom (VIa, b). Consequently, nucleophilic attack of the benzyl alcohol on the phosphorus atom becomes slower than the rearrangement of ethyl group and 4-ethoxyphenyl (*N*-diethyl)phosphoroamidate was predominantly formed (Eq. (5)).

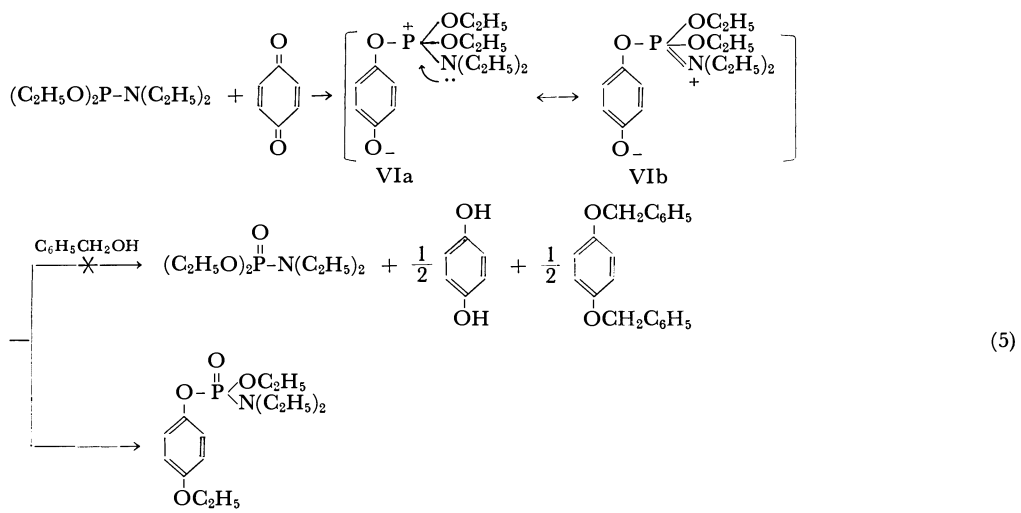

(5)

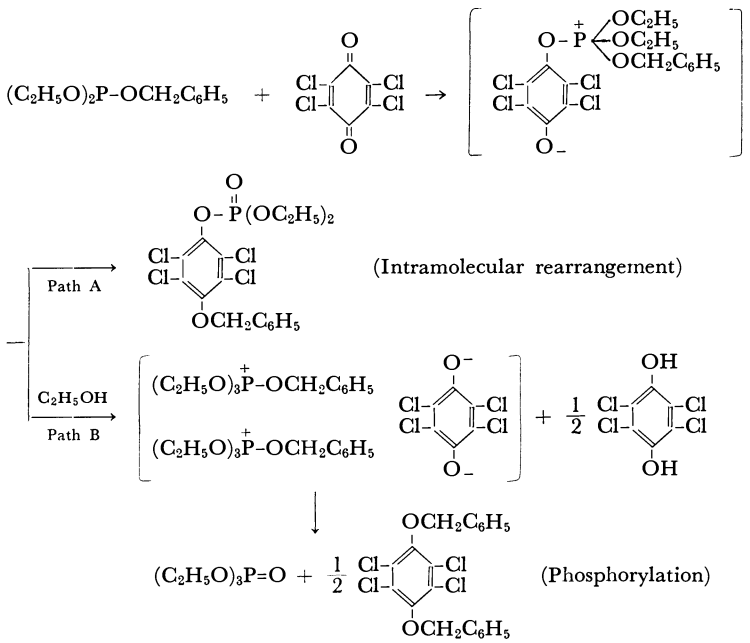

(6)

As shown above, the reactions of *p*-quinones with trivalent phosphorus compounds in the presence of benzyl alcohol show close resemblance to those of diethyl azodicarboxylate and either benzyl or allyl alcohol.[1] Thus, the reaction of diethyl benzyl phosphite with 2, 3, 5, 6-tetrachloroquinone and ethyl alcohol was attempted with the assumption that the ethyl alcohol may be phosphorylated to give triethyl phosphate[1] (Eq. (6), Path B). However, contrary to our expectation, the main product of the reaction was 4-benzyloxy-2, 3, 5, 6-tetrachlorophenyl diethyl phosphate (68%) and triethyl phosphate was obtained only in 16% yield. This observation shows that the intramolecular rearrangement of the benzyl group of an intermediate (Eq. (6), Path A) take place more easily than the displacement of the aryloxy anion by the ethoxy anion (Eq. (6), Path B).

Experimental

Triethyl phosphite, tri-*n*-butyl phosphite and *p*-quinones were obtained from commercial sources. The solvents and alcohols were purified and dried by ordinary procedures. Diethyl benzyl phosphite was prepared by the procedure given in literature.[5]

Oxidation of Triethyl Phosphite by Means of *p*-Benzoquinone and Benzyl Alcohol. A solution of triethyl phosphite (8.30 g, 0.05 mol) in 10 m*l* of benzene was added drop by drop to a stirring solution of *p*-benzoquinone (5.40 g, 0.05 mol) and benzyl alcohol (5.40 g, 0.05 mol) in 100 m*l* of benzene at room temperature under nitrogen. Immediately, quinhydrone began to precipitate. After the reaction mixture was kept standing for 6 days at room temperature, quinhydrone was removed by filtration (0.32 g, 5.8%, mp 166—167°C, a mixture melting point with an authentic material was not depressed). The solvent was evaporated from the filtrate and hydroquinone dibenzyl ether thus formed was removed by filtration (3.17 g, 44%, an analytical sample was obtained by recrystallization from alcohol, mp 126—127°C. Found: C, 82.68; H, 6.39%). The filtrate was fractionated to give triethyl phosphate (7.30 g, 80%, bp 51—83°C/2 mmHg, redistillation nallowed the boiling point to 62—64°C/3 mmHg). The triethyl phosphate was shown to be identical with the authentic sample by comparison of infrared spectra. The residue of the fractionation was solidified on standing and washed with 10 m*l* of benzene-petroleum (1 : 1) to give hydroquinone (1.95 g, 71%).

Similarly, tributyl phosphate was obtained by the reaction of tri-*n*-butyl phosphite with *p*-quinone and benzyl alcohol.

Oxidation of Triethyl Phosphite by Means of 2, 3, 5, 6-Tetrachloroquinone and Benzyl Alcohol. A solution of triethyl phosphite (1.66 g, 0.01 mol) in 10 m*l* of benzene was added drop by drop to a stirring mixture of 2, 3, 5, 6-tetrachloroquinone (2.46 g, 0.01 mol) and benzyl alcohol (1.08 g, 0.01 mol) in 30 m*l* of benzene at room temperature. A red color appeared instantaneously together with dissolution of the quinone and faded after *ca.* 15 min. The mixture was refluxed for 100 min. After removal of the solvent, 2, 3, 5, 6-tetrachlorohydroquinone dibenzyl ether was obtained by filtration (0.95 g, 44%). An analytical sample was obtained by recrystallization from benzene, mp 174°C (Found: C, 55.37; H, 3.50%). Triethyl phosphate was obtained by fractionation of the filtrate (1.30 g, 72%). The residual oil which solidified on standing was taken up in benzene-ether (1 : 1). The solution was extracted with 5% aqueous sodium hydroxide. The aqueous solution was acidified to give 2, 3, 5, 6-tetrachlorohydroquinone (0.62 g, 50%, mp 234°C, undepressed by the admixture with an authentic sample).

5) F. W. Hofmann and R. J. Ess, *J. Am. Chem. Soc.*, **78**, 5817 (1956).

Reaction of Diethyl (*N*-Diethyl)phosphoroamidite with *p*-Benzoquinone and Benzyl Alcohol. A solution of diethyl (*N*-diethyl)phosphoroamidite (1.93 g, 0.01 mol) in 10 m*l* of benzene was added to a solution of *p*-benzoquinone (1.08 g, 0.01 mol) and benzyl alcohol (1.08 g, 0.01 mol) in 20 m*l* of benzene. Immediately, the orange color of the solusolution changed to a deep red. The solution was refluxed for 2 hr. After the solvent was removed, the residue was fractionated to give recovered benzyl alcohol (0.96 g, 89%, bp 100—104°C/14 mmHg, redistillation gave bp 100—101°C/8 mmHg) and ethyl 4-ethoxyphenyl (*N*-diethyl)phosphoroamidate (2.08 g, 69.0%, bp 120—130°C/0.03 mmHg. An analytical sample was obtained by redistillation, bp 115—120°C/0.05 mmHg).

Found: N, 4.42%. Calcd for $C_{14}H_{24}NO_4P$: N, 4.65%.

Reaction of Diethyl Benzyl Phosphite with 2, 3, 5, 6-Tetrachloroquinone and Ethyl Alcohol. A solution of diethyl benzyl phosphite (2.28 g, 0.01 mol) in 10 m*l* of benzene was added to the mixture of 2, 3, 5, 6-tetrachloroquinone (2.46 g, 0.01 mol) and ethyl alcohol (2 m*l*) in 40 m*l* of benzene. The solution was allowed to stand for 24 hr at room temperature. After the removal of the solvent, the residue was fractionated to give triethyl phosphate (0.29 g, 16%, bp 69—74°C/2 mmHg) and 2, 3, 5, 6-tetrachlorohydroquinone (0.11 g, 8.9%) deposited on the inner wall of condenser. The remaining oil crystallized on standing (3.20 g, 67.6%, mp 68—86°C, an analytical sample was obtained by recrystallization from ether, mp 95—96°C). The crystalline compound was shown to be 4-benzyloxy-2, 3, 5, 6-tetrachlorophenyl diethyl phosphate on the bases of elemental analysis and its conversion into 2, 3, 5, 6-tetrachlorohydroquinone monobenzyl ether as outlined below.

Found: C, 42.84; H, 3.87%. Calcd for $C_{17}H_{17}Cl_4O_5P$: C, 43.07; H, 3.59%.

Reaction of 4-Benzyloxy-2, 3, 5, 6-tetrachlorophenyl Diethyl Phosphate with Sodium Ethoxide. The white crystalline compound obtained in the above experiment was added to a solution of sodium ethoxide (0.12 g of sodium was dissolved in 5 m*l* of ethyl alcohol) and was refluxed for 1 hr. After removal of the solvent from the red colored solution, the residue was dissolved in water and acidified with hydrochloric acid. The mixture was filtered to give 2, 3, 5, 6-tetrachlorohydroquinone monobenzyl ether (mp 130—136°C). Recrystallization from benzene - petroleum ether gave an analytical sample, mp 136—138°C.

Found: C, 46.15; H, 3.10%. Calcd for $C_{13}H_8Cl_4O_2$: C, 46.16; H, 2.37%.

The authers wish to express their hearty thanks to members of Analytical Room, this Laboratory, for microanalyses.

BULLETIN OF THE CHEMICAL SOCIETY OF JAPAN VOL. 41 464—468 (1968)

Studies of Aminosugars. XVIII. Syntheses of Amino Derivatives of Schardinger α-Dextrin and Raffinose[1]

Sumio UMEZAWA and Kuniaki TATSUTA

Department of Applied Chemistry, Faculty of Engineering, Keio University, Koganei-shi, Tokyo

(Received September 25, 1967)

In continuing our study of the relationship between structural and biochemical characteristics of aminoglycosides, amino-deoxy derivatives of polysaccharides have been synthesized. The six primary hydroxyl groups of Schardinger α-dextrin and the three primary hydroxyl groups of raffinose have successfully been replaced by amino groups respectively, to give hexa-(6-amino-6-deoxy)-cyclohexaglucan (α-1, 4) (IV) and 1'', 6, 6''-triamino-1'', 6, 6''-trideoxyraffinose (X). Their structures were confirmed by their NMR and IR spectra and by the studies of their chemical reactions. It has been found that hexa-(6-amino-6-deoxy)-cyclohexaglucan (α-1, 4) showed significant antitumor activity.

In a previous paper[2] the syntheses of several amino derivatives of disaccharides were reported.

The present paper is concerned with an extension of our study on aminosaccharides and reports the syntheses of amino-deoxy derivatives from the natural polysaccharides with α-anomeric configuration, *i. e.*, Schardinger α-dextrin and raffinose.

Schardinger α-dextrin[3] (I) is a kind of cyclic dextrins and contains eighteen hydroxyl groups, six out of which are primary and the others are secondary. On preferential tosylation of I with *p*-toluenesulfonyl chloride, followed by purification

1) Part XXXIV of "Studies of Antibiotics and Related Substances," by Sumio Umezawa.

2) S. Umezawa, T. Tsuchiya, S. Nakada and K. Tatsuta, This Bulletin, **40**, 395 (1967).

3) D. French, M. L. Levine, J. H. Pazur and E. Norberg, *J. Am. Chem. Soc.*, **71**, 353 (1949).

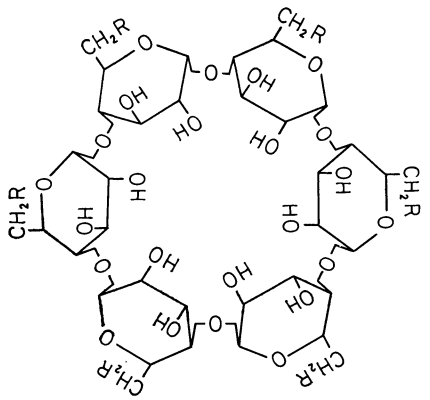

I : R = OH (Schardinger α-dextrin)

II : R = OTs

III : R = N_3

IV : R = NH_2

V : R = NHAc

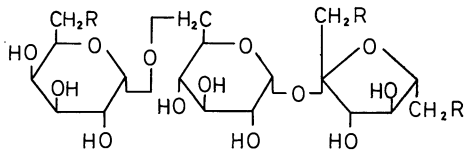

VI : R = OH (Raffinose)

IX : R = N_3

X : R = NH_2

XI : R = NHAc

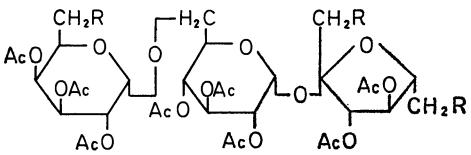

VII : R = OTs

VIII : R = N_3

by column chromatography, hexa-(6-*O*-tosyl)-cyclohexaglucan (α-1, 4) (II) was obtained in a 12.2% yield. Though the preparation of II was previously reported by W. Lautsch, *et al.*,[4] the product has not been purified by chromatography and seemed to be the mixture of partially tosylated products. In the next step, the replacement of the tosyloxy groups of II with azido groups was carried out by heating II in dimethylformamide with sodium azide, thus affording hexa-(6-azido-6-deoxy)-cyclohexaglucan (α-1, 4) (III) in a 52% yield. The azide compound (III) was finally converted to hexa-(6-amino-6-deoxy)-cyclohexaglucan (α-1, 4) (IV) by catalytic hydrogenation with platinum oxide in aqueous methanol in a yield of 60%. The structure of IV was confirmed by the fact that the hydrolysis of IV with hydrochloric acid gave only 6-amino-6-deoxy-D-glucose on paper chromatogram, and furthermore by the nuclear magnetic resonance spectrum of the hexa-*N*-acetylated derivative (V) of IV. The signal at τ 8.07 (singlet) with a relative intensity of 3 may be ascribed to eighteen *N*-acetyl protons, and the doublet at τ 4.99 with a relative intensity of 1 may be assigned to six anomeric protons.

Raffinose (VI) was preferentially tosylated and acetylated to give 2, 2', 3, 3', 3'', 4, 4', 4''-octa-*O*-acetyl-1'', 6, 6''-tri-*O*-tosylraffinose (VII) in a 40% yield. The three tosyloxy groups of VII were then replaced by azido groups similarly as has been described in the preparation of III to give 2, 2', 3, 3', 3'', 4, 4', 4''-octa-*O*-acetyl-1'', 6, 6''-triazido-1'', 6, 6''-trideoxyraffinose (VIII). Treatment of VIII with sodium methoxide in methanol gave the de-*O*-acetylated product (IX), which was finally hydrogenated with platinum oxide to give 1'', 6, 6''-triamino-1'', 6, 6''-trideoxyraffinose (X). Structural evidences for X were obtained by the determination of NMR spectrum of the tri-*N*-acetylated derivative (XI) of X, and by means of the periodate oxidation of XI, where five moles of periodate were consumed for one mole of XI.

Experimental

Thin-layer Chromatography, Silica-gel Column Chromatography, and Paper Chromatography. Thin-layer chromatography was conducted by the use of silica gel (Daiichi Pure Chemicals Co.); the prepared plate was activated at 110°C and then stored in a desiccator. The spray reagent used was concentrated sulfuric acid. Solvent systems used: benzene-ethanol (4 : 1) (Solvent A); benzene-ethanol (3 : 1) (Solvent B); methanol-chloroform (5 : 2) (Solvent C); benzene-ethyl acetate (8 : 5) (Solvent D), and chloroform-ethanol (1 : 1) (Solvent E). Silica-gel column chromatography was carried out by the use of silica gel (Kanto Chemical Co.) activated at 110°C before use. Paper chromatography was conducted by the descending technique on Toyo filter paper No. 50, and the substances were detected by the use of ninhydrin spray (0.25% in pyridine). Solvent system used: *n*-butanol - pyridine - water - acetic acid (6 : 4 : 3 : 1) (Solvent F).

General Procedure for Nuclear Magnetic Resonance Spectrometry. The NMR spectrum was determined at a frequency of 60 Mcps with a Japan

4) W. Lautsch, R. Wiechert and H. Lehmann, *Kolloid-Zeitschrift*, **135**, 134 (1954).

Electron Optics JNM-C-60 spectrometer in deuterium oxide. Sodium 2, 2-dimethyl-2-silapentane-5-sulfonate was used as an internal reference in the sample. Peak positions are given in τ-values.

Hexa-(6-*O*-tosyl)-cyclohexaglucan (α-1, 4) (II). To a suspension of Schardinger α-dextrin anhydride [cyclohexaglucan (α-1, 4), I, 2.43 g, 2.50 mmol] in dry pyridine (35 m*l*) cooled at $-15°C$, *p*-toluenesulfonyl chloride (4.40 g, 23.1 mmol) was added; the mixture was then stirred at $-15°C$ for 1 hr and allowed to stand overnight at 0°C, at 5°C for 5 hr and at room temperature for 3 days. After the addition of a small volume of water, the solution was left for 30 min. The resulting solution was poured into a large volume of ice and water. The precipitate was collected by a centrifuge and washed with water; yield 2.7 g (S, 10.12%). Thin-layer chromatography with Solvent A proved the product to be composed of six components, with R_f-values of 0.66, 0.53, 0.39, 0.23, 0.09 and 0.00. This product was dissolved in a solvent mixture of benzene-ethanol (4 : 1) and chromatographed on a silica-gel column (49×540 mm) with the same solvent. After about 600 m*l* of eluate, fractions (15 g each) were tested by thin-layer chromatography. Each substance having the corresponding R_f value was recrystallized from methanol, and their yields and S-contents (%) were summarized as follows:

R_f value	Fraction No.	Yield mg	S-content %
0.66	5—16	965	11.49
0.53	18—26	204	11.15
0.39	27—34	88	10.51
0.23	33—45	572	10.36
0.09	45—64	250	9.57

As the substance at the origin seemed to be less tosylated than the substance having an R_f 0.09, it was not further investigated. The substance having an R_f 0.23 had mp 184—188°C (decomp.), $[\alpha]_D^{17}$ +101° (*c* 0.72, chloroform) [lit.,[4] mp 174°C, $[\alpha]_D^{20}$ +95° (*c* 1, chloroform)]; IR spectrum (KBr disk): 3440 (νOH), 2930 (νCH), 1600 (phenyl), 1175 (sulfonate) cm^{-1}.

Found: C, 49.64; H, 5.49; S, 10.36%; mol wt (Vapor pressure osmometer), 1970. Calcd for $(C_{13}H_{16}O_7S)_6$: C, 49.36; H, 5.10; S, 10.14%; mol wt 1898.

On the basis of these data, it seemed reasonable to assume that the product (R_f 0.23) was regarded as II, which contained six tosyloxy groups; Yield 572 mg (12.2%).

Hexa-(6-azido-6-deoxy)-cyclohexaglucan (α-1, 4) (III). To a solution of II (1.14 g) in dry *N*, *N*-dimethylformamide (11 m*l*) sodium azide (1.6 g) was added; the suspension was then vigorously agitated at 135°C for 6.5 hr. The resulting dark solution was filtered, and the filtrate was evaporated and coevaporated with toluene to give the residue, which showed essentially a single spot (R_f 0.20) on thin-layer chromatography with Solvent B. The residue was dissolved in a solvent mixture of benzene-ethanol (3 : 1) and chromatographed on a silica-gel column (49×325 mm) with the same solvent. After about 400 m*l* of eluate, fractions (15 g each) were tested by thin-layer chromatography. The substance having an R_f 0.20 was eluted in the fractions of tube Nos. 4—18; these fractions were combined and evaporated to yield 350 mg (52%) of III as a slightly yellow solid, which was used for the next step without further purification; IR spectrum (KBr disk): 3400 (νOH), 2920 (νOH), 2105 (azide) cm^{-1}, no sulfonate band.

Hexa-(6-amino-6-deoxy)-cyclohexaglucan (α-1, 4) (IV). A sample (350 mg) of III was dissolved in 75% aqueous methanol (24 m*l*) and hydrogenated with platinum oxide (160 mg) under 3 atm of hydrogen-pressure at 30—40°C for 4 hr. After removal of the catalyst, the filtrate was treated with active charcoal and evaporated to give a base of IV (260 mg). The aqueous solution of the base was neutralized with hydrochloric acid to pH 2 and evaporated to dryness. Recrystallization of the residue from aqueous ethanol gave crystalline hexahydrochloride of IV; yield, 240 mg (60%); mp 214°C (decomp.), $[\alpha]_D^{17}$ +103° (*c* 0.67, water). On paper chromatography with Solvent F, hexahydrochloride of IV showed a single spot with an R_f 0.01. IR spectrum (KBr disk): 3400—3300 (νOH, NH), 2910 (νCH), 1600 (δ_{as} NH_3^+), 1500 (δ_s NH_3^+) cm^{-1}.

Found: C, 36.91; H, 6.48; N, 6.71%. Calcd for $(C_6H_{11}O_4N \cdot HCl)_6$: C, 36.47; H, 6.12; N, 7.09%.

A small quantity of IV was heated with 3 N hydrochloric acid for 3 hr in a boiling water bath, and the hydrolyzate was paper chromatographed with Solvent F. Detections by ninhydrin and ammoniacal silver nitrate colorations showed only a spot corresponding to 6-amino-6-deoxy-D-glucose*1 as monosaccharide, respectively.

Hexa-(6-acetamido-6-deoxy)-cyclohexaglucan (α-1, 4) (V). To a stirred suspension of IV base (80 mg) in dry methanol (2 m*l*) acetic anhydride (0.3 m*l*) was added; the mixture was stirred for 1 hr and allowed to stand overnight at room temperature. After evaporation, the aqueous solution of the residue was treated with active charcoal and evaporated to give a solid, which was recrystallized from water by adding ethanol; yield, 70 mg (69%); mp 135—137°C (decomp.), $[\alpha]_D^{19}$ +92° (*c* 0.79, water).

On thin-layer chromatography with Solvent C, the product V showed a single spot with an R_f value of 0.21. NMR spectrum data: τ 4.99 (doublet, J= 2.9 cps, 6 protons, anomeric hydrogen), 8.07 (singlet, 18 protons, *NAc*); IR spectrum (KBr disk): 3380—3300 (νOH, NH), 2920 (νCH), 1645 (amide I), 1550 (amide II) cm^{-1}.

Found: C, 46.97; H, 6.31; N, 6.52%. Calcd for $(C_8H_{13}O_5N)_6$: C, 47.29; H, 6.45; N, 6.89%.

2, 2′, 3, 3′, 3″, 4, 4′, 4″-Octa-*O*-acetyl-1″, 6, 6″-tri-*O*-tosylraffinose (VII). To a solution of raffinose anhydride (VI, 1.01 g, 2.00 mmol) in dry pyridine (30 m*l*), Drierite (anhydrous calcium sulfate, 1.2 g) was added; the mixture was then allowed to stand for 30 min. After the mixture had been cooled to $-15°C$, *p*-toluenesulfonyl chloride (1.34 g, 7.06 mmol) was added in one portion, and the mixture was kept at $-15°C$ for 1.5 hr, at 0°C for 1 day and then at 5°C for 2 days. Acetic anhydride (4.5 m*l*) was added to the resultant cold solution, and the solution was again

*1 The specimen of 6-amino-6-deoxy-D-glucose was obtained from the hydrolyzate of kanamycin.

set aside overnight at room temperature. After the addition of a small volume of water, the solution was left for 30 min. The reaction mixture was then poured into a large volume of ice and water. The precipitate which separated was collected by a centrifuge and washed with water, yielding 2.1 g of a crude product. Thin-layer chromatography with Solvent D proved the product to be composed of two components, with R_f values of 0.48 (main) and 0.36 (minor). This product was dissolved in a solvent mixture of benzene - ethyl acetate (8 : 5) and chromatographed on a silica-gel column (47×220 mm) with the same solvent. After about 110 m*l* of eluate, fractions (15 g each) were tested by thin-layer chromatography. The substance having an R_f 0.48 appeared in the fractions of tube Nos. 24—34; these fractions were combined and evaporated under reduced pressure, and the residue was recrystallized from ethanol affording VII; yield, 1.04 g (40%), mp 90—93°C, $[\alpha]_D^{17}$ +95° (*c* 0.70, chloroform); IR spectrum (KBr disk): 2950 (νCH), 1755 (ester), 1600 (phenyl), 1370 (OAc), 1175 (sulfonate) cm^{-1}.

Found: C, 51.05; H, 5.31; S, 7.20%. Calcd for $C_{55}H_{66}O_{30}S_3$: C, 50.69; H, 5.10; S, 7.38%.

2, 2′, 3, 3′, 3″, 4, 4′, 4″-Octa-*O*-acetyl-1″, 6, 6″-triazido-1″, 6, 6″-trideoxyraffinose (VIII). A suspension of sodium azide (4.0 g) in dry *N, N*-dimethylformamide (55 m*l*)was stirred with VII (5.5 g) at 130°C for 7 hr. The solvent was then removed from the dark solution by distillation and codistillation with toluene under reduced pressure. As a part of the acetyl groups of VII had been found to be removed by the above procedure, the dark residue obtained was acetylated with acetic anhydride (40 m*l*) and dry pyridine (110 m*l*) for 2 days. After filtration, the filtrate was evaporated to a syrup, which, on thin-layer chromatography with Solvent D, showed two spots with R_f values of 0.72 (main) and 0.60 (minor). The syrup was then dissolved in a solvent mixture of benzene - ethyl acetate (8 : 5) and chromatographed on a silica-gel column (54×630 mm) with the same solvent. After about 830 m*l* of eluate, fractions (15 g each) were tested by thin-layer chromatography. The substance having an R_f 0.72 was eluted in the fractions of tube Nos. 46—60; these fractions were combined and evaporated to give a solid, which was recrystallized from aqueous ethanol affording VIII; yield, 1.48 g (38%); mp 180—184°C (decomp.), $[\alpha]_D^{17}$ +131° (*c* 0.63, chloroform); IR spectrum (KBr disk): 2930 (νCH), 2105 (azide), 1755 (ester), 1375 (OAc) cm^{-1}.

Found: C, 44.98; H, 5.13; N, 13.32%. Calcd for $C_{34}H_{45}O_{21}N_9$: C, 44.59; H, 4.95; N, 13.77%.

1″, 6, 6″-Triazido-1″, 6, 6″-trideoxyraffinose (IX) A suspension of VIII (380 mg) in dry methanol (7.6 m*l*) was treated with 0.75 N methanolic sodium methoxide (0.6 m*l*) at room temperature for 5 days. After neutralization to pH 7 with Amberlite IRC 50 (H form) (previously washed with methanol), the solution was evaporated to give the residue, which showed two spots with R_f values of 0.71 (minor) and 0.61 (main) on thin-layer chromatography with Solvent E. The residue was then dissolved in the same solvent system and chromatographed on a silica-gel column (27× 230 mm) with the same solvent. After about 40 m*l* eluate, fractions (3 g each) were tested by thin-layer chromatography. The substance having an R_f 0.61 was eluted in the fractions of tube Nos. 29—54; these fractions were combined and evaporated to give a solid of IX; yield, 132 mg (55%); mp 80—83°C (decomp.), $[\alpha]_D^{17}$ +117° (*c* 0.71, water); IR spectrum (KBr disk): 3370 (νOH), 2930 (νCH), 2110 (azide) cm^{-1}.

Found: C, 37.20; H, 5.27%. Calcd for $C_{18}H_{29}O_{13}N_9$: C, 37.31; H, 5.04%.

1″, 6, 6″-Triamino-1″, 6, 6″-trideoxyraffinose (X). A solution of IX (107 mg) in 50% aqueous ethanol (10 m*l*) was hydrogenated with platinum oxide (40 mg) under 3 atm of hydrogen-pressure at 35—40°C for 4 hr. After removal of the catalyst, the filtrate was evaporated and the aqueous solution of the residue was passed through a column (6×110 mm) of Dowex 1X2 (OH form). The ninhydrin-positive eluate, which was evaporated to give a base of X, was neutralized with hydrochloric acid to pH 2 and evaporated to dryness. Recrystallization of the residue from water-acetone gave crystalline trihydrochloride of X; yield, 76.8 mg (68%); mp 139—141°C (decomp.), $[\alpha]_D^{17}$ +114° (*c* 0.68, water). On paper chromatography with Solvent F, trihydrochloride of X showed a single spot with an R_f 0.02. IR spectrum (KBr disk): 3370—3260 (νOH, NH), 2900 (νCH), 1610 (δ_{as} NH_3^+), 1505 ($\delta_s NH_3^+$) cm^{-1}.

Found: C, 35.55; H, 6.57; N, 6.89%. Calcd for $C_{18}H_{35}O_{13}N_3 \cdot 3HCl$: C, 35.39; H, 6.27; N, 6.88%.

1″, 6, 6″ - Triacetamido - 1″, 6, 6″ - trideoxyraffinose (XI). To a suspension of X base (82 mg) in dry methanol (0.85 m*l*) acetic anhydride (0.25 m*l*) was added; the mixture was treated as has been described in the synthesis of V. The product was recrystallized from water by adding acetone; yield, 66 mg (64%); mp 142—144°C (decomp.), $[\alpha]_D^{17}$ +123° (*c* 0.65, water). On thin-layer chromatography with Solvent C, the product XI showed a single spot with an R_f value of 0.44. NMR spectrum data: τ ~8.0 (three singlets, 9 protons, NAc-1″, 6, 6″), 4.57 (doublet, 1 proton, H-1′, J=3 cps), 5.07 (doublet, 1 proton, H-1, J=2.5 cps); IR spectrum (KBr disk): 3400—3300 (νOH, NH), 2930 (νCH,) 1650 (amide I), 1555 (amide II) cm^{-1}.

Found: C, 45.48; H, 6.86; N, 6.70%. Calcd for $C_{24}H_{41}O_{16}N_3$: C, 45.93; H, 6.58; N, 6.70%.

The Periodate Oxidation of XI. An accurately-weighed sample (32.5 mg) of XI was dissolved in a mixture of a 0.1 N sodium acetate buffer solution (pH 4.7, 10m*l*) and a 0.1 M sodium metaperiodate solution (5.26 m*l*); the oxidation was then carried out at 0°C in the dark. Iodometric titrations with sodium arsenite[5] showed that the periodate consumption in moles per mole of XI was (time in hr, moles of oxidant consumed per mole of XI): 0.5, 3.16; 3.0, 4.17; 6.0, 4.37; 24.0, 4.55; 48.0, 4.99; 96.0, 5.00.

Preliminary Bioassay. It is noteworthy that the daily intraperitoneal injection of 100 mg/kg of the amino-deoxy derivative (IV) of Schardinger α-dextrin inhibited the ascites increase and prolonged the survival period of mice bearing ascites-type of Ehrlich carcinoma by intraperitoneal route. The compound IV also inhibited the growth of *Bacillus subtilis* PCI 219 completely at a dilution of 1 : 500, but showed no inhibition against *M. pyogenes var. aureus* 209p, *E. coli* and *Mycobacterium tuberculosis* 607 in a dilution of 1 : 1000. Compound

5) J. M. Bobbitt, "Advances in Carbohydrate Chemistry," Vol. 11, Academic Press, New York (1956), pp. 1—14.

X did not show any activity against the above-mentioned test organisms and carcinoma.

The authors are indebted to Mr. Saburo Nakada for his microanalysis, to Mr. Kiyohiko Suo for his technical assistance, to Mrs. Setsuko Iriyama for her antibacterial assay, and to Dr. Kyuji Abe, Manager of the Biology Research Laboratories of Tanabe Seiyaku Co., for antitumor assay.

BULLETIN OF THE CHEMICAL SOCIETY OF JAPAN VOL. 41 468—475 (1968)

Photolysis of Nitrite Esters bearing Nitrogen on the β-Carbon

Hiroshi SUGINOME, Masakazu MURAKAMI and Tadashi MASAMUNE

Department of Chemistry, Faculty of Science, Hokkaido University, Sapporo

(Received October 2, 1967)

The results of photolysis of a number of nitrite esters derived from jervine, in which the respective β-carbon of nitrite group bears nitrogen, are described. It has been found that in these nitrites when a nitrogen on β-carbon was in the amide group, the irradiation caused the cleavage of α, β-single bond to the nitrite group. The reaction is exemplified by photolysis of 3*O*, *N*-diacetyl-22, 27-imino-11-oxojerva-5, 13(17)-diene-3β, 23β-diol 23-nitrite ester (Ic) to afford an aldehyde II. When a nitrogen on β-carbon of nitrite was tertiary (*e.g.*, XIb), however, no photoinduced fission of carbon-carbon bond in these nitrites was observed and the starting alcohol recovered unchanged. These results coupled with others, *e.g.*, the result of photolysis of 3*O*-acetyl-*N*-benzoyl-22, 27-imino-11-oxojerva-5, 12-diene-3β, 23β-diol 23-nitrite ester (IIIf) indicate the selective cleavage of acyl-nitrogen bond followed by acidic hydrolysis to an aldehyde during chromatography, as shown in the scheme V to VIII. It is noted that this reaction is contrasted with the reported results with regard to photolysis of nitrites bearing oxygen in place of nitrogen.

The study of the photolysis of organic nitrites has received considerable attention over the past 7 years largely because of its synthetic utility.[2] Alkoxy radicals generated from nitrites were found to react in a variety of ways, depending on detailed structures around the nitrite group.

Our interest in this photochemical transformation is primarily a synthetic one and in this communication we describe some observations on a new mode of transformation.

22,27-Imino-11-oxojerva-5, 13(17)-diene-3β,23β-diol (Ia)[3] which was prepared by Birch reduction of jervine[4] was partially acetylated to yield the corresponding 30, *N*-diacetyl derivative (Ib) in 48% yield. The evidence for the introduction of an acetyl group at 3β-hydroxyl of Ia was provided by steric considerations and the disappearance of a band at 1050 cm^{-1} in its infrared pectrum which is characteristic of a Δ^5-3β-hydroxyl group.[5] This was converted on treatment with nitrosyl chloride in pyridine[6] into the corresponding nitrite (Ic). This was unstable[7] and was readily hydrolyzed to regenerate the alcohol Ib. This nitrite in benzene was immediately photolysed (150 W high pressure mercury arc lamp) under the conditions commonly used for the Barton reaction.[8] After about one hour no nitrite remained unchanged as indicated by a specific color test.[9] The

1) Photoinduced Transformations. IV. Part of this work has been briefly reported. H. Suginome, M. Murakami and T. Masamune, *Chem. Commun.*, 343 (1966). Part III. H. Suginome, T. Tsuneno and T. Masamune, *Tetrahedron Letters*, **1967**, 4605.

2) For reviews see A. L. Nussbaum and C. H. Robinson, *Tetrahedron*, **17**, 35 (1962) and M. Akhtar in "Advances in Photochemistry," Vol. II, ed. by W. A. Noyes, G. S. Hammond and J. N. Pitts, Jr., Interscience Publishers, New York, N. Y. (1964), p. 263.

3) The configurations at C-22 and C-23 of jervine have recently been revised. J. W. Scott, L. J. Durham, H. A. P. deJongh, U. Burckhardt and W. S. Johnson, *Tetrahedron Letters*, **1967**, 2381. In this paper, a series of compounds derived from jervine will be formulated on the basis of this revised formula.

4) T. Masamune, M. Takasugi, M. Gohda, H. Suzuki, S. Kawahara and T. Irie, *J. Org. Chem.*, **29**, 2282 (1964).

5) T. Masamune, Y. Mori, M. Takasugi and A. Murai, *Tetrahedron Letters*, **1964**, 913.

6) R. H. Pickard and H. Hunter, *J. Chem. Soc.*, **1923**, 434.

7) All nitrites described in this paper were found to be very unstable to moisture and this seems to be general for nitrites substituted by nitrogen on the β-carbon of nitrite group. Similar instability has recently been reported on the nitrites substituted by oxygen in place of nitrogen. A. L. Nussbaum, R. Wayne, E. Yuan, O. Zagneetko Sarre and E. P. Oliveto, *J. Am. Chem. Soc.*, **87**, 2451 (1965).

8) D. H. R. Barton, J. M. Beaton, K. E. Geller and M. M. Pechet, *J. Am. Chem. Soc.*, **82**, 2640 (1960); **83**, 4076 (1961).

9) F. Feigl, "Spot Tests in Organic Analysis," Elsevier Publ. Co., New York, N. Y. (1960), p. 178.

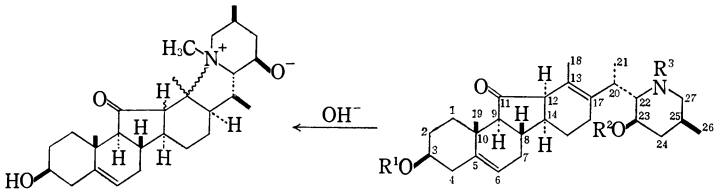

(IX) (I)

a. $R_1=R^2=R^3=H$; b. $R^1=R^3=Ac$, $R^2=H$;
c. $R^1=R^3=Ac$, $R^2=NO$; d. $R^1=R^2=R^3=COC_6H_5$;
e. $R^1=R^2=H$, $R^3=Me$; f. $R^1=Ac$, $R^2=H$, $R^3=Me$;
g. $R^1=Ac$, $R^2=NO$, $R^3=Me$

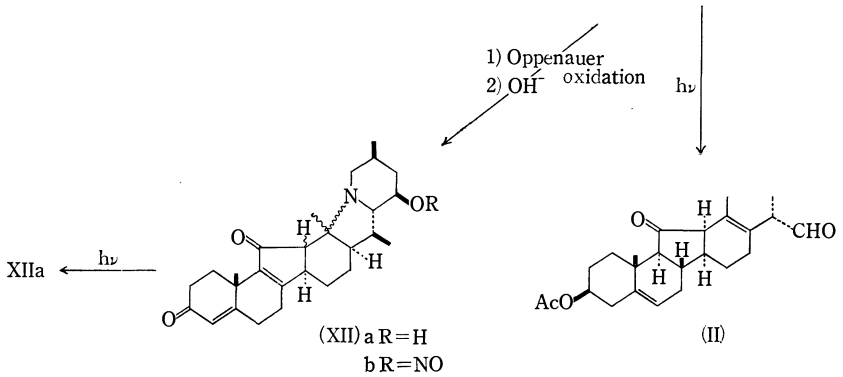

(XII) a R=H
b R=NO

(II)

examination of the product by TLC showed this to be rather a complex mixture, and this was then subjected to chromatographic separation on the column of silicic acid. The least polar fraction which was eluted with a mixed solvent of benzene and ether crystallized on evaporation of the solvent, and had mp 150—152°C, after purification. A structure II could be assigned to this substance on the following basis. Elemental analysis and mass spectrometry (M^+ 384) indicated a molecular formula $C_{24}H_{32}O_4$, corresponding to the loss of nitrogen moiety in Ib. In the NMR spectrum of the compound Ib, signals due to *N*-acetyl, *O*-acetyl, 18- and 19-methyl groups appeared as singlets at τ 8.00,*1 τ 8.03,*1 τ 8.15 and τ 9.03, respectively, and those due to 21- and 26-methyl groups as a coincident broad doublet centered at τ 8.83 (J=6.6). However, the NMR spectrum of II retained only three singlets at τ 7.99, τ 8.16 and τ 9.05, which are attributable to *O*-acetyl, 18- and 19-methyl groups, respectively. A doublet in II was exactly a half of that of the corresponding doublet of Ib, indicating that either the 21-methyl or the 26-methyl had been removed from the starting diacetyl derivative Ib. Moreover, the NMR spectrum of II showed the presence of an aldehydic proton as a doublet centered at τ 0.56 (J=4.2). The IR spectrum of the product also showed the presence of typical aldehyde bands[10] at 2697, 2799 and 1740 cm^{-1} (shoulder) and a notable feature of this IR spectrum was the absence of a band due to an *N*-acetyl group. Only the structure II reasonably accommodates all the spectral data and the molecular formula mentioned above.

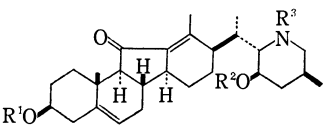

(III)

a. $R^1=R^2=H$, $R^3=H$
b. $R^1=R^3=Ac$, $R^2=H$
c. $R^1=Ac$, $R^2=NO$, $R^3=Ac$
d. $R^1=R^2=H$, $R^3=COC_6H_5$
e. $R^1=Ac$, $R^2=H$, $R^3=COC_6H_5$
f. $R^1=Ac$, $R^2=NO$, $R^3=COC_6H_5$

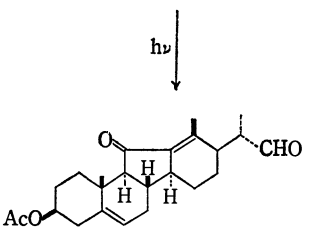

(IV)

In a similar manner, the isomeric 3*O*, *N*-diacetyl derivative IIIb was prepared by partial

*1 These two signals are assigned to *N*- and *O*-acetyl groups but which is *O*-acetyl or *N*-acetyl was not determined.

10) S. Pinchas, *Anal. Chem.*, **27**, 2 (1955).

acetylation of *N*-acetyl-22, 27-imino-11-oxojerva-5, 12-diene-3β, 23β-diol[11] (IIIa) in good yield. The nitrite was again unstable and was immediately photolyzed in benzene. Examination of the product by thin layer chromatography showed that the composition of the product was noticeably simpler than that from the photolysis of Ic. Column chromatography with silicic acid enabled us to isolate a single compound IV as the least polar material in 13% yield.

The compound, which was analyzed for a formula $C_{24}H_{32}O_4$, melted at 192—194°C and had the bands at 1699 cm^{-1} (α, β-unsaturated C=O), 1727 cm^{-1} (*O*-acetyl), 1628 cm^{-1} (conjugated C=C) and 2700 and 1727 cm^{-1} (aldehyde) in its infrared spectrum. The NMR spectrum of this clearly indicated the compound to be an aldehyde. It showed signals corresponding to C-19 methyl at τ 8.93, C-21 methyl at τ 9.12 (doublet, J=6.6), *O*-acetyl at τ 7.97 and C-18 methyl at τ 7.85. A signal due to aldehydic proton appeared at τ 0.18 as doublet (J=1.4 cps). From these results it is clear that the compound is correctly formulated as IV.

The course of this reaction apparently involves the formation of imino-intermediates VII followed by acid hydrolysis during separation by chromatography on silicic acid. The following sequence V-VIII may be proposed for this photochemical fragmentation.

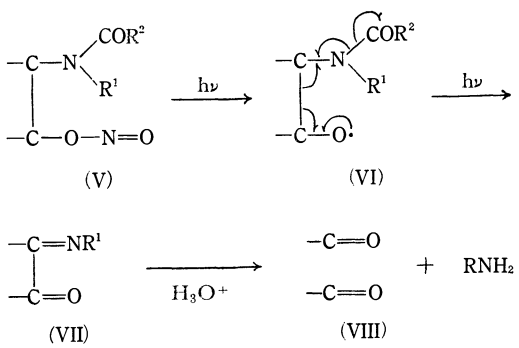

In the scheme shown the photochemical excitation of the system V generates an alkoxyl radical VI which collapses in a variety of ways to afford stable species, one being a process to lead to VII in which the acyl-nitrogen linkage would most probably be cleaved. In order to confirm this fission of acyl-nitrogen bond, we attempted to examine the photolysis of the nitrite Ig in which the nitrogen has a methyl group in place of an acetyl substituent. Although Birch reduction of *N*-methyl jervine[12] gave rise to a well-defined compound Ie having mp 185.5—189°C, the selective acetylation for the C-3 hydroxyl group to afford If proved to be difficult, owing to the facile migration of the 13(17) double bond to the α, β-position of 11-carbonyl, as shown by the appearance of the absorption at 1626 cm^{-1} in the crude product from acetylation, and subsequent interaction between the α, β-unsaturated double bond and the basic nitrogen to afford partly the cyclic product during acetylation procedure. Actually, the compound Ie was very easily convertible into a compound with base which is formulated as a zwitterion IX from its spectral and analytical data and by analogy of the reaction.[4,13] In the infrared spectrum the compound IX showed the bands at 1734 cm^{-1} and 3440 and 3630 cm^{-1} due to a five-membered ring ketone and a hydroxyl stretching vibration, respectively. Treatment of IX in acetic acid with aqueous potassium iodide afforded the highly crystalline hydriodide.

Furthermore, in the NMR spectrum of the starting compound Ie, three singlets due to *N*-methyl, C-19 methyl and C-18 methyl appeared at τ 7.76, τ 9.06 and τ 8.09. But all these peaks in the compound IX shifted to τ 7.84, τ 8.97 and τ 8.26, respectively.

The synthesis of the compound of type If was equally unsuccessful in isomeric 22, 27-imino-11-oxojerva-8, 13(17)-diene series in which a double bond is located at the 8-position instead of the 5-position in If and in this cyclopentenone system there seemed some possibility of affording the compound of type If. 5α, 6-Dihydroisojervine was oxidized selectively at 3-position to yield the corresponding 3-ketone X.[4] However, attempted *N*-methylation with methyl iodide and potassium hydroxide led exclusively to a weak tertiary base XIa as experienced in the analogous compounds.[4,13] The structure XIa was evident from its IR and the NMR spectra.

We then considered the use of nitrite of the hexacyclic base XIa or XIIa, in which the β-carbon of the nitrite group has a tertiary nitrogen, to obtain more insight into the process from V to VIII. As already cited, the formation of this type of compound was first observed by Wintersteiner and Moor.[13] Birch reduction product Ia of jervine was submitted to Oppenauer oxidation to yield the corresponding Δ^4, 3-ketone. Crude Δ^4, 3-ketone gave rise to a tertiary base XIIa which was treated with nitrosyl chloride in pyridine in the usual manner. After work-up as usual, an unstable nitrite, mp 143—146°C, XIIb was obtained in excellent yield. This was immediately photolyzed in dry benzene without further purification. The photolyzed product consisted solely of the starting alcohol XIIa and no other noticeable products were produced as revealed by thin-layer

11) T. Masamune, K. Orito and A. Murai, This Bulletin, **39**, 2503 (1966).
12) K. Saito, H. Suginome and M. Takaoka, This Bulletin, **11**, 172 (1936).
13) O. Wintersteiner and M. Moor, *J. Am. Chem. Soc.*, **75**, 4938 (1953).

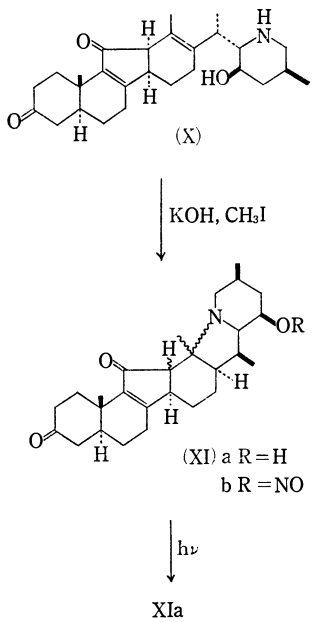

chromatography. The hexacyclic base XIa described above was also converted into the corresponding nitrite XIb and the nitrite was photolyzed. This likewise gave the original alcohol XIa exclusively.

These results demonstrate that in a photochemically excited system, ·O-C-C-N-alkyl, as that from XIb or XIIb, *N*-alkyl bonds are stable under the conditions of the Barton reaction and that acyl-nitrogen linkage is selectively cleaved in the scheme shown in V-VIII.

In order to probe further into the effect of *N*-substituents, *N*-benzoyl analogue of IIIc was newly synthesized. 22, 27-Imino-11-oxojerva-5, 13(17)-diene-3β, 23β-diol (Ia) was treated with benzoic anhydride to afford its crude tribenzoyl derivative Id. This was hydrolyzed to yield the corresponding *N*-benzoyl derivative IIId, mp 230.5—232.5°C. The *N*-benzoyl derivative IIId was submitted to partial acetylation to yield the corresponding 3*O*-acetate IIIe, mp 144.5—146°C. Conversion of this into the corresponding nitrite IIIf mp 206—208°C and the photolysis of the nitrite gave a mixture of the products. Column chromatography of the product afforded the aldehyde IV, which was identical with the specimen obtained from the photolysis of the nitrite IIIc, and also a small amount of benzoic acid. The nature of the reaction which leads to the formation of benzoic acid has not been fully understood. But this result supplements the evidence for the occurrence of acyl-nitrogen fission.

Moreover, we tried to confirm this acyl-nitrogen cleavage by studying some simpler system. *N*-Acetyl-3-hydroxy-5-methylpiperidine[14] XIIIa was converted into the corresponding unstable nitrite XIIIb. However, the photolysis of this nitrite gave rise to a complex mixture of amines which was characterized only by qualitative tests and we have not been successful in isolating any single amine.

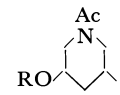

XIIIa R=H
b R=NO

Although the cleavage reaction described here has obviously limited synthetic value, it may provide a useful synthetic route to certain aldehydes which are inaccessible by other procedures.[15]

It has been reported by Barton and coworkers[16] that in a number of nitrites vicinally substituted by an oxygen-bearing moiety, photolysis leads to an oxidative fission of carbon-carbon bond. In these cases the oxygen-bearing moieties could be carbonyl, hydroxyl-bearing tertiary carbon and ethyleneacetal groups. However, when the group was acetoxyl-bearing carbon, *i. e.*, the nitrite of 4-pregnene-3-one-17α, 20β-diol 20-acetate in which we have a system Ac-O-C-C-O-N=O, no carbon-carbon bond cleavage was observed and the starting alcohol was recovered unchanged. Moreover, several similar cases in the nitrite photolysis have been reported. For example, Kwok and Wolff[17] have reported that O-radical generated from the nitrite ester of 5α-androstane-2β, 3α, 17β-triol-3, 17-diacetate performed the normal Barton reaction. Moreover, Barton and his colleagues have reported[18] that the nitrite of 12α-hydroxy oleanolic acid acetate lactone was capable of achieving the normal Barton reaction. In these nitrites, ONO group is equally in the system

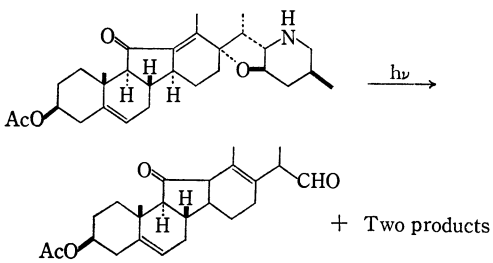

14) This compound was prepared by K. Orito in this laboratory through the catalytic hydrogenation of the corresponding aromatic amine, acetylation of the piperidine obtained and subsequent hydrolysis.

15) R. W. Franck and W. S. Johnson, *Tetrahedron Letters*, **1963**, 545; R. W. Franck, G. P. Rizzi and W. S. Johnson, *Steroids*, **1964**, 464.

16) A. L. Nussbaum, E. P. Yuan, C. H. Robinson, A. Mitchell, E. P. Oliveto, J. M. Beaton and D. H. R. Barton, *J. Org. Chem.*, **27**, 20 (1962).

17) R. Kwok and M. E. Wolff, *ibid.*, **28**, 423 (1963).

18) D. H. R. Barton, P. G. Sammes and M. Silva, *Tetrahedron*, Suppl. No. 7, 57 (1966).

AcO–C–C–ONO and no products from carbon-carbon bond cleavage were obtained.[19]

The observed difference in the photolytic behavior between Ac–N–C–C–ONO system and Ac–O–C–C–ONO is of considerable interest. It may be noted that the difference in photolytic behavior between the two systems is parallel to the difference of the bond energy of O–C and N–C.

Nearly simultaneously with our preliminary publication[1] Jeger and his colleagues published[20] the results of the photolysis of *O*-acetyljervine which seem to be relevant to the problem discussed here. On irradiation with light of 253.7 mμ, *O*-acetyljervine gave a mixture of the products from which they isolated three compounds. One of these is an aldehyde which is, in all probability, identical with the aldehyde IV obtained by us during the photolysis of the nitrite IIIc.

It is to be noted that they have found *N, O*-diacetyljervine to be photochemically inert, since they postulated[21] a similar process to ours for the formation of this aldehyde. As in the photolysis of *O*-acetyljervine different energy source and solvent (20 W, low pressure mercury arc lamp, 16 hr, dioxane) were employed, it would be difficult to assess this difference in the results.

Experimental

All melting points were determined on a Yanagimoto-type hot-stage and uncorrected. Unless stated otherwise, infrared spectra were determined in Nujol using an Nihonbunko DS-402G type spectrophotometer. NMR spectra were determined on a Japan electron optics 3H 60 high resolution NMR spectrometer in deuteriochloroform solution using tetramethylsilane as an internal reference. The course of reactions and the progress in column chromatography were followed by thin layer chromatography on Merck silica gel G.

3*O*, *N*-Diacetyl-22, 27-imino-11-oxojerva-5, 13(17)-diene-3β, 23β-diol (Ib). 22, 27-Imino - 11 - oxojerva-5, 13(17)-diene-3β, 23β-diol[4] (Ia) (4.038 g) and freshly distilled acetic anhydride (2.003 g) in dry pyridine (7.14 g) were set aside at room temperature. After 24 hr, a further amount of acetic anhydride (0.201 g) was added and the mixture was set aside for an additional 24 hr and heated for 10 min on a water bath. Benzene was added to the cooled solution and the solvents were evaporated by a rotatory evaporator. To the residue, there was added 10% aqueous sodium carbonate solution (20 ml) and the mixture was extracted with chloroform (60 ml, 40 ml, 40 ml, successively). The chloroform solution was washed with water (50 ml,) dried with sodium sulfate and evaporated. The residue was chromatographed on silicic acid (80 g, Mallinckrodt, 100 mesh) eluting with benzene-ether mixtures with increasing amounts of ether to give, successively, 3*O*, 23*O*, *N*-triacetyl derivative (295 mg), a mixture of tri- and diacetyl derivatives (331 mg), 3*O*, *N*-diacetyl derivative (2.3 g). The latter was recrystallized from ethyl acetate and *n*-hexane to yield Ib (2.07 g), mp 112—134°C. This was again purified from ether. mp 159—161°C. $[\alpha]_D^{18}$ +41.4° (*c* 2.4, methanol). IR: ν_{max} 1733 cm^{-1} (O-Ac and 11-C=O), 3400 cm^{-1} (broad, C23-OH), 1625 cm^{-1} (N-Ac), NMR: τ 9.03 (C-19 methyl), τ 8.15 (C-18 methyl), τ 8.03 and τ 8.00 (O- and N-Ac). Found: C, 72.51; H, 8.87; N, 2.48%. Calcd for $C_{31}H_{45}O_5N$: C, 72.76; H, 8.86; N, 2.74%.

3*O*, *N*-Diacetyl-22, 27-imino-11-oxojerva-5, 13(17)-diene-3β, 23β-diol 23-Nitrite (Ic). To 3*O*, *N*-diacetyl 22, 27 - imino -11- oxojerva-5, 13(17)-diene-3β, 23β-diol (Ib) (202 mg) in dry pyridine (0.95 g) there was added a mixture of nitrosyl chloride and pyridine at −30—−35°C until the solution persisted orange color. The solution was allowed to stand for 20 min at −17—−40°C and the reaction was then quenched with ice water. The resultant precipitates of the nitrite were filtered, washed with water and dried at room temperature under vacuum to afford 212 mg of crude nitrite Ic, mp 87—90°C (decomp.). This nitrite was unstable and was positive in the color reaction with diphenylamine-sulfuric acid.[9] Owing to the presence of *N*-acetyl absorption, a double band due to N=O stretching frequency in the infrared spectrum was not clear. However, two bands (768 and 795 cm^{-1}), which are most probably due to N–O stretching,[22] were descernible.

After a few hours a thin layer chromatogram of this nitrite showed the appearance of a spot of significant amount of the starting material. Therefore, this nitrite was immediately used in the next step without further purification.

Photolysis of the Nitrite Ester (Ic). The nitrite ester Ic (212 mg) in dry benzene (10 ml) at 15°C and under an atmosphere of dry nitrogen was irradiated with a 150-W high pressure mercury arc lamp for 67 min. After removal of a small amount of precipitation, the dark brown solution was concentrated to dryness and the residue was chromatographed on silicic acid (6 g) with benzene containing an increasing amount of ether. The least polar product (50 mg), eluted with benzene and ether, crystallized on evaporation of the solvent. This was washed with *n*-hexane and recrystallized from aqueous ethanol to yield aldehyde II (22 mg) mp 149.5—152°C. IR: ν_{max} 1731 cm^{-1} (O-Ac and 11-C=O) 2697 cm^{-1}, 2799 cm^{-1} and 1740 cm^{-1} (shoulder) (aldehyde) NMR: τ 9.05 (C-19 methyl) τ 8.16 (C-18 methyl) τ 8.83 (doublet, J=6.6) (C-21 methyl), τ 7.99 (O-acetate) and τ 0.56 (doublet, J=4.2) (aldehyde). Found: C, 75.47; H, 8.62%. Calcd for $C_{24}H_{32}O_4$: C, 74.97; H, 8.39%.

3*O*, *N*-Diacetyl-22, 27-imino - 11 - oxojerva - 5, 12-diene-3β, 23β-diol (IIIb). *N*-Acetyl-22, 27-imino-11-oxojerva-5, 12-diene-3β, 23β-diol (2.477 g) and acetic anhydride (0.576 g) in dry pyridine (2.19 g) were set aside for 22 hr at room temperature and then heated for 10 min on the water bath. To this solution there was added acetic anhydride (200 mg) and the solution was

19) As Kwok and Wolff have quoted, there is naturally a possibility that both hydrogen abstraction and oxidative fission occurred competitively in their case and only the product of abstraction was isolated.

20) G. Bozzato, K. Schaffner and O. Jeger, *Chimia.*, **20**, 114 (1966).

21) G. Bozzato, Ph. D. Thesis, E. T. H. Zürich (1966). We are grateful to Professor O. Jeger for the correspondence and sending the thesis by Dr. G. Bozzato.

22) P. Tarte, *Bull. Soc. Chem. Belges*, **60**, 227 (1951).

again heated for 30 min. After addition of benzene, the solvent was removed and to the residue were added water (30 m*l*) and 10% aqueous sodium carbonate (20 m*l*) and this was extracted with chloroform (50 m*l*, 40 m*l* and 40 m*l*, successively). The chloroform layer was washed with water (70 m*l*) and dried over magnesium sulfate. After evaporation of the solvent, the residue (3.03 g) was chromatographed on silicic acid (49 g). Elution with a mixture of benzene-ether with an increasing amount of ether afforded 3*O*, 23*O*, *N*-triacetyl-22, 27-imino-11-oxojerva-5, 12-diene-3β-, 23β-diol (0.227 g), a mixture of di- and triacetyl derivatives (38 mg) 3*O*, *N*-diacetyl-22, 27-imino-11-oxojerva-5, 12-diene-3β, 23β-diol (IIIb) (1.31 g) and a mixture of di- and monoacetyl derivatives (0.805 g) successively. The diacetyl derivative was recrystallized from aqueous ethanol to yield pure IIIb (0.741 g) mp 217.5—220°C. IR: ν_{max} 1645 cm^{-1} (N-Ac), 1697 cm^{-1}(11-C=O), 1733 cm^{-1} (O-Ac) 3505 cm^{-1} (OH) NMR: τ 9.25 (J=6.0) (C-26 methyl) τ 8.95 (C-19 methyl), τ 8.73 (J=6.0) (C-21 methyl), τ 7.92 (C-18 methyl), τ 8.00 and τ 7.83 (N-Ac and O-Ac). Found: C, 72.95; H. 8.94; N, 2.84%. Calcd for $C_{31}H_{45}O_5N$: C, 72.76; H, 8.86; N, 2.74%.

3*O*, *N*-Diacetyl-22, 27-imino-11-oxojerva-5, 12-diene-3β, 23β-diol Nitrite (IIIc). Compound IIIb (201 mg) was dissolved in dry pyridine and treated with nitrosyl chloride-pyridine mixture at −30°C until the solution persisted greenish yellow color. This was set aside for 7 min and poured into ice water. The resultant precipitates were collected by filtration to yield nitrite IIIc, 261 mg, mp 212—214°C (decomp.). This was unstable, and, dried for 4 hr under vacuum, was used immediately for the next photolysis.

Photolysis of Nitrite Ester (IIIc). The nitrite ester IIIc (261 mg) in dry benzene (12 m*l*) at 14°C and under an atmosphere of dry nitrogen was irradiated with a 150-W high pressure mercury arc lamp (Daikakogyo HLVA type, Japan) for 2 hr and 10 min. The residue was chromatographed on silicic acid (7 g). The least polar product (23 mg), eluted with benzene, crystallized on evaporation of the solvent. This was recrystallized from aqueous ethanol (17 mg) mp 192—194°C.[23] IR: ν_{max} 1699 cm^{-1} (α, β-unsaturated C=O), 1727 cm^{-1} (O-Ac and aldehyde) 1628 cm^{-1} (C=C) 2700 cm^{-1} (aldehyde). NMR: τ 8.97 (C-19 methyl) τ 9.12 (C-21 methyl) (J=6.6) τ 7.97 (O-Ac) τ 7.85 (C-18 methyl), τ 0.18 (J=1.4 cps) (aldehyde). Found: C, 75.03; H, 8.31%. Calcd for $C_{24}H_{32}O_4$: C, 74.97; H, 8.39%.

The Preparation of XIa. 5α, 6-Dihydroisojervone[4] (X) (200 mg), potassium hydroxide (63 mg) and methyliodide (82 mg) in ethanol (8 m*l*) were heated at 72°C for 95 min in a sealed tube. After the removal of ethanol, the residue was extracted with chloroform (20 m*l*) and water (10 m*l*). The organic layer was washed and dried. After the removal of the chloroform, the residue was recrystallized from acetone to yield 42 mg of XIa, mp 235—236°C (decomp.). The residue gave a further 84 mg of XIa by the preparative T.L.C. NMR: C-19 and C-18 methyls, τ 8.71 and τ 8.76. IR: 1703 cm^{-1} (six membered ketone), 1685 and 1635 cm^{-1} (CO-C=C), 3470 cm^{-1} (OH) Found: C, 75.93; H, 9.10; N, 3.54%. Calcd for $C_{27}H_{39}O_3N$: C, 76.19; H, 9.24; N, 3.29%.

The Preparation and Photolysis of Nitrite (XIb). The alcohol XIa (84 mg) in pyridine (1 m*l*) was treated with nitrosyl chloride in pyridine at −25°C in the usual manner. The nitrite obtained softened at 90°C and melted at 160°C with decomposition (63 mg). IR: 1713 cm^{-1} (six membered ketone), 1695 and 1640 cm^{-1} (CO-C=C). The nitrite (63 mg) in benzene (13 m*l*) was photolyzed in the usual manner for 90 min. After the removal of the solvent, T. L. C. revealed that the product was solely the starting alcohol XIa.

The Preparation of XIIa. (Experiments by N. Sato). 22, 27-Imino-11-oxojerva-5, 12-diene-3β, 23β-diol (Ia) (3.7 g) was dissolved in 500 m*l* of dry toluene and 150 m*l* of the solvent was removed by distillation. To this solution, there was added 40 m*l* of cyclohexanone and then 60 m*l* of the solvent was distilled to remove a trace of water. A solution of 3.7 g of aluminum isopropoxide in 19 m*l* of dry toluene was added. The reaction mixture was refluxed for 6.5 hr. On cooling, 10 m*l* of water was added to the solution and the precipitate was removed by filtration. To the filtrate there was added 2 N aqueous hydrochloric acid (50 m*l*) and the salt (3.0 g) formed was collected by filtration. The salt was dissolved in water (2.5 *l*) and the aqueous solution was extracted with ether. The aqueous solution was made up to pH 8.0 with 2 N aqueous ammonia, extracted with chloroform (total volume, 700 m*l*), washed with water and dried over sodium sulfate. After evaporation, 3.4 g of crude Δ^4, 3-ketone was obtained. This was purified by making the complex (2.0 g) with chloroform. The complex (1.0 g) was immediately submitted to cyclization with base to yield XIIa. The chloroform complex in 5% methanolic potassium hydroxide was refluxed for 1 hr. The resultant compound was extracted with ether. The ethereal solution was washed with water and dried over sodium sulfate. After evaporation of the solvent, the residue was recrystallized from ethanol to yield XIIa mp 222—224°C. IR: 1728 cm^{-1} (five membered ring ketone), 1655 and 1616 cm^{-1} (α, β-unsaturated ketone). UV λ_{max} 232 mμ (ε; 9800) (ethanol) NMR τ 8.81 and τ 8.70 (C-19 and C-18 methyls). Found: C, 76.31; H, 9.22; N, 3.41%. Calcd for $C_{29}H_{39}O_3$: C, 76.19; H, 9.24; N, 3.29%.

The Nitrite XIIb. Compound XIIa (200 mg) in pyridine (1 m*l*) was treated with nitrosyl chloride in pyridine at −30°C until dark green color persisted. The reaction mixture was poured into ice water. The resultant precipitate was collected by filtration and dried under vacuum. Mp 143—146°C (204 mg). T.L.C. gave only one spot. IR: 1730 cm^{-1} (five membered ketone), 1671 and 1638 cm^{-1} (α, β-unsaturated ketone) 1618 cm^{-1} (weak) 1660 cm^{-1} (shoulder), 795 and 802 cm^{-1} (doublet) and 675 cm^{-1} (-O-NO).

Photolysis of the Nitrite (XIIb). The nitrite (204 mg) in dry benzene (15 m*l*) was irradiated under an atmosphere of dry nitrogen at 14—16°C. After 68 min. no nitrite remained unchanged. The residue (233 mg) gave only one spot on T.L.C. This was dissolved in methanol. To the solution there was added ether and *n*-hexane to yield the crude alcohol XIIa. This was again recrystallized from acetone, mp 222—224°C.

23) In our preliminary communication,[1] the melting point of this was described as mp 167—171°C.

N-Benzoyl-22, 27-imino-11-oxojerva-5, 12-diene-3β, 23β-diol (IIId). 22, 27-Imino-11-oxojerva-5, 13-(17)diene-3β, 23β-diol (2.38 g) and benzoic anhydride (4.65 g) in dry pyridine (20 ml) were set aside overnight at room temperature. Then, the reaction mixture was further heated for 1 hr on a water bath. After the removal of pyridine under reduced pressure, there was added aqueous 5% sodium carbonate (80 ml). This was extracted with chloroform (100 ml, 50 ml, and 50 ml, successively).

The combined organic layer was washed with water (100 ml, twice) and dried over sodium sulfate. The residue (7.7 g) in 6% methanolic potassium hydroxide (50 ml) was refluxed for 1.5 hr under nitrogen atmosphere. After 30 min, solid appeared in the solution and methanol (20 ml) was added. The solution was further refluxed for 1 hr and cooled. The crystals that appeared were collected by filtration. A total amount of 2.32 g of crude benzoyl derivative IIIc was obtained. After purification from methanol, it melted at 230.5—232.5°C. $[\alpha]_D^{18}$ −8.2 (*c* 2.0, pyridine) IR: 1623 cm^{-1} (*N*-benzoyl), 1703 cm^{-1} (C=O). NMR: MeOH τ 6.49 C-18 methyl, τ 7.79 C-19 methyl, τ 8.93, phenyl proton, τ 2.62. Found: C, 75.74; H, 8.64; N, 2.29%. Calcd for $C_{33}H_{45}O_6N\frac{1}{2}MeOH$: C, 75.65; H, 8.65; H, 2.58%.

3O-Acetyl-N-benzoyl-22, 27-imino-11-oxojerva-5, 12-diene-3β, 23β-diol (IIIe). To *N*-benzoyl-22, 27-imino-11-oxojerva-5, 12-diene-3β, 23β-diol (1.01 g) in pyridine (20 ml) there was added acetic anhydride (2 ml) at −10°C. The reaction mixture was set aside for four days at −5°C. To the reaction mixture, methanol was added and the mixture was heated for 2 hr on a water bath. The solvent was removed and to the residue water was added and this was extracted with chloroform (50 ml, 50 ml and 30 ml).

The chloroform solution was washed and dried. After the removal of the solvent the residue was chromatographed on alumina (Merck, standard, 25 g). Elution with benzene containing an increasing amount of ether gave diacyl derivative (231 mg), the mixture of di- and mono-acetyl derivatives (110 mg) and desired 3*O*-acetyl derivative IIIe (680 mg, 62%). The mono-acetyl derivative was recrystallized from aqueous ethanol (644 mg) mp 144.5—146°C. $[\alpha]_D^{18}$ −67.7° (*c* 2.1, methanol). IR: 1629 cm^{-1} (Ph–C=O), 1705 cm^{-1} (C=C–C=O) and 1735 cm^{-1} (–O–$COCH_3$) 3400 cm^{-1} (broad, OH). Found: C, 72.89; H, 8.51; N, 2.28%. Calcd for $C_{36}H_{47}O_5N\cdot H_2O$: C, 73.06; H, 8.35; N, 2.37%. After purification from aqueous ethanol, diacetate had mp 233—235°C. IR: 1633 cm^{-1} (benzoyl), 1702 cm^{-1} (C=C–C=O) and 1739 cm^{-1} (–$OCOCH_3$). Found: C, 73.66; H, 8.06; N, 2.76%. Calcd for $C_{38}H_{49}O_6N$: C, 74.11; H, 8.02; N, 2.27%.

The Nitrite (IIIf). 3*O*-Acetyl-*N*-benzoyl-22, 27-imino-11-oxojerva-5, 12-diene-3β, 23β-diol (336 mg) in dry pyridine (4 ml) was treated with nitrosyl chloride-pyridine mixture at −40°C until the solution persisted blue color. This was set aside for 22 min and poured into ice water (500 ml). The resultant precipitates of the nitrite were collected by filtration, washed with water and dried at room temperature under vacuum (344 mg), mp 206—208°C (decomp.). This nitrite was positive for the nitrite color reaction with diphenylamine-sulfuric acid and was unstable.

Photolysis of the Nitrite Ester. The nitrite ester (334 mg) above in dry benzene (18 ml) at room temperature and under an atmosphere of dry nitrogen was irradiated with a 150 W high pressure mercury arc lamp for 85 min. After this period the color reaction disclosed complete disappearance of the nitrite. After removal of the solvent under reduced pressure, the oily residue was chromatographed on silicic acid (10 g). Elution with benzene and then benzene containing ether (0.5 vol%) gave 38 mg of the least polar fraction (A). Then, the column was eluted with ethyl acetate-methanol mixture. Eluate (B) (287 mg) was obtained. Tritulation of (A) above with ether gave 42 mg of the residue. This was dissolved in ether (20 ml) and extracted with 5% aqueous sodium hydrogen carbonate (1.5 ml) and water (3 ml). Ethereal layer was washed with water and dried over sodium sulfate. Removal of ether yielded 17 mg of the residue (C). Aqueous layer was acidified to pH 1 with 1 N hydrochloric acid and extracted with ether. From this ethereal solution, benzoic acid (2 mg) was obtained. Preparative thin layer chromatography of the eluate (B) afforded 39 mg of aldehyde as the least polar fraction. Recrystallization of this from aqueous ethanol afforded the aldehyde IV, 15 mg, mp 189—192°C. IR and NMR spectra of this aldehyde were completely superimposable with that obtained from IIIc.

N-Methyl-22, 27-imino-11-oxojerva-5, 13(17)-diene-3β, 23β-diol (Ie). To a solution of liquid ammonia (300 ml) containing lithium (474 mg) there was added *N*-methyljervine[12] (3.92 g) in tetrahydrofuran (70 ml). A further amount of tetrahydrofuran (30 ml) was added while stirring. The mixture was stirred for 35 min and the blue color of the reaction mixture disappeared after this period. A further amount of lithium (30 mg) was added. Ammonium chloride (5 g) was added and the resulting colorless solution was kept at room temperature to remove ammonia and then tetrahydrofuran was removed under reduced pressure. To the residue there was added water (100 ml) and this was extracted with chloroform (four times, the total volume 450 ml). The chloroform layer was washed with water (150 ml), dried and evaporated. The residue was recrystallized from methanol. Crude Ie (2.59 g) was obtained in three crops. This was further recrystallized from methanol. Mp 185.5—189°C $[\alpha]_D^{18}$ +30.8° (*c* 2.5, pyridine). IR: 3400 cm^{-1}(OH), 1731 cm^{-1} (five membered C=O). NMR: τ 7.76 (N–Me), τ 8.09 (C-18 methyl) τ 9.06 (C-19 methyl). Found: C, 76.07; H, 9.87; N, 3.13%. Calcd for $C_{28}H_{43}NO_3$: C, 76.15; H, 9.81; N, 3.17%.

The Preparation of the Compound (IX). The compound Ie (292 mg) in methanol (10 ml) and 5% methanolic potassium hydroxide (2 ml) was refluxed for 2 hr under an atmosphere of dry nitrogen. To the reaction mixture methanol (10 ml) and 5% methanolic potassium hydroxide (2 ml) were again added and this was refluxed for 1 hr. After the removal of methanol, the residue was washed with water (30 ml) and dried (237 mg). This was recrystallized from methanol (156 mg). Mp 275—302°C (decomp.). IR: 3400 cm^{-1} (OH), 1731 cm^{-1} (five membered ketone). NMR: τ 7.84 (N–Me) τ 8.26 (C-18 methyl) τ 8.95 (C-19 methyl). Found: C, 75.95; H, 9.92; N, 3.01%. Calcd for $C_{28}H_{43}O_3N$: C, 76.15; H, 9.81; N, 3.17%.

The hydriodide was obtained as follows: the zwitterion IX (126 mg) in acetic acid (0.3 ml) was admixed with

aqueous potassium iodide (20%, 0.4 m*l*). The highly crystalline hydriodide deposited immediately. This was collected by filtration and recrystallized from ethanol to yield colorless needles, (73 mg) mp 300°C. Found: C, 59.19; H, 7.89; N, 2.43%. Calcd for $C_{28}H_{44}O_3NI$: C, 59.04; H, 7.79; N, 2.46%.

The authors are grateful to Mr. S. Shimokawa for the measurements of NMR spectra and to the staff of the laboratory for microanalyses, the Faculty of Pharmaceutical Science of Hokkaido University, for the elemental analyses.

BULLETIN OF THE CHEMICAL SOCIETY OF JAPAN VOL. 41 475—478 (1968)

Analyses of Organic Soils Extracted from Naturally-soiled Cloths

Teruo TSUNODA

Central Research Laboratory, Hitachi, Ltd., Kokubunji, Tokyo

(Received April 22, 1967)

The analyses of organic soils extracted from naturally-soiled chloths were carried out by IR spectroscopy, gas chromatography, thin-layer chromatography (TLC), and gel filtration. The fatty-acid constituents involved in organic soil were determined by gas chromatography. The presence of triglycerides, cholesterol and its ester, and such hydrocarbons as paraffin and squalene in organic soil was also found by means of TLC. In gel filtration, two peaks were found in elution diagrams of the detergent solution after washing naturally-soiled cloths. The ultraviolet spectra, which were measured for the effluent corresponding to each peak, indicated that the nitrogen compound involved in each effluent is probably a protein-lipid complex such as lipoprotein. The nitrogen content in each effluent was also determined by the micro-Kjeldahl method. A smaller nitrogen content was given for the effluent corresponding to the first peak than for that of the second peak. The nitrogen compound involved in the effluent for the first peak was harder to remove from cloths than that for the second peak.

Knowledge concerning natural soils adhering on cloths is necessary in order to investigate the detergency mechanism. The natural soils may be divided into two main groups; one is an inorganic soil for which dirt floated in an atmosphere is considered to be the main constituent, while the other is an organic soil consisting of skin fats.

A study has been made by Brown[1] of the amount and composition of the organic soil adhering to domestically-soiled fabrics. However, the constituents have not been shown in detail for each component involved in the organic soils. Bey[2] has reported the results of his analysis of skin-surface lipids which were transferred on to textiles or underwear during wearing. Oldenroth *et al.*[3] have also reported similar analytical results for organic soils extracted from underwear. The composition of human foream sebum and of adult human-hair fat have been determined by Wheatly[4] and Nicolaides *et al.*[5] respectively. Further, the compositions of human surface lipids have been reported in detail by Nicolaides *et al.*[6]

With the recent advance in the separation techniques of lipid mixture, such as gas and thin-layer chromatography, it has become possible to determine the constituents of natural lipids in detail. The purpose of this work is to determine the composition of organic soils extracted from naturally-soiled collars with such techniques as infrared spectroscopy, gas and thin-layer chromatography (TLC), and gel filtration.

Experimental

Two kinds of organic soils were prepared for analysis. Sample 1 and Sample 2 were prepared by extraction with methylene chloride for the soiled cloths supplied by the Lion Fat and Oil Co. and with petroleum ether for the soiled cloths prepared in our laboratory in a manner similar to that described by Tomiyama *et al.*[7] The two samples were essentially similar.

The composition of free fatty acid involved in the organic soil was determined by a Hitachi F6-D gas

1) C. B. Brown, *Research*, **1**, [7] 46 (1947).
2) K. H. Bey, *Am. Perfumer and Cosmetics*, **79**, [8] 35 (1964).
3) K. Kind and O. Oldenroth, *Waschere-Tech u-Chem*, **1**, [5] 9, 13 (1948); O, Oldenroth, *ibid.*, **10**, 430 (1957); O. Oldenroth and K. Nettelnstroth, *Melliand Textilber.*, **45**, 79 (1964).
4) V. R. Wheatley, *Seifen-Oele-Fette Wachse*, **81**, 214 (1955).
5) N. Nicolaides and R. C. Foster, *J. Am. Oil Chem. Soc.*, **33**, 404 (1956).
6) N. Nicolaides and R. E. Kellum, *ibid.*, **42**, 685 (1965); N. Nicolaides, *ibid.*, 691; N. Nicolaides and Thomas Ray, *ibid.*, 702; N. Nicolaides, *ibid.*, 708.
7) S. Tomiyama and M. Iimori, *ibid.*, **42**, 449 (1965).

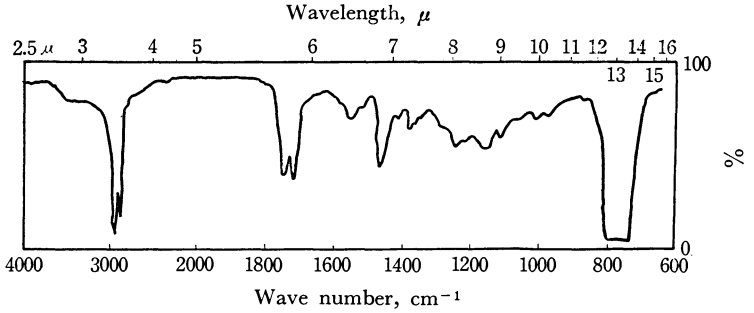

Fig. 1. IR spectrum of CCl_4 solution of a organic soil extracted from naturally soiled cloths (Sample 2).

chromatograph (with a flame-ionization-type detector) using a Golay column B. D. S. 45 m in length. The methylation[8] was performed by refluxing Sample 2 with a 5% HCl - methanol solution at 100°C for several hours.

The lipid components were detected by the TLC method. Silica gel (Wako gel B-O, Wako Pure Chemical Ind., Ltd.) was used as the adsorbent. The commercial solvents and reagents were used without purification. The adsorbent layer was produced on a 20×20 cm clean glass plate with a thickness of about 250 μ and equipped with an applicator (Yamato TL-1, Yamato Sci. Co., Ltd.), and then activated by heating in an oven at 110—120°C for 1—2 hr. After 10 m*l* of a dilute methylene chloride solution of each sample had been applied to the adsorbent layer with a microsyringe, the chromatoplate was dipped up to the depth of 1 cm into some developing solvent in a covered-glass vessel. The identification was carried out by heating the plate at 120—180°C in an oven after spraying it with concentrated H_2SO_4.

The Sephadex gel filtration technique was also attempted in order to find the nitrogen compounds involved in natural soils. Completely-swollen Sephadex G-100 gel after been in a 1% NaCl aqueous solution for 2 days was packed in the column 2.5 cm in diameter and 45 cm in height. After 10 m*l* of the sample solution had been added to the column, 0.1% NaCl aqueous solution was poured in from the top of the column. Nitrogen compounds in the effluents were detected by measuring the absorbance at 280 mμ with a Hitachi Perkin-Elmer spectrophotometer, 139.

Results and Discussion

Infrared Spectrum. The infrared spectrum of Sample 2 in a carbon tetrachloride solution is shown in Fig. 1. (A similar spectrum was obtained for Sample 1.) The IR spectrum exhibited characteristic peaks at 1740 cm^{-1} and 1710 cm^{-1} and a broad peak in the 1300—1100 cm^{-1} region which can not seen in the spectrum of the solvent. The peaks at 1740 cm^{-1} and 1300—1100 cm^{-1} were identical with those of the triolein, but that at 1710 cm^{-1} could not be observed in the triolein spectrum. The peaks at 1740 and 1710 cm^{-1} may be identified as, respectively, the stretching vibration in carbonyl groups in glyceride molecules such as triolein and that in free fatty acid molecules. Since the infrared spectrum shown in Fig. 1 was essentially identical with that of triolein except for the peak at 1710 cm^{-1}, it can be estimated that such triglycerides as triolein are present in naturally-soiled cloths. On the other hand, the existence of the peak at 1710 cm^{-1} indicates that free fatty acids are also present in the samples.

Gas Chromatography. A gas chromatogram of the fatty acid in Sample 2 is shown in Fig. 2. The results show that most of the fatty acids involved in this organic soil have carbon numbers from 14 to 18 in their molecules. For the C_{14} fatty acids, the peak height of saturated acid was greater than that of unsaturated fatty acids. In the C_{16} fatty acids, both are of equal height. On the contrary,

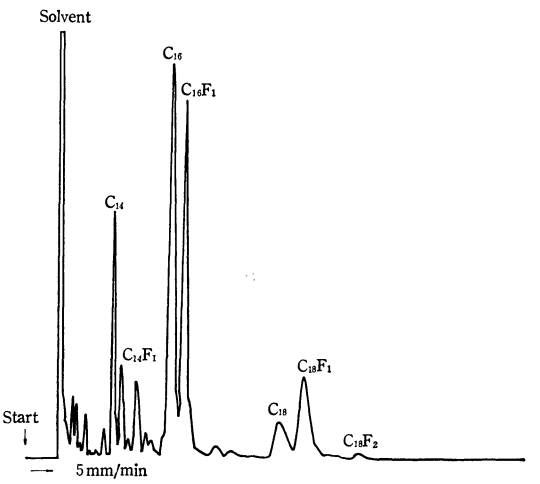

Fig. 2. Gas chromatographic analysis of fatty acids involved in a organic soil extracted from naturally soiled cloths.
Sample 2. 4 μ*l*, column: Golay B. D. S. 45 m, Oven temp.: 170°C, Injection block: 300°C, Carrier gas: N_2, Flow rate: 0.7 kg/cm², Attenuation: 10×4, Chart speed: 5 mm/min, Instrument: No. F6-D.

8) H. Schlenk and J. L. Gellerman, *Anal. Chem.*, **32**, 1412 (1960).

the order of peak height mentioned above was reversed in the case of C_{18} fatty acids. A similar result has been reported by Bey.[2] It is interesting that the ratio of the amount of unsaturated fatty acids to that of saturated acids increases with the increase in carbon number.

Thin-layer Chromatograph (TLC). By preliminary experiments it was found that the cyclohexane and a solution consisting of 1-nitropropane and *n*-hexane can be successfully used as solvents for the detection of nonpolar lipids, such as squalene and paraffin, and polar lipids, such as glycerides, cholesterol, and its stearate. It may be seen in Figs. 3 (solvent: cyclohexane) and 4 (solvent: solution consisting of 1-nitropropane and *n*-hexane) that paraffin, squalene, triglycerides, cholesterol, and its esters are involved in natural organic soils.

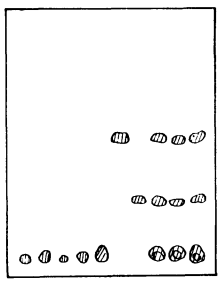

Fig. 3. Thin layer adsorption chromatographic separation of hydrocarbon involved in organic soils.
Solvent is cyclohexane.
a: Stearic acid b: Glycerin monostearate
c: Tristearin d: Cholesterol
e: Cholesterol stearate
f: Paraffin g: Squalene
h: Mixture of a—g lipids
i: Sample 1 j: Sample 2

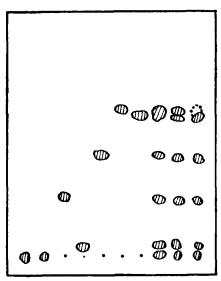

Fig. 4. Thin layer adsorption chromatographic separation of cholesterol, cholesterol ester and triglyceride involved in organic soils.
Solvent is *n*-hexane 180 cc + 1-nitropropane 20 cc solution.
a: Stearic acid b: Glycerin monostearate
c: Tristearin d: Cholesterol
e: Cholesterol stearate
f: Paraffin g: Squalene
h: Mixture of a—g lipids
i: Sample 1 j: Sample 2

Gel Filtration. Figure 5 shows the elution curves obtained for: (a) the distilled water, (b) the sodium dodecylbenzene sulfonate (NaBS) aqueous solution after washing the naturally-soiled cloths, and (c) a 0.1 wt% egg albumin aqueous solution containing 0.05 wt% NaBS.

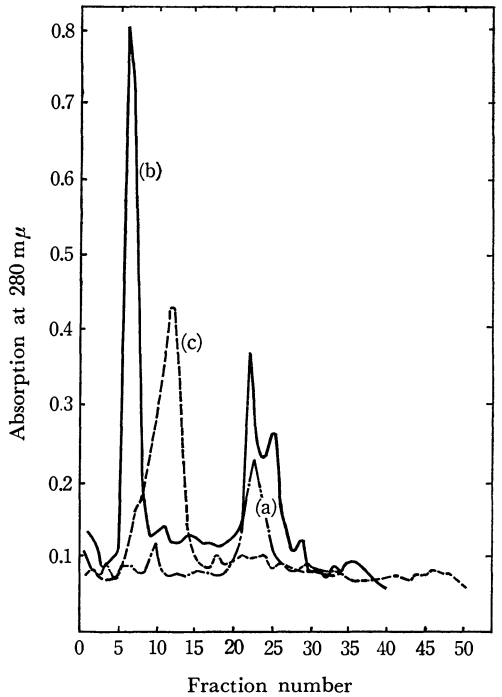

Fig. 5. The elution curve obtained for the distilled water (a), the NaBS aqueous solution after washing the naturally soiled cloths (b) and 0.1% NaBS (c).

A single peak appeared in fraction number 23 in the elution curve (a). On the other hand, two peaks were found in fractions number 6—8 and 22—26 in the elution curve (b). The heights of these peaks increase with the increase in the concentration of NaBS.

From a comparison of (b) with (c) in Fig. 5, we may find that the substance corresponding to the first peak in the curve (b) has a larger molecular size, while the substance corresponding to the second peak has a smaller molecular size, than the egg albumin molecule.

The nitrogen compound involved in the effluents of fractions number 6—8 could be removed from cloths only when a detergent solution was used for washing. Such interactions between proteins and detergents have been reported by Aoki *et al.*[9]

9) K. Aoki, *J. Am. Chem. Soc.*, **80**, 4904 (1958); K. Aoki and J. Hori, *ibid.*, **81**, 1885 (1959); K. Aoki, *Yushi*, **16**, [11] 21 (1963); **17**, [2] 26 (1964); **17**, [3] 12 (1964); **17**, [4] 20 (1964).

and by others.[10]

The Ultraviolet Spectra. Figure 6 shows the ultraviolet spectrum for each effluent corresponding to the first and second peaks in the elution curve (b) in Fig. 5, along with those of egg albumin and β-lipoprotein. The spectrum of egg albumin showed the characteristic absorption due to the polypeptide bond at 280 mμ, but a smaller plateau was found at 270 mμ in that of β-lipoprotein. In the spectrum of each effluent, the characteristic absorption found in egg albumin was not observed, but the inflection point near 270 mμ and the plateau in the region from 240 to 270 mμ were found for each effluent corresponding to the first and second peaks in Fig. 5, curve (b). The nitrogen compound involved in each effluent is not considered to be pure protein, but a protein-lipid complex such as lipoprotein.

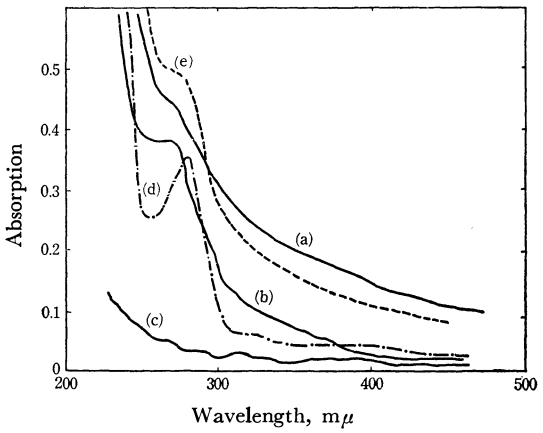

Fig. 6. Ultraviolet spectra.
- a : Effluent corresponding to first peak in curve (b) in Fig. 5.
- b : Effluent corresponding to second peak in curve (b) in Fig. 5.
- c : Effluent corresponding to fraction number 45 in Fig. 5.
- d : 1% egg albumin.
- e : β-Lipoprotein.

The nitrogen contents involved in the two effluents corresponding to the first and second peaks and egg albumin, as determined by the micro-Kjelder method, were 5.40, 13.50, and 65.60 γN/ml respectively.

The author wishes to express his hearty thanks to Professor I. Hara of Tokyo Medical and Dental University for his valuable discussions and for supplying the β-lipoprotein. He is also grateful to Mr. K. Komeji of Tokyo Metropolitan University and Mr. I. Kashiwa of Lion Fat and Oil Co. for supplying the cholesterol stearate and naturally-soiled cloth respectively. Grateful acknowledgment is also made to Mr. N. Ichiki for his gas chromatographic analysis of fatty acids and to Miss M. Imagawa for her assistance in the experimental work.

10) H. P. Lundgren, *J. Am. Chem. Soc.*, **63**, 2854 (1941); F. W. Putnam and H. Neurath, *ibid.*, **66**, 692 (1944); F. W. Putnam and H. Neurath, *ibid.*, **66**, 1992 (1944).

BULLETIN OF THE CHEMICAL SOCIETY OF JAPAN VOL. 41 479—485 (1968)

The Zinc Oxide-Copper Catalyst for Carbon Monoxide-Shift Conversion. II. The Catalytic Activity and the Catalyst Structures

Hiroshi UCHIDA,*1 Masaaki OBA, Norio ISOGAI*2 and Toji HASEGAWA

Government Chemical Industrial Research Institute, Tokyo, Shibuya-ku, Tokyo

(Received August 28, 1967)

Structures of the zinc oxide-copper catalysts, whose catalytic activity in carbon monoxide-shift conversion had been determined, were investigated by X-ray diffraction technique, mercury- and helium-volume measurement, and electron microscopy. The electron microscopic observations were conducted in two ways; one on a catalyst sample after the activity test and the other on a raw sample while undergoing specified treatments in a reaction chamber attached to the electron microscope. On the basis of models of particle geometry obtained from the electron microscopic images, the results on pore volume, average diameters of pores and particles, all dependent on the method of preparation and the chemical composition, are explained. The models and the observed dependency of the specific activity of copper surface on the copper content indicate that the finer copper particles, whether patch-like or massive, show the higher specific activity. The fine copper particle is apt to be oxidized more readily than the well-grown particle.

The preceding paper[1] described how the preparation method and the chemical composition of zinc oxide-copper catalysts are related to their catalytic activity in carbon monoxide-shift conversion. The catalysts studied were a series of catalysts of varying copper contents prepared by kneading zinc oxide powder with copper hydroxide cake (the kneaded series) and a couple of catalysts of an approximate copper content prepared by the impregnation and the coprecipitation method. Practicable catalysts could be produced only by the kneading process provided they contained appropriate amounts of copper. As regards the kneaded series, a model of particle geometry that copper forms its own particles among the original zinc oxide powders was tentatively proposed and successful in an attempt of explaining the observed dependency of catalytic activity on the chemical composition, but exact knowledge on structures of the catalysts is still lacking. In the present study, the catalyst structures will be investigated, the results of which may be used for an understanding of the catalytic activity from the structural viewpoint of the catalysts.

Experimental

Table 1 presents the method of preparation and the chemical composition of catalysts repeatedly. Experimental methods used for investigating catalyst structures include X-ray diffraction technique, mercury- and helium-displacement method, and electron microscopy.

The X-ray diffraction diagram for a powdered sample of the catalyst was obtained with an X-ray diffractometer of the Geigerflex D-3F type. The nickel filtered Cu$K\alpha$ radiation from a sealed-off tube with berylium windows was used. The tube was operated at 40 kV and 18 mA. The volumes by the mercury- and helium-displacement method were determined on catalyst grains after they had been used in the activity test for carbon monoxide-shift conversion.

TABLE 1. METHOD OF PREPARATION AND CHEMICAL COMPOSITION OF CATALYSTS

Catalyst No.	Method of preparation	Cu/Zn atomic ratio
1	Kneading[a)]	ZnO
2	Kneading[a)]	0.09
3	Kneading[a)]	0.25
4	Kneading[a)]	0.45
5	Kneading[a)]	0.68
6	Kneading[a)]	0.90
7	Kneading[a)]	1.98
8	Kneading[a)]	2.95
9	Kneading[a)]	9.70
10	Kneading[a)]	Cu
21	Impregnation	0.34
22	Coprecipitation	0.40

a) Zinc oxide powder was kneaded with a copper hydroxide cake into a pasty mixture, which was dried at 150°C, pelleted, and heat-treated in the air at 250°C. A series of catalysts 1—10 with be designated as the kneaded series.

*1 Present address: Faculty of Engineering, Nagoya University, Chikusa-ku, Nagoya.

*2 Present address: Japan Gas Chemical Co., Enoki-cho, Niigata.

1) H. Uchida, N. Isogai, M. Oba and T. Hasegawa, This Bulletin, **40**, 1981 (1967).

The size and shape of particles of a catalyst sample after the activity test were examined under an electron microscope of the JEM-6A type. Moreover, changes in shape of particles were pursued under the electron microscope on a dried paste (the sample after drying at 150°C a pasty mixture of oxide or hydroxide of zinc and copper hydroxide) while the paste was undergoing such treatments as heating in the air and subsequent reduction in hydrogen. In particular cases, the paste was oxidized finally in the air. These treatments were conducted in a reaction chamber attached to the electron microscope.

The reaction chamber is schematically drawn in Figs. 1A and 1B. The chamber is a stainless steel cylinder (C) (110 mm diameter by 100 mm long) and attached to the electron microscope by way of an air-lock (L). It is equipped with two valves, one (V) for introduction of a reactant gas (hydrogen or air) at a constant feed rate (10 *l*/hr) at atmospheric pressure and another (V') either for withdrawal of the gas at atmospheric pressure or for evacuation. A holding device (A, for details see Fig. 1B showing another side of 1A) of a sample is centrally held in the chamber by means of a perforated stainless steel rod (R) inserted from top of the chamber. Through the perforation pass an insulated Pt-Pt·Rh thermocouple and two insulated nichrome wires leading to a nichrome wire heater (I). A stainless steel sample holder (H), which is similar in dimension to the one as conventional in the electron microscopic observation and which has small ceramic protruding parts around its supporting drim, is mounted vertically in a notched steatite cylinder having a steatite drim (J). The nichrome wire heater (I) is wound along the notch. The steatite drim is fixed to the rod (R) one over another together with a stainless steel plate (K), into which a stainless steel tube for protection of the heater is screwed. A horizontally movable rod (M) with a fork at the end carries the sample holder, while the holder being hung by the ceramic protruding parts, into and out of the electron microscope through the air-lock open.*3

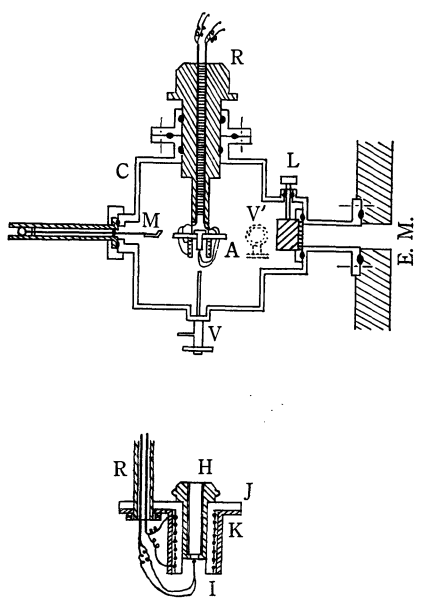

Fig. 1. Schematic diagram of reaction chamber.
Above: Fig. 1A, below: Fig. 1B

The sample was ground in a mortar to powder. The powder was sprinkled by means of an adsorbent cotton over an evaporated silica film supported on a stainless steel mesh, which was then placed at bottom in the sample holder. The temperature at which the sample was undergoing progressive reduction processes in hydrogen or oxidation in the air was measured with the Pt-Pt·Rh thermocouple just below the mesh. The electron microscopic observations were conducted at time intervals after the successive treatments of a short period.

Results

The X-Ray Diffraction Diagram. The raw copper hydroxide cake gave a complicated diffraction diagram, indicating the presence of basic copper hydroxide, $Cu_2(OH)_3(NO_3)$, in addition to that of copper hydroxide. However, no more sign other than oxides of copper and zinc appeared in the diagram of the finished sample.*4 This reveals rapid decomposition of both the basic hydroxide and the hydroxide into the oxide by a simple heat-treatment in the air at 250°C. After having been used in the activity test, all the samples including catalysts 21 (the impregnated catalyst) and 22 (the coprecipitated catalyst) gave sharp diffraction lines due to zinc oxide and copper in addition to very weak and diffused lines due to copper oxide (*e. g.* Ref. Fig. 2 for catalyst 4). Lattice constants of the zinc oxide were found to be $a=3.255$—3.285 Å and $c=1.60$ Å, while the constant of copper $a=3.618$—3.628 Å, the values being identical with the literature values.

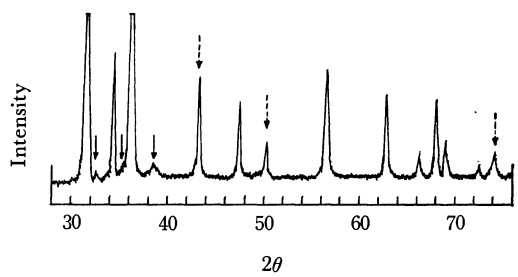

Fig. 2. X-Ray diffraction diagram of catalyst 4 after use in activity test.
The arrows indicate the lines due to copper oxide.

The Total Pore Volume and the Porosity. The mercury-volume and the helium-volume (hereafter denoted by V_{Hg} and V_{He} respectively) of catalyst grains are presented in Fig. 3 as a function of the catalyst chemical composition expressed

*3 Details of procedures for the observation will be described elsewhere.

*4 Refer to the foot note of Table 1.

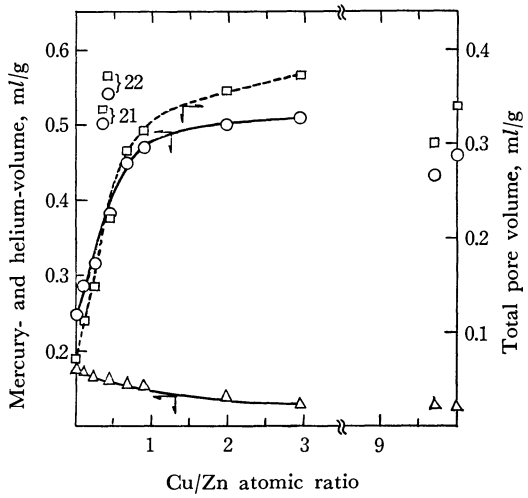

Fig. 3. Mercury- and helium-volume and total pore volume as function of Cu/Zn atomic ratio.
○: V_{Hg}, △: V_{He}, □: V_{po}

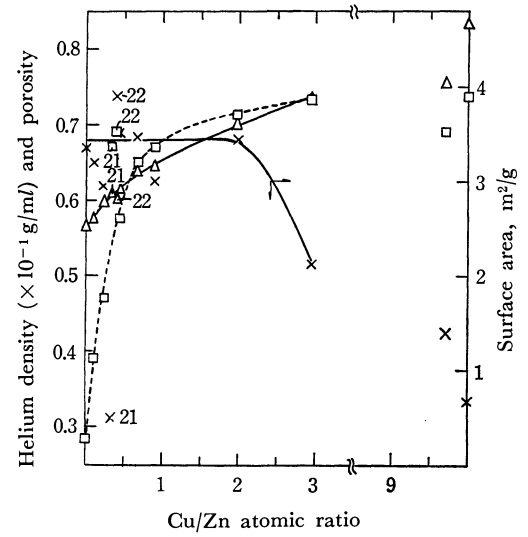

Fig. 4. Helium-density, porosity, and specific surface area plotted against Cu/Zn atomic ratio.
□: porosity, △: ρ_t, ×: S

by the Cu/Zn atomic ratio. The total pore volume (V_{po}) was then obtained as the difference between V_{Hg} and V_{He}, while the porosity (θ) as the ratio of V_{po} to V_{Hg}. The V_{po} and the θ are plotted in Figs. 3 and 4 against the Cu/Zn atomic ratio respectively. These two plots similarly rise rapidly with the ratio in the initial range below 1, less steeply in the intermediate range. In the final range of high ratios (probably >5), the V_{po} turns to fall, whereas the θ remains almost constant. The V_{po} values of catalysts 21 and 22 are much larger than those of catalyst 4, the corresponding catalyst (the catalyst approximate in copper content) of the kneaded series.

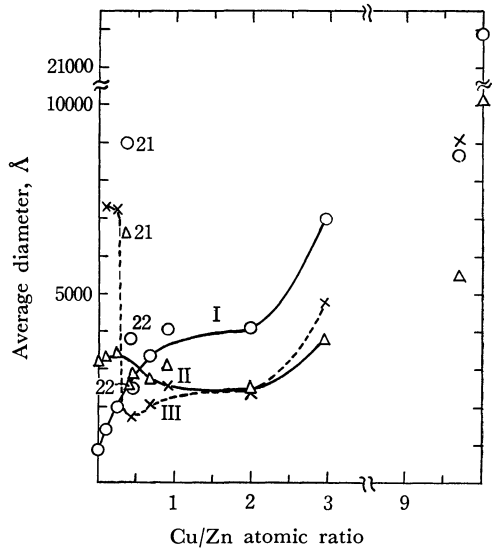

Fig. 5. Average diameters of pores and particles as function of Cu/Zn atomic ratio.
○ (I): $\bar{d}_{po}$, △ (II): $\bar{d}_{pa}$, × (IIII): $\bar{d}_{paCu}$ calculated on the basis of model II in the preceding paper.

The Average Diameter of Pores and Particles. On the assumption of cylindrical pores the average pore diameter ($\bar{d}_{po}$) was claculated by the equation of $\bar{d}_{po}=4V_{po}/S$, where S was the specific surface area of catalyst, on the assumption of spherical or cubic particles the average particle diameter ($\bar{d}_{po}$) was calculated by the equation of $\bar{d}_{pa}=6/\rho_t S$, where ρ_t was the true density or $1/V_{He}$ (Ref. the plot in Fig. 4). Plots of the $\bar{d}_{po}$ and the $\bar{d}_{pa}$ against the Cu/Zn atomic ratio are shown in Fig. 5 (the plots I and II respectively). As the copper content increases, an initial rapid rise in the plot of $\bar{d}_{po}$ is followed with a slower rise. In contrast, the plot of $\bar{d}_{pa}$ first rises very slowly, turns to fall at a ratio of *ca.* 0.3, and finally rises again after passing through a minimum at a ratio of 2.0. For both of these plots, the rises in the range of very high ratios seem not so rapid.

The $\bar{d}_{po}$ and $\bar{d}_{pa}$ values of catalysts 21 and 22 do not fit the respective plots of the kneaded series; as compared with catalyst 4, these two catalysts show the $\bar{d}_{po}$ values somewhat large, but the $\bar{d}_{pa}$ value is slightly small for catalyst 22 and considerably large for catalyst 21.

The Electron Microscopic Image. Figure 6-(a) presents an electron micrograph of powders of the raw zinc oxide, while electron micrographs of catalysts 2, 4, and 8 after the activity test are shown in (b), (c), and (d), of the same figure respectively. On these latter micrographs, it is difficult to immediately distinguish between zinc oxide

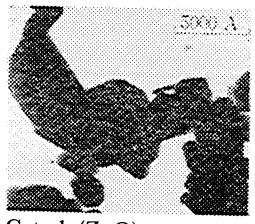

(a) Cat. 1 (ZnO)

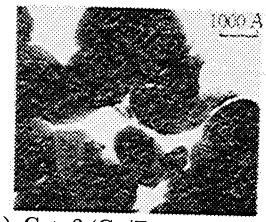

(b) Cat. 2 (Cu/Zn=0.09) after use in activity test

(c) Cat. 4 (Cu/Zn=0.45) after use in activity test

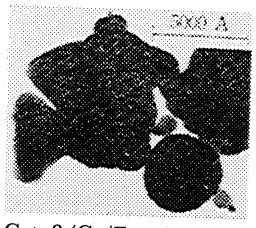

(d) Cat. 8 (Cu/Zu=2.95) after use in activity test

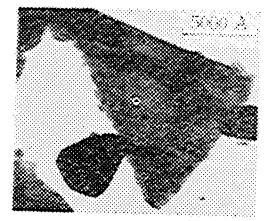

(e) Cat. 8 (Cu/Zn=2.95), dried paste

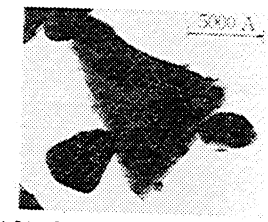

(f) Cat. 8, after heating of sample of (e) in air at 250°C for 5 min

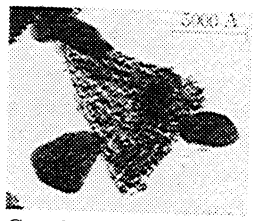

(g) Cat. 8, after reduction of sample (f) in H_2 at 180°C for 5 min

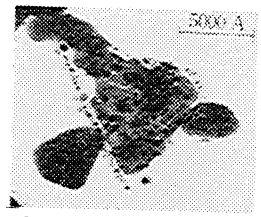

(h) Cat. 8, after further reduction of sample of (g) in H_2 at 350°C for 5 min

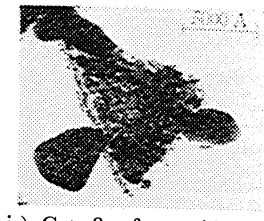

(i) Cat. 8, after oxidation of sample of (h) in air at 200°C for 2 min

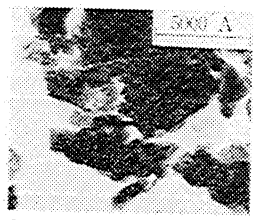

(j) Cat 21 (impregnated cat., Cu/Zn=0.34), after heating dried sample in air at 250°C for 5 min

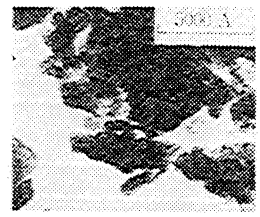

(k) Cat. 21 after reduction of sample of (j) in H_2 at 250°C for 5 min and at 400°C for 5 min

(l) Cat. 22 (coprecipitated cat., Cu/Zn=0.40), after heating dried sample in air at 250°C for 5 min

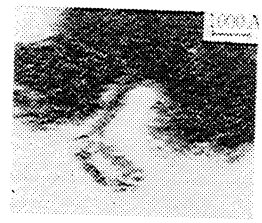

(m) Cat. 22 after reduction of sample of (l) in H_2 at 250°C for 5 min at 400°C for 5 min

Fig. 6. Electron micrographs [(a)—(m)].

and copper, but further insight into this can be obtained by refering to a series of micrographs (e)-(h), which illustrate changes in size and shape of both a copper hydroxide particle and a zinc oxide powder of a dried paste (the paste for preparation of catalyst 8) while the paste is under going the specific treatments in the reaction chamber.

In contrast to the pracitcally non-porous zinc oxide powder of distinct contour, the copper hydroxide particle in the dried paste is characterized by its thin plate-like structure of a comparatively large dimension [Ref. (e)]; a part of this plate seems to have been torn into pieces, which lie on the surface of the zinc oxide powder. On heating at 250°C, the plate-like particle shrinks a little with simultaneous production of a large number of extremely fine copper oxide particles within [Ref. (f)]. When reduced with hydrogen at 180°C for a short period, these fine particles exhibit considerable mobility and grow to irregularly shaped particles of several hunderd Å in width [Ref. (g), conveniently designated as the primary particles hereafter]. On futher reduction at a higher temperature of 350°C, large majority of these primary particles stick together to form a plate-like aggregate (the secondary particle) of copper occupying a slightly smaller area than before, while a part of them is left behind along periphery of the previous plate-like particle [Ref. (h)]. This aggregate is rather inhomogeneous in structure. Meanwhile, the pieces of copper oxide having lied on the surface of a zinc oxide powder are reduced *in situ* to form patches of copper. It should be emphasized that the primary particles of copper do not tend to stick to the zinc oxide powder. The zinc oxide powder preserves its size and shape throughout these treatments, and this is also true even for the catalyst smaple after the activity test [Ref. (b) and (c)].

On the basis of information available on a series of micrographs (e)-(h), it is possible to state that the particle image with an obscure contour in the series (b)-(d) represents a copper particle. It has appeared, accordingly, that copper in the sample after the activity test often forms, in addition to its massive particles, its thin, small flakes lying flat on the surface of zinc oxide powder. This is particularly the case with catalysts containing relatively small amounts of copper [Ref. (b) and (c)]; as the copper content is increased progressively, the massive particles increase in number at the expense of the thin flakes, insofar as the copper content remains within a certain limit [compare (b) with (c)]. However, matters are different for catalyst 8 of a high copper content [Ref. (d)]; the zinc oxide powder in the sample after the activity test is seemingly covered, at least partially, with layers of copper and frequently a few of these powders collect together to form an irregularly shaped, much larger aggregate [Ref. (d)].

The electron micrographs of catalysts 21 and 22 after the activity test appear quite different from that of catalyst 4; the particle is as large as that of catalyst 4, but shows too homogeneous a structure to permit a distinction to be made between zinc oxide and copper.*5 Although the original zinc oxide powder is not at all disintegrated by having been kneaded with a copper hydroxide cake, the powder is disintegrated at some depth from periphery by impregnation with a copper nitrate solution [Ref. (j)], and copper produced by reduction in this region is disperesed homogeneously in zinc oxide [Ref. (k)]. With catalyst 22, mutual dispersion between the two components is finer in degree than with catalyst 21, before as well as after reduction [Ref. (l) and (m), and also compare (m) with (k)]. The pronounced particle growth taking place with these two catalysts during the activity test may perhaps be due to a some less stable structure of the particles, but nothing more decisive can be said.

Upon oxidation with air at 200°C for a short period, the copper aggreagte (the secondary particle) in (h) for catalyst 8 is readily back in size and shape to the previous aggregate in (g). No trasformation of this kind, however, was observed for such a well grown copper particle with a smoothed, sharply outlined contour of the same catalyst as shown in (d), even though the particle had been oxidized at a higher temperature of 300°C.*5 These findings reveal that the secondary particle which is an aggregate of the small primary particles with uneven surfaces is oxidized more easily than the massive, large particle with a smoothed surface.

Discussion

The Total Pore Volume and the Average Pore Diameter. In the light of the results of the electron microscopic observations, an attempt will be here made to explain the trends in the changes of V_{po} and $\bar{d}_{po}$ with the copper content for the catalysts of the kneaded series (Ref. Fig. 3 and the plot I in Fig. 5 respectively). If the catalyst contains not so large a amount of copper, the greater part of copper exists, immediately after reduction, as the plate-like aggregates among the zinc oxide powders, and each of these aggreagates transforms *in situ,* with shrinking, to a massive particle after the catalysts have been used in the activity test, whereas each of the original zinc oxide powders remains unaltered in size and shape. Accordingly, the larger the copper content is the larger is the V_{po}, which has been produced within original matrix of zinc oxide powders by the shrinking of aggreagates. Since the $\bar{d}_{po}$ is related to the V_{po} through the equation of $\bar{d}_{po}=4V_{po}/S$,

*5 The electron micrograph is not presented here in order to reduce number of micrographs.

the $\bar{d}_{po}$ is to change in the same way as the V_{po} does if the S differes little with copper content. This is, in fact, the case with this series of catalysts (Ref. the plot I in Fig. 4). If the catalyst, however, contains a very large amount of copper, the zinc oxide powder becomes covered with layers of copper after the activity test and, as a consequence, more easily sinter with each other to grow to large aggregates. This results in the V_{po} decreasing with the copper content (Ref. Fig. 3). In spite of this decrease in the V_{po}, the $\bar{d}_{po}$ in this range still decreases, which fact may come from the S decreasing more rapidly with the copper content (Ref. the plot in Fig. 4) than the V_{po}.

The abnormally high V_{po} values of catalyst 21 and 22, as compared with that of catalyst 4, can not be explained on the basis of the results of electron microscopic observations alone. This may perhaps be ascribed to the difficulty in finishing the raw paste to pellets as dense as those of the kneaded series.

The Average Particle Diameter. The previous particle model (model II in the preceding paper[1]) by no means accounts for the initial slow rise in the plot of $\bar{d}_{pa}$ (Ref. the plot II in Fig. 5). The model was conveniently proposed in order to explain the change in the specific activity of copper surface with varying copper contents, and it was assumed that, for every catalyst studied, particles consisting of copper alone were distributed among the original zinc oxide powders. However, the previous model has proved to agree only incompletely with the models of particle geometry presented in this paper. Provided the catalysts contain not a very large amount of copper, portion of copper exists as patches on the surface of zinc oxide powder, while another portion as massive particles. According to this model, the copper added is to contribute for enlarging the $\bar{d}_{pa}$ rather than reducing it, which is justified with the initial rise in the plot. In the range of moderate copper contents, the previous model has proved to be almost true; the $\bar{d}_{pa}$ is then likely to decrease as the copper content is increased, because the copper particles, which are small in size as compared with the zinc oxide powders, increase in number. The previous model differs again in the range of sufficiently large copper contents; the original zinc oxide powder is covered with layers of copper. This may bring about easier particle growth by agglomeration, and hence a rise in the plot of $\bar{d}_{pa}$. Neither the previous model fails to explain this rise, but the present explanation, being based on a more concrete model, is preferable.

In the preceding paper,[1] the surface area of copper per 1 g of catalyst, S_{Cu}, was calculated on the basis of the previous model. However, this model has proved to agree with the electron microscopic images only for the catalysts of moderate copper contents, and the S_{Cu} values might, in general, have been subject to considerable error except for the above-stated catalysts. In fact, calculation of the average diameter, $\bar{d}_{paCu}$, of copper particles by $\bar{d}_{paCu}=6/S_{Cu}\rho_{Cu}$ (ρ_{Cu}, the copper density$=8.92$) using the previous S_{Cu} values results in unreasonably large values with the catalysts of a very small copper content (Ref. the plot **III** in Fig. 5). The previously calculated values of S_{Cu} must have been underestimated for any of the catalysts containing either a very small or a very large amount of copper, because the calculation of S_{Cu} for this was conducted without consideration of the copper surface area due to patches or layers of copper on a zinc oxide powder. Unfortunately, it is difficult, however, to evaluate accurate extents of adjustment from the data available.

The Structure of Copper Responsible for the High Specific Activity. In the preceding paper,[1] the specific activity of copper surface (the activity per unit of area of the copper surface) at a reaction temperature, *e. g.*, of 180°C, k'_{Cu180}, was obtained by the equation of $k'_{Cu180}=k_{180}/\rho_b S_{Cu}$, where k_{180} was the rate constant*6 at 180°C per unit of volume of the catalyst bed, and ρ_b is the catalyst bed density, on the reasonable assumption that only the copper surface is effective in the reaction. The k'_{Cu180} values obtained by the use of the previous S_{Cu} values were very high in the range of very small copper contents, fell rapidly and then gradually with the copper content.[1] In this connection, the k'_{Cu180} values in each of the two extreme ranges of either very small (the lower range) or very large copper contents (the upper range) should be more or less reduced from the previous values owing to the k'_{Cu} values having been underestimated, whereas the values in the range between these extremes (the intermediate range, 0.4—2.0 in the Cu/Zn atomic ratio) are to vary little from the previous values. Nevertheless, the decreasing trend of k'_{Cu180} with the copper content is likely to be retained, though only qualitatively, over the whole range studied; even though the k'_{Cu180} value in the two extreme ranges is reduced, the decreasing trend of the k'_{Cu180} with the copper content in the upper range is not affected substantially and at the same time any downward bend is scarcely suspected with the plot of the k'_{Cu180} rising with the decreasing copper content in the lower range, where the activation energy of reaction is lowering with the decreasing copper content.[1] This and the present models of particle geometry indicate that the finer copper particles, whether patch-like or massive, are responsible in structure for the higher specific activity.

*6 The k was calculated by the aid of the rate equation of Kul'kova-Temkin.[2]

Taking into account the finding that the finer copper particles are oxidized more easily, it may be concluded that the copper surface participates in the reaction to the extent that the surface is apt to be oxidized. This may lend another support, though not directly, to the view of Temkin *et al.*[2,3] on the reaction rate over an iron oxide, who proposed a mechanism according to which the gaseous components react with oxidized and reduced surface sites as expressed by the following scheme:

$$CO + (O) = CO_2 + (\ )$$

$$H_2O + (\ ) = H_2 + (O)$$

where ( ) and (O) designate reduced and oxidized site respectively.

The poor and unstable activity, in spite of the mutual dispersion between zinc oxide and copper, of catalysts 21 and 22 is explained only with difficulty. A probable explanation for this may be that too fine a dispersion, in turn, causes copper to be included into interior of the particle and a small extent of copper becomes available on the particle surface.

2) N. V. Kul'kova and M. I. Temkin, *Zhur. Fiz. Khim.*, **23**, 695 (1949).

3) G. G. Shchibria, N. M. Morozov and M. I. Temkin, *Kinetika i Kataliz*, **6**, 1057 (1965).

BULLETIN OF THE CHEMICAL SOCIETY OF JAPAN VOL. 41 485—492 (1968)

Effect of Pressure on Graphitization of Carbon. I. Heat Treatment of Soft Carbon under 1, 3 and 5 kbar

Tokiti NODA,*1 Kanichi KAMIYA and Michio INAGAKI

Faculty of Engineering, Nagoya Universisty, Nagoya

(Received October 4, 1967)

Polyvinylchloride coke was heat-treated under the quasi-hydrostatic pressure of 1, 3, and 5 kbar by using a simple piston cylinder type high pressure apparatus. The process of graphitization under pressure was studied kinetically by analyzing the profile of the (002) diffraction line. It was found that the accelerating effect of pressure on the graphitization of carbon became more pronounced at higher pressure. The process of graphitization under 3, and 5 kbar seemed to take place in at least two stages. In the first stage, the profile of the (002) line shifted simply from the position of the original line to 26.0° in 2θ, which corresponded to a c_0-spacing of 6.85 Å. In the next stage, a new component, having a c_0-spacing of about 6.72 Å, appeared in addition to the first component, having a c_0-spacing of 6.85 Å. Therefore, the profiles of the (002) line became composite. Under 1 kbar, however, no composite profiles were observed and the c_0-spacing decreased gradually with heat treatment. Approximate values for the activation energy and activation volume for graphitization under 3—5 kbar were estimated to be 80—120 kcal/mol, and −7——9 cc/mol, respectively.

It has been reported that the graphitizing cokes, such as petroleum coke and polyvinylchloride coke, graphitized very rapidly at around 1500°C under a pressure of 10 kbar.[1] Profiles of the (002) diffraction line of the cokes heat-treated at 1400—1500°C under 10 kbar were found to be composite, while no composite profiles were found with heat treatment of the same cokes under a reduced pressure of 10^{-2} Torr.[1] A kinetic study of the graphitization could not be carried out at a pressure as high as 10 kbar, because of the high rate of graphitization.

In the present work, the heat treatment of polyvinylchloride coke under pressures of 1, 3, and 5 kbar was carried out for various durations at various temperatures, in order to learn the effect of pressure on the graphitization of carbon, and also to obtain more precise information on the composite profile of (00*l*) diffraction.

Experimental

Sample and Apparatus. The sample used was a graphitizing coke PV-7, which was also used in previous work.[1] The coke was prepared by carbonizing polyvinylchloride at 680°C, and was examined spectroscopically and found to contain only negligible amounts of inorganic impurities. The coke had a paricle size in the range of 0.1 to 0.4 mm.

The high pressure apparatus used was of a simple piston-cylinder type. It was made of tool steel, having a hardness of R. C. 64, and a bore diameter of 24 mm.

*1 Present address: Mie University, Tsu, Mie-ken.

1) T. Noda and H. Kato, *Carbon*, **3**, 289 (1965).

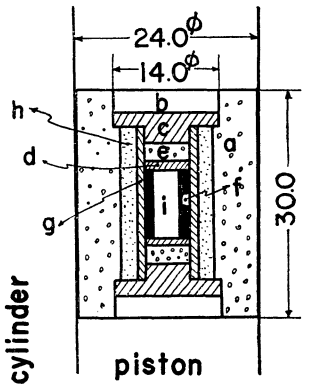

Fig. 1. Arrangement of the specimen cell.
a : pyrophyllite holder, b : metal disk (14φ-3 mm), c : graphite terminal plate (14φ-2mm), d : graphite plate (6φ-1mm), e : pyrophyllite disk (6φ-2.5mm), f : glassy carbon tube (6φ·4φ-10mm), g : graphite heater (8φ·6φ-21mm), h : boron nitride, i : sample

Such a piston-cylinder type apparatus made of tool steel has been known to last up to 10 kbar at room temperature.[2] The whole apparatus was immersed in water for cooling during the experiment. The arrangement of the specimen cell is shown in Fig. 1. Boron nitride (h in the figure) was placed between a graphite heater and pyrophyllite in order to prevent chemical reaction between them. A glassy carbon tube (f in the figure) played the role of preventing contamination of the sample. A heating current was passed through the pistons into a graphite tube heater. The pistons were insulated from the cylinder by a composite sheet of asbestos and Myler film. The temperature of the central part of the sample was evaluated from the relation between heating input power and temperature, which had been determined beforehand up to about 1200°C using a chromel-alumel thermocouple. The relations between input power and temperature were determined at different pressures and are shown in Fig. 2. A thermocouple inserted in the specimen probably makes a heat sink which may cause a small decrease in the temperature of the specimen. In most of the actual runs, no thermocouple was inserted in the specimen, and therefore the heat treatment temperature of the specimen could be a little higher than the temperature estimated from the input power. However, the difference may be within the error of temperature measurement, because the input power for the melting of platinum under 5 kbar (1800°C[3]) with in same arrangement was exactly on the extrapolated straight line of the upper part of the curve for 5 kbar.

There was a very large temperature gradient in the specimen along the axial direction of the graphite heater, the temperature of the end part of the specimen being about 10% lower than that of the central part. The temperature of the specimen was controlled manually by regulating the input power. The error in

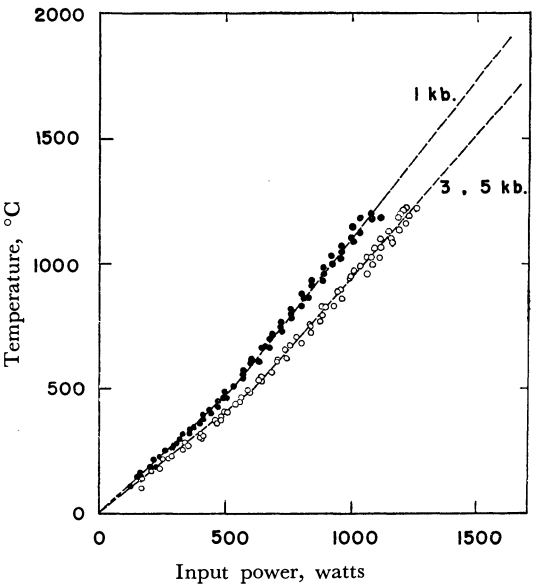

Fig. 2. Relations between input power and temperature under different pressures.

the determination of the heat treatment temperature was estimated to be ±50°C at 2000°C from the scattering of the points in the relation between input power and temperature, and from the variation of input power regulation. The heating rate was about 1000°C/min and the specimen was cooled down to room temperature within a few minutes by cutting off the power. The maximum temperature which was attainable depended strongly on the arrangement of the specimen cell. By using the arrangement shown in Fig. 1, a temperature up to 1800°C was attained under 1 kbar, and 2000°C under 5 kbar.

The pressure was transmitted through pyrophyllite, so that quasi-hydrostatic pressure was applied to the sample. The pressure was calibrated by use of the phase transition of neutral ammonium fluoride, which occurs at 3.7 kbar with a volume change of about 28%,[4] The error in the pressure measurement was estimated to be ±0.2 kbar from the scattering of four independently measured values of the phase transition.

The heat treatments of the sample were carried out at temperatures ranging from 1100°C to 1900°C for 3 to 90 min under 1, 3, and 5 kbar. The central part (about 1 mm thick) of the heat-treated specimen was used for the X-ray diffraction analysis, in order to avoid ambiguity caused by the temperature gradient along the specimen.

Analysis of X-Ray Diffraction Profiles. The profiles of the (002), and (004) diffraction lines for the heat-treated specimen were measured by using a recording X-ray diffractometer and Ni-filtered Cu$K\alpha$ radiation. Most of the profiles obtained were composite, as can be seen in Figs. 3b), and c). All the composite profiles appear to have two peaks at around 26.0° and 26.5° in 2θ. The occurrence of a composite profile indicates that there must be more than one independent range to produce coherent scattering of X-rays,

2) T. Noda, H. Kato, T. Takasu, A. Okura and M. Inagaki, This Bulletin, **39**, 829 (1966).
3) W. Paul, "Solid under Pressure," McGraw-Hill, New York (1963), p. 175.
4) R. Stevenson, *J. Chem. Phys.*, **34**, 346 (1963).

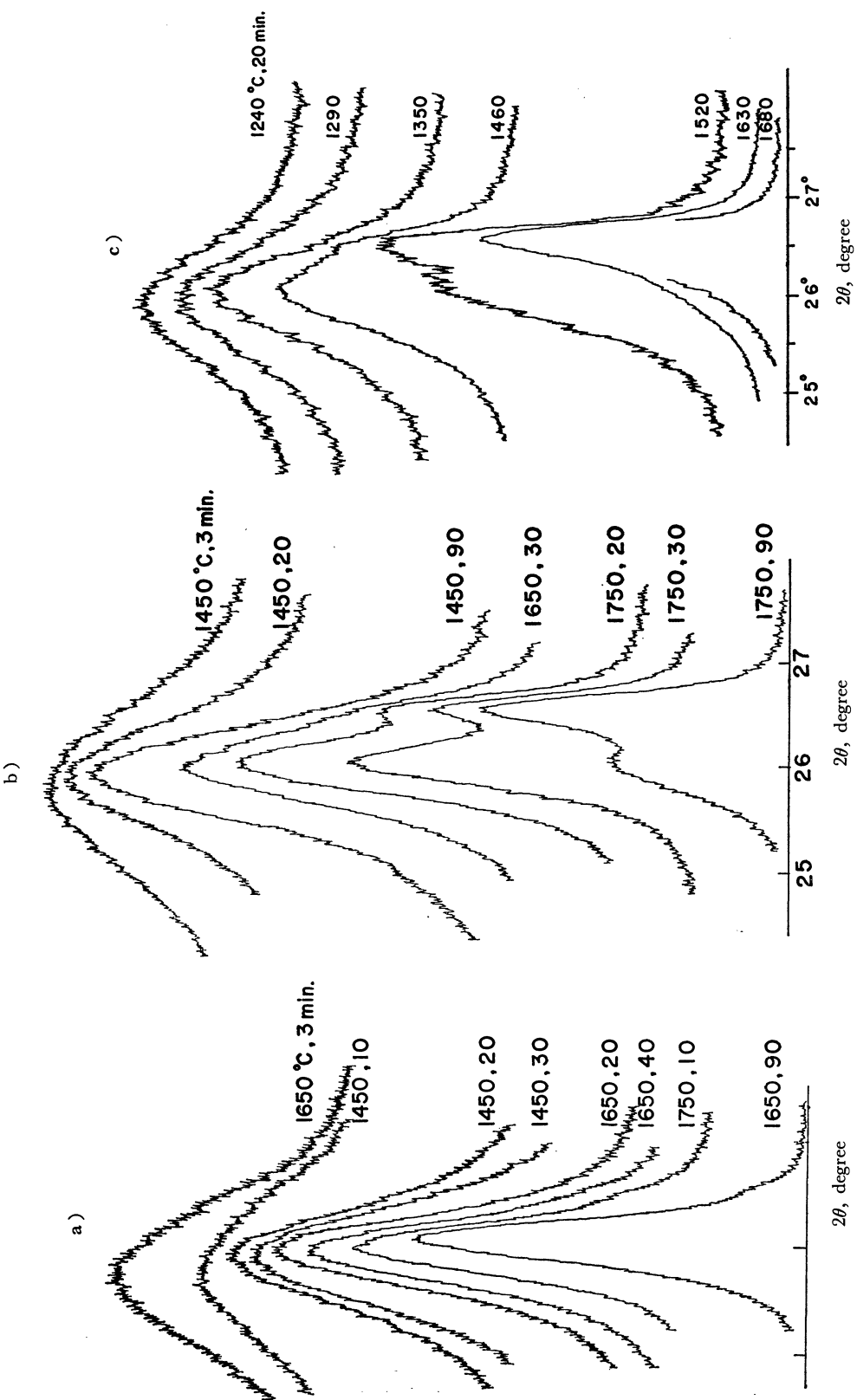

Fig. 3. Changes of the profile of (002) diffraction line a) under 1 kbar, b) under 3 kbar, c) under 5kbar.

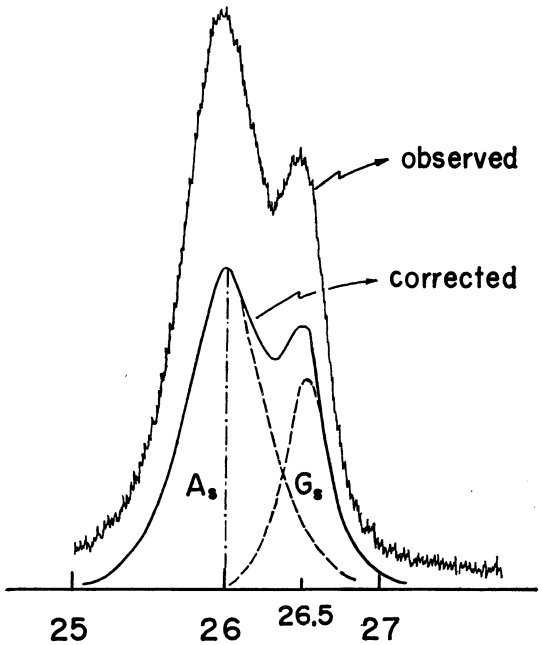

Fig. 4. Schema of separation of composite profile.

and therefore the composite profile can be separated into its component profiles.[5] The procedure for the separation of an observed composite profile into its component profiles is illustrated in Fig. 4. After correction for the Lorentz-polarization, atomic scattering and absorption factors by the conventional method,[6] the profile on the low angle side is folded at 26.0°, the reason for which will be described later. When the component profile at 26.0° is subtracted from the composite profile, the balance gives an almost symmetrical and sharp peak at around 26.5°. The components, correspond to the separated profiles at 26.0°, and at 26.5°, are designated as A_s, and G_s, respectively.*2 The areas under the separated component profiles were measured by using a planimeter, and the ratio of the area of the profile of the component G_s to the total area of the composite profile was calculated. This area ratio is sensitive to the preferred orientation of the crystallite in the specimen used for X-ray measurement. The correction of the area ratio for the preferred orientation was carried out by using the calibration curve, because the quantity of specimens for X-ray measurement was so small that direct measurement of the preferred orientation of crystallites in the specimen could not be carried out. The calibration curve was determined by using known mixtures of two kinds of petroleum cokes, one treated at 1600°C, and the other treated at 3200°C, which have the same diffraction angles as those of the component profiles, 26.0°, and 26.5°, respectively.

Results

Profiles of the (002) diffraction line for specimens heat-treated under 1 kbar are shown in Fig. 3 a). The diffraction angle of the line increased and its half-width decreased with increase in heat treatment temperature (HTT) and residence time, similar to the changes for heat treatments under room or reduced pressure. Changes of the (002) profile under 3 kbar are shown in Fig. 3 b). At low temperature and short residence time for heat treatment, the diffraction angle and half-width of the line changed the same as in the case of 1 kbar. When the diffraction angle of the line reached to

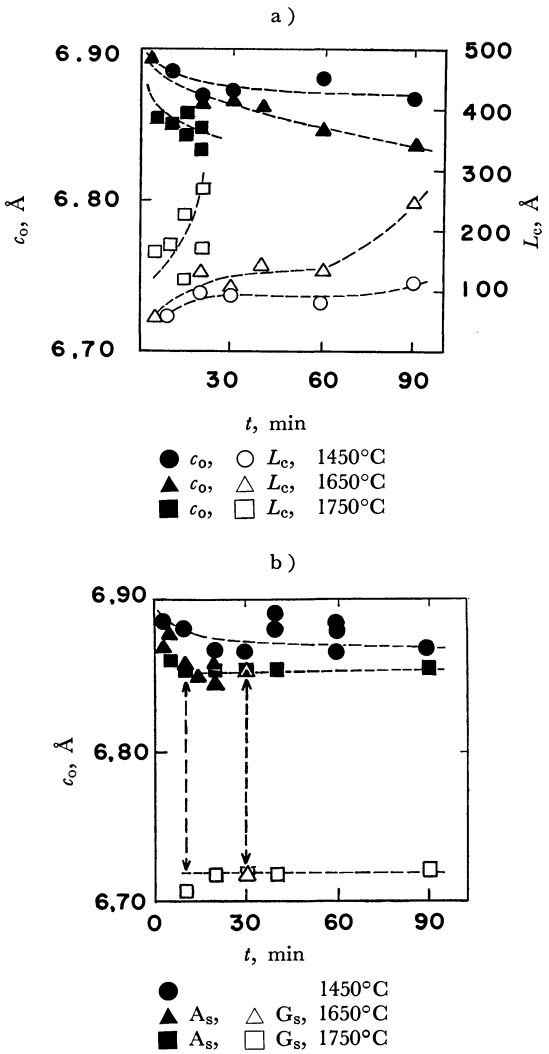

Fig. 5. Changes of c_o-spacing and crystallite size L_c with residence time.
a) under 1 kbar, b) under 3 kbar.

5) T. Noda and M. Inagaki, "Proceedings of the Fifth Conference on Carbon Vol. I," Pergamon Press, London (1962), p. 559.
6) W. R. Ruston, *Fuel*, **32**, 53 (1953).
*2 For a hard carbon heat-treated under 5 kbar, the authors found a similar composite profile, which seemed to consist of two components. In the present work, the components of soft carbon were distinguished from those of hard carbon by using a suffix "s," because they might not have the same structures.

26.0°C, however, a new sharp peak for the component G_s appeared at 26.5°, overlapping the profile for the component A_s. With further heat treatment, this sharp profile for G_s developed without appreciable change in the diffraction angle. Almost the same changes in the profile of the (002) diffraction line were observed under 5 kbar (Fig. 3 c)), but the change occured at lower temperature, or in a shorter time than in the case of 3 kbar. In the heat treatments under 3, and 5 kbar, the diffraction angle of the profile for the component A_s stayed unchanged at 26.0° after the appearance of the profile for the component G_s. This is the reason why the position of the profile for A_s was fixed at 26.0° when the observed composite profile was separated into its component profiles, as illustrated above.

Changes in the c_0-spacing and crystallite size L_c of the specimens heat-treated under 1 kbar with residence time are shown in Fig. 5 a). Comparing these changes with those of the same coke under reduced pressure,[1] the accelerating effect of pressure on graphitization of carbon becomes very evident. In Fig. 5 b), the changes in the c_0-spacing of the specimens heat-treated under 3 kbar with residence time are shown. Under 3 kbar, the component G_s was observed to appear in 30 min at 1650°C, and in 10 min at 1750°C, while at 1450°C no indication of the component G_s was observed in 90 min. The crystallite size of the component A_s increased gradually from 100 to 200 Å, while that of the component G_s was about 300 Å. Change in the content of the component G_s with residence time is shown in Fig. 6. The content of G_s increased to about 50% in 90 min at 1750°C. Changes in the c_0-spacing of the components A_s and G_s of the specimens heat-

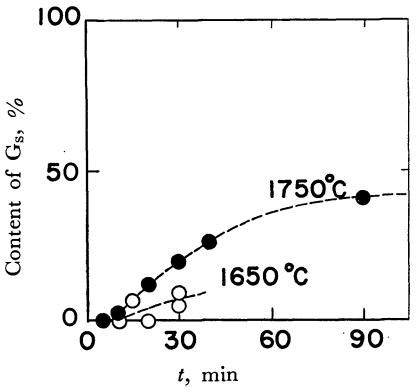

Fig. 6. Changes of content of the component G_s with residence time under 3 kbar.

treated under 5 kbar with HTT for various residence times are shown in Fig. 7 a). The c_0-spacing of the component A_s decreased to 6.85 Å around 1600°C in 3 min, around 1350°C in 20 min, and around 1300°C in 60 min. Changes in the content of the component G_s with HTT under 5 kbar are shown in Fig. 8 a) The intersection of these curves with the abscissa, or the temperature at which the component G_s begins to appear, should be about the same as those at which the c_0-spacing of the component A_s reaches 6.85 Å. The shape of the curves appears to be the same for different residence times, and they may be superimposed by translation along the abscissa. Such a superimposed curve for a residence time of 10 min is shown in Fig. 8 b). It is evident that the superimposition works quite well. Therefore, the curves for c_0-HTT and L_c-HTT were translated by the same amount. The superimposed curves make it easier

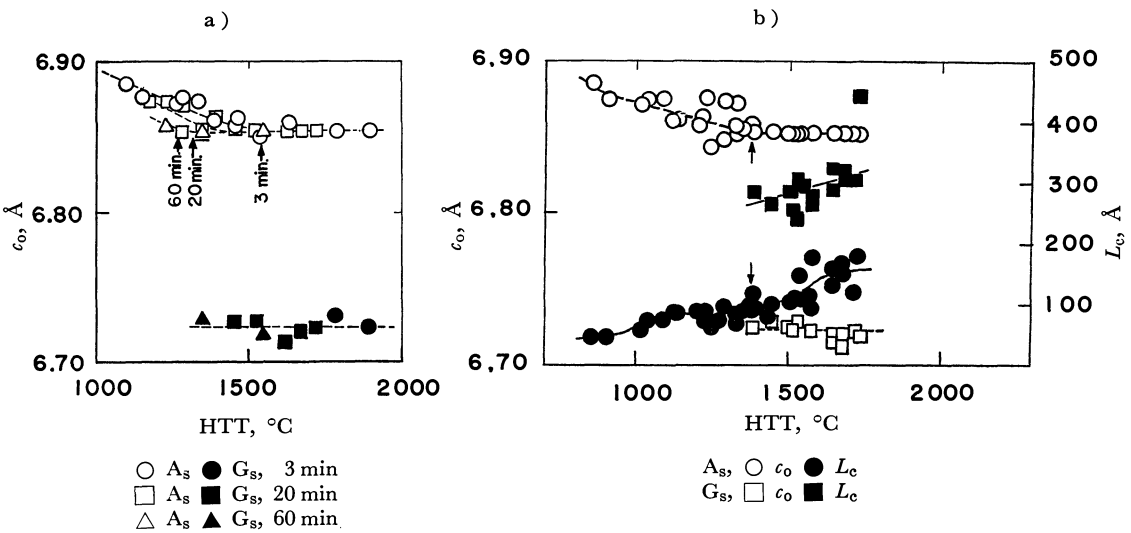

Fig. 7. Changes of c_0-spacing and crystallite size L_c with HTT under 5 kbar.
a) for different residence times, b) superimposed curve for the residence time of 10 min

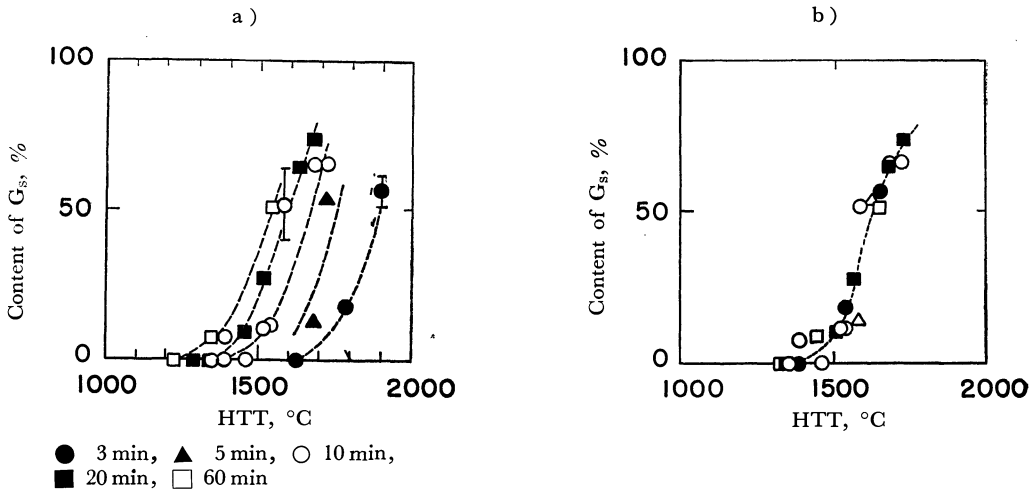

Fig. 8. Changes of content of the component G_s with HTT under 5 kbar.
a) for different residence times b) superimposed curve for the residence time of 10 min

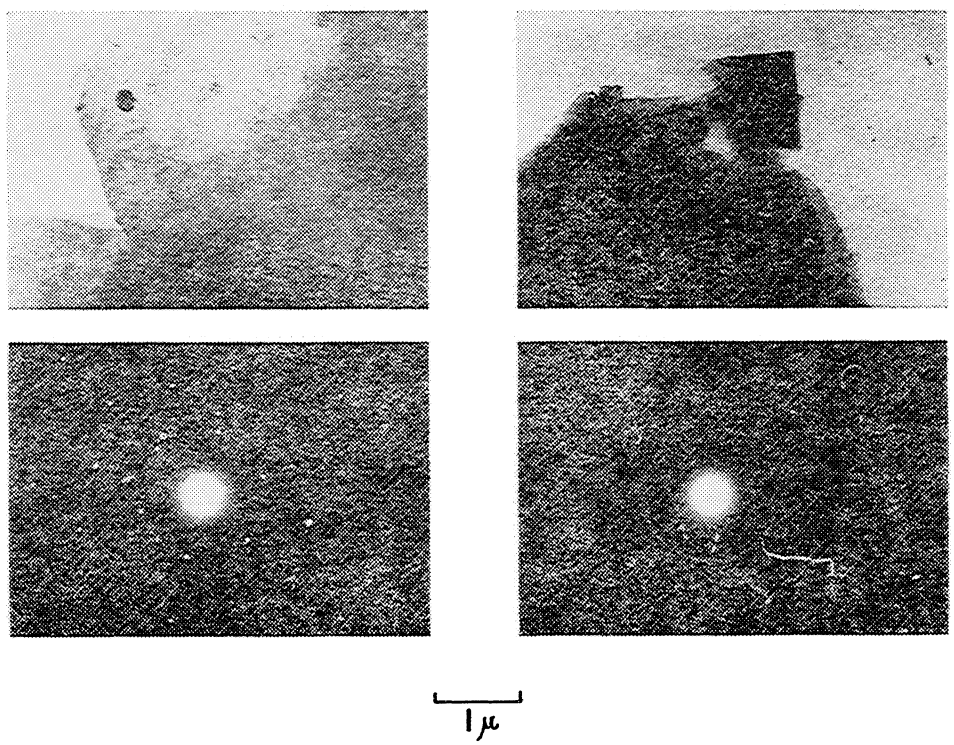

Fig. 9. Electron micrographs and electron diffraction patterns for the specimen heat-treated at 1720°C under 5 kbar.

to view the general trends of the changes in c_0 and L_c with HTT (Fig. 7 b)).

From these figures, it can be seen that the graphitization of carbon under 3, and 5 kbar seems to proceed as follows. In the early stage of graphitization, there is one component A_s, of which the c_0-spacing decreases from the original value of 6.91 Å to 6.85 Å, and the crystallite size L_c increases to about 100 Å. In the next stage, the component G_s appears, and its content increases rapidly with increase in temperature and residence time for heat treatment. The c_0-spacing of the components A_s, and G_s remain unchanged at 6.85, and 6.72 Å, respectively. The crystallite sizes L_c of the

components A_s, and G_s are about 150—200 Å, and 300 Å, respectively.

Discussion

In a previous work,[1] composite profiles were also obtained in cases where a rapid change in the c_0-spacing was observed. It was suggested that there might be a possibility that each specimen used for X-ray study was a mixture of carbons heat-treated at different temperatures because of the steep temperature gradient in the specimen In the present work, pyrophyllite disks (e in Fig. 1) were inserted between the specimen chamber and the graphite terminal plates in order to minimize the temperature gradient in the specimen. Even in this modified arrangement a temperature difference was observed between the end and the central parts of the specimen, the temperature of the end part being about 10% lower than that of the central part, as mentioned previously. In addition to the temperature gradient, the pressure gradient along the specimen must be taken into account. The pressure at the end part of the specimen may be a little higher than that at the central part. The (002) profile of the end part of the specimen of which the central part had a composite profile was also composite, and its only difference from the central part was the degree of the developement of the component G_s, the content of G_s for the end part being smaller than that for the central part. This seems to show that temperature and pressure gradients along the specimen were not the cause of the occurence of a composite profile. The temperature difference itself affected the content of the component G_s. In other words, the structural change in the specimen under pressure was properly reflected in the diffraction profile.

In the graphitization process of PV-7 under a pressure of 3—5 kbar, there exist the components G_s and A_s side by side in the one specimen. In the early stage, there is only one component A_s, of which the mean c_0-spacing gradually decreases to 6.85 Å and the crystallite size L_c increases a little. In the next stage, in which the c_0-spacing of the component A_s has reached 6.85 Å, the component A_s begins to transform into the component G_s, and the main change at this stage is the increase in the content of the component G_s. The c_0-spacing of the component A_s stays unchanged at 6.85 Å, and its crystallite size L_c also remains unchanged at around 150—200 Å through this stage. The c_0-spacing of 6.85 Å is a little but evidently smaller than that of the so-called turbostratic structure, 6.88 Å. If the c_0-spacing of one component is assumed to be 6.88 Å, the balance of the profile becomes strongly un-symmetrical, and it is necessary to assume it consists of more than two components. The c_0-spacing of the component G_s is 6.72 Å and its crystallite size L_c is around 300 Å. The spacing of the component G_s measured from the (004) diffraction line is also 6.72 Å, and is clearly not 6.71 Å. Even though this spacing of 6.72 Å is a little larger than the spacing of natural graphite, 6.708 Å, specimens having a high content of the component G_s were found by X-ray diffraction to have a three dimensional structure, and by electron microscope and microdiffraction to contain flaky particles of which diffraction pattern was of the perfect six-fold symmetry of single crystal (Fig. 9a)). In the same specimen, however, some other particles showed continuous diffraction rings (Fig. 9b)). It is known that the c_0-spacing of the cokes graphitized as highly as possible can hardly be reduced to that of natural graphite.[7]

Phenomenally, the change in profile in the second stage of graphitization under a pressure of 3—5 kbar is similar to the so-called two-, or three-phase graphitization of non-graphitizing or hard carbons. The occurence of a composite profile,

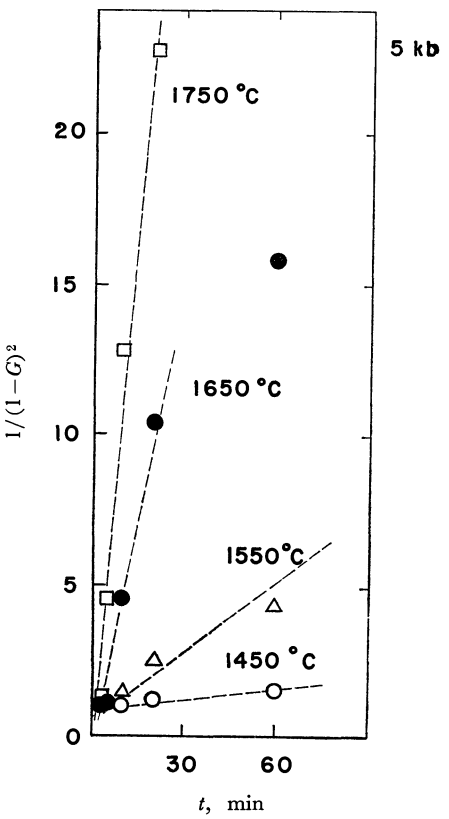

Fig. 10. Relations between content G of the component G_s and residence time t.

7) T. Noda and M. Inagaki, This Bulletin, **37**, 1709 (1964); T. Noda and H. Matsuoka, *Kogyo Kagaku Zasshi (J. Chem. Soc. Japan, Ind. Chem. Sect.)*, **63**, 465 (1960); P. L. Walker and G. Imperial, *Nature*, **180**, 1184 (1957).

which was composed of the components G_s and A_s, indicates that ranges having graphitic and non-graphitic structures have a sufficient extent to produce independent coherent scattering of X-ray in one specimen.

Under 1 kbar, no composite profile was observed and the c_0-spacing decreased continuously to 6.78 Å without the appearance of the second peak for the component G_s. This means that not a sufficient extent of lattice, having graphitic structure to produce coherent X-ray scattering, was formed in the specimen by the treatment, so that only a homogeneous decrease of the c_0-spacing was observed.

From these experimental results, it can be concluded that the accelerating effect of pressure on the graphitization of carbon increases with pressure. However, the graphitization process above 3 kbar seems to be different from that below 3 kbar. For experiments under 3, and 5 kbar, an approximate relation between the content, G, of the component G_s, and residence time t was investigated, although the accuracy of the measurements of temperature and pressure of heat treatment were not good enough, and also experimental data was not abundunt enough for a quantitative kinetic analysis of graphitization under pressure. A relatively good linearity between $1/(1-G)^2$ and t was obtained (Fig. 10). By using the experimental rate constant, the activation energy was calculated to be 80—120 kcal/mol, and the activation volume -7——9 cc/mol at temperature of 1650—1750°C.

The authors wish to thank Tokai Electrode Mfg. Co. for supplying the graphite materials used, and Professor K. Mihama, Department of Applied Physics, Faculty of Engineering, Nagoya University, for taking the electron micrographs.

NOTES

Thermal Decomposition of Ammonium Molybdoselenite and Its Iron Salt

the Late Sarju PRASAD and Virendra Nath GARG

Chemical Laboratories, Banaras Hindu University, Varanasi, India

(Received November 11, 1965)

The previous work[1] on the preparation of unsaturated heteropoly salts of selenium and molybdenum has now been extended to a study of the solid-state decomposition reactions of ammonium molybdoselenite and its iron salt at high temperatures. In the present communication thermogravimetric analysis (T. G. A.) and differential thermal analysis (D. T. A.) are used in conjunction with infrared spectroscopy to study the nature of the decomposition of the compounds by observing (a) the loss of water molecules, (b) the loss of volatile material, and (c) the breakdown by pyrolysis as the temperature is increased.

Experimental

The ammonium molybdoselenite and its iron salt of the composition: $3(NH_4)_2O \cdot 2SeO_2 \cdot 5MoO_3 \cdot 30H_2O$ and $Fe_2O_3 \cdot 2SeO_2 \cdot 5MoO_3 \cdot 24H_2O$ were prepared from seleneous acid and molybdic acid as has been described earlier.[1]

The T. G. A. studies were carried out by a Stanton Thermobalance (high-temperature model) with a 10-mg sensitivity. A heating rate of 3°C per min was employed, with a sample size ranging from 150—170 mesh. The loss in weight was within 2% of the theoretical values in all cases. The apparatus of differential thermal analysis employed in this work consists of an analytical furnace, a transformer, and recording equipment. The specimen holders, made of sintered alumina, have the dimensions $1'' \times 3/4'' \times 1/4''$. A heating rate[2] of 10°C per min was employed, with a sample size ranging from 100—120 mesh. For D. T. A. study the sample was well mixed with extra-pure alumina (E. Merck's) and tightly packed in one cell, whereas alumina alone as a reference material was placed in the other.

The infrared spectrum was recorded on a Perkin-Elmer Infracord apparatus in a potassium bromide medium by the disk method. The spectra are between 2—15 μ.

Results and Discussion

The T. G. A. curve of ammonium salt reveals that the compound loses 13 molecules of water at 120°C, and the rest in the temperature range from 230 to 320°C. The anhydrous ammonium salt thus obtained at 320°C is brown and gives the test for ammonia. It is insoluble in cold or strong acids and alkalies. Its insolubility shows that it is an interstitial solid solution in which selenium atoms are closely packed in the interstices of molybdenum atoms, this theory is supported by the D. T. A., in which an exothermic peak is obtained at 330°C which can be attributed to the lattice transition. The gradual cooling curve from high to low temperatures reveals no peak, thus indicating the irreversibility of the process.

After further heating the decomposition of the compound formed occurs mainly in the 330—420°C temperature range, with a loss of selenium dioxide and an oxidation of the ammonia released; this is confirmed by the strong exothermic peak at 390—420°C in the D. T. A. curve. The nitrogen atmosphere gives a normal endothermic peak, thereby showing that there is no oxidation of ammonia. It may be concluded that ammonia is either oxidized or decomposed at the surface of

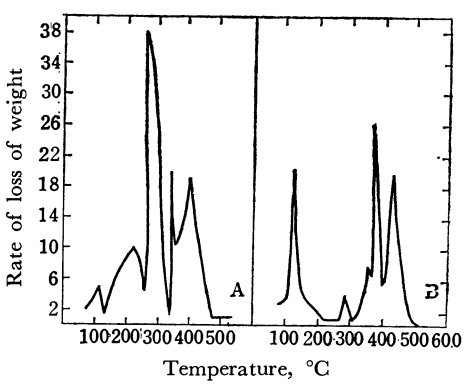

Fig. 1. Thermogravimetric analysis curves of ammonium selenitomolybdate (A) and ferric selenitomolybdate (B).

1) S. Prasad and V. N. Garg, This Bulletin, **38**, 1533 (1965).
2) S. Prasad and V. N. Garg, *Indian J. Chem. (communicated)*.

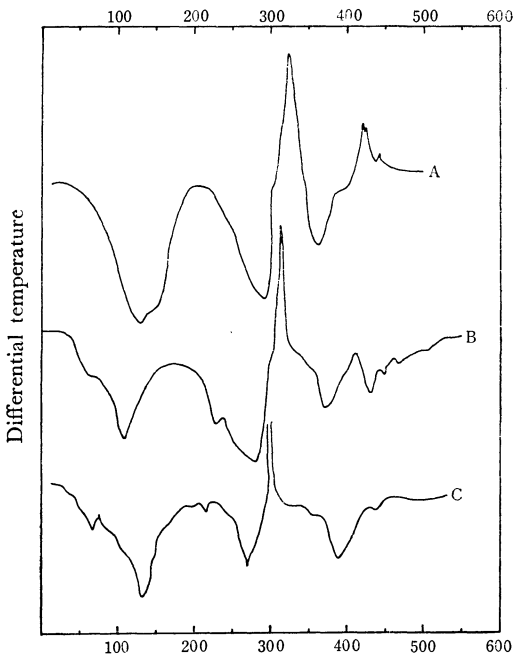

Fig. 2. Differential thermal analysis curves of Ammonium molybdoselenite in air (A) and in atmosphere of nitrogen (B) and ferric molybdoselenite in air (C).

molybdenum oxide through its catalytic action.[3]

In the case of iron molybdoselenite the T. G. A. curve shows a distinct region at 140°C where loss occurs due to 17 water molecules. Afterwards a flat plateau, corresponding to the iron salt with 7 water molecules, is obtained; these molecules are lost in the temperature range of 270—290°C. The two endothermic peaks, with maxima around 135°C and 280°C respectively, correspond to the dehydration of the compound. The exothermic peak at 310°C is interesting because no significant weight losses were noted in the T. G. A. curve in this temperature range; it can be attributed to the lattice transition, as in the ammonium salt. One endotherm, that at 360°C, may be due to the escape of selenium dioxide.

In the infrared spectra one peak is observed in the 3 μ region (3450—3400 cm^{-1}); this peak is due to the O–H stretching vibration of water. In the 6 μ region a weak absorption band appears at

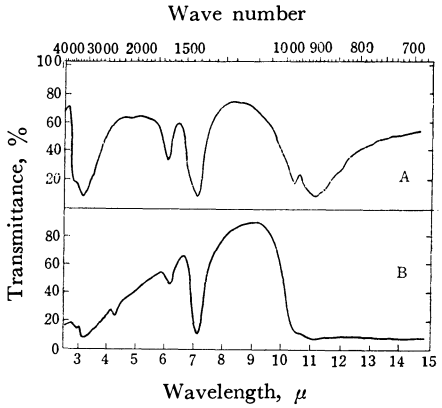

Fig. 3. Infrared spectra of ammonium molybdoselenite (A) and heated ammonium molybdoselenite (B).

1640—1620 cm^{-1} which corresponds to the bending mode of water. It has been found that on dehydration, these bands are fully or partially eliminated and that the overall spectrum is considerably altered. The introduction of water molecules into the lattice usually results in a rearrangement of the packing and in the adoption of a different crystalline form. The water molecules may form hydrogen bonding with some part of the anions and, consequently, their vibrational frequencies, may be affected. The regions of the absorption of Se–O and Mo–O[4] linkages are so close that, in the compounds, the absorption bands of the two overlap to a considerable extent to form a broad band about 900 cm^{-1}. In the case of ammonium salt, the absorbances at 3100 cm^{-1} and 1400 cm^{-1} are characteristic of the ammonium ion.

The authors are grateful to the authorities of the Banaras Hindu University for providing the necessary facilities and to the Director, C. B. R. I., Roorkee, for his kind permission to V. N. G. to work there. Our grateful thanks are also due to Dr. V. S. Ramachandran and Dr. N. G. Dave, C. B. R. I., Roorkee, for their helpful suggestions, and to Mr. K. P. Agarwal, C. D. R. I., Lucknow, for IR spectra. One of the authors (V. N. G.) wishes to thank the Council of Scientific and Industrial Research, New Delhi, for its financial assistance.

3) E. Ma, This Bulletin, **37**, 171 (1964).

4) Landolt - Börnstein, "Physikalisch - Chemische Tabellen," 2 Teil (1951).

Aminobutadienes. IX.[1] The Synthesis of 2-Phthalimidomethyl-1, 3-butadiene

Kenichi MURATA and Akira TERADA*[1]

Government Industrial Research Institute, Osaka, Midorigaoka, Ikeda, Osaka

(Received March 30, 1967)

In previous papers of this series, we reported that 1-phthalimido-,[2] 1-succinimido-,[2] and 1-(2-oxopyrrolidino)-1, 3-butadienes[1] were synthesized from 1, 3-butadiene, and that 2-phthalimido- and 2-succinimido-1, 3-butadienes[3] were derived either from ethyl α-oxyiminoacetoacetate or D-threonine. Among these monomers, 1-phthalimido- and 1-succinimido-1, 3-butadienes are easily polymerized in the presence of either radical[4] or cationic initiators,[5] while 2-phthalimido-1, 3-butadiene is very easily polymerized by radical initiators,[6] but not cationic ones.[6] The monomer reactivity ratios and Alfrey-Price *Q-e* values were determined by copolymerizations with styrene.[6,7]

In this paper, we wish to report on the synthesis of 2-phthalimidomethyl-1, 3-butadiene (VII) from isoprene.

The addition reaction of hypochlorous acid to isoprene was carried out by passing carbon dioxide gas into a liquid of isoprene and bleaching powder dispersed in a large amount of water. The main product was a fraction with a boiling point of 52—54°C/27 mmHg. The elemental analysis and infrared spectrum showed that this product was 1-chloro-2-methyl-3-buten-2-ol (I), and not either the 1, 4-, 3, 4-, or 1, 2, 3, 4-addition product. From the remaining part, white crystals melting at 81.5—83°C were separated. These crystals were found by elemental analysis to be isoprene dichlorohydrine. The infrared spectrum of this dichlorohydrine reveals the bands of primary and tertiary alcohols. On the other hand, this dichlorohydrine does not have the α, β-glycol unit in its structure, because it is negative on periodic acid oxidation, and its melting point does not agree with that of 1, 4-dichloro-2-methyl-2, 3-butandiol (mp 106.5°C).[8] Therefore, this dichlorohydrine

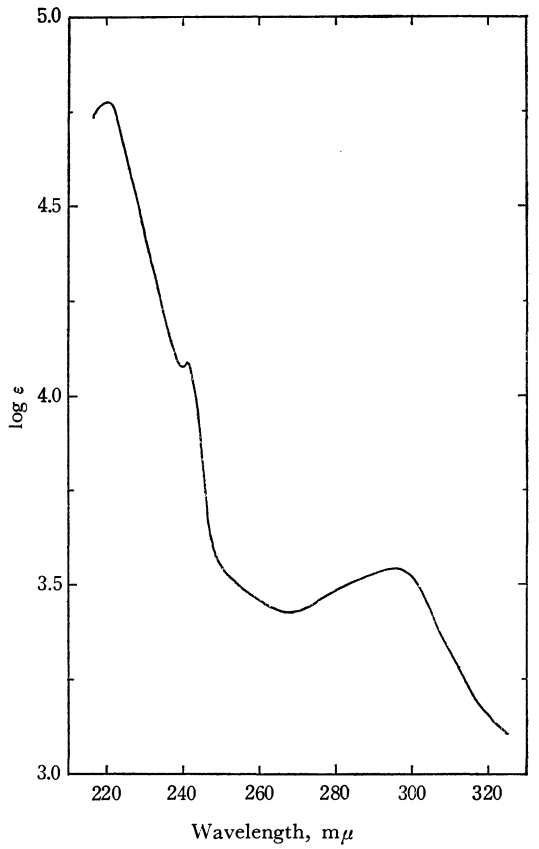

Fig. 1. Ultraviolet absorption spectrum of 2-phthalimidomethyl-1, 3-butadiene (VII) in ethanol. λ_{max} 219.5 mμ (ε 6.23×10^4); 240.5 mμ (1.28×10^4); 294 mμ (3.56×10^3).

was confirmed to be 1, 3-dichloro-2-methyl-2, 4-butandiol (II).

The dehydrochlorination of I by using alkali was easily carried out to give 1, 2-epoxy-2-methyl-3-butene (III), bp 80—82°C. III can also be obtained by the reaction of isoprene with perbenzoic acid.[9]

1-Amino-2-methyl-3-buten-2-ol (IV) was then prepared by the ammonolysis of III, according to the method of Ettlinger.[10]

*1 Present address: Department of Industrial Chemistry, Kyushu Institute of Technology, Tobata-ku, Kita-kyushu.

1) Paper VIII: K. Murata and A. Terada, This Bulletin, **40**, 414 (1967).
2) A. Terada and K. Murata, *Nippon Kagaku Zasshi (J. Chem. Soc. Japan, Pure Chem. Sect.)*, **83**, 490 (1962).
3) A. Terada and S. Takahashi, *ibid.*, **83**, 485 (1962).
4) A. Terada and K. Murata, *J. Polymer Sci., A-1*, **5**, 2219 (1967).
5) K. Murata and A. Terada, *Makromol. Chem.*, **109**, 260 (1967).
6) K. Murata and A. Terada, *J. Polymer Sci., A-1*, **4**, 2989 (1966).
7) K. Murata and A. Terada, This Bulletin, **39**, 2494 (1966).
8) W. J. Jones and H. G. Williams, *J. Chem. Soc.*, **1934**, 835.
9) R. Pummerer and W. Reindel, *Ber.*, **66**, 335 (1933).
10) M. G. Ettlinger, *J. Am. Chem. Soc.*, **72**, 4792 (1950).

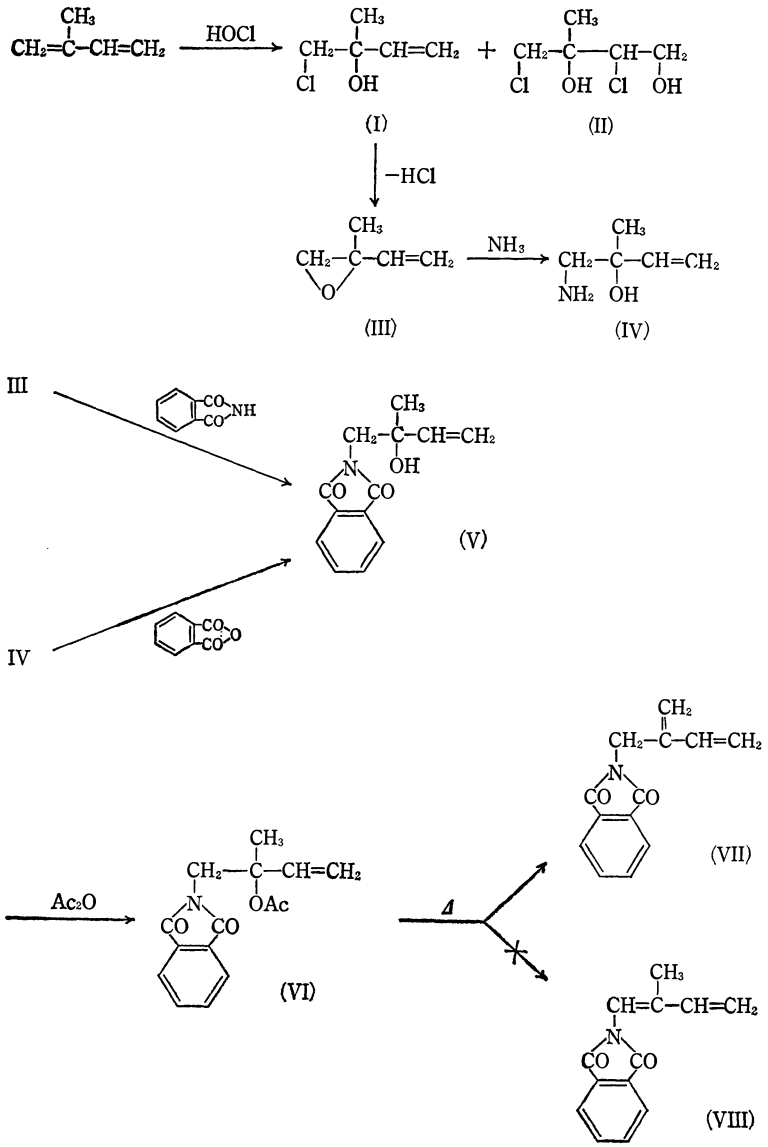

Scheme 1. The synthetic route of 2-phthalimidomethyl-1, 3-butadiene.

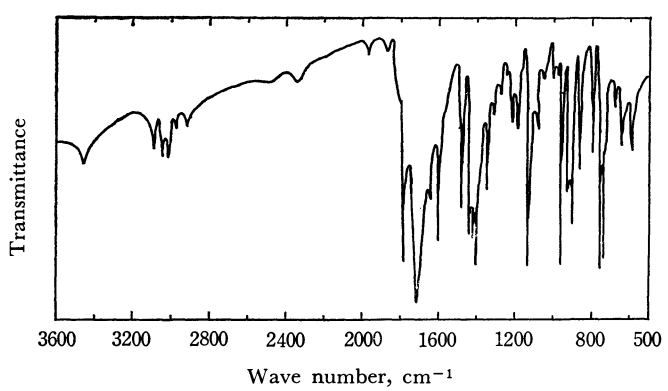

Fig. 2. Infrared absorption spectrum of 2-phthalimidomethyl-1, 3-butadiene (VII) in KBr disk.

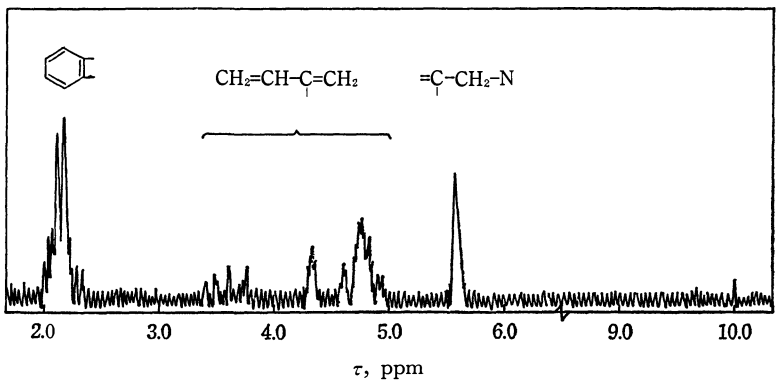

Fig. 3. NMR spectrum of 2-phthalimidomethyl-1, 3-butadiene (VII) in carbon tetrachloride at 60 Mc.

2-Methyl-1-phthalimido-3-buten-2-ol (V), mp 102—103°C, was obtained in a theoretical yield by the condensation reaction of IV with phthalic anhydride at 200°C. Although this intermediate, V, could also be prepared by the direct addition of phthalimide to III at 150°C using an alkali catalyst, the yield was very poor due to the difficult solubility of phthalimide in III.

The acetylation of V was carried out according to the ordinary method to give 2-acetoxy-2-methyl-1-phthalimido-3-butene (VI), mp 71—72°C.

The pyrolysis of VI at 550°C gave colorless crystals with a melting point of 114.5—116°C. The ultraviolet absorption spectrum is shown in Fig. 1, in which a strong absorption maximum appears at 219.5 mμ, almost the same position as those of isoprene (220 mμ),[11] 2-phthalimido-1, 3-butadiene (219 mμ),[3] and 2-succinimido-1, 3-butadiene (219.5 mμ),[3] all of which have been characterized as 2-substituted-1, 3-butadienes. On the other hand, 1-substituted-1, 3-butadienes, such as 1-phthalimido-1, 3-butadiene, 1-succinimido-1, 3-butadiene, and 1-(2-oxopyrrolidino)-1, 3-butadiene, show different absorption maxima, at 278.5,[2] 248,[2] and 268.5 mμ[1] respectively. The infrared absorption spectrum reveals a conjugated diene band at 1600 cm^{-1}, shown in Fig. 2, and the NMR spectrum in Fig. 3 shows methylene protons at 5.57 ppm, but no methyl protons.

The crystalline product prepared by the deacetylation of VI should be either 2-phthalimidomethyl-1, 3-butadiene (VII) or 2-methyl-1-phthalimido-1, 3-butadiene (VIII); from the results of the ultraviolet and NMR spectra, it is concluded that the product is VII.

Finally, a Diels-Alder reaction of VII with maleic anhydride gave 4-phthalimidomethyl-1, 2, 3, 6-tetrahydrophthalic anhydride.

Experimental

The infrared spectra were measured with a Perkin-Elmer spectrophotometer, model 221, and a Hitachi infrared spectrophotometer, model EPI-S. The NMR and ultraviolet spectra were recorded with a Varian NMR spectrometer, model A-60, and a Hitachi recording spectrophotometer, model EPS-2, respectively.

The Addition of Isoprene with Hypochlorous Acid. Into a dispersed solution of 50 g of isoprene, 100 g of bleaching powder (available chlorine 60%) and 1.0 g of Nonion N-1000 (Nissan Oils and Fats Co., Ltd.) in 1.2 *l* of water, 40 *l* of carbon dioxide gas was passed under stirring for 2 hr at 0—5°C. The reaction mixture was filtered to remove calcium carbonate, and then saturated with sodium chloride and extracted four times with ether. The combined ether extract was dried over calcium chloride. Then, after the ether had been removed, the residue was distilled through a Widmer column (length 200 mm) under a vacuum; 33.3 g (37.6%) of 1-chloro-2-methyl-3-buten-2-ol (I) was thus obtained as a colorless liquid with a boiling point of 52—54°C/27 mmHg.

Found: C, 49.66; H, 7.69%. Calcd for C_5H_9OCl (I): C, 49.81; H, 7.52%.

IR: 3470 (OH); 1175 (tertiary alcohol); 1870, 1410, 1290, 990, 927 (vinyl); 752 cm^{-1} (C-Cl).

After the I had been distilled out, the liquid residue was allowed to stand for a long time at room temperature; then a small amount of crystals was separated. When those crude crystals were recrystallized from benzene, isoprene dichlorohydrine was obtained as white crystals with a melting point of 81.5—83°C. This dichlorohydrine did not react with periodic acid.[12]

Found: C, 34.55, 34.80; H, 5.90, 6.02%. Calcd for $C_5H_{10}O_2Cl_2$ (II): C, 34.70; H, 5.78%.

IR: 3330 (OH); 1175 (tertiary alcohol); 1280, 1075 (primary alcohol); 724 cm^{-1} (C-Cl).

The Dehydrochlorination of I. To 200 g of 50% aqueous sodium hydroxide, 85.0 g of I was added, drop by drop, with a thorough agitation at about 130°C over a 3.0 hr period. In the course of this reaction, the reaction product was distilled with water; the distillate was separated into two phases, in both of which sodium chloride was then saturated. The upper organic layer was separated, dried over calcium chloride,

11) H. Brooker, L. K. Evans and A. E. Gillam, *J. Chem. Soc.*, **1940**, 1453.

12) R. L. Shriner, R. C. Fuson and D. Y. Curtin, "The Systematic Identification of Organic Compounds," John Wiley and Sons, New York, N. Y. (1956), p. 129.

and distilled to yield 43.0 g (72.4%) of 1,2-epoxy-2-methyl-3-butene (III), bp 80—82°C. Lit., bp 81°C/735 mmHg.[9]

IR: 1860, 1425, 1300, 988, 915 (vinyl); 1233, 883 cm^{-1} (epoxide.)

The Ammonolysis of III. Into 500 g of ammonia water (concentration 28%), 36.3 g of III was added, drop by drop, under stirring at 5—10°C. After the addition had been finished, the mixture was stirred for 48 hr at room temperature. The excess ammonia water was removed through a Widmer column under a vacuum, and finally 20.6 g (47.1%) of 1-amino-2-methyl-3-buten-2-ol (IV) was distilled out at 50—54°C/4.5—6 mmHg.

IR: 3500 (OH); 3420—3300, 1618 (primary amine); 1170 (tertiary alcohol); 1870, 1655, 1427, 1305, 1000, 925 cm^{-1} (vinyl).

The Condensation of IV with Phthalic Anhydride. A mixture of 6.0 g of IV and 8.8 g of phthalic anhydride was slowly heated to 200°C, and then kept for half an hour at this temperature in order to remove 1.0 m*l* of water. The crude product (14.0 g) crystallized when it came to room temperature. Recrystallization from water gave 2-methyl-1-phthalimido-3-buten-2-ol (V) as colorless needles with a melting point of 102—103°C.

Found: C, 67.50, 67.67; H, 5.80, 5.83; N, 6.05%. Calcd for $C_{13}H_{13}O_3N$ (V): C, 67.52,; H, 5.67; N, 6.06%.

IR: 3520 (OH): 1770, 1705 (C=O, phthalimido); 1610 (phenyl); 1180 (tertiary alcohol); 1867, 1655, 1411, 1300, 998, 928 (vinyl); 725, 712 cm^{-1} (*o*-disubstituted benzene).

The Addition of Phthalimide to III. A mixture of 8.4 g of III and 14.7 g of phthalimide, plus 5 drops of 30% aqueous potassium hydroxide as a catalyst, was heated in a sealed tube for 24 hr at 150°C. After standing for one day, the reaction product was extracted with benzene; a solid residue (8.7 g) remained. The recrystallization of this residue from water gave colorless needles with a melting point of 230—233°C. These crystals were confirmed to be phthalimide by a mixed-melting-point test with an authentic sample.

After the benzene had been removed from the extract, the oily residue was subjected to distillation under a vacuum; it thus gave a fraction with a boiling point of 163—165°C/3 mmHg, 6.3 g (27%). This fraction slowly crystallized on standing. Recrystallization from water gave colorless needles, mp 102—105°C. These crystals were confirmed to be V by a mixed-melting-point test.

The Acetylation of V. To 4.0 g of V, 25 m*l* of acetic anhydride and 0.5 g of anhydrous sodium acetate as a catalyst were added; the mixture was then refluxed for 10 hr. After the excess acetic anhydride had been removed under a vacuum, the oily residue was poured into a large amount of cold water and neutralized with sodium bicarbonate. Then crude crystals appeared; they were dried after washing with water. Recrystallization from benzene - petroleum benzine gave 2-acetoxy-2-methyl-1-phthalimido-3-butene (VI) as colorless crystals, mp 71—72°C.

Found: C, 65.92, 66.01; H, 5.65, 5.71; N, 5.10%. Calcd for $C_{15}H_{15}O_4N$ (VI): C, 65.92; H, 5.53; N, 5.13%.

IR: 1770, 1725 (C=O, phthalimido); 1750 (C=O, ester); 1235 (acetate); 1610 (phenyl); 1650, 1395, 1300, 980, 940 (vinyl); 725, 710 cm^{-1} (*o*-disubstituted benzene).

The Pyrolysis of VI. A solution of 20.0 g of VI in 60 m*l* of acetone was pyrolyzed under a nitrogen atmosphere by being dropped into a reaction tube of porcelain (ϕ 20 mm, length 500 mm) kept at 550°C[13] in an electric furnace (ϕ 30 mm, length 230 mm). The dropping time needed was 2.3 hr. The pyrolyzate was then poured into cold water, neutralized with sodium bicarbonate, and extracted with benzene. The extract was dried over anhydrous sodium sulfate. After the benzene had been removed under a vacuum, the remaining part crystallized. By extraction with hot petroleum benzine and letting the mixture stand in a refrigerator, crude crystals (4.5 g) of mp 92—109°C were obtained; they were then recrystallized from petroelum benzine to give 2-phthalimidomethyl-1, 3-butadiene (VII) as colorless crystals, mp 114.5—116°C. The ultraviolet and NMR spectra are shown in Figs. 1 and 3 respectively.

Found: C, 73.23; H, 5.25; N, 6.44%. Calcd for $C_{13}H_{11}O_2N$ (VII): C, 73.22; H, 5.20; N, 6.57%.

IR (Fig. 2): 1770, 1700 (C=O, phthalimido); 1870, 1400, 1305, 958, 912 (vinyl); 1615 (phenyl); 1600 (conjugated diene); 725, 710 cm^{-1} (*o*-disubstituted benzene).

The Diels-Alder Reaction of VII with Maleic Anhydride. A solution of 0.27 g of VII and 0.14 g of maleic anhydride in 10 m*l* of benzene was refluxed on a water bath for 2 hr. After the benzene had been removed, the residue was crystallized by letting it stand overnight. Recrystallization from benzene-petroleum benzine gave 4-phthalimidomethyl-1, 2, 3, 6-tetrahydrophthalic anhydride as white crystals, mp 146—147.5°C.

Found: C, 65.73, 65.78; H, 4.25, 4.45; N, 4.36, 4.33%. Calcd for $C_{17}H_{13}O_5N$: C, 65.59; H, 4.21; N, 4.50%.

IR: 1850 (C=O, five-membered cyclic anhydride); 1770, 1720 (C=O, phthalimido); 1610 (phenyl); 721, 710 cm^{-1} (*o*-disubstituted benzene).

The authors are indebted to Professor Shizunobu Hashimoto of Doshisha University and Dr. Isao Shiihara of this Institute for their helpful suggestions, and to Noboru Kito, M. Sc. of the University of Colorado for his NMR spectrum measurements.

13) This temperature was measured in the central part of the tube by a thermo-couple.

The Alkaline Sulfide Reduction of Aromatic Nitro Compounds. XIII. The Processes in the Alkaline Sulfide Reduction of Aromatic Nitro Compounds*[1]

Shizunobu HASHIMOTO and Junzo SUNAMOTO*[2]

Department of Applied Chemistry, Doshisha University, Karasuma-imadegawa, Kamikyo-ku, Kyoto

(Received April 26, 1967)

Goldschmidt and Larsen have presented evidence[1] that the reduction of sodium *m*-nitrobenzenesulfonate by an aqueous hydro sulfide saturated with hydrogen sulfide gives the corresponding nitroso, *N*-phenylhydroxylamino, and an anilino compound, but the anilino compound was not produced *via* the *N*-phenylhydroxylamino compound. Recently, Cope and Brown have suggested the formation of *N*-phenylhydroxylamine by gas chromatography in the reduction of nitrobenzene with an aqueous monosulfide containing ammonium chloride (pH=10.5).[2] On the other hand, in an earlier paper dealing with the kinetics of the aqueous monosulfide and with hydrosulfide reductions of sodium *m*-nitrobenzenesulfonate, we have suggested[3] that the monosulfide and hydrosulfide must be essentially identical in their reactions, a fact related to the hydrolytic equilibrium of the monosulfide.

The present investigation was undertaken to determine the alkaline sulfide reduction process of aromatic nitro compounds.

Table 1 shows the reduction products of nitro, nitroso, *N*-phenylhydroxylamino, azoxy, and azo compounds with the aqueous monosulfide or disulfide. The nitro compound gave only the corresponding amine, VI, with both sulfides. The nitroso compound gave VI together with VII, the product ratio of VI to VII being approximately unity in the monosulfide reduction. In the disulfide reduction, however, the yield of VII became much higher than that of VI. The monosulfide reduction of the *N*-phenylhydroxylamino compound was very slow under the conditions shown in Table 1; traces of VI and of VIII, the acidic rearrangement product of III, were detected on the paper chromatogram. On the other hand, in the disulfide reduction of III, the formation of VI and VII were observed, and the reduction rate of III became rather higher. Anlike the nitroso and *N*-phenylhydroxylamino compounds, the azoxy and azo compounds were reduced to give only the corresponding VII, derived from hydrazo compound. A small amount of VI given by the disproportionation of the hydrazo compound[4] was also detected.

The reduction of the nitro and nitroso compounds with the aqueous monosulfide and disulfide are shown in Fig. 1, while those of azoxy and azo compounds are shown in Fig. 2. The reduction rate of the nitro compound with an aqueous disulfide was very different from that with an aqueous

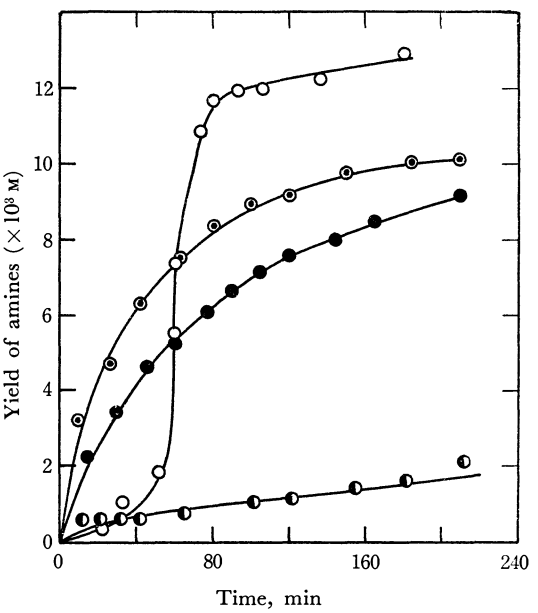

Fig. 1. Aqueous monosulfide and disulfide reduction of sodium *m*-nitro- and *m*-nitrosobenzene sulfonate at 35.0°C.
○: (Ar-NO_2)=1.429×10⁻² M
(Na_2S)=6.571×10⁻² M
●: (Ar-NO_2)=1.563×10⁻² M
(Na_2S_2)=1.926×10⁻² M
◐: (Ar-NO)=1.430×10⁻² M
(Na_2S)=13.14×10⁻² M
⊙: (Ar-NO)=1.430×10⁻² M
(Na_2S_2)=6.571×10⁻² M

*1 Presented at the 17th Annual Symposium on Organic Reaction Mechanisms of the Chemical Society of Japan, Tokyo, November 8, 1966.

*2 Present address: Department of Organic Synthesis, Faculty of Engineering, Kyushu University, Hakozaki, Fukuoka.

1) H. Goldschmidt and H. Larsen, *Z. physik. Chem.*, **71**, 437 (1910).

2) O. J. Cope and R. K. Brown, *Can. J. Chem.*, **40**, 2317 (1962).

3) S. Hashimoto and J. Sunamoto, This Bulletin, **39**, 1207 (1966).

4) S. Hashimoto and J. Sunamoto, *Yuki Gosei Kagaku Kyokaishi (J. Synth. Org. Chem. Japan)*, **24**, 1025 (1966).

Table 1. Reduction products in aqueous monosulfide or disulfide solution of sodium *m*-nitrobenzene sulfonate and its reduction intermediates

Starting material and its concn. $\times 10^2$ M	Reducing agent and its concn. $\times 10^2$ M	Reduction condition °C	Reduction condition min	Reduction product*
I: 1.429	M: 6.571	35	180	VI
I: 1.563	D: 1.926	35	250	VI
II: 1.430	M: 13.14	35	270	VI and VII
II: 1.430	D: 6.571	35	330	VI $\gg$ VII
III: 1.514	M: 7.669	35	300	Almost unreacted, VI, (VIII)
III: 5.00	D: 23.00	98	30	VI $\gg$ VII
IV: 0.758	M: 7.669	35	300	VI (VII)
IV: 0.714	D: 6.571	35	280	VI (VII)
V: 0.740	M: 13.14	35	350	VI (VII)
V: 0.740	D: 6.571	35	270	VI (VII)

* The products given by the other processes besides the reduction, as described in the text, are shown in parentheses.

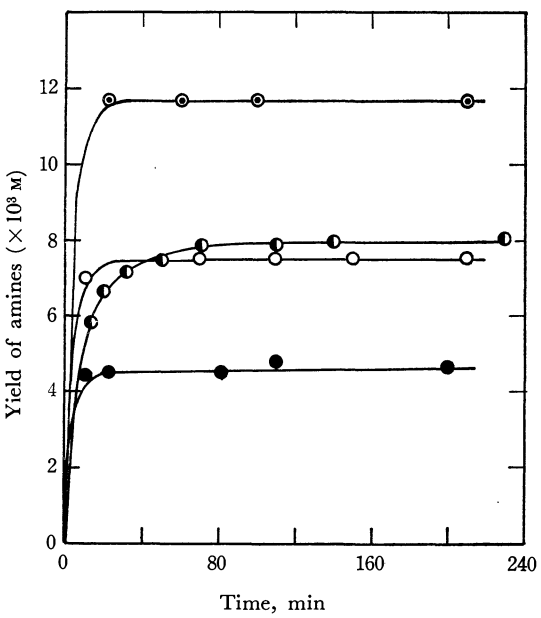

Fig. 2. Aqueous monosulfide and disulfide reduction of disodium *m*, *m'*-azoxy- and *m*, *m'*-azobenzene disulfonate at 35.0°C.
○: (Ar-N(O)=N-Ar) = 0.758×10^{-2} M
(Na_2S) = 7.669×10^{-2} M
◐: (Ar-N(O)=N-Ar) = 0.714×10^{-2} M
(Na_2S_2) = 6.571×10^{-2} M
●: (Ar-N=N-Ar) = 0.740×10^{-2} M
(Na_2S) = 13.14×10^{-2} M
⊙: (Ar-N=N-Ar) = 0.740×10^{-2} M
(Na_2S_2) = 6.571×10^{-2} M

monosulfide.[3,5] Anlike the monosulfide reduction of the nitro compound, that of the nitroso compound had no induction period and its reduction rate was much slower throughout the reaction. On the other hand, the disulfide reduction of the nitroso compound proceeded at approximately the same rate as that of the nitro compound. The monosulfide reduction rate of the *N*-phenylhydroxylamino compound was much lower than that of the nitroso compound, but the disulfide reduction rate was the same as those of the nitro and nitroso compounds. Our findings concerning the reduction rates listed above are consistent with the results obtained by Cope and Brown,[2] although our point of view was somewhat different from theirs. In the reduction of the azoxy and azo compounds, no comparable differences in the reduction rates were observed between the monosulfide and the disulfide reduction. In these cases, the initial reduction rates were rather high, and the reactions reached an apparent equilibrium rather early.

On the basis of the data thus obtained, it seems most reasonable to conclude that, in the alkaline sulfide reductions of sodium *m*-nitrobenzenesulfonate, but not the hydrogen sulfide reduction, methanilic acid will be directly produced from the nitro compound upon the attack of the disulfide on the positively-charged nitrogen of the nitro group[6] and upon the subsequent rapid interchange between hydrogen and oxygen, as is shown in Eq. (1):

$$\mathrm{Ar\text{-}\overset{+\delta}{N}{=}O} \xleftarrow{(S\text{-}S)^{2-}} \mathrm{Ar\text{-}N(O)\text{-}N\text{-}Ar} \quad \mathrm{Ar\text{-}\underset{\downarrow}{\overset{}{N}}{=}\underset{\downarrow}{O}} \quad \mathrm{Ar\text{-}\underset{-\delta}{O}} \quad + \quad \mathrm{H_2O} \rightarrow \mathrm{Ar\text{-}NH_2} + S_2O_3^{2-} \qquad (1)$$

No nitroso, *N*-phenylhydroxylamino, azoxy, or azo compounds is intermediately produced during the course of the reduction of the nitro compound. In the monosulfide or the hydrosulfide reduction, the disulfide is produced by the radical oxidation

5) S. Hashimoto and J. Sunamoto, This Bulletin, **39**, 100 (1966).

6) M. Hojyo, Y. Takagi and Y. Ogata, *J. Am. Chem. Soc.*, **82**, 2459 (1960).

of the monosulfide or the hydrosulfide with light, oxygen, and so forth.[5,7,8]

Experimental

Materials. The sodium monosulfide (M) and disulfide (D), sodium *m*-nitrobenzenesulfonate (I), sodium *m*-nitrosobenzenesulfonate (II), disodium *m,m'*-azoxybenzenedisulfonate (IV), and disodium *m,m'*-azobenzenedisulfonate (V) were the same as those used in previous papers.[3,5] The sodium *m*-(*N*-phenylhydroxylamino)benzenesulfonate (III) was prepared by the zinc reduction of the corresponding nitro compound, I; the sulfonate thus obtained, when recrystallized from aqueous methanol, was found to be chromatographically pure. Their purities were exactly determined before use by the usual reduction-diazometry.

Rate Measurement. The procedure for the rate measurements and analyses were the same as in the method described earler.[3,5]

When a nitroso, azoxy, or azo compound was reduced by aqueous alkaline sulfide, the corresponding hydrazo compound was obtained. After the benzidine rearrangement of the hydrazo compound with hydrochloric acid, the amine produced was determined by diazometry. When *m*-(*N*-phenylhydroxylamino)benzenesulfonate was reduced by aqueous monosulfide under the same conditions as those used in the reduction of the nitro or nitroso compound, the reduction rate of the former was much slower and most of the reactant was recovered.

The reaction was also followed by paper chromatography. The chromatograms were developed with *n*-butanol containing concentrated hydrochloric acid (4 : 1 by vol.). The R_f values and the detections were as follows: *m*-aminobenzenesulfonate (VI), $R_f=0.30$, reddish orange upon diazotization and coupling with α-naphthol-4-sulfonate (method A) or orange, with *p*-dimethylaminobenzaldehyde (method B); *m,m'*-benzidinedisulfonate (VII), $R_f=0.05$, red, with A or orange, with B; III, $R_f=0.22$, yellow, with B; and 2-hydroxy-5-aminobenzenesulfonate (VIII), $R_f=0.13$, dull red, with A or yellow, with B. No other materials were observed.

7) Part XI: S. Hashimoto, J. Sunamoto and K. Sato, This Bulletin, **40**, 2860 (1967).

8) Part XII: S. Hashimoto, J. Sunamoto and A. Aoki, *ibid.*, **40**, 2867 (1967).

A New Method for the Quantitative Verification of the Butadiene-Styrene Copolymer

Koichi IRAKO, Shiro ANZAI and Akira ONISHI

Central Research Laboratory, Bridgestone Tire Company, Kodaira, Tokyo

(Received May 19, 1967)

A new method to separate the homopolymer from butadiene-styrene copolymerization product, a "two-layer extraction method," has been developed.

Many new catalyst systems and copolymerization techniques (random, block or graft *etc.*) have previously been employed in the preparation of the butadiene-styrene copolymer.

It is important to characterize these products and identify the copolymer in the light of the evaluation of catalyst systems, copolymerization methods, and the physical properties of the products. Several solvent-extraction methods and fractional extraction methods have been employed in order to verify the existence of the copolymer and to separate a homopolymer from the copolymerization product. By these methods, however, a quantitative treatment was difficult. Moreover, the selection of a solvent and a nonsolvent was troublesome.

We have now succeeded in making a quantitative separation of the homopolymer from copolymerization products by a "two-layer extraction method," using *n*-hexane and *N*, *N*-dimethylformamide (DMF); the separation is accompanied by a dioxane extraction.

The butadiene-styrene copolymerization product (1.0 g) was dissolved or suspended in *n*-hexane (200 m*l*) under stirring for *ca.* 50 hr; then the solution or the suspension was placed in a 500 m*l* separating funnel and 100 m*l* of DMF was added. The funnel was shaken for *ca.* 15 min and then left standing for 1 hr, after which two layers, (the *n*-hexane layer(upper) and the DMF layer (lower)), were separated. The polymer (A) dissolved in the DMF layer and the polymer (B) dissolved or suspended in the *n*-hexane layer were isolated and dried under a vacuum. The polymer (B) was then further extracted with dioxane to

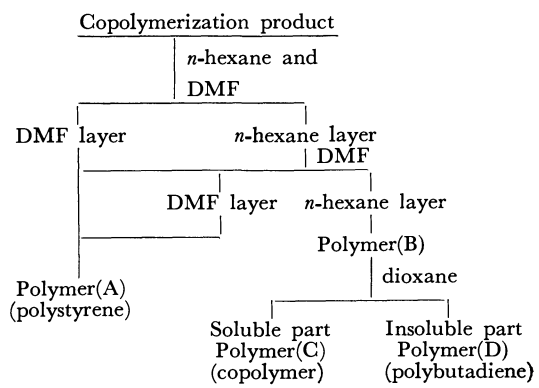

separate a dioxane-insoluble part (C) from a dioxane-soluble part (D).

The separation of homopolystyrene from the copolymerization product can be effectively carried out by the "two-layer extraction method" using *n*-hexane and DMF. Table 1 shows the results obtained by applying this method to a mixture of polystyrene and polybutadiene, or to each homopolymer. It is evident from the table that the homopolymers were separately extracted by the respective solvents, *i. e.*, polybutadiene by the *n*-hexane and polystyrene by the DMF.

Next, this method was applied to butadiene-styrene copolymerization product, and the copolymerization efficiency was determined by the following equation:

TABLE 1. EXTRACTION RESULTS OF HOMOPOLYMERS AND POLYBUTADIENE-POLYSTYRENE MIXTURES BY THE TWO LAYERS METHOD

No.	Polymer mixture				Polymer A		Polymer B		Recovered[3]
	PBD[1] part		PST part		DMF soluble part		*n*-Hexane part		
	wt %	$[\eta]$	wt %	$[\eta]$	wt %	St %[2]	wt %	St %	wt %
1-1	100	3.07	—	—	0	0	97.3	0	97.3
-2	—	—	100	0.082	99.5	100	0	0	99.5
-3	75	3.20	25	0.688	24.1	100	73.0	0	97.1
-4	75	3.20	25	0.082	23.8	100	72.5	0	96.3
-5	75	1.17	25	0.688	20.6	100	75.0	0	95.6
-6	75	1.17	25	0.082	20.0	100	76.5	0	96.5
-7	75	2.08[4]	25	0.082	20.2	100	72.6	0	92.8
-8	90	3.39	10	0.082	10.3	100	85.7	0	96.0

1) Cis 1, 4 polybutadiene (cis content 95.8%)
2) Styrene content was measured by IR analysis. Thus, we prepared various compositions of mixture of polystyrene and polybutadiene which had a similar microstructure to the sample to be analyzed, plotted $DCH_2(2930\,cm^{-1})/DC_6H_5(700\,cm^{-1})$ and each composition from the IR chart of each polymer mixture, and determined styrene content of each sample from this calibration curve.
3) Methanol soluble part has not been recovered.
4) Li catalyzed polybutadiene (cis content, 35.4%)

TABLE 2. EXTRACTION RESULTS OF VARIOUS TYPE OF BUTADIENE-STYRENE COPOLYMERIZATION PRODUCTS BY THE TWO LAYERS METHOD

No.	Polymerization catalyst	Copolymer type	Commercial brand	Styrene content %
2-1	Radical type (emulsion)	random	SBR 1502 (JSR)	25.3
-2	Li type (solution)	random	Duradene (Firestone)	24.2
-3	Li type (solution)	random	Solprene 1204 (Phillips)	25.0
-4	Li type (solution)	block	Solprene 1205 (Phillips)	28.7
-5	$Co(acac)_2$-$Al_2Et_3Cl_3$*1	random	—	9.3
-6	$TiCl_4$-$AlEt_3$*1	random	—	28.4

No.	Polymer A DMF soluble part wt %	Polymer B *n*-hexane part St %	Recovered*2 %	Copolymerization efficiency %
2-1	trace	25.3	91.80	≒100
-2	trace	24.0	97.30	≒100
-3	trace	25.0	96.17	≒100
-4	0.13	28.7	95.28	≒100
-5	4.0	5.9	94.60	57.0
-6	24.28	5.8	95.50	14.5

*1 Copolymerization was conducted at 40°C.
*2 Methanol soluble part has not been recovered.

TABLE 3. EXTRACTION RESULTS OF POLYBUTADIENE-BUTADIENE-STYRENE COPOLYMER MIXTURE BY THE DIOXANE METHOD

No.	Polymer	Styrene content %	Polymer C Dioxane soluble part		Polymer D Dioxane insoluble part	
			wt %	St %	wt %	St %
3-1	SBR 1502 (JSR)	24.5	100	24.5	—	—
-2	Polybutadiene-copolymer*1 mixture (5 : 5)	8.7	51.0	11.7	49.0	1.8
-3	Copolymer*1	14.4	100	14.4	—	—

Extraction condition

Polymer: 1.0 g; Solvent: dioxane 30 m*l*; Extraction time: 50 hr at 25°C.

*1 Copolymer obtained by $Ni(acac)_2$-BF_3Et_2O-$AlEt_3$ catalyst system (Japanese Pat. 42-7795) was used after two layers extraction method.

Copolymerization efficiency(%) =

$$\frac{S_T - S_H}{S_T} \times 100 = \frac{S_C}{S_T} \times 100$$

S_T: total styrene content (%)
S_H: homopolystyrene content (%)
S_C: copolymerized styrene content (%)

The results obtained are shown in Table 2.

We also found that dioxane extraction after the removal of homopolystyrene could be used to separate polybutadiene from a copolymer-polybutadiene mixture. Some results of the dioxane extraction are shown in Table 3.

The "two-layer extraction method" is also effective for a liquid-liquid extraction. This method is especially recommended for the isolation of a graft copolymer from the reaction products. The method described above was also applied to an isoprene-styrene copolymerization product. Similar quantitative extraction results were obtained. This method may also be applied to other conjugated diolefin-vinyl compound copolymerization products, such as butadiene-acrylonitrile, butadiene-methylmethacrylate, and isoprene-methylmethacrylate.

Surface Activity and Some Optical Properties of Na-1-acylaminonaphthalene-5-sulfonates in Solutions

Yoshinori MUSHA, Akio OKAGAWA and Tamotsu KONDO

Faculty of Phamaceutical Sciences, Science University of Tokyo, Funakawara-machi, Shinjuku, Tokyo

and Masuzo NAGAYAMA

Research Laboratory, Lion Fat & Oil Co., Ltd., Hirai, Edogawa-ku, Tokyo

(Received May 19, 1967)

Previous papers[1,2] have reported on the syntheses, properties, and possible applications in basic research and industry of new surface-active agents, which are fluorescent as well as surface-active in aqueous solutions.

There are two ways, in principle, of synthesizing a compound of this kind. First, a strong surface activity can be given to certain fluorescent dyes or intermediates by introducing one or more long-chain alkyl radicals into the dye or intermediate molecules. Secondly, some surface-active agents can be chemically modified to exhibit fluorescence by reaction with appropriate fluorescent reagents.

From the physicochemical point of view, however, the compounds obtained so far are not necessarily suitable for basic research in colloid and interface science, for some of them are subject to light-catalyzed cis-trans isomerization,[1] while others are hardly soluble in water at pH values around 7 or at room temperatures.[2]

In the present study, therefore, an attempt has been made to prepare the compounds by the first method without the shortcomings mentioned above. Thus, a homologous series of Na-1-acylaminonaphthalene-5-sulfonates has been synthesized from 1-naphthylamino-5-sulfonic acid (Laurent's acid) and acyl chlorides. Some properties of these compounds have also been studied.

1) T. Kondo, A. Okagawa and M. Nagayama, *Kogyo Kagaku Zasshi (J. Chem. Soc. Japan, Ind. Chem. Sec.)*, **68**, 2125 (1965).
2) S. Muto, T. Kondo and M. Nagayama, *Yukagaku (J. Japan Oil Chemists' Soc.)*, **15**, 26 (1966).

Experimental

Materials. Acyl chlorides were prepared from thionyl chloride and *n*-fatty acids by the usual method. The purity of all the *n*-fatty acids used was estimated to be more than 99.5% by gas chromatography. Laurent's acid was purchased from K & K Laboratories, Inc., Plainview, N.Y., U.S.A. This material was said to have a purity of about 95%.

Preparation and Purification. The reaction of acyl chloride with Laurent's acid easily gave the desired compound. As an example, the reaction of decanoyl chloride with Laurent's acid will be described below.

9.6 g (0.04 M) of Laurent's acid were dissolved in 150 m*l* of water, with the addition of sodium carbonate to make the resultant solution slightly alkaline. The reaction was initiated by simultaneously dropping 9.5 g (0.05 M) of decanoyl chloride dissolved in 20 m*l* of acetone and of an aqueous 5% sodium carbonate solution into the solution of the sodium salt of Laurent's acid obtained above. An hour was sufficient for the reaction to be completed at room temperature.

The product was purified by dry-column-chromatography[3] as follows. A column made of silica gel (Wako 100—200 mesh) was used. The column was filled with dry packing by slowly pouring in the absorbent while tapping the column. Appropriate quantities of silica gel and a methanolic solution of the product were mixed, and the solvent was evaporated to dryness, thus leaving the silica gel covered with the product. Then the column was loaded by pouring the silica gel on top of the packed column and covering it with a filter paper. The development was done by allowing a chloroform-methanol mixture (2 : 1, v/v) to move down the column. When the solvent reached the bottom of the column, the chromatogram was stopped at this point and the content of the column was extruded. The part exhibiting a violet fluorescence was cut off and treated with the same solvent as had been used in the development. The extracted product was precipitated out of the solution by evaporating the solvent under atmospheric pressure. The precipitate was collected and recrystallized at least two times from methanol, and once from water. The final product was obtained as a white powder; the yield was slightly less than 10%.

The high purity of the compounds thus obtained was checked by thin-layer-chromatography, which gave only one spot on the chromatogram.

In Table 1 are listed the results of the elemental analyses of the homologous compounds. Octanoyl, decanoyl, and dodecanoyl compounds are abbreviated as C_8, C_{10} and C_{12} compounds respectively.

Table 1. Elemental analyses

	C_8		C_{10}		C_{12}	
	Calcd	Found	Calcd	Found	Calcd	Found
C	58.27	59.23	60.13	60.27	61.80	62.39
H	5.97	6.01	6.56	6.51	7.07	7.42
N	3.77	3.74	3.53	3.56	3.27	3.12

Ultraviolet Absorption and Fluorescence Spectra. The ultraviolet absorption spectra were recorded on a Hitachi Model EPA-3A spectrophotometer. The wavelengths in these measurntemes ranged from 210 to 350 mμ.

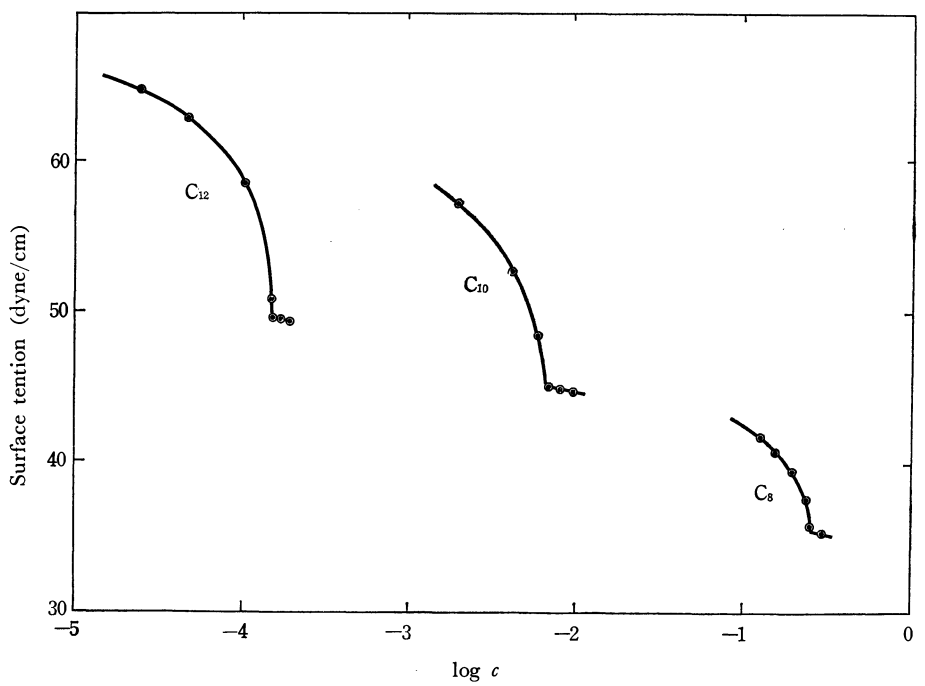

Fig. 1. Surface tension of aqueous solutions of the homologous compounds at 50°C.

3) B. Loev and K. M. Snader, *Chem. & Ind.*, **1965**, 15.

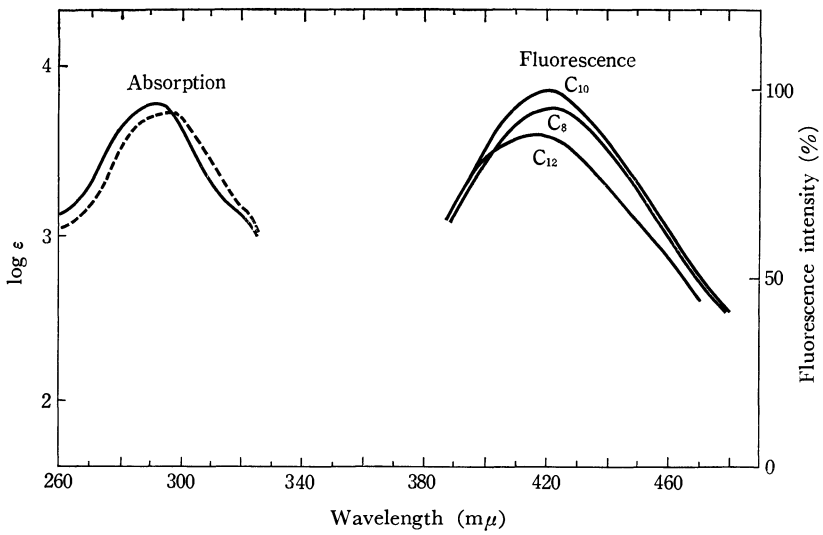

Fig. 2. Ultraviolet absorption and fluorescence spectra of the homologous compounds in water (——) and in methanol (- - -).

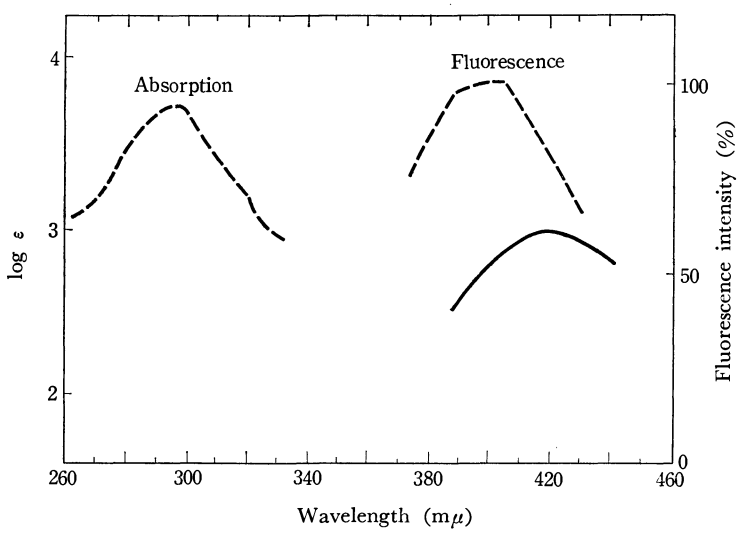

Fig. 3. Ultraviolet absorption and fluorescence spectra of C_{10} compound in methanol (——) and water (- - -)

The fluorescence spectra were obtained with a Hitachi Model ESP-2 spectrophotometer, with attachements for fluorescence measurements. The concentration of all the aqueous and methanolic solutions of the compounds used for the measurements was 5×10^{-5} M.

Surface-tension Measurements. The surface tensions of aqueous solutions of these compounds were measured by the drop-weight method, using a micrometer syringe at 50°C. Necessary precautions were taken to give the equilibrium values in these measurements.

Results and Discussion

Figure 1 gives the sulface tension *vs.* concentration curve for aqueous solutions of the homologous compounds. The concentration at the inflection point on each curve was taken as the CMC. The CMC values for the C_8, C_{10}, and C_{12} compounds were estimated from this figure to be 2.7×10^{-1}, 6.6×10^{-3}, and 1.5×10^{-4} M respectively.

The relation between the CMC and the hydrophobic chain length of the compounds is expressed by the equation: $\log \mathrm{CMC}=5.87-0.80N$, where N is the carbon atom number in a long hydrophobic chain. This means that the CMC of our compounds varies with the hydrophobic chain length in the manner of geometric progression, as does that of many common surface-active agents.

The UV absorption and fluorescence spectra are shown in Figs. 2 and 3. With the exception

of fluorescence spectra in water, only one curve is presented in these figures, since the remaining spectra were independent of the chain length. The reason why the fluorescence spectra in water vary with the carbon atom number in an alkyl chain has not been yet established. In the UV absorption spectra, the primary band appeared at about 225 mμ, and for ordinary naphthalene derivatives. The secondary band occured at 290 mμ in water and at 300 mμ in methanol. The peak of the fluorescence spectra was at 420 mμ in water, while it was located at 400 mμ in methanol.

From the experimental results presented above, the homologous compounds may be designated as fluorescent surface-active agents.

Some applications of these compounds in colloid and interface science are now being studied.

The Reduction of Schiff Bases with Aluminum Amalgam

Tatsuo TAKESHIMA, Motomu MURAOKA, Hiroe ASABA and Masataka YOKOYAMA

Department of Chemistry, Faculty of Science, Chiba University, Yayoi-cho, Chiba
The Second Laboratory of Organic Chemistry, The Institute of Physical and Chemical Research, Yamato-machi, Saitama

(Received June 7, 1967)

There are several common methods for the reduction of Schiff bases. Among them, the catalytic hydrogenation seems, in general, to be the most preferred, in part because of its neutral nature.

In the present experiment, aluminum amalgam, which almost fits the neutral conditions, was found to be an effective agent for this reduction. The aluminum amalgam was easily made in the usual way. The reduction was carried out under an atmospheric pressure and at room temperature. In addition, the treatment of the reaction product involved no troublesome manipulation.

The Schiff bases used were conveniently prepared by refluxing ketone with primary amine in the presence of potassium fluoride. Few new secondary amines were obtained besides the known ones.

All of the hydrochlorides of amines obtained showed several typical infrared absorption of NH_2^+ in the region of 2800—2000 cm^{-1} (stretching) and at ~1587 (deformation).[1]

Of the amines prepared, the known ones were identified as hydrochlorides (for melting point,[2] see Table 2). The assignment of the structure of the new amines was based on the results of the elemental analysis and the infrared spectra of the hydrochloride, and on the course of the synthesis. The structures of the Schiff bases prepared were deduced from the course of the synthesis and from the fact that the amines were reduced to the corresponding secondary amines.

The reduction of the Schiff bases was also carried out by means of lithium aluminum hydride. However, this method was not favorable from the standpoint of either the manipulation or the yield.

Experimental

Procedure. The Schiff bases were prepared by refluxing a mixture of the reactants in a ketone: amine ratio of 1 (mol): 1 (mol) in the presence of excess anhydrous potassium fluoride. The secondary amines were obtained by reducing the Schiff bases with an aluminum amalgam in the usual way. The amalgam was prepared by immersing aluminum foil, cut into pieces, in a dilute solution of mercuric chloride (less

1) KBr disk.

2) The melting point of the hydrochloride of VIIA was not depressed on admixture with an authentic specimen; T. Takeshima, T. Hayashi, M. Muraoka and T. Matsuoka, *J. Org. Chem.*, **32**, 980 (1967).

3) A few specimens of the Schiff base prepared were analyzed with respect to the nitrogen content. The Schiff bases were unstable, especially when exposed to air. The specimens were purified gas chromatographically (NpGS (1.5%)/Shimalite) just before the analyses.

4) W. D. Emmons, *J. Am. Chem. Soc.*, **79**, 5739 (1957).

5) a) G. Mignonac, *Ann. Chim.*, **(11) 2**, 225 (1934); b) V. E. Haury, EL Cerrito and S. A. Ballard, U. S. Pat. 2418173 (Apr. 1, 1947); c) E. D. Bergmann, E. Zimkin and S. Pinchas, *Rec. Trav. Chim.*, **71**, 168 (1952); d) H. L. Wehrmeister, *J. Org. Chem.*, **25**, 2132 (1960); e) R. E. Miller, *ibid.*, **25**, 2126 (1960); f) R. Mayer and Jentzsch, *J. Prakt. Chem.*, **23**, 83 (1964).

6) K. Jewers and J. McKenna, *J. Chem. Soc.*, **1958**, 2209.

7) G. F. Grail, L. E. Tenenbaum, A. V. Tolstoouhov, C. J. Duca, J. F. Reinhard, F. E. Anderson and J. V. Scudi, *J. Am. Chem. Soc.*, **74**, 1313 (1952).

8) a) A. Skita and F. Keil in Part with E. Baesler and L. Boente, *Ber.*, **61B**, 1682 (1928); b) G. Wittig and H. D. Frommeld, *ibid.*, **97**, 3548 (1964).

9) a) G. Breuer and J. Schnitzer, *Monatsh.*, **68**, 301 (1936); b) E. T. Borrows, B. M. C. Hargreaves, J. E. Page, J. C. L. Resuggan and F. A. Robinson, *J. Chem. Soc.*, **1947**, 197; c) C. W. Kruse and R. F. Kleinschmidt, *J. Am. Chem. Soc.*, **83**, 213 (1961).

10) D. G. Norton, V. E. Haury, F. C. Davis, L. J. Mitchell and S. A. Ballard, *J. Org. Chem.*, **19**, 1054 (1954).

Table 1. Schiff bases prepared

Starting substances	The Schiff bases prepared	Bp °C/mmHg	Yield %	Anal. (Found, N%)[3]	Reported Bp °C/mmHg
Acetone *n*-Hexylamine	*N*-Isopropylidene-hexylamine	71—74/17	*ca.* 70	9.31	53—55/5[4]
Acetone Cyclohexylamine	*N*-Isopropylidene-cyclohexylamine (IIS)[10]	67—69/17	*ca.* 40		180.6/760[10]
Methyl ethyl ketone *n*-Hexylamine	*N*-*s*-Butylidene-hexylamine (IIIS)	85—86/16	*ca.* 70	9.15	
Methyl ethyl ketone Cyclohexylamine	*N*-*s*-Butylidene-cyclohexylamine (IVS)	84—86/18	*ca.* 40	8.93	
Cyclohexanone *n*-Hexylamine	*N*-Cyclohexylidene-hexylamine (VS)	111—116/7	*ca.* 65		
Cyclohexanone Cyclohexylamine	*N*-Cyclohexylidene-cyclohexylamine (VIS)[5b,c,d,e,f]	99—104/6	*ca.* 60	7.86	135.7/20[5b] 136—137/15[5c] 92— 94/ 2[5d] 93— 95/ 2[5e] 135—140/17[5f]
2-Methylcyclo-hexanone, Cyclo-hexylamine	*N*-2-Methylcyclo-hexylidene-cyclo-hexylamine (VIIS)	114—115/7	*ca.* 50		
Cyclopentanone *n*-Hexylamine	*N*-Cyclopentylidene-hexylamine (VIIIS)	89—91/5	*ca.* 80		
Cyclopentanone Cyclohexylamine	*N*-Cyclopentylidene-cyclo-hexylamine (IXS)[5f,6]	92—94/5	*ca.* 60		

Table 2. Secondary amines prepared

Starting substances	The amines prepared	Bp °C/mmHg	Yield %	Appearance and mp (°C) of the hydrochloride	Reported mp of the hydro-chloride, °C
IS	*N*-Isopropylhexyl-amine (IA)[7]	57—59/12	54	Colorless long plates (from dioxane) 147—148	
IIS	*N*-Isopropylcyclohexyl-amine (IIA)[8]	60—62/15	54	Colorless square plates (*n*-amyl alcohol) 208—209	204—205[8a]
IIIS	*N*-*s*-Butylhexyl-amine (IIIA)	74—75/12	63	Colorless long plates (from dioxane) 167	
IVS	*N*-*s*-Butylcyclohexyl-amine (IVA)[8a]	79/15	55	Colorless square plates (from dioxane) 212—213	211[8a]
VS	*N*-Cyclohexylhexyl-amine (VA)[9]	87—93/13	34	Colorless plates (from *n*-amyl alcohol) 241—242	240[9b]
VIS	*N*-Cyclohexylcyclo-hexylamine (VIA)	103—104/6	57	Colorless needles (from ethanol) 334—335 (in sealed tube)	
VIIS	*N*-2-Methylcyclohexyl-cyclohexylamine (VIIA)	119/11	55	Colorless square plates or cubic crystals (from *n*-amyl alcohol) 246—245 (in sealed tube)	
VIIIS	*N*-Cyclopentylhexyl-amine (VIIIA)	95—100/11	44	Colorless plates (from *n*-amyl alcohol) 210 (in sealed tube)	
IXS	*N*-Cyclopentylcyclo-hexylamine (IXA)[6]	130/33	59	Colorless plates (from *n*-amyl alcohol) 276—277 (in sealed tube)	

than 1%) for a short time; the amalgamated aluminum was then collected, washed with water and then ethanol, and used immediately. An example is described below.

Preparation of IS. A mixture of acetone (30 g, *ca.* 0.5 mol), *n*-hexylamine (50 g, *ca.* 0.5 mol) and potassium fluoride (80 g, *ca.* 1.3 mol) was refluxed for *ca.* 12 hr. When the reaction mixture, freed from the inorganic portion, was then distilled (preferably in an atomosphere of nitrogen), a fraction distilling at 71—74°C/17 mmHg was collected; colorless liquid with a characteristic smell, yield *ca.* 55 g (*ca.* 70%).

Preparation of IA. A mixture of IS (10 g), an aluminum amalgam (10 g), and methanol (70 m*l*) was shaken under cooling with water. After *ca.* 10

Table 3. Analyses of the amine hydrochlorides

		Calcd (%)				Found (%)			
		C	H	N	Cl	C	H	N	Cl
IA·HCl	$C_9H_{22}NCl$	60.14	12.34	7.79	19.73	60.13	12.08	7.85	18.85
IIA·HCl	$C_9H_{20}NCl$	60.82	11.34	7.88	19.95	61.17	11.06	7.86	20.15
IIIA·HCl	$C_{10}H_{24}NCl$	61.98	12.48	7.23	18.30	61.82	12.26	7.19	18.50
IVA·HCl	$C_{10}H_{22}NCl$	62.63	11.57	7.31	18.49	62.76	11.36	7.33	18.78
VA·HCl	$C_{12}H_{26}NCl$	65.57	11.92	6.37	16.13	65.75	11.76	6.30	16.67
VIA·HCl	$C_{12}H_{24}NCl$	66.18	11.11	6.43	16.28	66.51	11.38	6.85	15.95
VIIA·HCl	$C_{13}H_{26}NCl$	67.35	11.31	6.04	15.30	67.26	11.29	6.33	15.19
VIIIA·HCl	$C_{11}H_{24}NCl$	64.20	11.76	6.81	17.23	64.20	11.90	6.80	17.28
IXA·HCl	$C_{11}H_{22}NCl$	64.84	10.89	6.86	17.40	65.14	10.73	6.96	16.29

min, the initial evolution of heat subsided. Then water (*ca.* 12 ml) was added, portion by portion, over a period of *ca.* 10 hr with shaking at room temperature. When the reaction was complete, an aqueous solution of sodium hydroxide (100 g of a 25% soln.) was added to dissolve the aluminum hydroxide produced. The whole was then filtered, sodium chloride was added, and the mixture was extracted with ether. The extract was concentrated, dried over potassium hydroxide, and distilled. A fraction which distilled at 57—59°C/12 mmHg was collected; colorless liquid, yield 5.4 g (*ca.* 54%).

The hydrochloride of the amine was prepared by passing dry hydrogen chloride into a solution of the amine in ether. The precipitates produced were recrystallized from hot dioxane to give long, colorless plates, mp 147—148°C.

The authors are grateful to Dr. Hiroshi Midorikawa for affording facilities for the present work.

Preparation of 1 : 1- and 2 : 1-Telomers of Allyl Acetate Using the Azeotropic Mixture with Carbon Tetrachloride[1)]

Masao Ōkubo

Government Industrial Research Institute, Nagoya, Kita-ku, Nagoya

(Received June 15, 1967)

Recently, several relations were observed between the structure and the reactivity of carboxylic acid esters of allylic alcohols in their γ-ray induced telomerization with carbon tetrachloride.[2-4)]

In this paper, the results will be reported on an investigation to confirm the effect of temperature, the elevation of which caused an increase in the yield of 1 : 1-telomer as had been observed in the preliminary experiment.[2)] In consequence, an apparatus was devised to increase the yields of 1 : 1- and 2 : 1-telomers and to decrease simultaneously the yield of the 3 : 1-telomer of allyl acetate.

Experimental

Irradiation at an Elevated Temperature. By modifying the Soxhlet's extractor, an apparatus was constructed as shown in Fig. 1. A solvent of a suitable boiling point in the Flask 2 was heated to boiling by the Heating Mantle 1, and the temperature inside the Glass Mantle 4 could be maintained to be constant. A sample solution was introduced into the Ampoule 5, on the top of which is connected the U-Tube 6 containing a suitable amount of carbon tetrachloride to prevent the sample solvent from its escaping and, at the same time, to avoid the danger of an unexpected violent reaction. This apparatus was placed at a given distance from the γ-ray source 8. Methanol, bp 65°C, was used as the heating solvent, and the Flask is protected from γ-ray by the Pb-Block 9.

By this device, the strength of γ-ray falls only slightly, and the Ampoule can be placed, if necessary, at the least distance from the γ-ray source.

Irradiation of Circulated Sample. Again by modifying the Soxhlet's extractor, the other apparatus was constructed as shown in Fig. 2. A mixture of allyl acetate and carbon tetrachloride in the Flask 2 is heated to boiling by the Heating Mantle 1. The vapor of the azeotropic mixture goes through the Side

1) γ-Ray Induced Telomerization Reactions between Allylic Compounds and Carbon Tetrachloride. V; Part IV: M. Ōkubo, This Bulletin, **40**, 1672 (1967).
2) M. Ōkubo, *Nippon Kagaku Zasshi (J. Chem. Soc. Japan, Pure Chem. Sect.)*, **87**, 1191 (1966).
3) M. Ōkubo, *ibid.*, **87**, 1196 (1966).
4) M. Ōkubo, *ibid.*, **88**, 212 (1967).

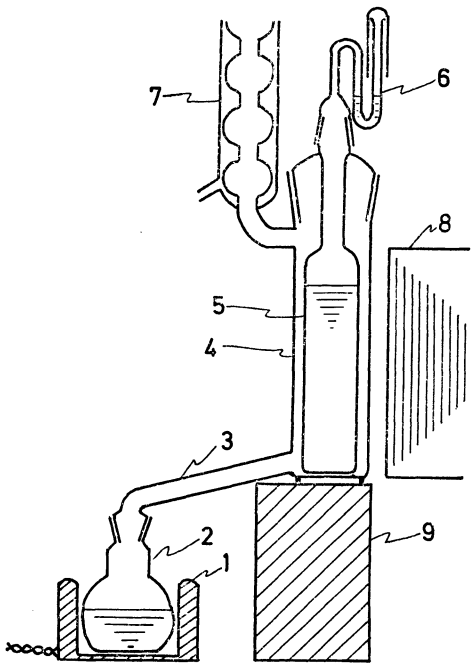

Fig. 1. The apparatus for irradiation at an elevated temperature.

1 Heating mantle	2 Flask
3 Side tube	4 Glass mantle
5 Ampoule	6 U-tube
7 Condenser	8 γ-Ray source
9 Pb-block	

Tube 3 and the Glass Mantle 4, and then to the Condenser 7. The liquefied azeotrope comes down through the Long Funnel 6 and fills up the Reaction Tube 5 and is irradiated. The produced telomers and the unreacted materials run over the top of 5, passing through 3, and comes back to 2. The telomers are stored in 2, and protected from γ-ray by the Pb-Block 9. The unreacted azeotrope is brought to 5 and is irradiated again. So, this method is named the circulation technique in this paper.

The concentration of allyl acetate in the Reaction Tube 5 changes gradually, and it was determined by the titration with a KBr-$KBrO_3$ aqueous solution before and after the irradiation. Then, the remaining solution in 5 was put back into 2, and the resulting total solution was titrated to determine the overall consumption of ally acetate.

Results and Discussion

Effect of Temperature. Using the apparatus of Fig. 1, a solution of the molar ratio of 1/5 (allyl acetate, 0.0667 mol, and CCl_4, 0.333 mol) was irradiated at the dose rate of 5.5×10^4 R/hr, at 65°C. Table 1 lists this result together with the results of the preceding experiments at 25°C.[1] From these data, it can be seen that the elevation of the temperature makes the reaction faster, and the lowering of the initial concentration of the allyl ester causes an increase in % consumption of C=C bond. Furthermore, both of these changes of the reaction condition favor the yields of 1 : 1- and 2 : 1-telomers. Since these changes of the reaction condition may accelerate the chain transfer of the propagating radical to CCl_4, the above result is ascribed to the acceleration of the step (1) and, at the same time, to the relative retardation of the step (2).

$$\begin{aligned} &Cl_3C\text{-}CH_2\text{-}\dot{C}H \\ &\qquad\quad | \\ &\qquad CH_2O\text{-}OCOCH_3 \end{aligned} + CCl_4 \longrightarrow \begin{aligned} &Cl_3C\text{-}CH_2\text{-}CHCl \\ &\qquad\quad | \\ &\qquad CH_2O\text{-}OCOCH_3 \end{aligned} + \cdot CCl_3 \qquad (1)$$

$$\begin{aligned} &Cl_3C\text{-}CH_2\text{-}CH\text{-}CH_2\text{-}\dot{C}H \\ &\qquad\quad |\qquad\quad | \\ &\qquad CH_2\quad CH_2 \\ &\qquad |\qquad\quad | \\ &\qquad OCOCH_3\ OCOCH_3 \end{aligned} + \begin{aligned} &CH_2\text{=}CH \\ &\qquad\quad | \\ &\qquad CH_2 \\ &\qquad\quad | \\ &\qquad OCOCH_3 \end{aligned} \longrightarrow \begin{aligned} &Cl_3C\text{-}(\text{-}CH_2\text{-}CH\text{-})_2\text{-}CH_2\text{-}\dot{C}H \\ &\qquad\qquad\quad |\qquad\quad | \\ &\qquad\qquad CH_2\quad CH_2 \\ &\qquad\qquad |\qquad\quad | \\ &\qquad\qquad OCOCH\ OCOCH_3 \end{aligned} \qquad (2)$$

From the above observation, the increase in the yields of 1 : 1- and 2 : 1-telomers is expected when the irradiation is carried out at higher temperatures and lower concentrations.*1 However, the apparatus of Fig. 1 does not seem to fit for this purpose, since, besides the necessity of an heating solvent, a voluminous reaction tube is required to contain the large volume of a diluted solution of CCl_4. To avoid these inconveniences, the circulation technique was adopted and the apparatus of Fig. 2 was devised.

Results of Circulation Technique. Allyl acetate, 80 g, and CCl_4, 246 g (molar ratio of 1/2), were introduced into the Flask 2 in Fig. 2. The voltage applied on the Heating Mantle was controlled so that the azeotropic mixture came down from the Condenser at a rate of *ca.* two drops per second. In this condition, the molar ratio of the solution inside the Reaction Tube was found to be 1/7.5. After irradiation for 170 hr, it came down to 1/19. The results are shown in Table 2.

The reaction temperature was nearly the boiling point of CCl_4, 76°C. The production ratios of 3 : 1-telomer in Table 2 resemble the ratio obtained in the experiment of 1/5 molar ratio at 65°C, but are slightly higher than that obtained in the experiment of 1/10 molar ratio at 25°C in Table 1. Therefore, the concentration lowering by half is considered to be more effective than the temperature elevation by 40 or 50 degrees for the increase in the

*1 Both of 1 : 1- and 2 : 1-telomers can be isolated easily by distillation under the reduced pressure, and the 2 : 1-telomers of allyl carboxylates have been shown to give a trichloroethyl derivative of tetrahydrofurfuryl alcohol in good yields.[3]

Table 1. Effects of temperature and concentration in the telomerization of allyl acetate

Molar ratio[a)]	Irradn. temp. °C	Irradn. hours hr	C=C consumption %	Telomer production ratios[b)]		
				1 : 1	2 : 1	3 : 1
1/2	25	120	74	1	10.0	7.5
1/5	25	72	85	1	5.7	2.6
1/10	25	48	87	1	2.9	0.74
1/5	65	43—48	85—90	1	3.4	0.93

a) The molar ratio of allyl acetate to CCl_4.
b) Telomer production ratios were calculated by dividing the moles consumed for 2 : 1- and 3 : 1-telomers with those for 1 : 1-telomers, respectively.[2)]

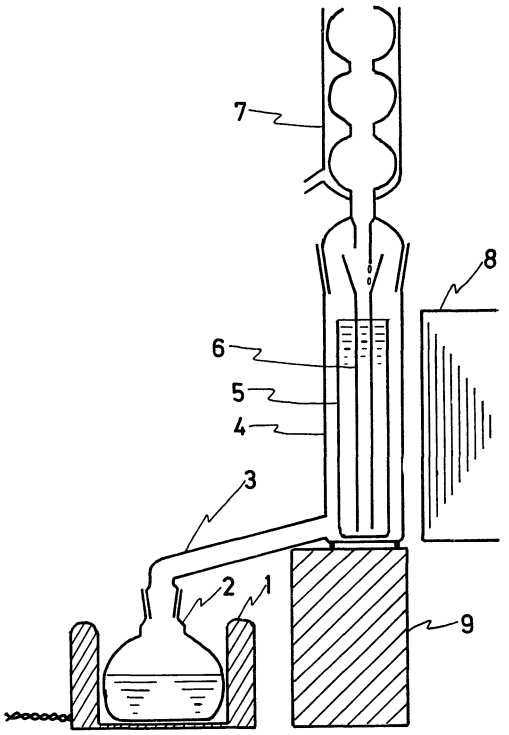

Fig. 2. The apparatus for irradiation of circulated sample

1 Heating mantle 2 Flask
3 Side tube 4 Glass mantle
5 Reaction tube 6 Long funnel
7 Condenser 8 γ-Ray source
9 Pb-block

yields of 1 : 1- and 2 : 1-telomers. But, it is remarkable that, notwithstanding the use of the mixture as high molar ratio as 1/2, the content of 1 : 1- and 2 : 1-telomers reached 80.3% by weight of the total products, and therefore, this technique was shown to be useful for preparing these telomers.

Table 2. Irradiation of the circulated mixture
allyl acetate, 80 g; CCl_4, 246 g

Irradn. hours hr	C=C consumption %	Telomer production ratios		
		1 : 1	2 : 1	3 : 1
120	40	1	3.3	1.3
170	82	1	3.9	1.3

The advantages of this method are: that the concentrated solutions can be used and, therefore, a large quantity of the allyl ester can be treated at once; and that, as mentioned already, the heating of the reacting sample can be performed automatically without the heating solvent.

A disadvantage, the slightly higher yield of the 3 : 1-telomer than that obtained in the case of the molar ratio of 1/5 at 65°C, may be partly due to the fact that the concentrated solution of the allyl ester in the Flask 2 is irradiated continuously during the experiment with scattered γ-rays and, moreover, with weak γ-rays which have passed through the Pb-Block.

One of the well-known undesirable features of the telomerization reaction in general is that the telomer of a particular molecular weight cannot be prepared exclusively when a concentrated solution of taxogen is used. The present method suggests one of the directions to overcome this difficulty.

The author is indebted to Mr. Keichi Nunome of the present institute for operating the γ-ray irradiator. He also offers his gratitude to Professor Ryozo Goto of Kyoto University for his encouragement throughout the work.

The Photochemical Cleavage of Friedelin

Takahiko TSUYUKI, Shûzô YAMADA and Takeyoshi TAKAHASHI

Department of Chemistry, Faculty of Science, The University of Tokyo, Hongo, Bunkyo-ku, Tokyo

(Received July 29, 1967)

We wish to report the formation of a series of compounds (II—VI) on the photolysis of friedelin.

A boiling solution of friedelin[1] (I; 1.00 g) in ethanol was irradiated with a high pressure mercury lamp under a nitrogen atmosphere for 9 hr. The reaction products were separated by preparative thin layer chromatography (TLC). The main product was 3, 4-seco-ester*1 (II, R=Et; 732 mg). The formation of 4-isofriedelin*1 (III; 49 mg), 3β-friedelanol[1] (IV; 11 mg), 3α-friedelanol[2] (V; 86 mg) and 3, 4-seco-acid*1 (II, R=H; 2 mg) was confirmed. A hydrocarbon (VI; 25 mg) was also isolated besides friedelin (I; 135 mg). The hydrocarbon (VI) showed two peaks on gas-liquid chromatography (GLC), though this compound gave only one spot on TLC (silica gel-silver nitrate). One of the peaks was shown to be due to 3-norfriedelane*1 (VIa) and the other would be due to 3-nor-4-isofriedelane (VIb) (*Cf.* Experimental). However, no isolation of VIb has yet been furnished. The structure III was confirmed by alkaline isomerization to I.

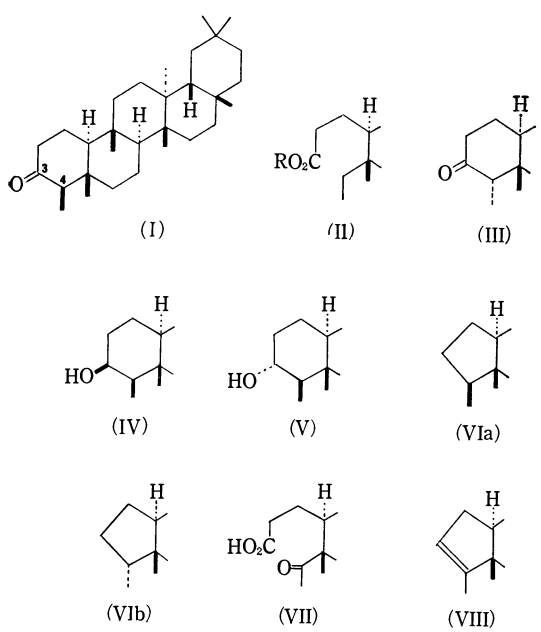

Friedelin (I; 1.00 g) in acetic acid-water (9 : 1) was heated under reflux and was photolyzed under the same condition as above for 27 hr. The product was mainly the acid (II, R=H; 883 mg) accompanied with the hydrocarbon mixture (VIa and VIb: 20 mg) and friedelin (I; 28 mg).

In ethanol solution, the formation of II (R=Et and H) and of hydrocarbons (VIa and VIb) could be interpreted by the known photochemical reaction processes.[3] The formation of III would be explained by recombination of a diradical formed by α-cleavage (between positions 3 and 4) of I. A part of recovered friedelin (I) should be resulted from diradical recombination of alternative fashion. Furthermore, the photoreduction was concomitant to form a pair of friedelanols (IV and V).[4] In the aqueous acetic acid solution, the formation of II (R=H) was predominant.

Experimental

Photochemical Cleavage of Friedelin in Ethanol. The suspension of friedelin (1.00 g) in ethanol (600 m*l*) was heated under reflux with bubbling of nitrogen for 30 min. The solution was then irradiated with a high pressure mercury lamp (100 W) under a nitrogen atmosphere for 9 hr. Repeated separation of the products by preparative TLC (SiO_2 and SiO_2-$AgNO_3$) afforded the compounds (I)—(VI).

3, 4-Seco-ester (II, R=Et). 3, 4-Seco-ester was recrystallized from ethanol and then from acetone, mp 116.0—116.7°C.

Found: C, 81.40; H, 11.85%. Calcd for $C_{32}H_{56}O_2$: C, 81.29; H, 11.94%. This material was identical with the authentic sample in mp, TLC and IR spectrum. The authentic sample was obtained from friedonic acid (VII).[2b,5] Huang-Minlon reduction of VII yielded 3, 4-seco-acid (II, R=H), mp 211°C.

Found: C, 80.77; H, 11.78%. Calcd for $C_{30}H_{52}O_2$: C, 81.02; H, 11.79%.

Esterification (EtOH-H_2SO_4) and recrystallization from ethanol and then from acetone gave the ester (II, R=Et), mp 116.3°C.

4-Isofriedelin (III). 4-Isofriedelin was recrystallized from petroleum ether, mp 257.5°C, $\nu_{C=O}$ 1706 cm^{-1}. The solution of III in dioxane was heated under reflux with sodium methoxide in methanol under a nitrogen atmosphere for 6 hr. GLC examination (Diasolid

1) E. J. Corey and J. J. Ursprung, *J. Am. Chem. Soc.*, **78**, 5041 (1956), and related papers.
2) a) N. L. Drake and S. A. Shrader, *ibid.*, **57**, 1854 (1935). b) N. L. Drake and W. P. Campbell, *ibid.*, **58**, 1681 (1936).
*1 Refers to a new compound.
3) *Cf.* R. O. Kan, "Organic Photochemistry," McGraw-Hill, New York (1966), pp. 71—93, 222—223.
4) *Cf.* G. Quinkert, B. Wegement, F. Homburg and G. Cimbollek, *Chem. Ber.*, **97**, 958 (1964).
5) L. Ruzicka, O. Jeger and P. Ringnes, *Helv. Chim. Acta*, **27**, 972 (1944).

H-523, 240°C) revealed that the most of III (t_R=36.6 min) isomerized to I (t_R=41.1 min). The isomerized product was purified by preparative TLC and recrystallization from petroleum ether. The IR spectrum, mp, mixed mp and R_f value on TLC were identical with those of friedelin (I).

3-Norfriedelane (VIa) and 3-Nor-4-isofriedelane (VIb). The hydrocarbon fraction was recrystallized from chloroform-methanol, mp ~210°C.

Found: C, 87.11; H, 12.49%. Calcd for $C_{29}H_{50}$: C, 87.36; H, 12.64%. The IR spectrum and R_f value on TLC (SiO_2-$AgNO_3$) were identical with those of the authentic 3-norfriedelane. However, two peaks appeared at t_R=12.5 and 13.4 min on GLC (Diasolid H-523, 240°C). The authentic 3-norfriedelane (VIa) was prepared as follows: Hydrogenation (5% Pd-C/AcOEt) of 3-norfriedelene[2b] (VIII) proceeded mainly from α-side to afford the sole product, 3-norfriedelane*[1] (VIa), mp 224°C (Found: C, 87.15; H, 12.41%. Calcd for $C_{29}H_{50}$: C, 87.36; H, 12.64%), which gave a single peak at t_R=13.4 min on GLC under the same condition, described above.

Photochemical Cleavage of Friedelin in Aqueous Acetic Acid. Friedelin (1.00 g) in acetic acid-water (9 : 1) (600 m*l*) was irradiated at reflux temperature under nitrogen with a high pressure mercury lamp (100 W) for 27 hr. Working up as before and 883 mg of the 3, 4-seco-acid (II, R=H), mp 214.5—215.0°C, 20 mg of the hydrocarbon mixture (VIa and VIb), mp ~212°C, (Found: C, 87.40; H, 12.77%. Calcd for $C_{29}H_{50}$: C, 87.36; H, 12.64%) and 28 mg of friedelin (I) were obtained.

Polymerization of Alkoxyacetylenes

Sun'ichi NOZAKURA,* Manabu TAGAYA*[1],* Heimei YUKI** and Shunsuke MURAHASHI**

* *Department of Polymer Science, Faculty of Science, Osaka University, Toyonaka, Osaka*

** *Department of Chemistry, Faculty of Engineering Science, Osaka University, Toyonaka, Osaka*

(Received August 3, 1967)

Acetylene and its derivatives are known to undergo polymerization to linear polymers or cyclic oligomers depending on the polymerization conditions.[1] Alkoxyacetylene gives an interesting linear polymer which is susceptible to chemical transformations because of its unsaturated ether structure. There have been, however, only a few reports on its polymerization. Phenoxyacetylene has been polymerized thermally to a cross-linked polymer.[2] Ethoxyacetylene has been reported to give a cyclic trimer in the presence of $Ni(CO)_2(PPh_3)_3$.[3]

Since alkoxyacetylene was expected to polymerize cationically by analogy with vinyl ether, the polymerization of methoxy- and isobutoxyacetylene were attempted in the presence of Friedel-Crafts catalysts and soluble Ziegler catalysts, which were known to be effective for acetylene.

Monomers were prepared according to a known procedure.[4] Methoxyacetylene, bp 23.5°C; isobutoxyacetylene, bp 46.0—47.0°C/135 mmHg, n_D^{20} 1.4022.

The cationic polymerization was carried out in either *n*-hexane or methylene chloride (20 m*l*) at −78°C for 3 hr, using 2 m*l* of isobutoxyacetylene and a 0.1 mol equivalent of a catalyst. The polymerization was then quenched by the addition of methanol, followed by evaporation; this gave a 39% yield with $TiCl_4$ in methylene chloride, a 55% yield with BF_3 (saturated), and a 18% yield with $AlBr_3$. Catalysts such as $BF_3 \cdot Et_2O$, $SnCl_4$ and VCl_3 gave yields of only a few percentage points. The polymerizations in *n*-hexane resulted in lower yields than those in methylene chloride.

Soluble complex catalysts composed of transition-metal acetylacetonate and triisobutylaluminum (1 : 1) were found to be very effective. Polymerizations were carried out in benzene (20 m*l*) at 30°C for 3 hr, using 2 m*l* of isobutoxyacetylene and a 0.1 mole quivalent of the complex catalysts. These polymerizations were stopped by the addition of methanol, and the whole contents were evaporated. The yields were calculated using the correction of the catalyst residue, the following yields being found for the given acetylacetonate: Fe^{3+} 92, Cr^{3+} 91, Co^{3+} 89, VO^{2+} 81, Ni^{2+} 59, Co^{2+} 46, Cu^{2+} 42, V^{3+} 25, TiO^{2+} 16, Zr^{4+} 0, Mn^{3+} 0, Zn^{2+} 0%. It is interesting to note that Cr^{3+}, Fe^{3+} and Cu^{2+} had scarcely been at all effective in the polymerization of acetylene.[5]

---

*1 Present address: Research Centre of Osaka Gas Co., Ltd., Konohana-ku, Osaka.

1) E. M. Smolin and D. S. Hoffenberg "Encyclopedia of Polymer Science and Technology," Vol. I, ed. by H. F. Mark, N. G. Gaylord and N. M. Bikales, Interscience Publishers, New York, N. Y. (1964), p. 46.

2) T. L. Jacobs and W. P. Tuttle, Jr., *J. Am. Chem. Soc.*, **71**, 1313 (1949).

3) L. S. Meriwether, E. C. Colthup, G. W. Kennerly and R. N. Reusch, *J. Org. Chem.*, **26**, 5155 (1961).

4) J. F. Arens, "Advances in Organic Chemistry," Vol. 2, ed. by R. A. Raphael, E. C. Taylor and H. Wynberg, Interscience Publishers, New York, N. Y. (1963), p. 117.

5) S. Kambara, M. Hatano and T. Hosoe, *Kogyo Kagaku Zasshi (J. Chem. Soc. Japan, Ind. Chem. Sect.)*, **65**, 720 (1962).

The cationic polymers were viscous or tacky semisolids, in color ranging from a light brown to a reddish brown, and in molecular weight ranging around 500—600. The absence of IR absorption bands of trisubstituted benzene and NMR resonance due to aromatic hydrogen suggests a negligible formation of cyclic trimers, if any.*2

The polymers which were obtained with the Ziegler catalysts were partly soluble in methanol. The soluble part was a reddish-brown, tacky solid and resembled the cationic polymer. The insoluble part was a brown-to-black powder. Both the parts contained an inorganic ingredient originating from the catalyst, and purification was found to be difficult. For example, when a 0.1 mol equivalent of $Fe(acac)_3$-$Al(i\text{-}Bu)_3$ (1 : 1) to the monomer was used, the soluble part of the poly(isobutoxyacetylene) was found to contain 8.6% ash, and the insoluble part, 10.6%. The Al/Fe atomic ratio in the latter was found to be 0.31. Upon treatment with aqueous 2 N HCl, the polymer was almost free from ash, which amounted to only 0.28% in the soluble part and 0.51% in the insoluble part. Unfortunately, however, the treatment was accompanied by a chemical modification of the polymer, as will be mentioned below.

A crude poly(methoxyacetylene) showed in its infrared apectrum a broad band of a polyconjugated double bond around 1560 cm^{-1} (s), an ether linkage at around 1080(s), and an olefinic C-H bond at 820 cm^{-1}(m). On treatment with 2 N HCl, all these bands diminished in intensity, and new bands appeared around 1715(s), 1660(s) and 1600(s) cm^{-1}; these bands are considered to be due to various kinds of carbonyls. Poly(isobutoxyacetylene) showed essentially the same spectral change and weight loss of 20% upon treatment with 2 N HCl, followed by heat-treatment at 90°C. As a volatile product of the treamtent, isobutanol was identified by gas chromatography. Hence, the spectral change may be interpreted by the following reaction scheme:

$$-\underset{\underset{OR}{|}}{CH}=\underset{\underset{OR}{|}}{C}-\underset{\underset{OR}{|}}{CH}=\underset{\underset{OR}{|}}{C}- \rightarrow -CH_2-\overset{\overset{O}{\|}}{C}-\underset{\underset{OR}{|}}{CH}=\underset{\underset{OR}{|}}{C}- \rightarrow$$

$$-CH_2-\overset{\overset{O}{\|}}{C}-CH_2-\overset{\overset{O}{\|}}{C}-$$

In fact, the methanol-insoluble part of poly(methoxyacetylene) after the treatment with 2 N HCl showed the following analytical data, which correspond to those where 3/5 of the enol-ether structure was converted into ketone.

Found: C, 60.61; H, 5.40%. Calcd for $[(C_3H_4O)_2(C_2H_2O)_3]_n$: C, 60.50; H, 5.88%.

The halogenation of the polymers was attempted in chloroform at room temperature, 75—93% of the theoretical value of chlorine and 56—68% of that of bromine were introduced, a process accompanied by a slight evolution of hydrogen halide. The halogenated polymers were soluble in acetone and benzene. The molecular weight of the chlorinated poly(methoxyacetylene) were found by vapor-pressure osmometry to be 560 and 800 for the soluble and insoluble parts respectively, and the chlorine contents, 41.74 and 49.79% respectively.

The hydrogenation of the crude poly(isobutoxyacetylene) was attempted using Pd or Pt on carbon as a catalyst or with tri-*n*-butylboron,[6] but no hydrogenation was observed. Diels-Alder reactions with maleic anhydride or maleimide in refluxing toluene gave negative results.

*2 When ethoxyacetylene was treated with $TiCl_4$ in benzene at 40°C for 3 hr, there was obtained a polymer in a 51% yield; from this a cyclic trimer (13%, mp 35—36°C) was isolated by alumina-column chromatography.

6) F. L. Ramp, E. J. Dewitt and L. E. Trapasso, *J. Org. Chem.*, **27**, 4368 (1962).

The Infrared Spectra of *p*-Substituted Benzenediazonium Cations

Katsumi TABEI and Chihiro ITO

Tokyo College of Pharmacy, Kashiwagi, Shinjiku-ku, Tokyo

(Received August 8, 1967)

The infrared spectra of some aromatic diazonium cations have already been measured by several authors and the change of the diazonium group stretching frequency by the introduction of a substituent into the aromatic nucleus was discussed with reference to the change of N-N bond order.[1,2] However, any other vibration than the diazonium stretching one has never been studied.

In the present report, the infrared spectra of twenty kinds of *p*-substituted benzenediazonium cation were measured in the form of solid chloromercurate to study the aryl carbon - nitrogen bond (Ar-N) stretching vibration in relation to the electronic effect of a *p*-substituent.

In an aromatic diazonium cation, the aryl carbon-nitrogen bond stretching vibration appeared in the frequency region 1300—1400 cm^{-1}, and the above assignment was made with reference to that of nitrobenzenes[3] and phenyl isocyanides[4].

The wave numbers of the characteristic absorption band of diazonium cation, $\nu_{N\equiv N}$ and ν_{Ar-N} were listed in Table 1.

From the data of Table 1, it was shown that an electron-donating *p*-substituent increases the wave number of ν_{Ar-N} and decreases that of $\nu_{N\equiv N}$.

An electron-attracting *p*-substituent, on the other hand, seems to be rather less effective upon the above two absorption bands.

By plotting the wave numbers of ν_{Ar-N} and $\nu_{N\equiv N}$ against Hammett's σ_p value for the substituent in Figs. 1 and 2, it can be clarified that there is almost a linear correlation between them, and that the straight line was distorted as represented by the dotted line above the region of plus σ_p value.

The high frequency shift of the aryl carbon-nitrogen bond stretching vibration by the substitution of an electron-donating group can be explained in the same way as described in the case of the diazonium group stretching band,[5,6] that is, the substitution of an electron-donating group at the para position of the benzene ring increases the contribution of the polarized structure (II) to the ground state (I), namely it decreases the N≡N bond order and at the same time increases the aryl carbon - nitrogen (Ar-N) bond order.

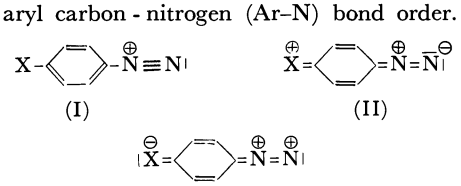

(I) (II)

(III)

The break in the linear correlation by the substitution of a strong electron-attracting group, on the other hand, may be partly interpreted by taking the polarized structure (III) into consideration.

Since an increase in the contribution of the structure (III) to the ground state (I) increases the aryl carbon - nitrogen (Ar-N) bond order and

TABLE 1. IR SPECTRA OF *p*-SUBSTITUTED BENZENEDIAZONIUM SALTS

No.	*p*-Substituent	Hammett σ_p*	dp (°C)	ν_{Ar-N} (cm^{-1})	$\nu_{N\equiv N}$ (cm^{-1})
1	NO_2	+0.78	98	1316	2280
2	CN	+0.63	97—98	1309	2270
3	$COCH_3$	+0.52	95—96	1312	2275
4	$COOC_2H_5$	+0.45	106	1320	2270
5	COOH	+0.27	109	1320	2275
6	I	+0.28	120	1310	2260
7	Cl	+0.23	120—121	1314	2265
8	Br	+0.23	117—118	1314	2250
9	CHO	+0.22	108—110	1319	2275
10	C_6H_5	+0.01	109	1325	2250
11	H	0.00	—**	1314	2260
12	C_2H_5	−0.15	87—89	1332	2250
13	CH_3	−0.17	107—108	1324	2255
14	OC_2H_5	−0.25	119	1340	2230
15	OCH_3	−0.27	120	1342	2235
16	OH	−0.46	155—156	1385	2235
17	NH_2	−0.66	157—159	1365	2165
18	$N(CH_3)_2$	−0.83	146—148	1394	2155
19	$NHCOCH_3$		137—138	1340	2245
20	NHC_6H_5		114—115	1328	2240

* H. H. Jaffé, *Chem. Revs.*, **53**, 191 (1953).

** This double salt does not show sharp decomposition temperature. 100—130°C of dp is reported in the literature; O. A. Reutov and Yu. G. Bundel, *Chem. Abstr.*, **48**, 623 (1954).

1) M. Aroney, R. J. W. Le Fèvre and R. L. Werner, *J. Chem. Soc.*, **1955**, 276.
2) K. B. Whetsel, G. F. Hawkins and F. E. Johnson, *J. Am. Chem. Soc.*, **78**, 3360 (1956).
3) R. D. Kross and V. A. Fassel, *ibid.*, **78**, 4225 (1956).
4) I. Ugi and R. Meyr, *Chem. Ber.*, **93**, 239 (1960).
5) K. B. Whetsel, G. F. Hawkins and F. E. Johnson, *J. Am. Chem. Soc.*, **78**, 3360 (1956).
6) M. Sukigara and S. Kikuchi, This Bulletin, **40**, 1077 (1967).
7) A. N. Nesmejanow, *Ber.*, **62**, 1010 (1929).

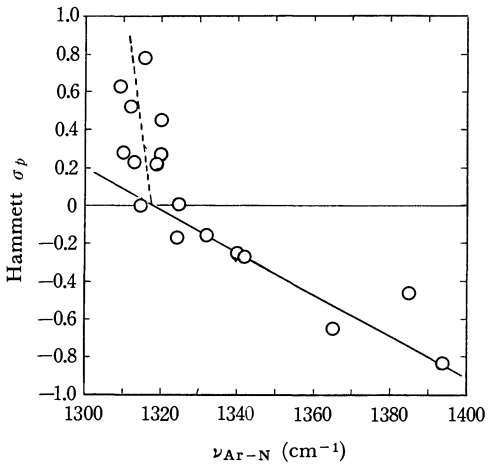

Fig. 1. Plot of aryl carbon-nitrogen bond stretching frequency *vs.* Hammett's σ_p constant for the corresponding *p*-substituent.

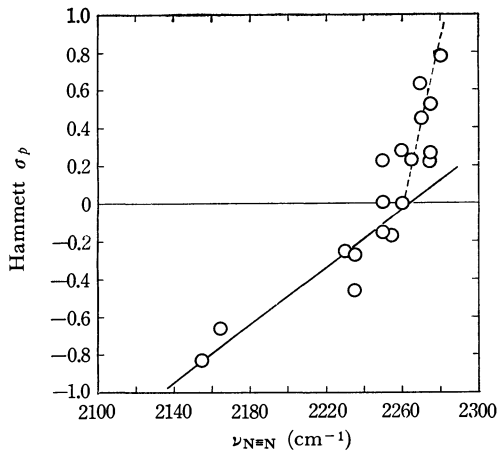

Fig. 2. Plot of diazonium group stretching frequency *vs.* Hammett's σ_p constant for the corresponding *p*-substituent.

at the same time, decreases the N≡N bond order, the substitution of a strong electron-attracting group shifts the aryl carbon - nitrogen (Ar-N) stretching vibration to the higher frequency side and at the same time, shifts that of the diazonium group to the lower frequency side. However, the above contribution of the structure (III) by the substitution of a strong electron-attracting group is less important than that of structure (II), because there is an unstable, doubly positive charged N=N bonding in the former structure.

The net effect of a strong electron-attracting group upon the characteristic infrared absorption bands of diazonium cation seems to be small and then the absorption band of ν_{Ar-N} and $\nu_{N\equiv N}$ of the diazonium salts having a strong electron-attracting group at para position of benzene nucleus appears in the narrow frequency regions 1310—1320 cm^{-1}, and 2260—2280 cm^{-1}, respectively.

Experimental

Preparation of Diazonium Double Salts. The preparation of the mercuric chloride double salt of *p*-substituted benzenediazonium chlorides was carried out following the method of Nesmejanow[7]; The diazotization of an arylamine was done by a usual method with the corresponding amount of moles of sodium nitrite in 20% hydrochloric acid solution at 0—5°C.

The diazotized solution was filtered and then poured into a solution of one and a half times as much as the corresponding amount of moles of mercuric chloride in 20—30 m*l* of cooled concentrated hydrochloric acid. The mixture was stirred at 0—5°C for ten minutes or so.

After precipitation of the double salt, the crystal was collected on a glass-filter, washed with cooled water, ethanol and ether, in that order, and dried in a vacuum desiccator. The yield of dried double salt was 10—60%.

Infrared Spectra of Diazonium Double Salts. The infrared spectra of the double salts were measured by using a JASCO DS-301 infrared spectrophotometer in a KBr disk. The wave numbers of $\nu_{N\equiv N}$ and ν_{Ar-N} are listed in Table 1.

The authors wish to express their deep gratitude to Miss Michiko Hayama of Tokyo College of Pharmacy for her infrared measurement.

π-Allylic Palladium Complexes from Methyl Sorbate

Akira KASAHARA and Taeko IZUMI

Department of Chemistry, Faculty of Liberal Arts and Science, Yamagata University, Yamagata

(Received August 15, 1967)

The reaction of sodium chloropalladite with conjugated diolefin in alcohols has been shown to result in the formation of alkoxy-π-allylic palladium complexes.[1,2] Thus, butadiene in methanol gaves the chloro-bridged 4-methoxy-π-butenyl complex, $[Pd_2Cl_2(C_4H_6OCH_3)_2]$,[1] while the reaction of cycloocta-1, 3-diene with sodium chloropalladite in methanol gives rise to di-μ-chlorodi-(4-methoxy-cyclooct-2-enyl)-dipalladium. When this is heated, *in situ*, the methanol is eliminated and an unsaturated complex, di-μ-chlorodi-(cycloocta-2, 4-dienyl)-dipalladium, is formed.[2]

This paper will describe the application of this reaction to methyl 2, 4-hexadienoate (methyl sorbate).

Results and Discussion

The treatment of methyl sorbate with sodium chloropalladite in methanol at room temperature for 20 hr gave two products, $[C_{16}H_{26}O_6Cl_2Pd_2]$ (mp 122—125°C) as the major product and $[C_{14}H_{18}O_4Cl_2Pd_2]$ (mp 116—119°C); the I and IIA structures respectively were assigned to these productes on the basis of their infrared and NMR spectra. The dimeric nature of these compounds was supported by the molecular-weight determinations, and by their reacting with pyridine to give readily-soluble monomeric derivatives (*cf.* Fig. 1).

The infrared spectrum of the major product (I) showed the presence of methoxy group at 2820 and 1097 cm^{-1} and an uncoordinated ester carbonyl group at 1728 cm^{-1}. The allylic structure of this complex was also supported by an examination of its NMR spectrum, which showed a doublet at 8.63 τ (3H, J=6 cps) for methyl protons on C_5, a singlet at 6.63 τ (3 H) for methoxy protons on C_4, a multiplet at 6.57 τ (1 H) for the proton on C_4, a doublet at 6.47 τ (1 H, $J_{1,2}$=10 cps) for the allylic proton on C_1, a singlet at 6.31 τ (3 H) for methyl protons of the ester group, a double doublet at 6.00 τ (1 H, $J_{2,3}$=10 cps and $J_{3,4}$=2 cps) for the allylic proton on C_3, and a triplet at 3.90 τ (1 H, J=10 cps) for the allylic proton on C_2. These spectral data suggest that

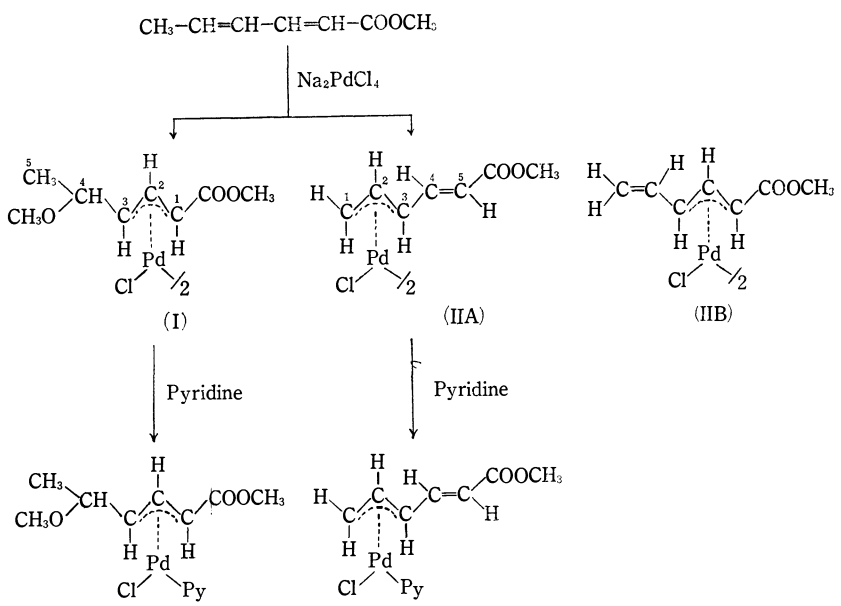

Fig. 1

1) S. D. Robinson and B. L. Shaw, *J. Chem. Soc.*, **1963**, 4806.

2) a) S. D. Robinson and B. L. Shaw, *ibid.*, **1964**, 5002. b) M. R. Churchill, *Chem. Commun.*, **1965**, 625; *Inorg. Chem.*, **5**, 1608 (1966).

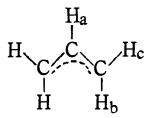

Fig. 2

the major product (I) is di-μ-chlorodi-[1-carbomethoxy-3-(1'-methoxyethyl) -π-allyl]-dipalladium. In addition, the proton on the center carbon atom (C_2) of the π-allyl system couples with the two trans protons on C_1 and C_3; their coupling constants were found to be both 10 cps. In the simple π-allyl complex (*cf.* Fig. 2), the trans coupling constant ($J_{a,b}$) between the proton on the center carbon and the proton on the terminal carbon is 11 cps and the cis coupling constant ($J_{a,c}$) is 7 cps.[3] Thus, it may be concluded that the orientation of the methoxyethyl and carbomethoxy groups in I is "*syn.*"

On the other hand, the minor product, [$C_{14}H_{18}O_4Cl_2Pd_2$], was less stable than the major product (I); it gradually decomposed in a solution to give a palladium mirror. In the infrared spectrum of this complex, there were no bands in the regions between 2810—2840 and 1080—1110 cm^{-1}, suggesting the absence of a methoxy group.[2a] Furthermore, the spectrum did not show the characteristic absorption bands due to a vinyl group. The ultraviolet absorption spectrum in ethanol did, however, show a strong absorption band at 211 mμ, suggesting the presence of a double bond conjugated with the ester group. These spectral data favor the conjugated structure (IIA) rather than the vinylic structure (IIB), formed simply by the loss of methanol from the structure (I). This structure was also supported by an examination of its NMR spectrum, which showed a doublet at 6.98 τ (1 H, $J_{1,2}=1.05$ cps) for the allylic terminal "*anti*" proton on C_1, a double doublet at 6.47 τ (1 H, $J_{3,4}=13$ cps and $J_{2,3}=10$ cps) for the allylic proton on C_3, a singlet at 6.33 τ (3 H) for methyl protons of the ester group, a doublet at 5.83 τ (1 H, $J_{1,2}=6.5$ cps) for the allylic "*syn*" proton on C_1, a multiplet at 4.04 τ (1 H) for the allylic center proton on C_2, a doublet at 3.74 τ (1 H $J_{4,5}=18$ cps) for the olefinic proton on C_5, and a double doublet at 2.60 τ (1 H, $J_{4,5}=18$ cps and $J_{3,4}=13$ cps) for the olefinic proton on C_4. The complex (IIA) seems to be derived from methyl sorbate by the activation of allylic hydrogen at the terminal methyl group, followed by eliminating hydrogen chloride,[4] rather than from the complex (I) by the loss of methanol, followed by a 1, 3 shift of the palladium atom.

Experimental

All the melting points are uncorrected. The infrared spectra were measured in KBr disks with a Hitachi EPI-S infrared spectrometer, while the ultraviolet absorption spectra were measured with a Hitachi recording spectrophotometer, model EPS-3T. The NMR spectra were recorded by a Varian Model A-60 instrument in deuterochloroform, using tetramethylsilane as an internal standard.

Reaction of Methyl Sorbate with Sodium Chloropalladite. Methyl sorbate (2.52 g) was added to a suspension of sodium chloropalladite trihydrate (7.0 g) in methanol (50 m*l*). After 20 hr, the metallic palladium thus deposited was removed by filtration, and then the brown filtrate was evaporated to dryness under reduced pressure. Chromatography in chloroform on an alumina column gave two complexes. The first complex eluted was di-μ-chlorodi-[1-carbomethoxy-3-(1'-methoxyethyl)-π-allyl]-dipalladium (1.10 g, 16.5 %). Recrystallization from cyclohexane gave yellow needles, mp 122—125°C (decomp.). λ_{max}^{EtOH}: 213 mμ (log ε 2.66). IR spectrum (KBr): 2820 (OCH_3), 1728 (ester), and 1098 cm^{-1} (OCH_3).

Found: C, 32.14; H, 4.77%; mol wt, 595 (in benzene). Calcd for $C_{16}H_{26}O_6Pd_2Cl_2$: C, 32.08; H, 4.67%; mol wt, 598.

The second complex eluted was di-μ-chlorodi-[1-(2'-carbomethoxy-ethenyl)-π-allyl]-dipalladium (0.09 g, 1.7%), yellow needles. Mp 116—119°C (decomp.). λ_{max}^{EtOH} 211 mμ (log ε 4.47). IR spectrum: 1720 cm^{-1} (ester).

Found: C, 31.22; H, 3.41%; mol wt, 529 (in benzene). Calcd for $C_{14}H_{18}O_4Pd_2Cl_2$: C, 31.43; H, 3.36%; mol wt, 534.

The Preparation of Chloro-(π-allyl)-pyridine-palladium Complexes. A solution of the chloro-bridged palladium complex (0.05 g) in dichloromethane (5 m*l*) was treated with a solution of pyridine (5% excess) in ether. After 10 min, the solvent was removed under reduced pressure, after which chromatography on alumina using chloroform afforded the expected product. The complexes below were prepared in this manner.

Chloro-[1-carbomethoxy-3-(1'-methoxyethyl)-π-allyl]-pyridine-palladium. Yellow crystal. Mp 128—132°C (decomp.).

Found: C, 41.47; H, 4.68; N, 3.81%. Calcd for $C_{13}H_{18}O_3NPdCl$: C, 41.25; H, 4.75; N, 3.70%.

Chloro-[1-(2'-carbomethoxy-ethenyl)-π-allyl]-pyridine-palladium. Yellow crystal. Decomp. p. 78—84°C (without melting).

Found: C, 41.85; H, 4.22; N, 4.18%. Calcd for $C_{12}H_{14}O_2NPdCl$: C, 41.59; H, 4.07; N, 4.04%.

3) M. L. Green and P. L. Nagy, "Advances in Organometallic Chemistry," Vol. II, ed by F. G. A. Stone and R. West, Academic Press, New York (1964), p. 331.

4) Recently, the preparations of π-allyl palladium complexes from α, β-conjugated carbonyl compounds have been reported.[5]

5) a) G. W. Parshall and G. Wilkinson, *Chem. & Ind.*, **1962**, 261; *Inorg. Chem.*, **1**, 896 (1962). b) J. Tsuji, S. Imamura and J. Kiji, *J. Am. Chem. Soc.*, **86**, 4491 (1964); J. Tsuji and S. Imamura, This Bulletin, **40**, 197 (1967). c) A. Kasahara, K. Tanaka and K. Asamiya, *ibid.*, **40**, 351 (1967).

A Study of the Charge-Transfer Complexes. VI. A Question on the Concept of the Weak Charge-Transfer Complexes*1

Taku MATSUO and Osamu HIGUCHI*2

Department of Organic Synthesis, Faculty of Engineering, Kyushu University, Hakozaki, Fukuoka

(Received August 18, 1967)

In the recent years, several criticisms have been made on the reliability of the equilibrium constant (K) and the extinction coefficient (ε) for weak charge-transfer (CT) complex as estimated by the Benesi-Hildebrand (B-H) equation or the modified ones.[1-4] The disbelief in the B-H equation has mainly come from the three facts: (1) the dependence of the K-value on the ratio between the concentrations of donor and acceptor molecules,[1] (2) the variation of the K-value with the wavelength of the absorption band which the B-H equation is applied to,[2,3] and (3) the inconsistent relationship between the K- and ε-values.[1,4] All of these criticisms may be summarized to indicate that the basic assumptions inherent to the B-H equation do not hold in the actual cases of weak CT complexes. In other words, the fundamental concept of weak CT complexes might have been in error. Dewar and Thompson, in this connection, have lately emphasized that the appearance of CT absorption band does not necessarily mean that the CT interaction is the main driving force in the formation of molecular complexes.[5] The present authors have reached similar conclusions as described below.

The CT absorption bands of tetracyanoethylene (TCNE) complexes with *p*-methylanisole (I) and *t*-butyl *p*-tolyl ether (II) have been measured in carbon tetrachloride. The ordinary B-H equation has been used to obtain the K- and $K\varepsilon$-values for the complexes as summarized in Figs. 1 and 2. If the K-values at the absorption maxima are compared, as usual, the TCNE complex with II is more stable than that with I. As to the CT bands themselves, on the other hand, the absorption maximum for the complex II is at considerably larger wave numbers than that for the complex I. This is a very peculiar situation. On the basis of the ordinary concept of CT complexes, it is expected that the more stable the complex becomes, the smaller the wave numbers at the absorption maximum are. The apparent contradiction to the expectation, as observed here, may be easily understood however if the associations are essentially due to the van der Waals forces as suggested by Dewar and Thompson.[5] If this assumption is correct, the CT absorption is expected to occur simply because the pair of donor- acceptor molecules are held at close distance where CT forces contribute additional stabilizing effects on the association. In the present case, the relative importance of CT interaction in the association may be considerably different between the two complexes.

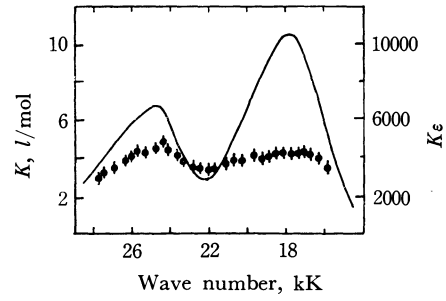

Fig. 1. The K- and $K\varepsilon$-values for TCNE complex of *p*-methylanisole. ●, K; —, $K\varepsilon$. The short, vertical line across the dot represents the standard deviation for the K.

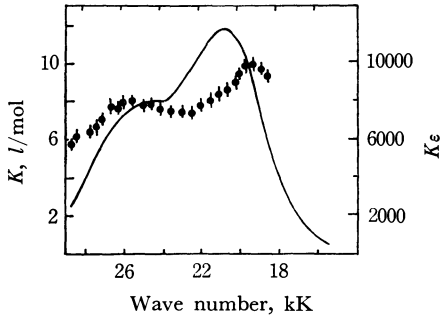

Fig. 2. The K- and $K\varepsilon$-values for TCNE complex of *t*-butyl *p*-tolyl ether. ●, K; —, $K\varepsilon$.

*1 Contribution No. 138 from the Department of Organic Synthesis, Faculty of Engineering, Kyushu University.

*2 Present address: Research Institute of Osaka-Gas Co., Ltd., Torishima-machi, Konohana-ku, Osaka-shi.

1) P. H. Emslie, R. Foster, C. A. Fyfe and I. Horman, *Tetrahedron*, **21**, 2843 (1965).
2) R. Foster and I. Horman, *J. Chem. Soc.* (B), **1966**, 171.
3) G. D. Johnson and R. E. Bowen, *J. Am. Chem. Soc.*, **87**, 1655 (1965).
4) S. Carter, J. N. Murrell and E. J. Rosch, *J. Chem. Soc.*, **1965**, 2048.
5) M. J. S. Dewar and C. C. Thompson, Jr., *Tetrahedron, Suppl.* No. 7, 97 (1966).

One of the present authors has found, in his study of the NMR solvent effects also, that the CT forces are merely complementary ones in the interaction between solvent benzene and polar solute such as maleic anhydride or *p*-benzoquinone.[6,7] It should be recalled further that the heats of formation for the weak CT complexes are of the order of a few kcal/mol, in general. Therefore, one can hardly distinguishes the energy of weak CT interaction from that of van der Waals interaction.

On the basis of the above discussion, the present authors propose a revised model for weak CT complexes as follows. The donor and acceptor molecules at close distance may be held each other mainly by the van der Waals-type forces. Then, the configurations (or mutual orientations) of the pair will follow a statistical distribution. The most stable configuration in the distribution is not necessarily the most favored one from the view points of CT interactions. The apparent CT bands in solution are considered to be originated from such assembly of the associated species. In short, the spectra may not be taken to represent a simple, rigid complex. The three problems about the B-H equation, as described in the beginning, have appeared to be reasonably solved by Foster and his associates who have assumed that the absorption of CT complexes deviates*3 from Beer's law.[1,2] It is suggested here that the deviation occurs simply because the relative importances among the configurations of the associated species vary with the change in the environment.

Experimental

Chemicals. *p*-Methylanisole and *t*-butyl *p*-tolyl ether were prepared from *p*-cresol by the use of dimethyl sulfate and *t*-butyl alcohol (together with concentrated sulfuric acid), respectively. The products were repeatedly purified by fractional distillations, and were identified by the IR and NMR spectra. The purities were proven to be above 99% by the gas chromatography. TCNE were prepared from malononitrile by the method of Carboni (mp 199—200°C).[8] Carbon tetrachloride was purified by the standard procedure.

Measurements. The spectra were measured under the temperature regulation (25±0.5°C) with a Hitachi model EPS-2U recording spectrophotometer. The *K*- and K_ε-values were obtained by the least-square-mean method as applied to the B-H equation.

6) Y. Nakayama and T. Matsuo, *Kogyo Kagaku Zasshi (J. Chem. Soc. Japan, Ind. Chem. Sect.)*, **69**, 1925 (1966).

7) T. Matsuo, *Can. J. Chem.*, **45**, 1829 (1967).

*3 The magnitude of the deviation has been suggested to depend on the wavelength.

8) R. A. Carboni, "Organic Syntheses," Coll. Vol. IV, p. 877 (1963).

On the Hydrothermal Behavior of the Solutions of Some Metal Complexes Observed by Means of Visual Autoclaving

Tominosuke KATSURAI and Kôzô SONE

Pilot Laboratory, Hiratsuka-Kanagawa and Department of Chemistry, Faculty of Science, Shizuoka University, Shizuoka

(Received August 28, 1967)

Visual autoclaving, a method of direct observation of autoclaving process, was worked out for the purpose of following the hydrothermal changes which take place during the course of autoclaving. The method turned out to be very effective, and the principal achievements so far obtained are (1) discovery of new examples of thermochromism,[1-3] (2) establishment of optimum concentration effect in hydrothermal precipitation,[4] (3) synthesis of a new magnetic compound Fe_3S_4, identified with the new mineral *greigite*, thiospinel of iron.[5,6] Study by means of this method is in progress. Some recent results which do not seem to have been reported so far are given in the following.

1. Ethylenediaminetetracetate (EDTA) Complexes. In order to see the effect of EDTA, a representative chelate-forming agent, on the hydrothermal behavior of heavy ions, *ca.* 0.1 M solutions of the chelate complexes of EDTA with bivalent Mn, Co, Ni, Cu, Zn, Pb, Hg and tervalent Fe were subjected to autoclaving at 200°C for one

1) T. Katsurai and M. Tanaka, *Kolloid-Z.*, **158**, 58 (1958).
2) T. Katsurai and K. Sone, *ibid.* **164**, 70 (1959).
3) M. Tanaka and T. Katsurai, *Naturwissenschaften*, **48**, 48 (1961).
4) T. Katsurai, *Kolloid-Z.*, **170**, 58 (1960); R. G. Robins, *J. Inorg. Nucl. Chem.*, **29**, 433 (1967).
5) S. Yamaguchi and T. Katsurai, *Kolloid-Z.*, **170**, 147 (1960).
6) B. J. Skinner, R. C. Erd and F. S. Grimaldi, *Am. Mineralogist*, **49**, 543 (1964); R. A. Berner, *J. Geol.*, **72**, 293 (1964); M. Uda, *Am. Mineralogist*, **50**, 1487 (1965).

hour.*[1] No noticeable change was observed in the solutions except in that of Hg(II) complex. No thermochromism was observed in the solutions of the complexes of Co(II), Ni(II) and Cu(II). This behavior is different from that of the simple salts of these bivalent metals, indicating the higher hydrothermal stability of the complex compounds. The stabilization caused by EDTA is particularly notable in the case of the Fe(III) complex, if we recall the fact that the solutions of the simple salts as well as those of the cyano-complexes of Fe(II) and of Fe(III) undergo decomposition above 100°C.[7]

A peculiar decomposition takes place in the case of Hg(II) complex. The colorless and transparent 0.1 M solution changes into a white suspension at 130°C. Coagulation is accelerated with the rise of temperature, and the suspension separates finally into two phases, *viz.* the shining Hg drops at the bottom and the brown supernatant liquid. Contrary to this, the 0.1 M solution of $HgCl_2$ remains intact at 200°C. This suggests that chelate formation diminishes the hydrothermal stability of the solution. In connection with this, it should be mentioned that the formation of metallic gold takes place when a Au(III) salt reacts with EDTA at room temperature.[8]

II. Halogeno-complexes of Some Noble Metals. In order to study the hydrothermal stability of noble-metal complexes, the 0.01 M and 0.1 M solutions of the following compounds were autoclaved up to 200°C and the resulting change was observed: Hexachloroplatinic(IV) acid $H_2[PtCl_6]$, potassium hexachloroplatinate(IV) $K_2[PtCl_6]$, tetrachloroauric(III) acid $H[AuCl_4]$, potassium tetrachloroaurate(III) $K[AuCl_4]$. It was found that all the solutions are thermochromic. The yellow color of these solutions turns red above 140°C. The change is enhanced with the rise of temperature. On cooling the colorations return to the original state. The change is thus reversible with respect to temperature.

The cause of the thermochromism might be attributed to the partial reversible hydrolysis of these chloro-complexes. We realize the facts herewith that the color of the solution of platinum(IV) chloride $H_2[Pt(OH)_2Cl_4]$ changes from greenish yellow to orange red with the progress of hydrolysis and that the solution of gold(III) chloride $H[Au(OH)Cl_3]$ is reddish yellow.[9] We see thus that the thermochrmomism of these noble-metal complexes and that of the solutions of Co(II), Ni(II) and Cu(II) chlorides are caused by different mechanisms. In the latter case, the cause is attributed to the formation of chloro complexes at elevated temperatures.

It should be added that the solutions of potassium tetrachloroplatinate(II) $K_2[PtCl_4]$ and potassium tetrachloropalladate(II) $K_2[PdCl_4]$ are both unstable above 100°C, and dark brown precipitates are formed at *ca.* 150°C.

*[1] The general formulas of the reagents: $Na_2Me^{II}(EDTA)\cdot 3\text{-}4H_2O$, $NaFe^{III}(EDTA)\cdot 2\text{—}3H_2O$. "Dotite" products were used.

7) T. Katsurai and T. Watanabe, *Sci. Papers Inst. Phys. Chem. Research (Tokyo)*, **13**, 89 (1930); **14**, 189 (1930).

8) W. A. Hynes, L. K. Yanowski and J. E. Ransford, *Mikrochem. ver. Microchim. Acta*, **35**, 160 (1950).

9) J. W. Mellor, A Comprehensive Treatise on Inorganic and Theoretical Chemistry, **3**, 592 (1923); **16**, 296 (1937).

Base-Catalyzed Polymerization of *p*-Vinyl Benzamide

Hiroyuki NAKAYAMA, Tsutomu SOGO, Toshinobu HIGASHIMURA and Seizo OKAMURA

Department of Polymer Chemistry, Kyoto University, Sakyo-ku, Kyoto

(Received September 5, 1967)

Recently, it has been reported[1,2] that *p*-vinyl benzamide [I] was polymerized by a basic catalyst to give the proton transfer type polymer [II]. In these studies, alkali metals and their alkoxides were used as catalyst. The object of this paper is to elucidate the effect of catalyst and solvent on the polymerization of *p*-vinyl benzamide.

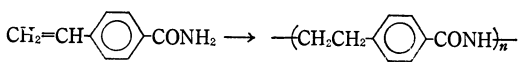

[I] [II]

p-Vinyl benzamide was synthesized from β-phenylethyl alcohol through *p*-carboxy-β-phenylethyl bromide[3] and *p*-vinyl benzoic acid[4]. The crude product was recrystallized from petroleum

1) K. Kojima, N. Yoda and C. S. Marvel, *J. Polymer Sci.*, A1-**4**, 1121 (1966).
2) S. Negishi and Y. Tamura, International Symposium on Macromolecular Chemistry (Tokyo-Kyoto) Preprints, **II**, 34 (1966).
3) E. L. Foreman and S. M. McElvain, *J. Am. Chem. Soc.*, **62**, 1435 (1940).
4) E. Osawa, K. Wang and O. Kurihara, *Makromol. Chem.*, **83**, 102 (1965).

Table 1. Polymerization of *p*-vinyl benzamide

Catalyst mmol/*l*		Solvent	$[M]_0$ mol/*l*	Time hr	Temp. °C	Polymer yield[a] %	*D*-ratio[b]	η_{sp}/c[c]
PhMgBr	32	Toluene	0.27	3	120	23	0	—
PhMgBr	32	Toluene	0.14	10	120	49	0	0.14
PhMgBr	32	Pyridine	0.29	3	120	6	0.07	—
PhMgBr	32	Pyridine	0.14	10	120	12	0.04	—
PhMgBr	32	Pyridine	0.07	5.5	120	31	0	—
n-BuLi	13	Toluene	0.27	10	80	3	0.10	—
n-BuLi	13	Toluene	0.27	10	100	4	0.07	—
n-BuLi	13	Toluene	0.14	10	120	12	0.09	0.34
n-BuLi	13	Pyridine	0.28	10	80	4	—	—
n-BuLi	13	Pyridine	0.26	10	100	4	0.13	—
n-BuLi	13	Pyridine	0.14	20	120	17	0.11	—

a) Acetone-insoluble product b) *D*-ratio; $D_{1500\ cm^{-1}}/D_{1660\ cm^{-1}}$

c) Inherent viscosity of a polymer was measured in conc. H_2SO_4 (1w/v%) after heating of the solution at 100°C for 1 hr.

ether/acetone mixture and benzene to give colorless powder, mp 171—172°C (Lit.[5] 168°C).

Catalyst was added to the test tube containing monomer, solvent and inhibitor for radical polymerization (*N*-phenyl-*β*-naphthylamine: 10 mg/10 m*l* solution) and then the test tube was sealed in a nitrogen atmosphere. After polymerization at constant temperature, the mixture was poured into a large amount of acetone. The polymer was removed by filtration, washed with acetone and dried at 40°C for 48 hr in vacuum.

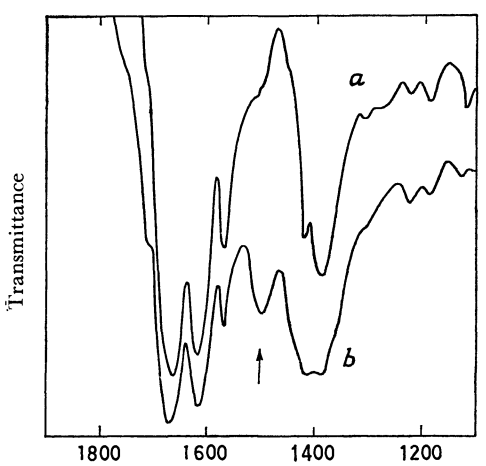

Fig. 1. IR spectra of poly(*p*-vinyl benzamide).
a: Polymer obtained by PhMgBr in toluene at 120°C. (D ratio=0)
b: Polymer obtained by BuLi in pyridine at 100°C. (D ratio=0.13)

5) D. Faulkner, C. E. Hollis and J. N. Mihe, Brit. Pat., 676376 (1952).

The results of polymerization catalyzed by *n*-butyllithium (*n*-BuLi) and phenylmagnesium bromide (PhMgBr) in toluene and pyridine are summarized in Table 1. It is estimated that the product is a polymer as the inherent viscosity of products was larger than 0.1. Moreover, the real values of inherent viscosity might be higher than the observed values since the polymer was to some extent decomposed in conc. H_2SO_4 at 100°C.

IR spectra of polymers obtained by two different polymerization conditions, that is, by *n*-BuLi in pyridine and by PhMgBr in toluene, are different in the absorption at about 1500 cm^{-1} as shown in Fig. 1. The absorption at 1500 cm^{-1} corresponds to secondary amide and the existence of this absorption shows that polymers contain the proton transfer unit [III]. On the other hand, the absence of the absorption at 1500 cm^{-1} indicates that the repeating unit of polymers may be the vinyl unit [IV].

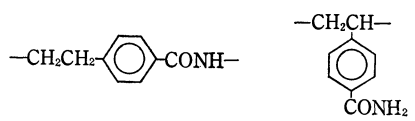

[III] [IV]

In this paper, the fraction of the proton transfer unit [III] in polymer was not measured quantitatively, but could be compared qualitatively by *D*-ratio[6] which was defined as a ratio of optical densities at 1500 to 1660 cm^{-1}. Hence, *D*-ratio of the polymer which consists of only the vinyl unit [IV] is zero, and *D*-ratio is higher if the polymer contains larger amount of the proton transfer

6) H. Nakayama, T. Higashimura and S. Okamura, *Kobunshi Kagaku (Chem. High Polymers, Japan)*, **23**, 433 (1966).

unit [III]. In fact, *D*-ratio of vinyl polymer obtained by heat polymerization was zero. *D*-Ratio of the polymer[2] consisting of almost the proton transfer unit [III] was 0.7 according to our calculation.

The *D*-ratios of polymers shown in Table 1 suggest the following facts. In the use of PhMgBr as a catalyst, the polymer was obtained by vinyl polymerization in toluene, but proton transfer polymerization occured to some extent in pyridine. In the case of *n*-BuLi, the proton transfer unit was present in the resultant polymer, and the polymer obtained in pyridine seemed to contain larger amount of the proton transfer unit than that in toluene.

These results are summarized as follows. First, the fraction of the proton transfer unit was very much smaller in the case of *p*-vinyl benzamide than in the case of acrylamide or methacrylamide under the same polymerization condition. Second, in the base-catalyzed polymerization of *p*-vinyl benzamide, there were the polymerization conditions under which proton transfer polymerization did not proceed. These facts may be due to that intramolecular proton transfer might hardly occur in the polymerization of *p*-vinyl benzamide containing *p*-phenylene group between an ethylenic double bond and amide group.

Mass Spectrometric Studies of α, β-Epoxyketones

Shini-ichi SASAKI, Hidetsugu ABE and Koji NAKANISHI

Department of Chemistry, Tohoku University, Katahira-cho, Sendai

and Yasuhiro ITAGAKI and Eiji WATANABE

Japan Electron Optics Laboratory Co., Ltd., Akishima, Tokyo

(Received September 7, 1967)

The mass spectra of epoxy compounds have already been published in some detail[1a-1d] and have proven to be of diagnostic use in the structure determination of natural compounds.[1a] We now extend our studies to several α, β-epoxyketones:

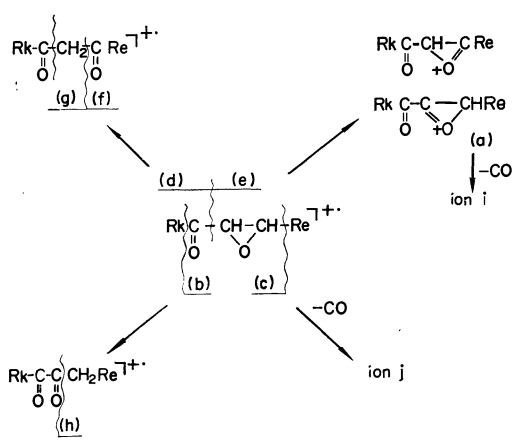

Scheme 1.

chalcone oxide (1), monodeuterated chalcone oxide (2), 2, 3-benzochalcone oxide (3), 4-methoxychalcone oxide (4), 1, 2-epoxy-1-phenyl-3-butanone (5), 2, 3-epoxy-1-phenyl-1-butanone (6) and *cis*- and *trans*-dypnone oxide (7 and 8).

The characteristic peaks observed in the spectra of these compounds are listed in Table 1 in which R_k and R_e represent the aromatic or aliphatic group adjacent to the carbonyl and epoxide group, respectively. The fragmentation of epoxy compounds are summarized in Scheme 1.

α, β-Epoxyketones (1—6), excepting the two dypnone oxides (7 and 8), lose one hydrogen radical to give ion (a), and groups R_k and or R_e to form ions (b) and (c), respectively. The CO-epoxide bond is also cleaved to afford cations (d) and (e). For instance, chalcone oxide (1) produces rather weak peaks at *m/e* 223 (M-1)(a), *m/e* 147 (M-C_6H_5)(b) and/or (c), *m/e* 119 (M-C_6H_5CO) (e) and a base peak at *m/e* 105 (C_6H_5CO) (d) as shown in Scheme 2, which is similar to that encountered in aromatic epoxides.[1b]

Ions (f) and (g) obviously arise from the β-diketone forms produced by rearrangement; similar ions (h) owe their geneses to the rearranged α-diketone form. It should be noted that the peaks (f) and (g) are not present in dypnone oxides, in which rearrangement to a β-diketone is not possible because of the extra methyl group. Furthermore, the spectrum of chalcone oxide (1) closely resembles

1) a) Y. Itagaki, T. Kurokawa, H. Moriyama, S. Sasaki and Y. Watanabe, *Chem. & Ind.*, **1965**, 1654; S. Sasaki, Y. Itagaki, H. Moriyama, K. Nakanishi, E. Watanabe and T. Aoyama, *Tetrahedron Letters*, **1966**, 623. b) E. H. Audier, J. F. Dupin, M. Fetizon and Y. Hoppilliard, *Tetrahedron Letters*, **1966**, 2077. c) N. S. Issacs, *Canad. J. Chem.*, **44**, 395 (1966). d) J. Baldas and Q. N. Porter, *Chem. Commn.*, **1966**, 571.

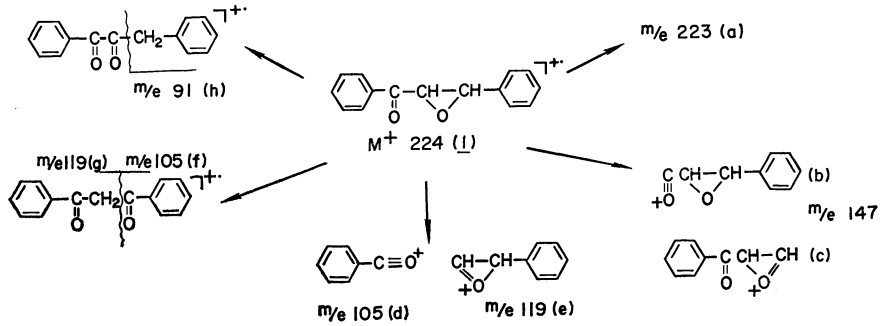

Scheme 2.

that of dibenzoylmethane[2] which corresponds to the rearranged β-diketone form. The formation of ions *m/e* 105 (f) and *m/e* 135 (f) in the mass spectra of (3) and (4), respectively, also support the occurence of the rearrangement mechanism. The composition of ions *m/e* 155 (d) and *m/e* 105 (f) of (3), and *m/e* 105 (d) and *m/e* 135 (f) of (4) was determined by high resolution mass spectrometry (Scheme 3).

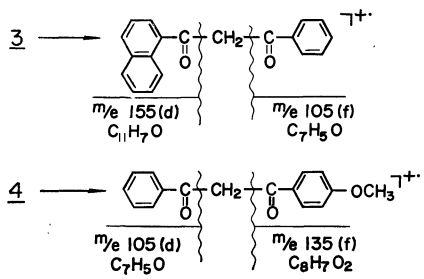

Scheme 3.

The ion *m/e* 105 decomposes further by successive elimination of carbon monoxide and acetylene to *m/e* 77 and *m/e* 51 as evidenced by appropriate metastable ions (*m/e* 56.5 and 33.8, respectively) in every case.

Compounds (5) and (6) carry alkyl groups, but their mass spectral fragmentations are almost identical with those of the chalcone oxides (1—4). The formation of ion *m/e* 105 (f) in (5), and ions *m/e* 43 (f) and 119 (g) in (6) are again due to hydrogen migration to form the corresponding β-diketones (Scheme 4).

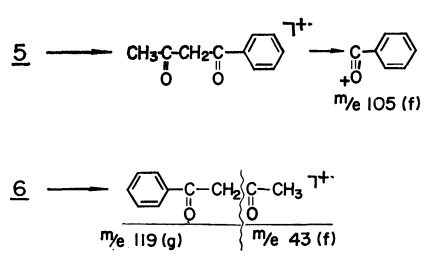

Scheme 4.

The conversion of epoxyketones to α-diketones is observed in the spectra of (1—5), in which tropylium ions are found at *m/e* 91, 92, 91, 121 and 91, respectively (Scheme 5).

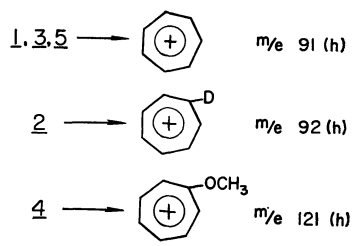

Scheme 5.

Similarly the *cis* and *trans* dypnone oxide (7 and 8), which give identical spectra, also rearrange to the corresponding α-diketone to give the ion (h) at *m/e* 105. The fact that the base peak at *m/e* 105 also involves the benzoyl ion (d) as well indicated by measurements of high resolution mass spectrometry (Scheme 6).

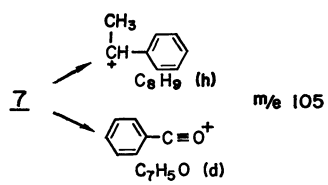

Scheme 6.

Finally, the spectra of α, β-epoxyketones (1—5, 7 and 8) show ions corresponding to the loss of HCO and CO from the molecular ion. For instance, the ions *m/e* 195 (M-CHO) and *m/e* 196 (M-CO) appear in the spectrum of chalcone oxide (1). The geneses of these peaks are accounted for by the repulsion of carbon monoxide[3] from the M-1 ion and carbon monoxide from the molecular ion.

2) J. H. Bowie, D. H. Williams, S.-O. Lawesson and G. Schroll, *J. Org. Chem.*, **31**, 1384 (1966).
3) J. H. Bowie, R. Grigg, D. H. Williams, S.-O. Lawesson and G. Schroll, *Chem. Commn.*, **1965**, 403.

TABLE 1. CHARACTERISTIC PEAKS OF α,β-EPOXYKETONES. Relative intensity % of the base peak are enclosed in parentheses

$R_kC(=O)CH(O)CHR_e$	M-1 (a)	M-R_k (b)	M-R_e (c)	$R_kC{\equiv}O^+$ (d)	M-$R_kC{\equiv}O$ (e)	$R_eC{\equiv}O^+$ (f)	M-$R_eC{\equiv}O$ (g)	$R_eCH_2^+$ (h)	M-CHO (i)	M-CO (j)
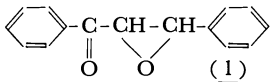 (1)	223 (4)	147*1′ (2)	147*1′ (2)	105*2 (100)	119 (1)	105*2′ (100)	119 (1)	91 (13)	195 (2)	196 (1)
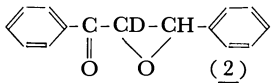 (2)	M-H 224 (18) M-D 223 (8)	148*3 (3)	148*3′ (3)	105*4 (100)	120*5 (2)	105*4′ (100)	120*5′ (2)	92 (7)	196 (1)	197 (1)
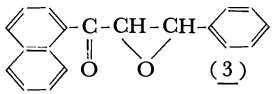 (3)	273 (11)	147 (2)	197 (2)	155 (97)	119 (3)	105 (32)	169 (3)	91 (12)	245 (2)	246 (2)
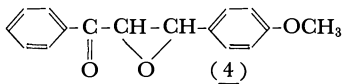 (4)	253 (2)	177 (7)	—	105 (100)	149 (9)	135 (5)	— —	121 (50)	225 (1)	226 (3)
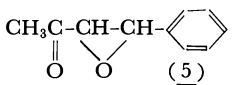 (5)	161 (8)	147 (5)	85 (5)	43 (95)	—	105 (10)	—	91 (100)	133 (4)	134 (1)
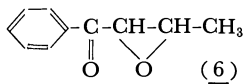 (6)	161 (16)	—	147 (12)	105 (100)	—	43 (5)	119 (1)	29 (9)	—	—
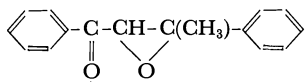 trans (7), cis (8)	—	—	—	105*6 (100)	133 (2)	—	—	105*6′ (100)	209 (2)	210 (12)

The ions marked with *1 and *1′ have the same mass units and are most probably originated from different parts of the molecular ion. Then the same mass and intensity are listed in this table. The pairs of ions marked with *2, *2′; *3, *3′; *4, *4′; *5, *5′ and *6, *6′ are listed in this manner.

Experimental

All the samples were synthesized according to known procedures. For instance, 4-methoxychalcone oxide (4) was prepared by the epoxidation of 4-methoxychalcone with alkaline hydrogen peroxide.[4] Monodeuterated chalcone oxide (2) was synthesized by the condensation of ω-d_3-acetophenone and benzaldehyde, following the epoxidation with hydrogen peroxide, mp 52—54°C.

Mass spectra were obtained with a Hitachi RMU-6D Mass Spectrometer, with an energy of 70 eV and an 80 μA ionizing current. The temperature of ion source was 250°C. High resolution mass spectra were dedetermined with a JMS-OIS Mass Spectrometer. The temperature of ion source 130—150°C, ionizing voltage 25—40 eV, ion accl. volt. 7.5 kV, and exposure 3×10^{-11} coulomb.

4) E. Weitz, A. Scheffer, *Ber.*, **54**, 2335, 2339 (1921).

Exact masses and compositions of ions

2,3-Benzochalcone oxide (3)

m/e observed	*m/e* calculated	composition
155.048	155.049	$C_{11}H_7O$
105.033	105.034	C_7H_5O

4-Methoxychalcone oxide (4)

m/e observed	*m/e* calculated	composition
105.034	105.034	C_7H_5O
135.046	135.044	$C_8H_7O_2$

Dypnone oxide (7)

m/e observed	*m/e* calculated	composition
105.070	105.070	C_8H_9
105.033	105.034	C_7H_5O

The authors (S.S. and K. N.) are grateful to the Toyo Rayon Company for the grant to purchase the RMU-6D mass spectrometer.

Composition of Fayalite and Its Standard Free Energy of Formation

Kenzo KITAYAMA and Takashi KATSURA

Department of Chemistry, Faculty of Science, Tokyo Institute of Technology, Ookayama, Meguro-ku, Tokyo

(Received September 19, 1967)

Data on fayalite (Fe_2SiO_4) stability have previously been studied by Schenck, Franz, and Laymann[1] at 900°C, and by Cirilli[2] at 900, 1000, and 1100°C, both controlled by the CO_2/CO equilibria in a gas phase co-existing with fayalite, silica, and metallic iron. These data have summarized by Richardson, Jeffes, and Withers,[3] and they proposed a linear free energy equation on the basis of the data obtained by Schenck *et al.* Pitzer and Brewer[4] also calculated the free energy function of fayalite based on H°_{298}. Recently Taylor and Schmalzried[5] determined the free energy of formation of fayalite by electromotive-force measurements between 900 and 1100°C, and they recalled a complication met with the formation of solid solutions at high temperatures.

Schwerdtfeger and Muan[6] determined the equilibrium ratio of CO/CO_2 of a gas phase co-existing with fayalite, silica and metallic iron, and calculated the standard free energy of formation of fayalite at temperatures of 1000, 1100, and 1150°C. Berliner and Shapovalova[7] determined the equation, $\Delta G^\circ = -135{,}320 + 33.20\,T$, for the reaction (3) which will be seen in later, on the basis of the reduction of fayalite by H_2 gas.

The present objectives are first to ascertain whether or not there exists an appreciable composition range in fayalite within the ternary system FeO-Fe_2O_3-SiO_2, and then to determine the standard free energy of formation of fayalite at temperatures slightly below the solidus after finding an equilibrium oxygen partial pressure obtained by a CO_2/H_2 gas mixture.

Experimental

Reagent grade chemicals are served as starting materials. Ferric oxide is heated at 900°C and silicic acid is heated at 1300°C for several hours in a global furnace. The desired amounts of the dry oxides are mixed and ground for several hours. Approximately a 20 g of each mixture is then heated in a platinum crucible in the globar furnace at 1300°C for 10—24 hr. The sintered mass is re-ground and re-heated at the same temperature for several hours. From the new sintered mass cut a disc weighing approximately 2 g and with a central bore for suspending the disc by

1) Von R. Schenck, H. Franz and A. Laymann, *Z. anorg. u. allgem. Chem.*, **206**, 129 (1932).
2) V. Cirilli, *Gazz. Chim. Ital.*, **76**, 331 (1946).
3) F. D. Richardson, J. H. E. Jeffes and G. Withers, *J. Iron Steel Inst.*, **166**, 213 (1950).
4) K. S. Pitzer and L. Brewer, "Thermodynamics," 2nd Ed., McGraw-Hill, New York (1961).
5) R. W. Taylor and H. Schmalzried, *J. Phys. Chem.*, **68**, 2444 (1964).
6) K. Schwerdtfeger and A. Muan, *Trans. AIME*, **236**, 201 (1966).
7) L. D. Berliner and R. D. Shapovalova, *Zh. Fiz. Khim.*, **40**, 2905 (1966).

means of a thin platinum wire from one beam of an analytical balance.

Pellets consisting of fayalite-silica mixtures are kept at chosen constant temperature and chosen levels of oxygen partial pressure until equilibrium is attained.

Composition changes of the sample in response to changes in oxygen partial pressure are determined by both thermogravimetric and wet chemical analyses of quenched samples. Phases present are determined by microscopic and X-ray examination of quenched samples. The apparatus used in this study are the same as those used in a previous work.[8]

For determining the free energy of formation of fayalite, reagent grade chemicals are used without purification as starting materials. Ferric oxide is reduced to ferrous at 1200°C in an atmosphere consisting of CO_2/H_2 mixed gas ($CO_2/H_2=1$). The ferrous oxide is stoichiometrically mixed with silica to prepare fayalite. The mixtures are melted in the same atmosphere at 1300°C in a 80% platinum - 20% rhodium container which is previously saturated with iron. The melts are quenched and pulverized in an agate mortar. The powder (fayalite) is mixed with silica to avoid excess free iron oxide. The mixture is again melted, quenched and pulverized. The fayalite-silica powder is caked at 1154°C in the CO_2-H_2 atmosphere in the same container.

The standard quenching technique is adopted for the present study under controlled atmospheric conditions. The cakes are kept at chosen temperature and chosen levels of oxygen partial pressure. After 24 hr, these samples are quenched and metallic iron separated is ascertained by microscopic and dilute hydrochloric acid method. After repeating the procedure, a CO_2/H_2 ratio just appearing the metal iron is determined at four temperatures. The oxygen partial pressures corresponding to the CO_2/H_2 ratio are measured directly by a solid electrolyte. Details of the measurement have been reported by Katsura and Hasegawa.[9]

Results and Discussion

Composition of Fayalite. The FeO content of fayalite present in sample A through D after equilibration at various oxygen partial pressures at 1125, 1156, and 1170°C are listed in Table 1. Within the limit of experimental error (±0.4 mol%), the composition of fayalite is constant and corresponds to the formula $2FeO \cdot SiO_2$ around 1150°C

Free Energy of Formation of Fayalite. Phase equilibrium studies previously reported for the system Fe-Si-O (Bowen and Schairer[10]: Darken[11]: Muan[12]) are useful for defining the

TABLE 1. COMPOSITION OF FAYALITE AS A FUNCTION OF OXYGEN PRESSURE AT VARIOUS TEMPERATURES

Temp. °C	Mixture	Starting composition (mol%) Fe_2O_3	Starting composition (mol%) SiO_2	Time hr	log P_{O_2} atm	Mole% FeO in Mixture	Calculated Mole% FeO in Fayalite phase
1125	A	44.4	55.6	41	−10.62	61.1	66.3
				18	−11.56	61.3	66.4
				15	−12.32	61.3	66.4
				12	−12.73	61.3	66.4
	C	36.1	63.9	12	−12.75	53.0	66.6
				12	−12.80	53.0	66.6
1156	A	44.4	55.6	41	−11.57	61.2	66.3
				29	−12.43	61.4	66.6
	C	36.1	63.9	18	−11.28	53.0	66.6
				10	−11.52	53.0	66.6
				11	−11.67	53.0	66.6
				12	−12.16	53.0	66.6
1170	A	44.4	55.6	38	−10.11	61.1	66.3
	B	41.1	58.9	25	−12.08	58.2	66.4
				14	−12.33	58.3	66.5
	D	27.3	72.7	28	−11.39	42.8	66.4
				17	−12.34	42.9	66.7
				9	−12.40	42.9	66.7

8) T. Katsura and S. Kimura, This Bulletin, **38**, 1664 (1965).
9) T. Katsura and M. Hasegawa, *ibid.*, **40**, 561 (1967).
10) N. L. Bowen and J. F. Schairer, *Am. J. Sci.*, **24**, 177 (1932).
11) L. S. Darken, *J. Am. Chem. Soc.*, **70**, 2046 (1948).
12) A. Muan, *Trans. AIME*, **7**, 965 (1955).

TABLE. 2. OXYGEN PARTIAL PRESSURE $P_{O_2}(1)$ AND $\Delta G°(1)$ TOGETHER WITH PREVIOUS DATA AT VARIOUS TEMPERATURES

Temperature °C	log $P_{O_2}(1)$ atm present study	$\Delta G°(1)$ kcal			
		present study	Schenck	Taylor	Schwerdtfeger
1129	−13.40±0.05	−86.0±0.3	−87.1	−86.2	−86.6
1144	−13.14	−85.2	−86.6	−85.7	−86.1
1160	−12.87±0.01	−84.4±0.1	−86.0	−85.2	−85.5
1174	−12.77±0.02	−84.6±0.1	−85.5	−84.7	−85.0

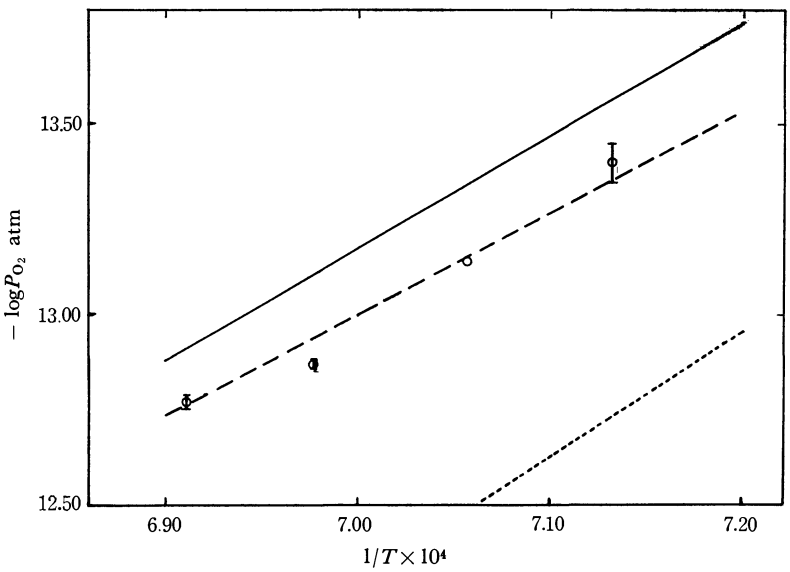

Fig. 1. Relation between oxygen partial pressures and reciprocal absolute temperatures in the present study. Schenck's data and Darken and Gurry's data for Eq. (2) are also represented for comparison.
—— from Schenck *et al.*, ····· from Darken and Gurry, ---- present study

upper temperature limit for the present investigation. An application of the phase rule to the various phase assemblages show that in composition area, where three crystalline phases coexist in equilibrium with, the oxygen pressure of the gas phase must be fixed. For instance, in the two areas where silica (tridymite) + fayalite + iron and fayalite + wüstite + iron coexist in equilibrium, different oxygen partial pressures, $P_{O_2}(1)$ and $P_{O_2}(2)$ respectively, prevail at equilibrium. The standard free energy changes, $\Delta G°(1)$ and $\Delta G°(2)$, are determined from the oxygen partial pressures in the isothermal invariant equilibrium as follow:

$$2Fe + SiO_2 + O_2 = Fe_2SiO_4 \quad (1)$$

$$K = a_{Fe_2SiO_4}/a^2_{Fe_2}\cdot a_{SiO_2}\cdot P_{O_2}(1)$$

$$\Delta G°(1) = 2.303\boldsymbol{R}T\log P_{O_2}(1)$$

and

$$1.90Fe + O_2 = 2Fe_{0.95}O \quad (2)$$

$$\Delta G°(2) = 2.303\boldsymbol{R}T\log P_{O_2}(2)$$

By substracting of Eq. (2) from Eq. (1) the standard free energy of formation of fayalite according to the equation

$$0.1Fe + 2Fe_{0.95}O + SiO_2 = Fe_2SiO_4 \quad (3)$$

is calculated as:

$$\Delta G°(3) = 2.303\boldsymbol{R}T\log P_{O_2}(1)/P_{O_2}(2)$$

The experimental results obtained are summarized in Table 2 together with Schenck's, Taylor's and Schwerdtfeger's data for comparison, while they are illustrated graphically in Fig. 1 with the width of experimental errors.

The standard free energy changes of reaction (1) are −86.0, −85.2, −84.4 and −84.6 kcal at temperatures 1129, 1144, 1160 and 1174°C, respectively. The values at each temperature in Table 2 and Fig. 1 are a mean for three experimental results except for the value at 1144°C, and we get an equation as a function of temperature:

$$\Delta G°(3) = -122{,}000+26.0\,T \text{ (cal)}$$

by means of the method of least squares.

The oxygen partial pressures for Eq. (2) obtained from Darken and Gurry's data[13] is shown in the second column of Table 3. Using these values for Eq. (2) and the present results for Eq. (1), $\Delta G°(3)$, that is the standard free energy of formation of fayalite relative to the oxide components SiO_2 and wüstite, is easily calculated. In the Table 3, $\Delta G°(3)$ is indicated at various temperatures together with other two experimental results. $\Delta G°(3)$ varies between -2.8 and -3.4 kcal in the present temperature range. Except for the value at 1160°C, the change in free energy of formation of fayalite relative to oxides is nearly constant (about -3.3 kcal) regardless of the temperature in this experiment. According to recent tabulations by Kelley,[14] $\Delta G°(3)$ varies approximately linearly between -2.3 and -1.7 kcal in the temperature range 1000 to 1150°C. His values are very larger than those in Table 3. The present value, -3.3 kcal, is in fairly good agreement with Taylor's.

Table 3. Oxygen partial pressures for Eq. (2) and $\Delta G°(3)$ together with previous data at various temperatures

Temp. °C	log $P_{O_2}(2)$ atm*	$\Delta G°(3)$, kcal		
		Present study	Taylor	Schwerdtfeger
1129	−12.87	−3.4	−3.6	−4.0
1144	−12.66	−3.1	−3.6	−4.0
1160	−12.45	−2.8	−3.6	−3.9
1174	−12.26	−3.4	−3.5	−3.8

* from Darken and Gurry

The authors wish to express their sincere gratitude to Professor Arnulf Muan, the Pennsylvania State University, who initiated the present study. The authors also thank Professor Iwaji Iwasaki, Tokyo Institute of Technology, for the encouragement throughout the study.

13) L. S. Darken and R. W. Gurry, *J. Am. Chem. Soc.*, **67**, 1398 (1945).
14) K. K. Kelley, *U. S. Bur. Mines, Rept. Invest.* No. 5901 (1962).

SHORT COMMUNICATIONS

A New Monocyano Cobalt(III) Complex

Nobufumi MAKI, Takahiro ITOH and Shukichi SAKURABA

Department of Chemistry, Faculty of Engineering, Shizuoka University, Johoku, Hamamatsu

(Received December 4, 1967)

Previously, dicyano-cobalt(III) complex, K-$[Co(CN)_2dg_2]\cdot 3/2H_2O$, was reported to have been prepared and reduced to a cobalt(I) complex polarographically.[1,2]

In the present communication, the preparation of the monocyanobis(dimethylglyoximato)ammine-cobalt(III) complex, $[Co(CN)dg_2(NH_3)]\cdot 1/2H_2O$ (trans-form), is described and was found to undergo stepwise reduction to a cobalt(0) complex at the dropping mercury electrode (DME).

The complex was prepared by the following method: To 15.0 g of $[Co(CN)(OH_2)(NH_3)_4]Cl_2$[3] in 150 m*l* of water was added 14.4 g dimethylglyoxime. The mixture was heated on a water bath (85°C) for three hours. The reaction proceeds, evolving ammonia, according to the following:

$$[Co(CN)(OH_2)(NH_3)_4]^{2+} + 2dgH \rightarrow [Co(CN)dg_2(NH_3)] + 3NH_3.$$

Every half hour during the reaction, 5—7 g of ammonium acetate was added to the solution. In total, 20 g of ammonium acetate was used. Lustrous orange-yellow needle-shaped crystals (17.2 g) separated from solution when it was allowed to stand. The product was filtered and washed with 80% ethanol to eliminate traces of unreacted dimethylglyoxime. The yield was above 82%. The complex was recrystallized from hot water (85°C) containing acetic acid.

Found: Co, 17.41; C, 32.08; N, 24.83; H, 5.43%. Calcd for $[Co(CN)dg_2(NH_3)]\cdot 1/2H_2O$: Co, 17.37; C, 31.83; N, 24.77; H, 5.64%.

The complex gave rise to the well-defined waves of three steps in 0.5 M sodium sulfate supporting electrolyte containing 0.007% Triton X100 at the DME (Fig. 1). For each, the limiting current was diffusion-controlled. The diffusion current and the concentration of the complex was linearly related in the concentration range between $5\cdot10^{-4}$ and 10^{-3} M. The first, second and third waves, each corresponding to an acceptance of one electron, represents the reduction of Co(III)→Co(II), Co(II)→Co(I) and of Co(I)→Co(0), respectively.

Table 1 shows the half-wave potentials of the

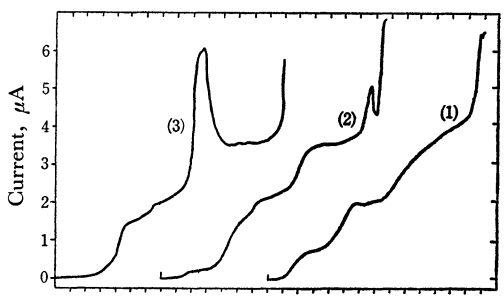

Fig. 1. The current-potential curves for the [Co-(CN)$dg_2(NH_3)$] complex obtained at 10^{-3} M in 0.5 M Na_2SO_4 solution (25°C).
(1) No suppressor
(2) In the presence of 0.0035% Triton X100
(3) 0.0070% Triton X100
Measured from −0.40 V *vs.* SCE.

TABLE 1. HALF-WAVE POTENTIALS OF THE WAVES FOR THE MONOCYANO-COBALT(III) COMPLEXES (25°C)

Complex	$E_{1/2}$ of 1st wave	$E_{1/2}$ of 2nd wave	$E_{1/2}$ of 3rd wave
$[Co(CN)dg_2(NH_3)]$*	−0.65	−0.80	−1.05
$[Co\,dg_2(NH_3)_2]^+$	−0.43	−0.83	−1.05
$[Co(CN)_2dg_2]^-$	−1.12($Co^{III}\rightarrow Co^{I}$)		

* 0.0035% TritonX100 0.5 M Na_2SO_4 supporting salt
V *vs.* SCE.

waves for the cobalt(III) complexes of the monocyano-series in 0.5 M sodium sulfate solution. The oscillopolarogram obtained with a Polaroscope P 576 indicates three cuts on both the cathodic and anodic branches. Namely, the process of oxidation occurs in three steps, almost the same as in reduction. This implies that the cobalt(0) complex exists in solution.

The net processes of the electrode reaction in the following are considered to be most plausible:

$$\begin{array}{ccc} [Co^{III}(CN)dg_2(NH_3)] & & \\ \downarrow & & \\ [Co^{II}(CN)dg_2(NH_3)]^- & \rightarrow & [Co^{I}(CN)dg_2(NH_3)]^{2-} \\ \downarrow & & \downarrow \\ [Co^{II}(CN)dg_2(OH_2)]^- & \rightarrow & [Co^{0}dg_2]^{2-} \\ & & \downarrow \\ & & Co \end{array}$$

1) N. Maki, This Bulletin, **38**, 2013 (1965).
2) N. Maki, *Nature*, **188**, 227 (1960).
3) H. Siebert, *Z. anorg. u. allgem. Chem.*, **327**, 63 (1964).

The Absolute Configuration of the Tris(trimethylenediamine)cobalt(III) Ion, $(-)_D$-[Co tn_3]$^{3+}$

Yoshihiko SAITO, Teruo NOMURA and Fumiyuki MARUMO

The Institute for Solid State Physics, The University of Tokyo, Roppongi, Minato-ku, Tokyo

(Received December 4, 1967)

In a series of our investigation on the absolute configurations of tris(bidentate)cobalt(III) complex ions,[1-3] the absolute configuration of tris(trimethylenediamine)*1cobalt(III) ion, [Co tn_3]$^{3+}$, has been determined. The crystal structure of $(-)_D$-tris(trimethylenediamine)cobalt(III) bromide monohydrate, $(-)_D$-[Co tn_3]$Br_3 \cdot H_2O$, has been determined by three-dimensional Fourier methods.[4] The final R-value is 0.113 for 1890 observed reflections. The crystals were kindly supplied by Dr. Woldbye of the Technical University of Denmark. They are monoclinic with the space group $P2_1$: $a=16.274\pm0.009$ Å, $b=7.863\pm0.015$ Å, $c=9.489\pm0.005$ Å and $\beta=126.42°\pm0.06°$ (Cu$K\alpha$=1.5418 Å). A perspective drawing of the complex ion is presented in Fig. 1. The complex ion has

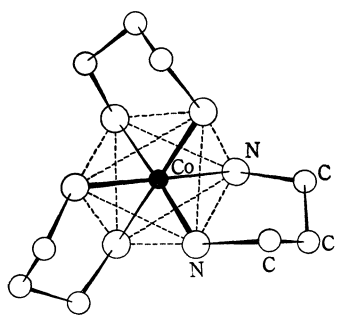

Fig. 1. A perspective drawing of the complex ion, $(-)_D$-[Co tn_3]$^{3+}$.

approximately a three-fold axis of rotation through the central cobalt atom. The three six membered Co-tn rings are nearly identical and take chair form. The chelate ring is rather flattened out, clearly owing to the strong H-H repulsion. Bond angles ∠CoNC are much larger than the normal tetrahedral angle, the average value being 117.4°. But the average value of ∠NCC and ∠CCC is 112.8°. The avarage ∠NCoN is 94.5°. The bond distances within the chelate ring are quite normal.

The absolute configuration of the complex ion was determined by using absorption edge technique.[5]

Some of the calculated intensities and observed relations between $I(hkl)$ and $I(\bar{h}\bar{k}l)$, the latter being equivalent to $I(\bar{h}\bar{k}\bar{l})$ because of the symmetry of the space group, are compared in Table 1.

TABLE 1. DETERMINATION OF THE ABSOLUTE CONFIGURATION

Indices $h\ k\ l$	$F_c^2(hkl)$	obs.	$F_c^2(\bar{h}\bar{k}l)$
1 1 $\bar{2}$	2284	>	2174
1 3 3	380	>	369
2 3 3	374	>	310
2 3 $\bar{3}$	394	>	319
5 2 $\bar{5}$	576	<	654
$\bar{3}$ 1 2	1287	<	1707
$\bar{4}$ 1 3	331	<	534
$\bar{5}$ 1 4	241	>	161

From these accordances in the table, it may be found that the complex ion, [Co tn_3]$^{3+}$, shown in Fig. 1 corresponds to the laevorotatory form with respect to the Na D lines. Thus the absolute configuration of $(-)_D$-[Co tn_3]$^{3+}$ can be represented by Δ according to the nomenclature proposed at the Meeting of the Commission on Inorganic Nomenclature of IUPAC, held at Beckenried, Switzerland in 1966. This configuration is enantiomeric to that assigned on the basis of the sign of the prominent Cotton effect.[6] The ORD and CD of [Co tn_3]$^{3+}$ have already been measured by Woldbye.[8] A simple empirical rule[8] relating the sign of the longer wavelength CD band and the absolute configuration of the chelate ring about the metal atom seems to hold in this case, too.

*1 tn: 1, 3 diaminopropane, $H_2N(CH_2)_3NH_2$

1) Y. Saito, K. Nakatsu, M. Shiro and H. Kuroya, *Acta Cryst.*, **8**, 729 (1955), This Bulletin, **30**, 795 (1957).
2) Y. Saito, H. Iwasaki and H. Ota, *ibid.*, **36**, 1543 (1963).
3) H. Iwasaki and Y. Saito, *ibid.*, **39**, 92 (1966).
4) T. Nomura, F. Marumo and Y. Saito, *ibid.*, To be published.
5) J. M. Bijvoet, A. F. Peerdeman and A. J. van Bommel, *Nature*, **168**, 271 (1951).
6) R. D. Gillard and G. Wilkinson, *J. Chem. Soc.*, **1964**, 1368.
7) F. Woldbye, ORD of transition metal complexes, European Research Office, U. S. Army, Frankfurt a. M. (1959), Record of Chemical Progress, **24**, 197 (1963).
8) A. J. McCaffery, S. F. Mason and B. J. Norman, *Chem. Commn.*, **1965**, 49.

Vinyl Polymerization. 205.*[1] Polymerization of Methyl Methacrylate in the Presence of Cellulose Triacetate and Water

Minoru IMOTO, Kiichi TAKEMOTO and Tadashi TANIMOTO

Department of Applied Chemistry, Faculty of Engineering, Osaka City University, Sumiyoshi-ku, Osaka

(Received December 6, 1967)

In the series of our papers, we have shown that some sorts of macromolecule could initiate the polymerization of methyl methacrylate (hereafter abridged as MMA) by radical mechanism in the presence of water. It was concluded that the effective macromolecules contained -OH or -NHCO- groups.[1-7] In the present communication, the polymerization of MMA was carried out with the system of the partially or completely acetylated cellulose and water. The polymerization was found to be able to be initiated even with cellulose triacetate in which no -OH groups were contained.

Partially and completely acetylated cellulose fibers with different grade of acetylation were prepared by the reaction of commercial tissue paper (99.0% α-cellulose) in benzene with a mixture of acetic acid, acetic anhydride and sulfuric acid.

The reaction was carried out under stirring at 40°C in the range of 2—48 hr. Degree of acetylation was measured by alkaline hydrolysis.[8]

Polymerization was carried out in sealed tubes in dark, in the same manner as described earlier.[1] 0.2 g of acetylated cellulose, 10.0 m*l* of water and 4.68 g of MMA were charged in each tube, and the reaction was carried out for 5 hr at 85°C.

Figure 1 shows the results of the polymerization of MMA initiated with this system. It can be seen from the figure that the polymerization could proceed even in the case where cellulose triacetate having no hydroxy groups was chosen as a macromolecule, and that the total conversion resulted in almost the same amount as these by partially acetylated cellulose. These results differed from the case of polymerization initiated with water and partially hydrolyzed polyvinyl acetate system, where the completely acetylated polyvinyl acetate and completely hydrolyzed polyvinyl alcohol showed no initiating abilities.[9]

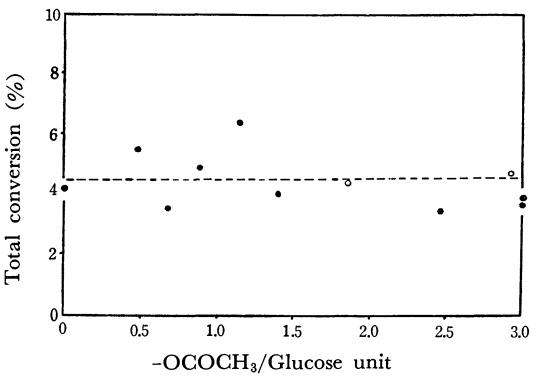

Fig. 1. Polymerization of MMA in the presence of acetylated cellulose fiber and water: Relationship between total conversion and the degree of acetylation of cellulose (85°C, 5 hr).
● Averaged value in two measurements,
○ Value in one measurement,
◐ Acetylation was repeated twice.

In 1961, Ceresa carried out a block copolymerization based on the vapor phase swelling of cellulose acetate (degree of acetylation 1.35 per glucose unit) with acrylonitrile.[10] Differed from his experiment, a large amount of water was present in our reaction system. Although the initiation mechanism by the system of cellulose or cellulose triacetate and water is not yet clear, it may be sure that the Ceresa's mechanism could not be applied to the present experiment from the formerly mentioned considerations[1-7] which include the homogeneous initiation of MMA in the presence of water and low molecular polyvinyl alcohol or soluble starch.

*1 Part 204 of the series: H. Yano, K. Takemoto and M. Imoto, *J. Macromolecular Chem.*, in press.

1) M. Imoto, M. Kondo and K. Takemoto, *Makromolekulare Chem.*, **89**, 165 (1965).
2) M. Imoto, M. Kondo and K. Takemoto, *Kogyo Kagaku Zasshi (J. Chem. Soc. Japan, Ind. Chem. Sect.)*, **68**, 1302 (1965).
3) M. Kondo, K. Yamada, K. Takemoto and M. Imoto, This Bulletin, **39**, 536 (1966).
4) M. Imoto, K. Takemoto and M. Kondo, *Makromolekulare Chem.*, **98**, 74 (1966).
5) M. Imoto, K. Takemoto and T. Otsuki, *ibid.*, **104**, 244 (1967).
6) M. Imoto, K. Takemoto, H. Azuma, N. Kita and M. Kondo, *ibid.*, **107**, 188 (1967).
7) T. Nakaya, H. Sutoh, K. Takemoto and M. Imoto, *Kogyo Kagaku Zasshi (J. Chem. Soc. Japan, Ind. Chem. Sect.)*, **70**, 1949 (1967).
8) "Cellulose Handbook," ed. by H. Sobue, Asakura Shoten, Tokyo (1958), p. 295, 307.
9) M. Imoto, K. Takemoto, A. Okuro and M. Izubayashi, *Makromolekulare Chem.*, in press.
10) R. J. Ceresa, *Polymer*, **2**, 213 (1961).

Insertion of Isonitrile into Alkyl-Nickel Bonds

Yasuhiro YAMAMOTO, Hiroshi YAMAZAKI and Nobue HAGIHARA

The Institute of Scientific and Industrial Research, Osaka University, Sakai, Osaka

(Received December 7, 1967)

There are many examples of the insertion reactions of carbon monoxide and olefins into transition metal-carbon σ-bonds. On the other hand, there has been no such example of isonitriles, although they are known as ligands similar to carbon monoxide.

In the course of our studies of the catalytic polymerization of isonitriles with transition metal complexes,[1] we found that cyclohexyl isocyanide could be inserted into nickel-carbon σ-bonds. Now we wish to report on the stable complexes derived from such reactions.

The treatment of triphenylphosphine-π-cyclopentadienyl methyl nickel[2] in benzene with cyclohexyl isocyanide at room temperature gave a red-brown solution. After the evaporation of the solvent, the residue was separated on an alumina column, using benzene-ether (2 : 1) as the eluant. The red-brown fraction was then concentrated, and the residue was crystallized from hexane to give red-brown crystals (I) (mp 72.5—73.5°C (decomp). Found: C, 67.08; H, 8.66; N, 7.70%. Calcd for $C_{20}H_{30}N_2Ni$: C, 67.24; H, 8.47; N, 7.84%.). The IR spectrum of I (KBr disk) showed the existence of a carbon-nitrogen triple bond (2140 cm^{-1}) and a double bond (1618 cm^{-1}). The NMR spectrum*1 indicated the existence of a cyclopentadienyl group (singlet at 4.72 τ, 5H), a methyl group (singlet at 7.73 τ, 3H), and a cyclohexyl group (broad bands at 6.36 τ, 2H and $\sim$8.5 τ, 20H). It was concluded from these results that I was π-cyclopentadienyl(cyclohexyl isocyanide)(methylcyclohexyliminomethyl)nickel, π-$C_5H_5Ni(C{\equiv}NC_6H_{11})(C(CH_3){=}NC_6H_{11})$. I is fairly stable to air in the solid state and is soluble in most organic solvents. The reaction of I with moist air gave *N*-cyclohexyl acetamide.

Similar red-brown compounds were also prepared by the reaction of cyclohexyl isocyanide and other triphenylphosphine-π-cyclopentadienylalkylnickel compounds.

π-$C_5H_5Ni(C{\equiv}NC_6H_{11})(C(C_6H_5){=}NC_6H_{11})$: Yield, 85%. Mp 113—114°C (decomp). IR: 2140 cm^{-1} (N≡C), 1589 cm^{-1} (C=N). Found: C, 71.46; H, 7.72; N, 6.70%. Calcd for $C_{25}H_{32}N_2Ni$: C, 71.62; H, 7.69; N, 6.68%.

π-$C_5H_5Ni(C{\equiv}NC_6H_{11})(C(p\text{-}CH_3C_6H_4){=}NC_6H_{11})$: Yield, 72%. Mp 99.0—101.5°C (decomp). IR: 2140 cm^{-1} (N≡C), 1589 cm^{-1} (C–N). Found: C, 71.92; H, 8.00; N, 6.19%. Calcd for $C_{26}H_{34}N_2Ni$: C, 72.07; H, 7.92; N, 6.19%.

π-$C_5H_5Ni(C{\equiv}NC_6H_{11})(C(p\text{-}ClC_6H_4){=}NC_6H_{11})$: Yield, 89%. Mp 126—128°C (decomp). IR: 2135 cm^{-1} (N≡C), 1587 cm^{-1} (C=N). Found: C, 66.19; H, 7.14; N, 6.39%. Calcd for $C_{25}H_{31}N_2ClNi$: C, 66.18; H, 6.89; N, 6.17%.

π-$C_5H_5Ni(C{\equiv}NC_6H_{11})(C(n\text{-}C_4H_9){=}NC_6H_{11})$: Yield, 68%. Mp 51—53°C (decomp). IR: 2140 cm^{-1} (N≡C), 1618 cm^{-1} (C=N). Found: C, 68.68; H, 9.14; N, 7.31%. Calcd for $C_{23}H_{36}N_2Ni$: C, 69.19; H, 9.09; N, 7.02%.

No reaction of cyclohexyl isocyanide with *o*-tolyl or mesityl nickel compounds was observed, suggesting steric hindrance by the ortho methyl group.

The reaction of *t*-butyl isocyanide with triphenylphosphine-π-cyclopentadienylphenylnickel proceeded to give tris(*t*-butyl isocyanide)triphenylphosphinenickel and biphenyl, without forming any complex of the I type. Detailed studies are now in progress.

1) Y. Yamamoto, T. Takizawa and N. Hagihara, *Nippon Kagaku Zasshi (J. Chem. Soc. Japan, Pure Chem. Sect.)*, **87**, 1355 (1966).

2) H. Yamazaki, T. Nishido, Y. Matsumoto, S. Sumida and N. Hagihara, *J. Organometal. Chem.*, **6**, 86 (1966).

*1 Measured in $CDCl_3$, tetramethylsilane as the internal standard.

The Total Synthesis of Kanamycin C

Sumio UMEZAWA, Shinkiti KOTŌ, Kuniaki TATSUTA and Takayuki TSUMURA

Department of Applied Chemistry, Faculty of Engineering, Keio University, Koganei-shi, Tokyo

(Received December 14, 1967)

Kanamycin C[1] is a member of kanamycin congeners and composed of paromamine and 3-amino-3-deoxy-D-glucose. We wish to report a synthesis of this antibiotic. Since we have synthesized paromamine[2] (I), the combined achievements constitute the first total synthesis of kanamycin C (VIII).

Tri-*N*-carbobenzoxyparomamine (II), mp 258°C (decomp.), $[\alpha]_D^{18}$ +64.5° (*c* 0.67, DMF), was treated with 2, 2-dimethoxypropane and *p*-toluenesulfonic acid in *N*, *N*-dimethylformamide (DMF) to give the diisopropylidene derivative(III). Benzylation of III with benzyl bromide in the presence of barium oxide and barium hydroxide in DMF gave IV, which, by deacetonation, gave V. When partially acetonated, V gave monoisopropylidene-monobenzyl derivative (VI); mp 239—241°C, $[\alpha]_D^{18}$ +75° (*c* 0.63, DMF).

The condensation of VI with 3-acetamido-2, 4, 6-tri-*O*-benzyl-3-deoxy-α-D-glucopyranosyl chloride[3] [mp 143—144°C (decomp.), $[\alpha]_D^{23}$ +78° (*c* 1.0, $CHCl_3$)] in a mixture of benzene-dioxane in the presence of mercuric cyanide and Drierite gave the condensation product. After removal of the all protecting groups, the resulting free base was dinitrophenylated and *O*-acetylated. The product was chromatographed on a silica-gel column with a solvent system (A): toluene-MEK (2 : 1), to afford yellow crystals of VII; 15% over-all yield from VI; mp 208—211°C (decomp.), $[\alpha]_D^{18}$ +285° (*c* 0.75, acetone).

On the other hand, kanamycin C[1] was dinitrophenylated and acetylated to give hepta-*O*-acetyltetra-*N*-(2, 4-dinitrophenyl)-kanamycin C; mp 208—211°C (decomp.), $[\alpha]_D^{18}$ +299° (*c* 0.64, acetone). On TLC with a solvent system (A), the synthetic product VII and the above-mentioned derivative of natural kanamycin C showed identical mobilities andt heir IR spectra were superimposed. Hydrolysis of VII with methanolic ammonia followed by treatment with Dowex 1×2 (OH) gave a crude

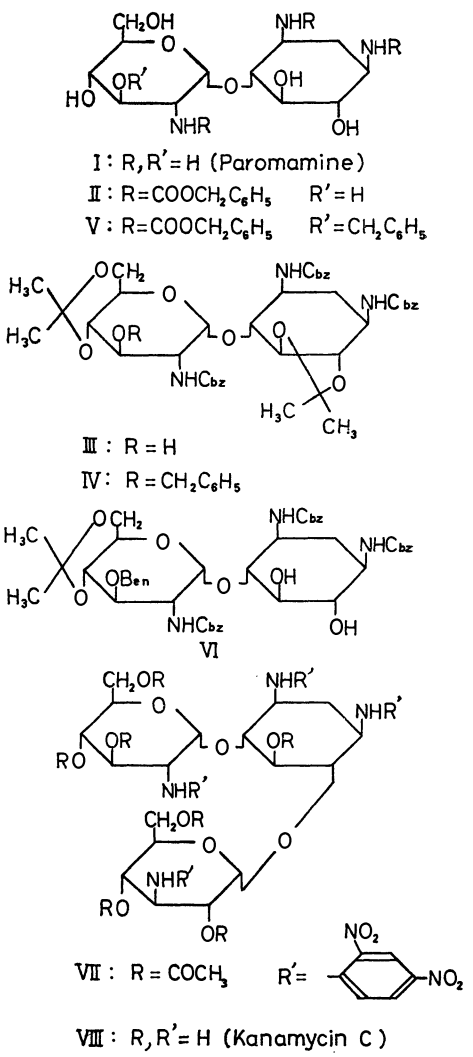

free base, which was purified by column-chromatography to give VIII; $[\alpha]_D^{18}$ +139° (*c* 0.50, water). The natural kanamycin C showed $[\alpha]_D^{18}$ +145° (*c* 0.58, water) [lit.,[1] $[\alpha]_D^{20}$ +126° (water)]. Paper chromatography and IR spectra showed that VIII was identical with the natural kanamycin C. The antibiotic spectra and minimal inhibitory concentrations of the synthetic product VIII against test organisms were in agreement with those of the natural kanamycin C.

1) K. Maeda, M. Ueda, K. Yagishita, S. Kawaji, S. Kondo, M. Murase, T. Takeuchi, Y. Okami and H. Umezawa, *J. Antibiotics*, **A10**, 228 (1957); J. W. Rothrock, R. T. Goegelman and F. J. Wolf, *Antibiotics Annual*, **1958/59**, 796; M. Murase, *J. Antibiotics*, **A14**, 367 (1961).

2) S. Umezawa and S. Kotō, This Bulletin, **39**, 2014 (1966); *J. Antibiotics*, **A19**, 88 (1966).

3) This compound have been reported by S. Umezawa *et al.* at the 20th Annual Meeting of the Chemical Society of Japan, Tokyo, March, 1967.

The Electron Spin Resonance of Mn^{2+} Ion in the Aqueous Solution of Surfactant

Masaji MIURA, Akinori HASEGAWA and Yasuyoshi MICHIHARA

Department of Chemistry, Faculty of Science, Hiroshima University, Higashisenda-machi, Hiroshima

(Received December 18, 1967)

Manganese ion is one of the typical paramagnetic ions and a number of ESR studies on this ion have been published. Most of them have dealt with it in solid; a minute amount of cation in solid is displaced with Mn^{2+} ion, and the magnitude of the crystal field and its symmetry are estimated through the ESR spectrum of Mn^{2+} ion. The method of spin label of cation with Mn^{2+} ion is expected to be applied not only to solid but to electrolytic solution.

It is well-known that cation plays an important role in the formation of surfactant micelle. So Mn^{2+} ion was added to the aqueous solution of surfactant and the effect of counterion in the solution was evaluated through the ESR spectrum of Mn^{2+} ion.

Theory of the ESR spectrum of Mn^{2+} ion in liquid solution has been recently presented by Garrett and Morgan in terms of solvent-fluctuation-induced relaxation.[1] They have shown that each of six hyperfine lines consists of five transitions of $\Delta m_S=1$, the line width of $m_I=-5/2$ is broadest and that of $m_I=1/2$ is narrowest, and that the latter is approximately proportional to the correlation time τ_C for solvent fluctuation.

Sodium dodecyl sulfate (SDS) and sodium decyl sulfate (NaDS) were employed as surfactant in this study. Each of them was added to the aqueous solution of 1×10^{-3} M $Mn(NO_3)_2$. The solution thus obtained was sealed in a capillary of glass and ESR measurements were carried out.

The ESR spectrum of Mn^{2+} ion in the aqueous solution is affected by the concentration of SDS. The variation in the line width accompanied with the concentration of SDS is shown in Fig. 1. When the concentration of SDS is below 3×10^{-3} or above 13×10^{-3} M, the line width is practically unaffected by the concentration. But line width increases with the concentration in the range from 3×10^{-3} to 13×10^{-3} M. As the line width of $m_I=1/2$ is proportional to the correlation time τ_C, τ_C increases up to 1.7 times in this region.

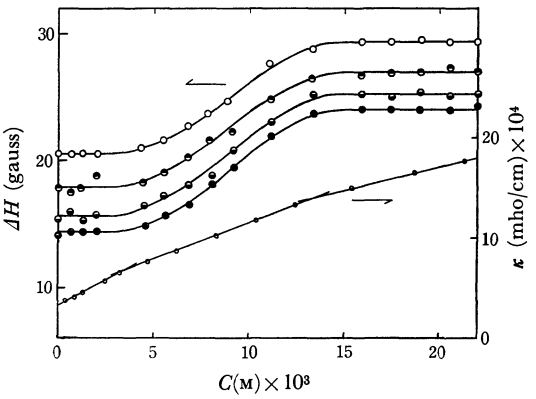

Fig. 1. The dependences of the line width (large circles) and the specific conductivity (smaller circle) on the concentration of SDS at 50°C.
○— $m_I=-5/2$, ◔— $m_I=-3/2$,
◒— $m_I=-1/2$, ●— $m_I=1/2$

Conductivity measurements were carried out in order to determine the CMC (critical micelle concentration). The specific conductivity-concentration curve broke at two points as is seen in Fig. 1. The concentrations corresponding to these two points are the first and second CMC_s from the side of the lower concentration of SDS, respectively, and agree well with the concentrations at which the line width of ESR of Mn^{2+} changes.

Similar experiments were also done on NaDS. Coincidence between CMC_s and the concentrations at which ESR line width changes was also found here. The correlation time increases in the range from the first CMC, 3×10^{-2} M, to the second CMC, 7×10^{-2} M, and that at the concentration above the second CMC is about 0.93 times of that in case of SDS.

The increase in the correlation time may be interpreted as that Mn^{2+} ion is bound to the surfactant micelle.

The details of this investigation will be published later.

1) B. B. Garrett and L. O. Morgan, *J. Chem. Phys.*, **44**, 890 (1966).

Synthesis of Tris(*N*-isopropyl-*C*-substituted salicylideneiminato)cobalt(III) Complexes

Shoichiro YAMADA, Emiko OHNO and Kuniko YAMANOUCHI

Institute of Chemistry, College of General Education, Osaka University, Toyonaka, Osaka

(Received December 22, 1967)

Numerous cobalt(III) complexes of the Co(X-sal.R)$_3$ type (Formula I)*1 have been reported, but Co(X-sal. *iso*-C_3H_7)$_3$ has never been synthesized up to the present.[1] Thus it has currently been believed that the steric condition arising from the isopropyl groups does not allow the formation of the complexes of this type.[2,3] This statement is no longer correct, as the present authors have succeeded in synthesizing the complexes of the Co(X-sal. *iso*-C_3H_7)$_3$ type, where X denotes 5-NO_2 and 5-Br.

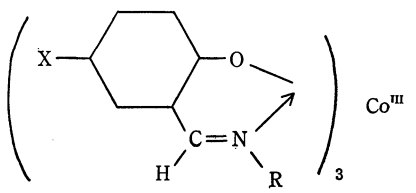

Formula I

A typical method of preparation was as follows. To a solution of Co(X-sal. *iso*-C_3H_7)$_2$ (0.01 mol) and the ligand (0.01 mol) in ethanol (20 m*l*) was added with stirring a 30% solution of H_2O_2 (5 m*l*) drop by drop at about 60°C. The solution was kept at this temperature for about twenty minutes and then allowed to stand overnight at about 5°C. A crystalline precipitate which separated was filtered, and recrystallized from ethanol, chloroform or acetone. Dark-green crystals of Co(X-sal. *iso*-C_3H_7)$_3$ were obtained in good yield. The complexes of the Co(X-sal. *n*-C_3H_7)$_3$ were prepared as dark-green crystals by a method similar to that previously reported.[2]

Analytical data of these complexes, which are given in Table 1, agree with the above formulae. The fact that the complexes prepared are diamagnetic indicates that they are cobalt(III) complexes of a low-spin type. The complexes with R=*iso*-C_3H_7 show clear melting points which are different from those of the corresponding complexes with R=*n*-C_3H_7, as given in Table 1. The infrared spectra of the complexes with R=*iso*-C_3H_7 are different from the spectra of the complexes with R=*n*-C_3H_7, the latter showing bands due to C–C stretching vibrations of the *n*-propyl group at about 1000 to 1100 cm^{-1}, where no absorption band appears for the complexes with R=*iso*-C_3H_7.

Two configurations, a *mer*- and a *fac*-form, are possible for the complexes of the Co(X-sal. R)$_3$ type, but only the *mer*-form has been isolated for all the previously synthesized complexes.[4] It is, therefore, most likely that the complexes prepared in the present work are also of the *mer*-form. The maxima of d-d bands of Co(X-sal. *iso*-C_3H_7)$_3$ are nearly equal to the maxima of Co(X-sal. *n*-C_3H_7)$_3$, for which the *mer*-form is usually found.

It seems to be significant that the complexes which have been claimed to be incapable of existence are isolated as pure crystals. The result of the present work clearly demonstrates that the extent of the steric hindrance is not great enough to forbid the formation of the complexes of the Co(X-sal. *iso*-C_3H_7)$_3$ type, although it is true that there may be more or less remarkable steric hindrance.

TABLE 1. ANALYTICAL DATA OF Co(X-sal·R)$_3$

X	R	mp (°C)		C	H	N (%)
NO_2	*i*-C_3H_7	243.5—245	Found	52.40	4.90	12.22
	n-C_3H_7	216.5—218	Found	52.56	4.74	12.21
			Calcd	52.94	4.89	12.35
Br	*i*-C_3H_7	227.5—229	Found	46.47	4.12	5.20
	n-C_3H_7	232.5—234	Found	46.45	4.31	5.33
			Calcd	46.44	4.25	5.37

*1 The complexes represented by Formula 1 are abbreviated as Co(X-sal·R)$_2$ in the present communication.

1) S. Yamada, *Coordin. Chem. Rev.*, **1**, 415 (1966).
2) H. Nishikawa and S. Yamada, This Bulletin, **37**, 1154 (1964).
3) A. Chakravorty and R. H. Holm, *Inorg. Chem.*, **3**, 1521 (1964).
4) M. Ciampolini, F. Maggio and F. P. Cavasino, *ibid.*, **3**, 1188 (1964).

Particle Size Dependence of the Magnetic Heat Capacity of $Ni(OH)_2$ Crystal at Low Temperatures

Michio SORAI, Akio KOSAKI, Hiroshi SUGA and Syûzô SEKI

Department of Chemistry, Faculty of Science, Osaka University, Toyonaka, Osaka

(Received December 26, 1967)

The heat capacities of $Ni(OH)_2$ crystals with three kinds of particle sizes [*i. e.* (1) (~20 Å)×(~130 Å), (2) (30—1000 Å)×(200—10000 Å), and (3) (0.2—0.5 μ)×(1—3 μ), where we designate their particle size as (average distance in <001> direction)×(distance in <100> direction)] have been measured in the temperature region form 1.5 to 300°K. Each of these crystals showed a heat capacity anomaly associated with the spin ordering of the metal ions at 23.0±0.1°K, 24.25±0.05°K, and 24.80±0.05°K for the $Ni(OH)_2$-(1), -(2), and -(3), respectively.

The magnetic heat capacities of these substances were separated from the total heat capacities by a rather reasonable method. The reduced plots of the magnetic heat capacities thus obtained are shown in Fig. 1. The magnetic entropies of the Ni-salts associated with the spin ordering effect agreed well with the value of 9.134 J/°K·mol from $R\cdot\ln(2S+1)$ where $S=1$ for the spin of the Ni^{2+} ion, and about 50% of this was acquired in the region above the Néel point, T_N, indicating the characteristic behaviours due to much stronger two-dimensional interactions predicted from their layer lattice structures (the CdI_2-type).

The variation of the transition temperatures form sample to sample observed in the Ni-salts may be the largest effect ever known[1] and clearly regarded as the particle size effects on the magnetic heat capacity. Additional effect of the particle size could be observed in the rounding of the heat capacity maxima with decreasing size of the crystal particles (see Fig. 1). This particle size effect has long been one of the unsolved problems which could help to fulfill the gaps between theory and experiment.

The particle size effect was also reflected in the surface heat capacities. The excess heat capacity was estimated to be about 1.2 J/°K·mol at 100°K for $Ni(OH)_2$ with the surface area of 314 m^2/g. This magnitude of excess heat capacity is the largest effect ever known and is compared with the data for NaCl, MgO, and BeO crystals[2] in Fig. 2.

The detailed results and discussions will be published in due course.

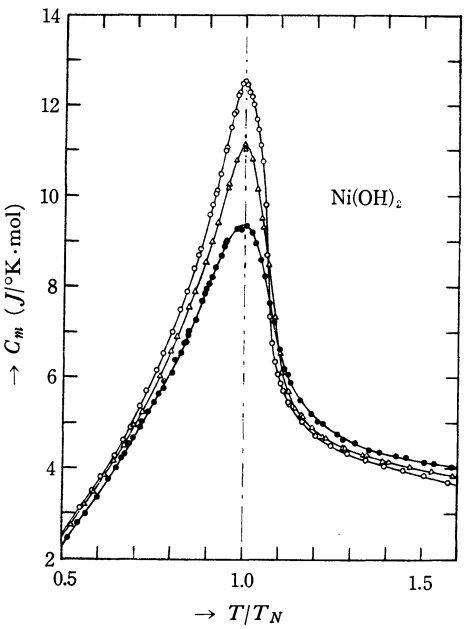

Fig. 1. The magnetic heat capacity C_m *versus* reduced temperature curves for $Ni(OH)_2$ with different crystal sizes. ●, the $Ni(OH)_2$-(1); △, the $Ni(OH)_2$-(2); ○, the $Ni(OH)_2$-(3)

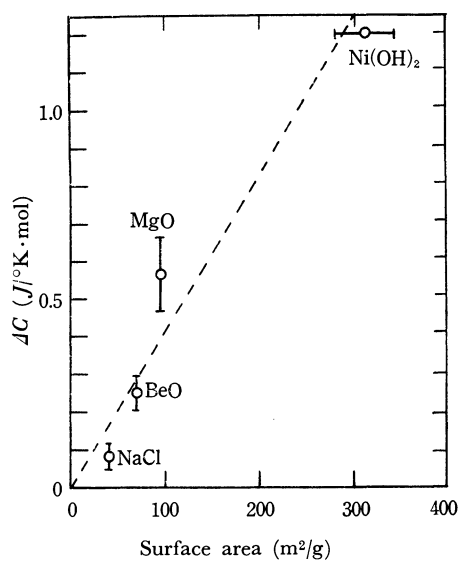

Fig. 2. The excess heat capacity ΔC for several kinds of crystals at 100°K as a function of surface area per unit mass.

1) D. T. Teaney, "Critical Phenomena," ed. by M. S. Green and J. V. Sengers, Natl. Bur. Stands., Washington, D. C. (1966), p. 50; B. E. Keen, D. P. Landau and W. P. Wolf, *J. Appl. Phys.*, **38**, 967 (1967).

2) A. C. Victor, *J. Chem. Phys.*, **36**, 2812 (1962).

Resolution of Optically Active Tris(1, 10-phenanthroline)vanadium(II) Complex

Ichiro FUJITA, Masayuki SHIMIZU, Youkoh KAIZU, Yasuo TORII and Hiroshi KOBAYASHI

Department of Chemistry, Tokyo Institute of Technology, Ookayama, Meguro-ku, Tokyo

(Received January 10, 1968)

Resolution of the optically active complexes with easily oxidized metal ions such as vanadium-(II) has never been reported. However inert gas atmosphere makes it possible to prepare and resolve them. Recently we succeeded in preparation and resolution of tris(1, 10-phenanthroline)vanadium(II) diperchlorate under the complete inert gas atmosphere.

This complex was obtained by the following procedure.[1] 0.001 mol vanadous solution prepared by electrolytic reduction of $VOSO_4$ was mixed with 0.003 mol 1, 10-phenanthroline (phen) and the mixed solution was stirred until it turned dark blue showing the formation of $[V(phen)_3]^{2+}$ ion. Then this solution was added the saturated solution of 1 g potassium antimonyl-*d*-tartrate as resolving agent. After the less soluble diastereomer was precipitated, the $(-)_{589}[V(phen)_3]^{2+}$ ion was precipitated as the perchlorate salt by the addition of ammonium perchlorate solution. The whole procedure was carried out in nitrogen gas. Solvent water was freed from oxygen by nitrogen bubbling. For the measurements of UV and visible absorption spectrum and circular dichroism (CD),*1 vacuum distilled methanol was used.

The absorption spectrum and also the CD curve resemble to those of $[Fe(phen)_3](ClO_4)_2$.[2] The observed spectra are shown in Fig. 1. The observed absorption intensity in UV region of vanadium complex is almost the same magnitude as those of the corresponding iron and nickel complexes. The observed CD intensity in the same region of vanadium complex is rather lower than those of the iron complex and nickel one,

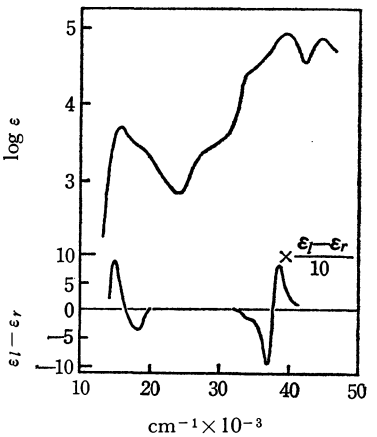

Fig. 1. Electronic absorption spectrum and CD curve of $(-)_{589}$-$[V(phen)_3](ClO_4)_2$.

while the CD intensity of the iron complex is comparable with that of the nickel one. The lower intensity of the vanadium complex might be interpreted as partial resolution. Any trial of the resolution of the vanadium complex could not get the corresponding values of the iron and nickel complexes, as far as potassium antimonyl-*d*-tartrate is used as resolving agent. Resolution using other resolving agents is being carried out. The CD curve of the less soluble diastereomer has not been obtained because of its insolubility.

The half-life of racemization assuming the first-order reaction is about 63 min in methanol at a room temperature. This value is as twice as that the iron complex and much less than that of the nickel complex.[3] When this complex was partially oxidized, the racemization became too fast to be measured.

Whole details will be published elsewhere.

1) F. P. Dwyer and E. C. Gyarfas, *J. Proc. Roy. Soc. N. S. Wales*, **85**, 135 (1951).

*1 Dr. T. Samejima kindly allowed us to use his CD instrument.

2) J. Hidaka and B. E. Douglas, *Inorg. Chem.*, **3**, 1180 (1964).

3) F. Basolo and R. G. Pearson, "Mechanisms of Inorganic Reactions," John Wiley and Sons, Inc., New York, N. Y. (1958), p. 260.

The Excluded Volume Effect of Very-long-chain Molecules

Keizo SUZUKI

Department of Chemistry, Tokyo Kyoiku University, Otsuka, Tokyo

(Received December 26, 1967)

The problem of the excluded volume effect upon the shape of the chain molecule was set twenty years ago[1] and has not been completely solved yet.[2] The approach by Monte Carlo simulation using an electronic computer has led to rather meagre results because of the extraordinarily poor yield of the overlapless form of the long chain; reliable results have been obtained only on chains with a few hundred bonds.[3]

The present author has found a new program to make the overlapless forms in a good yield, producing 8192-bond chains on a diamond lattice. Some results are shown in Table 1, where N is the number of the bonds, r is the radius of the gyration of the chain, a is the bond longth, and α is the exponent in the formula:

$$\langle r^2 \rangle = KN^{\alpha},$$

and is calculated by the equation:

$$\alpha = (\log \langle r^2{}_{2N} \rangle - \log \langle r^2{}_{N} \rangle)/\log 2.$$

Table 1

N	$\langle r^2 \rangle / a^2$	α	Yield (%)
1	0.2500	1.052	100
2	0.5185	1.092	100
4	1.105	1.145	94
8	2.444	1.19±0.01	87
16	5.560	1.20±0.01	78
32	12.78	1.20±0.01	71
64	29.31	1.20±0.01	62
128	67.37	1.19±0.01	56
256	153.4	1.19±0.02	50
512	350.3	1.17±0.04	46
1024	787.0	1.15±0.05	40
2048	1740	1.11±0.10	36
4096	3747	1.08±0.13	27
8192	7943		

With the increase in N, α increases at first but gradually decreases after passing a maximum value, 1.20. The previous studies did not find the decrease because they did not reach this region. Theoretically the exponent, α, can not go under 1; it probably approaches 1 very slowly, as previously expected by the present author.[4]

The scheme of the program to make overlapless chains with equal probability is as follows:

1 MAKE AN M-BOND CHAIN AT RANDOM. ($M=64$, for example)
2 IF THERE IS AN OVERLAP, GO TO 1.
3 $N=M$.
4 IF ANOTHER N-BOND CHAIN IS NOT STORED, STORE THE NEW CHAIN AND GO TO 1.
5 CONNECT THE STORED CHAIN TO THE NEW CHAIN AND MAKE A $2N$-BOND CHAIN.
6 IF THERE IS AN OVERLAP, OUTPUT AND CLEAR BOTH THE N-BOND CHAINS, AND GO TO 1.
7 $N=2N$, AND GO TO 4.

Full programs will appear elsewhere. The last column of Table 1 shows the average yield in getting an overlapless $2N$-bond chain by connecting two N-bond chains. The yield decreases with the increase in N, but it must converge to a finite value of not less than 1/9.

1) P. J. Flory, *J. Chem. Phys.*, **17**, 303 (1949); K. Suzuki, This Bulletin, **22**, 8 (1949).
2) Z. Alexandrowicz, *J. Chem. Phys.*, **46**, 3789 (1967).
3) P. H. Verdier, *ibid.*, **45**, 2118 (1966).
4) K. Suzuki, Thesis, The University of Tokyo (1957).

BULLETIN OF THE CHEMICAL SOCIETY OF JAPAN VOL. 41 539—542 (1968)

Studies of the ζ-Potential of Natural and Synthetic Fibers in Dye Solutions. XVIII. ζ-Potential and Surface Dyeability of Heat-Set Nylon 6 Fiber in an Acid Dye Solution

Toshiro SUZAWA and Tomoyuki SAITO

Department of Applied Chemistry, Faculty of Engineering, Hiroshima University, Senda-machi, Hiroshima

(Received June 12, 1967)

In order to ascertain the relation between the change in the fibrous fine structure and the dyeability of nylon 6 fiber caused by its heat-setting, the ζ-potential, the surface dye adsorption, and the total dye adsorption of the heat-set nylon 6 fiber in an acidic solution (pH 3.0) of acid dye—Orange II were determined. The crystallinity and the birefringence of the fiber increase in the order of the untreated, the wet-heat-treated, and the dry-heat-treated fiber. The isoelectric points of the untreated, the wet-heat-treated, and the dry-heat-treated fiber are pH 5.4, pH 4.6, and pH 2.8 respectively. With the increase in the dye concentration, the sign of the ζ-potential of the untreated and the wet-heat-treated fiber in a dye solution change from positive to negative because of the electrostatic bonds between the NH_3^+ of the fiber and the dye anion, RSO_3^-, while the ζ-potential of the dry-heat-treated fiber increases its negative value because of the van der Waals' forces between the fiber and the dye. The surface dye adsorption, as calculated from the difference between the surface charge density, $\Delta\sigma$, of the system with dye and that without dye, increases in any case as the dye concentration increases. The total dye adsorption increases as the dye concentration increases and attained the plateau regions at higher dye concentrations. The surface dye adsorptions become smaller in the order of the untreated, the dry-heat-treated, and the wet-heat-treated fiber. The total dye adsorptions become smaller in the order of the wet-heat-treated, the untreated, and the dry-heat-treated fiber. The differences in behavior among the fibers may be attributed to the adsorption of the dye to the loosely-packed portions in the amorphous region of the wet-heat-treated fiber, in addition to the differences in crystallinity and birefringence among the fibers. Moreover, the surface areas covered by adsorbed dye molecules, which were calculated from the reciprocal of the slope of the surface dye adsorption *vs.* the total dye adsorption curve of each fiber, were 1.8, 4.0, and 0.6×10^6 cm²/g fiber in the order of the untreated, the wet-heat-treated, and the dry-heat-treated fiber.

In manufacturing synthetic fibers such as polyamide nylon fibers, heat-setting is the usual processing practice. It is known that this treatment causes changes in the fibrous fine structure.

Hitherto, several articles on the relation between the changes in the fibrous fine structure and the dyeability of nylon 6 fiber caused by the heat-setting treatment have been published,[1] but few reports on the relation between the changes in the fine structure and the dyeability of the surface of the nylon 6 fiber caused by the heat-setting treatment are to be found. In this report the dyeability of the heat-treated nylon 6 fiber surface in an acid dye solution will be studied in relation to the ζ-potential, the surface dye adsorption, and the total dye adsorption in order to ascertain the influence of the changes in the fine structure upon the dyeability of the fiber surface.

1) *E.g.*, A. Koshimo and T. Kakishita, *Chem. High Polymers Japan*, **19**, 506 (1962).

Experimental

Fiber. Nylon 6 filaments (manufactured by the Toyo Rayon Co., Ltd.) were extracted with ethanol for about 24 hr at room temperature, and then dried in air. Three kinds of fiber were used. Some of the filaments were heat-treated as follows, while the rest were untreated specimens.

TABLE 1. NYLON 6 FIBERS USED

Fiber	Method of heat-treatment
Untreated fiber	(Draw ratio 4, 200 denier)
Wet-heat-treated fiber	Untreated fiber was treated 30 min in hot water (100°C) without tension
Dry-heat-treated fiber	Untreated fiber was treated 30 min in air at 170°C without tension

(All specimens were composed of 30 filaments)

Dye. The acid dye Orange II (I), which had been purified by recrystallization from an aqueous solution, was used.

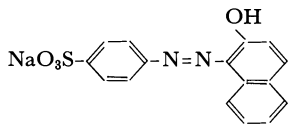

(I)

ζ-Potential. The ζ-potential was measured by the method of the streaming potential, described in previous papers.[2] The dye solution was kept at pH 3.0 at 25°C with hydrochloric acid. Sodium chloride was added to the solution in order to prevent any influence of the ionic strength on the ζ-potential; its concentration was 10^{-4} mol/*l*.

Surface Charge Density and Surface Dye Adsorption. The surface charge density, σ, and the surface dye adsorption were calculated by method described in previous papers.[3]

Total Dye Adsorption, Crystallinity, Birefringence, Intrinsic Viscosity and End Groups. These values were measured and determined by the methods described in a previous paper.[3b]

Results and Discussion

End Groups, Crystallinity, Birefringence, and Intrinsic Viscosity of Nylon 6 Fiber. The values determined are shown in Table 2.

The end amino group decreased and the end carboxylic group increased in the order of the untreated, the wet-heat-treated, and the dry-heat-treated fiber. The intrinsic viscosity of the untreated fiber and that of the wet-heat-treated fiber were almost the same. However, the intrinsic viscosity of the dry-heat-treated fiber was about half of that of two former fibers; this result suggests that the decrease in the degree of polymerization is caused by the dry-heat-treatment. The crystallinity and the birefringence increase in the order of the untreated, the wet-heat-treated, and the dry-heat-treated fiber. These results suggest some change in the fine structure of these fibers, especially an increase in the crystalline region and in the degree of orientation.

The Isoelectric Point of Fiber. The ζ-potential of the fiber in solutions of hydrochloric acid or sodium hydroxide of various concentrations was measured in order to ascertain the influence of the pH on ζ. The results are shown in Fig. 1.

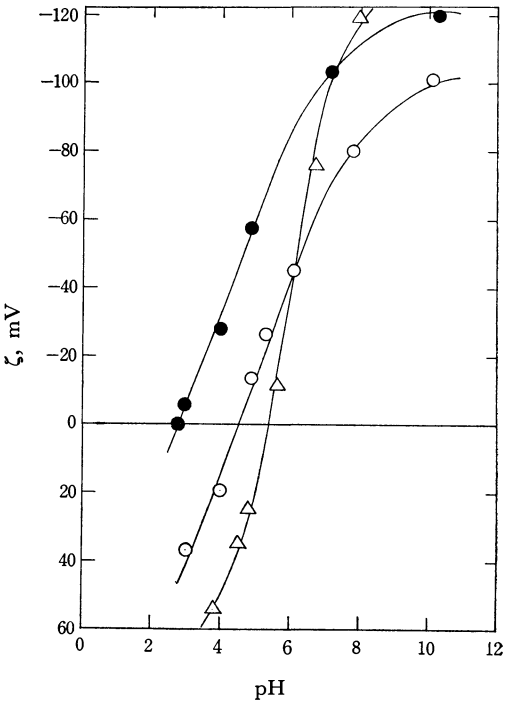

Fig. 1. Influence of pH on ζ-potential of heat-set nylon 6 fibers.
△: Untreated fiber
○: Wet-heat-treated fiber
●: Dry-heat-treated fiber

The ζ-potential of any fiber is positive in an acidic solution and negative in an alkaline one. From these results, it was found that the isoelectric points of the untreated, the wet-heat-treated, and the dry-heat-treated fiber are pH 5.4, pH 4.6, and pH 2.8 respectively. These differences in the isoelectric point among the fibers correspond to the differences in the end amino group and the end carboxylic group with the fibers, differences which are caused by the heat-treatment.

ζ-Potential with Dye Concentrations. The ζ-potential of the fiber *vs.* dye concentration curves

TABLE 2. END GROUPS, CRYSTALLINITY, BIREFRINGENCE AND INTRINSIC VISCOSITY OF THE NYLON 6 FIBERS USED

Fiber	End amino group (mol/g fiber) $\times 10^5$	End carboxylic group (mol/g fiber) $\times 10^5$	Crystallinity %	Birefringence $\times 10^3$	$[\eta]$
Untreated fiber	5.02	6.65	39.5	51.4	1.12
Wet-heat-treated fiber	4.28	7.92	42.5	53.2	1.10
Dry-heat-treated fiber	1.39	12.27	53.7	57.6	0.54

2) T. Suzawa, *Kogyo Kagaku Zasshi (J. Chem. Soc. Japan, Ind. Chem. Sect.)*, **62**, 232 (1959); **63** 1069 (1960).

3) a) T. Suzawa, *ibid.*, **63**, 148 (1960); b) T. Suzawa, T. Saito and H. Shinohara, This Bulletin, **40**, 1596 (1967).

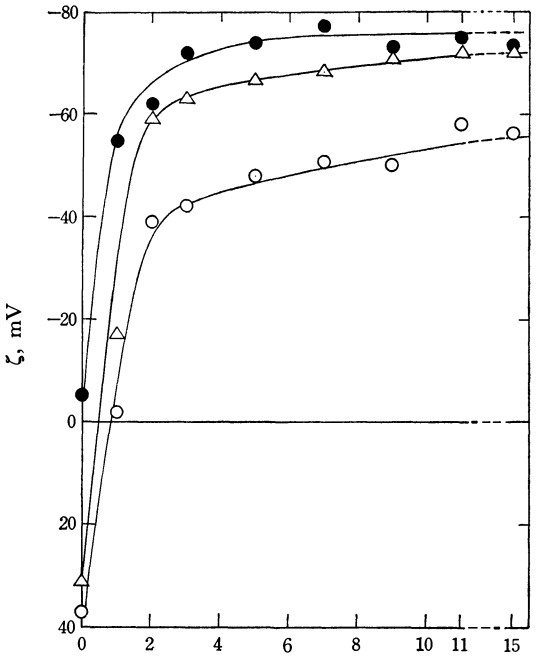

Fig. 2. ζ-Potential of the fibers with Orange II concentration.
△: Untreated fiber
○: Wet-heat-treated fiber
●: Dry-heat-treated fiber

are shown in Fig. 2. The ζ-potential was measured every hour on the hour; the values recorded in Fig. 2 are the equilibrium values, to which the potentials were approximated after four hours of immersion.

As the ζ *vs.* dye concentration curves in Fig. 2 show, the ζ-potentials of the untreated and the wet-heat-treated fiber are positive in a solution without dye, while the ζ-potential of the dry-heat-treated fiber is negative in the same solution. Such behavior may be expected from the dissociation of the NH_3^+ groups of the fiber in the former and that of the COO^- groups in the latter, because the pH of the solution used is smaller in the former, and larger in the latter, than the pH corresponding to the isoelectric point of the fiber.

Upon the addition of dye to this system, the ζ-potentials of the untreated and the wet-heat-treated fiber changed from positive to negative, while the ζ-potential of the dry-heat-treated fiber increased in its negative value. These facts may possibly be attributed to the formation of the electrostatic bond between the NH_3^+ of the fiber and the dye anion RSO_3^- in the former, and to the van der Waals' force between the fiber and the dye in the latter, because the pH of the dye solution used is smaller in the former, and larger in the latter, than the pH corresponding to the isoelectric point of the fiber. The ζ *vs.* dye concentration curves change rapidly in the range of concentrations smaller than 3×10^{-4} mol/*l*, and then the ζ-potentials (negative) approximate the saturated value.

Surface Dye Adsorption with Dye Concentration. The surface dye adsorptions increase with the dye concentration, as Fig. 3 shows.

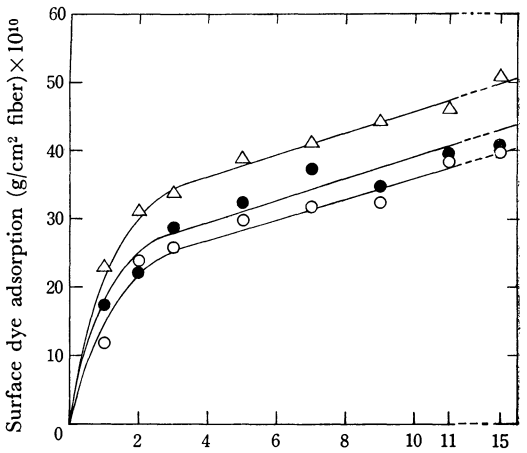

Fig. 3. Surface dye adsorption with Orange II concentration.
△: Untreated fiber
○: Wet-heat-treated fiber
●: Dry-heat-treated fiber

Throughout the range of dye concentrations, these values become smaller in the order of the untreated, the dry-heat-treated, and the wet-heat-treated fiber. This means that the surface of the untreated fiber, with a smaller crystallinity, a lower degree of orientation, and more end amino groups, adsorbs more dye than that of the dry-heat-treated fiber, with a larger crystallinity, a higher degree of orientation, and fewer end amino groups. Of course, this fact may also be related to the fact that the pH of the solution used is larger than the pH of the isoelectric point of the dry-heat-treated fiber.

In the case of the wet-heat-treatment, the intermolecular hydrogen bonds between the polymer-chain molecules of a fiber are broken by water molecules and the swollen, loosely-packed portions are formed in the amorphous region of the fiber.[1] The dyes adsorbed on these loosely-packed portions in the amorphous region cause the decrease in the dye concentration of the dye solution. This decrease in the dye concentration of the solution in the case of the wet-heat-treated fiber then gives rise to the decrease in the surface dye adsorption.

Therefore, it may be attributed to the adsorption of the dye to these loosely-packed portions in the amorphous region in the case of the wet-heat-treated fiber that the surface dye adsorption of the

wet-heat-treated fiber becomes smaller than that of the dry-heat-treated fiber, in spite of the smaller crystallinity and the lower degree of orientation of the former.

Total Dye Adsorption with Dye Concentration. The total dye adsorptions increase with the dye concentration, as Fig. 4 shows. Moreover, the plateau regions are attained at higher dye concentrations. The total dye adsorptions decrease in the order of the wet-heat-treated, the untreated, and the dry-heat-treated fiber. This means that the untreated fiber, with a smaller crystallinity, a lower degree of orientation, and more end amino groups, adsorbs more dye than does the dry-heat-treated fiber, with a larger crystallinity, a higher degree of orientation, and fewer end amino groups. Of course, this fact may also be related to the fact that the pH of the solution used is larger than the pH of the isoelectric point of the dry-heat-treated fiber. Moreover, the adsorption of the dye to the loosely-packed portions in the amorphous region of the wet-heat-treated fiber may be supposed to be the reason why the total dye adsorption of the wet-heat-treated fiber becomes larger than that of the untreated fiber, in spite of the larger crystallinity and the higher degree of orientation of the former.

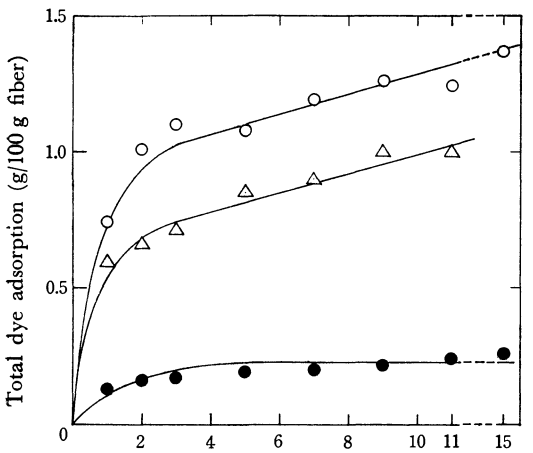

Fig. 4. Total dye adsorption with Orange II concentration.
△: Untreated fiber
○: Wet-heat-treated fiber
●: Dry-heat-treated fiber

Surface Area Covered by Adsorbed Dye Molecules on Fiber. The surface dye adsorption *vs.* the total dye adsorption curves were found to be linear, as Fig. 5 shows. These slopes are considered to be reciprocals of the surface area covered by adsorbed dye molecules on the fiber. These surface areas, as calculated from Fig. 5, are shown in Table 3.

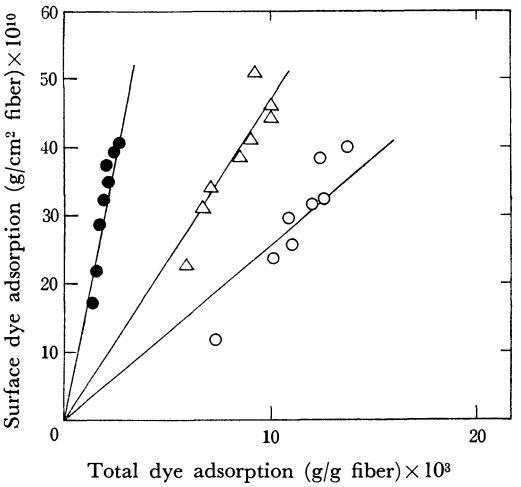

Fig. 5. Relation between surface dye adsorption and total dye adsorption.
△: Untreated fiber
○: Wet-heat-treated fiber
●: Dry-heat-treated fiber

TABLE 3. SURFACE AREA COVERED BY DYE MOLECULES ON FIBER

Fiber	Surface area (cm^2/g fiber)
Untreated fiber	1.8×10^6
Wet-heat-treated fiber	4.0×10^6
Dry-heat-treated fiber	0.6×10^6

The surface area of the wet-heat-treated fiber is twice of that of the untreated fiber, while that of the dry-heat-treated fiber is 1/3 that of the untreated fiber. The large surface area of the wet-heat-treated fiber is supposed to be caused by the loosely-packed portions in its amorphous region. Moreover, the small surface area of the dry-heat-treated fiber may possibly be attributed to its larger crystallinity and higher degree of orientation, and also to be related to the fact that the pH of the solution used is larger than the pH of its isoelectric point.

The authors wish to thank the Toyo Rayon Co., Ltd., for providing the fiber and for the measurement of its birefringence.

BULLETIN OF THE CHEMICAL SOCIETY OF JAPAN VOL. 41 543—547 (1968)

High Pressure Copolymerization of Styrene and Vinyl Acetate with Vinyl Chloride

Tatsuya IMOTO and Yoshiaki OGO

Osaka City University, Sugimoto-cho, Sumiyoshi-ku, Osaka

and Hideo NAKAMOTO

Mitsubishi Rayon Co., Ltd., Misono-cho, Otake-shi, Hiroshima

(Received July 3, 1967)

The radical copolymerization of vinyl chloride and styrene, and that of vinyl chloride and vinyl acetate, were investigated in an acetone solution at 50°C under high pressures of up to 3000 kg/cm^2. The monomer reactivity ratios of these copolymers were not affected by the pressure, while their molecular weights and overall rates of copolymerization increased with the pressure. The increments of the four rate constants of the growing chain of copolymerization (k_{11}, k_{12}, k_{21}, and k_{22}) with the pressure are all of the same order. In such a case, ΔV^*_{11} is ΔV^*_{12}, and ΔV^*_{22} is ΔV^*_{21} (ΔV^*_{ij} is the activation volume in which the i radical reacted with the j monomer). The conclusion drawn from our previous works, that the monomer reactivity ratios of the copolymerization between nonconjugated monomers are independent of the pressure was supported by the experimental results of this report.

Radical copolymerization under high pressures has been studied by several groups of workers in recent years, but the great majority of works on high-pressure copolymerization have dealt with the effect of the pressure on the monomer reactivity ratio in the copolymerization system.

In the copolymerization processes, there are four possible ways in which a monomer can add:

$$M_1\cdot + M_1 \xrightarrow{k_{11}} M_1\cdot$$

$$M_1\cdot + M_2 \xrightarrow{k_{12}} M_2\cdot$$

$$M_2\cdot + M_1 \xrightarrow{k_{21}} M_1\cdot$$

$$M_2\cdot + M_2 \xrightarrow{k_{22}} M_2\cdot$$

where $M_1\cdot$ and $M_2\cdot$ represent chains ending in the M_1 and M_2 monomer units respectively, and where the parameters, $r_1=k_{11}/k_{12}$ and $r_2=k_{22}/k_{21}$, are defined as monomer reactivity ratios.

Zutty and Burkhart[1] investigated the copolymerizations of styrene and acrylonitrile, and of methyl methacrylate and acrylonitrile, under high pressures of up to 1000 kg/cm^2; they reported that their individual monomer reactivity ratios increase with the pressure.

On the other hand, the monomer reactivity ratios in the styrene - vinyl acetate and styrene - *n*-butyl vinylether systems were found in our previous experiment[2] not to change with the pressure.

Many investigations of high-pressure radical copolymerization have been undertaken in order to explain these disagreements. We investigated a series of copolymerizations under high pressure[3-8]; the most reasonable conclusion to be drawn from the available results was that the reactivity ratios of the copolymerization of the nonconjugated vinyl monomer with styrene did not vary with the pressure.

However, the vinyl acetate and *n*-butyl vinylether used in our previous work are monomers with the lowest reactivity of all the vinyl compounds. Therefore, the constancy of the reactivity ratios in copolymerizations under high pressure may be attributed to their original reactivities. The present investigation was undertaken to determine their effect by means of the copolymerization of vinyl chloride (VC) with a considerable reactivity among various conjugated monomers and styrene (St) or vinyl acetate (VAc).

Experimental

Styrene and vinyl acetate were distilled under a vacuum just before use. Benzoylperoxide (BPO), used as initiator, was purified by precipitating it from a chloroform solution into methanol, dried *in vacuo* at

1) N. L. Zutty and R. D. Burkhart, *J. Polymer Sci.*, **57**, 793 (1962).

2) T. Imoto and H. Asai, *Nippon Kagaku Zasshi (J. Chem. Soc. Japan, Pure Chem. Sect.)*, **85**, 152 (1964).
3) T. Imoto and H. Asai, *ibid.*, **84**, 871 (1963).
4) T. Imoto and H. Asai, *ibid.*, **85**, 155 (1964).
5) T. Imoto and H. Asai, *ibid.*, **85**, 247 (1964).
6) T. Imoto and H. Asai, *ibid.*, **85**, 252 (1964).
7) T. Imoto and H. Asai, *ibid.*, **85**, 312 (1964).
8) T. Imoto and H. Asai, *ibid.*, **85**, 347 (1964).

room temperature, and stored in the dark. Vinyl chloride was purified with sodium hydroxide and dried with calcium chloride.

The acetone used as a solvent, the BPO, and the distilled vinyl monomer were placed in a polyethyrene tube with a capacity of 15 m*l*, and the tube was immersed in dry ice - methanol bath at −40°C. Purified gaseous vinyl chloride was introduced and liquified in the tube. Then the tube was immediately immersed in a high-pressure autoclave at 50°C.

The copolymer mixture thus obtained was precipitated into a large amount of methanol as a precipitant, dried completely *in vacuo* at room temperature, and its polymerization yield determined.

The compositions of the copolymers were calculated from the chloride contents as measured by Schöniger's flask-combustion method; then the reactivity ratios were evaluated by the Fineman-Ross method,[9] in which the $F=[M_1]/[M_2]$ and $f=d[M_1]/d[M_2]$ terms are connected by the following equation:

$$\frac{F}{f}(f-1)=r_1\frac{F^2}{f}-r_2 \qquad (1)$$

where $[M_1]$ and $[M_2]$ are the respective concentrations of the two monomers. Plotting the values of $F/f(f-1)$ *versus* F^2/f, r_1 and r_2 can be evaluated from, respectively, the slope and intercept of the straight line expressed by Eq. (1).

The pressure of the reaction system was measured by pressure guages (Bourdon tube and/or strain guage) directly connected to autoclaves.

Results and Discussion

Pressure Dependence of Monomer Reactivity Ratios. The experimental data for the St-VC and VC-VA systems are summarized in Tables 1 and 2. The monomer-polymer composition curves obtained at a 5% total conversion,

TABLE 1. St-VC COPOLYMERIZATION IN EACH PRESSURE AT 50°C

Pressure kg/cm²	St in monomer mol%	Polymerization hr	Conversion wt%	Chlorine content %	St in polymer mol%
1	12.0	64.0	5.30	10.00	82.40
	35.6	24.0	7.71	2.34	95.88
	52.1	16.5	9.78	1.73	95.96
	55.71	24.0	11.50	1.41	97.60
	60.8	20.0	9.20	1.40	97.54
	73.3	6.2	4.28	0.70	98.77
1000	9.0	45.0	7.20	17.10	69.90
	41.3	28.9	1.65	2.24	95.35
	46.0	23.0	10.60	2.50	95.60
	51.0	2.8	1.90	1.56	96.26
	63.5	3.5	1.95	1.16	97.96
	66.0	5.7	3.12	1.18	97.92
	75.7	—	—	0.68	98.80
3000	16.0	16.0	8.61	9.90	82.60
	27.3	3.5	3.88	4.57	91.95
	40.0	4.0	7.50	2.73	96.05
	50.7	3.0	4.76	2.34	95.87
	57.0	2.7	8.63	1.69	97.03
	66.0	2.0	4.78	1.13	98.01
	82.0	2.0	6.22	0.83	98.54

TABLE 2. VC-VA COPOLYMERIZATION IN EACH PRESSURE AT 50°C

Pressure kg/cm²	VC in monomer mol%	Polymerization hr	Conversion wt%	Chlorine content %	VC in polymer mol%
1	34.0	3.5	4.3	27.0	47.6
	45.0	3.5	6.1	34.1	60.2
	56.0	3.5	3.4	40.3	71.0
	88.0	2.0	3.0	52.4	92.3
1000	52.0	3.5	25.0	37.6	66.3
	68.0	3.5	23.2	45.3	79.8
	77.0	1.5	6.7	48.6	85.6

9) M. Finemann and S. D. Ross, *J. Polymer Sci.*, **5**, 269 (1950).

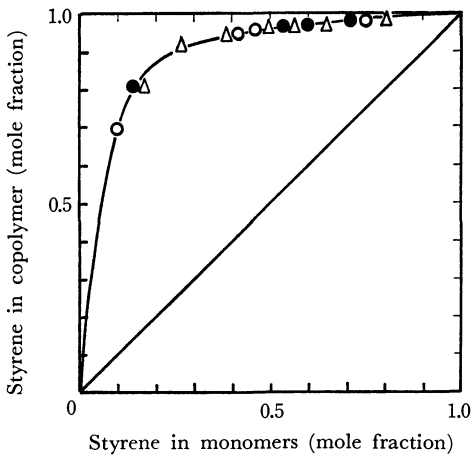

Fig. 1. Copolymer composition curve for St-VC system (50°C).
-△-: 3000 kg/cm², -○-: 1000 kg/cm²
-●-: 1 kg/cm²

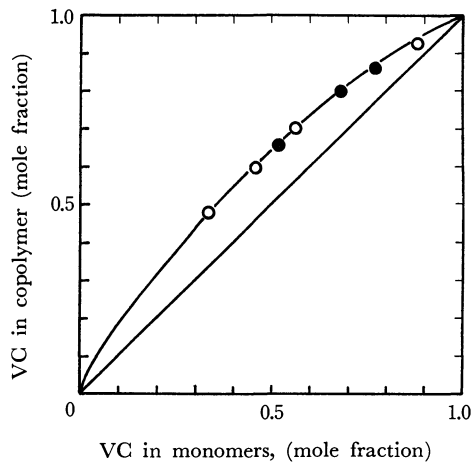

Fig. 2. Copolymer composition curve for VC-VA system.
-○-: 1000 kg/cm², -●-: 1 kg/cm²

regardless of the reaction period under each pressure for the two systems, are shown in Figs. 1 and 2. In addition, the plots obtained by the Fineman-Ross method are illustrated in Figs. 3 and 4.

As Figs. 1 and 2 show, the copolymer compositions under high pressures form the same line as that of the atmosphere, within the limits of experimental error. The fact suggests that the copolymer compositions are quite independent of the pressure for the St-VC and VC-VA systems; that is the monomer reactivity ratios are not affected by the pressure.

The values of r_1 and r_2 evaluated from the slope and the intercept in Figs. 3 and 4 are summarized in Table 3. The values agree with those obtained by other workers[10,11] and show that the styrene monomer has a much greater tendency than does

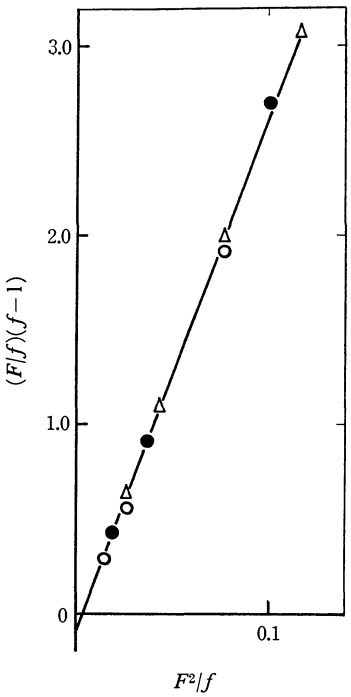

Fig. 3. Finemann-Ross plots for St-VC system.
-△-: 3000 kg/cm², -○-: 1000 kg/cm²,
-●-: 1 kg/cm²

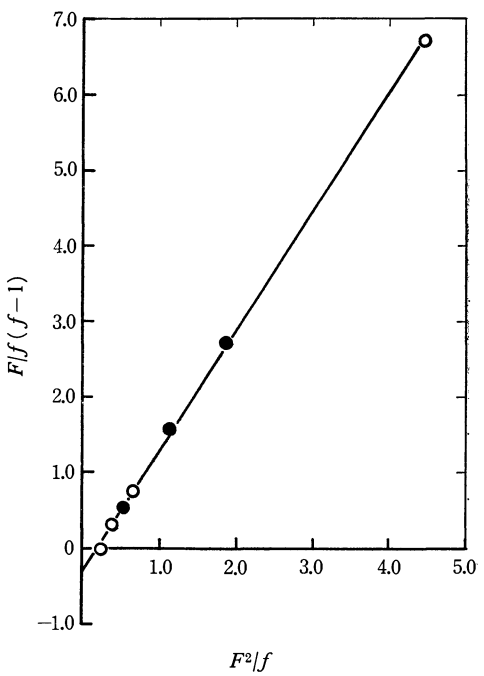

Fig. 4. Finemann-Ross plots for VC-VA system.
-○-: 1000 kg/cm², -●- 1 kg/cm²

10) E. Ham, E. C. Chapin and R. G. Fordyce, *J. Am. Chem. Soc.*, **70**, 538 (1948).
11) F. R. Mayo, C. Walling, F. M. Lewis and W. F. Hulse, *ibid.*, **70**, 1523 (1948).

vinyl chloride to add either to a styrene-free radical or to a vinyl chloride-free radical.

The results of the studies of the high-pressure copolymerization of the St-VC system lend some support to our previous conclusion about the pressure effect on copolymerization. Moreover, the conclusion may be extended as follows by considering the above findings regarding the VC-VA system: "The reactivity ratios of the copolymerization between nonconjugated monomers are also independent of the pressure. Therefore, the pressure affects only the copolymerization of a pair of conjugated monomer."

The effect of the pressure on the rate of chemical reactions can be related to the volume change from reactants to the transition state with Van't Hoff's expression:

$$\left(\frac{\mathrm{d}\ln k}{\mathrm{d}P}\right)_T = -\frac{\Delta V^*}{RT} \qquad (2)$$

where ΔV^* is an activation volume.

Assuming that ΔV^* does not vary with the pressure, Eq. (2) leads to:

$$\ln\frac{(k)_p}{(k)_1} = -\frac{\Delta V^*}{RT}(P-1) \fallingdotseq -\frac{\Delta V^*}{RT}P \qquad (3)$$

where $(k)_p$ and $(k)_1$ are the rate constants at P kg/cm^2 and atmosphere respectively.

By substituting r_1 and r_2 into Eq. (3), the following equations are obtained:

$$\ln\frac{(r_1)_p}{(r_1)_1} = \frac{\Delta V^*_{11} - \Delta V^*_{12}}{RT}P \qquad (4)$$

$$\ln\frac{(r_2)_p}{(r_1)_1} = \frac{\Delta V^*_{22} - \Delta V^*_{21}}{RT}P \qquad (5)$$

where $(r)_p$ and $(r)_1$ are the reactivity ratios at P kg/cm^2 and atmosphere respectively. ΔV^*_{ij} is the activation volume for the addition of the j monomer to a chain ending in the i radical.

The constancy of the reactivity ratios with the pressure leads to $\Delta V^*_{11}=\Delta V^*_{12}$ and $\Delta V^*_{22}=\Delta V^*_{21}$. This fact indicates that the two rate constants, k_{11} and k_{12}, similarly increase with the pressure.

In the case of styrene, since ΔV^*_{11} has been known to be -11.5 cc/mol from the data of Nicholson and Norrish,[12] the activation volume of the propagation reaction between the styryl radical and the vinyl chloride molecule, ΔV^*_{12}, may be -11 cc/mol.

Effect of Pressure on the Overall Copolymerization Rates in the St-VC System. The overall copolymerization rates in each pressure are shown in Fig. 5. St and VC are not easy to copolymerize and require a long time to produce VC-rich compositions (see Table 1).

The overall copolymerization rates are markedly accelerated by the pressure and become larger with an increase in the initial styrene mole fraction. This behavior is related to the activation volumes of styrene and vinyl chloride in homopolymerizations. The overall copolymerization rates at each pressure with 50 mol percent of styrene are illustrated in Table 4.

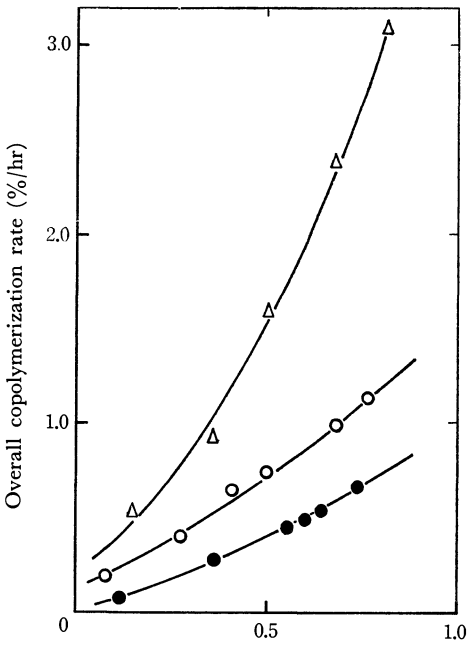

Fig. 5. Effect of pressure on the overall copolymerization rates for St-VC system (50°C).
-△-: 3000 kg/cm^2, -○-: 1000 kg/cm^2,
-●-: 1 kg/cm^2

TABLE 3. THE MONOMER REACTIVITY RATIOS FOR THE SYSTEM OF St-VC AND VC-VA

System	r_1	r_2
St-VC	28	0.08
Ham *et al.*[10]	34	0.077
VC-VA	1.60	0.30
Mayo *et al.*[11]	1.68±0.08	0.23±0.02

TABLE 4. THE OVERALL COPOLYMERIZATION RATES IN EACH PRESSURE AT 0.5 mol%

Pressure kg/cm^2	Rate %/hr	Ratio of rates $(R)_p/(R)_1$
1	0.4	—
1000	0.8	2.0
3000	1.6	4.0

According to the transition-state theory, the following relation is given;

$$k_{11} = kT/h \exp(\Delta S^*_{11}/R)\exp(-\Delta H^*_{11}/RT) \qquad (6)$$

where k is Boltzman's constant, h is Planck's

12) A. E. Nicholson and R. G. W. Norrish, *Discussions Faraday Soc.*, **22**, 97, 104 (1956).

constant, ΔS^* is the activation entropy, and ΔH^* is the activation enthalpy. By substituting $r_1=k_{11}/k_{12}$ for Eq. (6), we have:

$$r_1 = \exp[(\Delta S_{11}^* - \Delta S_{12}^*)/\boldsymbol{R}] \times \exp[-(\Delta H_{11}^* - \Delta H_{12}^*)/\boldsymbol{RT}] \quad (7)$$

Since the activation enthalpies, ΔH^*, are almost invariable with the pressure,[13] the pressure dependence of the reactivity ratios may be attributed to the increment of the relative activation entropies $(\Delta S^*_{11}-\Delta S^*_{12})$.

Therefore, the relative activation entropies at high pressures, $(\Delta S^*_{11}-\Delta S^*_{12})_p$, would be equal to that of the atmosphere, $(\Delta S^*_{11}-\Delta S^*_{12})_1$, in the copolymerization of the nonconjugated monomer and styrene.

Effect of Pressure on the Molecular Weight of the Copolymer. The molecular weights of the copolymer in the St-VC system were not measured directly, but the intrinsic viscosity $[\eta]$ was determined as a approximate indication, whose relation to the copolymer composition is shown in Fig. 6.

Although the reason why these curves rise abruptly at higher styrene contents cannot be explained briefly, the increase in $[\eta]$ with the pressure can be recognized in the figure. This behavior must be due to the acceleration of the chain growth by the pressure.

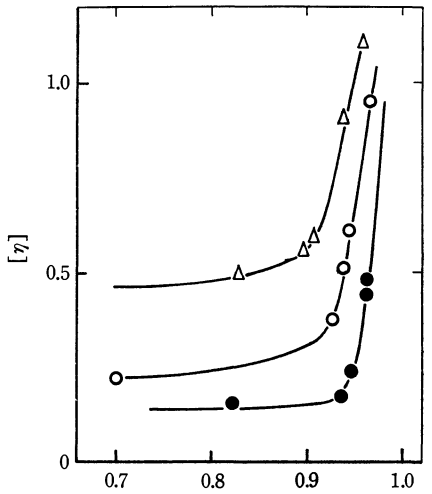

Fig. 6. Effect of pressure on the intrisic viscosity in toluene solution (30°C).
-△-: 3000 kg/cm², -○-: 1000 kg/cm², -●-: 1 kg/cm²

13) C. Walling and J. Pellon, *J. Am. Chem. Soc.*, **79**, 4782 (1957).

BULLETIN OF THE CHEMICAL SOCIETY OF JAPAN VOL. 41 548—555 (1968)

Studies of Poly-2-vinylpyridine. V. Temperature Dependence of the Intrinsic Viscosity and Osmotic Pressure of an Ethanol Solution

Shizuo ARICHI

Department of Chemistry, Faculty of Science, Kumamoto University, Kurokami-machi, Kumamoto

(Received July 17, 1967)

The viscosity of a series of 10 fractions of poly-2-vinylpyridine and the osmotic pressure of a fraction of the same polymer in ethanol were measured at several temperature. The temperature coefficients of the intrinsic viscosities of all the fractions measured were found to be completely negative. The Mark-Houwink equations for molecular-weight-homogeneous samples were obtained in ethanol at 10, 25, 40, and 65°C. The Flory constant, $K=[\eta]_\theta/M^{1/2}$, obtained by the method of Fixman was found to be 13.0×10^{-4} at 25°C; this value is considerably larger than those estimated from the intrinsic viscosity data of this polymer in non-acidic solvents. The K value lowered to an ordinary level when it contained 2.7 N of dry ammonia in ethanol at 25°C. The values of the thermodynamic interaction parameters for dilution, ψ_1 and θ, were obtained from the viscosity data; the former was negative, but nearly zero (−0.02), while the latter was unusually large (397°C). The excess molar entropy of dilution obtained from the measurements of the temperature dependence of the osmotic pressure was found to be negative, but almost zero, which was in accordance with the value of ψ_1 described above; the excess molar heat of dilution obtained in the same way was found to be completely negative. Thus, the exhothermic interaction and negative excess entropy for dilution in this system were studied somewhat quantitatively.

In preceding papers[1-4] some results of the investigation of the solution properties of poly-2-vinylpyridine have been reported as a part of a series of studies of this polymer. Recently, several other papers concerning the solution properties of this polymer[5] and of a related polymer, poly-2-methyl-5-vinylpyridine[6,7] have also been reported. These papers have indicated that the Flory constants, $K=[\eta]_\theta/M^{1/2}$, of polyvinylpyridine homologues are exceptionally larger in alcohols or chloroform than those in the other solvents.[3,4,6,7] It has been also suggested that the thermodynamic interactions of polyvinylpyridine homologues with alcohols are peculiar; for example, in the cases of poly-4-vinylpyridine and poly-2-vinylpyridine, it has been suggested qualitatively that the contributions of enthalpy and entropy to the relative polymer-solvent interaction in alcohols are negative.[2,8]

The present investigation was intended to clarify more completely the solvent effects on the unperturbed dimension, and the thermodynamic interactions between poly-2-vinylpyridine and ethanol, by measuring the temperature dependence of the intrinsic viscosity of a series of fractions in ethanol, and also by measuring the temperature dependence of the osmotic pressure of a fraction in the same solvent.

Experimental

Materials. The poly-2-vinylpyridine fractions used in the viscosity and osmotic pressure measurements were all the same to those used in a previous study.[3] The ethanol was refluxed with freshly-burned calcium oxide and was then carefully distilled with the apparatus described in a previous paper.[1] Ethanol and methanol containing dry ammonia were prepared by introducing ammonia gas into these solvents. The ammonia gas was generated by slightly warming 32% ammonia water and was dried with soda lime, potassium hydroxide, and phosphorus pentoxide successively. The concentration of ammonia was determined by titration with hydrochloric acid.

Viscosity and Osmotic Pressure. The viscosity measurements were carried out with Ubbelohde-type capillary viscometers. The flowing volume was about 2 ml, and the flow time of ethanol for one of viscometers at 10, 25, 40, and 65°C were 187.5, 141.8, 109.5 and 74.3 sec, respectively. Nearly the same flow time was required for the other three viscometers. All the solutions were filtered through a glass filter immediately

1) S. Arichi, S. Mitsuta, N. Sakamoto and H. Murata, This Bulletin, **39**, 428 (1966).
2) S. Arichi, H. Matsuura, Y. Tanimoto and H. Murata, *ibid.*, **39**, 439 (1966).
3) S. Arichi, *ibid.*, **39**, 439 (1966).
4) S. Arichi, *J. Sci. Hiroshima Univ., Ser. A-II*, **29**, 97 (1965).
5) A. J. Hyde and R. B. Taylor, *Polymer*, **4**, 1 (1963).
6) G. B. Gechele and L. Crescentini, *J. Polymer Sci.*, **A-3**, 3599 (1965).
7) C. Garbuglio, L. Crescentini, A. Mula and G. B. Gechele, *Makromol. Chem.*, **97**, 97 (1966).
8) A. G. Boyes and U. P. Strauss, *J. Polymer Sci.*, **22**, 463 (1956).

before measurement. The initial concentrations of the solution ranged from 0.5 to 2.5 g/d*l* according to the molecular weight of the fractions measured; they were determined by the weight method at 25°C and were corrected for thermal expansion or contraction. The kinetic-energy correction was neglected.

The measurements of osmotic pressure were carried out with an apparatus of the type proposed by Sands and Johnson.[9] The detailed procedure and the complete construction of the equipment were described in their paper. Almost the same equipment was constructed; fifteen measurements could be carried out at the same time in the same water bath using a turntable. The membranes used were gel cellophane, # 300, kindly supplied by the Tokyo Cellophane Co., Ltd. At least 10 hr were required to attain equilibrium, regardless of the concentration of the solution, at 15°C. The lowering of height difference, $h-h_0$, between the head in the measuring capillary, h, and that in the reference capillary, h_0, after the equilibrium had been attained were not observed during the 15 days the solution was kept at 15°C. With an increase in the temperature, the linear line in $h-h_0$ *versus* the time plots inclined slightly, but when measurements were continued for at least 10 days, a sufficiently accurate extraporation to zero time could be made.

Results and Discussion

The Mark-Houwink Equation. The results of viscosity measurements for a series of fractions at 10, 25, 40, and 65°C in absolute ethanol are summarized in Table 1, while plots of the intrinsic viscosity number, $[\eta]$, *versus* the temperature are shown in Fig. 1. The fraction numbers in Table 1 and Fig. 1 correspond to those described in a previous paper,[3] where the measurement of the weight-average and the number-average molecular weight, M_w and M_n, for each fraction are described. The slopes of the line in Fig. 1, namely, the temperature coefficients of the intrinsic viscosity, are all negative, in contrast to the case in ordinary polymer-solvent systems.

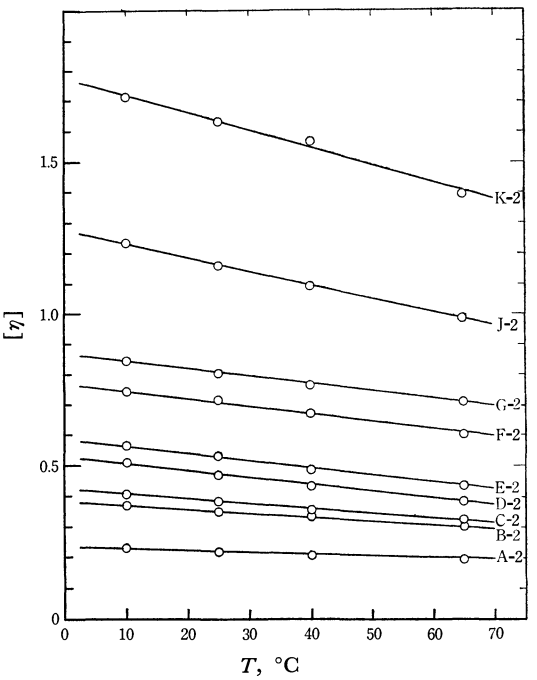

Fig. 1. Plots of intrinsic viscosity of poly-2-vinyl-pyridine fractions in ethanol *vs.* temperature.

Figure 2 shows plots of $[\eta]$ at four temperatures against M_w in double logarithmic scales. The Mark-Houwink equation at each temperature was obtained by the method of least squares as follows:

$$[\eta] = 1.03\times10^{-4} M_w^{0.746} \quad \text{at } 10°C$$
$$[\eta] = 1.09\times10^{-4} M_w^{0.729} \quad \text{at } 25°C$$
$$[\eta] = 0.99\times10^{-4} M_w^{0.733} \quad \text{at } 40°C$$
$$[\eta] = 1.06\times10^{-4} M_w^{0.718} \quad \text{at } 65°C$$

TABLE 1. THE WEIGHT AVERAGE MOLECULAR WEIGHT AND THE INTRINSIC VISCOSITY NUMBER AT VARIOUS TEMPERATURE FOR A SERIES OF FRACTIONS OF POLY-2-VINYLPYRIDINE IN ABSOLUTE ETHANOL, AND IN ETHANOL CONTAINED 2.7 N DRY AMMONIA

Fraction No.	M_w $\times10^{-4}$	$[\eta]$ in ethanol at				$[\eta]$ in ethanol contained 2.7 N NH_3 at 25°C
		10°C	25°C	40°C	65°C	
A-2	3.40	0.231	0.219	0.210	0.199	0.160
B-2	6.28	0.370	0.354	0.332	0.300	0.225
C-2	7.27	0.409	0.384	0.356	0.325	0.259
D-2	9.30	0.511	0.466	0.440	0.385	0.280
E-2	12.01	0.562	0.526	0.484	0.437	0.398
F-2	16.05	0.747	0.713	0.678	0.601	—
G-2	21.95	0.849	0.800	0.767	0.712	0.528
J-2	30.75	1.235	1.156	1.096	0.986	0.815
K-2	52.06	1.715	1.637	1.577	1.397	0.932
M-1	81.29	2.487	2.205	2.075	1.825	1.642
L-1	84.97	—	—	—	—	1.785

9) G. D. Sands and B. L. Johnson, *Anal. Chem.*, **19**, 261 (1947).

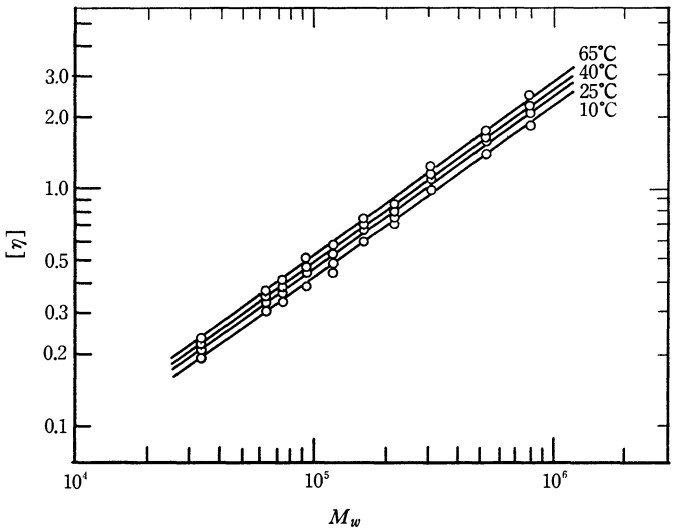

Fig. 2. Log-log plots of intrinsic viscosity of poly-2-vinylpyridine fractions in ethanol *vs.* weigt average molecular weight at 10, 25, 40 and 65°C.

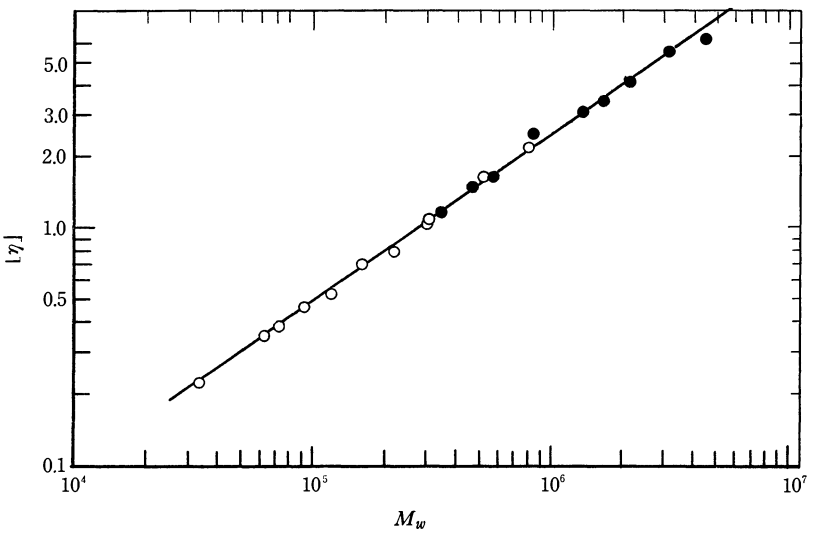

Fig. 3. Log-log plots of intrinsic viscosity of poly-2-vinylpyridine fractions in ethanol *vs.* weight average molecular weight at 25°C; (●): data obtained by Hyde and Taylor,[5] (○): data obtained in this study.

The Mark-Houwink equation for poly-2-vinylpyridine in absolute ethanol has already been reported by Hyde and Taylor[5] as follows:

$$[\eta] = 2.8\times 10^{-4} M_w^{0.66} \qquad \text{at } 25°C$$

The values of the two constants in this equation seem to be considerably different from those in our equation at the same temperature described above. However, if all the data for $[\eta]$ and M_w obtained by Hyde and Tailor and those obtained in this study are plotted together, the relation between $\log [\eta]$ and $\log M_w$ are sufficiently represented by a linear line for a very wide range of molecular weight, as is shown in Fig. 3. The line is consistent with the following equation, obtained by the method of least squares:

$$[\eta] = 1.50\times 10^{-4} M_w^{0.703} \qquad \text{at } 25°C$$

with the point of the lowest-molecular-weight sample, $M_w=8.6\times 10^4$, in the data of Hyde and Taylor being excepted.

The Mark-Houwink equations for the molecular-weight-homogeneous samples were obtained in the

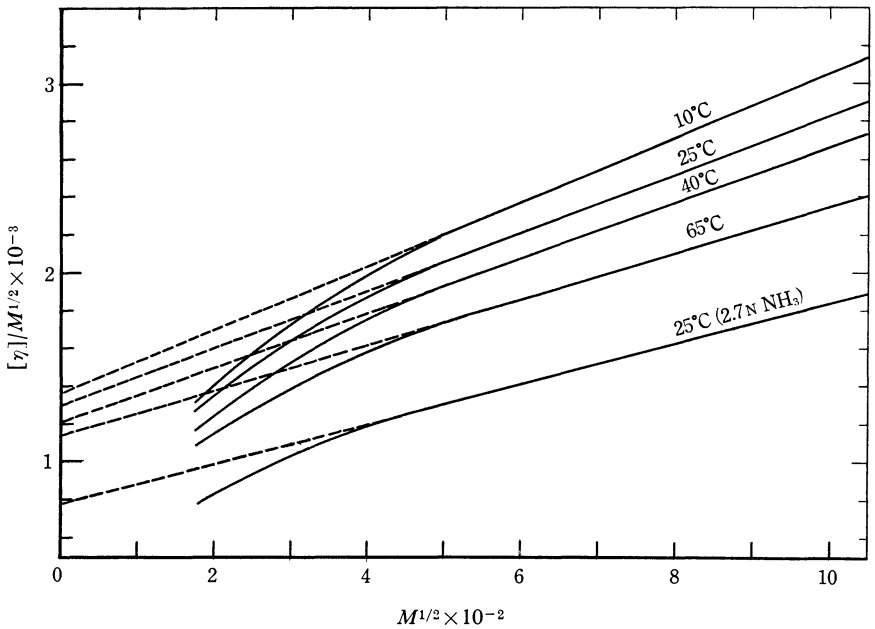

Fig. 4. Plots of $[\eta]/M^{1/2}$ *vs.* $M^{1/2}$ for poly-2-vinylpyridine in ethanol at 10, 25, 40 and 65°C and of those in ethanol contained ammonia (2.7 N) at 25°C.

same manner as before,[3] assuming that the molecular-weight distribution of each fraction is represented by the logarithmic normal-type molecular-weight-distribution function[10]:

$$w(M) = MA \exp\{-p^2(\ln M/M_0)^2\}$$

where the parameters are the same as in a previous paper.[3] The results are as follows:

$$[\eta] = 1.10\times10^{-4} M^{0.740} \quad \text{at } 10°C$$
$$[\eta] = 1.18\times10^{-4} M^{0.729} \quad \text{at } 25°C$$
$$[\eta] = 1.06\times10^{-4} M^{0.733} \quad \text{at } 40°C$$
$$[\eta] = 1.15\times10^{-4} M^{0.718} \quad \text{at } 65°C$$

These equations were used for the following evaluations of the Flory constants and of the thermodynamic interaction parameters.

The Flory Constant. The Flory constant, K, is defined by the following equations:

$$[\eta]_\theta = KM^{1/2} \tag{1}$$
$$K = \Phi_0(\langle L^2\rangle_0/M)^{3/2} \tag{2}$$

where $[\eta]_\theta$ and $\langle L^2\rangle_0$ are the intrinsic viscosity and the mean square of the end-to-end distance of a polymer molecule in the θ-solvent respectively; M, the molecular weight, and Φ_0, the universal constant (2.87×10^{21} for the molecular-weight-homogeneous polymer). The values of K were estimated according to the equation of Stockmayer and Fixman:[11]

$$[\eta]/M^{1/2} = K + 0.51\Phi_0 BM^{1/2} \tag{3}$$

where B is the long-range-interaction parameter. In spite of recent attempts to improve the graphical method for obtaining the unperturbed dimension, the Stockmayer and Fixman relation is still recommended as the most versatile form.[12]

Plots of the left-hand side of Eq. (3) against $M^{1/2}$ are drawn in Fig. 4. The calculations were carried out for a number of pairs of ideal values of M and $[\eta]$ obtained from the Mark-Houwink equation for molecular-weight-homogeneous poly-2-vinylpyridine in ethanol at each temperature described previously. The full lines show the range of molecular weight over which the original Mark-Houwink equations can be applied. Although the samples used in this study have quite a large inhomogeneity of molecular-weight distribution about their average values,[3] the corrected values of K may be obtained by the way of plotting shown in Fig. 4. A similar plotting method has been used by Gechel and others[7] in obtaining the value of K.

Because the lines in Fig. 4 show an appreciable downward curvature in the low-molecular-weight region, where, unfortunately, it is most important to extrapolate the lines to zero molecular weight, the values of K at each temperature were estimated by the extrapolation of the linear part of the lines in the relatively higher molecular-weight region.

10) R. Koningsveld and C. A. F. Tuijinman, *J. Polymer Sci.*, **39**, 445 (1959).

11) W. H. Stockmayer and M. Fixman, *ibid.*, *C*-**1**, 137 (1963).

Recently, the deviation from linearity in the Fixman plots has been discussed by several authors.[12,13] Berry[14] has proposed a new approximate expression instead of Eq. (3). However, most of these discussions have been based on the data of considerably higher-molecular-weight samples in good solvents. In this study, the molecular weights of the samples are not so large (less than 10^6), and the expansion coefficients, α_η, were mostly less than 1.4. Consequently, no correction has been applied further.

The values of K estimated from Fig. 4 are shown in Table 2; they are extraordinary large when compared with those estimated from the data in non-alcoholic solvents.[4] Gechel and others[6,7] reported just the same situation as to the trend of downward curvature shown in Fig. 4, and as to the estimation of the large value of K from the intrinsic viscosity data of poly-2-methyl-5-vinylpyridine in methanol and chloroform. They attributed these results to the association of solution components due to the polarity of the solvents.

TABLE 2. THE FLORY CONSTANT, K, OBTAINED FROM Fig. 4 FOR POLY-2-VINYLPYRIDINE AT VARIOUS TEMPERATURE

Temp. (°C)	Solvent	$K\times10^4$
10	Ethanol	13.7
25	Ethanol	13.0
40	Ethanol	12.2
65	Ethanol	11.5
25	Ethanol - 2.7 N NH_3	7.9

Attempts were made to clarify the effect of the acidity of methanol and ethanol on the values of the intrinsic viscosity of poly-2-vinylpyridine fractions in these solvents. Figure 5 shows the plots of the intrinsic viscosity of poly-2-vinylpyridine fractions in methanol and ethanol containing varying amounts of ammonia *versus* the concentration of ammonia in these solvents.

The sensitive lowering of the intrinsic viscosity with the increase in the concentration of ammonia, namely, with the decrease in the acidity of the solvent, is shown in Fig. 5. The plots of the intrinsic viscosity of the fractions in ethanol contained 2.7 N of dry ammonia *versus* M_w at 25°C; for purposes of comparison, those in absolute ethanol at 25°C *versus* M_w are shown in Fig. 6. The Mark-Houwink equation for the fractions of molecular-weight-homogeneous poly-2-vinylpyridine in ethanol containing 2.7 N dry ammonia were obtained in the same way as before to be as follows:

$$[\eta] = 0.64\times10^{-4} M^{0.74} \quad (4)$$

The lowest line in Fig. 4 resulted from the combination of Eq. (3) and Eq. (4); the value of K was estimated to be 7.9×10^{-4}, which is very close to the values obtained from the data of the intrinsic viscosity in non-acidic solvents.

The results obtained above are considered to be sufficient to show that the unperturbed dimension of poly-2-vinylpyridine in alcohols is influenced by the acidity of solvents.

Parameters for Thermodynamic Interaction. The thermodynamic interaction parameters for dilution, ψ_1 and θ, were obtained using

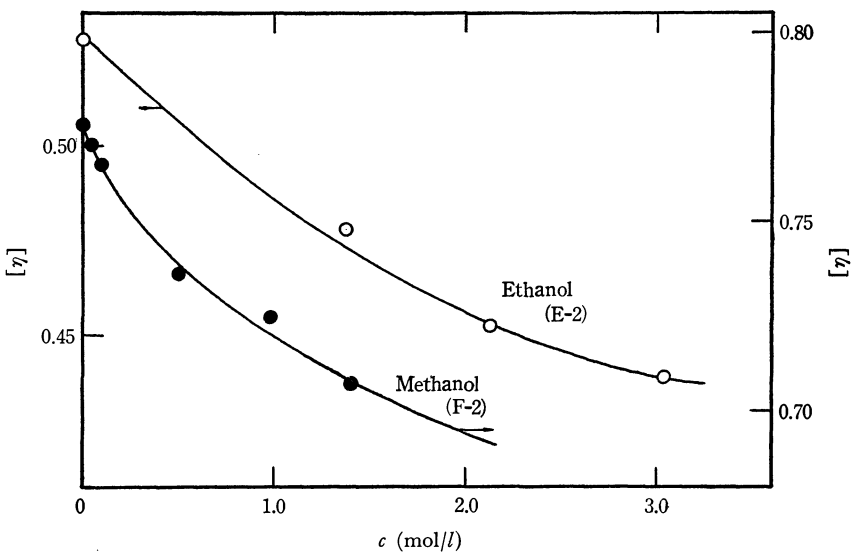

Fig. 5. Plots of intrinsic viscosity of poly-2-vinylpyridine fractions *vs.* concentration of ammonia contained in solvent at 25°C; (○): data for the fraction E-2 in ethanol, (●): data for the fraction F-2 in methanol.

12) J. M. G. Cowie, *Polymer*, **7**, 487 (1966).
13) H. Inagaki, H. Suzuki, M. Fujii and T. Matsuo, *J. Phys. Chem.*, **70**, 1718 (1966).
14) G. C. Berry, *J. Polymer Sci., B-4*, 161 (1966)

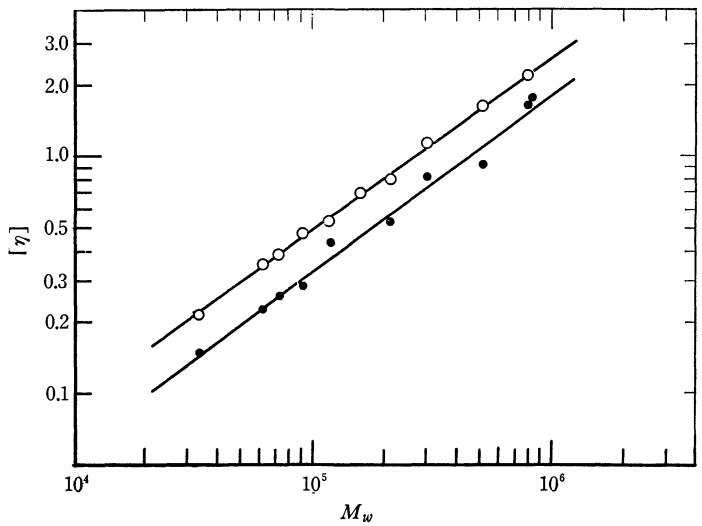

Fig. 6. Log-log plots of intrinsic viscosity of poly-2-vinylpyridine fractions in absolute ethanol (○), and in ethanol contained ammonia (2.7 N) (●), *vs.* weight average molecular weight at 25°C.

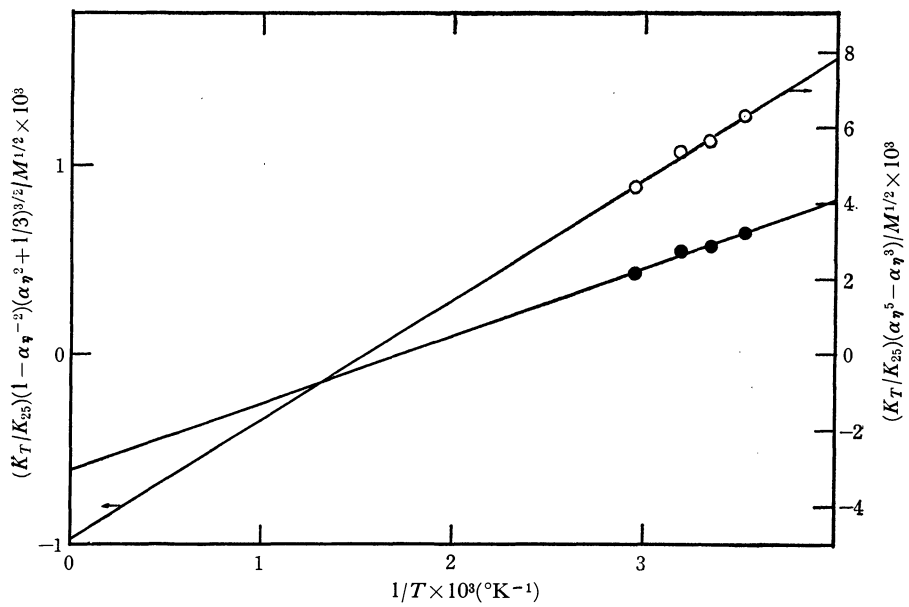

Fig. 7. Plots of $(K_T/K_{25})(\alpha_\eta^5-\alpha_\eta^3)/M^{1/2}$, (●), and $(K_T/K_{25})(1-\alpha_\eta^{-2})(\alpha_\eta^2+1/3)^{3/2}/M^{1/2}$, (○), *vs.* $1/T$ for poly-2-vinylpyridine in ethanol.

the data of the intrinsic viscosities at four different temperatures. The basic equations used for this purpose were the equation of Flory and Fox[15] and that of Kurata and Stockmayer:[16]

$$(K_T/K_{25})(\alpha_\eta^5-\alpha_\eta^3)/M^{1/2} = 2C_M\psi_1(1-\theta/T) \quad (5)$$

$$(K_T/K_{25})(1-\alpha_\eta^{-2})(\alpha_\eta^2+1/3)^{3/2}/M^{1/2} = (2^5/3^3)1.10C_M\psi_1(1-\theta/T) \quad (6)$$

where:

$$\alpha_\eta^3 = [\eta]/[\eta]_\theta$$

and

$$C_M = ((3^3/2^{5/2}\pi^{3/2})v^2/N V_1)(M/\langle L^2\rangle_0)^{3/2}$$

and where K_T and K_{25} are the Flory constants at T°C and 25°C respectively; v, the specific volume

15) P. J. Flory and T. G. Fox, *J. Am. Chem. Soc.*, **73**, 1904 (1951).
16) M. Kurata and W. H. Stockmayer, *Fortsch. Hochpolymer. Forsch.*, **3**, 196 (1963).

of the polymer; V_1, the molar volume of the solvent, and N, the Avogadro number.

With the aid of the Mark-Houwink equations for the molecular-weight-homogeneous samples at each temperature, we calculated the values of $[\eta]$ and $[\eta]_\theta$ and, consequently, the α_η value for an ideal polymer fraction whose molecular weight $M=10^6$; the values of the left-hand side of Eq. (5) and Eq. (6) are plotted against $1/T$ in Fig. 7. Apparently the slopes of the lines are the reverse of those for ordinary polymer-solvent systems. The values of ψ_1 and θ obtained by the method of least squares are summarized in Table 3.

TABLE 3. THE THERMODYNAMIC INTERACTION PARAMETERS FOR DILUTION OF POLY-2-VINYLPYRIDINE IN ETHANOL

Method	ψ_1	θ (°C)
Flory and Fox, Eq. (5)	−0.02	287
Kurata and Stockmayer, Eq. (6)	−0.02	397

The values of the entropy parameter obtained by the two equations are both very small, but negative, while the theta temperatures thus evaluated are unusually high. Such an anomaly as the occurrance of precipitation upon the heating of the solution can be predicted when the solution process is characterized by a negative excess entropy.[17]

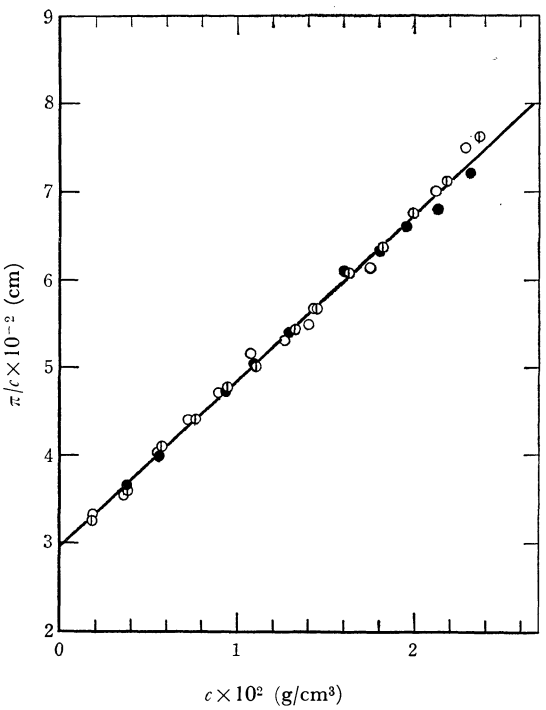

Fig. 8. Plots of reduced osmotic pressure *vs.* concentration of poly-2-vinylpyridine fraction, E-2, in ethanol at 15°C (ⓘ), 30°C (●), and 45°C (○).

The extraordinariness of the thermodynamic interaction between polyvinylpyridine and ethanol was further studied by investigating the temperature dependence of the second and the third virial coefficient, A_2 and A_3, of this polymer-solvent system.[18]

Figure 8 shows plots of the reduced osmotic pressure, π/c, *versus* the concentration, c. In spite of the measurements of the osmotic pressure over the range of very wide concentration, the temperature dependence of π/c is very small, as may be seen in Fig. 8; however, the data were treated with the method of Flory and Krigbaum,[19] assuming that the following equation is valid for this polymer-solvent system:

$$(\pi/c)^{1/2} = (\pi/c)_0^{1/2}[(1+\Gamma_2/2)c] \qquad (7)$$

The values of A_2 and A_3 were calculated from the values of $(\pi/c)_0$ and Γ_2 as evaluated by the method of least squares; they are plotted against the temperature in Fig. 9.

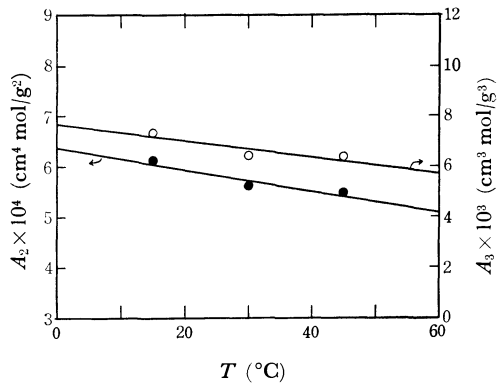

Fig. 9. Plots of osmotic the second, (●), and the third virial coefficient, (○), *vs.* temperature for poly-2-vinylpyridine fraction, E-2, in ethanol.

The excess thermodynamic functions of dilution for this system at 25°C were calculated by the following equations:

$$\Delta\mu_1^E/c^2V_1 = -RT(A_2 + A_3c)$$
$$\Delta h_1^E/c^2V_1 = RT^2\{(\partial A_2/\partial T) + (\partial A_3/\partial T)c\}$$
$$T\Delta s_1^E/c^2V_1 = RT\{A_2 + T(\partial A_2/\partial T) + A_3c + T(\partial A_3/\partial T)c\}$$

where $\Delta\mu_1^E$ represents the excess free energy of dilution; Δh_1^E, the excess molar heat of dilution, and Δs_1^E, the excess molar entropy of dilution. The results are summarized in Table 4.

Here again, it was confirmed that the contributions of both enthalpy and entropy to the relative polymer-solvent interaction in this system are

17) H. Morawetz, "Macromolecules in Solution," Interscience Publishers, N. Y. (1965).
18) K. Takamizawa, This Bulletin, **39**, 1186 (1966).
19) P. J. Flory, *J. Chem. Phys.*, **17**, 1347 (1949); P. J. Flory and W. R. Krigbaum, *ibid.*, **18**, 1086 (1950).

TABLE 4. THE EXCESS THERMODYNAMIC FUTNCTIONS OF DILUTION FOR POLY-2-VINYLPYRIDINE IN ETHANOL AT 25°C (cal cm³/g²)

$c \times 10^2$ g/100 cm³	$\Delta\mu_1^E/c^2V_1$	$\Delta h_1^E/c^2V_1$	$T\Delta s_1^E/c^2V_1$
0	−0.346	−0.376	−0.030
1	−0.387	−0.433	−0.046
2	−0.428	−0.489	−0.061

negative, indicating a very strong specific interaction between polymer and solvent upon their being mixed, and also, a very high degree of order in the packing of ethanol molecules and of the polymer segments (this is probably due to the hydrogen bond formation).[17]

The existence of some exhothermic interaction between poly-2-vinylpyridine and aliphatic alcohols or chloroform, and the resulting possibility of hydrogen-bond formation between the polymer and solvent, has been already suggested by investigations of the data of the intrinsic viscosity in many solvents at a constant temperature, 25°C, and those of the precipitation measurements of this polymer in mixed solvents consisting of alcohol and hexane, and of chloroform and hexane.[2] However, the parameters and the functions for the relative thermodynamic interactions between poly-2-vinylpyridine and absolute ethanol obtained by the data of the temperature dependence of intrinsic viscosity and osmotic pressure in this study confirm more directly and quantitatively the suggestions described above.

The author wishes to express his thanks to Professor Daisei Yamamoto of this University for his continued advice and encouragement in this work.

BULLETIN OF THE CHEMICAL SOCIETY OF JAPAN VOL. 41 555—563 (1968)

Effect of the Ionic Strength on the Behavior of Sodium Chondroitin Sulfate C in Aqueous Solutions*1

Masayuki NAKAGAKI and Kiyoshi IKEDA*2

Faculty of Pharmaceutical Science, Kyoto University, Sakyo-ku, Kyoto

(Received July 26, 1967)

Viscosity and light-scattering investigations were carried out in aqueous sodium chloride solutions at 25°C on a sample of sodium chondroitin sulfate C from shark cartilage. The weight-average molecular weight of 74000 was obtained. The molecular dimensions, obtained from the viscosity-partial specific volume, from the light scattering-partial specific volume, and from the light scattering-viscosity, were found to fit well for a long-rod model with a length of about 800 Å and a diameter of about 10 Å at the infinite ionic strength.

Sodium chondroitin sulfate is known to be an unbranched linear anionic polyelectrolyte. It has been considered that the molecule is fully stretched at a very low ionic strength by intramolecular electrostatic repulsion, but that it begins contracting with the increase in ionic strength because of the suppression of the repulsive force by ion-pair formation or by the electrostatic screening effect of the ion atmosphere, until at last it becomes randomly coiled.[1]

Chondroitin sulfate has three isomers, as is schematically illustrated in Fig. 1.[2] The B type of chondroitin sulfate has an axial carboxyl and sulfonic group, the A type, an equatorial carboxyl and an axial sulfonic group, and the C type, an equatorial carboxyl and sulfonic group. These differences in primary structure are considered to influence the behavior of the molecules in aqueous solutions. It has been known, actually, that the solubility in aqueous ethanol[3] is greater for the A and C types than for the B type; the value of pK_a on the potentiometric titration curve[3] is larger for the B type than for the A type, and the affinity of Ca^{2+} and Mg^{2+} under physiological conditions is greater for the B type than for the A type.[4] Furthermore, the affinity of a trivalent cation,

*1 This paper was presented at the 19th Annual Meeting of the Chemical Society of Japan, Yokohama, March, 1966.

*2 Present address of K. I.: Department of Chemistry, Faculty of Science, Kwansei Gakuin University, Nishinomiya.

1) M. B. Mathews, *Arch. Biochem. Biophys.*, **43**, 181 (1953).

2) M. B. Mathews, *ibid.*, **104**, 394 (1964).

3) M. B. Mathews, *Biochim. Biophys. Acta*, **35**, 9 (1959).

4) E. Buddecke and R. Drezenick, *Z. Physiol. Chem.*, **327**, 49 (1962).

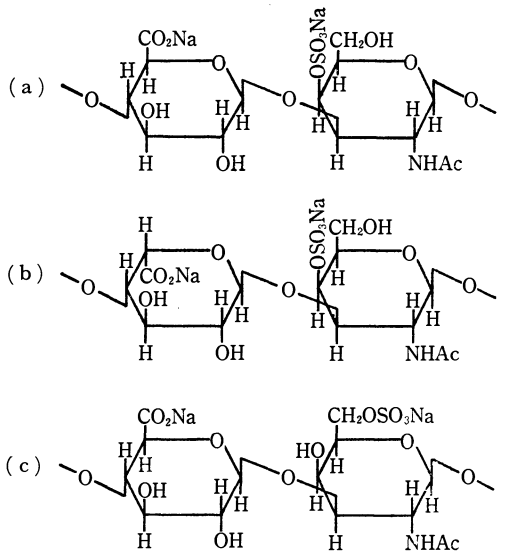

Fig. 1. Schematic illustration of disuccharide units of sodium chondroitin sulfates.
(a) A type; (b) B type; (c) C type

$Co(NH_3)_6^{3+}$, is greater for the B type than for the A type at a fixed ionic strength.[5] At a very low pH, where the ionization of carboxyl groups is mostly suppressed, there is not so large a difference in the affinity for $Co(NH_3)_6^{3+}$ among the three types of chondroitin sulfates at a low ionic strength; with an increase in the ionic strength, the affinity increases in the order of B>A>C types.[2] Further, only the B type of chondroitin sulfate is resistant to testicular hyaluronidase and possesses anticoagulant properties.[6]

It may be supposed from these facts that the C-type chondroitin sulfate has the least flexible structure of the three isomers, while the B type is the most flexible molecule. Recent studies of optical rotatory dispersion[7] have shown that a Cotton effect exists on the ultraviolet ORD curve with the C-type chondroitin sulfate, and an induced Cotton effect in the visible region is observed for the complex of this polymer with acridine orange. Comparing this phenomenon with other, similar phenomena shown by the helical polyglutamic acid,[8] tobacco mosaic virus,[9] and DNA,[10] chondroitin sulfate C may be supposed to have a helical structure at a suitable ionic strength.

In this paper, the effects of the ionic strength on the behavior of sodium chondroitin sulfate C prepared from shark cartilage is discussed quantitatively on the basis of viscosity measurements and light-scattering (Zimm-plot method) experiments.

Experimental

Materials and Solvent. The sodium chondroitin sulfate of the C type was kindly furnished by the Seikagaku-Kogyo Co., Ltd.,[11,12] the preparation being extracted from shark cartilage, fractionated, and carefully purified to remove any electrolyte except sodium chloride. The molecular weight of this preparation was 50000, as determined by the results of the terminal analysis, using D-galactosamine hydrochloride as a standard. The water content was 5.46%, and the specific viscosity of a one percent solution of this preparation was 2.03 at 30°C in a physiological solution of sodium chloride. Table 1 shows this preparation contained scarcely any diffusible ion species other than sodium ions.

For the purpose of serial experiments, a 1% stock solution was prepared by the dry-weight method and kept in a refrigerator. Water was distilled and refined by the ion-exchange method for the viscosity measurements. For light scattering, this water was distilled again with an all-glass unit.

Viscosity Measurements. The viscosity was measured at 25°C with a dilution viscometer of the Ubbelohde type. The filtering of the solution was omitted, because the solution was filtered automatically in the course of the experiment by the glass filter attached to the viscometer. The ionic strength and pH were adjusted with sodium chloride, sodium hydroxide, and hydrochloric acid.

Refractive Increment, dn/dc. The refractive increment, dn/dc, was measured with a Shimadzu electrophotometric differential refractometer at 25°C; the calibration was done by referring to a potassium chloride solution.[13] So as to remove errors due to the difference between the temperature of the solution and that of the solvent, and also because of the existence of bubbles, reading was carried out an hour after setting.

Light-scattering Measurements. A Shimadzu electrophotometric light-scattering photometer was employed. All the measurements were done with an unpolarized light of the 436 mμ wavelength, *in vacuo* and at the constant temperature of 25°C, controlled with circulated water. The apparatus was calibrated with the reduced scattering intensity at a 90° angle of benzene,[14] $R_{90}=48.5\times10^{-6}$. For this purpose, a reagent-grade commercial product of benzene was distilled twice with sodium metal, and filtered directly into the cell through a Cella Filter (Mittel) under pressing. A cylindrical glass was used as a solution cell, and its illuminated volume was corrected with a fluorescein solution. The solution and the solvent

5) M. B. Mathews, *Biochim. Biophys. Acta*, **37**, 288 (1960).
6) J. A. Cifonelli, J. Ludowieg and A. Dorfman, *J. Biol. Chem.*, **233**, 541 (1958).
7) A. L. Stone, *Biopolymers*, **3**, 617 (1965).
8) L. S. Streyer and E. R. Blout, *J. Am. Chem. Soc.*, **84**, 1411 (1961).
9) N. S. Simmons and E. R. Blout, *Biophys. J.*, **1**, 55 (1960).
10) D. F. Bradley, I. Tinoco, Jr., and R. W. Woody, *Biopolymers*, **1**, 239 (1963).
11) T. Furuhashi and K. Uchida, *Seikagaku*, **33**, 537 (1961).
12) M. B. Mathews, *Biochim. Biophys. Acta*, **58**, 92 (1962); the specimen used in our study was also employed in his study.
13) A. Kruis, *Z. Phys. Chem.*, **34B**, 13 (1936).
14) C. L. Carr, Jr., and B. H. Zimm, *J. Chem. Phys.*, **18**, 1616 (1950).

Table 1. Analysis of sodium chondroitin sulfate C (N104)
(by Mr. T. Furuhashi,[11] Seikagaku Co., Ltd.)

		Method
pH	6.0	1% in distilled water
Uronic acid (as a glucronic acid)	38.46%	Dische's treatment using carbazole
Hexosamine (as a galactosamine)	33.88%	Modified Elson-Mogan procedure (Boas procedure)
Ester sulfate (SO_4)	20.94%	Chelate method
Total nitrogen	2.78%	Micro Kjeldahl method
Sodium ion	9.28%	Chelate titration
Potassium ion	negative	Ammonium oxalate method
Free sulfuric ion	negative	Nephelometry using barium sulfate
Chloric ion	negative	Direct titration using mercurous nitrate
Peptide or protein	negative	Biuret reaction
$[\alpha]_D^{28}$ (1% in water)	−13.4	Hitachi model POB polarimeter
Paper electrophoresis	one spot	0.1 M acetate buffer (pH 6), 12 v/cm, 90 min dying with toluidine blue

were optically clarified with Membrane Filter No. 15 under pressure. The pressure was given by the air, which was washed by passing a dilute alkaline solution and distilled water through it. The solution was prepared at each concentration by direct dilution in the cell, and the decrease in the concentration was determined by weighing the whole cell. The density decrease of the solution with dilution was neglected in this case. By measuring the refractive index of the solution before and after the filtration, it was confirmed that there is no appreciable decrease in the polymer concentration in the course of the filtration. The ionic strength and the pH were adjusted by the same method as has been described for the viscosity measurements. The scattering intensity was read about an hour later after setting.

Results

The relation between the reduced viscosity and the polymer concentration are shown in Fig. 2 at various ionic strengths. As the ionic strength was decreased, an unusual phenomenon characteristic of polyelectrolytes was observed at low concentrations. Nevertheless, extrapolation to zero concentration was possible except in the case of an extremely low ionic strength. The value of $[\eta]$ thus obtained decreased with an increase in the ionic strength. At a fixed ionic strength, the value of $[\eta]$ was largest in a neutral solution, middle in an alkaline solution, and the smallest in an acidic solution.

The results of light scattering are shown in Figs. 3, 4, 5, and 6. The experimental data were analyzed according to the equation for a two-component system:[15]

$$\frac{Kc}{R_\theta} = \frac{1}{M_w}\left(1+\frac{16\pi^2}{3\lambda^2}\langle\bar{S}^2\rangle \sin^2(\theta/2)\right) + 2A_2c \qquad (1)$$

and

$$K = 2\pi^2 n_0^2 (dn/dc)^2/(\lambda_0^4 N) \qquad (2)$$

R_θ is the reduced scattering intensity of the solution at a scattering angle of θ, from which the term of the solvent is subtracted. c is the polymer concentration, M_w is the weight-average molecular weight of the molecule, dn/dc is the refractive index of the medium, and λ_0 is the wavelength *in*

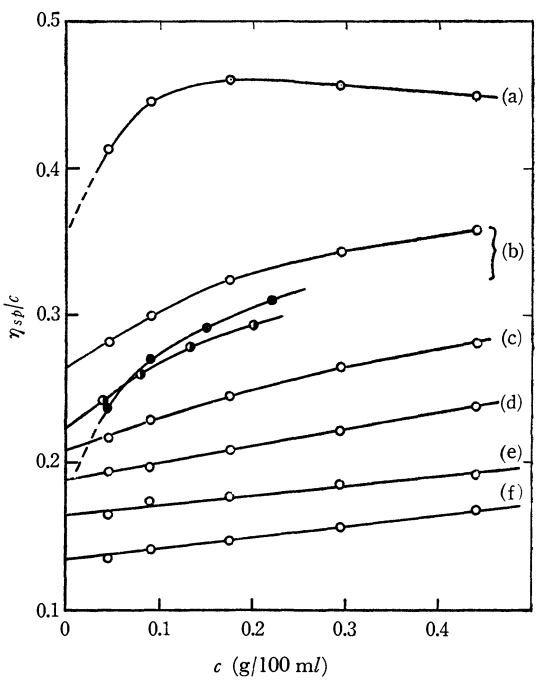

Fig. 2. Viscosity data for sodium chondroitin sulfate C obtained by dilution at a fixed ionic strength at 25°C.
(a), J=0.0035; (b), J=0.01 (○, pH 5.4; ●, pH 2.7; ◑, pH 11.5); (c), J=0.025; (d), J=0.05; (e), J=0.2; (f), J=1.0

15) B. H. Zimm, *ibid.*, **16**, 1099 (1948).

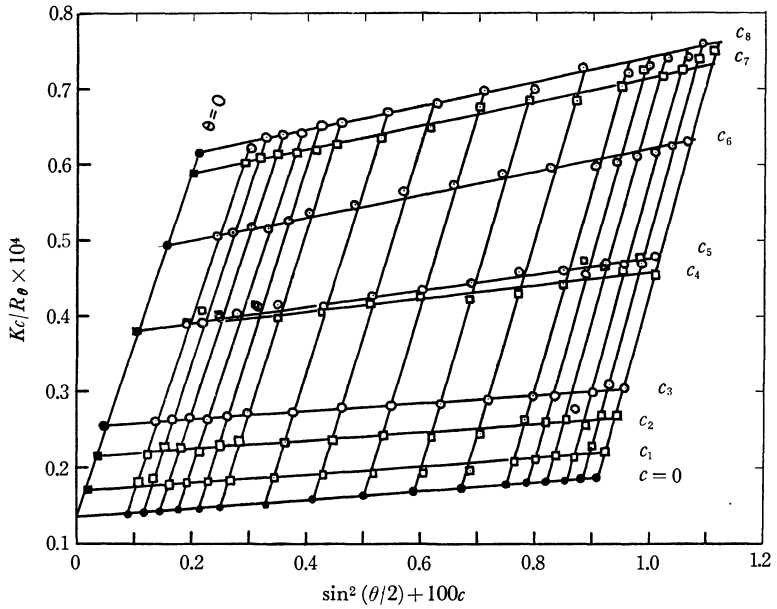

Fig. 3. Zimm plot for sodium chondroitin sulfate C in 0.01 M NaCl (pH 5.4) at 25°C. Polymer concentration: c_1, 0.01646%; c_2, 0.0341%; c_3, 0.04817%; b_4, 0.09824%; c_5, 0.1011%; c_6, 0.1545%; c_7, 0.2014%; c_8, 0.2112%

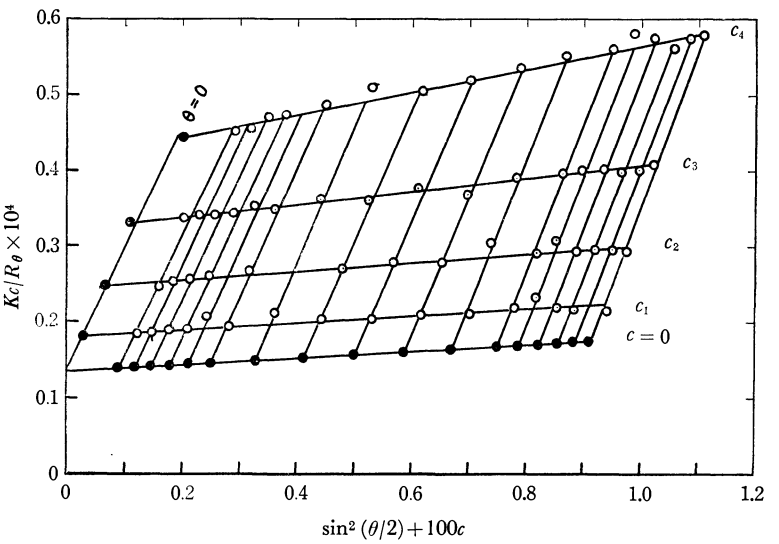

Fig. 4. Zimm plot for sodium chondroitin sulfate C in 0.01 M NaCl (pH 3.5) at 25°C. c_1, 0.03089%; c_2, 0.06355%; c_3, 0.1124%; c_4, 0.2014%

vacuo (4360 Å was used in this experiment). The wavelength, λ, in the medium is related to λ_0 as follows:

$$\lambda = \lambda_0/n_0 \tag{3}$$

$\langle\bar{S}^2\rangle$ is called the mean-square radius of gyration, which is the mean-square distance between the center of gravity and the respective mass element in the molecule; from it the molecular dimensions can be estimated. The following relation exists in the case of a long, rigid rod:[16]

$$\langle\bar{S}^2\rangle = L^2/12 \tag{4}$$

where L is the length of the rod. In the case of a randomly coiled molecule:

$$\langle\bar{S}^2\rangle = R^2/6 \tag{5}$$

where R is the root mean-square end-to-end distance of the flexible molecule.

In the Zimm plots of Figs. 3—6, the Kc/R_θ is

16) T. Neugebauer, *Ann. Phys.*, **42**, 509 (1943).

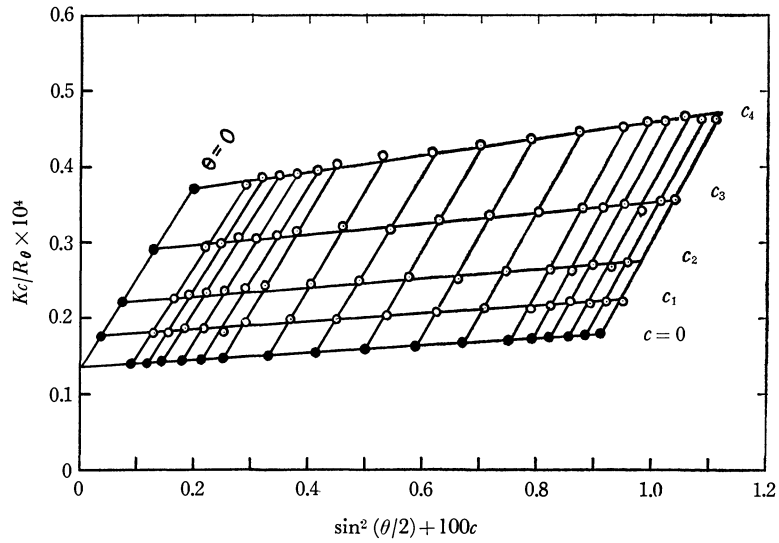

Fig. 5. Zimm plot for sodium chondroitin sulfate C in 0.025 M NaCl at 25°C. c_1, 0.03919%; c_2, 0.0764%; c_3, 0.1306%; c_4, 0.2014%

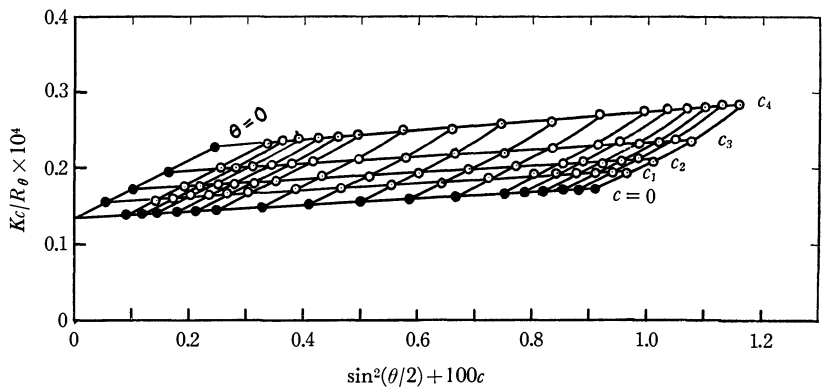

Fig. 6. Zimm plot for sodium chondroitin sulfate C in 0.2 M NaCl at 25°C. c_1, 0.05507%; c_2, 0.1028%; c_3, 0.1653%; c_4, 0.2464%

plotted as a function of $\sin^2(\theta/2)+100\,c$, where the value of 100 is an arbitrarily-selected constant. In Fig. 3, the open circles and squares are referred to independent experiments in order to show the reproducibility of the data. The refractive increment, dn/dc, was constant in every case within the limits of experimental error; its averaged value, 0.155, was used throughout.

On the basis of Eq. (1), the molecular weight was calculated from the intercept of the $c=0$ and $\theta=0$ lines on the ordinate; the mean-square radius of gyration, $\langle S^2 \rangle$ from the ratio of the initial slope of the $c=0$ line to the intercept on the ordinate, and the second virial coefficient, from the initial slope of the $\theta=0$ line. The results are collected in Table 2.

A constant molecular weight of 74000 was obtained in every case, and both the mean-square radius of gyration and the second virial coefficient decreased with an increase in the ionic strength or with a decrease in the pH of the solution at a fixed ionic strength. On the other hand, the molecular weight, estimated from the viscosity data according to this equation:[17]

$$[\eta] = 3.1\times10^{-4}\overline{M}_w{}^{0.74} \qquad (6)$$

was 80000 in a 0.15 M phosphate buffer (pH 7.0) containing 0.2 M NaCl at 25°C. The relation in Eq. (6) has been obtained for the A-type chondroitin sulfate; the molecular weight obtained from Eq. (6) is known to accord fairly well with that obtained from the results of terminal analysis for A-type molecule. However, the former is two or three times larger than the latter for the C type. In our case, the molecular weight determined by the

17) M. B. Mathews, *Arch. Biochem. Biophys.*, **61**, 367 (1965).

TABLE 2. EXPERIMENTAL RESULTS OF VISCOSITY AND LIGHT SCATTERING MEASUREMENTS FOR SODIUM CHONDROITIN SULFATE C IN VARIOUS IONIC STRENGTHS AT 25°C

J	0.0035	0.01*	0.025	0.05	0.2	1.0	∞
$[\eta]$	3.55	2.66	2.08	1.88	1.64	1.35	1.25
$[\eta]^{2/3}/[\eta]_\infty^{2/3}$	2.005	1.654	1.404	1.313	1.198	1.055	1.000
$\langle\bar{S}^2\rangle\times10^{14}$	—	848	744	—	641	—	580
$\langle\bar{S}^2\rangle/\langle\bar{S}^2\rangle_\infty$	—	1.462	1.283	—	1.105	—	1.000
$\langle\bar{S}^2\rangle^{1/2}$ (Å)	—	291	273	—	253	—	241
$A_2\times10^3$	24.5	11.5	5.88	—	1.9	—	1.3

$dn/dc = 0.155$, $\bar{M}_w = 74000$

* $\langle\bar{S}^2\rangle$ and $[\eta]$ at $J=0.01$ (pH 3.5 or 2.7) is in the same order as that at $J=0.2$ as seen from Figs. 13 and 2, respectively. A_2 at $J=0.01$ (pH 3.5) is 8.00×10^{-3}.

results of terminal analysis is 50000, while that obtained from the viscosity is 80000, according to Eq. (6). The value of 80000 is about 1.6 times as large as the value of 50000. The molecular weight, 74000, obtained by light scattering is rather closer to the value, 50000, by the results of terminal analysis.

Discussion

Treatment as a Flexible Coil. The intrinsic viscosity tabulated in Table 2 is plotted as a function of the reciprocal root of the ionic strength, $1/\sqrt{J}$, in Fig. 7; then the intrinsic viscosity, $[\eta]_\infty$, at the infinite ionic strength was estimated. In the same manner, the mean square of the radius of gyration, $\langle\bar{S}^2\rangle$, from light scattering is plotted as a function of $1/\sqrt{J}$ in Fig. 8, and $\langle\bar{S}^2\rangle_\infty$ was estimated at the infinite ionic strength.

On the other hand, the second virial coefficient, A_2, in Table 2 is plotted against the reciprocal ionic strength, $1/J$, and the reciprocal root of the ionic strength, $1/\sqrt{J}$, in Figs. 9 and 10 respectively. As the A_2 value is small at the infinite ionic strength, it can be considered that the medium is practically

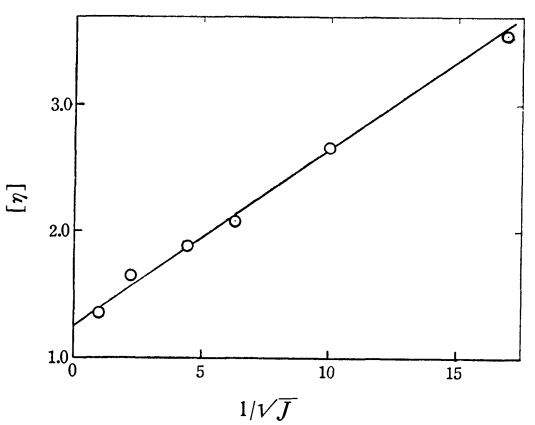

Fig. 7. Intrinsic viscosity of sodium chondroitin sulfate C plotted against reciprocal root of ionic strength $1/\sqrt{J}$.

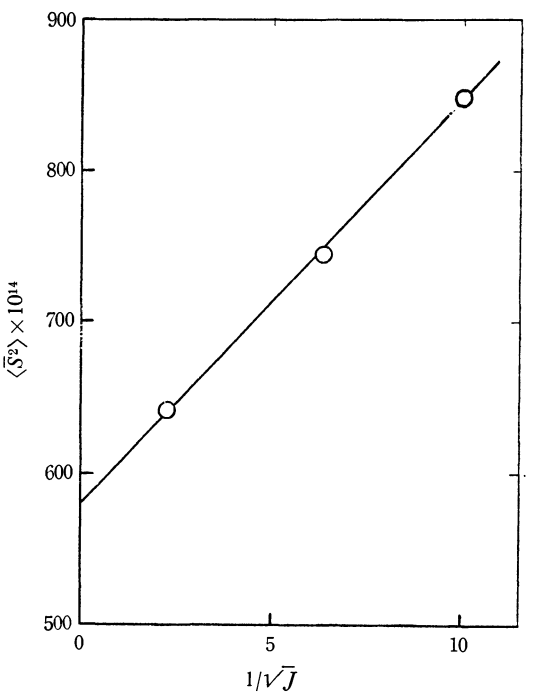

Fig. 8. Mean square radius of gyration $\langle\bar{S}^2\rangle$ plotted against reciprocal root of ionic strength $1/\sqrt{J}$.

a θ solvent at the ionic strength, and $[\eta]_\infty$ and $\langle\bar{S}^2\rangle_\infty$ may be regarded as $[\eta]_\theta$ and $\langle\bar{S}^2\rangle_\theta$ respectively.

The expansion factor of the macromolecule, α, is defined as the ratio of the radius of gyration to that in the θ solvent:

$$\alpha = \langle\bar{S}^2\rangle^{1/2}/\langle\bar{S}^2\rangle_\theta^{1/2} \quad (7)$$

Flory[18] has defined it as:

$$\alpha = [\eta]^{1/3}/[\eta]_\theta^{1/3} \quad (8)$$

Therefore, α^2 corresponds to $[\eta]^{2/3}/[\eta]_\infty^{2/3}$ or

18) P. J. Flory, "The Principles of Polymer Chemistry," Cornell Univ. Press (1953); P. J. Flory and T. G. Fox, *J. Am. Chem. Soc.*, **73**, 1904 (1951).

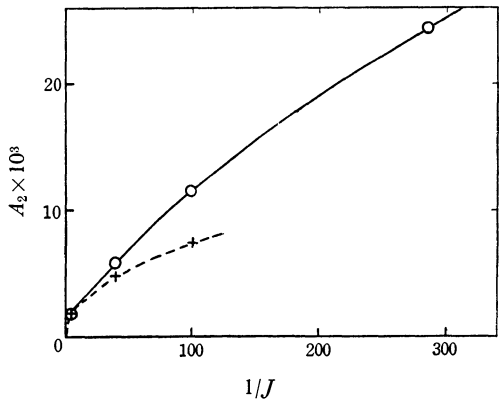

Fig. 9. Second virial coefficient A_2 plotted against reciprocal ionic strength $1/J$.
○, Experimental
+, Theoretical value by Eq. (10)

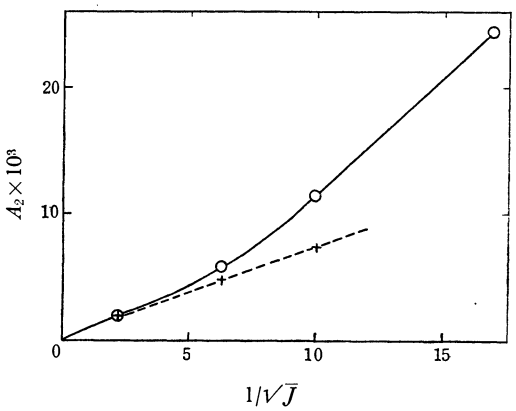

Fig. 10. Second virial coefficient A_2 plotted against reciprocal root of ionic strength $1/\sqrt{J}$.
○, Experimental
+, Theoretical value by Eq. (10)

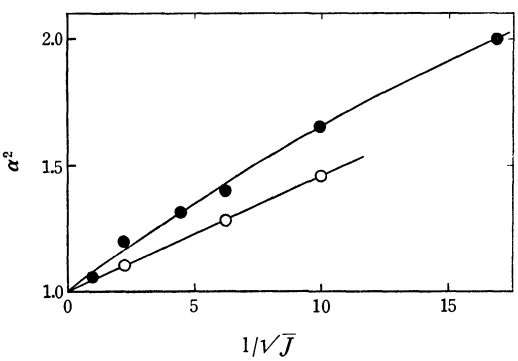

Fig. 11. Expansion factor α^2 obtained from viscosity (●) and light scattering (○), plotted against $1/\sqrt{J}$.

$\langle\bar{S}^2\rangle/\langle\bar{S}^2\rangle_\infty$. These quantities are plotted as a function of $1/\sqrt{J}$ in Fig. 11. With the decrease in ionic strength, the α^2 value obtained from the intrinsic viscosity increases more steeply than that obtained from light scattering. The discrepancy between the two curves can easily be expected to be even more severe when α is estimated from another relation obtained recently[19]:

$$\alpha \doteqdot [\eta]^{1/2.43}/[\eta]_\theta^{1/2.43} \tag{9}$$

The second virial coefficient calculated theoretically on the basis of the light-scattering data ($\langle\bar{S}^2\rangle$, $\bar{M}_w$, and α) and the following Flory relation,[19] is plotted as a function of $1/J$ and $1/\sqrt{J}$, together with the experimental second virial coefficient, in Figs. 9 and 10 respectively.

$$A_2 = (16\pi N/3^{3/2})[\langle\bar{S}^2\rangle^{3/2}/\bar{M}_w{}^2]\ln[1+(\pi^{1/2}/2)(\alpha^2-1)] \tag{10}$$

There is a large difference between the theoretical and experimental results here. It may, however, be meaningless to discuss the virial coefficient further, since no clear explanations have been obtained for many polyelectrolytes, such as sodium carboxymethyl cellulose,[20] sodium polyphosphate,[21,22] and potassium polyvinyl sulfonate.[22,23]

Considering a flexibly-coiled molecule as a sphere, the intrinsic viscosity (ml/g) of the spherical molecule can generally be expressed as follows:

$$[\eta] = 2.5\cdot\frac{4}{5}\cdot R_e\cdot\frac{N}{M} \tag{11}$$

where R_e is the effective radius of the sphere. By Kirkwood and Riseman's treatment,[24] the radius, R_e, is related to the radius of the gyration of the flexible coil of an adequately large degree of polymerization as follows:

$$R_e = 0.875\langle\bar{S}^2\rangle^{1/2} \tag{12}$$

Accordingly, the root mean-square radius of gyration $\langle\bar{S}^2\rangle^{1/2}$ is obtained through Eqs. (11) and (12) as 130 Å at the infinite ionic strength by consulting the value given in Table 2, $[\eta]=125$. On the other hand, the value of 241 Å was obtained as the value of $\langle\bar{S}^2\rangle^{1/2}$ from light scattering. In view of these facts, this molecule can not be considered as a flexible coil of a spherical shape.

Treatment as an Ellipsoid or a Rigid Rod. The intrinsic viscosity, $[\eta]$ (ml/g), is related to the hydrodynamic volume, V_h, molecular weight, M, and Avogadro's number, N, by:

19) T. A. Orofino and P. J. Flory, *J. Phys. Chem.*, **63**, 283 (1959).
20) H. J. Trap and J. J. Harmans, *ibid.*, **58**, 757 (1954); N. S. Schneider and P. Doty, *ibid.*, **58**, 762 (1954).
21) U. P. Straus and P. Ander, *J. Am. Chem. Soc.*, **80**, 6494 (1958); U. P. Straus and P. L. Wineman, *ibid.*, **80**, 2366 (1958).
22) N. Ise, *J. Phys. Chem.*, **67**, 382 (1963).
23) H. Eisenberg and E. Casassa, *J. Polymer Sci.*, **47**, 29 (1960); H. Eisenberg and D. Woodside, *J. Chem. Phys.*, **36**, 1844 (1962).

TABLE 3. MOLECULAR DIMENSIONS OF CHONDROITIN SULFATE C ESTIMATED FROM INTRINSIC VISCOSITY-PARTIAL SPECIFIC VOLUME, LIGHT SCATTERING-PARTIAL SPECIFIC VOLUME AND INTRINSIC VISCOSITY-LIGHT SCATTERING

J		0.01	0.025	0.2	∞
a (Å)	vis.	507	461	420	380
	L.S.	504	473	438	422
b (Å)	vis.	5.27	5.52	5.80	6.08
	L.S.	5.28	5.46	5.67	5.78
f	vis.	96.2	83.5	72.4	62.5
	L.S.	95.5	86.6	77.2	73.0
L (Å)	vis.	1014	922	840	760
	L.S.	1008	946	876	843
D (Å)	vis.	8.61	9.01	9.47	9.93
	L.S.	8.62	8.92	9.26	9.44
$\langle\bar{S}^2\rangle^{1/2}$	vis.	293	266	243	219
	L.S.	291	273	253	241
	f(vis.)	293	267	244	220
	f(L.S.)	293	268	245	222

$$[\eta] = \nu\frac{N}{M}V_h \tag{13}$$

Moreover, V_h is connected with the partial specific volume, $\bar{v}_2$, of the solute by:

$$V_h = \frac{M}{N}(\bar{v}_2 + \delta_1 v_1^\circ) \tag{14}$$

where v_1° is the specific volume of the pure solvent and δ_1 is the adsorption coefficient of the solvent to the solute. The ν in Eq. (13) is expressed by Simha[25] for prolate ellipsoids with the axial ratio, f, as follows:

$$\nu = \frac{f^2}{15(\ln 2f - 3/2)} + \frac{f^2}{5(\ln 2f - 1/2)} + \frac{14}{15} \tag{15}$$

The values of ν have been computed and tabulated by Scheraga[26] for various f values. According to Eqs. (13), (14) and (15), the hydrodynamic volume and the axial ratio can be estimated from the experimental values of $[\eta]$, M, and $\bar{v}_2$, supposing $\delta_1 = 0$. If the molecules are thus assumed to be prolate ellipsoids, the two semi-axes, a and b, of the ellipsoid can be obtained from the values of the hydrodynamic volume and the axial ratio according to these equations:

$$V_h = \frac{4}{3}\pi ab^2 \tag{16}$$

$$f = a/b \tag{17}$$

If the molecules are, on the other hand, assumed to be rigid rods with the same volume and length as the ellipsoid, then the length, L, and the diameter, D, of the rod will be:

$$L = 2a \tag{18}$$

$$D = (2/3)^{1/2}2b \tag{19}$$

and the radius of gyration will be:

$$\langle\bar{S}^2\rangle^{1/2} = L/12 \tag{20}$$

The results obtained in this manner are shown in Table 3 on the lines designated as (vis.) and in Fig. 12 for various ionic strengths, J.

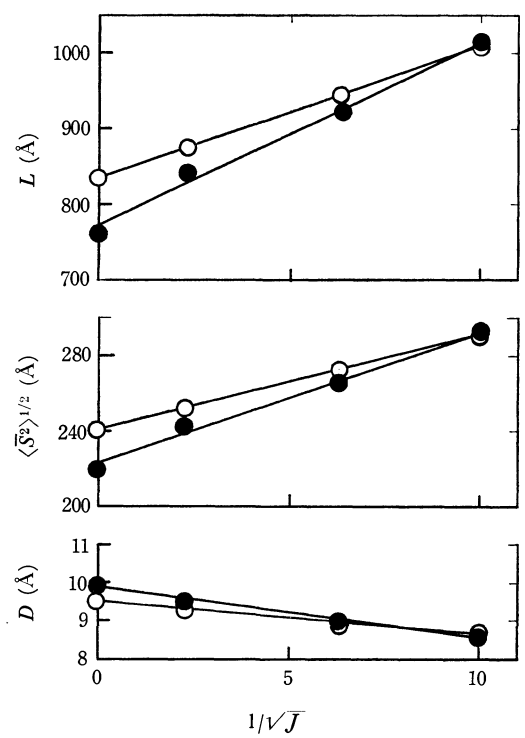

Fig. 12. Molecular dimensions of chondroitin sulfate C obtained, assuming a rigid rod.
○, light scattering-partial specific volume
●, intrinsic viscosity-partial specific volume

25) R. Simha, *J. Phys. Chem.*, **44**, 25 (1940); J. W. Mehl, J. L. Oncley, and R. Simha, *Science*, **92**, 132 (1940).
26) H. A. Scheraga, *J. Chem. Phys.*, **23**, 1526 (1955).

On the other hand, the length, L, and the diameter, D, of the rod can also be calculated from the radius of gyration by light-scattering experiments and from the molecular volume obtained from the specific volume, according to Eq. (20) and this equation:

$$V_h = \pi(D/2)^2 L \qquad (21)$$

These results, too, are shown in Table 3, on the lines designated as (L. S.) and in Fig. 12 for various values of the ionic strength, J.

As for the radius of gyration, it has been shown that the $\langle \bar{S}^2 \rangle^{1/2}/([\eta]M)^{1/3}$ quantity can be expressed as a function of the axial ratio, f, only.[27] Therefore, the value of $\langle \bar{S}^2 \rangle^{1/2}$ can be calculated by using the values of the axial ratio, f(vis.) or f(L. S.), together with the $[\eta]$ values and with $M=74000$. These results, shown in Table 3, show a fairly good agreement with each other.

As Fig. 12 shows, the results from the viscosity-partial specific volume and from the light scattering-partial specific volume show a certain disagreement with each other when the ionic strength is large. Even at the infinite ionic strength, however, the radius of gyration, 241 Å, obtained from light scattering, is much closer to the value as a rigid rod (219 Å) than to the value as a flexible coil (130 Å).

When we assume that the length of a repeating disuccharide unit is of the order of 10 Å, the residue weight, 490, and the molecular weight, 74000, will give a rough estimate of 1500 Å for the length of the polymer chain. Accordingly, the rod length of 843 Å obtained from light scattering or that of 760 Å obtained from the intrinsic viscosity must mean that the molecule is two-fold, if the polymer chain is assumed to be extended in full. If the polymer is, however, assumed to have a helical structure, as has been emphasized in an optical rotatory dispersion experiment,[7] sodium chondroitin sulfate C can probably be considered to be a helical rod with 5.0—5.6 Å of pitch per repeating disuccharide unit.

Consideration at Finite Polymer Concentrations. The slopes on the plot of Kc/R_θ against $\sin^2(\theta/2)$ at various concentrations:

$$g = \mathrm{d}(Kc/R_\theta)/\mathrm{d}\sin^2(\theta/2) \qquad (22)$$

are considered to be related to the dimentions of the solute.

They are plotted against the polymer concentration in Fig. 13. It is apparent that the magnitude

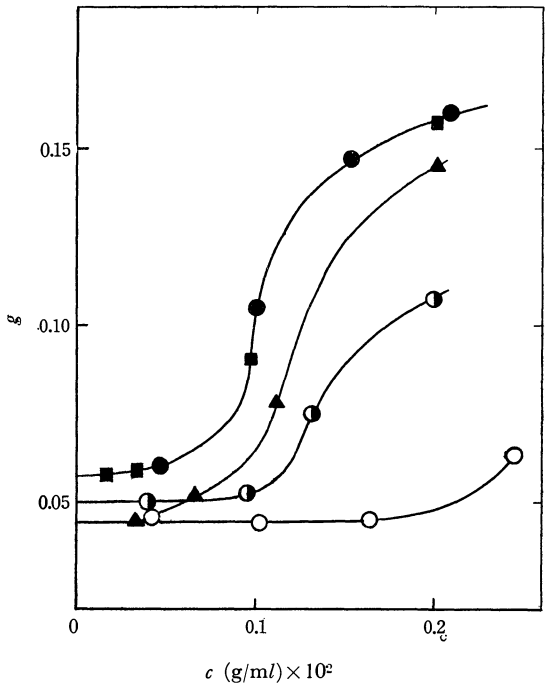

Fig. 13. Slopes on the plot of Kc/R_θ *vs.* $\sin^2(\theta/2)$ at various polymer concentrations.
● and ■, $J=0.01$; ▲, $J=0.01$ (pH 3.4); ◑, $J=0.025$; ○, $J=0.2$

of the slope is unchanged up to a certain critical polymer concentration, and then steeply increases. It reaches a limiting value, when the ionic strength is low. This phenomenon can probably be considered to be related to its unusual viscosity behavior at low polymer concentrations, and also to the metachromatic color change,[28,29] observed at higher polymer concentrations. Furthermore, the chondroitin sulfate C is known to develop a non-Newtonian viscosity. It is, however, not sure at present that this behavior of chondroitin sulfate C is due to its rod shape, to the association of the molecules, or to the orientation of the highly-charged, rod-like macromolecules.

The authors wish to express their thanks to the Seikagaku Kogyo Co., Ltd., for furnishing the material and to Mr. Tamotsu Furuhashi for his analysis of the preparation.

27) R. B. Martin, "Introduction to Biophysical Chemistry," McGraw-Hill Book Co., New York (1964).

28) A. N. Levine and M. Schubert, *J. Am. Chem. Soc.*, **74**, 91 (1952); A. N. Levine and M. Schubert, *ibid.*, **74**, 5702 (1952).

29) M. D. Schoenberg and R. D. Moore, *Biochim. Biophys. Acta*, **83**, 42 (1964).

BULLETIN OF THE CHEMICAL SOCIETY OF JAPAN VOL. 41 564—569 (1968)

The Solution Properties of Nonionic Oligosoaps Derived from Nonylphenol Formaldehyde Resin

Yutaka ISHIGAMI and Hideo NARASAKI

Government Chemical Industrial Research Institute, Tokyo, Shibuya-ku, Tokyo

(Received July 28, 1967)

Nonionic oligosoaps (mol wt 6200 and 9700), consisting of a short polymer chain with chemically-attached soap-like groups, have been prepared from nonylphenol formaldehyde resin (mol wt 2000) by condensing 11 and 20 mol of ethylene oxide per nonylphenol ring making up the resin. Light-scattering, surface-tension, and vapor-pressure-depression measurements have been carried out. These oligosoaps formed agregates in water; the micellar weights were 81000 (11 mol condensate) and 70700 (20 mol), respectively, much as with the cationic oligosoap derived from polyallyl chloride reported elsewhere. The aggregation number, the dependence of the micellar weight on the sodium chloride concentration, the small surface area per molecule, in water, and the nonaggregation in nonaqueous solutions are discussed. It is noteworthy that these oligosoaps behave like monosoaps in various ways.

In a preceding paper,[1] we reported that a cationic polysoap (quaternization product (formura weight, 2770) of *N*-dodecyl-piperidine with polyallyl chloride (mol wt, 650)), consisting of a short polymer chain with chemically-attached soap-like groups (designated as "*oligosoap*" below) formed a micelle in water. It seems that such an oligosoap generally forms a micelle in aqueous media. The occurence of this phenomenon in a nonionic oligosoap was ascertained in the present investigation.

Regarding an aqueous solution of ethylene-oxide condensates of alkylphenol formaldehyde resin, Yamashita[2] mentioned that the critical micelle concentration (CMC) of a dimeric resin derivatives was lower than that of the corresponding alkylphenol derivative (monosoap). Hayano *et al.*[3] reported that even those surfactants equal to the dimer did not show the CMC when treated by the method of determining the CMC for nonionic surfactants developed by Ross *et al.*

The present situation of the problem of the aggregation of these nonionic oligosoaps is similar to the early studies of the micelle formation of polyoxyethylated nonionic monosoaps. Namely, the physicochemical properties of the nonionic surfactant solutions changed gradually over a relatively wide surfactant concentration range depending upon the presence of a wide range of molecular sizes and impurities. Therefore, the CMC's of these surfactants were not definite and, further, differed from method to method among the CMC determination methods. On the other hand, numerous papers on the physicochemical properties of Pluronic polyol homologues in aqueous and nonaqueous media have appeared.[4,5] The present authors are especially interested in whether these polyols form a micelle or not.

Experimental

Determination of Molecular Weight Using a Vapor-pressure Osmometer (VPO). Determinations were carried out with a Mechrolab vapor-pressure osmometer, Model 302, at 37°C. The instrument was calibrated with solutions of benzil and methyl linolate over a concentration range of 0.004—0.05 mol solute/kg solvent. Steady readings of the resistance in ohms (ΔR) of these solutions were attained for more than 5 min in benzene and 15 min in *n*-butanol. The ΔR of the unknowns (oligosoaps) were divided by the weight concentration (C), and these quotients were plotted against C. The molecular weights were obtained by dividing the cali- bration constant by $(\Delta R/C)_{c\to 0}$.

Light Scattering (LS). Light-scattering measurements were carried out at a room temperature of about 21°C with a wavelength of 436 mμ, using a Shimadzu photoelectric light-scattering photometer. Scattered light was observed at 90°, 45°, and 135° relative to the incident beam. The optical clarification of the solution to be examined was made by centrifuge at 21000 g and filtration with an ultrafine sintered glass filter. Aqueous solutions were prepared by diluting an original solution volumetrically. After these solutions had been

1) Y. Ishigami and H. Narasaki, This Bulletin, **38**, 1852 (1965).
2) Y. Yamashita, *Yushi*, **14**, No. 11, 79 (1961).
3) W. Hayano, K. Kitagawa, T. Arai and K. Hattori, *Yukagaku (J. Japan Oil Chemists, Soc.)*, **13**, 33 (1964).
4) I. R. Schmolka and A. J. Raymond, *J. Am. Oil Chemists' Soc.*, **42**, 1088 (1965); C. W. Dwiggins, Jr., R. J. Bolen and H. N. Dunning, *J. Phys. Chem.*, **64**, 1175 (1960), *etc.*
5) J. M. G. Cowie and A. F. Sirianni, *J. Am. Oil Chemists' Soc.*, **43**, 572 (1966).

allowed to stand overnight, they were filtered by the filter directly into a light-scattering cell and measured. *n*-Butanol solutions were measured by successive dilutions of an original solution by filtering the solvent directly into the cell. The details have been given elsewhere.[1]

As a check on the entire calibration, the weight-average molecular weight ($\overline{M}_w$) of a standard polystyrene, Styron 683-7, supplied by the Asahi-Dow Co., was estimated by Hamashima and Hattori[6] by means of this instrument to be 234000; this value is in good agreement with the $\overline{M}_w$ values of 227000 for a column-fractionation method and 256000 for an ultracentrifuge.

Surface Tension. The surface-tension measurements were carried out by the drop-weight method in a thermostat maintained at 30.0±0.2°C, using the correction of Harkins and Brown.[7] More than two minutes were allowed for the formation of each drop of the solution in a saturated atmosphere (*cf.* Fig. 4).

Reagents. Nonylphenol was supplied by the Sanyo Yushi Kogyo Co.; the *p*- and *o*-nonylphenol contents were approximately 75% and 25%, respectively.[8] The benzene was dehydrated with sodium, and the *n*-butanol was dehydrated with calcium oxide. Methyl linolate supplied by Tanabe and Hashimoto,[9] was prepared from safflower oil; its minimum purity was found to be 98% (contained less than 2% methyl oleate) by gas chromatographic analysis. The other materials were reagent-grade materials.

Preparation of Oligosoaps. A mixture of 165 g (0.75 mol) of nonylphenol, 22.5 g (0.75 mol) of paraformaldehyde, and 225 m*l* of toluene were introduced, with 1.5 g of *p*-toluene sulfonic acid, into a two-necked 500 m*l*-flask, to which there were a reflux condenser and a thermometer. The reaction mixture was heated under reflux on an oil bath for 2.5 hr, and the resulting water was removed. The nonylphenol formaldehyde resin was then isolated by running the solution into stirred 90% methanol. The resin was purified by dissolving it in toluene and by adding this solution to 90% methanol; then it was dried at 60°C for 50 hr in a vacuum. The yield of the resin obtained was 44.5 g; its molecular weight was found to be $2.0\times10^3\pm100$ by means of VPO (the degree of number-average addition-condensation was 8.6).

Nonionic oligosoaps were prepared as follows, 15 g of the nonylphenol formaldehyde resin and 0.15 g of metallic sodium were dissolved in 45 g of xylene, after which ethylene oxide (EO) gas which had been dried through the layer of pellet pottasium hydroxide was bubbled into the solution at 120°C. The resulting products were poured into a 1 : 2 ether- *n*-hexane mixture. The precipitates were redissolved in methanol, and the solution was then treated with a great deal of *n*-hexane. An additional dissolution and precipitation were carried out. The oligosoaps were dried at 60°C for 50 hr in a vacuum. The EO contents of the compounds were determined by the weight increase in the EO condensation reaction. The oligosoap had the average EO chain lengths of 10.8 and 19.8 respectively per nonylphenol ring making up the nonylphenol formaldehyde resin molecule. These are abbreviated as NF-11 and NF-20 below. The corresponding molecular weights of these oligosoaps were $6.2\times$ and 9.7×10^3, respectively. A monosoap, NP-18, was similarly prepared from nonylphenol; it had an average EO chain length of 18.4 per mol.

Results and Discussion

Light Scattering of Aqueous Solutions. The reduced-intensity *vs.* oligosoap-concentration curves are shown in Fig. 1. The CMC's of the aqueous oligosoap solutions (NF-11: $6\times$; NF-20: 5×10^{-6} mol/*l*) corresponding to the sharp breaks on these curves are in good agreement with the inflection points (CMC: both, 2×10^{-6} mol/*l*) observed in the surface-tension *vs.* log-concentration curves, as is shown in Fig. 3. These CMC values (the order of 10^{-6} mol/*l*) of the oligosoaps are much smaller than that found for the monosoap (the order of 10^{-4} mol/*l*). The Debye plots of the oligosoaps in aqueous solutions are illustrated in Fig. 2. These CMC's and the micellar weights of these oligosoaps are given in Table 1. The micellar weights and the aggreagation numbers in water were 81000 and 13.0 in NF-11, and 70700 and 7.3 in NF-20.

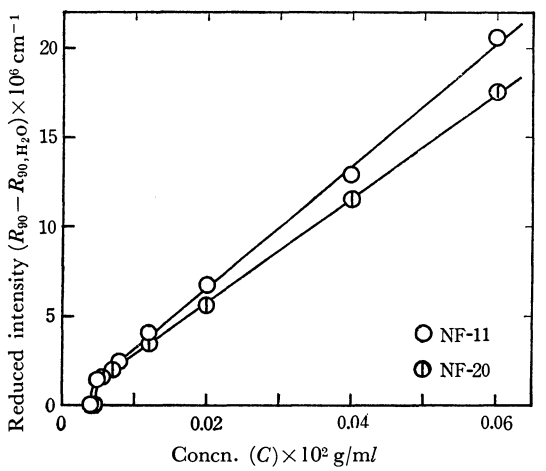

Fig. 1. Reduced intensity *vs.* concentration curves in water. (Wavelength 436 mμ, 21°C)

It was found that these nonionic oligosoaps formed aggregates in aqueous solution, much like the cationic oligosoap derived from polyallyl chloride already reported.[1] The micellar weights and the aggregation numbers of the cationic oligosoap were 18800 and 7.0 in water, 32300 and 11.8 in a 0.3 M aqueous sodium chloride solution. Taking account of the contribution of the presence of the

6) M. Hamashima and S. Hattori, *Tokyo Kogyo Shikenjo Hokoku (Reports of The Government Chemical Industrial Research Institute, Tokyo)*, **62**, 247 (1967).
7) W. D. Harkins and F. E. Brown, *J. Am. Chem. Soc.*, **41**, 499 (1919).
8) H. Narasaki, *Kogyo Kagaku Zasshi (J. Chem. Soc. Japan, Ind. Chem. Sect.)*, **66**, 391 (1963).
9) K. Tanabe and T. Hashimoto, *Yukagaku (J. Japan Oil Chemists' Soc.)*, **16**, 611 (1967).

Table 1. The micellar properties of the nonionic oligosoaps in water and aqueous sodium chloride solutions as determined by light scattering

	NaCl mol/l	CMC mol/l $\times 10^6$	$\overline{M}_w$[b] $\times 10^{-3}$	n[c]	A_2[d] mol·cm^3/g$^2 \times 10^4$	dn/dc[e] ml/g
NF-11	0	6	81.0	13.0	0.4	0.172
	0.1	5	77.1	12.4	−0.2	0.169
	0.5	3	82.3	13.3	−0.5	0.169
	1.0	2	95.1	15.3	−4.9	0.169
	2.0[a]	<2	177.9	28.6	−3.7	0.169
NF-20	0	5	70.7	7.3	1.6	0.158
	0.1	4	68.2	7.0	1.8	0.158
	0.5	2	63.1	6.5	1.2	0.158
	1.0	1	58.8	6.0	0.9	0.158
NP-18	0	200	52.0	51	1.6	0.146

a) Dissymmetry is 1.04. The others are 1.00.
b) Weight-average micellar weight.
c) Aggregation number. The molecular weights of NF-11 and NF-20 employed in the calculation were 6210 and 9720, respectively.
d) Second virial coefficient.
e) Refractive index increment, $\Delta n/\Delta(C-\mathrm{CMC})$.

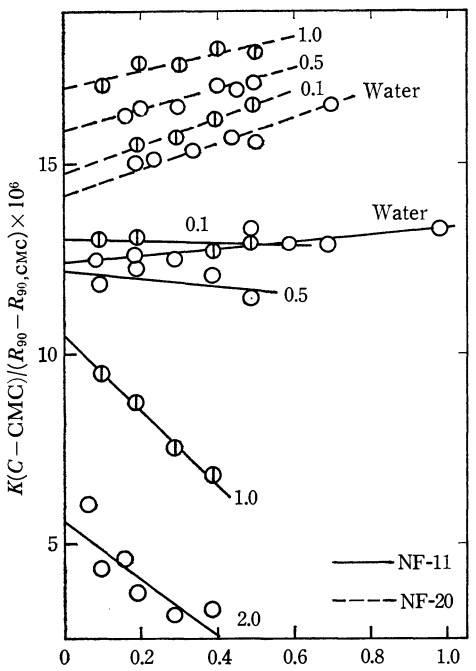

Fig. 2. Light scattering of the oligosoaps in water and aqueous sodium chloride solution (wavelength 436 mμ, 21°C). Numericals in this figure show the concentration of sodium chloride (mol/l).

molecular-weight distribution for $\overline{M}_w$, or account of the possibility of the presence of a small number of very large particles to be mentioned below, the aggregation numbers of these oligosoaps may be smaller than the results shown in Table 1. In this manner, we concluded that these oligosoaps formed aggregates even in quite lower oligosoap concentration ranges, and that the aggregation numbers of these oligosoaps were relatively small.

The Effect of Added Sodium Chloride on Light-scattering Results. The effect of added sodium chloride on the CMC's and the micellar weights of the oligosoaps are included in Fig. 2. and Table 1. The micellar weight of NF-11 increased with an increase in the salt concentration except for the case of the 0.1 M salt concentration; namely, the aggregate grew from 81000 in water to 177900 (dissymmetry 1.04) in 2 M salt concentration. At the same time, the second virial coefficient (A_2) decreased gradually with an increase in the salt concentration.

This behavior was reversed for NF-20. A decrease in the micellar weight was observed with an increase in the salt concentration. The A_2 was little affected by the salt.

On the other hand, the CMC's of both NF-11 and NF-20 declined upon the addition of salt, although the CMC values are too low to estimate accurately. Such a behavior of NF-20 was different from the well-known fact that the addition of salt causes a decrease in the CMC and an increase in the micellar weight in ordinary ionic monosoaps.

Related results have been reported for polyoxyethylene alkyl ether by Becher,[10] and Schick *et al.*[11] Becher theorized that the added salts had no appreciable shielding effect on the micellar charge of higher EO condensates, whereas a

10) P. Becher, *J. Colloid Sci.*, **17**, 325 (1962).
11) M. J. Schick, S. M. Atlas and F. R. Eirich, *J. Phys. Chem.*, **66**, 1326 (1962).

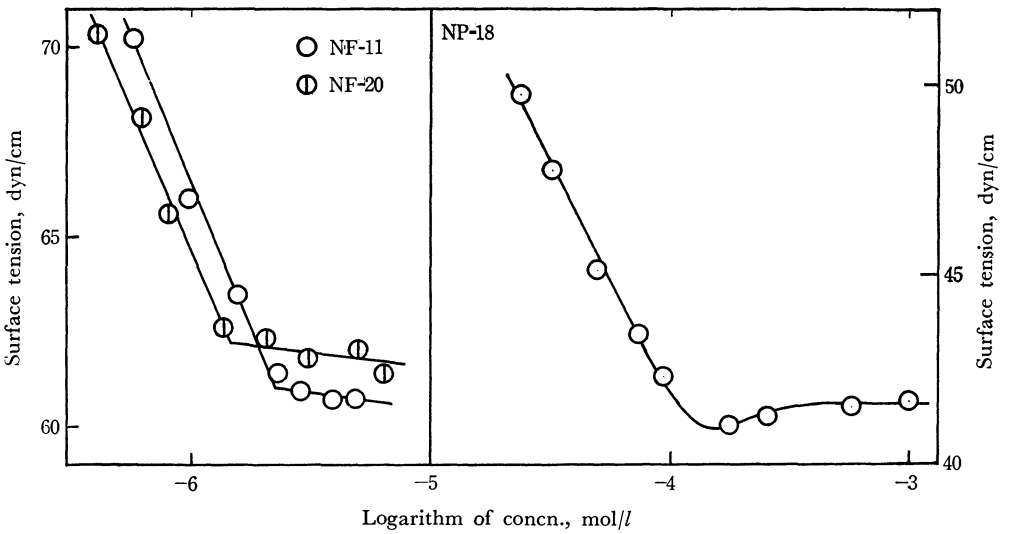

Fig. 3. Surface tension *vs.* logarithm of concentration curves at 30°C by the drop-weight method.

significantly larger charge on a single molecule (produced by the formation of hydronium ion) was smeared out into the interior of a micelle if the extension of the EO chains was at all great. Consequently, the effect of the added salt would be to lower the double-layer potential of the individual monomer molecules and render their incorporation into the micelle easier. In another way, this would seem to indicate that the dehydration effect of the added salt was minor for the higher EO condensates. For the lower EO condensates, he considered the result to be incipient coacervation rather than the formation of large micelles upon the addition of salt. Thus, he explained why the micellar weight of higher EO condensates remained unchanged upon the addition of salt in his cases. However, he did not explain why it decreased in other cases.

Schick *et al.* postualted that the increased length and lower solubility of EO chain enhanced the absorption of Na^+ to such an extent that it increased the overall solubility of the nonionic surfactant. In this case, they did not take the decrease in the CMC value into consideration.

Further, Becher pointed out that the EO contents in each EO condensate homologue in which the apparent size of the micelle did not increase upon the addition of salt, were about 70—75% of the EO by weight per molecule. The EO contents of NF-11 and NF-20 were 68 and 79% respectively. Therefore, the solution behavior of the oligosoaps under consideration here was consistent with Becher's results. It is noteworthy that these phenomena can be seen in the oligosoaps as well as in monosoaps.

From the viewpoint of the steric configuration of the oligosoaps, adjacent *p*-nonylphenol rings connected with a methylene group can not exist on the same plane because of the steric hindrance between the O atom of the 1-position and the *m*-H, or between the *m*-H of the nonylphenol ring themselves. This is true in the case of *o*-nonylphenol. Therefore, the aggregates of these oligosoaps perhaps form a crowded and interpenetrated structure in aqueous solutions. Namely, the aggregates may easily form intramolecular and intermolecular interpenetrated structures between the lyophilic and the EO groups making up these oligosoaps. Therefore, Becher's smearing-out effect of the charges into the aqueous portion of the micelle can take place, in NF-11 as well as in NF-20, because such interpenetrated structures can form in both NF-11 and NF-20 independent of the EO chain lengths of these oligosoaps. However, the results observed did not support this. Presumably we can interpret this phenomenon by the possibilities that there are two patterns in the hydration of the EO chain, for lower and higher EO condensates, or that the effect of the added salt concentration on the micellar weight of any EO condensate homologues can be divided into two regions which are combined at such a minimum micellar weight as for 0.1 M salt in the case of NF-11. The A_2 of NF-11 became negative and that of NF-20 remained positive upon the addition of salt, as is tabulated in Table 1. This appears to support this assumption that the hydrations of these micellar surface layers are different from one another.

Moreover, it would seem to be possible for us to consider separately the effect of added salt on a single molecule and on a micelle in explaining this phenomenon.

Surface-tension Results. The relations of the surface tension (γ) *vs.* the logarithm of concentration (C) are given in Fig. 3. The apparent

surface tension *vs.* the time required for each drop formation curves as determined by the drop-weight method are shown in Fig. 4. There are evident inflection points at about 2×10^{-6} mol/*l*, corresponding probably to the CMC and then a gentle descent of the γ follows.

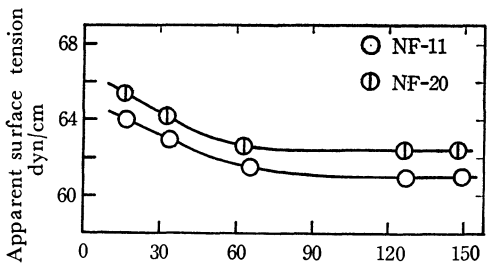

Fig. 4. Apparent surface tension *vs.* the time required for each drop formation curves at 30°C by the drop-weight method NF-11 : 2.90×10^{-6} mol/*l*; NF-20: 2.06×10^{-6} mol/*l*.

In view of the presence of the molecular-weight distribution in the oligosoaps under consideration here, the selected adsorption of smaller members of the molecules at the air-solution interface is, of course, to be expected. However, these oligosoaps show evident inflection points in the γ-log *C* plots and make straight lines below the concentration of the inflection points in the aqueous solutions. Therefore, in order to compare them approximately with monosoaps, we estimated the surface excess (Γ) and the corresponding surface area per molecule (A) of the oligosoaps at the air-solution interface from the slopes below the concentration of the inflection points by applying Gibbs adsorption isotherm, $\Gamma=-d\gamma/(\boldsymbol{R}T\,d\ln C)$, and $A=10^{16}/\boldsymbol{N}\Gamma$, where $\boldsymbol{R}$ is the gas constant; T is the absolute temperature; and $\boldsymbol{N}$ is the Avogadro number. The results obtained are listed in Table 2; they are of the same order of magnitude as that of monosoap, which is consistent with the findings concerning the cationic oligosoap reported on previously.[1] Moreover, the A values of NF-11 and NF-20 are almost the same. The small A values can be explained if the smaller molecules included in the oligosoaps are selectedly adsorbed at the air-solution interface at higher densities as a result of the Van der Waals attractive force.

Table 2. Surface tension results in water

	CMC mol/*l* $\times10^6$	Γ[a] mol/cm^2 $\times10^{10}$	A[b] Å^2/mol
NF-11	2	3.00	55
NF-20	2	2.58	64
NP-18	150	2.21	75

a) Surface excess calculated from the slopes of γ-log *C* plots below the CMC.
b) Corresponding surface area per molecule.

The Properties of Nonaqueous Solutions. The molecular weights of the nonionic oligosoaps under consideration here were determined in benzene and *n*-butanol by means of vapor-pressure depression (VPO) and light-scattering (LS) measurements. The results obtained are summarized in Table 3. The number-average molecular weight

Table 3. The molecular weights in nonaqueous solutions as determined by vapor pressure depression and light scattering

	$M(w, inc)$[a] $\times10^{-3}$	VPO $\bar{M}_n\times10^{-3}$		LS[c] $\bar{M}_w\times10^{-3}$
		benzene	*n*-butanol	*n*-butanol[d]
NF-11	6.2_1	7.0±0.5	5.4±0.5	18.6
NF-20	9.7_2	9.5±0.7	—[b]	25.9

a) Molecular weight determined by the weight increase in the ethylene oxide condensation reaction.
b) Turbid in the concentration range capable of determination.
c) Light scattering measurements in benzene were not made because dn/dc values were small and scattered.
d) NF-11: $A_2=1.6\times10^{-4}$, $dn/dc=0.106$
NF-20: $A_2=1.6\times10^{-4}$, $dn/dc=0.096$

($\bar{M}_n$) of NF-11 was 7000 (9500 in NF-20) in benzene and 5400 in *n*-butanol, as determined by means of VPO. These values were in tolerable agreement with the molecular weights ($M(w, inc)$) of 6200 in NF-11 and 9700 in NF-20 as determined from the weight increase in the EO condensation reaction. Therefore, it can be said that these oligosoaps did not form an aggregate in these solvents. The weight-average molecular weights ($\bar{M}_w$) of NF-11 and NF-20 were 18600 and 25900 in *n*-butanol, respectively, as determined by means of LS. Although the light-scattering results in *n*-butanol would suggest the formation of an aggregate, it would be possible to suppose that the oligosoaps did not aggregate; this seems possible because of approximate agreement with $\bar{M}_n$ and $M(w, inc)$, and because of the presence of molecular-weight distribution. It may be suggested that the difference between $\bar{M}_n$ and $\bar{M}_w$ is partly caused by a polydispersity in the micellar weight. Some reports have appeared to support this assumption.

Corkill, Goodman, and Walker[12] have shown that the $\bar{M}_w$ of Aerosol OT by LS diminishes in toluene with the time of aging after the preparation of the solution, at last reaching the same level as the $\bar{M}_n$ obtained by VPO, which remained constant independent of the solution's age. This phenomenon was attributed to a very small number

12) J. M. Corkill, J. F. Goodman and T. Walker, *Trans. Faraday Soc.*, **61**, 589 (1965).

of very large aggreagtes, which were formed by small quantities of water (or impurities) in the fresh solutions.

Cowie and Sirianni[5] showed that the $\overline{M}_w$'s of Pluronic polyol homologues were larger for the values determined from LS than for those determined from ultracentrifuge in water, butyl chloride, and dioxane. They explained this phenomenon by postulating the presence of a small number of large clusters which could be observed by LS but which were disrupted under the influence of the strong force field experienced in the ultracentrifuge, or by postulating the presence of a very broad spectrum of molecular sizes in the system. Therefore, nonaggregation of these oligosoaps is conceivable.

As has been mentioned above, it is noteworthy that such an oligosoap behaves like a monosoap in various ways. This indicates that such an oligosoap molecule is not as immobile as might be expected from its crowded and interpenetrated molecular structure.

The authors wish to express their hearty thanks to Dr. Toshio Kamata of our Institute for his valuable advice.

BULLETIN OF THE CHEMICAL SOCIETY OF JAPAN VOL. 41 569—572 (1968)

Determination of the Self-diffusion Coefficient of Nickel Atoms in Nickel Sulfide

Kazuo FUEKI, Yasuo OGURI and Takashi MUKAIBO

Department of Industrial Chemistry, Faculty of Engineering, The University of Tokyo, Hongo, Tokyo

(Received August 24, 1967)

The self-diffusion coefficient of ions or atoms in such crystals as halides, oxides and sulfides can be determined from the rate of the diffusion-controlled solid-state reaction as well as by the tracer method. In the present study, the self-diffusion coefficient of nickel atoms in nickel sulfide was determined from the rates of the sulfidation and desulfidation of nickel sulfide in H_2S-H_2 gas mixtures. The results agreed well with the data obtained by the previous investigators employing the tracer technique.

Although the self-diffusion coefficients of atoms in halides, oxides, sulfides and other crystals have been measured by tracer methods, it is also possible to determine them from the kinetic data of diffusion-controlled solid-state reactions, such as the parabolic oxidation of metals and sintering reactions. This paper will deal with the determination of the self-diffusion coefficient of nickel atoms in nickel sulfide from the kinetic data of the sulfidation and desulfidation of nickel sulfide.

The Ni-S binary system has several phases: Ni_3S_2, $Ni_3S_{2+\delta}$, Ni_6S_5, $Ni_{1-\delta}S$, NiS_2 and so on. The stability region for these sulfides has been established by Rosenquvist,[1] Leine and Laffitte,[2] and by other investigators. According to the result of the previous investigators, nickel monosulfide is a metal-deficient compound and is expressed by the formula $Ni_{1-\delta}S$, where δ is the metal deficit, varying from 0 to 0.05. In the present study, the sulfidation and desulfidation of this sulfide in H_2S-H_2 mixtures were followed by the gravimetric method, and the self-diffusion coefficient of nickel atoms was determined.

In order to confirm the predominant migrating species in nickel sulfide, a marker study was also carried out. Nickel atoms were found to be the predominant migrating species.

Experimental

Marker Study. A high-purity nickel specimen, $10\times30\times0.1$ mm, on both surfaces of which a slurry of fine Cr_2O_3 particles had been placed, was dried and then sulfidized in H_2S at 550°C until the nickel had been completely converted to nickel sulfide. The nickel is electrolytic Ni, 99.98% pure (impurities: 0.013% Co, 0.001% Cu, 0.002% C, 0.0003% S). After the sulfidation, the specimen was mounted in resin and sectioned in order to observe the location of Cr_2O_3

1) T. Rosenquvist, *J. Iron Steel Inst.*, **176**, 37 (1954).
2) G. Leine and M. Laffitte, *Compt. Rend.*, **256**, 3306 (1963); M. Laffitte, *Bull. Soc. Chim. France*, **1959**, 1223.

markers. The positions of the markers were determined by means of a metallographic microscope and X-ray microanalyzer.

Kinetic Study of the Sulfidation and Desulfidation of Nickel Sulfide. Purification of Gases. Hydrogen sulfide gas, 99.9% pure, was supplied by the Suzuki Shokan Co. The gas was passed through a $Mg(ClO_4)_2$ column, and then a tube filled with porcelain pieces was heated at 500°C to convert the oxygen impurity into water vapor by the following reaction:

$$2H_2S + O_2 \longrightarrow 2H_2O + S_2$$

The gas was then dried again by passing it through a $Mg(ClO_4)_2$ column and stored in a bulb.

Hydrogen was passed through a $Mg(ClO_4)_2$ column on a Pd-asbestos catalyst in order to remove oxygen in the form of water vapor. The gas was then stored.

Apparatus. The apparatus used for the rate measurement of the sulfidation and desulfidation is shown in Fig. 1. A is a magnetic device used to raise and lower the specimen, suspended with the quartz fiber, and also to transfer them to and from the beam of the Gulbransen microbalance, C. H is the circulation pump for the gas, and G is a mercury manometer.

Specimens. The nickel sulfide specimens employed for the measurements of the sulfidation and desulfidation rates and for the determination of the metal deficit were prepared in the following manner. Nickel coupons, $10\times30\times0.1$ mm, were taken from a rolled sheet of highly-pure nickel, polished chemically with a mixture of nitric acid and sulfuric acid, and annealed in hydrogen (10 mmHg) for 4 hr at 550°C. A finished and weighed nickel specimen was then hung from a quartz spring balance and sulfidized in hydrogen sulfide (400 mmHg) for about 5 hr at 550°C. When the weight indicated the complete sulfidation of the nickel into nickel sulfide, the sulfidized specimen was quenched, annealed for a sufficient length of time in a H_2S-H_2 gas mixture of a desired composition in order to obtain a specific metal deficit of nickel sulfide, and weighed.

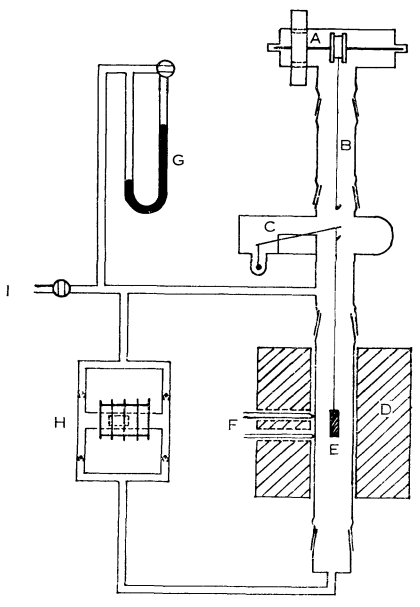

Fig. 1. Schematic diagram of apparatus.

From the weights before and after the sulfidation, the metal deficit of the nickel sulfide specimen was calculated. The thickness of the specimen was determined by means of a micrometer.

Experimental Procedure. A nickel sulfide specimen of a known composition was suspended from a chain by means of a fine quartz fiber, and the entire system was evacuated. Then a H_2S-H_2 gas mixture of a desired composition was introduced into the system and circulated by a circulation pump in order to keep its composition uniform. After the temperature of the furnace had attained the reaction temperature, the specimen was lowered to the heated zone, transferred, together with the quartz fiber, to the beam of the balance, and the weight change was followed by observing a marked point on the beam by means of a cathetometer. During the run the gas mixture was circulated except for those intervals when cathetometer readings were made. After the weight had reached the equilibrium value, the specimen and the quartz fiber were transferred to the chain and raised to the initial position, and the weight of the specimen was determined.

Results and Discussion

Marker Study. A section of a specimen completely converted to nickel sulfide is shown in Fig. 2. The markers are located at the center of the compact sulfide layer. It may be concluded from these results that the formation of nickel sulfide proceeded by means of the outward migration of nickel atoms. Since nickel sulfide is a metal-deficient compound, it is considered that nickel atoms migrate *via* nickel vacancies.

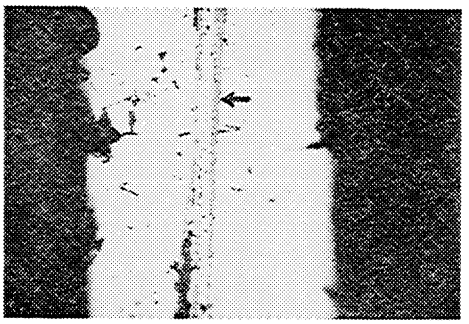

Fig. 2. Section of NiS. ← shows the Marker

Kinetic Study. Figure 3 shows some typcial weight change - time curves of sulfidation. In the figure, M_t is the weight change at the time t and M_∞ is the weight change after sufficient time has lapsed. When the total pressure of the gas mixture was changed while the other conditions, such as the thickness and the metal deficit of sulfide and the pressure ratio of H_2S to H_2, were kept constnat, the values of M_t/M_∞ obtained at a certain temperature lie on the same curve, which is only dependent on the temperature. This means that the reaction is controlled by the diffusion, because

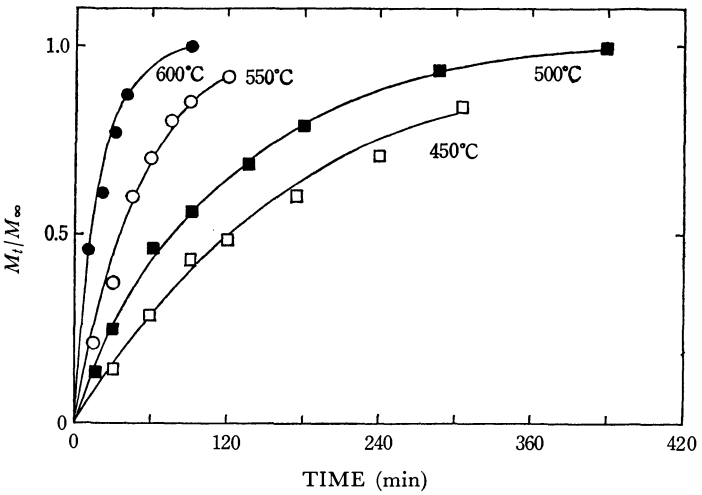

Fig. 3. Typical weight change time curves.
600°C=0.007 → 0.013 500°C=0.008 → 0.018

the rate of the diffusion-controlled reaction depends not on the total pressure but on the pressure ratio.

If a nickel sulfide slab is exposed to a H_2S-H_2 gas mixture which has sulfur with a higher activity than the sulfide, the specimen is sulfidized and the weight is increased. In this case sulfide atoms and nickel vacancies are introduced into sulfide at the gas-sulfide interface. Since nickel atoms migrate in nickel sulfide predominantly *via* nickel vacancies, as has been found in the marker experiment, nickel vacancies introduced at the gas-sulfide interface diffuse inwards. The rate equation for this process is:

$$\frac{\partial C_\square}{\partial t} = D_\square \frac{\partial^2 C_\square}{\partial x^2} \tag{1}$$

where $C_\square$ and $D_\square$ are the concentration and the self-diffusion coefficient of nickel vacancies respectively.

Solving the equation under the boundary conditions:

$$\left.\begin{aligned} C_\square &= C_\square^\circ \text{ for } -l < x < l \text{ and } t = 0 \\ C_\square &= C'_\square \text{ for } x = \pm l \text{ and } t > 0 \end{aligned}\right\} \tag{2}$$

one can obtain this equation:

$$\frac{C_\square - C_\square^\circ}{C'_\square - C_\square^\circ} = 1 - \frac{4}{\pi}\sum_{n=0}^{\infty}\frac{(-1)^n}{(2n+1)} \times \exp\left\{\frac{-D_\square(2n+1)^2\pi^2 t}{4l^2}\right\} \times \cos\frac{(2n+1)\pi x}{2l} \tag{3}$$

where $C_\square^\circ$ is the vacancy concentration before the reaction, $C'_\square$ is the vacancy concentration at the gas-sulfide interface during the reaction, and $2l$ is the thickness of the sulfide slab. The replacement of the concentrations by M_t and M_∞ and integration with regard to x yields:

$$\frac{M_t}{M_\infty} = 1 - \sum_{n=0}^{\infty}\frac{8}{(2n+1)^2\pi^2} \times \exp\left\{\frac{-D_\square(2n+1)^2\pi^2 t}{4l^2}\right\} \tag{4}$$

Omitting the higher terms of the series, one obtains:

$$-\ln\left(1 - \frac{M_t}{M_\infty}\right) = \frac{\pi D_\square t}{4l^2} \tag{5}$$

Figure 4 shows the plot of $-\log(1-M_t/M_\infty)$

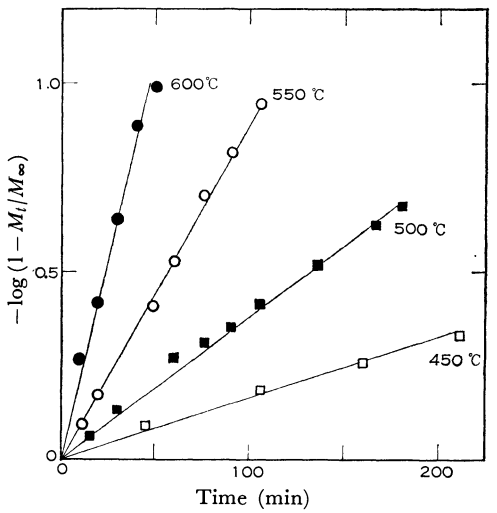

Fig. 4. Plot of $-\log\left(1-\frac{M_t}{M_\infty}\right)$ *vs.* time.
600°C=0.007 → 0.013
550°C=0.007 → 0.018
500°C=0.008 → 0.018
450°C=0.009 → 0.016

vs. t. A linear relationship is obvious. From the slope of the plot, $D_{\square}$, the self-diffusion coefficient of nickel vacancies is determined. When nickel atoms diffuse by the vacancy mechanism, the following relationship exists:

$$D_{\square}C_{\square} = DC \qquad (6)$$

where D and C are the self-diffusion coefficient and the concentration of nickel atoms respectively, accordingly, D can be determined from $C_{\square}/C$ and $D_{\square}$.

Since $C_{\square}$ and C are related to the metal deficit, δ, by the following equation:

$$\delta = \frac{C_{\square}}{C_{\square}+C}$$

and since $C_{\square}$ is small enough to be neglected, we obtain:

$$\delta \fallingdotseq \frac{C_{\square}}{C}$$

The metal deficit determined gravimetrically is given in Fig. 5 as a plot of δ *vs.* $\log(P_{H_2S}/P_{H_2})$.

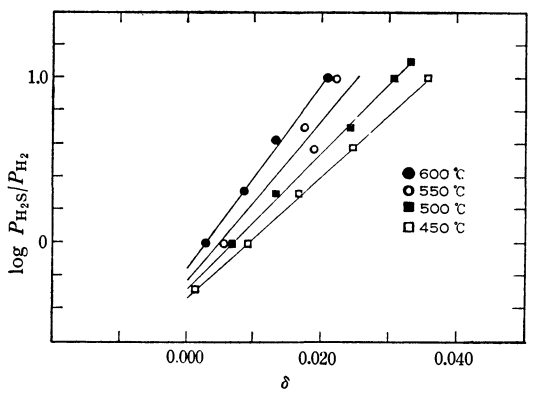

Fig. 5. Metal deficit of nickel sulfide as a function of temperature and P_{H_2S}/P_{2H}.

This result agrees well with the equilibrium data of Rosenquvist.[1] It can easily be seen that $C_{\square}/C$ ranges from 0 to 0.05. Assuming that $C_{\square}/C$ is the avarage of the initial and final values, we can obtain the D values by Eq. (6). These values are summarized in Table 1. Figure 6 shows the

Table 1

Temp °C	Change in δ	$C_{\square}/C$	$D_{\square}\times 10^7$ (cm²/sec)	$D\times 10^9$ (cm²/sec)
600	0.007→0.013	0.010	1.45	1.45
	0.013→0.008	0.011	1.61	1.69
550	0.018→0.005	0.012	0.470	0.541
	0.007→0.018	0.013	0.511	0.638
500	0.008→0.018	0.013	0.236	0.307
	0.018→0.008	0.013	0.241	0.313
450	0.009→0.016	0.013	0.0977	0.127

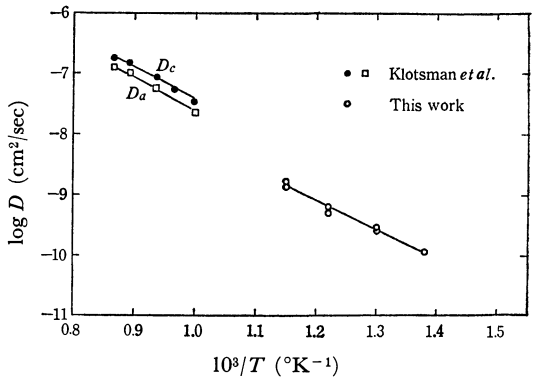

Fig. 6. Arrhenius plot of diffusion coefficient.

Arrhenius plot for the self-diffusion coefficient of nickel in nickel sulfide. The open circles indicate the data of this work. The present data are expressed by the equation:

$$D = 3.2\times 10^{-4} \exp\left(\frac{-21300}{RT}\right) \text{cm}^2/\text{sec} \qquad (7)$$

For comparison, the data obtained by Klotsman and his collaborators,[3] who employed the tracer method, are indicated by closed circles and squares in the same figure. The diffusion coefficients obtained by Klotsman and his collaborators are about three times higher than those extrapolated from the present data. They used nickel sulfide with a metal deficit of 0.03, while in the present work a deficit of 0.010—0.013 was employed. Since the diffusion coefficient is proportional to the vacancy concentration, the difference in diffusion data must be due to the difference in vacancy concentration of the sulfide employed in the experiments.

Summary

(1) The diffusivity of nickel was found, by means of a marker experiment on the sulfidation of nickel, to be much higher than that of sulfur.

(2) The rates of the sulfidation and desulfidation of nickel sulfide in H_2S-H_2 atmospheres were determined gravimetrically, and the diffusion coefficients of nickel vacancies were calculated.

(3) The metal deficit of nickel sulfide was determined as a function of the partial pressure ratio of H_2S to H_2 and of the temperature.

(4) From the concentrations and diffusion coefficients of nickel vacancies, the self-diffusion coefficients of nickel atoms were obtained.

The values agreed well with those determined by previous investigations employing the tracer technique.

3) S. M. Klotsman, A. M. Timofeyev and I. Sh. Trakhtenberg, *Physics of Metals and Metallography*, **16**, 92 (1963).

BULLETIN OF THE CHEMICAL SOCIETY OF JAPAN VOL. 41 573—576 (1968)

Adsorption Behavior of Hydrogen and Carbon Monoxide over Zinc Oxide in the Mixed Gas Adsorption and during the Methanol Decomposition Reaction*1

Susumu TSUCHIYA and Tadao SHIBA

Tokyo Institute of Technology, Ookayama, Meguro-ku, Tokyo

(Received September 4, 1967)

Adsorption of hydrogen and carbon monoxide at the different situations has been investigated with zinc oxide which is the principal component of ordinary methanol synthesis catalysts. In the simultaneous adsorption of hydrogen and carbon monoxide the mutual interaction was also observed. The results were explained as the displacement effect as well as the enhancement took place in a certain region of the partial pressures. Adsorption measurements during the decomposition reaction suggest that in initial state the adsorbed species are mostly the adsorbed methanol and that the step of the decomposition of it is the rate-determining step of the overall reaction. The mechanism of methanol synthesis over zinc oxide is suggested to proceed in the similar way as on the three component catalyst previously used.

In the previous papers,[1-4] adsorption behaviors of hydrogen and carbon monoxide in the mixed gas adsorption and during the methanol synthesis and decomposition reaction over three component methanol synthesis catalyst have been investigated in the relation to the mechanism of the methanol synthesis. The rate-determining step of the synthesis of methanol was suggested to be the process of the Eley-Rideal type hydrogenation of the surface complex. The mutual influence of the chemisorption of hydrogen and carbon monoxide has been observed, and the facts suggest that the adsorption behavior both in the mixed gas adsorption and that during the reaction can not be estimated from the single gas adsorption.

In this work, the similar investigations as previously[1-4] reported, have been carried out with zinc oxide in order to obtain further informations on the mechanism of the methanol synthesis and decomposition, because zinc oxide is the principal component of the three component methanol synthesis catalyst previously[1-4] used.

Experimental

The apparatus employed and method were the same as was previously reported.[1-4] Known amounts of the reactants were introduced into the system, the extent of the reaction was followed by pressure measurement. The amount of gas adsorbed on the catalyst surface was estimated by material balance of reactants introduced and the partial pressure and composition of the circulating gas. The composition of the circulating mixture was determined by gas chromatography. Due allowance was made for the analytical samples removed from the apparatus. The amount of gas adsorbed on the catalyst, including the surface complex, was obtained in terms of either the adsorbed hydrogen or the carbon monoxide.

The zinc oxide catalyst (13.7 g) employed was obtained by calcining zinc hydroxide at 300°C, which was precipitated from zinc nitrate solution by ammonium hydroxide. Before each run, the catalyst was evacuated for 10 hr at 400°C. The experimental results were satisfactorily reproducible.

Results and Discussion

Simultaneous Adsorption. Typical results of simultaneous chemisorption of hydrogen and carbon monoxide on the zinc oxide catalyst are shown in Figs. 1 and 2. Pure hydrogen was first introduced into the reaction system. A marked acceleration of hydrogen chemisorption at the addition of carbon monoxide was thus observed, as shown in Fig. 1. An enhanced adsorption of carbon monoxide by the presence of hydrogen was also observed when hydrogen was added to carbon monoxide as shown in Fig. 2, where pure carbon monoxide was first introduced and then hydrogen was admitted. In both cases of hydrogen and carbon monoxide, the enhanced adsorption of the pre-admitted gas by the addition of the other gas were also observed over zinc oxide, as well as over the three component methanol synthesis catalyst.[2] The mutual enhancement of the

*1 This paper was presented at the Annual Meeting of the Catalysis Society of Japan, Osaka, October, 1964.

1) S. Tsuchiya and T. Shiba, This Bulletin, **38**, 1726 (1965).
2) S. Tsuchiya and T. Shiba, *J. Catalysis*, **4**, 116 (1965).
3) S. Tsuchiya and T. Shiba, *ibid.*, **6**, 270 (1966).
4) S. Tsuchiya and T. Shiba, This Bulletin, **40**, 1086 (1967).

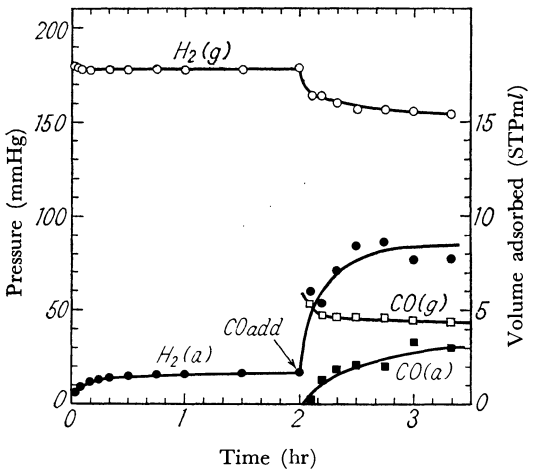

Fig. 1. Effect of carbon monoxide addition on the adsorption of hydrogen at 250°C.

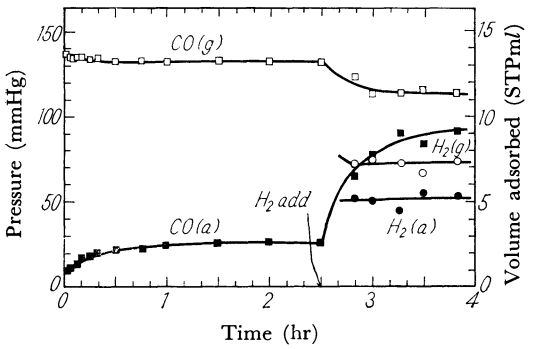

Fig. 2. Effect of hydrogen addition on the adsorption of carbon monoxide at 250°C.

adsorption was complicatedly varied by the added gas and the ratio of hydrogen to carbon monoxide.

The mutual interaction of the adsorption of hydrogen and carbon monoxide is shown more quantitatively in Fig. 3. The amounts of adsorption of hydrogen pre-admitted increased by the addition of the carbon monoxide, but the amounts of the increments rather decreased, when the pressure of carbon monoxide added increased. These results suggest that a part of the hydrogen adsorbed was displaced by carbon monoxide added. The similar results were observed when the same was done replacing carbon monoxide with hydrogen. It is consequently suggested that the mutual enhancement as well as displacement of the chemisorption of hydrogen and carbon monoxide take place on zinc oxide. The mutual enhancement effect might be due to the creation of additional sites as was suggested by Nagarjunan, Sastri and Kuriacose[5] and the displacement would

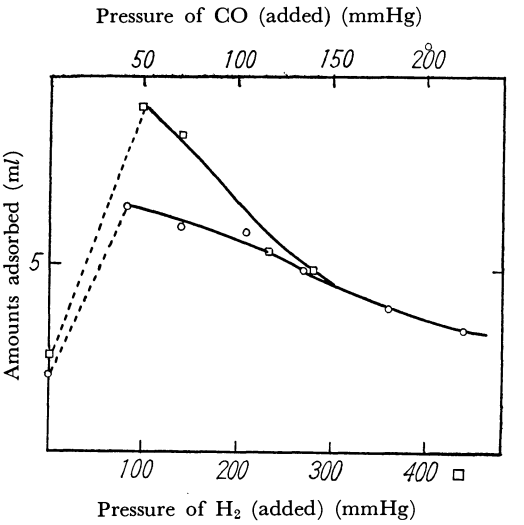

Fig. 3. Mutual interaction in the adsorption of hydrogen and carbon monoxide.

occur when the amounts of gas were in excess of the total sites.

The adsorption isotherms of hydrogen and carbon monoxide, are shown in Figs. 4 and 5, respectively. The mixed adsorption isotherms were obtained by introducing the mixtures of the $2H_2$: 1CO gases. The adsorption was more enhanced at 250°C than at 300°C.

Using the BET method for nitrogen adsorption at −190°C, the surface area and volume of gas which gives a complete monolayer v_m of the catalyst were estimated to be 6.7×10^5 cm^2 and 15 m*l*, respectively. As Figs. 4 and 5 show, in some

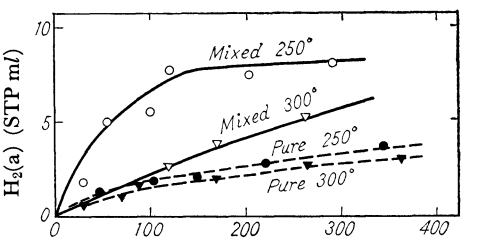

Fig. 4. Adsorption isotherms of hydrogen.

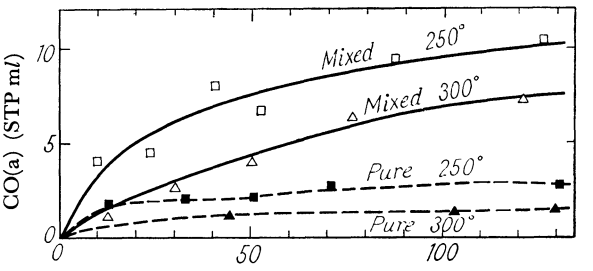

Fig. 5. Adsorption isotherms of carbon monoxide.

5) T. S. Nagarjunan, M. V. C. Sastri and J. C. Kuriacose, *J. Catalysis*, **2**, 223 (1963).

cases the sum of the amounts of hydrogen and carbon monoxide adsorbed exceeded v_m to some extent, which suggests the formation of surface complex from hydrogen and carbon monoxide, coupling with the fact that zinc oxide has the catalytic activity for methanol synthesis from hydrogen and carbon monoxide.

Decomposition Reaction. Typical result of the decomposition of methanol is shown in Fig. 6. As the decomposition proceeded, the partial pressure of methanol decreased with time, and those of hydrogen and carbon monoxide increased, while the ratio of adsorption of hydrogen to carbon monoxide changed.

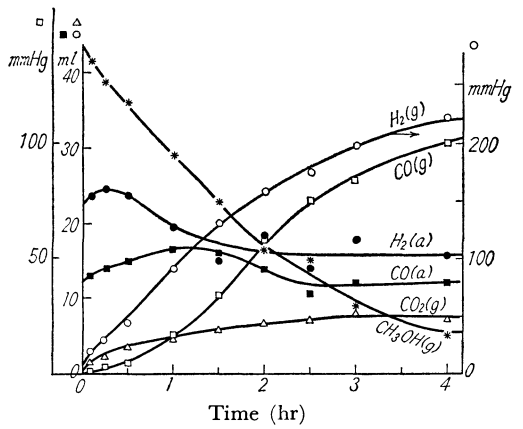

Fig. 6. Adsorption measurements during the methanol decomposition at 250°C.

At the initial stage, the ratio of the sum of the amounts of hydrogen adsorbed to that of carbon monoxide adsorbed, which include those in the surface complex formed from them, was nearly two. The adsorbed species on the zinc oxide is probably suggested to be CH_3OH at the initial stage of the reaction as was previously[3] concluded over the three component methanol synthesis catalyst. The results that the change of the ratio of hydrogen to carbon monoxide adsorbed during the course of the methanol decomposition, is explained in terms of the existence of "free hydrogen" and "free carbon monoxide" which was suggested previously,[4] as well as the surface complex.

If the decomposition of methanol over a zinc oxide and over a three component methanol synthesis catalyst proceeds in the same way as proposed previously,[3] the mechanism of the reaction would be as given by Scheme A.

The authors previously[3,4] expressed hydrogen adsorbed as $H_2(a)$, which include both atomic and molecular ones.

However, the hydrogen adsorbed might be atomic becaurse the hydrogen and deuterium equilibration reaction took place over a zinc oxide.[6]

The amounts of adsorption during the decomposition of methanol were always greater than those in the adsorption from the mixture $2H_2 : 1CO$; the amounts of the adsorption both of hydrogen and of carbon monoxide from the mixture were less than 10 m*l* even at 200 mmHg pressure. The results suggest that not all of the species adsorbed on the catalyst—hydrogen, carbon monoxide, and any intermediate complex formed from hydrogen and carbon monoxide—were in equilibrium with hydrogen and carbon monoxide in the gas phase, and that the process of the adsorption of methanol (process 1) can not be the rate-determining step of the reaction.

As shown in Fig. 7, the ambient pressure of hydrogen did not decrease when methanol was abruptly removed from the system during the reaction, and the amount of methanol in the trap stayed constant during the trapping. The facts suggest that the major part of the adsorbed species, hydrogen, carbon monoxide, and the complex formed from them, on the catalyst is not in equilibrium with the methanol in the gas phase; otherwise,

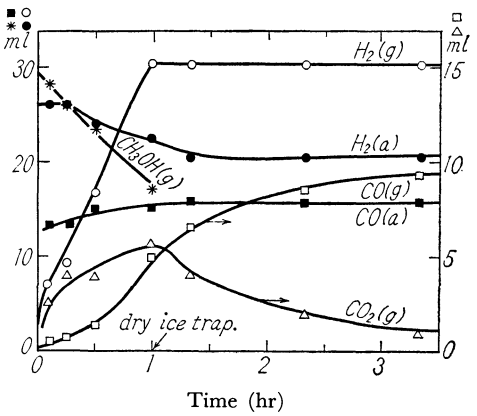

Fig. 7. The effect of methanol elimination during the decomposition reaction.

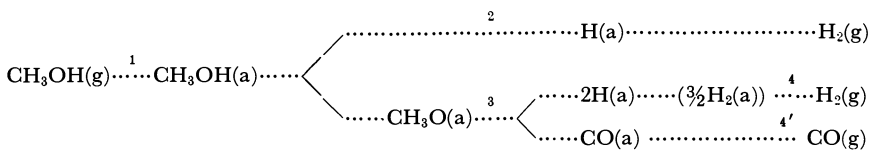

Scheme A.

6) E. Molinari and G. Parravano, *J. Am. Chem. Soc.*, **75**, 5233 (1953).

the major part of them would rapidly be desorbed to be caught by the trap. Neither of the processes of the desorption of hydrogen nor carbon monoxide (processes 3, 4, and 4') are accordingly suggested to be the rate-determining step of the reaction. Consequently, the rate-determining step is suggested to be the process of the dissociation of adsorbed complex (process 2). The suggestion conforms to the conclusion previously[1-4] reported in the case of the reaction over the three component methanol synthesis catalyst.

The results for decomposition of various amounts of methanol are shown in Fig. 8, where the pressure of methanol is plotted against time. The pressures at time zero were, however, estimated from the amounts of methanol introduced and the volume of the reaction system. The initial decreases in the methanol pressure represented by the upper dotted lines were followed by the linear part of the decreases in the pressure, represented by solid lines. The initial rate of the pressure decrease in the solid line range was almost independent of the methanol pressure; deviation from linearity, however, occured at later time.

The initial rapid decrease in the methanol pressure represented with the upper dotted lines can be considered to be due to the adsorption of methanol as menthioned above. Hence the order of methanol decomposition reaction is approximately zero and the rate of the reaction would be roughly expressed by Eq. (1), since the solid lines would show the methanol decomposition reaction.

$$r \doteqdot k \qquad (1)$$

The results agreed with those observed previously.[3] The apparent activation energy of the decomposition reaction was estimated to be 27.8 kcal/mol from the Arrhenius plots of k.

A curve considered to be an adsorption isotherm of methanol was obtained as shown with a solid line for 250°C in Fig. 9. The ambient pressure of methanol was obtained by extraporating the pressure-time curve in Fig. 8 to time zero (lower dotted lines), and the adsorbed amount was estimated from the mass balance between the amount of the methanol introduced and that in the gas phase at that time, because the methanol only adsorbed on the surface. It is thus shown in Figs. 8 and 9 that the nearer the amounts of methanol initially adsorbed approach v_m in BET equation (see Fig. 9), the nearer the reaction order comes to zero (see Fig. 8). At 150°C the decomposition of methanol was not observed, so the curve

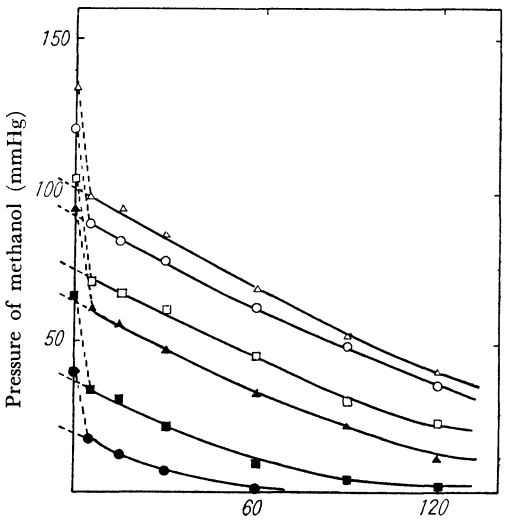

Fig. 8. The methanol decomposition at various initial pressure at 250°C.

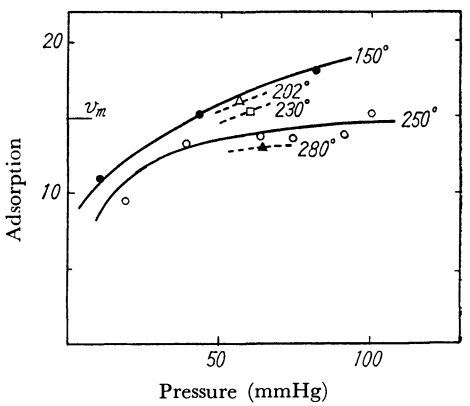

Fig. 9. Relation between adsorbed and gaseous methanol.

was obtained by means of the usual manner for the adsorption measurement.

As for the mechanism and kinetics of the methanol decomposition, it is consequently concluded that the process of the dissociation of the adsorbed methanol into the adsorbed intermediate complex and hydrogen is the rate-determining step of the overall reaction as on the three component catalyst. The mechanism of methanol synthesis on zinc oxide is thus suggested to proceed in the similar way as on the three component catalyst.

BULLETIN OF THE CHEMICAL SOCIETY OF JAPAN VOL. 41 577—582 (1968)

Faradaic Impedance of Fast Electrode Processes as Measured by an Impedance Bridge Using an Inductor

Takuma TANAKA and Hideo IMAI

Department of Chemistry, Faculty of General Education, Hiroshima University

(Received September 12, 1967)

An impedance bridge using an inductor in parallel with the cell is proposed for accurate measurement of kinetic parameters of fast electrode processes. The theory and method of analysis are given in detail. Its applicability was proved up to at least 50 kc, and possibly at higher frequencies. The kinetic parameters obtained by this method for the electrode reaction $Cd^{2+}+2e=Cd(Hg)$ in M Na_2SO_4 at the D. M. E. were $\alpha=0.17$, and $k^\circ=0.064$ cm/sec (25°C).

A conventional impedance bridge[1] for measurement of faradaic impedance is composed of resistors and capacitors, and the faradaic impedance is replaced by a series or parallel R-C network. This type of a.c. bridge has shown its usefulness in evaluating kinetic parameters of electrode processes, although it can not be applied to measurement at frequencies higher than several ten thousands cps due to its low response. The reason can easily be understood from the fact that the faradaic impedance is in parallel with the differential capacity, and that the impedance of the latter is very small at higher frequencies.

However, high frequency is necessary in order to evaluate the kinetic parameters of fast electrode processes.*1

For capacity measurement, Melik-Gaikazyan[2] recommended the use of a very small inductance in series with the cell, and Lorenz suggested the use of a T-bridge.[3] In this paper it is tentatively proposed to use an inductor*2 in parallel with the cell in an a.c. bridge in order to improve its applicability at higher frequencies. The inductor used was in parallel with the cell so as to be in resonance with the capacitive component of the electrode-solution double layer so that the impedance of the imaginary component will be infinite. (The series resonant circuit was also investigated, with the details omitted here because of its complexity for practical use.) It was found that this improved a.c. bridge can be used up to at least 50 kc. The method of analysis is described in detail with an application to the fast electrode process, $Cd^{2+}+2e=Cd(Hg)$, at the dropping mercury electrode.

Experimental

Reagents and Solution. All the reagents were of analytical grade. The solution contained 0.5 mM Cd^{2+} (weighed as $CdSO_4 \cdot H_2O$) in M Na_2SO_4 as the supporting electrolyte. Purified nitrogen was used for deaeration, and measurement was carried out in a nitrogen atmosphere. Temperature was kept constant at 25±0.1°C.

Electrode and Cell. The working electrode was a dropping mercury electrode (DME), and it was made of capillary tubing used in a usual Hg-thermometer. In the top of the capillary (17 cm in length) a Pt wire (0.012 cmϕ, 5 cm in length) was inserted, and the upper part of the capillary was constricted in order to give an appropriate flow rate of mercury. The lifetime of the D. M. E. was about 6 sec in the open circuit. A hammer was used to give drops at 4.0 sec intervals. The resistance of the DME was as small as 4.5 Ω. The auxiliary electrode was a smooth Pt cylinder, and a saturated-Hg_2SO_4 electrode (SSE) was used as the reference.

Generation of Reductant *in situ*. A potentiometer circuit (P in Fig. 1A) was used to give an optional

1) D. C. Grahame, *J. Am. Chem. Soc.*, **68**, 301 (1946); **71**, 2975 (1949); *J. Phys. Chem.*, **61**, 701 (1957); J. E. B. Randles, *Trans. Faraday Soc.*, **50**, 1246 (1954); J. Shön, W. Mehl and H. Gerischer, *Z. Electrochem.*, **59**, 144 (1955).

*1 When diffusion is the sole mode of mass transfer, the average flux of the reducing species diffusing toward a plane electrode is given by $2C^*(D/\pi t)^{1/2}$, where C^* is the bulk concentration of the reducing species, D the diffusion coefficient, and t the time elapsed since the beginning of the electrolysis. In a process with mixed control by both mass- and charge-transfer, this conclusion is qualitatively valid, and diffusion is no longer rate-determining for a measurement with very short electrolysis time, or at a sufficiently high frequency, the concentration gradient in the diffusion layer being steep enough. Thus the evaluation of kinetic parameters of fast charge transfer processes inherently necessitates measurement in a very short time interval, or the application of high frequency.

2) V. I. Melik-Gaikazyan, *Zhur. Fiz. Khim.*, **26**, 560 (1952); V. I. Melik Gaikazyan and P. Dolin, *Doklady Akad. Nauk S. S. S. R.*, **66**, 409 (1949).

3) W. Lorenz, *Z. physik. Chem. Neue Folge*, **26**, 424 (1960).

*2 The authors are indebted to Professor T. Kambara of Hokkaido University for his suggestion to use an inductor in series with the cell in order to improve the sensitivity of an a. c. polarograph.[4]

4) T. Kambara and K. Hasebe, *Rev. Polarography (Japan)*, **13**, 132 (1966).

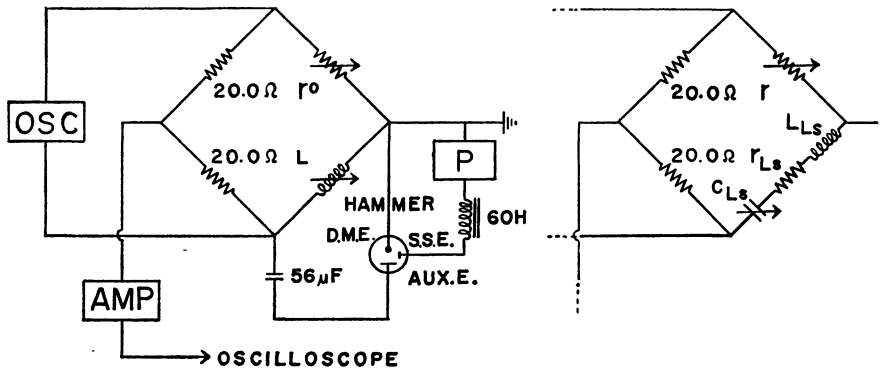

A B

Fig. 1. A: Bridge circuit for the faradaic impedance measurements. OSC, audio-generator; P, potentiometer; AMP, selective amplifier.
B: Bridge circuit for the measurement of the real (r_{Ls}) and imaginary (L_{Ls}) components of the inductor L in resonance with the cell.

electrode potential. Thus the reductant was generated *in situ*, and the concentrations of the oxidant (C_O) and reductant (C_R) at the pre-electrode layer can be calculated from polarographic theory, *i. e.*,

$$C_O = C_O^*\left(1-\frac{i}{i_d}\right) \quad (1)$$

$$C_R = C_O^*\left(\frac{D_O}{D_R}\right)^{1/2}\cdot\frac{i}{i_d} \quad (2)$$

where C_O^* is the bulk concentration of the reducing species, i the current flowing at a given potential, i_d the diffusion-controlled current, and the D's are the diffusion coefficients. The current was recorded by a Shimadzu Model RP-3 polarograph.

A. C. Bridge. The a. c. voltage applied to the cell was about 5 mV peak to peak and was supplied from an audio-generator, Trio Model AG-10 (OSC in Fig. 1A). The frequency was calibrated by a crystal oscillator (15 kc). The out-put of the bridge was fed to a selective amplifier (AMP in Fig. 1A), Yokogawa-Hewlett-Packard, Model AL-11, and was detected by a synchro-oscilloscope, Iwasaki Model SS-5302 with a plug-in amplifier, Model SP-30H-A.

The bridge circuit is shown in Fig. 1, where a variable inductor (L in Fig. 1, 400 μH—1 mH) was connected in parallel with the cell. A large capacitor (56 μF) was used in series with the cell in order to shut off the potentiometer circuit. The two resistors in the two arms of the bridge were 20.0 Ω and inductanceless. A variable resistor ($r°$ in Fig. 1) used for balancing the bridge was composed of a decade box (0.1 Ω—1.1 kΩ in 4 stages) and a manganin wire (0.01 Ω—0.1 Ω) with a sliding contact.

The bridge balance was detected at the maximum size of the mercury drop. The surface area of the DME was calculated by means of the following equation:

$$S(\mathrm{cm}^2,\ 25°\mathrm{C}) = 0.00852\ (mt)^{2/3}, \quad (3)$$

where m is the rate of flow of mercury in mg/sec, and t the life-time of the DME (=4.0 sec using the hammer).

Theoretical

Equivalent Circuit of the Cell. The equivalent circuit of the cell components is illustrated in Fig. 2A, where r_{cap} is the capillary resistance, r_e the solution resistance, r_s, and C_s the series resistive, and capacitive components of the faradaic impedance, respectively, and C_l the differential capacity of the double layer. The total impedance

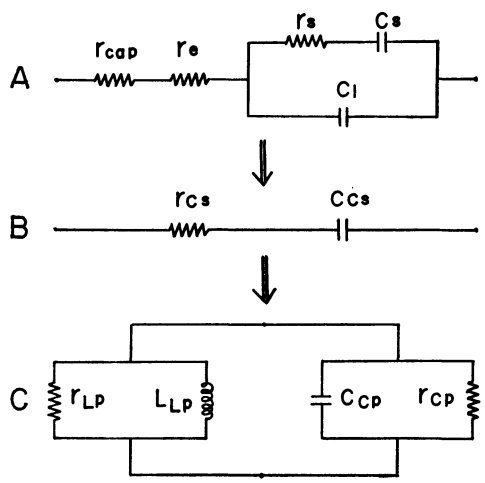

Fig. 2. Conversion scheme of the equivalent circuit of the cell.
A: Equivalent circuit of the overall cell circuit: r_{cap}, capillary resistance; r_e, solution resistance; r_s and C_s; series resistive and capacitive components of the faradaic impedance, respectively; C_l, differential capacity of the double layer.
B: Equivalent simple series circuit.
C: Equivalent simple parallel circuit of the cell and inductor in a resonant condition: The suffix, C or L represents the cell or inductor, respectively.

(Z) of this cell circuit is represented by:

$$Z = Z_{\text{real}} + \frac{1}{j} Z_{\text{Imaginary}} \tag{4}$$

with

$$Z_{\text{real}} = r_{\text{cap}} + r_e + \left(\frac{1}{\omega C_l}\right)^2 \frac{r_s}{r_s^2 + \left(\frac{1}{\omega C_s} + \frac{1}{\omega C_l}\right)^2} \tag{5}$$

and

$$Z_{\text{imaginary}} = \frac{1}{\omega C_l} - \left(\frac{1}{\omega C_l}\right)^2 \frac{\frac{1}{\omega C_s} + \frac{1}{\omega C_l}}{r_s^2 + \left(\frac{1}{\omega C_s} + \frac{1}{\omega C_l}\right)^2} \tag{6}$$

In Eqs. (5) and (6), r_{cap} and r_e can be determined separately, and C_l at a given potential can also be determined by using the base line shown in the plot of C_{Cs} *versus* E (Fig. 5).

Conversion to an Equivalent Simple Series Circuit of the Cell. In order to evaluate r_s and C_s in Eqs. (5) and (6), a conversion of the equivalent circuit in Fig. 2A to an equivalent simple series circuit as shown in Fig. 2B was made. Then the total impedance (Z) in Eq. (4) becomes:

$$Z = r_{\text{Cs}} + \frac{1}{j\omega C_{\text{Cs}}} \tag{7}$$

with $$Z_{\text{real}} = r_{\text{Cs}} \tag{8}$$

and $$Z_{\text{imaginary}} = \frac{1}{\omega C_{\text{Cs}}} \tag{9}$$

Equations (5), (6), (8) and (9) lead to the following expressions for r_s and $1/\omega C_s$;

$$r_s = \left(\frac{1}{\omega C_l}\right)^2 \frac{r_{\text{Cs}} - r_{\text{cap}} - r_e}{(r_{\text{Cs}} - r_{\text{cap}} - r_e)^2 + \left(\frac{1}{\omega C_l} - \frac{1}{\omega C_{\text{Cs}}}\right)^2} \tag{10}$$

$$\frac{1}{\omega C_s} = \left(\frac{1}{\omega C_l}\right)^2 \frac{\frac{1}{\omega C_l} - \frac{1}{\omega C_{\text{Cs}}}}{(r_{\text{Cs}} - r_{\text{cap}} - r_e)^2 + \left(\frac{1}{\omega C_l} - \frac{1}{\omega C_{\text{Cs}}}\right)^2} - \frac{1}{\omega C_l} \tag{11}$$

Inductor in Resonance with Cell. In the circuit shown in Fig. 1A the inductor is in parallel with the cell, and at the null point of the bridge the cell and inductor are in a resonant condition. The condition is taken into account by the conversion of the equivalent circuit given in Fig. 2B into the equivalent parallel circuit given in Fig. 2C. In Fig. 2C the inductor is also represented by an equivalent parallel circuit.

The resonant condition, in general, is given by

$$\omega L = \frac{1}{\omega C} \tag{12}$$

Accordingly, one is lead to the following relationship,

$$\omega L_{\text{Lp}} = \frac{1}{\omega C_{\text{Cp}}} \tag{13}$$

and

$$\frac{1}{r^\circ} = \frac{1}{r_{\text{Lp}}} + \frac{1}{r_{\text{Cp}}} \tag{14}$$

These parallel components are equivalent to the series components given in Fig. 2B, so that

$$r_{\text{Cs}} = \frac{\frac{1}{r_{\text{Cp}}}}{\left(\frac{1}{r_{\text{Cp}}}\right)^2 + (\omega C_{\text{Cp}})^2} \tag{15}$$

$$\frac{1}{\omega C_{\text{Cs}}} = \frac{\omega C_{\text{Cp}}}{\left(\frac{1}{r_{\text{Cp}}}\right)^2 + (\omega C_{\text{Cp}})^2} \tag{16}$$

Evaluation of Inductive and Resistive Components of the Inductor in Resonance with the Cell. The series inductive (L_{Ls}) and resistive (r_{Ls}) components of the inductor in resonance with the cell were measured by the impedance bridge shown in Fig. 1B. Under a series resonant condition, that is, at bridge balance, the following equation holds,

$$\omega L_{\text{Ls}} = \frac{1}{\omega C_{\text{Ls}}} \tag{17}$$

Conversion of Eq. (17) into a parallel equivalent circuit leads to the following expression;

$$\frac{1}{r_{\text{Lp}}} = \frac{r_{\text{Ls}}}{r_{\text{Ls}}^2 + \left(\frac{1}{\omega C_{\text{Ls}}}\right)^2} \tag{18}$$

Combining Eqs. (14), and (18), one obtains

$$\frac{1}{r_{\text{Cp}}} = \frac{1}{r^\circ} - \frac{1}{r_{\text{Lp}}} \tag{19}$$

and $$\omega C_{\text{Cp}} = \frac{\frac{1}{\omega C_{\text{Ls}}}}{r_{\text{Ls}}^2 + \left(\frac{1}{\omega C_{\text{Ls}}}\right)^2} \tag{20}$$

Method of Analysis of Experimental Data. The values of r°, r_{Ls}, and C_{Ls} can be directly determined by experiment. By using these data, C_{Cp} is calculated by Eq. (20), and $1/r_{\text{Cp}}$ is calculated by Eqs. (18) and (19). Then r_{Cs} and $1/\omega C_{\text{Cs}}$ are evaluated from Eqs. (15) and (16). Finally, r_s and $1/\omega C_s$ can be evaluated from Eqs. (10) and (11), using the values for r_{cap}, r_e, and C_l.

Results and Discussion

Variation of Bridge Component Values with Frequency. The bridge was composed of inductanceless resistors, and moreover, precaution was paid to the arrangement of the circuit in order to avoid any possible stray capacity. But the rather high resistance of the inductor may introduce bad effect. Figure 3 shows the direct reading of a standard resistor (20.0 Ω), and a capacitor (1.0000 μF) network which replaces the cell circuit in Fig. 1A. The variation in component values with frequency was fairly large. The ratio of the direct reading to the standard value at each frequency was used for calibration.

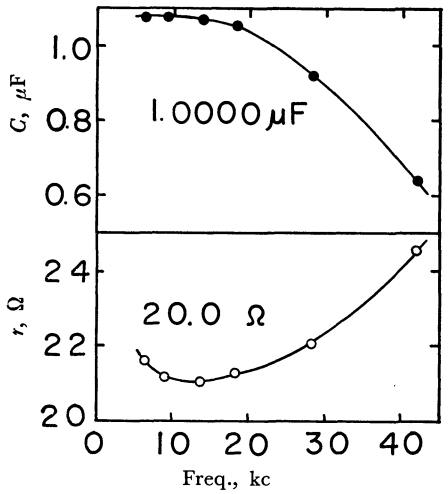

Fig. 3. Frequency dependence of direct reading values of the series $R(20.0\,\Omega)-C(1.0000\,\mu F)$ network.

Application to the Electrode Process $Cd^{2+}+2e=Cd(Hg)$ at the DME. The ability of this improved impedance bridge was tested by a fairly rapid electrode process, $Cd^{2+}+2e=Cd(Hg)$ in M Na_2SO_4 at the DME. The electrode process was assumed to involve no kinetic complication. Cd(II) ions (5×10^{-7} mol/cm^3) developed a well-defined polarographic wave in M Na_2SO_4. The half-wave potential was -1.020_5 V *vs.* SSE. The reductant (Cd(Hg)) was generated *in situ* by the application of a d.c. potential to the working electrode. The concentrations of the oxidant and reductant at the pre-electrode layer were calculated by Eqs. (1) and (2), using the polarographic data. The values, $D_O=0.72\times10^{-5}$ cm^2/sec and

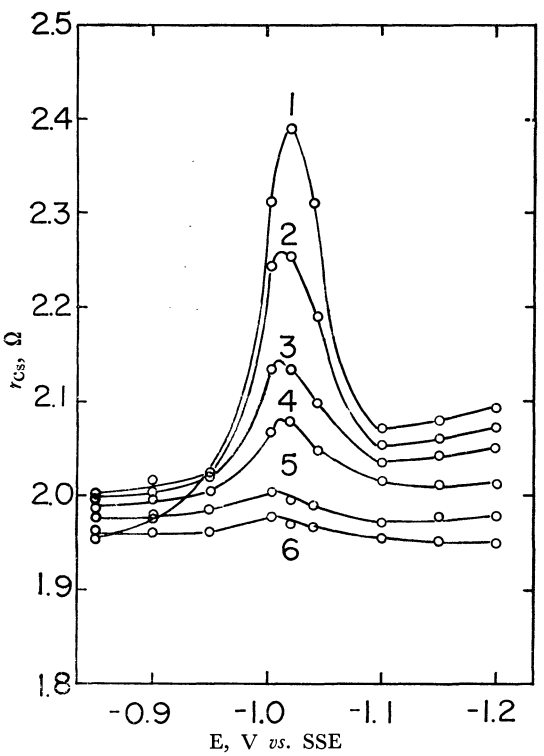

Fig. 4. Variation of the equivalent simple series resistive component (r_{Cs}) with potential at frequencies, 6.42 kc (Curve 1), 9.12 kc (Curve 2), 13.92 kc (Curve 3), 18.45 kc (Curve 4), 28.25 kc (Curve 5), and 41.99 kc (Curve 6).

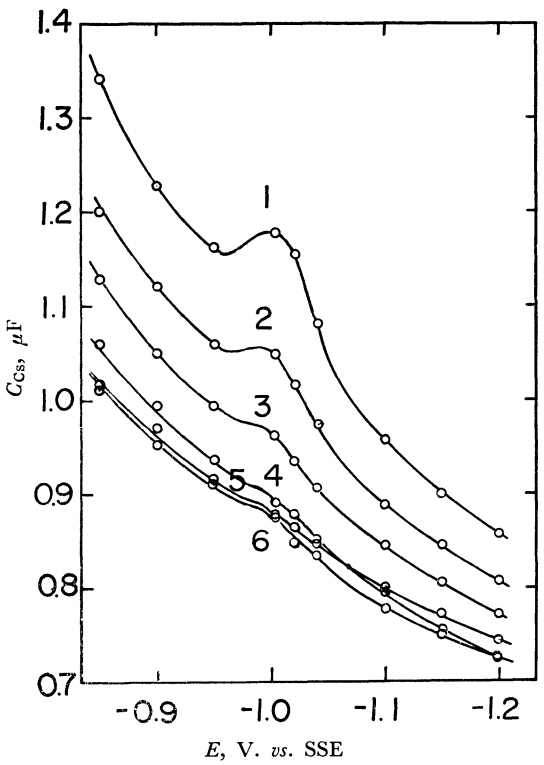

Fig. 5. Variation of the equivalent simple series capacitive component (C_{Cs}) with potential at frequencies, 6.42 kc (Curve 1), 9.12 kc (Curve 2), 13.92 kc (Curve 3), 18.45 kc (Curve 4), 28.25 kc (Curve 5), and 41.99 kc (Curve 6).

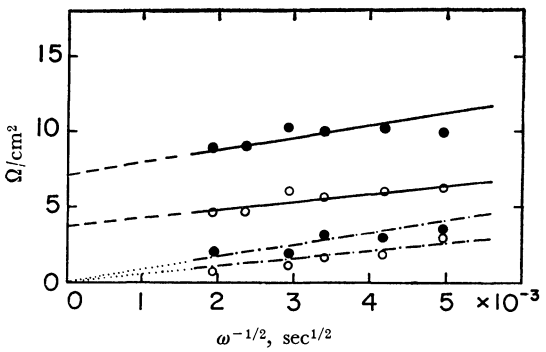

Fig. 6. Plot of the series components, r_s and $1/\omega C_s$, of the faradaic impedance *versus* $\omega^{-1/2}$ for the electrode reaction, $Cd^{2+}+2e=Cd(Hg)$ in M Na_2SO_4 at 25°C: —●— r_s at $E_{3/4}$, -·●·- $1/\omega C_s$ at $E_{3/4}$, —○— r_s at $E_{1/4}$, -·○·- $1/\omega C_s$ at $E_{1/4}$.

$D_R=1.63\times10^{-5}$ cm²/sec[5] were used for calculation.

Figures 4 and 5 show the variation of r_{Cs} and C_{Cs}, evaluated at frequencies of 6.42, 9.12, 13.92, 18.45, 28.25 and 41.99 kc with potential. Irregularities in the base line of the curves in Figs. 4 and 5 are attributed to the variation in the surface area of the DME in each measurement.

The values obtained for the series components, r_s and $1/\omega C_s$, of the faradaic impedance were plotted against $\omega^{-1/2}$ in Fig. 6.

According to theory on faradaic impedance[6]

$$r_s = \frac{RT}{nF}\left\{\frac{1}{I^\circ}+\frac{1}{2^{1/2}nF\omega^{1/2}}\left(\frac{1}{C_O D_O^{1/2}}+\frac{1}{C_R D_R^{1/2}}\right)\right\} \quad (21)$$

$$\frac{1}{\omega C_s} = \frac{RT}{nF}\left\{\frac{1}{2^{1/2}nF\omega^{1/2}}\left(\frac{1}{C_O D_O^{1/2}}+\frac{1}{C_R D_R^{1/2}}\right)\right\}, \quad (22)$$

where I° is the exchange current density, and ω the radial frequency. In accordance with this theory, the plots of r_s and $1/\omega C_s$ *versus* $\omega^{-1/2}$ gave straight lines as shown in Fig. 6. The value of I° was obtained from the intercept of the plot as:

$$I^\circ = \frac{RT}{nF}\frac{1}{(r_s)_{\omega^{-1/2}\to 0}} \quad (23)$$

and the numerical values of r_s extrapolated to infinite frequency were 3.5, 4.8 and 7.5 Ω at $E_{1/4}$, $E_{1/2}$ and $E_{3/4}$ respectively.

The transfer coefficient (α) was evaluated through use of the equation of Laitinen, Tischer, and Roe,[7] *i. e.*,

$$\frac{\partial \ln\left(\frac{I^\circ}{C_O}\right)}{\partial \ln\left(\frac{C_R}{C_O}\right)} = \alpha \quad (24)$$

Figure 7 shows the plot of $\log(I^\circ/C_O)$ *versus* $\log(C_R/C_O)$. From the slope of the plot the value of α was found to be as great as 0.17.

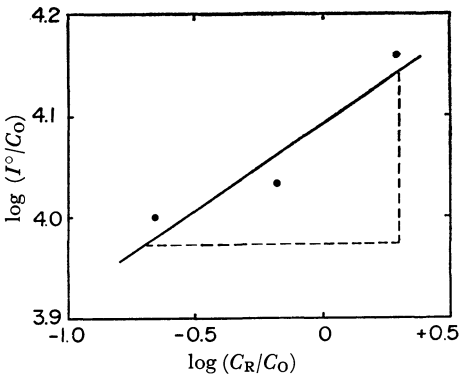

Fig. 7. Plot of $\log(I^\circ/C_O)$ *versus* $\log(C_R/C_O)$. The inclination $=\alpha=0.17$

The heterogeneous rate constant (k°) of the electrode reaction was computed by the following equation,

$$I^\circ = nFk^\circ C_O^{1-\alpha} C_R^{\alpha} \quad (25)$$

The kinetic parameters evaluated by this method are illustrated in Table 1, and related values previously reported are given in Table 2.

Table 1. Kinetic parameters of the electrode reaction, $Cd^{2+}+2e=Cd(Hg)$, in M Na_2SO_4 at the D.M.E. (25°C)

Electrode potential, V *vs.* SSE	$(r_s)_{\omega^{-1/2}\to 0}$ Ω/cm²	I° A/cm²	α	k° cm/sec
$E_{1/4}=-1.001_5$	3.5	0.0037		0.066
$E_{1/2}=-1.020_5$	4.8	0.0027	0.17	0.060
$E_{3/4}=-1.040_5$	7.0	0.0018		0.066
mean				0.064

In Table 2 the values of k° are comparatively low in most cases of the hanging mercury drop electrode. Moreover, the values show a trend to decrease with the lapse of time after the electrode is put into the solution. The authors ascribed this trend to the contamination of the electrode surface by the adsorption of surface active materials.

In the case of the DME, the electrode surface

5) M. von Stackelberg and V. Toome, *Z. Elektrochem.*, **58**, 226 (1954); H. Strehlow, Dissertation, Bonn (1949).

6) D. C. Grahame, *J. Electrochem. Soc.*, **99**, 370 (1952).

7) H. A. Laitinen, R. P. Tischer and D. K. Roe, *J. Electrochem. Soc.*, **107**, 546 (1960).

TABLE 2. VALUES REPORTED FOR THE HETEROGENEOUS RATE CONSTANT FOR $Cd^{2+}+2e=Cd(Hg)$ IN SULFATE SOLUTION

Supporting electrolyte	Temp. °C	k° cm/sec		Ref.
0.5 M Na_2SO_4	—	0.042	Hanging drop	(8)
0.5 M Na_2SO_4	20	0.026	Hanging drop, Voltage step	(9)
—	0	0.0038	Hanging drop after 2 hr	(10)
—	0	0.037	Hanging drop after 20 min	(10)
—	0	~0.2	DME	(10)
0.5 M Na_2SO_4	25	0.25	DME*,**	(11)
0.5 M K_2SO_4	22	~0.08	Radiofreq. polarograph	(12)
1 M Na_2SO_4	25	0.045	Hanging drop, Current step	(13)
1 M Na_2SO_4	25	~0.3	DME**	(11)
1 M Na_2SO_4	25	~0.1	DME**	(11)
1 M Na_2SO_4	—	0.0137 0.0116 0.067 0.051	Hanging drop, Potential-step-integral method	(14)

Unless otherwise noted, the measurement was carried out by the a. c. method.
* Calculated from data of frequencies up to 1 kc. ** An incorrect equation was used for the calculation, which was later admitted to be incorrect by Breyer and Bauer.[15]

is renewed every 2 or 3 sec, so that the contamination is much smaller than in the case of the hanging mercury drop. Thus, the values of k° obtained by the DME were much higher, as shown in Tables 1 and 2. Some data obtained by the faradaic impedance method with the DME, in Table 2, however, were computed from measurements at frequencies up to 1 kc, and the authors pointed out the discrepancy between the experimental data and the theory at frequencies higher than 1 kc.[11,16] This discrepancy seems to be attributed to the lack of correction for the bridge components in the high frequency range (*cf.* Fig. 3).

When diffusion is the sole mode of mass-transfer, the average flux of the reducing species toward a plane electrode is given by $2C_O^*(D/\pi t)^{-1/2}$, t being the electrolysis time. In a process with mixed control by both mass- and charge-transfer, this conclusion is qualitatively valid, and diffusion is no longer rate-determining for measurements in sufficiently short time intervals or at a sufficiently high frequency of electrolysis. Accordingly, the reason is well understood why our datum ($k^\circ=0.064$ cm/sec) shows fairly good agreement with Barker's datum[12] ($k^\circ=\simeq 0.08$ cm/sec), which has been obtained by the faradaic rectification method at very high frequencies (500 kc). It is worth consideration that in the faradaic rectification method the accuracy of determining the kinetic parameters is low due to the uncertainty in evaluating the radio-frequency voltage applied to the electrode-solution interface,[17] while the faradaic impedance method is sufficiently accurate so as to give at least three significant figures in the measurement of the bridge components. Our datum also shows good agreement with some data obtained by Christie *et al.*,[14] who used a modified potential-step method. In view of this agreement, the general feature of our method appears well substantiated.

The authors wish to express their hearty gratitude to Professor Herbert A. Laitinen for his interest and reading of the manuscript. Support by the Scientific Research Fund of the Ministry of Education is gladly acknowledged.

8) H. Gerischer, *Z. Elektrochem.*, **57**, 604 (1953).
9) W. Vielstich and P. Delahay, *J. Am. Chem. Soc.*, **79**, 1874 (1957).
10) P. Delahay and I. Trachtenberg, *ibid.*, **80**, 2094 (1958); *J. Electrochem. Soc.*, **105**, 433 (1958).
11) H. H. Bauer, D. L. Smith and P. J. Elving, *J. Am. Chem. Soc.*, **82**, 2094 (1960).
12) G. C. Barker, *Anal. Chim. Acta*, **18**, 118 (1958).
13) T. Berzins and P. Delahay, *J. Am. Chem. Soc.*, **77**, 6448 (1955).
14) J. H. Christie, G. Lauer and R. A. Osteryoung, *J. Electroanal. Chem.* **7**, 60 (1964).
15) B. Breyer and H. H. Bauer, "Alternating Current Polarography and Tensammetry," Interscience/John Wiley, New York (1963), p. 43.
16) J. E. B. Randles and K. W. Somerton, *Trans. Faraday Soc.*, **48**, 937, 951 (1952).
17) H. Imai and P. Delahay, *J. Phys. Chem.*, **66**, 1108 (1962). For a review, see H. Imai, *Rev. Polarography (Japan)*, **10**, 209 (1962).

BULLETIN OF THE CHEMICAL SOCIETY OF JAPAN VOL. 41 583—593 (1968)

Thermodynamic Properties and Phase Transitions of Sodium Cyanide Crystal*[1]

Takasuke MATSUO, Hiroshi SUGA and Syûzô SEKI

Department of Chemistry, Faculty of Science, Osaka University, Toyonaka, Osaka

(Received October 6, 1967)

The heat capacities of the sodium cyanide crystal were measured from 14 to 310°K by an adiabatic calorimeter. The two anomalous regions reported by Ziegler *et al.* are confirmed. The entropy changes associated with these anomalies is explained by proposing structural changes at the transition points. Analysis of the lattice heat capacity gives the average librational frequency of the cyanide ion at the lowest temperatures as 210 cm^{-1} in the Einstein approximation. For the higher temperature range, the cyanide ions may be described as undergoing a hindered rotation, with a barrier height of approximately 2 kcal/mol. The upper-phase transition is discussed in terms of a model based on the coexistence of the two crystalline phases. The lower transition and the analogous one reported previously for potassium cyanide are interpreted together as order-disorder phenomena with respect to the behavior of the cyanide ions. The thermodynamic functions of the crystal are also calculated by the graphical integration of the heat capacity data.

In a previous paper we reported the results of a thermal study of the potassium cyanide crystal.[1] Investigations of the sodium cyanide crystal along the same line of study will be presented in this paper. The present crystal has the same rod-like shaped anion as potassium cyanide as its constituent, so that in order to simulate the rock-salt structure observed at room temperature, the cyanide ion must be either rotating or randomly-orientated along one of the eight body-diagonal directions of the rock-salt-type lattice. Verweel and Bijvoet[2] investigated the structure by the X-ray diffraction method and interpreted their results in terms of the spherical rotation model of the cyanide ion. By the use of the same technique, Siegel[3] attempted to settle whether the dynamical or the statical model was more realistic. He could not, however, arrive at any definite conclusion, although he succeeded in detecting the presence of a new crystal phase of sodium cyanide. Verweel and Bijvoet found that, on cooling, the crystal is transformed into an orthorhombic modification at about 290°K. Messer and Ziegler[4] measured the heat capacity of the salt from 100°K to 350°K and observed an anomalous heat capacity at the corresponding temperature, 287°K, associated with an entropy change of approximately $R\ln 4$. They also concluded, by estimating the oscillation-rotation heat capacity of the cyanide ions, that their motion is rather restricted in the cubic phase and highly hindered in the orthorhombic phase.

For the potassium salt, Elliot and Hastings[5] suggested a free rotation model on the basis of their neutron diffraction data. More recently, after the completion of our study, Sequeira[6] published a short note in which he showed that even with the neutron diffraction, the dynamical and the statical states are indistinguishable as long as one employs a powdered sample. NMR[7] and infrared[8] studies have also been reported on these problems.

A theoretical treatment of the phase changes of these salts was carried out by Matsubara and Nagamiya[9]; they found that the potential barrier hindering the rotation of the cyanide ion is about 1.2 kcal/mol in the cubic phase and 6 kcal/mol in the orthorhombic phase for the sodium salt.

Besides the phase transition mentioned above, Messer and Ziegler observed another anomalous region in the heat capacity with its maximum value

*1 Read before the 17th Annual Meeting of the Chemical Society of Japan, 1964, Tokyo, and presented partially at The International Symposium on the Reactivity of Solids, 1966, Aberdeen, Scotland.

1) H. Suga, T. Matsuo and S. Seki, This Bulletin, **38**, 1115 (1965).

2) H. J. Verweel and J. M. Bijvoet, *Z. Krist.*, **100**, 201 (1939).

3) L. A. Siegel, *J. Chem. Phys.*, **17**, 1146 (1949;) Y. Shin'naka, *J. Phys. Soc. Japan*, **22**, 669 (1967).

4) C. E. Messer and W. T. Ziegler, *J. Am. Chem. Soc.*, **63**, 2610 (1941).

5) N. Elliot and J. Hastings, *Acta Cryst.*, **14**, 1018 (1961).

6) A. Sequeira, *ibid.*, **18**, 291 (1965).

7) C. K. Coogan and H. S. Gutowsky, *J. Chem. Phys.*, **40**, 3419 (1964).

8) Y. Sato, *J. Phys. Soc. Japan*, **20**, 275 (1965).

9) T. Matsubara and T. Nagamiya, *Sci. Papers from Osaka Univ.*, No. **14** (1949).

at 172°K. The estimated entropy change is approximately $R\ln 2$, so they inferred that this anomaly is associated with a kind of ordering process with respect to the end-for-end rearrangement of the cyanide ions.

The present investigation aims at: (1) the extension of the temperature region of the heat capacity measurement down to the temperature of liquid hydrogen, (2) the analysis of the thermal motion of the cyanide ion using the low temperature heat capacity data and (3) the interpretation of the heat capacity anomalies in comparison with the analogous phenomena in the potassium cyanide crystal reported on previously.

Experimental

The sample employed was purified by the recrystallization of commercial sodium cyanide (Kantoh Kagaku, an extra pure reagent) twice from an absolute methyl alcohol, following the method by Thompson.[10] The dominant impurity detected by infrared absorption was found to be carbonate ions, which amounted to 0.3 percent. The weight of the specimen used for the measurement was 19.375 g, or 0.4027 mol, taking NaCN=49.008 g/mol. The buoyancy correction was not made. The apparatus and the procedure used for the measurement were the same as have been reported previously.[1,11]

Experimental Results

The observed heat capacity values are listed in Table 1 in chronological order; they are illustrated in Fig. 1. They are expressed in terms of the thermochemical calorie, equal to 4.1840 absolute joules. The ice point is taken as 273.15°K. The heat capacity values listed in the table are the ratios of the increase in enthalpy, ΔH, to the rise in temperature ΔT. The temperature given for each point is the arithmetic mean of the initial and the final temperatures.

As is shown in the figure, the lower anomaly was found to start at 70°K. The transition temperatures given by Messer and Ziegler[4] coincide very well with the present data. Their heat capacity values above 100°K are, however, lower by about 1 percent.

In Table 2 the heat capacity, the entropy, the enthalpy, and the Gibbs energy functions are given for the rounded temperatures. They were obtained by fitting a smooth curve on the observed values of the heat capacity, extrapolating it to 0°K, and integrating it graphically. The contribution from the extrapolated region below 15°K to the entropy amounts to 0.050 cal/mol degK. Around the upper phase transition, a direct summation of the input energy was carried out. The estimated error in

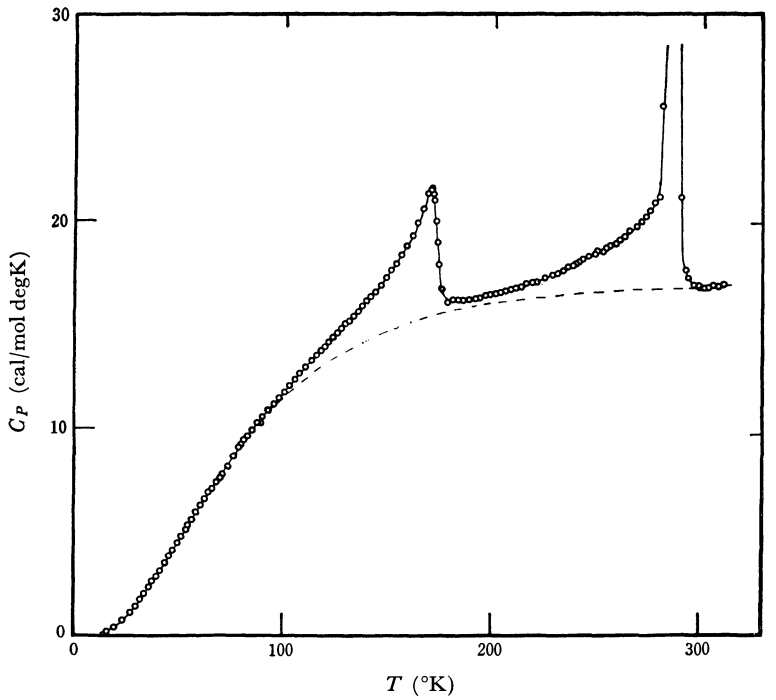

Fig. 1. Heat capacity *versus* temperature curve of NaCN crystal.

10) M. R. Thompson, *J. Res. Natl. Bur. Std.*, **6**, 1051 (1931).

11) H. Suga and S. Seki, This Bulletin, **38**, 1000 (1965).

TABLE 1. SELECTED VALUES OF HEAT CAPACITY FOR NaCN CRYSTAL

$T_{av.}$ (°K)	$\Delta H/\Delta T$ (cal/mol degK)	ΔT	$T_{av.}$ (°K)	$\Delta H/\Delta T$ (cal/mol degK)	ΔT
116.61	13.51	2.070	175.01	17.88	1.375
118.67	13.71	2.040	176.84	16.70	2.299
122.69	14.15	1.992	179.14	16.04	2.331
128.70	14.80	1.976	181.60	16.16	2.603
134.52	15.40	1.919	184.19	16.16	2.599
140.34	16.10	1.968	189.54	16.19	2.911
			192.06	16.21	2.901
15.53	0.180	3.428	194.72	16.24	2.895
16.02	0.202	3.872	197.36	16.39	2.648
20.42	0.461	1.753	202.15	16.47	2.576
23.15	0.700	1.569	207.26	16.60	2.558
27.10	1.081	2.390	212.34	16.72	2.540
33.83	1.970	2.168	217.37	16.91	2.516
37.75	2.559	1.768	222.36	17.05	2.499
41.37	3.076	1.734	226.31	17.25	2.476
44.76	3.662	1.812	232.25	17.42	2.447
48.47	4.289	1.709	237.11	17.71	2.418
52.58	4.973	1.925	241.84	17.90	2.394
56.53	5.595	2.060	244.20	18.14	2.372
60.81	6.281	2.087	247.29	18.24	2.369
66.33	7.090	1.957	251.98	18.35	2.333
70.24	7.560	2.081	255.69	18.72	2.313
74.11	8.158	2.777	260.25	18.86	2.298
79.38	9.079	2.564	264.74	19.20	2.267
83.21	9.612	2.447	270.27	19.64	2.228
88.28	10.26	2.525	274.61	20.14	2.162
93.47	10.87	2.576	278.96	20.86	2.130
98.58	11.45	2.586	281.05	21.09	2.111
103.67	12.01	2.491	282.98	25.51	1.840
108.91	12.65	2.626	284.49	40.32	1.289
116.55	13.16	2.101	286.57	59.47	0.927
120.69	13.93	2.016	287.21	127.9	0.464
124.70	14.36	2.022	287.55	189.4	0.320
128.70	14.80	1.976	287.72	300.3	0.206
132.61	15.20	1.937	287.78	245.0	0.250
136.42	15.63	1.898	288.09	220.3	0.277
140.34	16.11	1.968	288.31	205.2	0.297
144.88	16.55	2.562	288.62	136.7	0.436
147.43	16.89	2.537	289.05	108.2	0.542
152.39	17.59	2.449	289.79	58.74	1.058
157.20	18.35	2.373	289.93	40.52	1.281
162.06	19.23	2.639	291.32	21.68	2.064
164.89	19.85	2.579	293.39	17.59	2.379
167.51	20.60	2.509	294.84	17.15	2.420
169.98	21.34	2.444	297.24	16.90	2.441
170.02	21.32	1.224	299.67	16.84	2.444
170.24	21.49	1.215	302.12	16.70	2.456
171.80	21.61	1.210	304.56	16.74	2.450
172.45	21.29	1.220	306.99	16.84	2.440
173.02	21.00	1.235	309.41	16.80	2.441
173.69	19.93	1.277	311.83	16.88	2.431
174.30	18.93	1.328			

TABLE 2. THERMODYNAMIC PROPERTIES OF NaCN CRYSTAL*

T(°K)	$C°_P$	$S°$	$(H°-H°_0)/T$	$-(G°_0-H°_0)/T$
5	(0.005)**	(0.002)	(0.001)	(0.001)
10	(0.043)	(0.014)	(0.010)	(0.004)
15	0.166	0.050	0.038	0.012
20	0.433	0.129	0.099	0.030
30	1.443	0.477	0.363	0.114
40	2.903	1.085	0.809	0.276
50	4.540	1.908	1.391	0.517
60	6.156	2.878	2.049	0.829
70	7.587	3.938	2.741	1.197
80	9.135	5.048	3.440	1.608
90	10.469	6.205	4.151	2.054
100	11.621	7.368	4.840	2.528
120	13.853	9.686	6.159	3.527
140	16.037	12.100	7.413	4.687
160	18.819	14.409	8.646	5.763
171.9±0.2	Lower transition			
190	16.208	17.428	10.028	7.400
210	16.666	19.071	10.637	8.434
230	17.353	20.616	11.189	9.427
250	18.302	22.100	11.718	10.282
270	19.636	23.554	12.239	11.315
288.1±0.1	Upper transition			
289.15	16.831	27.654	15.039	12.615
305	16.704	28.018	15.042	12.976

* All values in units of cal/mol degK.
** Values in the parentheses were obtained by extrapolation of the C_p curve to 0°K.

the C_v is about 1 percent at the temperature of liquid hydrogen and 0.4 percent at room temperature.

Discussion

Thermal Motion of the Cyanide Ion. The method of analyzing the heat capacity data is essentially the same as that used for the potassium cyanide crystal in the previous paper.[1] The observed heat capacity was transformed into the apparent Debye temperature, as shown in Fig. 2. We can see here that the presence of the transitions is more conspicuous than in the C_P-T curve itself. By a rather arbitrary interpolation of the normal Debye temperature below and above the transition regions, the anomalous heat capacities were estimated. This procedure is a convenient means of minimizing the ambiguity in separating the effect of the transition from the total heat capacity. In the present case of sodium cyanide, however, the anomalous effect due to the phase transitions contributes to the total heat capacities over considerably wide ranges of temperature, so we assumed three reasonable kinds of normal Debye temperature, as shown in Fig. 2 by A, B, and C. From these normal Debye temperatures, the normal heat capacity was calculated. This procedure may be convenient but not rigorous, since we are assuming a continuous temperature dependence of the normal heat capacity, even at the upper transition, where the crystalline field symmetry surrounding the cyanide ion changes abruptly from orthorhombic to octahedral. At the present stage of our knowledge, however, we have to content ourselves with the approximate procedure adopted here.

The normal heat capacity thus obtained comes from 6 N translational degrees of freedom of both the kinds of ions, and from 2N torsional degrees of freedom and N internal degrees of freedom of the cyanide ions (N, Avogadro constant).

In order to get more detailed knowledge about the motion of the ion, we first tried to estimated the torsional frequency of the cyanide ion. For this purpose, we adopted the following procedure. First, we subtracted the contribution of the internal vibration of the cyanide ion from the total heat capacity by using the Einstein function of the wave number, 2085 cm^{-1}.[12] Then, by taking a rather arbitrary value of the parameter, the C_P values were transformed to C_V by applying the approximate relation, $C_P-C_V=1.1\times10^{-5}C_P^2T$.[4] These C_V values yielded the Debye temperature, which is plotted in Fig. 3 (curve a), where only 6 N degrees of freedom are taken into account. The decline

12) F. A. Miller and C. H. Wilkins, *Anal. Chem.*, **24**, 1253 (1952).

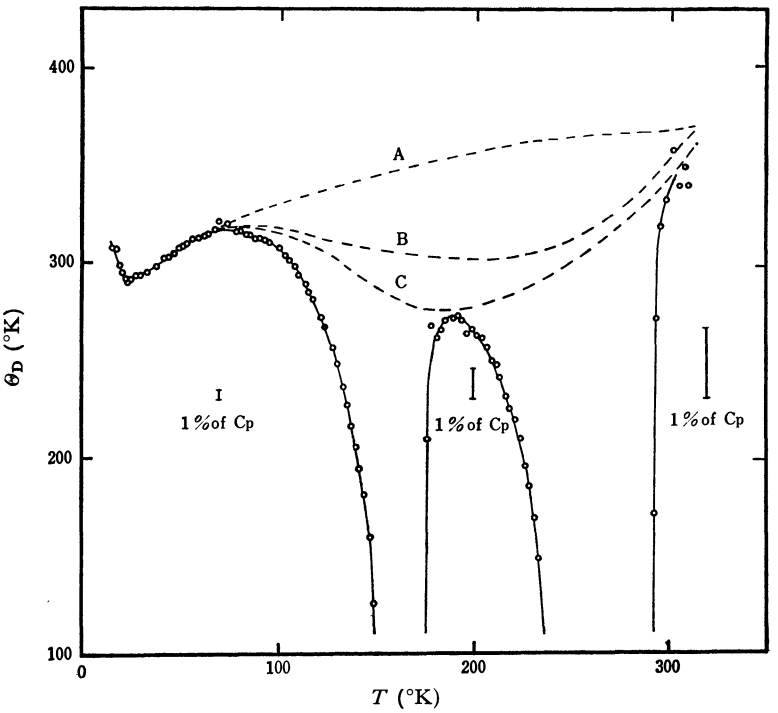

Fig. 2. Apparent Debye temperature of NaCN crystal.
-○-: observed, - - -: A, B and C: assumed.

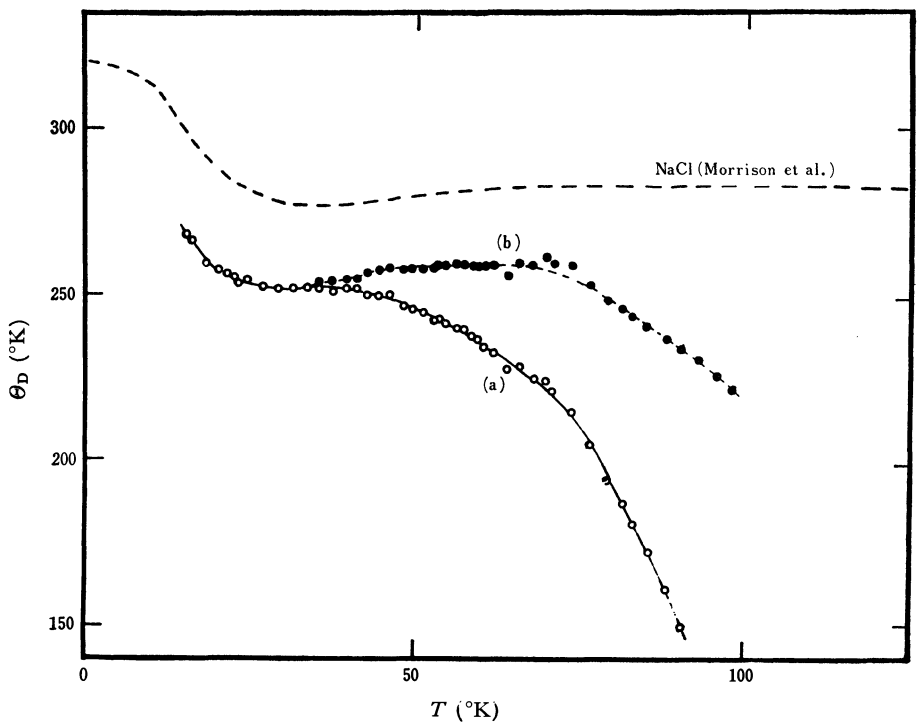

Fig. 3. Debye temperatures of NaCl and NaCN crystals.
- - -: NaCl, -○-: NaCN, assuming 6N degrees of freedom
-●-: NaCN, allowing for the two Einstein oscillators

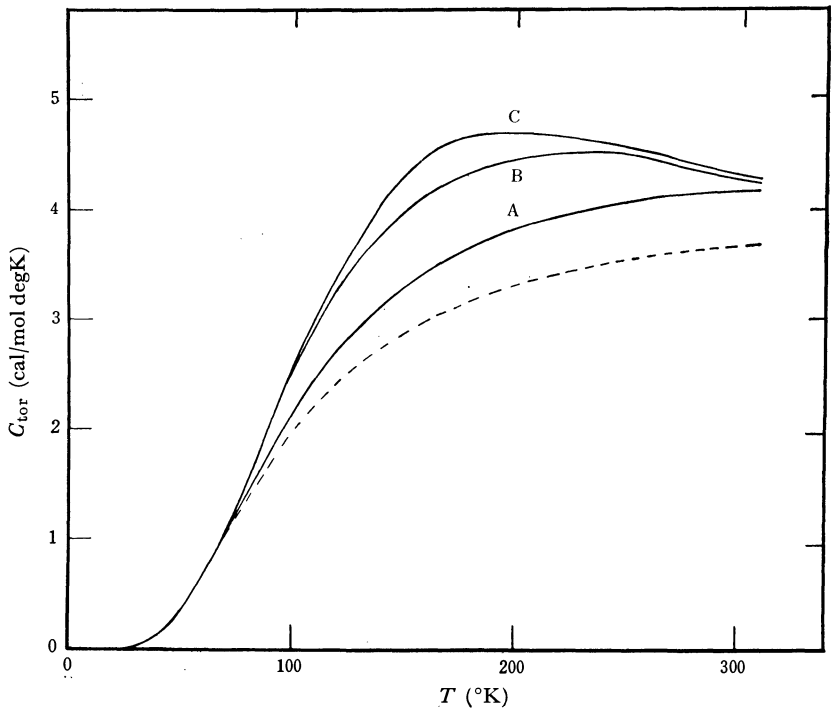

Fig. 4. Torsional heat capacity of CN^- ion in NaCN crystal.
——: A, B and C corresponding to the three estimations of the normal heat capacity
– – –: to two simple harmoic oscillators of wave number 210 cm^{-1}

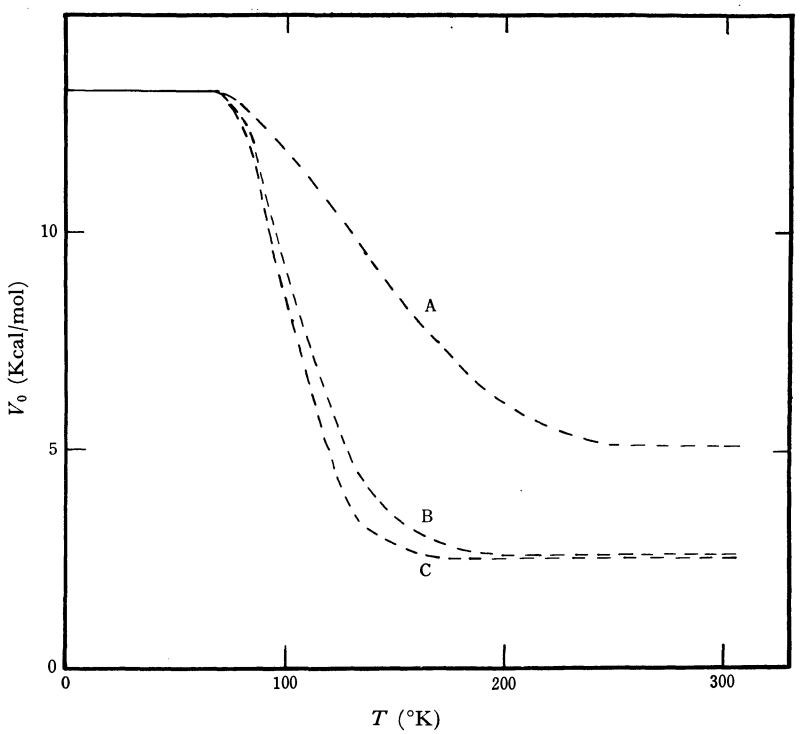

Fig. 5. Potential barrier hindering the rotational motion of the CN^- ion in the NaCN crystal as derived from the heat capacity analysis. The meaning of A, B and C is the same as in Fig. 4.

of the curve above 40°K comes from the neglect of the $2N$ degrees of torsional freedom. Therefore, if we assume further that the temperature dependence of the translational Debye temperature is similar to that of the sodium chloride crystal,[13] we can estimate the torsional frequency by a trial-and-error calculation. With one and the same wave number of 210 cm^{1-} for the two degrees of freedom of the torsional motion, we obtained the most reasonable variation of the translational Debye temperature, as is shown in Fig. 3, curve b. This wave number may be looked upon as a kind of average value of two frequencies of an anisotropic, two-dimensional oscillator. Although the angular dependence of the potential energy of the cyanide ion in the crystal may be very complicated, for simplicity, we assume it to be $V=(1/2)V_0(1-\cos 2\theta)$, where θ is the polar angle from the equilibrium direction of the cyanide ion. Then V_0, which yields the torsional frequency of 210 cm^{-1} in the harmonic approximation, is calculated to be 13 kcal /mol. Extending the Debye temperature of the translational modes to higher temperatures, meanwhile keepting it parallel with that of NaCl, we can estimate the torsional heat capacity for all the temperature range (see Fig. 3) The results are plotted in Fig. 4. Above 70°K, no combination of two harmonic oscillators can produce the torsional heat capacity. This implies that the harmonic approximation fails around that temperature. Pitzer and Gwinn's treatment extend to two-dimensional motion by Stepakoff and Coulter[14] shows that the heat capacity of a hindered rotator can be larger than R per degree of freedom. Following this method, we can evaluated the V_0 from the experimental torsional heat capacity. The values of V_0 thus obtained are plotted in Fig. 5, in which the curves A, B and C correspond, respectively, to the three variations of the normal Debye temperature assumed in Fig. 2. The estimated V_0 value changes from 13 kcal/mol at the lowest temperatures to 2—3 kcal/mol at the higher temperatures. This is remarkable in view of the fact that there occurs no significant change in the crystal structure at the lower transition; it deserves further investigations, both theroetical and experimental. The high-temperature value may be compared with that of 1.8 kcal/mol derived by Sato[8] with combination of infrared data and Coogan and Gutowsky's result obtained by NMR.[7] (In passing, it might also be mentioned that the theoretical values of the barrier height given by Matsubara and Nagamiya are 6 kcal/mol in the orthorhombic and 1.2 kcal/mol in the cubic phases. These values represent the difference between the maximum and the minimum values of the hindering potentials, whose functional forms are different from those adopted here.)

Mechanism of the Phase Transitions. The temperatures, enthalpies, and entropy changes of the transitions are summarized in Table 3. Here, a "case B" estimation of the normal heat capacity was made. The entropy change of the upper transition amounts to approximately $R\ln 4$.

Table 3. Temperatures, enthalpies and entropies of transitions in NaCN crystal

	T °K	ΔH (cal/mol)	ΔS (cal/mol degK)
Lower transition	171.9±0.2	177.2±3.0	1.21±0.02
Upper transition	287.7±0.1	783.7±8.0	2.80±0.02

This implies that a kind of randomization in the alignment of the cyanide ions takes place at this transition point. Matsubara and Nagamiya treated this transition as a first order one. This treatment might be supported by the hysteresis phenomenon in the heat-capacity measurement found by Messer and Ziegler, and by the results of differential thermal analysis made in this laboratory. The heat-capacity peak is so sharp that 80 percent of the whole enthalpy change occurs in rather narrow range of 5°C for both the Na- and K-salts, although no latent heat effects were detected experimentally.

In principle, a first-order phase transition takes place at a definite temperature which is determined by the equality of the free energies of the two phases involved. Consequently, the heat capacity would behave normally at all but one temperature, where it would go on to infiinity. Experimentally, however, a number of phase transitions are known to occur over a finite temperature range. In some cases, *e. g.*, where the Ising model is an adequate picture, the phase transition is intrinsically diffused. In others, structurally different crystalline phases have to be in equilibrium with each other at the transition point, as is the present case; this gives rise to interfacial and strain energies in the crystal. As a result, the two phases can coexist over a finite range of temperature, since these variables provide extra degrees of freedom in the sense of the Phase Rule.[15] These ideas were used in quantitative calculations by Tobolsky, Kozak, and Canter.[16]

As has been mentioned above, the heat-capacity anomaly at the upper transition is over a temperature range of about 5°C for NaCN. For KCN also, the anomaly around 168°K takes place with a comparable diffuseness, as has been reported previously.[1] Seeking an explanation of this behavior,

13) J. A. Morrison and D. Patterson, *Trans. Faraday Soc.*, **52**, 764 (1956).
14) G. L. Stepakoff and L. V. Coulter, *J. Phys. and Chem. of Solids*, **24**, 1435 (1963).
15) A. Ubbelohde, *Quart. Rev.*, **11**, 246 (1957).
16) A. V. Tobolsky, J. J. Kozak and N. H. Canter, *Phys. Rev.*, **138**, A651 (1965).

we tried to apply the Tobolsky model of diffuse phase transitions to the present cases. The relevant parameters involved in the theory were determined with the experimental values of the transition temperature, the entropy of transition, and the maximum value of the heat capacity at the transition temperature. The last quantity was quite difficult to evaluate precisely, since at the critical temperature the thermal equilibrium in the calorimeter was achieved very slowly. To minimize the uncertainty due to the sluggishness of the transition in the experimental heat capacity, an extrapolation method was applied to the temperature change of the calorimeter after heating it, assuming an exponential decrease in the temperature.

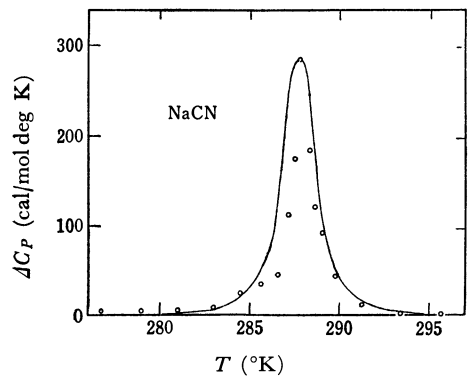

Fig. 6. Anomalous heat capacity at the upper transition of NaCN crystal.
○: observed, —: theoretical

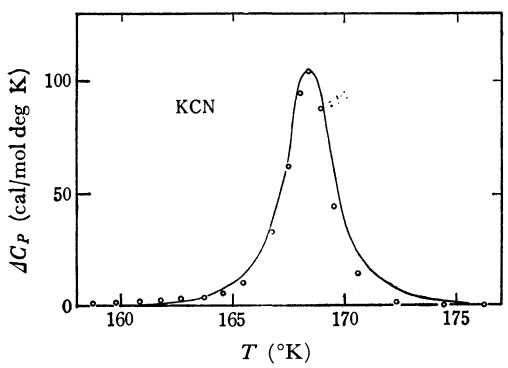

Fig. 7. Anomalous heat capacity at the upper transition of KCN crystal.
○: observed, —: theoretical

In Figs. 6 and 7, the calculated heat capacity is shown for NaCN and for KCN respectively, together with the experimental points. As may be seen in the figures, the heat-capacity anomalies are reproduced with reasonable success. The interfacial energy parameters are $\Delta G_K = 6.33$ kcal/mol and 3.07 kcal/mol for NaCN and KCN respectively. Here, ΔG_K indicates the molar Gibbs energy difference of the domain boundary from that of the bulk crystal in the orthorhombic modification.

One important point to be added is that the two crystalline phases co-exist in both these salts over the corresponding temperature ranges. Cimino, Parry, and Ubbelohde[17] showed by the X-ray Laue photographic method that orthorhombic and cubic phases can coexist in KCN at around 168°K. The symmetry relation of the coexisting domains was later discussed in detail by Cimino and Parry.[18] For NaCN, the coexistence of the two phases was observed at around 285°K by Nitta and Oda[19] by the use of the X-ray powder method. In concluding the discussion of the upper phase transition of the two salts, it might be said that if one disregards the difficulty arising from the hysteresis phenomenon, the coexistence model provides a reasonably satisfactory picture of the upper phase transition of NaCN and KCN crystals. For the hysteresis phenomena, however, one would have to take into account nucleation and other aspects of the transition. This is a problem still to be investigated.

Let us now proceed to the discussion of the lower phase transition. Figure 8 shows the anomalous part of the heat capacity at the lower transition as a function of T/T_c (T_c: temperature corresponding to the heat capacity maximum), together with that of KCN. A theoretical curve is also plotted; it will be explained later.

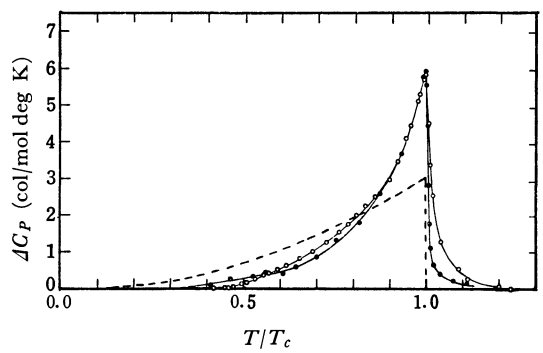

Fig. 8. Anomalous heat capacity at the lower transition of NaCN and KCN crystals.
-●-: NaCN, -○-: KCN, - - -: theoretical

Now we should like to treat these lower transitions of both the salts from the same point of view. Nagamiya presented a molecular field theory of order-disorder transition which includes Pauling's, Frenkel's and Weiss' treatments as extreme cases. In this theory the potential curve described in

17) A. Cimino, G. S. Parry and A. R. Ubbelohde, *Proc. Roy., Soc.*, **A252**, 445 (1959).
18) A. Cimino and G. S. Parry, *Nuov. Cim.*, **19**, 971 (1961).
19) I. Nitta and T. Oda, unpublished work read before the 63th Annual Meeting of the Chemical Society of Japan (1941).

TABLE 4. THERMAL EFFECTS AT THE LOWER TRANSITION OF NaCN and KCN CRYSTALS COMPARED WITH THE WEISS APPROXIMATION VALUES

		ΔH (cal/mol)	ΔS (cal/mol degK)	ΔC (cal/mol degK)
NaCN (T_c=171.9°K)	Obs.	177	1.21	5.9
	Calc.	171	1.38	3.0
KCN (T_c=82.9°K)	Obs.	95	1.32	5.8
	Calc.	83	1.38	3.0

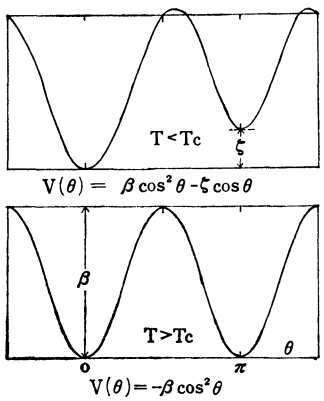

Fig. 9. Hindering potential in Nagamiya's theory of phase transition.

Fig. 9 is assumed for the molecular field, where β is a parameter related to the potential barrier height, and where ζ is an order paramater proportional to the population difference between the two potential minima. Equating β to the V_0 determined by the heat capacity analysis, ζ_0(=ζ at 0°K) can be evaluated by using the observed transition temperature. This treatment gives ζ_0=400 cal/mol for NaCN and 180 cal/mol for KCN. Thus, in either crystal β/ζ_0=30; this essentially corresponds to the Weiss case. Hereafter, therefore, we will adopt the Weiss model throughout. Another reason for using the Weiss model, which is less realistic than Nagamiya's, is that the latter gives 2 cal/mol degK per degree of freedom for the heat capacity, even at the temperature of absolute zero, since the treatment is classical. The Weiss model is originally a static one, but actually the ions oscillate even at the lowest temperature. This difference can be shown to be negligible for the present cases, because of the strong force constant and the large moment of inertia of the oscillator. The enthalpy, the entropy, and the heat capacity jump based on the Weiss model are listed in Table 4. The theoretical curve in Fig. 8 is also calculated by the Weiss approximation. If we keep in mind the fact that the observed value is C_P while the theoretical one is C_V, the agreement seems to be rather satisfactory, since the volume effect usually sharpens transitions.

Finally, we should like to proceed to a discussion of the ionic interaction in relation to the crystal structure at the lowest temperature. According to Verweel and Bijvoet,[2] no significant change in structure occurs at the lower transition for NaCN, even though they observed an unusual contraction of the b-axis around 170°K without being aware of any transition effect. This effect was later shown by Messer and Ziegler[4] to correspond to the lower phase transition. In KCN also, as has been described in a previous paper, no change was detected by the powder X-ray photographs. In view of these results and the small difference in the atomic-scattering factors of carbon and nitrogen atoms, it may be that the transition is of a order-disorder type with respect to the sense of the cyanide ions. If we assume some specific interactions between the ions as the origin of the energy difference between the two orientations of the anions at 0°K, we may obtain the lowest energy configuration as the plausible structure in the lowest temperature phase. The possible types of interaction may be dipolar interaction and steric effect. Considering the fairly spheroidal shape of the cyanide ion and its short range nature, we can neglect the steric effect and retain only the dipolar term as we consider the mechanism of the phase transition.

The energy difference between the two orientations of the cyanide ion at 0°K, 2ζ, arises, then, from the interaction of the electric dipole of the ion with the local electric field, E, produced at the position of the ion by the array of all other dipoles in the crystal. The local field in a dipole array may be written as:

$$E = \sum_i \frac{3(\vec{\mu}_i \cdot \vec{r}_i)\vec{r}_i - r_i^2 \vec{\mu}_i}{r_i^5},$$

where r_i and μ_i are the position vector and the moment of the ith dipole respectively. The summation can be extended over all the dipoles present. For the explicit calculation, let us resort to the approximate method of Lorentz.

Let E be written as:

$$E = E_1 + E_2 + E_3$$

Here, E_1 is the electric field due to the dipoles within a certain spherical region in the crystal; E_2,

TABLE 5. LOCAL ELECTRIC FIELD IN NaCN AND KCN CRYSTALS*

	Configuration	E_1	E_2	E_1+E_2	E'
NaCN	Polar	-0.95×10^{22}	8.87	7.92	6.77
	Antipolar (A)**	−1.61	0	−16.1	−0.66
	Antipolar (B)	5.46	0	5.46	5.79
KCN	Polar	0.28	6.03	6.31	5.62
	Antipolar (A)	0.35	0	0.35	0.02
	Antipolar (B)	4.61	0	4.61	4.61

* In units of the dipole moment in cgs esu.

** The antipolar configurations (A) and (B) are the typical ones for the body centered orthorhombic cell as shown in Fig. 10. For detailed discussion of dipolar lattice, see Luttinger and Tisza, *Phys. Rev.*, **70**, 954 (1947); **72**, 257 (1947).

the cavity field produced by the charges which appear on the inside surface of the cavity left by the sphere, and E_3, the contribution from the charge on the outer surface of the crystal. If the crystal has not net polarization as a whole, then $E_2=E_3=0$ and only the contribution from the dipoles within the sphere is operative. On the other hand, if it has a net polarization, P, E_2 is equal to $(4/3)\pi P$ for a cubic crystal and E_3 is $-(4/3)\pi P$ for a spherical specimen and zero for a long, cylindrical specimen. E_1 was calculated by summing up the contribution from about 50 dipoles within a sphere. For three representative configurations, the results of calculation are summarized in Table 5. In the table E' represents the local field at the center of a long specimen ($12\times15\times250$ Å^3) polarized along the longest axis, calculated for the sake of comparison. If, as is usually assumed, there were some mechanisms supplying charges to the outer surface of the specimen, then $E_3=0$ for any shape of the crystal and the polar configuration would have the lowest energy. Or, following the discussion by Kittel,[20] the polar structure would be the most stable by forming long domains.

If we assume that this polar configuration is realized in the lowest temperature, we can estimate the dipole moment of the cyanide ion in the crystal as follows. By equating the interaction energy to kT_c, we get $\mu=0.55$D for NaCN and 0.42D for KCN. Although, at present, we unfortunately have no experimental data to compare with these values, their order of magnitude seems quite reasonable. We may mention here a recent calculation of the electronic structure of some cyanide compounds by Yonezawa, Kato and Konishi,[21] who used a semiempirical self-consistent field method. Their result was 0.49D for the dipole moment of the cyanide ion, a value which compares favorably with our experimental values, although their calculation refers to the free ion.

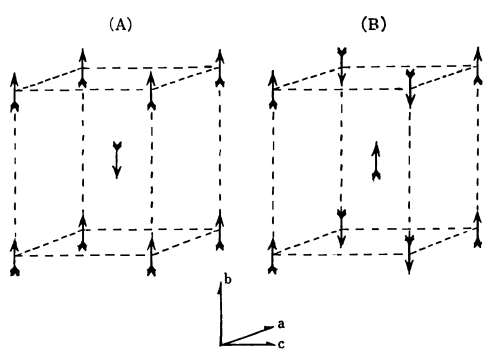

Fig. 10. Typical antipolar configurations of the CN^- dipoles in the lowest temperature phase of NaCN and KCN crystals.

The difference between the two values derived from Na- and K-salt, however, seems to point to the approximate nautre of our treatment; we can not expect the electronic structure in the two salts to be really different. We observed little difference in the infrared fundamental bands of the cyanide ion in the Na- and K-salts, while for thallium cyanide,[22] which is believed to be in electronically-different state, the C-N stretching band is greatly shifted. Accordingly, the difference between the two values may be accounted for more reasonably as a consequence of neglecting the steric, induced polarization and other effects. As may be seen in Table 5, the antipolar configuration, B, must be taken into consideration if the above-mentioned condition favoring the polar structure is in competition with other factors. Therefore, our results are not conclusive. In order to determine the structure of the lowest-temperature phase of the two salts, further experiments, such as neutron diffraction, far-infrared absorption, or dielectric measurements using single crystals, together with a more precise theoretical treatment of molecular interactions in crystals, are much desired.

20) C. Kittel, *Phys. Rev.*, **82**, 965 (1951).

21) H. Kato and T. Yonezawa, Proceedings of a Symposium on Molecular Structures, Osaka (1966) 53; T. Yonezawa, H. Kato and H. Konishi, This Bulletin, **40**, 1071 (1967).

22) Unpublished.

Summary

The heat capacity of the NaCN crystal was measured from 14 to 310°K by using an adiabatic calorimeter. Two anomalous regions were confirmed, at 171.9±0.2°K and 287.7±0.1°K. The estimated entropy changes of these anomalies were approximately equal to $R\ln 2$ and $R\ln 4$, respectively. These values may be interpreted in terms of a step-by-step randomization process of the orientation of the cyanide ions.

By analyzing the observed heat capacities, the contribution from the torsional motion of the cyanide ion was derived on several assumptions. It was shown that, below 70°K, the separated torsional heat capacity can be reproduced by a two-dimensional harmonic oscillator with the average wave number of 210 cm^{-1}, a value which corresponds to a barrier height of 13 kcal/mol. At higher temperatures it may be compared to those of a hindered rotator with a barrier height of 2—3 kcal/mol. This behavior is quite similar to that of KCN.

By integrating the heat capacity data, $S°$, $(H°-H°_0)/T$, and $-(G°-H°_0)/T$ were calculated.

The upper phase transitions of NaCN and KCN conform rather well to the coexistence model of diffuse phase transition proposed by Tobolsky and others.

As to the relative orientation of the cyanide ions in the lowest-temperature phase, the lattice energy was evaluated for both NaCN and KCN, and the most stable configuration was inferred to be polar. These considerations, coupled with the observed transition temperatures, yield estimates of the magnitude of the dipole moment of the anion in the crystal, 0.55D for NaCN and 0.42D for KCN.

BULLETIN OF THE CHEMICAL SOCIETY OF JAPAN VOL. 41 593—600 (1968)

On the Glass Transition Phenomenon of Isopentane*[1]

Masayasu SUGISAKI, Keiichiro ADACHI, Hiroshi SUGA and Syûzô SEKI

Department of Chemistry, Faculty of Science, Osaka University, Toyonaka, Osaka

(Received October 14, 1967)

Heat capacity measurement of isopentane was carried out for crystalline, liquid, glassy, and supercooled liquid states in the temperature region between 13 and 300°K. The glass transition phenomenon of isopentane was found around 65°K with drastic heat capacity change of 68.20 J/mol degK. This glass transition phenomenon is tentatively interpreted in terms of the Adam and Gibbs theory. The value of T_g/T_2, the ratio of glass transition temperature T_g, and the temperature of disappearance of the configurational entropy of the supercooled liquid T_2, for isopentane was found to be 1.30 which is concordant with the value cited by Adam and Gibbs. The residual entropy at absolute zero of the glassy isopentane was shown to be 14.06 J/mol degK. In addition the irreversible production of entropy during the glass transition intervals was found to be 0.08 J/mol degK. It is concluded that the neglect of the irreversible production of entropy leads no significant error in determing the residual entropy.

Recently, Turnbull and Cohen[1] have empirically found that the substance which satisfy the condition that the ratio T_b/T_m, of their normal boiling to their normal melting temperature is equal to or larger than 1.8 are easily supercooled. On the basis of this empirical rule they suggest that the substances which fulfill this condition may have much glass-forming tendency, if the liquid is cooled rapidly far below their melting point with no occurrence of crystallization.

There have been known many kinds of pure substances showing glass transition phenomenon. They may be classified into, (1) network glasses such as SiO_2 and other nonmetallic oxides, (2) inorganic and organic polymers, (3) hydrogen bonded substances, (4) low molecular weight materials, *etc.*[2] In order to study the essential feature of the glassy state from theoretical as well as experimental points of view, it seems much desirable to investigate the simple low molecular weight substances. For such purpose we have undertaken to study the glassy state in relation to

*1 This paper was read before the 19th Annual Meeting of the Chemical Society of Japan, Yokohama, March, 1966.

1) D. Turnbull and M. H. Cohen, *J. Chem. Phys.*, **29**, 1049 (1958).

2) "Progress in Solid-State Chemistry," Vol. 3, ed. by H. Reiss, Pergamon Press Inc., New York (1967), p. 407.

its crystalline phase by use of the method of heat capacity measurement, and really found a characteristic heat capacity jump associated with the occurrence of the glass transition phenomenon.

Experimental

Apparatus. The adiabatic Nernst-type calorimeter[3] used in our laboratory was partly modified, so that rapid cooling may be easily carried out. For this purpose, liquid nitrogen or liquid hydrogen is able to be charged directly into the space between the outer and inner adiabatic shields as is shown in Fig. 1. Measurements of temperature were made with platinum resistance thermometer calibrated in terms of International Temperature Scale between 90 and 500°K and the provisional scale of the National Bureau of Standards between 11 and 90°K.[3]

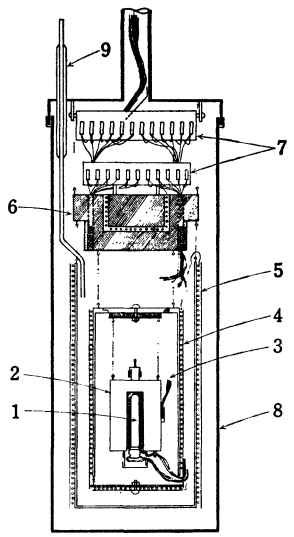

Fig. 1. Description of adiabatic calorimeter.
1) platinum resistance thermometer, 2) sample container, 3) thermo-couple, 4) inner shield, 5) outer shield, 6) copper block, 7) lead connector, 8) vacuum jacket, 9) transfer tube.

Sample. The commercial extra pure isopentane (Nakarai Chemicals, Ltd.) was purified by fractional distillation, and then distilled twice under high vacuum (10^{-6} mmHg). Impurities contained in each fraction were detected by gas chromatography technique and the purest fraction was employed for the heat capacity measurements. The amount of the impurities present in the sample was determined to be 0.014 mol percent by making use of thermo-analytical method as is described later.

Heat Capacity Measurements. Measurements of the heat capacities were made on a sample with single loading (0.2433 mol) which was sealed in a gold calorimeter cell, for the crystalline, liquid, glassy, and supercooled liquid states in the temperature region from 13 to 300°K. The reported values are based on a molecular weight 72.152 g and ice point is taken to be 273.15°K.

Our preliminary observation by differential thermal analysis clarified that cooling rate of 10°C/min was sufficient to supercool the liquid isopentane far below its melting point without any occurrence of crystallization. Consequently, liquid hydrogen was directly transferred into the space between outer and inner shields (see Fig. 1), in order to satisfy this cooling condition. From the results of the heat capacity measurements, it was found that the whole amount of the sample was completely superocooled down to 20°K without any occurrence of crystallization.

Furthermore, in order to determine the purity of the sample, detailed measurements of melting point and enthalpy analysis of melting, were also performed.

Experimental Results

Heat Capacity of Crystalline and Liquid States. The results of heat capacity measurements are listed in Table 1A for crystalline and liquid states, and are shown by hollow circles in Fig. 2. These values agree with those reported by Guthrie and Huffman[4] in 1943. They reported the nonexistence of the appearance of anomalous heat capacity of liquid state in the temperature region between 170—250°K which was first reported by Schumann and Aston (1942).[5] This fact coincides with our results.

The data of melting point in relation to mole fraction of the melt, and the heat of fusion, obtained from the results of heat capacity measurements, are shown in Table 2, and the relationship between melting point and inverse molten fraction is given in Fig. 3. The value obtained for the melting point of 100% pure isopentane is found to be 113.36±0.05°K.

From the melting curve, the amount of impurities in the sample was found to be 0.014 mol percent.

Heat Capacities of Glass and Supercooled Liquid. The results of the heat capacity measurements in the glassy and the supercooled liquid states of isopentane are shown in Table 1B, and shown by filled circles in Fig. 2. There appears a sharp rise of heat capacity at about 65°K which is characteristic to glass transition phenomenon of supercooled liquid. These results indicate that isopentane can be supercooled far below its melting point and can be transformed into a glassy state. It may be noted that the differences of the heat capacities between the crystalline and glassy states are smaller near 30°K in each side, similar to that of glycerol.[6]

The amount of heat capacity of the supercooled

3) H. Suga and S. Seki, This Bulletin, **38**, 1000 (1965).

4) G. B. Guthrie, Jr., and H. M. Huffman, *J. Am. Chem. Soc.*, **65**, 1139 (1943).

5) S. C. Schumann, J. G. Aston and Malcolm Sagenkahn, *ibid.*, **64**, 1039 (1942).

6) G. E. Gibson and W. F. Giaque, *ibid.*, **45**, 93 (1923).

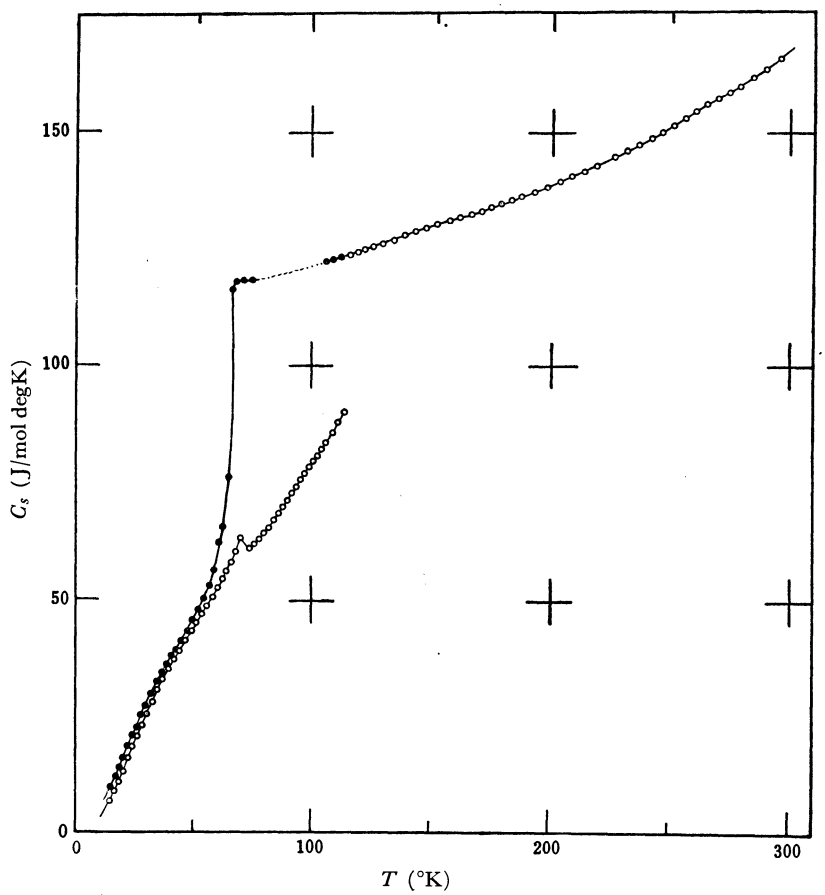

Fig. 2. Heat capacity curve of isopentane.

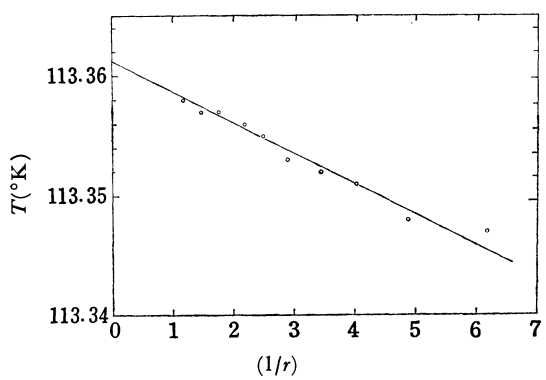

Fig. 3. Melting curve of isopentane.

liquid just above the glass transition point is nearly equal to the twice of that for the crystalline state. This fact is rather common feature at glass transition of almost all supercooled liquids.[7] When the supercooled liquid which had experienced glass transition, was heated up to above the glass transition temperature, the crystallization takes place at about 75°K. This crystallization phenomenon was observed experimentally with the start of gradual heat evolution effect. The heat capacity measurements, a little below the melting point were made with the supercooled liquid obtained by means of careful slow cooling. It was possible

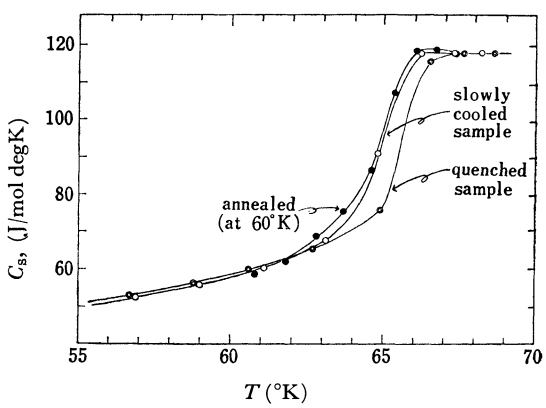

Fig. 4. Heat capacity of isopentane during the glass transition intervals.
●: annealed sample at 60°K, ○: slowly cooled one, ◎: quenched one

7) R. O. Davies and G. O. Jones, *Proc. Roy. Soc.*, **A217**, 26 (1953).

for about 10°C below the melting point, and the temperature region where the heat capacity measurements were impossible is shown by dotted line in Fig. 2. Detailed measurements were also made in the glass transition intervals for various samples which had experienced the different thermal treatments. The results are shown in Fig. 4 and double circles represent the data for the quenched sample which was quenched to 25°K from room temperature during six minutes. The series of measurements for this quenched sample were made from 13°K to 68°K. After this series of measurements have finished at 68°K, the sample was slowly cooled down to 43°K during 4 hr.

The results with this slowly cooled sample are depicted by a series of circle in the Fig. 4.

Finally, this sample was again cooled down to 60°K from 68°K during 25 min and annealed for about 20 hr at this temperature. The filled circles are for this sample.

This series of measurements was continued to the temperature region above the glass transition

TABLE 1A. MOLAR HEAT CAPACITIES OF ISOPENTANE (CRYSTAL AND LIQUID) IN J/mol degK.

T (°K)	C_s	T (°K)	C_s	T (°K)	C_s	T (°K)	C_s
Series 1		72.61	62.931	140.72	127.89	208.79	140.08
		74.54	60.829	142.94	128.34	211.41	140.56
14.99	6.414	76.46	61.513	145.15	128.74	214.02	141.13
16.87	8.624	78.35	62.634	147.36	129.00	216.63	141.81
18.61	10.848	80.20	64.840	149.56	129.23	219.22	142.33
20.40	12.928	82.01	65.343	151.77	129.76	221.81	142.91
22.51	15.736	83.91	66.851			226.66	144.24
24.49	18.259	85.90	68.121	Series 5		229.22	144.74
26.40	20.447	87.86	69.683			231.76	145.56
28.34	22.632	89.78	71.167	155.44	130.38	234.30	146.13
30.31	25.200	91.67	72.520	157.62	130.64	236.83	146.74
32.67	27.777	93.53	73.888	159.79	130.80	239.47	147.22
35.12	30.402	95.37	75.232	161.96	131.21		
37.37	32.686	97.18	76.654	164.13	131.31	Series 7	
39.68	34.908	98.96	77.920	165.68	131.76		
42.07	36.936			168.44	132.24	234.70	145.95
44.42	38.989	Series 3		170.58	132.58	237.12	146.76
46.88	41.136			172.73	133.05	239.52	147.65
49.31	43.106	97.20	75.764	174.86	133.52	241.91	148.30
51.64	44.892	98.95	78.217	177.00	133.88	244.29	148.78
53.86	46.681	100.68	79.152	179.12	134.28	246.65	149.49
56.09	48.520	102.40	80.558	181.24	134.63	249.01	150.11
58.32	50.428	104.11	81.997	183.36	134.92	251.36	150.88
60.48	52.357	105.77	83.456	185.47	135.31	253.72	151.64
62.57	54.188	107.40	84.532			256.07	152.41
64.16	55.726	109.02	85.962	Series 6		258.39	153.12
66.15	57.753	110.61	88.151			260.69	153.83
68.12	60.251	112.13	96.408	165.68	131.76	262.99	154.60
70.10	63.005	113.36	123.38	168.23	132.24	265.28	154.96
72.04	62.502	114.83	124.83	171.13	132.68	267.57	155.65
74.00	60.598			173.88	133.13	269.84	156.59
75.95	61.336	Series 4		176.62	133.69	272.10	157.25
77.86	62.457			179.35	134.27	274.36	157.95
79.74	63.896	119.70	124.51	182.07	134.76	276.46	158.56
		121.53	124.63	184.78	135.25	278.85	159.13
Series 2		123.36	124.92	187.49	135.73	281.68	160.16
		125.19	125.05	190.18	136.21	284.50	161.05
60.18	51.999	127.23	125.52	192.87	136.76	287.30	161.92
62.43	54.179	129.50	125.62	195.54	137.28	290.08	162.98
64.60	56.669	131.76	125.99	198.21	137.83	292.85	164.17
66.69	58.302	134.01	126.42	200.87	138.36	295.61	165.15
68.72	60.140	136.25	127.02	203.52	138.99	298.34	166.17
70.69	63.533	138.49	127.66	206.16	139.38		

Table 1B. Molar heat capacities of isopentane (glass and supercooled liquid) in J/mol deg K

T (°K)	C_s	T (°K)	C_s
Glass		54.90	50.016
		56.92	52.436
Series 1		58.99	55.676
		61.08	60.210
15.60	9.398	63.09	67.832
17.34	11.707	64.82	90.959
19.06	13.834	66.20	117.61
20.61	15.779	67.30	117.66
22.59	18.289	68.24	117.68
24.47	20.546		
26.28	22.764	Series 3	
28.14	24.850		
30.05	26.976	60.79	57.671
32.34	29.462	61.75	60.944
34.73	31.882	62.77	65.565
36.93	34.042	63.70	72.107
38.99	35.852	64.98	82.561
41.03	37.612	65.37	96.907
43.08	39.302		
45.33	41.103	Supercooled liquid	
47.78	43.325		
50.33	45.659	66.02	116.34
52.54	47.773	66.69	117.47
54.67	50.115	67.35	117.62
56.72	52.939	68.31	117.79
58.79	56.253	69.59	117.78
60.61	61.971	70.85	117.60
62.71	65.400	72.12	118.07
64.92	75.800	73.39	117.78
66.54	116.04	74.67	118.13
67.66	117.79		
68.62	117.87	Series 4	
Series 2		105.96	122.38
		107.45	122.49
45.88	41.615	108.93	122.71
48.30	43.630	110.41	122.97
54.60	45.630	111.89	123.03
52.79	47.810		

temperature, until the heat evolution due to the crystallization was observed.

While the crystallization proceeds, the adiabatic condition of the calorimeter was watched to be satisfied. When the heat evolution effect has ceased at 106.2°K, the temperature of the crystalline phase was determined accurately. This procedure was necessary in order to determine the enthalpy of the glassy state on the basis of the enthalpy of the crystalline states as will be given in the next section.

Enthalpy Curves of the Glass and the Supercooled Liquid. The enthalpy curves of the glass and the supercooled liquid, calculated with the results of the heat capacity data are shown in Fig. 5.

Table 2. Heat of fusion of isopentane

T (°K) Melting point	$\int \Delta C_P dT$ Heat input J/mol	$1/r$ Inverse of pre-melting fraction
113.341	601.9	8.73
113.347	820.7	6.19
113.348	1039.8	4.88
113.351	1258.7	4.03
113.352	1477.7	3.44
113.353	1759.3	2.89
113.355	2041.0	2.49
113.356	2322.5	2.19
113.357	2885.5	1.76
113.357	3448.1	1.47
113.358	4339.7	1.17

(Heat of fusion 5140±2 J/mol)

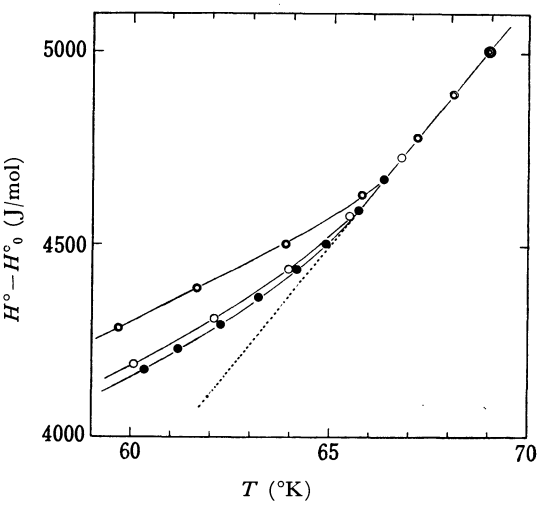

Fig. 5. Enthalpy curve of isopentane near the glass transition point.
●: annealed sample at 60°K, ○: slowly cooled sample, ◎: quenched sample

Each curve represents the various samples which had experienced different thermal treatments.

In the case of quenched sample, the enthalpy value of the supercooled liquid deviates from the equilibrium curve at about 66.5°K, and transforms into the glassy state. For slowly cooled sample, the curve deviates from the equilibrium value at the temperature 1°C lower than that for the quenched sample. The effect of annealing is really found in the enthalpy curve in such a way that the enthalpy curve of glass comes below the slowly cooled one. The triple circle near 69°K which is taken as the reference point for evaluation of absolute enthalpy of the glass was determined as the intersection of the curve for supercooled liquid and the isenthalpy straight line at 106.2°K of the enthalpy curve for crystalline state. The enthalpy curve of the crystalline state is easily

TABLE 3A. THERMODYNAMIC PROPERTIES OF ISOPENTANE (CRYSTALLINE AND LIQUID STATES) IN J/(mol degK)

T	$C_P°$	$S°$	$(H°-H°_0)/T$	$-(G°-H°_0)/T$
5	(0.255)	(0.085)	(0.063)	(0.021)
10	(2.030)	(0.655)	(0.499)	(0.155)
15	6.430	2.236	1.667	0.569
20	12.47	4.893	3.596	1.297
30	24.76	12.32	8.642	3.678
40	35.21	20.93	14.03	6.903
50	43.60	29.71	19.12	10.59
60	51.92	38.38	23.88	14.50
70	63.08	47.12	28.59	18.53
80	63.88	55.43	32.79	22.64
90	71.25	63.38	36.65	26.72
100	78.72	71.27	40.48	30.78
110	86.81	79.14	44.32	34.82
113.36		Fusion		
120	124.42	134.19	92.78	41.41
140	127.74	153.59	97.51	56.08
160	130.97	170.87	99.01	71.86
180	134.38	186.48	104.96	81.52
200	138.17	200.83	100.08	92.74
220	142.50	214.20	110.01	104.19
240	147.63	226.81	113.84	112.97
260	153.60	238.85	116.66	122.19
280	159.62	250.46	119.52	130.94
300	166.82	261.70	122.42	139.28

Values in parentheses are extrapolated by means of Debye function.

TABLE 3B. THERMODYNAMIC PROPERTIES OF ISOPENTANE (GLASSY AND SUPERCOOLED LIQUID STATES) IN J/(mol degK)

T	$C_P°$	$S°-S°_0(\mathrm{gl})$*	$(H°-H°_0(\mathrm{gl}))/T$	$-(G°-H°_0(\mathrm{gl}))/T$
5	(0.365)	(0.122)	(0.091)	(14.09)
10	(2.880)	(0.977)	(0.735)	(14.30)
15	8.660	2.951	2.373	14.64
20	15.03	6.315	4.733	15.65
30	26.95	14.73	10.21	18.58
40	36.75	23.88	15.67	22.27
50	45.13	32.97	20.72	26.31
60	58.77	42.16	25.70	30.52
70	117.28	55.45	38.60	30.91
80	118.63	71.21	48.52	36.75
90	119.98	85.26	56.38	42.94
100	121.33	97.72	62.81	48.97
110	122.67	108.68	68.19	54.55

$S°_0(\mathrm{gl})=14.06$ J/(mol degK); $H°_0(\mathrm{gl})-H°_0(\mathrm{c})=2673$ J/mol.
The values between 70 and 110°K are evaluated by means of interpolation using equation $C_P=107.82+0.1351T$ (J/mol degK).
* (gl) indicates glassy state.

obtained by graphical integration of their heat capacity data.

Thermodynamic Properties of Isopentane. The values of heat capacity, entropy, and also the enthalpy and Gibbs energy functions of isopentane at selected temperature were listed for the liquid crystalline, glassy, and supercooled liquid states in Table 3.

Discussion

The heat capacities of isopentane have been measured by three investigators,[4,5,8] nevertheless, the occurrence of the glassy state of this compound

8) G. S. Parks, H. M. Huffman and S. B. Thomas, *J. Am. Chem. Soc.*, **52**, 1032 (1930).

had not been known by any authors. As is described already, we have succeeded in obtaining the glassy state of the present material. The relation of the normal boiling to its normal melting points of isopentane is equal to 2.70. This fact is concordant with the Turnbull-Cohen empirical rule[1] for obtaining glassy state by supercooling method; *i. e.*, the ratio should be equal to or larger than 1.8. The ratio $T_b/T_m=2.15$ for *n*-pentane suggests that this liquid might have also the tendency to be supercooled, whereas the crystallization has always occurred as far as our observation is concerned.

Now, in liquid isopentane two kinds of origin associated with the relaxation phenomenon may be considered, one is due to the degree of freedom of the internal rotation with respect to intramolecular C-C bond, and the other is due to the change of intermolecular configuration which is related to the shear and/or volume viscosity of liquid isopentane. Concerning the liquid state of isopentane, there is investigation with ultrasonic absorption technique by Young and Petrauskas.[9] Their results suggest that around 150°K the relaxation time with respect to the degree of freedom of internal rotation is longer than that for intermolecular configurational change. It is not clear, however, how is the relation between these two types of relaxation times for supercooled liquid near 65°K. We may safely conclude, anyhow, that ΔC_P, the increment of heat capacity at the glass transition point, is mainly associated with intermolecular configurational change, since the difference between the contributions due to the intramolecular rotation in the supercooled liquid and in the glass, may be too small to explain this ΔC_P.

Turning to the phenomenological interpretation of the glass transition phenomenon of supercooled liquid, there exist two kinds of opposite opinions. One is such that the glass transition occurs at temperature where a certain kind of thermodynamical quantity takes critical value; *i. e.*, the glass transition is like a second order phase transition.[10,11] The other is such that the glass transition may be interpreted as the relaxation phenomenon due to the degree of freedom of molecular motions.[12]

According to Adam and Gibbs, the relaxation time of a system can be uniquely related to the configurational entropy of the system. This idea is based on the resolution of the well-known Kauzmann's paradox.[13] This theory shows explicitly the existence of temperature at which the configurational entropy of the system has critical value and it is called T_2, a glass transition temperature in the sense of thermodynamical equilibrium. According to their theory, the actual glass transition temperature T_g can be related to T_2 in the following equation;

$$S_{\text{config}}(T_g) = \int_{T_2}^{T_g} \Delta C_P/T \, dT, \text{ and}$$

$$S_{\text{config}}(T_g) \equiv \Delta S_0 = (S_{\text{glass}} - S_{\text{cryst}})_{T=0}$$

From our results of the heat capacity measurements, ΔS_0 and ΔC_P are known, so the ratio T_g/T_2 can be calculated.

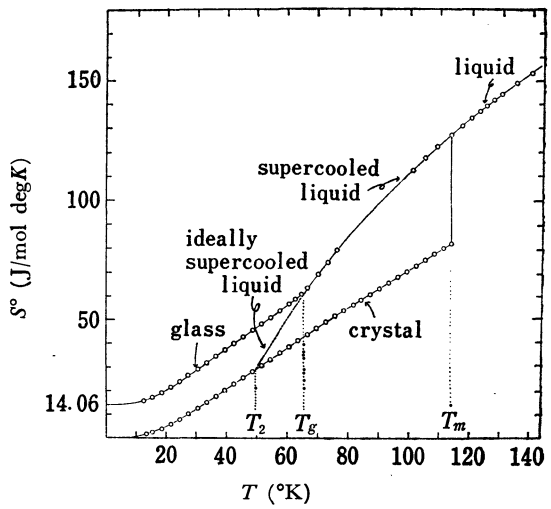

Fig. 6. Entropy diagram of isopentane.

Figure 6 shows the entropy diagram of isopentane calculated from the data of the heat capacity measurements. From this entropy diagram, it is clear that T_2 (the temperature at which the configurational entropy disappears) situates at about 50°K. Consequently, the following relations are obtained,

$$T_g/T_2=65/50=1.30$$

and $$T_g-T_2=65-50=15 \ (°K)$$

The relation, $T_g/T_2=1.30$, is corresponding to the average value of many substances cited by Bestul and Chang[14] and Adam and Gibbs.[11]

The consistency of the present results with Adam and Gibbs' theory seems to suggest that a certain kind of thermodynamical relation takes part in the glass transition phenomenon of the supercooled liquid.

Finally a few comments will be given concerning the irreversible phenomenon taking part in a glassy state.[7,15]

9) J. M. Young and A. A. Petrauskas, *J. Chem. Phys.*, **25**, 943 (1956).
10) M. Goldstein, *ibid.*, **39**, 3369 (1963).
11) G. Adam and J. H. Gibbs, *ibid.*, **43**, 139 (1965).
12) M. L. Williams, R. F. Landel and J. D. Ferry, *J. Am. Chem. Soc.*, **77**, 3701 (1955).
13) W. Kauzmann, *Chem. Revs.*, **43**, 219 (1948).
14) A. B. Bestul and S. S. Chang, *J. Chem. Phys.*, **40**, 3731 (1964).
15) A. B. Bestul and S. S. Chang, *ibid.*, **43**, 4532 (1965).

Near below the glass transition temperature, we can observe usually an exothermic effect due to the stabilization phenomenon of the glassy state into a supercooled liquid.

This stabilization gives rise to an irreversible entropy production within the system. It is well known that a residual entropy of the glassy state generally involves the excess entropy due to these irreversible phenomenon. Davies and Jones[7] suggested the possibility that this entropy production can be estimated by considering the heat conduction between a system of configurational part and a system of lattice, each of which is in different temperatures. Consequently, the irreversible production of entropy can be expressed very simply by the following expression,

$$\Delta S_{\mathrm{Irr.}} = \Delta C_P (1/\bar{T} - 1/T)\Delta T$$

where ΔC_P is the heat capacity of configurational part, T the temperature of a lattice, and $\bar{T}$ fictive temperature of a configurational system.

In order to estimate this quantity, the drift of temperature of the sample in the calorimeter was measured for long time during the glass transition intervals. This drift corresponds to the time derivative of T, or $\bar{T}$. Analysing the results of drift curve for quenched sample, $\Delta\bar{T}$ was found to be -0.0892°C with the assumption that configurational heat capacity is equal to that of the lattice. Taking the following data $\bar{T}=65$°K, $T=60$°K, $\Delta C_P=16.3$ cal/mol degK, we get $\Delta S_{irr}=.0.019$ cal/mol degK which is very small compared with the residual entropy at absolute zero, $\Delta S_0=3.36$ cal/mol degK.

We can safely conclude that the neglect of the irreversible production of entropy leads to no significant error on determing the residual entropy.

Summary

1) The results of the heat capacity measurements of isopentane were given for crystalline, liquid, glassy and supercooled liquid states in the temperature region between 13 and 300°K.

2) The glass transition phenomenon of isopentane was found near 65°K with the drastic change of heat capacity of 16.3 cal/mol degK.

3) The residual entropy of the glassy isopentane at absolute zero was found to be 3.36 cal/mol·degK.

4) The irreversible production of entropy during the glass transition intervals was estimated to be 0.019 cal/mol degK.

BULLETIN OF THE CHEMICAL SOCIETY OF JAPAN VOL. 41 600—603 (1968)

Extraction-Photometric Determination of Osmium with Thenoyltrifluoroacetone

Asha V. RANGNEKAR and S. M. KHOPKAR

Department of Chemistry, Indian Institute of Technology, Bombay-76, India

(Received June 21, 1967)

The study of the liquid-liquid extraction of some platinum group elements (A. V. Rangnekar and S. M. Khopkar, *Bull. Chem. Soc. Japan*, **38**, 1696 (1965); **39**, 2169 (1966)), with fluorinated β-diketones showed that, osmium reduced to trivalent state with hydroxylamine hydrochloride forms a red chelate with 2-thenoyltrifluoroacetone, TTA. The chelate is readily extracted in benzene giving strong absorbance at around 440 mμ.

The thiocarbonilide[1] complex of osmium is extracted with ether, where as complex with ephedrine hydrochloride[2] was extracted in carbon tetrachloride. Thiourea[3,4] was used for extraction and colorimetric determination of osmium. Such complex was extracted in chloroform and measured at 480 mμ. The osmium was found to be in the trivalent state with composition of the extractable[5] species as $[Os(NH_2\text{–}CS\text{–}NH_2)_6]^{3+}$. The other extracting agents include; thiosemicarbazide,[6] 1-naphthylamine -3, 5, 7-trisulphonic acid,[7] mercaptobenzimidazole[8] and *o*-(β-benzoylthiourido)benzoic acid.[9] Unfortunately these methods

1) W. Singleton, *Ind. Chem.*, **3**, 121 (1927).
2) S. O. Thompson, F. E. Beamish and M. Scott, *Ind. Eng. Chem. Anal. Ed.*, **9**, 421 (1937).
3) E. B. Sandell, *ibid.*, **16**, 342 (1944).
4) G. H. Ayres and W. N. Wells, *Anal. Chem.*, **22**, 317 (1950).
5) R. D. Sauerbrunn and E. B. Sandell, *J. Am. Chem. Soc.*, **75**, 3554 (1953).
6) W. Geilmann and R. Neeb, *Z. Anal. Chem.*, **156**, 420 (1957).
7) E. L. Steel and J. H. Yoe, *Anal. Chim. Acta*, **20**, 205 (1959).
8) B. C. Bera and M. M. Chakraborty, *Anal. Chem.* **38**, 1419 (1966).
9) A. K. Majumdar and S. K. Bhawal, *Anal. Chim. Acta*, **35**, 479 (1966).

are not rapid. An attempt is made in this paper to present a rapid method for the extraction-photometric determination of osmium at micro-levels with TTA.

Experimental

Apparatus and Reagents. A type SP-4 quartz spectrophotometer, Cambridge pH meter, wrist action flask shaker. TTA (E. Merck and Co.) 0.015 M solution in benzene. A stock solution of osmium was prepared from osmic acid as by Ayres' method.[4] On standardisation[3,10] it was found to contain 58.8 μg of osmium per m*l*. Hydroxylamine hydrochloride (B. D. H) 5% aqueous solution.

General Procedure. An aliquot of the solution (294 μg of osmium) was taken, 10 m*l* of 5% hydroxylamine hydrochloride was added to reduce osmium to trivalent state, the pH of the solution was then adjusted to pH 4.5 with 0.01 N sodium hydroxide, and 0.01 N sulphuric acid. The final volume of the solution was made upto 20 m*l* and the solution was then transferred to separatory funnel. Ten millilitres of 0.015 M TTA-benzene was added and it was shaken for about 10 min. After allowing the solution to settle and separate, organic phase was stripped into 10 m*l* volumetric flask. The absorbance of the colored complex was measured at 440 mμ. The amount of osmium was computed from the calibration curve.

Results and Discussion

Absorption Spectrum. The absorption spectrum of Os(III)-TTA complex (Os = 1.545×10^{-4} M) shows strong absorbance at 430 mμ (Fig. 1). Although the reagent blank shows significant absorbance at 420 mμ, it is negligible at 430 mμ. All absorbance measurements were therefore made at 440 mμ. The molar absorptivity is 1.42×10^2 at 440 mμ on the basis of osmium contents.

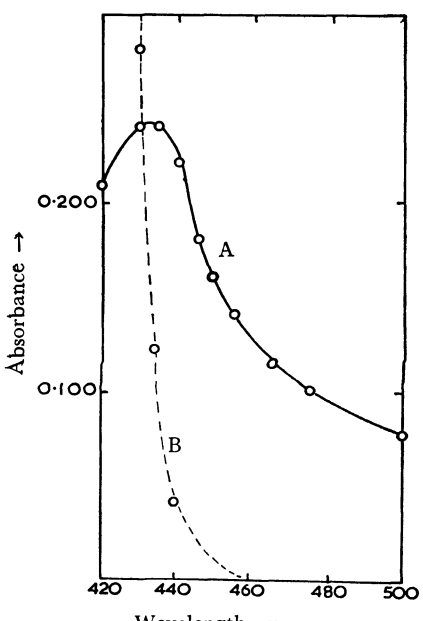

Fig. 1. Absorption spectra of osmium-TTA complex.
A Os(III)-TTA complex *vs.* reagent blank Os(III) = 1.545×10^{-4} M at pH 4.5
B Reagent blank *vs.* benzene at pH 4.5 TTA = 1.5×10^{-3} M

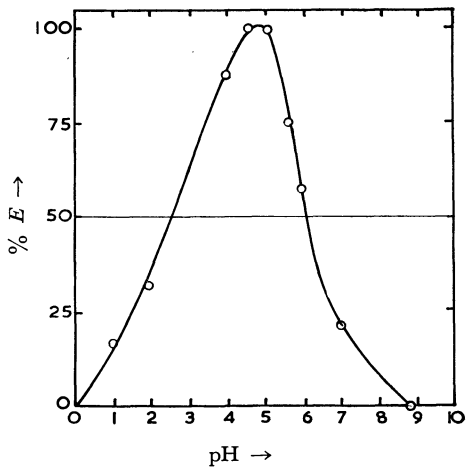

Fig. 2. Percentage extraction of osmium as the function of pH.

The Effect of pH Value. The extraction of osmium was carried out from pH 1.0—10.0 with TTA. (Fig. 2). The distribution ratio (*D*) was calculated as before[11,12] (Table 1). Between pH region of 3.5 to 5.5, more than 80% osmium is

Table 1. Extraction as the function of pH

pH	*E* %	*D*
0.5	7.5	0.176
1.0	17.5	0.424
1.5	25.0	0.660
2.0	32.5	0.752
2.5	50.0	2.000
3.0	62.5	3.330
3.5	72.0	8.100
4.0	87.5	14.000
4.5	100.0	∞
5.0	100.0	∞
5.5	75.0	6.000
6.0	57.5	2.710
6.5	30.0	0.857
7.0	22.5	0.602
7.5	12.5	0.286
8.0	7.5	0.176
8.5	5.0	0.105
9.0	0.0	—

10) A. K. De, "Separation of Heavy Metals," Pergamon Press, London (1961), p. 237.
11) A. V. Rangnekar and S. M. Khopkar, This Bulletin, **38**, 1696 (1965).
12) A. V. Rangnekar and S. M. Khopkar, *ibid.*, **39**, 2169 (1966).

Table 2. Beer's law curve

Osmium μg	Absorbance at mμ		
	430	435	440
58.8	0.040	0.040	0.045
88.2	0.055	0.070	0.110
117.6	0.100	0.100	0.095
176.4	0.140	0.140	0.135
235.2	0.190	0.180	0.175
294.0	0.230	0.230	0.220
352.8	0.270	0.270	0.265
441.0	0.300	0.300	0.320

Table 3. Effect of reagent concentration
Os=294 μg pH=4.5

Concentration M	Volume of reagent ml	Absorbance at 440 mμ
0.0015	10.0	0.000
0.0075	10.0	0.010
0.0150	5.0	0.100
0.0150	7.5	0.220
0.0150	10.0	0.220
0.0250	10.0	0.230
0.0500	10.0	0.240

extracted, but at pH 4.5 the extraction is quantitative. The $pH_{1/2}$ is 2.6 and 6.0.

Beer's Law Curve. The different amounts of osmium were extracted pH 4.5 (Table 2) and measured at 430, 435 and 440 mμ. The system conforms to Beer's law over the concentration range of 2.9 to 22 μg of osmium per ml at 440 mμ.

The Effect of Reagent Concentration. The osmium (294 μg) was extracted at pH 4.5 with varying concentration of the reagent (Table 3). The results indicate that 10 ml of 0.015 M TTA is quite adequate for quantitative extraction.

Stability of the Color. The absorbance of the colored complex was measured at lapsed interval of 30 min. Probably the complex decomposes after 6 hr. Therefore it is recommended to measure the absorbance within first 4 hr of complex formation.

Period of Shaking. The variation in period of shaking from 30 sec to 30 min revealed that the complex is quantitatively extracted within 10 min of shaking.

The Effect of Salting-out Agents. The sulphates of alkali and alkaline earth metals were used as the salting-out agents (Table 4). The results showed none of them have any pronounced effect upon the process of extraction.

The Effect of Diverse Ions. The effect of the presence of several ions on the extraction behaviour was studied (Table 5). About 5 mg of cadmium, tin(II), platinum(IV), palladium, rhodium, iridium, gold, manganese, cobalt(II),

Table 4. Effect of salting-out agents

Salting -out agent	Molarity M	Absorbance at 440 mμ
Li_2SO_4	1	0.120
	2	0.095
Na_2SO_4	1	0.220
	2	0.175
$(NH_4)_2SO_4$	1	0.140
	2	0.080
K_2SO_4	1	0.110
	2	0.100

Table 5. Effect of diverse ions

Foreign ion	Added as	Amount added, μg	Absorbance at 440 mμ
None	—	—	0.220±0.010
Tl^+	Tl_2SO_4	3000	0.200
Cu^{2+}	$CuSO_4 \cdot 5H_2O$	5000	Color
Cd^{2+}	$3CdSO_4 \cdot 8H_2O$	5000	0.220
Sb^{3+}	$SbCl_3 \cdot 3H_2O$	2500	0.220
Bi^{3+}	$Bi(NO_3)_3$	2000	0.150[a]
Sn^{2+}	$Sncl_2 \cdot 2H_2O$	2500	0.220
Pt^{4+}	H_2PtCl_6	5000	0.220
Pd^{2+}	$PdCl_2 \cdot 2H_2O$	5000	0.210
Rh^{3+}	$RhCl_3 \cdot 3H_2O$	5000	0.210
Ir^{3+}	$IrCl_3 \cdot 3H_2O$	2500	0.195
An^{3+}	$HAuCl_4$	5000	0.210
Fe^{3+}	$FeCl_3$	5000	Color[a]
U^{6+}	$UO_2(NO_3)_2 \cdot 2H_2O$	5000	Color[b]
Zr^{4+}	$Zr(NO_3)_4 \cdot 2H_2O$	1500	0.150[b]
Th^{4+}	$Th(NO_3)_4 \cdot 4H_2O$	1500	0.150[a]
Ce^{4+}	$Ce(SO_4)_2 \cdot 2H_2O$	5000	Color[b]
Zn^{2+}	$ZnSO_4 \cdot 7H_2O$	1800	0.210
Mn^{2+}	$MnCl_2 \cdot 4H_2O$	5000	0.210
Co^{2+}	$CoCl_2 \cdot 6H_2O$	5000	0.220
Ni^{2+}	$NiSO_4 \cdot 7H_2O$	500	0.195
Ca^{2+}	$CaCl_2 \cdot 2H_2O$	500	0.205
Mg^{2+}	$MgSO_4 \cdot 7H_2O$	500	0.205
Li^+	LiCl	1000	0.220
AsO_3^{3-}	Na_3AsO_3	5000	0.220
TeO_3^{2-}	Na_2TeO_3	1200	0.205
$Formate^-$	HCOOH	1000	0.200
$Tart^{3-}$	Tartaric Acid	5000	0.220
Cit^{3-}	Citric acid	5000	0.220
$Ascorb^{2-}$	Ascorbic acid	2500	0.225
$EDTA^{4-}$	EDTA (Na_2-salt)	5000	0.220

a) Interference eliminated by masking with EDTA at pH 2.0.
b) Interference eliminated by forming anionic complex with citrate at pH=6.0.

arsenite, tartrate, citrate, and EDTA do not interfere. Similarly about 1 mg of antimony, zinc, lithium, tellurite, formate can be tolerated. The ions showing interference are thorium, bismuth, zirconium, cerium, uranium and iron; but their

interference can be easily eliminated by complexation with suitable masking agents.

From twenty determinations, it was observed that the absorbance of the solution ranged from 0.210 to 0.230. The standard deviation is $\pm 1.1\%$. As little as 1.33 μg of osmium per m*l* can be detected.

Summary

2-Thenoyltrifluoroacetone forms orange red chelate with trivalent osmium, the chelate which shows strong absorbance at 440 mμ. Beer's law is obeyed over the concentration range of 2.9 to 22 μg of osmium per m*l*. The color of the complex is stable. Large number of cations as well as anions are tolerated.

We are thankful to Council of Scientific and Industrial Research (India) for sponsering this project and awarding Senior Research Fellowship to one of us (A. V. R.).

BULLETIN OF THE CHEMICAL SOCIETY OF JAPAN VOL. 41 603—605 (1968)

Chemical Studies of Minerals Containing Rarer Elements from the Far East District. LXI. Yttrofluorite from Suishoyama, Kawamatamachi, Fukushima Prefecture, Japan

Keiji UETANI,* Yoshiko OGIMURA,** Akira KATO* and Kozo NAGASHIMA***

* *Department of Geology, National Science Museum, Ueno Park, Tokyo*
** *Department of Chemistry, Faculty of Science, The University of Tokyo, Hongo, Tokyo*
*** *Department of Chemistry, Faculty of Science, Tokyo Kyoiku University, Otsuka, Tokyo*

(Received September 1, 1967)

A very rare yttrium mineral, yttrofluorite, from granite pegmatite found at Suishoyama, Fukushima Prefecture, was studied. Chemical analysis: Ca 35.50%, $\sum$ Rare earths 18.84%, Mg 0.42%, Fe 0.34%, Al 0.15%, Mn 0.08%, F (remainder) 44.67%. Cell constant calculated from the X-ray powder data: $a_0=5.500$ Å. Specific gravity: 3.51 (measured), 3.62 (calculated). Refractive index: $n=1.454$. The distribution pattern of lanthanide elements studied by the X-ray fluorescent method disclosed that the mineral is poor in cerium group lanthanide, rich in yttrium group with maxima at dysprosium and erbium. The mineral occurs as aggregates of small crystals in spessartine garnet embeded in large crystals of feldspars.

In spite of the many detailed chemical studies of pegmatite minerals from Japan, yttrofluorite was hitherto not reported, except for one[1] from Yamaguchi-mura, Nagano Prefecture, which was assumed because of the high refractive index (although the sample was too small to be analyzed).

Suishoyama pegmatite, Kawamata-machi, Fukushima Prefecture, is found in a Mesozoic biotite granite body, has a zonal arrangement of felsic minerals, and has been worked for quartz and feldspar for many years. The pegmatite is also well-known for the production of many rare element minerals, such as abukumalite (type locality), yttrialite, fergusonite, tengerite, thorogummite, allanite, uraninite, zircon, gadolinite, keilhauite, thalenite,[2] and some secondary uranium minerals such as autunite, torbernite, zeunerite, and a mineral[3] very close to uranophane, but which has higher refractive indices and larger d values obtained from X-ray powder diffraction.

The mineral herein described was collected from a waste outside the quarry, so the mode of occurrence or the paragenesis of minerals is not certain. The mineral usually occurs as irregularly shaped, fine grained agglomerate in spessartine garnet of a dark red brown color, and contains a small amount of yttrium group rare earths. The largest aggregate reaches 3 cm in size, but individual grains are too small to see with the naked eye.

The spessartine garnet is usually embeded in potash feldspars. This occurrence of yttrofluorite is very similar to that of tengerite[4] in Suishoyama pegmatite suggesting a close relationship between these two minerals.

1) H. Shibata, *J. Geol. Soc. Japan*, **46**, 558 (1939). (in Japanese)
2) K. Nagashima and A. Kato, This Bulletin, **39**, 925 (1966). Literatures describing these minerals from Suishoyama are cited in this paper.
3) K. Nagashima, A. Kato and M. Chiba, *Chigaku-kenkyu*, **17**, Nos. 10, 11, 12, p. 95 (1966). (in Japanese)
4) T. Iimori, *Sci. Pap. Inst. Phys. Chem. Research*, **34**, 832 (1938).

The mineral yttrofluorite is also important as an example of a complete assemblage of rare earth elements in which the yttrium earths are of the same abundance as the cerium earths. This kind of complete assamblage is known as "yttrofluorite type" (Goldschmidt and Thomassen[5]). However, as shown by Semenov,[6] the distribution of rare earth elements in fluorite is quite variable. In Dana's "System of Mineralogy,"[7] both yttrofluorites rich in yttrium group rare earths, $\sum Y_2O_3$ 17.35%, $\sum Ce_2O_3$ 1.68%, and those rich in cerium group rare earths, $\sum Y_2O_3$ 8.10%, $\sum Ce_2O_3$ 16.45% are described.

Optical and X-Ray Powder Studies

As the grains composing the aggregates are so small, clevages characteristic of fluorite is hardly observable with the naked eye. The color of the aggregates, and that of the powder is gray. The refractive index is 1.454. The value is much higher than that of the usual fluorite, and agrees with values, 1.4572, 1.4425, or 1.4483 for yttrofluorites of other localities.[7]

X-Ray powder diffraction measurements were made on a Norelco X-ray Diffractometer. The diffraction data are compared with those of pure artificial calcium fluoride in Table 1. D values and intensities of the present mineral are very close to those of calcium fluoride, but the d values of the mineral are definitely a little larger than those of artificial fluorite suggesting substitution of calcium by larger rare earth elements. From the d values, a_0 was calculated to be 5.500 Å.

Chemical Composition

Chemical analyses were carried out on the hand-picked material. Fluoride was not analyzed directly, but determined by subtracting analyzed

TABLE 1. X-RAY POWDER DATA

(1) Artificial CaF_2		(2) Yttrofluorite from Suishoyama				
d Å	I	d Å	I	Q_{obs}	Q_{calcd}	hkl
3.153	94	3.171	100	0.0995	0.0992	111
—	—	2.751	2	0.1321	0.1323	200
1.931	100	1.943	60	0.2648	0.2645	220
1.647	35	1.658	10	0.3637	0.3637	311
—	—	1.586	2	0.3974	0.3968	222
1.366	12	1.375	6	0.5292	0.5290	400
1.253	10	1.262	3	0.6281	0.6282	331
—	—	1.230	1	0.6615	0.6613	420
1.150	16	1.123	6	0.7935	0.7935	422
ASTM, No. 4-0864 Cu/Ni radiation a_0=5.4626 Å		Cu/Ni radiation a_0=5.500 Å				

TABLE 2. CHEMICAL ANALYSIS

	%	%/Formula weight		×0.9154 (=1/1.092)
Ca	35.50	0.8857		0.811
∑R.E.*	18.84	0.1762		0.161
Fe(III)	0.34	0.0061	1.0924	0.005
Al	0.15	0.0056		0.005
Mn	0.08	0.0015		0.001
Mg	0.42	0.0173		0.016
F (remainder)	44.67	2.3511		2.152
Total	100.00			

* Mean atomic weight = 99.7

5) V. M. Goldschmidt and L. Thomassen, *Vidensk. Skrifter I. Mat.-naturv. Klaase*, **1924**, No. 5.
6) E. I. Semenov, *Geohkimiya*, **1958**, 452.
7) C. Palache, H. Berman and C. Frondel, "Dana's System of Mineralogy," 7th ed., Vol. II, John Wiley, New York (1951), p. 32.

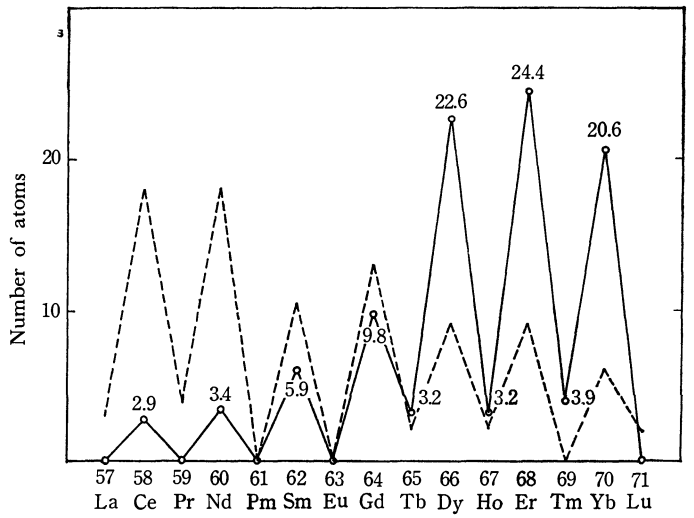

Fig. 1. Distribution of rare earth elements.

—— Yttrofluorite type observed (this work) Total lanthanoids=100 atoms
---- Yttrofluorite type (by V. M. Goldschmidt and Thomassen)

cations from 100%. The average atomic weight of the rare earth elements was determined by titrating the weighed mixed oxides with an EDTA standard solution after dissolving them in hydrochloric acid.

The results of the analyses are given in Table 2, together with the molecular ratios of the components. The experimental formula of the yttrofluorite from Suishoyama calculated on the bases of $\sum$ cation=1.00 is $(Ca_{0.8107}, \sum R.E._{0.1613}, Mg_{0.0158}, Fe, Al, Mn)_{1.00}F_{2.1524}$. The content of rare earth elements as fluoride is 28%, and the atomic ratio of rare earth elements to calcium reaches 1 : 5.04. This ratio is almost the same as that for the yttrofluorite from Hundholmen, Norway, in which (Y, Ce) : Ca is 1 : 6.0, and the yttrofluorite (more correctly cerium fluorite) from Fahlum, Sweden, in which the ratio is 1 : 5.2.

The Distribution Pattern of Rare Earth Elements

The distribution of lanthanum series elements was determined by the X-ray fluorescent technique. Cerium, neodymium, samarium, gadolinium, terbium, dysprosium, holmium, erbium, thulium, and ytterbium (with the maxima at dysprosium and erbium) were found. Lutetium may be present, but could not be confirmed due to the overlapping diffractions of other spectra. A quantitative estimation, with the relative error of less than 10%, is given in Fig. 1, in which the atomic % of the elements is plotted. In the figure, the yttrofluorite type distribution pattern of rare earth elements by Goldschmidt and Thomassen[5] is also shown. As seen in the figure, the present mineral is richer in yttrium group rare earths than the so called yttrofluorite type. The higher concentration of the yttrium group in the mineral might be a reflection of the high concentration of yttrium group rare earths in the original solution of the Suishoyama pegmatite.

Specific Gravity

When divalent calcium ions in fluorite are substituted by trivalent rare earth ions, excessive fluoride ions are thought to enter the interstitial sites in the fluorite structure. This type of structural model is called the interstitial model. There could be another model —a vacant cation model— in which 1/3 of the lattice points of substituted calcium are left vacant. The phase relationship of the YF_3-CaF_2 system was studied by Short and Roy.[8] They also compared the measured specific gravity of a CaF_2-YF_3 solid solution with theoretical values calculated on the basis of the interstitial fluoride model, and the vacant cation model, and showed a beautiful agreement between the measured, and interstitial model values.

The specific gravity of the present yttrofluorite measured by the pycnometric technique is 3.51. The calculated value, adopting the interstitial model, and the concentration, and mean atomic weight of rare earth elements is 3.62. The difference may be explained by the fine, powdery nature of the specimen.

The authors wish to express their thanks to Dr. Kinichi Sakurai and Mr. Otokichi Nagashima for their interest in this work, and their help in collecting the mineral.

8) J. Short and R. Roy, *J. Phys. Chem.*, **67**, 1860 (1963).

BULLETIN OF THE CHEMICAL SOCIETY OF JAPAN VOL. 41 606—609 (1968)

Conductance Behavior of Some Hexa-amminecobalt(III) Complexes and Their Ion Association in Aqueous Solutions

Shunzo KATAYAMA and Reita TAMAMUSHI

The Institute of Physical and Chemical Research, Yamato-machi, Saitama

(Received September 7, 1967)

The conductance behavior of some hexa-amminecobalt(III) complexes in dilute aqueous solutions at 25°C was studied in association with the ion-pair formation of hexa-amminecobalt(III) ions. The equivalent conductivities were analyzed according to the Onsager theory, and the thermodynamic formation constants, K, of the ion-pairs, $[Co(NH_3)_6]^{3+}\cdot A^{z}{}_{A}{}^{-}$, were determined. The log K values obtained are 1.4_0 (perchlorate), 1.6_3 (nitrate), 1.6_5 (bromide), 1.3_8 (iodide), and 3.2_5 (oxalate). These values were compared with the formation constants calculated from the spectroscopic data, and discussed in terms of Bjerrum's theory on ion association.

The measurement of electric conductivity of dilute solutions provides a valuable method of studying the outer-sphere ion association of inert complexes. The conductance behavior and the ion association of hexa-amminecobalt(III) chloride,[1,2] sulfate,[2] trimetaphosphate,[3] and tetrametaphosphate[3] in aqueous solutions were studied by Hartley and Donaldson and by Jenkins and Monk. In our previous papers,[4,5] the equivalent conductivities of nitroamminecobalt(III) complexes in dilute aqueous solutions were discussed in terms of the Onsager theory, and the ion-pair formation constants of $[Co(NH_3)_6]^{3+}\cdot Cl^-$ and $[Co(NO_2)(NH_3)_5]^{2+}\cdot Cl^-$ were determined. The present study deals with the conductance behavior and the ion-pair formation of hexa-amminecobalt(III) perchlorate, nitrate, bromide, iodide, and oxalate in dilute aqueous solutions at 25°C.

Experimental

The samples of hexa-amminecobalt(III) chloride, bromide, and iodide were prepared according to the procedure described in the literature.[6] Hexa-amminecobalt(III) perchlorate, nitrate, and oxalate were obtained by adding perchloric acid, nitric acid, and ammonium oxalate, respectively, to the aqueous solutions of hexa-amminecobalt(III) chloride. These samples were carefully purified by three recrystallizations from their aqueous solutions containing a few drops of acetic acid. The purity of the samples was examined by the conventional chemical analysis of the components; the results were in very good agreement with the theoretical values.

The solutions of different concentrations were carefully prepared by using the conductivity water of low specific conductance ($<2\times10^{-7}\Omega^{-1}\,cm^{-1}$) in an atmosphere of purified nitrogen gas. The electric conductivities were measured by the same apparatus as described in the previous papers.[4,5] The resistance readings of the conductivity cell were calibrated by the substitution method using a precision decade resistance box (Dekastat RS-624, Electro Scientific Industries; accuracy, ±0.005%), and their reproducibility was better than 0.1%. All measurements were carried out in a water-thermostat of 25.000±0.005°C.

Results

The hexa-amminecobalt(III) complexes are subjected to the slow decomposition in aqueous solutions; therefore, the conductivities were measured at different times after the preparation of the solution, and the equivalent conductivities at time zero, which were determined by the extrapolation of the measured conductivities against time, were used in the following discussion.[4,5]

The limiting equivalent conductivities, Λ°, of the complexes were determined by Onsager's method of extrapolation[7]: the Λ° of each complex gave consistent values of the limiting ionic equivalent conductivity, λ°, of hexa-amminecobalt(III) ion. The results are summarized in Table 1.

The relation between the equivalent conductivity, Λ, and the concentration, c (equiv./l) was analysed according to the limiting equation of Onsager,[7]

$$\Lambda = \Lambda^\circ - bc^{1/2} \qquad (1)$$

where b is a theoretical constant. Figures 1 and 2 show the plot of Λ against $c^{1/2}$; the broken lines

1) G. S. Hartley and G. W. Donaldson, *Trans. Faraday Soc.*, **33**, 457 (1937).
2) I. L. Jenkins and C. B. Monk, *J. Chem. Soc.*, **1951**, 68.
3) C. B. Monk, *ibid.*, **1952**, 1317.
4) S. Katayama, *Rept. I. P. C. R.*, **42**, 243 (1966).
5) R. Tamamushi, T. Isono and S. Katayama, This Bulletin, **40**, 334 (1967).
6) W. C. Fernelius (ed.), "Inorganic Syntheses," II, McGraw-Hill, New York (1946), p. 216.
7) L. Onsager, *Physik. Z.*, **28**, 277 (1927).

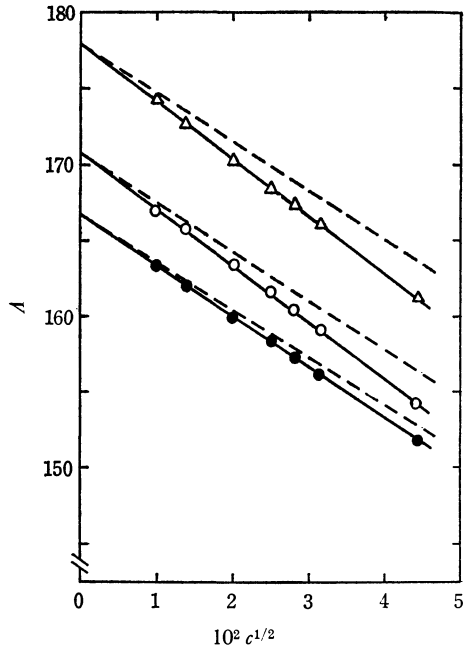

Fig. 1. The Onsager plots of hexa-amminecobalt-(III) perchlorate (-●-), nitrate (-○-), and bromide (-△-) in aqueous solutions at 25°C.

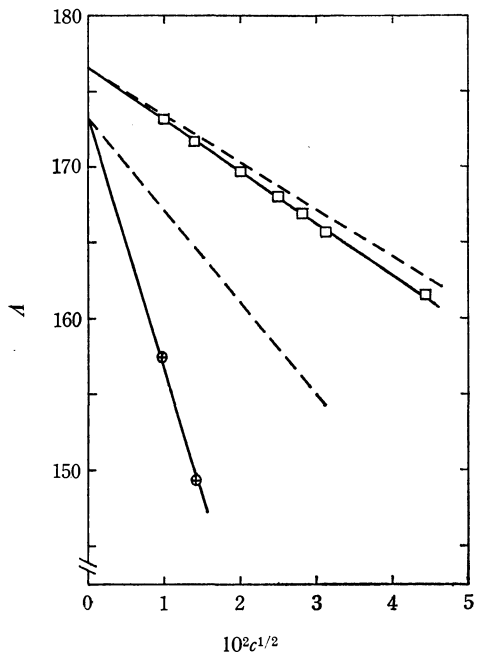

Fig. 2. The Onsagar plots of hexa-amminecobalt-(III) iodide (-□-) and oxalate (-⊕-) in aqueous solutions at 25°C.

represent the theoretical Onsager lines calculated by Eq. (1). The equivalent conductivity of hexa-amminecobalt(III) oxalate gave a large deviation from the theoretical Onsager value even at very low concentrations. A small but significant deviation was also observed with the complexes of $[Co(NH_3)_6]A_3$ type.

Discussion

The deviation of the Λ *vs.* $c^{1/2}$ plot from the theoretical Onsager line in dilute solutions is considered to be due to the outer-sphere association of the complex cation, $[Co(NH_3)_6]^{3+}$, with the anion represented by A^{z_A-},

$$[Co(NH_3)_6]^{3+} + A^{z_A-} \rightleftarrows [Co(NH_3)_6]^{3+}\cdot A^{z_A-} \quad (2)$$

The degree of dissociation of the possible ion-pairs was determined from the conductivity data according to the successive approximation method of Jenkins and Monk,[2] and the concentration formation constants, K_c, of the ion-pairs were calculated at each concentration. In the present calculation, the λ° values of the ion-pairs were estimated from $\lambda^\circ([Co(NH_3)_6]^{3+})$ according to the following equation,

$$\frac{\lambda^\circ(\text{ion-pair})}{\lambda^\circ([Co(NH_3)_6]^{3+})} = \frac{|z|}{3} \quad (3)$$

where z is a net charge of the ion-pair; the equation is obtained from the Stokes' law by neglecting the ion-size effect on the mobility. This estimation of λ°(ion-pair) is rather arbitrary, but it is shown by calculation that a considerable change in λ°(ion-pair) does not affect the derived value of K_c appreciably.[8]

By using the modified Debye-Hückel equation suggested by Guggenheim[9] for the activity coefficient of an ion, the relation between the thermodynamic and the concentration formation constants, K and K_c, is given by the relation,[10]

$$\log K_c + A'\frac{I^{1/2}}{1+I^{1/2}} = \log K + CI \quad (4)$$

where I is the ionic strength, A', a coefficient obtained theoretically from the Debye-Hückel constant and the ionic charges of the ions involved in the ion-pair formation, and C, an arbitrary parameter. The thermodynamic formation constant of each ion-pair was determined by extrapolating the plot of $[\log K_c + A'I^{1/2}/(1 + I^{1/2})]$ against I to infinite dilution (Fig. 3). In Table 2 the present results are compared with the $\log K$ values obtained by Tanaka and his coworkers from the spectroscopic data.[11]

8) C. B. Monk, "Electrolytic Dissociation," Academic Press, London (1961), pp. 132—133.
9) E. A. Guggenheim, *Phil. Mag.*, **19**, 588 (1935).
10) See for example: G. H. Nancollas, "Interactions in Electrolyte Solutions," Elsevier, Amsterdam (1966), pp. 80—81.
11) N. Tanaka, Y. Kobayashi and M. Kamada, Preprints for the 20th Annual Meeting of the Chemical Society of Japan (1967), p. 30; This Bulletin, **40**, 2839 (1967).

TABLE 1. THE LIMITING EQUIVALENT CONDUCTIVITY, $\Lambda°$, OF HEXA-AMMINECOBALT(III) COMPLEXES AND THE LIMITING IONIC EQUIVALENT CONDUCTIVITY, $\lambda°$, OF HEXA-AMMINECOBALT(III) IONS IN AQUEOUS SOLUTIONS AT 25°C

Complex	$\Lambda°$	$\lambda°([Co(NH_3)_6]^{3+})$
$[Co(NH_3)_6](ClO_4)_3$	166.7	99.3
$[Co(NH_3)_6](NO_3)_3$	170.7	99.3
$[Co(NH_3)_6]Cl_3$	175.8[4,5]	99.5,[4,5] 99.2,[2] 101.9[1]
$[Co(NH_3)_6]Br_3$	177.6	99.5
$[Co(NH_3)_6]I_3$	176.5	99.7
$[Co(NH_3)_6]_2(SO_4)_3 \cdot 5H_2O$	179.2[2]	99.2[2]
$[Co(NH_3)_6]_2(C_2O_4)_3 \cdot 4H_2O$	173.2	99.0

TABLE 2. THERMODYNAMIC FORMATION CONSTANTS OF THE ION-PAIR, $[Co(NH_3)_6]^{3+} \cdot A^{z_A-}$, IN AQUEOUS SOLUTIONS AT 25°C

A^{z_A-}	Thermodynamic formation constant, log K		
	Conductivity	Spectroscopy[11]	Bjerrum's theory
ClO_4^-	1.4_0	—	1.7_8
NO_3^-	1.6_3	—	1.7_9
Cl^-	1.5_5[4,5], 1.49[2]	0.96 ± 0.1	1.8_1[4,5]
Br^-	1.6_5	0.96 ± 0.1	1.8_2
I^-	1.3_8	0.47 ± 0.2	1.8_2
SO_4^{2-}	3.5_6[2]	3.26 ± 0.01	3.1_5
$C_2O_4^{2-}$	3.2_5	—	3.1_0

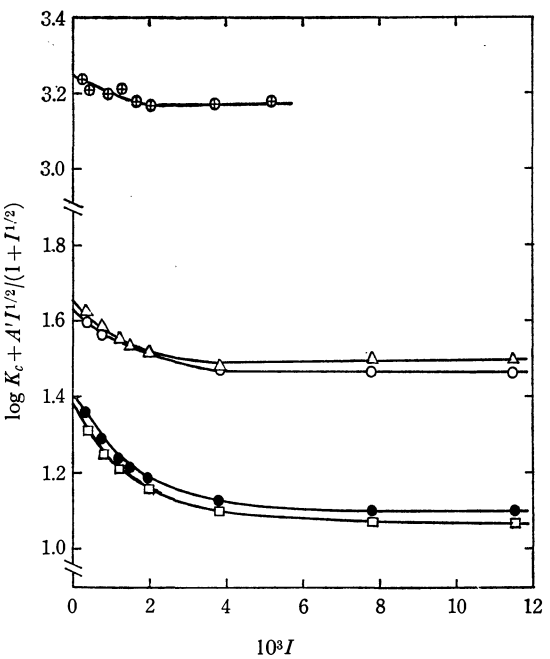

Fig. 3. The determination of thermodynamic formation constants of hexa-amminecobalt(III) perchlorate (-●-), nitrate (-○-), bromide (-△-), iodide (-□-), and oxalate (-⊕-).

If the distance of closest approach of the two ions of an ion-pair is assumed to be equal to the sum of their Stokes radii, the association constant of the ion-pair can be estimated by Bjerrum's theory.[12] The last column of Table 2 presents the log K values calculated theoretically.

In the present analysis of the conductivity data, the deviation of the measured equivalent conductivities from the theoretical Onsager values was entirely attributed to the ion-pair formation of one complex cation with an anion in the solution. Accordingly, the formation constants thus determined may be considered to involve the possible but small contribution from the ion-pairs containing more than one anions. The method of analysis is based upon the assumption that the free ions quantitatively obey the limiting equation of Onsager[7] in dilute solutions, the assumption which, unfortunately, has not been fully examined with higher charge-type electrolytes. Because of this uncertainty involved in the present treatment when applied to the determination of association constants of higher charge-type ions, the results obtained should be subjected to a critical discussion. However, a relatively good agreement of the log K values obtained by the conductivity method with those estimated from Bjerrum's theory (Table 2) suggests that the conductivity method gives reliable information on the ion-pair formation of hexa-amminecobalt(III) ions due to the electrostatic interaction.

A significant difference in the log K values

12) See for example: Ref. 8, pp. 272—275.

determined by the conductivity and spectroscopic methods (Table 2) is supposed to be due to the following reason. The conductometric determination of formation constants is based upon the change in the transport properties of ionic species under electric fields, the properties are not very specific to a particular type of ion interaction. On the other hand, the spectroscopic determination is based upon the change in the charge-transfer spectra; the spectroscopic properties are more specific to the short-range interaction than the transport properties. According to Tanaka and his coworkers, the spectroscopic behavior in the ultraviolet region is expected to give the information on the ion association due to the short-range interactions, and the formation constants determined by this method may be smaller than those obtained from the conductivity data.[11]

The perchlorate ion is usually assumed not to form appreciable ion-pairs with most cations in aqueous solutions. In the present study, however, the ion-pair formation of a perchlorate ion with a hexa-amminecobalt(III) ion was observed, the formation constant of which is of the same order of magnitude as that of iodide ion. This effect of the perchlorate ion must be remembered in the study of ion association in solutions containing relatively large amounts of perchlorate ions.

BULLETIN OF THE CHEMICAL SOCIETY OF JAPAN VOL. 41 609—613 (1968)

The Coprecipitation and Spectrophotometric Determination of Iron as 8-Hydroxyquinolinate

Tsunenobu SHIGEMATSU, Masakazu MATSUI, Megumu MUNAKATA and Takayuki SUMIDA

Institute for Chemical Research, Kyoto University, Sakyo-ku, Kyoto

(Received September 16, 1967)

The coprecipitation and spectrophotometric method, which is likened to the solvent extraction and spectrophotometric method, was applied to the following system for the first time; ferric ion was coprecipitated as 8-hydroxyquinolinate with an organic coprecipitant, and was determined spectrophotometrically after the precipitate was dissolved with an organic solvent. The effect of the ligand concentration on the pH *vs.* absorbance curve in the present method was apparently similar to that for solvent extraction. A nearly constant absorbance was obtained above pH 4 at a ligand concentration of 4×10^{-3} M. Over 100 mg of *o*-phenylphenol, an almost quantitative coprceipitation was obtained, though the absorbance decreased gradually as the coprecipitant was increased. The effect of diverse ions was also examined. Titanium(IV), vanadium(V) and molybdenum(VI) interfered considerably, while others have little effect on the absorbance. The method was applied to the determination of trace amounts of iron in natural waters and reagent grade sodium chloride.

The coprecipitation method for trace metal ions with organic coprecipitants has been developed for the chemical separation of radioisotopes, and the chemical enrichment of trace elements in natural water and biological materials.[1-3] Compared with inorganic coprecipitants, such as ferric hydroxide, organic coprecipitants have several advantages such as they are easily eliminated from the precipitate by ashing. This fact is of use especially in the treatment of radioactive solutions, and they are very selective, free from trace elements, and easy to filter.

Kuznetsov[2] has studied several types of organic coprecipitation processes for over 35 elements, and compared them to extraction by solid extractants. Tappmeyer and Pickett[4] have investigated the coprecipitation mechanism of metal 8-hydroxyquinolinates with organic coprecipitants and indicated that the factors influencing the

1) H. V. Weiss and M. G. Lai, *Anal. Chem.*, **32**, 475 (1960); H. V. Weiss, M. G. Lai and A. Gillespie, *Anal. Chim. Acta*, **25**, 550 (1961); H. V. Weiss and M. G. Lai, *ibid.*, **28**, 242 (1963).

2) V. I. Kuznetsov, in "Radioisotopes in Scientific Research," Vol. II (ed. R. C. Extermann), Pergamon Press, London (1958), pp. 264—283.

3) S. Hirano, A. Mizuike and Y. Ujihira, *Bunseki Kagaku (Japan Analyst)*, **12**, 160 (1963); Y. Ujihira, *Nippon Kagaku Zasshi (J. Chem. Soc. Japan, Pure Chem. Sect.)*, **84**, 642 (1963); *Bunseki Kagaku (Japan Analyst)*, **14**, 399 (1965); Y. Ujihira and E. Niki, *Nippon Kagaku Zasshi (J. Chem. Soc. Japan, Pure Chem. Sect.)*, **87**, 620 (1966).

4) W. P. Tappmeyer and E. E. Picket, *Anal. Chem.*, **34**, 1709 (1962).

coprecipitation of these metal chelates with organic coprecipitants like β-naphthol and phenolphthalein were the same as those that influenced solvent extraction. They also noted a similarity between the plots calculated by employing the equilibrium considerations of solvent extraction, and the plots experimentally determined showed good agreement. In our previous paper,[5] the influence of organic coprecipitants on the coprecipitation efficiency of six metals was examined, and it was found that organic coprecipitants with hydroxyl groups such as *o*-phenylphenol or α-naphthol were excellent for coprecipitation. Also it was suggested that a metal ion could be determined spectrophotometrically if the precipitate containing the coprecipitated metal chelate was filtered and dissolved in a suitable organic solvent. This new method is likened to the "solvent extraction and spectrophotometric method." It is expected that the method has the advantages of easiness in chemical treatment, and of good selectivity on chemical separation, which are observed in the extraction method, and a high concentrating efficiency, which is observed in the coprecipitation method.

In the present work, the main object is to examine whether ferric ion is coprecipitated as 8-hydroxyquinolinate with such an organic coprecipitant as *o*-phenylphenol, and is determined spectrophotometrically after the precipitate is dissolved with a suitable organic solvent.

Experimental

Reagents. A standard stock solution of iron was prepared by dissolving the pure metal in 6 N perchloric acid, by adding a few drops of 30% hydrogen peroxide solution, by fuming with concentrated perchloric acid repeatedly and by diluting with deionized water. Reagent grade *o*-phenyplhenol was purified by reduced pressure distillation. 8-Hydroxyquinoline was dissolved in dilute hydrochloric acid.

The other chemicals were chemically pure or reagent grade materials.

Apparatus. A SV 50 Shimadzu automatic recording spectrophotometer was used for the measurement of absorption spectra. For quantitative measurement, a Model 139, Hitachi manual spectrometer was used with absorption cells having a path length of 1.00 cm. pH measurements were performed with a Hitachi-Horiba Model M-3 pH meter.

Procedure. An aliquot of a ferric perchlorate solution containing 11.2 μg of iron per m*l* was taken. Then 2 m*l* of 0.1 M 8-hydroxyquinoline and 5 m*l* of buffered solution (1.0 M NaAc-HAc) were added to the solution. The pH of the solution was then adjusted to the desired pH by the addition of 1 M hydrochloric acid, or 1 M sodium hydroxide. The aqueous phase was finally diluted to 50 m*l* with water. The solution after the pH adjustment was transferred to a 100 m*l* Erlenmeyer flask. Then 0.25 g of *o*-phenylphenol which was ground with the same quantity of sodium chloride in an agate mortar was added to it. After the flask was properly stoppered, it was shaken for 30 min and the solution allowed to settle. The solid phase was carefully filtered with a glass filter and dissolved with a suitable organic solvent, followed by dilution to 10 m*l*. After the solution was filtered through filter paper, the absorbance was measured against a blank solution.

Results and Discussion

Choice of Organic Coprecipitant and Organic Solvent. *o*-Phenylphenol was selected as an organic coprecipitant because it is more stable toward color change over long periods and in alkaline solution than α-naphthol; that is, color change hinders the measurement of absorbance. There are a few methods of treatment for *o*-phenylphenol to increase its efficiency of coprecipitation. The first is the method of crushing the coprecipitant in an agate mortar. The second is that of crushing it together with the same quantity of sodium chloride in the mortar. The third is that of dissolving it in an alkaline solution, followed by fine recrystallization in an acidic solution. In this study, the second method was chosen because of high efficiency, good reproducibility, and an easy method of coprecipitation.

Several kinds of organic solvents were tested in order to examine the easiness of dissolving the precipitate into them, and the final absorbance. The absorbance was measured at 0.620, 0.612, 0.597, 0.510 and 0.470 for benzene, methylisobutylketone, cyclohexane, amylalcohol and benzylalcohol, respectively. Benzene and methylisobutylketone are better than the others in both absorbance and solubility. Methylisobutylketone was used for the present purpose as it is more nonvolatile than benzene. As the chelate reagent does not coprecipitate in the present system, methylisobutylketone containing 2×10^{-3} M of 8-hydroxyquinoline was used to make the 8-hydroxyquinolinate stable.

Absorption Spectra. The absorption spectra for the methylisobutylketone solutions of ferric 8-hydroxyquinolinate containing 0.2, and 5 g of *o*-phenylphenol are compared in Fig. 1. The spectra have their maximum absorptions at 465, and 580 mμ, and as described later, they are slightly affected by the amount of coprecipitant. As the reagent and coprecipitant blank at 465 mμ shows scarcely any absorbance, the absorbance was measured throughout the experiment at that wavelength.

The Effect of pH and the Concentration of Reagent. To establish the optimum pH value of the aqueous phase for the coprecipitation of iron, the dependence of the absorbance of the organic phase on the pH values was studied. In Fig. 2, the absorbance of the organic phase measured at

5) M. Matsui, M. Munakata and T. Shigematsu, *Bull. Inst. Chem. Res., Kyoto Univ.*, **45**, 273 (1967).

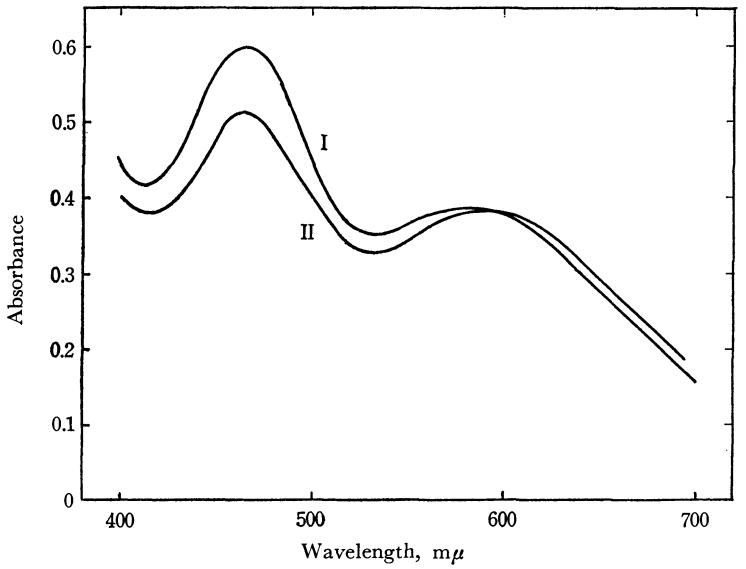

Fig. 1. Absorption spectra of ferric oxinate in methylisobutylketone. *o*-Phenylphenol: I 250 mg, II 5 g, 8-Hydroxyquinoline: 4×10^{-3} M Fe(III): 2×10^{-5} M in aqueous phase, Volume: aqueous phase 50 m*l*, organic phase 10 m*l*, pH: 4.50.

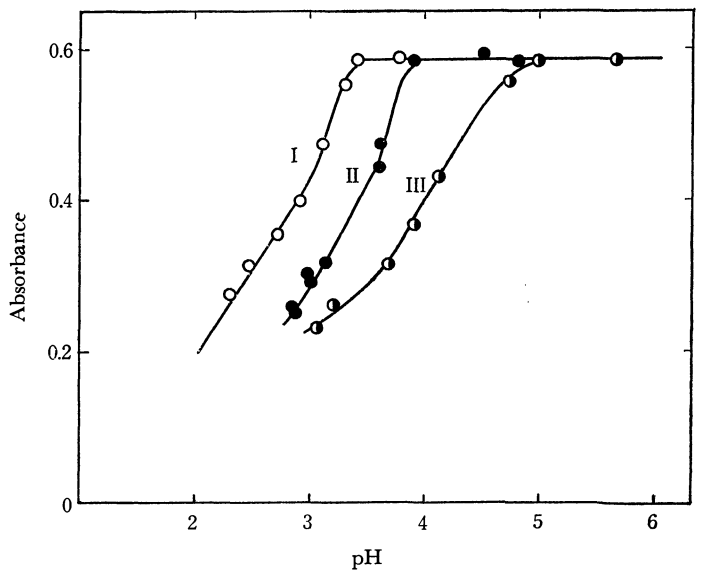

Fig. 2. Effect of pH and reagnet concentration. 8-Hydroxyquinoline: I 1×10^{-2} M, II 4×10^{-3} M, III 4×10^{-4} M. Others are same to in Fig. 1.

465 mμ was plotted against pH. The effect of the concentration of 8-hydroxyquinoline on the pH *vs.* the absorbance curve in the coprecipitation was similar to that in solvent extraction. That is, the chelate coprecipitated in the more acidic range of the solution as the concentration of the reagent became high. However, the shapes of the pH *vs.* absorbance curves of the present work were not so ideal as those of the solvent extraction. This fact shows that in the present system it is difficult to reach a state of true thermodynamic equilibrium. A nearly constant absorbance was obtained above pH 4 when the concentration of the reagent was 4×10^{-3} M. The pH value and reagent concentration were kept at 4.50, and 4×10^{-3} M, respectively, throughout the experiments.

The Effect of the Amount of Coprecipitant. The effect of the amount of *o*-phenylphenol on the

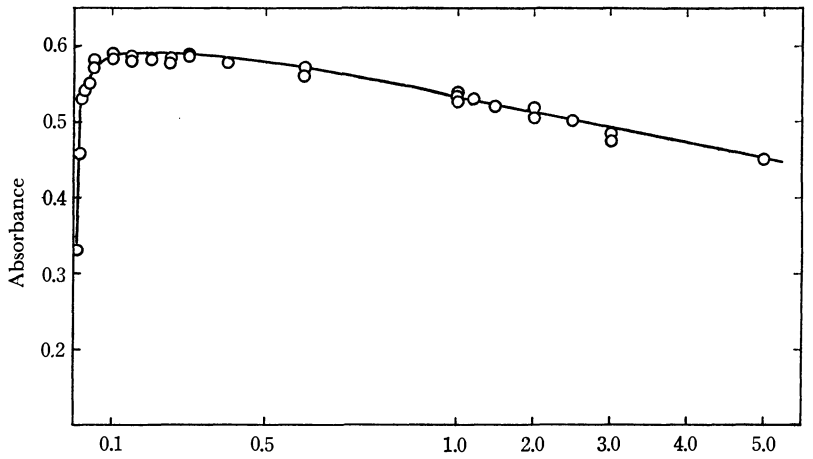

Fig. 3. Effect of *o*-phenylphenol.

absorbance of the organic phase was studied. As shown in Fig. 3, the absorbance of the organic phase increased rapidly until 100 mg of coprecipitant, had a nearly constant value from 100 to 400 mg, and decreased gradually as more coprecipitant was added. The gradual decrease in the absorbance does not mean the lowering of coprecipitation efficiency, but rather the fall in the absorption coefficient of the chelate probably is due to the solvation effect of the polar coprecipitant. This may be seen from the following: The absorbances in the coprecipitation method were identical for any certain of coprecipitant above 250 mg with those in the extraction method (where the same quantity of coprecipitant was added into the methylisobutylketone phase), by which iron was extracted quantitatively. This showed the quantitative coprecipitation of any amount of coprecipitant. Also, the solvation effect was suggested from the absorption spectra in Fig. 1, where there was almost no change in absorption intensity but some change in energy at the longer wavelength, though the absorbance at 465 mμ decreased as precipitant increased. Thus, 250 mg of *o*-phenylphenol was used throughout the experiments.

The Effect of Standing and Shaking Time. The absorbance of the methylisobutylketone solution of ferric 8-hydroxyquinolinate was measured at 465 mμ at appropriate intervals of time to examine the effect of the standing and shaking time. As shown in Fig. 4, little influence of the standing time was observed upon the absorvance of the organic phase. Similarly, the absorbance was almost constant for 5 min and over of shaking time.

Coprecipitation of the Chelate Reagent. To examine the coprecipitation of the reagent with coprecipitant, the following procedure was adopted. Two milliliters of 0.1 M 8-hydroxyquinoline and 1 m*l* of buffer solution was taken in an Erlenmeyer flask. The solution was then adjusted to pH 4.50 and diluted to 50 m*l* with water. The absorbance of the solution was measured at 410 mμ. After the solution was treated according to the process used in this study, the absorbance of the filtrate was measured at the same wavelength, and the procedure was repeated. The corresponding absorbances were 0.591, 0.602 and 0.597. This result indicates that the reagent was scarcely coprecipitated with the coprecipitant.

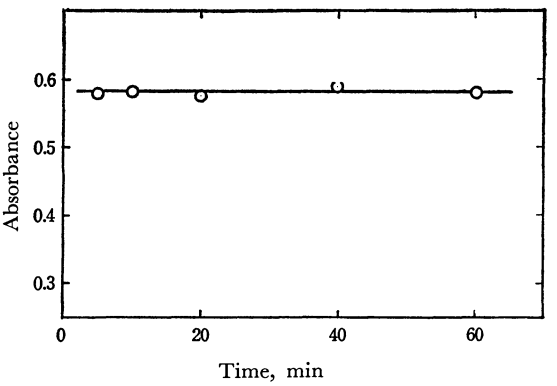

Fig. 4. Effect of shaking time.
pH: 4.5 Wavelength: 465 mμ

Calibration Curves. A calibration curve was made by coprecipitating different amounts of iron with 0.25 g of *o*-phenylphenol as a 8-hydroxyquinoline chelate. The absorbance of the solution at 465 mμ was measured against a blank. A good linear relationship was obtained by plotting the absorbance of the solution against the concentration of iron added in the aqueous solution, as shown in Fig. 5. The other curve in Fig. 5

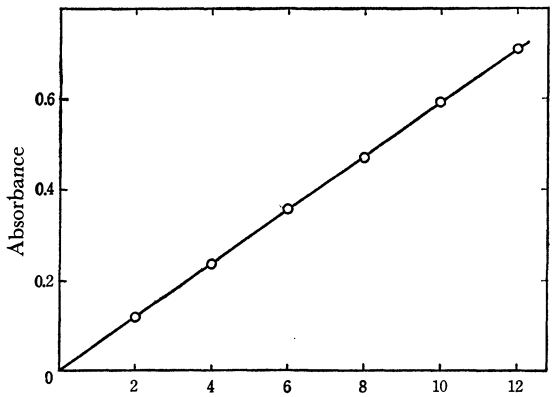

Fig. 5. Calibration curve of ferric oxinate.
pH: 4.5 Wavelength: 465 mμ

was made by extracting iron with 8-hydroxyquinoline into a 10 m*l* portion of methylisobutylketone with 0.25 g of the coprecipitant from 50 m*l* portions of the aqueous solution. As these calibration curves are in good agreement, it is considered that the coprecipitation of iron is almost quantitative.

Table 1. Effect of diverse ions

Ion	Added, mg	Fe found,* μg
Al(III)	0.1	51
Ba(II)	10	50
Ca(II)	10	50
Cd(II)	0.5	49
Ce(IV)	0.7	50
Co(II)	0.01	50
	0.1	81
Cr(III)	0.1	50
	0.5	53
Cu(II)	1.0	54
Hg(II)	0.5	50
In(III)	0.1	52
Mg(II)	10	50
Mn(II)	0.5	50
Mo(VI)	0.5	84
Ni(II)	0.1	53
Pb(II)	1.0	50
Sb(III)	0.1	51
Sn(IV)	0.5	48
Sr(II)	10	50
Ti(IV)	0.2	84
V(II)	0.5	94
Zn(II)	0.5	49

* 50 μg of ferric ion was taken.

The Effect of Diverse Ions. The effect of diverse ions was examined with a solution containing 50 μg of iron and diverse ions. The pH value of the solution was adjusted to 4.50. Of the 21 cations tested, titanium(IV), vanadium(V) and molybdenum(VI) gave a positive error, while common di- and tervalent cations had little effect on absorbance, as shown in Table 1.

Applications. The effect of the volume of the solution, and the amount of coprecipitant on the absorbance of the organic phase was examined in order to determine iron in natural water, and in reagent grade sodium chloride. As shown in Table 2, a nearly quantitative recovery was obtained when the coprecipitant increased as the volume of the sample solution increased.

Table 2. The effect of the volume of the solution and the amount of coprecipitant

Volume m*l*	Carrying reagent g	Percent copptn.
100	0.25	99
200	1.0	101
500	1.5	100
1000	3.0	102

Filtered sea and fresh water were acidified to pH 1 with concentrated hydrochloric acid (Sea water was collected in the open sea off Shirahama, Wakayama Pref., and fresh water from Lake Biwa.). Aliquots of these waters were put into Erlenmeyer flasks and 3 g of *o*-phenylphenol was added. These samples were treated according to the procedure used in this study. The results of the determination of iron in aliquots and commercial reagent sodium chloride (guaranteed reagent, and chemical pure grade) are shown in Table 3. These values were determined by the method of standard addition. The method provides several important advantages over the usual method of determination of trace elements in extremely dilute solutions described previously.

Table 3. The assay of iron in natural waters and sodium chloride

Sea water (Shirahama)	7.0×10^{-6} g/*l*
	6.8×10^{-6}
	7.7×10^{-6}
Fresh water (Biwako)	12.0×10^{-6}
	12.4×10^{-6}
Reagent grade NaCl,	
Guaranteed reagent	7.0×10^{-6} %
Chemical pure reagent	2.0×10^{-6}

BULLETIN OF THE CHEMICAL SOCIETY OF JAPAN VOL. 41 614—619 (1968)

A New Anion Exchanger Containing Cobalticinium Cation

Takuji Ito* and Tadao Kenjo**

*Department of Chemistry, Tokyo Institute of Technology, Ookayama, Meguro-ku, Tokyo
**Graduate School of Science and Engineering, Tokyo Institute of Technology, Ookayama, Meguro-ku, Tokyo

(Received September 27, 1967)

A New type of anion-exchanger, polymeric olygomethylene cobalticinium cation, was synthesized and its ion-exchange properties and stability toward heat and reagents were investigated in comparison with those of the ion-exchange resins. The preparative method of the exchanger was the same as that for polymeric olygomethylene ferrocene; hexamminecobalt(II) chloride was added to the product of α, ω-dicyclopentadienyl alkane with sodium. Although the pure products could not be obtained, the substance extracted with water showed several peaks common to a cobalticinium cation in IR spectra. The content of cobalt in tetraphenyl borate was 0.175 mmol/g, which corresponded to 91% trimethylene cobalticinium tetraphenyl borate. The saturated ion-exchange capacity of the eschanger was 1.75 meq/g, which was half the theoretical value. This discrepancy could be attributed to the shortage of cobalt according to the results of chemical analysis and magnetic susceptibility measurements. Although ion-exchange resins lose their exchange capacity by heating at 150°C in air, this exchanger was thermostable decreasing to only 70% in ion-exchange capacity. The ion-exchange capacity of the exchanger in hydrothermal water at 220°C decreased to 55—35%, while that of resins drops to as low as 20%. The selectivity coefficient for various anions became smaller in the order; $ClO_4^- > I^- > ClO_3^- > BrO_3^- > Br^- > Cl^- > IO_3^- > F^-$. This tendency was the same as that for ion-exchange resins.

The ion-exchange group as well as the structure of net-works influences the properties of ion-exchangers, such as stability toward high temperature and reagents, and selectivity for ions.

Quaternary ammonium salt type resin has been used most generally during the past decade. However, this type of resin is not stable at high temperature. This weak point can be attributed to the property of quaternary ammonium salt.

Inorganic ion-exchangers such as zirconium oxide, thorium oxide[1] and bismuth hydroxide were synthesized and their properties have been investigated from the point that these inorganic materials are stable at high temperature. In spite of many studies, some weak points, *e. g.*, lower ion-exchange capacity, lower exchange rate, lower reversibility of ion-exchange and higher solubility in acid or akaline solution, have not been improved.

Recently, dicyclopentadienyl metal compounds were found.[2,3] Some of them (compounds of Co(III), Rh(III) and Ir(III)) exist as stable cations in an alkaline medium as well as in water, and do not decompose at high temperature.[2,3] Accordingly, it is expected that a polymer containing these salts exhibits more thermostable properties than the quaternary ammonium type resin. Since the compound of Rh(III) and Ir(III) can not readily obtained, a polymer containing cobalticinium cation (π-dicyclopentadienyl cobalt-(III) cation) was synthesized. The synthesis of the polymer was made according to that of polymeric olygomethylene ferrocene.[4] The reaction steps and the probable structure of the product are as follows;

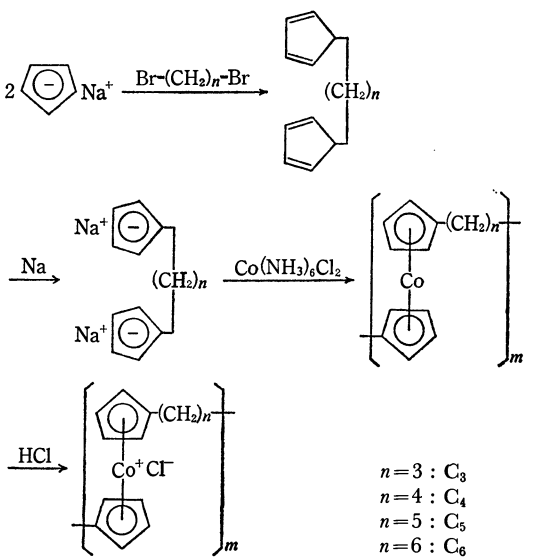

1) C. B. Amphlett, L. A. Mcdonald and M. J. Redman, *J. Inorg. & Nucl. Chem.*, **6**, 236 (1958).
2) G. Wilkinson and F. A. Cotton, "Progress in Inorganic Chemistry," Vol. 1, ed. by F. A. Cotton, International Publishers, New York, N. Y. (1959), p. 13.
3) J. A. Page and G. Wilkinson, *J. Am. Chem. Soc.*, **74**, 6149 (1952).
4) A. Littringhaus and W. Kullick, *Makromol. Chem.*, **44/46**, 669 (1961).

Experimental

Synthesis of Polymeric Olygomethylene Cobaltocene. Four kinds of α, ω-dibromoalkanes were used; 1, 3-dibromopropane, 1, 4-dibromobutane, 1, 5-dibromopentane and 1, 6-dibromohexane. After the reaction of α, ω-dicyclopentadienyl alkane with sodium metal was completed, the reaction mixture was cooled to 0°C and hexamminecobalt(II) chloride (75 g) added. The temperature was raised gradually in a water bath. Ammonia gas began to evolve at about 25°C. The temperature was maintained until the evolution ceased. Finally the reaction was completed by refluxing for 2 hr. Unreacted sodium and sodium compounds were decomposed with methanol. Solvent was removed by evaporation under reduced pressure after the mixture was centrifuged. The precipitates were extracted with 300 m*l* benzene, and the resulting solutions separated with a centrifuge. Benzene was removed by evaporation under reduced pressure.*1

An aqueous layer was separated and washed with benzene several times. Tetraphenyl borate solution was added to the aqueous solution. Resulting precipitates were dried at 110°C. The cobalt content was 0.175 mmol/g. The theoretical cobalt content calculated from the formula, $Co(C_5H_4)_2(CH_2)_3(C_6H_5)_4B$, is 0.192 mmol/g.

Samples for measurement of IR and UV spectra were prepared from the preceeding aqueous solution after converting to a triiodide, or hydroxide form.

The precipitate obtained from benzene solution was treated with 1 N hydrochloric acid, washed with water and dried at 60°C. Then it was ground and sieved to two kinds of mesh size; 50/100 mesh and 100/200 mesh. The exchangers were conditioned by alternate treatment with 2 N HCl and 2 N NaOH. After washing with distilled water, it was converted to the desired salt forms.

Preparation of Cobaltocene and Cobalticinium Salts. Cobaltocene was prepared in accordance with the method of Cordes,[5] from sodium cyclopentadienide and hexamminecobalt(II) chloride. Cobalticinium salts were obtained by treating cobaltocene with dilute hydrochloric acid and purified by recrystallization of the picrate. The desired salt forms were obtained by anion exchange resin columns.

Measurements of Ion-exchange Capacity, pH-titration Curves, Selectivity Coefficient and Ion-exchange Rate. Ion-exchange capacities at different pH, and pH-titration curves were measured in a 0.1 M (KCl+HCl) solution of constant ionic strength. The volume of the solution was 25 m*l*, and the amount of sample, 0.250 g. After equilibration, pH measurements were made with a pH-meter with a glass electrode. Adsorption capacities were measured from the decrease in the concentration of chloride ion, which was determined potentiometrically by titration with silver nitrate solution. pH-titration curves for cobalticinium hydroxide and polymeric tetramethylene cobalticinium hydroxide were measured by titrating 50 m*l* of 0.146 N solution of cobalticinium hydroxide, and 50 m*l* of 0.124 N solution of polymeric tetramethylene cobalticinium hydroxide with 0.1 N HCl, respectively.

Selectivity coefficients for ions of SCN^-, I^-, Br^- and Cl^- were measured on exchangers of the NO_3 form, and others on exchangers of the Cl form. Measurements were carried out at 25.00±0.01°C. Neutral salt solutions (0.1 M) were added to a certain amount of the exchangers. After 24 hr, halogenide ion, and thiocyanate ion concentrations were determined by the method previously mentioned. The selectivity coefficient (K_B^A) was computed according to the definition:

$$K_B^A = \left(\frac{m_B}{m_A}\right)_r \Big/ \left(\frac{m_A}{m_B}\right)_w ,$$

where m_B is meq. of B^- and m_A is that of A^-, the subscript r refers to the phase of the exchanger, and w the phase of the external solution. The amount of m_A and m_B in the exchanger can be obtained from the amount of ions adsorbed, and the saturated capacity.

The ion-exchange rate was measured at 25.00±0.01°C. After ion-exchangers of the OH form (100/200 mesh) were added to 100 m*l* of 0.1 N HCl with stirring, the decrease in concentration of Cl^- ion was determined by the method previously mentioned. The fractional attainment of equilibrium was computed as the fraction of ion adsorbed at a given time to the amount of ion adsorbed after equilibration.

Measurements of Stability toward Temperature and Reagents. Stability toward heat was measured by heating exchangers of the OH form in an oven, or in hydrothermal water in an autoclave. After treatment, the ion-exchange capacity was measured. Stability toward reagents was measured by treating exchangers of the OH form with hydrochloric, sulfuric and nitric acids of varying concentrations at room temperature for 24 hr. After the adsorbed ions were eluted with 5 N NaOH, the exchangers were washed with water, dried at 60°C, and the ion-exchange capacities measured.

Analysis of Cobalt and Measurement of IR and UV Spectra. Cobalt was determined by the gravimetric method as Co_3O_4, or by chelatometric titration with 0.01 N EDTA using XO as indicator, after cobaltocene was destroyed with fuming perchloric acid. UV spectra were recorded on an EPS-2 Hitachi recording spectrophotometer, and IR spectra on an EPI-S2 Hitachi spectrophotometer with a KBr disk.

The magnetic susceptibility of the pentamethylene cobalticinium compound was measured by the Guoy method using water ($\kappa = -0.72 \times 10^{-6}$ c.g.s. unit/g) as a standard.

Results and Discussion

The IR spectrum of polymeric tetramethylene cobalticinium triiodide exhibits 5 peaks common to those of cobalticinium triiodide, as shown in Fig. 1. The UV spectrum in Fig. 2 shows that the peaks of the polymer shift to longer wavelength relative to cobalticinium ion.

The ion-exchange of Cl^- ion from 0.1 N HCl on the exchanger of the OH form is rapidly attained, almost at the same rate as with the ion-exchange

*1 Ferrocene compounds were separated from organic impurities (hydrocarbons) by oxidation with $FeCl_3$ solution. The compounds of cobaltocene, however, were very difficult to separate in this manner owing to the formation of an emulsion of benzene and water.

5) J. F. Cordes, *Chem. Ber.*, **95**, 3084 (1962).

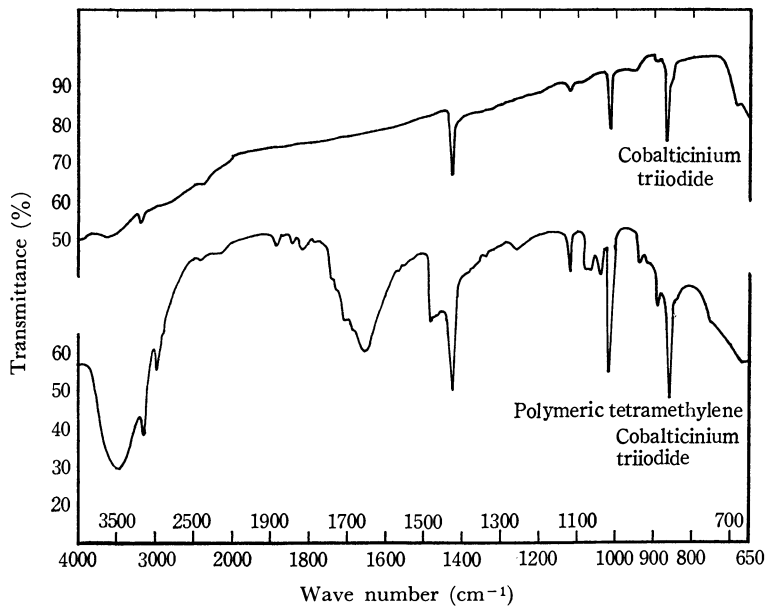

Fig. 1. IR spectra of polymeric tetramethylene cobalticinium triiodide and cobalticinium triiodide.

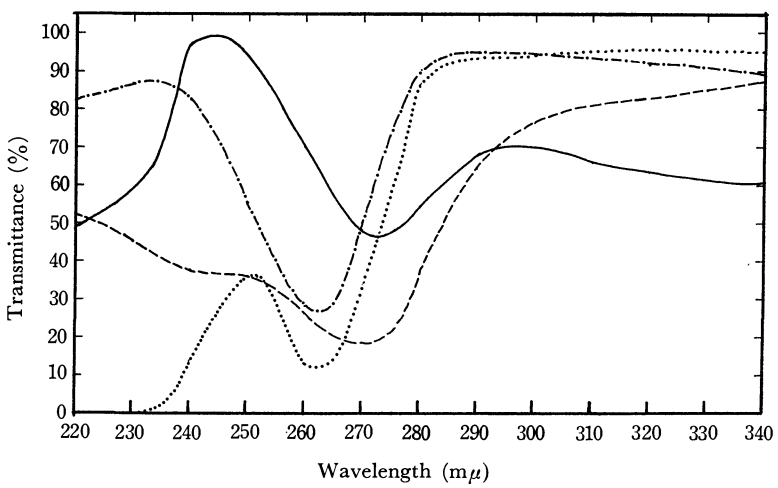

Fig. 2. UV spectra of polymeric pentamethylene cobalticinium salts and cobalticinium salts.

—— Soluble polymer —— Solid polymer dispersed
—·— Cobalticinium picrate ····· Cobalticinium iodide

resin (Fig. 3). One day therefore is enough to attain ion-exchange equilibrium.

Table 1. Saturated ion-exchange capacities of polymeric olygomethylene cobalticinium salts and cobalt content

	C_3	C_4	C_5	C_6
Ion-exchange capacity (meq/g)	1.036	1.209	1.241*2	1.020
Cobalt content (meq/g)	1.350	1.460	1.504	1.385

The saturated ion-exchange capacity of these compounds was 1.75 meq/g from Fig. 4. This is half the value calculated from the formula weight of the polymer, $(C_5H_4)_2Co(CH_2)_5OH$. The comparison of cobalt content with saturated ion-exchange capacities after alternate treatment with

*2 The saturated ion-exchange capacity was different in different batches. The values shown in Fig. 4 are for the highest one. A small decrease in the capacity was observed when the ion-exchanger was treated with hydrochloric acid as shown in following section.

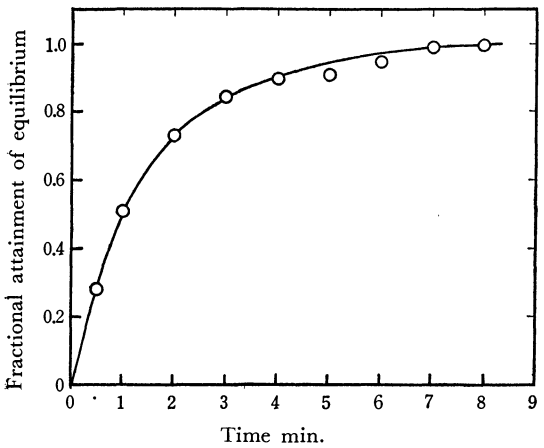

Fig. 3. Rate of attainment of ion-exchange equilibrium of the polymeric pentamethylene cobalticinium (OH form).

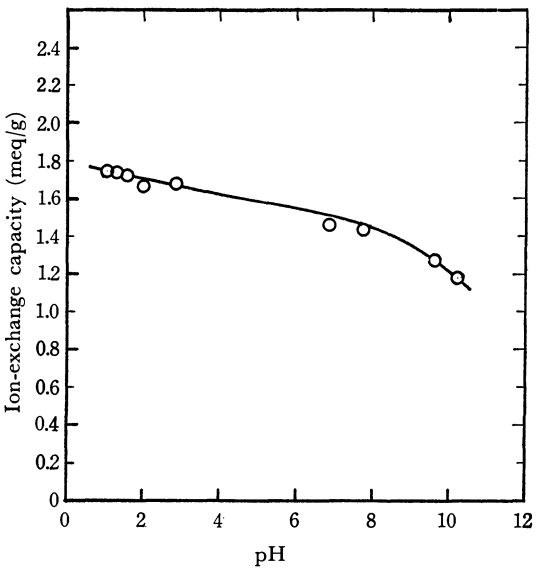

Fig. 4. pH dependence of the ion-exchange capacity of the polymeric pentamethylene cobalticinium (OH form).

hydrochloric acid and sodium hydroxide is shown in Table 1.

The magnetic susceptibility of the pentamethylene cobalticinium compound was 1.3×10^{-6} c.g.s.unit/g, whereas that of cobaltocene was 6.8×10^{-6} c.g.s. unit/g,[2] and cobalticinium ion was found to be diamagnetic.[2] Therefore, this weak paramagnetism of the compound suggests that the discrepancy between the saturated ion-exchange capacity and the cobalt content may be attributed to cobaltocene which is not oxydized to cobalticinium ion.

A discrepancy between the saturated ion-exchange capacity, and the value calculated from the formula weight indicates the presence of organic impurities. Although it is unknown what the impurities are, the main impurity could be supposed to be α,ω-dicyclopentadienyl alkane which did not react with sodium. Although these impurities decreased

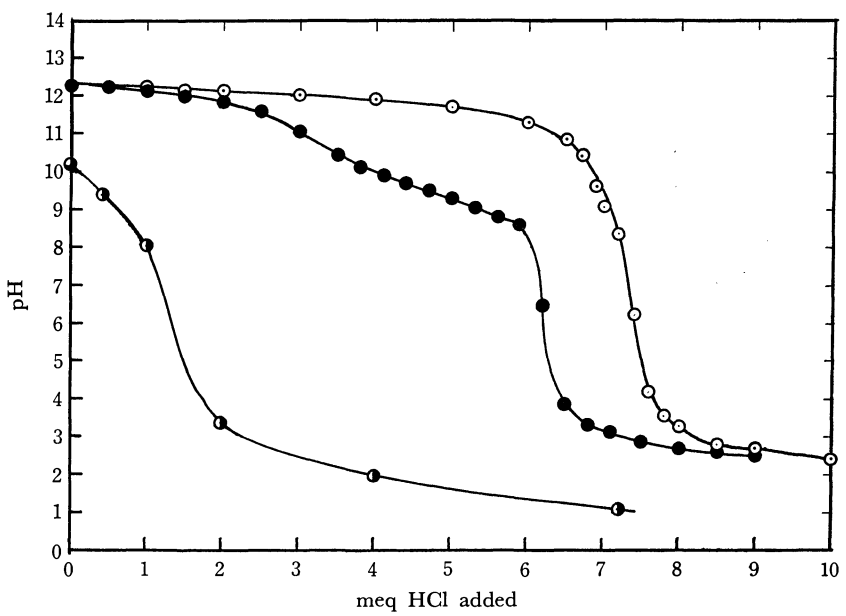

Fig. 5. Titration curves of polymeric olygomethylene cobalticinium hydroxide and cobalticinium hydroxide.

○ Cobalticinium hydroxide
● Soluble tetramethylene cobalticinium hydroxide
◑ Solid pentamethylene cobalticinium hydroxide

the saturated ion-exchange capacity, they also decreased the solubility of the exchanger.

Ion-exchange capacity does not change greatly with pH, as may be seen in Fig. 4. This fact suggests that the exchanger is of a strong base type. Although cobalticinium hydroxide is a very strong base, it seems to become weaker with polymerization, as can be seen from the comparison of the pH-titration curve of cobalticinium hydroxide with that of polymeric tetramethylene hydroxide (Fig. 5).

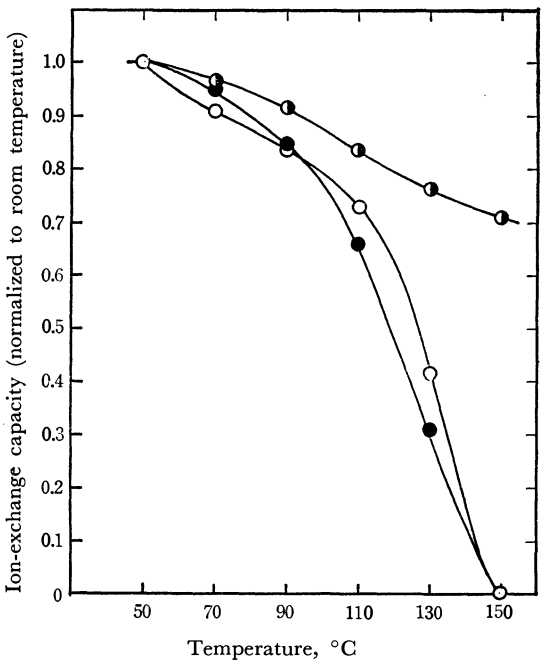

Fig. 6. Decreases of the ion-exchange capacities with temperature in air.

- ◐ Polymeric pentamethylene cobalticinium (OH form)
- ● Dowex 1 X-2 (OH form)
- ○ Amberlite IRA-410 (OH form)

Decreases in ion-exchange capacities with temperature in air are given in Fig. 6. Resins were decomposed completely at 150°C, while this exchanger decreased to 70% in ion-exchange capacity. Decreases in ion-exchange capacity in water are shown in Fig. 7. The exchanger did not decrease so greatly as ion-exchange resin in capacity. The resins were more stable toward heat in water than in air. This fact may be explained as being due to the sensitivity of the quaternary ammonium ion to air. From the fact that cobalt hydroxide was detected in water after heating in the autoclave, it is apparent that the cobalticinium ion decomposes to the hydroxide and hydrocarbons. As for the stability of other forms of exchangers to heat, salt forms were more stable than the OH form. After heating at 205°C for

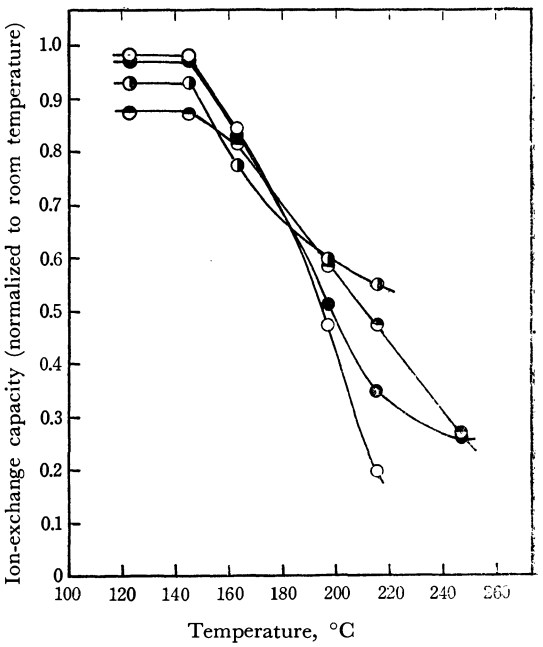

Fig 7. Decrease of the ion-exchange capacities with temperature in hydrothermal water.

- ○ Dowex 1 X-2 (OH form)
- ◓ Polymeric tetramethylene cobalticinium (OH form)
- ● Polymeric pentamethylene cobalticinium (OH form)
- ◑ Polymeric hexamethylene cobalticinium (OH form)

Table 2. Decrease of ion exchange capacity of the polymeric olygomethylene cobalticinium salts by alternate treatments of mineral acids and sodium hydroxide solution

Concentration of acid (N)	C_3	C_4	C_5	C_6
		HCl		
0	1.181	1.405	1.511	1.200
0.1	1.084	1.284	1.383	1.122
1	1.006	1.291	1.416	1.072
5	1.101	1.300	1.339	1.138
ca. 12	1.122	1.251	1.244	1.080
		H_2SO_4		
1	1.079	1.342	1.431	0.993
9	1.071	1.324	1.463	0.971
18	1.067	1.331	1.418	0.967
		HNO_3		
1	0.931	1.265	1.337	0.895
6	0.704	0.979	1.232	0.882
13	0.438	0.687	0.753	0.433

1 hr in hydrothermal water, the capacity of the OH form decreased to 0.327 meq/g, while that of the Cl form, and the NO_3 form decreased to

Table 3. The effect of repetition of alternate treatment of 0.1 N HCl and 5 N NaOH on the ion-exchange capacities of polymeric olygomethylene cobalticinium salts

Number of acid-base treatment	C_3	C_4	C_5	C_6
0	1.251	1.416	1.511	1.372
1	1.084	1.322	1.403	1.122
2	1.020	1.270	1.366	0.943
3	1.039	1.270	1.348	0.912
4	1.062	1.228	1.247	0.903
5	1.046	1.262	1.307	0.896
6	1.029	1.209	1.272	0.909

0.764 meq/g, and 0.784 meq/g, respectively, under the same conditions.

The decrease in ion-exchange capacity with treatment by reagents is shown in Table 2. Hydrochloric, and sulfuric acids do not affect the exchangers as seriously as nitric acid. Possibly, nitric acid liberates cobalticinium cation from the polymer by destroying the olygomethylene links.

After a rather large decrease in the ion-exchange capacity due to the first treatment with acid, the anion-exchange capacity remained almost constant after several alternate treatments with acid and sodium hydroxide, as shown in Table 3. This means that almost all ions adsorbed were eluted with sodium hydroxide.

As for the influence of the number of carbon chains connecting cobalticinium cations, compounds with carbon chains of 4 or 5 are the most stable toward reagents (Table 2). As the number increases, however, grinding the sample becomes difficult owing to the increase of elasticity. From the point of practical application, compounds with carbon chains of 4 or 5 are the most suitable.

The selectivity coefficient of this exchanger is summarized in Table 4. The order of the coefficient is the same as that for resins. The properties of the cobalticinium salts are therefore nearly the same as those of the quaternary ammonium ion.

Table 4. Selectivity coefficients for various anions

	Dowex 1 X-1		Dowex 1 X-8		Amberlite IR-4B		Amberlite IR-45		C_5	
	K_{NO_3}	X_{NO_3}	K_{NO_3}	X_{NO_3}	K_{NO_3}	X_{NO_3}	K_{NO_3}	X_{NO_3}	K_{NO_3}	X_{NO_3}
SCN^-	3.95	0.120	4.69	0.079	2.16	0.196	1.53	0.155	3.08	0.200
I^-	3.59	0.122	3.43	0.100	1.23	0.270	1.01	0.205	2.14	0.283
NO_3^-	1	—	1	—	1	—	1	—	1	—
Br^-	0.764	0.315	0.763	0.275	0.625	0.372	0.470	0.317	0.303	0.708
Cl^-	0.366	0.430	0.243	0.453	0.455	0.418	0.219	0.439	0.048	0.935
	K_{Cl}	X_{Cl}	K_{Cl}	X_{Cl}	K_{Cl}	X_{Cl}	K_{Cl}	X_{Cl}	K_{Cl}	X_{Cl}
ClO_4^-	88.1	0.029	56.3	0.014	8.70	0.038	5.46	0.056	36.1	0.0475
I^-	7.79	0.135	5.04	0.070	2.99	0.108	2.38	0.126	25.3	0.035
ClO_3^-	2.45	0.164	3.35	0.097	2.05	0.143	2.43	0.122	4.46	0.164
Cl^-	1	—	1	—	1	—	1	—	1	—
BrO_3^-	0.939	0.208	0.918	0.241	1.67	0.439	1.21	0.198	1.25	0.220
IO_3^-	0.425	0.411	0.198	0.480	1.63	0.168	0.528	0.317	0.202	0.242
F^-	0.287	0.404	0.0856	0.706	0.409	0.365	0.288	0.412	0.129	0.313

X_{Cl} and X_{NO_3}=equivalent fraction in the exchanger phase.

BULLETIN OF THE CHEMICAL SOCIETY OF JAPAN VOL. 41 620—623 (1968)

Solvent Extraction of Cadmium(II) from Aqueous Chloride and Bromide Solutions by Tri-*n*-octylamine

Hiroto WATANABE and Kunihiko AKATSUKA

Department of Industrial Chemistry, The Muroran Institute of Technology, Muroran

(Received October 11, 1967)

The distribution of cadmium(II) between dilute hydrochloric or hydrobromic acid solution and tri-*n*-octylamine dissolved in a number of diluents has been measured for several cadmium(II) loadings and amine concentrations. Diluents investigated are *n*-hexane, cyclohexane, benzene, xylene, toluene, carbon tetrachloride, chloroform, chlorobenzene and *o*-dichlorobenzene. The results show that all the species extracted into various diluents are present in the form of bis(tri-*n*-octylammonium)tetrahalocadmium(II). The specific ability of each diluent in extracting cadmium(II) from acidic halide solutions is approximately correlated with the dielectric constant of the pure diluent, suggesting that the dissociation of ion paired alkylammonium salt in the organic phase is responsible for the extraction.

It has been shown in our previous papers[1,2] that the formation of binegatively charged thiocyanate complexes is responsible for the extraction of iron(III) and cobalt(II) from acidic thiocyanate media with tri-*n*-octylamine in various organic diluents. The influence of diluents on the extraction of these metal ions was approximately correlated with the dielectric constant of the diluents. A similar study was carried out in the present investigation for the extraction of cadmium(II) from hydrochloric or hydrobromic acid solutions with tri-*n*-octylamine.

It is well known that cadmium(II) easily forms halo-complexes which are extractable into an organic phase with amines dissolved in various diluents,[3-6] and is generally accepted that the cadmium(II) species thus extracted is the tetrahalo-complexes of cadmium(II).[7,8] The present investigation was undertaken to obtain further information about the diluent influence on the extraction behavior of cadmium(II).

Experimentals

Apparatus. An Iwaki-V-S Shaking Unit was employed to carry out the equilibration. A Hitachi Model-139 Spectrophotometer was used to determine the concentration of cadmium(II) spectrophotometrically

Reagents. All reagents used were of analytical grade, and were further purified, if necessary. Tri-*n*-octylamine obtained from Kao Soap Co., Ltd. was converted to the chloride or bromide form by equilibrating the amine solution (0.1 N) in an appropriate dilutent twice with an equal volume of 0.5 N hydrochloric or hydrobromic acid. Then, the organic phase was separated and diluted to cover the concentration range studied. The concentration of the alkylammonium salt dissolved in various diluents was determined by potentiometric titration with a standard sodium hydroxide solution in ethanol medium.

The stock solution of cadmium(II) bromide was obtained by precipitation of the cadmium(II) hydroxide and subsequent dissolution in hydrobromic acid.

Diluents used and their dielectric constants in Debye Units were as follows[9]: *n*-hexane (1.9), cyclohexane (2.0), xylene, benzene (2.3), toluene (2.4), carbon tetrachloride (2.2), chloroform (5.0), chlorobenzene (5.8) and *o*-dichlorobenzene (9.9). The xylene used in this study was a mixture of three isomers and hence the dielectric constant was not given above.

Procedure. For all operations, 20 m*l* each of amine-halide solution and cadmium(II) halide solution were mixed together in a 100 m*l* glass separatory funnel and the mixture was equilibrated at room temperature. Fifteen minute shaking period at a rate of 120 strokes per minute was more than adequate. Then, the aqueous phase was filtered through paper to remove entrained organic phase. Aliquot portions were taken

1) H. Watanabe and M. Murozumi, This Bulletin, **40**, 1006 (1967).
2) H. Watanabe and K. Akatsuka, *Anal. Chim. Acta*, **38**, 542 (1967).
3) G. Nakagawa, *Nippon Kagaku Zasshi (J. Chem. Soc. Japan, Pure Chem. Sect.)*, **81**, 1533 (1960).
4) T. Suzuki and T. Sotobayashi, *Bunseki Kagaku (Japan Analyst)*, **12**, 910 (1963).
5) S. Hirano, A. Mizuike and Y. Iida, *ibid.*, **11**, 1127 (1962).
6) T. Suzuki and T. Sotobayashi, *ibid.*, **13**, 1103 (1964); *Nippon Kagaku Zasshi (J. Chem. Soc. Japan, Pure Chem. Sect.)*, **87**, 587 (1966).
7) A. A. Morozov and N. A. Kisel, *Chem. Abstr.*, **63**, 12392c (1963).
8) T. Sato, K. Abe and H. Baba, Preprints for the 20th Annual Meeting of the Chemical Society of Japan, Tokyo (1967), II, 105.
9) International Critical Tables of Numerical Data, Physics, Chemistry and Technology, Vol. VI (1929). (McGraw Hill Book Company, Inc.).

and the cadmium(II) content in the aqueous phase was determined either spectrophotometrically with 4-(2-pyridylazo)resorcinol or complexometrically with Eriochrome Black T as an indicator. Spectrophotometric determination of cadmium(II) with 4-(2-pyridylazo)resorcinol has not yet been reported, but the following procedure used in our preliminary experiments is adequate both in the sensitivity and in the reproducibility for the purpose of the present investigation. One m*l* of aqueous 4-(2-pyridylazo)-resorcinol solution (2.5×10^{-3} M) is added to the aliquot of the aqueous phase. Adjusting the pH to 9.8 with a sodium hydroxide solution and a borate buffer solution prepared by the standard method, the orange color was developed and the solution was diluted to 25 m*l* with pure water. The absorbance was measured at 495 mμ in a 10 mm quartz cell using a reagent blank as a reference. Beer's law was followed up to 2 mg/*l* of cadmium(II) in the 20 m*l* of aqueous phase.

The amount of cadmium (II) in the organic phase was calculated by material balance.

Results

The effects of amine concetration on the distribution of cadmium(II) between both phases were examined at fixed concentrations of cadmium(II) and hydrochloric or hydrobromic acid. The distribution ratio, q, is defined as the total concentration of cadmium(II) in the organic phase divided by that in the aqueous phase,

$$q = \sum[\mathrm{Cd}]_o/\sum[\mathrm{Cd}]_w$$

where subscripts o, w stand for the organic and aqueous phase respectively. Figures 1 and 2 summarize the results on the various diluents. It is apparent that there is a close relationship between the extractability of the amine and the dielectric constant of the diluents. On the influence of diluents the order of increasing extractability agrees fairly well with those obtained by previous studies[1,2] for the extraction of iron(III) and cobalt(II) from acidic thiocyanate media.

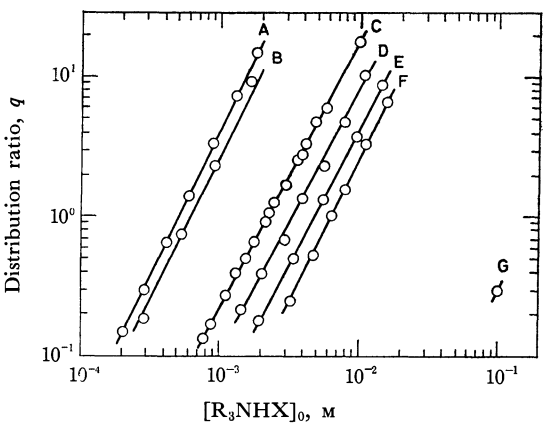

Fig. 1. Distribution of cadmium(II) as a function of amine concentrations from 0.50 N hydrochloric acid; 4.54×10^{-5} M total cadmium.
(A) *n*-hexane, (B) cyclohexane, (C) benzene, toluene, xylene, (D) chlorobenzene, (E) *o*-dichlorobenzene, (F) carbon tetrachloride, (G) chloroform

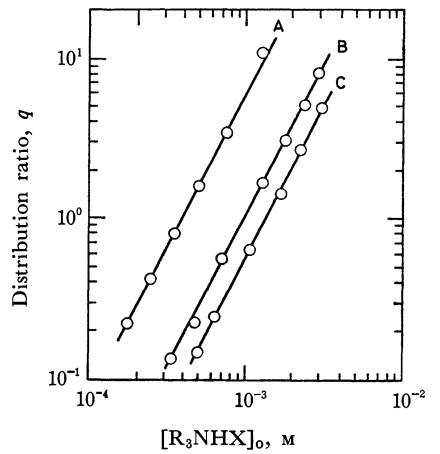

Fig. 2. Distribution of cadmium(II) as a function of amine concentrations from 0.10 N hydrobromic acid; 4.54×10^{-5} M total cadmium.
(A) benzene, (B) chlorobenzene, (C) *o*-dichlorobenzene

To determine the stoichiometry of the organic cadmium(II) species by measuring the maximum loading number which is the maximum equivalents of amine per mole of cadmium(II) in organic phase, loading curves were determined in a fixed concentration of amine (5×10^{-3} M) dissolved in cyclohexane and toluene. The results are shown in Figs. 3 and 4, which indicate a maximum $\sum[\mathrm{Cd}]_o/\sum[\mathrm{Amine}]_o$ for conditions of maximum loading being close to 0.5.

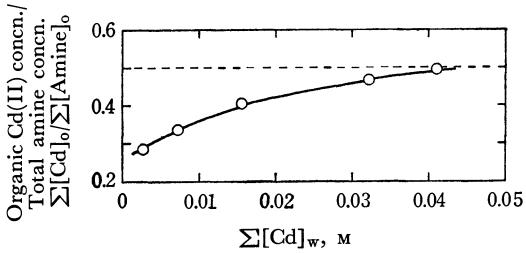

Fig. 3. Loading curve; 4.86×10^{-3} M tri-*n*-octylamine in cyclohexane, 0.5 N hydrochloric acid in aqueous phase.

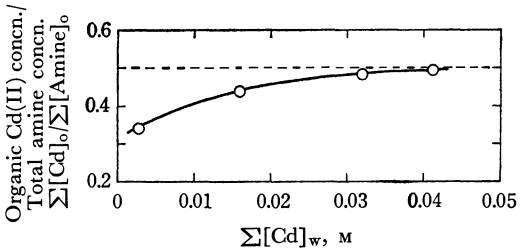

Fig. 4. Loading curve; 5.06×10^{-3} M tri-*n*-octylamine in toluene, 0.5 N hydrochloric acid in aqueous phase.

Discussions

In the present investigation, where the acids used are not over 0.5 N, the extraction of the excess acid by tri-*n*-octylamine can be assumed to be negligibly small.[10,11] Thus, the reaction between the amine in various diluents and hydrochloric or hydrobromic acids can be written as:

$$R_3N + H^+ + X^- \rightleftharpoons R_3NHX \qquad (1)^{12}$$

where R_3N refers to the tri-*n*-octylamine and R_3NHX indicates its ammonium salt form. As it has been indicated by several authors,[11,13] the equilibrium constant of reaction (1) is in the order of magnitude 10^6. Therefore, under the conditions of the present study, one equivalent of amine combines with one equivalent of hydrochloric or hydrobromic acid and the species, R_3NHX, is formed in the organic phase almost quantitatively.

The simplest generalized equation for the extraction of cadmium(II) can be written as follows:

$$mR_3NHX + CdX_2 \rightleftharpoons (R_3NH)_mCdCl_{2+m} \qquad (2)$$

Assuming that the amine salts exist as monomeric species and that the activity coefficients of each species in both phases are essentially unchanged throughout the experiments, the corresponding mass action law expression in terms of concentration is derived as

$$K_m = [(R_3NH)_mCdX_{2+m}]_o / [R_3NHX]_o^m[Cd^{2+}][X^-]^2\beta_2 \qquad (3)$$

where β_2 denotes the cumulative formation constant of the aqueous species, CdX_2. Then the distribution ratio, q, may be expressed in terms of K_m;

$$q = A\sum_{m=1}^{M} K_m[R_3NHX]_o^m \qquad (4)$$

where A denotes $\beta_2[X^-]^2/(1+\sum_{n=1}^{4}\beta_n[X^-]^n)$. If halide concentration $[X^-]$ in aqueous phase is kept constant, the product of $[R_3NHX]_o$ by the derivative of q with respect to $[R_3NHX]_o$ is given by;

$$dq[R_3NHX]_o/d[R_3NHX]_o = A\sum_{m=1}^{M} mK_m[R_3NHX]_o^m \qquad (5)$$

Using Eq. (3), we can now introduce the average number of amine molecules combined with cadmium(II) halo-complexes in the organic phase.

$$\bar{m} = \sum_{m=1}^{M} mK_m[R_3NHX]_o^m / \sum_{m=1}^{M} K_m[R_3NHX]_o^m \qquad (6)$$

From Eqs. (4) and (5), the average number of combined amines, $\bar{m}$, can be written as follows:

$$\bar{m} = d\log q / d\log [R_3NHX]_o \qquad (7)$$

Equation (7) shows that, if halide concentration $[X^-]$ is kept constant, the slope of the $\log q$ *vs.* $\log[R_3NHX]_o$ gives the average number of amine molecules combined with halide complex of cadmium(II) in the organic phase. As shown in Figs. 1 and 2, log-log plots of q *vs.* $[R_3NHX]_o$ for different diluents at a fixed concentration of the aqueous hydrochloric or hydrobromic acid yield straight lines of slope ~ 2 within the experimental error. This means that only a single species is extracted and the binegatively charged CdX_4^{2-} complexes are formed in the organic phase.

In Eqs. (4) and (7), $[X^-]$ and $[R_3NHX]_o$ denote the equilibrium concentrations. As the total concentration of cadmium(II) is in the order of magnitute of 10^{-5} M, the analytical concentrations of the amine ($>10^{-4}$ M) and the hydrohalic acids ($>10^{-1}$ M) are large enough and they can be assumed to be kept unchanged throughout the extraction.

The results in Figs. 1 and 2 are confirmed by the loading curves shown in Figs. 3 and 4. The maximum loading numbers indicate two equivalents of amine per mole of cadmium(II) in cyclohexane and toluene and presumably in other diluents. From these results it is concluded that the charge of the cadmium complex extracted is -2 and hence the species present is CdX_4^{2-}.

The influences of diluents on the extraction of cadmium(II) from the same aqueous phase by tri-*n*-octylamine are also shown in Figs. 1 and 2. These figures indicate that the extractability is correlated approximately with the dielectric constant of diluent; the smaller the value of dielectric constant, the larger the extractability. In the present results, the diluent effect is not so apparent compared with the previous ones on the extraction of iron(III) and cobalt(II) from acidic thiocyanate solutions, that is, in Fig. 1 benzene, toluene and xylene behave identically and carbon tetrachloride shows smaller extractability than that of aromatic diluents irrespective of the comparable magnitude of the dilelectric constant. However, in a series of the diluents of similar structures it can be said that the extractability is lowered with increasing dielectric constant except for nitrobenzene in the aromatic diluents which was examined in the previous study.[2] From the examination of the Eq. (1), Diamond *et al.*[13] reported that the alkylammonium salts dissociate in nitrobenzene. Assuming that the alkylammonium salt behaves as a Bjerrum type ion pair, the increase of the dissociation of $R_3NH^+X^-$ would occur with increasing the dielectric constant of the diluent. In other diluents the ion paired alkylammonium salt presumably dissociates to a smaller extent depending

10) A. S. Wilson and J. A. Wogman, *J. Phys. Chem.*, **66**, 1552 (1962).
11) U. Bertocci and G. Rolandi, *J. Inorg. Nucl. Chem.*, **23**, 323 (1961).
12) X^- denotes chloride or bromide ions.
13) J. J. Bucher and R. M. Diamond, *J. Phys. Chem.*, **69**, 1565 (1965).

on the dielectric constant of the diluent. From such considerations in the medium of smaller dielectric constants such as *n*-hexane or benzene, ion paired alkylammonium salts will not appreciably dissociate and hence the activity coefficient of amine salts should be unity under these experimental conditions. This may be an important factor illustrating the high extractability for these diluents. On the contrary, as a result of the dissociation of the ion pairs in the medium of the larger dielectric constant, the activity of amine salt is considered to be smaller than in the previous case, irrespective of the increased solvation by the dipole of the diluent molecules.

Such consideration may lead to the conclusion that the higher the dielectric constants is the lower is the extractability. However, as it has been shown in our previous paper,[2] nitrobenzene has the high extractability which is comparable to that of cyclohexane. In this case the interaction between the dipole of the dilutent molecules and the ion paired alkylammonium salt must be strong enough compared with other diluents used in the present study. Therefore, if strong dissociation may occur, the activity coefficient of amine salt would be approximately unity because of the strong affinity of nitrobenzene to the ion pairs. In a series of our researches the alkylammonium cation is tri-*n*-octylammonium ion, so the small difference in behavior between the thiocyanate, chloride and bromide systems must be due to the anion size. From such considerations it is evident that the dissociation of the ion paired alkylammonium salt and the solvating properties of the diluent molecules to the ion pairs are the important factors goverining the extraction of metal ions.

The authors wish to express their thanks to Professor Masayo Murozumi of The Muroran Institute of Technology for his encouragement and valuable discussions and to Professor Masaichi Nagayama, Dr. Katsumi Goto and Mr. Takao Yotsuyanagi of The Hokkaido University for their helpful discussions and for citicizing the manuscript. We are also indebted to Mr. Sakae Matsumura for assistance with part of the experimental work.

BULLETIN OF THE CHEMICAL SOCIETY OF JAPAN VOL. 41 623—626 (1968)

The Photochemical Reduction of Hydrazobenzene*1

Shizunobu HASHIMOTO, Junzo SUNAMOTO*2 and Syunpei NISHITANI

Department of Appied Chemistry, Doshisha University, Kamikyo-ku, Kyoto

(Received April 26, 1967)

Hydrazobenzene was irradiated with an ultraviolet light in *n*-hexane under a nitrogen atmosphere. The products were azobenzene, aniline, and a trace of semidines. The yield of azobenzene was usually larger than that calculated on the basis of the disproportionation of hydrazobenzene, while the yield of aniline was less. The reactions were followed by the determination of the disappearance of hydrazobenzene and that of the formation of azobenzene. On the basis of the available data, in the photochemical reaction of hydrazobenzene it was assumed that the formation of azobenzene was not due to the disproportionation, but to the oxidation of hydrazobenzene, and that no fission of the N–N bond of hydrazobenzene occurred to give azobenzene.

Hydrazobenzene and its derivatives partly disproportionate to give the aromatic amine and the aromatic azo compound in the acid-catalyzed benzidine rearrangement,[1] as in Eq. (1):

$$2\,\text{Ar-NHNH-Ar} \rightarrow \text{Ar-N=N-Ar} + 2\,\text{Ar-NH}_2 \quad (1)$$

The thermal reaction of hydrazobenzene has also been studied by Stiegliz and Crume,[2] who have presented evidence that the rate of this reaction was given by the first-order equation with respect to the concentration of hydrazobenzene and was according to the processes shown in Eqs. (2) and (3):

$$\text{Ar-NHNH-Ar} \rightarrow \text{Ar-N:} + \text{Ar-NH}_2 \quad (2)$$

*1 Presented at the 19th Annual Meeting of the Chemical Society of Japan, Tokyo, April, 1966.

*2 Present address; Department of Organic Synthesis, Fuculty of Engineering, Kyushu University, Hakozaki, Fukuoka.

1) *Cf.*, for example, M. J. S. Dewar, "Molecular Rearrangement," Part One, de Mayo, ed., Interscience Publishers, New York (1963), p. 323.

2) J. Stiegliz and O. Crume, *Ber.*, **46**, 911 (1923).

$$Ar\text{-}N: \rightarrow Ar\text{-}N{=}N\text{-}Ar \quad (3)$$

On the other hand, Weiss has observed qualitatively the formation of azobenzene and aniline by irradiation with an ultraviolet light (2300—2700 Å) on a methanol solution of hydrazobenzene.[3]

The present investigation was undertaken in order to examine in detail the photochemical reaction of hydrazobenzene, which was irradiated with an ultraviolet light (2537 Å) in *n*-hexane.

Result and Discussion

Azobenzene Formation and Hydrazobenzene Disappearance. Hydrazobenzene was irradiated with an ultraviolet light in *n*-hexane at different temperatures. The results obtained are shown in Fig. 1. Clearly, the yield of azobenzene is dependent upon the reaction temperature and on

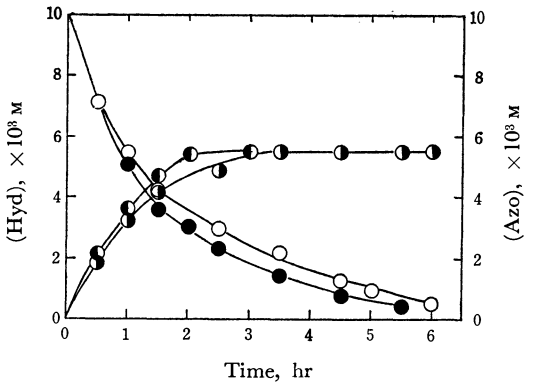

Fig. 1. The disappearance of hydrazobenzene at 35.0°C. (○) and at 45.5°C (●), and the formation of azobenzene at 35.0°C (◑) and at 45.5°C (◐) are indicated.

TABLE 1. THE PER CENT YIELDS OF AZOBENZENE IN THE PHOTOCHEMICAL REACTION OF HYDRAZOBENZENE

Temp. °C	Initial concn. of hydrazobenzene ×10³M				
	10	8	6	5	4
9.0±0.1	—	—	77	80	83
17.6±0.1	—	65	70	—	77
35.0±0.1	55	56	60	64	67

the initial concentration of hydrazobenzene, as Table 1 shows; as the reaction temperature becomes lower, the yield of azobenzene increases. In every run azobenzene was produced in an amount larger than that calculated on the basis of the disproportionation of hydrazobenzene. The aniline formation proceeded further after the azobenzene formation terminated. The formation of aniline was semiquantitatively identified by paper chromatography throughout the reaction. Therefore, it seems most reasonable to assume that there may be another process for the aniline formation, independent of the azobenzene formation. In addition, there seems certainly to be some kind of intermediate for the aniline formation. This intermediate may easily return to hydrazobenzene in the dark or during the determination of the hydrazobenzene. Unfortunately, we can not estimate the structure of this intermediate from the available experimental evidence.

The relation between the concentration of hydrazobenzene and the rates of the formation of azobenzene has been plotted, the rate of the formation of azobenzene was, thereby, given by this first-order equation (Eq. (4)):

$$\frac{d(Azo)}{dt} = k'_1(Hyd) \quad (4)$$

where (Azo) is a concentration of azobenzene, (Hyd) is that of hydrazobenzene, and k'_1 is an apparent rate constant. On the other hand, the rate of disappearance of hydrazobenzene is given by a second-order equation in the initial stage and by a first-order equation in the final stage, in which azobenzene is no longer produced, only aniline:
in the initial stage;

$$-\frac{d(Hyd)}{dt} = k'_2(Hyd)^2 \quad (5)$$

in the final stage;

$$-\frac{d(Hyd)}{dt} = k'_3(Hyd) \quad (6)$$

All the experimental data and the rate constants are given in Table 2.

N-N Fission of Hydrazobenzene. Holt and Hughes have reported[4] that no fission of the N-N bond of hydrazobenzene occurred in the pyrolysis of ^{15}N-labeled hydrazobenzene. In order to examine the N-N fission in the present reaction, *n*-hexane solutions of 4-chlorohydrazobenzene and of 4-methoxyhydrazobenzene were each irradiated under the same conditions as those used for hydrazobenzene above, and the products were identified by thin-layer chromatography (silica gel). No disubstituted or unsubstituted azobenzene was ever detected, only the corresponding monosubstituted azobenzene; that is, 4-chloroazobenzene and 4-methoxyazobenzene were obtained, respectively, together with a small amount of their cis isomers. Therefore, no N-N fission leading to the formation of an azo compound occurs in the present reaction.

Effects of Reaction Products. A definite amount of azobenzene or aniline was added from the beginning of the reaction. However, such

3) J. Weiss, *Trans. Fraday Soc.*, **36**, 856 (1940).

4) P. F. Holt and B. P. Hughes, *J. Chem. Soc.*, **1953**, 1666.

TABLE 2. THE APPARENT REACTION RATE CONSTANTS FOR THE PHOTOCHEMICAL REACTION OF HYDRAZOBENZENE IN *n*-HEXANE

Initial concn. (Hyd) $\times 10^3$ M	Temp. °C	Apparent rate constant k'_1 $\times 10^3$ min^{-1}	k'_2 l mol^{-1} min^{-1}	k'_3 $\times 10^5$ min^{-1}
10	35.0	7.14	1.43	7.37
10	45.5	7.95	2.03	8.86
10[a]	35.0	7.14	1.43	—
10[b]	35.0	7.14	1.43	7.39
10[c]	35.0	7.14	1.43	7.39
10[d]	35.0	0	0	0
8	17.6	3.50	0.75	—
8	35.0	9.21	2.18	7.20
8	45.5	10.55	3.15	9.76
6	9.0	2.57	0.95	—
6	17.6	4.37	1.53	—
6	35.0	12.90	4.11	8.10
6	45.5	15.60	5.00	9.01
5	9.0	3.15	1.37	—
5	17.6	—	—	—
5	35.0	14.60	0.83	7.85
5	45.5	—	—	—
4	9.0	4.03	2.01	—
4	17.6	6.50	2.45	—
4	35.0	20.00	9.73	7.38
4	45.5	21.00	12.70	—

a) In *n*-heptane.
b) 1×10^{-4} mol of azobenzene was added.
c) 2×10^{-4} mol of aniline was added.
d) In the dark.

additions had no effects on the reaction (see Table 2). It is, therefore, clear that the azobenzene and aniline produced in the course of the reaction never reacted photochemically under our reaction conditions and had no inner-filter effect. Moreover, although hydrogen gas produced together with azobenzene in the present reaction, it was found that hydrazobenzene gas also had no effects on the reaction, and that no further reduction of azobenzene by hydrogen gas occured. In order to examine the possible formation of new products by radical-chain transfer to a solvent, the solvents used were examined by gas chromatography before and after the reaction (Shimadzu GC-50, DOP column 2.25 m long, H_2, 110 ml/min, at 51°C). However, no new products were observed on the gas chromatogram.

Assumption of Reaction Scheme. It is very difficult to estimate the reaction course on the basis of only the results obtained above. If the simplest case is assumed, however, without any deactivation processes of the photoexited molecules, the following processes are probable:

$$\text{Hyd} \xrightarrow{h\nu} \text{Hyd}^* \quad (7)$$

$$\text{Hyd}^* \longrightarrow \text{Ar-}\dot{\text{N}}\text{-NH-Ar} + \text{H}\cdot \quad (8)$$

$$\left.\begin{matrix}\text{Ar-}\dot{\text{N}}\text{-NH-Ar}\\ \text{Ar-NH-}\dot{\text{N}}\text{-Ar}\end{matrix}\right\} \rightarrow \left\{\begin{matrix}\text{Ar-N=N-Ar}\\ \text{Ar-NHNH-Ar}\end{matrix}\right. \quad (9)$$

$$2\text{H}\cdot \rightarrow \text{H}_2 \quad (10)$$

$$\text{Hyd} \underset{\text{in the dark, } -2\text{H}}{\overset{h\nu,\ +2\text{H}}{\rightleftarrows}} \text{(Intermediate)} \xrightarrow{h\nu} \text{Aniline} \quad (11)$$

First, hydrazobenzene absorbs the ultraviolet light and is excited. The monoradical (Ar-$\dot{\text{N}}$-NH-Ar)[5] may thereby be produced *via* the excited hydrazobenzene. Subsequently, azobenzene may be formed by the disproportionation of the monoradical. In the initial stage, the azobenzene formation may occur parallel to the aniline formation. When the hydrazobenzene has disappeared, however, the azobenzene formation may spontaneously terminate and only the aniline formation from the intermediate may proceed. The rate equations of the hydrazobenzene disappearance and the azobenzene formation, derived from the proposed reactions ((7)—(11)) on the basis of the stationary-state assumption for the concentrations of the

5) J. K. S. Wan, L. D. Hess and J. N. Pitts, Jr., *J. Am. Chem. Soc.*, **80**, 2069 (1964).

monoradical and the hydrogen radical, fit Eqs. (4), (5), and (6), obtained from the kinetic measurements.

Experimental

Materials. The hydrazobenzene was prepared from nitrobenzene by the usual method and used after careful purification (mp 126°C). *trans*-Azobenzene was prepared by the air oxidation of hydrazobenzene and was recrystallized from methanol (mp 67°C). The solvent used were obtained commercially and were purified by the usual method; *n*-hexane, bp 68.5°C, $n_D^{20}=1.3750$; *n*-heptane, bp 98.5°C, $n_D^{20}=1.3877$. They were completely deaerated and were replaced by nitrogen. The reagents of an analytical grade were obtained commercially and were used without any special pretreatment.

Identification of Products. The photochemical reaction of hydrazobenzene was carried out under the same conditions as those used in the kinetic experiments; after irradiation of a sufficient duration in *n*-hexane, the resulting solution was submitted to paper chromatography according to the method given in the literature.[6] After careful examination, the following products were identified: *p*-semidine (R_f 0.22, violet), aniline (R_f 0.43, red), *o*-semidine (R_f 0.80, reddish violet), and azobenzene (R_f 0.98, yellow). The yields of azobenzene, aniline, *o*-semidine, and *p*-semidine were 56 mol%, 40 mol%, 0.25 mol%, and 0.25 mol% respectively on the basis of the hydrazobenzene.

Procedures for Rate Measurement. About 100 m*l* of a *n*-hexane or *n*-heptane solution of hydrazobenzene was placed in a 200 m*l* four-necked flask equipped with a reflux condenser, an outlet tube, a nitrogen-inlet tube, and a low-pressure mercury vapor lamp (2537 Å, 15 W). The flask was immersed for five minutes at a given temperature in a thermostat regulated and flushed by nitrogen. The reaction begun by the irradiation. At appropriate time intervals, samples were pressed out by nitrogen and were submitted to iodometry and photometry as follows.

Analytical Procedures. The unchanged hydrazobenzene was determined by iodometry modified from the method of Stieglitz and Crume.[2] Although the effects of coexistent materials, such as azobenzene, aniline, or a small amount of semidines, were investigated in detail, there is no interference by them with the determination of hydrazobenzene in this procedure. The probable error in the determination of hydrazobenzene was ±0.02%.

The azobenzene produced was determined by the usual photometry on a Erma Type-5 photometer, since azobenzene has the characteristic absorption bands in the visible region. However, a calibration curve prepared with *trans*-azobenzene could not be used for the determination of the azobenzene produced in the course of the reaction, because *trans*-azobenzene isomerizes to give the *cis*-isomer upon irradiation.[7] Therefore, the calibration curve was corrected by the use of irradiated azobenzene in a state of cis-trans equilibrium. The calibration curves were in good accordance with Beer's law.

6) S. Hashimoto, I. Shinkai and J. Sunamoto, *Kogyo Kagaku Zasshi (J. Chem. Soc. Japan, Ind. Chem. Sect.)*, **69**, 290 (1966).

7) S. Yamashita, H. Ono and O. Toyama, This Bulletin, **35**, 1849 (1962).

BULLETIN OF THE CHEMICAL SOCIETY OF JAPAN VOL. 41 626—628 (1968)

The Synthesis of Agarobiose*[1]

Susumu HIRASE, Choji ARAKI[2]* and Kiyoshi ARAI

Department of Chemistry, Faculty of Industrial Arts, Kyoto Technical University, Matsugasaki, Kyoto

(Received May 13, 1967)

Agarobiose, 3, 6-anhydro-4-*O*-β-D-galactopyranosyl-L-galactose, was synthesized by a series of reactions involving the condensation of 1, 2-*O*-isopropylidene-3, 6-anhydro-L-galactopyranose with tetra-*O*-acetyl-α-D-galactosyl bromide, deacetylation with sodium methoxide, and the hydrolytic removal of the *O*-isopropylidene group. The resulting disaccharide, and its osazone and dimethyl acetal were identical with the corresponding authentic samples obtained naturally.

Agarobiose is a disaccharide which has been obtained from agar by a partial acid hydrolysis.[1] The structure has been dientified as 3, 6-anhydro-4-*O*-β-D-galactopyranosyl-L-galactose (I) on the basis of chemical evidence.[2,3] The idsaccharide was later isolated in the forms of diethyl thioacetal

*1 This paper was reported in outline by one of the authors (C. A.) at the 5th International Seaweed Symposium, Halifax, Canada, August, 1965.

*2 Present address: Shijonawate Women's College, Daito-shi, Osaka Prefecture.

1) C. Araki, *Nippon Kwagaku Kwaisi (J. Chem. Soc. Japan)*, **65**, 533 (1944).

2) C. Araki, *ibid.*, **65**, 627 (1944).

3) S. Hirase and C. Araki, This Bulletin, **27**, 105 (1954).

and dimethyl acetal from agar[3,4] and the polysaccharide of the red seaweed *Gloiopeltis furcata*.[5] The present paper will deal with the synthesis of the disaccharide.

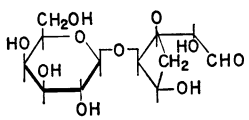

(I)

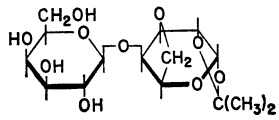

(IV)

The starting compound, 1, 2-*O*-isopropylidene-3, 6-anhydro-L-galactopyranose (II), prepared by the condensation of 3, 6-anhydro-L-galactose (III) with acetone in a manner previously reported,[6] was allowed to condense with tetra-*O*-acetyl-*α*-D-galactopyranosyl bromide in chloroform in the presence of silver oxide and anhydrous calcium sulfate. The deacetylation of the product with sodium methoxide and subsequent purification on a cellulose-powder column gave crystalline 1, 2-*O*-isopropylidene-3, 6-anhydro-4-*O*-*β*-D-galactopyranosyl-L-galactose (IV). The removal of the *O*-isopropylidene group with dilute sulfuric acid yielded 3, 6-anhydro-4-*O*-*β*-D-galactopyranosyl-L-galactose (I) in an amorphous form. This disaccharide was then converted to the crystalline phenylosazone. Furthermore, IV was treated with dilute methanolic hydrogen chloride to give the dimethyl acetal of I. These derivatives were identical with those prepared from natural agarobiose.

Experimental

General Procedure. Solutions were evaporated under reduced pressure at about 40°C. Paper chromatography was performed on Toyo Filter Paper No. 51 using a 1-butanol - acetic acid - water (4 : 1 : 2 v/v) mixture. The chromatographic spray reagent used was *o*-aminophenol in ethanol acidified with phosphoric acid.[7]

1, 2-*O*-Isopropylidene-3, 6-anhydro-L-galactopyranose (II). III (4.5 g), obtained by the hydrolysis of the dimethyl acetal,[8] was shaken in a mixture of acetone (300 m*l*) and concentrated sulfuric acid (3 m*l*) with anhydrous cupric sulfate (30 g) at room temperature for 5 hr. The mixture was then filtered, neutralized with sodium carbonate, and re-filtered. The filtrate was evaporated to a syrup, which was then dissolved in water (30 m*l*). An insoluble oil was removed by filtration with charcoal, and the filtrate was repeatedly extracted with chloroform. The evaporation of the extracts gave a mobile syrup (3.0 g) which crystallized on standing. The product was recrystallized twice from ether-hexane (1 : 1 v/v); yield 1.2 g; mp 91—92°C, $[\alpha]_D^{20}$ −26.8° (*c* 1.17, water). The values reported for the enantiomorph are mp 92°C and $[\alpha]_D^{14}$ +26.94° (water).[6]

Found: C, 53.28; H, 6.89%. Calcd for $C_9H_{14}O_5$: C, 53.46; H, 6.98%.

1, 2-*O*-Isopropylidene-3, 6-anhydro-4-*O*-*β*-D-galactopyranosyl-L-galactopyranose (IV). A mixture of II (3.0 g), silver oxide (7.5 g), Drierite[9] (15 g), and some pieces of glass beads was shaken in chloroform (60 m*l*) for 1 hr. Tetra-*O*-acetyl-*α*-D-galactopyranosyl bromide[10] (6.2 g) was then added, and the resulting mixture was shaken at room temperature for 24 hr. The mixture was filtered, and the filtrate was evaporated to dryness. The residue (7 g) was dissolved in a mixture of absolute methanol (50 m*l*) and a 0.1 N sodium methoxide solution (5 m*l*), and left at room temperature for 3 hr. The neutralization of the solution with carbon dioxide and subsequent evaporation afforded a syrup, which was then taken up in water (20 m*l*) and washed with chloroform (recovery of II: 1.2 g). The aqueous layer of the extraction was evaporated to a syrup (4.9 g), which was then repeatedly extracted with boiling acetone. The syrup (3.0 g) obtained on the evaporation of the extract showed several spots on a paper chromatogram. This syrup was chromatographed on a cellulose-powder column (4×35 cm) using a 1-butanol - water (6 : 1 v/v) mixture. Fractions of 14 m*l* were collected and monitored by paper chromatography. A compound with R_f 0.49 was obtained as a syrup (1.8 g). Crystallization was effected by dissolving it in acetone (5 m*l*), and by adding ethyl acetate (5 m*l*) and then ether (5 m*l*); yield 1.3 g, mp 173—175°C. Two recrystallizations from an acetone - ethyl acetate (1 : 2 v/v) mixture gave IV in prisms; mp 175—177°C, $[\alpha]_D^{16}$ −24.8° (*c* 1.29, water), $[\alpha]_D^{16}$ −35.0° (*c* 1.03, methanol).

Found: C, 49.62; H, 6.52%. Calcd for $C_{15}H_{24}O_{10}$: C, 49.45; H, 6.64%.

Agarobiose (I). The compound IV (0.20 g) was heated with 0.02 N sulfuric acid (10 m*l*) at 100°C. The optical rotation of the solution changed from $[\alpha]_D$ −25.5° to a constant value of $[\alpha]_D$ −18.0° within 45 min. The solution was then neutralized with barium carbonate and filtered, and the filtrate was evaporated to dryness. The residue was dissolved in methanol, filtered, and then evaporated to give a colorless, amorphous solid (I) (0.15 g), $[\alpha]_D^{15}$ −15.9° (*c* 0.82, water). It reduced a Fehling solution at room temperature and restored the color to a Schiff reagent.

Phenylosazone: mp 220—221°C, $[\alpha]_D^{16}$ −136.2° (5 min)→−109.2° (44 hr, *c* 0.42, pyridine-methanol (2 : 3 v/v)). (For the reported physical constants, see Refs. 3 and 4.) The melting point was not depressed on admixture with an authentic sample of natural origin.

Found: C, 57.88; H, 5.74; N, 11.11%. Calcd for $C_{24}H_{30}O_8N_4$: C, 57.36; H, 6.02; N, 11.15%.

Agarobiose Dimethyl Acetal. The compound IV (0.30 g) was refluxed with 0.5% methanolic hydrogen

4) C. Araki and S. Hirase, *ibid.*, **27**, 109 (1954).
5) S. Hirase, C. Araki and T. Ito, *ibid.*, **31**, 428 (1958).
6) C. Araki and K. Arai, *Nippon Kwagaku Kwaisi (J. Chem. Soc. Japan)*, **63**, 1720 (1942).
7) S. Hirase, C. Araki and S. Nakanishi, This Bulletin, **26**, 183 (1953).
8) C. Araki, *Nippon Kwagaku Kwaisi (J. Chem. Soc. Japan)*, **65**, 725 (1944).
9) Anhydrous calcium sulfate of the W. A. Hammond Drierite Co., Ohio, U. S. A.
10) W. T. Haskins, R. M. Hann and C. S. Hudson, *J. Am. Chem. Soc.*, **64**, 1852 (1942).

chloride (15 m*l*) for 30 min. The solution was neutralized with silver carbonate, filtered, and evaporated to a syrup, which was then crystallized from a methanol-acetone (1 : 2 v/v) mixture; yield 0.22 g, mp 163—165°C, $[\alpha]_D^{16}$ −29.4° (*c* 1.17, water). (For the reported physical constants, see Refs. 4 and 5.) The melting point was not depressed on admixture with an authentic sample of natural origin.

Found: C, 42.25; H, 7.11; OCH_3, 16.58%. Calcd for $C_{14}H_{26}O_{11}$: C, 45.40; H, 7.08; OCH_3, 16.76%.

The authors are grateful to the Ministry of Education for a grant-in-aid for Scientific Research.

BULLETIN OF THE CHEMICAL SOCIETY OF JAPAN VOL. 41 628—633 (1968)

Synthesis of Pyridoxine. II. The Preparation of Pyrrole Derivatives

Masuo MURAKAMI, Kozo TAKAHASHI, Jun MATSUMOTO, Kazuharu TAMAZAWA, Kiyoshi MURASE, Hidenori IWAMOTO and Masaru IWANAMI

Central Research Laboratory, Yamanouchi Pharmaceutical Co., Ltd., Azusawa-cho, Itabashi-ku, Tokyo

(Received June 16, 1967)

A new method for the synthesis of 2-acetyl-3, 4-diethoxycarbonylpyrrole and its derivatives by the Diels-Alder reaction is described, and the reaction mechanism of their formation is discussed.

In the previous paper,[1] we reported that 5-ethoxycarbonyloxy-4-methyloxazole (I) reacted with diethyl fumarate (II) to give 4, 5-diethoxycarbonyl-3-hydroxy-2-methylpyridine (III). Investigating this reaction furthermore, we found an isomer of III was produced as by product. The isomer III was also obtained by treatment of the intermediate (V), shown in Scheme 1, in the aftermentioned reaction, with ethanolic hydrochloric acid only in 10—20% yield, but the yield of IV was increased to 50—60%, when the ethanolic hydrochloric acid was replaced by aqueous hydrochloric acid as shown in Table 1.

In this paper, we will confirm the structure of IV as 2-acetyl-3, 4-diethoxycarbonylpyrrole and discuss the reaction mechanism. Although the synthesis of pyridine derivatives by the Diels-Alder reaction has been reported by a number of workers,[2] the formation of pyrrole derivatives as described here has never been noticed.

The compound IV is a weakly acidic substance and insoluble in both diluted hydrochloric acid and sodium bicarbonate solution. An ultraviolet (UV) spectrum of IV had absorption maxima at 281 mμ (log $\varepsilon = 4.712$) in ethanol. The nuclear magnetic resonance (NMR) spectrum of IV had two triplets at δ 1.31 and 1.40 (6H), a singlet at 2.41 (3H), two quartets at 4.26 and 4.42 (4H), a doublet at 7.53 (H) and a broad peak at about 10.50 (H) (ppm, $CDCl_3$). On treatment with D_2O, the doublet at δ 7.53 due to an aromatic proton collapsed to a singlet, which indicated

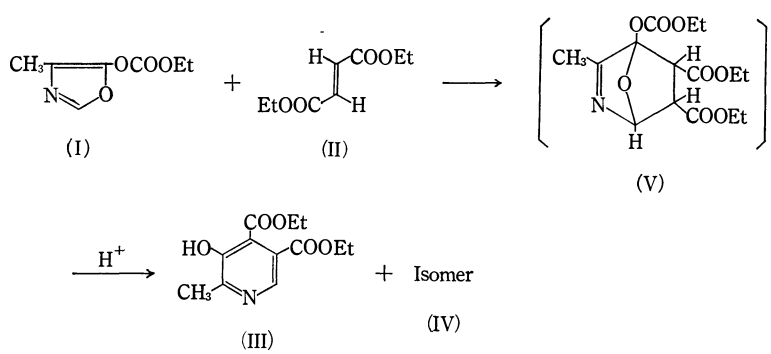

Scheme 1.

The products from the Diels-Alder reaction.

1) M. Murakami and M. Iwanami, This Bulletin, **41**, 726 (1968).

2) Kondratéva, *Izv. Akad. Nauk SSSR*, 484 (1959); E. E. Harris and R. A. Firestone, *J. Org. Chem.*, **27**, 2705 (1962); Rosche Co., Brit. Pat. 971361 (1962).

TABLE 1. THE REACTION OF 5-ETHOXYCARBONYLOXY-4-METHYL OXAZOLE (I) WITH DIETHYL FUMARATE (II)

Exp. No.	Reaction conditions: Temp. °C	Time hr	Molar ratio of II to I	Method of decomposition of adduct (V)	Products and yield, %: III*	IV
A-1	100	2	4	8 N HCl - EtOH	48.6	12.6
A-2	90	6	2	8 N HCl - EtOH	48.8	19.5
B-1	100	2	4	10% HCl - H_2O	17.4	50.0
B-2	90	6	2	10% HCl - H_2O	11.1	54.0

* as hydrochloride

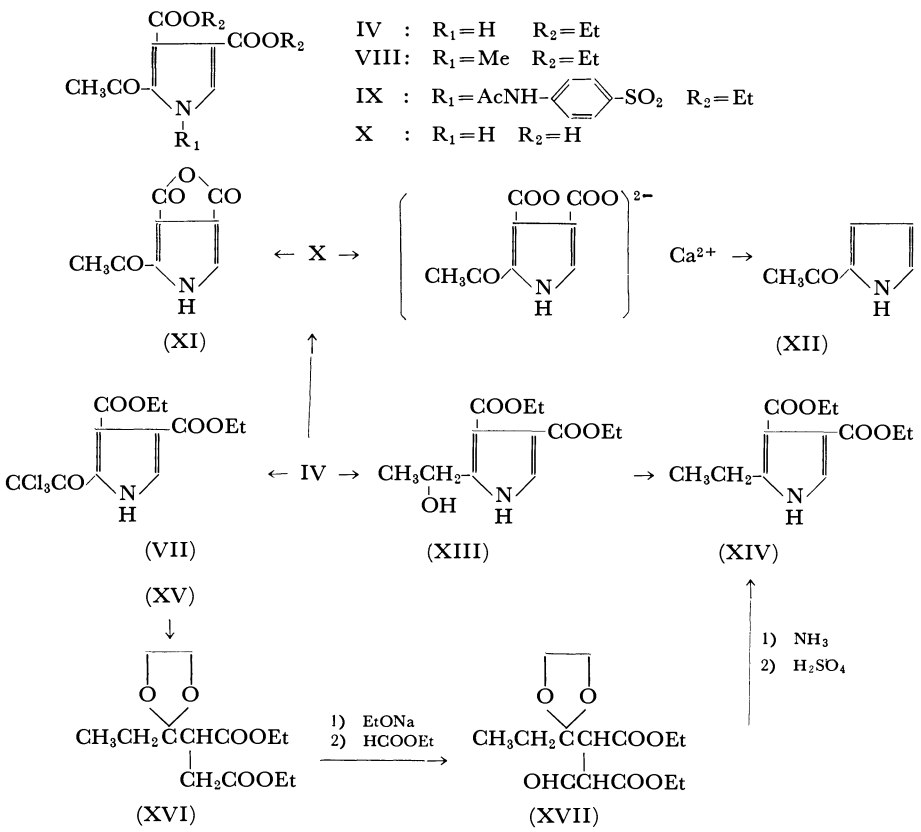

Scheme 2.

The derivatives from the isomer (IV) and authentic compound synthesis route.

that the aromatic proton was adjacent to =NH or –OH group. The infrared (IR) spectrum of IV had the absorption bands at 3260 (=NH), 1700, 1280 (–CO–) and 1670, 1360 (C=O) (cm^{-1}, KBr). The presence of an acetyl moiety was ascertained both by the formation of 2, 4-dinitrophenylhydrazone (VI) and a positive iodoform test. Chlorination of IV with phosphorus pentachloride gave the trichloro compound (VII). The NMR spectrum of VII showed no signal at δ 2.41, indicating the CH_3CO– group of IV had been chlorinated to CCl_3CO–. The reaction of IV with diazomethane gave colorless crystals (VIII). The IR spectrum of VIII showed no absorption band at 3260 cm^{-1}, suggesting the absence of =NH group. The presence of =NH group in IV was ascertained also by the formation of its *p*-acetoaminobenzenesulfonamide derivative (IX). Alkaline hydrolysis of IV gave the corresponding dicarboxylic acid (X), proving that IV is an ester. Refluxing of X in acetic anhydride yielded 2-acetyl-3, 4-dicarboxylpyrrole anhydride (XI), the structure of which was confirmed by the characteristic absorption bands of anhydride at 1850 and 1790 cm^{-1} in the IR spectrum. This fact indicated that two –COOH groups in X were situated vicinal to each other. Decarboxylation of the calcium salt of X gave 2-acetylpyrrole (XII). Reduction of IV with sodium borohydride gave a

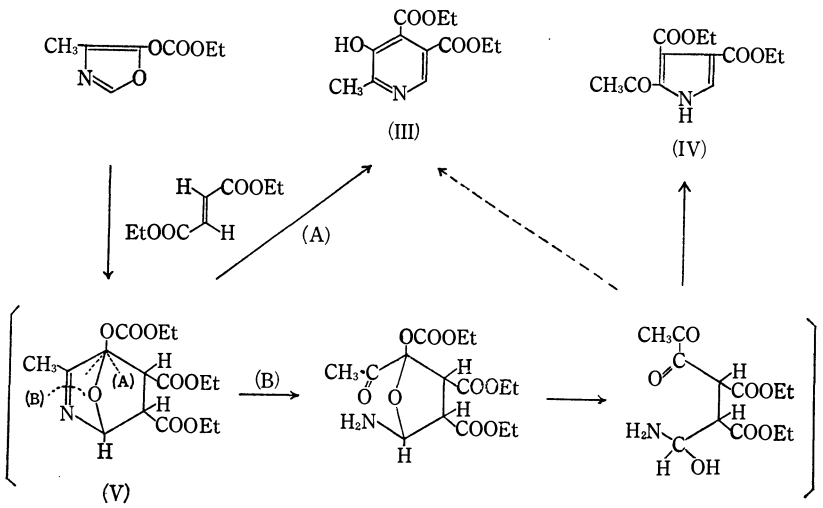

Scheme 3.

The mechanism of pyridine and pyrrole derivatives formation in this reaction.

Table 2. The reaction of 5-ethoxy-4-methyl oxazole (XVIII) and 2, 4-dimethyl-5-ethoxy oxazole (XIX) with diethyl fumarate (II)

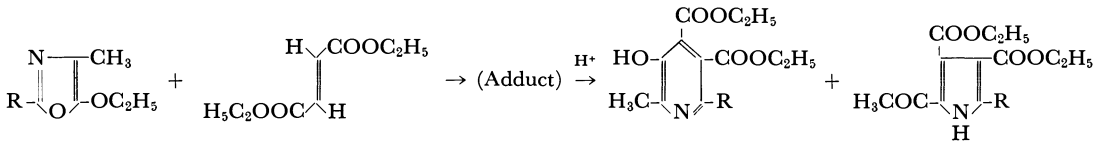

R	Oxazole	Method of decomposition of adduct	Products and yield, %			
			Pyridine deriv.*		Pyrrole deriv	
H	XVIII	8 N HCl - EtOH	III	80	IV	trace
H	XVIII	10% HCl - H_2O	III	30	IV	45
CH_3	XIX	10% HCl - H_2O	XX	80	XXI	10

* as hydrochloride

secondary alcohol XIII, which in turn was transformed into 3, 4-diethoxycarbonyl-2-ethylpyrrole (XIV) by hydrogenation over palladium-charcoal in methanol under acidic condition. This compound XIV was identified with the authentic sample which was prepared from diethyl propionyl succinate (XV) by the method of Kornfeld.[3] (Scheme 2)

Next we examined the NMR spectrum of the reaction mixture of the Diels-Alder reaction and noticed that there was no signal of ring proton as I, III and IV. On the basis of this result, it was presumed that V is considerably stable in the course of the Diels-Alder reaction and is decomposed only by the addition of acid to give pyridine and pyrrole derivatives. As shown in Scheme 3, V would be decomposed by two different pathes (A) and (B). When ethanolic hydrochloric acid was added to V, the oxygen bridge of V would be cleaved to III according to the process A. When aqueous hydrochloric acid was added to V, the hydrolysis of -CH=N- bond of V would predominantly occur to give IV *via* B. The reaction of 5-ethoxy-4-methyloxazole (XVIII) or 2, 4-dimethyl-5-ethoxyoxazole (XIX) with diethyl fumarate (II), or XVIII with diethyl maleate also gave the corresponding pyrrole derivatives as shown in Table 2.

Experimental

The Diels-Alder Reaction (Pyrrole Derivatives): The Reaction of 5-Ethoxycarbonyloxy-4-methyloxazole (I) with Diethyl Fumarate (III). *A) Decomposition of the Reaction Mixture, Adduct (V), with Ethanolic Hydrochloric Acid. A-1)* A mixture of I (8.6 g) and II (34.5 g, 4 equiv.) was heated at 100°C for 2 hr. After cooling, 8 N ethanolic hydrochloric acid (50 m*l*) was added and the mixture was allowed to stand for 30 min at room temperature, then the ethanol was

3) E. C. Kornfeld and R. G. Jones, *J. Org. Chem.*, **19**, 1671 (1954).

removed *in vacuo*. When ether (100 m*l*) was added to the resulting residue, 4, 5-diethoxycarbonyl-3-hydroxy-2-methylpyridine (III) was precipitated as hydrochloride, which was collected by filtration, 7.0 g (48.6%), mp 147—148°C (decomp.).

Found: C, 49.70; H, 5.58; N, 5.07%. Calcd for $C_{12}H_{15}O_5N \cdot HCl$: C, 49.74; H, 5.57; N, 4.84%.

The mother liquor was washed with water, 5% aqueous sodium bicarbonate and water successively, and dried over anhydrous magnesium sulfate. The solvent, ether and excess II, was removed by evaporation to afford pale yellow oily residue. The residue was dissolved in a small volume of benzene and by addition of petroleum ether, 2-acetyl-3, 4-diethoxycarbonylpyrrole (IV) was precipitated. The product was recrystallized from benzene - petroleum ether to give the pale yellow crystals, mp 101—102°C (2.6 g, 12.6%).

Found: C, 57.21; H, 5.92; N, 5.48%. Calcd for $C_{12}H_{15}O_5N$: C, 56.91; H, 5.97; N, 5.53%.

A-2) A mixture of I (2.0 g) and II (4.0 g, 2 equiv.) was heated at 90°C for 6 hr and the reaction mixture was treated as above. The yield of the hydrochloride of III was 1.65 g (48.8%) and the yield of IV was 0.6 g (19.5%).

B) Decomposition of the Adduct (V) with Aqueous Hydrochloric Acid. B-1) A mixture of I (17.0 g) and II (69.0 g, 4 equiv.) was heated at 100°C for 2 hr. After cooling, 10% aqueous hydrochloric acid (50 m*l*) was added to the reaction mixture and it was allowed to stand for 30 min at room temperature. The resulting solution was extracted with ether and the ether layer was washed with 5% aqueous hydrochloric acid, water, 5% aqueous sodium bicarbonate and water succesively, and dried over anhydrous magnesium sulfate. The solvent, ether and excess II, was removed by evaporation to afford pale yellow oily residue. The residue was treated as described in A-1) to give IV, yield 12.5 g (50%). The aqueous layer was neutralized with sodium bicarbonate, and was extracted with ether. After the ether solution was washed with water and dried over anhydrous magnesium sulfate, gaseous dry hydrogen chloride was bubbled into the ethereal solution. The compound III was deposited as hydrochloride, yield 5 g (17.4%).

B-2) A mixture of I (1.6 g) and II (3.2 g, 2 equiv.) was heated at 90°C for 6 hr and the reaction mixture was treated as described in B-1). The compound IV was yielded 1.27 g (54%) and III was also obtained as hydrochloride, yield 0.3 g (11.1%).

The Reaction of 5-Ethoxy-4-methyloxazole (XVIII) with Diethyl Fumarate (II). A mixture of XVIII (2.0 g) and II (5.0 g) was heated at 90°C for 1.5 hr and the reaction mixture was decomposed with 10% aqueous hydrochloric acid (5 m*l*). Treatment of the solution obtained according to the same method as in B-1) yielded IV, 1.8 g (45%) and III, 1.4 g (30%) as hydrochloride. When the reaction mixture was decomposed with 8 N ethanolic hydrochloric acid and the resulting solution was treated by the same method as in A-1), III was obtained as hydrochloride in the yield of 80% and IV in a trace amount.

Instead of II, when the diethyl maleate as dienophile was reacted with XVIII, the results were similar to those mentioned before.

The Reaction of 2, 4-Dimethyl-5-ethoxyoxazole (XIX) with Diethyl Fumarate (II). A mixture of XIX (1.0 g) and II (1.35 g) was heated at 80°C for 1 hr. After removing the excess II *in vacuo*, aqueous hydrochloric acid (20 m*l*) was added to the resulting mixture. After stirring for 20 min, ethanol (10 m*l*) was added to the solution, and homogeneous solution thus obtained was stirred for further 10 min. The solution was evaporated *in vacuo* until ethanol was largely removed and the remaining aqueous phase was extracted twice with chloroform (50 m*l*). The chloroform layer was washed with 5% aqueous sodium bicarbonate and water, and dried over anhydrous magnesium sulfate. The solvent was removed by evaporation to yield an oily residue. On addition of 8 N ethanolic hydrochlorio acid, the pyridine derivative, 3, 4-diethoxycarbonyl-2, 6-dimethyl-5-hydroxypyridine (XX), was precipitated as hydrochloride. After collecting the product by filtration, *n*-hexane was added to the mother liquor, 2-acetyl-3, 4-diethoxycarbonyl-5-methylpyrrole (XXI) was precipitated, which was recrystallized from benzene - *n*-hexane to afford colorless needles, mp 103—104°C. Yield 200 mg.

Found: C, 58.64; H, 6.21; N, 5.69%. Calcd for $C_{13}H_{17}O_5N$: C, 58.42; H, 6.41; N, 5.24%. IR (KBr-Wafer): 3300 (=NH); 1652 cm^{-1} (C=O)

The aqueous layer, after being extracted with chloroform, was neutralized with 5% aqueous sodium bicarbonate and extracted with ether. The extract was washed with water and dried over anhydrous magnesium sulfate. Gaseous hydrogen chloride was passed into this ethereal solution to give XX as hydrochloride, mp 150°C (decomp.). The total yield of XX as hydrochloride was 1.8 g (80%).

Found: C, 51.69; H, 6.00; N, 4.85%. Calcd for $C_{13}H_{17}O_5N \cdot HCl$: C, 51.40; H, 5.97; N, 4.61%.

The Reaction of the Isomer (IV). 2, 4-Dinitrophenylhydrazone of IV (VI). To a solution of IV (0.5 g) in 95% ethanol, 2, 4-dinitrophenylhydrazine sulfuric acid solution was added. After heating at 50°C for several min, the reaction mixture was allowed to stand overnight at room temperature. The precipitated crystals were collected and recrystallized five times from 95% ethanol. The compound VI was obtained as monohydrate of orange needles, yield 0.7 g. After drying over phosphorus pentoxide at 100°C for 6 hr *in vacuo*, VI changed into anhydrous red crystals, mp 195°C (decomp.).

Found: C, 49.84; H, 4.55; N, 16.29%. Calcd for $C_{18}H_{19}O_8N_5$: C, 49.88; H, 4.42; N, 16.16%.

3, 4-Diethoxycarbonyl-2-trichloroacetylpyrrole (VII). A mixture of IV (0.4 g), phosphorus oxychloride (5 m*l*) and phosphorus pentachloride (1.5 g) was heated at 120°C for 4 hr. After phosphorus oxychloride was removed, water was added to the oily residue and the mixture was extracted with ether. The ethereal extract was dried over anhydrous magnesium sulfate and evaporated *in vacuo* to give white crystals. Recrystallization of the product from benzene afforded VII (0.2 g), needles, mp 195°C (decomp.). Found: Cl, 30.38%. Calcd for $C_{12}H_{12}O_5NCl_3$: Cl, 29.83%.

2-Acetyl-3, 4-diethoxycarbonyl-1-methylpyrrole (VIII). Into an ethereal solution of diazomethane which was prepared from *N*-nitrosomethyl urea (4 g), 2.0 g of IV was dissolved and the mixture was allowed to stand overnight at room temperature. VIII was deposited

from the solution as white needles, mp 117—118°C. Yield 1.4 g.

Found: C, 58.54; H, 6.35; N, 5.43%. Calcd for $C_{13}H_{17}O_5N$: C, 58.42; H, 6.41; N, 5.24%. IR (KBr-Wafer): 1660 cm^{-1} (C=O). NMR ($CDCl_3$): singlet (3H) at δ 3.90 ($N-CH_3$).

1-(*p*-Acetoaminobenzenesulfonyl)-2-acetyl-3,4-diethoxycarbonylpyrrole (IX). To a suspension of the sodium salt of IV (1.53 g) in anhydrous pyridine (10 m*l*), *p*-acetoaminobenzenesulfonyl chloride (1.8 g) was added at room temperature. After stirring for 2 hr, the reaction mixture was poured into water and extracted with chloroform. The extract was washed with 5% aqueous hydrochloric acid, water, 5% aqueous sodium bicarbonate and water successively, and dried over anhydrous magnesium sulfate. Evaporation of the solvent left a crude product of IX, which was recrystallized from chloroform-ether to give 1.6 g of IX mp 179—180°C. Found: C, 53.28; H, 4.82; N, 6.23%. Calcd for $C_{20}H_{22}O_8N_2S$: C, 53.33; H, 4.92; N, 26.2%.

2-Acetyl-3,4-dicarboxylpyrrole (X). The compound IV (3.0 g) was dissolved in 20% aqueous sodium hydroxide (20 m*l*) and the solution was refluxed for 1.5 hr. The reaction mixture was cooled with ice-water and then strongly acidified with conc. hydrochloric acid. The precipitated product was collected and recrystallized from water. After drying over phosphorus pentoxide at 100°C for 6 hr, 2.0 g of X was obtained as yellow platelets, mp 210°C (decomp.).

Found: C, 48.72; H, 3.66; N, 7.42%. Calcd for $C_8H_7O_5N$: C, 48.74; H, 3.58; N, 7.11%.

2-Acetyl-3,4-dicarboxylpyrrole Anhydride (XI). A mixture of X (500 mg), acetic anhydride (6 m*l*) and glacial acetic acid (2 m*l*) was heated at 140°C for 4 hr. After cooling, the solvent was removed *in vacuo*. The residue was dissolved in ether and an insoluble product was removed. The ethereal solution was evaporated to give the crude product of XI, which was recrystallized from ethyl acetate to afford pale yellow needles, mp 196—197°C (decomp.). Yield 360 mg.

Found: C, 53.62; H, 2.82; N, 8.10%, Cacld for $C_8H_5O_4N$: C, 53.64; H, 2.81; N, 7.82%. IR (KBr-Wafer): 1850, 1790 cm^{-1} (-CO-O-CO-)

2-Acetylpyrrole (XII). To an aqueous solution of X (1.0 g), calcium carbonate (0.5 g) was added and heated at 110°C. The slurry was dried up to give the calcium salt of X, which was heated over an alcohol lamp under reduced pressure (15—20 mmHg) to give dark yellow oily product. This material was fractionally distilled under the same pressure to afford pale yellow oily product, which was crystallized to give white needles of XII, mp 90—91°C. Yield 50 mg.

Found: N, 12.62%. Calcd for C_6H_7ON: N, 12.84%. IR (KBr-Wafer): 3240 (=NH), 1640 cm^{-1} (C=O).

3,4-Diethoxycarbonyl-2-(α-hydroxyethyl)pyrrole (XIII). To a methanolic solution of IV (5.0 g), sodium borohydride (2.0 g) was added in portionwise at 5—10°C for 20 min. The reaction mixture was neutralized to pH 7 with 10% aqueous hydrochloric acid and methanol was largely removed, and the remaining aqueous phase was extracted with ether. After the ethereal solution was dried over anhydrous magnesium sulfate, the solvent was distilled off and the residue was recrystallized from benzene to afford white crystal of XIII, mp 109—110°C. Yield 4.5 g.

Found: C, 56.45; H, 6.65; N, 5.68%. Calcd for $C_{12}H_{17}O_5N$: C, 56.46; H, 6.71; N, 5.49%.

3,4-Diethoxycarbonyl-2-ethylpyrrole (XIV). To a methanolic solution of XIII (500 mg), conc. hydrochloric acid (0.1 m*l*) and 5% palladium charcoal (1.2 g) were added and hydrogenation was carried out at room temperature. After the reaction was over, the catalyst was filtered off and the filtrate was evaporated *in vacuo* at or below 40°C. The oily residue was extracted with ether, washed with water, 5% aqueous sodium bicarbonate and water successively, and dried over anhydrous magnesium sulfate. After removing the solvent, colorless oily residue was dissolved in a small amount of benzene, and *n*-hexane was added until the solution became turbid. The resulting mixture was allowed to stand several days in a freezer. The product XIV was crystallized as white prisms, which was recrystallized from benzene-*n*-hexane, mp 106—107°C. Yield 90 mg.

Found: C, 60.15; H, 7.10; N, 6.16%. Calcd for $C_{12}H_{17}O_4N$: C, 60.24; H, 7.16; N, 5.86%.

The structure of XIV was identified with an authentic sample prepared from diethylpropionyl succinate (XV).

3,4-Diethoxycarbonyl-2-ethylpyrrole (XIV) from Diethylpropionyl Succinate (XV). Diethyl-1-(α-ethylenedioxy)propyl Succinate (XVI). A mixture of diethylpropionyl succinate (XV) (10 g), ethylene glycol (10 m*l*), *p*-toluenesulfonic acid (0.7 g) and benzene (350 m*l*) was refluxed for 25 hr. The benzene solution was washed with 5% aqueous sodium bicarbonate, dried over anhydrous magnesium sulfate and fractionally distilled under reduced pressure to give XVI, bp 115—120°C/0.3 mmHg. Yield 4 g.

Diethyl-1-(α-ethylenedioxy)propyl-2-formyl Succinate (XVII). Finely divided sodium (0.35 g) was suspended in 10 m*l* of absolute ether, and absolute ethanol (0.1 m*l*) was added with stirring. A mixture of XVI (3.5 g) and ethyl formate (1.45 g) was added dropwise to the ethereal solution during 1 hr and the reaction mixture was allowed to stand overnight. Ice and water were added to the solution, the aqueous layer was separated and acidified with 10% aqueous sulfuric acid at or below 0°C. The aqueous layer was extracted twice with ether (20 m*l*) and the extract was dried over anhydrous magnesium sulfate. After removing the solvent, the oily residue was distilled under reduced pressure at 120°C to afford XVII 0.9 g. The crude product was sufficiently pure for cyclization.

3,4-Diethoxycarbonyl-2-elthylpyrrole (XIV). A solution of crude XVII (0.75 g) in 5 m*l* of absolute ether was mixed with ammoniac ethanol (0.6 m*l*). The mixture was stirred for 10 min and evaporated under reduced pressure to remove ether and ethanol. The residual oily product was mixed with 2 m*l* of concentrated sulfuric acid keeping the temperature below 55°C. After 5 min, the sulfuric acid solution was poured onto 10 g of ice with stirring. The mixture was extracted twice with 10 m*l* of ethyl acetate and the extract was washed with 5% aqueous sodium bicarbonate, dried over anhydrous magnesium sulfate and the solvent was evaporated. The residual product was extracted with boiling water. After cooling the extract, the deposited white crystalline product was collected and dried over phosphorus pentoxide *in vacuo*.

Recrystallization from benzene-*n*-hexane afforded XIV as white needles, mp 106—107°C. Yield 120 mg.

Found: C, 60.41; H, 7.27; N, 5.78%. Calcd for $C_{12}H_{17}O_4N$: C, 60.24; H, 7.16; N, 5.86%.

The authors wish to express their gratitude to the staffs of the analysis labolatory of this faculty for elemental analyses, infrared and nuclear magnetic resonance spectra measurements.

BULLETIN OF THE CHEMICAL SOCIETY OF JAPAN VOL. 41 633—635 (1968)

Chemical Synthesis of *O*-Ethyl-L-homoserine, a New Amino Acid Produced by *Corynebacterium Ethanolaminophilum*

Yoshikatsu MUROOKA, Tokuya HARADA and Yoshiharu IZUMI*1

Institute of Scientific and Industrial Research, Osaka University, Sakai, Osaka

(Received June 22, 1967)

The synthesis of *O*-ethyl-DL-homoserine (V) was achieved by the condensation of β-ethoxyethylbromide (II) with diethyl acetoaminomalonate (III) and by the successive hydrolysis of diethyl ethoxyethylacetoaminomalonate (IV) with hydrochloric acid. The optical resolution of *O*-ethylhomoserine was performed enzymatically using papain. The *O*-ethyl-L-homoserine (VIII) obtained by the resolution was shown to be identical with the amino acid formed ethanol by *Corynebacterium ethanolaminophilum*, sp.nov.

In a previous paper,[1] *Corynebacterium ethanolaminophilum*, strain E17, was reported to form new amino acids when grown in a well-aerated medium containing ethanol, *n*-propanol, or *n*-butanol. The chemical properties and structures of these compounds were investigated by Murooka and Harada; the amino acids formed from ethanol, *n*-propanol, and *n*-butanol were assumed to be, respectively, *O*-ethylhomoserine (Compound E), *O*-propylhomoserine and *O*-butylhomoserine on the basis of a study of the infrared spectrum and the nuclear magnetic resonance spectrum and on the basis of an elemental analysis.

In the present paper, in an attempt to identify the structures of these compounds, the DL- and L-forms of *O*-ethylhomoserine were prepared by the process described in the following scheme (a preliminary account of part of this work has already appeared):[2]

$$\underset{\text{I}}{CH_3\text{-}CH_2\text{-}O\text{-}CH_2\text{-}CH_2\text{-}OH} \xrightarrow{PBr_3}$$

$$\underset{\text{II}}{CH_3\text{-}CH_2\text{-}O\text{-}CH_2\text{-}CH_2Br} \xrightarrow[NaOC_2H_5]{HC(COOC_2H_5)_2NHCOCH_3} \underset{\text{III}}{}$$

$$\underset{\text{IV}}{CH_3\text{-}CH_2\text{-}O\text{-}CH_2\text{-}CH_2\text{-}C(COOC_2H_5)_2\text{-}NHCOCH_3} \xrightarrow{HCl}$$

$$\text{DL-}CH_3\text{-}CH_2\text{-}O\text{-}CH_2\text{-}CH_2\text{-}CHNH_2\text{-}COOH \quad \underset{\text{V}}{}$$

$$\downarrow C_6H_5CH_2OCOCl$$

$$\underset{\text{IV}}{\text{DL-}CH_3\text{-}CH_2\text{-}O\text{-}CH_2\text{-}CH_2\text{-}CH(NH\text{-}CO\text{-}O\text{-}CH_2\text{-}C_6H_5)\text{-}COOH}$$

$$\downarrow \text{papain},\ C_6H_5NH_2$$

$$\text{L-}CH_3\text{-}CH_2\text{-}O\text{-}CH_2\text{-}CH_2\text{-}CH(NH\text{-}CO\text{-}O\text{-}CH_2\text{-}C_6H_5)\text{-}CONHC_6H_5$$

$$\downarrow HCl$$

$$\text{L-}CH_3\text{-}CH_2\text{-}O\text{-}CH_2\text{-}CH_2\text{-}CHNH_2\text{-}COOH$$

The optical rotatory value of the L-compound (VIII) obtained was $[\alpha]_D^{30}$ −14° (*c* 2.5, water); this value was accordant with that[1] of the compound formed from ethanol by the bacterium. The infrared spectrum of the *O*-ethyl-L-homoserine (VIII) obtained by the optical resolution was identical with that of the bacterial product, while that of the racemate was rather different from that of the L-compound (Fig. 1). Thus, it was confirmed that Compound E was *O*-ethyl-L-homoserine. The syntheses of *O*-propylhomoserine and *O*-butylhomoserine are in progress.

Experimental

β-Ethoxyethylbromide (II). β-Ethoxyethanol (I) was brominated with phosphorus tribromide by the

*1 Institute for Protein Research, Osaka University, Osaka.

1) Y. Murooka and T. Harada, *Agr. Biol. Chem.*, **31**, 1035 (1967).

2) T. Harada, Y. Murooka and Y. Izumi, *Biochem. Biophys. Res. Commun.*, **28**, 485 (1967).

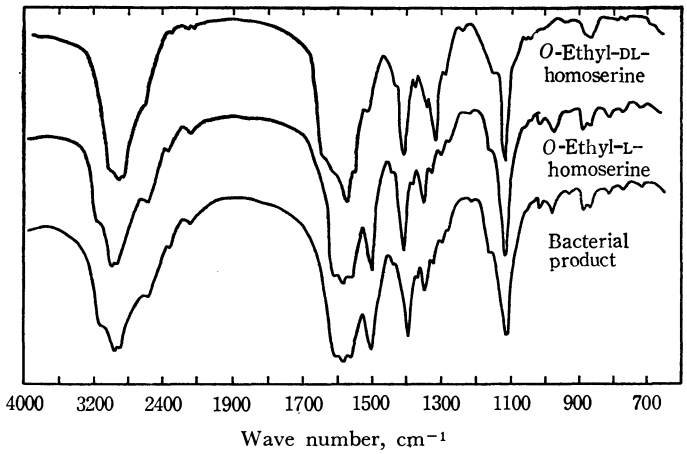

Fig. 1. Comparison of infrared spectra (in KRS-5) of bacterial product and synthetic DL- and L-*O*-ethylhomoserine.

procedure of Harrison and Diehl.[3]

***O*-Ethyl-DL-homoserine (V).** To 700 m*l* of an ethanolic solution of sodium ethylate (prepared from 30 g of sodium), 217 g of III and 1 g of potassium iodide were added. To the reaction mixture, 212 g of II were then added with heating over a 4-hr period, after which the reaction mixture was heated for a further 3 hr. The reaction mixture was removed from the sodium bromide by filtration, and the filtrate was evaporated to dryness. The residue was hydrolyzed with 1.5 *l* of 10% hydrochloric acid for 7 hr. The hydrolysate was evaporated to dryness *in vacuo* to remove the hydrochloric acid. The residue was dissolved in 300 m*l* of water and adjusted to pH 6.0 with sodium hydroxide. This solution was evaporated to dryness *in vacuo*, and the residue was extracted with 500 m*l* of 80% methanol. The solution was concentrated *in vacuo*, and the residue was dissolved with 50 m*l* of hot water. This solution was stored in a cold room, and then the crude material was collected and washed with aqueous acetone. The concentration of acetone was increased from 40% to 80%. The crystals which formed were dissolved in 100 m*l* of water, and a pure crystalline material was precipitated by the addition of 200 m*l* of acetone; yield, 95 g; mp 262°C.

Found: C, 49.25; H, 8.85; N, 9.58%. Calcd for $C_6H_{13}NO_3$: C, 48.96; H, 8.90; N, 9.52%.

Carbobenzoxy-*O*-ethyl-DL-homoserine (VI). Sodium hydroxide (50 g) in 100 m*l* of water and 63 g of carbobenzoxy chloride in 50 m*l* of dioxane were simultaneously added to a 400 m*l* aqueous solution of 50 g of V and 13 g of sodium hydroxide at 5°C over a period of about 3 hr. Stirring was then continued for another hour at the same temperature. The reaction mixture was washed twice with 150 m*l* of ether, and the aqueous layer was acidified to pH 3 with 5 N hydrochloric acid. The resulting oily precipitate was extracted with 300 m*l* of ethyl acetate. The ethyl acetate layer was extracted with 400 m*l* of 3.4% sodium bicarbonate solution.

The aqueous layer was acidified again and reextracted with 300 m*l* of ethyl acetate. The organic layer was washed twice with 30 m*l* of water to remove hydrochloric acid and dried over anhydrous sodium sulfate. The solution was then concentrated *in vacuo*. After the solution had been cooled in an ice bath, crystalline carbobenzoxy-*O*-ethyl-DL-homoserine appeared. The crystalline material was dissolved into 50 m*l* of benzene, after which 10 m*l* of petroleum ether were added to the solution. White, crystalline carbobenzoxy-*O*-ethylhomoserine was collected and dried in air; yield, 82 g; mp 65—66°C.

Found: C, 59.86; H, 6.77; N, 4.99%. Calcd for $C_{14}H_{19}NO_5$: C, 59.77; H, 6.81; N, 4.98%.

Carbobenzoxy-*O*-ethyl-L-homoserine Anilide (VII). The procedure was a modification of the method of Bergmann and Fraenkel-Conrat.[4]

An enzyme solution was prepared from 20 g of papaya latex by extraction with a mixture of 40 m*l* of a 0.5 M citrate buffer (pH 5.5) and 60 m*l* of water, and the suspension was filtered after incubation for one hour. Then 80 g of VI, 28 g of aniline, and 1 g of potassium cyanide were dissolved in 500 m*l* of water at 40°C. The solution was mixed with a papain-buffer solution at pH 7.0, and then the pH was adjusted to 5.5 with citric acid. After about ten minutes incubation at 38°C, synthetic anilide separated out as an oily material. It was dissolved by adding water to the incubated mixture, and the pH was readjusted to 5.5 with citric acid. After two days storage, 28 g of crude anilide separated out as crystals. These were filtered and washed with water and methanol. The crude material was recrystallized from 70 m*l* of aqueous ethanol (60%) (as white crystals); yield, 25 g; mp 105°C.

Found: C, 67.38; H, 6.83; N, 7.93%. Calcd for $C_{20}H_{24}N_2O_4$: C, 67.39; H, 6.79; N, 7.86%.

***O*-Ethyl-L-homoserine (VIII).** Twenty-five grams of VII were hydrolyzed with 10% hydrochloric acid for 7 hr. The lower layer of benzyl chloride separated off and was discarded. The upper layer was washed with ether and evaporated to dryness. The residue was dissolved in water and passed through Dowex

3) G. C. Harrison and H. Diehl, "Organic Syntheses," Coll. Vol. III, p. 370 (1955).

4) M. Bergmann and H. Fraenkel-Conrat, *J. Biol. Chem.*, **119**, 707 (1937).

50 (H^+ form). VIII was eluted with 2% aqueous ammonia from the exchanger, and the eluted solution was evaporated to dryness. The residue was recrystallized from aqueous ethanol (50%); yield, 4 g; mp 261°C. $[\alpha]_D^{30}$ −14° (*c* 2.5, water).

Found: C, 48.74; H, 9.37; N, 9.42%. Calcd for $C_6H_{13}NO_3$: C, 48.96; H, 8.90; N, 9.52%.

The authors wish to thank Miss Kiku Koike for the elemental analyses.

BULLETIN OF THE CHEMICAL SOCIETY OF JAPAN VOL. 41 635—640 (1968)

Episulfones. III. Reductive Cleavage of Episulfones by Complex Metal Hydrides

Shoichi MATSUMURA, Toshikazu NAGAI and Niichiro TOKURA

Department of Applied Chemistry, Faculty of Engineering, Osaka University, Higashinoda, Osaka

(Received July 15, 1967)

The reduction of *cis*-stilbene episulfone (I) by such a complex metal hydride as lithium borohydride, sodium borohydride, or lithium aluminum hydride gave dibenzylsulfone (V) selectively as a result of the unusual cleavage of the carbon-carbon single bond. Comparing the difference between lithium aluminum hydride and lithium borohydride or sodium borohydride in various solvent systems, we suggest that particular solvent effects are operating in the present reaction. The reduction of I with lithium aluminum hydride resulted in a low yield (0—10%) of V, while the reduction with lithium borohydride afforded V in a 45% yield. The reduction of styrene episulfone (II) gave no carbon-carbon cleavage product, but it did give a carbon-sulfur fission product, yielding sulfinic acid salt (VIII). The formation of VIII is interesting compared with the reduction of styrene oxide by lithium aluminum hydride. Tetraphenylethylene episulfone (III) produced a carbon-carbon cleavage product, 1, 1, 3, 3-tetraphenyl dimethyl sulfone (XI), in a 68% yield. A reaction mechanism for the reductive cleavage reaction has been proposed on the basis of the above-mentioned results. In addition, we observed that diborane was evolved by the reaction of sulfur dioxide with lithium- or sodium borohydrides.

Much work has been done on the reactivity of heteroatom-containing three-membered ring compounds, for example, epoxides, episulfides, and aziridines. However, the reactions of three-membered rings containing a sulfone group (episulfones) have not yet been studied, except for base-catalyzed reactions.[1,2]

It is very interesting to investigate the physical and chemical behavior of episulfones.

In previous papers[3,4] the present authors have reported the alkaline cleavage of *cis*-stilbene episulfone (I) and the reduction of I by complex metal hydrides. In this paper, we wish to report on the reduction of such episulfones as *cis*-stilbene episulfone (I), styrene episulfone (II), and tetraphenylethylene episulfone (III) by complex metal hydrides. (The episulfones isolated before have been few[1-3,5] because it is difficult to synthesize them because of their unstability.)

Selective Reduction by Complex Metal Hydrides. Reduction of I with complex metal hydrides were carried out under various conditions; the results are summarized in Table 1. The yields of dibenzylsulfone (V) and *cis*-stilbene (VI) obtained totalled almost 100%. No sulfinic acid salt was detected. Therefore, it can be said that the carbon-carbon bond cleavage occurs selectively, without any carbon-sulfur bond fission[6] (Eq. (1)).

1) a) N. P. Neureiter, *J. Am. Chem. Soc.*, **88**, 558 (1966); b) L. A. Paquette, *Chem. Commn.*, **1966**, 471.

2) G. Hesse, E. Reichold and S. Majmudar, *Chem. Ber.*, **90**, 2106 (1957).

3) Part I: N, Tokura, T. Nagai and S. Matsumura, *J. Org. Chem.*, **31**, 349 (1966).

4) Part II: S. Matsumura, T. Nagai and N. Tokura, *Tetrahedron Letters*, **1966**, 3929.

5) a) H. Staudinger and F. Pfenniger, *Ber.*, **49**, 1941 (1916); b) L. V. Vargha and E. Kovacs, *ibid.*, **75**, 794 (1942); c) G. Opitz and K. Fischer, *Angew. Chem.*, **77**, 41 (1965); d) S. Rossi and S. Mairona, *Tetrahedron Letters*, **1966**, 263; e) L. A. Carpino and R. H. Rynbrandt, *J. Am. Chem. Soc.*, **88**, 5682 (1966).

6) The stereospecific formation of *cis*-stilbene from I was the result of thermal decomposition.[3] Though I is stable below its dec. pt. (87—88°C) in a pure state without a solvent, it has been found that I decomposes to give *cis*-stilbene in some yield, even at room temperature, if it is dissolved in such solvents as are listed in Table 1. The yield of the olefin from this decomposition in a solvent seems to depend on the solvent used and on the coexistence of a metal cation, though its quantitative relationship is not clear.

TABLE 1. REDUCTION OF *cis*-STILBENE EPISULFONE (I) BY COMPLEX METAL HYDRIDES

Entry	Reducing agent[a)]	Solvent	Temp. °C	Products (mol%)	
				Dibenzyl-sulfone (V)	*cis*-Stilbene (VI)
1	$LiAlH_4$	Tetrahydrofuran	15	0	89
2	$LiAlH_4$	Diethyl ether	15	10	65
3	$LiAlH_4$	Diglyme[b)]	15	12	77
4	$LiAlH_4$	Tetrahydrofuran	70	4	77
5	$LiBH_4$	Tetrahydrofuran	15	47	40
6	$LiBH_4$	Diethyl ether	15	43	58
7	$LiBH_4$	Diglyme	15	48	28
8	$LiBH_4$	Tetrahydrofuran triethylamine	15	29	65
9	$NaBH_4$	Tetrahydrofuran[c)]	15	33	66
10	$NaBH_4$	Diglyme	15	49	50
11	$NaBH_4$	Dimethyl sulfoxide	20	44	61
12	$NaBH_4$	Methanol	15	0	85
13	BH_3[d)]	Tetrahydrofuran	15	0	60[f)]
14	AlH_3[e)]	Tetrahydrofuran	15	0	83
15	H_2AlCl[e)] $HAlCl_2$[e)]	Tetrahydrofuran	15	0	100
16	LiH	Tetrahydrofuran	15	0	100
17	NaH	Tetrahydrofuran	15	0	100

a) A molar ratio of I to the reducing agents of 1 : 2 was used.
b) Diethylene glycol dimethyl ether.
c) Suspension of sodium borohydride in tetrahydrofuran was used.
d) Diborane was generated externally in the reaction flask by adding diglyme saturated with sodium borohydride to boron fluoride etherate. (H. C. Brown and B. C. Subba Rao, *J. Am. Chem. Soc.*, **81**, 6428 (1959).) Excess diborane was used in this reaction.
e) AlH_3, H_2AlCl and $HAlCl_2$ were prepared by the method of Ashby. (E. C. Ashby and J. Prather, *J. Am. Chem. Soc.*, **88**, 749 (1966).) In these reactions, we directly used them prepared from lithium hydride and aluminum chloride in ether.
f) Yield was based on 1,2-diphenyl ethanol obtained.

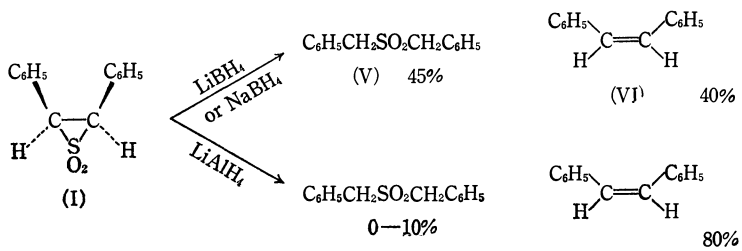

(1)

Remarkable solvent effects on the reductive cleavage were observed (Table 1). Thus, no dibenzylsulfone (V) was produced when I was treated with lithium aluminum hydride in tetrahydrofuran at room temperature. When diethyl ether or diglyme was used as the solvent, however, V was formed under the same conditions.

This reason might be that tetrahydrofuran forms a complex[7,8)] with lithium aluminum hydride (Fig. (A)), thus prohibiting the reactions more or less due to steric reasons. In ether and diglyme, which are weaker bases than tetrahydrofuran, such complexes are dissociated at room temperature, so the yields of V are more in these solvent than in tetrahydrofuran.

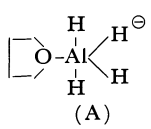

(A)

When tetrahydrofuran,[9)] diethyl ether, diglyme, and dimethyl sulfoxide (Entries 5-11) were treated

7) E. Wiberg and A. Jahn, *Z. Naturforsch.*, **11b**, 489 (1956).
8) D. Nafstein and C. Vogel, *J. Am. Chem. Soc.*, **88**, 1576 (1966).
9) The decrease in the yield of V in tetrahydrofuran may be ascribed to the low solubility of sodium borohydride.

with lithium borohydride or with sodium borohydride, V was produced in very similar yields. Thus, the suggestion has been made that the interactions of lithium borohydride or sodium borohydride with these solvents are diminished.[10] In methyl alcohol, on the contrary, sodium borohydride reacts with the solvent to give[11] sodium tetramethoxyboron, $NaB(OCH_3)_4$ before reduction; thus V is not produced (Entry 12). In the reduction of I in the presence of triethylamine, no marked decrease in the yield of V was observed.

This remarkable difference in reactivity between the aluminum- and boro-hydrides can be explained by the fact that aluminum can expand its octet to form A, while boron cannot.[8]

Recently, many workers have discussed the solvent effects on reductions by complex metal hydrides. Eliel *et al.*[12] concluded that sodium borohydride in inert solvents brings about the same steric results as does lithium aluminum hydride in ether, and Dauben[13] postulated that the borohydride species has a greater effective size than the aluminum hydride anion. Wheeler and Huffman[14] claimed that neither borohydride ion nor aluminum hydride ion is solvated.

Contrary to the above suggestions, we have concluded that the marked solvent effect on reduction by alkaline aluminum hydride is due to a complex formation such as A.

The present authors investigated the reductions of styrene episulfone (II) and tetraphenylethylene episulfone (III), formulated below;

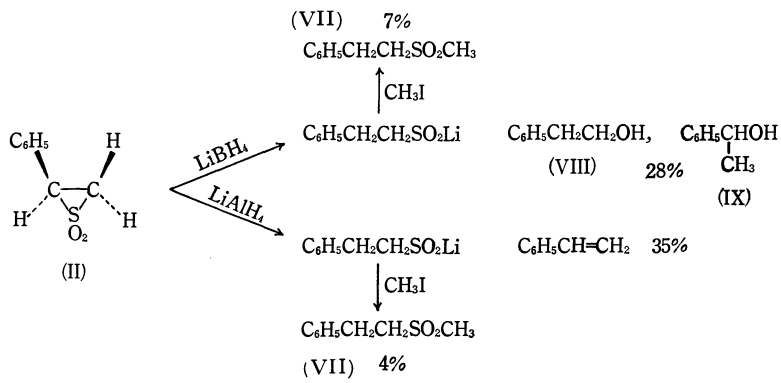

(2)

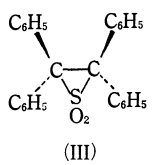
(III)

$\xrightarrow[\text{or } NaBH_4]{LiAlH_4}$ $(C_6H_5)_2CHSO_2CH(C_6H_5)_2$ (3)

(XI) 68%

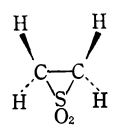
(IV)

$\xrightarrow{LiAlH_4}$ $(C_2H_4S)_n$ (4)

To clarify the driving force of the carbon-carbon bond cleavage of I, we reduced styrene episulfone (II) by lithium aluminum hydride and lithium borohydride in diethyl ether at 0°C, but the carbon-carbon bond cleavage product was not detected, even after careful alumina-column chromatography. Instead, β-phenylethyl sulfinic acid salt, which was identified as β-phenylethyl methyl sulfone (VII) by the reaction with methyl iodide, was formed, indicating a carbon-sulfur bond cleavage.

It is interesting to note that the normal cleavage product, α-phenylethyl methyl sulfone, was not detected in the reaction mixtures. In the reduction of styrene oxide by lithium aluminum hydride or lithium borohydride, it has been observed[15] that the former gives only α-phenylethyl alcohol, while the latter, on the other hand, gives α- and β-phenylethyl alcohols in a ratio of 74 : 26.[15] This difference may arize from the greater size of the aluminum hydride anion species. In the case of styrene episulfone (II), however, both reducing agents gave abnormal products. The explanation for this unusual reaction is that the carbon-carbon bond length of the episulfone is longer than that of epoxides, thus relaxing the steric prohibition.[16]

During the reaction using lithium borohydride

10) Lithium borohydride forms a 1 : 1 complex with diethyl ether, but this complex dissociates at the reaction stage. (E. Wiberg, H. Hoth and R. Uson, *Z. Naturforsch.*, **11b**, 490 (1956).

11) R. E. Davis and J. A. Gottbrath, *J. Am. Chem. Soc.*, **84**, 895 (1962).

12) H. Haubenstock and E. L. Eliel, *ibid.*, **84**, 2368 (1962).

13) W. G. Dauben, G. J. Forken and D. S. Noyce, *ibid.*, **78**, 2579 (1956).

14) D. M. S. Wheeler and J. W. Huffman, *Experientia*, **16**, 516 (1960).

15) R. Fuchs and C. A. Van der Werf, *J. Am. Chem. Soc.*, **76**, 1631 (1954); *ibid.*, **78**, 5612 (1956).

16) We are now studying the physical properties of the episulfone by means of the NMR and UV spectra.

as a reducing agent, we observed that the hydroboration of styrene occurred: α-(IX) and β-phenylethyl alcohol (VIII) were produced in a ratio of about 20 : 80; this ratio was the same as that obtained by the usual hydroboration of styrene.[17a,b]

Such an evolution of diborane is interesting, we first assumed as follows: the produced sulfinic acid salt can not form a complex with diborane, which is different from the behavior of carbanion or oxoanion. Accordingly, the diborane could react with styrene in the case of the present reduction (Eq. (5)):

$$\left.\begin{aligned} &R^{\ominus}M^{\oplus} + BH_3 \rightarrow R\text{-}\overset{\ominus}{B}H_3\ M^{\oplus} \\ &RO^{\ominus}M^{\oplus} + BH_3 \rightarrow R\text{-}O\text{-}\overset{\ominus}{B}H_3\ M^{\oplus} \\ &RSO_2^{\ominus}M^{\oplus} + BH_3 \not\rightarrow R\text{-}SO_2\text{-}\overset{\ominus}{B}H_3\ M^{\oplus} \end{aligned}\right\} \quad (5)$$

However, as will be described below, we discovered a new route to the formation of diborane by the reaction of lithium borohydride or sodium borohydride with sulfur dioxide. Therefore, this hydroboration must mainly come from the diborane[18] formed by the reaction of the borohydride with sulfur dioxide, which is obtainable from the episulfone. (In the case of lithium aluminum hydride, allane (AlH_3) might be formed, but in our study this reaction did not occur.)

The reduction of tetraphenylethylene episulfone (III) by lithium aluminum hydride or sodium borohydride gave 1, 1, 3, 3-tetraphenyl dimethyl sulfone (XI) in good yields. The formation of XI showed the occurrence of carbon-carbon bond fission, though it was sterically much hindered.

Previously, Hesse *et al.*[2] found that ethylene episulfone (IV) was reduced to give polyethylene sulfide (XII) by lithium aluminum hydride, indicating that no carbon-carbon cleavage of the compound occurred.

To summarize the above results, both *cis*-stilbene episulfone (I) and tetraphenylethylene episulfone (III) gave products formed by selective carbon-carbon-bond fission by complex metal hydrides. On the other hand, neither styrene episulfone (II) nor ethylene episulfone (IV) have the carbon-carbon bonds cleavage products; only the carbon-sulfur bond was cleaved.

From these results, it seems that at least two phenyl groups are required for the carbon-carbon bond fission.[19] An inductive effect of phenyl groups weakens the carbon-carbon bonds, and a resonance effect of the groups may act to stabilized the resonance forms (B and C) mentioned below. Also, the steric effect by the phenyl groups would make the carbon-carbon bond longer; as a result, the carbon-carbon bond is more vulnerable to attack by nucleophiles.

The driving force for these reactions cannot be the carbanion stabilization of an intermediate or transition state.[20] If this were the case, the carbon-carbon bond of styrene episulfone would be cleaved, giving a carbanion almost identical (formation of benzyl carbanion formed by attack at the α-carbon) to the case of *cis*-stilbene episulfone (I).

The driving force for the reductive cleavage of the carbon-carbon bond should include a relief of the strain.

Thermally, carbon-carbon bond would be stronger than carbon-sulfur bonds, for sulfur dioxide is evolved by the thermal decomposition of episulfones, affording olefins.[6] However, the carbon-carbon bonds have a π-character; in other words, they have a double-bond character according to the Walsh model.[21] Therefore, if carbon-carbon bonds were weakened by such electron-withdrawing substituents as sulfone and phenyl groups in this case, the carbon-carbon bonds would be attacked by nucleophiles.

Let us now discuss the mechanism of these reactions in the case of I. We proposed, in a previous report,[4] a four-centered reaction mechanism for the reduction by lithium borohydride, sodium borohydride, and lithium aluminum hydride (Eq. (6));

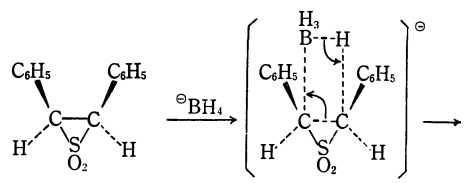

(I)

$$C_6H_5CH(\overset{\ominus}{B}H_3)SO_2CH_2C_6H_5 \xrightarrow{H_2O} C_6H_5CH_2SO_2CH_2C_6H_5 \quad (6)$$

(V)

The following mechanism would also be attractive:

17) a) H. C. Brown and G. Zweifel, *J. Am. Chem. Soc.*, **82**, 4708 (1960). Review: G. Zweifel and H. C. Brown, "Org. Reactions," Vol. 13, John Wiley and Sons, New York (1963), p. 1. b) In the case of the *cis*-stilbene episulfone (I) reduction, 1, 2-diphenylethanol was not formed because of the short reaction time.

18) We will report on the reaction in the near future.

19) G. W. Griffin *et al.* recently reported the photocleavage of phenyl-substituted cyclopropane in ionic fashion to give substituted propanes. This reaction proceeded by a photochemical process, not by heating. On the other hand, in our study, episulfones gave carbon-carbon bond cleavage products more easily, even at room temperature. This difference may be ascribed to the higher energy of the ground state of episulfones. (G. S. Irving, R. C. Petterson, I. Sarkar, H. Kristinsson, C. S. Aaron, G. W. Griffin and G. J. Boudreaux, *J. Am. Chem. Soc.*, **88**, 5675 (1966)).

20) B. Franzus and E. I. Snyder, *ibid.*, **87**, 3423 (1965).

21) M. Pomerantz *et al.* have reported on the electronic structure and reactivity of bicyclobutanes, showing a π-character in the peripheral and bridgehead bonds (M. Pomerantz and W. Abrahamson, *J. Am. Chem. Soc.*, **88**, 3970 (1966)).

Three-membered rings involving the electron-withdrawing groups, such as tetracyanoethylene oxide,[22] 1, 2-diphenylaziridine,[23] and cyclopropanones,[24] react with olefins, acetylenes, and dienes by 1, 3-dipolar or 1, 3-diradical concerted mechanisms, resulting in carbon-carbon bonds fission. Similarly, the present reaction might occur by a promotion of the episulfone to activated species B and C, which then react with complex metal hydrides by a 1, 3-dipolar-type reaction.

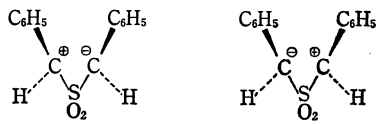

(B) (C)

There also is another mechanistic route to give V, *i. e.*, the S_N2 type, as shown by epoxide reduction[25] (Eq. (7)):

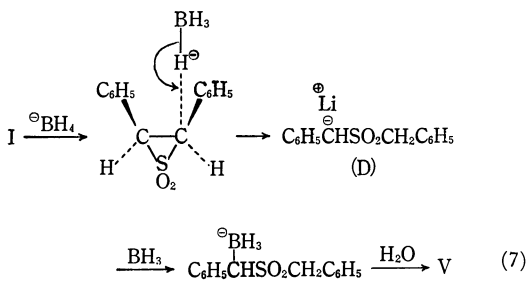

(7)

There is no clear reason to exclude these mechanisms, since stereochemical and kinetical data are lacking.[26,27] Solvent effects also give no suggestion about the problem. Since the carbanion leading to the formation of V could not be trapped, the fast attack on the carbanion by the liberating hydrogen, as shown in Eq. (8), could not be omitted. The backside-attack mechanism of the reagent due to its complex formation with sulfone group may, however, be ruled out, for borane (BH_3) did not give V at all, though borane would more easily attack the oxygen atom of the sulfone group.

There remains a question of the fate of the liberated sulfur dioxide (liberated by thermal decomposition).

It is noteworthy that sulfur dioxide reacts selectively with lithium borohydride or sodium borohydride to give diborane, without reacting with alkyl lithium (D). To investigate the reductive-cleavage mechanism, the authors added triethylamine to the reaction mixture. The products were V, VI, and, interestingly, triethylamine borane (XIII). If sulfur dioxide did not react with lithium borohydride or sodium borohydride, triethylamine borane would not be formed, since the carbanion (D) would be stronger base than triethylamine, giving no XIII.[28] In addition, the reaction of sulfur dioxide with complex borohydride to give borane was verified (Eq. (8)):

$$4LiBH_4 + SO_2 \xrightarrow{THF} 2BH_3 + Li_2S + 2LiOBH_3 + 2H_2 \quad (8)$$

The formation of diborane by this method was confirmed by the hydroboration of styrene, and the lithium sulfide liberated was ascertained by a reaction with Pb $(OAc)_2$ to form PbS.[29]

The results of the new route to borane formation and the subsequent use of diborane in sulfur dioxide will be reported elsewhere in detail.

Experimental[30]

Materials. The solvents were purified as follows. Tetrahydrofuran, diethyl ether, dimethyl sulfoxide and triethylamine were obtained from Wako Pure Chemicals. The tetrahydrofuran was purified by refluxing it with sodium for two days. It was then treated with lithium aluminum hydride, and distilled. The diethyl ether was dried over sodium and distilled over lithium aluminum hydride. The dimethyl sulfoxide was refluxed for 10 hr over calcium hydride and distilled at reduced pressure. The triethylamine was distilled over potassium hydroxide pellets. The diglyme (diethylene glycol dimethyl ether) (Aldrich Chemical Co., Inc.) was first distilled over calcium hydride, and then over lithium aluminum hydride.

Lithium borohydride (98%), lithium aluminum hydride, sodium borohydride, lithium hydride, sodium

22) W. J. Linn, *J. Am. Chem. Soc.*, **87**, 3665 (1965).
23) a) A. Padwa and L. Hamilton, *Tetrahedron Letters*, **1965**, 4363; b) A. E. Pohland, R. C. Badger and N. H. Cromwell, *ibid.*, **1965**, 4369; c) R. Huisgen, W. Scheer, G. Szeimies and H. Huber, *ibid.*, **1966**, 397, 405.
24) a) N. J. Turro, G. W. Byers and P. A. Leermaker, *J. Am. Chem. Soc.*, **86**, 955 (1964); b) P. A. Leermaker, G. Vesley, N. J. Turro and D. C. Neckers, *ibid.*, **86**, 4213 (1964); c) N. J. Turro, P. A. Leermaker, H. R. Wilson, D. C. Neckers, G. W. Byers and G. F. Vesley, *ibid.*, **87**, 2613 (1965).
25) The borohydride ion, which is more ionic in character than the aluminum hydride ion, yields more V. This suggests that a transition state, such as B or C, may be favored by a more ionic reagent.
26) R. E. Parker and N. S. Lsaacs, *Chem. Revs.*, 737 (1959).
27) A few examples of supposed four-centered transition states by sodium borohydride have appeared. CF. F. G. Bordwell and M. L. Douglass, *J. Am. Chem. Soc.*, **88**, 993 (1966); R. E. Dessay and E. Grannen, Jr., *ibid.*, **83**, 3953 (1961).
28) The carbanion (D) is a stronger base, since α-chlorobenzyl benzyl sulfone treated with triethylamine did not give stilbene.[3]
29) The reaction of diborane with KOH has recently been reported by Jolly and Schmitt (W. J. Jolly and T. Schmitt, *J. Am. Chem. Soc.*, **88**, 4282 (1966)).
30) All melting points and boiling points are uncorrected. The infrared absorption spectra were determined on a Hitachi infrared spectrophotometer. The nuclear magnetic resonance spectra were run on a Nihondensi spectrometer at 60 Mc. Tetramethylsilane was used as an internal standard, and chloroform-d was used as the solvent (Chiba Ltd.). V. p. c. analysis was carried out on a Yanagimoto, Model GCS-100, instrument.

hydride, and aluminum chloride were obtained commercially. All these compounds were used without further purification.

Liquid sulfur dioxide was donated by Seitetsu Kagaku and was used after having been dried over phosphorus pentoxide for at least one day.

cis-Stilbene episulfone (I) was synthesized as has been described in a previous report;[3] a phenyldiazomethane solution[31] (about 0.05 mol in 300 m*l* ether) in a 1-*l* Erlenmeyer flask had a sulfurous acid solution added (6%) over a five-minute period. The solid obtained on cooling was filtered and recrystallized from ether-benzene at about 50°C. Mp 87—88°C (dec.).

Styrene episulfone (II) was obtained by the method of Opitz;[5c] in a three-necked, 500 m*l*, round-bottomed flask, equipped with a reflux condenser, a stirrer, and a dropping funnel, there were placed about 0.05 mol of diazomethane and 7.0 g of triethylamine in 100 m*l* of ether. In a dropping funnel there were placed about 11.0 g benzylsulfonyl chloride in 300 m*l* of ether. The solution was then added slowly, over a period of 30 min, to diazomethane triethylamine solution, with the temperature maintained at −30°C (dry ice - triclene bath). After the addition, the solid (triethylammonium chloride) was filtered off and the mother liquor was concentrated by distillation under reduced pressure as fast as possible. The resulting solid (6.5 g (0.039 mol)) was filtered off, washed once with cold ether, and used without further purification; mp 40°C (dec.) (yield 70%). Styrene episulfone was too unstable to be stored it at noom temperature and dried it in a round-bottom flask kept at 0°C (ice bath) by pumping.

Tetraphenylethylene episulfone (III) was synthesized by the method of Staudinger *et al.*[5a] Because of its poor stability, III was used as soon as it had been dried for 30 min in a desiccator.

Reduction of *cis*-Stilbene Episulfone (I) by $LiAlH_4$, $LiBH_4$ and $NaBH_4$ (General Procedure). In a three-necked, 200 m*l*, round-bottomed flask, equipped with a reflux condenser and a stirrer, there were placed 0.04 mol of complex metal hydride and 100 m*l* of a solvent. To a well-stirred suspension, there were then added 0.02 mol of *cis*-stilbene episulfone (I) under nitrogen. After 4 hr at room temperature (15° C), the reaction mixture was added to 100 m*l* of ice-water and extracted twice with 150 m*l* of ether. After the combined ether layer had been dried over anhydrous sodium sulfate, the ether was removed under reduced pressure. The white precipitate was washed with ether to give dibenzylsulfone (V).[32] V was identified by comparison with an authentic specimen; mp 148—149°C. IR ν_{max}^{KBr} 1302, 1286, 1125, 1113 cm^{-1} (SO_2-stretching). NMR $\tau=5.9$ ppm (methine). The residue (liquid) was *cis*-stilbene, identified as before.[3] No product was obtained from the water layer.

Reduction of Styrene Episulfone (II) by $LiBH_4$. In a three-necked flask there was placed 0.764 g (0.035 mol) of lithium borohydride in 150 m*l* of anhydrous ether. To this solution there were then added 2.894 g (0.0172 mol) of styrene episulfone (II). The mixture was stirred at 0°C for 3 hr, and then poured over ice water. It was extracted with ether and dried over Na_2SO_4, after which the ether was evaporated under reduced pressure.

Remaining was a liquid (1.96 g). G. l. c. analysis at 170°C on a PEG 6000 column showed the formation of α- and β-phenylethyl alcohol in the ratio of 20 : 80.[33]

The water extract was refluxed with methyl iodide (10 g) for two days, and was then extracted with ether. The evaporation of the solvent gave 0.210 g (0.00114 mol) of white crystals (VII) (mp 87—88°C). β-Phenylethyl methyl sulfone (VII) was identified by comparison with an authentic sample.[33]

Reduction of Styrene Episulfone (II) by $LiAlH_4$. Using the technique described above, 0.954 g (0.0261 mol) of lithium aluminum hydride in a 150 m*l* ether solution was added to 3.177 g (0.0189 mol) of styrene episulfone, and the reaction mixture was stirred at 0°C for 3 hr. After having been treated as above, a liquid (0.832 g) remained; it was identified as styrene by g. l. c. analysis (PEG 6000 at 70°C). The water extract was refluxed with methyl iodide (10 g) for two days; it was then extracted with ether to give α-phenylethyl methyl sulfone (0.135 g (0.0011 mol)), which was identical with an authentic sapecimen.

Reduction of Tetraphenylethylene Episulfone (III) by $NaBH_4$ or $LiAlH_4$. To 150 m*l* of a tetrahydrofuran solution containing 0.280 g (0.0074 mol) of sodium borohydride, there was added tetraphenylethylene episulfone (III) (1.127 g (0.00285 mol)) at room temperature (15°C).

The reaction mixture was stirred for 6 hr and then poured into water. The ether extract, after drying, gave 0.59 g of white crystals, which were recrystallized from benzene petroleum ether (30—60°C) to give 1, 1, 3, 3-tetraphenyl dimethyl sulfone (XI) (mp 185—186°C (dec.)).

Found: C, 78.40; H, 5.42%. Calcd for $C_{26}H_{22}O_2S$: C, 78.37; H, 5.57%.

NMR $\tau=2.5$ ppm (phenyl), 4.78 ppm (methine: singlet).

IR ν_{max}^{KBr} 1312, 1130 cm^{-1} (SO_2-stretching).

When treated with lithium aluminum hydride, (III) give a 28% yield of (XI). The residual, tar-like substance was not identified.

Reduction of (I) by $LiBH_4$ or $NaBH_4$ in the Presence of Triethylamine. To a stirred solution of 0.463 g (0.0212 mol) of lithium borohydride and 1.40 g (0.0139 mol) of triethylamine in 100 m*l* of tetrahydrofuran, 2.287 g (0.00937 mol) of *cis*-stilbene episulfone (I) were added, after which the reaction mixture was stirred for 4 hr at room temperature and then decomposed by water. After the residue had been treated as in the above procedure, dibenzylsulfone (V) (0.601 g (0.00244 mol)) and triethylamine-borane (0.580 g (0.00504 mol)) were produced; they were identified by comparison with authentic specimens.[34]

IR ν_{B-H} 2300 cm^{-1}, bp 76°C/4 mmHg.

The residual *cis*-stilbene was identified by the coincidence of the IR spectra.

The authors are indebted to the Seitetsu Kagaku Company, Ltd., for its gift of liquid sulfur dioxide.

31) R. J. Mohrbacker and N. H. Cromwell, *J. Am. Chem. Soc.*, **79**, 401 (1957).
32) E. C. Leonard, Jr., *J. Org. Chem.*, **27**, 1921 (1962).
33) W. E. Truce and J. A. Simms, *J. Am. Chem. Soc.*, **78**, 2756 (1956); The NMR spectra of the α-form were clearly different from those of the β-form.
34) E. C. Ashby, *J. Am. Chem. Soc.*, **81**, 4791 (1961).

BULLETIN OF THE CHEMICAL SOCIETY OF JAPAN VOL. 41 641—646 (1968)

The Autoxidation of Toluene Catalyzed with Cobalt Monobromide in Acetic Acid

Koichiro SAKOTA, Yoshio KAMIYA and Nobuto OHTA

Department of Fuel Technology, The University of Tokyo, Hongo, Tokyo

(Received August 17, 1967)

The kinetics of cobalt-catalyzed autoxidation of toluene have been studied in acetic acid in the presence of sodium bromide. The reaction is found to proceed of apparent zero-order in the concentration of toluene for a long duration and of first-order in its initial concentration and of second-order in cobalt ion concentration. In case of ethylbenzene or cumene the rate of oxidation is of first-order in its concentration. This zero-order dependence is explained as a result of the co-oxidation of toluene and its intermediate reaction product, benzaldehyde. A reaction scheme is proposed, which has been shown to be consistent with experimental data by solving out the rate equations simultaneously with a computer, co-oxidation of toluene and benzaldehyde being taken into consideration.

The profound accelerating effect of the bromide on the rate of the autoxidation of aromatic hydrocarbons catalyzed by cobalt salt in organic acid media has been recognized and commercially in practice. Several papers have been published on this reaction mechanism after Revens' paper in 1959. Recently Hay and Blanchard[1] made some experimentals to examine the elementary reactions. We also have made kinetical experimentals treating with tetralin and ethylbenzene to obtain the detail of the reaction mechanism and extended our study to the oxidation of *p*-xylene under its low conversions. The characteristics of the cobalt-catalyzed autoxidation of methylbenzenes in the presence of bromide were as follows.

The rate of oxidation of methylbenzenes keeps constant for a long duration in spite of the decrease of their concentrations, even though the rates are of first-order dependence with respect to their initial concentrations. There are many complexities in the oxidation of methylbenzenes, since the aromatic aldehydes produced as intermediate products of reaction are easily oxidized and the reaction turns into co-oxidation of toluene and benzaldehyde. In this paper we studied the oxidation of toluene kinetically in detail in stead of *p*-xylene to avoid the difficulties caused by the number of the intermediate products which prevent us from satisfactory kinetical analysis when high conversions are attained. The co-oxidation reaction of toluene and benzaldehyde was taken into consideration.

Results and Discussion

The Effects of Hydrocarbons. The oxygen uptake took place after a few minutes of induction period, when toluene was oxidized with oxygen in acetic acid solution with cobalt acetate and sodium bromide as catalysts. It was observed that the rate of oxidation was increased by a factor of about 300 in the presence of bromide. As is observed in Fig. 1, there is a long duration where the rates of the consumption of toluene and of the accumulation of benzaldehyde kept constant. We regard these phenomena characteristic in the oxidation of methylbenzenes in a cobalt bromide - acetic acid-system. Kinetical experiments were made to obtain the accounts. The fact that so much of benzaldehyde was accumulated may be partly attributed to the low temperatures of reaction but

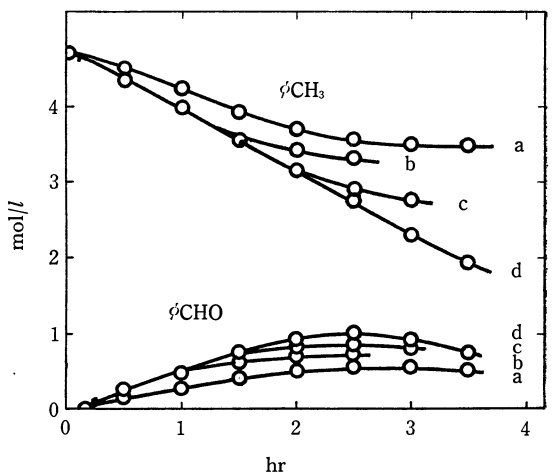

Fig. 1. Oxidation of toluene at 80°C.
Co: 2.0×10^{-2} mol/*l*
NaBr: a, 2.0×10^{-2}; b, 4.0×10^{-2}; c, 8.0×10^{-2}; d, 1.6×10^{-1} mol/*l*

1) A. S. Hay and H. S. Blanchard, *Can. J. Chem.*, **43**, 1306 (1965).

strongly suggests that the reaction of the hydrogen abstraction from toluene is more profoundly accelerated than that from benzaldehyde by the catalysis of bromide. It was observed in this case that the stronger the C-H bond, the more profoundly catalyzed the hydrogen abstraction reaction from the hydrocarbons, say, in the case of ethylbenzene (*ca.* 30 fold) and of tetralin (*ca.* 4 fold). This may be explained from the difference of the degree of the C-H bond rupture in the transition state of the hydrogen abstraction stage by peroxy radicals and by cobalt-bromide complexes. The profound effect of bromide implies that cobalt-bromide complex is more active than peroxy radicals. So the stretching of C-H bond in transition state is thought to be larger for peroxyradicals than for cobalt-bromide complex. The larger the stretching of a C-H bond, the more the contribution of the C-H bond energy to the activation energy of the process. And the order of acceleration by bromide was observed as *p*-toluic acid > toluene > ethylbenzene > tetralin. The bond formation between peroxyradical and toluene, ROO···H-CH_2-ϕ, may be less favoured than between bromide and toluene, Co-Br···H-CH_2-ϕ, because bromine atom is more capable of covalent bond formation and less oriented to form a bond due to the presence of d-orbitals and its larger size than oxygen. These properties may explain that the activation energy of the reaction catalyzed by bromine is less affected by the bond energy of the C-H bond to be broken. Benzaldehyde is oxidized into perbenzoic acid *via* benzoyl radical. Perbenzoic acid suffers homolytic decomposition by cobalt salt to give radicals. These radicals can abstract the hydrogen atom from toluene or increase the concentration of the active cobalt complex, which can also abstract hydrogen atom from toluene. In other words, benzaldehyde can accelerate the consumption of toluene—co-oxidation of toluene and benzaldehyde—. The behaviors of benzaldehyde explain qualitatively the apparent zero-order dependence of the rate of toluene consumption on the concentration of toluene. It was observed also in case of *p*-xylene and *p*-toluic acid that the profile of the reaction was the same as in case of toluene. To determine the effect of the concentration of the hydrocarbon, the initial concentration of toluene was varied. As presented in Fig. 2, the variation of the initial concentration of toluene with constant concentrations of cobalt acetate and sodium bromide showed first-order dependence of the rate of toluene consumption and of accumulation of benzaldehyde. It follows from this fact the hydrogen abstraction stage is the rate-determining step. Benzaldehyde and benzoic acid were produced mainly, with a little amount of benzyl alcohol. The concentration of peroxidic compounds was less than 10^{-3} mol/*l*. Ethlbenzene and cumene were oxidized to give acetophenone mainly. In either case, the rates of oxygen uptake and of consumption of hydrocarbon were proportional to the concentration of their own during the oxidation, namely the rate of oxidation is of first-order with respect to the concentration of hydrocarbon in contrast to the case of toluene (Fig. 3).

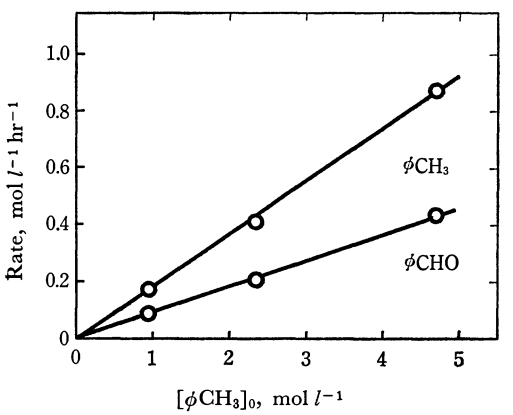

Fig. 2. The rates of toluene consumption and of accumulation of benzaldehyde at 80°C with 2×10^{-2} mol/*l* cobalt, 4×10^{-2} mol/*l* sodium bromide.

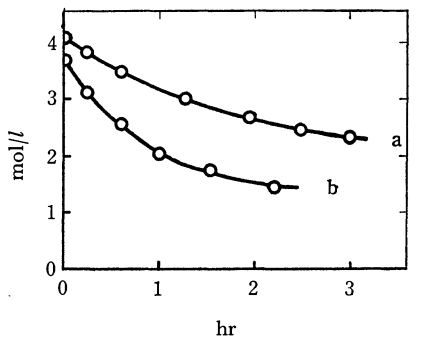

Fig. 3. Oxidation of ethylbenzene and cumene at 80°C with 2×10^{-2} mol/*l* cobalt and 4×10^{-2} mol/*l* sodium bromide.
a, ethylbenzene; b, cumene

This difference of the reaction profile is ascribed to the difference between the stability of benzaldehyde and acetophenone against oxidation. The facts above make it necessary that the oxidation of toluene is treated kinetically as co-oxidation when high conversions of toluene are reached. In general, it might be said in the oxidation of aromatic hydrocarbons in cobalt bromide - acetic acid-system that: (1) the oxidation of the hydrocarbons with only primary hydrogens in the side chains, proceeds of apparent zero-order dependence on the concentration during the oxidation and shows first-order dependence on the initial concentration of the hydrocarbons to be oxidized, (2) the oxidation of hydrocarbons with secondary and/or

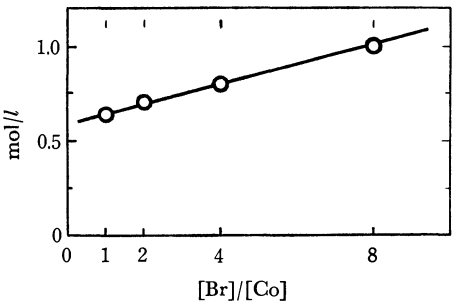

Fig. 4. The maximum amount of benzaldehyde accumulated *vs.* ratio of sodium bromide to cobalt.

tertiary hydrogens in the side chains, is of first-order dependence on the concentration and gives corresponding ketones as oxidation products.

The Effect of The Concentration of Sodium Bromide. As mentioned above the bromide seems to catalyze the process where toluene is oxidized into benzaldehyde, and the amount of bromide added has a profound effect on the oxidation rate (Figs. 1 and 4). The rate of toluene consumption increased continuously as the concentration of bromide increased until the ratio of [bromide]/[cobalt acetate] attained near two and kept constant when the ratio became higher than two. We conclude from the facts mentioned above and other papers[2,3] that the catalytic species is cobalt monobromide. It seems, however, that our proposed reaction mechanism may be insufficient to explain the length of the duration where the rate of toluene consumption kept constant and the maximum amount of accumulated benzaldehyde became larger according to the increase of the amount of the added bromide. But these behaviors can be fully understood from the data in Fig. 5. The line (a) stands for the change of the concentration of the bromide anion and has good correspondence to the toluene consumption curve. It implies that bromine atoms were consumed proportionally to the extent of the reaction. When bromide was analyzed quantitatively after the reaction solution was diluted with alkaline solution and refluxed sufficiently, the values obtained were equal to the initial concentration of bromide (the line (b)). Bromine atom seems to be consumed as benzyl bromide. The number of toluene molecule oxidized per one bromine atom was about 25. This number is temperature dependent and becomes larger at higher temperatures because organic bromides may be decomposed to regenerate bromine atoms. The electronic spectra of the reaction solution are shown in Fig. 6. Optical density readings were taken at the reaction temperature. Oxygen feed and time count were started when the temperature of the solution reached the designated value. The decrease in the optical densities at 14.5 kK corresponded satisfactorily to the change of the concentration of the bromide anion shown in Fig. 5. The increases in optical densities in the ultraviolet region are due to the increase in the concentration of benzaldehyde formed. The shape of the electronic spectra changed and had a stronger resemblance to that of cobaltous acetate after the consumption of bromine atom. The reaction rate also began to tail off according to the decrease of the concentration of the bromide. Now it was understood easily that the more the added amount of bromide, the longer the length of the duration where the sufficient amount of bromide anion is present to maintain the catalytic activities of the cobalt-bromide complex.

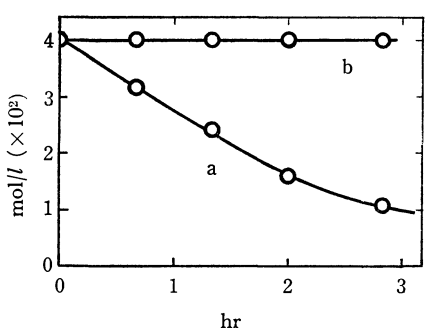

Fig. 5. Concentration of bromide anidn *vs.* reaction time at 80°C with 2×10^{-2} mol/*l* cobalt.

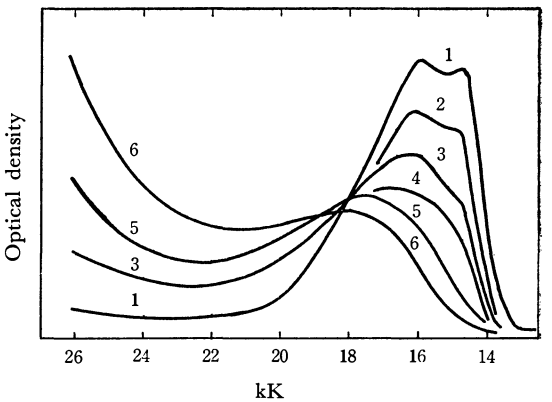

Fig. 6. Electronic spectra of reaction solution at 80°C with 5×10^{-3} mol/*l* cobalt and 1×10^{-2} mol/*l* sodium bromide.
1: 0 min; 2: 25 min; 3: 65 min; 4: 85 min; 5: 105 min; 6: 120 min

The Effect of Cobalt Concentration. The dependence of the rate of oxygen uptake was shown in Fig. 7. At the concentrations from 5×10^{-3} to 4×10^{-2} mol/*l* of cobalt acetate, the rate of oxygen uptake was of second-order with respect to the

2) Y. Kamiya, *Kogyo Kagaku Zasshi (J. Chem. Soc. Japan, Ind. Chem. Sect.)*, **69**, 897 (1966); Y. Kamiya, *Tetrahedron*, **22**, 2029 (1966).
3) Y. Kamiya, J. Nakajima and K. Sakoda, This Bulletin, **39**, 2211 (1966).

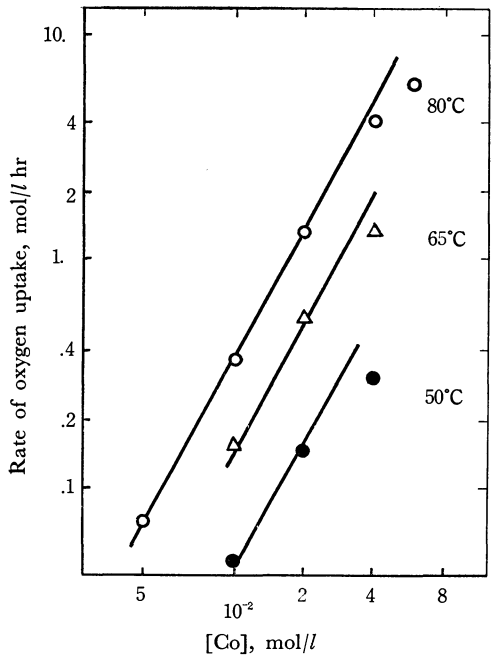

Fig. 7. The rates of oxygen uptake *vs.* concentration of cobalt acetate at $[NaBr]/[Co(OcA)_2 \cdot 4H_2O]=2$.

concentration of cobalt salt, showing some departure from linearity at high concentrations of cobalt salt. This may be partly due to the limitation of solubility of sodium bromide to maintain the ratio of [bromide]/[cobalt acetate] higher than about two, which assures the maximum concentration of cobalt monobromide. If the cobalt ion only affects the catalysis of decomposing hydroperoxides, the rate of toluene consumption will be of less first-order to the concentration of cobalt acetate assuming a bi-molecular termination process. Since the decomposition of hydroperoxide by cobalt ions in glacial acetic acid (referred to as (Co)) is expressed as follows[4] under the conditions employed here.

$$\text{hpo} + 2(\text{Co}) \longrightarrow \text{radicals}$$

The second-order dependence to cobalt ion implies the following reactions with participation of cobalt ion into propagation steps.

$$\phi CH_3 + \text{Co(III)Br}^- \longrightarrow \phi CH_2\cdot + \text{Co(II)BrH} \quad (1)$$

$$\phi CH_2\cdot + O_2 \longrightarrow \phi CH_2OO\cdot \quad (2)$$

$$\phi CH_2OO\cdot + \text{Co(II)BrH} \longrightarrow \phi CHO + \text{Co(III)Br} + H_2O \quad (3)$$

Benzaldehyde can behave like initiator. So the concentration of active species which are capable to abstract hydrogen atom from methyl groups may increase, as the concentration of benzaldehyde increases. It seems inadequate to apply stationary state treatment in this system when the amount of benzaldehyde accumulated is considerable. Co-existence of active species, such as $\phi CH_2OO\cdot$, $\phi COOO\cdot$ and Co(III)Br^-, and the occurrance of cross-termination prevent from solving out equations directly to show the second-order dependence on cobalt concentration, the apparent zero-order dependence on toluene concentration, *etc.*

The Cobalt-Bromide Complexes. It has been reported that $Co(H_2O)_6^{2+}$, $Co(H_2O)_4Cl_2$ are octahedral and $CoBr_4^{2-}$ is tetrahedral. Cobalt acetate will be changed into $CoBr^+$(Oh), $CoBr_2$(Oh),$\cdots CoBr_4^{2-}$(Td) step by step according to the addition of bromide. The absorption band at 14.5 kK in Fig. 8 is considered to be caused by the transition $^4T_1 \leftarrow {}^4A_2$ of $CoBr_4^{2-}$, because it has the strongest intensity and is located at the longest wavelength and the intensity at 14.5 kK decreased continuously according to the extent of the reaction (Fig. 6). The bands around 16 kK may be the bands splitted and shifted of that of cobalt acetate at 18.7 kK by the lowering of the symmetry caused by the coordination of bromide anion to cobalt ion. The Co–Br bond is expected to be more covalent than the Co–OAc bond from the values of nephelauxetic ratios and nuclear quadrupole resonance data and so on. This covalency will make the electron transfer easier from bromide anion to cobaltic cation which is formed *via* oxidation of Co(II) by hydroperoxides or peroxyradicals. This tranfer will stabilize the Co(III) state and as a result, give the radical character to the bromine ligated to the Co(III). And the bromine may gain the ability of hydrogen abstraction. Because of the presence of *d*-orbitals and its larger size, bromine is less oriented and easier for hydrogen to form a bond with than oxygen in acetate or cobalt ion is. This favours the bond formation with hydrogen atom of alkyl groups.

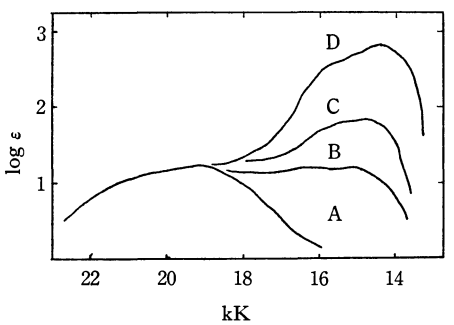

Fig. 8. Electronic spectra of cobalt acetate in the presence of sodium bromide in acetic acid solution.
[sodium bromide]/[cobalt acetate]:
A, 0; B, 0.5; C, 2.0; D, 100

4) Y. Kamiya and K. U. Ingold, *Can. J. Chem.*, **41**, 2020 (1964).

The Reaction Mechanism. The detailed mechanism of initiation steps is not still fully explained but we gave some discussions in other papers.[2,3] When the reaction proceeds to some extent and the concentration of benzaldehyde becomes considerable, the initiation reaction (12) is predominant over other initiation processes. When benzylhydroperoxide is decomposed catalytically by cobalt ion, benzyloxy and benzylperoxy radicals are formed in equal amount. Benzyloxy radical abstracts hydrogen and become benzylalcohol. If benzylperoxy radical became benzylhydroperoxide, benzylalcohol would be accumulated to considerable amount. Because benzylalcohol was rather stable and oxidized at the rate of 5% of that of toluene. But little amount of benzylalcohol was detected in experiments. This suggests thatthe contribution of the reaction (4) is small. An alternative mechanism below, where benzaldehyde is formed from benzylhydroperoxide without formation of benzylalcohol,

$$\phi CH_2OOH + Co(II) \rightarrow [\phi CH_2O\cdots Co(III)] + OH^- \rightarrow \phi CHO + Co(II) + H^+ + OH^-$$

$$\phi CH_2OOH + Co(III) \rightarrow [\phi CH_2OO\cdots Co(II)] + H^+ \rightarrow \phi CHO + Co(III) + OH^- + H^+$$

may not be operative. Because it may be unreasonable that above reactions proceed without migration of radicals formed from hydroperoxide out of the solvent cage around the cobalt ion. The reaction (3) is probable. The following elementary reactions will explain the experimental observations after the initial stage of the reaction.

$$\phi CH_3 + Co(III)Br \xrightarrow{k_1} \phi CH_2\cdot + Co(II)BrH \quad (1)$$

$$\phi CH_2\cdot + O_2 \xrightarrow{k_2} \phi CH_2OO\cdot \quad (2)$$

$$\phi CH_2OO\cdot + Co(II)BrH \xrightarrow{k_3} \phi CHO + Co(III)Br + H_2O \quad (3)$$

$$\phi CH_2OO\cdot + \phi CH_3 \xrightarrow{k_4} \phi CH_2OOH + \phi CH_2\cdot \quad (4)$$

$$\phi CH_2OO\cdot + \phi CHO \xrightarrow{k_5} \phi CH_2OOH + \phi CO\cdot \quad (5)$$

$$\phi CHO + Co(III)Br \xrightarrow{k_6} \phi CO\cdot + Co(II)BrH \quad (6)$$

$$\phi CO\cdot + O_2 \xrightarrow{k_7} \phi COOO\cdot \quad (7)$$

$$\phi COOO\cdot + Co(II)BrH \xrightarrow{k_8} \phi COOOH + Co(III)Br \quad (8)$$

$$\phi COOO\cdot + \phi CH_3 \xrightarrow{k_9} \phi COOOH + \phi CH_2\cdot \quad (9)$$

$$\phi COOO\cdot + \phi CHO \xrightarrow{k_{10}} \phi COOOH + \phi CO\cdot \quad (10)$$

$$\phi CH_2OOH + Co_2 \xrightarrow{k_{11}} \text{radical} \rightarrow 2Co(III)Br \quad (11)$$

$$\phi COOOH + Co_2 \xrightarrow{k_{12}} \text{radical} \rightarrow 2Co(III)Br \quad (12)$$

$$\phi COOOH + \phi CHO \xrightarrow{k_{13}} 2\phi COOH \quad (13)$$

$$2\phi CH_2OO\cdot \xrightarrow{k_{14}} \phi CHO + \phi CH_2OH \quad (14)$$

$$2\phi COOO\cdot \xrightarrow{k_{15}} (\phi COO)_2 + O_2 \quad (15)$$

$$\phi CH_2OO\cdot + \phi COOO\cdot \xrightarrow{k_{16}} \phi CHO + \phi COOH + O_2 \quad (16)$$

The equilibrium below exists and reactions (3) and (1) are expressed as follows.

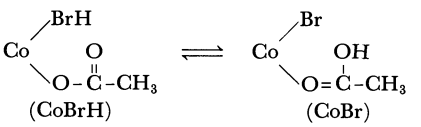

reaction (3):

$$\phi CH_2OO\cdot + Co(II)BrH \longrightarrow$$

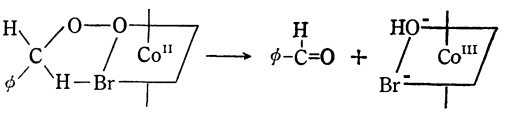

reaction (1):

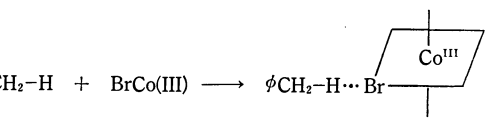

Benzoyloxy radical has not hydrogen atom and cannot proceed *via* reaction (3), so might be converted to perbenzoic acid.

$$\phi COOO\cdot + HBrCo(II) \rightarrow \phi COOOH + BrCo(III)$$

The reactions (2) and (7) are very fast, therefore can be simplified as follows.

$$\phi CH_3 + Co(III)Br \xrightarrow{k_1'} \phi CH_2OO\cdot + Co(II)BrH$$

$$\phi CHO + Co(III)Br \xrightarrow{k_6'} \phi COOO\cdot + Co(II)BrH$$

Above reactions are rewritten as ordinary differential equations.

$$-d[\phi CH_3]/dt = k_1'[\phi CH_3][Co(III)Br] + k_4[\phi CH_3][\phi CH_2OO\cdot] + k_9[\phi CH_3][\phi COOO\cdot]$$

$$d[\phi CH_2OO\cdot]/dt = k_1'[\phi CH_3][Co(III)Br] - k_3[\phi CH_2OO\cdot][Co(II)BrH] - k_5[\phi CHO][\phi CH_2OO\cdot] + k_9[\phi CH_3][\phi COOO\cdot] - 2k_{14}[\phi CH_2OO\cdot]^2 - k_{16}[\phi CH_2OO\cdot][\phi COOO\cdot]$$

$$d[\phi CHO]/dt = k_3[\phi CH_2OO\cdot][Co(II)BrH] - k_5[\phi CHO][\phi CH_2OO\cdot] - k_6'[\phi CHO][Co(III)Br] - k_{10}[\phi CHO][\phi COOO\cdot] - k_{13}[\phi CHO][\phi COOOH] + k_{14}[\phi CH_2OO\cdot]^2 + k_{16}[\phi CH_2OO\cdot][\phi COOO\cdot]$$

$$d[\phi COOO\cdot]/dt = k_5[\phi CHO][\phi CH_2OO\cdot] + k_6'[\phi CHO][Co(III)Br] - k_8[\phi COOO\cdot][Co(II)BrH] - k_9[\phi CH_3][\phi COOO\cdot] - 2k_{15}[\phi COOO\cdot]^2 - k_{16}[\phi CH_2OO\cdot][\phi COOO\cdot]$$

$$d[\phi COOOH]/dt = k_8[\phi COOO\cdot][Co(II)BrH] + k_9[\phi CH_3][\phi COOO\cdot] + k_{10}[\phi CHO][\phi COOO\cdot] - k_{12}[\phi COOOH][Co(II) + Co(III)]^2$$

$$d[Co(III)Br]/dt = -k_1'[\phi CH_3][Co(III)Br] + k_3[\phi CH_2OO\cdot][Co(II)BrH] - k_6'[\phi CHO][Co(III)Br] + k_8[\phi COOO\cdot][Co(II)BrH] + 2k_{12}[\phi COOOH][Co(II) + Co(III)]^2$$

As the concentration of benzaldehyde become higher according to the consumption of toluene, the concentration of perbenzoic acid may increase. Perbenzoic acid is decomposed to give radicals. This increase may raise the rate of initiation step and compensate the decrease of toluene concentration to keep the rate of toluene consumption constant for a long time. But this explanation is only qualitative. Above simultaneous six first-order ordinary differential equations have been solved after Runge-Kutta Gill's method with a OKITAC 5090 electronic computer to see the dependence on the initial concentration of the toluene and cobalt salt. The meaningful results may be obtained in spite of some arbitraliness of the values of rate constants used.

The values of rate constants were changed little by little in order that the curves of the concentrations of toluene and benzaldehyde against reaction time have stronger resemblance to those obtained in experiments. One set of the rate constants which gave satisfiable calculation results are as follows.

k_1': 1×10^{-2}, k_3: 1, k_4: 1×10^{-5}, k_5: 5×10^{-5}, k_6': 1.5×10^{-2}, k_8: 2, k_9: 1×10^{-4}, k_{10}: 2×10^{-4}, k_{12}: 2×10^{1}, k_{13}: 5×10^{-3}, k_{14}: 3×10^{-1}, k_{15}: 3×10^{-1}, k_{16}: 3×10^{-1}, $mol^{-1}\,l^{-1}\,sec^{-1}$ except k_{12} ($mol^{-2}\,l^{2}\,sec^{-1}$)

According to the assumed predominance of the reaction (12) in initiation steps mentioned above, the initial conditions for intermediates, $\phi CH_2OO\cdot$, ϕCHO, $\phi COOO\cdot$, $\phi COOOH$, Co(III)Br, were given as 5×10^{-3}, 5×10^{-2}, 2×10^{-4}, 2×10^{-3}; $1—4\times10^{-3}$, mol l^{-1}, respectively.

The calculation results suggest that above elementary reactions are consistent with the observations: the apparent zero-order dependence of the rate of toluene consumption on the concentration of toluene in the solution, and the constancy of the ratio of $d[\phi CH_3]/d[\phi CHO]$ in the earlier stage of the reaction and the first-order dependence on the initial concentration of toluene and the second-order with respect to the concentration of cobalt acetate. The ratio of k_1' to k_6' suggests that the oxidation of toluene was more efficiently catalyzed than that of benzaldehyde.

Experimental

Reagents. Hydrocarbons such as toluene, were washed with sulfuric acid till the solutions were not colored and with alkaline solution, then distilled as usually. Acetic acid, cobalt acetate and sodium bromide of guaranteed grade were used without further purification.

Reaction Vessels. All runs were carried out in a 50 m*l* glass flask connected to the oxygen reservoir and the pressure was kept constant automatically in a thermostatted water bath. All measurements of absorption spectra were made by means of a Hitachi EPS-2 spectrophotometer, using 10 mm quartz cell mounted in a thermostated cell holder under temperature controll to ±0.5°C. The cells are equipped with a condenser, a oxygen inlet tube and a glass thermister to controll the reaction temperature automatically. The solution was stirred by oxygen gas.

Analysis. Quantitative analysis was made by gas chromatography and polarography, under the conditions—polyethylene glycol 6000, 20 wt%, on Flusin-T; and 50% alcoholic McIlvaine buffer solution, respectively. The concentration of bromide was determined by potentiometric titration with a siver electrode coated with argentous bromide by a standard argentous nitrate solution.

BULLETIN OF THE CHEMICAL SOCIETY OF JAPAN VOL. 41 647—652 (1968)

Macro Rings. I. Syntheses of a Novel Class of Compounds with a Chain of Alternating Benzene Rings and Methylene Groups[1]

Takahiko INAZU and Tamotsu YOSHINO

Department of Chemistry, Faculty of Science, Kyushu University, Hakozaki, Fukuoka

(Received August 22, 1967)

As starting materials for the synthesis of a macrocyclic compound, I, bridged diphenylmethane derivatives of the general formula p-$XC_6H_4CH_2(C_6H_4CH_2)_mC_6H_4X$-$p$ were synthesized; X is hydrogen or $(CH_2)_nCOOR$ (n=0—3), m=2 or 3, and R=hydrogen or alkyl.

Because of the possibility of forming clathrate compounds and other charge-transfer complex, a macrocyclic compound constructed of four or five benzene rings and intervening methylene bridges attached to their para positions is of particular interest.

In the hope of synthesizing a paracyclophane such as I carrying four or five benzene rings, the cyclization of a chain compound with the same number of benzene rings in its molecule has been attempted several times,[2,3] all these attempts have been unsuccessful. As a result of a preliminary experiment, it seemed necessary for a compound to be cyclized to have both an appreciable solubility in an inert solvent suitable for ring closure and some crystallizability in order to avoid difficulty of isolation. For the purpose of finding an accessible and suitable material for the synthesis, bridged diphenylmethane derivatives of the general formula p-$XC_6H_4CH_2(C_6H_4CH_2)_mC_6H_4X$-$p$ were synthesized; X stands for hydrogen or $(CH_2)_n$·COOR (n=0—3), m means 2 or 3, and R represents hydrogen or alkyl.

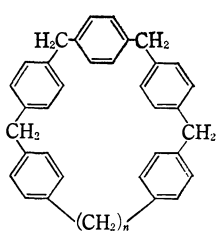

I

Fig. 1

Esters of dicarboxylic acids derived from p-bis(p-benzylbenzyl)benzene, Vb—f, were synthesized as shown in Fig. 2 by the Friedel-Crafts acylation of 4-substituted diphenylmethanes, II, with terephthaloyl chloride to terephthalophenone derivatives, III, and either by the Wolff-Kishner reduction of III and subsequent esterification or by the formation of thioketals, IV, and subsequent desulfurization with Raney nickel. Their characteristic infrared absorption bands over the 2000—1660 cm^{-1} range obviously showed that the Friedel-Crafts acylation products, III, and the reduction products, V and VI were para-substituted compounds.

Although the Friedel-Crafts acylation of p-dibenzylbenzene VIII with p-ethoxycarbonylbenzoyl chloride yielded, as is shown in Fig. 3, p-bis[p-(p-ethoxycarbonylbenzoyl)benzyl]benzene, IX, which might be reducible to Vb, this route seemed to be less general than that illustrated in Fig. 2.

The p-dibenzylbenzene, VIII, has been obtained by the Friedel-Crafts reaction of benzyl chloride and benzene, but it has also been reported that the product was accompanied by other isomers and that the separation was fairly difficult because of the similarity of boiling point, melting point and other characteristics between these isomers.[4] The p-dibenzylbenzene, VIII, was prepared in a pure state either by the Friedel-Crafts alkylation of benzene with p-xylylene chloride, using sulfuric acid as a catalyst, or by the Grignard-coupling reaction of phenylmagnesium bromide with p-xylylene chloride.

Dimethyl bis(p-benzylphenyl)methanedipropionate, XII, was synthesized as shown in Fig. 4. The condensation of p-substituted diphenylmethane, IId, with chloral gave a DDT-type compound, X. The hydrolysis and decarboxylation of X according to the method of Bergmann[5] led to XI, which was then esterified to XII.

Of all the reactions leading to cyclic compounds, the acyloin condensation of diester is one of the

1) Presented in part at the 17th Annual Meeting of the Chemical Society of Japan, Tokyo, April, 1964.
2) J. J. Randall, *Dissertation Abstr.*, **20**, 2568 (1960).
3) C. F. Koelsch and C. E. Bryan, *J. Am. Chem. Soc.*, **67**, 2041 (1945).
4) T. Zinke, *Ber.*, **6**, 119 (1873).
5) A. B. Galun, A. Kaluszyner and E. D. Bergmann, *J. Org. Chem.*, **27**, 1246 (1962).

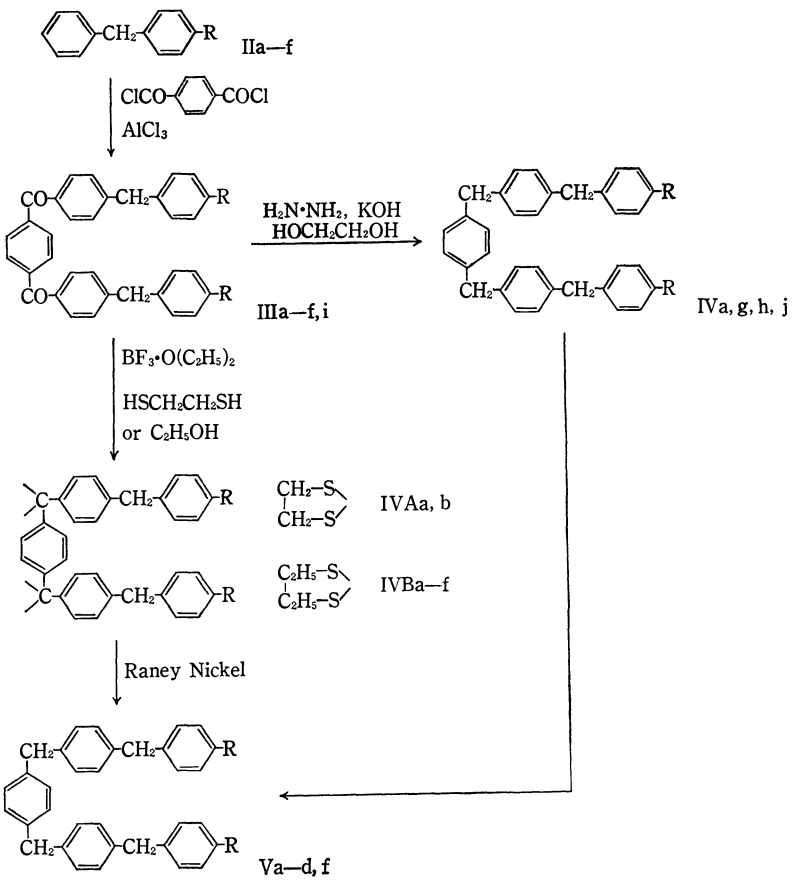

Fig. 2

R: a=H, b=$COOC_2H_5$, c=$CH_2COOC_2H_5$, d=$(CH_2)_2COOC_2H_5$, e=$CO(CH_2)_2COOCH_3$, f=$(CH_2)_3COOCH_3$, g=COOH, h=$(CH_2)_2COOH$, i=$CO(CH_2)_2COOH$, j=$(CH_2)_3COOH$.

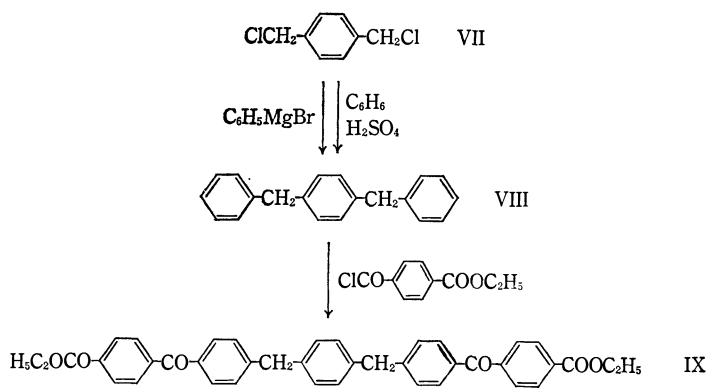

Fig. 3

most popular methods, especially when a satisfactory yield is needed. However, acyloin condensation is usually inapplicable to a compound with a carboxylate group or an acetate group attached to a benzene ring. The Blomquist cyclization method,[6] utilizing the intramolecular condensation of a bifunctional ketene derived from a dicarboxylic acid chloride, is also unsuitable for a compound with an chloroformyl group substituted in

6) A. T. Blomquist and R. D. Spencer, *J. Am. Chem. Soc.*, **70**, 30 (1948).

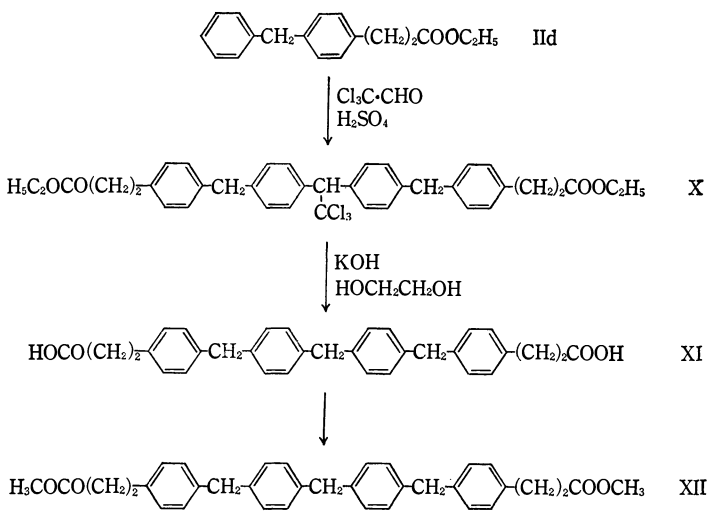

Fig. 4

a benzene ring. For the purpose of obtaining a compound adaptable to cyclization by acyloin or a like reaction, the synthesis of the diphenylmethane derivative, XX, carrying three benzene rings and two cyclohexane rings was carried out as shown in Fig. 5 in a way analogous to that outlined in Fig. 2.

4-Benzylcyclohexanecarboxylic acid, XV, obtained by the reduction of diphenylmethane-4-carboxylic acid, XIV, with sodium and isoamyl alcohol, was confirmed to be identical with the *trans*-4-benzylcyclohexanecarboxylic acid derived from *trans*-hexahydroterephthalic acid, by a comparison of the melting points, infrared spectra, and thin-layer chromatograms of the two anilides.[7]

As a result of the present work, some synthetic procedures for obtaining a compound to be cyclized have been found to be disadvantageous because of either a poor over-all yield or a tedious separation of an intermediate difficult to crystallize or of an end product.

Experimental

All melting points are uncorrected. The physical properties and analytical data of the products are summarized in Table 1.

4-Substituted Diphenylmethanes (IIb—f). *The Ester IIb.* A haloform-reaction product of 4-acetyldiphenylmethane was esterified with ethanol and sulfuric acid.

The Ester IIc was prepared by the hydrolysis[8] and esterification of the 4-cyanomethyldiphenylmethane derived from 4-chloromethyl diphenylmethane.

The Ester IId was prepared by the hydrolysis, decarboxylation, and esterification of the condensation product of 4-chloromethyldiphenylmethane and diethyl sodiomalonate.[8,9] The ester IId was also obtained by the hydrolysis and esterification of a thiomorphoride which had been derived, by a modified Willgerodt reaction, from 4-propionyldiphenylmethane.[10]

The Ester IIe was prepared by the Friedel-Crafts acylation of diphenylmethane with β-methoxycarbonylpropionyl chloride.[11]

The Ester IIf was prepared by the reesterification of the Wolff-Kishner reduction product of IIe.

Terephthalophenone Derivatives (IIIb). To a stirred mixture of 9.2 g of terephthaloyl chloride[3] and 27.5 g of anhydrous aluminum chloride in 100 m*l* of carbon disulfide, there was added slowly, at room temperature, 21.0 g of ethyl 4-diphenylmethanecarboxylate. After the addition, the mixture was stirred for 5 hr at room temperature, left to stand overnight, and refluxed with stirring for 5 hr. After the distillation of the carbon disulfide, the residue was poured onto crushed ice and water. The white solid which deposited was collected by filtration and washed with water, dilute hydrochloric acid, and again with water. Recrystallization from ethanol gave 23.2 g of colorless crystals, mp 162—164°C. An analytical sample was recrystallized from a benzene-ethanol mixture to give colorless needles.

The Thioketal (IVAb). To a mixture of 10.0 g of the keto ester, IIIb, and 4 m*l* of ethanedithiol in 150 m*l* of benzene, 4 m*l* of boron trifluoride etherate were added, after which the mixture was refluxed for 2 hr. After it had then stood for 3 hr at room temperature, 50 m*l* of methanol were added. The removal of the solvent gave 12.0 g of a pale yellow, crystalline powder, which was then washed with acetone and ethanol. An analytical sample was recrystallized from benzene-ethanol mixture.

7) T. Inazu and T. Yoshino, unpublished data.
8) C. Maquin and H. Gault, *Compt. rend.*, **234**, 629 (1952).
9) C. Maquin and H. Gault, *J. recherches centre natl. recherche sci., Labs. Bellevue*, **No. 34**, 57 (1956) (*Chem. Abstr.*, **51**, 2667e (1957)).
10) D. J. Cram and M. F. Antar, *J. Am. Chem. Soc.*, **80**, 3103 (1958).
11) J. Cason, "Organic Syntheses," Coll. Vol. III, p. 169 (1955).

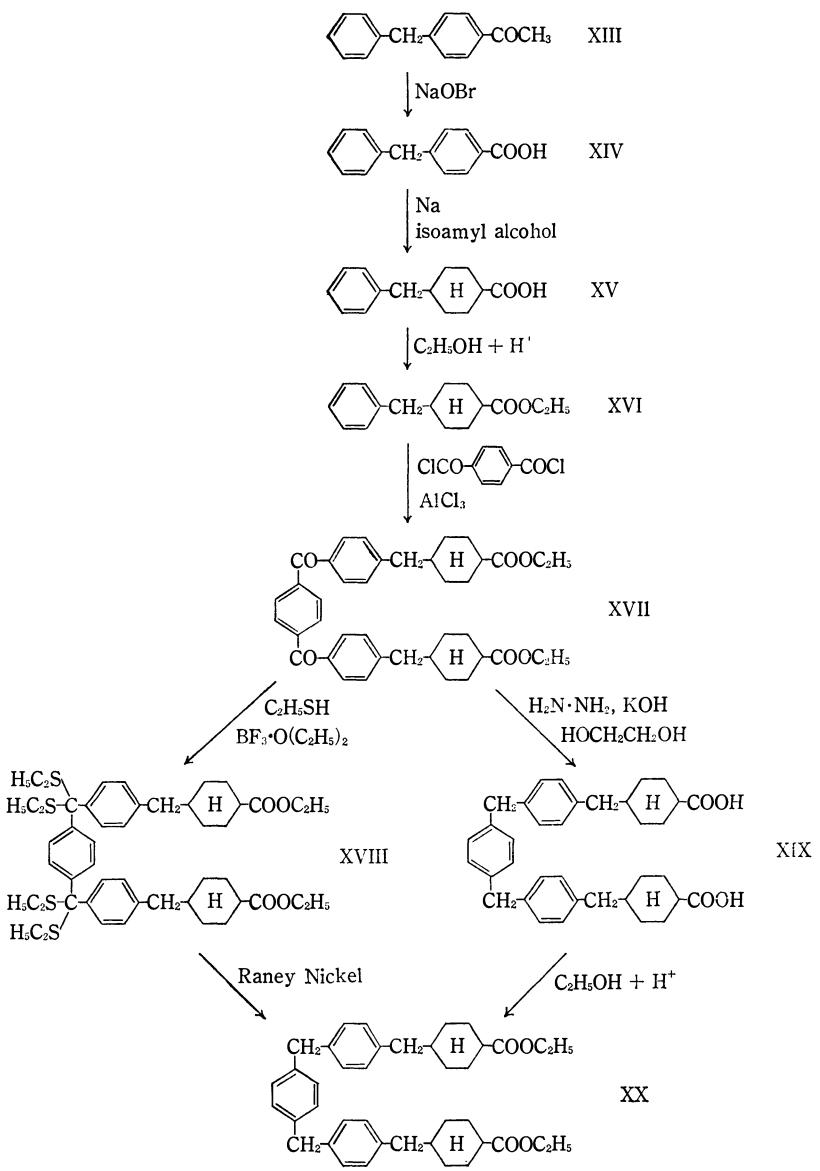

Fig. 5

The Ester (Vb). The thioketal, IVBb, obtained from 1.0 g of the keto ester, IIIb, was refluxed for 16 hr with an excess of Raney nickel in a benzene-ethanol mixture, after which the catalyst was filtered off. The concentration of the filtrate gave 500 mg of colorless crystals, which were recrystallized from a benzene-ethanol mixture, mp 140—141°C.

Carboxylic Acid (VIj). A mixture of 40 m*l* of 90% hydrazine hydrate, 40 g of potassium hydroxide, 250 m*l* of ethylene glycol, and 10 g of keto acid, IIIi, was refluxed for 12.5 hr. After cooling, the deposit, consisting of 5 g of the potassium salt of VIj, was recrystallized from acetic acid to give needles of free acid, mp 225—229.5°C. The potassium salt was converted to free acid during the recrystallization.

The Ester (Vf). Carboxylic acid, VIj (14.5 g, dissolved in benzene), was esterified with methanol and sulfuric acid, and then recrystallized from a benzene-ethanol mixture to give 13.7 g of colorless crystals, mp 133.5—135°C.

***p*-Dibenzylbenzene (VIII).** *Method A*: A mixture of 10 g of *p*-xylylene chloride,[12] 5 m*l* of sulfuric acid, and 100 g of benzene was refluxed for a few days. After the removal of the acid, the mixture was distilled to remove the benzene, and then fractionated under diminished pressure. The first fraction removed, boiling at 125°C/5 mmHg, was an unchanged chloride amounting to 2.5 g; the successive fraction, boiling at 185°C/5 mmHg, was collected to give 3.4 g of colorless crystals, which were recrystallized from ethanol to give VIII, mp 85—86.5°C (reported mp 86°C).[4]

12) T. Azumi and M. Hayashi, *Kōgyō Kagaku Zassi (J. Chem. Soc. Japan, Ind. Chem. Sect.)*, **55**, 476 (1952).

TABLE 1.

Compd.	mp or bp	Cryst. solv.	Cryst. form	Formula	Analyses, % Found C	Found H	Calcd C	Calcd H	Yield %
IIb	161.5—163°C (3 mmHg)		liq						82
IIc	179—181.5°C (4 mmHg)		liq						88
IId	170—178°C (3 mmHg)		liq						
IIe	213.5—216°C (3 mmHg)		liq						49
IIf	190—194.5°C (5.5 mmHg)		liq						31[a]
IIg	159—161°C	W-E	w.n.						97[b]
IIIa	107—111.5°C	E	w.c.	$C_{34}H_{26}O_2$	87.53	5.55	87.53	5.62	16
IIIb	162—164°C	E-B	w.n.	$C_{40}H_{34}O_6$	78.77	5.67	78.67	5.61	81
IIIc	101—103°C	E	w.n.	$C_{42}H_{36}O_6$	78.76	5.93	78.97	6.00	35
IIId	99—101°C	E	w.c.	$C_{44}H_{42}O_6$	79.39	6.32	79.25	6.35	33
IIIe	102—103°C	E-B	w.n.	$C_{44}H_{38}O_8$	75.99	5.65	76.06	5.51	40
IIIf	128.5—129°C	M	w.c.	$C_{44}H_{42}O_6$	79.19	6.54	79.25	6.35	
IIIi	231—232°C (decomp.)	AcOH	w.n.	$C_{42}H_{34}O_8$[p]	75.03	5.32	74.65	5.22	55
IVAa	148°C[c]	E-B	py.p	$C_{38}H_{34}S_4$	73.83	5.52	73.74	5.54	98
IVAb	144—146°C	E-B	w.c.	$C_{44}H_{42}O_4S_4$	69.13	5.68	69.26	5.55	96—99
IVBa	121—123°C	E-PB	py.c.	$C_{42}H_{46}S_4$	74.39	7.12	74.31	6.83	76
IVBb—f[d]									
Va[e]	127—128.5°C	E	w.c.						
Va[f]	123.5—125.5°C	E	w.c.	$C_{34}H_{30}$	92.81	7.23	93.11	6.89	47
Vb[g]	140—141.5°C	E-B	w.c.	$C_{40}H_{38}O_4$	82.45	6.62	82.44	6.57	58
Vc	133—134.5°C	E-B	w.c.	$C_{42}H_{42}O_4$	82.57	7.15	82.59	6.93	31
Vd	127.5—129°C	E	w.p.	$C_{44}H_{46}O_4$	82.74	7.13	82.72	7.26	29
Vf	133.5—135°C	E-B	w.c.	$C_{44}H_{46}O_4$	82.73	7.28	82.72	7.26	14
Vf[h]		E-B	w.c.						91
VIg	>290°C	AcOH	w.p.	$C_{36}H_{30}O_4$[q]	81.51	5.82	81.41	5.80	100
VIh		AcOH	w.c.	$C_{40}H_{38}O_4$	79.67	6.49	79.01	6.63	38
VIj	225—229.5°C	AcOH	w.n.	$C_{42}H_{42}O_4$	82.23	7.12	82.59	6.93	96
VII[i]	100°C	E	w.n.						
VIII[j]	85—86.5°C	E	w.pr.	$C_{20}H_{18}$	92.81	7.03	92.81	6.98	23
VIII[k]	85.5—87°C	E	w.pr.						68
IX	121—126.5°C	E	w.n.	$C_{40}H_{34}O_6$	78.52	5.84	78.67	5.61	26
X[d]									
XI[l]	212—213°C	E	w.p.	$C_{33}H_{32}O_4$[p]	79.12	6.56	79.01	6.63	7
XII	122—122.5°C	M	w.n.	$C_{35}H_{36}O_4$	80.93	6.82	80.74	6.97	95
XIII	161—167°C (3 mmHg)		liq						60
XV	80°C	M-W	w.n.	$C_{14}H_{18}O_2$	77.01	8.23	77.03	8.31	70
XVI	148°C (2.5 mmHg)		liq	$C_{16}H_{22}O_2$	77.75	8.78	78.01	9.00	80
XVII	162°C	Ac-PB	w.p.	$C_{40}H_{46}O_6$	76.99	7.39	77.14	7.45	16
XVIII[d]									57
XIX	219.5°C[m]	Ac-W	w.p.	$C_{36}H_{42}O_4$[q]	79.20	7.94	78.94	7.91	31
XX[n]	107.5—110°C	E	w.c.	$C_{40}H_{50}O_4$	80.45	8.68	80.77	8.47	63
XX[o]	107.5—110°C	E	w.c.						57

a) from diphenylmethane. b) by haloform reaction, lit. mp 158°C. c) sintered at 140°C.
d) not isolated in pure state. e) by the Wolff-Kishner reaction of IIIa.
f) *via* thioketal IVBa. g) from ketone IIIb. h) from VIj. i) footnote 12.
j) by the Friedel-Crafts reaction. k) by the Grignard reaction. l) from ester IId.
m) sintered at 207°C. n) from XIX. o) from ketone XVII *via* XVIII.
p) as a hydrate with a half molecule of water. q) as a hydrate with one fourth molecule of water.
Ac=acetone, AcOH=acetic acid, B=benzene, c=crystals, E=ethanol, liq=liquid, M=methanol, n=needles, PB=petroleum benzin, p=powder, pr=prisms, py=pale yellow, w=white, W=water.

Method B: A solution of 10 g of *p*-xylylene chloride in 80 m*l* of benzene was added to a solution of phenylmagnesium bromide in 60 m*l* of ether. The mixture was refluxed and then distilled to remove the ether. After the solution had been left standing overnight, crushed ice and dilute hydrochloric acid were added. An oily substance which separated from the organic layer was distilled at 140—185°C/4 mmHg to give 7.6 g of colorless crystals, which were recrystallized to give colorless plates, mp 85.5—87°C.
No melting-point depression was observed when this substance was admixed with a sample prepared by the method A.

Keto Ester (IX). To a stirred mixture of 25.5 g of powdered anhydrous aluminum chloride and 15 g of *p*-ethoxycarbonylbenzoyl chloride[13] in 50 m*l* of carbon disulfide, there was added a solution of 10 g of *p*-dibenzylbenzene VIII in 80 m*l* of carbon disulfide. After additional stirring for 2 hr at room temperature, the mixture was refluxed for 21 hr, and decomposed with dilute hydrochloric acid and crushed ice after the removal of the carbon disulfide by distillation. The deposit was extracted with benzene to yield 5.6 g of colorless crystals. An analytical sample was recrystallized from ethanol to give colorless crystals, mp 121—126.5°C.

Carboxylic Acid (XI). To a stirred mixture of 2.75 g of freshly-prepared anhydrous chloral and 10.0 g of the ester IId, 25 m*l* of concentrated sulfuric acid were added, drop by drop, under cooling. After additional stirring for 3.5 hr, the mixture was poured onto crushed ice. The pale pink, gummy deposit was refluxed with a solution of potassium hydroxide in 100 m*l* of ethylene glycol for 14 hr, and then poured onto crushed ice and acidified with dilute hydrochloric acid. The deposit afforded XI as a pale brown powder (600 mg); this powder was crystallized from ethanol to give a crystalline powder with a mp 212—213°C.

***trans*-4-Benzylcyclohexanecarboxylic Acid (XV).** Into a solution of 60 g of 4-benzylbenzoic acid, XIV, obtained from 4-acetyldiphenylmethane, XIII, by haloform reaction and dissolved in 1250 m*l* of isoamyl alcohol, there were stirred, portion by portion, 148.9 g of sliced sodium. The mixture was refluxed with stirring for 3 hr, and then cooling water was added. After the removal of the isoamyl alcohol by steam distillation, the solution was neutralized and extracted with ether. The usual treatment gave 42 g of colorless needles, mp 79—80°C. An analytical sample was recrystallized from a methanol-water mixture.

13) J. B. Cohen and H. S. de Pennington, *J. Chem. Soc.*, **113**, 63 (1918).

BULLETIN OF THE CHEMICAL SOCIETY OF JAPAN VOL. 41 652—655 (1968)

Macro Rings. II.[1] Synthesis of [2.1.1.1.1]Paracyclophane

Takahiko INAZU and Tamotsu YOSHINO

Department of Chemistry, Faculty of Science, Kyushu University, Hakozaki, Fukuoka

(Received August 22, 1967)

A macrocyclic compound which incorporates five benzene rings and intervening methylene bridges as parts of a large ring structure, [2.1.1.1.1]paracyclophane I ($n=2$), was synthesized and then compared with a corresponding open-chain analog, X.

Because of its ability to form clathrates or charge-transfer complexes, a macrocyclic compound, I, furnished with an empty space of an appropriate size at the center of its molecule is of particular interest.

Although several attempts have been made to synthesize paracyclophane with four or five benzene rings by an intramolecular cyclization reaction, these attempts have all resulted in failure.[2,3]

As an initial step of the present investigation, [2.1.1.1.1]paracyclophane I ($n=2$) was synthesized. This may be the first example of a paracyclophane constructed with five benzene rings and intervening methylene bridges. As the result of several preliminary experiments, the Wurtz reaction was adopted for the synthesis of the paracyclophane.

The yield of a macrocyclic compound by the usual Wurtz reaction is generally poor, but the modified Wurtz reaction using sodium adduct of tetraphenylethylene has been proved to be useful for improving the yield of cyclization. It has also been verified that the improved, intramolecular Wurtz-type reaction is appreciable to a large ring formation from a compound with two distant halogen atoms in a chain molecule.

Although a chain compound of the benzyl-bromide type, IX, seemed to be a reactive material, an attempt to cyclize the compound IX was thwarted because of the compound's insufficient solubility in tetrahydrofuran at room temperature. This difficulty was surmounted by using the corresponding compound of the benzyl-chloride type, VIII, in place of the bromide, IX.

1) T. Inazu and T. Yoshino, This Bulletin, **41**, 647 (1968).
2) J. J. Randall, *Dissertation Abstr.*, **20**, 2568 (1960).
3) C. F. Koelsch and C. E. Bryan, *J. Am. Chem. Soc.*, **67**, 2041 (1945).

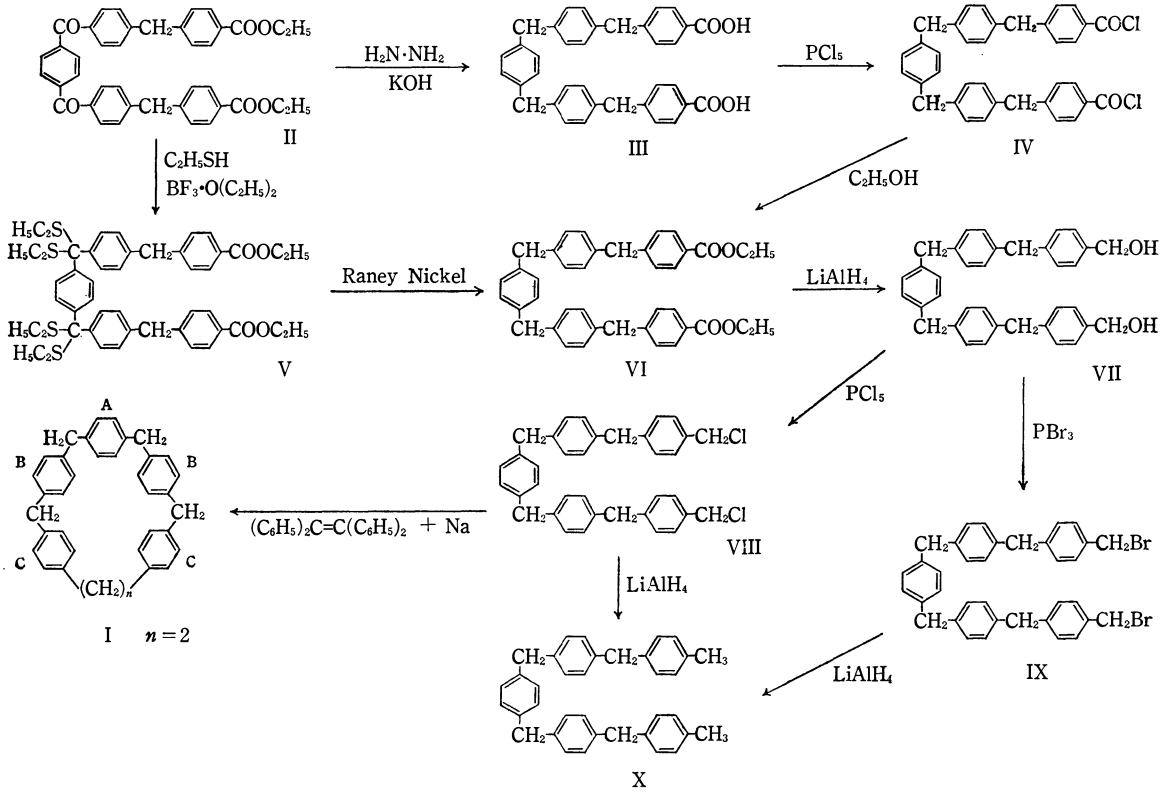

Fig. 1

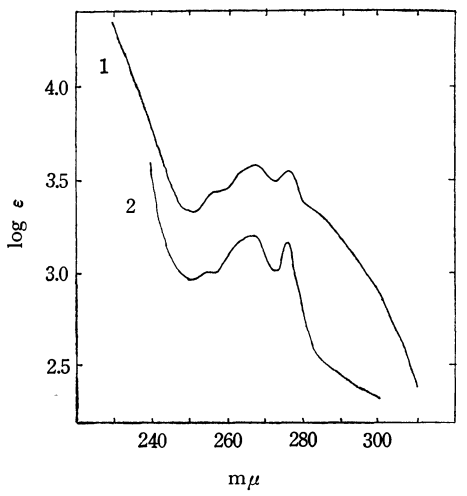

Fig. 2. Ultraviolet spectra of [2.1.1.1.1]paracyclophane I and the open chain analog X in C_2H_5OH.

Curve 1: compound I (λ_{max}: 267.5 mμ, log ε=3.58)
Curve 2: compound X (λ_{max}: 267.5 mμ, log ε=3.20)

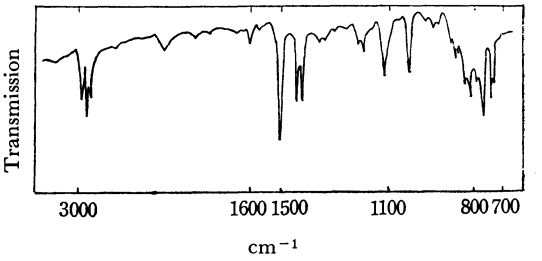

Fig. 3. Infrared spectrum of [2.1.1.1.1]paracyclophane I in KBr disk.

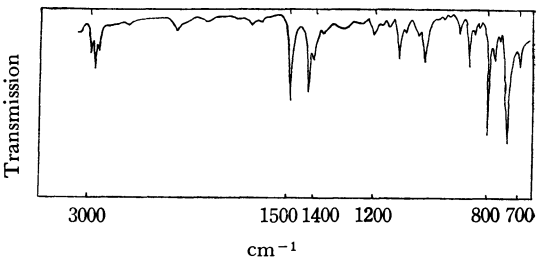

Fig. 4. Infrared spectrum of the open chain analog X in KBr disk.

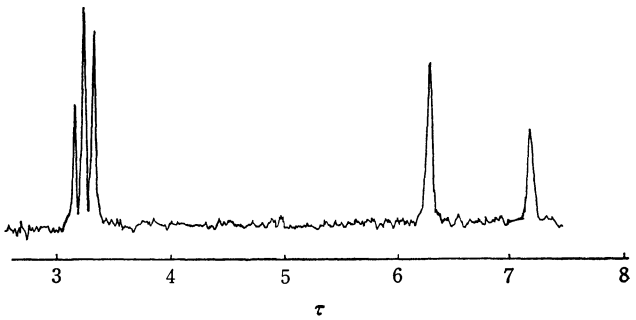

Fig. 5. The NMR spectrum of [2.1.1.1.1]paracyclophane I.

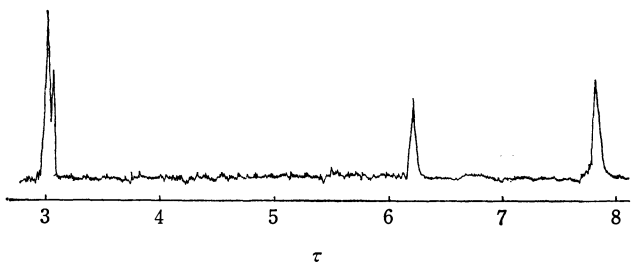

Fig. 6. The NMR spectrum of the open chain analog X.

The synthetic route is outlined in Fig. 1. A keto ester, II,[1] was converted to another ester, VI, either by the desulfurization of a thioketal, V, with Raney nickel, or by the Wolff-Kishner reduction to an acid, III, followed by esterification *via* acid chloride, IV. The ester VI was reduced with lithium aluminum hydride, and the resulting carbinol, VII, was treated with phosphorus tribromide or phosphorus pentachloride to give, respectively, a bromide, IX, or a chloride, VIII. This bromide and this chloride were each then reduced with lithium aluminum hydride to a compound, X. This compound was synthesized as a reference compound which served as a chain analog of the cyclophane, I, for a comparison of their spectra.

With the aid of a modified high-dilution technique, [2.1.1.1.1]paracyclophane, I, was obtained as colorless crystals by the intramolecular condensation of the chloride VIII with the sodium adduct of tetraphenylethylene in tetrahydrofuran at room temperature under a nitrogen atmosphere; this was done according to the method of Müller and Röscheisen.[4]

The close resemblance of the ultraviolet spectrum of the compound I to that of a corresponding chain compound, X, reveals that benzene rings of the compound I are probably planar, unlike the distorted non-planar rings in [2.2]paracyclophane.[5] This fact was anticipated from our having been able to assemble a molecular model of the macrocyclic compound, I, without any strain.

The NMR spectrum of the compound I was in accord with that assumed tentatively for the cyclic structure: $\tau=7.13$ singlet (ethylene protons), $\tau=6.26$ singlet (methylene protons), and three singlets (benzene ring protons) at $\tau=3.13$, 3.20, and 3.29. Each of the peaks for protons of the benzene ring and methylene and ethylene groups was a singlet; this suggests that the conformation of the cyclic compound, I, may be flexible, without any rigid fixation, in a solution at room temperature. In the NMR spectra, the peak for methylene protons in the cyclic compound, I, was found to shift upfield by 0.14 ppm from that for the methylene protons of diphenylmethane. Peaks for benzene the rings A, B, and C in the cyclic compound, I, were also found to shift upfield by 0.17, 0.24, and 0.33 ppm respectively from those for benzene protons in diphenylmethane. These upfield shift is attributable to the fact that protons of the cyclophane I may be a little more shielded by transannularly-situated benzene rings than are protons of diphenylmethane.

Although no marked difference was observed between the IR spectra of the cyclic compound, I, and that of the chain analog, X, the results of the molecular-weight determination excluded the possibility of the compound I being a polymer. The cyclic structure of the compound I being different from that of the chain compound, X; this

4) E. Müller and Röscheisen, *Chem. Ber.*, **90**, 543 (1957).
5) D. J. Cram and H. Steinberg, *J. Am. Chem. Soc.*, **73**, 5691 (1951).

fact was confirmed by the NMR spectrum, as has been described above.

Experimental

All melting points are uncorrected. The ultraviolet spectra were measured on a Hitachi EPS-3T spectrophotometer. The infrared spectra were measured on a Hitachi EPI-S2 spectrophotometer. The NMR spectra were recorded on a Varian Associates A-60 model, using tetramethyl silane as the internal standard and carbon tetrachloride as the solvent.

***p*-Bis[*p*-(*p*-carboxybenzyl)benzyl]benzene (III).** A mixture of 20 g of a keto ester, II, 80 m*l* of 80% hydrazine hydrate, 60 g of potassium hydroxide, and 240 m*l* of ethylene glycol was refluxed for 17.5 hr. After cooling, the mixture was neutralized with concentrated hydrochloric acid to give 17.2 g (almost a theoretical yield) of a white powder, mp above 290°C. Found: C, 81.51; H, 5.82%. Calcd for $C_{36}H_{34}O_4 \cdot \frac{1}{4}H_2O$: C, 81.41; H, 5.80%.

***p*-Bis[*p*-(*p*-chloroformylbenzyl)benzyl]benzene (IV).** A mixture of 24.5 g of the acid, III, and 70 g of phosphorus pentachloride in 200 m*l* of chloroform was refluxed for 3 hr; after the solvent and phosphoryl chloride had been removed by distillation under reduced pressure, pale pink crystals were obtained in an almost theoretical yield.

***p*-Bis[*p*-(*p*-ethoxycarbonylbenzyl)benzyl]benzene (VI).** To a solution prepared by dissolving the acid chloride, IV, derived from 24.5 g of the acid, III, in 100 m*l* of chloroform, 100 m*l* of ethanol was added, little by little under cooling, and the mixture was refluxed for 30 min. The removal of the chloroform by distillation gave 20.3 g (74.5%) of colorless crystals, which were confirmed to be identical with a smaple prepared from the compound II *via* a thioketal, V, by a comparison of their infrared spectra and melting points.

***p*-Bis[*p*-(*p*-hydroxymethylbenzyl)benzyl]benzene (VII).** A solution of 7.8 g of the ester VI in 200 m*l* of tetrahydrofuran was added, at room temperature, to a mixture of 1.9 g of lithium aluminum hydride in 100 m*l* of tetrahydrofuran placed in a flask fitted with a reflux condenser, after which the mixture was refluxed for 1¾ hr with stirring. After being cooled and treated with hydrochloric acid, the mixture was distilled under diminished pressure to remove the solvent. The residue gave 6.4 g (96% yield) of a white powder, which was recrystallized from tetrahydrofuran to give a white crystalline powder, mp 203—205°C. Found: C, 86.53; H, 7.04%. Calcd for $C_{36}H_{34}O_2$: C, 86.71; H, 6.87%.

***p*-Bis[*p*-(*p*-chloromethylbenzyl)benzyl]benzene (VIII).** A mixture of 6.4 g of the diol, VII, 25 g of phosphorus pentachloride, and 150 m*l* of chloroform was refluxed for 3 hr, and then distilled under diminished pressure to remove the chloroform and phosphoryl chloride. The residue gave a white crystalline mass, which was recrystallized from tetrahydrofuran to give 5.05 g (73.5% yield) of colorless crystals, mp 182.5—183°C. Found: C, 80.47; H, 6.02%. Calcd for $C_{36}H_{32}Cl_2$: C, 80.74; H, 6.02%.

***p*-Bis[*p*-(*p*-bromomethylbenzyl)benzyl]benzene (IX).** A mixture of 1.0 g of the diol VII and 12 m*l* of phosphorus tribromide was refluxed for 3.5 hr and then, after the addition of 50 m*l* of chloroform, refluxed for an additional 5 hr. After cooling, the whole was poured onto crushed ice. The evaporation of the chloroform gave 1.3 g (almost a theoretical yield) of a white crystalline powder, mp 191°C (dec.). Found: C, 69.38; H, 5.36%. Calcd for $C_{36}H_{32}Br_2$: C, 69.24; H, 5.17%.

***p*-Bis[*p*-(*p*-methylbenzyl)benzyl]benzene (X).** A suspension of 500 mg of the bromide, IX, in 100 m*l* of tetrahydrofuran was stirred, drop by drop, into a mixture of lithium aluminum hydride in 40 m*l* of tetrahydrofuran at room temperature; after stirring for an additional 1.5 hr, the mixture was refluxed for 2 hr. After cooling, the mixture was treated with water and then with dilute hydrochloric acid. The removal of the tetrahydrofuran under reduced pressure gave a pale yellow powder, which was recrystallized from an ethanol-benzene mixture to give 240 mg (65% yield) of a white crystalline powder, mp 153°C. Found: C, 91.86; H, 7.41%. Calcd for $C_{36}H_{34}$: C, 92.66; H, 7.34%.

[2.1.1.1.1]Paracyclophane (I). Into a dark-violet solution of an adduct of sodium and 1.8 g of tetraphenylethylene in 100 m*l* of tetrahydrofuran, there was stirred a solution of 2.0 g of the chloride, VIII, in 400 m*l* of tetrahydrofuran; the addition was made *via* a modified Hershberg dropping funnel[6] at room temperature, under a nitrogen atmosphere, and over a period of 14.5 hr. After being left standing for several hours, the mixture was distilled to remove the tetrahydrofuran; then water and ethanol were added to give 3.5 g of a pale yellow powder, which was collected by filtration and then subjected to fractional crystallization from a benzene-ethanol mixture to give 87 mg of colorless crystals, mp 257°C. Found: C, 92.73; H, 6.96%; mol wt, 495 (Rast). Calcd for $C_{36}H_{32}$: C, 93.06; H, 6.94%; mol wt, 464.62.

6) E. B. Hershberg, "Organic Syntheses," Coll. Vol. II, p. 129 (1943).

BULLETIN OF THE CHEMICAL SOCIETY OF JAPAN VOL. 41 656—660 (1968)

The Effect of Hydrogen Bonding on the Rates of Inversion of 1-Hydroxy-5, 7-dihydrodibenz[*c*, *e*]oxepin

Michinori Ōki, Hiizu Iwamura and Toshiaki Nishida*[1]

Department of Chemistry, Faculty of Science, The University of Tokyo, Hongo, Tokyo

(Received August 25, 1967)

The rates of inversion of 1-hydroxy-5, 7-dihydrodibenz[*c*, *e*]oxepin (I) and its methyl ether (II) have been measured by NMR line-shape method in several solvents. The activation parameters for inversion of II are insensitive to the change in solvents, while the activation energy of I in strongly proton-accepting DMSO is clearly smaller by one kcal/mole than that of I in $CDCl_3$ and those of II. The solvent effect may be due partly to the enhanced mesomerism of the biphenyl system as the result of hydrogen bonding and partly to the inhibition of the intramolecular O–H$\cdots\pi$ interaction which will otherwise stabilize the non-planar ground state in the inert solvents.

NMR spectroscopy has lately been applied to the study of rates of the restricted rotation of biphenyls with the rate constants of 1 to 10^3 sec^{-1} by observing the temperature-dependent signal shape of the dissymmetrically disposed methylene protons which are originally diastereomeric but tend to be equalized by mutual exchange of their magnetic environments through rotation around the pivot bond of the biphenyl skeleton.[1-5] Before the advent of this NMR technique of kinetics, rates of the restricted rotation and inversion of biphenyl derivatives had solely been measured by following rates of racemization of the optically active biphenyls through polarimetry.[6,7] Although some criticisms have been thrown on both theoretical and practical conformities of the kinetic parameters obtained by the two independent methods,[8,9] the equivalence between them has been demonstrated experimentally by comparing directly the kinetic results derived from the two methods with the same rate process.[5,10] It has also been demonstrated that the solvent effect on the rates of biphenyl inversion is rather small as far as there is no special solute-solvent interaction.[4,5,11] In the present paper the NMR method is developed to explore the effect of solvents on the rates of inversion of 1-hydroxy-5, 7-dihydrodibenz[*c*, *e*]oxepin (I) and its methyl ether (II), where strong solute-solvent interaction may be expected to take place in the former through hydrogen bonding when a suitable solvent is used.

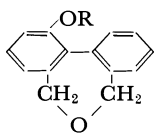

I (R=H)

II (R=CH_3)

Experimental

Materials and Solvents. *1-Hydroxy-5, 7-dihydrodibenz[c, e]oxepin (I).* Preparation of this compound was described elswhere.[12]

1-Methoxy-5, 7-dihydrodibenz[c, e]oxepin (II). I was methylated with dimethyl sulfate as usual to give an oil, bp 153°C/2 mmHg. Found: C, 79.44; H, 6.33%. Calcd for $C_{15}H_{14}O_2$: C, 79.62; H, 6.24%.

All the solvents were of spectro-grade containing enough TMS to make the reference signals of comparable intensity to those of CH_2 resonances investigated. To dimethyl-d_6 sulfoxide was added 5% w/w acetone-d_6 in order to lower the freezing point.

Spectral Measurements. The NMR spectra were obtained on a Varian A-60 spectrometer operating at 60 Mc/sec and equipped with a variable temperature accessory. TMS was used as the internal reference,

*1 Present address: Department of Chemistry, The Johns Hopkins University, Baltimore, Md., U. S. A.

1) W. L. Meyer and R. B. Meyer, *J. Am. Chem. Soc.*, **85**, 2170 (1963).
2) M. Ōki, H. Iwamura and N. Hayakawa, This Bulletin, **36**, 1542 (1963); **37**, 1865 (1964).
3) R. J. Kurland, M. B. Rubin and W. B. Wise, *J. Chem. Phys.*, **40**, 2426 (1964).
4) I. O. Sutherland and M. V. J. Ramsay, *Tetrahedron*, **21**, 3401 (1965).
5) M. Ōki and H. Iwamura, *ibid.*, **24**, 2377 (1968).
6) R. Kuhn and O. Albrecht, *Liebigs Ann.*, **455**, 272 (1927).
7) D. M. Hall and M. M. Harris, *J Chem. Soc.*, **1960**, 490.
8) H. S. Gutowsky, *J. Chem. Phys.*, **25**, 1228 (1956).
9) D. M. Hall and T. M Poole, *J. Chem. Soc.*, **1966**, 1034.
10) While the preparation of this paper, the authors became aware of a report confirming the soundness of the kinetic measurements by NMR line shapes by comparing with the rate of equilibration of isomeric *N*-benzyl-*N*, 2, 4, 6-tetramethylbenzamides (A. Mannschreck, A. Mattheus and G. Rissmann, *J. Mol. Spectry.*, **23**, 15 (1967)).
11) B. M. Graybill and J. E. Leffler, *J. Phys. Chem.*, **63**, 1461 (1959).
12) M. Ōki and H. Iwamura, *J. Am. Chem. Soc.*, **89**, 576 (1967).

and the calibration of the spectrometer checked by the usual side-band technique. Temperature reading was calibrated by examining the CH_3 and OH signal separation of a methanol sample as prescribed in the instruction manuals, and the reading is accurate to ± 2.0°C.

Within the measurement of a given sample, the strength of the radiofrequency was held sufficiently small and the spectra were assured of being far below saturation by observing no lowering in the peak intensity on a slight raising of the r.f. field. Since the apparent amplitude of the normal signals decreases as the temperature is raised mainly because of the thermal expansion of the solvent and the consequent apparent dilution, the recorder gain was adjusted to attain the desired amplitude of the signals. Each resonance was swept three times in turn without altering the controls. The usual sweep rate was 1 cps/sec.

The exchange broadening of the two interacting nuclear spin resonance signals has been written down by Alexander.[13] Under slow-exchange limit at lower temperature, the observed change in the line-width w is correlated to the life-time τ by Eq. (1);

$$\tau = \frac{1 \pm J_{AB}/\sqrt{\delta_{AB}^2 + J_{AB}^2}}{\pi(w - w_0)} \qquad (1)^{5}$$

At the very point of the coalescence of the AB-quartet signal, τ_c is given by Eq. (2) when natural line-width in the absence of exchange, w_0, is negligible.

$$\tau_c = \frac{\sqrt{2}}{\pi\sqrt{\delta_{AB}^2 + 6J_{AB}^2}} \qquad (2)^{2,3}$$

Above the coalescence temperature, the width of the coalesced singlet relative to that at $\tau=0$ can again be used to calculate τ from Eq. (3);

$$\tau = \frac{2(w - w_0)}{\pi\delta_{AB}^2} \qquad (3)^{4,5}$$

Equations (1) to (3) were employed to calculate the exchange life-time from the observed change in the line shapes. The line-width in the absence of the exchange, w_0, was read directly from the CH_2 signals at enough low (−20°C) and/or high (150°C) temperature where $\tau=\infty$ and $\tau=0$ hold approximately.

Results and Discussion

In every solvent examined, both I and II at the lower temperature show double AB-quartet signals due to the presence of two pairs of the methylene groups. In Tables 1 and 2 are shown the spectral parameters. The quartet at the higher applied magnetic field can be assigned to the methylene protons attached to the benzene ring carrying the hydroxyl group and the methoxyl group in I and II, respectively. The assignment bases upon the fact that the aromatic methyl signal of *m*-methylanisole resonates at τ 7.77 which is located at the higher field than that of toluene, τ 7.66,[14] but the reverse assignment does not affect the following discussion. From the fact that the chemical shifts of the four protons on a pair of methylene groups can be differentiated, it

Table 1. The methylene proton spectra of I at the lower temperatures

Solvent	δ ppm[a]	δ_{AB} cps	J_{AB} cps	t °C
$CDCl_3$[b]	4.31	27.4	11.2	−20
	4.41	19.1	11.0	
DMSO[c]	4.15	35.9	11.5	0
	4.25	29.0	11.3	

Table 2. The methylene proton spectra of II at the lower temperatures

Solvent	δ ppm	δ_{AB} cps	J_{AB} cps	t °C
C_2Cl_4	4.15	23.8	11.2	−20
	4.21	16.5	11.1	
$CDCl_3$	4.26	27.4	11.2	−10
	4.36	19.3	11.2	
DMSO[c]	4.16	39.0	11.5	0
	4.24	31.5	11.4	

a) center of the AB-quartet from TMS.
b) 0.11 mol/*l*.
c) Dimethyl-d_6 sulfoxide added 5% w/w acetone-d_6.

is concluded that at these temperatures specified in Tables 1 and 2 the two benzene rings in I and II are fixed as non-planar in the sense of NMR and that the rate of restricted rotation around the pivot bond (Eq. (4)) should be less than a few times in a second.

At enough elevated temperatures, the methylene groups show two singlet signals at the center of the original pair of AB-quartets. In these circumstances, the thermal motion is active enough to bring the rates of inversion (Eq. (4)) faster than 10^3 sec^{-1}, and thus the two methylene protons on the same carbon atom cannot be distinguished.

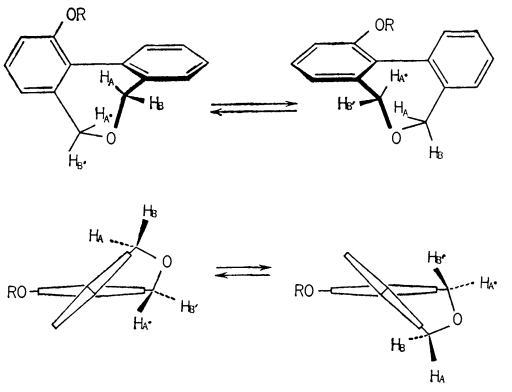

(4)

In the intermediate temperature, as the temperatures is raised, the line-width of the quartet broadens at first with the two outer lines broadening more rapidly than the two inner lines. The broadened signals coalesce gradually to a singlet, and then the peak intensity of the singlet increases at the expense of the line-width. Some typical

13) S. Alexander, *J. Chem. Phys.*, **37**, 967 (1962).
14) C. Heathcock, *Canad. J. Chem.*, **40**, 1865 (1962).

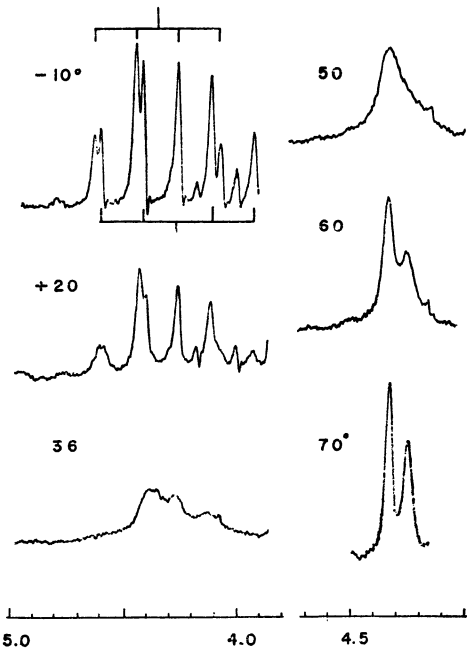

Fig. 1. NMR spectra of CH_2 protons of II in $CDCl_3$ at various temperatures.

experimental curves are shown in Fig. 1. Two pairs of AB-quartet overlap rather heavily on a 60 Mc/sec NMR chart, and therefore the estimated error of the coalescence temperature (T_c) is ±5°C. In Table 3 are shown the approximate T_c's of the spectra. It is to be emphasized that, in a given sample, an AB-quartet of a smaller δ_{AB} has the lower T_c. I in DMSO is unique in that it has rather low T_c's with respect to the greater δ_{AB}. The data are indicative of the lower activation energy for inversion than those in the other systems.

Table 3. The coalescence temperature (T_c) of the AB-quartets and the life-time (τ_c) at the temperature

	Solvent	δ_{AB} cps	T_c °C	τ_c 10^{-3} sec
I	$CDCl_3$	27.4	48	11.6
		19.1	40	13.6
	DMSO	35.9	20	9.9
		29.0	10	11.2
II	C_2Cl_4	23.8	50	12.4
		16.5	40	14.2
	$CDCl_3$	27.4	46	11.6
		19.3	40	13.4
	DMSO	39.0	45	9.4
		31.5	38	10.7

Equations (1) to (3) were employed to calculate the exchange life-time τ at the intermediate temperature ranges which are listed in Tables 4 and 5. The Arrhenius activation energy E_a and the frequency factor A for the exchange process (Eq. (4)) were obtained from the best fitting line

Table 4. Experimental line-widths and exchange life-times for I in chloroform-d and dimethyl-d_6 sulfoxide

Temp. °C	w for inner lines[a]		w for outer lines[a]		w for coalesced line[b]		τ msec
	h[c]	l	h	l	h	l	
			$CDCl_3$ (w_0=1.20 cps)				
0	1.45	1.45	1.80	—			714
10	1.80	1.70	—	—			325
50					—	6.00	8.42
60					5.30	3.50	3.74
70					3.15	2.30	1.78
			DMSO (w_0=1.10 cps)				
36					5.60	4.00	2.21
50					2.80	2.20	0.84
70					1.60	1.50	0.27_2
90					1.20	1.15	0.042_9
120					1.15	1.12	0.018_3

a) Data treated by Eq. (1).
b) Data treated by Eq. (3).
c) h and l stand for the AB-quartets at the higher and the lower applied magnetic field, respectively.

15) From the ultraviolet spectral data, the dihedral angle between the two benzene rings is estimated to be about 45°[12] (H. Suzuki, This Bulletin, **32**, 1340, 1350, 1357 (1959); **33**, 109 (1960)).

TABLE 5. EXPERIMENTAL LINE-WIDTHS AND EXCHANGE LIFE-TIMES FOR II IN TETRACHLOROETHYLENE, CHLOROFORM-d AND DIMETHYL-d_6 SULFOXIDE

Temp. °C	w for inner lines		w for outer lines		w for coalesced line		τ msec
	h	l	h	l	h	l	
			C_2Cl_4 (w_0=1.20 cps)				
0	1.60	1.60	1.80	2.30			467
10	1.80	1.85	—	3.30			247
60					4.05	3.10	3.69
70					2.60	2.15	1.80
80					2.00	1.60	0.91_5
90					1.60	1.40	0.45_8
100					1.50	1.30	0.27_6
			$CDCl_3$ (w_0 = 1.20 cps)				
0	1.50	1.50	1.90	1.70			662
10	1.80	1.80	2.10	—			338
20	2.20	2.00	3.00	—			211
50					—	6.00	8.21
60					6.50	3.80	4.4_7
70					2.90	2.10	1.4_9
			DMSO (w_0 = 1.05 cps)				
50					6.00	4.00	2.07
70					3.35	2.45	0.93
80					2.20	1.65	0.43_3
90					1.55	1.40	0.23_5
100					1.35	1.25	0.12_6
120					1.15	1.15	0.05_3

TABLE 6. ACTIVATION PARAMETERS FOR THE INVERSION OF I AND II IN SEVERAL SOLVENTS

	Solvent	E_a kcal/mol	log A
I	$CDCl_3$	16.9±1.0	13.6±0.8
	DMSO	15.6±1.2	13.6±0.9
II	C_2Cl_4	17.0±1.0	13.5±0.8
	$CDCl_3$	16.9±1.0	13.5±0.8
	DMSO	17.2±1.4	13.7±1.0

determined by the method of least squares.[16] The results are summarized in Table 6. Although the number of solvents examined is quite limited, they cover wide varieties of the solvent properties; dielectric constant, polarity, basicity, viscosity,[17] *etc.* From the data obtained for II in Table 6, it follows again that the kinetic parameters for inversion are, within the experimental error, almost independent of the solvents.[18] Because the energy of activation for inversion of biphenyls such as II may be regarded to be governed by the non-bonded repulsion and the ring-strain in the activated state for the process, and because they are rather insensitive to the intermolecular interaction, the indifference to the change in solvent is not unreasonable.

To the contary, the activation parameters for the inversion of I in $CDCl_3$ and DMSO are decidedly different. Since DMSO is famous for its strong proton-accepting ability for phenols,[19] the hydrogen bonding must be playing some role. Two mechanisms may then be considered to be operative. Firstly, the strong hydrogen bonding between the hydroxyl group of I and DMSO will

16) The probable errors in the values of E_a and log A thus determined are ±0.3 kcal/mol and ±0.2, respectively. For a more realistic estimate of the uncertainty in these kinetic paramaters, each point was marked as a rectangle corresponding to the uncertainty of the point; two straight lines with maximum and minimum slopes were drawn in such a manner as to pass through each rectangle. The probable errors thus obtained are listed in Table 6.

17) A change in viscosity of the medium will contribute to the width of the NMR lines investigated and may affect the activation parameters, but the contribution of this relaxation width is discarded from the constancy of the width of other lines in the same molecule, *e. g.*, that of CH_3O signal.

18) Graybill and Leffler[11] examined the rates of racemization of dimethyl *o, o'*-dimethoxydiphenate in 23 solvents. The rates vary by about a factor of two and the activation energy has a range of 2.1 kcal/mol. There is a general tendency for the ester to racemize more rapidly in polar solvents and the alcoholic proton donor solvents ratard the racemization, although the latter solvents have not been tested for the present examples.

19) A. Wagner, H. J. Becjer and K.-G. Kottenhahn, *Chem. Ber.*, **89**, 1708 (1956); S. Ghersetti and A. Lusa, *Spectrochim. Acta*, **21**, 1067 (1965).

reduce the electronegativity of the hydroxyl oxygen and the consequent conjugation between the two benzene rings. This contribution III stabilizes the planar conformation corresponding to the activated state for inversion more than the non-planar ground state. In effect E_a will be reduced relative to that of non-hydrogen bonded cases.

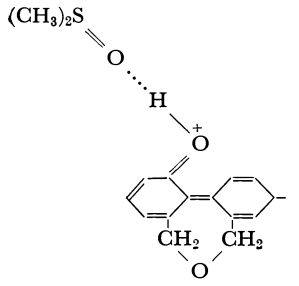

III

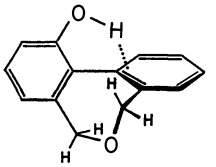

IV

Secondly, it has been shown by the infrared spectroscopy of the ν_{O-H} region that there is an intramolecular interaction between the hydroxyl group and the π-electrons on the benzene ring (IV) in the ground state of I in non-associative solvents, while no such intramolecular O–H$\cdots\pi$ interaction takes place in the planar 2-hydroxybiphenyl derivatives which may represent a model for the activated state for inversion.[12] The ground state of I in $CDCl_3$ is, therefore, stabilized with respect to the activated state by the energy of that interaction which is expected to be of the order of 1.5 kcal/mol.[20] Since DMSO is a powerful proton acceptor[19] and the hydroxyl group in I is essentially deprived of the intramolecular O–H$\cdots\pi$ interaction in this solvent, the ground state of I is not stabilized relative to the excited state. Accordingly E_a for inversion should be smaller in DMSO than in $CDCl_3$ by the amount of the energy of that O–H$\cdots\pi$ interaction (IV). The observed value is compatible with that obtained by the IR measurements.[12,20]

The experiments are now in progress to separate the contribution of the two factors.

20) M. Ōki and H. Iwamura, This Bulletin, **34**, 1395 (1961).

BULLETIN OF THE CHEMICAL SOCIETY OF JAPAN VOL. 41 660—664 (1968)

Kinetic Studies of the Oxidation of Benzils with Peroxyacetic Acid in Acetic Acid

Yoshiaki FURUYA and Iwao URASAKI

Department of Industrial Chemistry, Faculty of Engineering, Kumamoto University, Kumamoto

(Received September 4, 1967)

The oxidation of benzils with peroxyacetic acid in the presence of sulfuric acid in acetic acid has been studied kinetically. The rate of the consumption of peroxyacetic acid has been found to be the sum of the four terms shown in the following equation:

$$-\mathrm{d}[AcO_2H]/dt = \{k_d + k_t[H_2SO_4]\}[AcO_2H] + \{k_2 + k_2'[H_2SO_4]\}[Bz_2][AcO_2H]$$

It is considered that the first and second terms correspond to the decomposition of peroxyacetic acid itself and to the acid-catalyzed reversible transformation of peroxyacetic acid to acetyl peroxide, while the third and fourth terms represent, respectively, the non- and the acid-catalyzed oxidations of benzils with peroxyacetic acid. In both non- and acid-catalyzed oxidations, a probable mechanism passing through benzoic anhydride is postulated.

When the α-diketones are treated with oxidizing agents, such as hydrogen peroxide,[1] potassium periodate[2] and peroxyacetic acid,[3] the corresponding carboxylic acids are obtained. One mechanism of the reaction has already been discussed[1] briefly on the basis of the synthetic results. The present authors have now followed the reaction of benzils with peroxyacetic acid by iodometry and will here discuss a probable mechanism.

Experimental

Materials. Peroxyacetic acid was prepared by the reaction of acetic anhydride with hydrogen peroxide in the presence of sulfuric acid.[4] The benzils were prepared by means of the benzoins[5] obtained from the

1) J. E. Leffler, *J. Org. Chem.*, **16**, 1785 (1951).
2) V. J. Shiner and C. R. Wasmuth, *J. Am. Chem. Soc.*, **81**, 37 (1959).
3) J. Böeseken and G. Slooff, *Rec. trav. chim.*, **49**, 91 (1930).
4) T. W. Findley, D. Swern and J. T. Scanlan, *J. Am. Chem. Soc.*, **67**, 413 (1945).
5) R. Adams and C. S. Marvel, "Organic Syntheses," Coll. Vol. I, p. 94 (1956).

corresponding aldehydes, and were then recrystallized from methanol; benzil,[6] mp 95.5—96°C (lit., 94—95°C); *p*-tolil,[7] mp 103—104°C (lit., 104—105°C); *p*-anisil,[8] mp 133.5—134°C (lit., 133°C). Benzoic anhydride was recrystallized from a mixture of benzene and petroleum ether; mp 43—43.5°C. Benzoic acid was recrystallized from water; mp 122.5—123°C.

Reaction Products Criterion. A mixture (20 m*l*) of benzil (0.1 M), peroxyacetic acid (0.5 M), and sulfuric acid (0.2 N) in acetic acid was heated at 70°C for 10 hr, and then allowed to stand 2 days at room temperature. The reaction mixture was poured into water (100 m*l*). The product extracted with chloroform (30 m*l*) was identified as benzoic acid by the mixed-melting-point method; yield 90%, mp and mmp 122—122.5°C. The evolution of oxygen gas during the reaction was found by means of gas chromatography employing a Hitachi gas chromatograph, model KGL-2A, operated with a 3-m column packed with molecular sieve 13X and using helium with a flow rate of 25 m*l*/min at 38°C. The retention time was 2.5 min for oxygen and 3.2 min for nitrogen. The formation of acetyl peroxide was observed by paper chromatography under the same conditions as have been previously reported.[9]

Typical Run for the Rate Measurements. A solution of 1 m*l* of *ca.* 1 M peroxyacetic acid in acetic acid was poured into a solution of 9 m*l* of 0.11 M benzil in acetic acid to start the reaction after the two solutions had attained a temperature equilibrium at 70°C. Aliquots (each 1 m*l*) were taken out at appropriate time intervals and introduced to 100 m*l* of an ice-cooled aqueous solution of *ca.* 0.06% potassium iodide. The iodine liberated by peroxyacetic acid was quickly titrated with 0.01 N sodium thiosulfate in order to estimate the concentration of the remaining peroxyacetic acid.

Results and Discussion

The initial rate of the reaction satisfied the first-order equation in the concentration of the remaining peroxyacetic acid, as is illustrated in Table 1.

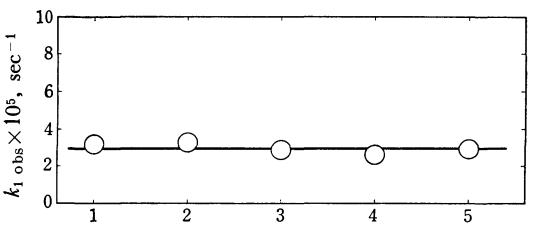

Fig. 1. Plots of $k_{1\,obs}$ *vs.* initial concentration of peroxyacetic acid in acetic acid at 70°C.
Initial concn. of benzil: 0.1 M
Concn. of H_2SO_4: 0.12 N

The $k_{1\,obs}$ rate constant with a varying initial concentration of peroxyacetic acid kept a settled value, as is shown in Fig. 1. As is illustrated in

$$-d[AcO_2H]/dt = k_{1\,obs}[AcO_2H]$$

Table 1. Typical rate data for the consumption of peroxyacetic acid in the oxidation of benzil with peroxyacetic acid in acetic acid at 70°C
Nominal initial concn. of CH_3CO_3H: 1×10^{-1} M
Concn. of $(C_6H_5CO)_2$: 1×10^{-1} M
Concn. of H_2SO_4: 3.0×10^{-2} N

Time min	$(a-x)\times10^2$ M	$\frac{a}{a-x}$	$k_{1\,obs}\times10^5$ sec^{-1}
0	10.06	1.000	
60	9.28	1.084	2.25
120	8.59	1.170	2.18
180	7.90	1.273	2.23
240	7.23	1.391	2.29
300	6.67	1.508	2.28
360	6.10	1.648	2.31
420	5.59	1.799	2.33
480	5.13	1.960	2.34
			Av. 2.28

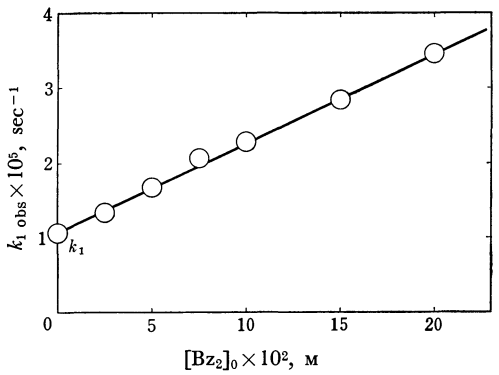

Fig. 2. Plots of $k_{1\,obs}$ *vs.* initial concentration of benzil in acetic acid at 70°C.
Initial concn. of CH_3CO_3H: 0.1 M
Concn. of H_2SO_4: 0.030 N

Table 2. The effect of acidity on the rate constants for the first- and second-order reactions at 70°C
Initial concn. of CH_3CO_3H: 1×10^{-1} M

$[H_2SO_4]$ M	$-H_0$[10]	$k_1\times10^5$ sec^{-1}	$k_{2\,obs}\times10^4$ M^{-1}sec^{-1}
0	—	0.74 ($=k_d$)[a]	1.00 ($=k_2$)[a]
0.015	0.72	1.07	1.19
0.04	1.18	1.74	1.48
0.06	1.37	1.94	1.83
0.08	1.50	2.51	2.09
0.10	1.60	2.96	2.23

a) The values of k_d and k_2 were estimated by extrapolation in Fig. 3.

6) H. T. Clarke and E. E. Dreger, "Organic Syntheses," Coll. Vol. I, p. 87 (1956).
7) R. Stierlin, *Ber.*, **22**, 376 (1889).
8) M. Bösler, *ibid.*, **14**, 323 (1881); A. T. Mason and L. A. Dryfoos, *J. Chem. Soc.*, **63**, 1300 (1893).
9) Y. Ogata, Y. Furuya, J. Maekawa and K. Okano, *J. Am. Chem. Soc.*, **85**, 961 (1963).

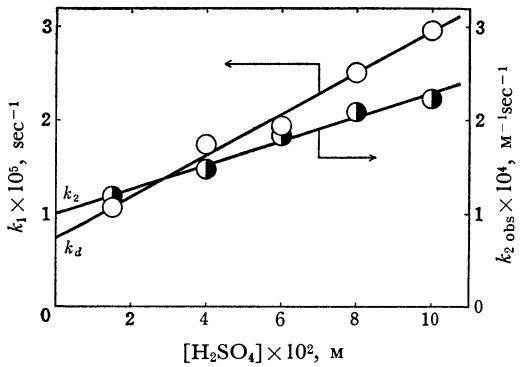

Fig. 3. Effect of the acidity of medium on the rate constants at 70°C.
Initial concn. of CH_3CO_3H: 0.1 M

Fig. 2, however, the plots of $k_{1\,obs}$ *vs.* the initial concentration of benzil gave a straight line, which satisfied the following equation:

$$k_{1\,obs} = k_1 + k_{2\,obs}[Bz_2]$$

The plots of k_1 and $k_{2\,obs}$ *vs.* the concentration of sulfuric acid gave straight lines, as Table 2 and Fig. 3 show; these lines followed the accompanying equations, respectively:

$$k_1 = k_d + k_t[H_2SO_4]$$

and $$k_{2\,obs} = k_2 + k_2'[H_2SO_4]$$

The plots of $\log(k_1 - k_d)$ and $\log(k_{2\,obs} - k_2)$ *vs.* H_0[10] gave straight lines with slopes of -0.94 and -0.95 respectively (Fig. 4). From these results,

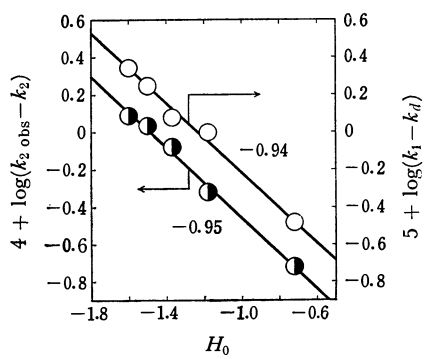

Fig. 4. Plots of $\log(k_1 - k_d)$ and/or $\log(k_{2\,obs} - k_2)$ *vs.* H_0 in acetic acid at 70°C.

it may be considered that the proton participates once before the rate-determining step in both the acid-catalyzed first-order and second-order reactions.

Finally, the rate equation is expressed as:

$$-d[AcO_2H]/dt = \{k_d + k_t[H_2SO_4]\}[AcO_2H] + \{k_2 + k_2'[H_2SO_4]\}[Bz_2][AcO_2H]$$

10) N. F. Hall and W. F. Spengeman, *J. Am. Chem. Soc.*, **62**, 2487 (1940).

Table 3. Substituent effect for the oxidation of benzil with peroxyacetic acid in acetic acid at 70°C
Initial concn. of CH_3CO_3H: 1×10^{-1} M

Benzils	$k_2 \times 10^5$ M^{-1}sec^{-1}	$k_2' \times 10^3$ M^{-2}sec^{-1}
Benzil	10.0	1.29
p-Tolil	3.2	2.45
p-Anisil	1.5	2.81

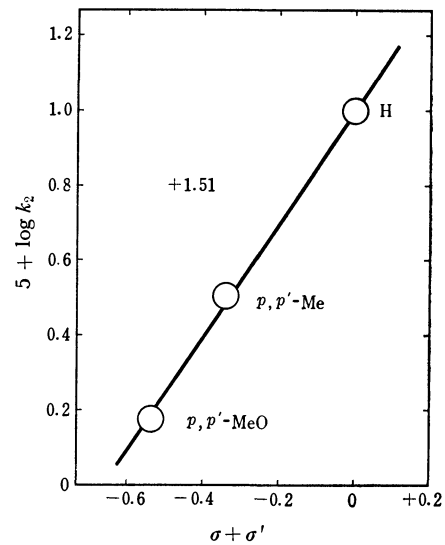

Fig. 5. Hammett plots for the non-catalyzed oxidation of substituted benzil to the corresponding benzoic acid in acetic acid at 70°C.

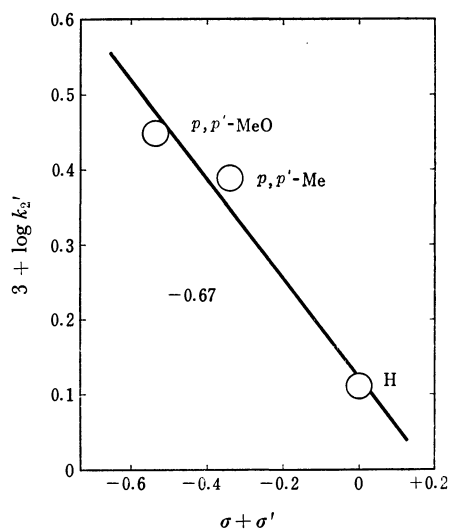

Fig. 6. Hammett plots for the acid-catalyzed oxidation of substituted benzil in acetic acid at 70°C.

It may be considered from the reaction products that the first, second, third, and fourth terms represent the decomposition of peroxyacetic acid itself,[11] the acid-catalyzed reversible transformation of peroxyacetic acid to acetyl peroxide,[9] and the non-catalyzed and the acid-catalyzed oxidation of benzils with peroxyacetic acid respectively. In this paper, only the third and fourth terms have been dealt with.

The introduction of an electron-releasing group into the benzil retarded the non-catalyzed oxidation of benzil and accelerated the acid-catalyzed oxidation (Table 3), and Hammett's plot gave positive and negative ρ-values of $+1.51$ and -0.67 respectively, as shown in Fig. 5 and/or 6.

On the oxidation of benzil with hydrogen peroxide in benzene, Leffler obtained an oily matter which gave benzoic acid by hydrolysis.[1] Thus, a reaction mechanism passing through acid anhydride has been suggested. The reaction scheme in Leffler's fashion is described as:

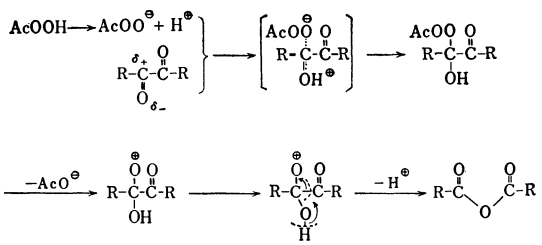

The mechanism consists of three steps, such as the addition of peroxyacetic acid to the carbonyl group of benzil, the elimination of the acetoxy anion from the adduct, and the deprotonation. Neither the step 1 nor 2 is the rate-determining step in this reaction, since the step 1 is the protonation and the step 2 should have a $-\rho$ value. Only the deprotonation could satisfy the experimental results shown in Fig. 5. It has not been confirmed by Leffler that the deprotonation is the rate-determining step. For these reasons, Leffler's scheme is unbelievable. A more probable mechanism is considered to be as follows:

(I) (II)

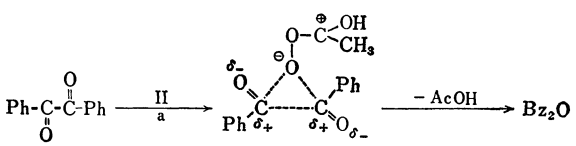

From the results such as the second-order in the concentrations of benzil and peroxyacetic acid and/or the positive ρ-value in the Hammett plots of $\log k_2$ *vs.* $\sigma+\sigma'$, the step a is probably the rate-determining step in the non-catalyzed oxidation of benzil with peroxyacetic acid, and the non-catalyzed oxidation is probably a nucleophilic attack by negative oxygen of peroxyacetic acid, II. If the reaction is an electrophilic attack of peroxyacetic acid, I, the value of ρ must be negative.

On the other hand, it is presumed that protonation to a substrate occurs once before the rate-determining step in the acid-catalyzed oxidation, as has been described above. In fact, the absorption maximum of benzil in acetic acid at 260 mμ decreases with an increase in the acidity. This phenomenon is probably due to the protonation to the carbonyl group of benzil.

Also, the acid-catalyzed reaction is probably a nucleophilic attack of peroxyacetic acid, II, because the k_2'/k_2 ratio is nearly 10. As the positivity on the carbonyl carbon in protonated benzil is much larger than that in free benzil induced by only the polarity of the C–O bond of the carbonyl group, the rate of the acid-catalyzed reaction will be ten times larger than the non-catalyzed one. A nucleophilic attack on the positive carbonyl carbon atom of free or protonated benzil by positive oxygen of peroxyacetic acid can not be considered. The existence of protonated benzil was observed by the ultraviolet spectrophotometry described above.

These results suggest this probable mechanism in the acid-catalyzed oxidation of benzil:

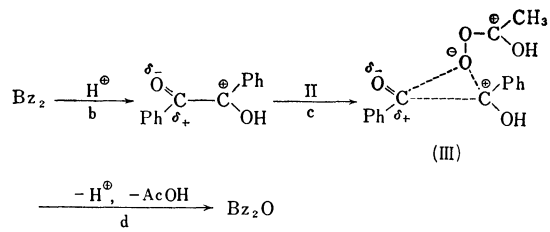

(III)

If the deprotonation determines the reaction, Hammett's plot of $\log k_2'$ *vs.* $\sigma+\sigma'$ is expected to give a positive ρ-value. It cannot be supposed that the elimination of acetic acid from the transition state, III, is influenced by a substituted group on the benzene ring. The step c probably determines the reaction rate.

The negativity of a carbonyl oxygen atom in benzil is increased by an electron-releasing group. Thus, the concentration of protonated benzil is enlarged with an increase in the electron-releasing degree. In other words, the equilibrium constant, K, for the protonation to benzil is enlarged with an increase in the electron-releasing force.

$$Bz_2 + H^{\oplus} \overset{K}{\rightleftharpoons} Bz_2H^{\oplus}$$

11) T. Suzuki, I. Iwamoto and S. Suzuki, *Nippon Kagaku Zasshi (J. Chem. Soc. Japan, Pure Chem. Sect.)*, **83**, 1212 (1962).

$$Bz_2H^{\oplus} + AcO_2H \xrightarrow{k}$$

$$[Bz_2H^{\oplus}] = K[H^{\oplus}][Bz_2]$$

$$v_{(acid\ cat)} = k[Bz_2H^{\oplus}][AcO_2H]$$
$$= kK[H^{\oplus}][Bz_2][AcO_2H]$$

$$\therefore\ k_2' = kK$$

On the other hand, the rate constant, k, for the reaction of protonated benzil with peroxyacetic acid may decrease with an increase in the electron-releasing degree, since the positivity of a carbonyl carbon atom in protonated benzil will be decreased by an electron-releasing group. However, the proportion of the diminution in the positivity of carbonyl carbon in protonated benzil caused by an electron-releasing group is not so great as to have a considerable influence upon the reaction rate. Thus, the influence of a substituent on the equilibrium constant, K, may be much larger than that on the k rate constant. Consequently, the acid-catalyzed rate constant, k_2', which is equal to the product of k by K, will be increased by an electron-releasing group with a Hammett ρ-value of -0.67. By means of these hypotheses, the kinetic findings can be explained without difficulty.

The value of 3×10^{-3} sec^{-1} was obtained as the rate constant for the hydrolysis of benzoic anhydride in the presence of 0.027 N sulfuric acid at 70°C. The value divided by the calculated concentration of water in the reaction solvent is about two hundred times larger than the value of $k_{2\ obs}$ obtained under the same reaction conditions. Hence, the step of the hydrolysis of benzoic anhydride is undoubtedly not the rate-determining step.

The oxidation is a sort of Baeyer-Villiger reaction.

The non- and acid-catalyzed oxidations may be summarized as follows:

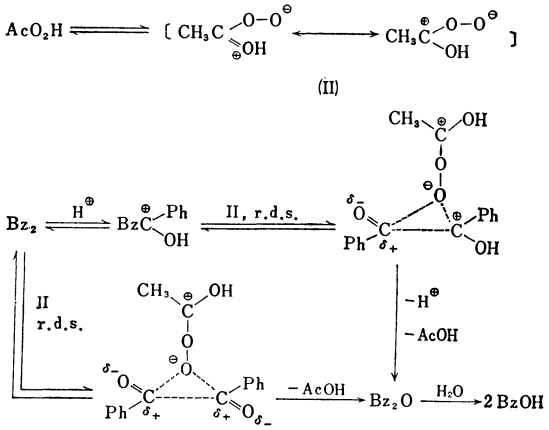

BULLETIN OF THE CHEMICAL SOCIETY OF JAPAN VOL. 41 664—668 (1968)

Thermal Transformation of Alkali Salts of Aromatic Carboxylic Acids. V.[1] Reaction of Potassium and Sodium Salts of Naphthoic Acids

Yasuhiko DOZEN

Government Industrial Research Institute, Osaka, Ikeda-shi, Osaka

(Received September 6, 1967)

The cadmium fluoride-catalyzed thermal transformation of potassium and sodium salts of naphtoic acids has been investigated. At the initial reaction stage both potassium and sodium α-naphthoate gave naphthalene and naphthalene-1, 2- and 1, 3-dicarboxylates, which were converted to naphthalene-2, 3- and 2, 6-dicarboxylates. The products composition, however, differed between potassium and sodium salts. Potassium β-naphthoate gave naphthalene and naphthalene-1,2- and 2,3-dicarboxylates, which were then further converted to naphthalene-2, 6-dicarboxylate. On the other hand, sodium β-naphthoate gave naphthalene and naphthalene-1, 2- and 2, 3-dicarboxylates. In the presence of potassium cyanate, potassium α- and β-naphthoates gave a high yield of naphthalene-2, 6-dicarboxylate. The mechanism of the reaction was discussed.

Raecke[2,3] found that potassium α- and β-naphthoates gave naphthalene-2, 6-dicarboxylate in the presence of a catalyst under carbon dioxide pressure and under heating at a high temperature. The reaction conditions have been studied by Yamashita, Enomoto, Ebisawa, and Kato,[4] **and**

1) Part IV: Y. Dozen, This Bulletin, **40**, 1218 (1967).

2) B. Raecke (to Henkel & Cie, G. m. b. H.), German Pat. 953072 (1956); Brit. Pat. 744721 (1956); U. S. Pat. 2823231 (1958).

3) B. Raecke, *Angew. Chem.*, **70**, 1 (1958).

4) J. Yamashita, K. Enomoto, H. Ebisawa and S. Kato, *Yuki Gosei Kagaku Kyokaishi (J. Soc. Org. Syn. Chem. Japan)*, **20**, 501 (1962).

Table 1. Reaction products of α-naphthoate

Run No.	Condition		Product (mol%)							
	Temp. °C	Time hr	Naphthalene[a]	Naphthoic acid		Naphthalene dicarboxylic acid[a]				
				α-	β-	1,2-	2,3-	1,3-	2,6-	2,7-
From potassium salt										
1	325	1	22	78	—	10	1	—	—	—
2	345	1	53	35	12	0.6	1.4	12	4	—
3	385	1	79	—	24	—	8	—	34	—
4[b,c]	370	1	99	—	27	—	—	—	47	—
5[b,c]	370	4	100	—	10	—	—	—	64	—
From sodium salt										
6	290	1	33	61	—	10	5	6	0.3	0.2
7	320	1	63	8	19	24	28	1	4	2
8[c]	345	1	73	—	21	—	23	—	6	—
9	385	1	66	—	20	12	24	—	7	—
10	385	3	61	—	21	—	25	1	9	—

a) The yield was based on the disproportionation of naphthoate.
b) Potassium cyanate (7.0 g) was added.
c) The acid II fraction (see Experimental part) was not treated for the large contamination with the resinous substance.

Table 2. Reaction products of β-naphthoate

Run No.	Condition		Product (mol%)					
	Temp. °C	Time hr	Naphthalene[a]	Naphthoic acid		Naphthalene dicarboxylic acid[a]		
				α-	β-	1,2-	2,3-	2,6-
From potassium salt								
1[b]	380	1	11	—	80	—	18	—
2	430	2	31	—	34	Trace	9	43
3[b,c]	380	1	26	—	68	—	6	14
4[b,c]	380	4	25	—	43	—	5	44
5[c]	395	10	31	—	30	1	4	78
From sodium salt								
6	385	1.5	38	—	58	4	30	—
7	445	1.5	30	—	48	Trace	33	—
8	445	5	33	—	44	Trace	29	—
9[b,d]	450	5	28	—	44	—	37	—

a) The yield was based on the disproportionation of naphthoate.
b) The acid II fraction (see Experimental part) was not treated for the large contamination with the resinous substance.
c) Potassium cyanate (7.0 g) was added.
d) Zink chloride instead of cadmium fluoride was added.

an improvement of the reaction apparatus has been reported by Dorschner, Markworth, and Plenz.[5]

In the previous paper,[1] it has been reported that potassium methylbenzoates gave *o*-, *m*-, and *p*-directed disproportionation products, while sodium methylbenzoates gave an *o*-directed one. It was also observed in 1965 that sodium β-naphthoate gave naphthalene-2, 3-dicarboxylate. At that time, similar results were reported by McNelis,[6] and Patton and Son.[7] This paper will report the results of more detailed studies of the difference in orientation between potassium and sodium salts of naphthoic acids in the disproportionation.

5) O. Dorschner, H. Markworth and J. Plenz (to Metallgeselschaft A.-G.), German Pat. 1155770 (1963).

6) E. McNelis, *J. Org. Chem.*, **30**, 1209 (1965).
7) J. W. Patton and M. O. Son, *ibid.*, **30**, 2869 (1965).

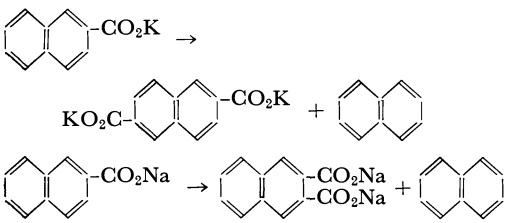

Table 1 shows the reaction products from potassium and sodium salts of α-naphthoic acid. Both salts, in each case, gave naphthalene and naphthalene-1, 2- and 1, 3-dicarboxylates as the primary product at a low temperature. With a rise in the temperature, however α-naphthoate disappeared, and β-naphthoate, naphthalene-2, 3-, 2, 6-, and 2, 7-dicarboxylates were produced. The potassium salt gave the 2, 6-isomer predominantly, while the sodium salt gave the 2, 3-isomer as the main product.

In the presence of potassium cyanate and potassium carbonate, potassium α-naphthoate gave a higher yield of naphthalene-2, 6-dicarboxylate than in the absence of potassium cyanate. This may be explained in terms of direct carboxylation with potassium carbonate, as has been reported in the reactions of potassium benzoate, potassium carbonate, and potassium cyanate.[8]

Table 2 shows the reaction products from potassium and sodium salts of β-naphthoic acid. Potassium β-naphthoate gave naphthalene-2, 3-dicarboxylate at low temperatures and 2, 6-isomer at high temperatures. In the presence of potassium cyanate, the yield of 2, 6-isomer was increased. On the other hand, sodium β-naphthoate gave naphthalene-2, 3-dicarboxylate selectively.

These results indicate that α-naphthoate is disproportionated to naphthalene-1, 2- and 1, 3-dicarboxylates in the initial stage of the reaction, and then a thermally-unstable α-carboxyl group of these acids is decarboxylated or cross-disproportionated to β-naphthoate. Thermally-stable naphthalene-2, 3- and 2, 6-dicarboxylates may be produced by the disproportionation of β-naphthoate or by the cross-disproportionation of β-naphthoate and another carboxylate, as shown in Chart 1. The facts that potassium β-naphthoate gave naphthalene-2, 3- and 2, 6-dicarboxylates, and that sodium β-naphthoate was converted to naphthalene-2, 3-dicarboxylate, may be explained in terms of the difference in thermal stability between the potassium and sodium salts of naphthalene-2, 3-dicarboxylate.

McNelis[6] reported the decarboxylation-recarboxylation mechanism for the reaction of potassium β-naphthoate to naphthalene-2, 6-dicarboxylate. In the reaction of potassium benzoate, a similar mechanism has been discussed by Furuyama[9] using deuterated or radioactive benzoate. In the reaction of potassium phthalates and benzoate under an atmosphere of radioactive carbon dioxide, it has been reported by Riedel and Kienitz[10] that the quantity of $^{14}CO_2$ incorporated into the molecules of benzene carboxylates was lower than the calculated value. This reaction was further investigated by Ratusky and Sorm[11] in a thin-layer state of carboxylates with perfect mixing; there results suggest the decarboxylation-recarboxylation mechanism.

When the decarboxylation - recarboxylation mechanism is involved in the reaction, the α-hydrogen of the naphthalene ring, which is more reactive than the β-hydrogen, will be abstracted by the carbanion which is produced by the decarboxylation of β-naphthoate, and α-naphthoate

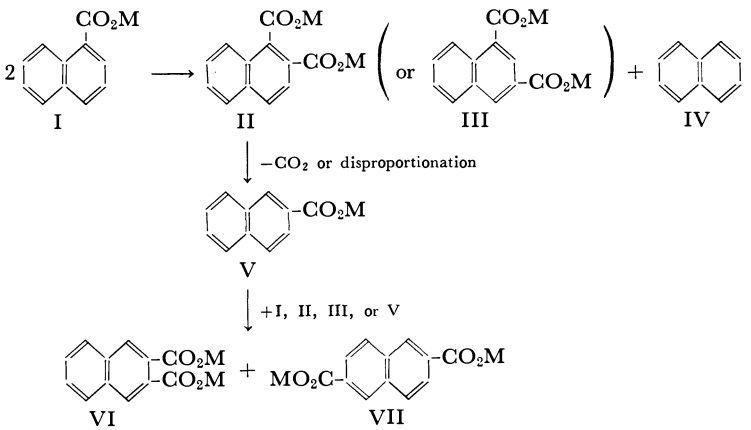

Chart 1

8) Y. Dozen and S. Fujishima, *Yuki Gosei Kagaku Kyokaishi (J. Soc. Org. Syn. Chem. Japan)*, **25**, 155 (1967).
9) S. Furuyama, This Bulletin, **40**, 1212 (1967).
10) O. Riedel and H. Kienitz, *Angew. Chem.*, **72**, 738 (1960).
11) J. Ratusky and F. Sorm, *Chem. & Ind. (London)*, **1966**, 1798.

will be obtained as the reaction product. α-Naphthoate, however, could not be detected in the reaction product of the β-naphthoate (see Table 2). This fact may be explained by the intermolecular disproportionation mechanism.

Experimental[12]

Materials. α-Naphthoic acid was prepared by the Grignard reaction of α-bromonaphthalene[13]; mp 161—162°C (benzene). β-Naphthoic acid was synthesized by the hypobromite oxidation of β-acetylnaphthalene,[14] which had been prepared by the Friedel-Crafts reaction of naphthalene and acetyl chloride[15]; mp 183—184°C (EtOH).

General Method. A naphthoic acid was neutralized with aqueous potassium (or sodium) hydroxide to pH 7.0—7.5. The solution was then evaporated to dryness and further dried under a vacuum (*ca.* 5 mmHg) at 150—180°C. The alkali salt of naphthoic acid (15.0 g) was mixed with cadmium fluoride (1.0 g) and potassium (or sodium) carbonate (5.0 g). The mixture was dried under a vacuum (*ca.* 5 mmHg) at 150—180°C, charged in a rotary autoclave (160 m*l*, 60 rpm), and allowed to react under the pressure of carbon dioxide (initial pressure of 40 kg/cm² gauge). The warm-up period was *ca.* 1 hr. After cooling, the reaction product was extracted with ether (Soxhlet) to remove the naphthalene, which was identified by means of its melting point. The ether-insoluble substance was dissolved in hot water (500 m*l*). The solution was neutralized with hydrochloric acid to pH 6—7, treated with active carbon, and further acidified to pH 1. The precipitate was filtered while hot and dried (Acid I). The aqueous solution was evaporated to dryness, and the residue was extracted with ethanol to give an acidic substance (Acid II).[16]

Analysis. Each fraction of Acid I and II (1—2 g) was converted to silver salt, and the salt was esterified with methyl iodide in benzene. After the evaporation of the solvent, the residue was dissolved in chloroform and analyzed by vapor-phase chromatography. α- and β-Naphthoates were analyzed with 25% Silicone DC 550 on Shimalite (30—60 mesh; 4 mmφ × 1.5 m; column temperature, 190°C; flow rate of He, 50 m*l*/min), and naphthalene dicarboxylates were determined with 15% Silicone DCHV Grease on Celite 545 (Nishio Kogyo Co., Ltd.) (40—60 mesh; 4 mmφ × 1.5 m; column temperature, 220°C; flow rate of He, 50 m*l*/min). The retention times of the authentic samples are shown in Fig. 1. The analytical data of the esters derived from an authentic mixture of α-naphthoic (24.8 wt%), β-naphthoic (26.7%), naphthalene-2, 3-dicarboxylic (23.5%), and 2, 6-dicarboxylic (25.0%) acids gave 21.8, 29.5, 23.4 and 25.4 wt% respectively.

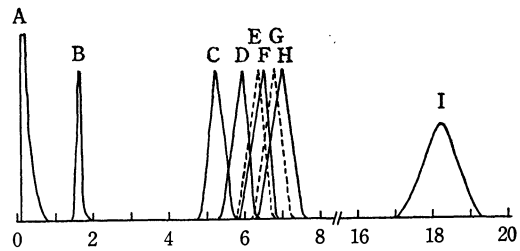

Fig. 1. Vapor-phase chromatogram of methyl esters of naphthalene carboxylic acids.

15% silicon DCHV grease on celite 545
column temperature, 220°C
flow rate of He, 50 m*l*/min
A Solvent ($CHCl_3$)
B α- and β-Naphthoates
C 1, 2-Dicarboxylate
D 2, 3-, 1, 4- and 1, 8-Dicarboxylates
E 1, 3- and 1, 5-Dicarboxylates
F 1, 7-Dicarboxylate
G 2, 6- and 1, 6-Dicarboxylates
H 2, 7-Dicarboxylate
I 1, 3, 5-Tricarboxylate

Identification of the Reaction Products. *Naphthalene-2, 6-dicarboxylic Acid.* The dimethyl ester obtained from the reaction product of potassium β-naphthoate (430°C for 1.5 hr) or α-naphthoate (Table 1, run 5) was recrystallized from ethyl acetate or benzene to give dimethyl naphthalene-2, 6-dicarboxylate; mp 189.0—189.5°C (lit., mp 187—188°C[17]).

Naphthalene-2, 3-dicarboxylic Acid. The reaction products of sodium β-naphthoate (445°C for 1.5 hr) were extracted with ether (Soxhlet, 8 hr); the insoluble substance (1.5 g) was then treated with acetic anhydride to give 0.9 g of naphthalene-2, 3-dicarboxylic anhydride; mp 245—246°C (lit., mp 246°C[18]).

Found: C, 72.59; H, 2.74%. Calcd for $C_{12}H_6O_3$: C, 72.72; H, 3.05%.

The infrared spectrum had acid anhydride bands at 1841 and 1764 cm^{-1}.

Naphthalene-1, 2-dicarboxylic Acid. The ester of the Acid II fraction obtained by the reaction of potassium α-naphthoate (Table 1, run 7) was recrystallized from methanol to give dimethyl naphthalene-1, 2-dicarboxylate (mp 78—82°C), which was identified by a mixed-melting-point determination and by a comparison of the infrared spectra with those of an authentic sample (see the next paragraph).

Naphthalene-1, 3-dicarboxylic Acid. The ester obtained from the reaction product of potassium α-naphthoate Table 1, run 2) was distilled to remove the methyl naphthoates. The residue had all the peaks of the infrared spectrum appearing in dimethyl naphthalene-1, 3-dicarboxylate, but all attempts to isolate it failed.

12) All melting points are corrected. Vapor-phase chromatography, infrared spectroscopy, and micro analysis were performed using a Shimadzu G. C-1B, a Hitachi Infrared Spectrophotometer EPI-SII (in Nujol), and a Yanagimoto C. H. N. Corder MT-1 apparatus respectively.

13) H. Gilman, N. B. St. John and F. Schulze, "Organic Synthesis," Coll. Vol. II, p. 425 (1948).

14) M. S. Newman and H. L. Holmes, *ibid.*, p. 428.

15) T. Immediate and A. R. Day, *J. Org. Chem.*, **5**, 516 (1940).

16) This fraction was more or less contaminated with a resinous substance.

17) M. Freund and K. Fleischer, *Ann.*, **402**, 68 (1913).

18) H. Meyer and K. Bernhauer, *Monatsch.*, **53/54**, 750 (1929).

Synthesis of Dimethyl Naphthalene Dicarboxylates as the Standard Sample of the Vapor-phase Chromatography.[19] *1, 2-Isomer.* 1, 2-Dicyanonaphthalene (mp 190.5—191.5°C; lit., mp 190°C[20]) was synthesized by the method of Brandbrook and Linstead[20] from 2-aminonaphthalene-1-sulfonic acid (Tobias Acid), and the nitrile was hydrolyzed to naphthalene-1, 2-dicarboxylic acid. The dimethyl ester had a melting point of 84—85°C (MeOH) (lit., mp 85°C[20]).

1, 3-Isomer. Brandbrook and Linstead[20] have reported that they prepared naphthalene-1, 3-dicarboxylic acid (mp 267—268°C) by the hydrolysis of 1, 3-dicyanonaphthalene (mp 179°C), which had been synthesized by the reaction of sodium 3-cyanonaphthalene-1-sulfonate and potassium ferrocyanide. The physical constants of these substances as prepared by the following route, however, differ from those reported by Brandbrook and Linstead.

A) 2, 4-Dibromo-1-naphthylamine (mp 115—117°C (EtOH); lit., mp 116—118°C[21]), which had been prepared by the method of Consden and Kenyon,[21] was converted to 1, 3-dibromonaphthalene (mp 61—62°C (EtOH); lit., mp 64°C[22]) by the method of Meldra.[22] The dibromonaphthalene (6.1 g, 0.021 mol), cuprous cyanide (5.0 g, 0.056 mol), and dimethyl formamide (30 ml) were heated at 180—185°C for 4 hr by a method similar to that of Friedman and Shechter[23] to give 1, 3-dicyanonaphthalene (0.8 g); mp 226.5—227.5°C (EtOH).

Found: C, 81.11; H, 3.48; N, 15.44%. Calcd for $C_{12}H_6N_2$: C, 80.87; H, 3.39; N, 15.72%.

The dinitrile was hydrolyzed with aqueous sulfuric acid to give naphthalene-1, 3-dicarboxylic acid (0.7 g); mp>300°C. The methyl ester has a melting point of 105—106°C (EtOH).

Found: C, 69.12; H, 4.73%. Calcd for $C_{14}H_{12}O_4$: C, 68.84; H, 4.95%.

B) 1, 3-Dimethylnaphthalene (bp 100°C/4 mmHg; lit., bp 129°C/9 mmHg[24]) was prepared by the method of Balaban and Barabas[24] from acetyl acetone and benzyl magnesiumchloride. A mixture of dimethylnaphthalene (7.2 g), sodium bichromate (22 g), and water (40 ml) was heated at 250—260°C for 22 hr in an autoclave by a method similar to that of Friedman, Fishel, and Shechter[25] to give naphthalene-1, 3-dicarboxylic acid. The dimethyl ester had a melting point of 104.5—105.5°C. It was identified by a mixed-melting-point determination and by a comparison of the infrared spectrum with that of the sample obtained in A).

1, 4-Isomer. Naphthalene-1, 4-dicarboxylic acid was prepared from 1, 4-dicyanonaphthalene (mp 207.5—208.5°C (EtOH); lit., mp 208°C[20]), which had been prepared by the method of Brandbrook and Linstead[20] from 1-aminonaphthalene-4-sulfonic acid (Naphthionic Acid). The dimethyl ester had a melting point of 65—66°C (dil. AcOH) (lit., mp 67°C[20]).

1, 5-Isomer. 1, 5-Dicyanonaphthalene was synthesized from disodium naphthalene-1, 5-disulfonate and potassium ferrocyanide by a method similar to that of Brandbrook and Linstead[20]; mp 263—264°C (EtOH) (lit., mp 263°C[20]). The dinitrile was converted to the corresponding acid, which gave dimethyl naphthalene-1, 5-dicarboxylate (mp 116—117°C (EtOH); lit., mp 119°C[20]).

1, 6-Isomer. 1, 6-Dicyanonaphthalene was prepared by the method of Brandbrook and Linstead[20] from 1-aminonaphthalene-6-sulfonic acid (1, 6-Cleve's Acid); mp 210—211°C (EtOH) (lit., mp 211°C[20]). The nitrile was hydrolyzed to acid. The dimethyl ester had a melting point of 97—98°C (aq. MeOH) (lit., mp 98°C[20]).

1, 7-Isomer. 1, 7-Dicyanonaphthalene was prepared from 1-aminonaphthalene-7-sulfonic acid (1, 7-Cleve's Acid); mp 166—167°C (EtOH) (lit., mp 167°C[20]). The nitrile was hydrolyzed to acid, which gave dimethyl naphthalene-1, 7-dicarboxylate (mp 89—90°C (aq. EtOH); lit., mp 90°C[20]).

1, 8-Isomer. Dimethyl naphthalene-1, 8-dicarboxylate was prepared from naphthalic acid; mp 102—103°C (MeOH) (lit., mp 104°C[20]).

2, 3-Isomer. Naphthalene-2, 3-dicarboxylic anhydride, which had been obtained by the reaction of sodium β-naphthoate, was converted to dimethyl naphthalene-2, 3-dicarboxylate; bp 191—192°C/6 mmHg, mp 48—50°C (lit., mp 47°C,[20] 50—51°C[26]).

2, 6-Isomer. Dimethyl naphthalene-2, 6-dicarboxylate was prepared from the corresponding dicarboxylic acid, which had been obtained by the reaction of potassium β-naphthoate; mp 189.0—189.5°C.

2, 7-Isomer. 2, 7-Dicyanonaphthalene was obtained by the reaction of disodium naphthalene-2, 7-disulfonate and potassium ferrocyanide by a method similar to that of Brandbrook and Linstead[20]; mp 264°C (AcOH) (lit., mp 267°C[20]). The nitrile was hydrolyzed to an acid, which gave dimethyl naphthalene-2, 7-dicarboxylate (mp 135—136°C (EtOH); lit., mp 135°C[20]).

The author is indebted to Professor Haruo Shingu, Kyoto University, for his help and encouragement, and to (Mrs.) Shizu Fujishima of our laboratory for her assistance in the microanalysis.

19) The ester of the carboxylic acid was synthesized by the reaction of the silver salt of the carboxylic acid and methyl iodide.

20) E. F. Brandbrook and R. P. Linstead, *J. Chem. Soc.*, **1936**, 1739.
21) R. Consden and J. Kenyon, *J. Chem. Soc.*, **1935**, 1594.
22) R. Meldra, *Ber.*, **12**, 1963 (1879).
23) L. Friedman and H. Shechter, *J. Org. Chem.*, **26**, 2522 (1961).
24) A. T. Balaban and A. Barabas, *Chem. & Ind. (London)*, **1967**, 404.
25) L. Friedman, D. L. Fishel and H. Shechter, *J. Org. Chem.*, **30**, 1453 (1965); "Oxidation in Organic Chemistry," Part A, K. B. Wiberg Ed., Academic Press, New York (1965), p. 90.
26) D. N. Burge and N. L. Allphin, *Chem. Eng. Data*, **8**, 458 (1963).

BULLETIN OF THE CHEMICAL SOCIETY OF JAPAN VOL. 41 669—672 (1968)

Ribonuclease T_1 Peptides. II. Synthesis of a Protected Pentapeptide Corresponding to Sequence 12—16

Michinori WAKI, Nobuo Mitsuyasu, Tetsuo KATO, Satoru MAKISUMI and Nobuo IZUMIYA

Laboratory of Biochemistry, Faculty of Science, Kyushu University, Hakozaki, Fukuoka

(Received September 16, 1967)

A protected pentapeptide corresponding to sequence 12—16 of ribonuclease T_1, namely benzyloxycarbonyl-L-seryl-L-seryl-L-seryl-β-*t*-butyl-L-aspartyl-L-valine ethyl ester (XI), was synthesized by coupling of benzyloxycarbonyl-seryl-serine azide with a tripeptide ester, seryl-β-*t*-butyl-aspartyl-valine ethyl ester, which is derived from benzyloxycarbonyl-seryl-β-*t*-butyl-aspartyl-valine ethyl ester by the hydrogenolysis. The hydrogenolysis and the subsequent treatment with trifluoroacetic acid of the protected pentapeptide ester (XI) yielded a neutral pentapeptide ester, seryl-seryl-seryl-aspartyl-valine ethyl ester, as a crystalline product.

The synthesis of the protected *N*-terminal undecapeptide (1—11) of ribonuclease T_1 containing asparagine residue in the 3rd position was previously reported.[1] In the present paper, we will describe the synthesis of the protected pentapeptide corresponding to sequence 12—16, that is benzyloxycarbonyl-L-seryl-L-seryl-L-seryl-β-*t*-butyl-L-aspartyl-L-valine ethyl ester (XI).

This pentapeptide sequence possesses several functional groups, three hydroxyl ones of serine and an acidic one of aspartic acid, in a rather short peptide, so the preparation of this peptide derivatives seemed to be interesting as an object of organic synthesis.

In the synthesis of the protected pentapeptide (XI), we first selected a route involving the coupling of benzyloxycarbonyl-seryl-seryl-serine azide derived from the corresponding hydrazide (VI) with β-*t*-butyl-aspartyl-valine ethyl ester (VIII). However, the coupling reaction did not afford the desired product (XI); it was found that the product isolated was benzyloxycarbonyl-seryl-seryl-serine amide. In this connection, it would be noteworthy that several workers have reported the formation of acylamino acid or peptide amide from the corresponding azide during the peptide synthesis.[2]

The successful synthesis of the desired product (XI) was performed through the sequence of reactions as shown in Fig. 1. Benzyloxycarbonyl-seryl-serine ethyl ester (II) was prepared by coupling benzyloxycarbonyl-serine azide obtained from the corresponding hydrazide[3] using isoamyl nitrite[4] with serine ethyl ester (I). The dipeptide ester (II) obtained was converted to the hydrazide (III) by the treatment with hydrazine. Benzyloxycarbonyl-β-*t*-butyl-aspartyl-valine ethyl ester (VII) was prepared by coupling benzyloxycarbonyl-β-*t*-butyl-aspartic acid[5] with valine ethyl ester[6] using dicyclohexylcarbodiimide[7] as a coupling reagent or by the mixed anhydride method.[8] The oily product (VII) was hydrogenated to yield the dipeptide ester hydrochloride (VIII·HCl), which was then coupled with benzyloxycarbonyl-serine azide derived from the corresponding hydrazide[3] to give the protected tripeptide ester (IX). This protected peptide ester (IX) was subjected to hydrogenolysis to yield the tripeptide ester (X), which was coupled with benzyloxycarbonyl-seryl-serine azide derived from III as the same manner used for the preparation of II. This coupling gave the desired protected pentapeptide ester (XI) as a crystalline product.

Thus we could prepare the protected pentapeptide ester (XI) by coupling of benzyloxycarbonyl-dipeptide azide derived from III with the tripeptide ester (X). In this connection, it should

1) M. Ohno, T. Kato, N. Mitsuyasu, M. Waki, S. Makisumi and N. Izumiya, This Bulletin, **40**, 204 (1967).

2) E. Schröder and K. Lübke, "The Peptides," Vol. I, Academic Press, New York and London (1965), p. 84.

3) J. S. Fruton, *J. Biol. Chem.*, **146**, 463 (1942); G. Riley, J. H. Turnbull and W. Wilson, *J. Chem. Soc.*, **1957**, 1373.

4) J. Honzl and J. Rudinger, *Collection Czech. Chem. Commun.*, **26**, 2333 (1961); E. Wünsch and A. Zwick, *Chem. Ber.*, **99**, 101 (1966).

5) E. Schröder and E. Klieger, *Liebigs Ann.*, **673**, 208 (1964); R. Schwyzer and H. Dietrich, *Helv. Chim. Acta*, **44**, 2003 (1961); E. Wünsch and A. Zwick, *Z. Physiol. Chem.*, **328**, 235 (1962).

6) T. Kato, S. Makisumi, M. Ohno and N. Izumiya, *Nippon Kagaku Zasshi (J. Chem. Soc. Japan, Pure Chem. Sect.)*, **83**, 1151 (1962).

7) J. C. Sheehan and G. P. Hess, *J. Am. Chem. Soc.*, **77**, 1067 (1955).

8) J. R. Vaughan, Jr., and R. L. Osato, *ibid.*, **73**, 5553 (1951).

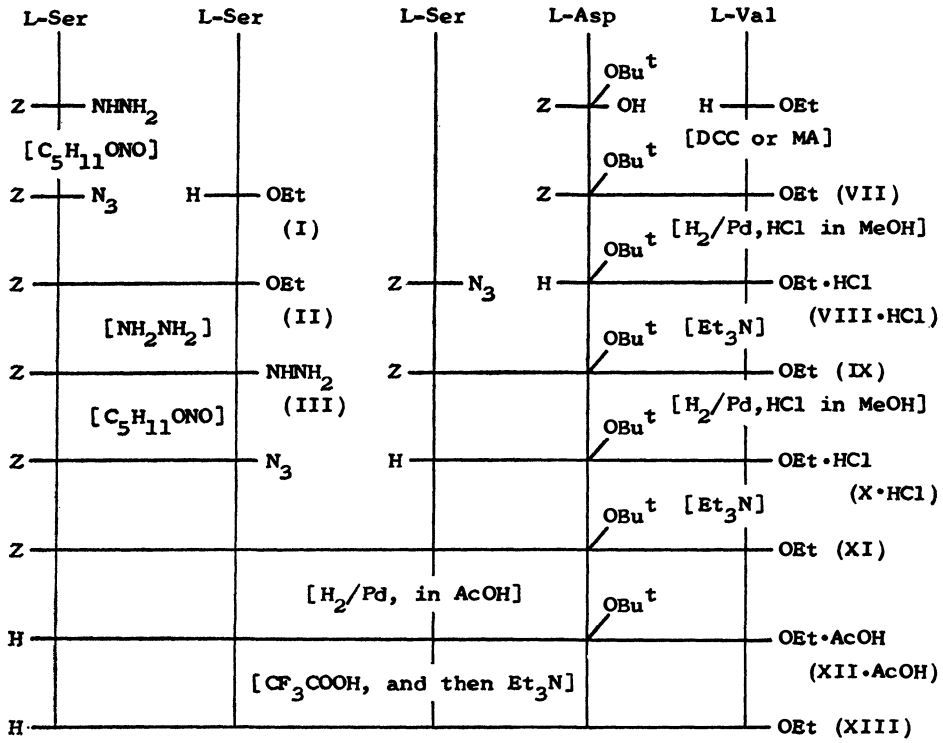

Fig. 1. Schematic diagram of synthesis of the pentapeptide ester. Z-, Benzyloxycarbonyl; -OBu^t, *t*-butyl ester; DCC, dicyclohexylcarbodiimide; MA, mixed anhydride method.

be pointed out that Hofmann *et al.*[9] reported the successful synthesis of the protected hexapeptide *t*-butyl ester (sequence 15—20 of ribonuclease A) by coupling of benzyloxycarbonyl-seryl-serine azide with threonyl-seryl-alanyl-alanine *t*-butyl ester and Scoffone *et al.*[10] similarly prepared the protected pentapeptide ester (sequence 16—20 of ribonuclease A) from benzyloxycarbonyl-seryl-threonine azide and seryl-alanyl-alanine *t*-butyl ester.

The protected pentapeptide ester (XI) was hydrogenated in a solvent of acetic acid to remove the benzyloxycarbonyl group, and the pentapeptide ester acetate (XII·AcOH) obtained was then treated with trifluoroacetic acid to remove the β-*t*-butyl group. The resulting pentapeptide ethyl ester (XIII) was obtained as a crystalline product. The homogeneity of the peptide (XIII) was ascertained by paper and thin-layer chromatography and the expected molar ratio of the constituent amino acids was observed in the acid hydrolysate of XIII by the amino acid analysis. Furthermore, the stereospecific purity of the peptide (XIII) was ascertained by the digestion with leucine aminopeptidase.

9) K. Hofmann, W. Hass, M. J. Smithers and G. Zanetti, *ibid.*, **87**, 631 (1965).
10) E. Scoffone, F. Marchiori, R. Rocchi, G. Vidali, A. M. Tamburro, A. Scatturin and A. Marzotto, *Tetrahedron Letters*, **9**, 943 (1966).

Experimental

All the melting points are uncorrected. The paper and thin-layer chromatographies were carried out on Toyo Roshi No. 52 paper and on Merck silica gel G, respectively. Spots of materials possessing a free amino group on a thin-layer plate were detected by spraying ninhydrin, and those of the amino group-blocked materials, by spraying 47% hydrobromic acid and then ninhydrin.

L-Serine Ethyl Ester *p*-Toluenesulfonate (I·TsOH). This compound was prepared according to the general procedure of Kato *et al.*[6] A suspension of L-serine (10.51 g) and *p*-toluenesulfonic acid monohydrate (19.02 g) in a mixture of ethanol (60 m*l*) and carbon tetrachloride (300 m*l*) was refluxed for 48 hr, and the water liberated was removed as an azeotropic mixture. The reaction mixture was then evaporated to dryness *in vacuo* to give an oily product; yield, 30.66 g (100%); R_f 0.67.[11]

Benzyloxycarbonyl-L-seryl-L-serine Ethyl Ester (II). To a chilled (−5°C) solution of benzyloxycarbonyl-serine hydrazide[3] (5.06 g, 20 mmol) in dimethylformamide (60 m*l*) containing 12.12 m*l* of 3.3 N hydrogen chloride in ethyl acetate, there were stirred isoamyl nitrite[4] (2.34 g, 20 mmol). After 10 min, triethylamine (5.6 m*l*, 40 mmol) was added. To the solution was added a mixture of I·TsOH (6.11 g, 20 mmol) and

11) The R_f value of the thin-layer chromatography with Merck silica gel refers to a solvent system of *n*-butanol-acetic acid-pyridine-water (4 : 1 : 1 : 2, v/v).

triethylamine (2.8 ml, 20 mmol) in dimethylformamide (40 ml). The reaction mixture was then stirred for 2 days at 0°C and evaporated *in vacuo*. The residue was dissolved in ethyl acetate (120 ml), and the solution was washed successively with a 4% sodium bicarbonate solution, 3% hydrochloric acid and water, dried over sodium sulfate, and then evaporated *in vacuo*. The crystalline residue was collected with the aid of ether-petroleum ether. It was recrystallized from ethyl acetate-petroleum ether; yield, 5.0 g (71%); mp 127—129°C; $[\alpha]_D^{22}$ −8.3° (*c* 1, methanol); R_f 0.82.[11]

Found: C, 54.10; H, 6.26; N, 7.95%. Calcd for $C_{16}H_{22}O_7N_2$: C, 54.23; H, 6.26; N, 7.91%.

Benzyloxycarbonyl-L-seryl-L-serine Hydrazide (III). A solution of II (3.18 g, 9 mmol) and hydrazine hydrate (1.09 ml, 22.5 mmol) in ethanol (20 ml) was allowed to stand overnight at room temperature. The excess hydrazine was evaporated *in vacuo*, and the resulting crystals were collected by filtration with the aid of cold ethanol. It was recrystallized from hot water; yield, 1.96 g (64%); mp 221—222°C (decomp.); $[\alpha]_D^{25}$ −30.0° (*c* 1, N hydrochloric acid); R_f 0.75.[11] Hofmann *et al.* had prepared this compound (III) previously from benzyloxycarbonyl-seryl-serine methyl ester with hydrazine; mp 221—222°C (decomp.); $[\alpha]_D^{20}$ −30.5° (*c* 1, N hydrochloric acid).[9]

Benzyloxycarbonyl-L-seryl-L-seryl-L-serine Ethyl Ester (IV). III (1.26 g, 3.7 mmol) in dimethylformamide (8 ml) containing 2.24 ml of 3.3 N hydrogen chloride in ethyl acetate was treated with isoamyl nitrite (432 mg, 3.7 mmol) for 10 min, and then triethylamine (1.03 ml, 7.4 mmol) as described above. To this solution was added a mixture of I·TsOH (1.13 g, 3.7 mmol) and triethylamine (0.51 ml, 3.7 mmol) in dimethylformamide (20 ml). The mixture was stirred for 3 days at 0°C and then evaporated *in vacuo* to a small volume. The precipitate which formed upon the addition of water was collected (the mother liquor was set aside for further isolation of IV), washed with a small amount of 4% sodium bicarbonate solution, 3% hydrochloric acid and water, and dried; yield, 0.43 g.

The mother liquor was extracted with chloroform, and the extract was washed with water, and dried. The filtrate was evaporated, and the residual syrup was solidified by the addition of ether and petroleum ether; yield, 0.56 g. The combined product (0.99 g) was recrystallized from methanol - ether - petroleum ether; yield, 0.90 g (56%); mp 184—185°C; R_f 0.77.[11]

Found: C, 50.95; H, 6.24; N, 9.30%. Calcd for $C_{19}H_{27}O_9N_3 \cdot \frac{1}{2}H_2O$: C, 50.66; H, 6.27; N, 9.33%.

Benzyloxycarbonyl-L-seryl-L-seryl-L-serine Methyl Ester (V). To a chilled solution of III (0.96 g, 2.8 mmol) in a mixture of glacial acetic acid (10 ml) and water (15 ml), there were stirred 6 N hydrochloric acid (1.13 ml) and a 0.4 M sodium nitrite solution (7.05 ml). After 5 min, the azide was extracted with ethyl acetate (100ml), and the organic layer was washed with a 4% sodium bicarbonate solution and water, and dried. The filtrate was added to a mixture of serine methyl ester hydrochloride[12] (0.44 g, 2.8 mmol) and triethylamine (0.4 ml) in dimethylformamide (20 ml). The mixture was stirred for 2 days at 0°C and evaporated *in vacuo*. The precipitate which formed upon the addition of 2% hydrochloric acid was collected, and washed with water and dried; yield, 0.37 g (30%); mp 195—196°C; R_f 0.73.[11]

Found: C, 50.76; H, 6.06; N, 9.79%. Calcd for $C_{18}H_{25}O_9N_3$: C, 50.58; H, 5.90; N, 9.83%.

Benzyloxycarbonyl-L-seryl-L-seryl-L-serine Hydrazide (VI). To a solution of IV (358 mg, 0.81 mmol) in methanol (6 ml), hydrazine hydrate (0.16 ml, 3.24 mmol) was added and the solution was allowed to stand for 2 days at 30°C. The reaction mixture was then evaporated *in vacuo*. The resulting crystals were collected with the aid of cold ethanol; yield, 327 mg (92%); mp 232—234°C (decomp.); R_f 0.68.[11]

Found: C, 47.48; H, 5.99; N, 16.06%. Calcd for $C_{17}H_{25}O_8N_5$: C, 47.77; H, 5.90; N, 16.39%.

VI was also prepared from V (261 mg, 0.61 mmol) and hydrazine hydrate (0.59 ml) by the same procedure as described above; yield, 157 mg (60%); mp 233—234°C (decomp.); R_f 0.68.[11]

Benzyloxycarbonyl-β-*t*-butyl-L-aspartyl-L-valine Ethyl Ester (VII). *a) Mixed Anhydride Method.* To a chilled solution of benzyloxycarbonyl-aspartic acid β-*t*-butyl ester[5] (404 mg, 1.25 mmol) and triethylamine (0.175 ml) in tetrahydrofuran (6 ml), isobutylchloroformate (0.164 ml, 1.25 mmol) was added. After 15 min, a mixture of valine ethyl ester *p*-toluenesulfonate[6] (397 mg, 1.25 mmol), triethylamine (0.175 ml) and chloroform (3 ml) was added to the solution. The reaction mixture was allowed to stand overnight and then evaporated to dryness *in vacuo*. The residual oil was dissolved in ethyl acetate (15 ml), and the solution was washed successively with 0.5 M citric acid, a 4% sodium bicarbonate solution and water, dried over sodium sulfate, and then evaporated to dryness *in vacuo*. The product was obtained as an oil; yield, 483 mg (86%); R_f 0.94.[11]

b) Dicyclohexylcarbodiimide Method. To a solution of the dicyclohexylammonium salt of benzyloxycarbonyl-aspartic acid β-*t*-butyl ester[5] (4.04 g, 8 mmol), valine ethyl ester *p*-toluenesulfonate[6] (2.54 g, 8 mmol) in chloroform (80 ml) was added dicyclohexylcarbodiimide[7] (1.65 g, 8 mmol) at 0°C. The reaction mixture was stirred for 1 hr at 0°C and then kept overnight in a refrigerator. The mixture was evaporated *in vacuo*, and ethyl acetate (100 ml) was added to the residue. After the insoluble dicyclohexylurea was filtered off, the filtrate was treated following the same procedure as described above; yield of the oily VII, 3.17 g (88%); R_f 0.94.[11]

β-*t*-Butyl-L-aspartyl-L-valine Ethyl Ester Hydrochloride (VIII·HCl). A solution of VII (3.38 g, 7.5 mmol) in methanol (20 ml) was hydrogenated in the presence of palladium black at 0°C. After 5 min, 0.408 N methanolic hydrogen chloride (18.38 ml) was added and hydrogenolysis was continued for 2 hr at 0°C. The filtrate from the catalyst was evaporated to dryness *in vacuo* at room temperature, and the yield of the oily product was 2.44 g (92 %). The oily product was crystallized upon the standing in a refrigerator for several days. A portion (352 mg) of this crystal was recrystallized from methanol-ether; yield, 226 mg; mp 147—148°C; R_f 0.77.[11] This sample was dried over phosphorus pentoxide for 2 hr at 45°C and 2 mmHg for the analysis.

Found: C, 50 40; H, 8 24; N, 7.95%. Calcd for

12) S. Guttmann and R. A. Boissonnas, *Helv. Chim. Acta*, **41**, 1867 (1958).

$C_{15}H_{28}O_5N_2 \cdot HCl \cdot \frac{1}{4}H_2O$: C, 50.41; H, 8.04; N, 7.83%.

Benzyloxycarbonyl-L-seryl-β-*t*-butyl-L-aspartyl-L-valine Ethyl Ester (IX). This compound was obtained by the same procedure as described for the preparation of II. Benzyloxycarbonyl-serine hydrazide (1.77 g, 7 mmol) and VIII·HCl (2.47 g, 7 mmol) afforded 2.28 g of the crude product. It was recrystallized from methanol-ether-petroleum ether; yield, 2.07 g (55%); mp 134—137°C; $[\alpha]_D^{25}$ −29.0° (*c* 1, methanol); R_f 0.96.[11]

Found: C, 57.96; H, 7.37; N, 8.01%. Calcd for $C_{26}H_{39}O_9N_3$: C, 58.08; H, 7.31; N, 7.82%.

L-Seryl-β-*t*-butyl-L-aspartyl-L-valine Ethyl Ester Hydrochloride (X·HCl). IX (1.85 g, 3.4 mmol) was subjected to hydrogenolysis in the presence of palladium black using 0.408 N methanolic hydrogen chloride (8.48 m*l*) as has been described in the case of VIII·HCl. The product was obtained as an oil; yield, 1.41 g (94%); R_f 0.76,[11] 0.94.[13]

Benzyloxycarbonyl-L-seryl-L-seryl-L-seryl-β-*t*-butyl-L-aspartyl-L-valine Ethyl Ester (XI). This compound was prepared by the same procedure as described for the preparation of II. III (1.17 g, 3.4 mmol) and X·HCl (1.50 g, 3.4 mmol) gave 2.14 g of the crystalline product. It was recrystallized from methanol-ether; yield, 1.62 g (67%); mp 174—175°C; $[\alpha]_D^{25}$ −26.4° (*c* 0.3, methanol); R_f 0.91.[11]

Found: C, 52.74; H, 6.96; N, 9.63%. Calcd for $C_{32}H_{49}O_{13}N_5 \cdot H_2O$: C, 52.66; H, 7.04; N, 9.60%.

L-Seryl-L-seryl-L-seryl-β-*t*-butyl-L-aspartyl-L-valine Ethyl Ester Acetate (XII·AcOH). XI (107 mg, 0.15 mmol) in acetic acid (5 m*l*) was subjected to hydrogenolysis in the presence of palladium black at 0°C. The filtrate from the catalyst was evaporated to dryness *in vacuo* at room temperature and the oily residue was triturated with ether. The hygroscopic powder was collected by filtration; yield, 91 mg (95%). The homogeneity was ascertained by the chromatographies; R_f 0.74,[11] 0.83,[13] 0.24.[14]

L-Seryl-L-seryl-L-seryl-L-aspartyl-L-valine Ethyl Ester (XIII). XII·AcOH (73 mg) was dissolved in trifluoroacetic acid (2.5 m*l*) and the solution was left to stand for 30 min at room temperature. The solution was evaporated to dryness *in vacuo* to yield a hygroscopic solid. The residue was dissolved in water and the solution was neutralized with the addition of triethylamine (*ca.* 0.025 m*l*). Then, the solution was evaporated to dryness and the remaining crystals were collected by filtration with the aid of ethanol; yield, 40 mg (67%); mp 182—183°C; $[\alpha]_D^{25}$ −22.7° (*c* 0.15, acetic acid); R_f 0.51,[13] 0.02;[14] amino acid ratios in acid hydrolysate, $Ser_{2.9}Asp_{1.0}Val_{1.1}$.[15]

Found: C, 44.57; H, 6.80; N, 12.90%. Calcd for $C_{20}H_{35}O_{11}N_5 \cdot H_2O$: C, 44.52; H, 6.91; N, 12.98%.

The digestion of XIII by leucine aminopeptidase was carried out by the procedure of Hofmann and Yajima.[16] The paper chromatography[13] of the digest revealed the presence of only three ninhydrine-positive components with R_f values identical with those of authentic samples of aspartic acid (R_f 0.20), serine (0.28) and valine (0.58).

13) The R_f value of the paper chromatography refers to the same solvent system described.[11]

14) The R_f value of the thin-layer chromatography with Merck silica gel refers to a solvent system of chloroform-methanol (5 : 1, v/v).

15) The authors are indebted to Mr. Kosaku Noda for the amino acid analysis.

16) K. Hofmann and H. Yajima, *J. Am. Chem. Soc.*, **83**, 2289 (1961).

BULLETIN OF THE CHEMICAL SOCIETY OF JAPAN VOL. 41 673—676 (1968)

S-Alkylthioamidium Salt. II.[1] The Reactions of S-Alkylthioamidium Iodides with Mercuric Compounds

Tatsuaki YAMAGUCHI, Katsuhiko INOMATA and Teruaki MUKAIYAMA

Laboratory of Organic Chemistry, Tokyo Institute of Technology, Ookayama, Meguro-ku, Tokyo

(Received September 18, 1967)

The reactions of S-alkylthioamidium iodides with some mercuric compounds have been studied. Mercuric carboxylates were found to react with S-alkylthioamidium iodides giving the corresponding acid anhydrides and amides in good yields along with alkylmercaptomercuric iodide. In addition, it was established that the reaction of mercuric cyanide with the iodides afforded α-dimethylaminomalononitriles by the elimination of alkylmercapto mercuric iodide. Further, α-morpholino-β-phenylacrylonitrile was obtained in 87% yield by treating S-ethylthiophenylacetomorpholidium iodide with silver cyanide.

In the previous paper, the reaction of *N, N*-dimethylbenzamide diethylmercaptole with mercuric acetate has been reported to yield *N, N*-dimethylbenzamide, acetic anhydride and mercury ethylmercaptide.[2]

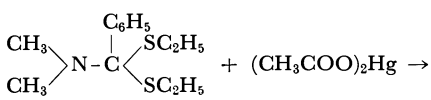

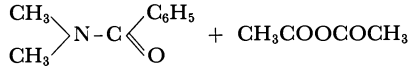

+ $(C_2H_5S)_2Hg$

In connection with this reaction, S-ethylthioamidium iodide (I) and its analogs (II and III) were tried to react with mercuric carboxylates in order to find a more convenient method for the preparation of acid anhydride.

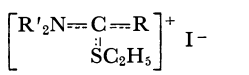

Ia R=C_6H_5 R′=CH_3
Ib R=CH_3 R′=CH_3
Ic R=H R′=CH_3
Id R=C_6H_5 R′$_2$=O
Ie R=$CH_2C_6H_5$ R′$_2$=O

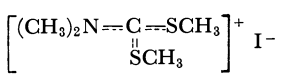

II

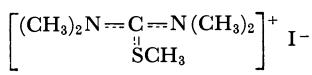

III

When mercuric carboxylate was added to a solution of *N, N*-dimethyl-S-ethylthiobenzamidium iodide (Ia) in acetonitrile at room temperature, a yellowish or colorless clear solution was obtained at first with a slight heat evolution, and in a few minutes a white precipitate of ethylmercaptomercuric iodide was separated from the solution. Since the ethylmercapto mercuric iodide (C_2H_5SHgI), which is 1 : 1 adduct[3] of mercury ethylmercaptide and mercuric iodide, is quite insoluble in almost all solvents, it can be easily separated by filtration. From the filtrate, corresponding acid anhydrides and *N, N*-dimethylbenzamide were obtained in good yields. Mercuric salts of aromatic carboxylic acids were less reactive toward Ia than aliphatic one, and a higher temperature was necessary to obtain the anhydrides in better yields. Lower yield of benzoic anhydride against that of the amide will be due to the hydrolysis of the reactive intermediate by the water of crystallization of mercuric benzoate; indeed, free benzoic acid was also isolated in 19% yield. The results of the reaction of S-alkylthioamidium iodides with some mercuric carboxylates are summarized in Table 1.

The reaction may be considered to proceed as follows. A nucleophilic attack of carboxylate anion upon the central carbon atom of S-alkylthioamidium ion might be assisted by ^+HgOCOR, which readily abstracts the ethylthio group attached to the same carbon atom;[2] for, by the separate experiment, it was established that sodium carboxylate did not react with S-alkylthioamidium iodide at all under the similar condition. Subsequently, acyloxyimmonium type intermediate would be resulted. The intermediate, in turn,

1) Part I: T. Mukaiyama, T. Yamaguchi and H. Nohira, This Bulletin, **38**, 2107 (1965).
2) T. Yamaguchi and T. Mukaiyama, *ibid.*, **40**, 1952 (1967).
3) K. A. Kofmann and W. O. Rabe, *Z. Anorg. Chem.*, **17**, 26 (1898).

TABLE 1. THE REACTION OF *S*-ALKYLTHIOAMIDIUM IODIDES WITH MERCURIC CARBOXYLATES

$$\left[R'_2\overset{+}{N}=\underset{\underset{SR''}{|}}{C}-R\right] I^- + Hg(OCOR''')_2 \rightarrow R'''COOCOR''' + R'_2N-\underset{\underset{O}{\|}}{C}-R + R''SHgI$$

S-Alkylthio-amidium iodide	Mercuric carboxylate	Temp. °C	Time hr	Anhydride %	Amide %	R''SHgI %
Ia	$(CH_3COO)_2Hg$	RT	2	85	85.5	93
Ia	$(C_3H_7COO)_2Hg$	RT	2	80	86	96
Id	$(C_3H_7COO)_2Hg$	RT	2	86	82	97
Ia	$((CH_3)_2CHCOO)_2Hg$	RT	4	81	80	94
Ia	$(C_6H_5COO)_2Hg$	RT	4	27	66	—
Ia	$(C_6H_5COO)_2Hg$	50	4	42	88	95
Ia	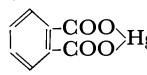	50	4	53	62	89
II	$(C_3H_7COO)_2Hg$	RT	2	73	72	88
II	$(C_6H_5COO)_2Hg$	RT	2	25	45	75

RT=room temperature

TABLE 2. THE REACTION OF *S*-ALKYLTHIOAMIDIUM IODIDES WITH MERCURIC OXIDE

$$\left[R'_2\overset{+}{N}=\underset{\underset{SR''}{|}}{C}-R\right] I^- + HgO \rightarrow R'_2N-\underset{\underset{O}{\|}}{C}-R + R''SHgI$$

	R	R'_2N	R''	Temp. °C	Time hr	Yield, % R'_2NCOR	Yield, % $R''SHgI$
Ia	C_6H_5	$(CH_3)_2N$	C_2H_5	RT	5	69	92
Ia	C_6H_5	$(CH_3)_2N$	C_2H_5	80	2	71	84
Id	C_6H_5		CH_3	RT	5	92	94
II	SCH_3	$(CH_3)_2N$	CH_3	RT	7	57	89
III	$N(CH_3)_2$	$(CH_3)_2N$	CH_3	80	5	66	—

RT=room temperature

would act as a strong acylating agent[4] toward another carboxylate anion to form acid anhydride and amide.

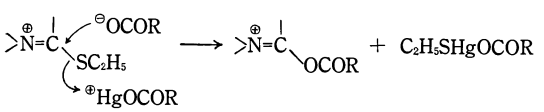

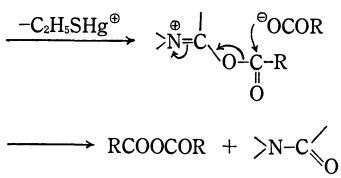

Next, the reactions of I, II or III with mercuric oxide were studied. When a suspension of mercuric oxide in acetonitrile was treated with I, II or III, the corresponding *N, N*-disubstituted amides, *N, N*-dimethyl-*S*-methylthiolcarbamate and *N, N, N', N'*-tetramethylurea, respectively, were obtained in good yields along with alkylmercaptomercuric iodide (Table 2). It is noted that Id is the most reactive toward mercuric oxide and III is less reactive than I and II. The poor reactivity of III may be due to its high resonance-stabilization of the structure, which retards the nucleophilic attack of mercuric oxide on the central carbon atom.

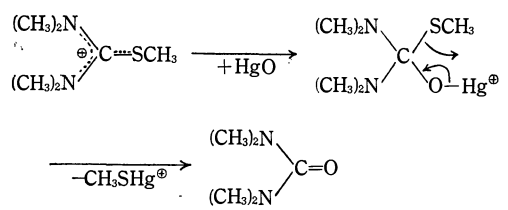

In addition, it was found that α-dimethylamino-malononitriles (IVa, b, c) were afforded in good yields by treating Ia, Ib or Ic with equimolar

4) H. K. Hall, *J. Am. Chem. Soc.*, **78**, 2717 (1956).

Table 3. α-Dimethylaminomalononitriles

$$(CH_3)_2N-C(R)(CN)_2$$

	R	Yield %	Bp °C/mmHg	n_D^{25}		Elemental analyses, % C	H	N
IVa	C_6H_5	92	99/4	1.5102	Found	71.67	6.02	22.50
					Calcd	71.35	5.95	22.70
IVb	CH_3	39	76—77/20	1.4287	Found	58.31	7.02	33.92
					Calcd	58.71	7.37	34.12
IVc	H	63	85/15	1.4331	Found	55.32	6.18	38.65
					Calcd	55.05	6.42	38.53
V	CH_3S	60	102/23	1.4732	Found	46.92	5.89	27.29
					Calcd	46.45	5.81	27.10

amount of mercuric cyanide in acetonitrile at room temperature. Similarly, II reacted with mercuric cyanide giving α-dimethylamino-α-methylthiomalononitrile (V) in 60% yield. They were identified by elemental analyses and infrared spectra. The results are listed in Table 3.

$$\text{I or II} + Hg(CN)_2 \xrightarrow[-R''SHgI]{} (CH_3)_2N-C(R)(CN)_2$$

IVa R=C_6H_5
IVb R=CH_3
IVc R=H
V R=SCH_3

Further, Ia was found to react with silver cyanide in acetonitrile at room temperature giving 61% yield of α-dimethylamino-α-ethylthiophenylacetonitrile (VI) along with silver iodide. On the other hand, when Ie was treated with silver cyanide under the same condition, the evolution of ethyl mercaptan was observed and α-morpholino-β-phenylacrylonitrile (VII) was obtained in 87% yield. The elimination of ethyl mercaptan may be explained by considering the similar pathway, shown in the reaction of Ib with sodium ethylmercaptide giving ketene *N, S*-acetal.[5]

$$\text{Ia} + AgCN \xrightarrow[-AgI]{} (CH_3)_2N-C(C_6H_5)(CN)-SC_2H_5$$

VI

$$\text{Ie} + AgCN \xrightarrow[-AgI]{} \left(O(CH_2)_2N-C(CH_2C_6H_5)(CN)-SC_2H_5\right) \xrightarrow{-C_2H_5SH} O(CH_2)_2N=C(CN)-CHC_6H_5$$

VII

$$\text{Ib} + C_2H_5SNa \xrightarrow[-NaI]{} \left((CH_3)_2N-C(CH_3)(SC_2H_5)-SC_2H_5\right) \xrightarrow{-C_2H_5SH} (CH_3)_2N-C(SC_2H_5)=CH_2$$

Experimental[6]

Materials. *S*-Alkylthioamidium iodides (Ia—e) were prepared from the corresponding thioamides and alkyl iodides as described previously.[1] Their melting points, yields and analyses are listed in Table 4.

Table 4. *S*-Alkylthioamidium iodides

	Mp °C	Yield %		Elemental analyses, % C	H	N
Ia	130.5—132	92.5	Found	41.36	5.23	4.42
			Calcd	41.12	4.98	4.36
Ib	92—94	94	Found	28.46	5.82	5.99
			Calcd	27.82	5.41	5.41
Ic	107—108	91	Found	24.85	5.09	5.81
			Calcd	24.50	4.93	5.71
Id[11]	152—153	94	Found	41.09	4.76	4.06
			Calcd	41.25	4.58	4.02
Ie	126—127	51	Found	44.35	5.26	3.77
			Calcd	44.56	5.31	3.71

N, N, S, S'-Tetramethyldithiocarbamidium iodide[7] (II) was obtained in 93% yield, when the mixture of the corresponding dithiocarbamate and methyl iodide was

5) T. Mukaiyama, S. Aizawa and T. Yamaguchi, This Bulletin, **40**, 2641 (1967).
6) Melting points and boiling points are uncorrected.
7) This compound has been reported to melt at 95—96°C by K. Hartke, E. Schmidt, M. Castillo and J. Bartulin, *Chem. Ber.*, **99**, 3268 (1966).
8) J. Braun and K. Weissback, *Ber.*, **63**, 2846 (1930).

allowed to stand at room temperature for a day long; mp 77—78°C (decomp.).

Found: C, 21.52; H, 4.49; N, 4.83%. Calcd for $C_5H_{12}INS_2$: C, 21.66; H, 4.33; N, 5.05%.

N, N, N', N'-Tetramethyl-*S*-methylthiuronium iodide (III) was synthesized by the reaction of the corresponding thiourea, prepared by the thermal decomposition[8] of *N, N, N', N'*-tetramethylthiuram disulfide, and methyl iodide in refluxing acetone; mp 172—173°C.

Found: C, 26.59; H, 5.81; N, 10.10%. Calcd for $C_6N_{15}IN_2S$: C, 26.28; H, 5.48; N, 10.21%.

Mercuric salts of isobutyric, *n*-butyric, benzoic and phthalic acid were prepared by the method described in the literature.[9] Mercuric acetate, mercuric cyanide, mercuric oxide and silver cyanide were obtained from commercial sources.

Reaction of Ia with Mercuric Isobutyrate. To a solution of Ia (6.42 g, 0.02 mol) in acetonitrile (40 m*l*) was added 7.50 g (0.02 mol) of mercuric isobutyrate in portions. Immediately, a clear solution was obtained with a slight heat evolution, and in a few minutes a white precipitate began to separated from the solution. The reaction mixture was then stirred at room temperature for 4 hr. The precipitate of ethylmercaptomercuric iodide (mp 180°C decomp.) was filtered and washed with acetonitrile. It weighed 7.30 g (94%). After the solvent had been evaporated from the filtrate, the residue was distilled under reduced pressure giving 2.56 g (81%) of isobutyric anhydride and 2.39 g (80%) of *N, N*-dimethylbenzamide.

By a similar procedure, the other mercuric carboxylates were converted to the corresponding acid anhydrides by Ia or II. The reaction conditions and results are summarized in Table 1.

Reaction of Id with Mercuric Oxide. Into a stirred suspension of mercuric oxide (2.17 g, 0.01 mol) in 40 m*l* of acetonitrile was added 3.49 g (0.01 mol) of Id in portions. The yellow color of mercuric oxide disappeared gradually. After the stirring had been continued for 5 hr at room temperature, the resulting white precipitate of methylmercaptomercuric iodide (mp 186.5°C decomp.) was filtered and washed with acetonitrile. It weighed 3.51 g (94%). The filtrate was concentrated and distilled under reduced pressure to give 1.75 g (92%) of benzomorpholide; bp 140—141°C/1.5 mmHg, mp 74—75°C (lit.[10] 74°C).

Similarly, *N, N*-dimethyl-*S*-methylthiolcarbamate and *N, N, N', N'*-tetramethylurea were obtained by the reaction of II or III with mercuric oxide (Table 2).

Reaction of Ia with Mercuric Cyanide. To a solution of Ia (16.05 g, 0.05 mol) in acetonitrile (100 m*l*) was added 12.63 g (0.05 mol) of mercuric cyanide. The mixture was stirred at room temperature for 2 hr and the resulting white precipitate of ethylmercaptomercuric iodide was filtered off (18.56 g, 96%). After the acetonitrile had been evaporated from the filtrate, distillation of the residual liquid gave 8.47 g (92%) of α-dimethylaminophenylmalononitrile (IVa); bp 98.5—99.5°C/4 mmHg. The elemental analysis (Table 3) and infrared spectrum of the product were found to be consistent with the structure assigned.

Reaction of Ia with Silver Cyanide. A suspension of Ia (16.05 g, 0.05 mol) and silver cyanide (6.70 g, 0.05 mol) in acetonitrile (100 m*l*) was stirred at room temperature for 2 hr. After the resulting pale yellow precipitate of silver iodide had been filtered off, the filtrate was concentrated and distilled to yield 6.76 g (61%) of α-dimethylamino-β-ethylthiophenylacetonitrile (VI); bp 113°C/1.5 mmHg, n_D^{23} 1.5366. This compound was identified by comparing the infrared spectrum with the authentic sample.[2]

Reaction of Ie with Silver Cyanide. When a suspension of Ie (3.62 g, 0.01 mol) and silver cyanide (1.29 g, 0.01 mol) in acetonitrile (50 m*l*) was stirred at room temperature, the evolution of ethyl mercaptan was observed and a pale yellow precipitate of silver iodide was separated. After the stirring had been continued for 4 hr, the precipitate was filtered off and the filtrate was concentrated to give a solid, which was then recrystallized from ethanol as colorless needles, mp 100—100.5°C, yield 87%. This compound had the correct analysis for α-morpholino-β-phenylacrylonitrile (VII) and the infrared absorption at 2220 cm^{-1}, assigned for C≡N bond.

Found: C, 72.67; H, 6.28; N, 12.78%. Calcd for $C_{13}H_{14}N_2O$: C, 72.87; H, 6.59; N, 13.08%.

NMR $\delta_{TMS}^{CDCl_3}$: 2.85 (triplet, 4H, $-N(CH_2-)_2$), 3.65 (triplet, 4H, $O(CH_2-)_2$), 5.92 (singlet, 1H, $-CH=$), 7.15—7.34 (multiplet, 5H, phenyl).

The authors are indebted to Mr. Masaru Koizuka and Miss Kazuko Isojima for elemental analyses.

9) T. Mukaiyama, H. Nambu and I. Kuwajima, *J. Org. Chem.*, **28**, 917 (1963).

10) R. Fusco and S. Rossi, *Tetrahedron*, **3**, 209 (1958).

11) D. A. Peak and F. Stansfield, *J. Chem. Soc.*, **1952**, 4070.

BULLETIN OF THE CHEMICAL SOCIETY OF JAPAN VOL. 41 677—683 (1968)

Reaction of Allylbenzene with *n*-Butyllithium in Tetrahydrofuran

Yoshio OKAMOTO and Heimei YUKI

Department of Chemistry, Faculty of Engineering Science, Osaka University, Toyonaka, Osaka

(Received September 22, 1967)

The reaction products between allylbenzene and *n*-butyllithium in tetrahydrofuran at 60°C were fractionated and investigated by elementary analysis, a molecular-weight determination, and a study of the IR, UV, and NMR spectra. The products were hydrocarbons and alcohols, the latter of which were formed by the reaction of the carbanions with tetrahydrofuran. The main products were 3-phenylheptene-2, 5-methyl-6-phenyldecane, 5-phenyl-5-heptene-1-ol, 5-phenyl-5-vinylnonane-1-ol, and 5-phenyl-5-vinylnonane-1, 9-diol. 3-Phenylheptene-1 was not obtained. In the resonance structures of allyl anions, a and b, $Ph\text{-}\bar{C}R\text{-}CH{=}CH_2$ (a) ↔ $Ph\text{-}CR{=}CH\text{-}CH_2^-$ (b), the reaction with tetrahydrofuran took place only in the form a. The observed results are correlated with those of the anionic polymerization of *trans*-β-methylstyrene reported previously.

Recently, the present authors have examined the anionic polymerization of *trans*-β-methylstyrene.[1] In the polymerization of this monomer with *n*-butyllithium in tetrahydrofuran at room temperature, a benzyl-type living anion (B) was easily converted into an allyl-type anion (A) by a chain-transfer reaction to the monomer. At a high temperature such as 60°C, the anions A and B further changed to inactive anions which possessed no reactivity to the monomer; this resulted in the cessation of the polymerization reaction. The anions A and B had absorption maxima at 340 and 398 mμ respectively, while the inactive anions had theirs at 510 and 570 mμ. The species having a λ_{max} at 510 mμ was supposed to be an anion C, but the species showing a λ_{max} at 570 mμ (anion D) was not confirmed.

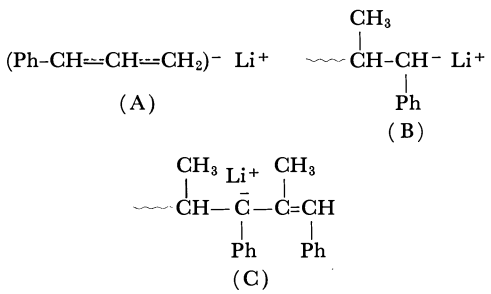

On the other hand, only the anion D was formed in the reaction of allylbenzene with *n*-butyllithium at 60°C in tetrahydrofuran.[1]

This paper will be concerned with investigations of the reaction of allylbenzene with *n*-butyllithium carried out in order to determine the structure of the anion D.

1) Y. Okamoto, H. Yuki and S. Murahashi, This Bulletin, **41**, 197 (1968).

Experimental and Results

Materials. *Allylbenzene.* This was prepared from phenylmagnesium bromide and allyl chloride,[2] and was purified by fractional distillation. Bp 72—73°C/39 mmHg. The purity was checked by gas chromatography.

Tetrahydrofuran (THF). Tetrahydrofuran was refluxed first over sodium and then over lithium aluminum hydride. The solvent was distilled onto sodium-potassium alloy and benzophenone, from where it was transferred into a reaction vessel on a vacuum line.

n-Butyllithium (n-BuLi). According to the method of Gilman,[3] *n*-BuLi was prepared in THF. The concentration was determined by double titration.[4] The presence of the unchanged *n*-butyl chloride, which was used for the preparation of *n*-BuLi, was not detected by gas chromatography, while the formation of *n*-octane was observed.

Reaction. The reaction was carried out under dry nitrogen in a glass vessel equipped with a three-way stopcock. To a solution of allylbenzene (13 g, 0.11 mol) in THF (200 ml), *n*-BuLi (0.11 mol) was added with a syringe over a ten minute period at room temperature. As soon as the *n*-BuLi was added, the solution turned red and generated gas and white precipitates. The reaction mixture was then allowed to stand at 60°C for 48 hr. During this time, the solution turned gradually red-purple. The reaction was terminated by adding methanol after the white precipitates

2) E. B. Hershberg, *Helv. Chim. Acta*, **17**, 351 (1934).
3) H. Gilman and B. J. Gaj, *J. Org. Chem.*, **22**, 1165 (1957).
4) H. Gilman and A. H. Haubein, *J. Am. Chem. Soc.*, **66**, 1515 (1944).

had been isolated under dry nitrogen. The white precipitates must have been lithium hydride because they showed flame-test results characteristic of lithium and reacted with methanol violently. The THF was then removed from the reaction mixture. The residue was dissolved in diethyl ether and washed with water. The ethereal layer was dried over magnesium sulfate, and then the ether was removed to give 16 g of an oily product.

Fractionation of Reaction Mixture. The above product was first separated into fractions by distillation under nitrogen, and subsequently the fractions were treated by column chromatography with activated alumina, using *n*-hexane, benzene, and methanol as eluents. The results are summarized in Table 1. The fractions eluted with *n*-hexane were hydrocarbons, while those eluted with benzene and methanol were alcohols.

Table 1. Fractionation of reaction product

Fraction	Distillation Bp /1.5 mmHg °C	Yield g	Yield %	Column chromatography Eluent	Recovery %
F1H	48— 52	0.3	2	Hexane	90
F2H				Hexane	63
F2B	77—104	1.6	10	Benzene	2
F2M				Methanol	33
F3H				Hexane	35
F3B	104—114	1.4	9	Benzene	46
F3M				Methanol	19
F4H				Hexane	56
F4B	114—154	2.9	18	Benzene	1
F4M				Methanol	43
F5H	154—160	2.0	13	Hexane	54
F5M				Methanol	46
F6	Residue	7.8	49	—	—

Measurement. *Molecular Weight and Elementary Analysis.* The molecular weight was measured on a Mechrolab Vapor Pressure Osmometer, Model 301 A, using a benzene solution for the hydrocarbon and an ethanol solution for the alcohol. The elementary analyses and the molecular weights of the fractions are listed in Tables 2 and 3.

Infrared Spectrum. The spectrum was obtained with a Nihon Bunko Model IR-S Spectrometer in a liquid state. The hydrocarbons showed the absorption bands at 1945, 1860, and 1800 cm^{-1} due to a mono-substituted benzene, at 2960 and 1380 cm^{-1} due to a methyl group, and at 2925 cm^{-1} due to a methylene group. The alcohols showed the absorptions due to a hydroxy group at 3300 and 1050 cm^{-1}, besides the absorption bands due to a mono-substituted benzene and a methylene group.

Table 2. Elementary analyses and molecular weights of hydrocarbons

Fraction number	Elementary analysis C%	H%	Molecular weight	Molecular formula
F1H	89.00	11.24	185	$C_{13}H_{19.1}$
F2H	87.64	11.88	230	$C_{17}H_{27.7}$
F3H	90.04	10.49	279	$C_{22}H_{30.5}$
F4H	89.44	10.10	300	$C_{22}H_{29.5}$
F5H	—	—	349	—

Table 3. Elementary analyses and molecular weights of alcohols

Fraction number	Elementary analysis C%	H%	Molecular weight in EtOH	Molecular formula
F2M	81.43	9.57	192	$C_{13}H_{18.3}O_{1.09}$
F3B	81.91	10.68	244	$C_{17}H_{26.4}O_{1.15}$
F4M	79.01	10.27	248	$C_{17}H_{26.0}O_{1.73}$
F5M	77.56	9.90	259	$C_{17}H_{25.9}O_{2.06}$

Electronic Spectrum. The measurements were made with a Hitachi EPS-2 Spectrophotometer using cyclohexane solutions for the hydrocarbons and ethanol solutions for the alcohols. The respective characteristics of the IR and UV spectra are summarized in Tables 4 and 5. In these tables, the molar extinction coefficient, ε_{max} is based on the observed molecular weight of each fraction.

NMR Spectrum. The NMR spectrum was taken in a carbon tetrachloride solution with a JNM-4H-100 Spectrometer (Japan Electron Optics Laboratory Co., Ltd.) at 100 Mc/sec, using tetramethylsilane as an internal standard. The spectra of the fractions F1H, F2H, F2M, and F3B are shown in Figs. 1, 2, 3, and 4 respectively.

Table 4. Characteristics of IR, UV, and NMR spectra of hydrocarbons

Fraction number	IR[a] 835 cm^{-1}	IR[a] 910 cm^{-1}	UV λ_{max} (mμ)	UV ε_{max}	NMR[b] H_{al}/H_{ar}
F1H	Strong	Weak	242	4300	3.4
F2H	Weak	Medium	242	1090	4.5
F3H	Weak	Weak	—	—	1.3
F4H	Weak	Weak	—	—	2.2

a) 835 cm^{-1}: $R_1R_2C{=}CHR_3$, 910 cm^{-1}: $CH_2{=}CH{-}$.
b) The ratio of the numbers of aliphatic proton to aromatic proton.

TABLE 5. CHARACTERISTICS OF IR, UV, and NMR SPECTRA OF ALCOHOLS

Fraction number	IR (cm^{-1})[a]			UV		NMR[b] H_{al}/H_{ar}
	835	910	3300	λ_{max}	ε_{max}	
F2M	Medium	Medium	Strong	243	6300	2.8
F3B	Weak	Strong	Strong	253	356	4.3
F4M	Weak	Strong	Strong	—	—	4.4
F5M	Weak	Strong	Strong	—	—	4.4

a) 835 cm^{-1}: $R_1R_2C{=}CHR_3$, 910 cm^{-1}: $CH_2{=}CH{-}$, 3300 cm^{-1}: $-OH$.
b) The ratio of the numbers of aliphatic proton to aromatic proton.

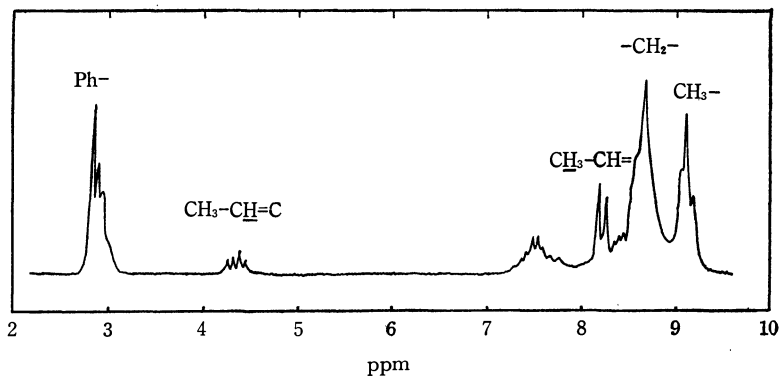

Fig. 1. NMR spectrum of fraction F1H.

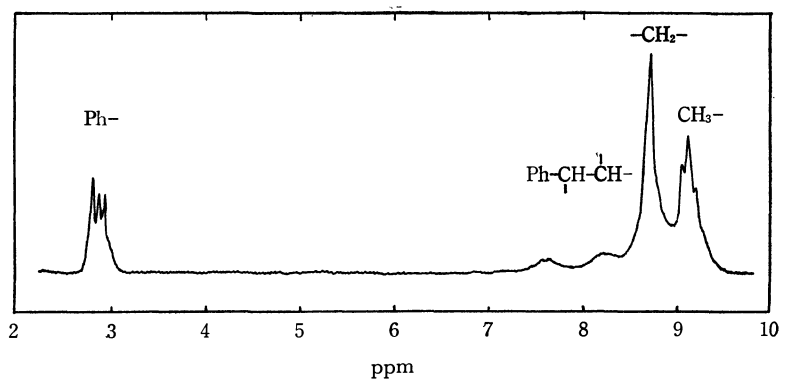

Fig. 2. NMR spectrum of fraction F2H.

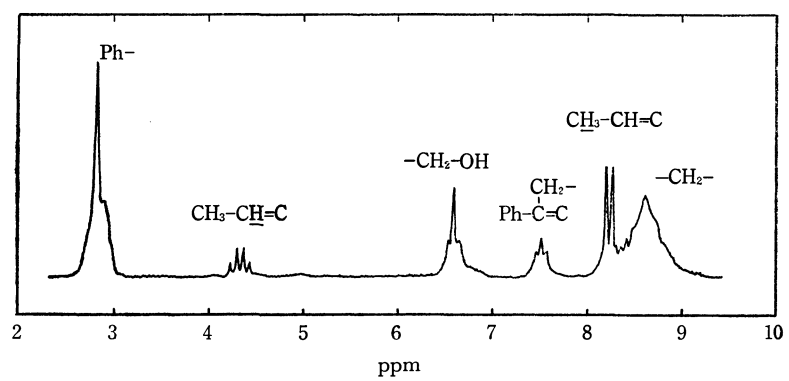

Fig. 3. NMR spectrum of fraction F2M.

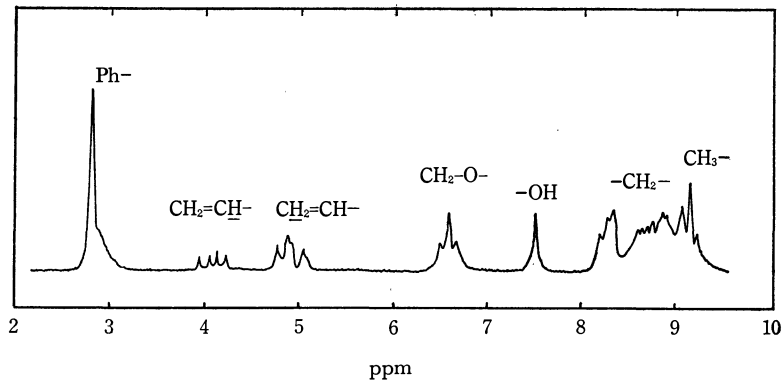

Fig. 4. NMR spectrum of fraction F3B.

Table 6. Hydrocarbons as probable products in the reaction

Molecular formula	Structural formula	Composition C%	Composition H%	Molecular weight	H_{al}/H_{ar} [a]	Remark
$C_{13}H_{18}$	Ph-CH(-C_4H_9)-CH=CH_2	89.6	10.4	174	2.60	Ia
$C_{13}H_{18}$	Ph-C(-C_4H_9)=CH-CH_3	89.6	10.4	174	2.60	Ib
$C_{17}H_{28}$	Ph-CH(C_4H_9)-CH(C_4H_9)-CH_3	87.8	12.2	232	4.60	II

a) The ratio of the numbers of aliphatic protons to aromatic protons.

Table 7. Alcohols as probable products in the reaction

Molecular formula	Structural formula	Composition C%	Composition H%	Molecular weight	H_{al}/H_{ar} [a]	Remark
$C_{13}H_{18}O$	Ph-CH(-$(CH_2)_4$-OH)-CH=CH_2	82.1	9.57	190	2.60	Va
$C_{13}H_{18}O$	Ph-C(-$(CH_2)_4$-OH)=CH-CH_3	82.1	9.57	190	2.60	Vb
$C_{13}H_{18}O$	Ph-CH=CH-CH_2-$(CH_2)_4$-OH (C_4H_9)	82.1	9.57	190	2.60	Vc
$C_{17}H_{26}O$	Ph-C(C_4H_9)-CH=CH_2	82.8	10.6	246	4.20	VIa
$C_{17}H_{26}O$	Ph-C(C_4H_9)=CH-CH_2-$(CH_2)_4$-OH	82.8	10.6	246	4.20	VIb
$C_{17}H_{26}O_2$	Ph-C($(CH_2)_4$-OH)-CH=CH_2	77.8	9.99	262	4.20	VIIa
$C_{17}H_{26}O_2$	Ph-C($(CH_2)_4$-OH)=CH-CH_2-$(CH_2)_4$-OH	77.8	9.99	262	4.20	VIIb

a) The ratio of the numbers of aliphatic protons to aromatic protons.

Probable Products of the Reaction. Tables 6 and 7 list some compounds which seem to be produced in this reaction. The alcohols listed in Table 7 were considered to be produced by the reactions of carbanions with THF. Their molecular formulae, structural formulae, elementary analyses, and molecular weights, and the ratios of the numbers of aliphatic protons to aromatic protons (H_{al}/H_{ar}) in them are also shown in the tables. From these characteristic features the structure of the compound contained in each fraction was estimated to be one of those included in Tables 6 and 7.

Determination of the Structure. *Fraction F1H.* The elementary analysis and the molecular weight of the fraction F1H were most similar to those of 3-phenylheptene-1 (Ia in Table 6) or 3-phenylheptene-2 (Ib). The IR spectrum showed a strong absorption due to a three-substituted olefin, $>C=CH-$, at 835 cm^{-1}; the NMR spectrum also indicated the existence of a $>C=CH-CH_3$ structure by the peaks at 8.2 and 4.3 ppm (Fig. 1). In the UV spectrum a strong absorption due to the conjugation between a benzene ring and a C=C double bond was observed at the same wavelength as that of the absorption of 3-phenylhexene-2 (λ_{max} 242 mμ, ε_{max} 4700 in cyclohexane).[5] These results showed that this fraction consisted mostly of Ib. However, the absorptions at 8.7 and 9.1 ppm in the NMR spectrum, attributed to the methylene and methyl groups respectively, are too strong if 3-phenylheptene-2 is the only component of the fraction. It seems that the fraction may also contain an other compound, probably 5-methyl-6-phenyldecane (II in Table 6); if so, the elementary analysis, the molecular weight, and the H_{al}/H_{ar} ratio show that the ratio of Ib to II will be about 2. The clear separation into these two components could not be attained by further fractionations, however.

Fraction F2H. The molecular formula of the fraction F2H was consistent with that of 5-methyl-6-phenyldecane. The IR spectrum showed the absence of an olefinic double bond, and the chemical shift and the relative area of each peak (Ph : $>CH-$: $-CH_2-$: CH_3-=5.0 : 2.2 : 11.3 : 8.8) in the NMR spectrum also supported the above consistence.

Fractions F3H and F4H. Both the fractions showed the absence of a C=C double bond in their IR and NMR spectra. Judging from the molecular weight and H_{al}/H_{ar}', III and IV might be suggested as the components of both the fractions, whose difference may be that of the relative amounts of these compounds.

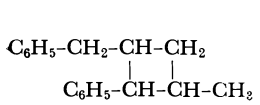

III

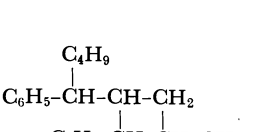

IV

Fractions F5H and F6. These fractions were composed of higher-molecular-weight products, the structures of which were not determined in this study.

Fraction F2M. The elementary analysis and the molecular weight of this fraction were similar to those of 5-phenyl-6-heptene-1-ol (Va in Table 7), 5-phenyl-5-heptene-1-ol (Vb), or 7-phenyl-6-heptene-1-ol (Vc). The NMR spectrum showed the respective absorptions at around 4.3 and 8.2 ppm for an olefinic proton and methyl protons in a $CH_3-CH=C$ unit and no absorption due to a *n*-butyl group, suggesting that this fraction consisted of Vb. The relative intensities of the peaks (Ph: C=CH– : $-CH_2OH$: $-CH_2-C=C$: CH_3- : $-CH_2-$= 5.0 : 1.0 : 3.0 : 2.0: 2.7 : 4.4) in the NMR spectrum were consistent with the above estimation. The IR and UV spectra also gave the same conclusion.

Fractions F2B and F3B. The molecular formula of the fraction F3B was most in accord with 5-phenyl-5-vinylnonane-1-ol (VIa in Table 7) or 7-phenyl-6-undecene-1-ol (VIb). Both IR and NMR spectra strongly suggested the existence of a vinyl group. The similarity of the UV spectrum with that of allylbenzene indicated that this fraction was VIa. The structure of VIa was also confirmed by the chemical shift and the relative intensities of the peaks (Ph : $CH_2=CH-$: $-CH_2O-$: $-OH$: $-CH_2-$: CH_3-=5.0 : 2.9 : 2.0 : 1.0 : 12 : 3.2) in the NMR spectrum. The IR spectrum of the fraction F2B was very similar to that of the fraction F3B.

Fractions F3M and F5M. The structure of 5-phenyl-5-vinylnonane-1, 9-diol (VIIa in Table 7) and that of 5-phenyl-5-undecene-1, 11-diol (VIIb) might be assigned to the fraction F5M on the basis of the elementary analysis and the molecular weight. The NMR and IR spectra indicated that this fraction was compound VIIa, for it contained a C=C double bond, but only a vinyl group. The IR spectrum of the fraction F3M was similar to that of the fraction F5M.

Fraction F4M. The data suggest that this fraction consists of almost equal amounts of VIa and VIIa present in the fractions F2B and F5M respectively.

Discussion

The compounds identified as the main products in the reaction between allylbenzene and *n*-BuLi were found to be Ib, II, Vb, VIa, and VIIa, listed in Tables 6 and 7. The following reactions may be suggested as the processes by which these compounds are formed.

5) D. J. Cram, F. A. Elhufez and H. Weingartner, *ibid.*, **75**, 2293 (1953).

$$\mathrm{Ph\text{-}CH_2\text{-}CH{=}CH_2} \xrightarrow[-C_4H_{10}]{C_4H_9^-\ Li^+} \begin{cases} \mathrm{Ph\text{-}\overset{-}{C}H\text{-}CH{=}CH_2} & (a_1) \\ \quad\downarrow\uparrow & \\ \mathrm{Ph\text{-}CH{=}CH\text{-}CH_2^-\ Li^+} & (b_1) \end{cases} \quad (1)$$

$$\mathrm{Ph\text{-}CH_2\text{-}CH{=}CH_2} \xrightarrow{C_4H_9^-\ Li^+} \mathrm{Ph\text{-}\underset{\displaystyle C_4H_9}{\underset{|}{C}}H\text{-}CH{=}CH_2} + \mathrm{LiH} \quad (2)$$

(Ia)

$$\mathrm{Ph\text{-}\underset{\displaystyle C_4H_9}{\underset{|}{C}}H\text{-}CH{=}CH_2} \xrightarrow[-RH]{R^-\ Li^+} \begin{cases} \mathrm{Ph\text{-}\underset{\displaystyle C_4H_9}{\underset{|}{\overset{-}{C}}}\text{-}CH{=}CH_2} & (a_3) \\ \quad\downarrow\uparrow & \\ \mathrm{Ph\text{-}\underset{\displaystyle C_4H_9}{\underset{|}{C}}{=}CH\text{-}CH_2^-\ Li^+} & (b_3) \end{cases} \quad (3)$$

$$\mathrm{Ph\text{-}\underset{\displaystyle C_4H_9}{\underset{|}{C}}{=}CH\text{-}CH_2^-\ Li^+} \xrightarrow{RH} \mathrm{Ph\text{-}\underset{\displaystyle C_4H_9}{\underset{|}{C}}{=}CH\text{-}CH_3} + R^-\ Li^+ \quad (4)$$

(Ib)

$$\mathrm{Ph\text{-}\underset{\displaystyle C_4H_9}{\underset{|}{C}}{=}CH\text{-}CH_3} \xrightarrow[2)\ RH]{1)\ C_4H_9^-\ Li^+} \mathrm{Ph\text{-}\underset{\displaystyle C_4H_9}{\underset{|}{\overset{\displaystyle C_4H_9}{\overset{|}{C}}}}H\text{-}CH_3} + R^-\ Li^+ \quad (5)$$

(II)

$$\mathrm{Ph\text{-}\overset{-}{C}H\text{-}CH{=}CH_2} \xrightarrow{\diagup\!\!\!

Although it has been known that organolithium compounds more or less easily decompose in ether solvents at room temperature,[3] the processes have not been studied in detail. Recently several groups have found that alkyllithium compounds react with THF to give alcohols. Rembaum *et al.*[9] reported the following reaction:

$$C_2H_5^- Li^+ + \boxed{\quad O \quad} \rightarrow C_2H_5\text{-}(CH_2)_4\text{-}O^- Li^+$$

Fetters *et al.*[10] investigated the reaction of polystyryl anion with THF and found it to be as follows:

$$\sim\sim CH_2\text{-}\underset{\underset{Ph}{|}}{CH}^- Li^+ + \boxed{\quad O \quad} \rightarrow$$

$$\sim\sim CH_2\text{-}\underset{\underset{Ph}{|}}{CH}\text{-}(CH_2)_4\text{-}O^- Li^+$$

In the reaction of allylbenzene with *n*-BuLi, an anion, a_1, formed by the process (1) reacts with THF to give an alcoholate, as is shown in the process (6). The alcoholate Va thus produced may isomerize to Vb through the processes (7) and (8) just the same as is isomerized Ia to Ib. On the other hand, the alcohol derived from the anion b_1 in the process (1) was not detected at all. The anions a_3 and a_7 in the processes (3) and (7) also react with THF to give alcoholates, VIa and VIIa, through the processes (9) and (10) respectively. In these cases the isomerizations of VIa and VIIa do not proceed because of the lack of a hydrogen atom at the 3-position in each compound. Moreover, the corresponding alcohols can not be derived from the anions b_3 and b_7 in the processes (3) and (7).

The above results show that, in the resonance structures of the allyl anions, a and b;

$$\underset{(a)}{Ph\text{-}\bar{C}R\text{-}CH{=}CH_2} \leftrightarrow \underset{(b)}{Ph\text{-}CR{=}CH\text{-}CH_2^-}$$

the form b is more stable than a; in other words, the form a is more reactive with THF to give an alcohol.

The allyl anions formed here reacted with THF to give alcohols in good yields, while a lot of allyllithium compounds abstract a proton from THF to yield alkanes.[11] This may be caused by the difference in the reactivity between these organolithium compounds.

At the present time, from the results of this study alone it seems to be difficult to determine the structure of the above-mentioned anion, D, having a λ_{max} at 570 mμ. However, it has been found that many of the anions derived from allylbenzene were converted into the alcoholate anions by the reaction with THF. In the anionic polymerization of *trans*-β-methylstyrene, the allyl anion, A, is formed by the chain transfer to the monomer. Therefore, the same reaction of the anion A with THF should also occur to produce alcoholate anions in this anionic polymerization at high temperatures, this reaction being one of the main causes why the polymerization ceases.

The poly-β-methylstyrene obtained by the anionic polymerization has no C=C double bond in the chain, and the structure of cyclic butane was proposed as that of the terminal unit.[1] The existence of compounds III and IV, the supposed components of the fractions F3H and F4H, may be connected with this saturated chain terminal, although the structures of III and IV have, so far, not been exactly determined.

9) A. Rembaum, S. P. Siao and N. Indictor, *J. Polymer Sci.*, **56**, S17 (1962).
10) L. J. Fetters, *ibid.*, **B2**, 425 (1964).
11) H. Gilman and G. L. Schwebke, *J. Organometal. Chem.*, **4**, 483 (1965).

BULLETIN OF THE CHEMICAL SOCIETY OF JAPAN VOL. 41 684—691 (1968)

Organic Catalysts. IV.[1] The Role of the Iron as an Oxidation Catalyst in Copper-Iron-Polyphthalocyanine

Hiroo INOUE, Yasuji KIDA and Eiji IMOTO

Department of Applied Chemistry, College of Engineering, The University of Osaka Prefecture, Sakai, Osaka

(Received September 22, 1967)

The role of the iron in copper-iron-polyphthalocyanine in the catalytic action in the oxidation of acetaldehyde ethylene acetal and cyclohexene was investigated on the basis of the inhibition of the reaction by the treatment of copper-iron-polyphthalocyanine with iron-binding agents and oxidizing agents. The catalytic action of copper-iron-polyphthalocyanine decreased or disappeared upon the addition of 2-phenylimidazole and pyridine to the reaction system, and upon the treatment with bromine or concentrated hydrochloric acid in the presence of air. However, the reduction of the oxidized copper-iron-polyphthalocyanine with ascorbic acid or sodium thiosulfate recovered the catalytic activity. Furthermore, the catalytic activities of iron-metal-polyphthalocyanines (metal; V, Cr, Mn, Co, Ni, Cu and Zn) and copper-metal-polyphthalocyanines (metal; V, Cr, Co, Ni and Zn) in the oxidation of acetaldehyde ethylene acetal were investigated. The former groups showed the catalytic actions, but no catalytic actions were observed in the latter groups. The catalytic activities of iron-metal-polyphthalocyanines increased with a decrease in the activation energy of the electrical conductivity of the polymer. From these results, it was presumed that the Fe(II) ions located in the conjugated system act as active sites for the activation of oxygen and for the decomposition of peroxide.

Copper-iron-polyphthalocyanine, which has a unit structure similar to the structure of an iron or copper porphyrin in biological oxygenases, shows a remarkable acceleration in the oxidation of acetaldehyde ethylene acetal with oxygen.[1)]

The copper-iron-polyphthalocyanine has a sensitive catalytic activity related to its electronic and stereochemical structure. Furthermore, the action of the iron ion in the activation of oxygen and in the decomposition of peroxide may be interpreted in terms of the electronic character of the iron ion with the assistance of coordination chemistry.

In this paper, we will describe the role of the iron ion in polyphthalocyanine in the catalytic action. Our conclusions are based on the following results: 1) the inhibition of the reaction by iron-binding agents, such as pyridine and 2-phenylimidazole; 2) the disappearance of the catalytic activity upon treatment with an oxidizing agent, such as bromine or hydrochloric acid in the presence of oxygen; 3) the requirement of a reducing agent, such as ascorbic acid, for the catalytic activity, and 4) the effect on the catalytic activity of the coexistence of vanadium, chromium, manganese, cobalt and zinc instead of copper with the iron in the polyphthalocyanine structure.

Experimental

Preparation of Metal Polyphthalocyanine. *Iron- and Copper-Iron-Polyphthalocyanine (Fe-poly PC and Cu-Fe-poly PC).* Cu-Fe-poly PC was prepared according to the method described in a previous paper,[1)] except that the reaction temperature was 175°C instead of 190°C. Fe-poly PC was prepared under various conditions: at different temperatures, with different solvents, and with different amounts of anhydrous ferric chloride. The results are shown in Table 1. The results of the elementary analyses of the Fe-poly PC and Cu-Fe-poly PC obtained are shown in Table 2.

Iron- and Copper-Metal-Polyphthalocyanine (Fe-M-poly PC and Cu-M-poly PC). Fe-M- and Cu-M-poly PC were prepared according to a method, A, described in the previous paper.[1)] However, the reaction temperatures for the preparation of the metal polyphthalocyanines in this paper were changed according to the kinds of metal ions coexisting with the iron ion. The reaction mixture turned green. For all the experiments, the product, 1.2—1.4 g of an infusible bluish or greenish-black powder, was obtained from the starting materials of 4.26×10^{-4} mol of anhydrous ferric chloride, 4.22×10^{-4} mol of metal salt, and 4.21×10^{-3} mol of 1, 2, 4, 5-tetracyanobenzene.

The properties and the conditions for the preparation of all the polymers obtained here are summarized in Tables 5 and 6.

Treatment of Metal Polyphthalocyanines (Cu-Fe-Poly PC and Fe-Poly PC (No. 1)). *By Bromine.* Into a solution of 5 g of potassium bromide and 10 m*l* of bromine in 100 m*l* of distilled water, 0.5 g of metal polyphthalocyanine was added; the mixture was then stirred at room temperature for 9 hr. After filtering off, the precipitate was washed sequentially with distilled water, methanol, and ether, and was dried over calcium chloride under a reduced pressure of 10 mmHg,

1) Part III of this series: H. Inoue, Y. Kida and E. Imoto, This Bulletin, **40**, 184 (1967).

TABLE 1. THE CONDITIONS OF THE PREPARATIONS OF Cu-, Fe- AND Cu-Fe-POLY PC

Polymer	Material, g			Solvent[a]	Reaction temperature, °C
	T. C. B.[b]	$CuCl_2$	$FeCl_3$		
Cu-Poly PC	1.5	0.67	0.00	E. G.	175
Cu-Fe-poly PC	1.5	0.11	0.14	E. G.	175
Fe-poly PC (No. 1)	1.5	0.00	0.67	E. G.	175
Fe-poly PC (No. 2)	1.5	0.00	0.67	E. G.	190
Fe-poly PC (No. 3)	1.5	0.00	0.48	E. G.	175
Fe-Poly PC (No. 4)	1.5	0.00	0.67	D. E. P.	190

a) The amount of the solvent is 16 g.
E. G. and D. E. P. mean ethylene glycol and diethyl phthalate, respectively.
b) T. C.B. means 1, 2, 4, 5-tetracyanobenzene.

TABLE 2. THE ELEMENTARY ANALYSES OF Cu-, Fe- AND Cu-Fe-POLY PC

Polymer	Elementary analysis, %				
	C	H	N	Cu	Fe
Cu-poly PC	50.7	2.13	18.3	11.6	0.0
Cu-Fe-poly PC	54.5	2.22	21.6	3.8	2.8
Fe-poly PC (No. 1)	46.7	2.76	14.2	0.0	12.6
Fe-poly PC (No. 2)	54.6	2.70	16.9	0.0	—
Fe-poly PC (No. 3)	50.8	2.80	18.0	0.0	—
Fe-poly PC (No. 4)	55.5	2.11	20.5	0.0	—

thus yielding 0.5 g of the powder.

By Ascorbic Acid. A solution of 2 g of ascorbic acid in 40 m*l* of distilled water was adjusted to pH 4 with sodium acetate; then into the solution there was added 0.5 g of the polymer treated by bromine, and the mixture was stirred under a nitrogen atmosphere for 2 hr at room temperature. After filtering off, the precipitate was washed and dried as has been described above.

By Sodium Thiosulfate. Into 100 m*l* of a 0.5 N sodium thiosulfate solution there was added 0.2 g of the polymer treated by bromine, and then the mixture was stirred at room temperature for one day. After filtering off, the precipitate (about 0.2 g) was washed and dried as has been described above.

By Concentrated Hydrochloric Acid. A solution of 0.4 g of the polymer in 300 m*l* of concentrated hydrochloric acid was heated while being stirred at 90°C for 1.5 hr according to Linstead's method, in which Fe(II) phthalocyanine is oxidized by air to Fe(III) phthalocyanine.[2] After the reaction, the precipitate was washed and dried by the method described above.

Oxidation of Acetaldehyde Ethylene Acetal and Cyclohexene with Oxygen. *Materials.* Acetaldehyde ethylene acetal and cyclohexene were prepared according to the methods described in the literature[3,4] and were purified before use by distilling them repeatedly through a Vigreux column over sodium under a nitrogen atmosphere. Acetaldehyde ethylene acetal; n_D^{25} 1.3960, bp 85°C, and cyclohexene; n_D^{25} 1.4465, bp 83°C. The absence of peroxide was confirmed by an iodine-starch test.

Apparatus and Procedure. The oxidation of acetaldehyde ethylene acetal or cyclohexene was carried out by stirring a suspension of 30 mg of the polymer in 5 m*l* of acetaldehyde ethylene acetal or cyclohexene at the atmospheric pressure of oxygen at 30°C using the same apparatus and procedure as have been described in a previous paper.[1]

Analyses of the Oxidation Products. The oxidation products, ethylene glycol monoacetate, 2-cyclohexenol, and 2-cyclohexenone, were analyzed with a gas chromatograph, Yanagimoto GCG-5DH, in which polyethylene glycol-6000 was used as an adsorbent and helium gas as a carrier gas. The results were similar to those described previously.[1]

The Measurement of the D. C. Resistivity. The d. c. resistivity of the polymer was measured in an applied electric field of 100—200 V/cm under a pressure of 1000 kg/cm² *in vacuo* according to a method described in a previous paper.[5] The electrical resistivity (ρ) at an ascending temperature (T) was identical with that at a descending temperature, and a linear relationship between log ρ and $1/T$ was observed. The resistivities of the polymers, as typical organic semiconductors, fit the following equation;

$$\rho = \rho_0 \exp(\Delta\varepsilon/2\boldsymbol{k}T)$$

where $\Delta\varepsilon$ is the energy gap and $\boldsymbol{k}$, the Boltzmann constant.

2) P. A. Barrett, D. A. Frye and R. P. Linstead *J. Chem. Soc.*, **1938**, 1157.
3) H. Hibbert and J. A. Timm, *J. Am. Chem. Soc.*, **46**, 1283 (1924).
4) A. Lapworth and J. A. MacRae, *J. Chem. Soc.*, **1922**, 1699.
5) H. Inoue, S. Hayashi and E. Imoto, This Bulletin, **37**, 336 (1964).

Results and Discussion

Properties of the Polymers. *Cu-, Fe-, and Cu-Fe-Poly PC.* Cu-, Fe-, and Cu-Fe-poly PC are insoluble in any organic solvents, but are soluble in concentrated sulfuric acid, giving a green color. The elementary analyses, the ratio of carbon to nitrogen (C/N ratio), the ratio of copper to iron (Cu/Fe ratio), and the electrical conductivities of Cu-, Fe- and Cu-Fe-poly PC are summerized in Tables 2 and 3. These results and, furthermore, the visible absorption spectra of the polymers are identical with those of the phthalocyanine polymer of Type A described previously.[1] The infrared absorption spectra of the polymers differed from those of the previously-prepared polymers[1] only in the absorption of the -CN group, 2200 cm^{-1}. Therefore, the structure of the polymers obtained here must be of a phthalocyanine type, with end groups of -CN and -CONHCO-. Furthermore, the degree of the polymerization of the phthalocyanine unit of Cu-Fe-poly PC is presumed to be larger than that of Cu- and Fe-poly PC on the basis of the C/N ratios and the electrical conductivities, which are shown in Table 3.

The electron spin resonance spectra of the polymers were measured in the air at room temperature. The results are shown in Fig. 1. The electron spin resonance spectra of Fe-poly PC (No. 1—4) have no absorption. These facts indicate that the central iron ion of Fe-poly PC has an oxidation state of +2 and a coordination number of 6.[6] On the other hand, the electron spin resonance spectra of Cu- and Cu-Fe-poly PC have absorptions at the g values of 2.072 and 2.055 respectively. Therefore, the central iron and copper ions of Cu- and Cu-Fe-poly PC must have oxidation states of +2 and coordination numbers of 6 and 4 respectively. Furthermore, in the case of Cu-Fe-poly PC only, one more absorption was observed, as shown in Fig. 1. This must be based on the free electron in the conjugated system of the polymer. This fact may mean that

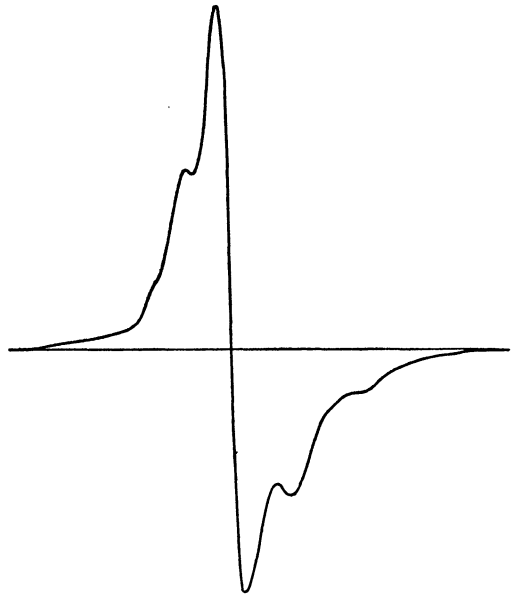

Fig. 1. ESR spectrum of Cu-Fe-poly PC (g: 2.055).

Cu-Fe-poly PC has a larger degree of polymerization of the phthalocyanine unit than that of Fe- or Cu-poly PC.

Fe- and Cu-Fe-Poly PC Treated with Bromine, Ascorbic Acid, and Sodium Thiosulfate. The treatment of Cu-Fe-poly PC and Fe-poly PC with bromine resulted in an increase in the halogen content from 0.85 to 4.07%; the halogen content was then recovered almost quantitatively to 0.78% by treatment with ascorbic acid or sodium thiosulfate, as shown in Table 4. By treatment with bromine and then with ascorbic acid, no significant differences in the C/N ratios, the infrared absorption spectra, the visible absorption spectra, and the electron spin resonance spectra of the polymers were observed from those of the untreated polymers, although some variations in the electrical conductivities were observed. This means that the phthalocyanine structure of the polymers, and

TABLE 3. THE VALUES OF C/N RATIO, Cu/Fe RATIO, $\Delta\varepsilon$ AND ρ_{20} OF Cu-, Fe- AND Cu-Fe-POLY PC

Polymer	C/N ratio[a]	Cu/Fe ratio[a]	Electrical properties	
			$\Delta\varepsilon$, eV	ρ_{20}, Ω-cm
Cu-poly PC	3.24	—	1.00	1.6×10^{8}
Cu-Fe-poly PC	2.95	1.18	0.35	5.0×10^{5}
Fe-poly PC (No. 1)	3.84	—	0.58	1.6×10^{6}
Fe-poly PC (No. 2)	3.78	—	0.55	2.2×10^{6}
Fe-poly PC (No. 3)	3.28	—	0.62	1.3×10^{6}
Fe-poly PC (No. 4)	3.16	—	—	—

a) C/N ratio $= \frac{14\times C\%}{12\times N\%}$, Cu/Fe ratio $= \frac{55.6\times Cu\%}{63.5\times Fe\%}$

6) A. B. P. Lever, *J. Chem. Soc.*, **1965**, 1821.

Table 4. The values of the halogen content, C/N ratio, $\Delta\varepsilon$ and ρ_{20} of Fe- and Cu-Fe-poly PC treated with bromine, ascorbic acid or concentrated hydrochloric acid plus air

Treatment	Halogen, %	C/N ratio	Electrical properties	
			$\Delta\varepsilon$, eV	ρ_{20}, Ω-cm
Cu-Fe-poly PC				
Untreated	0.85	2.95	0.35	5.0×10^{5}
Bromine	4.07[a)]	2.89	0.72	2.1×10^{6}
Ascorbic acid	0.78	2.90	0.53	1.2×10^{6}
Fe-poly PC (No. 3)				
Untreated	—	3.28	0.62	1.3×10^{7}
Conc. HCl plus air	—	3.66	0.89	3.5×10^{7}

a) This is the chlorine plus bromine contents.

Table 5. The conditions of the preparations and the elementary analyses of Fe-M- and Cu-M-poly PC

Polymer	Metal salt	Reaction temp. °C	Elementary analysis, %			
			C	H	N	Ash
Fe-V-poly PC	V_2O_5	180	53.7	2.18	21.6	—
Fe-Cr-poly PC	$CrCl_3\cdot6H_2O$	175	51.2	1.80	19.5	—
Fe-Mn-poly PC	$MnCl_2\cdot xH_2O$	185	50.9	2.30	19.6	—
Fe-Co-poly PC	$CoCl_2$	180	54.1	2.51	20.6	—
Fe-Ni-poly PC	$NiCl_2$	175	52.4	2.13	20.7	—
Fe-Zn-poly PC	$ZnCl_2$	175	53.5	2.60	20.5	—
Fe-Pd-poly PC	$PdCl_2$	175	49.7	2.30	19.7	—
Fe-Sn-poly PC	$SnCl_2\cdot2H_2O$	180	49.8	2.49	20.8	—
Fe-Cd-poly PC	$CdCl_2$	210	50.6	2.26	18.1	—
Cu-V-poly PC	V_2O_5	180	56.5	2.03	22.3	9.9
Cu-Cr-poly PC	$CrCl_3\cdot6H_2O$	180	53.8	2.63	20.9	6.9
Cu-Mn-poly PC	$MnCl_2\cdot xH_2O$	180	54.9	2.36	22.7	6.5
Cu-Co-poly PC	$CoCl_2$	180	57.5	2.22	22.7	10.0
Cu-Ni-poly PC	$NiCl_2$	180	57.0	2.15	23.8	11.0
Cu-Zn-poly PC	$ZnCl_2$	180	55.7	2.36	22.0	—
Mn-poly PC	$MnCl_2\cdot xH_2O$	180	54.6	2.34	19.8	11.0

both the oxidation states and the coordination numbers of the central metal ions do not change with the treatment with bromine and ascorbic acid. Moreover, the bromine treatment may form a complex between bromine and the central iron ion (1), or between bromine and the nitrogen atom of the pyrrole of the phthalocyanine structure (2).

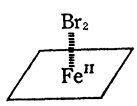

(1)

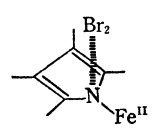

(2)

Fe- and Cu-Fe-Poly PC Treated by Air in Concentrated Hydrochloric Acid. The oxidation of the central iron ions of Fe- and Cu-Fe-poly PC by air was carried out in concentrated hydrochloric acid as has been described before. The polymer obtained from Fe-poly PC showed properties similar to those of the untreated Fe-poly PC in respect to the C/N ratios, the electrical conductivities, and the infrared absorption spectra (Table 4). However, the infrared absorption spectrum of the polymer obtained from Cu-Fe-poly PC showed an increase in the absorption of the –CONHCO– group with a decrease in that of the –CN group. This means that some of the –CN groups were changed to –CONHCO– groups in the process of the treatment with concentrated hydrochloric acid. In the case of both Fe- and Cu-Fe-poly PC, the electron spin resonance spectra showed absorption at the g value of 2.051 in the existence of the Fe(III) ion.

Fe-M- and Cu-M-Poly PC. The polyphthalocyanines containing various metals (M) with iron or copper (Fe-M- or Cu-M-poly PC) were bluish

or greenish-black powders; those powders were insoluble in any organic solvents, but were soluble in concentrated sulfuric acid. The results of the elementary analyses (Table 5), the C/N ratios (Table 6), and the infrared absorption spectra of Fe-M- and Cu-M-poly PC were similar to those of Cu-Fe-poly PC. On the other hand, the visible absorption spectra of Fe-M-poly PC, observed by the use of a KBr disk method, showed differences from those of Cu-M-poly PC, which have two absorption maxima, at about 720—740 mμ and 880—900 mμ. Most of the Fe-M-poly PC's showed an absorption maximum at 570—580 mμ besides those at 720—740 mμ and 880—900 mμ. Among the Fe-M-poly PC's, the absorption maxima of Fe-Zn-poly PC and Fe-Mn-poly PC at 750 mμ, and of Mn-poly PC at 770 mμ and 935 mμ, were shifted toward the longer wavelength side by 10—30, 50, and 55 mμ respectively as compared with those of the other Fe-M-poly PC's. The values of ρ_{20} and $\Delta\varepsilon$ of the electrical conductivity were in the range of 10^4—10^8 ohm-cm and 0.4—1.3 eV respectively (Table 6). The values of the electrical resistivities of Cu-M-poly PC and Mn-poly PC were lower than those of Fe-M-poly PC. Mn-poly PC showed the highest electrical conductivity, ρ_{20}-3.4×10^3 ohm-cm.

Table 6. The values of C/N ratio, $\Delta\varepsilon$ and ρ_{20} of Fe-M- and Cu-M-poly PC

Polymer	C/N ratio	Electrical properties	
		$\Delta\varepsilon$, eV	ρ_{20}, Ω-cm
Fe-V-poly PC	2.90	1.20	2.2×10^8
Fe-Cr-poly PC	3.06	1.30	1.1×10^9
Fe-Mn-poly PC	3.02	0.87	7.0×10^5
Fe-Co-poly PC	3.06	0.83	2.3×10^6
Fe-Ni-poly PC	2.95	0.87	4.1×10^6
Fe-Zn-poly PC	3.05	0.66	1.1×10^7
Fe-Pd-poly PC	2.95	0.42	5.0×10^5
Fe-Sn-poly PC	2.79	1.20	5.5×10^8
Fe-Cd-poly PC	3.26	1.30	2.1×10^8
Cu-V-poly PC	2.83	0.61	1.3×10^4
Cu-Cr-poly PC	3.00	0.65	3.5×10^5
Cu-Mn-poly PC	2.82	0.59	1.1×10^4
Cu-Co-poly PC	2.96	0.70	1.7×10^5
Cu-Ni-poly PC	2.80	0.83	2.5×10^5
Cu-Zn-poly PC	2.96	0.64	1.4×10^7
Mn-poly PC	3.22	0.53	3.4×10^8

Oxidations of Acetaldehyde Ethylene Acetal and Cyclohexene. *Catalytic Actions of Fe-Poly PC and Cu-Fe-Poly PC.* The oxidations of acetaldehyde ethylene acetal and cyclohexene by Fe-poly PC and Cu-Fe-poly PC with oxygenat 30°C were carried out as has been described previously.[1] The catalytic ability of Fe-poly PC depends on the synthetic conditions, that is, on the reaction temperature and on the ratio of anhydrous ferric chloride to 1, 2, 4, 5-tetracyanobenzene, as shown in Fig. 2. There were some difficulties in preparing the catalytically active Fe-poly PC as compared with the case of Cu-Fe-poly PC. Although the (No. 1 and 3) Fe-poly

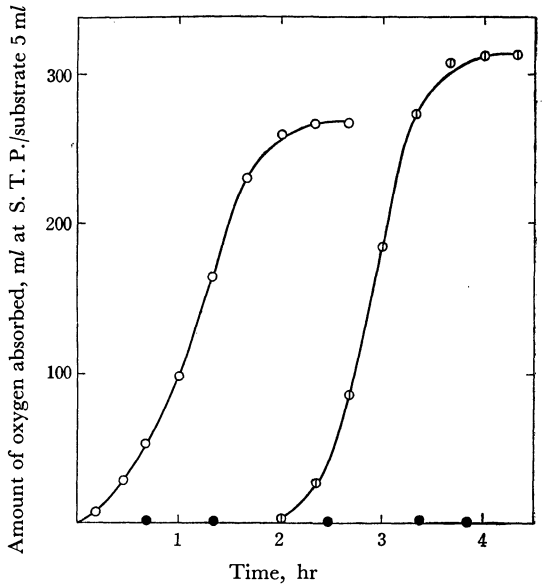

Fig. 2. The catalytic activity of Fe-poly PC prepared under the different conditions: Fe-poly PC; 30 mg.
○ No. 1 ◑ No. 3 ● No. 2 and 4

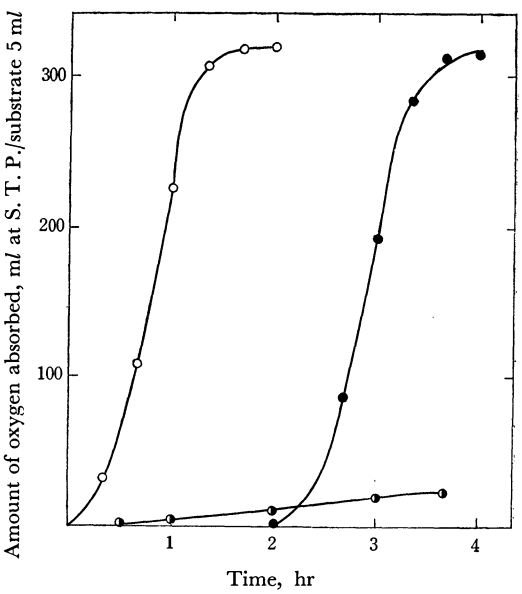

Fig. 3. The effect of *t*-butylhydroperoxide on the oxidation of acetaldehyde ethylene acetal in the presence of Fe-poly PC at 30°C: Fe-poly PC; 30 mg.
○ *t*-BuOOH (0.5 m*l*) plus Fe-poly PC
● Fe-poly PC alone
◑ *t*-BuOOH alone (0.5 m*l*)

PC's showed catalytic activity in the oxidation of acetaldehyde ethylene acetal, the (No. 2 and 4) Fe-poly PC's did not show any activity. The (No. 3) Fe-poly PC showed a long induction period in the oxidation of acetaldehyde ethylene acetal, but the induction period disappeared upon the addition of *t*-butyl hydroperoxide to the reaction system (Fig. 3). Thus, the catalytic action of the (No. 3) Fe-poly PC is not effective in the activation of oxygen, but it is effective in the decomposition of the peroxide formed in the oxidation process. Remarkable differences in catalytic activity between Fe-poly PC and Cu-Fe-poly PC were observed in the case of the oxidation of cyclohexene. As shown in Fig. 4, even Fe-poly PC (No. 1), which showed a significant catalytic action in the oxidation of acetaldehyde ethylene acetal, showed a longer induction period for the oxygen absorption than that of Cu-Fe-poly PC. These facts must mean that the catalytic action of Cu-Fe-poly PC in the oxidation of acetaldehyde ethylene acetal and cyclohexene is more effective than that of Fe-poly PC.

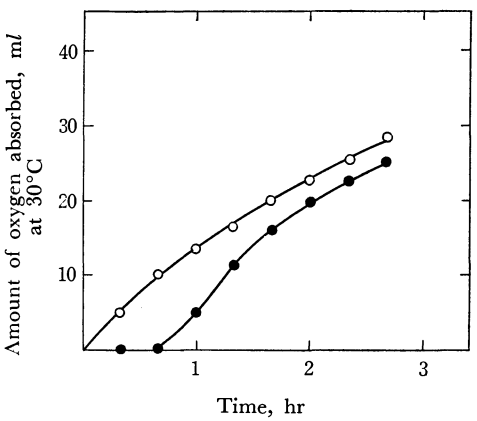

Fig. 4. The oxidation of cyclohexene in the presence of Fe- and Cu-Fe-poly PC: Catalyst; 30 mg.
○ Cu-Fe-poly PC ● Fe-poly PC (No. 1)

Effects of Various Treatments on the Catalytic Activities of Fe- and Cu-Fe-Poly PC. Cu-Fe-poly PC and Fe-poly PC treated with bromine showed no catalytic action in the oxidation of acetaldehyde ethylene acetal. However, the catalytic action was recovered to some extent by the reduction of bromine in Fe- and Cu-Fe-poly PC by ascorbic acid or sodium thiosulfate. The rate and the total amount of oxygen absorption into the system are shown in Fig. 5. Thus, bromine acts as an inhibitor of the catalytic action of Fe- and Cu-Fe-poly PC in the oxidation of acetaldehyde ethylene acetal. Probably this inhibition is caused by the formation of a complex between bromine and the polymer, as has been assumed previously.

The oxidation of acetaldehyde ethylene acetal

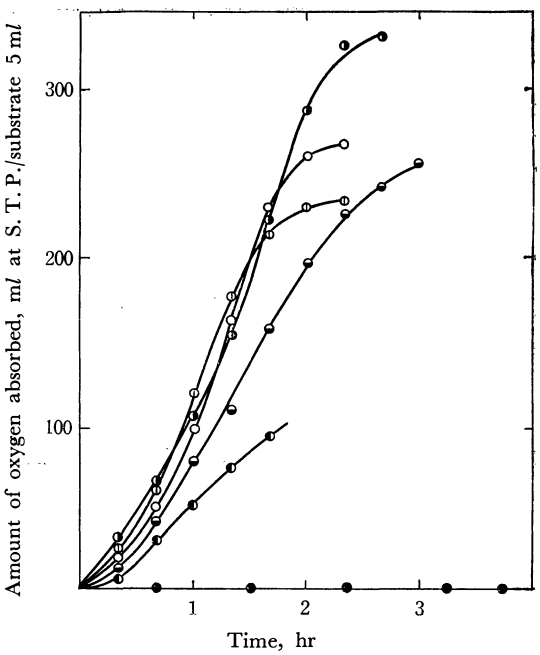

Fig. 5. The changes of the catalytic activities of Fe- and Cu-Fe-poly PC by the treatments of bromine and ascorbic acid: Catalyst; 30 mg.
◑ Cu-Fe-poly PC ○ Fe-poly PC
● Fe- and Cu-Fe-poly PC treated with Br_2
◒ Cu-Fe-poly PC treated with Br_2 and followed by ascorbic acid
◐ Cu-Fe-poly PC treated Br_2 and followed by sodium thiosulfate
ⓘ Fe-poly PC treated with Br_2 and followed by ascorbic acid

by Fe- and Cu-Fe-poly PC treated with concentrated hydrochloric acid and air showed the induction period of the oxygen absorption of 4 or 5 hr, as shown in Fig. 6. This indicates that the change of the Fe(II) to the Fe(III) ion in Fe- or Cu-Fe-poly PC upon treatment of concentrated hydrochloric acid and air results in a lowering of the catalytic activity in the activation of oxygen in the oxidation process. That is, the Fe(II) ion should be involved in Fe- and Cu-Fe-poly PC in order to contribute effectively to the acceleration of the oxygen absorption in the oxidation of acetaldehyde ethylene acetal. Furthermore, the addition of 2-phenylimidazole or pyridine to the reaction system containing Fe- or Cu-Fe-poly PC resulted in an increase in the induction period for oxygen absorption or a decrease in the rate of oxygen absorption. The effect of the inhibition by 2-phenylimidazole was greater than that by pyridine (Figs. 7 and 8). This may be caused by the stronger ligand field of 2-phenylimidazole as compared with that of pyridine. In the case of Fe-poly PC, the induction period increased proportionally with an increase in the amount of 2-phenylimidazole added, as shown in Fig. 9. The

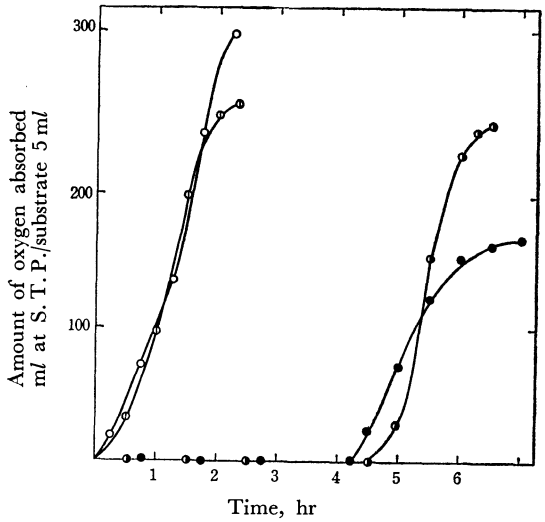

Fig. 6. The changes of the catalytic activities of Fe- and Cu-Fe-poly PC by the treatment of concentrated hydrochloric acid plus air: Catalyst; 30 mg.
○ Cu-Fe-Poly PC ⓘ Fe-poly PC
● Cu-Fe-poly PC treated with conc. HCl plus air
◑ Fe-poly PC treated with conc. HCl plus air

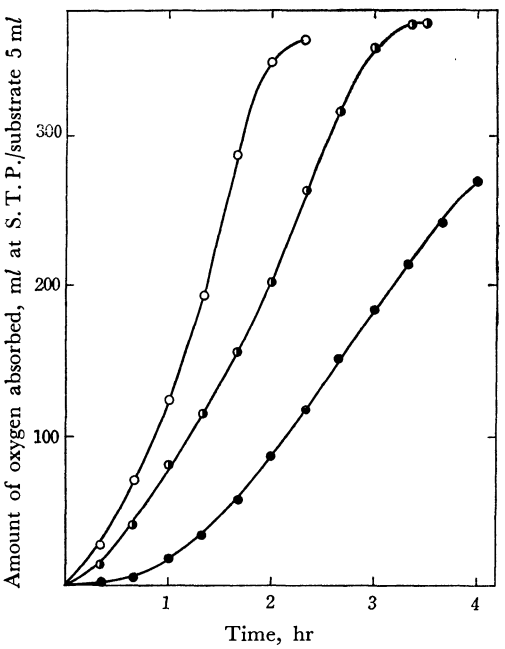

Fig. 7. The effect of pyridine on the oxidation of acetaldehyde ethylene acetal in the presence of Cu-Fe-poly PC: Catalyst; 30 mg.
The amount of the added pyridine: ○ none, ◑ 0.1 ml and ● 1.0 ml

decrease in the catalytic activity of Fe-poly PC with 2-phenylimidazole was larger than in the case of Cu-Fe-poly PC (Fig. 9). This may represent the difference between the properties of Fe- and Cu-

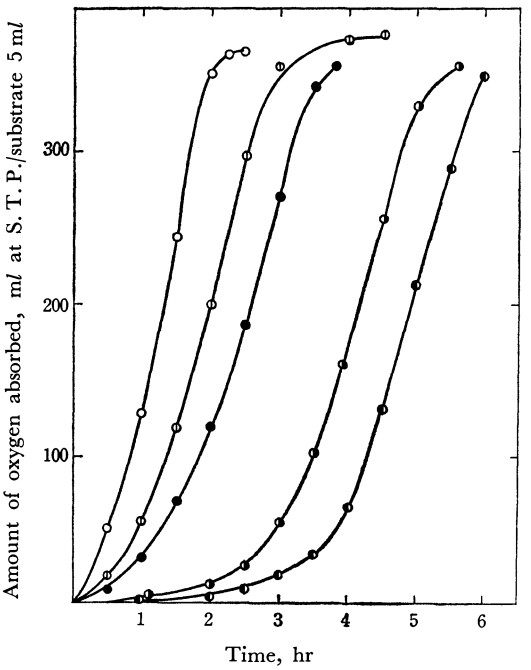

Fig. 8. The effect of 2-phenylimidazole on the oxidation of acetaldehyde ethylene acetal in the presence of Cu-Fe-poly PC: Catalyst; 30 mg.
The amount of the added 2-phenylimidazole: ○ none, ⓘ 4.29 mg, ● 5.90 mg, ◑ 8.16 mg and ◐ 10.14 mg

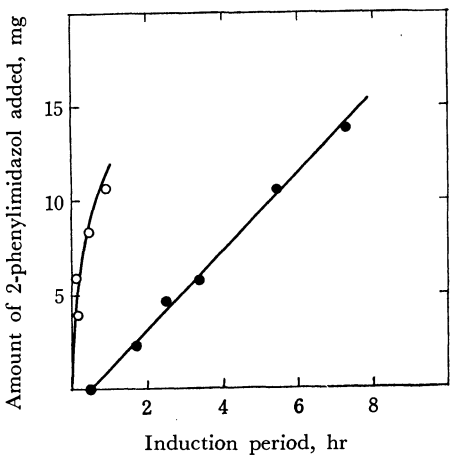

Fig. 9. Relationship between the amount of 2-phenylimidazole added and the induction period: Catalyst; 30 mg.
Acetaldehyde ethylene acetal: 5 ml
○ Cu-Fe-poly PC ● Fe-poly PC (No. 1)

Fe-poly PC as a catalyst, that is, the difference in the electronic properties of the Fe(II) ions located in the conjugated system. Thus, the electronic property of the Fe(II) ion conjugated with the π electron of the ligand seems to be important in making it an active site for the

activation of oxygen.

Oxidation of Acetaldehyde Ethylene Acetal in the Presence of Fe-M-Poly PC or Cu-M-Poly PC. As shown in Fig. 10, Fe-M-poly PC (M; Cr, V, Co, Ni and Zn), Cu-Mn-poly PC, and Mn-poly PC all showed catalytic activity in the oxidation of acetaldehyde ethylene acetal with oxygen, while Cu-M-poly PC did not. Therefore, the iron and manganese ions contained in the polyphthalocyanine polymer must play important roles in the catalytic action, probably as active sites. Furthermore, in the case of Fe-M-poly PC (M; Cr, V, Mn, Co, Ni and Cu), there was a linear relationship between the catalytic activity (the rate of oxygen absorption) and the activation energy ($\Delta\varepsilon$) of the electrical conductivity of Fe-M-poly PC, as shown in Fig. 11. That is, the catalytic activity of Fe-M-poly PC increases with a decrease in the $\Delta\varepsilon$ value of Fe-M-poly PC, namely, with an increase in the conjugated system of the π electron. Thus, the electronic property of an iron or manganese ion, which is modified by the conjugation of the π electron of ligand and the electronic property of the other metal ion coexisting with the iron or manganese ion, seems to contribute effectively to the catalytic action of Fe-M-poly PC.

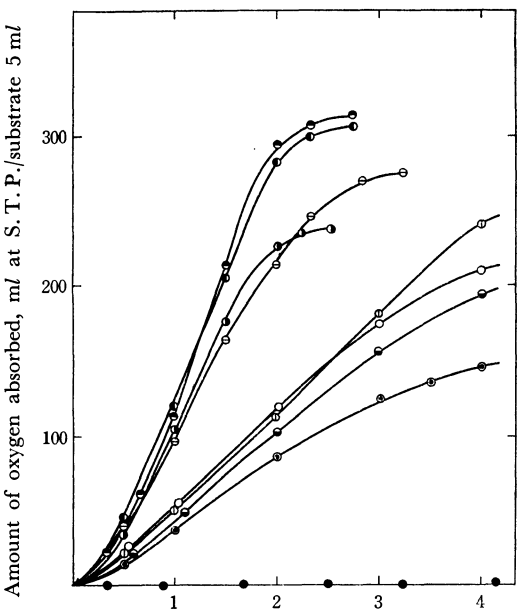

Fig. 10. The oxidation of acetaldehyde ethylene acetal in the presence of Fe-M- and Cu-M-poly PC: Catalyst; 30 mg.
○ Fe-V- ◑ Fe-Co- ◒ Cu-Mn- ● Cu- and Cu-M-poly PC (M: V, Cr, Co, Ni and Zn)
◐ Fe-Cr- ◓ Fe-Ni- ⊙ Mn-
⊖ Fe-Mn- ◓ Fe-Cu-

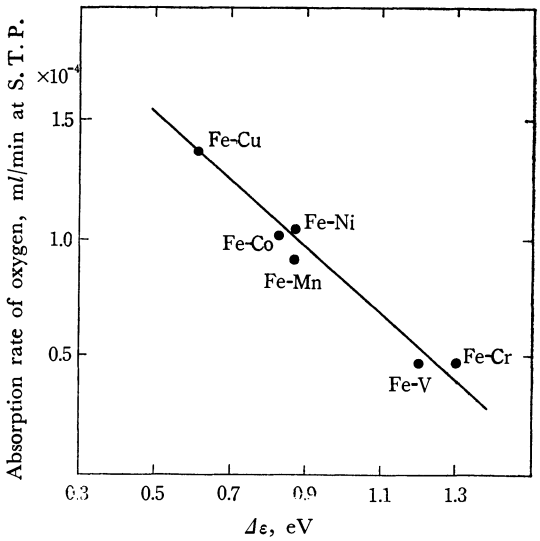

Fig. 11. Relationship between the absorption rate of oxygen in the oxidation of acetaldehyde ethylene acetal in the presence of Fe-M-poly PC and the value of $\Delta\varepsilon$ of Fe-M-poly PC: Fe-M-poly PC; 30 mg.
Acetaldehyde ethylene acetal; 5 ml

BULLETIN OF THE CHEMICAL SOCIETY OF JAPAN VOL. 41 692—696 (1968)

Organic Catalysts. V.[1] Specific Catalytic Properties of Copper-Iron-Polyphthalocyanine in the Oxidation of Aldehydes

Hiroo INOUE, Yasuji KIDA and Eiji IMOTO

Department of Applied Chemistry, College of Engineering, The University of Osaka Prefecture, Sakai, Osaka

(Received September 22, 1967)

Copper-iron-polyphthalocyanine showed a specific catalysis for the oxidations of the substituted benzaldehydes and the saturated aldehydes with oxygen. The catalytic activity of copper-iron-polyphthalocyanine was solvent-dependent: tetrahydrofuran, ethanol, acetonitrile, ethyl acetate and anisole inhibited the oxidation of benzaldehyde by copper-iron-polyphthalocyanine and oxygen, while benzene and acetone resulted in catalytic oxidation. Benzaldehyde and the saturated aliphatic aldehydes in benzene were oxidized catalytically with copper-iron-polyphthalocyanine and oxygen to afford the corresponding peroxy acids and acids in quantitative yields. Furthermore, oxygen was absorbed with no induction period; the rate of oxygen absorption was in the range of 8—13 m*l*/min. On the other hand, the unsaturated aliphatic aldehydes, cinnamaldehyde and acrolein, were oxidized with a very slow rate of oxygen absorption in spite of the existence of copper-iron-polyphthalocyanine in the reaction system. *p*-Methylbenzaldehyde and *p*-chlorobenzaldehyde were oxidized by copper-iron-polyphthalocyanine and oxygen in induction periods of about 8 and 15 min respectively, thus affording the corresponding peroxy acids and acids. However, no oxidations of *p*-nitrobenzaldehyde, *p*-hydroxycarbonylbenzaldehyde, *p*- and *m*-hydroxybenzaldehyde, *p*- and *m*-methoxybenzaldehyde and *p*-dimethylaminobenzaldehyde with copper-iron-polyphthalocyanine and oxygen were observed.

The autoxidations of aldehydes to carboxylic acids have been shown by a large number of investigators to be catalyzed by metal ions and peroxy acids.[2] It is the purpose of this paper to describe the specific catalytic activities of copper-iron-polyphthalocyanine in the oxidations of a series of aliphatic and aromatic aldehydes. The series of aldehydes chosen for investigation includes benzaldehyde, monosubstituted benzaldehydes (*p*-substituents: $-NO_2$, $-Cl$, $-CH_3$, $-OH$, $-OCH_3$ and $-N(CH_3)_2$, and *m*-substituents: $-OH$ and $-OCH_3$), and saturated and unsaturated aliphatic aldehydes.

Experimental

Materials. All of the aldehydes used here were of a commercial grade and had been purified by recrystallization or by distillation before use. It was confirmed by gas chromatography that aldehydes contain no impurity after purification. The absence of peroxide was confirmed by an iodine-starch test. Copper-polyphthalocyanine (Cu-poly PC), iron-polyphthalocyanine (Fe-poly PC), and copper-iron-polyphthalocyanine (Cu-Fe-poly PC), which were used as the catalysts for the oxidations of aldehydes, were prepared by the method (A)[3] or by the method used to prepare Fe-poly PC (No. 1)[1] in previous papers.

Oxidation. In most of the experiments, the oxidations of aldehydes were carried out by the same apparatus and procedure as have been described in the previous paper.[3] For the measurement of the rate of oxygen absorption, 5 m*l* of a solution of aldehyde at 6×10^{-1} M in an organic solvent, such as benzene, was oxidized at the atmospheric pressure of oxygen at 30°C. The oxidation products were determined after the oxygen absorption had been completed. The time-course investigation of the amounts of the oxidation products was carried out by using 450 m*l* of a solution of benzaldehyde at 6×10^{-1} M in benzene. 5-m*l* portions of the reaction mixture were pipetted out at appropriate time intervals, and the oxidation products were determined.

Analyses. The peroxy acids and acids formed in the oxidation process were identified by means of the iodine-starch test, the infrared absorption spectrum, and gas chromatography. The peroxy acid was determined by iodometric titration, the unreacted aldehyde by 2, 4-dinitrophenylhydrazone method. The formed acid was calculated by subtracting the sum of the amounts of peroxy acid and the unreacted aldehyde from the initial amount of the aldehyde.

Results and Discussion

Oxidation of Benzaldehyde. *The Catalytic Properties of Cu-, Fe- and Cu-Fe-Poly PC.* Fe-, Cu- and Cu-Fe-poly PC showed catalytic activity in the oxidation of benzaldehyde with oxygen. As

1) Part IV of this series: H. Inoue, Y. Kida and E. Imoto, This Bulletin, **41**, 684 (1968).
2) J. P. Mcnesby and C. A. Heller, *Chem. Revs.*, **54**, 325 (1954).
3) H. Inoue, Y. Kida and E. Imoto, This Bulletin, **40**, 184 (1967).

Fig. 1 and Table 1 show, a remarkable difference in the catalytic activity for Fe-, Cu-, and Cu-Fe-poly PC was observed. The oxidation of benzaldehyde in the presence of Cu-poly PC as a catalyst proceeded very slowly, with a rate of oxygen absorption of 0.7 ml/min in the stationary state after an induction period of about 10 min; the oxidation percentage of benzaldehyde at the reaction time of 107 min was about 60%.

In the case of Fe-poly PC, the oxygen absorption was started after an induction period of about 2 min and reached to completion after a reaction time of 25—30 min, with a rate of oxygen absorption of 8.1 ml/min in the stationary state.

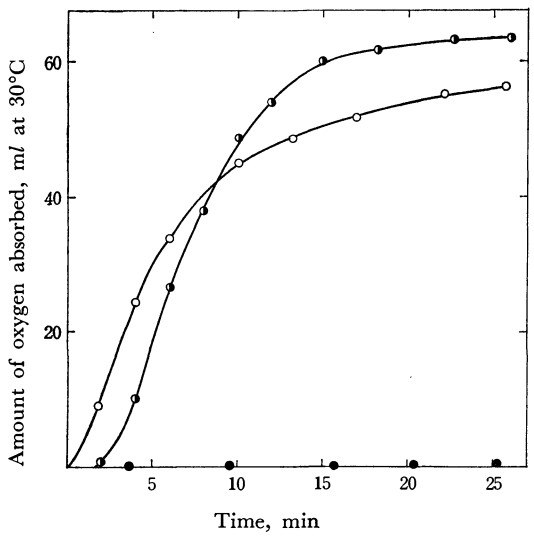

Fig. 1. The oxidation of benzaldehyde in the presence of Cu-, Fe- or Cu-Fe-poly PC : Catalyst ; 50 mg.
○ Cu-Fe-poly PC, ◑ Fe-poly PC,
● Cu-poly PC.

The catalytic action of Cu-Fe-poly PC differed from those of Cu- and Fe-poly PC in the initial state of the oxygen absorption. As shown in Fig. 1, the oxygen absorption started as soon as Cu-Fe-poly PC and benzaldehyde are mixed in benzene. There was, however, no significant difference in the rate of oxygen absorption in the stationary state between the cases of Fe- and Cu-Fe-poly PC. Thus, the action of Cu-Fe-poly PC seems to be characteristic of the activation of oxygen in the initial state of the oxidation process.

As shown in Table 1, peroxybenzoic acid and benzoic acid were obtained as the oxidation products. In all cases of Fe-, Cu-, and Cu-Fe-poly PC, the amount of the oxidized benzaldehyde was identical with the sum of the amounts of benzoic acid and peroxybenzoic acid produced. The catalytic efficiency (the reaction percentage of benzaldehyde per unit of weight of the catalyst until the oxygen absorption becomes constant) of each catalyst for the oxidation of benzaldehyde was higher than that of acetaldehyde ethylene acetal described previously.[1] No significant difference in the molar ratio of peroxybenzoic acid to benzoic acid, however, was observed in the cases of Cu-, Fe-, and Cu-Fe-poly PC.

Variations in the Amounts of Products in the Reaction Course. The amounts of the products, peroxybenzoic acid and benzoic acid, were determined by taking out portions of the reaction mixture at appropriate times during the oxidation of benzaldehyde. These results are shown in Fig. 2.

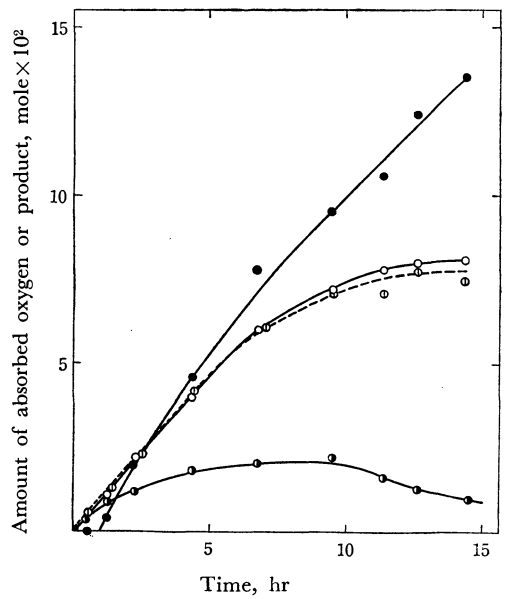

Fig. 2. The amounts of oxygen absorbed and the oxidation products in the oxidation course of benzaldehyde : Cu-Fe-Poly PC ; 0.3 g. Benzaldehyde solution ; 450 ml (6×10^{-1} M in benzene).
○ Absorbed oxygen, ◑ C_6H_5COOOH,
● C_6H_5COOH,
① $C_6H_5COOOH+\frac{1}{2}C_6H_5COOH$.

The absorption of oxygen was observed as soon as benzaldehyde and Cu-Fe-poly PC were mixed in benzene at an atmospheric pressure of oxygen at 30°C, and it increased linearly with the reaction time. After a reaction time of 7 hr, the rate of oxygen absorption decreased, however, until the absorption of oxygen stopped after a reaction time of about 15 hr.

The amount of peroxybenzoic acid produced increased with an increase in the amount of oxygen absorbed, and reached a constant after a reaction time of 3 hr. After staying almost constant for several hours, it started to decrease when the rate of oxygen absorption decreased.

On the other hand, another product, benzoic acid, was not produced even after a reaction time of 2 hr after the absorption of oxygen started.

After 2 hr, the amount of the benzoic acid started to increase with the reaction time. Even after the absorption of oxygen had become almost constant, the production of benzoic acid was observed. In the reaction mixture, no water or other compounds were produced. Furthermore, during the course of the oxidation, the amount of oxygen absorbed was identical with the sum of the amount of peroxybenzoic acid produced and half the amount of benzoic acid produced.

These facts show that the catalytic oxidation of benzaldehyde by Cu-Fe-poly PC with oxygen proceeds *via* the reaction steps represented by the following equation:

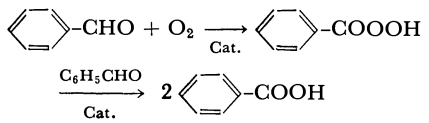

The catalyst contributes to the activation of oxygen, giving perbenzoic acid through the reaction of the activated oxygen and benzaldehyde, and to the decomposition of perbenzoic acid, thus giving benzoic acid quantitatively by the reaction of peroxybenzoic acid and benzaldehyde. Furthermore, the catalytic oxidation processes seem to indicate the character of Cu-Fe-poly PC as an oxidation catalyst.

The Effects of Solvents on the Oxidation of Benzaldehyde. The Fe(II) ion of Cu-Fe-poly PC acts as an active site for the activation of oxygen and for the decomposition of peroxide in the oxidation process. The catalytic activity of Cu-Fe-poly PC may be affected by the kind of solvent, since the Fe(II) ion may be solvated or coordinated by the solvent. The influence of solvents in the catalytic oxidation of benzaldehyde by Cu-Fe-poly PC with oxygen were investigated. As the solvents, benzene, acetone, ethyl acetate, tetrahydrofuran, acetonitrile, ethanol, and anisole were chosen. These results are shown in Fig. 3 and Table 1. Benzaldehyde in benzene or acetone containing Cu-Fe-poly PC was oxidized with oxygen to peroxybenzoic acid and benzoic acid, but no

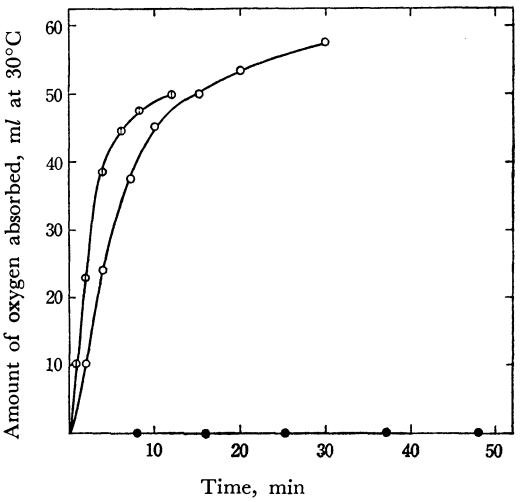

Fig. 3. Influence of solvent in the oxidation of benzaldehyde: Cu-Fe-Poly PC; 50mg,
① acetone, ○ benzene and ● tetrahydrofuran, acetonitrile, ethyl acetate, ethanol and anisole.

oxidation of benzaldehyde with oxygen was observed in tetrahydrofuran, ethanol, acetonitrile, ethyl acetate, or anisole, despite the presence of Cu-Fe-poly PC. The disappearance of the catalytic activity of Cu-Fe-poly PC when the latter solvents were used may be caused by the solvation or the coordination of the solvent to the Fe(II) ion as an active site, or by solvation to the Fe(II)$\cdots O_2$ intermediate. Furthermore, these phenomena must be related to the inhibition of pyridine and 2-phenylimidazole for the catalytic action of Cu-Fe-poly PC in the oxidation of acetaldehyde ethylene acetal, an inhibition described previously.[1]

The Oxidations of Monosubstituted Benzaldehydes. The oxidations of *p*-substituted benzaldehydes by peroxybenzoic acids are affected by the electron-donating or electron-withdrawing power of the substituent, although the rate of oxidation is independent of the Hammett substituent

TABLE 1. THE CATALYTIC ACTION OF Cu-, Fe- AND Cu-Fe-poly PC IN THE OXIDATION OF BENZALDEHYDE

Catalyst	Rate of oxygen[a] absorption, ml/min	Yield, %[b]	
		C_6H_5COOOH	C_6H_5COOH
Cu-poly PC	0.7[c]	34	26
Fe-Poly PC	8.1[c]	58	42
Cu-Fe-poly PC	8.1[c]	61	39
	11.0[d]	14	86
	0.0[e]	0	0

a) This is the rate of the oxygen absorption at the stationary state at 30°C.
b) The yield is the value for the initial amount of benzaldehyde.
c) The solvent: benzene.
d) The solvent: acetone.
e) The solvent: tetrahydrofuran, acetonitrile, ethanol and ethyl acetate, respectively.

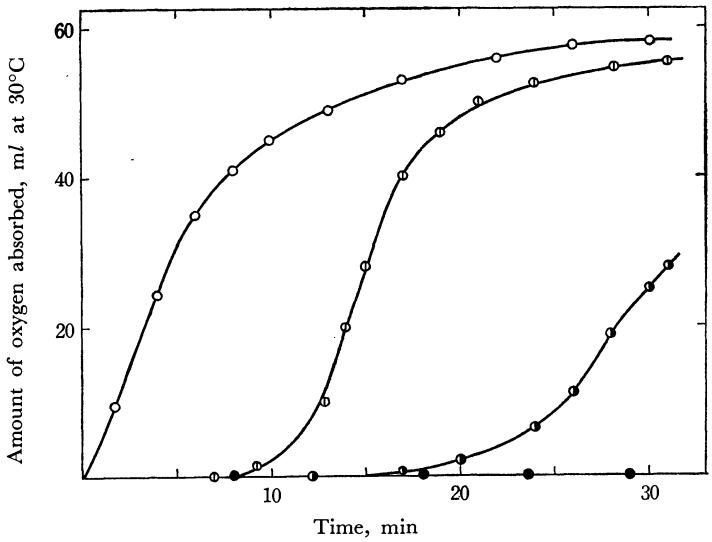

Fig. 4. The oxidation of monosubstituted benzaldehydes in the presence of Cu-Fe-poly PC : Cu-Fe-poly PC; 50mg.

○ Benzaldehyde, ⓘ *p*-CH_3–, ◑ *p*-Cl- (5×10^{-1} M, Cu-Fe-poly PC 20 mg), ● *p*-$(CH_3)_2N$–, *p*-HO–, *p*-CH_3O–, *p*-O_2N–, *p*-HOOC–, *m*-HO–, *m*-CH_3O– and *o*-HO-benzaldehyde.

constant.[4] The substituent effects on the catalytic oxidations of monosubstituted benzaldehydes by Cu-Fe-poly PC were also investigated. The oxidations of the monosubstituted benzaldehydes (*p*-substituents: $-NO_2$, –Cl, $-CH_3$, –OH, $-OCH_3$ and $-N(CH_3)_2$, and *m*-substituents: –OH and $-OCH_3$) with oxygen in the presence of Cu-Fe-poly PC were carried out under the same conditions as in the case of benzaldehyde. These results are shown in Fig. 4. *p*-Methylbenzaldehyde and *p*-chlorobenzaldehyde were oxidized catalytically by Cu-Fe-poly PC and oxygen to give the corresponding peroxy acids and acids, with induction periods of 8 min or 15 min respectively, while no oxidations of the other monosubstituted benzaldehydes were observed. That is, the catalytic effect of Cu-Fe-poly PC on the oxidation of monosubstituted benzaldehyde with oxygen was independent of the electron-donating or electron-withdrawing power of the substituent, and monosubstituted benzaldehydes, the substituents of which may coordinate to the Fe(II) ion, seem not to be oxidized by Cu-Fe-poly PC and oxygen. This is probably caused by the inhibition of the activation of oxygen in the oxidation processes; these facts seem to be related to the findings regarding the solvent effects on the catalytic action of Cu-Fe-poly PC.

The Oxidations of Aliphatic Aldehydes. Investigation was extended to the oxidations of aliphatic aldehydes, propionaldehyde, *n*-butyraldehyde, caprylaldehyde, 2-ethylcaproaldehyde, crotonaldehyde, cinnamaldehyde, and acrolein with Cu-Fe-poly PC and oxygen. The relation between the amount of oxygen absorbed and the

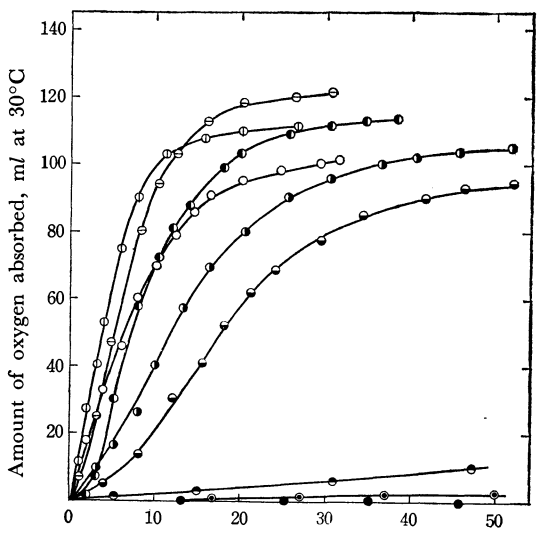

Fig. 5. The oxidation of aliphatic aldehydes in the presence of Cu-Fe-poly PC: Cu-Fe-poly PC; 30mg.

○ Propionaldehyde, ⓘ *n*-butyraldehyde, ◑ caprylaldehyde, ⊖ 2-ethylcaproaldehyde, ◒ crotonaldehyde, ◓ cinnamaldehyde, ⊙ acrolein, ◐ benzaldehyde.

4) W. Cooper, *J. Chem. Soc.*, **1952**, 2408; C. G. Swain, W. H. Stockmeyer and J. T. Clarke, *J. Am. Chem. Soc.*, **72**, 5426 (1950).

TABLE 2. THE OXIDATION OF ALIPHATIC ALDEHYDES IN THE PRESENCE OF Cu-Fe-poly PC[a]

Aldehyde	Rate of oxygen[b] absorption, ml/min	Yield, %[c]	
		Peroxy acid	Acid
Propionaldehyde	7.7	29	55
n-Butyraldehyde	13.0	44	52
Caprylaldehyde	4.8	47	48
2-Ethylcaproaldehyde	12.0	52	45
Acrolein	0.1	1[d]	1
Crotonaldehyde	3.7	38[d]	40
Cinnamaldehyde	0.5	5[d]	3

a) Aldehyde; 10 m*l* (6×10^{-1} M in benzene) and Cu-Fe-poly PC ; 30 mg.
b) This is the rate of the oxygen absorption at the stationary state at 30°C.
c) The yield is the value for the initial amount of benzaldehyde.
e) The reaction time ; 1 hr.

reaction time in the oxidation of each of the aliphatic aldehydes is shown in Fig. 5. Cu-Fe-poly PC showed a remarkable catalytic action in the oxidations of the saturated aliphatic aldehydes; the oxidations gave the corresponding peroxy acids and acids as the oxidation products in nearly quantitative yields (Table 2). On the other hand, the unsaturated aliphatic aldehydes, cinnamaldehyde and acrolein, were oxidized very slowly in spite of the presence of Cu-Fe-poly PC in the reaction system. Crotonaldehyde was oxidized, however, more easily than acrolein and cinnamaldehyde. These facts were similar to those of the case of metal-salt-catalyzed oxidation of unsaturated aldehydes in acetic acid.[5]

5) W. F. Brill and F. Lister, *J. Org. Chem.*, **26**, 565 (1961).

BULLETIN OF THE CHEMICAL SOCIETY OF JAPAN VOL. 41 696—701 (1968)

Concurrent Oxygen Exchange and Racemization Reactions of Diaryl Sulfoxides in Concentrated Sulfuric Acid[1)]

Shigeru OAE and Norio KUNIEDA

Department of Applied Chemistry, Faculty of Engineering, Osaka City University, Sumiyoshi-ku Osaka

(Received September 25, 1967)

When diaryl sulfoxides are dissolved in concentrated sulfuric acid at 0°C, characteristic bluish colored solutions are obtained, from which the starting sulfoxides can be recovered quantitatively upon quenching with a large amount of water. When ^{18}O-labeled and optically active sulfoxides are used, one observes the concurrent oxygen exchange and racemization reactions of the sulfoxides. The kinetic behaviors of these reactions have been studied in detail using various substituted diaryl sulfoxides. The rate of the oxygen exchange was found to be identical to that of the racemization while the rates of the racemization were nicely correlated with the Hammett acidity functions (H_0) (Slope$=1.07$). Meanwhile the polar effect of subsituents on the rates of both oxygen exchange and racemization was found to be very small. From these results possible mechanisms for these reactions have been discussed.

The sulfur-oxygen linkage in sulfoxides is known to be considerably weaker than that of sulfones and there are number of reactions which involve the facile cleavage of the sulfur-oxygen bond of sulfoxides.[2)] In the meantime, sulfoxides, being of pyramidal structure, have been resolved to pairs of optical isomers when the two substituents on the sulfur atom are different. An interesting reaction,

1) Paper XX on Sulfoxides.

2) For details see Chapter 4 of "Sulfur Bonding," by C. C. Price and S. Oae, Ronald Press., N. Y. (1962).

in these connection, is the concurrent oxygen exchange and racemization reactions of sulfoxides, which have attracted considerable attentions at various laboratories in recent years.[3] Previously, we have reported that sulfoxides undergo an oxygen exchange reaction in concentrated sulfuric acid and the concurrent racemization also takes place when (+)-*p*-aminophenyl *p'*-tolyl sulfoxide is used.[4] Based on a few observations such as the complete lack of oxygen exchange in sulfones, aromatic *N*-oxides and phosphine oxide, rough kinetics and stereochemical data, *etc.*, the mechanism involving the nucleophilic attack of sulfoxide on sulfuric acid was tentatively suggested as a working hypothesis, however, more careful kinetic studied were critically needed in order to elucidate a plausible mechanism for the reaction.

We now have compiled substantial amounts of kinetic data on the concurrent oxygen exchange and recemization reactions of diaryl sulfoxides and hence would like to report our further observations and comments concerning the nature of the reactions.

Results and Discussion

Sulfoxides used for this kinetic study are ^{18}O-labeled diaryl sulfoxides and optically active aryl-*p*-tolyl sulfoxides, and all of the sulfoxides were nicely recovered almost quantitatively and in no case the formation of the respective sulfones or sulfides was noticed.

At first careful kinetic experiments were conducted on the rates of both oxygen exchange and racemization reactions using (+)-*p*-tolyl phenyl sulfoxide in 95.5% sulfuric acid. The results, shown in Table 1, clearly reveal that the rate of the oxygen exchange is identical to that of the racemization ($k_{ex}/k_{rac}=0.97$), suggesting that the reaction proceeds through a SN_1 like S–O bond cleavage at the rate-determining step.[5] The energy and entropy of activation of this reaction are found to be 27.4 kcal/mol and +21.5 e. u., respectively. The positive value of the entropy of activation also favors the rate determining SN_1 like cleavage of S–O bond of the sulfoxide. Since our preliminary investigation has shown that the reaction is very fast in sulfuric acid of a high concentration and almost nil in a sulfuric acid of less than 85% concentration at a low temperature,[6] the rates of racemization were carefully measured in sulfuric acids of various concentrations. The results are shown in Table 2 and Fig. 1.

Table 1. Rate constants of ^{18}O-exchange and racemization of *p*-tolyl phenyl sulfoxide[a] in 95.5% sulfuric acid

Run No.	sec^{-1}
1	$k_{exchange}=3.22\pm0.15\times10^{-4}$ [b]
2	$k_{racemization}=3.32\pm0.20\times10^{-4}$ [b]
3	$=1.21\pm0.04\times10^{-4}$ [c]
4	$=7.25\pm0.27\times10^{-4}$ [d]

a) Sulfoxide=0.1 mol/*l*
b) at 5°C c) at 0°C d) at 10°C

Table 2. Rate constants of racemization of (+)-*p*-tolyl phenyl sulfoxide[a] in sulfuric acid of various concentrations at 5°C

Run No.	H_2SO_4 (%)	$k_{rac}\times10^4$, sec^{-1}	$\log k_{rac}+H_0$ [b]
5	91.8	1.16±0.10	−12.45
6	93.3	1.68±0.10	−12.42
7	94.4	2.58±0.06	−12.38
8	95.5	3.32±0.20	−12.40
9	96.3	4.48±0.28	−12.38

a) Sulfoxide=0.1 mol/*l*.
b) The H_0 values of these were used the values given by Paul and Long; Ref. 7.

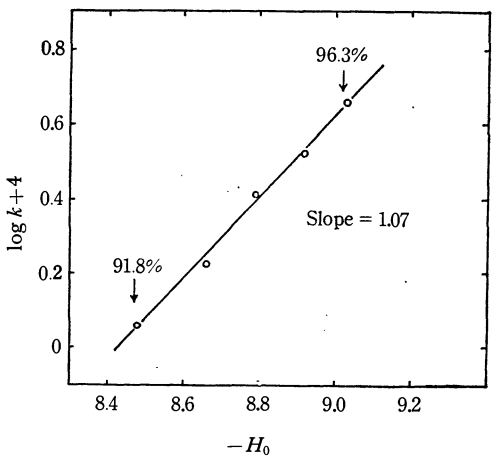

Fig. 1. The rate constants of racemization of (+)-*p*-tolyl phenyl sulfoxide protted against H_0.

3) a) The hydrogen chloride-catalyzed racemization; K. Mislow, T. Simmons, J. T. Mellilo and A. L. Ternay, *J. Am. Chem. Soc.*, **86**, 1452 (1964). b) The oxygen exchange and racemization reactions in dinitrogen tetroxide; S. Oae, N. Kunieda and W. Tagaki, *Chem. & Ind.*, **1965**, 1790. c) The oxygen exchange and racemization reactions in acetic anhydride; S. Oae and M. Kise, *Tetrahedron Letters*, **1967 (No. 15)**, 1409.

4) S. Oae, T. Kitao, Y. Kitaoka and S. Kawamura, This Bulletin, **38**, 546 (1965).

5) D. Samuel and B. L. Silver, "Oxygen Isotope Exchange Reactions of Organic Compounds," in "Advances in Physical Organic Chemistry," Vol. 3, ed. by V. Gold, Academic Press, London and N. Y. (1965), p. 129.

6) It will be discussed later in this paper.

7) M. A. Paul and F. A. Long, *Chem. Revs.*, **57**, 1 (1957).

As shown in Table 2 and Fig. 1, the rates are nicely correlated with the Hammett acidity functions (H_0) (Slope=1.07).[8] This means that the protonated species are involved in the transition state of the reaction, indicating that the reaction follows the A-I type mechanism of the Zucker-Hammett's hypothesis.[9] Meanwhile it have been shown by Gillespie and Passerini[10] and us[11] through the cryoscopic measurement and the ^{18}O-tracer experiment that sulfoxides ionize in concentrated sulfuric acid in the following manner (Eq. (1)).

$$\underset{\underset{O}{\downarrow}}{R\text{-}S\text{-}R} + H_2SO_4 \rightleftharpoons \underset{\underset{OH}{|}}{R\text{-}\overset{+}{S}\text{-}R} + HSO_4^- \qquad (1)$$

[A]

(Cryoscopic i-facter=2)

Therefore, the hydroxysulfonium ion [A] formed by the protonation of the sulfoxides in sulfuric acid in the preequilibrated ground state will probably pick up another proton from sulfuric acid before reaching the transition state of the reaction where the partial cleavage of the S–O bond will take place, as in the reduction of dimethyl sulfoxide with hydroiodic acid.[12]

There are a few ways conceivable for the cleavage of the S–O bond that fit in these observations, as shown by Eq. (2).

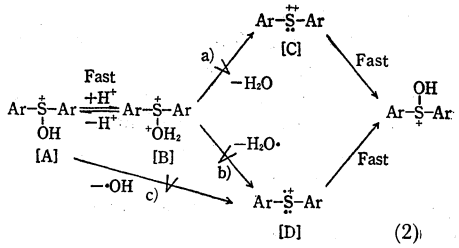

(2)

Path a is the heterolysis of the S–O bond involving the rate-determining formation of the doubly positive charged "sulfidonium ion" [C] intermediate. By the ^{18}O-tracer experiment and the freezing-point measurement the formation of the diaryl sulfidonium ion was excluded, but this *path a* is still attractive if one assumes that the formation of the sulfidonium ion [C] is the slow rate-determining step and that the sulfidonium ion [C] hydrolyzes to give the protonated sulfoxide [A] or [B] in the subsequent fast step.

Path b and *c* is the homolysis to form the cation radical intermediate [D]. The several ESR studies of the sulfur-containing aromatic compounds have been done. Schmidt[13] has reported that the concentrated sulfuric acid solutions of some aryl sulfoxides are paramagnetic. Especially well-studied are the sulfuric acid solutions of thianthrene oxide and phenoxathin oxide, *etc.*[14] We could

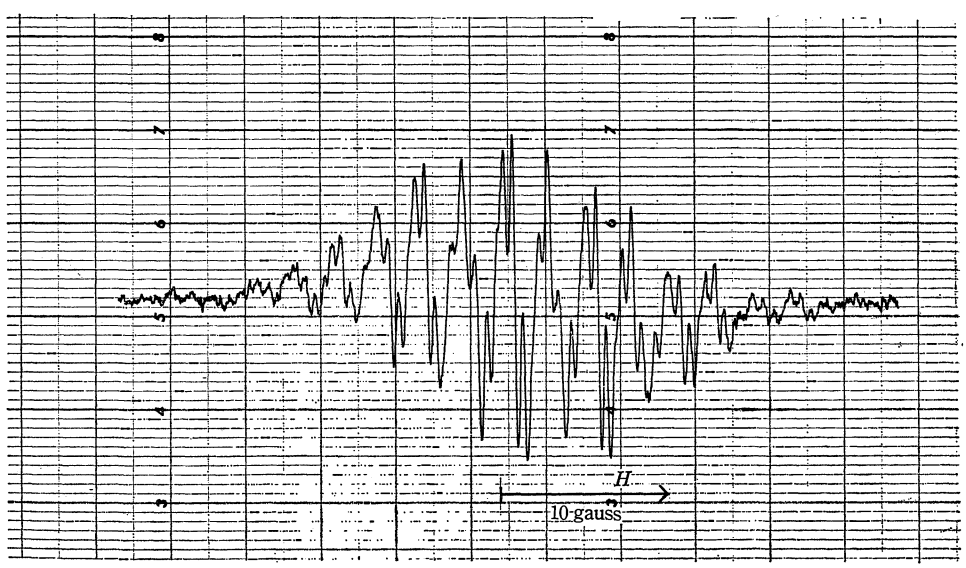

Fig. 2. The ESR spectrum of a 0.2 M solution of *p*, *p'*-ditolyl sulfoxide in 96.3% sulfuric acid.

8) When the H_0 values of Jorgenson and Hartter were used the slope of this correlation was 0.89; M. J. Jorgenson and D. R. Hartter, *J. Am. Chem. Soc.*, **85**, 878 (1963).

9) M. A. Paul and F. A. Long, *Chem. Revs.*, **57**, 935 (1957).

10) R. J. Gillespie and R. C. Passerini, *J. Chem. Soc.*, **1956**, 3850.

11) S. Oae, T. Kitao and Y. Kitaoka, This Bulletin, **38**, 543 (1965).

12) J. H. Krueger, *Inorg. Chem.*, **5**, 132 (1966).

13) U. Schmidt, K. Kabitze and K. Markau, *Angew. Chem.*, **72**, 708 (1960); U. Schmidt, *ibid.*, **76**, 629 (1964).

14) H. J. Shine and L. Piette, *J. Am. Chem. Soc.*, **84**, 4798 (1962) and their successive papers.

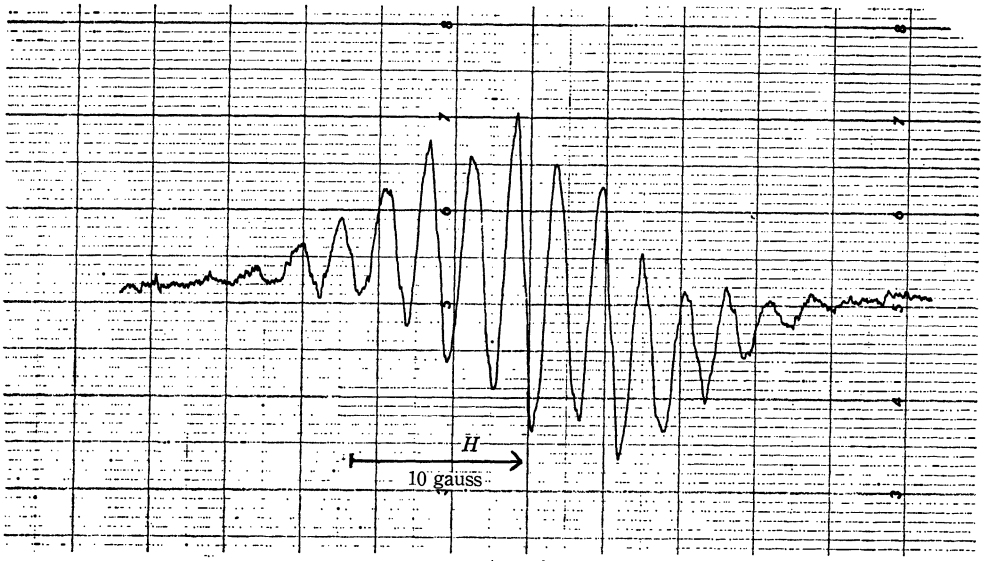

Fig. 3. The overmodulated ESR spectrum of a 0.4 M solution of *p,p'*-ditolyl sulfoxide in 96.3% sulfuric acid.

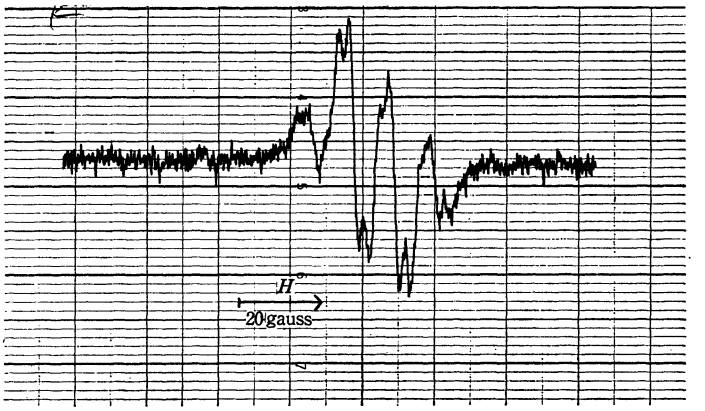

Fig. 4. The ESR spectrum of a 0.1 M solution of *p*-tolyl phenyl sulfoxide in 96.3% sulfuric acid.

detect no noticeable ESR signal from the solution of diphenyl sulfoxide in our previous work.[4] Recently, Shine and co-workers[15] have also reported that no noticeable ESR signal was found from the solution of diphenyl sulfoxide, but noticeable ESR signals were found from 96% sulfuric acid solutions of *p, p'*-substituted diphenyl sulfoxides when *p, p'*-substituents are good electron donating groups such as $-OCH_3$, $-CH_3$ and -OH, and ascribed it to the existence of the positive ion radicals.

We have also repeated the ESR measurements of *p*-tolyl phenyl, *p, p'*-ditolyl and *p, m'*-ditolyl sulfoxides in 96.3% sulfuric acid, and found that the same ESR signal with 15 major lines from the blue solution of *p, p'*-ditolyl sulfoxide as that of Shine. The 15 lines ESR spectra of the solution which are shown in Fig. 2 and Fig. 3 decay in a relatively short time, indicating the short life of this cation radical. The solutions of *p*-tolyl phenyl and *p, m'*-ditolyl sulfoxides gave very weak ESR signals which have no satisfactory hyperfine structure and *g* values of these were 2.0082 and 2.0080, respectively (Fig. 4 and Fig. 5). The one day old solution of *p*-tolyl phenyl sulfoxide gave a simple singlet ESR signal, but we do not know the origin of this signal. However, these ESR results suggest that the path involving the homolytic cleavage to form a incipient cation radical intermediate [D] is a likely possibility.

If the reaction follows the *path a*, the rate would

15) H. J. Shine, M. Rahman, H. Seeger and G.-S. Wu, *J. Org. Chem.*, **32**, 1901 (1967).

16) E. L. Eliel, "Substitution at Saturated Carbon Atoms" in "Steric Effects in Organic Chemistry," ed. by M. S. Newman, John Wiley and Sons, N. Y. (1965), p. 88.

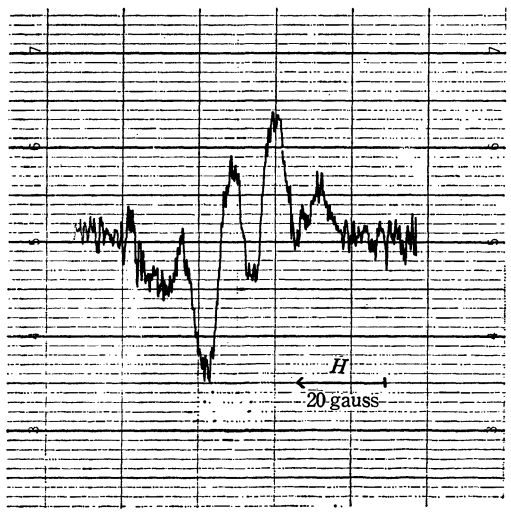

Fig. 5. The ESR spectrum of 0.15 M solution of *p*, *m'*-ditolyl sulfoxide in 96.3% sulfuric acid.

be markedly effected by polar substituents like the SN_1 type reactions of benzhydryl compounds,[16] on the other hand, the effect of polar substituents would be very small when the reaction proceeds through the path of homolytic cleavage. The rates of both oxygen exchange and racemization of several substituted diaryl sulfoxides were measured and the results are tabulated in Table 3.

TABLE 3. RATE CONSTANTS OF ^{18}O-EXCHANGE AND RACEMIZATION OF R_1-⟨⟩-SO-R_2

Run No.	Sulfoxide[a] R_1	R_2	(sec^{-1}) $k_{ex}\times10^4$	$k_{rac}\times10^4$
10	H	*p*-CH_3-C_6H_4	3.22±0.25	3.32±0.20
11	H	*p*-Cl-C_6H_4	1.52±0.03	
12	H	C_6H_5	1.11±0.03	
13	CH_3	*p*-Cl-C_6H_4		2.77±0.33
14	CH_3	*m*-CH_3-C_6H_4		2.53±0.32
15	CH_3	C_6H_5		2.38±0.10
16	CH_3	*p*-NH_2-C_6H_4		1.62±0.10
17	CH_3	Mesityl		0.268±0.013
18	CH_3	*o*-Cl-C_6H_4		0.236±0.013

a) Sulfoxide=0.1 mol/*l*
Run No. 10—12; in 95.5% sulfuric acid at 5°C.
Run No. 13—18; in 96.7% sulfuric acid at 0°C.

Inspection of the kinetic data reveals clearly that the polar effect of substituents on the rates of both oxygen exchange and racemization is very small in comparison with that of the typical SN_1 type reactions. For example, the substitution of *p*-methyl group accelerates the rate of oxygen exchange by only less than two fold while the electron-withdrowing *p*-chloro group also gave a small acceleration. These tendencies are shown equally in the racemization reactions. These rather small polar effects seem to favor the homolytic cleavage for the reaction.

The rates of racemization of *p*-tolyl *o*-chlorophenyl sulfoxide and *p*-tolyl mesityl sulfoxide were found to be about ten fold slower than that of *p*-tolyl phenyl sulfoxide. The marked rate retardation by ortho substituents is perhaps due to the steric hindrance of protonation to form the corresponding diprotonated intermediates.

Reaction with Dilute Sulfuric Acid at Higher Temperature. Although our earlier paper reported that the oxygen exchange was almost nil in a sulfuric acid of less than 85% concentration at around 0°C, we have found that diaryl sulfoxides racemize readily in a sulfuric acid of less than 85% concentration when the reaction was carried out at a considerably higher temperature. For example, *p*-tolyl phenyl sulfoxide was found to be racemized in 82% sulfuric acid at 40—50°C. Both the energy (ΔE=21.6 kcal/mol) and entropy (ΔS=−7.5 eu) of activation of this reaction were quite different from those of the lower temperature reaction. Apparently, the mechanism of this reaction is different from that at the lower temperature and similar to those in polychloroacetic acid[17] and phosphoric acid[18] in which the reaction is presumed to depend on pK_a of the medium used and not on the Hammett acidity function. Detailed discussion on these reactions will be the subject in our forthcoming paper of this series.

Experimental

Materials. *^{18}O-Labeled Diaryl Sulfoxides* were prepared by the oxidation of the corresponding sulfides with bromine complex of pyridine and ^{18}O-enriched water (1.63 atom% ^{18}O) in acetic acid by the same procedure as described in our previous paper.[19] Diphenyl sulfoxide; mp 71°C, 0.85_2 atom%. Phenyl-*p*-tolyl sulfoxide; mp 71—71.2°C, 0.72_0 atom%. Phenyl *p*-Cl-phenyl sulfoxide; mp 45—46°C, 0.95_2 atom%.

Optically Active Aryl p-Tolyl Sulfoxides were prepared from (−)menthyl (−)-*p*-toluenesulfinate according to the method developed by Andersen.[20] *p*-CH_3-C_6H_4-SO-R; (R, mp, $[\alpha]_D$(c); *l*=1 in absolute ethanol). Phenyl, 91.5, +27.2°(3.65). *p*-Cl-phenyl, 80—80.5, +25.9°(2.85). *o*-Cl-phenyl, 89—89.5, −120.7°(1.43). *m*-Tolyl, 63.5—64, +25.1°(3.10). *p*-NH_2-phenyl, 150.5−151, +105.3°(2.21). Mesityl, 107—107.5, −265.0°(2.00).

Kinetic Procedure of the Oxygen Exchange and Racemization Reactions of Diaryl Sulfoxides. In order to compare the rate constants of all the sulfoxides, both oxygen exchange and reacemization reactions were carried out under identical conditions.

17) S. Oae, M. Yokoyama and M. Kise, unpublished work.
18) S. Oae and N. Kunieda, unpublished work.
19) S. Oae, Y. Onishi, S. Kozuka and W. Tagaki, This Bulletin, **39**, 364 (1966).
20) K. K. Andersen, *Tetrahedron Letters*, **1962 (No. 3)**, 93.

An ^{18}O-labeled or an optically active sulfoxide was dissolved in a sulfuric acid, in such a way as to maintain the concentration of the sulfoxide just about 0.1 mol/*l*, at a preset temperature (0±0.06, 5±0.08 or 10±0.08°C). An aliquot portion (5.0 m*l*) of the solution was taken up from time to time for 5—7 times and was quenched with ice water. The precipitate formed was extracted with carbon tetrachloride, and the carbon tetrachloride solution was washed with water, 10% aqueous solution of sodium carbonate and water, respectively, and dried over anhydrous sodium sulfate. Finally, carbon tetrachloride was distilled *in vacuo* and then the sulfoxide recovered was subjected to the ^{18}O-analysis or the optically active measurement. The mass-spectrometric analysis was carried out with the carbon dioxide gas and the atom% ^{18}O was calculated from the mass peak heights 44 and 46 according to the following equation.

$$\text{Atom\% } ^{18}O = \frac{\text{Peak 46/Peak 44}}{2 + \text{Peak 46/Peak 44}}$$

The rate constants of the oxygen exchange and racemization were calculated from the following equations. For oxygen exchange; $\log \alpha_0 - \alpha/\alpha_t - \alpha = kt/2.303$, where α_0 and α_t are the atom% ^{18}O at times 0 and t, respectively, and α is the atom% ^{18}O of natural CO_2, and for racemization; $\log \beta_0/\beta = kt/2.303$, where β_0 and β are the rotatory powers at times 0 and t, respectively.

Typical Runs of Kinetics.

Polarimetric Run.

No. 2. *p*-Tolyl phenyl sulfoxide; Sulfoxide=0.1 M in 95.5% H_2SO_4 at 5°C.

Time (min)	0	5.2	10.2	15.3	25.2	30.2
$[\alpha]_D$	21.04°	18.80°	17.00°	15.50°	13.83°	12.10°

$k_1 = 3.32 \pm 0.20 \times 10^{-4}$ sec^{-1}

No. 18. *o*-Chlorophenyl *p*-tolyl sulfoxide; Sulfoxide=0.1 M in 96.7% H_2SO_4 at 0°C.

Time (min)	0	10.3	40.2	60.4	80.2	110.3
$[\alpha]_D$	−113.6°	−111.9°	−107.2°	−103.4°	−102.1°	−96.5°

$k_1 = 2.36 \pm 0.13 \times 10^{-5}$ sec^{-1}

Exchange Run

No. 1. *p*-Tolyl phenyl sulfoxide; Sulfoxide=0.1 M in 95.5% H_2SO_4 at 5°C.

Time (min)	0	5.2	10.4	15.3	20.2	25.2	35.2
α_t (atom%)	0.65_4	0.61_0	0.57_1	0.52_7	0.51_5	0.50_6	0.46_3

$k_1 = 3.22 \pm 0.25 \times 10^{-4}$ sec^{-1}

No. 12. Diphenyl sulfoxide; Sulfoxide=0.1 M in 95.5% HS_2O_4 at 5°C.

Time (min)	0	10.2	20.2	30.2	50.3
α_t (atom%)	0.84_3	0.80_8	0.76_1	0.74_8	0.65_7

$k_1 = 1.11 \pm 0.03 \times 10^{-4}$ sec^{-1}

($\alpha = 0.20_7$ atom%)

ESR Spectra. The ESR spectra of 96.3% sulfuric acid solutions of the sulfoxides were measured with JES-3BSX type spectrometer of Japan Electron Optics Lab. using a capillary sample cell of aqueous type (0.75 mmϕ) with 100 Kc field modulations at room temperature.

BULLETIN OF THE CHEMICAL SOCIETY OF JAPAN VOL. 41 702—707 (1968)

Syntheses and Reactions of Nitrogen- and Sulfur-Analogs of 2-Piperazinone[1]

Kuniyoshi MASUZAWA

Kyorin Pharmaceutical Co., Ltd., Ukima, Kita-ku, Tokyo

and Mitsuo MASAKI and Masaki OHTA

Laboratory of Organic Chemistry, Tokyo Institute of Technology, Ookayama, Meguro-ku, Tokyo

(Received September 25, 1967)

2-Piperazinone oxime, 2-piperazinoneimine, and 2-piperazinethione were synthesized. The reaction mixture of ethylenediamine and glycolonitrile was treated with an excess amount of hydroxylamine in methanol to give 2-piperazinone oxime in a 53% yield. 2-Piperazinone oxime was easily reduced to 2-piperazinoneimine, which was then treated with hydrogen sulfide to yield 2-piperazinethione. Some reactions of these compounds are described.

Many methods of synthesizing 2-piperazinones have been developed since the derivatives were found to possess some pharmacological activities.[2] However, no variation in the exocyclic oxo-group has ever been reported.[3] It thus appeared of interest to obtain nitrogen- or sulfur-analogs of 2-piperazinone.

The present paper will describe the syntheses of 2-piperazinone oxime (VIIIa), 2-piperazinoneimine (IIIb), and 2-piperazinethione (XV), and their reactivities.

Strong *et al.* reported the synthesis of 2-piperazinone by the reaction of ethylenediamine (I) with formaldehyde and sodium cyanide in an aqueous solution.[2a] This reaction was postulated to involve, as an intermediate, *N*-(2-aminoethyl)glycinonitrile (IIIa) or cyclic amidine (IIIb), which would be hydrolyzed to afford 2-piperazinone. Thus, the isolation of the intermediate (III) might be possible, provided the reaction of I with glycolonitrile (II) was carried out in a non-aqueous medium. When I was treated with an equimolar amount of II in methanol at room temperature for 2 days, a yellow, oily material was obtained. The infrared absorption spectrum of the oil showed a medium absorption band at 1660 cm^{-1} characteristic of the carbon-nitrogen double bond, while a control measurement of infrared absorption spectrum showed that the initial mixture of I and II exhibited no band at 1660—1630 cm^{-1} in the region for the carbon-nitrogen double bond. The oil was treated with sulfuric acid in methanol to yield pale yellow crystals with a melting point of 205—208°C (decomp.). The elementary analysis of the product indicated the empirical formula, $C_4H_9N_3 \cdot H_2SO_4$, corresponding to the sulfate (IV) of III. A thin-layer chromatogram (TLC) of IV showed two spots. The R_f value (0.31) of one spot was found to be identical with that of an authentic 2-piperazinoneimine sulfate prepared by another route, described below. From these observations as well as the following reactivities, it seemed reasonable to assume that the above products (III) consisted of IIIb and another substance (IIIa).[4] When II was treated with an excess amount of I in methanol at 55—60°C, *N, N'*-bis-cyanomethylethylenediamine (V) was obtained as the sole isolated product. This was characterized by means of its infrared absorption spectrum and by conversion into a dibenzoyl derivative (VI) (Chart I).

In order to examine the reactivities of III, the reaction of III with hydroxylamine was attempted. When the reaction mixture of I and II (III) was treated with an excess amount of hydroxylamine in methanol, a slightly exothermic reaction occurred with an evolution of ammonia, and colorless crystals with a melting point of 171—173°C were obtained. The product gave an intense purple color with an aqueous solution of

1) Presented in part at 19th Annual Meeting of the Chemical Society of Japan, Yokohama, March, 1966.

2) a) J. S. Strong, W. E. Craigant and V. T. Elkind (of Rohm and Hass Co.), U. S. Pat. 2649450 (Aug. 18, 1953). b) S. R. Aspinall, *J. Am. Chem. Soc.*, **62**, 1202 (1940). c) R. L. Hodgson, I. R. C. Bick and D. J. Cram, *ibid.*, **76**, 1137 (1954). d) A. P. Phillips (to Burroughs Wellcome & Co. (U. S. A.), Inc.), U. S. Pat. 2958693 (Nov. 1, 1960). e) M. Masaki and M. Ohta, This Bulletin, **36**, 922 (1963). f) O. E. Fancker, S. Hayao and W. G. Strycker, *J. Med. Chem.*, **7**, 154 (1964). g) K. Masuzawa, M. Masaki and M. Ohta, *Chem. Pharm. Bull. Japan*, **14**, 194 (1966).

3) Only one British Patent (Rohm & Hass Co.; 875135 (Aug. 16, 1961)) has referred to 4-substituted 2-piperazinethiones; unfortunately, neither the synthetic method nor their properties have been recorded.

4) The other substance, with a R_f value of 0.58, might be IIIa, but it was not further investigated.

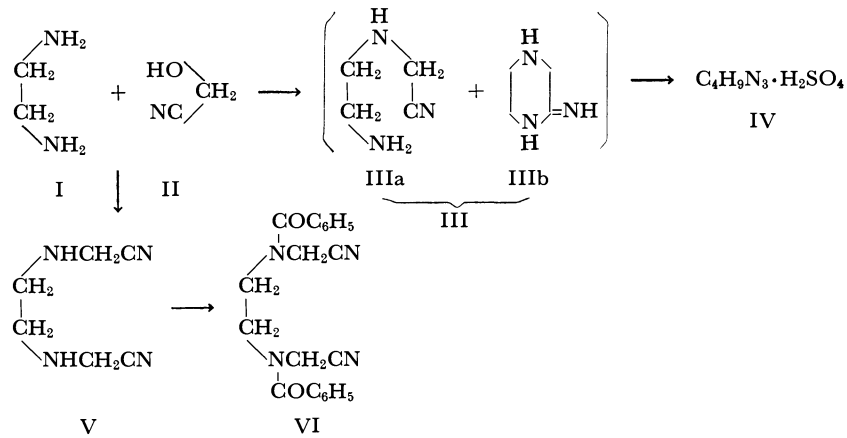

Chart I

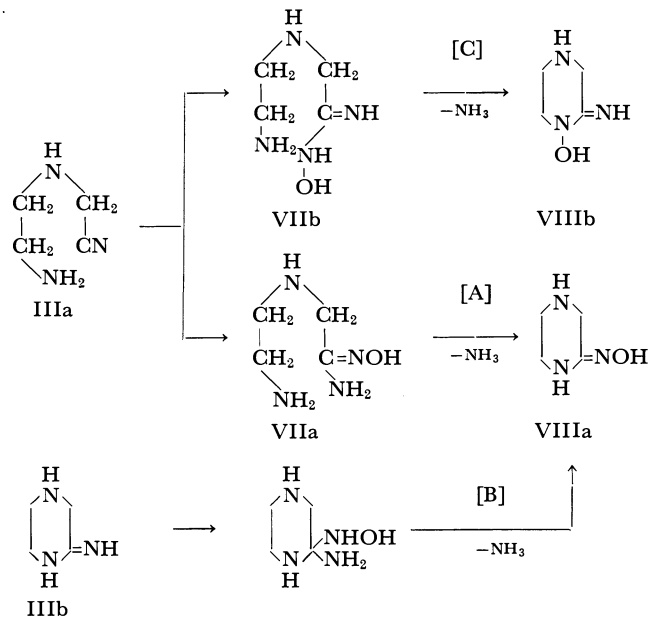

Chart II

ferric chloride and exhibited a strong infrared absorption band at 1660 cm^{-1}, which might be ascribed to the carbon–nitrogen double bond of amidoxime.[5] This observation and the elementary analysis indicate the structure of 2-piperazinone oxime (VIIIa) or 1-hydroxy-2-piperazinoneimine (VIIIb) for the product. Compound VIIIa would be formed from the reaction of either IIIa or IIIb with hydroxylamine (Course A or B), while VIIIb might be derived only from the reaction of IIIa and hydroxylamine (Course C) (Chart II).

However, only the structure VIIIa was supported by the following reactions. The product (VIIIa) was treated with 3N hydrochloric acid and methanol to afford methyl *N*-(2-aminoethyl)glycinate dihydrochloride (IX), which was isolated in a form combined with water. On the treatment of VIIIa with benzoyl chloride, a dibenzoyl derivative (X) was obtained, while treatment with tosyl chloride gave a tritosyl derivative (XI). The infrared absorption spectrum of the dibenzoyl derivative showed strong absorption bands in the ester region. The amidoximes have been known to react with nitrous acid or alkyl nitrite, yielding the corresponding amide.[6] The reaction of VIII with nitrous acid or amyl nitrite was next attempted, since it was expected to yield 4-nitroso-2-piperazinone (XII). All attempted reactions, however,

5) C. L. Bell, C. N. V. Nambury and L. Bauer, *J. Org. Chem.*, **29**, 2873 (1964).

6) T. Wieland and D. Grimm, *Chem. Ber.*, **96**, 275 (1963).

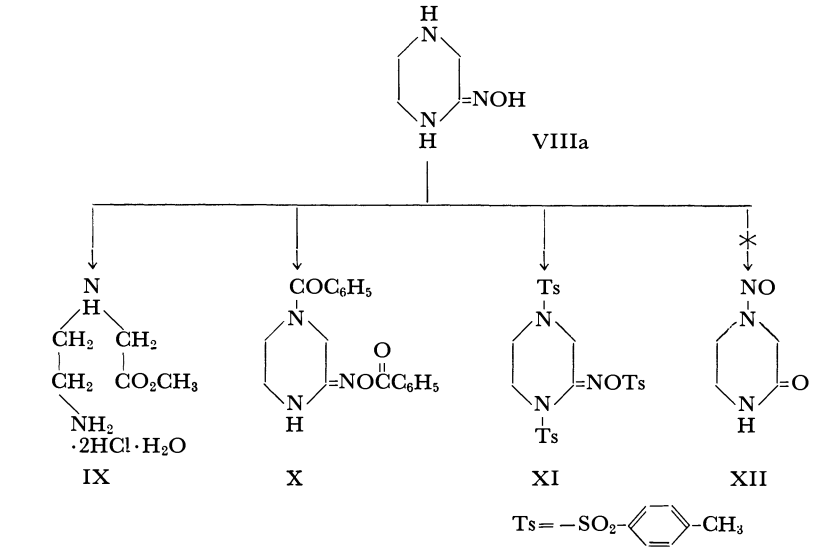

Chart III

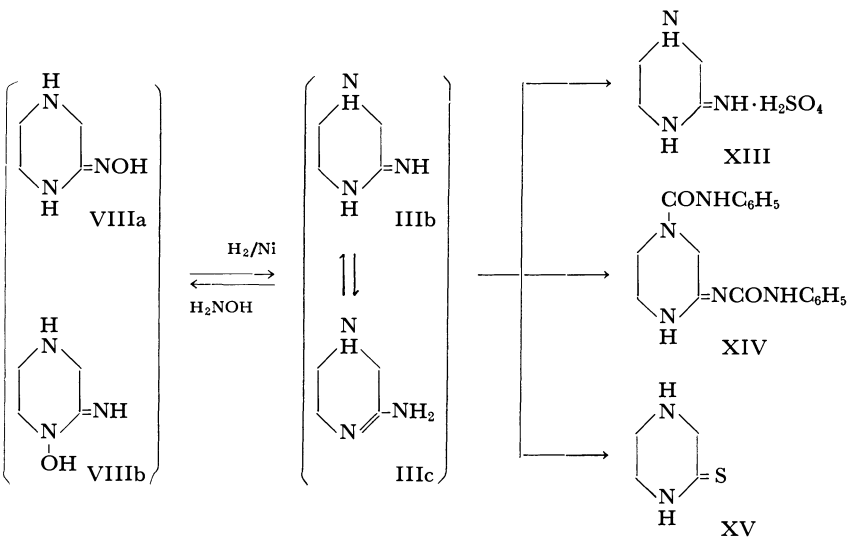

Chart IV

resulted only in the formation of a viscous oily substance, which gave a positive Lieberman test but which was unidentified, while the authentic XII was obtained in the form of crystals by the treatment of 2-piperazinone with amyl nitrite in *n*-butanol (Chart III).

Barber *et al.* have reported that the catalytic reduction of amidoxime gave the corresponding amidine.[7] The amidoxime (VIIIa) was hydrogenated at room temperature in the presence of Raney-nickel to give, as expected, 2-piperazinone-imine (IIIb) which was characterized by means of its infrared absorption spectrum and by conversion into the crystalline sulfate (XIII) or the crystalline phenylureido derivative (XIV). Compound XIII had a melting point of 212°C (decomp.) and gave a spot (R_f 0.31) on thin-layer chromatogram. When the reduction product was again treated with hydroxylamine in methanol at room temperature, ammonia was evolved and the amidoxime (VIII) was obtained in a 46% yield.[8] The amidoxime produced was identified by a comparison of its infrared absorption spectrum and by a mixed-melting-point determination with the original amidoxime (VIIIa). This fact excludes the alternative structure (VIIIb) for the amidoxime

7) H. J. Barber and A. D. H. Self (of May & Baker, Ltd.), U. S. Pat. 2375611 (May 8, 1945).

8) The yield was calculated from the first material (VIIIa) used for reduction.

(VIIIa), because an easy transformation between the amidoxime (VIIIb) and the amidine (IIIb) would be impracticable under the above mild conditions.

When the cyclic amidine (IIIb) was treated with hydrogen sulfide, 2-piperazinethione (XV) was obtained in a 20% yield. The structure of XV was confirmed by its infrared absorption spectrum and by elementary analysis. In an attempt to prepare XV by another route, 2-piperazinone was directly treated with phosphorus pentasulfide in benzene or toluene, but no definite product could be obtained (Chart IV).

In a further investigation of the reactivities of III, the methanolic solution of III was treated with *N*-phenylhydroxylamine at 60°C; a small quantity of yellow needles (XVI) was thus obtained. The reaction of IIIb, prepared by the reduction of VIIIa, with *N*-phenylhydroxylamine also gave XVI. The elementary analysis of the product (XVI) showed the empirical formula $C_{10}H_9N_3$, which may suggest that XVI is 2-anilinopyrazine. Thus, 2-anilinopyrazine was synthesized by the reaction of 2-chloropyrazine with an excess amount of aniline.

However, the chemical properties of XVI apparently differed from those of 2-anilinopyrazine and the structure of XVI remains unidentified.

Experimental[9]

Ethylenediamine (I). Commerical anhydrous ethylenediamine was dried over metallic sodium. The dried ethylenediamine was then filtered and distilled; bp 116—117°C.

Glycolonitrile (II) was prepared by the published procedure[10] and had a bp of 97—99°C/15 mmHg (lit.[10] bp 99—100°C/17 mmHg).

Reaction of I with II. a) A solution of II (2.0 g) in methanol (3 m*l*) was added, drop by drop, to a solution of I (2.1 g) in methanol (3 m*l*), and the mixture was allowed to stand at room temperature for 2 days. After the solvent and the starting materials had been removed under reduced pressure from the reaction mixture, an oily product (III) was obtained. Its infrared spectrum showed an absorption band at 1660 cm^{-1} (m). The oily product (III) was converted to a crystalline solid by adding a solution of sulfuric acid in methanol. The solid was collected to give 6.8 g (98.5% yield) of brown crystals, which, after recrystallization from aqueous methanol, afforded a mixture of 2-piperazinoneimine sulfate (IIIb) and an unidentified compound as pale yellow crystals, mp 205—208°C (decomp.). TLC[11] R_f=0.58 and 0.31.

Found: C, 24.03; H, 5.82; N, 22.12%.

b) A mixture of I (12.0 g) and II (5.7 g) in methanol (30 m*l*) was warmed, with stirring, at 55—60°C for 5 hr. The mixture was then concentrated under reduced pressure to give a syrup which was distilled under reduced pressure to yield *N, N'*-bis-cyanomethylethylenediamine (V) as a viscous liquid (2.73 g, 27.3%), bp 133—135°C/1 mmHg. IR (liquid): 3300 (–NH–) and 2200 cm^{-1} (–CN).

N, N'- Bis-benzoyl - *N, N'*- bis - cyanomethylethylenediamine (VI), mp 142—144°C (from ethanol), was also prepared.

IR (KBr disk): 2240 (–CN) and 1665 cm^{-1} (–CONH–).

Found: C, 68.93; H, 5.37; N, 15.96%. Calcd for $C_{20}H_{18}N_4O_2$: C, 69.35; H, 5.24; N, 16.18%.

2-Piperazinone Oxime (VIIIa). A solution of hydroxylamine [from the hydrochloride (10.4 g) and sodium (3.4 g) in methanol (160 m*l*)] was stirred into a solution of III (corresponding to 0.1 mol) in methanol (20 m*l*) at room temperature. The mixture was then kept at room temperature for 2 days, by which time the evolution of ammonia had ceased. The solution was concentrated under reduced pressure to yield a brown syrup. The syrup solidified spontaneously upon standing. The product was recrystallized from isopropyl alcohol to give 6.1 g (53%) of colorless plates, mp 171—173°C. The crystals are very soluble in water and give an intense purple color with an aqueous ferric chloride solution. IR (KBr disk): 3380 and 3320 (–NH–), 3180—2800 (broad band) and 1660 cm^{-1} (>C=N–).

The NMR spectrum exhibited a multiplet in the τ 6.7—7.1 region (4H) and a singlet at τ 6.6 (2H).[12]

Found: C, 41.97; H, 8.11; N, 36.74%. Calcd for $C_4H_9N_3O$: C, 41.72; H, 7.88; N, 36.50%.

Methyl *N*-(2-Aminoethyl)glycinate Dihydrochloride (IX). A solution of VIIIa (0.5 g) in 3 N hydrochloric acid (14.5 m*l*) was heated at 80°C for 3 hr, and the resultant solution was concentrated to dryness under reduced pressure. On adding methanol (4 m*l*) to the residue, 0.8 g (82.8%) of colorless needles was obtained. A portion of the product was recrystallized from methanol and analyzed; mp 188—190°C (decomp.).[13]

IR (KBr disk): 3480(OH), 3000—2500 (broad band) and 1720, 1250 cm^{-1} (–$COOCH_3$).

Found: C, 27.09; H, 7.37; N, 13.10%. Calcd for $C_5H_{12}N_2O_2 \cdot 2HCl \cdot H_2O$: C, 26.92; H, 7.23; N, 12.55%.

Dibenzoyl Derivative (X) of VIIIa. This derivative (mp 190—191.5°C (from ethanol)) was obtained as colorless needles.

Found: C, 66.86: H, 5.30; N, 13.00%. Calcd for $C_{18}H_{17}N_3O_3$: C, 67.17; H, 5.42; N, 13.16%.

IR (KBr disk): 3320(–NH–), 1725 and 1250 ($OCOC_6H_5$), 1660—1620 cm^{-1} (=NCO– and –CN).

1, 4-*O*-Tritosyl-2-piperazinone Oxime (XI). A solution of tosyl chloride (3.8 g) in dioxane (30 m*l*) and a solution of sodium hydroxide (0.8 g) in water

9) All the melting points are uncorrected. The infrared spectra of the samples were measured on a Hitachi spectrophotometer, Model EPI S II.

10) D. T. Mowry, *J. Am. Chem. Soc.*, **66**, 371 (1944).

11) TLC: Solvent system: *n*-Butanol(4) - Acetic acid(2) - Water (1). Adsorbent: Silica gel (Wakogel 10). Sample: 2.5—5 μg (0.01 m*l* applied to plates). Detection: A solution of 1 g of *p*-dimethylaminobenzaldehyde in 100 m*l* of a mixture of 35% hydrochloric acid (50 m*l*) and ethanol (50 m*l*).

12) The NMR spectrum was kindly determined by the Japan Electron Optics Lab. Co. on its Model G-60 at 60 Mc in a deuterium oxide solution, sodium dimethylsila pentasulfonate being used as the internal standard.

13) T. S. Moore, M. Boyle and V. M. Thorn, *J. Chem. Soc.*, **1929**, 51.

(10 ml) were alternatively stirred into a solution of VIIIa (1.2 g) in water (12 ml). The temperature of the mixture was then raised from 15°C to 30°C. After the addition had been completed, the mixture was stirred for several more hours, and then the pale yellow solution was allowed to stand overnight, thus yielding 0.7 g of XI as amorphous crystals, mp 206—209°C. The analytical sample was recrystallized from ethanol to give colorless plates, mp 210—211°C. The infrared absorption spectrum of XI showed no absorption band in the regions for both the amino group and the hydroxyl group.

Found: C, 51.74; H, 4.53; N, 6.90%. Calcd for $C_{25}H_{27}N_3O_7S_3$: C, 51.97; H, 4.71; N, 7.27%.

4-Nitroso-2-piperazinone (XII). A mixture of 2-piperazinone (3 g) and amyl nitrite (4 g) in *n*-butanol (30 ml) was heated on a water bath for 2 hr, and the resultant solution was allowed to stand overnight at room temperature. The precipitate (XII) was then collected and recrystallized from ethanol to give yellow plates, mp 124—125°C. The yield was 2.7 g (70%).

Found: N, 32.77%. Calcd for $C_4H_7N_3O_2$: N, 32.55%.

2-Piperazinoneimine Sulfate (XIII). A solution of VIIIa (1.5 g) in ethanol (70 ml) was shaken with Raney-nickel (1.0 g) at a pressure of 100 kg/cm² of hydrogen at room temperature for 1 hr. The catalyst was then removed by filtration, and sulfuric acid (1.0 g) in ethanol (20 ml) was added to the filtrate in order to precipitate a crystalline substance, which, after recrystallization from methanol-water, afforded the sulfate of IIIb as colorless needles, mp 212°C (decomp.). The yield was 1.9 g (76.0%).

IR (KBr disk): 3300—2500 (broad), 1660 (>C=N–) and 1120 cm^{-1} (sulfate).

Found: C, 24.08; H, 5.76; N, 21.00%. Calcd for $C_4H_9N_3 \cdot H_2SO_4$: C, 24.37; H, 5.63; N, 21.32%.

2-(*N*-Phenylcarbamoyl)imino-4-phenylcarbamoylpiperazine (XIV). The ethanolic solution obtained by the reduction of VIIIa (0.38 g) was evaporated to give IIIb (0.3 g) as an oil, which was used directly in the following reaction. The crude IIIb (0.3 g) and phenyl isocyanate (0.95 g) in chloroform (20 ml) were heated under refluxing for 4 hr. The resultant clear solution was passed through an activated alumina column. The column was then washed with ethanol (50 ml). The evaporation of the ethanolic eluate yielded a brown-yellow solid, which was recrystallized from *n*-butanol-ligroin to give 0.3 g (30%) of XIV as colorless needles, mp 172—173°C.

IR (KBr disk): 3370—3270 (–NH–, broad) and 1700, 1660—1640 cm^{-1} (–NHCO–).

Found: C, 64.18; H, 5.68; N, 21.23%. Calcd for $C_{18}H_{19}N_5O_2$: C, 64.08; H, 5.68; N, 20.76%.

Reaction of IIIb with Hydroxylamine. A solution of hydroxylamine [from the hydrochloride (0.42 g) and sodium (0.13 g) in methanol (8 ml)] was added to a solution of IIIb (0.4 g prepared from VIIIa) in ethanol (40 ml). The mixture was kept at 40°C for 5 hr, by which time the evolution of ammonia had ceased, and then warmed at 60°C for 1 hr. The solution was concentrated under reduced pressure to give a yellow solid. The product was recrystallized from isopropyl alcohol to yield 0.2 g of 2-piperazinone oxime (VIIIa) as colorless plates, mp 171—172°C, the melting point showed no depression in a mixing test with the VIIIa synthesized by the reaction of III (obtained by the reaction of I with II) with hydroxylamine.

2-Piperazinethione (XV). A solution of IIIb (1.95 g, prepared from VIIIa) in ethanol (125 ml) was saturated with hydrogen sulfide under cooling. The resultant yellow solution was allowed to stand at room temperature overnight, and then heated at 80°C for 4 hr. On cooling, the sulfur which separated from the solution was removed by filtration; the filtrate was concentrated under reduced pressure to give a viscous liquid. The oil solidified spontaneously upon standing. The product was recrystallized from isopropyl alcohol to give colorless prisms (0.45 g, 20%), mp 155—156°C (decomp.).

IR (KBr disk): 3200, 3150 and 3050(–NH) and 1585 cm^{-1} (–NHCS–).

Found: C, 41.64; H, 6.87; N, 24.32%. Calcd for $C_4H_8N_2S$: C, 41.37; H, 6.94; N, 24.13%.

Reaction of III (Obtained from I and II) with *N*-Phenylhydroxamine. A solution of *N*-phenylhydroxylamine[14] (1.8 g) in methanol (10 ml) was added, drop by drop, to a solution of III (corresponding to 0.0016 mol) in methanol (4 ml) at room temperature. When the mixture was warmed at 60°C with stirring, a yellow solid soon began to separate. After 5 hr, the mixture was concentrated under reduced pressure to yield an oily brown product. This oily product slowly solidified. The solid was collected, washed with isopropyl alcohol, and recrystallized from a small amount of benzene to yield yellow prisms (0.4 g; mp 265°C (decomp.)). The product (XVI) was soluble in dilute hydrochloric acid; it showed ultraviolet absorptions at $\lambda_{max}^{dioxane}$ 235 mμ (ε=13000) and 293 mμ (ε=10700).

IR (KBr disk): 3400, 1660, 1630, 1240 and 1250 cm^{-1}.

Found: C, 70.01; H, 5.24; N, 24.80%. Calcd for $C_{10}H_9N_3$: C, 70.15; H, 5.30; N, 24.55%.

Reaction of IIIb (Obtained from VIIIa) with *N*-Phenylhydroxylamine. A solution of *N*-phenylhydroxylamine (1.0 g) in ethanol (10 ml) was added to a solution of IIIb (0.92 g) in ethanol (60 ml), and the mixture was heated at 80°C for 5 hr, by which time the evolution of ammonia had ceased. Removal of the solvent yielded the product as a syrup, which was dissolved in hot isopropyl alcohol (4.5 ml); the solution was then filtered. The filtrate was allowed to stand in a refrigerator. After 2 days, the crystals were collected by filtration and washed with a small portion of benzene to give 0.62 g of XVI as yellow prisms, mp 265—266.5°C (unchanged by admixture with the XVI obtained by the reaction of III with *N*-phenylhydroxylamine).

2-Anilinopyrazine. A mixture of 2-chloropyrazine[15] (1.0 g) and aniline (4.0 g) was heated, with stirring, at 160°C for 7 hr. After the mixture had been kept overnight at room temperature, the aniline hydrochloride which had separated was filtrated off. Benzene (30 ml) was added to the filtrate. The benzene layer was washed twice with water, dried over anhydrous sodium sulfate, and evaporated under reduced pressure in order to recover the original aniline and benzene.

14) O. Kamm, "Organic Syntheses," Coll. Vol. I, 2nd ed., p. 445 (1941).

15) G. W. H. Cheeseman, *J. Chem. Soc.*, **1960**, 242.

When carbon tetrachloride was added to the residue small needles slowly crystallized out. The product was collected (0.5 g, 33.4%) and recrystallized from ethanol-isopropyl ether to give yellowish plates, mp 132—133°C; the crystal showed ultraviolet absorptions at λ_{max}^{EtOH} 275 mμ (ε=23000) and 345 mμ (ε=6000).

IR (KBr disk): 3270 and 3200 (-NH-), 1630 and 1520 cm^{-1}.

Found: C, 69.85; H, 5.09; N, 24.38%. Calcd for $C_{10}H_9N_3$: C, 70.15; H, 5.30; N, 24.55%.

BULLETIN OF THE CHEMICAL SOCIETY OF JAPAN VOL. 41 707—712 (1968)

Synthesis and Reactions of Functional Polymers. XXXIV. Low Polymerization of Ethylene Oxide with Sodium *N*, *N*-Dimethyldithiocarbamate in Dipolar Aprotic Solvents*[1]

Takeshi NAKAI and Makoto OKAWARA

Research Laboratory of Resources Utilization, Tokyo Institute of Technology, Ookayama, Meguro-ku, Tokyo

(Received October 9, 1967)

The low polymerization of ethylene oxide with sodium dimethyldithiocarbamate in a homogeneous system was studied. This reaction was verified as proceeding through a step-by-step addition mechanism, due to the enhanced nucleophilicity of the dithiocarbamate anion in dipolar aprotic solvents. The solvent effects and the catalyses of various dithiocarbamate salts were also examined. Epichlorohydrin was reacted with this salt in dimethylformamide to afford a polymer with a dithiocarbamate moiety through both ring-opening and substitution processes.

In previous papers[1] we have reported that polymers containing a dithiocarbamate moiety are effective as photosensitive resins. We prepared these polymers exclusively by polymer reactions since no monomer with a moiety has been readily available and since the radical polymerization of the monomers did not produce polymers of a high molecular weight. For example, *S*-vinyl-*N*, *N*-dialkyldithiocarbamates (I) were found to be polymerized with a radical initiator to give polymers of a low molecular weight, a low weight arising from the radical-stabilizing effect of the sulfur atom attached to the vinyl group (the *Q*-value for *N*, *N*-diethyl derivative is 0.45[2]). Thus, attempts have been made to prepare 1-*N*, *N*-dialkylthiocarbamylthio-2, 3-epoxy propane (II) by the reaction of epichlorohydrin (EPCl) with sodium dithiocarbamate and to produce a polymer by the ionic polymerization of the epoxide. As yet, however, we have not succeeded in the preparation of II.

During the course of our work on the reaction of EPCl with sodium dithiocarbamate in various solvents, it was found that epoxides were readily polymerized with sodium dithiocarbamate in dimethylformamide (DMF) at room temperature. This led us to our present study of the catalysis and of the solvent effect on the polymerization of ethylene oxide. It may be noted that this is in direct contrast to the observation that the transient dithiocarbamate anion (III) from triethylamine and carbon disulfide reacts with epoxides at 150°C under pressure, resulting in the formation of the corresponding ethylene trithiocarbonates *via* the episulfides, as is shown below,[3] just as in the well-known reactions of the alkylxanthate anion (⊖SCSOR) with epoxides at room temperature.[4]

*1 Presented at the 15th Annual Meeting of the Society of Polymer Science of Japan, Nagoya, May, 1966. Part XXIII: T. Nakagawa and M. Okawara, *J. Polymer Sci.*, in press.

1) a) M. Okawara, H. Yamashina, K. Ishiyama and E. Imoto, *Kogyo Kagaku Zasshi (J. Chem. Soc. Japan, Ind. Chem. Sect.)*, **66**, 1383 (1963); b) M. Okawara, K. Morishita and E. Imoto, *ibid.*, **69**, 761 (1966); c) M. Okawara, M. Ori, T. Nakai and E. Imoto, *ibid.*, **69**, 766 (1966); d) M. Okawara and T. Nakai, *Bull. Tokyo Inst. Technol.*, **78**, 1 (1967). For photochemical behaviors of various dithiocarbamates, also see a) M. Okawara, T. Nakai, K. Morishita and E. Imoto, *Kogyo Kagaku Zasshi (J. Chem. Soc. Japan, Ind. Chem. Sect.)*, **67**, 2108 (1964); b) M. Okawara, T. Nakai and E. Imoto, *ibid.*, **69**, 973 (1966); c) E. H. Hoffmeister and D. S. Tarbell, *Tetrahedron*, **21**, 35, 2857 (1966).

2) T. Nakai, K. Shioya and M. Okawara, *Makromol. Chem.*, **108**, 95 (1967).

3) J. A. Durden, Jr., H. A. Stranburg, Jr., and W. H. Catlette, *J. Am. Chem. Soc.*, **82**, 3082 (1960).

4) a) C. C. J. Culvenor, W. Davies and K. H. Pausacker, *J. Chem. Soc.*, **1946**, 1050; b) L. Owen *et al.*, *ibid.*, **1960**, 1024, 1030; c) C. G. Overberger and A. Drucker, *J. Org. Chem.*, **29**, 360 (1964).

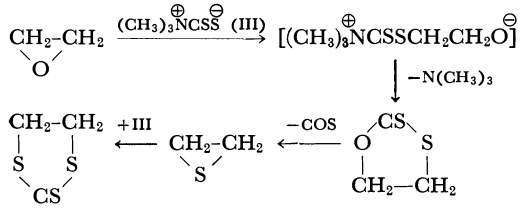

On the other hand, although many earlier studies[5] of base catalyzed polymerization of epoxides have been carried out in heterogeneous systems, little information is available on the polymerization in a homogeneous system. Recently, however, Price and his co-workers[6] have reported the polymerization of epoxides with potassium *t*-buthoxide in dimethyl sulfoxide (DMSO).

This paper will describe how ethylene oxide can be polymerized with sodium dimethyldithiocarbamate in DMF at room temperature by means of a step-by-step addition mechanism.

Results and Discussion

Preliminary Experiments. Initially we attempted to react 2 mol of dithocarbamate salt with 1 mol of various epoxides in DMF, since we expected that the dithiocarbamate anion would react with epoxides in the same manner as the xanthate does.[4] Contrary to our expectations, however, many viscous materials were obtained, accompanied by a violent generation of heat, while the expected ethylene trithiocarbonates were not obtained at all. The presence of a non-volatile residue, after a portion of the liquid phase had been heated on a steam bath, was taken to be a positive criterion of polymerization. Thus, ethylene oxide (EO) and propylene oxide (PO) were reacted with about 5 mol% of sodium dimethyldithiocarbamate hydrate (MDTC) in DMF or in bulk at room temperature, resulting in the formation of viscous polymers of a low molecular weight, as is shown in Table 1. This led us to a detailed study of the polymerization of EO with MDTC.

Effect of MDTC Concentration on the Rate of Polymerization and on the Molecular Weight of the Resulting Polymer. In order to examine the mechanism for the initiation process of this polymerization, EO was polymerized in DMF at 30°C in the presence of various amounts of MDTC. As Fig. 1 shows the time-conversion curves were straight up to 80% of conversion.

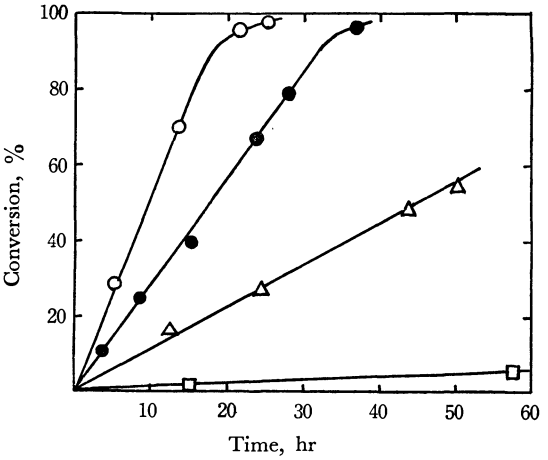

Fig. 1. Time-conversion curves.
EO 10.0 g; DMF 8.0 g; Temp. 30°C
MDTC=1.5 g (○), 0.8 g (●). 0.4 g (△) and 0.8 g (DMF none) (□)

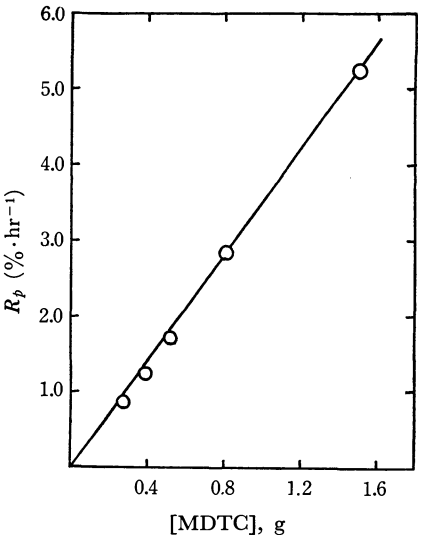

Fig. 2. Relationship between concentrations of MDTC and rates of polymerization.

The dependence of the rate of polymerization (R_p) on the concentration of MDTC is shown in Fig. 2. The relationship between the molecular weight of the resulting polymer and conversion is given in Fig. 3. These experimental results indicate the following facts; (i) the rate of polymerization is proportional to the concentration of MDTC; (ii) the molecular weight of the polymer increases gradually with conversion and (iii) the molecular weight of the polymer at the definite conversion increases with a decrease in the initial concentration of MDTC. These facts lead to the reasonable conclusion that this ring-opening polymerization proceeds through the anionic multistage polymerization mechanism, which is generally

5) For example, see a) L. E. St. Pierre and C. C. Price, *J. Am. Chem. Soc.*, **78**, 3432 (1956); b) G. Gee, W. C. E. Higgins and G. T. Merrall, *J. Chem. Soc.*, **1959**, 1345; c) E. C. Steiner, R. R. Pelletier and R. O. Trucks, *J. Am. Chem. Soc.*, **86**, 4678 (1964).

6) C. C. Price, C. D. Carmelite, R. Yamamoto and Y. Atarashi, International Symposium on Macromolecular Chem., Tokyo-Kyoto, Preprints I, p. 208 (1966).

Table 1. Polymerization of epoxides with MDTC*1

Epoxide, g		MDTC mol%	DMF ml	Product		
				Yield,*2 g	η_{rel} *3	Mol wt*4
EO	15.0	4.9	10	13.5	1.15	456
EO	14.3	3.2	0	4.3	1.11	374
PO	11.0	6.0	7	6.8	6.8	
PO	13.3	5.1	0	2.5		

*1 Temp.: room temperature Reaction time: 55 hr

*2 The product was isolated by the following procedure: the reaction mixture was poured into a large amount of ethyl acetate to form the precipitate, unreacted MDTC, which was then filtered off. The filtrate was distilled up to 80°C under 2 mmHg, giving a viscous residue in the flask, which was weighed.

*3 4% dioxane solution

*4 $[\eta]$ $(ml \cdot g^{-1}) = 0.083\, M^{0.59}$ (Ref. 5b; also see Experimental Section).

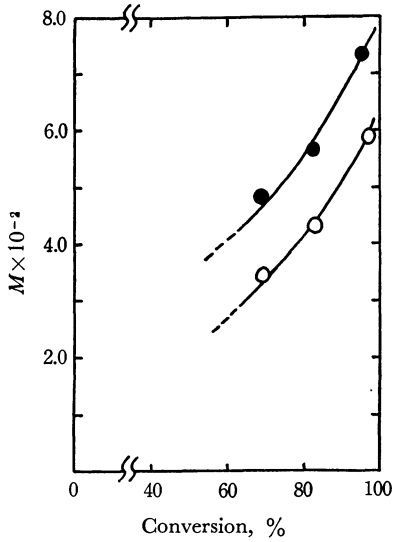

Fig. 3. Relationship between mol. wt. of polymers and conversions.
MDTC=0.8 g (●) and 1.5 g (○)

accepted for the ring-opening polymerization of epoxides with various anionic catalysts.[7] Consequently, the initiation and propagation reactions would be as follows:

$$Me_2NCSS^{\ominus}(Na^{\oplus}) + C_2H_4O \rightarrow$$

$$Me_2NCSSCH_2CH_2O^{\ominus}(Na^{\oplus})$$

$$Me_2NCSS(CH_2CH_2O)_{n-1}CH_2CH_2O^{\ominus}(Na^{\oplus}) \xrightarrow{C_2H_4O}$$

$$Me_2NCSS(CH_2CH_2O)_nCH_2CH_2O^{\ominus}(Na^{\oplus})$$

The IR spectrum (Fig. 4) of the resulting polymer shows absorptions of a double bond and of carbonyl groups, the formation of which might arise from the chain transfer or side reactions. The decolorization of bromine in carbon tetrachloride with the polymer also indicates the presence of the double bond. The treatment of the polymer with 2, 4-dinitrophenylhydrazine did not give the hydrazone, indicating that the polymer does not contain any ketone or aldehyde group. No further attempts were made to examine the chain-transfer reaction or to analyze the end groups.

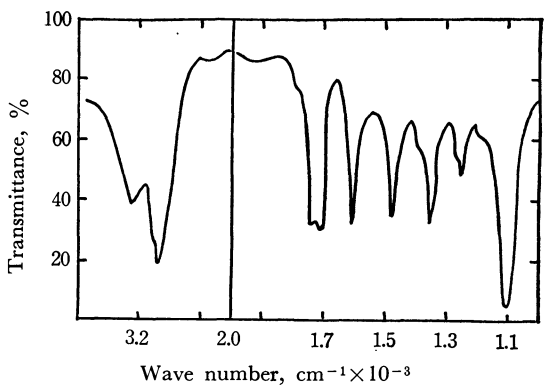

Fig. 4. IR spectrum of poly(EO) (liquid film).

According to Kagiya's equation[8] for successive high polymerizations, we tentatively calculated the catalytic activity coefficient (α), which denotes the number of active sites of MDTC:

$$\alpha = \frac{m \cdot M_p}{M \cdot C}$$

where m and M are molecular weights of the monomer and of the resulting polymer respectively, where M_p is the polymerized monomer (mol), and where C is the amount of MDTC (mol).

Table 2 indicates the α-values of MDTC thus obtained. It is surprising that the values ranged

7) For example, see a) S. Perry and H. Hibbert, *Can. J. Research*, **8**, 102 (1933); *J. Am. Chem. Soc.*, **62**, 2599 (1940); b) S. D. Holland, Brit. Pat., 821203 (1959).

8) a) T. Kagiya, M. Hatta and K. Fukui, *Kobunshi Kagaku (Chem. High Polymer)*, **20**, 737 (1963); b) T. Kagiya, T. Sano and K. Fukui, *Kogyo Kagaku Zasshi (J. Chem. Soc. Japan, Ind. Chem. Sect.)*, **67**, 951 (1964); **68**, 1141 (1965).

TABLE 2. THE CATALYTIC ACTIVITY COEFFICIENT OF MDTC

C mol×10³	Time hr	M_p mol×10³	M	α
4.5	24	154	559	2.7
	28	179	568	3.0
	42	222	738	2.9
8.3	13	154	351	2.3
	17	181	450	2.2
	22	225	555	2.1

from 2 to 3; this variation cannot be reasonably explained at present. Alternatively, the application of the equation to low polymerizations remains in some doubt, since this equation has been originally devised for high-polymerization reactions.

Solvent Effect. It may be reasonably expected that the rate of polymerization is dependent on the nucleophilicity of the catalyst, varying with the nature of the solvent used. Thus, polymerizations were carried out in various aprotic solvents; the results are shown in Table 3.

TABLE 3. POLYMERIZATION IN VARIOUS SOLVENTS

Solvent	Dielectric constant	Polymerized monomer, g	Solubility of MDTC
DMF	37.6	8.4	soluble
DMSO	45.0	5.1	
CH_3CN	39.5	3.8	partially sol.
Acetone	21.2	0.5	insoluble
Dioxane	2.2	0.9	

EO 10.0 g; MDTC 0.5 g; Temp. 30°C; Time 65 hr; Solvent g

As expected, polymerization was accelerated in dipolar aprotic solvents in the following order: DMF>DMSO>CH_3CN, while the reaction was not accelerated in dioxane and acetone, in which MDTC is insoluble. This observation leads to the important conclusion that the major factor influencing the polymerization under homogeneous conditions is the enhanced nucleophilicity of the dithiocarbamate anion[9] in dipolar aprotic solvents; this is in agreement with many other observations[10] of nucleophilic substitutions and base-catalyzed reactions in these media. In the present case the catalysis of MDTC can be solely explained by the enhanced nucleophilicities of the thio anion in the initiation process and of the oxy anion in the propagation.

Catalysis of Various Dithiocarbamate Salts. Furthermore, we investigated the catalysis of various dithiocarbamate salts; the results are given in Table 4. It is not surprising that dithiocarbamate salts of bivalent metals, which are soluble in ordinary organic solvents, exhibit a small accelerating effect, or none at all, on this polymerization, since the metal-sulfur bonds in these dithiocarbamates are well-known to be chelate, not ionic bonds, and so the degree of the following dissociation is very small in solution.

$$M(SCSNR_2)_2 \rightleftarrows M^{2+} + 2R_2NCSS^-$$

It was also found that the ammonium salt of dithiocarbamate did not exhibit the catalysis on this polymerization; this implies a serious effect of the counter cation on the propagation process.

TABLE 4. CATALYSIS OF VARIOUS DITHIOCARBAMATE SALTS

Catalyst	polymerized monomer, g
$NaSCSNMe_2 \cdot 2H_2O$(MDTC)	6.6
$NaSCSNEt_2 \cdot 2H_2O$	7.7
$Nn(SCSNMe_2)_2$	2.7
$Zn(SCSNBu_2^n)_2$	0
$Ni(SCSNBu_2^n)_2$	2.0
$Et_2NHHSCSNEt_2$	0

EO 10.0 g; Catalyst 0.88 mol%; Temp. 30°C; Time 66 hr; DMF 8.0 g

Reaction of Epichlorohydrin with MDTC. Next, we attempted the reaction of epichlorohydrin (EPCl) with a small excess of MDTC in DMF. A DMF solution of MDTC was stirred into a DMF solution of EPCl to generate heat and to produce a precipitate (NaCl). After 20 hr, the mixture was poured into a large amount of water to give a white precipitate. The polymer obtained was soluble in DMF, DMSO, and acetonitrile, and was purified by reprecipitation (DMF-H_2O) to afford a white powder, which exhibited a negative Beilstein test. The reaction in DMSO gave a similar polymer. The experimental results are shown in Table 5.

Figure 5 indicates that the polymer exhibits characteristic bands of *S*-alkyl dithiocarbamate in the range from 1490 to 1375 cm^{-1} (–S–CS–N$\langle$), and ether linkage at 1140 cm^{-1} ($\rangle$C–O–C$\langle$). The IR spectrum of this polymer was essentially identical with that of the polymer obtained by the reaction of epichlorohydrin rubber (V) (prepared by the Nihon Zeon Co.) with MDTC in a mixture of DMF and toluene, except in the range from 1700 to 1650 cm^{-1}. These observations indicate that the reaction of EPCl with MDTC involves the following two processes in affording the polyether

9) Dithiocarbamate anions are ranked with the strongest nucleophiles in aqueous solutions: R. E. Davis, "Survey of Progress in Chemistry," Vol. 2, ed. by A. Scott, Academic Press Inc., New York, N. Y. (1964), p. 189; R. E. Davis, H. Nakshbendi and A. Ohno, *J. Org. Chem.*, **31**, 2702 (1966).

10) For example, see a) D. J. Cram, C. A. Kingsbury and B. Rickborn, *J. Am. Chem. Soc.*, **83**, 3688 (1961); b) C. C. Price and W. H. Synder, *ibid.*, **83**, 1773 (1961); c) W. M. Weaver and J. D. Huchinson, *ibid.*, **86**, 261 (1964).

Table 5. Reactions of EPCl with MDTC at room temperature

EPCl g (mol)	MDTC mol	Solvent ml	Time hr	Product: Yield, g	Product: Elemental[a] analysis (%)	Product: $[\eta]^{30°C}_{DMF}$
9.3 (0.1)	1.8 DMF	50	20	19.0	C, 38.01; N, 7.55 H, 5.91; S, 37.74	—
4.7 (0.05)	0.08 DMF	50	19	8.3[b]	C, 37.01; N, 7.71 H, 6.00; S, 40.01	0.040
4.7 (0.05)	0.08 DMSO	50	21	12.2[c]	—	0.035

a) Calcd for $(C_6H_{11}NOS_2)_n$; C, 40.68; H, 6.21; N, 7.91; S, 36.13%.
b) Softing point 75—80°C c) Softing point 68—75°C

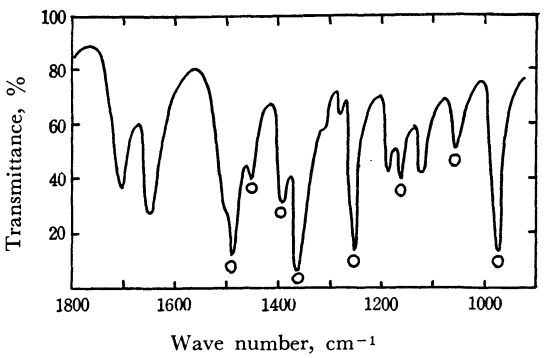

Fig. 5. IR spectrum of product from EPCl and MDTC (KBr disk). The sign ○ denotes the adsorption band observed CH_3-$SCSN(CH_3)_2$.

IV containing the dithiocarbamate moiety: the nucleophilic substitution (S_N) reaction on the chloromethyl carbon atom, and the ring-opening polymerization of the epoxy group. As is shown below, Chart, there are two possible mechanisms for the formation of the polymer IV. The first mechanism involves the initial polymerization of the EPCl catalyzed by MDTC, as has been verified above, followed by the S_N reaction (pathway a). The other consists of pathway b, which involves the initial formation of II, followed by the polymerization of II with MDTC. It seems reasonable to assume that pathway a is operative, since heat was usually evolved in the initial stage of the reaction and since EPCl reacted with less than 100 mol% of MDTC to give a viscous polymer, which exhibited a positive Beilstein test.

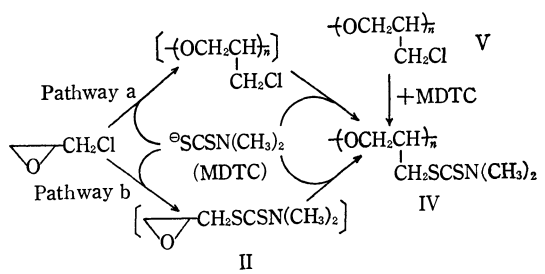

Figure 5 also indicates that the polymer IV exhibits two carbonyl bands, at 1700 and 1650 cm^{-1}. The former cannot be assigned, but the band was also observed for the polymer obtained by the polymerization of EO with MDTC (see Fig. 4). The latter band is assigned to the thiolcarbamate structure (-S-CO-N<) (1650 cm^{-1} for various *S*-alkyl *N, N*-dimethylthiolcarbamates); its formation can reasonably be explained by the following reaction sequence, involving the 1, 3-dithianylium ion (VI), through anchimerism by the dithiocarbamate function:[11]

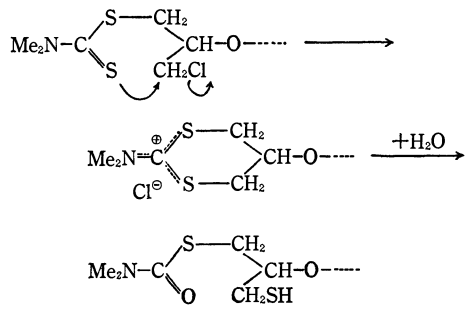

The formation of the thiolcarbamate structure also provides another evidence for the initial polymerization of EPCl with MDTC (pathway a). Further, the equimolar reaction of EPCl with sodium *N, N*-diethyldithiocarbamate in dioxane or benzene did not give any polymeric materials, but a distillable liquid, bp 118—120°C/0.15 mmHg; n_D^{30} 1.5420. (Found: S, 31.09%. Calcd for $C_8H_{15}NOS_2$: S, 31.22%). This unidentified compound also exhibits a same strong carbonyl band at 1650 cm^{-1}. This observation gives another support to anchimerism by the dithiocarbamate function.

Experimental

Materials. *Sodium N, N-Dimethyldithiocarbamate Hydrate (MDTC).* Commercial MDTC was washed several times with chloroform and then dried *in vacuo*.

11) T. Nakai, Y. Ueno and M. Okawara, *Tetrahedron Letters*, No. 39, 3831 (1967).

According to the reported method,[12] it was determined that this salt contained two molecules of coordinated water. The other dithiocarbamate salts used were available commercially and were employed without further purification.

Epoxides and Solvents. EO and PO were purified by distillation over solid potassium hydroxide. EPCl was purified by distillation. The solvents employed were purified by the usual methods.

Polymerization Procedure. A purified, anhydrous monomer and the solvent were added to a given amount of MDTC in a hard-glass tube at −78°C. The tube was then sealed and immersed in the stirring-thermostat adjusted at 30°C. After a given interval, the tube was removed from the thermostat and opened at −78°C. The unreacted monomer was readily removed on the steam-bath. From the decrease in the weight observed, the weight of the polymerized monomer was calculated.

Procedure of Isolating the Polymer. Anhydrous benzene (*ca* 80 m*l*) was added to the reaction mixture, and the precipitate formed was removed off using the centrifuge. The benzene and the solvent were removed by heating the clear solution to 80°C under reduced pressure (1 mmHg), thus producing a viscous residue. Viscosity measurements were made in dioxane solutions with an Ostwald viscometer at 30°C. The molecular weight of the polymer was calculated using Gee's equation,[5b] $[\eta]$ $(ml \cdot g^{-1}) = 0.083 M^{0.59}$. It has been verified that molecular weights ranging from 300 to 5100 can be determined by this equation, although no high precision is claimed.

Reaction of EPCl with MDTC. To a solution of 4.7 g (0.05 mol) of EPCl in 15 m*l* of DMF, 15 g (0.08 mol) of MDTC in 35 m*l* of DMF were added, little by little, at room temperature; the mixture was then stirred for 19 hr at room temperature. The white precipitate formed (NaCl) weighed 2.8 g (0.05 mol). The mixture was stirred into a large amount of water to give a white precipitate, which was collected by filtering and then dried *in vacuo* (yield 8.3 g). The product was purified by reprecipitation (DMF-H_2O). The reaction conditions and the results of individual experiments are shown in Table 5.

IR Spectra. The IR spectra were measured using a Hitachi Model EPI-2 Infrared Spectrometer.

12) D. G. Clarke *et al.*, *Anal. Chem.*, **23**, 1842 (1957).

BULLETIN OF THE CHEMICAL SOCIETY OF JAPAN VOL. 41 712—716 (1968)

Azetidines. IV. The Reaction of 1-*t*-Butylazetidinyl-3 Tosylate with Amines and Mercaptans[1]

Teng-yueh CHEN,[2] Hiroshi KATO and Masaki OHTA

Laboratory of Organic Chemistry, Tokyo Institute of Technology, Ookayama, Meguro-ku, Tokyo

(Received October 21, 1967)

3-Amino and 3-mercapto-azetidine derivatives were prepared by the reaction of 1-*t*-butylazetidinyl-3 tosylate with ammonia, primary and secondary amines, and mercaptans. Ring cleavage was observed when the tosylate was reacted with compounds of higher acidity, such as thiobenzoic acid.

In a previous communication,[1] we reported that a nitrile group could be introduced onto the azetidine ring by the reaction of 1-*t*-butylazetidinyl-3 tosylate (I) and potassium cyanide; the nitrile was then hydrolyzed to 1-*t*-butylazetidine-3-carboxylic acid in fairly good yield.

This result suggests that tosylate I is a promising starting material for the preparation of a wide variety of azetidine derivatives. In this communication we report the preparation of amino and mercapto derivatives of azetidine by the reaction of I with amines and mercaptans.

When 1-*t*-butylazetidinyl-3 tosylate (I) was allowed to react with dimethylamine, 1-*t*-butyl-3-dimethylaminoazetidine (IIa) was obtained in 40% yield. The NMR spectrum of IIa (Fig. 1) exhibits two singlets at τ 9.01 (9H) and 7.90 (6H) and a complex multiplet between 6.5—7.3 (5H), corresponding to the *t*-butyl group, the dimethylamino group and the ring protons respectively. The treatment of I with piperidine and morpholine likewise afforded the corresponding amino derivatives, 1-*t*-butyl-3-(1-piperidino)-azetidine (IIb) and 1-*t*-butyl-3-(1-morpholino)-azetidine (IIc). The reaction of I with methanolic ammonia also gave the expected derivative, 1-*t*-butyl-3-aminoazetidine (IId), but in lower yield. The infrared spectrum of IId shows a characteristic bands of a primary amino group at 3360 and 3280 cm^{-1} and a NH bending band at 1610 cm^{-1}. The NMR spectrum of IId (Fig. 1) which consists of a nine-proton singlet at τ 9.05 for the *t*-butyl

1) Part III: T. Chen, T. Sanjiki, H. Kato and M. Ohta, This Bulletin, **40**, 2401 (1967).

2) On leave of absence from National Tsing Hua University, Taiwan, The Republic of China.

group, a two-proton broad singlet at 8.19 for the amino group and two complex multiplets at 7.05—7.35 (2H) and at 6.40—6.75 (3H) for the cis and trans protons of the methylene group plus the methine proton, agrees with the assigned structure (IId), if not prove it.

The reaction of I and cyclohexylamine, a primary amine, gave directly the disubstituted derivative, di-(1-*t*-butylazetidinyl-3)-cyclohexylamine (III) as an oil, which was purified by conversion to its trihydrochloride monohydrate. The hydrochloride shows bands of an OH and N^+H groupings at 3500—3280 and 2800—2400 cm^{-1}. When I was treated with a large excess of cyclohexylamine,

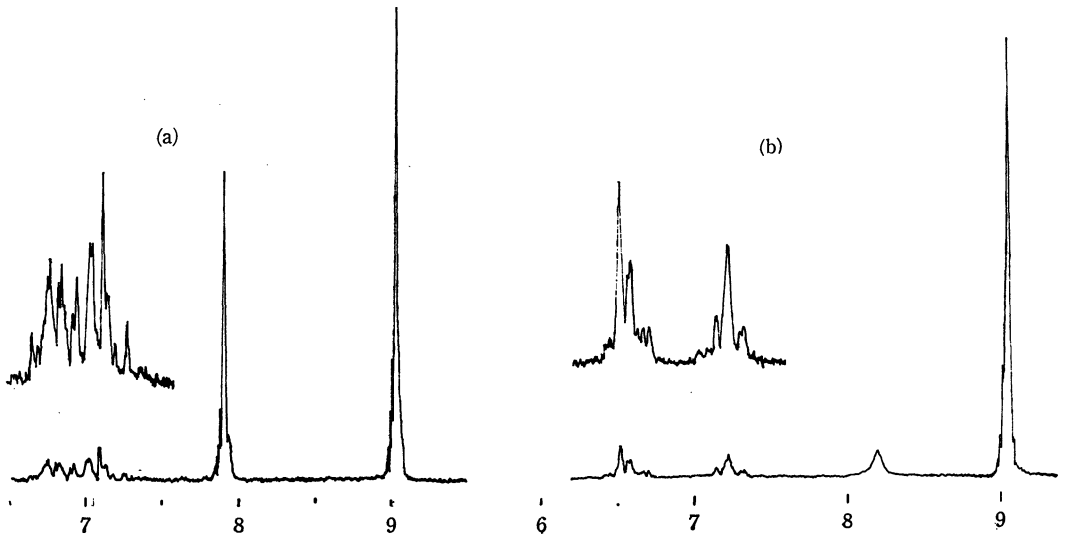

Fig. 1. The NMR spectrum of 1-*t*-butyl-3-dimethylaminoazetidine (a) and 1-*t*-butyl-3-amino-azetidine (b).

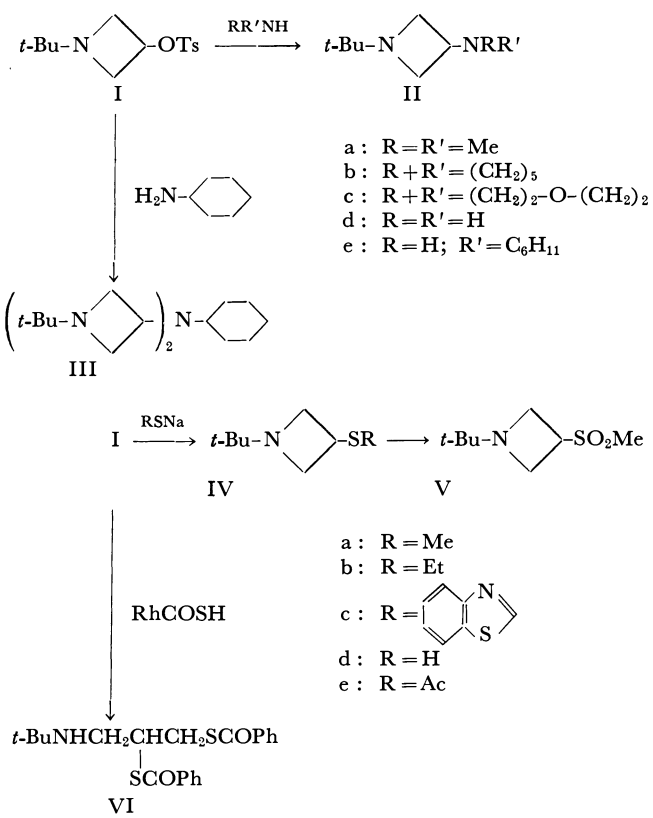

however, mono-substituted derivative IIe was obtained. Compound IIe was also a liquid but it could be crystallized in the form of its monohydrate. The infrared spectrum of IIe monohydrate shows a broad band of an OH group between 3500—3200 cm^{-1} and a band of an NH group at 3260 cm^{-1}.

The reaction of I with methyl mercaptan, ethyl mercaptan, and 2-mercaptobenzothiazole in ethanol in the presence of sodium ethoxide proceeded smoothly to give the corresponding sulfide, 1-*t*-butyl-3-methylthioazetidine (IVa), 1-*t*-butyl-3-ethylthioazetidine (IVb) and 1-*t*-butyl-3-(2-benzothiazolylthio)azetidine (IVc) respectively in good yields. Permanganate oxidation of IVa gave the corresponding sulfone V as a solid. The NMR spectrum of IVa consists of two sharp singlets at τ 9.12 (9H) corresponding to the *t*-butyl group and 8.00 (3H) corresponding to the methyl group, and a complex multiplet between 6.50 and 7.10 (5H) for the ring protons.

The reaction of I and potassium hydrogen sulfide in methanol was also tried with a hope of obtaining 1-*t*-butylazetidine-3-thiol (IVd). The crude reaction product was treated with acetic anhydride and distilled to give two components. The minor, lower boiling fraction shows a carbonyl absorption band at 1695 cm^{-1} and the elemental analysis was in agreement with the composition of 1-*t*-butyl-3-acetylthioazetidine (IVe). The major component, a highly viscous higher boiling liquid shows two carbonyl absorption bands at 1695 (acetylthio) and 1640 (amide) cm^{-1}, suggesting this component to be a ring cleavage product, but attempts of its purification failed. The ring cleavage reaction may have taken place at the stage of treatment with acetic anhydride rather than at the stage of treatment with potassium hydrogen sulfide.

The reaction of I with an excess of thiobenzoic acid in the presence of potassium carbonate also provided a ring cleavage product as a highly viscous oily substance which was purified by conversion to its hydrochloride. The infrared spectrum of the base shows a weak band at 3320 cm^{-1} (NH), a strong band of a carbonyl group at 1660 cm^{-1} and no absorption due to an SH group was found around 2600 cm^{-1}. The infrared spectrum of its hydrochloride shows a group of bands between 2800—2500 cm^{-1} besides the carbonyl band at 1660 cm^{-1}. These spectral data, as well as the results of elemental analyses suggest its structure to be VI rather than VII.

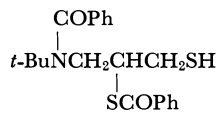

VII

This ring cleavage reaction may be considered to proceed through a protonated azetidinium salt (VIII; R=TsO or PhCOS) followed by an attack of an thiobenzoate anion to the ring, as is shown as follows:

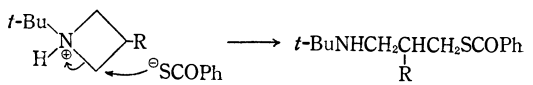

VIII

There have been ample examples[3] of such a mode of ring cleavage of azetidine ring.

The reaction of I with thioacetic acid also gave a highly viscous intractable substance. The infrared absorption spectrum of this crude substance was almost identical with that of the high boiling product obtained by acetic anhydride treatment of the reaction product of I and potassium hydrogen sulfide, but trials of its purification failed.

From the results described above, it may be concluded that amino and mercapto groups can be introduced to the 3 position of azetidine ring by the reaction of an azetidinyl-3 tosylate with an appropriate amine or mercaptan, but the reaction of the tosylate with compounds of higher acidity such as thiobenzoic acid leads to ring cleavage product.

Experimental[4]

1-*t*-Butyl-3-dimethylaminoazetidine (IIa). To a solution of 6 m*l* (0.07 mol) of dimethylamine in 20 m*l* of methanol were added 5 g (0.017 mol) of I and 2.7 g (0.02 mol) of potassium carbonate successively with cooling and stirring. After stirring for five hours at room temperature, the mixture was allowed to stand overnight. After removal of the precipitate by filtration, the filtrate was concentrated under reduced pressure, and was diluted with 40 m*l* of water and filtered again to remove unchanged I. The filtrate, after being saturated with potassium carbonate, was extracted with ether, and the ether extract was dried over sodium sulfate. Distillation under reduced pressure afforded 1 g (40% yield) of colorless liquid boiling at 60—64.5°C/20 mmHg. n_D^{25} 1.4232, IR: 2960—2780, 1460, 1360 and 1240 cm^{-1}. The NMR spectrum is shown in Fig. 1 (a).

Found: C, 68.99; H, 12.69; N, 17.57%. Calcd for $C_9C_{20}N_2$: C, 69.17; H, 12.90; N, 17.93%.

Picrate of IIa melted once at 133—135°C, then solidified and melted again at 220—251°C with decomposition.

3) See for example: a) C. F. Gibbs and C. S. Marvel, *J. Am. Chem. Soc.*, **57**, 1137 (1935); b) C. Mannich, and G. Baumgarten, *Ber.*, **70**, 210 (1937); c) R. C. Elderfield and H. A. Hageman, *J. Org. Chem.*, **14**, 605 (1949); d) R. C. Elderfield and C. Ressler, *J. Am. Chem. Soc.*, **72**, 4059 (1950); e) W. B. Wheatley and L. C. Cheney, *ibid.*, **74**, 1359 (1952); f) A. Müller, E. Funder-Fritzchse, W. Konar and E. Rintersbacher-Wlasak, *Monatsh.*, **84**, 1206 (1953); g) V. R. Gaertner, *Tetrahedron Letters*, **1967**, 343.

4) The general conditions for the measurements of physical constants and spectra were the same as described in Part I, T. Chen, H. Kato and M. Ohta, This Bulletin, **40**, 1964 (1967).

Found: C, 47.06; H, 6.20; N, 18.19%. Calcd for $C_{15}H_{23}N_5O_7$: C, 46.75; H, 6.02; N, 18.17%.

The following compounds were obtained by a similar method as described above.

1-*t*-Butyl-3-(1-piperidino)azetidine (IIb). (55% yield) Bp 64—67°C/1.5 mmHg, n_D^{25} 1.4678. IR: 2980—2660, 1460, 1360 and 1240 cm^{-1}.

Found: C, 73.27; H, 12.48; N, 14.38%. Calcd for $C_{12}H_{24}N_2$: C, 73.41; H, 12.32; N, 14.27%.

Picrate of IIb: partially melted at 150°C, then solidified and melted again at 202—225°C with decomposition.

Found: C, 50.55; H, 6.56; N, 15.96%. Calcd for $C_{18}H_{27}N_5O_7$: C, 50.81; H, 6.40; N, 16.46%.

1-*t*-Butyl-3-(1-morpholino)azetidine (IIc). (90% yield—crude). Very hygroscopic colorless prisms, mp 43—45°C (from petroleum ether). IR: 2980—2800, 1480, 1360, 1240 and 1120 cm^{-1}.

Found: C, 66.30; H, 11.20; N, 13.76%. Calcd for $C_{11}H_{22}N_2O$: C, 66.62; H, 11.18; N, 14.13%.

Dipicrate of IIc: mp 223—230°C (decomp.).

Found: C, 42.54; H, 4.30; N, 17.30%. Calcd for $C_{23}H_{28}O_{15}N_8$: C, 42.07; H, 4.29; N, 17.06%.

1-*t*-Butyl-3-aminoazetidine (IId). This was prepared in 35% yield by treatment of 10 g of I with 40 m*l* of saturated methanolic solution of ammonia for a week at room temperature. Colorless liquid, bp 55—61°C/13.5 mmHg, n_D^{25} 1.4545, IR: 3360, 2380, 1610, 1480, 1360 and 1240 cm^{-1}. The NMR spectrum is shown in Fig. 1 (b).

Found: C, 64.72; H, 12.65; N, 21.93%. Calcd for $C_7H_{16}N_2$: C, 65.57; H, 12.58; N, 21.85%.

p-Nitrobenzamide of IId: mp 163.5—165°C.

Found: C, 60.49; H, 6.58; N, 15.42%. Calcd for $C_{14}H_{19}O_3N_3$: C, 60.63; H, 6.91; N, 15.15%.

Monopicrate of IId: Mp 245—250°C (decomp.).

Found: C, 43.95; H, 5.50; N, 19.26%. Calcd for $C_{13}H_{19}N_5O_7$: C, 43.69; H, 5.36; N, 19.60%.

Dipicrate of IId: Mp 224—228°C (decomp.).

Found: C, 38.49; H, 3.80; N, 19.28%. Calcd for $C_{19}H_{22}N_8O_{14}$: C, 38.91; H, 3.78; N, 19.10%.

***N*, *N*-Di-(1-*t*-butylazetidinyl-3)cyclohexylamine (III).** This was obtained in *ca.* 60% yield by the reaction of 0.02 mol of I and 0.04 mol of cyclohexylamine.

Trihydrochloride monohydrate of III: Mp 194—196°C (white needles from ethanol). IR: 3480, 3440, 3300, a group of absorption between 2800—2400, 1470, 1430 and 1380 cm^{-1}.

Found: C, 53.02; H, 10.41; N, 9.53%. Calcd for $C_{20}H_{44}N_3OCl_3$: C, 53.50; H, 9.80; N, 9.36%.

1-*t*-Butyl-3-cyclohexylaminoazetidine (IIe). This was prepared in *ca.* 22% yield by the reaction of 5.8 g (0.02 mol) of I and 30 m*l* of cyclohexylamine.

Monohydrate of IIe: Colorless plates, mp 37—39°C (from hexane), IR: a broad peak between 3500—3200, 3260, 1448, 1360 and 1240 cm^{-1}. This substance melted to a liquid when kept in a desiccator, which resolidified to give the monohydrate when allowed to stand in the open air.

Found: C, 68.67; H, 12.16; N, 12.54%. Calcd for $C_{13}H_{28}N_2O$: C, 68.37; H, 12.36; N, 12.27%.

Dipicrate of IIe: mp 199.5—202°C (decomp.).

Found: C, 44.92; H, 4.98; N, 16.24%. Calcd for $C_{25}H_{32}N_8O_{14}$: C, 44.90; H, 4.82; N, 16.76%.

1-*t*-Butyl-3-methylthioazetidine (IVa). To a solution of *ca.* 0.1 mol of sodium methylmercaptide in 50 m*l* of ethanol was added 11.5 g (0.04 mol) of I and the mixture was stirred for a day at room temperature and was allowed to stand overnight. It was then treated in the same way as in the reaction of I and secondary amines. 4.7 g (74% yield) of colorless liquid was obtained. Bp 80—83°C/13 mmHg, n_D^{25} 1.4741. IR: 2980—2820, 1480, 1430, 1360, 1250 and 1080 cm^{-1}. NMR(τ): 9.12 (singlet, 9H); 8.00 (singlet, 3H); 6.50—7.10 (multiplet, 5H).

Found: C, 60.46; H, 11.00; N, 8.34%. Calcd for $C_8H_{17}NS$: C, 60.34; H, 10.76; N, 8.80%.

Picrate of IVa: Mp 165—167.5°C.

Found: C, 43.39; H, 5.12; N, 14.60%. Calcd for $C_{14}H_{20}N_4O_7S$: C, 43.30; H, 5.19; N, 14.43%.

The following sulfides were prepared by the same method as described above:

1-*t*-Butyl-3-ethylthioazetidine (IVb). (63% yield) Bp 95—102°C/22 mmHg, n_D^{25} 1.4705, IR: 3000—2820, 1480, 1450, 1360, 1250 and 1080 cm^{-1}.

Found: C, 61.91; H, 11.05; N, 8.00%. Calcd for $C_9H_{19}NS$: C, 62.39; H, 11.05; N, 8.09%.

Picrate of IVb: Mp 134—135°C.

Found: C, 44.60; H, 5.29; N, 14.14%. Calcd for $C_{15}H_{22}O_7N_4S$: C, 44.77; H, 5.51; N, 13.93%.

1-*t*-Butyl-3-(2-benzothiazolylthio)azetidine (IVc). (41% yield). White fine crystals (from petroleum ether), mp 48—49°C. IR: 3053, 2900, 2834, 1450, 1366, 1240 1000 and 765 cm^{-1}.

Found: C, 60.62; H, 6.66; N, 10.42%. Calcd for $C_{14}H_{18}N_2S_2$: C, 60.42; H, 6.52; N, 10.07%.

Picrate of IVc: Mp 144.5—145.5°C.

Found: C, 46.99; H, 4.27; N, 14.01%. Calcd for $C_{20}H_{21}N_5O_7S_2$: C, 47.33; H, 4.17; N, 13.80%.

Reaction of I and Potassium Hydrogen Sulfide. Hydrogen sulfide was saturated to a solution of 5 g of potassium hydroxide in 50 m*l* of methanol. To the above solution, 11.5 g (0.04 mol) of I was added and the mixture was processed according to the method described above. To the residue obtained by removal of the solvent was added with cooling 12 m*l* of acetic anhydride and the solution was warmed on a water bath for three hours. After setting aside at room temperature overnight, the reaction mixture was poured into water, made alkaline with potassium carbonate and was extracted with ether. The extract was concentrated and the residual oil was distilled to give 0.8 g of a colorless liquid, bp 44—56°C/1.5 mmHg, and 2 g of a light yellow viscous liquid, bp 142—152°C/1.5 mmHg.

Low boiling fraction: n_D^{25} 1.4805, IR: 3000—2820, 1695, 1480, 1360, 1240, 1120 cm^{-1}.

Found: C, 58.02; H, 9.65; N, 7.52%. Calcd for $C_9H_{17}NOS$: C, 57.73; H, 9.15; N, 7.48%.

Picrate of low boiling fraction: mp 168—170°C.

Found: C, 43.11; H, 4.78; N, 14.46%. Calcd for $C_{15}H_{20}N_4O_8S$: C, 43.27; H, 4.84; N, 13.46%.

High boiling fraction: n_D^{25} 1.4850, IR: 3000—2800, 1695, 1640, 1480, 1390, 1360, 1230 and 1130cm^{-1}.

Methyl 1-*t*-Butylazetidinyl-3 Sulfone (V). To a solution of 2 g (0.0125 mol) of IVa in 20 m*l* of glacial acetic acid was added dropwise with stirring a solution of 2.5 g (0.016 mol) of potassium permagnate in 25 m*l* of water. The mixture was stirred for half an hour at room temperature and then for another half an hour at 40—50°C. The precipitate was filtered off and the filtrate was treated with an aqueous sodium bisulfite.

Extraction with ether and removal of the solvent afforded 1.9 g of crude solid, which was recrystallized from ether to give 0.7 g (29% yield) of colorless plates, mp 46—48.5°C. IR: a group of absorption between 1330—1200 and 1140 cm^{-1}.

Found: C, 50.18; H, 9.15; N, 7.11%. Calcd for $C_8H_{17}NO_2S$: C, 50.25; H, 8.96; N, 7.33%.

Picrate of V: Mp 188—190.5°C.

Found: C, 40.27; H, 4.91; N, 13.31%. Calcd for $C_{14}H_{20}N_4O_9S$: C, 40.00; H, 4.79; N, 13.33%.

Reaction of I and Thiobenzoic Acid. To a solution of 10 g (0.07 mol) of thiobenzoic acid in 9 m*l* of dimethylformamide was added successively 1.6 g (0.01 mol) of potassium carbonate and 5.8 g (0.02 mol) of I and the mixture was stirred for six hours and was set aside overnight. The reaction mixture was then diluted with 30 m*l* of water, made strongly alkaline with potassium carbonate and was extracted with ether. A reddish brown viscous oil remained after removal of the solvent. The oil was dissolved again in ether and treated with dilute hydrochloric acid. A light colored precipitate (3.9 g) was obtained, which was recrystallized from ethanol-hexane to give white needles, mp 160—166°C. IR: 3060, 2800—2500, 2420, 1660 cm^{-1}.

Found: C, 59.45; H, 6.35; N, 3.22%. Calcd for $C_{21}H_{26}NO_2S_2Cl$: C, 59.50; H, 6.18; N, 3.30%.

A light-colored viscous oil was recovered by neutralization and extraction of the above hydrochloride. IR: 3320, 3060, 1660 cm^{-1}. (No absorption due to SH was observed.)

Found: C, 65.58; H, 6.63; N, 3.83%. Calcd for $C_{21}H_{25}NO_2S_2$ (VI): C, 65.10; H, 6.50; N, 3.83%.

We are indebted to Miss Mizuko Yoshida for the measurement of the NMR spectra.

BULLETIN OF THE CHEMICAL SOCIETY OF JAPAN VOL. 41 716—721 (1968)

A Study on Mixed Vanadium Catalysts for the Ammoxidation of Xylene

Masatomo Ito, Hazime Tanaka and Akira Matsumoto

The Central Research Laboratory, Showa Denko K. K., Tamagawa, Ohta-ku, Tokyo

(Received September 23, 1967)

The phase composition and the physicochemical properties of an antimony-vanadium catalyst and a chromium-vanadium catalyst for the ammoxidation of xylene were studied by X-ray diffraction method, differential thermal analysis, infrared absorption analysis and ESR measurement. An antimony-vanadium catalyst consisted essentially of $SbVO_4$ which contained no double covalent bond V=O, while a chromium-vanadium catalyst consisted essentially of a chemical compound which was different from $CrVO_4$. $SbVO_4$ and $CrVO_4$ were hard to be reduced with ammonia at 400°C, while a chemical compound in the chromium-vanadium system was reducible. The activity and the selectivity of reaction were affected by the nature and the distribution of metal ions and oxygen ion on surface.

The kinetic study of the vapor-phase ammoxidation of xylene over a vanadium oxide catalyst and mixed vanadium catalysts, an antimony-vanadium catalyst and a chromium-vanadium catalyst, showed that the rate and the selectivity of the reaction were affected by the adsorbability and the reactivity of related reactants.[1] A basic study on mixed vanadium catalysts for the ammoxidation of xylene was, therefore, of interest in order to gain a better understanding of the reaction processes which take place on the catalyst surface.

The present study is an attempt to clarify the physicochemical properties of mixed vanadium catalysts for the ammoxidation of xylene.

Experimental

Sample Preparation. Catalyst samples, which were free of carrier, were prepared by mixing a solution of vanadyl oxalate with a solution of chromium oxalate or a solution of vanadyl tartarate with a solution of antimonyl tartarate in the desired proportions. After evaporating the mixture to dryness on a steam bath the sample was calcinated in air for periods up to 2 days.

Physical Measurement. The powder-type X-ray diffraction patterns of samples were recorded using a Rigaku Denki model D-2F Geigerflex with a copper target.

The infrared absorption spectra of samples were recorded using a JASCO model IR-S infrared spectrophotometer and preparing the samples in the form of KBr pressed discs (1 mg sample in 0.5 g KBr).

The differential thermal analysis curves for the samples were run in air heating at a rate of 10°C/min using a Shimadzu model DT-1A differential thermal analyzer.

The ESR absorption spectra of samples were measured at room temperature by using the same apparatus and procedure employed in a previous work.[2]

1) M. Ito and K. Sano, This Bulletin, **40**, 1321 (1967).

2) H. Tanaka and A. Matsumoto, *ibid.*, **39**, 876 (1966).

The oxygen loss during the reduction of samples with ammonia was determined at 400°C by using a Shimadzu thermal balance. Weighed powdered sample (0.3 g) was heated to 400°C in a nitrogen atmosphere and ammonia was then introduced at a rate of 200 cc/min.

Results

Antimony-Vanadium System. The differential thermal analysis curves of the mixtures of an antimonyl tartarate and a vanadyl tartarate are shown in Fig. 1. Taking account of the X-ray diffraction patterns (Fig. 2) of samples which were

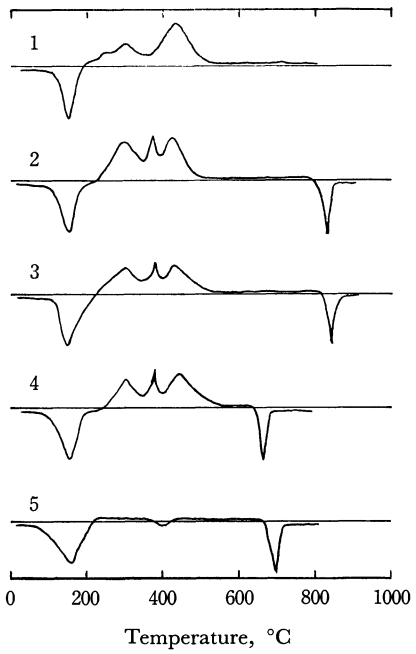

Fig. 1. Differential thermal analysis curve of the mixture of antimonyl tartarate and vanadyl tartarate.
Sb/V ratio: 1) 1/0, 2) 2/1, 3) 1/1, 4) 1/2, 5) 0/1

treated in air at desired temperature for 4 hr, they were interpreted in the following way. The endothermic peak in the range from 100 to 200°C and the following exothermic peak in the range from 200 to 300°C were ascribed to the dehydration and the decomposition of tartarates respectively. Two exothermic peaks at 300 and 420°C in an antimonyl tartarate were seemed to indicate the formation of antimony trioxide(cubic type) and tetraoxide (orthorombic type) respectively. In mixed tartarate samples a new crystal phase was formed below 300°C. This new crystal phase was in good agreement with one which was prepared by treating the equimolar mixture of antimony trioxide and vanadium pentoxide in a sealed Pt tube at 700°C.[3]

3) R. S. Roth and J. L. Waring, *Am. Mineral.*, **48**, 1348 (1963).

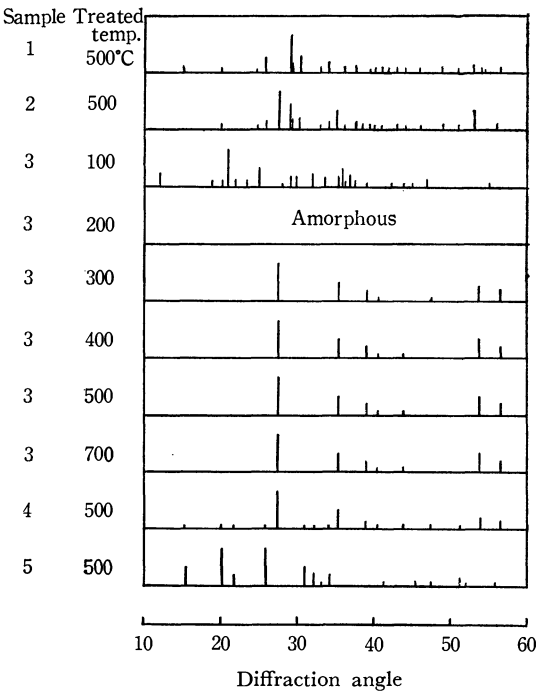

Fig. 2. X-Ray diffraction pattern of antimony-vanadium sample.
Sb/V ratio: 1) 1/0, 2) 2/1, 3) 1/1, 4) 1/2, 5) 0/1

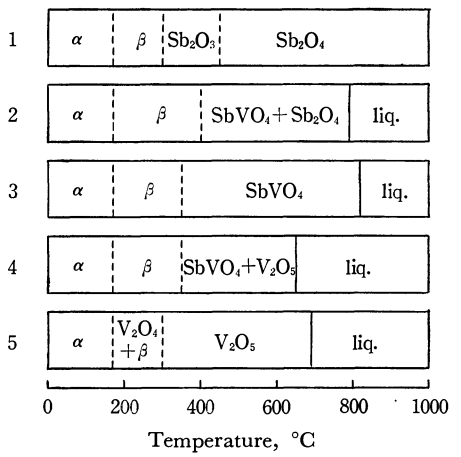

Fig. 3. Phase diagram in antimony-vanadium system.
Sb/V ratio: 1) 1/0, 2) 2/1, 3) 1/1, 4) 1/2, 5) 0/1

The exothermic peaks near 400°C were seemed to be ascribed to the crystallization of this chemical compound and the temperature at the last peak was regarded the melting point.

In view of above results, the phase diagram in this system is presented in Fig. 3. The α-phase was the crystalline of tartarates and the β-phase was the amorphous intermediate.

Infrared absorption spectra of the samples are shown in Fig. 4. The mixed sample in the atomic

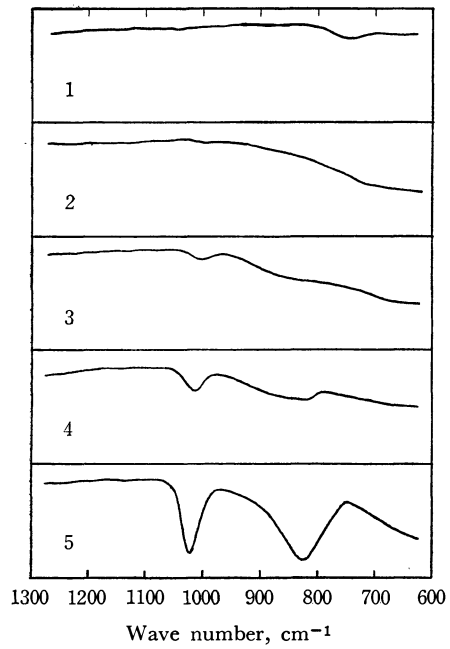

Fig. 4. Infrared absorption spectrum of antimony-vanadium sample heat-treated at 500°C for 4 hr.
Sb/V ratio: 1) 1/0, 2) 2/1, 3) 1/1, 4) 1/2, 5) 0/1

ratio of 1 : 1 had only a very weak absorption near 1000 cm^{-1}. This indicates that $SbVO_4$ contains no double covalent bond V=O.

The heat-treated samples of this system except Sb_2O_4 gave a single broad ESR absorption spectrum. Figure 5 shows the variation of the ESR intensity of the sample in the atomic ratio of 1 : 1 with heat treatment. The intensity of ESR signal decreased with an increase in treated temperature, while the width increased. The *g*-value,

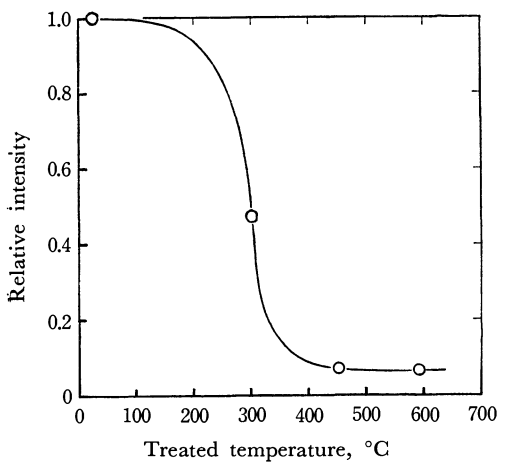

Fig. 5. Variation of the ESR intensity of antimony-vanadium sample in the atomic ratio of 1:1 with heat treatment.

Table 1. ESR constants of antimony-vanadium sample heat-treated at 480°C

Sb/V Ratio	*g*-Value	Width *ΔHmsl*	Relative signal intensity[b]
98/2	1.96	240 gauss	
10/1	1.97	270	0.00008
2/1	a	500	0.0023
1/1	1.98	500	0.04
1/2	1.96	500	0.007
1/10	1.98	95	
0/1	1.98	85	0.0008

a : very broad signal
b : relative intensity to vanadyl tartarate

ΔHmsl and relative intensity of ESR signal of samples heat-treated at 480°C are listed in Table 1. The signal intensity passed through a maximum at the atomic ratio of 1 : 1. Further details on the ESR study in this system will be reported in a separate paper.

Chromium-Vanadium System. The differential thermal analysis curves of the mixtures of a chromium oxalate and a vanadium oxalate are shown in Fig. 6. The X-ray diffraction patterns of samples, which were treated in air at desired temperature for 4 hr, at shown in Fig. 7. The endothermic and the following exothermic peaks near 400°C were seemed to be the decomposition of oxalates. The exothermic peaks in the mixed oxalate sample in the range from 500 to

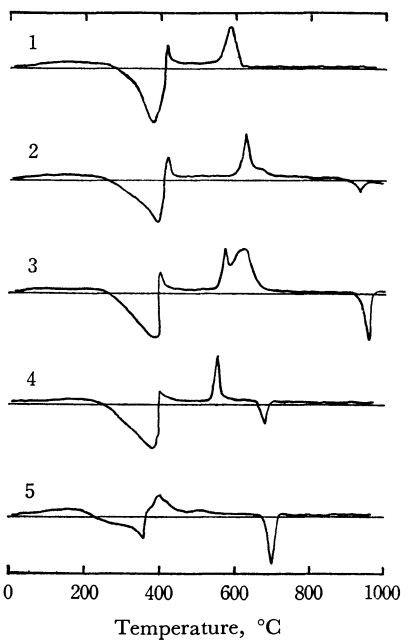

Fig. 6. Differential thermal analysis curve of the mixture of chromium-oxalate and vanadium oxalate.
Cr/V ratio: 1) 1/0, 2) 2/1, 3) 1/1, 4) 1/2, 5) 0/1

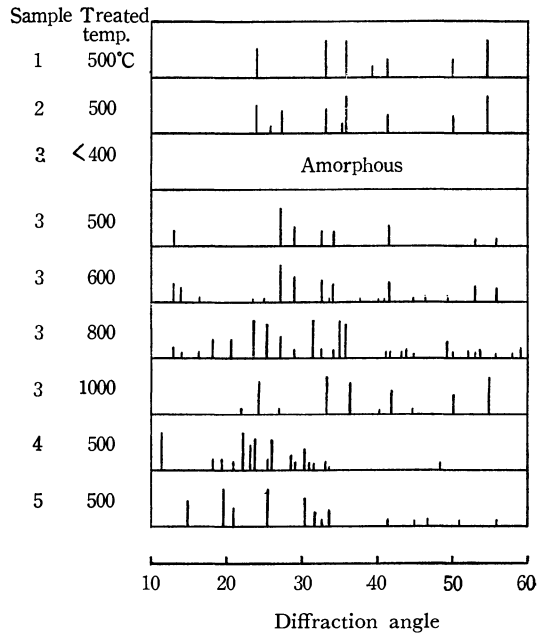

Fig. 7. X-Ray diffraction pattern of chromium-vanadium sample.
Cr/V ratio: 1) 1/0, 2) 3/1, 3) 1/1, 4) 1/3, 5) 0/1

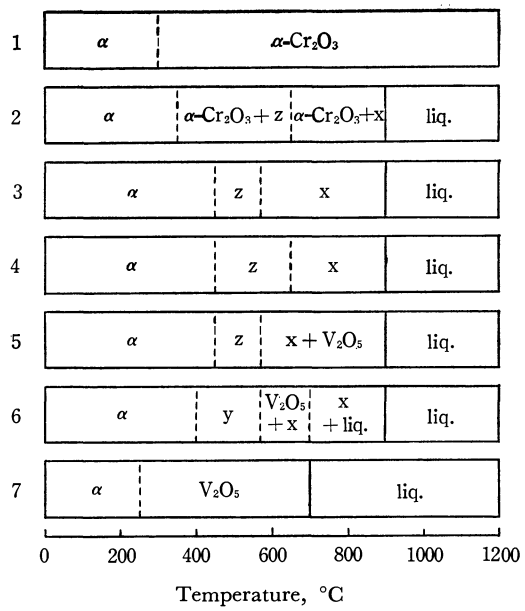

Fig. 8. Phase diagram in chromium-vanadium system.
Cr/V ratio: 1) 1/0, 2) 3/1, 3) 3/2, 4) 1/1, 5) 2/3, 6) 1/3, 7) 0/1

620°C were seemed to be ascribed to the formation of x-phase compound which was in good agreement with $CrVO_4$ described by Brandt.[4] The last endothermic peak was regarded the melting point.

The X-ray diffraction pattern also showed that there were two new phase present in mixed samples. When the atomic ratio of chromium to vanadium was near 1 : 3, the y-phase was present in the range from 400 to 600°C. This phase could be obtained by the heat-treatment of chromium metavanadate[5,6] at 500°C. When the atomic ratio was near 1 : 1, the z-phase was present and was stable up to a higher temperature at the atomic ratio of 1 : 1. In view of above observation and the result by Amiel and his co-workers,[7] the phase diagram in this system is presented in Fig. 8.

Infrared absorption spectra of the heat-treated samples are shown in Fig. 9. The spectra of mixed samples differed from that of V_2O_5 and Cr_2O_3. In the atomic ratio of 1 : 1 the spectra showed remarkable change by the temperature of heat treatment. The spectrum of a brownish black amorphous material obtained by the heat treatment at 400°C was similar to one of chromium orthovanadate obtained by precipitating chromic nitrate solution with sodium orthovanadate and

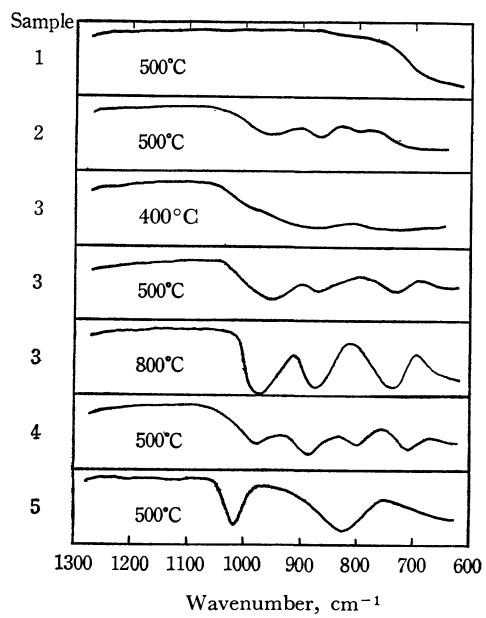

Fig. 9. Infrared absorption spectrum of chromium-vanadium sample heat-treated at desired temperature for 4 hr.
Cr/V ratio: 1) 1/0, 2) 3/1, 3) 1/1, 4) 1/3, 5) 0/1

heating the precipitate at 400°C. In the spectrum of a grayish black crystal powder obtained by the heat treatment at 500°C three broad absorption bands were observed at 950, 870 and 740 cm^{-1}. The spectrum of a yellowish brown crystal powder obtained by the heat treatment at 800°C showed

4) K. Brandt, *Arkiv. Kemi. Mineral Geo.*, **17A** (6), 1 (1943).
5) J. Amiel, D. Olivier and M. Dessolin, *Compt. Rend.*, **264**, 1045 (1967).
6) D. Olivier, *ibid.*, **264**, 1176 (1967).
7) J. Amiel, D. Colaitis and D. Olivier, *ibid.*, **263**, 224 (1966).

three very strong absorption bands at 970, 880 and 740 cm^{-1}. This observed change in the spectra is seemed to be ascribed to the formation of the chemical compounds, in good agreement with phase analysis described above.

The heat-treated samples in this system gave a single broad ESR absorption spectrum. Figure 10 shows the variation of the ESR intensity of the sample in the atomic ratio of 1 : 1 with heat treatment. The intensity of ESR signal passed through a minimum at the sample heat-treated at 500°C, while the sample heat-treated at 800°C gave a very intense signal with a *g*-value of 1.98 and a width of 90 gauss. The *g*-value, *ΔHmsl* and relative intensity of ESR signal of samples heat-treated at 500°C are listed in Table 2. The sample in the atomic ratio of 1 : 1 gave a broad signal with a weak intensity.

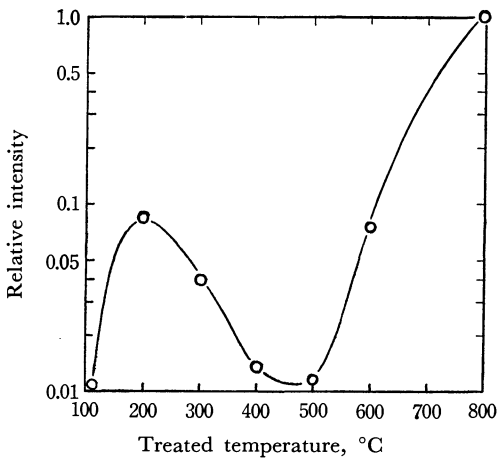

Fig. 10. Variation of the ESR intensity of chromium-vanadium sample in the atomic ratio of 1:1 with heat treatment.

Table 2. ESR constants of chromium-vanadium sample heat-treated at 500°C

Cr/V Ratio	*g*-Value	Width *ΔHmsl*	Relative signal intensity[a]
1/0	1.97	600 gauss	0.004
3/1	1.97	260	0.05
1/1	1.98	600	0.01
1/3	1.98	250	0.05
0/1	1.98	70	0.0008

a : relative intensity to vanadyl oxalate

Permanganate titration indicated also that the sample heat-treated in the range from 400 to 500°C presented no vanadium in the V^{4+} state.

Reduction of Sample with Ammonia. In Fig. 11 the thermogravimetric analysis curves treated with ammonia at 400°C are shown. Vanadium pentoxide was very reducible under the given condition, while mixed samples were hard to be reduced. However the z-phase in the chromium-vanadium system was reducible. The phase analysis by X-ray diffraction method and infrared absorption analysis showed that each mixed sample treated with ammonia retained the original composition. These results indicate that mixed samples have no covalent double bond V=O to be easily reducible.

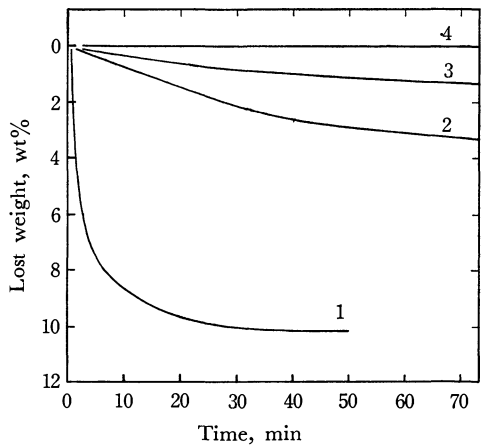

Fig. 11. Thermogravimetric analysis curve of sample in the treatment with ammonia at 400°C.
Sample:
1) V_2O_5
2) chromium-vanadium (1:1) treated at 500°C
3) antimony-vanadium (1:1) treated at 500°C
4) chromium-vanadium (1:1) treated at 800°C

Phase Composition of Used Catalysts. The fresh catalysts used for the ammoxidation of xylene[1] consisted essentially of V_2O_5, $SbVO_4$ and z-phase for a vanadium oxide catalyst, an antimony-vanadium catalyst and a chromium-vanadium catalyst respectively. X-Ray diffraction patterns for used catalysts showed that a vanadium oxide catalyst consisted essentially of V_2O_4, while mixed catalysts retained the original composition even after prolonged usage.

Discussion

Roth and Waring[3] and Brandt[8] have shown that $SbVO_4$ has the rutile structure with the metal ions randomly distributed. Taking account of the results for infrared absorption analysis, ESR measurement and reactivity with ammonia, it is suggested that the nature of vanadium ion in $SbVO_4$ is similar to one of V_2O_4.[9]

The chromium-vanadium system is more complicated. Brandt has shown that x-phase, that is $CrVO_4$, has a defect spinal structure having the vanadium atoms in tetrahedral coordination.[4]

8) K. Brandt, *Structure Reports*, **9**, 178 (1942—4).
9) K. Narita, *Nihon Butsuri Gakkaishi (J. Applied Phys. Japan)*, **20**, 748 (1965).

The very intense absorption bands of infrared spectrum and the intense signal of ESR indicate also that octahedral chromium ion and tetrahedral vanadium ion are regularly distributed. The metal ions in $CrVO_4$ are also not reduced under reaction conditions.

The infrared absorption spectrum of amorphous phase was similar to one of amorphous chromium metavanadate. The amorphous phase is, therefore, seemed to have the polyanion of VO_3^-.

On the other hand X-ray diffraction pattern indicates that the structure of z-phase is quite different from one of x-phase. Ioffe and his co-workers[10,11] have obtained the similar compound by heat-treating the mixture of vanadyl oxalate and chromic acid at 400°C, but X-ray diffraction pattern is not in agreement with one of the z-phase of this work. The infrared absorption spectrum of z-phase was similar to one of x-phase rather than one of amorphous phase, but each absorption band of its spectrum was broad and considerably weak. The absorption band near 1000 cm^{-1} also shifted to the longer wavelength than one of x-phase. The ESR absorption spectrum of 1 : 1 sample heat-treated in the range from 400 to 500°C was similar to one of Cr_2O_3 which had a single broad signal. Furthermore the z-phase was reducible with ammonia at 400°C differing from x-phase. The surface of the catalyst consisting of z-phase is seemed to become partially reduced under reaction condition. In view of above results, the z-phase is seemed to have the transitional structure with the elongated double convalent bond V=O.

A vanadium oxide catalyst, a chromium-vanadium catalyst and an antimony-vanadium catalyst had similar activity in the ammoxidation of xylene as described in the previous paper,[1] while a chromium-vanadium catalyst in which x-phase was one of major constituent of catalyst had a little catalytic activity in this reaction. These observations indicate that the nature and the distribution of metal ions and oxygen ion on catalyst surface affect the catalytic activity and the selectivity of reaction. It is difficult to expect the relationship between the adsorbability of reactant and the selectivity of reaction, but it may be assumed that the addition of more electronegative metal ions affects the electronic property of vanadium ion functioning as an adsorption center.[12,13]

Ioffe and his co-workers[10,11] showed that a chromium-vanadium catalyst in the atomic ratio of 1 : 1 had low activity and selectivity for the oxidation of benzene to maleic anhydride. An antimony-vanadium catalyst and a chromium-vanadium catalyst had an activity for the oxidation of *o*-xylene to phthalic anhydride, but the selectivity to phthalic anhydride showed less than 35%. Furthermore the relationship between the catalytic activity and the physical property of mixed catalysts for the ammoxidation of xylene are different from that for the oxidation of benzene.[11] These results suggest that the oxidative dehydrogenation is more significant than the formation of carboxylic acid for the mechanism of ammoxidation.[14]

The authers wish to thank Messrs. Hideo Ichinokawa, Tadashi Aoki, Nobuhisa Goto and Ken-ichi Sano for their valuable discussion.

10) I. I. Ioffe, Z. I. Ezhkova and A. G. Lyubarskii, *Kin. & Cat.*, **3**, 165 (1962).
11) Z. I. Ezhkova, I. I. Ioffe, V. B. Kazanskii, A. V. Krylova, A. G. Lyubarskii and L. Ya. Margolis, *ibid.*, **5**, 753 (1964).
12) L. Ya. Margolis, "Advance in Catalysis," Vol. 14 Academic Press Inc., London (1963), p. 429.
13) L. Ya. Margolis, A. V. Krylova and E. S. Aleksandrova, *Kin. & Cat.*, **7**, 59 (1966).
14) M. Ito and K. Sano, *Yuki Gosei Kagaku Kyokaishi (J. Soc. Org. Syn. Chem. Japan)*, **25**, 329 (1967).

NOTES

Polymerization of Styrene by Ceric *n*-Dodecylbenzene Sulfonate in the Presence of Alcohol or a Carbonyl Compound

Kyoji KAERIYAMA

The Textile Research Institute of Japanese Government, Sawatari, Kanagawa-ku, Yokohama

(Received June 10, 1967)

The present investigation was undertaken to seek for a better co-catalyst for the polymerization of styrene by organoceric compounds. As an organoceric compound ceric *n*-dodecylbenzene sulfonate[1] was used. From the results of the similar studies by Iwakura *et al.*[2] and Ogiwara *et al.*,[3] in the present paper alcohols and carbonyl compounds were selected as the co-catalysts.

To a solution of 22 g of ceric ammonium nitrate dissolved in 200 cc of 0.1 N aqueous nitric acid, a solution of 27.6 g of sodium *n*-dodecylbenzene sulfonate in 200 cc of water was added. The yellow precipitate was then separated by filtration and dried *in vacuo* at 40°C. This precipitate will hereafter be referred to as ceric *n*-dodecylbenzene sulfonate (CDBS) according to the reference.[1] The yield was 41.9 g. When CDBS was burned in a crucible, 21.14% of the CDBS (in weight) remained as an ash. This ash was presumed to be ceric dioxide. In addition to the bands observed in the IR spectra of sodium *n*-dodecylbenzene sulfonate, the IR spectra of CDBS contain a band at 1380 cm^{-1}, assignable to the nitric ion, and a shoulder at 3150 cm^{-1}, assignable to the ammonium ion. These data show that 1.03 of the nitric ions in the original ceric diammonium hexanitrate were replaced by *n*-dodecylbenzene sulfonic ions. CDBS is soluble in ethyl acetate, methyl ethyl ketone, benzene, styrene, and diethyl ether, while it is insoluble in methyl, ethyl, amyl, *n*-octyl alcohol, and in acetone.

Polymerization was carried out *in vacuo* at 60°C for 48 hr. The concentration of CDBS in the polymerization mixture were expressed by the concentration of ceric ions. The results are shown in Table 1. Judging from the low conversions for such a long polymerization time, it can be said that the catalytic activity is low. It was an unexpected feature that ketone and aldehyde were better co-catalysts than alcohol. When ketones are used, radicals may be formed by the elimination of α-hydrogen atoms, because benzophenone, which has no α-hydrogen atoms, shows no catalytic activity. As for aldehyde, radicals may be formed, at least partly, by the elimination of aldehyde-hydrogen atoms, because benzaldehyde does show catalytic activity.

Table 1. Polymerization in the presence of various co-catalysts

Co-catalyst	mol/*l*	Conversion %
Methyl alcohol	1.0	1.81
Ethyl alcohol	0.50	1.8
Ethyl alcohol	1.0	2.2
Ethyl alcohol	1.5	1.6
Cyclohexanone	0.50	8.4
Cyclohexanone	1.0	11.3
Cyclohexanone	1.5	13.4
Cyclohexanone	2.0	12.7
Diethyl ketone	1.0	10.2
Caproic aldehyde	0.50	8.35
Caproic aldehyde	1.0	9.14
Benzaldehyde	1.0	3.46
Acetophenone	1.0	12.3
Acetone	1.0	5.4
Methyl ethyl ketone	1.0	10.8
Benzophenone	0.50	0
Ethyl acetate	1.0	0.31
Diethyl ether	1.0	0.33
—		0

CDBS: 4.43×10^{-3} mol/*l*
Styrene: 1.0 mol/*l*
Solvent: benzene

If the termination reaction is a combination of polymer radicals and if a steady state is assumed,

$$fk_i[Ce^{IV}\text{-complex}] - 2k_t[Mn\cdot]^2 = 0$$

the rate of polymerization can be expressed as follows:

1) S. Kaizerman, N. Plainfield and G. Mino, U. S. Pat. 2922801.
2) Y. Iwakura, T. Kurosaki and Y. Imai, *J. Polymer Sci.*, **A3**, 1185 (1965).
3) Y. Ogiwara, Y. Ogiwara and H. Kubota, Preprints for the 20th Annual Meeting of the Chemical Society of Japan (April, 1967), 4P213.

$$-d[M]/dt = k_p[Mn\cdot][M]$$
$$= k_p(fk_i/2k_t)^{1/2}[Ce^{IV}\text{-complex}]^{1/2}[M]$$

The rate of polymerization is proportional to the square root of the concentration of the Ce^{IV}-complex. If the termination reaction is the reaction of the polymer radical with the Ce^{IV}-complex and if a steady state is assumed,

$$fk_i[Ce^{IV}\text{-complex}] - k_t'[Mn\cdot][Ce^{IV}\text{-complex}] = 0$$

then

$$-d[M]/dt = fk_ik_p/k'_t[M]$$

Thus, the rate of polymerization is independent of the concentration of the Ce^{IV}-complex.

As shown in Fig. 1, when diethyl ketone or cyclohexanone was used, the rate of polymerization was proportional to the square root of the concentration of CDBS; therefore the termination reaction was a combination of polymer radicals: when ethyl alcohol was used, the rate of polymerization was independent of the concentration of CDBS; therefore, the termination reaction was a reaction of the polymer radical with CDBS.[2,4,5] When caproic aldehyde was used, the rate of polymerization increased with a decrease in the concentration of CDBS. This phenomenon may be interpreted in terms of the change in the dissociation constant of the complex of Ce^{IV} and aldehyde.

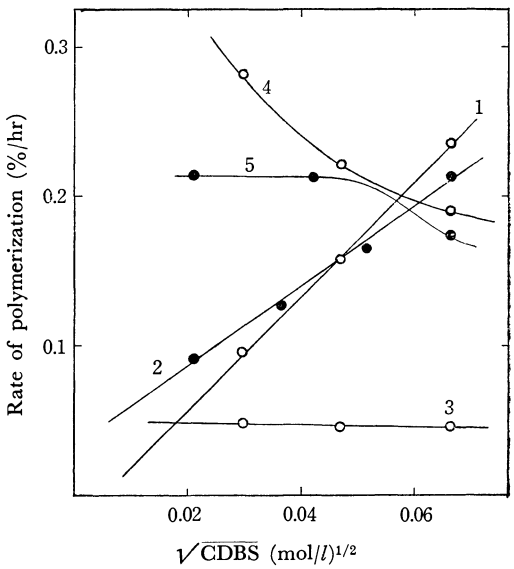

Fig. 1. Rate of polymerization *vs.* square root of the concentration of CDBS.
1 Cyclohexanone (1.0 mol/*l*)
2 Diethyl ketone (1.0 mol/*l*)
3 Ethyl alcohol (1.0 mol/*l*)
4 Caproic aldehyde (1.0 mol/*l*)
5 Caproic aldehyde (0.5 mol/*l*)

Further investigations are in progress on other organoceric compounds.

4) S. Kimura and M. Imoto, *Makromol. Chem.*, **42**, 140 (1960).
5) V. S. Ananthanarayanan and M. Santappa, *J. Appl. Polymer Sci.*, **9**, 2437 (1965).

Self-heating of a Thermistor in Temperature Measurements

Satohiro TANAKA

Government Chemical Industrial Research Institute, Tokyo, Shibuya-ku, Tokyo

(Received June 16, 1967)

The electrical resistances of a thermistor have found wide application as thermometric parameters. For this purpose, suitable resistance bridges are used to measure the resistance or unbalanced voltages of the bridges due to the variation in resistance accompanying a change in the ambient temperatures to be measured. Usually, the sensitivity of the bridge is improved as the bridge voltage is increased; however, this improvement encounters self-heating or rises in the temperature of the resistance thermometer element due to the dissipation of the electrical power produced in the element. At first, there is difference in temperatures between that of the thermometer element and the ambient medium. Secondly, a considerable deviation from the simple $\exp(b/T)$ law for thermistors is anticipated. For instance, Hutchinson and White[1] showed that, above a certain value of bridge voltage, unsatisfactory results were obtained in calorimetry. Therefore, it is necessary to clarify the effect before proceeding to precise measurements in thermometry.

If we assume a thermal equilibrium between the heat due to electrical power dissipation, W, produced in a thermistor element and the thermal leakage, which is proportional to the difference between the temperature, T, of the thermistor element and the ambient temperatures T_0 (Newton's law of cooling): then

1) W. P. Hutchinson and A. G. White, *J. Sci. Instrum.*, **32**, 309 (1955).

$$h(T - T_0) = W = V^2/R \quad (1)$$

where h is the heat transfer coefficient between the thermistor element and the ambient medium, R is the electrical resistance of the thermistor, and V is the voltage across the thermistor. Further, we assume a usual $\exp(b/T)$ temperature-variation law of the resistance:

$$R=A\exp(B/T), \quad (2)$$

where A and B are experimentally-determined constants. Then, from Eq. (1), the temperature, T, of the thermistor element is given by the equation:

$$T = T_0 + (V^2/hR), \quad (3)$$

and the temperature differences, ΔT, between the element and the ambient medium, by:

$$\Delta T = T - T_0 = V^2/hR. \quad (4)$$

By substituting the T from (3) into (2), one obtains:

$$R = A \exp\left\{B\Big/\left(T_0 + \frac{V^2}{hR}\right)\right\}. \quad (5)$$

If the temperature rise, ΔT, of the thermistor element due to electrical-heat dissipation is small compared to T_0 and T ($\Delta T \ll T_0$, T), Eq. (5) can be approximated as follows:

$$R = R_0 - \frac{BV^2}{hT_0^2}, \quad (6)$$

where R_0 is a extrapolated resistance value as $V\rightarrow 0$ on the straight portion of the plots in Fig. 1, an explanation of which will be given later.

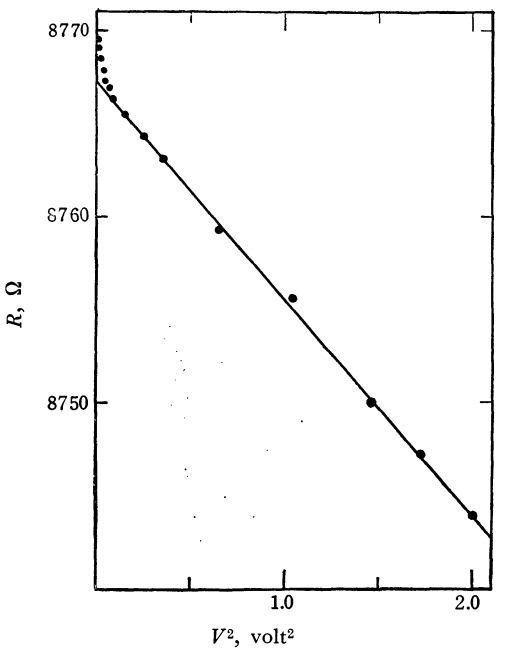

Fig. 1. Variation of electrical resistances with squares of voltage across thermistor at 25.00°C in water.

Experimental

Measurements were done on a bead-type OS41B-2 thermistor manufactured by Ōizumi Seisakusho, Ltd. The bead is coated with a skin film of glass to protect it. A d. c. Wheatstone bridge was used for the measurements of the resistance of the thermistor, and a National FM-5 primary cell was used for the power supply to the bridge. The thermistor was immersed in a thermostat held constant at ±0.002°C for extended periods of time. The signal from the bridge was amplified by a d. c. current amplifier (Ōkura AMl001B), the output of which was used to derive a recorder (Yokogawa LER-12). The bridge voltage was varied and measured by a conventional d. c. voltmeter. The measurements were carried out at 25, 35, 40, and 45°C.

Results and Discussion

The results of the measurements are shown in Fig. 1. This figure shows that Eq. (6) is valid except in low voltages across the thermistor. The slope of the plot in Fig. 1, together with the measurements of the variation in the resistance of the thermistor with the temperature, allows the constants A, B, and h to be approximately obtained; the values are:

$$A = 3.76\times 10^{-2}\ \Omega,$$
$$B = 3.69\times 10^{3}\text{°K} \quad (7)$$

and

$$h = 3.54\times 10^{-3}\ \text{W°K}^{-1},$$

where A and B are evaluated by assuming a simple relation, $R_0=A\exp(B/T)$, of the R values and h extrapolated from Eq. (6).

The effects of the variation in the voltage across the thermistor during temperature measurements are examined on this thermistor, the constants of which are given by (7) as follows:

1. The differences in temperature, ΔT, between that of the thermistor element and that of the ambient medium are evaluated from Eq. (4) as, for example, 7.05×10^{-3} ° (V=0.5 V) and 3.22×10^{-2} ° (V=1.0 V) on this thermistor.

2. The variation, ΔT, in the temperature of the thermistor due to the variation, ΔV, in voltage across the thermistor is given by:

$$\Delta T = (2V/hR)\Delta V \quad (8)$$

on the basis of Eq. (1). The variation in voltage must be maintained, if the variation in temperature should be kept less than ΔT, as follows:

$$(\Delta V/V)\times 100 < (hR/2V^2)\cdot\Delta T\times 100\%. \quad (9)$$

If the values of $\Delta T=10^{-5}$° and V=0.5 V are taken, Eq. (9) gives:

$$(\Delta V/V)\times 100 < 0.062\% \quad (10)$$

on the above-mentioned thermistor.

3. Let us now determine the errors in the temperature measurements caused by the self-heating of thermistor, if the simple $\exp(b/T)$ law of the thermistor is used. For this purpose, some numerical calculations were carried out on a model thermistor; in these calculations Eq. (5) was assumed to be valid, and the A, B and h constants were given by Eq. (7). Now let us see the temperature differences, δT, between the temperature, $T°$, obtained by using a simple $R=a\exp(b/T)$ law for this thermistor and that, T, given by Eqs. (5) and (7). The a and b constants can be determined by $R=a\exp(b/T)$ if the resistances are given as $R_1=10500\ \Omega$ and $R_2=7000\ \Omega$, and corresponding temperatures as T_1 and T_2 by Eq. (5), substituting the resistance values, R_1 and R_2. Then, using these values of a and b, the temperature, $T°$, is calculated for an arbitrary resistance, R, and for temperature differences, δT, between the $T°$ and T values given by Eqs. (5) and (7) for the same resistance, R. Figure 2 shows the temperature differences, $\delta T=T°-T$, thus calculated for various values of voltage, V, across the thermistor. Deviations from the true values of the temperature increase with the voltage across a thermistor, as shown in Fig. 2, if a thermistor whose calibration has been carried out at about 20 and 30°C using

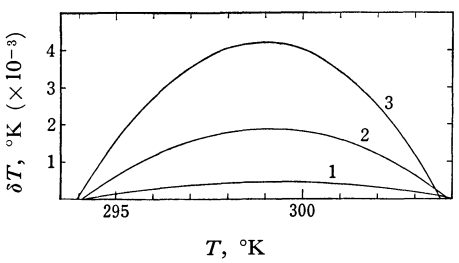

Fig. 2. Temperature differences $\delta T=T°-T$. T are given by Eqs. (5) and (7). $T°$ are calculated using relation $R=a\exp(b/T)$. Voltage V across the thermistor are $1V$ (1), $2V$ (2) and $3\,V$ (3).

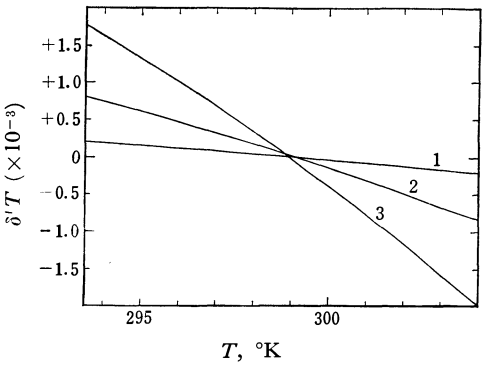

Fig. 3. First derivatives $\delta' T$ of δT with respect to T. $\delta' T$ are thought to be errors in measurements of temperature variations. Voltage V across the thermistor are $1V$ (1), $2V$ (2) and $3V$ (3).

$R=a\exp(b/T)$ is used to measure an absolute temperature between about 20 and 30°C.

A thermistor is generally used to measure temperature variations rather than absolute temperatures. Therefore, errors in the measurement of temperature variations should be examined. These errors may be defined as first derivatives, $\delta' T$, of δT with respect to T; they are shown in Fig. 3 for various voltages, V. Figures 2 and 3 also show an upper-limit value of voltage across the thermistor, a value which must not be exceeded for a desired degree of precision in the measurement of absolute temperatures and temperature variations when a simple $\exp(b/T)$ law is used.

The author wishes to acknowledge the interest and discussions of Dr. Kazuo Amaya, Mrs. Kazuko Sasaki, Mr. Ichirō Takeda and Dr. Tomoyoshi Kudō of this Institute. He also wishes to Mr. Masahiro Funazaki for tracing the figures in this manuscript, and Mr. Kaneharu Matsuo and Mr. Ryōichi Motohashi of Tōa Dempa Kōgyō, Ltd., for their suggestions.

Synthesis of Pyridoxine. I. Synthesis of 4-Methyl-5-ethoxycarbonyloxyoxazole

Masuo MURAKAMI and Masaru IWANAMI

Central Research Laboratory, Yamanouchi Pharmaceutical Co., Ltd., Azusawa-cho, Itabashi-ku, Tokyo

(Receved June 16, 1967)

Recently, Firestone *et al.*[1] reported the synthesis of pyridoxine by the Diels-Alder reaction of 4-methyl-5-alkyoxyoxazole with various dienophiles followed by acid treatment and reduction. They prepared the oxazoles from alanine through three steps, but the yield of the last step was very low.[2] In the present paper, We describe an efficient synthetic method of 4-methyl-5-ethoxycarbonyl-oxyoxazole (I) as well as its Diels-Alder reaction.

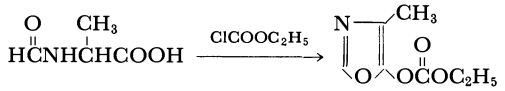

(I)

(1)

Compound I was obtained in 80% yield by treatment of *N*-formylalanine (1 mol) with ethyl chlorocarbonate (2 mol) in the presence of triethylamine at −10——20°C. The structure of I was confirmed by the elemental analysis and the spectral data.

A synthetic method of oxazole by the reaction of acylamino acid with ethyl chlorocarbonate has never been reported, except the report on the synthesis of 2-methyl-4-benzal-5-oxazolone (II) by the reaction of α-acetoaminocinnamic acid (III) with ethyl chlorocarbonate.[3] This result suggests that 4-methyl-5-oxazolone (IV) was intermediately formed and its enolized form, 4-methyl-5-hydroxyoxazole (V), further reacted with ethyl chlorocarbonate to form I.

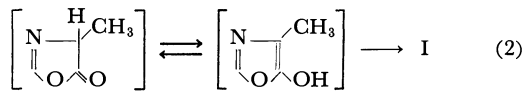

(IV) (V)

(2)

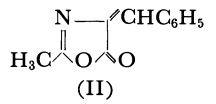

(II)

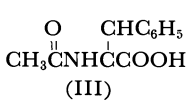

(III)

Although, IV could not be isolated, this mechanism may be supported by the following fact: 2-methyl-4-benzyl-5-oxazolone (VI)[4] was converted into 2-methyl-4-benzyl-5-ethoxycarbonyloxy-oxazole (VII) by treatment with ethyl chloro-carbonate under the same conditions.

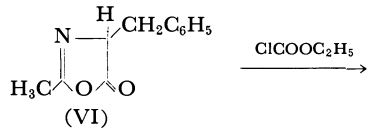

(VI)

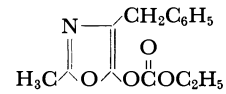

(VII)

(3)

As 4-methyl-5-alkoxyoxazole, I underwent the Diels-Alder reaction with various dienophiles. The resulting adducts were converted into pyridine derivatives on acid treatment: *e. g.*, by reaction with diethyl maleate, dimethyl thiofumarate or maleimide, I gave 2-methyl-3-hydroxy-4, 5-disubstituted pyridines. These pyridines were converted into pyridoxine by reduction. The reaction of I with maleic anhydride gave ethyl 2-methyl-3-hydroxypyridine-5-carboxylate accompanying with decarboxylation. But that of I with fumaronitrile in acetic acid produced 2-methyl-3-hydroxy-4, 5-dicyanopyridine, which was converted into pyridoxine by reduction.

Experimental

4-Methyl-5-ethoxycarbonyloxyoxazole (I). To a suspention of 10 g of formylalanine in 50 m*l* of chloroform, 18 g of triethylamine was added. The solution was cooled at −10——20°C. To the solution, 18.8 g of ethyl chlorocarbonate was added drop by drop at −10——20°C under stirring. After being kept for 2 hr at the same temperature, the reaction mixture was washed succesively with water, 1% hydrochloric acid and water, and dried over anhydrous magnesium sulfate. The solvent was removed from the reaction mixture to give an oily residue, which was distilled under reduced pressure to give 11.8 g of I, bp 80—82°C/5—6 mmHg, λ_{max} 1780 cm^{-1} (carbonic ester $\nu_{C=O}$), τ ($CDCl_3$): 8.60 (3H, triplet), 7.85 (3H, singlet), 5.70 (2H, quartet), and 2.39 (1H, singlet).

Found: C, 49.08; H, 5.47; N, 8.46%. Calcd for

1) Merck Co., British Pat. 966804. R. A. Firestone, E. E. Harris and W. E. Reuter, *Tetrahedron*, **23**, 943 (1967).

2) Merck Co., British Pat. 880595.

3) M. Brenner and K. Rufenacht, *Helv. Chim. Acta*, **37**, 203 (1954).

4) M. Bergmann, F. Stern and C. Witte, *Ann.*, **499**, 277 (1932).

$C_6H_9NO_4$: C, 49.12; H, 5.30; N, 8.18%.

Similarly, VII (170—171°C/7 mmHg, yield 6.2 g) was obtained from the reaction of VI[4] (6.1 g) with ethyl chlorocarbonate (3.1 g) in the presence of triethylamine (2.9 g).

Found: C, 64.44; H, 5.67; N, 5.31%. Calcd for $C_{13}H_{13}NO_4$: C, 64.36; H, 5.79; N, 5.36%.

The Reaction with Diethyl Maleate, Diethyl Fumalate or Dimethyl Thiofumarate. A mixture of 0.85 g of I and 1.7 g of diethyl maleate was heated at 120°C for 6 hr. After cooling, 20 m*l* of ethyl alcohol and 1 m*l* of 5 N ethanolic hydrochloric acid were added to the solution. The substance, which was obtained by evaporation of ethanol from the reaction mixture, was recrystallized from acetone to give 1.2 g of 2-methyl-3-hydroxy-4, 5-diethoxy carbonylpyridine, mp 149°C. It was identified with an authentic sample[5] by the mixed melting point.

Similarly, I reacted with diethyl fumarate to give 60% of 2-methyl-3-hydroxy-4, 5-diethoxycarbonylpyridine, and with dimethyl thiofumarate to give 1.2 g of 2-methyl-3-hydroxy-4, 5-dicarboxylic acid methyl thioester hydrochloride, mp 210—212°C.

Found: C, 40.53; H, 4.29; N, 4.79%. Calcd for $C_{10}H_{11}NO_3S_2$: C, 40.88; H, 4.12; N, 4.77%.

The Reaction with Maleic Anhydride. A solution of 1.7 g of I and 1.2 g of maleic anhydride in 20 m*l* of benzene was heated under refluxed for 30 min. After cooling, 2 m*l* of 5 N ethanolic hydrochloric acid was added to the solution. The solvent was evaporated at reduced pressure. The oily residue was dissolved in water and extracted with ether. After drying over anhydrous magnesium sulfate, the ether was removed. The residue was recrystallized from ethyl acetate to give 0.8 g of 2-methyl-3-hydroxy-5-ethoxycarbonylpyridine, mp 205—207°C.

Found: C, 59.65; H, 6.00; N, 7.25%. Calcd for $C_9H_{11}NO_3$: C, 59.70; H, 6.08; N, 7.44%.

5) E. E. Harris and R. A. Firestone, *J. Org. Chem.*, **27**, 2075 (1962).

The Reaction with Maleimide. A solution of 2.0 g of I and 1.0 g of maleimide in benzene was heated under reflux for 4 hr. The solvent was removed under reduced pressure. The residue was recrystallized from ethyl acetate to give 1.8 g of 2-methyl-3-hydroxypyridine-4, 5-dicarboximide, mp 250—252°C.

Found: C, 53.93; H, 3.49; N, 15.50%. Calcd for $C_8H_5NO_3$: C, 53.93; H, 3.40; N, 15.73%.

The Reaction with Fumaronitrile. A mixture of 1.0 g of I and 2.0 g of fumaronitrile was dissolved in 4 m*l* of acetic acid in a sealed tube. After heating at 140°C for 3 hr, the solvent was removed from the reaction mixture to give an oily residue, which was taken up in ether. The ethereal layer was dried over anhydrous magnesium sulfate and the ether was evaporated to give 0.6 g of 2-methyl-3-hydroxy-4, 5-dicyanopyridine, mp 189—191°C. It was identified with an authentic sample[5] by the IR spectra and the mixed melting point.

2-Methyl-3-hydroxy-4, 5-diaminomethylpyridine Trihydrochloride. A mixture of 1.3 g of 2-methyl-3-hydroxy-4, 5-dicyanopyridine and 1.0 g of palladium charchoal (1 : 10) was suspended in 100 m*l* of methanol. The reduction was carried out for 6 hr under hydrogen of the atomospheric pressure at room temperature. After absorption of 4 mol of H_2 was over, the catalyst was filtered off and 1 m*l* of 5 N methanolic hydrochloric acid was added to the filtrate. The solvent was removed from the reaction mixture to give 1.7 g of 2-methyl-3-hydroxy-4, 5-diaminomethylpyridine trihydrochloride, mp 296°C dec. (lit., 296°C dec.)[5] It was identified with an authentic sample by the IR spectra.

Pyridoxine Hydrochloride. To a solution of 4.9 g of 2-methyl-3-hydroxy-4, 5-diaminomethylpyridine trihydrochloride dissolved in 80 m*l* of 2 N hydrochloric acid, 1.7 g of sodium nitrite in 10 m*l* of water was added in small portions at room temperature. After stirring for 4 hr, the solvent was evaporated *in vacuo* below 40°C. Pyridoxine hydrochloride was obtained from the residue by recrystallization from dilute ethanol, mp 206—208°C. It was identified with an authentic sample by the mixed melting point and IR spectra.

Hydrogenation, Hydrogenolysis, or Isomerization of Dienes and Monoenes Catalyzed by the Nickel Cyanide Complex

Taiichi MIZUTA, Hiroshi SAMEJIMA and Takao KWAN

Faculty of Pharmaceutical Sciences, The University of Tokyo, Hongo, Tokyo

(Received June 28, 1967)

The hydrogenation, hydrogenolysis, and isomerization of allene, butadiene, isoprene, butene, and some of their derivatives were studied in an aqueous solution containing the nickel cyanide complex and excess sodium borohydride. The catalytic behavior of the nickel cyanide complex appeared to be somewhat different from that of the cobalt cyanide complex reported on in previous works.[1-5]

The catalyst formation was as follows. A tetracyanonickelate(II) complex, $Ni(CN)_4^{2-}$, dissolved in an aqueous solution gave a homogeneous red solution, accompanied by the evolution of hydrogen

1) J. Kwiatek, I. L. Mader and J. K. Seylor, "Advances in Chemistry Series, Reaction of Coordinated Ligands and Homogeneous Catalysis," A. C. S. (1963).
2) T. Mizuta and T. Kwan, *Nippon Kagaku Zasshi (J. Chem. Soc. Japan, Pure Chem. Sect.)*, **86**, 1010 (1965).
3) T. Suzuki and T. Kwan, *ibid.*, **86**, 713 (1965).
4) T. Suzuki and T. Kwan, *ibid.*, **86**, 1342 (1965).
5) T. Mizuta and T. Kwan, *ibid.*, to be published.

TABLE 1. THE REACTION OF DIENES AND MONOENES WITH SODIUM BOROHYDRIDE IN THE PRESENCE OF THE NICKEL CYANIDE COMPLEX $T=0°C$

Substrate	Product, %			
	Isopentane	2-Me-1-Butene	2-Me-2-Butene	3-Me-1-Butene
$CH_2=C-CH=CH_2$ CH_3	0	21	79	trace
	Butane	1-Butene	*trans*-2-Butene	*cis*-2-Butene
$CH_2=CH-CH=CH_2$	trace	14	65	21
$CH_3CH=CH-CH_2Cl$	6	18	59	17
$CH_3-CH=CH-CH_2OH$	6	70	17	7
$CH_2-CH-CH=CH_2$ OH	trace	1	65	34
	Propane		Propylene	
$CH_2=C=CH_2$	20		80	
$CH_2=CH-CH_2Cl$	21		79	
$CH_2=CH-CH_2Br$	21		79	
$CH_2=CH-CH_2I$	23		77	
$CH_2=CH-CH_2NCS$	25		75	
$CH_2=CH-CH_2OCOCH_3$	27		73	
$(CH_2=CH-CH_2)_2S$	23		77	
$CH_2=CH-CH_2OH$	4		96	
$CH_2=CH-CH_2NH_2$	6		94	
$(CH_2=CH-CH_2)_2O$	3		97	

gas when excess sodium borohydride was added. The UV absorption peaks shifted from 268 and 285 mμ to 318 and 475 mμ. A red crystalline compound was isolated and subjected to the IR absorption measurement. The spectra appeared to agree entirely with that reported by El-Sayed and Sheline,[6] who studied the IR spectrum and the structure of the hexacyanodinickelate (I) complex, $K_4[Ni_2(CN)_6]$. The addition of allene, butadiene, or isoprene made the color of the solution change from red to yellow. The UV absorption measurements showed maxima at 303 mμ (allene), 315 mμ (butadiene), and 302 mμ (isoprene).

The apparatus and procedure for the measurement of the reaction were almost the same as those reported previously.[3,5] The reaction took place rapidly and was completed within ten to thirty minutes, depending on the kind of substrates at 0°C, when the amount of the substrate was not greater than that of the complex. The products were usually collected after thirty minutes' contact and were analyzed by gas chromatography. Their compositions are shown in Table 1, where the substrates investigated are listed in the first column.

As is shown in Table 1, isoprene gave three olefins, with no paraffin, just as in the case of the cobalt cyanide complex with a CN/Co molar ratio of less than five.[4] Butadiene and butenyl derivatives also gave rise to three olefin isomers. Table 1 shows also that the reductive elimination of a substituted group, such as halogen or hydroxyl, takes place. In this connection it is of interest to note that the distribution of the three isomers produced is sensitive to the kind and the position of the substituted group.

Allene and allyl derivatives gave both propane and propylene, proving that the nickel cyanide complex is active in both hydrogenation and hydrogenolysis. As has already been reported,[3] the cobalt cyanide complex yielded propylene exclusively from allyl halides. Again, the selective formation of propane and propylene appeared to depend on the kind of substituted group; that is, both allyl alcohol and allyl amine gave more propylene than allyl halides. It should be mentioned that the rate of the reaction is faster with allyl halides than with allyl alcohol or amine.

When 1-butene or *cis*-2-butene was introduced,

TABLE 2. THE ISOMERIZATION OF 1-BUTENE IN THE PRESENCE OF $Ni(CN)_4^{2-}$-$NaBH_4$ $T=0°C$
4 mmol of $Na_2Ni(CN)_4\cdot 3H_2O$
36 mmol of $NaBH_4$
1 mmol of 1-butene in 100 m*l* of H_2O

Time min	1-Butene	*trans*-2-Butene	*cis*-2-Butene	Butane
0	100	0	0	0
10	50	27	14	9
20	45	30	15	10
40	40	34	16	10
120	28	44	17	11
Equilibrium	3	75	22	—

6) M. F. El-Sayed and R. K. Sheline, *J. Am. Chem. Soc.*, **72**, 702 (1956).

Table 3. The isomerization of *cis*-2-butene in the presence of $Ni(CN)_4^{2-}$-$NaBH_4$, $T=0°C$
The composition of the reacting solution is the same as that of Table 2.

Time min	*cis*-2-Butene	1-Butene	*trans*-2-Butene	Butane
0	100	0	0	0
10	65	trace	35	trace
60	60	1	38	1
120	55	2	41	2
180	53	2	43	2

the isomerization of the butene took place, and a small amount of *n*-butane was formed. The results are shown in Tables 2 and 3. The isomerization of butenes was not detectable with the cobalt cyanide complex.[3] It can be seen from Tables 2 and 3 that *trans*-2-butene, thermodynamically most stable, surpasses the other isomer during the course of the reaction. The rate of the isomerization seems much slower than that of the hydrogenation of butadiene, but faster than the rate of formation of butane.

Let us now discuss some of the results. The hydrogenation of acetylene or butadiene in the presence of the nickel cyanide complex and sodium amalgam has been reported briefly.[7,8] Little is known, however, about the mechanism of the reaction. We have already shown[4] that isoprene is hydrogenated almost exclusively to 2-methyl-2-butene by the cobalt cyanide complex only when the CN/Co molar ratio is kept below five. In other words, two-site coordination[9] is necessary for isoprene to be hydrogenated to 2-methyl-2-butene.

The hydrogenation of isoprene and butadiene by sodium borohydride in the present case yielded 2-methyl-2-butene and *trans*-2-butene, respectively, as the major products. Therefore, it seems reasonable to assume that the same sort of interaction is operative between dienes and the nickel cyanide complex. Thus, it is tentatively suggested that the nickel cyanide complex forms a π-allyl type of intermediate, such as:

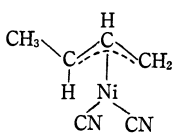

The addition of a hydrogen atom to the less hindered terminal methylene may produce *trans*-2-butene, although it is not certain whether the hydrogen atom comes directly from sodium borohydride or from nickel hydride.

It is of interest to note that butenyl chloride and butenyl alcohol react at different rates and give different distributions of the butene isomers produced. The difference can probably be explained as follows. Butenyl chloride loses its chlorine atom easily and gives a π-allyl type intermediate, for it gave almost the same distribution of the olefins formed as did butadiene. On the other hand, butenyl alcohol may form a π-type intermediate complex without losing its hydroxyl group.

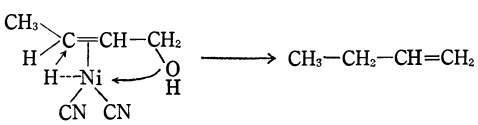

If the hydrogen atom attacks the γ-carbon of the intermediate, followed by the elimination of the hydroxyl group, 1-butene may be expected to form mainly, as was the case. The dominant formation of *trans*-2-butene from CH_3-CH(OH)-CH=CH_2 can also be explained if a similar sort of mechanism is assumed.

7) M. S. Spencer and D. A. Dowden, U. S. Pat. 2966534 (1960).
8) M. G. Burnett, *Chem. Commn.*, 507 (1965).
9) T. Suzuki and T. Kwan, *Nippon Kagaku Zasshi (J. Chem. Soc. Japan, Pure Chem. Sect.)*, **87**, 395 (1966).

Cyclizations of Acetylene Derivatives with Tri-β-styrylchromium*[1]

Masao SATO and Yasumasa ISHIDA

Tokyo Institute of Technology, Ookayama, Meguro-ku, Tokyo

(Received July 13, 1967)

It is known that triorganochromium compounds are decomposed rapidly by either the acidic hydrogen of acetylene or monosubstituted acetylenes to give no cyclization product,[1] and that those materials cyclize disubstituted acetylenes to give two types of products,[1-3] hexasubstituted benzene derivatives and condensed products in which two molecules of the acetylene are combined with one of the groups attached to chromium by hydrogen abstraction. In these reactions, an unsym-disubstituted acetylene derivative has not been used as the acetylene derivative.

In cyclizations with tri-β-styrylchromium, 1, 2, 4-triphenylbenzene was obtained from phenylacetylene, *i. e.*, monosubstituted acetylene. Moreover, 1, 2, 4-trimethyl-3, 5, 6-triphenylbenzene was produced, with no 1, 3, 5-trimethyl-2, 4, 6-triphenylbenzene, from methylphenylacetylene, *i. e.*, unsym-disubstituted acetylene. In these reactions no condensed product was obtained.

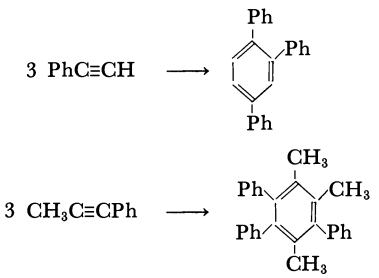

It seems that the tri-β-styrylchromium compound is stabilized by a great conjugated system of the styryl group to be stabilized against the acidic hydrogen of phenylacetylene.

The reason why 1, 2, 4-triphenylbenzene is produced from phenylacetylene, while 1, 2, 4-trimethyl-3, 5, 6-triphenylbenzene is produced from methylphenylacetylene, is probably as follows: two molecules of the acetylene derivative approach a chromium compound along the direction of less resistance, forming a 1, 4-disubstituted cyclobutadiene complex or a 1, 4-disubstituted butadiene biradical, and then the third acetylene molecule reacts with the complex or the biradical formed above to produce a 1, 2, 4-trisubstituted benzene derivative.

Experimental

Cyclization of Phenylacetylene with Tri-β-styrylchromium. A tetrahydrofuran solution of β-styrylmagnesium bromide (63 m*l*, 40.4 mmol) was added, under nitrogen at −75°C, to 5.0 g (13.3 mmol) of chromium trichloride tristetrahydrofuranate[4] suspended in 200 m*l* of tetrahydrofuran. This solution changed rapidly from deep purple to brown. After the mixture had been stirred for 1 hr at −75°C, 4.4 m*l* (40.4 mmol) of phenylacetylene were added to the solution obtained above. The reaction mixture was allowed to warm to 20°C over a 2 hr period and then refluxed for 6 hr. After the solvent had been evaporated *in vacuo*, the residue was hydrolyzed with ice water and the organic products were extracted with benzene. The brownish residue obtained from the benzene solution was dissolved in a minimum amount of benzene and chromatographed on 80 g of activated alumina. Elution with 150 m*l* of *n*-hexane gave 2.6 g of a white crystalline material. The recrystallization of this material from *n*-hexane gave 1, 2, 4-triphenylbenzene melting at 120°C (lit.[5] mp 119—120°C). The present sample was identical in all respects with an authentic sample.

Found: C, 93.65; H, 6.32%. Calcd for $C_{24}H_{18}$: C, 94.12; H, 5.88%. Further elution with 150 m*l* of *n*-hexane gave 2.1 g of 1t, 4t-diphenylbutadiene-(1, 3) melting at 152.5°C (lit.[6] mp 152°C).

Found: C, 92.84; H, 7.12%. Calcd for $C_{16}H_{14}$: C, 93.15; H, 6.85%. Finally, elution with 300 m*l* of benzene gave intractable tars which were not investigated further.

Cyclization of Methylphenylacetylene with Tri-β-styrylchromium. A tetrahydrofuran solution of β-styrylmagnesium bromide (94 m*l*, 60.4 mmol) was added, under nitrogen at −75°C, to 7.5 g (20 mmol) of chromium trichloride tristetrahydrofuranate suspended in 250 m*l* of tetrahydrofuran. After the mixture had been stirred for 1 hr at −75°C, 22 m*l* (180 mmol) of methylphenylacetylene were added to the solution. This reaction mixture was allowed to warm to 20°C over a 2-hr period and then refluxed for 6 hr. Then, the tetrahydrofuran and the unreacted methylphenylacetylene were evaporated *in vacuo*. The residue was hydrolyzed with ice water, and the organic products

*1 The essence of this paper was presented at the 20th Annual Meeting of the Chemical Society of Japan, Tokyo, April, 1967.

1) H. Zeiss, Organometallic Chemistry, Am. Chem. Soc. Monograph No. 147, Reinhold, New York, 1960, p. 411.

2) W. Herwig, W. Metlesics and H. Zeiss, *J. Am. Chem. Soc.*, **81**, 6203 (1959).

3) H. P. Throndsen, W. Metlesics and H. Zeiss, *J. Organometal. Chem.*, **5**, 176 (1966).

4) R. P. A. Sneeden and H. Zeiss, *J. Organometal. Chem.*, **4**, 355 (1965).

5) C. G. Overberger and J. M. Whelan, *J. Org. Chem.*, **24**, 1155 (1959).

6) M. Tsutsui and M. N. Levy, *Z. Naturforsch.*, **21b**, 823 (1966).

were extracted with benzene. The brownish residue obtained from the benzene solution gave, by chromatography on activated alumina, 1.8 g of 1t, 4t-diphenylbutadiene-(1, 3) and 7.1 g of white crystalline of 1, 2, 4-trimethyl-3, 5, 6-triphenylbenzene melting at 224°C (lit.[7] mp 225—227°C).

Found: C, 93.10; H, 6.85%. Calcd for $C_{27}H_{24}$: C, 93.06; H, 6.94%. The remainder was intractable tars which were not investigated further.

Cyclization of Diphenylacetylene with Tri-β-styrylchromium. A tetrahydrofuran solution of β-styrylmagnesium bromide (118 m*l*, 60.7 mmol) was added to 7.5 g (20 mmol) of chromium trichloride tristetrahydrofuranate and 3.6 g (20 mmol) of diphenylacetylene in 250 m*l* of tetrahydrofuran under nitrogen at −75°C. After it had been stirred for 1 hr at −75°C, the reaction mixture was allowed to warm to 20°C over a 2 hr period and then refluxed for 15 hr. After the solvent had been evaporated *in vacuo*, the residue was hydrolyzed with ice water and the organic products were extracted with benzene. The brownish residue obtained from the benzene solution gave, by chromatography on activated alumina, 1.77 g of 1t, 4t-diphenylbutadiene-(1, 3) and 3.10 g of white crystalline of hexaphenylbenzene melting at 415°C (lit.[3] mp 408—415°C). The present sample was identical in all respects with an authentic sample.

Found: C, 93.94; H, 5.80%; mol wt, 520 (osmotic pressure in benzene). Calcd for $C_{42}H_{30}$: C, 94.38; H, 5.62%; mol wt, 534.

7) W. Huebel and C. Hoogzand, *Chem. Ber.*, **93**, 103 (1960).

Raman Spectra of DNA in Aqueous Solution

Koichi HIRANO

Department of Natural Sciences, Faculty of Education, Tohoku University, Kawa-uchi, Sendai

(Received July 21, 1967)

The infrared absorption spectra of DNA and polynucleotide have been studied by several workers,[1-3] but little work has been reported on the Raman spectra of an aqueous solution of DNA. In this note the author will report on the Raman spectra of an aqueous solution of DNA.

The calf-thymus DNA was purchased from the Sigma Chemical Co. The concentrations used were *ca.* 2 mg/25 m*l* tris buffer solution at pH=7.4. In order to cancel out the background due to the solvent molecules, tris buffer solutions were used as the reference substances. Before measurement the solutions were centrifuged at 1×10^4 g for 60 min. All the measurements were made at room temperature. The excitation wavelengths were in the vicinity of 260 mμ and of 400 mμ. A slightly-modified Hitachi photoelectric spectrofluorometer was used for both the selection of the excitation ray and the analysis of the scattering spectrum. No fluorescence was observed in these measurements. To obtain the Raman spectra, the correction for Rayleigh scattering was made by the use of Eq. (1)[4,5]:

$$\left.\begin{aligned} &I_{\theta=(\pi/2)}(\lambda) = \\ &\left\{\frac{2\pi^2n_0^2}{Nr^2\lambda^4}\right\}\left(\frac{dn}{dc}\right)^2 CM^2 2/z^2\{z-1+e^{-z}\}I_0(\lambda) \\ &z = 2/3\left\{\frac{2\pi Rn_0}{\lambda}\right\}^2 \sin^2\left(\frac{\pi}{4}\right) \end{aligned}\right\} \quad (1)$$

where $I_{\theta=(\pi/2)}(\lambda)$ is the relative intensity of the Rayleigh scattering in the direction of $\theta=\pi/2$; $I_0(\lambda)$ the relative intensity of the incident ray; λ, the wavelength; r, the constant determined from the instrument; N, the Avogadro number; c, the concentration of the sample solution (g/m*l*); M, the molecular weight; R, the end-to-end distance of the random-coiling DNA,[6] and n_0 and n, the refractive indices of the solvent and of the solution, respectively.

The corrected scattering spectrum of DNA

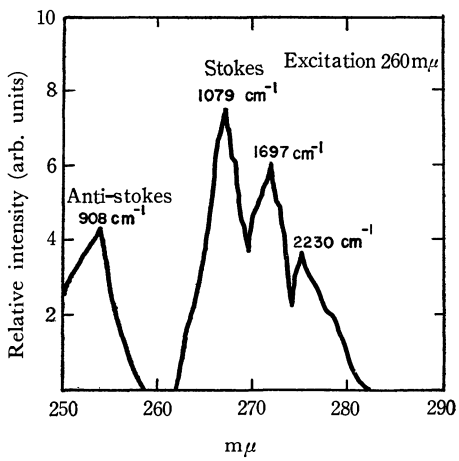

Fig. 1. Raman spectrum of DNA solution.

1) R. S. Morgan and E. R. Blout, *J. Am. Chem. Soc.*, **81**, 4625 (1959).
2) M. Tsuboi, *Seibutu-Buturi*, **3**, 95 (1963).
3) E. M. Bradbury, W. C. Price and G. R. Wilkinson, *J. Mol. Biol.*, **3**, 301 (1961).
4) L. Rayleigh, *Proc. Roy. Soc. (London)*, **A90**, 218 (1914).
5) P. Debye, *J. Phys. Colloid Chem.*, **51**, 18 (1947).
6) M. E. Reichmann, S. A. Rice, C. A. Thomas and P. Doty, *J. Am. Chem. Soc.*, **76**, 3047 (1954).

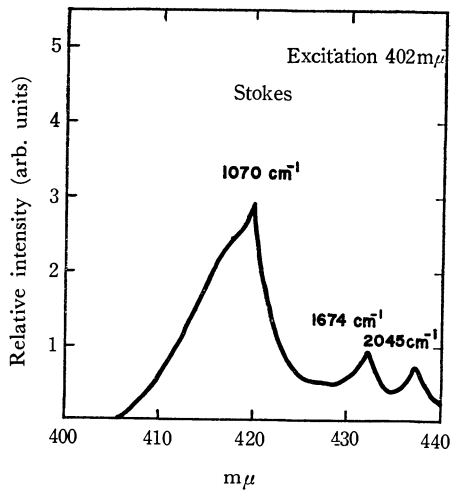

Fig. 2. Raman spectrum of DNA solution.

excited at 260 mμ is illustrated in Fig. 1, in which four frequencies, $\tilde{\nu}_1 \simeq 908\ cm^{-1}$, $\tilde{\nu}_2 \simeq 1079\ cm^{-1}$, $\tilde{\nu}_3 \simeq 1697\ cm^{-1}$ and $\tilde{\nu}_4 \simeq 2230\ cm^{-1}$, are characteristic. In Fig. 2 a similar spectrum excited at 402 mμ is displayed. From the figure it is obvious that three frequencies, $\tilde{\nu}_2 \simeq 1070\ cm^{-1}$, $\tilde{\nu}_3 \simeq 1674\ cm^{-1}$ and $\tilde{\nu}_4 \simeq 2045\ cm^{-1}$, are very similar to those of Fig. 1. These facts lead us to the conclusion that the corrected scattering spectra presented here are the Raman spectra of DNA in solution. That the anti-Stokes line, $\tilde{\nu}_1 \simeq 908\ cm^{-1}$, was not observed in the spectra may be attributed to the error arising from the correction of Rayleigh scattering, because the spectral intensity of the scattering ray deviates from the Gaussian distribution. On the basis of these results, the Raman frequencies of DNA in a tris buffer solution were estimated to be as shown in Table 1. The assignment of the frequencies listed in Table 1 based on the data of the infrared spectra of the purine base,[7] poly-A, DNA,[8,9] and on the Raman spectra of dimethyl phosphate anions.[10]

Table 1. Raman frequencies of DNA in an aqueous solution

	Frequency, cm^{-1}	Assignment
$\tilde{\nu}_1$	908	Sym. [OPO] stretching
$\tilde{\nu}_2$	1070—1079	Sym. $[PO_2]^{-1}$ stretching
$\tilde{\nu}_3$	1674—1697	C=C, C=N stretching in the purine ring
$\tilde{\nu}_4$	2045—2230	?

The Raman frequencies listed in Table 1 correspond well to the infrared absorption maxima of poly-A or DNA.[2] On the contrary, the chart produced by the commercial Raman spectrophotometer did not give any significant frequencies for these solutions. Therefore, the measurement of the Raman scattering described here would be a very useful tool for the study of macrobiomolecules in solution.

7) C. H. Willits, J. C. Decius, K. Diele and B. E. Christensen, *ibid.*, **77**, 2569 (1955).
8) M. Tsuboi, *Prog. Theoret. Phys., Supple.*, **17**, 99 (1961).
9) M. Tsuboi, *J. Am. Chem. Soc.*, **79**, 1351 (1957).
10) T. Shimanouchi, M. Tsuboi, Y. Kyogoku and J. Duchesen, ed., "The Structure and Properties of Biomolecules and Biological Systems," Interscience Publishers, London (1964), p. 476.

ESR Studies of Naphthalene-alkali Metal Ion Pairs. The Effect of Alkali Ions on the Proton-coupling Constants and the Structure of the Ion Pairs

Masamoto IWAIZUMI,* Masayasu SUZUKI,** Taro ISOBE* and Hiroshi AZUMI**

* *Chemical Research Institute of Non-Aqueous Solutions, Tohoku University, Katahira-cho, Sendai*

** *Department of Chemistry, Faculty of Science, Tohoku University, Katahira-cho Sendai*

(Received August 8, 1967)

Following the work of Adam and Weissman[1] and Atherton and Weissman,[2] a number of ESR investigations of radical anion-alkali metal ion pairs have been reported. In the pioneering work of Atherton and Weissman, they suggested that in naphthalene-alkali metal ion pairs the equilibrium position of the alkali ion was situated above the nodal plane of the lowest antibonding molecular orbital of naphthalene, *i. e.*, above the 9—10 bond; they suggested this on the basis of an examination of the temperature dependence of the alkali metal hyperfine splittings. Although they found no variation in the proton-coupling constants on the formation of the ion pair, thereafter a few examples showing a variation in the proton coupling

1) F. C. Adam and S. I. Weissman, *J. Am. Chem. Soc.*, **80**, 1518 (1958).
2) N. M. Atherton and S. I. Weissman, *ibid.*, **83**, 1330 (1961).

TABLE 1. THE COUPLING CONSTANTS OF THE NAPHTHALENE RADICAL ANION*

Solvent	Cation	Proton coupling constant (in gauss)		Metal coupling constant (in gauss)
		a_α	a_β	a_M
Dioxane	Li	4.792	1.788	1.213
Dioxane	Na	4.871	1.857	1.295
Dioxane	K	4.861	1.837	—
DMF	Li, Na, K	4.906	1.812	—

* the values at 24°C.

TABLE 2. THE EFFECT OF CATIONS ON THE PROTON COUPLING CONSTANTS

	Observation (in gauss)*1			Calculation (in gauss)	
	$Naph^-$-Li^+	$Naph^-$-Na^+	$Naph^-$-K^+	Model A*2	Model B*3
a_α	−0.114	−0.035	−0.045	−0.176	−0.349
a_β	−0.024	+0.045	+0.025	+0.205	+0.003

*1 The values were obtained by taking the difference between the proton coupling constants observed in dioxane and in DMF; $a_{diox.}-a_{DMF}$.

*2 The cation was assumed to be above the center of the molecular plane of the radical anion and at a distance of 3.5 Å from it.

*3 The cation was assumed to be hopping rapidly from the position above the center of the one benzene ring to that of the other benzene ring. The distance between the two ions was taken to be 2.8 Å.

constants with alkali ions have been reported.[3] In this paper we wish to report the effect of the ion pair formation on the proton-coupling constants observed for the naphthalene-alkali ion system in dioxane. As is well known, dioxane is a good solvent for the formation of ion pairs; we could observe significant changes in the proton-coupling constants, changes attributable to the effect of the alkali ion in the solvent. Through an examination of these data in terms of the MO method, we will estimate the structure of the ion pairs.

Table 1 gives the observed proton-coupling constants of the naphthalene radical anion in dioxane, together with the data observed in dimethylformamide (DMF). As the table shows, in dioxane the proton-coupling constants varied significantly with the alkali ions, while no variation was observed in DMF. In DMF, the radical anions showed no alkali metal hyperfine splittings, either. The negligible cation effect on the proton-coupling constants and the lack of the alkali metal coupling constant suggest that the radical anion may exist as a "free" anion, or as "a weak ion pair" (a solvent-separated ion pair) in which the radical anion is scarcely perturbed at all by the cation. Hence, one may estimate the effect of the formation of the ion pair on the proton-coupling constants by taking the difference between the proton-coupling constants observed in dioxane and in DMF. Table 2 shows the difference between the coupling constants observed in these two solvents. It shows that the proton-coupling constant at the α position may decrease on the formation of the ion pair with a sodium or potassium ion, while that at the β position may increase. Interestingly, however, on the formation of the ion pair with a lithium ion, the proton-coupling constants at both the α and β positions decrease, the coupling constant at the α position more extensively than is the case for the ion pair with sodium or potassium ion, while that at the β position does so only slightly.

To account for these observations and to obtain information on the structure of the ion pairs, we examined the interaction between the two ions in terms of the MO method. The details of the method used for the calculations have been described in a previous paper.[3b] For the present paper the proton-coupling constants were calculated from the spin densities using Colpa and Bolton's relation.[4]

In the naphthalene-alkali metal ion pairs, the most plausible structure for the ion pairs may be that in which the equilibrium position of the alkali ion is just above the center of the molecular plane of the radical anion. As is shown in Fig. 1, the MO calculation admittedly suggests that such an ion-pair structure may be most likely when the distance between the two ions is larger than about 3.5 Å.

3) a) A. H. Reddoch, *J. Chem. Phys.*, **43**, 3411 (1965). b) M. Iwaizumi, M. Suzuki, T. Isobe and H. Azumi, This Bulletin, **40**, 1325 (1967).

4) J. P. Colpa and J. R. Bolton, *Mol. Phys.*, **6**, 273 (1963).

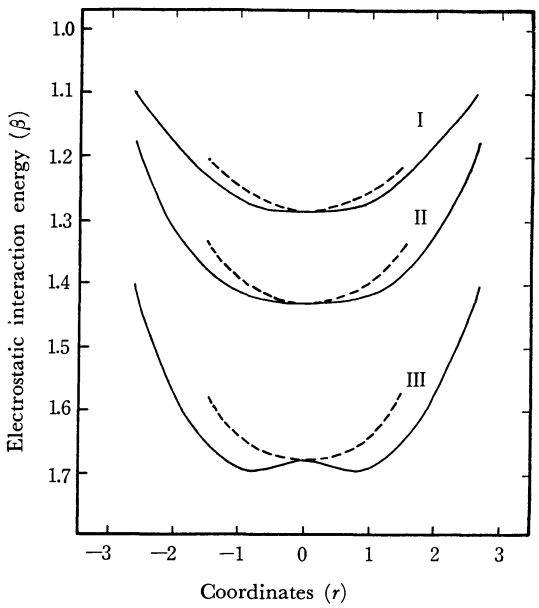

Fig. 1. Electrostatic interaction within Naphthalene-alkali metal ion-pair.
The origin of the coordinates is taken at the center of the anion molecule. Solid lines correspond to x coordinate (long axis) and dotted lines to y coordinate (short axis). The coordinates are in unit of r, a C–C bond length (1.39 Å). The distance between the two ions is taken as I: 4.0 Å, II: 3.5 Å and III: 2.8 Å, respectively.

Then, we attempted to calculate the proton-coupling constants in the presence of the cation, assuming that the alkali ion is placed just above the center of the molecular plane and at a distance of 3.5 Å from it. The results are shown in Table 2 (model A). As the table shows, the qualitative behavior of the calculations is in good agreement with the observation for the ion pairs with sodium and potassium ions rather than for the ion pair with a lithium ion; *i. e.*, the calculation predicts well the decrease in the α proton-coupling constant and the increase in the β proton-coupling constant.

As has been noticed above, the ion pair with a lithium ion shows a different behavior in the proton-coupling constants from in the cases of the ion pairs with sodium and potassium ions. This fact may imply that the structure of the ion pair is somewhat different from those of the ion pairs with a sodium or potassium ion. As it is, one may notice that in Fig. 1 the double minima occur well in the potential as the distance between the two ions becomes shorter. Since the lithium ion can approach the molecular plane more closely, it may be expected that with the lithium ion we can see a potential with double minima. Therefore, the calculation for the proton-coupling constant was attempted on the assumptions that the equilibrium position of the alkali ion is above the center of the benzene ring and that the alkali ion migrates rapidly back and forth between the two equilibrium positions above the anion molecule, so as to average the coupling constants of the protons at positions symmetrical to the short axis of the molecule. As Table 2 (model B) shows, the calculation predicts well the qualitative change in the effect of the cation upon going from the ion pair with a sodium or potassium ion to that with a lithium ion. Although the changes in the proton-coupling constants calculated are rather large compared to the observed ones, considering the nature of the calculation the results of the calculation are rather satisfactory. Therefore, one may conclude that the most likely structure of the naphthalene-sodium or -potassium ion pair in dioxane is that in which the equilibrium position of the alkali ion is situated above the center of the molecular plane of the naphthalene radical anion, while in the case of the ion pair with a lithium ion in dioxane the equilibrium position of the lithium ion may be rather above the benzene ring and the lithium ion may migrate between the two equilibrium positions.

In the case of the naphthalene-potassium system in dioxane, no potassium hyperfine splitting was observed. However, in view of the fact that the proton-coupling constants are affected by the potassium ion in a way similar to the case of the sodium ion, an ion pair must be formed. The lack of a splitting from the potassium ion is probably due to the small magnetogyric ratio of ^{39}K.

Recently, Smid *et al.*[5] reported that the naphthalene sodium metal ion pair in dioxane must be a contact ion pair. Our conclusion regarding the ion pair with a lithium ion may suggest that the naphthalene-lithium metal ion pair is also a contact ion pair in dioxane.

The numerical calculations were carried out on the NEAC 2230 at the Computer Center, Tohoku University.

The authors wish to express their appreciation to Miss Akie Sakai for her help throughout this work.

5) T. E. Hogen-Esch and J. Smid, *J. Am. Chem. Soc.*, **88**, 307 (1966).

On the Formation of Benzonitrile from Benzaldehyde and Ammonia. III. A Role of the Existing Base[1,2]

Akira MISONO, Tetsuo OSA and Seiichiro KODA

Department of Industrial Chemistry, Faculty of Engineering, The University of Tokyo, Hongo, Bunkyo-ku, Tokyo

(Received August 15, 1967)

In the preceding paper,[1] the authors reported on the mechanism of the oxidative formation of benzonitrile from benzaldehyde and ammonia in a methanol solution with oxygen catalyzed by some copper compounds. It was assumed that the aldehyde and ammonia reacted to produce benzilideneimine, from which was produced the corresponding nitrile oxidatively. Though it was observed that the basicity played an important role in the oxidation step, its exact role remained ambiguous to be made clear in this paper. The rates of the formation of benzonitrile against various concentrations of cupric chloride as a main catalyst with the concentration of sodium hydroxide being kept constant were observed and are shown in Fig. 1. The reaction rates were almost independent on the concentration of cupric chloride in the region where the concentration of cupric chloride was over a certain limit. From the consideration of this result and of the experimental results reported in the preceding paper,[1] such as

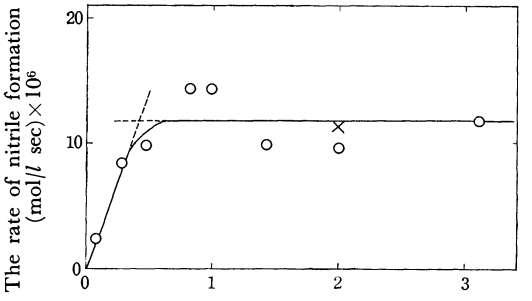

Fig. 1. The dependence of the reaction rate on the concentration of cupric chloride.
Initial conditions:

$CuCl_2$	0.095—3.11 mmol
NaOH	3.00 mmol
NH_3	103 mmol
Benzaldehyde	30 mmol
Solvent ($+NH_3$)	100 ml
Reaction temperature	29.5±0.2°C

×: the corrected value from the datum in the preceding paper[1] according to the equation;

$$\text{the rate} \propto \frac{[NH_3][\text{benzaldehyde}]}{([NH_3]+[\text{Benzaldehyde}])}$$

the first-order dependence of the reaction rate upon the concentration of cupric hydroxide as the catalyst (the basicity of the system may be proportional to the concentation of cupric hydroxide), the linear relation of the reaction rate to the concentration of sodium hydroxide and the relation between the basicity and the activity of catalysts, the rate-determining step of the formation of the nitrile would be the deprotonation of benzilideneimine and the oxidation reaction of the formed anion or the corresponding sodium salt would be sufficiently fast. Of course, in the case when the concentration of cupric ion is very small, the rate-determining step may be alternatively the oxidation step of the formed anion.

To investigate on this oxidation step further, the oxidation of the sodium derivative of benzophenoneimine was tried. This stable N-unsubstituted imine was selected in place of the unstable benzilideneimine. Though some difference may be between these two imines, the reaction may begin at the position of the imino-group (=N–H) in both of the imines. The sodium derivative of benzophenoneimine, which was prepared from benzophenoneimine and sodium amide in benzene (or tetrahydrofuran), was oxidized with suspended cupric chloride after the removal of unreacted sodium amide. The oxidation reaction seemed to proceed rapidly, judging from the observation that the characteristic deep red color of the sodium derivative disappeared immediately after the contact of the derivative with the oxidant. The corresponding oxidative dimerization product, benzophenone azine was obtained in an about 70% yield. The fact that a complex of benzophenoneimine with cuprous chloride, $CuCl\cdot Ph_2C{=}NH$, was detected as a by-product may mean that the oxidation step is an one-electron transfer reaction. Benzophenoneimine may be resulted from the hydrolysis of the sodium derivative, as a trace of water could exist in the oxidant or the solvent. The oxidation reaction of the sodium derivative may proceed much faster than the oxidation reaction of the parent imine by cupric chloride, judging from the fact that the complex of benzophenoneimine with cupric chloride, $CuCl_2\cdot 2Ph_2C{=}NH$, is observed to be stable at room temperature.[3] Potassium permanganate and manganese dioxide

1) Part I: A. Misono, T. Osa and S. Koda, This Bulletin, **40**, 912 (1967).
2) Part II: *ibid.*, **40**, 2875 (1967).
3) A. Misono, T. Osa and S. Koda, *ibid.*, **41**, 373 (1968).

also oxidized the sodium derivative to the ketazine in gross yields of 51% and 22%, respectively. Palladium chloride and silver nitrate also oxidized the sodium derivative to the ketazine, though not quantitatively observed. As for other oxidants, Morton[4] oxidized the sodium derivative to benzophenone oxime by air and to benzophenone azine by iodine in a yield of 17%. From the consideration of the above stated observations, the oxidation of the imines may plausibley proceed as follows.

$$PhCH{=}NH \xrightarrow{base} PhCH{=}N^- \xrightarrow{Cu^{II}} \text{(rate-determining)}$$

$$PhCH{=}N\cdot \xrightarrow{oxidation} PhCN$$

$$Ph_2C{=}NH \xrightarrow[NaNH_2]{} Ph_2C{=}N\cdot Na \xrightarrow[Oxidant]{} Ph_2C{=}N\cdot \rightarrow (Ph_2C{=}N)_2$$

Experimental

The Oxidation of Benzaldehyde and Ammonia with Oxygen Catalyzed by Cupric Chloride and Sodium Hydroxide. The materials and the reaction apparatus were all the same as in the preceding paper.[1] The procedure were also same except the following treatments before the start of the reaction; the methanol containing ammonia and sodium hydroxide was introduced in the flask and was stirred for 15 min. Then the introduction of oxygen gas was started. When 10 min passed after the beginning of the introduction of oxygen, the given amount of cupric chloride was added to at one time. When additional 5 min passed, benzaldehyde was introduced to start the reaction.

The Oxidation of the Sodium Derivative of Benzophenoneimine. All treatments were carried out at room temperature under dried nitrogen before the oxidation products were separated by filtration.

Oxidation by Cupric Chloride in Benzene. In 20 m*l* of benzene, 1 g (26 mmol) of sodium amide and 1.890 g (10.4 mmol) of benzophenoneimine (prepared from phenylmagnesium bromide and benzonitrile,[5] bp 146.5—148°C/7.5 mmHg) were agitated for 1 hr. Then, undissolved substances were separated and washed with 10 m*l* of benzene. The filtrate together with the washing was added to 2.708 g (20.1 mmol) of cupric chloride (prepared through dehydration by thionyl chloride from commercial cupric chloride dihydrate[6]) and the mixture was stirred for 3 hr. Then 20 m*l* of benzene was added to the mixture, and the resulted mixture was filtered. After stripping off benzene, 1.281 g (gross yield, 68%, mp 148—156°C) of yellow solid of benzophenone azine became available (recry. from ethanol. mp 164.5°C, lit.[7] 164°C. Its infrared spectrum agreed with that of an authentic sample.). In this process, small amount of $CuCl\cdot Ph_2C{=}NH$ was precipitated from benzene solution by adding *n*-hexane. Its infrared spectrum agreed with that of an authentic sample.[3] Found: C, 55.57; H, 3.87; N, 5.00%. Calcd for $CuCl\cdot C_{13}H_{11}N$: C, 55.71; H, 3.96; N, 5.00%.

In tetrahydrofuran as a solvent, benzophenone azine was obtained in a 72% yield after a similar treatment.

Oxidation by Potassium Permanganate. In 20 m*l* of benzene, 1 g of sodium amide and 1.905 g (10.5 mmol) of benzophenoneimine were agitated together for 1 hr, and treated similarly. The filtrate was added to 1.591 g (10.1 mmol) of potassium permanganate. The mixture was stirred for 2.5 hr and then kept for 40 hr at standing. The resulted mixture was treated similarly. Solids with little liquids remained after the removal of benzene. The mixture was again dissolved in 100 m*l* of ethanol with 10 m*l* of benzene. The solution was concentrated, then the resulting precipitate was separated at −30°C. The precipitate, 0.959 g (51%, mp 160.5—161.5°C) in weight, proved to be benzophenone azine (recry. from ethanol, 164.8°C). From the filtrate, 0.769 g (40%) of yellow liquid, which was mainly benzophenoneimine, contaminated with a little benzophenone, judging from its infrared spectrum, was obtained.

The oxidation by activated manganese dioxide (prepared from potassium permanganate[8]) of the sodium derivative of benzophenoneimine for 3 hr yielded benzophenone azine in a 22% gross yield after similar treatments.

4) A. A. Morton and J. R. Stevens, *J. Am. Chem. Soc.*, **53**, 2769 (1931).

5) P. L. Pickard and T. L. Tolbert, "Organic Syntheses," **44**, 51 (1964).

6) A. R. Pray, "Inorganic Syntheses," **5**, 153 (1957).

7) J. Guenzet, *Compt. rend.*, **251**, 2970 (1960).

8) J. Attenburrow, A. F. B. Cameron, J. H. Chapman, R. M. Evans, B. A. Hems, A. B. A. Jansen and T. Walker, *J. Chem. Soc.*, **1952**, 1094.

Organotin Compounds of the $R_2SnO \cdot SnR'_2X_2$ and $H(R_2SnO)_3OH \cdot SnR'_2X_2$ Mixed Types

Taichi HARADA

The Institute of Physical and Chemical Research, Yamato-machi, Saitama

(Received August 16, 1967)

The characteristic nature of R_3SnX, *i. e.*, its property of combining with one or two R_3SnOH and forming $R_3SnOH \cdot SnR_3X$ or $(R_3SnOH)_2 \cdot SnR_3X$,[1,2] was found first; for it 5 or 6 coordination bond linkings were first introduced to organotin chemistry by the present author.[3-6] Then this conception is extended to the formation of many complexes of the type $R_2SnO \cdot SnR_2X_2$*1 (I) and $H(R_2SnO)_3OH \cdot SnR_2X_2$ (II) types and, further, to the mixed-type compound:[7] $R_2SnO \cdot SnR'_2X_2$ (III) and $H(R_2SnO)_3OH \cdot SnR'_2X_2$ (IV), and also $(Me_2SnO)_2 \cdot SnMe_2Cl_2$ (V), in which the $(Sn-O)_2$ ring is present.[3,5] Recently, Rochow *et al.*[8] proposed a dimeric conception for I; then Okawara[9-11] proposed one for the compound of the I type where $X=OSiMe_3$ and the II type. The existence of III and IV, therefore, is very important in checking whether or not I, II, and V can be formulated by the dimeric hypothesis. The present investigation was carried out again with some new compounds of the R_2SnO and R'_2SnX_3 types, and of $3R_2SnO$ and R'_2SnX_2 compounds in the R°OH (R°=alkyl) solvent.

Experimental

Preparations. 1) n-$Pr_2SnO \cdot SnEt_2Br_2$[7] prepared by fusion. Both Et_2SnO and n-Pr_2SnBr_2, as well as n-Pr_2SnO and Et_2SnBr_2, in an exact mole ratio of 1 : 1, were fused at 110°C under exactly the same conditions; a melting point of 102—103°C was thus obtained for the former (A) and one of 104—105°C when crystallized from n-butyl alcohol, but the latter (B) gave a melting point of 83—84°C, which, upon its crystallization from the alcohol, was elevated to (87→93→97) 101°C. These two substances, A and B, are the same; *i. e.*, they gave the same amount of n-Pr_2Sn upon reduction with the Na-equivalent to Br_2 in liquid ammonia.[12] The process will be described later.

Other compounds of a similar type, 2) $Et_2SnO \cdot SnMe_2Cl_2$, 3) n-$Bu_2SnO \cdot Sn$$n$-$Pr_2Cl_2$, and 4) n-$Bu_2SnO \cdot SnMe_2Cl_2$, were also prepared.

The results of the analysis of the halogen contents, and the melting points or decomposition points are gives in Table 1. It is interesting to note here that n-$Bu_2SnO \cdot SnMe_2Cl_2$ (or this composition) could not be obtained by the action of n-Bu_2SnCl_2 on Me_2SnO as the case of n-Bu_2SnCl_2 on Et_2SnO.

Molecular Weight. The molecular weight of this mixed-type compound was not determined, but those of $Et_2SnO \cdot SnEt_2Br_2$ with higher concentrations in freezing benzene were obtained as 763, 900, and 947 at 5.000, 4.000, and 3.240 (by weight %) respectively. As has been shown above, the molecular weight decreases with the concentration or increases with the dilution (just as with n-$Bu_2SnO \cdot Sn$$n$-$Bu_2Br_2$,[13] Et_2SnI_2,[14] $SnCl_4$[14] and tetraalkyl ammonium halides[14]). Therefore, the compound may associate little or not at all at a point of saturation where a crystal sppears. On the other hand, $Me_2SnO \cdot SnMe_2(OAc)_2$[7] (which gives the 460 cm^{-1} band) indicates the reversing tendency (as do tetraalkyl ammonium nitrates[14]). Furthermore, the molecular weight of $H(Et_2SnO)_3OH \cdot SnEt_2(OAc)_2$[3] increases rapidly with the lapse of time, tripling in weight. Indeed, none of the halogen compounds in question except n-$Bu_2SnO \cdot Sn$$n$-$Pr_2Cl_2$ (Table 2) show the ring $(Sn-O)_n$ band[15] in the infrared spectrum. Therefore, there remains some uncertainty in determining whether they are in a monomer form or in a dimer on the base of these data only.*1

$(Me_2SnO)_2 \cdot SnMe_2Cl_2$. The electric conductivity of this compound, formed between $(Me_2SnO)_2$ and Me_2SnCl_2, was measured. From the results (Table 3), the compound may be considered to be $[(Me_2SnO)_2 \cdot SnMe_2]Cl_2$, since there are three ions and it gives an infrared 467 cm^{-1} ring band.[15] It is insoluble in organic solvent, Therefore, the molecular weight was not determined.

1) C. A. Kraus and T. Harada, *J. Am. Chem. Soc.*, **47**, 2416 (1925).
2) T. Harada, This Bulletin, **14**, 472 (1939).
3) T. Harada, *Sci. Paps. I. P. C. R.*, **35**, 290 (1939).
4) *Ibid.*, **36**, 504 (1939).
5) *Ibid.*, **38**, 146 (1940).
6) *Ibid.*, **57**, 25 (1963).
*1 To determine the location of the halogens and to determine whether the monomeric or dimeric structure is correct for the $Me_2SnO \cdot SnMe_2Cl_2$ and $Et_2SnO \cdot SnEt_2Br_2$-type compounds, some researchers (including the present author) of the Institute of Physical and Chemical Research are making X-ray analyses under the guidance of Professor Yoshihiko Saito of the Institute of Solid State Physics, The University of Tokyo.
7) T. Harada, *Sci. Paps. I. P. C. R.*, **43**, 178 (1947).
8) M. P. Brown, R. Okawara and E. G. Rochow, *Spectrochim. Acta*, **16**, 595 (1960).
9) R. Okawara, *Proc. Chem. Soc.*, **1961**, 383.
10) R. Okawara and M. Wada, *Organometal Chem.*, **1**, 81 (1963).
11) R. Okawara, *Nippon Kagaku Zasshi (J. Chem. Soc. Japan, Pure Chem. Sect.)*, **86**, 543 (1965).
12) T. Harada, This Bulletin, **4**, 266 (1929).
13) D. L. Alleston, A. G. Davies, M. Hancock and R. F. M. White, *J. Chem. Soc.*, **1963**, 5468.
14) P. Walden, Molekulargrossen von Elektrolyten," Leipzig (1923).
15) T. Shimanocuhi, I. Nakagawa, H. Kyogoku and M. Ishii, XIXth IUPAC London, AB4-24 (1963); Symp. Organometallic Compounds, Nagoya City, Oct. 13th, 1963.

Table 1. Prepared compounds (in the reaction ratio: $1 \leqq 1$)

Solvent	Reaction product	Found (Calcd) Halogen, %	C, %	H, %	Mp or dp °C	Yield %
i-PrOH	$Et_2SnO \cdot SnMe_2Cl_2$	17.28(17.20)	17.21(17.46)	3.91(3.80)	191—192	
	$Me_2SnO \cdot SnEt_2Cl_2$*	17.09(17.20)	17.72(17.46)	3.82(3.80)	181—182	
	(By boiling in water these gave $H(Et_2SnO)_3OH \cdot SnEt_2Cl_2$ and insub. subs.)					
n-BuOH	*n*-$Pr_2SnO \cdot SnEt_2Br_2$	28.78(28.67)	21.65(21.53)	4.39(4.34)	104—105	
	$Et_2SnO \cdot Sn$*n*-Pr_2Br_2*	28.65(28.67)	21.73(21.53)	4.29(4.34)	101	
i-PrOH	*n*-$Bu_2SnO \cdot Sn$*n*-Pr_2Cl_2	13.50(13.52)	32.21(32.04)	6.04(6.15)	103	90
	n-$Pr_2SnO \cdot Sn$*n*-Br_2Br_2*	13.53(13.52)	(32.04)	(6.15)	102	84
i-PrOH	*n*-$Bu_2SnO \cdot SnMe_2Cl_2$	15.17(15.13)	25.66(25.61)	4.97(5.12)	95— 96	50
then recrysz. by acetone	(From this mother liquor *n*-$Bu_2SnO \cdot Sn$*n*-Bu_2Cl_2 (10%) was obtained.)					
i-PrOH	Me_2SnO + *n*-Bu_2SnCl_2 → dispropt. products (*n*-$Bu_2SnO \cdot Sn$*n*-Bu_2Cl_2 and other)					
n-BuOH then, 1 : 1 (EtOH : H_2O)	$H(Et_2SnO)_3OH \cdot SnMe_2I_2$		16.89(16.82)	3.92(3.83)	180—200	
	$H(Et_2SnO)_3OH \cdot SnMe_2CI_2$	8.79(8.69)	20.89(20.59)	5.08(4.69)	221—223	
Water	$(Me_2SnO)_2 \cdot SnMe_2Cl_2$	12.95(12.93)	13.09(13.11)	3.25(3.30)	—	
i-PrOH	3*n*-Bu_2SnO + Me_2SnCl_2 → cryst. $\xrightarrow{EtOH/H_2O}$ $H($*n*-$Bu_2SnO)_3OH \cdot Sn$*n*-Bu_2Cl_2					
	Anal. for this	6.77(6.64)	36.02(35.97)	6.78(6.98)	120—125**	

* Does not represent the linking nor structure but represent the reactants of R'_2SnO and R_2SnX_2.

** Reported melting point 109—121 °C.[10]

Table 2. IR bands found in the region 350—800 cm^{-1} (KBr)

1.	$Me_2SnO \cdot SnMe_2(OAc)_2$:	435(vw), 460(s, shp), 620(w), 655(w), 685(w), 784(ms)
2.	$H(Et_2SnO)_3OH \cdot SnMe_2I_2$:	360(ms, shld), 410(ms, shld), 434(s), 530(s), 570(s), 630(s), 687(s), 790(s)
3.	$H(Et_2SnO)_3OH \cdot SnMe_2Cl_2$:	375(ms), 415(ms), 510(ms), 547(s), 584(s), 650(s), 695(s), 795(m)
4.	$(Me_2SnO)_2 \cdot SnMe_2Cl_2$:	467(s), 520(s), 550(s), 576(s), 705(m), 780(s)
5.	$Et_2SnO \cdot SnMe_2Cl_2$:	428(?, vw), 503(ms), 527(ms), 560(s), 605(s), 700(m), 800(s)
6.	*n*-$Bu_2SnO \cdot SnMe_2Cl_2$:	400(?, vw), 425(?, vw), 530(s), 560(s), 610(s), 700(m), 800(ms)
7.	*n*-$Bu_2SnO \cdot Sn$*n*-Pr_2Cl_2:	400(m), 420(m), 535(s), 600(s), 687(s), 780(w)
8.	$(Me_3SnOH)_2 \cdot SnMe_3I$:	480(s), 520(ms), 553(s), 565(s), 780(s)
9.	$(Me_3SnOH)_2 \cdot SnMe_3Cl$:	490(ms), 530(m), 557(ms), 570(?, m, shld), 784(m)

Compounds 1 and 4 prepared in water as solvent in which OH group does not enter in their molecules.

Table 3. Conductance of $(Me_2SnO)_2 \cdot SnMe_2Cl_2$ in water at 25°C (± 0.01)

$M = 0.0001$	0.0002	0.0005	0.0010	$\mu = 221.28$	208.41	197.45	193.22
$C = 0.0002$	0.0004	0.0010	0.0020	$\Lambda = 110.64$	104.21	96.78	96.61

M=mol. conc. μ=mol. conduc.
C=equiv. conc. Λ=equiv. conduc.

Reduction of $H(Et_2SnO)_3OH \cdot SnMe_2I_2$[6] in Liquid Ammonia. Compound (3.000 g) with the Na-equivalent to I_2 in liquid ammonia gave a 1/3 equivalent of (very roughly) Et_2Sn (0.35 g, free from the Me_2Sn group) upon being freed by 0.5 N HCl - aqueous alcohol (50/50 by volume). On the other hand, *n*-$Pr_2SnO \cdot SnEt_2Br_2$ (3.000 g) gave *n*-Pr_2Sn (1.0 g, free from the Et_2Sn group), but not $(Cl$*n*-$Pr_2Sn)_2$ nor $(ClEt_2Sn)_2$; $Et_2SnO \cdot SnEt_2Br_2$ (6.000 g) gave Et_2Sn (1.8 g) upon a similar treatment. This may be explained as follows:

$$n\text{-}Pr_2SnO \cdot SnEt_2Br_2 \xrightarrow{2Na} n\text{-}Pr_2SnO \cdot SnEt_2$$

$$\longrightarrow n\text{-}Pr_2Sn \cdot OSnEt_2$$

$$(\text{or} \longrightarrow n\text{-}Pr_2Sn + Et_2SnO)$$

$$\xrightarrow{2HCl} n\text{-}Pr_2Sn + Et_2SnCl_2.$$

For $H(Et_2SnO)_3OH \cdot SnMe_2I_2$, the same explanation can be given.

Discussion

On Formation and Stability. The linking of $R_2SnO{\cdot}SnR'_2X_2$ where R (*e. g.*, R=*n*-Bu) is larger than R' (*e. g.*, R'=Me) usually takes place along the model "streaming-down bridge" (*e. g.*, $Me_2SnO—Bu_2SnX_2$); it is somewhat difficult against the stream →, and it is impossible or very difficult to jump over one or more bridges to the left, as shown below with the arrow (←-⊗--):

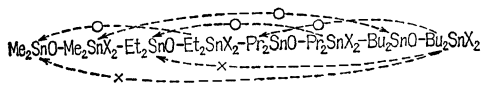

where the arrow --⊖→ in dicates a possibility of linkings, of greater or lesser difficulty, whereas linking ←-⊗-- is impossible or very difficult. In comparison, R_2SnX_2 (R=*n*-Bu) is somewhat organic, whereas R'_2SnX_2 (R'=Me) is of an inorganic nature for solvents, causing the formation of disporportionate products when R_2SnX_2 is subjected to reaction on R'_2SnO. The *n*-$Bu_2SnO{\cdot}SnMe_2Cl_2$ compound clearly differes from the mixture of *n*-$Bu_2SnO{\cdot}Sn$*n*-Bu_2Cl_2 and $Me_2SnO{\cdot}SnMe_2Cl_2$ toward heat; it melts at 95—96°C (clearly or almost clearly) with a mild decomposition above the melting point; it gradually becomes very opaque, perhaps because of the formation of a mixture of the two chlorides, whereas the mixture (in an exact mole ratio of 1 : 1) melts partially at about 102°C, giving two layers (liquid of the former and solid of the latter), leaving the solid of the latter on the bottom of the capillary tube readily. A tendency more or less similar is seen in the case of $Et_2SnO{\cdot}Me_2Cl_2$. When the compound is heated at or near 140°C under a reduced pressure, it gives pure *n*-Bu_2SnCl_2 (as in the case of *n*-$Bu_2SnO{\cdot}Sn$*n*-Bu_2Cl_2). Therefore, the change may take as follows:

$$n\text{-}Bu_2SnO{\cdot}SnMe_2Cl_2 \xrightarrow[\text{heat}]{\text{Partially}} n\text{-}Bu_2SnCl_2 + OSnMe_2,$$

as in the case of the liquid ammonia method described above.

On the Migration of X_2. The oxide having the $R_2Sn\langle{}^{O}_{O}\rangle SnR_2$[15] skeleton is affected by two molecules of R'_2SnX_2, forming a new structural product, $R_2SnO{\cdot}SnR'_2X_2$ (which polymerizes[5] loosely in a solvent) at a moderate dilution. In the both X_2's are unstable and, hence, may migrate very mildly from the tin of the larger alkyltin to the tin of the smaller alkyltin; *e. g.*, $Me_2SnO{\cdot}SnEt_2Cl_2$, $Et_2SnO{\cdot}Sn$*n*-Pr_2Br_2, and *n*-$Pr_2SnO{\cdot}Sn$*n*-Bu_2Cl_2, as in the cases of the liquid ammonia treatments, give $Et_2SnO{\cdot}SnMe_2Cl_2$, *n*-$Pr_2SnO{\cdot}SnEt_2Br_2$, and *n*-$Bu_2SnO{\cdot}Sn$*n*-Pr_2Cl_2, respectively. Thus, the two reactions, that between R'_2SnO and R_2SnX_2 and that between R_2SnO and R'_2SnX_2, should give only one compound as the stable product. Therefore, the difference in the melting points of the two products (Table 1) prepared by the two different reactions is due to the degrees of purity. This is shown by X-ray diffraction patterns; *e. g.*, the product (mp 103°C) prepared by the action of *n*-Pr_2SnCl_2 on *n*-Bu_2SnO appeared to be pure, whereas the product (mp 102°C) prepared by the action of *n*-Bu_2SnCl_2 on *n*-Pr_2SnO appeared to be slightly impure. On the other hand, in the reaction between Me_2SnO and *n*-Bu_2SnCl_2 in a solvent, the *n*-Bu_2SnO formed in the migration of X_2 readily combines with the free *n*-Bu_2SnX_2 to form the most stable linking products (disproportionate products). The reaction between *n*-Bu_2SnO and Me_2SnX_2 proceeds fairly normalily, giving *n*-$Bu_2SnO{\cdot}SnMe_2X_2$. In a very dilute solution, this mixed-type compound, the oxide, and the halogens are freely move, giving a mixture of the most stable compounds. The stability in question, therefore, depends completely on the energy level between R'_2Sn– and –SnR_2 in the linkings.

Mode of Formation. For the formation mechanism of the compounds of the II type, Davies *et al.*[13] Proposed the following hydrolytic mechanism:

$$R_2SnX_2 \rightarrow R_2SnXOH \rightarrow$$
$$XR_2Sn\text{-}O\text{-}SnR_2X \rightarrow XR_2Sn\text{-}O\text{-}SnR_2OH$$

the latter two dimerise readily in non poler solvents. On the other hand, the present author[5,6] has proposed the following mechanism:

$$R_2SnO \xrightarrow[\substack{2R°OH\\(\text{alcohol})}]{2HX} R_2SnX_2 \xrightarrow{R_2SnO}$$
$$R_2SnO{\cdot}SnR_2X_2 \xrightarrow{2R_2SnO} R°(R_2SnO)_3OR°{\cdot}SnR_2X_2.$$

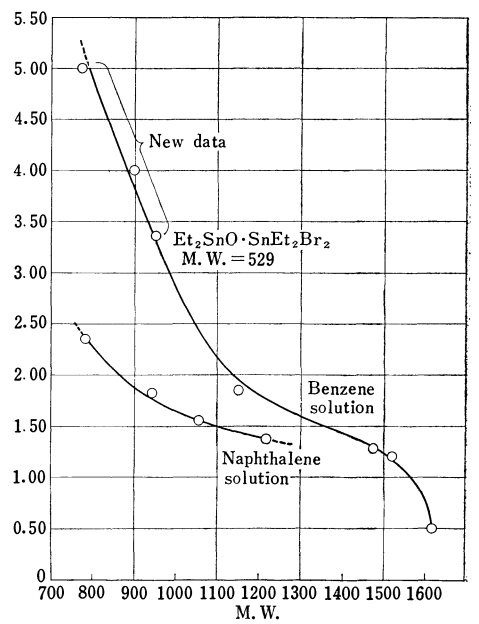

Fig. 1

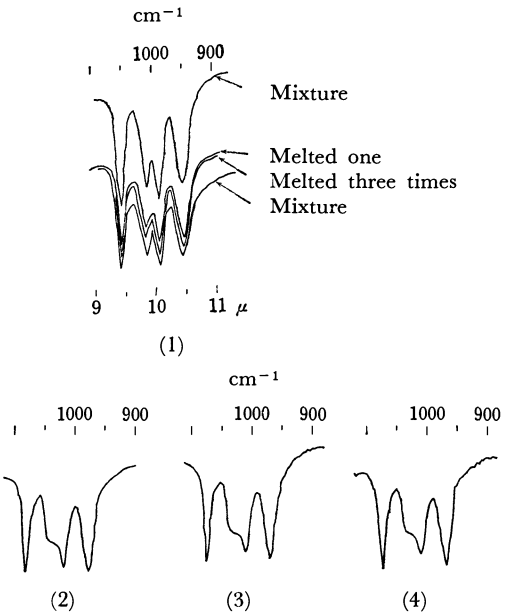

Fig. 2. Infrared spectral bands (Nujol).
(1) Mixture of exact mole ratio (1 : 1) of $Et_2SnO \cdot SnEt_2Br_2$ and n-$Pr_2SnO \cdot Sn$$n$-$Pr_2Br_2$ in powdered states. (2) Crystal obtained from n-Pr_2O and $Et_2 \cdot SnBr_2$ ($1<1$) mixture in alcohol, recrystallized. (3) Crystal obtained from exact mole ratio (1 : 1) mixture (Fig. 1) in 99% alcohol. (4) Fused substance of exact mole ratio (1 : 1) mixture of n-Pr_2SnO and Et_2SnBr_2.

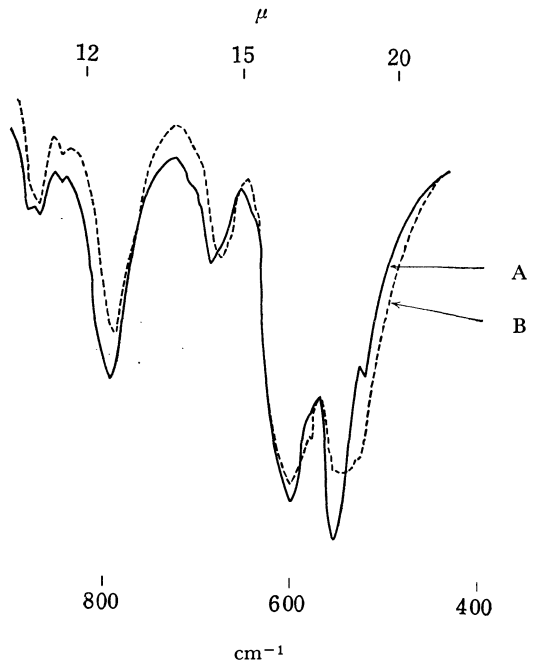

Fig. 3

A: n-$Bu_2SnO \cdot SnMe_2Cl_2$
B: Mixture of n-$Bu_2SnO \cdot Sn$$n$-$Bu_2Cl_2$ and $Me_2SnO \cdot SnMe_2Cl_2$ in exact mole ratio 1 : 1

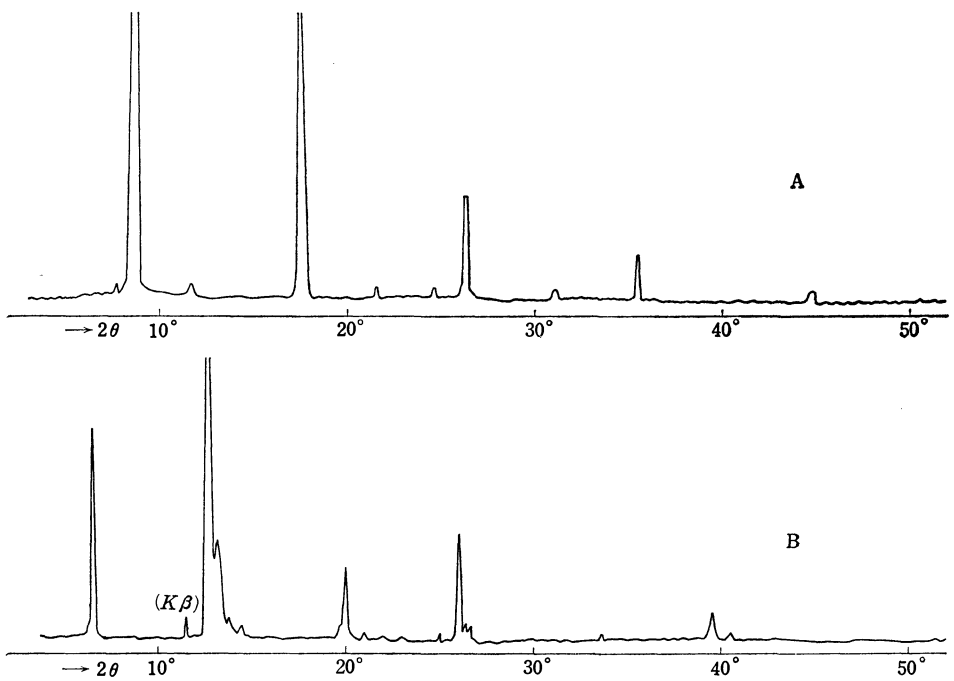

Fig. 4. X-Ray diffraction pattern.
A: n-$Bu_2SnO \cdot MeSnCl_2$ B: $Me_2SnO \cdot Me_2SnCl_2$ - n-$Bu_2SnO \cdot n$-Bu_2SnCl_2 mixture

If we accepted the former mechanism and applied it to mixed type compounds, it should give (XR_2Sn-O-SnR'_2OH). In fact, however, no such compound was formed. However, the latter mechanism accounts for the formation of mixed-type compounds, which can be represented as follows:

$$3R_2SnO + R'_2SnX_2 + 2R°OH \rightarrow$$

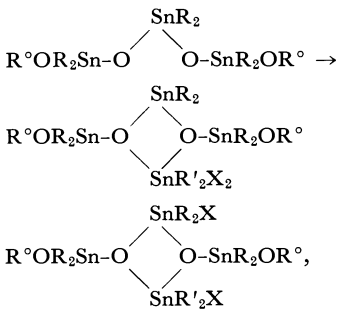

$$\text{or}\quad R°OR_2Sn\text{-}O\quad O\text{-}SnR_2X\quad SnR'_2X,$$

which gives the free OH band[11] in the case of R°=H, R'=R.

This $>SnR_2X$ linking is possible, but improbable judging from the results of the Na-liquid ammonia treatment and from the formation of R_2SnS and SnR_2X_2 (but not XR_2Sn-S-SnR_2X) upon H_2S treatment; it may differ from the structure of $(Me_3SiOMe_2Sn)_2O$[16] pointed out by Poller *et al.*[17] Very recently Davies *et al.*[18] have prepared several mixed-type compounds, $R_2SnO{\cdot}SnR'_2Cl_2$, $R_2SnO{\cdot}SnR'_3Cl$, $R_2SnO{\cdot}SnCl_4$, *etc.* They reported that the degree of association of these compounds is slight.

16) Wm. J. Considine, G. A. Baum and R. G. Jones, *J. Organometal Chem.*, **3**, 308 (1965).
17) R. C. Poller and J. A. Spillmann, *ibid.*, **7**, 259 (1967).
18) A. G. Davies and P. G. Harrison, *ibid.*, **7**, 13 (1967).

On Infrared Spectral Bands. In the region of 800—4000 cm^{-1}, bands of *n*-$Bu_2SnO{\cdot}SnMe_2Cl_2$ and a mixture*2 (in an exact mole ratio of 1 : 1) of the two compounds *n*-$Bu_2SnO{\cdot}Sn$*n*-Bu_2Cl_2 and $Me_2SnO{\cdot}SnMe_2Cl_2$ are the same, but in the 400—800 cm^{-1} region the first compound gives bands at 530, 558, 608, 643, 698, and 780, while the mixture gives a broad band (530—570) and others at 607, 683 and 780. In the case of *n*-$Pr_2SnO{\cdot}SnEt_2Br_2$, shoulder bands (Nujol) appear at 995 and 1020, but in the case of a mixture (exact mole ratio of 1 : 1) of *n*-$Pr_2SnO{\cdot}Sn$*n*-Pr_2Br_2 and $Et_2SnO{\cdot}SnEt_2Br_2$, there are sharp individual bands at 995 and 1020 cm^{-1}. These are listed in Table 2 and illustrated in Fig. 2. For *n*-$Pr_2SnO{\cdot}SnEt_2Br_2$, see Fig. 3.

The author is grateful to Professor Saburo Nagakura of The University of Tokyo, and to Dr. Hiroshi Midorikawa and Dr. Tetsuzo Atoda, chief chemists of The Institute of Physical and Chemical Research, for their encouragement. He also greatly indebted to Dr. Isaburo Hori, Dr. Kiyoko Yamamoto, Mr. Iwami Higashi, and Mr. Shunzo Katayama of The Institute of Physical and Chemical Research, who partly helped him with this study. Finally, thanks are due to the Sankyo Organic Chemicals Co., Ltd., Kawasaki, for supplying some organotin materials for this work. This work was carried out partly at the laboratory of the Takaido Chemical Co., Ltd., Itabashi, Tokyo, and partly at The Institute of Physical and Chemical Research.

*2 X-Ray diffraction analysis shows these two substances to be quite different from each other. (Fig. 4A and B) The same is true in the case of *n*-$Bu_2SnO{\cdot}Sn$*n*-Pr_2Cl_2 (mp 103°C).

Delta- and Theta-Al_2O_3 under Hydrothermal Conditions

Goro YAMAGUCHI and Wen-Chau CHIU

Department of Industrial Chemistry, Faculty of Engineering, The University of Tokyo, Hongo, Tokyo

(Received August 18, 1967)

In a previous paper,[1] Yamaguchi *et al.* reported that under hydrothermal conditions, γ-Al_2O_3 obtained from the dehydration of boehmite was deformed further, more tetragonally, but not inverted into δ-Al_2O_3. In this experiment the authors treated η- and γ-Al_2O_3, with various origins, under hydrothermal conditions.

1) G. Yamaguchi and H. Yanagida, This Bulletin, **35**, 1896 (1962).

Preparation of Standard Samples

In order to compare and discriminate the polymorphs, standard samples were prepared.

Preparation and Identification of η-Al_2O_3. Commercial fine gibbsite was heated in vacuum at 900°C for 30 min. The X-ray diffraction pattern of this product is given in Fig. 1a showing the character of η-Al_2O_3.

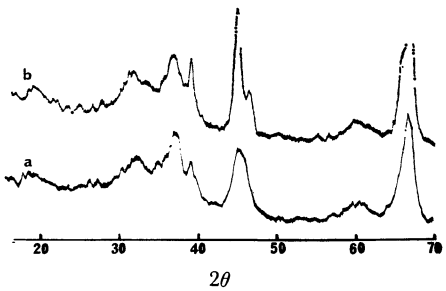

Fig. 1. X-ray diffraction patterns of η-Al_2O_3 (a) and γ-Al_2O_3 (b).

Preparation and Identification of γ-Al_2O_3. Well crystallized boehmite obtained hydrothermally from gibbsite was treated again under hydrothermal conditions (500°C, 50 atm) for 20 hr. The X-ray diffraction pattern of this product is given in Fig. 1b, showing the character of γ-Al_2O_3.

Preparation and Identification of δ-Al_2O_3. Well crystallized boehmite obtained hydrothermally from gibbsite was heated in air at a heating rate of 5°C/min, up to 1000°C, and kept there for 1 hr. The X-ray diffraction pattern of this product is given in Fig. 2a, showing the character of δ-Al_2O_3.

Preparation and Identification of θ-Al_2O_3. Bayerite, obtained by aging alumina gel[2] in conc. NH_3 aqueous solution, was heated in air at a heating rate 5°C/min, up to 1100°C, and kept there for 1 hr. The X-ray diffraction pattern of this product is given in Fig. 2b, showing the character of θ-Al_2O_3.

The characters of the X-ray diffraction pattern of these polymorphs are summarized in Table 1.

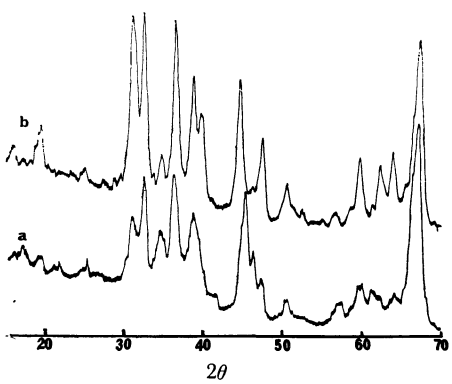

Fig. 2. X-ray diffraction patterns of δ-Al_2O_3 (a) and θ-Al_2O_3 (b).

Hydrothermal Treatment of η- and γ-Al_2O_3

Starting materials were as follows:

1. η-Al_2O_3 A. Bayerite, obtained by treating alumina gel with conc. NH_3 aqueous solution at room temperature for 3 days, was heated and dehydrated in air at 800°C for 1 hr.

2. η-Al_2O_3 B. Bayerite, obtained by hydrolyzing sodium aluminate aqueous solution (NaOH 3.5 mol/l, Na/Al=1.35) at 15°C for 3 days, was heated and dehydrated in air at 800°C for 1 hr.

3. η-Al_2O_3 C. Nordstrandite, obtained by treating alumina gel with a 5% ethylenediamine

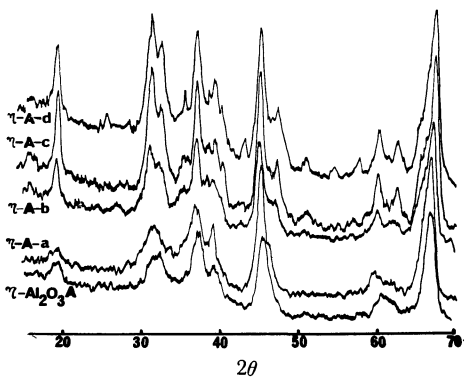

Fig. 3. X-ray diffraction patterns of products from η-Al_2O_3 A.

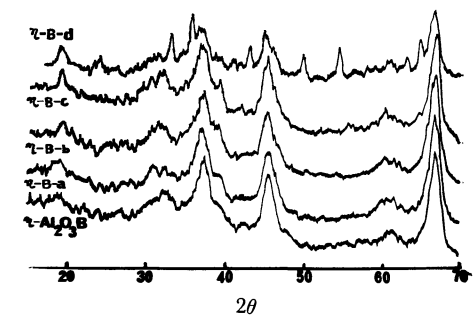

Fig. 4. X-ray diffraction patterns of products from η-Al_2O_3 B.

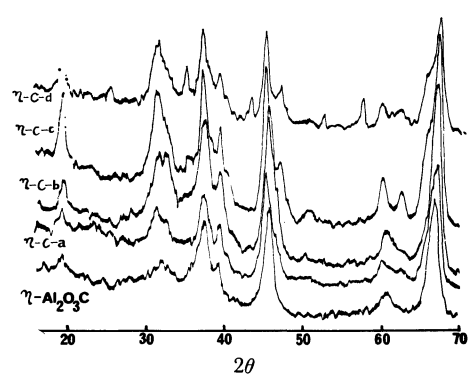

Fig. 5. X-ray diffraction patterns of products from η-Al_2O_3 C.

2) G. Yamaguchi and W. This Bulletin, Feb. (1968).

TABLE 1. CHARACTER OF DIFFRACTION PATTERN OF Al_2O_3 POLYMORPHS, ( ) SHOWS SPINEL INDEX

2θ range	η	γ	δ	θ
67—68	(440) singlet	(440) doublet	(440) doublet	doublet
59—64	(333) (511) broad	(333) (511) broad	two peaks	three peaks
45—48	(400) singlet	(400) doublet	(400) doublet and one more small peak	two or three peaks
ca. 39	(222) singlet	(222) singlet	(222) singlet	singlet
36—38	(311) broad	(311) broad	two peaks	two peaks
34—35	—	—	one peak	small one peak
31—32	(220) broad	(220) broad	two peaks	two peaks

TABLE 2. STARTING MATERIALS, HYDROTHERMAL CONDITIONS AND PRODUCTS

Starting material	Notation	Hydrothermal condition			Product
		Temp. °C	Pressure atm	Period hr	
η-Al_2O_3 A	η-A-a	450	50	20	γ
	η-A-b	450	110	20	δ or θ
	η-A-c	500	40	175	θ
	η-A-d	500	50	20	$\theta+(\alpha)$
η-Al_2O_3 B	η-B-a	400	50	20	γ
	η-B-b	450	30	20	γ
	η-B-c	500	30	20	γ
	η-B-d	500	50	20	$\gamma+(\alpha)$
η-Al_2O_3 C	η-C-a	400	50	20	γ
	η-C-b	450	70	45	γ
	η-C-c	500	50	20	γ
	η-C-d	500	130	20	δ or $\theta+(\alpha)$
η-Al_2O_3 D	η-D-a	400	50	20	γ
	η-D-b	450	90	20	γ
	η-D-c	500	70	20	γ
	η-D-d	500	90	20	$\gamma+(\alpha)$
η-Al_2O_3 E	η-E-a	450	70	20	η
	η-E-b	450	130	20	γ
	η-E-c	500	80	20	γ
	η-E-d	500	200	20	$\gamma+\alpha$
η-Al_2O_3 F	η-F-a	400	40	20	η
	η-F-b	450	70	45	η
	η-F-c	500	70	45	γ
	η-F-d	500	130	20	$\gamma+(\alpha)$
γ-Al_2O_3	γ-a	400	50	20	γ; $a=7.98$ $c=7.78$
$a=7.94$	γ-b	450	90	45	γ; $a=7.98$ $c=7.73$
$c=7.85$	γ-c	520	50	20	γ; $a=7.99$ $c=7.72$
	γ-d	520	70	20	$\gamma+(\alpha)$ $a=8.00$ $c=7.72$

α α-Al_2O_3, γ γ-Al_2O_3, δ δ-Al_2O_3, η η-Al_2O_3, θ θ-Al_2O_3, ( ) small amout

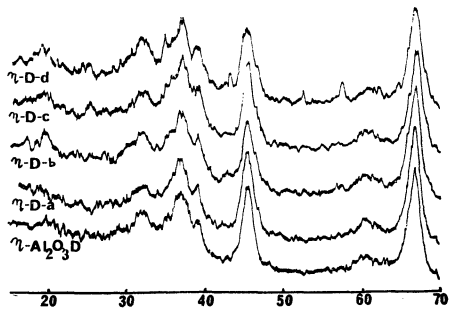

Fig. 6. X-ray diffraction patterns of products from η-Al_2O_3 D.

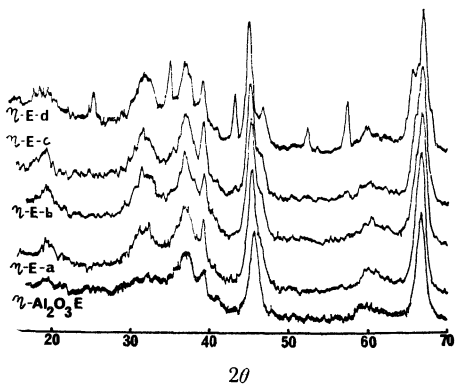

Fig. 7. X-ray diffraction patterns of products from η-Al_2O_3 E.

aqueous solution at 40°C for 2 days, was heated and dehydrated in air at 700°C for 1 hr.

4. η-Al_2O_3 D. Commercial gibbsite was heated and dehydrated in vacuum at 900°C for 0.5 hr.

5. η-Al_2O_3 E. Well crystallized boehmite was heated and dehydrated in vacuum at 900°C for 0.5 hr.

6. η-Al_2O_3 F. Bayerite, obtained by treating alumina gel with conc. NH_3 aqueous solution at room temperature for 3 days, was heated and dehydrated in vacuum at 800°C for 1 hr.

7. γ-Al_2O_3. Well crystallized boehmite was heated in air at 650°C for 0.5 hr.

These materials were treated under hydrothermal conditions and examined by an X-ray diffraction method. Results are given in Table 2, and Fig. 3 through Fig. 9.

Conclusion and Discussion

1. Similar to the previous paper, 1) γ-Al_2O_3, obtained from the dehydration of well crystallized boehmite was deformed further, more tetragonally, but not inverted into δ- or θ-Al_2O_3. As for η-

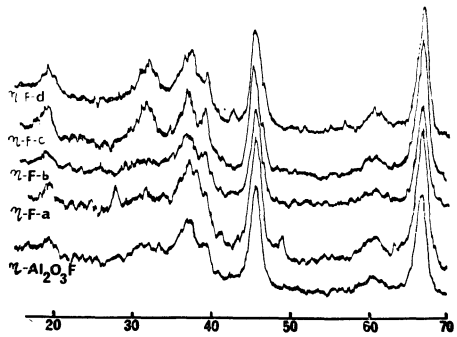

Fig. 8. X-ray diffraction patterns of products from η-Al_2O_3 F.

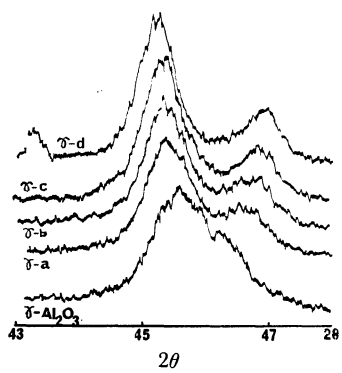

Fig. 9. X-ray diffraction peaks of (400) and (004) of γ-Al_2O_3 under hydrothermal condition.

Al_2O_3 however, some was only deformed into γ-Al_2O_3, while the rest was inverted into θ-Al_2O_3 before being finally inverted into α-Al_2O_3; η-Al_2O_3 A, and C belonged to the latter.

2. Before the formation of θ-Al_2O_3, η-Al_2O_3 A, and C seemed to pass through an intermediate phase like δ-Al_2O_3 but the X-ray diffraction pattern of this intermediate phase was not correctly coincident with that of standard δ-Al_2O_3 (Fig. 2a). Interpretation of this phenomenon can not be accomplished before the structural problem of δ-Al_2O_3 and θ-Al_2O_3 is clarified. Whether or not δ-Al_2O_3 and θ-Al_2O_3 are considered to be of different phases is a problem which is now being investigated by the present authors.

3. Among η-Al_2O_3 specimens obtained from different origins, there were two types. One was hardly inverted into θ-Al_2O_3, and the other was easily inverted under hydrothermal conditions. This difference seems to be due to a delicate structural difference, but the explanation is left as a future problem.

Photo-Claisen Rearrangement. The Photochemical Rearrangement of Allyl Phenyl Ethers*[1]

Gen KOGA and Noriko KIKUCHI*[2]

Department of Chemistry, Ibaraki University, Mito

and Nobuo KOGA

Department of Chemistry, Yokohama City University, Kanazawa-ku, Yokohama

(Received August 18, 1967)

Two years ago, Woodward and Hoffmann presented an ingenious theory in an attempt to interpret the stereochemical cours of the so-called "electrocyclic" and "sigmatropic" transformations.[1] They suggested[1b] that the photo-Claisen rearrangement reported to give a para-rearrangement product[2] would serve as an example of the [3, 5] sigmatropic transformation. Another example of the photo-Claisen rearrangement had previously been reported to give only a para-rearrangement product.[3]

Although this interpretation of the photo-Claisen rearrangement was highly attractive, the following facts seemed to us conflicting enough to warrant a thorough reinvestigation of the photo-rearrangement of allyl phenyl ethers:

(1) An eight-membered cyclic transition state these systems seems sterically impossible.

(2) γ-^{14}C-Allyl 2, 6-dimethylphenyl ether has been shown to rearrange to 4-α- and 4-γ- ^{14}C-allyl-2, 6-dimethylphenols.[2]

$$(CH_3)_2C_6H_3\text{-}OCH_2CH\overset{*}{=}CH_2 \rightarrow \overset{*}{C}H_2\text{=}CH\overset{*}{C}H_2\text{-}C_6H_2(CH_3)_2OH$$

(3) Several related systems, phenyl esters,[4] acyl anilides,[5] phenoxyacetic acid,[6] and ethyl phenyl carbonate,[7] have been reported to rearrange photochemically to ortho- and para-rearrangement products.

The recent publication of a communication[8] dealing with an investigation closely related to ours prompts us to publish our own results.

Experimental

Materials. The allyl phenyl ethers for the photoreaction were purified by rectification until no appreciable impurity was observed by glc.

Reaction Procedure. A 5% solution of a sample in isopropyl alcohol was irradiated with an immersion-type 10W low-pressure mercury lamp (Ricoh Kagaku Sangyo Co., UVL300Q) under a nitrogen atmosphere. After irradiation, most of the solvent was removed under reduced pressure, and the residual mixture was analyzed by glc.

Identification of Products. *o*- and *p*-Allylphenols, 2-allyl-3, 5-dimethylphenol, *trans-o*- and *-p*-but-2-enylphenols, and *o*- and *p*-(1-methyl-prop-2-enyl)phenols were identified by a comparison of their retention times with those of authentic sample. 4-Allyl-3, 5-dimethylphenol was isolated from the reaction mixture by means of preparative glc and was identified spectrometrically. Two unknown peaks in the gas chromatogram of the reaction mixture from *trans*-but-2-enyl phenyl ether were tentatively assigned to *cis-o*- and *-p*-but-2-enylphenols on the basis of their having been formed by the irradiation of their trans-isomers.

Analyses. The samples were analyzed by the use of a Hitachi K-23 gas chromatograph. A 1-meter Celite-545 (60—80 mesh) column with 33% Silicon KF-54 was used. The results in the table are given as the percentage ratio of the peak area.

Results and Discussion

As shown in the table, all the compounds rearranged to give ortho- and para-rearrangement products in addition to the parent phenols of the starting ethers. Some unidentified products were also present. *trans*-But-2-enyl phenyl ether was shown to give *o*- and *p*-but-2-enyl and *o*- and *p*-(1-methylprop-2-enyl)phenols. The results are consistent with those of Schmid[2] and clearly indicate that the rearrangement does not proceed

*1 A preliminary account of this investigation has been presented at the 19th Annual Meeting of the Chemical Society of Japan, Tokyo, March, 1966; Abstr., Vol. 3, p. 209.

*2 Present address: Sagami Chemical Research Center, Sagamihara, Kanagawa.

1) a) R. B. Woodward and R. Hoffmann, *J. Am. Chem. Soc.*, **87**, 395 (1965); b) *ibid.*, **87**, 2511 (1965); c) R. Hoffmann and R. B. Woodward, *ibid.*, **87**, 4389 (1965).

2) K. Schmid and H. Schmid, *Helv. Chim. Acta*, **36**, 687 (1953).

3) M. S. Kharasch, G. Stampa and W. Nudenberg, *Science*, **116**, 309 (1952).

4) a) H. Kopsa, *J. Org. Chem.*, **27**, 2293 (1962); b) J. C. Anderson and C. B. Resse, *J. Chem. Soc.*, **1963**, 1781; c) W. M. Horspool and P. L. Pauson, *ibid.*, **1965**, 5162; d) R. A. Finnegan and J. J. Mattice, *Tetrahedron*, **21**, 1015 (1965).

5) D. Elad, D. V. Rao and V. I. Stenberg, *J. Org. Chem.*, **30**, 3252 (1965).

6) D. P. Kelly and J. T. Pinhey, *Tetrahedron Letters*, **1964**, 3427.

7) C. Oac and S. Tsutsumi, This Bulletin, **37**, 1392 (1964).

8) D. P. Kelly, J. T. Pinhey and R. D. G. Rigby, *Tetrahedron Letters*, **1966**, 5953.

Table 1. Analyses of products

(1) Allyl phenyl ether

Time of irradiation (hr)	Starting material	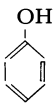	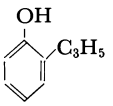	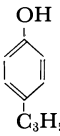
12	84.2%	2.3%	7.3%	6.3%
24	68.6	4.9	14.3	12.3
48	39.6	10.2	26.8	23.4

(2) Allyl 3,5-dimethylphenyl ether

Time of irradiation (hr)	Starting material	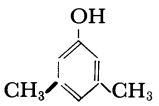	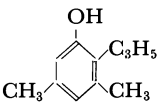	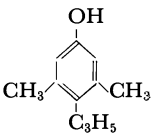
12	81.5%	3.9%	8.8%	5.8%
24	67.5	7.3	15.2	10.0
48	36.5	14.7	29.4	19.4

(3) *trans*-But-2-enyl phenyl ether

Time of irradiation (hr)	Starting material	Phenols (%)						
		I	*o*-II	*p*-II	*o*-III	*o*-IV	*p*-III	*p*-IV
24	77.3%	3.7	3.6	3.7	4.7	1.2	4.6	1.2
48	53.3%	8.6	6.6	6.9	9.1	3.4	8.3	3.8

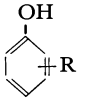

(I) R = -H
(II) -CHCH=CH_2 (CH$_3$)
(III) -CH_2CH=CHCH$_2$ (*trans*)
(IV) -CH_2CH=CHCH$_2$ (*cis*)

via a cyclic process, but probably involves a radical or an ionic recombination of two fragments.

The products do not seem to undergo further rearrangement; in each case, the ortho/para ratio of the products*3 was unchanged during the irradiation. In fact, as has been reported by Kelly *et al.*,[8] these phenols are quite stable to any irradiation except for trans-cis isomerisation.

In the rearrangement of but-2-enyl phenyl ethers, the ratio of (1-methylprop-2-enyl)phenols to but-2-enylphenols was about 0.6. Although some steric factors may be responsible for the observed ratio, this value strongly suggests that the reaction mechanism is a radical process. If the reaction proceeded through an ionic path, the fragmentation would lead to a phenoxide anion and an allyl cation, and from the reported data of the SN1 reaction of crotyl and methylallyl substrates, the ratio would be expected to be about 0.1—0.2.[9]

The ortho/para ratio of the products is 1.1 for allyl phenyl ether, 1.5 for allyl 3, 5-dimethylphenyl ether, and 1.0 for but-2-enyl phenyl ether, showing in each case a slight preference for the attack on the para-position. Although somewhat different results have been previously reported,[8] the discrepancy may be ascribed to the differences in the experimental conditions. Steric factors seem to be operative in the rearrangement of allyl 3, 5-dimethylphenyl ether.

To ascertain whether the rearrangement is intra- or inter-molecular, a mixed solution of allyl 3, 5-dimethylphenyl ether and *trans*-but-2-enyl phenyl ether, each 5% in isopropyl alcohol, was irradiated. The products were analyzed both as free phenols and as their methyl ethers. Other than the rearrangement products expected for each component separately, no trace of crossed products could be detected, a clear indication of the intramolecular nature of the reaction. The mechanism of the photo-Fries rearrangement has been suggested[4a] to be a radical recombination within a solvent cage. Arenesulfonyl anilides have also been shown to rearrange photochemically *via* an intramolecular process.[10] Thus, as in the preceding cases, the photo-rearrangement of allyl phenyl ethers can most consistently be interpreted by a radical recombination mechanism within a solvent cage.

*3 Although the ratio of the peak area was used for the isomer ratio without calibration throughout the discussion, the error seems to be small, as was found to be the case with *o*- and *p*-allylphenols.

9) A. G. Catchpole and E. D. Hughes, *J. Chem. Soc.*, **1948**, 4.

10) H. Nozaki, T. Okada, R. Noyori and M. Kawanishi, *Tetrahedron*, **22**, 2177 (1966).

On the Estimation of Alloy Film Thickness by X-Ray Fluorescent Spectroscopy

Kichinosuke HIROKAWA and Hidehiro GOTÔ

The Research Institute for Iron, Steel and Other Metals, Tohoku University, Sendai

(Received August 23, 1967)

For the simultaneous determination of alloy film thickness and its composition, several methods in which experimental equations were employed have been proposed.[1-3] In the present report it shall be shown that thickness of a binary alloy film can be easily obtained with two experimental absorption parameters, when the composition of the film is known.

Usually the X-ray intensity from a film of thickness z is given by Eq. (1),

$$I_z = \int_{\lambda_{\min}}^{\lambda_{\text{edge}}} \int_0^z \frac{I_0(\lambda)\rho_j Q(\lambda)}{\sin\beta} \cdot \exp\left\{-\left(\frac{\sum \mu^j{}_{(\lambda)} W_j}{\sin\alpha} + \frac{\sum \mu^j{}_f W_j}{\sin\beta}\right)z\right\} \mathrm{d}z \cdot \mathrm{d}\lambda \quad (1)$$

where α is the incident angle of primary X-rays; β is the emergent angle of fluorescent X-rays; $Q(\lambda) = \mu_j/\rho_j W_j K_j w_j R_p{}^j$ (μ_j/ρ_j is the mass absorption coefficient of element j; W_j is the weight fraction of element j ; K_j is the term $(r_j-1)/r_j$ in which r_j is the ratio of absorption coefficient at the K discontinuity, *i. e.*, r_j is the K jump for j : w_j is the fluorescent yield of j; $R_p{}^j$ is the intensity ratio of the measured p line of element j, which belongs to the K series, to the total intensity of K lines, *i. e.*, the fraction of the measured p line in the characteristic X-ray series which the p line belongs to); $\mu^j{}_{(\lambda)}$ is the absorption coefficient of j for the incident ray of wavelength λ; $\mu_f{}^j$ is the absorption coefficient of j for the fluorescent beam; $I_0(\lambda)$ is the primary X-ray intensity; I_z is the X-ray intensity from a film of thickness z; ρ_j is the density of the element j.

To obtain an exact expression for fluorescent X-ray intensity, of course, Eq. (1) must be integrated with respect to the wavelength λ, together with respect to thickness z. However, if we assume that $I_0(\lambda)$ and $\mu_{(\lambda)}$ are constant at the definite experimental condition,[4] the approximate expression for the intensity ratio of X-rays from a film to that from the bulk sample with a constant composition A_j is given by Eq. (2):

$$-\ln\left(1 - \frac{I_z{}^{A_j}}{I_\infty{}^{A_j}}\right) = \left(\frac{\sum \mu_i{}^{A_j} W_{Aj}}{\sin\alpha} + \frac{\sum \mu_A{}^{A_j} W_{Aj}}{\sin\beta}\right)z \quad (2)$$

The approximate X-ray intensity ratio of an element A in an alloy film to the pure element A can be also obtained by Eq. (3),

$$-\ln\left(1 - \frac{\rho_{AA}}{\rho_{Aj}} \cdot \frac{1}{W_A} \cdot \frac{I_z{}^A}{I_\infty{}^A} \cdot \frac{\dfrac{\sum \mu_i{}^A W_A}{\sin\alpha} + \dfrac{\sum \mu_A{}^A W_A}{\sin\beta}}{\dfrac{\mu_i{}^A}{\sin\alpha} + \dfrac{\mu_A{}^A}{\sin\beta}}\right) = \left(\frac{\sum \mu_i{}^A W_A}{\sin\alpha} + \frac{\sum \mu_A{}^A W_A}{\sin\beta}\right)z \quad (3)$$

where ρ_{AA} is the density of pure element A, and ρ_{Aj} is the density of the alloy. When Eq. (3) is applied to an element A in a binary alloy AB, Eq. (4) can be derived:

$$-\ln\left\{1 - \frac{I_z{}^A}{I_\infty{}^A} \cdot \frac{\rho_{AA}}{\rho_{AB}}\left[1 - \frac{\left(\dfrac{\mu_i{}^B}{\sin\alpha} + \dfrac{\mu_A{}^B}{\sin\beta}\right)W_B}{\left(\dfrac{\mu_i{}^A}{\sin\alpha} + \dfrac{\mu_A{}^A}{\sin\beta}\right)W_A}\right]\right\} = \left\{\left(\frac{\mu_i{}^A}{\sin\alpha} + \frac{\mu_A{}^A}{\sin\beta}\right)W_A + \left(\frac{\mu_i{}^B}{\sin\alpha} + \frac{\mu_A{}^B}{\sin\beta}\right)W_B\right\}z \quad (4)$$

Equation (4) was applied to a nickel-iron alloy (81.5% Ni) film. The experimental conditions were the same as described in previous reports.[1,2] In this case it is necessary to get the $\mu_i{}^A$ and $\mu_i{}^B$ values. Fortunately, in this experiment the value of $\mu_i{}^{Ni}$ or $\mu_i{}^{Fe}$ could be obtained by the applica-

TABLE 1. EXPERIMENTAL AND CALCULATED VALUES OF X-RAY INTENSITY RATIO OF Ni AND Fe IN Ni-Fe ALLOY FILMS

Thickness μ	$I_z{}^{Ni}/I_\infty{}^{Ni}$		$I_z{}^{Fe}/I_\infty{}^{Fe}$	
	Exp.	Calcd.	Exp.	Calcd.
0.2	0.044	0.042	0.015	0.009
0.4	0.077	0.079	0.021	0.017
0.6	0.114	0.126	0.038	0.025
1.23	0.228	0.223	0.087	0.046
2.35	0.345	0.351	0.138	0.074

1) K. Hirokawa and H. Gotô, *Z. anal. Chem.*, **190**, 309 (1962).
2) K. Hirokawa and H. Gotô, *ibid.*, **193**, 346 (1963).
3) K. Hirokawa and H. Gotô, *ibid.*, **199**, 89 (1964).
4) a) H. T. Beattie and R. M. Brissey, *Anal. Chem.*, **26**, 980 (1954). b) J. Sherman, "Advances in X-Ray Analysis," Vol. 1, ed. by W. M. Mueller, Plenum Press, New York (1960), p. 244. c) K. Hirokawa and H. Goto, *Nippon Kagaku Zasshi (J. Chem. Soc. Japan, Pure Chem. Sect.)*, **87**, 383 (1966).

tion of Eq. (2) to a nickel or iron film; the value of μ_i^{Ni} was 1750, and that of μ_i^{Fe}, 977. Using these values, the X-ray intensity ratios of nickel and iron were calculated with Eq. (4). These results were shown in Table 1 together with the experimental results. From this experiment it was recognized that the thickness of a binary alloy film could be easily obtained from the X-ray intensity ratio of an element in the film to that of the pure element.

However, for the element that receives inter-element effects from accompanying elements in the film, or from backing materials, of course, the correction for these effects must be considered, as for iron in the nickel-iron alloy film used in this experiment. For the normal case, the calculated results are in good agreement with experimental values, as nickel in this experiment.

The Preparation of Several Tetrakis(triorganosiloxymethyl)methanes

Toshio TAKIGUCHI, Minoru ABE and Yukio MORIMURA

Department of Synthetic Chemistry, Kiryu College of Technology, Gunma University, Tenjin-cho, Kiryu

(Received September 2, 1967)

As regards the organosilyl or silylene derivatives of pentaerythritol (hereinafter called PET), very little has been said in the literature.[1-3]

In our investigations involving the reactions of PET with triorganochlorosilanes, some tetrakis-triorganosilyl derivatives of PET with the formula of $(R_3SiOCH_2)_4C$(hereafter R_3PET) were isolated in a pure form. They are tetrakis(trimethylsiloxymethyl)methane (Me_3PET), terakis(dimethylbutylsiloxymethyl)methane (Me_2BuPET), tetrakis-(dimethylphenylsiloxymethyl)methane (Me_2Ph-PET), tetrakis(diphenylbutylsiloxymethyl)methane (Ph_2BuPET), and tetrakis(triphenylsiloxymethyl)-methane (Ph_3PET), the last four being new compounds.

They were obtained from the reaction of PET either with the corresponding triorganochlorosilanes or with aminosilanes according to the following schemes.

$$(HOCH_2)_4C + 4R_3SiCl \rightarrow (R_3SiOCH_2)_4C + 4HCl$$

or $$(HOCH_2)_4C + 4R_3SiNH_2 \rightarrow (R_3SiOCH_2)_4C + 4NH_3$$

The products were all soluble in toluene and dioxane, and were found to be quite stable towards hydrolysis in the absence of ionic catalysts.

Experimental

Triorganochlorosilanes. A pure sample of trimethylchlorosilane (bp 58°C) was obtained from the Shin-etsu Chemical Industrial Co. Dimethylbutylchlorosilane (bp 139—140°C), dimethylphenyl chlorosilane (bp 76—78°C/2 mmHg), and diphenylbutylchlorosilane (bp 129°C/1 mmHg) were prepared by the Grignard route.[4] Triphenylchlorosilane (mp 98—99°C) was isolated from a high-boiling residue[5] of the direct synthesis of phenylchlorosilanes. They were further purified by conventional methods immediately before use.

Triorganoaminosilanes. Hexamethyldisilazane (bp 121°C), dimethylbutylaminosilane (bp 128°C), dimethylphenylaminosilane (bp 142°C/3 mmHg), diphenylbutylaminosilane (bp 139°C/1.5 mmHg), and triphenylaminosilane (mp 60°C, bp 156°C/1.8 mmHg) were prepared from the reaction of dried gaseous ammonia with the corresponding chlorosilanes dissolved in ether; the yields were consistently 85—88%.

The Preparation of R_3PET. Typical procedures will be described in detail, using the preparations of Me_3PET and Ph_3PET as examples.

Me_3PET: When a mixture of trimethylchlorosilane (0.44 mol, 47.7 g) and PET (0.1 mol, 13.6 g) was gently refluxed, PET gradually dissolved with the evolution of hydrogen chloride, and the temperature rose to 120°C after 30 hr. The resultant substance was then fractionated and a fraction boiling at 105—115°C/1 mmHg was collected. The further purification of the product was effected by fractional vacuum distillation, giving pure Me_3PET, mp 27.5—28.5°C, bp 110°C/1 mmHg (lit.[2] bp 128—129°C/5 mmHg) in a yield of 77% (mean).

Found: Si, 26.4; C, 48.52; H, 10.54%; mol wt, 418 (determined cryoscopically in dioxane). Calcd for $C_{17}H_{44}O_4Si_4$: Si, 26.4; C, 48.06; H, 10.44%; mol wt, 425.

Several modifications of the above procedure, using some organic bases (aniline, *N*, *N*-dimethylaniline, pyridine, *etc.*) as a hydrogen-chloride acceptor and toluene as a reaction medium unfailingly gave identical products in similar yields.

1) L. W. Breed, W. J. Haggerty, Jr. and J. Harvey, *J. Org. Chem.*, **25**, 1804 (1960).
2) M. M. Sprung and L. S. Nelson, *ibid.*, **20**, 1750 (1955).
3) B. N. Dolgov, G. Vinter, V. A. Komarov, N. P. Kharitonov and Y. I. Khudobin, *Izvest. Akad. Nauk SSSR, Ser. Khim.*, **1963**, 2146; *Chem. Abstr.*, **60**, 9305c (1964).
4) T. Takiguchi and M. Abe, *Kogyo Kagaku Zasshi (J. Chem. Soc. Japan, Ind. Chem. Sect.)*, **66**, 625 (1963).
5) T. Takiguchi and M. Abe, *ibid.*, **68**, 679 (1965).

Another effective method of preparing the product was by the reaction of PET with hexamethyldisilazane; here, there was a consistent yield of 83—86%.

Ph_3PET: When a mixed sample of triphenylaminosilane (0.44 mol, 123.4 g) and PET (0.03 mol, 4.1 g) was gently heated, a reaction occured with the evolution of ammonia. After the addition of PET (0.07 mol, 9.5 g) to the mixture, portion by portion, over a 1-hr period, the whole was further maintained at 160—170°C for 6 hr. After the resultant substance had stood, there was obtained a transparent viscous liquid from which a white crystalline mass, melting at 255—267°C, was obtained by the extraction of impurities with hexane. The recrystallization of the crude product from hexane-dioxane (1 : 1) gave 82 g (70%) of pure Ph_3PET, mp 285°C, as fine cubic crystals.

Found: Si, 9.6; C, 77.73; H, 5.15%; mol wt, 1165. Calcd for $C_{77}H_{68}O_4Si_4$: Si, 9.6; C, 79.07; H, 5.86%; mol wt, 1170.

Ph_3PET was readily soluble in dioxane, soluble in hot toluene, soluble only with difficulty in boiling benzene, and insoluble in ether, hexane, and ethanol. This was also found highly resistant to hydrolysis and was recovered quite unchanged after prolonged boiling with water.

The preparation of this compound from a direct reaction between PET and triphenylchlorosilane was also attempted; however, this attempt failed because of the presumably lower reactivity of triphenylchlorosilane. The yield of the tetrakis-derivatives always remained below 20%, even when an organic base was used as a hydrogen-chloride acceptor, the majority of the by-product being partially triphenylsilyl-substituted PET with hydroxyl groups.

Other Tetrakis-derivatives. Me_2BuPET (bp 155°C/1 mmHg), Me_2PhPET (bp 224°C/0.1 mmHg), and Ph_2BuPET (mp 76°C, bp 332°C/0.1 mmHg) were prepared by procedures similar to those used for Me_3PET or Ph_3PET. Throughout all the preparations, reactions with aminosilanes proved to be more advantageous than those with chlorosilanes, both in the marked simplicity of the procedure and in the higher yield of tetrakisderivatives.

Me_2BuPET Found: Si, 18.5; C, 58.95; H, 12.61%; mol wt, 575. Calcd for $C_{29}H_{68}O_4Si_4$: Si, 18.9; C, 58.73; H, 11.56%; mol wt, 593.

Me_2PhPET Found: Si, 16.5; C, 65.89; H, 7.97%; mol wt, 665. Calcd for $C_{37}H_{52}O_4Si_4$: Si, 16.7; C, 66.02; H, 7.97%; mol wt, 673.

Ph_2BuPET Found: Si, 10.2; C, 75.78; H, 7.96%; mol wt, 1075. Calcd for $C_{69}H_{84}O_4Si_4$: Si, 10.3, C, 76.05; H, 7.77%; mol wt, 1090.

The products thus obtained were all readily soluble in dioxane and were soluble in acetone, toluene and boiling benzene. The compounds with methyl groups were soluble in hot hexane and ethanol. They were all fairly resistant to solvolysis in the absence of an ionic catalyst. However, the addition of a few drops of acid or alkali to the boiling ethanolic solution readily decomposed it to the original PET and the ocrresponding hexaorganodisiloxanes.

IR Absorption Spectra and X-Ray Powder Patterns. All the products were well defined and were characterized by their IR spectra. The X-ray powder diffraction data were also recorded for crystalline products by using Cu$K\alpha$ radiation filtered by Ni.

IR Spectra

Me_3PET 745(m) 840(vs) 870(vs) 906(s) 1070(vs) 1170(m) 1260(vs) 1305(w) 1460(w) 1475(w) 2870(w) 2920(m) 2965(s)

Me_2BuPET 745(m) 785(s) 840(vs) 883(s) 905(m) 963(w) 998(w) 1023(m) 1073(vs) 1171(m) 1192(m) 1257(vs) 1340(w) 1375(w) 1466(m) 2875(s) 2925(vs) 2965(vs)

Me_2PhPET 670(s) 740(s) 785(vs) 840(vs) 905(m) 996(m) 1065(vs) 1120(vs) 1170(m) 1193(m) 1263(vs) 1305(w) 1320(w) 1407(w) 1427(s) 1460(w) 1470(m) 1487(w) 1593(m) 2895(m) 2935(s) 2980(vs) 3035(m) 3095(m)

Ph_2BuPET 700(vs) 735(vs) 783(w) 819(vs) 835(m) 853(w) 873(w) 961(w) 995(m) 1028(s) 1058(vs) 1116(vs) 1171(m) 1190(m) 1268(w) 1305(w) 1340(w) 1376(w) 1425(vs) 1458(m) 1485(w) 1566(w) 1589(m) 2880(s) 2935(vs) 2995(s) 3065(m) 3095(m)

Ph_3PET 700(vs) 740(vs) 815(vs) 838(s) 852(m) 920(w) 974(w) 996(m) 1028(s) 1066(vs) 1116(vs) 1156(w) 1190(m) 1268(w) 1308(w) 1328(w) 1380(w) 1425(vs) 1468(w) 1485(m) 1566(w) 1589(m) 2885(m) 2935(m) 3030(s) 3065(vs) 3090(vs)

X-Ray Powder Diffraction Data

Me_3PET	d,kX:	9.51	8.35	8.19	8.04	7.44	6.71
		5.95	5.22	5.04	4.44	4.08	3.72
	I/I_0:	0.43	0.35	0.51	0.49	0.19	0.33
		0.45	0.47	1.00	0.69	0.35	0.18
Ph_2BuPET	d,kX:	15.11	13.59	11.05	10.05	7.50	
		6.76	5.01	4.90	4.65	4.55	4.48
		4.04					
	I/I_0:	0.11	1.00	0.16	0.13	0.16	1.00
		0.28	0.12	0.23	0.16	0.23	0.11
Ph_3PET	d,kX:	13.19	10.65	8.76	7.56	7.31	6.71
		6.61	5.01	4.70	4.44	4.19	3.93
	I/I_0:	0.17	0.35	0.49	0.33	0.24	0.44
		0.45	0.55	0.42	1.00	0.44	0.65

The authors' thanks are due to the Shin-estu Chemical Industrial Co. for the supply of the chlorosilanes used in the present work.

Some Reactions of Di-π-cyclopentadienyldiphenyltitanium

Haruo MASAI, Kenkichi SONOGASHIRA and Nobue HAGIHARA

The Institute of Scientific and Industrial Research, Osaka University, Suita, Osaka

(Received September 7, 1967)

In the course of our study of the isomerization of olefin catalyzed by $(\pi\text{-}C_5H_5)_2Ti(C_6H_5)_2$ and related complexes,*1 it was found that the isomerization was inhibited by diphenylacetylene and carbon monoxide (CO). These phenomena were studied in some detail in relation to the investigation of the mechanism of the isomerization, and the following results were obtained.

When $(\pi\text{-}C_5H_5)_2Ti(C_6H_5)_2$ was refluxed in benzene with diphenylacetylene under nitrogen, a new organotitanium complex (I) was obtained. The dark green crystals of the complex (I), having the empirical formula, $C_{30}H_{24}Ti$, are stable in air at room temperature. For the determination of the structure of this complex, the reactions described below have been investigated.

By the reaction of I with aq. HCl in $CHCl_3$, $(\pi\text{-}C_5H_5)_2TiCl_2$ and triphenylethylene were isolated in good yields. This result suggests the existence of a $(\pi\text{-}C_5H_5)_2Ti$ fragment in I.

The complex (I) easily reacted with pressured CO at room temperature to afford 2, 3-diphenylindone in good yields. An attempt to isolate the organotitanium fragment was, in this case, unsuccessful.

The decomposition of the complex (I) by iodine in benzene gave *cis*-1-iodo-1, 2-diphenyl-2-(*o*-iodophenyl)-ethylene in good yields.

These facts lead us to the structure (A), namely, *Ti*-di-π-cyclopentadienyl-2, 3-diphenylbenztitanacyclopentadiene.

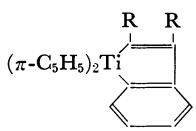

(A) (R=C_6H_5)

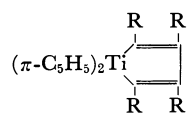

(B) (R=C_6H_5)

An analogous complex (B) has been prepared by us[1] and by Vol'pin *et al.*[2] independently. We obtained the complex (B) from the reaction of $(\pi\text{-}C_5H_5)_2Ti(CO)_2$ with diphenylacetylene.

The structure of the complex (I) is also supported by the NMR spectrum, which shows a sharp singlet at τ 3.9 and a multiplet centered at τ 3.4. The former is assignable to the cyclopentadienyl protons, and the later to the aromatic protons. The relative intensities observed are 10 and 13.5 (calcd for the structure (A): 10 and 14) respectively.

The infrared spectrum of I shows no bands due to Ti-H and coordinated C≡C stretching absorptions.

An attempt to prepare the analogous complex from the reaction of $(\pi\text{-}C_5H_5)_2Ti(CH_3)_2$ with diphenylacetylene by the similar procedure was unsuccessful.[3] Therefore, it is not likely that the complex (I) is formed through the insertion of acetylene in the Ti-alkyl bond. It seems more reasonable to describe the route of the formation of the complex (I) as follows:

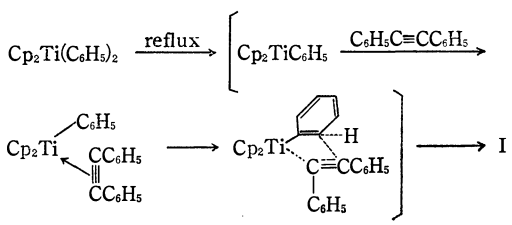

(Cp = π-C_5H_5)

The complex (I) was not attacked by atmospheric hydrogen at the reflux temperature in benzene, while diphenyl and dimethyl derivatives easily reacted under the same conditions.[4] This might be due to the stability of the titanacyclopentadiene ring caused by the partial double-bond character of the Ti-C σ-bond.

When $(\pi\text{-}C_5H_5)_2Ti(C_6H_5)_2$ was reacted with pressured CO at room temperature, benzophenone was isolated in good yields. It is considered that CO should initially coordinate to the vacant orbital of Ti. The insertion of CO in the Ti-phenyl bond will occur in the next step, and finally another phenyl group will migrate to the acyl group, producing benzophenone.

Experimental

$(\pi\text{-}C_5H_5)_2Ti(C_6H_5)_2$ was prepared by the method reported by Summers *et al.*[5]

Synthesis of I. A solution of 0.5 g of $(\pi\text{-}C_5H_5)_2Ti(C_6H_5)_2$ and 0.28 g of diphenylacetylene in 10 ml

*1 H. Masai, K. Sonogashira and N. Hagihara, *Mem. Inst. Sci. and Ind. Res., Osaka Univ.*, **25**, (1968), in press.

1) K. Sonogashira and N. Hagihara, This Bulletin, **39**, 1178 (1966).

2) M. E. Vol'pin, V. A. Dubovitskii and O. V. Nogina, *Dokl. Akad. Nauk S. S. S. R.*, **151**, 1100 (1963).

3) H. Masai, K. Sonogashira and N. Hagihara, unpublished results.

4) K. Clauss and H. Bestian, *Ann.*, **654**, 8 (1962).

5) L. Summers, R. H. Uloth and A. Holms, *J. Am. Chem. Soc.*, **77**, 3604 (1954).

of benzene was refluxed under nitrogen for 1 hr. The orangecolored solution turned dark green. The solution was then purified by column chromatography, using alumina under nitrogen. A dark green band eluted by benzene was collected. After the removal of the benzene, 0.18 g of crude, dark green crystals were obtained (46%). An analytical sample was obtained by recrystallization from CH_2Cl_2 - petroleum ether, mp 227—228°C.

Found: C, 83.64; H, 5.58%; mol wt (cryoscopic method in benzene using a Dampfdruckosmometer des Dr-Ing Herbert Knauer), 435. Calcd for $C_{30}H_{24}Ti$: C, 83.33; H, 5.59%; mol wt, 432.

The NMR spectrum of I in CCl_4 was recorded by a Varian A-60 spectrometer, using TMS as the internal standard.

The infrared spectrum was taken with a KBr tablet.

This complex was hydrogenated in Hershberg's apparatus in benzene at a reflux temperature. No hydrogen was absorbed.

Reaction of I with Aq. HCl. To a solution of 0.4 g of I in 15 m*l* of $CHCl_3$, an excess of aq. HCl was added. The color of the $CHCl_3$ layer immediately changed to red. The organic layer was then separated, and the aqueous layer was extracted by $CHCl_3$. After the removal of the $CHCl_3$, the residual mass was extracted by petroleum ether. Fine red crystals remained in the flask. The infrared spectrum of these crystals, obtained by the KBr method, was thoroughly coincident with that of authentic $(\pi\text{-}C_5H_5)_2TiCl_2$[6] (0.199 g, 70%).

The extract was purified by chromatography over alumina. After the evaporation of the solvent, white crystals were obtained, and the crystals were recrystalized from petroleum ether. The melting point and the infrared absorption spectrum of these crystals were identical with those of authentic triphenylethylene[7] (0.166 g, 70%), mp 72.5—73.5°C. Found: C, 93.63; H, 6.51%; mol wt (by vapor pressure osmometer, Dampfdruckosmometer des Dr-Ing Herbert Knauer), 256.8. Calcd for $C_{20}H_{16}$: C, 93.61; H, 6.29%; mol wt, 256.3.

Carbonylation of I. A solution of 0.068 g of I in 10 m*l* of benzene was reacted with CO under 200 atm at room temperature for 7 hr. An orange-yellow solution containing a yellow precipitate was thus obtained. This reaction mixture was chromatographed over alumina and eluted with benzene. After the removal of the benzene, 0.03 g of ruby-red crystals was obtained and recrystallized from benzene-petroleum ether. The melting point and the infrared spectrum of these crystals were identical with those of authentic 2, 3-diphenylindone[8] (70%), mp 156.5—157.5°C.

Found: C, 89.28; H, 5.07%. Calcd for $C_{21}H_{14}O$: C, 89.33; 5.00%.

Decomposition of I by Iodine. To a solution of 0.2 g of I in 10 m*l* of benzene, an excess of an iodine solution in benzene was gradually added at room temperature. After the addition, the mixture was left for 1 hr. After the removal of the solvent, the residue was extracted by petroleum ether, and the extract was chromatographed. A slightly-colored solution eluted by petroleum ether was thus obtained. After the removal of the solvent, 0.15 g of yellowish crystals recrystalized from benzene-petroleum ether were obtained. The melting point of these crystals was identical with that of *cis*-1-iodo-1, 2-diphenyl-2-(*o*-iodophenyl)-ethylene found in the literature[9] (64%), mp 172—173°C. Found: C, 47.33; H, 2.70%. Calcd for $C_{20}H_{14}I_2$: C, 47.27; H, 2.78%.

Carbonylation of $(\pi\text{-}C_5H_5)_2Ti(C_6H_5)_2$. A solution of 3.2 g of this complex in 20 m*l* of benzene was reacted with CO by a procedure similar to that used in the case of I. After the removal of the solvent, the residue was extracted by petroleum ether. The extract was concentrated in a vacuum, and then the residual liquid was distilled. A colorless liquid of benzophenone was thus obtained (bp 118°C/3 mmHg). The infrared spectrum in CCl_4 was coincident with that of authentic benzophenone (1.5 g, 83%).

Found: C, 85.00; H, 5.64%. Calcd for $C_{13}H_{10}O$: C, 85.69; H, 5.53%.

2, 4-Dinitrophenylhydrazone of this sample showed the same melting point as that of authentic benzophenone 2, 4-dinitrophenylhydrazone, mp 247—248°C.

Found: C, 62.94; H, 3.66; N, 15.45%. Calcd for $C_{19}H_{14}N_4O_4$: C, 62.98; H, 3.39; N, 15.45%.

6) R. B. King, "Organometallic Syntheses," Vol. I, Academic Press, New York, N. Y. (1965).

7) H. Adkins and W. Zartman, "Organic Syntheses," Coll. Vol. II, p. 606, (1959).

8) C. F. H. Allen, J. W. Gate, Jr., and J. A. VanAllan, *ibid.*, Coll. Vol. III, p. 353 (1955).

9) J. J. Eisch and W. C. Kaska, *J. Am. Chem. Soc.*, **84**, 1501 (1962).

Radical Copolymerization of *m*-Bromostyrene with Liquid Sulfur Dioxide*[1]

Masashi IINO, Takeshi MASUDA and Niichiro TOKURA

Department of Applied Chemistry, Faculty of Engineering, Osaka University, Higashinoda, Miyakojima-ku, Osaka

(Received September 12, 1967)

The simple olefins, such as ethylene, propylene, and butenes, readily form alternating copolymers with sulfur dioxide from a wide range of feed compositions by means of a radical initiator.

Styrene also reacts with sulfur dioxide by means of a radical initiator and forms a 2 : 1 copolymer (molar ratio of styrene unit to sulfur dioxide unit) from a wide range of feed compositions above room temperature.[1,2] The fact that the resulting copolymers are not alternating but 2 : 1 copolymers suggests that the propagation reaction can not be elucidated by the ordinary mechanism of copolymerization.

Thus, Barb[1] has given an interpretation involving reversible propagation steps and the inclusion of sulfur dioxide in the copolymer only by the reaction of a growing chain with a 1 : 1 styrene-sulfur dioxide complex, which can be shown to be present spectroscopically.

However, as an entirely equivalent scheme can be derived without invoking any complex participation,[3] Barb's postulation appears to be uncertain.

Concerning this problem, we have investigated the copolymerization of various styrene derivatives with sulfur dioxide.[4] We have found that *p*-isopropylstyrene[4b] or *p*-methylstyrene,[4a] whose substituent is an electron-donating group, forms a 2 : 1 copolymer like that in the case of styrene, but *p*-nitrostyrene,[4c] with an electron-withdrawing group, does not form a 2 : 1 copolymer.

The results in the case of *p*-nitrostyrene are thus different from those in the case of styrene, but *p*-nitrostyrene reacts with sulfur dioxide heterogeneously, unlike as in the case of styrene; therefore, it is possible to consider that this abnormality in the *p*-nitrostyrene - sulfur dioxide system is due to its heterogeneity.

To elucidate this problem we have investigated the copolymerization of *m*-bromostyrene with sulfur dioxide, because *m*-bromostyrene, whose substituent, *m*-Br, was electron-withdrawing, as in the case of *p*-nitrostyrene, has reacted with sulfur dioxide homogeneously.

Experimental

Styrene, α, α'-azobisisobutyronitrile (AIBN), and liquid sulfur dioxide were purified by a method similar to that described in a previous paper.[4]

m-Bromostyrene was prepared from *m*-bromobenzaldehyde.[5] Elementary analysis: Found: C, 52.78; H, 4.11; Br, 43.36%. Calcd for C_8H_7Br: C, 52.48; H, 3.82; Br, 43.68%.

Bp 76.5—78.0°C/11 mmHg; n_D^{17}, 1.5882. The *m*-bromostyrene thus obtained was distilled twice in a nitrogen atmosphere at a reduced pressure.

The *n*-hexane used in the measurement of the ultraviolet spectra was purified in the usual way.

The method of the copolymerization was similar to that described in a previous paper.[2]

The compositions of the copolymers were determined from the results of elementary analyses of carbon. The ultraviolet spectra of a *m*-bromostyrene-liquid sulfur dioxide mixture were measured in *n*-hexane by using a pressure cell.

Results and Discussion

Copolymerization of *m*-Bromostyrene and Liquid Sulfur Dioxide. The radical copolymerization of *m*-bromostyrene with sulfur dioxide was carried out at 50°C, using AIBN as an initiator, and was stopped at a low conversion (below 7%).

As is shown in Fig. 1, the sulfur dioxide contents (mol%) in the resulting copolymers vary with the feed composition but are all below that (about 33 mol%) in the case of styrene.

The *e* value (*Q-e* scheme) of styrene, *m*-bromostyrene, and *p*-nitrostyrene are −0.8, −0.21, and 0.39 respectively.[6] The sulfur dioxide contents (mol%) of the copolymers obtained at 50°C from an equimolar feed composition in the case of styrene, *m*-bromostyrene, and *p*-nitrostyrene are 33, 24, and 8 respectively.

Therefore, it may be concluded that styrene derivatives, having an electron-withdrawing substituent and a larger *e* value than styrene, have no tendency toward constant copolymer compositions, and that the sulfur dioxide contents in the

*1 Polymerization in Liquid Sulfur Dioxide. Part XXVII.

1) W. G. Barb, *Proc. Roy. Soc.*, **A212**, 66, 177 (1952).

2) N. Tokura and M. Matsuda, *Kogyo Kagaku Zasshi (J. Chem. Soc. Japan, Ind. Chem. Sect.)*, **64**, 501 (1961).

3) C. Walling, *J. Polymer Sci.*, **16**, 315 (1955).

4) a) N, Tokura, M. Matsuda and Y. Ogawa, *ibid.*, **A-1**, 2965 (1963). b) N. Tokura, M. Matsuda and K. Arakawa, *ibid.*, **A-2**, 3355 (1964). c) M. Iino, I. Otsuka and N. Tokura, *Kogyo Kagaku Zasshi (J. Chem. Soc. Japan, Ind. Chem. Sect.)*, **69**, 115 (1966).

5) J. H. Brown and C. S. Marvel, *J. Am. Chem. Soc.*, **59**, 1176 (1937).

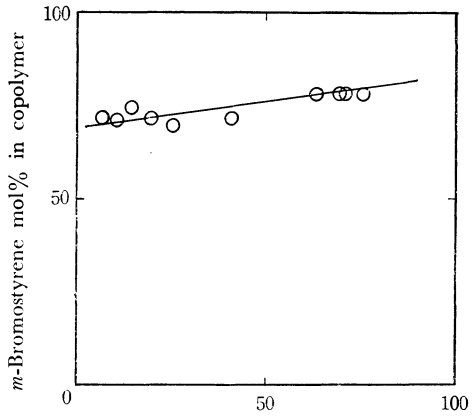

Fig. 1. Copolymer composition curve for *m*-bromostyrene - sulfur dioxide system.
Poly temp., 50°C; $[AIBN]_0$, 3.0×10^{-2}—3.0×10^{-1}(mol/*l*).

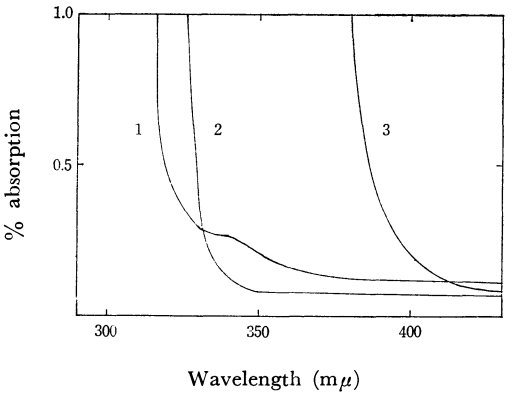

Fig. 2. Ultraviolet absorption for *m*-bromostyrene-sulfur dioxide system.
(1) *m*-Bromostyrene, 5.8 (mol/*l*)
(2) Sulfur dioxide, 5.6 (mol/*l*)
(3) *m*-Bromostyrene 5.8 (mol/*l*)) + sulfur dioxide(5.6(mol/*l*))
Solv., *n*-hexane; Cell depth, 0.4 mm; Room temperature.

copolymers are lower than that in the case of styrene.

Ultraviolet Spectra of the *m*-Bromostyrene-Liquid Sulfur Dioxide Mixture. It is well known that sulfur dioxide forms a charge-transfer complex with some olefins, in which complex sulfur dioxide acts as an electron acceptor and olefin, as an electron donor.[7] In Fig. 2 the ultraviolet spectra of *m*-bromostyrene, sulfur dioxide, and *m*-bromostyrene - sulfur dioxide mixture are shown. It may be seen in Fig. 2 that a complex is formed in the *m*-bromostyrene - sulfur dioxide mixture, because there is a large shift in the absorption of the mixture in comparison with that of *m*-bromostyrene or sulfur dioxide only in the same concentration as in the mixture.

From the above results, in the *m*-bromostyrene - sulfur dioxide system a charge-transfer complex is formed as in the case of styrene; however, the compositions of the copolymers vary with the feed compositions, unlike the case of styrene.

As has previously been described, in the case of the *p*-nitrostyrene - sulfur dioxide system, the compositions of the copolymers vary with the feed compositions; the results of the ultraviolet spectra of the *p*-nitrostyrene - sulfur dioxide mixture suggest that no charge-transfer complex is formed.[4c]

Therefore, it may be concluded that, in the radical copolymerization of sulfur dioxide with styrene or its derivative (and perhaps also in that of sulfur dioxide with another olefin), the formation of a charge-transfer complex is not related to the constancy of the compositions of the copolymers when the feed compositions are varied.

The authors wish to thank the Seitetsu Kagaku K. K. for its gift of liquid sulfur dioxide.

6) L. J. Young, *J. Polymer Sci.*, **54**, 411 (1961).
7) D. Booth, F. S. Dainton and K. J. Ivin, *Trans. Faraday Soc.*, **55**, 1293 (1959).

Oxidation of Graphite by Carbon Dioxide - Carbon Monoxide Gas Mixtures

Shigeru YAMAUCHI and Takashi MUKAIBO

Department of Industrial Chemistry, Faculty of Engineering, The University of Tokyo, Hongo, Bunkyo-ku, Tokyo

(Received September 14, 1967)

Graphite has been considered to be oxidized by carbon dioxide by the following mechanism[1];

$$C + CO_2 \underset{i_2}{\overset{i_1}{\rightleftarrows}} C(O) + CO \quad (1)$$

$$C(O) \xrightarrow[i_3]{} CO \quad (2)$$

where i_1, i_2, and i_3 are rate constants and C(O) is the surface oxide.

From Eqs. (1) and (2) the over-all oxidation rate is expressed as follows;

$$R = i_1 P_{CO_2}/(1 + (i_2/i_3)P_{CO} + (i_1/i_3)P_{CO_2}) \quad (3)$$

In this study the over-all oxidation rates were measured in the carbon dioxide - carbon monoxide gas mixtures and the values of rate constants, i_1, i_2 and i_3 for elementary reactions were determined at temperatures from 1100°C to 1175°C. Activation energies for elementary reactions were determined and discussed in connection with the surface oxide.

Experimental

Two types of high purity artificial graphite made from petroleum coke were used. In the course of preparation, graphites A and B were heat-treated at 2400°C and 3000°C, respectively. Both kinds of graphite did not contain any metallic impurities more than 1 ppm, as determined by the spectroscopic analysis.

Results and Discussion

Equation (3) is rewritten in the form;

$$1/R = (1/i_3) + (i_2/i_1 \cdot i_3)(P_{CO}/P_{CO_2}) + (1/i_1)(1/P_{CO_2}) \quad (4)$$

Equation (4) shows that: (1) If the rates are measured at various total pressures with a constant ratio of (P_{CO}/P_{CO_2}), the plot of $1/R$ *vs.* $1/P_{CO_2}$ gives the value of $1/i_1$. (2) The intercept on the axis of $1/R$ (of the above straight line) gives the value of $1/R^\circ = (1/i_3) + (i_2/i_1 \cdot i_3)(P_{CO}/P_{CO_2})$. Moreover, the plot of $1/R^\circ$ *vs.* P_{CO}/P_{CO_2} gives a straight line and the slope gives the value of $(i_2/i_1 \cdot i_3)$ and the intercept on the axis of $1/R^\circ$ gives the value of $1/i_3$. The value of the above slope should coincide with the value of a slope when $1/R$ is plotted against

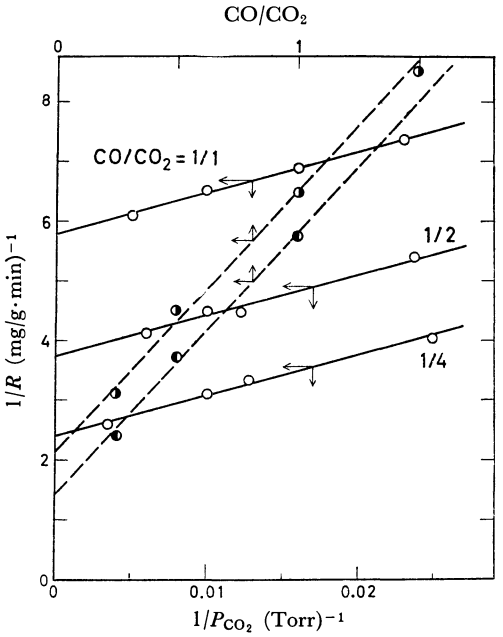

Fig. 1. Plot of $1/R$ *vs.* $1/P_{CO_2}$ and $1/R$ *vs.* P_{CO}/P_{CO_2} of graphite A at 1150°C.
-○-: plots of $1/R$ *vs.* $1/P_{CO_2}$ at constant ratios of P_{CO}/P_{CO_2}
-◑-: plot of $1/R^\circ$ *vs.* P_{CO}/P_{CO_2}
-◐-: plot of $1/R$ *vs.* P_{CO}/P_{CO_2} (P_{CO_2} = 100 Torr)

P_{CO}/P_{CO_2} at a constant partial pressure of carbon dioxide.

The plots of $1/R$ *vs.* $1/P_{CO_2}$ and $1/R$ *vs.* (P_{CO}/P_{CO_2}) are shown in Fig. 1. The values of i_1, i_2 and i_3 are calculated from the values of $1/i_1$, $1/i_3$ and $i_2/i_1 \cdot i_3$. They are shown in Figs. 2 and 3 as Arrhenius plots. The values of activation energies are also given in these figures.

The value of $\Delta H_1 = E_1 - E_2$ gives the enthalpy change of the reaction (1). The values of ΔH_1 obtained in this study are 24 kcal/mol and 20 kcal/mol for graphites A and B, respectively.

Assuming the value of ΔH_1 to be 25 kcal/mol, the enthalpy of formation of surface oxides is calculated as follows.

$$\Delta H^\circ_{f,C(O)} = \Delta H_1 - \Delta H^\circ_{f,CO} + \Delta H^\circ_{f,C} + \Delta H^\circ_{f,CO_2} = 42 \text{ kcal/mol}$$

Bull and co-workers[2] reported the value of the

1) P. L. Walker, Jr., F. Rusinko, Jr. and L. G. Austin, Advances in Catalysis, Vol. 11, Academic Press, New York (1959), p. 133.

2) H. I. Bull, M. H. Hall and W. E. Garner, *J. Chem. Soc.*, **19**, 837 (1931).

heat of adsorption of oxygen on the surface of carbons to be 100 kcal/mol. If the adsorption results in the formation of surface oxide, the heat of formation of this surface oxide is 50 kcal/mol. $\Delta H^\circ_{f,C(O)}$ determinedk inetically in this study seems to meet this value.

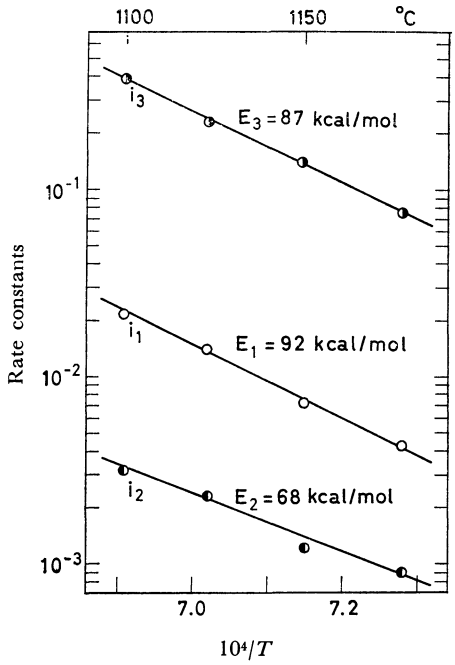

Fig. 2. Arrhenius plots of the rate constants of graphite A.

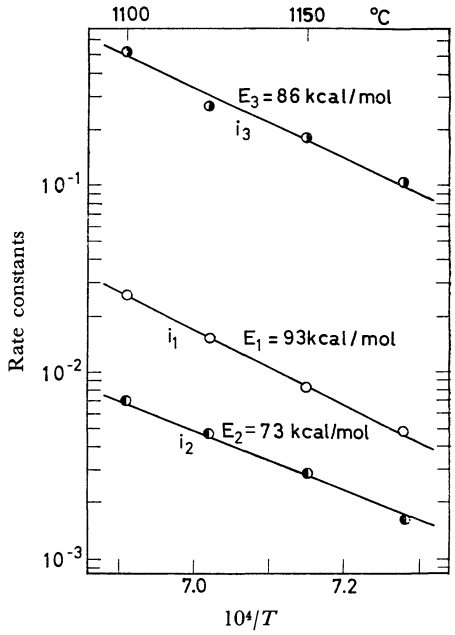

Fig. 3. Arrhenius plots of the rate constants of graphite B.

Effect of Chlorine on the Oxidation of Graphite by Carbon Dioxide

Shigeru YAMAUCHI, Takashi MUKAIBO and Tadao IKEDA

Department of Industrial Chemstry, Faculty of Engineering, The University of Tokyo, Hongo, Bunkyo-ku, Tokyo

(Received September 14, 1967)

In the previous papers[1-3] the effects of iodine and bromine on the oxidation of graphite were reported to be an accelerating one. This note reports the experimental results on the effect of chlorine on the oxidation of graphite by carbon dioxide.

Experimental

High purity artificial graphite made from petroleum coke and graphitized at 2400°C was used. The results of a spectroscopic analysis showed that this graphite contained only 0.05 ppm Mg and 0.5 ppm Si as impurities. Impurities other than Mg and Si were not found.

The chlorine gas was fed from a bomb at a constant flow rate and the partial pressure of chlorine was determined by the ratio of the flow rate of chlorine to that of carbon dioxide. The apparatus and the experimental procedures were the same as described in detail in a previous paper.[1]

Results

As shown in Fig. 1, the oxidation rate increased rapidly during an initial period following the supply of chlorine gas into the carbon dioxide gas stream and then gradually decreased to a steady value. This steady value was considered to be that of oxidation rate affected by the presence of

1) T. Mukaibo and S. Yamauchi, *Carbon*, **3**, 87 (1965).
2) S. Yamauchi and T. Mukaibo, *ibid.*, **4**, 455 (1966).
3) S. Yamauchi, T. Mukaibo and M. Hirano, *ibid.*, **5**, 243 (1967).

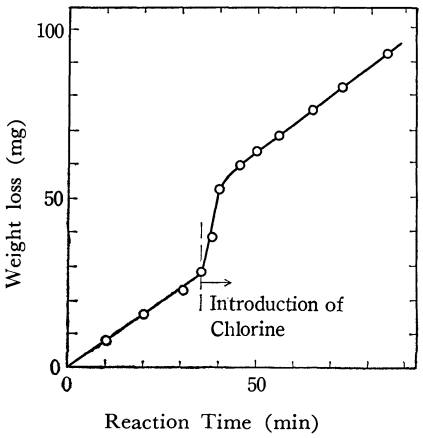

Fig. 1. Weight loss *vs.* time curve (1100°C).

chlorine gas.

The oxidation rate was markedly affected by the partial pressures of chlorine gas as shown in Fig. 2. Oxidation rates accelerated by iodine and bromine are also presented in Fig. 2 in order to compare the effect of halogenous gases. It is seen that the oxidation rate has a maximum point at 0.9 Torr in the case of bromine and 0.1 Torr in the case of chlorine, respectively. Any maximum point was not observed in the case of iodine at the partial pressure of 0.3 to 10 Torr.

The most remarkable observation in Fig. 2 is that the effect of chlorine at the partial pressures above 3.5 Torr is an inhibiting one, although an accelerating effect was observed on the effect of iodine and bromine.

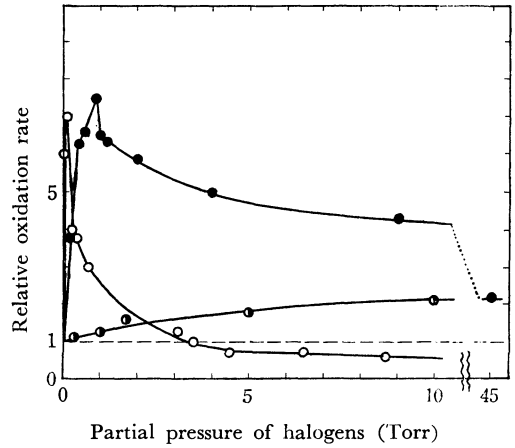

Fig. 2. The dependence of oxidation rates on the partial pressure of halogens.

The relative oxidation rate is defined as a ratio of oxidation rate affected by halogens to that in pure carbon dioxide. If the value of the relative oxidation rate is larger than unity, the effect of halogens is accelerating and if the value is smaller than unity, the effect is inhibiting.

○: chlorine (at 1100°C)
●: bromine (at 1145°C)
◑: iodine (at 1145°C)

Preparation of 1-Choro-1-fluoroethylenes *via* Chlorofluorocarbene

Hiroki YAMANAKA, Teiichi ANDO and Wataru FUNASAKA

Department of Industrial Chemistry, Faculty of Engineering, Kyoto University, Sakyo-ku, Kyoto

(Received October 11, 1967)

It has already been reported that chlorofluorocarbene reacts with triphenylphosphine to yield chlorofluoromethylenetriphenylphosphorane, and that the ylid reacts with benzophenone to give 1-chloro-1-fluoro - 2, 2 - diphenylethylene.[1] This paper will deal with the synthesis of some other 1-chloro-1-fluoroethylenes by a modification of this method.

Chlorofluorocarbene was generated by the addition of methanol to a mixture of sodium hydride and methyl dichlorofluoroacetate.[2] After it had been allowed to react with triphenylphosphine, the reaction mixture was treated, without the isolation of the ylid, with a carbonyl compound. The reaction scheme is shown below, and the results are summarized in Table 1.

$$CFCl_2COOCH_3 + CH_3OH/NaH \rightarrow :CFCl$$

$$:CFCl + Ph_3P \rightarrow Ph_3P{=}CFCl$$

$$Ph_3P{=}CFCl + RCOR' \rightarrow RR'C{=}CFCl + Ph_3PO$$

The main product obtained from an aldehyde or an unsymmetrical ketone gave a gas chromatogram composed of two peaks, indicating the formation of two geometrical isomers. Unfortunately, however, the retention times of the isomers under the conditions employed were too close to each other to make the gas chromatographic separation of the

1) A. J. Speziale and K. W. Ratts, *J. Am. Chem. Soc.*, **84**, 854 (1962).
2) T. Ando, H. Yamanaka, S. Terabe, A. Horike and W. Funasaka, *Tetrahedron Letters*, **1967**, 1123.

TABLE 1. REACTION OF CHLOROFLUOROMETHYLENETRIPHENYLPHOSPHORANE WITH CARBONYL COMPOUNDS

Carbonyl compound	Product	Yield %	Bp °C/mmHg	n_D^t (t, °C)	$\nu_{C=C}$ cm^{-1}	C, %		H, %	
						Calcd	Found	Calcd	Found
cyclo-$(CH_2)_5CO$	cyclo-$(CH_2)_5C$=CFCl	25	68—70/80	1.4627 (21)	1688	56.58	56.69	6.78	6.82
PhCOMe	PhC(Me)=CFCl	8	75—80/25	—	1665	63.36	63.47	4.73	4.80
PhCHO	PhCH=CFCl[4]	40	79—80/26	1.5293 (22) [a] 1.5330 (22) [b]	1665 [a] 1666 [b]	61.36	61.61	3.86	4.06
p-ClC_6H_4CHO	*p*-ClC_6H_4CH=CFCl[4]	63	93—96/12	1.5606 (19)	1663	50.30	50.50	2.67	2.72
p-$MeOC_6H_4CHO$	*p*-$MeOC_6H_4CH$=CFCl[4]	40	97—104/7	1.5533 (23)	1663	57.92	57.89	4.32	4.54
o-$MeOC_6H_4CHO$	*o*-$MeOC_6H_4CH$=CFCl	50	92—93/6	1.5404 (22)	1660	57.92	58.02	4.32	4.25
$PhCOCF_3$	PhC(CF_3)=CFCl	40	60—61/25	1.4603 (21) [a] 1.4549 (21) [b]	1660 [a] 1668 [b]	48.13	48.23	2.24	2.26
p-$FC_6H_4COCF_3$	*p*-$FC_6H_4C(CF_3)$=CFCl	45	44—45/35	1.4473 (22)	1660	44.56	44.85	1.66	1.71
p-$ClC_6H_4COCF_3$	*p*-$ClC_6H_4C(CF_3)$=CFCl	41	85—86/14	1.4788 (24)	1663	41.73	41.67	1.56	1.79
p-$MeC_6H_4COCF_3$	*p*-$MeC_6H_4C(CF_3)$=CFCl	38	65—70/16	1.4628 (21)	1665	50.34	50.67	2.96	3.23
p-$MeOC_6H_4COCF_3$	*p*-$MeOC_6H_4C(CF_3)$=CFCl	36	98—100/11	—	1665	47.17	47.05	2.77	2.74

a) For the *anti*-isomer. b) For the *syn*-isomer.

TABLE 2. PARAMETERS OF THE ^{19}F NMR SPECTRA OF 1-CHLORO-1, 3, 3, 3-TETRAFLUORO-2-ARYLPROPENES[a]

anti-form: 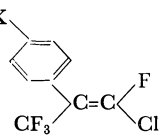

syn-form: 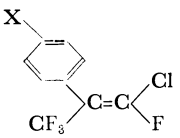

X	Configration	Chemical shift, ppm[b] δ_{-CF_3}	Chemical shift, ppm[b] $\delta_{=CF}$	Coupling constant between $-CF_3$ and $=CF$, cps
H	anti	20.33	17.52	13.0
	syn	20.42	15.03	23.1
Me	anti	18.48	15.32	13.0
	syn	18.53	13.45	25.4
MeO	anti	19.47	16.15	12.5
	syn	19.45	14.25	25.4
Cl	anti	18.82	17.04	13.5
	syn	18.93	15.13	24.0
F	anti	19.05	16.97	13.0
	syn	19.09	14.94	25.4

a) Measured on a JNM C-60 NMR spectrometer at 56.446 Mc (20—40% in CCl_4).
b) Downfield from external trifluoroacetic acid.

TABLE 3. COMPETITION REACTION

Carbonyl compounds	Products and their ratio
PhCHO + PhCOMe	PhCH=CFCl (100) + PhC(Me)CFCl (0)
PhCHO + $PhCOCF_3$	PhCH=CFCl (54) + $PhC(CF_3)$=CFCl (46)
PhCHO + *p*-ClC_6H_4CHO	PhCH=CFCl (37) + *p*-ClC_6H_4CH=CFCl (63)
PhCHO + *p*-$MeOC_6H_4CHO$	PhCH=CFCl (74) + *p*-$MeOC_6H_4CH$=CFCl (26)
$PhCOCF_3$ + PhCOMe	$PhC(CF_3)$=CFCl (100) + PhC(Me)=CFCl (0)

isomers feasible,[3] except in the following two cases.

The product obtained from benzaldehyde (β-chloro-β-fluorostyrene) was successfully separated, by preparative gas chromatography (TCP 10%, 80°C, He 30 ml/min) into two isomers, the *anti*- (Ia) and the *syn*-form (Ib). The structures of the isomers were determined by their proton NMR spectra,[4] and the ratio of Ia to Ib (57 : 43) was determined by gas chromatography before distillation. The *anti*-isomer had a longer retention time than the *syn*-isomer.

Similarly, the product from α, α, α-trifluoroacetophenone (1 - chloro - 1, 3, 3, 3 - tetrafluoro-2-phenylpropene) could also be separated into *anti*-(IIa) and *syn*- (IIb) isomers (PEG 6000 10%, 120°C, He 30 ml/min). The ratio of IIa to IIb was 52 : 48, the *anti*-isomer again possessing a longer retention time.

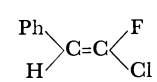

(Ia)

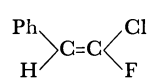

(Ib)

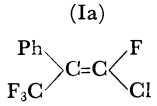

(IIa)

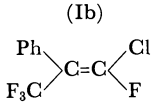

(IIb)

The structural assignments of the ethylenes derived from aryl trifluoromethyl ketones, including IIa and IIb, were made by means of their fluorine NMR spectra, based on the fact that the coupling constant between $-CF_3$ and =CF in the $-C(CF_3)$=CF– system is larger when they are cis to each other than when they are trans.[5] The NMR data are shown in Table 2.

Table 3 shows the results of the competition reactions which were carried out in order to examine the relative reactivities of carbonyl compounds toward chlorofluoromethylenetriphenylphosphorane. As is evident from the table, the ylid reacts with aldehydes or with ketones having electron-withdrawing groups more rapidly than with ketones having electron-releasing groups. Analogous results have been obtained with dichloromethylenetriphenylphosphorane.[1]

3) As judged from the areas of the NMR signals and/or the half-height widths of the gas chromatographic peaks, the ratio of the isomers formed was estimated to be approximately 50 : 50 in all of these cases.
4) T. Ando, F. Namigata, M. Kataoka, K. Yachida and W. Funasaka, This Bulletin, **40**, 1275 (1967).
5) J. W. Emsley, J. Feeney and L. H. Sutcliffe, "High Resolution NMR Spectroscopy," Vol. 2, Pergamon Press, London (1966), p. 909.

As compared with the other methods for preparing 1-chloro-1-fluoroethylenes,[6] the method described in this paper seems to have the advantages of being simpler and of wider applicability, although the yields are not always satisfactory.

Experimental

General Procedure for Preparing 1-Chloro-1-fluoroethylenes. A mixture of 0.2 mol of triphenylphosphine, 0.25 mol of sodium hydride, 0.25 mol of methyl dichlorofluoroacetate,[4] and 100 m*l* of dry petroleum ether (bp 60—70°C) was placed in a 200-m*l*, four-necked flask equipped with a stirrer, a thermometer, a gas inlet tube for introducing nitrogen, and a reflux condenser. To the mixture was added, under an atmosphere of nitrogen, 0.25 mol of methanol at 25—30°C (3—5 hr), and then 0.25 mol of a carbonyl compound at the same temperature (0.5 hr). After the reaction mixture had been allowed to stand at 60—80°C for 10 hr, it was cooled to room temperature and poured into 100 m*l* of water. The organic layer was separated from the aqueous layer, the aqueous layer was extracted twice with 50 m*l* portions of ether, and the combined organic layer was dried over anhydrous sodium sulfate. The distillation of the organic layer gave the desived ethylene (8—63%), the unchanged carbonyl compound (10—25%), and an unidentified product whose bp was a little higher than that of the ethylene. The ethylenes were identified by elemental analysis as well as by IR and /or NMR spectroscopy.

Competition Reaction. A mixture of two different carbonyl compounds (each 0.017 mol) was gradually added, at 25°C (0.5 hr), to a reaction mixture containing chlorofluoromethylenetriphenylphosphorane, which had been obtained, in the way described above, from 0.017 mol of triphenylphosphine, 0.02 mol of sodium hydride, 0.02 mol of methyl dichlorofluoroacetate, 0.02 mol of methanol, and 20 m*l* of benzene. The reaction mixture was kept at 60—80°C for 10 hr, and then cooled to room temperature. The ratio of the olefinic products was determined, without distillation, by gas chromatography with TCP, Apiezon Grease L, PEG 4000, or Silicone Grease as the liquid phase. All the olefins were assumed to have the same molar response under the conditions employed.

The authors wish to express their gratitude to Dr. Hiroshige Muramatsu of the Government Industrial Research Institute, Nagoya, for his measurements of the fluorine NMR spectra.

6) See Ref. 4, and the references cited therein.

Stabilities of Rare Earth Chelates of 5-Sulphosalicylic Acid

C. R. KANEKAR

Tata Institute of Fundamental Research, Colaba, Bombay 5, India

and N. V. THAKUR and S. M. JOGDEO

Bhabha Atomic Research Centre, Trombay, Bombay 74, India

(Received September 16, 1967)

The spectrophotometric and potentiometric study of complex formation between gadolinium ions and 5-sulphosalicylic acid (SSA) has been reported in an earlier paper.[1] It was observed that at pH lower than 7, the reaction between the metal ion and the ligand results in the formation of a protonated complex of the type MHL in equilibrium with the usual ML complex; between pH 7 and 9, however, ML_2 species are predominantly present in solution. We have now studied the reaction of SSA with other rare earths. The data of stability constants obtained will be discussed in this paper in terms of the bonding in these complexes.

Experimental

The stability constants were determined at 20°C and at constant ionic strength of 0.1 M. The technique used for the potentiometric and the spectrophotometric measurements was similar to that described earlier.[1] The spectrophotometric measurements were made at pH 6.0 which was much below the pH of hydrolysis in each case. The spectra of all the rare earth complexes with this ligand were similar; two maxima were observed. The wavelengths corresponding to them are given in Table 1. At the wavelength of 340 mμ and the concentration chosen, the metal perchlorate had negligible absorption. The ligand, however, had finite absorption and during the evaluation of the stability constants the values of the optical density were corrected for this absorption by Beer's law.

The results obtained for all the rare earth complexes were remarkably similar. In the range of pH investigated (5 to 10), both 1 : 1 and 1 : 2 complexes are formed with this ligand. Below pH 7, the reaction is of the type

$$M+HL \overset{k}{\rightleftharpoons} MHL \overset{k'}{\rightleftharpoons} ML+H$$

The equilibrium constants k and k' have been evaluated in each case by exactly the same manner as described

1) N. V. Thakur, S. M. Jogdeo and C. R. Kanekar, *J. Inorg. Nucl. Chem.*, **28**, 2297 (1966).

Table 1. Wavelengths of maximum absorption in the ultraviolet for rare earth complexes of SSA at pH 6.0

Metal ion	Wavelength of maximum absorption, mμ	
Ce^{3+}	252	308
Pr^{3+}	254	310
Nd^{3+}	252	310
Sm^{3+}	254	317
Eu^{3+}	252	314
Gd^{3+}	252	315
Tb^{3+}	254	318
Dy^{3+}	253	317
Ho^{3+}	253	317
Er^{3+}	253	317
Tm^{3+}	254	319
Yb^{3+}	253	316
Lu^{3+}	253	319

in the previous paper[1] using both potentiometric and spectrophotometric data. The values of k were also calculated independently from the potentiometric data alone assuming the equilibrium of MHL and ML and this served as a further check on the reliability of the previous calculations.

The values of the stability constant (K_1) for the reaction $M+L \rightleftharpoons ML$ have been calculated using the relation

$$K_1 = k \cdot k' \cdot K_1^H$$

where K_1^H is the first proton ligand stability constant ($10^{11.72}$), involving the phenolic group. The values of K_2 for the reaction $ML+L \rightleftharpoons ML_2$ have been also calculated. The data of k, k', K_1, K_2 and $(K_1 \cdot K_2)$ are given in log units in Table 2.

Discussion

There is considerable evidence that rare earths form compounds involving ionic bonds and that the "f" orbitals are not generally involved in bond formation as they are considerably shielded from the influence of the ligand orbitals. If bonds are ionic, one expects Born's energy relationship to be valid and that, for the complexes of various rare earths, the values of stability constants should increase linearly with e^2/r where r is the radius of the rare earth ion. Such a relationship has been tested for a number of rare earth complexes.[2-5] Moeller *et al.*[6] have reviewed the present state of our knowledge on this subject.

Briefly, the work so far reported indicates that, although the bonding may be predominantly ionic in all the rare earth complexes and the electrostatic description may be fairly adequate for the complexes of the cerium earths, other factors such as steric effect, crystal field stabilisation, the coordination of water molecules in addition to that of the ligand around the rare earth ion and the possibility of $f\pi$-$p\pi$ bonding may be important in the formation of complexes of heavier rare earths. In the light of the previous work the data of the stability constants for SSA complexes can now be examined. The data obtained in this work for k, K_1 and K_2 for various rare earth sulphosalicylates have been plotted in Fig. 1 against e^2/r. For this purpose the values of crystal radii given by

Table 2. Stability constants of rare earth-SSA complexes at 20°C and constant ionic strength (0.1 M)

Metal ion	pk'	$\log k$	$\log K_1$	$\log K_2$	$\log K_1 \cdot K_2$
Ce^{3+}	6.82	1.93	6.83	5.57	12.40
Pr^{3+}	6.63	1.99	7.08	5.61	12.69
Nd^{3+}	6.42	2.09	7.39	5.62	13.01
Sm^{3+}	6.30	2.23	7.65	5.93	13.58
Eu^{3+}	6.11	2.26	7.87	6.03	13.90
Gd^{3+}	6.20	2.06	7.58	6.07	13.65
Tb^{3+}	5.77	2.47	8.42	6.19	14.61
Dy^{3+}	5.35	2.42	8.29	6.60	14.89
Ho^{3+}	5.55	2.23	8.40	6.75	15.15
Er^{3+}	5.69	2.12	8.15	6.30	14.45
Tm^{3+}	5.65	2.27	8.34	6.61	14.95
Yb^{3+}	5.67	2.30	8.35	6.81	15.16
Lu^{3+}	5.76	2.47	8.43	7.03	15.46

2) R. Harder and S. Chaberek, *J. Inorg. Nucl. Chem.*, **11**, 197 (1959).
3) E. J. Wheelwright, F. H. Spedding and G. Schwarzenbach, *J. Am. Chem. Soc.*, **75**, 4196 (1953).
4) L. C. Thompson, *J. Inorg. Nucl. Chem.*, **24**, 1083 (1962).
5) D. Fleischer and J. E. Powell, USAEC-IS-1121, Ames Laboratory, Iowa State University of Science and Technology (1965).
6) T. Moeller, D. F. Martin, L. C. Thompson, R. Ferrus, G. R. Feistel and W. J. Randall, *Chem. Revs.*, **65**, 1 (1965).

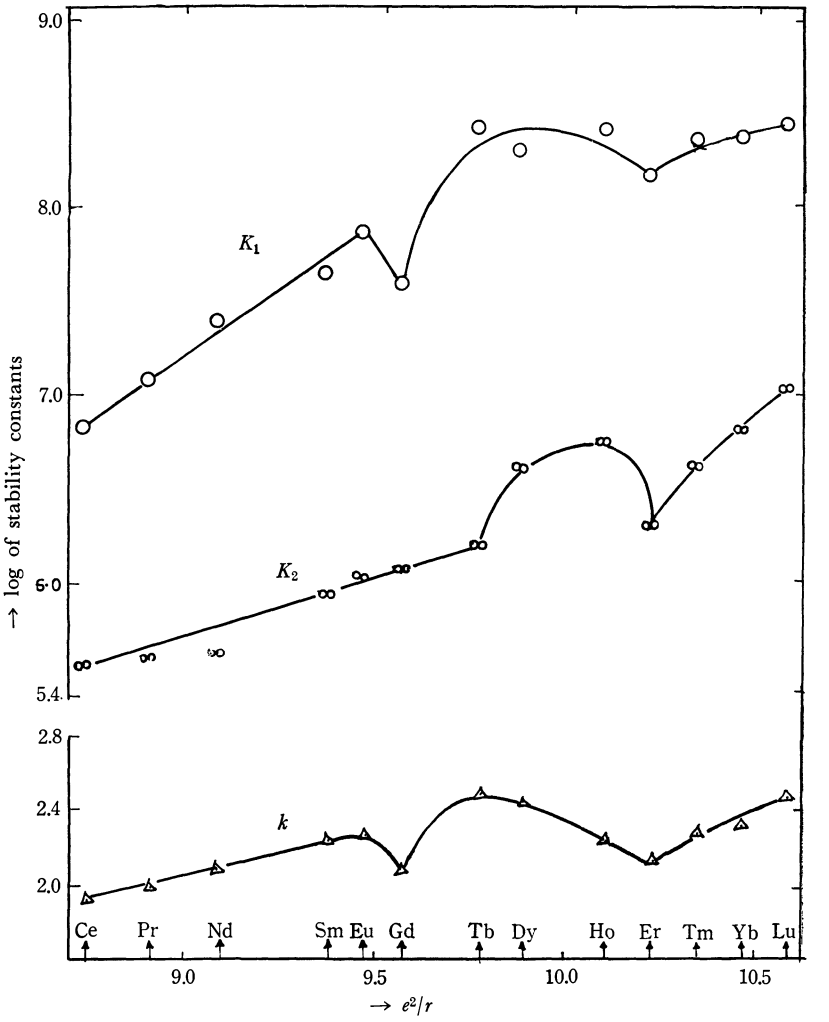

Fig. 1. Graph of stability constants (log units) for rare earth-SSA complexes as a function of ionic potential e^2/r.

Zachariasen[7] have been used. It is seen that the stability constants show in general a monotonic increase with decreasing ionic radius and the increase is approximately linear for the cerium earths (Ce^{3+} to Eu^{3+}). For complexes of rare earths heavier than gadolinium, however, the relationship between log of the stability constant and e^2/r is definitely non-linear. The observed stability constants for the rare earths heavier than gadolinium are in general less than expected from the extrapolation of the straight line observed for the complexes of the lighter rare earths. The progressively smaller radii of these rare earths may impose an increasing steric hindrance to the ligands and thus effect may partly account for the decrease. In the SSA complexes there are only two possible bonding sites and the chelate ring would utilise both these points. If the steric effect is to be operative there should be a change in the number of coordinated atoms. One is, therefore, led to speculate that the number of water molecules coordinated to the rare earths heavier than gadolinium in SSA complexes may be different from the number attached in complexes of the lighter rare earths. This speculation cannot be tested as the data for $\Delta H°$ and $\Delta S°$ for the formation of these complexes is not available. It is reasonable to expect that the steric effect, if present, should be pronounced for the formation of 1 : 2 complex because two chelate rings have to be formed. However, the ratios of K_1/K_2 for the heavier rare earth complexes are not appreciably different from the corresponding ratios for the complexes of the lighter rare earths. It appears, therefore, that the steric effect alone cannot account for the observed departure from the Born relationship and

7) W. H. Zachariasen in G. T. Seaborg and J. J. Katz, eds., "The Actinide Elements," McGraw Hill Book Co., New York (1954), Chap. 18

other factors must be considered. One of them appears to be the interaction of the 4-f orbitals with the ligand orbitals. This may produce different degrees of stabilisation for the various rare earth complexes. To test whether such interactions are significant in rare earth complexes of SSA, it is necessary to study the magnetic susceptibilities of these complexes in the solid state. Such work is in progress.

The values of log k for the SSA complexes are comparatively lower than Fleischer's data[5] for ethylglycolates (EG), ethylmethylglycolates (EMG) and diethylglycolates (EEG) (Ce^{3+} to Lu^{3+} log k (EG) 2.45—3.14; (EMG) 2.47—3.45; (EEG) 2.05—3.25; (SSA) 1.93—2.47). This is probably because SSA complex involves a six membered ring while glycolates form five membered rings.

Our thanks are due to Shri S. Fareeduddin, Head, Chemical Engineering Division, Bhabha Atomic Research Centre, Trombay for his keen interest and encouragement.

SHORT COMMUNICATIONS

Gas Chromatography of Rare Earth Chelates of Pivaloyltrifluoroacetone

Tsunenobu SHIGEMATSU, Masakazu MATSUI and Kei UTSUNOMIYA

Institute for Chemical Research, Kyoto University, Sakyo-ku, Kyoto

(Received January 24, 1968)

The gas chromatography of rare earth chelates of a new β-diketone, pivaloyltrifluoroacetone (PTA) was investigated. The trifluoromethyl group enhances the volatility of these chelates and the *t*-butyl one shows the shielding effect to weaken the intermolecular bonding. By these effects, rare earth PTA chelates were eluted in the gas phase as well as dipivaloylmethane[1] and 1,1,1,2,2,3,3-heptafluoro-7, 7-dimethyl-4, 6-octanedione (fod)-chelates.[2]

PTA was synthesized by condensation of ethyl trifluoroacetate with pinacolin with sodium methoxide. The crude product was purified by converting it into the copper chelate, which was dissolved in ether, decomposed in 10% sulfuric acid, and distilled (bp 39—41°C/17 mmHg). Tris PTA chelates of the following rare earth elements were prepared; Sc, Y, Lu, Yb, Er, Dy, Tb, Gd, Eu, Sm and Nd. The column (75 cm × 3 mm i. d. stainless steel) was packed with 5% (W/W) silicone grease on 60—80 mesh Chromosorb W. The chromatograms of these metal chelates were obtained, of which a typical example was shown in Fig. 1. The order of elution is the same with that of increasing ionic radius of the central metal. The thermogravimetric curves are shown in Fig. 2. They approach 100% weight loss of the chelates, except the case of $Nd(PTA)_3$. Figure 2 indicates that the volatility of the chelate increases with decrease in the ionic radius of rare earth metal ion.

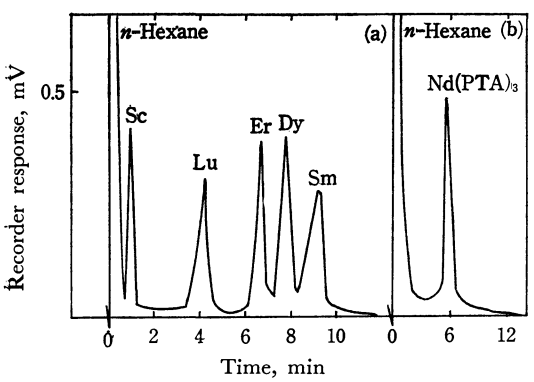

Fig. 1. Chromatograms of some rare earth PTA chelates.
a) The separation of $Sc(PTA)_3$, $Lu(PTA)_3$, $Er(PTA)_3$, $Dy(PTA)_3$ and $Sm(PTA)_3$. Column tem.: programmed from 150 to 260°C at 12°/min. Injection port temp.: 280°C. Helium flow rate: 50 ml/min.
b) Chromatogram of $Nd(PTA)_3$. Column temp.: programmed from 200 to 270°C at 12°/min. Injection port temp.: 320°C. Helium flow rate: 43 ml/min.

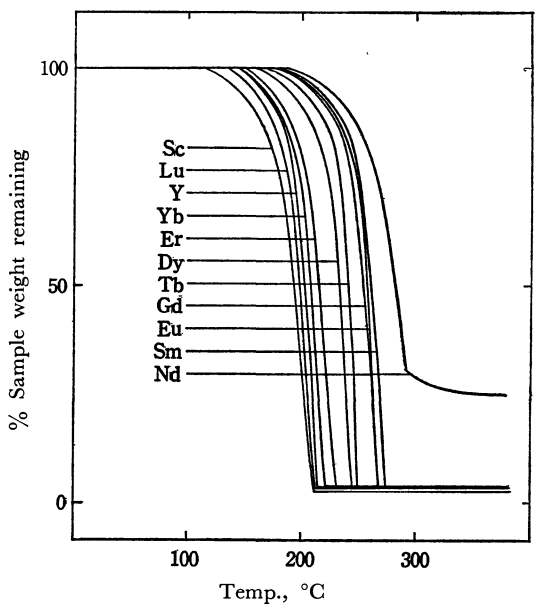

Fig. 2. Thermogravimetric curves of rare earth PTA chelates.

1) K. J. Eisentraut and R. E. Sievers, *J. Am. Chem. Soc.*, **87**, 5254 (1965).
2) C. S. Springer, Jr. D. W. Meek and R. E. Sievers, *Inorg. Chem.*, **6**, 1105 (1967).

The Temperature Dependence of Absorption Spectra of Cation Radicals of Benzidine and *N, N, N,' N'*-Tetramethyl-benzidine and Their Dimerization in Solution

Katsuo TAKEMOTO, Hiroshi MATSUSAKA, Shigeki NAKAYAMA, Keisuke SUZUKI and Yuzuru OOSHIKA

Faculty of Science, Kwansei Gakuin University, Nishinomiya

(Received December 20, 1967)

Detailed spectroscopic studies of cation radicals of *p*-phenylenediamine and its methyl derivatives have already been reported,[1-4] but those of benzidines have not yet been obtained. In the present letter, the absorption spectra of the cation radicals of benzidine (I) and *N, N, N', N'*-tetramethyl-benzidine (II) are reported.

Bromides of radicals, which were obtained by oxidation of their parent bases by bromine, were used for this study. Alcoholic solutions of the two radicals were stable enough to obtain quantitative spectrophotometric data below 0°C, although they gradually decomposed at room temperature.

Spectra of the alcoholic solution of II are shown in Fig. 1. Spectra of the solution of I (not shown here) are very similar to those of II except that the A band of II is shifted towards longer wavelengths compared with the corresponding band of I. This red shift of II is perhaps due to the hyperconjugation effect of the methyl groups. Therefore, we suppose that the A band has a transition moment oriented towards the longer molecular axis.

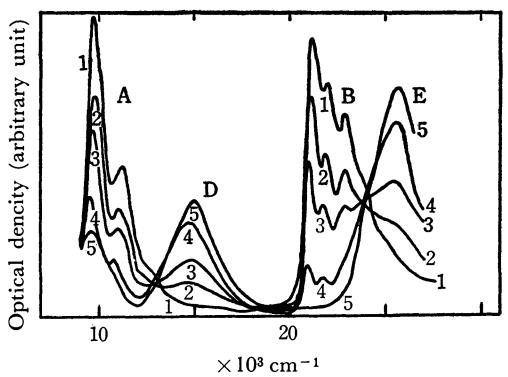

Fig. 1. Spectra of *N, N, N', N'*-tetramethyl-benzidine radical in ethanol.
Curve 1: 25°C, 2: −47°C, 3: −56°C, 4: −77°C, 5: −117°C

The temperature dependent spectra of II were analyzed by assuming an equilibrium $nR^+ \rightleftarrows R_n^{n+}$. Intensity data at each temperature are best fitted by assuming n values between 2.0 and 2.3. Therefore, it is concluded that the radicals form dimers as in the case of phenylenediamines at low temperature. The heat of dimerization of II is estimated to be 13 kcal/mol from the above analysis.

A similar analysis of I leads to the same conclusion, but the data contain greater experimental error. The heat of dimerization of I agreed with that of II within the error (±1 kcal/mol).

It is interesting to add that the heat of dimerization of tetramethyl-*p*-phenylenediamine radical (5 kcal/mol) is smaller than that of *p*-phenylenediamine (8 kcal/mol).

The spectra of solids of I and II are compared with those of their solutions at low temperature in Fig. 2. The solid spectra are very different from those of the solutions at room temperature (the monomer spectra), and have some resemblance to those at low temperature (the dimer spectra). The bands of the solids are, however, shifted towards the red. These suggest that the radicals in the solids interact strongly with each other and exist as dimers of some kind.

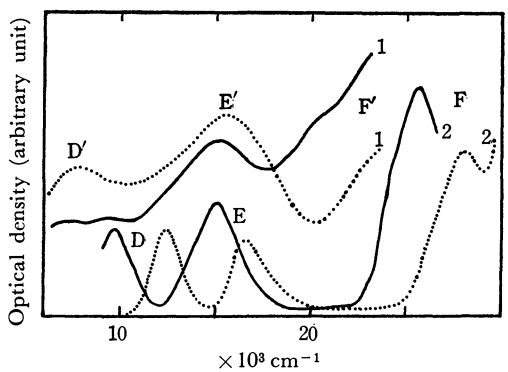

Fig. 2. Spectra of solids and low temperature solutions of benzidine cation radical (·····) and *N, N, N', N'*-tetramethyl-benzidine cation radical (——).
Curve 1: solids (25°C), 2: solutions (about −117°C)

More detailed experimental and theoretical research is now in progress in this laboratory.

1) K. Uemura, S. Nakayama, Y. Seo, K. Suzuki and Y. Ooshika, This Bulletin, **39**, 1348 (1966).
2) T. Sakata and S. Nagakura, *Technical Report of ISSP. Ser. A*, No. 244 (1967).
3) G. T. Pott and J. Kommandeur, *J. Chem. Phys.*, **47**, 395 (1967).
4) Y. Nakato, N. Yamamoto and H. Tsubomura, This Bulletin, **40**, 2480 (1967).

Copper(II) Catalyzed Oxidation of Molybdenum(V) in Aqueous Solutions*1

Yukichi YOSHINO, Toshio TAKEUCHI, Hisashi KINOSHITA and Shin UCHIDA

Department of Chemistry, College of General Education, The University of Tokyo, Komaba, Meguro-ku, Tokyo

(Received December 27, 1967)

Molybdenum(V) with the $4d^1$ electronic structure has been the subject of a number of recent studies from the viewpoints of magnetic susceptibility,[1] ESR,[2] electronic spectra[3] and redox enzyme activity.[4] In connection with these studies, it has been generally believed that molybdenum(V) in aqueous solutions is easily oxidized to molybdenum(VI) by atmospheric oxygen.[5] During the course of investigating stabilization of molybdenum(V) by complex formation, we have found that the oxidation of molybdenum(V) is strongly catalyzed by the presence of metal cations, such as copper(II) and iron(III).

In order to clarify the nature of this reaction, kinetic measurements were carried out as follows. Standard molybdenum(V) solutions prepared by reduction of sodium molybdate(VI) solutions with mercury[6] were used in the preliminary experiments. In the later runs, solid complex, $(NH_4)_2MoOCl_5$, prepared after Klason's method[7] was conveniently employed. Copper(II) and iron(III) solutions were prepared from JIS*2 special grade copper(II) sulfate pentahydrate and iron(III) alum, respectively. Other chemicals were all of JIS special grade and used after purifying by recrystallization or distillation. Thrice-distilled water was used for all experiments. Just before each run, a certain amount of $(NH_4)_2MoOCl_5$ was weighed out and dissolved in the acetate buffer solutions of appropriate pH and temperature. All experiments were conducted with dissolved molybdenum(V) concentration of about 2×10^{-4} M. The oxidation reaction was followed spectrophotometrically by measuring extinction at 320 mμ which is at the maximum of the absorption spectrum of molybdenum(V) species.

After a number of preliminary runs, it was found that, under the conditions given above, the rate of catalytic oxidation of molybdenum(V) was independent of the kind of standard molybdenum(V) species employed, and small amounts of anions, such as acetate, chloride, perchlorate, sulfate and nitrate, had no effect on the oxidation rate.

The results of systematic experiments showed that the rate of oxidation of molybdenum(V) was first order with respect to the concentration of molybdenum(V), when other conditions were kept the same. In the range of pH 2.4—5.2, the rate was inversely proportional to the square of hydrogen ion concentration.

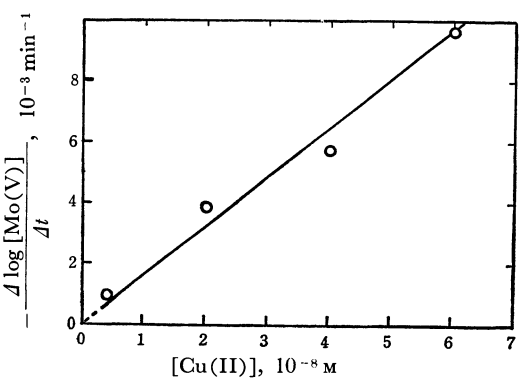

Fig. 1. A plot of the rate of oxidation of molybdenum(V) *vs.* concentration of copper(II).
0.01M acetate buffer, pH: 5.1, 25°C. Initial concentration of molybdenum(V): 2×10^{-4}M

As is seen from Fig. 1, it was also confirmed that under a definite condition the rate is proportional to the concentration of copper(II). In an extreme case where the concentration of copper(II) is less than 10^{-9} M, almost no oxidation of molybdenum(V) was seen to take place. It appeared that the rate is independent of the partial pressure of oxygen.

From the above-mentioned results, the experimental rate law may be expressed as follows:

$$-d[Mo(V)]/dt = k[Mo(V)][Cu(II)]/[H^+]^2.$$

The value of the apparent rate constant k was estimated as *ca.* 2×10^{-4} M min^{-1} at 25°C.

*1 Read before the 17th Symposium on the Coordination Chemistry, Hiroshima, 1967.

1) L. Sacconi and R. Cini, *J. Am. Chem. Soc.*, **76**, 4239 (1954).
2) C. R. Hare, I. Bernal and H. B. Gray, *Inorg. Chem.*, **1**, 831 (1962); R. D. Dowsing and J. F. Gibson, *J. Chem. Soc., (A)*, **1967**, 655.
3) G. P. Haight, Jr., *J. Inorg. Nucl. Chem.*, **24**, 663 (1962).
4) J. T. Spence and M. Heydanek, *Inorg. Chem.*, **6**, 1489 (1967).
5) R. L. Pecsok and D. T. Sawyer, *J. Am. Chem. Soc.*, **78**, 5496 (1956); J. T. Spence and J. Y. Lee, *Inorg. Chem.*, **4**, 385 (1965).
6) N. H. Furman and W. M. Murray, Jr., *J. Am. Chem. Soc.*, **58**, 1689 (1936).
7) W. G. Palmer, "Experimental Inorganic Chemistry," Cambridge University Press, Cambridge, England (1954), p. 408.

*2 Japanese Industrial Standards.

Electron Spin Resonance Study of Carbamoyl Radical*[1]

Teijiro YONEZAWA, Isao NODA and Takashi KAWAMURA

Faculty of Engineering, Kyoto University, Sakyo-ku, Kyoto

(Received January 24, 1968)

An ESR study is made of intermediate radicals in the oxidation of amides with hydroxyl radical in aqueous solution by using rapid flow technique with hydrogen peroxide and titanous chloride redox system. The ESR spectrum attributed to acyl type radical is observed. The ESR parameters of the radical from formamide are $g=2.00167$, $a_N=21.8$ gauss (one nitrogen nucleus), $a_H=30.8$ gauss (one proton), and $a_H=1.3$ gauss (one proton). Smith and Wood[1] observed the same spectrum and assigned the radical to HCONH (π electron radical). But we identify it as NH_2CO (carbamoyl σ electron radical) according to the following consideration.

One of characteristics of the spectrum is that the g value is smaller than that of free spin (2.00232). Unusually small g values are observed for some σ electron radicals such as vinyl (2.00220)[2a] and formyl (2.0009)[2b] radicals, on the other hand g value of the π electron radical is generally larger than 2.00232.[3] So the radical from formamide is considered to be a σ electron radical with a configuration I, II, or III.

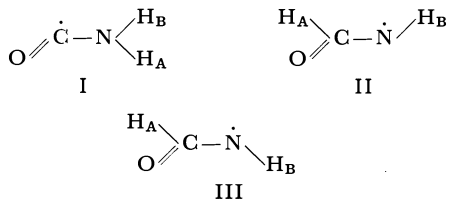

I II III

Isotropic hyperfine coupling (hfc) constants and g values of the radicals with structures I, II, and III are calculated with the extended Hückel method.[4,5] The calculated g value[3] for I is 2.00131, for II 2.00427, and for III 2.00984. In Table 1 the calculated hfc constants[4b] are compared with the observed ones.

TABLE 1. CALCULATED hfc CONSTANTS

	a(N)	a(H_A)	a(H_B)
(I)	8.0	31.3	3.1
(II)	1.9	115.9	4.3
(III)	30.2	92.0	33.5
Observed	21.8	30.8	1.3

Only the calculated g value for I is smaller than the g value of free spin (2.00232), and shows a good agreement with the observed value. The calculated hfc constants for I also agree with the observed ones. In view of the above bases it can be concluded that the observed radical is carbamoyl σ electron radical.

These calculated results suggest that in the carbamoyl radical the larger one of the hfc constants of the two protons is due to the *trans* proton to the odd electron orbital and the smaller one to the *cis* proton.

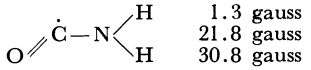

This assignment is consistent with those of vinyl[2a] and iminoxy[6] radicals.

N-Alkyl substituted carbamoyl radicals as well as other π electron radicals formed in the oxidation of amides will be reported in near future.

*1 Presented at the Sixth Symposium on ESR, Kyoto, Oct., 1967.

1) P. Smith and P. B. Wood, *Can. J. Chem.*, **44**, 3085 (1966).

2) a) E. L. Cochran, F. J. Adrian and V. A. Bowers, *J. Chem. Phys.*, **40**, 213 (1964); b) F. J. Adrian, E. L. Cochran and V. A. Bowers, *ibid.*, **36**, 1661 (1962).

3) A. J. Stone, *Mol. Phys.*, **6**, 509 (1963).

4) a) R. Hoffmann and W. N. Lipscomb, *J. Chem. Phys.*, **36**, 2179, 3489 (1962); b) G. A. Petersson and A. D. McLachlan, *ibid.*, **45**, 628 (1966).

5) In the extended Hückel calculation, the orbital exponent of the Slater type atomic orbital for hydrogen is set equal to 1.2. The calculated results show that in all the structures the odd electron occupies a σ orbital.

6) W. M. Fox and M. C. R. Symons, *J. Chem. Soc., (A)*, **1966**, 1503.

BULLETIN OF THE CHEMICAL SOCIETY OF JAPAN VOL. 41 767—773 (1968)

A Measure of the Electron-donating Power and Electron-accepting Power of Liquid Organic Compounds

Tsutomu KAGIYA, Yūzō SUMIDA and Tokuji INOUE

Faculty of Engineering, Kyoto University, Sakyo-ku, Kyoto

(Received July 20, 1967)

A quantitative study has been made of the measurement of the electron-donating nature and the electron-accepting nature of various liquid organic compounds. The position of the O–D or C=O absorption band of a liquid compound which contained a small quantity of methanol-d or of acetophenone was measured by means of an infrared spectrophotometer. The relative magnitude of the electron-donating nature or of the electron-accepting nature of the compound was compared by a measurement of the perturbation which it produced on the O–D vibrational band of methanol-d or on the C=O vibrational band of acetophenone. The electron-donating power or the electron-accepting power of a compound is defined as the relative difference (counted as wave numbers) of the O–D or the C=O absorption band observed in the compound from that in benzene. From the results, it was found that, in a homologous series, the electron-donating power decreased with an increase in the ionization potential in the gaseous phase, or with an increase in the pK_b value in the liquid phase, and that it increased linearly with the co-ordination power to diethyl zinc. It was also found that the electron-accepting power increased with an increase in the electron affinity in the gaseous phase and decreased with an increase in the pK_a value in the liquid phase. Moreover, the various liquid organic compounds, classified into four typical groups, were considered on the basis of their electron-donating and electron-accepting power.

It has previously been reported[1,2] that the solvent effect in ionic polymerization was dependent on the relative magnitude of the electron-donating power or on that of the electron-accepting power of the monomer and solvent used.

On the other hand, Gordy *et al.* have made a study of the proton-attracting properties of various liquid compounds,[3] while the relative acceptor strengths of some inorganic halides have been reported on by Lappert *et al.*[4]

The purpose of this report was to evaluate the relative magnitude of the electron-donating nature or the electron-accepting nature of various liquid organic compounds on the basis of the infrared spectral data. The O–D or the C=O vibrational band of the compounds containing a small amount of methanol-d or acetophenone were measured by means of an infrared spectrophotometer. On the basis of these data, a measure of the electron-donating power and of the electron-accepting power of liquid organic compounds was proposed.

Experimental

Materials. The aromatic and aliphatic hydrocarbons, esters, ethers, nitriles, amines, ketones, aldehydes, amides, imines, lactones, sulfoxides, nitro compounds, and inorganic halides were all obtained commercially and were purified by the usual method. Methanol-d, bp 64.5—65.0°C; acetophenone, bp 202°C/750 mmHg.

Apparatus and Method. The infrared spectra of the O–D band of methanol-d or of the C=O band of acetophenone in the mixture were determined with a Hitachi EPI-2 infrared spectrophotometer (resolving power: 3 cm^{-1} at 10 μ; slit width: 0.03 mm at 10 μ), equipped with a sodium chloride prism; the cell used was 0.010 cm, thick. A small quantity of methanol-d or acetophenone was added to a solution of 1.0 m*l* of the liquid organic compound in a 2.0 m*l* weighing bottle. The concentration of acetophenone was 0.1 mol/*l* while that of methanol-d was 0.4 mol/*l*, because the position of the O–D vibrational band was not clear when the concentration of methanol-d was lower than 0.4 mol/*l*. After having been shaken for 10 min at room temperature (18 ± 3°C), the mixture was used for the measurement of the infrared spectrum. The error in the measured shifts of the O–D band is not more than ±1 cm^{-1}, whereas that of the C=O band is ±0.3 cm^{-1} (with the scale up). The electronic properties of various liquid organic compounds were then compared by a measurement of the different perturbations which they caused in the O–D vibrational band of methanol-d or in the C=O vibrational band of acetophenone in the mixture.

Results and Discussion

The positions of the monomeric O–D and C=O vibrational bands of various liquid organic compounds are listed in Table 1, together with the

1) A. V. Tobolsky and C. E. Rogers, *J. Polymer Sci.*, **38**, 205 (1959).
2) Yu Spirin, A. A. Arest-Yakubovich, D. K. Polyakov and S. S. Mendrev, *ibid.*, **58**, 1181 (1962).
3) W. Gordy and S. C. Stanford, *J. Chem. Phys.*, **9**, 204 (1941).
4) M. F. Lappert, *J. Chem. Soc.*, **1962**, 542.

TABLE 1. ELECTRON-DONATING POWERS AND ELECTRON-ACCEPTING POWERS OF LIQUID ORGANIC COMPOUND

No.	Compound	Position of O-D band ν_D (cm^{-1})	Electron-donating power $\Delta\nu_D$ (cm^{-1})	Position of C=O band ν_A (cm^{-1})	Electron-accepting power $\Delta\nu_A$ (cm^{-1})
	Aromatic hydrocarbons and derivatives				
1	Benzene	2668	0	1690.2	0
2	Toluene	2666	2	1691.1	−0.9
3	Ethylbenzene	2664	4		
4	Styrene	2666	2	1689.2	1.0
5	α-Methylstyrene	2664	4		
6	*p*-Methylstyrene	2666	2		
7	Chlorobenzene	2670	−2	1689.3	0.9
8	Bromobenzene	2669	−1	1689.5	0.7
9	*o*-Dichlorobenzene	2679	−11	1687.4	2.8
10	*m*-Dichlorobenzene	2683	−15	1688.5	1.7
	Aliphatic hydrocarbons and derivatives				
11	*n*-Hexane	2667	1		
12	*n*-Heptane	2668	0		
13	Carbon tetrachloride	2689	−21	1691.0	−0.8
14	Chloroform	2685	−17		
15	Methylene chloride	2680	−12		
16	Ethylene chloride	2666	2		
	Nitro compounds				
17	Nitromethane	2662	6	1685.4	4.8
18	Nitroethane	2660	8	1686.6	3.6
19	Nitrobenzene	2647	21	1681.2	9.0
	Nitriles				
20	Acetonitrile	2619	49	1688.3	1.9
21	Propionitrile	2616	52		
22	Acrylonitrile	2631	37	1688.0	2.2
23	Benzonitrile	2630	38		
	Esters				
24	Methyl acetate	2632	36		
25	Ethyl acetate	2629	39		
26	Methyl chloroacetate	2641	27		
27	Methyl dichloroacetate	2645	23		
28	Methyl propionate	2635	33		
29	Ethyl propionate	2636	32		
30	Methyl isobutyrate	2636	32		
31	Vinyl acetate	2647	21		
32	Methyl acrylate	2638	30		
33	Ethyl acrylate	2635	33		
34	Methyl metacrylate	2631	37		
	Lactones				
35	β-Propiolactone	2634	34		
36	γ-Butyrolactone	2602	66		
37	ε-Caprolactone	2586	82		
	Ketones				
38	Acetone	2604	64		
39	Methyl ethyl ketone	2611	57		
40	Diethyl ketone	2612	56		
41	Methyl vinyl ketone	2579	89		
42	Cyclohexanone	2602	66		

TABLE 1 (Continued)

No.	Compound	Position of O–D band ν_D (cm^{-1})	Electron-donating power $\Delta\nu_D$ (cm^{-1})	Position of C=O band ν_A (cm^{-1})	Electron-accepting power $\Delta\nu_A$ (cm^{-1})
43	Acetophenone	2612	56		
	Ethers				
44	Diethyl ether	2590	78	1693.6	−3.4
45	Di-*n*-propyl ether	2595	73		
46	Diisopropyl ether	2593	75	1694.2	−4.0
47	Ethyl *n*-butyl ether	2591	77	1693.5	−3.3
48	Ethyl vinyl ether	2637	31	1690.4	−0.2
49	*n*-Butyl vinyl ether	2635	33		
50	Isobutyl vinyl ether	2635	33		
51	Diallyl ether	2602	66		
52	1,2-Dimethoxyethane	2597	71	1691.7	−1.5
53	Anisole	2642	26	1688.8	1.4
54	Phenetole	2643	25		
55	Propylene oxide	2609	59	1690.8	−0.6
56	Epichlorohydrin	2623	45	1687.0	3.2
57	Styrene oxide	2617	51		
58	3,3-Bischloromethyloxetane	2590	78	1689.0	0.8
59	Furan	2664	4		
60	Tetrahydrofuran	2578	90	1690.0	0.2
61	1,3-Dioxolane	2610	58		
62	2-Methyl-1,3-dioxolane	2607	61		
63	4-Methyl-1,3-dioxolane	2612	56		
64	2-Phenyl-1,3-dioxolane	2612	56		
65	4-Chloromethyl-1, 3-dioxolane	2625	43		
66	Tetrahydropyran	2575	93	1696.1	−5.9
67	1,4-Dioxane	2591	77	1690.0	0.2
	Aldehydes				
68	Acetaldehyde	2589	79		
69	Propionaldehyde	2583	85		
70	*n*-Butyraldehyde	2585	83		
71	Acrolein	2546	122		
72	Crotonaldehyde	2593	75		
73	Benzaldehyde	2615	53		
	Amines				
74	Ethylamine	2435	233		
75	*n*-Propylamine	2438	230		
76	Di-*n*-propylamine	2426	242		
77	Triethylamine	2430	238	1695.0	−4.8
78	Aniline	2510	158		
79	*N*-Methylaniline	2517	151		
80	*N*, *N*-Dimethylaniline	2520	148		
81	Pyridine	2500	168		
82	α-Picoline	2485	183		
83	γ-Picoline	2508	160		
84	4-Ethylpyridine	2489	179		
85	*o*-Toluidine	2523	145		
86	Piperidine	2428	240		
87	4-Vinylpyridine	2475	193		
	Imines				
88	Ethylenimine	2431	237		
89	*N*-Phenylethylenimine	2482	186		

TABLE 1. (continued)

No.	Compound	Position of O-D band ν_D (cm^{-1})	Electron-donating power $\Delta\nu_D$ (cm^{-1})	Position of C=O band ν_A (cm^{-1})	Electron-accepting power $\Delta\nu_A$ (cm^{-1})
	Amides				
90	*N,N*-Dimethylformamide	2561	107		
91	*N,N*-Dimethylacetamide	2555	113		
	Sulfoxides				
92	Dimethyl sulfoxide	2527	141	1682.0	8.2
	Inorganic Halides				
93	Zinc chloride			1618.0	72.2
94	Tin chloride			1582.0	108.2
95	Antimony pentachloride			1565.0	125.2

chemical structures of the compounds. The positions of the O–D vibrational band vary from about 2400 to 2700 cm^{-1} with the kind of compound, and the Lewis bases, such as the ethers and amines, shift to lower frequencies because of the formation of hydrogen bonds. In the C=O band, on the other hand, the Lewis acids which form the coordination bonds with another atom having an electron-pair cause a greater shift to a lower frequency.

Electron-donating Power and Electron-accepting Power. It is considered that the electron-donating nature of liquid compounds corresponds to the proton-attracting force and that the electron-accepting nature is the electron-pair-attracting force. On the basis of the considerations described above, we propose that the electron-donating power or the electron-accepting power of a liquid organic compound is to be defined as the relative difference (counted as wave numbers) of the O–D or the C=O absorption band observed in the compound from that in benzene, chosen as a reference compound.

Electron-donating Power:

$$\Delta\nu_D = \nu_D(\text{benzene}) - \nu_D(\text{compound})$$

Electron-accepting Power:

$$\Delta\nu_A = \nu_A(\text{benzene}) - \nu_A(\text{compound})$$

From the above definition, it can be said that the greater the $\Delta\nu_D$ or the $\Delta\nu_A$ value, the stronger is the proton-attracting force or the electron-pair-attracting force.

Examination of $\Delta\nu_D$ Values. The $\Delta\nu_D$ as defined above expresses the electron-donating power in the state of aggregation. On the other hand, since the ionization potential is the smallest energy which is necessary for taking a valence electron from a gaseous atom or molecule, it is reasonable to consider that the ionization potential is related to the electron-donating power. The relation between the $\Delta\nu_D$ values of several typical liquids and the ionization potentials[5,6] in the gaseous phase is shown in Fig. 1. That the $\Delta\nu_D$ values decreased with an increase in the ionization potentials was observed in any homologous series of aliphatic and aromatic hydrocarbons, ethers, esters, or ketones.

A regular relationship was also observed between the $\Delta\nu_D$ and pK_b values[7] of various aliphatic

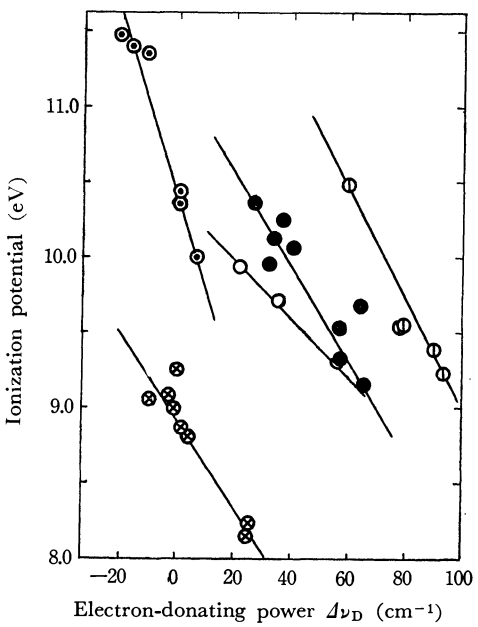

Fig. 1. Relation between the ionization potentials and the electron-donating powers ($\Delta\nu_D$) of various organic compounds.
⊗ Unconjugated aromatic compounds
○ Conjugated aromatic compounds
⊙ Aliphatic compounds
● Esters and ketones
Ⓘ Ethers

5) K. Watanabe, *J. Chem. Phys.*, **26**, 542 (1957).
6) F. I. Vipesov and B. P. Kurbatov, *Dokl. Akad. Nauk, SSSR*, **140**, 1364 (1961).
7) N. F. Hall and M. R. Sprinkle, *J. Am. Chem. Soc.*, **54**, 3469 (1932).

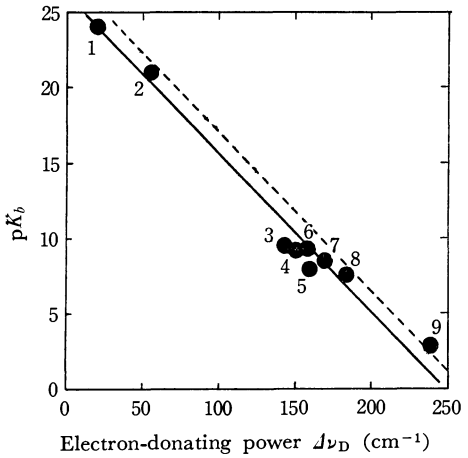

Fig. 2. Relation between the pK_b values of various aromatic and aliphatic amines and the electron-donating powers ($\Delta\nu_D$).

--- Gordy work $pK_b = -0.102\Delta\nu_D + 26.8$
—— Present work $pK_b = -0.102\Delta\nu_D + 26.3$
1 Nitrobenzene, 2 Acetophenone, 3 *o*-Toluidine
4 Methylaniline, 5 *γ*-Picoline, 6 Aniline,
7 Pyridine, 8 *α*-Picoline, 9 Triethylamine

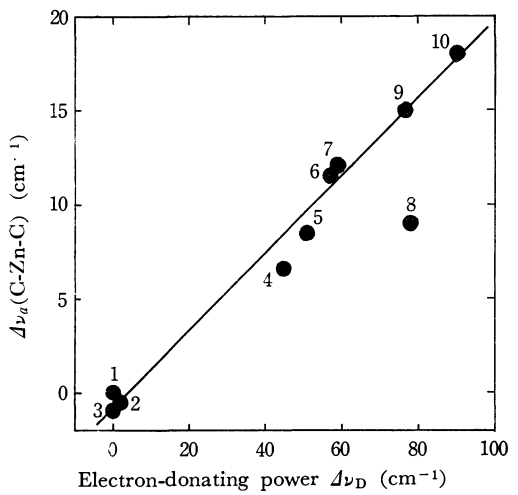

Fig. 3. Relation between the co-ordination powers to diethyl zinc and the electron donating powers.

1 Benzene, 2 Toluene, 3 *n*-Heptane,
4 Epichlorohydrin, 5 Styrene oxide,
6 Ethylene oxide, 7 Propylene oxide,
8 Diethyl ether, 9 Dioxane,
10 Tetrahydrofuran

and aromatic amines. Figure 2 shows that the larger the $\Delta\nu_D$ value is, the smaller is the pK_b value of the liquid organic compound.

On the other hand, Ishimori and Tsuruta have spectrally investigated the co-ordination power of cyclic ethers to diethyl zinc, which is regarded as an electrophilic compound.[8] It may be inferred that the ether having the stronger co-ordination

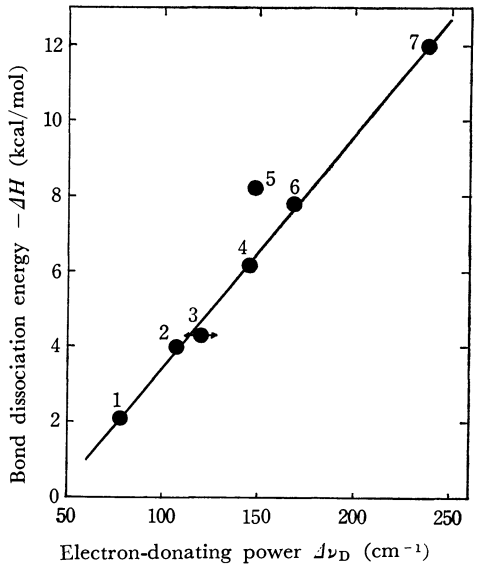

Fig. 4. Relation between the bond dissociation energies of the charge transfer complexes (I_2-electron donors) and the electron donating powers ($\Delta\nu_D$) of the electron donors.

1 Diethyl ether, 2 *N*, *N*-Dimethylformamide,
3 Ethanol, 4 *o*-Toluidine,
5 *N*, *N*-Dimethylaniline, 6 Pyridine,
7 Triethylamine

power to diethyl zinc has the larger electron-donating power. Figure 3 shows that the co-ordination power to diethyl zinc increases linearly with the $\Delta\nu_D$ value.

Moreover, since it is considered that the hydrogen bond formed between the methanol-d molecule and the solvent molecule is due to the charge transfer, the $\Delta\nu_D$ value may be expected to be related to the bond dissociation energy of the charge-transfer complex[9] formed between the iode molecule and the electron-donor molecule. In order to discuss this relation, we tried to plot the $\Delta\nu_D$ values of the electron donors against the bond dissociation energies of the charge-transfer complexes. As Fig. 4 shows, the energies of the bond dissociation of the charge-transfer complexes are in better correlation with the $\Delta\nu_D$ values than with the ionization potentials.

From these results, it may be concluded that the $\Delta\nu_D$ value expresses quantitatively the electron-donating power in both the gaseous and liquid phases.

8) M. Ishimori and T. Tsuruta, *Kogyo Kagaku Zasshi (J. Chem. Soc. Japan, Ind. Chem. Sect.)*, **70**, 378 (1967).
9) P. A. D. de Maine, *J. Chem. Phys.*, **26**, 1192 (1957); C. Reid and R. S. Mulliken, *J. Am. Chem. Soc.*, **76**, 3869 (1954); S. Nagakura, *ibid.*, **80**, 520 (1958); H. Tsubomura, *ibid.*, **82**, 40 (1960); H. Tsubomura and R. P. Lang, *ibid.*, **83**, 2085 (1961).

Examination of $\Delta\nu_A$ Values. The $\Delta\nu_A$ value of liquid compound is defined above as the electron-accepting power in the state of aggregation. On the other hand, the electron affinity of a compound is defined as the energy generated when its molecule absorbs an electron; this has been regarded as a measure of the electron-accepting power in the gaseous phase. Scarcely no experimental values of the electron affinities have, however, been reported. In order to evaluate the electron affinity, the energy ($\varepsilon_{lv}=\alpha-\eta_{lv}\beta$, α, $\beta<0$) of the lowest unoccupied σ level was used, since it is reasonable to consider that the smaller the coefficient (η_{lv}) of β in the energy of the lowest unoccupied level, the greater is the electron affinity, *i.e.*, the electron-accepting power of the compound in the gaseous phase. Figure 5 shows that the $\Delta\nu_A$ values decrease with an increase in the η_{lv} values.[10]

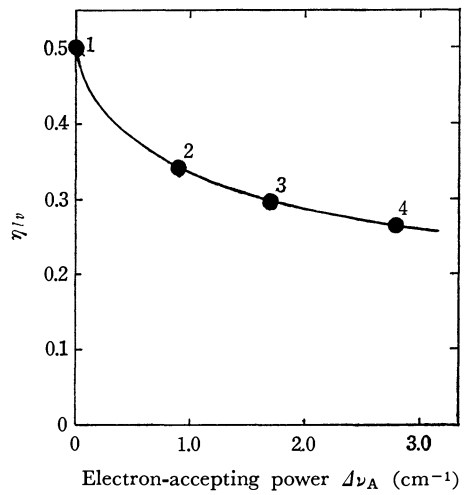

Fig. 5. Relation between the energies of the lowest unoccupied σ level and the electron-accepting powers ($\Delta\nu_A$) of aromatic halides.

$\varepsilon_{lv}=\alpha-\eta_{lv}\beta$. 1 Benzene, 2 Chlorobenzene, 3 *m*-Dichlorobenzene, 4 *o*-Dichlorobenzene

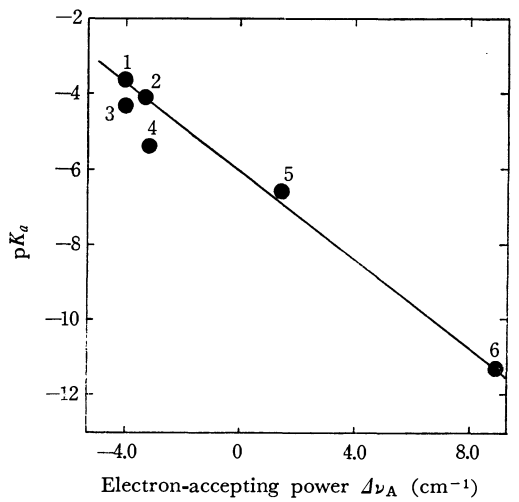

Fig. 6. Relation between the pK_a values of various ethers and the electron-accepting power ($\Delta\nu_A$).

1 Tetrahydropyran, 2 Diisopropyl ether, 3 *n*-Butyl ethyl ether, 4 Di-*n*-butyl ether, 5 Anisole, 6 Nitrobenzene

On the other hand, a linear relation was found to exist between the $\Delta\nu_A$ values and the pK_a values[11] of various ethers and aromatic compounds, as is shown in Fig. 6. The $\Delta\nu_A$ values of liquid compounds decrease with an increase in the pK_a values.

From these results, it may be concluded that the $\Delta\nu_A$ values express quantitatively the electron-accepting power in both the gaseous and liquid phases.

A Consideration of Liquid Organic Compounds on the Basis of the Electron-donating Power and the Electron-accepting Power. It is well known that Lewis bases like the ethers employed in the Grignard reaction and in the S_N2 reaction are the nucleophilic solvents, that the nitro compounds employed in the Friedel-Crafts reaction and Lewis acids are electrophilic solvents, and that the hydrocarbons have scarcely no ionization power. From these facts, the liquid organic compounds have been classified qualitatively into the following four groups: (1) amphoteric liquids,

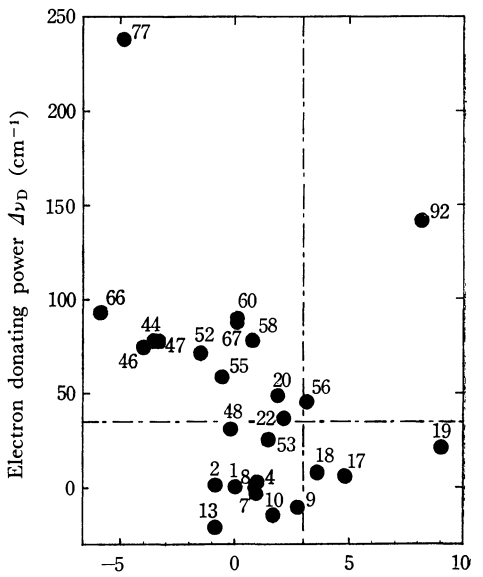

Fig. 7. Relation between the electoron-donating power ($\Delta\nu_D$) and the electron-accepting power ($\Delta\nu_A$) of various liquid organic compounds. The number of a point represents the number in Table 1.

10) K. Fukui, K. Morokuma, H. Kato and T. Yonezawa, This Bulletin, **36**, 217 (1963).
11) E. M. Arnett and C. Y. Wu, *J. Am. Chem. Soc.*, **84**, 1684 (1962).

(2) nucleophilic liquids, (3) electrophilic liquids and (4) non-philic liquids.

Little attention has, however, been paid to the quantitative consideration of the liquid compounds on the basis of the electronic features, in spite of the importance of this approach. In Fig. 7 we have plotted the relation between the $\Delta\nu_D$ values and the $\Delta\nu_A$ values of various liquid organic compounds. As Fig. 7 shows, the electron-donating power is more dominant than the electron-accepting power in most liquid organic compounds. In view of the classification on the basis of the results shown in Fig. 7, it is reasonable to take a point, with a $\Delta\nu_D$ value of 35 cm^{-1} and a $\Delta\nu_A$ value of 3 cm^{-1} as the standard point. In the amphoteric liquids the $\Delta\nu_D$ and $\Delta\nu_A$ values are both larger than the standard point, while, in the non-philic liquids both are smaller. The nucleophilic liquids have larger $\Delta\nu_D$ values and smaller $\Delta\nu_A$ values, while the electrophilic liquids have smaller $\Delta\nu_D$ values and larger $\Delta\nu_A$ values than the standard point. This quantitative classification, based on the electronic features of liquid organic compounds, seems useful as an unifying interpretation for many kinds of experimental results.

The authors are grateful to Professor Kenichi Fukui for his valuable suggestions while carrying out this study and to Mr. S. Nakao and Mr. K. Ueda for their technical assistance. They also wish to thank Sumitomo Atomic Energy Industries, Ltd., for supplying the materials and equipment used in this work.

BULLETIN OF THE CHEMICAL SOCIETY OF JAPAN VOL. 41 773—778 (1968)

A Study of the Nucleophilic Solvation Based on the Theory of Chemical Equilibrium

Tsutomu KAGIYA, Yūzō SUMIDA and Tokuji INOUE

Faculty of Engineering, Kyoto University, Sakyo-ku, Kyoto

(Received July 20, 1967)

The nucleophilic solvation to a deuterium atom in a methanol-d molecule has been quantitatively studied by using the infrared spectroscopic data of the O–D vibrational band. The position of the O–D band did not change in spite of the variation in the methanol-d concentration in solutions of a single solvent, whereas the area of the O–D peak changed in proportion to the first-order of the methanol-d concentration. From these results, it has been concluded that the area of the O–D band corresponds to the concentration of the methanol-d solvated. In a binary solvent system, which consisted of components with substantial differences in the electron-donating power, two positions of the O–D peak were observed at positions identical to those in the component examined in a single solvent system, and the area of each O–D peak changed with the composition of the system. These results led to the conclusion that the nucleophilic solvation of each component in the binary system took place competitively and individually. From the quantitative treatment of the results on the basis of the theory of chemical equilibrium, the equilibrium constant of the nucleophilic solvation of a solvent to methanol-d was calculated. The following empirical formula was obtained between the electron-donating powers and the nucleophilic equilibrium constants of various solvents:

$$\log K_{\mathrm{D}} = -\frac{3.67}{1 + 8.14 \times 10^{-3} \Delta\nu_{\mathrm{D}}} + 2.16.$$

It is well known, regarding an ionic reaction in solution, that the reaction rate is markedly affected by the kind of solvent, and by the characteristic features of the solvation. Scarcely no quantitative studies of solvation have, however, been reported.

On the other hand, Gordy *et al.* have made a study of the proton-attracting properties of various liquid compounds, using methanol-d as an indicator.[1] In a previous paper[2] the electron-donating power ($\Delta\nu_{\mathrm{D}}$) and the electron-accepting power ($\Delta\nu_{\mathrm{A}}$) of liquid compounds have been measured, and it has been found that the electron donating power of a liquid organic compound is more dominant than the electron-accepting power.

1) W. Gordy and S. C. Stanford, *J. Chem. Phys.*, **9**, 204 (1941).

2) T. Kagiya, Y. Sumida and T. Inoue, This Bulletin, **41**, 767 (1968).

The purpose of the present investigation is to study quantitatively the nucleophilic solvation, also making a theoretical treatment of the data on the position and the area of the O–D band of methanol-d in solution.

Experimental

Materials. Tetrahydrofuran, benzene, nitroethane, ethyl propionate, phenetole, triethylamine, pyridine, and methanol-d were obtained commercially. All but methanol-d were purified by the usual methods.

Apparatus and Method. A typical infrared spectroscopic experiment was carried out as follows. A small quantity (0.4 mol/*l*) of methanol-d was added to 1.0 m*l* of the solvent, which consisted of one or two components, in a weighing bottle (2.0 m*l*). After the bottle had then been shaken for 10 min at room temperature (18±3°C), the infrared spectra of the O–D absorption band of methanol-d in the mixture were determined with a Hitachi EPI-2 infrared spectrophotometer (resolving power: 3 cm^{-1} at 10 μ, slit width: 0.03 mm at 10μ) equipped with a sodium chloride prism. The thickness of the cell used in this experiment was 0.010 cm.

Evaluation of the Integrated Intensity of the O-D Absorption Band. The O–D vibrational curve ought theoretically to be symmetrical. In most of the compounds in which the O–D vibrational band shifted to a lower frequency, symmetrical absorption bands were observed (Fig. 1(a)). On the other hand, asymmetrical O–D absorption bands were observed in some compounds which had small shifts (Fig. 1(b)). It may be considered that the phenomenon is caused by the overlapping of the unassociated and associated bands (2400—2500 cm^{-1}). Similarly, two O–D absorption bands in the binary solvent system were observed as asymmetrical bands by the overlapping of two unassociated absorption bands due to each solvent (Fig. 1(c)). Therefore, we estimated the integrated intensity of the unassociated O–D absorption band using the method of the half-value-width. For example, the integrated intensity of a symmetrical band (a) was evaluated as a triangular area (△ABC). In an asymmetrical band (b) or (c), each integrated intensity was separately determined, using each shoulder without an overlapping (*i.e.*, 2△DEF, 2△GIK and 2△HJL). We then took the average values of several measurements (maximum experimental errors: ±1.5%).

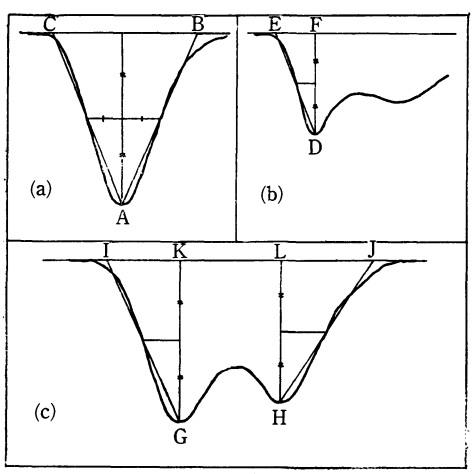

Fig. 1. Evaluation method of the integrated intensity of O–D absorption band.
(a) Single-solvent system; a symmetrical band
(b) Single-solvent system; an asymmetrical band
(c) Binary-solvent system

Results and Discussion

In a Single-solvent System. Since it was observed that the solvent which shifted the O–D band to a lower frequency had the stronger integrated intensity (area) of the O–D band, the

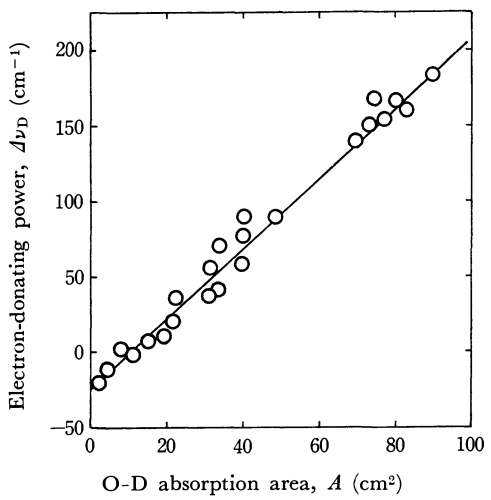

Fig. 2. Relation between the electron-donating powers ($\Delta\nu_D$) and the areas of O–D absorption bands (A).

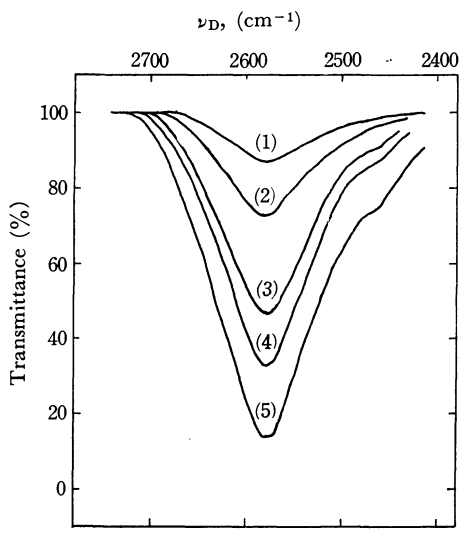

Fig. 3. Infrared spectra of O–D absorption bands in tetrahydrofuran systems.
CH_3OD concentration: (1) 0.085, (2) 0.18, (3) 0.40, (4) 0.58, (5) 0.97 (mol/*l*)

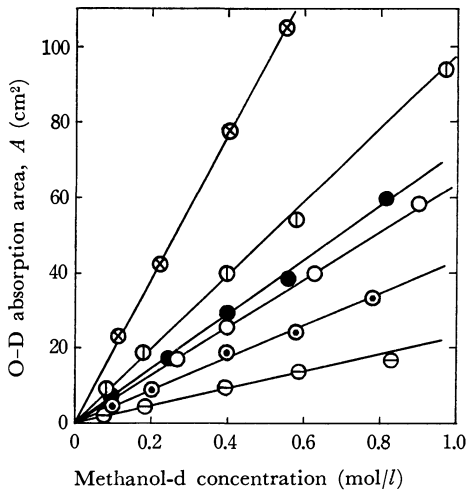

Fig. 4. Relation between the areas of O-D absorption bands and the concentration of CH_3OD in single solvent systems.
⊖ Benzene, ⊙ Nitroethane, ○ Phenetole,
● Ethyl propionate, ⓘ Tetrahydrofuran,
⊗ Triethylamine

positions of the O–D band in various solvents were plotted against the total area (*cf.* Fig. 2). A linear relation was found to exist between the position and the area of the O–D band at the same concentration (0.40 mol/*l*) of methanol-d; that is, the electron-donating power ($\Delta\nu_D$) proposed by us[2] increased as the area (A) increased.

The influence of the methanol-d concentration on the position and the area of O–D peak was also studied. The infrared spectra of tetrahydrofuran systems with various concentrations of methanol-d are shown in Fig. 3. It is evident that the position of the O–D absorption band does not change, regardless of the variation in its concentration, whereas its area increases with the concentration of methanol-d. Such features were also observed in other solvent systems. As shown in Fig. 4, this linear relation between the area of the O–D band and the methanol-d concentration was found to exist in various solvents. Therefore, the following equation was obtained:

$$A = \alpha(CH_3OD)_0 \qquad (1)$$

where $(CH_3OD)_0$ is the concentration of methanol-d in a pure solvent, and α is a constant, its exact nature depending on the kind of solvent. The area of the band depending only on the kind of solvent increases with the concentration of methanol-d. This fact suggests that the area of the O–D band corresponds to the concentration of the methanol-d solvated. This led to the following relation:

$$A = \frac{1}{\beta}(CH_3O\text{–}D\cdots nS) \qquad (2)$$

where $(CH_3O\text{–}D\cdots nS)$ is the concentration of methanol-d solvated by n molecules of the solvent, and β is a proportional constant.

On the basis of the above considerations, the nucleophilic solvation of a solvent to methanol-d may be quantitatively studied on the basis of the theory of chemical equilibrium; that is, the solvent, methanol-d, and solvated methanol-d are considered to be in equilibrium:

$$CH_3OD + nS \overset{K_D}{\rightleftharpoons} CH_3O\text{–}D\cdots nS \qquad (3)$$

K_D is the equilibrium constant. The concentration of methanol-d solvated in the equilibrium state is expressed by Eq. (4):

$$(CH_3O\text{–}D\cdots nS) = \frac{K_D(S)^n(CH_3OD)_0}{1 + K_D(S)^n} \qquad (4)$$

The parentheses indicate the concentration of each component in equilibrium. Using Eqs. (2) and (4), Eq. (5) is given as follows:

$$A = \frac{K_D(S)^n(CH_3OD)_0}{\beta(1 + K_D(S)^n)} \qquad (5)$$

Consequently, it is found that the constant (α) in Eq. (1) corresponds to $K_D(S)^n/\beta(1+K_D(S)^n)$ in Eq. (5).

In a Binary-solvent System. As a sample of a binary solvent system consisting of components with large differences in the electron-donating power, the infrared spectra in the tetrahydrofuran-nitroethane system are shown in Fig. 5. It is evident from Fig. 5 that the positions of the two O–D bands do not change in spite of the variation in the composition of the system, while the areas of the two bands do markedly vary with the composition. Moreover, the position of each

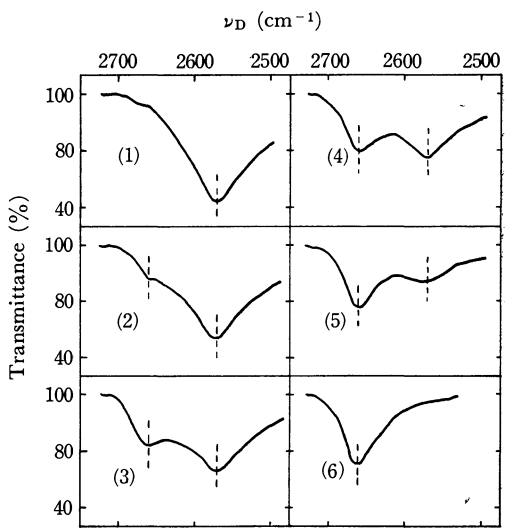

Fig. 5. Infrared spectra of the O–D absorption bands in tetrahydrofuran-nitroethane systems.
Tetrahydrofuran : Nitroethane (volume ratio)
(1) 1 : 0, (2) 3 : 1, (3) 1 : 1, (4) 1 : 3,
(5) 1 : 19, (6) 0 : 1

of the two peaks is identical with that due to tetrahydrofuran or nitroethane in a single-solvent system. Similar features were observed in other binary systems. If both components, S_1 and S_2, simultaneously solvate to one molecule of methanol-d, the position of the O-D band might be different from the position of each O-D peak appearing in the single solvent (S_1 or S_2) and might be observed between them. The experimental results, however, did not agree with this prediction. This fact leads to the conclusion that each component in a binary-solvent system solvates to each molecule of methanol-d individually and competitively.

On the basis of these findings, the solvation may be considered to consist of the following equilibrium reactions:

$$CH_3OD + nS_1 \overset{K_{D1}}{\rightleftharpoons} CH_3O\text{-}D\cdots nS_1 \qquad (6)$$

$$CH_3OD + mS_2 \overset{K_{D2}}{\rightleftharpoons} CH_3O\text{-}D\cdots mS_2 \qquad (7)$$

where n or m is the number of solvent molecules coordinating to a deuterium atom of methanol-d, and K_{D1} or K_{D2} is the equilibrium constant of each reaction. $CH_3O\text{-}D\cdots nS_1$ and $CH_3O\text{-}D\cdots mS_2$ indicate the state of methanol-d solvated by n molecules of the component S_1 and by m molecules of the component S_2 respectively. From the reactions (6) and (7), Eqs. (8) and (9) are obtained as follows:

$$(CH_3O\text{-}D\cdots nS_1) = \frac{K_{D1}(S_1)^n(CH_3OD)_0}{1 + K_{D1}(S_1)^n + K_{D2}(S_2)^m} \qquad (8)$$

$$(CH_3O\text{-}D\cdots mS_2) = \frac{K_{D2}(S_2)^m(CH_3OD)_0}{1 + K_{D1}(S_1)^n + K_{D2}(S_2)^m} \qquad (9)$$

As has been described previously, the concentration of the solvated methanol-d can be evaluated as the area of the O-D absorption band; that is $(CH_3O\text{-}D\cdots nS_1)$ may be expressed by $\beta_1 A_1$. A_1 is the area due to the component S_1. By substituting the relation described above into Eqs. (8) and (9), and by taking the ratio of Eq. (8) to Eq. (9), Eq. (10) is given:

$$\frac{(CH_3O\text{-}D\cdots nS_1)}{(CH_3O\text{-}D\cdots mS_2)} = \frac{\beta_1 A_1}{\beta_2 A_2} = \frac{K_{D1}(S_1)^n}{K_{D2}(S_2)^m} \qquad (10)$$

Equation (10) shows that a straight line exists between $\beta_1 A_1/\beta_2 A_2$ and $(S_1)^n/(S_2)^m$.

Since the interaction force that we are considering is a kind of hydrogen bonding, it seems reasonable to consider that the solvation number of methanol-d is unity in all systems, *i. e.*, that $n=m=1$. Moreover, in order to simplify Eq. (10), it is assumed that β is a constant independent of the kind of solvent. Using the above considerations, Eq. (10) is expressed as Eq. (11):

$$\frac{A_1}{A_2} = \frac{K_{D1}(S_1)}{K_{D2}(S_2)} \qquad (11)$$

As shown in Fig. 6, we tried to plot A_1/A_2 against $(S_1)/(S_2)$ in all binary systems. In view of this fact, it may be concluded that the solvation number is unity and that β is a constant which is independent of the kind of solvent used. A straight-line slope indicates the relative ratio of the equilibrium constant of the solvent for a standard solvent. The ratios of the equilibrium constants of various solvents against tetrahydrofuran as a standard solvent are listed in Table 1.

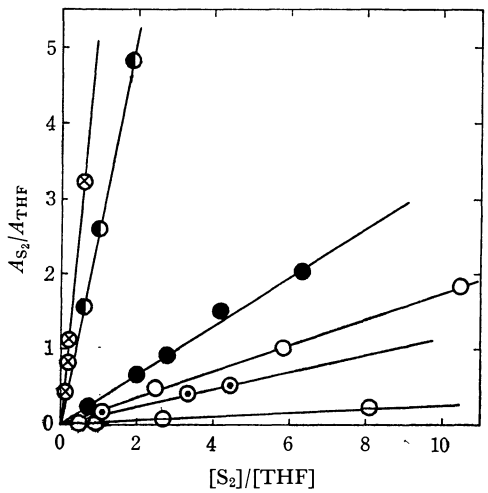

Fig. 6. Relation between the area ratios of O-D bands and the mol ratios of solvents S_2 in tetrahydrofuran-solvent S_2 systems.
Solvent S_2: ⊖ Benzene, ⊙ Nitroethane, ○ Phenetole, ● Ethyl propionate, ◐ Pyridine, ⊗ Triethylamine

Using Eqs. (8) and (11), we can obtain an equation by which the equilibrium constant can be calculated. When we substitute Eq. (11) into the reciprocal of Eq. (8), Eq. (12) is given as:

$$(S_1)\left(1 + \frac{A_2}{A_1}\right) = \frac{(CH_3OD)_0}{\beta}\frac{(S_1)}{A_1} - \frac{1}{K_{D1}} \qquad (12)$$

From Eq. (12), it may be expected that there is a linear relation between $(S_1)(1+A_2/A_1)$ and $(S_1)/A_1$, that its slope is constant in any kind of solvent at the same concentration of methanol-d, and that the value of the armature gives the reciprocal of the equilibrium constant. In Figs. 7 and 8, the propriety of Eq. (12) is confirmed in two cases, a tetrahydrofuran-solvent S_2 system and an ethyl propionate-solvent S_2 system. It may be seen in the two figures that a linear relationship exists between $(S_1)(1+A_2/A_1)$ and $(S_1)/A_1$. The values of the equilibrium constants of typical compounds are listed in Tables 1 and 2. The results in Table 1 show that the values $(K_{D2}/K_{D,THF})_{Fig.}$ obtained from the slope of the line in Fig. 6 agree well with

TABLE 1. RATIOS OF NUCLEOPHILIC EQUILIBRIUM CONSTANTS OF SOLVENTS AGAINST TETRAHYDROFURAN

Solvent	$\left(\frac{K_{D_2}}{K_{D,THF}}\right)_{Fig.}$	K_D (l/mol)	$\left(\frac{K_{D2}}{K_{D,THF}}\right)_{Calc.}$
Benzene	0.030_4	0.036_9	0.035_1
Nitroethane	0.11_0	0.058_5	0.055_7
Phenetole	0.17_5	0.17_8	0.17_0
Ethyl propionate	0.32_5	0.32_0	0.30_4
Tetrahydrofuran	1.00	1.0_5	1.00
Pyridine	2.6_3	2.6_8	2.5_5
Triethylamine	5.5_0	6.1_0	5.8_1

TABLE 2. EQUILIBRIUM CONSTANT OF NUCLEOPHILIC SOLVATION TO METHANOL-D

	Compound	$\Delta\nu_D$ (cm^{-1})	K_D (l/mol)	ΔG_D (kcal/mol)
	Aromatic Hydrocarbons			
1	Benzene	0	0.036_9	1.9_1
2	Ethylbenzene	4	0.044_0	1.8_0
3	Styrene	2	0.032_0	1.9_9
4	α-Methylstyrene	4	0.041_2	1.8_5
5	p-Methylstyrene	2	0.038_1	1.8_9
	Esters			
6	Ethyl acetate	39	0.31_7	0.66_4
7	Ethyl propionate	32	0.32_0	0.65_9
8	Methyl isobutyrate	32	0.32_2	0.65_5
9	Vinyl acetate	21	0.13_4	1.1_6
10	Ethyl acrylate	33	0.30_0	0.69_6
11	Methyl metacrylate	37	0.33_4	0.63_4
	Lactones			
12	β-Propiolactone	34	0.25_8	0.80_2
13	γ-Butyrolactone	66	0.70_1	0.20_5
14	ε-Caprolactone	82	0.97_4	0.016_0
	Ketones			
15	Methyl ethyl ketone	57	0.51_4	0.38_5
16	Methyl vinyl ketone	89	1.0_2	-0.010_7
	Ethers			
17	Diethyl ether	78	0.72_5	0.18_6
18	Ethyl vinyl ether	31	0.15_8	1.0_7
19	Phenetole	25	0.17_8	0.99_8
20	p-Methoxystyrene	28	0.11_4	1.2_6
21	Propylene oxide	59	0.45_5	0.45_5
22	Epichlorohydrin	45	0.35_2	0.60_5
23	Styrene oxide	51	0.41_4	0.51_0
24	3,3-Bischloromethyloxetane	78	0.89_1	0.066_1
25	Tetrahydrofuran	90	1.0_5	-0.028_0
26	1,3-Dioxolane	58	0.54_8	0.34_8
27	4-Methyl-1,3-dioxolane	56	0.53_8	0.35_8
28	Tetrahydropyran	93	1.4_3	-0.20_6
	Amines			
29	Pyridine	168	2.6_3	-0.57_0
30	Triethylamine	238	6.1_0	-1.0_4
	Nitriles			
31	Propionitrile	52	0.29_3	0.71_0
32	Acrylonitrile	37	0.19_2	0.95_5
	Nitro Compounds			
33	Nitroethane	8	0.058_5	1.6_4

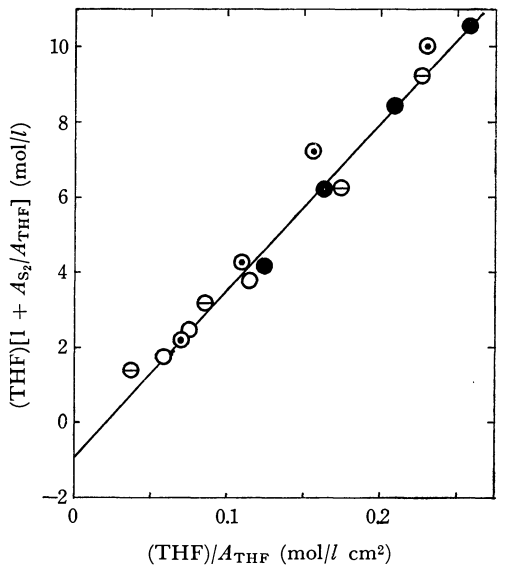

Fig. 7. Calculation method of nucleophilic equilibrium constant of tetrahydrofuran to CH_3OD.
Solvent S_2: ⊖ Benzene, ⊙ Nitroethane,
○ Phenetole, ● Ethyl propionate

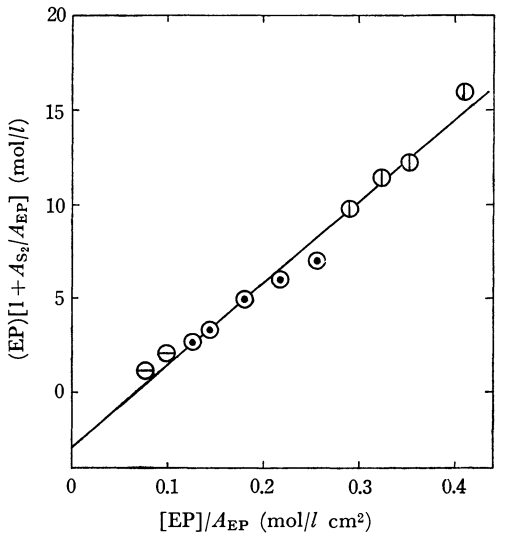

Fig. 8. Calculation method of nucleophilic equilibrium constant of ethyl propionate to CH_3OD.
Solvent S_2: ⊖ Benzene, ⊙ Nitroethane,
① Tetrahydrofuran.

the values $(K_{D2}/K_{D,THF})_{Calc.}$ calculated by means of the K_D values, so we can approximately estimate the unknown K_D value by measuring the $K_{D2}/K_{D,THF}$ value.

It may also be seen in Table 2 that the equilibrium constant increases with the electron-donating power of the solvent. With the purpose of considering this relation, we plotted the equilibrium constants against the electron-donating powers; we thus obtained the following empirical formula:

$$\log K_D = -\frac{3.67}{1 + 8.14 \times 10^{-3} \Delta\nu_D} + 2.16 \quad (13)$$

This empirical formula shows that the equilibrium constant of nucleophilic solvation to methanol-d can be quantitatively estimated by measuring the shift of the O–D vibrational band of methanol-d.

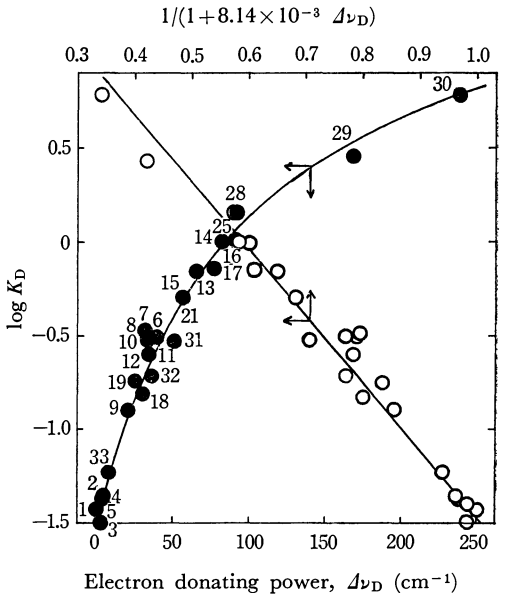

Fig. 9. Relation between the nucleophilic equilibrium constants of solvents and the electron-donating powers.
The number of a point represents the number in Table 2.

On the other hand, as has been reported previously, the shift of the O–D band is linearly related to the co-ordination power to diethyl zinc as an electrophilic compound. On the basis of these facts, it may be concluded that the equilibrium constant of the solvation to methanol-d can be used as a measure of the force of the general nucleophilic co-ordination to electrophilic compounds.

BULLETIN OF THE CHEMICAL SOCIETY OF JAPAN VOL. 41 779—782 (1968)

A Definition of Selectivity of Nucleophilic Solvation in a Binary Solution

Tsutomu KAGIYA, Yūzō SUMIDA and Tokuji INOUE

Faculty of Engineering, Kyoto University, Sakyo-ku, Kyoto

(Received July 26, 1967)

This is the third paper of a series in which the behavior of nucleophilic solvation is investigated by a measurement of the position and the area of the O-D vibrational band of methanol-d. In a binary solution which consisted of two components remarkably different in electron-donating power, the relation between the mol fraction (n_1) of the S_1 component and the area fraction (N_1) of S_1 was not a straight line, but a concave or convex curve. This fact suggests that a component co-ordinates selectively to a deuterium atom in a methanol-d molecule. The following definition of the selectivity of nucleophilic solvation to methanol-d as a cation model of the S_2 component to the S_1 component is proposed:

$$(S^{S_2}_{S_1})_D = \sqrt{\left(\frac{dN_2}{dn_2}\right)_{n_2=0} \Big/ \left(\frac{dN_1}{dn_1}\right)_{n_1=0}}$$

The selectivity of the S_2 solvent to the S_1 solvent was considered in detail in connection with the equilibrium constant of the nucleophilic solvation to methanol-d of the solvent; the selectivity was also found to be defined as the ratio of the equilibrium constants of the solvents used. Since there was a correlation between the equilibrium constants and the electron-donating powers, it was concluded that the selectivity of an S_2 solvent to a standard solvent, S_1, could be quantitatively estimated by measuring only the position of the O-D vibrational band of methanol-d in each solvent.

It has previously been reported in connection with ionic copolymerization that the monomer reactivity ratios are significantly affected by the kind of solvent and catalyst used;[1,2] the systematic interpretation is difficult even in the simplest cases.[3] Recently, Overberger and Kamath have tried to explain this phenomenon on the basis of the preferential solvation of the growing ion pair by the more polar monomer in nonpolar solvents.[4] This concept of the preferential solvation makes it possible to explain qualitatively many experimental results.[5,6] There have been, however, few quantitative investigations of the preferential solvation.

In the first paper of this series,[7] the electron-donating power ($\Delta\nu_D$) and the electron-accepting power ($\Delta\nu_A$) of liquid organic compounds have been defined by using methanol-d and acetophenone as indicators. The second paper[8] was undertaken to make clear the characteristic behavior of the nucleophilic solvation in single or binary systems on the basis of the theory of chemical equilibrium.

The main purpose of the present work is to define the selectivity of nucleophilic solvation to the methanol-d of the solvent in a binary solution and to consider it in connection with the equilibrium constant of the nucleophilic solvation to the methanol-d of the solvent. It has been found that the selectivity defined is equal to the ratio of the equilibrium constants of the two components in a binary solution.

Experimental

The experimental technique is the same as that used before[8] and so will not be described here.

Results and Discussion

As has been described previously,[8] in a binary solvent system consisting of two components remarkably different in electron-donating power, it was observed that the position of neither O-D absorption bands changed in spite of the variation in the composition of the system, while the area

1) C. G. Overberger, R. J. Ehrig and D. Tanner, *J. Am. Chem. Soc.*, **76**, 772 (1954).
2) A. V. Tobolsky and R. J. Boudreau, *J. Polymer Sci.*, **51**, S53 (1961).
3) B. D. Phillips, T. L. Hanlon and A. V. Tobolsky, *ibid.*, **A2**, 4231 (1964).
4) C. G. Overberger and V. G. Kamath, *J. Am. Chem. Soc.*, **85**, 446 (1963).
5) C. S. Marvel and J. F. Dunphy, *J. Org. Chem.*, **25**, 2209 (1960).
6) S. Okamura, T. Higashimura and K. Takeda, *Kobunshi Kagaku*, **18**, 389 (1961).
7) T. Kagiya, Y. Sumida and T. Inoue, This Bulletin, **41**, 767 (1968).
8) T. Kagiya, Y. Sumida and T. Inoue, *ibid.*, **41**, 773 (1968).

of each band changed remarkably with the composition. It was therefore concluded that the nucleophilic solvation to methanol-d of each component in a binary system took place competitively and individually.

On the other hand, with such a system, it may also be that a component with a strong electron-donating power preferentially solvates to a deuterium atom in a methanol-d molecule. With the purpose of considering this phenomenon, the area of each O-D band due to one of the two components was measured in tetrahydrofuran (THF=S_1, $\Delta\nu_D=90$) - solvents (S_2) systems by the half-value-width method.[8] Benzene ($\Delta\nu_D=0$), nitroethane (8), phenetole (25), ethyl propionate (32), pyridine (168), and triethylamine (238) were employed as the S_2 solvents. From the experimental results obtained, the relation between the mol fractions (n_{THF}) of THF and the area fractions (N_{THF}) of THF was plotted in Fig. 1. The

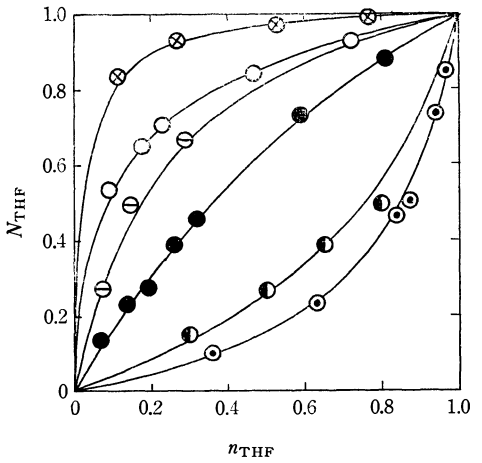

Fig. 1. Relation between the area fractions of O-D bands and the mol fractions of solvents in binary solvent systems containing 0.40 mol/l methanol-d.
Standard solvent: Tetrahydrofuran
Solvent S_2: ⊗ Benzene, ○ Nitroethane, ● Ethyl propionate, ⊖ Phenetole, ◐ Pyridine, ⊙ Triethylamine

$$n_{THF} = \frac{(THF)}{(THF) + (S_2)} \quad (1)$$

$$N_{THF} = \frac{A_{THF}}{A_{THF} + A_2} \quad (2)$$

parentheses indicate the concentration of the component, and A is the area of an O-D absorption band due to the component.

It is apparent from Fig. 1 that N_{THF} increases with an increase in n_{THF}. The n_{THF}-N_{THF} curves do not give straight lines, but vary convexly or concavely, depending on the kind of S_2 solvent; that is, N_{THF} values in the same mol fraction of THF are remarkably dependent on the electron-donating powers of S_2. In the case of using an S_2 whose electron-donating power is weaker than that of THF, for example, in the tetrahydrofuran-benzene and tetrahydrofuran-nitroethane systems, the N_{THF} value increases precipitously upon the addition of a small amount of tetrahydrofuran to a single S_2 solvent. In the contrary case, N_{THF} increases slowly. Similar features were also observed in ethyl propionate-S_2 solvents systems (Fig. 2). These facts indicate that one component with a strong electron-donating power solvates to methanol-d selectively.

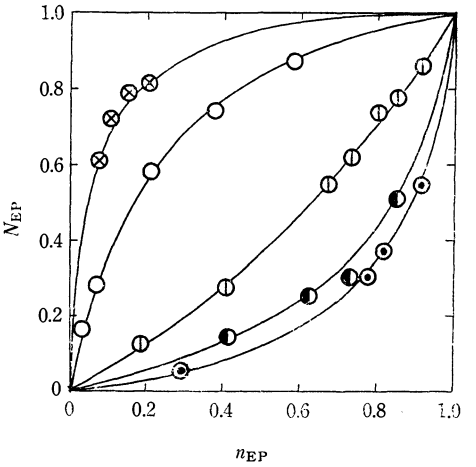

Fig. 2 Relation between the area fractions of O-D bands and the mol fractions of solvents in binary solvent systems containing 0.40 mol/l methanol-d.
Standard solvent: Ethyl propionate
Solvent S_2: ⊗ Benzene, ○ Nitroethane, ① Tetrahydrofuran, ◐ Pyridine, ⊙ Triethylamine

In order to investigate quantitatively the behavior of selective solvation, the selectivity $(S_{S_1}^{S_2})_D$ of nucleophilic solvation to methanol-d of an S_2 solvent to an S_1 solvent is defined as follows:

$$(S_{S_1}^{S_2})_D = \sqrt{\left(\frac{dN_2}{dn_2}\right)_{n_2=0} \Big/ \left(\frac{dN_1}{dn_1}\right)_{n_1=0}} \quad (3)$$

This definition is given graphically in Fig. 3, where the slope of the tangent line at the origin (0, 0) or the spot (1, 1) on the n_1-N_1 co-ordinates corresponds to the square of the denominator or the numerator in Eq. 3.

With the use of tetrahydrofuran or ethyl propionate as a standard solvent S_1, the selectivities of various solvents to the standard solvent were calculated by Eq. (3); they are listed in Table 1. It is obvious that the selectivity of benzene or of nitroethane to tetrahydrofuran is about 1/30 or 1/20, whereas that of triethylamine to tetrahydrofuran is about 6.

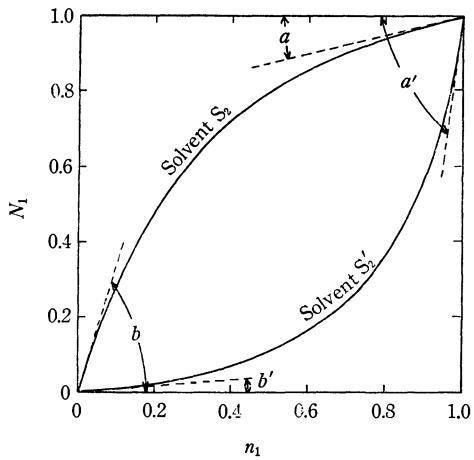

Fig. 3. Graphical evaluation of the selectivity of nucleophilic solvation of solvent S_2 to solvent S_1.

$$(S^{S_2}_{S_1})_D = \sqrt{\left(\frac{dN_2}{dn_2}\right)_{n_2=0} \Big/ \left(\frac{dN_1}{dn_1}\right)_{n_1=0}} = \sqrt{\frac{a}{b}}\ ,\quad \sqrt{\frac{a'}{b'}}$$

It may be also considered from Table 1 that the selectivity is closely correlated to the electron-donating power. On the other hand, it has previously been reported that the electron-donating power ($\Delta\nu_D$) is good relation with the equilibrium constants of solvents.[8] Consequently, a correlation also seems to exist between the selectivities and the equilibrium constants of solvents. Therefore, the selectivity of solvents was considered in detail in connection with the equilibrium constant. The square of the numerator $(dN_2/dn_2)_{n_2=0}$ in Eq. (3) is expressed as the following formula:

$$\left(\frac{dN_2}{dn_2}\right)_{n_2=0} = \lim_{n_2\to 0}\frac{N_2}{n_2} = \lim_{(S_2)\to 0}\frac{1+(S_1)/(S_2)}{1+A_1/A_2} \qquad (4)$$

In the second paper,[8] a linear relationship through the point of origin was observed to exist between the area ratio and the concentration ratio of two components, and it was found that the slope corresponded to the ratio of the equilibrium constants of the two solvents:

$$\frac{A_1}{A_2} = \frac{K_{D1}(S_1)}{K_{D2}(S_2)} \qquad (5)$$

When we place the relationship of Eq. (5) into Eq. (4), Eq. (4) is simplified as follows:

$$\lim_{(S_2)\to 0}\frac{1+(S_1)/(S_2)}{1+A_1/A_2} = \lim_{(S_2)\to 0}\frac{1+(S_1)/(S_2)}{1+K_{D1}(S_1)/K_{D2}(S_2)} = \frac{K_{D2}}{K_{D1}} \qquad (6)$$

Table 1. Selectivities of nucleophilic solvation of solvents S_2 to tetrahydrofuran or ethyl propionate

Solvent S_2	$\Delta\nu_D$ (cm^{-1})	$(S^{S_2}_{THF})_D$	$(S^{S_2}_{EP})_D$
Benzene	0	0.034_2	0.11_4
Nitroethane	8	0.054_4	0.18_2
Phenetole	25	0.17_2	—
Ethyl propionate	32	0.32_0	1.00
Tetrahydrofuran	90	1.00	3.1_3
Pyridine	168	2.6_1	7.1_5
Triethylamine	238	5.7_0	$13._5$

Table 2. Selectivities of nucleophilic solvation of solvents S_2 to tetrahydrofuran

Solvent S_2	K_D (l/mol)	$(S^{S_2}_{THF})_D$	$\frac{K_{D2}}{K_{D,THF}}$	$(S^{S_2}_{EP})_D(S^{EP}_{THF})_D$
Benzene	0.036_9	0.034_2	0.035_1	0.036_5
Nitroethane	0.058_5	0.054_4	0.055_7	0.058_3
Phenetole	0.17_8	0.17_2	0.17_0	—
Ethyl propionate	0.32_0	0.32_0	0.30_5	0.32_0
Tetrahydrofuran	1.0_5	1.00	1.00	1.0_0
Pyridine	2.6_8	2.6_1	2.5_5	2.2_9
Triethylamine	6.1_0	5.7_0	5.8_1	4.3_2

Table 3. Selectivities of nucleophilic solvation of solvents S_2 to ethyl propionate

Solvent S_2	K_D (l/mol)	$(S^{S_2}_{EP})_D$	$\frac{K_{D2}}{K_{D,EP}}$	$(S^{S_2}_{THF})_D(S^{THF}_{EP})_D$
Benzene	0.036_9	0.11_4	0.11_5	0.10_7
Nitroethane	0.058_5	0.18_2	0.18_3	0.17_0
Ethyl propionate	0.32_0	1.00	1.00	1.0_0
Tetrahydrofuran	1.0_5	3.1_3	3.2_8	3.1_3
Pyridine	2.6_8	7.1_5	8.3_8	8.1_7
Triethylamine	6.1_0	$13._5$	$19._1$	$17._8$

By the same method, the square of the denominator $(dN_1/dn_1)_{n_1=0}$ is given by Eq. (7):

$$\left(\frac{dN_1}{dn_1}\right)_{n_1=0} = \frac{K_{D1}}{K_{D2}} \tag{7}$$

Consequently, the selectivity of an S_2 solvent to an S_1 solvent is defined as the following equation by using Eqs. (3), (6) and (7):

$$(S^{S_2}_{S_1})_D = \frac{K_{D2}}{K_{D1}} \tag{8}$$

Equation (8) shows that the selectivity so defined can be calculated by using the ratio of the equilibrium constants. In order to confirm the propriety of Eq. (8), the selectivities of the S_2 solvents to tetrahydrofuran calculated by the various methods are listed in Table 2. Column 3 shows the value obtained by Eq. (3), column 4 the ratio of the equilibrium constants of the two solvents, and column 5 the value calculated by the following equation:

$$\text{column } 5 = (S^{S_2}_{EP})_D \times (S^{EP}_{THF})_D = 0.320(S^{S_2}_{EP})_D \tag{9}$$

It is evident from the results shown in Table 2 that the observed values of selectivity are in good accordance with the calculated values.

Similarly, the selectivities of S_2 solvents to ethyl propionate are listed in Table 3. The observed values accord well with the calculated values. This fact indicates that the relationship of multiplication or division plays a part in the selectivity.

On the other hand, it has previously been concluded that the equilibrium constant of the nucleophilic solvation to methanol-d can be used as a measure of the force of the general nucleophilic co-ordination to the electrophilic compounds.[8] It has now also been found that the equilibrium constants are related to the electron-donating powers as follows:

$$\log K_D = -\frac{3.67}{1+8.14\times 10^{-3}\,\Delta\nu_D} + 2.16 \tag{10}$$

These facts make reasonable the conclusion that the selectivity of the co-ordination of an S_2 solvent to a standard solvent, S_1, can be estimated by using Formula (10) and Eq. (8).

The authors are grateful to Professor Kenichi Fukui for his valuable suggestions while carrying out this study.

BULLETIN OF THE CHEMICAL SOCIETY OF JAPAN VOL. 41 782—785 (1968)

The Structure-Stability Relationship of the Metal Ion Complexes of Unsaturated Compounds. III.[1] The Effects of Polar Substituents on the Silver Ion - Olefin Complexation

Takayuki FUENO,*[1] Okitsugu KAJIMOTO*[1] and Junji FURUKAWA

Department of Synthetic Chemistry, Kyoto University, Sakyo-ku, Kyoto

(Received September 9, 1967)

The equilibrium constants for the formation of silver ion complexes of various vinyl compounds in water were determined at 25°C by the distribution method. It has been found that the equilibrium constants obtained are closely related to the Hammett sigma meta values of the relevant substituents, the reaction constant being $\rho = -5.07$ with the correlation coefficient $r = 0.974$. The results have been interpreted in terms of the inductive effect of the substituents as the most dominant contribution to the stabilities of these complexes.

The polar effect of substituents in the argentation (silver ion complexation) equilibria of unsaturated compounds was first discussed by Andrews ant Keefer[2] for benzene derivatives in terms of the Hammett ρ-σ relation. We also reported the results of similar studies for the case of ring-substituted styrenes,[3] and presented a theoretical interpretation of the observed substituent effects.[1] For olefinic compounds, however, available experimental data, though may be numerous, only indicate the importance of inductive, steric and structural strain effects of alkyl

*1 Present address: Faculty of Engineering Science, Osaka University, Toyonaka, Osaka.

1) Part II: T. Fueno, T. Okuyama and J. Furukawa, This Bulletin, **39**, 2094 (1966).

2) L. J. Andrews and R. M. Keefer, *J. Am. Chem. Soc.*, **72**, 3113 (1950).

3) T. Fueno, T. Okuyama, T. Deguchi and J. Furukawa, *ibid.*, **87**, 170 (1965).

groups on the relative stabilities of the complexes.[4-9] No work has ever been reported as to the role of polar substituents in the Ag^+-olefin complex stabilities.

In the present work we have measured argentation equilibrium constants of several "polar" vinyl compounds in water at 25°C, in order to compare the electronic contributions of various substituents to the stabilities of the ethylene complexes. It has been found that the equilibrium obeys the Hammett relation, provided the sigma meta values are used for the polar groups. Thus, the ease of complexation of an ethylenic bond appears to be governed primarily by the inductive effect of its neighboring groups.

Experimental

Materials. Silver nitrate and potassium nitrate were of the best grade commercially available. Carbon tetrachloride was washed successively with aqueous sodium hydroxide and water, dried over potassium carbonate and fractionally distilled. Most of the vinyl compounds studied were commercially obtained and purified by standard procedures. Phenyl vinyl ether was prepared by the methods of McElvain and Fajardo-Pinzón.[10] All these substrate compounds were checked for purity by gas chromatography before use.

Equilibrium Measurements. Equilibrium constants, K_1 and K_2, for the formation of the silver ion complexes in the aqueous phase

$$Ag^+ + M = AgM^+,$$

$$K_1 = [AgM^+]/[Ag^+][M] \quad (1)$$

$$Ag^+ + AgM^+ = Ag_2M^{2+}$$

$$K_2 = [Ag_2M^{2+}]/[Ag^+][AgM^+] \quad (2)$$

were measured at 25°C by the distribution method.[4] The polar olefins, M, were allowed to distribute between water and carbon tetrachloride by vigorously stirring the mixtures for 20 hr. The aqueous layer contained silver nitrate, whose concentration was in the range 0.1 to 0.6 M. The ionic strength of the layer was fixed at unity by the addition of a required amount of potassium nitrate. The initial concentration of the olefins dissolved in the organic layer was 1.0 M.

The constants, K_1 and K_2, may be related to an apparent equilibrium constant K in the following manner:

$$K = (k - k_0)/k_0[Ag^+] = K_1 + K_1K_2[Ag^+] \quad (3)$$

Here, k_0 is the distribution coefficient of an olefin between the aqueous and organic layers measured in the absence of the Ag^+ ions, while k is a similar coefficient measured in the presence of the ions. Measurements of the values of K for varying silver-ion concentrations, $[Ag^+]$, permit the evaluation of both K_1 and K_2 for each olefin.

The magnitudes of k as well as k_0 were obtained from the initial concentration of olefin in the organic layer and its concentration in either organic or aqueous layer after distribution. In the case of unsaturated hydrocarbons, the total concentrations of these compounds, both free and complexed, in the aqueous phase were determined by the spectrophotometric method. The procedure adopted was the same as had been described previously.[3] In the case of polar olefins, on the other hand, the decreases in their concentrations in the organic layer were measured by gas chromatography. The conventional half-height width method was found to suffice for this purpose, insofar as the volume ratio between the organic and aqueous layers was so adjusted as to suit such measurements.

Results

The values of K were measured for various vinyl compounds at varying silver ion concentrations. In evaluating the K-values, the concentration, of the silver ion $[Ag^+]$, which remained intact in the aqueous phase was assumed to be equal to its initial concentration. In other words, the variations in the concentration of free silver ions, which were caused by the formation of the complexes, were assumed to be negligibly small compared with the initial concentration. It was ascertained that this approximation introduced practically no error into the values of K.

If the presumptions underlying Eq. (3) are basically correct, then, for a given substrate, plots of K against $[Ag^+]$ should give a straight line with the intercept K_1 and the slope K_1K_2. Such linear

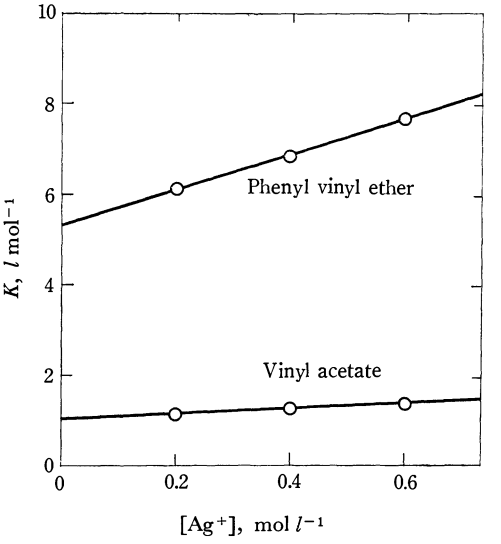

Fig. 1. Examples of the plots of K *vs.* $[Ag^+]$.

4) S. Winstein and H. J. Lucas, *ibid.*, **60**, 836 (1938).
5) a) H. J. Lucas, R. S. Moore and D. Pressman, *ibid.*, **65**, 227 (1943). b) H. J. Lucas, F. W. Billmayer and D. Pressman, *ibid.*, **65**, 230 (1943). c) F. R. Hepner, K. N. Trueblood and H. J. Lucas, *ibid.*, **74**, 1333 (1952). d) K. N. Trueblood and H. J. Lucas, *ibid.*, **74**, 1338 (1952).
6) L. J. Andrews and R. M. Keefer, *ibid.*, **71**, 3644 (1949); **72**, 5034 (1950).
7) J. G. Traynham and J. R. Olechowski, *ibid.*, **81**, 571 (1959).
8) M. A. Muhs and F. T. Weiss, *ibid.*, **84**, 4697 (1962).
9) R. J. Cvetanović, F. J. Duncan, W. E. Falconer and R. S. Irwin, *ibid.*, **87**, 1827 (1965).
10) S. M. McElvain and B. Fajardo-Pinzón, *ibid.*, **76**, 650 (1945).

TABLE 1. THE EQUILIBRIUM CONSTANTS FOR ARGENTATION OF SOME VINYL COMPOUNDS IN WATER AT 25°C

Compound	Substituent	k_0	K_1, l mol^{-1}	K_2, l mol^{-1}	r	σ_m
Ethylene	H[a)]	2.9×10^{-2}	85.3	0.15	—	0
Propylene	CH_3[a)]	6.8×10^{-3}	87.2	0.11	—	−0.069
Styrene	C_6H_5	5.59×10^{-4}	19.1	1.5	10	0.06
Ethyl vinyl ether	OC_2H_5	8.7×10^{-2}	13.0	0.6	20	0.115[b)]
Phenyl vinyl ether	OC_6H_5	1.10×10^{-3}	5.26	0.77	10	0.252
Vinyl acetate	$OCOCH_3$	4.5×10^{-2}	1.03	0.37	25	0.39
Methyl acrylate	$COOCH_3$	6.0×10^{-2}	0.37	0.28	25	0.37
Methyl vinyl ketone	$COCH_3$	0.47	0.42	—	2	0.376

a) Ref. 5d.
b) The value for the methoxy group was used.

relations were substantiated with sufficient precision with all the compounds studied here. Typical examples of such linearities are shown in Fig. 1.

The values of K_1 and K_2 obtained for the various vinyl compounds at 25°C are given in Table 1. Also listed in Table 1 are the distribution constant, k_0, of each compound between 1 N aqueous potassium nitrate solution and carbon tetrachloride and the volume ratio, r, between the aqueous and organic layers adopted for the distribution experiments of each compound.

Discussion

A number of workers[1-9] have already noted that the argentation equilibria of unsaturated compounds are sensibly influenced by the electronic, steric and strain factors of substituents. Among others, Muhs and Weiss[8] studied a large number of olefins by the gas chromatographic technique and extended detailed discussion of the steric and strain effects involved. As for the electronic contribution of substituents, the demonstrations that the relative stabilities of the silver ion complexes formed from substituted benzenes[2] and styrenes[3] obey the Hammett relation are noteworthy. In general cases, these factors join together in a complicated manner, and it is often extremely difficult to assess their relative importances in a simple yet general manner. All that has been possible to do is to isolate one major contributing factor or two, which may be different depending on the type of the substrate structures.

In an effort to disentangle the effects of polar substituents on the stabilities of the olefin complexes under study, we have plotted in Fig. 2 the values of log K_1 against the Hammett σ_m values of the substituents. The result was that the log K_1 was linearly related to the σ_m, though only roughly. The slope of the linear correlation was $\rho=-5.07$, and the correlation coefficient was $r=0.974$. As for the varia tions of the K_2 values with substituents, on the other hand, no simple generalization was possible to make.

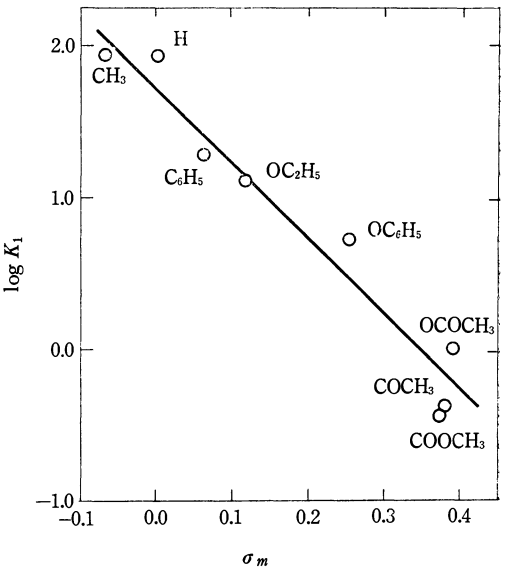

Fig. 2. Plots of log K_1 *vs.* σ_m for the silver ion complexation equilibria of some vinyl compounds in water at 25°C.

The finding that a linear relation holds between log K_1 and σ_m is not grossly fortuitous. The linearity may be rationalized as follows:

First of all, if the electronic effect of substituents is the most predominant contribution to the relative stabilities of polar olefin complexes, it will be nothing odd to expect that the values of log K_1 will be correlated, to a first approximation, with the Hammett sigma values of the substituents. One may inquire at the second step why then the stabilities should be functions of the sigma meta rather than sigma para values. Perhaps, the most plausible answer to this question may be given in terms of the inductive effect of the polar substituents. The view that the σ_m values of polar groups are associated primarily with their inductive effects is of wide acceptance, even though the way how the

effect would come into play and the extent to which it might contribute to the σ_m relative to the resonance contribution are still debatable.[11-14] No doubt, the argentation of vinyl compounds involves the interactions of the silver ion with the α-carbon just as well as the β-carbon of the vinyl linkage. Thus it is very likely that, in the case of vinyl compounds, the availability of the α-β bond for the complexation is greatly influenced by the inductive effect of its neighboring polar groups, and hence is correlated with their σ_m value.

The reaction constant, -5.07, obtained for a series of vinyl compounds as above is considerably larger in magnitude than the values of -1.6[2] and -0.766[3] which have previously been reported for ring-substituted benzenes and styrenes, respectively.[15] It may be said that the sensitivity of substrates toward the variation of substituents decreases in the order: ethylene > benzene > styrene. This order of sensitivity is readily understandable qualitatively in view that the polar effect of substituents should diminish with the increase in the distance between the substituents and the reaction center.

The above arguments, however, do not necessarily imply that the steric effect of substituents is wholly unimportant. For instance, one may clearly notice the importance of such an effect when he compares the K_1-values of heavily substituted ethylenes with those of the monosubstituted.[4,8,9] In the series of polar vinyl compounds studied here, possible steric effects of the various polar groups are apparently overshadowed by the more dominant contributions of their inductive effects. Hence, the steric effect is more conspicuous between ethylene derivatives of different degrees of substitution than between those that belong to the identical type of substitution but carry different substituent groups. Thus, it may be concluded that, so far as the silver ion complexation of vinyl compounds is concerned, the relative stabilities of the complexes formed is controlled most influentially by the inductive effect of the polar groups.

11) H. H. Jaffé, *J. Chem. Phys.*, **20**, 279, 285, 1554 (1952); **21**, 415 (1953).
12) M. J. S. Dewar and P. J. Grisdale, *J. Am. Chem. Soc.*, **84**, 3539, 3548 (1962).
13) Y. Yukawa, Y. Tsuno and M. Sawada, This Bulletin, **39**, 2274 (1966).
14) T. Fueno, T. Okuyama and J. Furukawa, *ibid.*, **39**, 569 (1966).
15) The difference is significant, even though we admit that we have chosen sigma meta values somewhat deliberately in correlating the log K_1 of vinyl compounds with Hammett's substituent constants.

BULLETIN OF THE CHEMICAL SOCIETY OF JAPAN VOL. 41 785—790 (1968)

The Structure-Stability Relationship of the Metal Ion Complexes of Unsaturated Compounds. IV.[1,2] Argentation Equilibria of Alkenyl Alkyl Ethers

Takayuki FUENO,*1 Okitsugu KAJIMOTO,*1 Tadashi OKUYAMA and Junji FURUKAWA

Department of Synthetic Chemistry, Kyoto University, Sakyo-ku, Kyoto

(Received September 9, 1967)

The equilibrium constants, K, for the formation of 1 : 1 Ag^+ - alkenyl alkyl ether complexes were measured in the temperature range 10 to 30°C by the gas chromatographic method. It has been found (1) that *cis* isomers have the values of K several times greater than those of the corresponding *trans* isomers, (2) that the K-value tends to diminish with the increasing degree of β-substitutions, (3) that, in a series of *cis* ethers, K increases as the β-alkyl substituent becomes bulkier, and (4) that the variation of the alkoxy groups causes little change in the K-value. The difference in the K-values between the *cis* and *trans* complexes is found to be ascribable mainly to their difference in the enthalpy changes, ΔH, accompanying the complexation. These trends have been discussed on a thermodynamic ground in comparison with those already noted for olefins.

The relations between the stability of the Ag^+-olefin complexes and the structure of the olefins have already been investigated and discussed to a considerable extent by several groups of workers.[3]

*1 Present address: Faculty of Engineering Science, Osaka University, Toyonaka, Osaka.

1) Part III: The preceding article.

2) Presented in part at the IUPAC International Symposium on Macromolecular Chemistry, Tokyo—Kyoto, September, 1966.

3) See, for example, Refs. 4, 5 and 6 and the papers cited therein.

Until recently, however, such investigations have never been extended to include "polar" olefins, *i. e.*, those olefinic compounds bearing polar groups. In the preceding paper of this series,[1] we have dealt with some vinyl compounds and reached the conclusion that the inductive effect of the substituents is of primarily importance to the relative stabilities of the complexes.

In the present communication, we treat the silver ion complexation equilibria of various alkenyl alkyl ethers, $R_1R_2C{=}CR_3(OR_4)$, with particular attention to the effect of the geometrical structures on the stabilities of the complexes formed. In measuring the equilibrium constants, we have utilized the gas chromatographic technique which has recently been developed by Muhs and Weiss.[4] This technique has greatly facilitated the comparison of the complexation abilities of *cis* and *trans* ethers as well as the examination of the temperature dependences of the equilibrium constants. Despite a possible influence of a large polarization of the carbon-carbon double bond in unsaturated ethers, the equilibrium data obtained for these compounds have manifested general features similar to those already recognized for olefins.[4-6] Apparently, the difference in the mesomeric effects of various alkoxy groups on the complexation is overshadowed by the difference in other contributions such as the inductive and steric effects of various alkyl groups present as well as the effect of the substrate structure.

Experimental

Materials. Silver nitrate, acetone and hexene-1 were of the best grade commercially available and were used without further purification. Ethylene glycol was obtained commercially and fractionally distilled immediately before use. Alkyl ethers were prepared by the methods described elsewhere[7] and were checked for purity by gas chromatography. Geometrical isomers of the ethers, when these occurred, were not separated. In all cases, the ethers were rich in *cis* isomer.

Equilibrium Measurements. The equilibrium constants for the Ag^+-olefin complex formation in ethylene glycol were measured by the gas chromatographic method developed by Muhs and Weiss.[4] It will be advantageous to briefly duplicate the principle here.

The distribution coefficient of the sample between liquid and vapor phases can be expressed as[4]

$$H = \frac{3}{2} \cdot \frac{(P_i/P_o)^2-1}{(P_i/P_o)^3-1} \cdot \frac{Ft_r}{V_L} \quad (1)$$

where P_i and P_o are the inlet and outlet pressures, respectively; F is the carrier gas flow rate; V_L is the volume occupied by liquid phase at the column temperature; and t_r is the retention time. The distribution coefficient varies with the Ag^+ concentration in the liquid phase as a result of complex formation. Thus, from the distribution coefficient, H_0, measured for a column without the Ag^+ ions and a similar coefficient, H, observed for an Ag^+-containing column, the equilibrium constant, K, for the complexation can readily be evaluated:[5]

$$K = [\text{Ether-Ag}^+]/[\text{Ether}][\text{Ag}^+] = (H-H_0)/H_0[\text{Ag}^+] \quad (2)$$

A Yanagimoto gas chromatograph model 3DH was operated at the column temperatures 10, 20 and 30°C with the hydrogen flow of 80 ml/min. A thermal conductivity detector and a soap bubble flowmeter were used. Special cautions were taken to minimize the scatters in the observed retention times which arose when the sample sizes were not strictly constant. The sample size finally adopted was 0.4 μl. The values of K obtained as above were fairly well reproducible, irrespective of the Ag^+ concentration not greater than 1.0 M. Mixtures of a given pair of geometrical isomers were subjected to the equilibrium measurements as such, but their retention times recorded separately. This expedience proved to introduce no error into the final results.

Preparation of Columns. Yanagimoto Celite 545 (80—100 mesh) was immersed in a silver nitrate solution in ethylene glycol diluted with acetone. The mixture was stirred until it attained homogeneity. Acetone was then evaporated off at room temperature. The ratio of the liquid phase to the support was 3 : 10 by weight. A weighed amount of packing was placed in a 1-m stainless steel column of 5 mm in diameter. Columns required *ca.* 9 g of packing. Three columns with 0, 0.5 and 1.0 M silver nitrate were prepared.

Results

Operating Conditions. Preliminary measurements of the equilibrium constants, K, indicated that the measured K-values were markedly dependent upon both the flow rate and the sample size adopted. Therefore, the effects of these factors had to be examined quantitatively in order to establish a routine operating condition.

For hexene-1, which showed relatively large variation in K with operating conditions, the following trends were observed:

The value of K tended to decrease considerably with the increasing sample size, whereas it slightly increased as the flow rate became greater. In magnitude, the effect of the sample size was the more appreciable, as may be seen in Fig. 1.

In such situations, it would be the most reasonable procedure in principle to extrapolate the K-values to both the zero flow rate and the zero sample size. Practically, however, a number of runs would then necessarily have to be performed for

4) M. A. Muhs and F. T. Weiss, *J. Am. Chem. Soc.*, **84**, 4697 (1962).
5) R. J. Cvetanovic, F. J. Duncan, W. E. Falconer and R. S. Irwin, *ibid.*, **87**, 1827 (1965).
6) a) S. Winstein and H. J. Lucas, *ibid.*, **60**, 836 (1938). b) L. J. Andrews and R. M. Keefer, *ibid.*, **72**, 3113 (1950). c) J. G. Traynham and M. F. Sehnert, *ibid.*, **78**, 4024 (1956).
7) T. Okuyama, T. Fueno, H. Nakatsuji and J. Furukawa, *ibid.*, **89**, 5826 (1967).

TABLE 1. DATA FOR THE ARGENTATION EQUILIBRIA OF ALKENYL ALKYL ETHERS, ALKENYL $\begin{matrix} R_1 \\ R_2 \end{matrix}\!\!>\!C=C<\!\!\begin{matrix} R_3 \\ OR_4 \end{matrix}$

No.[a]	Compound				K, l mol^{-1}			$-\Delta H$[b] kcal mol^{-1}	$-\Delta S$[c] e. u.
	R_1	R_2	R_3	R_4	10°	20°	30°		
1	H	H	H	C_2H_5	9.08	6.72	5.55	4.4	11.0
2	H	H	H	n-C_4H_9	8.72	7.76	5.66	3.7	8.8
3	H	H	H	i-C_4H_9	8.77	6.83	5.56	4.0	9.8
4c	H	CH_3	H	C_2H_5	4.00	3.13	2.55	3.9	11.0
4t	CH_3	H	H	C_2H_5	0.67	0.54	0.47	3.2	12.1
5c	H	C_2H_5	H	C_2H_5	5.62	4.24	3.13	4.5	12.6
5t	C_2H_5	H	H	C_2H_5	0.95	0.73	0.63	3.3	12.0
6c	H	i-C_3H_7	H	C_2H_5	5.98	4.46	3.48	4.7	12.9
6t	i-C_3H_7	H	H	C_2H_5	0.77	0.59	0.50	3.5	12.9
7c	H	CH_3	H	i-C_4H_9	3.58	2.86	2.34	3.7	10.4
7t	CH_3	H	H	i-C_4H_9	0.77	0.60	0.55	2.8	10.6
8	CH_3	CH_3	H	C_2H_5	0.27	0.21	0.17	3.5	15
9	H	H	CH_3	CH_3	9.51	7.35	—	4.7	12

a) The suffixes c and t refer to *cis* and *trans*, respectively.
b) Probable error of each entry does not exceed 0.2 kcal mol^{-1}.
c) Accurate only to within ±0.6 e. u.

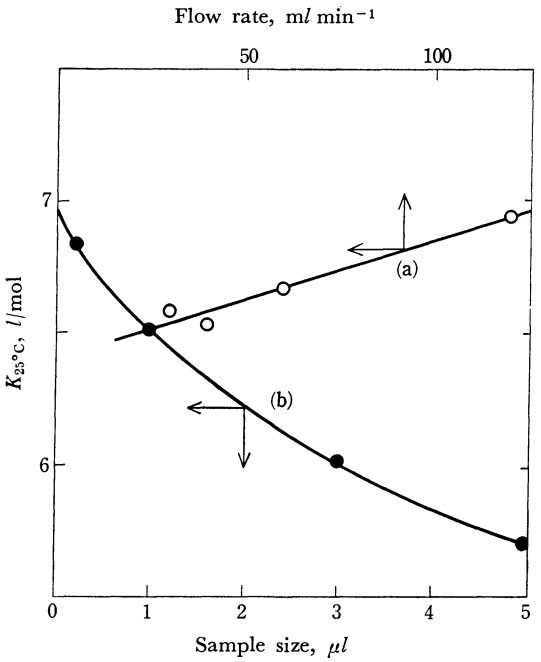

Fig. 1. Variations of K for hexene-1 (a) with the flow rate at constant sample size 1.0 μl and (b) with the sample size at constant flow rate 40 ml min^{-1}.

each compound under study, which might lead to undesirable deterioration of the column packings, introducing even more crucial experimental errors into the final results. Furthermore, experiments with too slow a flow rate coupled with a small sample size would make it extremely difficult to get precise retention times because of the large broadening as well as the small height of the sample peaks.

Under these circumstances, we have decided to compromise the cumbers by adopting such operating conditions that the relative magnitudes of the equilibrium constants for the various compounds to be examined were not seriously affected. The choices of the flow rate ranging from 40 to 80 ml/min and the sample size in the range 0.4 to 1.0 μl met this requirement. The flow rate and the sample size finally adopted as the routine conditions were 80 ml/min, and 0.4 μl, respectively, as has been specified in the experimental section.

Equilibrium Constants. The equilibrium constants were calculated from Eqs. (1) and (2). In obtaining the distribution constant, H, at a given Ag^+ concentration at a given temperature, three independent measurements were performed for each compound. The reproducibility of the equilibrium constants, K, was satisfactory. The values of K listed in Table 1 are the averages of the three independent measurements at each of the temperatures 10, 20 and 30°C. It was observed that at both 20 and 30°C alkenyl alkyl ethers were liable to suffer solvolysis during the distribution measurements in the column containing silver nitrate. Yet, the peaks of the reactant ethers and the products were separated sufficiently far to enable the recordings of the retention times of the ethers with fair accuracy. Above 40°C, however, the alkenyl alkyl ethers were consumed to a considerable extent so that the measurements of H were hardly feasible.

The changes of enthalpy, ΔH, and entropy, ΔS, in complexation were evaluated from the K-values given in Table 1. Plots of the logarithms

of K against the reciprocal of temperature were satisfactorily linear for all the unsaturated ethers investigated. An example of such plots is shown in Fig. 2. The values of ΔH and ΔS obtained in the temperature range 10 to 30°C are given in the final two columns of Table 1.

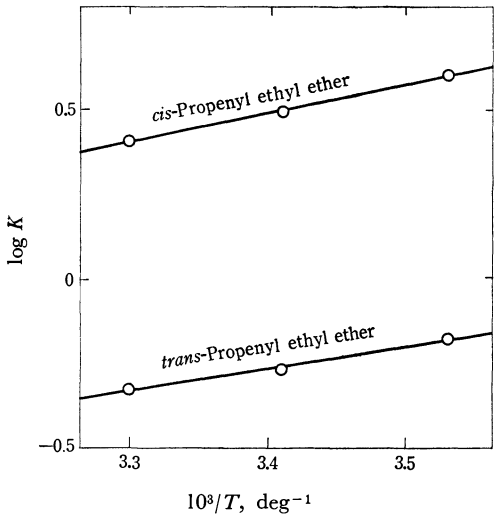

Fig. 2. Temperature dependence of log K for the silver ion complexation of *cis*- and *trans*-propenyl ethyl ethers (4c and 4t).

Discussion

Effects of Alkyl Substitutions. From the equilibrium constants listed in Table 1, the following generalizations can be made for the silver ion complexation of alkenyl alkyl ethers:

(1) The *cis* isomers have K values several times greater than those of the corresponding *trans* isomers.

(2) The K values largely decrease with the increasing degree of β-substitutions.

(3) As the substitutent on the β-position varies in the order CH_3, C_2H_5 and i-C_3H_7, the value of K of *cis* ethers increases asymptotically in this order.

(4) The K-value varies little when the ethoxy group is replaced by the isobutoxy or n-butoxy group.

The features (1) and (2) are in agreement with those already noted in the olefin complexation and may most simply be interpreted in terms of the adverse steric effect of the alkyl substituents.[4,5,8] However, the effect appears, in some cases, to be coupled with the favorable inductive effect of the alkyl groups. Perhaps, the order of the effects of β-alkyl groups $CH_3 < C_2H_5 < i$-C_3H_7 mentioned in the item (3) is a result that the latter contribution outweighs the former. It is noteworthy in this connection that the K-values of the olefin homologs have been reported to *decrease* in this same order in one case[4] while they show a maximum in another,[5] as in the case of our *trans* ethers, depending on the environments where the measurements of K have been made. This coupling of the two opposing contributions may also be a factor underlying the item (4).*2

In order to gain further insights into the nature of the complexation, it will no doubt be more advantageous to discuss the structure-stability relation in terms of the thermodynamic quantities, ΔH and ΔS. Thus, in Fig. 3, the values of ΔH for the various alkenyl alkyl ethers were plotted against the ΔS-values. It may be seen in Fig. 3 that the plotted points fall on a group of parallel straight lines which were drawn according to the types of β-substitution. We have found a similar relationship to hold (Fig. 4) between the ΔH and ΔS values for olefins which have recently been reported by Cvetanović *et al.*[5],*3 The slopes of these straight lines (*i. e.*, the isokinetic temperatures) corresponded to 310 and 350°K for the ethers and the alkenes, respectively.

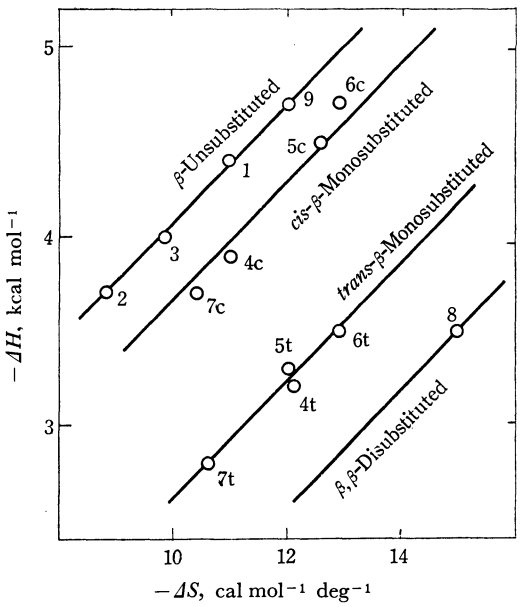

Fig. 3. Plots of ΔH *vs.* ΔS for the silver ion complexation equilibria of α, β-unsaturated ethers in ethylene glycol.
The numbers 1—9 refer to the unsaturated ethers listed in Table 1.

The families of linear ΔH-ΔS relationships in Figs. 3 and 4 may permit the following considerations:

First, since the isokinetic temperatures are only slightly above the temperatures at which the

8) R. F. Hepner, K. N. Trueblood and H. J. Lucas, *JAm. Chem. Soc.*, **74**, 1333 (1952).

*2 The finding that an α-methyl group produces no appreciable influence on the K-value (No. 9) may also have some bearing on this coupling effect.

*3 The essential feature is discernible, even though the number of the experimental points is limited.

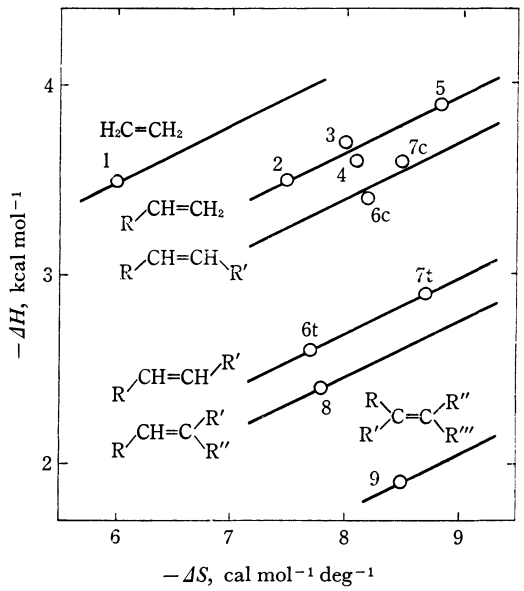

Fig. 4. Plots of ΔH *vs.* ΔS for the silver ion complexation equilibria of olefins in ethylene glycol. Data were taken from Ref. 5. The numbers 1—9 refer to the following olefins: 1, $CH_2=CH_2$; 2, $CH_3CH=CH_2$; 3, $C_2H_5CH=CH_2$; 4, *n*-$C_3H_7CH=CH_2$; 5, *i*-$C_3H_7CH=CH_2$; 6, $CH_3CH=CHCH_3$; 7, $C_2H_5CH=CHCH_3$; 8, $(CH_3)_2C=CHCH_3$; 9, $(CH_3)_2C=C(CH_3)_2$.

complexation studies have been carried out, it may not be quite proper to decide which of the two effects, enthalpy or entropy, is the more important factor to control the different complexation abilities of different alkenes or ethers of a given type of β-substitution. In fact, a closer examination of the thermodynamic data shows that the differentials in ΔH and $-T\Delta S$ between given pairs of substrate compounds are subject to complete cancellation between each other within the limit of experimental errors. As a consequence, no generalizations can possibly be made as to the relative importance of the two contributions in the temperature range studied.

Second, for compounds which belong to different classes of β-substitution, the relative importance of the enthalpy and entropy terms can be asscssed more easily. In particular, the greater stabilities of the complexes formed from *cis* ethers as compared with those from the corresponding *trans* isomers are evidently due to the greater enthalpy loss (*i. e.*, the greater heat evolution) of the former upon complexation.

Third and finally, one should be cautioned against a risk of ascribing different complexation abilities of arbitrarily selected two alkenes or ethers to a difference in either enthalpy or entropy effect in a simple and general manner. By the same token, it should be realized that the complex stability is by no means directly associated with the strength of the complexation bonds. This phase of the problem has previously been emphasized by us[9,10] in regard to the substituent effects in the silver ion complexation of aromatic hydrocarbons.

In the coordination of the silver ions with the double bond of olefins, there seems to be a favorable space (line, surface or volume) around the double bond for the ions to be located. As this space gets narrowed by the increasing substitution of alkyl groups, the degree of freedom of the coordinated silver ions would decrease correspondingly and, as a consequence, the loss of entropy would become larger to that extent. In the case of the tri- and tetra-substitutions, the silver ion may rather experience hindrance against approaching the most favorable space, so that the complexation bond would become the weaker.

Effects of the Geometrical Structure. As has already been mentioned, the difference in stability between the complexes of *cis* and *trans* ethers may most simply be interpreted in terms of the difference in adverse steric effect of substituents. The steric hindrance to complex formation by the two bulky groups, one being a β-alkyl group and the other an alkoxy group, may be greater when they are *trans* to each other.[8] Thus, *cis* isomers may tend to give more stable complexes. Incidentally, this interpretation implicitly assumes that the difference in the free energies of geometrical isomers is a less important factor than that of the resulting complexes.

Alternatively, it may also be conceivable that the energy difference between the Ag^+-complexes of the geometrically isomeric substrates is small as compared to the difference in total energy between the substrate molecules themselves. If this is true, the isomers which are less stable in total energy will experience larger enthalpy loss upon complexation, thus forming more stable complexes. The greater heat of complexation of *cis* ethers may thus be ascribable, for instance, to the relief of strain[4,10] of the two bulky groups *cis* to each other, when the complex is formed.

It is not quite an easy task to decide which of the above two interpretations is more plausible. However, it may be pointed out with some emphasis that the latter view receives support from the results of independent studies of the relative stabilities of the geometrical isomers of olefins as well as alkenyl ethers. Specifically, studies of the geometrical isomerization equilibria of both olefins[12]

9) T. Fueno, T. Okuyama, T. Deguchi and J. Furukawa, *ibid.*, **87**, 170 (1965).
10) T. Fueno, T. Okuyama and J. Furukawa, This Bulletin, **39**, 2094 (1966).
11) R. B. Turner, D. B. Nettleton and M. Perelman, *J. Am. Chem. Soc.*, **80**, 1430 (1958).
12) a) D. M. Golden, K. W. Egger and S. W. Benson, *ibid.*, **86**, 5416 (1964). b) K. W. Egger and S. W. Benson, *ibid.*, **87**, 3311 (1965); *ibid.*, **88**, 236 (1966).

and alkenyl alkyl ethers[13] have shown that the *cis* isomers are less stable than the corresponding *trans* isomers by approximately 1 kcal mol^{-1}. The energy difference roughly checks with the difference in the heats of complexation observed.

Thus, so far as the relative stabilities of the silver ion complexes of the *cis* and *trans* isomers of olefins or ethers are concerned, the concept of steric hindrance of bulky groups affecting the ΔH to different extents appears to be improbable. We feel that it is rather through the ΔS term that the steric effect of bulky groups influences the complexation to different extents depending on their placements, *cis* and *trans*. That is, the spatial limitation imposed on the location of the silver ion in the complexes of *trans* isomers perhaps has reflected in larger losses of entropy than would be expected if no such limitation existed. Thus, the entropy losses of *trans* isomers may well become comparable in magnitude with those of *cis* isomers, despite the smaller enthalpy losses of the former. This violation of the compensation rule between ΔH and ΔS must be an origin of such a separation of the ΔH-ΔS linear relationships for the two isomers as has been shown in Figs. 3 and 4.

13) T. Okuyama, T. Fueno, J. Furukawa and Y. Yonezawa, to be published.

BULLETIN OF THE CHEMICAL SOCIETY OF JAPAN VOL. 41 790—795 (1968)

Solvent Effects on the Proton Magnetic Resonance Spectra of 2,3-Dichlorobutane and the Problem of Rotational Isomers

Shoichi KONDO,*1 Eijiro TAGAMI,*2 Kazuyoshi IIMURA and Masatami TAKEDA

Department of Chemistry, Faculty of Science, Science University of Tokyo, Shinjuku-ku, Tokyo

(Received September 28, 1967)

Effect of solvent on the coupling and magnetic shielding constants of *meso* and *racemic* 2,3-dichlorobutanes has been examined using proton magnetic resonance (PMR). The iterative method of spectrum analysis is applied to the simple sub-state in order to improve the computation speed and the computer capacity. The variations in the coupling constants for the *meso* configuration are to some extent correlated with the population as a function of dielectric constant ε of solvent using an Onsager model. The coupling constants of the *racemic* configuration were almost independent of the solvent dielectric constant. The estimated chemical shift dependence on ε of the reaction field does not adequately describe the experimental data.

The PMR spectra of 2,3-dichlorobutane have been studied by Bothner-By *et al.*,[1] but further investigation seems worthwhile concerning the change in spectra with solvent polarity. A molecule having rotational isomers is known to have various populations in solution, since the relative energies of these isomers are considerably affected by the medium. This is due to the fact that the polar isomer, which corresponds to a higher energy in the gaseous state than the nonpolar isomer, is stabilized in solution by the action of a reaction field induced by the surrounding polar medium. In this paper, the effect of solvent on the population, obtained from the vicinal coupling constant, and on the chemical shift will be discussed in terms of reaction field theory.

Experimental

The preparation and characterization of the *meso* and *racemic* 2,3-dichlorobutanes will be described elsewhere. PMR spectra were taken on a Varian A-60 as 5 and 10% wt/vol solutions in solvents with different dielectric constants and recorded over a temperature range of −60 to 40°C.

The spectrum was calculated as a $X_3AA'X_3'$ system. The Hamiltonian matrix is factorized to reduce it to minimal dimensions by taking advantage of magnetic equivalence.[2] The spectrum of a $X_3AA'X_3'$ system is made up of a superposition of four sub-spectra $Q_XD_AD_{A'}Q_{X'}$, $Q_XD_AD_{A'}D_{X'}$, $D_XD_AD_{A'}Q_{X'}$ and $D_XD_AD_{A'}D_{X'}$. A nomenclature has been developed for the sub-states corresponding to the possible values

*1 Present address: Département de Génie Chimique, Faculté des Sciences, Université Laval, Québec 10e, Canada.

*2 Present address: Japan Synthetic Rubber Co., Yokkaichi, Mie.

1) A. A. Bothner-By and C. Naar-Colin, *J. Am. Chem. Soc.*, **84**, 743 (1962).

2) R. C. Ferguson and D. W. Marquart, *J. Chem. Phys.*, **41**, 2087 (1964).

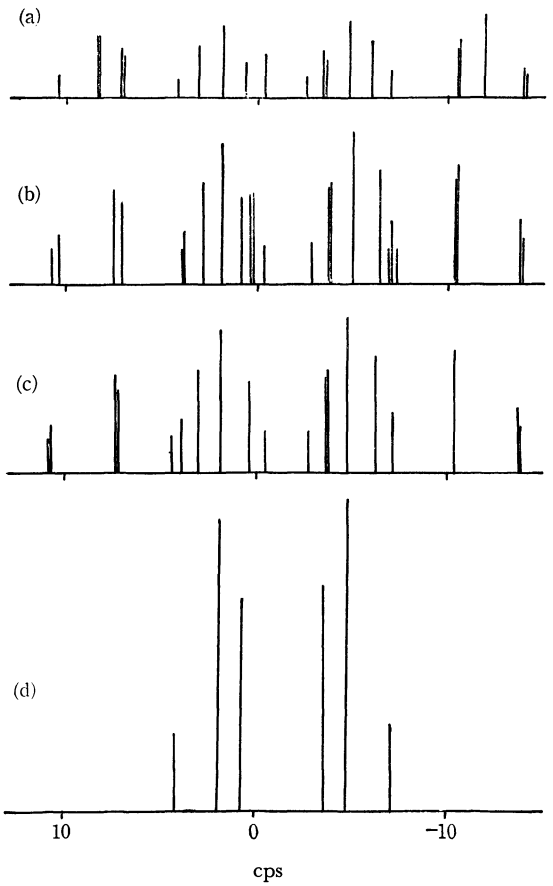

Fig. 1. " Stick spectra " of each substate.
(a) $Q_XD_AD_A'Q_X'$ (b) $Q_XD_AD_A'D_X'$
(c) $D_XD_AD_A'Q_X'$ (d) $D_XD_AD_A'D_X'$

of I in which the state with $I=1/2$, $3/2$ is known as a doublet, quartet (abbreviated to D and Q). Each spectrum is weighted by the factor 1, 2, 2 and 4, respectively. In Fig. 1, dividing the methine proton spectrum into contributions from sub-spectra, it is seen that a $X_3AA'X_3'$ system contains lines at the same position as in $D_XD_AD_A'D_X'$. An iterative method is used for the

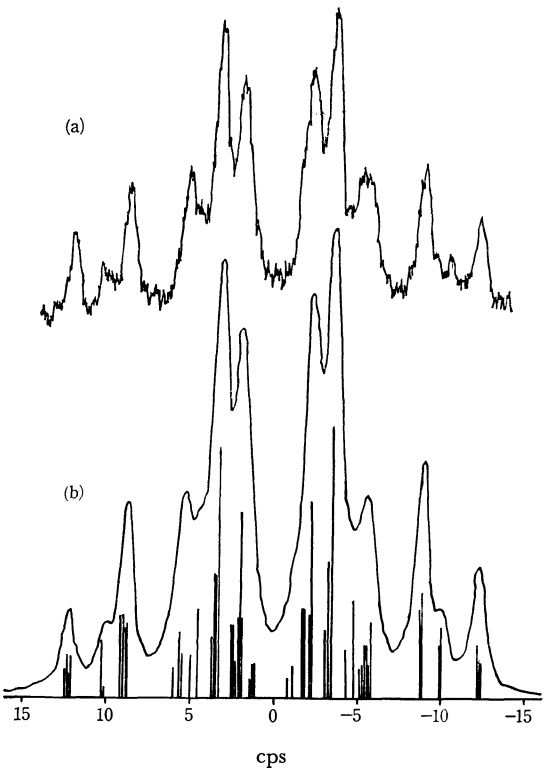

Fig. 2. *Racemic* 2,3-dichlorobutane in carbon tetrachloride.
(a) Observed methine proton spectrum
(b) Calculated spectrum (line width = 0.4 cps) and " Stick spectrum "

$D_XD_AD_A'D_X'$ system only to obtain improvements in computation speed, computer program capacity and convenience of use. Calculations of PMR spectra were carried out on an IBM 1620 computer using Fortran II_D.

The final calculated spectra obtained by this method agreed very closely with the observed spectra. As an example of the fit achieved, a methine proton spectrum of *racemic* 2,3-dichlorobutane in carbon tetrachloride is compared with the calculated spectra in Fig. 2.

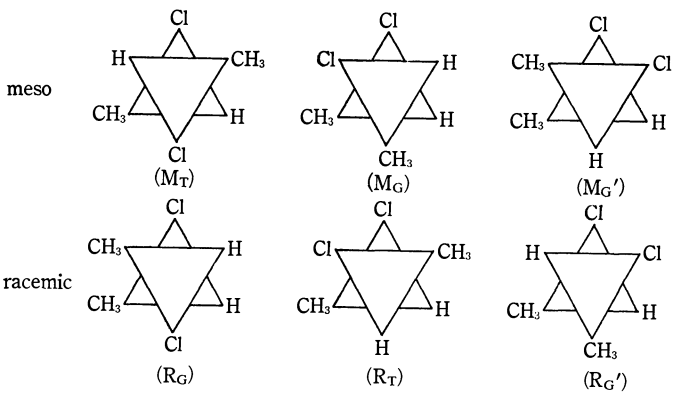

Fig. 3. The possible conformations for *meso* and *racemic* 2,3-dichlorobutanes.

TABLE 1. SOLVENT EFFECTS ON COUPLING CONSTANTS AND CHEMICAL SHIFTS OF 2,3-DICHLOROBUTANE

Compound	Solvent	$J_{AA'}$	ν_{CH_3}	ν_{CH}	P_{MT} or $P_{RG'}$
meso	1. CCl_4	7.7	99	237	0.63
	2. C_6H_6	6.3	95	216	0.48
	3. C_2Cl_4	7.8	99	238	0.64
	4. CS_2	7.2	97	234	0.58
	5. $CHCl_3$	6.5	98	243	0.50
	6. CH_2Cl_2	5.9	96	247	0.43
	7. $(CH_3)_2CO$	5.2	95	256	0.35
	8. $C_6H_5NO_2$	5.4	94	250	0.38
	9. CH_3CN	4.9	93	255	0.33
racemic	1. CCl_4	3.4	92	251	0.16
	3. C_2Cl_4	3.3	91	250	0.14
	4. CS_2	3.3	92	244	0.14
	5. $CHCl_3$		95	254	
	7. $(CH_3)_2CO$		94	263	
	8. $C_6H_5NO_2$	3.2	92	252	0.13
	9. CH_3CN		93	259	
		in cps			

Note: P_{MT} and $P_{RG'}$ indicates the populations of M_T in *meso* and of $R_{G'}$ in *racemic* configurations, respectively.

Results and Discussion

Estimation of Population of Rotational Isomers from the Vicinal Coupling Constants. The values of chemical shifts and coupling constants $J_{AA'}$ for various solvents are shown in Table 1. Three different rotational isomers are possible for both *meso* and *racemic* 2,3-dichlorobutane as shown in Fig. 3.

1) Experimental Results of meso 2,3-Dichlorobutane. The *meso* configuration has two effective conformations, the trans (M_T) and gauche (M_G), ($M_{G'}$) existing in two mirror-image forms. First, we shall attempt to obtain some information concerning the molecular conformation of the isomers in solution from the values of the vicinal coupling constants, $J_{AA'}$, of *meso*-DCB which is solvent dependent. $J_{AA'}$ may be regarded as an average value, given by

$$J_{AA'} = P_T J_T + P_G J_G, \qquad P_T + P_G = 1 \qquad (1)$$

where P_T and P_G are the populations of M_T and ($M_G + M_{G'}$), respectively, and J_T and J_G are the coupling constants for 60° and 180° dihedral angles between the methine protons. In Table 1 the populations obtained at 29°C, are summarized, assuming $J_T = 11$ c/s and $J_G = 2$ c/s.*3 As can be seen in Fig. 4, there is a fair correlation between the population and the dielectric constant of the solvent, except for benzene solution. Thus, the populations are shown to be given by the following experimental equation, as shown in Fig. 4.

$$\log (P_G/P_T) = -0.66 + 2.0(\varepsilon - 1)/(2\varepsilon + 1)$$

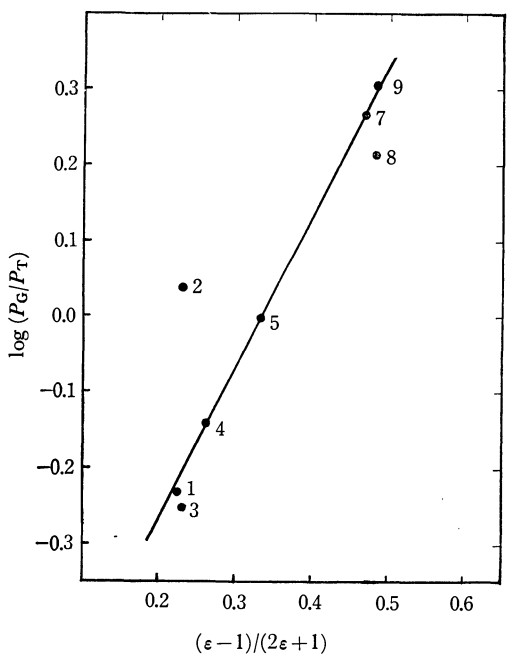

Fig. 4. The possible conformations for *meso* and *racemic* 2,3-dichlorobutanes.

*3 We have adopted these values instead of $J_T = 11$c/s and $J_G = 1$c/s, which are used by Bothner-By *et al.*,[1b] taking account of the theoretically calculated values of $J_T = 9.2$c/s and $J_G = 1.7$c/s for substituted ethanes (see M. Karplus, *J. Chem. Phys.*, **30**, 6 (1958)), and the recent experimental values of $J_T = 13.6$ c/s and $J_G = 2.6$ c/s used for the conformational analysis of amino acid (see H. Ogata, Y. Arata and S. Fujiwara, *J. Mol. Spectroscopy*, **23**, 76 (1967)), and of $J_T = 10$ c/s and $J_G = 2$ c/s used for studying the PMR spectra of 2, 4-dichloropentane (see T. Shimanouchi, M. Tasumi and Y. Abe, *Makromol. Chem.*, **86**, 43 (1965)).

TABLE 2. CONFORMATIONAL ENERGIES (in kcal/mol)

	M_T	M_G	$M_{G'}$	R_T	R_G	$R_{G'}$
Steric interaction (ΔE_1)	1.67	1.96	1.96	1.69	2.10	1.79
Dipole interaction (ΔE_2)	1.56	2.72	2.72	2.72	1.56	2.72
Total energy	3.23	4.68	4.68	4.41	3.66	4.51

$\Delta E(M_G - M_T) = 1.45$ $\Delta E(R_{G'} - R_T) = 0.10$
$\Delta E(R_T - R_G) = 0.75$

2) Estimation of Influence of Solvent upon Population of Rotational Isomers.[3,4] If M_T and M_G are considered to be in simple equilibrium, their relative proportions should be in accordance with the expression

$$P_G/P_T = 2(Z_G/Z_T)\exp(-\Delta E/\boldsymbol{R}T) \quad (2)$$

in which Z_T and Z_G are the partition functions of the two isomers, and the factor 2 is introduced to account for the mirror-image isomerism of the gauche form. It is a well known fact that the energy difference between rotational isomers ΔE changes considerably in the transition from gas to liquid, and is dependent on solvent. The energy of this change, ΔE_{reac}, was calculated by taking Onsager's field[5] as the reaction field,

$$\Delta E_{reac} = \Delta E_{gas} - \Delta E_{solu} = (\varepsilon-1)\mu^2/(2\varepsilon+1)a^3$$
$$\Delta E_{solu} = \Delta E_{gas} - (\varepsilon-1)\mu^2/(2\varepsilon+1)a^3 \quad (3)$$

where ΔE_{gas} and ΔE_{solu} are the energy differences between the gauche and trans forms referred to the gaseous state and to the solution, respectively; μ is the dipole moment of the gauche form, and a the radius of the solute molecule. If the solute molecular radius is estimated from the density and molecular weight of the liquid solute, and by assuming a perfect packing of the spheres, ΔE will be approximately

$$\Delta E = \Delta E_{gas} - (4\pi \boldsymbol{N}d/3M)\mu^2[(\varepsilon-1)/(2\varepsilon+1)] \quad (4)$$

combining with Eq. (2) and substituting numerical values, we obtain at 30°C

$$\log(P_G/P_T) = \log 2(Z_G/Z_T) - (\Delta E_{gas}/2.303\boldsymbol{R}T) + 2.16[(\varepsilon-1)/(2\varepsilon+1)] \quad (5)$$

Here the dipole moment of conformation M_G is approximated by vector addition of bond moment taken from C-Cl (1.86 D). The resultant dipole moment for M_G is 3.08 D.[6]

Furthermore, ΔE_{gas} can be calculated considering two factors; ΔE_1, which results from interactions between non-bonded atoms and groups, and ΔE_2, from the interaction of neighboring dipoles. ΔE_1 has been calculated assuming interactions in accordance with Lennard-Jones type potentials, and ΔE_2 calculated using a point dipole approximation.[7] The calculated results are also given in Table 2.

3) Comparison with the Experimental Results. To compare this estimate with the experimental results, the energy difference between the two isomers is evaluated to be 1.4 kcal/mol with M_T being the more stable form by extrapolating the line in Fig. 4 to $\varepsilon=1$, and assuming equal partition functions for M_T and M_G in the liquid state. The agreement between the observed and calculated values of ΔE_{gas} is gratifying, considering the assumptions involved in the calculation of energy difference. The slope predicted by Eq. (5) agrees closely with the observed values, 2.0. An abnormal phenomenon in the benzene solution was observed, and this "benzene effect" is assumed to be due to the fact that the molecule associates with the solvent molecule by affinity between the hydrogen atoms of the benzene ring and halogen atoms in 2,3-dichlorobutane as follows[8]:

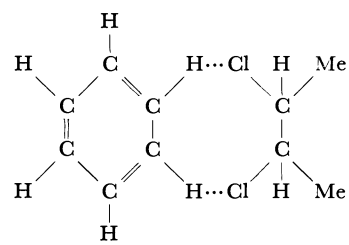

4) Interpretation of PMR Spectra of Racemic 2,3-Dichlorobutane. For *racemic* 2,3-dichlorobutane, the coupling constants $J_{AA'}$ are almost independent of the dielectric constant of the solvents within the limits of detection as can be seen in Table 1. This result is in direct contrast to that for the *meso*-2,3-dichlorobutane. The complexity introduced by consideration of three different isomers makes determination of the energy differences between isomers from $J_{AA'}$ of the spectra difficult. The situation is further complicated by the fact that the superposed peaks in the methyl spectrum render accurate measurements very difficult. As shown in Table 2, R_G is assumed to be the lowest in energy in the gaseous state. The energy difference between R_G and the two other conformers was con-

3) A. Wada, *J. Chem. Phys.*, **22**, 198 (1954).
4) E. B. Whipple, *ibid.*, **35**, 1039 (1961).
5) L. Onsager, *J. Am. Chem. Soc.*, **58**, 1486 (1936).
6) To be published.
7) I. Miyagawa, *Nippon Kagaku Zassi (J. Chem. Soc. Japan, Pure Chem. Sect.)*, **75**, 1169 (1954).
8) S. Mizushima, Y. Morino and K. Higasi, *Sci. Papers Inst. Phys. Chem. Research*, **25**, 153 (1934).

sidered to be about 0.8 kcal/mol. Since R_T and $R_{G'}$ are polar the energy in solution is stabilized by reaction fields. This energy of stabilization is calculated from Eq. (3) by use of the parameters $\mu=3.0$ D and $(\varepsilon-1)/(2\varepsilon+1)=0.25$ for nonpolar solvents. The value of 0.75 kcal/mol obtained indicates that the energy of each isomer seems to be comparable in nonpolar solvents. As the stabilized energy is 1.38 kcal/mol in acetonitrile which is the most polar solvent used, the energy difference between these and R_G becomes 0.6 kcal/mol which corresponds to a variation of 1 c/s in $J_{AA'}$. It seems to be detectable in the spectra. In contrast to PMR data, the populations of $R_{G'}$ in carbon disulfide and acetonitrile from infrared data are 24% and 43%, respectively.[6] A change of more than 1 c/s in $J_{AA'}$ is expected because of the difference of 20% in the population obtained from IR. Since accuracy is within ± 0.1 c/s, this is considerably different from the result shown in Table 1 that a slight change in $J_{AA'}$ was observed between polar and nonpolar solvents. We have at present no good explanation for this disagreement, but this problem should be worth further investigation.

Solvent Effects on Chemical Shift. The formation of an X-H bond causes an increase in the charge between the two nuclei, and an electric field E applied in the bond direction will draw this excess charge away from the hydrogen nucleus, thus decreasing its shielding coefficient. The magnitude of the decrease is given by the following equation[9]:

$$\sigma = -2\times 10^{-12}E\cos\theta - 10^{-18}E^2 \qquad (6)$$

where θ is the angle between the X-H axis and E.

This experiment was designed to test qualitatively the validity of Eq. (6) at different protons of *meso*-2,3-dichlorobutane. The chemical shifts of methyl and methine protons are plotted *versus* a function of ε at 29°C in Fig. 5.

If the reaction field is adequately given by Eq. (3) and the population is independent of the ε of the solvent, these curves would be straight lines with the slope for methyl and methine protons of gauche form -0.1 and -0.3 ppm, respectively. Instead of straight lines, however, smooth curves with an opposite slope are obtained. The curvature of the curve for the methine proton may be due to the fact that populations of the gauche form become larger as the ε of the solvent increases. The fact that the curve for σ_{CH_3} bends in the opposite direction indicates that the reaction field along the C-CH_3 bond must have a sign opposite to that along the C-H bond, which is not true considering the molecular structure of the gauche form. Even if the estimated reaction field changes in magnitude and direction at each methyl and methine proton, it does not adequately describe the experimental chemical shift dependence on ε.

Thus, long range shielding by carbon-carbon single bonds must be considered.[10] The two

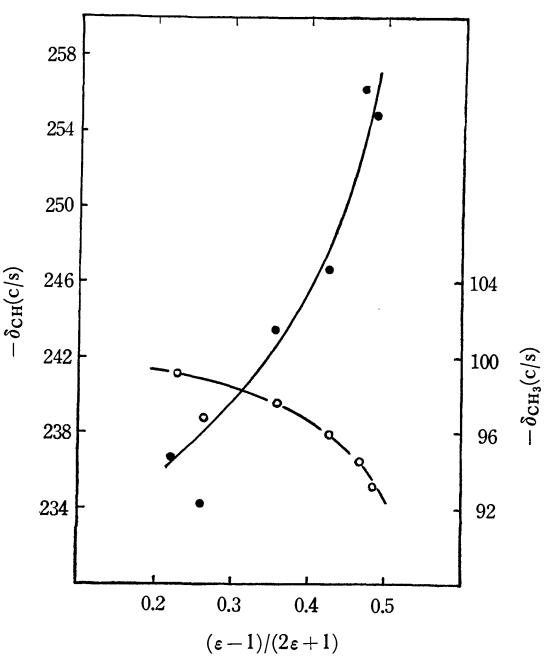

Fig. 5. δ values against the dielectric function.
Solid circles indicate methine proton.
Open circles indicate methyl proton.

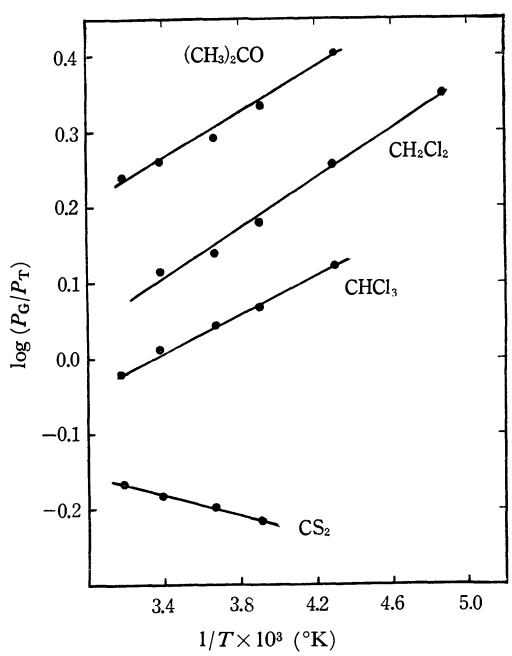

Fig. 6. Variation of population in *meso* 2,3-dichlorobutane as a function of temperature for different solvents.

9) A. D. Buckingham, *Can. J. Chem. Eng.*, **38**, 300 (1960).
10) A. G. Mority and N. Sheppard, *Mol. Phys.*, **5**, 361 (1962).

forms of the molecule differ in that for M_T, the C-CH_3 bonds are gauche to the methine proton and for M_G, trans and gauche to the methine proton. The chemical shift difference is 0.11 ppm with the methine proton of the M_T to high field. Similarly, for the methyl group, the other C-CH_3 bond is trans to the methyl group in M_T, and gauche in M_G. The predicted shift is 0.15 ppm with the M_T to low field. This is also in fair agreement with the observed shifts for methyl and methine protons. The qualitative agreement is sufficient to support the assumption that the chemical shifts are primarily caused by the anisotropy of the C-C bond due to the difference in population of rotational isomers in each solution, rather than by the reaction field from the polar effect of the solvent. The contributions to the shielding of a nucleus from the two factors appear to be additive.

Temperature Dependence of Isomer Ratio. Figure 6 shows the populations of the trans and gauche forms in solvents as a function of temperature. It will at once be clear that the curves of populations in polar solvents is of opposite slope to that in nonpolar solvents. This result suggests that M_G is preferred in solvents of high dielectric constants. This is coincident with the tendency of solvent effects observed in the preceding section.

BULLETIN OF THE CHEMICAL SOCIETY OF JAPAN VOL. 41 795—799 (1968)

The Behavior of Radical Anion of Acridine as Revealed from ESR Studies

Shigeya NIIZUMA, Michio OKUDA and Masao KOIZUMI

Department of Chemistry, Faculty of Science, Tohoku University, Katahira-cho, Sendai

(Received October 16, 1967)

Nature of acridine anions produced by the addition of alkali metals to the tetrahydrofuran solutions of acridine has been studied by means of ESR and VU spectra. In excess of acridine (A), a green species G is produced. This has been identified as A^-Na^+ (or A^-K^+ *etc.*). A^-Na^+ gives under suitable conditions, ESR spectra with hfs consisting more than fifty lines. This species reverts to acridine upon addition of a small quantity of water or ethanol. With the fall of temperature, the intensity of ESR spectra of G decreases remarkably and accompanied with it, UV spectra of G also decline with no change of the spectral shape. $\log I$ *vs.* $1/T$ plots where I is either the intensity of UV absorption or of the ESR signal are satisfactorily linear; this has been interpreted to be due to a large equilibrium constant of the process, $2A^-Na^+ \rightleftarrows (Na^+A^-)_2$ in which $(Na^+A^-)_2$ is a colorless diamagnetic substance. This interpretation has led to the value of enthalpy of dissociation of $(Na^+A^-)_2$ as *ca.* 14 kcal. When sodium is in excess, a diamagnetic violet species is produced. This has been assigned as $Na^+A^{2-}Na^+$. The chemical processes pertaining to A^-Na^+ and $Na^+A^{2-}Na^+$ can be summarized as follows:

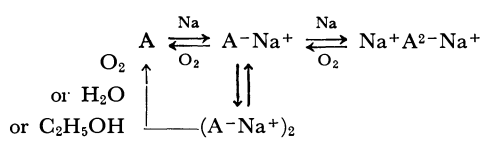

In a series of papers on the photoreduction of acridine reported by one of the present authors (M. K.) and his collaborators, it was established that semiquinone or half-reduced radical of acridine is formed in the irradiated alcoholic solution.[1] In connection with these studies, it is interesting to study the chemical nature of the various forms of half-reduced acridine such as neutral radical and radical anion by means of an ESR technique in addition to UV measurement.

This paper reports the behavior of radical anion which is produced by treating acridine with alkali metals in tetrahydrofuran (THF). Hitherto, there seems to be no papers on the ESR spectra which were decisively attributed to acridine radical anion, although some reports were made on other *N*-heterocyclics.[2,3] Carrington[4] said, by the

1) A. Kira, S. Kato and M. Koizumi, This Bulletin, **39**, 1221 (1966).

2) R. L. Ward, *J. Am. Chem. Soc.*, **83**, 3623 (1961).

3) R. Pointean, J. Favede and P. Delhaes, *J. Chim. Phys.*, **61**, 1129 (1964).

4) A. Carrington and J. D. Santos-Veiga, *Mol. Phys.*, **5**, 21 (1962).

analogy with pyridine which upon contact with sodium in DME (dimethoxyethane) or THF, yields dipyridyl anion, that acridine radical anion, being also unstable, might convert to a dimeric form. Kuwata *et al.*[5] found that acridine, upon contact with metallic sodium in THF, gives a diamagnetic substance red in color, and the solution, when heated, turns blue and gives broad ESR spectra consisting of a single line with $\Delta H_{msl}=$ 13G and $g=2.003$. They suggested that this is due to a radical anion of acridine. Russel *et al.*[6] reported in a paper dealing with some radical anions existing in a 1 : 1 solution of some unsaturated and its dihydro compounds in $(CH_3O)_2SO$ containing *t*-Bt-OK), that electron transfer occurs between acridine and acridan. No remark was made, however, on the ESR spectra.

In the present paper, we would like to report the following findings; 1) Radical anion of acridine, A^- gives under suitable conditions, ESR spectra with hfs consisting more than fifty lines. 2) A^- transforms to dianion A^{2-} when the quantity of sodium is in excess. 3) The intensity of ESR decreases remarkably at lower temperatures; this suggests the existence of a dimerization (or polymerization) equilibrium of the type $2A^-Na^+ \rightleftarrows (A^-Na^+)_2$.

Experimental

A Nippon-Denshi P-10 type ESR spectrometer was used; its characteristics are X-band, 100 kc field modulation and H_{011} mode of cavity. The constancy of temperature was maintained within $\pm 2°C$ by streaming through a cavity either nitrogen gas (from the liquid nitrogen) for low temperatures or hot air for high temperatures.

Materials. First grade tetrahydrofuran (THF) from Wakojunyaku was refluxed with sodium for several hours, distilled and then stored *in vacuo*. Na-K-alloy was added to the stock solvent to remove a trace of water. Sodium and potassium were made free from surface contamination by dropping fused metals down through a capillary *in vacuo*. Lithium was not specially purified. Acridine was purified by a usual method.

UV Spectra of the Solution in Contact with Alkali Metals. Several mg of acridine dissolved in 2 m*l* of degassed THF was brought into contact with *ca.* 0.2—0.4 g sodium through a breakable seal. The solution gradually turned green in several to ten and several minutes and finally became violet after a long time. The two species will be designated as G and V. Essentially similar results were obtained with both potassium and lithium. The absorption spectra are shown in Figs. 1 and 2. Table 1 gives the comparison of the

TABLE 1. PEAK POSITIONS OF THE ABSORPTION SPECTRA FOR G AND V SPECIES (at room temp)

	G	V
Reduction by K	599, 626 mμ	545, 580 mμ
Reduction by Na	590, 619	545, 570

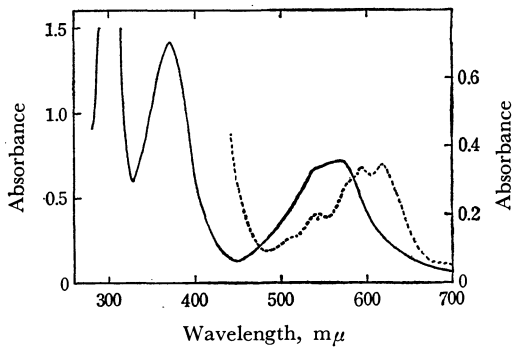

Fig. 1. Absorption spectra of G and V species (see text) (in contact with metallic sodium).
Dotted line, G species (right ordinate)
Solid line, V species (left ordinate)

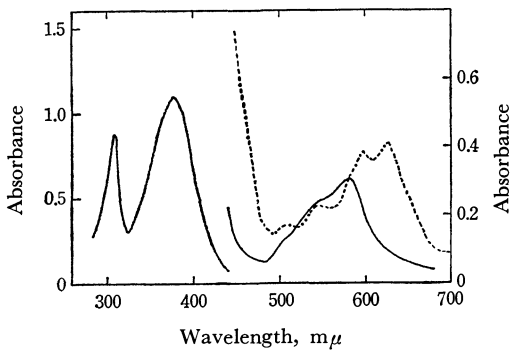

Fig. 2. Absorption spectra of G and V species (see text) (in contact with metallic potassium).
Dotted line, G species (right ordinate)
Solid line, V species (left ordinate)

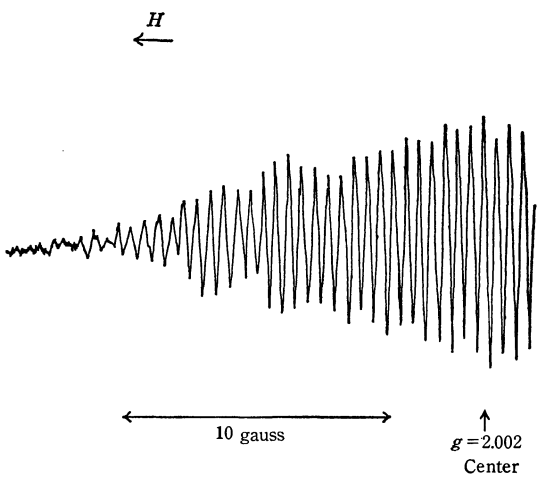

Fig. 3. ESR spectrum of acridine anion radical from acridine with metallic sodium.

5) K. Kuwata, T. Ogawa and K. Hirota, This Bulletin, **34**, 291 (1961).
6) G. A. Russel, E. G. Janzen and E. T. Strom, *J. Am. Chem. Soc.*, **84**, 4155 (1962).

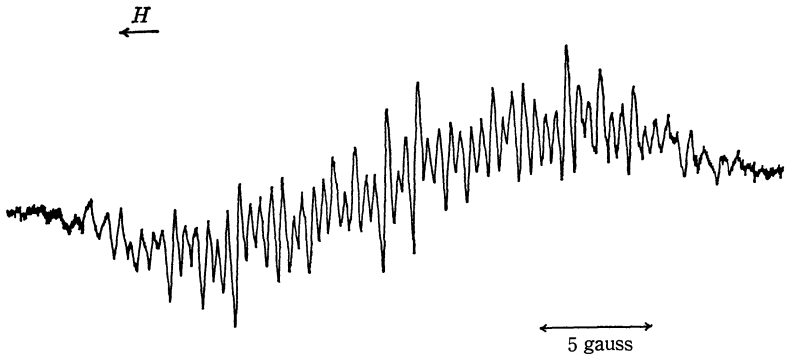

Fig. 4. ESR spectrum of acridine anion radical from acridine with metallic potassium.

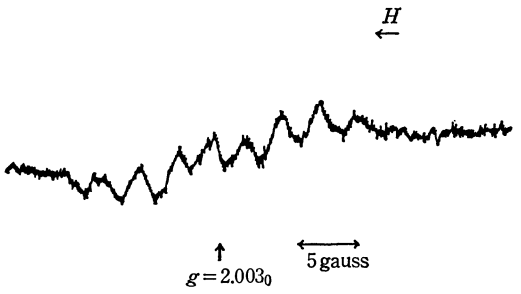

Fig. 5. ESR spectrum of acridine anion radical from acridine with metallic lithium.

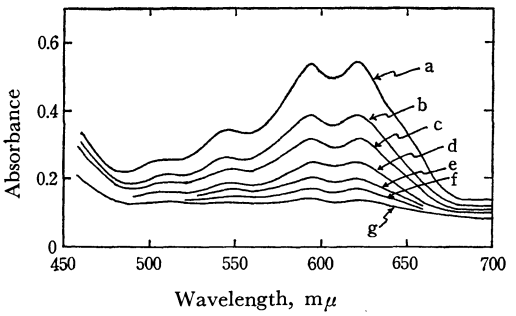

Fig. 6. Temperature change in absorption spectra of G species (produced from acridine with metallic sodium).

a : 20°C e : −24°C
b : 4°C f : −32°C
c : −3°C g : −47°C
d : −11°C

peak positions of G and V for the longest wavelength absorption in the case of sodium and potassium.

It was established that as long as unreacted acridine exists, only G is produced and that the production of V occurs as soon as acridine disappears.

Behavior of Green Species. Species G displays ESR spectra which are shown in Figs. 3—5. Upon addition of a very small quantity of water or ethanol, it transformed entirely to acridan; this was confirmed by UV spectra. G is photochemically stable; any slight change does not occur by 5890 Å illumination. The influence of temperature change on the intensity of ESR (produced by the addition of sodium) was investigated. It increases with the rise of temperature from −42 to ~77°C; at −63°C the signal was scarcely detected. Hfs in the ESR spectra at 77°C is essentially the same as the ones at ordinary temperatures except for fine details. This implies that one radical species is responsible to ESR spectra. At extremely low temperatures, the solution becomes colorless and is accompanied with the appearance of a white precipitate. This precipitate is redissolved by the introduction of air or by warming the solution. Figure 6 shows the temperature change of UV spectra.

As seen from the figure, the intensity at −47°C decreases nearly ten times as that at 20°C without any change in the spectral shape. Thus the intensity change in the absorption spectra runs parallel with that in the ESR signal. The determination of ε for G was performed by measuring the ESR signal and UV spectra at the same temperature and by using the radical concentration evaluated from the former. The value obtained is ε (at 620 mμ) $=6900\pm500$ M^{-1}cm^{-1}.

Behavior of Violet Species. The following observations were made on the samples treated with sodium. ESR signals decrease as G transforms to V and no signal is observed in the solution containing only species V. V is stable both thermally (from room temperature up to +70°C) and photochemically. The introduction of air causes the change V→ G→acridine to occur. From the change of UV spectra observed when the air is introduced to the solution containing only V species, it is concluded that V transforms to acridine at one to one ratio. This enables one to evaluate ε_{570} of V as 4600 ± 300 M^{-1}cm^{-1}. The temperature effect on the absorption spectra is shown in Fig. 7. For the sample treated with potassium, such temperature effect is given as the change with time, after the solution which had been kept in the dry ice bath was put out of the bath. The complicated change in both cases suggest that more than two species or two states may exist in thermal equilibrium. The present result is somewhat similar to the one reported by Smid[7] for fluorene radical anion.

Finally, it may be worthwhile to add that the temperature effect on the absorption spectra of the solution

7) T. E. Hogen-Esch and J. Smid, *J. Am. Chem. Soc.*, **88**, 307 (1966).

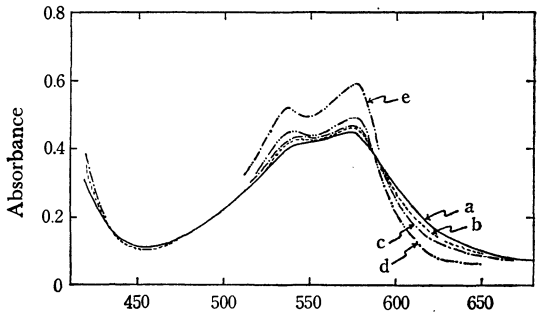

Fig. 7a. Temperature change in absorption spectra of V species (produced from acridine with metallic sodium).
a : 26°C d : −70°C
b : −9°C e : −108°C
c : −33°C

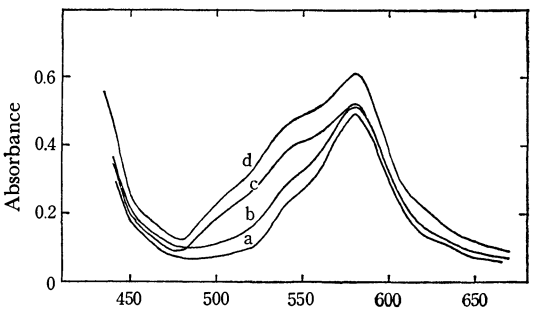

Fig. 7b. Change of the absorption spectra of V species (produced from acridine with metallic potassium) with time, after the solution was put out of the dry ice bath;
a : *ca.* 0—2 min
b : *ca.* 2—4 min
c : *ca.* 4—6 min
d : *ca.* 20 min after

containing both V and G, appears to be mere superposition of that on the solution containing only V or G alone.

Discussion

By the analogy with the general behavior of aromatic compounds in contact with alkali metals, there is scarcely any doubt that G species is a radical anion A^- (or A^-Na^+) produced by the electron transfer from alkali metals to acridine. The finding that the admittance of air transforms G into acridine is thought to negate the formation of diacridyl anion, which is expected to yield diacridan. It is most reasonable to identify V species as dianion A^{2-}, since V species is diamagnetic and is produced only in the existence of excess alkali metals. It is interesting to compare the above behavior with that of pyridine. According to Ward,[2] pyridine, when treated with alkali metals in DMF solutions, changes to a reddish violet substance in a short time but after a long time, becomes a yellow substance, the former being paramagnetic and the latter diamagnetic. In this case, however, the paramagnetic species was identified as dipyridyl anion on the basis of hfs of its ESR spectra. Thus one can say that acridine radical

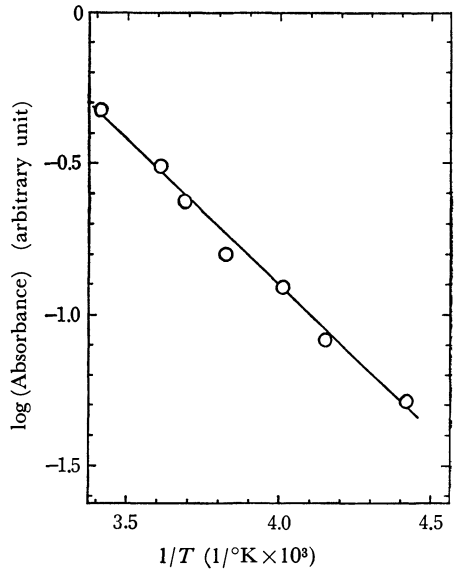

Fig. 8a. log (Absorbance) *vs.* $1/T$ plot of G species. Absorbance, at 619 mμ (ε_{max})

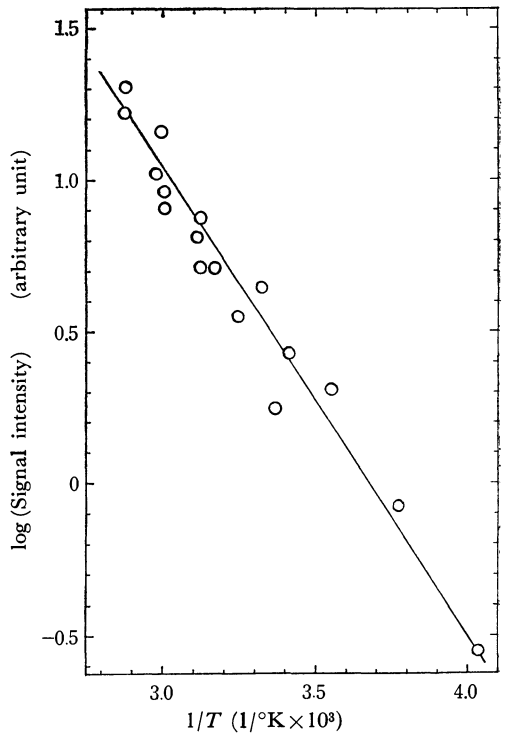

Fig. 8b. log (Signal intensity of ESR) *vs.* $1/T$ plot of G species.

anion is more stable than pyridine radical anion.

The effect of temperature on the intensity of both ESR spectra and of the visible absorption spectra, clearly indicates that the paramagentic G species is in thermal equilibrium with another diamagnetic species (having no absorption spectra in the visible region), the formation of the former being favored by the rise of temperature. It is most plausible to attribute this equilibrium to the following process

$$2A^{-}Ma^{+} \rightleftarrows (A^{-}Na^{+})_2 \qquad (1)$$

or to an association of higher degree. A white precipitate obtained at lower temperatures may be $(A^{-}Na^{+})_2$ or the higher associate. This is consistent with the finding that it is redissolved upon the introduction of air. Figure 8 gives a logarithmic plot of the intensity in the absorption spectra and in the ESR signal (Curie law is taken into consideration) against the reciprocal temperature. The linear relationship holds for the both plots although the slopes are somewhat different. This suggests that the equilibrium constant of (1) is quite large; if this is assumed, the heat of dissociation for the (1) process is estimated to be $\sim$14 and $\sim$9 kcal respectively from ESR and UV data. Perhaps the former value is more reliable.

In conclusion, the chemical processes related with the acridine radical anion in the THF solution (containing sodium, for instance) may be summarized as follows:

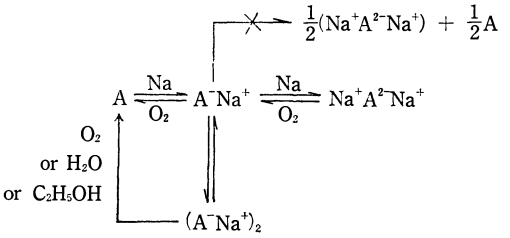

A species represented as $(A^{-}Na^{+})_2$ may alternatively be a higher associate or a mixture of various associates.

Analysis of the HFS is not yet thoroughly successful. Judging from the entire width, the McConnell's Q-value seems to be much larger than 23 gauss. It appears that the unpaired spin densities evaluated on the basis of a simple LCAO method assuming $\alpha_N=\alpha_C+\chi\beta_{CC}$, $\beta_{CN}=\beta_{CC}$, $\chi=$ 0.8 or 0.6 or 0.4, cannot give a satisfactory interpretation. The exact analysis is now being attempted, which will be published in near future.

BULLETIN OF THE CHEMICAL SOCIETY OF JAPAN VOL. 41 799—802 (1968)

Initiation Step of Methane Pyrolysis*[1]

Takayuki YANO and Kenji KURATANI

Institute of Space and Aeronautical Science, The University of Tokyo, Komaba, Meguro-ku, Tokyo

(Received October 16, 1967)

Equimolar mixtures of CH_4 and CD_4 were pyrolyzed at 1560°K by a reflected shock wave. From the isotope distribution of H_2, HD and D_2 which are components of the product in early stage, the initiation step of methane pyrolysis is concluded to be the splitting to a methyl radical and a hydrogen atom.

Recently, the vacuum ultraviolet photolysis[1] and the radiolysis[2] of methane were recognized to begin with the decomposition to a methylene radical and a hydrogen molecule. The reaction mechanism of the methane pyrolysis, especially the initiation step of this reaction, however, has not been settled yet and two hypotheses have been discussed during these thirty years. One of which[3] suggested the same mechanism as proposed in the case of the ultraviolet photolysis and the radiolysis, while the splitting to a methyl radical and a hydrogen atom was assumed by the others.[4]

It is the purpose of this paper to study the thermal

*1 Presented at the 20th Annual Meeting of the Chemical Society of Japan, Tokyo, April, 1967.

1) D. J. Walker and R. A. Back, *J. Chem. Phys.*, **38**, 1527 (1963); P. Ausloos, R. Gordon, Jr., and S. G. Lias, *ibid.*, **40**, 1854 (1964).

2) P. Ausloos and S. G. Lias, *ibid.*, **38**, 2207 (1963); V. Aquilanti, *J. Phys. Chem.*, **69**, 3434 (1965).

3) L. Kassel, *J. Am. Chem. Soc.*, **54**, 3949 (1932); L. Belchetz and F. K. Rideal, *ibid.*, **57**, 1168 (1935); V. Kevorkian, C. E. Heath and M. Boudart, *J. Phys. Chem.*, **64**, 964 (1960).

4) F. O. Rice, M. D. Dooley, *J. Am. Chem. Soc.*, **57**, 2747, (1934); G. B. Skinner and R. A. Ruehrwein, *J. Phys. Chem.*, **63**, 1736 (1959); P. S. Shantarovich and B. V. Pavlov, *Zhur. Fiz. Khim.*, **30**, 811 (1956).

decomposition of the equimolar mixture of methane and tetradeuteromethane around 1560°K using a single pulse shock tube and to decide which of these two aforementioned hypotheses is correct.

Experimental

The shock tube used in this study is similar to a magic hole type developed at Cornell University[5] (the detail of this tube will be described in near future). Mixtures of 6% each of CH_4 and CD_4 in argon were heated by the reflected shock wave to 1560+30°K for dwell times of about 1 msec. The reaction mixture was withdrawn to an evacuated vessel and its composition was determined by the gas chromatographic analysis. Isotope mixtures of hydrogen molecules were separated using an alumina column coated with $MnCl_2$ of 5 m length at 77°K and detected by a cathalometer (He was used as carrier gas.) Hydrocarbons were separated by a 3 m activated charcoal column at 150°C and analyzed by a flame ionization detector. CH_4 and CD_4 were supplied by Takachiho Chemicals Co. and Merck respectively, and used without further purification.

Results and Discussion

It is well known that methane is converted into ethane in the early stage of the reaction and ethane formed is decomposed further into ethylene, acetylene, *etc.* in the later stage. The presence of one mole of ethane in products corresponds to the formation of one mole of hydrogen, and similarly the findings of one mole each of ethylene and acetylene are equivalent to the production of two and three moles of hydrogen respectively. Therefore, it is the proper requirement to suppress the occurence of the secondary reactions such as ethylene and acetylene formations in order to study the initiation step of methane pyrolysis in terms of the isotopic distribution of the produced hydrogens. The another restriction is concerned with the deviation from the ideal behavior of gases behind a reflected shock wave. The use of high dilution with argon is essential to avoid this difficulty, but the limitation by the sensitivity of our analytical apparatus should be also taken into account. From these reasons, the aforementioned experimental conditions about temperature range, dwell time and concentration of reactants were adopted.

In order to confirm the experimental accuracy, yields of reaction products of three experimental runs are compared and mass balances in regard to hydrogen are testified. In Table 1 $\sum H_2$ means sum of observed values of H_2, D_2 and HD, and $\sum(C_2H_6+2C_2H_4+3C_2H_2)$ corresponds also to the total yield of hydrogen expected from the formation of these hydrocarbons. The agreement between these two values is satisfactory and we believe that analytical accuracy of our experiment is sufficient, though the chromatographic separation of the small amount of H_2, HD, and D_2 is rather troublesome, since the tailing of an individual peak interferes the distinct separation between the adjacent peaks.

In Table 2, experimental results on additional runs as well as the above described runs are summarized. The relative yields of HD and D_2 to H_2 are shown in this table along with those of ethylene and acetylene to ethane. As shown in Table 2 there are considerable scatters of experimental values, but the average value of the relative yields of H_2 : HD : D_2 is estimated to be 1 : 1.7 : 0.6. As already pointed out, hydrogen molecules are produced not only by the primary process from methane to ethane but also by the secondary processes from ethane to ethylene and acetylene, and

TABLE 1. MASS BALANCES OF PRODUCTS (VOLUME PER CENT IN PRODUCTS)

Run No.	H_2	D_2	HD	$\sum H_2$	C_2H_6	C_2H_4	C_2H_2	$\sum(C_2H_6+2C_2H_4+3C_2H_2)$
20	0.014	0.026	0.011	0.051	0.015	0.009	0.004	0.045
21	0.017	0.028	0.014	0.060	0.025	0.008	0.005	0.056
22	0.015	0.023	0.012	0.050	0.019	0.007	0.003	0.044

TABLE 2. RELATIVE YIELDS OF PYROLYZED PRODUCTS AT $T_5=1560\pm30$°K AND DWELL TIME FOR 1 msec

Run No.	HD/H_2	D_2/H_2	C_2H_4/C_2H_6	C_2H_2/C_2H_6	$1-R$
16	1.6	0.6	1.11	0.32	0.56
17	1.6	0.5	0.60	0.17	0.65
18	1.7	0.4	0.76	0.21	0.63
19	1.7	0.5	0.63	0.22	0.63
20	1.9	0.8	0.63	0.26	0.62
21	1.6	0.8	0.33	0.19	0.62
22	1.5	0.8	0.38	0.18	0.63

5) J. E. Klepeis, Thesis, Graduate School of Aeronautical Eng., Cornell University (1961); A Lifshitz, S. H. Bauer and E. L. Resler, Jr., *J. Chem. Phys.*, **38**, 2056 (1963).

the contribution of the primary process relative to the overall reaction is represented by the ratio $(1-R)$, where

$$R = [(C_2H_4) + 2(C_2H_2)]/[(C_2H_6) + 2(C_2H_4) + 3(C_2H_2)]. \quad (1)$$

If we assume the elimination of molecular hydrogen in the initiation step, then the following reaction scheme corresponding to the primary process will be formulated,

$$CH_4 \rightarrow CH_2 + H_2$$
$$CH_2 + CH_4 \rightarrow CH_3 + CH_3$$
$$CH_3 + CH_3 \rightarrow C_2H_6$$

That is, from this scheme only H_2 and D_2 are produced. Then, even if we further assume the elimination of atomic hydrogen from any step among the processes from ethane to ethylene and acetylene, the observed high yield of HD cannot be explained, since the contribution of the primary process relative to the overall reaction is rather large and the values of $(1-R)$ exceed 0.6 in all experimental runs.

From this consideration, we conclude qualitatively that the initiation steps of methane pyrolysis are the elimination of atomic hydrogen,

$CH_4 \rightarrow CH_3 + H$ yields of H atom a mol

and

$CD_4 \rightarrow CD_3 + D$ yields of D atom b mol

To explain the observed values of $H_2 : HD : D_2$ semiquantitatively, it is necessary to take into account the isotope effect on the reaction rates. If we assume the relative rate of the first step is equal to $a : b$, the amounts of hydrogen molecules produced from the primary processes will be represented as follows,

$H + CH_4 \rightarrow H_2 + CH_3$ yield of H_2 $a/2$,
$H + CD_4 \rightarrow HD + CD_3$ yield of HD $a/2$,
$D + CH_4 \rightarrow HD + CH_3$ yield of HD $b/2$,
$D + CD_4 \rightarrow D_2 + CD_3$ yield of D_2 $b/2$.

That is, in the primary processes the relative yields of $H_2 : HD : D_2$ are given as

$$H_2 : HD : D_2 = a : a+b : b, \quad (2)$$

and the methyl radicals produced both in the initiation steps and the abstraction reactions will be combined together to form ethanes. The isotopic distributions of the latters are

$$C_2H_6 : CH_3CD_3 : C_2D_6 = (3a+b)^2 : 2(3a+b)(a+3b) : (a+3b)^2. \quad (3)$$

As it is well known,[6] on the way of the secondary processes from ethane to ethylene, a hydrogen atom is removed from the parent molecule by the following mechanism,

$$C_2H_6 \rightarrow CH_3 + CH_3 \quad (R1)$$
$$CH_3 + C_2H_6 \rightarrow CH_4 + C_2H_5 \quad (R2)$$
$$C_2H_5 \rightarrow C_2H_4 + H. \quad (R3)$$

Here we assume tentatively that these reaction steps are independent on the presence of a large amount of methane in order to simplify the algebraic treatment. Therefore, from an ethane molecule a hydrogen atom is removed and an ethylene molecule is produced. The hydrogen atom produced in the step (R3) reacts with a large excess of methane, and it is converted to the molecular hydrogen,

$$H(D) + CH_4(CD_4) \rightarrow (H_2, HD, D_2) + (CH_3, CD_3). \quad (R4)$$

In our experiment, not only ethylene but also acetylene are produced step by step,

$$C_2H_6 \rightarrow C_2H_4 \rightarrow C_2H_2. \quad (R5)$$

As acetylene is formed from ethylene, the quantity of ethylene, which is equivalent to the amount of the hydrogen atom formed in process (R3), must be the sum of the observed values of ethylene and acetylene. Of course, in a process $C_2H_4 \rightarrow C_2H_2$, atomic or molecular hydrogen may be produced. But in our experiment, the yield of acetylene is relatively small compared with those of ethane and ethylene, and the amount of hydrogen formed in the process from ethylene to acetylene is omitted from the following discussions.

If we assume that the isotope effect on the process (R3) is negligible, H and D atoms are formed in proportion to the hydrogen isotopic distribution in ethane molecules. Since the relative yields of the isomeric ethanes are represented by Eq. (3), the distribution of H and D atoms in ethanes is given by

$$H : D = (3a + b)(4a + 4b) : (a + 3b)(4a + 4b) = (3a + b) : (a + 3b). \quad (4)$$

Therefore, the isotopic distributions of the hydrogen molecules produced by the process (R4) will be represented as

$$H_2 : HD : D_2 = (3a+b) : (3a+b)+(a + 3b) : (a+3b) = (3a+b) : (4a+4b) : (a+3b). \quad (5)$$

On the other hand, if we assume the same isotope effect on the process (R3) as that on the splitting of methane to a methyl radical and a hydrogen atom, the amounts of the hydrogen atoms liberated in the process (R3) are given as

$$H : D = a(3a+b) : b(a+3b),$$

and the ratios of hydrogen molecules produced by

6) B. S. Benson, "The Foundations of Chemical Kinetics," McGraw-Hill Co., New York (1960), p. 349.

(R4) process are expressed as

$$H_2 : HD : D_2 = a(3a+b) : a(3a+b)+b(a+3b) : b(a+3b). \quad (6)$$

The observed isotopic distributions of hydrogen molecules should be expressed as the sum of the contributions of the primary and secondary processes. That is, in the former case, where the isotope effect in the secondary process is ignored, the relative yields of hydrogens are given by combining Eqs. (2) and (5),

$$\begin{aligned} H_2 : HD : D_2 &= (1-R)a/[2(a+b)] + R(3a+b)/[8(a+b)] : \\ &\quad (1-R)(a+b)/[2(a+b)] + R4(a+b)/ \\ &\quad [8(a+b)] : \\ &\quad (1-R)b/[2(a+b)] + R(a+3b)/[8(a+b)] \\ &= [4a-R(a-b)]/[8(a+b)] : 1/2 : \\ &\quad [4b-R(b-a)]/[8(a+b)] \end{aligned}$$

and in the latter case, where the same isotope effect in the secondary process as in the primary process is assumed, the ratios are expressed by combining Eqs. (2) and (6),

$$\begin{aligned} H_2 : HD : D_2 &= (1-R)a/[2(a+b)] + Ra(3a+b)/ \\ &\quad [2(3a^2+2ab+3b^2)] : \\ &\quad (1-R)(a+b)/[2(a+b)] + \\ &\quad R(3a^2+2ab+3b^2)/[2(3a^2+2ab+3b^2)] : \\ &\quad (1-R)b/[2(a+b)] + Rb(a+3b)/ \\ &\quad [2(3a^2+2ab+3b^2)] \\ &= (1-R)a/[2(a+b)] + Ra(3a+b)/ \\ &\quad [2(3a^2+2ab+3b^2)] : \\ &\quad 1/2 : \\ &\quad (1-R)b/[2(a+b)] + Rb(a+3b)/ \\ &\quad [2(3a^2+2ab+3b^2)]. \end{aligned}$$

The experimental results shown in Table 2 are interpreted by these equations and the values of $a : b$ are determined as nearly equal to 1 : 0.6—0.7 in both cases. If we assume that the ratio of the isotopic rate constants k_H/k_D of the initiation step is expressed by the zero-point energy difference of the reaction coordinates of this process,

$$a/b = k_H/k_D = \exp[-(h\nu_D - h\nu_H)/2\boldsymbol{k}T]$$

and take the values of $\nu_H = 3000\ cm^{-1}$, $\nu_D = 2200\ cm^{-1}$, the ratio of a/b at 1560°K is calculated as 1/0.69, and agrees with the observed values. However, this calculation is an approximate one, and we are planning to obtain the more accurate ratio taking into account the differences in partition functions. The result will be reported in near future.

BULLETIN OF THE CHEMICAL SOCIETY OF JAPAN VOL. 41 802—809 (1968)

Rectification Effects Using Polyelectrolyte Solutions

Kunitoshi SHIMIZU, Manabu SENŌ and Hiroshi NOZAKI

The Institute of Industrial Science, The University of Tokyo, Azabu Roppongi, Tokyo

(Received October 18, 1967)

The rectifying properties of liquid junctions of polyelectrolyte solutions are examined and discussed. In the case of liquid junctions between aqueous solutions of poly(styrene-sulfonic acid) and poly(2-vinyl-*N*-*n*-butylpyridinium hydroxide), the rectification effects greatly depend on the concentrations of the polyelectrolytes and on the frequencies of the voltages applied, that is, rectification effects can not be found when the concentrations of polyelectrolytes are lower than 0.68×10^{-3} equivalents per liter and when the frequencies of the alternating voltages are higher than 200 cps. The mechanism of rectification can be explained to some extent by a semiconductor analogy. In the case of liquid junctions between poly(styrene-sulfonic acid) and poly(2-vinyl-*N*-*n*-butylpyridinium bromide), the static current *versus* voltage curves have strong hysteresis loops. The rectification effects can be slightly observed when alternating voltages with frequencies lower than 100 cps are applied. In this case, however, the mechanism of rectification can not be explained by the semiconductor analogy.

Reiss[1] and Fuller[2] have pointed out that the electron excess and the electron defficiency in a semiconductor correspond to the proton excess and the proton defficiency in an aqueous solution

1) H. Reiss, *J. Chem. Phys.*, **21**, 1209 (1953).

2) C. S. Fuller, *Rec. Chem. Progr.*, **17**, 75 (1956).

respectively. An *n*-type semiconductor is strongly analogous to an alkaline solution, containing highly mobile hydroxide ions together with corresponding cations so large as to be entirely immobile, while a *p*-type semiconductor is analogous to an acid solution, containing highly mobile protons together with corresponding anions so large as to be entirely immobile.

In view of these analogies, we may make electrolytic junctions in polyelectrolyte solutions corresponding to *p-n* junctions in semiconductors.

As a matter of fact, Lovreček,[3] Läuger,[4] Senō[5] and others[6] found rectification effects using cation-exchange membranes and anion-exchange membranes. In linear polyelectrolyte systems, however, only Lovreček[3] has observed rectifying effects, and he has reported only very simple data.

In the present investigations, electrolytic liquid junctions separating the solutions of a polyacid and a polybase by a milipore filter (a cellulose-acetate membrane) were prepared and their rectifying properties were examined. Further, the rectifying properties of liquid junctions between the salt of a polybase and of a polyacid were examined.

Experimental

Materials. *Poly(styrene-sulfonic Acid) (PVSA).* This product was prepared by a method in the literature[7]; one molecule of this product (molecular weight: 100000) has 420 sulfonic groups.

Poly(2-vinyl-N-n-butylpyridinium Bromide) (NBPB). From 2-vinylpyridine, poly(2-vinyl pyridine) was obtained according to a procedure previously reported.[8] NBPB was synthesized from poly(2-vinyl pyridine) by a method in the literature.[9] The product was analyzed for Br titmetrically[10] and for N by the micro-Dumas method. Found: Br, 21.2%; N, 8.0%. One molecule of NBPB (molecular weight: 15000) has 44 bromide atoms. The conductance of aqueous solutions of this NBPB at 25°C is given in Table 1, where C is the equivalent of bromide per liter and L is the observed specific conductance. The figures in the fourth column would be the equivalent conductance if the effect of the acidity were corrected. The fifth column shows the equivalent conductance, in which the effect of acidity is corrected by R. M. Fuoss' method.[9]

Poly(2-vinyl-N-n-butylpyridinium Hydroxide) (NBOH). An aqueous solution of NBOH was prepared by treating an NBPB aqueous solution with an anion-exchange resin (OH-form).

Apparatus and Procedure for Measurement. Figure 1 shows a block diagram of the apparatus used for the measurement of the currents *versus* the applied voltages.

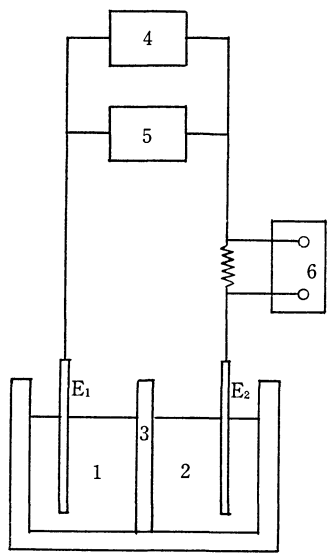

Fig. 1. Apparatus.

1. PVSA aqueous solution, the concentration of which is C_p.
2. NBOH (or NBPB) aqueous solution, the concentration of which is C_h (or C_{Br}).
3. Milipore filter (pore radius, 10 mμ).
4. Voltage source.
5. Voltmeter.
6. Osciloscope or X-Y recorder.

E_1 and E_2: Platinum electrodes.

The aqueous solutions of NBOH (or NBPB) and of PVSA were separated by a thin porous membrane (thickness: 0.1 mm, pore radius: 10 mμ), and a platinum electrode was immersed in each of the solutions. A constant voltage was supplied by a battery, and an alternating voltage was supplied by an ultra-low-frequency oscillator (10^{-3}—10^{3} cps), Toa-Dempa CR-IE, through a pair of electrodes, E_1 and E_2. The electric current was measured with an X-Y recorder or an osciloscope.

Table 1. Conductance of NBPB in water at 25°C

$C\times10^2$	$L\times10^3$	pH	Λ_{uncorr}	Λ
1.36	0.872	3.22	66.8	46.8
0.68	0.503	3.34	81.5	49.7
0.17	0.158	3.80	97.5	54.8
0.085	0.0817	4.09	100.0	57.3
0.021	0.0217	4.72	107.0	66.6

C: equiv/l L: $\mho$/cm

3) B. Lovreček, A. Despic and J. O'M. Bockris, *J. Phys. Chem.*, **63**, 750 (1959).
4) V. P. Läuger, *Ber. Buns. Phys. Chem.*, **68** (No. 6), 534 (1964).
5) M. Senō and T. Yamabe, This Bulletin, **37**, 668 (1964).
6) T. Teorell, *Z. Physik, Chem., Neue Folge*, **15**, 385 (1958).
7) H. H. Roth, *Ind. Eng. Chem.*, **49**, 1820 (1957).
8) A. Katchalsky, K. Rosenheck and B. Altmann, *J. Polymer Sci.*, **23**, 955 (1957).
9) R. M. Fuoss and U. P. Strauss, *ibid.*, **3**, 246 (1948).
10) S. Hirano, "Kogyo Bunseki Kagaku Zittsuken," Kyoritsu Shuppan, Tokyo (1963), p. 229.

Results

NBOH-PVSA Systems. *Static Voltage-Current Characteristics.* The system in which E_2 is the positive electrode and E_1 is the negative electrode was much more resistant to the direct current than when voltages with the reverse polarity were applied. The curves of the currents *versus* the voltages are shown in Figs. 2 and 3.

The data given in Figs. 2 and 3 were read 30 sec after the voltage was applied. The curves in Fig. 2 were measured while the concentration of NBOH (C_h) was maintained at a constant value (1.36×10^{-2} equivalents per liter), while the concentrations of PVSA (C_p) were varied from 1.36×10^{-2} to 0.68×10^{-3} equivalents per liter. The curves in Fig. 3 were measured while C_p was maintained at a constant value (1.36×10^{-2} equivalents per liter) and the C_h values were varied from 1.36×10^{-2} to 0.68×10^{-3} equivalents per liter.

The curves in Figs. 2 and 3 are well reproduced by the following equation:

$$J = J_s(\exp(\alpha eV/kT) - 1) \qquad (1)$$

where J is the electric current, V is the applied voltage, k is the Boltzmann constant, e is the charge of the electron, α is a parameter that shows the effective portion of an applied voltage, and J_s is an experimental parameter. The experimental

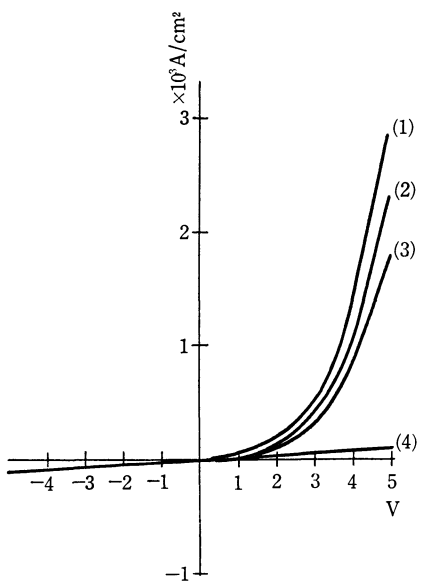

Fig. 2. Current plots *versus* constant voltages in NBOH-PVSA systems.

(1): $C_h=1.36\times10^{-2}$, $C_p=1.36\times10^{-2}$
(2): $C_h=1.36\times10^{-2}$, $C_p=1.02\times10^{-2}$
(3): $C_h=1.36\times10^{-2}$, $C_p=0.68\times10^{-2}$
(4): $C_h=1.36\times10^{-2}$, $C_p=0.068\times10^{-2}$
All values are in equiv/*l*.

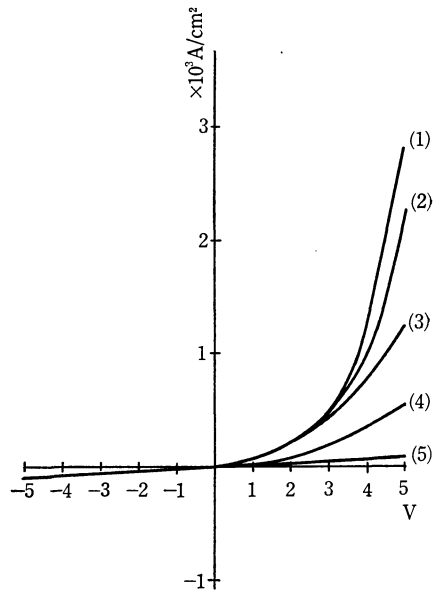

Fig. 3. Current plots *versus* constant voltages in NBOH-PVSA systems.

(1): $C_h=1.36\times10^{-2}$, $C_p=1.36\times10^{-2}$
(2): $C_h=1.02\times10^{-2}$, $C_p=1.36\times10^{-2}$
(3): $C_h=0.68\times10^{-2}$, $C_p=1.36\times10^{-2}$
(4): $C_h=0.272\times10^{-2}$, $C_p=1.36\times10^{-2}$
(5): $C_h=0.068\times10^{-2}$, $C_p=1.36\times10^{-2}$
All values are in equiv/*l*.

TABLE 2. THE EXPERIMENTAL VALUES OF J_s AND α IN NBOH-PVSA SYSTEMS

$C_h\times10^2$	$C_p\times10^2$	$J_s\times10^5$	$\alpha\times10^2$
1.36	1.36	2.65	2.20
1.36	1.02	3.76	2.00
1.36	0.68	4.90	1.70
1.02	1.36	3.76	1.95
0.68	1.36	5.73	1.05
0.272	1.36	8.63	0.97

C_h, C_p: equiv/*l* J_s: Coulomb/cm² sec

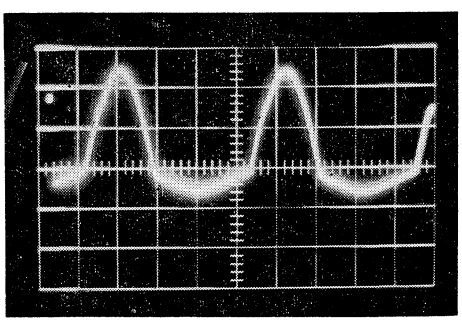

Fig. 4. Rectification of alternating sine-wave current in NBOH-PVSA systems.
$C_h=C_p=1.36\times10^{-2}$ equiv/*l*
Frequency : 0.1 cps

parameters, J_s and α, can be directly decided from the curves in Figs. 2 and 3; they are shown in Table 2.

Alternating Voltage-Current Characteristics. The rectification phenomena are effective when alternating voltages of ultra low frequencies are applied to the systems. The rectification ratio becomes poorer with an increase in the frequency. An example is shown in Fig. 4. The dependency of the rectification ratio on frequencies is illustrated in Fig. 5.

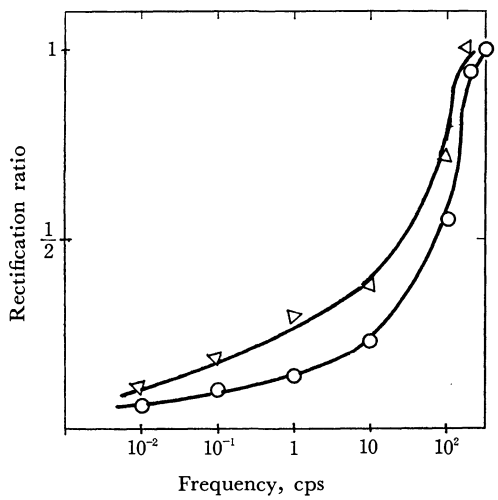

Fig. 5. Dependence of rectification ratio on frequencies in NBOH-PVSA systems. (Rectification ratio stands for the current ratio of the backword against the forward direction.)

○: $C_h=C_p=1.36\times10^{-2}$ equiv/l
△: $C_h=C_p=0.68\times10^{-2}$ equiv/l

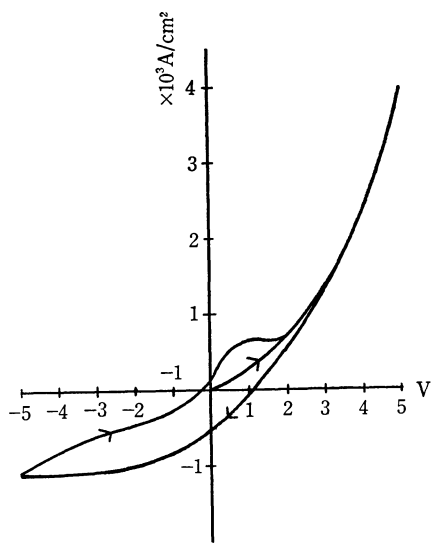

Fig. 6. Current plots *versus* constant voltages in NBPB-PVSA systems.
$C_{Br}=C_p=1.36\times10^{-2}$ equiv/l

From Fig. 4 we can see that the backward current is not very small. As is shown in Fig. 5, when frequencies are higher than 200 cps, the rectification ratio becomes unity, whatever concentrations of NBOH and PVSA are employed.

NBPB-PVSA Systems. *Static Voltage-Current Characteristics.* The static voltage-current characteristics of the NBPB-PVSA systems are similar to those of the NBOH-PVSA systems, but when the voltage was applied in an inverse direction, the voltage-current curve shows a remarkable hysteresis loops. A typical voltage-current curve is shown in Fig. 6.

The data given in Fig. 6 were read 30 sec after the voltages were applied. Figure 6 was obtained when we started from the application of a forward-bias voltage.

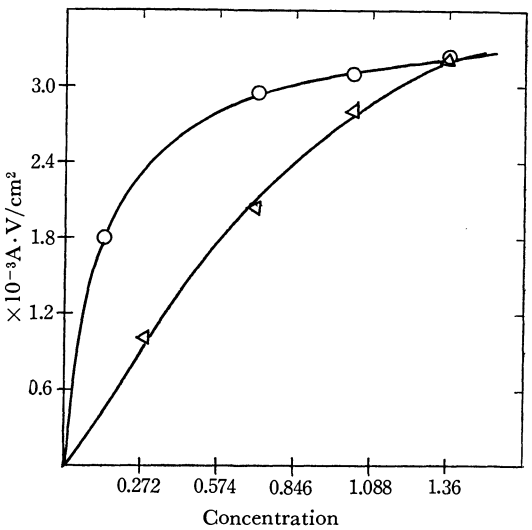

Fig. 7. Dependence of the areas of hysteresis loops on the concentrations of polyelectrolytes.

○: C_{Br} is maintained at the constant value (1.36×10^{-2} equiv/l) and C_p is varied.
△: C_{Br} and C_p are varied under the condition of $C_{Br}=C_p$.

TABLE 3. THE EXPERIMENTAL VALUES OF J_s AND α IN NBPB-PVSA SYSTEMS

$C_{Br}\times10^2$	$C_p\times10^2$	$J_s\times10^4$	$\alpha\times10^2$
1.36	1.36	2.40	1.34
1.36	1.02	2.25	1.23
1.36	0.68	3.70	1.10
1.36	0.136	3.30	0.84
1.02	1.36	2.70	1.25
0.68	1.36	2.30	1.10
0.272	1.36	4.70	1.07
0.136	1.36	3.30	0.68
1.02	1.02	2.50	1.18
0.68	0.68	3.15	0.93
0.272	0.272	7.00	0.34

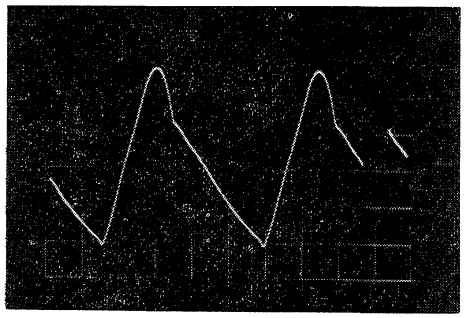

Fig. 8. Rectification of alternating sine-wave current in NBPB-PVSA systems.
$C_{Br}=C_p=1.36\times10^{-2}$ equiv/l
Frequency: 0.1 cps

The areas of the loops decrease with a decrease in the concentrations of NBPB and PVSA. The dependency of the areas of loops on the concentrations of NBPB and PVSA is shown in Fig. 7.

The experimental values of J_s and α are shown in Table 3.

Alternating Voltage-Current Characteristics. Slight rectification effects were observed when frequencies lower than 100 cps were applied. An example is shown in Fig. 8. The rectification characteristics were not reproducible.

Theoretical

Theoretical considerations of the electrolytic rectification in double-membrane systems have been made by several authors. Katchalsky,[11] Ohki[12] and Läuger[4] developed the theory from the point of view of membrane phenomena. Senō[5] and Oshida[13] treated it as a semiconductor analogy. We also consider the electrolyte-membrane junction as a *p-n* junction in semiconductors.

NBOH-PVSA Systems. The potential profile of protons in the transient region is shown in Fig. 9.

The electrolytic current of the protons is given by the so-called Nernst-Planck equation:

$$J_p = e\mu_p C_p \mathrm{d}\varphi/\mathrm{d}x + eD_p \mathrm{d}C_p/\mathrm{d}x \qquad (2)$$

where μ_p: the mobility of the protons, C_p: the concentration of the protons, D_p: the diffusion coefficient of the protons, and φ: the electrical potential. In the absence of a bias voltage, the electric current equals zero. Then the solution of the above equation is as follows:

$$C_p(x) = C_{p,0}\,\mathrm{epx}(-e\varphi/kT) \qquad (3)$$

where $C_{p,0}$ is the concentration of the proton at $\varphi=0$.

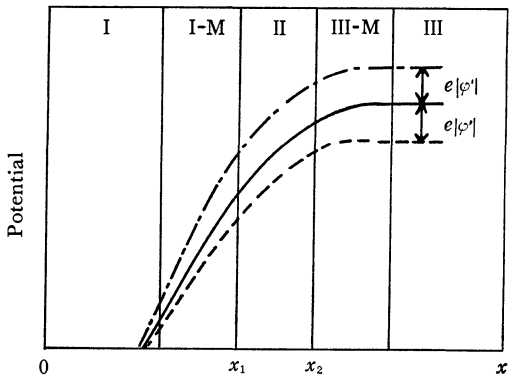

Fig. 9. Potential curve for protons.
I: PVSA aqueous solution. II: Membrane. III: NBOH aqueous solution. I-M, III-M: transition region. Steady line: no applied voltage. Dotted line: forward bias voltage. Chain line: inverse bias voltage.

When a forward voltage is applied, the potential barrier in the transient region becomes lower, as is shown by the dotted line in Fig. 9. As a result, the diffusional current (the second term of Eq. (2)) surpasses the driving current (the first term of Eq. (2)) and protons diffuse from the membrane region into the III-M region. Then the concentration of protons in the III-M region becomes:

$$C_p = C_{p,3} + \Delta C_p \qquad (4)$$

where the subscript 3 refers to the NBOH region.

As soon as the protons enter into the III-M region, the excess protons disappear as a result of the formation of water molecules with hydroxide ions.

The rate of this coupling reaction, R, is:

$$R(x) = \overleftarrow{r}C_pC_{h,3} = \overleftarrow{r}C_{p,3}C_{h,3} + \overleftarrow{r}C_{h,3}\Delta C_p(x)$$
$$= g + \overleftarrow{r}C_{h,3}\Delta C_p(x) \qquad (5)$$

where C_h is the concentration of hydroxide ions, $g=\overleftarrow{r}C_{p,3}C_{h,3}$ is the exchange velocity in the dissociation equilibrium of water, and $\overleftarrow{r}$ is the rate constant of the coupling reaction of protons and hydroxide ions. Under such circumstances, the diffusional flow of protons is expressed by Fick's second law:

$$\partial C_p/\partial t = D_p\partial^2 C_p/\partial x^2 \qquad (6)$$

The change of C_p in the III-M region is as follows:

$$\partial C_p/\partial t = R(x) - g \qquad (7)$$

Then, from Eq. (6) and Eq. (7), we get the following equation:

$$D_p\partial^2 C_p/\partial x^2 = R(x) - g \qquad (8)$$

If we accept $x=\infty$; $C_p=C_{p,3}$ as the boundary condition, then the solution of Eq. (8) becomes as follows:

11) A. Katchalsky and O. Kedem, *Biophys. J.*, **2**, 53 (1962).
12) S. Ohki, *J. Phys. Soc. Japan*, **20**, 1674 (1965).
13) I. Oshida, "Ekitai no Denki Bussei," Maki Shotten, Tokyo (1964), p. 317.

$$C_p(x) = C_{p,3} + C'\exp(-(x-x_2)/L_p) \quad (9)$$

where $L_p=\sqrt{D_p/\overleftarrow{r}C_{h,3}}$ is the mean distance which protons proceed in the III-M region untill their disappearance and where C' is the integral constant. Therefore, the current carried by the protons is given by:

$$J_p(x_2) = -eD_p(\mathrm{d}C_p/\mathrm{d}x)_{x_2} = eD_p(C_p(x_2)-C_{p,3}) \quad (10)$$

From Boltzmann's distribution law (we suppose that the concentration distribution of protons obeys Boltzmann's law just as in Eq. (3), even if the electric current is not equal to zero.*1), we get Eq. (11).

$$C_p(x_2) = C_{p,3}\exp(e\varphi'/kT) \quad (11)$$

These relations lead to the following expression:

$$J_p(x) = (eD_pC_{p,3}/L_p)\{\exp(e\varphi'/kT)-1\} = (eD_pC_{p,3}/L_p)\{\exp(\alpha eV/kT)-1\} \quad (12)$$

where α is a parameter which shows the effective portion of applied voltage,

$$\varphi' = \alpha V \quad (13)$$

Exactly the same procedure is used for hydroxide ions. Therefore, the total current is expressed by:

$$J = e(D_pC_{p,3}/L_p + D_hC_{h,1}/L_h)\{\exp(\alpha eV/kT)-1\} \quad (14)$$

where the subscript h refers to hydroxide ions, the subscript p refers to protons, and the subscript 1 refers to the PVSA region.

When a reverse bias voltage is applied, the density of protons at $x=x_2$ decreases by a ratio of $\exp(-e\alpha|V|/kT)$. As a result, protons diffuse out from the region III. However, this current is small and soon attains saturation because of the low density of protons in this region.

NBPB-PVSA Systems. Here also we adopt the above procedure, in which the role of hydroxide ions is to be displaced by bromide ions. Then the relation of the electric current *versus* the voltage is expressed by:

$$J = e(D_pC_{p,3}/L_p + D_{Br}C_{Br}/L_{Br})\{\exp(\alpha eV/kT)-1\} \quad (16)$$

where the subscript Br represents bromide ions.

Discussion

NBOH-PVSA Systems. Currents *versus* voltages curves are expressed by Eq. (14). Comparing Eq. (1) and Eq. (14), we get the following relation:

$$J_s = e(D_pC_{p,3}/L_p + D_hC_{h,1}/L_h) \quad (17)$$

Considering the dissociation equilibrium of water, we get the following equation:

$$C_{p,1}C_{h,1} = C_{p,3}C_{h,3} = K_w \quad (18)$$

where K_w is the ionic product of water.

Then Eq. (17) and Eq. (18) lead to:

$$J_s = eK_w\sqrt{\overleftarrow{r}}\ (\sqrt{D_h/C_{p,1}} + \sqrt{D_pC_{h,3}}) \quad (19)$$

From Eq. (19) we can calculate the values of J_s. Then the calculated values of $J_s/(J_s)_{1,1}$, where $(J_s)_{1,1}$ is the value of J_s at $C_{p,1}=C_{h,3}=1.36\times10^{-2}$ equivalents per liter, and the experimental values of $J_s/(J_s)_{1,1}$ are compared in Table 4.

Table 4. Comparison of $\{J_s/(J_s)_{1,1}\}_{calc}$ with $\{J_s/(J_s)_{1,1}\}_{exp}$ in NBOH-PVSA systems

$C_h\times10^2$	$C_p\times10^2$	$\{J_s/(J_s)_{1,1}\}_{calc}$	$\{J_s/(J_s)_{1,1}\}_{exp}$
1.36	1.36	1.00	1.00
1.36	1.02	1.07	1.35
1.36	0.68	1.18	1.85
1.02	1.36	1.09	1.42
0.68	1.36	1.23	1.54
0.272	1.36	1.68	3.26

We can see from Table 4 that the calculated values show characteristics similar to the experimental values, although no quantitative coincidence is found.

When a backward-bias voltage is applied, the electric current is independent of the concentrations of NBOH and PVSA (as is clear from Figs. 2 and 3). On the other hand, Eq. (14) shows that it must depend on the concentrations of NBOH and PVSA. Therefore, when a backward-bias voltage is applied, the diffusional mechanism can not be adopted as the conduction mechanism.

Therefore, it may be supposed that, while a backward-bias voltage is being applied, the electric currents are controlled not by the rate of diffusion, but by the rate of the dissociation of water in the transient region.

$$H_2O \underset{\overleftarrow{r}}{\overset{\overrightarrow{r}}{\rightleftharpoons}} H^+ + OH^-$$

*1 When the electric current is not equal to zero, we get the following solution from Eq. (2):

$$C_p(x) = \exp\left(-e\int_0^x \mathrm{d}\varphi\right)\left\{\int_0^x (-J/eD_p) \times \exp\left(e/kT\int_0^{x'}(\partial\varphi/\partial x'')\mathrm{d}x''\right)\mathrm{d}x' + C_{p,1}\right\} \quad (15)$$

Then we must use Eq. (15) as the concentration distribution function. However, when a bias voltage is not applied, the potential difference in the transient region, $\Delta\varphi=(kT/e)\times\ln(C_{p,1}/C_{p,3})$, is about 0.6 V at $C_{p,1}=C_{h,3}=1.36\times10^{-2}$ equivalents per liter, and when a bias voltage ($V\leq5$ V) is applied, the effective portion of the applied voltage in the transient region is found from Table 2 to be of the order of 10^{-2}. Then the potential difference does change not so much that we must not adopt Boltzmann's law instead of Eq. (15) as the concentration distribution function.

where $\vec{r}$ and $\overleftarrow{r}$ are the rate constants in each direction. In the absence of a bias voltage, the rate of dissociation equals that of the recombination reaction:

$$\vec{v} = \vec{r}_0[H_2O] = \overleftarrow{v} = \overleftarrow{r}_0[H^+][OH^-] = g \quad (20)$$

where g is the exchange velocity, and $\vec{r}_0$ and $\overleftarrow{r}_0$ are the rate constants in each direction in the absence of a bias voltage. In the presence of a bias voltage $(-V)$, the potential of the reactants (H_2O) increases by δG_1^*, and that of the products ($H^+ + OH^-$) decreases by δG_2^*, while the potential at the transition state remains constant (ΔG^*), then

$$\delta G_1^* + \delta G_2^* = \boldsymbol{N}e V \quad (21)$$

where $\boldsymbol{N}$ is the Avogadro number.

The rates of the reactions in the forward and backward directions becomes as follows:

$$\vec{v} = \vec{r}[H_2O] = \boldsymbol{kT}/\boldsymbol{h}\exp\{-(\Delta G^* - \delta G_1^*)/\boldsymbol{RT}\}[H_2O] = g\exp(\delta G_1^*/\boldsymbol{RT}) \quad (22)$$

$$\overleftarrow{v} = \overleftarrow{r}[H^+][OH^-] = \boldsymbol{kT}/\boldsymbol{h}\exp\{-(\Delta G^* + \delta G_2^*)/\boldsymbol{RT}\}[H^+][OH^-] = \overleftarrow{r}_0[H^+][OH^-]\exp(-\delta G_2^*/\boldsymbol{RT}) \quad (23)$$

The H^+ and OH^- produced by the electric field are quickly caused to migrate by the electric field. Therefore, the concentrations of H^+ and OH^- would not be influenced by the electric field.

Then the total rate of the reaction is:

$$v = \vec{v} - \overleftarrow{v} = g[\exp(\delta G_1^*/\boldsymbol{RT}) - \exp(-\delta G_2^*/\boldsymbol{RT})] = g[\exp(\beta e V/\boldsymbol{kT}) - \exp\{-(1-\beta)eV/\boldsymbol{kT}\}] \quad (24)$$

where β is the so-called transfer coefficient.

$$\delta G_1^* = \boldsymbol{N}\beta e V, \quad \delta G_2^* = \boldsymbol{N}(1-\beta)eV \quad (25)$$

Therefore, the electric current is as follows:

$$J = eg[\exp(\beta eV/\boldsymbol{kT}) - \exp\{-(1-\beta)eV/\boldsymbol{kT}\}] \quad (26)$$

The J derived from Eq. (26) does not depend on the concentrations of NBOH and PVSA.

Therefore, it can be considered that when a forward-bias voltage is applied, the current *versus* voltage curves are decided by Eq. (14), while when a backward-bias voltage is applied, the current *versus* voltage curves are decided by Eq. (26).

The dynamic characteristics are shown in Fig. 5. From Fig. 5 we can see that the rectification effect becomes poorer as the frequencies become higher. The primary cause is probably the contribution of the capacitance of the systems.[5] The contribution of the relaxation effect of the ionic atmosphere can be neglected, because the Wien effect and the Falkenhagen effect will appear at the frequencies higher than 10^7 cps.[14]

NBPB-PVSA Systems. Just as in the NBOH-PVSA systems we can get the following equation instead of Eq. (19):

$$J_s = eK\sqrt{r'}(\sqrt{D_{Br}/C_{p,1}} + \sqrt{D_p/C_{Br}}) \quad (27)$$

where $K = K_{HBr}[HBr]$, where K_{HBr} is the dissociation constant of HBr, and where r' is the rate constant of the dissociation equilibrium of HBr. In Table 5 the values of $J_s/(J_s)_{1,1}$ calculated using Eq. (27) are compared with the experimental values.

TABLE 5. COMPARISON OF $\{J_s/(J_s)_{1,1}\}_{calc}$ WITH $\{J_s/(J_s)_{1,1}\}_{exp}$ IN NBPB-PVSA SYSTEMS

$C_{Br}\times 10^2$	$C_p\times 10^2$	$\{J_s/(J_s)_{1,1}\}_{calc}$	$\{J_s/(J_s)_{1,1}\}_{exp}$
1.36	1.36	1.00	1.00
1.36	1.02	1.05	0.98
1.36	0.68	1.13	1.61
1.36	0.136	1.69	1.43
1.02	1.36	1.11	1.17
0.68	1.36	1.27	1.00
0.272	1.36	1.82	2.05
0.136	1.36	2.47	1.43
1.02	1.02	1.16	1.09
0.68	0.68	1.40	1.35
0.272	0.272	1.88	3.05

From Table 5 it is clear not only that the values of $[J_s/(J_s)_{1,1}]_{calc}$ do not agree quantitatively with those of $[J_s/(J_s)_{1,1}]_{exp}$, but also that the qualitative tendency of the calculated values does not agree with that of the experimental values.

This disagreement and the hysteresis of the current *versus* voltage curves (Fig. 6) may be caused by the high degrees of the dissociation of hydrogen bromide and by the acidity of NBPB.

Another experiment was then carried out. At first a backward-bias voltage $(-V)$ was applied for 60 sec (while a backward-bias voltage is being applied, only the dissociation reaction of water occurs in the membrane region); the current after 60 sec was denoted I_{60}. Then suddenly we applied the forward-bias voltage (V) for 30 sec, after which we again applied $-V$ until the current became equal to I_{60} (in the transient region, at first the HBr accumulated by the forward current would begin to flow out). We then again applied the forward-bias voltage (V) for 60 sec, followed by the backward-bias voltage until the current equaled to

14) H. S. Harned and B. B. Owen, "The Physical Chemistry of Electrolytic Solutions," Reinhold Pub. Corp., New York (1950), p. 211.

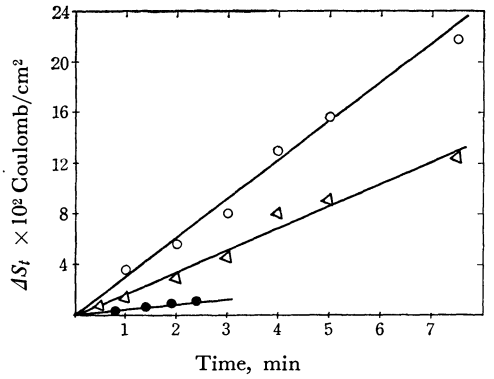

Fig. 10. The change of the backward electric quantities by the forward electric quantities. $C_{Br}=C_p=1.36\times10^{-2}$ equiv/l

I_{60}. Then we applied the forward-bias voltage for 120 sec, and so on.

In Fig. 10 the $\Delta S_t(=S_t-S_0)$-t curves are shown, where S_t are the electric quantities carried by the backward currents, which flowed after the forward-bias voltage was applied for t sec, until the currents became equal to I_{60}. S_0 is the electric quantities which flowed while we first applied the backward voltage. ΔS_t indicates the extra electric quantities caused by applying the forward voltage and corresponds to the quantities of HBr accumulated in the transient region.

Figure 10 shows that the relation between ΔS_t and t is linear. This means that hysteresis is caused by the HBr accumulated in the membrane region.

While a forward-bias voltage is applied, HBr is accumulated in the transient region. When a backward-bias voltage is applied thereafter, the electric current is at first carried by H^+ and Br^-, and then, when the accumulated HBr has disappeared, the H_2O may begin to dissociate into H^+ and OH^-. Thus, the greater the quantity of HBr in the transient region, the larger the areas of the hysteresis loops.

BULLETIN OF THE CHEMICAL SOCIETY OF JAPAN VOL. 41 809—813 (1968)

Low Frequency Bands and Barrier to Internal Rotation in Pentafluoroethane

Susumu KINUMAKI and Muneteru KOZUKA

Chemical Research Institute of Non-Aqueous Solutions, Tohoku University, Sendai

(Received October 18, 1967)

The infrared absorption spectra of gaseous and liquid CF_3CHF_2 were examined in the region from 500 to 60 cm^{-1}. The Raman spectrum of the liquid at room temperature was also photographed. In the gas-phase spectrum, bands were observed at 414, 363, 306, 246, 216 and 82 cm^{-1}. The contour of the medium-intensity band at 82 cm^{-1} was consistent with that to be expected for torsional oscillation. This frequency would correspond to a triple cosine barrier of 4.4 kcal/mol.

Although infrared and Raman spectra of CF_3CHF_2 have already been studied by Nielsen, Moran and Moran[1] in 1954, the detection and assignment of low frequency bands remain incomplete.

Of low frequency bands, the torsion band, which is expected to be observed as the lowest fundamental, is especially interesting in connection with the barrier height of the internal rotation of the molecule. Ward and Ward[2] have pointed out that the barrier height of CH_3CHF_2 was lower than either that of CH_3CH_2F or CH_3CF_3 by 0.2—0.3 kcal/mol, and suggested that, in general, an ethane-like molecule containing the CHX_2 (X: halogen) group might have an abnormally low barrier. Recently, Tipton, Britt and Boggs[3] measured the microwave spectrum of CF_3CHF_2, and calculated the torsional frequency 74 cm^{-1}, and the corresponding barrier height 3.51 kcal/mol, on the basis of the relative intensity method. The latter, which was considerably less than either 4.2 kcal/mol for CF_3CH_2F or 4.35 kcal/mol for CF_3CF_3, led us to favor the suggestion of Ward and Ward. Furthermore, Tipton *et al.* mentioned that their calculated torsional frequency 74 cm^{-1}, was in good agreement with the infrared frequency 73.3 cm^{-1},

1) J. R. Nielsen, H. H. Moran and N. B. Moran, *J. Chem. Phys.*, **23**, 329 (1955).

2) C. R. Ward and C. H. Ward, *J. Mol. Spectr.*, **12**, 289 (1964).

3) A. B. Tipton, C. O. Britt and J. E. Boggs, *J. Chem. Phys.*, **46**, 1606 (1967).

observed by Clague and Danti.[4] However, in the present investigation it was found that the center of the torsion band was located at 82 cm^{-1}, which corresponds to a barrier height of 4.4 kcal/mol, while the absorption maximum of the lower wing was located at 74 cm^{-1} (see Fig. 2). Hence, we reinvestigated the barrier height of the molecule, referring to the theory of Scott and Scheraga[5] concerning the origin of the barrier, and the barrier heights of the chlorine-substituted ethanes reported by Allen, Brier and Lane[6] (see Table 3).

Experimental

The sample of pentafluoroethane, bp −48.5°C, was obtained through the courtesy of Dr. R. J. Plunkett, the E. I. du Pont de Nemours and Company. It was purified by vapor-phase chromatography and dried with phosphorus pentoxide.

The infrared absorption spectra of the gas and the liquid at room temperature were obtained in the region from 500 to 60 cm^{-1} with a Hitachi model FIS-I vacuum, grating, double-beam spectrometer. The gas was contained in a long-path cell built especially for this instrument; its path length was variable in increments of 1.2 m up to 6 m. For the liquid-state spectrum, a polyethylene liquid cell was used, whose effective path length was obscure because of infiltration of the sample into the polyethylene. A spectrum of the sample imprisoned in polyethylene was the same as that of the liquid in the frequency region higher than 200 cm^{-1}, at least, in which the KRS-5 cell could also be used. The Raman spectrum of the liquid at room temperature was photographed with a Yuki-Gosei model RL-II spectrograph of linear dispersion 19 Å/mm at 4358 Å.

All the absorption bands observed are summarized in Table 1. Infrared spectra are shown in Fig. 1.

In order to ascertain the purity of the sample and the correctness of the vibration analysis, an infrared spectrum of the gas between 4000 and 400 cm^{-1} was also obtained with a Perkin-Elmer model 125 grating, double-beam spectrometer.

Table 1. Far infrared and Raman spectra of pentafluoroethane
(at room temperature)

Infrared		Raman liquid	Interpretation
Gas	Liquid		
414 m	410 m	413 wd	a'' fundamental
363 m	361 m	362 msh	a' fundamental
306 w	304 m	—	829−523=306 a'
246 s	246 s	250 vw	a' fundamental
216 m	218 m	—	1359−1143=216 a''
82 m	90 m	92 w	a'' fundamental

s : strong, m: medium, w: weak, vw: very weak
wd: weak and diffuse, msh: medium sharp

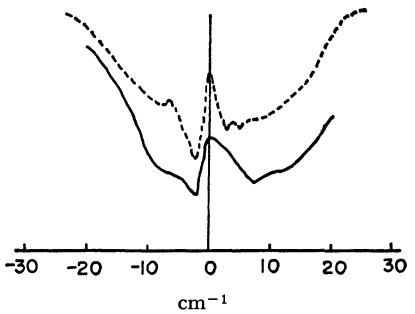

Fig. 2. The contour of the 82 cm^{-1} band.
——: Observed
----: Calculated (with the method of Badger and Zumwalt)

Discussion

Bands in the Region from 500 to 100 cm^{-1}. The CF_3CHF_2 molecule may be assumed to have the symmetry C_s, and the 18 normal vibrations divide themselves into 11 of species a' and 7 of species a''. In the frequency region lower than 500 cm^{-1}, it is expected that there are two fundamentals for each of the species a' and a''. They are the CF_3 symmetric deformation mode, two CF_3 degenerate deformation modes, and the torsional mode.

The molecule is an asymmetric top. The principal moments of inertia, calculated from microwave data by Tipton *et al.*,[3] were 136.92, 208.86 and 251.93 amu.$Å^2$. The axis of the intermediate moment is perpendicular to the symmetry plane. From Badger and Zumwalt's curves,[7] it is found that the a'' fundamentals should have type B contours with a doublet separation of 4.6 cm^{-1}, whereas the a' fundamentals should have contours that are hybrids between type A and C.

In the infrared spectrum of the gas, the medium-intensity band at 414 cm^{-1} has a typical contour of type B and a weak and diffuse counterpart in the Raman spectrum. It is undoubtedly an a'' fundamental. The band at 363 cm^{-1} appears to have PQR structure, and the corresponding Raman band is sharp. It was therefore identified with an a' fundamental. The weak, diffuse and structureless bands at 306 and 216 cm^{-1} had no counterparts in the Raman spectrum. They could be interpreted as difference bands, that is, 829(a')−523(a')= 306 cm^{-1}(a') and 1359(a') − 1143(a'')=216 cm^{-1}(a''), respectively. These higher frequency bands were assigned in the present study independently of the previous work by Nielsen *et al.*,[1]

4) A. D. H. Clague and A. Danti, Proc. Intern., Symp. Mol. Struct. Spectry. (Columbus Ohio, 1965), to be published.
5) R. A. Scott and H. A. Scheraga, *J. Chem. Phys.*, **42**, 2209 (1965).
6) G. Allen, P. N. Brier and G. Lane, *Trans. Faraday Soc.*, **63**, 824 (1967).
7) R. M. Badger and L. R. Zumwalt, *J. Chem. Phys.*, **6**, 711 (1938).

in which the 829 cm^{-1} band was not assigned to any fundamental. Also, Nielsen *et al.* observed a band at 270 cm^{-1}, and assigned it to an a'' fundamental. However, we could detect no absorption band around 270 cm^{-1} in both infrared and Raman spectra. It should be noted that they had no information concerning the purity of their sample.

The population factor for the excited levels of any low frequency fundamental, such as that at 246 cm^{-1}, will be rather large at room temperature. Indeed, the contour of this band has a slightly diffused structure. Its corresponding Raman band at 250 cm^{-1} was weak, but distinct. With somewhat less certainty, it was interpreted as an a' fundamental.

It is well known that in the frequency region higher than 250 cm^{-1}, liquid-phase data is shifted to the lower frequency side of the corresponding vapor-phase data, whereas in the frequency region lower than 250 cm^{-1}, the reverse is the case.[8] Our data also show this feature.

The 82 cm^{-1} Band. This medium-intensity band was only one band that could be detected in the gas-phase infrared spectrum between 120 and 60 cm^{-1}. In the liquid-state data, it was shifted toward a higher frequency of 90 cm^{-1}, and was a comparatively strong band having its Raman counterpart in a weak, diffuse line, at 92 cm^{-1}.

For reference, infrared torsional frequencies for related compounds are collected in Table 2.

The contour of the perpendicular-type torsional fundamental, calculated by the method of Badger and Zumwalt,[7] and shown in Fig. 2, also includes contributions from five "hot bands" which originate from excited vibrational states of the torsion (quantum numbers $v=1, 2, \cdots, 5$). These have a marked effect on the band contour of the torsional frequency, since the population factor $\exp(-h\nu/kT)$ for the excited torsional states is relatively large, and further, the anharmonicity of the cosine potential results in the centers of the hot bands somewhat displaced from that of the $v=0\rightarrow1$. Thus the $v=1\rightarrow2$ band falls 1.2 cm^{-1} below the $v=0\rightarrow1$ band. The rotational structure was expected to be beyond the limit of resolution of the instrument, and no evidence of such structure was found. The observed contour of the 82 cm^{-1} band is consistent with the interpretation of this as the torsional fundamental. Apparently, the absorption minimum of the calculated total band contour resulted in the same wave number as that of the $v=0\rightarrow1$ transition.

For a rough consideration of the intensity of the band, the harmonic oscillator approximation is satisfactory. The dipole moment of the molecule being 1.54 D,[9] it is conjectured that the torsional fundamental will be a band of medium-intensity, or a slightly weaker band than that of CF_3CH_2F (about 2.0 D).

Barrier. Using the method of solving the wave equation for internal rotation,[10,11] the observed torsional frequency 82 cm^{-1}, and the molecular parameters reported by Tipton *et al.*[3] gave a value of 4.4 kcal/mol as the barrier height of the molecule, in which the tables of Blanch and Rhodes[12] were used to obtain the reduced barrier from the difference in the Mathieu's eigenvalues.

The barrier heights for the molecules formed by the successive substitution of fluorine for hydrogen in

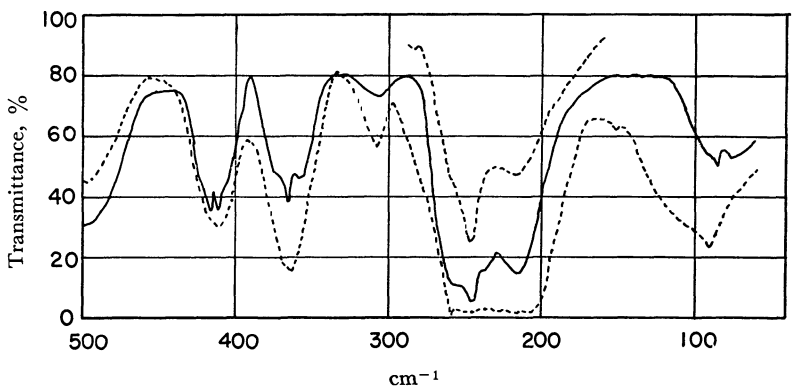

Fig. 1. Far infrared spectra of CF_3CHF_2.
——: Gas, 4.8 m cell, 50 mmHg (room temperature)
----: Liquid, polyethylene cell (room temperature)

8) G. A. Crowder and D. W. Scott, *J. Mol. Spectr.*, **16**, 122 (1965).
9) C. P. Smyth, "Dielectric Behavior and Structure," McGraw-Hill Book Company, Inc., New York (1955).
10) D. R. Herschbach, *J. Chem. Phys.*, **31**, 91 (1959).
11) C. C. Lin and J. D. Swalen, *Rev. Mod. Phys.*, **31**, 341 (1959).
12) G. Blanch and I. Rhodes, *J. Wash. Acad. Sci.*, **45**, 166 (1955).

TABLE 2. BARRIER HEIGHTS OF THE FLUORINE-SUBSTITUTED ETHANES

Molecule	Torsional frequency cm^{-1}	V_3 calc.* kcal/mol	V_3 exptl. kcal/mol	Experimental method
CH_3CH_3		3.29	2.87±0.12[a]	Thermodynamic
CH_3CH_2F	241	3.31	3.31±0.02[b]	Microwave
			3.30[c]	Infrared
CH_3CHF_2	235	3.33	3.18±0.01[b]	Microwave
			3.70±0.60[d]	Microwave
			3.2[e]	Infrared
CH_3CF_3		3.35	3.70±0.45[d]	Microwave
			3.5±1.4[f]	Microwave
CF_3CH_2F	120	3.62	4.2[g]	Infrared
CF_3CHF_2	82	4.02	4.4[h]	Infrared
			3.51±0.10[i]	Microwave
CF_3CF_3		4.35	4.35[j]	Electron diffraction

* The values were calculated with the method of Scott and Scheraga.[5]
a) K. S. Pitzer, *Discussions Faraday Soc.*, **10**, 66 (1951).
b) D. R. Herschbach, *J. Chem. Phys.*, **25**, 358 (1956).
c) S. Kinumaki and M. Kozuka, unpublished work.
d) Ref. 5.
e) S. Kinumaki and S. Onodera, unpublished work.
f) H. Mindew and B. P. Dailey, *Phys. Rev.*, **82**, A338 (1951).
g) A. Danti and J. L. Wood, *J. Chem. Phys.*, **30**, 582 (1959).
h) This investigation.
i) A. B. Tipton, C. O. Britt and J. E. Boggs, *J. Chem. Phys.*, **46**, 1606 (1967).
j) E. L. Pace, *ibid.*, **16**, 74 (1948).

TABLE 3. BARRIER HEIGHTS OF THE CHLORINE-SUBSTITUTED ETHANES*

Molecule	V_3, kcal/mol
CH_3CH_3	(3.0)
CH_3CH_2Cl	3.7
CH_3CHCl_2	3.3—3.7
CH_3CCl_3	(2.8) 5.8**
CH_2ClCCl_3	10.0
$CHCl_2CCl_3$	14.2
CCl_3CCl_3	17.5

* All the data were cited from the paper of Allen *et al.*,[6] except the one marked with double stars.
** This value was derived from the cold-neutron study by J. J. Rush (*J. Chem. Phys.*, **46**, 2285 (1967)).

ethane are given in Table 2. In the third column of the table, theoretical values calculated by the method of Scott and Sheraga[5] are listed. In the fourth one, experimental values are collected, which were obtained by each experimental method written in the fifth column.

In the method of calculating the barrier from the infrared or Raman data, it is not taken into account that the infrared torsional frequency is shifted by coupling with other molecular vibrations. Hence, it was checked that, in CH_3CH_2F and CH_3CHF_2, the barrier heights calculated from infrared data were almost equal to those obtained from microwave data. In these molecules, it is supposed that the torsional vibration is quite pure, because the torsional vibrations in the trans configuration of 1,1-dichloro-[13,14] and 1,1-dibromoethane[15] have the potential energy distribution of 90 and 80%, respectively. Consequently, if it may be supposed that the degree of mixing of molecular vibrations is almost equal in CF_3CH_2F and CF_3CHF_2, the experimental barrier heights of these molecules would be as reliable, at least, as the relative values.

According to Scott and Scheraga,[7] the origin of the internal rotation barrier in ethane-like molecules is mainly attributed to two effects, exchange interactions of the electrons in bonds adjacent to the bond about which internal rotation occurs, and nonbonded or van der Waals interactions. They used a modified Buckingham or "6-exp" potential to calculate the nonbonded interaction, and developed a method for obtaining the constants in the 6-exp potential for any pair of atoms based on experimentally available parameters for inert gases. For the exchange interactions, the theory proposed by Pauling was

13) T. Miyazawa and K. Fukushima, Preprints for the 16th Annual Meeting of the Chemical Society of Japan (April, 1963), 1S14.
14) T. Miyazawa and K. Fukushima, *J. Mol. Spectr.*, **15**, 308 (1965).
15) S. Kanno and T. Miyazawa, Preprints for the 16th Annual Meeting of the Chemical Society of Japan (April, 1964), 1X02.

adopted,[16,17] who showed that, in a molecule of the type $(X_1\ X_2\ X_3)X_4\text{-}X_5(X_6\ X_7\ X_8)$, U_0, which would be the barrier height in the absence of nonbonded interaction, should be a constant for each class of molecules having the same atoms, X_4 and X_5, regardless of the substitutent atoms X_1, X_2, X_3, X_6, X_7 and X_8. For example, there would be a single U_0 for ethane and all the substituted ethanes, another U_0 for disilane and all its substituted derivatives and another U_0 for acetaldehyde and its halogen derivatives, *etc.* From the above theories, it follows that the difference in the barrier heights of the halogenoethane molecules considered in the present study should be due mainly to the difference in the effects of nonbonded interactions. Since the effect of the H···H nonbonded interaction is comparable to that of H···F and H···Cl in magnitude,[5] both the experimental and theoretical data in Tables 2 and 3 show that the barrier in each of CH_3CHF_2 and CH_3CHCl_2 is almost equal to, or, within the experimental error, slightly less than that of CH_3CH_2F and CH_3CH_2Cl. On the other hand, the X···X (X: F or Cl) nonbonded interaction has an effect so much larger than that of H···H, that either CF_3CHF_2 or CCl_3CHCl_2 has a higher barrier than CF_3CH_2F or CCl_3CH_2Cl. Consequently, we were led to the conclusion that the CHX_2 (X: halogen) group had no unique property; that is, the barrier height of an ethane-like molecule containing this group was not abnormally low, although it is inconsistent with the suggestion by Ward and Ward.[2]

The torsional frequency 74 cm^{-1}, calculated by Tipton *et al.*, and corresponding to a barrier of 3.51 kcal/mol, seems to us to be abnormally low. Here, it should be recalled that their values were calculated by a relative intensity method, which was based on the microwave spectrum of only one kind of isotopic species of the molecule, and frequently led to considerable errors.

The authors wish to express their indebtness to Dr. R. J. Plunkett of the E. I. du Pont de Nemours and Company for the gift of the sample. Thanks are also due to Dr. F. Watari of Tohoku University for the measurement of the Raman spectrum.

16) L. Pauling, *Natl. Acad. Sci.* (U. S.), **44**, 211 (1958).
17) L. Pauling, "The Nature of the Chemical Bond," 3rd ed., Cornell University Press, Ithaca, New York (1960), p. 130.

BULLETIN OF THE CHEMICAL SOCIETY OF JAPAN VOL. 41 813—817 (1968)

Thermal Decomposition of Hexamethylene Tetramine

Yoshitomo IWAKAMI and Masao TAKAZONO

Industrial Research Institute of Kanagawa Prefecture, Kanazawa-ku, Yokohama

and Toshikazu TSUCHIYA

Government Chemical Industrial Research Institute, Tokyo, Shibuya-ku, Tokyo

(Received October 28, 1967)

In order to get information about the mechanism of the thermal decomposition of hexamethylene tetramine (hexa), hexa was decomposed thermally in a vacuum vessel, and the composition of the gas thus produced was determined with a mass spectrometer. The main products found were ammonia and a carbon-rich solid residue. The carbon in the carbon-rich residue seems to act as a catalyst for the decomposition.

In a thermal decomposition product of phenol resin, one of the present authors (T. T.) has found an appreciable amount of ammonium compounds.[1] The origin of the compounds was inferred to be the hexamethylene tetramine (hexa) which is added to resol or novolak, the precursory products of the resin, as a hardening reagent of the resin. The purpose of the present study is to confirm the origin of the ammonium compounds mentioned above and to clarify the thermal decomposition mechanism of hexa.

Stranski *et al.*[2] reported on the thermal decomposition of hexa. They investigated the total pressure of the decomposition gas produced in the presence (180—250°C) and in the absence (250—

1) H. Hoshino, N. Wasada and T. Tsuchiya, This Bulletin, **39**, 1809 (1966).

2) I. N. Stranski, G. Klipping, A. F. Bogenschurtz, H. J. Heinrich and H. Maennig, *Advances in Catalysis*, **9**, 409 (1957).

500°C) of the solid phase, and found that in both systems the decomposition has similar characteristics and that the ratio of the final pressure to the initial pressure increases with the temperature. They did not study the compounds produced by the decomposition.

Experimental

The hexa was a G. R.-grade substance obtained from the Tokyo Kasei Kogyo Co., Ltd. The hexa was heated in a vacuum ampoule. Figure 1 shows the hard glass ampoule used for thermal decomposition. About 0.5 g of hexa was into the ampoule, A, through the side tube, B. After the ampoule had been evacuated for about an hour at room temperature with a diffusion pump, it was sealed off at C. The volume of the ampoule was about 13 m*l*. In each of the pyrolysis experiments, the furnace was first preheated to the required temperature. Then the ampoule containing the sample was placed in the furnace up to the dotted line, D (Fig. 1), for an hour. At the end of this period the furnace was quickly evacuated and cooled. After cooling, the ampoule was attached to a mass spectrometer through the common joint, E, for analysis. The experiments were carried out at temperatures of 200, 270, 300 and 400°C.

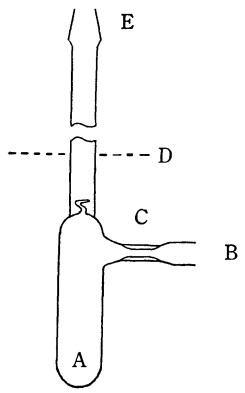

Fig. 1. Ampoule for thermal decomposition.

As the amount of ammonia, which is the main component of the products, as is shown in Table 1, reached a nearly constant value after about an hour of heating at 300°C, we fixed the heating time at one hour in the following experiments.

Besides the gaseous products, the samples treated at temperatures higher than 300°C gave a dark carbonaceous product. The gas products were analyzed with a CEC 21-103C mass spectrometer. The gaseous fraction was cooled in a liquid nitrogen trap. The gaseous and the trapped materials at a certain temperature were analyzed separately. The accuracy of analysis was better than ±5%. The total amount of gas produced was measured with a gas burette and a mercury manometer. The residue obtained in pyrolysis at temperatures higher than 270°C was out-gassed thoroughly, washed with water and alcohol, dried, and weighed. The treated residue was inferred, from its color and for a reason which shall be discussed later, to consist in the main of carbon and shall be referred to as "residual carbon."

Results and Discussion

Figure 2 shows the amount of residual carbon and total gas produced as functions of the decomposition temperature. The figure indicates that hexa begins to decompose at approximately 270°C. At 400°C, the weight percentages of the products are: residual carbon, 60%; gaseous compounds, 33%, and water- or alcohol-soluble material, 7%. Table 1 shows the amount of gaseous products formed per mole of hexa on thermal treatment. Because the *m/e* 28 peak was rather weak and because accurate analysis from *m/e* 14 and *m/e* 12 was impossible, we assumed that the peak is composed of CO^+ and of N_2^+ ions. Each of the gas products at various temperatures (P-T curve) is shown in Fig. 3.

From the data given in Table 1 and Fig. 2, the overall composition of the products at 400°C, other than the gaseous species shown in Table 1, is estimated to be $C_{5.9}H_{6.1}N_{2.1}$. About 12% of

TABLE 1. COMPOSITION OF GASES PRODUCED FROM 1 mol OF HEXAMETHYLENE TETRAMINE AT VARIOUS DECOMPOSITION TEMPERATURES

Component	200°C	270°C	300°C	400°C
Trimethylamine	1.75×10^{-4}	5.43×10^{-3}	1.31×10^{-2}	2.12×10^{-3}
Dimethylamine	—	—	1.80×10^{-2}	9.67×10^{-3}
Methylamine	—	—	1.11×10^{-1}	3.67×10^{-2}
Propionitrile	—	—	—	4.05×10^{-5}
Acetonitrile	4.66×10^{-5}	2.18×10^{-3}	1.64×10^{-3}	5.93×10^{-3}
Ethylene imine	4.51×10^{-5}	2.18×10^{-3}	—	—
Water	3.74×10^{-3}	5.43×10^{-3}	8.18×10^{-3}	9.67×10^{-3}
Ammonia	1.26×10^{-3}	1.056	1.447	1.806
Methane	4.01×10^{-5}	1.53×10^{-2}	3.64×10^{-2}	4.08×10^{-2}
Hydrogen	—	2.19×10^{-3}	3.62×10^{-3}	4.13×10^{-3}
Carbon dioxide	5.23×10^{-4}	2.87×10^{-6}	—	1.35×10^{-5}
Nitrogen and carbon monoxide	2.87×10^{-4}	3.86×10^{-3}	2.71×10^{-3}	6.88×10^{-3}

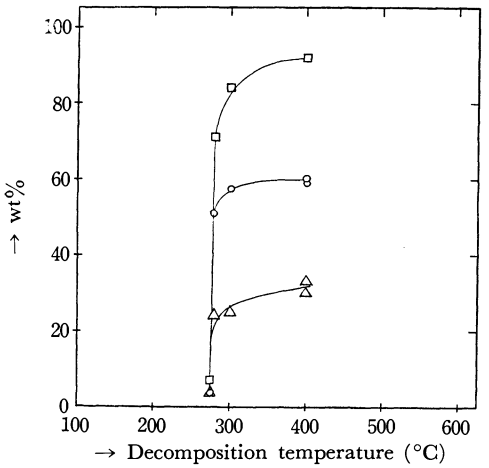

Fig. 2. Decomposition temperature *versus* gas product and residual carbon.
○ Residual carbon, △ Gas products,
□ Summation of residual carbon and gas products.

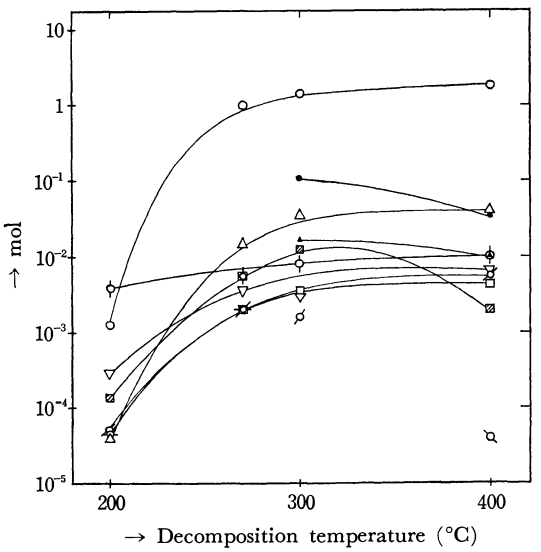

Fig. 3. Amount of gases produced from 1 mol of hexa *versus* decomposition temperature.
○ Ammonia, △ Methane, □ Hydrogen,
● Methylamine, ▲ Dimethylamine,
▨ Trimethylamine, ◇ Ethylene imine,
♂ Acetonitrile, ◇ Water, ▽ Nitrogen and carbon monoxide, ♀ Propionitrile.

the $C_{5.9}H_{6.1}N_{2.1}$ is soluble in water or in alcohol; the remaining 88% was inferred to be residual carbon. The hydrogen atom is considered to be present in the main in the soluble substances. The main component of the residual carbon is, therefore, the carbon atom, though it is shown from the material balance that at least 24% of the weight of the residual carbon is composed of hydrogen and nitrogen atoms. We assume that at least a part of the residual carbon is bulk carbon.

As is seen in Fig. 3, the P-T curves of various products may be divided into two types, *i. e.*, those which show a tendency toward saturation (Type 1; the curves for ammonia, methane and hydrogen), and those which have a maximum (Type 2, the curves for methylamines). We will ignore the behavior of carbon dioxide, because its amount is very small. The compounds of Type 1 are considered to be the final products of the decomposition because they show saturation and because they are stable, low-molecular-weight compounds. The compounds of Type 2 are inferred to be intermediate products which can decompose further when heated to higher temperatures.

As the decomposing temperature increases, the molecular weight of the gaseous products tends to drop (Table 1). This phenomenon suggests the possibility that the compounds produced will decompose further into compounds of lower molecular weights as the temperature rises. The shape of the P-T curves of Type 2 is compatible with this inference. In order to check it, each of the compounds of a higher molecular weight in Table 1, *i. e.*, trimethylamine, dimethylamine, methylamine, propionitrile, acetonitrile, and ethylene imine, was heated individually and the decomposition products were investigated. The three amines were obtained from the Tokyo Kasei Kogyo Co., Ltd., as a 40% aqueous solution, and were dried with caustic potash and distilled under reduced pressure. The two nitriles and the imine were guaranteed reagents obtained from the same company as the amines, and were used without further purification. About 0.1 m*l* of each of these reagents was directly distilled under reduced pressure into the glass ampoule shown in Fig. 1; the ampoule was then treated just as in the case of hexa, and each reagent was decomposed at 300°C for an hour. The compositions of the gaseous compounds produced are shown in Table 2. The 1st column in the table shows the samples treated, and the 1st row shows the decomposition products. Though trimethylamine and propionitrile were not decomposed, the other compounds were more or less decomposed into lighter compounds. The common products from all the reagents were ammonia and methane. Other than these products, acetonitrile and ethylene imine gave hydrogen and nitrogen. In addition to these products, ethylene imine gave hydrogen cyanide and an appreciable amount of methylamine.

From Table 2, it may be seen that some of the compounds, for instance, ethylene imine, produced from hexa under lower decomposition temperatures (Table 1) decompose further, when heated to higher temperatures, into compounds of a lower molecular weight. The behavior of ethylene imine, for instance, which was found at temperatures below 270°C but which could not be detected

TABLE 2. DECOMPOSITION PRODUCTS OF REAGENTS (DECOMPOSED AT 300°C, WITHOUT ACTIVE CARBON)

Component	Reagent					
	Trimethyl-amine	Dimethyl-amine	Methyl-amine	Propio-nitrile	Aceto-nitrile	Ethylene-imine
Trimethylamine	100	—	—	—	—	—
Dimethylamine	—	97.5	—	—	—	—
Methylamine	—	—	89.9	—	—	66.0
Propionitrile	—	—	—	100	—	—
Acetonitrile	—	—	—	—	96.5	—
Ethyleneimine	—	—	—	—	—	6.1
Ammonia	—	1.5	9.2	—	0.8	11.5
Methane	—	1.0	0.9	—	0.2	5.4
Hydrogen	—	—	—	—	1.4	3.2
Nitrogen	—	—	—	—	1.1	5.2
Hydrogen cyanide	—	—	—	—	—	2.6

TABLE 3. DECOMPOSITION PRODUCTS OF REAGENTS (DECOMPOSED AT 300°C, WITH ACTIVE CARBON)

Component	Reagent					
	Trimethyl-amine	Dimethyl-amine	Methyl-amine	Propio-nitrile	Aceto-nitrile	Ethylene-imine
Trimethylamine	1.9	—	—	—	—	—
Propionitrile	—	—	—	65.1	—	—
Acetonitrile	—	—	—	14.6	96.4	—
Ammonia	20.9	20.2	58.9	1.0	—	54.6
Methane	33.8	44.4	23.9	—	—	10.4
Hydrogen	5.5	8.8	1.5	—	—	2.7
Nitrogen	17.9	8.6	7.6	15.0	3.6	8.7
Ethane	20.0	18.0	8.1	—	—	23.7
Ethylene	—	—	—	4.3	—	—

at temperatures higher than 300°C, can be elucidated by the results given in Table 2.

On the other hand, trimethylamine, which tends to decrease from 300°C with an increase in the temperature (Table 1), does not decompose at 300°C (Table 2). However, as has been described, residual carbon was obtained when hexa was treated above 270°C. The primary products produced under a lower heating temperature may decompose further in the presence of residual carbon. In order to estimate the influence of the catalytic action of the residual carbon on the decomposition reaction, the following experiment was carried out.

Instead of residual carbon, a commercial active carbon was used. The active carbon powder obtained from Takeda Yakuhin Kogyo (pure grade "Shirasagi") was heated at 360°C for 2 hr in a vacuum obtained with a diffusion pump. The sample substance (0.05 m*l*) was distilled, under a reduced pressure, into an ampoule which contained 0.1 g of the treated carbon at room temperature; then the system was heated by just the same procedure as has been described before, and the gas produced was analyzed. The temperature of the furnace was 300°C. All of the sample materials studied were found to have been decomposed thermally into ammonia, methane, hydrogen, nitrogen, and ethane. The results are shown in Table 3. We can see that trimethylamine and propionitrile, which were not decomposed at 300°C without active carbon, decompose when treated with active carbon. Ethane and ethylene are detected in the decomposition products when samples are heated with active carbon (Table 3), while the two compounds were not found in the case of a reaction without active carbon (Table 2). We cannot decide from this experiment whether or not the decomposition mechanism differs essentially according as active carbon is present during the decomposition, because the production of ethane or ethylene can depend on the degree of decomposition. The actual experimental conditions of the thermal decomposition of hexa are considered to be intermediate between the two extreme conditions, under which the results of Table 2 and Table 3 have been obtained.

Figure 4 shows the potential pathways of the thermal decomposition of hexa deduced from Table 2 and Table 3. The actual pathways of

the production of lighter substances, such as nitrogen, methane, ammonia, and hydrogen, produced at higher temperatures may not necessarily follow the course suggested. They can be produced, for instance, directly from hexa. However, at least a part of these lighter compounds can legitimately be considered to be produced *via* intermediate products, such as trimethylamine and dimethylamine, because all these compounds, except for ethylene imine, are contained in the decomposition product of hexa at higher temperatures and can be shown to decompose into the lighter substances at these temperatures.

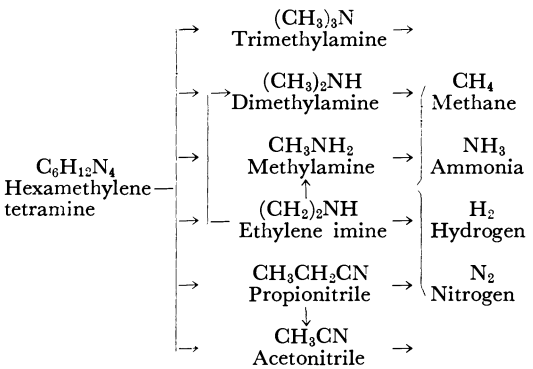

Fig. 4. Potential pathway of thermal decomposition of hexa.

We cannot expect to obtain direct information about the mechanism of the decomposition reaction of hexa itself from the results of the present experiment, because the primary thermal decomposition products of hexa react further with each other under the present experimental conditions and the information we get is the overall result of these primary and secondary reactions.

Based on these experimental results, however, the following possible profile of the reactions can be inferred. When heated to 200°C, a part of the hexa is decomposed and small amounts of ammonia, trimethylamine, acetonitrile, ethylene imine and methane are produced. The amounts of the last three substances are just the same. This suggests that their formations are closely related to each other. At 270°C, the amount of ammonia increases markedly, and hydrogen comes out for the first time. The carbon-rich solid phase is produced, it acts more or less as a catalyst for the following reactions, again promoting the production of the solid phase itself. At 300°C, the P-T curves for ammonia and methane are nearly saturated, monomethylamine and dimethylamine appear for the first time, ethylene imine disappears completely, and the trimethylamine curve reaches its maximum. The appearance of methylamine and dimethylamine and the disappearance of ethylene imine seem to have some interrelation. Ethylene imine gives methylamine, as is shown in Table 2, and the reaction of ethylene imine with hydrogen, which is detected at this temperature, as is shown in Fig. 3, would probably give dimethylamine at this stage of the reaction. Between 300 and 400°C, methylamine, dimethylamine and trimethylamine decrease, while ammonia and methane increase slightly. The increments of the latter compounds are approximately equal to the amounts of those substances expected, from Table 3, to be produced from the decrements of the former compounds.

The amount of water detected is about 0.1% of the weight of the charged hexa. Much should not be inferred from this result, because water molecule is known to be adsorbed on various parts of the gas-handling manifold and of the mass spectrometer. However, from the amount detected and its behavior, the water appears to originate mainly from that adsorbed on the hexa. The small *m/e* 28 peak is considered to be due mainly to nitrogen, as there is no source of carbon monoxide.

From the present results, the hexa, dipped in phenol resin, may be considered to be the origin of the ammonium compounds found in the thermal decomposition product of the resin.

BULLETIN OF THE CHEMICAL SOCIETY OF JAPAN VOL. 41 818—823 (1968)

Structure and Reactivity of α, β-Unsaturated Ethers. IV.[1] The Effects of Ring Substituents on the Acid-Catalyzed Hydrolysis Rate of Phenyl Vinyl Ether

Takayuki FUENO

Faculty of Engineering Science, Osaka University, Toyonaka, Osaka

and Itaru MATSUMURA, Tadashi OKUYAMA and Junji FURUKAWA

Department of Synthetic Chemistry, Kyoto University, Sakyo-ku, Kyoto

(Received October 30, 1967)

The rates of hydrolysis of various ring-substituted phenyl vinyl ethers, $CH_2=CHOC_6H_4X$, have been measured in 80 : 20 dioxane-water containing hydrochloric acid as catalyst. The ring substituents investigated include H, *p*-CH_3O, *m*-CH_3O, *p*-CH_3, *m*-CH_3, *p*-Cl and *m*-Cl. The reaction was first order with respect to both the acid and the ethers. It has been found that the effect of substituents on the hydrolysis rates obeys the Hammett $\rho\sigma$ relationship with the reaction constant $\rho = -2.21$ at 35°C. These results are compatible with the previous conclusion that the acid-catalyzed hydrolysis of alkenyl ethers involves the rate-determining protonation of the ethers at their β-carbon atom, to form intermediate oxycarbonium ions. It has been shown that the observed substituent effect can be rationalized from the π-electronic energy changes of the ethers on protonation, which have been calculated by an empirical molecular orbital method.

It is generally accepted that the acid-catalyzed hydrolysis of α, β-unsaturated ethers involves irreversible protonation of the β-carbon atom of the unsaturated bond.[2-6] In a previous paper (Part I) of this series,[7] we investigated the kinetic courses of hydrolysis of various alkenyl alkyl ethers, $R_1R_2C=CH(OR_3)$, and presented direct evidence that the protonation step is rate-determining. It was also shown that the relative reactivities of the various ethers may best be interpreted in terms of the conjugative stabilities of the intermediate carbonium ions that are formed on the transfer of a proton from a hydronium ion to the ethers.

In the present communication, we will report the rates of hydrolysis of several ring-substituted phenyl vinyl ethers in an acidic dioxane-water medium in the temperature range 25 to 45°C. From the outset, we may assume, in analogy to the hydrolysis mechanism of alkenyl alkyl ethers, that the reaction under question will proceed according to the scheme:

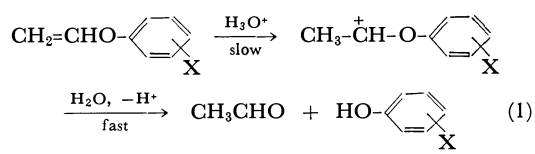

(1)

where the first protonation step is rate-determining. The rate data obtained have shown that the effects of substituents on the hydrolysis rates nicely fit the Hammett $\rho\sigma$ relationship with the reaction constant, ρ, ranging from -1.89 to -2.26, depending on the reaction temperature selected. That the observed substituent effects are compatible with the mechanism (1) appears to be justifiable from the linear correlation which has been found to hold between the Hammett σ constants and the β-carbon localization energies of the phenyl vinyl ether derivatives as calculated by an empirical molecular orbital method.

Experimental

Materials. Phenyl vinyl ether (PVE) and its *p*-CH_3O, *m*-CH_3O, *p*-CH_3, *m*-CH_3, *p*-Cl and *m*-Cl derivatives were prepared from ethylene dibromide and appropriate substituted phenols according to the method of McElvain and Fajardo-Pinzón.[8]

1) Part III: T. Okuyama, T. Fueno, J. Furukawa and K. Uyeo, *J. Polymer Sci., A1*, in press.
2) L. A. Kiprianova and A. F. Rekasheva, *Dokl. Akad. Nauk SSSR*, **142**, 589 (1962).
3) D. M. Jones and N. F. Wood, *J. Chem. Soc.*, **1964**, 5400.
4) P. Salomaa, A. Kankaanperä and M. Lajunen, *Acta Chem. Scand.*, **20**, 1790 (1966).
5) T. H. Fife, *J. Am. Chem. Soc.*, **87**, 1084 (1965).
6) A. J. Kresge and Y. Chiang, *J. Chem. Soc. (B)*, **1967**, 58.
7) T. Okuyama, T. Fueno, H. Nakatsuji and J. Furukawa, *J. Am. Chem. Soc.*, **89**, 5826 (1967).
8) S. M. McElvain and B. Fajardo-Pinzón, *ibid.*, **67**, 650 (1945).

TABLE 1. SOME PHYSICAL CONSTANTS AND THE ELEMENTAL ANALYSIS DATA OF PHENYL VINYL ETHERS[a]

Substituent	Elemental analysis, % C	Elemental analysis, % H	Boiling point °C/mmHg	Specific gravity[b] d_4^{25}	Refractive index[b] n_D^{25}
H	79.44	6.89	54/17	0.974	1.5209
	(79.97)	(6.71)	(54—55/17)[d]	(0.9770)[f]	(1.5224)[g]
p-CH_3O	71.81	6.73	91.0—91.5/12	1.048	1.5275
	(71.98)	(6.71)	—	—	—
m-CH_3O	72.10	6.93	96/13	1.051	1.5300
	(71.98)	(6.71)	—	—	—
p-CH_3	81.65	7.57	72.5/17	0.956	1.5169
	(80.56)	(7.51)	(75/18)[d]	(0.9587)[f]	(1.5168)[g]
m-CH_3	80.93	7.71	71/16	0.957	1.5180
	(80.56)	(7.51)	(74/20)[d]	—	(1.5183)[g]
p-Cl[c]	62.20	4.72	85.5—86.5/19	1.137	1.5398
	(62.15)	(4.56)	(83—86/10)[e]	(1.0039)[e]	(1.5404)[g]
m-Cl[c]	61.97	4.68	82.5—83.5/17	1.138	1.5390
	(62.15)	(4.56)	—	—	(1.5401)[g]

a) The figures in parentheses are either the calculated or literature values.
b) The literature values are all for 20°C.
c) Analysis of Cl: Calcd. 22.93. Obsd. *p*-Cl, 22.84; *m*-Cl, 22.86.
d) Ref. 10. e) Ref. 11. f) Ref. 12. g) Ref. 13.

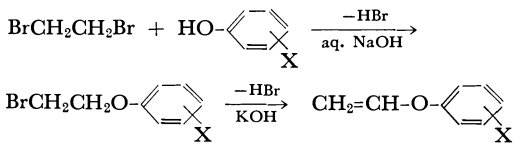

(2)

Syntheses of the intermediate β-bromophenetole derivatives were carried out by heating a mixture of ethylene dibromide, sodium hydroxide and phenols in boiling water for 10 hr. The phenetoles were separated from the aqueous layer and distilled. Their boiling points were as follows: H, 90—94°C/5.5 mmHg; *p*-CH_3O, 125.5°C/6 mmHg; *m*-CH_3O, 93°C/2.5 mmHg; *p*-CH_3, 87°C/3 mmHg; *m*-CH_3, 94—99°C/2.5 mmHg; *p*-Cl, 102—105°C/3 mmHg; *m*-Cl, 110.5—112.5°C/3 mmHg.

The phenetole derivatives were then subjected to dehydrobromination by heating in the presence of an equal amount (in weight) of powdered potassium hydroxide in a copper flask at *ca.* 200°C. The resulting PVE derivatives were collected in a glass flask, distilled over calcium hydride and stocked in the dark under a nitrogen atmosphere.

Gas chromatography of the ethers prepared as above indicated that they were over 99.5% pure. The ethers were also checked for isomeric purity by both infrared and NMR spectroscopies. Some physical constants of these ethers are summarized in Table 1, together with their elemental analysis data.

Tetralin, which was used as an internal standard for gas chromatography, was of the best grade commercially available. Dioxane of guaranteed grade was further purified by a conventional method.

Kinetic Measurements. Hydrolysis was carried out in 80% aqueous dioxane containing 0.2 N hydrochloric acid at 25, 35 and 45°C, thermostatically maintained.

The initial concentrations of the reactant ethers were typically *ca.* 1.5×10^{-2} M. The courses of the hydrolysis reactions were pursued by gas chromatographic determinations of the ethers remaining in the reaction mixtures. Details of the procedures for the rate measurements were the same as those described previously.[7]

Product Identifications. Phenyl vinyl ethers are expected to give acetaldehyde and the corresponding phenols on hydrolysis. For the case of the nonsubstituted PVE, the formations of these products were confirmed by gas chromatography; their retention times were in perfect agreement with those of the authentic samples. The products were also identified by the routine procedures of qualitative analysis. Tollens' reagent[9a] and an aqueous ferric chloride solution[9b] were used to identify acetaldehyde and phenol, respectively; both reagents gave positive results.

Experimental Results

Kinetic Data. The hydrolysis of phenyl vinyl ethers (PVE) was found to be first order with respect to both ether and acid. The first-order decay of the reactant ether, as is seen in Fig. 1, proved to hold uniformly down to over 80% conversions for all the PVE derivatives investigated.

9) a) R. L. Shriner, R. C. Fuson and D. Y. Curtin, "The Systematic Identification of Organic Compounds," John Wiley and Sons, Inc., New York (1956), p. 112; b) *ibid.*, p. 162.
10) W. Reppe *et al.*, *Ann.*, **601**, 81 (1956).
11) M. Ban, H. Yamamoto and S. Otsuka, *Nippon Kagaku Zassi (J. Chem. Soc. Japan, Pure Chem. Sect.)*, **77**, 176 (1956).
12) M. F. Shostakovskii and M. S. Burmistrava, *J. Applied Chem. (USSR)*, **15**, 260 (1942); *Chem. Abstr.* **37**, 2336 (1943).
13) Y. L. Frolov and A. v. Kalabina, *Spectroskopiya, Metody Primenenie Akad. Nauk SSSR, Sibirsk. Old*, 171, 173 (1964); *Chem. Abstr.*, **62**, 5156 (1965).

The first-order rate constants, k_1, were exactly proportional to the concentration of hydrochloric acid, as may be seen in Fig. 2. These results preclude the possibility that the phenols which were produced on hydrolysis may partake in the kinetics to any appreciable extent as acid catalysts, whether as the Brönsted-type or as the general acid catalyst.

The second-order rate constants, defined as $k_2=k_1/[\mathrm{HCl}]$, were measured for the various PVE derivatives at varying temperatures. The results are given in Table 2, where it may be seen that electron-releasing substituents enhance the reactivity of PVE, while electron-attracting ones lower it.

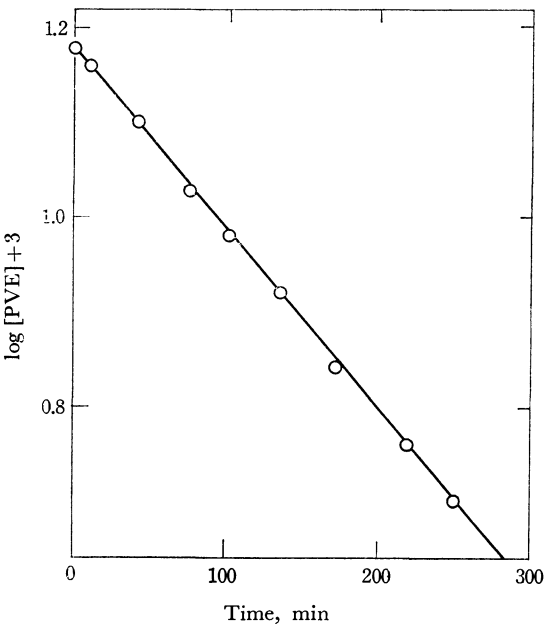

Fig. 1. First-order plots for the hydrolysis of phenyl vinyl ether.
The initial concentration, 1.53×10^{-2} M.
[HCl], 0.2 N. Temperature, 35°C.

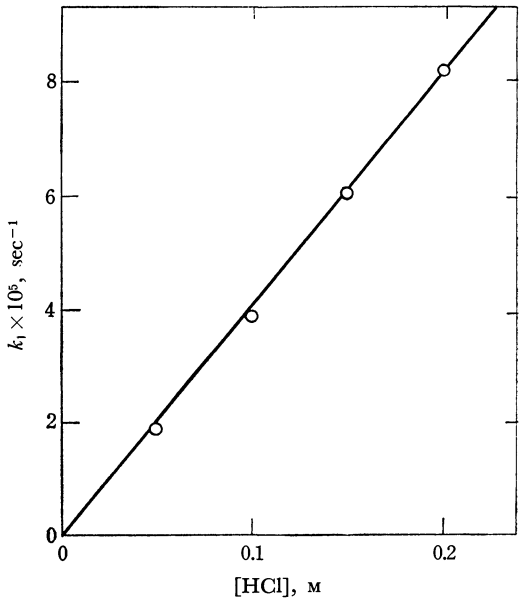

Fig. 2. Linear dependence of the first-order rate constant of the phenyl vinyl ether hydrolysis on the hydrochloric acid concentration.
Temperature, 35°C.

From the k_2 values listed in Table 2, the heats and entropies of activation, $\Delta H^{\neq}$ and $\Delta S^{\neq}$, at 35°C were evaluated in a usual manner. The linearities of the plots of $\log(k_2/T)$ *vs.* $1/T$ were satisfactorily good for all the PVE derivatives studied here. The activation parameters obtained are included in Table 2.

Free Energy Correlations. In Fig. 3 the logarithms of the rate constants, k_2, listed in Table 2 have been plotted against Hammett's σ values. The plots are satisfactorily linear at every temperature studied.

TABLE 2. THE SECOND-ORDER RATE CONSTANTS AND THE ACTIVATION PARAMETERS OF THE ACID-CATALYZED HYDROLYSIS OF VARIOUS PHENYL VINYL ETHER DERIVATIVES

Substituent	Hammett's σ	$10^4_i k_2$, l mol^{-1} sec^{-1}			$\Delta H^{\neq}_{308}$,[a] kcal mol^{-1}	$\Delta S^{\neq}_{308}$[b] e. u.	$\delta\Delta E$[c] $-\gamma^2/\beta$
		25°C	35°C	40°C			
p-CH_3O	−0.268	4.35	14.1	36.9	19.5	−8.3	0.0334
p-CH_3	−0.170	2.46	8.41	22.4	20.2	−7.0	0.0225
m-CH_3	−0.069	1.34	5.19	14.1	21.8	−2.8	0.0135
H	0	1.01	4.01	10.9	21.9	−3.0	0
m-CH_3O	0.115	0.85	3.44	9.03	21.8	−3.6	−0.0196
p-Cl	0.227	0.31	1.16	3.98	23.5	−0.3	−0.0450
m-Cl	0.373	—	0.52	2.06	26.1	6.6	−0.0483

a) The probable errors do not exceed 0.3 kcal mol^{-1}.
b) Accurate only to within ±1.0 e. u.
c) The relative stabilities of carbonium ions, $XC_6H_4O\overset{+}{C}HCH_3$, as calculated by the empirical molecular orbital theory. See the text.

Table 3. The reaction constants, ρ, the correlation coefficients, r, and the standard deviations, s, of the Hammett plots

Temperature °C	$\sigma_{m\text{-}CH_3O}=0.115$			$\sigma_{m\text{-}CH_3O}=0.060$		
	ρ	r	s	ρ	r	s
25	−2.138	0.982	0.084	−2.261	0.997	0.035
35	−2.158	0.984	0.096	−2.209	0.996	0.059
45	−1.889	0.992	0.066	−1.925	0.999	0.020

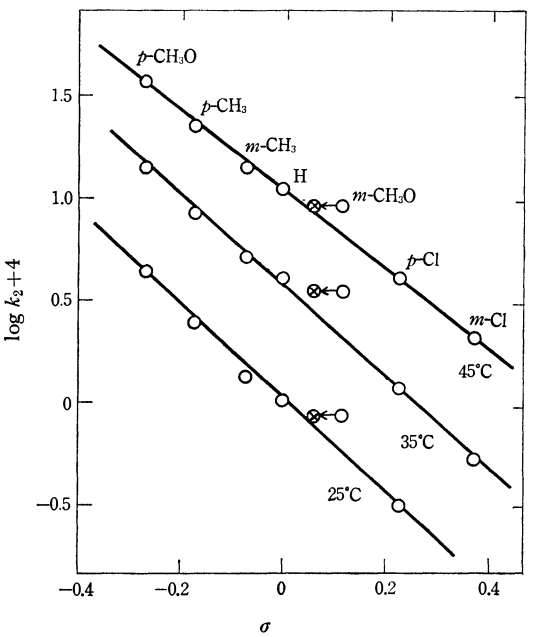

Fig. 3. The Hammett correlations of the acid-catalyzed hydrolysis rates of ring-substituted phenyl vinyl ethers.
The crossed circles are plots for the m-CH_3O group, for which a special value (0.060) has been adopted.

It is noticeable, however, that the m-CH_3O points uniformly deviate from linearity. Yet, these points become aligned with the others if we use the "special" σ value, 0.060, that Taft recommended for the m-CH_3O group in the free energy correlations of the reactions in nonaqueous and mixed solvents.[14] Such an improvement in the Hammett correlation by use of the value 0.060 for the m-CH_3O group has also been noted recently by Ceska and Grunwald for the ionization equilibria of anilines in acetic acid.[15]

The least squares treatments of the linearities of Fig. 3 have led to the reaction constants, ρ, which are given in Table 3. Also listed in Table 3 are the correlation coefficients, r, of the plots, and their standard deviations, s,[16] from the regression lines.

For the sake of comparison, the two σ values, 0.115 and 0.060, have been used for the m-CH_3O group. Although the number of points included in the correlations is only modest, the linearities may be regarded as sufficiently good, especially when the m-CH_3O group is allowed to have the value 0.060.

The Extrathermodynamic Relation. It is known that in a series of reactions a change of substituent tends to cause $\Delta H^{\neq}$ and $\Delta S^{\neq}$ to vary in the same direction. This extrathermodynamic relation[17] between $\Delta H^{\neq}$ and $\Delta S^{\neq}$ is often linear so as to permit the quantitative assessment of the relative importances of the two quantities governing the observed substituent effects.

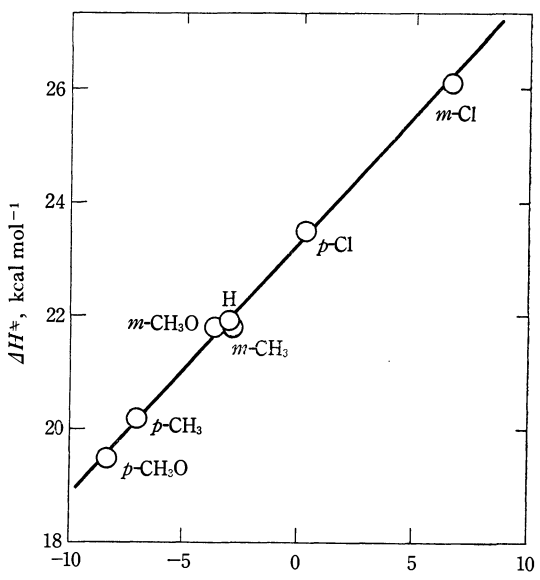

Fig. 4. Plots of $\Delta H^{\neq}$ *vs.* ΔS.

In our present series of reactions, such a linear, compensating relationship between $\Delta H^{\neq}$ and $\Delta S^{\neq}$ is indeed discernible with fair precision, as may be seen in Fig. 4. The isokinetic temperature, defined as the slope of the linearity, has been found to be 465°K. Thus we may draw the conclusion

14) R. W. Taft, *J. Phys. Chem.*, **64**, 1805 (1960).
15) G. W. Ceska and E. Grunwald, *J. Am. Chem. Soc.*, **89**, 1371 (1967).
16) H. H. Jaffé, *Chem. Revs.*, **53**, 191 (1953).
17) J. E. Leffler and E. Grunwald, "Rates and Equilibria of Organic Reactions," John Wiley and Sons, Inc., New York (1963), pp. 315—402.

that the observed substituent effects are primarily enthalpy-controlled.

Empirical Molecular Orbital Considerations

It is a widely accepted view that the sigma values of para substituents are more or less subject to a variation in magnitude, depending on the type of reaction being investigated. This nonlinearity of free energy correlations is believed to arise from the different extents of direct conjugation between substituents and reaction centers in the transition states of different reaction types.

We have previously reported that such a multiplicity of substituent constants, as represented by σ°, σ, σ^+ and σ^-, can be interpreted on a unified ground in terms of the π-electron energy changes as calculated by the empirical molecular orbital method for the activation processes of relevant side-chain reactions of benzene derivatives.[18] In the following, we will apply an analogous treatment to the hydrolyses of ring-substituted PVE's and examine whether or not the general trends of the observed substituent effects may be justifiable.

We will be primarily concerned with the difference in the total π-electronic energies between reactants, XC_6H_4Y, and intermediates, XC_6H_4Y'. Here, X is a substituent, and Y and Y' are the side-chain reaction centers in the initial and intermediate states, respectively, which are $-O-CH=CH_2$ and $-O-\overset{+}{C}H-CH_3$ in the present instance. In conformity with our previous treatments,[18] the energy difference under question may be expressed as

$$\begin{aligned} &E(XC_6H_4Y') - E(XC_6H_4Y) \\ &\quad = [E(XC_6H_5) + E(Y') - DE'] \\ &\qquad - [E(XC_6H_5) + E(Y) - DE] \\ &\quad = [E(Y') - E(Y)] - (DE' - DE) \end{aligned} \tag{3}$$

where E's are the π-electronic energies of the compounds or groups specified in the parentheses, and where DE and DE' are the delocalization energies of the two states due to the linkage of XC_6H_5 with Y and Y' to form XC_6H_4Y and XC_6H_4Y', respectively. The delocalization energies can be computed from the following familiar expression that Dewar[19] derived by a perturbation technique:

$$DE = 2\left\{\sum_i^{occ}\sum_j^{un} - \sum_i^{un}\sum_j^{occ}\right\} \frac{c_{ir}^2 c_{js}^2}{m_i - m_j}\left(-\frac{\gamma^2}{\beta}\right) \tag{4}$$

The notations involved in Eq. (4) are the same as have been described previously.[18]

Since, in Eq. (4), the difference between E (Y') and E (Y) is constant for a given reactive side chain, the difference between the delocalization energies, defined as

$$\Delta E = DE' - DE \tag{5}$$

should be a quantity which may be regarded as a measure of the effects of substituents on the stabilities of the intermediate carbonium ions. Thus, it is to be expected that the greater the ΔE, the more stable is a carbonium ion, $XC_6H_4O\overset{+}{C}HCH_3$, and hence the greater is the reactivity of its parent PVE derivative, $XC_6H_4OCH=CH_2$.

Perturbation calculations of ΔE have been carried out for the various phenyl vinyl ethers. The molecular orbital functions and energies of monosubstituted benzenes as unperturbed systems were the same as those used previously.[18] The integral parameters adopted for the composite groups Y and Y' were as follows:

For $-O-CH=CH_2$, the Coulomb integral parameters were $k_O=0.5$, $k_{C\alpha}=0.1$ and $k_{C\beta}=0$, and the resonance integral parameters were $h_{C-O}=0.5$ and $h_{C=C}=1$. For $-O-\overset{+}{C}HCH_3$, these parameters were $k_O=0.5$, $k_{C\alpha^+}=0.3$ and $h_{O-C}=0.5$. The value of $k_{C\alpha^+}=0.3$, which was most crucial to the calculated results, was simply a sum of $k_{C^+}=0.2$ that was adopted previously for a side chain $-\overset{+}{C}(CH_3)_2$ and $k_{C\alpha}=0.1$ that was assumed for the α-carbon of an ether in the initial state. Variations of the other parameters caused no material changes in the general trends of the calculated results.

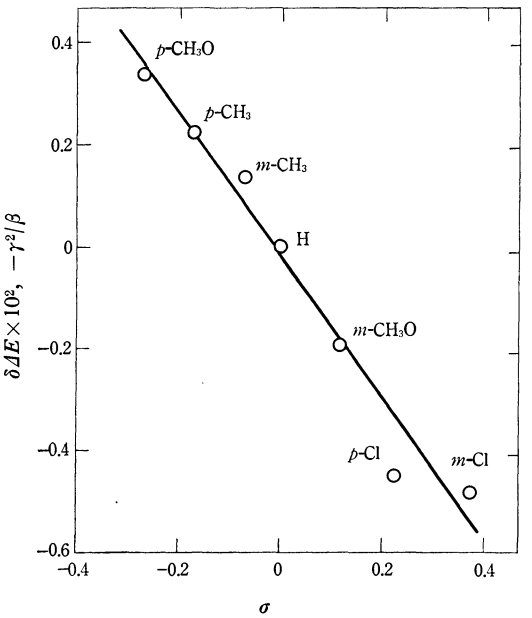

Fig. 5. Linear variation of the relative stabilities, $\delta\Delta E$, of the carbonium ions, $XC_6H_4O\overset{+}{C}HCH_3$, as calculated by the empirical molecular orbital theory, with the Hammett σ values of the substituents, X.

18) T. Fueno, T. Okuyama and J. Furukawa, This Bulletin, **39**, 569 (1966).
19) M. J. S. Dewar, *J. Am. Chem. Soc.*, **74**, 3341 (1952).

The delocalization energy differences, ΔE, obtained for the various PVE's were as follows: 0.0552 (p-CH_3O), 0.0443 (p-CH_3), 0.0353 (m-CH_3), 0.0218 (H), 0.0022 (m-CH_3O), -0.0232 (p-Cl) and -0.0265 (m-Cl) in units of $-\gamma^2/\beta$. Denote by $\delta\Delta E$ each value of ΔE relative to that (0.0218) obtained for the unsubstituted PVE. The $\delta\Delta E$ may then be regarded as a measure of the relative stabilities of the carbonium ions, $XC_6H_4O\overset{+}{C}HCH_3$, taking the unsubstituted ion as the standard. These values of $\delta\Delta E$ have been found to be proportional to the Hammett σ values of the substituents, as may be seen in Fig. 5. These results of calculation rationalize the observation that the effects of substituents on the rates of the acid-catalyzed hydrolysis of phenyl vinyl ethers obey the Hammett correlation, in which the original Hammett σ values have been used for substituents.

Discussion

The observed Hammett correlations, coupled with molecular orbital considerations, allow us to postulate that the Hammett σ value of the ring substituents is an adequate measure of the relative stabilities of the various intermediate carbonium ions, $XC_6H_4O\overset{+}{C}HCH_3$. The intervention of an oxygen atom between the benzene ring and the charged center suppresses direct conjugation between them, which otherwise would have permitted the correlation of $\log k_2$ with Brown's σ^+ values,[20] as in the case of the acid-catalyzed hydration of styrene derivatives.[21]

Perhaps the following are the best pictorial representations of the origin of the different effects of para $-R$ substituents on the stabilities of the carbonium ions formed from styrene and phenyl vinyl ether:

For ions formed from styrene derivatives,

For ions formed from phenyl vinyl ether derivatives,

In the latter ions, the strong electron demand of the electron-deficient carbon is saturated by the migration toward it of the lone pair electrons of the neighboring oxygen, leaving no valency available to permit direct conjugation between the substituent and the side chain group.

Nonetheless, the oxygen atom certainly transmits the mesomeric effect of substituents onto the reaction center, even though only slightly. Otherwise, $\log k_2$ would have been better correlated with Taft's normal substituent constants, σ°.[14] Conjugation between the ring and the extracyclic vinyl linkage through the oxygen atom in phenyl vinyl ethers is also evidenced by the observed effect of ring substituents on the NMR chemical shifts of the β-protons of the ethers.[22] In our specific series of reactions, then, the stabilizations of the initial states and the intermediate cations due to such conjugations must have been of proper amount to just cancel each other, leading, as a net result, to the substituent effects which have been observed to conform to the Hammett σ constants.

20) H. C. Brown and Y. Okamoto, *ibid.*, **80**, 4979 (1958).

21) W. M. Schubert, B. Lamm and J. R. Reeffe, *ibid.*, **86**, 4727 (1964), have reported that the acid-catalyzed hydration of styrene derivatives involves the rate-determining protonation of the vinyl linkage, the effects of ring substituents thus conforming to the σ^+ values.

22) O. Kajimoto and T. Fueno, Abstracts of the papers presented at the Symposium on the Hammett Relationship, October 1967, Kyoto, p. 51.

BULLETIN OF THE CHEMICAL SOCIETY OF JAPAN VOL. 41 824—827 (1968)

Effects of Heating Temperature and Irradiation on the Catalytic Activities of Active Carbons for Phosgene Synthesis

Shoichi SATO*1 and Yukio YONEDA

Department of Synthetic Chemistry, Faculty of Engineering, The University of Tokyo, Bunkyo-ku, Tokyo

(Received November 4, 1967)

The kinetic factors for phosgene synthesis over thermal and irradiated sucrose carbons were examined in particular regard to their dependences on the heating temperature and irradiation. Gamma-irradiation on carbons prepared at 900 or 1000°C produced new active sites with E_A of 11—12 kcal/mol. An explanation is suggested of the effects of heating temperature and irradiation on the catalysts; the catalytic activity is most reasonably related to the degree of growth of the network structure of carbons. In the case of carbons prepared by heating at 900 or 1000°C and having the structure grown to the largest extent, a high dose of gamma-rays presumedly destroys most efficiently the thermally generated active sites and forms sites with a high activation energy. Free radicals and peripheral atoms which also comprise characteristics of amorphous carbons seem to behave independently of catalytic activities and are supposed to have no direct relation to the activities.

The ionizing radiation has been known to affect the catalytic activity of metals, oxides and other salts.[1,2] None has been reported, however, about the irradiation effect on active carbon, which has a unique structural character among inorganic catalysts with its disorderly layered ring networks, peripheral atoms and free radicals. It is well known that carbons catalyze phosgene synthesis from carbon monoxide and chlorine as well as some other reactions.[3] No relation has yet been reported between the catalytic activity for this synthesis and other nautres of the catalysts.

We will report about catalytic activities of sucrose carbons prepared by evacuation within a range of temperatures, the effect of irradiation and some related behaviors of the carbons.

Experimental

Catalysts. Reagent grade sucrose was heated in air at around 350°C, crashed and heated twice, then ground to pass between 20 and 80 mesh (Primary Carbon, Pri. C.). Pri. C. was evacuated below 10^{-3} mmHg in a quartz tube for 20 hr at temperature (T) between 500 and 1000°C, at intervals of 100°C (C^T catalysts). Each C^T: catalyst was heated in an ampoule at 450°C for an hour in a helium stream and sealed while it was still hot. The ampoules were gamma-irradiated at room temperature with a ^{60}Co source at a dose rate of 1.0×10^6 R/hr to a total dose of 1.0×10^8 R (C^{T*} catalysts).

Catalytic Activity Measurements. The flows of tank chlorine (electrolytic) and of carbon monoxide (gas chromatographically pure) were mixed after being measured by flowmeters filled with concd. sulfuric acid and were introduced into a glass U-tube reactor of 6 mm I. D.; the tail gas was pulsed into a gas chromatographic system. A catalyst, 0.1—1 g, was placed on glass wool in the reactor, preheated to 450°C in the helium stream (about 20 ml/min) and kept for over an hour. Then the helium flow was stopped and chlorine flow (about 20 ml/min) was admitted for over 4 hr at the same temperature. The reactor was cooled to the reaction temperature (100—220°C) in the chlorine stream, then carbon monoxide was introduced in order to begin the reaction. The reaction products were analyzed over 100 min after the start of the reaction. The flow rates of both reactants were about 40 ml/min throughout the experiment. Such a pretreatment, without which no catalysis for the reaction was detectable, secured the constancy and reproducibility of the catalytic activity.

A fixed amount of the tail gas (2 ml), containing carbon monoxide, chlorine and the sole reaction product, phosgene, of less than 10% was analyzed by a gas chromatographic system after Runge[4] with a minor modification for convenience. The system was composed of a thermal conductivity cell with platinum filaments, a 4.5 m long glass tube analyzing column of 6 mm I. D. packed loosely with about 50 g of polytetrafluoroethylene powder*2 on which trichlorinated diphenyl*3 was carried in weight ratio of 1/20, and a

*1 On leave from Takasaki Radiation Chemistry Research Establishment, Japan Atomic Energy Research Institute (1963—1965). Present Address; Takasaki Laboratory, JAERI, Tokai-mura, Ibaraki-ken.

1) E. H. Taylor, *Nucleonics*, **20**, 53 (1962); *J. Chem. Educ.*, **36**, 396 (1959).

2) R. Coekelbergs, A. Crucq and A. Frennet, *Advan. in Catalysis*, **13**, 55 (1962).

3) J. W. Hassler, "Active Carbon," Chemical Pub. Co., New York, N. Y. (1951).

4) H. Runge, *Z. anal. Chem.*, **189**, 111 (1962).

*2 Polyflon M-11, 32—60 mesh, The Daikin Kogyo Co., Ltd.

*3 Kanechlor-300, The Kanegafuchi Chemical Co., Ltd.

1 m long glass tube with Molecular Sieve 5A for desiccating helium carrier gas. All parts were connected with polyvinyl chloride tubes and set in a wooden case lined inside with aluminum plates. The analysis was done at a helium flow rate of 50 ml/min and a bridge current of 80 mA at room temperature. The retention times were 0, 2.0 and 6.6 min for carbon monoxide, chlorine and phosgene, respectively. The analytical accuracy and reproducibility were satisfactory. The system was operated without any trouble for one year.

B. E. T. Surface Areas. Specific surface areas of C^T catalysts were measured by the B. E. T. method with nitrogen.

Infrared Spectra of Catalysts. The infrared spectra of the carbon catalysts, ground into fine powder, were observed by the KBr pellet method in the wavelength range, 650—4000 cm^{-1}.

Results and Discussions

Surface Area. Specific surface areas of C^T catalysts are shown in Table 1. The data show a drastic change of the catalyst structures by heating.

Elementary Analysis. It was reasonably expected that the contact of the carbon with chlorine at 450°C and perhaps with phosgene up to 220°C may cause considerable change in its structure and elementary composition. Carbon blacks[5] were reported to react with chlorine with the maximum uptake at 400—500°C, nearly total content of hydrogen being substituted. However, our results of the elementary analysis of the carbons before and after use, does not exhibit any general relationship among components. Atomic ratios of the components, hydrogen, oxygen and chlorine (C=1.000) are shown in Table 1.

The increase of the specific surface area as the heating temperature of carbons was raised from 500 to 700°C corresponds to a loss of hydrogen and oxygen. The decrease of the surface area at higher heating temperature (800—1000°C) is accompanied with a loss of hydrogen but not with that of oxygen.

After use as the catalyst, the carbons were hydrogenated, deoxygenated and chlorinated. The dehyderogenation was severe for low temperature carbons. A remarkable deoxygenation was however, limited to occur to C^{500} alone, and beyond C^{600} the oxygen content with regard to carbon remains almost unchanged. The degree of chlorination is not associated with that of dehydrogenation, though the chlorine content is comparable to the hydrogen content before reaction for higher temperature carbons. Considering that conditions of the pretreatment and the reaction were common to all samples, the rather small divergence of the amount of the chlorine introduction into carbons, which is in remarkable contrast to a large change in the B. E. T. surface areas, suggests that chlorine does not necessarily combine with or substitute peripheral atoms but rather attacks peripheral and even inner carbon atoms with equal probability; one chlorine atom corresponds with 13—19 carbon atoms. That is, chlorine may react with carbon atoms to the same extent although they are present in a variety of imperfect polycondensed system.

Infrared Spectra. IR spectra of chars and coals have been observed and several assignments[6-8] have been made for characteristic absorption.

The spectra of some of our samples were examined in order to find any relation between the catalytic activities and the structures of the catalysts.

The low temperature carbon C^{500} did not show perceptible absorption before and after reaction in the wave number range 550—800 cm^{-1} ($\nu_{\phi-Cl}$= 702 cm^{-1}) or at around 950 and 1100 cm^{-1} (ν_{C-Cl} in RCOCl), in spite of the large uptake of chlorine by the catalyst. The appearance of the

Table 1. B.E.T. surface areas and elementary compositions of C^T catalysts

Catalyst	Surface area m^2/g*	Elementary composition**	
		Before use	After use***
Pri. C.	—	$C_1H_{0.604}O_{0.245}$	—
C^{500}	121	$C_1H_{0.430}O_{0.076}$	$C_1H_{0.248}O_{0.043}Cl_{0.063}$
C^{600}	378	$C_1H_{0.373}O_{0.044}$	$C_1H_{0.186}O_{0.037}Cl_{0.053}$
C^{700}	418	$C_1H_{0.194}O_{0.043}$	$C_1H_{0.089}O_{0.030}Cl_{0.080}$
C^{800}	384	$C_1H_{0.129}O_{0.029}$	$C_1H_{0.043}O_{0.023}Cl_{0.081}$
C^{900}	195	$C_1H_{0.093}O_{0.026}$	$C_1H_{0.061}O_{0.041}Cl_{0.062}$
C^{1000}	90.3	$C_1H_{0.067}O_{0.025}$	$C_1H_{0.052}O_{0.027}Cl_{0.063}$

* For catalysts before use.
** Oxygen content was given by subtraction.
*** Catalysts were kept in a desiccator after use over a month.

5) H. P. Boehm, U. Hofmann and A. Clauss, "Proc. 3rd. Conf. on Carbon," 1957, Pergamon Press, New York, N. Y. (Pub. 1959), p. 241.
6) R. A. Friedel, "Proc. 4th. Conf. on Carbon," 1959, Pergamon Press, New York, N. Y. (Pub. 1960), p. 321.
7) R. A. Friedel and J. A. Queiser, *Anal. Chem.*, **28**, 22 (1956).
8) J. K. Brown, *J. Chem. Soc.*, **1955**, 744; *ibid.*, 752.

absorption due to R-Cl group was neither observed for the high temperature carbon C^{1000} after its use as the catalyst.

The pile irradiation was reported to have an effect on the IR spectra of carbons simply to make them diffuse.[6] In our case, gamma-rays were likewise proved to have the similar effect on the spectrum of the carbon C^{1000}.

Dependences of Kinetic Constants on Heating Temperature and Irradiation. A rate equation was reported for phosgene synthesis over a commercial carbon catalyst by Potter and Barron.[9] Their results were found to obey either the mechanism of the surface reaction of molecular carbon monoxide with molecular chlorine or that with atomic chlorine, but they rejected the atomic chlorine mechanism because of the reaction temperature (31—99°C) and some other factors. However, a re-examination[10] of their data showed that rates could be expressed simply in the form;

$$\text{Rate} = k p_{CO} p_{Cl_2}^{1/2} \qquad (1)$$

where k is the rate constant per unit catalyst weight.

In our work, the almost constant partial pressures of the reactants made no significant difference in quality of the kinetic canstants whichever nearly linear[9] or square root[10] dependence of the rate on chlorine pressure might be adopted. Considering our higher reaction temperatures employed, we adopted the expression of reaction rate given in Eq. (1).

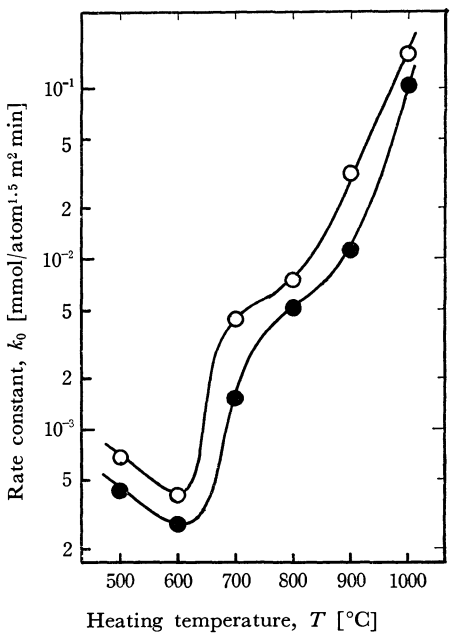

Fig. 1. Rate constants per unit area.
○ Unirradiated catalysts (C^T)
● Irradiated catalysts (C^{T*})

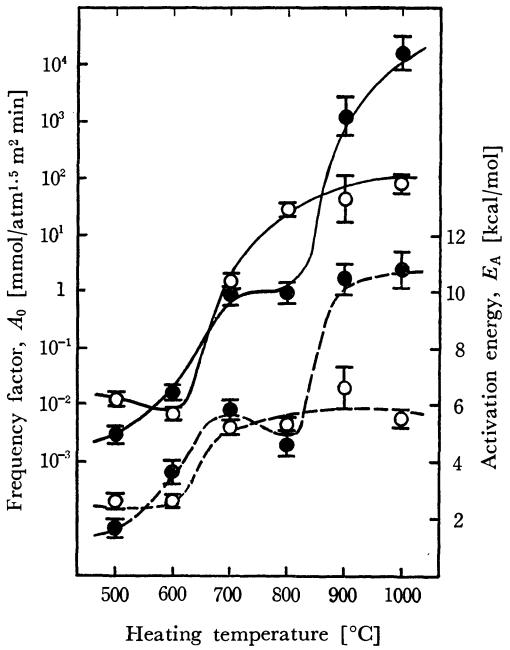

Fig. 2. Frequency factors and activation energies. ○ Unirradiated catalysts ● Irradiated catalysts
Full line Frequency factors
Broken line Activation energies

Rate constants per unit area, k_0, at 180°C are plotted against the heating temperature, T, in Fig. 1, where k_0 is k/S, and S is the specific area. The rate constant, k, at 180°C increases monotonously as the heating temperature is raised, while k_0 exhibits a slight decrease with T from 500°C to 600°C. Since C^{600} has the surface area three times as large as that of C^{500}, it is shown that the newly developed surface on C^{600} may have a smaller catalytic activity. With the heating temperature increased from 600°C to 700°C, both k and k_0 increase about tenfold, whereas the surface area is scarcely changed.

Gamma-irradiated carbons (C^{T*}) have always lower k and k_0 than the corresponding catalysts (C^T), as shown in Fig. 1. But an apparent parallelism of temperature dependences of the rate constants of the two catalyst groups may not have any significance. Analyses of k_0 values by separating them into frequency factors, A_0, and activation energies, E_A, reveal a definite dissimilarity between the two groups.

The A_0 values of C^T catalysts (Fig. 2) increase with the increasing heating temperature, but at higher heating temperatures they seem to be saturated. Those of C^{T*} catalysts do not show such a saturation, and A_0 of C^{1000*} exceeds that of C^{1000} by more than two orders of magnitude.

9) C. Potter and S. Barron, *Chem. Eng. Progr.*, **47**, 473 (1951).
10) S. Weller, *Am. Inst. Chem. Eng. J.*, **2**, 59 (1956).

The A_0 values of lower temperature carbons are less affected by irradiation.

The activation energies of C^T group can be classified into two groups. Both C^{500} and C^{600} have activation energies of about 2—3 kcal/mol and higher temperature catalysts about 5—6 kcal/mol. The general feature of C^{T*} carbons is similar to C^T ones for heating temperatures lower than 800°C, however C^{900*} and C^{1000*} have activation energies nearly doubled.

Changes in A_0 and E_A by the irradiation indicate that to lower (T=500 and 600°C) and middle (T=700 and 800°C) temperature carbons the gamma-dose of 1.0×10^8 R gives only a vague effect, the quality and the quantity of catalytic sites being not greatly affected.

The disappearance of the saturation of A_0 and the remarkable increase of E_A upon irradiation for higher heating temperature (900 and 1000°C) carbons will be associated with the destruction of some of the thermally generated sites and with the creation, by gamma-irradiation, of new sites of different nature which may not be produced by any thermal treatment of the carbons.

Conclusions

Characteristics of structure of amorphous carbons are peripheral atomic groups, free radicals and π-electron systems. Free radicals do not disappear but are indeed produced by pile-irradiation in 90% carbon coals which behave much alike the carbons from carbohydrates.[6] If the catalytic activity is to be related with free radicals, irradiation should enhance the activities of carbons. Moreover, succrose carbons have a maximum concentration of free spins when heated around 600°C,[11] although C^{600} is not active as shown in Fig. 1. It is clear from the results of elementary analyses that the increasing tendency of the catalytic activity with increasing heating temperature can not be related to the content of any component nor to the change in the content of C^T carbons. The measurement of the IR spectra could not point out any special bonding in carbons, which is positively responsible for the catalytic activity. The only remaining possible explanation for the effect of structure for the catalysis seems to be the correlation of the catalytic activity to the growth of the condensed ring system.

The radiation is able to destroy the π-electron system through bond ruptures, resulting certainly in an activity decrease. Atomic displacements of 0.35—0.7 per 10^4 atoms occurred in the graphite sample pile-irradiated to about 10^8 rad.[12] This leads to the radiation yield of the atomic displacement, G_d=0.03—0.05. For polystyrene, the most stable polymer to radiation, the G-value of C–C splitting by electron irradiation[13] could be estimated to about 0.04. Also C–H splitting yield in carbons could be assumed from some reported radiolytic yields; for n-hexane, $G(C_6H_{13})=5.5$,[14] for cyclohexane, $G(C_6H_{11})=7.2$,[15] and for benzene, twice of $G(H_2)$ is about 0.08.[16]

There would be a possibility to explain the radiation effect by correlating the varied activity directly with the radiation induced point defects. The broken bonds might be associated with the irradiation effect. But the radiolytic yield is too low. For carbon with a surface area of 100 m^2/g, about 8% of the total carbon atoms exist on the surface, if only the (001) planes were exposed on particles of graphite structure. If any speculative mechanism allowed radiation damage to occur preferentially on surface atoms, 1.6% of the surface atoms (0.13% of the total atoms) could be damaged by doses of 10^8 R through a process with G=1.

This value is not recognized as sufficient so long as the catalytic action of the carbons is related simply to atomic lattice points. However, when a considerably developed carbon network as a whole is thought effective for the catalysis, the damaged several tenths percents of the total carbon atoms may suffice the observed radiation effect on the reaction rate.

11) L. S. Singer, W. J. Spry and W. H. Smith, "Prod. 3rd. Conf. on Carbon," 1957, Pergamon Press, New York, N. Y. (Pub. 1959), p. 121.

12) G. R. Hennig, "The Effects of Radiation on Materials," ed. by J. J. Harwood, H. H. Hausner, J. G. Morse and W. G. Rauch, Reinhold Pub. Corp., New York, N. Y. (1958), p. 226.

13) A. R. Schulz, R. I. Roth and G. B. Rathmann, *J. Polymer Sci.*, **22**, 495 (1956).

14) H. A. Dewhurst, *J. Phys. Chem.*, **61**, 1466 (1957); **62**, 15 (1958).

15) H. A. Dewhurst, *ibid.*, **63**, 813 (1959).

16) R. H. Schuler, *ibid.*, **60**, 381 (1956).

BULLETIN OF THE CHEMICAL SOCIETY OF JAPAN VOL. 41 828—832 (1968)

Study of Motion of D_2O in $Ba(ClO_3)_2D_2O$ by Transient NMR

Takehiko CHIBA*1 and Yoshinobu KAKIUCHI

The Institute for Solid State Physics, The University of Tokyo, Roppongi, Minato-ku, Tokyo

(Received November 6, 1967)

Deuteron spin lattice relaxation time T_1 and the reorientation rate of D_2O have been measured at various temperatures on a single crystal of $Ba(ClO_3)_2D_2O$ by transient nuclear magnetic resonance method. Temperature dependence of T_1 is similar to that of corresponding proton resonance but three to four orders of magnitude smaller than the latter. From the slope of log T_1 *vs.* $1/T$ curve, activation energy of reorientation of D_2O of 6.5—6.8 kcal/mol is obtained in agreement with that from line width transition. Theoretical values of T_1 minima were in good agreement with the observed. Direct measurement of reorientation rate is made by observing a signal recovery from saturation of one of the two deuteron sites of D_2O due to the exchange with unsaturated spins at the other site. The Arrhenius plot of the reorientation rate down to -170°C determined in this manner smoothly connects to that derived from the line width transition. A revision of the previous treatment of line width change is described and the reorientation rates of $Ba(ClO_3)_2D_2O$ are re-evaluated according to this method. A satisfactory agreement is found among the conclusions from the three different types of experiment, T_1, the line width transition and the directly measured reorientation rate. The motion is a random reorientation of D_2O with a rate governed by an activation process of 7 kcal/mol.

In a deuteron magnetic resonance the splitting due to a deuteron quadrupole coupling is usually of the order of 100 kc/sec. If a motion that interchanges two deuterons with different electric field gradient (EFG) components in the direction of H_0 is rapid enough, one gets a splitting corresponding to the averaged EFG of these two deuterons. Thus in hydrates a rapid reorientation of D_2O about its bisector causes the averaged spectra at high temperatures, while at low temperatures the spectra correspond to the stationary deuterons. From the line width change at both the slow and fast exchange limits, the reorientation rate of deuterons can be obtained employing the theory of motional narrowing process.[1] The method has an advantage over the usual line width transition due to dipole interactions in that the separation between the lines can be made as large as 200 kc/sec. However, because of insufficient signal-to-noise ratio usually encountered in deuteron resonances, observation of the broadening process is rather limited to a narrow range of temperatures and the presence of the dipole structure of the lines often imposes additional difficulty in extracting the rate of exchange. An activation energy of 6.5 kcal/mol for the reorientation in $Ba(ClO_3)_2D_2O$ determined in this way is somewhat larger than 5.0 kcal/mol for $Ba(ClO_3)_2H_2O$ determined from the temperature dependence of spin-lattice relaxation time, T_1, by Silvidi *et al.*[2]

It seems therefore worthwhile to study the motion by different method and compare the resulting value of reorientation rate with those obtained from the line width change for $Ba(ClO_3)_2 \cdot D_2O$ to examine whether the latter method gives the correct value. The present paper describes the measurements of T_1 and the reorientation rate in D_2O in this suitably simple system. The whole procedure of the present experiment and analysis are similar to the work of Schmidt and Uehling[3] of KD_2PO_4. A refined treatment of the line width transition for the derivation of exchange rate is also given.

Experimental

Single crystals of $Ba(ClO_3)_2D_2O$ are prepared as in the previous study.[1] All measurements were made using a pulse method. The pulse apparatus is of coherent type using Blume's gate circuit[4] operated at a frequency of crystal-controlled 10 Mc. Programmed pulses are furnished by the combination of Tektronix type 162, and 163 generators. The sample coil in a probe is incorporated in a single coil arrangement. Signal was detected by PA-620-L preamplifier and WA-600-D wideband amplifier of Arenberg Ultrasonic Laboratory Inc. Recovery time of the apparatus is about 15 μs. Rf field strength used was such that width of 90° pulse for D was about 15 μs.

*1 Present address: Department of Chemistry, Nihon University, Sakurajosui, Setagaya-ku, Tokyo.

1) T. Chiba, *J. Chem. Phys.*, **39**, 947 (1963).
2) A. A. Silvidi and J. W. McGrath, *ibid.*, **41**, 105 (1964).
3) V. H. Schmidt and E. A. Uehling, *Phys. Rev.*, **126**, 447 (1962).
4) R. Blume, *Rev. Sci Instr.*, **32**, 554 (1961).

Results and Discussion

Measurement of T_1. $Ba(ClO_3)_2D_2O$ crystal is monoclinic. Bisector of D_1OD_2 is a two-fold axis parallel to the crystallographic b axis.[5] D has nearly axially symmetric EFG about the D-O direction.[1]

For a deuteron nuclear spin $I=1$, therefore, an inclusion of a quadrupole interaction gives three unequally-spaced Zeemen levels. If only one of the two transitions (say, $m=1\rightarrow0$) is saturated, the recovery to the equilibrium cannot in general be represented by a single exponential function. If $P_1 \neq P_2$ as is generally the case, where P_1 is the thermal transition probability of $\Delta m=\pm1$ and P_2 is that of $\Delta m=\pm2$, unique T_1 can be defined only when three levels become equidistant as

$$1/T_1 = 2P_2 + P_1 \qquad (1)$$

Therefore, the measurement of T_1 is to be made for the crystal orientation where the quadrupole splitting is zero. Moreover, in the present case, because of the rapid exchange motion of D_1 and D_2 at high temperatures, in order to be able to observe T_1 for a wide temperature range the crystal orientation must be so chosen that the quadrupole splitting vanishes both for D_1 and D_2. There are two directions specified as direction I and II in Fig. 1 where this condition is met. The observed T_1 in these directions at various temperatures are

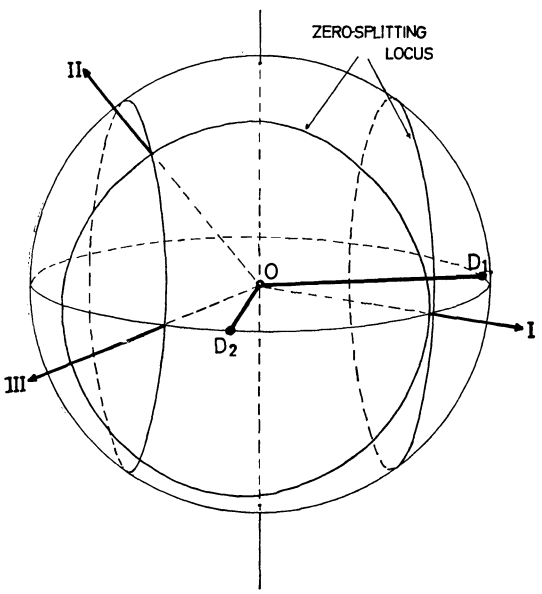

Fig. 1. Directions of magnetic field relative to the orientation of the D_2O molecule in the present study: Direction I and II for the measurement of T_1, Direction III for the direct measurement of jump rate.

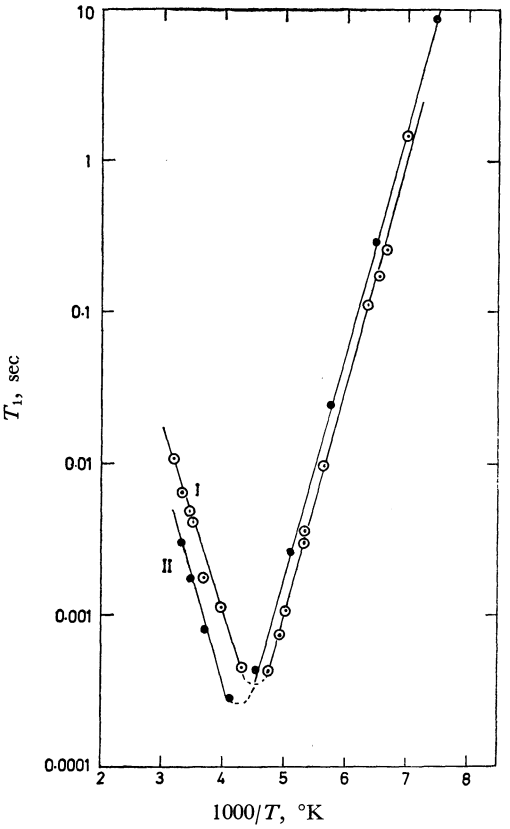

Fig. 2. Temperature dependence of T_1.
⊙ Measured in Direction I.
● Measured in Direction II.

plotted in Fig. 2. A typical V-shaped curve indicates that the reorientation with the jump rate ν_j governed by Arrhenius equation is a principal relaxation mechanism. The activation energy (in kcal/mol) is obtained from the slopes at the high and low temperature sides of the T_1 minimum as,

H_0 direction	High temp. side	Low temp. side	Averaged
I	6.1	6.9	6.5
II	6.85	6.8	6.8

These values are in good agreement with that of 7.0 kcal/mol from the line width transition.

The curve is similar to the one obtained from the proton resonance in $Ba(ClO_3)_2H_2O$ by Silvidi and McGrath,[2] but T_1 is 3 to 4 orders of magnitude smaller in the present case indicating predominant quadrupolar relaxation mechanism of deuteron. Theoretical values of T_1 minimum are calculated as follows.

The matrix elements of quadrupole interaction Hamiltonian are given as

$$(m\pm1\,|\,\mathscr{H}_Q\,|\,m) = \frac{eQ}{4I(2I-1)} \times (2m\pm1)[(I\pm m+1)(I\mp m)]^{1/2}(\varphi_{xz}\mp i\varphi_{yz}) \qquad (2)$$

5) G. Kartha, *Acta Cryst.*, **5**, 845 (1952).

$$(m\pm2|\mathscr{H}_Q|m) = \frac{eQ}{8I(2I-1)} \times [(I\pm m)(I\mp m-1)(I\pm m-1)(I\pm m+2)] \times (\varphi_{xx}-\varphi_{yy}\mp 2i\varphi_{xy}) \quad (3)$$

where φ's represent the matrix elements of EFG tensor. The z axis is taken along H_0. φ's which are different for the D_1 and D_2 of D_1OD_2, fluctuate with the random flip of D_2O, and cause relaxation among different m levels.

Denoting the mean lifetime of a deuteron in one of the site by τ, the autocorrelation function of the fluctuating φ can be written as

$$\langle\varphi(0)\varphi^*(t)\rangle = \varphi_\Delta^2 \exp(-2t/\tau), \quad (4)$$

where

$$\varphi_\Delta = [\varphi(D_1) - \varphi(D_2)]/2, \quad (5)$$

and $\varphi(D_1)$ and $\varphi(D_2)$ are φ at D_1 and D_2 respectively. Corresponding spectral density $J(\omega)$ is given by

$$J(\omega) = |\varphi_\Delta|^2 j(\omega), \quad (6)$$

$$j(\omega) = 4\tau/(1 + 4\omega^2\tau^2). \quad (7)$$

The transition probabilities of $1\rightarrow0$ and $1\rightarrow-1$ due to this motion are

$$P_1 = \hbar^2|A_1|^2 J(\omega), \quad (8)$$

$$P_2 = \hbar^2|A_2|^2 J(\omega), \quad (9)$$

where A_1 and A_2 represent spin parts of (2) and (3), respectively. T_1 is given by Eq. (1). To calculate T_1 in the direction I, the quadrupole coupling tensor $(eQ/h)q$ of D in the principal axis system as determined in Ref. 1 is transformed into the coordinate system where the z axis is along H_0 and the x axis perpendicular to the molecular plane. By the 180° flip motion the yz element changes as $\varphi_{yz}\rightarrow-\varphi_{yz}$. All the other elements are unchanged by the motion. $|(eQ/h)\varphi_{yz}| = 167$ kc/sec. Then from (1), (2), (6), and (8)

$$1/T_1 = (1/8\hbar^2)(167\times10^3h)^2 j(\omega). \quad (10)$$

Similarly in the direction II, when transformed into the coordinate system where z is along H_0 and x along bisector of D_2O, only the xy and xz elements of EFG tensor change by the flip motion, namely,

$$\varphi_{xy} \rightarrow -\varphi_{xy} \quad \text{and} \quad \varphi_{xz} \rightarrow -\varphi_{xz}.$$

$$|(eQ/h)\varphi_{xy}| = 117 \text{ kc/sec},$$

and $$|(eQ/h)\varphi_{xz}| = 119 \text{ kc/sec},$$

T_1 in this case will be,

$$1/T_1 = (1/8\hbar^2)(119\times10^3h)^2 j(\omega) + (1/4\hbar^2)(117\times10^3h)^2 j(2\omega). \quad (11)$$

The T_1 minimum and corresponding ν_j from (10) and (11) are 0.45 msec and 3.1×10^7 sec^{-1} for the direction I, and 0.24 msec and 4.5×10^7 sec^{-1} for the direction II respectively. Observed T_1 minimum values are about 0.4 msec and 0.3 msec

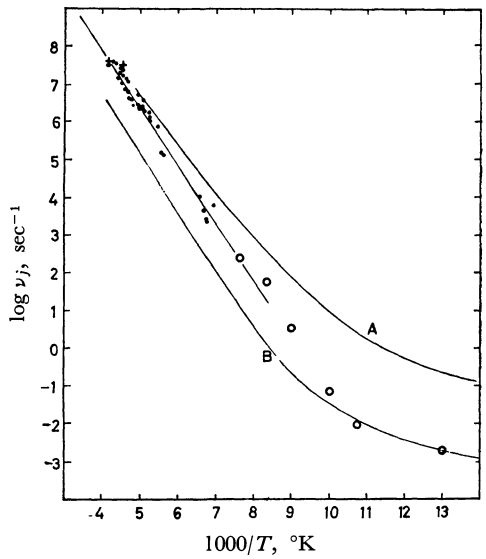

Fig. 3. Temperature dependence of jump rate ν_j determined from T_1 minimum, +, from direct measurement, ○, and from the line width change, ●. Curves A and B are theoretical ones from quantum mechanical tunneling process with potential barrier of 6.17 and 7.61 kcal/mol, respectively.

for the directions I and II, respectively. The agreement between the calculated and the observed is quite satisfactory. The parallel shift of the curve I from curve II of Fig. 2 is in the right direction, but a few times larger than that expected from the theory. ν_j at the T_1 minima are indicated in Fig. 3 of ν_j *versus* $1/T$ curve.

Direct Reorientation Rate Measurement. The rate of reorientation or the jump rate of a deuteron from the site 1 to site 2 can be directly measured in the following experiment, if one observes a recovery from saturation of a signal of site 1 by diffusion of site 2 spins, which has been kept in thermal equilibrium. Suppose the crystal is oriented in such a way that the signal of site 1 is unsplit, while that of site 2 has large splitting. We apply two 90° pulses in succession at the Larmor frequency. The first pulse saturates site 1 line. Then the magnitude of the Bloch decay signal after the second pulse shows a recovery due to the diffusion of unsaturated spins from the site 2 to site 1 by reorientation in addition to the recovery by spin-lattice relaxation. The method is applicable when T_2 is much shorter than this recovery time, that is, the two successive Bloch decay signals can be well separated. Also the rf pulse strength H_1 should be such that $\gamma H_1 \ll 2\pi\Delta\nu$, where $\Delta\nu$ is the frequency difference between the two sites, in order that the rf pulse has negligible effect on the site 2 nuclei. Direct measurement of τ, the lifetime in one of the sites, $(\tau = 1/\nu_j)$, is made when $\tau \ll T_1$ and $\tau \ll T_{12}$, the latter being the condition

that the cross-relaxation time T_{12} due to spin flip between the two sites should be negligible. This method has been applied to study the jump rate between bonds of deuterons in KD_2PO_4 by Schmidt and Uehling.[3] The relation of jump rate with recovery time constant given in Appendix I of their paper exactly applies to the present case, and the recovery time constant $=\tau/2=1/2\nu_j$. In order to avoid the error due to possible nonlinearity in the observed signal amplitude, they used the following method. Three 90° pulses are applied in succession, the time interval being t_1 between the first and second pulses, and t_2 between the first and third. t_1 is varied while t_2 is fixed at a value $t_2 \gg \tau$. t_1 is so adjusted that the Bloch decay signals after the second and the third pulses are made to have equal height. Then τ is given by $t_1=(\ln 3)\tau$. We used this method, and also two 90° pulse sequence, where the signal height following the second pulse is compared with the first one to observe the exponential growth. The measurement was done with H_0 in the direction III shown in Fig. 1, where site 1 line is at the Larmor frequency and $\Delta\nu$ is about 150 kc/sec. In $Ba(ClO_3)_2D_2O$, lines of stationary water molecule are observed below -120°C, and this is well below the temperature of the T_1 minimum. Since quadrupole relaxation due to reorientation is a principal relaxation mechanism, and the quadrupole interaction is only a small perturbation to the Zeeman energy, the inequality $T_1 \gg \tau$ holds. Therefore, the direct measurement of jump rate is applicable below -120°C. At very low temperatures, however, T_1 gets so large that it is necessary to irradiate the crystal with γ ray to bring T_1 to the workable range. Thus after this treatment, T_1 measured at direction I is about 90 sec at liquid nitrogen temperature, and stays nearly constant up to the temperature where relaxation due to the motion becomes appreciable (~ -140°C). The observed recovery is found to be much faster than 90 sec except at liquid nitrogen temperature where it becomes comparable to 90 sec. With this sample, we can conclude that the condition $\tau \ll T_1$, T_{12} is valid down to -170°C since T_{12} should be nearly constant, and T_1 due to paramagnetic centers is also rather insensitive to temperature variation, whereas the observed recovery gets much longer at the liquid nitrogen temperature. To estimate τ at the liquid nitrogen temperature, the observed recovery curve is compared with the calculated one with various τ values assuming $T_1=90$ sec, same as in direction I. If τ of 5 min at liquid nitrogen temperature thus obtained is correct, a bend in the plot of $\log \nu_j$ *vs.* $1/T$ would show a departure from the Arrhenius equation, and indicate quantum mechanical tunnel effect. ν_j calculated from the tunnelling process shown in the figure suggests that such a bend is quite probable.

Since the lines are narrow while $\Delta\nu$, the separation between the lines of D_1 and D_2, is large, the cross-relaxation between D_1 and D_2 is probably ineffective. It should be definitely ineffective from the formalism of Bloembergen *et al.*[6] However, to get an experimental justification for excluding cross-relaxation process at liquid nitrogen temperature, we measured the recovery at the crystal orientation where $\Delta\nu$ is about 80 kc/sec. Unless the recovery rate changes drastically, the cross-relaxation could be neglected.*2 In this case the recovery at liquid nitrogen temperature is found to be shorter by a factor of about 3 than the other case. However, that this is not due to the cross-relaxation is seen from the fact that the recovery toward a full intensity is observed instead of one half as expected from the cross-relaxation process. This shortening of recovery can be understood as the T_1 diminution due to cross-relaxation to the Ba nuclei which have short T_1 due to a quadrupole interaction. Using a quadrupole coupling tensor for ^{135}Ba and ^{137}Ba by Nakamura and Enokiya[7] the transition frequencies of Ba in the present experiment are calculated. The result turned out that one of the transitions falls in fact almost at 10 Mc. The whole task for such an experiment is rather involved. Moreover, transition frequencies of Ba resonances depend in a complex manner on crystal orientation, and the Ba quadrupole coupling and its temperature dependence have been determined only at higher temperatures, which situation makes the estimation of exact transition frequencies in the present experiment difficult. For this reason no further experiment on this line is made.

Values of ν_j determined in the present work are to be compared with those from the line width change. In the following a revision of the previous treatment[1] of line width transition will be described.

A random motion of atoms has an effect both on the quadrupole splitting and on dipole structure. It would be possible to derive a reorientation rate by comparing the observed broadened spectra with the numerically calculated one at each particular case taking into account the effect of motion on both quadrupole and dipole interaction in an exact fashion according to the theory of motional broadening.[8] However, poor quality of the observed line shape prevents the analysis of detailed line shape, and also the fact that the observations have to be made at various orientations of the crystal (that is, various values of quadrupole and dipole interactions) which requires much

*2 The authors are indebted to Professor C. P. Slichter for suggesting this measurement.

6) N. Bloembergen, S. Shapiro, P. S. Pershan and J. O. Artman, *Phys. Rev.*, **114**, 445 (1959).
7) S. Nakamura and H. Enokiya, *J. Phys. Soc. Japan*, **18**, 183 (1963).
8) A. Abragam, "The Principles of Nuclear Magnetism," Chapter X, Section II—IV, Oxford University Press, Oxford (1961).

too laborious calculations, this exact method seems to be impractical.

Generally signal-to-noise ratio of the broadened spectra is such that, 1) spectra can only be observed at the fast and slow exchange limits of the quadrupole broadening, 2) the only quantity which can be measured with a reasonable accuracy is the signal amplitude of the derivative curve between the points of maximum and minimum slopes of the absorption line. This signal amplitude will be denoted by S.

Since in general practice, one measures the line broadening where the quadrupole interaction is much larger than the dipole interaction the effect of motion upon the dipole width is relatively small (particularly so in the 180° flip of a water molecule where the intramolecular dipole interaction is unaffected by the motion). The change in dipole line width should therefore take place at the temperature range different from those of quadrupole structure. It may then be permissible to assume that the dipole width is invariant under the present condition of observation.

To derive an exact effect on quadrupole broadening it is, however, necessary to separate this effect from the dipole structure. Since S depends on the line width strongly (as the inverse square of the width if the dipole width is absent*3) the following procedure will be used.

A width between the maximum slopes, $\Delta\nu_{ms0}$, and a signal intensity S_0 is defined at the point where the exchange motion is either sufficiently rapid or sufficiently slow so that practically no motional broadening is involved in the line shape.

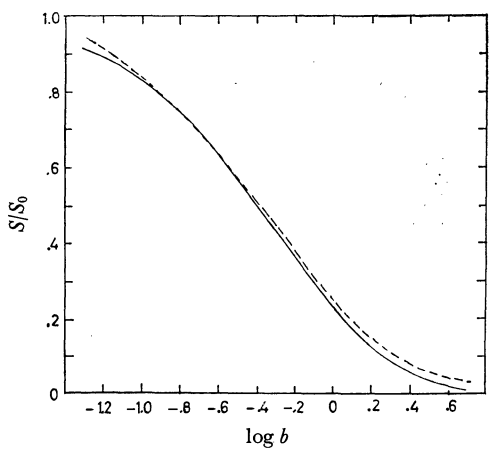

Fig. 4. Diminution of derivative signal intensity (S/S_0) due to broadening.
—— Gaussian line (half width $(\ln 2)^{1/2}$) broadened inhomogeneously by Lorentzian curve (half width b).
---- Lorentzian line (half width 1) broadened to half width $1+b$.

*3 Previous treatment (Ref. 1) is inadequate since $S/N \propto 1/\Delta\nu$ is assumed.

Numerical calculation of line shape is made, assuming a Gaussian dipole line shape (half maximum half width $(\ln 2)^{1/2}$) and each component of it is further broadened by a Lorentzian line shape of a given width (half maximum half width b). Then S/S_0 has a dependence on the line width parameter b as shown in Fig. 4. From the observed S/S_0, b is read off. $\Delta\nu_M$ $(=1/(2\pi T_2'))$, the half width due to motion) is obtained as,

$$\Delta\nu_M = \Delta\nu_{ms0} \times b/\sqrt{2},$$

a factor $1/\sqrt{2}$ coming from the normalization.

S and S_0 are obtained at different temperatures, and the signal height may therefore vary with temperature, according to various factors such as sensitivity of the instrument, the relaxation time, the Boltzmann factor, and the thermal noise, but difference between the temperatures of observation of S and S_0 is usually not so large to give serious effect.

If the original line is approximately Lorentzian with T_2 as in the case of certain paramagnetic substances, added breadth by motion can be separated by use of the similar curve also shown in Fig. 4, through the formula $\Delta\nu_M = \Delta\nu_{ms0} \times b \times 2\sqrt{3}$. $\Delta\nu_M$ is related to the jump rate in the case of 180° flip of a water molecule as $\Delta\nu_M = \nu_j/2\pi$ for the slow exchange limit, and $\Delta\nu_M = (\pi/4) \times (\Delta\nu^2/\nu_j)$ for the fast exchange limit.

The above procedure is applied to the case of $Ba(ClO_3)_2D_2O$. In Fig. 3 is shown the revised result including some added experimental points. The activation energy is 7.0 kcal slightly higher than the previous value, and the pre-exponential factor is 10^{14-15}.

As shown in Fig. 3, a satisfactory agreement is found among the experimental results of T_1, line width and jump rate, interpreted as due to random 180° flip of D_2O with a rate $\nu_j \propto \exp(-\Delta E/\boldsymbol{R}T)$, ΔE being 7 kcal/mol. Such a simple picture of the motion is probably true in case of this crystal. In this connection it is interesting to note that the good agreement of the frequency of twisting mode of D_2O derived from the recent neutron scattering experiment on this compound by Prask and Boutin[9] with those from ΔE with the assumption of cosine type potential.

Finally, it may safely be said that the present results give also a support to the reliability of deriving activation energy of the motion from the line width transition of quadrupole splitting by the procedure described above.

We are grateful to Assistant Professor Kiyoshi Kume of Tokyo Metropolitan University for many helpful comments for the construction of the pulse apparatus.

9) H. J. Prask and H. Boutin, *J. Chem. Phys.*, **45**, 699 (1966).

BULLETIN OF THE CHEMICAL SOCIETY OF JAPAN VOL. 41 833—837 (1968)

Electron Spin Resonance Study on Ultraviolet Light Irradiated Benzene Adsorbed on Silica Gel and Alumina

Tadayoshi TANEI*1

Department of Chemistry, Faculty of Science, Kyoto University, Sakyo-ku, Kyoto

(Received November 9, 1967)

Benzene adsorbed on silica gel was irradiated at 77°K with ultraviolet light. Three kinds of samples, with different degree of adsorption, were examined. ESR spectra were strongly dependent on the amount of benzene adsorbed and three different spectra were observed; (1) six-line spectrum with a splitting value of 6 gauss, assigned to phenyl radical, (2) seven-line spectrum with a splitting value of 4.5 gauss, assigned to benzene cation radical, and (3) apparent nine-line spectrum with 2.4 gauss splitting due to benzene dimer cation radical. Upon raising temperature, benzene cation radical was found to transform into benzene dimer cation radical. In UV-irradiated benzene-alumina system, cyclohexadienyl radicals were observed in addition to the ion radicals. It is suggested that the above reaction may be occurred by two photon absorption process involving the excitation of triplet benzene.

Photochemical studies on benzene have been carried out in various organic rigid glasses, mainly by optical spectroscopic methods. Gibson *et al.*[1] showed an evidence that benzene was photochemically decomposed in the rigid glasses of EPA and 3-methyl perfluoropentane to produce hexatriene-1,3,5 and diphenyl, respectively. Subsequently, Porter[2] and Leach *et al.*[3] independently investigated these reactions and led to a conclusion of the formation of substituted hexatriene. Migirdicyan[4] made an attempt to observe photochemical intermediates of benzene in organic rigid glasses by the method of electron spin resonance, but failed to observe any intermediate signal from benzene.

In the previous paper,[5] we reported that an ESR spectrum, consisting of six lines with the splitting value of 6 gauss, was observed from benzene irradiated with ultraviolet light from high-pressure mercury lamp at 77°K. In relation to this investigation, the present work was undertaken in order to obtain more insight in unstable photochemical intermediates from UV-irradiated benzene and to examine its reaction mechanism, using the method of ESR. We obtained an evidence that benzene adsorbed on silica gel can be photoionized by UV-irradiation at 77°K and that, when alumina is used as an adsorbent, hydrogen addition reaction to benzene ring can take place in addition to photo-ionization. A subsequent conversion reaction of benzene cation radical has also been investigated. On the basis of these experimental results, a photochemical reaction mechanism of benzene has been presented.

Experimental

Materials. Benzene was obtained from two commercial sources, Dotite spectrosol benzene manufactured by the Dojindo Research Laboratories Co., Ltd., and Merck's spectro-grade benzene. These samples were purified by recrystallization according to the method of Kanda *et al.*[6] In some experiments, benzene was purified in the presence of Na-K alloy through repeated freezing and thawing *in vacuo*. Hexadeuterobenzene of Merck (purity: 99%) was used without further refining. Silica gel from Mallinckrodt Chemical Works (100 mesh silica gel) was heated *in vacuo* for about 5 hr at 413 to 773°K. In some experiments, the silica gel was washed with special grade concentrated hydrochloric acid and distilled water, immediately before its use. Silica powder was obtained from ground quartz ampoules. Activated alumina for chromatographic adsorption from Nakarai Chemical Company Ltd. was used without further refining. It was heated *in vacuo* at 573°K for about 5 hr.

Adsorption Procedures. The adsorption apparatus was made modifying a vacuum transfer apparatus by Lewis *et al.*[7] and was connected to vacuum line. All samples were treated in the adsorption apparatus and subsequently the vapor was led to adsorbent in the ESR ampoule. The amount of adsorption of

*1 Present address: Sekisui Chemical Company Ltd., Research Laboratory, Hirose 25, Shimamoto-cho, Mishima-gun, Osaka Prefecture.

1) G. E. Gibson, N. Blake and M. Kalm, *J. Chem. Phys.*, **21**, 1000 (1953).

2) I. Norman and G. Porter, *Proc. Roy. Soc. (London), Ser. A*, **230**, 399 (1955).

3) S. Leach and E. Migirdicyan, *J. Chim. Phys.*, **54**, 643 (1957); *ibid.*, **58**, 409 (1961); *ibid.*, **58**, 416 (1961).

4) E. Migirdicyan, *ibid.*, **63**, 543 (1966).

5) T. Tanei, This Bulletin, **40**, 2456 (1967).

6) Y. Kanda and R. Shimada, *Spectrochim. Acta*, **17**, 7 (1961).

7) I. C. Lewis and L. S. Singer, *J. Chem. Phys.*, **43**, 2712 (1965).

benzene was not measured, but controlled by the following three procedures. 1) ESR quartz ampoule was cooled by liquid nitrogen for a moment (Sample-1). 2) Silica gel was exposed to benzene vapor for about 5 to 10 min at room temperature (Sample-2). 3) Sample-2 was pumped off at 323 to 333°K for about 2 to 3 hr (Sample-3).

Light Source and Irradiation. Either high-pressure mercury lamp (Toshiba 400W) or low pressure mercury lamp (Toshiba germicidal lamp) was used. As the filters were used Toshiba UV-25, UV-D25 and UV-29, respectively. γ-Irradiation was performed with Co-60 (700 Ci) at 77°K.

ESR Measurement. Spectra were recorded on a Varian V-4560 EPR spectrometer with 100kc modulation at 77°K and at higher temperatues up to about 173°K by using the Varian liquid nitrogen and variable temperature accessories.

Results

Benzene-Silica Gel Adsorption System. ESR spectra of UV-irradiated Sample-1, Sample-2 and Sample-3 are shown in Fig. 1. The effective wavelength to produce these spectra was found in the region from 2300 Å to 2600 Å by using filters. It is demonstrated that the spectra are strongly dependent on apparent amount of adsorption of benzene. UV-Irradiated hexadeuterobenzene, corresponding to Sample-2 and Sample-3,

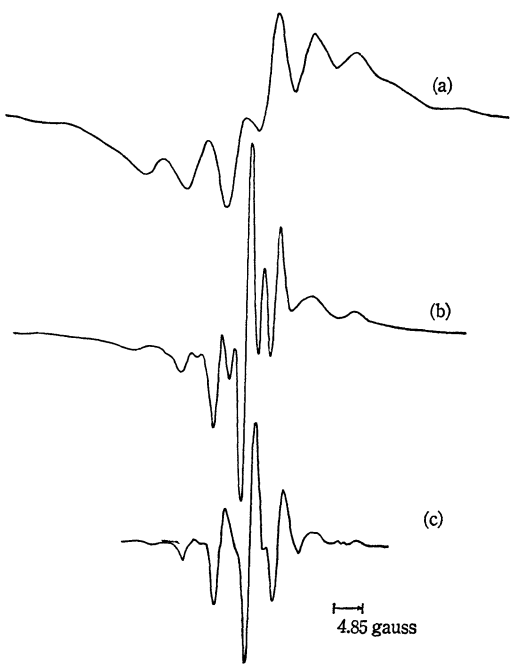

Fig. 1. ESR spectra of UV-irradiated benzene adsorbed on silica gel. The alphabetical marks in the figure, (a), (b) and (c), corresponds to Sample-1, Sample-2 and Sample-3 (see Experimental in this paper), respectively. UV-irradiation was performed for 100 min at 77°K.

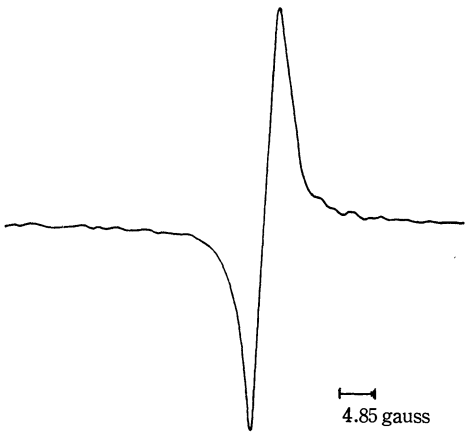

Fig. 2. ESR spectrum of UV-irradiated hexadeuterobenzene adsorbed on silica gel. UV-irradiation was performed for 100 min at 77°K.

gave only a singlet spectrum with ΔH_{msl} value of 3.4 gauss (see Fig. 2). Irradiated silica gel without adsorbed benzene gave no ESR signal, nor did adsorbed benzene without irradiation.

On raising temperature, these spectra change as shown in Figs. 3 to 5. In the spectrum of Sample-1 (see Fig. 3), a sharp component of the splitting 2.4 gauss appears in the central part. The seven-line spectrum of Sample-3 (see Fig. 5) gradually disappears and an apparent nine-line spectrum, with the intensity ratio of 1 : 2 : 5 : 8 : 14 : 8 : 5 : 2 : 1 and the splitting value of 2.4 gauss, appears, when the sample was kept at dry ice - methanol temperature. The behavior of Sample-2 (see Fig. 4) is also analogous to those of Sample-1 and Sample-3.

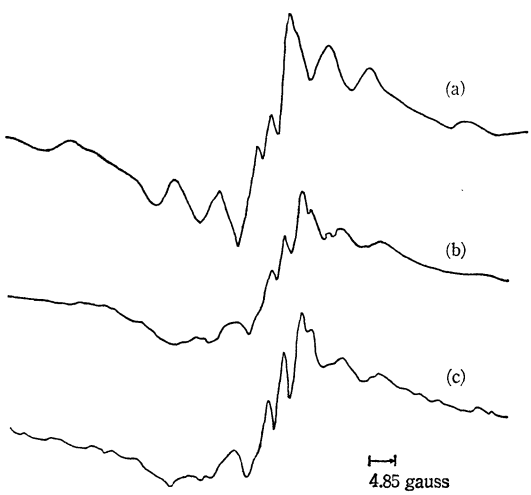

Fig. 3. Change with increasing temperature of ESR spectrum of Sample-1. Spectra were recorded at the temperatures of 77°K (a), 123°K (b) and 153°K (c).

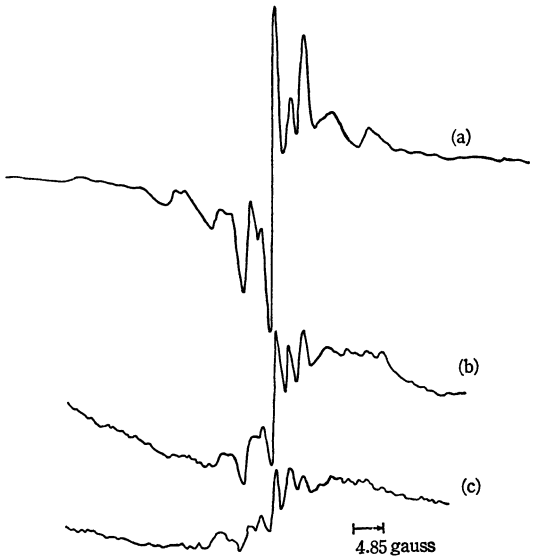

Fig. 4. Change with increasing temperature of ESR spectrum of Sample-2. Spectra were recorded at the temperatures of 77°K (a), 128°K (b) and 173°K (c).

The spectrum of Sample-1 mainly consists of six lines with the splitting value of 6 gauss (see Fig. (1 a)), which is essentially the same as the six-line spectrum[5] observed from UV-irradiated polycrystalline benzene at 77°K. The spectrum of Sample-2 is a superposition of the six-line spectrum and some sharp line spectrum in the central part, with the splitting value of 2.4 gauss (see Fig. 1(b)). The spectrum of Sample-3 is a sharp seven-line one, with the intensity ratio of 1 : 5 : 16 : 24 : 15 : 4.5 : 1, and its splitting value is approximately 4.5 gauss (see Fig. 1(c)).

From the UV-irradiated mixture of benzene with ground silica powder was observed a poorly resolved six-line spectrum, with the splitting value of 6 gauss, which is quite similar to the six-line spectrum of UV-irradiated polycrystalline benzene.

To summarize, we have observed three different spectra from UV-irradiated benzene adsorbed on silica gel. One is the six-line spectrum of 6 gauss separation (Fig. 1(a)). The second one is the seven-line spectrum of 4.5 gauss splitting (Fig. 1(c)) and the third one is the apparent nine-line spectrum of 2.4 gauss splitting (Fig. 5(c)).

Benzene-Alumina Adsorption System. The ESR spectrum of UV-irradiated benzene-alumina system (see Fig. 6) consists of a triplet of about 47 gauss splitting, each component with further quartet splitting of about 10.5 gauss, and in addition, it has a six-line component analogous to the benzene-silica gel system in the central part. The triplet spectrum of about 47 gauss splitting can be ascribed to the cyclohexadienyl radical.[8,9]

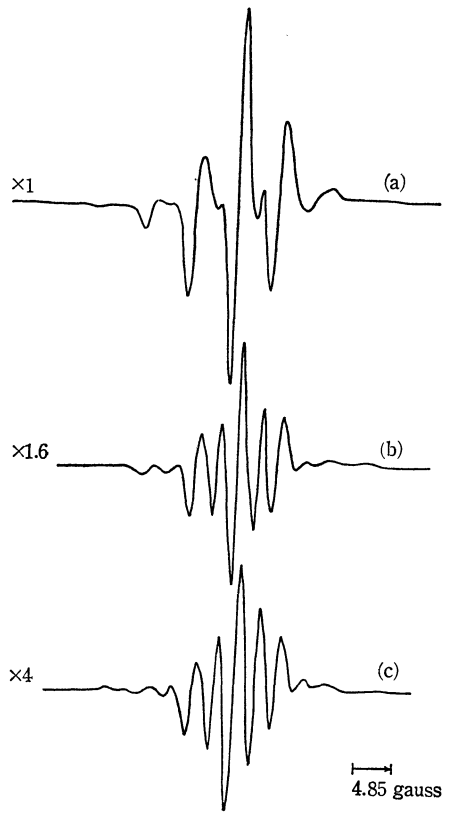

Fig. 5. Change with increasing time of ESR spectrum of Sample-3 kept at dry ice - methanol temperature.
(a) sample kept at 77°K. (b) sample kept at dry ice - methanol temperature for 57 min. (c) sample kept at dry ice - methanol temperature for 16 hr.
In this figure, numerical figures represent the relative sensitivity of spectrometer.

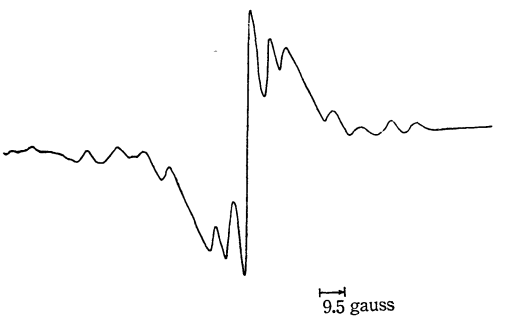

Fig. 6. ESR spectra of UV-irradiated benzene adsorbed on alumina. This sample corresponds to Sample-2. UV-irradiation was performed for 75 min at 77°K.

8) S. Ohnishi, T. Tanei and I. Nitta, *J. Chem. Phys.*, **37**, 2402 (1962).
9) H. Fisher, *Kolloid Z.*, **180**, 64 (1962).

Appearance of this triplet component is in contrast with the benzene - silica gel system. Upon subsequent γ-irradiation at 77°K, increase in triplet component was observed.

Discussion

Interpretation of ESR Spectra. According to the presentation in the preceding paper,[5] the six-line spectrum of 6 gauss splitting in Fig. 1(a) can be interpreted as the phenyl radical. The seven-line spectrum of 4.5 gauss splitting (Fig. 1(c)) can be assigned to the benzene cation radical. The splitting value is found to be 25% larger than that of the benzene anion radical. The difference between negative and positive ion radicals of alternant aromatic hydrocarbons has been studied by many workers from experimental and theoretical points of view.[7,10-17] Bolton *et al.*[12] have predicted that proton hyperfine coupling constants of positive ions should be larger than those of corresponding negative ions as a result of difference in charge density and obtained the following equation.

$$a_H^{\pm} = (Q\rho \pm K\rho^2) \qquad (1)$$

a_H: the hyperfine coupling constant between electron and an aromatic proton
ρ: the spin density on the adjacent carbon atom
Q: a constant charateristic for an aromatic C–H bond
K: excess charge density

Lewis *et al.*[7] have measured the proton coupling constants of cation radicals of alternant aromatic hydrocarbons and concluded that hyperfine coupling constants of cation radicals are 25% larger than those of corresponding anion radicals. Their empirical values of Q and K in the Eq. (1) are 32.2 and 16, respectively.

The experimental result in the present work is found to agree quite well with the general tendency ascertained as for the difference between corresponding anions and cations. However, we have to use a different set of Q and K values. Namely, Q should be 25 and K be 15, in the Eq. (1). Most recently, in an independent work of the present study, Edlund *et al.*[18] have observed the ESR spectrum of the benzene cation radical from γ-irradiated benzene adsorbed on silica gel. Their splitting value is found to be in accord with the present value.

As shown in Fig. 5, benzene cation radical gradually decays and changes to show an apparent nine-line spectrum, on being preserved at dry ice-methanol temperature. The splitting value of nine-line spectrum corresponds to one half of that of benzene cation radical. On the basis of these data, it seems the most reasonable to assume that the apparent nine-line spectrum is responsible for the benzene dimer cation radical $(C_6H_6)_2^+$, in which the spin density on carbon atom should be 1/12 and its theoretical spectrum should consist of 13 lines with the intensity ratio of 1 : 12 : 66 : 220 : 495 : 792 : 924 : 792 : 495 : 220 : 66 : 12 : 1. The above ratio indicates that the intensities of outer peaks become almost negligible as compared with those of the central part. Therefore, its relation seems to be consistent with the experimental fact that only the nine lines, with the intensity ratio of 1 : 2 : 5.4 : 8.1 : 14 : 8.1 : 5.4 : 2 : 1, were observed from the benzene dimer cation radical. The central intensity ratio in the experimental nine-line spectrum, however, seems to be rather higher in comparison with the theoretical intensity ratio. Its difference is probably due to the overlapping of the initial seven-line spectrum still just remaining in the central part of the nine-line spectrum. Edlund *et al.*[18] have also observed this nine-line spectrum from γ-irradiated benzene adsorbed on silica gel.

The spectrum shown in Fig. 1(b) can be interpreted as an overlapping of six-line spectrum in Fig. 1(a), seven-line spectrum in Fig. 1(c) and nine-line spectrum in Fig. 5(c).

In benzene-alumina system (Fig. 6), one can interpret that cyclohexadienyl radicals are produced in addition to phenyl and benzene ion radicals.

Bubnov *et al.*[19] have observed ESR spectra from ultraviolet light irradiated "benzene-phosphoric acid matrix" (benzene concentration; 2×10^{-2} mol/l) at 77°K. And very recently, Carter *et al.*[20] have observed the seven-line and nine-line spectrum from UV-irradiated "benzene-sulfuric acid matrix" and the six-line spectrum from UV-irradiated polycrystalline benzene, while we are preparing the present manuscript.

Photochemical Reactions of Adsorbed Benzene. Photo-ionization of benzene derivatives has been observed in various media by many

10) S. Aono, *Progr. Theor. Phys. (Kyoto)*, **21**, 779 (1954).
11) J. Higuchi, *J. Chem. Phys.*, **39**, 3455 (1963).
12) J. P. Colpa and J. R. Bolton, *Mol. Phys.*, **6**, 273 (1963).
13) J. R. Bolton, *J. Chem. Phys.*, **43**, 309 (1965).
14) G. Giacommeti, P. L. Nordio and M. V. Pavan, *Theret. Chim. Acta*, **1**, 404 (1963).
15) A. Carrington, *Quart. Rev.*, **17**, 67 (1963).
16) S. I. Weissman, E. DeBoer and J. J. Conradii, *J. Chem. Phys.*, **26**, 963 (1957).
17) G. J. Hoijtink and W. P. Weijland, *Rec. Trav. Chim.*, **76**, 836 (1957).
18) D. Edlund, P. O. Kinell, A. Lund and A. Shimizu, *J. Chem. Phys.*, **46**, 3679 (1967).
19) N. N. Bubnov, V. V. Voevodskii, N. V. Fok and B. N. Sheltztov, *Opt. Spectry. (USSR)*, **11**, 78 (1961).
20) M. K. Carter and G. Vincow, *J. Chem. Phys.*, **47**, 292 (1967).

workers[21-25] and its mechanism has been interpreted by two photon absorption process involving an excitation of triplet state. In the case of photo-ionization of adsorbed benzene, the absorption of one photon, with the energy of 4.75 to 5.37 eV, would be energetically insufficient to photoionize benzene, because the first ionization potential of benzene corresponds to 9.2 eV. In the radiolysis of hydrocarbons adsorbed on silica gel, an increase in G values has been confirmed.[26] Moreover, it has also been reported that some catalytic sites are generated in silica gel irradiated with ionizing radiation.[27] In the photolysis, however, such a phenomenon has never been reported. Accordingly, it seems reasonable to assume that silica gel, generally well known as a physical adsorbent, would only act as a trapping site for very unstable paramagnetic species. As a trapping site in silica gel, one can suppose OH group, by which π-type hydrogen bond can be formed between benzene and silica gel surface.[28,29] From such a point of view, the photochemical reactions in benzene - silica gel system could be interpreted in terms of the following processes involving an excitation of triplet state benzene.

$$C_6H_6(\text{ads}) \xrightarrow{2h\nu} C_6H_6^+ + e \qquad (2)$$

$$C_6H_6^+ + C_6H_6 \rightarrow \{C_6H_6 \cdots C_6H_6\}^+ \qquad (3)$$

In the process (2), photo-ionization is induced by two photon absorption to lead to the formation of benzene cation radical. Namely, two photon absorption mechanism in benzene could be attained through transitions between the following excited states.

$$^1A_{1g} \xrightarrow{h\nu} {}^1B_{2u}(4.84\,\text{eV}) \qquad {}^1B_{2u} \rightarrow {}^3B_{1u}(3.7\,\text{eV})$$

$$^3B_{1u} \xrightarrow{h\nu} {}^3E_{2g}(8.4\,\text{eV})$$

In fact, triplet-triplet absorption in benzene has been successfully observed in organic rigid glasses of isopentane and 3-methyl-pentane at 77°K by Godfrey *et al.*[30] in recent years. Furthermore, the experimental fact that UV-irradiation at dry ice-methanol temperature gave no paramagnetic species and the emittance of phosphorescence at 77°K seem to suggest that the photo-excitation of $^3B_{1u}$ state plays a very important role in photo-ionization of benzene. The energy of $^3E_{2g}$ state, theoretically calculated by Pariser,[31] is approximately comparable to the benzene ionization potential energy.

Benzene cation radical is known as very unstable paramagnetic species. In the process (3), benzene cation, weakly adsorbed in polylayer state, and with more mobility, is followed by dimerization with surrounding benzene molecules to produce benzene dimer cation.

The process of the phenyl radical formation can not be reasonably explained from the present experimental results, although Carrington *et al.*[32] have suggested a possibility of phenyl radical being produced from benzene cation by ring proton detachment. According to the prediction by Carrington *et al.*,[32] the six-line spectrum of Fig. 1(a) can be responsible for the phenyl radical, the unpaired electron being localized on the carbon σ orbital.

The observation of cyclohexadienyl radicals in benzene-alumina system is rather different from the result in benzene - silica gel system, where cyclohexadienyl radicals can hardly be observed. This phenomenon can be reasonably interpreted as being responsible for the catalytic activity of alumina for the hydrogenation.[33]

The author wishes to thank Professors Hiroyuki Hatano and Shunichi Ohnishi for their helpful discussions and encouragement during this work. Thanks are also due to Professor Isamu Nitta for his favor to provide Varian V-4560 EPR spectrometer and to Professor Keiji Kuwata for his interest.

21) G. N. Lewis and D. Lipkin, *J. Am. Chem. Soc.*, **64**, 2801 (1942).
22) K. D. Cadogan and A. C. Albrecht, *J. Chem. Phys.*, **43**, 2550 (1965).
23) G. E. Johnson, W. M. McClain and A. C. Albrecht, *ibid.*, **43**, 2911 (1965).
24) W. A. Gibbons, G. Porter and M. I. Savadatti, *Nature*, **206**, 1355 (1965).
25) H. Tsubomura, N. Yamamoto, K. Kimura, T. Sato, H. Yamada, M. Kato, G. Yamaguchi and Y. Nakato, This Bulletin, **38**, 2021 (1965); N. Yamamoto, Y. Nakato and H. Tsubomura, *ibid.*, **39**, 2603 (1966).
26) H. W. Kohn, *J. Phys. Chem.*, **68**, 3129 (1964).
27) C. Barter and C. D. Wagner, *ibid.*, **69**, 491 (1965).
28) M. Okuda, *Nippon Kagaku Zasshi (J. Chem. Soc. Japan, Pure Chem. Sect.)*, **82**, 1118 (1961).
29) A. V. Kiselev, *Dokl. Akad. Nauk., USSR*, **120**, 834 (1958).
30) T. S. Godfrey and G. Porter, *Trans. Faraday Soc.*, **62**, 7 (1966).
31) R. Pariser, *J. Chem. Phys.*, **24**, 250 (1956).
32) A. Carrington, F. Pravnieks and M. C. R. Symons, *J. Chem. Soc.*, **1959**, 947.
33) J. H. Sinfelt, *Ind. Eng. Chem.*, **58**, 18 (1967).

BULLETIN OF THE CHEMICAL SOCIETY OF JAPAN VOL. 41 838—843 (1968)

Synthesis of Chelating Agents. V.*1 1,2,3-Triaminopropanehexaacetic Acid and Its Acid Dissociation Scheme*2

Mitsumasa MIYAZAKI,*3, *4 Yoshiki MORIGUCHI and Keihei UENO

Department of Organic Synthesis, Faculty of Engineering, Kyushu University, Hakozaki, Fukuoka

(Received October 30, 1967)

1,2,3-Triaminopropane-*N,N,N',N',N'',N''*-hexaacetic acid (TAPHA) was synthesized by the carboxymethylation of 1,2,3-triaminopropane. The acid dissociation scheme of the ligand was studied by means of potentiometric titration, infrared absorption spectroscopy and proton nuclear magnetic resonance spectroscopy. It is found that TAPHA exists as a zwitter ion in aqueous solution, in which protons attach to each nitrogen atom of 1- and 3-carbon, and that the dissociations of first four and the last two steps correspond to the dissociations of carboxylic protons and ammonium protons, respectively. The stepwise proton dissociation constants of the ligand is determined as $pK_1 \approx 2$, $pK_2 = 2.43$, $pK_3 = 3.52$, $pK_4 = 4.30$, $pK_5 = 8.26$ and $pK_6 = 9.88$ ($\mu = 0.1$, 25°C).

Many multidentate complexanes such as EDTA, DTPA (diethylenetriaminepentaacetic acid)[1] and TTHA (triethylenetetraminehexaacetic acid[2]) have been synthesized and the relationships between their structures and chelating behaviors have been discussed in various ways. In our laboratories, our efforts have been focused to the syntheses of multidentate complexanes with a hope of finding the ligands with high metal ion specificity, and some of the results have been published in the previous papers of this series.[3]

This paper is to report on the synthesis of the new ligand, 1,2,3-triaminopropane-*N,N,N',N',N'',N''*-hexaacetic acid (TAPHA), and on the acid dissociation scheme of this ligand. TAPHA has been synthesized in 84% yield from 1,2,3-triaminopropane by the alkaline condensation of three moles of bromoacetic acid per mole of triamine, followed by the repeated carboxymethylation with sodium cyanide and formaldehyde.

Before going into the investigation on the chelating behavior of the ligand, the acid dissociation scheme of TAPHA has been investigated by the conventional potentiometry, the infrared absorption spectroscopy and the proton nuclear magnetic resonance spectroscopy. A microscopic picture of the acid dissociation scheme of this nonadentate hexabasic acid has been establsihed from these results.

During the course of our investigation, a British Patent has been published on the synthesis of TAPHA just after we have succeeded in the synthesis, but no detailed procedure of the synthesis nor detailed chelating behavior of this ligand was available.[4]

Experimental

Synthesis of Ligand. 1,2,3-Triaminopropane-*N,N,N',N',N'',N''*-hexaacetic acid (TAPHA) was synthesized by the carboxymethylation of 1,2,3-triaminopropane.

1,2,3-Triaminopropane (IV).[5] The triamine was synthesized from allyl chloride (I) *via* allylamine (II)[6] and 1-amino-2,3-dibromopropane hydrobromide (III)[7] succesively. The crude triamine was purified by vacuum distillation, bp 89—90°C/15 mmHg. The triamine was identified by the melting point and elementary analysis of tribenzoyl derivative, and IR spectra of free amine. The purity of the triamine determined by the perchloric acid titration in acetic acid, was 97.4%.

TAPHA (VI). The alkaline condensations of chloroacetic acid or bromoacetic acid with triamine (IV) have been tried in various conditions. The reaction

*1 Paper IV; N. Okaku, K. Toyota, Y. Moriguchi and K. Ueno, This Bulletin, **40**, 2326 (1967).

*2 Contribution No. 146 from the Department of Organic Synthesis, Kyushu University.

*3 Taken in part from the thesis of Master of Engineering, Kyushu University of M. M.

*4 Present Address: Amagasaki Plant, Dainippon Ink Chem. Ind. Ltd., Amagasaki-shi.

1) a) E. J. Durham and D. P. Ryskiwich, *J. Am. Chem. Soc.*, **80**, 4812 (1958); b) G. Anderegg, P. Nägeli, F. Müller and G. Schwarzenbach, *Helv. Chim. Acta*, **42**, 827 (1959); c) S. Chaberek, A. E. Frost, M. A. Doran and N. J. Bicknell, *J. Inorg. Nucl. Chem.*, **11**, 184 (1959).

2) a) J. H. Grimes, A. J. Huggard and S. P. Wilford, *J. Inorg. Nucl. Chem.*, **25**, 1225 (1963); b) T. A. Bohigian and A. E. Martell, *Inorg. Chem.*, **4**, 1264 (1965).

3) N. Okaku, K. Toyota, Y. Moriguchi and K. Ueno, This Bulletin, **40**, 2326 (1967).

4) J. R. Geigy A. G. Brit. Pat. 926351; *Chem. Abstr.*, **59**, 11264f (1963).

5) J. E. Sutton, *Roy. Australian Chem. Inst. J. & Proc.*, **17**, 232 (1900).

6) A. Clavier, *Bull. Soc. Chim. France*, **1954**, 646.

7) C. Paal and C. Hermann, *Ber.*, **22**, 3076 (1889).

with chloroacetic acid gave no desired product, but gave unidentified partially carboxylated products. The reactions with bromoacetic acid gave TAPHA in very low yield (less than 3.5%). The repeated carboxymethylation of triamine with sodium cyanide and formaldehyde[8] gave also TAPHA, but still in low yield (less than 6.1%). The best result was obtained by the alkaline condensation of three moles of bromoacetic acid with one mole of triamine, followed by the repeated carboxymethylation with sodium cyanide and formaldehyde. The condition of the typical run is as follows.

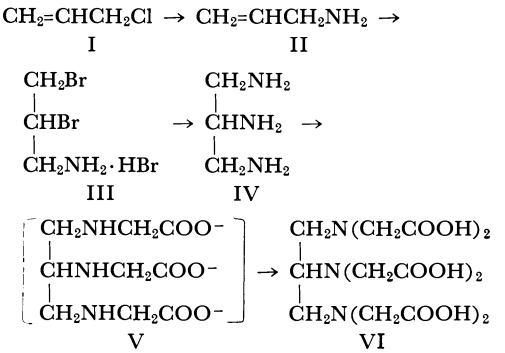

Plate 1

In a 300 m*l* reaction flask, a solution of 94.2 g (1.0 mol) of monochloroacetic acid in 70 m*l* water was neutrized to phenolphthalein with 10 N sodium hydroxide solution below 15°C. To this solution, 17.8 g (0.20 mol) of triamine (IV) was added with stirring, and the mixture was heated to 30—45°C. The pH of the mixture was maintained at 10—11 (red to phenolphthalein) by adding sodium hydroxide solution intermittently. It took 25—35 hr to consume theoretical amount of alkali. After then, another 5 m*l* of 10 N sodium hydroxide solution was added and the reaction mixture was heated at 45°C for an additional hour. In a 500 m*l* three-necked flask fitted with a stirrer, a dropping funnel and a distilling column, the above reaction mixture (V) was placed with 6.8 g of sodium hydroxide and 43.6 g (0.89 mol) of sodium cyanide. To this solution, 70 m*l* of aqueous solution containing 0.10 mol of formaldehyde was dropped continuously with stirring at 25°C for 5 hr. After the addition of formaldehyde, the reaction mixture was distilled at reduced presure below 60°C. After 70 m*l* of distillate was obtained, 100 m*l* of water was added to the residue and the distillation was continued under the same condition until 100 m*l* of water distilled. Then the reaction mixture was cooled to 25°C and another formaldehyde solution was dropped slowly into it. After addition of formaldehyde the distillation was repeated again. This process was repeated for eight times. The total amount of formaldehyde added was 0.80 mol. Finally, the pH of the reaction mixture was adjusted to about 1 with 6 N HCl. After keeping the solution in an refrigerator overnight, the white precipitate was separated by filtration, washed with water and was dried at reduced pressure overnight (55.7 g). An additional amount (20.6 g) of the product was obtained by concentrating the filtrate. Total yield 76.3 g (84% for triamine (IV)). The crude product was purified by repeated recrystallization from hot water. When it was dried in vacuum over phosphorus pentoxide or silica gel at 120°C overnight, monohydrate was obtained as white crystalline powder that was slightly soluble in cold water and decomposed at 233.5—230°C.

Found: C, 39.85; H, 5.51; N, 9.16%; mol wt, 458 (Neut. equiv.). Calcd for $C_{15}H_{25}O_{12}N_3 \cdot H_2O$: C, 39.56; H, 5.53; N, 9.23%; mol wt, 455.

Measurement of Infrared Absorption Spectra. The spectra were recorded with a Nippon Bunko Model DS 301 double-beam spectrophotometer equipped with sodium chloride optics. The spectra of free ligand as well as its sodium salts were studied in solid phase by Nujol mull method (Fig. 1). The spectra were also measured in a deuterium oxide solution as a function of pD using a cell with calcium fluoride windows. The p*d* of the solution was adjusted by adding sodium deuteroxide solution which was prepared by dissolving metallic sodium in deuterium oxide. Three characteristic absorption bands of 1720, 1625—1630, 1590 cm^{-1} were assigned to $=NCH_2COOH$, $=N^+HCH_2COO^-$, $=NCH_2COO^-$ respectively,[9] and their spectra at various pD values are reproduced in Fig. 2.

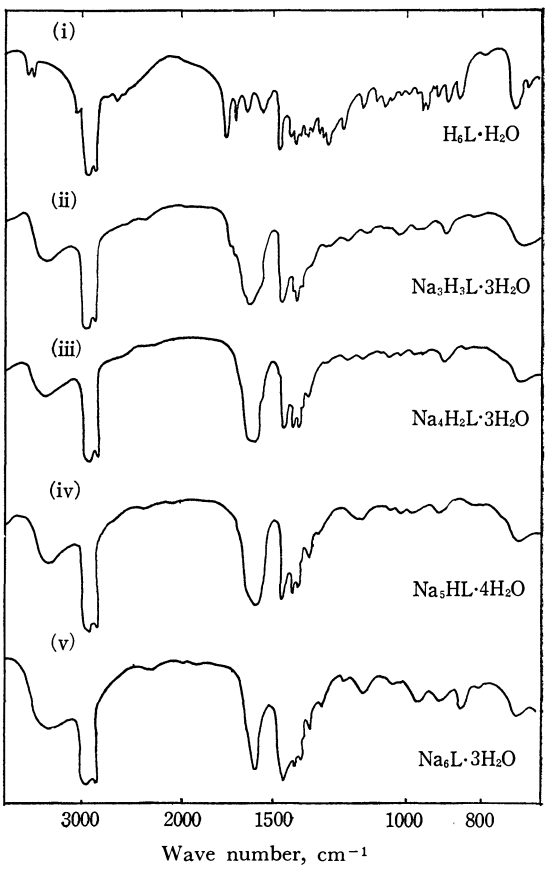

Fig. 1. Infrared spectra of TAPHA free acid and its sodium salts in Nujol mull.

8) R. Smith, J. L. Bullock, F. C. Bersworth and A. E. Martell, *J. Org. Chem.*, **14**, 355 (1949).
9) Y. Tomita, T. Ando and K. Ueno, *J. Phys. Chem.*, **69**, 404 (1965).

Measurements of Proton Nuclear Magnetic Resonance Spectra. The spectra were studied as a function of pH with a Varian A-60 high resolution spectrometer equipped with a 60 Mc oscillator. *t*-Butylalcohol was used as an internal reference (τ= 8.78 ppm). The pH of the aqueous solution was adjusted by the careful addition of 5 N nitric acid to 1 m*l* of 0.5 M TAPHA stock solution (pH≒12), which was prepared by dissolving free acid in aqueous potassium hydroxide solution. The pH of sample solutions was measured with a Hitachi-Horiba Model P pH meter equiped with a micro glass electrode.

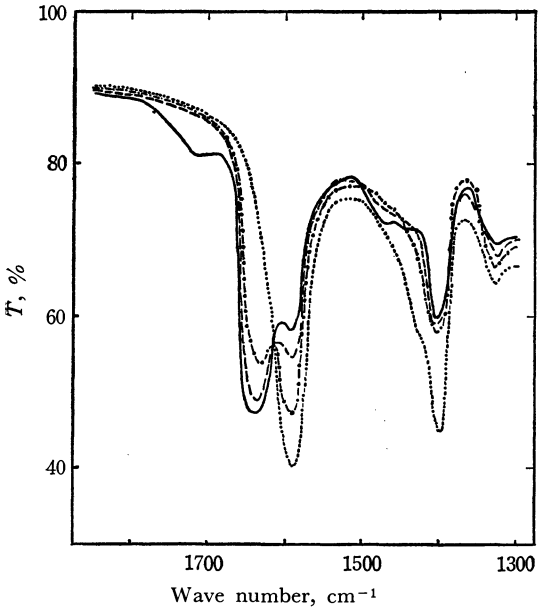

Fig. 2. Infrared spectra of TAPHA in D_2O at various pD values; ——, pD=4.4; - - -, pD= 5.8; -·-·-, pD=8.4; ····, pD≒14.

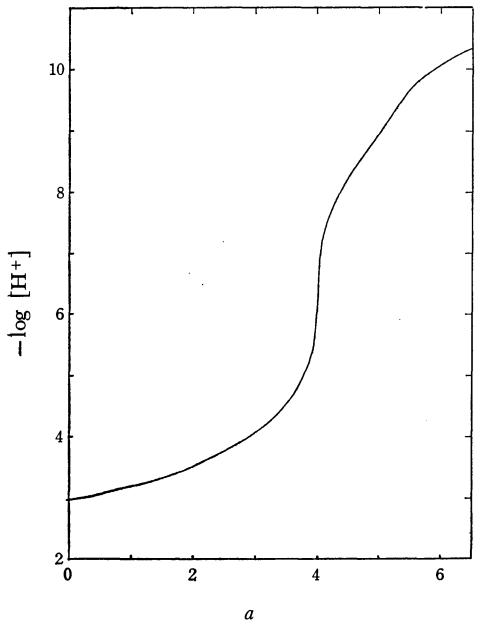

Fig. 3. pH titration curve of TAPHA (5×10^{-4} M) at 25°C in 0.1 M KNO_3.

Measurements of Acid Dissociation Constant. The same apparatus as described in our previous paper was employed.[3] The measurements were carried out at 25±0.1°C in aqueous solution of ionic strength μ=0.1 with KNO_3. For the determination of acid dissociation constant, a 200 m*l* of 5—6×10^{-4} M solution of the ligand was titrated with carbonate free 1×10^{-1} N potassium hydroxide solution. The pH meter was a Hitachi-Horiba Model P and was calibrated under a constant ionic stregnth (0.1) by refering to hydrogen ion concentration calculated from the acetic acid - potassium hydroxide system. A typical result of the titration is shown in Fig. 3.

Calculation of Acid Dissociation Constants

It is seen from Fig. 3 that the dissociations of first four steps are clearly separated from the last two steps. Thus, the calculation of dissociation constants of first four steps and last two steps can be conducted separately.

In general, when the successive acid dissociation constants of *m*-basic acid are defined by Eq. (1), these constants can be calculated from a set of *m* equations as expressed by Eq. (2) using *m* numbers of data of a pH titration curve.[10]

$$\left.\begin{aligned} K_1 &= [H][H_{m-1}L]/[H_mL] \\ K_2 &= [H][H_{m-2}L]/[H_{m-1}L] \\ &\vdots \\ K_m &= [H][L]/[HL] \end{aligned}\right\} \quad (1)$$

$$(1-n_i)[H]_i/K_m + (2-n_i)[H]_i^2/K_mK_{m-1} + \cdots + (m-n_i)[H]_i^m/K_mK_{m-1}\cdots K_1 - n_i = 0 \quad (2)$$

where

$$n_i = m - a_i + ([OH]_i - [H]_i)/L_t \quad (3)$$

and a_t and L_t represent the moles of alkali added per mole of ligand at *i*th datum in a pH titration curve and total concentration of ligand respectively. In this paper, the equation for solving Eq. (2) is expressed as the matrixes of Eqs. (4) and (5) and the calculation were carried out at the Computation Center of Kyushu University with a program of Gauss-Jorden method.

$$\begin{vmatrix} J_{11} & J_{12} & J_{13} & J_{14} & n_1 \\ J_{21} & J_{22} & J_{23} & J_{24} & n_2 \\ J_{31} & J_{32} & J_{33} & J_{34} & n_3 \\ J_{41} & J_{42} & J_{43} & J_{44} & n_4 \end{vmatrix} \qquad a_i \leqq 4 \quad (4)$$

$$\begin{vmatrix} J_{11} & J_{12} & n_1 \\ J_{21} & J_{22} & n_2 \end{vmatrix} \qquad 4 < a_i \leqq 6 \quad (5)$$

in which, elements of the matrixes are expressed by Eqs. (3) and (6).

10) G. Schwarzenbach, *Helv. Chim. Acta*, **33**, 947 (1948).

Table 1. Acid dissociation constants of TAPHA and related complexanes
$\mu=0.1$ (KNO_3), 25°C

	pK_1	pK_2	pK_3	pK_4	pK_5	pK_6	Ref.
TAPHA	≈2	2.43 ±0.14	3.52 ±0.01	4.30 ±0.01	8.26 ±0.02	9.88 ±0.03	
EDTA	1.99	2.67	6.16	10.23			12
TMDTA	2.0	2.67	7.91	10.27			11
DTPA	1.6	2.64	4.27	8.60	10.58		1b
TTHA	2.42	2.95	4.16	6.16	9.40	10.19	2b

TMDTA: Trimethylenediaminetetraacetic acid
DTPA: Diethylenetriaminepentaacetic acid
TTHA: Triethylenetetraaminehexaacetic acid

$$J_{ij} = (j-n_i)[H]^i \quad (6)$$

For Eq. (4), $m=4$; $i, j=1, 2, 3, 4$

For Eq. (5), $m=6$; $i, j=1, 2$

The results are shown in Table 1 along with those of other complexanes of related structure.

Results and Discussion

As shown in Fig. 3, there is a marked pH jump at $a=4$, so it is expected that the nature of the acid dissociation of the first four steps are quite different from those of the last two steps, and that TAPHA exists as zwitter ion in aqueous solution. If one compares the acid dissociation constants of TAPHA with those of the other complexanes (Table 1), it is clear that the first four and the last two steps correspond to the dissociations of the carboxylic protons and ammonium protons respectively.

This view is also confirmed from the pD dependence of infrared absorption spectra of TAPHA in deuterium oxide solution. The characteristic absorption bands of TAPHA in deuterium oxide solution over a range of 1800—1300 cm^{-1} are reproduced in Fig. 2. Three bands at 1720, 1630—1625 and 1590 cm^{-1} can reasonably be assigned to $\bar{\nu}_{C=O}$ of $=NCH_2COOH$, $=\overset{+}{N}HCH_2COO^-$ and $=NCH_2COO^-$ groups respectively.[9] In the pD region which corresponds to the pH region on the titration curve at $a>4$, a weak band at 1720 cm^{-1} disappeared completely, indicating the dissociation of carboxylic proton. It was also noticed that a strong band at 1630 cm^{-1} increased in its intensity with an increase of pD, indicating the deprotonation from ammonium nitrogens at higher pH region. Because of the poor solubility of TAPHA in water at low pH region, the dissociation in acidic solution could not be followed by the solution spectra. However, these results show that the acid dissociations of the first four steps correspond to those of carboxylic protons and the last two dissociation steps are related with the deprotonation from ammonium groups.

Thus, it may be concluded that, in aqueous solution, TAPHA takes a zwitter ion structure, in which only two of three basic nitrogens exist as protonated state. Then, we can write two possible structures for TAPHA, the one having two α-ammonium carboxylate groups at 1- and 2-positions (VIIb) and the other having two α-ammonium carboxylate groups at 1- and 3-positions (VIIa). These two structures resemble with EDTA and TMDTA (trimethylenediaminetetraacetic acid) respectively with regard to their relative positions of protonated nitrogen atom.

Now, it has been known that $\Delta pK_{4-3}(=pK_4-pK_3)$ of TMDTA (2.36)[11] is smaller than that of EDTA (4.07),[12] while the pK_4 values being about the same. This indicates that the dissociation of third step, which is a deprotonation from one of two protonated nitrogen atoms, occurs more easily in EDTA than in TMDTA. This effect can be explained by the electrostatic repulsion between protons on two positive nitrogens, which are closer in EDTA, receiving stronger repulsive force between them. The similar effect has been also observed for trimethylenediamine (1,3-diaminopropane) and 1, 2-diaminopropane. ΔpK_{2-1} for trimethylenediamine (1.76)[13] is smaller than that of 1,2-diaminopropane (2.87).[14] If one compares these values with ΔpK_{6-5} of TAPHA which corresponds to ΔpK_{4-3} of EDTA or TMDTA, and ΔpK_{2-1} of the diamines, the value for TAPHA (1.62) is rather closer to those of TMDTA and trimethylenediamine than those of EDTA and 1,2-diaminopropane. This result may suggest that TAPHA will take the structure VIIa rather than VIIb.

A more direct confirmation on the zwitter ion structure of TAPHA in aqueous solution was undertaken by the proton nuclear magnetic spectroscopy. The pH dependence of chemical shift

11) G. Schwarzenbach and H. Ackermann, *ibid.*, **31**, 1029 (1948).
12) G. Schwarzenbach and H. Ackermann, *ibid.*, **30**, 1798 (1947).
13) G. Schwarzenbach, B. Maissen and H. Ackermann, *ibid.*, **35**, 2333 (1952).
14) F. Basalo, R. K. Murmann and Y. T. Chen, *J. Am. Chem. Soc.*, **75**, 1478 (1953).

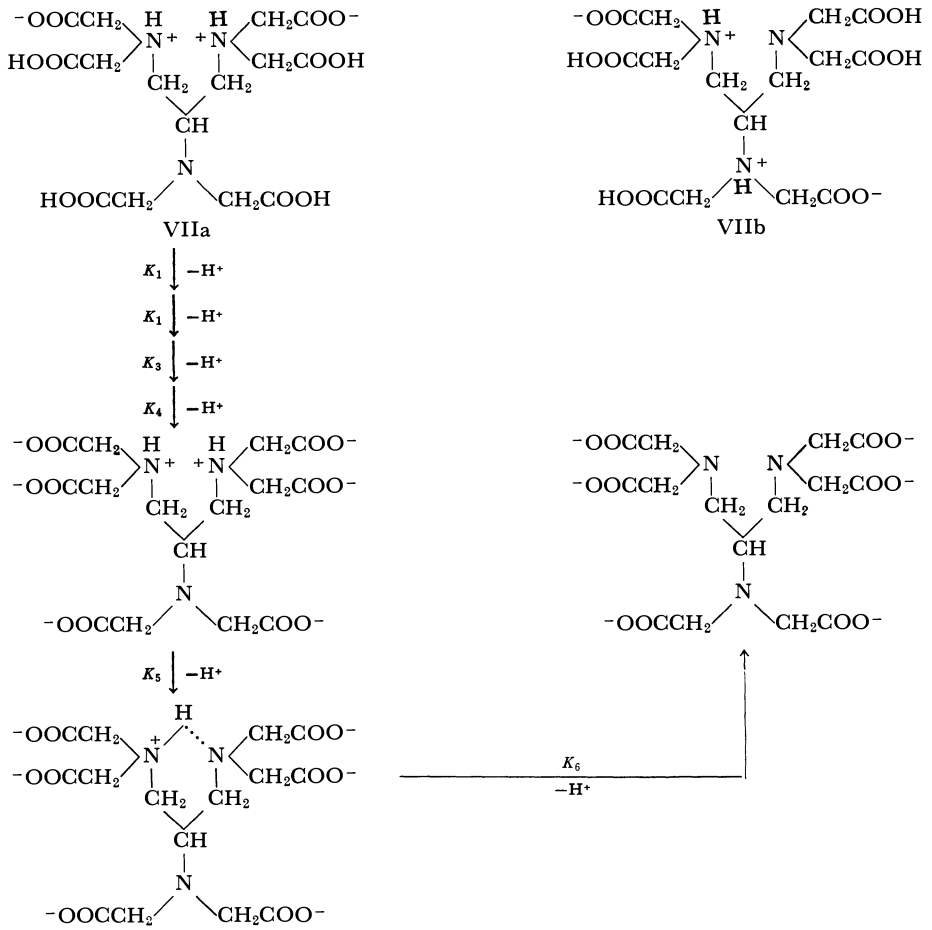

Plate 2

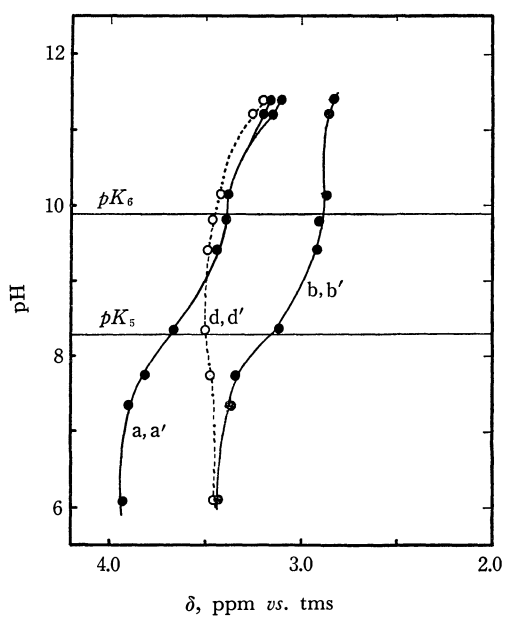

Fig. 4. Chemical shifts of TAPHA at various pH values.

(δ) of TAPHA is shown in Fig. 4. The spectra were assigned by refering to the data of various complexanes which were reported by Reilley *et al.*[15]

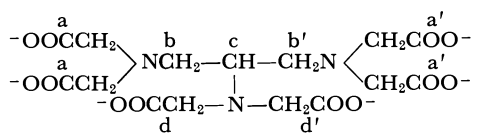

As TAPHA is not soluble enough in water at pH lower than 6, the deprotonation process from carboxyl groups could not be followed. The assignment of methyne proton (–CH–) at c-position was also difficult because the corresponding peak was too weak to be distinguished from noise at the concentration level investigated.

As shown in Fig. 4, the peak of methylenic protons at a, a′ and b, b′ position shift markedly over the pH range of 8—10. On the other hand, a very slight shift was observed for the peak of d, d′ methylenic protons. As it is expected that the chemical shifts of a(a′), b(b′) and d(d′)

15) J. L. Sudmeier and C. N. Reilley, *Anal. Chem.*, **36**, 1698 (1964).

methylenic protons are mainly influenced by protonation to its neighboring basic nitrogen atom or carboxylate ion, a most reasonable conclusion is that, when the pH of solution increased from 8 to 10, the deprotonation occures on the nitrogen atoms attached to 1- and 3-carbons. It is also expected from the NMR spectra that TAPHA takes VIIa structure, since the peaks of a- and a'-protons could not be differentiated and no splitting was observed on this peak. If TAPHA would take VIIb structure, which is no longer symmetric with regard to 2-carbon, the peaks due to a, a' and d, d' protons probably split each other.

In view of above facts, the most reasonable scheme of the acid dissociation of TAPHA may be expressed as shown in Plate 2.

Authors are grateful to the Ministry of Eductation for its financial support.

BULLETIN OF THE CHEMICAL SOCIETY OF JAPAN VOL. 41 843—849 (1968)

Copper Catalyzed Oxidation of As(III) by Peroxydisulphate

A. P. BHARGAVA and Y. K. GUPTA

Department of Chemistry, University of Rajasthan, Jaipur, India

(Received May 17, 1967)

A kinetic study of the oxidation of As(III) by peroxydisulphate catalyzed by Cu(II) has been made. The rate has been measured by estimating As(III) by the permanganate. The data follow the rate expression,

$$-\frac{d[As(III)]}{dt} = \frac{k'[Cu(II)]^{1/2}[S_2O_8^{2-}][As(III)]}{1 + K_2[As(III)]}$$

A chain mechanism has been suggested in which the decomposition of peroxydisulphate is the chain initiating step. Cu(II) and As(III) participate in the chain propagating steps. Allyl acetate and Mn(II) inhibit the reaction. The mechanism also involves a complex formation between Cu(I) and As(III) with an equilibrium constant, K_2, having a value of about 1475 M^{-1} at 35°C. Energy and entropy of activation have been found to be 24190 calories and +10.46 e. u. respectively.

Universality of Ag^+ as a catalyst in peroxydisulphate oxidations is very well known[1] and there is probably no species of lower oxidation state which the higher valent silver so formed can not oxidise. If there is no reducing substance, the medium itself, whether it is water, alcohol, dioxane or any other solvent, is oxidised.[2,3] The use of copper(II) as a catalyst, however, is limited to a particular type of reactions. The catalysed reactions reported so far are those of thiosulphate,[4-6] oxalate,[7,8] 2-propanol[9] and hydrogen peroxide.[10] Some catalytic activity of Cu(II) has also been found in the persulphate oxidations of phenylacetic and aliphatic acids.[11]

Gupta and Ghosh[12] found that Cu(II) catalyses the oxidation of As(III) by persulphate, and based on this catalytic activity, there appeared a paper[13] on the determination of As(III). Recently Woods and coworkers[14] have investigated the kinetics of this oxidation. This study is mainly based on the assumption of As(IV) as an intermediate and that Cu(II) is reduced to Cu(I) which is subsequently oxidised back to Cu(II) by peroxydisulphate. This mechanism is more or less similar to the one adopted by Morgan[5] in the oxidation of thiosulphate. Another mechanistic view involving the

1) D. A. House, *Chem. Revs.*, **62**, 185 (1962).
2) H. G. S. Sengar and Y. K. Gupta, *J. Ind. Chem. Soc.*, **43**, 223 (1966).
3) H. G. S. Senger and Y. K. Gupta, Communicated.
4) C. V. King and O. F. Steinbach, *J. Am. Chem. Soc.*, **52**, 4779 (1930).
5) L. B. Morgan, *Trans. Faraday Soc.*, **42**, 169 (1946).
6) C. D. Bisht and S. P. Srivastava, *Z. Anal. Chem.*, **188**, 23 (1962).
7) R. S. Bhakuni and S. P. Srivastava, *Z. Physik. Chem.*, **213**, 129 (1960).
8) E. Ben-Zvi and T. L. Allen, *J. Am. Chem. Soc.*, **83**, 4352 (1961).
9) D. L. Ball, M. M. Crutchfield and J. O. Edwards, *J. Org. Chem.*, **25**, 1599 (1960).
10) H. S. Samant and S. P. Srivastava, *Proc. Natl. Acad. Sci. (India)*, **27A**, 282 (1958).
11) R. G. R. Bacon and R. W. Bott, *Chem. & Ind.*, **1953**, 1285.
12) Y. K. Gupta and S. Ghosh, *J. Inorg. Nucl. Chem.*, **11**, 62 (1959).
13) G. Prasad and Y. K. Gupta, *Z. Anal. Chem.*, **198**, 173 (1963).
14) R. Woods, I. M. Kolthoff and E. J. *Meehan, Inorg. Chem.*, **4**, 697 (1965).

transient formation of Cu(III) is held by Ben-Zvi and Allen[8] and Srivastava[7,10] in the oxidation of oxalate and hydrogen peroxide. Ball and coworkers[9] on the other hand assume the formation of both Cu(III) and Cu(I) to explain their results. In view of two differing views, though not opposed, it appeared to us that the problem is still worth investigation. Some work on As(III) in this laboratory was done three years back and it was therefore, thought worthwhile to begin an investigation with As(III). In fact the investigation has been extended to the oxidation of other related compounds also and the results will appear in subsequent papers.

Experimental

Potassium sulphate, copper sulphate, arsenious oxide and all other chemicals used were of B. D. H. Analar or E. Merck G. R. quality. Stock solutions of 0.1 M arsenious acid was prepared by dissolving the requisite amount of arsenious trioxide, sufficient to give a little more than 0.1 M acid, in boiling water. After cooling it was filtered and standardised against standard permanganate solution.[15] It was found and as reported[12,16] earlier that the results were reproducible within 5% only when the same stock solution of arsenious acid was used and that the rate constants changed within a factor of ten if different solutions of arsenious acid were used. Hence wherever the results have been compared the same stock solution has been used. No definite reason could be assigned for this behaviour but it appeared that some impurity to which the reaction is very much susceptible, enters into the solution of As(III) or the distilled water while it is being prepared and the amount of this impurity is always changing. However, this explanation has to be accepted with slight reservation because this type of behaviour in peroxydisulphate oxidations is reported only in a few cases *e. g.* oxalate,[17] thiosulphate[4] and arsenious acid.[12,16]

Apart from the impurities, peroxydisulphate oxidations are susceptible to a small extent to the nature of the glass vessel and hence all the vessels and apparatus used were of pyrex glass. The medium was redistilled water, the second distillation being done, in presence of permanganate. Peroxydisulphate solution was always freshly prepared and its concentration checked, by Eckardt's[18] or arsenite[19] method.

All the reactions have been carried out at 35°C unless otherwise mentioned, in a thermostat and peroxydisulphate was always added at the end. There was no reaction between copper sulphate and arsenious acid or precipitation in acid solutions of the concentration employed. Ten millilitres of the reaction mixture were pipetted out at suitable intervals of time, and the concentration of the unreacted arsenious acid was determined by titration against a standard permanganate solution. Peroxydisulphate or copper sulphate did not interfere with the titration. The reaction was completely checked by inhibiting chloride ions.[29] All solutions were prepared in freshly boiled and cooled double distilled water from day to day except that of As(III). The reaction rates are different in presence and absence of oxygen as reported by Woods and coworkers.[14] A few experiments were carried out in an atmosphere of nitrogen and the rate was found to be slightly faster than the situation when reactions are carried out in boiled and cooled distilled water as stated above, but the rates were quite different if the solutions are air or oxygen saturated. Bacon[11] has reported large induction periods in peroxydisulphate polymerisation reactions in oxygen saturated solutions. Inhibiting action of air is much less than that of oxygen. The importance of absence or presence of oxygen or air becomes much less in presence of a reducing substance. In no case we could observe an induction period even though the solutions were not completely free of air.

A literature survey reveals that air does not readily oxidise As(III) in acid solution[21] even in presence of Cu(I) or Cu(II) which have been regarded as catalysts.[22,23] These oxidations take place only in alkaline medium. In view of the fact that the nature of the reaction in ordinary solutions is not different than in nitrogen saturated systems, we thought it convenient to work in air atmosphere. Another reason which led us to do so was the fact that the results were less reproducible in case when nitrogen gas was flushed through the reaction mixture, probably because nitrogen gas itself brings some impurities with it.

Results and Discussion

The reaction is first order with respect to peroxydisulphate and some of these first order plots are

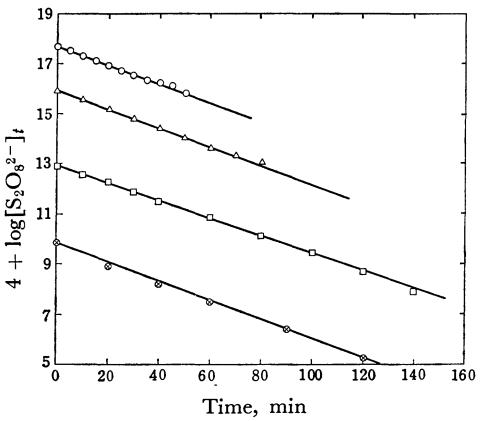

Fig. 1. Effect of change of $[S_2O_8^{2-}]$; $[NaClO_4] = 0.2$ M; $[HClO_4] = 0.2$ M; $[As(III)] = 0.02$ N; $[CuSO_4] = 1 \times 10^{-4}$ M.
○ 0.06 N $S_2O_8^{2-}$ △ 0.04 N $S_2O_8^{2-}$
□ 0.02 N $S_2O_8^{2-}$ ⊗ 0.01 N $S_2O_8^{2-}$

15) D. E. Metzler, R. J. Mye and E. H. Schift, *Ind. Eng. Chem., Anal. Ed.*, **16**, 625 (1944).
16) D. D. Misra and Y. K. Gupta, This Bulletin, **32**, 1306 (1959).
17) C. V. King, *J. Am. Chem. Soc.*, **50**, 2089 (1928).
18) Le Blank Eckardt, *Chem. News*, **81**, 38 (1900).
19) Y. K. Gupta and S. Ghosh, *Anal. Chim. Acta*, **17**, 379 (1957).
20) Y. K. Gupta, *J. Ind. Chem. Soc.*, **36**, 643 (1959).
21) D. Ya Evdokimov, *Ukrain Khim. Zhur.*, **26**, 132 (1960); *Chem. Abstr.*, **54**, 15864 e. (1960).
22) Y. Kato and T. Murakami, *J. Soc. Chem. Ind., Japan*, **33**, 226 (1930); *Chem. Abstr.*, **24**, 44516(1930).
23) W. Reinders and S. I. Vles, *Rec. Trav. Chim.*, **44**, 29 (1925); *Chem. Abstr.*, **19**, 15232 (1925).

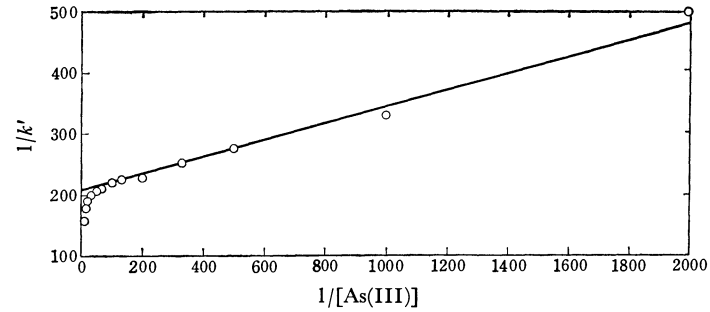

Fig. 2. $[S_2O_8^{2-}]=0.02$ N; $[CuSO_4]=1\times10^{-4}$ M; $[NaClO_4]=0.2$ M; $[HClO_4]=0.2$ M.

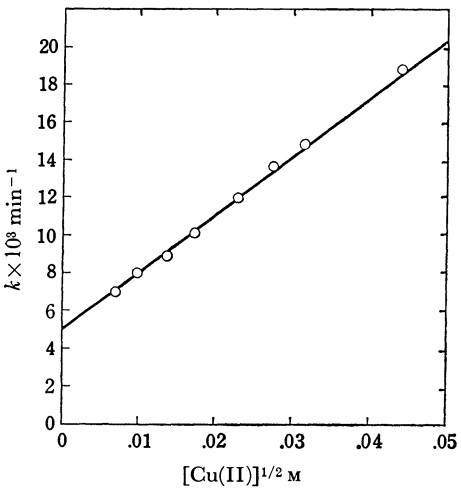

Fig. 3. $[S_2O_8^{2-}]=0.02$ N; [As(III)=0.02 N; $[NaClO_4]=0.2$ M; $[HClO_4]=0.2$ M.

shown in Fig. 1. The order with respect to reducing substance, aresenite is not zero, as found in the other silver catalyzed oxidations *i.e.* of Mn(II),[24] hydrazine,[25] Ce(III),[26] Cr(III),[27] Tl(I),[2] *etc.* and for the concentrations employed in the investigation, is found to be 0.17 by van't Hoff's differential method. A plot of the reciprocal of the observed rate constant *vs.* reciprocal of the arsenite concentration gives a straight line not passing through the origin (Fig. 2). The rate has one half order dependence on the concentration of the catalyst, $CuSO_4$ (Fig. 3). The rate law, therefore, should be of the form,

$$-\frac{d[As(III)]}{dt}=\frac{[Cu^{2+}]^{1/2}[S_2O_8^{2-}][As(III)]}{1+K_2[As(III)]}$$

For the same concentration of Cu^{2+} and high As(III), the rate law assumes the form:

$$-\frac{d[As(III)]}{dt}=k'[S_2O_8^{2-}]$$

with k' as the observed first order rate constant. However, whether k' will have uniformly the same values or not would depend on the relative magnitudes of 1 and K_2[As(III)]. K_2 has a value of 1475 (as will be found later) and, therefore, for concentrations of As(III), 1×10^{-2} M and above, 1 may be neglected in comparison to the term K_2[As(III)] and for constant concentration of [Cu(II)], the rate will be first order with respect to $[S_2O_8^{2-}]$. For low concentrations of As(III) such as 1×10^{-4} M or less the second term of the denominator may be neglected and the order with respect to As(III) would be one. The combined total order for As(III) and $[S_2O_8^{2-}]$ would be two. If, however, $[S_2O_8^{2-}]$ is in excess over that of [As(III)], the reaction would be of pseudo first order. Such low concentrations of [As(III)] could not be employed because of the difficulty in its determination. However, for concentrations of 1×10^{-3} or 5×10^{-4} M of As(III), we do find this tendency to give pseudo first order straight lines with respect to As(III).

The first order plots with respect to peroxydisulphate for As(III) concentration 1×10^{-3} to 7.5×10^{-3} M deviate from the straight line relationship towards the end of the reaction, but the tendency becomes less and less as the concentration of As(III) is increased and we have good first order plots for 7.5×10^{-3} M concentration or above (Fig. 1). For concentrations, 2×10^{-3}, 3×10^{-3} and 5×10^{-3} M, *etc.* of As(III), good half order plots with respect to As(III) are also obtained, but for 1×10^{-3} or 5×10^{-4} M a tendency for first order reaction is indicated. These half order plots and the tendency of some of them indicating first order reaction are shown in Fig. 4. Woods and coworkers[14] have also reported the order of 1/2 for $1—2\times10^{-3}$ M As(III). They did not investigate a wider range of concentration and hence failed to notice the rate being a complex function of As(III) concentration.

Effect of Ionic Strength. The ionic strength was changed by varying the concentration of sodium perchlorate at constant $HClO_4$ concentration. A plot of log k' *vs.* $\sqrt{\mu}$ gives a straight line with a slope of -1.18. Although this would

24) Y. K. Gupta and S. Ghosh, *J. Inorg. Nucl. Chem.*, **9**, 178 (1959).
25) A. O. Dekker and D. M. Yost, *J. Am. Chem. Soc.*, **59**, 2129 (1937).
26) W. H. Cone, *ibid.*, **67**, 78 (1945).
27) D. M. Yost, *ibid.*, **48**, 152 (1926).

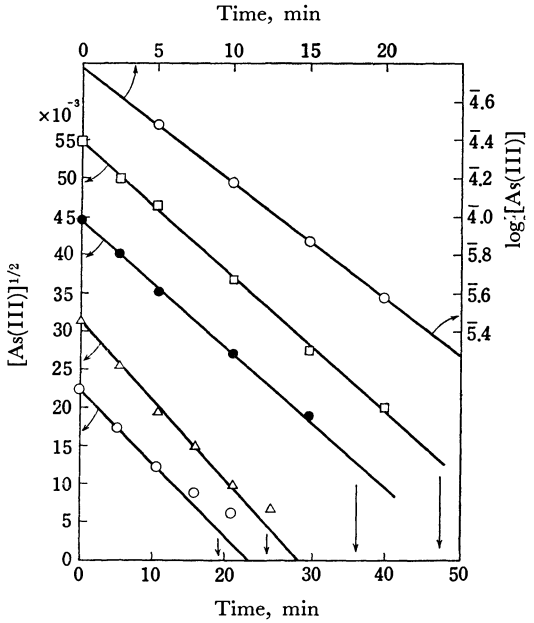

Fig. 4. $[S_2O_8^{2-}]=0.02$ N; $[NaClO_4]=0.2$ M; $[HClO_4]=0.2$ M; $[CuSO_4]=1\times10^{-4}$ M; half order plots ○, 5×10^{-4} N [As(III)]; △, 1×10^{-3} N [As(III)]; ●, 2×10^{-3} N [As(III)]; □, 3×10^{-3} N [As(III)]; first order plot ○, 5×10^{-4} N [As(III)].

indicate a slow reaction step involving ions of unit opposite charge,[28] the reaction is quite complicated (the rate determining step being preceded by a number of steps) to draw any such conclusion, particularly when the ionic strengths are not in the range in which Debye-Hückel theory is applicable.

Effect of Hydrogen Ions. The concentration of hydrogen ions was varied with the help of perchloric acid at almost constant ionic strength (0.2 M $NaClO_4$). The rate slightly decreases by increasing the concentration of perchloric acid as shown in Table 1.

TABLE 1

$[As(III)]=1\times10^{-2}$ M; $[S_2O_8^{2-}]=1\times10^{-2}$ M; $[CuSO_4]=1\times10^{-4}$ M; $[NaClO_4]=2\times10^{-1}$ M

$[HClO_4]$, M×10⁻²	0	0.5	1	2	4
$k'\times10^2$ min⁻¹	1.996	1.90	1.81	1.675	1.37

Increase in the concentration of perchloric acid involves a small increase in the ionic strength also but the change in the rate constant is not much. It, therefore, appears that the effect of hydrogen ion concentration reaches a limiting value. This would happen if arsenious acid which is almost unionised, is involved in an equilibrium like

$$H_3AsO_3 \rightleftarrows H_2AsO_3^- + H^+ .$$

28) A. A. Frost and R. G. Pearson, *Kinetics and Mechanism*, **1961**, 151.

All reactions were, therefore, studied in a high concentration *e. g.* 0.2 M $HClO_4$ where small changes in $[H^+]$ would be without any effect. Similarly ionic strength was kept constant by adding 0.2 M $NaClO_4$. Table 2 brings out the fact that the effect of perchloric acid in higher concentration range is equivalent to that of decrease in ionic strength. The concentrations of perchlorate and perchloric acid have been changed so that the ionic strength does not change. It was found that the rate constants also are reasonably constant.

TABLE 2

$[As(III)]=1\times10^{-2}$ M; $[S_2O_8^{2-}]=1\times10^{-2}$ M; $[CuSO_4]=1\times10^{-4}$ M

$[NaClO_4]$, M×10	1	1.5	2	2.5	3	3.5
$[HClO_4]$, M×10	3	2.5	2	1.5	1	0.5
$k'\times10^3$ min⁻¹	7.16	7.05	8.06	7.37	7.78	8.05

At low concentrations of perchloric acid the first order plots deviated a lot from the straight line towards the end of the reaction, but this tendency decreased as the concentration of perchloric acid was increased. No such tendency was noticed if the concentration of perchloric acid is 0.1 M and above. This behaviour is in some way connected with the different forms of As(III) in which it can exist in solution.

Effect of Reaction Products. Bisulphate and As(V) are the products of the reaction, but they do not seem to affect the rate (Table 3).

TABLE 3

$[As(III)]=1\times10^{-2}$ M; $[S_2O_8^{2-}]=1\times10^{-2}$ M; $[CuSO_4]=1\times10^{-4}$ M; $[HClO_4]=2\times10^{-1}$ M; $[NaClO_4]=2\times10^{-1}$ M

$NaHSO_4$, M×10²	0.5	1	2	5	10
$k'\times10^3$ min⁻¹	5.25	5.29	5.18	5.08	5.11

Similarly added disodium hydrogen arsenate (5×10^{-3}, 1×10^{-2} and 2×10^{-2} M) had absolutely no effect on the rate. The rate determining step is, therefore, not a mass law term.

Energy and Entropy of Activation. Table 4 gives the rate constants at different temperatures.

A plot of log k' *vs.* $1/T$ gives a straight line from the slope of which the energy of activation was calculated and found to be 24190 calories. The entropy of activation was found to be +10.46 e.u.

TABLE 4

$[As(III)]=1\times10^{-2}$ M; $[S_2O_8^{2-}]=1\times10^{-2}$ M; $[CuSO_4]=1\times10^{-4}$ M; $[HClO_4]=2\times10^{-1}$ M; $[NaClO_4]=2\times10^{-1}$ M

Temperature, °C	25	30	35	40
$k'\times10^3$ min⁻¹	2.245	4.50	8.06	14.69

TABLE 5

$[As(III)]=2\times10^{-2}$ M; $[S_2O_8^{2-}]=2\times10^{-2}$ M; $[CuSO_4]=1\times10^{-4}$ M; $[HClO_4]=2\times10^{-1}$ M; $[NaClO_4]=2\times10^{-1}$ M

$[MnSO_4]$, M$\times10^3$	0	1	2	4	6	50	100	200
$k'\times10^4$ min^{-1}	80	16.31	4.35	1.73	1.67	0.84	0.83	0.83

Effect of Manganous Ions. Mn(II) has been found to be an anticatalyst in the silver catalysed peroxydisulphate oxidations of oxalate,[29] formate,[30] As(III),[16] citrate,[31] tartrate,[31] malonate[31] and also in the uncatalysed oxidation of As(III).[20] This behaviour of Mn(II) is also found in the present reaction. Table 5 gives the rate constants for different concentrations of manganous sulphate.

It is observed that as the concentration of Mn(II) is increased, the rate constants appreciably decrease. For 100×10^{-3} M Mn(II), the rate constant has the value which is comparable to that of the rate constant for the decomposition of peroxydisulphate which at 35°C calculated from the data of Kolthoff and Miller,[32] is 5.49×10^{-5} min^{-1}. It is thus found that Mn(II) acts in such a way that it checks all the steps of the catalysed reaction and only thermal decomposition of peroxydisulphate can take place. Incidentally here we come across the main difference between the silver catalysed reactions[31] and this copper catalysed reaction. In the former case the rate approaches a limiting value (0.3—0.5 min^{-1}) as the concentration of Mn(II) is increased. This points to a two term rate law in case of Ag(I) catalysed reactions. One of them is a non-chain process and the other is a chain mechanism which is altogether stopped in presence of sufficient concentration of Mn(II). In case of copper(II) catalysed reaction which as we shall see, is a chain reaction, the catalytic activity of Cu(II) is completely masked by the presence of sufficient Mn(II).

Allyl Acetate Inhibition. A few reactions were studied in presence of allyl acetate to see whether the reaction is a chain process or not. As the permanganate reacts with allyl acetate, the reaction could not be followed by estimating the arsenite with permanganate. In all such experiments alcoholic iodine was used to estimate the arsenite iodometrically. Preliminary work in connection with such titrations, showed that peroxydisulphate and allyl acetate do not interfere. Following the kinetics in this way the rate constant was found to be 1.56×10^{-2} min^{-1} (with 0.2 M $NaClO_4$ and no $HClO_4$) which is reasonably of the same order of magnitude as the value (1.99×10^{-2} min^{-1}) obtained by the permangnate method under almost similar conditions.

Rate inhibition by allyl acetate is very well known.[8,33] It has been shown by Kolthoff and coworkers[34] that allyl acetate is a highly efficient captor of sulphate radicals. Since peroxydisulphate has been reported to initiate polymerisation of vinyl compounds[35,36] through the sulphate ion radical,[37] it seems reasonable that the allyl acetate reacts with sulphate ion radical and its presence is confirmed by the incorporation of ^{35}S from ^{35}S labelled peroxydisulphate into polymer chains. The very marked inhibition in the present investigation by allyl acetate is indicative of a chain reaction involving sulphate free radicals. In presence of 0.5 or 0.2 M allyl acetate, there is almost no change in the concentration of As(III) even after 150 min. The rate constant in presence of 0.1 M allyl acetate is 3.58×10^{-5} min^{-1}. This rate is even lower than the thermal decomposition[23] of $S_2O_8^{2-}$ according to the following reaction:

$$S_2O_8^{2-} \xrightarrow{k} 2SO_4^-$$
$$(k=5.49\times10^{-5}\ \text{min}^{-1}\ \text{at}\ 35°C)$$

because it is here $-d[As(III)]/dt$ which is being measured and so sulphate ion radicals will be captured by allyl acetate leaving none or few SO_4^- for the oxidation of As(III). If it were possible to estimate peroxydisulphate in such a case, $-d[S_2O_8^{2-}]/dt$ will have a value of 5.49×10^{-5} at 35°C. At higher concentrations of allyl acetate, As(III) is not at all oxidised, but $S_2O_8^{2-}$ will decompose with a rate constant of 5.49×10^{-5} min^{-1}.

It is, therefore, obvious that neither As(III) nor Cu(II) participates in the chain initiating reaction which is the homolytic cleavage of $S_2O_8^{2-}$, but they are definitely involved in chain propagating steps. Allyl acetate cuts off all these chains by taking away the sulphate free radical.

Comparison with Reported Results. The notable point of difference observed in the present investigation and between that in the work of

29) Y. K. Gupta and S. Ghosh, *J. Inorg. Nucl. Chem.*, **11**, 320 (1959).
30) Y. K. Gupta and R. K. Nigam, *J. Ind. Chem. Soc.*, **37**, 125 (1960).
31) H. G. S. Senger and Y. K. Gupta, Communicated, 1966.
32) I. M. Kolthoff and I. K. Miller, *J. Am. Chem. Soc.*, **73**, 3055 (1951).
33) K. B. Wiberg, *J. Am. Chem. Soc.*, **81**, 252 (1959).
34) I. M. Kolthoff, E. J. Meehan and E. M. Karr, *ibid.*, **75**, 1439 (1953).
35) J. H. Mertz and W. A. Waters, *Disscussions Faraday Soc.*, **29**, 179 (1947).
36) J. W. L. Fordham and H. L. Williams, *J. Am. Chem. Soc.*, **73**, 1634 G, 4855 (1951).
37) P. Bartlett, E. J. Meehan and E. M. Carr, *ibid.*, **3**, 216 (1948).

Woods and coworkers is that the rate is not independent of arsenite concentration at low Cu(II) concentration, although the effect is not much. A two hundred fold change in As(III) concentration (5×10^{-4}—1×10^{-2} M) increases the rate approximately only three times (1.94×10^{-3}—6.33×10^{-3}). The change in k' is so small that the earlier workers failed to notice this. Apart from this, the more important fact is the increase in the order of As(III) as its concentration is lowered in conformity with the linear relationship of Fig. 2. These workers also report a half order dependence on As(III) when the concentration of the latter is approximately 1×10^{-3} M. In spite of the conditions which were by no means identical, under which the two investigations have been made the values of the rate constant (2.25×10^{-3} min^{-1}) found by us compare remarkably well with that of Woods and coworkers[14] (2.7×10^{-3} min^{-1}) both at 25°C.

These workers further report that the rate constant tends to a limiting value at higher concentration of Cu(II) (1×10^{-3} M and more). In our case, though the rate constant at higher [Cu(II)] was less than that expected no limiting value was reached even for 5×10^{-3} M Cu(II). It appears that the reason for the limiting value is the formation of a turbidity of copper arsenite in absence of sufficient hydrogen ions. We did not notice any such limiting tendency because we used higher (0.2 M) concentration of perchloric acid.

Mechanism. Any proposed mechanism must incorporate (a) the first order character in respect of peroxydisulphate (b) half order dependence on Cu(II) concentration (c) variation of order from 0 to 1 with respect to As(III) (d) inhibition by Mn(II) and allyl acetate.

We postulate sulphate ion free radicals and As(IV) as intermediate as was done by Woods and coworkers.[14] Sulphate ion free radicals are now well known to be formed by the thermal and photochemical decomposition of peroxydisulphate.[32,35,38-40] Similarly the intermediate formation of As(IV) now seems to be well founded. Woods and coworkers[41,42] have found it in the induced oxidation of As(III) by $S_2O_8^{2-}$-Fe(II) and Fe(II)-H_2O_2 systems. Daniels and Weiss[43] proposed the production of As(IV) by the reaction of hydroxyl radical with As(III) to occur during the oxidation of arsenite by the action of X-rays. In the photochemically induced oxidation of As(III) also, Daniel[44] concluded the existence of As(IV). Csyani postulated its intermediate formation in the titration[45] of As(III) by $S_2O_8^{2-}$-H_2O_2 mixture and also in the induced induction[46] of chlorate by As(III).

We propose the following mechanism:

$$S_2O_8^{2-} \xrightarrow{k_1} 2SO_4^- \quad (1)$$

$$SO_4^- + \text{As(III)} \xrightarrow{k_2} SO_4^{2-} + \text{As(IV)} \quad (2)$$

$$\text{As(IV)} + \text{Cu(II)} \xrightarrow{k_3} \text{As(V)} + \text{Cu(I)} \quad (3)$$

$$2\text{Cu(I)} \overset{K_1}{\rightleftarrows} \text{Cu}^0 + \text{Cu(II)} \quad (4)$$

$$\text{Cu(I)} + \text{As(III)} \overset{K_2}{\rightleftarrows} [\text{Cu}^{\text{I}}\text{As}^{\text{III}}] \quad (5)$$

$$[\text{Cu}^{\text{I}}\text{As}^{\text{III}}] + S_2O_8^{2-} \xrightarrow{k_4} \text{Cu}^{3+} + \text{As(III)} + 2SO_4^{2-} \quad (6)$$

$$\text{Cu}^{3+} + \text{As(III)} \xrightarrow{k_5} \text{Cu}^+ + \text{As(V)} \quad (7)$$

$$\text{Cu}^0 + S_2O_8^{2-} \xrightarrow{k_6} 2SO_4^{2-} + \text{Cu(II)} \quad (8)$$

$$SO_4^- + \text{As(IV)} \xrightarrow{k_9} SO_4^{2-} + \text{As(V)} \quad (9)$$

If $k_3>k_2$, k_5 and $k_6>k_4$; $k_2[SO_4^-][\text{As(III)}]>k_9[SO_4^-][\text{As(IV)}]$ (because the steady state concentration of SO_4^- and As(IV) both will be small) and K_1 and K_2 are rapid equilibria, the rate of decrease of As(III) is given by the equations,

$$-\frac{d[\text{As(III)}]}{dt} = k_5[\text{As(III)}][\text{Cu}^{3+}] + k_2[SO_4^-][\text{As(III)}]$$

$$= \frac{K_2}{K_1^{1/2}} \frac{k_4[\text{Cu(II)}]^{1/2}[\text{As(III)}]}{1+K_2[\text{As(III)}]} + \frac{k_1}{2}[S_2O_8^{2-}]$$

k_1 is of the order[32] of 1×10^{-5}—10^{-6} min^{-1} and hence can be neglected in comparison to the first term:

$$-\frac{d[\text{As(III)}]}{dt} = \frac{K_2}{K_1^{1/2}} \frac{k_4[\text{Cu(II)}]^{1/2}[\text{As(III)}]}{1+K_2[\text{As(III)}]}[S_2O_8^{2-}]$$

The above expression has the same form as the experimental rate law provided the concentrations of Cu(I), Cu(II) and Cu^0 and also the complex of Cu(I) are very small and the only significant species of copper in solution is Cu(II). Cu(II) is not known to form any complex with arsenite and a spectrophotometric investigation in the range 600—750 mμ also indicated no complex formation. In the above mechanism a complex

38) M. S. Tsao and W. K. Wilmarth, *J. Phys. Chem.*, **63**, 346 (1959).
39) P. D. Bartlett and T. D. Cotman, *J. Am. Chem. Soc.*, **71**, 1419 (1949).
40) I. M. Kolthoff, A. I. Medatia and H. P. Raaen, *ibid.*, **73**, 1733 (1951).
41) R. Woods, I. M. Kolthoff and E. J. Meehan *ibid.*, **85**, 2385 (1963).
42) R. Woods, I. M. Kolthoff and E. J. Meehan, *ibid.*, **86**, 1698 (1964).
43) M. Daniels and J. Weiss, *J. Chem. Soc.*, **1950**, 2467.
44) M. Daniels, *J. Phys. Chem.*, **66**, 1473 (1962).
45) L. J. Csyani, *Disscussions Faraday Soc.*, **29**, 146 (1960).
46) L. J. Csanyi and M. Szabo, *Talanta*, **1**, 359 (1958).

formation between Cu(I) and As(III) has been postualted although there is no direct evidence for it. However substituted arsine complex of Cu(I) has been reported by Cass and coworkers.[47] Cu(I) complex of peroxydisulphate itself has been postulated by Chaltkyan and Beileryan[48] in the oxidation of Cu(I) by persulphate, and a complex of Cu(I) and thiosulphate by Morgan[5] in the oxidation of the latter by peroxydisulphate. The existence of tripositive copper is now beyond doubt, though the knowledge about it is limited. Sneed, Maynard and Brasted[49] report quite a few complex compounds of Cu(III) and Latimer[50] has given its approximate oxidation potential. Of particular mention in this study is the fact that a series of complex salts containing tripositive copper has been prepared by peroxydisulphate oxidation.[51] The disproportionation reaction of cuprous ion (step 4) postulated to explain half order dependence on Cu(II) is well known in aqueous solution.[52,53] The equilibrium constant for the reaction (4) is 1.2×10^6 and thus the concentration of Cu (I) or Cu(I) complex is very small. The oxidation of zerovalent copper to cupric ion (step 8) is also known.[54]

From the intercept (=205) and the slope (=0.139) of the straight line in Fig. 2, the value of K_2, the equilibrium constant for the complex formation (step 5) of the mechanism is found to be approximately 1475. With this value of K_2, it can now be easily understood that 1 can be neglected as compared to K_2[As(III)] in the denominator of the above rate expression. This would give a zero order dependence on As(III). For sufficiently low concentrations of As(III) (10^{-4} M or less), K_2[As(III)] can be neglected as compared to one, giving first order dependence on As(III). It has already been mentioned earlier about this tendency. From the interecept which is equal to $K_1^{1/2}/K_4$[Cu(II)]$^{1/2}$, the approximate value of k_4 can be calculated, provided we know K_1 at 35°C. Its value at 25°C (1.2×10^6) is known from the works of Fenwick[52] and Heinerith[53], but we have no straight line at 25°C corresponding to Fig. 2. However, the intercept for a corresponding straight line plot at 25°C would be within a factor of two or three and this would give a value of approximately 150 to 270 for k_4.

We have assumed the following chain terminating step in the mechanism.

$$SO_4^- + As(IV) \rightarrow SO_4^{2-} + As(V) \quad (9)$$

The other probable chain breaking steps,

$$Cu(I) + SO_4^- \rightarrow Cu(II) + SO_4^{2+} \quad (10)$$

$$Cu(I) + Cu(III) \rightarrow 2Cu(II) \quad (11)$$

have not been considered important because the increase in the concentration of Cu(II), produces an almost expected increase in the rate (Fig. 3), though at higher concentrations of Cu(II) than those employed, these chain breaking steps are likely to become important.

In presence of Mn(II), SO_4^- oxidises it to Mn(III) and the latter oxidises As(III) instantaneously. Thus no chains are initiated and the rate decreases considerably. Allyl acetate also takes away the sulphate ion radical but it does not oxidise As(III) at all and hence in presence of its sufficient concentration, no decrease in concentration of As(III) would be found. Peroxydisulphate, however, would decrease at the same rate as that of its thermal decomposition.

47) R. C. Cass, G. E. Coates and R. G. Hayter, *Chem. & Ind.*, **1954**, 1845; *J. Chem. Soc.*, **1955**, 4007.
48) O. A. Chaltkyan and N. M. Beileryan, *Izvest. Akad. Nauk, Armyan, S. S. S. R., Khim. Nauki*, **11**, No. 1, 13 (1958); *Chem. Abstr.*, **52**, 18054 (1958).
49) M. C. Sneed, J. L. Maynard and R. C. Brasted, "Comprehensive Inorganic Chemistry," Vol. II, D. Van Nostrand Co. Inc., New York (1954), p. 111—113.
50) W. M. Latimer, "Oxidation Potentials," Prentice Hall, New York (1938), Chapt. 11.
51) L. Malatesta, *Gazz. Chim. Ital.*, **71**, 476, 580 (1941).
52) F. Fenwick, *J. Am. Chem. Soc.*, **48**, 860 (1926).
53) Heinerth, *Z. Elektrochem.*, **37**, 61 (1931).
54) G. C. Bond, B. M. Hilland R. Tennison, *J. Chem. Soc.*, **1959**, 33.

BULLETIN OF THE CHEMICAL SOCIETY OF JAPAN VOL. 41 850—854 (1968)

Distribution of Some Minor Elements in Sulfide Ores from the Hitachi Mine, Ibaraki Prefecture, Japan

Shuichi HAMADA, Ryuji SATO and Toshiaki SHIRAI

Department of Chemistry, Faculty of Science, Science University of Tokyo, Kagurazaka, Shinjuku-ku, Tokyo

(Received July 14, 1967)

The contents of some minor elements in copper-bearing ores from the Fujimi ore deposit No 5, the Hitachi mine, were determined. The selenium content in 46 samples was found to vary from 0.5 to 117 ppm. Though selenium seems to be concentrated in the ores rich in chalcopyrite, that is not always the case, as there are pyrite-rich ores with higher selenium contents than those rich in chalcopyrite. The average value of the atomic ratio of Se/S in the pyrite ores was calculated to be 3.48×10^{-5}; this value was larger than those found for the ores from the Minenosawa and the Chichibu mines, and about the same as those found for the ores from the Nakase, the Ashio, and the Hanaoka mines. The variations with depth in the atomic ratios of Se/S and Co/Ni are closely related to each other. The atomic ratio of Se/S increased with an increase in that of Co/Ni. It has been concluded that selenium is concentrated in the pyrite ores of the high-temperature-type rather than in those of the low-temperature-type. The mercury content was small in general, but a large content of mercury was observed at the depth where the values of the atomic ratios of Se/S and Co/Ni were at their maxima.

Several papers about the selenium content in sulfide ores have been published.[1-6] For example, Takimoto and Minato compared the selenium content in sulfide ores from several mines in Japan, and discussed the correlation between the selenium contents and the formation temperatures of the ores.

In the present paper, the distribution of such minor elements as selenium, nickel, cobalt, and mercury in the sulfide ores from the Hitachi mine will be reported.

Geology of the Hitachi Mine[7] and Sampling of Ores. Rocks of the paleozoic strata occupy the major part of this region, although igneous rocks lie in the northwestern part, as is shown in Fig. 1. The major part of the paleozoic strata consists of dynamo-metamorphosed greenschist and siliceous schist. Granodiorite intruded upon the paleozoic strata at the northwestern part of this region.

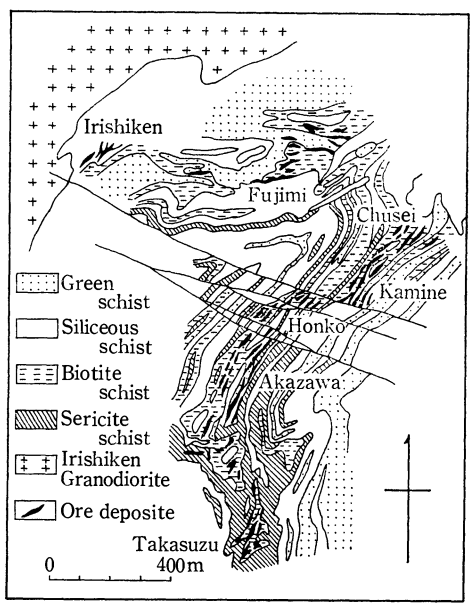

Fig. 1. Geology of Hitachi mine.

The vicinity in contact with this igneous rock suffered thermal metamorphism. The area of the ore deposits is the polymetamorphosed area which suffered both dynamic and thermal metamorphisms.

The ores were obtained from the Fujimi ore deposit No. 5, which suffered a strong thermal metamorphism by the northwestern granodiorite. The samples were obtained at vertical intervals of

1) K. Takimoto and T. Minato, *Nippon Kogyo Kaishi (J. Min. Inst. Japan)*, **68**, 405 (1952).
2) K. Takimoto, T. Minato, T. Okuda and T. Tokita, *Suiyo Kaishi (Trans. Min. Met. Alumni Assoc.)*, **12**, 287 (1954).
3) K. Takimoto, T. Minato and S. Hirono, *Ganseki Kobutsu Koshogakkaishi (J. Japanese Assoc. Min. Petr. Econ. Geol.)*, **42**, 161 (1958).
4) T. Minato, *Suiyo Kaishi (Trans. Min. Met. Alumni Assoc.)*, **14**, 301 (1961).
5) K. Takimoto and T. Minato, *Kozan Chishitsu (Min. Geol.)*, **11**, 331 (1961).
6) T. Shirai, S. Hamada, H. Takahashi and I. Saruyama, *Nippon Kagaku Zasshi (J. Chem. Soc. Japan, Pure Chem. Sect.)*, **86**, 196 (1965).
7) Section of Exploration of the Hitachi Mine, *Kozan Chishitsu (Min. Geol.)*, **12**, 1 (1962).

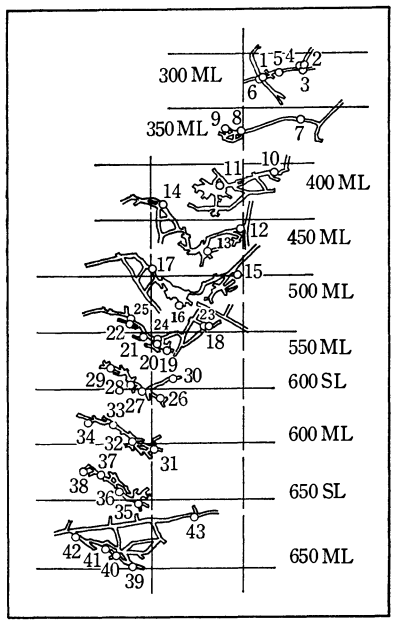

Fig. 2. Locality of ores at Fujimi ore deposit No. 5.

fifty or twenty-five meters over the range from 300 ML to 650 ML.*1 The sampling points are shown in Fig. 2. The ores mainly consisted of intimate aggregates of fine crystals of pyrite. Some of these contained chalcopyrite, pyrrhotite, and other materials. The pyrite ore was separated visually from the crushed sample, and the chalcopyrite ore, from the chalcopyrite-rich sample.

Experimental

Determination of Selenium. The selenium content was estimated by the colorimetric method using 3,3'-diaminobenzidine, as has been described in a previous paper.[6]

Determination of Sulfur. The sulfur content was estimated by the combustion method of JIS K 1331.

Determination of Metals. The iron content was estimated as ferric oxide by the usual gravimetric method. The copper content was estimated as cuprous thiocyanate by the gravimetric method for the high-copper-content ore, and by the polarographic method for the low-copper-content ore. The nickel, cobalt, and mercury contents were estimated by the colorimetric method as nickel dimethylglyoximate,[8] as the cobalt complex of Nitroso R salt,[9] and as mercury dithizonate[10-12] respectively.

*1 The symbol "ML (meter level)" is the depth measured from the base level of the Hitachi mine, 350 m above sea level. The symbol "SL (sublevel)" is 25 m above each ML.

8) E. B. Sandell, "Colorimetric Determination of Traces of Metals," Interscience Publishers, New York (1959), p. 665.

9) *Ibid.*, p. 409.

10) H. Irving, G. Andrew and E. J. Risdon, *J. Chem. Soc.*, **1949**, 537.

Results

The amounts and the atomic ratios of the several elements in the ores are listed in Table 1.

The selenium content in 46 samples was found to range from 0.5 to 117 ppm. The atomic ratio of Se/S in the chalcopyrite-rich ores was larger than that in the chalcopyrite-poor ores when the respective ores were separated from samples obtained at the same point. However, selenium can not be said to be always concentrated in the chalcopyrite-rich ores, because a higher content of selenium was observed in the pyrite-rich ores than in the chalcopyrite-rich ores.

The Contents of Nickel and Cobalt. The nickel content in the pyrite ores was usually about 10—50 ppm. The nickel content was lower than those in the pyrite ores from the Daikoku ore deposit, the Chichibu mine (20—110 ppm, 26 samples), and the Okutomi, the Taisho and the Himi ore deposits, the Tsushu mine (20—100 ppm, 7 samples), and was similar to that from the Kajika ore deposit, the Ashio mine (20—50 ppm, 6 samples).[13]

The cobalt content in the pyrite ores was estimated to range from 0.0 to 654 ppm. Unlike the nickel content in the ores, a wide fluctuation of the cobalt content was observed. The cobalt content in the pyrite ores was larger than in those from the Chichibu and the Tsushu mines (10—200 ppm and 20—150 ppm, respectively), and was quite large compared with that from the Ashio mine (10—30 ppm).

The Mercury Content. The mercury content in the ores was estimated to range from 0.0 to 176 ppm. No correlation could be found between the contents of copper and mercury.

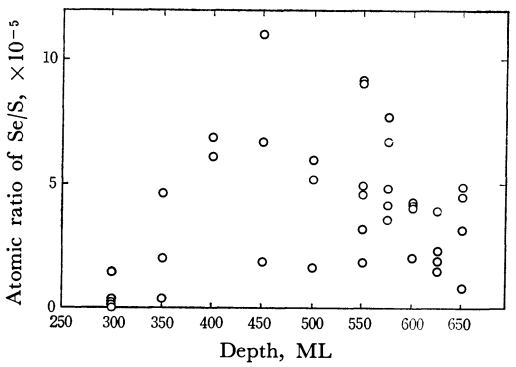

Fig. 3. Plot of atomic ratio of Se/S in pyrite ores against depth.

11) S. Uehara and S. Hamada, *Kogyo Kagaku Zasshi (J. Chem. Soc. Japan, Ind. Chem. Sect.)*, **63**, 1580 (1960).

12) T. Kato, N. Takei and A. Okaue, *Japan Analyst*, **5**, 689 (1956).

13) K. Takimoto, T. Minato and S. Hirono, *Ganseki Kobutsu Koshogakkaishi (J. Japanese Assoc. Min. Petr. Econ. Geol.)*, **50**, 118 (1963).

TABLE 1. CHEMICAL COMPOSITION OF SULFIDE ORES

Sampling point	Level	Cu %	Fe %	S %	Se ppm	Zn %	Ni ppm	Co ppm	Hg ppm	Se/S $\times 10^{-5}$	Co/Ni
1	300 ML	12.82	34.91	35.94	2.9	2.88	20.8	49.7	0.3	0.327	2.38
2	300 ML	tr.	48.59	49.25	0.5	0.83	33.6	30.8	0.0	0.04	0.91
3	300 ML	8.44	44.79	43.14	14.6	3.86	28.6	89.7	2.2	1.38	3.12
4	300 ML	0.046	47.83	48.02	3.1	1.75	22.6	8.1	0.0	0.262	0.36
5	300 ML	0.040	47.53	47.72	2.1	1.21	14.0	3.0	0.0	0.178	0.21
6	300 ML	2.14	47.13	46.61	16.2	2.41	24.4	1.2	19.7	1.41	0.05
7	350 ML	0.79	35.90	30.26	34.6	0.05	5.5	1.8	1.4	4.64	0.33
8	350 ML	0.077	45.59	45.26	4.5	2.94	12.2	1.8	5.3	0.404	0.15
9	350 ML	1.82	43.93	42.59	21.2	1.53	39.8	9.6	85.1	2.02	0.24
10	400 ML	0.10	49.16	47.76	81.1	tr.	17.3	297.0	9.1	6.89	17.1
11	400 ML	1.61	46.19	45.65	69.0	0.19	10.3	96.3	55.0	6.14	9.34
12	450 ML	1.87	45.11	43.07	116.6	0.07	9.0	445.3	112.8	11.0	49.4
13	450 ML	0.80	46.43	48.48	80.4	0.04	10.6	72.6	137.7	6.72	6.81
14	450 ML	0.013	46.49	44.67	20.9	0.37	20.0	70.0	2.0	1.90	0.54
15	500 ML	0.11	49.98	47.89	70.5	0.42	10.1	220.9	8.1	5.98	21.8
16-1	500 ML	3.28	46.35	43.52	18.0	0.21	48.3	97.7	10.6	1.68	2.02
16-2	500 ML	28.10	34.27	30.88	38.2	0.89	16.0	0.0	9.4	5.02	0.0
17	500 ML	2.73	46.10	40.25	51.8	0.12	43.2	73.5	176.2	5.22	1.69
18	500 ML	25.66	33.86	33.22	13.0	1.05	23.1	4.98	9.4	1.59	0.22
19	550 ML	27.82	34.69	33.23	44.3	0.71	14.7	6.18	12.4	5.42	0.42
20	550 ML	2.53	46.95	47.50	22.1	0.23	28.3	48.2	2.1	1.89	1.70
21	550 ML	1.58	47.77	49.64	39.5	0.16	31.3	103.4	0.0	3.23	3.29
22	550 ML	1.80	47.84	49.38	60.3	0.09	53.8	130.6	40.0	4.96	2.42
23	550 ML	0.058	45.87	47.33	107.1	0.03	1.8	422.4	7.0	9.19	231
24	550 ML	5.00	44.62	46.91	105.7	0.04	26.0	113.3	9.0	9.15	4.34
25	550 ML	0.90	46.84	50.45	57.3	0.02	25.0	49.4	2.0	4.61	1.97
26	600 SL	0.78	46.25	49.73	82.6	tr.	32.5	138.8	3.8	6.74	4.25
27	600 SL	0.67	47.83	50.48	60.3	0.06	15.9	142.1	2.6	4.85	8.90
28	600 SL	1.37	49.24	49.60	43.7	0.01	27.9	118.6	2.2	3.58	4.24
29	600 SL	0.45	47.75	51.45	52.8	tr.	12.5	98.9	11.1	4.17	7.88
30	600 SL	0.09	46.91	49.45	94.3	tr.	19.4	147.7	0.0	7.74	7.58
31-1	600 ML	0.68	48.36	50.10	51.4	0.33	35.3	58.9	3.4	4.17	1.66
31-2	600 ML	7.19	39.48	39.27	81.3	2.42	20.2	40.0	40.4	8.41	1.97
32	600 ML	0.89	48.73	48.16	24.4	0.13	20.1	83.4	1.4	2.06	4.13
33	600 ML	0.26	48.06	50.20	52.1	tr.	16.1	64.2	4.0	4.15	3.97
34	600 ML	0.41	47.83	48.96	50.7	tr.	34.7	119.3	2.1	4.20	3.42
35	650 SL	0.38	46.69	49.11	28.4	0.02	19.8	68.4	2.5	2.35	3.44
36	650 SL	0.53	46.77	49.78	23.4	0.04	25.2	76.7	1.5	1.91	3.03
37	650 SL	0.40	45.18	48.67	47.0	tr.	22.5	74.8	1.8	3.92	3.31
38-1	650 SL	0.98	47.97	47.87	17.8	0.03	33.7	91.5	4.0	1.51	2.70
38-2	650 SL	29.07	36.05	33.49	36.5	1.26	16.6	76.6	8.9	4.42	4.60
39	650 ML	1.29	47.97	47.34	36.5	0.28	26.4	75.1	7.6	3.13	2.83
40	650 ML	0.74	49.26	48.59	53.8	0.02	24.8	95.7	2.8	4.50	3.84
41	650 ML	0.78	49.75	49.57	59.9	0.02	38.3	141.4	5.9	4.91	3.68
42	650 ML	27.84	34.93	33.14	49.8	0.56	26.2	12.2	14.1	3.49	0.46
43	650 ML	0.01	48.81	48.44	10.2	1.33	20.4	8.5	2.8	0.854	0.41

The Relationship between the Depth and the Atomic Ratio of Se/S. The atomic ratio of Se/S in the pyrite ores changed within the range from 4×10^{-7} to 1.10×10^{-4}. The atomic ratio of Se/S in the pyrite ores was correlative with the depth within the range from 300 ML to 650 ML, as is shown in Fig. 3. The atomic ratios of Se/S at 300 ML were quite small, but the ratio increased with an increase in the depth, the maximum appearing at the depth of 450 ML—550 ML.

The Relationship between the Depth and the Atomic Ratio of Co/Ni. Figure 4 shows the relationship between the depth and the atomic ratio of Co/Ni. The values of the atomic ratio of Co/Ni were small at the upper part of the ore deposit, but they increased with an increase in the

depth. The maximum appeared at the depths from 450 ML to 550 ML, as with the atomic ratio of Se/S. Increases in the atomic ratio of Co/Ni with an increase in the depth were observed at the Chichibu mine (within the range of 120 m), the Tsushu mine (within the range of 150 m), and the Ashio mine (within the range of 100 m). The atomic ratio of Se/S in the pyrite ores increased with an increase in that of Co/Ni, as is shown in Fig. 5. The coefficient of the correlation of Fig. 5 is 0.70; therefore, the correlation is significant.

The Relationship between the Depth and the Mercury Content. The mercury content is generally very small, but quite a large content of mercury was observed at the depth of 450 ML—550 ML, in which range the maxima of the atomic ratios of Se/S and Co/Ni appeared, as is shown in Fig. 6.

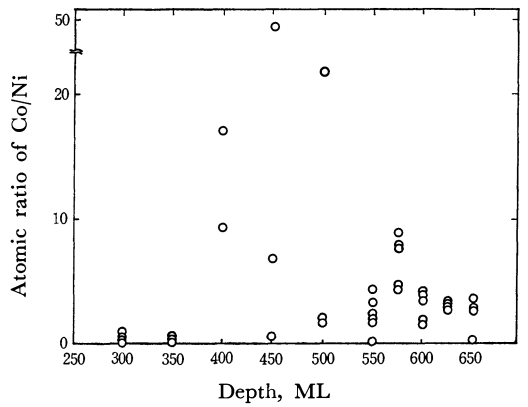

Fig. 4. Plot of atomic ratio of Co/Ni in pyrite ores against depth.

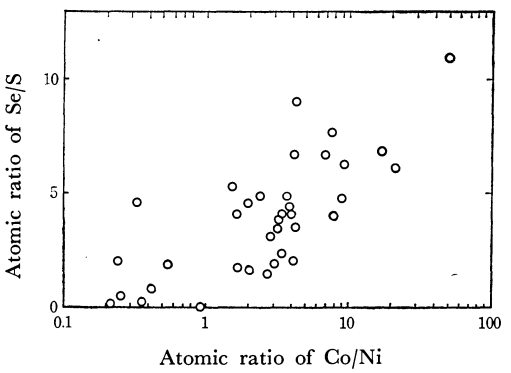

Fig. 5. Plot of atomic ratio of Se/S against atomic ratio of Co/Ni.

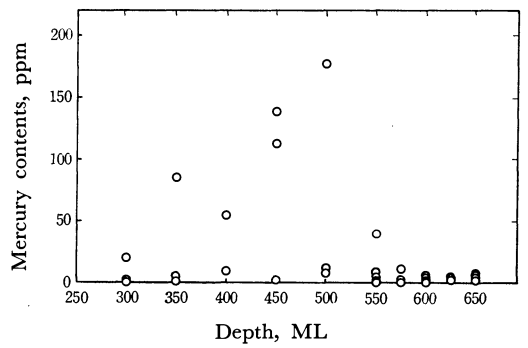

Fig. 6. Plot of mercury content in pyrite ores against depth.

Discussion

The atomic ratios of Se/S and Co/Ni are found to vary with the depth in the same manner at the Fujimi ore deposit No 5. This suggests that a certain correlation between the atomic ratios of Se/S and Co/Ni should exist. Carstens[14] reported that cobalt was concentrated in the pyrite ores of the high-temperature-type rather than in those of the low-temperature-type, and large values of the atomic ratio of Co/Ni were observed when the ore deposits were formed by the hydrothermal process. Hawley[15] described how large values of the atomic ratio of Co/Ni were observed in the pyrite ores of high formation temperatures when several pyrite ores of known formation temperatures were examined. Hegeman[16] stated that the values of the atomic ratio of Co/Ni became larger as the degree of metamorphism rises. The values of the atomic ratio of Co/Ni in the pyrite ores of the high-temperature-type from the lower part of the Daikoku ore deposit, the Chichibu mine, which is of contact-metasomatic origin (2.7—6.5), were larger than those of the low-temperature-type from the upper part of the ore deposit, which is of hydrothermal origin (0.2—1.6).[13] The formation or metamorphism temperatures of the lower part of the Fujimi ore deposit No. 5 were probably higher than those of the upper part, because the vertical distribution of the atomic ratio of Co/Ni showed a dependence on the depth. This is supported by the fact that sphalerite of the low-temperature-type exists in the upper part of the ore body and chalcopyrite of the high-temperature-type, in the lower part. Therefore, it may be considered that selenium is concentrated in the pyrite ores of the high-temperature-type rather than in those of the low-temperature-type; this conclusion agrees with Takimoto's results.[2,5]

Krauskopf[17] reported that mercury in vein fluid was transported as mercuric chloride or as free mercury and free sulfur in a high-temperature gas phase. In both case, merucry should be concentrated in the low-temperature-type ores. Therefore, the vertical distribution of mercury is

14) C. W. Carstens, *Kgl. Norske Videnskabs Selskabs Forh.*, **15**, 165 (1942).
15) J. E. Hawley, *Econ. Geol.* **47**, 260 (1952).
16) F. Hegeman, *Z. angew. Mineral*, **4**, 122 (1941).
17) K. B. Krauskopf, *Econ. Geol.*, **46**, 498 (1951).

contradictory to that of the atomic ratios of Se/S and Co/Ni on the temperature-type of the ores. This discrepancy has not yet been solved, because it is not evident whether the present distributions of selenium, cobalt, and nickel in pyrite ores at the Fujimi ore deposit were formed at the same time with that of mercury or not.

The authors are indebted to the authorities concerned of the Section of Exploration of the Hitachi Mine, Nippon Mining Co., Ltd., for helping our investigation.

BULLETIN OF THE CHEMICAL SOCIETY OF JAPAN VOL. 41 854—862 (1968)

Metal Complexes with Amino Acid Amides. I. Preparations and Electronic Spectra of the Nickel(II) and Palladium(II) Complexes

Takashi KOMORITA, Jinsai HIDAKA and Yoichi SHIMURA

Department of Chemistry, Faculty of Science, Osaka University, Toyonaka, Osaka

(Received July 31, 1967)

Several planar bis(amino-acid-amidato) complexes of nickel(II) and palladium(II) have been newly synthesized and characterized mainly spectroscopically. The geometrical structures of these $[M(N)_4]$-type complexes have been determined: palladium(II) produced both cis and trans complexes with L-alanine- and L-leucine-amidate ligands, while nickel(II) did only trans forms with glycine-, L-alanine- and L-leucine-amidates. Nickel(II) also produced cationic complexes, Ni(L-alanine-amide)$_2SO_4$ and its glycine amide analogue. The circular dichroism spectra and rotatory dispersion of the complexes containing optically active amino acid amide have been measured and discussed as for the assignments of the ligand field absorption bands of the diamagnetic planar complexes. A good correspondence was observed between the circular dichroism spectra of the nickel(II) and the palladium(II) complexes.

A number of reports[1-3] have been presented for the electronic structures of the tetracoordinated planar complexes with d^8 electron configuration. It seems, however, that the attempts have been less successfully carried out, partly because of the rather simple feature of the ligand field bands of these complexes and partly because of the lack of favorable series of complexes suitable to systematic studies. In these circumstances, it is thought of as desirable to study the circular dichroism (CD) and the rotatory dispersion (RD) of the planar complexes containing optically active ligands.[4,5]

It is well known that the bidentate ligand with amide or amidino groups, such as biuret, biguanide, oxamide or dicyandiamidine, is coordinated planarly to copper(II) or nickel(II) through its two nitrogen atoms;[6,7] an authentic example is the bis(biuretato)-cuprate(II) ion whose structure has been established by X-ray analysis of its potassium salt tetrahydrate.[8] The α-amino acid amide, such as L-alanine amide *etc.*, belongs to the category of ligands above shown and furthermore has one asymmetric carbon atom in the structure. Therefore the complexes of optically active α-amino acid amides will be excellently suitable for CD or RD studies of the planar complexes. Such complexes have not been isolated heretofore, except for a few copper(II) complexes, which have been prepared by Rising and Yang,[9] and Rosenberg.[10]

In the present paper, the preparations of several nickel(II) and palladium(II) complexes with glycine amide, L-alanine amide and L-leucine

1) G. Maki, *J. Chem. Phys.*, **28**, 651 (1958); **29**, 1129 (1958).
2) D. S. Martin, Jr., M. A. Tucker and A. J. Kassman, *Inorg. Chem.*, **5**, 1298 (1966).
3) H. Basch and H. B. Gray, *ibid.*, **6**, 365 (1967); F. A. Cotton and C. B. Harris, *ibid.*, **6**, 369 (1967).
4) B. Bosnich, *J. Chem. Soc. (A)*, **1966**, 1394; B. Bosnich, J. H. Dunlop and R. D. Gillard, *Chem. Commn.*, **1965**, 274.
5) H. Ito, J. Fujita and K. Saito, This Bulletin, **39**, 2056 (1966); and personal communication.
6) M. Kato, Y. Komuro and K. Sone, *Nippon Kagaku Zassi (J. Chem. Soc. Japan, Pure Chem. Sect.)*, **78**, 896 (1957).
7) Y. Kuroda, M. Kato and K. Sone, This Bulletin, **34**, 877 (1961).
8) H. C. Freeman, J. E. W. L. Smith and J. C. Taylor, *Acta Cryst.*, **14**, 407 (1961).
9) M. M. Rising and P. S. Yang, *J. Biol. Chem.*, **99**, 755 (1933).
10) A. Rosenberg, *Acta Chem. Scand.*, **11**, 1390 (1957).

amide*[1] are reported, and the electronic absorption and CD spectra of these complexes are discussed in relation to their geometrical structures.

Experimental

Preparation. *1) Glycine Amide, L-Alanine Amide and L-Leucine Amide.* These were derived from the corresponding amino acids by the similar methods described in literature.[11]

2) trans-Bis(glycine-amidato)nickel(II) Monohydrate: trans-[Ni(glya)$_2$]·H$_2$O. To the suspension of 2.43 g of [Ni(NH$_3$)$_6$](ClO$_4$)$_2$ in 20 m*l* of water was added 1.00 g of glycine amide, and the suspension was mechanically stirred for a few minutes. When the solution containing 0.54 g of sodium hydroxide and 5 m*l* of water was dropped into the suspension with stirring, the color of the mixture changed from blue to orange brown. After the mixture was stirred for several minutes and the residue, [Ni(NH$_3$)$_6$](ClO$_4$)$_2$, filtered off, the filtrate was cooled in an ice bath until the desired complex began to crystallize out as orange needles. The crystals obtained were washed with water-methanol mixture (1 : 1) and with methanol and then dried in air.

Found: C, 21.89; H, 5.24; N, 25.21%. Calcd for C$_4$H$_{12}$N$_4$O$_3$Ni: C, 21.56; H, 5.43; N, 25.14%.

An additional crop of the complex was obtained by adding methanol to the mother liquor which was concentrated by evaporation below 35°C. Total yield, 0.7 g.

This complex is soluble in water, but the solution is not very stable. It is slightly soluble in methanol, and insoluble in ethanol, acetone, benzene and chloroform.

In the preparation above, it is also possible to use nickel(II) acetate tetrahydrate instead of [Ni(NH$_3$)$_6$](ClO$_4$)$_2$.

3) trans-Bis(L-alanine-amidato)nickel(II): trans-[Ni(L-alaa)$_2$]. A solution of 0.46 g of sodium hydroxide in 4 m*l* of water was gradually added to a solution containing 1.41 g of nickel(II) acetate tetrahydrate and 1.00 g of L-alanine amide in 7 m*l* of water. After about 60 m*l* of methanol was added to the mixture, the resultant orange solution was filtered. By adding 30 m*l* of methanol and about 300 m*l* of ether to the filtrate, the complex desired was crystallized out as glistening orange plates. The crystals were filtered and washed with methanol-ether mixture and then with ether and dried *in vacuo* over calcium chloride. The complex was recrystallized by adding ether to its methanolic solution. Yield, 0.9 g.

Found: C, 31.26; H, 6.11; N, 24.26%. Calcd for C$_6$H$_{14}$N$_4$O$_2$Ni: C, 30.90; H, 6.06; N, 24.05%.

This complex is soluble in water, but the solution is not very stable. It is soluble in methanol and ethanol, but insoluble in other organic solvents.

4) trans-Bis(L-leucine-amidato)nickel(II): trans-[Ni(L-leua)$_2$]. To a solution containing 0.93 g of purified nickel(II) sulfate heptahydrate in 30 m*l* of water was added a solution of 1.00 g of L-leucine amide in 10 m*l* of water and then the mixture was mechanically stirred. A small fraction of the desired complex already began to deposit in this step. A solution of 0.31 g of sodium hydroxide in 10 m*l* of water was added drop by drop to the mixture with stirring. The orange microplates deposited were filtered out and washed with water, methanol and ether, and then dried *in vacuo* over calcium chloride. The yield was nearly quantitative.

Found: C, 45.10; H, 8.14; N, 17.60%. Calcd for C$_{12}$H$_{26}$N$_4$O$_2$Ni: C, 45.46; H, 8.27; N, 17.67%.

This complex is soluble in methanol, and insoluble in water and ethanol.

5) Bis(glycine-amide)nickel(II) Sulfate Sesquihydrate: Ni(glyaH)$_2$SO$_4$·1.5H$_2$O and Bis(L-alanine-amide)nickel(II) Ni(L-alaaH)$_2$SO$_4$. These complexes were prepared by adding methanol to an aqueous solution of nickel(II) sulfate containing glycine amide or L-alanine amide. After the desired complex began to appear, the resultant mixture was stirred mechanically for a few hours. The blue crystals were soluble in water and insoluble in methanol and ethanol. The complex sulfate with L-alanine amide was very hygroscopic.

Found: C, 14.73, 14.69; H, 4.75, 4.55; N, 16.33, 16.41%. Calcd for Ni(glyaH)$_2$SO$_4$·1.5H$_2$O=C$_4$H$_{15}$N$_4$O$_{7.5}$SNi: C, 14.56; H, 4.58; N, 16.98%.

Found: C, 21.01; H, 4.99; N, 15.18%. Calcd for Ni(alaaH)$_2$SO$_4$=C$_6$H$_{16}$N$_4$O$_6$SNi: C, 21.77; H, 4.87; N, 16.93%.

The elemental analysis data fluctuated slightly, and this may be caused by a partial hydrolysis of the ligands.

An attempt to obtain the complex salt with L-leucine amide was unsuccessful because of the precipitation of insoluble [Ni(L-leua)$_2$].

6) trans-Bis(glycine-amidato)palladium(II): trans-[Pd(glya)$_2$]. Palladium(II) chloride (2.86 g) was dissolved in 130 m*l* of water with stirring and filtered once. By adding a solution of 3.00 g of glycine amide in 20 m*l* of water to the dark brown solution, a light brown precipitate appeared. When an aqueous solution of 1.30 g of sodium hydroxide was dropped into the mixture, the light brown precipitate disappeared. Within several minutes after the dissolution of the precipitate, pale yellow fine needles began to appear. The mixture was mechanically stirred until the crystals did not increase further (about 20 min). The crystals filtered off mainly consisted of the pale yellow needle crystals. The second and third crops of crystals were fractionally obtained from the mother liquor by concentrating it to 10—20 m*l* *in vacuo* at about 30°C. These second and third crops were contaminated by another kind of pale yellow crystals which were prismatic. However, the two kinds of crystals have not been separated as yet. Recrystallization was repeated until the pure *needles* were obtained, by dissolving the crude complex in water and by evaporating the solution *in vacuo* at about 30°C. The needle crystals obtained were washed with cold water and dried *in vacuo* over phosphorus pentoxide. The yield was 1.6 g in total.

Found: C, 19.08; H, 4.16; N, 21.94%. Calcd for C$_4$H$_{10}$N$_4$O$_2$Pd: C, 19.02; H, 3.99; N, 22.19%.

This complex is moderately soluble only in water.

7) trans-Bis(L-alanine-amidato)palladium(II): trans-[Pd(L-alaa)$_2$]. Two grams of palladium(II) chloride was suspended in a solution of 2.00 g of L-alanine amide in 20 m*l* of water, and to this suspension was added a

*1 The following abbreviations are used in this paper: glyaH=glycine amide, alaaH=alanine amide, and leuaH=leucine amide.

11) P. S. Yang and M. M. Rising, *J. Am. Chem. Soc.*, **53**, 3183 (1931); G. Hillmann, *Z. Naturforsch.*, **1**, 682 (1946).

solution containing 0.90 g of sodium hydroxide in 5 m*l* of water with stirring. After the continuous stirring for about 2 hr, the palladium(II) chloride dissolved gradually. The insoluble materials were filtered off and the pale yellow filtrate was concentrated at about 30°C. When a pale yellow microplates began to separate, the mixture was diluted by adding 30 m*l* of ethanol. The whole of them was concentrated to about 10 m*l* by evaporation at about 30°C. The crystals deposited were gathered by filtration and washed with a small amount of ethanol. The mother liquor and the washings were kept for obtaining the cis complex in 8). The crude complex was recrystallized by concentrating its aqueous solution at about 30°C and then by adding methanol and ether to it. Yield, 0.7 g.

Found: C, 26.08; H, 4.96; N, 19.62%. Calcd for $C_6H_{14}N_4O_2Pd$: C, 25.68; H, 5.03; N, 19.97%.

This complex is soluble in water, slightly soluble in methanol and insoluble in ethanol.

8) cis-Bis(L-alanine-amidato)palladium(II) Monohydrate: cis-[Pd(L-alaa)$_2$]·H_2O. The combined mother liquor and washings from 7) was filtered once more. The filtrate was concentrated to half of its original volume under a reduced pressure and a few milliliters of methanol was added to the yellow solution. At this stage, a small amount of *trans*-[Pd(L-alaa)$_2$] and sodium chloride has precipitated. After those were filtered off, the desired complex, which is pale yellow, was formed by adding a large amount of ether to the filtrate. The crude complex obtained was dissolved in a small amount of methanol, and the solution was filtered. An appropriate amount of ether was added to the filtrate, and the vessel was scratched with a glass rod if necessary to obtain crystals. This purification procedure was repeated until a uniform mixture of the pure prisms was obtained. The crystals were washed with ether and dried *in vacuo* over calcium chloride. Yield, 0.6 g.

Found: C, 24.15; H, 5.34; N, 18.73%. Calcd for $C_6H_{16}N_4O_3Pd$: C, 24.13; H, 5.40; N, 18.76%.

This complex is very soluble in water, methanol and slightly soluble in ethanol.

9) trans-Bis(L-leucine-amidato)palladium(II): trans-[Pd(L-leua)$_2$]. Thirty milliliters of aqueous solution containing 1.25 g of potassium tetrachloropalladate(II) was added little by little to the solution of 1.00 g of L-leucine amide in 30 m*l* of water with stirring. A solution of 0.5 g of potassium hydroxide in 10 m*l* of water was added to the solution. The desired complex, pale yellow precipitate, began to deposit soon after. After the mixture was stirred for about 2 hr, the precipitate was filtered off, washed with water three times, and with methanol, and then with ether. This was dried *in vacuo* over calcium chloride. Yield, 0.7 g.

Found: C, 39.55; H, 7.15; N, 15.39%. Calcd for $C_{12}H_{26}N_4O_2Pd$: C, 39.51; H, 7.18; N, 15.36%.

This complex is very sparingly soluble in water, methanol and ethanol.

10) cis-Bis(L-leucine-amidato)palladium(II) Hexahydrate: cis-[Pd(L-leua)$_2$]·$6H_2O$. A mixture of 1.40 g of L-leucine amide in 10 m*l* of water and 0.45 g of sodium hydroxide in 15 m*l* of water were added to the suspension of 1.00 g of palladium(II) chloride in 10 m*l* of water with stirring. Being stirred for about 30 min until it became very pasty, the mixture was diluted with 60 m*l* of water. After the continuous stirring for 1 hr further, a mixed precipitate of cis and trans forms appeared: then it was filtered out (ppt. 1). After the mother liquor was concentrated to about 1/5 volume by evaporation at about 30°C, the solution was kept in a refrigerator overnight. A large amount of pale yellow fine needles (desired cis complex) were separated by filtration (ppt. 2).

The ppt. 1 was suspended in an appropriate amount of ethanol: in this procedure only the cis form dissolved. This extraction was repeated several times. When the combined extracts was kept in a refrigerator overnight, a small amount of trans form was deposited, which was discarded by filtration. The pale yellow filtrate was concentrated under reduced pressure at about 30°C until it became yellow syrup. From this syrup crystallization was started by scratching the vessel with a glass rod. This crude cis complex and the ppt. 2 obtained above were dissolved in an appropriate amount of methanol-water mixture (10 : 1). By concentrating the solution to 15 m*l* at about 30°C, a very small amount of the trans complex was deposited and then filtered off. Pure crystals of cis complex were obtained by concentrating the yellow filtrate to about 5 m*l*. The crystals, elongated rectangular plates, were gathered and washed with a little of ice water three times and dried in a desiccator over calcium chloride.

Found: C, 29.82; H, 8.03; N, 11.85%. Calcd for $C_{12}H_{38}N_4O_8Pd$: C, 30.48; H, 8.10; N, 11.85%.

The crystal form of the final product was different from that of ppt. 2, but the infrared absorption (IR) spectra of these two kinds of crystals agreed well with each other (in NaCl region) except for the bands due to crystalline water.

This complex is soluble in water, methanol and ethanol. It was noted that the cis forms of [Pd(L-alaa)$_2$] and [Pd(L-leua)$_2$] are more soluble in water and in alcohols than the corresponding trans forms.

Measurements. The following instruments were employed for the measurements: for the visible and ultraviolet absorption spectra, a Beckman DU spectrophotometer; for the diffuse reflectance spectra, a Hitachi EPU-2A spectrophotometer (in visible region) and a Hitachi EPS-3T recording spectrophotometer (in ultraviolet region); for the CD spectra, a Roussel-Jouan dichrographe; for the RD curves, a Yanagimoto recording spectropolarimeter Model-185; for the IR absorption spectra, a Model DS-402G infrared spectrophotometer of Japan Spectroscopic Co. (700—4000 cm^{-1}) and a Hitachi EPI-2 spectrophotometer (1300—1500 cm^{-1}); and finally for the nuclear magnetic resonance (NMR) spectra, a Japan Electron Optics JNM 3H-60 spectrometer using tetramethylsilane as an internal reference. All the measurements were made at room temperature.

Results and Discussion

1) Palladium(II) Complexes. The five palladium complexes obtained are classified into two groups, (A) and (B), on the basis of their absorption and diffuse reflectance spectra; (A) group consists of [Pd(glya)$_2$], [Pd(L-alaa)$_2$] and [Pd(L-leua)$_2$], and (B) group [Pd(L-alaa)$_2$]·H_2O and [Pd(L-leua)$_2$]·$6H_2O$. The spectral behavior of the complexes is the same in each group, but is

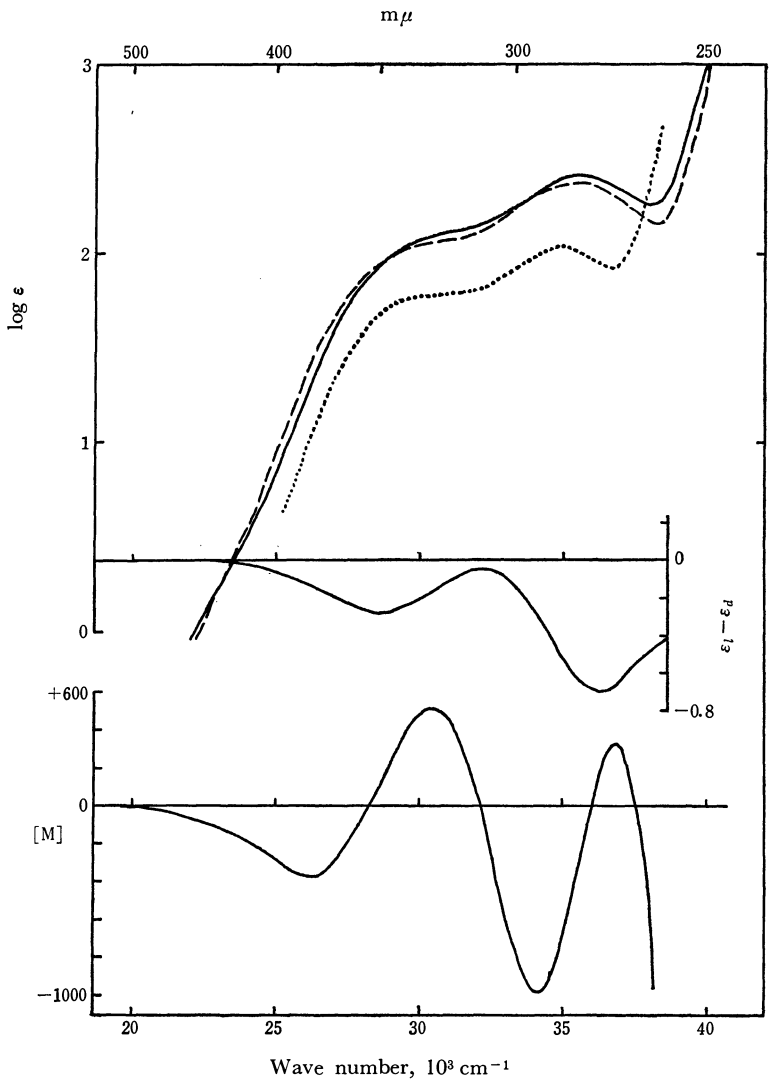

Fig. 1. Absorption and CD spectra, and RD of *trans*-[Pd(amino-acid-amidate)$_2$].
—— L-alaa complex in water; ---- glya complex in water; and ····· L-leua complex in the solid state.

remarkably different from that of the other group, as can be seen in Table 1 and Figs. 1—3.

The NMR spectra of (A) group's [Pd(L-alaa)$_2$] and of (B) group's [Pd(L-alaa)$_2$]·H_2O, in deuterium oxide, show only one kind of sharp doublet line due to the methyl protons of the ligands; τ-value of the former is 8.29 and that of the latter 8.16. This fact confirms, together with the results of the elemental analyses, that two coordinated alanine amidate ligands are not hydrolyzed. The IR spectra also support this conclusion (Table 2).

From these facts, it was concluded that the groups, (A) and (B), represent a couple of geometrical isomers, *i. e.*, cis and trans isomers concerning the two amino groups.

It may be expected that double bond character of the amidate's C–N bond is rich for the coordination type II or III in comparison with the type I.

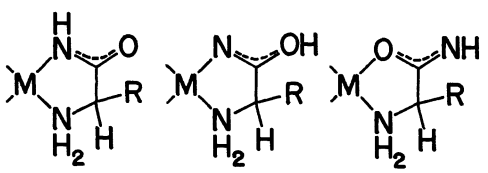

I II III

In IR spectra of the complexes (Table 2), very intense C–O stretching bands are observed at about 1600 cm^{-1} for both groups of complexes, (A) and (B). This behavior did not contradict[7] the theory that these palladium(II) complexes have structure I. A similar behavior of the amidate's C=O

TABLE 1. ABSORPTION MAXIMA OF THE COMPLEXES
(Wave numbers are give in $10^3\,cm^{-1}$ unit and the intensities, log ε, in parentheses)

Complex	Solvent or condition[a)]	Absorption maximum[b)]
trans-[Pd(glya)$_2$]	(S)	29.5, 34.3
	(W)	~30 sh (2.1), 35.3 (2.39)
trans-[Pd(L-alaa)$_2$]	(S)	~30 sh, 34.8
	(W)	~30 sh (2.1), 35.5 (2.41)
trans-[Pd(L-leua)$_2$]	(S)	~30 sh, 34.8
cis-[Pd(L-alaa)$_2$]·H$_2$O	(W)	~26.7 sh (1.3), 34.7 br (2.62)
	(Me)	~26.7 sh (1.4), 34.5 br (2.63)
cis-[Pd(L-leua)$_2$]·6H$_2$O	(W)	~26.7 sh (1.3), 34.8 br (2.63)
	(Et)	~26.7 sh (1.4), 34.8 br (2.65)
trans-[Ni(glya)$_2$]·H$_2$O	(S)	22.9
trans-[Ni(L-alaa)$_2$]	(S)	23.7
	(Me)	23.4 (1.77)
trans-[Ni(L-leua)$_2$]	(Me)	23.4 (1.82)
Ni(glyaH)$_2$SO$_4$·1.5H$_2$O	(S)	10.4, 13.6 sh, 15.9, ~27 br
	(W)	9.7 (0.86), 13.5 sh, 16.1 (0.73), 26.5 (0.97)
Ni(L-alaaH)$_2$SO$_4$	(W)	9.7, 13.5 sh, 16.0, 26.4

a) Abbreviations: S=solid, W=water, Me=methanol, and Et=ethanol.
b) sh=shoulder, br=broad band.

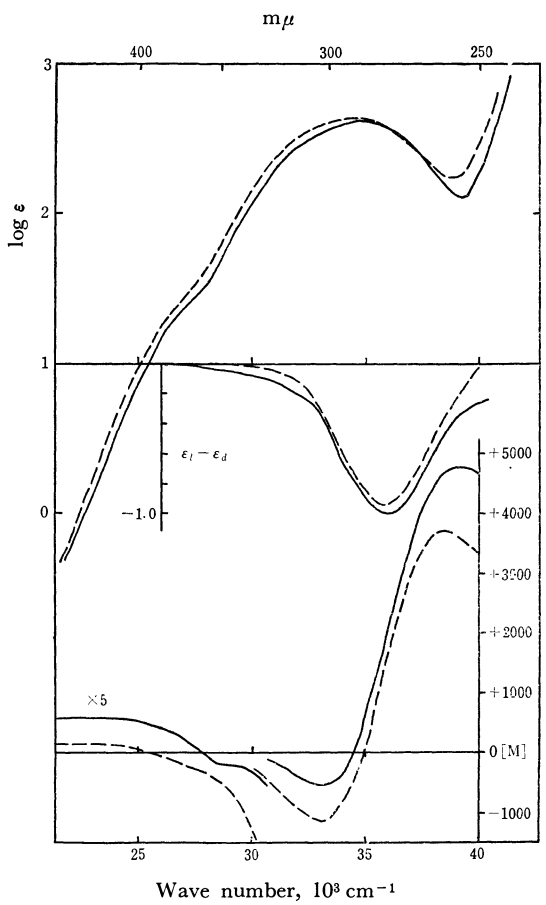

Fig. 2. Absorption and CD spectra, and RD of *cis*-[Pd(L-alaa)$_2$]·H$_2$O.
—— in water; and ---- in methanol.

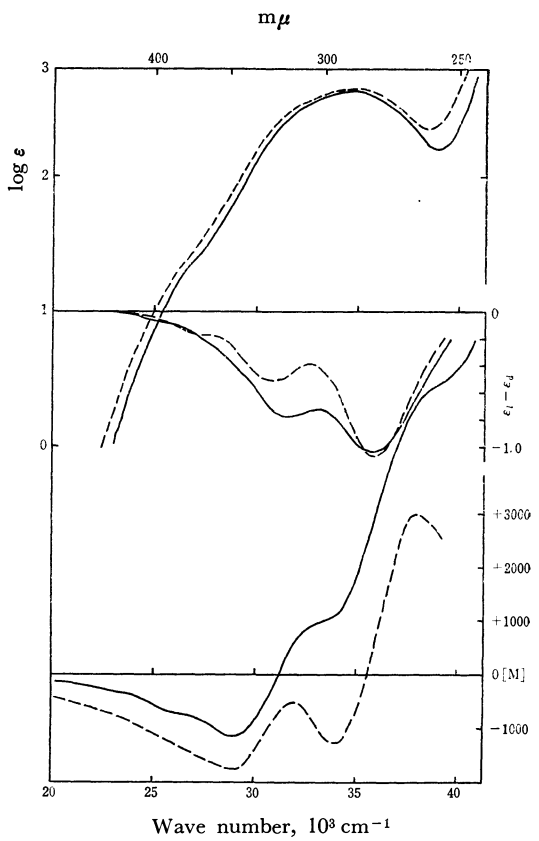

Fig. 3. Absorption and CD spectra, and RD of *cis*-[Pd(L-leua)$_2$]·6H$_2$O.
—— in water; and ---- in ethanol.

Table 2. IR data of the complexes in 3μ and 6μ regions, obtained with Nujol mull method (C-H Stretching bands are omitted in 3μ region)[a,b]

trans-[Ni(glya)$_2$]·H$_2$O	3328m, 3200s, 3120s, 1630s, 1580vs, 1552s
trans-[Pd(glya)$_2$]	3310sh, 3206s, 3110s, 1620sh, 1575vs, 1552s
trans-[Ni(L-alaa)$_2$]	3300s, 3166s, 3056s, 1597vs
trans-[Pd(L-alaa)$_2$]	3296s, 3158s, 3056s, 1629m 1584vs
cis-[Pd(L-alaa)$_2$]·H$_2$O	3320w, 3250m, 3200s, 3118s, 1630m, 1600sh, 1575vs, 1550sh
trans-[Ni(L-leua)$_2$]	3310m, 3170s, 3078s, 1616s, 1595s, 1555vs
trans-[Pd(L-leua)$_2$]	3312m, 3167s, 3072s, 1605s, 1587s, 1546vs
cis-[Pd(L-leua)$_2$]·6H$_2$O	3250sh, 3210s, 3110s, 1575vs

a) Abbreviations: s=strong, m=medium, w=weak, vs=very strong, and sh=shoulder.
b) Wave number in cm^{-1}.

stretching bands has been reported in several current papers, for example, for bis(biuretato)-cuprate(II),[12] bis(oxamidato)-cuprate(II) and -nickelate(II) complexes,[7] and bis(glycine-amidato)- and bis(L-leucine-amidato)-copper(II) complexes.[10]

Now, considering the absorption spectra, we find those of (B) group's complexes are quite similar to that of tetramminepalladium(II) ion,[13] as shown in Figs. 2 and 3. From the point of view of ligand field theory, it may be concluded that the complexes belonging to (B) group are cis form of the structure I, since the effective field symmetry is approximately D_{4h} in these cis complexes even by considering a moderate π-interaction between the metal d-orbitals and the ligand π-orbitals.

Another support for the geometrical structures can be furnished by comparing their absorption spectra with those of the [Pd(Cl)$_2$(N)$_2$]-type complexes of known geometrical structures. A trans complex, [Pd(Cl)$_2$(1-phenylethylamine)$_2$], has been reported[4] to show two "spin-allowed" ligand field bands at about 25500 and 30000 cm^{-1}, while a cis(N)-type complex, [Pd(Cl)$_2$(1-pn)], shows[5] a broad band at 26200 cm^{-1} with a weak shoulder at the lower wave number side. The comparison of these data with the spectra in Figs. 1—3 clearly shows that (A) group is trans and (B) group cis.

The solution absorption spectra of *trans*-[Pd(glya)$_2$] and *trans*-[Pd(L-alaa)$_2$] are quite similar to those in their solid states (Table 1). It may be concluded that the structures of these complexes in solution and in solid state are not very different each other. This conclusion may also be supported by the two cis complexes, though their absorption spectra slightly depended upon the solvents used (Figs. 2 and 3).

It seems likely that the σ-lone pair electrons of an amidate nitrogen alone do not give effects to the electronic structure of the complex much different from those of an amino nitrogen. Consequently, to explain the significant difference between the absorption spectra of cis and trans forms, it is necessary to consider π-interactions between the palladium 4d- and the ligand π-orbitals through metal-amidate linkages. By an inspection of the orbital overlaps, it is expected that the most sensitive one to this kind of π-interaction is the d_{xz}- or d_{yz}-orbital. If the antibonding effects are predominant, only the d_{xz}-orbital will be strongly instabilized in trans form, while both the d_{xz} and d_{yz} will be moderately instabilized in cis form. The d_{yz}-orbital of the trans form will be nearly non-interacted. Accordingly, the energy order, $\nu_4 > \nu_3' \sim \nu_4' > \nu_3$, is expected.*2 Thus the band at about 30000 (CD, 28700) cm^{-1} in *trans*-[Pd(L-alaa)$_2$] may be assigned to ν_3 while the band at about 34500 (CD, 36000) cm^{-1} in the cis form and one at 35500 (CD, 36400) cm^{-1} in the trans form to (ν_3', ν_4') and ν_4' respectively (Figs. 1 and 2).

The *cis*-[Pd(L-leua)$_2$] has two CD components at about 31300 and 36000 cm^{-1} corresponding to one broad ordinary absorption band at 24800 cm^{-1}. The component at 36000 cm^{-1} is considered to be a combined peak of ν_3' and ν_4' corresponding to 36000 cm^{-1} band of *cis*-[Pd(L-alaa)$_2$]. Therefore the CD component at 31300 cm^{-1} should be another component, ν_1' or ν_2', whose absorption component is also included in the lower wave number side of the broad absorption band at 34800 cm^{-1}. In the CD spectra of *cis*- and *trans*-[Pd(L-alaa)$_2$], the band at about 31000 cm^{-1} did not appear clearly, but it seems likely that a positive CD band is canceled out almost completely by the strong negative CD bands. These bands at about 31000 cm^{-1} may be ν_1 and ν_1', or ν_2 and ν_2'. Theoretically,[1-3] it is expected that the order is $\nu_1 > \nu_2$, and $\nu_1' > \nu_2'$. But the absorption and CD bands at the region lower than 27000 cm^{-1} in the cis complexes and the CD tail in lower wave numbers of the trans complex may be assigned to "spin-forbidden" ligand field transitions, judging from their band intensities. Also a theoretical consideration expects that the Cotton effect in

*2 ν_1, ν_2, ν_3 and ν_4 mean transitions $(z^2)\rightarrow(x^2-y^2)$, $(xy)\rightarrow(x^2-y^2)$, $(xz)\rightarrow(x^2-y^2)$ and $(yz)\rightarrow(x^2-y^2)$ in trans form respectively, and ν_i' ($i=1-4$) means corresponding transition in cis form. Here, (k) means a molecular orbital composed mainly of d_k-orbital. Coordinate systems adopted for cis and trans forms are different, as in Ref. 1.

12) K. Aida, Y. Musha and S. Kinumaki, *Inorg. Chem.*, **2**, 1268 (1963).
13) S. Yamada and R. Tsuchida, *Ann. Rept. Sci. Works, Fac. Sci. Osaka Univ.*, **4**, 79 (1956).

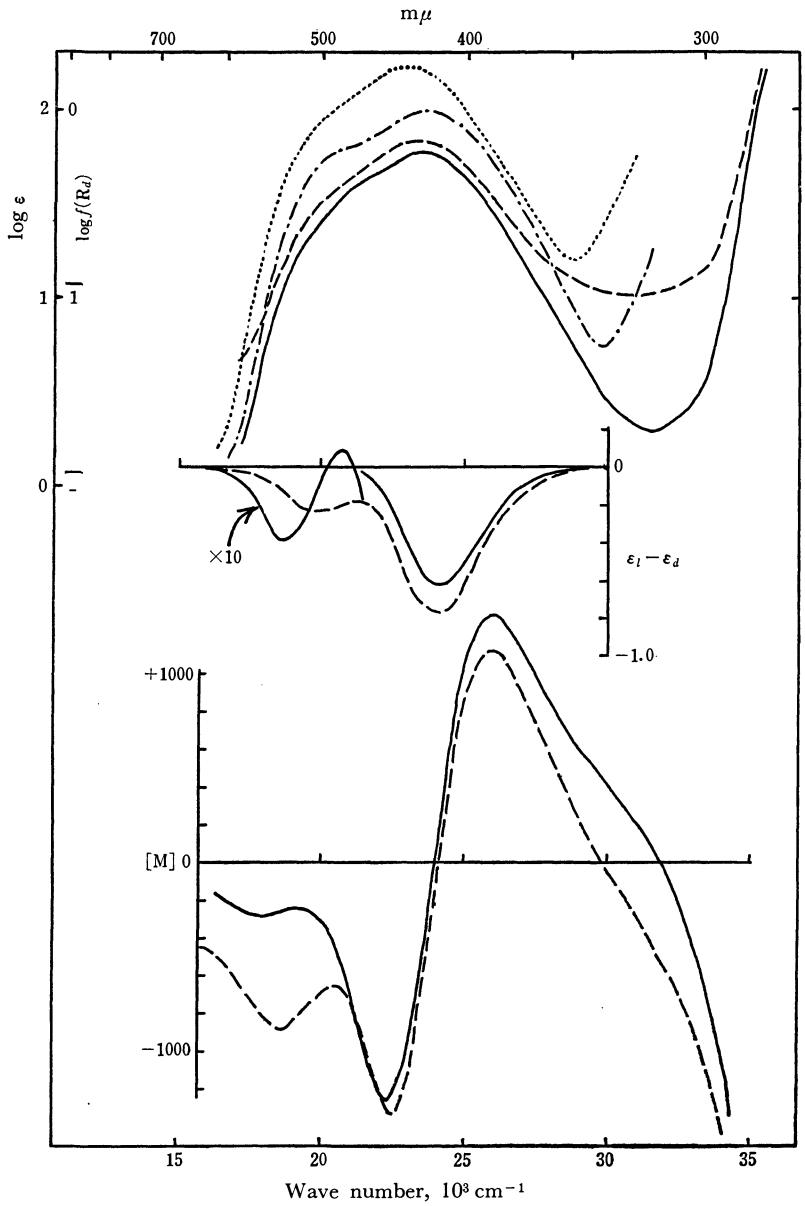

Fig. 4. Absorption and CD spectra and RD of *trans*-[Ni(amino-acid-amidate)$_2$]·xH$_2$O.
—— L-alaa complex in methanol; ---- L-leua complex in methanol; ····· glya complex in the solid state; and -·-·- L-alaa complex in the solid state. As for the x-values, see Table 2.

transitions ν_1 and ν_1' are forbidden under an appropriate approximation.*3 Therefore the present CD measurements suggest that the bands at about 31000 cm^{-1} are ν_2 and ν_2' and the transitions ν_1 and ν_1' are located in the region of higher wave numbers.

The ordering of d-levels assumed above (Table 3) agrees essentially with that proposed recently for tetrachloropalladate(II) ion.[3]

2) Bis(amino-acid-amidato)nickel(II) Complexes. The diffuse reflectance spectra of the three neutral nickel(II) complexes in their solid states are very similar to those of the diamagnetic planar [Ni(N)$_4$]-type complexes,[6,14] as may be seen in Fig. 4 and Table 1. Their IR spectra (Table 2 and Fig. 5) indicate that also the structure I is suitable to these complexes by the similar

*3 Pure d-orbitals can not produce magnetic moment for transitions ν_1 and ν_1' without configuration interaction.

14) D. M. L. Goodgame and L. M. Venanzi, *J. Chem. Soc.*, **1963**, 616, 5909.

TABLE 3. CD EXTREMA OF THE COMPLEXES AND THE TENTATIVE BAND ASSIGNMENTS FOR THEM
(Wave numbers are given in $10^3\,cm^{-1}$ unit and the intensities, $\varepsilon_l-\varepsilon_d$, in parentheses)

Complex	Solvent[a]	Observed extrema and their assignments			
		ν_3	ν_2 or ν_2'	ν_4	(ν_3', ν_4')
trans-[Pd(L-alaa)$_2$]	(W)	28.7 (−0.27)		36.4 (−0.69)	
cis-[Pd(L-alaa)$_2$]·H_2O	(W)				36.0 (−1.00)
	(Me)				35.9 (−0.96)
cis-[Pd(L-leua)$_2$]·$6H_2O$	(W)		31.5 (−0.77)		36.0 (−1.06)
	(Et)		31.1 (−0.50)		36.0 (−1.07)
trans-[Ni(L-alaa)$_2$]	(Me)	18.7 (−0.04)	20.8 (+0.01)	24.1 (−0.62)	
trans-[Ni(L-leua)$_2$]	(Me)	20.0 (−0.22)		24.1 (−0.77)	

a) Abbreviations: see Table 1.

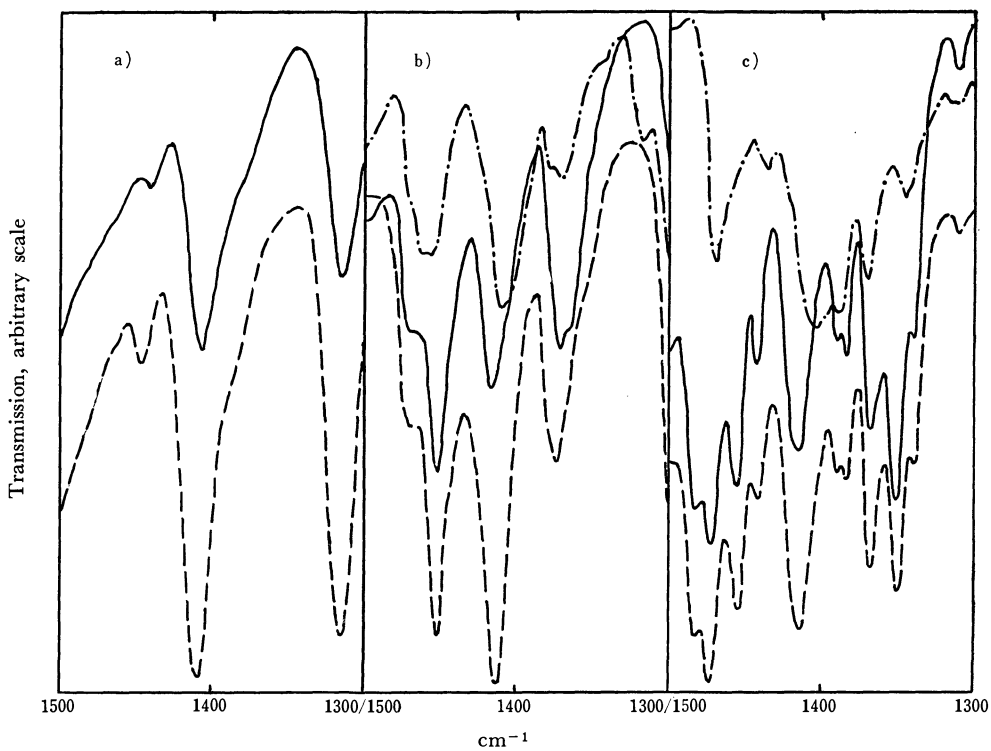

Fig. 5. IR spectra of the *cis*- and *trans*-[M(amino-acid-amidate)$_2$]·xH_2O in 1500—1300 cm^{-1} region (hexachlorobutadiene mull). a) glya-, b) L-alaa-, and c) L-leua-complexes; —— *trans*-Pd, ---- *trans*-Ni, and -·-·- *cis*-Pd complexes. As for the *x*-values, see Table 2.

reason for the palladium(II) complexes. Moreover, the IR spectra of the nickel(II) complexes show good correspondence to those of the trans palladium(II) complexes throughout NaCl region (700—4000 cm^{-1}). In Fig. 5 amidate's C–N stretching and C–H bending bands are shown; these kinds of bands have been believed to be less sensitive to the hydrogen bonding in crystal lattices. For instance, the spectra of [Ni(glya)$_2$]·H_2O and *trans*-[Pd(glya)$_2$] are very similar to each other in the region, 1300—1500 cm^{-1}. It may be concluded, therefore, that the remarkable difference between the IR spectra of the cis and the trans palladium(II) complexes in 1300—1500 cm^{-1} region should not be assigned to the difference due to the waters of hydration, but to the difference of geometrical configurations of the complexes. These observations strongly suggest that the three nickel(II) complexes concerned are the trans forms. It was confirmed, from the absorption data of Fig. 4 and in Table 1, that these trans structures were retained in their solutions also.

The band assignments of these nickel(II) complexes may be in parallel with those for the trans palladium(II) complexes. Thus the CD extrema of [Ni(L-alaa)$_2$], 18700, 20800 and 24100 cm^{-1},

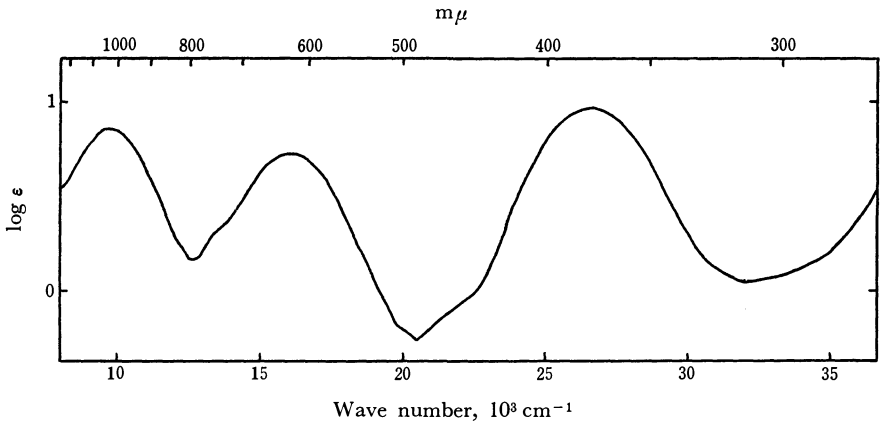

Fig. 6. Absorption spectrum of $Ni(glyaH)_2SO_4 \cdot 1.5H_2O$ in water.

are assigned to transitions ν_3, ν_2 and ν_4 respectively. It is most probable that the ν_2 band is hidden at about 21000 cm^{-1} in the CD spectrum of [Ni(L-leua)$_2$], since this complex should have an electronic structure which is not so different from that of [Ni(L-alaa)$_2$]. The rotatory strength of the band, which is assigned to ν_2 or ν_2', is strongly dependent upon the terminal alkyl groups of the ligands in both nickel(II) and palladium(II) complexes.

3) Bis(amino-acid-amide)nickel(II) Complexes. From the absorption spectra given in Table 1 and Fig. 6, it was inferred[15] that these two cationic complexes have approximately octahedral configurations, with spin triplet ground states, in the solutions and in the solid states. This hexacoordinated configuration will become possible by the coordination of sulfate ions or water molecules besides the amino acid amide ligands.

The structures of nickel(II) complexes with various amino acids[16,17] or with picoline amide,[18,19] which belong to $[Ni(N)_2(O)_4]$-type, have been studied previously, and it has been known that most of those complexes are of trans(N) structures. The absorption spectra of $Ni(glyaH)_2SO_4$ and $Ni(L\text{-}alaaH)_2SO_4$ in water (Table 1 and Fig. 6) are very similar to those of bis(glycinato)nickel(II) dihydrate[20] and of bis(picoline-amide)nickel(II) chloride dihydrate,[18] the structures of which have been determined by X-ray analyses.[16,19] In conclusion, it may be said that an oxygen of amide and an amino nitrogen are coordinated to nickel(II) in the blue complexes with glycine amide and with L-alanine amide.

It will be worthwhile to note that picoline amide, as amino acid amides, also produces a diamagnetic nickel(II) complex, bis(picoline-amidato)nickel(II) dihydrate,[18] the planar $[Ni(N)_4]$-structure of which has also been established by an X-ray analysis.[21]

The authors express their sincere thanks to Assistant Professor Tetsuo Shiba and Mr. Shuji Futakawa of Osaka University for their helpful suggestions about the preparations of amino acid amides. The authors wish to thank also Assistant Professor Fukiko Yamada of Kansai University for her measurements and discussion of the NMR spectra. Their thanks are also due to Dr. Seiko Komorita of Osaka University for her continuing interest.

15) C. K. Jørgensen, *Acta Chem. Scand.*, **10**, 887 (1956).
16) A. J. Stosick, *J. Am. Chem. Soc.*, **67**, 365 (1945).
17) T. Noguchi, This Bulletin, **35**, 99 (1961); P. Jose, *Acta Cryst.*, **17**, 24 (1964).
18) K. Yamasaki and M. Sekizaki, This Bulletin, **38**, 2206 (1965); M. Sekizaki and K. Yamasaki, *Nippon Kagaku Zasshi (J. Chem. Soc. Japan, Pure Chem. Sect.)*, **87**, 1053 (1966).
19) A. Masuko, T. Nomura and Y. Saito, This Bulletin, **40**, 511 (1967).
20) G. Maki, *J. Chem. Phys.*, **29**, 162 (1958).
21) Y. Nawata, H. Iwasaki and Y. Saito, This Bulletin, **40**, 515 (1967).

BULLETIN OF THE CHEMICAL SOCIETY OF JAPAN VOL. 41 863—874 (1968)

Spectroscopic Studies of Mixed Amine Carbonyl Complexes of d^6 Structure. II. Solvent Effect on the Ultraviolet and Visible Absorption Spectra of Diamine-tetracarbonyl Complexes of Chromium(0), Molybdenum(0) and Tungsten(0)

Hide SAITO, Junnosuke FUJITA and Kazuo SAITO

Chemistry Department, Faculty of Science, Tohoku University, Katahira-cho, Sendai

(Received August 11, 1967)

Absorption bands, especially metal to amine charge transfer bands of bipyridyl- and phenanthroline-tetracarbonyl chromium(0), molybdenum(0) and tungsten(0) are shifted in various solvents by less than 4500 cm^{-1}. The shift is discussed in accordance with McRae's equation, which was derived with the point-dipole approximation. The solvents can be classified into two groups, the alcohol and the ester group. When three constants corresponding to (1) the interaction between induced dipoles of the solute and of the solvent, (2) the interaction between permanent dipole of the solute and induced dipole of the solvent, and (3) the interaction between permanent dipoles of the solute and of the solvent, are duely chosen for the two groups of solvent individually, the experimental values are satisfactorily accounted for. Short range interactions, such as hydrogen bonding can be ignored.

Many studies have been made of the solvent effect (frequency shift) on visible and ultraviolet absorption spectra of π-conjugate organic compounds, and theoretical interpretation on the basis of simple electrostatic model, among them, seems quite successful.[1-5] On the other hand, little information is available concerning the solvent effect on absorption spectra of coordination compounds. Nakamoto *et al.* studied the absorption spectra of tervalent chromium and cobalt complexes in water, methanol and acetic acid.[6] The *d-d* transition bands exhibited red shift by less than 200 cm^{-1} and the extent increased in the order given. The intraligand transition bands, however, did not always give such a shift with a definite tendency. Alderdice[7] reported that the charge transfer band ($M\rightarrow\pi^*_{CO}$(1)C.T.)*1 of hexacarbonyltungsten(0) showed small blue shift in water and cyclohexane. Behrens and Harder[8] described that bisbipyridyl- and bisphenanthrolinedicarbonyl molybdenum(0) and tungsten(0) changed their colors according to the solvent and temperature.

We have found that several absorption bands of diamine-tetracarbonyl complexes of chromium(0), molybdenum(0) and tungsten(0) are shifted in various solvents. Especially the shift of the metal to diamine transition bands in the visible region is remarkable, *e.g.* shift by 3800 to 4500 cm^{-1} in acetonitrile and cyclohexane. In this paper the frequency shift of absorption bands of diamine-tetracarbonyl complexes of chromium(0), molybdenum(0) and tungsten(0) has been described and discussed on the basis of McRae's equation for solvent effect, which was derived with the point-dipole approximation.

Experimental

Preparation of the compounds was described elsewhere.[9] The solvents were carefully purified by the usual methods from commercial extra pure grade products. The absorption spectra were measured with Hitachi EPS-3 Automatic Recording Spectrophotometer at 20 to 25°C, with a slow scanning speed, (6 min 700—340 mμ, 360—210 mμ) and 1 cm quartz cells. Sparingly soluble compounds in *e.g.* cyclohexane, *n*-butyl ether and carbon tetrachloride were measured with 2, 5 or 10 cm quartz cells. The solution was filtered through a glass filter of G4 texture, whenever necessary.

1) Y. Ooshika, *J. Phys. Soc. Japan*, **9**, 594 (1954).
2) E. G. McRae, *J. Phys. Chem.*, **61**, 562 (1957).
3) W. W. Robertson, A. D. King, Jr., and O. E. Weigang, Jr., *J. Chem. Phys.*, **35**, 464 (1961).
4) T. Kubota and M. Yamakawa, This Bulletin, **35**, 555 (1962).
5) M. E. Baur and M. Nicol, *J. Chem. Phys.*, **44**, 3337 (1966).
6) K. Nakamoto, M. Kobayashi and R. Tsuchida, *ibid.*, **22**, 957 (1952).
7) D. S. Alderdice, *J. Mol. Spectry.*, **15**, 509 (1965).
*1 The abbreviations are the same as mentioned in Part I. (This Bulletin).
8) H. Behrens and N. Harder, *Chem. Ber.*, **97**, 426 (1964).
9) H. Saito, J. Fujita and K. Saito, This Bulletin, **41**, 359 (1968).

Results

The absorption curves are shown in Figs. 1 to 5 and the numerical data for the bands showing distinct shifts are summarized in Tables 1 to 4. The constancy of integrated intensities and the small change in shapes of the absorption band indicate that no substantial change occurs in the complexes themselves. The tungsten(0) compound $[W(CO)_4en]^0$ decomposed rapidly and its spectrum was not measured.

The bands generally show blue shifts to various extents according to the dielectric constant of solvents, and it appears reasonable to classify the solvents into two groups, the alcohol (solvents Nos. 1 to 7 in Tables 1 to 4) and the ester group (Nos. 8 to 13), because the correlation seems better within one particular group.

Application of McRae's Equation I. McRae[2] gave a theoretical equation for solvent effects on absorption spectra. His theory is based on a simple electrostatic model in which the solvent-solute interaction is only long-range dipole interaction. (Onsager's approximation) The equation in a simplified form[4] is as follows:

$$\tilde{\nu} = \tilde{\nu}_{gas} + (A + B)\frac{n^2 - 1}{2n^2 + 1} + C\left(\frac{D - 1}{D + 2} - \frac{n^2 - 1}{n^2 + 2}\right) \quad (1)$$

where $\tilde{\nu}$ is the wave number of bands in a given solution, and D and n are static dielectric constant, and refractive index of the solvent, respectively.

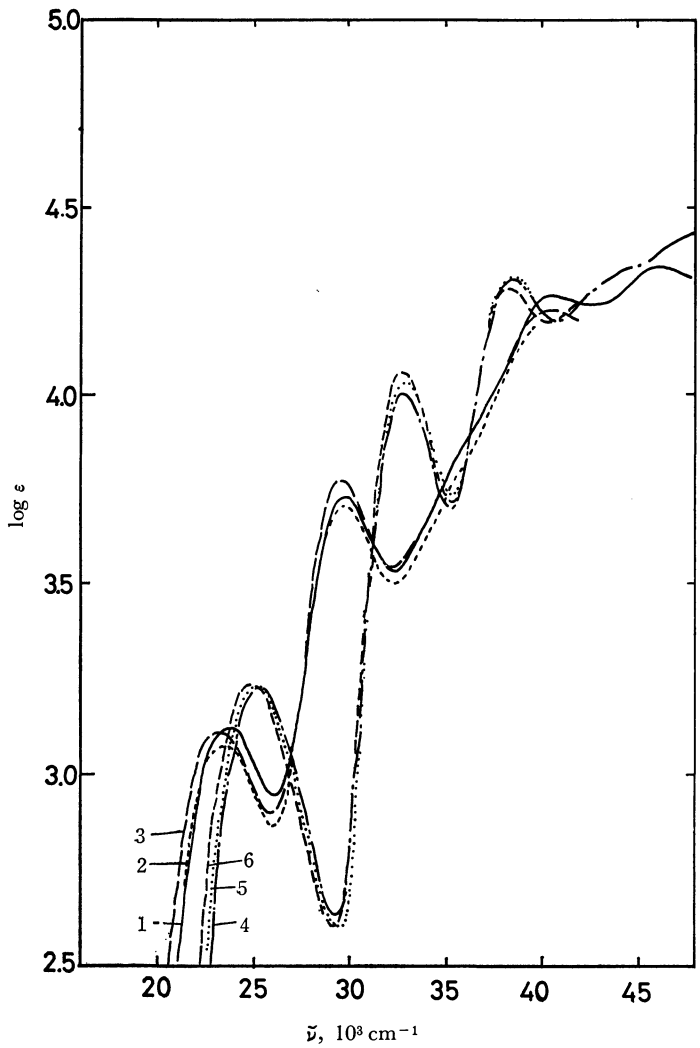

Fig. 1. Absorption spectra of ethylenediamine-tetracarbonyl chromium(0) and molybdenum(0) in some solvents:
$[Cr(CO)_4en]$ 1 —— in methanol, 2 ---- in methylacetate, 3 —— —— in *p*-dioxane;
$[Mo(CO)_4en]$ 4 — — — in methanol, 5 ····· in methylacetate, 6 — — in *p*-dioxane.

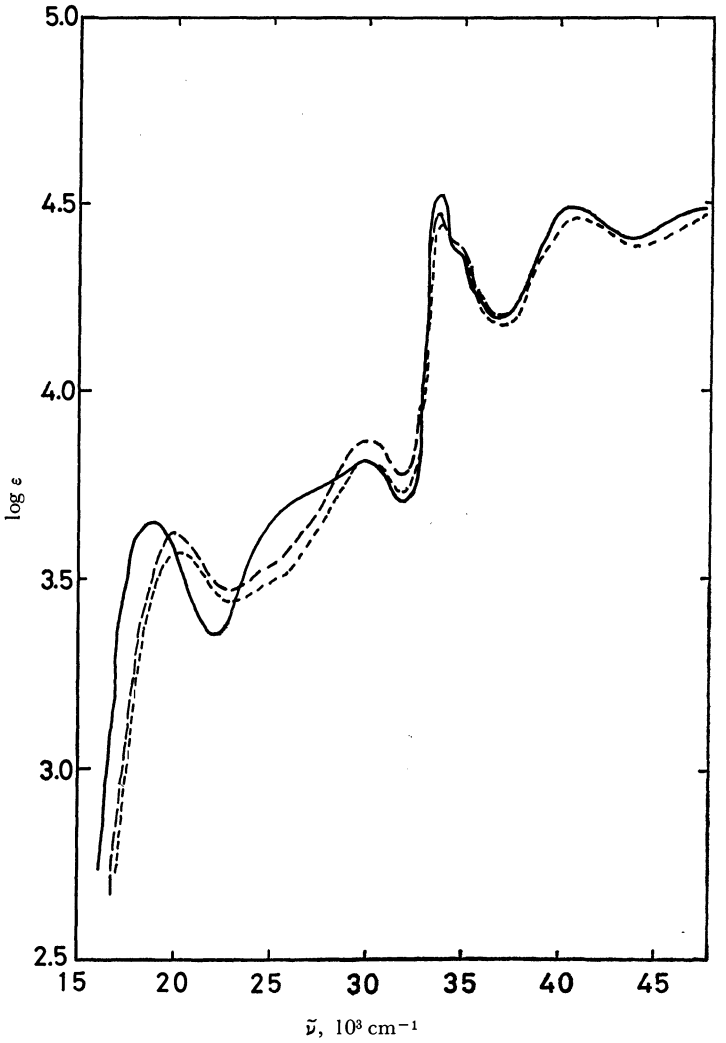

Fig. 2. Absorption spectra of bipyridyl-tetracarbonyl chromium(0) in some solvents: ---- in methanol, — — in methylacetate, —— in ethylether.

$\tilde{\nu}_{gas}$ denotes the wave number of bands of the compound in "vapor state," which is not subject to solvent effect. The term $A\cdot(n^2-1)/(2n^2+1)$ represents the induced dipole-induced dipole interaction (dispersion force). The term $B\cdot(n^2-1)/(2n^2+1)$ indicates the interaction between permanent dipole of the solute and induced dipole of the solvent (induced force). The last term shows interaction between permanent dipoles of the solute and the solvent (orientation force). Equation (1) ignores any short range interaction including hydrogen bonding, π-π interaction and short range dipole interaction, as if the cavity radius, a, of Onsager's approximation were equal in all solvents in an ideal case. The equation also excludes the interaction between permanent dipole of the solvent and induced dipole of the solute.

McRae gave different values to the "weighted mean wavelength" L_0, which is expressed by $A=-2.14\times10^{-14}\, fL_0/\tilde{\nu}a^3$ as the first approximation (f, integrated intensity, a, cavity radius) and involves the influence of all transitions of both solvent and solute. However, this value L_0 was assumed to be constant by several workers[3,4] and we have applied Eq. (1) to the M→π^*_{AA}C.T. bands of diamine-tetracarbonyl chromium(0) complexes, assuming that L_0 is constant for all solvents. The cavity radius, a, is also assumed to be constant. The constants n and D were taken from Landolt-Börnstein's tables. The values for n are those for Na-D line at 20°C and those of D at 20°C. The constants, $\tilde{\nu}_{gas}$, $(A+B)$ and C in Eq. (1) were determined by the least square method for the solvents Nos. 1 to 13 in Table 5. Then the expected wave number $\tilde{\nu}_{calcd}$ obtained from these values, should coincide with the observed value $\tilde{\nu}_{obs}$ if the shifts

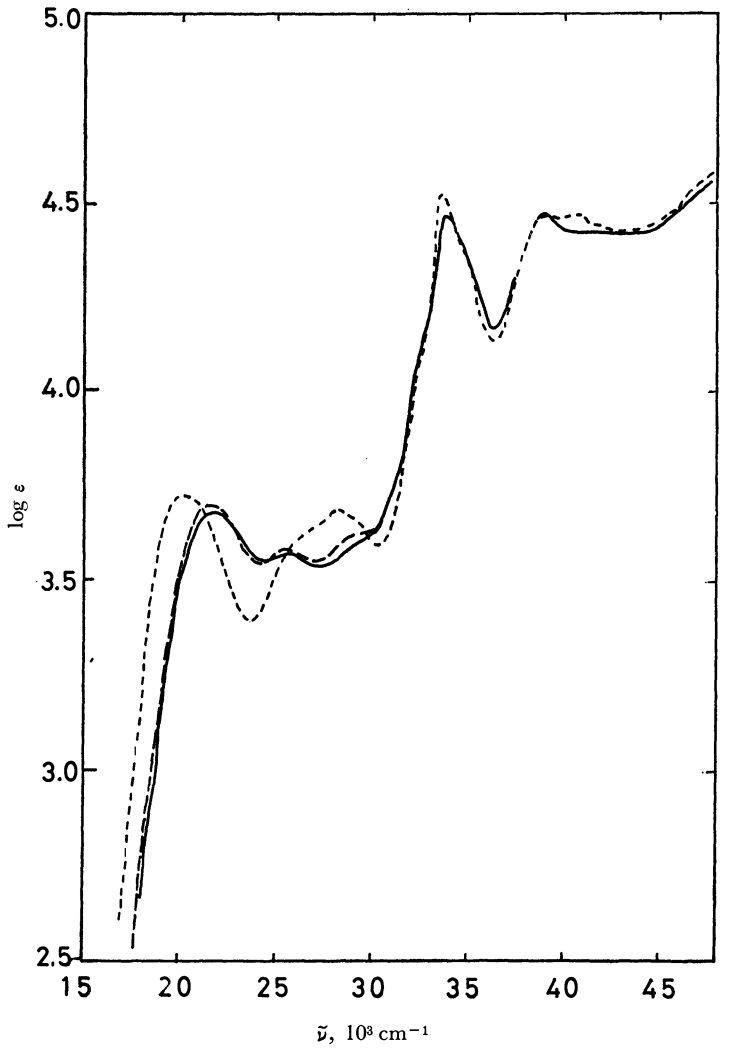

Fig 3. Absorption spectra of bipyridyl-tetracarbonyl molybdenum(0) in some solvents: —— in methanol, — — in methylacetate, - - - - in ethylether.

were accounted for by Eq. (1). The results are listed in Table 5 (analysis 1). The difference in wave number between the calculated and the observed, $\tilde{\nu}_{\text{calcd}}-\tilde{\nu}_{\text{obs}}$ amounts to 200 to 700 cm^{-1} (5 to 20 mμ), and it appears as if Eq. (1) cannot be applied to the present bands in its original form.

Application of McRae's Equation II. The difference $\tilde{\nu}_{\text{calcd}}-\tilde{\nu}_{\text{obs}}$ is, however, always positive for the alcohols, and always negative for the esters. Such a tendency suggests that different factors are operating in each solvent. The $\tilde{\nu}_{\text{gas}}$ of a given compound should be always the same, but A, B, and C can represent the terms operating differently according to the kind of solvent. These values are generally expressed as A', B' and C' henceforth and particular terms operating in the given solvent groups as A_a, B_a, C_a and A_e, B_e, and C_e, for the alcohol and the ester group, respectively. Thus Eq. (1) is modified as Eq. (2).

$$\tilde{\nu} = \tilde{\nu}_{\text{gas}} + (A' + B')\left(\frac{n^2-1}{2n^2+1}\right) + C'\left(\frac{D-1}{D+2} - \frac{n^2-1}{n^2+2}\right) \qquad (2)$$

The results for M$\rightarrow\pi^*_{\text{AA}}$(C. T. band of bipyridyl- and phenanthroline-tetracarbonyl chromium(0) are shown in Table 5 (analysis 2). The difference $|\tilde{\nu}_{\text{calcd}}-\tilde{\nu}_{\text{obs}}|$ in the alcohol and in the ester group are less than 60 and 100 cm^{-1}, respectively. All the $|\tilde{\nu}_{\text{calcd}}-\tilde{\nu}_{\text{obs}}|$ values obtained by this treatment for metal to amine charge transfer bands are less than 120 cm^{-1} (3 mμ) for molybdenum(0) complexes and less than 140 cm^{-1} (3.5 mμ) for tungsten(0) complexes. The reliability of the values $\tilde{\nu}_{\text{gas}}$ (A_a+B_a), (A_e+B_e), C_a and C_e is 80

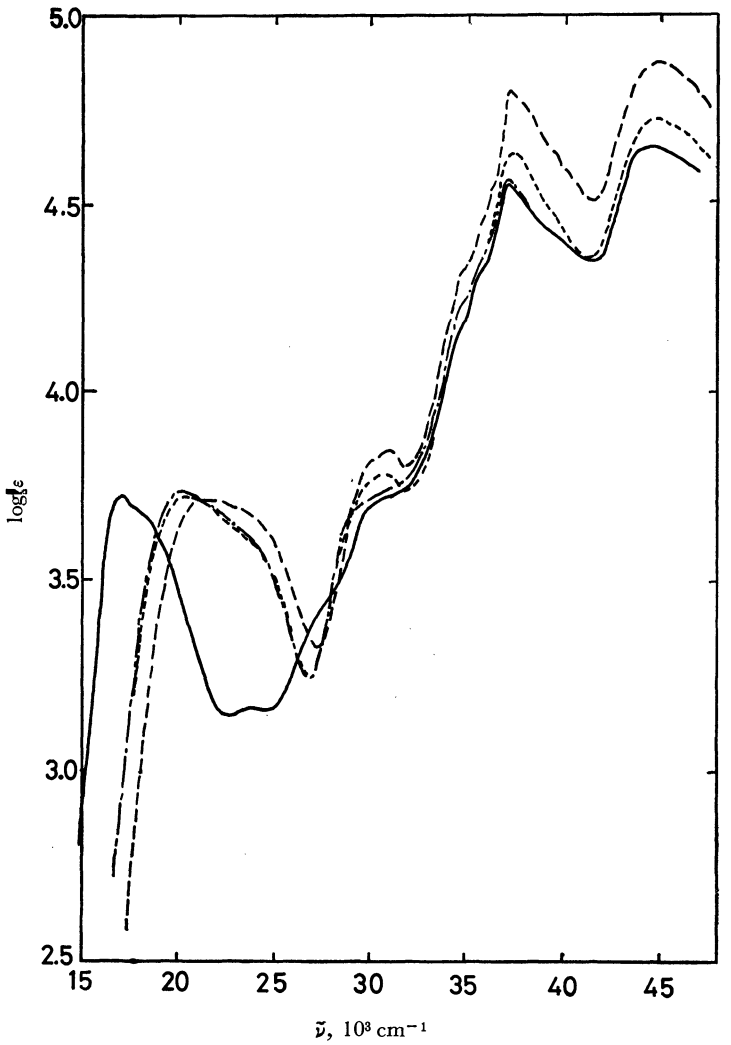

Fig. 4. Absorption spectra of phenanthroline-tetracarbonyl chromium(0) in some solvents: —— in cyclohexane, ---- in methanol, — - — in methylacetate, — — in acetonitrile (arbitrary scale intensity).

to 110 cm^{-1}. These constants are summarized in Table 7 and their meanings will be discussed in the following.

There would be no big difference among the physical properties of diamine-tetracarbonyl complexes with varying metals and amines except for the molecular radii, so that the interaction between a given solvent and a complex molecule would be very similar. Hence the difference in wave number of absorption maximum between any two complexes in a given solvent would be almost constant and equal to that in "vapor state." In Table 6 the mean differences in wave number among complexes in both groups of solvents and in "vapor state" are listed. They coincide well with one another.

The changes in values $A'+B'$, and C' in different solvent groups have similar trend for complexes with different central metals. The C_e value is always larger than the C_a but the difference is less than 30% relative corresponding to a shift less than 530 cm^{-1}. The absolute value for (A_a+B_a) is always larger than the (A_e+B_e), but the difference is even smaller (less than 15% relative).

Thus Eq. (2) seems to be applicable to the metal to amine charge transfer bands. The *d-d* transition, metal to carbonyl charge transfer ($M\rightarrow\pi^*_{CO}$[1] C. T.) and intraligand transition bands are shifted to a smaller extent in various solvents, but calculation has disclosed that Eq. (2) is more appropriately applied to all these bands than Eq. (1) is. The values $|\tilde{\nu}_{calcd}-\tilde{\nu}_{obs}|$ are less than 70, 100 and 50 cm^{-1}, for the *d-d* transition, the intra ligand transition and the metal to carbonyl charge transfer

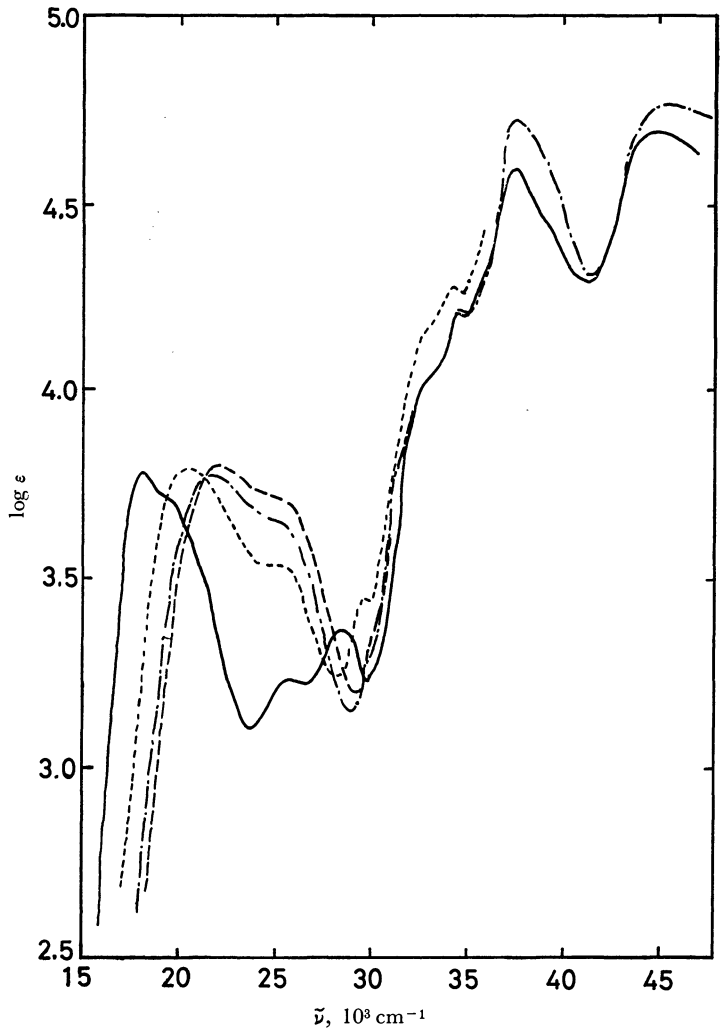

Fig. 5. Absorption spectra of phenanthroline-tetracarbonyl molybdenum(0) in some solvents: —— in cyclohexane (arbitrary scale intensity), - - - - in benzene, — - — in methanol, — — in acetone.

bands, respectively. The constants, $\tilde{\nu}_{gas}$ (A_a+B_a), C_a, (A_e+B_e), and C_e are listed in Table 7.

Discussion

It has been made clear that the shifts of the bands of these compounds are reasonably expressed by McRae's model of a simple electrostatic interaction in such solvents as alcohols, esters, ethers, acetonitrile and acetone. From the data in Tables obtained by Eq. (1) the solvents are arranged in the order of increasing $\tilde{\nu}_{calcd}-\tilde{\nu}_{obs}$ values as follows:

toluene $\simeq$ benzene $\simeq$ *p*-dioxane $<$ chloroform $\leq$ acetic acid $\simeq$ the "esters" $<$ carbon tetrachloride $\simeq$ the "alcohols" $<$ cyclohexane

In carbon tetrachloride and cyclohexane solution, split components are observed in the metal to amine charge transfer bands, but the mean absorption maximum of phenanthroline-tetracarbonyl chromium(0) in cyclohexane is estimated to be about 17400 cm^{-1}. This value is compared to 17530 and 18180 cm^{-1} expected from A_a+B_a and C_a and A_e+B_e and C_e, respectively. On the other hand, the split components in carbon tetrachloride are less obvious, so that the splitting can be neglected. A similar result is also seen for molybdenum(0) and tungsten(0) complexes. Hence these two solvents can be regarded as belonging to the alcohol group.

The anomaly given in benzene and toluene solution would be due to π interaction between the aromatic diamine in the ligand sphere and the solvent molecule. Such an interaction has been known in *e. g.* pyridine *N*-oxide solution.[4] *p*-Dioxane has strong local dipole moments which are compensated in the whole molecule and does not

TABLE 1. NUMERICAL DATA OF ETHYLENEDIAMINE-TETRACARBONYL CHROMIUM(0) AND MOLYBDENUM(0) IN VARIOUS SOLVENTS

(maximum absorption, $10^3\,cm^{-1}$; molar extinction coeff. in parentheses, log ε)

No.	Solvent	[Cr(CO)$_4$en]			[Mo(CO)$_4$en]		
		$d\rightarrow d$	$M\rightarrow\pi^*_{CO}$	C.T.	$d\rightarrow d$	$M\rightarrow\pi^*_{CO}$	C.T.
1	Methanol	23.63 (3.12)	29.70 (3.73)	40.54 (4.26)	25.30 (3.23)	32.73 (4.00)	38.39 (4.30)
3	Isopropanol	23.50	29.52	40.52	25.27	32.66	38.43
4	*n*-Butanol	23.36	29.43	40.40	25.13	32.57	38.28
6	Ethylether	22.82	29.31	40.49	24.78	32.68	38.61
8	Acetonitrile	23.76	29.73	40.27	25.38	32.81	38.43
10	Methylacetate	23.30 (3.08)	29.67 (3.70)		25.06 (3.13)	32.79 (4.02)	38.43 (4.30)
11	Ethylacetate	23.18 (3.10)	29.57		24.98 (3.23)	32.75	
12	*n*-Butylacetate	23.11 (3.11)	29.54		24.87 (3.23)	32.69	
13	Isoamylacetate	23.09	29.50		24.83	32.66	
16	*p*-Dioxane	23.09 (3.11)	29.51 (3.77)	40.32 (4.22)	24.83 (3.23)	32.68 (4.06)	38.24 (4.28)

fit the point-dipole approximation. Chloroform is said[10] to form π-hydrogen bonding with benzene from NMR studies and such an interaction might also occur with diamine-tetracarbonyl complexes to result in anomaly in band shift.

Short Range Dipole Interaction. Solvents of the alcohol and the ester group obey McRae's formula with differing constants. The difference does not seem to come from any special interaction other than electrostatic. One of such special interactions could be hydrogen bonding, but this force cannot play a role, because ethers, cyclohexane and carbon tetrachloride belong to the alcohol group, whereas acetic acid having a greater acidity than alcohols belong to the other ester group.

The nature of interaction represented by C' in Eq. (2) might involve a kind of short range dipole interaction, which has similar factors to those of long range dipole interaction, but is subject to significant steric influence. The dipole moments of solvent molecules belonging to the "ester" and the "alcohol" group are 1.8 to 4 and less than 1.8 debyes, respectively. In the former group, the dipole moment originates mainly from the functional group $>C{=}O$ or $-C{\equiv}N$. On the other hand, dipole distribution of diamine-tetracarbonyl complexes is considered as shown in Fig. 6.

Although the contribution of the metal amine bond is quite big, that of the metal carbonyl bond is also appreciable owing to the metal to carbonyl back donation.[11,12] The latter bonding is formally similar to the functional groups, $>C{=}O$, and $-C{\equiv}M$,

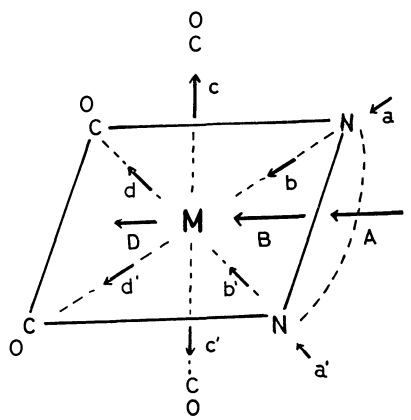

Fig. 6. Distribution of dipoles in metal diamine-tetracarbonyl complexes.

$\vec{a}$, $\vec{a}'$: Dipole moment of the ligand
$\vec{A} = \vec{a} + \vec{a}'$; en, $\simeq 2.0$;
py$_2$, bp, phen $\simeq 3.6$ Debyes
$\vec{b}$, $\vec{b}'$: nitrogen to metal ($\overrightarrow{N\text{-}M}$)
$\vec{B} = \vec{b} + \vec{b}'$; 5 to 6.2 Debyes
$\vec{c}$, $\vec{c}'$; metal to carbonyl (*trans*) ($\overrightarrow{M\text{-}CO}$)
$|\vec{c}| = |\vec{c}'|$; 0.5 to 0.8 Debyes,
$\vec{d}$, $\vec{d}'$: metal to carbonyl (*cis*) ($\overrightarrow{M\text{-}CO}$)
$\vec{D} = \vec{d} + \vec{d}'$; 0.7 to 1.1 Debyes (for estimations, *cf.* Refs. 11, 12)

so that the symmetry of dipoles M–CO corresponds well to that of R_1R_2CO and R–CN. When such a part of the molecule (M–CO) interacts with the solvent molecule by a simple short range dipole-dipole interaction, anti-parallel orientation would be far preferable to parallel both energetically and

10) L. W. Reeves and W. G. Schneide, *Canadian J. Chem.*, **35**, 251 (1957).
11) W. Strohmeier and H. Hellmann, *Chem. Ber.*, **97**, 1877 (1964).
12) W. Strohmeier and W. Langhauser, *Z. Phys. Chem., N. F.*, **28**, 268 (1961).

Table 2. Numerical data of metal to amine charge transfer bands of bipyridyl- and phenanthroline-tetracarbonyl complexes in various solvents
(maximum absorption, $10^3\,cm^{-1}$; molar extinction coeff. in round brackets, $\log\varepsilon$; integrated intensity in square brackets $f\times10^2$)

No.	Solvent	$[Cr(CO)_4bp]$	$[Mo(CO)_4bp]$	$[W(CO)_4bp]$	$[Cr(CO)_4phen]$	$[Mo(CO)_4phen]$	$[W(CO)_4phen]$
1	Methanol	(3.57) 20.11 [6.62]	(3.68) 21.60 [8.99]	(3.71) 20.98 [8.86]	(3.72) 20.37 [10.58]	(3.77) 21.68 [11.74]	(3.85) 21.01 [14.53]
2	Ethanol	(3.58) 19.68 [5.89]	(3.68) 21.14 [8.13]	20.49	(3.69) 19.90 [8.99]	(3.78) 21.22 [11.22]	(3.79) 20.48 [11.52]
3	Isopropanol	19.38	20.83	20.30	19.68	21.05	20.24
4	*n*-Butanol	19.18	20.67	19.97	19.50	20.76	20.06
5	Isopentanol	19.10	20.56	—	19.34	20.64	—
6	Ethylether	(3.65) 18.73 [6.79]	(3.72) 20.11 [8.69]	19.33	(3.72) 18.90 [9.37]	(3.81) 20.16 [10.23]	(3.85) 19.36 [12.21]
7	*n*-Butylketone	18.02	19.32	18.56	18.25	19.38	18.71
8	Acetonitrile	21.00 [6.97]*	22.47 [9.42]*	21.90	21.37 [9.46]*	22.63 [12.21]*	21.98 [14.79]*
9	Acetone	(3.60) 20.53 [6.32]	(3.69) 21.99 [8.04]	(3.71) 21.43	(3.73) 20.84 [10.06]	(3.79) 22.10 [11.57]	(3.85) 21.37 [13.98]
10	Methylacetate	(3.61) 19.97 [7.05]	(3.69) 21.42 [8.47]	(3.76) 20.74 [10.10]	(3.73) 20.25 [10.66]	(3.79) 21.50 [11.65]	(3.86) 20.76 [13.59]
11	Ethylacetate	(3.62) 19.69 [7.00]	(3.71) 21.11 [9.12]	(3.75) 20.39 [10.84]	(3.75) 19.98 [11.27]	(3.81) 21.22 [12.47]	(3.87) 20.44 [15.62]
12	*n*-Butylacetate	(3.61) 19.30 [6.28]	(3.70) 20.71 [8.17]	19.98	(3.74) 19.54 [9.76]	(3.79) 20.83 [11.87]	(3.88) 20.01 [14.32]
13	Isoamylacetate	19.12	20.55	19.75	(3.74) 19.45 [10.15]	(3.78) 20.67 [11.27]	(3.89) 19.88 [14.36]
14	Benzene	(3.62) 18.83 [6.62]	(3.69) 20.16 [8.05]	(3.75) 19.41 [9.29]	(3.72) 19.08 [8.94]	(3.79) 20.27 [10.49]	(3.91) 19.51 [14.10]
15	Toluene	(3.62) 18.66 [6.19]	(3.73) 19.99 [8.73]	19.22	(3.72) 18.93 [8.90]	(3.82) 20.11 [11.01]	(3.90) 19.36 [13.50]
16	*p*-Dioxane	19.26	20.65	19.92	(3.71) 19.58	20.84	20.07
17	Chloroform	(3.63) 19.08 [6.84]	(3.72) 20.41 [8.56]	(3.78) 19.69 [10.02]	19.42	20.60	19.84
18	CCl_4	17.21 [6.67]*	18.45 [7.87]*	—	17.49 [8.64]*	18.57 [10.79]*	18.13
19	Cyclohexane	—	—	—	16.95 [8.51]	18.10 [10.06]	17.64
20	Acetic acid	19.81	21.31	20.68	20.08	21.46	20.79

f values with * marks are estimated on the assumed $\log\varepsilon$ values
$[Cr(CO)_4bp]$, 3.60; $[Mo(CO)_4bp]$, $[Cr(CO)_4phen]$, 3.70; $[Mo(CO)_4phen]$, 3.80; $[W(CO)_4phen]$, 3.85.

TABLE 3. NUMERICAL DATA OF THE INTRA-LIGAND π-π ABSORPTION OF BIPYRIDYL- AND PHENANTHROLINE-TETRACARBONYL COMPLEXES IN VARIOUS SOLVENTS

(maximum absorption, $10^3\,cm^{-1}$; molar extinction coeff. in parentheses, log ε)

No.	Solvent	[Cr(CO)$_4$by]	[Mo(CO)$_4$bp]	[W(CO)$_4$bp]	[Cr(CO)$_4$phen]	[Mo(CO)$_4$phen]	[W(CO)$_4$phen]
1	Methanol	33.78 (4.44)	33.85 (4.46)	33.68 (4.44)	37.37 (4.67)	37.47 (4.72)	37.38 (4.69)
2	Ethanol	33.67	33.77 (4.47)	33.52	37.27 (4.69)	37.43 (4.75)	37.24 (4.63)
3	Isopropanol	33.61	33.68	33.48	37.29	37.34	37.19
4	*n*-Butanol	33.52	33.57	33.41	37.24	37.34	37.16
5	Isopentanol	33.52	33.56	—	37.20	37.29	—
6	Ethylether	33.58 (4.50)	33.61 (4.53)	33.41	37.13 (4.63)	37.31 (4.70)	37.31 (4.63)
7	*n*-Butylether	33.36	33.44	33.24	37.23	37.29	37.12
8	Acetonitrile	33.90	33.98	33.81	37.38	37.61	37.52
10	Methylacetate	33.72 (4.48)	33.78 (4.50)	33.60 (4.52)	37.34 (4.69)	37.52 (4.74)	37.31 (4.70)
11	Ethylacetate	33.67 (4.48)	33.73 (4.54)	33.53 (4.51)	37.31 (4.68)	37.44 (4.72)	37.27 (4.69)
12	*n*-Butylacetate	33.59 (4.46)	33.64 (4.55)	33.44	37.30 (4.65)	37.33 (4.70)	37.23 (4.64)
13	Isoamylacetate	33.56	33.60	33.41	37.29 (4.69)		37.23 (4.69)
14	Benzene	33.20 (4.44)	33.20 (4.51)	33.00 (4.51)			
15	Toluene	33.17 (4.43)	33.13 (4.53)	32.92			
16	*p*-Dioxane	33.50	33.51	33.32	37.17 (4.65)	37.27	37.24
17	Chloroform	33.49	33.90	33.33 (4.52)	37.19		37.02
18	CCl_4	33.34	33.28	—	37.16	37.19	37.02
19	Cyclohexane	—	—	—	37.22	37.31	37.05

TABLE 4. NUMERICAL DATA OF METAL TO CARBONYL CHARGE TRANSFER BANDS OF BIPYRIDYL- AND PHENANTHROLINE-TETRACARBONYL CHROMIUM(0) IN VARIOUS SOLVENTS

(maximum absorption $10^3\,cm^{-1}$; sh, shoulder; molar extinction coeff. in parentheses log ε)

No.	Solvent	[Cr(CO)$_4$bp]	[Cr(CO)$_4$phen]
1	Methanol	30.00 (3.84)	30.75 (3.78)
2	Ethanol	29.94	30.59 (3.72)
3	Isopropanol	29.90	30.63
4	*n*-Butanol	29.90	30.51
5	Isopentanol	29.90	30.58
6	Ethylether	29.90 (3.81)	30.45 (3.75)
7	*n*-Butylether	29.89	—
8	Acetonitrile	30.18	30.96
9	Acetone	30.03 (3.86)	—
10	Methylacetate	30.00 (3.86)	30.70 (3.82)
11	Ethylacetate	29.99 (3.86)	30.64 (3.83)
12	*n*-Butylacetate	29.89 (3.82)	30.53 (3.82)
13	Isoamylacetate	29.85	30.49 (3.81)
14	Benzene	29.94 (3.84)	30.44 (3.82)
15	Toluene	30.00 (3.84)	30.49 (3.81)
16	*p*-Dioxane	29.94	30.58 (3.80)
17	Chloroform	29.85	30.77
18	CCl_4	31.0 (sh)	30.0 (sh) 31.3 (sh)
19	Cyclohexane		27.0 (sh) 30.8 (sh)

sterically. (Here the term "energetic" represents the contribution of such an interaction where no steric effect is taken into consideration.) Such short range interactions could be expressed by $(\alpha+\beta+\gamma)$ so that the last term of Eq. (2) is multipled by $(1+\alpha+\beta+\gamma)$ (Fig. 6). The first term, α represents the effect around the two metal-carbonyl bonds on M–NN plane, the second, β, that around the two metal-carbonyl bonds across M–NN plane and the last, γ, that around the metal-amine bonds. γ does not seem to involve big steric effect. From the values of dipole moments of the solvent, it could be estimated that $\gamma_e > \gamma_a > 0$, for phenanthroline- and bipyridyl-tetracarbonyl complexes and $\gamma_e \geq \gamma_a \geq 0$ for ethylenediamine-tetracarbonyl complexes. Suffixes e and a stand for values for the ester and the alcohol group, respectively.

For $\alpha+\beta$, the steric effect seems to be quite

Table 5. Analysis of the absorption data of metal to amine charge transfer bands of bipyridyl- and phenanthroline-tetracarbonyl chromium(0) in various solvents by Eq. (1) and Eq. (2)
(The values are $\nu_{calcd}-\nu_{obs}$ in cm^{-1})

No.	Solvent	Analysis 1 (Eq. (1))		Analysis 2 (Eq. (2))*	
		[Cr(CO)$_4$bp]	[Cr(CO)$_4$phen]	[Cr(CO)$_4$bp]	[Cr(CO)$_4$phen]
1	Methanol	+440	+490	−10	−30
2	Ethanol	+360	+450	−10	+50
3	Isopropanol	+290	+380	+50	0
4	*n*-Butanol	+290	+280	+20	−10
5	Isopentanol	+200	+260	−60	−20
6	Ethylether	+490	+670	+50	+80
7	*n*-Butylether	+430	+440	−20	−50
8	Acetonitrile	−610	−600	−40	−70
9	Acetone	−490	−510	+80	+120
10	Methylacetate	−480	−490	−100	−90
11	Ethylacetate	−390	−420	−10	−20
12	*n*-Butylacetate	−380	−380	+20	+60
13	Isoamylacetate	−400	−450	+40	+10
14	Benzene	−1820	−1840	−2050 −1310	−2060 −1330
15	Toluene	−1570	−1600	−1800 −1060	−1820 −1100
16	*p*-Dioxane	−1350	−1460	−1790 −1130	−1930 −1250
17	Chloroform	−830	−920	−1100 −250	−1190 −300
18	CCl_4	+240	+180	−100 +600	−160 +550
19	Cyclohexane	—	+1040	—	+580 +1230
20	Acetic acid	−490	−500	−940 −100	−970 +90

* Analysis 2: For solvents Nos. 1 to 7, A_a, B_a and C_a values are used, whereas for Nos. 8 to 13, A_e, B_e and C_e are used. For Nos. 14 to 20, the upper values are calcd. with A_a, B_a and C_a and lower with A_e, B_e and C_e.

Table 6. Difference in wave number of $\tilde{\nu}_{obs}$ and calculated $\tilde{\nu}_{gas}$ of the metal to amine charge transfer bands between chromium(0) molybdenum(0) and tungsten(0) complex
(analysed by "analysis 2 in Table 5)

		Mo-Cr	Mo-W	W-Cr
[M(CO)$_4$bp]	ν_{obs}	1280	650	630
	ν_{gas}	1430	680	760
[M(CO)$_4$phen]	ν_{obs}	1180	420	760
	ν_{gas}	1270	730	520

important, but the energetic effect would be less so, because the absolute value of local dipole moment is rather small. Figure 7a illustrates the statistical dipole arrangement for the alcohol group solvent, where Onsager's approximation is applicable, *i. e.* $\alpha=\beta=0$. Figure 7b and 7c represent the cases where steric conditions are appreciable and short range interactions significant. A probable explanation is as follows.

The solvent molecules can orientate statistically as required by the overall dipole moment of the complex near the carbonyl ligands on the M–NN plane. On the other hand, such an orientation is hindered near those carbonyl groups in the plane across M–NN. Hence α is always positive, and β negative. The contribution of α would be slightly smaller in the case represented by Fig. 7b, than in the case represented by Fig. 7c, because the dipole moment of the whole complex is greater in the latter case, where the dipole of the amine ligand operates additive. By the same reason, the influence of β would be greater in the case Fig. 7b. Depending on whether the dipole moment of the whole complex molecule is greater or smaller than a certain value, $\alpha+\beta+\gamma$ has plus or minus sign. This value should be different for each central atom, because the cavity radius a and the dipole moment of M–CO are not expected to be equal in all the complexes. Ethylenediamine-, and bipyridyl- (or phenanthroline-) tetracarbonyl complex have dipole moments 8 to 10, and 9 to 11

TABLE 7. THE VALUES ν_{gas}, $A'+B'$ AND C' OBTAINED BY MODIFIED MCRAE'S EQUATION (cm^{-1})

	ν_{gas}	Alcohol group		Ester group	
		A_a+B_a	C_a	A_e+B_e	C_e
Metal to amine charge transfer					
[Cr(CO)$_4$bp]	22160	−23690	+2714	−20490	+3301
[Mo(CO)$_4$bp]	23440	−23840	+3063	−20040	+3479
[W(CO)$_4$bp]	22790	−24810	+3348	−21350	+3918
[Cr(CO)$_4$phen]	21980	−21840	+2874	−18670	+3627
[Mo(CO)$_4$phen]	23160	−22170	+3182	−18290	+3626
[W(CO)$_4$phen]	22740	−23720	+3130	−20650	+3858
d–d Transition					
[Cr(CO)$_4$en]	22440	−1364	+2017	+414	+1755
[Mo(CO)$_4$en]	24480	−585	+1326	−105	+1301
Intra ligand π–π transition					
[Cr(CO)$_4$bp]	34910	−8221	+378	−7607	+445
[Mo(CO)$_4$bp]	35070	−8766	+386	−8316	+509
[W(CO)$_4$bp]	34650	−7686	+466	−7315	+628
Metal to CO charge transfer					
[Cr(CO)$_4$en]	30300	−6972	+818	−4382	+289
[Cr(CO)$_4$phen]	31320	−5974	+628	−5492	+850

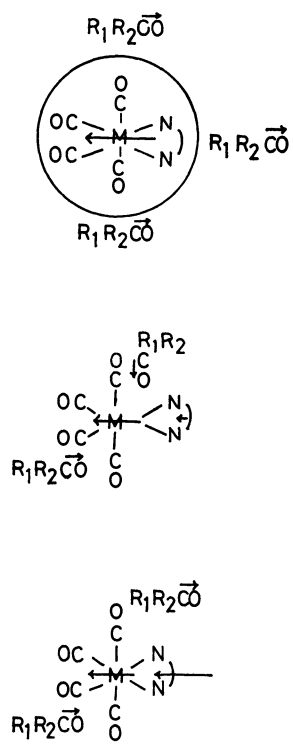

(a) Onsager's approximation

(b) Small dipole of ligand diamine

(c) Large dipole of ligand diamine

Fig. 7. Schematic representation of the orientation of organic carbonyl radical around polar metal carbonyl (M-CO) bonds.

Debyes, respectively.[12] From the values of C_a and C_e in Table 5, it might be concluded that Fig. 7b and 7c represent the cases of the ethylenediamine and the bipyridyl (or phenanthroline) complex respectively. Regardless of the nature of absorption bands, C_e is always greater than C_a for phenanthroline- and bipyridyl-tetracarbonyl complexes, whereas the reverse is true for ethylenediamine complexes.

The short range dipole interaction can induce the change of $A'+B'$ values expected from Onsager's approximation. The $-(A_a+B_a)$ value for the alcohol group is larger than $-(A_e+B_e)$ values for the ester group in all the absorption bands. The maximum value of $-A_a$ and $-A_e$ can be estimated from (A_a+B_a) and (A_e+B_e), respectively, by use of the following relationship,

$$B' = \frac{1}{\boldsymbol{hc}a^3}(M_g^2 - M_e^2) \leqq \frac{2M_g}{\boldsymbol{hc}a^3}(M_g - M_e) = C', \quad (M_g,\ M_e > 0) \tag{3}$$

where $\boldsymbol{h}$ stands for Planck's constant, $\boldsymbol{c}$ the light velocity, a the cavity radius, M_g the dipole moment of the ground state and M_e that of the excited Franck-Condon state for the transition in question.

When $-A$ value is to be approximated by $2.14\times 10^{-14} fL_0/\tilde{\nu}a^3$, the ratio of the L_0 values for the alcohol and the ester group solvents could be calculated from the estimated A_a and A_e values, and measured $\tilde{\nu}$, on the assumption that f is equal for these two group solvents. The value L_0 (alcohol)/L_0 (ester) is 1.2. Generally L_0 is regarded to be independent of the solvent; McRae's consideration[2] suggests that ester group would have greater L_0, because esters themselves have strong absorption bands in low frequency region. Such discrepancies seem to suggest that the short range interaction is significant in the dispersion and the

induced force, too. Such an interaction might be a kind of π-π interaction, although not necessarily due to orientation. Bauer and Nicol[5] reported on the solvent effect for the ^1L_a transition of naphthacene, which is due to the dispersion force and the Stark effect of solvent. In this case varying solvents behave differently (difference, $\simeq 100\ cm^{-1}$). This fact also suggests that the dispersion effect can differ from one solvent group to another.

Consideration on Individual Bands. The metal to amine charge transfer bands show red shift by 2000 to 4000 cm^{-1} as compared with $\tilde{\nu}_{gas}$, owing to the big contribution of dispersion force. On the other hand, *d-d* transition bands of ethylenediamine-tetracarbonyl chromium(0) [$Cr(CO)_4en$] show a blue shift by 400 to 1000 cm^{-1}, owing to big contribution of orientation force. It appears as if the influence of dispersion force is quite significant for most organic compounds. It seems that the extinction coefficient is small for the *d-d* transition of [$Cr(CO)_4en$] and the electrons move in the interior molecule behind polarizable ligands to give only little influence upon the solvent molecule.

The large *C* values for the *d-d* band of [$Cr(CO)_4en$] could be attributed to the facts that the difference of permanent dipole moment between the ground and the excited Franck-Condon state is large and that the *a* values are rather small. The large difference in $M_g - M_e$ could be accounted for by considering that the d_π electron is polarized to the carbonyl ligand in the ground states, but the extent is decreased by transition to the d_σ* level. In this level the electrons would be localized appreciably on the central metal and the state of σ-bonding in CO ligand would remain unchanged. This view seems to be further supported by infrared and dipole moment studies.[12,13] The dipole moment of the excited Franck-Condon state is estimated from the *C* values as shown in Table 8. The M_g is indirectly estimated from Strohmeier's data[12] by simple addition of vectors. The cavity radii are estimated by adding 1 to 2 Å to the molecular radii calculated from the bond distance of diethylenetriaminetetracarbonyl chromium(0).[14] The values in Table 8 seem reasonable.

Table 8. Dipole moments in the excited Franck-condon state estimated from *C* values (in Debye units)

	Assumed cavity radius		
	M_g	a(Å)	M_e
[$Cr(CO)_4en$]			
$d \rightarrow d$	8.3	4	2.4—2.7
		5	3.0—3.7
[$Cr(CO)_4bq$]			
$Cr \rightarrow \pi^*_{bp}$C.T.	9.3	5	1.6—3.0
		6	4.9—5.7
$\pi_{bp} \rightarrow \pi^*_{bp}$	9.3	5	8.3
		6	7.6
[$Cr(CO)_4phen$]			
$Cr \rightarrow \pi^*_{phen}$C.T.	9.3	5	1.0—2.6
		6	4.4—5.4

The change of the electron distribution would occur in same directions but to different extents, for the metal to amine charge transfer and for the intra-ligand transition. Hence we can compare the values in Table 8 directly. The big change of dipole moments between the ground and the excited Franck-Condon state agrees with the assignment.[9]

13) C. S. Kraihanzel and F. A. Cotton, *Inorg. Chem.*, **2**, 533 (1963).

14) F. A. Cotton and D. C. Richardson, *ibid.*, **5**, 1851 (1966).

BULLETIN OF THE CHEMICAL SOCIETY OF JAPAN VOL. 41 875—882 (1968)

The Reaction between Mercury(II) and Organic Compounds. IV.*[1] A Photometric Method for the Determination of Basic Amino Acids Precipitated with a Mercury(II) Perchlorate Precipitant and Some Properties of Their Products

Fumiaki KAI

Department of Chemistry, Faculty of Science, Kumamoto University, Kurokami-machi, Kumamoto

(Received October 2, 1967)

The particular reactivity of basic amino acids in presence of mercury(II) perchlorate gives white amorphous products (by X-ray powder diffraction). The structures of the products may be considered to be $[Arg\text{-}Hg]ClO_4 \cdot Hg(ClO_4)_2$, $[His\text{-}Hg]ClO_4 \cdot Hg(ClO_4)_2$ and $[Lys\text{-}Hg]ClO_4 \cdot Hg(ClO_4)_2$ on the bases of elemental analytical data and of infrared patterns showing the absorption bands of $\nu_{as}(Hg\text{-}O)$, $\nu(Hg\text{-}N)$ and perchlorate ions. The applicability of this peculiar reactivity to the separation and photometric determination of basic amino acids has been studied. The above mentioned products were obtained selectively as a mixture from a mixture of about twenty kinds of amino acids. The isolation of the mixture into each product could be performed satisfactorily by utilizing the different solubilities of the products in 10 N acetic acid containing sodium or potassium chloride (3.3 W/V %), and in an aqueous sodium hydroxide solution. Although the products showed characteristic ultraviolet absorption curves differing from those of the components, there were no absorption maxima in any case. The calibration curves, which followed Beer's law, could be obtained at any proposed wavelength. By using the calibration curves thus obtained, a very small amount of each basic amino acid could be determined spectrophotometrically in the 220—250 mμ region, within detection limits of about 10^{-5}—10^{-4} M. Constant absorbancies could be attained in the pH range of 1.5—10.7 of the sample solutions.

Numerous works of analyses of basic amino acids (Arg, His, and Lys) have hitherto been undertaken by many workers. The analyses, after the preparation of the derivatives of amino acids such as flavianate,[1] 3,4-dichlorobenzenesulfonate,[2] picrate,[3] and benzenesulfonate[4] are known as long-established techniques. Ion exchange resins,[5] electrophoresis,[6] various chromatographic techniques,[7] spectral reflectance,[8] and conductivity measurements[9] have also been used in recent years. Phosphotungstic acid[10] which is known specific for the simultaneous and preferential precipitant of basic amino acids, silver(I),[11] copper(II)[12] and mercury(II)[13] salts have been used as the coprecipitants of basic amino acids. Especially, mercury(II) chloride, acetate and sulfate had been used for the isolation of Asp, Glu, Cys, Met and Try besidese basic amino acids. However, in the separation of basic amino acids using mercury(II) salts by Warburg *et al.*,[13] His was almost exclusively obtained, while Arg and Lys were isolated by using silver salts.

*1 Presented in part at the 20th Annual Meeting of the Chemical Society of Japan, Tokyo, March, 1967.

1) A. Kossel and R. E. Gross, *Z. Physiol. Chem.*, **135**, 167 (1942).
2) H. B. Vickery, *J. Biol. Chem.*, **143**, 77 (1942).
3) E. E. Rice, *Biochem. Prep.*, **1**, 63 (1949).
4) E. V. McCollum and A. A. Rider, *J. Biol. Chem.*, **190**, 451 (1951).
5) F. Turba, *Ber.*, **74B**, 1829 (1941); J. W. Dubnoff, *J. Biol. Chem.*, **141**, 711 (1941); R. J. Block, *Proc. Soc. Exp. Biol. Med.*, **51**, 252 (1942); D. T. Englis and H. A. Fiess, *Ind. Eng. Chem.*, **36**, 604 (1944); C. S. Cleaver, R. A. Hardy and H. G. Cassidy, *J. Am. Chem. Soc.*, **67**, 1343 (1945); J. C. Winters and R. Kunin, *Ind. Eng. Chem.*, **41**, 460 (1949); J. E. Eastoe, *Biochem. J.*, **74**, 8 (1960); S. Jacobs, *ibid.*, **87**, 30 (1963).
6) G. N. Atfield and C. J. O. R. Morris, *ibid.*, **74**, 37 (1960); T. Shinoda and K. Satake, *J. Biol. Chem.*, **50**, 293 (1961); V. Jirgl, *Anal. Biochem.*, **13**, 381 (1965).
7) A. Darbre and K. Blau, *Biochem. J.*, **88**, 8 (1963); F. Lucas, J. T. B. Shaw and S. G. Smith, *Anal. Biochem.*, **6**, 335 (1963); J. G. Heathcote and K. Jones, *Biochem. J.*, **97**, 15 (1965); G. Barbiroli, *Microchim. Ichnoanal. Acta*, **4**, 652 (1965); *Chem. Abstr.*, **64**, 2402 (1966); El. Bujard and J. Mauron, *J. Chromatog.*, **21**, 129 (1966); S. M. Petrovic and S. E. Petrovic, *ibid.*, **21**, 313 (1966).
8) M. M. Frodyma and R. W. Frei, *ibid.*, **17**, 131 (1965); R. W. Frei, *Chem. Abstr.*, **64**, 10073 (1966).
9) A. Nieman, *Z. Anal. Chem.*, **205**, 403 (1964).
10) V. Slyke, *J. Biol. Chem.*, **22**, 281 (1915).
11) H. B. Vickery and R. J. Block, *ibid.*, **93**, 105 (1931); G. R. Tristram, *Biochem. J.*, **33**, 1271 (1939).
12) L. G. Brazier, *ibid.*, **24**, 1188 (1930); S. Town, *ibid.*, **22**, 1083 (1928).
13) G. L. Foster and D. Shemin, *Org. Syn.*, **18**, 43 (1938); O. Warburg and W. Christian, *Biochem. Z.*, **310**, 304 (1942).

In the previous paper[14] of this series,[14-16] the present author has shown that mercury(II) chloride as well as phosphotungstic acid reacted selectively and simultaneously with basic amino acids in various amino acids. He also suggested that instead of phosphotungstic acid, mercury(II) perchlorate, as well as chloride, could be utilized as selective precipitant.

The present investigation has been undertaken in order to establish the methods for the separation and determination of basic amino acids by mercury(II) perchlorate, and to discuss some properties of the resulting products.

The proposed methods are sufficiently rapid, precise, and accurate to be used for the selective and simultaneous separation and determination of a small amount of basic amino acids. Furthermore, there is no procedure, except that using phosphotungstic acid and that by mercury(II) chloride reported in the preceding paper,[14] for the selective and simultaneous separation of basic amino acids.

Experimental

Materials. All the amino acids were obtained from the Nippon Rikagaku Yakuhin Co., Ltd., while reagent-grade mercury(II) chloride was obtained commercially. Mercury(II) perchlorate was prepared from the chloride by a procedure similar to that reported previously.[15] All the other chemicals used were of an analytical or of a special grade; they were used without further purification. Solutions for the measurement of the absorption spectra were prepared using redistilled water.

Apparatus. The pH was measured with a glass electrode (Yokogawa type KPH-51A and Hitachi-Horiba type M-5). The ultraviolet absorption spectra and the absorbancies were recorded with a Hitachi recording spectrophotometer (EPS-2 type) and a Hitachi photoelectric spectrophotometer (EPU-2 type) with 10 mm cells respectively. The infrared spectra in the 4000—650 cm^{-1} and 700—200 cm^{-1} region were obtained using a Hitachi-Perkin Elmer (type 125) and a Hitachi EPI-L type spectrophotometer respectively. All the samples were examined as Nujol-mull.

The mercury contents in the products were determined by chelatometric titration or by colorimetric determination.[17] The pH was adjusted with dilute aqueous perchloric acid and sodium hydroxide solutions as occasion demands.

Procedure

The Selective Separation of Basic Amino Acids in a Mixture of Various Amino Acids. An aqueous solution of mercury(II) perchlorate below 10^{-2} M*2 was added to an acid sample solution (with $HClO_4$) composed of a mixture of about twenty kinds of amino acids. A dilute sodium hydroxide solution was then added, drop by drop, into the solution until the pH of the supernatant reached about 8.5. Thereby, the only basic amino acids were co-precipitated with mercury(II) perchlorate as [Arg-Hg]ClO_4·$Hg(ClO_4)_2$, [His-Hg]ClO_4·$Hg(ClO_4)_2$ and [Lys-Hg]ClO_4·$Hg(ClO_4)_2$. In order to certify the complete precipitation, a small aliquot of the supernatant was taken out and the same procedure was carried out again after the addition of a slight excess of mercury(II) perchlorate.

The Isolation of Each Basic Amino Acid from the Mixture. The isolation could be carried out by utilizing different solubilities of the precipitates under various experimental conditions.

His. Acetic acid (10 N) containing sodium chloride (3.3 W/V %) was added to a wet mixture of Arg, His and Lys as mercury salts. By shaking the mixture for a while at room temperature, only [His-Hg]ClO_4·$Hg(ClO_4)_2$ remained as it is, while [Arg-Hg]ClO_4·$Hg(ClO_4)_2$ and [Lys-Hg]-ClO_4·$Hg(ClO_4)_2$ were dissolved completely.

Arg and Lys. By adjusting the pH of the mother liquor separated from His to about 8, a mixture of [Arg-Hg]ClO_4·$Hg(ClO_4)_2$ and [Lys-Hg]ClO_4·$Hg(ClO_4)_2$ was reprecipitated. It was suspended in water, and then aqueous sodium hydroxide was added to the suspension until the pH reached to 12.1—12.3 at room temperature. When this suspension was heated to boil, only [Lys-Hg]ClO_4·$Hg(ClO_4)_2$ was dissolved, while [Arg-Hg]ClO_4·$Hg(ClO_4)_2$ remained at this pH; filtration was then carried out keeping the suspension hot, and the residue was washed with hot water at the pH 12.1. When the filtrate reached to room temperature, [Lys-Hg]ClO_4·$Hg(ClO_4)_2$ was reprecipitated.

Results and Discussion

The Structures and Some Properties of the Products. *Elemental Analysis.* The products were analyzed as follows:

Arg. Found: C, 8.01; H, 1.52; N, 6.99; Hg, 43.94; Cl, 13.51%. Calcd for $C_6H_{13}N_4O_{14}$·Hg_2Cl_3: C, 8.26; H, 1.49; N, 6.42; Hg, 45.98; Cl, 12.19%. Mp 206—208°C (decomp.).

His. Found: C, 9.06; H, 0.89; N, 4.56; Hg, 46.57; Cl, 13.45%. Calcd for $C_6H_8N_3O_{14}$·Hg_2Cl_3: C, 8.44; H, 0.94; N, 4.92; Hg, 47.0; Cl, 12.46%. Mp 215—218°C (decomp.).

Lys. Found: C, 6.10; H, 0.98; N, 3.20; Hg, 45.99; Cl, 14.78%. Calcd for $C_4H_9N_2O_{14}$·

14) F. Kai, This Bulletin **40**, 2297 (1967).
15) F. Kai, *ibid.*, **40**, 1136 (1967).
16) F. Kai, *Nippon Kagaku Zasshi (J. Chem. Soc. Japan, Pure Chem. Sect.)*, **86**, 1040 (1965).
17) K. Ueno, "Chelate Titration" (in Japanese), Nankodo, Tokyo (1964), p. 268; E. B. Sandell, "Colorimetric Determination of Traces of Metals," Interscience Publ., New York (1959), p. 621; F. D. Snell and C. T. Snell, "Colorimetric Method of Analysis," C. Van Nostrand Co., Philadelphia (1959), p. 63.

*2 At a higher concentration, the added mercury(II) perchlorate was apt to decompose to mercury oxide.

Hg_2Cl_3: C, 5.90; H, 1.11; N, 3.19; Hg, 49.24; Cl, 13.10%. Mp 188—190°C (decomp').

These analytical results indicate the ratio of 2 : 1 for mercury(II) perchlorate to basic amino acid in all the products. All of the products were amorphous (by X-ray powder diffraction).

Infrared Spectra of the Products and Relative Substances. Figures 1—3 give the infrared spectra of the precipitates (A—C) and related substances. In the spectra of the precipitates, the absorption bands

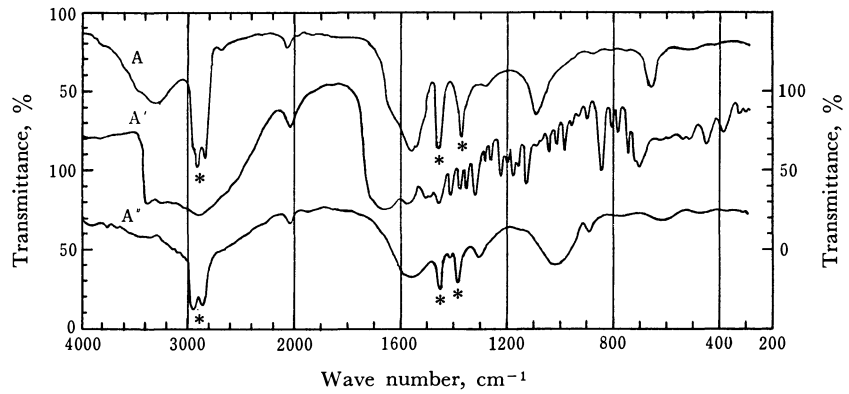

Fig. 1. Infrared spectra of Arg-mercury salt and relative compounds (Nujol).
A: $[Arg\text{-}Hg]ClO_4 \cdot Hg(ClO_4)_2$ A': Free Arg-hydrochloride
A'': Mixture of Arg and $Hg(ClO_4)_2$ (1 : 2) *, Absorption of Nujol

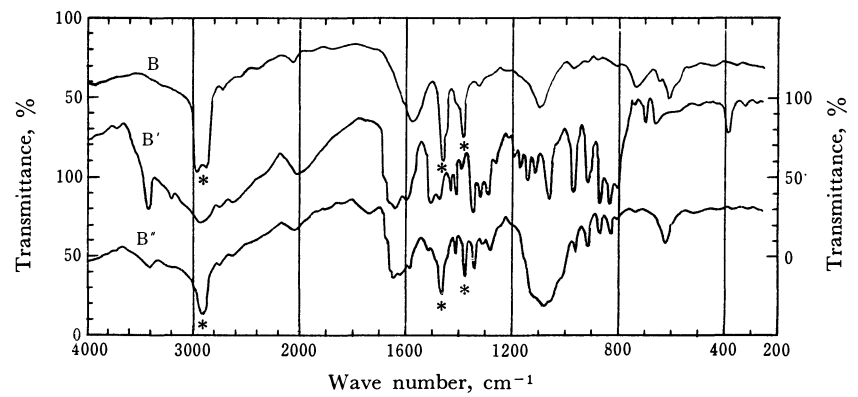

Fig. 2. Infrared spectra of His-mercury salt and relative compounds (Nujol).
B: $[His\text{-}Hg]ClO_4 \cdot Hg(ClO_4)_2$ B': Free His-hydrochloride
B'': Mixture of His and $Hg(ClO_4)_2$ (1 : 2) *, Absorption of Nujol

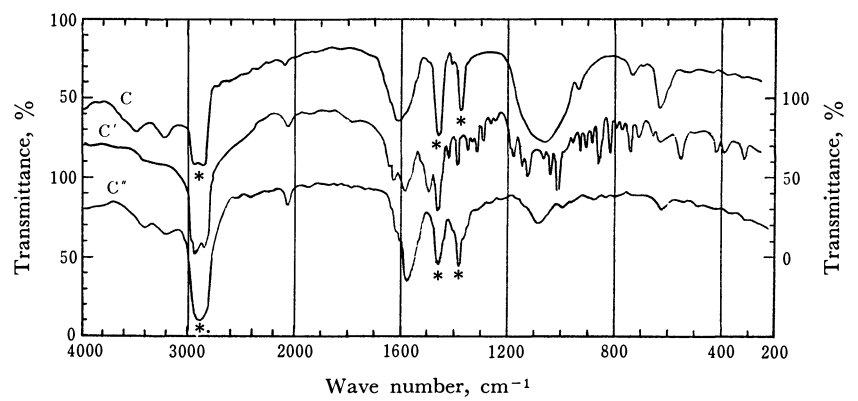

Fig. 3. Infrared spectra of Lys-mercry salt and relative compounds (Nujol).
C: $[Lys\text{-}Hg]ClO_4 \cdot Hg(ClO_4)_2$ C': Free Lys-hydrochloride
C'': Mixture of Lys and $Hg(ClO_4)_2$ (1 : 2) *, Absorption of Nujol

considered to be due to the ν_{as} (Hg–O)*3 shifted from the free carboxylic acid (A'—C') are shown in the 1565—1570 cm^{-1} region. The bands considered to be ν(Hg–N)[18] are seen at 624 cm^{-1} for A and B, and at 622 cm^{-1} for C. Strong absorptions due to the perchlorate ions[19] are seen at 1090 cm^{-1} for A, at 1100 cm^{-1} for B and at 1085 cm^{-1} for C. Although free amino acids (A'—C') as the components of the precipitates show many absorptions in the finger-print region, the precipitates give scarcely any absorptions in that region. Therefore, there is a possibility of the decomposition of the amino acids. However, since the stoichiometrical mixtures (A''—C'') of mercury(II) perchlorate and each basic amino acid (2 : 1) showed nearly the same absorption curves as those of A—C, the many absorptions in the finger-print region of A—C were considered to be hidden by the mercury(II) perchloarte which was predominant in quantity in the precipitates. As a result, the following structures of the precipitates are reasonable:

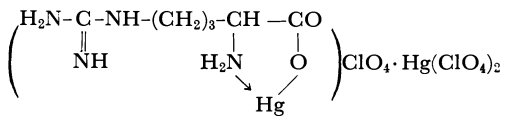

Abb. as $[Arg\text{-}Hg]ClO_4 \cdot Hg(ClO_4)_2$ (I)

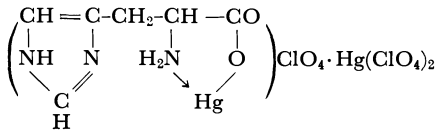

$[His\text{-}Hg]ClO_4 \cdot Hg(ClO_4)_2$ (II)

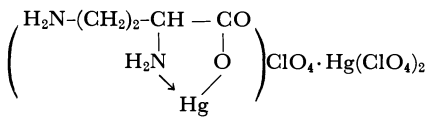

$[Lys\text{-}Hg]ClO_4 \cdot Hg(ClO_4)_2$ (III)

With respect to the II structure, the other structures shown below were considered possible:

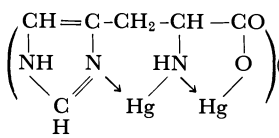

(II')

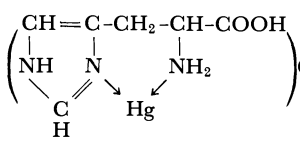

(II'')

However, II' was considered to be unstable and II''*4 was unreasonable because the carboxylic group was expected to be fully utilized by the bonding with mercury(II).

The Solubilities of the Precipitates. The precipitates were insoluble in water and in organic solvents (even in DMF), but were soluble in aqueous mineral acid and alkaline solutions. Therefore, the amphoteric properties of amino acids remained. The I, II and III are soluble in hot alkaline solutions at the pH values of 12.8—13.0, 13< and 12.1—12.3 respectively. The II structure is, however, apt to decompose into mercury oxide under these conditions. Accordingly, isolation using different solubilities in alkali was not employed. In an acetic acid containing chloride ions (KCl, NaCl), it was found that I and III were dissolved completely, while II remained insoluble. Concentrations up to 10 N of acetic acid and up to 2% (W/V) of sodium or potassium chloride in acetic acid were required for a thorough dissolution.

When sodium or potassium acetate was used in place of chloride, I and III were insoluble. Accordingly, the presence of chloride ions seems to be indispensable for the dissolution of I and III. The isolation of I and III could be carried out by treating a mixture of them, obtained again in the way described hitherto, by utilizing their different solubilities in a sodium hydroxide solution.

Application to the Quantitative Determination of Basic Amino Acids. *The Stoichiometric Study of the Components.* The yields of the products varied with the ratios of the components. The results are illustrated in Fig. 4. The concentrations of both mercury(II) perchlorate and a basic amino acid in the original standard aqueous solutions were 5×10^{-3} M; the volume of each amino acid solution used was kept at 10 ml, corresponding to 5×10^{-5} mol. Into this solution of mixtures, dilute aqueous sodium hydroxide was added drop by drop while stirring. The yields of the products at a given ratio of two components were determined by the spectrophotometric method, by analyzing the nitrogen content, and by observing a ninhidryne reaction in a small aliquot of the supernatant. As can be seen in this figure, at the ratio of 1.0 the yields of Arg, His and Lys were 35, 42 and 45% respectively. Furthermore, at the ratio of 2.0, which was considered to be the theoretical value for a complete precipitate formation, the yields were no more than 65—77%. On increasing the ratio,

*3 In a homologous metal such as zinc, it is said that the band of ν(Zn–O) appears at 1656 cm^{-1}; Y. Sano and H. Tanabe, *J. Inorg. Nucl. Chem.*, **8**, 119 (1958).

18) S. Mizushima, I. Nakagawa and D. M. Seeny, *J. Chem. Phys.*, **25**, 1006 (1956); K. Broderson and H. J. Becher, *Chem. Ber.*, **89**, 87 (1956); I. Nakagawa, R. B. Penland, S. Mizushima, T. J. Lane and J. V. Quagliano, *Spectrochim. Acta*, **9**, 199 (1957); E. P. Bertin, *J. Am. Chem. Soc.*, **80**, 525 (1958).

19) B. J. Hathaway and A. E. Underhill, *J. Chem. Soc.*, **1961**, 3091.

*4 The possibility of the homologous formula of II'' was pointed out in Ref. 15.

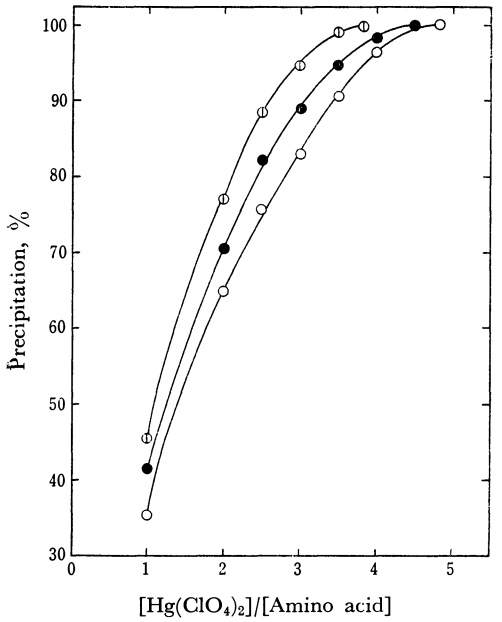

Fig. 4. Effect of varying ratio of component on precipitate formation.
-○- [Arg-Hg]$ClO_4 \cdot Hg(ClO_4)_2$
-●- [His-Hg]$ClO_4 \cdot Hg(ClO_4)_2$
-ⓘ- [Lys-Hg]$ClO_4 \cdot Hg(ClO_4)_2$
Original concn. of each component std. soln. was 5×10^{-3} M.

sufficient yields were obtained at the ratios of 3.8, 4.5 and 4.8 for Lys, His and Arg respectively. Therefore, more than five times as much mercury(II) perchlorate as each basic amino acid was required at least. The influence of excess mercury(II) perchlorate (about ten times as much mercury as each basic amino acid) on the precipitate formation was also studied. The formation, however, was not affected by the addition of excess mercury(II) perchlorate, and nor was any production of mercury oxide observed under these experimental conditions.

The Effect of pH on the Precipitate Formation. The yields of the products were affected by the pH of the sample solution. A dilute aqueous sodium hydroxide solution was added, drop by drop, to mixtures consisting of 2×10^{-4} M of each amino acid and 1.4×10^{-3} M of mercury(II) perchlorate. The results, shown in Fig. 5, suggest that the pH values of the solutions of mixtures which gave substantial yields were 7.8—7.9, 6.2—6.3 and 7.2—7.3 for Arg, His and Lys respectively. Therefore, in order to obtain substantially a mixture of the three kinds of precipitates, the pH of the solution was required to be at least 8.0. In order to obtain precipitates from a solution of more dilute amino acids, the effect of several organic solvents (methanol, ethanol, *n*- and isopropanol, acetone, dioxane, *etc.*), which are soluble in water, on the

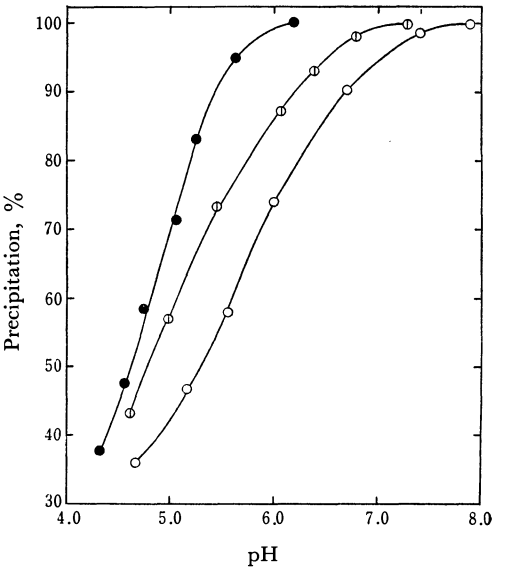

Fig. 5. Effect of pH on precipitate formation.
-○- [Arg-Hg]$ClO_4 \cdot Hg(ClO_4)_2$
-●- [His-Hg]$ClO_4 \cdot Hg(ClO_4)_2$
-ⓘ- [Lys-Hg]$ClO_4 \cdot Hg(ClO_4)_2$
Concn. of original std. soln.:
Amino acid $=2\times10^{-4}$ M
$Hg(ClO_4)_2=1.4\times10^{-3}$ M

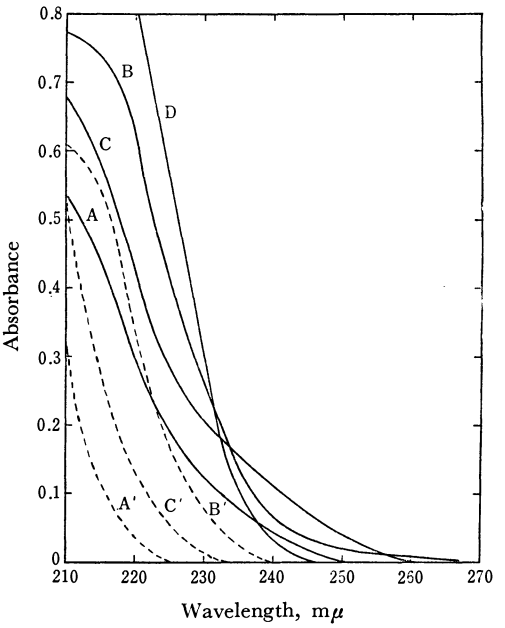

Fig. 6. Absorption spectra of the precpitates and their components in acidic aqueous solutions. (pH=2.1 with $HClO_4$)
A: [Arg-Hg]$ClO_4 \cdot Hg(ClO_4)_2$ (1×10^{-4} M)
B: [His-Hg]$ClO_4 \cdot Hg(ClO_4)_2$ (5×10^{-5} M)
C: [Lys-Hg]$ClO_4 \cdot Hg(ClO_4)_2$ (1×10^{-4} M)
A': Free Arg (1×10^{-3} M)
B': Free His (1×10^{-4} M)
C': Free Lys (1×10^{-2} M)
D: $Hg(ClO_4)_2$ (2×10^{-4} M)

formation of precipitates was investigated. The results made it clear that the formation of precipitates was facilitated by ethanol (ethanol: sample solution=1 : 1); thereby a small amount of basic amino acids could be precipitated from about a 10^{-5} M solution. This effect may presumably be explained by a reduction in the polarity of an aqueous sample solution.

Spectrophotometric Analyses. The ultraviolet absorption curves for the products and for their components are illustrated in Fig. 6. The spectra of the acidic solutions of I (curve A), II (curve B) and III (curve C) showed characteristic curves differing from those of the components, Arg (curve A'), His (curve B'), Lys (curve C') and mercury(II) perchlorate (curve D). As can also be seen from this figure, since the corresponding free amino acid content in these samples was as small as 1.9×10^{-5} M, 9.0×10^{-6} M and 1.4×10^{-5} M for Arg, His and Lys respectively, the proposed quantitative determination by the spectrophotometric method can be employed for a micro amount of basic amino acids.

Calibration Curves. The optimum wavelength for the quantitative determination must be ascertained, because there is no maximum in any of the absorption curves of the products. After many trials, the calibration curves in a good linear relationship at the proposed wavelength were obtained, as is shown below. The concentrations scaled in Figs. 7—9 show the calculated amounts of free amino acids in the corresponding mercury salts of basic amino acids.

Arg. The calibration curves on Arg in an acidic aqueous solution ($HClO_4$, pH 2.5), shown in Fig. 7, were obtained at a wavelength fixed arbitrarily in

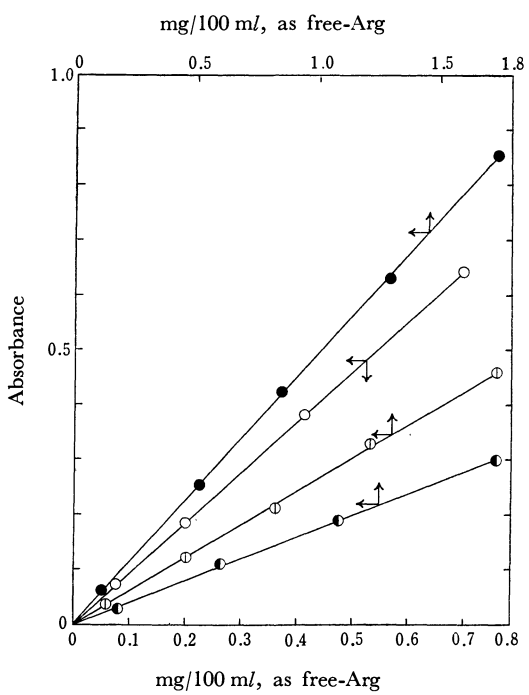

Fig. 7. Calibration curves on Arg, pH=2.5.
-○- 220 mμ -●- 230 mμ
-◑- 240 mμ -◐- 245 mμ

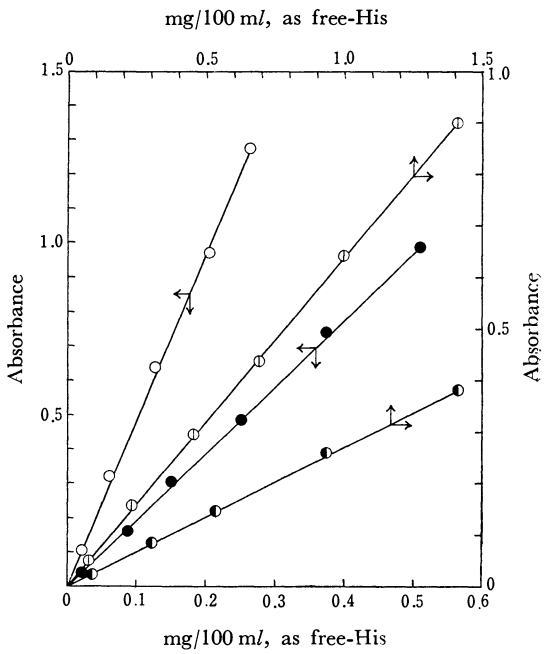

Fig. 8. Calibration curves on His, pH=2.0.
-○- 220 mμ -●- 230 mμ
-◑- 240 mμ -◐- 250 mμ

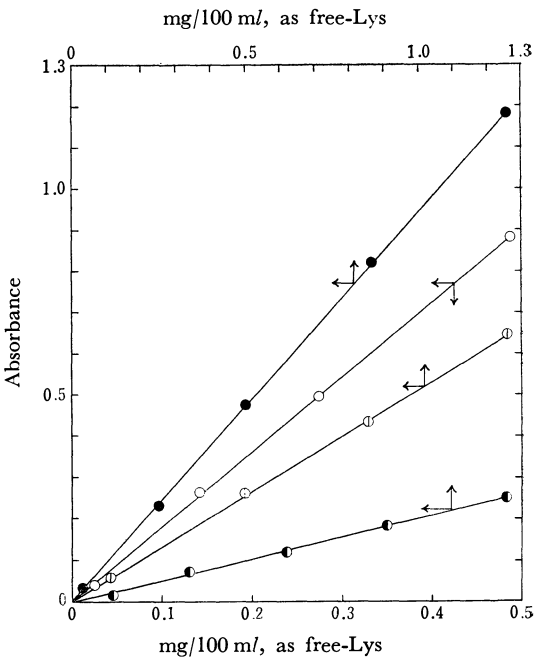

Fig. 9. Calibration curves on Lys, pH=2.3.
-○- 220 mμ -●- 230 mμ
-◑- 240 mμ -◐- 250 mμ

the region between 220—245 mμ. About 4×10^{-5} M of free Arg can be determined near 220 mμ, while about 1×10^{-4} M of free Arg can be determined in the 230—245 mμ region.

His. Figure 8 shows the curves of His (pH 2.0) in the range of 220—250 mμ. His up to 3.6×10^{-5} M in the 220—230 mμ and up to about 9.1×10^{-5} M in the 240—250 mμ region can be determined.

Lys. The curves for free Lys (pH 2.3) up to 3.5×10^{-5} M near 220 mμ and to 8.7×10^{-5} M in the 230—250 mμ region, shown in Fig. 9, have a fair linearity.

From these results, it was found that the quantitative determination of smaller amounts of basic amino acids may be carried out by the present calibration curves than those determined by using mercury(II) chloride[14] because the free basic amino acids contents in the products in this case of this perchlorate precipitant are lower than in those of chloride.

The Effect of the pH Value on the Absorbance of Sample Solutions. In order to study the effect of the pH on absorbancies, the pH of the sample solutions was adjusted to the required value with a dilute perchloric acid or a dilute sodium hydroxide solution.

Nevertheless these samples had been obtained at the pH values of 6—8 as described above (Fig. 5), at concentrations below 10^{-4} M of the sample solutions, there were, unexpectedly, neither any turbidity nor any conversion of the solution. The results are shown in Fig. 10. It was found that there are constant absorbancies extending over a wide range of pH values. His in the pH range of 1.5—8.5, Lys, in that of 2.5—10.7, and Arg, in that of 2.0—10.0 were determined at the respective constant absorbancies. Therefore, a precise set of pH values determined by a buffer solution was not necessary.

Recoveries by the Spectrophotometric Determination. The recoveries of basic amino acids by the present

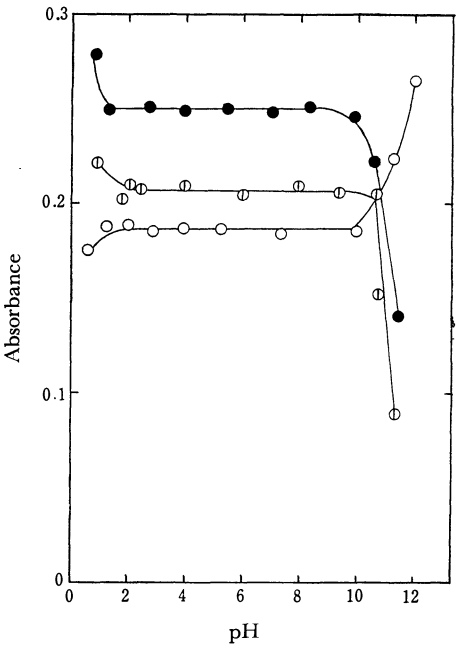

Fig. 10. Effect of pH on absorbancies.
-○- $[Arg\text{-}Hg]ClO_4\cdot Hg(ClO_4)_2$, 1×10^{-4} M at 225 mμ
-●- $[His\text{-}Hg]ClO_4\cdot Hg(ClO_4)_2$, 5×10^{-5} M, at 230 mμ
-○- $[Lys\text{-}Hg]ClO_4\cdot Hg(ClO_4)_2$, 1×10^{-4} M, at 230 mμ

method were examined; the data obtained are listed in Tables 1 and 2. Table 1 shows the results obtained when each aqueous testing solution was composed of a mixture of mercury(II) perchlorate and an individual basic amino acid, while Table 2 shows those obtained from an aqoeus solution of a mixture of mercury(II) perchlorate and all the basic amino acids. Sufficient recoveries were shown in all cases.

Further confirmation of the usefulness of the proposed method was obtained by measuring the

Table 1. Recoveries of a basic amino acid from an each aqueous solution by the spectrophotometric determination

Arg			His			Lys		
Added mg	Found mg	Recoveries %	Added mg	Found mg	Recoveries %	Added mg	Found mg	Recoveries %
0.5	0.4	80	0.5	0.6	120	0.5	0.5	100
1.0	1.1	100	1.0	1.0	100	1.0	1.0	100
1.5	1.3	87	1.5	1.2	81	1.5	1.7	113
2.0	1.9	95	2.0	1.9	95	2.0	2.2	110
2.5	2.6	104	2.5	2.7	108	2.5	2.4	96
3.0	3.2	107	3.0	2.9	97	3.0	3.1	103
3.5	3.7	106	3.5	3.5	100	3.5	3.3	94
4.0	4.1	102	4.0	4.2	105	4.0	3.9	98

Concentration of each original aqueous standard solution was 10^{-3} M.

TABLE 2. RECOVERIES OF A BASIC AMINO ACID FROM AN AQUEOUS SOLUTION CONTAINING MIXTURE OF BASIC AMINO ACIDS AND VARIOUS AMINO ACIDS

a									b								
Added mg			Found mg			Recoveries %			Added mg			Found mg			Recoveries %		
Arg	His	Lys	Arg	His	Lys	Arg	His	Lys	Arg	His	Lys	Arg	His	Lys	Arg	His	Lys
1.0	1.0	1.0	1.1	0.9	1.0	110	90	100	2.0	2.0	2.0	2.1	2.0	1.7	105	100	85
3.0	3.0	3.0	2.9	3.1	3.1	97	103	103	4.0	4.0	4.0	4.3	4.1	3.8	107	102	95
5.0	5.0	5.0	5.2	4.8	4.7	104	96	94	6.0	6.0	6.0	5.7	6.1	6.0	95	101	100
7.0	7.0	7.0	7.0	7.1	6.8	100	101	97	8.0	8.0	8.0	8.4	7.8	8.3	105	98	104

a : Obtained from a mixture of three kinds of basic amino acids.
b : Obtained from a mixture of various amino acids.
Concentration of each original aqueous standard solution was 10^{-3} M.

basic amino acids in an ovalbumin. By comparing the present results with the data reported by Folin *et al.*[20] and Wieland,[21] it was confirmed that the proposed method is sufficiently rapid, precise and accurate to be used for the preferential and simultaneous separation and determination of a small amount of basic amino acids.

The author wishes to express his deep gratitude to Professor Daisei Yamamoto of this University for his kind direction and encouragement throughout the course of this study. Thanks are also due to Dr. Minoru Nakamizo of the Goverment Industrial Research Institute, Kyushu, for his infrared spectral measurements.

20) O. Folin, *J. Biol. Chem.*, **56**, 377 (1922); O. Folin, *ibid.*, **51**, 393 (1922); E. G. Frame, J. A. Russell and A. E. Wilhelmi, *ibid.*, **140**, 255 (1943); N. H. Furman, G. H. Morrison and A. F. Wagner, *Anal. Chem.*, **22**, 1561 (1950).
21) T. Wieland and L. Wirth, *Ber.*, **76**, 823 (1943).

BULLETIN OF THE CHEMICAL SOCIETY OF JAPAN VOL. 41 882—888 (1968)

Spectrophotometric Determination of Formation Constants of Iron(III) Complexes with Chloride Ion in Dimethyl Sulfoxide*[1]

Goro WADA

Department of Chemistry, Nara Women's University, Nara

(Received October 4, 1967)

The formation constants of $FeCl^{2+}$ and $FeCl_2^+$ have been measured in dimethyl sulfoxide (DMSO) containing $Fe(ClO_4)_3$, NaCl, $HClO_4$ and $NaClO_4$. Some spectrophotometric methods giving the formation constants and molar extinction coefficients of the complexes were developed and gave, on the average, log $K_1=3.62$ and log $K_2=2.10$, at 0.02 M $HClO_4$ and an ionic strength of 0.10 M at 25°C. It is rather surprising that these values are only slightly larger than those in *N*-methylacetamide, which is expected, however, to give much smaller values than DMSO, due to its extraordinarily large dielectric constant. The species formed between Fe(III) and Cl^- ion is reasonably supposed to be a true complex bonded directly with each other and not an ion-pair association product. At higher concentrations of Fe(III), formation of polynuclear complexes can occur.

Dimethyl sulfoxide (DMSO) has recently come to be widely used as an advantageous medium for inorganic chemical reactions. Spectrophotometric and electron magnetic resonance studies showed that a small amount of tetrachloroferrate(III) ion was present in solution of iron(III) chloride in a number of organic solvents including DMSO, the formation being the smallest in the case of DMSO.[1] On the other hand, the predominant iron(III)

*1 Presented at the 20th Annual Meeting of the Chemical Society of Japan, Tokyo, No. 2B104, April, 1967.

1) T. B. Swanson and V. W. Laurie, *J. Phys. Chem.*, **69**, 244 (1965).

ion in DMSO was found to exist in the form of monochloroiron(III) complex ion in solutions of hexa-solvated iron(III) perchlorate and tetraethylammonium chloride at the concentration ratios of 1 and 2 between iron(III) and chloride ion when the concentration of iron(III) was 1.52×10^{-4} M.[2,3]

In an investigation of the electron transfer reaction between iron(III) and iron(II) in DMSO catalyzed by chloride ion, the formation constants for the chloride ion-containing complexes were required to be known in order to estimate the individual rate constants, which have been already reported.[4] Consequently, the present work was undertaken to obtain formation constants, and a couple of methods of calculation based on spectrophotometrically observed data were developed for the purpose.

Experimental

Materials. Commercial DMSO of analytical reagent grade was distilled under a reduced nitrogen atmosphere, shaken with activated alumina overnight, and redistilled under the same conditions. The purified DMSO contained water approximately at the concentration of 0.025 M at the highest, found using Karl Fischer reagent.

Crystals of $Fe(ClO_4)_3\cdot6DMSO$,[5] anhydrous sodium perchlorate and solutions of perchloric acid in DMSO were prepared by a procedure described previously.[6] Sodium chloride was twice recrystallized from water and dried.

Apparatus. A Beckman Model DU spectrophotometer with a thermostated cell compartment and quartz cells was used for the measurement of optical density.

Results and Calculations

Absorption Spectra. Figure 1 shows the absorption spectra of iron(III) species in the absence and the presence of chloride ion in DMSO. Curve A is the spectrum of $Fe(DMSO)_6^{3+}$ (written Fe^{3+} for simplicity), which agrees well with that of Drago and others.[3] Curve B represents the apparent spectrum of the mixture of Fe^{3+} and $Fe(DMSO)_5Cl^{2+}$ ($FeCl^{2+}$ for simplicity). By using the values of K_1 as will be obtained below, the true molar extinction coefficients of $FeCl^{2+}$ at various wavelengths were calculated from Curves A and B, and then Curve C was drawn as the true spectrum of $FeCl^{2+}$. There is an absorption peak at 340 mμ in the spectrum of $FeCl^{2+}$, whereas none

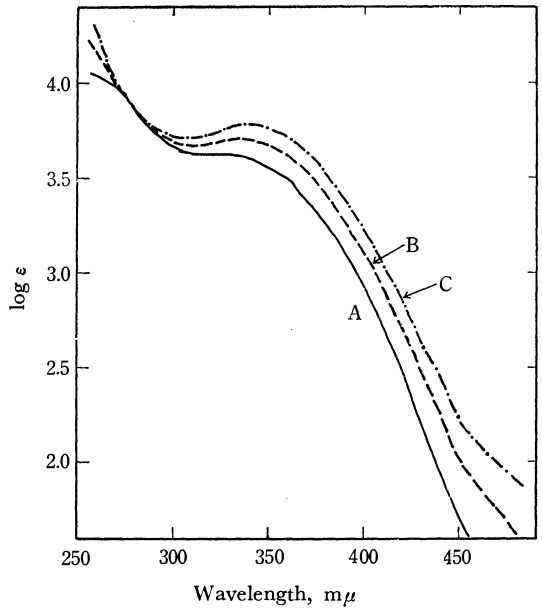

Fig. 1. Absorption spectra of Fe^{3+} and $FeCl^{2+}$ in DMSO, $[HClO_4]=0.02$ M, $\mu=0.10$, 25°C.
A: ——— Fe^{3+}
B: ——— $[Fe(III)]=7.0\times10^{-5}$ M, $[Cl]=6.3\times10^{-4}$ M
C: —·—· $FeCl^{2+}$

is observed in that of Fe^{3+}, and an isosbestic point at about 280 mμ is also recognized for the two spectra. The apparent spectra of iron(III) complexes in both solutions are not affected by acid concentration, indicating that the solvating DMSO molecule of iron(III) undergoes no appreciable solvolysis (proton donation), because DMSO is aprotic,[7] or rather slightly basic.[8]

Continuous Variation Method. Job's method of continuous variations[9] was used to indicate the formula of the prominent species, if any. Figure 2 shows the Job's curves at 450, 460 and 470 mμ with $C=[Fe(III)]+[Cl]=1.00\times10^{-2}$ M, $[HClO_4]=0.02$ M and $\mu=0.10$ M at 25°C, where [Fe(III)] and [Cl] stand for the total concentrations of iron(III) and chloride ion employed, respectively. The ordinate Y is defined as the difference between the observed optical density and the optical density which would have been obtained if no complex formation had occurred. At the wavelengths used here, absorption caused by the free ligand was negligible. The abscissa x is defined as $x=[Fe(III)]/C$.

Figure 3 shows the Job's curves at 400 mμ with $C_a=1.00\times10^{-3}$ M and $C_b=0.70\times10^{-3}$ M for

2) R. L. Carlson, Ph. D. Thesis, University of Illionis, 1962.
3) R. S. Drago, D. M. Hart and R. L. Carlson, *J. Am. Chem. Soc.*, **87**, 1900 (1965).
4) G. Wada and W. L. Reynolds, *Inorg. Chem.*, **5**, 1354 (1966).
5) J. Selbin, W. E. Bull and L. H. Holmes, Jr., *J. Inorg. Nucl. Chem.*, **16**, 219 (1961).
6) J. Menashi, W. L. Reynolds and G. Van Auken, *Inorg. Chem.*, **4**, 299 (1965).
7) T. B. Reddy, Ph. D. Thesis, University of Minnesota, 1960; I. M. Kolthoff and T. B. Reddy, *J. Electrochem. Soc.*, **108**, 980 (1961).
8) G. Wada and W. L. Reynolds, unpublished.
9) P. Job, *Ann. Chim.*, 10E series, **9**, 113 (1928); *ibid.*, 11E series, **6**, 97 (1936).

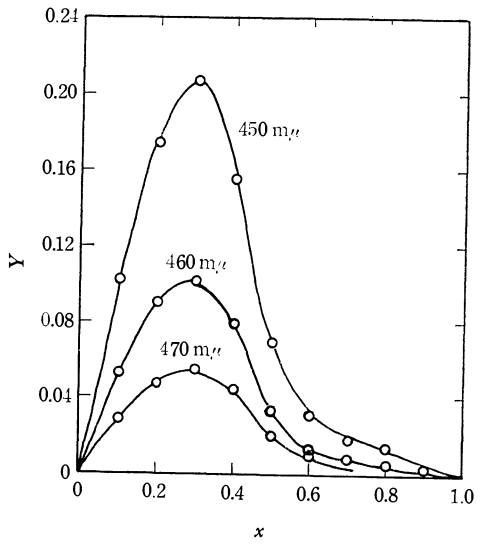

Fig. 2. Job's curves of Fe(III)+Cl⁻ system in DMSO. $C=1.00\times10^{-2}$ M, $[HClO_4]=0.02$ M, $\mu=0.10$, 25°C.

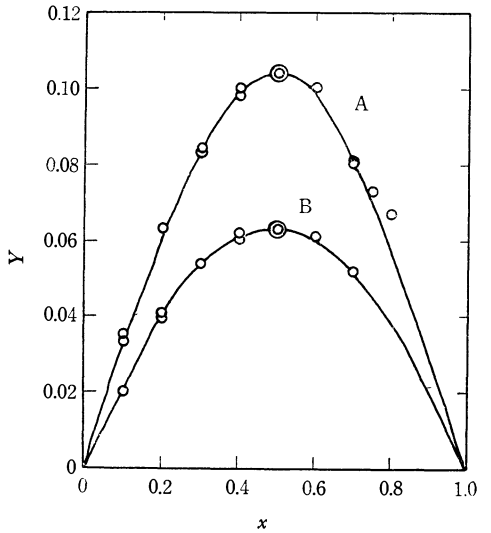

Fig. 3. Job's curves of Fe(III)+Cl⁻ systems in DMSO. $[HClO_4]=0.02$ M, $\mu=0.10$, 25°C, 400 mμ.
A: $C_a=1.00\times10^{-3}$ M B: $C_b=0.70\times10^{-3}$ M

Curves A and B, respectively, as well. Other conditions were the same as in Fig. 2. Quite similar plots to those in Fig. 3 but with smaller Y values, were obtained at 410 mμ, although they are omitted in the figure.

It would be reasonably concluded from Figs. 2 and 3 that, at a lower total concentration C, the 1 : 1 complex $FeCl^{2+}$ is predominantly formed, while, at a higher C, the system is more complicated, with the probable formation of polynuclear chloroiron(III) complexes, as well as polychloromononuclear iron(III) complexes. This is because the shift of the maximum point of Y from $x=0.5$ to approximately 0.3 as C is increased tenfold indicates the occurrence of polychloroiron(III) complexes, probably $FeCl_2^+$, and the sudden decrease in Y values at $x>0.4$ in Fig. 2 suggests the formation of polynuclear iron(III) complexes containing chloride ion, with smaller molar extinction coefficients than those of $FeCl^{2+}$ and $FeCl_2^+$, although their formulas are unknown.

In the following part of the text, simpler systems will be mainly taken into account, where $FeCl^{2+}$ plays the leading role, except as otherwise noted.

Calculation of K_1 from Job's Curves. In the system where simply $FeCl^{2+}$ complex is formed, Y and K_1 are expressed by the following relations, according to their definitions,

$$Y = \varepsilon_0[Fe^{3+}] + \varepsilon_1[FeCl^{2+}] - \varepsilon_0[Fe(III)] \quad (1)$$

$$K_1 = [FeCl^{2+}]/[Fe^{3+}][Cl^-] \quad (2)$$

in which ε_0 and ε_1 are the molar extinction coefficients of Fe^{3+} and $FeCl^{2+}$, respectively. By using the following relation

$$[Fe(III)] = [Fe^{3+}] + [FeCl^{2+}] \quad (3)$$

Eq. (1) is rewritten as

$$Y = (\varepsilon_1-\varepsilon_0)[FeCl^{2+}] \quad (4)$$

Method I of Common Y. In Fig. 3, consider a set of two points (x_a, Y) and (x_b, Y) on the Curves A and B, respectively, which have a common value of Y. Then, the following relation is established, where subscripts a and b correspond to the respective points on the Curves A and B,

$$K_1 = \frac{[FeCl^{2+}]_a}{[Fe^{3+}]_a[Cl^-]_a} = \frac{[FeCl^{2+}]_b}{[Fe^{3+}]_b[Cl^-]_b} \quad (5)$$

By solving Eq. (5),

$$[FeCl^{2+}]_a = [FeCl^{2+}]_b = \frac{x_a(1-x_a)C_a^2 - x_b(1-x_b)C_b^2}{C_a - C_b} \quad (6)$$

$$[Fe^{3+}]_a = x_aC_a - [FeCl^{2+}]_a \quad (7)$$

$$[Cl^-]_a = (1-x_a)C_a - [FeCl^{2+}]_a \quad (8)$$

and substituting for Eq. (5) the values from Eqs. (6), (7) and (8), the value of K_1 can be calculated. And ε_1 is also known from the following equation.

$$\varepsilon_1 = \frac{Y}{[FeCl^{2+}]_a} + \varepsilon_0 \quad (9)$$

Similar, but less complete methods have been reported by several researchers.[10] Table 1 shows an example of this method under the conditions $C_a=1.00\times10^{-3}$ M, $C_b=0.70\times10^{-3}$ M, $[HClO_4]=0.02$ M and $\mu=0.10$ M at 25°C and gives the

10) For instance, S. E. Turner and R. C. Anderson, *J. Am. Chem., Soc.*, **71**, 912 (1949); A. K. Mukerji and A. K. Dey, *J. Inorg. Nucl. Chem.*, **6**, 314 (1958); P. Sanyal, S. P. Sangal and S. P. Mushran, This Bulletin, **40**, 217 (1967).

Table 1. Derivation of K_1 and ε_1 by the method I of common Y

$C_a=1.00\times10^{-3}$ M, $C_b=0.70\times10^{-3}$ M, $[HClO_4]=0.02$ M, $\mu=0.10$ M at 25°C. $\varepsilon_0^{400}=845$, $\varepsilon_0^{410}=520$ $M^{-1}cm^{-1}$

λ mμ	Y	x_a	x_b	$K_1\times10^{-3}$ M^{-1}	$\varepsilon_1\times10^{-3}$ $M^{-1}cm^{-1}$
400	0.060	0.18	0.36	2.6	1.36
400	0.055	0.17	0.30	4.2	1.28
400	0.050	0.15	0.26	3.9	1.30
400	0.045	0.14	0.23	5.4	1.25
				Mean	1.30±0.05
410	0.035	0.16	0.31	2.2	0.88
410	0.030	0.14	0.24	3.7	0.81
				Mean 3.7±1.2	0.85±0.04

averaged values of $K_1=(3.7\pm1.2)\times10^3$ M^{-1} and $\varepsilon_1^{400}=(1.30\pm0.05)\times10^3$ $M^{-1}cm^{-1}$ and $\varepsilon_1^{410}=(0.85\pm0.04)\times10^3$ $M^{-1}cm^{-1}$.

In considering Y values for this method, such ranges of Y had better be avoided as where the differences between x_a and x_b are too small ($x_a<0.1$) or where the lower curve is too broad near its maximum point ($x_b>0.4$). In addition, only the left halves of the curves must be used, otherwise polynuclear iron(III) species might become effective.

Similarly, at the concentration of acid $[HClO_4]=0.07$ M, other conditions being the same, the method gave $K_1=(3.8\pm0.6)\times10^3$ M^{-1} and $\varepsilon_1^{400}=(1.24\pm0.02)\times10^3$ $M^{-1}cm^{-1}$. No dependence of K_1 upon acid concentration was recognized.

At 41.1°C and $[HClO_4]=0.02$ M, $K_1=(6.3\pm1.5)\times10^3$ M^{-1} and $\varepsilon_1^{400}=(1.29\pm0.02)\times10^3$ $M^{-1}cm^{-1}$ were obtained, which gave approximate values of $\Delta H_1=7$ kcal/mol and $\Delta S_1=40$ cal deg^{-1} mol^{-1}, in association with data at 25°C.

Other possible methods for obtaining K_1 from Job's curves will be described briefly in the following.

Method II Using Two Maxima. The Y values of the two maximum points on the two curves in Fig. 3 are denoted as Y_a^m and Y_b^m, respectively. At these points, as $[Fe^{3+}]=[Cl^-]$, the following relation holds.

$$K_1 = \frac{Y_a^m/(\varepsilon_1-\varepsilon_0)}{\{(C_a/2)-Y_a^m/(\varepsilon_1-\varepsilon_0)\}^2} = \frac{Y_b^m/(\varepsilon_1-\varepsilon_0)}{\{(C_b/2)-Y_b^m/(\varepsilon_1-\varepsilon_0)\}^2} \quad (10)$$

By solving this equation, the values of ε_1 and therefore K_1 will be obtained.

$$\varepsilon_1 = \frac{2(Y_a^m\sqrt{Y_b^m}-Y_b^m\sqrt{Y_a^m})}{C_a\sqrt{Y_b^m}-C_b\sqrt{Y_a^m}}+\varepsilon_0 \quad (11)$$

The results of the numerical calculation at $[HClO_4]=0.02$ M and $\mu=0.10$ M are that $K_1=3.1\times10^3$ M^{-1}, $\varepsilon_1^{400}=1.30\times10^3$ $M^{-1}cm^{-1}$ and $\varepsilon_1^{410}=0.81\times10^3$ $M^{-1}cm^{-1}$ at 25°C, and $K_1=6.7\times10^3$ M^{-1}, $\varepsilon_1^{400}=1.27\times10^3$ $M^{-1}cm^{-1}$ and $\varepsilon_1^{410}=0.79\times10^3$ $M^{-1}cm^{-1}$ at 41°C. This method is less accurate than the previous one.

Method III using a Single Curve. Taking a pair of points (x_1, Y_1) and (x_2, Y_2) on a single Job's curve, and defining the ratio $Y_1/Y_2=[FeCl^{2+}]_1/[FeCl^{2+}]_2$ as α, the following relation is established.

$$K_1 = \frac{\alpha[FeCl^{2+}]_2}{(x_1C-\alpha[FeCl^{2+}]_2)\{(1-x_1)C-\alpha[FeCl^{2+}]_2\}} = \frac{[FeCl^{2+}]_2}{(x_2C-[FeCl^{2+}]_2)\{(1-x_2)C-[FeCl^{2+}]_2\}} \quad (12)$$

Solving Eq. (12), a value for $[FeCl^{2+}]_2$ is obtained and therefore K_1.

$$[FeCl^{2+}]_2 = \left\{\frac{\alpha x_2(1-x_2)-x_1(1-x_1)}{\alpha(\alpha-1)}\right\}^{1/2}C \quad (13)$$

Then ε_1 is known from Eq. (9).

The results of the numerical calculation from 9 sets of data at $[HClO_4]=0.02$ M, $\mu=0.1$ M at 25°C when $C=1.00\times10^{-3}$ M are $K_1=(3.7\pm0.7)\times10^3$ M^{-1} and $\varepsilon_1^{400}=(1.28\pm0.03)\times10^3$ $M^{-1}cm^{-1}$.

Determination of K_1 and K_2 from Linear Relations of $\bar{\varepsilon}$. *Determination of* K_1. At concentrations of iron(III) and chloride ion low enough so that the amount of $FeCl_2^+$ formed is negligible, the apparent molar extinction coefficient of iron(III), $\bar{\varepsilon}$, is defined as

$$\bar{\varepsilon}[Fe(III)] = \varepsilon_0[Fe^{3+}] + \varepsilon_1[FeCl^{2+}] \quad (14)$$

By combining Eq. (14) with Eqs. (2) and (3), $\bar{\varepsilon}$ is expressed by a relationship linear with respect to $(\bar{\varepsilon}-\varepsilon_0)/[Cl^-]$.

$$\bar{\varepsilon} = \varepsilon_1 - \frac{1}{K_1}\frac{\bar{\varepsilon}-\varepsilon_0}{[Cl^-]} \quad (15)$$

Accordingly, plotting $\bar{\varepsilon}$ *vs.* $(\bar{\varepsilon}-\varepsilon_0)/[Cl^-]$ will give $-1/K_1$ as the slope and ε_1 as the intercept. Figure 4 shows this relation when $[Fe(III)]=3.00\times10^{-4}$ M and $[Cl]=8.0\times10^{-5}$—6.5×10^{-3} M were used at $[HClO_4]=0.02$ M and $\mu=0.10$ M at 25°C, observed at 400 mμ. As the concentration of chloride ion is raised, corresponding to a point moving from right to left on the abscissa, the observed $\bar{\varepsilon}$ goes off the straight line, indicating that the occurrence of $FeCl_2^+$ is no longer negligible. Only the linear part is to be taken account of so far as the calculation of K_1 is concerned. At first, [Cl] is used in place of $[Cl^-]$ and a rough value of K_1 is estimated from the slope. By using the first approximate K_1, a second approximate $[Cl^-]$ is calculated at the corresponding [Cl], and a more accurate straight line is drawn, followed by the recalculation of a more accurate K_1. On repeating the cycles until a self-consistent K_1 and $[Cl^-]$'s are obtained, the most reliable K_1 is finally decided. Actually, two cycles were enough for

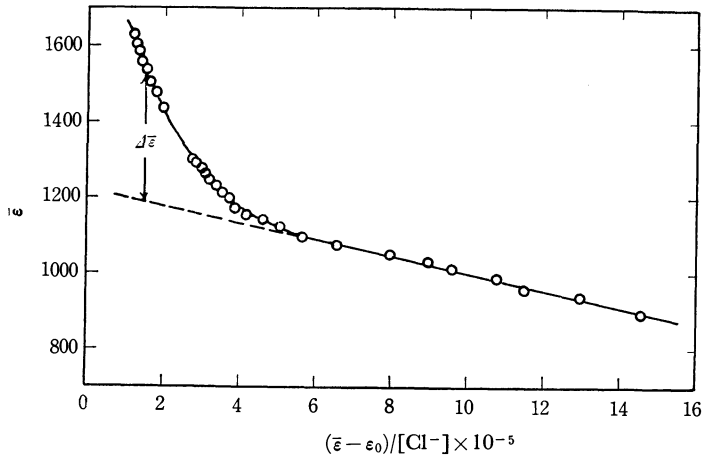

Fig. 4. The plot of $\bar{\varepsilon}$ *vs.* $(\bar{\varepsilon}-\varepsilon_0)/[Cl^-]$ at 400 mμ. $[HClO_4]=0.02$ M, $\mu=0.10$, 25°C.

the purpose. Computation for the slope and the intercept of a straight line was performed by the method of least squares.

As results, $K_1=(4.2\pm0.1)\times10^3$ M^{-1}, and $\varepsilon_1^{400}=(1.24\pm0.01)\times10^3$ M^{-1} cm^{-1}, both of which are in fairly good agreement with the values from Job's curves.

Determination of K_2. K_2 is defined as the stepwise formation constant of $FeCl_2^+$ in DMSO.

$$K_2 = [FeCl_2^+]/[FeCl^{2+}][Cl^-] \quad (16)$$

Equations (3) and (14) can be extended to the following, by taking the presence of $FeCl_2^+$ into account,

$$[Fe(III)] = [Fe^{3+}] + [FeCl^{2+}] + [FeCl_2^+] \quad (17)$$

$$\bar{\varepsilon}[Fe(III)] = \varepsilon_0[Fe^{3+}] + \varepsilon_1[FeCl^{2+}] + \varepsilon_2[FeCl_2^+] \quad (18)$$

in which ε_2 is the molar extinction coefficient of $FeCl_2^+$. Therefore, Eq. (15) is altered to

$$\varepsilon = \varepsilon_1 - \frac{1}{K_1}\frac{\bar{\varepsilon}-\varepsilon_0}{[Cl^-]} + (\varepsilon_2-\bar{\varepsilon})K_2[Cl^-] \quad (19)$$

with the third term on the right-hand side of Eq. (19), which causes the plot to deviate from a straight line at higher concentrations of chloride ion in Fig. 4, because ε_2 is larger than $\bar{\varepsilon}$. Consequently, the deviation $\Delta\bar{\varepsilon}$ is defined as the difference between the observed $\bar{\varepsilon}$ and hypothetical $\bar{\varepsilon}$ which would have been obtained if no $FeCl_2^+$ formation had occurred, and Eq. (19) can be rearranged into another form in terms of $\Delta\bar{\varepsilon}$.

$$\bar{\varepsilon} = \varepsilon_2 - \frac{1}{K_2}\frac{\Delta\bar{\varepsilon}(1+K_1[Cl^-])}{K_1[Cl^-]^2} \quad (20)$$

A plot of $\bar{\varepsilon}$ *vs.* $\Delta\bar{\varepsilon}(1+K_1[Cl^-])/K_1[Cl^-]^2$ will yield a straight line, whose slope and intercept indicate $-1/K_2$ and ε_2, respectively. In order to get the final correct values of K_2 and ε_2, a procedure similar to that in the case of K_1 has to be taken.

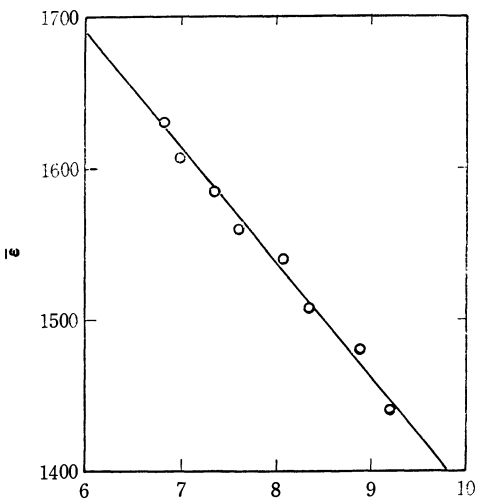

Fig. 5. The plot of $\bar{\varepsilon}$ *vs.* $\Delta\bar{\varepsilon}(1+K_1[Cl^-])/K_1[Cl^-]^2$ at 400 mμ.
$[HClO_4]=0.02$ M, $\mu=0.10$, 25°C

The linearity is obvious in Fig. 5 when $[Fe(III)]=1.50\times10^{-4}$ M and $[Cl]=(3.0\text{—}6.5)\times10^{-3}$ M were used at $[HClO_4]=0.02$ M and $\mu=0.10$ M at 25°C and 400 mμ. The results are $K_2=(1.33\pm0.05)\times10^2$ M^{-1} and $\varepsilon_2^{400}=(2.14\pm0.03)\times10^3$ M^{-1} cm^{-1}.

Other Complementary Methods. *Computer Method.* Collecting all the values of the optical density at many iron(III) and chloride ion concentrations as far as were measured, a high-speed digital computation yielded best fitted values of K_1 and K_2 along with the extinction coefficients as $K_1=(5.3\pm0.6)\times10^3$ M^{-1} and $K_2=(1.1\pm0.3)\times10^2$ M^{-1}, $\varepsilon_1^{400}=1180\pm16$ and $\varepsilon_2^{400}=2350\pm130$ M^{-1} cm^{-1}.[4,11]

11) Z. Z. Hugus, "Advances in the Chemistry of the Coordination Compounds," The Macmillan Co., New York, N. Y. (1961), p. 379.

TABLE 2. SUMMARY OF THE VALUES OF K_1, K_2, ε_1^{400} AND ε_2^{400} MEASURED BY VARIOUS METHODS $[HClO_4]=0.02$ M, $\mu=0.10$ M AT 25°C

Method	$K_1\times10^{-3}$, M^{-1}	$\varepsilon_1^{400}\times10^{-3}$, $M^{-1}cm^{-1}$	$K_2\times10^{-2}$ M^{-1}	$\varepsilon_2^{400}\times10^{-3}$ $M^{-1}cm^{-1}$
Job's I	3.7±1.2	1.30±0.05	—	—
Job's I	3.8±0.6*	1.24±0.02*	—	—
Job's II	3.1	1.30	—	—
Job's III	3.7±0.7	1.28±0.03	—	—
Linearity	4.2±0.1	1.24±0.01	1.33±0.05	2.14±0.03
Computer	5.3±0.6	1.18±0.02	1.1 ±0.3	2.35±0.13
Kinetic	5.4±1.0**	—	—	—

* $[HClO_4]=0.07$ M ** 20°C

TABLE 3. COMPARISON OF K_1, K_2, ΔH_1 AND ΔS_1 FOR THE FORMATION OF $FeCl^{2+}$ AND $FeCl_2^+$ IN WATER, NMA AND DMSO AT 25°C

Solvent	$\log K_1$	$\log K_2$	ΔH_1 kcal/mol	ΔS_1 cal/deg·mol	Dielectric constant
Water	1.48	0.65	8.5	35	80
NMA	2.88	1.11	—	—	178.9 (30°C)[15]
DMSO	3.62	2.10	7	40	46.7 (25°C)[7]

Kinetic Method. The electron transfer reaction between iron(II) and iron(III) in DMSO is accelerated by the presence of chloride ion. At very low concentrations of iron species, the apparent rate constant $\bar{k}$ is expressed by

$$\bar{k}[Fe(III)] = k_0[Fe^{3+}] + k_1[FeCl^{2+}] \qquad (21)$$

which is quite similar to Eq. (14) in appearance, except there are only k's instead of ε's. Accordingly a relationship corresponding to Eq. (15) is obtained as follows.[12]

$$\bar{k} = k_1 - \frac{1}{K_1}\frac{\bar{k}-k_0}{[Cl^-]} \qquad (22)$$

By applying 36 pieces of data measured by Wada and Reynolds,[4] K_1 and k_1 were found to be $K_1=(5.4\pm1.0)\times10^3$ M^{-1} and $k_1=176$ $M^{-1}sec^{-1}$ at $[HClO_4]=0.02$ M and $\mu=0.10$ M at 20°C. This is a convenient method to obtain k_1 without knowing K_1 separately measured in advance.

In Table 2, the values of K_1 and K_2 and ε_1 and ε_2 calculated by various methods are summarized together. In looking at the table, the agreement is good between the Job and the linearity methods with regard to K_1, although the computer and the kinetic methods give a little higher values. Besides this small discrepancy, K_2, ε_1^{400} and ε_2^{400} agree very well among their all measured values, respectively. Considering the accuracy and the reliability of the individual methods employed here, it seems safe to conclude that the most reasonable values are $\log K_1=3.62$ and $\log K_2=2.10$, and therefore $\log \beta_2=5.72$.

Discussion. The values of K_1, K_2, ΔH_1 and ΔS_1 in water[13] and in *N*-methylacetamide (NMA)[14] are listed in Table 3 together with those in DMSO. The decreasing dielectric constant of the solvent seems to favor increased formation of complex between iron(III) and chloride ion. This prevails in the cases of water and DMSO, where iron(III) ion is coordinated through oxygen atoms with the solvating molecules, as compared to nitrogen atoms in NMA. However, coordination through oxygen would favor increased dissociation of $FeCl^{2+}$ better than through nitrogen, considering the spectrochemical series of ligands. In fact, the larger values of K_1 and K_2 found in NMA than in water are really against expectation from the dielectric constant but due to the coordinating atom. The latter effect must be predominant over the former. The coincidence of ΔH_1 and ΔS_1 in water and DMSO seems to have come about rather by chance.

The electron transfer reaction between iron(II) and iron(III) in chloride ion-containing DMSO occurs through two paths.

$$Fe^{2+} + {}^*Fe^{3+} \rightarrow Fe^{3+} + {}^*Fe^{2+} \qquad (23)$$

$$Fe^{2+} + {}^*FeCl^{2+} \rightarrow FeCl^{2+} + {}^*Fe^{2+} \qquad (24)$$

The K_1 value obtained by the kinetic method means the formation constant of $FeCl^{2+}$ appearing in Reaction (24), which probably proceeds through the inner-sphere mechanism with an activated

12) J. C. Sheppard, *Nucl. Sci. Abst.*, **19**, 2431 (1965).

13) E. Rabinowitch and W. H. Stockmayer, *J. Am. Chem. Soc.*, **64**, 335 (1942).

14) W. L. Reynolds and R. H. Weiss, *ibid.*, **81**, 1790 (1959).

15) L. R. Dawson, R. H. Graves and P. G. Sears, *ibid.*, **77**, 1986 (1955); S. J. Bass, W. I. Nathan, R. M. Meighan and R. H. Cole, *J. Phys. Chem.*, **68**, 509 (1964).

complex bridged by a chloride ion.[4] Therefore, the approximate agreement between the K_1 values by the spectrophotometric and the kinetic methods, in other words, from independent sources of observation, will permit one to presume that the species of $FeCl^{2+}$ observed in the spectrophotometric method was the same as in the kinetic method, and accordingly, was not a mere association product between ions without liberating the solvating molecules to the ions, but a complex, in the true sense of the word, with a chloride ion, as a ligand, attached directly to the iron(III) ion.

The experimental part of the work was carried out at the Department of Chemistry, University of Minnesota, U. S. A. The author's sincere thanks are due to Professor Warren L. Reynolds for his helpful advice.

BULLETIN OF THE CHEMICAL SOCIETY OF JAPAN VOL. 41 888—892 (1968)

The Hydrogen Yields in the Radiolysis of Cysteine and Biscysteinatocobaltate(III) in 0.8 N Sulfuric Acid

Niro MATSUURA and Nobuyoshi SHINOHARA

Department of Pure and Applied Sciences, College of General Education, The University of Tokyo, Komaba, Meguro-ku, Tokyo

(Received October 13, 1967)

Radiation-induced oxidation of cysteine in an acid medium was studied by measuring the hydrogen yields at an initiation stage of radiolysis. In the deaerated system $G(H_2)=4.0$ along with the $G(-CySH)=7.1$ were observed and the results can be interpreted in terms of the yields of primary radicals from the radiolysis of water in 0.8 N sulfuric acid medium. From stoichiometric view point it is predicted that the radiolysis takes place through cysteine radical as intermediate to form cystine. In the aerated system on the other hand, the radiolysis of cysteine is much complicated. For a possible explanation satisfying all the G values obtained, 10.5 in the disappearance of cysteine, 4.0 in the formation of hydrogen peroxide and 0.4 in the hydrogen, the air oxidation of cysteine caused by the radicals, HO_2 and OH which produce H_2O_2 and O_2 by the radical recombination, is proposed as mechanism. The radiolysis of cysteine is greatly reduced by complexation with metallic ion as biscysteinatocobaltate(III) complex. The absence of hydrogen abstraction from cysteine by H atom, the isolation of cysteine from a ligand site and the extraordinary high G values in the disappearance of optical absorption of the complex can be cited as characteristics in the radiolysis of the biscysteinatocobaltate(III) complex. The intramolecular redox of the complex into Co(II) ion and cysteine is a best fit mechanism as over all reaction in the radiolysis of the biscysteinatocobaltate(III) complex.

In the literature so far appeared, the radiolysis of cysteine produces cystine along with some H_2S and alanine with G values around 3,[1-4] depending on the concentration of cysteine as solute. In the presence of dissolved oxygen from air the irradiated cysteine produces sulfate instead of H_2S.[1] A recent paper reported the formation of a lot of sulfur oxyacids and other several compounds as stable products from cystine in the radiolysis of its aerated solution.[5] The disagreement on the stoichiometric balance and therefore, on the resulted mechanism appears likely to be derived from the technique employed by different workers. In their studies secondary reaction intermediates are picked up to account for the radiolysis and make the interpretation rather complicated. One of our principal concerns is the establishment of stoichiometry with the primary reaction between the solute and the primary radicals from the radiolysis of solvent water. As an initiation of radiation-induced oxidation of cysteine an assumption was made of cysteine radicals CyS· as intermediate which was subsequently reformed to cystine as final stable product. In this investigation the cysteine oxidation to cystine at an earlier stage of radiolysis was confirmed by the hydrogen yields

1) A. J. Swallow, *J. Chem. Soc.*, **1952**, 1334.
2) S. L. Whitcher, *Nucleonics*, **11**, No. 8, 30 (1953).
3) P. Markakis and A. L. Tappel, *J. Am. Chem. Soc.*, **82**, 1613 (1960).
4) J. Parker, *J. Chem. Soc.*, **1963**, 2320.
5) J. W. Puradie, *J. Am. Chem. Soc.*, **89**, 226 (1967).

from the cysteine in 0.8 N sulfuric acid under γ irradiation in the presence and absence of dissolved oxygen.

Experimental

Materials. Triply distilled water was used for preparing samples throughout the experiments. Cysteine solution was prepared by dissolving an appropriate quantity of reagent grade cysteine (Wako Pure Chem. Ind. Ltd.) in 0.8 N sulfuric acid for acid medium radiolysis. The complex salt was prepared from cobalt(II) chloride by the method in Schubert's paper.[6] The purification by recrystallization was repeated three times. The analysis provided the composition of the complex together with theoretical values in parentheses: Co, 16.5% (17.6%); H, 4.57% (3.0%); C, 20.98% (21.4%); N, 8.09% (8.35%) corresponding to the formula $CoH(CyS)_2 \cdot 2H_2O$[7] All other reagents used, acids and salts, are of reagent grade.

Irradiation. Sample solutions were saturated with air or flashed with nitrogen in telextube and were irradiated with γ-rays from 60-Co source of one kilo curie facilitated by the Institute of Physical and Chemical Research. Dose rates were measured by Fricke Dosimeter taking the $G_{Fe^{3+}}$ value equal to 15.6, and the molecular extinction coefficient for Fe^{3+} $\varepsilon=2150$ at 304 mμ and 20°C was employed.

Analysis. Decrease of cysteine and increase of cystine in a solution caused by irradiation was determined by the polarographic method described in the published work.[8]

Spectrophotometric and polarographic measurements of biscysteinatocobaltate(III) is effected by the procedure as follows. A solution of 1×10^{-4} M biscysteinatocobaltate(III) was taken as reference and irradiated sample solutions were diluted to a concentration nearly same as above. Photoabsorption maxima of biscysteinatocobaltate(III) lie at the wavelengths of 276, 345 and 430 mμ. By differential spectrum method the decrease of absorption was measured against gamma doses at 276 mμ.

Analysis of Hydrogen and Hydrogen Peroxide. The amount of hydrogen evolved from irradiated liquid sample was determined by gas chromatographic method using a GC-1B type Shimadzu Gas Chromatograph to which a liquid-separating line and a precolumn consisting of Molecular Sieve was attached. A similar method has been reported in detail by one of present authors as well as Swinnerton *et al.*[9,10]

Hydrogen peroxide in the irradiated solutions was colorimetrically determined by titan yellow method known as common usage.

Result

The Yields of Hydrogen from Cysteine. The radiolysis of cysteine proceeds in linear function of absorbed γ dose. The slope of the curve drawn by the plots of the amount of cysteine lost against the received γ dose provides a G value for a given cysteine concentration. The G values thus obtained are dependent on the cysteine concentration, hardly attainable to a maximum value independent of the cysteine concentration. Then, an inverse-plots method is required to find such a maximum G value which is independent of the cysteine concentration. The estimated G values are available for establishing stoichiometric balance relation. Concerning the disappearance yields of cysteine, the G values from our earlier data[7] are represented by the formula in Table 1 as a function of cysteine concentration.

Table 1. G values of cysteine lost
[CySH] designates the concentration of cysteine in M

$G(-\mathrm{CySH})$	O_2 present $\dfrac{10.5}{1+(1/6.2\times10^3[\mathrm{CySH}])}$
$G(-\mathrm{CySH})$	O_2 absent $\dfrac{7.5}{1+(1/2.5\times10^3[\mathrm{CySH}])}$

Figure 1 shows the amount of hydrogen determined by gas chromatographic analysis towards the received γ dose in the radiolysis in the deaerated system. In the deaerated system the maximum $G(H_2)$ was determined at a cysteine concentration higher than 2×10^{-3} M from the curve shown in Fig. 2. In the aerated system, on the other hand, the hydrogen yields were found to be no more than 0.4 over all the range of cysteine concentration.

This means that there is no hydrogen derived from the hydrogen abstraction from cysteine by

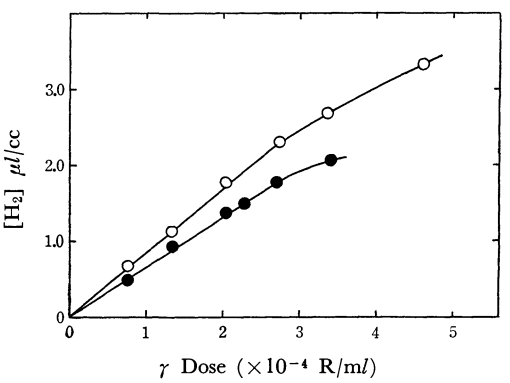

Fig. 1. Hydrogen evolution from deaerated cysteine solution.
Initial concentration of cysteine
○ 200×10^{-3} M, ● 2.00×10^{-4} M

6) M. P. Schubert, *ibid.*, **51**, 3851 (1931).
7) N. Matsuura and K. Muroshima, *Sci. Papers of College of General Education, Univ. Tokyo*, **14**, 197 (1964).
8) N. Matsuura, K. Muroshima and M. Takizawa, *Japan Analyst*, **13**, 324 (1964).
9) J. W. Swinnerton, V. J. Linnenbom and C. H. Cheek, *Anal. Chem.*, **34**, 483 (1962).
10) J. W. Swinnerton, V. J. Linnenbom and C. H. Cheek, *ibid.*, **34**, 1509 (1962).

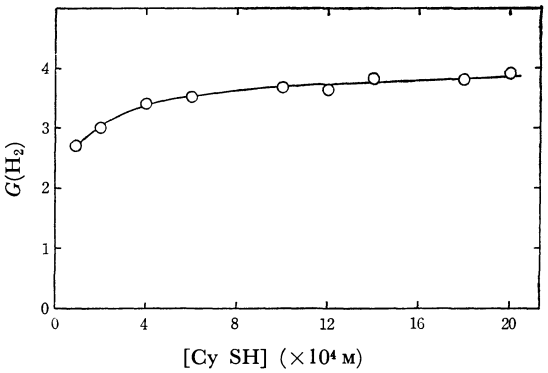

Fig. 2. $G(H_2)$ as function of cysteine concentration in deaerated system.
γ dose: 1.3×10^4 R/m*l*
Dose rate: 4.0×10^4 R/m*l*/hr

H atom and all of produced hydrogen is composed of unscavengeable H atom, whose yield is 0.4 in G value.

The Hydrogen Peroxide Yields in Aerated System. The determination of hydrogen peroxide yields is of much importance for the radiolysis of cysteine in the aerated system. The $G(H_2O_2)$ were 4.0 for the aerated system and 0.0 for the deaerated system. The dependency of the G values on cysteine concentration is illustrated in Fig. 3.

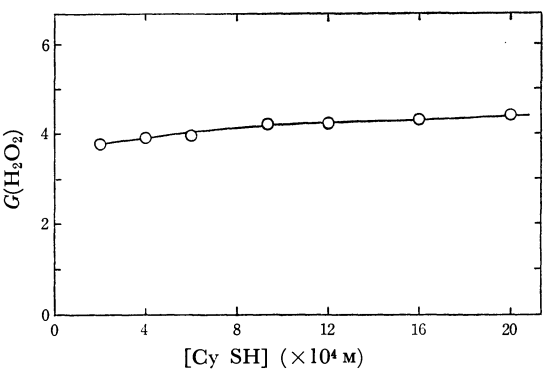

Fig. 3. $G(H_2O_2)$ as function of cysteine concentration (aerated system).
γ dose: 1.3×10^4 R/m*l*

The Hydrogen Yields from Biscysteinatocobaltate(III). The $G(H_2)$ are plotted in Fig. 4 against the concentration of the complex at a given γ dose of 2×10^4 R/m*l* or 1.2×10^{18} eV/m*l*. The observed G values did not exceed 0.4, corresponding to the primary molecular hydrogen yield. This fact suggests the chelated cysteine is no longer so sensitive to γ radiation as free cysteine is, even in deaerated system. In the radiolysis of this complex the G values with respect to the disappearance have been given by the formula in Table 2 established from our earlier data.[7]

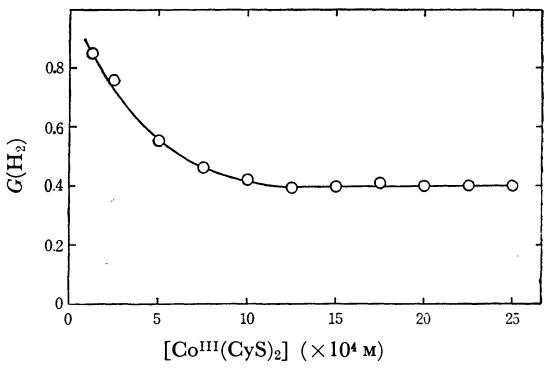

Fig. 4. Variation of $G(H_2)$ with the concentration of $Co^{III}(CyS)_2$ in deaerated system.

TABLE 2. G VALUES OF BISCYSTEINATOCOBALTATE(III) LOST
[$Co^{III}(CyS)_2$] designates the concentration of $Co^{III}(CyS)_2$ in M

$G(-Co^{III}(CyS)_2)$	O_2 present $\dfrac{12}{1+(1/5.5\times10^3[Co^{III}(CyS)_2])}$
$G(-Co^{III}(CyS)_2)$	O_2 absent $\dfrac{13}{1+(1/8.5\times10^3[Co^{III}(CyS)_2])}$

The Yields of Cysteine Liberation. In the radiolysis of biscysteinatocobaltate(III) a break point was observed as shown in Fig. 5A, indicating that there had been a secondary reaction accompanied by the retardation of radiolysis at a critical dose of 2×10^4 R/m*l*. The cause of secondary reaction, occuring in slower rate, could be ascribed to a primary radiolysis product as prohibitor toward the degradation of the complex. The presence of break point suggests that hydrogen abstraction from cysteine as ligand molecule was suppressed by the reduction of cobalt(III) complex to cobalt(II) which resulted in the liberation of

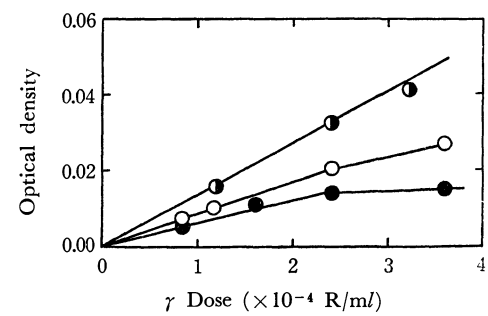

Fig. 5A. Disappearance of $Co^{III}(CyS)_2$ as function of received γ dose.
Initial concentration of $Co^{III}(CyS)_2$
● 1.00×10^{-4} M, ○ 6.00×10^{-4} M,
◑ 1.02×10^{-3} M

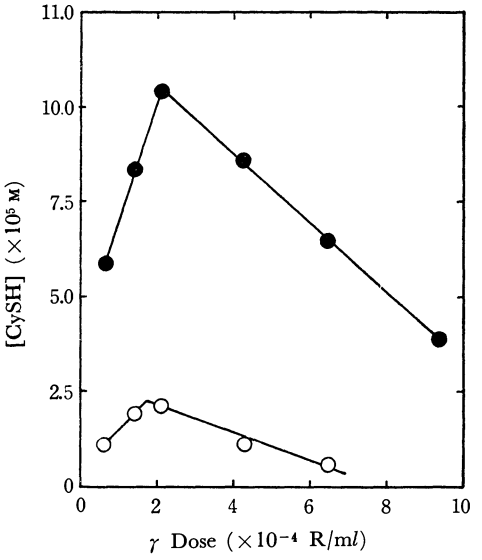

Fig. 5B. Liberation of cysteine from irradiated biscysteinatocobaltate(III) solution.
○ Aerated, ● Deaerated

cysteine from ligand position. The free cysteine thus liberated could be determined polarographically and by PCBM method[11] as function of received γ dose and a maximum yield was found at the corresponding critical dose cited above. The maximum yield of cysteine in the radiolysis of the complex, shown in Fig. 5B, can be accounted for by the loss of cysteine by oxidation after isolation from the complex in concurrence with the increase by isolation.

Discussion

Cysteine is regarded as one equivalent redox reagent when it is converted into cystine by the radiolysis in aqueous phase. If the final oxidation product of cysteine is assumed as cystine alone, so far as an earlier stage of radiolysis is concerned, the G values with regard to cysteine disappearance should be equal to the sum of primary radical yields, g_H+g_{OH}, attaining $3.6+2.9=6.5$ as a maximum G value in the deaerated system. The difference between the theoretical and experimental values, amounting to 1.0, is not small enough to be ignored as an experimental error. However, the observed $G(H_2)$ can account for the initiation of radiolysis by hydrogen abstraction to yield cysteine radical as intermediate product which forms stable cystine under our condition of the radiolysis at high scavenger concentration.

$$CySH + H(\text{or } OH) = CyS\cdot + H_2(\text{or } H_2O) \quad (1)$$

$$CyS\cdot + CyS\cdot = CyS : SCy \text{ (cystine)} \quad (2)$$

From Eqs. (1) and (2) the $G(H_2)$ is just equal to the sum $g_H+g_{H_2}=3.6+0.4=4.0$ in good agreement with the value experimentally found. The radiolysis in deaerated system gave no hydrogen peroxide which might be responsible to the shortage of the G value 1.0 as stated above. Since hydrogen peroxide is inert against cysteine because of its slow reaction rate, the oxidation of cysteine by hydrogen peroxide must be induced by the radiolysis through a certain reactive intermediate, like a cysteine radical. Nevertheless, a presumed value of $g_H+g_{OH}+2g_{H_2O_2}=3.6+2.9+1.6=8.4$ based on the two equivalent oxidation of H_2O_2 is too large to explain the experimental G value of 7.5.

As for the aerated system the stoichiometric relation is much more complicated, probably because of the dissolved oxygen taking part in the radiolysis of cysteine by the formation of some radical intermediate like a $CySO_2\cdot$ radical. In the aerated system the maximum G values were 10.5 with the $G(-CySH)$, 4.0 with the $G(H_2O_2)$ and 0.4 with $G(H_2)$. For possible explanation satisfying all these G values the schema (3) and (4), has to be introduced.

$$2CySH + HO_2(H+O_2) = CyS : SCy + \tfrac{1}{2}H_2O_2 + H_2O \quad (3)$$

$$2CySH + 2OH + \tfrac{1}{2}O_2 = CyS : SCy + H_2O_2 + H_2O \quad (4)$$

Under the assumption made for the schema (3) and (4) the stoichiometric balance between G values is quite self-consistent, because $G(-CySH)=2g_H+g_{OH}=2\times 3.6+2.9=10.1$, $G(H_2O_2)=(1/2)g_H+(1/2)\,g_{OH}+g_{H_2O_2}=4.1$ and $G(H_2)=g_{H_2}=0.4$. It is interesting to indicate that the reaction schema described in (3) and (4) are nothing but the recombination of radicals HO_2 and OH to H_2O_2 in the presence of cysteine as solute and the oxidation of cysteine by air oxygen induced by radiolysis.

The radiolysis of biscysteinatocobaltate(III) shows several characteristic features: the absence of hydrogen abstraction, the liberation of free cysteine from a ligand position and the high G value, 12—13, with regard to the disappearance of the complex. The latter yields are approximately twice as large as the sum of the primary radical yields $g_H+g_{OH}=6.5$. These facts could be interpreted in terms of the inner sphere reduction of the complex from Co(III) to Co(II) due to radicals H and OH.[13]

$$2Co^{III}(CyS)_2^- \xrightarrow{H,\ OH} 2Co^{2+} + 2CySH + CyS{:}SCy + H_2O \quad (5)$$

11) P. B. Boyer, *J. Am. Chem. Soc.*, **76**, 4331 (1954).

12) M. Haissinsky and M. Magat (edt.) Tables of selected Constants Radiolytic Yields, Pergamon (1963).

13) N. Matsuura, M. Muroshima and M. Takizawa, *Nippon Kagaku Zasshi (J. Chem. Soc. Japan, Pure Chem. Sect.)*, **85**, 268 (1964).

The reaction (5) is based on the one molecule cysteine liberation per one molecule of the complex lost at an earlier stage of radiolysis with a dose below the critical value of 2×10^4 R/m*l*. It is indicated that the overall reaction (5) is nothing but an intramolecular redox of the complex caused by the radicals.

Generally speaking, so far as maximum G values are concerned or secondary reactions are excluded that might occur between free radicals and an intermediate product of radiolysis, a quantitative stoichiometric balance holds well. As initiation of radiolysis in the system of cysteine or metal-cysteine complex, the major product is likely the cystine produced by the recombination of cysteine radical CyS. Namiki *et al.*[14] have evidenced a stationary mixture of cysteine and cystine in equilibrium attained by the radiolysis of either cysteine or cystine used as starting solute. A number of products different from cystine reported by several workers could be ascribed to the results involving secondary reaction products in a large γ-dose region.

The authors extend their thanks for the financial aid from the Radiation Research Funds defrayed by the Ministry of Education, Japan.

14) M. Namiki, The 9th Symposium on Radiation Chemistry (Osaka, Japan, 1966).

BULLETIN OF THE CHEMICAL SOCIETY OF JAPAN VOL. 41 892—896 (1968)

Crystalline Complexes of Allylamine and Propylamine with Copper(I) Chloride and Bromide

Tetsuya OGURA, Takeshi HAMACHI and Shinichi KAWAGUCHI

Department of Chemistry, Faculty of Science, Osaka City University, Sumiyoshiku, Osaka

(Received November 21, 1967)

Crystalline 1 : 1 and 1 : 3 complexes of allylamine and propylamine with copper(I) chloride and bromide were synthesized *in vacuo*. Equilibrium vapor pressures of these complexes were measured at several temperatures and the enthalpy of ligation of each amine molecule was determined. Both the thermochemical and infrared absorption data indicate that in the 1 : 1 complexes of allylamine the ligand molecule serves as a bidentate, but in the 1 : 3 complexes the second and third ligand molecules link to the metal only through the amino nitrogen atom.

The ability of simple aliphatic amines to form metal coordination compounds have been examined and found to decrease in the series[1] $NH_3 > RNH_2 > R_2NH > R_3N$. Recently Yoke and his collaborators reported copper(I) chloride complexes of triethylamine,[2] diethylamine[3] and ethylamine.[4] However, the unsaturated amine such as allylamine has not yet been employed as the coordinating ligand. In this paper we report crystalline complexes of copper(I) chloride and bromide with allylamine and propylamine which were synthesized by the same method as that previously adopted in the syntheses of copper(I) chloride complexes of acrolein[5] and allyl alcohol.[6]

Experimental

Materials. Copper(I) chloride and bromide were prepared by the ordinary method[5] and purified by the distillation *in vacuo*. Allylamine (abbreviated as am in this paper), $CH_2=CHCH_2NH_2$, and propylamine (abbreviated as pm) were dried with Molecular Sieves Type 3A, Linde Co. and the freshly distilled sample was used in each experiment.

Syntheses of Copper(I) Halide - Amine Complexes with the Mole Ratio of One to Three. Allylamine or propylamine (10—15 g) was distilled into an ampoule containing pulverized copper(I) chloride or bromide (1g). In each case the exothermic reaction occurred and colorless, transparent and bulky crystals grew up on copper(I) halide powder. The reaction

1) J. C. Bailar, Jr., and D. H. Busch, "The Chemistry of the Coordination Compounds," ed. by J. C. Bailar, Jr., Reinhold Publishing Co., New York, N. Y. (1956), p. 62; W. E. Hatfield and J. T. Yoke, III, *Inorg. Chem.*, **1**, 463 (1962).
2) J. T. Yoke, III, J. F. Weiss and G. Tollin, *Inorg. Chem.*, **2**, 1210 (1963).
3) J. R. Clifton and J. T. Yoke, III, *ibid.*, **5**, 1630 (1966).
4) J. R. Clifton and J. T. Yoke, III, *ibid.*, **6**, 1258 (1967).
5) S. Kawaguchi and T. Ogura, *ibid.*, **5**, 844 (1966).
6) T. Ogura, N. Furuno and S. Kawaguchi, This Bulletin, **40**, 1171 (1967).

mixture was kept standing overnight to complete the reaction, and the excess amine was then distilled back to the original ampoule. The copper(I) complex was dried completely without decomposition by keeping the two ampoules at 5 and 0°C respectively for 50 hr. The analytical data of four kinds of complexes thus prepared are as follows:

Found: Cu, 23.2; Cl, 13.1%. Calcd for $CuCl(C_3H_7N)_3$: Cu, 23.5; Cl, 13.1%.

Found: Cu, 20.1; Br, 25.2%. Calcd for $CuBr(C_3H_7N)_3$: Cu, 20.2; Br, 25.4%.

Found: Cu, 22.8; Cl, 13.0%. Calcd for $CuCl(C_3H_9N)_3$: Cu, 23.0; Cl, 12.8%.

Found: Cu, 19.3; Br, 24.5%. Calcd for $CuBr(C_3H_9N)_3$: Cu, 19.8; Br, 24.9%.

Syntheses of Copper(I) Halide-Amine Complexes with the Mole Ratio of One to One. The ampoule containing a copper(I) halide-amine complex with the mole ratio of one to three was kept at room temperature around 20°C and another empty one at 0°C which had been connected with each other and evacuated. The complex decomposed partially and expelled about two moles of amine per mole complex during standing overnight. The amine vessel was cooled with liquid nitrogen for further 24 hr and exactly two moles of amine was recovered. The copper(I) amine complexes prepared in this way showed the following analytical data.

Found: Cu, 40.1; Cl, 22.8% mp around 100°C. Calcd for $CuCl(C_3H_7N)$: Cu, 40.7; Cl, 22.7%.

Found: Cu, 31.8; Br, 39.8%; mp around 100°C. Calcd for $CuBr(C_3H_7N)$: Cu, 31.7; Br, 39.9%.

Found: Cu, 39.3; Cl, 22.6%; mp 22°C. Calcd for $CuCl(C_3H_9N)$: Cu, 40.1; Cl, 22.4%.

Found: Cu, 31.3; Br, 39.7%; mp 75°C. Calcd for $CuBr(C_3H_9N)$: Cu, 31.4; Br, 39.5%.

These copper(I) halide-amine complexes are all stable at room temperature. When they were heated to higher temperatures, 80—90% amine was recovered, but the quantitative dissociation could not be attained.

For comparison, copper(I) chloride complexes of deuterated amines, $CuCl(C_3H_5ND_2)$ and $CuCl(C_3H_7ND_2)$ were also prepared in the following way. Allylamine or propylamine (0.3 g) was distilled into heavy water (5 g) whose deuterium content was 99.8%. The solution was then distilled into an ampoule containing copper(I) chloride (0.2 g) and kept standing overnight. The complex was then dried at a temperature difference of room and dry ice temperatures as described above.

Vapor Pressure Measurement. The dried crystalline complex was prepared in an ampoule connected with a U-type mercury manometer. The equilibrium vapor pressure was measured at various temperatures by keeping the sample tube in appropriate thermostat baths.

Infrared Spectra. The infrared absorption spectra were measured with a Hitachi infrared spectrophotometer, EPI-2. The amine complex with the mole ratio of one to three is unstable and the crystalline specimen was mixed with Nujol and ground down quickly in a nitrogen atmosphere.

Results

Copper(I) halide complexes of allylamine and propylamine with the mole ratio of one to three are all colorless and transparent crystals, showing no difference in appearance. These compounds have appreciable vapor pressures and decompose spontaneously in an open atmosphere resulting in the complexes with the metal-ligand mole ratio of one to one. They are also very sensitive to air and change to deep blue color characteristic of the copper(II) amine complex.

Table 1. The vapor pressure data of the copper(I) halide complexes of allylamine and propylamine with the mole ratio of one to three

$CuCl(am)_3$	t, °C	5.4	9.6	20.7	28.1	
	P, cmHg	1.655	2.405	6.360	11.525	
	t, °C (calc)*	5.4	9.5	20.7	28.1	
	$\log P$ (cmHg) $= 11.401 - 3.115 \times 10^3/T$					(3)
$CuBr(am)_3$	t, °C	0	5.2	11.0	18.0	24.5
	P, cmHg	1.000	1.599	2.730	5.015	8.804
	t, °C (calc)*	0.1	5.1	10.9	17.9	24.6
	$\log P$ (cmHg) $= 11.488 - 3.140 \times 10^3/T$					(4)
$CuCl(pm)_3$	t, °C	0	5.2	11.0	19.0	25.2
	P, cmHg	1.956	2.950	4.653	8.853	13.450
	t, °C (calc)*	0.1	5.1	10.8	19.3	25.1
	$\log P$ (cmHg) $= 10.292 - 2.734 \times 10^3/T$					(5)
$CuBr(pm)_3$	t, °C	0	5.2	10.9	14.4	20.6
	P, cmHg	3.432	4.763	6.978	8.849	12.920
	t, °C (calc)*	0.2	5.0	10.8	14.5	20.6
	$\log P$ (cmHg) $= 8.815 - 2.264 \times 10^3/T$					(6)
Allylamine	t, °C	0	5.4	9.8	21.2	29.0
	P, cmHg	7.530	9.880	12.240	21.150	29.385
	t, °C (calc)*	−0.1	5.6	9.9	21.3	28.8
	$\log P$ (cmHg) $= 7.180 - 1.725 \times 10^3/T$					(7)

* Calculated by means of each equation (3)—(7), respectively.

TABLE 2. THE VAPOR PRESSURE DATA OF THE COPPER(I) HALIDE COMPLEXES OF ALLYLAMINE AND PROPYLAMINE WITH THE MOLE RATIO OF ONE TO ONE

CuCl(am)	t, °C	107.0	112.9	119.3	124.5		
	P, cmHg	0.228	0.315	0.636	0.939		
	t, °C	107.8	111.5	119.8	124.7		
	$\log P$ (cmHg) $= 13.838 - 5.517 \times 10^3/T$						(8)
CuBr(am)	t, °C	95.1	104.8	114.6	124.6		
	P, cmHg	0.117	0.235	0.639	1.507		
	t, °C*	95.9	103.4	114.7	124.9		
	$\log P$ (cmHg) $= 14.281 - 5.615 \times 10^3/T$						(9)
CuCl(pm)	t, °C	84.9	95.1	104.8	114.6	124.6	
	P, cmHg	0.624	0.988	1.661	2.772	4.554	
	t, °C*	85.9	94.2	104.2	114.2	125.0	
	$\log P$ (cmHg) $= 8.134 - 3.154 \times 10^3/T$						(10)
CuBr(pm)	t, °C	82.3	90.8	101.0	109.6	119.6	125.0
	P, cmHg	0.734	1.192	2.048	3.142	4.953	6.200
	t, °C*	82.1	90.9	100.9	110.0	119.7	124.7
	$\log P$ (cmHg) $= 8.530 - 3.079 \times 10^3/T$						(11)

* Calculated by means of each equation (8)—(11), respectively.

On the other hand copper(I) halide complexes of these amines with the mole ratio of one to one are fairly stable against air or heat just as the monoammine adduct of copper(I) chloride is.

The Vapor Pressure Data. The equilibrium vapor pressure of the copper(I) halide-amine system was determined at various compositions and the following two equilibria were found to exist:

$$CuX + RNH_2 = CuX(RNH_2) \quad (1)$$

$$\tfrac{1}{2}CuX(RNH_2) + RNH_2 = \tfrac{1}{2}CuX(RNH_2)_3 \quad (2)$$

where X represents Cl or Br, and R stands for C_3H_5 or C_3H_7. However, the copper(I) complex of the composition, $CuX(RNH_2)_2$ or $CuX(RNH_2)_{1.5}$ was not identified.

The equilibrium dissociation pressure of the copper(I) halide complexes of allylamine and propylamine with the mole ratio of one to three was determined at various temperatures. The results obtained are shown in Table 1 and represented by Eqs. (3) through (6).

The vapor pressure of the copper(I) halide-amine complexes with the 1 : 1 composition was lower and determined at temperatures higher than 100°C. The results are listed in Table 2 and reproduced by Eqs. (8) through (11). However, data for allylamine complexes might be less reliable than those for the above 1 : 3 complexes, since some kind of chemical change of the ligated allylamine (possibly disproportionation to ammonia and diallylamine or triallylamine) was noticed to occur when the complex was maintained at temperatures higher than 130°C for several days.

From Eqs. (3) through (11) the heat of formation of each complex referring to Eqs. (1) and (2) was calculated and listed in Table 3. The vapor pressure data of allylamine were not available in literature and determined for the specimen which had been specially purified by formation and decomposition of copper(I) chloride complex with the mole ratio of one to three. The results obtained are represented by Eq. (7) in Table 2. The boiling point of allylamine calculated by means of Eq. (7) is 54.8°C which coincides fairly well with the literature value[7] of 55—58°C. As the heat of vaporization of propylamine the value of 7.3 kcal·mol^{-1} due to Stull[8] was used for calculation in Table 3.

TABLE 3. THE CONSECUTIVE ENTHALPY OF FORMATION OF COPPER(I) HALIDE COMPLEXES OF ALLYLAMINE AND PROPYLAMINE CALCULATED FOR ONE MOLE OF GASEOUS AMINE*

Compound	ΔH kcal·mol^{-1}	Compound	ΔH kcal·mol^{-1}
CuCl(am)	−25.2 (−17.3)	$CuCl(am)_3$	−13.9 (−6.0)
CuBr(am)	−25.7 (−17.8)	$CuBr(am)_3$	−14.3 (−6.4)
CuCl(pm)	−14.4 (−7.1)	$CuCl(pm)_3$	−12.5 (−5.2)
CuBr(pm)	−14.1 (−6.8)	$CuBr(pm)_3$	−10.4 (−3.1)

* The value in a bracket refers to the enthalpy of formation from the liquid amine.

Infrared Spectra. The infrared spectra of these complexes are very complicated in comparison with those of free amines. Several characteristic absorption bands due to NH_2 group were assigned on the observation of their shifts by the deuteration. They are listed in Table 4 together with the stretching frequency of the double bond of allylamine.

7) "The Merck Index of Chemicals and Drugs," 7th ed., Merck Co., Inc., Rahway, New Jersey (1960), p. 36.

8) D. R. Stull, *Ind. Eng. Chem.*, **39**, 517 (1947).

Table 4. The infrared absorption bands (cm^{-1}) due to the amine group and double bond in the copper(I) halide complexes of allylamine and propylamine

Compound	$\nu(NH_2)$		$\delta(NH_2)$		$\nu(C=C)$
$C_3H_5NH_2$	3400	3310	1615	820	1645
$CuCl(C_3H_5NH_2)$	3240	3160	1605	630	1535
$CuCl(C_3H_5ND_2)$	2440	2380	1175		1535
$CuBr(C_3H_5NH_2)$	3260	3150	1580	610	1535
$CuCl(C_3H_5NH_2)_3$	3240	3160	1590	660	1645, 1535
$CuBr(C_3H_5NH_2)_3$	3240	3130	1590	610, 675	1645, 1535
$C_3H_7NH_2$	3390	3310	1615	810	
$CuCl(C_3H_7NH_2)$	3215	3135	1585	635	
$CuCl(C_3H_7ND_2)$	2430	2380	1180		
$CuBr(C_3H_7NH_2)$	3220	3140	1570	620	
$CuCl(C_3H_7NH_2)_3$	3220	3120	1585	625, 665	
$CuBr(C_3H_7NH_2)_3$	3220	3140	1570	620	

Propylamine has no way of coordination to the metal other than *via* nitrogen atom, and the remarkable shifts of the stretching and deformation frequencies of the NH_2 group by ligation indicate that this is the case. Allylamine, on the other hand, may be linked to copper(I) either by nitrogen atom or by the double bond. As shown in Table 4 coordinated allylamine shows similar shifts of $\nu(NH_2)$ and $\delta(NH_2)$ to the lower frequency side as propylamine does. This suggests that nitrogen atom of every allylamine molecule is used in bonding to copper(I). The stretching frequency of the double bond of allylamine in the 1 : 1 complex is lower by 110 cm^{-1} than that of the free amine. However, two peaks are observed at 1645 and 1535 cm^{-1} for the 1 : 3 complex, corresponding to the free and ligated double bond, respectively.

These results indicate that in the 1 : 1 complex every allylamine molecule is coordinated to copper(I) by both double bond and amine group, while in the 1 : 3 complex two kinds of allylamine molecules are contained, one acting as a bidentate and the other as a unidentate ligand which is linked solely by the amine group.

Discussion

Wilkins and Burkin[9] investigated the reactions of copper(I) halides with long-chain aliphatic amines such as *n*-octyl-, *n*-dodecyl- with *n*-octadecylamines, and identified $[CuBr(RNH_2)_2]_2$ and $[CuX(RNH_2)]_4$ where X is Cl, Br or I. Triethylamine was reported to form 1 : 1 complexes with copper(I) halides,[2] and diethylamine to form both 1 : 1 (tetrameric) and 1 : 2 (dimeric) complexes with copper(I) chloride. In the system of copper(I) chloride - ethylamine 1 : 1 and 1 : 2 complexes were isolated and 1 : 3 complex was noticed in the isothermal phase study at 0°C. In the present case 1 : 1 and 1 : 3 complexes were obtained for the copper(I) halides and allylamine or propylamine systems, but no indication of 1 : 2 complexes was observed.

As shown in Table 3 the enthalpy of formation of the 1 : 1 complex from solid copper(I) halide and liquid propylamine was determined as −7.1 kcal·mol^{-1} for the chloride complex and −6.8 kcal·mol^{-1} for the bromide complex, but the enthalpy of ligation of the second and third molecule of propylamine is −5.2 and −3.1 kcal·mol^{-1}, respectively. It is quite reasonable that the first ligand molecule coordinates to the metal atom more exothermically than the second or third one since more or less negative charge is brought in around the central metal by the ligand molecule. The fact is noticed that the heat evolved by ligation of propylamine to copper(I) bromide is a little less than that for copper(I) chloride. Bromine may make a more covalent bond and bring larger negative charge around the central metal than chlorine does, reducing the bond strength between copper(I) and the hard amine ligand.

The enthalpy of formation of $CuI(NEt_3)$ from CuI(s) and triethylamine(*l*) was reported[2] as −8.21 kcal·mol^{-1}, and ΔH for the second molecule of diethylamine(*l*)[3] and ethylamine(*l*)[4] ligating to each 1 : 1 copper(I) chloride complex was estimated as −7.8 and −6.65 kcal·mol^{-1}, respectively. These data together with our present ones indicate the possible region of values for the enthalpy of ligation of aliphatic amines to copper(I) halide. The observed values of ΔH for the second and third molecule of allylamine ligating to copper(I) chloride and bromide lie in this probable region suggesting that the ligand molecule in question coordinates to copper(I) through the amine group.

However, ΔH for the ligation of the first molecule of allylamine to copper(I) chloride or bromide is much more negative, and even more negative than those for other vinyl complexes as summarized in Table 5. This clearly indicates that the first

9) R. G. Wilkins and A. R. Burkin, *J. Chem. Soc.*, **1950**, 127.

molecule of allylamine coordinates to copper(I) atom with both the amino nitrogen atom and π-electrons of the double bond. In the case of allylamine ΔH's for copper(I) bromide are a little more negative than those for the chloride in contrast to the case of propylamine complexes. The softness of bromine in comparison with chlorine may enhance the bonding between copper(I) and the C=C double bond in which the contribution of back donation from metal to ligand is significant.

TABLE 5. THE ENTHALPY OF FORMATION OF 1:1 COPPER(I) CHLORIDE COMPLEX WITH SEVERAL VINYL COMPOUNDS AND THB SHIFT OF C=C STRETCHING FREQUENCY

Compound	$-\Delta H$ kcal·mol^{-1}	$\Delta\nu$(C=C) cm^{-1}	Ref.
CH_2=CH-CHO	11.8	90	5
CH_2=CH-CH_2OH	12.0	95	6
CH_2=CH-CN	14.9	100	10
CH_2=CH-CH_2NH_2	25.2	110	this study

The conclusion that in the tris(allylamine)-copper(I) complexes one ligand molecule coordinates to the metal with both nitrogen atom and the double bond but the second and third molecules only with nitrogen, is also supported by the infrared absorption data as mentioned already. Copper(I) usually prefers the coordination number four. If one of three molecules of allylamine is serving as a bidentate ligand, the 1 : 3 copper(I) halide complexes must be salts keeping the halide as outer-sphere anions. Some extensive studies such as the conductivity measurement of copper(I) halides in allylamine are desired but have not yet been performed.

There are summarized in Table 5 the enthalpy of formation of 1 : 1 copper(I) chloride complexes with several vinyl compounds together with the associated shift of C=C stretching frequency. A remarkable correspondence is noticed between these two properties. The X-ray analysis of the copper(I) chloride complex of acrolein revealed that each acrolein molecule is assuming the s-trans configuration and acting as a bridging ligand between two copper atoms.[11] On the other hand the allyl alcohol complex seems to exist as a dimer[12] with the chloride double bridge, the alcohol molecule acting as a chelating agent. In the present case the molecular weight of the 1 : 1 complex of copper halide with allylamine has not been determined owing to the lack of any suitable solvents, but it might be presumed by analogy with the allyl alcohol complex to exist as a dimer. Further information concerning the real structure must be offered by the X-ray analysis of this compound.

10) G. N. Schrauzer, *Chem. Ber.*, **94**, 1891 (1961).
11) Y. Kushi, T. Ogura, S. Kawaguchi and H. Kuroya, Presented at the 20th Annual Meeting of the Chemical Society of Japan, Tokyo, April, 1967.
12) In a previous paper (Ref. 6) copper(I) chloride was reported to exist as a monomer in boiling allyl alcohol, but further detailed measurements revealed that this rather preliminary observation was wrong. Copper(I) chloride exists as a dimer in allyl alcohol even at the boiling point just as at lower temperature.

BULLETIN OF THE CHEMICAL SOCIETY OF JAPAN VOL. 41 897—903 (1968)

A Kinetic Study of the Free-Radical Bulk Polymerization of Ethylene

Sueo MACHI, Takashi SAKAI, Fujio SUGANUMA and Tsutomu KAGIYA

Japan Atomic Energy Research Institute, Takasaki Radiation Chemistry Research Establishment, Takasaki, Gunma

(Received January 16, 1967)

The bulk polymerization of ethylene was carried out under mild conditions, *i. e.*, pressures of from 183 to 400 kg/cm^2 and temperatures of from 30 to 140°C, using azobisisobutyronitrile as an initiator. In polymerization at the low temperature of 40°C, both the polymerization rate and the molecular weight of the polymer formed increased with the reaction time. At the above temperature, the polymerization rate was shown to be proportional to the amount of initiator, and the molecular weight was found to be independent of it. Furthermore, both the polymerization rate and molecular weight were found to be proportional to the 2.5th power of ethylene fugacity. The dependencies of the polymerization rate and the molecular weight on the reaction time decrease with the rise in reaction temperatures from 30 to 100°C. A kinetical discussion indicated that the rate of termination is almost zero at 30—40°C, but that it increases with the temperature. The polymerization rate and the molecular weight were shown to be proportional to the 0.8 and 0.2th powers of the amount of the initiator. The activation energy of the initiation reaction was evaluated to be *ca.* 27 kcal/mol.

The free-radical polymerization of ethylene has usually been investigated under severe reaction conditions, such as high pressures from 800 to 2000 kg/cm^2 and high temperatures from 130 to 250°C.[1-5] Such conditions are also used in the industrial process. Recently, however, a few studies have been conducted under milder conditions, namely, under lower pressures and at lower temperatures.[6,7] The possibility of the existence of a long-lived polymer radical was first pointed out briefly by Buchdahl[8] in his discussion of the paper by Laird *et al.*[2] Lyubetzky *et al.*[7] studied the polymerization of ethylene at 70°C with azobisisobutyronitrile (AIBN) in benzene, and pointed out that the propagation reaction occurs with the living polymer radical in the polymer crystalline phase.

We have reported several characteristics of the low temperature free-radical bulk polymerization of ethylene in a previous paper.[9] This paper, a continuation of that earlier paper, will be concerned with the kinetic study of ethylene polymerization in bulk with AIBN, at temperatures of from 30 to 140°C and at pressures of from 100 to 400 kg/cm^2.

Experimental

Polymerization was carried out in a static, unstirred, stainless-steel (SUS-27) high-pressure vessel with a capacity of 100 m*l*. After the desired amount of crystalline AIBN had been introduced, the vessel was flushed out six times with ethylene (10 kg/cm^2). The vessel was then cooled in a methanol-dry ice bath, ethylene being introduced from a reservoir. The vessel was warmed to the desired reaction temperature, and a very small amount of ethylene was released from the vessel to adjust the reaction pressure. Since the polymerization was carried out to a low conversion, the pressure, which was measured by a Bourdon tube gauge, was almost constant throughout the reaction. A temperature constant within ±1°C was also maintained by an automatic controller. At the end of the reaction, the unpolymerized ethylene was purged and the vessel was opened. After the unchanged initiator had been extracted by using boiling acetone, the polymer yield was determined.

The ethylene used had been commercially obtained and was 99.9% pure (free of CO and H_2S), containing 21 ppm acetylene and 0.3 ppm oxygen. The density and fugacity of ethylene at a given pressure and temperature were known from Benzler's pressure-enthalpy diagram.[10] AIBN was purified by recrystallization

1) S. Kodama, I. Taniguchi, S. Yuasa, T. Ota and Y. Terada, *Kogyo Kagaku Zassi (J. Chem. Soc. Japan, Ind. Chem. Sect.)*, **57**, 439 (1954).
2) R. K. Laird, A. G. Morrell and L. Seed, *Discussions Faraday Soc.*, **22**, 126 (1956).
3) S. Kodama, Y. Matsushima, A. Ueyoshi, T. Shimidzu, T. Kagiya and K. Fukui, *J. Polymer Sci.*, **41**, 83 (1959).
4) R. O. Symcox and P. Ehrlich, *J. Am. Chem. Soc.*, **84**, 531 (1962).
5) R. H. Bretton and B. F. Dodge, *Chem. Eng. Progr.*, **58** (No. 8), 50 (1962).
6) H. N. Friedlander, *J. Polymer Sci.*, **58**, 455 (1962).
7) B. L. Erussalimsky, S. G. Lyubetzky, W. W. Mazurek, S. Ya. Frenkel and L. G. Shaltyko, *Polymer*, **3**, 639 (1962).
8) R. Buchdahl, *Discussions Faraday Soc.*, **22**, 150 (1956).
9) S. Machi, T. Sakai, M. Gotoda and T. Kagiya, *J. Polymer Sci.*, **B3**, 709 (1965).
10) H. Benzler and A. V. Koch, *Chem. Ingr. Tech.*, **27**, (No. 2), 71 (1955).

from acetone. The molecular weight of the polymer was determined from its intrinsic viscosity in tetralin at 130°C. Tung's formula[11] was used in the calculation of the molecular weight, because the polymer has little branching, like a low-pressure polyethylene.[9]

Results and Discussion

Polymerization at a Low Temperature. The experimental results are summarized in Table 1.

Figure 1 shows the changes in the polymer yield (*i. e.*, the amount of polymerized monomer) and the molecular weight with the reaction time. The polymer yield is found to be proportional to the second power of the time, and the molecular weight, to the first power. The polymerization rate and molecular weight increase with the time. Similar features have been found as distinct characteristics in the low temperature bulk polymerization of ethylene induced by radiation.[12,13] These facts suggest that the rate of termination is very small. The polymer radical, therefore, accumulates as AIBN decomposes to radicals, and the rate of polymerization increases. The steady increase in the molecular weight suggests that the rates of both termination and transfer are very small.

TABLE 1. RESULTS OF THE POLYMERIZATION AT 40°C

Ethylene pressure kg/cm²	Amount of AIBN mmol	Reaction time hr	Polymer yield g	Molecular weight $\overline{M}_n \times 10^{-4}$
400	0.980	1.5	0.24	11.3
		2.0	0.32	13.9
		3.0	0.76	23.7
		4.0	1.35	31.6
183	0.421	4.0	0.11	6.5
210			0.15	9.1
240			0.19	11.9
400			0.54	32.0
400	0.140	4.0	0.20	31.4
	0.412		0.54	32.0
	0.700		0.94	31.4
	0.980		1.35	31.6

Volume of reaction vessel, 100 m*l*

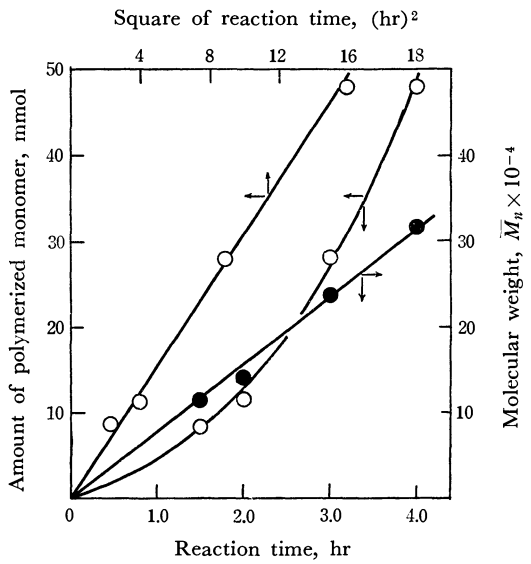

Fig. 1. Amount of polymerized monomer and polymer molecular weight *vs.* reaction time.
(Reaction conditions: temperature, 40°C; pressure, 400 kg/cm²; AIBN, 0.98 mmol)

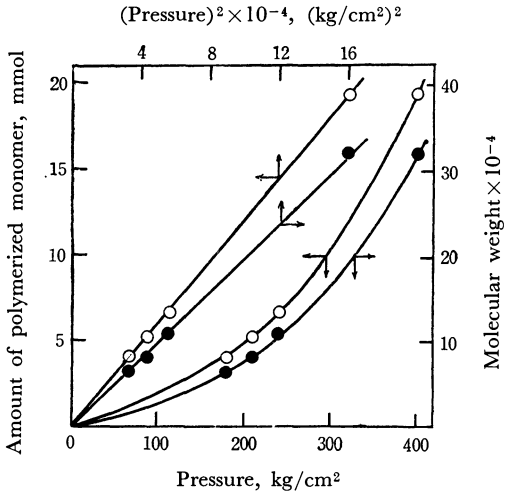

Fig. 2. Amount of polymerized monomer and polymer molecular weight *vs.* reaction pressure.
(Reaction conditions: temperature, 40°C; AIBN, 0.42 mmol; time, 4.0 hr)

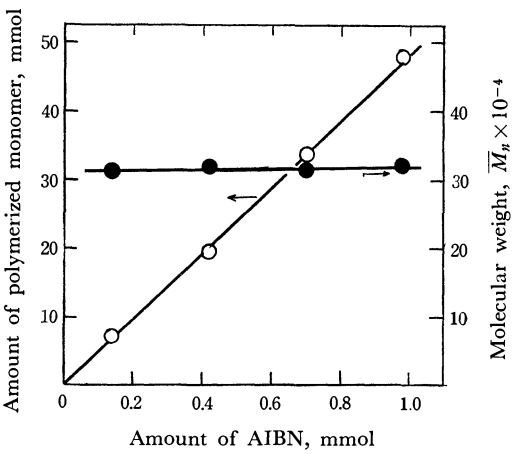

Fig. 3. Amount of polymerized monomer and polymer molecular weight *vs.* amount of initiator.
(Reaction conditions: temperature, 40°C; pressure, 400 kg/cm²; time, 4.0 hr)

11) L. H. Tung, *J. Polymer Sci.*, **24**, 333 (1957).

12) S. Machi, M. Hagiwara, M. Gotoda and T. Kagiya, This Bulletin **39**, 675 (1966).

13) S. Machi, M. Hagiwara, M. Gotoda and T. Kagiya, *J. Polymer Sci.*, **A-1**, **4**, 1517 (1966).

Figure 2 shows the effects of the ethylene pressure on the polymer yield and the molecular weight. Both the molecular weight and polymer yield increase rapidly with the ethylene pressure at a constant time. Their pressure exponents are found to be approximately two.

Figure 3 shows the influence of the amount of the initiator; the figure indicates that the polymer yield at a constant time is proportional to the number of moles of initiator added, and that the molecular weight of the polymer is independent of it. These facts are in contrast to the dependencies of the rate and molecular weight on the amount of the initiator in a polymerization where rapid bimolecular termination occurs.

The polymerization is considered to consist of the following steps:

Initiation

Decomposition of initiator $\quad I \xrightarrow{k_d} 2R\cdot \quad (1)$

Addition of a monomer $\quad R\cdot + M \xrightarrow{k_a} RM_1\cdot \quad (2)$

Propagation $\quad RM_1\cdot + M \xrightarrow{k_p} RM_2\cdot \quad (3)$

$\quad \vdots \quad \vdots \quad \vdots$

$\quad RM_{n-1}\cdot + M \xrightarrow{k_p} RM_n\cdot \quad (4)$

Transfer $\quad RM_n\cdot + Y \xrightarrow{k_{tr}} P_n + Y\cdot \quad (5)$

Termination $\quad RM_n\cdot + Z \xrightarrow{k_{t_1}} P_n \quad (6)$

$\quad RM_m\cdot + RM_n\cdot \xrightarrow{k_{t_2}} P_{m+n} \quad (7)$

The initiation step consists of two reactions, *i. e.*, the decomposition of the initiator, I, into free radicals, R·, and the addition of a monomer to form radicals, $RM_1\cdot$. Since the decomposition of AIBN has been shown to proceed *via* a first-order reaction independent of the reaction media, such as various organic solvents,[14,15] an aqueous solution of dioxane[16] and water[17] where AIBN is not soluble, a first-order decomposition is assumed in this system in the absence of a solvent. Thus, the rate of the primary radical formation at time t is:

$$d[R\cdot]/dt = 2k_dI_0 \exp(-k_dt) \quad (8)$$

where k_d represents the rate constant of the decomposition of the initiator, and where I_0 is the amount of the initiator at the initial stage. Some fraction of the primary radicals may initiate chains according to Eq. (2), and the other fraction tends to disappear through other reactions. The rate of the initiation of chain radicals is, therefore, given by:

$$R_i = d[RM_1\cdot]/dt = 2fk_dI_0\exp(-k_dt) \quad (9)$$

where f is the fraction of the radicals initiating polymerization chains, the so-called radical yield. Since the number of moles of polymer chains formed at a constant reaction time is independent of the ethylene pressure, as will be described below, the f fraction is not dependent on the monomer concentration.

At a low temperature of 40°C and at the initial stage, since the value of k_dt is much smaller than unity, R_i is approximately expressed as:

$$R_i = 2fk_dI_0 \quad (10)$$

Propagation proceeds by the addition of monomers to the chain radical to form the growing polymer radical, $RM_n\cdot$, which has n monomeric units. The rate of propagation, R_p, is:

$$R_p = k_p[RM\cdot]f_M \quad (11)$$

where [RM·] is the total concentration of radicals irrespective of size ($\sum_{n=1}^{\infty}[RM_n\cdot]$), and k_p, the rate constant of propagation. The ethylene fugacity, f_M, is used as a measured of ethylene activity under high pressure. The concentration of radicals at time t is given as the difference between initiation and termination:

$$[RM\cdot] = \int_0^t R_i dt - \int_0^t R_t dt \quad (12)$$

where R_t is the rate of termination. As has been mentioned above, the rate of termination is negligible. Thus:

$$[RM_n\cdot] \fallingdotseq \int_0^t R_i dt = 2fI_0\{1-\exp(-k_dt)\} \quad (13)$$

At low temperatures and at the initial stage of polymerization, Eq. (13) is approximately rewritten as:

$$[RM\cdot] \fallingdotseq 2fk_dI_0t \quad (14)$$

The rate of polymerization, which is essentially the same as the rate of propagation, is given by combining Eq. (11) and Eq. (14):

$$R \fallingdotseq R_p = R_p[RM\cdot]f_M = 2fk_dk_pI_0f_Mt \quad (15)$$

By integrating Eq. (15), the amount of the polymerized monomer, M_p, at time t is given:

$$M_p = fk_dk_pI_0f_Mt^2 \quad (16)$$

The experimental correlations described above between the amount of the polymerized monomer and the reaction time, as well as the amount of the initiator (that is, the amount of the polymerized monomer is proportional to the second power of the reaction time and to the first power of the amount of the initiator), have thus been shown to

14) C. G. Overberger, M. T. O'Shaughnessy and H. Shalit, *J. Am. Chem. Soc.*, **71**, 2661 (1949).
15) F. M. Lewis and M. S. Matheson, *ibid.*, **71**, 747 (1949).
16) K. S. Kwei, *J. Polymer Sci.*, **A3**, 2387 (1965).
17) S. Kodama, Y. Matsushima, A. Ueyoshi, T. Shimidzu, T. Kagiya, S. Yuasa, and K. Fukui, *ibid.*, **41**, 83 (1959).

coincide well with the theoretical equation (16) at the initial stage of polymerization.

The number of moles of polymer chains is calculated as the ratio of the moles of the polymerized monomer to the degree of polymerization of the polymer ($M_p/\overline{DP}_n$). Figure 4 indicates that the number of moles of polymer chains increase proportionally with the reaction time.

The relation between the amounts of the polymerized monomer and the molecular weights of the polymers formed at various ethylene fugacities

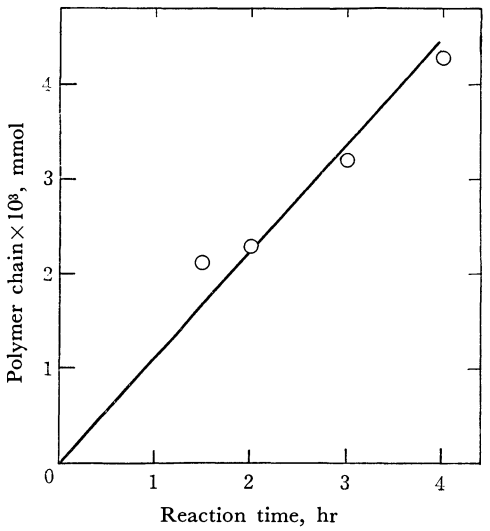

Fig. 4. Number of moles of polymer chains *vs.* reaction time.
(Reaction conditions : temperature, 40°C; AIBN, 0.98 mmol; pressure, 400 kg/cm²)

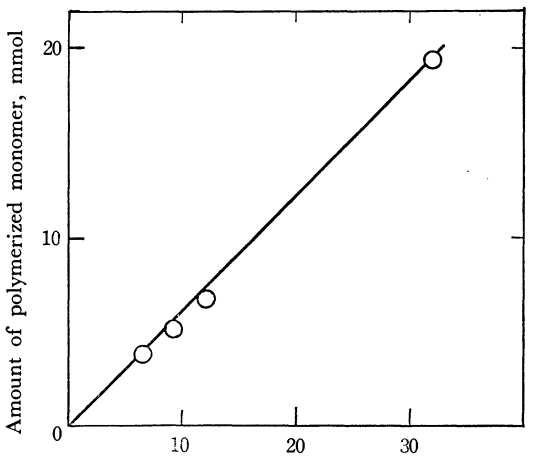

Fig. 5. Relation between amount of polymerized monomer and polymer molecular weight at various pressures.
(Reaction conditons: pressure, 138—400 kg/cm²; temperature 40°C; AIBN, 0.42 mmol)

is shown in Fig. 5. The fact that all the plots ride on the same straight line through the point of origin indicates that the number of moles of polymer chains formed at a constant time (*i. e.*, the initiation rate) is independent of the ethylene fugacity.

The effects of the ethylene fugacity on the polymer yield and the molecular weight are shown in Fig. 6, from which the fugacity exponents for them all are found to be the same, *i. e.*, 2.5. This demonstrates that the rate of propagation is linear to the 2.5 th power of the ethylene fugacity. The fugacity dependence of the propagation rate has also been determined to be *ca.* 2 by means of the two-stage polymerization method reported in other of our papers.[18,19] The reason for this high fugacity exponent of the propagation rate is not clear, but one possible reason is that the propagation is brought about by the addition of two or three associated monomer molecules, as will be described below.

The degree of the polymerization of the polymer ($\overline{DP}_n$) is given by the following equation when the termination and transfer are eliminated:

$$\overline{DP}_n = \int R_p dt \Big/ \int R_i dt = fk_dk_pI_0f_M t^2/2fk_dI_0t = 1/2 \cdot k_pf_M t \quad (17)$$

This equation means that the degree of polymerization is proportional to the reaction time and independent of the amount of initiator. The experimental facts, which are shown in Fig. 1 and Fig. 3, agree very well with Eq. (17). As for the dependence of the degree of polymerization on ethylene fugacity, however, the experimental results shown in Fig. 6 indicate that the exponent is *ca.* 2.5, which is higher than that expected from Eq. (17).

The empirical equations of the polymer yield and the degree of polymerization are thus obtained as follows:

$$M_p = k_1I_0f_M^{2.5}t^2 \quad (18)$$

$$\overline{DP}_n = k_2f_M^{2.5}t \quad (19)$$

The fact that the fugacity exponents of both the polymer yield and the degree of polymerization are higher than the theoretical values seems to be due to a higher-order dependence of the propagation rate on the monomer fugacity.

When ethylene reacts with a growing radical as associated form of n molecules, the rate of propagation is proportional to the fugacity of the associated

18) S. Machi, S. Kise, M. Hagiwara and T. Kagiya, *J. Polymer Sci.*, **B4**, 585 (1966).
19) S. Machi, S. Kise, M. Hagiwara and T. Kagiya, Mechanism of Propagation, Transfer, and Short-Chain Branching in the Free-Radical Bulk Polymerization of Ethylene, *ibid.*, in press.

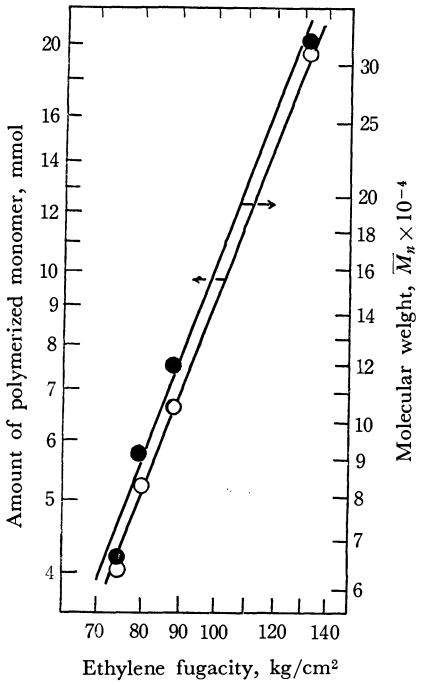

Fig. 6. Amount of polymerized monomer and polymer molecular weight *vs.* ethylene fugacity. (Reaction conditions are the same as for Fig. 2.)

monomers, which is proportional to the nth power of the monomer fugacity. The rate of propagation is thus given by Eq. (20) instead of Eq. (15):

$$R_p = k_p[\mathrm{RM}\cdot]f_M{}^n = 2fk_dk_pI_0f_M{}^nt \qquad (20)$$

By integrating (20) with t and by substituting Eq. (20) for R_p in Eq. (17), Eqs. (21) and (22) are obtained:

$$M_p = 2fk_dk_pI_0f_M{}^nt^2 \qquad (21)$$

$$\overline{DP}_n = 1/2\cdot k_pf_M{}^nt \qquad (22)$$

The fact that the observed exponent, n, is 2.5, as is shown in Eqs. (18) and (19), suggests that the propagation proceeds by the addition of associated monomers which consist of 2—3 units.

Effect of Reaction Temperature. The experimental results are listed in Table 2. The time-yield and time-molecular weight curves for the polymerizations at various reaction temperatures from 40 to 100°C are shown in Figs. 7 and 8 respectively. Figure 7 shows that the rate of polymerization is markedly accelerated with time at 30 and 40°C, but the acceleration becomes less remarkable with a rise in temperature. Figure 8 shows that the molecular weight of the polymer increases linearly with the time in the polymerization at 30—40°C, and when the temperature rises, the plots deviate from proportionality. These corresponding facts may indicate that the rate of chain termination increases with a rise in the temperature.

Table 2. Effects of reaction temperature on the polymer yield and molecular weight

Reaction temp. °C	Amount of AIBN mmol	Reaction time hr	Polymer yield g	Molecular weight $\overline{M}_n \times 10^{-4}$
30	0.700	4.0	0.14	15.9
		8.0	0.49	33.5
		14.0	1.47	57.0
55	0.140	1.0	0.14	13.7
		2.0	0.37	20.3
		3.7	0.85	27.5
65	0.140	1.0	0.32	6.1
		2.0	0.75	10.1
		4.0	1.92	13.6
100	0.140	1.0	2.44	1.2
		2.0	2.45	1.3
		4.0	2.44	1.1

Ethylene pressure, 400 kg/cm²; volume of reaction vessel, 100 m*l*

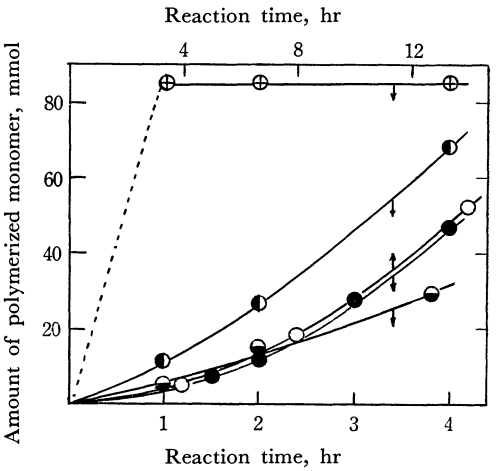

Fig. 7. Relation between amount of polymerized monomer and reaction time at various reaction temperatures.
(Reaction conditions: pressure 400 kg/cm²;
○: 30°C, AIBN 0.70 mmol,
●: 40°C, AIBN 0.98 mmol,
◒: 55°C, AIBN 0.14 mmol,
◐: 65°C, AIBN 0.14 mmol,
⊕: 100°C, AIBN 0.14 mmol)

The dependence of the polymer yield and the molecular weight on the amount of the initiator in the polymerization at the higher temperatures of 100 and 140°C is shown in Fig. 9 and Table 3. It is well known that the exponents of the initiator of the polymerization rate and the molecular weight are 0.5 and −0.5 in polymerization with a rapid second-order termination, and 1.0 and 0 in polymerization with a rapid first-order termination with respect to the radicals.

From the slope of the lines in Fig. 9, the exponents of this polymerization are found to be 0.8

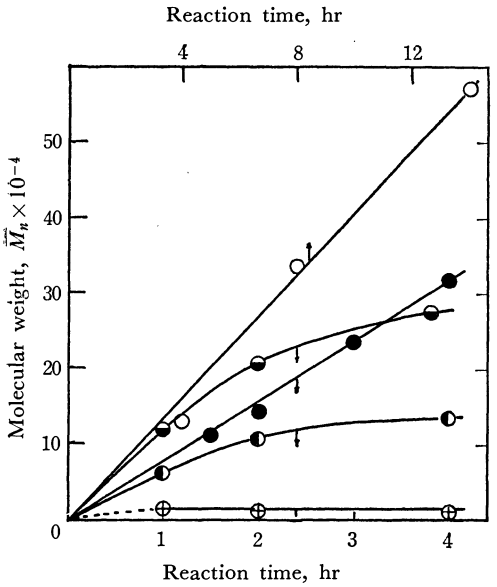

Fig. 8. Relation between polymer molecular weight and reaction time at various reaction temperatures.
(Reaction conditions and notes are the same as for Fig. 7.)

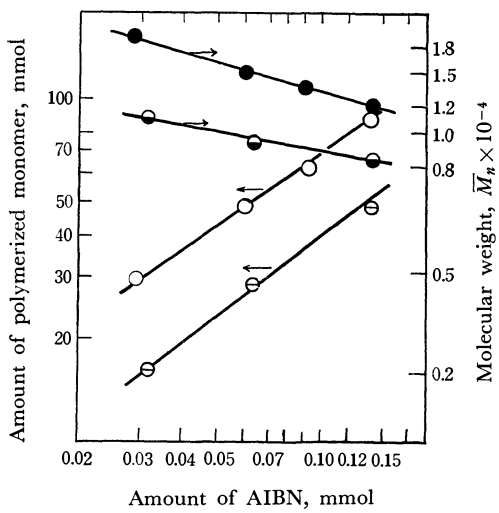

Fig. 9. Logarithmic plot of amount of polymerized monomer and polymer molecular weight *vs.* amount of initiator at higher temperatures.
(Reaction conditions: pressure, 400 kg/cm^2; time, 1.0 hr; temperatures, ○, ●: 100°C, ⊖, ◒: 140°C)

and −0.2, respectively, for the polymer yield and the molecular weight at a constant time. These high exponents indicate that the contribution of the first-order termination is larger than that of the second-order termination.

Considering the first-order termination and transfer reactions, and using the empirical rate equation of the propagation (Eq. (20)), Eqs.

TABLE 3. EFFECTS OF AMOUNT OF AIBN ON THE POLYMER YIELD AND MOLECULAR WEIGHT IN the POLYMERIZATION AT HIGHER TEMPERATURES

Reaction temp. °C	Amount of AIBN mmol	Polymer yield g	Molecular weight $\overline{M}_n \times 10^{-4}$
100	0.029	0.81	1.9
	0.061	1.34	1.5
	0.092	1.76	1.2
	0.140	2.44	1.2
140	0.032	0.46	1.1
	0.064	0.79	0.95
	0.140	1.34	0.85

Ethylene pressure, 400 kg/cm^2; reaction time, 1.0 hr; volume of reaction vessel, 100 m*l*

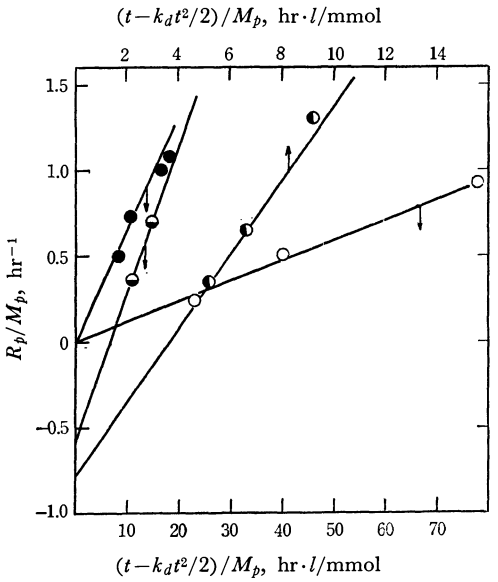

Fig. 10. R_p/M_p *vs.* $(t-k_dt^2/2)/M_p$ at the various reaction temperatures.
(Reaction conditions and notes are the same as for Fig. 7.)

(23) and (24) are derived for the polymer yield and the molecular weight; these equations can be used to evaluate the rates of termination and transfer reactions.[20]

$$R_p/M_p = 2fk_dI_0f_M^{2.5}(1/M_p)(t-k_dt^2/2) - k_t[Z] \quad (23)$$

$$1/\overline{DP}_n = 2fk_dI_0(1/M_p)(t-k_dt^2/2) + k_{tr}[Y]/k_pf_M^{2.5} \quad (24)$$

where Z is the substance by which the radical is deactivated, Y is the subtance with which the radical is transferred, and the ethylene fugacity exponent used is experimentally determined as

20) T. Kagiya, M. Izu, S. Machi and K. Fukui, This Bulletin, **40**, 1049 (1967).

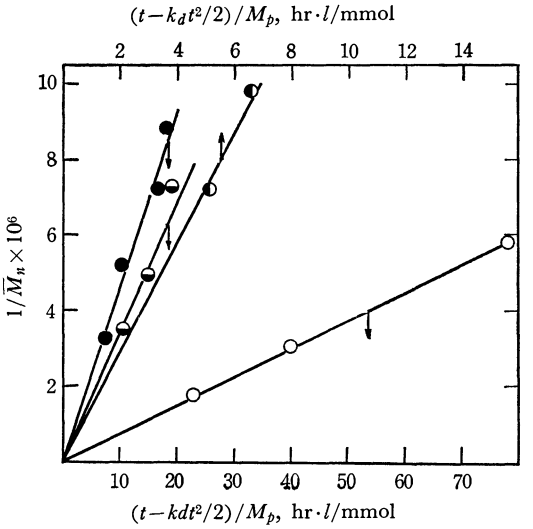

Fig. 11. $1/\overline{M}_n$ *vs.* $(t-k_dt^2/2)/M_p$ at the various reaction temperatures.
(Reaction conditions and notes are the same as for Fig. 7.)

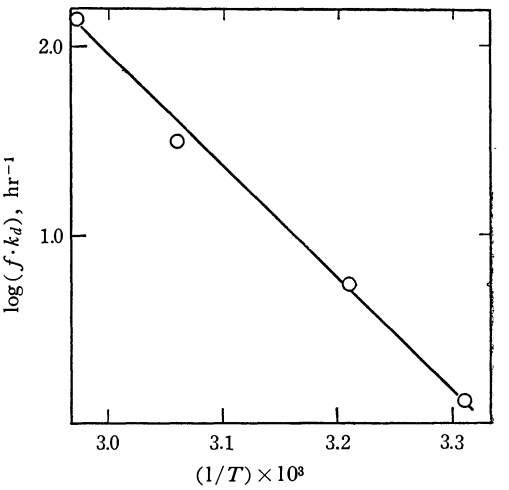

Fig. 12. Effect of temperature on the initiation rate constant, fk_d.

has been described above. The decomposition rate constant of AIBN, k_d, has been reported to be nearly constant, independent of the reaction media.[14-17] In the calculation of Eqs. (18) and (19), therefore, the value of k_d which was determined by Tobolsky[21] in benzene at various temperatures from 37 to 100°C was used. The plot of R_p/M_p against $(t-k_dt^2/2)/M_p$ according to Eq. (18) is shown in Fig. 10. The intercept on the axis of R_p/M_p gives the rate of termination $(k_t[Z])$. The rate of termination is thus shown to be approximately zero at 30 and 40°C and to increase with a rise in the temperature.

Figure 11 shows the plot of $1/\overline{M}_n$ against $(t-k_dt^2/2)M_p$ according to Eq. (19). Straight lines through the point of origin are obtained, their slopes corresponding to the rate of initiation. The correlation between the initiation rate and the temperature is shown in Fig. 12 as an Arrehenius plot. The activation energy of the initiation reaction is obtained as *ca.* 27 kcal/mol. The order of magnitude of the value is close to that of the decomposition of AIBN, *i. e.*, 30.8 kcal/mol.[14]

The fact that the lines in Fig. 11 pass through the point of origin indicates that the rate of the transfer reaction is approximately zero at temperatures from 30 to 65°C.

21) J. P. Van Hook and A. V. Tobolsky, *J. Am. Chem. Soc.*, **80**, 779 (1958).

BULLETIN OF THE CHEMICAL SOCIETY OF JAPAN VOL. 41 904—909 (1968)

The Gas-phase Oxidation of Propylene in an Inert Fluidized Bed Reactor under Pressure. The Effects of the Reaction Conditions on the Formation of Oxidation Products*1

Etsuro ECHIGOYA,*2 Mitsuo MASAI and Kiyoshi MORIKAWA

Research Laboratory of Resources Utilization, Tokyo Institute of Technology, Ookayama, Meguro-ku, Tokyo

(Received March 16, 1967)

The oxidation of propylene is studied in an excess-propylene atmosphere under pressure, using an inert fluidized bed reactor. The effects of the temperature, the pressure, and the concentration of oxygen on the reaction were examined. The so-called "negative temperature coefficient" is clearly observed with relation to the rate of the oxidation of propylene and the rates of the formation of acetaldehyde, propylene oxide, acrolein, carbon monoxide, methane, and ethylene. Therefore, the reaction courses involving these may be regarded as radical-chain reactions. Little effect of the pressure is observed. The molar fraction of oxygen exerts a profound effect on the yields of acetaldehyde, propylene oxide, and acrolein.

Many products such as aldehydes, epoxides, alcohols, and acids, are obtained in the course of the autoxidation of hydrocarbons in the gas phase.[1] In this paper, we will attempt to determine the reaction conditions which will give the optimum yields of acetaldehyde, propylene oxide, and acrolein.

Kamiya has reported that, in narrow tubular reactors, acetaldehyde, propylene oxide, acrolein, and allyl alcohol are produced in the oxidation of propylene under pressure with a small amount of oxygen.[2-4] On the other hand, propylene oxide has not been formed in the oxidation of propylene under reduced pressure.[1a]

A fluidized bed reactor has a large heat-transfer coefficient; therefore, the temperature gradient in the bed is almost negligible, except for the gas-inlet section, and the temperature in the reactor can be easily controlled and clearly defined. The fluidized bed reactor is therefore well-suited to the study of highly exothermic reactions, such as the autoxidation of propylene in a flow system.

In the present paper, the effects of the temperature, the pressure, and the molar fraction of oxygen on the reaction results are studied using a fluidized bed reactor with inert particles such as silicon carbide. In these experiments, the negative temperature coefficient is clearly observed, on the basis of this fact,[1b] a radical-chain mechanism is suggested for the formation of all the oxidation products except carbon dioxide. It is suggested that excess propylene is an important factor in producing good yields of acetaldehyde and propylene oxide, and also that acetaldehyde plays an important role in the formation reaction of propylene oxide.

Experimental

Materials. Propylene gas containing 5 mol% of propane, 1.3 mol% of ethane, and 0.2 mol% of C_4 hydrocarbons was supplied by the Nippon Petrochemicals Co., Ltd. The oxygen was obtained commercially. Fine particles of silicon carbide supplied by the Mitsui Mining and Smelting Co., Ltd., were washed by diluted nitric acid and water prior to the experiments.

Procedures. The flow sheet of the reaction apparatus is shown in Fig. 1. The propylene gas and oxygen were mixed after their flow rates had been measured and then introduced into the bottom of the reactor, R. The pressure of the product gas was reduced to a normal pressure by V, the reducing valve. The reduced gas was led to the cold traps, T_1 and T_2, and then to the wet gas meter. The linear velocity of the reactant gas was 1.5 cm/sec under the conditions of the oxidation experiments (on an empty-tube basis).

The reactor was made of stainless steel.*3 It was 56.3 mm i.d. and 700 mm long. The reactor contained 600 cc silicon carbide (greenish color) of 100—150 mesh (Tyler) as fluidizing particles, this is considered to be inert for this kind of reaction. The minimum fluidization velocity of the particle was measured as 1.13 cm/sec (on an empty tube basis), using nitrogen at a normal

*1 Presented at the 17 th Annual Meeting of the Chemical Society of Japan, Tokyo, April, 1964.

*2 Present address: Department of Chemical Engineering, Faculty of Engineering, Tokyo Institute of Technology.

1) V. Ya. Shtern, "The Gas-Phase Oxidation of Hydrocarbons," translated by M. F. Mullins, la) pp. 527—564, 1b) pp. 105—110, 480—492, Pergamon Press, Oxford (1964).

2) Y. Kamiya, *Sekiyu Gakkai Shi (J. Japan Petrol. Inst.)*, **5**, 18 (1962).

3) Y. Kamiya, *ibid.*, 398.

4) Y. Kamiya, *Bull, Japan Petrol. Inst.*, **5**, 13 (1963).

*3 JIS SUS 27, AISI 304, Austenite.

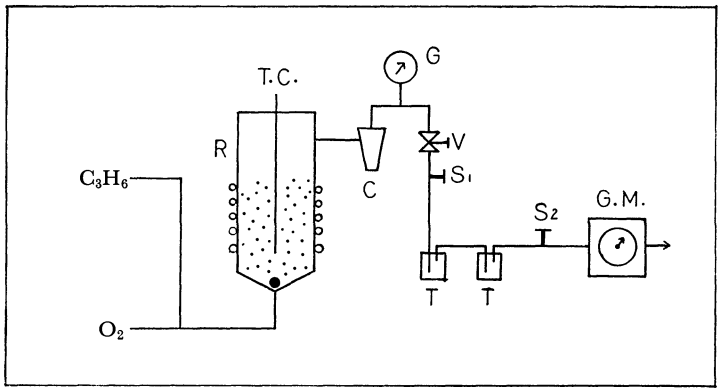

Fig. 1. Flow sheet of the reaction apparatus.
C, cyclon; G, Bourdon guage; G. M., wet gas meter; R, fluidized bed reactor; S_1 and S_2, sampling points; T, cold traps (−30—−10°C); T. C., thermocouple; V, needle valves.

temperature and pressure. The quiescent height of the fluidized bed was 320 mm. The reactor was heated electrically from outside, and controlled within ±5°C. No temperature gradient along the gas flow was observed except for the bottom gas-inlet section. The temperature was measured using chromel alumel thermocouples. The section from the outlet of the reactor to the sampling point, S_1, was kept at 100—120°C. The pressure of the reaction system was measured using a pressure gauge of the Bourdon type. The pressure was kept within ±0.1 kg/cm² by means of the pressure control valve, V.

Analysis. The product gas was analyzed in two gas chromatographs, using hydrogen as the carrier gas. Acetaldehyde, propylene oxide, and acrolein were analyzed using a 2.5 m dioctyl phthalate column (30 wt% on celite 545) at 80°C. The sample for this analysis was taken from S_1, using a glass syringe maintained at 40—50°C. The determinations of these three components were carried out precisely using absolute working curves calibrated every day. Oxygen, carbon monoxide, methane, and carbon dioxide were analyzed using a 2 m, activated charcoal column at 80°C. A fraction composed of oxygen plus carbon monoxide, and five fractions each composed of methane, ethane, ethylene, propane, and propylene respectively were separated using the 2.5 m column of activated alumina with 1.5 wt% squalane at 40°C. The samples for these two analysis were taken from S_2 by glass syringes.

Results and Discussion

The oxidation reaction was observed above 300°C. The temperature at the point 15 cm above the fluidizing surface was always kept under 240°C so as to minimize the oxidation reaction in the gas phase over the fluidizing surface; therefore, almost all the oxidation reaction is considered to proceed in the fluidizing bed.

Small amounts of polymerized substances were observed in every experiment, but they were not examined further, for the carbon balances of the oxidation experiments were almost entirely satisfactory, as Table 1 and Table 2 show. The acids were also not analyzed, because, Kamiya's results[3] indicate that acid formation is small.

Table 1. Carbon balances at 350°C

Press. atm	Carbon balances reacted gas/reactant gas
2.0	98.6 %
2.5	102
3.0	102
3.5	97.1
4.5	101

Table 2. Carbon balances at 350°C

Mol. fraction of O_2	Carbon balances reacted gas/reactant gas
0.10	101 %
0.15	102
0.20	94
0.25	91
0.30	90

The effects of the surface of the fluidizing particles are considered to be small on the basis of other data, which will be discussed in a later paper.

The experimental results described below are represented using a *yield* (%) of a product determined as follows:

$$yield = \frac{\text{moles of a product}}{\text{moles of propylene in feed}} \times 100$$

The Effect of the Pressure. The reactant gas consisted of 15 vol% oxygen and 85 vol% propylene gas. The experiments were carried out at the reaction temperatures of 300, 350, and 400°C in the pressure range of 1.5—4.5 atm. Figures 2—4 show the effects of the pressure on the yields of

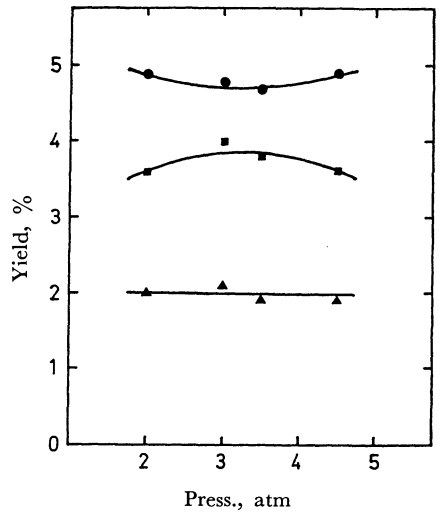

Fig. 2. Effect of press. on the yields of AA, PO and Acr at 300°C with mol fraction of O_2: 0.15.
● AA ■ PO ▲ Acr

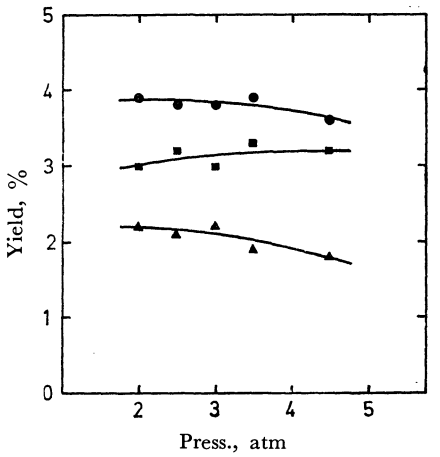

Fig. 3. Effect of press. on the yields of AA, PO and Acr at 350°C with mol fraction of O_2: 0.15.
● AA ■ PO ▲ Acr

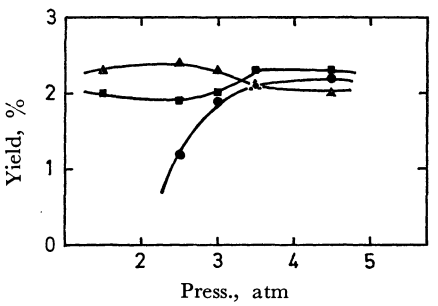

Fig. 4. Effect of press. on the yields of AA, PO and Acr at 400°C with mol fraction of O_2: 0.15.
● AA ■ PO ▲ Acr

acetaldehyde (AA), propylene oxide (PO), and acrolein (Acr).

At 300 and 350°C, little effect of the pressure is observed on the yields of AA, PO, and Acr, as Figs. 2 and 3 show. This observation differs markedly from that using narrow tubular reactors reported by Kamiya,[2-4] in his experiments the concentrations of AA and PO in the reacted gas showed steep maxima at 3—4 atm.*4 The yield of AA show a rapid decrease from 3 atm with the decrease in the pressure at 400°C, as is shown in Fig. 4. The yields of AA and PO decrease with a rise in the temperature, as may be seen by comparing Figs. 2—4.

A small effect of the pressure is observed on the conversion of propylene, as is shown in Fig. 5. The conversion of propylene at 400°C is lower than those at 300 and 350°C, as Fig. 5 shows. At 350°C the formation reactions of carbon monoxide, carbon dioxide, methane, and ethylene are also indifferent to the reaction pressure in the same pressure region. These results also differed markedly from those of Kamiya, his showed that the conversion of propylene and the concentrations of carbon monoxide, carbon dioxide, methane, and ethylene in reacted gas increased as the reaction pressure increased from 2 to 4 atm, reaching constant values beyond 4 to 6 atm at 315°C (1400

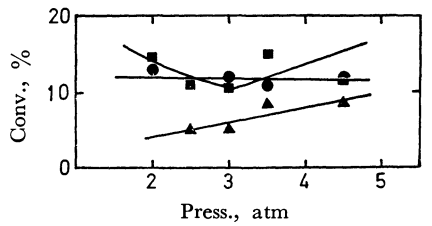

Fig. 5. Effect of press. on the conv. of C_3H_6 with mol fraction of O_2: 0.15.
● 300°C ■ 350°C ▲ 400°C

hr^{-1} of space velocity).[2] The rather slow rates of the oxidation reaction in the low-pressure region observed by Kamiya are very different from the present results, where the effect of reaction pressure is very small at 300 and 350°C. This difference is probably to be attributed to the effect of fluidizing particles, and/or to a difference in the surface area-to-volume ratio of the reactor, which is a measure of the wall effect of the reactor; this ratio differs by a factor of about seven. The reasons for considering the wall effect are as follows: the active species can easily reach the reactor wall rather than encounter propylene, *etc.* in Kamiya's narrow reactor (about 8 mm[2]) at a low pressure; when the pressure is sufficiently high, *i. e.*, above about 4 atm, the diffusion to the wall becomes minor.

*4 The yield and the concentration in the reacted gas show similar trends.

Therefore, result described above is observed. At present we have no clue by which to evaluate these two effects.

Table 1 shows good carbon balances of the oxidation experiments at 350°C.

The Effect of the Concentration of Oxygen. The experiments were carried out at 300, 350, and 400°C under 3 atm in the range of the molar fraction of oxygen from 0.1 to 0.35. The control of the reaction temperature and pressure became difficult with the increase in the molar fraction of oxygen in the reactant gas above 0.25 at 300 and 350°C. On the contrary, the reaction proceeded quietly at 400°C over the same range of concentration.

As Figs. 6—8 show, the yields of AA and PO increase at first, reach maxima and then decrease as the concentration of oxygen increases. A comparison of these figures indicates that the maximum yield of Acr probably shifts to the side of higher oxygen concentration. The yield of Acr decreases with a rise in the temperature (Figs. 6—8). The yields of AA and PO vary similarly with the change in the oxygen concentration (Figs. 6—8).

The yield of carbon monoxide increases as the concentration of oxygen increases and decreases as the temperature rises, as shown in Fig. 9. The

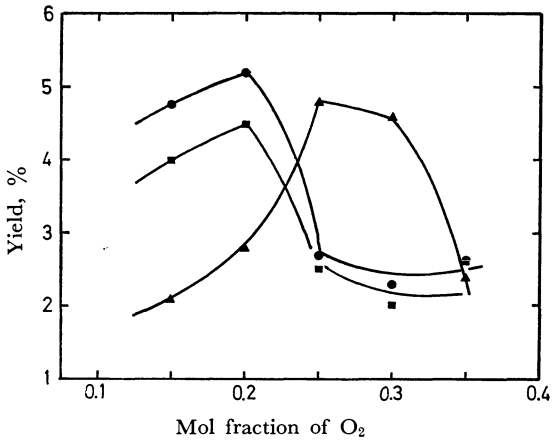

Fig. 6. Effect of O_2 conc. on the yields of AA, PO and Acr at 300°C under 3 atm.
● AA ■ PO ▲ Acr

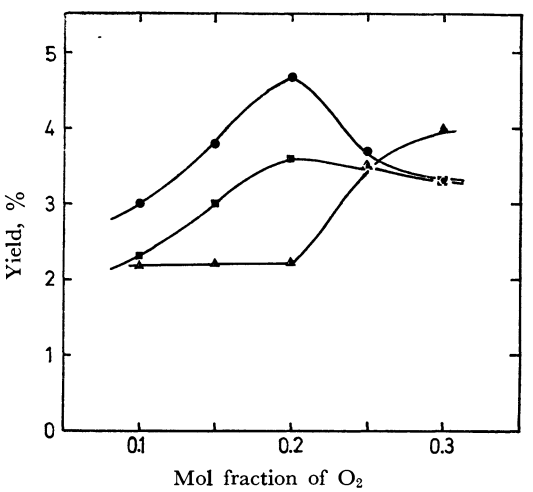

Fig. 7. Effect of O_2 conc. on the yields of AA, PO and Acr at 350°C under 3 atm.
● AA ■ PO ▲ Acr

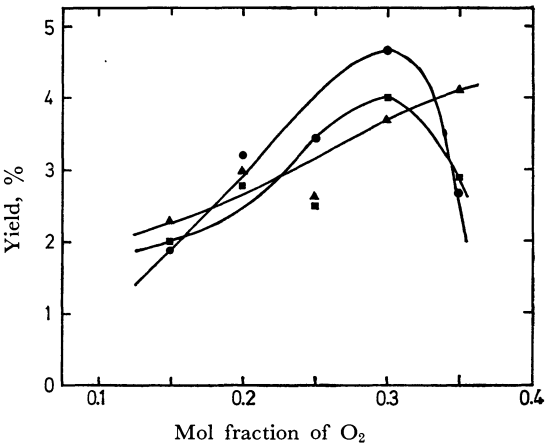

Fig. 8. Effect of O_2 conc. on the yields of AA, PO and Acr at 400°C under 3 atm.
● AA ■ PO ▲ Acr

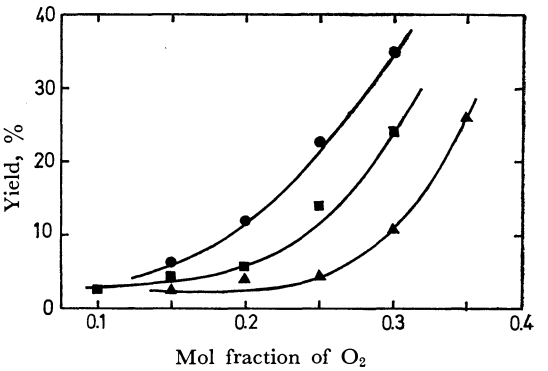

Fig. 9. Effect of O_2 conc. on the yield of CO under 3 atm.
● 300°C ■ 350°C ▲ 400°C

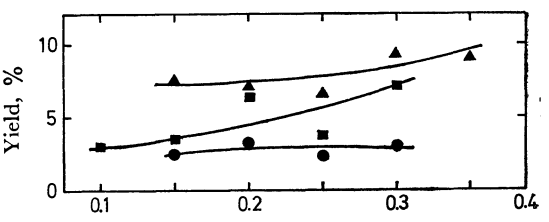

Fig. 10. Effect of O_2 conc. on the yield of CO_2 under 3 atm.
● 300°C ■ 350°C ▲ 400°C

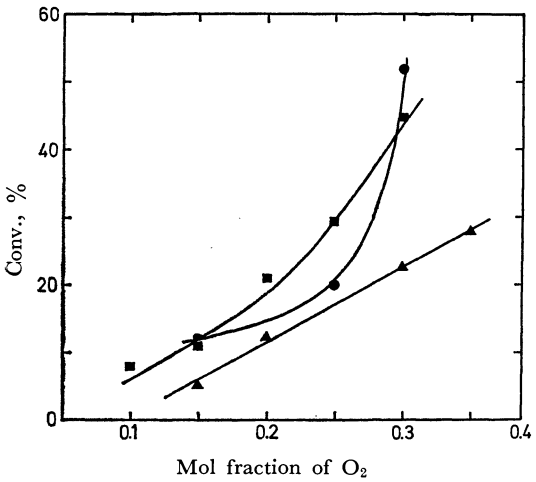

Fig. 11. Effect of O_2 conc. on the conv. of C_3H_6 under 3 atm.
● 300°C ■ 350°C ▲ 400°C

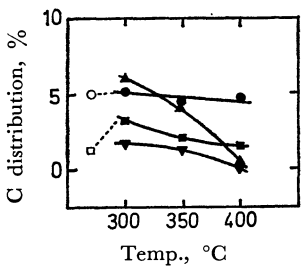

Fig. 12. Effect of temp. on the carbon distribution of hydrocarbons in products under 3 atm, with mol fraction of O_2: 0.20.
● C_3H_8 ■ C_2H_6 ▲ C_2H_4 ▼ CH_4
○ and □ correspond to the values in reactant gas for C_3H_8 and C_2H_6 respectively.

effect of the temperature on the yield of carbon dioxide is just the reverse, as shown in Fig. 10. The conversion of propylene increases as the concentration of oxygen increases and decreases with a rise in the temperature, as shown in Fig. 11. The formations of ethylene and methane decrease with a rise in the temperature, as Fig. 12 shows. At 350°C and 3 atm, the formations of methane and ethylene remain constant up to the molar fraction of oxygen of 0.2 and increase beyond this value. Propane retains its initial value (represented by an open circle in Fig. 12) within the limits of error. A comparison of the black square with the open square shows some formation of ethane, but it decreases as the reaction temperature rises, as shown in Fig. 12. It may be concluded, therefore, that propane and ethane, which are major impurities in propylene gas, do not play important roles in the oxidation reaction.

The trend of the effect of the oxygen concentration up to the molar fraction of oxygen, 0.2—0.25, at 300—350°C is nearly the same as that observed by Kamiya except for the yield of carbon dioxide.[3] His experiments were performed in the 7—24% range of oxygen content at 315°C between 3—6 atm, using a Pyrex reactor 12 mm in *i. d.* Kamiya's results show an increased formation of carbon dioxide with an increase in the oxygen concentration. In the present results, it is indifferent to the oxygen concentration up to a oxygen concentration of 0.25. This indicates that the existence of fluidizing particles (silicon carbide) prevents combustion reactions.

Table 2 shows the good carbon balances of the oxidation experiments at 350°C.

As has been described above, the yields of AA, PO, and Acr increase at first, reach maxima and then decrease with the oxygen concentration, as Figs. 6—8 show. In the increasing sector, the yields of AA and PO decrease as the temperature is raised. These yields *vs.* temperature relations are reversed in the decreasing sector of the said curves. The yields of carbon monoxide, methane, ethane, and ethylene decreased with a rise in the temperature (Figs. 9 and 12). It is known that propylene is a powerful inhibitor of the decomposition of a compound which contains the acetyl group,[5] and also that AA is easily decomposed by oxygen.[6] Therefore, AA is probably decomposed very easily in the range with high concentrations of oxygen. The combination of these two opposite effects may reasonably be expected to produce the maximum in the variation of the yield of AA against the concentration of oxygen. Therefore, up to an oxygen concentration which corresponds to the maximum yield of AA, species containing the acetyl group are decomposed to a lesser extent. It may be concluded from these results and discussion that the formation reaction of AA proceeds predominantly in the increasing sector of the curves, while the decomposition reaction of AA is enhanced in the decreasing sector of the curves (Figs. 6—8). In the decreasing sector of the curves for AA in Figs. 6—8, the temperature effect on the yield of AA is positive. In other words, there is a negative temperature coefficient of the decomposition of AA.

AA has been established to be a chain-branching agent in propylene oxidation at reduced pressures.[1] Imamura *et al.* obtained a relatively high selective production of PO by the direct addition of the oxidation products of AA to propylene;[7] they proposed that PO is formed by the addition of the

5) A. Maccoll, "Technique of Organic Chemistry," Vol. 8, 2nd Ed., Part 1, ed. by S. L. Friess, E. S. Lewis and A. Weissberger, Interscience, New York (1961), p. 472.
6) E. W. R. Steacie, "Atomic and Free Radical Reactions," 2nd Ed., Vol. 1, Reinhold, New York (1954), p. 211.
7) J. Imamura, N. Nagato, S. Sato and N. Ohta, *Kogyo Kagaku Zasshi (J. Chem. Soc. Japan, Ind. Chem. Sect.)*, **69**, 1863 (1966).

acetyl peroxy radical to the double bond of propylene and also by the reaction of peracetic acid with propylene.[7] Here, it can reasonably be estimated that the further predominant reaction of AA is the oxidation to the acetyl peroxy radical in the increasing sector and decomposition into the methyl radical and carbon monoxide in the decreasing sector. This assumption accords with the steep increase in the yield of carbon monoxide at a high oxygen concentration (Fig. 9). In the increasing sector, where AA is assumed to be converted into the acetyl peroxy radical, the formation reaction of PO may be the main course of the oxidation reaction. In the decreasing sector, where AA is estimated to decompose, the formation reaction of PO may become slight. Thus, the similar variation in the curves of AA and PO can be reasonably explained. Therefore, it may be suggested that AA plays an important role in the formation of PO.

Kamiya, Sekine and Yamakawa proposed that Acr is formed by the dehydration of allyl hydroperoxide in propylene oxidation.[8] It can be considered that the oxygen-catalyzed decomposition of AA efficiently increases the concentration of radicals (methyl and therefore, allyl) (*cf.* the discussion of Imamura *et al.*[7]). This increase in the said radicals will enhance the formation of the allyl peroxy radical by the reaction of the allyl radical and oxygen. Thus, the formation reaction of Acr will become the main course of the oxidation reaction as a result of the increased allyl peroxide which is formed by the reaction of the allyl peroxy radical and propylene. These considerations can explain the increasing yield of Acr in the decreasing sector. The decrease in the yield of Acr at higher oxygen concentrations may be ascribed to an increased combustion.

As has been discussed above, the variation in the curves for AA, PO, and Acr (Figs. 6—8) can thus be well explained. It may be concluded from the above discussion that a small amount of oxygen, in another words, a large excess of propylene, is an essential factor in producing high yields of AA and PO. This explains well why the formation of PO was not reported in past experiments,[1a] almost all of which were performed in an atmosphere with a relatively high partial pressure of oxygen and at a reduced reaction pressure. The reaction scheme mentioned to above will be discussed in detail in the next paper.

The so-called negative temperature coefficient is observed in the conversion of propylene and in the formations of AA, PO, Acr, carbon monoxide, methane, ethane, and ethylene. On the basis of the negative temperature coefficient,[1b] all the reactions of propylene oxidation may be considered to proceed through the radical-chain mechanism except for the formation reaction of carbon dioxide.

The authors wish to thank the Nippon Petrochemicals Co., Ltd., for supplying the propylene gas, and the Mitsui Mining and Smelting Co., Ltd., for supplying the silicon carbide.

8) Y. Kamiya, N. Sekine and Y. Yamakawa, *Sekiyu Gakkai Shi (J. Japan Petrol. Inst.)*, **8**, 951 (1965).

BULLETIN OF THE CHEMICAL SOCIETY OF JAPAN VOL. 41 910—919 (1968)

Mechanism of the Gas-phase Oxidation of Propylene in a Propylene-excess Atmosphere under Pressure*[1]

Mitsuo MASAI, Etsuro ECHIGOYA*[2] and Kiyoshi MORIKAWA

Research Laboratory of Resources Utilization, Tokyo Institute of Technology, Ookayama, Meguro-ku, Tokyo

(Received March 16, 1967)

The mechanism of the oxidation of propylene is studied through the addition of *t*-butyl hydroperoxide, acetaldehyde, or propionaldehyde to the reactant (propylene and oxygen), and also through the direct addition of the products of the ($C_3H_5Br+O_2$ or CH_3CHO+O_2) reaction to propylene. The following conclusions are reached: acetaldehyde and not propionaldehyde is responsible for chain-branching, acetaldehyde is formed from the allyl peroxy radical alone, propylene oxide is formed mainly by the reaction of the acetyl peroxy radical with propylene, the allyl peroxy radical probably contributes to the formation of propylene oxide, propionaldehyde, and acrolein in an equal extent, and the recombination of radicals is highly retarded in this propylene-excess system. On the basis of the data obtained, a plausible reaction scheme is proposed.

The data presented in a previous paper[1] have demonstrated the negative temperature coefficient[2,3a] in the conversion of propylene and in the yields of all the products except carbon dioxide, and have also demonstrated that excess propylene is essential to obtaining the high yields of acetaldehyde and propylene oxide in the thermal oxidation of propylene with an inert fluidized bed reactor under pressure.

The mechanism of the oxidation of hydrocarbons is generally known to be a degenerate branching process accompanying the negative temperature coefficient.[2,3a] Concerning the branching agent in the low-temperature oxidation of propylene, higher aldehydes contribute to the degenerate branching process according to Mulcahy and Ridge[4] and also according to Batten and Ridge.[5] Among the higher aldehydes, acrolein is not a branching agent according to Mullen and Skirrow.[6] It has been concluded that only acetaldehyde is responsible for the branching process,[3b,4-6] however, the role of propionaldehyde has not yet been discussed. And the formation of acetaldehyde through the isomerization of the allyl peroxy radical was discussed by Shtern and Polyak.[3b]

The features of the oxidation of propylene can be explained by the proposed formation of the unreactive allyl radical according to Mullen and Skirrow.[6]

Contrary to the results presented above[3b,4-6] propylene oxide is one of the major products in the propylene oxidation in a propylene-excess atmosphere under pressure.[1,7] The scheme of the reaction was duscussed first by Kamiya *et al.*[8] Some parts of the reaction scheme were elucidated using carbon-14-labeled propylene by White, Davis, and Hammack.[9] Propylene oxide and propionaldehyde were considered by Cvetanović[10] to be formed through the addition of an oxygen atom to the double bond of propylene. Oba and Sakai recently demonstrated that the methyl group of propylene was retained in the resulting propylene oxide.[11]

The purpose of the present work is to obtain some experimentally probable views on the main routes of the reaction. Two kinds of experiments will be described. In the first (Exp. A), *t*-butyl hydroperoxide, acetaldehyde, or propionaldehyde

*1 Part of this paper was presented at the 18 th Annual Meeting of the Chemical Society of Japan, Osaka, April, 1965, and part at the 19 th Annual Meeting of the Chemical Society of Japan, Yokohama April, 1966.

*2 Present address: Department of Chemical Engineering, Faculty of Engineering, Tokyo Institute of Technology.

1) E. Echigoya, M. Masai and K. Morikawa, This Bulletin, **41**, 904 (1968).

2) R. Ben-Aïm and M. Lucquin, "Oxidation and Combustion Reviews," Vol. 1, ed. by C. F. R. Tipper, Elsevier Pub. Co., Amsterdam (1965), p. 1.

3) V. Ya. Shtern, "The Gas-phase Oxidation of Hydrocarbons," translated by M. F. Mullins: 3a) pp. 105—110, 480—492; 3b) pp. 527—573, Pergamon Press, Oxford (1964).

4) M. F. R. Mulcahy and M. J. Ridge, *Trans. Faraday Soc.*, **49**, 906 (1953).

5) J. Batten and M. J. Ridge, *Australian J. Chem.*, **8**, 370 (1955).

6) J. D. Mullen and G. Skirrow, *Proc. Roy. Soc.*, **A244**, 312 (1958).

7) Y. Kamiya, *Sekiyu Gakkai Shi (J. Japan Petrol. Inst.)*, **5**, 18 (1962).

8) Y. Kamiya, N. Sekine and Y. Yamakawa, *ibid.*, **8**, 951 (1965).

9) E. R. White, H. G. Davis and E. S. Hammack, *J. Am. Chem. Soc.*, **87**, 1175 (1965).

10) R. J. Cvetanović, *Can. J. Chem.*, **36**, 623 (1958); S. Sato and R. J. Cvetanović, *ibid.*, **37**, 953 (1959).

11) S. Oba and W. Sakai, This Bulletin, **40**, 681 (1967).

is added to the reactant gas (propylene gas and oxygen); in the second (Exp. B), the oxidation products of allyl bromide or acetaldehyde are added directly to the propylene gas. The following conclusions are obtained: acetaldehyde and not propionaldehyde is the branching agent in this reaction; acetaldehyde is formed from the allyl peroxy radical; propylene oxide is formed mainly through the addition of the acetyl peroxy radical to the double bond of propylene; the allyl peroxy radical contributes to the formation of propylene oxide, propionaldehyde, and acrolein to an equal extent, and the recombination of radicals is highly retarded by the excess propylene. A plausible reaction scheme is proposed on the basis of the data obtained here.

Experimental

Materials. The propylene gas and oxygen have been described before.[1] The acetaldehyde was prepared by the depolymerization of paraldehyde and distilled just before use. Allyl bromide of a G. R. quality was obtained from the Tokyo Kasei Kogyo Co., Ltd. (Tokyo). *t*-Butyl hydroperoxide of a 70% purity was obtained from the Lucidol-Yoshitomi Co., Ltd. (Osaka). Propionaldehyde of an E. P. quality was obtained from the Tokyo Kasei Kogyo Co., Ltd. The silicon carbide has been described before.[1]

Reactors. Two kinds of reaction experiments were carried out using two different reactors.

For Exp. A. The oxidation experiments featuring the addition of *t*-butyl hydroperoxide, acetaldehyde, or propionaldehyde to the reactant gas (propylene and oxygen) were carried out in a fluidized bed reactor, shown in Fig. 1. The reactor was made of stainless steel*3 and had the following dimensions; 24.5 mm i. d. × 460 mm length. It contained 70 cc of silicon carbide (150—250 Tyler mesh) as a fluidizing powder. The quiescent bed height was 200 mm. The mixer (evaporator), made of steel had the following dimensions; 20 mm i. d. × 150 mm length. It contained quartz chips washed with diluted nitric acid.

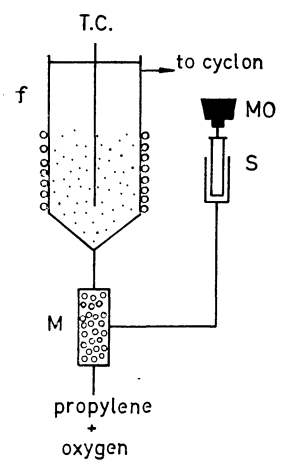

Fig. 1. Reactor for Exp. A.
f, fluidized bed reactor; M, mixer; MO, slow geared motor; S, syringe; T. C., thermocouple

*3 JIS SUS-27, AISI 304, Austenite.

For Exp. B. The reaction of propylene with the products of the $C_3H_5Br+O_2$ or CH_3CHO+O_2 reaction was carried out in the reaction apparatus shown in Fig. 2. The reactor, made of stainless steel,*3 consisted of two concentric tubes. The inner tubes, in which the oxidation of allyl bromide or acetaldehyde was carried out, had the following dimensions; 8 mm o. d. × 6 mm i. d. × 300 mm length. The outer tube, in which the reactions of propylene with the products from the inner tube were carried out, had the following dimensions; 24.5 mm i. d. × 360 mm length. The volume of the effective reaction zone in the inner tube was about 1.0 cc, while the volume of the effective reaction zone in the outer tube was about 46 cc. The reactor was heated from the outside; the temperature of the inner tube was higher than that of the outer tube by 5—10°C during the experiments.

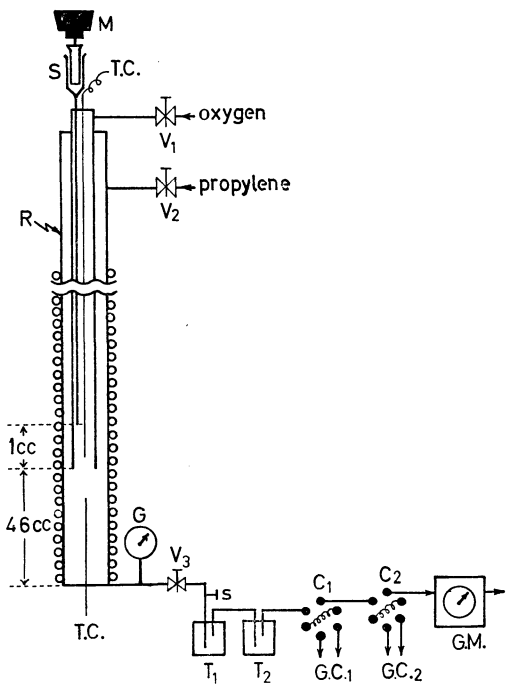

Fig. 2. Flow sheet of reaction apparatus for Exp. B.
C_1, C_2, sampling cock; G, press. guage (Bourdon type); G. C.$_1$, G. C.$_2$, gas chromatograph; G. M., wet gas meter; M, slow geared motor; R, reactor; S, syringe; s, sampling point; T. C., thermocouple; T_1, T_2, cold trap; V_1, V_2, V_3, needle valve

Procedures. *Exp. A* was carried out under 3.5 atm, using a reactant gas consisting of 80 vol% of propylene gas and 20 vol% oxygen. The linear velocity of the reactant gas was kept constant at 2.5 cm/sec on the empty-tube basis under the reaction conditions. The additives were fed into the mixer (kept about 80°C) by means of a glass syringe whose plunger was pushed at a constant speed using a slow-geared motor; the

additives were then mixed with the reactant gas. The concentrations of the additives varied a little as the reaction temperature changed; they were 0.61—0.83 vol% for acetaldehyde, 0.14—0.20 vol% for *t*-butyl hydroperoxide, and 0.55—0.65 vol% for propionaldehyde.

Exp. B was carried out under 3.0 atm. Propylene gas was passed through the outer tube. Allyl bromide (in Exp. B_1) or acetaldehyde (in Exp. B_2), which had been fed through the syringe needle was reacted with oxygen in the space (1.0 cc) of the inner tube. The reaction products from this space immediately reacted with propylene in the space (46 cc) of the outer tube. The flow rates of the reactants (at a normal temperature and pressure in the vapor phase) were as follows; allyl bromide, 1.14 *l*/hr, oxygen, 1.05 *l*/hr, and propylene gas, 4.26 *l*/hr, for the experiments (Exp. B_1) at 340 and 280°C, acetaldehyde, 1.17 *l*/hr, oxygen, 0.9 *l*/hr and propylene gas, 5.6 *l*/hr, for the experiment (Exp. B_2) at 280°C, and acetaldehyde, 1.17 *l*/hr, oxygen, 1.1 *l*/hr, and propylene gas, 5.8 *l*/hr, for the experiment (Exp. B_2) at 255°C.

Analysis. The reaction gas was analyzed gas chromatographically. An activated charcoal column of one meter long was used for oxygen, carbon monoxide, and methane at 50°C. A two-meter column containing activated alumina with 2 wt% of squalane was used for ethane and ethylene at 70°C (Exp. A) or 50°C (Exp. B). An eight meter column containing 30 wt% of acetonylacetone S on Celite 545 was used for oxygen + carbon monoxide + methane, ethane + ethylene, carbon dioxide, propane, and propylene at about 10°C. A three-meter column containing 30 wt% of Reoplex 400 on Celite 545 was used for acetaldehyde, propylene oxide, propionaldehyde, and acrolein at 70°C for Exp. A. A six-meter column containing 10 wt% of Reoplex 400 on Diasolid M was used at 50°C for Exp. B. All the packing materials except the Diasolid M were obtained from the Nishio Kogyo Co., Ltd. (Tokyo). The Diasolid M was obtained from the Nippon Chromato Kogyo Co., Ltd. (Tokyo).

The analytical procedures were the same as have been described before,[1] except that two sampling cocks were used for the analysis of the non-condensed gas sample in Exp. B.

Results and Discussion

The reactions studied are tabulated in Table 1.

Experiment A (Effect of a small amount of additives). In the case of Exp. A_0 (the oxidation experiment without additives), the oxidation reaction took place above 360°C.

Addition of t-Butyl Hydroperoxide. As Fig. 3 shows, the oxidation reaction took place above 300°C. Methane is much increased by the addition of *t*-butyl hydroperoxide, while there is only a small increase in ethane, as shown in Fig. 3. The increased methane formation shows the increased formation of the methyl radical. However, these methyl radicals probably contribute only a little to the formation of ethane by the recombination reaction. These observations show that the recombination of the radicals can be neglected in this reaction system because of the inhibiting effect of excess propylene, as the discussion of Mullen and Skirrow[6] has established.

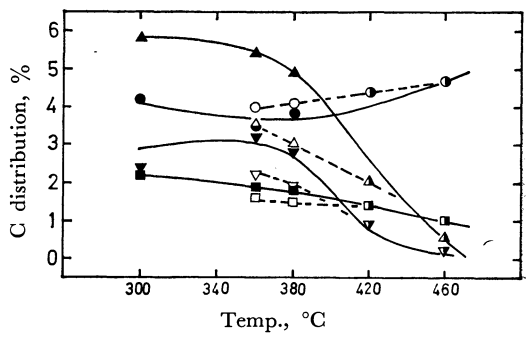

Fig. 3. Carbon distribution - temp. curves with the addition of *t*-butyl hydroperoxide; under 3.5 atm with mol fraction of O_2, 0.2 (exp. A_1).
-●- C_3H_8; --○-- C_3H_8 in Exp. A_0;
-■- C_2H_6; --□-- C_2H_6 in Exp. A_0;
-▲- C_2H_4; --△-- C_2H_4 in Exp. A_0;
-▼- CH_4; --▽-- CH_4 in Exp. A_0

Table 1. Reactions studied in this paper

Symbol	Additive	Reactor	Temp., °C	Amount of additive
Exp. A_0*	no additive	Fig. 1	360—460	
Exp. A_1	t-C_4H_9OOH	Fig. 1	300—460	0.14—0.20 vol%
Exp. A_2	CH_3CHO	Fig. 1	300—460	0.61—0.83 vol%
Exp. A_3	C_2H_5CHO	Fig. 1	360—460	0.55—0.65 vol%
Exp. B_0	no additive	Fig. 2	255, 280	
Exp. B_1	oxidation products of C_3H_5Br to C_3H_6	Fig. 2	340, 280	C_3H_5Br 1.14 *l*/hr,** O_2 1.05 *l*/hr, C_3H_6, 4.26 *l*/hr
Exp. B_2	oxidation products of CH_3CHO to C_3H_6	Fig. 2	280	CH_3CHO 1.17 *l*/hr,** O_2 0.9 *l*/hr, C_3H_6 5.6 *l*/hr
			255	CH_3CHO 1.17 *l*/hr,** O_2 1.1 *l*/hr, C_3H_6 5.8 *l*/hr

* Without special remarks, blank exp. (without additive) for exp. A_2 and A_3.
** At normal temperature and pressure in vapor phase.

Addition of Acetaldehyde or Propionaldehyde. As Figs. 4 and 7, 5 and 8, and 6 and 9 show, the oxidation reaction took place above 300°C upon the addition of acetaldehyde (AA); a good agreement is observed between the results of Exp. A_0 and Exp. A_2 (AA-added experiments) above 360°C. The chain-initiating radicals are easily produced by the addition of AA; therefore, the oxidation reaction took place at 300°C in Exp. A_2, unlike Exp. A_0. On the other hand, the amount of AA added is so small that the concentrations of the radicals in this reaction are not changed from those of Exp. A_0; therefore, the reaction courses and the results vary little upon the addition of AA above 360°C. Thus, AA may be concluded to be the branching agent in the case of excess propylene under pressure, as in the case of reduced-pressure experiments with a relatively low partial pressure of propylene.[3b,4-6] The apparent reaction times were kept constant in the Exp. A series; the results

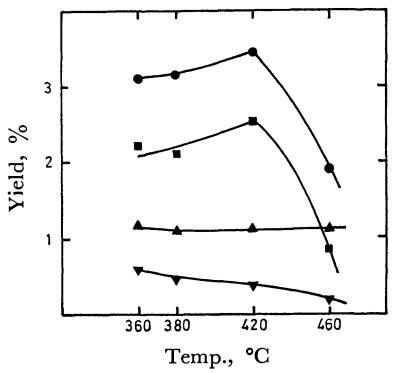

Fig. 4. Yield-temp. curves; under 3.5 atm with mol fraction of O_2, 0.2 (exp. A_0).
● AA ■ PO ▲ Acr ▼ PA

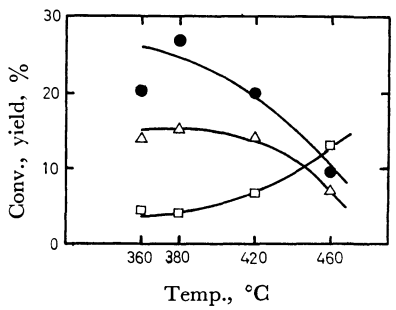

Fig. 5. Conv.- and yield-temp. curves; under 3.5 atm with mol fraction of O_2, 0.2 (exp A_0).
● conv. of C_3H_6 △ yield of CO
□ yield of CO_2

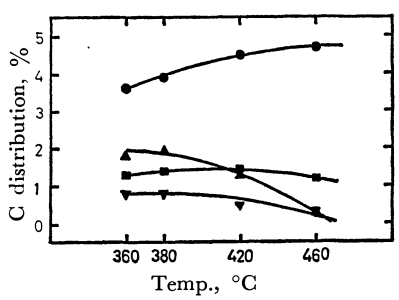

Fig. 6. Carbon distribution-temp. curves; under 3.5 atm with mol fraction of O_2, 0.2 (exp. A_0).
● C_3H_8 ■ C_2H_6 ▲ C_2H_4 ▼ CH_4

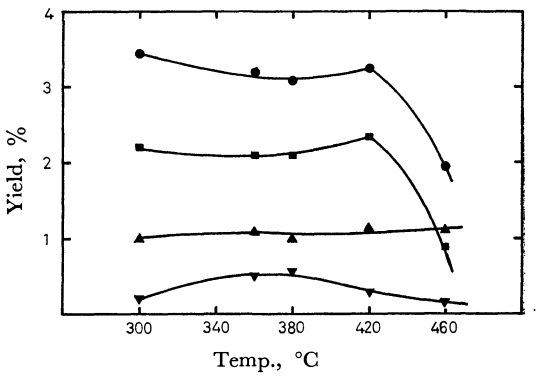

Fig. 7. Yield-temp. curves with the addition of AA; under 3.5 atm with mol fraction of O_2, 0.2 (exp. A_2).
● AA ■ PO ▲ Acr ▼ PA

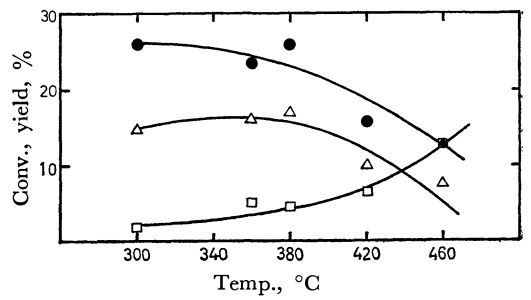

Fig. 8. Conv.- and yield-temp. curves with the addition of AA; under 3.5 atm with mol fraction of O_2, 0.2 (exp. A_2).
● conv. of C_3H_6 △ yield of CO
□ yield of CO_2

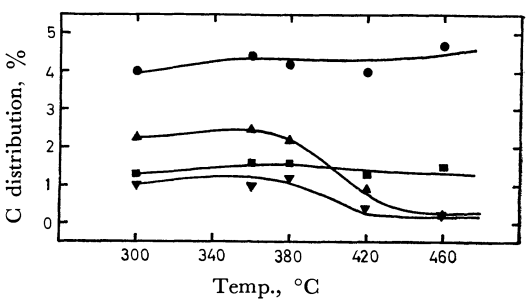

Fig. 9. Carbon distribution - temp. curves with the addition of AA; under 3.5 atm with mol fraction of O_2, 0.2 (exp. A_2).
● C_3H_8 ■ C_2H_6 ▲ C_2H_4 ▼ CH_4

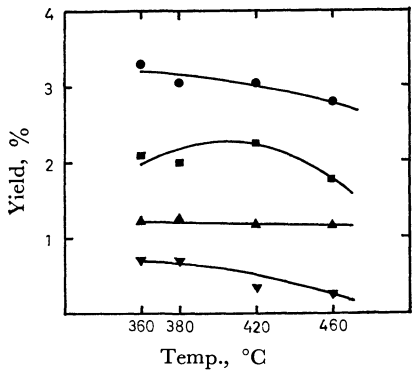

Fig. 10. Yield-temp. curves with the addition of PA; under 3.5 atm with mol fraction of O_2, 0.2 (exp. A_3).
▲ AA ■ PO ▲ Acr ▼ PA

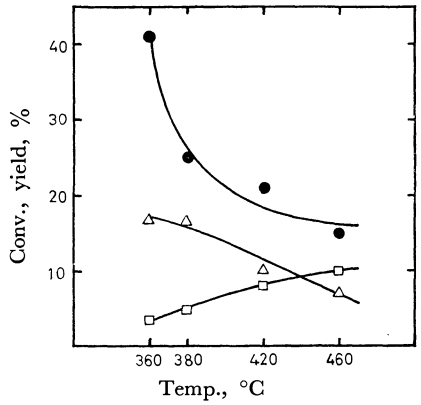

Fig. 11. Conv.- and yield-temp. curves with the addition of PA; under 3.5 atm with mol fraction of O_2, 0.2 (exp A_3).
● Conv. of C_3H_6 △ yield of CO
□ yield of CO_2

Table 2. The results of Exp. B

	Temp. of outer tube °C	React. time sec inner tube	React. time sec outer tube	Conv. of O_2 %	Conc. (vol %) in products flow AA	PO	PA	Acr	CO	CO_2	CH_4	C_2H_6	C_2H_4
Exp. B_1	340*	2.5	36	—	0.52	0.12	0.07	0.06	—	—	—	—	—
	280	2.7	40	20	0.52	0.06	0.06	0.04	2.6	2.0	0.51	0.13	0.20
Exp. B_2	280	2.8	34	52	—**	0.30	0.07	0.06	1.7	4.0	0.44	0.12	0.27
	255	2.8	34	51	—**	0.25	0.07	0.04	3.1	2.1	0.91	0.26	0.14

* The analysis of the gaseous products were failed.
** The analysis of AA was failed owing to the scale out of its peak.

of Exp. A_2 indicate that the induction period of this oxidation reaction was shortened by the addition of a small amount of AA between 300—360°C as has already been found in static experiments.[5,6]

Imamura *et al.* studied the addition of a large amount of AA in nearly the same reaction system as in Exp. A_2 at normal pressure.[12] They showed that the selectivity of acetic acid was four times that of PO (propylene oxide),[12] and also that acetic acid decreased and PO increased with a decrease in the amount of added AA.[12] In our work, the amount of added AA is very small, as shown in Table 1, and the rates of the oxidation reaction are found to be increased only a little, as has already been found in static experiments.[5,6] The addition of AA probably enhances the rates of all the reaction paths. The branching reaction is as follows.[17a]

$$CH_3CHO + O_2 \rightarrow CH_3\dot{C}O + \dot{O}OH$$

Figures 4 and 10, 5 and 11, and 6 and 12 show that upon the addition of propionaldehyde (PA) the oxidation reaction still takes place at 360°C (Exp. A_3) as in Exp. A_0, and also that the results of the two experiments Exp. A_0 and Exp. A_3 disagree with each other not only in the trend of the curves

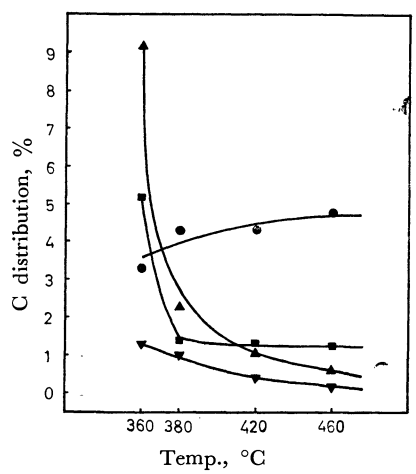

Fig. 12. Carbon distribution - temp. curves; with the addition of PA; under 3.5 atm with mol fraction of O_2, 0.2 (exp. A_3).
● C_3H_6 ■ C_2H_6 ▲ C_2H_4 ▼ CH_4

12) J. Imamura, N. Nagato, S. Sato and N. Ohta, *Kogyo Kagaku Zasshi (J. Chem. Soc. Japan, Ind. Chem. Sect.)*, **69**, 1863 (1966).

but also in the numerical values. Thus, PA is not the branching agent in this reaction.

Experiment B. Table 2 contains the results of Exp. B. Exp. B_0 did not take place at 255, 280, and 340°C. Therefore, the products shown in Table 2 must be formed by the reactions of the species produced in the inner tube.

Experiment B_1 $(C_3H_5Br+O_2)+C_3H_6$. At 280°C, the amount of AA formed is about ten times those of PO, PA, and acrolein (Acr) as Tables 2 and 3 show.

Table 3. Comparision of relative yield of AA, PO, PA and Acr in Exp. B with those in Exp. A_0 (The values of Acr in each experiment is taken as unity.)*

	Temp., °C	AA	PO	PA	Acr
Exp. A_0 (Fig. 4)	380	2.9	1.9	0.44	1
Exp. B_1**	340	8.7	2.0	1.2	1
Exp. B_1**	280	13	1.5	1.5	1
Exp. B_2**	280	—	5.0	1.2	1
Exp. B_2**	255	—	6.3	1.2	1

* Acr is observed to be relatively insensitive oxygenated product to the variations of experimental conditions in comparision with AA and PO as shown in the previous paper[1] and Figs. 4, 7 and 10 in this paper.

** Calculated from the data presented in Table 2.

In this case, allyl bromide is decomposed into the allyl radical and the bromine atom.[13] The allyl radical produced most likely reacts with oxygen to form the allyl peroxy radical in the inner tube of the reactor. The allyl peroxy radical has been considered to be the main active species in the homogeneous-gas-phase oxidation of propylene.[3b,6,8] The bromine atom which is converted into bromine or hydrogen bromide most likely affects the course of the reaction. Bromine is an especially active catalyst for the decomposition of AA, according to Fromherz.[14] Hurst, Skirrow and Tipper[15] discussed the result of the oxidation of butene containing hydrogen bromide, citing some Russian workers results reporting the decomposing action of hydrogen bromide on hydroperoxide. Thus, the decomposition of AA, allyl hydroperoxide, and perhaps the allyl peroxy radical should all be considered here. The products described in Table 2 are, then, formed by the succeeding reactions of the allyl peroxy radical and the allyloxy radical. The alkoxy radical produced from the decomposition of peroxide is considered to decompose according to the following reactions:[16]

$$CH_2{=}CHCH_2\dot{O} \rightarrow CH_2{=}\dot{C}H + CH_2O$$
$$\searrow\ CH_2{=}CHCHO + \dot{H}$$

The same kinds of products are obtained in Exp. B_1 and Exp. A_0, while the oxidation reaction did not take place in Exp. B_0. Therefore, the reaction paths in the oxidation of propylene are not extinguished in Exp. B_1 by the presence of bromine or hydrogen bromide; furthermore, these paths start from the same active species, which are present in Exp. B_1 and Exp. A_0. The active species must be the allyl peroxy radical, because this is produced almost only in the inner tube of the reactor (as Exp. B_0 shows, the oxidation reaction without an additive did not take place), and also because the presence of the allyl peroxy radical as an active species in the oxidation of propylene is generally accepted.[3b] The secondary reactions induced by the radicals from the inner tube can be neglected at 280°C, because only a low conversion of oxygen is observed, as shown in Table 2.

The yield of AA relative to PO, PA, and Acr in Exp. B_1 at 280°C is higher than that of Exp. A_0, as Table 3 shows.

The above discussion leads to the conclusion that only the allyl peroxy radical contributes to the formation of AA. Shtern and Polyak[3b] and Neiman *et al.*[3b] proposed, and demonstrated kinetically, the following scheme for the formation of AA:

$$CH_2{=}CHCH_2O\dot{O} \rightarrow \dot{C}H_2CH\text{-}CH_2$$
$$\qquad\qquad\qquad\qquad\qquad\quad |\quad |$$
$$\qquad\qquad\qquad\qquad\qquad\quad O{-}O$$
$$\rightarrow \dot{C}H_2CHO + HCHO$$
$$\dot{C}H_2CHO + C_3H_6 \rightarrow CH_3CHO + \dot{C}_3H_5$$

This scheme does not contradict the results of Exp. B_1 at 280°C. Thus, it is reasonable to conclude that AA is formed by the isomerization of the allyl peroxy radical, as in Shtern and Polyak's scheme. The following modification may be suggested for this scheme, considering the propylene excess atmosphere:

$$\dot{C}H_2CH\text{-}CH_2 + C_3H_6 \rightarrow CH_3CH_2\text{-}CH_2 + \dot{C}_3H_5$$
$$\quad |\quad |\qquad\qquad\qquad\qquad\quad |\quad |$$
$$\quad O{-}O\qquad\qquad\qquad\qquad\quad O{-}O$$
$$CH_3CH\text{-}CH_2 \rightarrow CH_3CHO + HCHO$$
$$\quad |\quad |$$
$$\quad O{-}O$$

The allyl peroxy radical is most likely to be formed

13) E. W. R. Steacie, "Atomic and Free Radical Reactions," 2nd ed., Vol. 1. Reinhold Pub. Corp., New York (1954), p. 260.

14) H. Fromherz, *Z. physik. Chem.*, **B25**, 301 (1934).

15) P. Hurst, G. Skirrow and C. F. H. Tipper, *Proc. Roy. Soc.*, **A268**, 405 (1962).

16) K. Maruyama, *Kagaku (Chemistry)*, **21**, (No. 11) 54 (1966).

according to the following scheme, as proposed by Shtern and Polyak[3b] for the oxidation of propylene;

$$CH_2{=}CHCH_3 + O_2 \rightarrow$$

$$CH_2{=}C\dot{H}CH_2 + \dot{O}OH$$

$$CH_2{=}C\dot{H}CH_2 + O_2 \rightarrow$$

$$CH_2{=}CHCH_2O\dot{O}$$

Contrary to the results of Exp. A_0, PO is formed in an amount comparable to PA and Acr at 280°C, as shown in Tables 2 and 3.*4 According to the above discussion concerning the formation of AA, allyl peroxy radical is the sole active oxygenated species formed in the inner tube, from which the oxygenated products are derived. The increased relative yield of PA in Exp. B_1 at 280°C may be compared with the small relative yield of PA in Exp. A_0 (Table 3). This fact strongly suggests that the reaction path to PA is emphasized by the presence of the allyl peroxy radical. The yield of PO is comparable to the yield of PA, as shown in Table 3. Cvetanović proposed the rearrangement of the oxygeneated biradical to PO and PA in the reaction of propylene and an oxgen atom as follows,[10] (he obtained almost equal amounts of PO and PA):

$$CH_2{=}CHCH_3 + O \rightarrow$$

$$CH_2\text{-}\dot{C}HCH_3 \rightarrow CH_2\text{-}CHCH_3$$

$$\dot{O}\cdot \qquad\qquad \diagdown\,O\,\diagup$$

$$\downarrow$$

$$CHCH_2CH_3$$

$$\|$$

$$O$$

Our results can also be explained well on the basis of Cvetanović's mechanism; *i. e.*, the allyl peroxy radical contributes to the formations of PO and PA to an equal extent. Since the allyl peroxy radical is the sole active species, as has been established above, the contribution of the allyl peroxy radical to the formation of Acr is considered to be feasible according to the discussion of Mullen and Skirrow.[6] The yield of Acr comparable to those of PO and PA (Table 3) suggests the same degree of contribution of the allyl peroxy radical to the reaction paths which produce the said three products. To summarize the above discussions, the allyl peroxy radical is the sole precursor of AA, and it also contributes to the formation of PO, PA, and probably Acr to almost equal extents. At a higher temperature (340°C), the amount of PO becomes greater than those of PA and Acr in Exp. B_1, as shown in Table 2. This result may be ascribed to the further reaction of AA, as will be discussed below.

Experiment B_2 $(CH_3CHO + O_2) + C_3H_6$. In the case of Exp. B_2, the amounts of PO produced are greater than those of PA and Acr at 225 and 280°C, as shown in Tables 2 and 3. As has already been described, at the same temperature of 280°C, the amount of PO produced is comparable to those of PA and Acr (Table 2) in Exp. B_1. In Exp. B_2, the relative amount of PO is greater than that in Exp. A_0 (Table 3). The concentration of AA in the inner tube in Exp. B_1 at 280°C should be much less than that of Exp. B_2. These facts show that the contribution of the oxidation product of AA to the formation of PO is superior to that of the allyl peroxy radical.

Here, AA is easily oxidized to the acetyl peroxy radical,[17a,18] its oxidation scheme is as follows;[17a,18]

$$CH_3CHO + O_2 \rightarrow CH_3\dot{C} + \dot{O}OH$$

$$\|$$

$$O$$

$$CH_3\dot{C} + O_2 \rightarrow CH_3CO\dot{O}$$

$$\|\qquad\qquad\|$$

$$O\qquad\qquad O$$

$$CH_3\dot{C} \rightarrow \dot{C}H_3 + CO$$

$$\|$$

$$O$$

In the propylene-excess atmosphere, the acetyl radical formed will react with propylene;

$$CH_3\dot{C} + C_3H_6 \rightarrow CH_3CHO + \dot{C}_3H_5$$

$$\|$$

$$O$$

Thus, it is reasonable to suggest that the most reactive radical in the above scheme—the acetyl peroxy radical—plays an important role in the main reactions in Exp. B_2.

Imamura *et al.* studied the same reaction system as in Exp. B_2 with lower oxygen under normal pressure at 180 and at 270°C.[12] Their reaction gas consisted of about 0.4 AA and about 0.2 air in the inner reactor and of about 0.4 propylene in the outer reactor.[12] They used a reactor, the reaction spaces of which were 135 m*l* for the inner reactor

*4 The data presented in Exp. B_1 of Table 2 show an increase in PO, PA and Acr with an increase in the temperature; this indicates a negligible interaction between these products and the allyl bromide or species derived from them. The known reactions of PO with allyl bromide, bromine and hydrogen bromide can be neglected under the conditions of Exp. B_1, such as the reaction time of 36—40 sec and the reaction tmeperature of 280—340°C [P. Bedos, *Compt. rend.*, **183**, 562 (1926); A. Rosowsky, "Heterocyclic Compounds with Three- or Four-membered Rings" (A. Weissberger, ed.), Part 1, Interscience Pub. New York (1964), pp. 436—455].

17) N. N. Semenov, "Some Problems in Chemical Kinetics and Reactivity," Japanese translation by T. Kwan and A. Matsuda, Vol. 1, 17a) p. 81, 17b) Chap. 7 § 2, 17c) Chap. 1 § 7, Iwanami Shoten, Tokyo (1963).

18) G. J. Minkoff and C. F. H. Tipper, "Chemistry of Combustion Reactions," Chap. 5, Butterworths Co., London (1962).

and 265 m*l* for the outer reactor; the outlet of the inner reactor had a narrow neck. They obtained considerable amounts of acetic acid, and peracetic acid and a small amount of PO. This supports the formation of the acetyl peroxy radical in Exp. B_2.

During the oxidation of propylene, PO retains the carbon skelton of propylene, according to the results of White, Davis and Hammack.[9] It has been proposed by Cvetanović[10] that PO is formed through the addition of an oxygen atom to the double bond of propylene. Oba and Sakai recently demonstrated that the methyl group of propylene is retained in PO in a homogeneous oxidation of propylene.[11] These results indicate that PO is formed by the addition of active species to the double bond of propylene. Concerning the active species which may introduce the oxygen atom to the double bond of propylene, there have been no definite discussions which have experimental support about gas-phase homogeneous reactions. Only the acetyl peroxy radical and acetyl hydroperoxide have been proposed by Imamura *et al.* on the basis of their experiments,[12] and they evaluated these reaction paths low because of the low selectivity of the PO formation. It is reasonable to assume that the molecular reaction of acetyl hydroperoxide with propylene is very much slower than the addition of the acetyl peroxy radical to the double bond of propylene in the gas-phase reaction,[17b] because the addition of a radical to the double bond generally always proceeds with a low activation energy.[17c]

Therefore, the following scheme may be concluded to hold for the route to PO in Exp. B_2; it is deduced from the results of Exp. B_2 already described and also from the discussions presented above:

$$CH_3\overset{\overset{\|}{O}}{C}O\dot{O} + CH_2{=}CHCH_3 \rightarrow$$

$$CH_3\overset{\overset{\|}{O}}{C}OOCH_2\dot{C}HCH_3$$

$$CH_3\overset{\overset{\|}{O}}{C}OOCH_2\dot{C}HCH_3 \rightarrow$$

$$CH_3\overset{\overset{\|}{O}}{C}O + CH_2\text{-}CHCH_3 \quad (\text{O bridging CH}_2\text{–CH})$$

PO is formed in Exp. B_1 in an amount comparable with those of PA and Acr, which are minor products in Exp. A_0 (Table 2, Fig. 4). Furthermore, the amount of PO formed in Exp. B_1 is distinctly small in comparision with that formed in Exp. B_2 (Table 2). These observations strongly indicate that the contribution of the allyl peroxy radical to the formation of PO is less than that of the acetyl peroxy radical. The route *via* the addition of the allyl peroxy radical is as follows:

$$CH_2{=}CHCH_2O\dot{O} + CH_2{=}CHCH_3 \rightarrow$$

$$CH_2{=}CHCH_2OOCH_2\dot{C}HCH_3$$

$$CH_2{=}CHCH_2OOCH_2\dot{C}HCH_3 \rightarrow$$

$$CH_2{=}CHCH_2\dot{O} + CH_2\text{–}CHCH_3 \quad (\text{O bridging CH}_2\text{–CH})$$

Thus, the route *via* the addition of the acetyl peroxy radical may be concluded to be the main route for the formation of PO in the gas-phase homogenous oxidation of propylene.*5 This conclusion accords with the discussion presented in the previous paper,[1] where the decomposition of the species containing an acetyl group was found to be retarded to some extent in an oxidation atmosphere with an excess of propylene.

The amount of PO increased at 340°C in comparison with the amount at 280°C in Exp. B_1 (Table 2); this fact indicates that the route *via* the acetyl peroxy radical becomes predominant as the amount of AA increases with a rise in the temperature. PO is regarded as a stable species under normal reaction conditions, according to the results of Kamiya.[19] The acetoxy radical produced will decompose as follows.[18] Here, Kamiya's results indicate the low formation of acetic acid in the same reaction system.[20]

$$CH_3\overset{\overset{\|}{O}}{C}O \rightarrow \dot{C}H_3 + CO_2$$

Two paths have been discussed for the formation of the methyl radical, *i. e.*, the decomposition of the acetyl radical and the decomposition of the acetyl oxy radical. On the basis of the low yield of methane, the methyl radical probably partly reacts with propylene to form methane and is partly burned to carbon dioxide. Therefore, it can not

*5 The activation energy of the $CH_3CHO+O_2\rightarrow CH_3\dot{C}O+\dot{O}OH$ reaction is 30 kcal/mol, and that of the $C_3H_6+O_2\rightarrow\dot{C}_3H_5+\dot{O}OH$ reaction is also about 30 kcal/mol or somewhat higher, according to the data tabulated in Semenov's book (N. N. Semenov, *loc. cit*, p. 268 and other parts). The reaction temperature is 360—460°C in Exp. A_0 and 255 or 280°C in Exp. B_2. These suggest that the concentration of the hydroperoxy radical in Exp. A_0 is not lower than that in Exp. B_2. A comparison of the yield of PO relative to those of PA and Acr in Exp. A_0 with that in Exp. B_2 reasonably suggest that the contribution of the hydroperoxy radical to the formation of PO is very small. On this point, Imamura *et al.* neglected the contribution of the hydroperoxy radical to the formation of PO, though they considered the formation of the hydroperoxy radical in their work.[12]

19) Y. Kamiya, *Sekiyu Gakkai Shi (J. Japan Petrol. Inst.)*, **5**, 573 (1962).

20) Y. Kamiya, *ibid.*, **5**, 398 (1962).

be decided which path is major. The allyloxy radical produced is considered to be energy-rich and to decompose as follows:[16]

$$CH_2=CHCH_2\dot{O} \rightarrow CH_2=\dot{C}H + HCHO$$

The formation of allyl alcohol is neglected, because it could not be detected in Exp. A_0.

Formation Reactions of PA and Acr. Comparable amounts of PO, PA and Acr were formed in Exp. B_1 at 280°C.

PA and Acr are also formed in Exp. B_2; this fact may be attributed to the secondary reaction by the allyl peroxy radical formed from radicals induced by the oxidation or decomposition of AA. This idea is supported by the higher conversion of oxygen (50%) in Exp. B_2 than that in Exp. B_1 (20%). According to the discussions presented in the preceding section (in Exp. B_1), the allyl peroxy radical is responsible for the formation of PA and probably of Acr also.

PA retains the carbon skelton of propylene during the reaction, according to the results of White, Davis and Hammack.[9] Cvetanović[10] has proposed that PA is formed through the isomerization of the oxygenated biradical which is formed by the addition of an oxygen atom to the double bond of propylene. Here, the following similar isomerization of the oxygenated radical may be suggested for the formation of PA:

$$CH_2=CHCH_2OOCH_2-\dot{C}HCH_3 \rightarrow$$

$$CH_2=CHCH_2OO\dot{C}H-CH_2CH_3$$

$$CH_2=CHCH_2OO\dot{C}H-CH_2CH_3 \rightarrow$$

$$CH_2=CHCH_2\dot{O} + HC\overset{\overset{\|}{O}}{C}H_2CH_3$$

It can be considered that an acetyl peroxy compound is more unstable than an alkyl peroxy compound. Therefore, this may be a reason for ruling out the route for the formation of PA*6 *via* the addition of an acetyl peroxy radical.

Acr may be formed by the following decomposition of the allyloxy radical,[16] as has been discussed above:

$$CH_2=CHCH_2\dot{O} \rightarrow CH_2=CHCHO + \dot{H}$$

The allyloxy radical is formed in line with the formation of part of PO (from allyl peroxy radical) and PA, as has been discussed above, so the yield of Acr should be less than twice the yield of PA. However, this is not satisfied in Exp. A_0 as shown in Fig. 4. This perhaps indicates that this reaction is minor. The yield of Acr in Exp. B_1 at 280°C is too low in view of the yields of PO and PA (Table 2). Therefore, this reaction is perhaps not feasible. The reaction *via* allyl hydroperoxide is considered to be feasible, however, the following reactions have been proposed by Mullen and Skirrow[6] and also by Kamiya, Sekine and Yamakawa[8] for the formation of Acr:

$$CH_2=CHCH_2O\dot{O} + C_3H_6 \rightarrow$$

$$CH_2=CHCH_2OOH + \dot{C}_3H_5$$

$$CH_2=CHCH_2OOH \rightarrow$$

$$CH_2=CHCHO + H_2O$$

The same scheme may be suggested for the formation of Acr.

Formation Reactions of Ethylene. White, Davis and Hammack[9] have proposed that ethylene is formed *via* the allyl radical. Ethylene is considered to be formed according to the following reactions, which are the competing reaction in the formation of AA by Shtern and Polyak:[3b]

$$CH_2=CHCH_2O\dot{O} \rightarrow CH_2=CH\dot{C}HOOH$$

$$CH_2=CH\dot{C}HOOH \rightarrow$$

$$CH_2=\dot{C}H + CO + H_2O$$

The same scheme may be suggested for the formation of ethylene.

Though $CH_2=\dot{C}H$ is also formed from the decomposition of the allyloxy radical, as has been described above, the reaction path through the isomerization of the allyl peroxy radical is considered to be predominant on the basis of the low contribution of the allyl peroxy radical to the formation of PO, and also on the basis of the low yield of PA in Exp. A_0. $CH_2=\dot{C}H$ most likely reacts with propylene to form ethylene.

Two paths have been discussed for the formation of carbon monoxide, *i.e.*, the decomposition of the acetyl radical and the decomposition of $CH_2=CH\dot{C}HOOH$. There is no experimental evidence, however, upon the basis of which to decide which path is major.

Formation Reaction of Water. It has been postulated that the hydroperoxy radical are formed in the course of the initiation reaction. The following reactions most likely proceed in the formation of water:

$$H\dot{O}O + C_3H_6 \rightarrow HOOH + \dot{C}_3H_5$$

$$HOOH \rightarrow 2\dot{O}H$$

$$\dot{O}H + C_3H_6 \rightarrow H_2O + \dot{C}_3H_5$$

The Scheme of the Oxidation of Propylene in a Propylene-excess Atmosphere. To summarize the above discussions, a reaction scheme is

*6 The yield of PA relative to Acr is lower in Exp. A_0 than that in Exp. B_1, where the concentration of the hydroperoxy radical is very small. Therefore, the contribution of the hydroperoxy radical to the formation of PA is neglected.

TABLE 4. THE PROPOSED REACTION SCHEME (main courses)

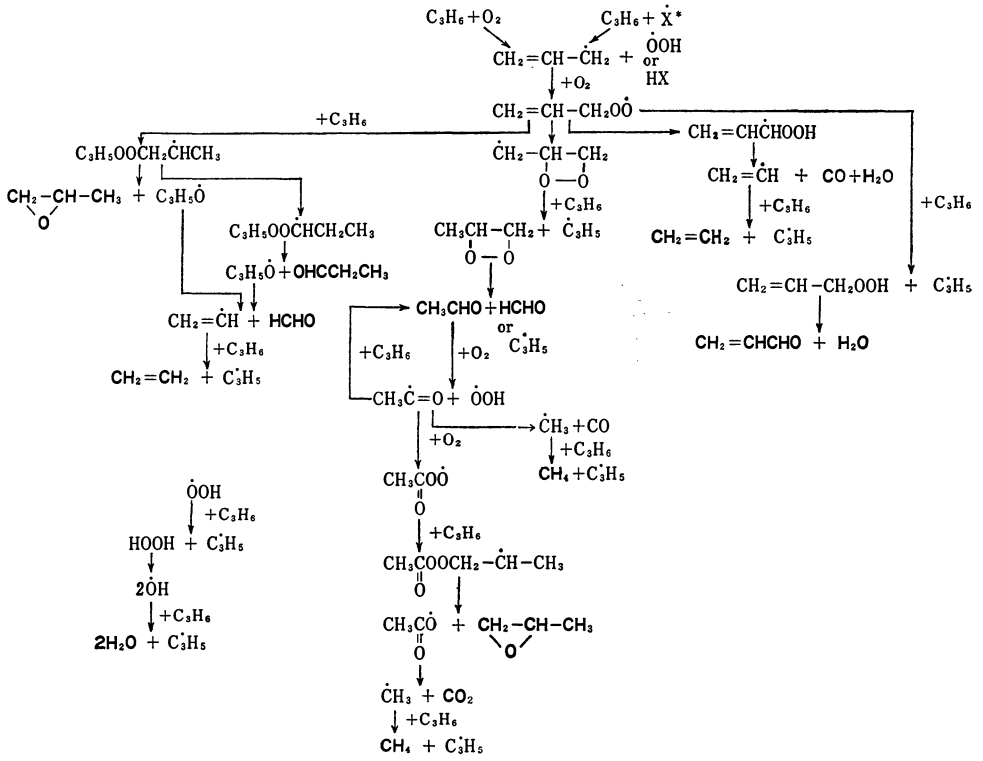

* $\dot{X}$: $\dot{C}H_2CHCH_2$ (O–O), $\dot{C}H_3$, $CH_3\dot{C}$ (=O), $CH_2=\dot{C}H$, $C_3H_5O\dot{O}$, $HO\dot{O}$ and $H\dot{O}$

presented in Table 4. Because of the propylene-excess atmosphere, propylene behaves as the hydrogen donor for the radicals, which are $\dot{C}H_3$ and $CH_2=\dot{C}H$.

The scheme presented in Table 4 is proposed for the main route of the oxidation of propylene. Though this scheme is supported by reasonable evidence in the main, other evidence will be necessary before this scheme can be regarded as a "theory" which can explain the phenomena accompanying the oxidation of propylene.

The authors wish to thank the Nippon Petrochemicals Co., Ltd., for supplying the propylene gas, and the Mitsui Mining and Smelting Co., Ltd., for supplying the silicon carbide.

BULLETIN OF THE CHEMICAL SOCIETY OF JAPAN VOL. 41 920—928 (1968)

Kinetic Study of the Gas-phase Oxidation of Propylene in a Propylene-excess Atmosphere under Pressure*1

Mitsuo MASAI, Etsuro ECHIGOYA*2 and Kiyoshi MORIKAWA

Research Laboratory of Resources Utilization, Tokyo Institute of Technology, Ookayama, Meguro-ku, Tokyo

(Received March 16, 1967)

Reaction-rate equations are derived for oxygen, acetaldehyde, propylene oxide, carbon monoxide, and ethylene on the basis of a plausible reaction scheme. These rate equations are shown to fit the experimental results obtained using a flow-type reactor. It seems most reasonable to conclude that the above reaction mechanism is correct. The type of flow of the reactant gas through the reactor used in this work can be practically regarded as a plug flow from the measurements of the resisdence time distribution using the pulse-tracer method.

In our earlier papers dealing with the gas-phase oxidation of propylene in a propylene-excess atmosphere under pressure using an inert fluidized bed reactor, it was shown that the formations of oxygenated products, such as acetaldehyde and propylene oxide, were favored in a propylene-excess atmosphere,[1] and a plausible reaction scheme was presented which fit the experimental results obtained well.[2]

The purpose of the present paper is to discuss kinetically the reaction scheme reported earlier.[2] It is necessary to obtain a reaction scheme which can elucidate all the main phenomena accompanying this reaction. The reaction scheme proposed in the previous paper[2] fit well the experimental results obtained there. However, because of the complexity of the reaction system, and also because of the lack of other suitable analytical methods, the kinetic study is still a powerful method by which to ascertain what is proceeding in the reaction system predominantly. Among the several papers published concerning the kinetic study of the oxidation of propylene,[3] only Kamiya, Sekine and Yamakawa employed a flow method; they showed that the rate of oxygen consumption is first-order with relation to the concentration of oxygen at the total pressures of 4 and 6 atm, and also that the rate constant in this rate equation is proportional to the -0.75th power of the surface area of the reactor wall.[4]

The flow-type reactor is considered to be suitable for use in following a rapid reaction. The residence-time distribution in the reactor was measured by means of the pulse-tracer technique;[5] the residence time distribution in the reactor used here is practically neglected in the experimental region, so the correct reaction time in this flow reactor can be easily calculated.

On the basis of the reaction scheme reported earlier by the present authors,[2] the reaction-rate equations for the initial reaction step are derived for oxygen, acetaldehyde, propylene oxide, carbon monoxide, and ethylene, the major components in this reaction system. These equations demonstrably fit the experimental results obtained here well. Therefore, it seems most reasonable to conclude that the proposed mechanism of the reaction is correct.

Experimental

Materials. The propylene gas and oxygen have been described before.[1]

Apparatus. The kinetic experiments were carried out in a usual flow-type reactor, 14.8 mm i. d. $\times$ 803 mm length and made of stainless steel*3; the reactor was mounted vertically, as shown in Fig. 1. The pressure in the reactor was controlled by a needle valve of stainless steel*3 at the bottom of the reactor. The inner surface of the reactor was polished nearly to a mirror surface, and the reactor was heated from outside by a fused metal bath.

Procedures. The kinetic experiments were carried out in the region of the low conversion of oxygen;

*1 Part of this paper was presented at the 19th Annual Meeting of the Chemical Society of Japan, Tokyo, April, 1966.

*2 Present address: Department of Chemical Engineering, Faculty of Engineering, Tokyo Institute of Technology.

1) E. Echigoya, M. Masai and K. Morikawa, This Bulletin, **41**, 904 (1968).

2) M. Masai, E. Echigoya and K. Morikawa, *ibid.*, **41**, 910 (1968).

3) V. Ya. Shtern, "The Gas-Phase Oxidation of Hydrocarbons," translated by M. F. Mullins, Pergamon Press, Oxford (1964), pp. 527—573.

4) Y. Kamiya, N. Sekine and Y. Yamakawa, *Sekiyu Gakkai Shi (J. Japan Petrol. Inst.)*, **8**, 951 (1965).

5) T. Miyauch, "Ryukei-Sosa To Kongo-Tokusei" (Operation of a Flow System and Characteristics of Mixing Phenomena), Zoku Shin Kagaku Kogaku Koza, Vol. 14, Nikkan Kogyo Shinbunsha Co., Tokyo (1962), p. 16.

*3 JIS SUS 32, AISI 316, Austenite

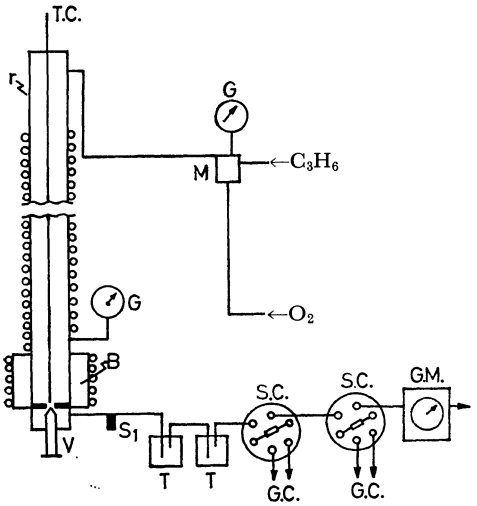

Fig. 1. Flow sheet of reaction apparatus.
B, fused metal bath; G, press. guage (Bourdon type); G. C., gas chromatograph; G. M., wet gas meter; M, gas mixer; r, reactor; S_1, sampling point; S. C., sampling cock; T, cold trap; T.C., thermocouple; V, press. control valve

i. e., the assumption of differential reactor nearly holds. The part of the reactor with temperatures higher than 360°C was regarded as a reaction space, on the basis of previously obtained results.[2] The volume change in the reaction was +3——4.9%, therefore, the volume change during the reaction was neglected. The temperature distributions through the reactor were similar for the same mean reaction temperatures. The mean reaction temperatures were evaluated by averaging the temperatures measured at 5—10 mm intervals along the gas flow with equation, $T_{aver}=(\sum T_i \times l_i)/(\sum l_i)$, where T_i is the measured temperature and l_i is the distance from the bottom of the reactor to the point where T_i was measured. The reaction rates were evaluated carefully from the gradient of the concentration *vs.* reaction time curves (Figs. 3—5, 7—12).

Analysis. The procedure was that described for Exp. B in an earlier paper.[2]

Rate Equations

The reaction scheme which was discussed in the earlier paper[2] was as follows:

0 $CH_2=CH-CH_3 + O_2 \rightarrow CH_2=CH-\dot{C}H_2 + H\dot{O}O$

1 $CH_2=CH-\dot{C}H_2 + O_2 \rightarrow CH_2=CH-CH_2O\dot{O}$

2a $CH_2=CH-CH_2O\dot{O} + C_3H_6 \rightarrow CH_2=CHCH_2OOCH_2\dot{C}HCH_3$

2b $CH_2=CHCH_2OOCH_2\dot{C}HCH_3 \rightarrow CH_2=CHCH_2OO\dot{C}HCH_2CH_3$

2c $CH_2=CHCH_2O\dot{O} + C_3H_6 \rightarrow CH_2=CHCH_2OOH + CH_2=CH\dot{C}H_2$

2d $CH_2=CHCH_2O\dot{O} \rightarrow \dot{C}H_2CHCH_2$ (O–O)

2e $\dot{C}H_2CHCH_2$ (O–O) $+ C_3H_6 \rightarrow CH_3CHCH_2$ (O–O) $+ CH_2=CH\dot{C}H_2$

2f $CH_2=CHCH_2O\dot{O} \rightarrow CH_2=CH\dot{C}HOOH$

3 CH_3CHCH_2 (O–O) $\rightarrow CH_3CHO + HCHO$

4a $CH_3CHO + O_2 \rightarrow CH_3\dot{C}O + H\dot{O}O$

4b $CH_3\dot{C}O + O_2 \rightarrow CH_3COO\dot{O}$ (O)

4c $CH_3COO\dot{O}$ (O) $+ C_3H_6 \rightarrow CH_3COOCH_2\dot{C}HCH_3$ (O)

5a $CH_3\dot{C}O \rightarrow \dot{C}H_3 + CO$

5b $CH_3\dot{C}O + C_3H_6 \rightarrow CH_3CHO + CH_2=CH\dot{C}H_2$

6a $CH_2=CHCH_2OOCH_2\dot{C}HCH_3 \rightarrow CH_2=CHCH_2O\dot{O} + CH_2CHCH_3$ (O)

6b $CH_3COOCH_2\dot{C}HCH_3$ (O) $\rightarrow CH_3CO\cdot$ (O) $+ CH_2CHCH_3$ (O)

7 $CH_2=CHCH_2OO\dot{C}HCH_2CH_3 \rightarrow CH_2=CHCH_2O\dot{O} + HCCH_2CH_3$ (O)

8 $CH_2=CHCH_2OOH \rightarrow CH_2=CHCHO + H_2O$

9 $CH_2=CH\dot{C}HOOH \rightarrow CH_2=\dot{C}H + CO + H_2O$

10 $CH_2=CHCH_2O\dot{O} \rightarrow CH_2=\dot{C}H + HCHO$

11 $CH_3C\dot{O}$ (O) $\rightarrow \dot{C}H_3 + CO_2$

12 $CH_2=\dot{C}H + C_3H_6 \rightarrow CH_2=CH_2 + CH_2=CH\dot{C}H_2$

13 $\dot{C}H_3 + C_3H_6 \rightarrow CH_4 + CH_2=CH\dot{C}H_2$

14 $H\dot{O}O + C_3H_6 \rightarrow HOOH + CH_2=CH\dot{C}H_2$

15 $HOOH \rightarrow 2\dot{O}H$

16 $\dot{O}H + C_3H_6 \rightarrow H_2O + CH_2=CH\dot{C}H_2$

17 $CH_2=CHCH_2O\dot{O} \rightarrow$ chain stop

Reaction (17) is postulated, because a wall effect was observed in our previous work; the oxidation reaction took place above 300°C with the reactor 56.3 mm in i. d.[1] and at 360°C with the reactor

24.5 mm in i. d.[2],*4 This strongly indicates the prolonged induction period for the 24.5 mm reactor discussed in Exp. A_0 of the previous paper.[2] The surface area-to-volume ratios of these reactors differ by a factor of about 2.3. Hence, the wall effect of these stainless steel reactors may be evaluated as stronger than that of the entire surface of the fluidizing particle (silicon carbide).*5 The induction period of a radical-chain reaction ends when a sufficient quantity of the branching agent is accumulated.[6] The branching agent of this reaction is acetaldehyde (AA), which, it has been proposed, is formed from the allyl peroxy radical.[2] Thus, the prolonged induction period can be attributed to the reduced rate of the accumulation of AA. The peroxy radical is considered to be decomposed rapidly on the metallic surface, according to the discussion of Walsh *et al.*[7] This must be the cause of the prolonged induction period with the reactor 24.5 mm in i. d. Therefore, reaction (17) is reasonable.

In the propylene-excess atmosphere under pressure, the probability of the encounter of radicals with propylene is very high, and propylene is assumed to react easily with radicals in the following two ways: the addition of radicals to the double bond, or the abstraction of hydrogen by radicals. Both these reactions produce other radicals. Therefore, the termination reactions in the gas phase is not considered here.

The following equations are obtained on the assumption of the stationary state of the concentrations of radicals. It is postulated that the stationary-state approximation can hold for the concentrations of peroxide molecules. In the initial step of the reaction, the concentrations of propylene and oxygen can be considered to be constant, the following kinetic equations are derived on this assumption.*6

In the following equations, the suffix of the rate constant k indicates a reaction described above, P, O, AA, PO, and C=C indicating propylene, oxygen, acetaldehyde, propylene oxide, and ethylene respectively.

The concentrations of main radicals are as follows:

$$[CH_2{=}CH{-}CH_2{-}O{-}\dot{O}] = 3[O](k_0[P] + k_{4a}[AA])/k_{17} \quad (1)$$

$$[CH_3{-}\dot{C}{=}O] = k_{4a}[AA][O]/G \quad (2)$$

$$[CH_2{=}CH{-}\dot{C}H_2] = 3F(k_0[P] + k_{4a}[AA])/k_1 \cdot k_{17} \quad (3)$$

where

$$G \equiv k_{4b}[O] + k_{5b}[P] + k_{5a}$$

$$F \equiv (k_{2a} + k_{2c})[P] + k_{2d} + k_{2f} + k_{17}$$

The concentrations of these radicals are positive functions of the concentration of AA, which was previously concluded to be the degenerate branching agent in this reaction.[2]

The rate of formation and the concentration of AA are as follows:

$$\frac{d}{dt}[AA] \equiv r_{AA} = \chi[P][O] + \varphi[AA] = \chi[P][O]\exp(\varphi t) \quad (4)$$

$$[AA] = \omega[\exp(\varphi t) - 1] \quad (5)$$

where

$$\varphi \equiv k_{4a}[O][(3k_{2d}/k_{17}) - (k_{4b}[O] + k_{5a})/G] \quad (6)$$

$$\chi \equiv 3k_0 \cdot k_{2d}/k_{17} \quad (7)$$

$$\omega \equiv \chi[P][O]/\varphi$$

Eqs. (4) and (5) show that the rate of the increase of AA is accelerated with the reaction time, and that the accumulations of the allyl, allyl peroxy and acetyl radicals are also accelerated with the reaction time, as may be seen from Eqs. (1)—(3).

Equations (8)—(11) are derived for O, PO, CO, and C=C respectively:

$$-\frac{d}{dt}[O] \equiv r_O = \alpha[O] + \gamma \cdot \omega(e^{\varphi t} - 1)[O] = \alpha[O] + \gamma[AA][O] \quad (8)$$

$$\frac{d}{dt}[PO] \equiv r_{PO} = \beta[P]^2[O] + \delta \cdot \omega(e^{\varphi t} - 1)[O] = \beta[P]^2[O] + \delta[AA][O] \quad (9)$$

$$\frac{d}{dt}[CO] \equiv r_{CO} = \theta[P][O] + \eta \cdot \omega(e^{\varphi t} - 1)[O] = \theta[P][O] + \eta[AA][O] \quad (10)$$

*4 The apparent reaction time is 21 sec for the experiment using the 56.3 mm reactor[1] and 8 sec for that with the 24.5 mm reactor.[2] It was confirmed further that the results of the reaction experiment with the 24.5 mm reactor varied only a little in the range of the apparent reaction time from 5 to 15 sec. This result indicates that the variation in the apparent reaction time in this order does not significantly affect the results of the reaction experiments using the fluidized bed reactor. Therefore, the above discussion about the length of the induction period is not disturbed by the variation in the apparent reaction time.

*5 A detailed discussion of the effect of several kinds of fluidizing particles will be published later.

6) N. N. Semenov, "Some Problems in Chemical Kinetics and Reactivity," Japanese translation by T. Kwan and A. Matsuda, Vol. 2, Chap. 12, Iwanami Shoten Co., Tokyo (1964).

7) D. E. Cheaney, D. A. Davis, A. Davis, D. E. Hoare, J. Prothesroe and A. D. Walsh, "Seventh Symposium (International) on Combustion (1958)," Butterworths Sci. Pub., London (1959), p. 183.

*6 In the derivation of these rate equations, the rate of the formation of the hydroxy radical was regarded as being first-order with regard to the concentration of hydrogen peroxide, considering the initial step of the reaction.

$$\frac{d}{dt}[C{=}C] \equiv r_{C=C} = \varepsilon[P][O] + \zeta\cdot\omega(e^{\varphi t} - 1)[O]$$
$$= \varepsilon[P][O] + \zeta[AA][O] \quad (11)$$

where:

$\alpha \equiv k_0[P] + (3\,k_0\cdot F[P])/k_{17}$

$\beta \equiv 3k_0\cdot k_{2a}\cdot k_{6a}/k_{17}(k_{2b} + k_{6a})$

$\gamma \equiv k_{4a}(1 + k_{4b}[O]/G + 3F/k_{17})$

$\delta \equiv k_{4a}[3k_{2a}\cdot k_{6a}[P]/k_{17}(k_{2b} + k_{6a}) + k_{4b}[O]/G]$

$\varepsilon \equiv \frac{3k_0}{k_{17}}(k_{2f} + k_{2a}[P])$

$\zeta \equiv \frac{3k_{4a}}{k_{17}}(k_{2f} + k_{2a}[P])$

$\eta \equiv k_{4a}(3k_{2f}/k_{17} + k_{5a}/G)$

$\theta \equiv 3k_0\cdot k_{2f}/k_{17}$

As has been shown above, an exponential term or the concentration of AA is present in all kinetic equations. Therefore, these equations may be considered to accord well with the results of the previous work[2] in which AA was demonstrated to be the branching agent in this reaction; also, the relations between the concentration of AA and the reaction rates for O, PO, CO, and C=C can be obtained from the reaction scheme discussed in that earlier paper.[2] The values of α, β, γ, δ, ε, ζ, η, θ, and χ should be positive. As has been shown by Semenov,[6] the reaction rates described above are subject to the value of φ, which can be either positive or negative.

These rate equations represent the well-known "S-shaped rate-*vs.*-time curves" which are characteristic of a degenerate branching reaction, if the value of φ is positive and relatively small, as has been described by Semenov.[6]

The reaction scheme described above can not be a full and precise description of a "perfect reaction mechanism," however, a complete elucidation of such a mechanism is impossible at present. The scheme described above should thus be considered as a description of the predominant course of the homogeneous gas-phase oxidation of propylene in a propylene-excess atomsphere under pressure. Therefore, if the kinetic equations here derived fit the experimental results well, the reaction scheme presented certainly obtains experimental support.

Results

Residence-time Distributions. Figure 2 shows the standard curves of the residence-time distribution function for the Peclet-Bodenstein numbers of 50 and 100; in the figure these curves are compared with the experimental results at the reaction times of 1.1 and 0.3 sec. Their Peclet-Bodenstein numbers are evaluated from Fig. 2 as 70 and 90. On the basis of these values, the residence-time (reaction-time) distribution can be practically neglected under the conditions of the kinetic experiments described below. Thus, the reaction time in this reactor can be easily calculated on the basis of the plug flow.

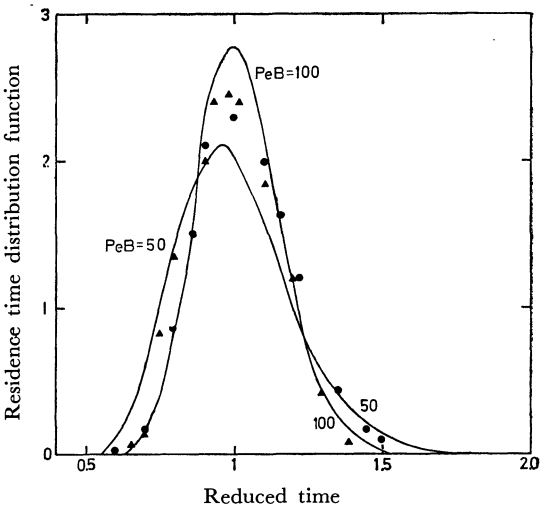

Fig. 2. Results of the measurement of residence time distribution.
▲ 1.1 sec ● 0.3 sec PeB, Peclet-Bodenstein no.

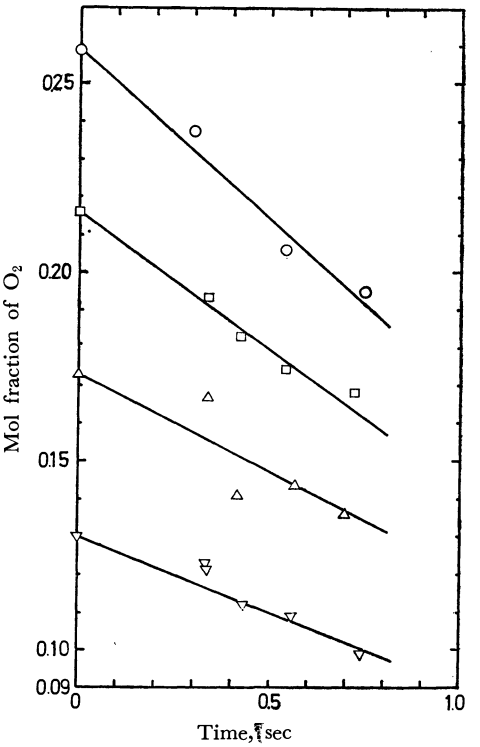

Fig. 3. Effect of the mol ratio (O_2/C_3H_6) on the comsumption of O_2 *vs.* reaction time correlation at 385°C under 3 atm.
○, O_2 0.26/C_3H_6 0.70 □, 0.22/0.74
△, 0.17/0.78 ▽ 0.13/0.82

The Effect of the Molar Ratio of Propylene to Oxygen. Experiments were carried out at 385°C, under 3 atm and with reaction times of 0.3—0.75 sec. The molar ratios of oxygen to propylene examined were 0.26/0.70, 0.22/0.74, 0.17/0.78, and 0.13/0.82; here, the molar fraction of propylene was regarded as roughly constant. The reaction rates were determined from the gradients of the straight lines shown in Figs. 3—5. The reaction order was determined from the gradients of plots, log (molar fraction of oxygen) *vs.* log (rate); Fig. 6 shows the plot of the rate of the comsumption of oxygen and the rates of the

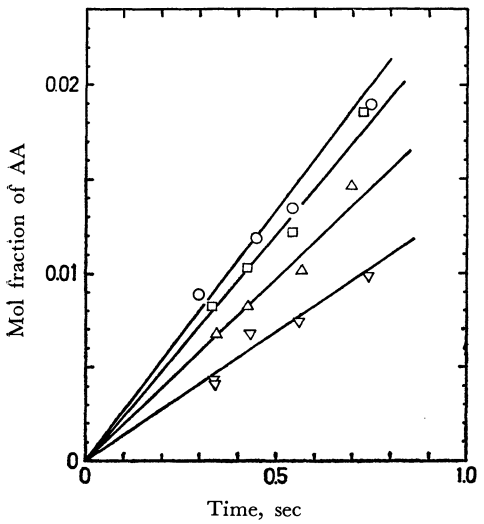

Fig. 4. Effect of the mol ratio (O_2/C_3H_6) on the yield of AA *vs.* reaction time correlation at 385°C under 3 atm.
○, O_2 0.26/C_3H_6 0.70 □, 0.22/0.74
△, 0.17/0.78 ▽, 0.13/0.82

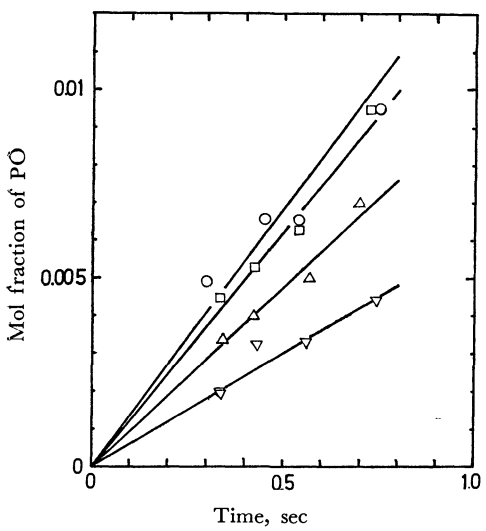

Fig. 5. Effect of the mol ratio (O_2/CH_6) on the yield of PO *vs.* reaction time correlation at 385°C under 3 atm.
○, O_2 0.26/C_3H_6 0.70 □, 0.22/0.74
△, 0.17/0.78 ▽, 0.13/0.82

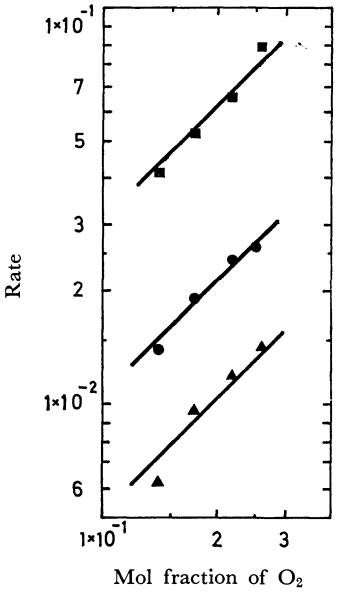

Fig. 6. Logarithmic plot; mol fraction of O_2 *vs.* the rate of the comsumption of O_2 (■) and the rate of the formation of AA (●) and PO (▲).

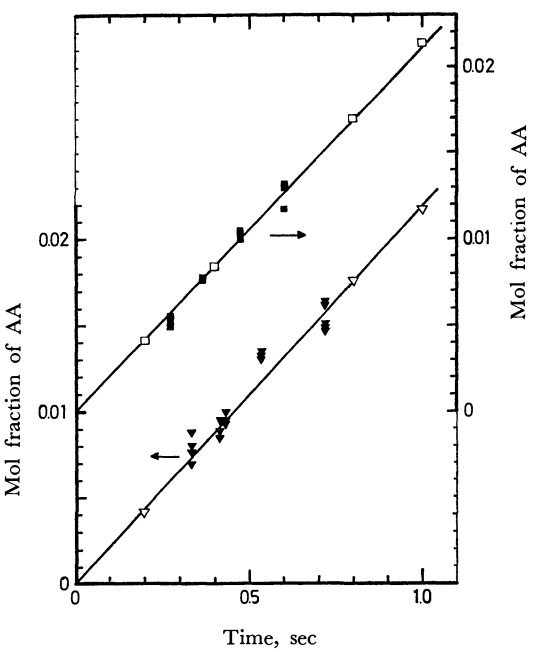

Fig. 7. Effect of temp. on the yield of AA *vs.* reaction time correlation at O_2 0.22/C_3H_6 0.74 under 3 atm.
■, measured at 374°C □, calc. from Eq. (5) for 374°C ▼, measured at 384°C ▽, calc. from Eq. (5) for 384°C

Table 1. Rate constants at 385°C under 3.0 atm

$-\frac{d}{dt}[O_2]=k_O[O_2]$	$\frac{d}{dt}[AA]=k_{AA}[O_2]$	$\frac{d}{dt}[PO]=k_{PO}[O_2]$
k_O, sec^{-1}	K_{AA}, sec^{-1}	k_{PO}, sec^{-1}
0.34	0.12	0.082

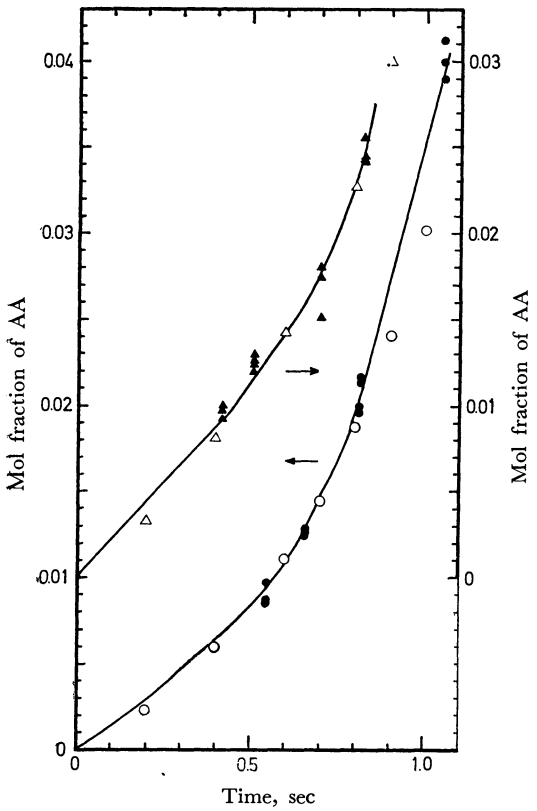

Fig. 8. Effect of temp. on the yield of AA *vs.* reaction time correlation at O_2 0.22/C_3H_6 0.74 under 3 atm.
▲, measured at 399°C △, calc. from Eq. (5) for 399°C ●, measured at 421°C ○, calc. from Eq. (5) for 421°C

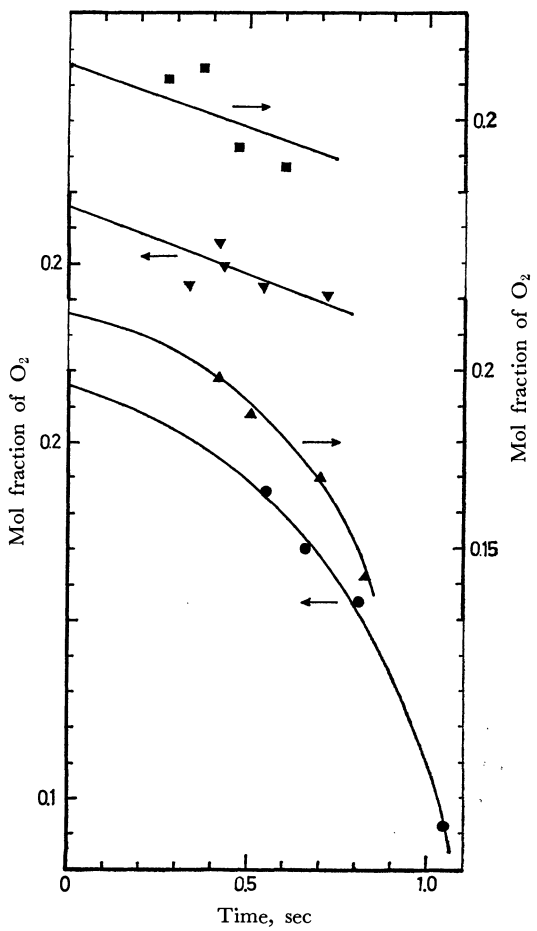

Fig. 9. Effect of temp. on the consumption of O_2 *vs.* reaction time correlation at O_2 0.22/C_3H_6 0.74 under 3 atm.
■, 374°C ▼, 384°C ▲, 399°C ●, 421°C

formation of AA and PO. The rate equations and rate constants obtained are shown in Table 1.

Effects of Temperature. Experiments were carried out under the following conditions: 3 atm, molar ratio of 0.22/0.74 (oxygen/propylene), and temperatures of 374, 384, 399, and 421°C. The results for AA are shown in Figs. 7 and 8, and those for O, PO, CO and C=C, in Figs. 9, 10 11 and 12 respectively. Equations (4)—(5) and (8)—(11) were applied to these results; the constants in these equations were determined using the observed values of molar fractions or the rates at the short reaction times measured at the two points which have different gradients on each curve. The concentration-*vs.*-time curves for AA are shown in Figs. 7 and 8; here the black points represent observed values and the open points represent values calculated using Eq. (5). Table 2 contains the constants in Eqs. (4)—(5) and (8)—(11). The observed and calculated concentrations of AA and rates are compared with each other in Table 3.

Discussion

On the Reaction Scheme. As is shown in Figs. 7 and 8, excellent agreements are obtained between the observed and calculated values for the concentration of AA. The small deviations

Table 2. Constants in rate equations

Temp. °C	φ	ω	$\alpha(\times 10^{-1})$*	$\beta(\times 10^{-2})$*	γ*
374	0.020	1.1	1.7	9.2	
384	0.020	1.0	1.8	10	
399	1.5	0.0098	0.60	0.085	35
421	1.9	0.0051	1.4	3.3	32

Temp. °C	δ*	$\chi(\times 10^{-2})$	ε*$(\times 10^{-2})$	ζ*	θ*$(\times 10^{-2})$	η*
374		13	3.3		30	
384		14	2.4	3.4	29	
399	5.1	9.3	2.8	1.6	5.7	20
421	5.1	6.2	0.61	2.8	11	15

* Owing to the straight lines in concentration *vs.* time plots for O, PO, CO and C=C at 374 and 382°C as shown in Figs. 8—11, the values of α and γ, β and δ, θ and η, ε and ζ, can not be obtained separatly as seen from Eqs. (8)—(11).

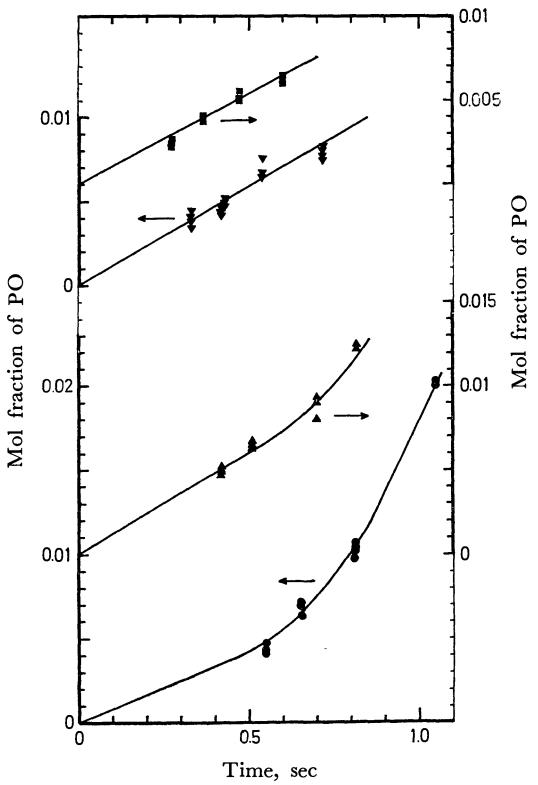

Fig. 10. Effect of temp. on the yield of PO *vs.* reaction time correlation at O_2 0.22/C_3H_6 0.74 under 3 atm.
■, 374°C ▼, 384°C ▲, 399°C ●, 421°C

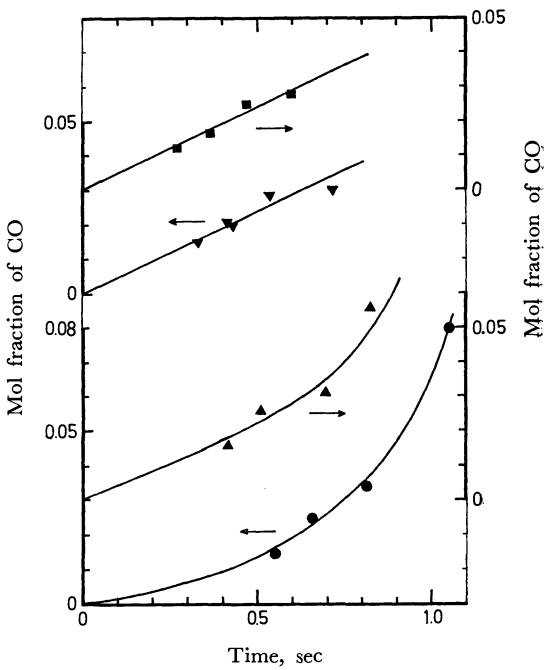

Fig. 11. Effect of temp. on the yield of CO *vs.* reaction time correlation at O_2 0.22/C_3H_6 0.74 under 3 atm.
■, 374°C ▼, 384°C ▲, 399°C ●, 421°C

which are observed in Fig. 8 at the longer reaction time can be ascribed to the failure of the postulation of the initial reaction step. Therefore, it may be concluded that Eq. (5) is suitable for describing the course of the change in the concentration of AA *vs.* the reaction time in the initial step of this reaction system.

As is shown in Table 3, the agreements between the observed and calculated values of r_O, r_{AA}, r_{PO}, r_{CO} and $r_{C=C}$ are satisfactory. It may be concluded, therefore, that Eqs. (4), (8), (9), (10) and (11) are quite satisfactory for describing the reaction rates in this reaction system for O, PO, AA, CO, and C=C. The first order rate equations obtained experimentally for O, AA and PO (Table 1) support this conclusion, because the exponential

TABLE 3. COMPARISON OF OBSERVED VALUES WITH THE CALCULATED VALUES

Conc. and rates	Reaction time sec	374°C		384°C		399°C		421°C	
		Obs.	Calc.	Obs.	Calc.	Obs.	Calc.	Obs.	Calc.
$[CH_3CHO]^*$ ($\times 10^{-2}$)	0.3	0.64	0.64	0.67	0.62	0.66	0.56	0.46	0.40
	0.5	1.1	1.1	1.1	1.1	1.1	1.1	0.82	0.83
	0.8	—	1.7	1.8	1.8	2.3	2.3	2.0	1.9
$-\frac{d}{dt}[O_2]^{**}$ ($\times 10^{-2}$)	0.3	3.6	3.6	3.8	3.8	5.5	5.5	6.0	5.8
	0.5	3.6	3.6	3.8	3.8	9.5	9.5	8.8	8.8
	0.8	3.6	3.6	3.8	3.8	23	18	16	16
$\frac{d}{dt}[CH_3CHO]^{**}$ ($\times 10^{-2}$)	0.3	2.1	2.1	2.2	2.2	2.2	2.5	1.8	1.8
	0.5	2.1	2.1	2.2	2.2	2.9	3.0	2.1	2.6
	0.8	2.1	2.1	2.2	2.2	6.7	4.9	5.2	4.6
$\frac{d}{dt}[CH_3\overset{\diagup O \diagdown}{C}HCH_2]^{**}$ ($\times 10^{-2}$)	0.3	1.1	1.1	1.2	1.2	1.2	0.62	0.83	0.83
	0.5	1.1	1.1	1.2	1.2	1.2	1.2	0.90	1.3
	0.8	1.1	1.1	1.2	1.2	2.5	2.5	2.4	2.5
$\frac{d}{dt}[CO]^{**}$ ($\times 10^{-2}$)	0.3	5.0	5.0	4.6	4.6	3.3	4.7	3.2	2.6
	0.5	5.0	5.0	4.6	4.6	5.6	5.2	4.6	4.8
	0.8	5.0	5.0	4.6	4.6	11	14	8.0	9.2
$\frac{d}{dt}[C_2H_4]^{**}$ ($\times 10^{-3}$)	0.3	5.3	5.3	8.8	5.8	6.5	6.9	3.4	3.7
	0.5	5.3	5.3	12	11	8.3	8.0	6.2	5.5
	0.8	5.3	5.3	—	—	12	14	12	16

* expressed in mol fraction ** expressed in (mol fraction)/(sec)

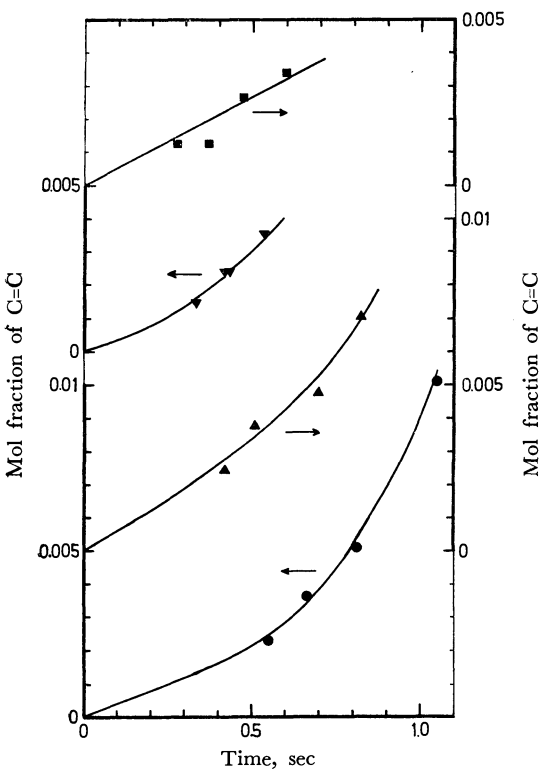

Fig. 12. Effect of temp. on the yield of C_2H_4 *vs.* reaction time correlation at O_2 0.22/C_3H_6 0.74 under 3 atm.
■, 374°C ▼, 384°C ▲, 399°C ●, 421°C

terms in Eqs. (4), (8) and (9) are not so large; when φt is small, as is shown in Table 2, these equations apparently become first-order rate equations. Thus all the kinetic equations derived have been proved to fit the experimental results.

Though many reaction schemes leading to the same rate equations are plausible, the authors' scheme has been supported by experiments and also by the results of many other authors' cited in the previous paper.[2] It seems, therefore, reasonable to conclude that the reaction scheme presented in this paper is a correct description of the main course of this reaction. In consideration of the values of the reaction rate constants (Tables 1 and 2) and the yields of the various oxidation products given in Figs. 4—6 of the previous paper,[2] the relative weight of the reaction paths may finally be considered to be as follows:

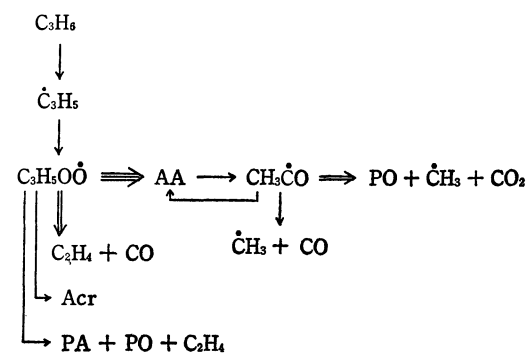

On the Slow Rate Period. From the above discussions, the characteristics of this reaction system can be represented in terms of the behavior of AA. In Fig. 8, for AA at 399 and 421°C a steep increase in AA formation is observed after a linear increase. This linear sector corresponds to the constant-reaction-rate region at the initial reaction time. As is shown in Fig. 7 for AA at 374 and 384°C, this linear sector continues to the end of the experiment; in this case, the values of φ are small, as shown in Table 2. The value of φ undergoes a sudden increase at some temperature between 384 and 399°C, as is also shown in Table 2.

In Eq. (4), the values of $\chi(\equiv 3k_0 \cdot k_{2d}/k_{17})$ decrease slowly with the rise of temperature, as shown in Table 2. Therefore, the $3k_{2d}/k_{17}$ term, in φ may also be considered to change slowly; moreover, it is reasonable to consider that $k_{4a}[O]$ the term in φ changes slowly. Thus, the sudden increase in φ may be attributed to the sudden decrease in the $(k_{4b}[O]+k_{5a})/(k_{4b}[O]+k_{5b}[P]+k_{5a})$ term in Eq. (6). Here, this term of φ may be written as $a/(a+k_{5b}[P])$. Therefore, the value of φ can increase rapidly upon the gradual increase in k_{5b} with the temperature. Thus, the difference between the kinetic curves of 374 and 384°C and those of 399 and 421°C can be reasonably explained.

The authors are indebted to Mr. Mitsuhiko Iwasaki for his advices on the pulse tracer technique and for his kind help for the digital computer calculation, also thank Nippon Petrochemicals Co., Ltd, for supplying the propylene gas.

BULLETIN OF THE CHEMICAL SOCIETY OF JAPAN VOL. 41 928—931 (1968)

Reactions of Triethylaluminum with α,β-Unsaturated Carbonyl Compounds

Yoshio BABA

Resources Research Institute, Kawaguchi, Saitama

(Received April 17, 1967)

The reactions of triethylaluminum and its various ether adducts with α,β-unsaturated ketone, aldehyde, ester, and methyleneanthrone have shown that the addition occurs mainly at the 1,2-positions of the carbonyl function, and not at the 1,4-positions as has been observed in the Grignard reaction. The mode of addition was discussed in view of the reactivity of the organometallic compound and the steric factor of the unsaturated carbonyl compounds.

A possible mode of the addition of organometallic compounds to unsaturated carbonyl compounds has been studied by many investigators.

Cologe[1] has proposed correlations between the structure of α,β-unsaturated ketones and the mode of addition in the reaction of a simple Grignard reagent.

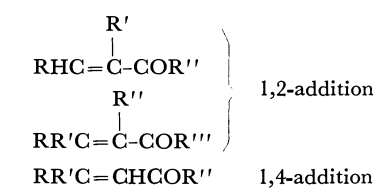

Gilman,[2] however, has reported that the reactivity of the organometallic compounds determines the direction of the addition. The relatively less reactive phenyl metallic compounds add to benzalacetophenone at the 1,4-positions, while the reactions with more reactive members afford 1,2-addition products.

Recently, Wittig[3-5] has proposed a mechanism of the addition reaction of organometallic compounds in which the mode of addition is effected by the ability of ate-complex formation. Thus, even though difficulty is encountered in the reaction of benzophenone with triphenylaluminum, the reaction of benzalacetophenone with triphenylaluminum proceeds readily to give the 1,4-addition product. The facile reaction of benzalacetophenone is interpreted as being due to the ability of ate-complex (I) formation, as is shown in Eq. (1):

1) J. Colonge, *Bull. Soc. Chim.*, (5), **2**, 754 (1935).
2) H. Gilman and R. H. Kirby, *J. Am. Chem. Soc.*, **63**, 2046 (1941).
3) G. Wittig, *Angew. Chem.*, **70**, 65 (1958).
4) G. Wittig and O. Bub, *Ann.*, **566**, 113 (1950).
5) A. Luettringhaus and K. Scholtis, *ibid.*, **557**, 70 (1941).

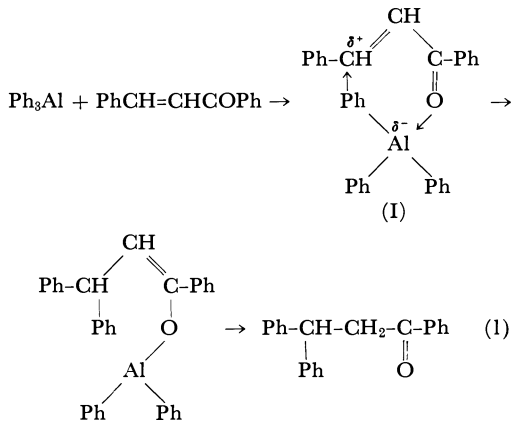

Phenylsodium or phenyllithium, however, reacts with the same α,β-unsaturated ketone to give the 1,2-addition product because of its lack of the ability to make an ate-complex intermediate.

The present work was undertaken to study the possible modes of addition in the reaction of triethylaluminum with unsaturated carbonyl compounds.

Experimental

All the reactions were carried out in an atmosphere of dry nitrogen. The melting points were measured on a micro hot stage and were not corrected.

Materials. Triethylaluminum purchased from the Ethyl Corp. was used without further purification. Commercial di-*n*-propyl ether (bp 90°C), diisopropyl ether (bp 68°C), di-*n*-butyl ether (bp 142°C), di-*n*-amyl ether (bp 186°C), diisoamyl ether (bp 172°C), cinnamaldehyde (bp 93—94°C/5 mmHg), benzalacetone (bp 112—113°C/5 mmHg, mp 41—42°C), ethyl cinnamate (bp 127—128°C/7 mmHg), crotonaldehyde (bp 102°C), mesityl oxide (bp 129°C), methyl crotonate (bp 127°C), and benzophenone (bp 150—151°C/5 mmHg) were purified by distillation. Methyleneanthrone (mp 146—147°C) was prepared from anthraquinone *via* anthrone.[6] Ethyl ethylenetetracarboxylate (mp 52.0—52.5°C) was synthesized from diethyl malonate *via* diethyl bromomalonate.[7]

Analytical Procedure. The C=C double bond and carbonyl group were analyzed according to the Lucas[8] and Iddles[9] methods respectively.

Reactions of Benzalacetone with Triethylaluminum and Its Various Ether Adducts. A 30-weight-percent solution of an aluminum compound in dry benzene containing 0.1 mol of triethylaluminum or its ether adducts was added drop by drop, to an ice-cooled solution of benzalacetone (0.05 mol) in dry benzene. The reaction mixture was, after standing for 0.5 hr in an ice-bath, refluxed for 1 hr. The crude product obtained by the usual method was distilled under reduced pressure. The carbonyl component in the distillate was extracted with a Girard reagent ($(C_5H_5N-\overset{+}{C}H_2CONHNH_2)Cl^-$). The amounts of unchanged ketone and 1,4-addition product were then determined by C=C double bond and carbonyl group analysis in the carbonyl fraction by the methods described in the "analytical procedure" section, while the amounts of alcohol produced by the 1,2-addition reaction and its dehydrated product produced in the course of the distillation were determined by active-hydrogen and C=C double bond analysis of the non-carbonyl fraction.

Reaction of Benzophenone with Triethylaluminum. The reaction of benzophenone (9.1 g, 0.05 mol) with 0.075 mol of triethylaluminum in a benzene solution (refluxed for 1 hr) yielded 9.2 g of an oily product distilled at 143—150°C/5 mmHg. The above product was mixed with phthalic anhydride (6.0 g) and 24 g of dry pyridine. After a 3 hrs' refluxing of the reaction solution, the pyridine was removed by distillation and the residue was dissolved in 30 m*l* of benzene. From the benzene solution, the mono ester of the phthalic acid of secondary alcohol was extracted with a 10% potassium hydroxide solution, while the benzene solution, after drying over calcium chloride, was evaporated to give 4.3 g (42%) of crystals (mp 90—92°C). The recrystallization of the crude crystal from petroleum ether gave plates, mp 93—94°C, which showed no depression in melting point upon the admixture of diphenylethylcarbinol (mp 93—94°C), prepared from ethylmagnesium bromide and benzophenone. The alkaline solution containing the mono ester of phthalic acid of the secondary alcohol was boiled for 5—10 min, and then the separated oil was extracted with benzene. The benzene solution was dried over calcium chloride and the benzene was evaporated. The crude crystals (mp 65—66°C, 4.7 g, 51%) were recrystallized from ethanol, mp 66—67°C, needles, the melting point was undepressed by admixture with benzhydrol.

Reaction of Methyleneanthrone with Triethylaluminum. A powdered methyleneanthrone (5.2 g, 0.025 mol) was added to a strirred solution of triethylaluminum (0.076 mol) in dry petroleum ether. The solid methyleneanthrone dissolved readily, and a faint-yellow-colored solution resulted. The reaction solution was stirred for 4 hr at room temperature and then treated by the usual method. The faintly-yellow-colored oily product (7.0 g) was mixed with a small amount of ethanol and then allowed to stand for several days at room temperature. The crystals which separated were collected by filtration and washed with ethanol. The crude crystal (1.7 g, 33.0%) was recrystallized from ethanol; mp 283—284°C, undepressed by admixture with anthraquinone. The chromic acid oxidation of the oily product yielded 9-ethylanthrol (mp 106—107°C, from ethanol).

Found: C, 80.39; H, 6.35%. Calcd for $C_{16}H_{14}O_2$: C, 80.65; H, 5.92%.

Reaction of Ethyl Ethylenetetracarboxylate with Triethylaluminum. The reaction of ethyl ethylenetetracarboxylate (12.9 g, 0.041 mol) with 0.184 mol of triethylaluminum yielded 5.5 g (42.2%) of crystals, mp 75—76°C, from ethanol; the crystals were identified as ethyl ethanetetracarboxylate by a mixed melting point determination with a sample prepared from

6) E. Barnett, *Ber.*, **59**, 767 (1926); "Organic Syntheses," Coll. Vol. I, p. 60 (1956).
7) "Organic Syntheses," Coll. Vol I, p. 245; II, p. 273 (1956).
8) H. Lucas and D. Pressman, *Ind. Eng. Chem., Anal. Ed.*, **10**, 140 (1938).
9) H. Iddles and C. Jackson, *ibid.*, **6**, 454 (1934).

ethylmagnesium bromide and ethyl ethylenetetracarboxylate according to the procedure reported by Hsing.[10]

Results and Discussion

The results of the experiments of benzalacetone with triethylaluminum and its various ether adducts shows that, as Table 1 indicates, in every case the 1,2-addition reaction constituted the principal reaction, whether the free triethylaluminum or its ether adducts, which are considered to have some influence on the ate-complex formation, were employed. On the basis of these data, it seems reasonable to infer that the mode of addition in the reaction of triethylaluminum with α,β-unsaturated ketone is not influenced by the ability of ate-complex formation, but is rather defined by the reactivity of organometallic compounds.

Thus, even in the reaction of organometallic compounds with the same metal atom, such as triethylaluminum and triphenylaluminum, the highly reactive member permits the 1,2-addition, while the compound with a lower reactivity gives the 1,4-addition product.

A higher reactivity of triethylaluminum as compared with triphenylaluminum was demonstrated by the reaction with benzophenone. Although benzophenone does not react with triphenylaluminum,[3] it reacts readily with triethylaluminum to give both the addition and reduction products, each in a 50% yield.

Bergman[11] has reported that the reaction of methyleneanthrone with ethylmagnesium bromide does not afford any of the alcohol expected from the normal Grignard reaction, but gives anthraquinone as the sole reaction product. Julian and Magnani[12] have studied this reaction and concluded that the reaction involves the 1,6-addition of ethylmagnesium bromide to the conjugated system in methyleneanthrone. They have verified the above mechanism by the isolation of the intermediate peroxide produced by the air oxidation of 1,6-addition product, and the formation of anthraquinone, by the decomposition of the peroxide, as shown in Eq. (2). They have also further disclosed that, in the case of a homolog of methyleneanthrone carrying a bulky group at the γ-position, benzalanthrone for example, the 1,6-addition is inhibited and the 1,2-addition is realized.

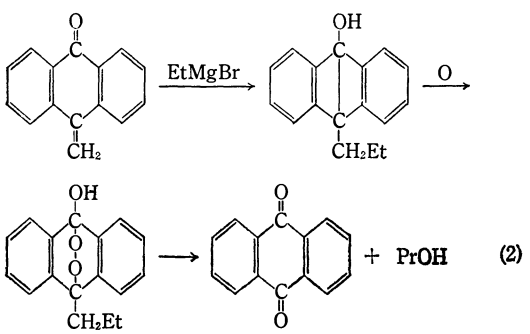

(2)

Methyleneanthrone reacted with triethylaluminum to give anthraquinone, an oxidative degradation product of the 1,6-addition product, in a 33% yield, but a substance carrying a hydroxyl group was obtained in a 32% yield as another product. A postulation that the alcohol (I) formation can be attributed to the 1,2-addition of al-Et to the conjugated system of methyleneanthrone was verified by the chromic acid oxidation of this alcohol to yield 9-ethylanthrol (II) (*cf.* Eq. (3)).

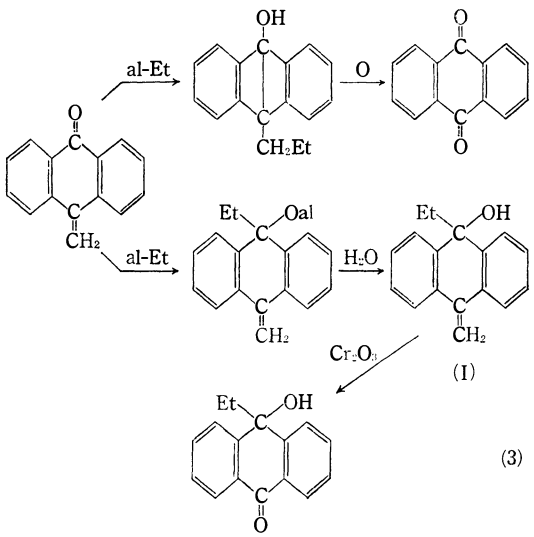

(3)

Thus it was found that triethylaluminum tends to add more readily to the carbonyl group of the conjugated system in methyleneanthrone than the corresponding magnesium compound, and that the mode of addition is defined both by the reactivity of the organometallic compound and by the steric factor of the unsaturated ketones.

The facile addition of trialkylaluminum to the carbonyl group in the unsaturated carbonyl compound could be verified from the reaction of triethylaluminum with the six α,β-unsaturated carbonyl compounds listed in Table 2; the 1,2-addition products were obtained as the major products.

A difficulty of the 1,2-addition of al-Et group to a carbonyl group in the unsaturated carbonyl compound was encountered in the reaction with ethyl ethylenetetracarboxylate. Hsing[10] has found that the reaction of ethyl ethylenetetracarboxylate with a large excess of ethylmagnesium bromide

10) C.-Y. Hsing and L.-T. Li, *J. Am. Chem. Soc.*, **71**, 774 (1949).
11) E. Bergman, *Ber.*, **63**, 1041 (1930).
12) P. L. Julian and A. Magnani, *J. Am. Chem. Soc.*, **56**, 2174 (1934).

TABLE 1. REACTIONS OF BENZALACETONE WITH TRIETHYLALUMINUM AND ITS ETHER ADDUCTS

Aluminum compd.	Ketone recovered (b)	Condensation product (a)	1,4-Addition product (b)	1,2-Addition product (b)
$AlEt_3$	1.9	17.8	8.1	69.2
$AlEt_3$-Et_2O	5.5	29.5	15.5	47.5
$AlEt_3$-Pr_2O-*n*	2.9	9.5	23.6	60.8
$AlEt_3Pr_2O$-*i*	1.5	11.5	2.9	81.9
$AlEt_3$-Bu_2O-*n*	1.8	13.2	24.7	57.2
$AlEt_3$-Am_2O-*n*	1.9	13.4	27.4	53.1
$AlEt_3$-Am_2O-*i*	3.1	14.1	20.6	58.1

(a) Weight percent (b) Theor. yield %

TABLE 2. REACTION OF TRIETHYLALUMINUM WITH UNSATURATED CARBONYL COMPOUNDS

Unsaturated carbonyl compd.	Unchanged compd. (b)	Condensation product (a)	1,2-Addition product (b)	1,4-Addition product (b)
$C_6H_5CH{=}CH{-}CHO$	0	2.5	99.3	0
$C_6H_5CH{=}CHCOOC_2H_5$	20.0	3.4	65.7	4.0
$C_6H_5CH{=}CHCOCH_3$	10.9	17.8	65.2	1.1
$CH_3CH{=}CHCHO$	0	4.8	91.6	1.0
$(CH_3)_2C{=}CHCOCH_3$	4.0	26.1	65.6	0.3
$CH_3CH{=}CHCOOCH_3$	20.0	6.7	58.4	10.9

(a) Weight percent (b) Theor. yield %

does not cause the addition of metalalkyl linkage to the carbonyl group of the ester, but yields the reduction product of the C=C double bond and the product derived from the addition of the metal-ethyl linkage to the C=C double bond in yield of 43% and 56% respectively. The reaction of this unsaturated ester with eight moles of triethylaluminum was found to give the same product as expected from the analogy of the corresponding Grignard reaction.

The author wishes to thank Dr. J. Yoshimura, Professor of Tokyo Institute of Technology, for his many helpful discussions and suggestions during this work, and Y. Koenuma for his assistance in the experimental work.

BULLETIN OF THE CHEMICAL SOCIETY OF JAPAN VOL. 41 932—936 (1968)

Catalytic Dehydrogenation of Secondary Alcohols with Reduced Copper. VI.[1] The Dehydrogenation of Isopropyl Alcohol (Part III)*[1]

Kazuaki KAWAMOTO, Yoshiharu NISHIMURA*[2] and Teruo HIRAKI

Institute of Commodities, Faculty of Economics, Kagawa University, Takamatsu

(Received May 12, 1967)

In order to determine whether the condensing activity of reduced copper is affected by the mode of preparation of the catalyst, the condensation of isopropyl alcohol to isobutyl methyl ketone, diisobutyl ketone, and isobutylmethylcarbinol was studied with catalysts prepared in different ways. It was found that the copper catalyst obtained by the hydrogen treatment of the oxide prepared from copper nitrate and an excess of sodium hydroxide was the most suitable catalyst for the condensation of isopropyl alcohol to isobutyl methyl ketone and diisobutyl ketone, and that the copper catalyst prepared with potassium carbonate was the most suitable catalyst for the dehydrogenation of isopropyl alcohol to acetone with no side reaction.

In a previous study,[2] it was found that isobutyl methyl ketone and diisobutyl ketone could be prepared in one step by passing isopropyl alcohol over various forms of copper catalysts heated at 220°C and 250°C, and that the relative amounts of the compounds in the reaction products depended not only upon the reaction temperature, but also upon the mode of preparation of the catalyst.

Adkins *et al.*[3] found that the nickel catalyst prepared by precipitation with ammonium carbonate was more active in the hydrogenation than those prepared with other precipitants (sodium hydroxide, sodium carbonate and sodium bicarbonate). Frolich *et al.*[4] reported that an active catalyst for the decomposition of methanol could be obtained by adding ammonia to a solution of copper nitrate.

Palmer[5] studied the influence of the reducing agents on the copper catalyst, which was used as the catalyst for the dehydrogenation of ethyl alcohol; he reported that the activity of the copper catalyst prepared with hydrogen was greater than those treated with methanol and with carbon monoxide.

No detailed study of the effect of solvents used in the preparation of copper catalysts on the dehydrogenation of a secondary alcohol have been reported.

The object of the present work is to discover how the precipitant, the solvent, and the reducing agent used in the preparation of a catalyst influence the activity and the selectivity of the catalyst, and to find the most suitable conditions and the best catalyst for the formation of isobutyl methyl ketone and diisobutyl ketone from isopropyl alcohol. Experiments were carried out at several temperatures between 185°C and 325°C; four different precipitants, six solvents, and three reducing agents were used.

Experimental

Preparation of Catalysts. The precipitates (Cu VII—Cu XXIV) were prepared as shown in Table 1. As a typical run, Cu XV was prepared as follows: A solution of 30 g of cupric nitrate hexahydrate in 900 m*l* of distilled water was kept at 22°C. An ammonia solution prepared from 12 g of ammonia (30%) and 300 m*l* of distilled water was brought to the same temperature and added rapidly to the stirred copper nitrate solution. After the mixture had been stirred at this temperature for 30 min, the precipitate was washed well with distilled water by decantation, collected on a glass filter, dried in an electric oven at 105°C for the time given in the table, powdered in an agate mortar, and finally stored in a stoppered bottle.

The precipitates were reduced in the following ways. When hydrogen was used as the reducing agent, the hydrogen was passed at the rate of 750—900 m*l* per hour over 10 g of the precipitate; the reduction temperature was always below 185°C. In the case of the reduction of the precipitate with isopropyl alcohol vapor, the isopropyl alcohol was charged at the rate of 10—11 g per hour, while the reduction temperatures were 185, 220, 250 and 325°C. In the case of the reduction of the precipitate with carbon monoxide, the flow rate of carbon monoxide was 800—900 m*l* per hour, and the reduction temperature was always below 140°C.

1) K. Kawamoto, This Bulletin, **34**, 799 (1961).

*1 The major part of this research was presented at the Chugoku Shikoku Local Meeting of the Chemical Society of Japan, Matsuyama, November, 1963.

*2 Present address: Department of Chemistry, Faculty of Education, Kagawa University, Takamatsu.

2) K. Kawamoto, This Bulletin, **34**, 161, 795 (1961).

3) H. Adkins and L. W. Covert, *J. Phys. Chem.*, **35**, 1684 (1931); L. W. Covert and R. Connor, *J. Am. Chem. Soc.*, **54**, 1651 (1932).

4) P. K. Frolich, M. R. Fenske and D. Quiggle, *ibid.*, **51**, 61 (1929).

5) W. G. Palmer, *Proc. Roy. Soc.*, **A99**, 412 (1921).

Table 1. Preparation of precipitates

Precipitate	Precipitant and amount		Solvent: Alcohol and volume		Solvent: Distilled water	Time of drying
		g		ml	ml	hr
Cu VII	NaOH	15			300	20
Cu IX	K_2CO_3	25			500	10
Cu XV	NH_4OH	12			300	20
Cu XVI	$(NH_4)_2CO_3$	16			300	20
Cu XVII	NaOH	15	CH_3OH	300		20
Cu XVIII	NaOH	15	C_2H_5OH	300		20
Cu XIX	NaOH	15	*n*-C_3H_7OH	250	50	20
Cu XX	NaOH	15	*n*-C_4H_9OH	250	50	20
Cu XXI	NaOH	15	*i*-C_3H_7OH	250	50	20
Cu XXII	NaOH	15	*s*-C_4H_9OH	250	50	20
Cu XXIII	K_2CO_3	25	CH_3OH	300	200	10
Cu XXIV	K_2CO_3	25	C_2H_5OH	300	200	10

Apparatus and Procedure. The apparatus employed was similar to that used in the previous investigation, with the exception that an electrically heated furnace was used. A definite amount (10 g) of the precipitate was placed in the Pyrex reaction tube (18 mm in inside diameter and 1 m in length), which was set in an electrically heated furnace of the horizontal type. The furnace was heated to the reduction temperature and kept at this temperature for the period of reduction. The reducing agent was passed through the tube at a regular velocity; the resulting catalyst was then heated to the reaction temperature. Experiments were performed at 185, 220, 250, 300, and 325°C under ordinary pressure, and isopropyl alcohol was passed through the tube at a constant flow rate. The reaction products coming out of the reaction tube were removed by being passed through a condenser cooled with ice water, supplemented by two traps which were cooled with ice. The volume of gas evolved was determined by allowing it to displace the water from a 2 *l* graduated cylinder. All the values given in the present research are averages of two to three measurements under constant reaction conditions.

Analysis of the Products. The reaction products (acetone, isobutyl methyl ketone, diisobutyl ketone, and isobutylmethylcarbinol) were identified by comparing them with authentic samples obtained by gas chromatography. In addition, the reaction products were dried with anhydrous sodium sulfate and then fractionally distilled, and the constituents of the cut were identified by their boiling points, densities, refractive indices, and the formation of the corresponding derivatives. All derivatives for the identification of the reaction products were made by the Shriner, Fuson, and Curtin method.[6] Acetone was present in a fraction boiled at 56—56.5°C. From this fraction, the 2,4-dinitrophenylhydrazone, mp 128°C, and the semicarbazone, mp 187°C were obtained. The fraction of isobutyl methyl ketone gave the semicarbazone, mp 133—133.5°C, and the 2,4-dinitrophenylhydrazone, mp 93.5—94°C. The fraction of diisobutyl ketone gave the 2,4-dinitrophenylhydrazone, mp 92—92.5°C, and the semicarbazone, mp 122—122.5°C. The fraction of isobutylmethylcarbinol gave the phenylurethane, mp 142—143°C. No formation of unsaturated or hydroxy ketones, such as mesityl oxide, phorone or diacetone alcohol, were detected in the reaction products of any of the experiments. The gaseous product, when analyzed by gas chromatography, has found to be hydrogen. The reaction products were analyzed quantitatively by gas chromatography using a Shimadzu-Type GC-2B and a Shimadzu-Type CG-2C apparatus. A 5-m column of PEG-6000 was used at an operating temperature of 100°C and at a flow rate of 22.0 ml/min of helium. For the determination of water, a 3-m column packed with Shimalite F impregnated with PEG-1000 was used at 100°C with a hydrogen carrier at 11.5 ml/min. Further, the content of acetone was determined by the hydroxylamine method.[7]

Results and Discussion

The influence of the precipitant, the solvent, and the reducing agent used in the preparation of catalyst on the activity and the selectivity of the copper catalyst is summarized in Tables 2 and 3; the amounts of reaction products given in these tables are reproducible within 1 per cent. The evolution of gas measured at intervals of 15—20 min was found to be constant during the reaction time. Therefore, it was concluded that the sustained activity of the catalyst held over the period of the operation. Little dehydration of isopropyl alcohol to propylene seems to occur at temperatures below 325°C.

Influences of the Precipitants and the Solvents on the Dehydrogenating Activity and the Condensing Activity of Reduced Copper. As shown in Table 2, the dehydrogenating activity and the condensing activity of a copper catalyst vary considerably with the sort of precipitant and

6) R. L. Shriner, R. C. Fuson and D. Y. Curtin, "The Systematic Identification of Organic Compounds," John Wiley & Sons, New York (1956).

7) M. Katsuno, *Kogyo Kagaku Zasshi (J. Chem. Soc. Japan, Ind. Chem. Sect.)*, **46**, 112 (1943).

TABLE 2. INFLUENCES OF THE PRECIPITANTS AND THE SOLVENTS ON THE DEHYDROGENATING ACTIVITY AND THE CONDENSING ACTIVITY OF REDUCED COPPER
(Reaction temp.: 250°C)

Precipitant		NaOH							K_2CO_3			NH_4OH	$(NH_4)_2CO_3$
Precipitate		Cu VII	Cu XVII	Cu XVIII	CuXIX	Cu XX	Cu XXI	Cu XXII	Cu IX	Cu XXIII	Cu XXIV	Cu XV	Cu XVI
Solvent		H_2O	CH_3OH	C_2H_5OH	n-C_3H_7OH	n-C_4H_9OH	i-C_3H_7OH	s-C_4H_9OH	H_2O	CH_3OH	C_2H_5OH	H_2O	H_2O
Isopropyl alcohol	g	38.8	38.6	39.0	39.4	39.3	38.6	38.6	39.2	39.4	39.2	38.8	38.8
Velocity	g/hr	11.7	11.4	9.8	12.1	11.8	12.5	12.1	11.5	12.3	10.8	10.0	8.4
Reaction product	g	34.6	34.7	34.9	35.2	35.0	34.9	34.7	35.9	35.9	35.9	34.6	35.0
Composition of reaction product													
Acetone	%	47.6	54.7	55.8	84.8	84.4	86.1	85.9	90.2	79.8	80.3	81.1	58.8
Isobutyl methyl ketone	%	19.8	16.7	16.4	T	T	T	T	0	0	0	2.6	12.5
Diisobutyl ketone	%	16.0	13.4	13.6	T	T	T	T	0	0	0	2.1	10.3
Isobutylmethylcarbinol	%	2.1	1.6	1.7	0	0	0	0	0	0	0	0.2	1.4
Unidentified product	%	0.8	0.9	0.7	0	0	0	0	0	0	0	0	0.6
Water	%	7.9	6.5	6.5	0	0	0	0	0	0	0	1.0	4.9
Unreacted alcohol	%	5.8	6.2	5.3	15.2	15.6	13.9	14.1	9.8	20.2	19.7	13.0	11.5
Gas collected	l	9.11	9.71	10.11	12.11	11.89	11.93	11.98	12.80	11.34	11.31	11.50	10.01

T: Trace

TABLE 3. INFLUENCES OF THE REDUCING AGENTS AND THE REACTION TEMPERATURES ON THE DEHYDROGENATING ACTIVITY AND THE CONDENSING ACTIVITY OF REDUCED COPPER

Precipitate		Cu VII												Cu IX	
Reducing agent		Isopropyl alcohol								Carbon monoxide					
Reduction temp. °C		185*	185	220*	220	250*	250	250	325*	325	140	140	140	140	140
Reaction temp. °C			250		250		250	325		325	220	250	300	250	300
Isopropyl alcohol	g	54.4	38.8	54.6	38.7	54.3	38.7	38.8	54.2	38.8	38.9	38.2	38.7	38.6	38.9
Velocity	g/hr	10.8	10.8	10.9	12.0	10.7	11.1	12.5	11.0	12.0	9.5	11.3	9.5	10.3	11.8
Reaction product	g	51.3	35.9	53.5	36.5	53.3	35.9	36.4	52.4	36.1	34.7	36.6	34.8	35.4	35.6
Composition of reaction product															
Acetone	%	58.0	82.6	72.5	82.2	78.8	83.9	95.5	92.4	96.1	59.4	46.7	83.5	74.3	92.5
Isobutyl methyl ketone	%	0	5.2	0	5.5	4.8	4.9	0	0	0	9.1	20.0	7.7	0	0
Diisobutyl ketone	%	0	1.2	0	1.3	1.2	1.2	0	0	0	3.9	17.0	2.0	0	0
Isobutylmethylcarbinol	%	0	0.5	0	0.5	0.4	0.4	0	0	0	1.6	2.4	0.3	0	0
Unidentified product	%	0	0	0	0	0	0	0	0	0	0.3	0.9	0.3	0	0
Water	%	4.4	1.2	4.2	1.3	5.5	1.1	0	4.4	0	2.8	8.2	1.8	0	0
Unreacted alcohol	%	37.6	9.3	23.3	9.2	9.3	8.5	4.5	3.2	3.9	22.9	4.8	4.4	25.7	7.5
Gas collected	l	9.27	11.87	12.91	12.06	15.33	11.96	13.67	19.37	13.56	9.25	10.13	12.76	10.91	13.11

* These columns show the products obtained when isopropyl alcohol was passed over the catalyst as the reducing agent at the temperatures described.

with the sort of solvent. Although the influence of the reaction temperature on the dehydrogenating activity of reduced copper is not listed in this table, at the highest reaction temperature (325°C) the catalyst prepared by the treatment with hydrogen of the precipitate (Cu IX) obtained by using potassium carbonate as a precipitant gave the highest yield of acetone (97.0%). The dehydrogenating activity of various copper catalysts is in the following order with respect to the precipitants: $K_2CO_3 > NaOH > (NH_4)_2CO_3 > NH_4OH$. Furthermore, it was found that the catalyst prepared by the treatment of Cu IX with hydrogen acted only to dehydrogenate isopropyl alcohol to acetone at all temperatures; the catalyst prepared by the treatment with hydrogen of the precipitates (Cu VII, Cu XV and Cu XVI) obtained by using sodium hydroxide, ammonia, and ammonium carbonate acted similarly at the highest temperature, but at lower temperatures (185—250°C) they gave not only acetone but also isobutyl methyl ketone, diisobutyl ketone, and isobutylmethylcarbinol. The copper catalyst prepared by precipitation with sodium hydroxide was more active in the condensation of isopropyl alcohol than those catalysts precipitated with ammonia and ammonium carbonate. The proportion of diisobutyl ketone in the condensation products increased with a rise in the reaction temperature.

From the fact that the copper catalyst obtained by using an excess of ammonium carbonate caused the condensation reaction, and that the copper catalyst prepared with an excess of potassium carbonate did not cause this reaction, it does not appear that this condensation was caused by traces of alkali contaminating the catalyst. Considering the information in the previous paper,[2] the formation of higher ketones in the present research seems to be attributable to the effect either of traces of water or of a lower oxide of copper in the catalysts.

When the precipitate prepared from ammonia water was used, the evolution of NO_2 gas in the course of reduction of the precipitate with hydrogen was noticed; this gas seems to be attributable to the nitrate ions remaining as an impurity in the precipitate. NO_2 gas tended to exert a strongly negative influence on the velocity of reduction, the reduction time being fifty hours. However, the gas had no appreciable change on the dehydrogenating activity.

Cu XVII and Cu XVIII, prepared in methyl alcohol and ethyl alcohol respectively as solvents, were nearly equal in their activity for the production of both the condensation product and acetone. When the reaction temperature was carried out at lower temperatures (220—250°C), Cu XX, prepared in butyl alcohol, had a relatively poor activity for the formation of the condensation product. However, at the reaction temperature of 220°C the copper catalysts obtained by the treatment with hydrogen of the precipitates (Cu XVII, Cu XVIII, Cu XIX, Cu XXI and Cu XXII) prepared in the other alcohols did give the condensation product. There was thus a marked difference in activity between the copper catalyst prepared in a higher alcohol and those prepared in lower alcohols with respect to the relative amount of condensation product formed. The maximum conversion to the higher ketones resulted when water was used as the solvent; the formation of the condensation product increased in the following order with respect to the solvent: water > methanol, ethanol > 2-propanol > 2-butanol > 1-propanol > 1-butanol. When the copper catalyst prepared in a higher alcohol was used at a low temperature, it gave a large quantity of unreacted alcohol. This seems to be caused by the adsorption of the higher alcohol on the catalyst. Because of the small extent of the condensation reaction, the degree of dehydrogenation was excellent over the catalyst prepared in the higher alcohol. When the copper catalysts obtained by the treatment with hydrogen of the precipitates (Cu XXIII and Cu XXIV) prepared with potassium carbonate in alcohols were used at 220—250°C, isopropyl alcohol yielded acetone and hydrogen, but not higher ketones. It has been found by Suito and Takiyama[8] that considerable differences in particle size occur with changes in the solvents used in preparing the precipitates. Accordingly, the dehydrogenating activity and the condensing activity of the copper catalyst is presumed also to depend on the particle size, which may vary with changes in the solvents.

Influence of Reducing Agents on the Dehydrogenating Activity and the Condensing Activity of Reduced Copper. The influence of the reducing agents and the reaction temperatures on the activity of the copper catalyst is shown in Table 3. The condensing activity of the copper catalyst varies considerably with the sort of reducing agent, the catalyst prepared by treatment with hydrogen showed the largest activity for condensation reaction. On the contrary, the reduction of the precipitate with isopropyl alcohol vapor, in place of hydrogen, prevented the formation of any condensation products. The fact that only a small amount of higher ketones was obtained when the catalyst reduced by isopropyl alcohol was used is interesting; probably, the most effective and simplest way to suppress the formation of condensation products is to use precipitates reduced with isopropyl alcohol. When the copper catalyst, prepared by treatment with sodium hydroxide followed by reduction with carbon monoxide, was used at 300°C, the condensation product was obtained, while the copper catalyst prepared with potassium

8) E. Suito and K. Takiyama, This Bulletin, **28**, 305 (1955).

carbonate acted only to dehydrogenate isopropyl alcohol to acetone at all temperatures.

The dehydrogenation activity of reduced copper catalysts depends also upon the temperature at which the oxide is reduced with the reducing agent and upon the velocity with which the reducing agent is passed over the oxide. The reduction of copper oxide with hydrogen is an exothermic reaction; the heat of reaction may accumulate on a part of the catalyst. Accordingly, this may cause sintering. On the other hand, when isopropyl alcohol was used as the reducing agent, the catalytic activity of dehydrogenation was not affected by the reducing temperature.

When isopropyl alcohol was passed over reduced copper, a small amount of isobutylmethylcarbinol was obtained. This compound is formed by the hydrogenation of isobutyl methyl ketone. Further, the present authors*[3] have found that the copper catalysts changed *l*-menthol to *l*-menthone, *d*-isomenthone, thymol, isomenthol and neomenthol, and allyl alcohol to acrolein, propargylaldehyde, propionaldehyde, and *n*-propyl alcohol, and the mixture of cyclohexene and hydrogen to cyclohexane. The reduced copper, therefore, is an effective catalyst for the hydrogenation.

Pease and Stewart[9] found that the addition of carbon monoxide to materials lowered the hydrogenation activity of a copper catalyst. When, however, the copper catalysts prepared by the reduction with carbon monoxide or hydrogen were used, isobutylmethylcarbinol was obtained. In this case, therefore, carbon monoxide seems to act somewhat as a poison with regard to the copper catalyst.

*[3] The results of their, investigation were presented at the 19th Annual Meeting of the Chemical Society of Japan, Yokohama, April, 1966; some of them were also presented at the 20th Annual Meeting of the Chemical Society of Japan, Tokyo, April, 1967.

9) R. N. Pease and L. Stewart, *J. Am. Chem. Soc.*, **47**, 1235 (1925).

BULLETIN OF THE CHEMICAL SOCIETY OF JAPAN VOL. 41 936—941 (1968)

The Chemiluminescence of Indole Derivatives. III. On the Mechanism of the Chemiluminescence of 2,3-Dimethylindole and 5-Substituted-2,3-dimethylindoles in the Dimethyl Sulfoxide-Alkali System

Noboru SUGIYAMA, Masamoto AKUTAGAWA and Hiroshi YAMAMOTO

Department of Chemistry, Tokyo Kyoiku University, Otsuka, Tokyo

(Received June 2, 1967)

A bright green light is observed on the treatment of a solution of 2,3-dimethylindole (I) and its hydroperoxide (II) in dimethyl sulfoxide (DMSO) with alkali (potassium *t*-butoxide or granular potassium hydroxide) under streams of oxygen and hydrogen respectively. The change in their ultraviolet and fluorescent spectra with the time and the chemiluminescent spectra is measured. The compound II is concluded to be the reaction intermediate of I; it decomposes to yield an excited singlet state of an *o*-acetamidoacetophenone anion (III*), a light emitting species in this reaction. The investigation, then extended to four 5-substituted-2,3-dimethylindoles, revealed that three of them displayed chemiluminescence through the same mechanism as in the case of I.

In relation to the luciferin of the bioluminescent marine organisms,[1-3] the chemiluminescence of indole derivatives is an especially interesting phenomenon; that of various simple indoles has recently been reported.[4-6]

We studied the relative light intensities of forty-one indole derivatives in the following two systems.[7]

(A) Sample-EtOH-KOH-H_2O_2-$K_3Fe(CN)_6$

(B) Sample-DMSO-KOH-AIR

We found that 2,3-dimethylindolenyl-3-hydroperoxide (II) emitted a bright flash of light in the B system. Although McCapra *et al.* suggested

1) Y. Kishi, T. Goto, Y. Hirata, O. Shimomura and F. H. Johnson, "Bioluminescence Conference at Hakone, 1965," ed. by F. H. Johnson and Y. Haneda, Princeton University Press, Princeton, New Jersey (1966), p. 88.

2) M. J. Cormier and C. B. Eckrode, *Biochim. Biophys. Acta*, **64**, 340 (1962).

3) M. J. Cormier and L. S. Dure, *J. Biol. Chem.*, **238**, 790 (1963).

4) G. E. Philbrook, J. B. Ayers, J. F. Garst and J. R. Totter, *Photochem. Photobiol.*, **4**, 869 (1965).

5) A. W. Berger, J. N. Driscoil and J. A. Pirog, *ibid.*, **4**, 1123 (1965).

6) E. H. White and M. J. C. Harding, *ibid.*, **4**, 1129 (1965).

7) N. Sugiyama, M. Akutagawa, T. Gasha, H. Yamamoto and Y. Saiga, This Bulletin, **40**, 347 (1967).

the intermediacy of a indolyl-3-hydroperoxide and a hydroperoxide decomposition mechanism accompanying a light emission,[8,9] the mechanism of the chemiluminescence has remained obscure.

In a preceding paper, we proposed a mechanism of the chemiluminescence of the indole derivative involving the hydroperoxide as an intermediate.[10] In the present paper, the mechanisms of 2,3-dimethylindole and 5-substituted-2,3-dimethylindoles will be discussed in detail in the light of the spectral studies.

Experimental

2,3,5-Trimethylindolenyl-3-hydroperoxide (VIIa). VIIa was prepared as follows. 2,3,5-Trimethylindole (200 mg) was dissolved in warm light petroleum (bp 60—80°C, 20 ml), and then a trace of benzoyl peroxide was added to the solution in the presence of atmospheric oxygen. After an hour the solution became opaque and then began to deposit crystalline hydroperoxide (140 mg), which was collected and recrystallized from a mixture of ethyl acetate and light petroleum to produce almost colorless prisms.

Mp 111.5°C (decomp.) Found: C, 69.34; H, 7.09; N, 7.44%. Calcd for $C_{11}H_{13}O_2N$: C, 69.09; H, 6.85; N, 7.33%.

UV: λ_{max}^{EtOH} mμ (log ε) 223 (4.24) 267 (3.59).

IR: ν_{KBr} cm^{-1} 3440, 3070, 2750, 1595, 1470, 860, 830

Attempted Preparation of 5-Chloro-2,3-dimethylindolenyl-3-hydroperoxide (VIIc). An ether - light petroleum solution of 5-chloro-2,3-dimethylindole (VIc) was oxidized with atmospheric oxygen as has been described above. After 20 hr a brown amorphous solid deposited out. This solid could not be recrystallized from any solvent, but it showed the characteristics of indolenine (*e. g.*, λ_{max} at approx. 230 and 260 mμ in the UV spectrum, and a positive starch-iodide test.).

Materials. The following derivatives were synthesized in our laboratory by the methods described in the literature.[11-15]

2,3-Dimethylindole (I)[11]: Recrystallized from ligroin, colorless leaflets, mp 107—108°C (Found: C, 82.69; H, 7.70; N, 9.63%).

UV: λ_{max}^{EtOH} mμ (log ε) 283 (3.8) 290 (3.75).

IR: ν_{KBr} cm^{-1} 3380, 2900, 1590, 1460, 760.

2, 3, 5-Trimethylindole (VIa)[12]: Recrystallized from alcohol, colorless plates, mp 120°C (Found: C, 82.51; H, 8.30; N, 8.78%).

UV: λ_{max}^{EtOH} mμ (log ε) 231 (4.39) 288 (3.82).

IR: ν_{KBr} cm^{-1} 3380, 2900, 2840, 1590, 1475, 870, 790.

5-Methoxy-2,3-dimethylindole (VIb)[13]: Recrystallized from alcohol, mp 109°C (Found: C, 75.54; H, 7.51; N, 7.99%).

UV: λ_{max}^{EtOH} mμ (log ε) 230 (4.41) 278 (3.90).

IR: ν_{KBr} cm^{-1} 3390, 2920, 2850, 1590, 1475, 870, 790.

5-Chloro-2,3-dimethylindole (VIc)[13]: Recrystallized from benzene, glistening white plates, mp 140—141.5°C Found: C, 66.15; H, 5.64; N, 7.72%.

UV: λ_{max}^{EtOH} mμ (log ε) 235 (4.49) 293 (3.80) 301 (sh.) (3.74).

IR: ν_{KBr} cm^{-1} 3400, 2900, 1575, 1470, 860, 800, 750.

5-Nitro-2,3-dimethylindole (VId)[13]: Recrystallized from benzene, golden needles, mp 187°C (Found: C, 63.35; H, 5.55; N, 14.65%).

2,3-Dimethylindolenyl-3-hydroperoxide (II)[14]: Recrystallized from ethyl acetate-light petroleum, colorless prisms, mp 103°C (Found: C, 67.7; H, 6.3; N, 7.9%).

UV: λ_{max}^{EtOH} mμ (log ε) 225 (4.11) 260 (3.46).

IR: ν_{KBr} cm^{-1} 3400, 3060, 2800, 1600, 1455, 780.

5-Methoxy-2,3-dimethylindolenyl-3-hydroperoxide (VIIb)[14]: Recrystallized from ethyl acetate - light petroleum, colorless needles, mp 109°C (decomp.) (Found: C, 63.96; H, 6.59; N, 6.49%).

UV: λ_{max}^{EtOH} mμ (log ε) 223 (4.19) 281 (3.82).

IR: ν_{KBr} cm^{-1} 3450, 3050, 2800, 1595, 1470, 870, 810.

o-Acetamidoacetophenone (III)[15]: Recrystallized from ethanol-water, long colorless needles, mp 74—75°C.

2-Acetamido-5-methylacetophenone (VIIIa): VIIa was dissolved in boiling water and the solution was kept at room temperature; then VIIIa slowly separated. Recrystallized from methanol, slightly yellow leaflets, mp 123.5—124.5°C.

VIIIa was also prepared by treating the indole with ozonized oxygen.[12] Recrystallized from methanol, mp 123.5—124.5°C.

2-Acetamido-5-methoxyacetophenone (VIIb)[14]: Recrystallized from light petroleum, long yellow needles, mp 91—91.5°C.

2-Acetamido-5-chloroacetophenone (VIIIc): VIc (0.3 g in AcOH (27 ml) + H_2O (2 ml)) was treated with ozonized oxygen at room temperature until the indole spot disappeared on T. L. C. The product was isolated by basification and extracted with ether. Recrystallized from methanol, almost colorless silky needles, mp 134—134.5°C.

Measurement of the Total Amount of Chemiluminescence. The total amount of light which was emitted when a solution of the sample was mixed with a solution of the alkali in the presence of oxygen was measured by a modified Moldel 139 Hitachi Photometer.

Table 1. Total light emission of I and II

Compd.	Concn.	Atmosphere	Total emission*
I	10^{-4} mol/l	Oxygen	31.1
II	10^{-4}	Hydrogen	36.1

* Area, arbitrary unit

8) F. McCapra, D. G. Richardson and Y. C. Chang, *Photochem. Photobiol.*, **4**., 1111 (1965).
9) F. McCapra and Y. C. Chang, *Chem. Commn.*, **1966**, 522.
10) N. Sugiyama and M. Akutagawa, This Bulletin, **40**, 240 (1967).
11) H. R. Snyder and C. W. Smith, *J. Am. Chem. Soc.*, **65**, 2452 (1943).
12) D. W. Ockenden and K. Schofield, *J. Chem. Soc.*, **1953**, 612.
13) D. W. Ockenden and K. Schofield, *ibid.*, **1957**, 3175.
14) R. J. S. Beer, T. Donavanik and A. Robertson, *ibid.*, **1954**, 4139.
15) N. J. Leonard and S. N. Boyd, Jr., *J. Org. Chem.*, **11**, 405 (1946).

TABLE 2. CHEMILUMINESCENCE AND FLUORESCENCE MAXIMA OF I AND II

Compound	Concn.	Atmosphere	Chemiluminescence maximum	Fluorescence* maximum
I	10^{-2} mol/*l*	Oxygen	520 mμ	520 mμ
II	10^{-3}	Hydrogen	520	520

* Fl. of reaction mixture

TABLE 3. RELATIVE TOTAL LIGHT EMISSION OF 5-SUBSTITUTED-2,3-DIMETHYLINDOLES

Compound	Total emission*
I	10
VIa	11
VIb	5.6
VIc	3.0
VId	10^{-5}

* Area, arbitrary unit
Condition: 10^{-3} mol/*l*, DMSO soln. 1 m*l* + 10^{-2} mol/*l*, *t*-BuOK DMSO soln. 1m*l* + O_2 stream

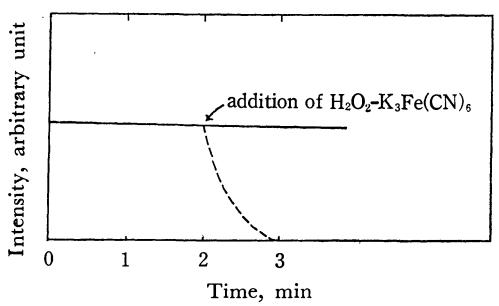

Fig. 1. Chemiluminescent curves of II.
10^{-3} mol/*l* in 0.1N ethanolic potassium hydroxide
- - - added 1 m*l* of 3% H_2O_2 - 3% $K_3Fe(CN)_6$ mixture

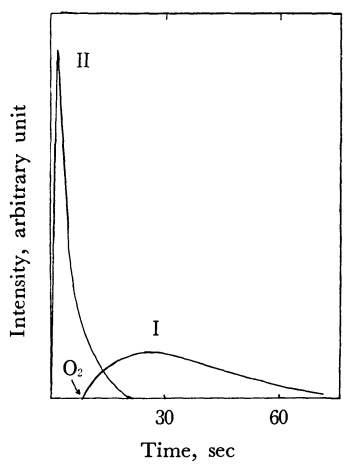

Fig. 2. Chemiluminescent curves of I and II.
10^{-4} mol/*l*, DMSO soln. 1 m*l* + 10^{-3} mol/*l*, BuOK DMSO soln. 1 m*l* + O_2(I) or Ar(II) stream

The change in the intensity of light with the time was recorded with a QPD 53 Hitachi Recorder, and the total emission was determined by the area of the emission curve. All measurements were carried out at 20°C.

One milliliter of a solution of a sample in DMSO (10^{-3} or 10^{-4} mol/*l*) was mixed with 1 m*l* of a potassium *t*-butoxide DMSO solution (10^{-2} or 10^{-3} mol/*l*) in an oxygen or argon stream, or 2 m*l* of a sample solution was added to 0.5 g of granular potassium hydroxide. The results are shown in Tables 1 and 3 and in Fig. 2.

Emission Spectra. In front of the slit of a spectrometer was set a test tube containing about 3 g of granular potassium hydroxide. Ten milliliters of the sample solution was at once added to this test tube. By means of a fine syringe needle, tiny bubbles of oxygen were continuously passed through this solution from the bottom of the test tube. Suddenly a brilliant emission of light was took place; it continued for a period of time. The emission spectrum of this light was measured.

Fluorescence Spectra. The fluorescence spectra were measured with a Hitachi Recording Spectrophotometer, Model EPS-2, equipped with an attachment for measuring the fluorescence spectrum. The 365 mμ line of a high-pressure mercury lamp was used for excitation. The chemiluminescent reaction was carried out by adding 10 m*l* of a solution of 2,3-dimethylindole (10^{-3} mol/*l*) in DMSO to an excess of granular potassium hydroxide in the oxygen stream. After periods of 1, 5, 10, and 30 min, 0.2 m*l* portions of this solution (solution A) were placed in a small Erlenmyer flask and diluted with 3.5 m*l* of the blank solution, which had been made by letting a quantity of DMSO stand with an excess of granular potassium hydroxide. These solutions were then used for the measurement of the fluorescence spectra.

In the case of 2,3-dimethylindolenyl-3-hydroperoxide (II), the chemiluminescent reaction was carried out in an argon stream and the fluorescence spectra was measured by the same procedure as above. The results are given in Fig. 4.

Ultraviolet Spectra. 0.2 m*l* of the solution A was diluted with 3 m*l* of ethanol after 0, 1/2, 5, and 30 min periods. These solutions were then used for the measurement of the ultraviolet spectra; the results are shown in Fig. 3.

Results and Discussion

Mechanism of the Chemiluminescence. In order to get accurate information about the chemiluminescence mechanism of indole derivatives, it is necessary to find a compound which posesses such desirable properties as being easily accesible in the pure state and showing a demonstrable intensity of light emission in a measureable period of time.

In addition, since the oxidation reaction is involved in the chemiluminescent reaction, it is even more important to be able to obtain an oxidation intermediate with the same properties.

It was found that 2,3-dimethylindole (I) and its hydroperoxide, 2,3-dimethylindolenyl-3-hydroperoxide (II), satisfy these requirements.

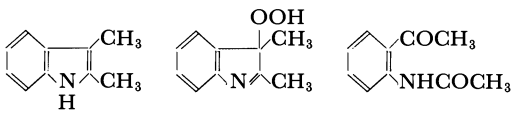

I II III

When **II** was dissolved in 0.1 N ethanolic potassium hydroxide, a weak light emission, detectable only by a photometer, continued for about six hours. However, when an oxidizing agent of the system A, a hydrogen peroxide-potassium ferricyanide solution, was added to the light-emitting ethanolic potassium hydroxide solution of II, the emission spontaneously disappeared, as shown in Fig. 1. Therefore, it is probable that, in the system A, II is not substantially connected with the light emission.

On the contrary, in the system B, II showed a bright flash of light, as has been previously reported.[7,10] Thus, it was assumed that **II** is an intermediate of the chemiluminescence of **I** in the system B.

This assumption was proved to be reasonable by the following results. When, under an oxygen atmosphere, 2-m*l* solutions of I and II in dimethylsulfoxide of a concentration of 10^{-4} mol/*l* were added to 0.5 g of granular potassium hydroxide, approximately equal amounts of light were emitted (Table 1). The emission period of I was longer than that of II, however, and the maximum intensity of I was lower than that of II (Fig. 2). Further, under a hydrogen atmosphere, the light emission was not observed in the case of I, although, in the case of **II**, a brilliant emission was observed. From these results, it seems probable that II is an intermediate and that the oxidation of I to II by oxygen is the rate-controlling step in the chemiluminescent reaction of I.

The emission spectra of both the solution of I (10^{-2} mol/*l*) and that of II (10^{-3} mol/*l*) appeared at 520 mμ, as shown in Table 2. This fact suggests that the same emitting species are concerned in the chemiluminescent reaction of I and II.

This was further supported by the following facts. After the light emission of the dimethylsulfoxide solution of I or II by potassium hydroxide was over, the ultraviolet absorption maxima of the

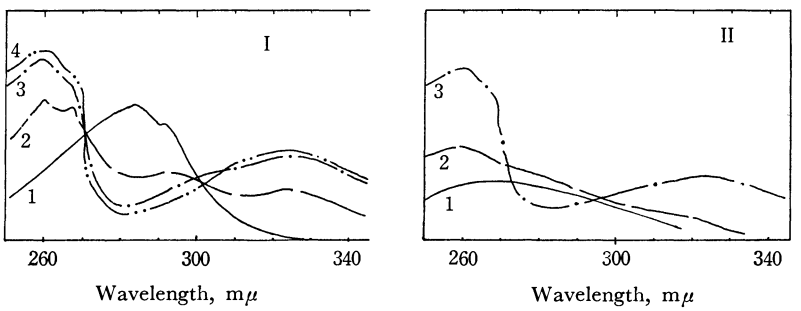

Fig. 3. The change of UV spectra of I and II in chemiluminescent reaction.
1: 0 min 2: 1/2 min 3: 5 min 4: 30 min

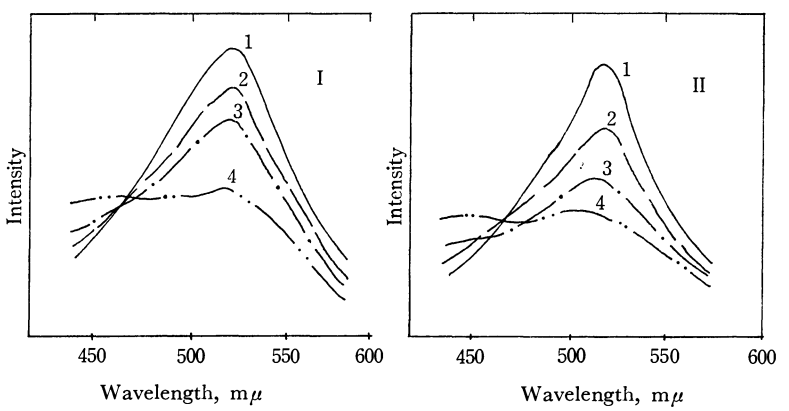

Fig. 4. The change of fluorescence spectra of I and II in chemiluminescent reaction.
1: 1 min 2: 5 min 3: 10 min 4: 30 min

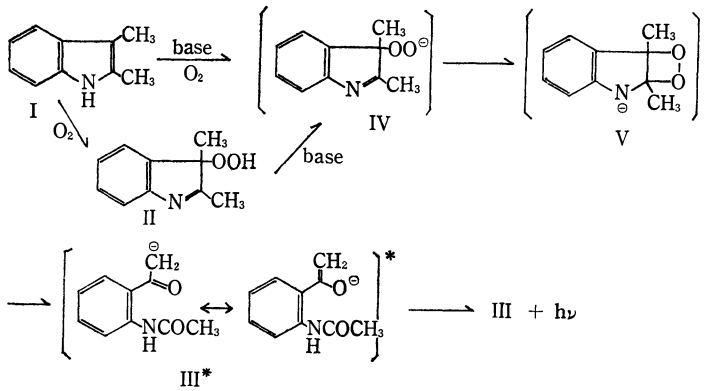

Fig. 5. Reaction scheme for the chemiluminescence of I.

solution of I (284 and 292 mμ) and that of II (260 mμ) both shifted to 259, 267 and 325 mμ, values which are consistent with those of *o*-acetamidoacetophenone (III).

Furthermore, the fluorescence spectra of I and II varied similarly with the time and showed a maximum at 520 mμ, which completely coincided with that of III. The fluorescence spectra and ultraviolet spectra in the chemiluminescent condition are summarized in Figs. 3 and 4.

Now it can be concluded that II is the intermediate of the chemiluminescent reaction of I, that the product of this chemiluminescent reaction is III, and that the emitting species of the chemiluminescent reaction of I and II are the same. The emitting species may be the excited singlet state of the *o*-acetamidoacetophenone anion (III*), because the maximum of the fluorescence spectra of III in the same condition as chemiluminescence coincided completely with that of the emission spectra of I and II, and with their fluorescence spectra after the chemiluminescent reaction.

From these results the mechanism of the chemiluminescent reaction of 2,3-dimethylindole in the dimethylsulfoxide-potassium hydroxide oxygen system shown in Fig. 5 may reasonably be formulated.

Compound I is changed to the hydroperoxide anion, IV, by oxygen and a base, such as potassium *t*-butoxide or granular potassium hydroxide. On the other hand, Compound II requires only a base to change to IV. IV converts to the four-membered cyclic peroxide V, a short-lived intermediate, which then decomposes to an excited *o*-acetamidoacetophenone anion (III*). An excited state of III falls to the ground state with the emission of light.

Chemiluminescence of 5-Substituted-2,3-dimethylindoles. We prepared four 5-substituted-2,3-dimethylindoles and measured the total amount of light, they emitted by treating 10^{-3} mol/*l* solutions in DMSO with potassium *t*-butoxide and oxygen. The indoles were found to decrease in chemiluminescence efficiency in the order; VIa>I>VIb>VIc>VId (Table 3).

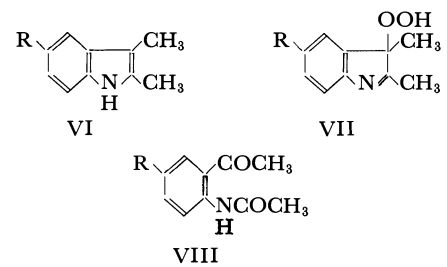

R=a: CH_3, b: CH_3O, c: Cl, d: NO_2

According to our experiment, 5-nitro-2,3-dimethylindole (VId) could not afford the hydroperoxide as II, and the chemiluminescence of VId was extremely weak.

The chemiluminescence maxima of indoles

Table 4. Chemiluminescence maxima of VI and VII

R of VI or VII	Chemiluminescence maxima of VI	Chemiluminescence maxima of VII
H	520 mμ	520 mμ
CH_3	532	532
CH_3O	548	546
Cl	532	—

Table 5. Fluorescence maxima

R of VI, VII or VIII	Fluorescence maxima of VI	VII	VIII
H	520 mμ	520 mμ	520 mμ
CH_3	531	531	532
CH_3O	549	546	546
Cl	532	—	533

* Under the same condition as chemiluminescent reaction.

(VIa, b, c) and the hydroperoxide (VIIa, b) are shown in Table 4. The hydroperoxide (VIIc) was too unstable to be obtained in the crystalline state. The fluorescence maxima of VI and VII after chemiluminescence and that of 5-substituted-2-acetamidoacetophenones (VIII) are shown in Table 5. After the chemiluminescent reaction of the solution of VI or VII, the solution was proved by T. L. C. to contain mainly VIII, which was also identified by a T. L. C. of the authentic samples. Thus VIII was the major product of the chemiluminescent reactions of both indoles (VI) and hydroperoxides (VII).

A good match was found between the chemiluminescence maxima of indoles (VI), those of the hydroperoxides (VII), and the fluorescence maxima of the major product (VIII). Therefore, it may be reasonably concluded that 5-substituted-2,3-dimethylindoles emitted light by the same mechanism as 2,3-dimethylindole.

BULLETIN OF THE CHEMICAL SOCIETY OF JAPAN VOL. 41 941—943 (1968)

Asymmetric Hydrogenation with Modified Raney Nickel.*1 IX

Yoshiharu IZUMI, Tadashi TANABE, Shinichi YAJIMA and Masami IMAIDA

Division of Organic Chemistry, Institute for Protein Research, Osaka University, Kita-ku, Osaka

(Received July 8, 1967)

The asymmetric hydrogenation catalysts were prepared from the Raney nickel catalyst by modifying it with L$_S$-3,3-dimethyl-2-hydroxybutyric acid and the corresponding amino acid, L-*t*-leucine, which have most methyl groups at the β-position. The asymmetric activities of the catalysts were measured by the hydrogenation of the methyl acetoacetate to methyl 3-hydroxybutyrate. The asymmetric activity of the catalyst modified with an aqueous solution of L$_S$-3,3-dimethyl-2-hydroxybutyric acid was very low, and the direction of asymmetric activity at pH 5.0 was inverted by the temperature of the modifying solution. However, there was a high asymmetric activity in the catalyst modified with L-*t*-leucine, and this activity was not so influenced by the temperature of the modifying solution. The aysmmetric activities of catalysts modified with α-hydroxy acids and the corresponding amino acids reported in this paper and the previous papers are compared, and the effect of the bulk of the α-alkyl substituent of the modifying reagent upon the asymmetric activity of the catalyst is discussed.

The asymmetric activities of Raney nickel catalysts, modified with various optically active amino acids or hydroxy acids, in the hydrogenation of methyl acetoacetate to methyl 3-hydroxy butyrate have previously been reported on by the present authors.[1-8]

The asymmetric activity of a modified Raney nickel catalyst was found to be influenced not only by the pH and temperature of the modifying solution,[1] but also by the structure of the modifying reagent. The "asymmetric activity" of a catalyst involves two factors. One is the direction of the asymmetric activity, which is expressed as the direction of the specific rotation, (+) or (−), of the hydrogenated product. The other is the degree of asymmetric activity, which is usually presented as the asymmetric yield. On modification at 0°C, the direction of the asymmetric activity of a catalyst is mainly controlled by the absolute configuration of the α-carbon of the modifying reagent. Catalysts modified with L-α-amino acids other than alanine, serine, proline, and cystine produce methyl D$_S$-3-hydroxybutyrate predominantly. However, on modification with L$_S$-2-hydroxy acids, methyl L$_S$-3-hydroxybutyrate is produced predominantly. However, the factor controlling the asymmetric yield has not been discussed. In the present work, *t*-leucine and 3,3-dimethyl-2-hydroxybutyric acid, which have a bulky *t*-butyl substituent on the α-carbon, were investigated as asymmetric modifying reagents, and the role of the alkyl group of the modifying reagent discussed in

*1 Presented in part at the 19th Annual Meeting of the Chemical Society of Japan, Tokyo, April, 1966.

1) H. Fukawa, Y. Izumi, S. Komatsu and S. Akabori, This Bulletin, **35**, 1703 (1962).
2) Y. Izumi, M. Imaida, H. Fukawa and S. Akabori, *ibid.*, **36**, 21 (1963).
3) Y. Izumi, M. Imaida, H. Fukawa and S. Akabori, *ibid.*, **36**, 155 (1963).
4) S. Tatsumi, M. Imaida, Y. Fukuda, Y. Izumi and S. Akabori, *ibid.*, **37**, 846 (1964).
5) Y. Izumi, S. Akabori, H. Fukawa, S. Tatsumi, M. Imaida, Y. Fukuda and S. Komatsu, Proc. of the 3rd Int. Cong. on Catalysis, **2**, 1364 (1964).
6) Y. Izumi, S. Tatsumi, M. Imaida, Y. Fukuda and S. Akabori, This Bulletin, **38**, 1206 (1965).
7) Y. Izumi, S. Tatsumi, M. Imaida, Y. Fukuda and S. Akabori, *ibid.*, **39**, 361 (1966).
8) Y. Izumi, S. Tatsumi and M. Imaida, *ibid.*, **39**, 2223 (1966).

Table 1. Optical rotation of modifying reagents

Modifying reagent	Optical rotation, $[\alpha]_D^{20}$	Value in literature
L-(+)-3,3-Dimethyl-2-hydroxybutyric acid	+4.5 (*c* 4, water)	—
L-(−)-*t*-Leucine	−9.5 (*c* 2, water)	−10.2 (*c* 4.3, water)[9]

comparison with the results reported in a previous paper.

Materials

Modifying Reagents.[*2] The optical rotations of the Ls(+)-3,3-dimethyl-2-hydroxybutyric acid and L-(−)-*t*-leucine used in this work are listed in Table 1.

Experimental

The preparation of the Raney nickel catalyst, the hydrogenation of methyl acetoacetate, and the measurement of the asymmetric activity of the catalyst were performed as has been described in a previous paper.[3]

Results and Discussion

Modification with Ls-3,3-Dimethyl-2-hydroxybutyric Acid (I). The Raney nickel catalyst was modified at 0°C or 100°C with an aqueous solution of Ls-3,3-dimethyl-2-hydroxybutyric acid (1) which had been adjusted to a specified pH with 1 N sodium hydroxide. The asymmetric activity of the catalyst modified at pH 3—12 and the neutralization curve of the 2% aqueous solution of 1 with 1 N sodium hydroxide (f=0.996) are shown in Fig. 1.

The optimum asymmetric activity of catalysts modified with 1 at 0°C was observed at pH 5.0. This pH value corresponds to the pH-jumping region of the neutralization curve of 1 observed with other hydroxy acids. The direction of asymmetric activity of the catalyst changed at the complete neutralization point.

On modification at 100°C, the catalyst showed its highest asymmetric activity at pH 3.2. The direction of the asymmetric activity of the catalyst modified at 100°C changed at a low pH value than in the case of modification at 0°C, this pH corresponded to the pH-jumping region in the titration curve. The values of the asymmetric activities of catalysts modified at 0°C and 100°C were both very low over the whole range of modifying pH values.

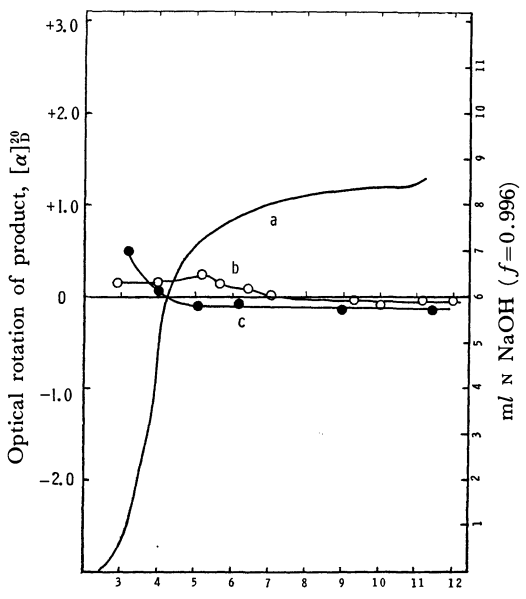

Fig. 1. Neutralization curve of 2% solution of (1) with N NaOH and effects of pH in modifications with (1) at 0°C and 100°C.
a Neutralization curve
b Modified at 0°C
c Modified at 100°C

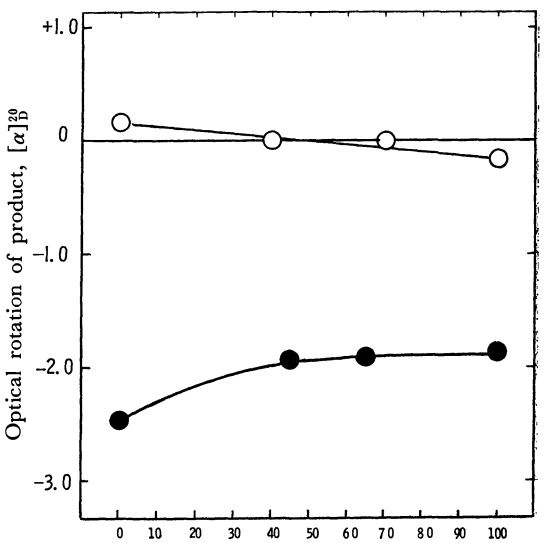

Fig. 2. Effect of modifying temperature.
○ Modified with L-3,3-dimethyl-2-hydroxybutyric acid (1) at pH 5.0
● Modified with L-*t*-leucine (II) at the isoelectric point

*2 The details of the preparation of these compounds will be reported in this Bulletin later.

9) N. Izumiya, S.-C. J. Fu, S. M. Birnbaum and J. P. Greenstein, *J. Biol. Chem.*, **205**, 221 (1953).

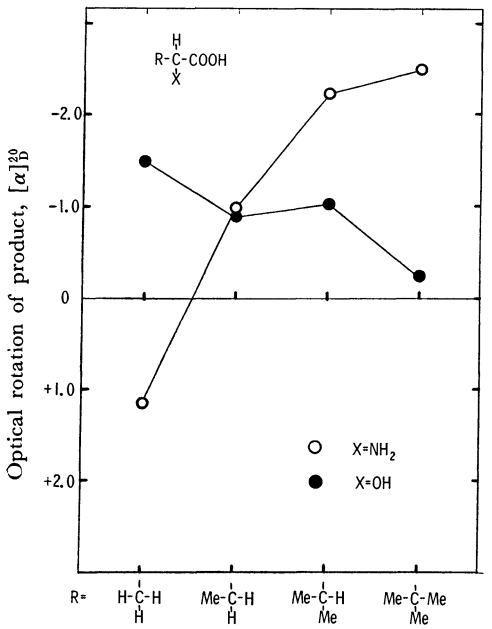

Fig. 3. Effect of substituent.

○ Modified at 0°C, isoelectric point
● Modified at 0°C, pH 5.0

The effect of the temperature of the modifying solution of 1 was studied at pH 5.0; the results are shown in Fig. 2. As is shown in Fig. 2, the asymmetric activity decreased with an increase in the modifying temperature, and the direction of asymmetric activity changed at about 50°C. Such an inversion of the direction of asymmetric activity by the modifying temperature has not been found in the modifications with β-substituted α-hydroxy acids reported in previous papers.[2]

Modification with L-*t*-Leucine (II). The asymmetric activity of the catalyst modified with an aqueous solution of L-*t*-leucine (2) at the isoelectric point (pH 6.2) was measured at various temperatures. The results are shown in Fig. 2. The asymmetric activity was fairly high, and the activity of the catalyst modified at 0°C was intermediate between the activities of the catalysts modified with L-valine and with L-alloisoleucine*3 at 0°C. The rough linear relation shown in Fig. 2 was also found between the asymmetric activity and the modifying temperature in catalysts modified with other α-amino acids, such as valine and isoleucine.

Effect of α-Alkyl Substituent on Asymmetric Activity of Catalyst. In order to make clear effect of the bulk of α-alkyl substituents in asymmetric modifying reagents on the asymmetric activities of catalysts, the asymmetric activities of the catalysts modified with α-hydroxy acids and the corresponding α-amino acids, reported in this paper and in previous papers,[2,3] are compared in Fig. 3. Figure 3 shows the asymmetric activities of the catalysts when the hydrogen atoms on the β-carbon of lactic acid or alanine are replaced with methyl groups, one by one. The catalysts were modified at 0°C, at the isoelectric point with amino acids, and at pH 5.0 with hydroxy acids. The asymmetric activity of the catalyst modified with amino acid increases with the increase in the bulk of the α-alkyl substituent, while, with hydroxy acids, the influence of the bulk of alkyl substituents is smaller than in the case in modifications with amino acids; asymmetric activity is the lowest with the acid having the most bulky alkyl substituent.

This research was supported by the Kawaken Fine Chemicals Co., Ltd., Tokyo.

*3 The asymmetric activity of this catalyst will be reported on later by the present authors.

BULLETIN OF THE CHEMICAL SOCIETY OF JAPAN VOL. 41 944—948 (1968)

Stereochemical Studies of Monoterpene Compounds. III.[1] Stereochemistry and Intramolecular Hydrogen Bonding of 1-Hydroxy-*p*-menth-3-en-2-one and Its Reduction Products[2]

Takayuki SUGA, Tsuyoshi SHISHIBORI and Tamon MATSUURA

Department of Chemistry, Faculty of Science, Hiroshima University, Hiroshima

(Received July 20, 1967)

1-Hydroxy-*p*-menth-3-en-2-one (1) was prepared from α-terpinene by the *t*-butyl chromate oxidation. *trans*- and *cis*-*p*-Menth-3-ene-1,2-diols (4 and 5), 1-hydroxyisocarvomenthone (2), and 1-hydroxycarvomenthone (3) were also prepared from the compound 1 by lithium aluminum hydride reduction or by hydrogenation. The configurations of these compounds, 1—5, were identified on the basis of chemical evidence, and then the preferred conformation was determined by infrared spectroscopy on the basis of the conception of intramolecular hydrogen bonding. 1 and 2 were found to exist predominantly in the hydrogen-bonded conformations, 1a and 2a, respectively. With respect to 3, the existence of the conformational equilibrium, 3a⇌3b, was demonstrated by the presence of the free and bonded hydroxyl bands. Moreover, 4 and 5 were proved to take the preferred conformations of 4a and 5a respectively.

The conformational analysis of monoterpene cyclic diols[3] and monoterpene hydroxyketones[4] has been investigated in order to clarify the correlation between the formation of the intramolecular hydrogen bond and the conformation of the hydroxyl group in these compounds. α-Hydroxycyclohexanone derivatives can take the intramolecularly hydrogen-bonded forms, c and d, in addition to two interconvertible, unbonded chair-forms, a and b.

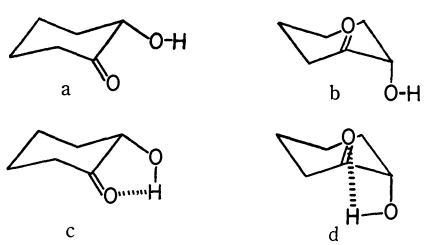

The conformer c contains intramolecular hydrogen bonding between the hydroxyl group and the lone-pair electrons on the carbonyl group (OH···O), whereas the hydroxyl group of the conformer d interacts with pi-electrons on the carbonyl group (OH···π). A characteristic hydroxyl-stretching absorption due to the OH···O-type hydrogen bond[4,5] gives a band at from 3480 to 3500 cm^{-1}. On the other hand, a band resulting from the OH···π interaction[5] appears at from 3600 to 3610 cm^{-1}. Hence, it is expected that the conformation of α-hydroxycyclohexanone derivatives may be determined on the basis of the conception of intramolecular hydrogen bonding. We wish to report here on the preparation of, and the correlation between the conformations and the intramolecular hydrogen bonding of, 1-hydroxy-*p*-menth-3-en-2-one (1), 1-hydroxyisocarvomenthone (2), 1-hydroxycarvomenthone (3), and *trans*- and *cis*-*p*-menth-3-ene-1, 2-diols (4 and 5).

Preparation and Configurations. 1-Hydroxy-*p*-menth-3-en-2-one (1) was prepared from α-terpinene by *t*-butyl chromate oxidation following a method previously reported.[6] The hydrogenation of 1 on palladium-charcoal gave a diastereoisomeric pair of ketols, 2 and 3, in the ratio of 2 to 1. In order to determine the configurations of 2 and 3, these ketols were further reduced with lithium aluminum hydride and then converted into *p*-menthane-1,2-diols, the configuration of which had already been established.[7] The ketol 2, was proved to be 1-hydroxyisocarvomenthone (2), since the reduction of 2 gave 1-hydroxyisocarvomenthol (6) and 1-hydroxyneoisocarvomenthol

1) Part II of this series: T. Suga, T. Shishibori and T. Matsuura, *J. Org. Chem.*, **32**, 965 (1967).
2) Partly presented at the 16th and 17th Annual Meetings of the Chemical Society of Japan, Tokyo, April, 1963 and 1964.
3) T. Suga, T. Shishibori and T. Matsuura, This Bulletin, **37**, 310 (1964).
4) T. Suga, T. Shishibori and T. Matsuura, *J. Org. Chem.*, **32**, 965 (1967).
5) M. Ōki and H. Iwamura, Preprints for the 20th Annual Meeting of the Chemical Society of Japan, Part III (April, 1967), p. 128.
6) T. Matsuura and T. Suga, *J. Org. Chem.*, **30**, 518 (1965).
7) P. R. Jefferies and B. Milligan, *J. Chem. Soc.*, **1956**, 4384.

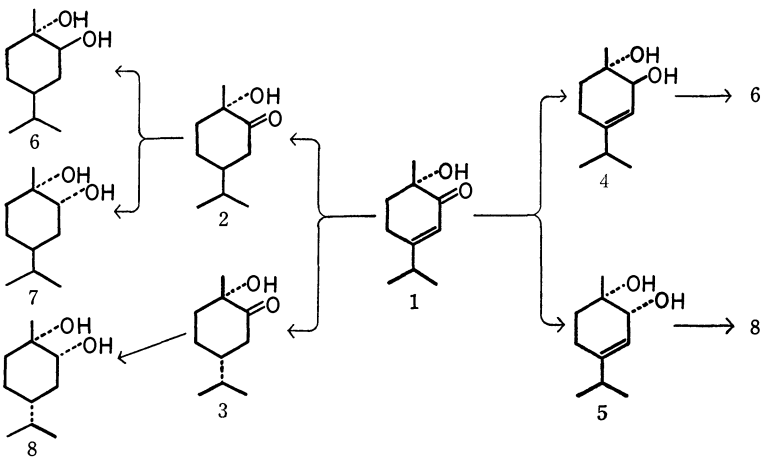

Scheme 1. The configurational assignment of 1-hydroxy-*p*-menth-3-en-2-one (1) and its reduction products.

(7). The reduction of 3 afforded 1-hydroxycarvomenthol (8), and so the ketol 3 must be 1-hydroxycarvomenthone (3).

The lithium aluminum hydride reduction of 1 gave the unsaturated diols 4, with a melting point of 57—58°C, and 5 with a melting point of 50—50.5°C, in the ratio of 3 to 1. The unsaturated diols, 4 and 5, were epimeric at the C-2 position, because both the diols were converted into the original ketone 1 on oxidation. The unsaturated diols 4 and 5 were further hydrogenated on palladium-charcoal in an attempt to assign the configuration of the hydroxyl groups; 4 gave a *trans*-diol, 1-hydroxyisocarvomenthol (6), and 5 yielded a *cis*-diol, 1-hydroxycarvomenthol (8). The unsaturated diols, 4 and 5, were thus proved to be *trans*- and *cis*-*p*-menth-3-ene-1,2-diols respectively.

Conformation and Intramolecular Hydrogen Bonding. As the configurations of the unsaturated hydroxyketone, 1, and its reduction products, 2, 3, 4 and 5, have been identified as above, the preferred conformation of these compounds was determined by considering a correlation between the hydroxyl-stretching absorption band and the distance of the intramolecular hydrogen bond.

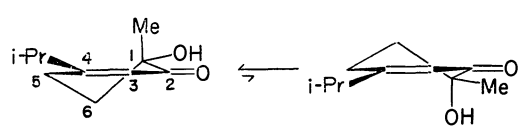

1a 1b

1-Hydroxy-p-menth-3-en-2-one. 1-Hydroxy-*p*-menth-3-en-2-one (1) can exist in two interconvertible conformations 1a and 1b, in which the carbonyl group and the carbon atoms at C-1, C-3, C-4, and C-5 are co-planer, whereas only the carbon atom at C-6 is apart from the plane.

The hydroxyl group of 1 is pseudo-equatorial in the conformer 1a and pseudo-axial in the conformer 1b. An examination of a Dreiding model[8] showed that the distance between the hydroxyl and carbonyl groups (OH···O) is *ca.* 2.1 Å in the conformer 1a and *ca.* 2.9 Å in the conformer 1b. Hence, an OH···O-type intramolecular hydrogen bonding can be expected in 1a, while the OH···π interaction is preferable in 1b. The infrared spectrum of the hydroxyl-stretching region of 1 showed a concentration-independent band at 3517 cm^{-1} (ε 82), which can be attributed to the OH···O-type bonded hydroxyl group. In addition to this principal band, a weak hydroxyl band, probably due to the OH···π interaction, was observed at 3603 cm^{-1} (ε 12) in a dilute solution. This weak band disappeared in a concentrated solution, and a new broad band resulting from the intermolecular hydrogen bond appeared at *ca.* 3400 cm^{-1}. These facts imply that, in a dilute solution, the unsaturated hydroxyketone 1 exists in the conformational equilibrium mixture 1a$\rightleftarrows$1b, in which the conformer 1a is preferred, and that, in a concentrated solution, the hydroxyl and carbonyl groups of the conformer 1b interact intermolecularly with other molecules.

1-Hydroxyisocarvomenthone and 1-Hydroxycarvomenthone. 1-Hydroxyisocarvomenthone (2) and 1-hydroxycarvomenthone (3) may take two interconvertible chair-forms (2a and 2b, and 3a and 3b, respectively). In the conformers 2a and 3b, with an equatorial hydroxyl group, OH···O intramolecular hydrogen bonding between the hydroxyl and carbonyl groups is possible, since the OH···O distance is estimated by means of the Dreiding model[8] to be *ca.* 2.1 Å. On the other hand, such bonding is considered to be difficult in the conformers 2b and 3a, because of the longer OH···O

8) "Dreiding Stereomodels," W. Büchi Manufacture of Glass Apparatus Flawil, Switzerland. The OH···O distance was estimated by using this model.

distance of *ca.* 3.2 Å and the unfavorable direction of the orbital of the lone-pair electrons on the carbonyl oxygen atom, making it difficult to form a OH···O-type hydrogen bond.

The infrared spectra of compound 2 revealed only a concentration-independent band at 3504 cm^{-1} (ε 100) due to the OH···O-type intramolecular hydrogen bond. This implies that the preferred conformation of 2 is the conformer 2a with an equatorial hydroxyl group, while that of the conformer 2b with a free axial hydroxyl group is not present or, if so, exists in a population so low as to make it impossible to observe its spectral band.

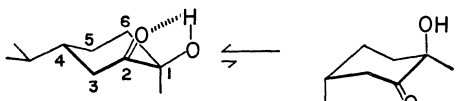

2a

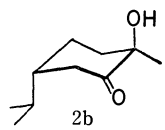

2b

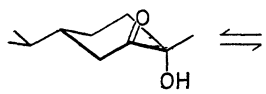

3a

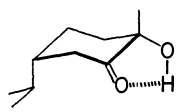

3b

On the other hand, compound 3 showed two peaks, at 3610 (ε 53) and 3502 cm^{-1} (ε 74), in a 0.005 M carbon tetrachloride solution. The former is attributed to the free hydroxyl group, and the latter, to the OH···O-type hydrogen bond. Upon an increase in the concentration of the solution, the frequency of the band due to intramolecular hydrogen bonding did not show any shift, whereas the strength of a newly-appeared band at *ca.* 3450 cm^{-1} resulting from an intermolecularly-hydrogen-bonded hydroxyl group, increased, in contrast to the decrease in the free hydroxyl band, which finally disappeared in the neat sample. These facts indicate that the conformational equilibrium 3a⇄3b exists in a dilute solution, and also that the free hydroxyl groups of the conformer 3a interact with each other in a concentrated solution.

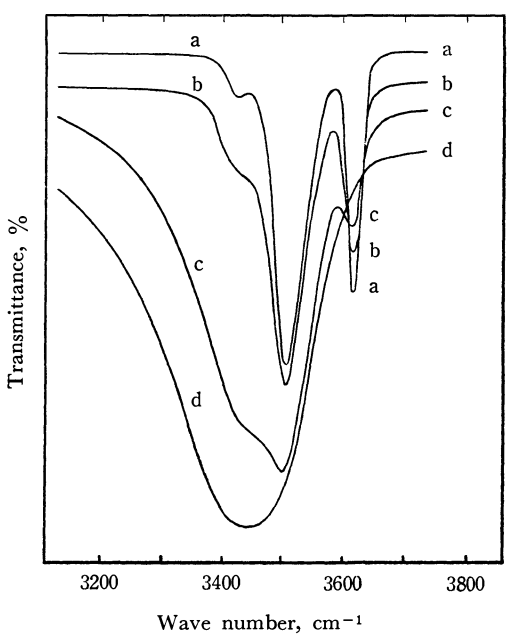

Fig. 1. Infrared spectra of 1-hydroxycarvomenthone (3) in a carbon tetrachloride solution of various concentration: a, 0.005 M; b, 0.05 M; c, 0.5 M; d, neat.

The difference in the conformational preference in the equilibrium mixture of the ketols 2 and 3 may be explained as follows. The difference in conformational free energy between the non-hydrogen-bonded form of the conformer 2a and the conformer 2b is expected to be of the value of *ca.* −1.1 kcal/mol.[9] In addition, the stabilization due to intramolecular hydrogen bonding between the hydroxyl and carbonyl groups in 2a can contribute to the conformational preference of the conformer 2a. Thus, the ketol 2 is thought to exist predominantly in the conformation 2a.

On the other hand, the difference in conformational free energy between the conformer 3a and the non-hydrogen-bonded form of the conformer 3b is expected to be of the value of *ca.* −3.1 kcal/mol.[9] If the stabilization due to intramolecular hydrogen bonding in 3b is sufficient to overcome the instabilization due to the steric repulsion among the 1,3-diaxial atoms and groups, the conformer 3b would be present. However, the stabilization due to intramolecular hydrogen bonding is expected to be of the value of $-\Delta G=1$ kcal/mol at room temperature, since the OH···O-type intramolecular hydrogen bond, forming a five-membered ring, results in a decrease in entropy ($-\Delta S=3.5$ e. u.), plus an enthalpy of the hydrogen bond ($-\Delta H=$ 2 kcal/mol).[12] Therefore, the 3a conformer with a free hydroxyl group, seems to exist preferentially in the conformational equilibrium 3a⇄3b.

trans- and cis-p-Menth-3-ene-1,2-diols. *trans-p*-Menth-3-ene-1,2-diol (4) may take three interconvertible half-chair forms, 4a—4c. Since the OH···O distances[8] are *ca.* 2.2 Å in 4b and 4c and *ca.* 4.0 Å in 4a, the intramolecular hydrogen bond is possible in 4b and 4c, which have equatorial

9) Estimated approximately by adding the corresponding values for a hydroxyl, a methyl, and an isopropyl groups, since such summation has been verified to be approximately correct in some cases.[10] The differences in free energy between the equatorial and axial forms of the hydroxyl, methyl and isopropyl groups are −0.7, −1.7 and −2.1 kcal/mol[11] respectively.

10) E. L. Eliel, N. L. Allinger, S. T. Angyal and G. A. Morrison, "Conformational Analysis," John Wiley & Sons, Inc., New York, N. Y. (1965), p. 58.

11) Ref. 10, p. 44.

12) L. P. Kuhn and R. A. Wires, *J. Am. Chem. Soc.*, **86**, 2161 (1964); C. Duculot, *Compt. rend.*, **241**, 1925 (1955).

and quasi-equatorial hydroxyl groups, but such a bond is impossible in the conformer 4a, which has axial and quasi-axial hydroxyl groups. The infrared spectrum of 4 in a dilute carbon tetrachloride solution exhibited only a band at 3616 cm^{-1} due to the free hydroxyl group. *trans*-diol 4 was thus found to exist predominantly in the conformation 4a.

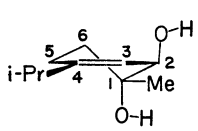

4a

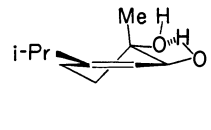

4b

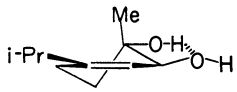

4c

cis-p-Menth-3-ene-1,2-diol (5) may take four interconvertible, internally-bonded half-chair forms, 5a—5d. Since each of the OH···O distances in 5a—5d is estimated to be 2.2 Å,[8] the intramolecular hydrogen bond is possible in all the conformers. The infrared spectrum of 5 showed two bands, at 3617 and 3578 cm^{-1}. The former was attributed to a free tertiary hydroxyl group, since the characteristic frequencies[13] for the unbonded tertiary hydroxyl group have been reported to be 3613—3619 cm^{-1}. The 3578-cm^{-1} band was assigned to an intramolecularly hydrogen-bonded hydroxyl group. Thus, *cis*-diol 5 would exist in the conformer 5a or 5b, in which the less basic secondary hydroxyl group is bonded to the oxygen atom of the more basic tertiary hydroxyl. However, the conformational preference in the equilibrium 5a$\rightleftarrows$5b can not be determined only on the basis of the $\Delta\nu$ in the infrared spectrum, because of the equality of the OH···O distances in 5a and 5b.

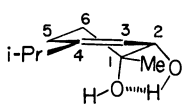

5a

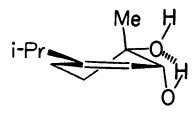

5b

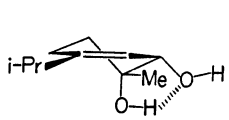

5c

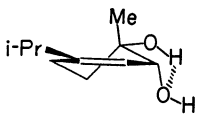

5d

The NMR spectra of the unsaturated diols 4 and 5 afforded further evidence for the conformational assignment described above. The carbinol proton on the C-2 position of the compounds 5 and 4 exhibited signals at δ 3.77 (doublet, J=3.4 cps, half-band width $W_{1/2}$=8 cps) and at δ 4.05 (broad singlet, $W_{1/2}$=6 cps) respectively, in a deuterochloroform solution. In general, the axial carbinol proton resonates at a higher magnetic field than does the equatorial carbinol proton, and the former has the wider half-band width than the latter.[14] According to this general rule, the carbinol proton on the C-2 position of the compound 4 is equatorial, and that of the compound 5 takes an axial conformation. Thus, it can be deduced that the unsaturated diol 4 exists predominantly in the conformation 4a. This result further supports the assignment resulting from the infrared spectrum measurement. Concerning the unsaturated diol 5, on the other hand, it was found that the conformation 5a seems to be preferential in such a conformational equilibrium, 5a$\rightleftarrows$5b, as is deduced from the infrared spectral data.

Experimental

1-Hydroxy-*p*-menth-3-en-2-one (1). The compound used in the present work was the same as that prepared from α-terpinene by *t*-butyl chromate oxidation in a previous paper[6]; it showed the follwoing properties: bp 99—100°C, n_D^{25} 1.4928, d_4^{25} 1.0074; ν_{max}^{neat} 3479, 1147 (OH), 3044, 1627, 878 (⟩C=CH–) 1430 (CH_2C=C); λ_{max}^{EtOH} 236 and 318 mμ (ε 13270 and 80); 2, 4-dinitrophenylhydrazone, mp 208—209°C, $\lambda_{max}^{CHCl_3}$ 392 mμ (ε 26000); phenylurethane, mp 132—132.5°C. The hydroxyl-stretching absorption frequencies in cm^{-1} (and the concentrationsin mol/*l*) were as follows: 3603, 3517 (0.005), 3603, 3517 (0.010), 3602, 3517, (0.05), 3602, 3515 (0.10), 3602, 3514 (0.25), 3601, 3510, (0.50), 3600, 3508 (1.0), 3480 (neat).

Catalytic Hydrogenation of 1. The unsaturated α-hydroxyketone 1 (2.84 g) in ethyl alcohol was hydrogenated in the presence of palladium-charcoal under an atmospheric pressure. The uptake of hydrogen amounted to 1.1 mol, and 1 was converted into a mixture of saturated hydroxyketones. The mixture was fractionated into two eluates by column chromatography on 200 g of silica gel with a mixture of *n*-hexane and ethyl acetate.

The first eluate (1.24 g) was 1-hydroxyisocarvomenthone (2): n_D^{25} 1.4627, d_4^{25} 0.9765; ν_{max}^{liq} 3494 (OH), 1712 (C=O), 1431 (CH_2CO), 1383, 1361 cm^{-1} (isopropyl). The hydroxyl-stretching absorption frequencies in cm^{-1} (and the molar concentration in a carbon tetrachloride solution) were as follows: 3504 (0.005), 3503 (0.050), 3502 (0.50), 3494 (neat).

The second eluate (0.92 g) was 1-hydroxycarvomenthone (3): n_D^{25} 1.4658, d_4^{25} 0.9852; ν_{max}^{liq} 3442 (OH), 1709 (C=O), 1425 (CH_2CO), 1384, 1360 (isopropyl). The IR spectra of 3 in the hydroxyl-stretching region

13) L. P. Kuhn, *J. Am. Chem. Soc.*, **74**, 2492 (1952); A. R. H. Cole, G. T. A. Müller, D. W. Thornton and R. L. S. Willix, *J. Chem. Soc.*, **1959**, 1218; A. R. H. Cole, P. R. Jefferies and G. T. A. Müller, *ibid.*, **1959**, 1222.

14) R. U. Lemieux, R. K. Kulling, H. J. Bernstein and W. G. Schneider, *J. Am. Chem. Soc.*, **80**, 6098 (1958).

are shown in Fig. 1; the ν_{OH} values in cm^{-1} (and the concentrations in mol/l) were as follows: 3610, 3502 (0.005), 3610, 3502 (0.050), 3608, 3494 (0.50), 3441 (neat).

Reduction of 2 with Lithium Aluminum Hydride. To 0.14 g of lithium aluminum hydride in 10 ml of dry ether, there was added, drop by drop, over a 1 hr period, a solution of 0.81 g of 2 in 5 ml of dry ether; the mixture was refluxed for 5 hr and then allowed to stand overnight. The reaction mixture, after it had been treated as usual, afforded 0.80 g of a mixture of diols, which was fractionated into two eluates by column chromatography on silica gel with a mixture of *n*-hexane and ethyl acetate. The initial eluate (0.29 g) was 1-hydroxyneoisocarvomenthol (7): mp 72—72.5°C (lit.[7] 72.5°C); ν_{OH} in a 0.0035 M carbon tetrachloride solution, 3619, 3581 cm^{-1} (lit.[15] 3618, 3580 cm^{-1}). The second eluate (0.39 g) was 1-hydroxyisocarvomenthol (6): mp 51—52°C (lit.[7] 53°C); ν_{OH} in a 0.0032 M carbon tetrachloride solution, 3617, 3597 cm^{-1} (lit.[15] 3618, 3597 cm^{-1}).

Reduction of 3 with Lithium Aluminum Hydride. Hydroxyketone 3 (0.77 g) in 5 ml of dry ether was reduced with 0.14 g of lithium aluminum hydride suspended in 10 ml of dry ether in the same manner as was 2. The purification of the crude product by chromatography on a silica gel column gave 0.55 g of 1-hydroxycarvomenthol (8): mono-3,5-dinitrobenzoate, mp 116—117°C (lit.[7] 117°C); ν_{OH} in a 0.0032 M carbon tetrachloride solution, 3628, 3588 cm^{-1} (lit.[15] 3628, 3586 cm^{-1}).

Reduction of 1 with Lithium Aluminum Hydride. To 0.35 g of lithium aluminum hydride in 15 ml of dry ether, there was added, drop by drop, a solution of 2.00 g of 1 in 4 ml of dry ether; the mixture was stirred for 8 hr at room temperature, and then allowed to stand overnight. This treatment gave 2.00 g of a mixture of unsaturated diols. The mixture was fractionated into two eluates by column chromatography on 100 g of silica gel with a mixture of isopropyl ether and ethyl acetate. The initial eluate (0.38 g) was the unsaturated diol 5, and the final eluate (1.23 g) was the unsaturated diol 4.

The unsaturated diol 5 showed the following properties: mp 50—50.5°C; ν_{max}^{KBr} 3383, 1047, 1021 (OH), 3021 (>C=CH-), 1667 (C=C), 1383, 1368 (isopropyl), 1428 cm^{-1} (CH_2C=C). The hydroxy-stretching absorption maximum in a 0.0032 M carbon tetrachloride solution appeared at 3619 and 3578 cm^{-1}. The NMR spectrum showed signals at δ 1.03 (doublet, J=6 cps, 6H, 9, 10-Me), δ 1.20 (singlet, 3H, 7-Me), δ 3.77 (doublet, J=3.4 cps, $W_{1/2}$=8 cps, 1H, C-2 H), and δ 5.40 (doublet, J=3.4 cps, 1H, C-3 H).

Found: C, 70.69; H, 10.77%. Calcd for $C_{10}H_{18}O_2$: C, 70.55; H, 10.66%.

The unsaturated diol 4 showed the following properties: mp 57—58°C; ν_{max}^{KBr} 3351, 1130, 1110 (OH), 3097, 1161, 845 (>CH=CH-), 1379, 1362 (isopropyl), 1431 cm^{-1} (CH_2C=C). The hydroxyl-stretching absorption maximum in a 0.0032 M carbon tetrachloride solution appeared at 3616 cm^{-1}. The NMR spectrum showed the signals at δ 0.99 (doublet, J=6 cps, 6H, 9, 10-Me), δ 1.14 (singlet, 3H, 7-Me), δ 4.05 (broad singlet, $W_{1/2}$=6 cps, 1H, C-2 H), and δ 5.25 (broad singlet, 1H, C-3 H).

Found: C, 70.74; H, 10.92%. Calcd for $C_{10}H_{18}O_2$: C, 70.55; H, 10.66%.

On oxidation with *t*-butyl chromate for 2.5 days at room temperature, both 4 and 5 were converted into the original unsaturated ketol 1. This was confirmed by a comparison of the infrared spectra.

Catalytic Hydrogenation of the Unsaturated Diol 4. The unsaturated diol 4 in methyl alcohol was hydrogenated in the presence of prereduced palladium hydroxide on calcium carbonate under an atmospheric pressure. The uptake of hydrogen amounted to 0.97 mol, and 4 was converted into 1-hydroxyisocarvomenthol (6): mp 52—52.5°C (lit.[7] 53°C); ν_{max}^{Nujol} 3322, 1069 cm^{-1} (OH); ν_{OH} in a 0.0043 M carbon tetrachloride solution, 3620 and 3602 cm^{-1} (lit.[15] 3618, 3597 cm^{-1}); di-*p*-nitrobenzoate, mp 163—164°C (lit.[7] mp 164°C).

Catalytic Hydrogenation of the Unsaturated Diol 5. The same treatment of 5 as has been described above afforded 1-hydroxycarvomenthol (8): mp 40—42.5°C; ν_{max}^{liq} 3368, 1035, 995 (OH), 1386, 1368 cm^{-1} (isopropyl); ν_{OH} in a 0.0043 M carbon tetrachloride solution, 3627 and 3588 cm^{-1} (lit.[15] 3628, 3586 cm^{-1}); mono-3, 5-dinitrobenzoate, mp 116.5—117°C (lit.[7] mp 117°C).

Measurement of the Infrared Spectra in the Hydroxyl-stretching Region. The infrared spectra were measured by a Hilger H-800 double-beam spectrophotometer under the following conditions: calcium fluoride prism; wave number accuracy at 3500 cm^{-1}: ± 3 cm^{-1}; temperature, 25°C; solvent, spectro-grade carbon tetrachloride.

The authors wish to express their hearty thanks to Professor Shô Itô of Tohoku University for his NMR spectra measurements.

15) A. R. H. Cole and P. R. Jefferies, *J. Chem. Soc.*, **1956**, 4391.

BULLETIN OF THE CHEMICAL SOCIETY OF JAPAN VOL. 41 949—953 (1968)

The Mechanism of the Alkaline Fusion of Halodiphenyl Sulfone and Halobenzenesulfinic Acids[1]

Naomichi FURUKAWA and Shigeru OAE

Department of Applied Chemistry, Faculty of Engineering, Osaka City University, Sumiyoshi-ku, Osaka

(Received August 5, 1967)

The alkaline fusion of 2-chlorophenyl phenyl sulfone afforded phenol, benzene and chlorobenzene. The initial step of the reaction appears to be the aromatic S_N2-type replacement of chlorine to form 2-hydroxyphenyl phenyl sulfone upon which the hydroxide ion further attacks both phenyl carbon-1 and the sulfur atom of the sulfone group to form the final products. The ^{14}C tracer experiment indicates that the preference of the nucleophilic-attacking site of the hydroxide ion appears to vary with the reaction temperature. A similar alkaline fusion of 2-bromo-4-tolyl phenyl sulfone gave not only benzene, bromotoluene, and phenol, but also *o*- and *m*-cresol, indicating that the reaction proceeds through a somewhat different path. Meanwhile, the alkaline fusion of 2-chlorobenzenesulfinic acid appears to proceed through the *o*-sulfinic benzyne formation; thus 2-bromo-4-tolylsulfinic acid gave equal amounts of *o*- and *m*-cresols.

Previously we have shown, mainly through ^{14}C and ^{18}O tracer experiments, that the alkaline fusion of benzenesulfonic acid proceeded through an aromatic S_N2-type reaction at the ring-carbon-bearing sulfonic acid group.[2] The same conclusion has been reached through studies of the careful isolation of products from substituted aromatic sulfonic acids.[3,4] Subsequently, the mechanism of the alkaline fusion of diphenyl sulfone has been studied by means of the ^{14}C-tracer technique[5]; this study suggests that the reaction proceeds through a simple SN2-type path, and not one involving benzyne formation. However, an unanswered question has remained as to the site of the nucleophilic attack of the hydroxide ion. The successful isolation of benzenesulfonic acid during the reaction by Ingold and Jessop[6] and the strong affinity of the negative hydroxide ion toward the positively-charged sulfur atom of the sulfone group seem to favor the nucleophilic attack of the hydroxide ion on the sulfone group, as is shown below Mechanism A:

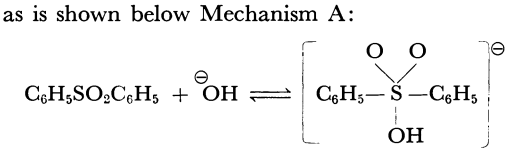

(Mechanism A)

Another mechanism, an aromatic S_N2 reaction on the carbon-atom-bearing sulfonyl group (Mechanism B), cannot be ruled out, however, since a similar alkaline fusion of benzenesulfonic acid is apparently a part of the aromatic S_N2 process, and benzenesulfinic acid has actually been isolated from the alkaline fusion of diphenyl sulfone.[7]

(Mechanism B)

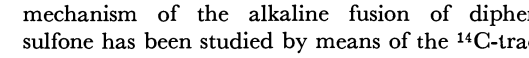

Although there is no easy way to make a choice between the above two mechanisms, the alkaline fusion of *o*-halophenyl phenyl sulfone is an interesting problem in this connection, since the process involving the initial nucleophilic attack of the hydroxide ion on the sulfone group (Mechanism I) may lead to the formation of a benzyne intermediate, as in the reaction of *o*-chlorobenzophenone with potassium amide,[8] and the products formed will be somewhat different from those expected from the attack on the carbon atom. A more clear-cut difference in the distribution of products will be observed when 2-halo-4-tolylsulfone is used, as in the aminolysis of *o*-halobenzophenone. Another interesting problem is the behavior of *o*-halobenzenesulfinate ion in the alkaline fusion, since it will be one of the intermediate formed if the reaction follows the mechanism B.

1) Phenols and Phenolic Esters. XIV.
2) S. Oae, N. Furukawa, M. Kise and M. Kawanishi, This Bulletin, **39**, 1212 (1966).
3) W. Pritzkow, P. Grothkoph, R. Hoering, H. Gross and W. Fuerhring, *Z. Chem.*, **5**, 300 (1965).
4) L. R. Buzbee, *J. Org. Chem.*, **31**, 3289 (1966).
5) S. Oae and N. Furukawa, This Bulletin, **39**, 2260 (1966).
6) C. K. Ingold and J. A. Jessop, *J. Chem. Soc.*, **1930**, 708.
7) Professor M. Kobayashi, unpublished.
8) J. F. Bunnett and B. H. Hrutfiord, *J. Org. Chem.*, **27**, 4152 (1962).

Thus, we have studied the alkaline fusion of 2-chlorophenyl phenyl sulfone, 2-bromo-4-tolyl phenyl sulfone, 2-chloro-benzenesulfinic acid, and 2-bromo-4-tolylsulfinic acid. The results we have obtained are somewhat different from what we anticipated, but they appear to suggest clearly that the nucleophilic attack of the hydroxide ion takes place at both the sulfone group and the aromatic ring carbon-1. By the use of 2-chlorophenyl phenyl-1'-^{14}C sulfone, the relative ratio of the nucleophilic attack of the hydroxide ion at the sulfone group and the aromatic ring carbon was estimated.

This paper will describe our experimental observations and discuss the mechanisms of these reactions.

Results and Discussion

The reaction was generally carried out by heating a mixture of a starting compound with an excess of potassium hydroxide at around 300°C for several minutes in a nickel crucible under a slow stream of nitrogen gas; the products were analyzed by introducing them to their corresponding known derivatives or by a comparison of their gas chromatographic behavior and infrared spectra with those of the authentic samples.

***o*-Halophenyl Phenyl Sulfone.** While the alkaline fusion of diphenyl sulfone takes place slowly at below 300°C, that of the *o*-halo derivative is quite facile. A similar phenomenon was observed in the aminolyses of *o*-halobenzophenone and benzophenone, where the *o*-chloro compound undergoes a much facile cleavage, apparently forming a benzyne intermediate.[8] It appears that the substitution of the electron-withdrawing chloro group facilitates the nucleophilic attack of hydroxide on the molecule. When the alkaline fusion of *o*-chlorophenyl phenyl sulfone was carried out, the products identified were phenol, benzene, and chlorobenzene. This means that unlike the aminolysis of *o*-halobenzophenone the reaction does not seem to proceed only through the formation of benzyne (Mechanism I), since the mechanism involving the formation of benzyne would require phenol and chlorobenzene to be the only products of this reaction. Actually, the formation of a small amount of chlorobenzene suggests that at least a portion of the nucleophilic attack of the hydroxide ion takes place on the sulfone group (Mechanism I).

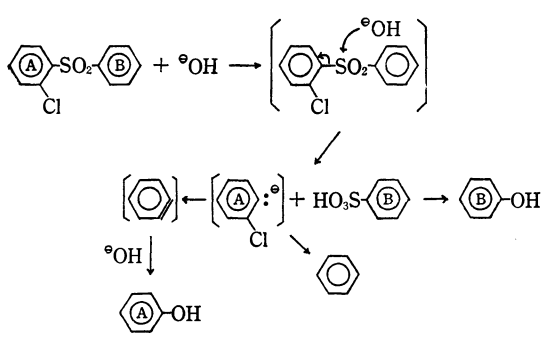

Mechanism I. Attack on the sulfone group.

The complete lack of catechol among the products suggests that the initial nucleophilic attack of hydroxide does not occur at the carbon-1 position of the A ring. This is rather strange, since the A ring would be more susceptible to nucleophilic attack because of its electron-withdrawing *o*-chloro group. However, since chloride is a better leaving group than the benzenesulfinate group, the initial nucleophilic attack on the A ring may take place at the 2-position, replacing chloride ion (Mechanism II).

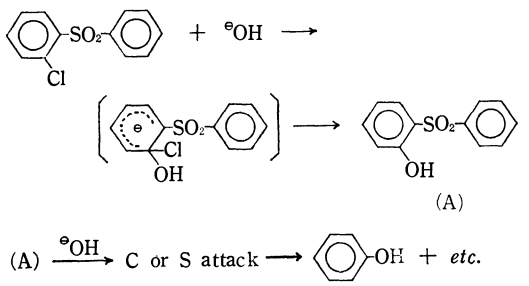

Mechanism II. Initial chloride replacement subsequent nucleophilic cleavage.

In fact, the *o*-chloro group is highly activated by the phenylsulfonyl group and is susceptible to nucleophilic attack.[9] When *o*-chlorophenyl phenyl sulfone was treated with aqueous potassium hydroxide in dimethyl sulfoxide, *o*-hydroxyphenyl phenyl sulfone was isolated in a high yield. Thus, *o*-hydroxyphenyl phenyl sulfone is a very likely intermediate in this reaction, and the lack of catechol formation may be ascribed to the negative field effect of the hydroxyl group, which suppresses the nucleophilic attack at the A ring. Another possible mechanism is the one that involves the prior formation of *o*-sulfonyl benzyne (Mechanism III). Though the formation of a small

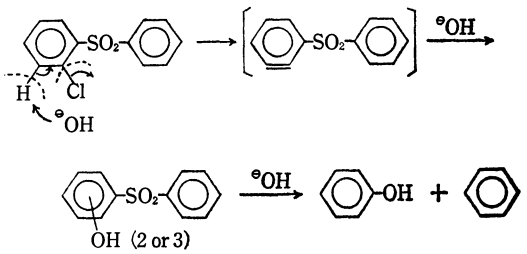

Mechanism III. Initial dehydrochlorination-addition subsequent nucleophilic cleavage.

9) S. Oae and Y. Khim, This Bulletin, **40**, 1716 (1967).

Table 1. The reaction conditions and the products

Compound	Products (yield %)	Reaction temp. °C
o-Cl-$C_6H_4SO_2Na$	C_6H_5OH (40)	260—330
p-Cl-$C_6H_4SO_2Na$	C_6H_5OH (70)	260—330
2,4-Br(CH_3)$C_6H_3SO_2Na$	*o*,*m*-$CH_3C_6H_4OH$* (70), C_6H_5OH	300—350
o-Cl-$C_6H_4SO_2C_6H_5$	C_6H_5OH (65), C_6H_5Cl, C_6H_6	260—300
2,4-Br(CH_3)$C_6H_3SO_2C_6H_5$	*o*,*m*-$CH_3C_6H_4OH$**, C_6H_5OH (60)	240—330

* The products ratio was 1 : 1 : 0.5 (*o*-cresol : *m*-cresol : phenol).
** *o*-cresol : *m*-cresol : phenol = trace : 7 : 1

amount of chlorobenzene cannot be explained by this mechanism, it is possible that a portion of the reaction may proceed through this process.

In order to test these possibilities, 2-bromo-4-tolyl phenyl sulfone was subjected to alkaline fusion. If the reaction follows the path of the III mechanism, one would expect to obtain nearly equal amounts of *o*- and *m*-cresols. As shown in Table 1, we did find *o*-cresol, but the amount was less than 1/20th that of *m*-cresol. The formation of such a small amount of *o*-cresol suggests that although a tiny fraction of the reaction actually goes through the III mechanism, it is by no means the major path of the reaction. The lack of *p*-cresol among the products is noteworthy, since it indicates that the initial benzyne formation through the nucleophilic attack of the hydroxide ion on the sulfone group does not occur in this reaction; however, the formation of a small amount of *m*-bromotoluene clearly suggests that the process involving the nucleophilic attack of the hydroxide ion on the sulfone group (Mechanism I) cannot be excluded. Moreover, the formation of 4-methylcatechol was not noticed in this reaction. Probably, here also, the major path of the reaction is the one involving the initial chloride replacement (Mechanism II).

Table 2. ^{14}C-tracer study

Compound	Reaction temp. °C	Activities cpm
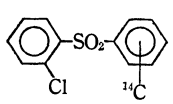	—	679
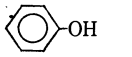	270	812
	270—290	806
	300—330	681
(as tribromide)		

As has been shown above, phenol was the major product of the alkaline fusion of *o*-chlorophenyl phenyl sulfone. In order to shed further light on the reaction, 2′-chlorophenyl phenyl-1-^{14}C sulfone was subjected to the alkaline fusion. If the source of phenol is limited to either A or B ring, the specific activity of the resulted phenol is expected to be either nil or twice the ^{14}C activitiy of the original sulfone. Indeed, as shown in Table 2, the phenol obtained was found to have nearly the same specific activity as that of the starting sulfone, suggesting that the phenol comes from both A and B rings nearly in the same extent. However, when the alkaline fusion was carried out at somewhat lower temperatures, the specific activity of the phenol formed was found to show a somewhat higher value, suggesting that there is a preference in attacking site in the nucleophilic attack of the hydroxide ion. If the portion of the reaction that proceeds through the I mechanism increases at lower temperatures, it will increase the activity of the phenol formed. However, detailed analyses of the preference of the attacking site of the hydroxide ion will have to await further investigation.

o-Halobenzenesulfinic Acids. In the foregoing discussion, the alkaline fusion of benzenesulfinate was presumed to give only benzene, as was reported previously.[10] In fact, when this reaction was repeated, we found only the formation of benzene. Undoubtedly the nucleophilic attack of the hydroxide ion takes place only at the sulfonyl group, as is illustrated below:

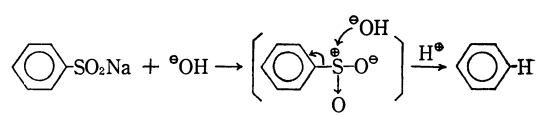

This desulfination is quite facile and is usually completed in a few minutes at around 300°C.

When *o*-chlorobenzenesulfinic acid was treated with an excess of potassium hydroxide, phenol was obtained, but the yield was not impressive; however, *p*-chlorobenzenesulfinic acid in the same reaction also afforded phenol in a much higher yield. In neither case chlorobenzene was isolated. The complete lack of chlorobenzene formation suggests that the nucleophilic attack in the sulfinate group to form chlorobenzene is not the initial process of this reaction; rather, the replacement of the chloro group by the hydroxide ion seems to follow the alkaline cleavage of the sulfinate group. This is clearly demonstrated in the alkaline fusion

10) R. Otto, *Ann*, **145**, 322 (1868).

of 2-bromo-4-toluenesulfinate, in which both *o*- and *m*-cresols were obtained as the main products; their yields were nearly equal. The results are shown in Table 1. The total absence of *p*-cresol suggests that the replacement reaction of bromine by hydroxyl takes place prior to the alkaline cleavage of the sulfinate group and that *m*-bromotoluene is not the intermediate, since the alkaline fusion of *m*-bromotoluene, presumably proceeding *via* the formation of benzyne,[11] would give not only *o*- and *m*-cresols, but also *p*-cresol. Thus, the equal distribution of *o*- and *m*-cresols suggests that the initial reaction is the dehydrobromination to form the benzyne intermediate, which upon the addition of hydroxide, forms both 2- and 3-hydroxytoluenesulfinates which in the succeeding step undergoes desulfination to afford *o*- and *m*-cresols, as is shown below:

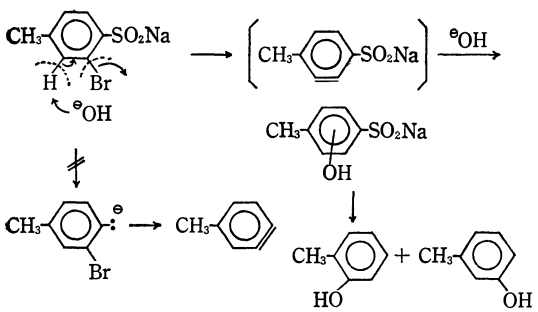

The formation of a small amount of phenol appears to be due to the demethylation of cresols during the alkaline fusion, though its mechanism is not fully understood.

Experimental

The Preparation of *o*-Halosulfinic Acid and *o*-Halosulfone. *o*-Chlorobenzene Sulfinic Acid. *o*-Chloroaniline (12.8 g) was diazotized with 7.6 g of sodium nitrite in a mixture of 16 m*l* of concentrated sulfuric acid and 200 m*l* of water. Into the diazotized solution sulfur dioxide gas was bubbled until the weight of the mixture increased by 50 g. Then copper powder was then added into the solution to decompose the diazotized compound. The precipitate was washed with ether three times. The filtrate was extracted with ether, and the combined ether solution was extracted with a 5% sodium hydroxide solution. The alkaline extract was acidified with concentrated hydrochloric acid. Thus, the sulfinic acid (12.5 g) was obtained in a 90% yield; mp 108—110°C.

o-Bromotoluenesulfinic acid was prepared similarly from 9.5 g of 2-bromo-4-methylaniline in a 72% yield; mp 115—117°C.

o-Chlorophenyl Phenyl Sulfone. *o*-Chlorophenyl phenyl sulfide (33 g), prepared by the reaction of thiophenolate with *o*-chlorobenzene diazonium sulfate, was oxidized with 47.4 g of potassium permanganate in 200 m*l* of acetic acid at a temperature below 50°C. The sulfone thus obtained was recrystallized from benzene - *n*-hexane. The yield was 30 g (80%); mp 106-107°C.

2-Bromo-4-tolyl Phenyl Sulfone. 2-Bromo-4-tolyl phenyl sulfide (10.1 g), prepared by the reaction of a 2-bromo-4-tolyl diazonium solution with thiophenolate, was oxidized with 12.0 g of potassium permanganate in 75 m*l* of acetic acid. After the reaction, the mixture was quenched with a large amount of water; then SO_2 gas was introduced to decompose the excess potassium permanganate. The gummy solid cake was dried and recrystallized from 95% ethanol. The yield was 10.5 g (90%) mp 112—113°C, after repeated recrystallizations from 95% ethanol. The sulfone has characteristic IR absorption bands at 1150 and 1350 cm^{-1}.

The Alkaline Fusion of Sulfinic Acid and Sulfone. *A Typical Example of Alkaline Fusion.* The alkaline fusion of *o*-chlorosulfinic acid was carried out as follows. Sodium *o*-chlorobenzenesulfinate (5.5 g) was added to molten potassium hydroxide (15 g) placed in a nickel crucible, at a temperature kept between 260—300°C under nitrogen stream. Vigorous foaming occurred immediately. After the addition, temperature was kept at 300—330°C for 5 min, and then the vessel was cooled rapidly with running water. The solidified mixture was dissolved into water and acidified with concentrated hydrochloric acid, and the aqueous solution was distilled with steam. Into the distillate bromine water was added until the solution turned slight yellow. The tribromide thus obtained was filtered and washed with water. The yield of tribromophenol was 2.0 g; mp 94°C.

In some cases, the distillate was extracted with ether and directly gas chromatographed. The conditions of G. L. C. were as follows: Temp., 130°C; H_2 35 m*l*/min; column, silicone grease coated on Celite 545, 2 m long.

The results of the alkaline fusion of the other sulfinic acids are listed in Table 1; the conditions were nearly the same.

The Alkaline Fusion of o-Chlorophenyl Phenyl Sulfone. *o*-Chlorophenyl phenyl sulfone (3.0 g) was mixed with 15 g of potassium hydroxide and heated in a nickel crucible at a temperature between 300—350°C with a silicone oil bath. The liquid was trapped and then analyzed by G. L. C. After several minutes of heating, the vessel was cooled. The solidified product was dissolved into water and acidified with concentrated hydrochloric acid. The acidified solution was then distilled with steam. The distillate was extracted with ether, and the etheral solution was dried over magnesium sulfate. After ether was removed, the residue was distilled. The yield was 1.46 g (91%). The products were analyzed by G. L. C., the conditions of which were the same as in the case of the sulfinic acid. The compounds identified were benzene and phenol; catechol could not be detected by G. L. C.

The Alkaline Fusion of 2-Bromo-4-tolyl Phenyl Sulfone. This compound was treated similarly; from 3.0 g of the sulfone, 0.6 g of phenols and 1.0 g of an unidentified solid were obtained.

The liquid products were analyzed by G. L. C.; benzene, toluene, phenol, *m*-cresol, and a tiny peak of *o*-cresol were found. The ratio of the products is shown in Table 1.

11) A. T. Bottini and J. D. Roberts, *J. Am. Chem. Soc.*, **79**, 1458 (1957).

o-Chlorophenyl Phenyl Sulfone with Potassium Hydroxide in DMSO. The sulfone (2.5 g) and 5.0 g of potassium hydroxide in 20 m*l* of DMSO containing 5 m*l* of water was refluxed over an oil bath for 24 hr. After cooling, the mixture was poured onto ice water. The aqueous solution was acidified with concentrated hydrochloric acid, and extracted with water. The ether extract was washed with water and dried over sodium sulfate. The ether was removed and the crystalline residue was recrystallized from benzene-*n*-hexane. The crystals were identified as *o*-hydroxyphenyl phenyl sulfone. The yield was 1.8 g (78.2%); mp 97—98°C.

2-Chlorophenyl Phenyl Sulfone-1-^{14}C. The synthesis of the sulfone was performed by the method described for unlabelled sulfone. From 2.0 g of aniline-1-^{14}C and *o*-chlorothiophenol prepared from *o*-chloroaniline and potassium xanthate, 2.5 g of 2'-chlorophenyl phenyl sulfide-1-^{14}C was obtained. The sulfide (2.5 g), when oxidized with potassium permanganate, gave 2.2 g of the titled sulfone. The alkaline fusion was performed as in the case of the unlabeled sulfone. The reaction conditions and products are listed in Table 1. The ^{14}C activity measurements were carried out by the Van Slyke wet combustion method by converting the samples as usual to barium carbonate pellets; the activities were recorded by a 2π gas-flow G. M. counter.

BULLETIN OF THE CHEMICAL SOCIETY OF JAPAN VOL. 41 953—959 (1968)

Polymerization and Isomerization of Allylbenzene and Propenylbenzene*1

Akihiko SHIMIZU,*2 Takayuki OTSU and Minoru IMOTO

Department of Applied Chemistry, Faculty of Engineering, Osaka City University, Sugimoto-cho, Sumiyoshi-ku, Osaka

(Received October 2, 1967)

In order to clarify the relationship between the isomerization and polymerization of α- and β-olefins by various types of catalysts, the isomerizations of allylbenzene and propenylbenzene during their polymerizations were studied. In the presence of cationic catalysts ($AlBr_3$, $BF_3O(C_2H_5)_2$, *etc*), neither the polymerization nor the isomerization of allylbenzene was observed, but propenylbenzene was found to be polymerized without the isomerization of the monomer to give a solid polymer which consisted substantially of a 1,2-structure, plus a minor unit of an isomerized structure. In the cases of the Natta catalysts [$TiCl_3$-$Al(C_2H_5)_3$, $Al/Ti \geq 2$], allylbenzene could easily be polymerized to a high-molecular-weight polymer with a 1,2-structure. During this polymerization, both positional and geometrical isomerizations of the unreacted monomer were observed, indicating that the propenylbenzene obtained from the isomerization did not participate in the polymerization of allylbenzene. It was also found that the polymerization and the positional isomerization of propenylbenzene by these catalysts did not occur.

In previous papers[1-3] it has been shown that some β-olefins, such as butene-2, pentene-2, and hexene-2, can be homopolymerized by the Natta catalyst to give high-molecular-weight polymers with a recurring unit of the corresponding α-olefins. As to the mechanism of the polymerization, it has been concluded that β-olefins were isomerized first to the corresponding α-olefins, which have less steric hindrance, and were then polymerized as α-olefins through a coordinated anionic mechanism. In such cases, it is characteristic that the isomerization of the unreacted monomer is observed, but that of a growing anion to give more stable anion species does not occur during the polymerization.

On the other hand, Kennedy and his co-workers[4] discovered and developed the isomerization polymerization of some branched α-olefins by cationic catalysts at lower temperatures. In this case, the isomerization of a growing cation, which is accompanied by a hydride shift to give a more stable carbonium ion, must occur during the polymerization, while no isomerization of the unreacted monomer is observed.

In order to clarify the relationship between the polymerization and isomerization of α-and β-olefins by various types of catalysts, we attempted to investigate the isomerizations of allylbenzene and propenylbenzene during their polymerizations in the present study. The polymerization of these

*1 Vinyl Polymerization. 184.

*2 Present address: Toyo Soda Co., Ltd., Tono-gun, Yamaguchi-ken.

1) A. Shimizu, T. Otsu and M. Imoto, *J. Polymer Sci.*, **3B**, 449 (1965).

2) A. Shimizu, T. Otsu and M. Imoto, *ibid.*, **3B**, 1031 (1965).

3) T. Otsu, A. Shimizu and M. Imoto, *ibid.*, **4A**, 1579 (1966).

4) J. P. Kennedy, *Fortschr. Hochpolym. Forsch.*, **3**, 508 (1964).

monomer is expected to give polymers with the following three types of recurring units:

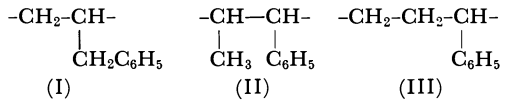

(I) (II) (III)

In 1935, Staudinger and Dreher[5] reported that, in the presence of boron trifluoride as a catalyst, propenylbenzene was polymerized to give a polymer with the structure III, but not the structure II. However, this experiment was reexamined in 1944 by Müller *et al.*[6] and the presence of a CH_3-C bond in the resulting polymer was established, negating Staudinger's findings.

Recently Murahashi, Nozakura, and their coworkers[7] found that propenylbenzene could be polymerized by a cationic mechanism to give the polymer with the structures II and III, and that the isomerization polymerization to the structure III was preferred by less acidic catalysts such as $BF_3O(C_2H_5)_2$, while the polymerization to the structure II was predominant with the BF_3 catalyst. They also reported that allylbenzene was polymerized by the BF_3 catalyst in methylene chloride at $-78°C$ to give a polymer which was somewhat different from the conventional polyallylbenzene I and polypropenylbenzene II. Similar results were independently reported by Kennedy.[8]

More recently, Murahashi, Nozakura, and their coworkers[9] pointed out that the polymer obtained by the cationic polymerization of allylbenzene contained the following two types of recurring units, IV and V:

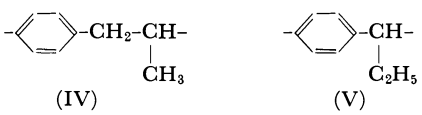

(IV) (V)

Experimental

Materials. The allylbenzene was prepared according to the procedure of Hershberg[10] by the reaction of allyl bromide with phenylmagnesium bromide; bp 60—61°C/27 mmHg, n_D^{20} 1.5144 (lit.[11]; n_D^{20} 1.5135 for the cis-isomer). From the gas chromatographic analysis (4-m tricresyl phosphate column), it was found that this compound was 97.5% pure.

The propenylbenzene was prepared by the procedure described by Overberger and Saunder[12] through the thermal decomposition of ethylphenylcarbinol; bp 71—74°C/27 mmHg, n_D^{20} 1.5505 (lit.[13]): n_D^{25} 1.5480 for the trans-isomer). This propenylbenzene was 99.1% pure and was found by gas chromatography to consist of 86.9% trans-isomers and 13.1% cis-isomers.

The boron trifluoride - diethyl etherate used as a catalyst was distilled under reduced pressure; bp 126—127°C. The metal halides, titanium tetrabutoxide, and aluminum alkyls were commercially obtained, and were used without further purification.

The *n*-heptane was purified by washing it thoroughly with concentrated sulfuric acid, followed by washing with distilled water until it was neutral, whereupon it was distilled over metallic sodium.

Polymerization Procedure. Cationic polymerizations by the $AlBr_3$ or $BF_3O(C_2H_5)_2$ catalyst were carried out in a sealed glass tube in methylene chloride or in toluene. The charging of the required amounts of reagents into the tube was performed in a dry nitrogen atmosphere.

Coordinated anionic polymerizations were also carried out by charging as follows: to a hard glass tube containing a given amount of titanium trichloride or vanadium trichloride in *n*-heptane, there was added, through a rubber cap using a hypodermic syringe, the required amount of a *n*-heptane solution of aluminum alkyl in a dry nitrogen atmosphere. The catalyst mixture thus obtained was aged for an hour at room temperature, after which the monomer was charged into this tube and the tube was sealed off.

After polymerization in a thermostat for a given period, the tube was opened and the unreacted monomer was recovered and its isomer distribution determined by gas chromatography. The contents of the tube were then poured into a large amount of a hydrochloric acid - isopropyl alcohol mixed solution in order to precipitate the polymer formed. The conversion was calculated from the weight of the dry polymer obtained.

Characterization of the Polymer. The infrared spectra of the resulting polymers were obtained on KBr disks or in thin liquid films. The ratio in the optical density of the band at 2960 to that at 2925 cm^{-1}, $D(CH_3/CH_2)$, was used as a measure of the methyl-to-methylene ratio, *i. e.*, the ratio of the structural units of II to I, or of II to III, in the polymer.[7]

The obtaining solid polymer was extracted with hot toluene, and its crystallinity was expressed by the amount of the insoluble fraction in hot toluene.

Results

Cationic Polymerization with $AlBr_3$ or $BF_3O(C_2H_5)_2$ Catalyst. The results obtained in the polymerization of allylbenzene and propenylbenzene by the $AlBr_3$ or $BF_3O(C_2H_5)_2$ catalyst are shown in Table 1, in which the isomer distribution of the recovered monomer after polymerization and the ratio of the optical densities, $D(CH_3/CH_2)$, of the resulting polymers are also indicated.

5) H. Staudinger and E. Dreher, *Ann.*, **517**, 73 (1935).
6) A. Müller, L. Toldy and Z. Racz, *Ber.*, **77**, 77 (1944).
7) S. Murahashi, S. Nozakura, K. Tsuboshima and Y. Kotake, This Bulletin, **37**, 706 (1964).
8) J. P. Kennedy, *J. Polymer Sci.*, **2A**, 5171 (1964).
9) S. Murahashi, S. Nozakura, Y. Kotake and T. Okamoto, Presented at the 14th Annual Meeting of the Polymer Society of Japan, May, 1965; Preprint, p. 66.
10) E. B. Hershberg, *Helv. Chim. Acta*, **17**, 352 (1934).
11) K. C. Frisch, *J. Polymer Sci.*, **41**, 359 (1959).
12) C. G. Overberger and J. H. Saunders, *Org. Synthesis*, **28**, 31 (1949).
13) C. G. Overberger, D. Tanner and E. M. Pearce, *J. Am. Chem. Soc.*, **80**, 4566 (1958).

TABLE 1. RESULTS OF CATIONIC POLYMERIZATION OF ALLYLBENZENE (AB) AND PROPENYLBENZENE (PB) WITH $AlBr_3$, OR $BF_3O(C_2H_5)_2$ CATALYST

Monomer	Temp. °C	Time hr	Conversion %	$D(CH_3/CH_2)$	Isomer distribution of monomer recovered after polymerization[a]		
					AB	*cis*-PB	*trans*-PB
$AlBr_3$ catalyst: $[AlBr_3]=7.7$ mmol/*l* in methylene chloride[b]							
AB	−78	458	0	—	100.0	0.0	0.0
AB	10—15	434	0	—	100.0	0.0	0.0
PB	−78	458	0.3	—	0.0	12.4	87.6
PB	10—15	434	0.1	—	0.0	12.8	87.2
$BF_3O(C_2H_5)_2$ catalyst: $[BF_3O(C_2H_5)_2=65.9$ mmol/*l* in bulk[c]							
AB	10—15	240	0.1	—	100.0	0.0	0.0
PB	10—15	240	8.6[d]	1.21	0.0	11.4	88.6
PB	0	71[e]	4.9[f]	1.00	0.0	12.0	88.0

a) Determined by gas chromatography. Values are wt%.
b) [Monomer]=2.63 mol/*l*.
c) [Monomer]=7.62 mol/*l*.
d) Colorless solid polymer having mol wt of 720 (Mechrolab vapor pressure osmometer).
e) [Monomer]=1.51 mol/*l* in toluene.
f) Colorless solid polymer.

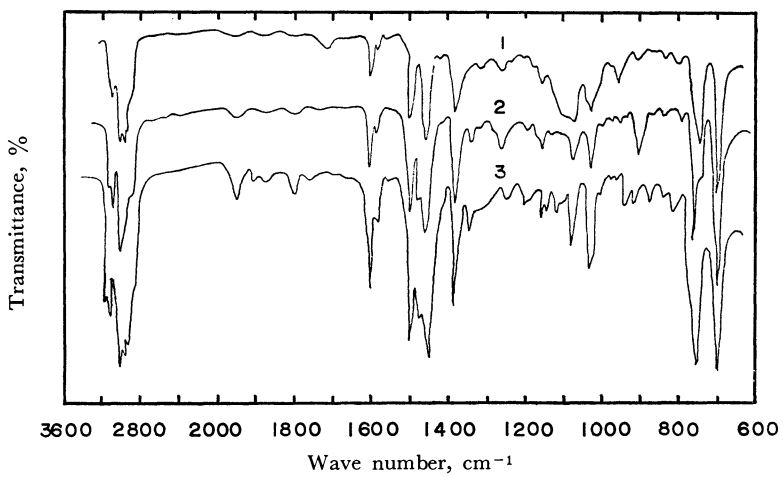

Fig. 1. Infrared spectra of polypropenylbenzene (film).
(1) Polymer obtained with $BF_3 \cdot O(C_2H_5)_2$ catalyst, (2) polymer obtained with $C_2H_5AlCl_2$-$TiCl_3$ catalyst, (3) polymer obtained with $TiCl_3$ catalyst.

As can be seen from this table, allylbenzene was neither polymerized nor isomerized by these catalysts during the reaction. However, propenylbenzene was polymerized by the $BF_3O(C_2H_5)_2$ catalyst, without the isomerization of the monomer, thus giving a colorless solid polymer which was soluble in benzene. The infrared spectrum of the obtaining polymer is shown in Fig. 1, where the $D(CH_3/CH_2)$ value was 1.00—1.21, indicating that the methylene group is present in the backbone of this polymer.

Polymerization with Catalyst Systems Containing $TiCl_3$. The results of the polymerization of allylbenzene by the catalyst systems of $TiCl_3$ alone and of $TiCl_3$-organoaluminum compounds are summarized in Table 2. By the addition of $TiCl_3$ alone, allylbenzene was found to be hardly polymerized at all and to be isomerized to propenylbenzene, giving a colorless viscous polymer. In its infrared spectrum, shown in Fig. 2, this polymer showed $D(CH_3/CH_2)$ values of 0.91—1.11, unmistakably confirming the presence of a methyl group attached to the backbone of this polymer.

In the presence of the binary systems of $TiCl_3$ and organoaluminum compounds, allylbenzene was readily polymerized to a solid polymer containing no methyl group ($D(CH_3/CH_2)=0$), as is indicated in Fig. 2. The polymer yields were found to depend upon the kind of organoaluminum compounds

TABLE 2. RESULTS OF POLYMERIZATION OF ALLYLBENZENE (AB) WITH THE CATALYST SYSTEMS CONTAINING $TiCl_3$ IN *n*-HEPTANE AT 80°C
$[TiCl_3]=50$ mmol, $[AB]=3.0$ mol/*l*

Catalyst system	Al/Ti molar ratio	Time hr	Conversion %	Toluene-insoluble polymer		$D(CH_3/CH_2)$	Isomer distribution of monomer recovered after polymerization		
				wt, %	mp, °C		AB	*cis*-PB	*trans*-PB
$TiCl_3$[a]	0	46	0.3	—	—	—	95.8	1.1	3.1
	0	158	2.4	—	—	1.11	89.0	1.3	9.7
$TiCl_3$-$Al(C_2H_5)_3$	0.5	3.5	20.1	48.3	208—211	0	98.3	0.0	1.7
	1	3.5	41.9	—	—	0	97.0	0.0	3.0
	2	3.5	49.7	52.7	211—216	0	91.2	1.6	7.2
	4	3.5	43.0	44.6	208—210	0	83.6	3.1	13.3
$TiCl_3$-$Al(C_2H_5)_2Cl$	2	7.5	12.7	—	175—181[b]	0	99.9	0.0	0.1
$TiCl_3$-$Al(C_2H_5)Cl_2$	2	24	20.4	0	50— 56	1.08	98.1	0.0	1.9
	2	68[c]	52.4	0	51— 58[d]	1.07	99.5	0.0	0.5
$TiCl_3$-$Al(i\text{-}C_4H_9)_3$	2	3.5	38.1	—	—	0	93.5	0.0	6.5

a) $[TiCl_3]=100$ mmol/*l*, $[AB]=1.0$ mol/*l*.
b) Determined for the unextracted polymer.
c) Polymerized at 10—15°C.
d) Mol wt was 1080.

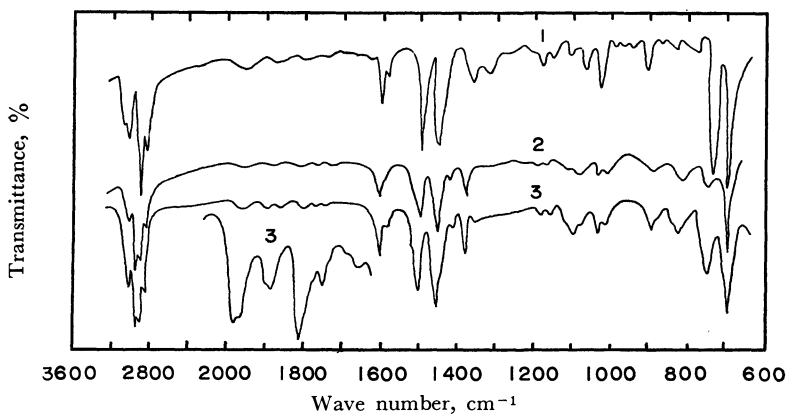

Fig. 2. Infrared spectra of polyallylbenzene (film).
(1) Polymer obtained with $(C_2H_5)_3Al$-$TiCl_3$ catalyst, (2) polymer obtained with $TiCl_3$ catalyst, (3) polymer obtained with $C_2H_5AlCl_2$-$TiCl_3$ catalyst.

and also on the Al/Ti molar ratios in the catalyst systems, indicating that the polymerization rate decreased with an increase in the cationic character of the catalyst systems (*i. e.*, from $Al(C_2H_5)_3$ to $Al(C_2H_5)Cl_2$ in the organoaluminum component, and from 2 to 0 in the Al/Ti molar ratio), while the $D(CH_3/CH_2)$ values in the resulting polymers increased from zero to 1.08 (see Fig. 2). In the case of the $TiCl_3$-$Al(C_2H_5)_3$ catalyst, it was also found that the positional isomerization of allylbenzene to propenylbenzene after the polymerization was accelerated upon an increase in the Al/Ti molar ratio.

Table 3 shows the results of the polymerization of propenylbenzene by these catalyst systems. It can be seen in this table that the polymerization of propenylbenzene by the $TiCl_3$ catalyst was observed, giving a yellowish oily product but without any positional isomerization to allylbenzene. This product was confirmed to be a dimer of propenylbenzene by a molecular-weight determination; it was showed an absorption band characteristic of the methylene group, *i. e.*, $D(CH_3/CH_2)=1.10$—1.33 (Fig. 1).

Table 3. Results of polymerization of propenylbenzene (PB) with the catalyst systems containing $TiCl_3$ in *n*-heptane at 80°C
$[TiCl_3]=50$ mmol/*l*, $[PB]=3.0$ mol/*l*

Catalyst system	Al/Ti molar ratio	Time hr	Conversion %	$D(CH_3/CH_2)$	Isomer distribution of monomer recovered after polymerization, wt%		
					AB	*cis*-PB	*trans*-PB
$TiCl_3$[a]	0	46	44.9[b]	1.10	0.0	4.3	95.7
	0	158	74.9	1.33	0.0	0.0	100.0
$TiCl_3$-$Al(C_2H_5)_3$	0.5	48	0	—	0.0	8.5	91.5
	2	48	0	—	0.0	4.1	95.9
$TiCl_3$-$Al(C_2H_5)_2Cl$	2	48	0	—	0.0	11.6	88.4
$TiCl_3$-$Al(C_2H_5)Cl_2$	2	48	21.4[c]	∞	0.0	12.5	87.5
$TiCl_3$-$Al(i\text{-}C_4H_9)_3$	2	48	0	—	0.0	7.5	92.5

a) $[TiCl_3]=100$ mmol/*l*, $[PB]=1.0$ mol/*l*.
b) Molecular weight of this polymer was 270.
c) Molecular weight of this polymer was 840.

Table 4. Results of polymerization of allylbenzene (AB) and propenylbenzene (PB) with the catalyst systems containing VCl_3 in *n*-heptane at 80°C
$[VCl_3]=50$ mmol/*l*, [Monomer] = 3.0 mol/*l*

Catalyst system	Al/Ti molar ratio	Monomer	Time hr	Conversion %	$D(CH_3/CH_2)$	Isomer distribution of monomer recovered after polymerization, wt%		
						AB	*cis*-PB	*trans*-PB
VCl_3	0	AB	158[a]	0	—	100.0	0.0	0.0
	0	PB	46[b]	0	—	0.0	12.7	87.3
VCl_3-$Al(C_2H_5)_3$	2	AB	0.5	20.1[c]	0	100.0	0.0	0.0
	2	PB	48	0	—	0.0	12.1	87.9
VCl_3-$Al(i\text{-}C_4H_9)_3$	2	AB	1.0	13.5	0	100.0	0.0	0.0
	2	PB	48	0	—	0.0	12.0	88.0

a) $[VCl_3]=93.1$ mmol/*l*, $[AB]=1.24$ mol/*l*.
b) $[VCl_3]=89.7$ mmol/*l*, $[PB]=1.50$ mol/*l*.
c) This polymer contained 36.4% of insoluble fraction (mp 212—215°C) in hot toluene.

Table 5. Results of polymerization of allylbenzene (AB) and propenylbenzene (PB) with the catalyst systems containing $Ti(OC_4H_9)_4$ in *n*-heptane at 80°C
$[Ti(OC_4H_9)_4]=50$ mmol/*l*, Al/Ti = 3.0, [Monomer] = 3.0 mol/*l*

Catalyst system	Monomer	Time hr	Conversion %	$D(CH_3/CH_2)$	Isomer distribution of monomer recovered after polymerization, wt%		
					AB	*cis*-PB	*trans*-PB
$Ti(OC_4H_9)_4$-$Al(C_2H_5)_3$	AB	24	5.9	0	65.9	6.6	27.5
	PB	48	1.1	0.94	0.0	3.6	96.4
$Ti(OC_4H_9)_4$-$Al(C_2H_5)_2Cl$	AB	24	0.6	0	99.8	0.0	0.2
	PB	48	0.7	—	0.0	12.9	88.1
$Ti(OC_4H_9)_4$-$Al(C_2H_5)Cl_2$	AB	24	0.7	—	100.0	0.0	0.0
	PB	48	0.1	—	0.0	12.9	88.1

In these binary catalyst systems, the geometrical cis-trans isomerization of propenylbenzene was observed, accelerating with a nincrease in the Al/Ti molar ratio, but no positional isomerization occurred. A solid polymer which has no absorption band for the methylene group was obtained when only the $C_2H_5AlCl_2$-$TiCl_3$ catalyst was used. These isomerizations and polymerizations were dependent on the cationic character of the catalyst system, as are those of allylbenzene.

Polymerization with Catalyst Systems Containing VCl_3. Table 4 shows the results of the polymerization of allylbenzene and propenylbenzene by the binary catalyst systems of VCl_3. As can be seen from this table, no isomerization occurred in any case. Allylbenzene was polymerized by VCl_3-trialkylaluminum catalysts to give a solid polymer whose infrared spectrum indicated no absorption band for the methyl group in the polymer.

Polymerization with Catalyst Systems Containing $Ti(OC_4H_9)_4$. The results of the polymerization of allylbenzene and propenylbenzene by the binary catalyst systems of $Ti(OC_4H_9)_4$ are summarized in Table 5, in which the isomerization of the monomer during the reaction and the $D(CH_3/CH_2)$ values of the resulting polymers are also shown. In these cases, both the isomerization and the polymerization were observed to be dependent upon the cationic character of the catalyst systems used. A viscous polymer from allylbenzene and an oily product from propenylbenzene were obtained by the use of the $Ti(OC_4H_9)_4$-$Al(C_2H_5)_3$ catalyst.

Discussion

As can be seen from Table 1, neither the polymerization nor the isomerization of allylbenzene was observed in the presence of the $AlBr_3$ catalyst or the $BF_3O(C_2H_5)_2$ catalyst. However, propenylbenzene was found to be polymerized by the latter catalyst to give a solid polymer whose molecular weight was 720. Although the infrared spectrum of the produced polymers showed intense absorption bands due to the methyl group at 2960, 2878, and 1380 cm^{-1}, weak absorption bands due to the methylene group were also observed at 2925 and 755 cm^{-1}, indicating that this polymer consisted of the structure II, with a minor unit of the I or III structure. In view of the results shown in Table 1 (no isomerization of the monomer takes place during the reaction), the participation of the allylbenzene isomerized from propenylbenzene to give the structual unit I was not considered in this polymerization. Although the isomerization of a growing cation of propenylbenzene leading to the structual unit III was considered, it might be impossible to find a driving force to cause this type of isomerization to proceed, as has been pointed out by Kennedy[8] and Murahashi *et al.*[14] No other evidence for the presence of such isomerized structures was obtained, and the possible mechanism for its production is also uncertain at the present time. Figure 1 shows that the structural unit IV in this polymer was not present.

No isomerizations of the monomer were observed in the polymerizations of allylbenzene and propenylbenzene by catalyst systems containing VCl_3. On the other hand, both isomerizations from allylbenzene to propenylbenzene and from *cis*-propenylbenzene to *trans*-propenylbenzene occurred in the presence of the catalyst systems including $TiCl_3$; these isomerizations were found to be accelerated upon increase in the Al/Ti molar ratio (*i. e.*, an increase in the anionic nature of the catalyst system). These results were in agreement with those observed in the isomerization of butene-2 by the same catalyst systems.[3]

However, the positional isomerization from propenylbenzene to allylbenzene did not occur in the polymerization of propenylbenzene by any of the catalyst systems used. This fact leads to the conclusion that the high-molecular-weight polyallylbenzene (I) from propenylbenzene is not obtained in the presence of the Natta catalyst, just as in the polymerization of butene-2 with isomerization to butene-1.[3] The experimental results coincided with this conclusion.

From Tables 1—4, it is clear that the polymerization activities of allylbenzene toward the Natta catalysts decrease greatly with a decrease in the Al/Ti molar ratio and with an increase in the substitution of the chloride component in organoaluminum compounds of the catalyst systems (*i. e.* an increase in the cationic nature). On the other hand, the polymerization of propenylbenzene was observed when the cationic nature of the catalyst systems used increased, and the resulting polymers were low in molecular weight.

As is shown in Fig. 2, the infrared spectra of the polyallylbenzene obtained through a coordinated anionic mechanism by the Natta catalysts showed a strong absorption band for the methylene group at 2925 cm^{-1}, but none for the methyl group. This result indicates that allylbenzene is polymerized by an ordinary anionic 1,2-addition mechanism to give a high-molecular-weight polymer with the non-isomerized structure (I). In this case, it is clear that propenylbenzene does not participate in the polymerization of allylbenzene, just as in the production of polybutene-1 from butene-2.[3]

Figure 2 shows, however, that the infrared spectra of the polymers obtained from allylbenzene by the $TiCl_3$-$Al(C_2H_5)Cl_2$ or $TiCl_3$ catalyst, which might induce cationic polymerization, showed the absorption bands characteristic of the methyl group

14) S. Murahashi, S. Nozakura, K. Tsuboshima and Y. Kotake, This Bulletin, **38**, 157 (1965).

of 2960, 2878, and 1380 cm^{-1}, that of the methylene group at 2925 cm^{-1}, and those of substituted benzene at 1700—2000 and 830 cm^{-1}. Accordingly, it can be concluded that the polymer is obtained not only by an ordinary 1,2-addition mechanism of allylbenzene and of the propenylbenzene which is isomerized from it, but also by the Friedel-Crafts-type addition mechanism[9] of a growing cation to the benzene nuclei of the monomer or of the polymer, leading to the recurring units, IV and V.

In the presence of the $TiCl_3$-$Al(C_2H_5)Cl_2$ catalyst, it was found that propenylbenzene is readily polymerized, giving a heptamer whose infrared spectrum showed a absorption band for the methyl group, but none for the methylene group or for substituted benzene, suggesting that this catalyst induces the cationic polymerization by an ordinary 1,2-addition mechanism, thus giving a polymer with the structure II.

BULLETIN OF THE CHEMICAL SOCIETY OF JAPAN VOL. 41 959—964 (1968)

Studies on Isothiazoles. III.[1] A Novel Ring Closure to Isothiazoles by the Reaction of α-Amino Ketones with Thionyl Chloride or Sulfur Monochloride

Takayuki NAITO, Susumu NAKAGAWA, Jun OKUMURA, Kiyoshi TAKAHASHI and Ken-ichi KASAI

Bristol-Banyu Research Institute Ltd., Meguro-ku, Tokyo

(Received October 5, 1967)

New compounds, 4-hydroxyisothiazoles, have been prepared by the reaction of α-amino ketones with thionyl chloride or sulfur monochloride, which is a novel procedure for cyclization to an isothiazole ring. Polar solvents, especially dimethylformamide (DMF), were preferable for this cyclization. The reaction hardly proceeded in a nonpolar solvent such as benzene, but was accelerated by an addition of a small amount of DMF.

Mononuclear isothiazoles have been unknown until Adams and Slack[2] obtained in 1956 isothiazole-4,5-dicarboxylic acid by oxidation of 5-aminobenzisothiazole. Since then, many isothiazole derivatives have been prepared by several routes: oxidative ring closure of β-iminothioamides[3] or β-iminothioketones,[4] reaction of olefins with sulfur dioxide and ammonia in the presence of activated alumina,[5] cyclization with liquid ammonia of the addition product from acetylenic ketones and thiosulfate or thiocyanate,[6] cyclization of dicyanoethylene-thiolate with sulfur, chlorine or chloramide,[7] treatment of dithiolium salts with ammonia[8] and reaction of nitriles with sulfur and morpholine.[9] Now we wish to report a novel procedure for formation of the isothiazole ring from open-chain compounds and the resulting products, 4-hydroxyisothiazoles, which have been hitherto undescribed.

1) Part II: T. Naito, S. Nakagawa and K. Takahashi, *Chem. Pharm. Bull.*, **16**, 160 (1968).

2) A. Adams and R. Slack, *Chem. & Ind. (London)*, **1956**, 1232.

3) a) A. Adams and R. Slack, *J. Chem. Soc.*, **1959**, 3061. b) J. Goerdeler and H. W. Pohland, *Chem. Ber.*, **94**, 2950 (1961); *ibid.*, **96**, 526 (1963). c) J. Goerdeler and H. Horn, *ibid.*, **96**, 1551 (1963). d) J. Goerdeler and U. Keuser, *ibid.*, **97**, 3106 (1964).

4) J. Goerdeler and W. Mittler, *ibid.*, **96**, 944 (1963).

5) a) F. Hübenett, F. H. Flock and H. Hofmann, *Angew. Chem.*, **74**, 654 (1962). b) F. Hübenett and H. Hofmann, *ibid.*, **75**, 420 (1963).

6) a) F. Wille, L. Capeller and A. Steiner, *Angew. Chem.*, **74**, 467, 753 (1962). b) M. S. Grant, D. L. Pain and R. Slack, *J. Chem. Soc.*, **1965**, 3842. c) M. Beringer, B. Prijs and H. Erlenmeyer, *Helv. Chim. Acta*, **49**, 2466 (1966). d) R. Raap, *Can. J. Chem.*, **44**, 1324 (1966).

7) a) W. R. Hatchard, *J. Org. Chem.*, **28**, 2163 (1963); *ibid.*, **29**, 660, 665 (1964). b) E. Soederback, *Acta Chem. Scand.*, **17**, 362 (1963). c) K. Hartke and L. Peshke, *Angew. Chem.*, **79**, 56 (1967).

8) a) D. Leaver and W. A. H. Robertson, *Proc. Chem. Soc.*, **1962**, 252. b) E. Fanghänel, *Z. Chem.*, **5**, 386 (1965). c) R. A. Olofson, J. M. Landesberg, R. O. Berry, D. Leaver, W. A. H. Robertson and D. M. McKinnon, *Tetrahedron*, **22**, 2119 (1966). d) G. Purrello, *Gazz. Chim. Ital.*, **96**, 1000 (1966).

9) A. Brund and G. Purrello, *Gazz. Chim. Ital.*, **96**, 986 (1966).

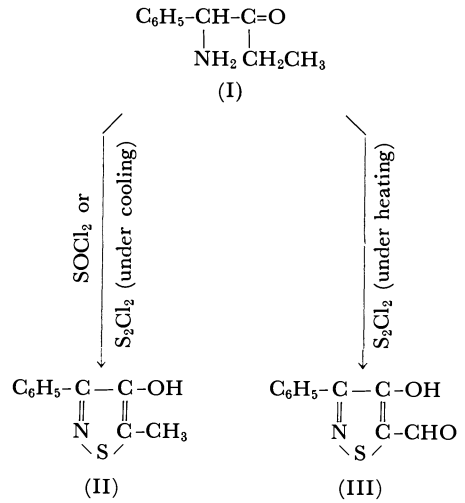

1-Amino-1-phenyl-2-butanone (I) readily reacted with thionyl chloride in dimethylformamide (DMF) to give an acidic product melting at 153—153.5°C, which showed the characteristics expected for those of 4-hydroxy-5-methyl-3-phenylisothizaole (II). The product is soluble in dilute sodium hydroxide, but insoluble in neutral or acid water. The IR spectrum shows a band at about 3200 cm^{-1}, but no band in the carbonyl region. Its NMR spectrum*1 in dimethylsulfoxide-d_6 has a singlet due to a phenolic hydroxyl proton at 9.62[10] together with a singlet of C_5-methyl protons at 2.46,[11] a multiplet due to meta- and para-protons of phenyl ring at 7.56—7.86 and a multiplet due to ortho-protons at 8.24—8.50. Acetylation of the product with acetic anhydride gave a neutral colorless oil, which showed a carbonyl band due to enol acetate at 1755 cm^{-1} in the IR spectrum. The NMR spectrum of the acetate in deuteriochloroform shows two methyl singlets at 2.24 and 2.34 and phenyl proton multiplets at 7.32—7.52 and 7.68—7.90. Methylation with diazomethane afforded a colorless oil which showed complete absence of hydroxy stretching band and appearance of new bands due to an aromatic ether at 1250 cm^{-1} and 1000 cm^{-1} in the IR spectrum. When I was allowed to react with sulfur monochloride in DMF under cooling, the same product (II) was obtained in 44% yield. However, the reaction under heating gave another acidic compound melting at 104—105°C, which was determined to be 5-formyl-4-hydroxy-3-phenylisothiazole (III). It shows a hydroxyl band at about 3400 cm^{-1} and a carbonyl band at 1655 cm^{-1}, and gives the corresponding 2,4-dinitrophenylhydrazone having an absorption maximum at 391 mμ. By acetylation the carbonyl band remains and the hydroxyl band disappears with an appearance of a new band due to enol acetate at 1770 cm^{-1}. The NMR spectrum of the acetate in carbon tetrachloride shows a methyl singlet at 2.46, multiplets of five phenyl protons at 7.54—7.82 and 7.94—8.18 and a singlet due to a formyl proton at 10.14.

TABLE 1. PREPARATION OF 4-HYDROXYISOTHIAZOLES

Starting ketone	Cyclization reagent, eq.	Method	Product	Yield, %
I	$SOCl_2$ 4	B	II	78
I	$SOCl_2$ 4	A	II	74
I	$SOCl_2$ 3	A	II	70
I	$SOCl_2$ 2	B	II	73
I	$SOCl_2$ 2	A	II	54
I	$SOCl_2$ 1	B	II	41
I	S_2Cl_2 4	B	III	34
I	S_2Cl_2 3	A	II	44
IV	S_2Cl_2 3	A	II	17
IV	$SOCl_2$ 4	B	*	—
VI	$SOCl_2$ 4	A	IX	22
VI	$SOCl_2$ 2	A	VIII	74
VI	S_2Cl_2 4	B	VII	43
VI	S_2Cl_2 3	A	VII	70
X	S_2Cl_2 3	A	VII	14
XIa	$SOCl_2$ 4	B	XIIa	66
XIa	S_2Cl_2 4	B	XIIa	37
XIb	$SOCl_2$ 2	A	XIIb	7
XIb	S_2Cl_2 2	A	XIIb	9
XIc	$SOCl_2$ 4	A	XIIc	7
XIc	S_2Cl_2 4	A	XIIc	19
XId	$SOCl_2$ 3	A	XIId	42

* An oxazole derivative (V) was obtained (see, experimental section).

The reaction of I with thionyl chloride was investigated under various conditions. As shown in Table 1, the reaction under cooling (Method A) gave more than 70% yield of the product (II) with three equivalents or more of thionyl chloride. The reaction without thermal control (Method B) proceeded with nearly the same yield as Method A when two equivalents or more of thionyl chloride was used, while the yield decreased considerably with an equimolar of the reagent. As shown in Table 4, the solvent, DMF, can be substituted by other polar solvents, but with decrease of the yield. The reaction in dimethylsulfoxide gave only an unidentified tarry product with mercaptan-like odor. A nonpolar solvent such as benzene was not suitable for this reaction, but the addition of a small amount of DMF accelerated the reaction considerably.

*1 All NMR spectra in this paper were run with a Varian A-60 spectrometer, for which the authors are indebted to Assistant Professor M. Goto and Dr. Urushibara of Gakushuin University. Chemical shifts are represented in ppm from an internal reference, TMS.

10) O. L. Chapman and R. W. King, *J. Am. Chem. Soc.*, **86**, 1256 (1964).

11) T. Naito, S. Nakagawa and K. Takahashi, *Chem. Pharm. Bull.*, **16**, 148 (1968).

TABLE 2. 4-HYDROXYISOTHIAZOLES

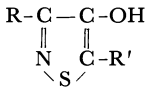

No.	R	R′	Mp., °C	λ_{max}^{EtOH} mμ(ε)	Molecular formula		Anal, % C	H	N	S	Cl
II	C_6H_5	CH_3	153—153.5	249(6500) 296(13700)	$C_{10}H_9NOS$	Calcd Found	62.79 62.79	4.74 4.40	7.32 7.09	16.78 17.28	
III	C_6H_5	CHO	104—105	235(21600) 284(7550) 342(9850)	$C_{10}H_7NO_2S$	Calcd Found	58.54 58.02	3.44 3.38	6.83 7.00	15.62 15.59	
VIII	C_6H_5	H	156—158	218(10700) 243.5(6500) 302(14000)	C_9H_7NOS	Calcd Found	61.00 61.01	3.98 3.66	7.91 7.58	18.09 18.35	
VII	C_6H_5	Cl	175(dec)	299(12800)	C_9H_6ClNOS	Calcd Found	51.07 51.59	2.86 2.82	6.62 6.57	15.09 14.61	16.69 16.93
XIIa	C_6H_5	C_6H_5	112.5—113.5	238(21500) 310(15400)	$C_{15}H_{11}NOS$	Calcd Found	71.12 71.81	4.38 4.68	5.53 5.92		
XIIb	CH_3	CH_3	106—108	217(4660) 269(6850)	C_5H_7NOS	Calcd Found	46.49 47.03	5.46 5.05	10.84 10.50		
XIIc	CH_3	Cl	150—155	225(3670) 271(6200)	C_4H_4ClNOS	Calcd Found	32.63 32.11	2.87 2.70	9.11 9.36	20.21 20.43	23.70 24.34
XIId	CH_3	C_6H_5	144—147	293(11900)	$C_{10}H_9NOS$	Calcd Found	62.79 62.70	4.74 4.96	7.32 7.51		
IX	C_6H_5	*	220—223	220(14750) 313(10600)	$C_{18}H_{12}N_2O_2S_3$	Calcd Found	56.23 56.64	3.44 3.12	7.29 7.47	25.02 25.30	

* 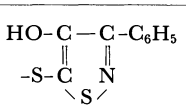

TABLE 3. 4-ACETOXYISOTHIAZOLES AND 4-METHOXYISOTHIAZOLES

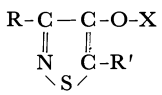

X	R	R′	Yield %	Bp °C/mmHg	$\nu_{C=O}$ cm^{-1}	λ_{max}^{EtOH} mμ(ε)	Molecular formula		Anal, % C	H	N
$COCH_3$	C_6H_5	CH_3	53	142—143/1.2	1775	272.5(16600)	$C_{12}H_{11}NO_2S$	Calcd Found	61.79 61.85	4.75 4.77	6.00 6.25
$COCH_3$	C_6H_5	CHO	60	mp 80—81.5	1770 1660	235(10000) 299(14500) 422(3800)	$C_{12}H_9NO_3S$	Calcd Found	58.29 58.10	3.67 3.72	5.67 5.75
$COCH_3$	C_6H_5	H	55	132—134/1.0	1780	239(5780) 275(14200)	$C_{11}H_9NO_2S$	Calcd Found	60.25 60.24	4.14 3.91	6.39 6.23
$COCH_3$	C_6H_5	Cl	79	mp 43—45	1785	218(15500) 275(14500)	$C_{11}H_8ClNO_2S$	Calcd Found	52.07 52.45	3.18 3.52	5.52 5.88
$COCH_3$	C_6H_5	C_6H_5	76	mp 72—73	1785	243(22000) 279(21000)	$C_{17}H_{13}NO_2S$	Calcd Found	69.13 69.82	4.44 4.99	4.74 4.88
$COCH_3$	CH_3	C_6H_5	57	132—134/1.2	1780	266(16800)	$C_{12}H_{11}NO_2S$	Calcd Found	61.79 62.06	4.75 4.93	6.00 5.90
CH_3	C_6H_5	CH_3	37	118/3	—	280(15800)	$C_{11}H_{11}NOS$	Calcd Found	64.39 64.30	5.40 5.36	6.83 7.22
CH_3	C_6H_5	H	54.5	124—126/0.7 (mp 58—61)	—	240(5700) 297.5(13300)	$C_{10}H_9NOS$	Calcd Found	62.80 62.96	4.74 4.52	7.32 7.25
CH_3	C_6H_5	Cl	61	115/1.0	—	217(16200) 283(14500)	$C_{10}H_8ClNOS$	Calcd Found	53.21 52.97	3.57 3.82	6.21 6.46

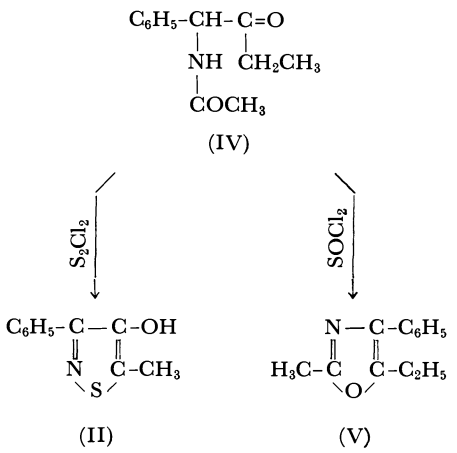

Treibs and Suter[12] have reported that 3-acetamido-2-butanone was reacted with thionyl chloride to give 2,4,5-trimethyloxazole. Similarly 1-acetamido-1-phenyl-2-butanone (IV) was dehydrated by thionyl chloride to afford 5-ethyl-2-methyl-4-phenyloxazole (V). The reaction with sulfur monochloride did not give the oxazole derivative (V) but the above-mentioned isothiazole (II) in 17% yield by cyclization accompanied with *N*-deacetylation.

1-Amino-1-phenyl-2-propanone (VI) was subjected to a similar reaction with sulfur monochloride either under cooling or under heating. In both cases, the product was the same chlorine-containing acidic compound, 5-chloro-4-hydroxy-3-phenylisothiazole (VII). The mass spectrograph*2

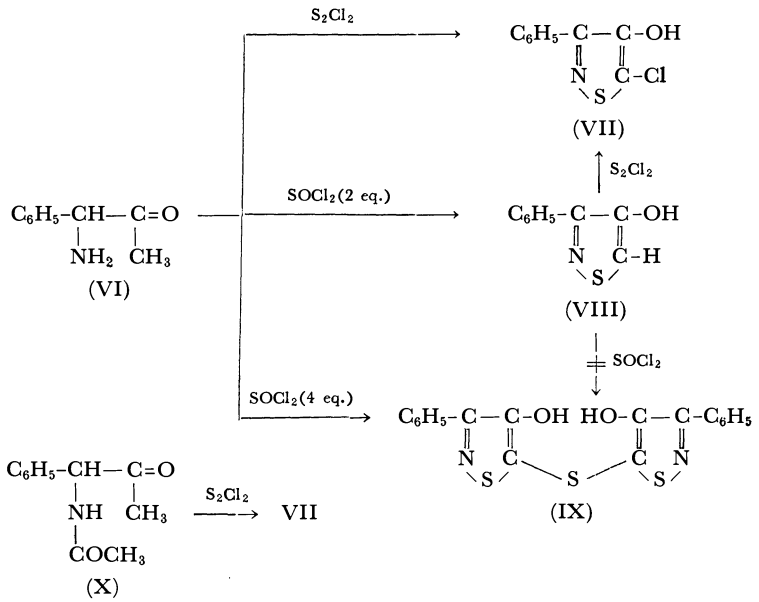

TABLE 4. PREPARATION OF 4-HYDROXY-5-METHYL-3-PHENYLISOTHIAZOLE (II) WITH 2.0 eq. OF THIONYL CHLORIDE IN VARIOUS SOLVENTS

Exp. No.	Solvent	Reaction condition	Yield (%)
(1)	DMF	overnight at room temp.	73
(2)	Nitromethane	overnight at room temp., then 25 hr at 65—70°C	40
(3)	Acetonitrile	overnight at room temp., then 7 hr at 30—40°C	30*
(4)	THF	overnight at room temp., then 2.5 hr at 50—60°C	55
(5)	Benzene	5 hr at 60°C	trace**
(6)	Benzene+DMF(0.18 g, 0.1 eq)	5 hr at 60°C	56
(7)	Benzene+DMF(1.82 g, 1.0 eq)	5.5 hr at 60°C	43
(8)	Benzene+DMF(3.7 g, 2.0 eq)	3 hr at 60°C	43

* 6.3% of the starting amino ketone was recovered.
** 83% of the starting amino ketone was recovered.

*2 Mass spectra were run with a Hitachi RMU-6 spectrometer by a heating inlet system (Chember voltage, 80 V; reservoir temp., 120°C; electron multiplier voltage 2000 V), for which the authors are indebted to Professor S. Hishida of Nihon University.

12) A. Treibs and W. Suter, *Chem. Ber.*, **84**, 96 (1951).

of VII showed a molecular peak at *m/e* 211/213 with characteristic isotopic abundance and the NMR spectrum in dimethylsulfoxide-d_6 solution indicated signals of phenyl protons and a phenolic hydroxyl proton. 1-Acetamido-1-phenyl-2-propanone (X) was reacted similarly with sulfur monochloride to afford VII by cyclization accompanied with *N*-deacetylation and chlorination.

The reaction of VI with 2 equivalents of thionyl chloride in DMF gave the expected product, 4-hydroxy-3-phenylisothiazole (VIII), which showed a singlet of C-5 proton at 8.12[11] along with singnals of phenyl protons and a phenolic hydroxyl proton. On the other hand the reaction with 4 equivalents of thionyl chloride gave another acidic product which showed a molecular peak at *m/e* 384. The structure was established as bis-(4-hydroxy-3-phenyl-5-isothiazole) sulfide (IX) by lack of C-5 proton and elemental analysis. It was found that a minor amount of VIII was also present in a reaction mixture of VI with sulfur monochloride under mild condition. Moreover, VIII was converted into VII by sulfur monochloride, while treatment with thionyl chloride gave neither VII nor IX, but the starting material (VIII) was recovered.

(XI) (XII)

a : R=R′=C_6H_5 a : R=R′=C_6H_5
b : R=R′=CH_3 b : R=R′=CH_3
c : R=CH_3, R′=H c : R=CH_3, R′=Cl
d : R=CH_3, R′=C_6H_5 d : R=CH_3, R′=C_6H_5

1-Amino-1,3-diphenyl-2-propanone (IXa) was expected to give 4-hydroxy-3,5-diphenylisothiazole (XIIa) as a sole product, because substitution or oxidation would be blocked in the 5-position in XIIa. In fact, none of by-product was obtained when XIa was allowed to react with thionyl chloride or sulfur monochloride under the condition same as that yielding the abnormal products such as IX, III and VII. 2-Amino-3-pentanone (XIb) was reacted similarly with either one of the cyclization reagents to afford 3,5-dimethylisothiazole (XIIb), although the yield was poor. Also, 3-amino-1-phenyl-2-butanone (XId) was cyclized to 4-hydroxy-3-methyl-4-phenylisothiazole (XIId) by thionyl chloride. On the other hand, the reaction with 3-amino-2-butanone (XIc) gave only a chlorine-containing product (XIIc).

Experimental

α-Amino Ketones. According to the procedure of Dakin and West,[13-17] α-amino ketones were prepared by heating an α-amino acid or α-acetamido acid with an acid anhydride in the presence of pyridine followed by hydrolysis of the resulting α-acylamido ketone with 6 N hydrochloric acid. The results and properties are shown in Table 5.

4-Hydroxyisothiazoles. 4-Hydroxyisothiazoles were prepared by the following two methods and the results are shown in Table 1. The properties and analyses of the products are shown in Table 2.

Method A. There was added 0.1—0.2 mol of thionyl chloride or sulfur monochloride to 50 m*l* of DMF below 0°C with stirring. To the stirred solution was added 0.05 mol of an appropriate α-amino ketone hydrochloride with cooling in an ice-salt bath to maintain the temperature below 10°C. After an exothermic reaction had ceased, the bath was removed and the stirring continued for two hours. The reaction mixture was allowed to stand overnight at room temperature, then poured into 100 m*l* of ice water and extracted with three 50-m*l* portions of ether. The combined ethereal extracts were washed with two 50-m*l* portions of water and then back-extracted with two 50-m*l* portions of 5% aqueous sodium hydroxide solution. The combined alkaline extracts were evaporated under reduced pressure to remove low boiling materials and then acidified whit 20% hydrochloric acid with cooling to give the product which was collected by filtration and recrystallized from ligroin or benzene-ligroin.

Method B. There was added 0.05—0.2 mol of thionyl chloride or sulfur monochloride to 50 m*l* of DMF below 0°C and the solution was mixed with 0.05 mol of an appropriate α-amino ketone hydrochloride in one portion. An exothermic reaction began soon and the temperature of the mixture rose to 50—80°C. When the reaction had ceased, the reaction mixture was heated on a water bath at 60—90°C for 1.5—2 hr, then allowed to stand overnight at room temperature. The product was isolated by the procedure described in Method A.

4-Acetoxyisothiazoles. Acetylation of 4-hydroxyisothiazoles was carried out with acetic anhydride by a usual manner. The yields and properties of the resulting 4-acetoxyisothiazoles are shown in Table 3.

4-Methoxyisothiazoles. 4-Hydroxyisothiazoles were converted into the corresponding 4-methoxy derivatives with diazomethane in ether. The yields and properties are shown in Table 3.

Reaction of 1-Acetamido-1-phenyl-2-butanone (IV) and Thionyl Chloride. To a cold suspension of 5 g (0.025 mol) of IV in 25 m*l* of ligroin was added 12 g (0.1 mol) of thionyl chloride in one portion. The mixture was stirred overnight at room temperature and heated at 80—90°C for four hours. The reaction mixture was evaporated under reduced pressure, the residual oxazolium salt was washed with three 30-m*l* portions of ether and added to 30 m*l* of water to convert it to the oily free oxazole. The oil was extracted with two 30-m*l* portions of ether and the extracts were washed with 30-m*l* of water, two 30-m*l* portions of 2.5% sodium

13) H. D. Dakin and R. West, *J. Biol. Chem.*, **78**, 91 (1928).

14) P. A. Levene and R. E. Steiger, *ibid.*, **79**, 95 (1928).

15) R. H. Wiley and O. H. Borum, *J. Am. Chem. Soc.*, **70**, 2005 (1948); "Organic Syntheses," Coll. Vol. 4, p. 5 (1963).

16) G. H. Cleland and C. Nieman, *J. Am. Chem. Soc.*, **71**, 841 (1949).

17) S. Searles and G. J. Cvejanovich, *ibid.*, **72**, 3200 (1950).

TABLE 5. α-AMINO KETONES (HYDROCHLORIDE)

Compd. No.	Yield** %	Mp °C	Lit. mp °C	$\nu_{C=O}$ cm^{-1}
I	(a) 86	166—170	***	1730
	(b) 76			
IV*	(b) 93	bp 162—169/3		1730, 1655
VI	(a) 81	205—207	204—208[13]	
			203[14]	
X*	(a) 90	100—102	103—104[13]	1715, 1640
			100—101[14]	
XIa	(b) 36	181—182(dec.)	****	1730
XIb	(b) 36	123—128(dec.)	128(dec.)[18]	1725
XIc	(a) 76	108—110(dec.)	111(dec.)[19]	1725
XId	(b) 13	143—145		1730

* *N*-Acetyl derivative.
** Overall yield from (a) α-amino acid or (b) α-acetamido acid.
*** Found: C, 59.83; H, 6.83; N, 7.44%. Calcd for $C_{10}H_{13}ON \cdot HCl$: C, 60.15; H, 7.07; N, 7.02%.
**** Found: C, 68.55; H, 6.22; N, 5.68%. Calcd for $C_{15}H_{15}ON \cdot HCl$: C, 68.83; H, 6.16; N, 5.35%.

hydroxide solution and finally with two 30-m*l* portions of water and then treated by active carbon. The filtrate was evaporated and the residue distilled under reduced pressure to give 1.9 g (41%) of V as a pale yellow oil boiling at 150—152°C/13 mmHg (lit.,[20] bp 146—148°C/12 mmHg). NMR (ppm, in CCl_4): 1.30 (3H, triplet), 2.42 (3H, singlet), 2.87 (2H, quartet), 7.25—7.75 (5H, multiplet).

Reaction of 4-Hydroxy-3-phenylisothiazole (VIII) with Sulfur Monochloride. To a stirred solution of 1.24 g (0.007 mol) of VIII in 10 m*l* of DMF was added dropwise 2.84 g (0.021 mol) of sulfur monochloride with cooling. The mixture was stirred for four hours and allowed to stand overnight at room temperature. The reaction mixture was poured into 100 m*l* of ice water and extracted with three 30-m*l* portions of ether. The combined ethereal solution was extracted with 5% sodium hydroxide solution and the aqueous extracts were acidified with hydrochloric acid to afford 1.09 g (74%) of white precipitate, which was identical to an authentic sample of VII by IR spectrum and acetylation.

Reaction of 4-Hydroxy-3-phenylisothiazole (VIII) with Thionyl Chloride. A solution of 1.24 g (0.007 mol) of VIII in 10 m*l* of DMF was allowed to react with 2.5 g (0.021 mol) of thionyl chloride by the procedure described above. Acidification with hydrochloric acid gave 0.98 g (79%) of the starting material (VIII) which was confirmed by mixed melting point and IR spectrum.

Reaction of 1-Amino-1-phenyl-2-butanone (I) and Thionyl Chloride in Various Solvents (Table 4). To a mixture of 5.0 g (0.025 mol) of I in 15 m*l* of an appropriate solvent listed in Table 4 was added dropwise 6.0 g (0.05 mol) of thionyl chloride at room temperature with stirring. An exothermic reaction occurred and the temperature rose to 30—40°C. The mixture was allowed to react under the condition shown in Table 4. In Exp. Nos. (1) and (2), the reaction mixture was a homogeneous solution and the product was isolated by the same procedure as Method A described above. In. Exp Nos. (3) and (5), the reaction mixture contained insoluble precipitate which was the unreacted starting ketone (I). The ketone was removed by filtration and the filtrate was worked up by the same procedure as Method A to give the product (II). In Exp. Nos. (4), (6), (7) and (8), the reaction mixture contained insoluble precipitate or oil, which appeared to be the isothiazolium salt by IR spectrum. The salt was collected by filtration or decantation and converted into, the corresponding isothiazole (II) by treating with cold water. The filtrate or the supernatant was poured into ice water and extracted with ether. To the ethereal extracts was added the crude II which was obtained from the isothiazolium salt. The solution was treated by the same procedure as described in Method A.

The authors wish to express their thanks to Dr. Koichi Iwadare and Mr. Eiji Iwadare of Banyu Pharmaceutical Co., Dr. Joseph Lein of Bristol Laboratories and Dr. Hiroshi Kawaguchi of this Institute for their valuable suggestions and encouragement throughout the present work. They are also grateful to Mr. Fumihide Sakai, Mr. Kenji Masuko and Mr. Yukio Narita for their fine assistance.

18) E. Jänecke, *Ber.*, **32**, 1095 (1899).
19) H. Künne, *ibid.*, **28**, 2036 (1895).
20) H. Bredereck and G. Theilig, *Chem. Ber.*, **86**, 96 (1953).

BULLETIN OF THE CHEMICAL SOCIETY OF JAPAN VOL. 41 965—971 (1968)

Studies on Isothiazoles. IV.[1] A New Synthetic Route to 4-Cyanoisothiazoles

Takayuki NAITO, Susumu NAKAGAWA, Jun OKUMURA, Kiyoshi TAKAHASHI, Kenji MASUKO and Yukio NARITA

Bristol-Banyu Research Institute Ltd., Meguro-ku, Tokyo

(Received October 5, 1967)

4-Cyanoisothiazoles have been prepared by a novel procedure which comprises the reac-reaction of β-cyano enamines with thionyl chloride or sulfur monochloride. The reaction proceeds favorably in nonpolar solvents or in the absence of solvent. However, the cyclization did not occur in dimethylformamide and instead an amidine derivative was isolated. The preparations of the corresponding isothiazole-4-carboxylic acids are also described briefly.

Direct preparation of 4-cyanoisothiazoles from open-chain compounds has been carried out by reaction of methacrylonitrile with sulfur dioxide and ammonia in the presence of activated alumina,[2] by oxidative ring closure of α-cyano-β-iminothioamides[3,4] and by cyclization of dicyanoethylene thiolates with sulfur,[5,6] chlorine[7] or chloramide.[8] However, 4-cyanoisothiazoles having alkyl or aryl group(s) at position(s) 3 and/or 5 have not been prepared by any of the above procedures, but by the substitution reaction of 4-bromoisothiazoles with cuprous cyanide.[9-12] The present paper reports a direct formation of 3- and/or 5-alkyl- or aryl-substituted 4-cyanoisothiazoles by heating β-cyano enamines with thionyl chloride or sulfur monochloride.

The starting enamines were prepared by Thorpe condensation[13,14] of the corresponding nitriles in the presence of (a) metallic sodium, (b) sodium amide or (c) sodium hydride as shown in Table 1. The IR spectra of the enamines showed three bands in a range of 3100—3600 cm^{-1} due to N-H stretching vibrations. This suggests that these compounds are present as an equilibrium mixture of two tautomers, β-cyano enamine (A) and β-imino nitrile (B). In this paper the compounds of this family are represented and named by formula (A).

$$\mathrm{R\text{-}CN + R'\text{-}CH_2CH_2\text{-}CN} \rightarrow \begin{array}{l} \mathrm{R\text{-}C(NH_2)=C(CH_2\text{-}R')\text{-}CN} \quad \text{(A)} \\ \updownarrow \\ \mathrm{R\text{-}C(=NH)\text{-}CH(CH_2\text{-}R')\text{-}CN} \quad \text{(B)} \end{array}$$

The preliminary experiments were carried out in dimethylformamide (DMF) with thionyl chloride and 1-amino-2-cyano-1-phenyl-1-butene (Ia) under similar conditions to the preparation of 4-hydroxyisothiazoles.[1] An exothermic reaction occurred, but no desired product was afforded. The only product isolated was a compound **III**, which has cyano (ν 2230 cm^{-1}), -C=N- (ν 1635 cm^{-1}), dimethylamino (3H singlet at 2.84*1 and 3H singlet at 3.03), ethyl (3H triplet at 1.15 and 2H quartet at 2.54; J=7.7 cps), =C-H (1H singlet at 7.12) and phenyl groups (5H multiplet centered at 7.37).

The reaction proceeded in the desired direction to give 4-cyano-5-methyl-3-phenylisothiazole (IIa)[12] when Ia was treated with thionyl chloride or sulfur monochloride in benzene, toluene, tetrahydrofuran, ligroin or solvent naptha, or without any solvent as shown in Table 2. Similarly, 1-amino-2-cyano-1-(2,6-dichlorophenyl)-1-butene (Ib) and 4-amino-3-cyano-3-heptene (Ic) gave 4-

1) Part III: T. Naito, S. Nakagawa, J. Okumura, K. Takahashi and K. Kasai, This Bulletin, **41**, 959 (1968).
2) F. Hübenett and H. Hofmann, *Angew. Chem.*, **75**, 420 (1963).
3) J. Goerdeler and H. W. Pohland, *Chem. Ber.*, **96**, 526 (1963).
4) J. Goerdeler and U. Keuser, *ibid.*, **97**, 3106 (1964).
5) W. R. Hatchard, *J. Org. Chem.*, **29**, 665 (1964).
6) E. Soderback, *Acta Chem. Scand.*, **17**, 362 (1963).
7) W. R. Hatchard, *J. Org. Chem.*, **29**, 660 (1964).
8) K. Hartke and L. Peshkar, *Angew. Chem.*, **79**, 56 (1967).
9) D. Buttimore, D. H. Jones, R. Slack and K. R. H. Wooldridge, *J. Chem. Soc.*, **1963**, 2032.
10) M. P. L. Caton, D. H. Jones, R. Slack and K. R. H. Wooldrigde, *ibid.*, **1964**, 446.
11) M. S. Grant, D. L. Pain and R. Slack, *ibid.*, **1965**, 3842.
12) T. Naito, S. Nakagawa and K. Takahashi, *Chem. Pharm. Bull.*, **16**, 148 (1968).
13) H. Baron, F. G. P. Pemery and J. F. Thorpe, *J. Chem. Soc.*, **85**, 1726 (1904).
14) G. A. Reynolds, W. J. Humphlett, F. W. Swamer and C. R. Hauser, *J. Org. Chem.*, **16**, 165 (1951).

*1 All NMR spectra were run in 10% solution of either carbon tetrachloride or deuteriochloroform with a Varian A-60 spectrometer, for which the authors are indebted to Assistant Professor M. Goto and Dr. Urushibara of Gakushuin University. Chemical shifts are represented in ppm from an internal reference, TMS.

Table 1. β-Cyano enamines $R-C(NH_2)=C(CN)-CH_2-R'$

No.	R	R′	Method	Yield %	Bp °C/mmHg [Mp* °C]	λ_{max}^{EtOH} mμ (ε)	ν_{NH} cm^{-1}	Molecular formula		Anal, % C	H	N
Ia	C_6H_5	CH_3	a b c	46 50 11	130/1	222 (21700) 287 (15200)	3190 3320 3480	$C_{11}H_{12}N_2$	Calcd Found	76.71 76.32	7.02 6.40	16.27 16.04
Ib	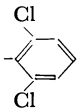	CH_3	a b	25 9.4	[127—129]	218 (sh) (14900) 266 (16300)	3240 3360 3500	$C_{11}H_{10}Cl_2N_2$	Calcd Found	54.79 55.11	4.18 4.37	11.62 11.69
Ic	n-C_3H_7	CH_3	a	29	140—142/7.5—9**		3280 3440 3540					
IVa	C_6H_5	H	a b	39 34	[102—103]	221.5 (12900) 233 (sh) (9700) 287 (8300)	3260 3380 3500	$C_{10}H_{10}N_2$	Calcd Found	75.92 75.75	6.37 6.40	17.71 17.32
IVb	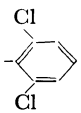	H	a b	28 22	[95—98]	218 (sh) (11200) 262 (12400)	3240 3380 3520	$C_{10}H_8Cl_2N_2$	Calcd Found	52.88 53.01	3.53 3.37	12.34 12.01

* Recrystallized from ligroin-benzene.
** H. Adkins and G. M. Whitman, *J. Am. Chem. Soc.*, **64**, 150 (1942); bp 137—142°C/7 mmHg.

TABLE 2. PREPARATION OF 4-CYANOISOTHIAZOLES

Starting enamine	Cyclization reagent	Solvent	Reaction time hr	Product Compd. No.	Product Yield, %
Ia	$SOCl_2$	benzene	3	IIa	15
Ia	$SOCl_2$	benzene	4	IIa	23
Ia	$SOCl_2$	toluene	4	IIa	31
Ia	$SOCl_2$	toluene	16	IIa	46
Ia	$SOCl_2$	tetrahydrofuran	4	IIa	8.5
Ia	$SOCl_2$	ligroin	4	IIa	18
Ia	$SOCl_2$	naphtha	18	IIa	41
Ia	$SOCl_2$	none	4	IIa	17
Ia	S_2Cl_2	toluene	16	IIa	12
Ia	S_2Cl_2	none	16	IIa	32
Ib	$SOCl_2$	toluene	48	IIb	55
Ib	S_2Cl_2	toluene	45	IIb	29
Ic	$SOCl_2$	benzene	20	IIc	7.5
IVa	$SOCl_2$	toluene	5	Va VIa	31 3.5
IVa	S_2Cl_2	toluene	5	Va VIa	42 trace
IVb	$SOCl_2$	toluene	10	Vb	40
IVb	S_2Cl_2	toluene	48	Vb	47

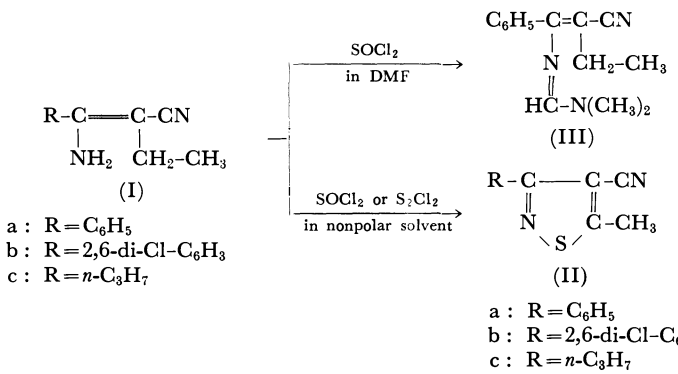

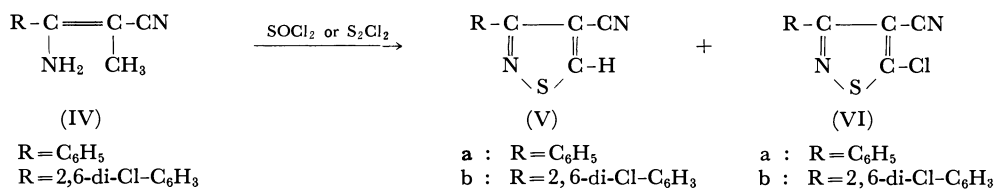

cyano-3-(2, 6-dichlorophenyl)-5-methylisothiazole (IIb) and 4-cyano-5-methyl-3-*n*-propylisothiazole (IIc), respectively.

The reaction of 1-amino-2-cyano-1-phenyl-1-propene (IVa) with thionyl chloride gave two kinds of cyanoisothiazoles, which were separated by an alumina column chromatography. The main product was the expected 4-cyano-3-phenylisothiazole (Va)[12] ($\nu_{C\equiv N}$ 2240 cm^{-1}; 5-H proton 9.30 ppm). The minor component was 5-chloro-4-cyano-3-phenylisothiazole (VIa) ($\nu_{C\equiv N}$ 2240 cm^{-1}; M^+ peak*2 at *m/e* 220 with the isotpe peak at *m/e* 222), which lacks the C-5 proton singlet in the NMR spectrum. Sulfur monochloride was allowed to react with IVa under similar conditions and Va was isolated, while VIa was detected by gas chromatography. In the reaction of 1-amino-2-cyano-1-(2,6-dichlorophenyl)-1-propene (IVb) with thionyl chloride or sulfur monochloride, 4-cyano-3-(2,6-dichlorophenyl)isothiazole (Vb) was isolated, but the 5-chloro derivative (VIb) was not detected.

*2 Mass spectrum was run with a Hitachi RMU-6 spectrometer by a heating inlet system (chamber voltage, 80 V; reservoir temp., 110°C; electron multiplier voltage, 2000 V), for which the authors are indebted to Professor S. Hishida of Nihon University.

TABLE 3. 4-CYANOISOTHIAZOLES

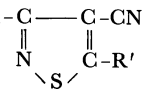

No.	R	R′	Mp °C	λ_{max}^{EtOH} mμ (ε)	$\nu_{C\equiv N}$ cm^{-1}	δ ppm	Molecular formula		Anal, % C	H	N	Cl
IIa	C_6H_5	CH_3	78*	264 (11300)	2280	2.73 (3H, s) 7.40—7.60 (3H, m) 7.97—8.17 (2H, m)						
IIb	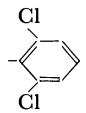	CH_3	124—125	257 (9000)	2260	2.80 (3H, s) 7.37 (3H, m)	$C_{11}H_6Cl_2N_2S$	Calcd Found	49.08 48.87	2.25 2.51	10.41 10.70	26.35 26.62
IIc	*n*-C_3H_7	CH_3	bp 73—76 (4.5—5.5 mmHg)	257.5 (6000) 262 (sh) (5600)	2260	0.99 (3H, t) 1.80 (2H, sex) 2.72 (3H, s) 2.87 (2H, t)						
Va	C_6H_5	H	54—55**	256.5 (11800) 273 (10500)	2260	7.45—7.65 (3H, m) 8.00—8.25 (2H, m) 9.30 (1H, s)						
VIa	C_6H_5	Cl	75—76	241.5 (20000)	2220	7.42—7.78 (3H, m) 7.96—8.26 (2H, m)	$C_{10}H_5ClN_2S$	Calcd Found	54.42 54.47	2.49 2.49	12.70 12.77	16.07 16.35
Vb	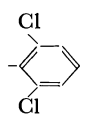	H	151—152	258.5 (9000)	2240	7.56 (3H, m) 9.50 (1H, s)	$C_{10}H_4Cl_2N_2S$	Calcd Found	47.17 47.39	1.58 1.30	10.98 10.87	27.80 27.71

* Ref. 12, mp 79—80°C ** Ref. 12, mp 54—55°C

TABLE 4. ISOTHIAZOLE-4-CARBOXYLIC ACIDS

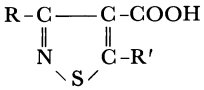

R	R'	Method	Yield %	Mp °C	λ_{max}^{EtOH} mμ (ε)	$\nu_{C=O}$ cm^{-1}	Molecular formula		Anal, % C	H	N	Cl
C_6H_5	CH_3	a	80	153—154*	264 (10000)	1670						
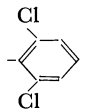	CH_3	b	81	213—213.5	255.5 (8400)	1670	$C_{11}H_7Cl_2NO_2S$	Calcd Found	45.85 46.27	2.45 2.19	4.86 4.94	24.61 24.54
n-C_3H_7	CH_3	a	14	83—84.5	257 (14000) 228 (sh) (7500)	1690	$C_8H_{11}NO_2S$	Calcd Found	51.87 51.63	5.99 5.72	7.56 7.26	
C_6H_5	H	a	78	165—166**	259 (10300)	1730						
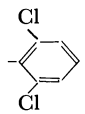	H	b	82	182—183	255 (7100)	1690	$C_{10}H_5Cl_2NO_2S$	Calcd Found	43.81 43.66	1.84 1.80	5.11 4.85	25.87 26.44

* Ref. 12, mp 153—154°C.
** Ref. 12, mp 165—166°C.

4-Cyanoisothiazoles prepared in the present study were readily converted into the corresponding isothiazole-4-carboxylic acids either (a) by heating with sulfuric acid followed by treatment with aqueous sodium nitrite, or (b) by hydrolysis with potassium hydroxide in aqueous ethylene glycol (Table 4).

Experimental

β-Cyano Enamines (Table 1). Representative examples of the preparation of β-cyano enamines, Ia—c and IVa, b, are given below.

a) A mixture of 105 g (1.0 mol) of benzonitrile and 70 g (1.0 mol) of *n*-butyronitrile in 500 m*l* of ether was added slowly to a dispersion of 23 g (1.0 atom) of metallic sodium in toluene under stirring over a period of about 2.5 hr at 20—30°C. The color of the mixture gradually turned to red. The reaction mixture was stirred for 6 hr at room temperature and allowed to stand overnight. Excess sodium was decomposed by adding water slowly under stirring. The ether layer was separated, washed with three 200-m*l* portions of saturated aqueous solution of sodium chloride and dried with anhydrous sodium sulfate. The solvent was evaporated and the residue distilled under diminished pressure to give 79 g (46%) of Ia.

b) To 200 m*l* of liquid ammonia containing about 0.1 g of ferric nitrate was added portionwise 4.8 g (0.21 atom) of sodium at −40 to −50°C. To the blue solution of sodium amide was added dropwise a solution of 20.6 g (0.2 mol) of benzonitrile and 13.8 g (0.2 mol) of butyronitrile in 100 m*l* of ether. After the addition was completed, liquid ammonia was replaced with 200 m*l* of dry ether and the solution was refluxed for three hours. To the reaction mixture was cautiously added 200 m*l* of water and the ether layer which separated was washed with four 200-m*l* portions of water, dried over anhydrous sodium sulfate and the solvent evaporated. The residue was distilled to give 17.1 g (50%) of Ia.

c) A 50% dispersion of sodium hydride in mineral oil (4.8 g, 0.1 mol) was mixed with 100 m*l* of dry benzene and to the stirred mixture was added a solution of 10.3 g (0.1 mol) of benzonitrile and 6.9 g (0.1 mol) of butyronitrile in 100 m*l* of dry benzene at 40—50°C. After the addition was completed, the mixture was stirred for 4 hr at 70°C, then cooled to room temperature and 200 m*l* of water was cautiously added dropwise. The benzene layer was distilled under reduced pressure and a fraction boiling at 100—160°C/1.5 mmHg was collected and redistilled to give 1.8 g (11%) of Ia.

2-Cyano-1-(*N*,*N*-dimethylforamidino)-1-phenyl-1-butene (III). To a stirred solution of 1.7 g (0.01 mol) of Ia in 15 m*l* of DMF was added dropwise 3.6 g (0.03 mol) of thionyl chloride. An exothermic reaction occurred and the temperature of the solution rose to about 50°C. After the exothermic reaction had ceased, stirring was continued for 4 hr. The reaction mixture was poured into ice-water, made alkaline by dil. sodium hydroxide solution and extracted with ether. The extracts were washed with water and dried over anhydrous sodium sulfate. The solvent was evaporated and the residue distilled under reduced pressure to give 1.1 g (48%) of III boiling at 163°C/1.0 mmHg, which solidified at room temperature. Recrystallization from ligroin gave colorless prisms melting at 50—52°C. λ_{max}^{EtOH} 309 mμ (ε 28000).

Found: C, 74.20; H, 7.95; N, 18.25%. Calcd for $C_{14}H_{17}N_3$: C, 73.97; H, 7.54; N, 18.49%.

4-Cyanoisothiazoles (Tables 2 and 3). To a solution of β-cyano enamine in an appropriate solvent shown in Table 2 was added 3—5 mol of thionyl chloride or sulfur monochloride in one portion. The mixture was refluxed for a certain period of time as shown in Table 2, then allowed to stand overnight at room temperature, poured into crushed ice and extracted twice with 50 m*l* of ether. The combined ethereal extracts were washed with water and dried over anhydrous sodium sulfate. The solvent was evaporated and the residue crystallized from ligroin (IIb and Vb) or distilled under reduced pressure (IIc).

The residue obtained by the reaction with Ia dissolved in ligroin. The solution was subjected to an alumina column chromatography and developed with ligroin followed with ligroin-benzene (1 : 1), the eluate being divided into 100—200 m*l* portions. Each of the fractions was evaporated into dryness. The residues were subjected to gas chromatography and the fractions which appeared to be rich in IIa were combined and crystallized from ligroin to give a pure sample of IIa.

The residue obtained by the reaction with IVa was dissolved in ligroin, chromatographed on an alumina column and eluted with ligroin. The eluate was collected in 50-m*l* portions, each fraction being analyzed by gas chromatography. The second and third fractions of the eluate were combined and evaporated to dryness to give a crystalline residue. Recrystallization from petroleum ether gave colorless needles of 5-chloro-4-cyano-3-phenylisothiazole (VIa). Evaporation of fractions No. 4—No. 10 and subsequent recrystallization from ligroin gave 4-cyano-3-phenylisothiazole (Va).

The results are shown in Table 2 and the properties and analyses of the products in Table 3.

Isothiazole-4-carboxylic Acids (Table 4). Hydrolysis of 4-cyanoisothiazoles was carried out by either one of the procedures illustrated in representative examples given below.

a) 5-Methyl-3-n-propylisothiazole-4-carboxylic Acid. A mixture of 0.52 g (0.00314 mol) of IIc and 15 m*l* of concentrated sulfuric acid was heated at 70—75°C for 6 hr and allowed to stand overnight at room temperature. The reaction mixture was cooled below 10°C and a solution of 0.27 g of sodium nitrite in 1 m*l* of water was cautiously added dropwise. The mixture was stirred for 20 min at 5—9°C, for 30 min at room temperature and finally for 30 min at 40°C. The reaction mixture was poured onto 40 g of crushed ice, insoluble material removed and the filtrate extracted with ether. The ethereal extracts were dried with anhydrous sodium sulfate, the solvent being evaporated. The residue was dissolved in aqueous sodium bicarbonate, washed with ether, treated with a small amount of active carbon and acidified with dilute hydrochloric acid to give 5-methyl-3-*n*-propylisothiazole-4-carboxylic acid which was recrystallized from benzene-ligroin (1 : 2).

b) 3-(2,6-Dichlorophenyl)-5-methylisothiazole-4-carboxylic Acid. A mixture of 2.3 g (0.0085 mol) of II, 1 g (0.018 mol) of potassium hydroxide, 1.8 m*l* of water and 9 m*l* of ethylene glycol was refluxed for 48.5 hr

and the reaction mixture was poured into 50 m*l* of water. A small amount of insoluble material was filtered off and the filtrate was acidified with dilute hydrochloric acid to separate 2.15 g of the crude acid. Recrystallization from ligroin-ethyl acetate gave 3-(2,6-dichlorophenyl)-5-methylisothiazole-4-carboxylic acid.

The authors wish to express their thanks to Dr. Koichi Iwadare and Mr. Eiji Iwadare of Banyu Pharmaceutical Co., Dr. Joseph Lein of Bristol Laboratories and Dr. Hiroshi Kawaguchi of this Institute for their valuable suggestions and encouragement throughout the present work.

BULLETIN OF THE CHEMICAL SOCIETY OF JAPAN VOL. 41 971—973 (1968)

The Structures and the Reactions of Acetyl- and Benzoylacrylic Acids and Their Esters

Noboru SUGIYAMA, Taketoshi GASHA, Hiroshi KATAOKA and Choji KASHIMA

Department of Chemistry, Tokyo Kyoiku University, Otsuka Tokyo

(Received October 9, 1967)

The Structures and properties of α,β-unsaturated γ-oxo acid, acetyl- and benzoylacrylic acid, and their esters are studied.

It can be considered that the α,β-unsaturated γ-oxo acid exists in three isomeric forms, the *trans*-form (A), the *cis*-form (B), and the angelica lactone form (C). Scheffold has established[1] that acetylacrylic acid (I) has two forms, A and C, which convert to each other. However, according to Shaw, the compound (mp 59°C)[2] produced by the reaction of I with diazomethane was not a simple methyl ester of I, but 5-methyl-5-methoxy-2,5-dihydro-2-oxofuran (III-C). The compound (mp 60.5°C),[3] synthesized from bromoacetone and triphenylphosphine carbomethoxymethylene, was a simple methyl ester of I, methyl acetylacrylate (III-A).

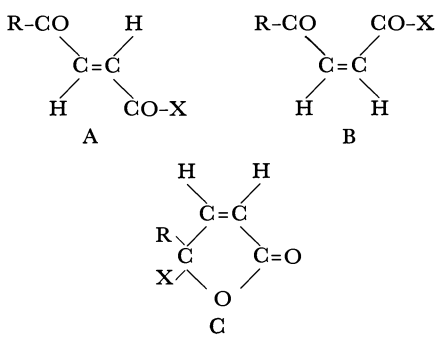

I: R=Me, X=OH IV: R=Ph, X=OMe
II: R=Ph, X=OH V: R=H, X=OH
III: R=Me, X=OMe VI: R=Me, X=Cl

1) R. Scheffold and P. Dubs, *Helv. Chim. Acta*, **50**, 798 (1967).
2) E. Shaw, *J. Am. Chem. Soc.*, **68**, 2510 (1946).
3) H. J. Bestmann, F. Seng and H. Schulz, *Chem. Ber.*, **96**, 465 (1963).

On the other hand, it has been reported that the compound obtained by the Friedel-Crafts reaction of maleic anhydride with benzene was benzoylacrylic acid of the A form.[4] Furthermore, one of the simplest α,β-unsaturated γ-oxo acids, fumaraldehydic acid (V), is not present in the form of V-A, but in the form of V-C, 5-hydroxy-2,5-dihydro-2-oxofuran.[5]

Thus, there still remain some uncertainties about the structures and properties of α,β-unsaturated γ-oxo acid and their derivatives. In spite of this situation, recently, several natural products with a partial structure of the A, B, or C form have been reported, for example, Cytochalasine A,[6] Pyrenopholin,[7] and (±)-2-acetamido-2,5-dihydro-5-oxofuran.[8,9]

This paper will describe the structure of typical substances, acetylacrylic acid (I), benzoylacrylic acid (II), methyl acetylacrylate (III) and methyl benzoylacrylate (IV), on the basis of chemical and spectral studies.

Results and Discussion

Acetyl- and Benzoylacrylic Acid. Scheffold described[1] how *trans* acetylacrylic acid (I-A) was

4) E. I. Becker and C. Miesse, "Organic Syntheses," Coll. Vol. III, p. 109 (1955).
5) N. Hellström, *Nature*, **187**, 146 (1960).
6) D. C. Aldridge, J. J. Armstrong, R. N. Speake and W. B. Turner, *Chem. Commn.*, **1967**, 26.
7) S. Nozoe, K. Hirai, K. Tsuda, K. Ishibashi, M. Shirasaka and J. F. Grove, *Tetrahedron Letters*, **1965**, 4675.
8) S. G. Yetes, H. L. Tookey, J. J. Ellis and H. Burkhardt, *Tetrahedron Letters*, **1967**, 621.
9) E. P. White, *J. Chem. Soc.*, **1967**, 346.

obtained from acetone and glyoxylic acid, and how the NMR spectrum of this acid showed the signal of olefinic protons at τ 3.20 (J=16.2 cps). The I compound, which we obtained by the elimination of hydrogen bromide from β-bromolevulinic acid,[10] showed the same NMR signal as I-A. The ultravioletspectrum showed λ_{max} 220 mμ.

Benzoylacrylic acid (II), which was obtained by the Friedel-Crafts reaction of maleic anhydride and benzene,[4] showed infrared absorption bands at 1700, 1670 and 1635 cm^{-1}, and no absorption between 1800 and 1750 cm^{-1}. In the ultraviolet absorption spectrum bands were observed at λ_{max} 238 mμ and λ_{max} 272 mμ. In the NMR spectrum, the signals of a pair of sharp doublets at τ 3.12 and 1.98 for the olefinic protons were observed. From the fact that the coupling constant, J=15.4 cps, of these olefinic proton signals is nearly equal to the J=16.2 cps of I-A, the structure of benzoylacrylic acid must be a II-A *trans* form.

Since the benzene ring and the remaining part of the molecule should be on the same plane as a result of the conjugation, two isomers, II-A′ and II-A″, are possible. However, inspection of the molecular model of II-A shows that II-A″ is not probable because of the steric hindrance between H_A and an ortho-H of the benzene ring. In II-A′, the deshielding effect of the benzene ring for H_B is expected to be present on account of its proximity to the benzene ring, but no such effect is expected for H_B in II-A″. From the NMR data for olefinic protons of methyl fumarate at τ 3.17,[11] the signal at τ 3.12 was assigned to H_A, and that at τ 1.98, to H_B. From the fact that H_B is more deshielded by the benzene ring, the II-A′ *trans* form is preferred as the structure of benzoylacrylic acid.

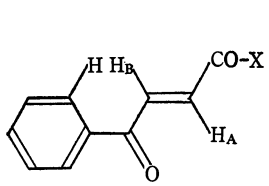

II-A′: X=OH
IV-A′: X=OMe

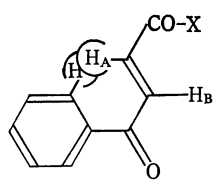

II-A″: X=OH
IV-A″: X=OMe

Methyl Acetylacrylate and Methyl Benzoylacrylate. *By the Elimination of Hydrogen Bromide.* Methyl acetylacrylate (III) was obtained by the elimination of hydrogen bromide from methyl β-bromolevulinate.[12] In the NMR spectrum of this product, an AB quartet signal for the olefinic protons, centered at τ 3.29 (J=15.4 cps), was observed. The infrared absorption spectrum showed carbonyl absorptions at 1725 and 1675 cm^{-1}, and no absorption in the region of the lactone carbonyl band. The ultraviolet absorption spectrum showed a λ_{max} of 220 mμ, similar to that of I-A. These data suggest that the structure of the product which we obtained by this method is in the III-A *trans* form.

By the elimination of hydrogen bromide from methyl β-bromo-β-benzoylpropionate, IV was prepared. In the NMR spectrum of IV we observed a pair of sharp doublets of the olefinic protons at τ 3.12 and 2.16 (J=15.4 cps). The infrared absorption spectrum of IV showed carbonyl absorption bands at 1725 and 1670 cm^{-1} and an olefinic double-bond absorption band at 1630 cm^{-1}, but no absorption band was observed in the lactone carbonyl region. Much as in II-A, the ultraviolet absorption spectrum of IV showed a λ_{max} value of 232 mμ and a λ_{max} value of 270 mμ. These results suggest that methyl benzoylacrylate was in the IV-A′ form.

By the Acid-Catalyzed Esterification. In the presence of sulfuric acid, II-A was esterified to IV.[13] The product was identified with IV-A′ on the basis of the spectral data and by thin-layer chromatography. In the case of the acid-catalyzed esterification of I-A, III-A was obtained in a 10% yield, and methyl α-methoxylevulinate,[14] in a 16% yield. These results suggest that the esterification of I-A and II-A by the acid catalyst occurs.

Isomerization. The treatment of III-A or IV-A with aqueous sodium hydroxide gave a hydrolyzed product, I-A or II-A. In the reaction mixture, the isomerized products were not detected. Thus, acetyl- and benzoylacrylic acids did not isomerize under the basic conditions.

It has been reported that I-A was isomerized by thionyl chloride to 5-methyl-5-chloro-2,5-dihydro-2-oxofuran (VI-C), which, in turn, was converted to I-C with an aqueous alkali.[1] Therefore, it is interesting to examine the reaction of II-A with thionyl chloride, followed by the reaction of methanol instead of an aqueous alkali.

In the NMR spectrum of the reaction mixture of II-A with thionyl chloride, followed by the reaction of methanol, we observed the signals corresponding to three substances, the normal esterified product, IV-A, and two anomalous products, 5-phenyl-5-methoxy-2,5-dihydro-2-oxofuran (IV-C) and methyl α-methoxy-β-benzoylpropionate. The molar ratio of these products was 49 : 21 : 30. The structure of IV-C was deduced from the spectral data. In the infrared absorption spectrum of IV-C absorption bands were observed at 1770 and 1630 cm^{-1}. The NMR spectrum showed olefinic proton signals at τ 3.98 and 2.82, J=5.5

10) L. Wolff, *Ann.*, **264**, 246 (1891).
11) N. S. Bhacca, L. F. Johnson and J. N. Shoolery, "Varian High Resolution NMR Spectra Catalog," Vol. I, ed by Varian associates, Palo Alto, California (1962), p. 213.
12) R. E. Lutz and G. W. Scott, *J. Org. Chem.*, **13**, 284 (1949).
13) H. Pauly, R. Gilmour and G. Will, *Ann.*, **403**, 119 (1914).
14) L. Birkofer and R. Dutz, *ibid.*, **608**, 7 (1957).

Table 1. The NMR spectra

Comp.	R	X	τ_{Ph}	τ_{Me}	τ_{OMe}	τ_{OH}	τ_{HA}	τ_{HB}	J_{AB}
I-A	Me	OH		7.60		0.27	3.20		16.2
II-A	Ph	OH	1.8—2.8			−1.36	3.12	1.98	15.4
III-A	Me	OMe		7.67	6.22		3.29		15.4
IV-A	Ph	OMe	1.9—2.8		6.19		3.21	2.16	15.4
II-B	Ph	OH	1.9—2.8			−0.92	3.70	2.90	12.0
III-B	Me	OMe		7.73	6.28		3.84		12.5
IV-B	Ph	OMe	2.0—2.8		6.42		3.76	3.13	12.0
I-C	Me	OH		8.23		4.41	3.91	2.77	6.0
IV-C	Ph	OMe	2.0—2.8		6.73		3.98	2.82	5.5

cps. The corresponding J value of I-C was 6 cps. These results suggest that II-A is partly esterified, but also partly isomerized to lactone.

Reaction of II-A with Diazomethane. When II-A was treated with diazomethane, neither IV-A nor IV-C was detected by thin-layer chromatography in the reaction mixture. The reaction of of diazomethane with carboxylic acid frequently does not lead to the expected methyl ester. For example, the reaction of diazomethane with I-A gave the isomerized product III-C,[2] while that with *trans-p*-bromobenzoylacrylic acid gave 4-(*p*-bromobenzoyl)-3-carbomethoxypyrazoline.[13] Thus, α,β-unsaturated γ-oxo acids do not afford the simple methyl ester by reaction with diazomethane.

Photoisomerization. By the photoreaction, the *cis* isomer (B) was produced from the *trans* isomer (A). The details of the photoreactions of α,β-unsaturated γ-oxo acid and their derivatives will be reported in another paper.

Experimental

Acetylacrylic Acid. This acid was prepared by the mehtod of Wolff[10] and was recrystallized from benzene to give colorless crystals, mp 125—126°C.

IR (KBr): 1700, 1670, 1625 cm^{-1}.

UV (EtOH): 220 mμ (ε 13800), 340 mμ (ε 40).

Benzoylacrylic Acid. This acid was prepared by the method of Becker,[4] and was crystallized from benzene to give colorless crystals, mp 95.5—96°C.

IR (KBr): 1700, 1670, 1635 cm^{-1}.

UV (EtOH): 238 mμ (ε 11000), 272 mμ (ε 8900).

Methyl Acetylacrylate. This was prepared by the method of Pauly[12] and was recrystallized from an ether and hexane (1 : 1 v/v) mixture, mp 58.5—60°C.

IR (KBr): 1725, 1675, 1645 cm^{-1}.

UV (EtOH): 220 mμ (ε 14400), 338 mμ (ε 40).

In the presence of sulfuric acid, acetylacrylic acid was esterified, and the product was identified on silica-gel thin-layer chromatography (Wakogel B-5) with a benzene and ethyl acetate (9 : 1 v/v) mixture.

Methyl Benzoylacrylate. This ester was prepared by two methods, by the method of Kohler[15] and by the esterification of the corresponding free acid in the presence of sulfuric acid. In both cases, the crude product was purified by chromatography on silica-gel (Merk 7734) with a benzene and ethyl acetate (9 : 1 v/v) mixture; mp 34°C.

IR (liquid film): 1725, 1670, 1630 cm^{-1}.

UV (EtOH): 232 mμ (ε 15400), 270 mμ (ε 9800).

Base-catalyzed Hydrolysis of III-A and IV-A. To a solution of the III-A or IV-A ester (100 mg) in methanol (2 m*l*), potassium hydroxide (25 mg) in water (1 m*l*) was stirred over a 2-hr period at room temperature. The reaction mixture was then worked up by the usual method, and the product was identified by thin-layer chromatography and by a study of its absorption spectrum.

Isomerization of II-A by Thionyl Chloride. One gram of II-A was dissolved in 2 m*l* of thionyl chloride, after which the mixture was kept for 10 min at 50°C. The mixture was then poured into excess methanol at 0°C. The ratio of the products in the reaction mixture was measured by means of the NMR spectrum and was found to be 49 : 21 : 30.

NMR ($CDCl_3$): τ 6.20 (1.5 H) ester methyl of IV-A. 6.29 (0.9 H) ester methyl of methoxypropionate. 6.59 (0.9H) methoxy of methoxypropionate. 6.71 (0.6 H) methoxy of IV-C.

Reaction with Diazomethane. Benzoylacrylic acid was reacted with diazomethane in ether in the usual manner. The reaction product was chromatographed on a thin layer of silica gel (Wakogel B-5) with a benzene and ethyl acetate (9 : 1 v/v) mixture. No spot corresponding to IV-A or IV-C was observed.

NMR Spectra. The NMR spectra were measured on a Hitachi H-60 High-resolution Nuclear Magnetic Resonance Spectrometer. The solvent was deuterochloroform, and TMS was used as the internal standard. The spectral data are listed in Table 1.

The authors wish to express their thanks to Mr. Kyuzaburo Furuhashi of Department of Chemistry, Tokyo Kyoiku University, for his measurement of the NMR spectra.

15) E. P. Kohler and H. Engelbrecht, *ibid.*, **41**, 764 (1919).

BULLETIN OF THE CHEMICAL SOCIETY OF JAPAN VOL. 41 974—979 (1968)

Selective Cleavage of Serine Peptides*1

Takeo KANEKO, Ikuko TAKEUCHI*2 and Toshishige INUI*3

Department of Chemistry, Faculty of Science, Osaka University, Toyonaka, Osaka

(Received October 11, 1967)

The treatment of *N*-benzyloxycarbonyl-L-alanyl-L-serine methyl ester (I) with phosgene afforded the corresponding *O*-chlorocarbonyl derivative (II), which was then cyclized to methyl L-3-(*N*-benzyloxycarbonyl-L-alanyl)-2-oxo-oxazolidine-4-carboxylate (III) accompanied with *N*-benzyloxycarbonyl-L-alanyl-3-chloro-L-alanine methyl ester (IV) by refluxing in xylene. By the mild alkaline hydrolysis of III, *N*-benzyloxycarbonyl-L-alanine and L-2-oxo-oxazolidine-4-carboxylic acid (V) were isolated as a result of the selective cleavage of the peptide bond in which an amino group of the serine residue participated. This method was also applied to three other serine peptides; the same results were obtained.

The method of the selective cleavage of proteins by enzymes is very valuable in the elucidation of their structure.[1,2] On the other hand, the use of the selective cleavage of peptide bonds on the special amino acid residue in proteins by chemical reagents is also important in achieving fragments different from those obtained by enzymes and so in determining their sequences. Recently, the techniques for the selective chemical cleavage on tyrosyl, tryptophyl, histidyl and methionyl peptides have been developed by Witkop and others.[1,3-6] N→O Acyl group migration with acid and subsequent hydrolysis induced selective cleavage on the serine or threonine residue in proteins.[7] Threonine peptides were cyclized with phosgene to their oxazolidone derivatives, the hydrolysis of which with a dilute alkali also afforded selective cleavage at the peptide linkage involving the amino group of the threonine residue.[8]

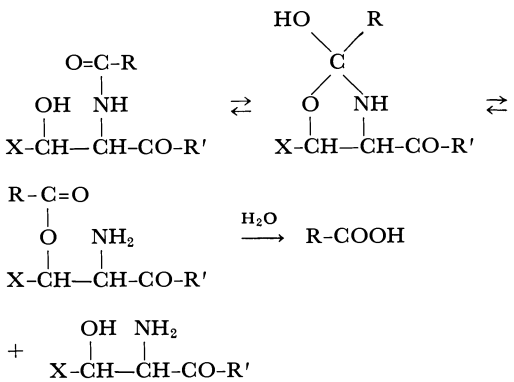

X=H: Serine, X=CH_3: Threonine

Another hydroxy-amino acid, serine, was also cyclized with phosgene to an oxazolidone derivative.[9]

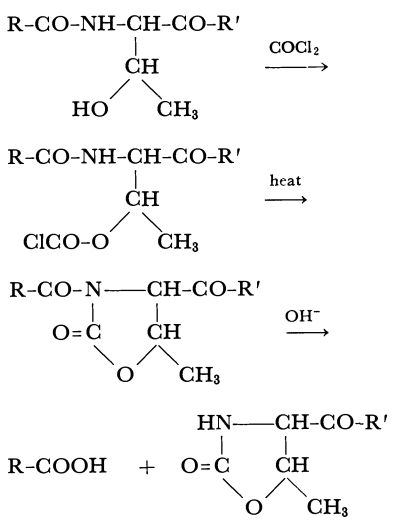

*1 Presented in part at the 17th Annual Meeting of the Chemical Society of Japan, Tokyo, April, 1964.

*2 Present address: Department of Chemistry, Faculty of Science, Kwansei Gakuin University, Nishinomiya, Hyogo.

*3 Present address: Institute of Chemistry, College of General Education, Osaka University, Toyonaka, Osaka.

1) B. Witkop, "Advances in Protein Chemistry," Vol. 16, Academic Press, New York (1961), p. 221.

2) S. Akabori and S. Mizushima, "Tampakushitsu Kagaku (Protein Chemistry)," Vol. 1, Kyoritsu Shuppan, Tokyo (1954), p. 25.

3) G. L. Schmir and L. A. Cohen, *J. Am. Chem. Soc.*, **83**, 723 (1961).

4) A. Patchoronik and B. Witkop, *ibid.*, **82**, 5923 (1960).

5) A. Patchoronik and S. Shltiel, *ibid.*, **85**, 2799 (1963).

6) W. B. Lawson, A. Patchoronik and B. Witkop, *ibid.*, **83**, 1509 (1961).

7) L. A. Cohen and B. Witkop, *Angew. Chem.*, **73**, 253 (1961); K. Iwai, *Nippon Kagaku Zasshi (J. Chem. Soc. Japan, Pure Chem. Sect.)*, **80**, 1066 (1959); **81**, 1302 (1960); **82**, 1088 (1961).

8) Short communication: T. Kaneko and T. Inui, This Bulletin, **36**, 1541 (1963). The details will be reported in this Bulletin later.

9) T. Kaneko and T. Inui, *Nippon Kagaku Zasshi (J. Chem. Soc. Japan, Pure Chem. Sect.)*, **82**, 1075 (1961).

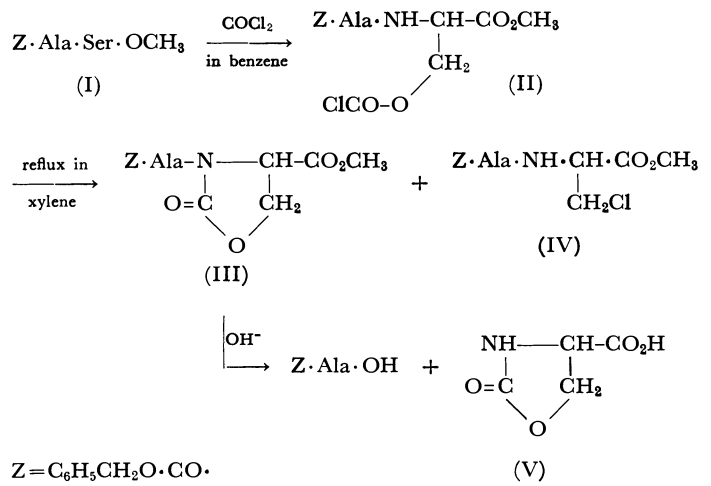

In a similar fashion, if serine peptides involving a peptide linkage between the amino group of the serine residue and the carboxyl group of another amino acid residue are cyclized with phosgene to the corresponding oxazolidone peptides at their serine residue, the peptides thus obtained will selectively be cleft in two parts at the amino group of the serine residue by alkaline hydrolysis. In order to investigate the selective cleavage of this type on serine peptides, *N*-benzyloxycarbonyl- L -alanyl- L -serine methyl ester (I), L-seryl-L-alanine (VI), *N*-benzyloxycarbonylglycyl-L-seryl-L-alanine methyl ester (VIII), and *N*-benzyloxycarbonyl- L -alanyl-L-alanyl-L-serine methyl ester (IX) were used as the model peptides in the present study.

I,[10] obtained from *N*-benzyloxycarbonyl-L-alanine and methyl L-serinate hydrochloride by using the *N*,*N'*-dicyclohexylcarbodiimide method, was converted with phosgene to the *O*-chlorocarbonyl derivative (II) by using the method of Bergel.[11] In threonine peptides, their *O*-chlorocarbonyl compounds were easily cyclized, under reflux in xylene, to the corresponding oxazolidone derivatives in good yields.[8] Under the same experimental conditions, II provided a crystal melting at 93—109°C; this was clarified as being a mixture of methyl L-3-(*N*-benzyloxycarbonyl-L-alanyl)-2-oxo-oxazolidine-4-carboxylate (II) and *N*-benzyloxycarbonyl-L- alanyl - 3 - chloro-L-alanine methyl ester (IV) by thin-layer chromatography with silica gel G (TLC) and by means of a study of the infrared spectra. The ratio of III to IV in the reaction mixture was established to be about two-to-one by an analysis of its infrared spectra. The separation of III from IV was achieved by using a column with silica gel and by eluting it with a mixture of benzene and methanol (19 : 1, v/v). The structure of III was confirmed by elemental analysis and by a study of its infrared spectra. On the other hand, the minor component, exhibiting a strongly positive Beilstein's test, was also confirmed to have IV by a study of its nuclear magnetic resonance spectra. Various conditions for cyclizing of II were then studied. The yield of the mixture which was obtained by the reflux of II in toluene was decreased to about two-thirds of that obtained under the above conditions, but the ratio of III to IV was increased to about eight-to-one. In another experiment, II was treated with an equivalent amount of pyridine in benzene; the product isolated was identified by TLC as IV, accompanied by a small amount of I.

The alkaline hydrolysis of III afforded *N*-benzyloxycarbonyl-L-alanine and L-2-oxo-oxazolidine-4-carboxylic acid (V) in yields of 89% and 68% respectively. The structures of the products isolated were confirmed by comparisons of their melting points, specific rotations, and infrared spectra with those of the corresponding authentic specimens. For comparison, the authentic V was prepared from L-serine by the method described for the cyclization of L-threonine.[12]

A peptide containing the serine residue as the amino terminal unit should be cyclized to an oxazolidone peptide without any change in the peptide bond. VI[13] was readily cyclized with phosgene to L-2-oxo-oxazolidine-4-carbonyl-L-alanine (VII) in an alkaline solution.

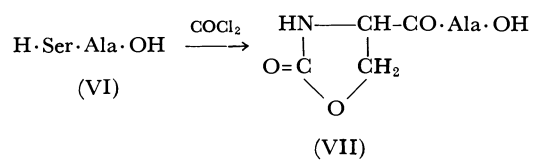

10) J. I. Harris and J. S. Fruton, *J. Biol. Chem.*, **191**, 143 (1951).
11) F. Bergel and R. Wade, *J. Chem. Soc.*, **1959**, 941.
12) T. Inui and T. Kaneko, *Nippon Kagaku Zasshi (J. Chem. Soc. Japan, Pure Chem. Sect.)*, **83**, 1078 (1961).
13) J. S. Fruton, *J. Biol. Chem.*, **146**, 463 (1942).

TABLE 1. RESULTS OF THE SELECTIVE CLEAVAGE OF SERINE PEPTIDES

Peptide	Oxazolidone derivative	Products isolated by alkaline hydrolysis (yields)	
I	III	Z·Ala·OH (89%)	V (68%)
VIII	XII	Z·Gly·OH (81%)	VII (40%)
IX	XIV	Z·Ala·Ala·OH (60%)	V (46%)

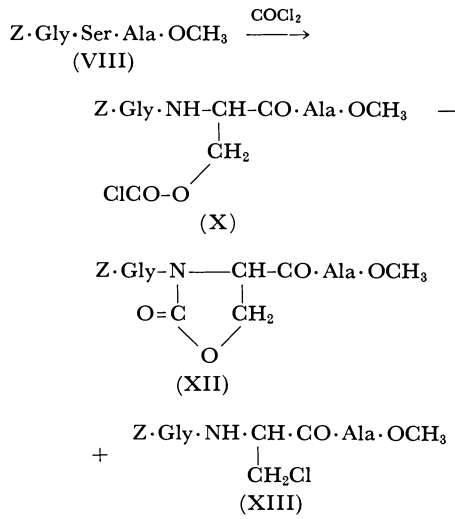

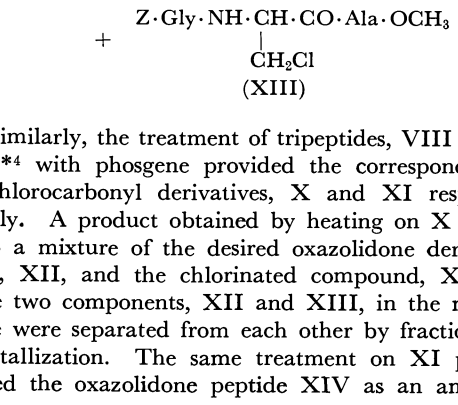

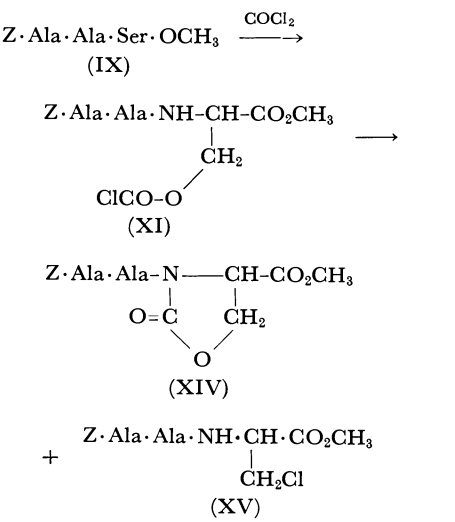

Similarly, the treatment of tripeptides, VIII and IX,*4 with phosgene provided the corresponding *O*-chlorocarbonyl derivatives, X and XI respectively. A product obtained by heating on X was also a mixture of the desired oxazolidone derivative, XII, and the chlorinated compound, XIII. The two components, XII and XIII, in the mixture were separated from each other by fractional crystallization. The same treatment on XI provided the oxazolidone peptide XIV as an amorphous solid (probably contaminated with a small amount of the chlorinated compound XV, for it gave a slightly positive Beilstein's test), which was used for the next step without further purification. The cleavage reactions of XII and XIV were also studied; the results were summarized in Table 1, plus those for III.

In conclusion, this selective cleavage of serine peptide occurs on the peptide linkage involving an amino group of the serine residue through its oxazolidone derivative without racemization.

Experimental*5

***N*-Benzyloxycarbonyl-L-alanyl-L-serine Methyl Ester (I).** A solution containing 22.3 g (0.10 mol) of *N*-benzyloxycarbonyl-L-alanine, 15.6 g (0.10 mol) of methyl L-serinate hydrochloride, and 14.0 m*l* (0.10 mol) of triethylamine in 225 m*l* of chloroform was treated with a solution of 20.6 g (0.10 mol) of *N,N'*-dicyclohexylcarbodiimide in 50 m*l* of chloroform. After the mixture had been stirred for 3 hr and then stood overnight at room temperature, the *N,N'*-dicyclohexylurea which precipitated was filtered off, and the filtrate was successively washed with water, dilute hydrochloric acid, and dilute aqueous sodium hydrogen carbonate solution. The dried solution was evaporated *in vacuo*, thus providing white crystals which were then recrystallized from ethyl acetate - petroleum ether. Yield, 22.5 g (70%), mp 134.5—135.5°C, $[\alpha]_D^{23.5}$ −17.7° (*c* 3.43, methanol), lit.,[10] mp 134—135°C.

Found: C, 55.80; H, 6.32; N, 8.64%. Calcd for $C_{15}H_{20}O_6N_2$: C, 55.55; H, 6.22; N, 8.64%.

***N*-Benzyloxycarbonyl-L-alanyl-*O*-chlorocarbonyl-L-serine Methyl Ester (II).** Phosgene was passed through a stirred suspension of 8.1 g (0.025 mol) of I and 3.0 g (0.025 mol) of *N,N*-dimethylaniline in 100 m*l* of benzene for 30 min at 5—10°C. After it had been stirred for 3 hr and then left to stand overnight below 20°C, the reaction mixture was bubbled with a stream of nitrogen (or carbon dioxide) until the excess phosgene had been removed, and then washed with dilute hydrochloric acid and water. The dried solution was evaporated *in vacuo*, thus providing white crystals which were then recrystallized by precipitation with the addition of petroleum ether to a solution of the product in a minimum amount of benzene. Yield, 7.6 g (79%), mp 93.5—94°C, $[\alpha]_D^{23}$ +20.1° (*c* 3.58, benzene).

Found: C, 49.76; H, 5.16; N, 7.63; Cl, 8.30%. Calcd for $C_{16}H_{19}O_7N_2Cl$: C, 49.68; H, 4.95; N, 7.24; Cl, 9.17%.

The treatment of a solution of II in benzene with an

*4 The preparations of these peptides, VIII and IX, will be described in Experimental section below.

*5 All melting points are uncorrected.

etheral solution of aniline gave the *N*-benzyloxycarbonyl-L-alanyl-*O*-(*N*-phenylcarbamoyl)-L-serine methyl ester; mp 146.3—146.8°C, $[\alpha]_D^{23.5}$ −7.8° (*c* 2.31, methanol).

Found: C, 60.02; H, 5.70; N, 9.40%. Calcd for $C_{22}H_{25}O_7N_3$: C, 59.58; H, 5.68; N, 9.48%.

Methyl L-3-(*N*-Benzyloxycarbonyl-L-alanyl)-2-oxo-oxazolidine-4-carboxylate (III) and *N*-Benzyloxycarbonyl-L-alanyl-3-chloro-L-alanine Methyl Ester (IV). A solution of 7.0 g (0.018 mol) of II in 70 m*l* of xylene was refluxed for 6 hr. The solution was then evaporated *in vacuo*, leaving an oil which was crystallized by seeding. Yield, 4.3—5.0 g, mp 93—109°C. It gave a positive Beilstein's test and exhibited two spots on TLC. The ratio of III to IV in the crystals was found to be 1.9—2.1 by an analysis of its infrared spectra.

A solution of 3.0 g of the crude product in 10 m*l* of hot benzene was adsorbed on a column (1.6×30 cm) with 30 g of silica gel, eluted with a mixture of benzene and methanol (19 : 1, v/v), and divided into four fractions by TLC.

The evaporation of the first fraction (170 m*l*) left no residue.

The second fraction (25 m*l*), exhibiting a single spot on TLC, was evaporated *in vacuo*, leaving III as white crystals. Yield, 1.1 g, mp 101.5—103°C. For analysis, it was also recrystallized from benzene - petroleum ether (3 : 1); mp 102.5—103.5°C, $[\alpha]_D^{23.5}$ −126.5° (*c* 3.09, methanol).

IR (Nujol mull): 1820, 1785 (C=O group in the oxazolidone ring); 1755 (C=O group in the ester); 1710 cm^{-1} (C=O group in the benzyloxycarbonyl group).

NMR (Chloroform solution): 1.46 (doublet, J=6.8 cps, CH_3 peak in the alanine residue); 3.82 ppm (singlet, CH_3 peak in the ester group).

Found: C, 54.99; H, 5.26; N, 8.02%. Calcd for $C_{16}H_{18}O_7N_2$: C, 54.85; H, 5.18; N, 8.00%.

The evaporation of the third fraction (20 m*l*) provided 0.8 g of a mixture of III and IV which melted at 95—108°C.

The evaporation of the fourth fraction (35 m*l*) provided 0.3 g of IV contaminated with a minor amount of III, as indicated by TLC. The recrystallization of the crude product, which melted at 120—134°C, from methanol and then from benzene raised the melting point to 150.5—151.3°C, $[\alpha]_D^{21.5}$ +14.1° (*c* 1.46, methanol).

IR (Nujol mull): 1655, 1530 (–CONH– group in the peptide bond); 1750 (C=O group in the ester); 1690 cm^{-1} (C=O group in the benzyloxycarbonyl group).

NMR (Chloroform solution): 1.26 (doublet, J= 7.2 cps, CH_3 peak in the alanine residue); 3.80 (singlet, CH_3 peak in the ester group); 3.91 ppm (doublet, J= 3.0 cps, $>CH_2$ peak in the $Cl{\cdot}CH_2{\cdot}CH<$ group).

Found: C, 52.73; H, 5.60; N, 8.31; Cl, 10.24%. Calcd for $C_{15}H_{19}O_5N_2Cl$: C, 52.56; H, 5.59; N, 8.17; Cl, 10.34%.

The refluxing of a solution of 3.7 g (0.0096 mol) of II in 40 m*l* of toluene for 6 hr provided another mixture of III and IV, in which the ratio of III to IV was 8.4. Yield, 1.7 g, mp 99—102°C.

L-2-Oxo-oxazolidine-4-carboxylic Acid (V). A solution of 4.2 g (0.04 mol) of L-serine in 80 m*l* (0.04 mol) of 0.5 N potassium hydroxide was treated with a solution of 4.8 g (0.048 mol) of phosgene in 20 m*l* of toluene in the presence of 8.3 g (0.06 mol) of anhydrous potassium carbonate for 3 hr at 0—5°C. The aqueous layer which separated from the toluene layer was acidified with 6 N hydrochloric acid to pH 1 and evaporated to dryness *in vacuo*. The residue was then extracted five times with hot ethyl acetate, and the dried extract was evaporated *in vacuo* to give crystals which melted at 116—117°C. Yield, 2.8 g (54%). Recrystallization from ethyl acetate - petroleum ether raised the melting point to 118.5—120°C, $[\alpha]_D^{22.5}$ −17.7° (*c* 3.44, water), lit.,[14] mp 118°C, $[\alpha]_D^{15}$ −10.95° (*c* 4.20, water).

Found: C, 36.80; H, 3.96; N, 11.03%. Calcd for $C_4H_5O_4N$: C, 36.65; H, 3.85; N, 10.69%.

Cyclohexylammonium salt; mp 155.0—155.8°C (decomp.), $[\alpha]_D^{19}$ −19.3° (*c* 3.11, water).

Found: C, 51.90; H, 8.12; N, 12.09%. Calcd for $C_{10}H_{18}O_4N_2$: C, 52.16; H, 7.88; N, 12.17%.

The hydrolysis of the sample of V with 6 N hydrochloric acid gave the L-serine; mp 214—215°C (decomp.), $[\alpha]_D^{21.5}$ +14.7° (*c* 2.91, 1 N hydrochloric acid).

Alkaline Hydrolysis of III. To a solution of 2.80 g (0.008 mol) of III in 40 m*l* of methanol 16.0 m*l* (0.016 mol) of 1 N potassium hydroxide were added, after which the reaction mixture was stirred for 1.5 hr at room temperature. After the evaporation of the methanol *in vacuo*, the residue was diluted with water and the aqueous solution was acidified with 8.5 m*l* of 1 N hydrochloric acid to pH 3.5. The separated oil was extracted with ethyl acetate. The dried extract was then evaporated to dryness *in vacuo*, leaving a crystalline *N*-benzyloxycarbonyl-L-alanine. Yield, 1.59 g (89%), mp 80—82.7°C and 86.0—87.3°C after recrystallization from chloroform - petroleum ether, $[\alpha]_D^{20.5}$ −13.0° (*c* 3.15, acetic acid); lit.,[15] mp 87°C, $[\alpha]_D^{27}$ −13.9° (*c* 2, acetic acid).

A mixed melting point with an authentic sample was not depressed.

An additional 8.5 m*l* of 1 N hydrochloric acid was added to the remaining aqueous solution. The residue, obtained by the evaporation of the acidic solution, was extracted three times with 20-m*l* portions of hot ethyl acetate; the evaporation of the combined extracts provided V as an oil which was crystallized by seeding. Yield, 0.71 g (68%), mp 95—103°C and 117—119°C after recrystallization from ethyl acetate - petroleum $[\alpha]_D^{20.5}$ −17.5° (*c* 3.43, water).

All the properties of the sample were identical with those of the cyclized product of L-serine.

L-Seryl-L-alanine (VI). This compound was prepared by the catalytic hydrogenation of 4.5 g (0.014 mol) of *N*-benzyloxycarbonyl-L-seryl-L-alanine [mp 157—158°C, $[\alpha]_D^{22.5}$ −12.5° (*c* 3, methanol)], which had been obtained from its methyl ester by hydrolysis with an equivalent amount of 1 N sodium hydroxide in methanol, with 0.5 g of 10% palladium on carbon in a mixture of 120 m*l* of methanol and 50 m*l* of water, according to the directions of Fruton.[13] Yield, 2.2 g (89%), mp 223—225°C (decomp.) after recrystallization from water-acetone, $[\alpha]_D^{24.5}$ −31.8° (*c* 6, 1 N hydrochloric acid), lit.,[13] $[\alpha]_D^{26}$ −30.4° (*c* 6, 1 N hydrochloric acid).

14) T. Saito, This Bulletin, **37**, 624 (1964).
15) M. Hunt and V. du Vigneaud, *J. Biol. Chem.*, **124**, 699 (1938).

Found: C, 40.99; H, 6.86; N, 15.85%. Calcd for $C_6H_{12}O_4N_2$: C, 40.90; H, 6.87; N, 15.90%.

L-2-Oxo-oxazolidine-4-carbonyl-L-alanine (VII). In the way similar to that described for the preparation of V, a solution of 3.7 g (0.021 mol) of VI in 44 m*l* (0.022 mol) of 0.5 N potassium hydroxide was treated with 25 g (0.025 mol) of a 10% solution of phosgene in toluene in the presence of 3.5 g (0.025 mol) of anhydrous potassium carbonate. The crude product which separated from the salt was dissolved in water, the aqueous solution was passed through a column of Dowex 50 (H^+ form), and the column was thoroughly washed with water. The combined aqueous solution was then evaporated to dryness *in vacuo* to give a syrup which was crystallized by the addition of petroleum ether to a methanol solution of the product. Yield, 2.5 g (60%), mp 178—181°C (decomp.). Recrystallization from ethanol - petroleum ether raised the melting point to 188—191°C (decomp.), $[\alpha]_D^{18}$ −28.3° (*c* 3, water).

Found: C, 41.43; H, 5.15; N, 13.96%. Calcd for $C_7H_{10}O_5N_2$: C, 41.58; H, 4.99; N, 13.86%.

Cyclohexylammonium salt; mp 196—197.5°C (decomp.) after recrystallization from methanol-ether.

Found: C, 51.83; H, 7.83; N, 14.12%. Calcd for $C_{13}H_{23}O_5N_3$: C, 51.81; H, 7.69; N, 13.95%.

***N*-Benzyloxycarbonylglycyl - L - seryl - L - alanine Methyl Ester (VIII).** A solution of 1.4 g (0.005 mol) of *N*-benzyloxycarbonylglycyl-L-serine methyl ester[10] [mp 96.5—98.5°C, $[\alpha]_D^{14.5}$ −4.0° (*c* 6, methanol)] and 0.5 m*l* of 85% hydrazine hydrate in 30 m*l* of ethanol was allowed to stand overnight at room temperature. The crystal, *N*-benzyloxycarbonylglycyl-L-serine hydrazide, which separated from the solution were collected by filtration. Yield, 1.3 g (93%), mp 220—221°C (decomp.) after recrystallization from ethanol-water, $[\alpha]_D^{13}$ −9° (*c* 1, acetic acid).

Found: C, 50.61; H, 5.97; N, 18.12%. Calcd for $C_{13}H_{18}O_5N_4$: C, 50.31; H, 5.85; N, 18.06%.

In a mixture of 50 m*l* of water, 5 m*l* of acetic acid, and 20 m*l* of 6 N hydrochloric acid, 3.1 g (0.010 mol) of the above hydrazide was dissolved and the resultant solution was cooled to −5°C. To the solution a cold 7-m*l* portion (0.010 mol) of a 10% aqueous sodium nitrite solution was added, and the mixture was stirred for 20 min at 0°C. The azide which separated from the reaction mixture was extracted with 250 m*l* of ethyl acetate, and the extract was washed with ice water, a 3% aqueous sodium hydrogen carbonate solution, and finally ice water below −5°C. To the cold, dried solution there was then added another cold, dried solution of methyl L-alaninate equivalent to 1.4 g (0.010 mol) of its hydrochloride in 20 m*l* of chloroform at 0°C. The reaction mixture was stirred for 2 hr below 5°C and allowed to stand overnight in a refrigerator. After washing with water, a 3% aqueous sodium hydrogen carbonate solution, 1 N hydrochloric acid, and water, the evaporation of the dried organic layer *in vacuo* provided 1.9 g (50%) of VIII. Mp 135.5—137°C after recrystallization from water, $[\alpha]_D^{11}$ −38.2° (*c* 3, methanol).

Found: C, 51.29; H, 6.33; N, 10.67%. Calcd for $C_{17}H_{23}O_7N_3 \cdot H_2O$: C, 51.12; H, 6.31; N, 10.52%.

***N*-Benzyloxycarbonylglycyl-*O*-chlorocarbonyl-L-seryl-L-alanine Methyl Ester (X).** In the same manner as has been described for the preparation of II, a solution of 3.9 g (0.01 mol) of VIII in 50 m*l* of anhydrous dioxane was treated with an excess of phosgene in the presence of 2.0 g (0.016 mol) of *N*,*N*-dimethylaniline below 10°C. After the excess phosgene had been removed, the reaction mixture was evaporated *in vacuo* and the residue was taken up with ethyl acetate. The ethyl acetate solution was washed with 0.1 N hydrochloric acid and water, and the dried solution was evaporated *in vacuo* to give an oil which was crystallized by adding petroleum ether. Yield, 3.2 g (73%), mp 126.5—127°C after recrystallization from acetone-petroleum ether, $[\alpha]_D^{18}$ −4.5° (*c* 0.7, dioxane).

Found: C, 49.39; H, 5.23; N, 8.93; Cl, 7.79%. Calcd for $C_{18}H_{22}O_8N_3Cl \cdot \frac{1}{2}C_3H_6O$: C, 49.25; H, 5.34; N, 8.89; Cl, 7.50%.

L-3-(*N*-Benzyloxycarbonylglycyl)-2-oxo-oxazolidine-4-carbonyl-L-alanine Methyl Ester (XII) and *N*-Benzyloxycarbonylglycyl-3-chloro-L-alanyl-L-alanine Methyl Ester (XIII). A solution of 4.8 g (0.010 mol) of X in 250 m*l* of toluene was refluxed for 4 hr under a stream of nitrogen and then evaporated to dryness *in vacuo*. The residue was extracted with chloroform, and the dried extract was again evaporated *in vacuo* to provide an oil which exhibited two spots upon TLC. From this oil, XII was separated as crystals by adding a small amount of petroleum ether and by scratching on the wall of the vessel. Yield, 1.2 g (27%), mp 155—160°C. Recrystallization from chloroform-petroleum ether and then from ethyl acetate - petroleum ether raised the melting point to 172.5—173°C, $[\alpha]_D^{14}$ −113.8° (*c* 0.9, methanol).

Found: C, 52.84; H, 5.17; N, 10.18%. Calcd for $C_{18}H_{21}O_8N_3$: C, 53.07; H, 5.20; N, 10.32%.

The mother liquor remaining after the filtration of XII was evaporated to dryness *in vacuo*, and to the residue there was added a large amount of petroleum ether in order to obtain XIII as another crystal, which was collected by filtration. Yield, 0.2 g, mp 137—139°C. Recrystallization from ethyl acetate - petroleum ether raised the melting point to 140.5—141°C. It gave a positive Beilstein's test.

Found: C, 51.19; H, 5.55%. Calcd for $C_{17}H_{22}O_6N_3Cl$: C, 51.06; H, 5.56%.

Alkaline Hydrolysis of XII. In a manner similar to that described for the hydrolysis of III, 1.0 g (0.0025 mol) of XII was hydrolyzed with a mixture of 5 m*l* (0.005 mol) of 1 N potassium hydroxide and 50 m*l* of methanol. After the evaporation of the solvent, the residue was diluted with water and acidified with 1 N hydrochloric acid to pH 3. From the ethyl acetate extract, 0.42 g (81%) of *N*-benzyloxycarbonylglycine was isolated, all the properties of which were identical with those of an authentic sample.

On the other hand, 0.2 g (40%) of VII was isolated from the aqueous solution as an oil which was purified as its cyclohexylammonium salt. No melting-point depression upon mixture with an authentic specimen obtained from the cyclized product of VI was observed.

***N*-Benzyloxycarbonyl-L-alanyl-L-alanyl-L-serine Methyl Ester (IX).** Seven and seven-tenths grams (0.025 mol) of *N*-benzyloxycarbonyl-L-alanyl-L-alanine hydrazide [mp 212—213°C, $[\alpha]_D^{18}$ −67.4° (*c* 1.84, 0.5 N hydrochloric acid)] were converted into its azide according to the directions of Erlanger.[16] To the cold,

16) B. F. Erlanger and E. Brand, *J. Am. Chem. Soc.*, **73**, 3508 (1951); E. Brand, B. F. Erlanger, H. Sachs and J. Polantnick, *ibid.*, **73**, 3510 (1951).

dried solution of the above azide in 200 ml of ethyl acetate-ether (1 : 1), there was added another cold, dried solution of methyl L-serinate equivalent to 6.1 g (0.039 mol) of its hydrochloride in a mixture of 45 ml of chloroform and 100 ml of ethyl acetate below 5°C. The reaction mixture was then stirred for 3 hr below 5°C and allowed to stand for 20 hr in a refrigerator. The crystals which separated were collected by filtration and washed with acetone, acetone-water (1 : 1), and finally acetone again. Yield, 6.4 g (65%), mp 197—198°C (sintered at 164°C). The melting point was unchanged after recrystallization from acetone. $[\alpha]_D^{16.5}$ −50.1° (*c* 3.53, methanol).

Found: C, 54.73; H, 6.54; N, 10.52%. Calcd for $C_{18}H_{25}O_7N_3$: C, 54.67; H, 6.37; N, 10.63%.

N-Benzyloxycarbonyl-L-alanyl-L-alanyl-O-chlorocarbonyl-L-serine Methyl Ester (XI). In a manner similar to that described for the preparation of II, 8.0 g (0.02 mol) of IX was converted to XI with phosgene in the presence of 2.4 g (0.02 mol) of *N,N*-dimethylaniline in 100 ml of anhydrous dioxane. Yield, 7.7 g (83%), mp 143.5—144.0°C (decomp.) after recrystallization from benzene, $[\alpha]_D^{12.5}$ −3.7° (*c* 2.72, dioxane).

Found: C, 50.34; H, 5.44; N, 9.24; Cl, 7.31%. Calcd for $C_{19}H_{24}O_8N_3Cl$: C, 49.84; H, 5.28; N, 9.18; Cl, 7.74%.

Methyl L-3-(N-Benzyloxycarbonyl-L-alanyl-L-alanyl)-2-oxo-oxazolidine-4-carboxylate (XIV). A solution of 10.0 g (0.022 mol) of XI in 130 ml of xylene was refluxed for 6 hr. The solvent was then evaporated *in vacuo*, leaving a syrup which was dissolved in 130 ml of ethyl acetate. The solution was treated with 3 ml of pyridine for 1.5 hr at room temperature under occasional shaking and then washed with dilute hydrochloric acid, a dilute aqueous sodium hydrogen carbonate solution, and water. The evaporation of the dried solution *in vacuo* provided a syrup, which was taken up with 50 ml of acetone. The decolorized solution was evaporated again to dryness *in vacuo* to give an amorphous solid. Yield, 6.2 g (67%). It gave a slightly positive Beilstein's test and exhibited a main spot, accompanied with two minor spots, upon TLC.

Alkaline Hydrolysis of XIV. In a way similar to that described for the hydrolysis of III, 4.67 g (0.011 mol) of the amorphous XIV was hydrolyzed with a mixture of 23.0 ml (0.023 mol) of 1 N potassium hydroxide and 75 ml of methanol. After the evaporation of the solvent, the residue was diluted with water and acidified with 1 N hydrochloric acid to pH 3. From the ethyl acetate extract, 1.96 g (60%) of crude *N*-benzyloxycarbonyl-L-alanyl-L-alanine were isolated, found to be contaminated with minor components upon TLC. It was purified and identified as its cyclohexylammonium salt*6 (0.73 g); mp 195—197°C (decomp.), $[\alpha]_D^{12}$ −34.7° (*c* 3.14, water).

V was isolated from the aqueous solution. Yield, 0.67 g (46%), mp 116—118°C after recrystallization from ethyl acetate-petroleum ether, $[\alpha]_D^{12}$ −17.8° (*c* 2.97, water). It was also identified as its cyclohexylammonium salt; mp 154—155°C (decomp.), $[\alpha]_D^{13.5}$ −19.8° (*c* 3.43, water).

The authors wish to express their thanks to the Ajinomoto Co., Inc., for supplying the amino acids.

*6 An authentic sample was prepared from *N*-benzyloxycarbonyl-L-alanyl-L-alanine[17] by the treatment of cyclohexylamine; mp 197—198°C (decomp.), $[\alpha]_D^{12}$ −35.0° (*c* 3.32, water). Found: C, 61.10; H, 8.00; N, 10.50%. Calcd for $C_{20}H_{31}O_5N_3$: C, 61.05; H, 7.94; N, 10.68%.

17) W. H. Stein, S. Moore and M. Bergmann, *J. Biol. Chem.*, **154**, 191 (1944).

BULLETIN OF THE CHEMICAL SOCIETY OF JAPAN VOL. 41 980—987 (1968)

Dihydroxyquinoxaline Studies. Solubility, Ionization Constant, and Chelating Behavior*[1]

Shoshichi OGUCHI

Department of Chemistry, Faculty of Education, The Tokyo Gakugei University, Koganei, Tokyo

(Received October 12, 1967)

The solubility, ionization constant, and chelating behavior of dihydroxyquinoxaline, mainly 5,8-dihydroxyquinoxaline (5,8-DHQ) derivatives, have been measured and will be discussed. The introduction of a hydroxyl group into quinoxaline greatly lowers the solubility. The order of the decreasing solubility of 2,3-disubstituted 5,8-DHQ in water (at 20°C) is: $O(CH_2)_2OC_2H_5 < H < OH < CH_3 < C_6H_5 < OC_2H_5 < Cl < SH < SC_2H_5$. For 5,8-DHQ the introduction of electron-repelling groups into 2,3-positions raises both the pK_{NH} and pK_{OH} values, while the introduction of electron-attracting groups into the same positions lowers both pK_{NH} and pK_{OH}. 5,8-DHQ and its derivatives form colored precipitates with metal ions, but some derivatives which have pK_{NH} values lower than zero fail to show any precipitation or coloration. 6,7-DHQ forms precipitate, and the precipitation colors distinctively with Cr(III) or Fe(II). The composition and stability constant (K) of copper(II) chelates of 5,8-DHQ and its derivatives in a dioxane-water (10 : 90 v/v) solution were studied spectrometrically. The copper chelate of 5,8-DHQ had a metal: ligand ratio of 1 : 1 and a log K value of 6.28 at pH 4.0. The structures of these copper chelates will be proposed.

It has been reported that 5,8-dihydroxyquinoxaline (5,8-DHQ) produces more deeply colored inner salts with many kinds of metallic ions[1] than 8-hydroxyquinoline, and that 5-hydroxyquinoxaline[2] and 5,8-DHQ[3] show a growth-inhibiting bacterial action. In this series of studies the author has attempted to find some useful knowledge about DHQ derivatives in the field of analytical chemistry and pharmaceutical science. Many derivatives of DHQ have been prepared,[4,5] and their solubility, ionization constants, and chelating behavior have been determined.

Experimental

Materials. All the reagents used in this work except 2,3,5,8-tetrahydroxyquinoxaline and 1,4-dimethyl-5,8-dimethoxy-2,3-dioxo-1,2,3,4-tetrahydroquinoxaline have been described previously[4,5] (see Table 1). Those two were prepared as follows.

2,3,5,8-Tetrahydroxyquinoxaline. A mixture of 2,3-dihydroxy-5,8-dimethoxyquinoxaline,[5] acetic acid, and hydrobromic acid (48%) was refluxed for 6 hr; then the mixture was poured into water and neutralized with aqueous ammonia. The precipitate thus formed was filtered and washed with water. The compound was hardly soluble in the organic solvents tested, even in pyridine or dimethylformamide. The compound was purified by repeated dissolutions in alkali and by reprecipitation by acetic acid. A colorless powder which does not melt below 360°C was produced. Yield, 75%.

Found: N, 14.37%. Calcd for $C_8H_6O_4N_2$: N, 14.43%.

1,4-Dimethyl-5,8-dimethoxy-2,3-dioxo-1,2,3,4-tetrahydroquinoxaline. 5,8-Dimethoxy-2,3-DHQ (1.5 g) was dissolved in a 2 N aqueous solution (60 m*l*) of sodium hydroxide and shaken with dimethyl sulfate (6 m*l*) for 2 hr. The reaction mixture was then cooled and extracted with chloroform. After the removal of the chloroform, the residue was repeatedly recrystallized from methanol. Yield, 1.1 g (65%). Colorless needles which melt at 180°C were produced. Found: C, 57.52; H, 5.38; N, 10.58%. Calcd for $C_{12}H_{14}O_4N_2$: C, 57.59; H, 5.64; N, 11.20%.

Apparatus and Procedure. Measurements of the absorbance in the visible and ultraviolet regions were made with a Hitachi EPU-2A spectrophotometer and an EPS-3T recording spectrophotometer, using quartz-stoppered cells with a light path of 10 mm.

pH Measurements were made with a Hitachi-Horiba Model P extension glass and calomel electrodes.

The first ionization constant of pK_{NH} quinoxaline derivatives, the so-called "*proton-gained* pK_a" value, was measured by the spectrometric method in a dioxane-water (10 : 90 v/v) solution in the usual manner.[6,7]

*1 Part V, Studies of Chelating Reagents Containing *N*-Heterocycles. Part IV: see Ref. 4.

1) S. Kawai, K. Kimura and T. Furuhata, *Proc. Japan Acad.*, **29**, 344 (1953).
2) S. K. Freeman and P. E. Spoerri, *J. Org. Chem.*, **16**, 438 (1951).
3) J. Adachi, *Nippon Kagaku Zassi (J. Chem. Soc. Japan, Pure Chem. Sect.)*, **76**, 311 (1955).
4) S. Oguchi, *ibid.*, **86**, 435 (1965).
5) S. Oguchi, *ibid.*, **86**, 319 (1965).
6) A. Albert and E. P. S. Serjeant, "Ionization Constants of Acids and Bases," Methuen & Co., London (1962), p. 69.
7) M. Iwazumi and H. Azumi, *Nippon Kagaku Zasshi (J. Chem. Soc. Japan, Pure Chem. Sect.)*, **84**, 694 (1963).

For the pH range from 1 to 9, a hydrochloric acid-formic acid buffer, acetate buffer, a phosphate buffer and a borax-potassium hydroxide buffer were used, in that order. For the compounds whose pK_a values lie below 1, hydrochloric acid or sulfuric acid was used and the pK_a values were calculated using the acidity function.[8,9] The first ionization constant of the pK_{OH} hydroxyl group, the so-called "*proton-lost* pK_a" value, was calculated from the data of the titration curve in a dioxane-water (50 : 50 v/v) mixture.[10,11] A mixed solvent was used because of the insolubility of DHQ in water.

The solubility in water was measured at 20±1°C spectroscopically and gravimetrically by the method Albert has reported.[12] A sample was dissolved in deoxidized water under a nitrogen stream at 100°C and left to stand at 20±1°C for one day under a nitrogen atmosphere before measurements.

Reactions with Metal Ions. The following metal ions were tested at pH 5.2 (A), 8.4 (B), and 12.4 (C) for precipitation and coloration: Mg(II), Ca(II), Cu(II), Cd(II), Hg(II), Al(III), Pb(II), Sn(II), Sn(IV), Th(IV), Zr(IV), Ce(IV), As(III), As(V), Cr(III), Mn(II), Fe(II), Fe(III), Co(II), Ni(II), Ag(I).

The degree of dissociation (α) and the stability constant (K) of chelate compounds were determined by the following formula, which was measured spectrophotometrically by the molar ratio method: $\alpha = (A_m - A_s)/A_m$, where A_m is the maximum extinction obtained from the horizontal portion of the curve and whose A_s is the extinction at the stoichiometric ratio. The stability constant, K, for a chelate compound, ML_n, was calculated by the following formula:[13,14] $K = (1-\alpha)/n^n C^n \alpha^{n+1}$, where C is the total concentration of the chelate in mol/*l*.

Results and Discussion

Solubility. The solubility of a number of quinoxaline derivatives has been determined; the results are shown in Table 1. The introduction of one hydroxyl group into quinoxaline lowers the solubility roughly 400 times. When two hydroxyl groups are introduced into quinoxaline, the solubility decreases from 1000 to 15000 times (Nos. 3—5). As Albert pointed in his study of pteridine[15] and purin series,[16,17] these decreases are probably to be attributed to unusually strong crystal lattice forces originating in the hydrogen bonding between the hydroxyl groups and the ring-nitrogen atoms of the neighbouring molecules of quinoxaline derivatives. These very hydrophilic groups in the organic molecules exert more attraction toward each other than toward water molecules. This is clearly demonstrated by the following facts. The alkoxyl derivatives or *N*-methyl derivatives of quinoxaline, which are not capable of forming hydrogen bonding, show a remarkable increase in solubility. 5-Methoxyquinoxaline is 22 times more soluble than 5-hydroxyquinoxaline (Nos. 1 and 2; see also Nos. 3 and 7, Nos. 4 and 8, and Nos. 10 and 19). *N,N'*-Dimethyl derivatives of 2,3-DHQ are 115 times more soluble than 2,3-DHQ (Nos. 5 and 31; see also Nos. 23 and 28), which exists predominantly in the diamide form in solution.[18] However, the *O*-methyl derivative (No. 9) of 2,3-DHQ (No. 5) shows an exceptionally smaller solubility than 2,3-DHQ.

Lipoid-solubilizing groups (*e.g.*, Me, Ph, Cl, OC_2H_5, and SC_2H_5) decreased the solubility of 5,8-dimethoxyquinoxaline (5,8-DMQ) and 5,8-DHQ. This phenomenon can be seen in the following compounds: Nos. 7 : 19, Nos. 3 : 10 (Me); Nos. 7 : 20, Nos. 3 : 11 (Ph); Nos. 7 : 26 Nos. 3 : 17 (Cl); Nos. 7 : 21, Nos. 3 : 12 (OC_2H_5), and Nos. 7 : 24 and Nos. 3 : 15 (SC_2H_5). The order of the decreasing solubility of 2,3-disubstituted 5,8-DHQ is: $O(CH_2)_2OC_2H_5 < H < OH < CH_3 < C_6H_5 < OC_2H_5 < Cl < SH < SC_2H_5$. Hydrophobic CH_3- and $(CH_3)_2N$- groups decrease the solubility of 5,8-DMQ, but the degree of decrease is small (Nos. 19 and 27). This phenomenon may be explained by the basicity increase of the ring nitrogen by electron-repelling groups, such as the CH_3 or $(CH_3)_2N$- group. The electron pair on the ring-nitrogen atom is able to form hydrogen bonds with water; this causes the 5, 8-DMQ to be more soluble in water than is expected from hydrophobic groups. The special insolubility of 6,7-DHQ and its derivatives may be attributed to a high crystal-lattice force between *o*-dihydroxyl groups and ring nitrogens. In harmony with this concept, 6,7-DHQ derivatives (Nos. 4, 32 and 33) do not melt below 360°C, but 6,7-DMQ and 2,3-dichloro-6, 7-DMQ (Nos. 8 and 35) melt at 151°C and 178°C respectively.

Ionization Constant. *a) pK_{NH} Value.* The results of the measurement of the pK_a values of quinoxaline and 8-hydroxyquinoline in aqueous dioxane are given in Tables 2 and 3. The pK_a values observed in a dioxane-water (10 : 90 v/v) solution are somewhat lower than those in water. This lowering effect is usually observed in mixed

8) M. A. Paul and F. A. Long, *Chem. Revs.*, **57**, 1 (1957).
9) K. N. Bascome and R. P. Bell, *J. Chem. Soc.*, **1959**, 1096.
10) A. Albert and E. P. Serjeant, "Ionization constants of Acids and Bases," Methuen & Co., London (1962), p. 16.
11) H. Freiser, R. G. Charles and W. D. Johnston, *J. Am. Chem. Soc.*, **74**, 1383 (1952).
12) A. Albert, D. J. Brown and G. Cheeseman, *J. Chem. Soc.*, **1952**, 4219.
13) T. Sakaguchi, K. Taguchi, S. Fukushima and N. Obi, *Yakugaku Zasshi*, **78**, 177 (1958).
14) Y. Kidani, *Chem. & Pharm. Bull. (Tokyo)*, **6**, 563 (1958).
15) A. Albert, D. J. Brown and G. N. H. Cheeseman, *J. Chem. Soc.*, **1951**, 474.
16) A. Albert and D. J. Brown, *ibid.*, **1954**, 2060.
17) A. Albert, "Heterocyclic Chemistry," Univ. of London Press. (Althlone), London (1959), p. 43.
18) G. W. H. Cheeseman, *J. Chem. Soc.*, **1958**, 108.

TABLE 1. SOLUBILITIES AND MELTING POINTS

No.	Quinoxaline deriv.	ml. of H_2O, which can dissolve 1g of the compd. (20°C)	Mp °C	Source*
	Quinoxaline	1.5	29—30	A
1	5-Hydroxy-	570	101—102	B
2	5-Methoxy-	25	100	C
3	5,8-Dihydroxy-	1700	237	D
4	6,7-Dihydroxy-	22100	360	E
5	2,3-Dihydroxy-	4700	360	F
6	2,3-Dimercapto-	5400	290—295(dec.)	G
7	5,8-Dimethoxy-	530	150	D
8	6,7-Dimethoxy-	2460	151	E
9	2,3-Dimethoxy-	12500	94	F
10	5,8-Dihydroxy-2,3-dimethyl-	4010	225	H
11	-2,3-diphenyl-	5900	176	I
12	-2,3-diethoxy-	12300	148	J
13	-2,3-bis(β-ethoxyethoxy)-	1280	65	J
14	-2,3-dihydroxy-	3270	360	K
15	-2,3-bis(ethylthio)-	41200	152	J
16	-2,3-dimercapto-	16800	360	L
17	-2,3-dichloro-	14300	244	C
18	-6,7-bis(ethoxycarbonyl)-	11480	149	J
19	5,8-Dimethoxy-2,3-dimethyl-	690	170	H
20	-2,3-diphenyl-	170000	227	I
21	-2,3-diethoxy-	130200	178	J
22	-2,3-bis(β-ethoxyethoxy)-	4500	114	J
23	-2,3-dihydroxy-	2400	325—329	J
24	-2,3-bis(ethylthio)-	145000	122	J
25	-2,3-dimercapto-	77000	261(dec.)	L
26	-2,3-dichloro-	24000	215	L
27	-2,3-bis(dimethylamino)-	970	117	J
28	-2,3-dioxo-1,4-dimethyl-1,2,3,4-tetrahydro-	1270	180	K
29	-2,3-bis(hydroxycarbonyl)-	670	186(dec.)	M
30	-2,3-bis(ethoxycarbonyl)-	1350	165	M
31	2,3-Dioxo-1,4-dimethyl-1,2,3,4-tetrahydro-	39	356—358	F
32	6,7-Dihydroxy-2,3-dichloro-	7500	360	L
33	-2,3-dimercapto-	8700	360	L

* Source—A: R. G. Jones and K. C. Mclaughin, "Organic Syntheses", **30**, 86 (195); B: 2); C: 19); D: 3); E: J. Ehrlich and M. T. Bogert, *J. Org. Chem.* **12**, 522 (1947); F: G. T. Newbold and F. S. Spring, *J. Chem. Soc.*, **1948**, 519; G: D. C. Morrison, A. Furst, *J. Org. Chem.* **21**, 470 (1956); H: S. Kawai, S. Tanaka and K. Ichikawa, *Nippon Kagaku Zasshi (J. Chem. Soc. Japan, Pure Chem. Sect.)*, **75**, 40 (1954); I: S. Kawai, J. Kosaka and M. Hatano, *Proc. Japan Acad.*, **30**, 774 (1954); J: 4); K: This paper; L: 5); M: S. Kawai, S. Oguchi, *et al.*, *Nippon Kagaku Zasshi (J. Chem. Soc. Japan, Pure Chem. Sect.)*, **80**, 778 (1959); N: S. Oguchi, *ibid.* **86**, 246 (1965).

TABLE 2. IONIZATION CONSTANTS (at 20°C)*1

Quinoxaline (in water)	0.60*2
(in 10 : 90 v/v dioxane-water)	0.30
8-Hydroxyquinoline	
(in water)	5.01*3
(in 10 : 90 v/v dioxane-water)	4.58
(in 50 : 50 v/v dioxane-water)	4.48*4

*1 Measured spectrometrically at ionic strength 0.1.
*2 Albert reported 0.56.[21]
*3 Albert reported 5.13.[22]
*4 Irving reported 4.48.[23]

solvents.[19,20] The values of 5-[24] and 6-hydroxyquinoxaline[22] (0.9 and 1.40 respectively; quinoxaline, 0.56[21]), which were determined in an

19) H. Irving and H. S. Rossotti, *Analyst*, **80**, 245 (1955).
20) A. Albert and E. P. Serjeant, "Ionization Constants of Acids & Bases," Methuen & Co., London (1962), p. 66.
21) A. Albert, "Physical Method in Heterocyclic Chemistry," Vol. 1, ed. by A. R. Katritzky, Academic Press, New York and London (1963), p. 76.
22) A. Albert and J. N. Phillips, *J. Chem. Soc.*, **1956**, 1294.
23) H. Irving and Mrs. H. Rossotti, *ibid.*, **1954**, 2910.
24) A. Albert and H. Hampton, *ibid.*, **1954**, 505.

TABLE 3. PHYSICAL PROPERTIES OF QUINOXALINE DERIVATIVES AND RELATED SUBSTANCES

Quinoxaline derivative	Ionization constants (at 20°C)				UV Absorption spectra	
	Proton gained pK_a (pK_{NH}) in dioxane-H_2O(10 : 90 v/v)*1	(mμ)*2	Proton lost pK_a (pK_{OH}) in dioxane-H_2O(50 : 50 v/v)*3	concn. (M)*4	Solvent	λ_{max}, mμ($\log_{10}\varepsilon$)
Quinoxaline	0.60(in H_2O)	334	—	—	EtOH	240(4.50), 325(3.80)*6
	0.30	332	—	—		
5-Hydroxy	0.9 (in H_2O)*5	—	9.29(in H_2O)*5	—	H_2O	251(4.37), 320(3.32)
5-Methoxy	—	—	—	—	H_2O	250(4.37), 324(3.39)
5,8-Dihydroxy	0.61	280	10.82	0.01	EtOH	265(4.50), 320(3.15) 402(3.09)
5,8-Dimethoxy	0.30	282	—	—	EtOH	263(4.56), 314(3.86) 399(3.42), 490(3.18)
6,7-Dihydroxy	0.89	380	—	—	H_2O	354(3.98)
5,8-Dihydroxy-2,3-dimethyl	1.65	284	11.36	0.01	EtOH	269(4.54), 377(3.09)
5,8-Dimethoxy-2,3-dimethyl	1.27	285	—	—	EtOH	265(4.57), 303(3.47) 365(3.25)
5,8-Dihydroxy-2,3-diphenyl	0.46	280	10.97	0.01	EtOH	260(4.27), 303(4.40) 360(3.51)
5,8-Dimethoxy-2,3-diphenyl	—	—	—	—	EtOH	262(4.21), 302(4.40) 345(3.62)
5,8-Dihydroxy-2,3-diethoxy	−1.88	275	10.04	0.01	Dioxane	237(3.85), 270(4.42) 315(3.56)
					EtOH	275(4.44)
5,8-Dimethoxy-2,3-diethoxy	−1.44	267	—	—	EtOH	265(4.50), 315(3.70)
2,3-Bis(β-ethoxyethoxy)-5,8-dihydroxy	−1.70	270	10.77	0.01	EtOH	275(4.51), 310(3.78)
2,3-Bis(β-ethoxyethoxy)-5,8-dimethoxy	−1.73	266	—	—	EtOH	265(4.50), 315(3.85)
2,3-Bis(ethylthio)-5,8-dihydroxy	−1.43	300	11.14	0.01	EtOH	304(4.55), 367(3.90)
2,3-Bis(ethylthio)-5,8-dimethoxy	−1.45	293	—	—	EtOH	223(4.43), 295(4.53) 414(2.80)
2,3-Bis(dimethylamino)-5,8-dimethoxy	1.93	387	—	—	Dioxane	290(4.42), 370(4.02)
2,3-Dichloro-5,8-dihydroxy	—	—	9.66	0.01	EtOH	279(4.13), 420(3.09)
2,3-Dichloro-5,8-dimethoxy	—	—	—	—	EtOH	279(4.61), 331(3.22) 397(3.20)
2,3-Bis(ethoxycarbonyl)-5,8-dimethoxy	—	—	—	—	EtOH	281(4.62), 342(3.21) 416(3.18)
2,3-Bis(ethoxycarbonyl)-6,7-dimethoxy	—	—	—	—	EtOH	227(4.43), 262(4.56) 365(4.20)
6,7-Bis(ethoxycarbonyl)-5,8-dihydroxy	0.62	280	9.28	0.01	EtOH	280(4.45), 340(3.45) 355(3.45)
2,3,5,8-Tetrahydroxy	1.66	279	—	—	EtOH	230(3.90), 238(3.66) 247(3.66), 285(4.01) 315(3.57), 440(2.24)
5,8-Dihydroxy-2,3-dimercapto	—	—	—	—	EtOH	317(3.81), 398(3.46)
2,3-Dimercapto-5,8-dimethoxy	—	—	—	—	EtOH	243(4.28), 309(4.30) 437(4.09)
6,7-dihydroxy-2,3-dimercapto	—	—	—	—	EtOH	275(4.51), 407(4.25)
6,7-Dimethoxy-2,3-dimercapto	−0.93	395	—	—	EtOH	239(4.32), 390(3.97)

*1 Measured spectrometrically. *2 Analytical wavelength *3 Measured potentiometrically at ionic strength 0.2. *4 Concentration of the substance. *5 Cited from Ref. 24.
*6 Cited from *J. Chem. Soc.*, **1956**, 123.

Table 4. Reactions with metal ions and ionization constants of 5,8-dihydroxyquinoxaline

Ligand	X=H Y=H	X=H Y=$COOC_2H_5$	X=CH_3 Y=H	X=OH Y=H	X=C_6H_5 Y=H	X=SC_2H_5 Y=H	X=$O(CH_2)_2OC_2H_5$ Y=H	X=OC_2H_5 Y=H	X=Cl Y=H
Metal formed precipitate in the buffer solution A, B, C*	Zn(II): C Fe(II): C Fe(III): A, B, C Ni(II): C Pb(II): C Cu(II): A, B, C	Fe(II): A Fe(III): A Cd(II): C Ni(II): B, C Mn(II): B, C Pb(II): A, B Th(IV): B, C Cu(II): A, B, C	Zn(II): C Co(II): C Fe(III): C Pb(II): C Cu(II): A	Zn(II): A, B Cd(II): C Fe(II): A Ni(II): B, C Cr(III): C Al(III): C Hg(II): A, B, C Ce(IV): C Cu(II): A, B Ag(I): B, C	Zn(II): C Cd(II): C Fe(II): C Co(II): C Pb(II): C Cu(II): A, B	Non	Non	Non	Non
pK_{NH}(20°C)	0.61	0.62	1.65	1.66	0.46	−1.43	−1.70	−1.88	—
pK_{OH}(20°C)	10.82	9.28	11.36	—	10.97	11.14	10.77	10.04	9.66

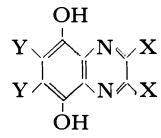

* A, B and C indicate precipitaion under pH 5.2, 8.4, 12.4 buffer solution, respectively. Three drops of buffer solution, one drop of metal ion solution (1000γ/ml) and one drop of 0.025—0.005M of reagent solution in ethanol.

aqueous solution by Albert, show that the hydroxyl groups in the phenyl nucleus of quinoxaline has some electron-repelling effect; this effect also exists in 5,8-DHQ (0.61) and 6,7-DHQ (0.89) and their *O*-methyl derivatives (Table 3). From Table 3 it can also be seen that the base-strengthening effect of the methoxyl group is somewhat weaker than that of the hydroxyl group. It has been reported[18] that the pK_a values of 2-methoxyquinoxaline (0.28 in water) and 2,3- DMQ (−1.15 in water) are considerably smaller than that of quinoxaline (0.56 in water); this fact suggests that the inductive effect is more effective than the mesomeric effect at 2 and/or 3 positions of quinoxaline. Similar effects are observed in the following compounds: 2,3-diethoxy-, 2,3-bis(ethoxyethoxy)- and 2,3-bis(ethylthio)-substituents of 5,8-DHQ and 5,8-DMQ. The pK_a values of the 2, 3-DHQ derivatives can be expected to be the same as that of 2-hydroxyquinoxaline because of their same partial structures. However, their pK_a values could not be determined by the spectrometric method, because their spectra did not change with the pH of medium as in the case of 2,3-DHQ. Electron-repelling substituents, such as methyl and dimethylamino groups, in the 2,3-position raise the pK_a values of 5,8-DHQ and 5,8-DMQ. Phenyl groups in the same positions lower the pK_a value. In 2,3-dichloro-5,8-DHQ, chlorine atoms are expected to have a base-weakening effect. However, its pK_a value could not be determined by the spectrometric method. The introduction of the alkoxycarbonyl group into the 6,7-positions of 5,8-DHQ induces hardly any appreciable effect on the pK_{NH} value.

b) pK_{OH} Value. By comparing the pK_a value of the 8-hydroxyquinoline anion (in dioxane-water 50 : 50 v/v, 10.80) with 5-hydroxyquinoxaline (9.29 in dioxane-water 50 : 50 v/v,)[23] the lowering effect of the pK_a value upon the further introduction of ring nitrogen may be seen. On the contrary, the further introduction of the hydroxyl group into the 8-position of 5-hydroxyquinoxaline raises the pK_a value (by an acid-weakening effect) (Table 3). The introduction of electron repelling substituents such as the methyl group into the 2,3-positions of 5,8-DHQ raises the pK_{OH} value (11.36), while the introduction of electron-attracting substituents, such as ethoxy and chloro groups, into the same positions, or that of the ethoxycarbonyl group into the 6,7-positions, lowers the pK_{OH} value (10.04, 9.66, and 9.28 respectively).

Chelating Behavior with Metal Ions. Reactions with metal ions are shown in Table 4. 5,8-DHQ and its derivatives formed a colorful precipitate, but some 2,3-disubstituted 5,8-DHQ failed to show any precipitation or coloration with metal ions in the buffer solution tested. Table 4 also shows the metal chelates and pK_{NH} and pK_{OH} values of 5,8-DHQ and its derivatives. According to Irving,[16] a linear relationship between $\log\beta$ (β: stability constant of the metal chelate) and the pK_{OH} of ligand exists for the chelate formation of 8-hydroxyquinoline and related compounds. Form Table 4, it is found that a close relationship exists between the precipitation of the meatl chelate of 5,8-DHQ derivatives and the pK_{NH} value of the ligand, but the pK_{OH} value has not special relation with the precipitation of the chelate. The basicity of a precipitate-forming ligand is higher than that of a ligand which does not form any precipitate. The limit of the value of pK_{NH} for causing the precipitation and coloration of chelates of 5,8-DHQ derivatives seems to lie near 0 — −1 (obtained in dioxane-water, 50 : 50 v/v).

2,3-DHQ and its 5,8- or 6,7-dimethoxy-derivatives fail to show any precipitation or coloration with metal ions. 6,7-DHQ, however, gives a distinct coloration and precipitations with Fe(II) and Cr(III) like catechol.[25,26] It is interesting to note that 2,3,5,8-tetrahydroxyquinoxaline can form precipitates with a larger number of metals (Table 4).

Kawai *et al.*[27] reported that the composition of copper chelates of 5,8-DHQ was not in accord with the molar ratio of metal : ligand=1 : 1, whose ratio was based on the assumed structure of Fig. 1.

Though 5,8-DHQ and its derivatives give precipitates with copper salt in an aqueous solution, in aqueous dioxane the copper chelates were kept in a colloidal solution. The composition of the copper chelate of 5,8-DHQ in a dioxane-water (10 : 90 v/v) solution was measured by the following two methods:

(1) Job's Continuous Variation Method: Fig. 3. The composition of the chelate was determined to be 1 : 1 (reagent : copper) at pH 4; 400 mμ.

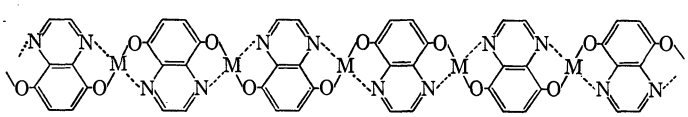

Fig. 1.

25) R. E. D. Clark and R. G. Nevile, *Chem. Educ.*, **36**, 390 (1959).
26) F. P. Dwyer and D. P. Mellor, "Chelating Agents and Metal Chelates," Academic Press, New York (1964), p. 106.
27) S. Kawai, H. Hamaguchi and M. Tatsumoto, *Bunseki Kagaku (Japan Analyst)*, **5**, 165 (1956).

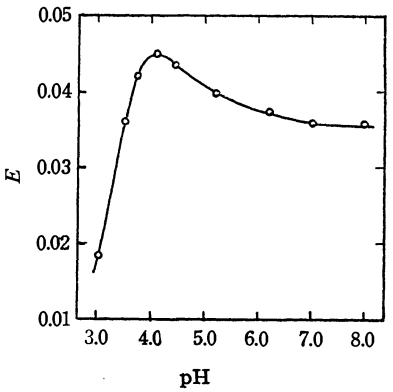

Fig. 2. Effect of pH on the absorbance of copper chelate of 5,8-DHQ. at 500mμ. Concn. of 5,8-DHQ: 2×10^{-4} M/l

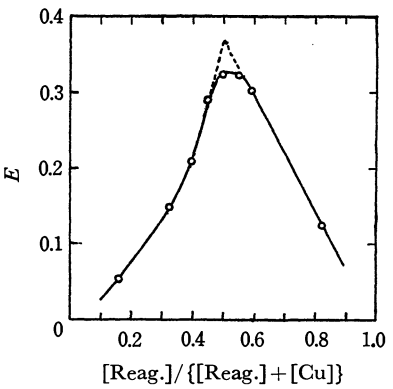

Fig. 3. Absorption curve of copper chelate of 5,8-DHQ (Continuous variation method).
Total concn.: 2.5×10^{-4} M/l, μ=0.1, pH 4.0 at 500 mμ

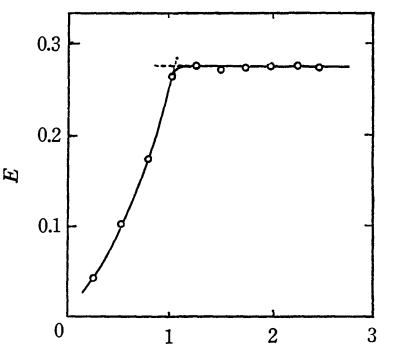

Fig. 4. Absorption curve of copper chelate of 5,8-DHQ (Molar ratio method).
Concn. of copper: 2×10^{-4} M/l, μ=0.1, pH 4.0 at 500 mμ

(2) Molar Ratio Method: Fig. 4. The composition of the chelate was found to be 1 : 1 (reagent : copper) at pH 4: 400 mμ.

By the same procedures, the compositions of

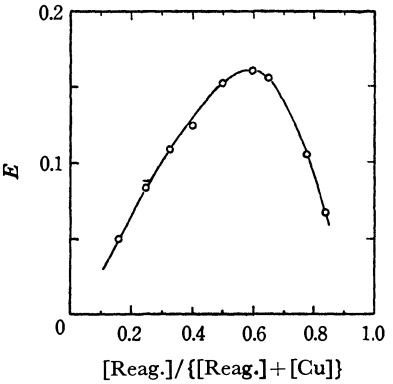

Fig. 5. Absorption curve of copper chelate of 6,7-bis(ethoxycarbonyl)-5,8-DHQ (Continuous variation method).
Total concn.: 2.5×10^{-4} M/l, μ=0.1, pH 6.2 at 625 mμ

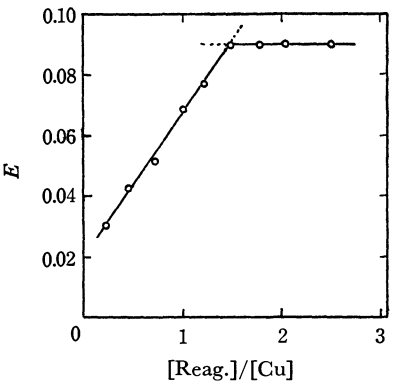

Fig. 6. Absorption curve of copper chelate of 6,7-bis(ethoxycarbonyl)-5,8-DHQ (Molar ratio method)
Concn. of copper : 1×10^{-4}M/l, μ=0.1, pH 6.2 at 625 mμ

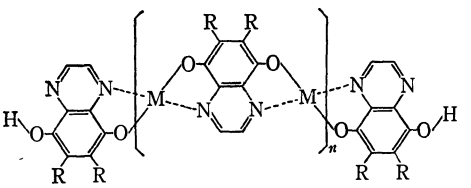

Fig. 7. R=H, 5,8-DHQ Cu chelate
R=$COOC_2H_5$, 2,3-Bis(ethoxycarbonyl)-5,8-DHQ Cu chelate n=1

TABLE 5. COMPOSITION, DEGREE OF DISSOCIATION (α) AND STABILITY CONSTANT (K) OF COPPER CHELATES OF 5,8-DHQ

Ligand	Composition Cu : Ligand	α	log K	pH
5,8-DHQ	1 : 1	0.05	6.28	4.0
6,7-Bis(ethoxy-carbonyl)-5,8-DHQ	2 : 3	0.01	10.73	6.2
2,3-Dimethyl-5,8-DHQ	could not be obtained			

the copper chelates of 5,8-DHQ derivatives were measured (Figs. 5 and 6). The compositions, the degrees of dissociation (α), and the stability constants (K) of the copper chelates calculated are shown in Table 5. The composition of the copper chelate of 2,3-dimethyl-5,8-DHQ could not be obtained by these procedures, however, because the absorbance of the mixed solution of cupric ions and the ligand varied rapidly and the precipitates separated.

From these chelate compositions (Table 5), the structures of chelates may be represented as in Fig. 7.

The author wishes to express his deep thanks to Professor Sin'iti Kawai and Professor Noboru Sugiyama for their encouragement and support. Grateful acknowledgement is also made to Professor Jisuke Seki for his helpful advice.

BULLETIN OF THE CHEMICAL SOCIETY OF JAPAN VOL. 41 987—992 (1968)

Reaction Rates in Binary Mixed Solvents. IV[1)]

Yasuhiko KONDO, Yoshitoshi HONJO and Niichiro TOKURA

Department of Applied Chemistry, Faculty of Engineering, Osaka University, Higashinoda, Miyakojima-ku, Osaka

(Received October 18, 1967)

Three cases of combinations of the solvation free-energy differences in two solvents, with respect to a reactant and an activated complex, have been proposed. The theoretical expressions for the rate constant and for the activation energy in binary mixed solvents have been derived for each model. From the theoretical calculations based on these models, it has been demonstrated that the behavior of a system in which the reaction rates are mainly dependent on the difference in the solvation energies of an activated complex can be distinguished from behavior of a system where the reaction rates are controlled by the difference in the solvation energies of a reactant. The reaction rates of the Menschutkin reaction in binary mixed solvents containing liquid sulfur dioxide as one component of the mixed solvent have been analyzed on the basis of these models.

According to the theory of the absolute reaction rates,[2)] a rate constant is expressed as the difference in the free energies between reactants and activated complexes. Therefore, the rate constants in a solution would be affected not only by the individual solvation of the reactants or an activated complex, but also by the combinations of these factors in several ways. In the theoretical treatment of the effects of solvents on reaction rates, these facts should be taken into consideration.

Some of the factors which influence the rates of a reaction in solution might be made clear by an analysis of the rate constants measured in pure solvents, but the study of other factors might have to depend on investigations of the rate constants measured in mixed solvents.

In previous studies[1)] the present authors have reported the theoretical treatment of the reaction rates in binary mixed solvents.

In this paper we will discuss theoretically what information can be obtained on the solvation of a solute from an analysis of the reaction rates measured in binary mixed solvents.

Discussion

The Model of a Solvation and Reaction Rates in Solution. The effects of solvents on the rates of a reaction in solution can be replaced by the dependence of the activation free energies on the nature of a solvent. If the influence of a solvent on the reaction rates in solution is assumed to be caused by its influence on the solvation of reactants and an activated complex, then the following combinations of the solvation free-energy differences (Fig. 1) can be considered as factors which make the reaction rates different in two solvents; the solvent in which the reaction proceeds more rapidly is expressed by the subscript 1. $\Delta F_4^{\neq}$ and $\Delta F_1^{\neq}$ stand for the activation free energy in the solvents 4 and 1 respectively.

Model I represents a system in which both a reactant and an activated complex are more solvated in the solvent 1 than in the solvent 4.

Model II is a system where an activated complex is more solvated in the solvent 1, while a reactant is more solvated in the solvent 4.

Model III stands for a system where both a

1) Part III: Y. Kondo and N. Tokura, This Bulletin, **40**, 1438 (1967).

2) S. Glasstone *et al.*, "The Theory of Rate Processes," McGraw-Hill Book Company, New York (1941).

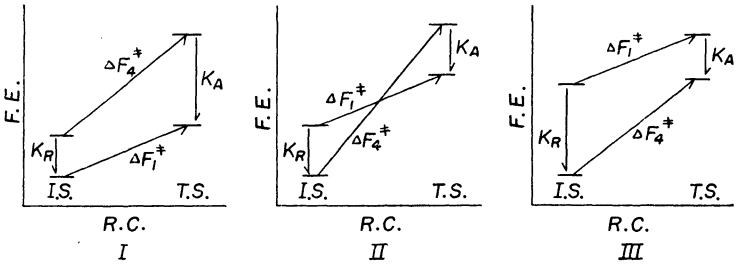

Fig. 1. The model of a solvation.

reactant and an activated complex are more solvated in the solvent 4 than in the solvent 1.

Any combination of the two solvents in which the rates of the same reaction are differentiated from each other should correspond to one of the three solvation models represented in Fig. 1.

Now, let us consider what variations should be introduced into the theoretical expressions for the rate constants and the activation energies in binary mixed solvents according to the solvation models presented above.

In previous papers[1] the authors have represented a system in which there are no specific interactions among the components by the construction of a regular solution, and have assumed the formation of an addition product as the model for a system in which attractive interactions are observed between the components. With the object of applying the above models to the three models mentioned previously, the following two assumptions will be made hereafter: 1) A system in which no specific interactions can be observed among the components constructs a regular solution, and 2) In the systems where a substantial difference in the solvation energies of a solute exists between the two solvents, we assume that the solute reacts to form an addition product with the solvent having the stronger solvating power, whereas the solute forms a regular solution with the other solvent, with the weaker solvating power.

Insofar as the above assumptions are adopted, the theoretical expressions for the rate constants and the activation energies in binary mixed solvents can be derived from suitable combinations of the expressions for Henry's constant in a regular solution and in an associated solution for all of the three models described previously.

The theoretical expressions for Henry's constant in binary mixed solvents and the relations between Henry's constants in pure solvents may be summarized as follows.

Shown below is a system in which the solute 2 constructs a regular solution with both of the two solvents, 1 and 4:[3]

$$\ln H_{2,\mathrm{mix}} = x_1 \ln H_{2,1} + x_4 \ln H_{2,4} - x_1 x_4 \alpha_{14} \quad (1)$$

$$(H_{2,1}/H_{2,4}) = \exp(\alpha_{21} - \alpha_{24}) \quad (2)$$

Shown below is a system in which the solute 2 reacts to form an addition product with the solvent 1, whereas it constructs a regular solution with the solvent 4:[1]

$$\ln H_{2,\mathrm{mix}} = x_1 \ln H_{2,1} + x_4 \ln H_{2,4} + x_1 \ln(K+1) - \ln(x_1 K + 1) - x_1 x_4 \alpha_{14} \quad (3)$$

$$(H_{2,1}/H_{2,4}) = \frac{1}{(K+1)} \exp(-\alpha_{24}) \quad (4)$$

Shown below is a system in which the solute 2 reacts to form an addition product with the solvent 4, whereas it constructs a regular solution with the solvent 1:

$$\ln H_{2,\mathrm{mix}} = x_1 \ln H_{2,1} + x_4 \ln H_{2,4} + x_4 \ln(K+1) - \ln(x_4 K + 1) - x_1 x_4 \alpha_{14} \quad (5)$$

$$(H_{2,4}/H_{2,1}) = \frac{1}{(K+1)} \exp(-\alpha_{21}) \quad (6)$$

The Theoretical Expressions for the Reaction Rate in Binary Mixed Solvents. In this paper the theoretical expressions will be derived for the general second-order reaction:

$$\mathrm{A} + \mathrm{B} \rightarrow \mathrm{M}^* \rightarrow \mathrm{Products}$$

For the sake of simplicity, the reactant A will be assumed to construct a regular solution with both of the two solvents, 1 and 4.

According to previous discussions,[1] the rate constant in a binary mixed solvent and the ratio of the rate constant in two sorts of pure solvents are expressed by Eqs. (7) and (8) respectively:

$$k_{\mathrm{mix}} = k_0 \left(\frac{H_{\mathrm{A,mix}} \times H_{\mathrm{B,mix}}}{H_{\mathrm{M}^*,\mathrm{mix}}}\right)\left(\frac{V_{\mathrm{mix}}}{RT}\right) \quad (7)$$

$$(k_1/k_4) = \left(\frac{H_{\mathrm{A},1}}{H_{\mathrm{A},4}}\right)\left(\frac{H_{\mathrm{B},1}}{H_{\mathrm{B},4}}\right)\left(\frac{H_{\mathrm{M}^*,4}}{H_{\mathrm{M}^*,1}}\right)\left(\frac{V_1}{V_4}\right) \quad (8)$$

Model I. Since, in this system, both a reactant and an activated complex are more solvated in the solvent 1, we assume that both the reactant B and an activated complex react to form addition products with the solvent 1.

The theoretical expression for the rate constant in a binary mixed solvent can then be derived by the substitution of Eq. (3) into Henry's constants of the solutes B and M* in Eq. (7).

3) J. P. O'Connell and J. M. Prausnitz, *Ind. & Eng. Chem. Fundamentals*, **3**, 347 (1964).

Accordingly, Eqs. (1) and (2) will be used for a solute, A, in all the equations.

$$\ln k_{mix} = x_1 \ln k_1 + x_4 \ln k_4 + \left\{x_1 \ln\left(\frac{K_R+1}{K_A+1}\right) - \ln\left(\frac{x_1K_R+1}{x_1K_A+1}\right) - x_1x_4\alpha_{14}\right\} + \ln V_{mix} - x_1 \ln V_1 - x_4 \ln V_4 \quad (9)$$

In Eq. (9), K_R and K_A stand for the equilibrium constants of a reactant and an activated complex respectively, when they form addition products with a particular solvent.

The ratio of the rate constant, (k_1/k_4), is given by the substitution of Eq. (4) into Henry's constants of solutes, B and M$^{\neq}$ in Eq. (8):

$$(k_1/k_4) = \exp(\alpha_{A1} - \alpha_{A4}) \times \exp(\alpha_{M^{\neq}4} - \alpha_{B4}) \times \left(\frac{K_A+1}{K_R+1}\right)\left(\frac{V_1}{V_4}\right) \quad (10)$$

The expressions for an activation energy are given by the differentiation of Eqs. (9) and (10) with respect to the temperature:

$$\Delta E^{\neq}_{mix} = x_1\Delta E_1^{\neq} + x_4\Delta E_4^{\neq} - x_1x_4\left\{\frac{\Delta H^\circ_R}{(1+1/K_R)(x_1+1/K_R)} - \frac{\Delta H^\circ_A}{(1+1/K_A)(x_1+1/K_A)}\right\} \quad (11)$$

$$(\Delta E_1^{\neq} - \Delta E_4^{\neq}) = \left\{\frac{\Delta H^\circ_A}{(1+1/K_A)} - \frac{\Delta H^\circ_R}{(1+1/K_R)}\right\} \quad (12)$$

where ΔH°_R and ΔH°_A stand for the enthalpy change of a reactant and an activated complex respectively, accompanied by the formation of addition products with a particular solvent.

Model II. Since an activated complex is more solvated in the solvent 1, while a reactant is more solvated in the solvent 4, we assume that an activated complex forms an addition product with the solvent 1 and that the reactant B forms an addition product with the solvent 4.

Thus, the theoretical expression for a rate constant is given by the substitution of Eqs. (3) and (5) for Henry's constants of an activated complex and the reactant B in Eq. (7):

$$\ln k_{mix} = x_1 \ln k_1 + x_4 \ln k_4 + \{x_4 \ln(K_R+1) - \ln(x_4K_R+1) - x_1 \ln(K_A+1) + \ln(x_1K_A+1) - x_1x_4\alpha_{14}\} + \ln V_{mix} - x_1 \ln V_1 - x_4 \ln V_4 \quad (13)$$

The ratio of the rate constant is given by the combination of Eqs. (2), (4), (6), and (8) as follows:

$$(k_1/k_4) = \exp(\alpha_{A1} - \alpha_{A4}) \times \exp(\alpha_{B1} + \alpha_{M^{\neq}4}) \times (K_A+1)(K_R+1)\left(\frac{V_1}{V_4}\right) \quad (14)$$

The expressions for an activation energy are given by the differentiation of Eqs. (13) and (14) with respect to the temperature:

$$\Delta E^{\neq}_{mix} = x_1\Delta E_1^{\neq} + x_4\Delta E_4^{\neq} + x_1x_4\left\{\frac{\Delta H^\circ_A}{(1+1/K_A)(x_1+1/K_A)} - \frac{\Delta H^\circ_R}{(1+1/K_R)(x_4+1/K_R)}\right\} \quad (15)$$

$$(\Delta E_1^{\neq} - \Delta E_4^{\neq}) = \left\{\frac{\Delta H^\circ_R}{(1+1/K_R)} + \frac{\Delta H_A^\circ}{(1+1/K_A)}\right\} \quad (16)$$

Model III. Since both a reactant and an activated complex are more solvated in the solvent 4, we assume that both the reactant B and an activated complex form addition products with the solvent 4.

The theoretical expressions for a rate constant and for the ratio of rate constants are given by combinations of Eqs. (1), (5), and (7) and of Eqs. (2), (6), and (8), respectively:

$$\ln k_{mix} = x_1 \ln k_1 + x_4 \ln k_4 + \left\{x_4 \ln\left(\frac{K_R+1}{K_A+1}\right) - \ln\left(\frac{x_4K_R+1}{x_4K_A+1}\right) - x_1x_4\alpha_{14}\right\} + \ln V_{mix} - x_1 \ln V_1 - x_4 \ln V_4 \quad (17)$$

$$(k_1/k_4) = \exp(\alpha_{A1} - \alpha_{A4}) \times \exp(\alpha_{B1} - \alpha_{M^{\neq}1}) \times \left(\frac{K_R+1}{K_A+1}\right)\left(\frac{V_1}{V_4}\right) \quad (18)$$

The expressions for an activation energy are given by the differentiation of Eqs. (17) and (18) with respect to the temperature:

$$\Delta E^{\neq}_{mix} = x_1\Delta E_1^{\neq} + x_4E_4^{\neq} + x_1x_4\left\{\frac{\Delta H^\circ_A}{(1+1/K_A)(x_4+1/K_A)} - \frac{\Delta H_R^\circ}{(1+1/K_R)(x_4+1/K_R)}\right\} \quad (19)$$

$$(\Delta E_1^{\neq} - \Delta E_4^{\neq}) = \left\{\frac{\Delta H^\circ_R}{(1+1/K_R)} - \frac{\Delta H^\circ_A}{(1+1/K_A)}\right\} \quad (20)$$

Since in the three sorts of combination the solvation of an activated complex and that of a reactant are taken into consideration at the same time, in the theoretical expressions for the rate constants, as well as those for the activation energies, there exist two sorts of parameters, which represent the solvations of a reactant and of an activated complex, *i. e.*, K_R and K_A for the rate constants, ΔH°_R and ΔH°_A, for the activation energies. However, these two parameters are related to one another by the theoretical expressions for the ratio of the rate constant, (k_1/k_4), or by those for the difference in the activation energies in pure solvents, $(\Delta E_1^{\neq} - \Delta E_4^{\neq})$.

Thus, there exists only one independent variable for the rate constant and for the activation energy

in binary mixed solvents. In order to compare the characteristics of these models, calculations have been made for the system where $(k_1/k_4)=100$, $(\Delta E_1^{\neq}-\Delta E_4^{\neq})=(-6.0)$ [kcal·mol^{-1}], $V_1=V_4=V_{mix}$, and all the interaction coefficients, α_{ij}, are zero. The results are shown in Figs. 2 and 3, while the parameters used in the calculations are summarized in Table 1.

In the limiting case of $K_R=0$, both the differences in the rate constants and in the activation energies in pure solvents should be dependent on the difference between the two solvents in the solvation of an activated complex.

Therefore, in this case the differences between the I and II models should vanish.

In the model I the curves approach Curve 3 in the order of 1→2→3, while in the model II they do so in the order of 5→4→3, as the values of K_R and $(-\Delta H_R^\circ)$ approach zero.

Similarly, in the limiting case of $K_A=0$, the influences of the solvents on the reaction rates in solution should be attributed to the differences between the two solvents in the solvation of a reactant.

Therefore, the differences between the models II and III should disappear. Then, in the model II the curves approach curve 9 in the order of 7→8→9, while in the model III they do so in the order of 11→10→9, as the values of K_A and $(-\Delta H^\circ_A)$ approach zero.

Curve 6 represents a system where $K_A=K_R$, and $\Delta H^\circ_A=\Delta H^\circ_R$. This is a system in which the solvation of an activated complex makes an contribution equivalent to that of a reactant to the

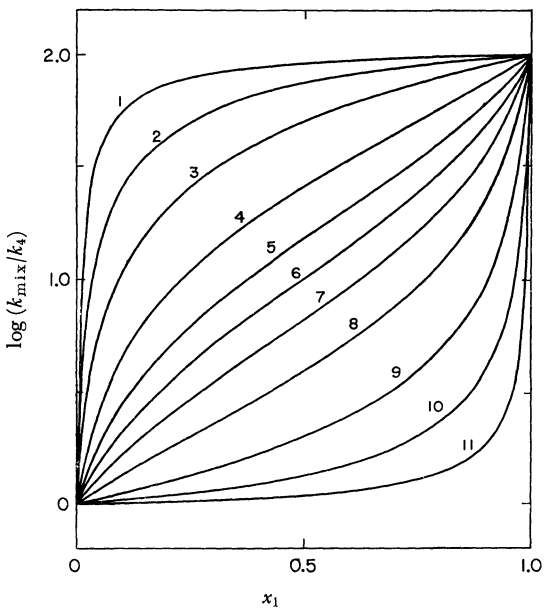

Fig. 2. The calculated values of $\log(k_{mix}/k_4)$ as a function of x_1.

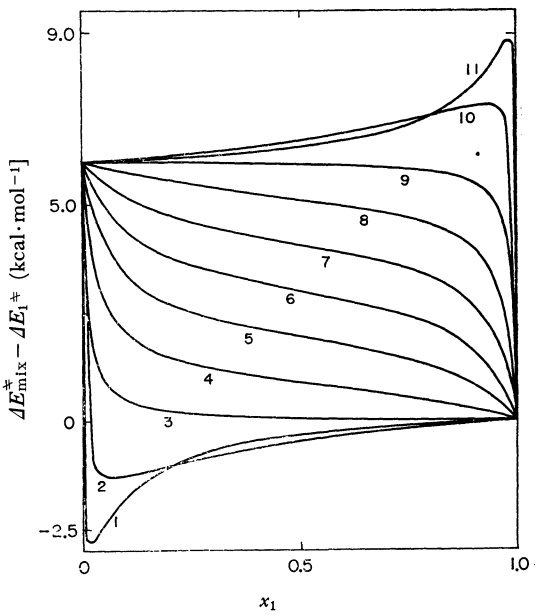

Fig. 3. The calculated values of $(\Delta E^{\neq}_{mix}-\Delta E_1^{\neq})$ as a function of x_1.

TABLE 1. THE PARAMETERS USED IN THE CALCULATIONS
$(k_1/k_4)=100$, $(\Delta E_1^{\neq}-\Delta E_4^{\neq})=(-6.0)$ [kcal·mol]

No.	The Model	K_A	K_R	$\Delta H^\circ_A/(1+1/K_A)$	$\Delta H^\circ_R/(1+1/K_R)$
1	I	1099	10.0	−10.0	−4.0
2	I	299	2.0	−8.0	−2.0
3	I or II	99	0	−6.0	0
4	II	32.33	2.0	−5.0	−1.0
5	II	15.66	5.0	−4.0	−2.0
6	II	9.0	9.0	−3.0	−3.0
7	II	5.0	15.66	−2.0	−4.0
8	II	2.0	32.33	−1.0	−5.0
9	II or III	0	99	0	−6.0
10	III	2.0	299	−2.0	−8.0
11	III	10.0	1099	−4.0	−10.0

The dimensions, ΔH°_A and ΔH°_R: [kcal·mol]

differences in the rate constants and the activation energies between the two solvents.

As the solvation of an activated complex exceeds that of a reactant in the contribution to the reaction rate, the positive deviation from linearity increases in the rate constants, while the negative deviation from linearity increases in the activation energies *i. e.*, in the order of 6→5→4. In contrast, as the solvation of a reactant exceeds that of an activated complex, the negative deviation from linearity increases in the rate constant, while the positive deviation from linearity increases in the activation energies, *i. e.*, in the order of 6→7→8.

In principle, it should be possible to determine, from the analysis of the reaction rates in binary mixed solvents, whether the differences in the rate constants and in the activation energies are due to the differences in the solvation of an activated complex or in the solvation of a reactant.

Comparison of the Theory with the Experimental Results. In previous papers[1,4] the

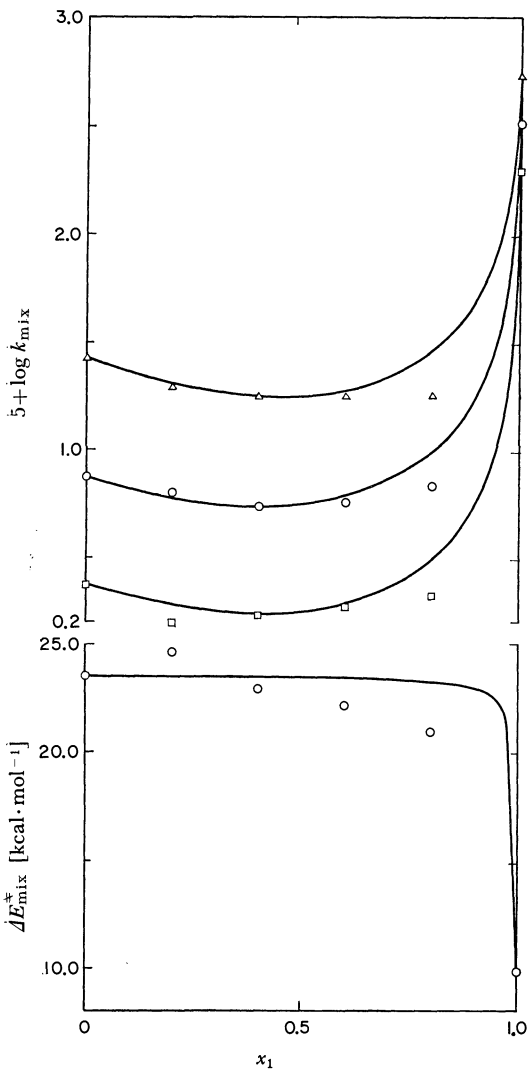

Fig. 4. Dependence of $\log k_{mix}$ and $\Delta E^{\neq}_{mix}$ for the reaction of triethylamine with methyl iodide in liq. SO_2 - benzene mixture upon mole fraction of benzene (x_1).
K_R=357, 30°C; K_R=186, 40°C; K_R=106, 50°C
α_{14}=0.973 (refered to the value for liq. SO_2-isoprene mixture[5])
□ (30°C), ○ (40°C), △ (50°C): experimental results, ——: calculated results based on model 9.

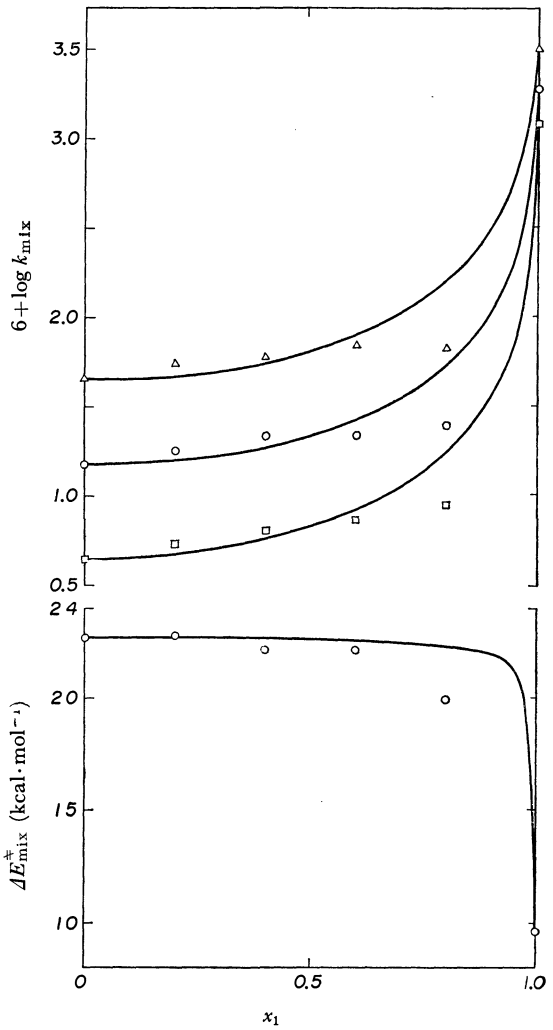

Fig. 5. Dependence of $\log k_{mix}$ and $\Delta E^{\neq}_{mix}$ for the reaction of dimethylbenzylamine with methyl iodide in liq. SO_2 - toluene mixture upon mole fraction of toluene (x_1).
K_R=287, 30°C; K_R=148, 40°C; K_R=80.2, 50°C
α_{14}=0.973 (refered to the value for liq. SO_2-isoprene mixture[5])
□ (30°C), ○ (40°C), △ (50°C): experimental results, ——: calculated results based on model 9.

4) Y. Kondo and N. Tokura, This Bulletin, **37**, 1148 (1964).
5) P. B. Ayscough, K. J. Ivin and J. H. O'Donnell, *Trans. Faraday Soc.*, **61**, 1601 (1965).

present authors have reported that, in most cases, positive deviations from linearity have been observed in the plots of $\log k_{mix}$ *vs.* the composition of a solvent, and that these positive deviations from linearity should correspond to a significant specific solvation of an activated complex due to a more polar solvent.

According to the models proposed by the present authors, large negative deviations from linearity should be observed in systems where there exists a significant specific solvation of a reactant due to a less polar solvent.

The experimental results of the Menschutkin reaction in mixtures of liquid sulfur dioxide and aromatic solvents are shown in Figs. 4 and 5.

These results can be explained semiquantitatively by Model No. 9 in Table 1, as shown by the smooth curves of Figs. 4 and 5. Since, in that model, only the interaction between a reactant and liquid sulfur dioxide has been taken into consideration, only one parameter, that is, K_R, can be determined from the analysis of the experimental results.

It has been suggested by two of the present authors[6] that the rate of the Menschutkin reaction in liquid sulfur dioxide is mainly dependent on the specific solvation of amines by liquid sulfur dioxide. The semiquantitative agreement of the experimental results in binary mixed solvents with the calculated results based on Model No. 9 would then be reasonable, since in that model the specific interaction between a reactant and liquid sulfur dioxide is emphasized as the main source of the effects of the solvent on reaction rates.

6) N. Tokura and Y. Kondo, This Bulletin, **37**, 133 (1964).

BULLETIN OF THE CHEMICAL SOCIETY OF JAPAN VOL. 41 992—996 (1968)

Solvent Effect under High Pressure. II[1]

Yasuhiko KONDO, Miyoji UCHIDA and Niichiro TOKURA

Department of Applied Chemistry, Faculty of Engineering, Osaka University, Higashinoda, Miyakojima-ku, Osaka

(Received October 19, 1967)

The activation volume of the reaction of triethylamine with ethyl iodide has been measured in four solvents. A linear relationship has been observed between the values of $\Delta V_0^{\neq}$ for the Menschutkin reaction in various solvents and the products of the compressibility and the molar volume of the pure solvent, as has been suggested in a previous paper. From the slope of the plots of $(-\Delta V_0^{\neq})$ *vs.* KV°, the product of the solvation number and the average pressure within the solvation shell of an activated complex has been calculated to be 2.6×10^3 (kg·cm^{-2}) according to a model proposed by the authors. An abnormal acceleration due to pressure has been observed for the reaction of triethylamine with ethyl iodide in *p*-xylene and dioxane at 30°C. This acceleration effects has been attributed to the partial freezing of the solvent under high pressure.

A study of the effects of solvents on an activation volume would throw some light on the effects of solvents on reaction rates and mechanisms.

In a previous report[1] the present authors proposed a relation between the activation volumes in a variety of solvents and the compressibilities of the solvents on the basis of the electrostriction theory. In the present paper, it will be established that the expression then proposed by the authors is useful for the description of the variation in the activation volumes for the reaction of triethylamine with ethyl iodide and of pyridine with methyl iodide[2] upon a change of solvents.

An abnormal acceleration effect of the rates of the Menschutkin reaction due to pressure was reported by the present authors in the previous paper.[1] Compared with the results of the reaction rates in frozen solutions obtained by Pincock *et al.*,[3] this abnormal acceleration due to pressure has been attributed to the partial freezing of the solution resulting from the rize of the freezing point with an increase in the pressure. In order to establish this phenomenon further, the same reaction has been treated in dioxane and *p*-xylene solvents under high pressures.

1) Part I: Y. Kondo, H. Tojima and N. Tokura, This Bulletin, **40**, 1408 (1967).

2) H. Hartmann, H. Kelm and G. Rinck, *Z. physik. Chem. N. F.*, **44**, 335 (1965).

3) R. E. Pincock and T. E. Kiovsky, *J. Am. Chem. Soc.*, **88**, 51 (1966).

Experimental

Materials. Triethylamine and ethyl iodide were purified by a method described earlier.[1] The solvents used were purified by known methods.[4]

Apparatus and Kinetic Procedure. The apparatus for kinetic runs under high pressure used in this experiment is that described in the previous paper.[1] As the reaction product, tetraethylammonium iodide, is insoluble in the solvents used in this experiment, the reaction rates were measured by batch processes with the use of polyethylene ampoules.

The activation volumes were evaluated by the graphical method developed by the authors, using Eqs. (1) and (2):

$$\log (k_p/k_1) = AP + BP^2 \quad (1)$$

$$\Delta V_0^{\neq} = -2.303\,ART \quad (2)$$

Typical runs under high pressures are represented in Table 1, while an example of the plot of $\log(k_p/k_1)/P$ *vs.* P is shown in Fig. 1.

The coefficients, A and B, of Eq. (1) for the reactions in various solvents are represented in Table 2.

Table 1. Rate constants under high pressures
Reaction: $(C_2H_5)_3N + C_2H_5I$, Solvent: *p*-Xylene
Reaction temp.: 45°C

P kg·cm^{-2}	$k_p \times 10^5$ l mol^{-1} sec^{-1}	k_p/k_1	$\{\log(k_p/k_1)/P\} \times 10^4$ kg^{-1} cm^2
1	0.6930	1	
300	1.135	1.638	7.143
300	1.201	1.733	7.960
600	1.880	2.713	7.223
900	2.733	3.944	6.621
900	2.748	3.965	6.647
1200	3.920	5.657	6.272
1500	5.425	7.828	5.958
1500	5.509	7.949	6.000

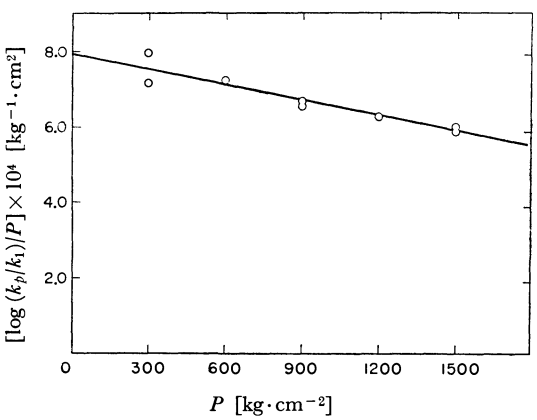

Fig. 1. Plot of $\log (k_p/k_1)/P$ *vs.* P for the reaction of ethyl iodide with triethylamine in *p*-xylene at 45°C.

4) "Technique of Organic Chemistry. VII. Organic Solvents," ed. by A. Weissberger, Interscience, New York (1955).

Table 2. Coefficients, A and B, of Eq. (1)
Reaction: $(C_2H_5)_3N + C_2H_5I$

Solvent	Reaction temp., °C	A kg^{-1}·cm^2	B kg^{-2}·cm^4
p-Xylene	45	7.93×10^{-4}	-1.34×10^{-7}
Dioxane	45	6.52×10^{-4}	-8.54×10^{-8}
Bromobenzene	25	6.15×10^{-4}	-8.47×10^{-8}
Chlorobenzene	25	6.50×10^{-4}	-1.06×10^{-7}

Results and Discussion

A Solvent Effect on an Activation Volume. Recently, the relationship between the thermodynamic activation parameters and the dielectric properties of the medium, considered as a continuum, has been discussed by Hartmann and his collaborators.[2,5,6]

In the previous report[1] the following expression for the effects of solvents on the activation volumes of the Menschutkin reaction has been derived on the basis of the assumption that the partial molar volume of the activated complex is expressed as a function of the molar volume of a pure activated complex and the electrostriction of a solvent molecule surrounding an activated complex, while the partial molar volume of a reactant is independent of the nature of the solvent:

$$\Delta V_0^{\neq} = \{V_{\neq} - (\bar{V}_A^{\circ} + \bar{V}_B^{\circ})\} - ZKV^{\circ}\Delta P \quad (3)$$

In Eq. (3), $V_{\neq}$, $\bar{V}_A^{\circ}$, $\bar{V}_B^{\circ}$, Z, K, V°, and ΔP stand for the molar volume of an activated complex in its pure state; the partial molar volume of the reactants, A and B; the solvation number of an activated complex; the compressibility and the molar volume of a pure solvent, and the average pressure within the solvation shell of an activated complex respectively.

The activation volumes obtained by the authors are represented in Table 3.

In Fig. 2 the activation volumes for the reaction of triethylamine with ethyl iodide and those for the reaction of pyridine with methyl iodide[2] are plotted against the values for KV° at 25°C.

For these two reactions there exists a similar correlation between the values for $\Delta V_0^{\neq}$ and those for KV°; in addition, the slopes of the lines, *i. e.*, the values for $Z\cdot\Delta P$, are like one another.

Since the values for $Z\cdot\Delta P$ stand for the product of the solvation number and the average pressure within the solvation shell of an activated complex, these values will vary depending on the structure of the activated complex or on the degree of the development of ionic charges during the course of the reaction, *i. e.*, on whether the ionic charges developed or decrease as the reaction proceeds.

5) H. Heydtmann, A. P. Schmidt and H. Hartmann, *Ber. Bunsenges. physik. Chem.*, **70**, 444 (1966).
6) H. Heydtmann, *Z. physik. Chem. N. F.*, **54**, 237 (1967).

TABLE 3. ACTIVATION VOLUMES AND COMPRESSIBILITIES OF THE SOLVENTS
Reaction: $(C_2H_5)_3N + C_2H_5I$

Solvent	Reaction temp. °C	$A\times10^4$ $cm^2\cdot kg^{-1}$	$KV°\times10^9$ [7] $cm^5\cdot dyn^{-1}\cdot mol^{-1}$	$-\Delta V_0^*$ $ml\cdot mol^{-1}$
p-Xylene	45	7.93	12.52*	49.3
Dioxane	45	6.52	—	40.5
Bromobenzene	25	6.15	7.05	35.8
Chlorobenzene	25	6.50	7.67	37.8
MeOH[1]	25	5.50	5.12	32.0
Nitrobenzene[1]	25	5.16	5.17	30.0
Benzene[1]	25	7.47	8.65	43.5

* The value for a compressibility, K, is that of *m*-xylene at 45°C.

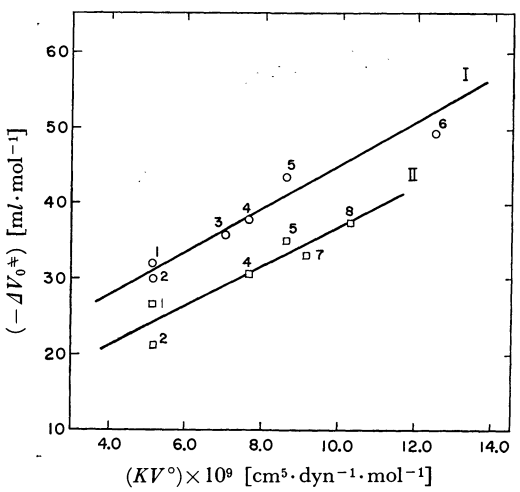

Fig. 2. Plot of $(-\Delta V_0^*)$ *vs.* $KV°$.
Curve I: $(C_2H_5)_3N + C_2H_5I$
Curve II: $C_5H_5N + CH_3I$
Solvent 1: MeOH, 2: $PhNO_2$, 3: PhBr, 4: PhCl, 5: Bz, 6: *p*-Xylene, 7: Acetone, 8: CCl_4

The values of $Z\cdot\Delta P$ for these two reactions, calculated from the slopes of Fig. 2, are about 2.6×10^3 (kg·cm^{-2}).

If we assume that the solvation number, Z, is equal to eight according to the theory of a non-electrolyte solution[8] or the solvation number of the quaternary ammonium salt in liquid sulfur dioxide measured earlier by the present authers,[9] a value of approximately 320 (kg·cm^{-2}) is obtained for the average pressure within the solvation shell of an activated complex.

In the estimation of the amount of the hydration of an electrolyte, the hydrated water within the hydration shell is assumed to be incompressible.[10]

The average pressure within the hydration shell of the alkali metal halides is calculated to be approximately 4300 (kg·cm^{-2}) from the measurement of the density and of the ultrasonic velocity in an electrolyte solution.[11]

The comparison of these results suggests that the activated complex is solvated to a lower extent than the ions of the reaction products.

Generally, ΔV_0^* has been treated as the sum of the two terms:[12]

$$\Delta V_0^* = \Delta V_1^* + \Delta V_2^* \qquad (4)$$

where ΔV_1^* is the change in the volume of the reacting particles during the formation of an activated complex and ΔV_2^* is the change in the volume of the solvent, resulting from the formation of the activated complex.

Since, in the model proposed by the authors, the first term on the right-hand side of Eq. (3) is independent of the nature of the solvent, whereas the second term is dependent, the former should correspond to the first term on the right-hand side of Eq. (4), whereas the latter should correspond to the second term.

Then, the value of ΔV_0^* obtained by extrapolating to zero the value of $KV°$ should represent ΔV_1^*, *i.e.*, the volume change of the reacting particles themselves.

Since the activation volume calculated on the basis of the Gonikberg model[13] should give the values of ΔV_1^* in Eq. (4), these values should correspond to the first term of Eq. (3), obtained by extrapolation.

7) C. D. Hodgmann, "Handbook of Chemistry and Physics," 44th Ed., Chemical Rubber Publishing Co., Cleveland (1962), pp. 2212—2218.
8) J. H. Hildebrand and R. L. Scott, "Regular Solutions," Prentice-Hall, Englewood Cliffs, N. J. (1962).
9) Y. Kondo, T. Goto, I. Suo and N. Tokura, This Bulletin, **36**, 1230 (1966).
10) J. O'M. Bockris, "Modern Aspects of Electrochemistry," Butterworths Scientific Publications, London (1954).
11) T. Yasunaga and T. Sasaki, *Nippon Kagaku Zasshi (J. Chem. Soc. Japan, Pure Chem. Sect.)*, **72**, 89 (1957).
12) S. D. Hamann, "Physico-Chemical Effects of Pressure," Butterworths Scientific Publications, London (1957).
13) M. G. Gonikberg, "Chemical Equilibria and Reaction Rates at High Pressures," 2nd Ed., Israel Program for Scientific Translations, Jerusalem (1963).

The values of $\Delta V_1^{\neq}$ extrapolated by the least-mean-square method from the experimental results shown in Fig. 2 are compared with the values calculated by Gonikberg *et al.*, in Table 4.

TABLE 4. THE VALUES OF $\Delta V_1^{\neq}$

Reaction	$\Delta V_1^{\neq}$ (Extrapolated) $ml \cdot mol^{-1}$	$\Delta V_1^{\neq}$ (Calcd by Gonikberg[13]) $ml \cdot mol^{-1}$
$C_5H_5N + CH_3I$	−10.7	− 9
$(C_2H_5)_3N + C_2H_5I$	−18.4	−24*

* The value for the reaction of triethylamine with isopropyl iodide.

It has been established that, for the reaction of pyridine with methyl iodide, the activation volume obtained by extrapolation is nearly equal to the calculated value.

Therefore, the extrapolation method mentioned above will be useful in resolving the values of $\Delta V_0^{\neq}$ measured in various solvents into their components, *i. e.*, $\Delta V_1^{\neq}$ and $\Delta V_2^{\neq}$, definitely.

An Abnormal Acceleration under High Pressure. In their previous study[1] the authors observed a greater acceleration effect of pressure for the rates of the Menschutkin reaction in benzene and nitrobenzene than was expected from the power-series treatment.

After being compared with the results of the reaction rates in frozen solutions by Pincock *et al.*,[3] this acceleration effect has been attributed to the partial freezing of the solvent which results from the rise in the freezing point with an increase in an external pressure.[1]

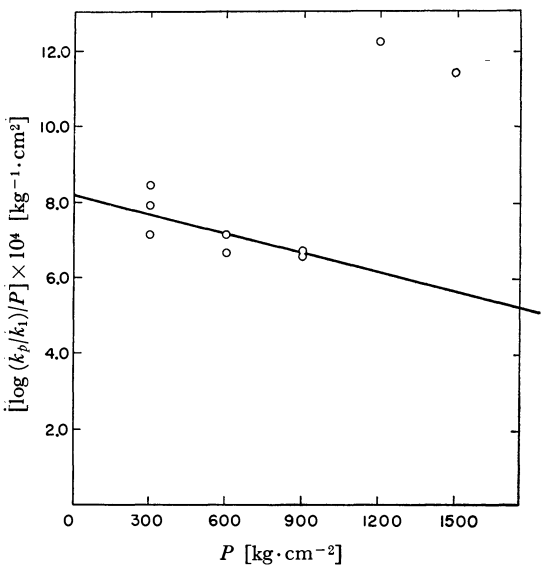

Fig. 3. Deviation from the linear relation between $\log (k_p/k_1)/P$ and P for the reaction of ethyl iodide with triethylamine in *p*-xylene at 30°C.

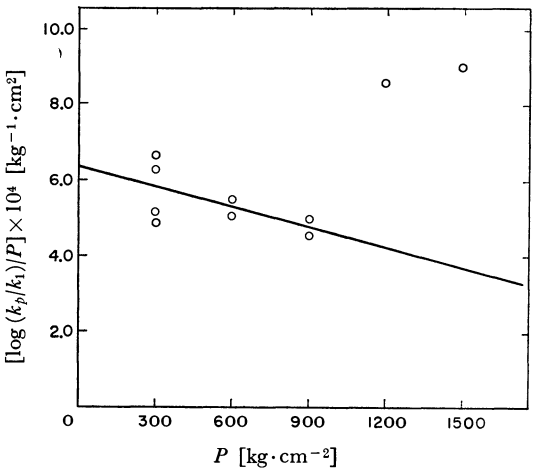

Fig. 4. Deviation from the linear relation between $\log (k_p/k_1)/P$ and P for the reaction of ethyl iodide with triethylamine in dioxane at 30°C.

In the previous study the experimental results in a high-temperature region were referred to the literature. With the object of obtaining the rate constants in both the low and high temperature regions; for the former the abnormal acceleration should be observed, but for the latter the plots of $\log (k_p/k_1)/P$ *vs.* P should be linear, the effects of the pressure on the rate constants of the Menschutkin reaction have been measured in two solvents, dioxane and *p*-xylene.

For the rate constants at 30°C large deviations from the linear relations of $\log (k_p/k_1)/P$ with the pressure have been found at the pressures of both 1200 and 1500 (kg·cm^{-2}) (see Figs. 3 and 4).

If this acceleration is caused by a freezing of the solvent similar to the phenomenon found by Pincock *et al.*,[3] the freezing points of these solvents at 1200 and 1500 (kg·cm^{-2}) should lie several degrees above the experimental temperature, *i. e.*, 30°C.

If we assume that the volume change on fusion per mole of a solvent, ΔV_f, is equal to ten percent of the molar volume of a pure solvent, on the basis of Eq.(5):

$$\left(\frac{dP}{dT}\right) = \left(\frac{\Delta H_f}{T\Delta V_f}\right) \tag{5}$$

the freezing points at 1000 (kg·cm^{-2}) are calculated to be 34°C and 30°C for *p*-xylene and dioxane respectively.

Therefore, in the region where the abnormal acceleration has been observed, *i. e.*, at 1200 and 1500 (kg·cm^{-2}), moderate portions of the solvent would be frozen.

Pincock *et al.*[3] examined the reaction of triethylamine with methyl iodide in frozen benzene solutions; they found that the reaction is accelerated

moderately and that the reaction in a frozen solution becomes a first-order reaction, in contrast to the second order in an unfrozen solution. They were able to explain their findings quantitatively by taking into account the fact that, if the reactants are soluble enough when the equilibrium is reached at a temperature above the eutectic temperature of the system, the reactants are rejected by the solid phase and become more concentrated in the unfrozen liquid region, and the fact that since, in this reaction, the reaction product, quaternary ammonium iodide, is insoluble in the solution, the walls of the reaction regions close in to hold the concentration of the remaining solute at a constant value.[3)]

As the reaction product of triethylamine with ethyl iodide, tetraethylammonium iodide, is almost insoluble in the solvents used in this experiment, the systems treated by the authors are similar to the system studied by Pincock *et al.*[3)]

The plots of log (concentration) against the time gave good straight lines for the reactions in the two solvents at the pressures of 1200 and 1500 (kg·cm^{-2}) (see Figs. 5 and 6).

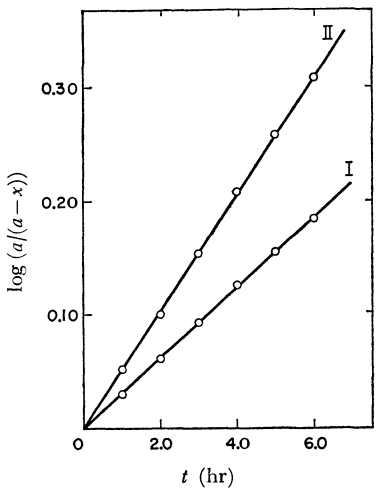

Fig. 5. First order plot for the reaction of ethyl iodide with triethylamine in *p*-xylene under high pressure at 30°C.
Curve I: at 1200 [kg·cm^{-2}]
II: at 1500 [kg·cm^{-2}]

However, at these pressures the plots of the reciprocal concentrations against the time were distinctly curved with equal concentrations of the reactants.

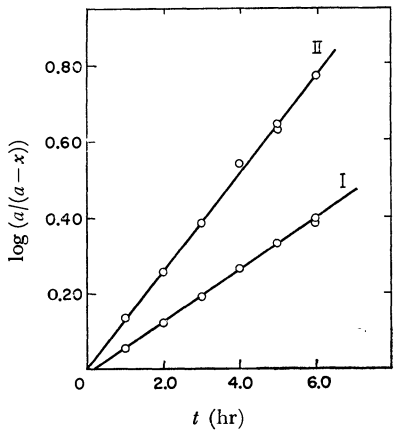

Fig. 6. First order plot for the reaction of ethyl iodide with triethylamine in dioxane under high pressure at 30°C.
Curve I: at 1200 [kg·cm^{-2}]
II: at 1500 [kg·cm^{-2}]

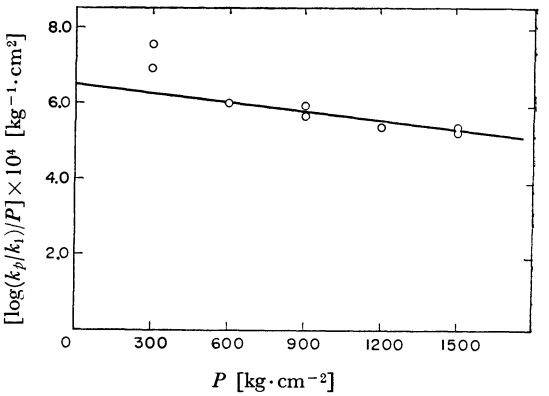

Fig. 7. Plot of log $(k_p/k_1)/P$ *vs.* P for the reaction of ethyl iodide with triethylamine in dioxane at 45°C.

The linear correlation can be expected to hold between $\log(k_p/k_1)/P$ and P over the region where no anomalous behavior such as the freezing of a solvent could be encountered at all.

The rate constants measured at a relatively high temperature, *i.e.*, 45°C, where the freezing of the solvent could not be expected even under the added pressures, show good correlations between log $(k_p/k_1)/P$ and pressure (see Figs. 7 and 1).

The facts mentioned above support the view that the abnormal acceleration observed in this experiment can be attributed to the freezing of the solvent under high pressures.

BULLETIN OF THE CHEMICAL SOCIETY OF JAPAN VOL. 41 997—1000 (1968)

The Acid-catalyzed Bromination of Aromatic Compounds with Potassium Bromate in Aqueous Acetic Acid

Yoshiaki FURUYA, Atsushi MORITA and Iwao URASAKI

Department of Industrial Chemistry, Faculty of Engineering, Kumamoto University, Kumamoto

(Received October 24, 1967)

Bromobenzene is obtained in a 64% yield when an aqueous acetic acid solution containing a catalytic amount of sulfuric acid is slowly added to an aqueous acetic acid solution of benzene and potassium bromate at 60°C. It seems, according to the synthetic data, that the formation of bromobenzene is accelerated by an electron-releasing group. The rate of the consumption of active oxygen has been expressed as follows:

$$v = k_2[BrO_3^-][C_6H_6] + k_3[BrO_3^-][C_6H_6]^2$$

Here, both k_2 and k_3 gave a straight line against $-\log(C_{BH^+}/C_B)$, with a slope of *ca.* -2. The reaction is accelerated by sulfuric acid and does not occur at all in the absence of the acid. The evolution of oxygen gas was not observed during the reaction, but the presence of peroxyacetic acid and/or acetyl peroxide in the reaction mixture was indicated by paper chromatography. A mechanism which involves the rate-determining attack of protonated hypobromous acid and/or protonated acetyl hypobromite on benzene has been suggested.

The heterogeneous bromination of benzene with potassium bromate in the presence of sulfuric acid is well-known[1]; however, no kinetical study has yet been made. We now wish to describe some findings regarding the mechanism of this reaction in a homogeneous system, using 50 vol% aqueous acetic acid as the solvent.

It is well known that there are two theories[2,3] as to the bromination of aromatic ring with molecular bromine in the presence of an electrophilic reagent. In the present reaction, however, the attacking species is not the bromine cation but protonated hypobromous acid and/or acetylbromite.

Experimental

Materials. The Potassium bromate was recrystallized twice from hot water and dried at 120°C for 2 hr. The benzene[4] was treated with concentrated sulfuric acid and diluted aqueous sodium hydroxide, washed with water, and then rectified after drying on phosphorus pentoxide; bp 80.0°C. The acetic acid was rectified; bp 117—119°C. The sulfuric acid used was of a guaranteed grade. Peroxyacetic acid was prepared by the reaction of acetic anhydride with hydrogen peroxide.[5] Acetyl peroxide was prepared by dropping water into a suspension of sodium peroxide in an ethereal solution of acetic anhydride.[6] Aqueous hypobromous acid was prepared by the addition of an aqueous solution of bromine to an excess of mercuric oxide suspended in water.[7] Acetyl hypobromite was prepared by mixing an acetic acid solution of bromine and a suspension of silver acetate in acetic acid.[8]

Preparation of Bromobenzenes. An aqueous acetic acid solution containing a catalytic amount of sulfuric acid was added slowly to an aqueous acetic acid solution of benzene and potassium bromate kept below 60°C; the heating was continued at the same temperature until the total reaction time reached 3.5 hr. The organic layer separated was washed with diluted aqueous sodium hydroxide and water, dried on calcium chloride, and then distilled, yielding bromobenzene, bp 156—157°C. The results, including those of the other brominations, are shown in Table 1. The yields were calculated on the basis of the original potassium bromate.

Reaction Products Criterion. Bromobenzene was identified by gas chromatography in comparison with an authentic sample. *p*-Chlorobromo- and *p*-dibromobenzene were identified by mixed melting point determinations; mp and mmp, 67°C and 89°C respectively.

A Typical Procedure for the Rate Measurements. A 50% aqueous acetic acid solution containing known amounts of benzene and potassium bromate was brought to a temperature equilibrium at 50°C. A known amount of the same aqueous acetic acid solution of sulfuric acid was then poured into the solution in order to start the reaction. Aliquots (1 m*l* each) were pipetted out at

1) F. Krafft, *Ber.*, **8**, 1044 (1875).
2) R. M. Keefer and L. J. Andrews, *J. Am. Chem. Soc.*, **78**, 255, 4549 (1956).
3) P. B. D. de la Mare and J. T. Harvey, *J. Chem. Soc.*, **1956**, 36; **1957**, 131, 923.
4) C. A. Kraus and R. A. Vingee, *J. Am. Chem. Soc.*, **56**, 511 (1934).
5) M. W. C. Smit, *Rec. trav. chim.*, **49**, 674 (1930).
6) J. R. Slagle and H. J. Shine, *J. Org. Chem.*, **24**, 107 (1959).
7) M. Christen and Hch. Zollinger, *Helv. Chim. Acta*, **45**, 2057 (1962).
8) M. Anber and J. Dostrovsky, *J. Chem. Soc.*, **1954**, 1105.

appropriate time intervals and poured into an ice-cooled aqueous solution of 50 ml of 0.02 N potassium iodide containing 1 N sulfuric acid. The iodine liberated by active oxygen was quickly titrated with a 0.01 N sodium thiosulfate solution.

Paper Chromatography of Reaction Mixture. A solution of the reaction products was developed with a mixture of diethyl ether and ethyl acetate (2 : 3 in vol) on acetylated Toyo Filter paper No. 54.[9] Two pink spots were observed upon spraying with a methanolic solution of 3% *p*-dimethylaminoaniline dihydrochloride. The values of R_f were found to be 0.64 and 0.83; these values agreed with those for authentic samples of peroxyacetic acid (0.66) and acetyl peroxide (0.82) respectively.

Measurement of the Isotope Effect. The rate constants, k_2 and k_3, were obtained from the plot of $k_{2\,obs}$ *vs.* the concentration of benzene on the reaction of various concentrations of benzene with 0.025 M potassium bromate in the presence of 3.0 N sulfuric acid in 50% acetic acid at 50°C. These constants, k_2 and k_3, were expressed as k_{2H} and k_{3H} for usual benzene, and as k_{2D} and k_{3D} for deuterobenzene, respectively.

Results and Discussion

Synthetic Results. The results of the bromination of benzene with potassium bromate in the presence of sulfuric acid are shown in Table 1. The substituent effect seems to suggest that the acid-catalyzed bromination involves an electrophilic attack on the benzene ring. The absence of sulfuric acid resulted in the complete recovery of benzene.

TABLE 1. BROMINATION OF SUBSTITUTED BENZENES IN AQUEOUS ACETIC ACID

Molar ratio, $C_6H_5X : KBrO_3 = 1.0 : 0.1$
Final concn. of sulfuric acid, 3.0 N
Solvent, 250 ml of aqueous acetic acid (50% in vol.)
Reaction temp., 60±2°C
Reaction time, 3—3.5 hr

Substituted group of C_6H_5X	Product	Yield, %
H[a]	—	0.0
H	C_6H_5Br	64.1
CH_3	CH_3-C_6H_4-Br[b]	70.1
Br	*p*-Br-C_6H_4-Br	36.0
Cl	*p*-Cl-C_6H_4-Br	28.7
NO_2	—	0.0

a) Without sulfuric acid
b) A mixture of *o*- and *p*-bromotoluenes

Kinetic Data. The bromination rate of benzene was followed by the iodometrical titration of the potassium bromate remaining in a reaction mixture. The initial rate data (up to 40—50% consumption) satisfied the following equation, as shown in Table 2.

TABLE 2. THE RATE DATA FOR THE CONSUMPTION OF ACTIVE OXYGEN IN THE ACID-CATALYZED BROMINATION OF BENZENE WITH POTASSIUM BROMATE IN 50% AQUEOUS ACETIC ACID AT 50°C

Initial concn. of $KBrO_3$, 2.48×10^{-2} M; C_6H_6, 4.00×10^{-2} M Concn. of sulfuric acid, 3.0 N

Time min	$[KBrO_3]$ $a-x$ $\times10^2$ M	$[C_6H_6]$ $b-x$ $\times10^2$ M	$\log\frac{a-x}{b-x}$	$k_{2\,obs}$ $\times10^3$ M^{-1} sec^{-1}
0	2.477	4.000	−0.2082	
30	2.015	3.538	−0.2445	3.05
50	1.735	3.258	−0.2738	3.31
80	1.427	2.950	−0.3154	3.38
120	1.142	2.665	−0.3680	3.36
150	0.969	2.492	−0.4103	3.40
180	0.854	2.377	−0.4445	3.31
				Av. 3.30

$$v = k_{2\,obs}[C_6H_6][BrO_3^-] \quad (1)$$

The apparent activation energy and entropy for the reaction in 50% acetic acid were calculated to be 22.3 kcal/mol and −4.01 e.u. respectively from the following average values of $k_{2\,obs}\times10^3$ M^{-1}sec^{-1}: 40°C, 0.833; 50°C, 2.85; and 60°C, 7.11, where the initial concentrations of benzene and potassium bromate were both 2.5×10^{-2} M and that of sulfuric acid was 3.0 N.

Under a definite initial concentration of benzene, the apparent second-order rate constant, $k_{2\,obs}$, slightly decreased with an increase in the initial concentration of potassium bromate, as is indicated in Table 3. Such a decrease in the rate may result from a decrease in the effective acidity in the reaction medium[10] with an increase in the concentration of potassium bromate, as is indicated

TABLE 3. THE CONSTANCY OF THE APPARENT SECOND-ORDER RATE CONSTANT WITH VARIOUS CONCENTRATION OF POTASSIUM BROMATE IN THE REACTION MIXTURE WITH 0.025 M BENZENE AND 3.0 N SULFURIC ACID AT 50°C

$[KBrO_3]$ $\times10^2$ M	$k_{2\,obs}$ $\times10^3$ M^{-1} sec^{-1}
1.99	2.94
2.50	2.85
3.03	2.82
4.05	2.78
5.02	2.68

9) J. Janoušek, *Faserforsch. u. Textiltech.*, **8**, 339 (1957).

10) To get experimental support for such an explanation, we tried to measure the acidity function (by the indicator method) for a given medium containing potassium bromate. However, this attempt was unsuccessful because of the fading of the indicator.

by the following equation:

$$\ln K_a = \ln K_c - 2A\mu^{1/2} + b\mu$$

Here, K_a and K_c are dissociation constants expressed by, respectively, activity and concentration in an equilibrium, $AH \rightleftarrows H^+ + A^-$; μ is the ionic strength of the medium, and A and b are constants. Hence, it is considered that the $k_{2\,obs}$ rate constant does not contain the concentration of potassium bromate.

On the other hand, the plot of $k_{2\,obs}$ against the initial concentration of benzene gave a straight line, with a definite slope which did not pass through the point of origin, as is shown in Fig. 1. Thus the rate equation would be given by:

$$v = \{k_2 + k_3[C_6H_6]\}[C_6H_6][BrO_3^-] \qquad (2)$$

The rate was also affected by the concentration of the acid catalyst. To obtain some information on the effective acidity, the indicator ratio (C_{BH^+}/C_B) at 415 mμ for each medium (without the bromate) were determined spectrophotometrically using *o*-nitroaniline. Since no accurate pK_a value

$$H_0 = pK_a - \log (C_{BH^+}/C_B) \qquad (3)$$

of *o*-nitroaniline in 50% acetic acid is available, we have plotted the values of $\log k_{2\,obs}$ against those of $-\log (C_{BH^+}/C_B)$ instead of H_0. As is illustrated in Fig. 2, a linear relationship with a slope of -1.81 was obtained. Therefore, both the k_2 and k_3 rate constants should involve the term of a square of proton activity. Thus, two corresponding paths yielding bromobenzene should involve protonation twice before each rate-determining step. On the other hand, the plots of $\log k_{2\,obs}$ *vs.* J_0[11] gave a straight line with a slope of -1.43. Thus, the attacking species are protonated hypobromous acid and protonated acetyl hypobromite, not the bromine cation.

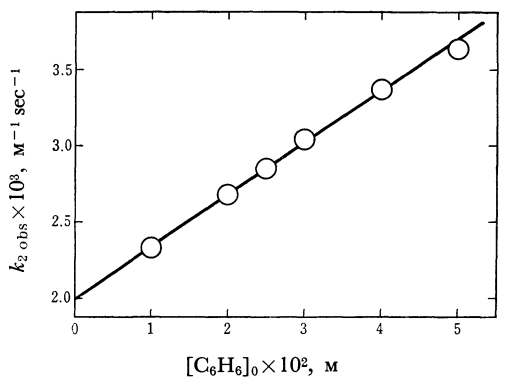

Fig. 1. The plots of $k_{2\,obs}$ *vs.* initial concentration of benzene in the bromination of benzene with 2.5×10^{-2} M potassium bromate in the presence of 3.0 N sulfuric acid at 50°C.

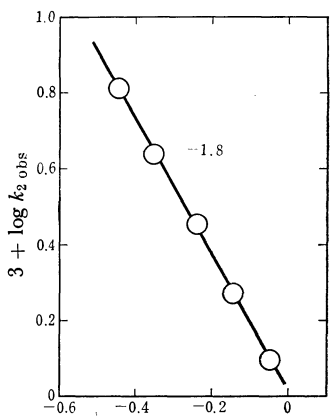

Fig. 2. The plots of $\log k_{2\,obs}$ *vs.* $-\log (C_{BH^+}/C_B)$ for the acid-catalyzed bromination of benzene with potassium bromate (both, 2.5×10^{-2} M) at 50°C.

The first participation of the proton would be the initial formation of bromic acid from the bromate anion:

$$KBrO_3 \overset{K_4}{\rightleftharpoons} K^+ + BrO_3^- \qquad (4)$$

$$H^+ + BrO_3^- \overset{K_5}{\rightleftharpoons} HBrO_3 \qquad (5)$$

The bromic acid thus formed may decompose to form hypobromous and perbromic acids, and the latter perhaps reacts with acetic acid to afford bromic acid and peroxyacetic acid:

$$3HBrO_3 \overset{K_6}{\rightleftharpoons} HOBr + 2HBrO_4 \qquad (6)$$

$$HBrO_4 + CH_3COOH \overset{K_7}{\rightleftharpoons} CH_3COOOH + HBrO_3 \qquad (7)$$

Acetyl peroxide will be formed by the reaction of peroxyacetic acid with acetic acid in the presence of sulfuric acid.[12] In fact, peroxyacetic acid and acetyl peroxide were detected by the paper chromatographic analysis of a reaction mixture. Unexpectedly, a mixture of the bromate and sulfuric acid in 50% acetic acid did not give any clear spots at the expected positions. This fact could be explained on the assumption that the equilibrium 6 lies too far to the left side. The addition of a substrate being brominated may cause the successive consumption of hypobromous acid, which is formed through Step 6, and the subsequent accumulation of peroxyacetic acid.

Previously, one of the present authors suggested the contribution of acetyl hypobromite as the active attacking species in the bromination of aromatic compounds with a mixture of peroxyacetic acid

11) These values were calculated from the results of N. C. Deno, J. J. Jaruzelski and A. Schriesheim, *J. Am. Chem. Soc.*, **77**, 3044 (1955).

12) Y. Ogata, Y. Furuya, J. Maekawa and K. Okano, *J. Am. Chem. Soc.*, **85**, 961 (1963).

and bromine in acetic acid.[13] A similar attack of acetyl hypobromite, which is thought to be formed from hypobromous and acetic acid, may also be expected in this bromination. Considering the effect of acidity on the rate, an activation of probable attacking species, such as hypobromous acid and acetyl hypobromite, by protonation would be necessary.

$$HOBr + H^+ \overset{K_8}{\rightleftharpoons} H_2\overset{\oplus}{O}Br \quad (8)$$

$$CH_3COOH + HOBr \overset{K_9}{\rightleftharpoons} CH_3COOBr + H_2O \quad (9)$$

$$CH_3COOBr + H^+ \overset{K_{10}}{\rightleftharpoons} CH_3\overset{\oplus}{C}(OBr)(OH) \quad (10)$$

$$C_6H_6 + H_2\overset{\oplus}{O}Br \overset{K_{11}}{\rightleftharpoons} \left[C_6H_5(H)(Br)\right]^{\oplus} + H_2O \quad (11)$$

(I)

$$C_6H_6 + CH_3\overset{\oplus}{C}(OBr)(OH) \overset{K_{12}}{\rightleftharpoons} I + CH_3COOH \quad (12)$$

When deuterobenzene was used as the substrate, the isotope effect was not observed for the rate constants, k_2 and k_3. The ratios of k_{2H}/k_{2D} and k_{3H}/k_{3D} were 1.05 and 1.07 respectively. Hence, the rate-determining step on the reaction is not the step of deprotonation from the σ-complex I, but the forming step of the complex. The reaction expressed by the first term in Rate Equation (2) may consist of Steps 5—12, while the reaction of the second term may involve the rate-determining attacks on benzene by the π-complex of benzene with hypobromous acid and/or acetyl hypobromite, which were formed by the following equilibria:

$$H_2\overset{\oplus}{O}Br + C_6H_6 \rightleftharpoons H_2\overset{\oplus}{O}Br\cdots C_6H_6 \quad (13)$$

$$CH_3\overset{\oplus}{C}(OBr)(OH) + C_6H_6 \rightleftharpoons CH_3\overset{\oplus}{C}(OBr)(OH)\cdots C_6H_6 \quad (14)$$

The suggested over-all mechanism can be charted as below:

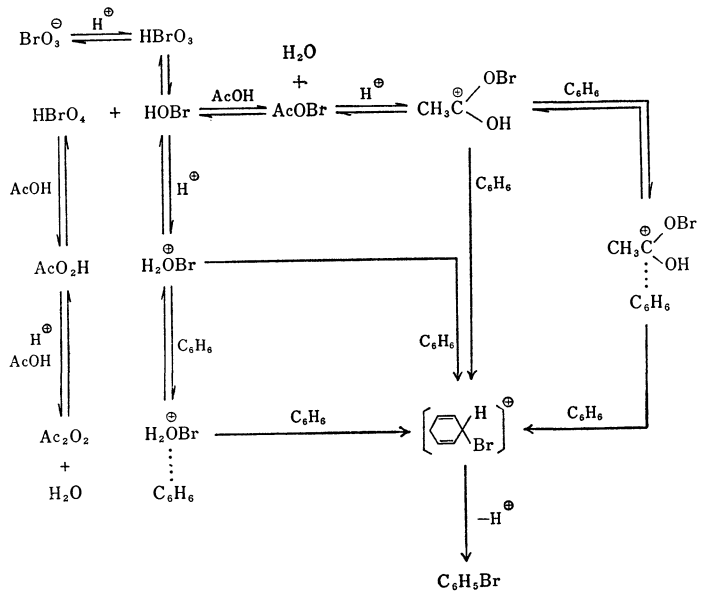

(Ac=CH_3CH)

The authors are indebted to Professor M. Okano for his helpful advice and Mr. M. Ishii and S. Miyazaki for their aids in performing these experiments.

13) Y. Ogata, Y. Furuya and K. Okano, This Bulletin, **37**, 960 (1964).

BULLETIN OF THE CHEMICAL SOCIETY OF JAPAN VOL. 41 1001—1005 (1968)

Thermal Rearrangement of Mixed Dithiocarbamic-Imidic Anhydrides*[1]

Koshin MIYAZAKI

Research Department of Takaoka Plant, Nippon Soda Co., Ltd. Mukaino-hommachi, Takaoka-shi, Toyama

(Received November 9, 1967)

The various mixed dithiocarbamic-imidic anhydrides with the formula R_2N–C(=S)–S–C(=N–Ph)–Ph (I) rearranged to thiobenzoyl-thioureas with the formula R_2N–C(=S)–N(–Ph)–C(=S)–Ph (II) when kept at an elevated temperature in an inert solvent. This rearrangement was found to be reversible, and it followed first-order kinetics. The value of the forward rate constant (k_1) in *o*-dichlorobenzene at 100°C increased in the order: R = CH_3 > C_2H_5 > *n*-C_3H_7 > *n*-C_4H_9, and a good correlation between log k_1 and σ^* for R was obtained. The rearrangement following mixture of $(CH_3)_2N$–C(=S)–S–C(=N–Ph)–Ph and $(C_2H_5)_2N$–C(=S)–S–C(=N–C_6H_5Cl-*p*)–Ph gave no crossed products. A probable reaction mechanism was proposed.

In an earlier paper,[1] the thermal rearrangement of *O*-aryl - *S* - (*N*,*N* - dimethyl-thiocarbamoyl)-*N*-arylthiolimidocarbonates to 1,1-dimethyl-3-aryl-3-(aryloxy-thiocarbonyl)-2-thioureas was reported. Since it was of interest to investigate further the scope of this kind of rearrangement, the thermal rearrangement of *N*,*N*-dialkyldithiocarbamic-*N*-(phenyl)benzimidic anhydrides with the formula R_2N–C(=S)–S–C(=N–Ph)–Ph (I), which are similar to the thiolimidocarbonates mentioned above, was tested; moreover, the kinetics of the rearrangement for various compounds I (R = CH_3, C_2H_5, *n*-C_3H_7, *n*-C_4H_9) have been studied in order to establish a reaction mechanism.

Results and Discussion

Synthesis of Mixed Dithiocarbamic-Imidic Anhydrides (I). The various anhydrides were synthesized by the reaction of an appropriate sodium *N*,*N*-dialkyldithiocarbamate with a proper *N*-(aryl)benzimidoyl chloride (Eq. (1)):

$$R_2N\text{–}\underset{\underset{S}{\|}}{C}\text{–SNa} + Cl\text{–}\underset{\underset{Ph}{|}}{C}\text{=N–Ar} \rightarrow R_2N\text{–}\underset{\underset{S}{\|}}{C}\text{–S–}\underset{\underset{Ph}{|}}{C}\text{=N–Ar} \quad (1)$$

(I)

Data on their physical constants, *etc.*, are given in Table 1.

Thermal Rearrangement. In order to examine the possibility of the thermal rearrangement of I, a pale yellow solution of I in *o*-dichlorobenzene, containing 1 mg I/ml, was kept at 100°C. Upon being heated, the solution gradually turned deep yellow. In order to analyze the reaction products, the resulting solution was submitted to thin-layer chromatography on silica gel and separated into two kinds of compounds. One kinds of compounds were compounds I unchanged, while the others were newly-formed deep yellow substances (II). The results of elemental analysis showed that the composition of the compounds II was just the same as that of I. In the infrared spectrum of the compounds II, however, no $\nu_{C=N}$ at *ca.* 1620 cm^{-1} was observed, and a strong absorption band appeared at *ca.* 1510 cm^{-1}; this band may be assignable to the thioureido group.[2] On the basis of these data, it seems reasonable to assume that I gave rise to the same kind of rearrangement to thiol-imidocarbonates as has been reported previously,[1] involving the migration of the thiocarbamoyl group, thus producing 1,1-dialkyl-3-aryl-3-(phenyl-thiocarbonyl)-2-thioureas (II) with the following structure:

$$R_2N\text{–}\underset{\underset{S}{\|}}{C}\text{–}\underset{\underset{Ar}{|}}{N}\text{–}\underset{\underset{S}{\|}}{C}\text{–Ph}$$

(II)

The compounds II formed by the thermal rearrangement of I are listed in Table 2.

Kinetics of the Rearrangement. Studies of the kinetics on the rearrangement for all the compounds I were successfully carried out by observing the development of the above-mentioned yellow color using photoelectric techniques. As a result, it was found that an equilibrium existed in these systems. The values of the equilibrium constants (K), given by the equation of $K = C_{II}/C_I$, where C_{II} and C_I are the concentrations of II and I respectively at the equilibrium, in *o*-dichlorobenzene at 100°C were 2.33 for I-1, 1.08 for I-2, 0.89 for I-3, and 0.82 for I-4, and fairly good first-order forward rate constants (k_1) were derived from the

*1 Presented at the 20th Annual Meeting of the Chemical Society of Japan, Tokyo, April, 1967.

1) A. Kaji and K. Miyazaki, *Nippon Kagaku Zasshi (J. Chem. Soc. Japan, Pure Chem. Sect.)*, **87**, 727 (1966).

2) H. M. Randall, R. G. Fowler, N. Fuson and J. R. Dangl, "Infra-red Determination of Organic Structure," Van Nostrand, New York (1949).

TABLE 1. MIXED DITHIOCARBAMIC-IMIDIC ANHYDRIDES

$$R_2N\text{-}\underset{\underset{S}{\|}}{C}\text{-}S\text{-}\underset{\underset{Ph}{|}}{C}\text{=}N\text{-}Ar$$

Compd. No.	R	Ar	Mp[a] °C	Appearance	Yield[b] %	Formula	Anal.[c] C(%) Found (Calcd)	H(%) Found (Calcd)	N(%) Found (Calcd)
I-1	CH_3	Ph	81—82	pale yellow needles[d]	66	$C_{16}H_{16}N_2S_2$	64.00 (64.00)	5.49 (5.33)	9.03 (9.33)
I-2	C_2H_5	Ph	91—92	pale yellow needles[d]	68	$C_{18}H_{20}N_2S_2$	65.60 (65.85)	5.39 (6.10)	8.39 (8.54)
I-3	n-C_3H_7	Ph	82—83	pale yellow prisms[e]	58	$C_{20}H_{24}N_2S_2$	67.10 (67.49)	6.30 (6.75)	7.77 (7.87)
I-4	n-C_4H_9	Ph	44—45	pale yellow needles[f]	55	$C_{22}H_{28}N_2S_2$	68.80 (68.75)	6.81 (7.28)	7.13 (7.28)
I-5	CH_3	4-Cl-C_6H_4	105—106	pale yellow needles[d]	65	$C_{16}H_{15}ClN_2S_2$	57.10 (57.40)	4.39 (4.49)	8.42 (8.39)
I-6	C_2H_5	4-Cl-C_6H_4	76—77	pale yellow needles[d]	70	$C_{18}H_{19}ClN_2S_2$	59.55 (59.59)	5.18 (5.24)	7.41 (7.72)

a) All melting points are uncorrected. b) Yield of the pure product.
c) All the compounds show a strong band at the region of *ca.* 1620 cm^{-1} which may be assigned to $\nu_{C=N}$.
d) From ethanol-acetone. e) From ethanol. f) From methanol.

TABLE 2. 1,1-DIALKYL-3-ARYL-3-(PHENYLTHIOCARBONYL)-2-THIOUREAS

$$R_2N\text{—}\underset{\underset{S}{\|}}{C}\text{—}N\text{—}\underset{\underset{S}{\|}}{C}\text{—}Ph$$
$$\qquad\qquad\quad\ \ |\qquad\ \ \|$$
$$\qquad\qquad\quad\ Ar$$

Compd. No.	R	Ar	Mp[a] °C	Appearance	Anal.[b] Found C(%)	Found H(%)	Found N(%)
II-1	CH_3	Ph	159—160	deep yellow needles[c]	64.00	5.38	9.54
II-2	C_2H_5	Ph	136—137	deep yellow needles[c]	65.70	5.95	8.31
II-3	n-C_3H_7	Ph	123—124	deep yellow needles[c]	67.30	6.39	8.31
II-4	n-C_4H_9	Ph	108—109	deep yellow needles[d]	68.75	6.94	6.95
II-5	CH_3	4-Cl-C_6H_4	140—141	deep yellow needles[c]	57.10	4.40	8.14
II-6	C_2H_5	4-Cl-C_6H_4	139—140	deep yellow plates[c]	59.30	5.26	8.00

a) All melting points are uncorrected.
b) In each compound, the molecular formula and the theoretical values for the elements are equal to those of the corresponding starting compound I in Table 1.
c) From ethanol-acetone. d) From ethanol.

slopes of the straight lines obtained by plotting $x_e \cdot \ln(x_e/(x_e-x))$ against the time in min, where x and x_e are the concentrations of II at time t and at equilibrium respectively.

Figure 1 shows the slopes of the straight lines obtained by plotting $x_e \cdot \ln(x_e/(x_e-x))$ *vs.* the time: the results are summarized in Table 3.

From these data, it is observed that the change of the reaction rate closely parallels the structure of the alkyl group in compound I. Figure 2 shows the slope of the straight line obtained by plotting $3+\log k_1$ *vs.* σ^* for R.

It is now desirable to determine whether the reaction is intermolecular or intramolecular in order to ascertain the mechanism of the rearrangement of I to II. If the reaction is supposed to be an intermolecular mechanism such as Scheme 1, the order of k_1 should be contrary to the experimental results shown in Table 3, because the polar

TABLE 3. FIRST-ORDER FORWARD RATE CONSTANTS (k_1) OF THE REARRANGEMENTS OF I TO II AT 100°C[a]

Compd. No.	$k_1 \times 10^2$ (min^{-1})	Relative rates
I-1	3.00	(1)
I-2	1.41	0.47
I-3	1.17	0.39
I-4	0.92	0.31

a) For all runs, solvent: *o*-dichlorobenzene; concentration: 1 mg I/m*l*.

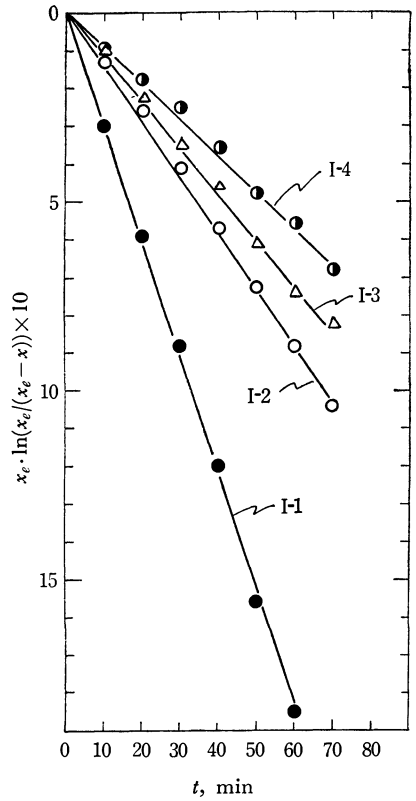

Fig. 1. The slopes of the straight lines obtained by plotting $x_e \cdot \ln(x_e/(x_e-x)) \times 10$ *vs.* time (min)

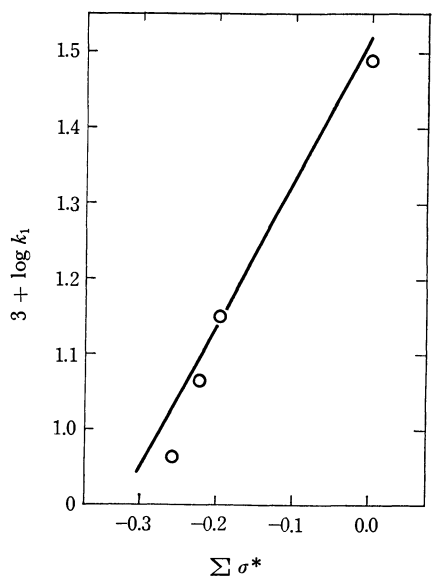

Fig. 2. The slope of the straight line obtained by plotting $3 + \log k_1$ *vs.* σ^*.

substituent constants (σ^*) of the alkyl group are 0.00 for CH_3, −0.10 for C_2H_5, −0.115 for *n*-C_3H_7, and −0.13 for *n*-C_4H_9[3]; thus, the stability of the *N,N*-dialkyl-thiocarbamoyl cation, which contributes to the reaction rate, should be increased in the order of R = *n*-C_4H_9 > *n*-C_3H_7 > C_2H_5 > CH_3.

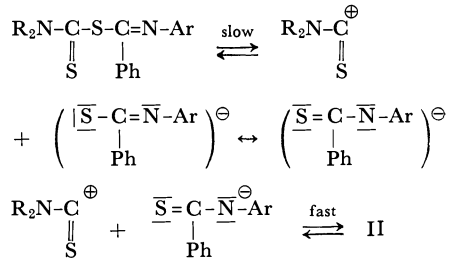

Scheme 1

Furthermore, the crossed products, such as II-2 and/or II-5, should be detected from the crossed reaction mixture of I-1 and I-6 if the rearrangement follows the intermolecular mechanism mentioned above. In order to ascertain this fact, the crossed reaction mixture obtained was compared with the specimens of II-2 and II-5 by thin-layer chromatography. However, the chromatograms of that reaction mixture eliminated the possibility of the formation of crossed products (Fig. 3).

Taking these results into consideration, it seems plausible to conclude that the rearrangement is not intermolecular, such as Scheme 1, but intramolecular.

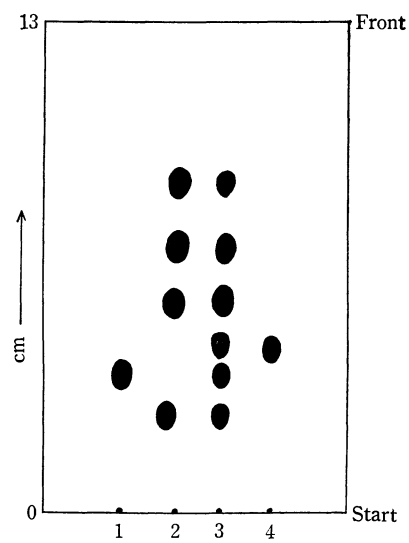

Fig. 3. Thin-layer chromatograms of the crossed reaction mixture.
1: II-5, 2: crossed reaction mixture, 3: mixture of I-1, I-6, II-1, II-2, II-5 and II-6, 4: II-2
Silica gel: WAKOGEL B-5F, Solvent: Benzene-*n*-Hexane-Glacial HOAc = 10 : 4 : 0.1 (vol%), Detection: UV-ray

3) R. W. Taft, Jr., "Steric Effects in Organic Chemistry," M. Newman, ed., John Wiley and Sons, New York (1956), Chapter 13, p. 619.

Consequently, the four-membered cyclic structure (Scheme 2) which may be formed by a nucleophilic attack of the ^2N atom of the imidocarbonyl group on the ^1C atom of the thiocarbonyl group can be considered as an intermediate in the rearrangement.

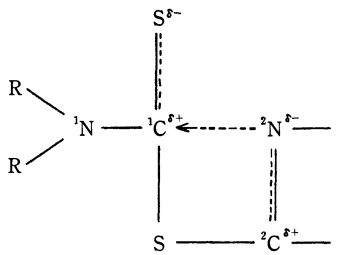

Scheme 2

The change in the rate of rearrangement with the nature of the alkyl groups can be explained by assuming as follows: The slope of the straight line in Fig. 2 shows that the rearrangement of I to II is a nucleophilic reaction ($\rho^* = 1.8$). Hence, it appears that the reaction rates depend on the reactivity of the electrophilic center on the ^1C atom. Accordingly, from a consideration of the mesomeric structure of the thiocarbamoyl group (Scheme 3), it can be supposed that a stronger electron-donating inductive effect of R, such as n-C_4H_9, can help to fill up the lack of electron density on the ^1C atom, thus resulting in a slower rate of the reaction. On the contrary, a weaker electron-donating effect of R, such as CH_3, results in a larger rate constant.

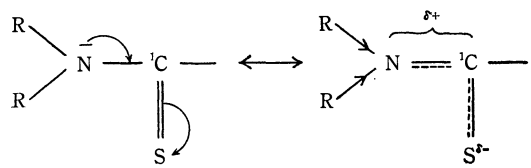

Scheme 3

Experimental

Materials. Sodium *N, N*-dialkyldithiocarbamates were prepared by the known method.[4] *N*-Phenyl- and *N*-(4-chlorophenyl)benzimidoyl chloride were prepared by the usual method.[5]

Mixed *N,N*-Dialkyldithiocarbamic-*N*-(phenyl)-benzimidic Anhydrides (I). The following general method was employed for the synthesis of the various compounds I.

A solution of sodium *N,N*-dialkyldithiocarbamate (0.05 mol) in 50 m*l* of acetone was cooled in an ice bath to a temperature of between 5 to 10°C, after which the proper *N*-(aryl)benzimidoyl chloride (0.05 mol) was gradually stirred in. After the addition had been completed, the mixture was warmed to 40°C for 5 min. It was then cooled to room temperature and poured into *ca.* 150 m*l* of cold water, by which the desired product was obtained as a pale yellow oil and crystallized spontaneously on standing. Recrystallization from a suitable solvent gave pale yellow crystals. The data are shown in Table 1.

1,1-Dialkyl-3-aryl-3-(phenyl-thiocarbonyl)-2-thioureas (II). A solution of I in an inert solvent (toluene, chlorobenzene, *o*-dichlorobenzene, *etc.* may be used) was heated on a boiling water bath for one to five hours,*2 after which the solvent was removed under reduced pressure. The crude product which remained was then purified by recrystallization or by chromatography on silica gel using as solvent benzene-*n*-hexane (2/1 v/v %).

Analytical Method. For the analysis of II in a mixture of I and II, it was advisable to use the absorbance at 452 mμ and to construct an absorbance-composition plot using a total concentration of the two components, I and II, of 100.0 mg/100.0 m*l* in *o*-dichlorobenzene. The calibration curves were obtained in this way. Since the rearrangement reactions were carried out at the same concentration, the composition of an unknown mixture could be determined by measuring the absorbance at 452 mμ and by reading the composition from the plot. The absorbance was determined with A. K. A. photo-electric-tube colorimeter (Kotaki-Seisakusho, Type No. 5-D).

Procedure for Kinetic Runs. To initiate a run, about 100 mg of I was weighed accurately. Next, in a 250 m*l* round-bottomed flask equipped with a sealed stirrer and a reflux condenser fitted with a calcium chloride drying tube, there was placed a suitable volume of *o*-dichlorobenzene (a G. R.-grade reagent was used after distillation) to make a solution of 100.0 mg I/100.0 m*l*; then the flask was immersed in a boiling water bath. When the inner temperature reached 100°C, the compound I already weighed was stirred into the flask. At appropriate intervals, a portion of the reaction mixture was taken out and cooled by immersion in cold water to room temperature. The absorbance was determined at 452 mμ, and the composition obtained from the plot. The data are shown in Fig. 1.

Equilibrium Constants (K). In the above run, the value of the equilibrium constant was derived from the analytical data of a reaction mixture heated until a constant absorbance was obtained. The values thus obtained were as follows:

$C_{II\text{-}1}/C_{I\text{-}1} = 70/30 = 2.33$, $C_{II\text{-}2}/C_{I\text{-}2} = 52/48 = 1.08$,

$C_{II\text{-}3}/C_{I\text{-}3} = 46.5/53.5 = 0.89$, $C_{II\text{-}4}/C_{I\text{-}4} = 45/55 = 0.82$

K Values Derived from Back Reactions. To confirm the K values obtained above, the following experiments were carried out: Pure accurately-weighed II (*ca.* 100 mg) was dissolved into *o*-dichlorobenzene to a concentration of 100.0 mg II/100.0 m*l*, after which the solution was heated on a boiling water bath. After 5 and/or 6 hr, a portion of the reaction mixture was

4) Houben-Weyl, "Methoden der organischen Chemie," **9**, Georg Thieme Verlag, Stuttgart (1955), p. 826.

5) W. M. Lauer and C. S. Benton, *J. Org. Chem.*, **24**, 804 (1959); P. A. Smith and N. W. Kalenda, *ibid.*, **23**, 1599 (1958).

*2 1.5 hr for I-1, 2 hr for I-2, 3 hr for I-3, and 4 hr for I-4.

taken up and analyzed. The absorbances of the reaction mixture at the two intervals were equal, indicating the reaction to be equilibrium. The values of C_{II}/C_{I} measured by this method were 2.33 for II-1, 1.08 for II-2, 0.89 for II-3, and 0.82 for II-4; these values were equal to the K values derived from the corresponding forward reaction.

The author wishes to express his sincere thanks to Professor Ryozo Goto of Kyoto University for valuable suggestions during this work, and also to Professor Aritsune Kaji of the same University for his continuing interest and encouragement.

BULLETIN OF THE CHEMICAL SOCIETY OF JAPAN VOL. 41 1005—1007 (1968)

Reaction of Aluminum Haloalkoxide with Diazomethane

Takeo SAEGUSA, Shimpei TOMITA and Takashi UESHIMA

Department of Synthetic Chemistry, Kyoto University, Sakyo-ku Kyoto

(Received November 16, 1967)

In the reaction of diazomethane with four aluminum haloalkoxides, $Al(OCH_2CF_3)_3$ (I), $Al(OCH_2CCl_3)_3$ (II), $Al(OCH_2CBr_3)_3$ (III), and $Al[OCH(CH_2Cl)_2]_3$ (IV), a methylene insertion into the aluminum-alkoxyl linkage was observed along with the polymethylene formation. By the methylene insertion, an organoaluminum compound with a haloalkoxymethyl-aluminum linkage is formed. Among aluminum alkoxides, these four haloalkoxides are distinguished by this methylene insertion. The usual aluminum alkoxides of unsubstituted alcohols do not undergo a methylene insertion reaction, but only the polymethylene formation. The difference in the reactivity towards diazomethane between the four haloalkoxides and usual alkoxides has been explained by the difference in acid strength.

In the course of our studies of the catalytic behavior of aluminum alkoxide in the polymerization of cyclic ethers,[1,2] we prepared five aluminum haloalkoxides,[3] $Al(OCH_2CF_3)_3$ (I), $Al(OCH_2CCl_3)_3$[4] (II), $Al(OCH_2CBr_3)_3$ (III), $Al[OCH(CH_2Cl)_2]_3$ (IV) and $Al(OCH_2CHCl_2)_3$ (V). In comparison with usual aluminum alkoxides, four haloalkoxides (I to IV) are characterized by a strong electron-accepting power of aluminum (Lewis acid strength), and by a marked tendency to dissociate to solvated monomers in a donor solvent.[3,4]

In the present study, we have found that four aluminum haloalkoxides of I to IV react with diazomethane to produce the linkage of al-CH_2OR by the insertion of a methylene group into the al-OR bond:

$$\text{al-OR} + CH_2N_2 \xrightarrow{-N_2} \text{al-}CH_2OR \qquad (1)$$

(R = $-CH_2CF_3$, $-CH_2CCl_3$, $-CH_2CBr_3$, $-CH(CH_2Cl)_2$)

In the reaction of diazomethane with the usual aluminum alkoxides of unsubstituted alcohols, the above insertion reaction was not observed. The difference in reactivity between the haloalkoxides and usual alkoxides has been explained by the difference in acid strength.

The reactions of the methylene insertion into aluminum-alkyl, -halide and, -hydrogen bonds by diazomethane have been known.[5-7] The present paper will describe a finding of the methylene insertion into the aluminum-alkoxyl bond.

Experimental

Reagents. Five aluminum haloalkoxides, I to V, were prepared and purified by the procedures given in previous papers.[3,4] Aluminum isopropoxide was a commercial reagent which was purified by distillation. Aluminum *t*-butoxide was prepared by the reaction of aluminum turning and *t*-butanol, and was purified by recrystallization from diethyl ether.

A toluene solution of diazomethane was prepared by treating *N*-nitroso-*N*-methylurea with an aqueous solution of KOH in toluene.[8]

The Reaction of Aluminum Alkoxide with Diazomethane. A toluene solution of diazomethane was added, drop by drop, into a toluene suspension or solution of an equimolar amount of aluminum alkoxide

1) H. Imai, T. Saegusa and J. Furukawa, *Makromol. Chem.*, **81**, 92 (1965).
2) T. Saegusa, T. Ueshima and S. Tomita, *Makromol. Chem.*, **107**, 131 (1967).
3) T. Ueshima, S. Tomita and T. Saegusa, to be published in This Bulletin,
4) T. Saegusa and T. Ueshima, *Inorg. Chem.*, **6**, 1679 (1967).
5) H. Hoberg, *Ann.*, **656**, 1, 15 (1956).
6) H. Hoberg, *Angew. Chem.*, **77**, 1084 (1965).
7) H. Hoberg, *Ann.*, **695**, 1 (1966).
8) F. Arndt, "Organic Synthesis," Coll. Vol. II, p. 165 (1943).

TABLE 1. REACTION OF ALUMINUM ALKOXIDE WITH DIAZOMETHANE

Al(OR)$_3$		mmol	(ml of toluene)	CH_2N_2/ml of mmol/ toluene	Reaction time hr	Polymethylene yield,[a] %	Methyl ethers	Yield[a] %
$Al(OCH_2CF_3)_3$	(I)	29.2	(10)	30.0/ 64	1/4	88	$CH_3OCH_2CF_3$	2.4
$Al(OCH_2CCl_3)_3$	(II)	46.3	(—)[b]	46.3/134	1/2	13	$DCH_2OCH_2CCl_3$	17.0
$Al(OCH_2CBr_3)_3$	(III)	5.9	(5)	5.9/ 15	1/6	79.5	$CH_3OCH_2CBr_3$	5.5
$Al[OCH(CH_2Cl)_2]_3$	(IV)	7.3	(5)	7.3/ 10	1/3	52.5	$CH_3OCH(CH_2Cl)_2$	4.0
$Al(OCH_2CHCl_2)_3$	(V)	16.3	(7)	16.3/ 22	7/6	96.5	$CH_3OCH_2CHCl_2$	0
$Al[OCH(CH_3)_2]_3$		34.0	(—)[b]	34.0/ 80	120	20	$CH_3OCH(CH_3)_2$	0
$Al[OC(CH_3)_3]_3$		43.7	(—)[b]	40.0/ 94	120	36	$CH_3OC(CH_3)_3$	0

a) Based on diazomethane.
b) Diazomethane solution was added to the solid aluminum alkoxide.

under a nitrogen atmosphere at 0°C. The reaction system was kept at 0°C until the gas evolution ceased and the yellow color of diazomethane faded away. Then the reaction mixture was subjected to evaporation at 50—60°C under 0.1 mmHg for 7—10 hr. The residue of the vacuum evaporation was treated with a dilute aqueous solution of HCl. The acid hydrolysis mixture was then extracted with diethyl ether or with toluene, and the extract was examined by v.p.c. analysis for the haloalkyl methyl ether, which should have been formed by the acid hydrolysis of the product of the methylene insertion reaction if the insertion had occurred. Haloalkyl methyl ethers were identified by a comparison of the retention time of the v.p.c. with those of the corresponding authentic samples. Two columns, silicone DC 550 and PEG 20000, were employed in the v.p.c. analysis. The solid insoluble residue of acid hydrolysis was extracted with hot xylene to isolate polymethylene.

In the case of $Al(OCH_2CCl_3)_3$ (II), the reaction with diazomethane was carried out by the same procedure, and the residue of vacuum evaporation was hydrolyzed with heavy water. Deutrated methyl ether, $DCH_2OCH_2CCl_3$, was isolated by means of a preparative v.p.c. technique, and was identified by means of its NMR spectrum using Varian A-60 Spectrometer. In the NMR spectrum of a CCl_4 solution, a singlet at 3.97 ppm downfield from TMS ($CCl_3\underline{CH_2}$-, area 1.00) and a triplet with components of an equal intensity centered at 3.60 ppm ($DC\underline{H_2}$- area 1.06) were observed. The chemical shifts of these absorptions were almost the same as those of the nondeutrated methyl ether, $CH_3OCH_2CCl_3$.

Results and Discussion

The results are summarized in Table 1.

The methylene insertion reaction produces an aluminum-alkyl bond, which was examined by the formation of the corresponding methyl ether (VI) in the acid hydrolysis of the reaction mixture.

$$\text{al-OR} + CH_2N_2 \xrightarrow{-N_2} \text{al-}CH_2OR \xrightarrow{H^+} \underset{\text{(VI)}}{CH_3OR} \quad (2)$$

As to the methyl ether formation, it has been established[9] that alcohol reacts with diazomethane, in the presence of aluminum alkoxide as the catalyst, to produce alkyl methyl ether. Therefore, the formation of haloalkyl methyl ether in the present study might be ascribed to the reaction of alcohol, which was possibly produced by the partial hydrolysis of aluminum haloalkoxide with impure moisture. This reaction route does not lead to the formation of the aluminum-alkyl bond. This possibility, however, has been definitely eliminated by the following two observations:

a. The hydrolysis of the reaction mixture with heavy water produced the deutrated methyl ether (VII):

$$\text{al-}OCH_2CCl_3 + CH_2N_2 \xrightarrow{-N_2}$$

$$\text{al-}CH_2OCH_2CCl_3 \xrightarrow{D_2O} \underset{\text{(VII)}}{DCH_2OCH_2CCl_3}$$

b. A reference experiment has shown that the vacuum evaporation of the reaction mixture before acid hydrolysis is quite effective in removing ether almost completely if it is present before the acid hydrolysis.

Thus, the production of haloalkyl methyl ethers in the acid hydrolysis of the reaction mixture is taken to indicate the occurrence of the methylene insertion.

Table 1 shows that the four aluminum haloalkoxides, I to IV, differ from others in their reactivity toward diazomethane. The former alkoxides react with diazomethane to form the linkages of alkoxymethylaluminum along with the formation of polymethylene. The alkoxide of V and the usual alkoxides of unsubstituted alcohols cause only the polymerization of methylene carbene from diazomethane.

Hoberg[5-7] has reported that, in the reactions of diazomethane with trialkylaluminums, alkylaluminum hydrides and alkylaluminum halides underwent the methylene insertion into aluminum-alkyl, -hydrogen, and -halogen bonds:

9) H. Meerwein and G. Hinz, *Ann.*, **484**, 1 (1930).

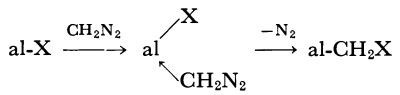

(X=alkyl, hydrogen, halogen)

It was also shown, however, that, in the reaction of alkylaluminum alkoxide with diazomethane, the methylene insertion into the aluminum-alkoxyl or the aluminum-alkyl bond did not take place. Only the formation of polymethylene occurred. The present study has indicated that $Al[OCH(CH_3)_2]_3$, $Al[OC(CH_3)_3]_3$, and V behave in almost the same manner as alkylaluminum alkoxide in their reaction with diazomethane, although $Al[OCH(CH_3)_2]_3$ and $Al[OC(CH_3)_3]_3$ have depressed catalytic activities for the polymethylene formation in comparison with Hoberg's alkylaluminum alkoxide and V. The present study is the first to observe the methylene insertion into the aluminum-alkoxyl bond, which is limited to haloalkoxides of aluminum.

The difference in the reactivity toward diazomethane between haloalkoxides and usual akloxides may reasonably be ascribed to the difference in acid strength. Hoberg[7] has suggested that the coordination of diazomethane onto aluminum was necessary prior to the methylene insertion. In this process, the aluminum compound acts as a Lewis acid.

By means of the Hammett indicator method as well as the extent of the shift of the infrared absorption of the xanthone carbonyl group, we have already shown that usual aluminum alkoxides and alkylaluminum alkoxides of unsubstituted alcohols are weaker acids than trialkylaluminums and alkylaluminum halides.[1] The four haloalkoxides, on the other hand, are shown to be stronger Lewis acids by the extent of the shift of the xanthone carbonyl band (Table 2). They are as strong as $AlEt_3$. Diazomethane coordinates onto haloalkoxides of strong acid, and hence the methylene insertion takes place. Unlike the four haloalkoxides, the haloalkoxide (V) does not undergo the methylene insertion reaction; this is explained by the finding that the alkoxide (V) is a much weaker acid than I—IV.

Table 2. Shift of carbonyl band of xanthone caused by aluminum alkoxides

$Al(OR)_3$	$\Delta\nu_{C=O}$ of xanthone
$Al(OCH_2CF_3)_3$	91
$Al(OCH_2CCl_3)_3$	90
$Al(OCH_2CBr_3)_3$	89
$Al[OCH(CH_2Cl)_2]_3$	91
$Al(OCH_2CHCl_2)_3$	0
$Al[OCH(CH_3)_2]_3$	0
$Al[OC(CH_3)_3]_3$	0
$AlEt_3$	88

BULLETIN OF THE CHEMICAL SOCIETY OF JAPAN VOL. 40 1008—1013 (1967)

The Rotatory Dispersion and Stereochemistry of Organic Compounds. XIV.[1] Nitrobenzylidene Derivatives of Diethyl *d*-Tartrate

Yojiro Tsuzuki, Motoo Koyama and Koko Tanabe

Department of Chemistry, Science University of Tokyo, Kagurazaka, Shinjuku-ku, Tokyo

(Received November 21, 1967)

Anomalous optical rotation has been observed not only with the ortho-nitrobenzylidene derivative of diethyl *d*-tartrate (Tsuzuki, *Bull. Chem. Soc. Japan*, **14**, 35 (1939); *Sci. Pap. I. P. C. Res. (Tokyo)*, **35**, 425, 466 (1939)), but also with some acetylated ortho-nitrophenyl glycosides of the β-type (Capon *et al.*, *J. Chem. Soc.*, **1961**, 5172; Montgomery *et al.*, *J. Am. Chem. Soc.*, **64**, 690 (1942); Snyder *et al.*, *ibid.*, **75**, 1758 (1953); Tsuzuki *et al.*, *Bull. Chem. Soc. Japan*, **40**, 1208 (1967)). To investigate this anomalous effect of the ortho-nitro group the authors have made rotatory dispersion studies on several derivatives of diethyl *d*-tartrate as well as its alkylidene derivatives. Of these compounds examined, the compound (I) with a nitro group in the ortho-position of the phenyl group shows a positive Cotton effect at about 340 mμ, and it has been found that the nitrophenyl group is optically active. Furthermore, in order to inquire into this anomaly the authors have observed the CD, UV and NMR spectra of these compounds, from which it is concluded that the conformations of the acetal rings of all the compounds are nearly equal, and the anomalous dispersion of the compound I at about 340 mμ is assumed to be due to the n→π* transition of the nitro group with a slight shoulder appearing at 325 to 350 mμ. In view of these facts it is considered that the ortho-nitro group is twisted from the plane of the benzene ring caused by the steric hindrance of the bulky acetal ring.

Many years ago one of the authors found in the course of studies on the optical activity of some benzylidene derivatives of diethyl tartrate that the optical rotation was deeply influenced by the position of nitro group,[2,3] namely, the meta- and para-nitrobenzylidene derivatives are normally laevo-rotatory, whereas the corresponding ortho-compound shows a large positive rotation; however, such inversion of rotation can never be observed with the benzylidene derivatives that carry *o,p*-directing hydroxyl group as well as halogen atoms even in the ortho-position.

A similar anomalous ortho-nitro effect has also been noticed with other series of compounds. Of late years a number of related papers appeared on the rotation of acetylated nitrophenyl glycosides of the β-type.[4-7] Mislow *et al.*[8] found that 2,2'-dinitrobiphenyls exihibit Cotton effects at 330 mμ, the sign of which is related with the absolute configuration. Nevertheless, the cause of the anomaly has not been elucidated.

With a view to inquiring into this anomalous effect of the ortho-nitro group the authors have made rotatory dispersion studies on several derivatives of diethyl *d*-tartrate as well as its alkylidene derivatives. In order to obtain information on the conformations of these compounds the authors have furthermore observed the circular dichroism (CD), ultraviolet absorption (UV) and nuclear magnetic resonance spectra (NMR). The compounds examined were in total sixteen:

Diethyl *o*-nitrobenzylidene-*d*-tartrate (compound I),
Diethyl *m*-nitrobenzylidene-*d*-tartrate (compound II),
Diethyl *p*-nitrobenzylidene-*d*-tartrate (compound III),
Diethyl 2,5-dimethylbenzylidene-*d*-tartrate (compound IV),

1) Part XIII: Y. Tsuzuki, K. Tanabe, M. Akagi and S. Tejima, This Bulletin, **40**, 628 (1967).
2) Y. Tsuzuki *ibid.*, **14**, 35 (1939).
3) Y. Tsuzuki, *Sci. Pap, I. P. C. Res. (Tokyo)*, **35**, 425 (1939); *ibid.*, **35**, 466 (1939).
4) B. Capon, N. G. Overand and M. Sobell, *J. Chem. Soc.*, **1961**, 5172.
5) E. M. Montgomery, N. K. Richtmyer and C. S. Hudson, *J. Am. Chem. Soc.*, **64**, 690 (1942).
6) J. A. Snyder and K. P. Link, *ibid.*, **75**, 1758 (1953).
7) Y. Tsuzuki and K. Tanaka, This Bulletin, **40**, 1208 (1967). Here it was shown by studying the NMR spectra of some anomeric tetra-*O*-acetyl-D-glucopyranosides that the anomalous optical rotatory power should not be attributed to the particular conformation of the aryl group, and in particular the anomaly of *o*-nitrophenyl glucosides seems rather to be attributable to a certain property of the nitro group, such as the field effect of the group exerted upon the anomeric center through space.
8) K. Mislow, M. A. W. Glass, E. O'Brien, P. Rutkin, D. H. Steinberg, J. Weiss and C. Djerassi, *J. Am. Chem. Soc.*, **84**, 1455 (1962).

Diethyl *m*-methylbenzylidene-*d*-tartrate (compound V),
Diethyl *p*-methylbenzylidene-*d*-tartrate (compound VI),
Diethyl *o*-iodobenzylidene-*d*-tartrate (compound VII),
Diethyl *p*-iodobenzylidene-*d*-tartrate (compound VIII),
Diethyl *o*-chlorobenzylidene-*d*-tartrate (compound IX),
Diethyl *p*-chlorobenzylidene-*d*-tartrate (compound X),
Diethyl methylidene-*d*-tartrate (compound XI),
Diethyl ethylidene-*d*-tartrate (compound XII),
Diethyl vinylidene-*d*-tartrate (compound XIII),
Diethyl benzylidene-*d*-tartrate (compound XIV),
Diethyl α-naphthylidene-*d*-tartrate (compound XV),
and
Diethyl 2-nitro-3,6-dimethylbenzylidene-*d*-tartrate (compound XVI).

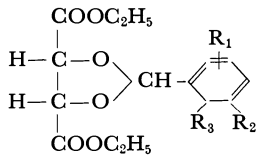

I $R_1=o\text{-}NO_2$; R_2, $R_3=H$
II $R_1=m\text{-}NO_2$; R_2, $R_3=H$
III $R_1=p\text{-}NO_2$; R_2, $R_3=H$
IV $R_1=o\text{-}CH_3$; $R_2=CH_3$; $R_3=H$
V $R_1=m\text{-}CH_3$; R_2, $R_3=H$
VI $R_1=p\text{-}CH_3$; R_2, $R_3=H$
VII $R_1=o\text{-}I$; R_2, $R_3=H$
VIII $R_1=p\text{-}I$; R_2, $R_3=H$
IX $R_1=o\text{-}Cl$; R_2, $R_3=H$
X $R_1=p\text{-}Cl$; R_2, $R_3=H$
XVI $R_1=o\text{-}CH_3$; $R_2=CH_3$; $R_3=NO_2$

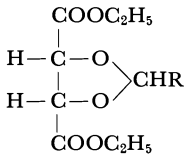

XI R=-H
XII R=-CH_3
XIII R=-CH_2=CH_2
XIV R=- 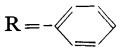
XV R=- 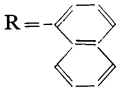

Fig. 1. Structures of derivatives of diethyl tartrate examined.

Results and Discussion

In Fig. 2 are shown the RD curves of the compounds I, II, III and XIV together with the CD curve of the compound I. The compound I with a nitro group in the ortho position of the phenyl group shows a positive rotation in the region above 350 mμ and, moreover, exhibits a number of Cotton

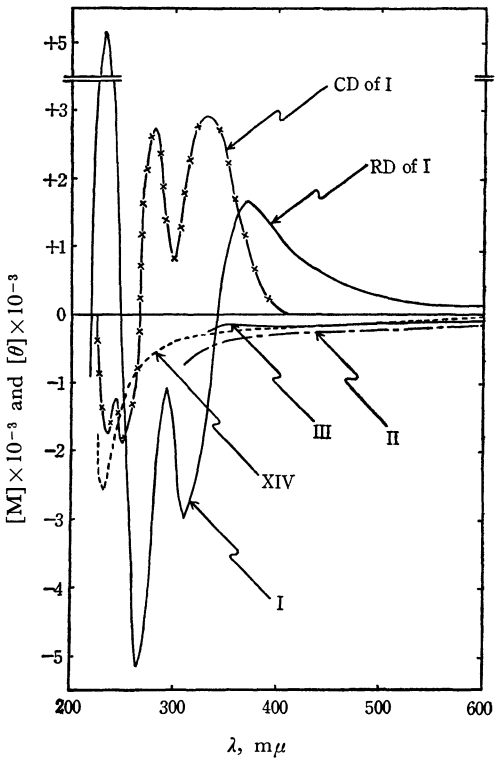

Fig. 2. RD of nitrobenzylidene derivatives and CD of I.

effects, namely two positive effects centered at 340 mμ and 280 mμ and a negative one near 248 mμ. The signs of these Cotton effects are supported by the CD curve I. On the other hand, the meta- and para-nitro derivatives (II and III) both exhibit negative plain RD curves with no anomaly near 340 mμ, which run just along their background curve XIV. The latter two compounds admitted of no RD measurement below 310 mμ due to the strong absorption.

In order to investigate whether the anomalous rotation of the compound I results from the distortion of the acetal ring effected by the steric hindrance due to the ortho-nitro group, the rotatory dispersions of the compounds IV—XVI were measured.

Figure 3 gives the RD curves of the compounds IV, V and VI, which carry a methyl group respectively on the ortho-, meta- and para-positions of the phenyl group. In Fig. 4 are shown the RD curves of the compounds VII, VIII, IX and X with a halogen atom occupying either the ortho- or para-position. Of these compounds no anomaly due to the ortho-substituent was observed. However, the *o*-iodo and *p*-chlorobenzylidene derivatives VII and X exhibit Cotton effects, though very weak, near 280 mμ. The other compounds, as are shown in Figs. 3 and 4, all exhibit negative plain curves in the region above 250 mμ, but the

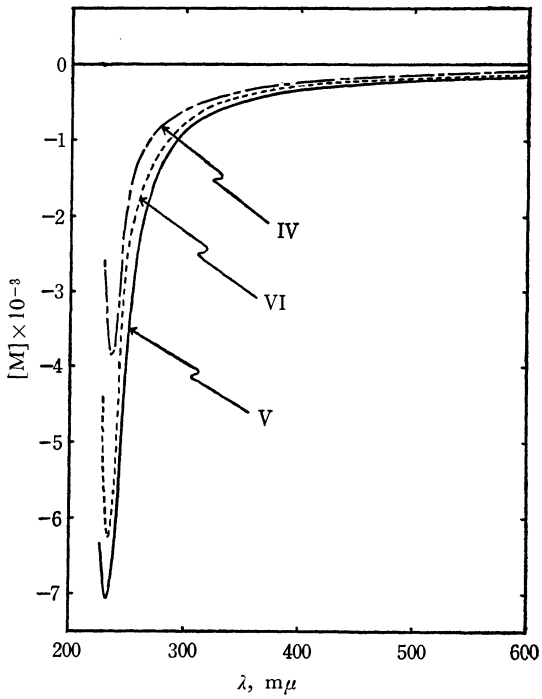

Fig. 3. RD of methylbenzylidene derivatives of diethyl tartrate.

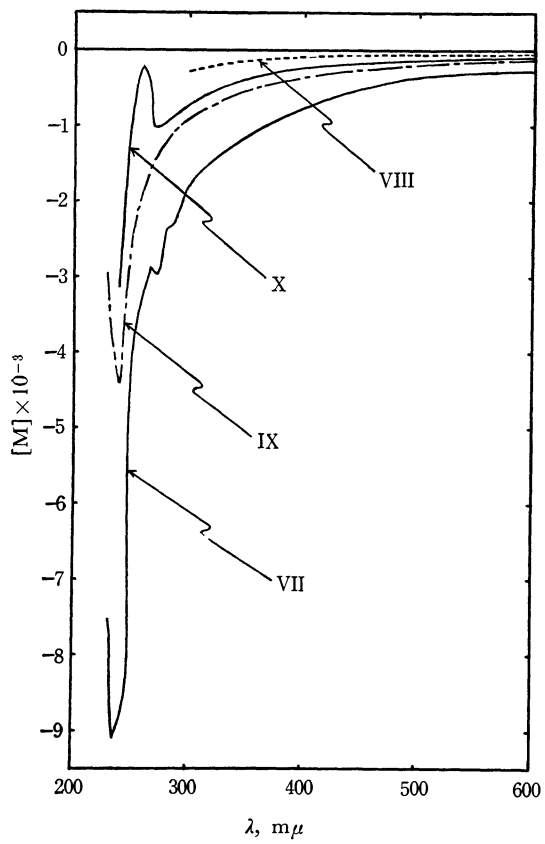

Fig. 4. RD of *o*- and *p*-halogenobenzylidene derivatives of diethyl tartrate.

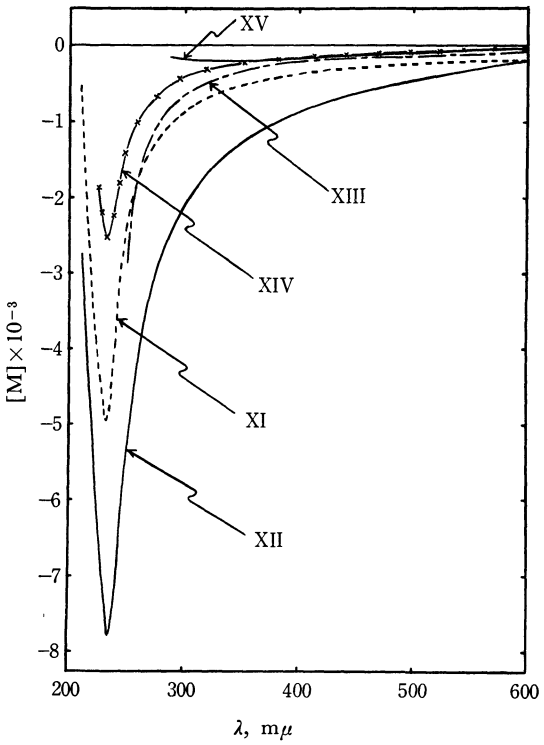

Fig. 5. RD of compounds XI—XV.

troughs appearing near 235 mμ are seen to show negative Cotton effects due to the carboxylate group.

In Fig. 5 are given the RD curves of the methylidene (XI), ethylidene (XII), vinylidene (XIII), benzylidene (XIV) and α-naphthylidene (XV) derivatives. These compounds exhibit negative plain curves in the region above 250 mμ and negative Cotton effects with troughs (near 235 mμ) similar in character to those shown in Figs. 3 and 4.

The RD curve of the compound XVI is illustrated in Fig. 6 together with the RD curves (I) and (IV) reproduced for comparison. In spite of the presence of ortho-nitro group, the compound XVI does not exhibit any Cotton effect near 340 mμ and the RD curve (XVI) runs closely along the background curve (IV) in the region above 340 mμ.

Furthermore, in view of the extraordinary optical rotation of *o*-nitrobenzylidene derivative (I), the conformation of the acetal ring was investigated by means of NMR spectrum. In the cases of R≠R', as may be seen in Fig. 7, the protons H_A and H_B are different in chemical environment, so that they interact to give a spin-spin coupling. From the coupling constant J_{AB}, as well as from Shimizu equation,[9]

$$J_{AB} = C + A|\cos\theta|,$$

9) H. Shimizu, "High Resolution Nuclear Magnetic Resonace," Maruzen, Tokyo (1962), p. 70.

where $C=0$ and $A=6.5+$ 1.5 cps in these cases, the angles, θ, of H_A–C–C–H_B can be calculated. The results are given in Table 1.

As may be seen in Table 1, the angles, θ, of the compounds are all in fairly good accordance with each other except for XVI. In other words, the stable conformations of the acetal rings of these compounds are nearly identical, where the two carboxylate groups of the tartrate are of the trans-form, and the acetal rings are, in all cases, of the half-chair form.

These compounds show in general negative rotations over all the wavelength range (Figs. 2, 3, 4, 5 and 6) but for the compound I. The fact that the angle, θ, of the compound XVI is considerably smaller than those of the others may be explained in terms of steric hindrance. It is thus concluded that the anomalous rotation of the *o*-nitrobenzylidene derivative (I) is not due to the distortion of the acetal ring that may be produced by the steric hindrance by the *o*-nitro group. It is, therefore, better to attribute this anomalous rotation to the property of the *o*-nitrophenyl group itself (Fig. 5).

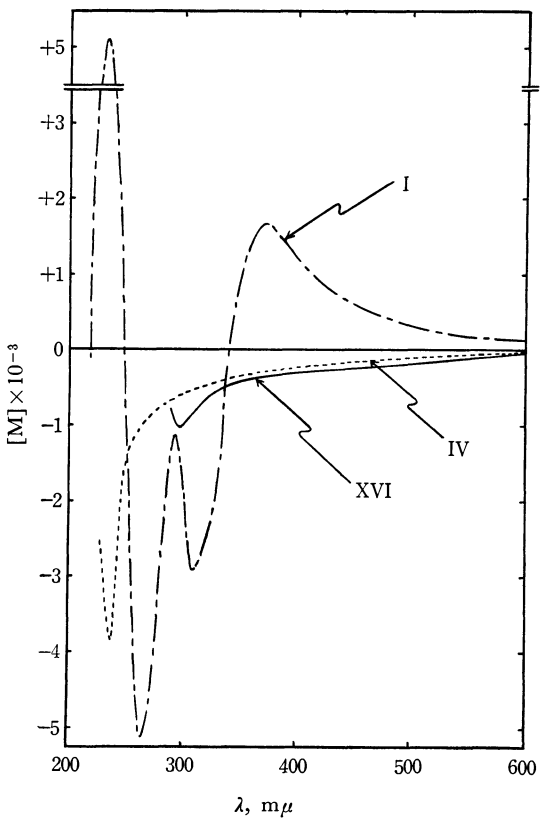

Fig. 6. RD of benzylidene derivatives of diethyl tartrate.

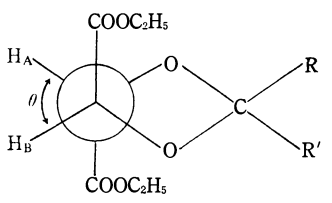

Fig. 7.

Table 1. NMR Data of the derivatives of ethyl *d*-tartrate at 25°C in CCl_4

Compound	Chemical shift of H_{AB}, ppm (δ)	J_{AB}-value, cps	θ
I	4.81	3.7	56°
II	4.83	3.9	54°
III	4.80	3.6	57°
IV	4.70	4.0	53°
V	4.71	3.8	55°
VI	4.70	3.8	55°
VII	4.77	3.6	57°
VIII	4.72	3.9	54°
IX	4.77	3.9	54°
X	4.71	4.3	48°
XII	4.51	3.9	54°
XIII	4.63	3.5	57°
XIV	4.76	3.9	54°
XV	8.88	3.8	58°
XVI	4.65	5.0	39°

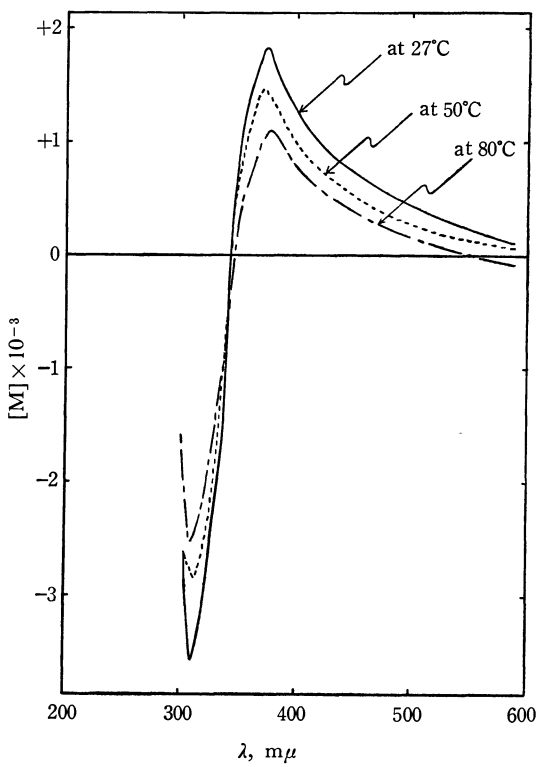

Fig. 8. Temperature variation of RD of I (in dimethyl formamide).

In addition, the authors have observed that the optical rotation of *o*-nitrobenzylidene derivative (I) varies with temperature: $[\alpha]_D^{27}$ +30.7°, $[\alpha]_D^{50}$ +20.9° and $[\alpha]_D^{80}$ −21.5° in dimethyl formamide, and with the increase of temperature the optical rotation tends to approach those of the *m*- or *p*-nitrobenzylidene derivatives, and have further noticed that the molecular amplitude of the Cotton effect near 340 mμ also diminishes with rise of temperature. The RD curves measured at 27, 50 and 80°C, of the compound I are shown in Fig. 8.

In view of these facts the ortho-nitro group must be twisted from the plane of the benzene ring by the steric hindrance of the bulky acetal ring, which may, on the other hand, be understood from the decrease of the strength of the UV absorption spectra. These can be regarded as charge transfer bands in view of Nagakura's report,[10] as is seen in Fig. 9; the compounds I and XVI each with a nitro group in the ortho-position of the phenyl group show $\varepsilon = 4.8 \times 10^3$ at 254 mμ and a shoulder at 243.6 mμ respectively, while the compounds II and III with a nitro group in the meta- and para-position show respectively $\varepsilon = 9.4 \times 10^3$ at 258.2 mμ and $\varepsilon = 10.2 \times 10^3$ at 260 mμ.

As may be seen in Fig. 6, the compound I could be measured down to 220 mμ, where the strong negative Cotton effect near 248 mμ appears to be due to the above-mentioned charge transfer band. In reality the UV spectra of the nitrobenzylidene derivatives have slight shoulders at 325—350 mμ due to the n–π^* transition that occurs possibly in the nitro group (Fig. 9). In the case of the compound I, this chromophore becomes optically active, but the compound XVI, in spite of its ortho-nitro group, does not exhibit any Cotton effect near 340 mμ. Furthermore, its UV absorption near 250 mμ is also very slight. However, the RD curve (XVI) also shows a Cotton effect near 290 mμ similar to the RD curve (I), although the former is very weak (see Fig. 6).

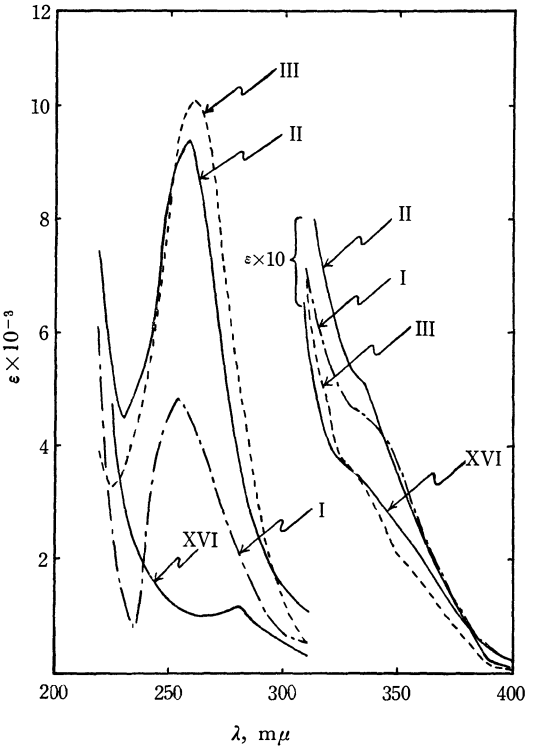

Fig. 9. UV spectra of nitrobenzylidene derivatives of diethyl tartrate.

According to the measurement and discussion by Nagakura *et al.*[10] of the absorption spectrum of nitromesitylene, the nitro group is twisted by 66.4° from the benzene ring plane and, accordingly, the conjugation between the mesityl and nitro groups must be prohibited to a great extent. Thus it is expected that the nitro group is in a similar manner twisted by about 30° in the *o*-nitrobenzylidene derivative (I) and by more than 66° in the 2-nitro-3,6-dimethylbenzylidene derivative (XVI).

These facts and considerations may lead to the conclusion that the anomalous positive rotation observed only in the *o*-nitrobenzylidene derivative is caused by its intense positive Cotton effect centered at 340 mμ, which dominates the positive sign of rotation further in the visible, and even if a nitro group is introduced in the ortho position, the nitro group cannot necessarily become optically active, as is seen in the compound XVI, which exhibit no anomalous rotation.

However, another important factor which induces the optical activity of the ortho-nitro group is to be sought for in the conjugation between the phenyl and nitro groups. The appearance of the Cotton effect at 260 mμ due to the charge transfer band shows that the *o*-nitro group is twisted unsymmetrically from the benzene ring plane under the influence of the unsymmetrical acetal ring, and the fact that molecular amplitude of the Cotton effect centered at 340 mμ distinctly decreases with rise of temperature may be interpreted in terms of the decrease of the unsymmetry of the twisted nitro group.

Anyhow, it must be admitted that further study will be needed to make clear the cause of the anomaly in rotation.

Experimental

The samples were all prepared according to the method described in the literature[11,12] at temperatures from 80 to 120°C. They were purified by recrystallization several times from ethyl alcohol or ethyl

10) S. Nagakura, M. Kojima and Y. Maruyama, *J. Mol. Spectry.*, **13**, 174 (1964).

11) Y. Tsuzuki, This Bulletin, **14**, 35 (1939).
12) Y. Tsuzuki, *ibid.*, **11**, 362 (1936).

alcohol-water, or by distillation in vacuum.

The rotatory dispersion was measured in ethyl alcohol at the temperatures 22 to 25°C in the wavelength region from 210 to 600 mμ with a Rudolph spectropolarimeter and JASCO optical rotatory dispersion recorder of the ORD/UV-5 type, and the circular dichroism was measured with the latter instrument. The NMR spectra were measured in carbon tetrachloride with tetramethylsilane as an internal reference with a Varian A-60 spectrometer. The ultraviolet absorption was measured in ethyl alcohol with a self-recording spectrophotometer of Hitachi EPU-II type.

Diethyl *o*-Nitrobenzylidene-*d*-tartrate (Compound I).[11] Colorless needles; mp 60°C. The RD was measured at 25°C in ethanol (*c* 0.701). $[\alpha]_{600}$ +38.3°, $[\alpha]_{589}$ +40.1°, $[\alpha]_{372}$ +493° (peak), $[\alpha]_{310}$ −879° (trough), $[\alpha]_{292}$ −324° (peak), $[\alpha]_{265}$ −1520° (trough), $[\alpha]_{231}$ +5120° (peak), $[\alpha]_{220}$ −914°. The RD by temperature variation of I was measured at 27, 50 and 80°C in dimethyl formamide and the concentrations were corrected, but the temperature dependence of the polarity of the solvent was ignored. $[\alpha]^{27}_{589}$ +30.7°, $[\alpha]_{500}$ +123°, $[\alpha]_{400}$ +368°, $[\alpha]_{375}$ +521° (peak), $[\alpha]_{310}$ −1050° (trough), $[\alpha]_{305}$ −777° (*c* 0.0978); $[\alpha]^{50}_{589}$ +20.9°, $[\alpha]_{500}$ +62.6°, $[\alpha]_{400}$ +282°, $[\alpha]_{370}$ +428° (peak), $[\alpha]_{310}$ −824° (trough), $[\alpha]_{305}$ −792° (*c* 0.0959); $[\alpha]^{80}_{589}$ −21.5°, $[\alpha]_{500}$ +43.0°, $[\alpha]_{400}$ +226°, $[\alpha]_{380}$ +333° (peak), $[\alpha]_{310}$ −742° (trough), $[\alpha]_{300}$ −473° (*c* 0.0930). The CD was measured at 25°C in ethanol (*c* 0.1301). $[\theta]_{410}$ +0°, $[\theta]_{330}$ −2890°, $[\theta]_{300}$ +832°, $[\theta]_{280}$ +2730°, $[\theta]_{250}$ −1900°, $[\theta]_{245}$ −1246°, $[\theta]_{235}$ −1724°, $[\theta]_{225}$ 0°.

Diethyl *m*-Nitrobenzylidene-*d*-tartrate (Compound II).[11] Colorless needles; mp 42—43°C. The RD was measured at 23°C (*c* 0.497). $[\alpha]_{600}$ −34.2°, $[\alpha]_{589}$ −35.6°, $[\alpha]_{400}$ −88.8°, $[\alpha]_{350}$ −142°, $[\alpha]_{310}$ −2110°.

Diethyl *p*-Nitrobenzylidene-*d*-tartrate (Compound III).[11] Pale yellow needles; mp 57—58°C. The RD was measured at 23°C (*c* 0.496). $[\alpha]_{600}$ −21.7°, $[\alpha]_{589}$ −22.3°, $[\alpha]_{400}$ −43.7°, $[\alpha]_{350}$ −30.9°, $[\alpha]_{234}$ −69.3°.

Diethyl 2,5-Dimethylbenzylidene-*d*-tartrate (Compound IV). Colorless crystals; bp 183—184°C/3 mmHg. The RD was measured at 23°C (*c* 0.505). $[\alpha]_{600}$ −30.3°, $[\alpha]_{589}$ −31.3°, $[\alpha]_{400}$ −83.2°, $[\alpha]_{350}$ −122°, $[\alpha]_{300}$ −200°, $[\alpha]_{236}$ −1800° (trough), $[\alpha]_{230}$ −1430°.

Diethyl *m*-Methylbenzylidene-*d*-tartrate (Compound V). Pale yellow liquid; bp 165—166°C/3 mmHg. The RD was measured at 23°C (*c* 0.598). $[\alpha]_{600}$ −42.1°, $[\alpha]_{589}$ −43.0°, $[\alpha]_{400}$ −104°, $[\alpha]_{300}$ −273°, $[\alpha]_{234}$ −2280° (trough), $[\alpha]_{223}$ −2060°.

Diethyl *p*-Methylbenzylidene-*d*-tartrate (Compound VI). Pale yellow liquid; bp 189.5—190°C/5 mmHg. The RD was measured at 23°C (*c* 0.497). $[\alpha]_{600}$ −38.8°, $[\alpha]_{589}$ −39.5°, $[\alpha]_{400}$ −94.2°, $[\alpha]_{300}$ −225°, $[\alpha]_{234}$ −2010° (trough), $[\alpha]_{230}$ −1420°.

Diethyl *o*-Iodobenzylidene-*d*-tartrate (Compound VII). Colorless needles; mp 34°C. The RD was measured at 23°C (*c* 0.503). $[\alpha]_{600}$ −65.7°, $[\alpha]_{589}$ −65.7°, $[\alpha]_{400}$ −180°, $[\alpha]_{280}$ −567°, $[\alpha]_{272}$ −707° (trough), $[\alpha]_{266}$ −697°, $[\alpha]_{236}$ −2160° (trough), $[\alpha]_{232}$ −1790°.

Diethyl *p*-Iodobenzylidene-*d*-tartrate (Compound VIII). Pale yellow liquid; bp 198°C/6 mmHg. The RD was measured at 22°C (*c* 0.708). $[\alpha]_{589}$ −4.93°, $[\alpha]_{400}$ −15.0°, $[\alpha]_{350}$ −26.9°, $[\alpha]_{300}$ −61.1°.

Diethyl *o*-Chlorobenzylidene-*d*-tartrate (Compound IX).[11] Colorless needles; mp 34—35°C. The RD was measured at 22°C (*c* 0.514). $[\alpha]_{589}$ −39.0°, $[\alpha]_{400}$ −106°, $[\alpha]_{300}$ −269°, $[\alpha]_{235}$ −1430° (trough), $[\alpha]_{230}$ −902°.

Diethyl *p*-Chlorobenzylidene-*d*-tartrate (Compound X).[11] Pale yellow liquid; bp 186—187°C/4 mmHg. The RD was measured at 22°C (*c* 0.519). $[\alpha]_{589}$ −26.7°, $[\alpha]_{400}$ −70.7°, $[\alpha]_{280}$ −314° (trough), $[\alpha]_{255}$ −103°, $[\alpha]_{240}$ −95.4°.

Diethyl Methylidene-*d*-tartrate (Compound XI).[12] Colorless liquid; bp 120—122°C/12 mmHg. The RD was measured at 23°C (*c* 0.577). $[\alpha]_{600}$ −77.5°, $[\alpha]_{589}$ −78.4°, $[\alpha]_{400}$ −112°, $[\alpha]_{300}$ −248°, $[\alpha]_{232}$ −2270° (trough), $[\alpha]_{210}$ −244°.

Diethyl Ethylidene-*d*-tartrate (Compound XII).[12] Colorless liquid; bp 132—134°C/17 mmHg. The RD was measured at 23°C (*c* 0.544). $[\alpha]_{600}$ −72.4°, $[\alpha]_{589}$ −74.6°, $[\alpha]_{400}$ −139°, $[\alpha]_{300}$ −388°, $[\alpha]_{264}$ −3340° (trough), $[\alpha]_{210}$ −1170°.

Diethyl Vinylidene-*d*-tartrate (Compound XIII). Colorless liquid; bp 169°C/36 mmHg. The RD was measured at 23°C (*c* 0.568). $[\alpha]_{589}$ −29.9°, $[\alpha]_{400}$ −83.6°, $[\alpha]_{300}$ −246°, $[\alpha]_{250}$ −1230°.

Diethyl Benzylidene-*d*-tartrate (Compound XIV). Colorless prisms; mp 48—49°C. The RD was measured at 23°C (*c* 0.703). $[\alpha]_{600}$ −18.0°, $[\alpha]_{589}$ −19.2°, $[\alpha]_{400}$ −52.4°, $[\alpha]_{300}$ −129°, $[\alpha]_{232}$ −866°, $[\alpha]_{227}$ −606°.

Diethyl α-Napththylidene-*d*-tartrate (Compound XV). Colorless needles; mp 63—64°C. The RD was measured at 22°C (*c* 0.498). $[\alpha]_{589}$ −19.3°, $[\alpha]_{450}$ −37.2°, $[\alpha]_{345}$ −54.1° (trough), $[\alpha]_{290}$ −39.0°.

Diethyl 2-Nitro-3,6-dimethylbenzylidene-*d*-tartrate (Compound XVI). Pale yellow needles; mp 46.5—47.5°C. The RD was measured at 23°C (*c* 0.507). $[\alpha]_{600}$ −26.0°, $[\alpha]_{589}$ −28.9°, $[\alpha]_{450}$ −56.7°, $[\alpha]_{350}$ −107°, $[\alpha]_{298}$ −291° (trough), $[\alpha]_{290}$ −234°.

The authors owe the Ministry of Education a grant.

BULLETIN OF THE CHEMICAL SOCIETY OF JAPAN VOL. 40 1014—1017 (1967)

Aminocyclitols. XVII. A Facile Synthesis of 2-Deoxystreptamine

Tetsuo SUAMI, Frieder W. LICHTENTHALER,* Seiichiro OGAWA, Yasuo NAKASHIMA and Hiroshi SANO

Department of Applied Chemistry, Faculty of Engineering, Keio University, Koganei-shi, Tokyo
**Institut für Organische Chemie, Technische Hochschule Darmstadt, 61 Darmstadt, Germany*

(Received November 21, 1967)

Bromination of *myo*-inosadiamine-1,3 dihydrochloride or its di-*N*-acetyl derivative with acetyl bromide and acetic anhydride yielded pentaacetyl-2-bromo-2-deoxy-*scyllo*-inosadiamine-1,3 (III), which upon reductive debromination afforded pentaacetyl-2-deoxystreptamine (IV). The configurations of the new compounds obtained were established by nuclear magnetic resonance and chemical evidences. A mechanism of the bromination reaction is presented, based on the configuration of the bromo-compound.

2-Deoxystreptamine has been found as a component of the antibiotics neomycin,[1] kanamycin,[2] paromomycin,[3,4] and gentamicin.[5]

The structure and configuration was established to be a 1,3-diamino-4,5,6-cyclohexanetriol with the all-trans configuration, by analogy of the stereochemistry of streptamine,[6] and this has been further confirmed by Lemieux by nuclear magnetic resonance (NMR) spectroscopy.[7]

In the present study we wish to report a two step synthesis of 2-deoxystreptamine from *myo*-inosadiamine-1,3.[8] When *myo*-inosadiamine-1,3 dihydrochloride (I)[9] or its di-*N*-acetyl derivative (II) are heated in a mixture of acetyl bromide and acetic anhydride in a sealed tube at 130—135°C for 6 hr, the identical products (mp 256.5—258°C dec.) are obtained in 48 and 16% yield. The structure and configuration of this product was established to be pentaacetyl-2-bromo-2-deoxy-*scyllo*-inosadiamine-1,3 (III) by elementary analysis, the NMR spectroscopic data and chemical evidence as described below.

The NMR spectrum of III in d_6-dimethylsulfoxide revealed two sharp signals at τ 8.04 (9H) and 8.23 (6H), which can be unequivocally assigned to three equatorial acetoxy groups and two equatorial acetamido groups on the basis of acetyl resonance ranges established for this solvent.[10] An axial acetoxy group, the resonance peak of which would be expected to appear between τ 7.80 and 7.86,[10] is not observed, thus establishing the preferential displacement of the axial hydroxyl group on C-2 by a bromide ion. The configuration of the bromo group, however, could not be deduced from the NMR spectrum, due to the rather complex multiplet patterns of the ring

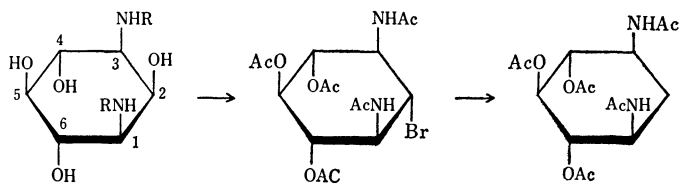

I R=H·HCl
II R=Ac

III IV

Scheme 1

1) F. A. Kuehl, Jr., M. N. Bishop and K. Folkers, *J. Am. Chem. Soc.*, **73**, 881 (1951).
2) H. Umezawa, M. Ueda, K. Maeda, K. Yagishita, S. Kondo, Y. Okami, R. Utahara, Y. Osato, K. Nitta and T. Takeuchi, *J. Antibiotics (Tokyo)*, **10A**, 181 (1957).
3) T. H. Haskell, J. C. French and Q. R. Bartz, *J. Am. Chem. Soc.*, **81**, 3480 (1959).
4) K. L. Rinehart, Jr., M. Hichens, A. D. Argoudelis, W. S. Chilton, H. E. Carter, M. Geordiadis, C. P. Schaffner and R. T. Schillings, *ibid.*, **84**, 3218 (1962).
5) M. J. Weinstein, G. M. Luedemann, E. M. Oden, G. H. Wagman, J. P. Rosselet, J. Marquez, C. T. Coniglio, W. Charney, H. Herzog and J. Black, *J. Med. Chem.*, **6**, 463 (1963).
6) J. R. Dyer, Ph. D. Theses (with H. E. Carter), University of Illinois, 1954.
7) R. U. Lemieux and R. J. Cushley, *Can. J. Chem.*, **41**, 858 (1963).
8) For a preliminary account see T. Suami and S. Ogawa, *Tetrahedron Letters*, **1967**, 2671.
9) S. Ogawa, T. Abe, H. Sano, K. Kotera and T. Suami, This Bulletin, **40**, 2405 (1967).
10) F. W. Lichtenthaler and P. Emig, "Carbohydrate Research," Vol. 6 (1968), in press.

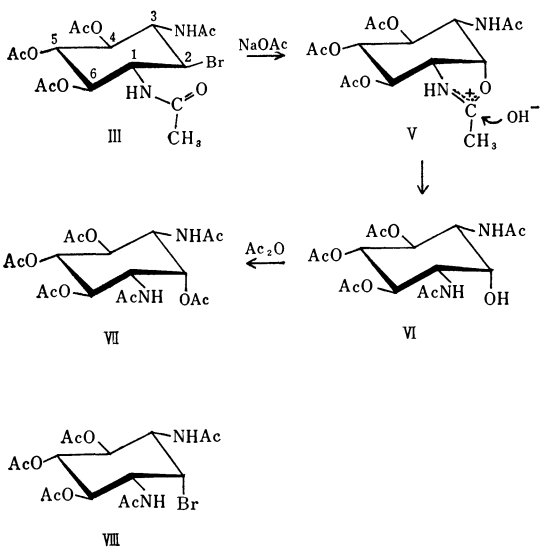

Scheme 2

protons.

Reductive debromination of III with Raney nickel under a hydrogen atmosphere (4 kg/cm²) in aqueous ethanol in the presence of Amberlite IR-4B afforded in 45% yield pentaacetyl-2-deoxystreptamine (IV), which was identified by comparison of mp, IR and NMR spectra with those of an authentic sample.[2]

On treatment of III with sodium acetate in aqueous 2-methoxyethanol followed by acetylation, hexaacetyl-*myo*-inosadiamine-1,3 (VII) is obtained in 62% yield. The stereoselectivity of this reaction can only be rationalized by proceeding *via* an oxazolinium intermediate[11,12] with subsequent cis-opening by water (V→VI). The formation of VI however requires an equatorial bromo group as in III, thus establishing its configuration. In the alternate configurational possibility with an axially oriented bromo group (VIII), an anchimeric assistance of the acetamido group is not possible and thus—under the same conditions—should give in a direct S_N2[13] displacement of the bromo group hexaacetyl-streptamine, contrary to the facts.

The mechanism of the bromination reaction is proposed as followings. The results found in the bromination of *myo*-inosadiamine-1,3 and *epi*-inosamine-2 (IX→X)[12] in a mixture of acetyl bromide and acetic anhydride give a strong evidence that the hydroxyl groups vicinal and in cis-position to an amino or acetamido group are preferentially displaced by bromine. Supporting this are the findings that streptamine dihydrochloride (XI) and di-*N*-acetyl-*myo*-inosadiamine-4,6 (XII), both having no *cis* amine-ol arrangement, fail to react with acetyl bromide in acetic anhydride, as evidenced by the isolation of the starting materials in the form of their hexaacetates. On the basis of these results, it seems obvious that any mechanism for the conversion of aminoinositols to bromo- or dibromo-derivatives with acetyl bromide and acetic anhydride must explain: (i) why the acetamido group is necessary for a facile bromination; (ii) why the *trans* amine-ol compounds fail to react and (iii) why an inversion of the configuration attends the replacement process. Of the many mechanisms considered, one involving what Boschan and Winstein[14] termed "front-side participation" seemingly meets the above described requirements.

As exemplified with *myo*-inosadiamine-1,3 or its di-*N*-acetyl derivative, the first step of the reaction is likely to be the formation of an intermediate XIII, generated by partial acetylation, since the axially oriented hydroxyl group on C-2 is less reactive towards acylation than the equatorial ones.[15,16] "Front-side participation" then yields an oxazolidine intermediate (XIV or XV) which is converted to an oxazolinium ion (XVI). Then XVI is opened by S_N2 attack of the bromide ion to give III.

This mechanistic course readily explains the facile formation of tetraacetyl-1,5-dibromo-1,5-dideoxy-*rac*-inosamine-6 (X) from *epi*-inosamine-2 as well as the inertness of *scyllo*-1,3- and *myo*-4,6-inosadiamines (XI and XII) towards this reaction.

A similar mechanistic course, with a participation of an acetoxy group, undoubtedly governs

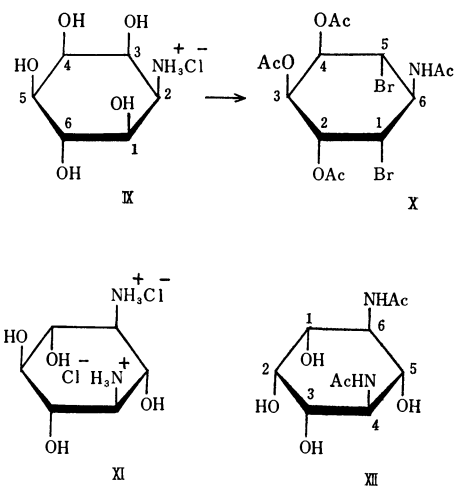

Scheme 3

11) G. E. McCasland, R. K. Clark, Jr., and H. E. Carter, *J. Am. Chem. Soc.*, **71**, 637 (1949).
12) T. Suami, S. Ogawa, Y. Nakashima and H. Sano, This Bulletin, **40**, 2958 (1967).
13) B. R. Baker and A. H. Haines, *J. Org. Chem.*, **28**, 442 (1963).
14) R. Boschan and S. Winstein, *J. Am. Chem. Soc.*, **78**, 4921 (1956).
15) E. L. Eliel, N. L. Allinger, S. J. Angyal and G. A. Morrison, "Conformational Analysis," Interscience Publishers, New York (1965), p. 72ff.
16) T. Suami, F. W. Lichtenthaler and S. Ogawa, This Bulletin, **39**, 170 (1966).

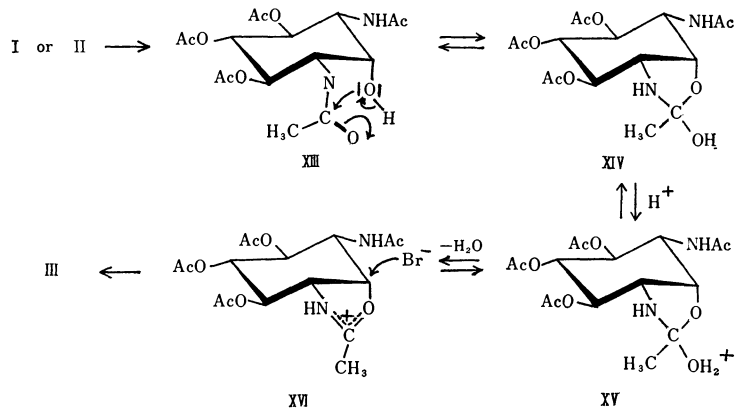

Scheme 4

the acetyl bromide-acetic anhydride bromination of *myo*- and *epi*-inositols, since it serves to explain the formation of 2-bromo-2-deoxy-*scyllo*-inositol and 1-bromo-1-deoxy-*rac*-inositol from the former[17] and of 5-bromo-5-deoxy-*allo*-inositol from the latter.[18]

Experimental

The melting points were determined in a liquid bath and are corrected. The infrared spectra were determined by pressed potassium bromide disks. The NMR spectra of the samples were determined at a frequency of 60 Mc with a Japan Electron Optics Laboratory JNM-C-60 spectrometer in deuteriochloroform or d_6-dimethylsulfoxide with tetramethylsilane as an internal standard. The peak positions are expressed by τ-values.

Pentaacetyl-2-bromo-2-deoxy-*scyllo*-inosadiamine-1,3 (III). a) A mixture of *myo*-inosadiamine-1,3 dihydrochloride (I) (882 mg),[9] acetyl bromide (1.2 m*l*) and acetic anhydride (2.6 m*l*) was heated in a sealed tube at 130—135°C for 6 hr. After cooling, 1.29 g of the crystalline precipitate was collected by filtration. The crude product was recrystallized from ethanol to give 586 mg of colorless needles melting at 256.5—258.5°C (dec.). The mother liquor was evaporated and the residue was acetylated with acetic anhydride (7.5 m*l*) and pyridine (7.5 m*l*) overnight at room temperature. After an excess amount of acetylating reagent had been removed, the residue was crystallized from ethanol giving 244 mg of colorless needles which was identical with the product in the first crop. The total yield was 48.3% (830 mg).

Found: C, 42.92; H, 5.06; N, 6.24; Br, 17.52%. Calcd for $C_{16}H_{23}N_2O_8Br$: C, 42.58; H, 5.14; N, 6.21; Br, 17.71%.

NMR: (d_6-DMSO) three equatorial acetoxy groups, τ 8.04(9H); two equatorial acetamido groups, τ 8.23 (6H).

b) Di-*N*-acetyl-*myo*-inosadiamine-1,3 (II, 644 mg)[19] was brominated in a mixture of acetyl bromide (0.8 m*l*) and acetic anhydride (1.7 m*l*) similarly as described above, giving 178 mg (16.1%) of III.

Hexaacetyl-*myo*-inosadiamine-1,3 (VII). A mixture of III (190 mg), sodium acetate (197 mg) and 90% aqueous 2-methoxyethanol (10 m*l*) was heated under reflux for 15 hr. Then the solution was evaporated under reduced pressure, and the residue was acetylated with acetic anhydride and pyridine. After an excess acetylating reagent was removed by evaporation, the residue was recrystallized from ethanol to yield 112 mg (61.6%) of colorless plates melting at 282—284°C. This product was identified with an authentic sample of hexaacetyl-*myo*-inosadiamine-1,3[19] by a mixed melting point determination and IR spectra.

Pentaacetyl-2-deoxystreptamine (IV). A 236 mg portion of III was hydrogenated in 50% aqueous ethanol (16 m*l*) with Raney nickel (1.5 spatulas) and Amberlite IR-4B (4 m*l*) under 4 kg/cm² of hydrogen pressure for 20 hr at 30°C. After the catalyst and the ion-exchange resin were removed by filtration, the filtrate was evaporated under reduced pressure. The residue was recrystallized from methanol, giving 87 mg (44.5%) of colorless prisms melting above 300°C. The product was identified with an authentic sample of pentaacetyl-2-deoxystreptamine which had been prepared from kanamycin[2] by IR and NMR spectra.

Bromination of Streptamine Dihydrochloride (XI). Streptamine dihydrochloride (1.00 g)[20] was heated in a mixture of acetyl bromide (1.5 m*l*) and acetic anhydride (2.5 m*l*) in a sealed tube as described above at 150—160°C. Hexaacetyl-streptamine (1.35 g) was recovered in 81.4% recovery, which was identified with an authentic sample[22] by IR spectra and its characteristic transition point at 248°C.

Bromination of Di-*N*-acetyl-*myo*-inosadiamine-4,6 (XII). Finely powdered di-*N*-acetyl-*myo*-inosadiamine-4,6 (1.00 g)[21,22] was heated in an acetyl bromide-acetic anhydride mixture as described above at 130—135°C. Then the reaction mixture was evaporated to dryness and the residue was recrystallized from ethanol

17) G. E. McCasland and E. C. Horswill, *J. Am. Chem. Soc.*, **75**, 4020 (1953).
18) G. E. McCasland, S. Furuta, L. F. Johnson and J. N. Shoolery, *ibid.*, **83**, 2335 (1961).
19) T. Suami and S. Ogawa, This Bulletin, **40**, 1295 (1967).
20) J. Fried, G. A. Boyack and O. Wintersteiner, *J. Biol. Chem.*, **162**, 391 (1946).
21) T. Suami and S. Ogawa, This Bulletin, **38**, 2026 (1965).

to give 1.02 g (62.0%) of the product melting at 270—274°C (dec.). This compound was identified with an authentic sample[22] of hexaacetyl-*myo*-inosadiamine-4,6 by IR spectra.

22) T. Suami and S. Ogawa, *ibid.*, **40**, 1925 (1967).

The authors are grateful to Professor Sumio Umezawa for his helpful advices, to Mr. Saburo Nakada for his elementary analyses, and to Dr. Keiji Kotera for the measurements of the NMR spectra. This research has been financially supported by a grant of the Japanese Ministry of Education.

BULLETIN OF THE CHEMICAL SOCIETY OF JAPAN VOL. 41 1017—1020 (1968)

Reduction Product and Leuco-form of Flavanthrone*1

Junji AOKI

Department of Chemistry, Faculty of Science, Toho University, Okubo, Narashino, Chiba

(Received October 11, 1967)

By reducing flavanthrone (II), 8,16-diazapyranthrene (V) (denoted as flavanthrene) was obtained. On the other hand, leucoflavanthrone dibenzoate was also prepared. Since these two substanses give nearly identical absorption spectra, the leucobenzoate is considered to have the VI formula (5,13-dibenzoyloxy-8,16-diazapyranthrene) and to belong to the same conjugated system as flavanthrene. Consequently, it may be considered that the leuco-form of flavanthrone corresponds to the IV formula (5,13-dihydroxy-8,16-diazapyranthrene) in which two carbonyl groups are reduced, but not the **III** formula (8-hydro-13-hydroxy-5-oxo-8,16-diazapyranthrene) previously presented. In addition, the leucobenzoate can also be synthesized by boiling the quinone with zinc dust and benzoyl chloride in *o*-dichlorobenzene containing pyridine. This method, devised by the author, is easy to perform and gives a good yield.

Flavanthrone (II) is a yellow vat color and is also the diaza compound equivalent to pyranthrone (I) in the field of the polycyclic system. Studies of this substance and of related compounds have already been carried out by Scholl *et al.*[1] There are, however, some doubtful points in their results. For example, the leuco-form was assigned the III formula, in spite of the fact that the IV formula is more reasonable. Furthermore, diazapyranthrene (V) which corresponds to the skeleton of flavanthrone, has not yet been synthesized.

The present investigation was undertaken in order to prepare this reduction product and the related compounds; it has been found during this work that the leuco-form of flavanthrone corresponds to the IV formula.

As is well known, the leuco compound is very unstable in air. It is, therefore, very difficult to isolate it, but it is possible to prepare a kind of ester, "leuco-ester," by adding acid chloride to the vat. The leuco-ester (VIII) may be considered to be a derivative of the corresponding hydrocarbon, since it is not a compound of a quinonoid form (VII) but belongs to a conjugated system of the

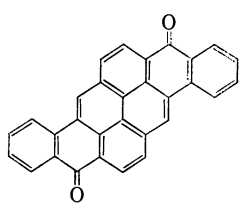

I

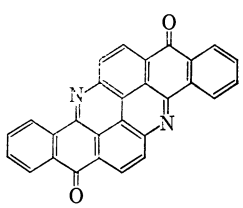

II

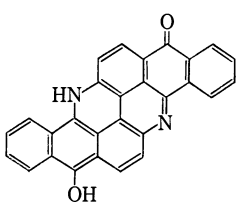

III

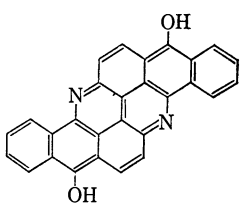

IV

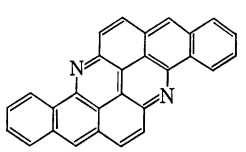

V

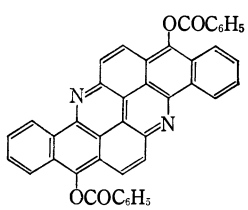

VI

*1 Presented at the 17th Annual Meeting of the Chemical Society of Japan, Tokyo, Aprill, 1964.

1) R. Scholl *et al.*, *Ber.*, **40**, 933 (1907); **41**, 2304, 2534 (1908); **44**, 1727 (1911).

Table 1. The wavelength (mμ) of the peaks in the absorption spectra of the hydrocarbons and their related leucobenzoates

Solvent: anthracene and its related benzoate, benzene; the others, 1,2,4-trichlorobenzene

Anthracene	311	325	341	359	378		
Leucoanthraquinone dibenzoate	324	339.5	356.5	375.5	396.5		
Pyranthrene	340	358	415	438	468		
Leucopyranthrone dibenzoate	342	360	423	448	480		
Violanthrene	347	365	385	409	434	462	496
Leucoviolanthrone dibenzoate	351	368	391.5	417	442	471	506
Leuco-16,17-dihydroxy-violanthrone tetrabenzoate	360	381	402	428	459	489	526
Flavanthrene	347	365	391	412	437	469	500
Leucoflavanthrone dibenzoate	348	367	395	416	442	475	508

hydrocarbon type (IX). In addition, it may be supposed that the ionization energy of the substituent ($-OCOC_6H_5$) is not small. It may, therefore, be considered that the absorption spectrum of the leuco-ester is about the same in appearance as that of the hydrocarbon and that the former appears in the region of somewhat longer wavelengths than the latter.

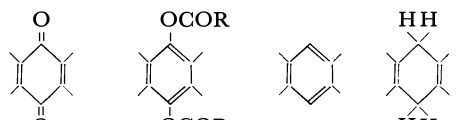

VII VIII IX X

The present author synthesized the lecuobenzoates of anthraquinone, pyranthrone, violanthrone, *etc.*,[2] examined their absorption spectra, and confirmed the suggestion mentioned above: these leucobenzoates gave absorption spectra nearly identical with those of the corresponding hydrocarbon, although they were somewhat red-shifted, as is shown in Table 1. These facts are not only useful for examining the structure of the leuco compound, but also give proof that the hydrocarbon*2 belongs to the aromatic hydrocarbon type (IX), but not its dihydro form (X).

Concerning flavanthrone (II), when the leucobenzoate was sysnthesized by the author's method, brown needles were obtained. On the other hand, when the zinc-dust fusion was applied to flavanthrone, a reduction product of the hydrocarbon type, a product which might be called "flavanthrene," was obtained as reddish brown needles which melted at 386—388°C. These two substances gave the absorption spectra shown in Fig. 1 and Table 1. By comparing these spectra, it may be found that the absorption spectrum of leucobenzoate is nearly identical with that of flavanthrene, although somewhat red-shifted.

As has been described above, this fact means that these two substanses belong to the same polycyclic conjugated system. The absorption band of flavanthrene is situated in a region of longer wavelengths than that of pyranthrene; the results of

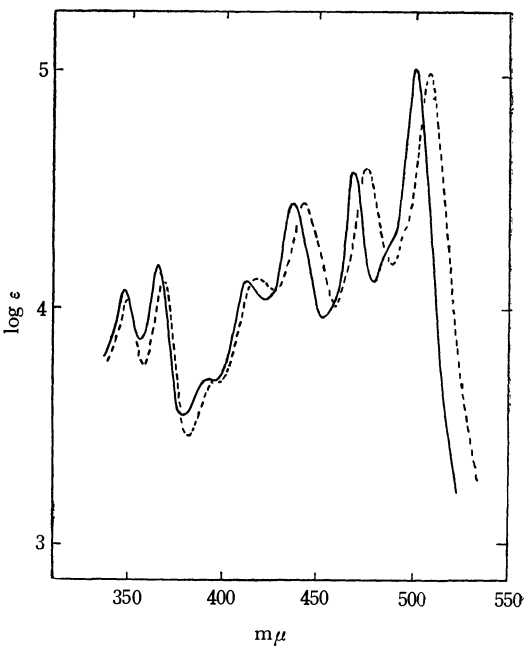

Fig. 1. Absorption spectra of flavanthrene and leucoflavanthrone dibenzoate (broken line) in 1,2,4-trichlorobenzene.

2) The synthesis of "leuco-ester" is generally carried out by adding acid chloride or acid anhydride to the vat, but a large excess of the reagent is necessary and still the yield is low. The following method, devised by the author, is easy to perform and gives a good yield.

A mixture of quinone (1 part), pyridine (1 part), and *o*-dichlorobenzene (30—50 parts) is refluxed, and then zinc dust (1 part) is added little by little. After several minutes, benzoyl chloride (1 part) is added, and the mixture is refluxed for 10—30 min; after cooling, the same volume of ethanol is added. After the mixture has stood overnight, the precipitate is collected and boiled with ethanol to remove the soluble impurities. Finally, it is recrystallized from a suitable solvent.

In addition, pyridine is indispensable for this reaction; indeed, more of it is necessary than the mole ratio of benzoyl chloride.

*2 Many kinds of condensed polycyclic hydrocarbons are prepared by the zinc-dust fusion of quinones. In this case, it is possible also to produce the dihydro compound.

the elementary analysis indicate that flavanthrene does not contain oxygen. From these facts, flavanthrene may be considered to be a compound with the V formula, 8,16-diazapyranthrene. Since the leucobenzoate corresponds to the derivative of flavanthrene and since the analysis indicates that it is dibenzoate, this ester may be considered to have the VI formula.

In addition, the author synthesized leucobenzoate by adding benzoyl chloride to the vat.*3 Since flavanthrone is readily vatted, the synthesis was carried out under six sets of conditions, from 20°C to 75°C; all the products gave absorption spectra identical with that of the ester described above.

These results mean that the author's method was useful in this case also and, further, confirm that the leuco-form of flavanthrone has the IV formula in which two carbonyl groups are reduced, not the III formula hitherto proposed.

Experimental

The melting points were measured in a liquid bath or in an air bath and are uncorrected.

Anthracene. The synthesis was carried out by the method described in Ref. 3. Colorless fine plates with a violet fluorescence were obtained by recrystallization from xylene. Mp 212.5°C (Ref. 3, 213°C).

Leucoanthraquinone Dibenzoate. A mixture of 5.0 g of anthraquinone, 5.0 g of zinc dust, 5.0 g of pyridine, and 200 m*l* of *o*-dichlorobenzene was refluxed for about 10 min. Then 5 g of benzoyl chloride was added, and boiling was continued for 30 min. After hot filtration, 200 m*l* of ethanol was added to the filtrate and the mixture was allowed to stand overnight. The crude product (5.2 g) was recrystallized from *o*-dichlorobenzene, giving pale yellow needles which melted at 292—293°C (Ref. 4, 293°C). This product is soluble in concentrated sulfuric acid with a yellow color.

Found: C, 80.62; H, 4.51%. Calcd for $C_{28}H_{18}O_4$: C, 80.37; H, 4.34%.

Pyranthrene. The synthesis was carried out by the method described in Ref. 5.

Leucopyranthrone Dibenzoate. Synthesis was carried out by the method described in Ref. 2 (pyranthrone: 2.0 g; *o*-dichlorobenzene: 80 m*l*). The crude product was recrystallized from trichlorobenzene, giving 1.4 g of fine, yellow-brown needles which colored at about 400°C but which did not melt below 450°C. This product is soluble in an organic solvent, giving a yellow color and a green fluorescence, while in a concentrated sulfuric acid solution it is blue.

Found: C, 85.86; H, 4.03%. Calcd for $C_{44}H_{24}O_4$: C, 85.70; H, 3.92%.

Violanthrene. The synthesis of the authentic sample has already been reported.[6]

Leucoviolanthrone Dibenzoate. The synthesis was carried out by a method similar to that used for pyranthrone. The crude product was recrystallized from *o*-dichlorobenzene, giving fine, red-brown needles which did not melt below 450°C, although they sintered at 358—364°C.*4 Although this product is hardly soluble in an organic solvent, its solution gives a yellow-green fluorescence, while a concentrated sulfuric acid solution shows a blue color.

Found: C, 86.71; H, 4.10%. Calcd for $C_{48}H_{26}O_4$: C, 86.47; H, 3.93%.

Leuco - 16, 17 - dihydroxyviolanthrone Tetrabenzoate. A mixture of 1.0 g of 16,17-dihydroxyviolanthrone dibenzoate,[6] 2 g of pyridine, 1.5 g of benzoyl chloride, and 200 g of *o*-dichlorobenzene was boiled, and then 1.0 g of zinc dust was added little by little. After the mixture had been refluxed for 10 min, the zinc dust was removed by hot filtration. The filtrate was concentrated and ethanol was added, whereupon 1.2 g of red crystals were obtained. They were recrystallized from chlorobenzene, giving fine, red leaflets which melted at 333°C (decomp.). This product is soluble in an organic solvent, giving a strong yellow fluorescence, while in a concentrated sulfuric acid solution it shows a violet-blue color.

Found: C, 82.02; H, 3.91%. Calcd for $C_{62}H_{34}O_8$: C, 82.11; H, 3.78%.

Flavanthrene (V). The synthesis was performed by the zinc-dust fusion of flavanthrone (II). A mixture of 1.0 g of flavanthrone, 1.0 g of zinc dust, 5 g of zinc chloride, and 1 g of sodium chloride was fused at 280—290°C for 10 min. After cooling, the reaction mixture was dissolved in water and the insoluble part was filtered off. Then, it was treated with an alkaline hydrosulfite solution and the unchanged material was removed as the soluble part. The excess of zinc dust was dissolved by treatment with a diluted hydrochloric acid solution. Yield, 0.90 g of a grey black powder. It was recrystallized from trichlorobenzene, giving 0.35 g of reddish-brown needles which melted at 386—388°C. This product is soluble in an organic solvent, giving a yellow color and a stronger and more yellowish-green fluorescence than pyranthrene, while in a concentrated sulfuric acid solution it is blue-green.

Found: C, 88.72; H, 3.82; N, 7.34%. Calcd for $C_{28}H_{14}N_2$ (V): C, 88.87; H, 3.73; N, 7.40%.

Leucoflavanthrone Dibenzoate (VI). *Method Performed in a Solvent.* A mixture of 0.5 g of flavanthrone, 0.6 g of zinc dust, 1 g of pyridine, and 50 m*l* of *o*-dichlorobenzene was refluxed for 10 min. Then, 0.6 g of benzoyl chloride was added, after which the reaction mixture was further refluxed for 30 min. After the mixture had then cooled, 50 m*l* of ethanol was added and the mixture was allowed to stand overnight. The precipitate was collected, and this crude product (1.05 g, containing zinc dust) was recrystallized from trichlorobenzene, giving 0.26 g of fine, brown needles which did not melt below 450°C, although they sintered at 358—362°C.*4 This product is soluble in an organic solvent with a strong yellowish-green fluorescence,

*3 The leucobenzoate prepared from a vat is an authentic sample equivalent to the actual leuco compound.

3) E. L. Martin, *J. Am. Chem. Soc.*, **58**, 1438 (1936).

4) Y. Nagai, Report of the Institute of Industrial Science, The University of Tokyo, **16** (Serial No. 104), 30 (1966).

5) E. Clar, *Ber.*, **72**, 1648 (1936).

6) J. Aoki, This Bulletin, **37**, 1356 (1961).

*4 It is considered that, during sintering, the original quinone with a high melting point is reproduced. Hence, the sintering may be regarded as a kind of decomposition.

while a concentrated sulfuric acid solution shows a green color.

Found: C, 80.93; H, 3.92; N, 4.41%. Calcd for $C_{42}H_{22}O_4N_2$ (VI): C, 81.54; H, 3.58; N, 4.53%. (Calcd for monobenzoate of III, $C_{35}H_{18}O_3N_2$: C, 81.70; H, 3.53; N, 5.44%)

Method Performed in a Vat. Flavanthrone (0.1 g) was vatted in 20 m*l* of an alkaline hydrosulfite solution (NaOH, 4%; $Na_2S_2O_4$, 2%). After the substance had then been kept at the reaction temperature (Table 2) for 20 min, 0.7 g of benzoyl chloride was added and the reaction mixture was further kept at the same temperature for 2 hr. Then, after cooling, the precipitate was filtered off and washed, successively, with an alkaline hydrosulfite solution and with water. Since it was inevitable that the crude product obtained by this method would contain considerable amounts of the unchanged material, further purification was carefully carried out by recrystallization from trichlorobenzene; the results shown in Table 2 were obtained.

Table 2. The results of vatting method

Reaction temp., °C	20	30	40	50	60	75
Yield, g	0.05	0.01	0.05	0.04	0.03	0.01

However, all of products gave absorption spectra identical with that of the sample prepared in a solvent.

The author wishes to express his thanks to Professor Saburo Nagakura, Professor Hiroo Inokuchi, and Dr. Yoshiya Harada of the Institute for Solid State Physics, The University of Tokyo, for their kind advice. He is also indebted to Mrs. Hisa Watanabe for her assistance.

NOTES

The Reaction of Triethylaluminum with Phthalic Anhydride

Yoshio BABA

Resources Research Institute, Kawaguchi, Saitama

(Received April 17, 1967)

In the Grignard reaction two different mechanisms have been proposed for the reaction with phthalic anhydride and for the reaction with ortho-disubstituted phthalic anhydride.

The present investigation of the reactions of triethylaluminum with phthalic anhydride, 4-methylphthalic anhydride, and 4,7-dimethylphthalic anhydride was undertaken in order to study the steric effect which has been observed in the case of Grignard reactions.

Experimental

All the reactions were carried out in an atmosphere of dry nitrogen. The melting points were measured on a micro hot stage and were not corrected.

Materials. Triethylaluminum purchased from the Ethyl Corp. was used without further purification. Commercial phthalic anhydride (mp 131—132°C) was purified by sublimation. 4-Methylphthalic anhydride (mp 115—116°C) was synthesized from piperylene-maleic anhydride adduct *via* 4-methyl-3,4,7,8-tetrahydrophthalic anhydride and the corresponding tetrabromide.[1] 4,7-Dimethylphthalic anhydride (mp 142—143°C) was prepared by the dehydration of the 3,5-dimethylfuran-maleic anhydride adduct.[1]

Reaction of Phthalic Anhydride with Triethylaluminum. A solution of triethylaluminum (11.1 g) in dry petroleum ether (bp 35—45°C) was added, drop by drop, at room temperature into a suspension of phthalic anhydride (14.8 g) in 100 m*l* of dry petroleum ether. The solid anhydride dissolved readily, resulting in a faintly brown-colored solution. After refluxing for 1.5 hr, the reaction mixture was cooled in an ice-bath, after which the aluminum compound was decomposed by adding 17.5 m*l* of ethanol. A solid precipitate, separated on the addition of 20 g of cracked ice, was collected by suction filtration. The filter cake was washed thoroughly with ether and poured into ice-cooled, diluted hydrochloric acid. The insoluble acid substance was extracted with ether. The unchanged phthalic acid which separated out when the crude oily product (13.4 g) was left standing, was collected by filtration; mp 189—191°C, 3.8 g (22.9%). The mother liquor was distilled under reduced pressure, and a fraction boiling at 150—160°C/5 mmHg (6.2 g) was collected; it solidified on standing, mp 72—73°C, from water; it showed no depression in melting point in a mixed melting point test with phthalide.

Reaction of 4,7-Dimethylphthalic Anhydride with Triethylaluminum. The reaction of 4,7-dimethylphthalic anhydride (6.2 g) with an equimolar amount of triethylaluminum under the conditions described above gave 5.4 g of a reaction product (mp

1) M. S. Newmann and C. D. McCleary, *J. Am. Chem. Soc.*, **63**, 1543 (1941).

67—69°C); practically no unchanged anhydride was obtained. The recrystallization of the crude crystal from diethyl ether-petroleum ether afforded prisms, mp 72—73°C. 3,6-Dimethyl-2-α-hydroxypropylbenzoic acid.

Found: C, 69.48; H, 7.97%. Calcd for $C_{12}H_{16}O_3$: C, 69.21; H, 7.75%.

Results and Discussion

In their study of the reactions of Grignard reagents with substituted phthalic anhydride, Newman and Lord[2] have reported that, although the steric hindrance of the ortho-substituted methyl group of 4-methylphthalic anhydride was observed in the reaction with phenylmagnesium bromide, 4,7-dimethylphthalic anhydride reacted smoothly with phenylmagnesium bromide to give the expected keto carboxylic acid in a 81% yield. From the results of this experiment they concluded that, in the reaction of 4,7-dimethylphthalic anhydride, the initial addition of the Grignard reagent to the carbonyl group of the anhydride is not realized because of the steric hindrance of both methyl groups on the 4,7-positions; the reaction appears to be initiated by the cleavage of the anhydride ring.

The reduction of 4,7-dimethylphthalic anhydride with lithium aluminum hydride, however, is reported to consist of the direct reduction of the carbonyl group of the anhydride, without the initial cleavage of the anhydride ring. Buchta and Loew[3] have reported that, because of the difficulty in addition of the hydrogen to carbonyl group caused by the steric hindrance of methyl groups on the 4,7-positions, the reduction of this anhydride with lithium aluminum hydride does not proceed to the formation of the corresponding diol (II) by one step and 4,7-dimethylphthalide (I) is produced in a 88% yield.

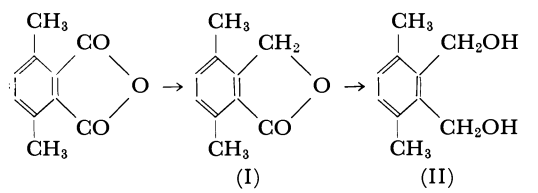

(I) (II)

(1)

Phthalic anhydride (III) is known to react with one mole of phenylmagnesium bromide to give keto carboxylic acid (IV)[4]:

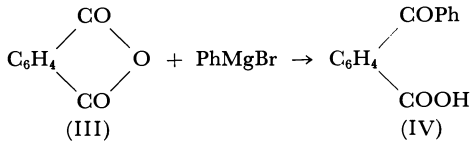

(III) (IV)

(2)

The reaction of III with an equimolar amount of triethylaluminum was found to give none of the keto acids expected from the analogy of the corresponding Grignard reaction, but afforded the reduction product or phthalide (V) in a 46.2% yield.

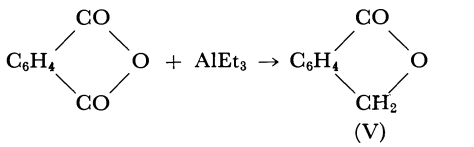

(V) (3)

4-Methylphthalic anhydride reacted with triethylaluminum under the same conditions as in the reaction with III to give unchanged anhydride in a 41% yield. From this apparent depression in the reactivity of 4-methyl homologue as compared with III, it might be concluded that the reaction of III and 4-methylphthalic anhydride proceeded through the direct addition of β-hydrogen of triethylaluminum to the carbonyl group.

The reaction of 4,7-dimethylphthalic anhydride with triethylaluminum found a parallel in the corresponding Grignard reaction rather than in the lithium aluminum hydride reduction. Unlike the reaction of III and 4-methyl homologue, 4,7-dimethylphthalic anhydride reacted readily with triethylaluminum under the same conditions as in the reactions with III and 4-methyl homologue, giving the product,

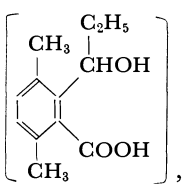

resulting from the addition of the ethyl group in a good yield; practically no unchanged anhydride was obtained.

2) M. S. Newmann and B. T. Lord, *J. Am. Chem. Soc.*, **66**, 733 (1944).
3) E. Buchta and G. Loew, *Ann.*, **597**, 123 (1955).
4) Bauer, *Ber.*, **38**, 240 (1905).

The Reaction of Triethylaluminum with Esters

Yoshio BABA

Resources Research Institute, Kawaguchi, Saitama

(Received April 17, 1967)

It is the aim of the present paper to study the difference in the reactivity appearing to be present between triethylaluminum and the Grignard reagent, through experiments with esters known to have a carbonyl group of a lower reactivity than that of aldehyde or ketone, and to study if the steric effect which has been recognized in the cases of the Grignard reactions could be observed.

Experimental

All reactions were carried out in an atmosphere of dry nitrogen. The melting points were measured on a micro hot stage and were not corrected.

Materials. Commercial methyl benzoate (bp 198—199°C) and methyl phenylacetate (bp 84—85°C/6 mmHg) were purified by distillation. Ethyl 2,4,6-triethylbenzoate (bp 143—144°C/7 mmHg) was synthesized from 1,3,5-triethylbenzene *via* 2,4,6-triethylbromobenzene, 2,4,6-triethylbenzoic acid, and acid chloride.[1] *p*-Tolyl 2,4,6-triethylbenzoate (bp 205—207°C/5 mmHg) was prepared from the corresponding acid chloride and *p*-cresol. Triethylaluminum purchased from the Ethyl Corp. was used without further purification.

Reaction of Methyl Benzoate with Triethylaluminum. Methyl benzoate (0.18 mol) was added, drop by drop, to a gently refluxing 25.0 wt% solution of triethylaluminum in dry petroleum ether ($AlEt_3$ 0.37 mol). After 3 hrs' refluxing, the reaction mixture was cooled in an ice-bath, and the aluminum compound was decomposed with a theoretical amount of ethyl alcohol; then the reaction mixture was poured into an ice-cooled diluted sodium hydroxide solution. The distillation of the crude product gave 25.3 g of an oily product with a boiling point of 95—98°C/16 mmHg. The separation of alcohols in the above fraction by the method described in a previous paper[2] gave 8.1 g (33.3%) of phenylethyl carbinol and 2.2 g (12.5%) of phenyldiethylcarbinol. 3,5-Dinitrobenzoate of phenylethylcarbinol, mp 67—68°C, from ethanol, undepressed by admixture with an authentic sample. The tertiary alcohol fraction was distilled with anhydrous oxalic acid, and the dehydration product was then oxidized with an aqueous alkaline permanganate solution. 2,4-Dinitrophenylhydrazone of the oxidation product, mp 191—192°C, from diluted ethanol, was identified as that of propiophenone by a mixed melting point determination with an authentic sample.

Reaction of Methyl Phenylacetate with Triethylaluminum. The reaction of this ester with two moles of triethylaluminum yielded benzylcarbinol (phenylurethane, mp 79—80°C, from ethanol) and benzyldiethylcarbinol (phenylurethane, mp 99.5—100°C from ethanol).

Reaction of Ethyl and the *p*-Tolyl Ester of 2,4,6-Triethylbenzoic Acid with Triethylaluminum. Ethyl 2, 4, 6-triethylbenzoate (0.05 mol) was mixed with triethylaluminum (0.114 mol) benzene solution and then the reaction solution was refluxed for 6 hr. The crude product was distilled under reduced pressure, and a fraction boiling at 127—129°C/4 mmHg (10 g) was collected. A solution of the above fraction (4 g) in 20 m*l* of glacial acetic acid was mixed with 2 m*l* of 60% sulfuric acid and the mixture was refluxed for 2 hr with stirring. The alkaline permanganate oxidation of the dehydration product gave 3.2 g of an acid substance, mp 113—114°C, from diluted ethanol, which was identified as 2, 4, 6-triethylbenzoic acid by a mixed melting point determination with an authentic sample. A reaction with the *p*-tolyl ester afforded the same product as that obtained in the above reaction.

Results and Discussion

Like Grignard reagents, triethylaluminum reacted with simple esters to give a corresponding secondary alcohol as a principal product, accompanied by tertiary alcohol. Methyl benzoate and methyl phenylacetate, for example, reacted with triethylaluminum to yield the corresponding secondary alcohol as a major product by the normal addition, followed by reduction, and a small amount of tertiary alcohol as a normal addition product.

It has been reported that, in a reaction with an aromatic ester carrying alkyl groups at both the ortho positions of the ester group, such as the mesitoic acid ester, the normal addition of a Grignard reagent to the carbonyl group of the ester function is completely inhibited and carboxylic acid or ketone is obtained as a reaction product instead of the normal product, tertiary alcohol. Fuson[3] has reported that a mesitoic acid ester (I) carrying an alkyl group as the alcohol component of the ester, for example, ethyl mesitoate, does not cause the normal addition reaction with the Grignard reagent, and the corresponding carboxylic acid is obtained as the sole reaction product. On the other hand, in the case of a mesitoic acid ester having an aryl group as the group, R, indicated in Eq. (1), for example, *p*-tolyl mesitoate, the alkyl Grignard reagent can

1) R. C. Fuson and J. Corse, *J. Am. Chem. Soc.*, **60**, 2065 (1938).
2) Y. Baba, This Bulletin, **41**, 928 (1968).
3) R. C. Fuson, E. M. Bottorff and C. B. Speck, *J. Am. Chem. Soc.*, **64**, 1450 (1942).

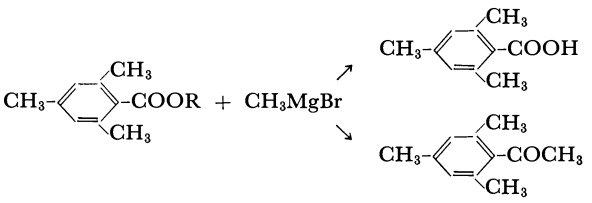

(1)

add to the carbonyl group of the ester, but the reaction product is a ketone consisting of the alkyl group of the Grignard reagent, instead of the corresponding tertiary alcohol expected from the normal addition reaction.

In the present study, it was found that ethyl 2,4,6-triethylbenzoate reacted with two molecular amounts of triethylaluminum to give neither carboxylic acid nor ketone, but a mixture of tertiary and secondary alcohols as the main reaction product. The analysis of the active hydrogen and secondary alcohol contents indicated that the secondary alcohol was the major product. That the reaction product mainly consisted of secondary alcohol was verified by the following facts. The oily product obtained from the reaction of ethyl 2,4,6-triethylbenzoate with triethylaluminum was subject to ready dehydration with 60% sulfuric acid, and the dehydration product gave the corresponding carboxylic acid, 2,4,6-triethylbenzoic acid, in a good yield by alkaline permanganate oxidation. This fact suggests that the reaction product might consist mainly of secondary alcohol or 2,4,6-triethylphenylethylcarbinol, as indicated in Eq. (2); thus, the reaction seems to proceed through the normal addition of one al-Et group to the carbonyl group of the ester followed by the reduction instead of the second normal addition of the second al-Et group.

The reaction of *p*-tolylester of 2,4,6-trisubstituted benzoic acid with triethylaluminum also differed from the corresponding Grignard reaction, the

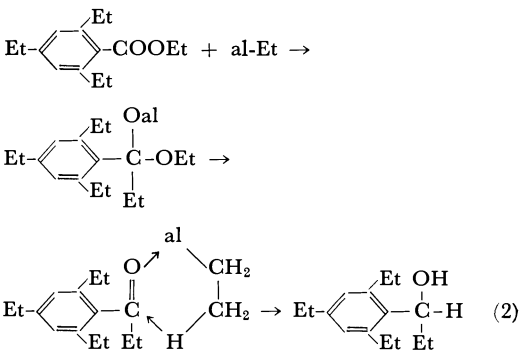

(2)

former reaction found a parallel in the reaction with the ethyl ester of 2,4,6-triethylbenzoic acid.

It may be concluded from the results of these experiments that, in the case of a simple ester, there is practically no difference between the reaction with trialkylaluminum and that with the Grignard reagent. In the case of a sterically hindered ester, however, the reaction with triethylaluminum proceeds through the normal addition or reduction reaction as observed in the reaction of a simple ester; none of the abnormal reactions expected from the analogy of the Grignard reaction take place.

The author wishes to thank Dr. J. Yoshimura, Professor of Tokyo Institute of Technology, for his many helpful discussions and suggestions during this work.

Continuous and Simultaneous Removal of Anions and Dissolved Oxygen from Water by an Ion Exchange Membrane Cell

Zdeněk MATĚJKA

Research Institute for Industrial Water Treatment, Prague, Czechoslovakia

(Received May 20, 1967)

Dissolved oxygen can be removed from anion-free water by an ion-exchange process[1] based on the interaction of dissolved oxygen with a sulfite form of a strongly basic anion exchange resin, according to the equation

$$2R_2SO_3 + O_2 \rightarrow 2R_2SO_4 \qquad (1)$$

On passing the treated solution through the column of the anion exchanger in a sulfite form, the content of dissolved oxygen is reduced below 10 ppb. This process is discontinuous. After exhaustion it is necessary to convert the resin to a sulfite form with a sodium sulfite solution. This process has now been carried out continuously in an electrolytic membrane cell.

Apparatus. A 4-compartment membrane cell (Fig. 1) has been used for experiments. Electric conductivity has been measured with a conductometer Radelkis Budapest. Dissolved oxygen has been estimated by the Töller method,[2] with a sensitivity as low as 10 ppb.

Procedure. Sulfite ions are transported under the influence of an applied electric potential from compartment III across membrane AM_1 into packed compartment II, and thus particles of resin are continuously converted into the sulfite form. Sulfate ions, resulting from the reaction (1), are transported across membrane AM_2 into anode compartment I. Treated water passes through the packed compartment II, and a continuous uptake of dissolved oxygen takes place in this compartment. It has been found that only such an amount of sulfite ions should be transported across membrane AM_1 which can be immediately absorbed by the given amount of resin in compartment II. Under these conditions, sulfite and sulfate ions are transported across packed compartment II toward membrane AM_2 preferably within the resin particles and do not remain in the solution.

When a greater number of sulfite ions than can be absorbed by the anion exchanger in compartment II are transported across membrane AM_1, they remain in solution and contaminate the deoxygenated effluent, increasing the electric conductivity of the deoxygenated water (Table 1, Run 1).

TABLE 1. SIMULTANEOUS REMOVAL OF DISSOLVED OXYGEN AND ANIONS FROM WATER

Run No.	SO_3^{2-} inlet concn. (equiv·l^{-1})	SO_3^{2-} flow rate (l·h^{-1})	Current density (mA·cm^{-2})	Effluent electric conductivity (m℧·cm^{-1})
1	0.025	0.75	7.7	10.0
2	0.025	0.54	7.7	5.5
3	0.025	0.47	7.7	2.5
4	0.011	2.70	2.3	5.5
5	0.011	2.70	2.75	1.8
6	0.011	2.70	4.0	1.3

Dissolved oxygen content of the outlet in all runs below 10 ppb.
Treated solution:
in runs No. 1—5: distilled water (electric conductivity 5.5 m℧·cm^{-1}, flow rate 1.0 l·h^{-1});
in run No. 6: 0.002 N H_2SO_4 solution, flow rate 0.7 l·h^{-1}; SO_3^{2-} outlet concentration = 0.0092 equiv·l^{-1}

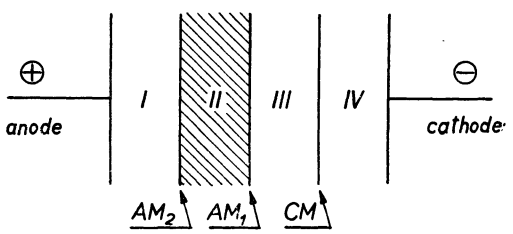

Fig. 1. 4-Compartment cell.

AM_1, AM_2: anion exchange membrane Permaplex A-20
CM: cation exchange membrane Permaplex C-20
Effective membrane area: 125 cm^2
Height of packed compartment: 25 cm
Width of packed compartment (distance of membranes): 0.3 cm
Material used: plexiglass
I: anode compartment
II: compartment packed with particles of the strongly basic anion exchange resin Zerolit FF (size 60—80 mesh)
III: SO_3^{2-} solution compartment
IV: cathode compartment

The number of sulfite ions transported across membrane AM_1 has been checked by evaluating the concentration polarisation, which causes a

1) V. Kadlec and A. Brodský, *Chem. listy*, **58**, 891 (1964).
2) K. Buriánek, *Energetika*, **7**, 21 (1957).

decrease in the transport numbers of the ions of the electrolyte.[3] A concentration polarisation arises under certain conditions (given by the concentration of the sulfite solution, flow rate and current density) on the surface of membranes AM_1 and CM in compartment III. The number of transported sulfite ions is, in this way, kept at the desired level. Contamination of effluent does not appear. Electric conductivity of deoxygenated water remains unchanged (Table 1, Run 2).

A strongly basic anion exchange resin in sulfite form in the column can be used for removing of dissolved oxygen from anion-free water only. Anions, present in the solution, displace, during the working period, sulfite ions into the effluent, causing both a capacity and efficiency decrease.

In the process of continuous removal of dissolved oxygen by the packed bed membrane cell, the presence of anions does not interfere. Resin in the packed membrane cell is continuously and simultaneously converted into sulfite and hydroxide forms and it is capable of the quantitative uptake of both dissolved oxygen and anions from water. By a variation in the conditions on which the concentration polarisation depends, one can vary the ratio of the functional groups converted into hydroxide and sulfite forms. It enables the treatment also of solutions which are rich in anions.

If the concentration of the sulfite solution, while passing through the cell, drops remarkably, the concentration polarisation increases and proceeds nonuniformly, *i. e.*, at the outlet increases more than at the inlet. Owing to this fact, some lower portions of the anion exchanger are converted into the hydroxide form only, and the removal of dissolved oxygen will cease. Therefore, the sulfite solution concentration can be reduced only slightly on passing the cell.

The results, obtained in experiments with distilled water and 0.002 N sulfuric acid solution are given in Table 1. It has been shown possible to reduce the dissolved oxygen content below 10 ppb, and simultaneously to remove all anions present in solution (electrical conductivity of the treated solution at the outlet $\kappa = 1.3\ m\mho \cdot cm^{-1}$) (Table 1, Run 6).

3) T. R. E. Kressman and F. L. Tye, *Discussions Faraday Soc.*, **21**, 185 (1956); N. W. Rosenberg and C. E. Tirrell, *Ind. Eng. Chem.*, **49**, 780 (1957); B. A. Cooke and S. J. van der Walt, *Electrochimica Acta*, **5**, 216 (1961).

Concurrent Oxygen Exchange and Racemization Reactions of Diaryl Sulfoxides in Phosphoric Acid*[1]

Norio KUNIEDA and Shigeru OAE

Department of Applied Chemistry, Faculty of Engineering, Osaka City University, Sumiyoshi-ku, Osaka

(Received October 6, 1967)

Several works have been reported on the acid-catalyzed oxygen exchange and racemization reactions of sulfoxides.[1)]

In this note, we wish to report that phosphoric acid[2)] can also cause the concurrent oxygen exchange and racemization reactions of various diaryl sulfoxides while recovering of the sulfoxides is quantitative when quenched with a large amount of water.

For a typical run, 100 mg of ^{18}O-labeled[3)] (0.97 atom% ^{18}O) or optically active[4)] ($[\alpha]_D=+27.1°$, $c=3.6$ $l=1$, in ethanol) *p*-tolyl phenyl sulfoxide was dissolved in 5.0 m*l* of 85% phosphoric acid, and the solution was kept for 2 hr at 120°C; then the resulting pale blue solution was diluted with 30 m*l* of normal water or 30 m*l* of ^{18}O-enriched water (0.45 atom% ^{18}O). The sulfoxide can be recovered as crystalline solid almost quantitatively from the aqueous solution, and its melting point and IR spectrum were found to be identical to those of the starting sulfoxide. The sulfoxides thus recovered under the two different conditions were found to be racemized and also incorporated with ^{18}O of the same concentration of ^{18}O as shown in Table 1.

*1 Paper XXI on "Sulfoxide."

1) a) In Sulfuric Acid: S. Oae, T. Kitao, Y. Kitaoka and S. Kawamura, This Bulletin, **38**, 546 (1965); S. Oae and N. Kunieda, *ibid.*, **41**, 696 (1968). b) In Hydrogen Chloride-Dioxane: K. Mislow, T. Simmons, J. Millow and A. L. Ternay, *J. Am. Chem. Soc.*, **86**, 1452 (1964). c) In Polychloroacetic Acid: S. Oae, M. Yokoyama and M. Kise, unpublished work.

2) Day and Cram have reported that (+)*p*-tolyl methyl sulfoxide was recemized in polyphosphoric acid; J. Day and D. J. Cram, *J. Am. Chem. Soc.*, **87**, 4398 (1965).

3) ^{18}O-Labeled sulfoxides were prepared by the oxidation of the corresponding sulfides with bromine complex of pyridine and ^{18}O-enriched water (1.63 atom%); S. Oae, Y. Onishi, S. Kozuka and S. Oae, This Bulletin, **39**, 364 (1966).

4) Optically active sulfoxides were prepared from (−)menthyl (−)-*p*-toluenesulfinate according to the method developed by Andersen; K. K. Andersen, *Tetrahedron Letters*, **1962**, 93.

Table 1. Oxygen exchange and racemization of *p*-tolyl phenyl sulfoxide in 85% phosphoric acid at 120°C

	^{18}O-Concentration (atom%)	Rotation $[\alpha]_D$ (in EtOH)
Starting sulfoxide	0.97	+27.1° (c=3.6 l=1)
Recovered sulfoxide		
Quenched with $H_2{}^{18}O$ (0.45 atom%)	0.28	
Quenched with H_2O	0.29	+3.8° (c=3.0 l=1)
Natural CO_2	0.21	

In order to understand the nature of these concurrent oxygen exchange and racemization reactions, we have compiled a substantial amount of kinetic data on the reactions of the diaryl sulfoxides. None of the sulfoxides used was found to undergo thermal racemization under the present condition. The kinetic data of both oxygen exchange and racemization are listed in Table 2.

Table 2. Rate constants of oxygen exchange and racemization of *p*-CH_3-C_6H_4-SO-R[3,4] in 85% phosphoric acid

No.	R[a]	Temp. °C	$k_r \times 10^4$ sec^{-1}	$k_{ex} \times 10^4$
1	C_6H_5	110	0.871±0.046	
2[b]	C_6H_5	120	1.98±0.11	1.93±0.11
3	C_6H_5	130	4.20±0.22	
4	*m*-CH_3-C_6H_4	120	1.91±0.08	
5[c]	*p*-Cl-C_6H_4	120	1.25±0.05	1.27±0.06
6	*o*-Cl-C_6H_4	120	0.543±0.013	

a) Sulfoxide=0.1 mol/l
b) k_{ex}/k_r=0.975, E_a=24.1 kcal, $\Delta S^{\neq}$=−15.7 e.u.
c) k_{ex}/k_r=1.02

The rate of the oxygen exchange was identical to that of the racemization (See; Run No. 2 and 5 of Table 2), which is presumed to suggest that the reaction proceeds through a S_N1 like S–O bond cleavage of the sulfoxide.[5] The whole pattern of substituent effects is quite similar to that of the concurrent oxygen exchange and racemization reactions of diaryl sulfoxides in sulfuric acid.[1a] Apparently, the diaryl sulfoxide dissociates in phosphoric acid to form the hydroxysulfonium ion,[6] and then the partial cleavage of the S–O bond will take place at the transition state. As for the cleavage of the S–O bond, two different ways are conceivable; the one is the heterolysis of the S–O bond to form the sulfidonium ion [A] and the other is the homolysis to form the radical cation [B].

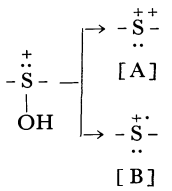

The very small polar effects of substituents on the rates of both oxygen exchange and racemization reactions seem to suggest that the reaction follows the homolytic cleavage.

Diphenyl sulfone was found not to undergo these reactions under the same reaction condition.

The detailed studies of these reactions and ESR measurements now in progress in our laboratory will shed further light on these problems.

Experimental

Kinetic Procedures of the Oxygen Exchange and Racemization Reactions of Diaryl Sulfoxides. An aliquot of ^{18}O-labeled[3] or an optically active[4] sulfoxide was dissolved in 85% phosphoric acid, maintaining the concentration of the sulfoxide to be 0.1 mol/l, at a preset temparature. An aliquot portion (5.0 ml) of the solution was taken up from time to time for 5—7 times and was quenched with ice water. Then the sulfoxide was recovered for both the ^{18}O-analysis and the optical activity measurement by the same procedure described in our previous paper.[1a]

5) D. Samuel and B. L. Silver, "Oxygen Isotope Exchange Reactions of Organic Compounds," in "Advances in Physical Organic Chemistry," Vol. 3, ed by V. Gold, Academic Press, London & N. Y. (1965), p. 129.

6) It is known that sulfoxides ionize in concentrated sulfuric acid to form the hydroxysulfonium ion: S. Oae, T. Kitao and Y. Kitaoka, This Bulletin, **38**, 543 (1965); R. J. Gillespie and R. C. Passerini, *J. Chem. Soc.*, **1956**, 3850.

Rotational Isomers in the Crystals of DL-α-Amino-n-butyric Acid

Tadayoshi ICHIKAWA, Yoichi IITAKA and Masamichi TSUBOI

Faculty of Pharmaceutical Sciences, The University of Tokyo, Hongo, Bunkyo-ku, Tokyo

(Received October 12, 1967)

For DL-α-amino-n-butyric acid, two crystalline modifications were previously found.[1] They were called as A- and B-forms. A-form is monoclinic, with the space group of $P2_1/a$, and with the unit cell dimensions: $a=9.85$ Å, $b=4.77$ Å, $c=11.94$ Å, $\beta=101°$, $Z=4$. B-form is tetragonal, with $P4_2/n$, $a=13.40$ Å, $c=5.82$ Å, and $Z=8$. By our recent X-ray analyses, it has now been established that all of the three rotational isomers (I, II, and III) shown in Fig. 1 are coexisting in the A-form crystal, whereas only one conformation (II in Fig. 1) is found in the B-form crystal.

Three-dimensional intensity data were collected from multiple-film equi-inclination Weissenberg photographs taken with filtered Cu$K\alpha$ radiation. For the A-form crystal, data of 809 reflections were used. First, the sharpened three-dimensional Patterson function was calculated. From this function, approximate coordinates of two oxygen atoms were estimated. The signs based upon these coordinates were used in the first three-dimensional Fourier synthesis. The coordinates of all the heavy atoms except those of the γ-carbon could be obtained in the Fourier map. In the course of the refinement, the γ-carbon atom was found to be distributed over the three positions corresponding to the three rotational isomers shown in Fig. 1. Therefore, the site occupancy factors of the γ-C in the three positions were set as parameters in the least squares refinement. After two cycles of full matrix least squares calculation with anisotropic temperature factors, the R factor dropped to 0.13. At the right end of Fig. 1, an electron density map of a section through the centers of the three possible methyl groups is given, which is obtained from the difference Fourier synthesis. This map shows how the methyl group (and two hydrogen atoms) on the β-carbon are distributed among the possible sites in the internal rotation around the C_α–C_β axis. The dihedral angles $C_\gamma C_\beta C_\alpha N$ determined are given in Table 1.

TABLE 1. DIHEDRAL ANGLES[a] $C_\gamma C_\beta C_\alpha N$ IN α-AMINO-n-BUTYRIC ACID

A-form	I	72.4°	(36%[b])
	II	−174.6	(40%)
	III	−53.8	(24%)
B-form		−176.0	

a) This angle is defined so that it is zero when C_β–C_γ bond comes at the eclipsed position with respect to the C_α–N bond. The positive direction is defined as that of the anticlockwise rotation of the C_β–C_γ bond, when viewed along the $C_\beta \rightarrow C_\alpha$ bond as shown in Fig. 1.

b) Normalized site occupancy factors as determined by the least squares calculation.

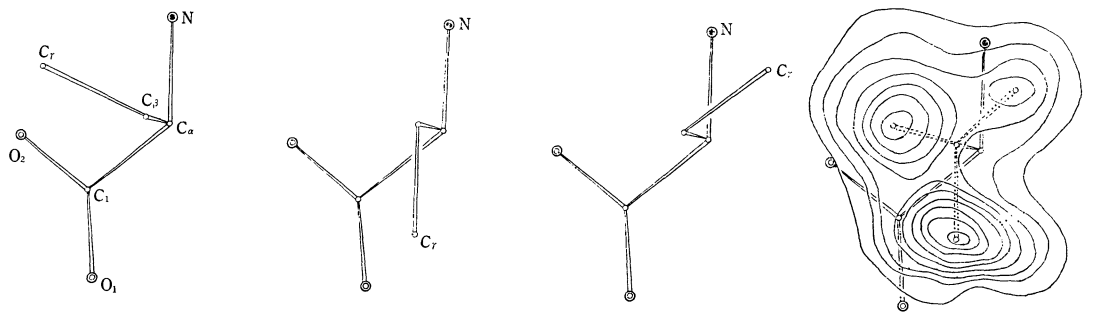

I II III Observed (A-form)

Fig. 1. Rotational isomers I, II, and III expected for α-amino-n-butyric acid. What is given at the right end is a section of the electron density map at the CH_3 group of A-form. This was obtained by a difference Fourier synthesis by the use of the structure factors calculated on the basis of all the heavy atoms except the γ-carbon. In this synthesis, there appeared three maxima corresponding to the three stable positions of C_γ, and this section was prepared through the plane determined by these three points. The figure is the projection along the c-axis of this section. Contours are drawn at 0.1, 0.2,···, 0.9 electron Å^{-3}.

1) M. Tsuboi, Y. Iitaka, S. Suzuki and S. Mizushima, This Bulletin, **32**, 529 (1959).

For the B-form crystal, intensities of 630 reflections were measured. The Harker section at $w=1/2$ allowed us to estimate only two-dimensional (x and y) coordinates of oxygen atoms and it was not possible to estimate the z parameters from the Patterson function. Accordingly, the analysis was started with two dimensional Fourier methods. After the x and y coordinates of all the heavy atoms (except C_γ) were determined, the approximate z coordinates of these atoms were estimated on the basis of a model-building. The first three-dimensional Fourier synthesis was made on the basis of the estimated coordinates of the two oxygen and one nitrogen atoms. All the carbon atoms including C_γ appeared at reasonable positions. C_γ appeared at the trans position to the NH_3^+ group, with the dihedral angle of $-176°$ (II of Fig. 1). It was ascertained that C_γ takes only this site by a three-dimensional difference Fourier synthesis based upon the coordinates of the heavy atoms except C_γ. After three cycles of least squares refinement with isotropic temperature factors, the R value reached 0.12.

More detailed crystallographic data as well as a full account of the crystal structures of the A- and B-forms of this amino acid will be given elsewhere.

This work was supported partly by a grant from the Ministry of Education, and partly by a grant from the United States Public Health Service GM 10024-04.

Potential Step Reduction of the Surface Oxide of Platinum Electrodes

Masaki Ioi

Department of Applied Chemistry, Faculty of Engineering, Osaka City University, Sumiyoshi-ku, Osaka

and Kazuo Sasaki

Department of Applied Chemistry, Faculty of Engineering, Hiroshima University, Sendamachi, Hiroshima

(Received October 24, 1967)

In previous papers,[1,2] we reported that the cathodic reduction of the surface oxide of a platinum electrode obeys a second order rate law with respect to the fractional coverage of the oxide. An empirical rate equation we proposed for the reaction concerned was

$$i = n\boldsymbol{F}kq^2 \exp(\alpha n\boldsymbol{F}E/\boldsymbol{R}T) \qquad (1)$$

where q is the quantity of the surface oxide to be reduced expressed in g atoms per square centimeter. Two constants in this equation were determined as $k=1.3$ cm^2 mol^{-1} sec^{-1} at 1.3 V SCE and $\alpha=0.26$.

The discussions therein made were mainly based on the results of cyclic voltammetry and chronopotentiometry. In this paper, we shall describe the results obtained by a potential step method.

Basic Concept. Generally, when an electrode reaction accompanied by a simultaneous detachement of an ad-layer at the electrode surface obeys one of the following rate equations

$$i = n\boldsymbol{F}k \exp(\alpha n\boldsymbol{F}E/\boldsymbol{R}T + \gamma q) \qquad (2)$$

$$i = n\boldsymbol{F}kq \exp(\alpha n\boldsymbol{F}E/\boldsymbol{R}T) \qquad (3)$$

or $$i = n\boldsymbol{F}kq^2 \exp(\alpha n\boldsymbol{F}E/\boldsymbol{R}T) \qquad (1)$$

then the current transient at a constant electrode potential should obey one of the following equations, respectively.

$$1/i = \gamma t/nF + 1/i_0 \qquad (2a)$$

$$i = i_0 \exp(-At); \qquad i_0 = nFAq_0 \qquad (3a)$$

or $$1/q = At + 1/q_0 \qquad (1a)$$

where A stands for $k \exp(\alpha n\boldsymbol{F}E/\boldsymbol{R}T)$ and q_0 is the total quantity of the surface oxide to be reduced (g atom/cm^2).

These equations will be examined in the following part of this paper.

Results. In order to confirm the validity of Eq. (1) and hence Eq. (1a), we carried out a series of experiments in 1 N sulfuric acid solutions. A potentiostaic rectangular pulse (repeating frequency: 1 cps, duty ratio: 1) was applied to the working electrode by means of NS-2 model pulse generator of Nichia-Keiki Co. The current transient was photographed using a 50 MC synchroscope (Model 502-A, Matsushita Communication Ind. Co.). Anodic pulse level was kept at 1.2 V against a saturated calomel reference electrode and the cathodic potential was varied between 0.2 to 0.4 V. A cross section of a 1 mm platinum wire sealed in a soft glass tube was used as the working electrode.

In Fig. 1, a typical current transient observed when the potential was stepped down from 1.2 to 0.4 V is shown. It was confirmed that Eq. (1a) best fitted for this curve. This is shown in

1) K. Ohashi, K. Sasaki and S. Nagaura, This Bulletin, **39**, 2066 (1966).
2) K. Sasaki and K. Ohashi, *Electrochim. Acta*, **12**, 366 (1967).

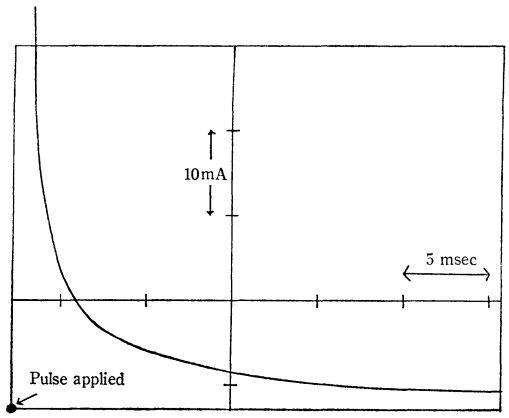

Fig. 1. The transient current for the reduction of surface oxide electrode potential stepped down from 1.2 V to 0.4 V SCE.

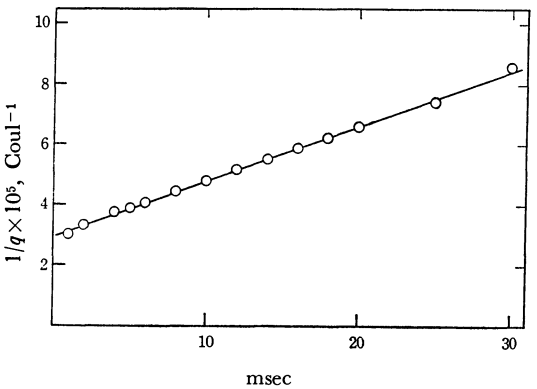

Fig. 2. Examination of Eq. (1a).

Fig. 2 where the reciprocal of the amount of the surface oxide to be reduced is plotted against time. According to Eq. (1a), the slope of the curve must be $k\exp(\alpha nFE/RT)$ so that the logarithmic expression of the slope is

$$\ln s = \ln k + \alpha nFE/RT \quad (4)$$

Accordingly, the transfer coefficient α should be determined from the determination of the slope at various cathodic potentials. The rate constant k will also be determined from the intersect of the $\ln s$ *vs.* E curve. This is shown in Fig. 3. The two constants determined from Fig. 3 were $\alpha = 0.25_5$ and $k = 2.8$ cm^2/mol sec at 1.3 V SCE, respectively. These are in good agreement with the values mentioned in the first of this paper.

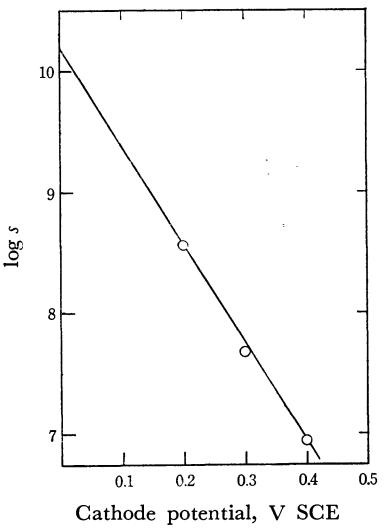

Fig. 3. Graphic representation of Eq. (4).

We are indeed grateful to Professor S. Nagaura for his constant encouragement. We are also grateful to Mr. K. Ohashi for his valuable discussions.

SHORT COMMUNICATIONS

Solvent Effects on ^{14}N Chemical Shifts in Formamides

Hirotake KAMEI

Electrotechnical Laboratory, Tanashi, Tokyo

(Received February 5, 1968)

Small chemical shifts in the ^{14}N resonance due to solvent effects have been lost in the experimental error in usual determinations.[1,2] In the present work, ^{14}N chemical shifts in formamide and its derivatives in acetone and methanol solutions were determined at various concentrations by a ^{1}H-{^{14}N} partial irradiating double resonance method. By this method, the chemical shifts can be determined more precisely than by direct, or usual indirect methods, and the small shifts are easily detectable.

Measurements were carried out on a JEOL JNM-3H-60 spectrometer equipped with a ^{1}H-{^{14}N} double resonance attachment.[3] The second radio-frequencies were measured which produced maximizations in the peak heights of the proton resonance lines. The nitrogen-14 resonance frequency of each sample was obtained from an average of the frequencies of the lines in a formyl proton multiplet. The reference was a 4.5 M solution of ammonium nitrate in 3 N aqueous hydrochloric acid. The nitrogen-14 resonance frequency of the ammonium ion was determined within ± 0.1 Hz. The chemical shifts of the amides were obtained relative to the ammonium ion and converted to the nitrate ion scale. The chemical shift of the ammonium ion relative to the nitrate ion has been taken as 353.5 ppm.[1] Extrapolated chemical shifts of amides at infinite dilution are given in Table 1.

TABLE 1. ^{14}N CHEMICAL SHIFTS IN FORMAMIDES
(In ppm referred to NO_3^-)

Compound	Chemical shifts		
	Neat	Infinite dilution acetone	Infinite dilution methanol
F	265.5±0.4	274±2.0	268±1.5
NMF	266.4±0.7	272±2.0	267±1.5
DMF	272.3±0.5	273±1.5	264±1.5
NEF	247.1±0.7	253±2.0	247±1.5
DEF	246.5±0.5	247±1.5	237±1.5

In the acetone solutions of formamide (F), *N*-methyl formamide (NMF) and *N*-ethyl formamide (NEF), high field shifts are observed on dilution. In the methanol solutions of *N,N*-dimethyl formamide (DMF) and *N,N*-diethyl formamide (DEF), the ^{14}N resonances are shifted to low field on dilution. Detectable dilution shifts are not found in methanol solutions of NMF and NEF, and in acetone solutions of DMF and DEF. These solvent shifts are attributed to the hydrogen bonding interaction involving the carbonyl oxygen of the amide. The amide group is generally represented by the canonical forms I and II.

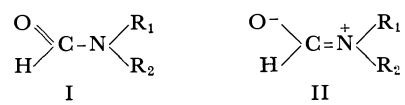

I II

It has been postulated that the ^{14}N chemical shifts is dominated by the paramagnetic term σ_p.[1] Because of the greater asymmetry of the electronic structure around the nitrogen nucleus, the ^{14}N resonance of form II would be expected to occur at lower field than that of form I. Hydrogen bond formation on carbonyl oxygen should increase the contribution of form II, and causes a low field shift. The effect of substituent on the chemical shift is also observed. The above facts indicate that chemical shifts at infinite dilution in inert solvents are needed for detailed discussions on substituent shifts.

1) D. Herbison-Evans and R. E. Richards, *Mol. Phys.*, **8**, 19 (1964).
2) P. Hampson and A. Mathias, *Mol. Phys.*, **11**, 541 (1966).
3) H. Kamei, *Japanese J. Appl. Phys.*, **4**, 212 (1965).

Unstable Intermediates. The Electronic Structures of Benzynes and Hetarynes

Teijiro YONEZAWA, Hideyuki KONISHI and Hiroshi KATO

Faculty of Engineering, Kyoto University, Sakyo-ku, Kyoto

(Received January 18, 1968)

Benzynes are known to be typical unstable intermediates on the basis of many experimental results.[1] Hetarynes, benzyne analogues derived from heteroaromatic compounds, such as 3,4-pyridyne,[2],*1 4,5-pyrimidyne[3] and 2,3-thiophyne[4] may also be supposed to be unstable intermediates. Calculations have been carried out for benzyne and 3,4-pyridyne by several authors,[5-8] but the electron interaction has never explicitly been taken into account in these treatments. In the present paper, calculations on these intermediates and their isomers are performed using a semi-empirical SCF MO method for valence electron systems previously reported on by us.[9] Here, however, our procedure is simplified by assuming the zero-differential overlap.*2

To estimate the unknown bond lengths of arynes, we utilize such a SCF procedure as has been proposed by Coulson,[5] a procedure which makes use of an empirical curve relating the bond order to the bond length.[10] In the present treatment, we use the following relation between the bond order and the total electronic energy, E_{AB}, of the AB bond:

$$E_{AB} = \sum_{r}^{A} \sum_{s}^{B} P_{rs}(H_{rs} + F_{rs})$$

where $\sum_{r}^{A}$ denotes the summation over all the valence AO's which belong to the A atom, and P_{rs}, H_{rs} and F_{rs} are, respectively, the bond order, the core-resonance integral, and Fock's operator between the rth and the sth AO's. The curve is obtained by plotting the E_{AB} values *vs.* the observed bond lengths, R_{AB}, for typical molecules (for example, C_2H_6, C_2H_4, C_6H_6, C_2H_2, *etc.* as to the carbon-carbon bonds). The iteration is repeated until a self-consistency between the initial R_{AB} and that graphically-obtained.

The bond lengths after iteration for the carbon-carbon "triple" bond, presumed to be so at the beginning of the calculations, are as follows (in Å units): 1.29 for benzyne, 3,4-pyridyne, and 2,3-pyridyne; 1.31 for 4,5-pyrimidyne; 1.26 for 2,3-thiophyne and 1.33 for 3,4-thiophyne. These bonds are probably triple bonds in view of their short lengths and large π and π' bond orders. Calculation shows further that the highest occupied (HO) and the lowest vacant (LV) molecular orbitals of arynes may be approximately described as linear combinations of nonbonding sp^2-type hybrids[11] of the carbon atoms in the C≡C bond.

TABLE 1. THE CALCULATED LOWEST TRANSITION ENERGIES (σ-σ^*) OF ARYNES (eV)

	State	Singlet	Triplet
Benzyne	B_2	3.73	1.65
3,4-Pyridyne	A′	3.44	1.82
2,3-Pyridyne	A′	3.13	1.60
4,5-Pyrimidyne	A′	2.56	1.46
2,3-Thiophyne	A′	2.80	0.85
3,4-Thiophyne	B_2	2.91	0.86

The calculated lowest transitions are the σ-σ^* type transitions between HO and LV levels mentioned above; the transition energies are presented in Table 1. In Table 1, it may be seen that the lowest triplet states of such arynes as thiophynes lie very close to the ground states. The calculated energies of n-π^* type transitions (4.20 eV for the pyridine $^1B_1$ state, 5.02 eV for the 3,4-pyridyne $^1A''$ state, and 5.95 eV for the 2,3-pyridyne $^1A''$ state) indicate that there exist blue shifts of the bands, taking pyridine as the basis. The larger shift in 2,3-pyridyne than in 3,4-pyridyne may be due to the stronger interaction between the lone pair on the nitrogen atom and the nonbonding sp^2-type hybrids on the carbon atoms. Full details will be published in the near future.

*1 This may also be called 3,4-dehydropyridine.

*2 Full details of the present treatment will be published in the near future.

1) H. Heaney, *Chem. Revs.*, **62**, 81 (1962).
2) Th. Kauffman, F.-P. Boettcher and J. Hansen, *Angew. Chem.*, **73**, 341 (1961).
3) H. C. van der Plas, *Tetrahedron Letters*, **1965**, 555.
4) G. Wittig, *Angew. Chem. Intern. Ed.*, **1962**, 415.
5) C. A. Coulson, *Chem. Soc. Special Publ. (London)*, **12**, 100 (1958).
6) R. Hoffmann and A. Imamura, private communication.
7) T. Yonezawa, H. Konishi, H. Kato, K. Morokuma and K. Fukui, *Kogyo Kagaku Zasshi (J. Chem. Soc. Japan, Ind. Chem. Sect.)*, **69**, 869 (1966).
8) H. L. Jones and D. L. Beveridge, *Tetrahedron Letters*, **1964**, 1577.
9) T. Yonezawa, K. Yamaguchi and H. Kato, This Bulletin, **40**, 536 (1967); H. Kato, H. Konishi and T. Yonezawa, *ibid.*, **40**, 1017 (1967).
10) C. A. Coulson, *Proc. Roy. Soc.*, **A169**, 413 (1939).
11) C. K. Ingold and G. W. King, *J. Chem. Soc.*, **1953**, 2702.

Novel Reactions of Iodosobenzene with Various Organic Compounds

Takao TAKAYA, Hiroji ENYO and Eiji IMOTO

Department of Applied Chemistry, School of Engineering, University of Osaka Prefecture, Sakai, Osaka

(Received January 24, 1968)

Little attention has so far been paid to the chemistry of iodosobenzene[1] with various organic compounds. When a solution of an alcohol (RCH_2OH, 10 mmol) and iodosobenzene (11 mmol) in dry dioxane (20 m*l*) was refluxed for 12 hr in a stream of nitrogen gas, the corresponding aldehydes (RCHO) were obtained in the following yields[2]: (R, %); (C_6H_5–, 85), (*p*-CH_3-C_6H_4–, 98), (*p*-CH_3O-C_6H_4–, 67), (*p*-Cl-C_6H_4–, 79), (C_6H_5CH=CH–, 88), (CH_2=CH–, 56), (H–, 40)[3], (CH_3–, trace)[3], (*n*-C_3H_7–, trace), and (2-furyl, 31). Glyoxal was obtained from ethylene glycol in a 15% yield. When 20 mmol of iodosobenzene were used to 10 mmol of benzyl alcohol, the yield of benzaldehyde was 86%. This result seems to show that the oxidation of benzaldehyde to benzoic acid does not proceed. In fact, when benzaldehyde was treated with iodosobenzene under similar conditions, benzaldehyde was recovered in a 90% yield.

Compounds other than primary alcohols were also oxidized by iodosobenzene under conditions similar to those described above. The results are summarized in Table 1.

Another interesting reaction of iodosobenzene is the dehydration of the dibasic acid of the *cis*-Ia[4] or Ib[4] type to the corresponding anhydride, IIa[4] or IIc, and that of 1,4-butanediol to tetrahydrofuran (see Table 1):

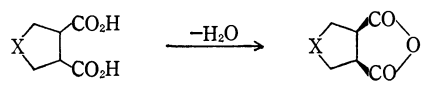

Ia: X=CH_2 IIa: X=CH_2
Ib: X=S
Ic: X=SO IIc: X=SO

After the *cis*-Ib (10 mmol) and iodosobenzene (20 mmol) in dioxane (20 m*l*) had been refluxed for 12 hr, the reaction mixture was evaporated to dryness *in vacuo* and the residue was recrystallized from acetone to give IIc in a 78% yield; mp 205—207°C. *trans*-Ib did not afford IIc, but instead the sulfoxide *trans*-Ic was obtained in a 27% yield; mp 170—171°C from ethanol-acetone. Similarly, *cis*-Ia gave the anhydride IIa in a 65% yield, but the use of *trans*-Ia resulted in its recovery in a 70% yield. Under the above reaction conditions, no formation of an anhydride, IIa or IIc, from *cis*-Ia or Ib was observed in the absence of iodosobenzene.

TABLE 1. OXIDATION OF COMPOUNDS OTHER THAN PRIMARY ALCOHOLS*1

A solution of compounds (10 mmol) and iodosobenzene (11 mmol) in dioxane was refluxed in each run.

Compound	Reaction time hr	Product	Method of isolation	Yield, %
$C_6H_5CH_3$	12	C_6H_5CHO	a	17
$C_6H_5CH_2Cl$	12	C_6H_5CHO	a	14
Cyclohexanol	12	Cyclohexanone	a	26
C_6H_5SH	2	$(C_6H_5S-)_2$	b	76
p-NO_2-$C_6H_4NH_2$	6	$(p\text{-}NO_2\text{-}C_6H_4N=)_2$	b	40
$(C_6H_5NH-)_2$	2	$(C_6H_5N=)_2$	b	100
HO-$(CH_2)_4$-OH	2	Tetrahydrofuran	c	40
Hydroquinone	12	Quinhydrone	b	98
Hantsch Ester	6	DLD*2	b	79

a) An acidic solution of 2,4-dinitrophenylhydrazine was added to the reaction mixture, and the precipitate thus obtained was separated, washed with hot water, dried, and then weighed.
b) The reaction mixture was evaporated to dryness, and the residue was purified by recrystallization.
c) The reaction mixture was subjected to distillation to give the liquid product.
*1 Except 1,4-butanediol.
*2 DLD=Diethyl 2,6-lutidine-3,4-dicarboxylate.

1) A. H. Ford-Moore (*J. Chem. Soc.*, **1949**, 2126) has reported that iodosobenzene is a reagent for the oxidation of sulfides to sulfoxides without further oxidation to sulfones. For the method of preparation, see H. J. Lucas, E. R. Kennedy and M. W. Formo, "Organic Syntheses," Coll. Vol. III, p. 483 (1955).

2) The yields were calculated from the weight of the 2, 4-dinitrophenylhydrazone in each run.

3) The reaction was carried out in the absence of a solvent.

4) T. Takaya, H. Yoshimoto and E. Imoto, This Bulletin, **40**, 2636, 2844 (1967).

A New Organometallic Compound with a Ga–Mn Bond

Satoru ONAKA, Toschitake IWAMOTO and Yukiyoshi SASAKI

Department of Chemistry, Faculty of Science, The University of Tokyo, Hongo, Tokyo

(Received February 7, 1968)

In this communication, we report a compound having a Ga–Mn bond, $Cl_2GaMn(CO)_5 \cdot C_4H_8O$, which was synthesized through a reaction between $GaCl_3$ and $NaMn(CO)_5$ in THF (tetrahydrofuran, C_4H_8O). This compound has a very intense absorption at 149 cm^{-1} in the far-infrared region, which suggests the presence of direct bonding between gallium and manganese. The method of synthesis is as follows: Equimolar amounts of gallium chloride and sodium pentacarbonylmanganate(−I) were separately dissolved in THF, and heated together at 30—40°C under dry nitrogen for 2 hr, and excess THF subsequently distilled off under reduced pressure. The residue was recrystallized from a mixture (1 : 5) of THF and *n*-pentane. A yellow crystalline powder was obtained. Yield 80%. Found: Cl, 17.57; Ga, 17.88; Mn, 12.51%. Calcd for $C_9H_8O_6Cl_2GaMn$: Cl, 17.42; Ga, 17.11; Mn, 13.48%. mol wt, Found: 441 (osmometry in methyl ethyl ketone). Calcd: 408.

TABLE 1. INFRARED ABSORPTION BANDS (cm^{-1})*

$Cl_2GaMn(CO)_5 \cdot THF$**	$Mn_2(CO)_{10}$[1-3]	Ga_2Cl_6[4]
2103 ms	2045 s	
2050 w	2012 s	
2035 m sh	1981 m	
2010 s		
1996 vs		
1991 vs		
193 w	120 m	274 vs
149 vs	113 m	123 s
	106 m	73 m

* Only absorption bands below 300 cm^{-1} are listed in the far-infrared region.

** Carbon tetrachloride solution in the carbonyl region, and the Nujol mull in the far-infrared region.

The compound is hygroscopic, but stable in a dry air. It is soluble in several organic solvents, especially in acetone. In solution it was unstable and decomposed in a day or two. Under conditions of 80°C and 0.1 mmHg, it decomposed without melting or sublimation. Thermogravimetry in a nitrogen atmosphere revealed a weight loss of about 60% in a temperature range of 80—220°C. The decrement is in fairly good agreement with the value of 52% calculated for the loss of one THF and five carbon monoxide molecules. The observed infrared absorption bands are shown in Table 1. In the carbonyl region, no absorption band due to bridging carbonyl was observed. The strong absorption band at 149 cm^{-1} can be assigned to a Ga–Mn stretching vibration from its position and intensity. Considering the analytical results, the molecular weight determined, the thermal decomposition behavior and the infrared spectrum, this compound may have the structure shown in Fig. 1. So far, a compound having a Ga–Mn bond has not been obtained. A detailed analysis of the infrared spectrum in the carbonyl region will be reported in following papers.

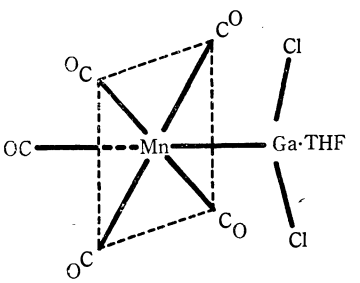

Fig. 1. The estimated structure of $Cl_2GaMn(CO)_5 \cdot THF$.

1) T. H. Brown and D. J. Darensbourg, *Inorg. Chem.*, **6**, 97 (1967).
2) M. A. Bennett and R. J. H. Clark, *J. Chem. Soc.*, **1964**, 5560.
3) P. N. Brier, A. A. Chalmers, J. Lewis and S. B. Wild, *ibid.*, **1967**, 1890.
4) A. Balls, J. A. Downs, N. N. Greenwood and B. P. Straughan, *Trans. Faraday Soc.*, **62**, 521 (1966).

Dipole Moment, Molecular Conformation and Crystal Structure of 1,4-Bis(dicyanomethylene)cyclohexane

Ariyuki AIHARA, Chikazu KITAZAWA and Fujiko IWASAKI

Department of Materials Science, University of Electro-Communications, Chofu, Tokyo

(Received February 20, 1968)

With the aim of obtaining some knowledge of the molecular conformation of 1,4-bis(dicyanomethylene)cyclohexane,*1 a dipole moment measurement in dioxane solution, and a three dimensional X-ray analysis of the crystal structure were carried out.

The increase in dielectric constant of the solution with concentration (0.416×10^{-3}—1.677×10^{-3} weight fractions) was measured at three temperatures with the use of a heterodyne-double-beat oscillator(1 MHz) constructed in this laboratory, and a pycnometer was used to determine densities. Values of total polarization were then calculated using both the Halverstadt-Kumlers and Guggenheim-Smiths equations. Dipole moment results obtained through the above procedures are shown in Table 1.

TABLE 1. DIPOLE MOMENT OF 1,4-BIS(DICYANOMETHYLENE)CYCLOHEXANE IN DIOXANE (Debye)

Temperature °C	μ(H-K procedure)	μ(G-S procedure)
40.2	2.14	2.31
50.1	2.20	2.36
59.9	2.42	2.53

As can be seen in the table, the dipole moments thus obtained are fairly large and also show a marked temperature dependence. Since the contribution from atomic polarization,[1] which is supposed to play a significant role in this case, has been neglected in calculating the dipole moment values, we must admit, apart from the possibility of a solvent effect, that these values might not necessarily represent the true dipole moment. Still, considering the symmetrical positions of the two dicyanomethylene substituents on the cyclohexane skeleton, and also the two possible conformations of the skeleton (a chair and a twisted-boat), the results obtained here seems to suggest that the molecule of 1,4-bis(dicyanomethylene)cyclohexane exists predominantly as a flexible twisted-boat form in solution. Molecules in a rigid chair conformation should exhibit a much smaller dipole moment temperature dependence,[1] if they showed any real moment due to distortion of molecular symmetry through solute-solvent interactions. The possibility of complex formation, such as a charge-transfer complex,[1,2] is also excluded in the light of the positive temperature dependence of the dipole moment.

Thus, it seems most probable that the molecule exists as a flexible twisted-boat conformer in solution, the libration of the two highly polar substituents on the central skeletion thereby giving rise to a larger value for the average dipole moment.

On the other hand, a three dimensional X-ray analysis of the crystal structure clearly revealed that the molecule of 1,4-bis(dicyanomethylene)-cyclohexane takes a chair conformation in the crystalline state. This fact is an interesting contrast with the case of 1,4-cyclohexanedione, where the molecule is known to behave as a flexible twisted-boat conformer, both in solution,[3-5] and in the crystal.[6,7] A strong interaction between adjacent molecules through highly polar and bulky dicyanomethylene substituents, in the 1,4-bis-(dicyanomethylene)cyclohexane crystal, must be responsible for the preference of the chair conformation to that of a flexible one which is more preferable for the 1,4-cyclohexanedione molecule because of the possible contribution of its high entropy term to decreasing the free energy.

Crystallographic data are as follows:

Monoclinic; Space group: $P2_1/n$
$a=10.625+0.005$ Å
$b=7.073+0.005$ Å
$c=7.250+0.005$ Å
$\beta=92.30+0.08°$
$Z=2$

Details will be published later in this Bulletin.

*1 The sample was kindly supplied by Professor H. Mikawa, Osaka University.

1) H. Huber and G. F. Wright, *Can. J. Chem.*, **42**, 1446 (1964).
2) H. Weiler-Feilchenfeld, I. Aganat and E. D. Bergmann, *Trans. Faraday Soc.*, **62**, 2084 (1966).
3) N. L. Allinger and L. A. Freiberg, *J. Am. Chem. Soc.*, **83**, 5028 (1961); N. L. Allinger, H. M. Blatter and L. A. Freiberg, *ibid.*, **88**, 2999 (1966).
4) A. Aihara, K. Chitoku and K. Higasi, This Bulletin, **35**, 2057 (1962).
5) M. V. Bhatt, G. Srinivasan and P. Neelakanatan, *Tetrahedron*, **21**, 291 (1965).
6) A. Mossel and C. Romers, *Acta Cryst.*, **17**, 1217 (1964).
7) P. Groth and O. Hassel, *Tetrahedron Letters*, **20**, 65 (1964).

BULLETIN OF THE CHEMICAL SOCIETY OF JAPAN VOL. 41 1035—1038 (1968)

The Electron Spin Resonance of Mn^{2+} Ion in Polyphosphate

Masaji MIURA, Akinori HASEGAWA and Masayuki WATANABE

Department of Chemistry, Faculty of Science, Hiroshima University, Higashisenda-machi, Hiroshima

(Received August 3, 1967)

A part of cation in polyphosphate was replaced with Mn^{2+} ion. Zero-field splitting parameter D due to the crystal field with axial symmetry was estimated according to Allen's method from the ESR spectrum of Mn^{2+} ion. The value of D changes with the change in the state of polyphosphate, crystalline or glassy. As the degree of polymerization of sodium polyphosphate glass decreases, the value of D increases and approaches to the value corresponding to the crystalline state. These phenomena were interpreted as due to the disorderness of glassy state. The value of D was found to change with the variation of the kind of cation in polyphosphate. This was explained in terms of the effective cationic field.

Many solid substances can have two states, that is, glassy and crystalline. Polyphosphate also has these two states.[1] Many phosphates having different kinds of cations and various degrees of polymerization are included under the name of polyphosphate. The characters of solid polyphosphate, therefore, are affected by these factors.

The environment of one of lattice points, atom or ion, is regular in crystalline state, whereas it is irregular in glassy state. So it is expected that the crystal field in solid polyphosphate is affected not only by the kind of cation and the degree of polymerization, but also by the state, glassy or crystalline. On the studies of the crystal field, the phenomena of the zero-field splitting in ESR spectrum offer many valuable informations.[2]

Allen has recently advanced the method by which zero-field splitting parameter D can be estimated from the relative intensities of the hyperfine structure of the ESR spectrum of Mn^{2+} doped in methanol and 12 N HCl, each of which can take two states, glassy and crystalline.[3]

In the present paper, a part of the cation of polyphosphate was replaced with Mn^{2+} and its ESR spectrum was observed. The zero-field parameter D due to the crystal field with axial symmetry in polyphosphate was estimated with Allen's method.

Theoretical

As Mn^{2+} ion has $S=5/2$ and $I=5/2$, the hyperfine and fine structures are expected to occur in its spectrum. The spin Hamiltonian, therefore, is given by

$$\mathscr{H} = g\beta\mathbf{H}\cdot\mathbf{S} + D[S_z^2 - \frac{1}{3}S(S+1)] + A\mathbf{S}\cdot\mathbf{I} \quad (1)$$

The first term of the right side represents the Zeeman effect and the next term indicates the fine structure interaction induced by the crystal field with axial symmetry. The last term shows the hyperfine interaction between the electron spin and the ^{55}Mn nuclear spin. The ESR spectra for glassy and polycrystalline states consist predominantly of hyperfine structures of the allowed transitions from $|-1/2m>$ to $|1/2m>$ state and the forbidden transitions from $|-1/2m>$ to $|1/2m+1>$ or $|1/2m-1>$ state, where $-1/2$ and $1/2$ denote the electronic spin magnetic quantum numbers and m is the nuclear spin magnetic quantum number.

For glassy and polycrystalline states, Allen[3] has derived the equation of the intensities of the allowed transitions by using the first-order perturbation theory.

$$I_m \propto 2 - \frac{A^2(35-4m^2)}{2(g\beta H)^2} - \frac{5.334D^2}{(g\beta H)^2} - \frac{D^2(34.14)(35-4m^2)}{(g\beta H)^2} + \frac{D^4(208)(35-4m^2)^2}{(g\beta H)^4} \quad (2)$$

Using $A=95$ gauss and $H=3245$ gauss and extrapolating the relation between the relative intensity and the D value to larger D value, Allen's graph was obtained as shown in Fig. 1. This graph gives the relation between the ratios of the intensity of the hyperfine line of $m=-5/2$ to those of $m=-1/2$ and $-3/2$ and the zero-field splitting parameter D. These intensities were estimated from the signal height of the first derivative, although the line width must be included in the interpretations of the intensity. As the line width is broadest in $m=$

1) M. Miura, A. Hasegawa and T. Fukui, This Bulletin, **39**, 1432 (1966).
2) B. Bleaney, H. R. S. and D. J. E. Ingram, *Proc. Roy. Soc.* (*London*), **A205**, 336 (1951).
3) B. T. Allen, *J. Chem. Phys.*, **43**, 3820 (1965).

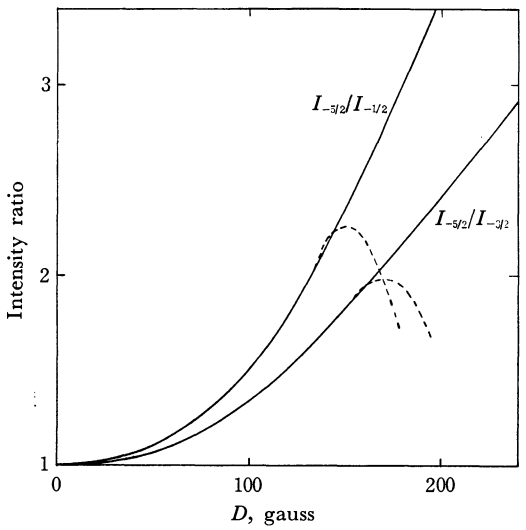

Fig. 1. Intensity ratios plotted against D. The dashed line shows the curve from Eq. (2), the solid line the extrapolated curve from the calculated curve up to $D=120$ gauss.

$-5/2$ line, the estimated value of D must become larger, if the line width is taken into account. These widths of the hyperfine structures, however, showed no detectable change in any cases. Accordingly, no substantial problems as to the line width remain at the discussion in this paper.

Experimental

Manganese hydrogen phosphate dihydrate ($MnHPO_4 \cdot 2H_2O$), which was used as the source of Mn^{2+} ion, was purified by the recrystallization from its aqueous solution. The salt was added to the aqueous solution of sodium dihydrogen phosphate dihydrate ($NaH_2PO_4 \cdot 2H_2O$), to give the molar ratio of the former to the latter of 10^{-4} : 1. The solution was evaporated to dryness. The product was heated at a temperature between 300 and 900°C in a furnace and then quenched with ice water.

Sodium polyphosphate melts at about 580°C. By the heat treatment at a temperature higher than 580°C, the glass of sodium polyphosphate was obtained, whereas by the treatment below its melting point, the crystal was gained. The crystal was also grown in the melt by slow cooling after heating at 900°C and seeding it.[1]

The samples used for studying the effects of crystallization water and polymerization on the D value were prepared by the following procedures. The crystal of $NaH_2PO_4 \cdot 2H_2O$ incorporated with Mn^{2+} ion was obtained by the recrystallization from the aqueous solution of their mixture. This crystal was evacuated and heated in a sample tube for ESR measurement. This treatment results in the elimination of water from the crystal following the polymerization of the orthophosphate. The amount of the water eliminated was determined gravimetrically. The progress of the polymerization was observed by paper chromatography.[4]

Polyphosphate glasses having various degrees of polymerization were prepared from $NaH_2PO_4 \cdot 2H_2O$ and disodium hydrogen phosphate dodecahydrate ($Na_2HPO_4 \cdot 12H_2O$) by varing their mixing ratio. The degree of polymerization was determined by the pH titration method.

The glass and the crystal of polyphosphates with different cations were obtained by heating and then quenching the mixtures of phosphoric acid (H_3PO_4) and the following orthophosphates: dilithium hydrogen phosphate (Li_2HPO_4), magnesium hydrogen phosphate trihydrate ($MgHPO_4 \cdot 3H_2O$), calcium hydrogen phosphate dihydrate ($CaHPO_4 \cdot 2H_2O$) and barium hydrogen phosphate ($BaHPO_4$). Potassium polyphosphate was prepared from potassium hydrogen phosphate (KH_2PO_4).

ESR measurements of these polyphosphates were carried out at room temperature, except for the case particularly denoted, by using the spectrometer described elsewhere.[5]

Results and Discussion

The Effect of the Concentration of Mn^{2+} Ion. The effect of the concentration of Mn^{2+} ion on the ESR spectrum was examined for sodium polyphosphate glass. When the relative concentration of Mn^{2+} ion to phosphorus atom was lower than 10^{-3}, the line width observed was practically constant. Therefore, the relative concentration of 10^{-4} was selected for Mn^{2+} ion in the present work. One of the ESR spectra was shown in Fig. 2.

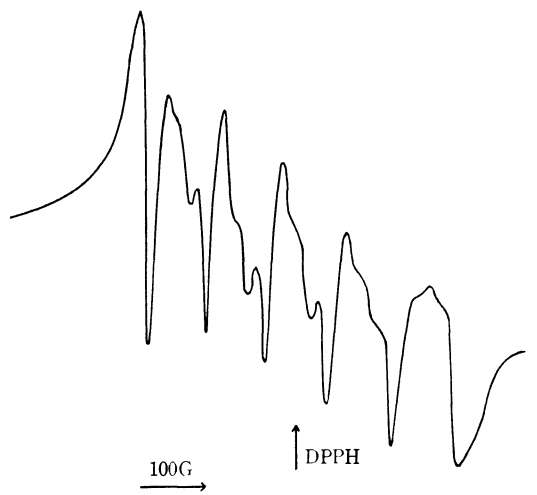

Fig. 2. ESR spectrum of Mn^{2+} in sodium polyphosphate glass.

The Effect of Heat Treatment Temperature on the Value of D. Sodium polyphosphate incorporated with Mn^{2+} ion was obtained by heating and quenching. The zero-field splitting parameter D of the Mn^{2+} ion estimated with Allen's graph is shown in Fig. 3 in relation to the heat treatment temperature. This figure shows that the parameter

4) H. Grunze and E. Thilo, *Sitzber. Deut. Akad. Wiss. Berlin, Kl. Math. Allgem. Naturw.*, **1953**, No. 5, p. 26 (1954).

5) A. Hasegawa and M. Miura, This Bulletin, **40**, 2553 (1967).

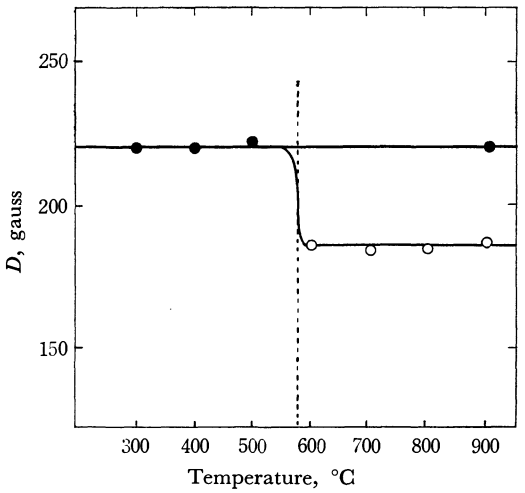

Fig. 3. The relation between D value and heat treatment temperature of sodium polyphosphate. ●: crystal; ○: glass. Dotted line shows the melting point.

D takes the value about 10% lower when treated above 580°C than that when heated below 580°C. This temperature is coincident with the melting point of sodium polyphosphate. By the treatment at a lower temperature than this, the crystal of sodium polyphosphate was obtained, whereas by that at higher temperature, the glass was obtained. The crystal of sodium polyphosphate was also obtained from the melt by cooling and seeding after heating at 900°C. The last crystal is known as Kurrol's sodium salt having very high degree of polymerization, *ca.* 10^4,[6] the D value of which is the same as that for the crystal obtained by heating at a temperature below the melting point. Thus, the D value depends largely on the state, crystalline or glassy, and has no relation to the degree of polymerization in case of the crystalline state.

The Effect of Water of Crystallization on the Value of *D*. The variation of the D value with the amount of the water of crystallization was investigated for $NaH_2PO_4 \cdot 2H_2O$ and the result obtained is given in Fig. 4.

The value of D increases first gradually, then abruptly with the progress of the elimination of water and finally takes a value which agrees with that for polyphosphate crystal. The water was removed by evacuating $NaH_2PO_4 \cdot 2H_2O$ in the initial stage at 50°C and finally at 260°C. Until almost all the crystallization water was eliminated, polymerization did not practically occurred, which was ascertained by a paper chromatographic method in both acidic and basic solvents.[4] The increase in the D value after the removal of all the crystallization water is due to the formation of pyrophosphate which was also ascertained by paper chromatography. The

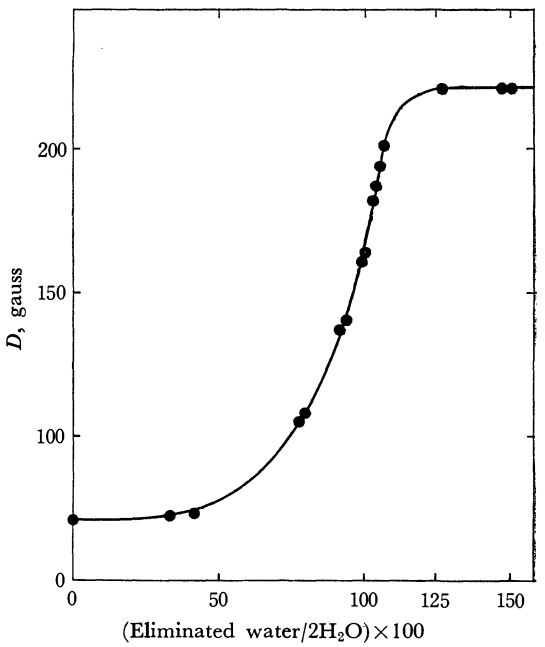

Fig. 4. The variation of D value with the elimination of water from $NaH_2PO_4 \cdot 2H_2O$. The positions of 50, 100, 125 and 150 on the abscissa mean the elimination of one of the crystallization waters and two of them and the formation of pyrophosphate and Kurrol's salt, respectively.

water of crystallization behaves to reduce the value of D. The water may coordinate to Mn^{2+} ion with high symmetry and shield the crystal field caused by phosphate anion from Mn^{2+} ion, resulting the decrease in the value of D.

The difference between the D values for the glass and the crystal of sodium polyphosphate, which is seen in Fig. 3, is due to the amount of distortion on Mn^{2+} ion. When Mn^{2+} ion exists as an impurity in infinite regular lattice of crystal, certain amount of perturbation may be exerted to lattice by Mn^{2+} ion. The lattice thus perturbed produces the distortion on Mn^{2+} ion. In glassy state, however, such perturbation and distortion may be weakened by lack of the regular structure.

The interpretation described above, however, may encounter the following criticism. As the random structure in glassy state gives the D value having some distribution, the value obtained with Allen's method is an average one. Whereas, the D value in crystalline state is directly evaluated with the method because of the lack of the distribution. The variation in the D value due to the difference of the state may depend upon the distribution.

The Effect of the Degree of Polymerization. The glasses having different degrees of polymerization were prepared and their D values were estimated (Fig. 5). The value increases with the decrease in the degree of polymerization. The value extrapolated to triphosphate was coincident with the value

6) M. Miura and Y. Kubota, *ibid.*, **40**, 466 (1967).

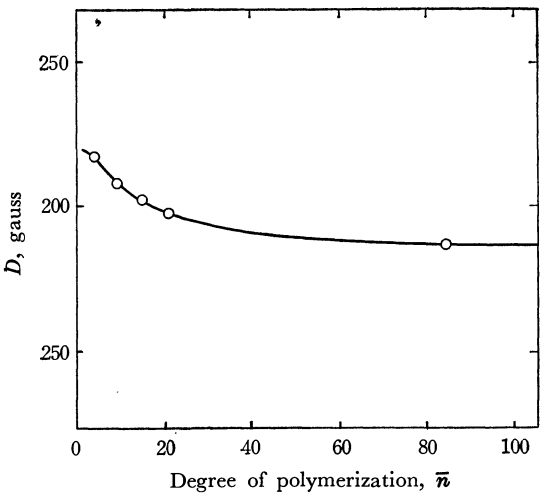

Fig. 5. The variation of D value with degree of polymerization of sodium polyphosphate glass.

obtained for the crystal of polyphosphate. This is closely correlated with the fact that the glass of triphosphate was not obtained by the method described here. The D value decreases accompanied with the increase in the degree of polymerization and approaches to the value for the glass in Fig. 3. This change, therefore, corresponds to the shift from crystalline state to glassy one, accompanied with the increase in the degree of polymerization of sodium polyphosphate glass. In the glass with low degree of polymerization, the environment of Mn^{2+} ion is considerably regular and is close to that in crystal.

The Effect of the Kind of Cation in Polyphosphate on the Value of D. The D values were also estimated for the glasses and crystals of polyphosphates having different kinds of cations. The

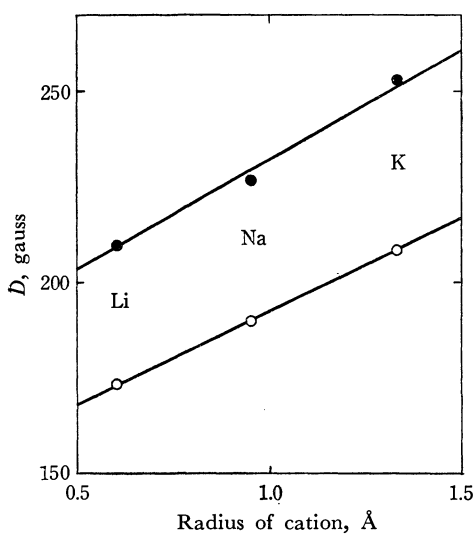

Fig. 6. The relation between D and radius of cation in alkali polyphosphate.
○: glass; ●: crystal

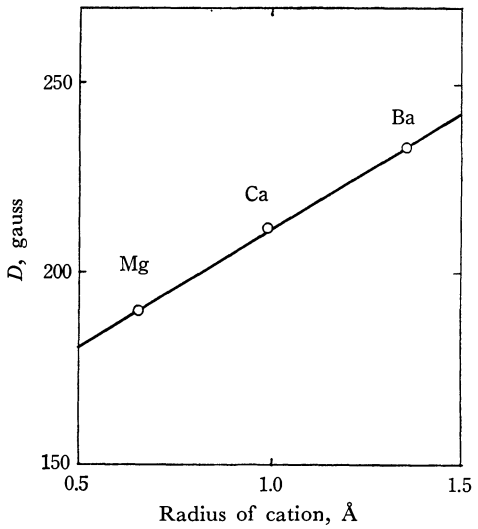

Fig. 7. The relation between D and radius of cation in alkaline-earth polyphosphate glass.

D values for the crystalline states of polyphosphates with alkaline earth cations could not be estimated owing to their peculiar spectra. The difference between the cases of alkali and alkaline earth cations, therefore, can be insufficiently discussed with these data. Almost linear relations, as shown in Figs. 6 and 7, exist between the value of D and radius of cation[7]; the decrease in radius of cation causes the decrease in the D value.

When cation with small radius strongly attracts the oxygen anions in polyphosphate by high effective cationic field, preferential coordination of the oxygen anion to Mn^{2+} ion is weakened. Thus, the center of the lone pair of oxygen may become more distant from Mn^{2+} ion and the value of D is considered to be reduced.

The Effect of Temperature on ESR Spectrum. ESR measurements of the glass and crystal of sodium polyphosphate were done at room temperature and the temperature of liquid nitrogen. ESR spectra obtained at both temperatures are essentially the same with each other. It may be concluded from this result that the value of D is not influenced by temperature and that the line width in the ESR spectrum of Mn^{2+} is not affected by relaxation mechanism.[8]

The authors wish to express their hearty thanks to Dr. B. T. Allen of University of Oregon Medical School for his kind answer to our question. Special thanks are also extended to Professor Junkichi Sohma of Hokkaido University for his valuable discussions.

7) L. Pauling, "Nature of Chemical Bond," 3rd Ed., Cornell University Press, Ithaca (1960).
8) R. Wilson and D. Kivelson, *J. Chem. Phys.*, **44**, 154 (1966).

BULLETIN OF THE CHEMICAL SOCIETY OF JAPAN VOL. 41 1039—1045 (1968)

Dissociation Pressures of Various Metallic Oxides

Kumasaburo KODERA, Isao KUSUNOKI and Shinkichi SHIMIZU*1

Department of Chemistry, Faculty of Science, Kyoto University, Sakyo-ku, Kyoto

(Received August 28, 1967)

Gases evolved during a vacuum heat treatment of various oxides were analyzed by means of an omegatron mass spectrometer. Carbon dioxide, carbon monoxide and water were detected as main gases evolved at lower temperatures. Oxygen due to thermal dissociation of ZnO, CdO, NiO, CuO, Cu_2O, and WO_3 was found at high temperatures. In the case of MoO_3, however, evolution of oxygen was not observed. The equilibrium pressures of the evolved gases over these oxides have been measured with a McLeod gauge and a Knudsen gauge. The oxygen dissociation pressures of ZnO, CdO, NiO, CuO, and Cu_2O were measured and compared with the calculated values.

The properties of metallic oxides were studied by many investigators from the various points of view. Especially, the semiconductivity of these oxides has been studied in relation to catalytic activities. However, the catalytic activity and the electrical conductivity of an oxide depend on the method of preparation and pretreatment.

In the case of *n*-type oxides (*e.g.*, ZnO, CdO, *etc.*), it is well known that the activity and conductivity are enhanced through a vacuum heat treatment. These effects may be attributed to the loss of oxygen from the stoichiometric composition. Baumbach and Wagner[1] found that the electrical conductivity of the oxides which were reduced by hydrogen or carbon monoxide depends on the equilibrium pressure of oxygen, and said that this is due to thermal dissociation accompanied with oxygen evolution represented by the following formula;

$$Zn^{2+}O^{2-} \rightleftarrows \frac{1}{2}O_2(g) + Zn^{+}(o) + e. \qquad (1)$$

However, thermal dissociation pressures of oxygen of these oxides are uncertain and few reports[2] have described the reason why non-stoichiometric oxides are produced at temperatures lower than their thermal decomposition temperatures.

Recently one of the present authors (I. K.)[3] pointed out that the loss of oxygen may be due to the reduction by impurity carbon contained in oxides, and in dirty vacuum the oxides may also be reduced by residual vapors of hydrocarbons. In the present work, we tried to obtain quantitative data about the dissociation pressures of oxygen of various oxides and to study the mechanism of dissociation.

The evolved gases during the heat treatment in vacuum were analyzed by an omegatron mass spectrometer. Up to the present, most of the investigators measured only the total pressure of the evolved gases, but it is very important to identify the gaseous species. In the present experiment, we found that carbon dioxide, carbon monoxide, and water were the main species evolved at lower temperatures, and that oxygen due to thermal dissociation of oxides such as ZnO, CdO, NiO, CuO, Cu_2O, and WO_3 was observed at higher temperatures.

Experimental

Figure 1 shows a schematic diagram of the apparatus, which is composed of two parts. Main part is made up of a decomposition cell made of fused quartz, and total pressure gauges. An omegatron mass spectrometer is in the other part. These parts are connected by a variable leak valve. The vacuum lines were constructed of molybdenum glass, and a copper sealed metal valve was used to cut off the main part from a pumping system. The apparatus was bakable at 450°C and its ultimate vacuum was 5×10^{-9} Torr. With liquid nitrogen traps no hydrocarbon was found in residual gases.

As a total pressure gauge a Knudsen gauge or a McLeod gauge was used. The Knudsen gauge of Klumb-Schwarz type was made in our laboratory[4] and calibrated with the McLeod gauge.

The omegatron tube, a modified simple box type with a rhenium electron emitter filament, was made by Mitsubishi Electronic Company. A large permanent magnet of about 4500 gauss with poles of 60 mm diameters and 35 mm gap was used. The resonance ion current of the omegatron was measured by a Takeda TR-84H vibrating reed electrometer. By combining these parts the following performance of the omegatron was obtained;

*1 Present address: Sumitomo Chemical Co., Ltd., Niihama, Ehime.

1) H. H. v. Baumbach and C. Wagner, *Z. physik. Chem.*, **B22**, 199 (1933).

2) B. Arghiropoulos, J. Elston, P. Hilaire, F. Juillet and S. T. Teichner, Proc. 4th International Symposium on Reactivity of Solids, 525 (1960); K. Torkar and F. Mostad, *Monatschrift der Chemie*, **93**, 657 (1962).

3) M. Onchi and I. Kusunoki, *Nippon Kadaku Zasshi* (*J. Chem. Soc. Japan, Pure Chem. Sect.*), **85**, 612, 617 (1964).

4) M. Onchi, K. Tominaga and N. Sasaki, *J. Vac. Soc. Japan*, **2**, 112 (1959); M. Onchi, Trans. 8th Natl. Vac. Symp. (1962, ed. L. E. Preuss, Pergamon Press), p. 544.

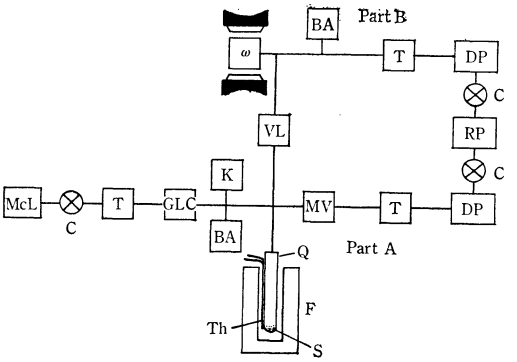

Fig. 1. Schematic diagram of the apparatus. (ω), omegatron; (BA), Bayard-Alpert gauge; (T), liquid nitrogen trap; (DP), oil diffusion pump; (RT), rotary pump; (VL), variable leak valve; (MV), metal valve; (K), Knudsen gauge; (GLC), greaseless cock; (McL), McLeod gauge, (C), cock; (Q), decomposition fused quartz cell; (Th), thermocouple; (F), furnace; (S), sample powder.

mass range: 1—500 a.m.u.,

resolution: 60 at $M/e = 60$,

measurable pressure range:

$$8 \times 10^{-5} — 5 \times 10^{-10} \text{ Torr.}$$

Samples of oxides were of extra pure grade and were used without further purification. In the decomposition cell 1 mmol of a powdered sample was placed and evacuated for a day in high vacuum at room temperature. After this treatment the main part of the apparatus, the volume of which is about 1 *l*, was cut off from the pump by the metal valve and the sample was heated in a furnace. The temperature was measured by a chromel-alumel thermocouple.

The total pressure of the evolved gases was measured by the McLeod gauge or the Knudsen gauge at regular intervals. Usually, after about a few hours it attained a stationary value. Then, the gas was introduced into the omegatron through the variable leak valve and analyzed. After the measurement, the apparatus was evacuated and the same procedure was repeated from room temperature up to 1200°C. The oxygen partial pressure evaluated from the omegatron measurement was taken to be the decomposition pressure of the oxide at the corresponding temperature. Confirmation of the equilibrium by varying the pressure or the temperature a little was not undertaken, because it would take unpractically long time for one run.

The oxide once heated to the highest temperature was cooled in vacuum and again the same procedure was repeated. In this second procedure, evolution of gases other than oxygen was reduced extremely, but the pressure of oxygen at the corresponding temperature was identical within the experimental error. This suggests that the equilibrium was not disturbed by the presence of the other gases.

Result and Discussion

Evolution of Carbon Monoxide and Carbon Dioxide.[3] All metallic oxides evolve large amount of carbon monoxide and carbon dioxide between 200 and 800°C. The gases adsorbed or combined with the oxides might constitute some fractions of the evolved gases. However, the main part of them seems to be produced by the reduction of metallic oxides by impurity carbon in them or by adsorbed or residual hydrocarbons on the oxide surface or in vacuum system, because the color and electrical conductivity of these oxides changed with carbon dioxide evolution. For example, the color of tungsten trioxide and molybdenum trioxide changed to dark gray after evolution of these gases. In our experiment performed in " hydrocarbon free " system, no hydrocarbon peak was observed in the spectra at any temperature. Therefore, the reduction by impurity carbon seemed to be more important than that by adsorbed or residual hydrocarbons, and the origin of non-stoichiometry of the metallic oxides should be attributed to the existence of some impurity carbon.

The Dissociation Pressure of Zinc Oxide. Mass spectra of evolved gases from zinc oxide at 600°C and 890°C are shown in Fig. 2. Above 750°C oxygen due to thermal decomposition begins to be observed. An example of the total equilibrium pressure of the evolved gases and its component is shown in relation to the temperature in Fig. 3. Above 900°C oxygen gas was a main component. In Fig. 4 the equilibrium pressures of oxygen are plotted

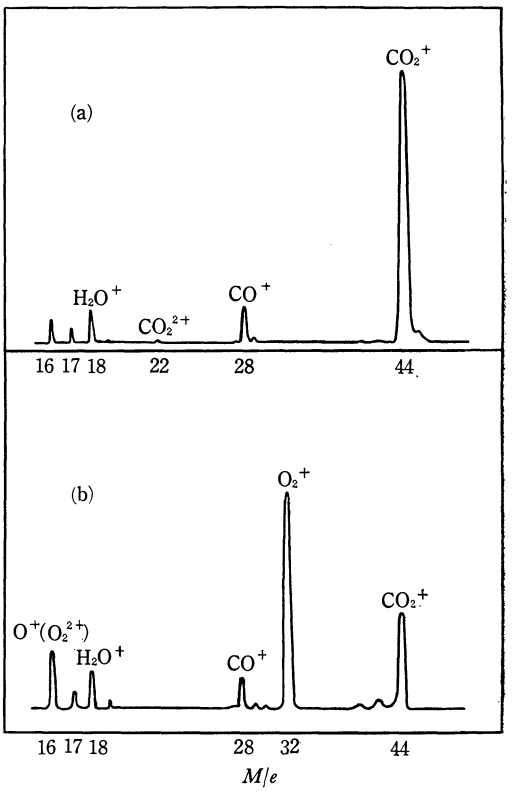

Fig. 2. Mass spectra of gases evolved from zinc oxide. (a) 600°C, (b) 890°C

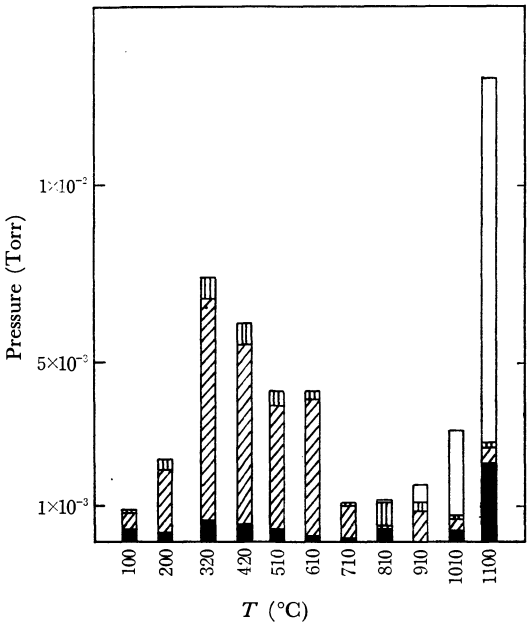

Fig. 3. Partial pressures of gases evolved from zinc oxide *versus* temperature.
□, oxygen; ▥, carbon monoxide; ▨, carbon dioxide; ■, water

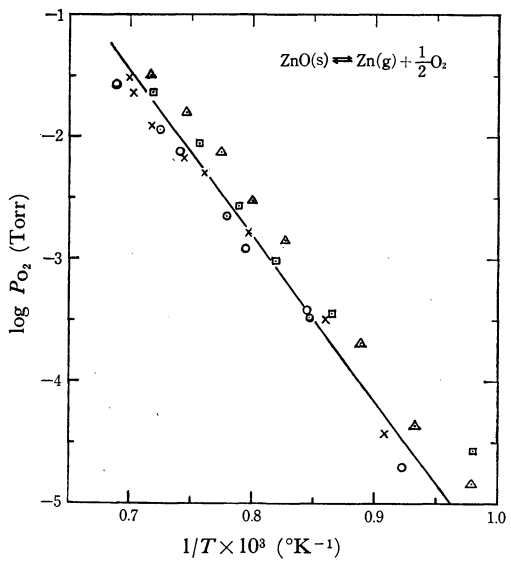

Fig. 4. Dissociation pressure of solid zinc oxide *vs.* $1/T$.
The values of different symbols show different runs.

against the reciprocal of the absolute temperatures. Then a good straight line, though the values by each run showed a little deviation from the line, was obtained. Over the range of 750—1200°C, the line is represented by the following equation;

$$\log P_{O_2}(\text{Torr}) = -\frac{13500}{T} + 8.01 \qquad (2)$$

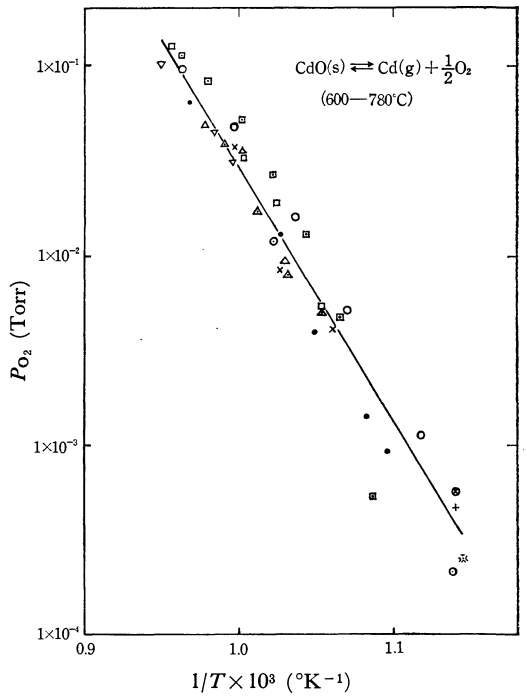

Fig. 5. Dissociation pressure of solid cadmium oxide *vs.* $1/T$.

If the following equilibrium is established at high temperature,

$$\text{ZnO(s)} \rightleftarrows \text{Zn(g)} + \frac{1}{2}\,\text{O}_2\,, \qquad (3)$$

the equilibrium constant ($K_p = P_{Zn} \cdot P_{O_2}{}^{1/2} \simeq 2P_{O_2}$) is represented by the relation;

$$\log K_p(\text{atm}^{3/2}) = -\frac{20250}{T} + 8.00\,, \qquad (4)$$

hence the value of standard free energy change, ΔG°, for the reaction, $\text{ZnO(s)} \rightleftarrows \text{Zn(g)} + \frac{1}{2}\text{O}_2$, is given by;

$$\Delta G^\circ(\text{cal}) = 92664 - 36.65T. \qquad (5)$$

On the other hand, the values of ΔG° for this reaction, which are obtained by combining the known values for other reactions, are as follows;

$$\Delta G^\circ(\text{cal}) = 112170 - 49.03T \qquad (6)^{5)}$$

or;
$$\Delta G^\circ(\text{cal}) = 114640 - 51.65T. \qquad (7)^{6)}$$

The difference of these values are not so large in the temperature range of measurement.

This result conflicts with Seeco's report[7] that an equilibrium constant for the dissociation of solid zinc

5) E. C. Truesdale and R. K. Waring, *J. Am. Chem. Soc.*, **63**, 1610 (1961).
6) J. A. Kitchener and S. Ignatowicz, *Trans. Faraday Soc.*, **47**, 1278 (1951).
7) E. A. Seeco, *Can. J. Chem.*, **38**, 596 (1960).

oxide into the gaseous elements was greater than that calculated from Eq. (6) by a factor of 10^8. One possible reason of this discrepancy might be due to the existence of other gases than oxygen. Because no instrument such as mass spectrometer to identify gaseous species was used in Seeco's experiment, it is not unreasonable to suppose that Seeco considered all the evolved gases as oxygen and overestimated its pressure.

The Dissociation Pressure of Cadmium Oxide. At lower temperatures (20—500°C) main components of the evolved gases were carbon dioxide, carbon monoxide, and water. The oxygen gas due to thermal decomposition was found above 500°C. In Fig. 5 the measured equilibrium pressures of oxygen are plotted against $1/T$. The straight line obtained can be represented by the following equation;

$$\log P_{O_2}\,(\text{Torr}) = -\frac{13800}{T} + 11.6 \qquad (8)$$

The pressure of oxygen is about twenty times as large as those of the other author's,[8] which were obtained by flow methods or calculated from thermodynamical data. This discrepancy may be attributable to the inhomogeneity of temperature in the experimental system. That is, as the cadmium has larger vapor pressure compared to other metals its vapor was condenced at the cold part of the apparatus and removed quickly from the dissociation cell before the equilibrium of $CdO(s) \rightleftarrows Cd(g) + \frac{1}{2}O_2$ was attained.

The Dissociation Pressure of Nickel Oxide. Nickel oxide is one of the important p-type oxide-semiconductor. However, there are few reports[9] published about the thermal decomposition. Johnson and Marshall obtained a vapor pressure equation of nickel oxide by measuring the rate of vaporization from a metallic nickel ring slightly oxidized its surface to nickel oxide. The value for the vapor pressure of nickel oxide is somewhat larger than the calculated dissociation pressure of nickel oxide. Therefore, they concluded that the dissociation of solid nickel oxide was negligible between 1438 and 1566°K. On the other hand, Brewer and Mastick[10] criticized Johnson and Marshall's conclusion, and concluded that vaporization by dissociation is the major process in case of nickel oxide.

In the present experiment, oxygen gas produced by thermal decomposition was identified with the omegatron and the formation of thick nickel deposit was observed on the wall of the colder part of the cell. A thin film of nickel oxide was also observed at the part of higher temperature. This might be explained by oxidation of the deposited metal film, *i.e.*, the same phenomenon observed in case of zinc oxide.[11] In Fig. 6 the dissociation pressure are plotted against $1/T$. When an untreated sample was examined, abnormally large pressures of dissociation with a maximum was observed, shown as curve A. On the contrary, the sample which was treated in vacuum at 1100°C for a few hours gave normal dissociation pressures, shown as curve B. Curves C and D were obtained from the samples with longer heat treatment in vacuum at 1100°C (for about 40 hr). The following equation for the dissociation pressure is obtained from the curve C;

$$\log P_{O_2}\,(\text{Torr}) = -\frac{23810}{T} + 11.33. \qquad (9)$$

Two processes of the dissociation of nickel oxide can be assumed as follows;

$$NiO(s) \rightleftarrows Ni(s) + \tfrac{1}{2}O_2,$$

$$Ni(s) \rightleftarrows Ni(g); \qquad (10)$$

or;

$$NiO(s) \rightleftarrows Ni(g) + \tfrac{1}{2}O_2. \qquad (11)$$

Equation (9) is in good agreement with the values calculated by the first process and not by the second process. Therefore, the standard free energy change

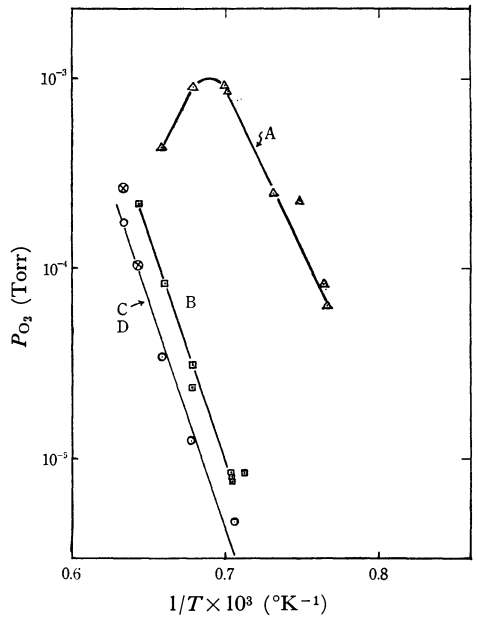

Fig. 6. Dissociation pressure of nickel oxide *vs.* $1/T$.
Curve A, from an untreated sample;
Curve B, C, D, from a vacuum-heat-treated sample.

8) A. Krupkowski, *Hotnicke Listy* (*tschech*), **3**, 357 (1948); J. G. F. Gilbert and J. A. Kitchener, *J. Chem. Soc.*, **1956**, 3919; W. B. Hinche, *J. Am. Chem. Soc.*, **55**, 1751 (1933); K. Ueno, *Nippon Kwagaku Kwaishi* (*J. Chem. Soc. Japan*), **62**, 990 (1941); Von O. Glemser and U. Stöcker, *Ber. Bunsenges. Physik Chem.*, **67**, 505 (1963).

9) J. Efemenko, *Chem. Abstr.*, **58**, 8612e (1963); H. W. Foote and E. K. Smith, *J. Am. Chem. Soc.*, **30**, 1344 (1908).

10) L. Brewer and D. S. Mastick, *J. Chem. Phys.*, **19**, 834 (1951).

11) K. Kodera, I. Kusunoki and S. Shimizu, *Nippon Kagaku Zasshi* (*J. Chem. Soc. Japan, Pure Chem. Sect.*), **86**, 814 (1965).

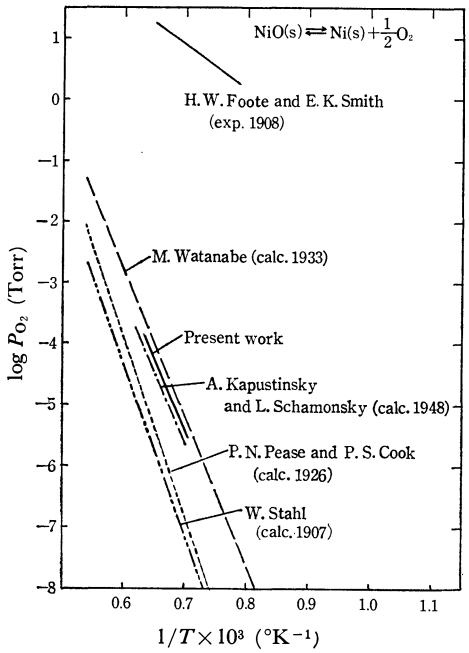

Fig. 7. Comparison of experimental and calculated pressures of oxygen in equilibrium with solid nickel oxide.

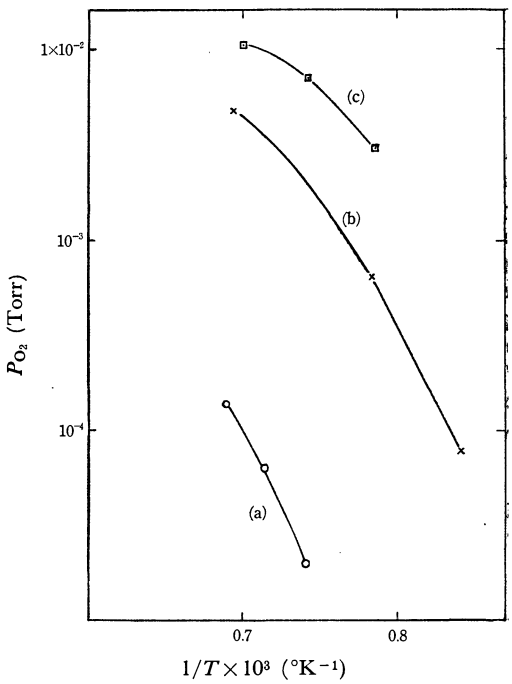

Fig. 8. Measured dissociation pressure in equilibrium with tungsten trioxide, (1), an untreated sample; (b), a sample treated in vacuum at 800°C for about 10 hr; (c), a sample treated in vacuum at 950°C for a couple of days.

of $NiO(s)\rightleftarrows Ni(s)+\frac{1}{2}O_2$ is obtained from Eq. (9);

$$\Delta G^\circ(\text{cal}) = 54500 - 19.35T,$$
$$1400^\circ\text{K} \leq T \leq 1570^\circ\text{K}. \qquad (12)$$

In Fig. 7 the oxygen dissociation pressure is compared with literature data, most of which are calculated from the thermodynamical data obtained by the reduction of nickel oxide. Foote and Smith[12] reported very large value for the dissociation pressures of nickel oxide. However, as they did not analyze the gases, it is possible that they mistook other gases as oxygen. The values obtained by our experiment are in good agreement with the calculated ones. Therefore, the curve C in Fig. 6 shows that the sample treated in vacuum has a stoichiometric composition. The curve A shows that the untreated sample had excess oxygen over the stoichiometric component.

Molybdenum Trioxide. Main species of evolved gases were found to be carbon dioxide and carbon monoxide. The evolution rate of carbon dioxide increased considerably above 200°C and its color changed to gray. Moreover, it was observed that molybdenum trioxide sublimed above 630°C. However, we could not detect any oxygen gas due to thermal decomposition.

Tungsten Trioxide. It has not been reported that oxygen due to thermal decomposition of tungsten trioxide was observed. However, the origin of non-stoichiometry of the oxide is often considered to

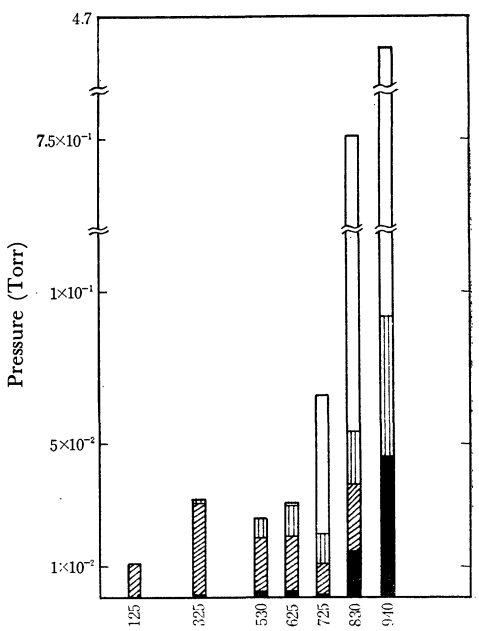

Fig. 9. Partial pressures of gases evolved from copper(II) oxide *vs.* temperature.
□, oxygen; ▨, carbon monoxide; ▨, carbon dioxide; ■, water

12) H. W. Foote and E. K. Smith, see Ref. 9.

be due to thermal dissociation.[13] In a previous paper, one of the authors (I. K.)[3] pointed out that the reduction of tungsten trioxide under vacuum heating at temperatures lower than 500°C was taken place by impurity carbon contained in the oxide.

In the present experiment, it was found that the sublimation of tungsten trioxide was accompanied with oxygen evolution above 950°C. Sometimes the oxygen dissociation pressure amounted to 1×10^{-2} Torr but the reproducibility of the measurement was not good among different runs. This may be due to the dissociation accompanied by sublimation. In Fig. 8 the examples of measured dissociation pressures are shown.

The Dissociation Pressure of Copper(I) and Copper(II) Oxides. In Fig. 9 the gaseous species evolved from copper(II) oxide are shown in relation to the temperature. Oxygen was observed above 590°C. Moreover, it was confirmed by X-ray analysis that copper(II) oxide transformed completely into cuprite (copper(I) oxide) under heat treatment in vacuum above 900°C. Therefore, the equilibrium of $2CuO(s)\rightleftarrows Cu_2O(s)+\frac{1}{2}O_2$ is only realized over the range of 600 to 900°C. In Fig. 10 the oxygen pressures are plotted against $1/T$. A good straight line is obtained over this range and the oxygen dissociation pressure is represented by;

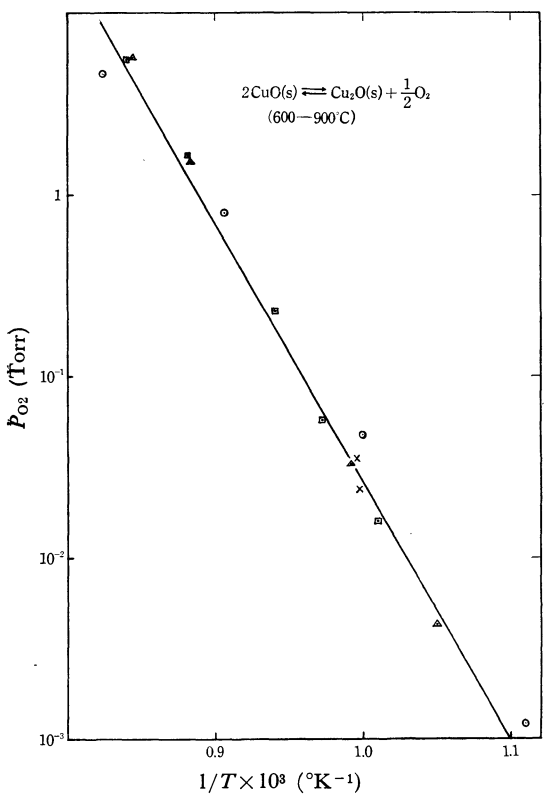

Fig. 10. Dissociation pressure of copper(II) oxide.

13) R. J. Ackermann and E. G. Rauch, *J. Phys. Chem.*, **67**, 2596 (1963).

$$\log P_{O_2}(\text{Torr}) = -\frac{14150}{T} + 12.61. \quad (13)$$

Therefore, the free energy change for the reaction of $2CuO=Cu_2O+\frac{1}{2}O_2$ is given by;

$$\Delta G^\circ(\text{cal}) = 32400 - 22.28T,$$
$$870^\circ\text{K} \leq T \leq 1170^\circ\text{K}. \quad (14)$$

Brewer and Mastick[10] thought that the stability of gaseous copper(II) oxide is proved by the measurement of the vapor pressure of solid oxide by Mack, Osterhof, and Krauer.[14] The vapor pressures of gaseous copper(II) oxide between 873 and 1223°K were higher by factors of 10^6—10^8 than those of gaseous copper which is in equilibrium with solid copper(II) oxide. However, we found only the deposit of cuprite and not that of copper(II) oxide. This observation shows copper(II) oxide does not vaporize.

In the present experiment, the sample of cuprite was prepared by heating of copper(II) oxide in vacuum at 900°C for a couple of days, and identified by X-ray analysis. Above 900°C cuprite began to deposit on the hot wall and then decomposed with oxygen evolution. In Fig. 11 the dissociation pressures of oxygen are plotted against $1/T$, and expressed by;

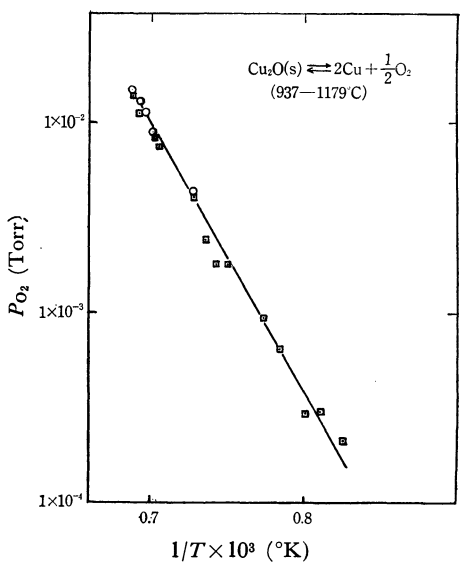

Fig. 11. Dissociation pressure of copper(I) oxide.

14) Mack, Osterhof and Krauer, *J. Am. Chem. Soc.*, **45**, 617 (1923).

15) W. Stahl, *Berg. Hütt. Zty.*, **40**, 127 (1890); E. Heyn, *Z. anorg. Chem.*, **39**, 1 (1904); R. E. Slade and F. D. Farrow, *Proc. Roy. Soc.*, **87**, A524 (1912); H. S. Roberts and F. H. Smyth, *J. Am. Chem. Soc.*, **43**, 1061 (1921); O. Kubaschewski and E. L. L. Evans, Metallurgical Thermochemistry, London (1956); W. Hofman and H. J. Schneider, *Tech. Wiss. Beich. Giessereiw u. Metallk*, **28**, 1567 (1960); V. V. Kondakov, D. I. Ryzhonkov and I. A. Titova, *Chem. Abstr.*, **58**, 7408b (1963).

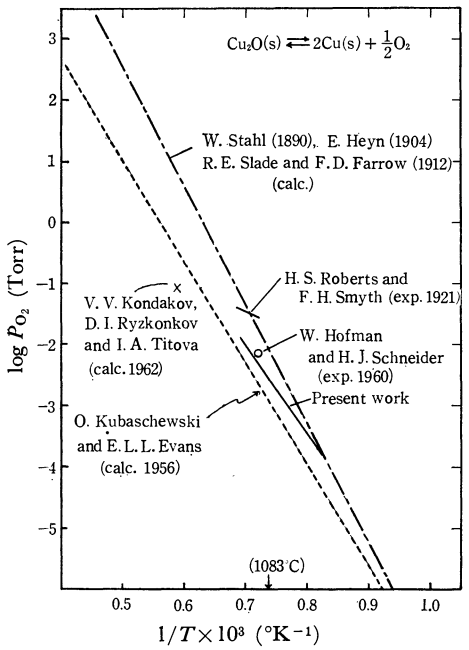

Fig. 12. Comparison of experimental and calculated pressures of oxygen in equilibrium with solid copper(I) oxide.

$$\log P_{O_2}\,(\text{Torr}) = -\frac{14100}{T} + 7.85. \qquad (15)$$

The free energy change for the reaction of $Cu_2O(s) = 2Cu(s) + \frac{1}{2}O_2$ or $Cu_2O(s) = 2Cu(l) + \frac{1}{2}O_2$ was given by;

$$\Delta G^\circ(\text{cal}) = 32200 - 11.4T,$$
$$1200^\circ\text{K} \leq T \leq 1420^\circ\text{K}. \qquad (16)$$

The melting point of copper is at 1083°C. However, we could not observe any change at this point. In Fig. 12 our result is compared with other author's values,[15] most of which were calculated from the thermodynamical data.

Summary

Carbon dioxide and carbon monoxide were often the main gaseous species evolved from various oxides at lower temperatures. Oxygen due to the thermal dissociation of tungsten trioxide was detected with the omegatron for the first time. In the case of nickel oxide, the excess oxygen contained in the p-type semiconductor was evolved at the first stage during a heat treatment in vacuum. Dissociation pressure of zinc oxide, cadmium oxide, nickel oxide copper(II) oxide, and cuprite were measured and were in good agreement with the calculated values from the standard free energy data.

The authors wish to thank Dr. Masaru Onchi for his valuable advice and one of authors (I. K.) is grateful for financial support from the Sakkokai Foundation.

BULLETIN OF THE CHEMICAL SOCIETY OF JAPAN VOL. 41 1046—1055 (1968)

Electronic Spectra and Electronic Structures of Benzonitrile *N*-Oxide and Its Derivatives

Masumi YAMAKAWA, Tanekazu KUBOTA, Hideko AKAZAWA and Itaru TANAKA

Shionogi Research Laboratory, Shionogi & Co., Ltd., Fukushima-ku, Osaka

(Received September 18, 1967)

The electronic spectra of 2,6-dimethylbenzonitrile *N*-oxide and its some derivatives were recorded in *n*-heptane and were compared with those of benzonitrile and phenylacetylene. The analyses of the electronic spectra of aromatic nitrile *N*-oxides were done by the following procedures. First, simple molecular orbitals (SMO) of benzonitrile and phenylacetylene were calculated using some parameters determined by the use of the overlap integrals and valence state ionization potentials. Then, by comparing the eigenvalues of the SMO thus obtained with the observed spectra the spectroscopic exchange integrals have been obtained for $^1A_1$ and $^1B_1$ bands, where interactions between two configurations were taken into consideration for the $^1B_1$ bands. The SMO of benzonitrile *N*-oxide was next calculated on reference to the physicochemical nature of aromatic nitrile *N*-oxides studied before. The parameters were chosen so as to fit with the observed values of dipole moments of benzonitrile *N*-oxide and its some methyl derivatives. Electronic spectra of the nitrile *N*-oxides were then analyzed using the above SMO's and spectroscopic exchange integrals. The substituent effect on the electronic spectrum of benzonitrile *N*-oxide was also discussed by the similar treatment. Characteristic strong band appearing in the near UV region was assigned to the $^1A_1$ band having a change transfer (CT) nature, where the CT from the oxygen atom to the residual conjugated system makes a larger contribution than that of the reverse direction. In addition, the physicochemical nature and reactivity of nitrile *N*-oxides were discussed on the basis of their molecular diagrams, which were obtained from the SMO's mentioned above.

In the previous papers,[1,2] the electronic spectra of substituted benzonitrile *N*-oxides and 9-anthronitrile *N*-oxide were recorded in various solvents and compared with those of the corresponding nitriles. In addition, molecular complexes of aromatic nitrile *N*-oxides with iodine, β-naphthol and phenol were studied quantitatively by electronic and infrared (IR) spectroscopic methods.[1-3] Discussions were made from the viewpoints of solvent and substituent effects on the above electronic spectra and of charge-transfer (CT) type complexing ability. It was concluded that the π-conjugated systems of benzonitrile *N*-oxide (BNO) are well illustrated as I,

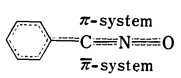

(I)

where the CNO group has a character of a partial triple bond consisting of π and $\bar{\pi}$ system (see I) This conclusion was led from the experimental evidences that (i) CT type complexing ability of aromatic nitrile *N*-oxides is very weak, (ii) the N–O stretching vibration, $\tilde{\nu}_{NO}$, appears at higher frequency than that of pyridine *N*-oxide, and (iii) substituted benzonitrile *N*-oxides exhibit an absorption band with high intensity ($\varepsilon > 10000$) in a near ultraviolet (UV) region where the corresponding nitriles do not show such a high intensity band. The absorption band pertinent to the nitrile *N*-oxides was found to undergo a blue shift with an increasing polarity of solvents, although the shift is small compared with some other kinds of tertiary amine *N*-oxides. It seems to be now interesting to examine the stated experimental results from theoretical points of view. The present paper describes the molecular orbital (MO) treatment of BNO and its derivatives to discuss the UV spectra and other physicochemical natures. The results will be compared with those of nitrones reported previously,[4,5] because benzylidene methylamine *N*-oxide (BMANO)[6] and BNO are isoelectronic on the π-electron system except for the presence of $\bar{\pi}$-system in BNO (see I).

1) M. Yamakawa, T. Kubota and H. Akazawa, This Bulletin, **40**, 1600 (1967).
2) T. Kubota, M. Yamakawa, M. Takasuka, K. Iwatani, H. Akazawa and I. Tanaka, *J. Phys. Chem.*, **71**, 3597 (1967).
3) T. Kubota, K. Ezumi, M. Yamakawa and Y. Matsui, *J. Mol. Spectroscopy*, **24**, 378 (1967).
4) T. Kubota and M. Yamakawa, This Bulletin, **36**, 1564 (1963).
5) T. Kubota, M. Yamakawa and Y. Mori, *ibid.*, **36**, 1552 (1963).
6) The structure is 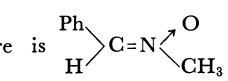 a typical nitrone.

Experimental

Measurement of electronic and IR spectra and the purification of solvents employed were the same as were described in the foregoing papers.[1,2]

Materials. In addition to the aromatic nitrile *N*-oxides reported already,[1] 4-dimethylamino-2,6-dimethylbenzonitrile *N*-oxide (DMABNO) was newly synthesized to get the spectra. DMABNO (new compound) was obtained by the reaction of the corresponding oxime with NaOBr according to Grundmann's method,[7] and was recrystallized several times with methanol: mp 134.0—136°C; IR, $\tilde{\nu}_{NO}=1341$ cm^{-1} and $\tilde{\nu}_{C\equiv N}=2287$ cm^{-1} in CCl_4. The above oxime, 4-dimethylamino-2,6-dimethylbenzaldoxime (new compound, mp 135.0—137.5°C, a mixture of syn and anti forms) was prepared by the reaction of hydroxylamine with the corresponding aldehyde (mp 82.5—83.5°C) which was obtained by Vilsmeyer-Haackschen's method[8] from *N*,*N*-dimethyl-3,5-dimethylaniline (125°C/37 mmHg) prepared by dimethylation of 3,5-dimethylaniline with trimethylphosphate ($(CH_3O)_3PO$).[9]

The nitrile, DMABN, corresponding to DMABNO was synthesized by the dehydration of 4-dimethylamino-2,6-dimethylbenzaldoxime mentioned above with acetic anhydride.[10,11] The pure material of DMABN, mp 89°C, was obtained by chromatograph passing through the alumina and by recrystalliation from petroleum ether; $\tilde{\nu}_{C\equiv N}=2213$ cm^{-1} (CCl_4). The main absorption maxima (mμ) and intensities (ε_{max}), latter being shown in parentheses, of DMABNO and DMABN in *n*-heptane are: 292.7 (22900), 229.0 (11500), and 206.8 (23000) for DMABNO and 282.3 (27600), 233.7 (14100), 227.2 (14700), 206.2 (19300), and 188.0 (17800) for DMABN. The purity of the samples was carefully checked on by elementary analyses and UV, IR, and NMR spectroscopic measurements. Commercial phenylacetylene (GR grade of Kanto Chemical Co.) and benzonitrile (special grade of Wako Chemical Co.) were first purified by repeated distillations. Then these were subjected to rectifying distillation through a good efficient column to collect the middle portions; bp 142.4°C and 46.0—46.5°C/5 mmHg for phenylacetylene (PA) and benzonitrile (BN), respectively.

Calculation and Experimental Results

As was mentioned in the introductory section of this paper the π-electronic structures of aromatic nitrile oxides and nitrones seem to bear some resemblance to each other. Therefore, the calculations of MO and transition energies were carried out with the similar treatment to that adopted to interpret the electronic spectra and electronic structures of BMANO.[4],*1 Namely, based on simple MO (SMO) calculation, and taking account of configuration interaction (CI) partly, the character of electronic spectra of BNO and its derivatives has been analyzed using the spectroscopic exchange integrals, β_s's, for the series of the following compounds,[14] in which the spectra of II[15] and III[16-18] were already analyzed by several authors.

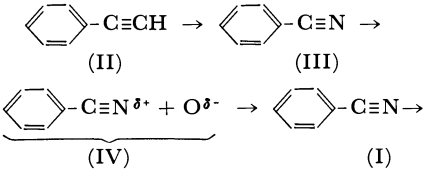

Hypothetical molecule, IV, is obtained by dividing I into the composite systems consisting of the oxygen atom, $O^{\delta-}$, and its residual part, IV. It seems to be valuable to compare the π energy level of the $O^{\delta-}$ with the levels of IV.

SMO Calculation of I—IV. First we evaluated the parameters for SMO calculations of II, III and IV. The parameters pertaining to an atom, X, and a bond, X=Y, are, respectively, expressed by k_X in the Coulomb integral $\alpha_X=\alpha+k_X\cdot\beta$, and by ρ_{XY} in the resonance integral $\beta_{XY}=\rho_{XY}\cdot\beta$. The valence state ionization potential (IP) due to a π electron of carbon and nitrogen atoms is insensitive for the change of σ-core hybridization from sp^2 to sp type[19,20] whether or not these atoms are neutral or cation.[19,20] Thus it may be allowed to assume that the k_X values for the atoms appearing in -C≡N and -C≡N$^{\delta+}$ (IV) bonds are the same as those reported previously for pyridine[21] and benzylidene methylamine[4] and its hypothetical molecule[4] 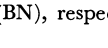 . That is, the values are as follows: $k_C=0$ and $k_N=0.5$ for C≡N bond, and in the case of IV $k_{N^{\delta+}}=1.6$ and

*1 This type of theoretical treatment was originally applied by Baba and Suzuki,[12] and Goodman and Shull[13] to the analyses of the electronic spectra of substituted aromatic hydrocarbons.

7) a) C. Grundmann and J. M. Dean, *Angew. Chem. Intern. Ed.*, **3**, 585 (1964); b) C. Grundmann and J. M. Dean, *J. Org. Chem.*, **30**, 2809 (1965).
8) C. Grundmann and J. M. Dean, *Angew. Chem.*, **77**, 966 (1965).
9) D. G. Thomas, J. H. Billman and C. E. Davis, *J. Am. Chem. Soc.*, **68**, 895 (1946).
10) L. F. Fieser and J. L. Hartwell, *ibid.*, **60**, 2555 (1938).
11) C. Grundmann and H. D. Frommeld, *J. Org. Chem.*, **30**, 2077 (1965).
12) H. Baba, This Bulletin, **34**, 76 (1961); H. Baba and S. Suzuki, *ibid.*, **34**, 82 (1961); *J. Chem. Phys.*, **32**, 1706 (1960).
13) L. Goodman and H. Shull, *ibid.*, **27**, 1388 (1957).
14) The comparison of the spectra of Ph-C≡N$^+$-H with those of BNO *etc.* seems to be interesting. However, our trial under various conditions to get the accurate spectra was not successful.
15) a) E. M. Layton, Jr., *J. Mol. Spectroscopy*, **5**, 181 (1960); b) J. R. Platt, *J. Chem. Phys.*, **19**, 101 (1951); c) J. F. Music and F. A. Matsen, *J. Am. Chem. Soc.*, **72**, 5256, 5260 (1950); d) A. K. Chandra, *ibid.*, **83**, 4177 (1961).
16) T. E. Peacock and P. T. Wilkinson, *Proc. Phys. Soc.*, **79**, 105 (1962).
17) H. E. Popkie and J. B. Moffat, *Can. J. Chem.*, **43**, 624 (1965).
18) K. Kimura and S. Nagakura, *Theort. Chim. Acta*, **3**, 164 (1965).
19) J. Hinze and H. H. Jaffé, *J. Am. Chem. Soc.*, **84**, 540 (1962).
20) J. Hinze and H. H. Jaffé, *J. Phys. Chem.*, **67**, 1501 (1963).

inductive effect $=(1/3)^n \times k_N{}^{\delta+}$ for carbon atoms. Adopting the Mulliken approximation,[22] $\rho_{C\equiv N}$ was estimated using Eq. (1), where $\beta_{C\equiv N}$ is for pyridine type C≡N bond. Here the relation $\beta_{C\equiv N} \approx \beta_{C=C\equiv}\beta$ was assumed, this assumption being commonly employed in our previous calculations of nitrone,[4] pyridine *N*-oxide and their related compounds[21b,c] and also in usual SMO calculation of *N*-heterocyclic compounds.[21a,23]

$$\rho_{C\equiv N} \approx \frac{\beta_{C\equiv N}}{\beta_{C=N}} \approx \frac{(1/2)\cdot K\cdot S_{C\equiv N}(IP_C{}^{sp}+IP_N{}^{sp})}{(1/2)\cdot K\cdot S_{C=N}(IP_C{}^{sp_2}+IP_N{}^{sp_2})} \propto \frac{S_{C\equiv N}}{S_{C=N}} \qquad (1)$$

It would be understood that Eq. (1) is satisfied, since $IP_{C\text{ or }N}{}^{sp} \approx IP_{C\text{ or }N}{}^{sp_2}$ is closely held for a π electron as was discussed before. The Mulliken Table[24] for overlap integrals, *S*'s, gave the values: $S_{C\equiv N}{}^{\pi} = 0.302$ at 1.15 Å (triple covalent bond length) and $S_{C=N}{}^{\pi} = 0.199$ at 1.37 Å, so that we got $\rho_{C\equiv N} = 1.52$. As a reference, this value should be referred to 1.50[16] and 1.35[17] for $\rho_{C\equiv N}$ estimated from the data in literatures.[16,17,25] We have now used the $\rho_{C\equiv N} = 1.50$ for C≡N and C≡C bonds in I, II, III, and IV for the sake of simplicity.[26]

Next our attention was paid to the parameters of ρ_{NO} and k_O in I. Keeping in mind the conclusion of previous studies[1,2] that the net electronic charge on the oxygen atom in nitrile oxides would be decreased because of a partial triple bond nature of an N→O bond in C≡N→O group, the following boundary conditions are expected. Namely, both the k_O and ρ_{NO} in the present case is larger than those of BMANO[4] and pyridine *N*-oxide,[21b,c] *etc.* The values of $k_O = 1.2$ for BMANO, $k_O = 0.8$ for pyridine *N*-oxide, and $\rho_{NO} = 1$ for both the compounds were already derived. Many calculations were carried out so as to fit with the observed dipole moments of BNO and 2,4,6-trimethylbenzonitrile *N*-oxide (TMBNO), *etc.* by using the various sets of k_O and ρ_{NO} under the above boundary conditions.[27] The best values were determined as $k_O = 1.55$ and $\rho_{NO} = 1.2$. The energy levels of MO's were thus calculated for I, II, III, and IV using the above mentioned parameters, and the results were drawn in Fig. 1 with the symmetry and numbering of each orbital.

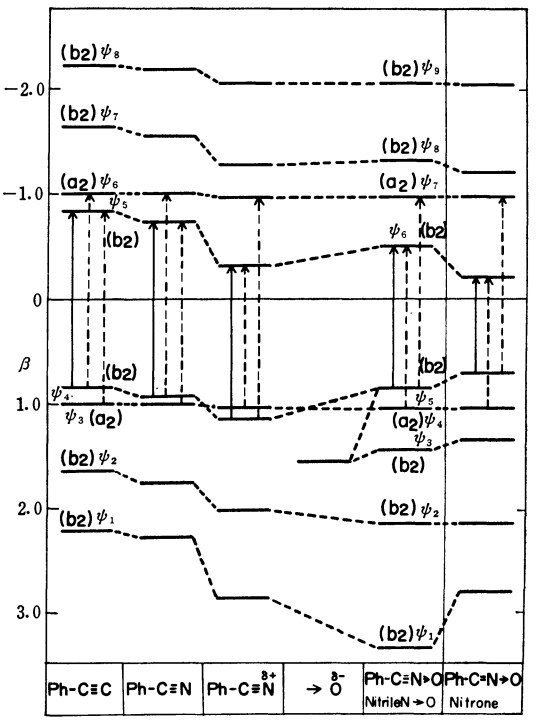

Fig. 1. The orbital energies and their numberings of phenyl acetylene, benzonitrile, and benzonitrile *N*-oxide and its composite ststems. The values of nitrone are cited from a previous paper[4] for comparison. Solid and broken vertical lines represent, respectively, $^1A_1$ and $^1B_1$ transitions responsible for near UV spectra. See "Appendix" for calculating conditions.

The present calculation of dipole moment has been based on the summation of σ and π moments. The values used for the former were cited from our previous paper[21c] and the latter values were taken from the present MO calculations. The molecular dimension of BNO was determined from molecular diagrams by employing the same treatment as in the previous work.[4] However, in the present molecule there are two π conjugated systems (π and $\bar{\pi}$) which are orthogonal to each other, and therefore MO calculation results for these two systems were taken into consideration to obtain the bond order and charge density. Although the bond length of the N→O bond (R_{NO}) is unknown, it was estimated as about 1.25 Å by the aid of N→O stretching frequency ($\tilde{\nu}_{NO} = \sim 1350\ cm^{-1}$) and $\tilde{\nu}_{NO}$-bond length relationship.[28] In the present study we used the

21) a) N. Mataga and K. Nishimoto, *Z. Physik. Chem. N. F.*, **13**, 140 (1957); b) T. Kubota, *Nippon Kagaku Zasshi* (*J. Chem. Soc. Japan, Pure Chem. Sect.*), **80**, 578 (1959); This Bulletin, **35**, 946 (1962); c) T. Kubota and H. Watanabe, *ibid.*, **36**, 1093 (1963).

22) R. S. Mulliken, *J. Chim. Phys.*, **46**, 497, 675 (1949); M. Wolfsberg and L. Helmholtz, *J. Chem. Phys.*, **20**, 837 (1952).

23) R. Daudel, R. Lefebvre and C. Moser, "Quantum Chemistry Methods and Application," Interscience Publishers, Inc., New York, N. Y. (1959), pp. 77, 211.

24) R. S. Mulliken, C. A. Rieke, D. Orloff and H. Orloff, *J. Chem. Phys.*, **17**, 1248 (1949).

25) In these papers[16,17] Pariser-Parr-Pople calculations of benzonitrile *etc.* were carried out. Using the data given therein, $\rho_{C\equiv N}$'s have been obtained from the ratio: $\beta_{C\equiv N}{}^{core}/\beta_{C=N}{}^{core}$.

26) When we calculate the $\rho_{C\equiv C}$ for a –C≡CH bond using the equation, $\rho_{C\equiv C} = [S_{C\equiv C}/S_{C=C}]$, the value of $\rho_{C\equiv C} = 1.38$ is led. A Streitwieser, Jr., "Molecular Orbital Theory for Organic Chemists," John Wiley & Sons, Inc., New York, London (1961), p. 105.

27) Here was included the inductive effect, $(1/3)^n \cdot k_N{}^{\delta+} = (1/3)^n \times 1.6$, in the calculations.

28) W. Lüttke, *Z. Elektrochem.*, **61**, 976 (1957).

value ranging from 1.21 to 1.30 Å tentatively, but uncertainty of the R_{NO} in this range resulted in only small differences in the calculated dipole moments. The lone pair moment ($\vec{\mu}_{1\cdot sp^2}$) of N atom in sp^2 hybridization was previously assessed 1.0 D.U.[21c] The N atom of C≡N group is, however, in sp hybridization, so that its lone pair moment ($\vec{\mu}_{1\cdot sp}$) was estimated to be 1.06 D.U. from the equation, $\vec{\mu}_{1\cdot sp} = [\vec{\mu}^{cal.}_{1\cdot sp}/\vec{\mu}^{cal.}_{1\cdot sp^2}] \times \vec{\mu}_{1\cdot sp^2}$. Here $\vec{\mu}^{cal.}_{1\cdot sp}$ and $\vec{\mu}^{cal.}_{1\cdot sp^2}$ are, respectively, the calculated lone pair moments for sp and sp^2 hybridized orbitals by the aid of the Slater orbital. Since both atoms of C≡N bond is in the sp type, the σ moment for the C≡N bond was here put as 0.00 D.U. because of the same reason as that for the C=N bond mentioned in the previous work.[21c] The σ-moment of the N→O dative bond assumed to be the same (4.55 D, see Ref. 21c) among three kinds of the bonds; aliphatic type $\rightarrow$N→O, pyridine *N*-oxide type $\gg$N→O, and nitrile *N*-oxide type ≡N→O; although some difference in the N-atom σ-donor orbital (that is, sp^3, sp^2, and sp orbitals in the above given order) would cause somewhat the variation of σ-electron distribution in the N→O σ bond itself as was discussed in Ref. 2. On the other hand, the non-bonding electrons at the oxygen atom in the N→O bond would be in almost no-hybridization[29] just like the oxygen atom in free carbonyl group,[30] so that no lone pair moment was supposed for the oxygen atom. Now, dipole moments of BNO, benzonitrile, and acetonitrile were calculated and compared with those observed.[31]

Evaluation of Spectroscopic Exchange Integrals, β_s's. In Fig. 2 are depicted the absorption spectra of PA, BN and 2,6-dimethylbenzonitrile *N*-oxide (DMBNO) in *n*-heptane. The band position of a quite strong band ($^1A_1$ under C_{2v}) appearing in 210—250 mμ region is considerably different to each other between PA and BN, but that the ^1L_b band ($^1B_1^-$ under C_{2v}) occurs in almost the same wavelength region for both compounds. As will be mentioned later it would be allowed that the β_s value ($\beta_s(^1A_1)$) for the former band ($^1A_1$) is evaluated on the basis of a single electronic configuration. However, this resulted in two relatively different $\beta_s(^1A_1)$ values for PA and BN, mainly because of different band ($^1A_1$) positions. Some difference in intramolecular interaction ability of -C≡CH and -C≡N groups with phenyl residue might be the principal origin for observed difference in the band ($^1A_1$) position, because the $^1A_1$ band in question is closely associated with the above mentioned intramolecular interaction. Hence, the $\beta_s(^1A_1)$ value was estimated from the observed band position of BN. This $^1A_1$ band will be mainly attributed to a one electron transition from ϕ_4 to ϕ_5, $^1\chi_{4\to5}$. Assuming the calculated energy difference ($^1\chi_{4\to5} = 1.653\,\beta$) to be equal to the observed value (5.510 eV) of BN, we get $\beta_s(^1A_1) = 3.33$ eV. This value will be used to discuss the $^1A_1$ bands in the UV spectra of BNO. It is worthwhile to point out that the other transitions having the symmetry $^1A_1$ seem to occur at much shorter wavelength than in $^1\chi_{4\to5}$, as is seen in Fig. 3, in which the calculated energy levels of excited states are shown. Therefore, the interaction of $^1\chi_{4\to5}$ transition with the other $^1A_1$ configurations would be small. The assumption to derive the above $\beta_s(^1A_1) = 3.33$ eV may be qualitatively allowed.

Next the evaluation of β_s for $^1B_1$ bands was carried out. The mutual interaction between two one-electron transitions, $^1\chi_{4\to6}$ and $^1\chi_{3\to5}$, may be the main origin for the $^1B_1$ bands appearing in near UV region. Assuming that the contribution to the $^1B_1$ bands from the other configurations might be neglected, two $^1B_1$ states, $^1B_1^-$ and $^1B_1^+$, of PA and BN are respectively written as Eqs. (2) and (3).

---

29) T. Kubota, M. Yamakawa and I. Tanaka, *J. Mol. Spectroscopy*, **20**, 226 (1966).

30) J. N. Murrell, "The Theory of the Electronic Spectra of Organic Molecules," Methuen & Co., Ltd., London (1963), p. 159.

31) Adopted molecular dimensions and experimental and calculated dipole moments are shown below.

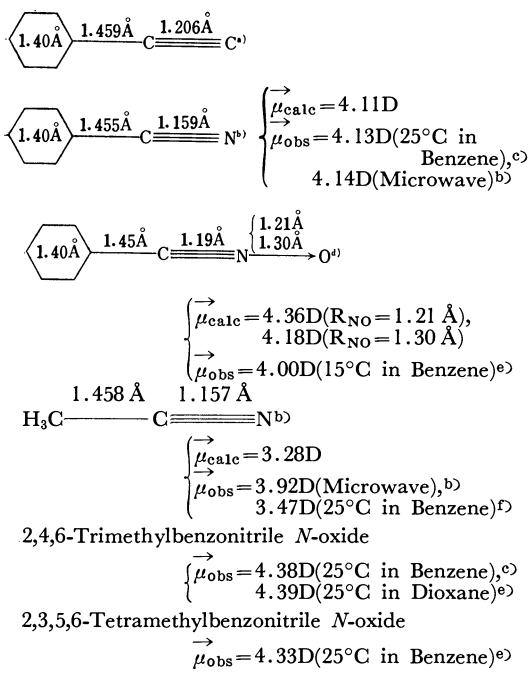

2,4,6-Trimethylbenzonitrile *N*-oxide

$\vec{\mu}_{obs}$=4.38D(25°C in Benzene),c)
4.39D(25°C in Dioxane)e)

2,3,5,6-Tetramethylbenzonitrile *N*-oxide

$\vec{\mu}_{obs}$=4.33D(25°C in Benzene)e)

a) L. E. Sutton, Ed., "Tables of Interatomic Distances and Configuration in Molecules and Ions," Special Publication No. 11, The Chemical Society, London (1958).

b) B. Bak, D. Christensen, W. B. Dixon, L. H. Nygaard and J. R. Andersen, *J. Chem. Phys.*, **37**, 2027 (1962).

c) Dipole moments for these compounds were measured by Dr. H. Watanabe and Miss N. Mōri, thanks of authors being due to them.

d) These values were estimated by using the order-length relation, *etc.* (see text).

e) G. Speroni, *Ricerca sci*, **27**, 1199 (1957).

f) J. W. Smith and L. B. Witten, *Trans. Faraday Soc.*, **47**, 1304 (1951).

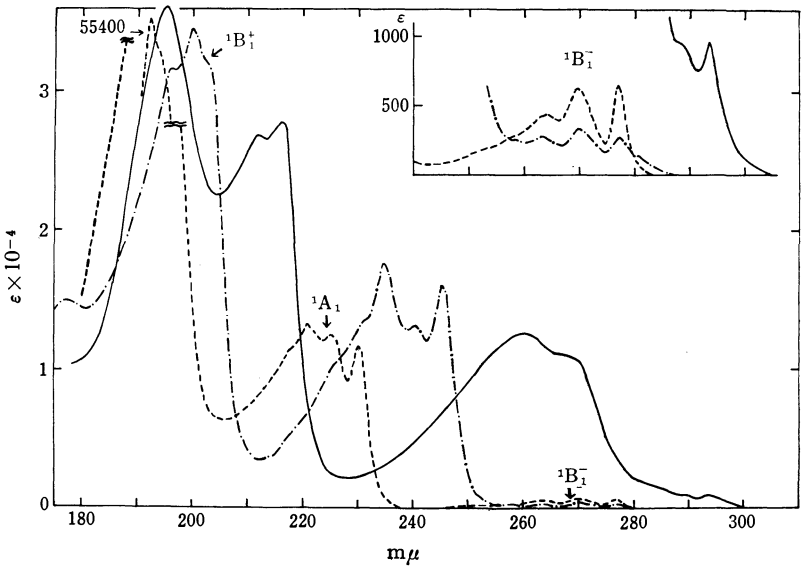

Fig. 2. Absorption spectra of phenylacetylene (—·—·), benzonitrile (------), and 2,6-dimethylbenzonitrile *N*-oxide (———) in *n*-heptane.

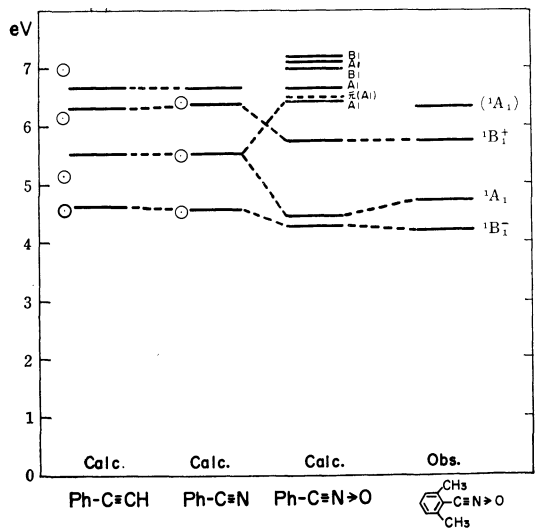

Fig. 3. The calculated and observed transition energies of the compounds indicated in this figure. Observed values for phenyl acetylene and benzonitrile are shown by circles.

$$(^1B_1^- \text{ or } ^1B_1^+) = \frac{1}{\sqrt{2}}(^1\chi_{3\to5} \mp {}^1\chi_{4\to6}) \qquad (2)$$

$$(^1B_1^- \text{ or } ^1B_1^+) = a^1\chi_{3\to5} \mp b^1\chi_{4\to6} \qquad (3)$$

Here, minus and plus signs on the right hand side of the equations stand for the $^1B_1^-$ and $^1B_1^+$, respectively. The interaction energy is given by $\mathscr{H}_{4\to6}^{3\to5} = \langle {}^1\chi_{4\to6}|\mathscr{H}|{}^1\chi_{3\to5}\rangle = 2\langle 36|G|54\rangle^{MO} - \langle 36|G|45\rangle^{MO}$. Using the one-center and two-center π-Coulomb repulsion integrals, which were already given by Eq. (5) in Ref. 4, $\mathscr{H}_{4\to6}^{3\to5}$ is calculated to be 0.8653 eV for PA and 0.8583 eV for BN. In the case of PA the $\mathscr{H}_{4\to6}^{3\to5}$ will be also given experimentally by the half of energy difference between the two absorption bands of 4.59 eV and 6.20 eV (see Fig. 4) under the above assumption to derive Eqs. (2) and (3). The value of 0.804 eV thus derived is a value consistent with the theoretical ones stated above.

Figure 4 shows the relation of the transition energy obtained by SMO calculation to the observed $^1B_1^-$ and $^1B_1^+$ bands. The spectroscopic exchange integral, $\beta_s(^1B_1)$, for $^1B_1$ state was evaluated to satisfy the observed values using the theoretical $\mathscr{H}_{4\to6}^{3\to5}$ values mentioned above and the SMO transition energies shown in Fig. 4. For the case of PA we obtained the $\beta_s(^1B_1) = 2.978$ eV and 2.911 eV for $^1B_1^-$ and $^1B_1^+$ excited states, respectively. The mean values is 2.945 eV. However, the spectrum of BN gave $\beta_s(^1B_1) = 2.983$ eV and 3.029 eV for $^1B_1^-$ and $^1B_1^+$ bands, respectively. The mean value results in 3.006 eV, and in this case the values of *a* and *b* for $^1B_1^-$ state in Eq. 3 were found to be 0.8142 and 0.5806, respectively. We would now understand that PA and BN give almost the same value of $\beta_s(^1B_1)$ as far as the $^1B_1^\mp$ bands are concerned. The value of $\beta_s(^1B_1) = 3.006$ eV was then used to discuss the spectra of BNO and its related compounds in relation to the choice for the $\beta_s(^1A_1)$ value mentioned before.

Calculation of Transition Energies and Oscillator Strength. Combination of the SMO calculation results and the values of $\beta_s(^1A_1)$ and $\beta_s(^1B_1)$ make it possible to calculate the transition energies and their oscillator strengths, f_{calc}, the latter being carried out by the standard method.[29,32] The re-

32) R. S. Mulliken and C. A. Rieke, *Repts. Progr. Phys.*, **8**, 231 (1941).

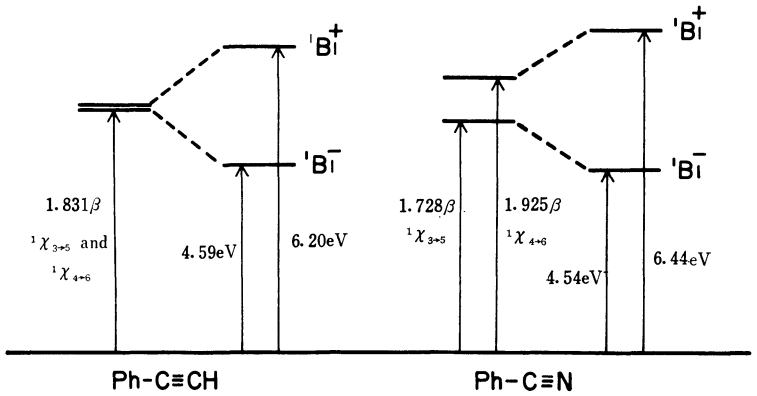

Fig. 4. The state energy splitting owing to the configuration interactions between two $^1B_1$ states yielded by SMO calculation, and the correlation, and the correlation with observed $^1B_1$ bands.

TABLE 1. THE CALCULATED AND OBSERVED VALUES OF TRANSITION ENERGIES, ΔE (IN eV), AND OSCILLATOR STRENGTHS, f, IN THE $^1A_1$ AND $^1B_1\pm$ STATES

		$\Delta E(^1B_1^-)$ eV	$f(^1B_1^-)$	$\Delta E(^1A_1)$ eV	$f(^1A_1)$	$\Delta E(^1B_1^+)$ eV	$f(^1B_1^+)$	The wave function of $^1B_1^-$ state
Ph-C≡C	Calcd.	4.609	0	5.540	1.058	6.340	0.862	$1/\sqrt{2}(^1\chi_{4\to6}-{}^1\chi_{3\to5})$
	Obs.	4.592	0.002—0.003	5.166	0.314	6.196	0.778[a]	
Ph-C≡N	Calcd.	4.583	0.0113	5.510	1.079	6.399	0.872	$0.5806^1\chi_{4\to6}-0.8142^1\chi_{3\to5}$
	Obs.	4.541	0.007	5.510	0.240	6.441	0.914[a,b]	
Ph-C≡N→O	Calcd.	4.311	0.0306	4.486	1.490	5.749	0.512	$0.8869^1\chi_{4\to6}-0.4619^1\chi_{5\to7}$
	Obs.[c]	4.224	0.009	4.775	0.258	5.766	0.308[a]	

a) The f value estimated experimentally is not very accurate, because the absorption bands corresponding to $^1B_1^+$ state overlapped quite strongly with the other absorption bands of higher transition energies.

b) See footnote 18. The value of $f_{obs}=1.6$ was reported[18] for the case where the integration was carried out over the three far UV bands in vapor phase; 6.61, (6.88), and 7.44 eV.

c) In addition to the absorption bands listed in this row another band with a high intensity was observed at 6.352 eV ($f_{obs}=0.768$, $\varepsilon=36100$).

sults for compounds I, II, and III are listed in Table 1 with the state functions obtained and with the observed transition energies. The transition moment, $\vec{Q}$, is given by

$$\vec{Q} = \langle \Psi_g(^1\Gamma)|\sum\vec{r}|\Psi_{exc}(^1\Gamma)\rangle,$$

where $\Psi_g(^1\Gamma)$ and $\Psi_{exc}(^1\Gamma)$ are singlet state wave functions in the ground and excited states, respectively (see Table 1). In Table 1 are included the oscillator strengths, f_{obs}, obtained experimentally from the recorded spectra by the aid of the equation: $f_{obs}=4.32\times10^{-9}\int\varepsilon(\tilde{\nu})d\tilde{\nu}$. The integrated intensity $\int\varepsilon(\tilde{\nu})d\tilde{\nu}$, was obtained using a planimeter from an enlarged absorption curve which was divided into each electronic transition component by the usual method.[29]

The Effect of Electron Donating Substituents on the Electronic Spectrum of 2,6-Dimethylbenzonitrile *N*-Oxide (DMBNO). It is of interest to elucidate theoretically the substituent effect on the UV spectrum of DMBNO. Some experimental results obtained here and reported in the foregoing paper[1] are shown in Table 2. The substituent effect was now introduced in the SMO calculation by such a way that k_x of Coulomb integral (α_x) for a substituent is varied in the range of 0.5—3.5, while ρ_{C-x} for the resonance integral (β_{C-x}) between a substituent and a benzene ring carbon atom to which the substituent is attached is assumed to be unity. Then many MO calculations were carried out using different values of the parameters. The calculation of transition energy is based on the same treatment as that in the preceding chapters except that $\beta_s(^1A_1)=3.55$ eV, which reproduces completely the 259.7 mμ band of DMBNO, is employed in stead of $\beta_s(^1A_1)=3.33$ eV mentioned before. Calculations were made using the above two $\beta_s(^1A_1)$ values, but the two $^1A_1$ curves calculated were nearly parallel to each other. That is, the two $\beta_s(^1A_1)$ values give almost the same results, as far as

TABLE. 2. OBSERVED TRANSITION ENERGIES (ΔE) AND ε_{max}'s IN *n*-HEPTANE, CALCULATED TRANSITION ENERGIES, AND THE COULOMB PARAMETERS, k_X, OF SUBSTITUENTS FOR MO CALCULATIONS OF 4-SUBSTITUTED-2,6-DIMETHYLBENZONITRILE *N*-OXIDES

X	k_X	$^1B_1^-$			$^1A_1$			$^1B_1^+$			$(^1A_1)$	
		ΔE (calc) eV	ΔE (obs)	ε_{max}	ΔE (calc) eV	ΔE (obs)	ε_{max}	ΔE (calc) eV	ΔE (obs)	ε_{max}	ΔE (obs)	ε_{max}
H	∞	4.31	4.224	968	4.775	4.775	12700	5.75	5.766	28000	6.352	36100
CH_3-	3.5	4.31	4.214	667	4.66	4.720	15000	5.64	5.687	27000	6.249	37300
Br-	2.5	4.32	4.229	1350	4.56	4.626	19000	5.56	5.732	25700	6.069	31000
CH_3O-	2.0	4.29	(4.188)[a]	(1300)[a]	4.46	4.628	17900	5.50	5.801	24700	6.122	34400
$(CH_3)_2N$-	1.2	4.16	—	—	4.06	4.235	22900	5.29	5.414	11500	5.996	23000

a) Since this band occurs as shoulder, the band position and intensity is not so accurate.

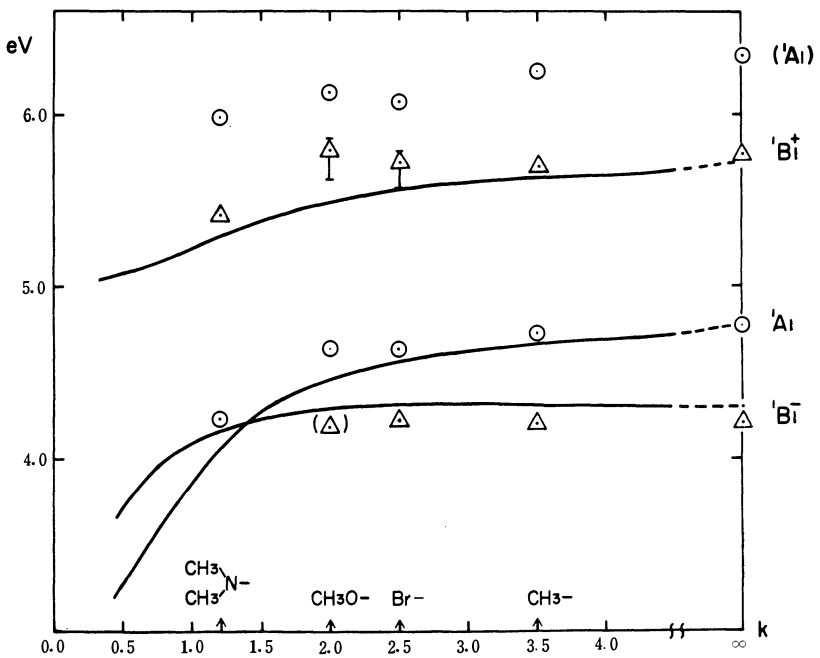

Fig. 5. The effect of substituents on the transition energies of 2,6-dimethylbenzonitrile *N*-oxide. Calculated and observed values are, respectively, shown by solid lines and by circles and triangles.

the comparison of magnitude of substituent effect is concerned. Altnough the present choice of the $\beta_s(^1A_1) = 3.55$ eV is somewhat arbitrary, we deem that it would lead to more satisfactory results in the investigation of the substituent effect and in the deviation of the calculated $^1A_1$ state energies from the observed ones when the 259.7 mμ band of DMBNO is taken as a standard. The results are shown in Table 2 and drawn in Fig. 5, in which the observed values are plotted at the following parameter positions:

$k_{N(CH_3)_2} = 1.2$, $k_{OCH_3} = 2.0$, $k_{Br} = 2.5$ and $k_{CH_3} = 3.5$.

These are determined by referring the values recommended by Baba,[12] and by Goodman and Shull.[13]

Discussion

Electronic Spectra of Benzonitrile *N*-Oxide and Its Related Compounds. As Table 1 shows, the comparison of the calculated and the observed results on the absorption spectrum of DMBNO indicates clearly that the 259.7 mμ band with high intensity should be assigned to $^1A_1$ band having the transition moment along the long axis of DMBNO (C_2 asis under C_{2v}). Now we may say that the $^1A_1$ band occurs in quite longer wavelength than in $^1A_1(^1L_a)$ band of benzonitrile, and thus would be thought to be a characteristic band for benzonitrile *N*-oxides. This is due to the fact that the 2pπ

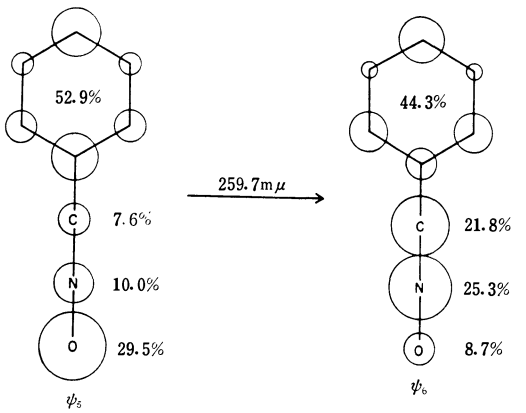

Fig. 6. The electron distribution in the highest occupied (ψ_5) and the lowest vacant (ψ_6) orbitals of benzonitrile *N*-oxide.

electrons of the oxygen atom coordinated to benzonitrile group can newly enter into π-conjugation, so that the charge transfer of $2p\pi$ electrons on the oxygen atom to the residual electron system, as well as the charge transfer of the reverse direction to the above, is brought about. In Fig. 6 we showed the change of orbital charge distribution caused by the $^1A_1$ (259.7 mμ) transition of DMBNO, which mainly consists of the $^1\chi_{5\to6}$ configuration. It is seen that the charge density on the oxygen atom decreases at the $^1\chi_{5\to6}$ excited state because of the charge transfer from the oxygen atom to the residual π-electronic system. However, calculations showed that the above charge transfer at the $^1A_1$ state is weaker than in the cases of BMANO[4,33] and pyridine *N*-oxide,[33] indicating that the solvent effect on the absorption band of nitrile *N*-oxides is less than that found in the case of nitrones and heterocyclic *N*-oxides, with which the considerable effect was observed.[1] The other two bands of DMBNO which appeared at 293.5 mμ and 215 mμ were assigned to $^1B_1^-$ (^1L_b, weak intensity) and $^1B_1^+$ (^1B_b, strong intensity) bands, respectively. The assignment was made by comparing the experimental results with the calculated ones as shown in Fig. 3. The band assignment made hitherto was consistent with that derived experimentally from the substituent- and solvent-effects and from the intensity consideration.[34] Tentative assignment of absorption bands appearing in far UV region are also given in Fig. 3. The assignment, however, would not be certain from the present study, because configuration interaction seems to play an important role for interpreting the electronic spectra in the above region. We suppose that the above band assignment, except for the one in far UV region, is also supported from the comparison of the calculated and experimental results concerning the substituent effect on the spectra of DMBNO, as is seen in Fig. 5. It is found there that the results of the calculation are parallel to the experimental ones at least semiquantitatively.

As was mentioned in the introduction of the present paper, nitrone and nitrile *N*-oxide have the π-electronic system similar to each other. The main difference in their UV spectra is the position of longer wavelength $^1A_1$ band. The band for nitrone occurs at longer wavelength than that of the corresponding nitrile *N*-oxide. For example, the $^1A_1$ band (259.7 mμ) of DMBNO in *n*-heptane appears at shorter wavelength than that (298.3 mμ)[5] of BMANO, a typical nitrone. It has been already known that the longer wavelength $^1A_1$ band is sensitive to substituents and shows an apparent red shift when electron donating power of substituents becomes stronger, as was reported for the system of mono-substituted benzenes.[12,13] The above difference in the $^1A_1$ band position between nitrone and nitrile *N*-oxide would be explained by the larger values of parameters k_O and ρ_{CN} for C≡N→O group, which make the separation of the lowest vacant and the highest occupied orbitals larger (see also Fig. 1).[35]

Molecular Diagrams and Physicochemical Natures of Nitrile *N*-Oxides. In connection with the analyses of the UV spectra discussed above it seems to be also valuable to make the discussion on the correlation between the molecular diagram and some physicochemical natures of nitrile *N*-oxides in the ground state. The molecular diagrams calculated for BN and BNO are designated in Fig. 7. Since these compounds have the two resonance systems, π and $\bar{\pi}$, their bond orders and charge densities are relatively different from those of benzylidenemethylamine and BMANO except for benzene part, where the above differences are not very large. Let us now consider the nature of –C≡N→O group. The π-bond order (0.779) of ≡N→O bond in BNO is much larger than that (0.406) of BMANO,[4] although partial bond order for π and $\bar{\pi}$ systems is less than the above 0.406. At the same time the C≡N bond order is also large (1.704), indicating that the bond exhibits a triple bond nature. These values should now be compared with those given by Wagner[36] who calculated the molecular diagram of fulminic acid, H–C≡N→O, by the method

33) T. Kubota and M. Yamakawa, This Bulletin, **35**, 555 (1962).

34) It is noted that the oscillator strengths calculated for $^1A_1$ band appearing in near UV region of PA, BN, and BNO are high from the quantitative viewpoint. The same tendency was also found for the calculated results of *p*-substituted DMBNO. Although MO calculation gives usually oscillator strength larger than that obtained experimentally, the above discrepancy would be ascirbed to the model of calculation which is not rigorous for the present case.

35) The spectral change similar to the above is naturally found between BN (225 mμ) and benzylidenemethylamine[5] (244.0 mμ), and between PA (240 mμ) and styrene (247.5 mμ).[4]

36) E. L. Wagner, *J. Chem. Phys.*, **43**, 2728 (1965).

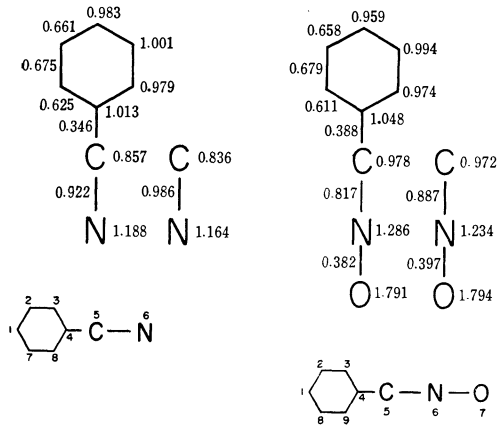

Fig. 7. Molecular diagrams of benzonitrile and its *N*-oxide.

of linear combination of group orbitals, and obtained the values: 0.939 and 1.729 for the π-bond order of N→O and C≡N bonds, respectively. Both his and our results seem to reflect the character of C≡N→O bond well. Therefore we may say that the stretching vibration of N→O bond, $\tilde{\nu}_{NO}$, of BNO occurs in higher frequency than in pyridine *N*-oxide, *etc.* Actually this prediction was verified experimentally as we discussed in the foregoing paper.[1]

It is known that $\tilde{\nu}_{NO}$ has the close correlation with N–O bond distance, R_{NO}. Using Lüttke's correlation curve[28] and also applying the Kharitonov's equation[37] which connects $\tilde{\nu}_{NO}$ and R_{NO}, the N–O bond distance was estimated to be 1.25 and 1.22 Å, respectively. On the other hand, the examination of the relation between $\tilde{\nu}_{NO}$ and R_{NO} reported for many aromatic and aliphatic amineoxides, oximes, nitroso compounds, *etc.*[1,4,5,38] led to $R_{NO}=1.28$—1.23 Å. Anyway it appears likely that R_{NO} of nitrile *N*-oxides in free state becomes relatively short.

Finally attention is directed to the π-electron density of BNO, *etc.* Comparing the molecular diagrams of BNO (see Fig. 7) and BMANO,[4] we can find that the charge distributions in the benzene ring are not very different between those of BNO and BMANO, but large change occurs in the part of C≡N→O group. Total π-electron net charges on the oxygen- and C_5 carbon-atoms (see Fig. 7) are +0.415 and +0.050 for BNO, but were +0.283 and +0.017 for the corresponding values of BMANO.[4] The increment of the positive net charge on the oxygen atom of BNO is responsible for weak complexing ability of aromatic nitrile *N*-oxides. Although the π net charge on the oxygen atom of C≡N→O group is positive, as has been discussed above, it is sure that the total charge on the oxygen atom is negative. This is because the N→O σ dative bond (σ moment, $\vec{\mu}_{NO}=4.55$ D.U.)[21c] shows a large shift of charge in the σ system. If we define $q_O=q_O^{\sigma}+q_O^{\pi}=(\vec{\mu}_{NO}/R_{NO})+q_O^{\pi}$, the value of $q_O\approx-0.368$ is derived. In addition to that, the net charge on the carbon atom of C≡N→O group (see Fig. 7) is positive and its value is considerably larger than that for C=N→O in BMANO, whereas the π net charge on nitrogen atom of C≡N→O is negative. These results may suggest that nitrile *N*-oxide group can also be expressed as a resonance formula, $-C^{\delta+}\equiv\ddot{N}-O^{\delta-}$. This fact seems to be the reason why nitrile *N*-oxides are rich in reactivity[39] and bring about easily the reaction of 1.3 dipole addition[39] unless bulky substituents prevent the reagent from coming closely enough to nitrile *N*-oxide groups.[7]

The authors wish to express their thanks to Professor Saburo Nagakura of the Institute for Solid State Physics, the University of Tokyo and to Professor Noboru Mataga of Osaka University for discussions.

Note Added in Proof: After the manuscript of this paper had been sent to the Chemical Society, we learned of two papers in which the N→O bond length (R_{NO}) of nitrile *N*-oxide group was reported. One is a paper by M. Winnewisser and H. K. Bodensch, *Z. Naturforsch.*, **A22**, 1724 (1967), in which they reported R_{NO} of H–C≡N→O molecule to be 1.207 Å based on the analyses of the microwave spectrum. Another paper by M. Shiro *et al.* in our laboratory showed R_{NO} of 4-methoxy-2,6-dimethylbenzonitrile *N*-oxide to be 1.249 Å by the method of X-ray analyses at about −140°C; the paper presented at the 21st Annual Meeting of the Chemical Society of Japan, Osaka, April 1968. The above R_{NO} values pertinent to nitrile *N*-oxide group are short and almost agree with theoretically predicted values reported in this paper.

Appendix

The MO's obtained here for BNO and its related compounds are listed below for the sake of comparison with those of BMANO and its related compounds.

37) Y. Y. Kharitonov, *Izvest. Akad. Nauk. S.S.S.R.*, **No. 11**, 1953 (1962).

38) a) L. E. Sutton, Ed., "Tables of Interatomic Distances and Configuration in Molecules and Ions," Special Publication No. 11, The Chemical Society, London (1958), p. M112, and b) its supplement (1965), pp. M24S, M25S, M119S, M126S, M127S, M137S, M138S and M155S; c) A. Caron, G. J. Palenik, E. Goldish and J. Donohue, *Acta Cryst.*, **17**, 102 (1964); d) K. Folting, W. N. Lipscomb and B. Jerslev, *ibid.*, **17**, 1263 (1964); e) N. B. H. Jonathan, *J. Mol. Spectroscopy*, **4**, 75 (1960); f) E. Ochiai and H. Mitarashi, *Ann. Rept. ITSUU Lab.*, **No. 13**, 19 (1963); g) W. Lüttke, *Z. Elektrochem.*, **61**, 302 (1957); h) H. W. Brown and G. C. Pimentel, *J. Chem. Phys.*, **29**, 883 (1958); i) Y. Matsui, *Nippon Kagaku Zasshi* (*J. Chem. Soc. Japan, Pure Chem. Sect.*), **83**, 990 (1962); i) H. Shindo, *Chem. Pharm. Bull.*, **6**, 117 (1958).

39) R. Huisgen, *Angew. Chem. Intern. Ed.*, **2**, 565 (1963); R. H. Wiley and B. J. Wakefield, *J. Org. Chem.*, **25**, 546 (1960).

Simple molecular orbitals of phenyl acetylene, benzonitrile, and benzonitrile *N*-oxide. Ψ and $\bar{\varepsilon}$ stand for the wave function and eigenvalue for π conjugated system (see Fig. 1 in text), respectively. Eigenvalue stands for the δ in the equation; $E=\alpha+\delta\cdot\beta$, and the calculating conditions are included in each table.

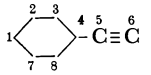

($\beta_{56}=1.5\,\beta$, $\beta_{45}=\beta$)

	Eigenvalue	Symmetry	C_{i1}	C_{i2}	C_{i3}	C_{i4}	C_{i5}	C_{i6}
ϕ_1	2.21380	b_2	+0.24551	+0.27176	+0.35610	+0.51658	+0.43140	+0.29230
ϕ_2	1.63042	b_2	−0.45136	−0.36795	−0.14856	+0.12574	+0.50213	+0.46196
ϕ_3	1.00000	a_2	0	−0.5	−0.5	0	0	0
ϕ_4	0.83116	b_2	+0.48580	+0.20189	−0.31800	−0.46619	+0.24851	+0.44850
ϕ_5	−0.83116	b_2	+0.48580	−0.20189	−0.31800	+0.46619	+0.24851	−0.44850
ϕ_6	−1.00000	a_2	0	−0.5	+0.5	0	0	0
ϕ_7	−1.63042	b_2	−0.45136	+0.36795	−0.14856	−0.12574	+0.50213	−0.46196
ϕ_8	−2.21380	b_2	−0.24551	+0.27176	−0.35610	+0.51658	−0.43140	+0.29230

$C_{i2}=\pm C_{i7}$; $C_{i3}=\pm C_{i8}$ (+ and − represent b_2 and a_2 orbitals respectively.)

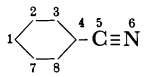

($\alpha_6=\alpha+0.5\,\beta$, $\beta_{56}=1.5\,\beta$, $\beta_{45}=\beta$)

	Eigenvalue	Symmetry	C_{i1}	C_{i2}	C_{i3}	C_{i4}	C_{i5}	C_{i6}
ϕ_1	2.27521	b_2	+0.19955	+0.22701	+0.31695	+0.49411	+0.49031	+0.41430
ϕ_2	1.74886	b_2	−0.43090	−0.37679	−0.22805	−0.02204	+0.41756	+0.50153
ϕ_3	1.00000	a_2	0	−0.5	−0.5	0	0	0
ϕ_4	0.92500	b_2	−0.51574	−0.23853	+0.29510	+0.51149	−0.11707	−0.41319
ϕ_5	−0.72824	b_2	−0.45606	+0.16606	+0.33513	−0.41012	−0.37160	+0.45382
ϕ_6	−1.00000	a_2	0	+0.5	−0.5	0	0	0
ϕ_7	−1.53893	b_2	−0.47625	+0.36646	−0.08770	−0.23149	+0.53165	−0.39113
ϕ_8	−2.18189	b_2	−0.27150	+0.29619	−0.37476	+0.52150	−0.38833	+0.21719

$C_{i2}=\pm C_{i7}$; $C_{i3}=\pm C_{i8}$ (+ and − represent b_2 and a_2 orbitals, respectively.)

$\bar{\varepsilon}_1=1.77069$ $\quad\bar{\psi}_1=0.64637\varphi_C+0.76302\varphi_N$

$\bar{\varepsilon}_2=-1.27069$ $\quad\bar{\psi}_2=0.76302\varphi_C-0.64637\varphi_N$

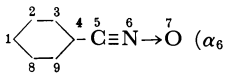

($\alpha_6=\alpha+1.6\beta$, $\alpha_7=\alpha+1.55\beta$, $\beta_{56}=1.5\beta$, $\beta_{67}=1.2\beta$, Ind.$=((1/3)^n\times 1.6)$)

	Eigenvalue	Symmetry	C_{i1}	C_{i2}	C_{i3}	C_{i4}	C_{i5}	C_{i6}	C_{i7}
ϕ_1	3.34037	b_2	+0.01373	+0.02293	+0.06240	+0.18184	+0.45043	+0.72179	+0.48378
ϕ_2	2.14272	b_2	−0.31002	−0.33214	−0.39512	−0.49119	−0.17528	+0.13935	+0.28213
ϕ_3	1.44351	b_2	+0.46001	+0.33201	+0.01272	−0.31441	−0.42363	−0.04754	+0.53574
ϕ_4	1.03954	a_2	0	−0.49506	−0.50489	0	0	0	0
ϕ_5	0.84945	b_2	−0.41450	−0.17605	+0.26842	+0.38822	−0.27578	−0.31700	+0.54300
ϕ_6	−0.49650	b_2	−0.37320	+0.09265	+0.32537	−0.27339	−0.46662	+0.50252	−0.29466
ϕ_7	−0.96084	a_2	0	+0.50489	−0.49506	0	0	0	0
ϕ_8	−1.29626	b_2	+0.50412	−0.32674	−0.07415	+0.42722	−0.48112	+0.30192	−0.12729
ϕ_9	−2.04459	b_2	+0.35619	−0.36413	+0.39548	−0.46780	+0.24830	−0.11481	+0.03833

$C_{i2}=\pm C_{i8}$; $C_{i3}=C_{i9}$ (+ and − represent b_2 and a_2 orbitals respectively.)

$\bar{\varepsilon}_1=3.26401$ $\quad b_1$ $\bar{\psi}_1=0.41032\varphi_C+0.74705\varphi_N+0.52302\varphi_O$

$\bar{\varepsilon}_2=1.18034$ $\quad b_1$ $\bar{\psi}_2=0.56354\varphi_C+0.24320\varphi_N-0.78948\varphi_O$

$\bar{\varepsilon}_3=-0.76135$ $\quad b_1$ $\bar{\psi}_3=0.71698\varphi_C-0.61868\varphi_N+0.32121\varphi_O$

BULLETIN OF THE CHEMICAL SOCIETY OF JAPAN VOL. 41 1056—1063 (1968)

Primary Processes in the Photoreduction of Acridine in Various Alcohols

Masao KOIZUMI, Yoshinori IKEDA and Hiroshi YAMASHITA

Department of Chemistry, Faculty of Science, Tohoku University, Katahira-cho, Sendai

(Received September 23, 1967)

The effect of the addition of biacetyl on the quantum yield of photoreduction of acridine in methanol, ethanol, *n*- and iso-propanol has been studied under the aerated and deaerated conditions. From the analysis of the results, the quantum yields for four mechanisms Φ^{S}_{M} (S means that a reactive state is singlet excited states, S*, and M denotes a molecular mechanism), Φ^{S}_{R} (R denotes a radical mechanism), Φ^{T}_{M} (T indicates that a reactive state is a state other than S* and T(π–π*), most likely T(n–π*) and Φ^{T}_{R} have been decided, assuming that oxygen does not deactivate T(n–π*). The values are

for methanol,	$\Phi^{S}_{M}(0.027)$	$\Phi^{S}_{R}(0.039)$	$\Phi^{T}_{M}(0.006)$	$\Phi^{T}_{R}(0.057)$
for ethanol,	$\Phi^{S}_{M}(0.043)$	$\Phi^{S}_{R}(0.067)$	$\Phi^{T}_{M}(0)$	$\Phi^{T}_{R}(0.019)$
for *n*-propanol,	$\Phi^{S}_{M}(0.030)$	$\Phi^{S}_{R}(0.036)$	$\Phi^{T}_{M}(0)$	$\Phi^{T}_{R}(0.022)$
for isopropanol,	$\Phi^{S}_{M}(0.03)$	$\Phi^{S}_{R}(0.058)$	$\Phi^{T}_{M}(0)$	$\Phi^{T}_{R}(0)$

The quenching constants of biacetyl on the fluorescence of acridine have been found to agree with the ones on the reaction at S* in all alcohols; the rate constants approximate diffusion controlled. In addition it has been confirmed by a flash method that biacetyl does not attack the T(π–π*) nor the semi-reduced acridine; this justifies the present method of analysis.

It is well known that acridine dissolved in some H-containing solvents, undergoes photoreduction and yields acridan, its derivatives or diacridan according to the experimental conditions.[1-5] Since all these products have no absorption from 350 to 400 mμ where the absorption of acridine is large, disappearance of acridine can be followed very accurately by the change in the optical density at 365 mμ and some interesting feature of the reaction was obtained from such kinetic studies.[6,7] Recent flash photolytic investigations performed by our group,[8] have revealed that two independent primary processes are involved in this photoreduction. One is a radical mechanism in which half-reduced acridine is formed as an intermediate, and the other is a mechanism in which acridan or its derivative (perhaps a compound in which a solvent fragment is attached to 9-position[3-5] is produced so quickly that no intermediate is observed by an ordinary flash technique. This mechanism was designated conventionally as a molecular mechanism.

Kellmann and Dubois, on the other hand, proposed that the reactive state of acridine in methanol is most likely the n–π* triplet state instead of the lowest π–π* triplet state.[9] They did not, however, exclude the possibility of singlet excited state participating in the reaction. We also confirmed by energy transfer experiments, using eosine as triplet energy acceptor, that the lowest triplet is not a reactive state.[10]

Under such status, we have planned to make the experiments which will make clear the contributions of singlet excited state and of n–π* triplet state to the entire reaction and the experiments which will decide for each state the contribution of radical and molecular mechanisms. Such experiments consist of investigating the effect of biacetyl (used as a triplet energy acceptor) concentration on the rate of photoreduction both in the absence and in the presence of oxygen. We have made such studies using methanol, *n*- and iso-propanol as H-containing solvents, and have obtained some interesting results. It was not a long while since we had finished the present experiments that a paper by Van der Donckt and Porter appeared,[11] which has raised some doubt on the conclusion of Kellmann and Dubois; they have

1) V. Zanker and P. Schmidt, *Z. physik. Chem. N.F.*, **17**, 11 (1958).
2) A. Kellmann, *J. Chem. Phys.*, **57**, 1 (1960).
3) M. Giurgea, G. Mihai, V. Topa and M. Musa, *J. Chimie Physique*, **61**, 619 (1964).
4) F. Mader and V. Zanker, *Chem. Ber.*, **97**, 2418 (1964).
5) H. Gyth, P. Cerutti and H. Schmid, *Helv. Chim. Acta*, **48**, 1395 (1965).
6) S. Kato, S. Minagawa and M. Koizumi, This Bulletin, **34**, 1026 (1961).
7) S. Niizuma and M. Koizumi, *ibid.*, **36**, 1629 (1963).
8) A. Kira, S. Kato and M. Koizumi, *ibid.*, **39**, 1221 (1966).
9) A. Kellmann and J. T. Dubois, *J. Chem. Phys.*, **42**, 2518 (1965); A. Kellmann, *J. Chimie Physique*, **63**, 936 (1966).
10) A. Kira, Y. Ikeda and M. Koizumi, This Bulletin, **39**, 1673 (1966).
11) E. Van der Donckt and G. Porter, *J. Chem. Phys.*, **46**, 1173 (1967).

claimed that an excited singlet state is an only reactive state in the photoreduction of acridine in *isopropanol*.

According to our present results, however, four alcohols behave more or less in different manner and in particular, isopropanol and methanol show distinctly different features in the effect of biacetyl on the photoreduction, which lead to the conclusion that the reactive states is in the former case only singlet excited state in agreement with Porter's conclusion, whereas in the latter case, are singlet and $T(n-\pi^*)$ state as Kellmann and Dubois proposed. Hence it seems timely to report the details of our experiments although we have not yet succeeded in interpreting the unexpected differences found in four kinds of alcohols.

Since Dubois and Kellmann's conclusion was based on the assumption that inhibiting action of biacetyl is due to the energy transfer according to $A^{T(n-\pi^*)}+B \rightarrow A+B^T$ (where A is acridine and B is biacetyl), it is desirable to examine whether biacetyl does not affect the lowest $T(\pi-\pi^*)$ of acridine by a different mechanism than energy transfer and further to examine whether it does not react with the half reduced acridine. Therefore we have investigated at first by the flash technique using methanol and ethanol as solvents, the effect of the addition of biacetyl on the decays of $T(\pi-\pi^*)$ of acridine and of the half reduced acridine. In addition, we have made investigations on the effect of the addition of biacetyl on the yield of $T(\pi-\pi^*)$, AH and AH_2, the results of which have supported the view of Kellmann and Dubois to some extent. These experiments are described in Part I. In Part II, the steady illumination experiments are described. The data, being more accurate than those from flash experiments, are analysed and interpreted on the basis of four alternative processes, and the quantum yields Φ_M^S, Φ_R^S, Φ_M^T and Φ_R^T (where S and T denote singlet excited state and $T(n-\pi^*)$ state and where M and R denote respectively molecular and radical) are separately decided.

Part I.*1 Flash Photolysis Studies

Experimental

Apparatus, procedures and samples are essentially similar as in the previous papers.[8,10] The decays and yields of $T(\pi-\pi^*)$ of acridine and of the half-reduced form of acridine were examined respectively at 440 and at 278 mμ (or in some cases as 520 mμ). The yield of acridan was investigated from the increase of optical density at 290 mμ. The concentration of acridine was always 4.8×10^{-5} M and the concentration of biacetyl was changed from zero to 1.1×10^{-2} M. By using a suitable filter only acridine was excited.

Results and Discussion

T-T Absorption Spectra of Biacetyl. Transient absorption spectra of biacetyl in methanol are shown in Fig. 1.

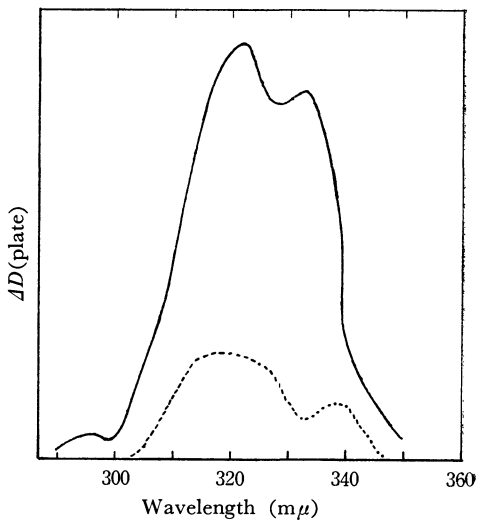

Fig. 1. Transient absorption spectra of biacetyl.
—— after 93 μsec, - - - after 360 μsec

The decay at 320 mμ is of the first order with a rate constant $k\simeq4\times10^3 sec^{-1}$. The comparison with the data in literatures[9,12,13] confirms that this species is the triplet state of biacetyl.

The Effect of the Addition of Biacetyl on the Decay of $T(\pi-\pi^*)$ of Acridine. The decay was not essentially affected by the addition of biacetyl up to 1.1×10^{-2}M. Some of the values of the first order rate constants are given in Table 1.

The Effect of the Addition of Biacetyl on the Decay of Half Reduced Acridine. The decay of half reduced acridine is second order and the rate

Table 1. Rate constant of the decay of $T(\pi-\pi^*)$, $k\times10^{-4}(sec^{-1})$

$[B]_M$	0	1.1×10^{-4}	1.1×10^{-3}	5×10^{-3}	1.1×10^{-2}
Methanl	1.1	1.1	1.1	1.1	1.1
	1.2	1.1	1.2	1.1	1.1
Ethanol	0.8	0.8	0.6	0.7	0.7
	0.9	0.8	0.7	0.7	0.8

*1 Experiments were made by Yamashita.

12) G. Porter and M. W. Windsor, *Proc. Roy. Soc.*, **A245**, 238 (1958).
13) H. L. J. Bäckström and K. Sandros, *Acta Chem. Scand.*, **12**, 823 (1958).

TABLE 2. RATE CONSTANT OF THE DECAY OF HALF-REDUCED ACRIDINE

	$[BA]_M$	0	1.1×10^{-4}	1.1×10^{-3}	5.0×10^{-3}	1.1×10^{-2}
$k\times10^{-8}$ (M^{-1} sec^{-1})	Methanol	4	4	3	4	4
	Ethanol exp. 1	4	3	4	5	3
	exp.	2	3	2	3	4

constant was evaluated from the plot of $1/D$ against t, D being measured at 520 mμ. The results are shown in Table 2. The analysis of the changes in the optical density at 278 mμ by the method employed in the previous paper,[8] also gave essentially the similar results. Thus the possibility of such a reaction AH+B→A+BH occurring, can safely be ruled out. The results given in Tables 1 and 2 justifies Kellmann and Dubois' interpretation of their results.

The Effect of [B] on the Yield of T(n–π^*) of Acridine. If the reactive state is T(n–π^*), then there is a possibility that the yield of T(π–π^*) is increased by the addition of biacetyl as inferred from the following reasoning. It is quite reasonable to presume that the intersystem crossing occurs *via* the following scheme,[14]

$$S^*(\pi\text{-}\pi^*) \rightarrow T(n\text{-}\pi^*) \xrightarrow{k_d'} T(\pi\text{-}\pi^*)$$
$$\Big\downarrow{\scriptstyle k_r'}$$
$$\longrightarrow \text{reaction}$$

In the absence of biacetyl, a portion of T(n–π^*) disappears through the reaction with the solvent; this portion, if biacetyl is present, will be affected by biacetyl according to $A^{T(n-\pi^*)}+B\rightarrow B^T+A$. The produced B^T then gives its excitation energy back again to acridine according to $B^T+A\rightarrow B+A^{T(\pi-\pi^*)}$ (The occurrence of such a process was demonstrated by Kellmann and Dubois and was reconfirmed by the present authors (see Part II).). Then the quantum yields of the production of T(π–π^*), $\phi_{\pi\pi}$ should be given by the following equations, provided biacetyl does not affect the intersystem crossing.

In the absence of B

$$\phi_{\pi\pi} = k_d'/(k_r'+k_d')\cdot\phi_{n\pi}.$$

In the presence of B

$$\phi_{\pi\pi} = (k_d'+k[B])/(k_r'+k_d'+k[B])\cdot\phi_{n\pi}.$$

The results are shown in Fig. 2, where the optical densities at 440 mμ immediately after flashing, are plotted against [B].

It seems that there is a slight increase at the largest biacetyl concentration, but in view of the crudeness of the data one should say rather that there is no essential effect. This suggests $k_r' \ll k_d'$. By the way, the optical densities at 440 mμ immediately after flashing in methanol, ethanol and isopropanol are respectively ~0.36, ~0.33 and ~0.37. Thus the yields are essentially the same in three alcohols. These data may be of some importance for the general discussion.

The Effect of [B] on the Yield of AH. The lifetime of singlet excited state of acridine in ethanol is 7.2×10^{-10} sec,[15] and that of T(n–π^*) was estimated by Kellmann and Dubois as ~10^{-8}sec. Therefore, if the reactive state were only S*, the addition of ~10^{-2}M of biacetyl would scarcely affect the yield of AH. On the other hand, if the reactive state were only T(n–π^*), the addition of this magnitude of biacetyl should decrease the yield to some extent. The yield of AH was estimated from the

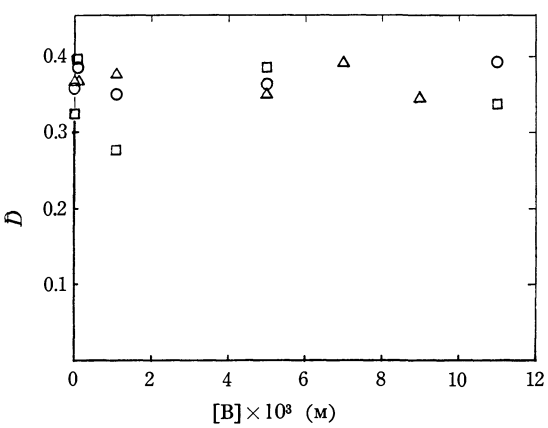

Fig. 2. Influence of the concentration of biacetyl on the yield of the lowest triplet of acridine (in terms of optical densities at 440 mμ).
○ methanol, □ ethanol, △ isopropanol

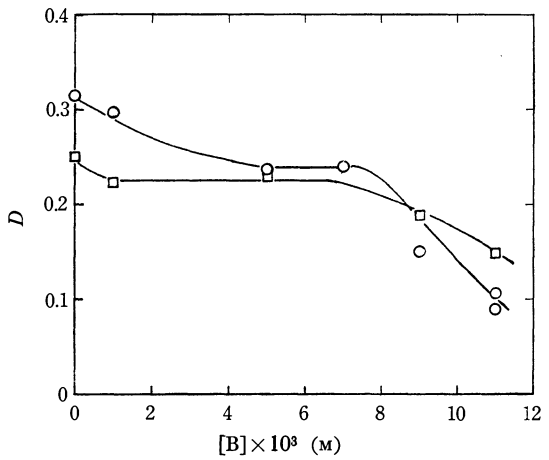

Fig. 3. Influence of the concentration of biacetyl on the yield of semi-reduced acridine (in terms of optical densities at 278 mμ).
○ methanol, □ ethanol

14) M. El-Sayed, *J. Chem. Phys.*, **38**, 2834 (1963).

15) H. Kokubun, to be published.

optical densities at 278 mμ directly after flashing. The results are shown in Fig. 3. Although the data are not very accurate, still there is a clear tendency that the yield decreases with the increase of [B]. At 5×10^{-3} M of B, the decrease in methanol and ethanol is approximately ~1/4 and 1/8 and at 1×10^{-2}M of B it is ~2/3 and 1/2. These results strongly suggest the participation of T(n–π^*) state in these two solvents.

The Effect of [B] on the Yield of AH_2. This was examined from the similar reasoning as above. The yield of AH_2 was evaluated from the optical density at 290 mμ a long time after flashing, D_∞^{290}. The results are shown in Fig. 4. The decrease in the yield of AH_2 by adding 5×10^{-2}M of biacetyl in methanol and ethanol are equally about 1/3 while at 1×10^{-2}M of the added biacetyl, it is respectively ~2/3 and 1/2. Although the above data are not very accurate, they lead us to suspect that T(n–π^*) as well as S* participates in the reaction. It may be added that the above data in combination with the oxygen effect on the yield of AH_2[8] enable us in principle, to evaluate Φ_M^S, Φ_R^S, Φ_M^T and Φ_R^T. But since it is difficult to get the exact data from the flash photolytic experiments, it seems wiser to leave the quantitative investigation to the steady light studies.

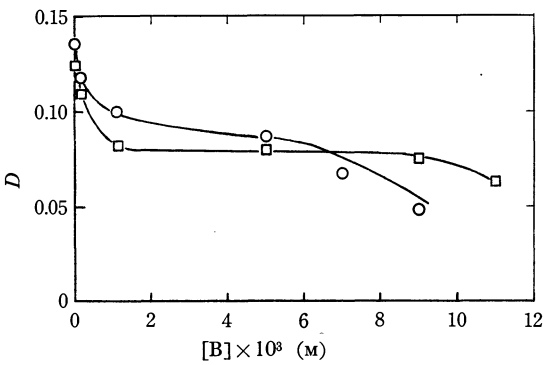

Fig. 4. Influence of the concentration of biacetyl on the yield of the product (in terms of optical densities at 290 mμ).
○ methanol, □ ethanol

Part II.*2 Steady Light Experiment

Preliminary Experiments for the Effect of the Addition of Biacetyl on the Photochemical Reduction of Acridine. Figure 5 shows a typical example of the spectral change when the deaerated solution of acridine, 1×10^{-4} M in methanol containing some quantity of biacetyl, is irradiated by 365 mμ. In the early stage of irradiation, the peak of acridine declines accompanied with the rise in the height of the peak at ~290 mμ. An isosbestic point is seen at ~325 mμ. The above behavior substantiates that the similar photoreduction as in the absence of biacetyl is occurring in the early stage. In the later stage, however, the absorption around 350 mμ gradually rises again and the absorption in the shorter wavelength region declines with no isosbestic point. This suggests the occurrence of some unknown reaction between biacetyl and acridan. Such a phenomenon was observed in all the alcohols investigated but it was most prominent in methanol. The similar phenomenon was observed in the air-saturated solution. It was checked that the alcoholic solution of biacetyl alone scarcely undergoes any reaction even by the irradiation for one hour.

Figure 6 gives some typical examples of the $\ln(e^{acd}-1)$ *vs.* t plots. In consistence with the above spectral change, the plots are satisfactorily linear in the early stage indicating the occurrence of a simple photoreduction of acridine whereas in the later stage they gradually deviate and finally show slow and apparently linear increase. The above results ensure us to investigate the retarding effect of biacetyl by

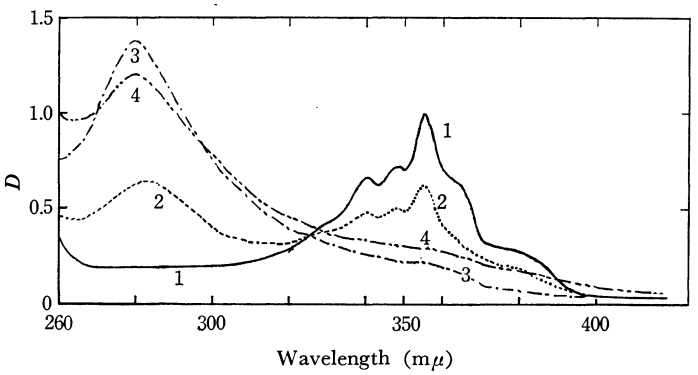

Fig. 5. Spectral change caused by the irradiation of the acridine solution of methanol containing biacetyl.
[acridine]$=1\times10^{-4}$ M [B]$=5\times10^{-3}$ M
1 before irradiation, 2 after 1 min irradiation, 3 after 6 min irradiation, 4 after 60 min irratiation

*2 The experiments were performed by Ikeda.

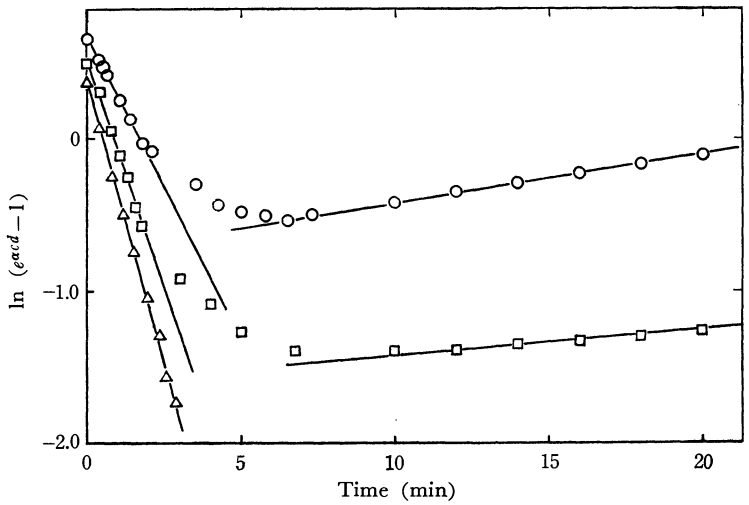

Fig. 6. $\ln(e^{acd}-1)$ *vs.* t plots (25°C).
[A]$=1\times10^{-4}$ M, ○ [BA]$=0$ M, □ [BA]$=2\times10^{-3}$ M, △ [BA]$=1\times10^{-2}$ M

comparing the initial slope of the $\ln(e^{acd}-1)$ *vs.* t plots.

The Effect of [B] on the Quantum Yield of Photoreduction. This was investigated for four kinds of alcohols and for both the aerated and deaerated solutions. Some corrections were made for the absorption of biacetyl when its concentration was high. The values of quantum yields for the four kinds of alcohol (in the absence of biacetyl) were redetermined and were found essentially the same as the previously reported ones.[6,7] In Fig. 7, some of the plots of Φ_0/Φ *vs.* [B] (Φ_0, the quantum yield in the absence of biacetyl) are given.*3

It is quite astonishing that the plots are essentially different in the four alcohols. Thus in methanol the plot clearly consists of two linear portions a and b, for both the aerated and deaerated conditions. In ethanol and *n*-propanol the similar curve as in methanol is obtained only in the deaerated solutions, but in the aerated solutions, the plot consists of a single straight line the slope of which is of the similar magnitude as the ones for the b-parts of the above mentioned plots. In the case of isopropanol the plot for both the aerated and deaerated solutions is satisfactorily reproduced by a single straight line.

From the above results, one may safely conclude that in the case of methanol, ethanol and *n*-propanol (for the latter two alcohols only in the deaerated condition) the two states participate in the reaction, whereas in isopropanol and the aerated solutions of ethanol and *n*-propanol only one state is involved in the reaction. It is most plausible that the latter state is a singlet excited state and the former two states are S* and T(n–π*). These conclusions agree with that of Kellmann and Dubois for methanol on one hand, and that of Porter for isopropanol.

Quenching Action of Biacetyl on the Fluorescence of Acridine. To confirm the participation of S* in the reaction further, the quenching action of B on the fluorescence of acridine has been studied and has been compared quantitatively with the retarding effect of B on the photoreduction (in the high concentration region of B). In Fig. 8, the emission spectra for the following three solutions are given (a) [A]$=1\times10^{-4}$ M, (b) [B]$=5\times10^{-2}$ M and (c) [A]$=1\times10^{-4}$ M, [B]$=5\times10^{-2}$ M. The absorption spectra of biacetyl are also dipicted for later consultation.

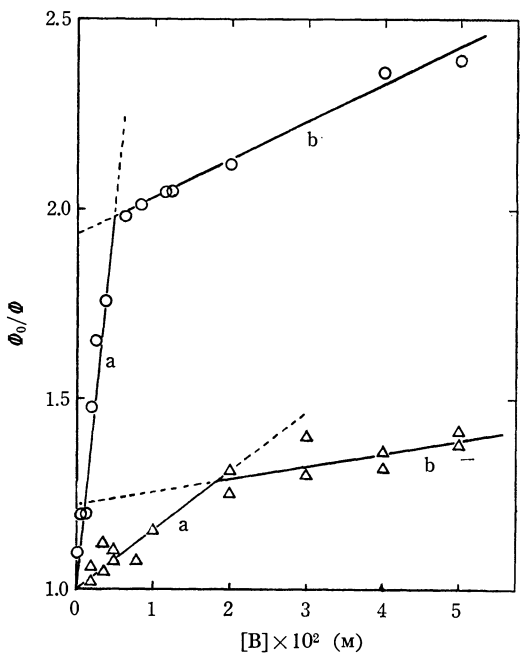

Fig. 7-1

*3 Comparing these results with the ones in the flash experiment, one may say that the effect of [B] agrees in the two cases for methanol but the disagreement for ethanol seems to exceed the experimental error

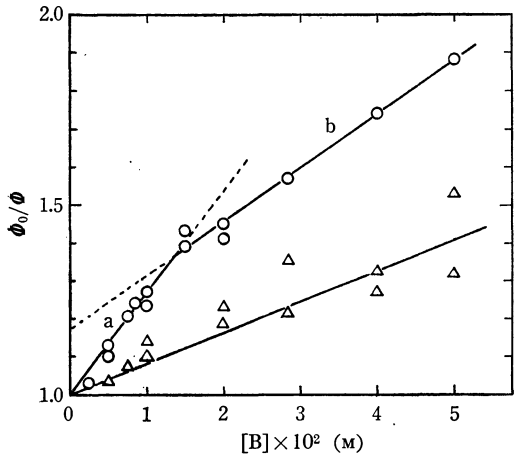

Fig. 7-2

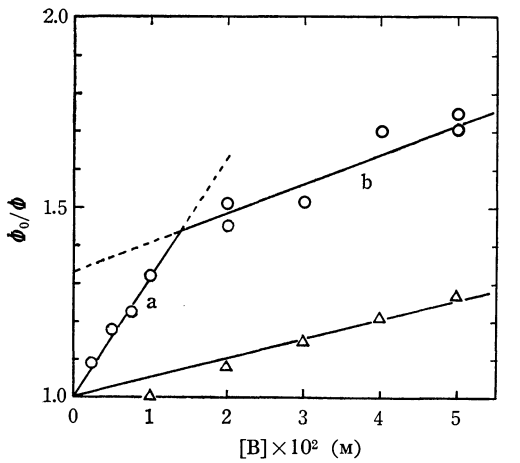

Fig. 7-3

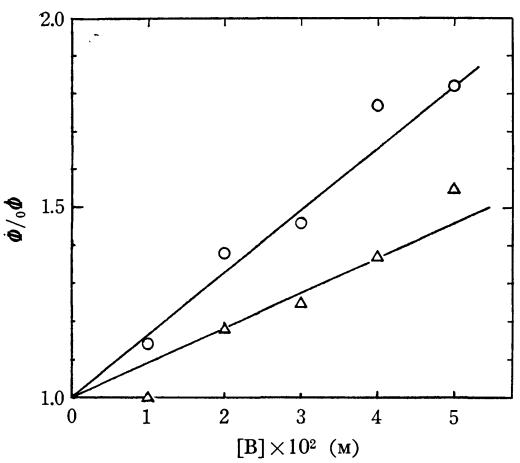

Fig. 7-4

Fig. 7. Plots of Φ_0/Φ against the concentration of biacetyl (25°C).
1 methanol, 2 ethanol, 3 *n*-propanol, 4 isopropanol

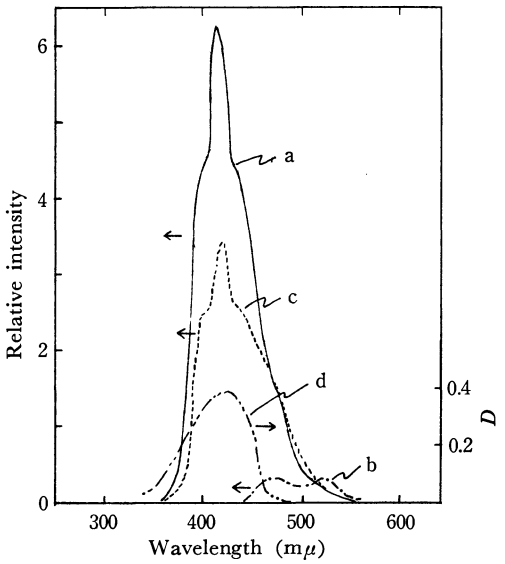

Fig. 8. Emission spectra of acridine, biacetyl and the mixture of the two in the deaerated methanol solution (exciting light, 365 mμ).
a) [A]=1×10⁻⁴ M, b) [B]=5×10⁻² M,
c) [A]=1×10⁻⁴ M, [B]=5×10⁻² M
d) absorption spectra of biacetyl.

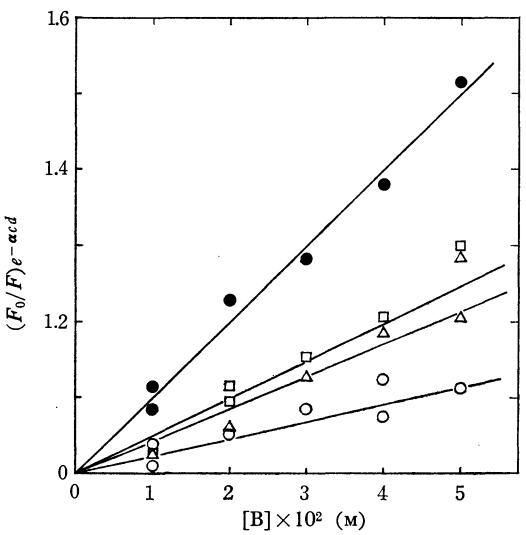

Fig. 9. Stern-Volmer plots for quenching of fluorescence of acridine by biacetyl.
○ methanol, □ ethanol, △ *n*-propanol, ● isopropanol

As is well known, the emission of B consists of fluorescence (shorter wavelength) and phosphorescence[16] (longer wavelength). It is apparent from the emission spectra of System C, that biacetyl quenches the fluorescence of acridine and that the phosphorescence of biacetyl is quenched by acridine. The latter

16) H. Bäckström and K. Sandros, *Acta Chem. Scand.*, **14**, 48 (1960).

phenomenon is due to the process $B^T + A \rightarrow B + A^{T(\pi-\pi^*)}$ as Kellmann and Dubois have established.[9] Systematic studies on the quenching action of B have been made at the emission peak, 410 mμ of acridine, choosing 365 mμ as an exciting light. Stern-Volmer plots for the four alcohols are shown in Fig. 9. The quantity for the ordinate, $(F_0/F)e^{-\alpha cd}$ contains a correction term, $e^{-\alpha cd}$ for the reabsorption of fluorescence by biacetyl (*cf.* Fig. 8) where α is the absorption coefficient of biacetyl at 410 mμ, where c is the concentration of biacetyl and where d is the length of fluorescence light path. d is approximated as 1/2 cm. From the slopes one can evaluate $k_Q\tau$; approximating τ as 10^{-9}sec for all the alcohols, one obtains the rate constant k_Q for the quenching process. The results are given in Table 3.

TABLE 3

		k_q ($M^{-1}sec^{-1}$)	k_Q ($M^{-1}sec^{-1}$)
Methanol	(dea)	1.2×10^{10}	0.3×10^{10}
	(aer)	0.4×10^{10}	
Ethanol	(dea)	1.4×10^{10}	0.7×10^{10}
	(aer)	0.8×10^{10}	
n-Propanol	(dea)	0.8×10^{10}	0.5×10^{10}
	(aer)	0.5×10^{10}	
Isopropanol	(dea)	1.7×10^{10}	1.0×10^{10}
	(aer)	0.9×10^{10}	

It is worthwhile to note that the k_Q-values are essentially the same for the aerated and deaerated solutions.

Quantitative Discussion about the Retarding Effect of B on the Photoreduction. Since the reaction occurring in the high concentration region of B is considered to be concerned with S*, the reaction scheme for it may be written as follows,

$$A + h\nu \rightarrow A^* \quad I_{ab}$$
$$A^* \rightarrow A \quad k_d$$
$$A^* + RH_2 \rightarrow Prod \quad k_r$$
$$A^* + B \rightarrow A + B \quad k_q$$

where A* is the singlet excited state of acridine. The following relations are derived straightforwardly.

$$\Phi = k_r/(k_r + k_d + k_q[B]) \quad (1)$$
$$\Phi_0 = k_r/(k_r + k_d) \quad (2)$$
$$\Phi_0/\Phi = 1 + (k_q/(k_d + k_r))[B] \quad (3)^{*4}$$

Since $k_r + k_d = 1/\tau$, k_q can easily be evaluated from the plots given in Fig. 7. The results are given in Table 3. The agreement between k_q and k_Q are satisfactory especially for the k-values for the aerated solutions. Somewhat larger k_q values for the deaerated solutions might be due to the participation of the T(n-π^*) state. Rate constants for the encounter-controlled reaction evaluated from the relation $k = 8RT/3000\eta$ for methanol, ethanol and *n*-propanol are respectively 1.2×10^{10}, 0.6×10^{10}, 0.3×10^{10} $M^{-1}sec^{-1}$. These values are close to those of k_q amd k_Q. Thus the above results lead to the conclusion that the part of the reaction occurring in the high concentration of biacetyl, is concerned with S* and that biacetyl quenches the reaction at an encounter-controlled rate.

The participation of T(n-π^*) state is very prominent only in the case of the deaerated methanol. Hence the accurate treatment can be made only on this case. If one assumes that biacetyl does not affect the intersystem crossing, equations corresponding to (1) and (2) are

$$\Phi = \frac{k_r'}{k_r' + k_d' + k_q'[B]}\varphi_{ST} \quad (1')$$

$$\Phi_0 = \frac{k_r}{k_r' + k_d'}\varphi_{ST} \quad (2')$$

where φ_{ST} is the quantum yield of intersystem crossing S*→T(n-π^*). The similar relation to (3) exactly holds also in this case. Making a suitable correction for the participation of the singlet excited state and assuming the calculated k_q' value, one can evaluate the lifetime of T(n-π^*). The result is 8.9×10^{-8}sec which agrees with the one proposed by Kellmann and Dubois.

Analyzing the experimental data along the above reasoning, the values of $(k_d+k_r)/k_r$ or $(k_d'+k_r')/k_r'\cdot\varphi_{ST}$ may be evaluated. The results are given in Table 4. The reliable value of φ_{ST} is still unknown. If one assumes $\varphi_{ST}\simeq0.3$,[*5] k_d' is several times larger than k_r' in the case of the deaerated methanol. In ethanol and *n*-propanol the ratio is considered to be still larger. This is consistent with the result obtained from the flash experiment, that

TABLE 4

		S* $(k_d+k_r)/k_r$	n-π^* $(k_d'+k_r')/k_r'\varphi_{ST}$
Methanol	(dea)	15	17
	(aer)	37	~170
Ethanol	(dea)	8.3	~ 50
	(aer)	23	—
n-Propanol	(dea)	15	~ 50
	(are)	33	—
Isopropanol	(dea)	11	—
	(are)	32	—

*4 In the presence of O_2, k_d+k_r should be replaced by $k_d''+k_r''$ with $k_r''<k_r$, but the sum of the two rate constants is the same.

*5 The maximum quantum yield for the photochemical reaction between acridine and acridan in benzene solution is ~0.25.[17] (In this case, the reactive state of acridine is T(π-π^*).) Furthermore, acridine-sensitized photooxidation of leucouranine in the aqueous solution leads to $\varphi_{ST}=0.24$ provided the efficiency for the reaction between T(π-π^*) of A and leuco-uranine is 1.[18]

17) This Bulletin, **40**, 2249 (1967).
18) *Ibid.*, **35**, 1875 (1962).

Tabee 5. Separate quantum yields of the four processes

	Φ_M^S	Φ_R^S	Φ_M^T	Φ_R^T	Φ_{total}
Methanol	0.027(20%) (0.009)	0.039(30%) (0.013)	0.006(5%) (0.002)	0.057(45%) (0.019)	0.128 (0.043)
Ethanol	0.043(30%) (0.022)	0.067(55%) (0.034)	0 (0)	0.019(15%) (0.010)	0.129 (0.065)
n-Propanol	0.030(35%) (0.015)	0.036(40%) (0.018)	0 (0)	0.022(25%) (0.011)	0.088 (0.044)
Isopropan-	0.03(35%) (0.031)	0.058(65%) (0.058)	0 (0)	0 (0)	0.089 (0.089)

the yield oi T(π-π*) is scarcely affected by the addition of biacetyl.

Evaluation of Φ_M^S, Φ_R^S, Φ_M^T and Φ_R^T. From the results given in Fig. 7, one can estimate these quantities if one assumes that T(n-π*) is not deactivated by oxygen contained in the aerated solution. Singlet excited state of acridine is not affected by oxygen as has been verified in the present experiment. That AH is not attacked by biacetyl is also verified by the present flash experiment.

Taking methanol for instance, the evaluation can be made in the following way. The quantum yield for the deaerated solution in the absence of biacetyl gives $\Phi_M^S+\Phi_R^S+\Phi_M^T+\Phi_R^T$. The aerated solution in the absence of biacetyl gives $\Phi_M^S+\Phi_M^T$, since oxygen quickly reverts semi-reduced acridine to acridine. The extrapolation of the b-part of the plot for the deaerated solution to [B]=0, gives $\Phi_M^S+\Phi_R^S$ and the similar extrapolation of b-part of the plot for the aerated solution gives Φ_M^S. From these values, each Φ can be determined separately. The results are given in Table 5. The second column for each alcohol is the respective value allotted to one α-H atom.

Although the data are not very accurate and still provisional, it is believed that the general feature will not be altered by more accurate experiments. Generally speaking, the singlet excited state makes a more important role than T(n-π*) for the photoreduction of acridine. There seems to be a tendency that more of the T(n-π*) reacts with alcohols with the increase of the number of α-hydrogen atoms. Molecular mechanism does not occur or scarcely occurs in T(n-π*) state. The reaction at S* increases in the order, methanol<ethanol<isopropanol for both molecular and radical mechanisms when the number of α-hydrogen is taken into account. This agrees with the general tendency of these alcohols when they act as hydrogen donors. Although conspicuous difference in methanol and isopropanol, *i.e.* the result that in methanol about 50% of the total reaction occurs at T(n-π*) whereas in isopropanol the entire reaction occurs at S*, cannot be interpreted in the present stage, one may say at least in the following way. Firstly, any reactions at singlet excited states may not affect the value of φ_{ST} so much since $\Phi_M^S+\Phi_R^S$ is rather small, *i.e.* $\sim$0.1 at most. In fact, as mentioned in Part I, the yield of T(π-π*) is essentially the same in methanol, ethanol and isopropanol. This is naturally expected if Φ_{ST}-(n-π*) is about equal and if T(n-π*) produced mostly goes to T(π-π*). The latter remark has been verified in the present experiment.

Hence, the cause for the difference in methanol and isopropanol should be sought in the step of reaction of T(n-π*) with an alcohol molecule. Steric effect might be a factor chiefly controlling the situation. To make clear the cause of this difference, it is desirable to extend such studies to other solvents. It is also desirable to make experiments using other triplet energy donors and acceptors. Further it is hoped that the reliable value of φ_{ST} is determined.

BULLETIN OF THE CHEMICAL SOCIETY OF JAPAN VOL. 41 1064—1067 (1968)

The Non-Newtonian Viscosity of Dilute Aqueous Solution of Methylcellulose

Naomichi Iso and Daijiro YAMAMOTO

Faculty of Agriculture, Meiji University, Ikuta, Kawasaki

(Received October 30, 1967)

The viscometric behavior of a dilute aqueous solution of methylcellulose was studied by tilting capillary viscometers. The intrinsic viscosity was obtained by the extrapolation of Martin's plots on the assumption that the plots were linear down to an infinite dilution. The intrinsic viscosity obtained increased with the rate of shear over the range of 200—1200 sec^{-1}. Huggins' constant, k', the temperature coefficient of the intrinsic viscosity, $d[\eta]/dT$, and the energy of the activation of flow, E_v, decreased with the rate of shear. From the data of $d[\eta]/dT$ and E_v thus obtained, it has seemed reasonable to assume that the methylcellulose chain has a relatively small flexibility and a strong tendency toward alignment with a flowing stream. This may be the main reason why the viscosity of the dilute aqueous solution of methylcellulose is non-Newtonian.

Methylcellulose is a kind of cellulose-ether used extensively in food products as a thickener, a stabilizer, a swelling agent, a coating agent, a molding agent, and a binder. During the course of an investigation into the viscosity of a concentrated methylcellulose solution,[1,2] our attention was called to the viscosity of a dilute solution of the same sample. Although the viscosity of a dilute solution of methylcellulose has been studied by several workers[3-5] in recent years, little attention has been paid to the non-Newtonian viscosity of the dilute solution.

On the other hand, the shear-rate dependence of the intrinsic viscosity of a high polymer solution has been investigated both theoretically and experimentally, and these results have been reviewed by several workers.[6-9] Most experiments and theories have found that the intrinsic viscosity decreased with the shear rate,[6,10-17] although theories which do not give a shear-rate dependence of the viscosity have been reported, too.[18-19] Furthermore, a few theories and experiments have shown that the intrinsic viscosity increases with the shear rate in some cases.[8,20,21]

The purpose of this study is to extend the investigation of the viscometric behavior of methylcellulose solutions to a low rate of shear and to a low concentration of the solution. The temperatures measured range from 25°C to 45°C, for it is found that a gelation of the solute takes place above about 50°C.[2] In that region the energy of the activation of the flow of the solution and the temperature dependence of the intrinsic viscosity have also determined in order to discuss the non-Newtonian viscosity of the solution.

Experimental

Materials. The methylcellulose was a product of Shinetsu Chemical Ind. (trade name, " Metolose 90 SH 15000 "). The manufacturer reported that the density was 1.31 g/cm^3; the degree of methylation of this sample was 1.08—1.42. The white powder of the sample was dissolved in distilled water without further purification; the concentration of the original solution was 0.3030 g/100 ml.

Viscosity Measurement. Four tilting capillary viscometers[22] were used. Each viscometer was a modification of the dilution suspended-level viscometer. The

1) D. Yamamoto, N. Iso and N. Ikawa, *Bull. Fac. Agr. Meiji Univ.*, **20**, 17 (1966).
2) D. Yamamoto, N. Iso and N. Ikawa, *ibid.*, **21**, 51 (1967).
3) K. Uda and G. Meyerhoff, *Makromol. Chem.*, **47**, 168 (1961).
4) K. Uda, *Nippon Kagaku Zasshi* (*J. Chem. Soc. Japan, Pure Chem. Sect.*), **82**, 1597 (1961).
5) W. Kuhn, P. Moser and H. Majer, *Helv. chim. Acta.*, **44**, 770 (1961).
6) A. Peterlin and M. Čopič, *J. Appl. Phys.*, **27**, 434 (1956).
7) E. Passaglia, J. T. Yang and N. J. Wegemer, *J. Polymer Sci.*, **47**, 333 (1960).
8) A. Peterlin, *J. Chem. Phys.*, **33**, 1799 (1960).
9) Y. Chikahisa, *Kobunshi* (*High Polymers, Japan*), **15**, 228 (1966).
10) R. Cerf, *J. Polymer Sci.*, **23**, 125 (1957).
11) Y. Ikeda, *J. Phys. Soc. Japan*, **12**, 378 (1957).
12) F. Bueche, *J. Chem. Phys.*, **22**, 1570 (1957).
13) T. W. Dewitte, *J. Appl. Phys.*, **26**, 889 (1955).
14) T. Takemura, *J. Polymer Sci.*, **28**, 185 (1958).
15) Y. H. Pao, *ibid.*, **61**, 413 (1962).
16) Y. Chikahisa and T. Fujiki, *J. Phys. Soc. Japan*, **19**, 2188 (1964).
17) N. Yamaguchi, *Sci. Papers I.P.C.R.*, **42**, 1 (1966).
18) P. E. Rouse, *J. Chem. Phys.*, **21**, 1272 (1955).
19) B. H. Zimm, *ibid.*, **24**, 269 (1956).
20) A. Peterlin and D. T. Turner, *ibid.*, **38**, 2315 (1963).
21) S. P. Burow, A. Peterlin and D. T. Turner, *Polymer*, **6**, 35 (1965).
22) E. Wada, *J. Polymer Sci.*, **16**, 305 (1954).

Table 1. The intrinsic viscosity, $[\eta]$ (100 ml/g), of dilute aqueous solution of methylcellulose and temperature coefficient of intrinsic viscosity, $d[\eta]/dT$

T (°C)	$g(F)$ (sec^{-1})						
	0	200	400	600	800	1000	1200
25	11.17	11.39	11.74	10.84	—	—	—
30	9.70	9.93	10.13	10.10	10.22	—	—
35	7.98	8.36	8.24	8.19	8.61	—	—
40	7.02	7.35	7.28	7.10	6.87	7.05	—
45	5.45	5.48	5.54	5.61	5.60	5.68	5.73
$-d[\eta]/dT$	0.28	0.29	0.31	0.30	0.31	—	—

capillaries of these viscometers ranged from 0.34 to 0.84 mm in diameter. Aqueous solutions of sucrose were used for the calibration of the viscometers, for Bingham and Jackson[23] have shown that an aqueous solution of sucrose is suitable for this purpose.

The relative viscosity, η_r, is given by the following equation:[17]

$$\eta_r = [4(t_s/t_0)/\{3 + (t_s/t_0)(dt_s/dt_0)\}] \times [1 + (V^2/\pi R^4 \boldsymbol{g} h)(1/t_0^2 - 1/t_s^2)], \quad (1)$$

where V is the total volume flowing in time t, while the suffixes s and 0 denote the solution and the solvent respectively. R is the radius of the capillary, h is the mean head of the liquid, and $\boldsymbol{g}$ is the acceleration due to gravity. The rate of shear at the capillary wall is expressed by:

$$g(F) = 4V/\pi R^3. \quad (2)$$

The intrinsic viscosity, $[\eta]_{g(F)}$, at a constant rate of shear is calculated from Martin's equation:[24]

$$\log(\eta_{sp}/c) = \log[\eta] + k[\eta]c, \quad (3)$$

where η_{sp} is the specific viscosity, c is the concentration of the solution, and k is a constant.

Results and Discussion

Figure 1 shows an example of the shear-rate dependence of the relative viscosity. As the figure shows, the viscometric behavior of the dilute solution of methylcellulose was non-Newtonian; this non-Newtonian behavior of the solution decreased with a decrease in the concentration of the solution. The values of $\log(\eta_{sp}/c)$ at a constant rate of shear were plotted against the concentration according to Martin's equation. An example of the plots of $\log(\eta_{sp}/c)$ *versus* c is shown in Fig. 2.

The intrinsic viscosity at a constant rate of shear was obtained by the extrapolation of each plot of $\log(\eta_{sp}/c)$ *versus* c to an infinite dilution. The values of $[\eta]_{g(F)}$ are shown in Table 1. As the table shows, all the intrinsic viscosities somewhat increased with the rate of shear over the range of 200—1200 sec^{-1} within the limit of experimental error. Although each plot of $\log(\eta_{sp}/c)$ *versus* c was linear, as Fig. 2

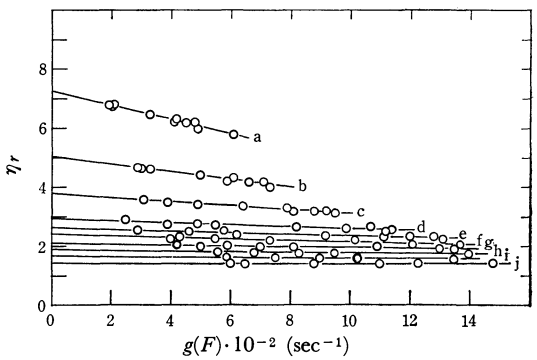

Fig. 1. Shear rate dependence of the relative viscosity of methylcellulose solution at 45°C; a, 0.3030 g/100 ml; b, 0.2424; c, 0.2020; d, 0.1731; e, 0.1515; f, 0.1359; g, 0.1212; h, 0.1010; i, 0.0866; j, 0.0606.

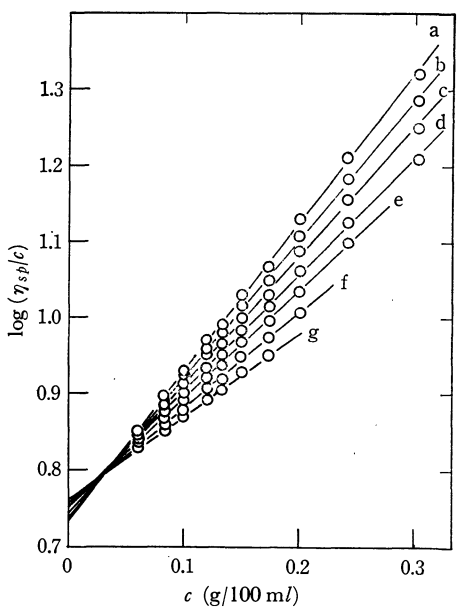

Fig. 2. Martin's plots of methylcellulose solution at 45°C; a, $g(F)=0$ sec^{-1}; b, 200; c, 400; d, 600; e, 800; f, 1000; g, 1200.

shows, $\log(\eta_{sp}/c)$ decreased with the rate of shear in this experimental range. Accordingly, the positive

23) G. W. Scott Blair, "Foodstuffs, Their Plasticity Fluidity and Consistency," North-Holland Pub. Co., Amsterdam (1953).

24) H. M. Spurlin, A. F. Martin and H. G. Tennet, *J. Polymer Sci.*, **1**, 63 (1946).

TABLE 2. HUGGINS' CONSTANT OF DILUTE AQUEOUS SOLUTION OF METHYLCELLULOSE

T (°C)	$g(F)$ (sec^{-1})						
	0	200	400	600	800	1000	1200
25	0.398	0.332	0.249	0.256	—	—	—
30	0.525	0.395	0.371	0.330	0.240	—	—
35	0.577	0.443	0.393	0.337	0.240	—	—
40	0.638	0.501	0.458	0.423	0.417	0.327	—
45	0.820	0.765	0.698	0.629	0.590	0.514	0.447

rate-shear dependence of $[\eta]_{g(F)}$ can be concluded to have been obtained on the assumption that Martin's plots are linear down to an infinite dilution. The positive rate-shear dependence of $[\eta]_{g(F)}$ obtained on this assumption was similar to those of aroclor solutions of polymethylmethacrylate,[21] although the highest value of the $[\eta]_{g(F)}/[\eta]_{g(F)=0}$ ratio in our case was 1.08 at 30°C, $g(F)=800$ sec^{-1}, while that in a polymethylmethacrylate solution was over 2.0. Peterlin[8] has predicted that, in an extreme case in which the usual flexible polymer molecule is very long and the solvent is extremely viscous, the intrinsic viscosity would be expected to increase with the shear gradient over a limited range. In our case, however, the first condition of the polymer molecule being very long was not met; the molecular weight of this methylcellulose was calculated to be about $(3—4)\times10^5$ by using the relationship between the intrinsic viscosity and the molecular weight reported in Ref. 4. The molecule with a molecular weight of about $(3—4)\times10^5$ cannot be considered to be very long. On the other hand, the viscosity of the solvent, water, is about 1 centi-poise at 20°C and so is not very large, either. Therefore, the shear-rate dependence of the intrinsic viscosity of a methylcellulose solution seems to be due to the small flexibility of the chain. In general, cellulose derivatives have a relatively extended form in solution and take the configuration of the free draining model. The increase in the intrinsic viscosity with the rate of shear is considered to come from the specific property of the cellulose derivative.

The constant, k, in Martin's equation is related to Huggins' constant, k', as $k=k'/2.3$. The values of k' obtained at constant $g(F)$ are shown in Table 2. These values decreased with $g(F)$ and increased with the temperature. Uda[4] has reported that the Huggins' constant of a dilute solution of methylcellulose decreased with the temperature over the range from 20°C to 45°C. However, his values were not those at a constant rate of shear. Since the flow time in the capillary decreases exponentially with an increase in the temperature and as, consequently, the rate of shear increases, the correction of the rate of shear may be necessary for any discussion of the temperature dependence of k'. Furthermore, the fact that the increase in k' comes from a decrease in solubility seems to support the positive temperature dependence of k'.

Generally the intrinsic viscosity of cellulose derivatives has a large negative temperature coefficient. Some workers[25-28] have attributed this behavior to the increase in the flexibility of chain, and others[4] to the decrease in the degree of hydration, with the increase in temperature. In view of the fact that the solubility decreased with the temperature, as has been described above, the latter interpretation seemed to be more reasonable. For the value of $-\mathrm{d}[\eta]/\mathrm{d}T$ where T is the temperature, values of 0.28—0.31 (100 ml/g·deg) were obtained over the range of the rate of shear from 200 to 800 sec^{-1}; these values are shown in Table 1. Since the value of $\mathrm{d}[\eta]/\mathrm{d}T$ decreased with the $g(F)$, the methylcellulose molecule in a dilute solution seems to be not sphere but an ellipsoid and it seems to correspond with the increase in intrinsic viscosity described above.

Kahn and Witnauer[29] pointed out that the energy of the activation of flow and the entropy of flow would be measures of the particle alignment in a solution; they treated their viscosity data according to the theory of rate process.[30]

According to Eyring's theory,[30] the viscosity is given by the following equation:

$$\eta = (\boldsymbol{N}\boldsymbol{h}/V)\exp(-\Delta S/\boldsymbol{R})\exp(E_v/\boldsymbol{R}T), \quad (4)$$

where $\boldsymbol{N}$ is Avogadro's number, $\boldsymbol{h}$ is Plank's constant, V is the molar volume of the solute, ΔS is the entropy of flow, $\boldsymbol{R}$ is the gas constant, E_v is the energy of the activation of flow, and T is the absolute temperature. From Eq. (4) we have:

$$\ln\eta = \ln(\boldsymbol{N}\boldsymbol{h}/V) - (\Delta S/\boldsymbol{R}) + E_v/\boldsymbol{R}T. \quad (5)$$

Some examples of the plots of $\log\eta$ *versus* $(1/T)$ are shown in Fig. 3. The values of E_v were calculated from the slopes of the plots. The values of E_v obtained are shown in Table 3. From Table 3 it is

25) L. Mandelkern and P. J. Flory, *J. Am. Chem. Soc.*, **74**, 2517 (1952).
26) H. Maeda, T. Kawai and K. Saito, *Chem. High Polymer (Japan)*, **15**, 610 (1958).
27) P. J. Flory, O. K. Spurr and D. K. Carpenter, *J. Polymer Sci.*, **27**, 231 (1958).
28) W. R. Moore and A. M. Brown, *J. Colloid Sci.*, **14**, 1, 343 (1959).
29) L. D. Kahn and L. P. Witnauer, *J. Biol. Chem.*, **241**, 1784 (1966).
30) S. Glasstone, K. J. Laidler and H. Eyring, "The Theory of Rate Processes," McGraw-Hill Book Co., Inc., New York (1941).

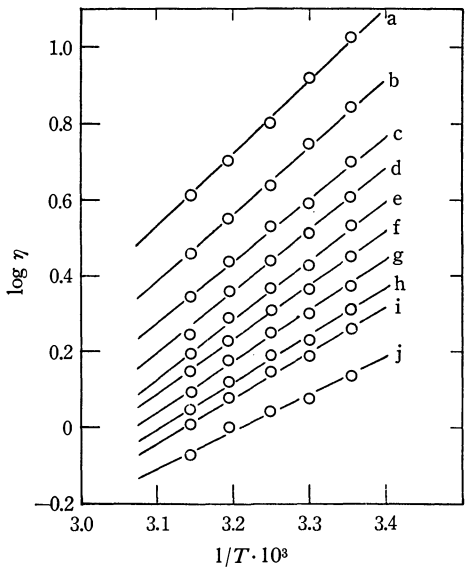

Fig. 3. Plots of $\log \eta$ of methylcellulose solution *versus* $1/T$ at $g(F)=200$ sec^{-1}; a, 0.3030 g/100 m*l*; b, 0.2424; c, 02020; d, 0.1731; e, 0.1515; f, 0.1359; g, 0.1212; h, 0.1010; i, 0.0866; j, 0.0606.

clear that a high energy is required for the flow in the high-concentration range and at a low rate of shear. The values of E_v obtained in this system were somewhat higher than the 5.8 kcal obtained in the aqueous solution of solubilized calf-skin collagen.[29] From these results, it seems that methylcellulose shows a strong tendency toward alignment with a flowing stream. The statement seems to be essentially consistent with the shear-rate dependence of $[\eta]$ and $\mathrm{d}[\eta]/\mathrm{d}T$ described above. For lack of the value of the molar volume of methylcellulose, however, the entropy of flow could not be discussed here. The effects of the molecular weight and the molecular-weight distribution on the non-Newtonian viscosity of the dilute solution are also awaiting discussion. The non-Newtonian viscosity of the dilute aqueous solution of methylcellulose, however, seems to come from the small flexibility of the chain and from a strong tendency toward alignment with a flowing stream.

Table 3. The energy of activation of flow of methylcellulose solution, E_v, (kcal)

c (g/100 m*l*)	$g(F)$, (sec^{-1})				
	0	200	400	600	800
0.0606	5.00	4.67	4.72	4.72	4.58
0.0866	6.10	5.68	5.55	5.09	5.04
0.1010	7.33	5.82	5.73	5.68	5.68
0.1212	7.88	6.32	6.19	5.91	5.96
0.1359	8.02	6.65	6.78	6.74	6.42
0.1515	8.11	7.24	7.20	7.10	—
0.1731	8.34	7.33	7.38	—	—
0.2020	8.80	7.65	7.61	—	—
0.2424	9.03	8.25	—	—	—
0.3030	9.72	8.80	—	—	—

The authors are grateful to Shinetsu Chemical Ind. for supplying the sample of methylcellulose (trade name " Metolose 90 SH 15000 ").

BULLETIN OF THE CHEMICAL SOCIETY OF JAPAN VOL. 41 1068—1073 (1968)

A Study of Charge-Transfer Complexes. VII. Interactions between the Alkyl- or Arylsubstituted Pyrroles and Chloranil or Tetracyanoethylene*1,*2

Taku MATSUO*3 and Hideto SHOSENJI

Department of Organic Synthesis, Faculty of Engineering, Kyushu University, Hakozaki, Fukuoka

(Received November 1, 1967)

The charge-transfer (CT) bands of complexes of alkylsubstituted pyrroles and chloranil or tetracyanoethylene (TCNE) were found to consist of two closely situated peaks. The peaks were assigned to transitions originated from the highest occupied, and second-highest occupied orbitals of the donor. The energy of the CT absorption band is hardly affected even by the presence of a bulky substituent such as a *t*-butyl group at the pyrrole nitrogen. Hence, the acceptor molecules were thought not to be close to the 1-position of the pyrryl group. In the case of 1-phenylpyrrole, the first CT bands are at almost the same positions as those of the corresponding complexes of 1-methylpyrrole. The bands show red shifts if methyl groups are introduced either on the pyrryl group or on the phenyl group, so that the planes of the two groups are twisted around the N-C bond between them. Thus the acceptor molecules were concluded to interact mainly with the pyrryl group.

The electronic spectra of pyrrole derivatives have been less investigated than those of benzene derivatives. The situation is the same for the intermolecular charge-transfer (abbreviated to CT hereafter) absorption bands of these compounds.[1] Only a few examples have been known of CT complexes of pyrrole derivatives.[3a,3b] In the present paper, the results of a systematic study on the nature of the CT absorption bands of alkyl- or aryl-substituted pyrroles will be described.

Results and Discussion

(A) Chloranil Complexes of Alkylpyrroles. The CT spectra of chloranil complexes of alkylpyrroles consist of two peaks, which overlap each other as shown in Fig. 1. The wave numbers for the peak positions are summarized in Table 1. In the case of chloranil complexes of *N,N*-dimethylaniline analogues, which will be described later, there are no signs of absorption bands within 10 kK of the first CT band. Therefore, the two peaks of the pyrrole complexes should be due to the intrinsic nature of the donor molecule. As suggested by several investigators,[3a,3b] the first and second CT bands of pyrrole complexes may be assigned to electronic transitions originated from the highest occupied, and

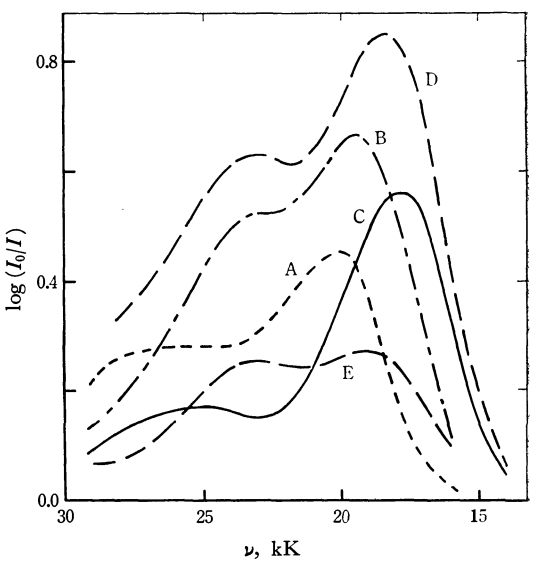

Fig. 1. The CT bands of the chloranil complexes of alkylpyrroles in carbon tetrachloride. The donors are indicated by the capital letters as the following: pyrrole (A), 1-methylpyrrole (B), 2-methylpyrrole (C), 3-methylpyrrole (D), 1-*t*-butylpyrrole (E). The concentrations of the acceptor are 0.0013 mol/*l*; the concentrations of the donors are 0.33 (A, C, D, E) or 0.073 mol/*l* (B).

*1 Previous paper: T. Matsuo and O. Higuchi, This Bulletin, **41**, 518 (1968); The contribution No. 144 from the Department of Organic Synthesis, Faculty of Engineering, Kyushu University.

*2 Presented in parts at the 20th Annual Meeting of the Chemical Society of Japan, Tokyo, April, 1967.

*3 The person whom any correspondence should be addressed to.

1) G. Briegleb, "Elektronen-Donator-Acceptor-Komplexe" Springer-Verlag, Berlin (1961).

2. A. R. Cooper, C. W. P. Crowne and P. G. Farrell, *Trans. Faraday Soc.*, **62**, 18 (1966).

3) a) R. P. Lang, *J. Am. Chem. Soc.*, **84**, 4438 (1962); b) Z. Yoshida and T. Kobayashi, The paper presented at the Discussion Meeting on the Molecular Structure, Osaka, October, 1966.

Table 1. The CT bands of the chloranil complexes of alkylpyrroles in carbon tetrachloride[a)]

Donor	The 1st band	The 2nd band
Pyrrole	20.1±0.1	26.2±0.5
1-Methylpyrrole	19.5±0.1	24.0±0.2
2-Methylpyrrole	17.8±0.1	25.3±0.5
3-Methylpyrrole	18.4±0.1	23.8±0.2
1-*t*-Butylpyrrole	18.9±0.1	22.9±0.2

a) The values are in kilokayser units.

second-highest occupied orbitals of pyrrole, respectively. The semiempirical SCF-LCAO-MO method of Pariser-Parr-Pople was utilized to study the π electronic structure of pyrrole by Solony *et al.*[4] According to the calculation, the highest occupied orbital of pyrrole is antisymmetric with respect to the C_2 axis of the molecule. The second highest occupied orbital, on the other hand, is symmetric with respect to the same axis. In other words, the nitrogen atom of the pyrrole molecule is involved in the second highest occupied orbitals but not in the highest occupied orbital. The separation between the energy levels of the two orbitals is estimated to be only 0.4 eV. The above assignment of the CT bands of pyrrole complexes is in good agreement with the predicted natures of the two occupied molecular orbitals; the second CT band is approximately 0.7 eV higher than the first band, and methyl substitution at a carbon atom causes an appreciably larger red shift of the first CT band than that at a nitrogen atom.

To a first order approximation, the effect of methyl substitution may be treated as an increase in the Coulomb integral for the atom to which the methyl group is attached. According to simple LCAO-MO theory, a variation in the Coulomb integral for the rth atom ($\delta\alpha_r$) is expected to cause the following change in the energy level of the ith orbital:

$$\delta\varepsilon_i = C_{ir}^2\delta\alpha_r + \sum_{k(\neq i)}^{n} \frac{(C_{ir}C_{kr})^2}{\varepsilon_i - \varepsilon_k}(\delta\alpha_r)^2 + \cdots \quad (1)$$

where ε_i and C_{ir} have the usual meaning. Using the coefficients (C_{ir}) obtained by Solony *et al.*,[4] the effect on the highest occupied orbital is calculated as summarized in Table 2. The experimental values for the red shifts of the first CT bands, as measured by taking unsubstituted pyrrole as standard, are also tabulated in the same table for comparison. The value of $\delta\alpha_r$ is positive for methyl substitution. It is clear, then, that the red shifts of the first CT bands correlated well with the perturbation effects of the methyl group on the highest occupied orbital.

Table 2. The effect of methyl substitution on the π energy levels of pyrrole molecule

Substitution position	C_{ir}^2	$\sum(C_{ir}C_{kr})^2/(\varepsilon_i-\varepsilon_k)$	Red shift of the 1st band
1	0.0	0.0	0.6±0.1 kK
2	0.34	0.12	2.3±0.1
3	0.16	0.12	1.7±0.1

In the case where 1-*t*-butylpyrrole is used as the π donor, the first CT band, as well as the second band, moves to lower wave numbers in comparison with the case of 1-methylpyrrole. The red shift may be explained as due to the fact that the inductive effect of the *t*-butyl group raises the π-energy levels of the pyrryl group. If the steric effect of the *t*-butyl group is of any importance, on the other hand, just the opposite shift will be expected because the increased donor-acceptor distance reduces the value of the electrostatic term C in the following equation:

$$h\nu_{CT} \cong I_p - E_A - C \quad (2)$$

Since the actual shifts are more or less bathochromic, the present authors speculate that the chloranil molecule is not close to the 1-position of the pyrryl group.

(B) Tetracyanoethylene Complexes of Alkylpyrroles. It is known that tetracyanoethylene (TCNE) reacts with pyrroles to form tricyanovinyl compounds.[5] In the present experiment, the CT bands were observed to decay with time. In return, new absorption bands appeared in the region between 300 and 500 mμ, which were due to the accumulation of reaction products. In the case of the

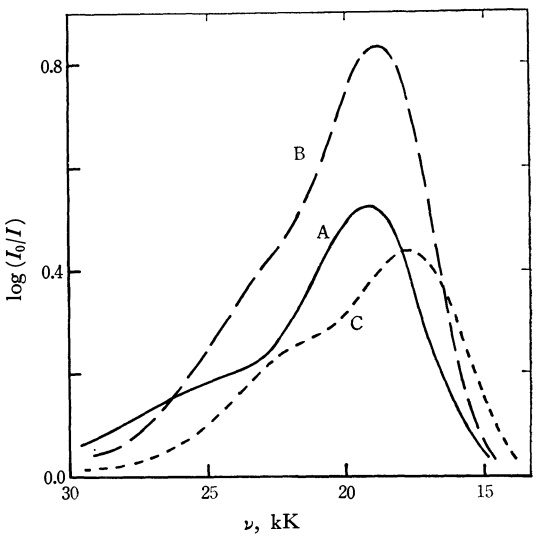

Fig. 2. The CT bands of the TCNE complexes of alkylpyrroles in *n*-hexane. The donors are indicated by the capital letters as follows: pyrrole (A), 1-methylpyrrole (B), 1-*t*-butylpyrrole (C). The concentrations of the acceptor are 3.0×10^{-4} mol/*l*; the concentrations of the donors are 0.10 (A), 0.15 (B) or 0.20 mol/*l* (C).

4) N. Solony, F. W. Birss and J. B. Greenshield, *Can. J. Chem.*, **43**, 1569 (1965).

5) a) G. N. Sausen, V. A. Engelhardt and W. J. Middleton, *J. Am. Chem. Soc.*, **80**, 2815 (1958); b) R. Bonnet and J. D. White, *J. Chem. Soc.*, **1963**, 1648.

TABLE 3. THE CT BANDS OF TCNE COMPLEXES OF ALKYLPYRROLES IN VARIOUS SOLVENTS[a,b]

Donor	In n-C_6H_{14}		In CCl_4		In $(CHCl_2)_2$	
	1st band	2nd band	1st band	2nd band	1st band	2nd band
Pyrrole	19.3	25.6	18.9	25.5	18.4	25.1
1-Methylpyrrole	18.9	23.8	18.5		18.0	
1-*t*-Butylpyrrole	17.8	22.5	17.3	22.1	17.0	

a) The values are in the same units as in Table 1.
b) The accuracies in the values of the absorption maxima for the first and the second CT bands are 0.1 and 0.2 kK, respectively.

TABLE 4. THE CT BANDS OF THE CHLORANIL AND TCNE COMPLEXES OF 1-PHENYLPYRROLE ANALOGUES WITH METHYL SUBSTITUENTS[a]

Donor	Chloranil complex[b]		TCNE complex[c]	
	1st band	2nd band	1st band	2nd band
1-Phenylpyrrole	20.9±0.1		18.4±0.1	31.8±0.2
1-*p*-Tolylpyrrole	20.3±0.1		18.1±0.1	30.3±0.1
1-*o*-Tolylpyrrole	19.0±0.1	24.7±0.2	16.1±0.1	23.2±0.2
1-(2′,6′-Xylyl)-pyrrole	19.0±0.2	25.1±0.1	16.0±0.2	22.0±0.1
1-Phenyl-2,5-dimethylpyrrole	15.8±0.1	23.0±0.1	d)	d)

a) The values are in the same units as in Table 1.
b) In carbon tetrachloride.
c) In tetrachloroethane.
d) The measurement was unsuccesful because the reaction was rapid.

2-methylpyrrole-TCNE system, the decay of the CT bands was so rapid that the complete spectra could not be followed even by using the fastest scanning speed. A solution of the 3-methylpyrrole-TCNE system also shows extraordinary behavior. The spectra are not only time dependent, but also consist of several sharp peaks indicating at least three species besides the component molecules. Thus, the location of the CT bands could not be definitely determined. A detailed study of this peculiar system is under way, and the results will be reported in the near future. The time dependences of the TCNE complexes of pyrrole, 1-methylpyrrole and 1-*t*-butylpyrrole are small enough to be measured without any appreciable change taking place during measurement, if measurement is made within five minutes of mixing the acceptor and donor components. The spectra thus measured in *n*-hexane are shown in Fig. 2. Analogous to the cases of chloranil complexes, one can observe two CT bands for each system. The second CT band, however, is much weaker than the first band, and the former appears just as a shoulder of the latter. Both the first and second bands show similar red shifts as the solvent is changed in the order of *n*-hexane, carbon tetrachloride and tetrachloroethane, as summarized in Table 3. The shapes of the spectra are quite alike in all solvents. Thus, it is suggested that the nature of the donor-acceptor interactions between TCNE and alkylpyrroles is essentially the same as that of the chloranil-alkylpyrrole system.

(C) Chloranil and TCNE Complexes of 1-Phenylpyrrole Analogues. On the basis of the size of the dipole moment, 1-phenylpyrrole has been suggested to have a nearly planar structure, where the π-electrons of the pyrryl group are easily delocalized to the phenyl group without much disturbance.[6] The suggested conformation may be reasonable because the van der Waals radii of the protons at the 1- and 1′-positions barely overlap each other. In the case of 1-phenyl-2,5-dimethylpyrrole, however, the dipole moment[6] and the electronic spectra[7,8] indicate that the dimethylpyrryl group and the phenyl group are twisted around the N–C bond axis joining the two groups. The electronic spectra of 1-(2′,6′-xylyl)-pyrrole also have been interpreted as indicating the presence of twisting around the N–C bond axis. This twisting is, of course, due to the steric hindrance exerted by the methyl groups. A more or less similar situation is expected for the conformation of 1-(*o*-tolyl)-pyrrole. These compounds were also used as the electron donors in the present experiment. The CT absorption spectra of the chloranil complexes are shown in Fig. 3. The wave numbers for the absorption maxima, together with those for the TCNE complexes, are summarized in Table 4. In either series, the

6) H. Kofod, K. E. Sutton and J. Jackson, *J. Chem. Soc.*, **1952**, 1467.
7) J. Davoll, *ibid.*, **1953**, 3802.
8) Y. Chiang, R. L. Hinman, S. Theodoropulos and E. B. Whipple, *Tetrahedron*, **23**, 745 (1967).

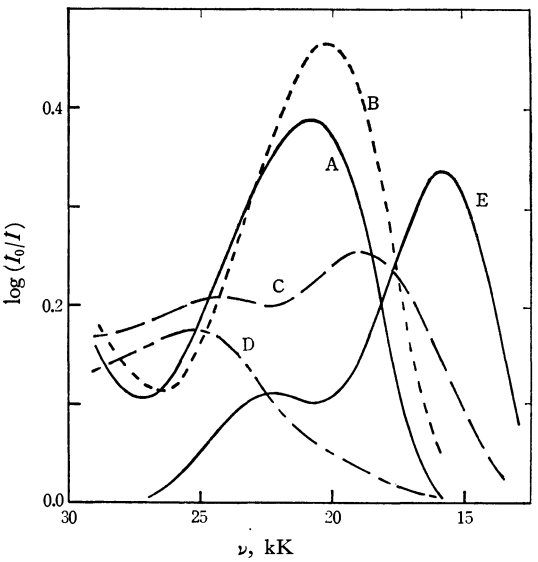

Fig. 3. The CT bands of the TCNE complexes of 1-phenylpyrrole analogues with methyl substituents in carbon tetrachloride. The donors are indicated by the capital letters as the following: 1-phenylpyrrole (A), 1-*p*-tolylpyrrole (B), 1-*o*-tolylpyrrole (C), 1-(2′,6′-xylyl)-pyrrole (D), 1-phenyl-2,5-dimethylpyrrole (E). The concentrations of the acceptor are 0.0013 mol/*l*; the concentrations of the donors are 0.33 (A, B, C, D) or 0.12 mol/*l* (E).

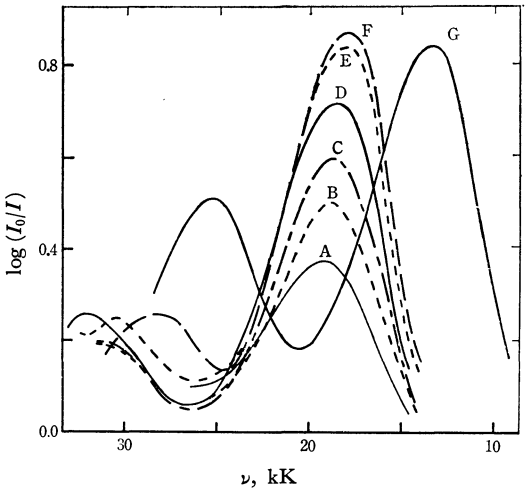

Fig. 4. The CT bands of the chloranil complexes of 1-(*p*-substituted phenyl)-pyrroles in the tetrachloroethane. The substituents are indicated by the capital letters as follows: acetyl (A), bromo (B), chloro (C), hydrogen (D), methyl (E), methoxy (F) and dimethylamino (G). The concentrations of the acceptor are 0.0020 mol/*l*; the concentrations of the donors are 0.10 (A, B, D, E, F), 0.12 (C) or 0.013 mol/*l* (G).

wave numbers for the absorption maxima of the first CT bands are in the following order: 1-phenyl-2,5-dimethylpyrrole < 1-(2′,6′-xylyl)-pyrrole < 1-(*o*-tolyl)-pyrrole < 1-(*p*-tolyl)-pyrrole ≈ 1-phenylpyrrole. It is interesting that the CT bands for donors with twisted conformations are at a lower energy than for those with planar structures. It should be noticed also that the first CT bands of 1-phenylpyrrole complexes are at almost the same positions as those of the corresponding complexes of 1-methylpyrrole. These observations appear to be against the general expectation that the ionization potential of an aromatic molecule decreases as the degree of conjugation is extended. An explanation may be the fact that the π-electrons of the pyrryl group are withdrawn to the more electronegative phenyl group. As a consequence, the energy level for the highest occupied orbital is lower than the case where conjugation between the two groups is forbidden. From this point of view, the rather large red shift of the first CT band for the chloranil complex of 1-phenyl-2,5-dimethylpyrrole may also be understood as due to the inductive effect of the methyl group on the π-electron system of the pyrryl group. Thus, it is suggested that the acceptor molecules interact mainly with the pyrryl group rather than with the phenyl group. In other words, the electronic state of the pyrryl group may be the most important factor determining the energy of the first CT band of the 1-phenylpyrrole analogues with alkyl substituents.

Table 5. The CT bands of the chloranil and TCNE complexes of 1-(*p*-substituted phenyl)-pyrroles[a)]

Substituent group	Chloranil complex[b)] 1st band	TCNE complex[c)] 1st band	TCNE complex[c)] 2nd band
Acetyl	21.4±0.1	19.2±0.1	
Bromo	21.4±0.1	18.8±0.1	29.4±0.3
Chloro	21.3±0.1	18.6±0.1	31.0±0.4
Hydrogen	20.9±0.1	18.4±0.1	31.8±0.2
Methyl	20.3±0.1	18.1±0.1	30.3±0.1
Methoxy	20.0±0.1	18.0±0.1	28.3±0.1
Dimethylamino	14.7±0.1	13.2±0.1	25.2±0.1

a) The values are in the same units as in Table 1.
b) In carbon tetrachloride.
c) In tetrachloroethane.

In order to obtain further information on the role of the phenyl group, the CT spectra of various 1-(*p*-substituted phenyl)-pyrrole complexes were also investigated (Fig. 4, Table 5). Since the variations of the first CT bands of the chloranil complexes in Table 5 are almost the same as those of the TCNE complexes, the substituent effects on the former may be taken as representative. For comparison, the first CT bands of the chloranil complexes of *p*-substituted *N*,*N*-dimethylanilines were also measured (Table 6, Fig. 5). As for substituents other than the *N*,*N*-dimethylamino group, the effects observed in the 1-(*p*-substituted phenyl)-pyrrole complexes are slightly less than those in the *p*-substituted aniline

Table 6. The CT bands of the chloranil complexes of *p*-substituted *N,N*-dimethylanilines in carbon tetrachloride[a)]

Substituent group	1st band
Acetyl	15.8±0.1 kK
Bromo	15.0±0.1
Chloro	15.2±0.1
Hydrogen	15.5±0.1
Methyl	14.9±0.1
Methoxy	13.9±0.1
Dimethylamino	11.2±0.1

a) There are no signs of absorption bands within 10 kK from the first CT bands in these systems.

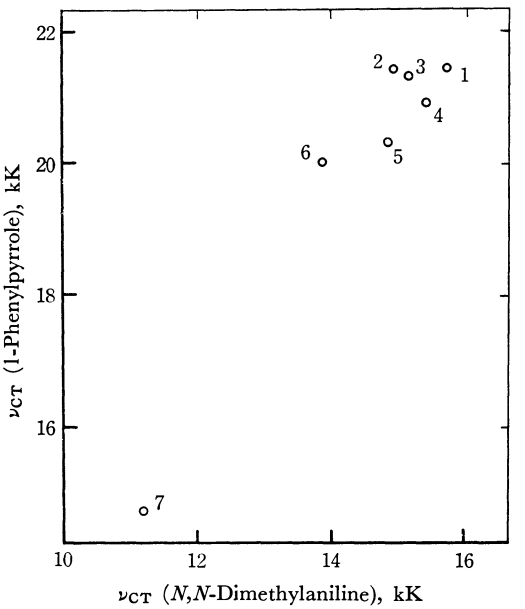

Fig. 5. The comparison of the first CT band of the chloranil complexes of 1-(*p*-substituted phenyl)-pyrrole with that of *p*-substituted *N,N*-dimethylaniline in carbon tetrachloride. The substituents are indicated by numbers as follows: acetyl (1), bromo (2), chloro (3), hydrogen (4), methyl (5), methoxy (6) and dimethylamino (7).

complexes. In the case of the dimethylamino group, the first CT bands are at considerably longer wavelengths than in the cases of other substituents. In comparison with the first CT bands of the chloranil complex of 1-phenylpyrrole, for example, the corresponding band of 1-(*p*-*N,N*-dimethylaminophenyl)-pyrrole is shifted to the longer wavelength side by 6.2 kK. The corresponding red shift in the *p*-*N,N*-dimethylaniline series, on the other hand, is only 4.3 kK. This interesting effect may be due to the fact that the *N,N*-dimethylaminophenyl group is a stronger electron donor than the pyrryl group, as may be seen by comparing the values in Table 1 with those in Table 6. As pointed out in the preceding paragraph, the acceptor molecules appear to be coordinated to the pyrryl group in 1-phenylpyrrole. The situation may be unchanged if the substituent at the phenyl group is either an electron-withdrawing or weakly electron-donating one. In the case of 1-(*p*-*N,N*-dimethylaminophenyl)-pyrrole, the electron-donating ability of the pyrryl group is exceeded by that of the substituent. As a consequence, the acceptor molecule may be coordinated to the *p*-*N,N*-dimethylamino group rather than to the pyrryl group.

Experimental

Measurements of the CT Spectra. Solutions of CT complexes were prepared by properly adjusting the concentrations of the donor (0.02—1.0 mol/*l*) and the acceptor molecules (0.00015—0.05 mol/*l*) in suitable solvents. The spectra were measured at room temperature (17—20°C) by the use of either a Bausch & Lomb Spectronic 505, or a Hitachi model EPS-2 recording spectrophotometer. The absorptions due to the donor and the acceptor were numerically subtracted from the recorded spectra to obtain the absorption bands of the pure complexes.

Materials. Carbon tetrachloride, *n*-hexane and tetrachloroethane were purchased from the Wako Pure Chemicals Co., Ltd., and purified by standard procedures. Chloranil (mp 292.5—293.0°C), pyrrole (bp 60—61°C/55 mmHg), 1-methylpyrole (bp 44.9°C/42.5 mmHg), *N,N*-dimethylaniline (bp 85°C/20 mmHg), *N,N*-dimethyl-*p*-aminoacetophenone (mp 108.2—108.7°C), *N,N*-dimethyl-*p*-bromoaniline (mp 55.2— 55.9°C), *N,N*-dimethyl-*p*-chloroaniline (mp 34.5—35.0°C), *N,N*-dimethyl-*p*-toluidine (bp 114—115°C/34 mmHg), *N,N*-dimethyl-*p*-anisidine (mp 48.0—48.5°C) and *N,N,N',N'*-tetramethyl-*p*-phenylenediamine (mp 51.0—52.0°C) were reagent-grade chemicals as supplied by the Wako Pure Chemicals Co., Ltd., and were repeatedly purified until they showed the melting points or boiling points given above. The following compounds were synthesized according to methods given in the references in parentheses: TCNE (Ref. 9, mp 199—200°C), 2-methylpyrrole (Ref. 10, bp 82.5°C/70 mmHg), 1-phenyl-2,5-dimethylpyrrole (Ref. 11, mp 51.5—52.5°C), 1-*p*-bromophenylpyrrole (Ref. 12, mp 96.2—96.5°C), 1-(*p*-*N,N*-dimethylaminophenyl)-pyrrole (Ref. 12, mp 152.5—153.2°C), 1-*o*-tolylpyrrole (Ref. 12,*4 bp 80°C/3 mmHg), 1-2',6'-xylylpyrrole (Ref. 12,*4 mp 47.2—47.6°C), 1-*p*-acetylphenylpyrrole (Ref. 12,*4 mp 120.0—121.0°C), 1-*t*-butylpyrrole (Ref. 13,*4 bp 65°C/38.5 mm-

9) T. L. Cairno, R. A. Carboni and D. D. Coffman, *J. Am. Chem. Soc.*, **80**, 2775 (1958).
10) A. J. Castro, J. F. Deck, M. T. Hugo, E. J. Lowe, J. P. Marsh, Jr., and R. J. Pfeifer, *J. Org. Chem.*, **20**, 668 (1955).
11) L. Knorr, *Ann.*, **236**, 290 (1886).
12) R. A. Jones, *Aust. J. Chem.*, **19**, 289 (1966).
13) The oral report by Altmann as quoted by L. Leichtenstein (*Ber.*, **14**, 933 (1881)).
*4 The materials used in the present syntheses are different from those in the references. The method, however, are essentially the same except for a little modification.

Hg), 1-phenylpyrrole (Ref. 13, mp 58.1—58.3°C), 1-*p*-chlorophenylpyrrole (Ref. 13,*4 mp 87.9—88.3°C), 1-*p*-tolylpyrrole (Ref. 13, mp 82.2—82.7°C) and 1-*p*-anisylpyrrole (Ref. 13,*4 mp 111.0—111.5°C). The synthesis of 3-methylpyrrole was accomplished by the alkali fusion of 3,5-dicarbethoxy-4-methyl-2-pyrrolecarboxylic acid, bp 76°C/53 mmHg. The purities of the above synthesized materials were determined by means of elementary analyses, NMR spectra and gas chromatography, where possible.

BULLETIN OF THE CHEMICAL SOCIETY OF JAPAN VOL. 41 1073—1087 (1968)

Phase Changes in Crystalline and Glassy-Crystalline Cyclohexanol*[1]

Keiichiro ADACHI, Hiroshi SUGA and Syûzô SEKI

Department of Chemistry, Faculty of Science, Osaka University, Toyonaka, Osaka

(Received November 6, 1967)

It has been known that cyclohexanol has low-temperature form (crystal-II) and high-temperature form (crystal-I) and that the supercooled crystal-I shows in its heat capacity curve an anomalous jump resembled to that associated with glass transition. In order to clarify whether this anomaly arises from relaxation phenomenon or not, we have reinvestigated the heat capacity of this substance from 14°K to 320°K and obtained the values of 8827 J/mol, 265.31°K, 1782 J/mol and 299.09°K for heat of transition, transition point, heat of fusion and melting point respectively. Comparing the ideal gas entropy of cyclohexanol calculated from thermal data and that from statistical-mechanical data, we have estimated that the residual entropy of the crystal-II is of zero and that the potential barrier of internal rotation of *OH* group is 7.0 kJ/mol. From these results, the residual entropy of the supercooled crystal-I amounts to 4.72 J/(mol deg K). We have discussed the glass transition of this crystal and proposed a new term **glassy crystal.** We have also studied the heat capacity of metastable phase (crystal-III) and obtained the results 244.8°K and 8640 J/mol for transition point and heat of transition. The residual entropy of the crystal-III has determined to be zero.

Thermal study of cyclohexanol crystal from liquid hydrogen temperature was first carried out by Kelley.[1)] He drew main two conclusions. First, this substance had two crystalline phases, the high-temperature phase (crystal-I) and the low-temperature one (crystal-II).*[2] The crystal-I was found to be supercooled easily and the heat capacity curve of the supercooled phase showed anomalous jump closely resembled to that associated with the glass transition of a supercooled liquid. Second, the supercooled crystal-I and the crystal-II had the same value of entropy at 0°K within the experimental error. In other words, the anomalous jump of the heat capacity curve of the supercooled crystal-I was considered to be second order transition in the sense of thermodynamics. Thereafter, Ôtsubo and Sugawara[2)] reinvestigated this anomaly of the heat capacity under the various annealing conditions and concluded that this anomaly was looked upon as a relaxation phenomenon associated with the glass transition. This stands in contrast to the conclusion by Kelley that the supercooled crystal-I is in the internal equilibrium state. However, they have given no discussion about the residual entropy which is a kind of measure for the degree of internal equilibrium. We have accordingly reinvestigated the low-temperature heat capacities of various crystalline phases accurately and also studied the kinetics of the relaxation in order to clarify the problem that the glass transition characteristic to amorphous state takes place also in the crystalline state in the sense of relaxation phenomenon. If this glass transition phenomenon is a real relaxation effect, the second conclusion of Kelley is contradicting to the fact of zero residual entropy. As to the substances which have been hitherto known to show the anomalous jump of the heat capacity similar to the glass transition in the crystalline state there are only *cis*-1,2-dimethylcyclohexane[3)] and the molecular compound

*1 Read before the 20th Annual Meeting of the Chemical Society of Japan (1967), Tokyo and partially presented at the symposium on New Investigations in Thermodynamics, Thermochemistry and Transport Properties (1967), Heidelberg.

1) K. K. Kelley, *J. Am. Chem. Soc.*, **51**, 1400 (1929).

*2 Following Smyth, Ôtsubo and Sugawara designated this modification as form-III and metastable one as form-II. We changed, however, this nomenclature as described in the text, since the metastable crystal-III in the text has lower transition point as described later.

2) A. Ôtsubo and T. Sugawara, *Sci. Rep. Res. Inst. Tohoku Univ.*, **A7**, 583 (1955).

3) H. M. Huffman, S. S. Todd and G. D. Oliver, *J. Am. Chem. Soc.*, **71**, 584 (1949).

between 2,3-dimethylbutane and 2,2-dimethylbutane.[4] It should be noted here that both of these substances and cyclohexanol belong to the so-called plastic crystals defined by Timmermans.[5] Aside from this problem, Ôtsubo and Sugawara also reported the occurrence of three kinds of metastable intermediate phases in the course of irreversible transformation from the supercooled crystal-I to the crystal-II. In the present study we have also studied the metastable crystalline phase (crystal-III) and the thermodynamic stability-relationship of the crystal-I, II and III were further determined in terms of Gibbs energy. On the basis of the data of the heat capacities, the vapor pressure and of the heat of vaporrization which were previously reported in this laboratory,[6] the residual entropies of the crystal-I, II and III have been determined by comparing the experimentally obtained entropies of ideal gas state with that calculated by statistical-mechanical method. The potential barrier of the internal rotation of *OH* group has been also estimated.

Experimental

Material. Commercial " Special-grade " cyclohexanol (Nakarai Chemicals) was fractionally distilled twice and further purified through vacuum distillation (10^{-3} mmHg) with baked calcium oxide. The calorimetric determination of the melting point (see below) revealed that the impurities in the sample were found to 0.025 mol% assuming no formation of a solid solution. Only a kind of impurity, presumably cyclohexanone, was detected by gas chromatography (Shimadzu Gas Chromatograph model GC-1B equipped with hydrogen flame ionization detector) and this impurity was calculated to be 0.02 mol% from the peak area of the chromatogram.

Apparatus. The heat capacity of cyclohexanol was measured between 14 and 320°K by the low-temperature adiabatic calorimeter with platinum resistance thermometer. The details of the apparatus, procedure, temperature scale and accuracy were previously described.[7] The purified sample was transferred into the cell of the calorimeter (whose capacity is about 30 cc) by vacuum distillation. The weight of the sample employed was 27.548 g and 1.3×10^{-4} mol of helium gas for heat exchange was introduced (about 1 atm in a room temperature).

For the preliminary study of the occurrence and the thermal properties of metastable crystalline phases, differential thermal analysis was carried out. The apparatus was previously reported[8] also.

The infrared spectra were obtained by a Nihon Bunko Co. Double-beam Spectrometer (model DS-402G) between 600 cm^{-1} and 4000 cm^{-1} and by a Hitachi Co. Spectrometer (model No. FIS-001) between 200 cm^{-1} and 600 cm^{-1}. In the measurement above 400 cm^{-1}, the sample which was the same as that used in the measurements of the heat capacity was put between the polished plates of KBr single crystal. Because of the high hygroscopy of this substance, the preparation of this sample was carried out in the dry nitrogen atmosphere.

Experimental Results

Studies of the Polymorphism of Cyclohexanol with Differential Thermal Analysis (D.T.A.). D.T.A. curves under various conditions are shown in Fig. 1. Run-1 is a cooling curve with the rate of -1.5°K/min. The peak at about 299°K corresponds to the freezing point of the crystal-I. Even with the more rapid cooling rate, the freezing point was observed always at the same point and supercooling of the liquid state has never been observed. On the other hand the crystal-I is easily supercooled and shows no remarkable anomaly due to the transition to other crystalline phase. However, irregular small anomalies seemingly due to the sluggish transitions from the supercooled crystal-I to other phases were observed below 200°K (see curve Run-1), so the glass transition*3 (the jump of the heat capacity of the crystal-1) was not clearly found. Run-2 shows a heating curve with the rate of about 1°K/min after the crystal-I was supercooled to about 80°K with cooling rate of -10°K/min. The anomaly due to the glass transition reported by Kelley and by Ôtsubo and Sugawara was observed about 150°K,

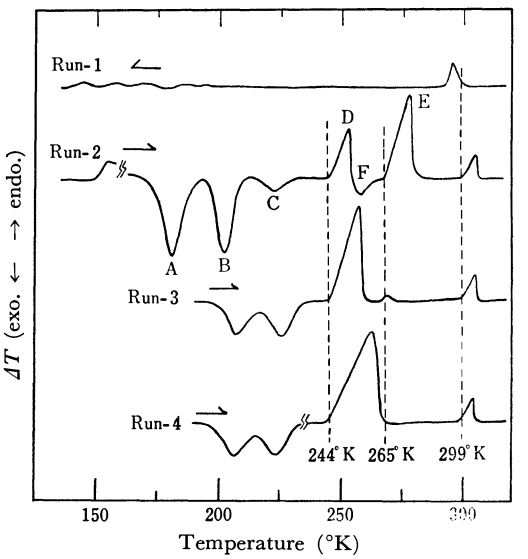

Fig. 1. D. T. A. curves of cyclohexanol. In Run-2 the mark ≀ shows the change of the sensitivity and in Run-4 the change of heating rate, respectively.

4) J. G. Aston, H. Segall and N. Fuscheillo, *J. Chem. Phys.*, **24**, 1061 (1956).
5) J. Timmermans, *J. Phys. Chem. Solids*, **18**, 1 (1961).
6) I. Nitta and S. Seki, *Nippon Kagaku Zasshi* (*J. Chem. Soc. Japan, Pure Chem. Sect.*), **69**, 141 (1948).
7) H. Suga and S. Seki, This Bulletin, **38**, 1000 (1965).
8) H. Suga, H. Chihara and S. Seki, *Nippon Kagaku Zasshi* (*J. Chem. Soc. Japan, Pure Chem. Sect.*), **82**, 24 (1961).

*3 As is described below, it has been confirmed that the anomalous jump of the heat capacity of the supercooled crystal-I at about 150°K is attributable to a relaxation phenomenon. Accordingly we call this anomaly as a glass transition in spite of the phenomenon observed in the crystalline state.

TABLE 1. SELECTED VALUES OF THE MOLAR HEAT CAPACITIES OF CYCLOHEXANOL

Mol wt=100.163 0°C=273.15°K

$T_{av.}$ (°K)	$\Delta H/\Delta T$ (J/mol degK)	ΔT (°K)
	Series 1	
	(Supercooled crystal-I)	
14.916	7.578	1.6084
16.558	9.326	1.6267
18.213	11.187	1.6023
19.904	12.965	1.7088
21.495	14.543	1.4181
23.161	16.325	1.8821
25.091	18.113	1.9276
26.924	19.869	1.7382
28.597	21.332	1.6031
30.309	22.946	1.8196
32.071	24.561	1.6902
33.717	26.064	1.5872
35.446	27.486	1.8534
37.255	28.862	1.7542
51.306	37.591	2.1472
53.406	38.645	2.0435
55.416	39.857	1.9787
57.367	41.063	1.9201
59.267	42.078	1.8718
61.114	43.246	1.8230
63.209	44.510	2.3645
65.372	45.690	1.9598
67.313	46.653	1.9190
69.216	47.594	1.8810
71.861	48.880	1.8261
75.483	50.813	1.8315
79.112	52.591	1.7729
82.604	54.455	1.7187
87.691	57.055	1.6499
90.954	58.568	1.6135
94.148	60.175	1.5789
96.873	61.421	1.7412
100.350	63.159	1.7724
103.900	65.041	1.8145
107.493	66.866	1.7766
111.010	68.669	1.7393
114.494	70.696	1.7783
118.019	72.449	1.7437
121.590	74.284	1.7878
124.109	76.065	1.7533
127.636	78.256	1.8403
131.342	80.186	1.8475
135.172	83.158	1.8891
139.106	86.239	1.9361
141.079	87.930	1.9095
143.059	90.652	1.8689
144.951	93.635	1.8277
146.873	97.632	1.9164
148.705	115.91	1.7476
150.416	118.70	1.6743
152.087	119.16	1.6684
153.753	119.54	1.6628
	Series 2	
	(Supercooled crystal-I)	
37.026	29.014	2.3613
39.313	30.741	2.2118
41.392	32.153	1.9372
43.291	33.402	1.8525
45.168	34.528	1.8925
47.236	35.766	2.2414
49.432	37.044	2.1495
51.543	38.235	2.0702
156.090	120.72	2.3207
158.404	121.78	2.3020
160.748	123.31	2.2757
	Series 3	
	(Supercooled crystal-I)	
248.488	153.20	1.8406
250.481	154.27	2.1467
252.619	155.77	2.1282
254.701	157.24	2.0350
256.728	158.52	2.0197
258.742	159.89	2.0085
260.743	161.27	1.9920
262.728	162.65	1.9779
	Series 4	
	(Supercooled crystal-I annealed at T°K)*	
	(T°K=144°K)	
144.394	90.283	1.8524
146.178	93.063	1.8120
147.911	97.441	1.8865
149.590	119.15	1.9756
151.317	120.83	1.9515
153.268	120.52	1.9510
155.216	120.87	1.9449
	(T°K=141°K)	
141.719	87.267	1.8660
143.544	89.041	1.8480
145.276	95.250	1.7557
147.127	95.018	2.0922
148.865	114.16	1.8436
150.525	123.02	1.8440
152.382	120.47	1.8693
	(T°K=137°K)	
137.924	84.885	0.3728
138.982	85.240	1.7463
140.767	86.605	1.8520
142.744	88.690	2.1733
144.816	91.651	2.1225
146.770	97.375	2.0355
148.569	109.31	1.8839
150.280	120.92	1.7493
152.187	120.36	2.0691
154.253	120.55	2.0634

(TABLE 1 continued)

$T_{av.}$ (°K)	$\Delta H/\Delta T$ (J/mol degK)	ΔT (°K)
	(T°K=133°K)	
134.745	82.760	2.2073
137.267	84.584	2.8462
140.066	86.901	2.7911
142.766	90.620	2.7101
145.339	97.136	2.5833
147.897	98.798	2.5475
151.268	119.16	4.4685
	Series 5	
	(Crystal-II)	
73.503	47.243	1.6829
76.823	48.800	1.6353
80.133	50.440	1.6459
83.379	52.073	1.6009
86.675	53.630	1.6497
90.037	55.118	1.6780
92.735	56.287	1.6719
96.633	57.834	1.9157
100.459	59.553	1.8779
104.178	61.106	1.8387
107.833	62.536	1.8262
111.417	64.209	1.7666
114.938	65.544	1.7751
118.449	67.007	1.7434
121.942	68.625	1.7887
125.563	69.900	1.7440
129.143	71.305	1.7944
132.827	72.930	1.8447
136.624	74.581	1.9013
140.403	76.239	1.8707
144.388	77.767	1.9386
148.084	79.298	1.9013
151.860	80.888	1.8728
155.582	82.387	1.8474
159.251	83.947	1.8215
162.940	85.345	1.8434
166.736	86.923	1.9084
171.779	89.121	1.8806
175.285	90.978	1.7977
178.978	92.850	1.8499
182.857	94.497	1.9704
186.760	96.506	1.9411
190.618	98.270	1.9151
194.432	99.823	1.8931
198.419	101.74	2.0188
202.429	103.78	1.9891
206.380	105.54	1.9633
210.284	107.33	1.9384
214.747	109.28	2.0613
221.066	112.26	2.0211
225.083	114.39	1.9941
229.056	116.56	1.9619
233.019	118.82	2.0492
237.092	120.68	2.0236
241.105	123.22	1.9927
245.110	125.82	2.0816
249.879	129.04	2.0410
253.926	131.90	2.0069
257.929	135.03	1.9718
261.832	138.79	1.9321
263.714	148.93	1.8351
265.004	449.49	0.7436
	Transition	
	(Crystal-I)	
267.788	165.97	1.8132
267.790	165.68	2.0040
269.787	167.06	1.9892
273.833	170.35	2.1563
278.534	174.13	2.0957
282.696	177.41	2.0649
286.790	181.52	2.0289
290.794	185.54	1.9880
294.742	189.78	1.9501
296.671	195.77	1.9043
297.887	288.86	0.5282
	(Fusion)	
300.058	213.41	0.1369
301.989	215.24	1.9455
303.830	217.67	1.9155
305.790	219.91	1.8889
307.669	221.50	1.8753
308.457	221.92	2.0810
310.791	223.74	2.5816
313.565	226.77	2.9658
316.509	230.62	2.9196
	Series 6	
	(Crystal-III)	
14.844	4.341	1.9244
17.071	6.249	2.3073
19.156	7.998	1.8017
20.815	9.620	1.5063
22.339	11.136	1.5150
23.778	12.556	1.3458
25.553	14.236	2.1957
27.619	16.194	1.9259
29.457	17.903	1.7403
31.274	19.536	1.8838
33.086	21.205	1.7384
35.028	22.885	2.1405
37.093	24.536	1.9896
39.019	26.067	1.8683
40.841	27.323	1.7736
42.927	28.779	2.4012
45.262	30.314	2.2654
47.471	31.708	2.1533
49.710	33.022	2.3241
51.961	34.347	2.1767
54.099	35.593	2.0963

(TABLE 1 continued)

$T_{av.}$ (°K)	$\Delta H/\Delta T$ (J/mol degK)	ΔT (°K)	$T_{av.}$ (°K)	$\Delta H/\Delta T$ (J/mol degK)	ΔT (°K)
56.163	36.744	2.0282	143.763	76.047	2.1497
58.162	37.852	1.9667	148.026	77.858	2.1137
60.100	39.017	1.9108	151.011	78.893	2.3922
61.989	40.086	1.8618	155.765	80.794	2.3695
63.831	41.096	1.8178	160.502	82.676	2.4450
65.628	42.080	1.7762	165.153	84.465	2.2702
67.439	43.018	1.8401	169.654	86.568	2.2323
69.268	43.612	1.8111	174.087	88.491	2.1980
70.555	44.177	1.4909	178.988	90.714	2.5178
74.568	46.128	2.1469	186.433	94.168	2.4298
78.946	48.195	2.3940	191.301	96.300	2.4105
83.717	50.444	2.2983	196.492	98.328	0.5804
88.232	52.562	2.2182	200.173	99.732	2.2459
92.605	54.433	2.1535	204.737	101.95	2.3919
96.858	56.106	2.0987	209.423	104.22	2.3118
101.001	58.018	2.0427	216.660	108.07	2.4669
105.045	59.723	1.9986	221.437	110.59	2.3454
108.936	61.175	2.2266	228.856	115.46	2.4593
113.354	63.014	2.1850	231.308	116.34	2.4438
117.907	64.914	2.2901		Series 7	
122.432	66.841	2.2369		(Crystal-III)	
126.849	68.850	2.1863	237.258	120.590	1.6191
131.181	70.588	2.1449	237.943	121.578	1.4400
135.431	72.362	2.1051	238.832	121.100	1.6145
139.603	74.186	2.0674	241.400	151.820	1.2001

* These specimens were anneald for 25 hr at respective temperatures. In the calculation of the heat capacities, anomalous temperature drift due to the stabilization (relaxation) is treated as if it were arizen from thermal leakages.

and there exist the exothermic irreversible transitions at about 180°K, 200°K, 220°K and 254°K (in Fig. 1, the peaks A, B, C and F, respectively) and the endothermic transitions at 244°K and at 265°K (peaks D and E, respectively). Ôtsubo and Sugawara studied these phase transformations by X-ray analysis in parallel with the thermal studies and concluded that peak A corresponded to the irreversible transition from the supercooled crystal-I to the metastable intermediate mixed crystalline phases and that peak B corresponded to the transition from these metastable phases to other metastable crystalline (crystal-III) or to low temperature form (crystal-II). But they did not find the existence of the peak C. The peaks D and E correspond to the transitions from the metastable crystal-III to the crystal-I and that from the crystal-II to the crystal-I, respectively. The exothermic anomaly F is probably the irreversible transition from the crystal-I occurred by III-I transition to the crystal-II. For the purpose of the measurement of the heat capacity of the metastable phase crystal-III, the condition of preparing the pure crystal-III was investigated by D. T. A. and the typical results are indicated by Runs 3 and 4. Run-3 is a heating curve of the supercooled crystal-I with the rate of about 1.1°K/min followed after rapid cooling from 280°K to 190°K with cooling rate of about −10°K/min. There exists a very small peak due to II-I transition at 265°K. But if one increase the heating rate from 1.1°K/min to 2.5°K/min at 235°K after the same cooling and heating operations as Run-3, the peak at 265°K is scarcely found as shown in Run-4. This fact may be explained in such a way that in Run-3 small peak of II-I transition appears because of the formation of the crystal-II between 244°K and 265°K due to the irreversible transition from I to II, although the almost pure metastable crystal-III is produced at 235°K. While in Run-4, it is considered that a detectable amount of the crystal-II was not produced on account of the rapid heating. For the measurement of the heat capacity of crystal-III, we prepared this modification by cooling the sample after stopping Run-3 around at 235°K.

Measurement of the Heat Capacities. The molar heat capacities are listed in Table 1 and plotted in Fig. 2, where are shown the data of Kelley and those of Ôtsubo and Sugawara for reference. Kelley's data agree well with our data for crystal-II between 14 and 65°K. They deviate, however, from −1.2 to −3% in the ranges between 65 and 170°K, from +1 to +5% between 180 and 230°K and more than 10% between 240 and 260°K, respectively.

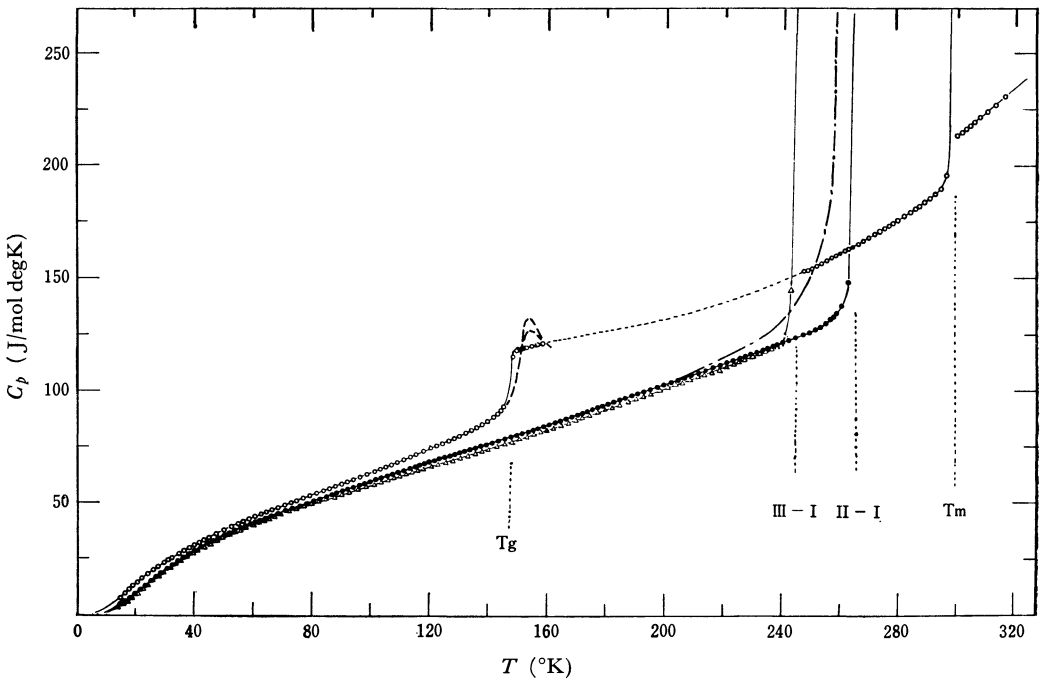

Fig. 2. The molar heat capacities of cyclohexanol.
—○— supercooled crystal-I, crystal-I and liquid
—●— crystal-II
—△— crystal-III
------ estimated heat capacity curve of supercooled crystal-I
——— Ôtsubo and Sugawara's data near T_g
– – – Kelley's data of crystal-II

For the crystal-I or the supercooled crystal-I, the smoothed values of his experiment agree fairly well with our data except for the region between 130 and 150°K, where the deviation is approximately +2%. Kelley's data for the crystal-II in the temperature region between 65 and 170°K coincide rather with the data of the crystal-III in the present measurement. Comparison with the data of Ôtsubo and Sugawara was not done because they did not give any numerical values. The heat capacities of the supercooled crystal-I below 160°K have been measured after the specimen was chilled with cooling rate of about −6°K/min from room temperatures and the heat capacities between 245 and 265°K have been measured after the specimen was slowly chilled with a cooling rate of −0.5°K/min from 310°K (liquid state) to 245°K. Crystal-II has been prepared as follows: The crystal-I supercooled below the glass transition temperature was heated up to about 255°K and slowly cooled from this temperature to about 240°K in 13 hr. The crystal-III (metastable phase) has been prepared after the condition investigated by D.T.A. as described above. In the course of the measurement of the heat capacities of this metastable phase, no remarkable irreversible transition to other phase was observed.

Thermal Data Associated with the Phase Transitions. The equilibrium temperatures during the fusion process are listed in Table 2. The temperatures of transitions are shown in Table 3 with those of Ôtsubo and Sugawara. The transition temperature of the crystal-III to the crystal-I could not be determined from the measurement of the heat capacity due to the sluggish irreversible transition from the crystal-I to the crystal-II, so we listed the value determined by D.T.A. Table 4, 5 and 6 summarize the data for the heat of transitions and of fusion together with the data of Kelley and of Ôtsubo *et al.* for comparison. As shown in Table 4 the heat of transition from the crystal-III to the crystal-I was

TABLE 2. THE EQUILIBRIUM TEMPERATURES DURING FUSION PROCESS

Fraction melted (%)	Temperature (°K)
25.01	298.729
34.11	298.790
43.46	298.833
52.97	298.864
62.54	298.889
82.37	298.929
92.08	298.946

Melting point of pure cyclohexanol under 1 atm pressure; 299.09±0.03°K, Mol% of impurity; 0.025%

Table 3. The tempepatures of transitions and fusion under the saturated vapor pressure

Phase change	This research	Kelley	Ôtsubo *et al.*
II—I	265.50±0.01	263.5	266
III—I	244.8 ±0.1		243
I—liquid	299.05±0.03*	297.0	298

* Corrected for pressure variation by using Clausius-Clapeyron's equation. Data of the volume increases on melting and on transition were taken from Ref. 19 and Ref. 6.

Table 4. Molar heat of transition from the crystal-II to crystal-I (unit; kJ/mol)

Temp. interval (°K)	Heat input	$\int C_p dT$	ΔH_t
260.817—271.077	10.9783	2.1563	8.823
259.555—268.181	10.5836	1.7527	8.830
		Mean	8.827±0.01
	Data by Kelley		8.201
	Data by Ôtsubo *et al.*		8.699

Table 5. Molar heat of transition from the crystal-III to the crystal-I (unit; kJ/mol)

Temp. interval (°K)	Heat input	$\int C_p dT$	ΔH_t
240.736—268.613	13.7693	5.8289	8.664
236.448—270.639	15.7898	7.0403	8.754
237.222—271.427	15.5911	7.0816	8.513
234.863—270.502	15.9060	7.2818	8.624
		Mean	8.64±0.1
	Data by Ôtubo *et al.*		8.4—8.8

Table 6. Molar heat of fusion (unit; kJ/mol)

Temp. interval (°K)	Heat input	$\int C_p dT$	ΔH
294.916—300.773	3.2816	1.4952	1.786
293.254—302.425	4.1349	2.3533	1.782
294.306—302.185	3.8112	2.0296	1.782
		Mean	1.783±0.002
	Data by Kelley		1.699
	Data by Ôtsubo *et al.*		1.70

obtained by measuring the enthalpy difference between the crystal-I above 265°K and the crystal-II, because of the instability of the crystal-I below 265°K.

The Entropy of Cyclohexanol in the Ideal Gas State from the Thermal Data. The molar entropy of cyclohexanol in the ideal gas state at 280°K is calculated by a third-law path *via* II-I transition and summarized in Table 7. The contribution below 14°K is determined by means of the Debye theory with 125°K for Θ_D and assuming 6 degrees of freedom. The data of the heat of sublimation and the vapor pressure were reported previously.[6] Due to the lack of the critical data or the virial coefficients of this material, the magnitude of the gas imperfection correction was estimated from the critical data of *n*-propanol, phenol and cyclohexane by using the Berthelot equation. The correction is, however, negligibly small due to the low vapor pressure at 280°K (0.149 mmHg).[6]

Table 7. The entropy in the ideal gas state from thermal data

Temp. (°K)	Contribution	ΔS (J/mol degK)
0—13.75	Debye extrapolation	1.30±0.08
13.75—265.51	$\int C_p(\mathrm{II}) d\ln T$	141.55±0.43
265.51	Transition (8827/265.51)	33.25±0.04
		176.10±0.55
265.51—280	$\int C_p(\mathrm{I}) d\ln T$	9.01±0.03
280	Sublimation (6.075×10^4/280)	217.0±1.0
280	Compression to 1 atm	−70.97±0.02
280	Correction to ideal gas	0.00±0.00
		331.1±1.6

The Entropy from Statistical Data and Residual Entropy of the Crystal-II. The Raman effect of this material was reported by Neelakantan[9] from 300 cm^{-1} to 4000 cm^{-1}. But a normal coordinate analysis was not carried out. Since the far-infrared spectra of this material have not been reported, we measured the infrared spectra down to 200 cm^{-1}. They are summarized in Table 8. The frequencies of the normal modes were estimated by comparison with those of cyclohexane which were assigned by Takahashi *et al.*[10] These are listed in Table 9. Measurements in the region from 200 cm^{-1} to 300 cm^{-1} were not reliable on account of the noise effect, so we considered that the weak absorptions at 220 cm^{-1} and 240 cm^{-1} corresponded to the normal mode of cyclohexane at 248 cm^{-1} which is of doubly degenerated skeletal vibration. Taking 1.54, 1.09, 1.43 and 0.96 Å for the *C–C*, *C–H*, *O–C* and *O–H* bond distances respectively and 109° for both of

Table 8. Observed frequencies of IR spectrum (unit; cm^{-1})

220 w, 240 w, 279 vw, 338 m, 395 m, 406 w, 454 w, 481 m, 556 m, 650 s(b), 786 m, 832 w, 843 m, 860 w, 888 m, 924 w, 970 s, 1025 m, 1033 w, 1070 s, 1138 m, 1172 m. (higher frequencies are omitted.)

s; strong, m; medium, w; weak, v; very, b; broad

9) P. Neelakantan, *Proc. Indian Acad. Sci.*, **A57** (2), 94 (1963).

10) H. Takahashi, T. Shimanouchi, K. Fukushima and T. Miyazawa, *J. Mol. Spectry.*, **13**, 43 (1964).

TABLE 9. ESTIMATION OF THE FREQUENCIES OF NORMAL MODES OF CYCLOHEXANOL BY COMPARING WITH THOSE OF CYCLOHEXANE

vib.	frequencies estimated	vib.	freq. of cyclohexane
220, 240	C-C-C bend.+torsion	248×2	C-C-C bend.+torsion
338	C-C-C bend.+torsion	381	C-C-C bend.+torsion
395, 406	C-C-C bend.+torsion	423×2	C-C-C bend.+torsion
454, 481, 556	C-C-C bend. (2) or C-C-C bend. (1)	522	C-C-C bend.
650	O-H out of plane vib.		
786		802	C-C str.
832		862×2	C-C str.
843		(778)	CH_2 rock. (calc.)
860		(923)	
888, 924	C-C str. (6) or CH_2 rock. (3) or C-O str. (1)		
970, 1025, 1033, 1048		1031×2	C-C str.
1200×9	CH_2 twist (5) and CH_2 rock. (2) and H-C-O bend. (1) and C-O-H bend. (1)		
1400×10	CH_2 wag. (5) and CH_2 scis. (5)		
3000×12	C-H str. (11) and O-H str. (1)		

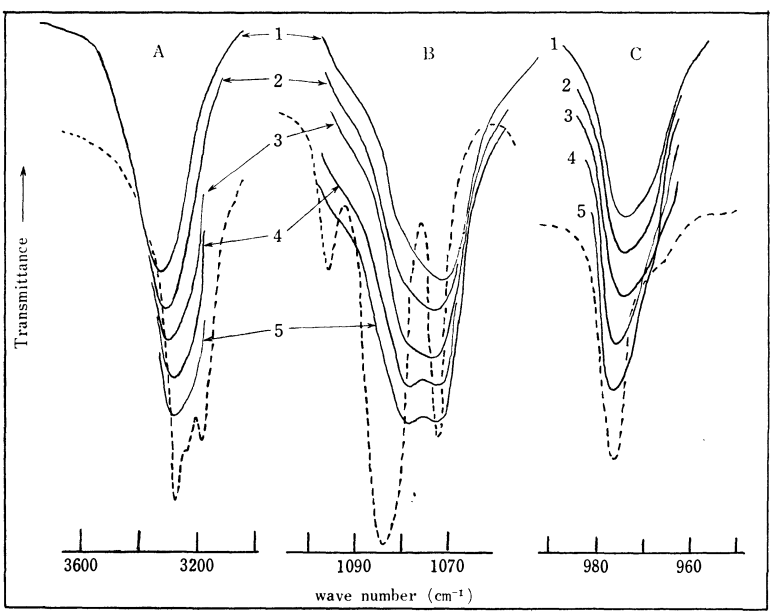

Fig. 3. Temperature dependence of the IR absorption. Full line for the crystal-I and the supercooled crystal-I.
Broken line for the crystal-III (at about 240°K)
A O-H stretching band
B C-O stretching band of equatorial form
C C-O stretching band of axial form
Crystal-I: 1, 301°K; 2, 276°K
Supercooled crystal-I: 3, 239°K; 4, 178°K; 5, 118°K

C-C-X (*X-H*, *C* or *O*) and *C-O-H* bond angles, one obtaines 3.63×10^{-113} g^3cm^6 for the product of three principal moments of inertia. This value is for the chair form with mean value of those for the axial (polar) and the equatorial conformations. The energy difference between the axial and the equatori-

al conformers was reported by Masschelein[11] as 1.57 ±0.21 kJ/mol from the temperature dependence of the intensity of infrared absorptions. The mixing entropy of both conformers was calculated by using this value. The value of this entropy amount is, however, somewhat ambiguous, since the result of our reinvestigation on the intensity of infrared absorption at low temperatures shows a little difference from that measured by Masschelein*4 (Fig. 3). Here, we have employed the value of the energy differences in the crystalline state in place of that in the gaseous state. As the mixing entropy is not so sensitive to the change of this value as far as the energy difference is smaller than RT, the error due to this ambiguity may be small. The entropy of internal rotation of *OH* group is left unknown and this value was determined so that the third-law entropy coincided with the statistical one. As shown in Table 10, it was found to be 6.9±2.9 J/(mol degK). Assuming the three-fold symmetry for hindering potential, the barrier height for internal rotation was then determined as 7.0 kJ/mol using the Pitzer and Gwinn table.[12] The value seems to be reasonable compared with those obtained for some aliphatic alcohols, *i.e.*, 3.3 kJ/mol for ethanol and 4.5 kJ/mol for methanol. These results constitute reasonably a third-law verification

Table 10. The entropy of gaseous state from statistical data (unit; J/mol degK)

Translation	164.97
Rotation	113.61±0.08
Vibration	40.23±1.2
Mixing isomers	5.34±0.05
Internal rot. of *OH* group	6.9 ±(2.9)
	331.1 ±1.3

Table 11. The third law entropy of the cpystal-I at 265.51°K *via* III-I transition

Temperature (°K)	Contribution	ΔS (J/mol degK)
0—13.75	Debye extrapolation	1.22±0.07
13.75—244.8	$\int C_p(\mathrm{III})\mathrm{d}\ln T$	127.04±0.38
244.8	Transition(8638/244.8)	35.29±0.4
244.8—265.51	$\int C_p(\mathrm{I})\mathrm{d}\ln T$	12.78±0.04
		176.33±0.8

11) W. Masschelein, *ibid.*, **10**, 161 (1961).

*4 Masschelein calculated the energy difference from the temperature dependence of the intensity of the bands at 1070 cm^{-1} and 970 cm^{-1} which were estimated to be those of the C–O stretching vibration of equatorial and axial forms, respectively. These absorption bands in the spectra of his measurement, however, did not show any such a splitting observed by us.

12) K. S. Pitzer and W. Gwinn, *J. Chem. Phys.*, **10**, 428 (1942).

Table 12. The difference of entropy of the supercooled crystal-I at 0°K and the crystal-I at 265.51°K

Temp.(°K)	Contribution	ΔS(J/mol degK)
0—13.75	Debye extrapolation	2.28±0.12
13.75—161.5	$\int C_p(\mathrm{I})\mathrm{d}\ln T$	100.28±0.30
161.5—245.5	$\int C_p(\mathrm{I})\mathrm{d}\ln T$*	56.47±0.51
245.5—265.51	$\int C_p(\mathrm{I})\mathrm{d}\ln T$	12.35±0.04
		171.4 ±1.0

* Calculated from Eqs. (1) and (2).

of the crystal-II. That is, we can safely conclude that the residual entropy of crystal-II is equal to zero.

Residual Entropies of Respective Phases. Calculations of the differences of entropies between that of the crystal-I at 265.51°K and those of the supercooled crystal-I, the crystal-II and the crystal-III at 0°K are shown in Table 11, 7 and 12, respectively. Since the supercooled crystal-I is unstable between 160 and 240°K, the heat capacity in this temperature region in Table 12 was calculated by using the following interpolation equations [unit; J/(mol degK)]:

$$C_p = 75.421 + 0.29368\mathrm{T} \quad (160—217°\mathrm{K}) \qquad (1)$$

and

$$C_p = 47.340 + 0.42290\mathrm{T} \quad (217—240°\mathrm{K}) \qquad (2)$$

These equations are derived based on our data and Kelley's value at 217°K and the error in determining the entropy is estimated to be ±0.5 J/(mol degK) in this temperature range. The contributions below 14°K were determined by using the Debye functions taking 102.3° and 127.6° for the Θ_D of the supercooled crystal-I and the crystal-III respectively. Comparison of Table 10, 6 and 11 shows that the residual entropy of the supercooled crystal-I amounts to 4.72±1.6 J/(mol degK) and that of the crystal-III −0.23±1.3 J/(mol degK). Accordingly, we may conclude that the crystal-III has actually no residual entropy. It may be noted that the crystal-III is in internal equilibrium notwithstanding that it is a metastable phase.

Finally based on the above data, the thermodynamic functions are calculated and these are listed in Table 13. Gibbs energies relationship of respective phases are shown in Fig. 4.

Discussion

Frozen-in State. What kind of degree of freedom would be involved in the relaxation process of the supercooled crystal-I is an interesting problem. In the ordinary glassy substances, they are usually

TABLE 13. THERMODYNAMIC FUNCTIONS OF CYCLOHEXANOL
unit; J/(mol degK)

T(°K)	C_p°	S °	$(H°-H_0°)/T$	$-(G°-H_0°)/T$
		(Crystal-II)		
5	(0.1912)	(0.0637)	(0.0478)	(0.0159)
10	(1.512)	(0.5093)	(0.3838)	(0.1256)
20	9.22	3.551	2.646	0.9045
30	19.13	9.180	6.502	2.678
40	27.84	15.93	10.80	5.134
50	34.73	22.91	14.92	7.986
60	40.85	29.78	18.74	11.04
70	46.02	36.49	22.28	14.21
80	50.49	42.92	25.52	17.40
90	55.10	49.14	28.56	20.58
100	59.35	55.17	31.43	23.74
110	63.60	61.02	34.15	26.87
120	67.79	66.73	36.78	29.95
130	71.67	72.32	39.32	33.00
140	76.02	77.79	41.79	36.00
150	80.10	83.17	44.20	38.97
160	84.22	88.47	46.58	41.90
170	88.38	93.70	48.91	44.79
180	93.18	98.89	51.24	47.66
190	97.89	104.05	53.57	50.48
200	102.54	109.19	55.90	53.29
210	107.18	114.56	58.23	56.33
220	111.78	119.40	60.56	58.84
230	117.03	124.48	62.90	61.58
240	122.57	129.58	65.27	64.31
250	129.22	134.71	67.69	67.02
260	136.93	139.92	70.20	69.72
265.51		Transition		
		(Crystal-I)		
270	167.40	178.89	105.90	72.92
280	175.16	185.12	108.23	76.89
290	184.55	191.42	110.70	80.72
299.09		Fusion		
		(Liquid)		
300	213.60	203.87	119.33	84.54
310	223.40	211.74	122.53	89.21
		(Crystal-III)		
		$S_0°=0$ $H_0°(\mathrm{III})-H_0°(\mathrm{II})=70.2$ J/mol		
5	(0.1676)	(0.0559)	(0.0444)	(0.0115)
10	(1.276)	(0.4743)	(0.3579)	(0.1164)
20	8.821	3.430	2.526	0.9045
30	18.37	8.847	6.441	2.435
40	26.75	15.33	10.37	4.962
50	33.18	22.02	14.32	7.706
60	38.93	28.58	17.94	10.64
70	44.13	34.99	21.37	13.62
80	48.70	41.18	24.49	16.69
90	53.32	47.18	27.44	19.74
100	57.56	53.02	30.24	22.78
110	61.67	58.70	32.92	25.78

Table 13 (continued)

T(°K)	$C_p°$	$S°$	$(H°-H_0°)/T$	$-(G°-H_0°)/T$
120	65.81	64.24	35.48	28.78
130	70.16	69.69	37.99	31.70
140	74.35	75.04	40.43	34.61
150	78.70	80.32	42.84	37.48
160	82.40	85.51	45.20	40.31
170	86.69	90.64	47.51	43.13
180	91.18	95.72	49.81	45.91
190	95.70	100.77	52.11	48.66
200	99.72	105.78	54.39	51.39
210	104.56	110.76	56.66	54.10
220	109.84	115.74	58.95	56.79
230	115.63	120.75	61.29	59.46
240	122.91	125.80	63.68	62.11
		(Supercooled crystal-I)		
		$S_0°=4.72$ J/mol degK $H_0°(\mathrm{I})-H_0(\mathrm{II})=4570$ J/mol		
5	(0.348)	(4.48)	(0.0870)	(4.75)
10	(2.716)	(5.64)	(0.692)	(4.95)
20	13.06	10.56	4.198	6.36
30	22.67	17.72	8.790	8.93
40	31.21	25.45	13.37	12.09
50	37.32	33.10	17.57	15.53
60	42.67	40.38	21.31	19.07
70	47.91	47.36	24.75	22.61
80	53.08	54.10	27.97	26.13
90	58.15	60.64	31.04	29.60
100	63.00	67.02	33.99	33.03
110	68.19	73.26	36.86	36.40
120	73.56	79.43	39.70	39.73
130	79.63	85.55	42.53	43.02
140	86.84	91.70	45.42	46.28
150	118.72	98.37	48.85	49.52
160	122.28	106.14	53.32	52.82
170	125.35	113.65	57.47	56.18
180	128.28	121.36	61.33	60.03
190	131.22	127.91	64.93	62.98
200	134.16	134.72	68.32	66.41
210	137.09	141.33	71.52	69.81
220	140.38	147.78	74.57	73.21
230	144.61	154.01	77.52	76.49
240	148.84	160.25	80.41	79.85
250	154.08	166.54	83.24	83.30
260	160.68	172.70	86.09	87.00

represented by a kind of quasi-particle "hole"[13,14] conventionally. Because the crystal-I has positional order (face-centered cubic),[15,16] the degree of freedom frozen in the glass transition of this crystal are expected as follows:

(a) Orientation of overall molecule,
(b) Number of the hydrogen bonds in the crystal,
(c) Orientation of *OH* group around a *C–O* bond,
(d) Tautomerism between the axial and the equatorial forms,
(e) Number of the defect.

We shall first discuss the contributions from the intramolecular terms (c) and (d). If it is assumed that the energy difference between the axial and the equatorial forms at T_g is equal to the value which

13) N. Hirai and H. Eyring, *J. Polymer Sci.*, **37**, 51 (1959).
14) B. Wunderlich, *ibid.*, **Pt. C, No. 6**, 137 (1963).
15) T. Oda, *X-rays*, **4**, 2 (1945).
16) T. Oda, *ibid.*, **5**, 26 (1948).

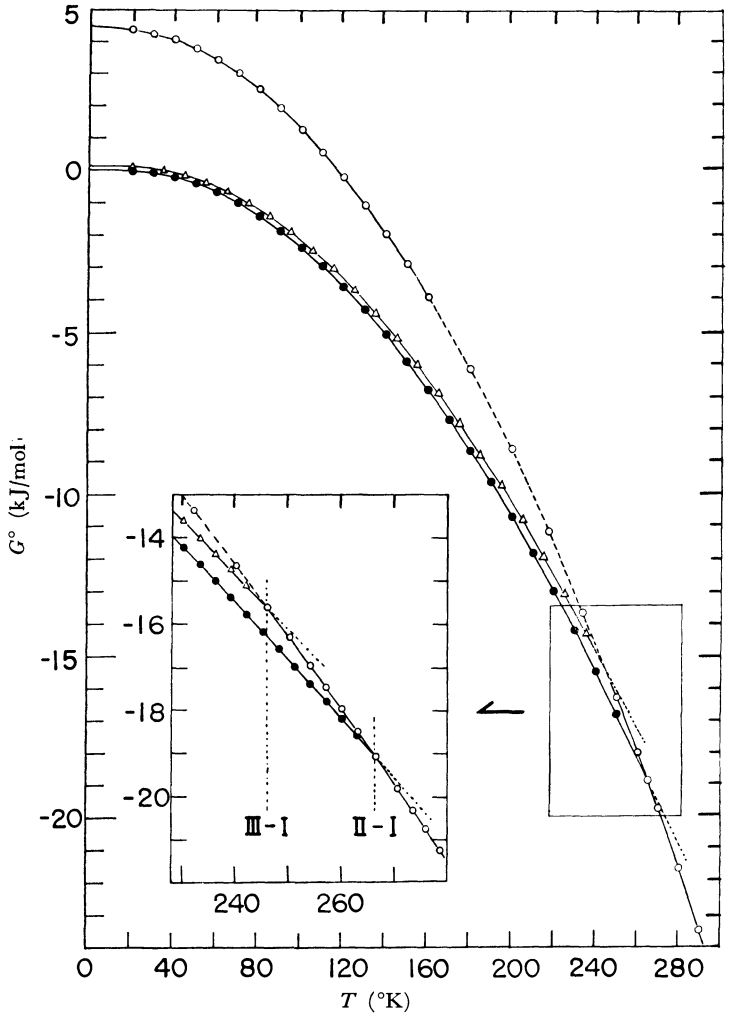

Fig. 4. Gibbs energies of respective phases.
—○— crystal-I and supercooled crystal-I
—●— crystal-II
—△— crystal-III

was reported by Masschelein and that this degree of freedom is frozen at T_g, the contribution of the mixing entropy of these tautomers to the residual entropy amounts to 4.5 J/(mol degK). This value seems to be large compared with the residual entropy (4.7 J/(mol degK)) and it may be considered that the energy difference will increase at low temperature. Focussing our attention to the intensity of the absorption of bands at 1070 cm^{-1} and at 970 cm^{-1} whose intensities had been studied by Masschelein, we reinvestigated the infra-red spectrum of supercooled crystal-I at low temperatures. The results are given in Fig. 3, where is also shown the temperature dependence of the *OH* stretching band. Masschelein assigned the bands at 1070 cm^{-1} and at 970 cm^{-1} to *C–O* stretching vibration of the equatorial and the axial forms, assuming these bands were single. However both of them are apparently composed of a pair of bands respectively and the individual bands of each pair show remarkable temperature dependence. Since it is very difficult to separate accurately the piled bands in two parts, we did not analyze the intensities of these bands quantitatively. From the fact that the bands do not change between 150°K and 80°K, it may be concluded that the degree of freedom of the tautomerism is frozen below T_g.

As to the contribution to the residual entropy of the orientation of the *OH* group for the rotation around a *C–O* bond, it should be also small. The quantitative discussion about it is, however, difficult at the present stage of our knowledge. If one attributes the residual entropy only to these intra molecular degrees of freedom ((c) and (d)), the jump of the heat capacity at T_g can not be explained, because these degrees of freedom offer the Schottky

heat capacity which is very small compared with the actual jump of the heat capacity at T_g.

We discuss now about the effects of (a) and (b). Meakins[17] and Corfield and Davies[18] have studied the dielectric dispersion of the crystal-I and also of supercooled one. Comparing with the results of cyclohexanone and chlorocyclohexane,*5 they concluded that the chains of hydrogen bonds are formed in this cyclohexanol crystal. If one extraporated the $\log(f_{max})$ *vs.* $1/T$ plots to low-temperature, the $1/f_{max}$ becomes from 1 sec to 1 hr at T_g, where the f_{max} indicated the frequency of maximum dispersion. Although these behaviors are also known in the ordinary glassy materials, this result shows that the orientation of the overall molecule is frozen at T_g. The careful examination of the possibility of the point defects in this crystal, as well as other plastic crystals by Staveley *et al.*,[19] has given no definite conclusion about the numbers of defects in these crystals. Accordingly, the role of the defects to the glass transition are still in question. In conclusion, we may only say that the residual entropy of the supercooled crystal-I may arise from frozen-in state partly of reorientational, and partly of conformational freedoms of the molecule in the lattice. The supercooled crystal-I below T_g is considered as a kind of new state of aggregation of pure material in the sense that the crystalline material has glass transition point and we should like to propose a term **glassy crystal** to this phase.

Debye Temperature. Debye temperatures of the supercooled crystal-I and the crystal-II are shown in Fig. 5. These calculations are based on the method of Wulff.[20] In Fig. 5, (1) and (2) are obtained by assuming 6 degrees of freedom. Debye temperatures due to 3 degrees of translational freedom are plotted in (3) and (4), where 3 degrees of torsional freedom are represented by a kind of Einstein function, whose average frequency is determined by a trial and error method. The lowering of the Debye temperature of the supercooled crystal-I above 90°K shows the existence of some configurational degrees of freedom which contribute to the heat capacity. Recently, Green and Scheie[21] determined the Debye temperature of the crystal-I between −40°C and 20°C from the study of the velocity of ultrasonic wave in the crystal. The result agrees fairly well with that of present low-temperature study. They have also reported that the velocity of ultrasonic wave in the crystal-III is larger than that in the crystal-II. This result is consistent with

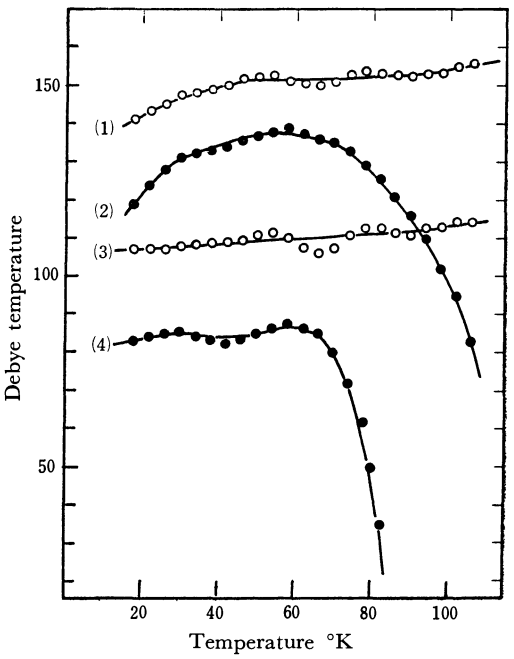

Fig. 5. Debye temperature of the supercooled crystal-I and the crystal-II.
(1) Crystal-II 6 degrees of freedom
(2) Supercooled crystal-I 6 degrees of freedom
(3) Crystal-II 3 degrees of freedom, $\omega=103$ cm^{-1}
(4) Supercooled crystal-I 3 degrees of freedom, $\omega=97$ cm^{-1}
Here, ω represents the frequency of the torsional vibration of overall molecule.

present result that the heat capacity of the crystal-III is smaller than that of the crystal-II.

Relaxation Phenomenon of the Supercooled Crystal-I. We have investigated the relaxation phenomena of the supercooled crystal-I below T_g with annealing treatment under different conditions. Figure 6 shows the contribution to the enthalpy from the degrees of freedom of configurations and conformations; in other words, the contributions from the intermolecular potential energy and intramolecular one. We call these terms conventionally configurational enthalpy. The experimental procedure for obtaining the configurational enthalpy $\Delta H_{conf.}$ is as follows: for instance, the difference of the total enthalpy between 155°K and 141°K is experimentally determined from the adiabatically supplied electric energies which is necessary to raise the temperature of the supercooled crystal-I from 141°K to 155°K. The increment of the kinetic energy and the energy of expansion due to the lattice vibration and internal vibration between 141°K and 155°K is calculated from the estimated heat capacity of vibrations that is represented by the following equation,

$$C_p \text{ (vib.)} = 22.81 + 0.41256T \text{ (J/mol degK)}. \quad (3)$$

This equation was determined so that the Debye

17) R. J. Meakins, *Trans. Faraday Soc.*, **58**, 1962 (1962).
18) G. Corfield and M. Davies, *ibid.*, **60** (**Pt. 1**), 10 (1964).
*5 They are also plastic crystals.
19) L. A. K. Staveley, P. F. Higgins and J. J. Virden, *J. Chem. Soc.* (*Suppl.* 1), **1964**, 5762.
20) C. A. Wulff, *J. Chem. Phys.*, **39**, 1227 (1963).
21) J. R. Green and C. E. Scheie, *J. Phys. Chem. Solids*, **28**, 383 (1967).

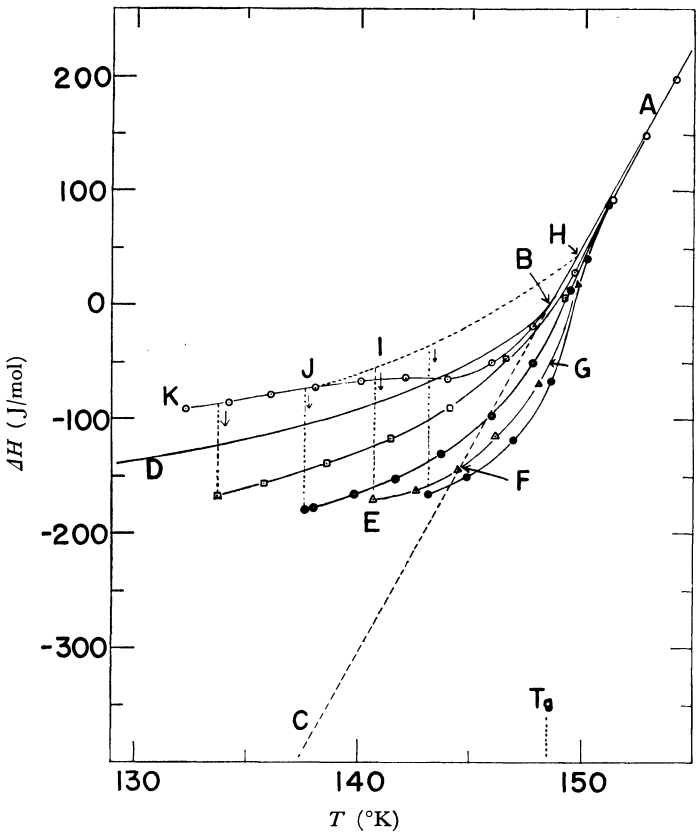

Fig. 6. Configurational enthalpy *vs.* temperature curves.

temperature calculated from above equation maintained nearly the same value as one at 90°K. The difference of the configurational enthalpy $\Delta H_{\text{conf.}}$ is determined by subtracting the increment of the kinetic energy from the total increment of enthalpy. Since the details about the origin of the anomalous heat capacity (C_p(obs)—C_p(vib)) is not known, it has some uncertainty whether this anomalous heat capacity is completely attributed to the degree of freedom of the configuration. Instead of this method, the $\Delta H_{\text{conf.}}$ is also calculable by the integration of the (C_p(obs)—C_p(vib)). In Fig. 6, curve A–B–C shows the estimated equilibrium curve assuming that the equilibrium heat capacity below T_g is represented by Eq. (1). A–B–D is obtained from the experimental heat capacity data (Table 1). In the measurement of the heat capacity of the supercooled crystal-I below T_g, the anomalous temperature drift due to the stabilization is treated as if the drift were arisen from thermal leakages.*6 This procedure below T_g provides the heat capacity eliminating the effect of relaxation. In other words, this heat capacity corresponds to the value for infinitely rapid measurement. If one takes this effect into consideration, the heat capacity curve shows a hump at T_g as shown by the data of Ôtsubo *et al.*, in Fig. 2. Accordingly, A–B–D shows the enthalpy changes for infinitely rapid heating. Other curves were determined from electric energy supplied under adiabatic condition. K–J–B–A shows the enthalpy increment when heated with the rate of about 1.5°K/hr as soon as cooled down to 130°K with the cooling rate of −6°K/min. The dotted line H–I–K is estimated curve for the cooling rate of −6°K/min. Annealing experiments were made at 144°K, 141°K, 137°K and 133°K for 25 hr, respectively, after cooling to these temperatures with cooling rate of −6°K/min from the liquid state at 300°K. For example, the enthalpy at 141°K changes from I to E in 25 hr and then traces the curve E–F–G upon heating. Assuming the exponential decay of enthalpy during the annealing period, the time constants (in hours) were calculated and summarized in Table 14. Here, it is assumed that the enthalpy at time zero lies on the curve A–H–I–J–K and on the curve A–B–C after infinite time. The Arrhenius plot of log τ against $1/T$ deviated from a straight line as shown in Fig. 7. The activation

Table 14. The time constants of the relaxation of the configurational enthalpy

Temperature (°K)	144	141	137	133
Time const. (hr)	11.9	32.3	60.4	125

*6 See Ref. 7.

energy calculated from the nearly straight portion of this curve is of 28.8 kJ/mol. As is well known, the relaxation time of dielectric or viscoelastic relaxation of supercooled liquid near T_g deviates from Arrhenius equation and is represented by the equation $\tau = \tau_0 \exp(E/(T-T_2))$, where T_2 is the temperature at which the relaxation time becomes infinite. But in these experiments, the deviation of the plot in Fig. 7 from the Arrhenius equation is the inverse to the deviation of the type of above equation. The origin of this result is apparently considered to be experimental error due to the incompleteness of adiabatic condition. But as shown in Fig. 7, the extent of this

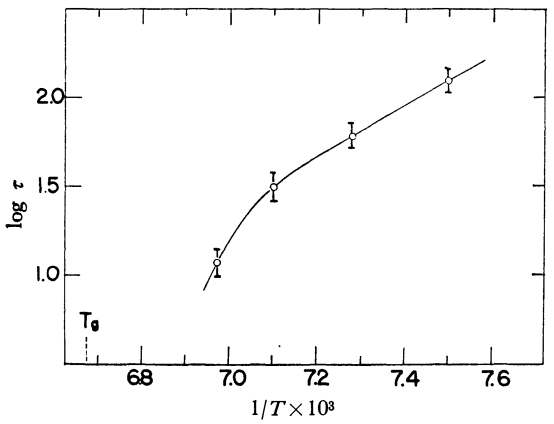

Fig. 7. $\log \tau$ *vs.* $1/T$ curve.
In this figure, $\overset{\top}{\underset{\perp}{\circ}}$ shows the limit of the experimentanl error due to incompleteness of adiabatic condition.

error is too small to change the behavior of the result. Another origin may be the ambiguity of the estimation of equilibrium curve (A–B–C). Assumption of exponential decay is also considered to be the possible source of the result. But if this result is accurate, it is seemingly explained by assuming the co-existence of different relaxation processes having respective characteristic time constants. The observed temperature drifts due to the stabilization also support this assumption. In general, the frozen-in state whose enthalpy is larger than that of equilibrium state should show the exothermic stabilization. Accordingly, behaviors of stabilization at all the points which are above the equilibrium curve (A–B–C) in Fig. 6 should be exothermic. But in this experiments, all the annealed specimen, *i.e.* at the points of ⊡, ◎, ● and ◬ in Fig. 6 showed net endothermic stabilization. This fact can be explained as follows: Although some degrees of freedom are frozen-in in this state, some other degrees of freedom which have shorter time-constant are already in equilibrium. So, when the temperature is raised up, the endothermic relaxation due to the degree of freedom having shorter relaxation time contributes largely to the stabilization.

T_2-Temperature. Gibbs and Adam[22] proposed a theory to solve the so-called Kauzmann's paradox[23] and the existence of a temperature denoted by T_2 where the relaxation time becomes infinite and the configurational entropy would vanish only if one supercooled a liquid infinitely slowly. Assuming that the heat capacity of the equilibrium state of glassy state corresponds to the extraporation of the heat capacity above T_g (Eq. (1)), we determined T_2 of the supercooled crystal-I to be 128°K. It is known that the ratio of T_g and T_2 of ordinary glassy substance is about 1.3, whereas the value amounts to 1.18 in this crystal.

Summary

(1) The heat capacities of cyclohexanol have been determined from 14°K to 320°K. The temperatures and the heats of transitions and of fusion for respective modifications were determined and the following results were obtained: *i.e.*, 265.50°K and 8827 J/mol for the phase transition of crystal-II—I, 244.8°K and 8638 J/mol for crystal-III—I and 299.05°K and 1782 J/mol for crystal-I—liquid.

(2) Comparing the entropy of ideal gas state calculated from thermal data with that from statistical-mechanical method, we have estimated that the residual entropy of the crystal-II is equal to zero and that the potential barrier of the internal rotation of *OH* group amounts to about 7.0 kJ/mol.

(3) Based on the estimation that the crystal-II has no residual entropy, the residual entropies of the supercooled crystal-I and of the crystal-III were determined. The residual entropy of the supercooled crystal-I amounted to 4.72 J/(mol degK) whereas that of the crystal-III was found to be zero within the experimental error.

(4) The Gibbs energies of the supercooled crystal-I, the crystal-II and of the crystal-III were calculated. From these results as well as that of the residual entropy, we can conclude that the crystal-III is of metastable but in the internal equilibrium state.

(5) It was confirmed that the anomalous jump of the heat capacity of the supercooled crystal-I at T_g ($\approx$150°K) arises from relaxation phenomena and the time constants in the relaxation process in enthalpy were determined.

(6) The origin of the residual entropy of the supercooled crystal-I was discussed and we proposed a new term **glassy crystal** for a crystalline material having glass transition temperature.

(7) Debye temperatures for the crystal-I and the crystal-II, and T_2 temperature were determined.

22) J. H. Gibbs and G. Adam, *J. Chem. Phys.*, **43**, 139 (1965).
23) W. Kauzmann, *Chem. Revs.*, **43**, 219 (1948).

BULLETIN OF THE CHEMICAL SOCIETY OF JAPAN VOL. 41 1088—1090 (1968)

Microwave Spectrum of *o*-Difluorobenzene*[1]

Aritada HATTA, Chiaki HIROSE and Kunio KOZIMA

Laboratory of Chemical Spectroscopy, Tokyo Institute of Technology, Ookayama, Meguro-ku, Tokyo

(Received November 9, 1967)

The microwave spectrum of *o*-difluorobenzene has been studied in the 7.8- to 28-Gc/sec region, R- and Q-branch transitions of the a-type being assigned for the lowest vibrational state. The rotational constants obtained are $A=3263.55$ Mc/sec, $B=2227.91$ Mc/sec, and $C=1323.87$ Mc/sec. Four possible sets of structural parameters were obtained. It seems probable that the angle made by two C–F bonds is larger than 60°. The value of the dipole moment obtained is 2.46 ± 0.03 D.

An electron diffraction investigation[1] has established that the molecule of *o*-dibromobenzene is planar or nearly planar, that the angle made by two C–Br bonds is larger than 60°, and that the opening of this angle may be due to the repulsive force between the bromine atoms. However, no such opening of the angle has been reported in the study of the microwave spectrum of *o*-fluorochlorobenzene.[2]

The present study was undertaken in the hope of determining the structure of *o*-difluorobenzene in detail, especially the angle made by two C–F bonds.[2]*

Experimental

The spectrum was measured over the frequency range from 7800 to 22600 Mc/sec with a conventional Stark-modulation microwave spectrometer, employing 110-kc/sec square-wave modulation. All measurements were made at room temperature. The frequencies were measured by comparison with a frequency standard which was monitored against the standard signals from Station JJY. The spectrum was displayed on an oscilloscope and, for weak absorptions, on a recorder.

o-Difluorobenzene was prepared from commercial *o*-fluoroaniline by the method of Schiemann and Pillarsky.[3]

Results and Discussion

Assignments of the spectrum were difficult because of the richness of the spectrum. Qualitative Stark patterns of the observed transitions were very helpful in identification. Since the C_2 axis coincides with the a-axis, only a-type transitions were observed.

The B and C rotational constants were calculated from the $1_{10}\rightarrow2_{11}$ and the $2_{21}\rightarrow3_{22}$ transitions, which occur at frequencies of $(3B+C)$ and $(3B+3C)$ respectively. The A constant was calculated from the observed Q-branch transitions. It is estimated that the A, B, and C rotational constants are accurate to ±0.015 Mc/sec. The rotational constants thus obtained agree with those of Nygaard *et al.* Since we used lower J-transitions in our determination than they did, the effect due to centrifugal distortion will be disregarded.

The measured frequencies and the assignments in the ground state are listed in Table 1, together with deviations between the measured frequencies and those calculated by the use of the rigid-rotor rotational constants given in Table 2. The agreement shown in Table 1 is such that it can be said that centrifugal distortion is not an important effect in the transitions studied. The transition frequencies and the rotational constants in terms of the geometrical parameters of the molecule were all calculated on a FACOM 222 digital computer.

The principal moments of inertia derived from the rotational constants are listed in Table 2. As is shown in Table 2, the inertia defect is 0.049 amu. Å^2 The small value of the inertia defect is strongly indicative of the planar configuration.

Since the molecule is planar, only two of these moments of inertia are independent. Therefore, a number of assumptions or approximations are required in order to extract any structural information. First of all, it may safely be assumed that the symmetry of the molecule is C_{2v}. Even if we assume that all the C–C bonds and all the C–H bonds are of equal length, and that the C–F bonds and the C–H bonds are located along the C–C–C angle bisectors,

---

*[1] Presented in part at the symposium on structural chemistry held by the Chemical Society of Japan, Osaka, Oct., 1966.

1) T. G. Strand, *J. Chem. Phys.*, **44**, 1611 (1966).

2) P. Kökeritz and H. Selén, *Arkiv Fysik*, **30**, 193 (1965).

*[2] While we were preparing this manuscript, we read a pre-publication copy of an article on the same topic written by L. Nygaard, E. R. Hansen, R. L. Hansen, J. Rastrup-Andersen, and G. O. Sørensen, an article which was kindly sent us by Professor Yonezo Morino of the University of Tokyo. The transitions measured were different from each other, and the lower J-transitions were obtained by us. For some of the R-branch transitions, those of our observed frequencies and assignments which agree with theirs are omitted in Table 1.

Note added in proof–Their article appeared in *Spectrochim. Acta*, **23**, 2813 (1967).

3) G. Schiemann and R. Pillarsky, *Ber.*, **62**, 3035 (1927).

TABLE 1. ASSIGNED GROUND-STATE TRANSITIONS OF *o*-DIFLUOROBENZENE

Transition	Observed* in Mc/sec	$\nu_{obs}-\nu_{calc}$	Transition	Observed* in Mc/sec	$\nu_{obs}-\nu_{calc}$
$1_{10} \rightarrow 2_{11}$	8007.7	+0.1	$6_{15} \rightarrow 7_{16}$	22585.5	−0.3
$2_{12} \rightarrow 3_{13}$	9092.7	+0.2	$7_{17} \rightarrow 8_{18}$	22507.2	+0.1
$2_{02} \rightarrow 3_{03}$	9422.8	0.0	$7_{35} \rightarrow 7_{34}$	8063.5	+0.2
$2_{21} \rightarrow 3_{22}$	10655.3	0.0	$4_{14} \rightarrow 4_{13}$	8333.5	0.0
$2_{11} \rightarrow 3_{12}$	11689.2	0.0	$9_{46} \rightarrow 9_{45}$	9206.6	−0.1
$2_{20} \rightarrow 3_{21}$	11887.8	−0.1	$4_{04} \rightarrow 4_{23}$	9474.0	0.0
$3_{13} \rightarrow 4_{14}$	11856.1	−0.1	$4_{13} \rightarrow 4_{32}$	9587.2	−0.1
$3_{03} \rightarrow 4_{04}$	11988.3	0.0	$6_{25} \rightarrow 6_{24}$	10118.4	0.0
$4_{32} \rightarrow 5_{33}$	18317.7	0.0	$5_{14} \rightarrow 5_{33}$	10348.1	+0.1
$4_{41} \rightarrow 5_{42}$	18604.7	+0.1	$5_{15} \rightarrow 5_{14}$	11343.3	−0.1
$4_{40} \rightarrow 5_{41}$	18809.0	+0.1	$8_{36} \rightarrow 8_{35}$	11735.5	0.0
$4_{31} \rightarrow 5_{32}$	19821.7	−0.1	$5_{05} \rightarrow 5_{24}$	11798.9	−0.2
$4_{22} \rightarrow 5_{23}$	19880.0	+0.3	$7_{25} \rightarrow 7_{44}$	13032.3	−0.1
$5_{24} \rightarrow 6_{25}$	19754.2	+0.3	$7_{26} \rightarrow 7_{25}$	13373.7	+0.2
$5_{14} \rightarrow 6_{15}$	20045.8	0.0	$6_{16} \rightarrow 6_{15}$	14181.2	−0.2
$5_{33} \rightarrow 6_{34}$	21669.0	0.0	$6_{06} \rightarrow 6_{25}$	14334.0	+0.1
$6_{25} \rightarrow 7_{26}$	22481.6	−0.1	$9_{36} \rightarrow 9_{55}$	15663.5	−0.3

* Maximum experimental uncertainty in the frequency measurements is ±0.2 Mc/sec

TABLE 2. ROTATIONAL CONSTANTS AND MOMENTS OF INERTIA

Rotational constant Mc/sec		Moments of inertia* amu·Å²	
A	3263.55	I_a	154.854
B	2227.91	I_b	226.838
C	1323.87	I_c	381.741
Asymmetry parameter $\kappa=-0.06785$		Inertia defect $\Delta=0.049$ amu·Å²	

* Conversion factor: 5.05375×10^5, corresponding to $^{12}C=12$ atomic weight scale.

we find that there are still four undetermined structural parameters. In addition, if we assume that the valency angle of carbon, ∠C–C–C, is 120°, three structural parameters, *i.e.*, the C–C distance, r_{C-C}, the C–H distance, r_{C-H}, and the C–F distance, r_{C-F}, remain to be determined. On these assumptions, however, we could not obtain any set of reasonable parameters to fit the observed moments of inertia.

Therefore, by assuming the values of the three bond lengths to be those reported by Kökeritz and Selén,[2] the valency angle α, ∠C–C–C, of the carbon atom to which the fluorine atom attaches and the angle, θ, made by two C–F bonds were determined. The parameters thus obtained are shown in Table 3 as set I. For the II, III, and IV sets, the values of r_{C-F} and α were determined by assuming that the C–F bond is located along the bisector of α, that the value of r_{C-C} is one of those reported previously,[2,4-6]

TABLE 3. STRUCTURAL PARAMETERS OF *o*-$C_6H_4F_2$

	Set I	Set II	Set III	Set IV
r_{C-C}	1.397*	1.395*	1.397*	1.402*Å
r_{C-H}	1.084*	1.084*	1.084*	1.084*Å
r_{C-F}	1.310*	1.313	1.308	1.294 Å
α	119°26′	119°20′	119°16′	119°7′
θ	60°22′	60°40′**	60°44′**	60°53′**

α: The valency angle of the carbon, ∠C–C–C, to which the F atom attaches.
θ: The angle made by two C–F bonds.
* Assumed by taking into account the data reported in Refs. 2, 4, 5, and 6.
** For these cases the C–F bonds are assumed to be along the bisectors of α.

and that the value of r_{C-H} is 1.084 Å. The parameters obtained are shown in Table 3 as the II, III, and IV sets.

The evaluation of $\partial R_j/\partial X_j$ was very useful in estimating the structural parameters, where R_j represents the jth rotational constant of the assumed structure and X_i is the ith structural parameter. All of the sets of the structural parameters were determined so as to get agreement between the calculated and observed values for the moments of inertia of I_a and I_b.

TABLE 4. STARK COEFFICIENTS AND DIPOLE MOMENT OF *o*-$C_6H_4F_2$

Transition		$\Delta\nu/E^2$(Mc/sec)/(V/cm)²×10⁵ observed	calculated
$1_{10} \rightarrow 2_{11}$	$M=0$	4.7±0.1	4.7
	$M=1$	−37.7±0.8	−38.0

$\mu=2.46\pm0.03$D

4) B. Bak, D. Christensen, L. Hansen-Nygaard and E. Tannenbaum, *J. Chem. Phys.*, **26**, 134 (1957); R. L. Poynter, *ibid.*, **39**, 1962 (1963).
5) E. Rosenthal and B. P. Dailey, *ibid.*, **43**, 2093 (1965).
6) H. Forest and B. P. Dailey, *ibid.*, **45**, 1736 (1966).

It is probable that the angle made by two C–F bonds is larger than 60°, inasmuch as the values of r_{C-C}, r_{C-F}, and r_{C-H} are not very different from those previously reported.

Stark effect coefficients were measured for the $M=0$ and 1 components of the $1_{10}\rightarrow 2_{11}$ transition. The data are shown in Table 4. The cell was calibrated using the $J=0\rightarrow 1$ transition of OCS, taking the dipole moment of OCS to be 0.7124 D.[7] The value of the dipole moment obtained is 2.46 ± 0.03 D. This value is in agreement with that of 2.38 D obtained by a solution method,[8] and slightly different from that of 2.59 ± 0.02 D obtained by Nygaard *et al.*

7) S. A. Marshall and J. Weber, *Phys. Rev.*, **105**, 1502 (1957).
8) E. Bergmann, L. Engel and S. Sándor, *Z. physik. Chem.*, **10B**, 106 (1930).

BULLETIN OF THE CHEMICAL SOCIETY OF JAPAN VOL. 41 1090—1096 (1968)

Radicals Produced by UV Irradiation of Acridan and Acridine in Glassy and Crystalline Medium at 77°K

Shigeya NIIZUMA and Masao KOIZUMI

Department of Chemistry, Faculty of Science, Tohoku University, Katahiracho, Sendai

(Received November 9, 1967)

Choosing two groups of solvent a) methanol, ethanol, isopropanol (glassy at liquid nitrogen temperature) and b) *t*-butanol, benzene, tetrahydrofuran (crystalline at liquid nitrogen temperature), ESR studies have been made on the irradiated solutions of A] acridine (A)+acridan (AH_2) (1 : 1), B] A alone, and C] AH_2 alone at 77°K. 1) 365 mμ irradiation of A] and B] in the solvents of a) group does not cause any photochemical reaction, whereas in the solvents of b) group, the $A^* + AH_2 \rightarrow 2AH\cdot$ reaction occurs. A resultant singlet ESR line has been assigned to AH·. 2) Irradiation of A] and C] with the entire output from a superhigh pressure mercury lamp gives, for solvents of group a), the ESR spectra which can be attributed mainly to alcohol radicals ($R\dot{C}HOH$) but gives electronic absorption spectra ascribed only to AH· ; for the solvents of group b) the results were almost the same as in 1).

In a series of papers dealing with the kinetics of the photoreduction of acridine, the participation of semi-reduced acridine, AH·, appears to be fully substantiated.[1-4] In particular, there is scarcely any doubt about the assignment of a transient species observed in flash experiments as AH·[1,4] in view of spectroscopic and kinetic evidence. However, the direct evidence for its radical nature is still lacking. ESR studies, although most promising for detecting a radical species, cannot be applied to the similar systems as employed in the kinetic studies, because the lifetime of AH· is too short. Hence, various attempts have been made to catch the ESR signal of AH· at liquid nitrogen temperature. At first, three kinds of alcohol, in which appreciable photoreduction of acridine occurs at room temperature, have been used as solvents. Irradiation by 365 mμ of the solutions of acridine and acridan as well as of acridine alone, has failed to give any sign of reaction. Irradiation of the solution of acridan by the total output from a superhigh pressure mercury lamp has given a certain species light brown in color, which is rather stable at liquid nitrogen temperature. The electronic spectra of this species agree with the ones in the flash experiment[1] and yet, the ESR spectra consist of the lines mainly originating from alcohol molecules.

Secondly, a group of solvents (benzene, *t*-butanol and tetrahydrofuran) which is known to take the crystalline form at liquid nitrogen temperature has been attempted with some success. It has been found that after dissolving acridine and acridan in these solvents at room temperature and irradiation with 365 mμ at liquid nitrogen temperature, the samples become colored in light brown and give ESR signals which are practically common to three solvents and are most likely attributed to AH·. The same signals as well as the same tint of color have been obtained with the samples containing only acridan on irradiation with a total output from a mercury lamp. We believe that most of the findings

1) A. Kira, S. Kato and M. Koizumi, This Bulletin, **39**, 1221 (1966).
2) A. Kira, Y. Ikeda and M. Koizumi, *ibid.*, **39**, 1673 (1966).
3) S. Niizuma, Y. Ikeda and M. Koizumi, *ibid.*, **40**, 2249 (1967).
4) A. Kira and M. Koizumi, *ibid.*, **39**, 2486 (1967).

obtained in the present investigation, are interesting from the standpoint of the reactivity of acridine and of acridan in general and of the sensitized decomposition of alcohols, not to speak of the confirmation of ESR spectra from AH·.

Experimental

ESR Spectrometer. A Nippon-Denshi P-10 type-ESR spectrometer was used.

Light Source. Light from a superhigh prssure mercury lamp (500 W and 100 W) was used without or with filters (in the latter case mainly 365 mμ but including 334 mμ).

Sample. *Benzene, Methanol and Isopropanol.* G. R. samples from Wako Junyaku were used without further purification.

Ethanol and t-Butanol. Reagents from Wako Junyaku were submitted to distillation. Tetrahydrofuran was distilled after refluxing over sodium. The solvent was kept over sodium and potassium metals. The concentrations of acridine and acridan were usually 10^{-2}—10^{-3} M. When the mixture of acridine and acridan was used, the composition was always 1 : 1.

Results

A) Glassy Medium. After having established that 365 mμ irradiation of the solution of acridine or of the solution of acridan and acridine in ethanol, methanol and isopropanol, did not cause any reaction, the samples were irradiated with the total output from a mercury lamp without filters. Since the results obtained are essentially the same as those in the solutions of acridan alone, both of them will be described here at the same place. It was checked that the irradiation of the solvents alone gives no appreciable signals under the similar conditions.

Methanol. A typical example for the deaerated solution is shown in Fig. 1. The radicals produced are quite stable at this temperature, the shape of the signal showing no change 1.5 hr after irradiation. In the presence of oxygen, the central three lines become somewhat unsymmetric. Three central lines (triplet) and the other two lines outside (doublet) are assigned to two different species, because the dependence on irradiation time of these two groups are different. Table 1 gives the relative height of the peak neighboring a central one and of the outermost peak, in reference to the height of the central peak. Figure 2 and 3 give respectively the build-up curves of the doublet and of the triplet. S-shape character for the former indicates that the doublet

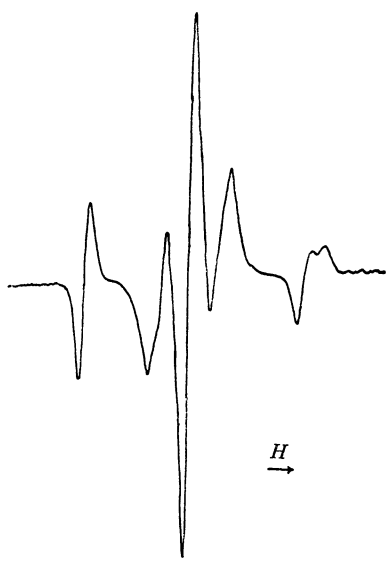

Fig. 1. ESR spectrum obtained by irradiating deaerated methanol solution of acridan for 25 min.

Table 1. Relative heights of the peaks as a function of irradiation time

Exp. No.	Time of irradiation min	Relative height of the peak: Neighbouring the central one	Relative height of the peak: Lying outermost
1	2	0.27	0.11
	14	0.27	0.22
	17	0.24	0.29
	25	0.26	0.33
2	25	0.24	0.36
	46.5	0.26	0.58
3	40	0.27	0.51
	50	0.28	0.38
	60	0.27	0.36

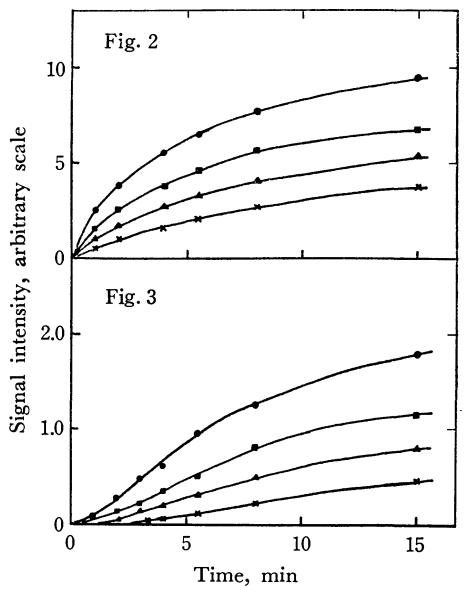

Fig. 2, 3. The build-up curves of the triplet (Fig. 2) and of the doublet (Fig. 3).
●: Irradiation without neutral filter (100% transmittance)
■: Irradiation with 61% neutral filter
▲: Irradiation with 46% neutral filter
×: Irradiation with 32% neutral filter

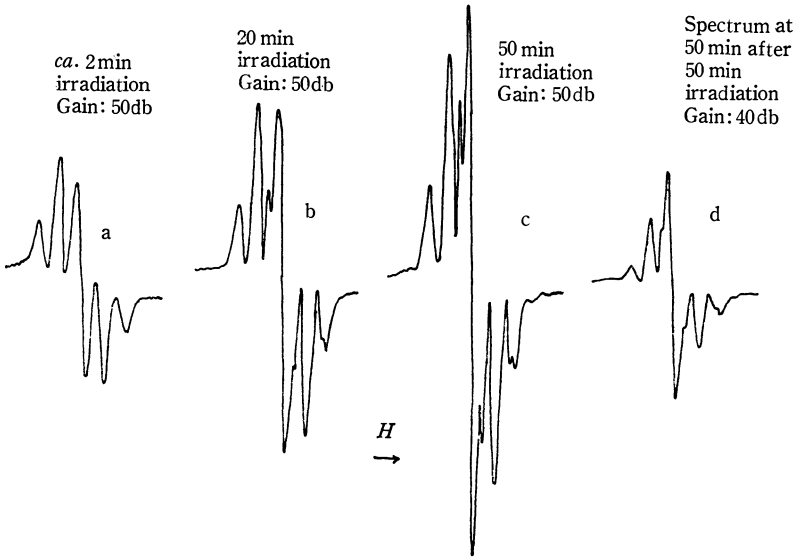

Fig. 4. ESR spectra obtained by irradiating acridan and acridine in deaerated ethanol.
a: *ca.* 2 min irradiation Gain: 50 db
b: 20 min irradiation Gain: 50 db
c: 50 min irradiation Gain: 50 db
d: Spectrum at 50 min after 50 min irradiation Gain: 40 db.

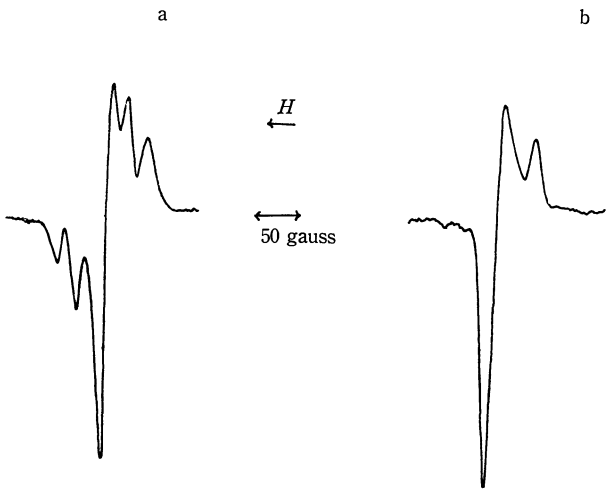

Fig. 5. ESR spectrum obtained by irradiating aerated ethanol solution of acridan.
a: When irradiated for a short time
b: When kept in the dark for 30 min after irradiation.

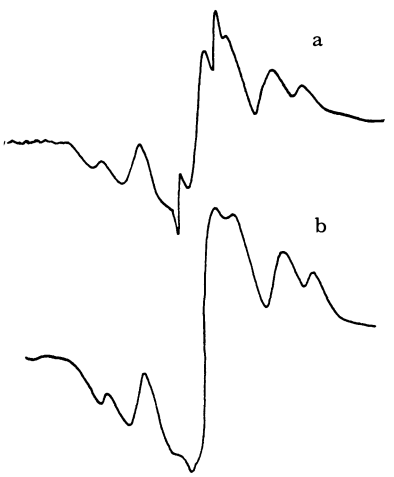

Fig. 6. ESR spectrum obtained from deaerated isopropanol solution of acridan.
a: When irradiated for a short time
b: When kept in the dark for four days after irradiation.

is produced not primarily but in the secondary reaction. Comparing the present results with the ones reported in the literature,[5-7] the triplet and the doublet may be assigned to methanol radical, $\cdot CH_2OH$ and formyl radical $H\dot{C}O$, respectively. The signal intensity of triplet is proportional to the light intensity, as is clear from Fig. 2. Therefore the main reaction is a one-photon process.

Ethanol. Figure 4 gives one example of the variation of the ESR spectra with the time of irradiation. Broadly speaking, the spectra consist of five lines which are due to $CH_3\dot{C}HOH$. The continued irradiation causes a slight but obvious change; an

5) Sr. P. J. Sullivan and W. S. Koski, *J. Am. Chem. Soc.*, **85**, 384 (1963).
6) V. E. Kholmogorov, E. V. Baranov and A. H. Terenin, *Dokl. Akad. Nauk. SSSR*, **149**, 142 (1963).
7) F. J. Adrian, E. L. Cochran and V. A. Bowers, *J. Chem. Phys.*, **36**, 1661 (1962).

additional line appears and becomes gradually larger in between the central and the next line. The height of the peaks at the initial stage is 1 : 2 : 4 : 2 : 1. ESR spectra labeled by d are the ones when c was kept in the dark for 50 min. It is seen that the two lines existing in the later stage have almost disappeared. In spite of this structural change, the integrated intensity remains the same within ±5%. At this stage, the height of the peaks is approximately in the ratio 1 : 3 : 5 : 3 : 1. It has been established that the signal intensity is proportional to the light intensity. A signal obtained in the aerated sample is unsymmetrical from the initial stage of irradiation (Fig. 5a); when it is kept in the dark for 30 min, it turns into a peroxide-like signal (Fig. 5b). The formation of peroxide is reasonable, but it is not certain whether the spectra are due to peroxide radical or $C_2H_5O\cdot$.[8,9] It is remarkable that 4 min irradiation of the deaerated solution dissolving 1×10^{-3} M of acridan produces $\sim2\times10^{-3}$ M of radical (at the stage of about half saturation).

Isopropanol. In the absence of oxygen, the signal at the initial stage of irradiation consists of septet attributable to $(CH_3)_2\dot{C}OH$[5,6] and small additional bands which decay very gradually in the dark. Figure 6 gives one example. The integrated intensity decreases about several percent in 1.5 hr.

Electronic Spectra for Alcoholic Solutions. In the ESR spectra the signals to be ascribed to AH· are lacking or very insignificant, but all the solutions, after having been irradiated, become light brown and show blue emission with a long duration suggesting the existence of AH··. Preliminary measurement of the absorption spectra has been attempted. Since the results are essentially the same for three alcohols, they will be described all together. Absorption spectra of the ethanol solution of acridine and acridan (both in 2.5×10^{-4}M) before irradiation are shown in Fig. 7. The spectra in methanol and isopropanol are quite similar. A large and broad peak around 280 mμ belongs to acridan. Other peaks are due to acridine. Figures 8 and 9 are the absorption spectra of the above solution after 30 min irradiation with the total output from a superhigh pressure mercury lamp at liquid nitrogen temperature. It is seen that the acridan absorption near 280 mμ has completely disappeared. A very sharp band near 280 mμ and the new bands appearing at 520—522 mμ and around 485 mμ agree with the bands which were assigned to AH· in the flash studies.[1,4] A remarkable change in the spectral shape in the region from 345—365 mμ indicates that AH· has an appreciable absorption in this region. It is worth while to add that a small peak near 570 mμ was lacking in the previous flash experiment where the solution of acridine in ethanol was used. Since the above changes are essentially

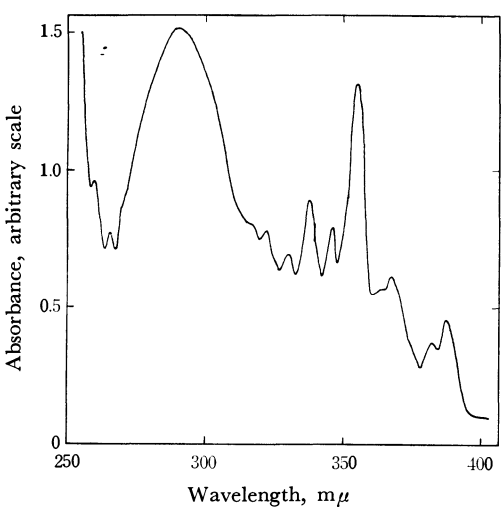

Fig. 7. UV absorption spectrum of deaerated acridine and acridan (both 0.25×10^{-3}mol/l) in ethanol at 77°K, before irradiation. It has no absorption in the visible region.

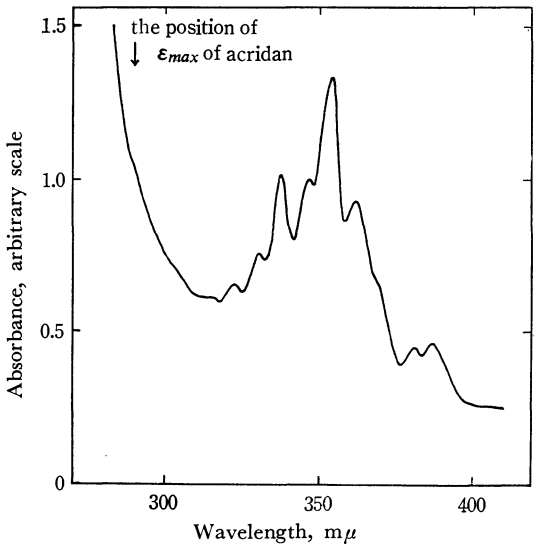

Fig. 8. UV absorption spectrum of deaerated acridine and acridan (both 0.25×10^{-3}mol/l) in ethanol at 77°K after 30 min irradiation.

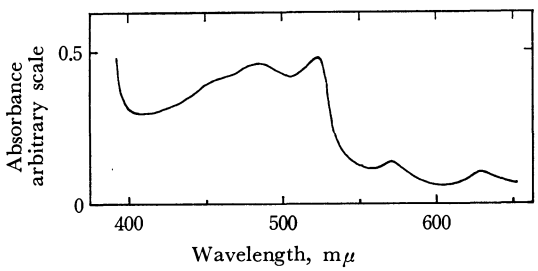

Fig. 9. Visible absorption spectrum of deaerated acridine and acridan (both 0.25×10^{-3}mol/l) in ethanol at 77°K after 30 min irradiation.

8) J. E. Bennett and A. Thomas, *Proc. Roy. Soc.*, **280**, 123 (1964).
9) Sr. P. J. Sullivan and W. S. Koski, *J. Am. Chem. Soc.*, **86**, 159 (1964).

common to methanol and isopropanol solutions, they are all interpreted to be concerned with acridan. Various radicals originating from alcohols which have been amply confirmed by ESR spectra, give no appreciable absorption from 250 to 600 mμ. When the irradiated solution was warmed up to room temperature and cooled again to 77°K, it gave essentially the same spectra as the ones of the non-irradiated solutions. This implies that acridine does not participate in the eventual reaction and that most of the half-reduced acridine in a fluid state, reconverts to either acridan or diacridan (The latter has the absorption spectra not differing so much from those of acridan.). It was checked that the 365 mμ irradiation of the above samples and the solutions of acridine alone for more than an hour, does not give any change in the absorption spectra.

B) Crystalline Medium. Benzene, *t*-butanol and THF are the solvents which have crystalline state at liquid nitrogen temperature. When the samples containing acridine and acridan in 1 : 1, were irradiated by 365 mμ at 77°K, they were colored in light brown and gave a prominent single ESR line. ΔH_{msl} values were 16.7, 17.5 and 22 for benzene *t*-butanol and THF, respectively. There is scarcely any doubt that these signals arise from the interaction of excited acridine and acridan, although there is some possibility of the participation of solvent molecules, because weak side bands depend upon the solvent used. Irradiation by a total emission from a mercury lamp gave essentially the same result. This may be due partly to the high intensity of 365 mμ of a light source. Of course it was checked that no signal was detected in the cases of solvents alone.

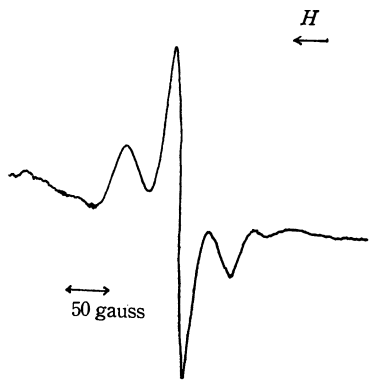

Fig. 10. ESR signal obtained by irradiating deaerated acridan and acridine in butanol at 77°K with 365 mμ of superhigh pressure mercury lamp.

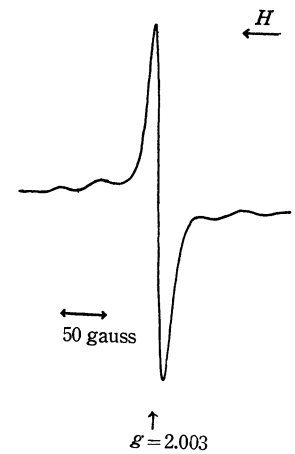

Fig. 11. ESR signal obtained by irradiating deaerated acridan and acridine in benzene at 77°K with 365 mμ of mercury lamp.

TABLE 2

	Solute		Medium	Irradiation from Hg lamp: 365 mμ	Irradiation from Hg lamp: Total output
A)	Acridine and acridan	a	Methanol	×⚹	◎○ (doublet & triplet)
		a	Ethanol	×	◎○ (quintet)
		a	Isopropanol	×	○ (septet)
		b	*t*-Butanol	○ (singlet)	○ (singlet)
		b	Benzene	◎○ (singlet)	○ (singlet)
		b	THF	◎○ (singlet)	◎○ (singlet)
B)	Acridine	a	Ethanol	×	×
		a	Isopropanol	×	
		b	Tetrahydrofuran	×	
		b	Benzene	×	×
C)	Acridan	a	Methanol		◎○ (doublet & triplet)
		a	Ethanol		◎○ (quintet)
		a	Isopropanol		◎○ (septet)
		b	*t*-Butanol		◎○ (singlet)
		b	Benzene		×⚹
		b	THF		○ (singlet)

○ Signal in the deareated condition
× No signal in the deaerated condition
◎ Signal in the aerated condition
⚹ No signal in the aerated condition

When THF and *t*-butanol containing acridan alone were irradiated by a mercury lamp without filters, they gave the similar signal as the above systems. In a very sharp contrast to *t*-butanol and THF, acridan solution of benzene did not give any ESR spectra.

t-Butanol. Figure 10 gives the ESR spectra obtained by irradiating with 365 mμ the deaerated solution of acridine and acridan. In the aerated system, the relative height of the central peak was somewhat low.

Benzene. As Fig. 11 shows, ESR spectra have four weak side bands in addition to a main line with $\Delta H_{msl}=16.7$ and $g=2.003$. The decay of the main line was measured at -95, -57 and -27°C. It increases with the rise of temperature, but the signal can be observed even near 0°C.

Tetrahydrofuran. Figure 12 gives the ESR spectra obtained by irradiating (without filters) the system of acridine and acridan in THF. In addition to a main single line, a broad absorption and a doublet 508 gauss apart, which is due to hydrogen atom, are apparently observed. Table 2 gives a brief summary of the present ESR studies.

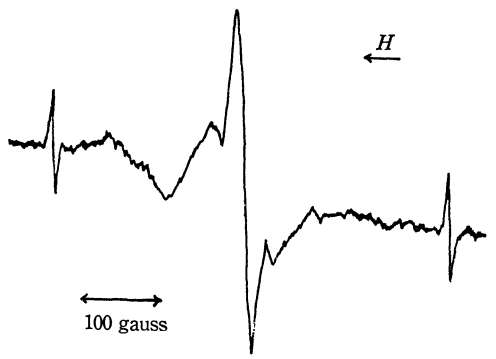

Fig. 12. ESR signal obtained by irradiating aerated acridine and acridan in tetrahydrofuran at 77°K with 365 mμ of mercury lamp.

It is to be noted that the results in glassy media and crystalline media are quite distinctive.

Discussion

It is well-known that acridine is photoreduced in various kinds of H-containing solvents in the fluid state. The reactive states of acridine, according to Kellmann *et al.*,[10] Porter *et al.*[11] as well as to our group,[12] are mainly singlet excited state and partly n-π^* triplet state, the lifetimes of which are respectively $\sim 10^{-10}$ and $\sim 10^{-8}$sec. Furthermore, we have established that part of the reaction goes *via* molecular mechanism without forming semiquinone,[1,12] and that acridine and acridan react photochemically (by 365 mμ) forming diacridan in benzene, the reactive state in this case being the lowest π-π^* triplet of acridine.[3,4]

In view of these results it is somewhat remarkable that no photochemical reaction (by 365 mμ) occurs at all in B) a) group at liquid nitrogen temperature. The reason may be that for the reaction to occur, reorientation of solvent molecules surrounding an excited acridine molecule is necessary and that at liquid nitrogen temperature such reorientation is impossible during the lifetime of the excited states. In the case of acridine and acridan, A) a) group, the two solute molecules are separated by solvent molecules so far apart that no reaction can occur. In crystalline medium on the other hand, acridine and acridan molecules (A) b) group) deposited from the medium, may be close to one another and in such a relative orientation to allow the reaction $A^*+AH_2 \rightarrow 2AH$ to occur. It is very natural that benzene and *t*-butanol with no easily detachable hydrogen, do not easily react with AH·. Thus the main ESR spectra are due to AH· (singlet).

Turning to the cases of irradiation without filters, the formation of AH· in alcohols, as verified by the electronic spectra, is due to the $AH_2 \rightarrow AH\cdot + H\cdot$ reaction. The produced hydrogen atom is expected to react with alcohol molecules, for instance according to $H\cdot + C_2H_5OH \rightarrow H_2 + CH_3\dot{C}HOH\cdot$. AH· is thought to be quite stable even photochemically, because the intensity of the electronic spectra, after reaching the saturation value, does not decrease by the continued irradiation. Thus the results from the electronic spectra implies that at liquid nitrogen temperature, AH· does not react thermally nor photochemically with any other radicals originating from alcohol or with alcohol molecules themselves. This leads to the expectation that in ESR the singlet line due to AH· should superpose on the signals of the radicals originating from alcohol molecules. It is difficult, however, to verify this unambiguously from the present data. There is also another problem, as to the quantity of radicals produced. If the production of all the radicals are initiated by such reactions, $AH_2 \rightarrow AH\cdot + H\cdot$, $H\cdot + C_2H_5OH \rightarrow CH_3\dot{C}HOH + H_2$, the finding that the quantity of the total radicals exceeds that of the original acridan even at a stage of half saturation, is difficult to understand. It seems necessary to consider that the formation of more than two radicals from one radical is occurring in secondary processes. Reactions such as $\dot{C}H_2OH \xrightarrow{h\nu} CH_2O + H\cdot \rightarrow \dot{C}HO + H\cdot + H\cdot$ which Sullivan *et al.*[13] suggested in the case of methanol, might be occuring. In the case of crystalline medium

10) A. Kellmann and J. T. Dubois, *J. Chem. Phys.*, **42**, 2518 (1965); A. Kellmann and J. T. Dubois, *J. Chimie Physique*, **63**, 936 (1966).

11) E. Van der Donckt and G. Porter, *J. Chem. Phys.*, **46**, 1173 (1967).

12) M. Koizumi, Y. Ikeda and H. Yamashita, This Bulletin, **41**, 1056 (1968).

13) P. J. Sullivan and W. S. Koski, *J. Am. Chem. Soc.*, **84**, 1 (1962).

containing only acridan Reaction, $AH_2 \rightarrow AH\cdot + H\cdot$ occurs in *t*-butanol and tetrahydrofuran just as in the case of alcohols but the reaction of atomic hydrogen with solvent molecules is not so significant as with alcohol molecules. Detection of a signal of atomic hydrogen in tetrahydrofuran also supports this conclusion. The absence of the reaction in benzene may be due to easy occurrence of the back reaction.

As to the radical species produced in the alcoholic solutions of acridan, there is no doubt that most of them are of the RC(OH)R′ type. There appears to be many problems about the secondary reactions that follow, which however, are out of the scope of the present aim. Our greatest concern is how the existent AH· radicals are affecting the observed ESR spectra. But the exact and quantitative answer to this problem also awaits further studies.

BULLETIN OF THE CHEMICAL SOCIETY OF JAPAN VOL. 41 1096—1104 (1968)

Infrared Spectra of Crystalline $CHCl_3$ and $CDCl_3$

Arata KIMOTO and Haruka YAMADA

Department of Chemistry, Kwansei Gakuin University, Nishinomiya

(Received November 9, 1967)

The infrared spectra for the fundamental absorption bands, ν_1, ν_2, ν_4 and ν_5, of $CHCl_3$ and $CDCl_3$ have been measured in polycrystalline films. For the C–H or C–D bending band a triplet has been observed in the pure crystal. The spectra of a mixed crystal ($CHCl_3$: $CDCl_3$) have also been studied over the entire concentration range. The space group of crystalline chloroform has been determined to be D_{2h}^{16}. The intensity of the band changes, going from the gas to the solid, depending on the symmetry species to which the vibrational mode belongs ; the A_1 bands increase in intensity, while the E bands decrease. The C–H stretching band shows an especially remarkable increase.

Recently the infrared spectra of chloroform in the solid state have been reported on by several investigators.[1-3] The crystal spectra observed so far, however, do not always agree with one another. For instance, a triplet was found for the C–H bending band by Lisitsa and Tsiashchenko,[1] while a doublet was found by Maklakov, Nikitin and Purkina[2] and by Denariez.[3] We have here studied carefully the infrared spectra of crystalline chloroform and deutero-chloroform, and obtained the definite spectra for the stable, well-annealed phase.

A qualitative analysis of crystalline spectra generally establishes only the site group of the molecule, but it can sometimes make possible the unique determination of the space group. In the present work, the spectra are also measured for the $CHCl_3$: $CDCl_3$ mixed crystals at various concentrations ; this is done to clarify the mechanism of the band splittings. The splittings observed in the crystal field can make it possible to determine the space group, when used in connection with the results of X-ray diffraction and the Raman spectra.

On the other hand, considerable attention has been paid to the infrared intensities in condensed phases.[4-11] The absolute intensities have already been measured for a number of simple molecules in the solid state. These studies attempted to compare the intensities in the solid state with those in the gaseous state. Large intensity changes are observed in benzene and ethylene, especially for the C–H stretching bands, while the intensity changes in carbon disulfide and carbon tetrachloride are relatively small and are interpreted as " ideal field effects." However, the observed intensity changes are not yet fully understood. The intensity behavior observed in chloroform may be useful in making theoretical progress on this problem, as our preliminary data[12] suggested.

1) M. P. Lisitsa and Iu. P. Tsiashchenko, *Opt. Spectry. (USSR)*, **6**, 396 (1959).
2) L. A. Maklakov, V. N. Nikitin and A. V. Purkina, *ibid.*, **15**, 178 (1963).
3) M. M. Denariez, *J. Chim. Phys.*, **62**, 323 (1965).
4) J. L. Hollenberg and D. A. Dows, *J. Chem. Phys.*, **37**, 1300 (1962) ; *ibid.*, **39**, 495 (1963).
5) G. M. Wieder and D. A. Dows, *ibid.*, **37**, 2990 (1962).
6) D. A. Dows, *Spectrochim. Acta*, **22**, 1479 (1966).
7) H. Yamada and W. B. Person, *J. Chem. Phys.*, **40**, 309 (1964).
8) H. Yamada and W. B. Person, *ibid.*, **41**, 2478 (1964) ; *ibid.*, **43**, 2519 (1965).
9) H. B. Friedrich and W. B. Person, *ibid.*, **39**, 811 (1963) ; H. B. Friedrich, H. Yamada and W. B. Person, *ibid.*, **43**, 4180 (1965) ; J. M. P. J. Verstegen, H. Goldring, S. Kimel and B. Katz, *ibid.*, **44**, 3216 (1966).
10) C. F. Cook, W. B. Person and L. C. Hall, *Spectrochim. Acta*, **23A**, 1425 (1967).
11) T. L. Brown, *J. Chem. Phys.*, **43**, 2780 (1965).
12) A. Kimoto and H. Yamada, This Bulletin, **40**, 243 (1967).

Experimental

Extra pure chloroform (Wako Pure Chemical Industries Ltd.) was washed with water in order to remove any alcohol present as a preservative. It was then dried over calcium chloride and distilled (bp 61.0—61.5°C). Deuterated chloroform was obtained from the Showa Denko, Ltd.; the purity stated was 99.8%. In the infrared spectrum of $CDCl_3$ some weak bands of $CHCl_3$ were discerned, from which the amount of $CHCl_3$ was estimated to be less than 0.7%. Commercial, extra-pure CS_2 and CCl_4 were used as solvents.

The technique for obtaining the spectrum has been described in the literature.[4-7] The sample in the gas phase was sprayed through a needle valve (VLV-II, Shinsei Sangyo Ltd.) onto a KRS-5 window, which was kept at the temperature of liquid nitrogen in a cold, glassy cell. Although the present study has been mostly concerned with sprayed samples, sample film was also made by cooling the liquid in a cold, metallic cell with KRS-5 windows. The temperature of the sample was determined to be 100°K in both of cases by use of a copper-constantan thermocouple.

The sample film was annealed as follows: after the sample film had been prepared at 100°K, it was gradually warmed 40 degrees and then again cooled down to 100°K. This process was repeated until the spectrum no longer showed any change. The spectrum varied with the deposition rate of the sample. The spectrum of the sample without annealing was slowly transformed to that of well-annealed film. That is, the slower the deposition, the better-annealed the film was obtained. The deposition rate, controlled by opening the needle valve, was 4—6 min per μ of thickness. The film thickness was measured from the interference fringes observed at 2.5 μ. The spectra of well-annealed films prepared by the two different methods coincided completely with each other. In order to detect any preferred orientation of the film, spectra were also measured in polarized light. No appreciable changes in the spectra were found, however.

The spectra were obtained using a Jasco DS-402G spectrometer in the 400—4000 cm^{-1} region. The spectral slitwidths were 0.7—1.0 cm^{-1} for ν_1, 0.8 cm^{-1} for ν_4, and 0.6—1.4 cm^{-1} for ν_2 and ν_5.

The index of refraction of the sample film was estimated to be $n^{100°K}=1.61$ for both $CHCl_3$ and $CDCl_3$; estimation was made from the Lorenz-Lorentz equation using the following values: [13]

$n_D^{288°K}=1.448$, $d^{288°K}=1.498$, $d^{100°K}=1.93$

for $CHCl_3$ and

$n_D^{293°K}=1.445$, $d^{293°K}=1.500$ and $d^{100°K}=1.95$

for $CDCl_3$.

The integrated absorption intensity was obtained from the curve of the absorbance *vs* the wave number, according to:

$$B = (\rho l)^{-1}\int \ln(T_0/T)d\nu \qquad (1)$$

where the concentration, ρ, was calculated to be 16.2 mol/*l* from the densities for both $CHCl_3$ and $CDCl_3$. Intensities in solutions were measured using a 0.1 mm cell with KRS-5 windows.

For the measurement of mixed crystals, the vapor of mixtures of $CHCl_3$ with $CDCl_3$ were deposited onto the cold substrate; the films deposited were also annealed. The ($CHCl_3/CDCl_3$) ratios were assumed to be equal to those in the liquid.

Results and Discussion

Figures 1 and 2 show the four fundamentals observed for crystalline $CHCl_3$ and $CDCl_3$. The dotted lines represent the curves of unannealed samples, and the solid lines, those of well-annealed samples. After annealing, the ν_1 and ν_2 bands belonging to A_1

Table 1. Observed frequencies for fundamental bands of chloroform (cm^{-1})

Band[a]	Gas[b]	Liquid	Solid[c]
$\nu_1(A_1)$	3034	3015	(3024) 3007
$\nu_4(E)$	1221	1216	1225 (1221) 1210 1206
$\nu_5(E)$	769	756	~765 756 ~738
$\nu_2(A_1)$	681	669	(677) 673

a) G. Herzberg, "Molecular Spectra and Molecular Structure," Vol. II, D. Van Nostrand Company, Inc., Princeton, N. J. (1945), p. 316.
b) J. Morcillo, J. Herranz and J. Biarge, *Spectrochim. Acta*, **15**, 110 (1959).
c) In parentheses are the bands which disappeared by annealing.

Table 2. Observed frequencies for fundamental bands of deutero-chloroform (cm^{-1})

Band[a]	Gas	Liquid	Solid[d]
$\nu_1(A_1)$	2262[b]	2260	(2260) 2250
$\nu_4(E)$	915[b]	909	911 902 898
$\nu_5(E)$	747[c]	732	~740 727 ~722
$\nu_2(A_1)$	651[a]	646	(655) 651

a) Ref. a in Table 1.
b) Ref. 3.
c) J. R. Madigan, F. F. Cleveland, W. M. Boyer and R. B. Bernstein, *J. Chem. Phys.*, **18**, 1081 (1950).
d) In parentheses are the bands which disappeared by annealing.

13) J. Timmermans, "Physico-Chemical Constants of Pure Organic Compounds," Elsevier Publishing Co., Inc., New York (1950); "Beilsteins Handbuch der Organischen Chemie," Drittes Ergängswerk, Band 1, System Nr. 1—15, Springer-Verlag, Heidelberg (1958).

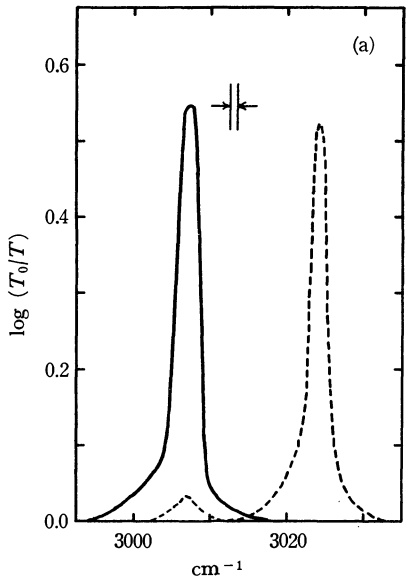

Fig. 1. (a), ν_1.

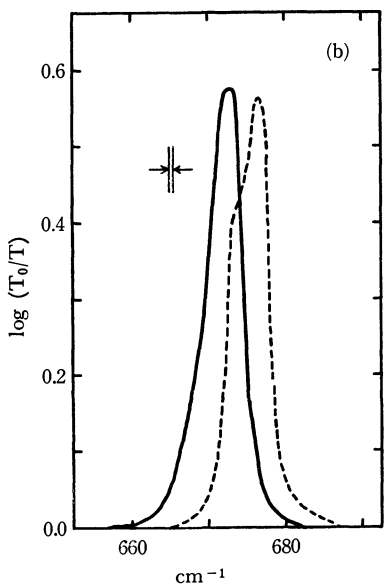

Fig. 1. (b), ν_2.

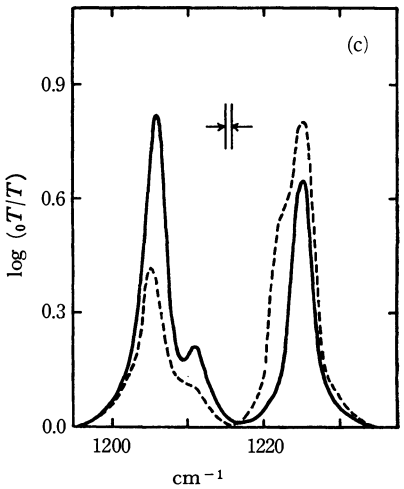

Fig. 1. (c), ν_4.

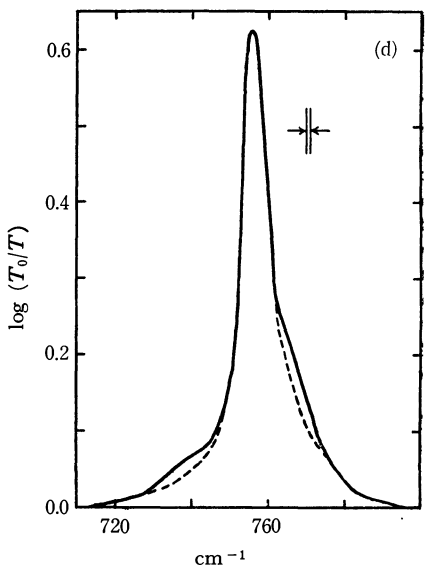

Fig. 1. (d), ν_5.

Fig. 1. Fundamental bands of crystalline $CHCl_3$.
—— annealed, - - - unannealed sample

species shift to the low-frequency side, while the ν_4 and ν_5 bands belonging to E species split into three components. Three peaks are clearly resolved in the ν_4, C–H bending band. The ν_1 and ν_2 bands are slightly asymmetric, suggesting that there are additional peaks on the low-frequency sides. The observed frequencies at the band peaks are listed in Tables 1 and 2.

In order to ascertain why the spectra obtained for the unannealed samples differed considerably from those for the well-annealed samples, a differential thermal analysis of $CHCl_3$ has been undertaken. No thermal anomaly, however, was detected over the 300—390°K temperature range, with the exception of that at the melting point, 209°K. This means that solid $CHCl_3$ does not show any phase transition. This is consistent with the results of the pure quadrupole resonance study by Gutowsky and McCall.[14] The spectra obtained for the unannealed samples, therefore, are those of the metastable or amorphous form, partly mixed with those of the stable form.

The C–H and C–D bending bands, ν_4(E), in the mixed crystals ($CHCl_3$: $CDCl_3$) are shown in Figs. 3

14) H. S. Gutowsky and D. W. McCall, *J. Chem. Phys.*, **32**, 548 (1960).

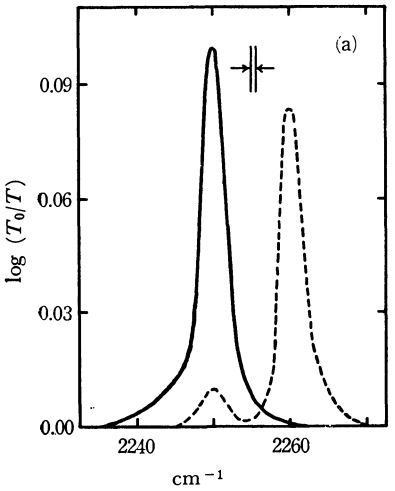

Fig. 2. (a), ν_1.

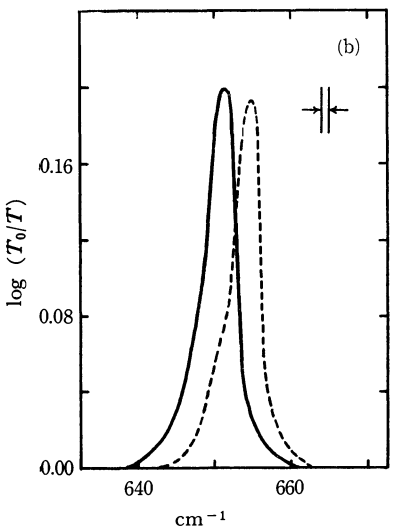

Fig. 2. (b), ν_2.

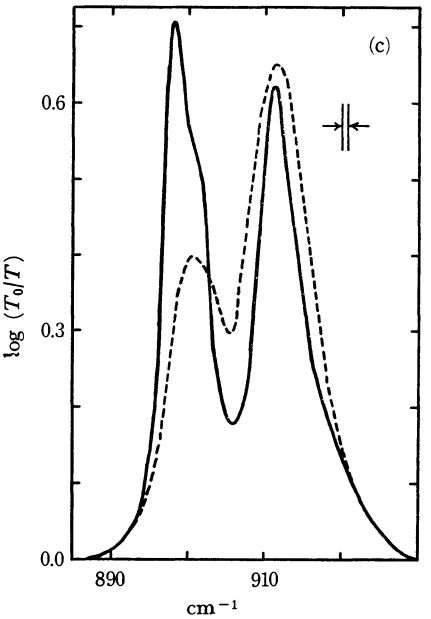

Fig. 2. (c), ν_4.

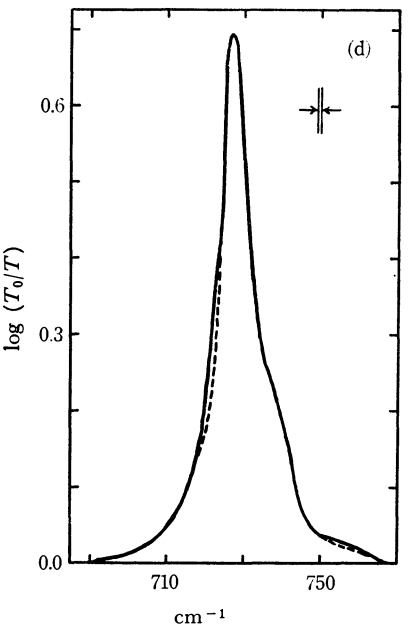

Fig. 2. (d), ν_5.

Fig. 2. Fundamental bands of crystalline $CDCl_3$.

and 4 at various concentrations. Figure 5 shows the frequencies of the absorption maxima in both the ν_4-$CHCl_3$ and ν_4-$CDCl_3$ regions for the mixtures of $CHCl_3$ and $CDCl_3$. In the mixed crystal four peaks are observed for the ν_4 bands. As the concentration of $CHCl_3$ decreases, the two inner peaks increase in intensity, while the two outer peaks decrease. When $CHCl_3$ was considerably diluted with $CDCl_3$ (97.4%), the two outer peaks disappeared and a complete doublet at 1213.8 and 1220.0 cm^{-1} was observed. The spacing of the two inner peaks remains almost constant at 6—8 cm^{-1}, independent of the concentration. Let us now designate the four peaks as ν_4^1, ν_4^2, ν_4^3, and ν_4^4 respectively, from high to low frequencies. Then ν_4^2 and ν_4^3 can be assigned to the components split by the site group or by removing the degeneracy in the crystal field, and ν_4^1, ν_4^3 and ν_4^4 in the pure $CHCl_3$ or $CDCl_3$, to the components split by the factor group. One of the factor group components overlaps with ν_4^3, the site group component. The four peaks observed in the mixed crystal, therefore, may be interpreted as a superposition of the components split by the site group upon those split by the factor group at various rates. The C–D bending band behaves in the same way as the C–H bending band, but its splitting is relatively small.

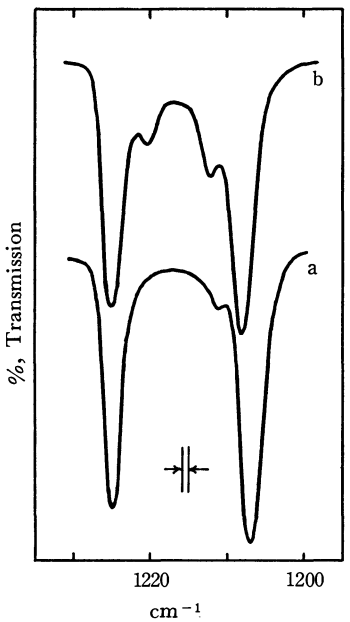

Fig. 3. a) $CDCl_3$ 7.2%, b) 23.2%.

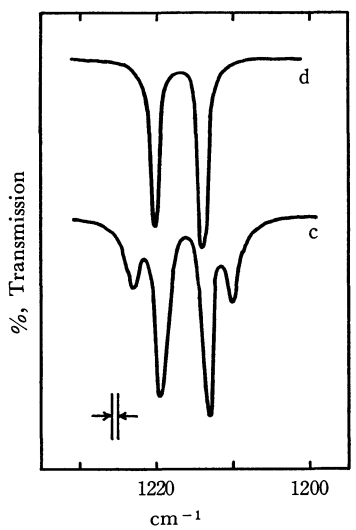

Fig. 3. c) 79.3%, d) 97.4%.

Fig. 3. Spectra in ν_4-$CHCl_3$ region for mixture of $CHCl_3$ and $CDCl_3$.

Although the spectra of the $CHCl_3$: $CDCl_3$ mixed crystal have already been reported by Maklakov *et al.*[2] and by Denariez,[3] their sets of results coincide with neither each other nor the present spectra. Maklakov *et al.*, observing a singlet at a very dilute solid solution, concluded that a factor-group splitting is predominant in crystalline $CHCl_3$. On the contrary, Denariez observed a doublet at the concentration of 1%, indicating that a site-group splitting is rather predominant. These differences may be caused by the use of unannealed or incompletely annealed films. In many cases, the crystal splittings observed are not in harmony with those theoretically predicted, even for simple molecules, because the

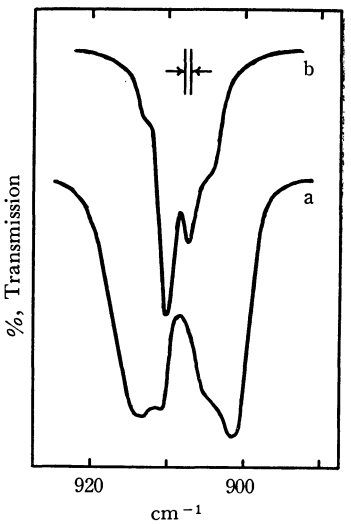

Fig. 4. Spectra in ν_4-$CDCl_3$ region for mixture of $CHCl_3$ and $CDCl_3$.
a) $CHCl_3$ 34.8% b) 94.5%.

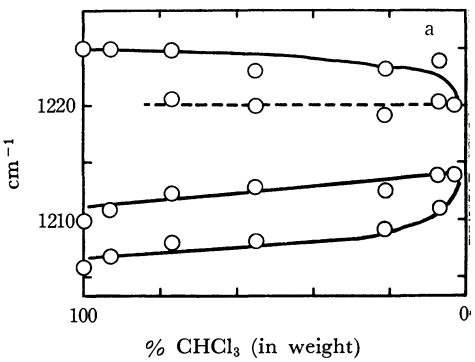

Fig. 5. a) Frequencies of absorption maxima in ν_4-$CHCl_3$ region for mixtures of $CHCl_3$ and $CDCl_3$.

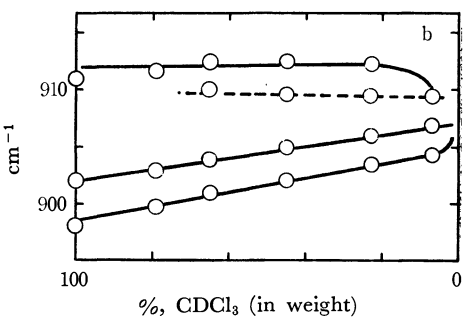

Fig. 5. b) Frequencies of absorption maxima in ν_4-$CDCl_3$ region for mixtures of $CHCl_3$ and $CDCl_3$.

natural abundance of isotopic molecules and sometimes the Fermi resonance[15] complicate the crystal spectra or because the magnitudes of the band splittings are small. However, the C–H bending band of $CHCl_3$ is not affected by these influences. Here it is a typical example for the site- and factor-group splittings.

The structure of crystalline chloroform may be inferred from the results of group theoretical analysis.[16] In the mixed crystal of $CHCl_3$ diluted by $CDCl_3$, the A_1 bands remain single, while the E bands split into two components. On the other hand, in the pure crystal the A_1 bands probably split into two components (if we count the asymmetric tail as a peak), while the E bands split clearly into three components. The unit-cell groups which explain these splitting are C_{2v}, D_{2h}, C_{3v}, *etc.* (20 altogether), all with the C_s-site symmetry. Referring to the Raman spectrum of crystalline $CHCl_3$,[17] we note that none of the peak frequencies of the infrared spectrum coincide with those of the Raman spectrum. This suggests that there exists a mutual exclusion between the infrared and Raman spectra, namely, the inversion symmetry in the unit-cell group.

An X-ray diffraction study of the chloroform single crystal has been made in our university,[18] and the possible space group has been found to be either C_{2v}^9 or D_{2h}^{16} with four molecules per unit-cell. While we were making this X-ray study, Fourme and Renaud[19] reported the crystal structure independently, giving the same space group. From the vibrational spectra described above, we can easily discard the possibility of C_{2v}^9 with the C_1 site symmetry. Consequently, the space group of crystalline $CHCl_3$ must be D_{2h}^{16} with the C_s site symmetry. The correlation diagram is shown in Fig. 6.

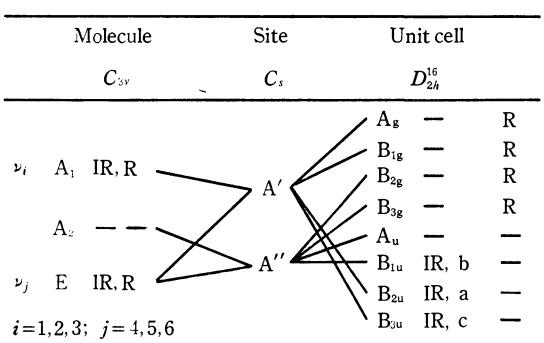

Fig. 6. Correlation diagram for crystalline $CHCl_3$.

15) For example, R. Kopelman, *J. Chem. Phys.*, **44**, 3547 (1966).

16) R. S. Halford, *ibid.*, **14**, 8 (1946); H. W. Winston and R. S. Halford, *ibid.*, **17**, 607 (1949); D. F. Hornig, *ibid.*, **16**, 1063 (1948).

17) M. Ito, *ibid.*, **40**, 3128 (1964). In this article only two components have been reported for the E species. In later works three components have been observed (private communication).

18) Y. Tomiie *et al.*; The cell dimension is determined to be a=7.14, b=9.80 and c=5.84 Å, Z=4.

Returning to Figs. 3 and 4 for the C–H and C–D bending vibration, ν_4, $\nu_4{}^4$ should be assigned to the B_{1u} component, since it is the strongest among the three peaks in the pure crystal. $\nu_4{}^1$ and $\nu_4{}^3$ are assigned to B_{3u} and B_{2u}, respectively or *vice versa*. $\nu_4{}^4$ is almost equal in intensity to the sum of $\nu_4{}^1$ and $\nu_4{}^3$. Thus, $\nu_4{}^1$, $\nu_4{}^3$ and $\nu_4{}^4$ correspond to the c, a, and b (or to be a, c, and b)-axis components of the crystal respectively, and the C–H bond of $CHCl_3$ lies on the ac plane. Taking the angle between the C–H bond and the a axis θ, the infrared intensities of B_{2u} (a) and B_{3u} (c) components are related as:

$$I(B_{2u})/I(B_{3u}) = \tan^2\theta,$$

if the oriented gas model can be assumed. The observed intensity ratio gives $\theta = 25°$. The parameters for the $CHCl_3$ crystal reported by Fourme and Renaud lead to a value of 14° for this angle. Notwithstanding the ambiguity in separating each component of the ν_4 band and the assumption of the oriented gas model, these are in good agreement. Assuming the molecular orientation shown in Fig. 7,[19] we may expect the B_{3u} (c) component of the A_1 band, as well as the B_{2u} (a) component of the E band, to be very weak. This may be the reason why the splittings of A_1 bands are not resolved clearly in the pure crystal.

The crystal structure of $CDCl_3$ is considered isomorphous to that of $CHCl_3$, since the same trends in band splittings are observed.

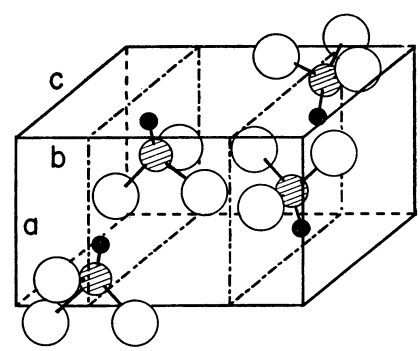

Fig. 7. Molecular orientation in the crystal. (After the structure given by Fourme and Renaud.)

As has been mentioned above, the band splittings may be well interpreted as the factor group for the pure crystals and as the site group for the dilutely-mixed crystals, in accordance with the crystal structure. It is of great interest for us what kind of forces give rise to such splittings of the bands; in other words, what kind of intermolecular potentials contribute to the splittings. As has been indicated by

19) R. Fourme and M. Renaud, *Compt. rend.*, **263B**, 69 (1966); The parameter for H atom z/c=0.7200 should be corrected to be 0.0720 (private communication).

Hexter[20] and Dows,[21] when the dipole-dipole interaction potential is predominant, the isotopic relation governing any particular factor group holds:

$$\frac{\Delta\nu_H}{\Delta\nu_D} = \frac{\nu_D}{\nu_H}\frac{I_H}{I_D} \qquad (2)$$

Here, $\Delta\nu$ represents the magnitude of band splitting, ν, the wavenumber, and I, the intensity of the band. $CHCl_3$ and $CDCl_3$ are denoted by the suffixes H and D respectively. Examining this formula for the ν_4 band, we must take $|\nu(B_{2u})-\nu(B_{3u})|$ as $\Delta\nu_H$ or $\Delta\nu_D$ for the factor-group splitting. The observed values are $\Delta\nu_H=15\ cm^{-1}$ and $\Delta\nu_D=9\ cm^{-1}$. Then, the left side in Eq. (2) gives 1.7, while the right side gives a quite different value, 0.23, using the gas-phase intensities. Even though we substitute I_H and I_D for the solid intensities, the right side still gives the same value. This suggests that some potential other than the dipole-dipole potential plays an important role in the splitting of the ν_4 band. Presumably atom-atom potentials, H···Cl interactions, contribute to the coupling of the ν_4 vibration, which is similar to the vibrations which arise primarily from hydrogen motions, of methylchloride[21,22] and ethylene.[23] On the other hand, the $\nu_5(E)$ of the C–Cl stretching vibration may split due to the dipole-dipole coupling, much as does the ν_3 of methyl chloride,[20-22] because the intensity of this band is extremely large. Detailed calculations of the splittings will be published elsewhere.

The absolute intensities of the fundamental bands in the crystals are given in Tables 3 and 4, while the intensities between different phases are compared in Tables 5 and 6. The maximum error involved in the intensity measurements is 15% for the solids. Lambert's law plots of $B\rho l$ *vs.* l are shown in Fig. 8. As for the solid intensities of $CHCl_3$, Lisitsa *et al.*[1] early reported values for the polycrystalline films

TABLE 3. ABSOLUTE INTENSITIES OF CRYSTALLINE CHLOROFORM

Band	ν_{max} (cm^{-1})	$\Delta\nu_{1/2}$ (cm^{-1})	B (darks)	
			This work	Lisitsa *et al.*[a]
$\nu_1(A_1)$	3007	3.5	1200	170
$\nu_4(E)$	1225 1210 1206	2.8 — 2.6	2700	320
$\nu_5(E)$	765 756 738	— 10.0 —	19000	3200
$\nu_2(A_1)$	673	5.0	1600	—

a) Ref. 1.

TABLE 4. ABSOLUTE INTENSITIES OF CRYSTALLINE DEUTERO-CHLOROFORM

Band	ν_{max} (cm^{-1})	$\Delta\nu_{1/2}$ (cm^{-1})	B (darks)
$\nu_1(A_1)$	2250	4.0	300
$\nu_4(E)$	911 902 898	6.0 — 6.1	8900
$\nu_5(E)$	740 727 722	— 10.4 —	20000
$\nu_2(A_1)$	651	5.2	1100

TABLE 5. ABSOLUTE INTENSITIES OF CHLOROFORM IN VARIOUS PHASES (darks)

Band	Gas[a]	Liquid	Solid	Solution CS_2
$\nu_1(A_1)$	44	707[b]	1200	559[b]
$\nu_4(E)$	4200	2900[c]	2700	3000
$\nu_5(E)$	27000	30000[c] 28600[d]	19000	24000
$\nu_2(A_1)$	600	—	1600	490

a) Ref. b in Table 1. See also, Ref. 26 and D. C. McKean, Dissertation, Oxford (1953).
b) R. E. Kagarise, U. S. Naval Research Laboratory Report, 5906(1963); See also, M. T. Forel, J. P. Leiknamand M. L. Josien, *J. Chim. Phys.*, **57**, 1103 (1960).
c) G. M. Irons and H. W. Thompson, *Proc. Roy. Soc. (London)*, **A298**, 160 (1967).
d) A. C. Gilby, J. Burr, Jr., W. Krueger and B. Crawford, Jr., *J. Phys. Chem.*, **70**, 1525 (1966).

TABLE 6. ABSOLUTE INTENSITIES OF DEUTERO-CHLOROFORM IN SOLID AND SOLUTION (darks)

Band	Solid	Solution	
		CS_2	CCl_4
$\nu_1(A_1)$	300	—	160
$\nu_4(E)$	8900	9500	9600
$\nu_5(E)$	20000	15200	—
$\nu_2(A_1)$	1100	490	540

obtained by cooling the liquid. Their values, shown in Table 3, are quite small, being only about 15% of the present values. As has been previously discussed for crystalline benzene,[24] measurement by cooling the liquid makes for considerable errors in determining the intensity, because the assumption that the product, ρl, of the concentration and the path length remains constant as it was frozen from the liquid to the solid will be in error.

20) R. M. Hexter, *J. Chem. Phys.*, **33**, 1833 (1960).
21) D. A. Dows, *ibid.*, **35**, 282 (1961).
22) D. A. Dows, *ibid.*, **33**, 1342 (1960).
23) D. A. Dows, *ibid.*, **36**, 2836 (1962).
24) H. Yamada and W. B. Person, *ibid.*, **38**, 1253 (1963).

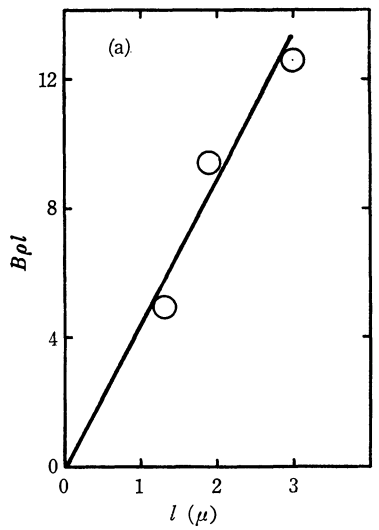

Fig. 8. (a) Lambert's law plots for ν_4 of crystalline $CHCl_3$.

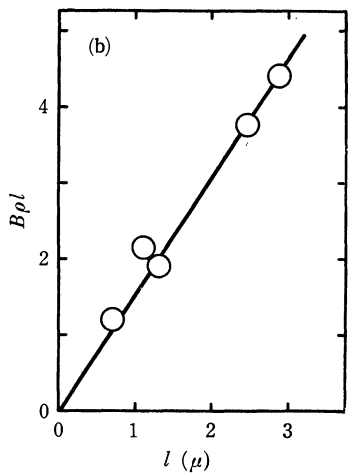

Fig. 8. (b) Lambert's law plots for ν_2 of crystalline $CDCl_3$.

For $CHCl_3$, the ν_1 and ν_2 bands increase in intensity going from the gas to the solid, while the ν_4 and ν_5 bands decrease. As may be seen from the Table 5, these trends can be roughly seen to be in order from the gas to the solution and to the solid. The increase in intensity for the ν_1 band of $CHCl_3$, going from the gas to the solid, is remarkable. However, most of this increase is observed when it goes from the gas to the solution. Some of the authors[25] who measured the intensity of the ν_1 band in dilute solutions (in CCl_4 and CS_2) attributed it to the effect of molecular association, similar to hydrogen bonding, though this point is not clear.

An interesting phenomenon has been reported that for this ν_1 vibration, the first overtone is much stronger in intensity than the fundamental band, suggesting an abnormal weakness of the fundamental ν_1 in the gas phase.[26]

In the crystal the interatomic distances between an H atom and its nearest Cl atoms are calculated from previously-reported data[19] to be as follows: molecule whose central carbon lies on the same C_s plane as the H atom), 3.12 Å for H···Cl (for a Cl atom of another molecule whose central carbon also lies in the same C_s plane), and larger than 3.7 Å for all others. Comparing these values with the van der Waals distance, 3.00 Å, for H···Cl, it seems that the hydrogen is surrounded by the three Cl atoms and that no special H···Cl linkage is formed. It is doubtful, therefore, that the observed intensity changes are due to any special association of the molecules.

At any rate, it is worth noting that the bands belonging to A_1 species of the molecule increase in intensity, while the bands belonging to E species decrease, going from the gas to the solid. That is, the intensity varies depending on the symmetry species of the vibrational mode. Since the molecular axis of chloroform coincides with the short axis of the molecular ellipsoid, the field effects predict that the intensity will increase for the A_1 modes and decrease for the E modes. Thus, the qualitative trends observed are the same as those expected from the field effects, though the magnitudes of the observed changes are considerably larger than those predicted. If we compare the intensities of $CDCl_3$ between the solution and the solid, the A_1 bands increase in intensity from the solution to the solid, while the E bands remain unchanged or decrease. Similar trends are observed in $CHCl_3$.

The intensity behavior observed in chloroform is quite different from those observed in benzene[4] and ethylene.[5] It also differs from those observed in CCl_4[10] and CS_2[7] where the "ideal field effects" is concerned. As for the C–H stretching bands, the intensity increases in $CHCl_3$ as well as in acetylene,[6] while it decreases in benzene and ethylene. If we interpret this behavior in terms of the "delocalization moment," M_D,[10] M_D should have the same sign as that of the intrinsic moment or exceed the intrinsic moment greatly.

We wish to thank to Professor K. Suzuki for his useful discussions, especially concerning the metastable phase. Thanks are also due to Professor S. Seki for making available the facilities of Osaka

25) C. M. Huggins and G. C. Pimentel, *ibid.*, **23**, 1244 (1955); S. Singh and C. N. R. Rao, *J. Phys. Chem.*, **71**, 1074 (1967); W. E. Thompson and G. C. Pimentel, *Z. Elektrochem.*, **64**, 748 (1960); See also, G. C. Pimentel and A. L. McClellan, "The Hydrogen Bond," H. W. Freeman and Company, San Francisco (1960), pp. 120, 197.

26) C. C. Robinson, S. A. Tare and H. W. Thompson, *Proc. Roy. Soc.*, **A269**, 492 (1962).

University for the differential thermal analysis, to Professor Y. Tomiie for his X-ray analysis, to Professor D. C. McKean for showing us his unpublished data on the gas-phase intensities, and to Professor M. Ito for showing us his detailed findings of the Raman spectra. We are also most grateful to Professor W. B. Person for his helpful correspondence and advice.

BULLETIN OF THE CHEMICAL SOCIETY OF JAPAN VOL. 41 1104—1109 (1968)

Electric Conductance and Density of Molten Salt Systems: $I_2 + SbI_3$, $SbBr_3 + SbI_3$, and $SbCl_3$

Kenji SAITO, Kazuhiko ICHIKAWA and Mitsuo SHIMOJI

Department of Chemistry, Faculty of Science, Hokkaido University, Sapporo

(Received December 4, 1967)

Measurements of electric conductance as a function of temperature have been made for the pure liquids; I_2, $SbCl_3$, $SbBr_3$ and SbI_3, and the mixtures; I_2+SbI_3 and $SbBr_3+SbI_3$, from 100 to 250°C. Furthermore, measurements of density by a pycnometric method as a function of temperature have also been made for these mixtures, from 100 to 300°C. The conductivities of these liquids lie in the range from 5×10^{-4} to 1×10^{-5} ohm^{-1} cm^{-1}, and are about 10^{-4} times lower than those of alkali halide melts. In these poorly-conducting pure liquids, the molecules may be considered as constituting a solvent in which slightly dissociated ions are contained. The negative temperature coefficient of conductivity for iodine is in marked contrast to the antimony halide melts, and may be interpreted in terms of the ionic conduction and electron hopping mechanism rather than the metallic one.

A few measurements concerning the electric conductance of pure molten iodine and antimony halides (or group VA metals) have been reported so far,[1-4] and some discrepancies in experimental data have been found. Furthermore, no full datum has been obtained for the electric conductance of mixtures of these antimony halides. The present communication reports the experimental results of density measurements for I_2+SbI_3 and $SbBr_3+SbI_3$ solutions, and of conductivity measurements for I_2+SbI_3, $SbBr_3+SbI_3$ and $SbCl_3$. The measurement of the conductivity of I_2+SbI_3 was made in order to investigate the change in transport properties of an iodine melt due to the addition of antimony iodide. This system is in striking contrast to the molten antimony+antimony halide mixture reported in an earlier paper.[5]

1) I_2: G. N. Lewis and P. Wheeler, *Z. Physik. Chem.*, **56**, 179 (1906); M. Rabinowitsch, *ibid.*, **119**, 83 (1926); W. A. Plotnikov, J. A. Fialkov and W. P. Tschalij, *ibid.*, **A172**, 307 (1935); D. J. Bearcroft and N. H. Nachtrieb, *J. Phys. Chem.*, **71**, 316 (1967).

2) $SbCl_3$: P. Walden, *Z. Anorg. Allgem. Chem.*, **25**, 219 (1900); Z. Klemensiewicz, *Bull. Acad. Cracow*, **487** (1908); G. Jander and K. H. Swart, *Z. Anorg. Allgem. Chem.*, **299**, 252 (1959).

3) $SbBr_3$: V. A. Izbekow and V. A. Plotnikow, *Z. Anorg. Allgem. Chem.*, **71**, 336 (1911); G. Hevesy, *Medd. Danske Selsk.*, **3**, 20 (1921); G. Jander and J. Weis, *Ber. Bunsenges. Physik. Chem.*, **61**, 1275 (1957).

4) SbI_3: G. Hevesy, *Medd. Danske Selsk.*, **3**, 17 (1921).

Experimental

Materials. Guaranteed reagent-grade $SbBr_3$ and $SbCl_3$ were dried under vacuum to remove surface and some hydrated water. All samples (guaranteed reagent-grade I_2, SbI_3, $SbBr_3$ and $SbCl_3$) were purified once or twice by distillation or sublimation *in vacuo*.

Apparatus and Procedure. Conductivity measurements were made with a Jones bridge,[6] constructed of the grounding circuit and measuring one. Alternating current was detected by a " tuned " null detector. The pyrex conductance cell[5] previously described was used with some modification. In particular, the sample of $SbCl_3$, distilled twice *in vacuo*, was directly distilled into the conductance cell through an extension tube, in order to prevent an apparent conductivity due to traces of moisture, and the cell was then sealed off under vacuum. Good precision was obtained by adjusting a variable condenser (0.45—0.70 μF) connected in parallel with the standard resistor. A pyconometric method[7] was used to measure the densities of liquid I_2+SbI_3 and $SbBr_3+SbI_3$ mixtures as a function of temperature and composition. The height of the liquid column was measured with a cathetometer within ±0.005 cm. In order to prevent condensation on the stem wall above the liquid, the top of the stem, which was fitted with a heating coil,

5) K. Ichikawa and M. Shimoji, *Trans. Faraday Soc.*, **62**, 3543 (1966).

6) G. Jones and R. C. Josephs, *J. Am. Chem. Soc.*, **50**, 1049 (1928).

7) F. J. Keneshea, Jr. and D. Cubicciotti, *J. Phys. Chem.*, **62**, 843 (1958).

was maintained at a temperature slightly higher (from 3 to 4°C) than the liquid temperature. The Archimedean method may be unsuitable because of the change in composition due to the appreciable vapour pressures of the samples of interest.

Results and Discussion

The specific conductance κ and the density d_t of I_2+SbI_3 and $SbBr_3+SbI_3$, and κ of $SbCl_3$ were measured over a temperature range from 100 to 350°C above their liquidus temperatures. The temperature dependence of conductivity for each system is shown in Figs. 1, 2 and 3. Table 1 shows the linear relations for the density of the mixtures I_2+SbI_3 and

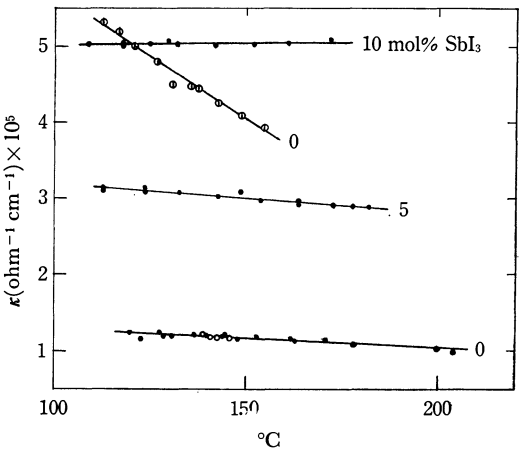

Fig. 1. Conductivity of I_2+SbI_3 solutions against temperature at various mol% SbI_3 compositions. ●, This work; ○, Bearcroft and Nachtrieb[1]; ◑, Rabinowitsch[1]

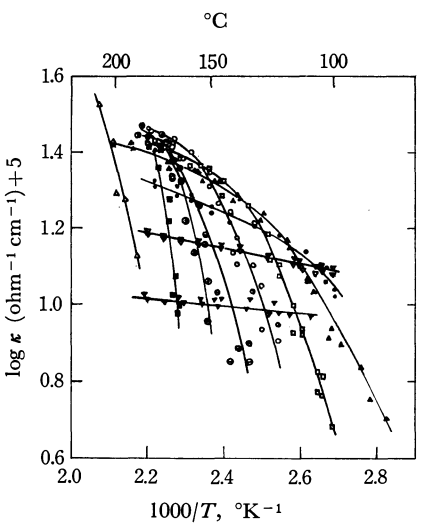

Fig. 2. Log conductivity of I_2+SbI_3 solutions against reciprocal temperature at various mole% SbI_3 compositions (▼: 20, ▽: 30, ●: 40, ▲: 50, □: 60, ○: 70, ⊖: 80, ⊙: 90, ◪: 95, △: 100 mol% SbI_3).

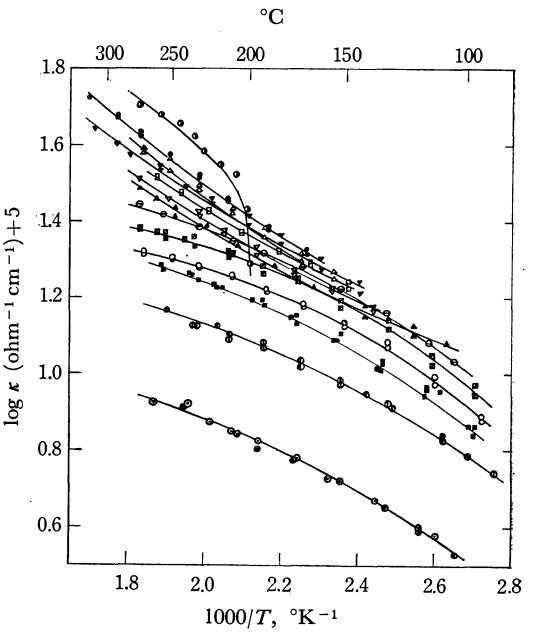

Fig. 3. Log conductivity of $SbBr_3+SbI_3$ solutions against reciprocal temperature at various mol% SbI_3 compositions (⊙: 0, ◑: 5, ■: 10, ○: 20, ◪: 30, ⊖: 40, ▲: 50, ▽: 60, □: 70, ▼: 80, △: 90, ●: 95, ◑: 100 mole% SbI_3).

Table 1. Density equations for I_2+SbI_3 and $SbBr_3+SbI_3$ mixtures

(A) I_2+SbI_3

Mole fraction SbI_3	$d_t=a-bt$ (g/cc) a	$b\times10^3$	Standard error g/cc	Exptl. temp. range, °C
0.000	4.203	2.797	0.042	118—184
0.200	4.190	2.490	0.063	99—226
0.400	4.176	2.205	0.053	113—222
0.600	4.376	2.433	0.027	137—192
0.800	4.423	2.160	0.067	97—235
1.000	4.588	2.483	0.073	182—322

(B) $SbBr_3+SbI_3$

Mole fraction SbI_3	$d_t=a-bt$ (g/cc) a	$b\times10^3$	Standard error g/cc	Exptl. temp. range, °C
0.000	3.762	2.510	0.080	100—256
0.200	3.888	2.152	0.074	106—281
0.400	4.078	2.568	0.091	94—280
0.600	4.208	2.377	0.102	93—280
0.800	4.373	2.490	0.079	153—285
1.000	4.588	2.483	0.073	182—322

$SbBr_3+SbI_3$. The experimental values (I_2; 3.727 g/cc at 170°C, $SbBr_3$; 3.260 at 200°C) obtained for pure I_2 and $SbBr_3$ are somewhat smaller than those (I_2; 3.796 at 170, $SbBr_3$; 3.416 at 200) of Billet,[8]

8) F. Billet, *L'Institute*, **23**, 292 (1855).

Table 2. Temperature dependence of specific and molar conductances of liquids I_2, $SbCl_3$, $SbBr_3$ and SbI_3

I_2			$SbCl_3$			$SbBr_3$			SbI_3		
t°C	$10^5\kappa$	$10^4\Lambda$	t°C	$10^5\kappa$	$10^3\Lambda$[a]	t°C	$10^5\kappa$	$10^3\Lambda$	t°C	$10^4\kappa$	$10^2\Lambda$
120	1.23	8.07	76	0.770	0.655	104	3.36	3.47	209	3.40	4.20
128	1.22	8.05	79	2.52	2.15	111	3.81	3.95	218	3.59	4.46
137	1.21	8.04	92	5.07	4.38	118	3.96	4.13	228	3.90	4.87
140	1.19	7.95	118	6.46	5.71	131	4.55	4.79	230	3.95	4.94
153	1.18	7.93	134	7.29	6.53	136	4.62	4.88	233	4.16	5.21
162	1.16	7.87	156	8.34	7.62	153	5.26	5.63	235	4.24	5.32
171	1.14	7.77	177	9.31	8.68	154	5.31	5.69	241	4.44	5.59
178	1.08	7.40	195	10.1	9.57	174	5.94	6.46	244	4.52	5.70
200	1.02	7.10	215	10.7	10.3	193	6.63	7.32	252	4.63	5.87
204	0.96	6.73	231	11.3	11.1	205	6.95	7.74	259	4.84	6.17
						209	7.07	7.90	264	4.90	6.26
						222	7.46	8.41	271	5.03	6.46
						240	8.19	9.37			
						261	8.34	9.71			

a) Density data[18]

Table 3. Exponential equation for conductivity of I_2+SbI_3 and $SbBr_3+SbI_3$ mixture

(A) I_2+SbI_3

Mole fraction SbI_3	$\kappa = \exp\left(\frac{-B}{T-T_0} - CT + E\right)$
0.200	$\kappa = \exp\{-86.4/(T-146)-8.89\}$
0.300	$\kappa = \exp\{-183/(T-152)-8.18\}$
0.400	$\kappa = \exp\{-461/(T-159)-6.90\}$
0.500	$\kappa = \exp\{-216/(T-165)-2.30\times10^{-2}T+9.66\}$
0.600	$\kappa = \exp\{-3839/(T-171)-4.606\times10^{-2}T+26.33\}$
0.700	$\kappa = \exp\{-6448/(T-178)-9.212\times10^{-2}T+56.79\}$
0.800	$\kappa = \exp\{-7370/(T-184)-9.212\times10^{-2}T+60.94\}$
0.900	$\kappa = \exp\{-6377/(T-190)-9.212\times10^{-2}T+57.46\}$
1.000	$\kappa = \exp\{-614.9/(T-197)-5.83\}$

(B) $SbBr_3+SbI_3$

Mole fraction SbI_3	$\kappa = \exp\left(\frac{-B}{T-T_0} - CT + E\right)$
0.000	$\kappa = \exp\{-640/(T-161)-2.07\times10^{-3}T-6.56\}$
0.050	$\kappa = \exp\{-575/(T-163)-1.61\times10^{-3}T-6.40\}$
0.100	$\kappa = \exp\{-633/(T-165)-2.30\times10^{-3}T-5.60\}$
0.200	$\kappa = \exp\{-758/(T-168)-4.61\times10^{-3}T-3.96\}$
0.300	$\kappa = \exp\{-576/(T-172)-2.30\times10^{-3}T-5.53\}$
0.400	$\kappa = \exp\{-500/(T-175)-1.15\times10^{-3}T-6.20\}$
0.500	$\kappa = \exp\{-438/(T-179)-6.93\}$
0.600	$\kappa = \exp\{-461/(T-182)-6.84\}$
0.700	$\kappa = \exp\{-474/(T-186)-6.68\}$
0.800	$\kappa = \exp\{-532/(T-190)-6.40\}$
0.900	$\kappa = \exp\{-532/(T-193)-6.36\}$
0.950	$\kappa = \exp\{-647/(T-195)-5.92\}$
1.000	$\kappa = \exp\{-615/(T-197)-5.83\}$

18) D. I. Juraflef, *Zh. Fiz. Khim.*, 13, (1939).

and Jander and Weis.[8] Table 2 shows the temperature dependence of the molar conductance Λ (or the product $\Lambda=\kappa V$ of the specific conductance κ and molar volume V) as well as κ for the pure melts I_2, $SbCl_3$, $SbBr_3$ and SbI_3. The specific conductance may be represented by the exponential function,

$$\kappa = \exp\left(\frac{-B}{T-T_0} - CT + E\right) \qquad (1)$$

which is almost similar to the equation due to Yaffe and Artsdalen,[9] though another expression which is a quadratic function[10] of temperature has often been employed. Two parameters (C and T_0) and two constants (B and E) in Eq. (1) are given in Table 3.

(A) Conductivities for Pure Melts. In poorly-conducting melts; I_2, $SbCl_3$, $SbBr_3$ and SbI_3, the molecules may be considered as constituting a solvent medium in which slightly dissociated ions (often univalent ions) exist, and with which they are in dynamic equilibrium with respect to the process of ionization. According to Jander *et al.*,[2,3] the fused $SbCl_3$ and $SbBr_3$ are regarded as a "waterlike ionizing solvent" for a considerable number of organic and inorganic compounds, especially for covalent ones. These melts may therefore be expected to obey Walden's rule[11] ($\Lambda\eta$=constant, with η the viscosity) to the extent to which the conditions for Stokes' law[12] holds. An estimate of the degree of dissociation, α, of the electrolytes which obey Walden's rule is possible using Greenwood and Martin's equation,[13]

$$\alpha = \frac{\Lambda\eta}{100}. \qquad (2)$$

From the values (see Table 4) calculated from Eq. (2), it may be seen that these pure melts are slightly dissociated, by about 5×10^{-8} per cent.

Table 4. Degree of dissociation α of some molten salt, such as $SbCl_3$, $SbBr_3$ and I_2

Salt	t°C	$10^3\,\Lambda$ ohm^{-1} cm^2 mol^{-1}	η cp	$10^5\,\alpha$
$SbCl_3$	150	7.06	1.01	7.1
$SbBr_3$	150	5.05	1.20	6.1
I_2	150	0.747	1.80	1.3

$SbCl_3$: viscosity data[19]
$SbBr_3$: viscosity data[19]
I_2 : viscosity data[20]

i) I_2 (see Table 2 and Fig. 1). Published values[1] for the conductivity of pure liquid iodine range from 0.092 to 1.68×10^{-4} ohm^{-1}cm^{-1} at 140°C. As seen in Fig. 1, our conductivity data for pure liquid iodine are in good agreement with the data of Bearcroft and Nachtrieb[1] (their work was presented shortly after our measurements had been completed, and their measurements were limited to the temperature range of 139—146°C). However, there exist large discrepancies between the above data and those reported by Rabinowitsch,[1] and it is of interest that the values for the I_2+10 mol% SbI_3 system in our work are similar to those of the I_2 melt of Rabinowitsch at 121°C (see Fig. 1). It is found to have negative temperature coefficient, or $d\kappa/dT=-3.1\times10^{-8}$ ohm^{-1} cm^{-1} deg^{-1} (-4.3×10^{-8}, Bearcroft and Nachtrieb, and -2.2×10^{-7}, Rabinowitsch). It is uncertain whether the conduction phenomena may be interpreted (Rabinowitsch[1]) in terms of the metallic conduction mechanism only, in view of the negative temperature coefficient obtained for the conductivities. It is desirable to investigate other transport properties, such as the Hall effect. Riggleman and Drickamer[14] proposed that a discontinuity in the slope of the resistance-pressure curve at 235 K bar represented the beginning of metallic conduction for solid iodine. The decrease in interatomic distance due to high pressure may bring about the transition from ionic conduction to metallic conduction. On the other hand, another point of view is that electron hopping occurs, as well as ionic conduction. Liquid iodine may consist of a neutral species nI_2 with I^-_{2n-1} and I^+ ions, through the reaction (Bearcroft and Nachtrieb[1])

$$nI_2 \rightleftarrows I^+ + I^-_{2n-1} \qquad (3)$$

just as in aqueous solution. As shown in Table 4, the degree of dissociation α of liquid I_2 is small, about one fifth of that of the antimony halide melts. It is well known that the ionization constant in aqueous solutions of some weak electrolytes often has a maximum at a particular temperature; that is to say, the heat content change on the ionization of weak electrolytes is often negative at high temperatures.[15] Then, it is of interest to examine whether or not an analogous result is obtained in liquid iodine containing partially auto-dissociated ions. The temperature dependence of the number density n_j, given by $n_j \propto \exp(-\Delta H_j/2RT)$, can be calculated from Eq. (3) for the chemical reaction (particularly for $n=1$), and from Greenwood and Martin's Eq. (2). Figure 4 shows that the calculated heat content change on ionization ΔH_j is negative and nearly independent of temperature in this temperature range (about -5.7 kcal·mol^{-1}). For such a slightly dissociated molecular melt, the temperature dependence of the

9) I. S. Yaffe and E. R. Artsdalen, *J. Phys. Chem.*, **60**, 1125 (1956).
10) See, *e.g.*, L. A. King and F. R. Duke, *J. Electrochem. Soc.*, **111**, 712 (1964).
11) P. Walden, *Z. Physik. Chem.*, **A157**, 389 (1931).
12) A. Einstein, *Ann. Physik*, **4**, 549 (1905).
13) N. N. Greenwood and R. L. Martin, *J. Chem. Soc.*, **1953**, 1427.
19) A. J. Batschinski, *Z. Physik. Chem.*, **84**, 643 (1913).
20) "Inter. Critic. Tables," Vol. VII, McGraw-Hill Comp., New York (1933), p. 212.
14) B. M. Riggleman and H. G. Drickamer, *J. Chem. Phys.*, **37**, 446 (1962).
15) R. A. Robinson and R. H. Stokes, "Electrolyte Solutions," Butterworths Pub., London (1959), p. 336.

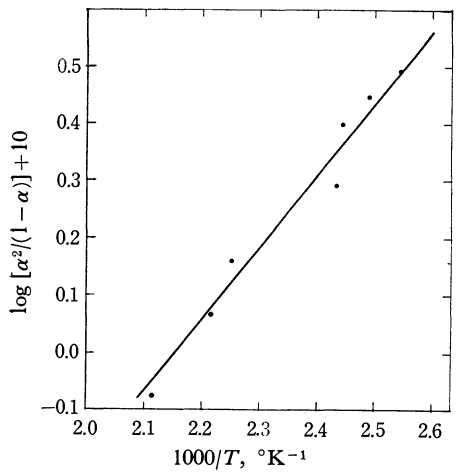

Fig. 4. Log $\alpha^2/(1-\alpha)$ as a function of reciprocal temperature for pure I_2 melt.

carrier concentration may be appreciable compared with that of the mobility due to ionic migration as well as electron hopping. For example, the negative temperature dependence for conductivities of HgI_2 have been interpreted in terms of such an ionic conduction mechanism.[16] Bearcroft and Nachtrieb[1] have recently proposed that I^- is transferred from I^-_{2n-1} ions to neighbouring I_2 molecules, and the mobility of I^- is large compared with that of I^+. It is to be noted that the surface self-diffusion coefficient D^* of species I^- for both mono- and multilayers of I_2 adsorbed on metals in the temperature range 145—235°C has an order of magnitude of 10^{-6} cm^2 sec^{-1} according to Arnikar and Mehta.[17] This charge transfer may also be interpreted in terms of the electron hopping mechanism proposed here.

ii) *$SbCl_3$* (see Table 2). According to previous papers,[2] the conductivity of pure $SbCl_3$ melt has been found to vary from 0.85×10^{-6} to 1.69×10^{-4} ohm^{-1} cm^{-1} immediately above the melting point, though it was not investigated as a function of temperature. Our experimental results (see Table 2), obtained as a function of temperature, lie in the midpoint of the above data. Jander and Swart[2] has proposed that electric conduction results from the self-dissociation reaction

$$SbCl_3 \rightleftarrows x SbCl_2^+ + x Cl^- \cdot (1-x)SbCl_3, \quad (4)$$

where $xCl^-\cdot(1-x)SbCl_3$ refers to xCl^- ion solvated by $(1-x)SbCl_3$ molecules. The observed conductivity κ is put equal to the sum of each conductivity. According to our formula for ionic conductivity,[5] the mobility μ_i of the ionic species i is

$$\mu_i \simeq (d_i^2 \nu_i Z_i e/kT)\exp[-B_i/(T-T_{0i}) - \Delta h_i/kT] \quad (5)$$

In view of the size and mass of each species contributing to the conductivity, the mobility of $SbCl_2^+$ may be much larger compared with that of $xCl^-(1-x)\cdot SbCl_3$. It seems that the conduudctivity κ may be nearly equal to $\kappa_{SbCl_2^+}$.

iii) *$SbBr_3$* (see Table 2). The specific conductance of molten $SbBr_3$ obtained in our investigation is smaller by about one tenth, compared with the data

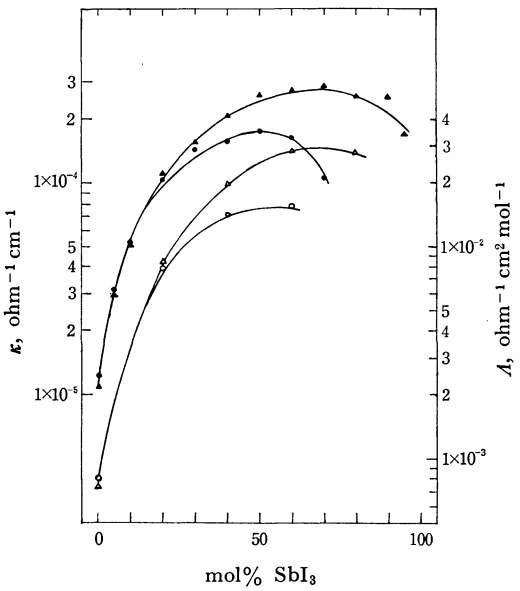

Fig. 5. Specific (● and ▲) and molar (○ and △) conductances of I_2+SbI_3 solutions (▲ and △ at 445°K, ● and ○ at 400).

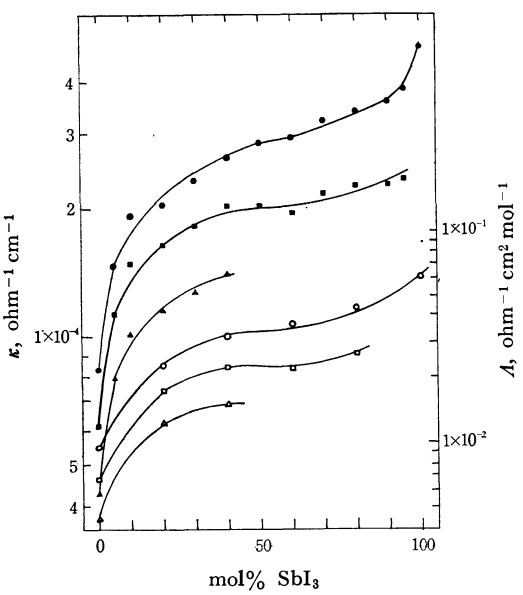

Fig. 6. Specific (●, ■ and ▲) and molar (○, □ and △) conductances of $SbBr_3+SbI_3$ solutions (● and ○ at 525°K, ■ and □ at 455, ▲ and △ at 400).

16) G. J. Janz and J. D. E. Mclutyre, *J. Electrochem. Soc.*, **109**, 842 (1962).
17) H. J. Arnikar and O. P. Mehta, *J. Phys. Chem. Solids*, **24**, 1633 (1963).

due to Hevesy,[3] in the range from 100 to 200°C. The values of κ due to Izbekow and Plotnikow,[3] and due to Jander and Weis[3] were respectively 2.25×10^{-5}, and 1.0×10^{-5} ohm^{-1}cm^{-1} at 100°C, though the temperature dependence of the conductivity was not observed by them. According to Jander and Weis,[3] slight dissociation should be considered, as for pure $SbCl_3$. Then, the species which contributes to the electric conduction may be chiefly $SbBr_2^+$, that is, $\kappa\simeq\kappa_{SbBr_2^+}$.

iv) *SbI_3* (see Table 2). The conductivities of molten SbI_3 are, within experimental accuracy, in agreement with those due to Hevesy.[4] The degree of self-dissociation in pure SbI_3 may be larger, by about ten times, relative to that for pure $SbCl_3$ or $SbBr_3$ in view of the difference between the conductivities of SbI_3, and those of $SbCl_3$ or $SbBr_3$.

(B) Conductivities for Mixtures of Molten Salts.

i) *I_2+SbI_3*. The composition variations in the specific and molar conductances Λ for I_2+SbI_3 are given in Fig. 5. It is of interest that the conductivities increase steeply within the region from 0 to 40 mol% SbI_3 as SbI_3 is added. This may be due to the dissociation of the dissolved SbI_3, as for aqueous electrolytes. With further increase in SbI_3 content, the value of κ has a weak maximum, and then falls monotonically.

ii) *$SbBr_3+SbI_3$*. The composition dependence of κ and Λ for $SbBr_3+SbI_3$ is shown in Fig. 6. The values of κ increase steeply over the range from 0 to 10 mol% SbI_3, because of the dissociation of SbI_3, as for the I_2+SbI_3 solution. With further increase in SbI_3 content, the value of κ increases monotonically.

For poorly-conducting melts, such as I_2+SbI_3, $SbBr_3+SbI_3$ and $SbCl_3$, which are only slightly dissociated, the degree of ionization is an important factor in analyzing the temperature dependence of the conductivities. Then the pre-exponential factor A_i, involved in Eq. (A11) in the previous paper due to Ichikawa and Shimoji,[5] should be regarded as the temperature dependent function since the value of A_i is proportional to the number density n_i of the ionic species i contributing to the conductivity.

BULLETIN OF THE CHEMICAL SOCIETY OF JAPAN VOL. 41 1109—1112 (1968)

A New Determination Method of Relative Rate Constants for Reactions with OH-radicals in Radiolysis of Aqueous Solutions*[1]

Makio MORITA and Masao FUJIMAKI

Department of Agricultural Chemistry, Faculty of Agriculture, The University of Tokyo, Hongo, Tokyo

(Received December 4, 1967)

Radioactivity of water increased linearly with dose when aqueous solution of ^{3}H-formate (2 μC_i/ml and 2×10^{-3} M) was irradiated with γ-rays in the presence of oxygen. The increase of the radioactivity was found to be reciprocally proportional to the non-labeled formate concentration where the amount of ^{3}H-formate was kept invariable. Addition of ferrocyanide and 2-propanol, effective OH-radicals scavengers, depressed the radioactivity increase to near zero. These facts show that the abstraction of tritium from ^{3}H-formate by OH-radicals causes the increase of the radioactivity of water. A competition method to measure relative rate constants for reactions with OH-radicals was deviced on the present results. Some values obtained by this method were in agreement with published data.

In measuring the relative rate constants for reactions with H atoms, Scholes and Simic[1] have established a competition method in the radiolysis of neutral aqueous systems using deuterioformate as a competitor. Formate undergoes the following reactions (1) and (2) by the attacks of H atoms and OH-radicals, respectively.

Hydrogen deuteride is evolved by the reaction (1) in this method and can be distinguished from the other source evolution of hydrogen.

$$HCO_2^- + H \xrightarrow{K_1} H_2 + CO_2^- \quad (1)$$

$$HCO_2^- + OH \xrightarrow{K_2} H_2O + CO_2^- \quad (2)$$

If tritiated formate ($^3HCO_2^-$) is used, H and OH attacks to formate will be indicated by formation of H^3H and H^3HO, respectively. Attempts were made to measure the rate constants for reactions with H and OH by using $^3HCO_2^-$ as a competitor, based

*1 This report was presented at the third Annual Meeting of Jap. Res. Assoc. Food Irradiation, Dec. 6th, 1967, as a part of "Radiation Chemistry of Foods, Part I."

1) G. Scholes and M. Simic, *J. Phys. Chem.*, **68**, 1738 (1964).

on detections of ^3H in H_2 and H_2O in the radiolysis of neutral aqueous solutions. The rate constants for reactions with OH could be readily measured in the presence of oxygen as a reducing species scavenger while those for reactions with H could not be obtained so readily as the former, because of much lower evolution of H^3H or much lower increase of radioactivity in the evolved hydrogen.

Experimental

The water used was triply distilled in a continuous Pyrex system (first from alkaline permanganate, second from acidic dichromate, and finally without any additive). Sodium ^3H-formate was supplied by the Radiochemical Centre (Amersham, England). Sodium formate, potassium ferrocyanide, sodium nitrite, potassium iodide, methanol, ethanol, 2-propanol, acetone, naphthalene, and dioxane (G. R. grade) were supplied by Kanto Chem. Co., Inc. (Tokyo) and were used as received. PPO (2,5-diphenyloxazole) and POPOP (1,4-bis-2-(5-phenyloxazolyl)-benzene) were Packard scintilater grade.

The stock solution of $^3HCO_2^-$ was 100 μCi/m*l* and 10^{-2} M, and was purified immediately prior to use as follows; to 2—5 m*l* of the stock solution was added 10—20 m*l* of water and the solution was lyophilyzed to dryness. This evaporation was repeated until the sublimed water showed desirably low radioactivity and the final residue of sodium formate was dissolved in water to make up the solution of the original concentration.

Solutions to be irradiated (2.5 m*l*, 20 μCi/m*l*, and 2×10^{-3} M formate) were made up of 0.5 m*l* of the stock solution and 2.0 m*l* water containing solutes tested. Irradiation of the solution was done in 5 m*l* Pyrex tubes (1.5 cm in outer diameter) fitted to standard taper joint covered with plastic film. Irradiation was carried out on ^{60}Co γ-ray source, the dose rate (2.4×10^{16} eV ml^{-1} min^{-1}) being determined by the Fricke dosimeter, taking $G(Fe^{III})=15.6$ and $\varepsilon_{(Fe^{III})}=2130$ at 305 mμ (22°C).

Prior to measuring radioactivity, water was sublimed under high vacuum from the irradiated solutions and condensed in dry ice-ethanol traps, and was passed through a small column (5—6 mm in diameter and 30—40 mm in length) packed with mixed ion exchangers (Amberlite IR 120-H and Dowex 2-OH, 1 : 1, completely dried at 100°C and stored in desiccator) at the top half and with charcoal (dried at 100°C) at the bottom half. A portion (0.1 m*l*) of the eluate from the column was mixed with 10 m*l* scintillator solution (7 g PPO, 0.3 g POPOP, and 100 g naphthalene in 1 *l* dioxane, 95 parts and water, 5 parts) and the radioactivity was determined on a liquid scintillation counter (Baird-Atomic, Inc., Liquid Scintillation Detector Model 845) at 0°C.

Results and Discussion

When the stock solution of $^3HCO^-_2$ was not purified, the count of the blank sample or the sample not irradiated was extremely high (47404 cpm/0.1 m*l*) as shown in Table 1, and if this sample were irradiated the count increase would not be, therefore, detectable. Three or four times repeated purifications described in the experimental section were required to lower the blank count to desirable level (1145 cpm/0.1 m*l*, after the four repeatings). However, after the purification, rapid increase of the blank count was observed with the lapse of time of the storage or the procedures.

Table 1. Effects of the purification and the pretreatment on blank count in the measurement of radioactivity (cpm/0.1 m*l*)

Repeating of sublimation	Sublimed water	Eluate from ion exchangers	Eluate from ion exchangers and charcoal
1	244358	128044	47404
4	63333	—	1037

This radiochemical impurities may occur from the decomposition of formate by β-radiation of tritium. The series of the procedures including the purification, γ-irradiation, and the measurement of the radioactivity was carried out within the short period of two or three days and the blank sample not irradiated was taken with irradiated one. It was necessary for the measurement of radioactivity to decrease the radioactivity not occurring from the irradiation to low level. For the sake, each of the three components of the pretreatment, sublimation of water, passage through ion exchangers, and passage through charcoal, was indispensable, since the former separated non-volatile materials to prevent the saturation of the latter two adsorbents, and the latter two decreased considerably the blank counts as shown in Table 1.

When the samples containing no additional solute were irradiated under the aerated condition with different doses, 1, 2/3, and $1/3\times7.2\times10^{17}$ eV ml^{-1}, a plot of count *vs.* dose made a straight line as shown in Fig. 1 and G (count-increase) was independent of dose. The linearity and the independent G (count-increase) suggested that the reaction concerning to the increase of count on irradiation was simple.

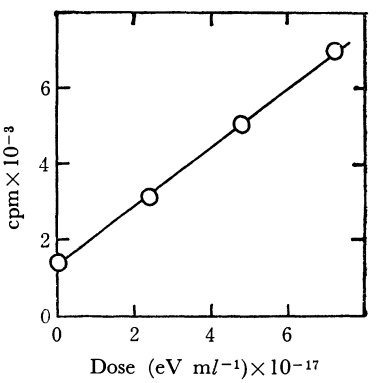

Fig. 1. Plot of count *vs.* dose.

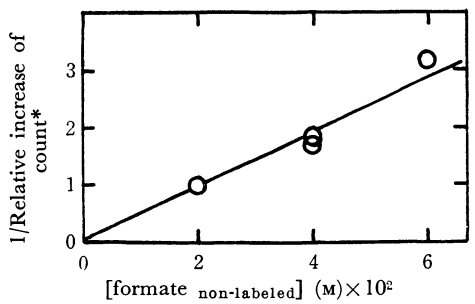

Fig. 2. Reciprocal proportion of count increase to the concentration of non-labeled formate.
* Count increase of the sample without additional non-labeled formate=1.00

Count decreased in reciprocal ratio with increase of the concentration of non-labeled formate, when the dose and the amount of $^3HCO_2^-$ were kept invariable, as shown in Fig. 2, in which 1/count-increase *vs.* [formate$_{non\text{-}labeled}$] was plotted. This reciprocal correlation implies that there is a simple competition between the reaction in which an active species removes tritium from $^3HCO_2^-$ to water and that in which the species is scavenged with non-labeled formate. When both $^3HCO_2^-$ and HCO_2^- are kept constant, the count increase may be, therefore, proportionate to the amount of the active species scavenged by non-labeled formate.

The count increase is probably caused by OH-radicals attack to $^3HCO_2^-$ as in the following reaction.

$$OH + {}^3HCO_2^- \rightarrow H^3HO + CO_2^- \qquad (2')$$

Count increase was effectively depressed to near zero by addition of ferrocyamide or 2-propanol of higher concentration (10^{-1} M) as shown in Table 2. They are known as effective scavengers for OH,[2-4] especially the former is a specific scavenger for OH. This depression of the count increase to near zero with ferrocyanide or 2-propanol may exclude the possibility that secondary species given by the reactions of reducing species, H and e^-_{aq}, with oxygen, HO_2, and O_2^-, contributed to the increase of count, because if these secondary species did so, ferrocyanide or 2-propanol should not reduce the count increase to near zero.

Table 2. Radioactivity in water from the irradiated solutions containing $^3HCO_2^-$

Exp. No.	Dose*	Solute added	(M)	Count	Count Increase (cpm/0.1 m*l*)
1	0	—		1465	—
1	1	—		6975	5510
1	1	$Fe(CN)_6^{4-}$	10^{-1}	1431	−34
2	0	—		1850	—
2	1	*i*-PrOH	10^{-1}	1817	−33

* 7.2×10^{17} eV ml^{-1}

Direct attack of e^-_{aq} to $^3HCO^-_2$ seems impossible under the aerated condition, since formate is known to be a poor scavenger for e^-_{aq}, while oxygen is much more effective one. It is calculated from the published datum[5] that the attack of H atoms to formate is decreased by oxygen under this experimental condition to about one tenth.

When 2-propanol was added to the solution in different concentrations, a plot of $\Delta count_0/\Delta count$ *vs.* [2-propanol]/[formate] is linear as shown in Fig. 3, where count increase is designated as Δ count, and Δ count$_0$ is that without 2-propanol added.
Assumption that the reaction (2) simply competes the reaction (3),

$$OH + (CH_3)_2CHOH \xrightarrow{K_3} (CH_3)_2\dot{C}OH + H_2O \qquad (3)$$

should lead to the following equation (i),

$$\frac{1}{G(\text{-formate})_{OH}} = \frac{1}{G(OH)}\left(1 + \frac{K_3}{K_2}\frac{[\text{2-propanol}]}{[\text{formate}]}\right) \qquad (i)$$

where $G(\text{-formate})_{OH}$ is $G(\text{-formate})$ by the attack of OH.

Moreover, assuming that the count increase is proportionate to the amount of degradation of non-labeled formate with OH, Eq. (i) should be modified as

$$\frac{1}{\Delta count} = \frac{1}{\Delta count_0}\left(1 + \frac{K_3[\text{2-propanol}]}{K_2[\text{formate}]}\right) \qquad (ii)$$

Table 3. Relative rate constants of some substances with OH-radicals

	this work	published data[4]
formate	1.00	1.00
2-propanol	4.5×10^{-1}	5.3×10^{-1}
ethanol[a]	5.3×10^{-1}	4.6×10^{-1}
methanol[b]	3.0×10^{-1}	2.7×10^{-1}
iodide[c]	3.8	3.6
nitrite[d]	3.0	1-5.2

a) ethanol=5×10^{-3} M and relative increase of count=0.430
b) methanol=8×10^{-3} M and relative increase of count=0.456
c) KI=8×10^{-4} M and relative increase of count=0.394
d) $NaNO_2=10^{-3}$ M and relative increase of count =0.397

2) J. K. Thomas, *Trans. Faraday Soc.*, **61**, 702 (1965).
3) J. Rabani and G. Stein, *ibid.*, **58**, 2150 (1962).
4) I. Kraljic and C. N. Trumbore, *J. Am. Chem. Soc.*, **87**, 2547 (1965).
5) J. Rabani, *J. Phys. Chem.*, **66**, 361 (1962).

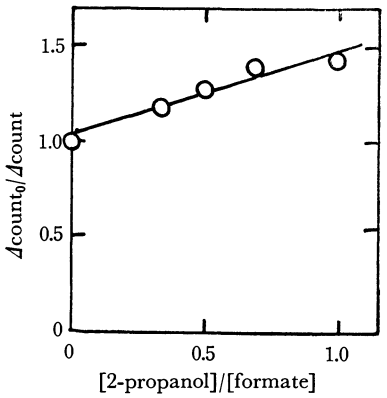

Fig. 3. Test of simple competition for OH radicals between formate and 2-propanol.

The slope of the straight line in Fig. 3 or the relative rate constant, $K=K_{(2\text{-propanol}+OH)}/K_{(\text{formate}+OH)}=0.45$, is in agreement with a published value, 0.53.[4]

The relative constants of ethanol, methanol, iodide, and nitrite were also calculated from data at each one concentration point and the listed in Table 3. They agree with published data, except the rate constant of nitrite, which has been reported as widely varied values, for the reactivity of nitrite to OH-radicals may markedly depend on pH.

In addition to the abstraction reaction (2′), an addition reaction of OH-radicals to $^3HCO_2^-$ may occur as in the reaction (4).

$$OH + {}^3HCO_2^- \rightarrow {}^3H(HO)\,C\langle^{O^-}_{O} \qquad (4)$$

When the other solute capable to scavenge OH is added to the system, the reaction (4) as well as (2′) will be depressed by simple competition for OH. Formation of H^3HO from the radical ion given by the reaction (4) will be, however, complicatedly influenced from the active species produced by the reactions concerning to the added solute. If the reaction (4) were not negligible in comparison with (2′), the total yield of H^3HO would not, therefore, obey simple competition rule in the presence of other solute. Results in Fig. 3 and Table 3 suggest that the reaction (4) may not, at least, be important, similarly as addition reaction in non-labeled formate may not be.[6-8]

The accuracy of this method is limited mainly by the error in the liquid scintillation counter measurement. The error seems to occur from the variation of counting efficiency by the incomplete stabilization of temperature. Consequently, the accuracy will be much more improved if the measurement is carried out on a counter set at more stabilized temperature.

We are indebted to Mr. Shinkichi Katsura for the operation of irradiation.

6) E. J. Hart, *J. Am. Chem. Soc.*, **73**, 68 (1951).
7) E. J. Hart, *ibid.*, **76**, 4198 (1954).
8) E. J. Hart, *ibid.*, **76**,, 4312 (1954).

BULLETIN OF THE CHEMICAL SOCIETY OF JAPAN VOL. 41 1113—1119 (1968)

The Crystal and Molecular Structure of an Isomer of Bis-(1,2-diethoxycarbonyl-ethyl)tin Dibromide

Mamoru YOSHIDA,*1 Tatzuo UEKI, Noritake YASUOKA, Nobutami KASAI,*2 Masao KAKUDO, Iwao OMAE, Shoichi KIKKAWA and Sumio MATSUDA

Department of Applied Chemistry, Faculty of Engineering, Osaka University, Yamada-Kami, Suita, Osaka

(Received December 4, 1967)

Low mp isomer of bis-(1,2-diethoxycarbonyl-ethyl)tin dibromide (mp 114—115°C) crystallizes in a monoclinic form: $a=11.85$, $b=20.24$, $c=9.79$ Å, $\beta=101.3°$; space group, $P2_1/a$; and four molecules are contained in a unit cell. Crystal structure was established by the heavy atom method. The coordination about the tin atom is nearly octahedral. Two bromine atoms attached to the tin atom are in *cis*-positions. Two ligands, 1,2-diethoxycarbonyl-ethyl groups, are both bound to the tin atom by carbon and oxygen, forming five-membered rings. These rings are rather puckered, and one is in *d*-form and another in *l*-form.

Present authors (S. M., S. K., and I. O.) obtained bis-(1,2-diethoxycarbonyl-ethyl)tin dibromide by the direct reaction between tin foil and diethyl bromosuccinate. From the reaction products they had two isomers isolated; their mp's being 114—115°C and 122—123°C respectively.[1)]

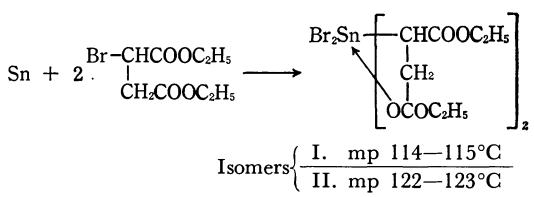

Isomers { I. mp 114—115°C / II. mp 122—123°C }

This paper describes the three-dimensional structure analysis of the isomer crystal I.

Experimental

The crystals were obtained by recrystallization from ethanol as colorless needles developed along the c axis. For the determination of the lattice parameters, oscillation and Weissenberg photographs were taken around the a, b, and c axes. Debye lines of aluminum were superposed on the Weissenberg photographs for calibration.

Layers 0 through 5 around the c axis were recorded by multi-film equi-inclination Weissenberg photographs with nickel-filtered Cu$K\alpha$ radiation. $0kl$ and $1kl$ reflections were also collected mainly for the use of the inter-layer scaling.

Intensities were estimated visually by using a calibrated standard scale. Lorentz and polarization corrections were carried out, but no absorption correction was made. 2109 non-zero reflections were finally obtained.

Crystal Data

Compound: Low mp isomer of Bis-(1,2-diethoxycarbonyl-ethyl)tin dibromide, $Br_2SnC_{16}H_{22}O_8$
mp=114—115°C,
MW=620.9

Unit Cell: (Cu$K\alpha$ radiation, $\lambda=1.5418$ Å)
$a=11.85$ Å, $Z=4$
$b=20.24$ Å, $U=2302.5$ Å^3
$c=9.79$ Å, $D_m=1.80$ g·cm^{-3}
$\beta=101.3°$, $D_x=1.79$ g·cm^{-3}

Space Group: $P2_1/a$
(uniquely determined from the systematic absences of reflections)

Determination and Refinement of the Structure

Crystal structure was established by the heavy atom method. From a three-dimensional Patterson function approximate parameters of tin and two bromine atoms were obtained. Positions of all the light atoms except hydrogen were then found in the three-dimensional Fourier maps, with phases based on the heavy atoms. Successive block-diagonal least-squares refinement was carried out on a HITAC 5020E computer at the University of Tokyo. After three cycles of refinement for heavy atoms, Sn and Br's, the discrepancy factor $R=\sum||F_o|-|F_c||/\sum|F_o|$ was reduced to 0.154. In this refinement unit weight for all the reflections was assigned. Refinement was then made for all of the non-hydrogen atoms and the following weighting scheme was applied in the least-squares refinements hereafter: 1.0 for $|F_o|>0.1$ and 0.1 for $|F_o|\leqq 0.1$.

*1 Present address: High Polymer Technical Service Laboratory, Showa Denko Co., Ohta, Tokyo.

*2 To whom the correspondence should be addressed.

1) S. Matsuda, S. Kikkawa and I. Omae, *Kogyo Kagaku Zasshi* (*J. Chem. Soc. Japan, Ind. Chem. Sect.*), **69**, 646 (1966).

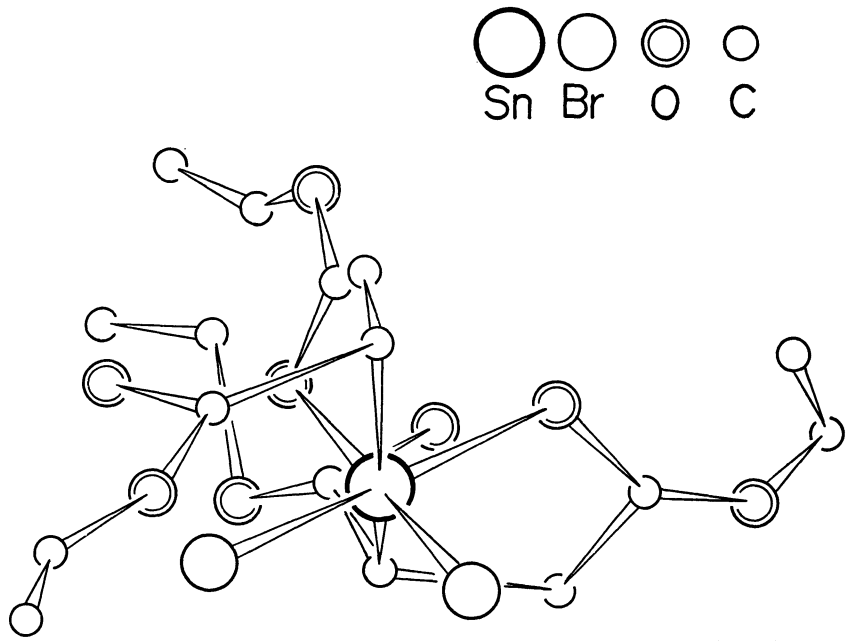

Fig. 1. Molecular structure of bis-(1,2-diethoxycarbonyl-ethyl)tin dibromide.

Table 1. Atomic positional and thermal parameters from the final least-squares refinement

Atom	x	y	z	β_{11}	β_{22}	β_{33}	β_{12}	β_{13}	β_{23}
Sn	0.1671	0.1295	0.4832	42	11	55	0	29	2
Br(1)	−0.0264	0.1516	0.5434	58	20	144	1	82	−13
Br(2)	0.2862	0.1143	0.7326	79	24	96	−4	−6	6
O(1)	0.332	0.096	0.381	2.8					
O(2)	0.415	0.007	0.314	4.3					
O(3)	0.125	−0.003	0.193	5.5					
O(4)	−0.032	0.027	0.283	3.3					
C(1)	0.339	0.041	0.381	3.8					
C(2)	0.274	−0.007	0.453	4.0					
C(3)	0.147	0.021	0.430	2.4					
C(4)	0.487	0.049	0.244	4.4					
C(5)	0.415	0.065	0.101	5.4					
C(6)	0.077	0.014	0.300	4.0					
C(7)	−0.108	0.024	0.128	5.5					
C(8)	−0.208	0.066	0.164	5.6					
O(10)	0.100	0.153	0.237	4.9					
O(20)	0.138	0.214	0.063	5.9					
O(30)	0.077	0.304	0.391	5.3					
O(40)	0.168	0.291	0.616	3.4					
C(10)	0.158	0.196	0.191	4.8					
C(20)	0.244	0.234	0.279	4.7					
C(30)	0.235	0.229	0.437	2.5					
C(40)	0.056	0.169	−0.043	5.0					
C(50)	−0.049	0.212	−0.048	7.8					
C(60)	0.150	0.279	0.489	3.0					
C(70)	0.077	0.331	0.668	4.6					
C(80)	0.129	0.352	0.810	5.1					

The values of anisotropic thermal parameters for heavy atoms are $\times 10^4$, and those for the light atoms are isotropic B in Å^2. The estimated standard deviation $\sigma(r)$ for Sn is 0.0025 Å and for Br about 0.004 Å.

TABLE 2. THE OBSERVED AND CALCULATED STRUCTURE FACTORS

K	FO	FC	K	FO	FC	K	FO	FC	K	FO	FC	K	FO	FC	K	FO	FC	K	FO	FC	K	FO	FC
H,L= 0 0			10	66	61	1*	0	16	13	75	76	1	133	-133	7	82	80	5	66	-61	5	163	180	13*	0	20
4	218	-212	11	98	-65	2	66	73	14*	0	-19	2	149	-149	8*	0	16	6	59	50	6	34	31	14*	0	33
6	190	180	12	46	-41	3*	0	-29	15	74	80	3	138	141	9*	0	-27	7	131	137	7	158	-164	15	71	-85
8	298	294	13	55	57	4*	0	-17	16	86	93	4	44	-42	10*	0	-18	8	88	-91	8	93	-91	16	58	48
10	35	-23	14	49	-39	5	50	-44	17	68	-81	5*	0	24	11	79	-82	9*	0	3	9	147	-143	H,L=	7	2
12	132	-129	15	41	48	6	50	-45	18*	0	6	6	130	-129	12*	0	-17	10	42	-26	10*	0	3	1	60	45
14	68	72	16	59	63	7	28	34	19	68	-62	7	99	-107	13	56	52	11	106	-103	11	73	73	2	79	-73
16	28	34	17	29	-29	8	57	58	20	67	-62	8	174	196	14	56	45	12	82	89	12	97	96	3	71	-66
H,L= 1 0			18*	0	12	9*	0	26	21	37	44	9	31	-41	15	55	58	13*	0	29	13	118	124	4*	0	-18
2	281	-298	19*	0	-36	10	38	35	H,L=	3	1	10*	0	8	H,L=	9	1	14*	0	31	14*	0	-23	5*	0	-6
3	142	-144	20	26	-36	H,L=	0	1	1	130	-130	11	69	65	1	38	39	15*	0	32	15	68	-59	6	75	68
4	42	-46	H,L=	6	0	0	213	-403	2	44	43	12	88	-87	2	76	-80	16	88	-74	16	70	-60	7	76	63
5	47	34	0	138	143	1	25	15	3	35	18	13*	0	32	3*	0	-5	17*	0	-9	17	58	-56	8*	0	0
6	229	227	1	134	129	2	36	33	4	30	17	14*	0	3	4*	0	11	18*	0	-15	18*	0	20	9	56	-49
7	222	206	2	29	-24	3	30	36	5	56	-54	15	39	-38	5*	0	-36	19*	0	-17	19	70	79	10	70	-70
8	47	44	3	87	86	4	215	222	6	48	-42	16	69	65	6	60	50	20	56	60	20*	0	8	11	71	-60
9	33	-24	4	192	-192	5	195	-180	7*	0	7	H,L=	6	1	7	79	79	H,L=	-1	2	21*	0	39	12*	0	-6
10	208	-186	5	81	-80	6	129	-115	8*	0	-21	0	214	-230	8*	0	-13	1	41	43	22*	0	-13	13*	0	37
11	99	-95	6*	0	18	7	129	-126	9	28	32	1	50	-35	9*	0	27	2	22	-21	23	30	-48	14*	0	47
12	23	-26	7	23	-27	8	231	-208	10	60	60	2	29	26	10*	0	-15	3	197	-227	H,L=	4	2	15*	0	47
13	60	61	8	81	81	9*	0	-8	11	78	-79	3	73	-76	11	39	-39	4	34	31	0	49	-28	16*	0	-3
14	99	101	9	91	92	10	91	77	12*	0	30	4	218	248	12*	0	12	5	75	-78	1	161	164	17*	0	-37
15	27	28	10	93	-95	11*	0	22	13	79	-77	5	62	66	13*	0	-22	6	42	-28	2	43	-38	18	49	-49
16*	0	23	11*	0	12	12	99	89	14	36	-42	6*	0	-5	14*	0	-15	7	104	107	3	73	67	H,L=	-7	2
17	50	-45	12	105	-100	13*	0	-6	15	85	81	7*	0	-3	15	50	58	8	35	36	4	65	68	1*	0	-28
18	66	-80	13*	0	-15	14	78	-69	16*	0	0	8	148	-152	H,L=	-9	1	9*	0	-17	5	102	-99	2*	0	18
19*	0	-24	14	41	44	15	51	-39	17*	0	33	9	49	-41	1	74	76	10	71	57	6	186	186	3	45	45
20*	0	16	15*	0	12	16	44	-28	18*	0	19	10	36	42	2*	0	12	11	69	-65	7	105	-103	4	46	37
21*	0	-1	16*	0	23	17	37	-34	19	104	-125	11*	0	9	3	74	-74	12	46	-44	8	116	-108	5	47	37
22	26	39	17*	0	-26	18	46	39	20*	0	17	12	101	106	4	65	-47	13*	0	1	9	87	78	6	49	-54
H,L=	2	0	18	49	-44	19*	0	20	21*	0	-9	H,L=	-6	1	5	76	-76	14	82	-79	10	34	-38	7*	0	17
0	72	-73	19*	0	0	20*	0	26	22*	0	-3	0	128	-134	6*	0	1	15*	0	32	11	62	61	8*	0	-7
1	177	-180	20	25	-27	21*	0	24	23	51	71	1	38	46	7	78	87	16*	0	48	12	119	122	9*	0	-31
2*	0	2	H,L=	7	0	22	33	-24	H,L=	-3	1	2	27	-19	8	55	55	17*	0	3	13	86	-79	10	94	88
3	84	81	1	105	111	H,L=	1	1	1	166	154	3*	0	-5	9	56	50	18	83	87	14	56	49	11*	0	-25
4	84	83	2	40	-38	1	87	-97	2	249	250	4	70	67	10	56	-10	19*	0	11	15*	0	-30	12*	0	25
5	155	138	3	84	-84	2	112	115	3	95	-78	5	66	-66	11	39	-67	20	48	-52	16	83	-88	13*	0	18
6	186	183	4	94	-49	3	90	86	4	117	-119	6	61	-62	12	39	-48	21*	0	0	17*	0	33	14	83	-87
7*	0	8	5	95	-52	4	97	91	5	166	-170	7	58	42	13*	0	-33	22	50	-65	18*	0	-5	15*	0	25
8	159	-143	6	80	79	5	32	-37	6	77	-63	8	56	-49	14*	0	19	23	46	-3	19*	0	34	16*	0	29
9	68	-61	7	93	98	6	192	-149	7	172	168	9	58	53	15	52	59	H,L=	2	2	20	74	78	17*	0	-8
10	113	-115	8	26	25	7	195	-184	8*	0	-2	10	78	78	H,L=	10	1	0	98	70	H,L=	-4	2	18	75	83
11	55	-47	9	94	66	8*	0	22	9	124	116	11	63	-58	0*	0	12	1	138	-136	0	86	-96	H,L=	8	2
12	125	123	10	68	-60	9	89	86	10	29	25	12	65	52	1	69	-65	2	65	-65	1	207	-236	0*	0	-27
13	109	107	11*	0	-21	10	95	81	11	62	-60	13*	0	8	2*	0	8	3	116	-123	2*	0	10	1*	0	-9
14	45	46	12	41	-34	11	111	105	12	57	-57	14	68	-68	3*	0	-30	4	171	-182	3	210	-223	2*	0	0
15*	0	5	13	29	-38	12	31	-40	13	92	-97	15	69	59	4*	0	1	5	100	91	4	41	34	3*	0	-12
16	90	-98	14	84	90	13	121	-119	14*	0	-24	16*	0	-25	5	69	85	6*	0	0	5	226	240	4*	0	3
17	72	-78	15	41	36	14	70	-74	15	100	100	17*	0	-14	6*	0	9	7	117	116	6	113	99	5*	0	7
18*	0	-20	16*	0	-5	15	52	-52	16*	0	-11	18	66	54	7*	0	-8	8*	0	15	7	111	117	6*	0	36
19*	0	-17	17*	0	23	16*	0	18	17	79	88	H,L=	7	1	8*	0	13	9	136	-134	8*	0	-9	7*	0	0
20	57	63	18	93	-64	17	55	59	18*	0	-12	1	64	-60	9	55	-60	10	61	-51	9	173	-172	8*	0	1
21	48	62	19*	0	-10	18	39	54	19	68	-73	2	106	107	H,L=	10	1	11	73	-62	10	56	-47	9	41	-41
22*	0	-17	20*	0	31	19*	0	30	H,L=	4	1	3	81	91	0	78	91	12*	0	20	11	48	-48	10*	0	-16
23*	0	4	21*	0	-15	20	38	-45	0	45	53	4	67	71	1	103	111	13	81	81	12	114	102	11	41	-27
24*	0	-28	22	29	42	H,L=	-1	1	1	68	-66	5	59	48	2*	0	-2	14*	0	-20	13	92	88	12	41	40
25*	0	-49	H,L=	8	0	1	65	-79	2	69	55	6	119	-122	3	68	66	15*	0	30	H,L=	5	2	13*	0	45
26	10	15	0	91	-48	2	199	-192	3*	0	-6	7	79	-80	4	68	-55	16*	0	-26	1	110	105	14*	0	8
H,L=	3	0	1	44	-46	3	130	136	4	81	-71	8	36	-44	5	88	-105	17	41	-54	2	165	180	15*	0	8
1	27	4	2*	0	-1	4	55	-62	5	85	81	9*	0	4	6*	0	-2	18*	0	25	3	140	-148	16*	0	-26
2	137	132	3	98	-63	5	274	282	6	75	-61	10	85	92	7*	0	-41	19*	0	-25	4	29	-35	17	48	-56
3	44	-34	4	65	67	6	199	178	7*	0	1	11	38	38	8*	0	59	20	52	29	5	61	-64	H,L=	8	2
4	82	-65	5	26	25	7	206	-187	8	99	93	12	39	35	9	68	77	H,L=	-2	2	6	136	-143	0	35	-36
5	33	22	6*	0	7	8	41	-41	9	118	-125	13*	0	14	10*	0	-3	0	33	42	7	116	127	1*	0	-14
6	79	-73	7	105	105	9*	0	12	10	64	70	14	79	-89	11*	0	23	1	68	76	8*	0	21	2*	0	7
7	37	-37	8	28	-29	10	174	-169	11	33	37	15*	0	-38	12*	0	-25	2	97	-100	9*	0	19	3*	0	-7
8	34	-24	9*	0	-19	11	96	96	12	99	-105	16*	0	-22	13	52	-54	3	83	75	10	135	144	4	72	76
9	55	-50	10*	0	-18	12*	0	-19	13	82	85	17*	0	7	H,L=	11	1	4	49	-49	11	85	-59	5*	0	25
10	62	64	11	102	-106	13*	0	39	14	38	-56	18	61	64	1*	0	10	5*	0	13	12*	0	-13	6	65	-58
11	66	68	12	51	43	14	78	74	15*	0	-23	H,L=	-7	1	2	55	-62	6	22	-23	13*	0	20	7*	0	-11
12*	0	7	13	91	59	15*	0	-21	16	79	88	1	69	-70	3*	0	14	7	106	-109	14	82	-74	8	78	-64
13	63	57	14*	0	4	16*	0	-15	17*	0	-54	2*	0	24	4*	0	26	8	45	-47	H,L=	-5	2	9*	0	28
14*	0	-5	15	64	69	17*	0	-13	18*	0	4	3*	0	29	5*	0	1	9*	0	29	1	144	154	10	70	57
15	114	-118	16	48	-38	18	69	-88	19*	0	-1	4*	0	-12	6	54	61	10	51	44	2	190	-210	11*	0	26
16	41	-30	17	45	-57	19*	0	9	20	63	-67	5*	0	8	7*	0	-20	11	178	179	3	131	-131	12*	0	19
17	51	-51	18*	0	9	20*	0	32	21	48	49	6*	0	13	8	37	-49	12	67	58	4*	0	17	13*	0	-16
18*	0	-11	19	39	-47	21*	0	20	H,L=	-4	1	7	97	-102	H,L=	-11	1	13	71	-65	5	143	-146	14*	0	-36
19	93	104	20*	0	22	22	35	51	0	92	-92	8*	0	23	1*	0	-46	14*	0	-27	6	166	172	15	40	-20
20*	0	7	21	29	41	H,L=	2	1	1	186	199	9*	0	-5	2	80	102	15	77	-80	7	85	79	H,L=	9	2
21*	0	9	H,L=	9	0	0	44	4	2*	0	-12	10	37	-45	3*	0	19	16	80	-67	8	89	-84	1*	0	-18
22*	0	3	1	88	-78	1	98	81	3	150	147	11*	0	17	4*	0	-3	17	82	73	9	73	74	2*	0	4
23	45	-70	2	48	69	2	72	61	4*	0	20	12*	0	-1	5	68	37	18	71	53	10	77	-66	3*	0	9
H,L=	4	0	3	69	73	3	59	-48	5	229	-229	13*	0	-6	6*	0	-77	19	71	60	11	95	-78	4*	0	-15
0	36	-33	4	28	-13	4	74	66	6	35	-35	14	80	83	7*	0	-14	20	69	64	12	75	73	5*	0	4
1	109	102	5	76	81	5	46	-43	7	80	-73	15*	0	-23	8*	0	36	21	53	-52	13	86	-80	6*	0	0
2	23	-19	6	97	-55	6	112	-100	8	39	-40	16	39	-44	9	38	-52	22	35	-40	H,L=	6	2	7*	0	-47
3*	0	-8	7	77	-89	7*	0	-16	9	160	161	17*	0	-13	H,L=	0	2	H,L=	3	2	0	200	224	8*	0	9
4	49	-48	8	41	46	8	25	12	10*	0	7	18	63	-63	0	92	97	1	80	-75	1*	0	-26	9*	0	-14
5	75	-70	9	99	-59	9	66	66	11	32	40	H,L=	8	1	1	29	-30	2	75	-77	2	32	-37	10*	0	-30
6	38	-27	10*	0	12	10	50	35	12*	0	-36	0	78	89	2	126	-153	3	74	62	3*	0	0	11*	0	31
7	28	16	11	91	55	11*	0	-19	13	88	-84	1*	0	0	3	25	0	4*	0	2	4	164	-169	12*	0	-28
8	21	-10	12*	0	-20	12	64	-56	14*	0	24	2*	0	13	4	119	-129	5	126	130	5*	0	-8	13*	0	5
9	138	135	13	90	55	13	102	-102	15*	0	4	3*	0	35	5	43	42	6	102	104	6	48	54	14*	0	19
10	46	-48	14*	0	20	14	35	-15	16*	0	28	4	72	-71	6	74	79	7*	0	-13	7	35	32	15	49	-55
11*	0	-3	15	94	-55	15	37	12	17	56	52	5*	0	-27	7*	0	-23	8*	0	22	8	122	134	H,L=	9	2
12	44	44	16*	0	11	16	54	49	H,L=	5	1	6*	0	-31	8	61	56	9	144	-149	9	37	23	1	54	-46
13	107	-111	17	33	-35	17	79	89	1*	0	-10	7	66	-56	9*	0	18	10	79	-75	10	54	-49	2*	0	-36
14*	0	-30	18*	0	-19	18*	0	-10	2	239	-235	8	67	64	10	115	-121	11	90	85	11	56	-54	3	67	76
15	49	51	19	27	41	19*	0	5	3	93	85	9*	0	33	11	62	48	12*	0	-31	12	70	-62	4	55	53
16	51	-45	H,L=	10	0	20	54	-55	4*	0	-24	10*	0	37	12	66	-58	13	112	117	13*	0	-6	5*	0	28
17	59	69	0*	0	-36	21	63	-72	5*	0	-18	11	69	62	13*	0	20	14	55	43	14	41	52	6*	0	19
18	29	32	1	83	105	H,L=	-2	1	6	192	191	12	69	-68	14	104	118	15	90	-85	H,L=	-6	2	7	69	-82
19*	0	-9	2*	0	23	0	119	118	7	111	-102	13	56	-53	15*	0	-20	16*	0	18	0	124	141	8	57	-52
20	48	37	3	66	72	1	123	-117	8	54	-52	14*	0	-28	16*	0	13	17	71	-60	1*	0	-18	9*	0	6
21	45	-43	4*	0	2	2	37	-30	9	56	43	15*	0	-34	17*	0	27	18*	0	-31	2*	0	0	10*	0	11
H,L=	5	0	5	93	-106	3	182	-165	10	116	-109	16*	0	31	18	71	-63	19	80	88	3	133	141	11	71	66
1*	0	7	6*	0	-12	4	25	-34	11	61	65	17	49	64	19*	0	4	20*	0	-19	4	121	-114	12	58	62
2	178	168	7*	0	-22	5	30	36	12*	0	-9	H,L=	-8	1	20*	0	-23	21*	0	29	5*	0	21	H,L=	10	2
3	83	-84	8*	0	-17	6	71	-63	13	65	-64	0*	0	4	21*	0	-33	22*	0	13	6	63	45	0	58	-49
4	39	-40	9	99	78	7	102	96	14	78	76	1*	0	-17	22	35	43	23	29	-52	7	86	-83	1*	0	33
5	20	21	10*	0	14	8	136	131	15*	0	-23	2*	0	-5	H,L=	1	2	H,L=	-3	2	8	127	133	2*	0	-8
6	103	-95	11*	0	22	9	107	-94	16*	0	-18	3*	0	-18	1	157	194	1	102	-112	9*	0	8	3*	0	3
7	72	62	12*	0	23	10	98	92	17*	0	12	4*	0	-12	2	65	-64	2*	0	-11	10*	0	-38	4*	0	37
8	105	98	13	46	-49	11	168	-182	18	38	-53	5*	0	8	3	147	-171	3	67	58	11	84	80	5	71	-73
9	75	-73	H,L=	11	0	12	111	-109	H,L=	-5	1	6	36	35	4	45	47	4	113	108	12	78	-74	H,L=	-10	2

TABLE 2. (Continued)

K	FO	FC	K	FO	FC	K	FO	FC	K	FO	FC	K	FO	FC	K	FO	FC	K	FO	FC
0	90	-112	6*	0	-23	14*	0	60	8	49	25	2*	0	-9	7*	0	-9	H,L=	1	5	2*	0	-24	8*	0	33
1	81	-75	7	122	-134	15*	0	-7	9*	0	4	3*	0	-4	8	89	84	1	48	-48	3	110	118	9*	0	39
2*	0	14	8*	0	18	16	49	-52	10*	0	28	4	121	126	9*	0	-12	2	145	140	4	30	33	10*	0	27
3	40	-50	9	163	171	H,L=	-9	3	11	70	-69	5	24	23	10*	0	10	3	60	61	5	169	-165	11	49	-64
4	57	71	10	78	55	1	66	-59	H,L=	10	3	6	26	-31	11*	0	22	4	57	-57	6	99	49	H,L=	10	5
5	71	89	11	92	94	2	177	205	0*	0	36	7	29	-22	12	79	-81	5	30	-20	7	51	-35	0*	0	0
6*	0	-13	12*	0	-23	3	109	109	1	49	-48	8	157	-152	13*	0	-19	6	93	-95	8	38	-31	1*	0	-17
7*	0	11	13	78	-76	4*	0	-26	2	49	3	9*	0	5	14*	0	10	7	70	-65	9	129	123	2*	0	2
8*	0	-45	14*	0	-20	5	89	76	3	49	-41	10*	0	-24	15*	0	-18	8	53	43	10	60	-58	3*	0	-25
9	58	-79	15*	0	-48	6	192	-196	4	49	-53	11*	0	10	16	93	90	9*	0	13	11*	0	5	4*	0	-4
10	71	16	16	49	51	7*	0	-11	H,L=	-10	3	12	81	80	17	64	62	10	59	42	12*	0	43	H,L=	-10	5
11*	0	20	H,L=	-2	3	8	54	55	0	49	52	H,L=	3	4	H,L=	7	4	11	88	93	13	83	-82	0	49	37
12*	0	20	0	26	31	9	40	-33	1	49	59	1	57	-55	1	98	108	12	46	-56	H,L=	5	5	1	70	73
13	38	51	1	95	59	10	103	103	2*	0	-19	2	41	-36	2*	0	-17	13*	0	-19	1*	0	-4	2	49	-35
H,L=	11	2	2	31	-19	11	76	69	3	49	46	3*	0	25	3	100	-99	14*	0	-34	2	95	-89	3	70	74
1*	0	-4	3	40	40	12*	0	-14	4*	0	-22	4	62	59	4*	0	11	15	70	-56	3*	0	4	4	50	-42
2	80	96	4	45	39	13	47	38	5	49	-71	5	46	40	5	78	-78	16*	0	28	4*	0	4	H,L=	0	6
3*	0	-2	5	25	-18	H,L=	6	3	6*	0	31	6*	0	-2	6*	0	22	17*	0	24	5	44	-41	0*	0	14
4*	0	-19	6	47	45	0	121	-120	7*	0	-12	7*	0	-9	7	93	94	18*	0	8	6	102	108	1*	0	-11
5*	0	4	7	67	56	1*	0	-17	8*	0	8	8	105	-109	H,L=	-7	4	19	48	58	7*	0	-6	2*	0	-2
6	77	-84	8	56	47	2*	0	30	9	70	74	9	87	-84	1*	0	2	H,L=	-1	5	8*	0	4	3	25	-20
H,L=	11	2	9*	0	3	3*	0	-11	H,L=	11	3	10*	0	6	2	74	62	1	40	-37	9*	0	41	4	32	-39
1*	0	22	10*	0	-9	4	73	70	1*	0	-26	11	42	48	3*	0	15	2	98	-107	10	99	-92	5	53	37
2	83	-104	11	68	-44	5*	0	38	2	81	-87	12	44	49	4*	0	11	3	41	47	11*	0	14	6	38	43
3*	0	15	12	83	-70	6	88	-98	3*	0	33	13	45	53	5	68	-64	4	41	-38	12*	0	-6	7*	0	-5
4*	0	11	13	76	62	7*	0	-8	4*	0	17	14*	0	-10	6	90	-98	5	60	60	13	90	-58	8	53	43
5*	0	-12	14	65	46	8	79	-58	5*	0	11	15	66	-75	7*	0	-8	6	118	126	14	49	68	9	41	36
6	82	86	15*	0	33	9*	0	-31	6	61	74	16	66	-60	8*	0	-29	7*	0	-6	H,L=	-5	5	10*	0	-31
H,L=	12	2	16	69	68	10	96	88	H,L=	0	4	H,L=	-3	4	9	76	67	8	61	59	1	70	-60	11	37	37
0	63	64	17	70	-78	11*	0	30	0	223	242	1	40	-36	10	90	88	9*	0	-27	2	56	49	12*	0	-23
1*	0	38	H,L=	3	3	12*	0	26	1	29	34	2	148	-174	11*	0	8	10	143	-143	3*	0	15	13	31	-35
2*	0	1	1	160	187	13*	0	7	2	17	-18	3	78	77	12*	0	20	11*	0	-1	4	77	-70	14	31	45
3*	0	22	2	49	39	14	70	-70	3	39	37	4*	0	5	13	47	-46	12*	0	-33	5	35	47	15*	0	-10
4	61	-68	3	72	-63	H,L=	-6	3	4	200	-220	5	59	62	14	105	-108	13	66	58	6	37	-34	16	44	44
H,L=	12	2	4	61	-60	0	165	-170	5*	0	-6	6	102	109	15*	0	4	14	97	118	7	68	-68	17	42	57
0*	0	52	5	104	-105	1*	0	47	6	54	47	7	69	-71	16*	0	14	15*	0	17	8	92	92	18*	0	-31
1*	0	-16	6*	0	14	2*	0	15	7	72	-78	8	73	-71	17*	0	36	16*	0	-12	9	43	-46	19	32	26
2*	0	10	7	86	85	3*	0	-24	8	187	200	9*	0	28	18	58	73	17*	0	0	10*	0	-2	20	29	-31
3*	0	11	8*	0	30	4	155	150	9*	0	-26	10	74	-72	H,L=	8	4	18	85	-92	11*	0	41	21	48	-48
4*	0	-52	9	146	160	5	53	-42	10	62	-51	11	88	93	0	80	50	19*	0	-10	12	83	-91	H,L=	1	6
5*	0	18	10*	0	23	6*	0	-5	11	77	72	12	41	50	1	93	-81	20*	0	16	13	49	47	1	32	33
6*	0	-24	11	61	-36	7	69	64	12	99	-98	13*	0	8	2*	0	0	21*	0	10	H,L=	6	5	2*	0	-5
7*	0	-13	12*	0	-32	8	141	-142	13*	0	-23	14*	0	12	3	81	-74	22	40	50	0	113	-100	3	38	-40
8	52	61	13	114	-124	9*	0	-6	14*	0	16	15	80	-72	4*	0	-16	H,L=	2	5	1*	0	-38	4	72	68
H,L=	0	3	14*	0	-8	10*	0	-29	15	79	-79	16*	0	-24	5	81	75	0	126	-109	2*	0	37	5	39	-39
0	150	-166	15	70	72	11	80	-79	16	66	62	17*	0	20	6*	0	20	1	77	77	3*	0	-43	6	40	39
1	32	-42	16*	0	38	12	95	95	17*	0	26	18*	0	-7	7	82	81	2*	0	-12	4	149	142	7	72	66
2*	0	20	17	50	74	13*	0	-12	18*	0	2	19	45	62	H,L=	-8	4	3*	0	-1	5*	0	16	8	62	-61
3	106	-109	H,L=	-3	3	14*	0	0	19	39	33	H,L=	4	4	0	134	-130	4*	0	-2	6*	0	-8	9*	0	11
4	145	174	1	78	71	15*	0	40	20	43	-44	0	98	93	1*	0	12	5	96	-101	7*	0	40	10*	0	17
5	24	-16	2	38	38	16	86	-90	21	40	-40	1*	0	25	2*	0	-10	6	35	-35	8	86	-87	11	59	-62
6	85	-78	3*	0	-16	H,L=	7	3	H,L=	1	4	2*	0	27	3	58	53	7*	0	-20	9*	0	-24	12	75	74
7	145	149	4	195	-112	1	89	-86	1	159	174	3*	0	13	4	138	131	8*	0	-4	10*	0	33	13*	0	-9
8	119	-120	5	72	-63	2*	0	-16	2	183	-225	4*	0	4	5*	0	-12	9	93	99	11	71	-62	14*	0	7
9*	0	19	6*	0	7	3	78	71	3	151	-166	H,L=	-4	4	6*	0	-51	10*	0	17	12	70	59	15	59	66
10	121	114	7	31	24	4*	0	-6	4	65	55	0*	0	-7	7	77	-85	11*	0	-39	H,L=	-6	5	16	44	-50
11	129	-127	8	121	121	5*	0	14	5	46	-43	1	123	-116	8	110	-106	12*	0	-9	0*	0	20	17*	0	24
12	82	64	9	36	37	6*	0	-11	6	146	155	2*	0	16	9*	0	17	13	84	-81	1*	0	15	18*	0	12
13*	0	14	10	38	37	7	95	-94	7	149	150	3	74	-70	10	46	39	H,L=	-2	5	2*	0	12	19	49	-53
14	91	-91	11	90	-87	8*	0	24	8	33	-34	4	48	-44	11	66	74	0	137	216	3*	0	-15	H,L=	-1	6
15	95	88	12	85	-83	9*	0	-4	9	35	38	5	123	132	12	47	54	1	25	22	4*	0	13	1	35	33
16	46	-49	13	63	-49	10*	0	32	10	112	-112	6	31	-41	H,L=	9	4	2	41	-42	H,L=	7	5	2*	0	7
17*	0	-22	14*	0	17	11	50	53	11	68	-70	7	31	-32	1	47	-45	3	92	-104	1	85	-75	3*	0	-9
18	41	44	15	48	81	H,L=	-7	3	12*	0	18	8*	0	-4	2*	0	-5	4	151	-180	2	85	68	4*	0	27
19	40	-45	16	70	79	1	54	44	13*	0	-11	9	139	-132	3	66	49	5*	0	-15	3	85	84	5	46	-49
20	38	31	17*	0	3	2	117	-112	14	63	54	10*	0	28	4*	0	-5	6*	0	-5	4*	0	-10	6	33	-34
21	36	28	18*	0	-11	3*	0	-37	15	65	47	11*	0	33	5	66	74	7	99	99	5	86	69	7	34	-40
H,L=	1	3	19	69	-80	4*	0	-25	16*	0	-6	12*	0	-23	H,L=	-9	4	8	151	142	6	86	-74	8	28	8
1	195	-257	H,L=	4	3	5*	0	8	17*	0	-4	13	77	70	1	152	-149	9*	0	-12	7	87	-79	9	29	31
2	144	178	0*	0	-40	6	84	74	18	33	-22	14*	0	-31	2	99	-99	10*	0	-8	8*	0	-9	10	68	69
3	162	187	1	97	-103	7*	0	13	19	39	-32	15*	0	-36	3	89	91	11	86	-81	9*	0	-15	11*	0	15
4	104	-106	2*	0	10	8*	0	45	H,L=	-1	4	16*	0	0	4*	0	29	12	101	-106	10	49	52	12	31	24
5	116	126	3	88	-91	9*	0	-2	1*	0	-1	17	66	-61	5	64	39	13*	0	21	11	49	55	13	50	-51
6	114	-118	4*	0	-3	10	141	-138	2	137	154	H,L=	5	4	6	103	60	14*	0	15	H,L=	-7	5	14	75	-80
7	139	-142	5	120	129	11*	0	-4	3	48	-49	1*	0	-17	H,L=	10	4	15	70	76	1*	0	-11	15*	0	-8
8	80	79	6*	0	-5	12*	0	-44	4*	0	2	2*	0	24	0*	0	-18	H,L=	3	5	2*	0	-22	16	44	35
9	114	-113	7	94	109	13*	0	16	5	58	47	3*	0	-30	1	45	47	1*	0	-1	3*	0	-24	17*	0	9
10	37	43	8	56	51	14	100	114	6	147	-146	4*	0	-27	2*	0	4	2	119	118	4*	0	10	18	58	67
11	79	81	9	41	-46	15*	0	-22	7*	0	-12	5*	0	20	3	49	59	3*	0	-11	5*	0	25	19	45	41
12	42	-53	10*	0	-18	16*	0	-10	8	62	-57	H,L=	-5	4	4*	0	20	4*	0	-24	6*	0	39	20	35	-45
13	44	45	11	64	-62	17*	0	-19	9	67	-62	1*	0	18	5	44	-45	5*	0	-11	7*	0	39	H,L=	0	7
14	54	-45	12	46	-50	18	78	-86	10	136	140	2	127	-123	H,L=	-10	4	6	78	-70	8*	0	-4	0	28	-21
15	51	-45	13*	0	40	H,L=	8	3	11*	0	-9	3*	0	5	0*	0	-19	H,L=	-3	5	9*	0	-38	1	40	-25
16	47	43	14*	0	17	0	95	-101	12	40	26	4	44	41	1	80	-78	1	82	85	10	69	-51	2	45	34
H,L=	-1	3	15*	0	58	1	47	45	13	42	40	5*	0	8	2*	0	16	2	195	212	H,L=	8	5	3	46	-37
1*	0	9	16	90	66	2*	0	-18	14	138	-140	6	114	114	3	81	-78	3	144	-153	0*	0	11	4	41	47
2	51	52	H,L=	-4	3	3	68	60	15*	0	11	7	35	44	4*	0	0	4	27	-26	1	50	47	5*	0	18
3	26	36	0	142	154	H,L=	-8	3	16*	0	1	8	91	-94	5	81	73	5	116	-117	2	50	24	6*	0	-11
4*	0	5	1	175	211	0	120	129	17*	0	-30	9*	0	28	6*	0	-38	6	148	-147	3	50	55	7	84	90
5	81	-74	2*	0	7	1*	0	-6	18	94	104	10	57	-52	7*	0	38	7	91	88	4*	0	-14	8*	0	-11
6	53	54	3	129	123	2*	0	5	19*	0	-2	11*	0	-40	8*	0	-3	8	52	50	5	50	-58	9*	0	-23
7	96	-97	4	70	-71	3*	0	-2	20*	0	-12	12	62	59	9	47	-75	9	55	47	H,L=	-8	5	10*	0	19
8	31	33	5	146	-149	4	146	-137	21*	0	5	13*	0	-14	H,L=	0	5	10	83	84	0	89	102	11	83	-87
9	102	98	6*	0	-22	5*	0	-23	22	49	-57	14*	0	15	0	137	-144	11	98	-95	1	44	-52	12	45	41
10	96	-94	7*	0	13	6*	0	17	H,L=	2	4	15	66	65	1*	0	25	H,L=	4	5	2*	0	-4	13	45	46
11*	0	0	8	72	79	7*	0	16	0*	0	14	H,L=	6	4	2*	0	-22	0	66	67	3	45	-48	14	38	-34
12*	0	11	9	146	153	8	95	103	1	134	-139	0	91	84	3	61	59	1*	0	25	4	79	-82	15	53	51
13	75	-73	10	96	96	9*	0	-17	2	25	25	1	57	53	4	109	122	2*	0	6	5*	0	10	16	29	-33
14	112	125	11*	0	-4	10	49	-48	3	158	-156	2	41	-41	5	56	-47	3*	0	2	6	67	70	17	39	-45
15*	0	-33	12	76	-73	11	49	-53	4	78	69	3	71	71	6*	0	-13	4	80	-72	7	68	65	18*	0	22
16*	0	-35	13	80	-73	12	90	-67	5	114	112	4	84	-90	7*	0	-3	5*	0	-42	8	69	73	19	41	-35
17*	0	32	H,L=	5	3	H,L=	9	3	6	104	104	5*	0	-24	8	137	-140	6	42	-49	H,L=	9	5	H,L=	1	7
18	87	-89	1	73	-67	1*	0	25	7	46	53	6	79	60	9*	0	-14	7*	0	-10	1*	0	28	1	76	-75
19*	0	7	2	73	-63	2*	0	27	8	60	-62	7*	0	-44	10*	0	27	8	78	72	2*	0	-10	2*	0	33
20*	0	47	3	112	112	3*	0	-37	9	136	-147	8*	0	43	11*	0	-17	9*	0	-14	3*	0	-18	3	97	89
21	64	-26	4	66	46	4*	0	24	10	67	-66	9*	0	41	12	78	75	10*	0	15	4*	0	0	4	43	-34
22	65	64	5	87	84	5*	0	-6	11*	0	-9	10	88	-84	13	47	42	11*	0	3	5*	0	-36	5	72	72
23	39	-6	6	70	56	H,L=	-9	3	12	74	69	H,L=	-6	4	14*	0	-13	12	86	-89	H,L=	-9	5	6	31	-34
H,L=	2	3	7	83	-71	1	80	74	13	76	74	0	80	73	15*	0	10	13*	0	23	1	117	112	7	80	-91
0	70	45	8	43	-51	2	93	94	14*	0	40	1	81	-82	16	50	-57	14*	0	-1	2*	0	43	8	59	57
1	203	227	9*	0	-3	3	94	-89	15*	0	-9	2*	0	38	17	40	-44	15*	0	9	3	118	-108	9	82	-81
2	79	70	10	45	-40	4	67	-50	16	47	-48	3*	0	-18	18*	0	5	16	48	65	4*	0	12	10*	0	-1
3	186	221	11	47	55	5*	0	-6	H,L=	-2	4	4	70	-61	19*	0	-10	H,L=	-4	5	5	49	-53	11	40	46
4*	0	19	12	48	59	6	84	-83	0	139	-169	5*	0	58	20	49	50	0	101	-88	6*	0	-13	12	46	-40
5	162	-170	13*	0	-8	7	85	90	1	25	-34	6*	0	-6	21	48	53	1	164	171	7	99	93	13	45	48

TABLE 2. (Continued)

K	FO	FC	K	FO	FC	K	FO	FC	K	FO	FC	K	FO	FC	K	FO	FC	K	FO	FC	K	FO	FC
14•	0	4	14	75	78	12	58	-68	14•	0	9	0	66	-67	6	32	-34	10	95	-65	14	21	8	10	26	36
15	53	-59	15•	0	10	13	-42	-47	15	38	46	1•	0	-14	7•	0	-33	11	38	-28	H,L=	1	10	11	20	27
16•	0	32	16•	0	-34	14•	0	-12	16•	0	2	2•	0	2	8•	0	8	12•	0	-10	1•	0	15	H,L=	0	11
17	47	-46	17•	0	6	15	48	-46	17	32	33	3•	0	-24	9•	0	-7	13•	0	6	2•	0	8	0•	0	13
18•	0	-10	18	45	-49	16	31	36	H,L=	-1	8	4	46	49	10•	0	14	14	47	58	3•	0	-13	1	41	-35
19	23	34	19•	0	-10	17	29	30	1	91	-80	5•	0	25	11	38	37	H,L=	0	10	4•	0	2	2•	0	3
H,L=	-1	7	20	34	44	H,L=	1	8	2	82	83	6•	0	26	12•	0	6	0•	0	7	5•	0	-18	3	41	-39
1	64	70	H,L=	0	8	1	67	60	3	62	62	7•	0	24	13•	0	16	1•	0	19	6•	0	-7	4•	0	-6
2•	0	-27	0	53	57	2	71	-74	4•	0	11	8	45	-42	14•	0	0	2•	0	4	7•	0	27	5	39	36
3•	0	-26	1	93	44	3	59	-58	5	44	38	9•	0	-30	15	53	-41	3•	0	14	8	21	-17	6•	0	-5
4•	0	-23	2•	0	-1	4	39	-20	6	100	-110	10•	0	-25	H,L=	-1	9	4•	0	0	H,L=	-1	10	7	26	30
5•	0	-11	3	94	53	5	75	-75	7	39	-38	11•	0	-10	1•	0	13	5•	0	-20	1•	0	-13	8•	0	0
6•	0	53	4	80	-63	6	60	66	8•	0	-4	12	50	55	2	82	-79	6•	0	-1	2•	0	37	9	23	-33
7	65	63	5	44	-44	7	64	76	9•	0	-29	13	39	41	3	58	-46	7•	0	-11	3•	0	37	H,L=	1	11
8•	0	-8	6	38	-34	8	39	-23	10	45	54	H,L=	1	9	4•	0	-15	8•	0	12	4•	0	4	1	48	-36
9•	0	30	7	82	-74	9	45	43	11•	0	25	1•	0	-15	5•	0	-21	9	26	25	5•	0	-2	2•	0	-16
10•	0	-34	8	48	45	10	39	-26	12•	0	0	2	47	49	6	91	95	10•	0	7	6•	0	-48	3	39	35
11•	0	-22	9•	0	24	11	38	-40	13•	0	21	3•	0	19	7•	0	30	11•	0	6	7•	0	-22	4•	0	-7
12•	0	13	10•	0	6	12•	0	4	14	59	-72	4•	0	1	8•	0	10	12•	0	-20	8•	0	11	5	38	44
13•	0	-12	11	49	55	13	36	-39	H,L=	0	9	5•	0	24	9•	0	-6	13•	0	-35	9•	0	17			

$R=0.116$ was obtained after 2 cycles. Anisotropic temperature factors were introduced at this stage, and three cycles of refinement gave the $R=0.098$.

Atomic and thermal parameters are listed in Table 1. In Table 2 listed are the observed and calculated structure factors.

Description of the Structure and Discussion

The molecular structure of the complex is shown in Fig. 1. The bond lengths and angles in the environment of tin atom are listed in Table 3. As seen in Fig. 1 and also in Table 3, the tin atom is coordinated by two bromine atoms in cis-positions as assumed before,[1] and also by two oxygen and two carbon atoms from 1,2-diethoxycarbonyl-ethyl groups. The coordination about the tin atom is a six-coordinated, distorted octahedron, and this may probably be the first structure of the six-coordinated organotin compounds analysed by means of X-ray diffraction.

Sn-Br distances are 2.52 and 2.59 Å respectively, and these values are close to the sum of the covalent radii of tin and bromine atoms, 2.54 Å. The deviations may be due to distortion of the configuration from the regular octahedron (Table 3) and also to different contacts between bromine atoms and other atoms in the adjacent molecules.

Two equal Sn–C distances, 2.26 Å, seem to be slightly longer than the sum of the covalent radii, 2.17 Å, and also longer than that in SnH_3CH_3,[2] 2.15 Å, in which the tin atom takes an usual tetrahedral configuration.

As regards the Sn–O bonds, the distances 2.44 and 2.46 Å are much longer than the sum of covalent radii, 2.06 Å. These Sn–O distances may be the longest values hitherto reported, and this suggests that the Sn–O are weak coordination bonds.

Two ligands, 1,2-diethoxycarbonyl-ethyl groups, are bound to the tin atom by carbon and oxygen atoms, forming rather puckered five-membered rings. Each pair of corresponding atoms in two rings deviate from the least-squares planes in a similar way (Fig. 2). C(3) and C(30) show the largest deviations from the planes, 0.35 and 0.31 Å respectively. The three planes Br(1)–O(10)–O(1)–Br(2), Br(1)–C(3)–O(10)–C(30), and C(3)–Br(2)–C(30)–O(10), all centered with tin, make dihedral angles,

TABLE 3. BOND LENGTHS AND ANGLES IN THE ENVIRONMENT OF Sn

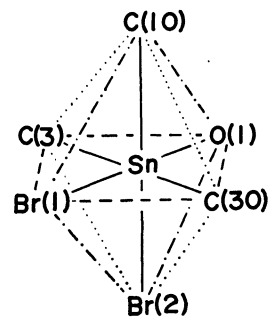

Br(1)-Sn-C(3)	100°	Sn-Br(1)	2.516 Å
O(1)-Sn-C(3)	72	Sn-Br(1)	2.588
O(1)-Sn-O(10)	78	Sn-O(1)	2.46
Br(1)-Sn-O(10)	93	Sn-O(10)	2.44
C(3)-Sn-O(10)	88	Sn-C(3)	2.26
C(30)-Sn-O(10)	72	Sn-C(30)	2.26
Br(1)-Sn-O(1)	168	Br(1)-Br(2)	3.88
C(3)-Sn-C(30)	148	-O(10)	3.61
O(10)-Sn-Br(2)	166	O(1)-Br(2)	3.61
Br(1)-Sn-C(30)	105	-O(10)	3.07
O(1)-Sn-C(30)	80	Br(1)-C(3)	3.65
O(1)-Sn-Br(2)	91	-C(30)	3.80
Br(1)-Sn-Br(2)	99	O(1)-C(3)	2.79
C(3)-Sn-Br(2)	97	-C(30)	3.03
C(30)-Sn-Br(2)	98	C(3)-O(10)	3.27
		-Br(2)	3.63
		C(30)-O(10)	2.75
		-Br(2)	3.67

The standard deviations of bonds in Sn-Br are 0.006 Å, in Sn-C 0.05 Å, in Sn-O 0.03 Å, Br-C 0.05 Å, Br-O 0.03 Å and C-O 0.05 Å. Those for the angles are of the order of 3°.

2) D. R. Lide, *J. Chem. Phys.*, **19**, 1605 (1951).

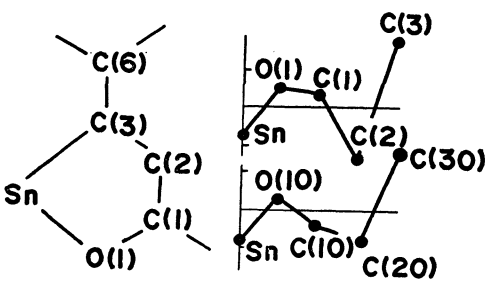

Fig. 2. Deviations of atoms from the least-squares planes in Sn-O(1)-C(1)-C(2)-C(3) and Sn-O(10)-C(10)-C(20)-C(30) rings.

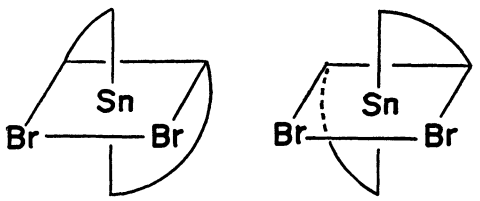

Fig. 3. Two optically active antipodes.

85°, 88°, and 91° each other. Some atoms in these planes show deviations more than 0.2 Å. The coordination configuration is the distorted octahedron as mensioned before. The bond lengths and angles in the ligands are shown in Table 4. The estimated standard deviations for these values are too big to discuss the dimensions of ligand groups in detail.

Table 4. The average bond lengths and angles in two ligand groups of molecule

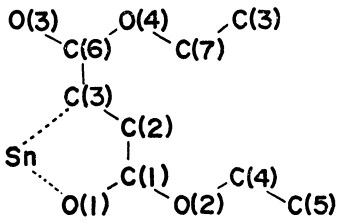

Sn-O(1)	2.45 Å	O(1)-Sn-C(3)	72°
Sn-C(3)	2.26	Sn-O(1)-C(1)	112
C(1)-O(1)	1.18	O(1)-C(1)-O(2)	123
C(1)-O(2)	1.34	O(1)-C(1)-C(2)	125
C(1)-C(2)	1.46	O(2)-C(1)-C(2)	113
C(4)-O(2)	1.52	C(1)-O(2)-C(4)	116
C(4)-C(5)	1.52	O(2)-C(4)-C(5)	103
C(3)-C(2)	1.57	C(1)-C(2)-C(3)	109
C(3)-C(6)	1.48	Sn-C(3)-C(2)	108
C(6)-O(3)	1.29	Sn-C(3)-C(6)	107
C(6)-O(4)	1.27	C(2)-C(3)-C(6)	117
C(7)-O(4)	1.56	C(3)-C(6)-O(3)	116
C(7)-C(8)	1.51	C(3)-C(6)-O(4)	118
		O(3)-C(6)-O(4)	126
		C(6)-O(4)-C(7)	117
		O(4)-C(7)-C(8)	100

The standard deviations for the bonds between light atoms are estimated to be 0.04—0.06 Å, and for angles about 4°.

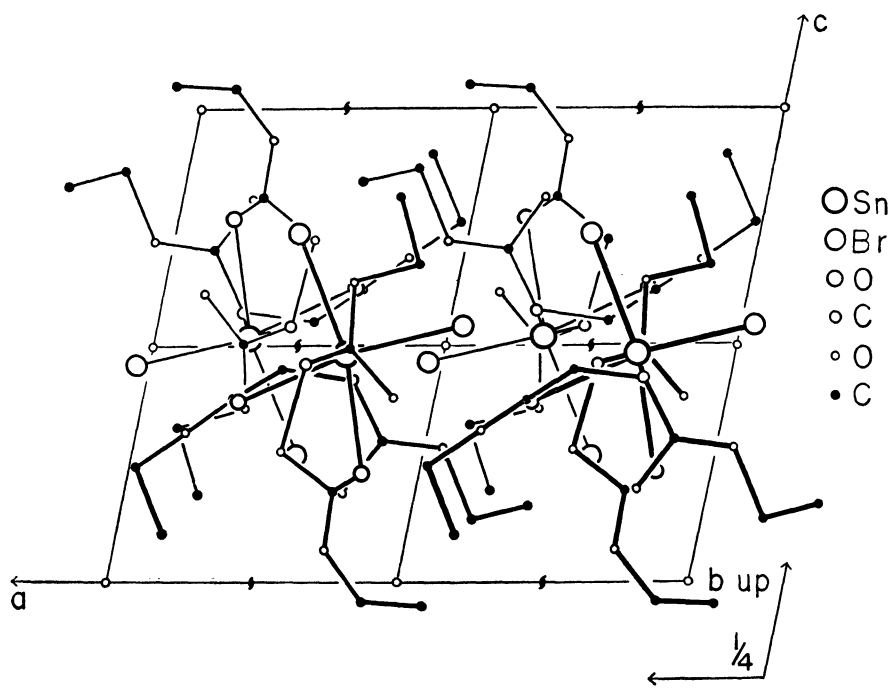

Fig. 4. Crystal structure of bis-(1,2-diethoxycarbonyl-ethyl)tin dibromide.

Both ligands in a molecule contain an asymmetric carbon atom, C(3) and C(30) respectively, of which one is in *d*-form and another in *l*-form, and the optical activity due to the asymmetric carbon atom does not exist. However, the whole molecule is still asymmetric and the molecule must possess the optical activity due to such molecular asymmetry. Since there are glide planes in the unit cell of this crystal (space group: $P2_1/a$) and since a unit cell contains four molecules, there are equal numbers of molecules of two optically active antipodes (Fig. 3) in the crystal. Therefore, the crystal, as a whole, exhibits no optical activity.

TABLE 5. SOME CLOSE INTERMOLECULAR ATOMIC CONTACTS IN THE CRYSTAL
(those less than 4.0 Å are listed)

Br(2)-C(70^{i})	3.79 Å	O(3)-C(7^{ii})	3.15 Å
O(1)-C(70^{i})	3.91	C(4)-C(8^{iii})	3.86
C(4)-O(30^{i})	3.38	Br(1)-C(40^{iv})	3.99
C(30)-Br(1^{i})	3.71	Br(2)-C(5^{iv})	3.77
O(1)-O(30^{i})	3.52	Br(2)-C(40^{iv})	3.99
C(20)-O(30^{i})	3.95	C(80)-C(50^{iv})	3.94
		C(80)-O(20^{iv})	3.72

Code for superscript
i $1/2+x,\ 1/2-y,\ z$
ii $-x,\ -y,\ -z$
iii $1+x,\ y,\ z$
iv $x,\ y,\ 1+z$

The crystal structure is shown in Fig. 4. There are not so many close intermolecular atomic distances. The shortest intermolecular contacts are O(3)-C(7^{ii}), 3.15 Å, and C(4)-O(30^{i}), 3.38 Å, and other contacts less than 4.0 Å are all listed in Table 5.

The three-dimensional structure analysis of another isomer crystal, II (mp 122—123°C), is now being carried out.

The authors are very much indebted to Miss Nobuko Kanehisa who joined them at the final stage of the refinement. Through this study, two computer programs in the UNICS,[3] HBLS IV and DAPH (both written by Professor T. Ashida) were used, for which the authors are very grateful. The present study was supported partly by a Scientific Research Grant from the Ministry of Education.

3) Tosio Sakurai Ed., UNICS, Japan Crystallographic Association (1967).

BULLETIN OF THE CHEMICAL SOCIETY OF JAPAN VOL. 41 1120—1125 (1968)

Hydrogen Formation in the Radiolysis of Liquid Olefins. The Role of Hot Hydrogen Atoms and Superexcited States

Yoshihiko HATANO, Shoji SHIDA and Shin SATO

Laboratory of Physical Chemistry, Tokyo Institute of Technology, Meguro-ku, Tokyo

(Received December 7, 1967)

The γ-radiolysis of liquid olefins was undertaken to obtain reliable evidence for a possible role of hot hydrogen atoms and superexcited states in radiation chemistry. The contribution of thermal hydrogen atoms may reasonably be excluded in this system. The effect of various electron or positive-ion scavengers on hydrogen formation in the radiolyses of liquid propylene and ethylene has been examined. The hydrogen formation is not appreciably affected by these additives, which indicates ionic species may not play an important role in the hydrogen formation. The liquid-phase radiolyses of C_3H_6-C_3D_6 and C_2H_4-C_2D_4 mixtures have also been investigated and compared with those previously reported of C_4H_8-1 - C_4D_8-1 and *trans*-C_4H_8 - 2-*trans*-C_4D_8-2 mixtures. The data indicate that the hydrogen from the olefins except ethylene may be formed for the most part by bimolecular processes. A large part of the hydrogen from liquid ethylene may be interpreted in terms of the molecular detachment of a hydrogen molecule, while from the other olefins it may be interpreted in terms of the hydrogen-atom abstraction reaction of hot hydrogen atoms formed by direct excitation which must at least partially involve superexcitation. To attempt quantitative substantiation of the above viewpoint a simple calculation has been made based on the so-called optical approximation. Calculated yields of the hydrogen formation are apparently in good agreement with observed ones.

The role of a hot hydrogen atom as a reaction intermediate in radiation chemistry has often been indicated complementarily by many authors,[1] who have presented little experimental confirmations of its role. Moreover, there have been some criticizing comments[2] on the hot-hydrogen-atom process. It has so far been difficult to distinguish the hot-hydrogen-atom process from bimolecular physical interactions or from the hydrogen-atom abstraction reaction by thermal hydrogen atoms. In a previous paper[3] on the radiolyses of liquid butene-1 and *trans*-butene-2, however, these difficulties as described above could appreciably be removed and evidence was presented for a possible role of hot hydrogen atoms in the radiation chemistry of hydrocarbons. Namely, the hydrogen formation was interpreted in terms of the hydrogen-atom abstraction reaction of hot hydrogen atoms formed by direct excitation which must, at least partially, involve superexcitation. The purpose of the present investigation is twofold: firstly to report new data on liquid propylene and ethylene and to compare these data with those previously reported[3] on liquid butene-1 and *trans*-butene-2, the result for ethylene being in striking contrast to those for the other olefins, and secondly to attempt quantitative substantiation based on the so-called optical approximation of the previous viewpoint.[3] Preliminary results of such work have already been reported,[4] and so the details are presented here.

Experimental

Materials. Research-grade propylene and ethylene from Takachiho Trading Co. were used after the usual degassing and trap-to-trap distillations. Gas-chromatographic analyses of the propylene and the ethylene showed no impurity except for less than 0.1% propane and 0.1% ethane, respectively.

Propylene-d_6 was synthesized from methylacetylene-d_4 by using a palladium catalyst. The methylacetylene-d_4 was obtained[5] from magnesium tricarbide by passing deuterium oxide vapor (99.8 at.% D) in an evacuated system over the carbide at 200°C which was prepared[6]

1) J. P. Manion and M. Burton, *J. Phys. Chem.*, **56**, 560 (1952); P. J. Dyne and W. M. Jenkinson, *Can. J. Chem.*, **38**, 539 (1960); V. V. Voevodskii and Yu. N. Molin, *Radiation Res.*, **17**, 366 (1962); T. J. Hardwick, *J. Phys. Chem.*, **66**, 1611 (1962); S. Z. Toma and W. H. Hamill, *J. Am. Chem. Soc.*, **86**, 1478, 4761 (1964); M. Cher, C. S. Hollingsworth and B. Browing, *J. Chem. Phys.*, **41**, 2270 (1964); J. Y. Yang and I. Marcus, *ibid.*, **42**, 3315 (1965); **43**, 1585 (1965); W. E. Falconer and R. Salovey, *ibid.*, **44**, 3151 (1966); P. J. Dyne and J. Denhartog, *Can. J. Chem.*, **44**, 461 (1966); L. A. Rajbenbach and U. Kaldor, *J. Chem. Phys.*, **47**, 242 (1967).

2) C. E. Klots, Y. Raef and R. H. Johnsen, *J. Phys. Chem.*, **68**, 2040 (1964); C. E. Klots, *J. Chem. Phys.*, **41**, 117 (1964).

3) Y. Hatano and S. Shida, *J. Chem. Phys.*, **46**, 4784 (1967).

4) Y. Hatano, S. Shida and M. Inokuti, *ibid.*, **48**, 940 (1968).

5) R. C. Lord and P. Venkateswarlu, *J. Chem. Phys.*, **20**, 1237 (1952).

6) W. H. C. Rueggeberg, *J. Am. Chem. Soc.*, **65**, 602 (1943).

by passing *n*-pentane vapor over a few grams of finely divided magnesium metal in a quartz tube heated to 700°C. The methylacetylene-d_4 was then treated with an equal volume of deuterium over 1 g of palladium catalyst[7] at 150°C until the calculated pressure fall had taken place. The catalyst was initially placed in an evacuated system at room temperature and reduced for 8 hr with deuterium at 180°C. The deuterium was replaced several times to remove any adsorbed hydrogen. The propylene-d_6 produced was used after a gas chromatographic purification and trap-to-trap distillations. No chemical impurity was detected by gas chromatography using dimethylsulfolane, benzyl ether, and $AgNO_3$-benzylcyanide columns operated at room temperature. The isotopic purity was determined mass spectrometrically to be 99 at.% D.

Ethylene-d_4 was synthesized from acetylene-d_2 by using a palladium catalyst in a way similar to the case of propylene-d_6. The acetylene-d_2 was obtained from calcium carbide by passing deuterium oxide vapor in an evacuated system over the purified carbide at room temperature. The ethylene-d_4 produced was used after a gas chromatographic purification and trap-to-trap distillations. No chemical impurity was detected by gas chromatography using squalane and $AgNO_3$-benzylcyanide columns operated at room temperature. The isotopic purity was determined mass spectrometrically to be again 99 at.% D.

Nitrous oxide (minimum purity: 99.9%), ammonia (>99.5%), and sulfur hexafluoride (>98.0%) were used without further purification. Carbon tetrachloride and methanol (spectral grade) were used after the usual degassing and distillation.

Irradiation. Measured amounts of propylene, ethylene, or the mixtures were sealed *in vacuo* at −196°C in glass ampules 5 mm in diameter and 50 mm long fitted with break-off-tips. The samples were irradiated in the facilities of Tokyo Institute of Technology (6 kCi ^{60}Co) at a dose rate of 6.9×10^{19} eV/g hr. Unless otherwise specified, samples were irradiated to a total dose of 4.3×10^{20} eV/g at −78°C using dry ice and methanol slushes. The dose rate was determined by Fricke dosimetry using $G(Fe^{3+})=15.6$.

Analysis. After irradiations, the sample tubes were attached to a vacuum line and the seals were broken. The products, noncondensable at −210°C, hydrogen and methane, were collected and measured by an analysis device composed of a Toepler pump, a gas burette, a a McLeod gauge, and a copper oxide furnace kept at 250°C. In this furnace, hydrogen was oxidized into water which was then trapped at −196°C.

In the case of isotopic experiments, the relative amounts of H_2, HD, and D_2 were determined with a Hitachi RMU-5 mass spectrometer.

Results

Figure 1 shows the variation of hydrogen formation as a function of the energy absorbed in the radiolyses of liquid propylene and ethylene at −78°C. The hydrogen formation is directly proportional to the energy absorbed; that is, the *G* value, the number of molecules formed per 100 eV of the energy absorbed in the system, is independent of the total energy absorbed. The *G* values of hydrogen formation in the radiolyses of pure liquid propylene and

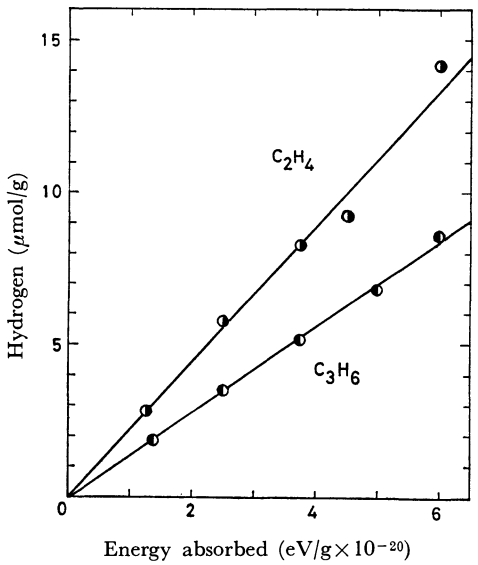

Fig. 1. Variation of hydrogen formation as a function of the energy absorbed in the radiolyses of liquid propylene and ethylene at −78°C.

Table 1. Effect of various electron or positive-ion scavengers on hydrogen formation in the radiolyses of liquid propylene and ethylene

System			$G(H_2)$
C_3H_6			0.82
C_3H_6 +	SF_6	4 mM	0.82
		20 mM	0.82
	N_2O	10 mM	0.78
		60 mM	0.82
	CCl_4	40 mM	0.78
		80 mM	0.86
		120 mM	0.74
	NH_3	0.1 M	0.82
		0.2 M	0.82
	CH_3OH	0.5 M	0.86
		1.0 M	0.94
C_2H_4			1.24
C_2H_4 +	SF_6	4 mM	1.30
		20 mM	1.30
	N_2O	10 mM	1.25
		60 mM	1.25
	CCl_4	40 mM	1.24
		80 mM	1.35
		120 mM	1.24
	CH_3OH	0.1 M	1.52
		0.2 M	1.42
		0.5 M	1.52
		1.0 M	1.47

7) T. Kabe and I. Yasumori, *Nippon Kagaku Zasshi* (*J. Chem. Soc. Japan, Pure Chem. Sect.*), **85**, 410 (1964).

ethylene at −78°C have been estimated as 0.82 and 1.24 from Fig. 1, respectively.

Various types of reagents possessing a high reactivity for ionic species, electrons or positive ions, were used. They were also selected on the basis of their ionization potentials being higher than that of propylene or ethylene. Table 1 shows the effect of various electron or positive-ion scavengers, *i.e.*, nitrous oxide, carbon tetrachloride, sulfur hexafluoride, ammonia, and methanol, on the hydrogen formation. The hydrogen formation is scarcely suppressed even at high concentrations above 100 mM of the electron scavengers and above 1 M of the positive-ion scavengers.

These results in Fig. 1 and Table 1 show a marked contrast to those in the radiolysis of saturated hydrocarbons as described in the previous paper,[3] in which a detailed comparison was made.

Table 2 shows the relative amounts of H_2, HD and D_2 evolved from the radiolyses of C_3H_6 - C_3D_6 and C_2H_4 - C_2D_4 mixtures. From the kinetic analysis as described previously,[3] when the value of

TABLE 2. ISOTOPIC COMPOSITION OF TOTAL HYDROGEN EVOLVED FROM THE LIQUID-PHASE RADIOLYSES OF C_3H_6-C_3D_6 AND C_2H_4-C_2D_4 MIXTURES

Mol%	Isotopic composition, %			D_2/HD
	H_2	HD	D_2	
C_3D_6				
0	100	0	0	—
1.40	99.2	0.68	0.14	0.21
1.84	98.6	1.19	0.25	0.21
2.70	98.0	1.63	0.38	0.23
5.50	95.6	3.58	0.87	0.24
11.5	90.5	7.56	2.02	0.27
C_2D_4				
0	100	0	0	—
0.96	99.2	0.39	0.47	1.2
1.79	98.6	0.62	0.77	1.2
3.65	96.9	1.25	1.80	1.4
4.03	97.0	1.29	1.84	1.4
5.53	95.6	1.76	2.63	1.5
8.81	92.7	2.92	4.46	1.5
12.9	90.7	3.56	5.70	1.6

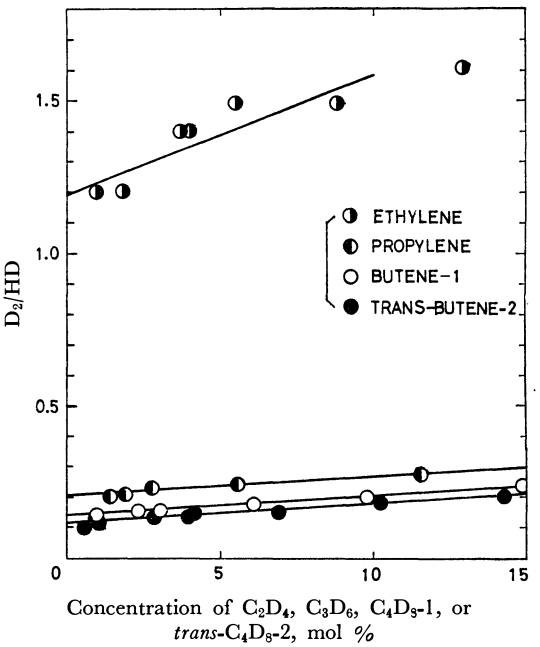

Fig. 2. D_2/HD *vs.* concentration of the perdeuterated olefins in the liquid-phase radiolyses of C_2H_4-C_2D_4, C_3H_6-C_3D_6, C_4H_8-1 - C_4D_8-1,[3] and *trans*-C_4H_8 - *trans*-2-C_4D_8-2[1] mixtures.

D_2/HD is extrapolated to zero concentration of C_3D_6 or C_2D_4, it is found to be one-half of the ratio of unimolecular to bimolecular processes in the hydrogen formation. Values of D_2/HD are listed in the last column of Table 2, and are plotted against the concentration of C_3D_6 or C_2D_4 in Fig. 2. The values of D_2/HD at zero concentration are determined to be, respectively, 0.20 and 1.2 for C_3H_6 - C_3D_6 and C_2H_4 - C_2D_4 mixtures. Thus, 71% and 29% of total hydrogen from propylene and ethylene, respectively, may be formed through bimolecular processes. The results for butene-1 and *trans*-butene-2, reported previously,[3] are also plotted in Fig. 2 and listed in Table 3 for ready comparison. Figure 2 or Table 3 shows that the result for ethylene is in striking contrast to those for the other olefins. For ethylene the bimolecular hydrogen formation is less important, while for the other olefins it is most important.

TABLE 3. PERCENTAGES OF UNIMOLECULAR (DENOTED BY I) AND BIMOLECULAR (II) PROCESSES FOR HYDROGEN FORMATION IN THE RADIOLYSIS OF LIQUID OLEFINS

Olefin	$G(H_2)$	$(D_2/HD)_0$[a]	I (%)	II (%)	$G(H')$[b]
trans-C_4H_8-2[c]	1.22	0.11	18	82	1.0
C_4H_8-1[c]	0.74	0.14	22	78	0.6
C_3H_6	0.82	0.20	29	71	0.6
C_2H_4	1.24	1.2	71	29	0.3

a) $(D_2/HD)_0$ means the value of D_2/HD extrapolated to zero concentration of the perdeuterated olefins.
b) H′ means the precursor for bimolecular hydrogen formation in the radiolysis of liquid olefins, probably a hot hydrogen atom.
c) Ref. 3.

Discussion of the Experimental Results

A fairly large quantity, about one molecule per 100 eV energy absorbed, of hydrogen formation has been observed in the radiolysis of some liquid olefins.[8-11] This cannot be explained by processes involving thermal hydrogen atoms, since for them olefins, RH_2, have a high reactivity; and the addition reaction (1) is dominant compared with the abstraction reaction (2):[12]

$$H + RH_2 \rightarrow RH_3 \quad (1)$$
$$\searrow$$
$$H_2 + RH. \quad (2)$$

Thus, Reaction (2) or thermal hydrogen atoms must be unimportant for hydrogen formation in the radiolysis of liquid olefins.

The hydrogen formation is scarcely suppressed by the addition of an appreciable concentration of various scavengers for ionic species, as shown in Table 1 and in the previous paper.[3] Consequently, from the discussion similar to that previously reported,[3] it seems reasonable to assume that ionic species, electrons and various positive ions, do not play an important role in the formation of observed hydrogen in the radiolysis of liquid olefins. The excited olefin molecule, RH_2^*, which is formed by recombination of the parent olefin ion and an electron may not be acting as a precursor for the product hydrogen, but rather as a precursor for a thermal hydrogen atom which will eventually be scavenged by olefin itself:

$$RH_2^+ + e^- \rightarrow RH_2^* \quad (3)$$
$$RH_2^* \rightarrow H + RH \text{ or } 2H + R \quad (4)$$
$$H + RH_2 \rightarrow RH_3. \quad (5)$$

The probability of hydrogen formation through various ion-molecule reactions in olefins may also be eliminated.

The most reasonable conclusion to be drawn from available data is that the excited olefin molecules RH_2' formed by direct excitation are essential to the hydrogen formation. Since, as described above, excited states which are formed by recombination of the parent olefin ion and an electron do not play an important role in the hydrogen formation, excited states lying below the ionization potential which are formed by direct excitation may also be of minor importance. Thus, the entities RH_2' may be in highly excited states lying above the ionization potential, which are called superexcited states.[13] The importance of direct excitation has never been indicated explicitly in the radiation chemistry. The hydrogen may be formed by the molecular detachment from RH_2',

$$RH_2 \rightsquigarrow RH_2' \quad (6)$$
$$RH_2' \rightarrow H_2 + R, \quad (7)$$

or by the hydrogen-atom abstraction reaction of a hot hydrogen atom H',

$$RH_2' \rightarrow H' + RH \quad (8)$$
$$H' + RH_2 \rightarrow H_2 + RH, \quad (9)$$

where a part of the highly excited states RH_2' may undergo the following autoionization:

$$RH_2' \rightarrow RH_2^+ + e^-. \quad (10)$$

The former is a unimolecular process and the latter bimolecular. Since, for ethylene, a greater part of the total hydrogen is formed by a unimolecular process as shown in Table 3, Reaction (7) is essential to hydrogen formation in the radiolysis of liquid ethylene. For the olefins except ethylene, on the other hand, Reactions (8) and (9) are important for the hydrogen formation as shown in Table 3.

It has well been known[14] from a mass spectrometric investigation that an ion of mono-olefin tends to rupture giving an allyl type ion fragment. Thus, particularly for propylene, the possibility of the following process giving a hot hydrogen atom might be considered:

$$C_3H_6^{+*} \rightarrow H' + C_3H_5^+, \quad (11)$$

where $C_3H_6^{+*}$ is an excited ion of propylene. As shown in Table 3, however, it can not be found for propylene to be characteristic of Reaction (11). Thus, the possibility of hot-hydrogen-atom formation through Reaction (11) may be eliminated.

Calculations and Their Discussion

The collisions of electrons, photons, or excited atoms with various molecules have been studied since long ago. Especially in recent years a number of studies have been made on the measurements of electron-energy loss or photoionization spectra providing significant information about the nature of higher excited states of molecules. And, moreover, theory is now able to provide at least an approximative quantitative description of the primary stage of radiolysis. A simple calculation has been made in this paper based on the optical approximation introduced by Platzman.[15]

The yield g_s, per 100 eV energy absorbed, of primary decomposition channel s may be estimated by the optical approximation. Thus, g_s can be taken

8) P. C. Kaufman, *J. Phys. Chem.*, **67**, 1671 (1963).
9) Y. Hatano, S. Shida and S. Sato, This Bulletin, **37**, 1854 (1964).
10) S. Sato, R. Yugeta, K. Shinsaka and T. Terao, *ibid.*, **39**, 156 (1966).
11) Y. Hatano and S. Shida, *ibid.*, **39**, 456 (1966).
12) K. R. Jennings and R. J. Cvetanović, *J. Chem. Phys.*, **35**, 1233 (1961).
13) R. L. Platzman, *Radiation Res.*, **17**, 419 (1962).
14) See, for example, F. H. Field and J. L. Franklin, "Electron Impact Phenomena," Academic Press Inc. Publishers, New York, N. Y. (1957), p. 174.
15) R. L. Platzman, *Vortex*, **23**, 372 (1962); R. L. Platzman, "Radiation Research 1966. Proceedings of the Third International Congress of Radiation Research, Cortina d'Ampezzo, Italy, 1966," ed. by G. Silini, North-Holland Publ. Co., Amsterdam (1967), p. 20.

as proportional to an effective dipole-matrix-element squared for s in atomic units:

$$M_s^2 = \int_{J_s}^{\infty} \phi_s(E) \frac{\boldsymbol{R}}{E} \frac{df}{dE} dE, \quad (12)$$

where E is the excitation energy in eV, $\boldsymbol{R}$ the Rydberg energy, df/dE the differential oscillator strength, $\phi_s(E)$ the probability of decomposition s upon excitation at E, and J_s the threshold excitation energy for s. Utilizing data on ionization, namely the W value (in eV) and M_i^2, the dipole matrix-element squared for ionization,[16]

$$M_i^2 = \int_{I}^{\infty} \eta(E) \frac{\boldsymbol{R}}{E} \frac{df}{dE} dE, \quad (13)$$

we may write[15]

$$g_s = \frac{100}{W} \frac{M_s^2}{M_i^2}. \quad (14)$$

In Eq. (13), I is the ionization energy and $\eta(E)$ is the probability of ionization upon excitation at E. Since the G value for hydrogen formation measured in our experiment is considered to represent the combined yield of hot hydrogen atoms and molecularly detached hydrogen:

$$RH_2' \rightarrow H' + RH \quad (15)$$

$$\searrow \; H_2 + R, \quad (16)$$

we can compare $G(H_2)$ with g_s calculated from Eqs. (12), (13), and (14) taking these two decomposition modes as the channel s.

In calculating g_s by numerical integrations in the above equations, we have relied upon the following sources of information. The differential oscillator strength df/dE is deduced from photo-absorption[17] and electron energy loss data.[18] The former has been mainly used and is shown in Fig. 3. The spectrum of butene-1 has not been reported in the region of large E. In the region of small E (<12 eV), however, it has been reported[17] that the spectrum of butene-1 is very similar to that of butene-2. Then, it is supposed that the quantity M_s^2 for butene-1 is nearly equal to that for butene-2. For ethylene, the data of Metzger and Cook somewhat differ from those of Schoen, which we have primarily relied upon.[17] The differential oscillator strength df/dE is proportional to the absorption cross section at E, and $\eta(E)$ is equal to the ratio of the ionization cross section to the total absorption cross section at E. The quantity M_i^2 is taken from ionization cross sections for fast electrons.[19] The W value is quoted

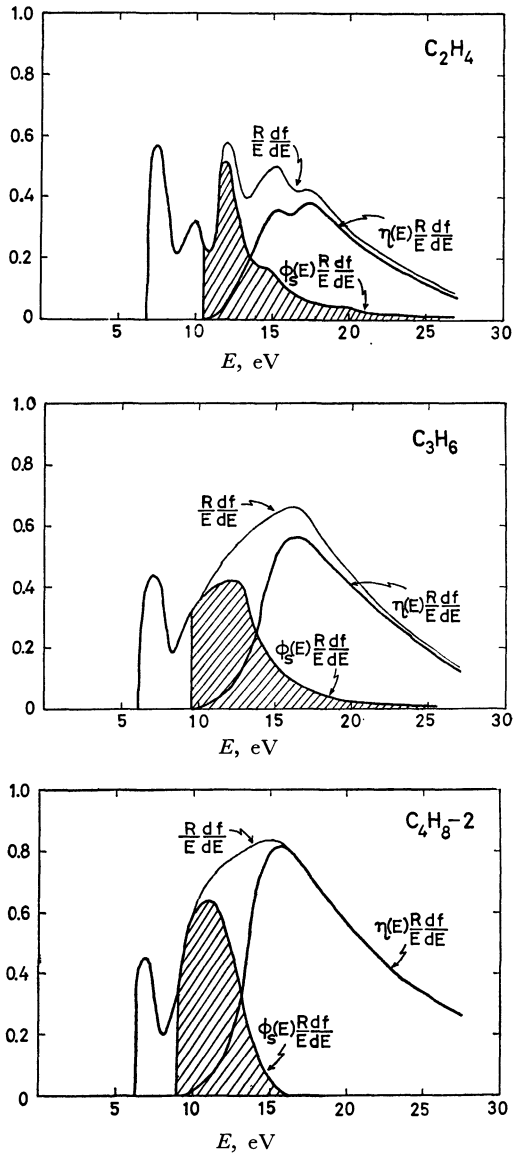

Fig. 3. Exitation spectra of olefins.

from the existing paper,[20] with an assumption that no artifacts disturbing total ionization such as the Jesse effect are operative. As to the probability $\phi_s(E)$ for the decomposition into a hot hydrogen atom and into a hydrogen molecule, lack of directly relevant information forces us to consider a reasonable model. Namely, we shall tentatively assume that the above decomposition corresponds to all the pathways, except for ionization, by which superexcited states decay:

$$\phi_s(E) = 1 - \eta(E), \quad I<E. \quad (17)$$

The highly exploratory nature of the model must be

16) R. L. Platzman, *J. Phys. Radium*, **21**, 853 (1960).
17) R. I. Schoen, *J. Chem. Phys.*, **37**, 2032 (1962); J. A. R. Samson, F. F. Marmo and K. Watanabe, *ibid.*, **36**, 783 (1962); M. Zelikoff and K. Watanabe, *J. Opt. Soc. Am.*, **43**, 756 (1953); J. T. Gary and L. W. Pickett, *J. Chem. Phys.*, **22**, 599 (1954); P. H. Metzger and G. R. Cook, *ibid.*, **41**, 642 (1964).
18) E. N. Lassettre and S. A. Francis, *J. Chem. Phys.*, **40**, 1208 (1964); K. J. Ross and E. N. Lassettre, *ibid.*, **44**, 4633 (1966).
19) B. L. Schram, M. J. van der Wiel, F. J. de Heer and H. R. Moustafa, *ibid.*, **44**, 49 (1966).
20) G. G. Meisels, *ibid.*, **41**, 51 (1964).

emphasized. Firstly, contribution of hot hydrogen atoms from excitation in the region $J_s<E<I$ are not included:

$$\phi_s(E) = 0, \quad J_s<E<I. \tag{18}$$

The value of J_s is difficult to be estimated *a priori*. A reasonable assumption, however, is that J_s is near I, because neutralization has been experimentally found not to contribute appreciably to the hydrogen formation as described in the last section. Secondly, other decomposition modes, C–C bond ruptures, have been disregarded. Presently available evidence does not seem to allow a conclusive statement as to this point,[21] although a recent study indicates the predominance of the C–H bond rupture in photolysis of ethylene at 11.6—11.8 eV.[22] Finally, influence of condensed phase on primary activation[15] has been neglected.

The results are listed in Table 4. Apparently g_s is in good agreement with $G(H_2)$. Although these results are still very tentative owing to approximate nature of estimation, they definitely lend some support to a significant role of superexcited states of hydrocarbons in the radiolysis.

In Table 4 the experimentally estimated yields of hot hydrogen atoms, $G(H')$, in the radiolysis of these olefins are also listed. As indicated in footnote 18 of the previous paper[3] it is a question whether the hot hydrogen atom H′ is a ground-state atom with appreciable kinetic energy or an electronically excited one. If we assume that H′ is electronically excited, its precursor requires at least about 14 eV of the excitation energy that is the sum of the C–H bond dissociation energy, about 4 eV, and the threshold energy, 10.2 eV, for the production of H(2P). Optical data in Fig. 3 show that superexcitation above 14 eV occupies relatively a small fraction of the absorption spectrum except in the case of ethylene. Thus, the majority of the hot hydrogen atoms in the other cases appears to be the ground-state atoms with kinetic energies rather than electronically excited ones.

Table 4. Comparison of calculated and observed hydrogen yields

	g_s	$G(H_2)$	$G(H')$
C_4H_8-2	0.7	1.2,[a] 1.0[b]	1.0[a]
C_4H_8-1	0.7	0.7[a]	0.6[a]
C_3H_6	0.8	0.8	0.6
C_2H_4	1.0	1.2	0.3
cyclo-C_6H_{10}	—	1.3[c]	—

a) Ref. 3.
b) Ref. 9.
c) Ref. 10.

As described in the last section, the experimental result for ethylene is in striking contrast to those for the other olefins. When, in Fig. 3, it is found for the spectrum of ethylene to be characteristic, it might be considered that the above two facts have some relations with each other.

The authors wish to thank Dr. M. Inokuti of Argonne National Laboratory for valuable suggestions. They are also indebted to Dr. H. Yamazaki of this Institute and Dr. K. Katsuura of Kurashiki Rayon Co. for their helpful discussions.

21) W. P. Jesse and R. L. Platzman, *Nature*, **195**, 790 (1962); G. G. Meisels, *ibid.*, **206**, 287 (1965).
22) R. Gorden, Jr., and P. Ausloos, *J. Chem. Phys.*, **47**, 1799 (1967).

BULLETIN OF THE CHEMICAL SOCIETY OF JAPAN VOL. 41 1126—1129 (1968)

Excitation from Superexcitation of Hydrocarbons. Estimation of Their Yields by the Optical Approximation

Yoshihiko HATANO

Laboratory of Physical Chemistry, Tokyo Institute of Technology, Meguro-ku, Tokyo

(Received December 7, 1967)

A simple calculation has been made based on the so-called optical approximation to obtain the yields of excitation from superexcitation of the hydrocarbons, methane, ethane, propane, *n*-butane, *n*-pentane, ethylene, propylene, butene-1, butene-2, 1,3-butadiene, acetylene, and cyclopropane. Their dipole-matrix-elements squared for excitation from superexcitation, M_d^2, have been found to be directly proportional to the number of carbon atoms in the hydrocarbons, and the ratio of M_d^2 to M_i^2, the dipole-matrix-element squared for ionization, is about 0.2. Thus, the yields, per 100 eV energy absorbed, of excitation from superexcitation are nearly equal to 0.8 for all the hydrocarbons described here.

A possible role of neutral fragments in radiation chemistry, which are formed by dissociation of superexcited molecules, was first suggested by Platzman.[1-3] Since then, however, little evidence has been presented for their role in radiation chemistry. On the other hand, reliable evidence has been required for the role of a hot hydrogen atom as a reaction intermediate in radiolysis.[4,5] Recently, however, evidence has been presented for a possible role of hot hydrogen atoms and superexcited states in radiation chemistry.[4-6] Namely, the hydrogen formation in the radiolysis of liquid olefins except ethylene is interpreted[4,5] in terms of the hydrogen-atom abstraction reaction of hot hydrogen atoms formed by direct excitation which must partially involve superexcitation. Moreover, a simple calculation has been made[6] based on the so-called optical approximation to attempt quantitative substantiation of the above viewpoint. In recent years studies have been made by Ausloos and his collaborators[7] of the primary decomposition processes in photolysis of various hydrocarbons at the photon energies a little higher than the ionization potential.

If, according to Platzman's theory, a polyatomic molecule AB receives energy of radiation, this energy may be utilized in direct ionization as

$$AB \rightarrow AB^+ + e^- \qquad (1)$$

with a probability δ, or in the formation of a superexcited state

$$AB \rightarrow AB' \qquad (2)$$

with a probability $(1-\delta)$. This is followed by

$$AB' \rightarrow AB^+ + e^-, \text{ pre-ionization,} \qquad (3)$$

$$\searrow A + B, \text{ "dissociation".}^{*1} \qquad (4)$$

It has been suggested[1] that the probability δ is much less than unity, and that there is, consequently, a real competition between Processes (3) and (4). The optical approximation introduced by Platzman[2,8] is now able to provide at least an approximative quantitative description of these processes. The yield g_d, per 100 eV energy absorbed, of the formation of the superexcited states followed by Process (4) may be estimated by the optical approximation. Namely, the yield g_d is taken as proportional to M_d^2, the dipole-matrix-element squared for excitation from superexcitation.*2 Thus, the role of the neutral fragments in radiation chemistry may be estimated by the quantity M_d^2. This paper presents the quantity M_d^2 for various hydrocarbons of which the optical spectra have already been known.

1) R. L. Platzman, *J. Phys. Radium*, **21**, 853 (1960).
2) R. L. Platzman, *Vortex*, **23**, 372 (1962).
3) R. L. Platzman, *Radiation Res.*, **17**, 419 (1962).
4) Y. Hatano and S. Shida, *J. Chem. Phys.*, **46**, 4784 (1967).
5) Y. Hatano, S. Shida and S. Sato, This Bulletin, **41**, 1120 (1968).
6) Y. Hatano, S. Shida and M. Inokuti, *J. Chem. Phys.*, **48**, 940 (1968).
7) P. Ausloos and S. G. Lias, "Preprints of International Conference on Photochemistry, München (1967)," Part I, p. 211, and the references therein.

*1 The term "dissociation" means any reorganization of atoms in the molecule which protects it against pre-ionization. The term, therefore, encompasses true dissociation, predissociation, and internal conversion.[2]

8) R. L. Platzman, "Radiation Research 1966. Proceedings of the Third International Congress of Radiation Research, Cortina d'Ampezzo, Italy, 1966," ed. by G. Silini, North-Holland Publ. Co., Amsterdam (1967), p. 20.

*2 The term "excitation from superexcitation" means formation of the superexcited states followed by the processes except for ionization, namely by the "dissociation" processes.[2]

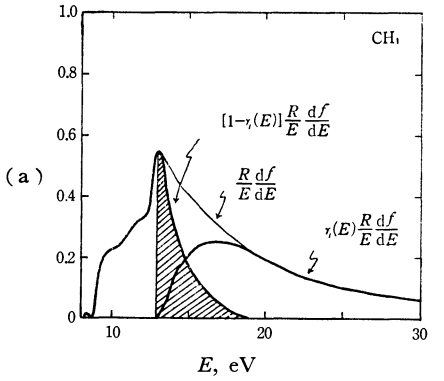

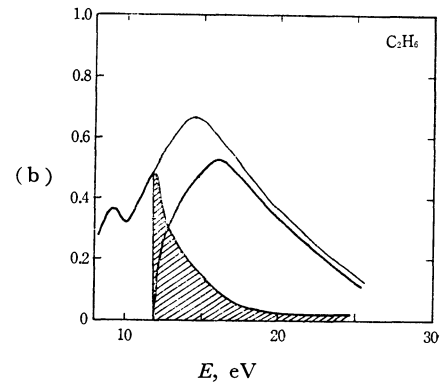

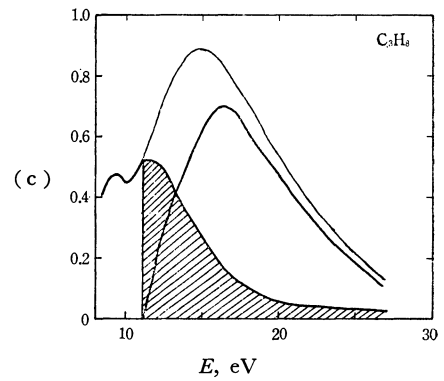

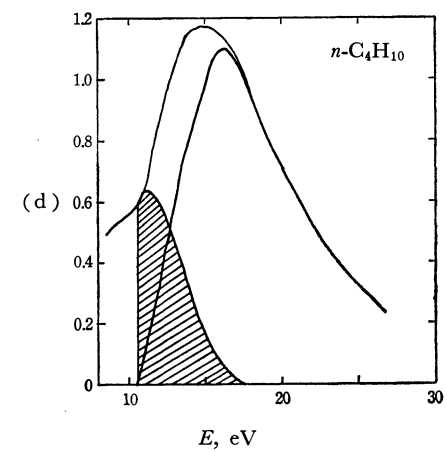

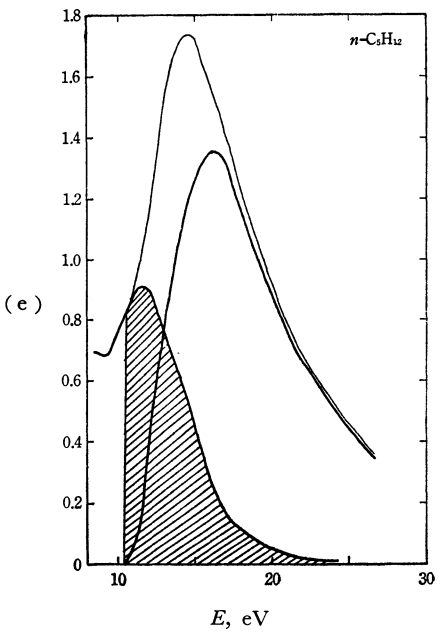

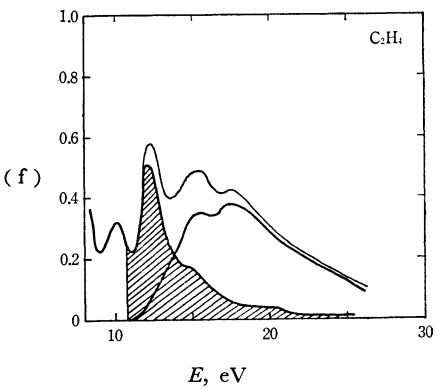

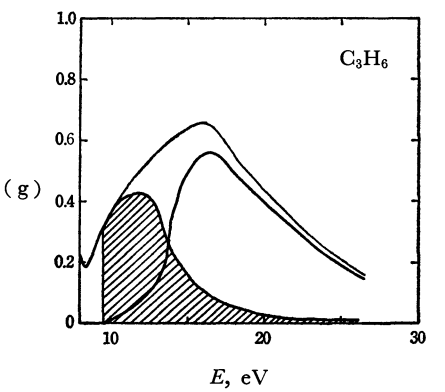

Fig. 1 (a)～(k). Excitation spectra of various hydrocarbons.

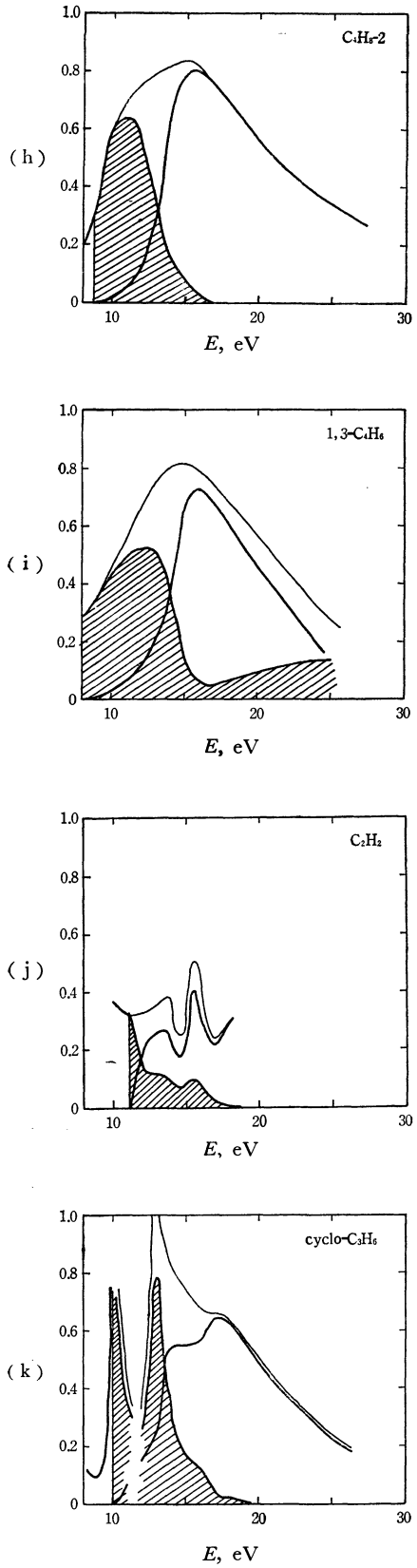

Calculation and Discussion

The yield g_d is proportional to the quantity M_d^2 (in atomic units):

$$M_d^2 = \int_I^\infty [1 - \eta(E)] \frac{\boldsymbol{R}}{E} \frac{df}{dE} dE, \qquad (5)$$

where E is the excitation energy, $\boldsymbol{R}$ the Rydberg energy, I the ionization energy, df/dE the differential oscillator strength, $\eta(E)$ the probability of ionization upon excitation at E. Now, attention has to be paid to a slight difference between the quantity M_d^2 in Eq. (5) and the quantity M_s^2 in the previous paper.[5,6] The latter is determined by the decomposition mode s, namely the threshold excitation energy J_s for s. Since, however, a reasonable assumption, $\phi_s(E) = 1 - \eta(E)$ at $I < E$ and $\phi_s(E) = 0$ at $J_s < E < I$ where $\phi_s(E)$ is the probability of decomposition s upon excitation at E, was introduced in the previous paper,[5,6] the value of the above two quantities have eventually been identical. Utilizing data on ionization, namely the W value and M_i^2, the dipole-matrix-element squared for ionization,[1] we may write $g_d = (100/W)(M_d^2/M_i^2)$.

In calculating M_d^2 by numerical integration in Eq. (5), we have utilized the following sources of information. The differential oscillator strength df/dE and the probability $\eta(E)$ are deduced from photoabsorption data[2,9,10] and are shown in Fig. 1

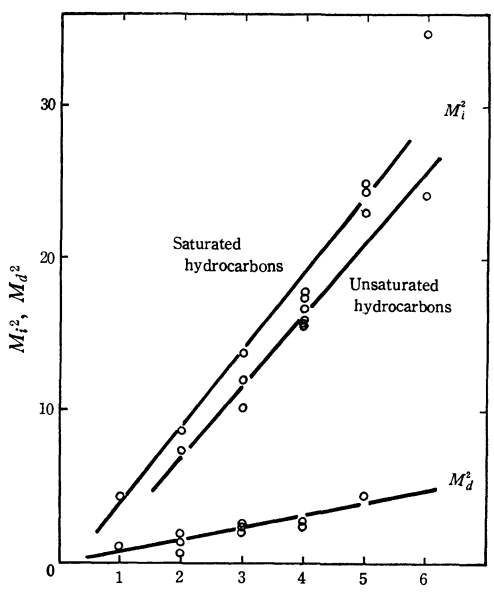

Fig. 2. Values of M_d^2 and M_i^2 for various hydrocarbons against the number of carbon atoms. The values of M_i^2 are quoted from the data by Schram *et al.*[11] Each circle corresponds to a particular hydrocarbon. Refer to Table 1.

9) R. I. Schoen, *J. Chem. Phys.*, **37**, 2032 (1962).
10) P. H. Metzger and G. R. Cook, *ibid.*, **41**, 642 (1964).
11) B. L. Schram, M. J. van der Wiel, F. J. de Heer and H. R. Moustafa, *ibid.*, **44**, 49 (1966).

TABLE 1. THE VALUES OF M_d^2 AND g_d FOR VARIOUS HYDROCARBONS.

	M_d^2	M_i^2 [a]	W, eV[b]	g_d
CH_4	1.0	4.28	26.7	0.9
C_2H_6	1.3	8.63	23.6	0.6
C_3H_8	2.6	13.8	23.4	0.8
n-C_4H_{10}	2.4	17.8	22.9	0.6
i-C_4H_{10}	—	17.4	23.0	—
n-C_5H_{12}	4.4	24.4	23.5[f]	0.8
i-C_5H_{12}	—	25.0	23.9	—
neo-C_5H_{12}	—	23.0	—	—
n-C_6H_{14}	—	34.8	23.4[f]	—
cyclo-C_3H_6	2	10.2	—	(0.9 if W=23)
C_6H_6	—	24.2	—	—
C_2H_4	1.9	7.32	25.9	1.0
C_3H_6	2.4	12.0	24.8	0.8
C_4H_8-1	2.7[c]	15.3	24.4	0.7
C_4H_8-2	2.7[d]	16.7[d], 15.5[e]	23.9[e]	0.7
C_4H_6-1,3	>4	15.9	—	(>1 if W=23)
C_2H_2	0.6	—	25.3	(0.4 if M_i^2=6)

a) Ref. 11 b) Ref. 12 c) See Ref. 5 d) *cis*-Butene-2 e) *trans*-Butene-2 f) Ref. 13

(a)—(k), all of which are drawn on the same scale. Thus, in the first instance, it has been found in these figures that the quantities M_d^2 increase with increasing the number of carbon atoms in the hydrocarbons, while that the oscillator-strength spectra of the hydrocarbons are almost in infinite variety. In the spectra of ethylene, acetylene, and cyclopropane, for example, the marked structures stand in contrast to the smoothness in the spectra of alkanes. The quantities M_d^2 estimated are listed in the first column of Table 1, and are plotted in Fig. 2 against the number of carbon atoms in the hydrocarbons. The data show that the quantities M_d^2 are directly proportional, still very roughly owing to the lack of more reliable basic data, to the number of carbon atoms in the hydrocarbons.*3 There has been, to the author's knowledge, no report with any result such as that shown in Fig. 2, although such result may be easily expected. The quantities M_i^2 taken from ionization cross sections for fast electrons measured by Schram *et al.*[11] are also plotted in Fig. 2. Although the quantities M_i^2 may also be determined by graphical integration in Fig. 1, it forces us to make a rough extrapolation of Schoen's data[9] to higher excitation energies. Figure 2 shows that the values of M_d^2/M_i^2 are nearly equal to 0.2 for all the hydrocarbons described here. Assuming that the W values of the hydrocarbons are equal to 25 eV, we get the values of g_d to be about 0.8. Namely, no peculiarity has been able to be found in the values g_d or M_d^2 at least for all the hydrocarbons under consideration. Going into details and using the W values quoted from the existing paper,[12,13] on the other hand, we get each one of the values g_d to be listed in the last column of Table 1.

Finally, we may add that more reliable and more accurate basic data such as df/dE, W, and $\eta(E)$ are greatly desirable.

The author wishes to thank Prof. S. Shida of this Institute for valuable suggestions. He is also indebted to Dr. S. Sato and Dr. H. Yamazaki of this Institute and Dr. M. Inokuti of Argonne National Laboratory for their helpful discussions.

12) G. G. Meisels, *ibid.*, **41**, 51 (1964).
13) P. Adler and H. K. Bothe, *Z. Naturforschg.*, **20a**, 1700 (1965).
*3 If M_d^2 and M_i^2 are plotted against the number of valence electrons in the hydrocarbons, better-fit lines are obtained for both the quantities.

BULLETIN OF THE CHEMICAL SOCIETY OF JAPAN VOL. 41 1130—1132 (1968)

Formation Constants of Maleatochromium(III) Complexes and Some Properties Thereof in the Solid State*[1]

Takeshi TOMITA, Eishin KYUNO and Ryokichi TSUCHIYA

Department of Chemistry, Faculty of Science, Kanazawa University, Kanazawa

(Received July 12, 1967)

The formation constants of the chromium(III) complexes with maleic acid have been determined by the pH method to be $\log k_1 = 5.4 \pm 0.1$, $\log k_2 = 3.0 \pm 0.1$, and $\log k_3 = 1.9 \pm 0.2$ at an ionic strength of $\mu = 0.1$ and at 25°C. We also attempted to prepare the solid of the chromium(III) complex with maleic acid. Though it was an amorphous solid to X-ray diffraction measurement, its composition was presumed to be $[Cr(mal^{*2})(OH)(H_2O)_3]$. After it had been dried in a desiccator for a few days, when it was exposed to moist air we observed the curious phenomenon that the solid was made jumping due to the absorption of water vapor.

The formation constants of the chromium(III) complexes with succinic and with phthalic acids have been reported by one of the present authors in earlier papers.[1,2] The curious jumping property of the latter complex in the solid state after it had been dehydrated was also noted.[2] In continuation of the above works, the formation constants of chromium(III) complexes with maleate have been determined. All the three anions described above can make similar coordination bonds to chromium(III) through the seven-membered chelate ring; there is only a fine structural difference originating from the ligand molecules themselves. The effect of such differences in the structure upon the formation constants of the chromium(III) complexes concerned will be discussed below.

Experimental

Formation Constant Measurement. The formation constants were determined by means of pH measurements in a mixed solution of hexaaquochromium(III) perchlorate and maleic anhydride at an ionic strength of $\mu = 0.1$ and at 25°C in a manner similar to that described in an earlier paper.[2] The maleic anhydride used as a ligand material was of a special grade and had been obtained from Wako Pure Chemical Industries, Ltd.

Attempt of Preparation of the Solid Maleatochromium(III) Complex. We attempted to prepare the maleatochromium(III) complex in the solid state by the procedure reported in an earlier paper.[2] To a mixed solution of 6 g (1/60mol) of chromium(III) nitrate nonahydrate and 5 g (1/20 mol) of maleic anhydride, we added 13 g (1/7 mol) of ammonium carbonate; the resulting solution was then evaporated to some extent until the film-like substance covering the surface of the solution began to appear. Then it was scooped on the filter and dried in the desiccator. About 2 g of the product were obtained. The product was amorphous to X-ray diffraction measurements.

The product showed the curious property of jumping when it was exposed to moist air, just as the phthalatochromium(III) complex did.[2] The analysis of the sample after it had absorbed enough water vapor gave the chromium content of 21.51%, a value of which is in good agreement with the calculated value, 21.93%, for the chemical formula, $[Cr(mal)(OH)(H_2O)_3]$.

Results and Discussion

Comparison of the Formation Constants of Maleatochromium(III) Complexes with Those of Phthalato- and Succinatochromium(III) Complexes. The relevant values of the first and second acid dissociation constants of maleic acid required for determining the formation constants of the complexes were taken from the literature—$pK_1 = 1.92$[3] and $pK_2 = 5.79$[4] respectively at an ionic strength of $\mu = 0.1$ and at 25°C.

The methods of calculating the average number of coordinated maleate anions as ligands per gram-ion of the chromium, $\bar{n}$, and the concentration of the non-coordinated anions, $p[A^{2-}]$, in solution, are the same as those described in an earlier paper.[5] The plots of $\bar{n}$ *vs.* $p[A^{2-}]$ for the maleatochromium(III) system are shown in Fig. 1, together with those for the succinato- and phthalatochromium(III) systems.

By applying the successive approximation method to the tentative values of the formation constants

*1 Presented in part at the 10th International Conference on Coordination Chemistry, Tokyo and Nikko, Japan, September, 1967.

*2 mal=maleate anion.

1) H. Muro and R. Tsuchiya, This Bulletin, **39**, 1589 (1966).

2) K. Higashi, K. Hori and R. Tsuchiya, *ibid.*, **40**, 2569 (1967).

3) N. E. Topp and C. W. Davies, *J. Chem. Soc.*, **1940**, 87.

4) M. Yasuda, K. Yamasaki and H. Ohtaki, This Bulletin, **33**, 1067 (1960).

5) K. Nagata, A. Umayahara and R. Tsuchiya, *ibid.*, **38**, 1059 (1965).

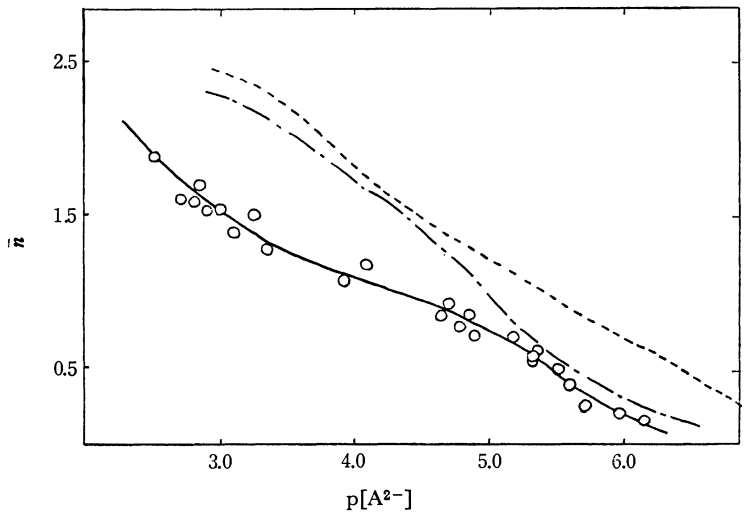

Fig. 1. Formation curve, $\bar{n}$ *vs.* p[A^{2-}].
——, in chromium(III)-maleate system
----, in chromium(III)-succinate system
—·—, in chromium(III)-phthalate system

TABLE 1. THE FORMATION CONSTANTS OF SUCCINATO-, PHTHALATO- AND MALEATOCHROMIUM(III) COMPLEXES, AT $\mu=0.1$ AND 25°C

	log k_1	log k_2	log k_3	pK_1	pK_2	Ref.
Succinato complex	6.42	4.57	2.86	4.00	5.21	1)
Phthalato complex	5.52	4.48	(2.5)	2.76	4.92	2)
Maleato complex	5.4	3.0	(1.9)	1.92	5.79	

(The numerals in parentheses are the values estimated by extrapolating the formation curve.)

obtained from the formation curve shown in Fig. 1, the step-by-step formation constants were obtained; they are listed in Table 1, together with those of the succinato- and phthalatochromium(III) complexes.

It is obvious from Table 1 that the formation constants of the maleato and phthalato complexes are rather smaller than those of the succinato complexes. This is due to the structural differences among the ligand molecules used.

The phthalate and maleate anions may be forced to hold the planar structure in a complex formation because of the presence of a benzene ring in the former and that of the double bond between two carbon atoms instead of the benzene ring between two carboxylate groups in the latter. Since the distance between two oxygen atoms which can coordinate to the metal ion in these two carboxylate anions is presumed to be about 1.6 Å on the basis of the crystal structure of the maleic acid,[6] a remarkable strain may be predicted to occur in the chelate formation when they coordinate to a metal ion using the above two oxygens as the bidentate ligand.

On the other hand, since the succinate anion[7] has neither a benzene ring nor a double bond between two carbon atoms within itself, the free rotation of the ethylene linkage placed between two carboxylate groups is possible without any steric hindrance. As a result, it may not always make a planar coordination structure. Therefore, in this case, little strain should appear in the chelate formation. It may be concluded that the difference in the original structure in the ligand coordinated to metal as mentioned above is the main contribution to the lower stability of the phthalato and maleato complexes than that of the succinato complexes.

When we compare the formation constants of the phthalato and maleato complexes in Table 1, we find that the latter are relatively smaller than the former. The phthalate and maleate must commonly form similar seven-membered planar chelate rings as a result of the double-bond character involved in their chelate rings.

6) M. Shahat, *Acta Cryst.*, **5**, 763 (1952).

7) J. S. Broadley, D. W. J. Cruickshank, J. D. Morrison, J. M. Robertson and H. M. M. Shearer, *Proc. Roy. Soc. (London)*, **251A**, 441 (1959).

Since, while the phthalate anion has a benzene ring, the maleate one has none, the double-bond character between the two carbon atoms combining with two carboxylate groups seems to be weaker in the former than in the latter. This results in the lesser electronic density at the oxygen atoms coordinating to metal in the latter than in the former. Therefore, it may be suggested that the basicity of the maleate anion is rather smaller than that of the phthalate. The values of the total acid dissociation constants of these acids given in Table 1 support this idea.

In short, the lesser stability of the maleato complexes than that of the phthalato complexes can be well explained by the facts that the acid dissociation constant of the maleic acid is smaller than that of the phthalic acid.

Jumping Property of the Solid Maleatochromium(III) Complex. The solid maleatochromium(III) complex prepared and dried in a desiccator showed jumping when it was exposed to moist air, as in an earlier experiment.[2] The fact that the phenomena took place as a result of the absorption of water vapor was ascertained by the presence of a stronger and broader absorption band in the range of 3200—3600 cm^{-1} of the IR spectra after jumping than before jumping.

It was observed that, even after the sample had absorbed water vapor enough to cause it to cease jumping, the jumping property re-appeared when it was again exposed to moist air.

The weight loss of the sample which had absorbed water vapor in the moist air and had ceased jumping was measured by the thermobalance; it is plotted in Fig. 2. The figure shows that a metastable dehydrated compound is formed by a weight loss of 20—24% at about 200°C; this is approximately consistent with the calculated value, 22.8%, for the following reaction:

$$[Cr(mal)(OH)(H_2O)_3] \xrightarrow{-2H_2O} [Cr(mal)(OH)(H_2O)].$$

It was also found that the sample which had thermally lost the water vapor in the amount corresponding to the expression in this equation began jumping again in the moist air, as in the case of the phthalatochromium(III) complex in the solid state reported on in an earlier paper.[2]

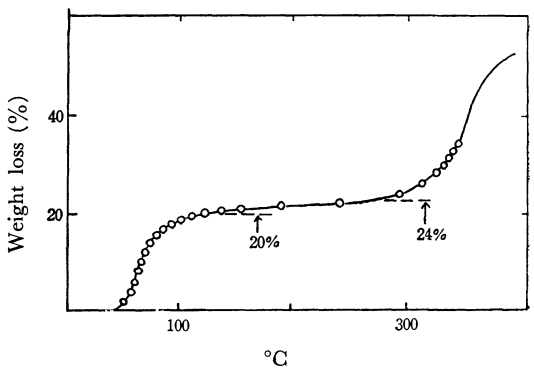

Fig. 2. Thermogravimetric curve of the solid maleatochromium(III) complex.

BULLETIN OF THE CHEMICAL SOCIETY OF JAPAN VOL. 41 1133—1139 (1968)

Bromine to Chlorine Ratios in Igneous Rocks

Tsutomu SUGIURA*1

Department of Earth Sciences, Nagoya University, Chikusa, Nagoya

(Received November 13, 1967)

Samples were decomposed by fusion with Na_2O_2 and benzoic acid in a Parr-bomb, then halogens were separated from other elements by distillation and determined colorimetrically; chlorine by the thiocyanate method and bromine by the rosaniline method. The chlorine and bromine contents of rocks cover a very wide range with no relation to the type of rock. The Br/Cl ratio, however, is in a relatively narrow range from 1×10^{-3} to 16×10^{-3} by weight, mostly from 1×10^{-3} to 6×10^{-3}, and evidently lower than those reported by previous investigators. The average Br/Cl ratio is $(3\pm2)\times10^{-3}$, about one-seventh of the value generally accepted for igneous rocks. The halogen content of quartz and feldspar is usually so small that it was not usually determined. The Br/Cl ratio in biotite seems to be rather small and certainly is smaller than 3×10^{-3} on the average. The Br/Cl ratios in volcanic rocks are similar to those in volcanic gases for any one volcano studied.

Sugiura *et al.*[1] (1963) reported that the Br/Cl ratio in volcanic gases is very alike at every volcano, and evidently smaller than the Br/Cl ratio in igneous rocks reported by Behne[2] (1953). This fact seemed interesting for the consideration of their behavior in volcanic emanations.

The bromine content of igneous rocks was first determined by Fellenberg and Lunde in 1926 (Behne,[2] 1953), and again by Selivanow[3] in 1940 and Behne in 1953. Behne's data had been accepted until Filby[4] (1964) reported the bromine contents of the standard rocks, granite G-1 and diabase W-1. His values are appreciably lower than the average values given by Behne.

Krasitseva[5] (1964) postulated that the Br/Cl ratio in ocean water has been decreasing through geologic time. One important fact supporting his hypothesis is that the average Br/Cl ratio in igneous rocks seems to be far higher than that in present-day ocean water.

From the above, it seems to be very important and urgent to obtain true average Br/Cl ratio for igneous rocks. In the present study, the author has determined the chlorine and bromine contents of volcanic and plutonic rocks. In order to examine the average Br/Cl ratio obtained the relations between the Br/Cl ratio in biotite and in coexisting quartz and feldspar, and also the ratios in volcanic rocks and volcanic gases from one volcano were investigated.

Experimental

Total Chlorine and Total Bromine. About 1 kg of rock sample was taken at each locality, and 50 to 100 g of sample crushed in a steel mortar and ground to approximately 200 mesh in an agate mortar, taking special precaution against any possibility of chlorine or bromine contamination. The powdered sample was decomposed by fusion with sodium peroxide, and chlorine and bromine separated from other elements by distillation. Chlorine was determined by the method of Iwasaki *et al.*[6] (1957), and bromine by a modification of the method of Hunter and Goldspink[7] (1954).

Separation of Chlorine and Bromine. The sample (1 to 3 g) was decomposed by fusion with 15 g of sodium peroxide and 0.5 g of benzoic acid in a Parr-bomb.*2 The cake was put into 100 m*l* of distilled water. The solution was condensed to about 50 m*l* on an electric heater, and transferred into a 150 m*l* distilling flask. Two milliliters and 50 m*l* of 2 N potassium hydroxide solution were added to trap A and trap B, respectively (Fig. 1). Forty milliliters of 14 N sulfuric acid and 10 *l* of 10% potassium permanganate solution were added to the distilling flask. The solution was heated to boiling and air bubbled in at the rate of 100 m*l*/min. Distillation was continued to obtain 50 m*l* of distillate. A half milliliter of 30% hydrogen peroxide was added to the distillate. The solution was boiled on a water-bath to decompose the surplus hydrogen peroxide, and made up to 5.0 m*l*.

Chlorine. One milliliter of the solution of chlorine

*1 Present address: Department of Chemistry, Aichi Kyoiku University, Higashi, Nagoya, Japan.

1) T. Sugiura, Y. Mizutani and S. Oana, *Earth. Sci. Nagoya Univ.*, **11**, 272 (1963).

2) W. Behne, *Geochim. et Cosmochim. Acta*, **3**, 186 (1953).

3) L. S. Selivanov, *Dokl. Akad. Nauk SSSR*, **28**, 809 (1940).

4) R. H. Filby, *Anal. Chim. Acta*, **31**, 434 (1964).

5) U. U. Krasitseva, *Geokhimiya*, No. 2, 171 (1964).

*2 "Peroxide Bomb Apparatus and Methods" published by Parr Instrument Company, 211 Fifty-third Street, Moline, illinois, U.S.A.

6) I. Iwasaki, T. Katsura, N. Sakato and M. Hirayama, *Nippon Kagaku Zassi* (*J. Chem. Soc. Japan, Pure Chem. Sect.*), **78**, 164 (1957).

7) G. Hunter and A. A. Goldspink, *Analyst*, **79**, 467 (1954).

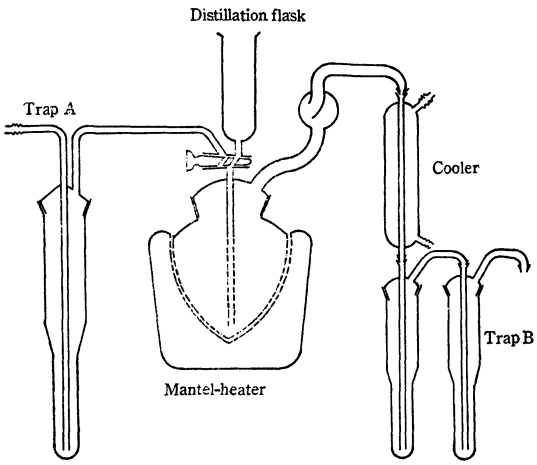

Fig. 1. Apparatus for distillation of chlorine and bromine.

and bromine, 1 m*l* of mercuric thiocyanate solution (0.3 g of $Hg(SCN)_2$ in 100 m*l* of C_2H_5OH) and 2 m*l* of ferric ammonium sulfate solution (6 g of $Fe_2(SO_4)_3(NH_4)_2SO_4 \cdot 24H_2O$ in 100 m*l* of 6 N NHO_3) were added to a 20 m*l* testtube, in that order. The volume of the solution was made up to 20 m*l* with distilled water and mixed well. The absorbance of this colored solution was measured at 460 mμ. Ten μg of chlorine in the colored solution can be determined within 10% by this colorimetric method, and chlorine in samples with more than 0.01% (100 ppm) chlorine can also be determined within 10%, by taking one-fifth of the distillate. The precision of this distillation method, which actually was examined in detail on the determination of bromine, is presented in Table 2.

Bromine. Four milliliters of the solution of chlorine and bromine, 1.0 m*l* of 1 N dihydrogen sodium phosphate solution (to adjust pH to about 6.3) and 0.5 m*l* of 1 N sodium hypochlorite solution (1 N NaClO in 0.1 N NaOH sol.) were added to a testtube which was kept in the boiling water for 15 min, and cooled with tap water for a few minutes. A half m*l* of 50% sodium formate solution was added. The testtube was again warmed in boiling water for 15 min, and cooled with tap water for 30 min. On the other hand, 0.5 m*l* of bromide-molybdate solution (0.15 g of KBr and 3.0 g of $(NH_4)_67Mo_7O_{24} \cdot 4H_2O$ in 100 m*l* of H_2O), 0.5 m*l* of rosaniline solution (0.006 g of $C_{20}H_{20}N_3OH$ in 100 m*l* of 2 N H_2SO_4 sol.) and 1 m*l* of 14 N sulfuric acid were put into a 20 m*l* flask in this order and mixed well. The above prepared solution was added slowly to this flask and stirred. After precisely 5 min, 10 m*l* of *t*-butyl alcohol ($(CH_3)_3COH$ containing 5% C_2H_5OH) was added and mixed well. After 5 min, 1 m*l* of 14 N sulfuric acid was added. The volume of the solution was made up to 20.0 m*l* with distilled water and mixed well. The absorbance of the colored solution was measured at 570 mμ. The smallest detectable amount of bromine in specimens is 0.5 μg, and the error in determination less than 0.5 μg. Hence, as 3 g of sample can be treated at a distillation, bromine in samples with more than 0.00002% (0.2 ppm) bromine can be determined with an error of less than 0.2 ppm. The relationship between the recovery of bromine and the volume of the distillate and precision of the determination are presented in Tables 1 and 2, respectively.

TABLE 1. RELATIONSHIP BETWEEN THE RECOVERY OF BROMINE AND THE WATER VOLUME DISTILLED

Analysis number	Watere volume distilled (m*l*)	Amount of bromine (μg)		Recovery (%)
		Added	Found	
1	5	2	0.8	40
2	10	2	1.6	80
3	10	2	1.0	50
4	20	2	1.6	80
5	20	10	9.5	95
6	30	2	1.8	90
7	30	2	1.4	70
8	40	2	1.6	80
9	40	2	1.9	95
10	50	2	2.0	100
11	50	2	1.7	85
12	50	1	0.8	80
13	50	1	1.1	110

TABLE 2. PRECISION OF THE ANALYTICAL METHOD

Analysis number	Amount of sample used (g)	Amount of chlorine and bromine determined (μg)	
		Chlorine	Bromine
14	2 g of No. 3	850	0.6
15	2 g of No. 3	880	0.8
16	3 g of No. 3	1310	1.0
17	3 g of No. 3	1240	0.8
18	3 g of No. 18	270	0.9
19	3 g of No. 18	340	1.2
20	3 g of No. 18	300	1.0
21	3 g of No. 18	280	0.7
22	2 g of No. 22	580	1.9
23	2 g of No. 22	580	1.4
24	3 g of No. 19	230	1.1
25	3 g of No. 19	240	0.7

Soluble Chlorine and Bromine. Two grams of sample per determination were soaked in 50 m*l* of water for 24 hr at room temperature, and stirred occasionally. One drop of concentrated nitric acid was added to the solution, and it centrifuged. The precipitate was soaked again in 50 m*l* of water containing one drop of concentrated nitric acid for 24 hr, and centrifuged. This procedure was repeated till the amount of leached chlorine in the water becomes negligibly small. The process usually was repeated two or three times. The amounts of chlorine and bromine leached in water were determined separately by the method described above.

Samples

Samples for the present study consist of 28 volcanic and 14 plutonic rocks collected from various parts of Japan. Rock species and localities of specimens are briefly described in Tables 3 and 4, to-

TABLE 3. CHLORINE AND BROMINE CONTENTS OF VOLCANIC ROCKS

Specimen number	Rock species	Locality	Total-Cl g/t	Soluble-Cl g/t	Total-Br g/t	Soluble-Br g/t	$\frac{\text{Total-Br}}{\text{Total-Cr}} \times 10^3$ (wt)	$\frac{\text{Soluble-Br}}{\text{Soluble-Cl}} \times 10^3$ (wt)
1	Basalt	Notoiida, Ishikawa Pref.	120	30	<0.2	—*	<2	—
2	Basalt	Tojinbo, Fukui Pref.	450	0	2.0	—	4	—
3	Basalt	Miharayama, Oshima, Tokyo Metropolitan	430	45	0.3	—	1	—
4	Basalt	Okada, Oshima, Tokyo Metropolitan	100	100	0.2	0.3	2	3
5	Basalt	Shidara, Okuwa, Aichi Pref.	150	40	0.5	—	4	—
6	Basalt	Shidara, Oidaira, Aichi Pref.	160	60	0.5	0.2	3	3
7	Sanukite	Shiraminezan, Kagawa Pref.	210	5	0.7	—	3	—
8	Andesite	Daisen, Tottori Pref.	200	30	0.5	—	3	—
9	Andesite	Yakeyame, Akita Pref.	180	10	<0.2	—	<2	—
10	Andesite	Usuzan, Hokkaido	200	40	0.8	—	4	—
11	Andesite	Issaikyoyama, Fukushima Pref.	140	45	0.8	—	6	—
12	Andesite	Chausudake, Tochigi Pref.	260	5	0.3	—	1	—
13	Andesite	Asahidake, Tochigi Pref.	80	5	0.2	—	3	—
14	Andesite	Kujyu-Ioyama, Oita Pref.	120	30	0.4	—	3	—
15	Andesite	Asosan, Kumamoto Pref.	430	35	1.3	—	3	—
16	Dacite	Tojinbo, Fukui Pref.	190	0	<0.2	—	<1	—
17	Dacite	Sanbeizan, Shimane Pref.	110	20	0.2	—	2	—
18	Dacite	Showashinzan, Hokkaido	100	20	0.3	—	3	—
19	Dacite	Ousu, Hokkaido	120	15	0.3	—	3	—
20	Dacite	Ogariyama, Usu, Hokkaido	50	10	<0.2	—	<4	—
21	Dacite	Kousu, Usu, Hokkaido	30	10	0.2	—	7	—
22	Pearlite	Horaiji, Aichi Pref.	290	50	0.8	—	3	—
23	Obsidian	Shirataki, Hokkaido	690	—	2.0	—	3	—
24	Pitch stone	Horaiji, Aichi Pref.	100	25	0.3	—	3	—
25	Pitch stone	Sosogi, Ishikawa Pref.	1020	40	5.5	—	5	—
26	Hyalolipalite	Kumano, Mie Pref.	90	—	1.4	—	16	—
27	Pyroclastic rock	Noto, Fukui Pref.	790	40	1.5	—	2	—
28	Pyroclastic rock	Shirataki Hokkaido	640	—	4.0	—	6	—

* Not detected

TABLE 4. CHLORINE AND BROMINE CONTENTS OF PLUTONIC ROCKS AND THEIR MINERALS

Specimen number	Rock species	Locality	Total-Cl g/t	Soluble-Cl g/t	Total-Br g/t	Soluble-Br g/t	$\frac{\text{Total-Br}}{\text{Total-Cl}} \times 10^3$ (wt)
29	Pegmatite	Ishikawa, Fukushima Pref.	40	0	0.2	—	5
	Biotite		100	30	0.2	—	2
	Quartz		10	—	—	—	—
	Feldspar		10	—	—	—	—
30	Pegmatite	Naegi, Gifu Pref.	—	—	—	—	—
	Biotite		2400	20	0.5	—	0.2
	Quartz		30	25	≦0.2	—	≦4
	Feldspar		50	30	≦0.2	—	≦7
31	Pegmatite	Ishikawa, Fukushima Pref.	20	—	—	—	—
	Muscovite		10	—	—	—	—
	Quartz+Feldspar		30	—	—	—	—
32	Granite	Ishikawa, Fukushima Pref.	10	—	—	—	—
	Biotite		20	—	—	—	—
	Quartz		10	—	—	—	—
	Feldspar		10	—	—	—	—
33	Granite	Naegi, Gifu Pref.	70	0	0.3	—	4
	Biotite		250	25	0.4	—	2
	Quartz+Feldspar		50	10	0.3	—	6
34	Granite	Yashirojima, Yamaguchi Pref.	100	10	≦0.2	—	≦2
	Biotite		200	5	≦0.2	—	≦1
	Quartz+Feldspar		80	20	≦0.2	—	≦3
35	Granodiorite	Taguchi, Aichi Pref.	90	—	—	—	—
	Biotite		700	—	—	—	—
	Quartz+Feldspar		10	—	—	—	—
36	Granite	Okazake, Aich Pref.	10	—	—	—	—
	Biotite		210	—	0.3	—	1
	Quartz+Feldspar		5	—	—	—	—
37	Granite	Tsunogawa, Yoshikigun, Gifu Pref.	40	—	≦0.2	—	≦5
	Biotite		1020	10	≦0.5	—	≦0.5
38	Quartzdiorite	Nakagawa, Shimoashikagara-gun Kanagawa Pref.	70	—	0.3	—	4
	Hornblende		200	—	0.4	—	2
	Quartz+Feldspar		5	—	—	—	—
39	Granite	Kadoshima, Yasuoka-mura, Nagano Pref.	30	10	0.3	—	10
	Biotite		280	10	≦0.5	—	≦2
40	Eclogite	Higashiakaishi, Ehime Pref.	20	—	—	—	—
	Pyroxene		70	—	≦0.5	—	≦7
	Garnet		10	—	—	—	—
41	Gabro	Murotozaki, Kochi Pref.	70	—	0.2	—	3
	Pyroxene		60	—	<0.5	—	<8
	Magnetite		90	—	0.2	—	2
	Plagioclase		80	—	<0.5	—	<6
42	Peridotite	Higashiakaishi, Ehime Pref.	40	—	0.2	—	5
	Pyroxene		70	—	<0.5	—	<7
	Olivine		10	—	—	—	—
	Spinel		75	—	<0.5	—	<7

gether with the chlorine and bromine contents. The analyzed minerals were roughly separated first with a magnetic separater, and then hand-picked under a microscope.

Result and Discussion

1) Br/Cl Ratios in Volcanic Rocks. Results of the determinations of chlorine and bromine in volcanic rocks are given in Table 3.

Kuroda and Sandell[8] (1953) and Iwasaki *et al*[6] (1957) have stated that the amount of water-soluble chlorine is generally very small compared with the total amount of chlorine in rocks which are fresh and not contaminated by sea-water. Also Iwasaki and Katsura[9] (1964) stated that the amount of water soluble chlorine in Hawaiian lavas is small and almost constant, and a rather large amount of the water-soluble chlorine found in rock specimens is supplied by sea-water. The present author determined the amount of water-soluble chlorine to see if the chlorine in rocks is due to secondary contamination. The results showed that the amount of water-soluble chlorine in rocks was within 30% of the total chlorine content, except in specimens Nos. 4 and 6. This percentage is normal for previously reported fresh rocks. Moreover, in the discussion of the Br/Cl ratio, such an amount of water-soluble chlorine does not seriously affect the ratio, even if almost all of this water-soluble chlorine is secondary. Most of the water-soluble chlorine in specimens No. 4 and No. 6 might be secondary, however, the Br/Cl ratio in them falls in the range for ordinary rocks. In Table 3, it is noticed that both chlorine and bromine contents are scattered over a wide range, from 30 to 1020 ppm for chlorine, and from 0 to 5.5 ppm for bromine. The abundance of these lements, however, does not show any marked relationship to the type of rock, as shown in Figs. 2 and 3. Some glassy rocks show much higher chlorine and bromine contents. These results coincide with what has been given by Iwasaki *et al.*[6] (1957) on the chlorine content of volcanic rocks in Japan, and by Kokubu[10] (1956) on fluorine. Figure 4 shows the relationship between chlorine and bromine contents. No distinct linear relationship is seen between them. Br/Cl ratios, however, are mostly involved in the range from 1×10^{-3} to 6×10^{-3}, apparently lower than those reported by Behne. On the average: 200 ± 100 ppm for chlorine, 0.3 ± 0.2 ppm for bromine and $(3\pm2)\times10^{-3}$ for Br/Cl ratio. A comparison of the values of Behne and those of the present author gives about the same value for chlorine, about one-tenth for bromine and about one-seventh for the Br/Cl ratio. This discrepancy for bromine is too large to be accounted for only by the difference in methods of determintion.

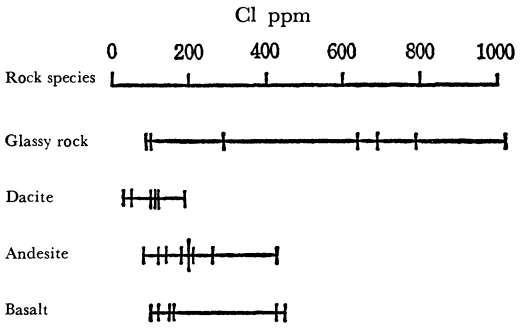

Fig. 2. Relationship between chlorine content of rocks and rock species.

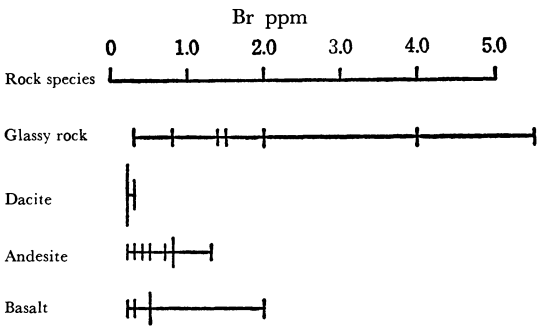

Fig. 3. Relationship between bromine content of rocks and rock species.

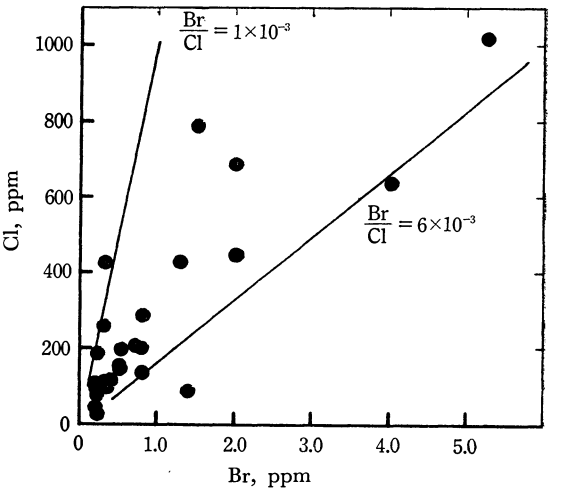

Fig. 4. Relationship between chlorine contents and bromine contents.

2) Br/Cl Ratios in Plutonic Rocks. The results are presented in Table 4, together with the chlorine and bromine contents of minerals in the rocks. Of plutonic rocks, only pegmatite, granite and a few other types of rocks have been analyzed, since it became clear in an early stage of this study

8) P. K. Kuroda and E. B. Sandell, *Anal. Chem.*, **22**, 1144 (1950).

9) B. Iwasaki and T. Katsura, This Bulletin, **37**, 1827 (1964).

10) N. Kokubu, *Kyushu Univ. Ser. C., Chemistry*, **2**, 95 (1956).

that the abundance of bromine in plutonic rocks is generally very small and the exact determination of bromine impossible for most specimens by the method employed. The chlorine content of the rocks analyzed, which contained negligibly small amounts of water-soluble chlorine and were believed to be uncontaminated by sea-water or other sources of contamination, is ordinarily 10—40 ppm, and a maximum of 100 ppm. The amount of chlorine in most rocks in this study is too small to be accurately determined. The situation is the same for bromine. The calculated Br/Cl ratios for these rocks are, of course, uncertain. However, the average Br/Cl ratio in plutonic rocks certainly is not as high as 21×10^{-3}, which was given by Behne. The highest value in any determination was 10×10^{-3}. The average Br/Cl ratio would then be the same as the average in volcanic rocks, $(3\pm2)\times10^{-3}$ or less.

3) Br/Cl Ratios in Biotite and Coexisting Quartz and/or Feldspar. Br/Cl ratios in plutonic rocks are still uncertain for most specimens. In order to examine the ratios obtained for these rocks, the author determined the Br/Cl ratios in biotite, and in quartz and feldspar coexisting with biotite. Biotite is considered to contain the greatest amount of chlorine in plutonic rocks, and is said to contain an appreciable amount of halogen in its crystal lattice. Chlorine and bromine in quartz and feldspar occur in quite a different manner from biotite. However, as shown in Table 4, bromine could not be determined accurately for most specimens, even for biotite containing a considerably high amount of chlorine. Yet, from these values, it was found that the Br/Cl ratio in these plutonic rocks is considerably smaller than the value reported by Behne, because the Br/Cl ratio in biotite, which seems to contain most of the chlorine found in these rocks, is certainly very small, 2×10^{-3} at maximum.

4) Relationship between the Br/Cl Ratios in Volcanic Rocks and in Volcanic Gases. Table 5 shows the chlorine and bromine contents and also the Br/Cl ratios in volcanic rocks and gases from a few volcanoes in Japan. For the Br/Cl ratio in volcanic gases, as mentioned above, it was confirmed in an earlier study[1] (1963) that they are more or less affected by many factors, and are usually in the range from 1×10^{-3} to 3×10^{-3} in weight ratio. The Br/Cl ratios in volcanic gases presented here are representative of the values obtained for each volcano in an earlier study[1] (1963). The Br/Cl ratio in rocks is somewhat larger than that in gases at Showashinzan, Fujusan and Issaikyoyama, while it is a little smaller than that at Chausuyama and Miharayama.

TABLE 5. THE CHLORINE AND BROMINE CONTENTS OF VOLCANIC ROCKS AND VOLCANIC GASES FOR 5 VOLCANOES IN JAPAN

Volcano		Cl, ppm	Br, ppm	Br/Cl×10³ (weigt)
Showashinzan	rock	90	0.3	3
	gas	856	1.1	1.2
Kujusan	rock	120	0.4	3
	gas	6250	7.6	1.2
Chausuyama	rock	260	0.3	1
	gas	429	0.6	1.4
Miharayama	rock	430	0.3	1
	gas	1640	2.8	1.7
Issaikyoyama	rock	140	0.8	6
	gas	239	0.5	2.4

5) Average Br/Cl Ratio in Igneous Rocks. Concerning the Br/Cl ratio in volcanic rocks, Kogarko and Gulyayeva[11] (1965) studied the halogen contents of the alkaline rocks of the Lovozero massif, and revealed that the chlorine and bromine contents of these rocks are normally in a linear log relationship independent of the rock species, and that the average Br/Cl ratio in the Lovozero rocks is about 1×10^{-3}. There are few determinations of the Br/Cl ratio in plutonic rocks. Filby[4] (1964) determined the bromine contents of standard rocks, granite G-1 and diabase W-1, by a neutron activation analysis developed by himself, and obtained values of 0.484 and 0.496 ppm for bromine of G-1 and W-1, respectively. These values are considerably lower than the averages for granites and basalts previously reported by Behne. The Br/Cl ratios of the standard rocks calculated with the chlorine contents determined by Kuroda *et al.*[12,13] (1950, 1951) are 5.7×10^{-3} for G-1, and 2.3×10^{-3} for W-1.

Most of the fluorine and chlorine in plutonic rocks is generally thought to exist in apatite or in minerals which contain OH^- in their crystal structure, replacing OH^-. This would be the case for bromine in rocks, also. The bromine to chlorine ratio, however, would be smaller in such minerals than in the liquid phase. The reason for this would be that the ionic radius of chlorine (1.81 Å) is closer to that of OH^- (1.40 Å) than that of bromine (1.96 Å), and the electron affinity of chlorine (3.82) is also stronger than that of bromine (3.54). It is realized that the Br/Cl ratio in biotite was very small in this study.

The Br/Cl ratio in volcanic rocks was roughly the same as that in volcanic gases at each volcano studied. However, as the Br/Cl ratio in volcanic gases has been reported to be $(1-3)\times10^{-3}$ in general, the average ratio obtained for volcanic rocks, $(3\pm2)\times10^{-3}$, is in rather good agreement with these values.

From the above, the average Br/Cl ratio obtained in this study is thought to be more reliable than previous values.

11) L. N. Kogaruko and L. A. Gulyayeva, *Geokhimiya*, No. 8, 1011 (1965).
12) P. K. Kuroda and E. B. Sandell, *Anal. Chem.*, **22**, 1144 (1950).
13) P. K. Kuroda and E. B. Sandell, *ibid.*, **22**, 1304 (1951).

Summary

1) Both chlorine and bromine contents of volcanic rocks are distributed over a wide range with no relation to rock types. The Br/Cl ratios, however, are restricted within a rather narrow range independent of their amounts in rocks, and the average value is $(3\pm2)\times10^{-3}$ by weight.

2) The average Br/Cl ratio in plutonic rocks is not so large as previously reported, but is the same as or less than the average in volcanic rocks.

3) The bromine contents of biotite, quartz and feldspar have not been determined accurately for most specimens, but it is certain that the Br/Cl ratio in biotite which contains most of chlorine in the rocks is very small.

4) The Br/Cl ratio in volcanic rocks and in volcanic gases at each volcano are nearly same in all volcanoes studied.

5) Taking account of these results together with the reports of Kogaruko and Gulyayeva[11] (1965), and others, the average Br/Cl ratio, $(3\pm2)\times10^{-3}$ in volcanic rocks seems to be more acceptable than the previous one, 21×10^{-3}.

Thanks are particularly due to Professor S. Oana, Department of Earth Sciences, Nagoya University who gave guidance throughout this study. Thanks are also due to Dr. N. Nakai, Department of Earth Sciences, Nagoya University for his valuable advice. The present author wishes to express his hearty thanks to Dr. Y. Mizutani, Department of Earth Sciences, Nagoya University who encouraged him with many useful suggestions and Mr. K. Shiraki who supplied him with many excellent samples.

BULLETIN OF THE CHEMICAL SOCIETY OF JAPAN VOL. 41 1139—1142 (1968)

Kinetics of Isotopic Exchange between 8-Quinolinol-^{14}C and Tris-8-quinolinolato Complexes of Tervalent Typical Elements

Kazuo SAITO, Michihiko TAKAHASHI, Yukio MIYAKAWA*[1] and Kazuyo MASUDA

Chemistry Department, Faculty of Science, Tohoku University, Katahira-cho, Sendai

(Received November 20, 1967)

Rate of isotopic exchange between 8-quinolinol-^{14}C and the 8-quinolinolato (oxinato) complexes of aluminum, gallium and indium has been studied in chloroform. Pure yellow complexes are precipitated by adding petroleum ether to the reaction mixture. The exchange rate decreased in the sequence In>Al>Ga, and a detailed kinetic study can be substantiated only with the gallium complex below 0°C. The rate is proportional to the concentration of the complex, but is independent of that of free 8-quinolinol (quinolH) and the Arrhenius activation energy is 18 kcal per mole. The reaction is accelerated by acid and presumably by water. It appears as if one of the ligands is present as unidentate under the given condition and the break of the remaining bond would be the rate determining step. Any reagent that can retard the recombination of the free end of unidentate ligand would catalyse the exchange reaction.

Typical elements of group III in the periodic table are regarded as substitution labile.[1] One of us, however, exemplified that trisacetylacetonato- and tris-8-quinolinolatoindium exchange radioactive indium at a measureable rate in chloroform at room temperature.[2] Recently we studied the isotopic exchange kinetics of trisacetylacetonatoaluminum in tetrahydrofuran.[3] The reaction mechanism was a dissociative nature and the break of unidentate ligand seemed to be the rate determining step. The reaction was accelerated by water and some kinds of organic acids, which appear to retard the recombination of the free end of unidentate acetylacetonate. It seems thus particularly interesting to examine the rate of isotopic exchange of 8-quinolinolato complexes, having a more rigid framework structure, and oxygen and nitrogen as coordinating atoms.

The solubility of tris-8-quinolinolato complexes of aluminum, gallium, indium and thallium(III) has been extensively examined in a variety of organic solvents, and it was found that the aluminum, gallium and indium complexes are precipitated in a pure state from their chloroform solutions by adding petroleum ether. However, the same procedure was not useful for obtaining pure thallium(III) complex, and

*[1] Present address: Kurosaki Plant, Mitsubishi Chem. Ind. Ltd., Kita-Kyushu.

1) M. Eigen, *Pure Appl. Chem.*, **6**, 105 (1963).

2) K. Saito and M. Tamura, *J. Inorg. Nucl. Chem.*, **13**, 334 (1960).

3) K. Saito and K. Masuda, This Bulletin, **41**, 384 (1968).

the exchange rate was studied with only the three kinds of complex. The precipitation is not affected by excessive ligand and some kinds of organic acid including *m*-toluic.

The rate of exchange decreased in the sequence indium, aluminum and gallium and detailed kinetic studies have been made only with the gallium complex below 0°C. The influence of the concentration of the complex, the free ligand and other ingredients has been carefully examined and a probable reaction mechanism posturated.

Experimental

Materials. 8-Quinolinol-^{14}C was synthesized by Scraup's method modified to suit for small scale preparation.[4] Aniline-^{14}C (0.1 mCi, 5.3 m*l*), glycerin (17.2 m*l*), nitrobenzene (3.5 m*l*), iron(II) sulfate (heptahydrate 2.0 g) and concentrated sulfuric acid (10.0 m*l*) were boiled for about five hours, cooled to about 100°C, and steam-distilled for 30 min, to remove unchanged nitrobenzene. The residual solution was neutralized with 40% sodium hydroxide solution (*ca.* 30 m*l*) and the quinoline steam-distilled together with remaining aniline. The organic layer of the distillate was treated with concentrated sulfuric acid (3.8 m*l*), cooled to 0—5°C, treated with excessive saturated sodium nitrite solution (5.0 m*l*), warmed on a steam bath for about an hour, and steam-distilled to remove volatile materials. The product treated with 40% sodium hydroxide solution (15.0 m*l*) and steam-distilled to collect crude quinoline, which was distilled and the dry colorless distillate (*ca.* 5 m*l*) was dropped into fuming sulfuric acid (10.0 m*l*) below 90°C. The darkcolored solution was warmed at 70°C for about 40 hr in anhydrous atmosphere, cooled and poured into cold water. Precipitated colorless prisms were filtered off, washed with water, recystallized from hot water and dried (6.27 g). Sodium hydroxide (12.0 g) and water (3 m*l*) were heated at 270°C with stirring, mixed with the quinoline 8-sulfonic acid powder, kept at the temperature for 10 min and chilled. The cake was broken, dissolved in an excess of hydrochloric acid (5 N 70 m*l*), neutralized, and steam-distilled. (Yeild 2.1 g 8-quinolinol-^{14}C)

8-Quinolinolato complexes of aluminum, gallium and indium were prepared by the method ordinarily used for gravimetric analysis, from commercial 8-quinolinol and appropriate salts of the metals.

Commercial chloroform was shaken with concentrated sulfuric acid, then 5% sodium hydroxide solution and water, dried with phosphorus pentoxide and distilled immediately before use.

m-Toluic acid was recrystallized from water and sublimed at 105°C at 5 mmHg. Commerical anisol was shaken with sodium hydroxide solution, dried with calcium chloride, refluxed with sodium and distilled. *p*-Terphenyl was recrystallized from xylene. *p*-Di-(5-phenyl-2-oxalozyl)-benzene (POPOP) was of scintillation grade and used without further purification. Other chemicals were of all chemically pure grade.

Experimental Procedure. Weighed amounts of the complex (65 to 250 mg) and the ligand (18 to 73 mg) were dissolved in 10 m*l* portions of chloroform separately (both $\simeq 10^{-2}$ M). Other reagents such as *m*-toluic acid were previously added to the solvent whenever necessary. Both solutions were kept in a bath at −5.0 or −20°C, and mixed after their temperature reached constant. At appropriate intervals, an aliquot ($\simeq$2 m*l*) was added to chilled petroleum ether (20 m*l*) to stop the reaction. Pure 8-quinolinolato complex was separated instantaneously free from excessive ligand. The precipitate was swiftly filtered off with filter paper, washed with petroleum ether, and dried at 110°C. The time required for this separation was about 2 min. Purity of the precipitate was checked by its absorption spectrum and the chemical analysis of the metal with EDTA. Absorption spectra of the reaction mixture disclosed that no reaction other than isotopic exchange was taking place in the reaction mixtures.

Measurement of Radioactivity. One mg of the precipitate was dissolved in 15.0 m*l* anisol, and mixed with 15.0 m*l* of anisol solution containing 0.02% POPOP and 0.8% *p*-terphenyl. The counting rate was measured by the scintillation technique with a coincidence liquid scintillation counter.[3] The 8-quinolinolato complexes have yellow color and provide quite significant quenching effect. The influence was examined with standard ^{14}C-benzoic acid and the inactive 8-quinolinolato complexes, to obtain calibration curves, with which the counting rate was duly corrected. The scintillation efficiency was *e.g.* 50.0% in the presence of 1.0 mg of the gallium complex in 30 m*l* of the liquid scintillator. The counting rate at the end of isotopic exchange reaction (infinite time) was calculated from that of the 8-quinolinol-^{14}C and the used amounts of the respective complexes.

Water contents in the chloroform and the reaction mixtures were determined by Karl Fischer titration. The ultraviolet absorption spectra were measured with Hitachi EPU-3 spectrophotometer and the infrared absorption spectra with Hitachi FIS-1, and EPI-2G spectrophotometer.

Results

The experimental data were treated with McKay's equation

$$R = -2.303\frac{3ab}{3a+b}\cdot\frac{\log(1-F)}{t} \qquad (1)$$

where a and b express the concentrations of the 8-quinolinolato complex (containing 3 mol of exchangeable ligands per mole) and 8-quinolinol, respectively. F is the fraction of reaction and t the lapse of time (in minutes). The plots of $\log(1-F)$ *vs.* t were all linear to permit the treatment with Eq. (1). The approximate rates of the ligand exchange of 8-quinolonolato complexes were as follows:

Indium complex, too rapid to be measured

Aluminum complex, half period ($t_{1/2}$), 10 min at −20°C, a=0.01 M

Gallium complex, measurably slow below 0°C.

Detailed kinetic studies were substantiated only with the gallium complex. About 10% zero-time exchange was observed throughout the studies with the gallium complex. The figure is reproducible and seems to be separation induced exchange. The

4) G. E. McCasland, *J. Org. Chem.*, **11** 277 (1946).

time zero of each kinetic run was taken as that the first aliquot was taken from the reaction mixture, *e.g.* 5 min after the mixing of the solutions. The experimental error involved in obtaining indiviual R values was less than 9%. The temperature deviated by less than 1°C from one kinetic run to another, but remained unchanged within an error less than 0.2°C during a given run.

The dependence of R on a and b is indicated in Fig. 1 and Table 1, respectively. They show that R is proportional to a and independent of b in the examined concentration ranges. Hence, R is expressed by Eq. (2).

$$R = k[\text{complex}] = ka \qquad (2)$$

The influence of water could not be examined. Saturated water concentration in chloroform at −20°C was 0.019 M. In the presence of more water, excessive water freezes on the surface of chloroform. The best dehydrated chloroform contained 0.016 M water immediately after distillation. However, even such a batch gave floating ice on the surface, whenever used as reaction medium, presumably owing to absorption of moisture from atmosphere. Thus the reaction mixture should be regarded as always saturated with water at the given temperature.

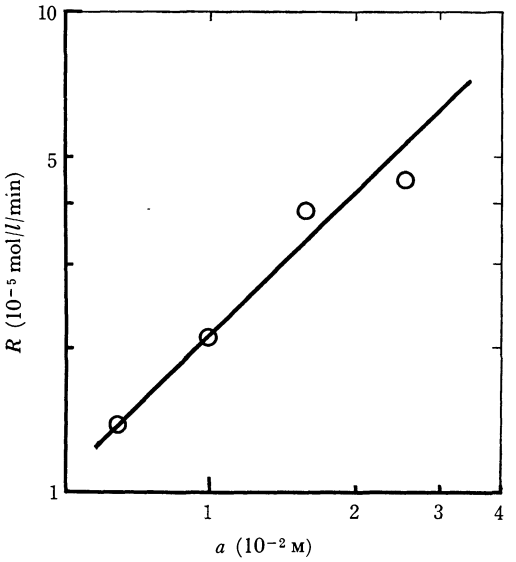

Fig. 1. Influence of the concentration of the gallium complex (a) on the exchange rate in chloroform. (−21.2°C, b=0.010 M)

Table 1. Influence of the concentration of free ligand (b) on the exchange rate of gallium in chloroform (a, 0.010 M)

t, °C	b, M	R,mol/ l /min
−5.0	0.010	2.1×10^{-4}
	0.030	1.8×10^{-4}
	0.040	1.9×10^{-4}
−20.2	0.010	2.4×10^{-5}
	0.016	2.6×10^{-5}
	0.025	2.6×10^{-5}

The temperature dependence of R was measured at −5.0, −10.4, −21.2°C. Arrhenius activation energy was 18.6 kcal per mole.

This reaction is catalyzed by acid, although the kinds of acid used for this examination were limited owing to the solubility. The influence of *m*-toluic acid upon R is shown in Fig. 2. Hence R is expressed as Eq. (3).

$$R = ka = a(k_0 + k_a[\text{acid}]) \qquad (3)$$

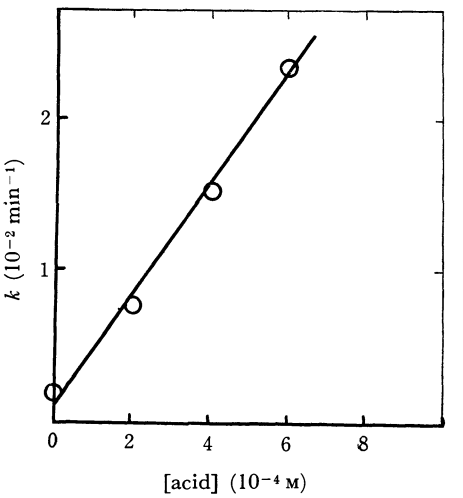

Fig. 2. Influence of the concentration of *m*-toluic acid on the exchange rate constant of gallium complex in chloroform. (−21.2°C, a=0.010 M)

Discussion

The mechanism would be of dissociative nature, because the exchange rate is independent of concentration of the free ligand. Since simultaneous break of two bonds, Ga–O and Ga–N, is not probable, we have to consider either that one of the ligands is present as unidentate and break of the remaining bond would be the rate-determining step, or that the break of one of the metal ligand bonds is the rate determining step and the liberation of unidentate ligand quite fast. In a kinetic study of isotopic exchange of trisacetylacetonato aluminum complex in THF, which gives similar kinetic formula, the two possible mechanisms were discriminated by examining the influence of water content upon the exchange rate.[3] In the present case, such a discrimination cannot be expected because we could not change the water content in chloroform. Hence Eq. (3) is only an apparent formula at a given concentration of water, in that the participation of water is not taken into consideration.

Nevertheless, the catalytic action of *m*-toluic acid could provide useful information. The proton could

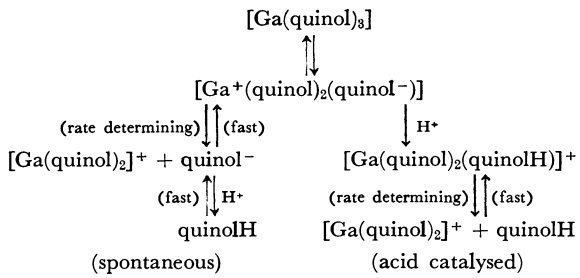

Fig. 3. Apparent mechanism of isotopic exchange for the gallium complex.

be transferred either to the free end of the unidentate ligand or to the coordinated oxygen. (Transfer to the negatively charged oxygen would be more feasible than to the nitrogen.) It remains again uncertain whether the proton is carried by the acid itself or by the hydronium ion, because the influence of water content upon the rate was neither known in the presence of acid. However, the proton would be more readily transferred to the negatively charged free end of unidentate ligand from the carrier, rather than the carrier reaches the co-ordinated oxygen atom making its way through the ligand sphere entangled with the bidentate chelates. Hence the plausible reaction mechanism would be postulated as seen in Fig. 3.

Eigen measured the exchange rate of coordinated water of various metal ions and found that the rate increases with increase in radii of ions with a given charge.[1] Hence the order of increasing reactivity among tervalent typical ions was aluminum, gallium, indium and thallium. The energy of hydration of the aquo complexes decreases in the same sequence and Eigen's order of reactivity is in accord with this order.

Our results are not consistent with his. The reason should be sought for in some factors characteristic of tris-8-quinolinolato complexes. If all the three complexes underwent isotopic exchange through similar dissociation mechanisms as exemplified by the gallium complex, their reactivity would be reflected, at least partly, in the stability of the tris complexes.

No reliable data are, however, available concerning the stability of tris-8-quinolinolato complexes of these metals. They form molecular lattice crystals and the solubility product[5] cannot be a good measure of stability. The shift of characteristic bands of the ligand in ultraviolet region due to complex formation was claimed to provide useful information concerning the stability of complexes with similar skeletal structure and symmetry.[6] Such a correlation cannot be always substantial, as exemplified by the comparison between the stability constants[7] and the absorption peaks of trisacetylacetonato complexes of these metals. The infrared absorption spectra in the region from 200 to 5000 cm^{-1} are too complicated for unambiguous band assignments to be made, and there is no concrete evidence that the force constant of metal-ligand bonds is simply interrelated with stability or lability of the complex.

Pritchard and Skinner compiled the electronegativity data of elements measured by various methods, and gave most probable values.[8] Since then, Allred and Rowchow[9] gave slightly different values obtained by electrostatic calculation, and Laubengayer *et al.*[10] compared the values for aluminum and gallium from proton magnetic resonance .data. All these estimations are consistent with one another in that the values for aluminum and indium are almost equal and that for gallium is significantly greater. Although the value for indium could become greater in some kinds of compound,[11] gallium seems always more electronegative than aluminum. If the reactivity of these complexes were governed by both the stability related to the electronegativity and the general reactivity represented in Eigen's experiment, the order of reactivity of tris-8-quinolinolato complexes, *i.e.* gallium < aluminum < indium, would not be very unreasonable.

The authors thank Nishina Memorial Foundation for grand in aid and Mrs. Yoshiko Doi (*née* Aizawa) for help in experiments.

5) S. Lacroix, *Anal. Chim. Acta*, **1**, 260 (1947).
6) E. Sekido, *Nippon Kagaku Zasshi* (*J. Chem. Soc. Japan, Pure Chem. Sect.*), **80**, 871 (1959).
7) R. M. Izatt, W. C. Fernelius, C. G. Haas, Jr., and B. P. Block, *J. Phys. Chem.*, **59**, 170 (1955).
8) H. O. Pritchard and H. A. Skinner, *Chem. Revs.*, **55**, 745 (1955).
9) A. L. Allred and E. G. Rowchow, *J. Inorg. Nucl. Chem.*, **5**, 264 (1958).
10) S. Brownstein, B. C. Smith, E. Ehrlich and A. W. Laubengayer, *J. Am. Chem. Soc.*, **81**, 3826 (1959).
11) R. C. Fay and T. S. Piper, *ibid.*, **85**, 500 (1963).

BULLETIN OF THE CHEMICAL SOCIETY OF JAPAN VOL. 41 1143—1146 (1968)

Kinetics and Mechanisms of Thermal Decomposition Reactions of Cobalt(III) Complexes. Hexammine-, Halogenoammine- and Oxalatoamminecobalt(III) Complexes

Nobuyuki TANAKA and Kenzo NAGASE*1

Department of Chemistry, Faculty of Science, Tohoku University, Katahira-cho, Sendai

and Saburo NAGAKURA

Institute of Solid State Physics, The University of Tokyo, Minato-ku, Tokyo

(Received November 29, 1967)

Kinetics of the thermal decomposition reactions of hexammine-,halogenoammine- and oxalatoamminecobalt(III) complexes in solid state has been studied by following the change in the cobalt(III) contents with time. It was found that the decomposition of these complexes was initiated by the change of the valence state of cobalt(III) to cobalt(II), and that these electron-transfer reactions were kinetically of a first order. The first-order rate constants, the activation energies and the frequency factors of these electron-transfer reactions were obtained. The values of the activation energies were found to increase in parallel with the increase in the difference between t_{2g} and e_g orbitals of the cobalt(III) complexes investigated. (The notations, t_{2g} and e_g, are used in the expression of an O_h-symmetry approximation for halogenoammine- and oxalatoamminecobalt(III) complexes.)

It has been reported that the thermal decomposition of cobalt(III) complexes in solid state is caused by the change of the valence state of cobalt(III) to cobalt(II); Tanaka and his co-workers[1-5] proposed that the decomposition of cobalt(III) and iron(III) complexes was initiated by an electron transfer from a ligand or an outer-sphere anion to the central metal(III) cation. Wendlandt *et al.*[6-8] also found the change of the valence state on the thermal decomposition of cobalt(III) and manganese(III) complexes.

In order to proceed a general consideration of the electron-transfer reactions on the thermal decomposition of cobalt(III) complexes, the present authors have undertaken the determination of the rates of these reactions. The activation energies and frequency factors were calculated from the first-order rate constants using the Arrhenius equation, and the mechanisms of the electron-transfer reactions were discussed.

Experimental

The apparatus and the procedure are described in a previous paper.[3] $[Co(NH_3)_6]X_3$(X=Cl, Br, I), $[Co(en)_3]Cl_3\cdot 3H_2O$, $[CoX(NH_3)_5]Y_2$(X, Y=Cl, Br), *trans*-$[CoCl_2(NH_3)_4]Cl\cdot H_2O$, $[Co(ox)(NH_3)_4]Cl$, $K[Co(ox)_2(NH_3)_2]\cdot H_2O$ and $M_3[Co(ox)_3]\cdot 3H_2O$(M=Na, K) were prepared according to the methods given in the literature (see Refs. 3 and 4).

Results

The preliminary measurements carried out with varied initial amounts of the samples had confirmed the relation given by the equation,

$$-dN/dt = kN \quad (1)$$

where N represents the number of cobalt(III) ions in the sample and k the first-order rate constant. Figure 1 shows the dependence of the reaction rate on the initial amount of the sample, indicating that the reaction follows the first-order rate law.

For the convenience of the treatment, Eq. (1) was modified to

$$\ln(1-x) = -kt \quad (2)$$

where x is the mole fraction of cobalt(II) in the sample. A plot of $\log(1-x)$ *versus* time was made for each complex at various temperatures, and nearly

*1 Present address: Department of Chemistry, College of General Education, Tohoku University, Kawauchi, Sendai.

1) N. Tanaka and M. Nanjo, This Bulletin, **37**, 1330 (1964).
2) N. Tanaka, M. Sato and M. Nanjo, *Sci. Repts. Tohoku Univ., Ser. I*, **48**, No. 1, 1 (1964).
3) N. Tanaka and K. Nagase, This Bulletin, **40**, 546 (1967).
4) N. Tanaka and M. Nanjo, *ibid.*, **40**, 330 (1967).
5) N. Tanaka, K. Nagase and S. Nagakura, *Inorg. Nucl. Chem. Letters*, **3**, 169 (1967); in press (1967).
6) W. W. Wendlandt and J. P. Smith, *J. Inorg. Nucl. Chem.*, **25**, 1267 (1963).
7) W. W. Wendlandt and E. L. Simmons, *ibid.*, **27**, 2317 (1965).
8) E. L. Simmons and W. W. Wendlandt, *ibid.*, **27**, 2325 (1965).

TABLE 1. KINETIC PARAMETERS FOR COBALT(III) COMPLEXES

Complex	$k\times10^5$, sec^{-1} (Temp., °C)	E_a kcal/mol	A sec^{-1}
$[Co(NH_3)_6]Cl_3$	1.87(165), 2.25(167), 3.61(172)	36.0	2×10^{13}
$[Co(NH_3)_6]Br_3$	2.35(155), 4.58(159), 6.12(165)	35.6	3×10^{13}
$[Co(NH_3)_6]I_3$	2.39(104), 3.39(109), 6.08(114)	29.4	3×10^{12}
$[CoCl(NH_3)_5]Cl_2$	2.88(155), 3.95(160), 6.40(167)	23.6	3×10^{7}
$[CoCl(NH_3)_5]Br_2$	1.78(132), 2.46(137), 3.80(142)	27.4	8×10^{9}
$[CoBr(NH_3)_5]Cl_2$	1.31(137), 2.19(144), 3.41(152)	22.6	1×10^{7}
$[CoBr(NH_3)_5]Br_2$	1.63(127), 2.31(132), 4.98(142)	24.0	2×10^{8}
trans-$[CoCl_2(NH_3)_4]Cl\cdot H_2O$	1.68(137), 2.66(142), 4.31(155)	19.6	4×10^{5}
$[Co(ox)(NH_3)_4]Cl$	1.12(164), 1.48(170), 3.09(178)	29.9	8×10^{9}
cis-$K[Co(ox)_2(NH_3)_2]\cdot H_2O$	1.60(110), 2.90(117), 4.08(121)	26.6	2×10^{10}
$Na_3[Co(ox)_3]\cdot 3H_2O$	1.69(51), 2.37(56), 3.65(61)	20.0	5×10^{8}
$K_3[Co(ox)_3]\cdot 3H_2O$	2.31(71), 4.03(76), 5.48(81)	20.8	4×10^{8}
$[Co(en)_3]Cl_3\cdot 3H_2O$	1.67(196), 1.99(199), 3.65(207)	34.9	2×10^{11}

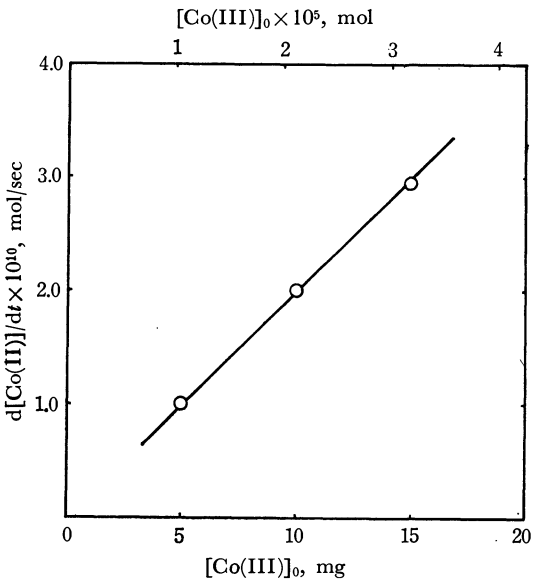

Fig. 1. Reaction rate as a function of the initial amounts of the sample ($[Co(III)]_0$) obtained with $K_3[Co(ox)_3]\cdot 3H_2O$ at 87°C.

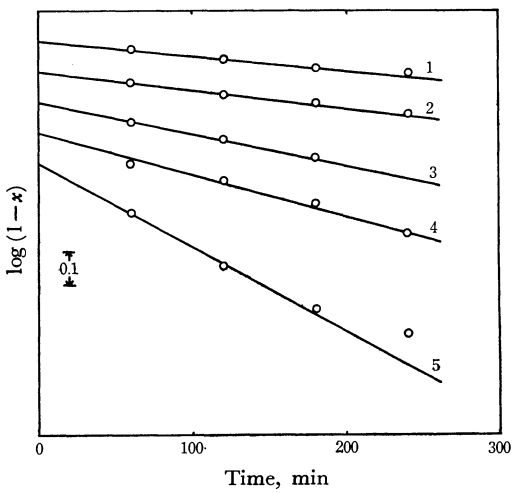

Fig. 2. Relation of $\log(1-x)$ *versus* time for $K_3[Co(ox)_3]\cdot 3H_2O$ at (1) 66, (2) 71, (3) 76, (4) 81 and (5) 87°C.

straight lines were obtained. The plots for $K_3[Co(ox)_3]\cdot 3H_2O$ are shown in Fig. 2 as an example. In the case of $[CoCl(NH_3)_5]Br_2$, $[CoBr(NH_3)_5]Cl_2$, $[CoBr(NH_3)_5]Br_2$ and $[Co(ox)(NH_3)_4]Cl$, the rate was considerably accelerated as the reaction took place and the plots showed a tendency of departing from the straight lines.

The first-order rate constants were determined from the plots of $\log(1-x)$ *versus* t at various temperatures, from which the activation energies and frequency factors were calculated. The kinetic parameters obtained are given in Table 1.

Discussion

The observed activation energies increase in parallel with the increase in the difference of e_g and t_{2g} levels, though they are somewhat lower than the transition energies of the A band of the absorption spectra of cobalt(III) complexes. This relation is shown in Fig. 3*1; the energies of the A bands are taken from the literatures.[9,10]

The cobalt(III) complexes investigated in this study have a singlet ground state and a triplet lowest excited state. Their symmetry notations are $^1A_{1g}$ and $^3T_{1g}$, respectively, in the expression of an O_h-symmetry approximation. The potential energy curves of the ground state of the cobalt(III) complexes and the lowest triplet state may be represented schematically with curves 1 and 2 in Fig. 4, respectively. The energy state given by curve 2 may

*1 Figure 1 in Ref. 5 should be replaced by this figure, in which the values of $\Delta E(^3T_{1g}-{}^1A_{1g})$ were recalculated.

9) M. Linhard and M. Weigel, *Z. Physik. Chem., N.F.*, **11**, 308 (1957).
10) J. Fujita and Y. Shimura, This Bulletin, **36**, 1281 (1963).

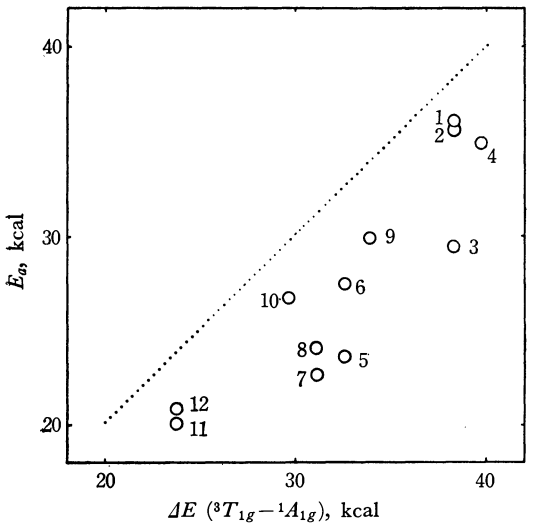

Fig. 3. Relation of the activation energies (E_a) *versus* the energy of the A band (ΔE) for
(1) $[Co(NH_3)_6]Cl_3$, (2) $[Co(NH_3)_6]Br_3$,
(3) $[Co(NH_3)_6]I_3$, (4) $[Co(en)_3]Cl_3\cdot 3H_2O$,
(5) $[CoCl(NH_3)_5]Cl_2$, (6) $[CoCl(NH_3)_5]Br_2$,
(7) $[CoBr(NH_3)_5]Cl_2$, (8) $[CoBr(NH_3)_5]Br_2$,
(9) $[Co(ox)(NH_3)_4]Cl$, (10) $K[Co(ox)_2(NH_3)_2]\cdot H_2O$,
(11) $Na_3[Co(ox)_3]\cdot 3H_2O$ and
(12) $K_3[Co(ox)_3]\cdot 3H_2O$.

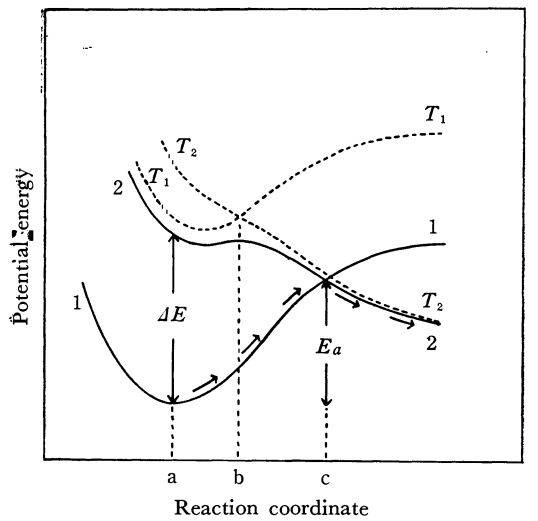

Fig. 4. Schematic potential energy diagram of cobalt complexes.

mainly consist of electron configurations T_1 and T_2 which are shown in Fig. 5.*2 The latter is the charge-transfer configuration in the sense that it is

*2 Besides these two configurations, T_3 configuration which is given in Fig. 5 may contribute to the lowest triplet state. Its energy, however, is undoubtedly higher than that of T_2 and the contribution of T_3 to the lowest triplet state may conceivably be small. Therefore, it may safely be disregarded in the qualitative consideration made in the present paper.

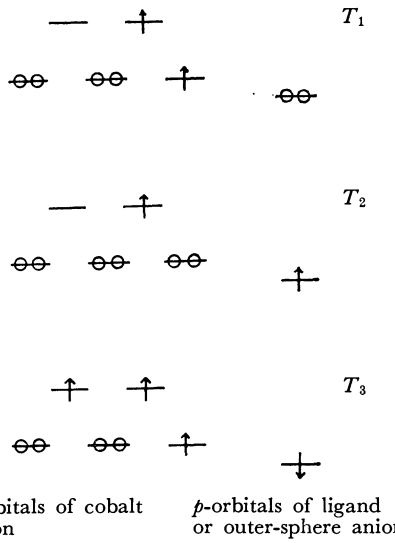

Fig. 5. Electron configurations of the triplet states of cobalt complexes.

brought about by an electron transfer from a ligand or an outer-sphere anion (X^-) to the central metal cation. The potential energy curves of T_1 and T_2 are also schematically shown in Fig. 4.*3 Curve 2 can be obtained as the result of the configuration interaction between T_1 and T_2.

At or near the point which corresponds to the equilibrium position of the reaction coordinate, T_1 is more stable than T_2, and therefore T_1 is the most important configuration in the lowest triplet state. With the increasing distance in the reaction coordinate, however, T_2 gradually approaches T_1, and they cross each other at point b. At more distant points, T_2 contributes to the lowest triplet state to a

*3 T_1 is stabilized by electrostatic interaction with decreasing distances between X^- and Co^{3+}. On the other hand, we can not expect the large electrostatic attraction in T_2 where X^- approaches Co^{2+}.

*4 It is difficult to discuss this point quantitatively, because the electron affinity of the central metal cation is very sensitive to its effective charge; namely 35.03 eV for Co^{3+}, 18.29 for Co^{2+} and 5.44 for Co^+. Let us now take as an example the case where X^- is an outer-sphere chloride anion. The energy difference between T_2 and T_1 in the infinite separation may be represented by $E_{T_2}-E_{T_1}=I_{X^-}-A_{Co^{\delta+}}+\Delta$, where I_{X^-} and $A_{Co^{\delta+}}$ are the ionization potential of X^- and the electron affinity of $Co^{\delta+}$, respectively, and Δ is the change in the electrostatic interaction energy between the central metal ion and ligands caused by the electron transfer. The value of Δ is also largely dependent on the δ value, because the positive charge on a ligand molecule, say NH_3, increases with the decreasing δ value.

In the case of $\delta=1$, Δ may be negative, because the electrostatic repulsion between $Co^{\delta+}$ and ligands with positive charge disappears, or at least decreases to a great extent, as the result of the electron transfer. $I_{X^-}-A_{Co^{\delta+}}$ is also negative for $\delta=1$, since $I_{X^-}=3.70$ eV and $A_{Co^+}=5.44$ eV. Therefore, $E_{T_2}-E_{T_1}$ turns out to have a negative sign and T_2 may be expected to be more stable than T_1 in the infinite separation. The above conclusion may conceivably be satisfied for the other δ values than 1.

greater extent than T_1. This may be inferred from the fact that, in the infinite separation between X^- and Co^{3+}, T_2 may conceivably be more stable than T_1.*4 From a similar reason, T_2 or curve 2 crosses curve 1 at point c in the reaction coordinate, as is shown in Fig. 4.

According to the potential energy curves shown in Fig. 4, the electron-transfer process leading to the decomposition of the complexes seems to occur passing through point c as is indicated by arrows given in Fig. 4. In other words, the transfer of the system from curve 1 to curve 2 occurs at point c being accompanied by the change in multiplicity and the electron transfer from a ligand or an outer-sphere anion to Co^{3+}.

In view of the different multiplicity in curves 1 and 2, the probability of the transfer will be small, and consequently the reaction will have a small transmission coefficient, which in turn will give a small value of the frequency factor. The observed frequency factors given in Table 1 support this consideration. The reactions which are kinetically of a first order have in usual the frequency factor of about 10^{13}.

The authors thank the Ministry of Education for the financial support granted for this research.

BULLETIN OF THE CHEMICAL SOCIETY OF JAPAN VOL. 41 1146—1151 (1968)

Activity Measurements in Orthosilicate and Metasilicate Solid Solutions. I. Mg_2SiO_4-Fe_2SiO_4 and $MgSiO_3$-$FeSiO_3$ at 1204°C

Kenzo KITAYAMA and Takashi KATSURA

Department of Chemistry, Faculty of Science, Tokyo Institute of Technology, Ookayama, Meguro-ku, Tokyo

(Received December 7, 1967)

The activity-composition relations in ortho-, and metasilicate solid solutions in the FeO-MgO-SiO_2 system are determined at 1204°C on the basis of the measurement of equilibrium oxygen partial pressures. Both the olivine and the pyroxene solid solutions show significant deviations from ideality. Using the present data, the standard free energy change of formation of ferrosilite (hypothetical compound, $FeSiO_3$) is calculated to be -41.7 ± 0.2 kcal/mol on the basis of the equilibrium between metallic iron and silica, and to be -1.6 ± 0.2 kcal/mol on the wüstite (" FeO ") and silica.

Recently, much efforts are being concentrated on the thermodynamic properties of ortho-, and metasilicate equilibria found in some ternary oxide systems at high temperatures under one atmospheric pressure. Of these, the relationship between activity and composition of the olivine-components (orthosilicate) and the pyroxene-components (metasilicate) is no doubt of the fundamental problem to exactly understand the stable co-existence of these solid solutions. Schwerdtfeger and Muan[1] have determined the activities of a component Fe_2SiO_4 in olivine and of a component $FeSiO_3$ in pyroxene solid solutions in the FeO-MnO-SiO_2 system at 1150°C on the basis of the CO_2/CO ratio in the gas phase in equilibrium with co-existing solid solutions, and concluded that both solid solutions behave ideally. In their Appendix, Darken and Schwerdtfeger[2] made clear statistically the expression of activity of the component Fe_2SiO_4 in the olivine solid solution to be written as $a_{FeSi_{0.5}O_2}$ as empirically had been accepted by many investigators. Masse, Rosen, and Muan[3] also published the activity-composition relations in Co_2SiO_4-Fe_2-SiO_4 solid solution at 1180°C, and showed a slightly positive deviation from ideality. Biggers and Muan[4] presented the relations in ortho-, and meta-silicate solid solutions found in the MnO-CoO-SiO_2 system at 1200 and 1250°C. On the basis of these results, Muan[5] emphasized the importance of the conjugation lines between co-existing solid solutions. However, the activity-composition relations to the olivine and pyroxene in the FeO-MgO-SiO_2 system has not yet been experimentally studied.

Generally, it has been assumed that the olivine composing of iron and magnesium may behave ideally, and the various thermodynamic calculations have

1) K. Schwerdtfeger and A. Muan, *Trans. AIME*, **236**, 201 (1966).
2) L. S. Darken and K. Schwerdtfeger, *ibid.*, **236**, 208 (1966).
3) D. P. Masse, E. Rosen and A. Muan, *J. Am. Ceram. Soc.*, **49**, 328 (1966).
4) J. V. Biggers and A. Muan, *ibid.*, **50**, 230 (1967).
5) A. Muan, *Am. Min.*, **52**, 797 (1967).

been made on the basis of the ideality. For instance, Bowen and Schairer[6] calculated the molal heat of fusion of fayalite (Fe_2SiO_4) and forsterite (Mg_2SiO_4) in their classical paper, and Lamberg and DeVore[7] also postulated the ideality to calculate the distribution constant of iron and magnesium in co-existing olivine and pyroxene by using mole fraction. Bradley[8] found that the olivine solid solution is ideal, on the basis of the molal heat of fusions of fayalite and forsterite. Sahama and Torgesson[9] also presented the linearity found in the relationship between the heat of solution and the Mg/Fe ratio in the natural forsterite-fayalite series by means of the solution calorimetry, and indicated that the replacement of Fe and Mg in the olivine structure is thermally perfect. They also stated that the replacement of Fe to Mg in orthorhombic pyroxene structure is perfect too.

The present objectives are to find the activity-composition relations in the olivine and the pyroxene solid solutions in the FeO-MgO-SiO_2 system and to confirm whether or not these solid solution aresideal just as expected by many investigators.

Methods of Calculation of the Activities

The approximate diagram for the subsolidus phase equilibria in the FeO-MgO-SiO_2 system is known from the study by Bowen and Schairer[6] under low oxygen partial pressures, and Fig. 1 shows an isothermal section at 1204°C. In this system, there exist three solid solution series; the oxide, MgO-FeO, the olivine, Fe_2SiO_4-Mg_2SiO_4, and the pyroxene, $FeSiO_3$-$MgSiO_3$. The oxide and olivine solid solutions are continuous, but the pyroxene solid solution is a limiting as shown in Fig. 1, because of the instability of ferrosilite in ordinary temperature and pressure. From the present study, we found a point A and a point B in Fig. 1 to be 62 mol% fayalite and 48 mol% ferrosilite at 1204°C, respectively. The activity-composition relation in the oxide solid solution, FeO-MgO, has already been studied by Hahn, Jr., and Muan[10] in the temperature interval from 1000 to 1300°C, and they concluded that the system showed a considerable positive deviation from the Raoult's law.

Based on Fig. 1, it may be convenient to calculate the activity of the component Fe_2SiO_4, $a_{FeSi_{0.5}O_2}$, in the olivine solid solution and the activity of the component $FeSiO_3$, a_{FeSiO_3}, in the pyroxene solid solution as follows:

1) The Activity of Fe_2SiO_4 in Composition Ranging from Pure Fe_2SiO_4 to a Point A. Consider the following reaction,

$$FeSi_{0.5}O_2 = Fe + \tfrac{1}{2}\,SiO_2 + \tfrac{1}{2}\,O_2 \qquad (1)$$

in which pure fayalite dissociates to metallic iron, silica, and oxygen gas. For this reaction, the equilibrium constant, K_1, is expressed as

$$K_1 = [a_{Fe} \cdot a_{SiO_2}^{1/2} \cdot P_{O_2}^{1/2}(1)]/a_{FeSi_{0.5}O_2\text{-}(p)} \qquad (2)$$

where a represents the activity of each component shown by subscripts, in which $FeSi_{0.5}O_2$-(p) means for pure fayalite, and where $P_{O_2}(1)$ implies an oxygen partial pressure. Since the composition of fayalite is stoichiometric as confirmed by Kitayama and Katsura,[11] then the equilibrium constant, K_1, may be written as

$$K_1 = P_{O_2}^{1/2}(1) \qquad (3)$$

In the case of the solid solution, the same treatment is applied as follows,

$$(FeSi_{0.5}O_2)_{ss} = Fe + \tfrac{1}{2}\,SiO_2 + \tfrac{1}{2}\,O_2 \qquad (4)$$

in which the fayalite component in the olivine dissociates to form pure metallic ion and pure silica as in the reaction (1). The subscript ss means a solid solution, and the equilibrium constant, K_4, is also expressed as

$$K_4 = P_{O_2}^{1/2}(4)/a_{(FeSi_{0.5}O_2)_{ss}\text{-}(1)} \qquad (5)$$

where the subscript $(FeSi_{0.5}O_2)_{ss}$-(1) means the limiting solid solution from pure fayalite to the point A. From Eqs. (3) and (5), we get the following relation by using pure fayalite as the standard state for the activity of $FeSi_{0.5}O_2$,

$$a_{(FeSi_{0.5}O_2)_{ss}\text{-}(1)} = P_{O_2}^{1/2}(4)/P_{O_2}^{1/2}(1) \qquad (6)$$

because K_4 is equal to K_1.

2) The Activity of Fe_2SiO_4 in Composition Ranging from the Point A to Pure Mg_2SiO_4. In this region, the reaction of olivine is different from that of Eq. (4). If we follow experimentally the appearance of metallic iron by changing the oxygen partial pressure, then olivine solid solution may first dissociate as follows,

$$(FeSi_{0.5}O_2)_{ss} = \tfrac{1}{2}\,Fe + \tfrac{1}{2}\,(FeSiO_3)_{ss} + \tfrac{1}{4}\,O_2 \qquad (7)$$

The equilibrium constant, K_7, is

$$K_7 = [a_{(FeSiO_3)_{ss}}^{1/2} \cdot P_{O_2}^{1/2}(7)]/a_{(FeSi_{0.5}O_2)_{ss}\text{-}(2)} \qquad (8)$$

where the subscript $(FeSi_{0.5}O_2)_{ss}$-(2) means the range from the point A to pure Mg_2SiO_4. The pyroxene thus appeared will subsequently decompose at an oxygen partial pressure defined by the following Eq. (9),

$$\tfrac{1}{2}\,(FeSiO_3)_{ss} = \tfrac{1}{2}\,Fe + \tfrac{1}{2}\,SiO_2 + \tfrac{1}{4}\,O_2 \qquad (9)$$

The equilibrium constant, K_9, is expressed as

6) N. L. Bowen and J. F. Schairer, *Am. J. Sci.*, **29**, 151 (1935).
7) H. Lamberg and G. DeVore, *J. Geol.*, **59**, 193 (1951).
8) R. S. Bradley, *Am. J. Sci.*, **260**, 550 (1962).
9) Th. G. Sahama and D. R. Torgesson, *J. Geol.*, **57**, 255 (1949).
10) W. C. Hahn, Jr., and A. Muan, *Trans. AIME*, **224**, 416 (1962).
11) K. Kitayama and T. Katsura, This Bulletin, **41**, 525 (1968).

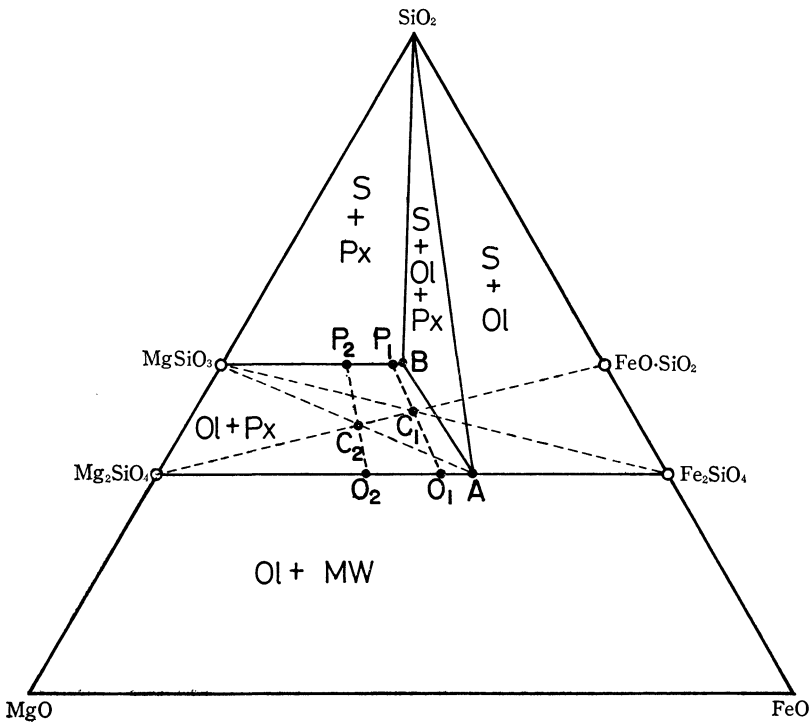

Fig. 1. The isothermal section for the system MgO-FeO-SiO_2 at 1204°C.
S: silica, Px: pyroxene, Ol: olivine, MW: magnesiowüstite

$$K_9 = P_{O_2}^{1/4}(9)/a_{(FeSiO_3)_{ss}}^{1/2} \qquad (10)$$

In the reaction (9), pure silica and iron appear as shown in Fig. 1, and there exists a relation, $K_4 = K_7 \cdot K_9$. Thus, we may obtain the Eq. (11), taking the pure fayalite as the standard state,

$$a_{(FeSi_{0.5}O_2)_{ss}} = [P_{O_2}^{1/4}(7) \cdot P_{O_2}^{1/4}(9)]/P_{O_2}^{1/2}(1) \qquad (11)$$

3) The Activity of $FeSiO_3$ in the Pyroxene Solid Solution. The activity of $FeSiO_3$ in the pyroxene solid solution is obtained by the same method as described above. As for the solid solution is concerned, the activity of $FeSiO_3$ is given by Eq. (10), taking an arbitrary composition as the standard state for the component $FeSiO_3$. If we want to take pure ferrosilite as the standard state, then we have to apply the extrapolation method. Here, we may apply the α-function method[12,13] to determine an oxygen partial pressure at which ferrosilite may decompose as shown in Eq. (9). After obtaining the oxygen partial pressure for pure ferrosilite, P_{O_2}(9-p), the activity of the component $FeSiO_2$ in pyroxene solid solution may be derived as

$$a_{(FeSiO_3)_{ss}} = P_{O_2}^{1/2}(9)/P_{O_2}^{1/2}(9\text{-p}) \qquad (12)$$

Experimental

Preparation of Olivine Solid Solution. Reagent grade chemicals are used. Ferric oxide is reduced to ferrous at 1200°C in an atmosphere of $CO_2/H_2 = 1$. After analyzing the ferrous content, the oxide is mixed with silica to prepare the stoichiometric fayalite having the Fe/Si ratio 1/2. The mixture is then heated at 1300°C to prepare the fayalite in the same atmosphere by using a Pt alloy (20%Rh) as a container which was previously saturated with iron. The melt is quenched and powdered. Forsterite is prepared as follows; Silica and magnesium oxide are stoichiometrically mixed and made uniform by using an alumina pot mill. The powder is heated at 1700°C by using a zirconia or a Pt alloy container. The quenched sample is powdered, and repeatedly heated at 1700°C. The iron content in fayalite and the magnesium in forsterite are analyzed by potassium permanganate and EDTA titration methods respectively. Both samples with various mole fractions are mixed to prepare the olivine solid solution.

About 5 g of each mixture is heated for 5 hr at 1200 to 1300°C by using a Pt alloy container under the atmosphere of $CO_2/H_2 = 1$. The prepared olivine solid solutions are checked by X-ray diffraction method and by chemical analysis. Yoder and Sahama,[14] and Eliseev[15] measured the d_{130} spacing of natural and

12) L. S. Darken and R. W. Gurry, "Physical Chemistry of Metals," McGraw-Hill, New York (1953), p. 264.
13) A. Muan, R. H. Nafziger and P. L. Roeder, *Nature*, **202**, 688 (1964).
14) H. S. Yoder, Jr., and Th. G. Sahama, *Am. Min.*, **42**, 475 (1957).
15) E. Eliseev, *Zapiski Vsesoyuz. Min. Obshchestva* **86**, 657 (1957) (Cited from the "Silicate Science," Vol. III, W. Eitel, Academic Press, New York (1965) p. 406.

synthetic olivines, and showed the linearity between the d_{130} value and the composition. The relationship between the d_{130} value and the composition by the present study is in good accordance with those of the literature.

Preparation of Pyroxene Solid Solution. The silica and magnesium oxide are thouroughly mixed by a pot mill to prepare enstatite ($MgSiO_3$). The mixture is repeatedly heated at 1700°C by using a Pt alloy container to make it homogeneous solution. The glass thus obtained is finally crystallized at 1200°C to get the monoclinic structure. Since ferrosilite cannot synthesize in the present conditions, then ferrous oxide is mixed with silica so as to maintain the Fe/Si ratio of 1 for the "ferrosilite." The mixture with various ratios of enstatite and "ferrosilite" are heated at 1200°C to prepare the homogeneous pyroxene solid solutions. The pattern of the X-ray diffraction of the solid solution is complicated, but systematically changes with increasing ferrosilite component. The problem of the structure of pyroxene has not yet been solved as summarized by Morimoto,[16] but Dr. Kushiro[17] found the proto-type pyroxene in the present samples.

Apparatus. The furnace, the gas mixer, the electric controller system for temperature are the same as those used in a previously study.[18] Mixed gases of CO_2 and H_2 are used to obtain the oxygen partial pressure.

Procedure. The standard quenching techniques are adopted under controlled atmospheric condition. A sample of either olivine or pyroxene solid solution is kept at 1204±2°C and at a desired level of the oxygen partial pressure. After 24 hr, the sample is quenched in the brass tube connected to the bottom of the furnace tube. Then an oxygen partial pressure, at which metallic iron appears in the sample, is determined. The presence of metallic iron is detected by dipping the sample into a dilute hydrochloric acid solution as previously described.[19]

A Direct Determination of the Oxygen Partial Pressure. The actual oxygen partial pressure of the gas phase is determined by a solid electrolyte cell, and the details of the design and the measurement were described by Katsura and Hasegawa.[20]

Results and Discussion

Determination of Conjugation Lines between Olivine and Pyroxene Solid Solution. In order to determine the activity of $a_{(FeSi_{0.5}O_2)\text{-}(2)}$, the conjugation lines between olivine and pyroxene solid solutions must be determined; for this purpose, various mixtures of Mg_2SiO_4 and "ferrosilite," or of Fe_2SiO_4 and $MgSiO_3$ are heated at 1204°C and at an oxygen partial pressure of $10^{-11.0}$ atm to avoid an appearance of metallic iron or ferric oxide. The samples are quenched after a reasonable period of time, and the d_{130} value of the olivine phase coexisting with pyroxene is measured to determine the composition of the olivine by comparing with the d_{130} of the standard. In order to criticise the reasonable period of time for the equilibrium state, different combinations of the two solid solution series, but with the same bulk composition are used just at the same conditions. Examples are illustrated in Fig. 1 as points C_1 and C_2. From the careful measurement of d_{130} value, it was found that 48 hr heating is sufficient to the equilibrium state throughout the study. The conjugation lines are, then, drawn so as to pass the two points, for example, C_1–O_1, or C_2–O_2 in Fig. 1 to determine the composition of pyroxene solid solution, P_1 or P_2. The result of the equilibrium co-existence of olivine and pyroxene solid solutions are graphically illustrated in Fig. 2.

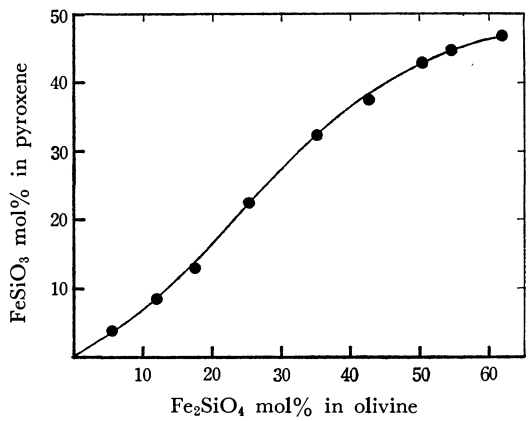

Fig. 2. The equilibrium composition between olivine and pyroxene solid solutions in terms of fayalite component in olivine and of ferrosilite component in pyroxene.

The Pyroxene Solid Solution. The values of the oxygen partial pressures of P_{O_2} (9) are given in Table 1, with the width of experimental errors. Activities calculated on choosing the composition of 48 mol% ferrosilite as an arbitrarily selected standard are also given in Table 1. The relationship between $[\log N_{FeSiO_3} - \frac{1}{2}\log P_{O_2}(9)]$ and $(1-N_{FeSiO_3})^2$, which is related to the α-function,[13] are illustrated in Fig. 3. An extrapolated value of $\log P_{O_2}$(9-p) for pure ferrosilite is determined to be -12.35 ± 0.03.

Table 1. Activity of pyroxene

N_{FeSiO_3}	$-\log P_{O_2}(9)$ (atm)	a_{FeSiO_3}*	a_{FeSiO_3}**
0.10	14.00±0.02	0.15±0.01	0.26±0.01
0.20	13.42±0.03	0.29±0.02	0.50±0.02
0.30	13.10±0.03	0.42±0.03	0.73±0.03
0.39	12.94±0.03	0.51±0.03	0.87±0.03
0.48	12.82±0.02	0.58±0.03	1.00

* Based on the pure ferrosilite as standard.
** Based on the composition 48 mo% ferrosilite as standard.

16) N. Morimoto, *Yogyo Kyokai Shi*, **74**, 3 (1966).
17) Private communication.
18) T. Katsura and S. Kimura, This Bulletin, **38**, 1664 (1964).
19) T. Katsura, B. Iwasaki, S. Kimura and S. Akimoto, *J. Chem. Phys.*, **47**, 4559 (1967).
20) T. Katsura and M. Hasegawa, This Bulletin, **40**, 561 (1967).

Activities calculated on the basis of choosing pure ferrosilite as standard are given in Table 1, and activity-composition relations are illustrated in Fig. 4, together with a curve for a_{MgSiO_3} calculated by a graphical integration of the Gibbs-Duhem equation. As may be seen in Fig. 4, the pyroxene system shows a significant positive deviation from ideality.

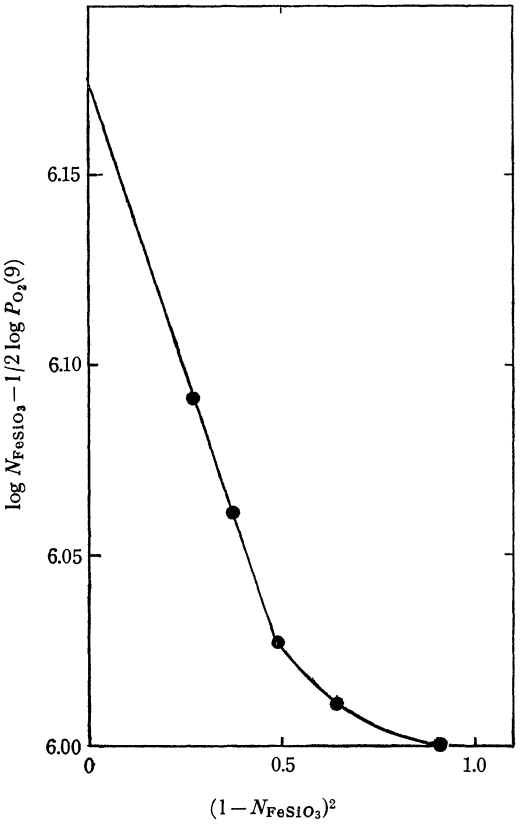

Fig. 3. Relationship between [log N_{FeSiO_3} − ½ log P_{O_2}(9)] and $(1-N_{FeSiO_3})^2$.

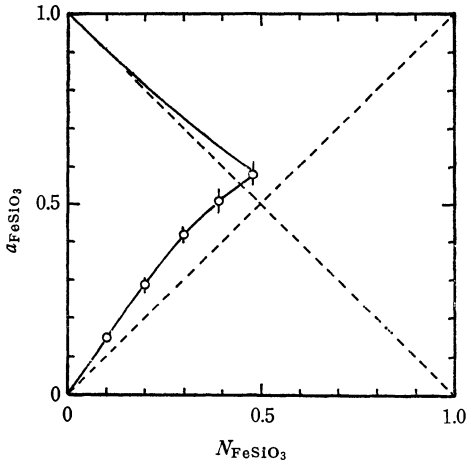

Fig. 4. Activity-composition relations in pyroxene solid solution at 1204°C.

Using the value of P_{O_2}(9-p), the standard free energy change of formation of ferrosilite, Fe(metal) + SiO_2(tridymite) + ½O_2 = $FeSiO_3$, is calculated to be −41.7±0.2 kcal/mol at 1204°C. Combining this with the value of the standard free energy change of formation of wüstite at 1204°C obtained by Darken and Gurry,[21] the free energy change of formation of ferrosilite from wüstite and silica is determined to be −1.6 kcal/mol. Akimoto *et al.*[22] gave the value of −1.4 kcal/mol at 1204°C on the basis of their high pressure synthesis of orthoferrosilite, Schwerdtfeger and Muan[1] gave −1.3±0.3 kcal/mol at 1150°C, and Muan *et al.*[13] gave −1.3±0.3 kcal/mol for the same reaction. Thus the present value is agreed well with those values obtained by different methods of determination.

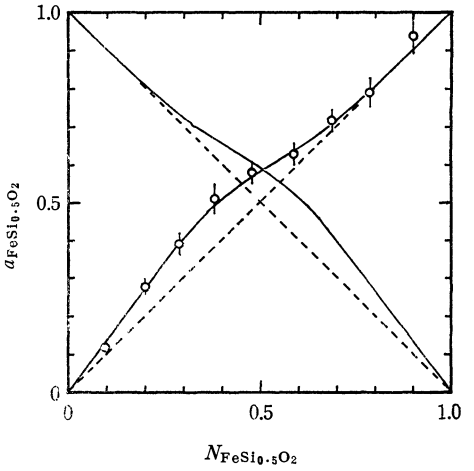

Fig. 5. Activity-composition relations in olivine solid solution at 1204°C.

The Olivine Solid Solution. The results for the olivine solid solution are given in Table 2. The values in the second and third columns are of the oxygen partial pressures of P_{O_2}(7) and P_{O_2}(4), respectively. The fourth column shows the composition of pyroxene co-existing with olivine with the composition in the first column, and obtained from Fig. 2. The fifth column shows the values of the P_{O_2}(9) obtained by interpolation of the values in Table 1.

The activity-composition relation in olivine solid solution is graphically illustrated in Fig. 5 with the experimental errors. A curve for $a_{MgSi_{0.5}O_2}$ is also drawn by a graphical integration of the Gibbs-Duhem equation. As may be seen in Fig. 5, the system displays a significant positive deviation from the ideality.

21) L. S. Darken and R. W. Gurry, *J. Am. Chem. Soc.*, **67**, 1398 (1945).
22) S. Akimoto, T. Katsura, Y. Syono, H. Fujisawa and E. Komada, *J. Geophys. Res.*, **70**, 5269 (1965).

TABLE 2. ACTIVITY OF OLIVINE*

$N_{Fe_2SiO_4}$	$-\log P_{O_2}(7)$ (atm)	$-\log P_{O_2}(4)$ (atm)	N_{FeSiO_3} (± 0.08)	$-\log P_{O_2}(9)$ (atm)	$a_{FeSi_{0.5}O_2}$
0.10	14.13±0.02		0.077	14.26±0.08	0.12±0.01
0.20	13.45±0.02		0.175	13.52±0.06	0.28±0.02
0.29	13.19±0.02		0.267	13.19±0.05	0.39±0.03
0.38	12.93±0.03		0.348	13.01±0.04	0.51±0.04
0.48	12.80±0.02		0.415	12.90±0.04	0.58±0.03
0.59	12.73±0.03		0.468	12.83±0.03	0.63±0.03
0.69		12.66±0.02			0.72±0.03
0.79		12.58±0.02			0.79±0.04
0.90		12.43±0.03			0.94±0.05

* The value of $-\log P_{O_2}(1)$ was determined to be -12.38 ± 0.02.[11]

The authors wish to express their hearty thanks to Mr. K. Hirota, Tokyo Institute of Technology, Mr. A. Kurabayashi, Unit leader of the Hitachi Electric Co., Ltd., and Dr. N. Ono, the Hitachi Electric Co., Ltd., without whose cooperation the determination of the actual oxygen partial pressures would have never been obtained. The authors also express their thanks to Dr. N. Morimoto, Osaka University, Dr. I. Kushiro, The University of Tokyo, and Professor I. Iwasaki, Tokyo Institute of Technology, who encouraged them throughout the study.

BULLETIN OF THE CHEMICAL SOCIETY OF JAPAN VOL. 41 1151—1153 (1968)

The Reaction of the Ester with Acyl Chloride in the Presence of Aluminum Chloride. VIII.[1] The Attempted Synthesis of the Carbethoxy Derivative of Polymalonylphenylene*[1]

Kiyotada MATSUI, Masatoshi MOTOI, Tetsuro NOJIRI and Kohtsuchi WAKABAYASHI*[2]

Department of Industrial Chemistry, Faculty of Technology, Kanazawa University, Kodatsuno, Kanazawa

(Received December 17, 1966)

The treatment of ethyl acetoacetate with terephthaloyl chloride in the presence of two equivalents of aluminum chloride in nitrobenzene at 55°C affords a polymer which may be designated as an aluminum chelate of the polymalonylphenylene derivative with some carbethoxy groups.

Recently we have reported that aluminum chloride is an effective agent for the acylation of active methylene group in compounds, such as diethyl malonate[2] or ethyl acetoacetate,[1,3] with acid chloride. For example, the reaction of ethyl acetoacetate with two equivalents of benzoyl chloride in the presence of a small amount of aluminum chloride in nitrobenzene at 35°C gave ethyl benzoylacetate, a small amount of ethyl benzoylacetoacetate, and traces of ethyl dibenzoylacetate and dibenzoylmethane. When the reaction was carried out by bubbling dry nitrogen gas into the reacting mixture, the yields of the above β-diketo esters and of dibenzoylmethane were increased and that of ethyl benzoylacetate was decreased. Under similar conditions, however, the use of a larger amount of aluminum chloride at the temperature of 55°C afforded dibenzoylmethane and its aluminum chelate in higher yields, besides small amounts of ethyl benzoylacetate, ethyl dibenzoylacetate, and tribenzoylmethane. Thus, the pathway of this reaction may be expressed as follows:

1) Part VII: T. Nojiri and K. Matsui, *Nippon Kagaku Zasshi* (*J. Chem. Soc. Japan, Pure Chem. Sect.*), **87**, 880 (1966).

*1 Presented at the 19th Annual Meeting of the Chemical Society of Japan, Yokohama, April, 1966.

*2 Present address: Teijin Co., Matsuyama Plant, Ehime.

2) H. Kaneyuki, This Bulletin, **35**, 519, 523, 713 (1962).

3) K. Matsui and T. Nojiri, *Nippon Kagaku Zasshi* (*J. Chem. Soc. Japan, Pure Chem. Sect.*), **86**, 531 (1965).

$$CH_3COCH_2COOC_2H_5 \rightleftarrows CH_3COCHCOOC_2H_5 \rightleftarrows C_6H_5CO$$

$$C_6H_5COCH_2COOC_2H_5 \rightleftarrows$$

$$(C_6H_5CO)_2CHCOOC_2H_5 \rightarrow (C_6H_5CO)_2CH_2 \rightleftarrows (C_6H_5CO)_3CH$$

In view of the above facts, the fact that the formation of di- and tri-benzoylated methane derivatives is accompanied by cleavages of carbon-carbon linkages suggests that ethyl acetoacetate may behave as a polyfunctional molecule toward acid chloride. It is the purpose of this paper to report the possibility of the formation of a polymer bearing the β-diketo structure, which will be formed by the above condensation reaction with terephthaloyl chloride.

Some reports on the synthesis of this kind of polymer have been published. Oda[4] and Furukawa *et al.*[5] prepared the polymer by treating ketene or diketene with aluminum chloride, but its purification was difficult owing to the contamination of aluminum. Nose *et al.*[6] also reported how polymers could be prepared from dimethyl terephthalate and the *p,p'*-diacetyl derivative of diphenyl ether or diphenylmethane by the use of metallic sodium.

When ethyl acetoacetate was treated with an equimolar amount of terephthaloyl chloride at 30°C by blowing nitrogen gas through the reaction mixture in the presence of a 0.5 equivalent of aluminum chloride in nitrobenzene, the resulting mixture was separated into ethyl *p*-carboxybenzoylacetate (I), diethyl terephthaloyldiacetate (II), an acidic (III) and a neutral polymer-like substance (IV), and a metal chelate polymer (V). Both III and IV are fusible, are soluble in ethanol or ether, and contain traces of aluminum, which combines to form a chelate more firmly than does aluminum chelating with dibenzoylmethane molecules.[1] In another run similar to the above, the viscous reaction mixture of the early stage was treated immediately with aqueous sodium hydroxide under the Schotten-Baumann conditions described in the Experimental section. The resulting mixture gave products similar to the above, but the acidic fraction, III, was of a relatively high molecular weight.

The infrared spectrum of III shows a broad absorption band, which corresponds to the β-diketo and carbethoxy absorption bands. Since this acylation reaction is often accompanied not only by a deacetylation reaction but also by a certain decarbethoxylation reaction, the structure of this substance is identified as that of a polymalonylphenylene derivative which does not contain as units, $-COCH_2COC_6H_4-$.
many carbethoxy groups as malonylphenylene

This substance was treated with aqueous sodium carbonate at room temperature in an attempt to hydrolyze its ester linkings. The infrared spectrum of the resulting product shows an absorption peak at 1362 cm^{-1} due to acetyl and the above-mentioned broad absorption, which is weakened in one region, as shown in Fig. 1. These features appear to be attributable to the ketonic hydrolysis of β-diketone linkings in the molecule. It should be noted that

TABLE 1. REACTION OF ETHYL ACETOACETATE WITH TEREPHTHALOYL CHLORIDE

Reactant: $CH_3COCH_2COOC_2H_5$ 1.9g (0.0146mol)
p-$C_6H_4(COCl)_2$ 3.0g (0.0148 mol)
Solvent: Nitrobenzene 15 m*l*, * 55 m*l*

$AlCl_3$ mol×10^2	Condition[a]		Product and yield (g)				
	Temp., °C	Time, hr	I	II	III	IV	V
3.0	55	24	s	s			2.5
0.75*	30	24	1.1	0.2			0.9
0.75	30	45	0.9	0.3	0.6 (440)	s	0.8
0.75	30	48	1.5	s	0.2 (630)	s	0.9
0.45[b]	30	48	0.3	s	0.6 (890) (450)[c]	0.1	0.8

I: p-$HOOCC_6H_4COCH_2COOC_2H_5$, II: p-$C_6H_4(COCH_2COOC_2H_5)_2$, III: Acidic polymer-like substance, IV: Neutral polymer-like substance, V: metal chelate polymer.
"s" means a small amount of product. ( ) indicates molecular weight.
a) Nitrogen gas was passed during the reaction except for the run at 55°C.
b) Reaction under Schotten-Baumann condition.
c) Molecular weight of hydrolyzed polymer.

4) R. Oda, S. Munemiya and M. Okano, *Makromol. Chem.*, **43**, 149 (1961).
5) J. Furukawa, T. Saegusa and N. Mise, *Kogyo Kagaku Zasshi* (*J. Chem. Soc. Japan, Ind. Chem. Sect.*), **65**, 254 (1962).
6) Y. Nose, M. Hatano and S. Kambara, *ibid.*, **69**, 566 (1966).

the substance partly undergoes fission, although all of its ester linkings may not be hydrolyzed. The yields of products and some molecular weights are summarized in Table 1.

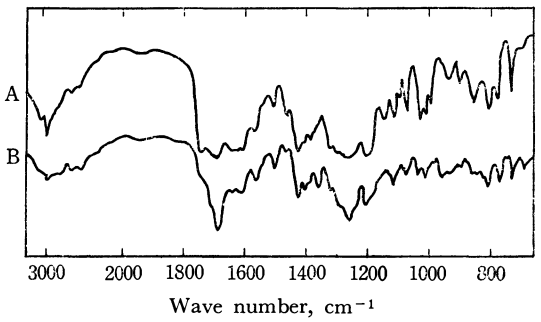

Fig. 1. Infrared spectra of carbethoxy derivative of polymalonylphenylene (KBr) (A) and its hyrdolyzed polymer (B).

When a similar treatment was carried out at 55°C in the presence of two equivalents of aluminum chloride but without passing nitrogen gas through, a vapor which seemed to be composed of carbon dioxide, hydrogen chloride, ethyl, and acetyl chloride bubbled out in a manner analogous to that in the reaction of ethyl acetoacetate with benzoyl chloride. The resulting product gave, in a very good yield, a polymer corresponding to V without any III and IV. It appears clear that this polymer was formed by the further condensation of the reaction intermediates corresponding to the substances, from I to V, though having its carbethoxy groups decreased markedly, as was expected from the above benzoylation reaction. The polymer is infusible, insoluble in ordinary organic solvents, swollen with ethanol on heating, and contains aluminum which can not be removed by any means. These findings suggest that aluminum is incorporated into stable intermolecular chelate linking to form the polymer. From the formation of tribenzoylmethane mentioned above, moreover, there is a possibility of a three-dimensional structure with some methine carbon atoms.

Experimental

Materials. The terephthaloyl chloride was prepared from phosphorus pentachloride and terephthalic acid which had been obtained by the hydrolysis of dimethyl terephthalate supplied by the Teijin Co., Ltd. Commercial ethyl acetoacetate was used after purification by distillation *in vacuo*.

Reaction of Ethyl Acetoacetate with Terephthaloyl Chloride. To a solution of aluminum chloride and terephthaloyl chloride in dry nitrobenzene, ethyl acetoacetate was added, and the mixture was kept in a thermostat at a given temperature. When it became gelatinous or viscous, the reaction mixture was poured into a mixture of hydrochloric acid and crushed ice. The aqueous solution containing aluminum chloride was removed from the organic layer by a centrifuge. The organic layer, after the removal of the nitrobenzene by steam distillation *in vacuo*, gave a solid which was then triturated with ether and filtered from an ether-insoluble chelate polymer. The filtrate was separated into an acidic and a neutral fraction by shaking with aqueous sodium bicarbonate. The former was extracted with hot water and purified by several reprecipitations from ethanol to water, thus giving an amorphous polymer-like substance. The hot-water extract obtained gave a crystal on cooling. Similarly, the latter, neutral fraction was separated into a crystal and a rather polymer-like substance by the use of ethanol and water. After the removal of the ether-insoluble substance which had formed during the above separations, the acidic, polymer-like substances generally melted at 120—130°C and the neutral, at 80—90°C. The molecular weights of the former were determined by the ebulioscopic method, using diethyl ether as a solvent.

Reaction under Schotten-Baumann Conditions. A viscous reaction mixture obtained as above was treated with ether (about 20 m*l*) and a 33% sodium hydroxide solution under conditions similar to those of the Schotten-Baumann reaction described in the literature.[7] The resulting mixture was separated into two layers by a centrifuge. Each layer was filtered to remove a rather insoluble substance. The organic layer gave a little viscous liquid on steam distillation *in vacuo*. The aqueous layer was then stirred into 6 N hydrochloric acid to give a solid of an acidic nature. The liquid and the solid were treated individually as above. A part of the acidic polymer-like substance was dissolved in aqueous sodium carbonate, left to stand for about 14 days at room temperature, and then acidified with hydrochloric acid to give a hydrolyzed polymer.

Ethyl p-Carboxybenzoylacetate (*I*). The crystal obtained from the acidic fraction was recrystallized from ethanol. Mp 151°C.

Found: C, 60.96; H, 4.96%. Calcd for $C_{12}H_{12}O_5$ C, 61.05; H, 5.12%. When refluxed with 20% sulfuric acid for 5 hr, this crystal gave colorless needles melting at 209—210°C (ethanol), (lit.,[8] mp 205°C of *p*-acetylbenzoic acid). Its methyl ester melts at 95—96°C (water) (lit.,[9] mp 92°C).

Diethyl Terephthaloyldiacetate (*II*). The neutral crystal was recrystallized from ethanol, mp 70°C (lit.,[10] mp 70°C). (Found: C, 63.01; H, 5.88%).

The authors are grateful to Mr. Yoshitaka Itatani of the Faculty of Pharmacy, Kanazawa University, for his elemental analysis.

7) J. M. Straley and A. C. Adams, "Organic Syntheses," Coll. Vol. IV, p. 415 (1963).
8) H. Rupe and A. Steinbach, *Ber.*, **43**, 3466 (1910).
9) R. Meyer, *Ann.*, **219**, 264 (1883).
10) L. Berend and P. Herms, *J. prakt. Chem.*, [2], **74**, 112 (1906).

BULLETIN OF THE CHEMICAL SOCIETY OF JAPAN VOL. 41 1154—1158 (1968)

Metal Ion-catalyzed Glycolysis of Terephthalonitrile

Takashi IKEDA, Michitoshi KITABATAKE, Masatomo ITO and Yoshitaka NOGUCHI

The Central Research Laboratory, Showa Denko K.K., Tamagawa, Ohta-ku, Tokyo

(Received June 2, 1967)

The effects of various metal compounds on the glycolysis of terephthalonitrile were studied in the presence of water at 185°C. The catalytically-active species were found to be metal ions. Their catalytic activities were correlated with the acid ionization constants, pK_a, of metal ions. The active catalysts were limited to the metal ions with pK_a values larger than 7. The study of the reaction mechanism suggests that, while one group of metal ions accelerates the formation of glycol and hydroxyl anions, the other involves catalytic acceleration through the coordination of metal ions. The metal ions with pK_a values of less than 7 showed no catalytic activities. These results were interpreted in terms of the tendency of the metal ions to form too stable coordination intermediates. Most of these metal compounds also served to inhibit the reactions. For a series of salts derived from a given metal, the catalytic activities were found to decrease with a decrease in their solubilities in water. On the other hand, metal oxides and hydroxides had high catalytic activities.

The glycolysis of nitriles to the corresponding esters is known to proceed under non-catalytic conditions. The reaction may also be catalyzed by acids and bases.[1] Recently the glycolysis of aromatic nitriles has been reported to be promoted by heavy metal salts and by oxides.[2,3] On the other hand, the metal ions are known to promote the hydrolyses of esters,[4] of amides,[5] and of Schiff bases,[6] and the glycolysis of esters.[7]

A basic study of the metal ion-catalyzed glycolysis of nitriles was, therefore, of interest in order to get a better understanding of the role of the metal ions in the metal-ion catalysis.

We will attempt in this paper to clarify the catalytic effects of metal compounds in the glycolysis of terephthalonitrile.

1) Distiller's Co., Brit. Pat. 800875 (1958).
2) Toyo Rayon K. K., Brit. Pat. 981703 (1965).
3) Showa Denko K.K., German Pat. to be published.
4) a) H. Kroll, *J. Am. Chem. Soc.*, **74**, 2036 (1952); b) M. L. Bender and B. W. Turnquest, *ibid.*, **79**, 1889 (1957); c) H. L. Conley, Jr., and R. B. Martin, *J. Phys. Chem.*, **69**, 2914, 2923 (1965); d) M. D. Alexander and D. H. Busch, *J. Am. Chem. Soc.*, **88**, 1130 (1966).
5) a) L. Meriwether and F. H. Westheimer, *J. Am. Chem. Soc.*, **178**, 5119 (1956); b) H. L. Conley, Jr., and R. B. Martin, *J. Phys. Chem.*, **69**, 2914 (1965).
6) a) G. L. Eichhorn and J. C. Bailar, *J. Am. Chem. Soc.*, **75**, 2905 (1953); b) G. L. Eichhorn and I. M. Trachtenberg, *ibid.*, **76**, 5183 (1954); c) G. L. Eichhorn and N. D. Marchand, *ibid.*, **78**, 2688 (1956).
7) a) W. Griel and G. Schnock, *J. Polymer Sci.*, **30**, 412 (1958); b) R. E. Wilfong, *ibid.*, **54**, 385 (1961); c) M. Sumoto, *Kogyo Kagaku Zasshi* (*J. Chem. Soc. Japan, Ind. Chem. Sect.*), **66**, 1663 (1963); d) K. Yoda, K. Kimoto and T. Toda, *ibid.*, **67**, 909 (1964); e) M. Sumoto and A. Kito, *Ohsaka Kogyo Gijutsushikenjo Kiho* (*Reports of the Government Chemical Industrial Research Institute, Osaka*), **12**, 214 (1961).

Experimental

Experimental Apparatus and Procedure. The reaction was carried out in a 100-m*l* three-necked glass flask equipped with a reflux condenser, a thermometer, and a nitrogen gas inlet; the flask was immersed in an oil bath with an electric heating system. During the reaction the reactants in this flask and an ammonia-absorbing solution prepared in another flask were stirred by the magnetic stirring device.

A typical example of the determination of reaction rate follows: 6.4 g of terephthalonitrile (0.05 mol), 93.0 g of ethylene glycol (1.5 mol), 1.8 g of water (0.1 mol), and 2.5×10^{-4} mol (as metal) of catalyst were added to the reaction vessel, which was then set in the oil bath preheated at 185°C. Nitrogen gas was bubbled into the reaction mixture at a rate of 40 m*l*/min. The nitrogen flux was introduced through a reflux condenser to the ammonia-absorbing solution kept at 25°C. The reaction was then carried out at 185°C.

The resulting ammonia, carried with the nitrogen flux, was absorbed into the sulfuric acid solution. The rate of the formation of ammonia was followed by the titration of a sulfuric acid solution at given intervals.

As the main reaction products, β-hydroxyethyl *p*-cyanobenzoate, and bis-β-hydroxyethyl terephthalate were obtained by the following reaction sequence:

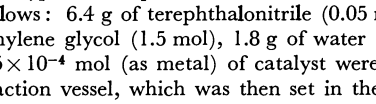

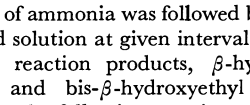

(1)

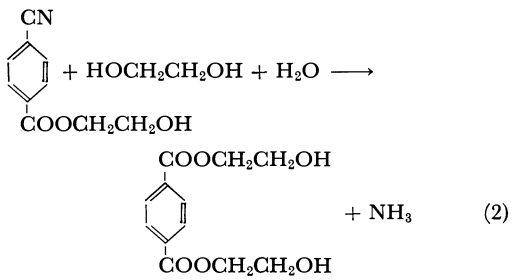

These products were analyzed by gas-liquid chromatography (column: 25 wt% of Apiezon L on Chromosorb W) for β-hydroxyethyl *p*-cyanobenzoate, and by fractionation and ultraviolet spectroscopy for bis β-hydroxyethyl terephthalate.

Materials. Terephthalonitrile (mp 224°C) was prepared by the ammoxidation of *p*-xylene and was purified by recrystallization from dioxane. Ethylene glycol (bp 197°C) used was of the reagent grade. The metal compounds were all extra pure, commercially-available products, with the exception of lead glyceroxide, which was prepared according to the procedure proposed by Nitschman.[8]

Results and Discussion

According to the kinetics of this reaction, which will be reported in a separate paper, the rate of the reaction of terephthalonitrile is not necessarily equal to the rate of the formation of ammonia, but the conversion of terephthalonitrile is parallel to the formation of ammonia. The catalytic activities of metal compounds can be correlated with the rate of the formation of ammonia.

The rates of formation of ammonia are shown in Fig. 1 for the different initial nitrile concentration; they are independent of the concentration of terephthalonitrile in the initial stage of the reaction, up to a 30% conversion to ammonia. This fact indicates that the rate of the formation of ammonia follows the first-order rate law with respect to the terephthalonitrile at a low range of conversion.

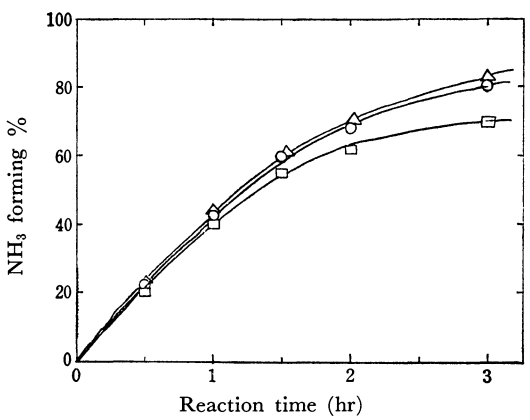

Fig. 1. Glycolysis of terephthalonitrile in the presence of lead acetate at various initial terephthalonitrile concentrations at 185°C.
Initial concentration of terephthalonitrile:
-△-; 0.0125 mol, -○-; 0.025 mol,
-□-; 0.05 mol,
Ethylene glycol 93.0 g; Water 1.8 g;
Lead acetate 0.47 g

On the other hand, the reaction proceeds considerably in the absence of any catalyst under the

Table 1. Rate constants for the glycolysis of terephthalonitrile in the presence of various catalysts at 185°C

Ethylene glycol 93.0 g; Terephthalonitrile 6.4g; Water 1.8 g; Catalyst 2.5×10^{-4} atomic equivalent on the basis of metal

Periodic Chart	Catalyst	K	$K-K_0$
	none	0.36	0
Ia	LiOAc	0.50	0.14
	NaOAc	0.50	0.14
	KOAc	0.47	0.11
IIa	$Mg(OAc)_2$	0.45	0.09
	$Ca(OAc)_2$	0.51	0.15
	$Sr(OAc)_2$	0.51	0.15
	$Ba(OAc)_2$	0.44	0.08
IIb	$LaCl_3$	0.21	−0.15
	La_2O_3	0.36	0.00
	$Ce(HCO_3)_3$	0.29	−0.07
	Ce_2O_3	0.36	0.00
	$Th(NO_3)_4$	0.14	−0.22
	$UO_2(OAc)_2$	0.24	−0.12
IVb	$TiOSO_4$	0.19	−0.17
	$ZrOCl_2$	0.17	−0.19
Vb	$VOSO_4$	0.21	−0.15
VIb	$Cr(OAc)_3$	0.29	−0.07
VIIb	$Mn(OAc)_2$	0.59	0.23
VIII	$Fe^{(III)}(OH)(OAc)_2$	0.36	0.00
	$Fe^{(II)}$-oxalate	0.47	0.11
	$Co(OAc)_2$	0.89	0.53
	$Ni(OAc)_2$	0.72	0.36
	$PdCl_2$	0.00	−0.36
Ib	$Cu(OAc)_2$	1.04	0.68
	Ag(OAc)	0.36	0.00
IIb	$Zn(OAc)_2$	0.61	0.25
	Zn(metal)	0.49	0.13
	$Cd(OAc)_2$	0.79	0.43
	HgOAc	0.21	−0.15
	$Hg(OAc)_2$	0.31	−0.05
IIIa	$Al_2O(OAc)_4$	0.40	0.04
	$Al(OC_3H_7)_3$	0.46	0.10
	$InCl_3$	0.29	−0.07
	Tl(OAc)	0.48	0.12
IVa	$Sn(OAc)_2$	0.26	−0.10
	$Pb(OAc)_2$	0.70	0.34
Va	$BiO(NO_3)$	0.33	−0.03
	Sb_2O_3	0.33	−0.03
	H_3PO_4	0.26	−0.10
VIIa	HCl	0.00	−0.36
IIIa	H_3BO_3	0.36	0.00

8) H. Nitschman, *Helv. Chim. Acta*, **66**, 759 (1935).

above conditions. The catalytic activities, therefore, have to be compared with the specific rate constants, $K-K_0$, adjusted by substracting the specific rate constants in the absence of any catalyst, K_0, from those in the presence of catalysts, K.

Table 1 lists the first-order specific rate constants obtained after the first 30% of the reaction for the glycolysis of terephthalonitrile in the presence of various catalysts.

The metal compounds with catalytic activities were those derived from metals which belong to the Ia, IIa, IIIa, VIIb, VIII, Ib, IIb, and IVa groups in the periodic charts of the elements.[9] Considering the reaction conditions and the results, it appears that the active species of the catalysts may be ascribed to the metal ions. Even the zinc metal itself showed catalytic activity, as Table 1 shows. From this fact, it appears that the effectiveness in this glycolysis can be ascribed to the metal ions in the final reaction state.

The catalytic activities in the glycolysis were found, with a few exceptions, to have a good correlation with the stability constants[10] of the oxine complex of metal ions. These correlations are shown in Fig. 2. From these facts, the coordinations of the reagent to metal ions may be considered to play an important role.

Accordingly, the electron affinity of the metal ions, which determines the coordinating tendency, may be closely related to the catalytic activity. By adopting the acid ionization constants[11,12] of the metal ions as a measure of the electron affinity of the metal

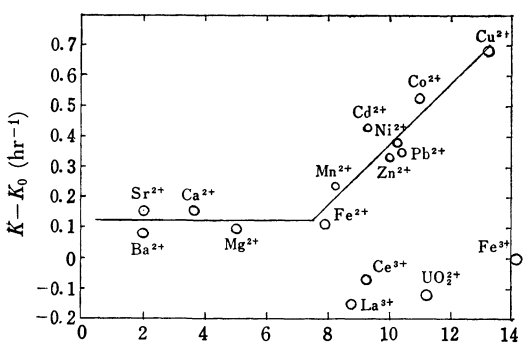

Fig. 2. Correlation between catalytic activities and stability constants of oxine complex of metal ions.

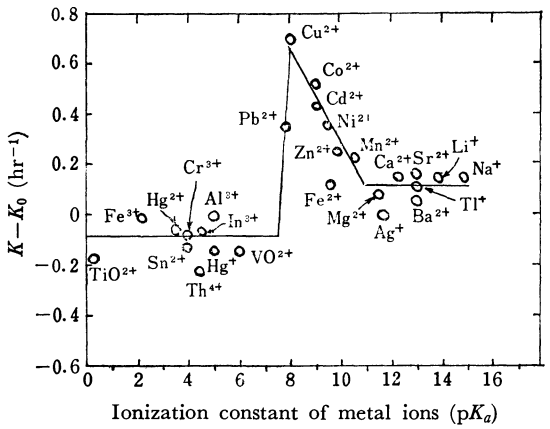

Fig. 3. Correlation between acid ionization constants (pK_a) and rate of the glycolysis of terephthalonitrile.

ions,[13] the aforementioned relationship may be illustrated as in Fig. 3. The catalytic activities as given by $K-K_0$ are distributed on volcano-type plots. The catalytically-active metal ions are limited to those having acid ionization constants, pK_a, larger than 7. They may be divided into two groups; one comprises alkali, alkaline earth, and thallium(I) metal ions derived from Ia, IIa, and IIIa, while the other includes the metal ions derived from VIIb, VIII, Ib, IIb, and IVa in the periodic chart of the elements.[9]

Metal ions of either group promote the reaction of glycolysis, but possibly by different reaction mechanisms. The former group seems to promote the reaction by accelerating the formation of glycol and hydroxyl anions, which promote the imidate formation and the imidate hydrolysis, as illustrated as follows:

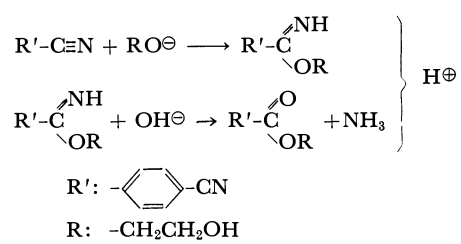

The latter group seems to promote the reaction by accelerating the formation of carbonium cations of the imidate through the coordination of metal ions:

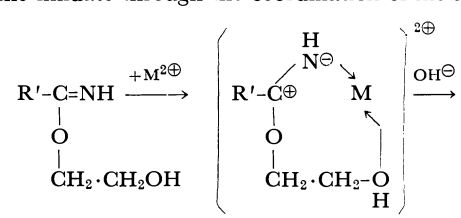

9) "The Merck Index of Chemicals and Drugs," 7th ed., Merck and Co., Inc., Rahway, New Jersey (1960).
10) K. Yamasaki and T. Inoue, "Sakuen" (Metal Complexes), Maruzen Publishing Co., Tokyo (1959), p. 434.
11) F. Basolo and R. G. Pearson, "Mechanisms of Inorganic Reactions," John Wiley & Sons, Inc., London (1958), p. 387.
12) A. Ringbom, "Complexation in Analytical Chemistry," Interscience Publishers, London (1963), p. 298.
13) K. Tanaka, A. Ozaki and K. Tamaru, *Shokubai (Catalysis)*, **6**, 262 (1964).

claimed that an excited singlet state is an only reactive state in the photoreduction of acridine in *isopropanol*.

According to our present results, however, four alcohols behave more or less in different manner and in particular, isopropanol and methanol show distinctly different features in the effect of biacetyl on the photoreduction, which lead to the conclusion that the reactive states is in the former case only singlet excited state in agreement with Porter's conclusion, whereas in the latter case, are singlet and $T(n-\pi^*)$ state as Kellmann and Dubois proposed. Hence it seems timely to report the details of our experiments although we have not yet succeeded in interpreting the unexpected differences found in four kinds of alcohols.

Since Dubois and Kellmann's conclusion was based on the assumption that inhibiting action of biacetyl is due to the energy transfer according to $A^{T(n-\pi^*)}+B \rightarrow A+B^T$ (where A is acridine and B is biacetyl), it is desirable to examine whether biacetyl does not affect the lowest $T(\pi-\pi^*)$ of acridine by a different mechanism than energy transfer and further to examine whether it does not react with the half reduced acridine. Therefore we have investigated at first by the flash technique using methanol and ethanol as solvents, the effect of the addition of biacetyl on the decays of $T(\pi-\pi^*)$ of acridine and of the half reduced acridine. In addition, we have made investigations on the effect of the addition of biacetyl on the yield of $T(\pi-\pi^*)$, AH and AH_2, the results of which have supported the view of Kellmann and Dubois to some extent. These experiments are described in Part I. In Part II, the steady illumination experiments are described. The data, being more accurate than those from flash experiments, are analysed and interpreted on the basis of four alternative processes, and the quantum yields Φ_M^S, Φ_R^S, Φ_M^T and Φ_R^T (where S and T denote singlet excited state and $T(n-\pi^*)$ state and where M and R denote respectively molecular and radical) are separately decided.

Part I.*1 Flash Photolysis Studies

Experimental

Apparatus, procedures and samples are essentially similar as in the previous papers.[8,10] The decays and yields of $T(\pi-\pi^*)$ of acridine and of the half-reduced form of acridine were examined respectively at 440 and at 278 mμ (or in some cases as 520 mμ). The yield of acridan was investigated from the increase of optical density at 290 mμ. The concentration of acridine was always 4.8×10^{-5} M and the concentration of biacetyl was changed from zero to 1.1×10^{-2} M. By using a suitable filter only acridine was excited.

Results and Discussion

T-T Absorption Spectra of Biacetyl. Transient absorption spectra of biacetyl in methanol are shown in Fig. 1.

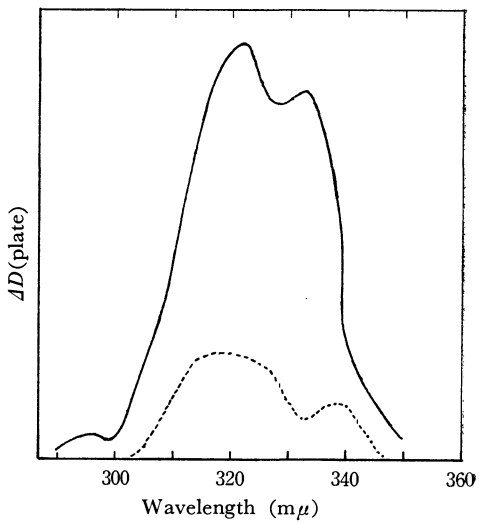

Fig. 1. Transient absorption spectra of biacetyl.
—— after 93 μsec, - - - after 360 μsec

The decay at 320 mμ is of the first order with a rate constant $k\simeq4\times10^3 sec^{-1}$. The comparison with the data in literatures[9,12,13] confirms that this species is the triplet state of biacetyl.

The Effect of the Addition of Biacetyl on the Decay of $T(\pi-\pi^*)$ of Acridine. The decay was not essentially affected by the addition of biacetyl up to 1.1×10^{-2}M. Some of the values of the first order rate constants are given in Table 1.

The Effect of the Addition of Biacetyl on the Decay of Half Reduced Acridine. The decay of half reduced acridine is second order and the rate

Table 1. Rate constant of the decay of $T(\pi-\pi^*)$, $k\times10^{-4}(sec^{-1})$

$[B]_M$	0	1.1×10^{-4}	1.1×10^{-3}	5×10^{-3}	1.1×10^{-2}
Methanl	1.1	1.1	1.1	1.1	1.1
	1.2	1.1	1.2	1.1	1.1
Ethanol	0.8	0.8	0.6	0.7	0.7
	0.9	0.8	0.7	0.7	0.8

*1 Experiments were made by Yamashita.

12) G. Porter and M. W. Windsor, *Proc. Roy. Soc.*, **A245**, 238 (1958).
13) H. L. J. Bäckström and K. Sandros, *Acta Chem. Scand.*, **12**, 823 (1958).

metal are quite applicable to that of the glycolysis of dimethyl terephthalate,[7c] it seems that the catalytic reaction mechanisms for this reaction are similar to those for the glycolysis of dimethyl terephthalate.

The reaction mechanisms and kinetics of the metal ion-catalyzed glycolysis of benzonitrile will be discussed in a succeeding paper.

The authors wish to thank Dr. Tajiro Oga and Messrs. Masashi Tanabe and Noriyoshi Aotsuka for their valuable discussions. Thanks are also given to Messrs. Masasuke Muto and Kazuharu Katagiri for their technical assistances.

BULLETIN OF THE CHEMICAL SOCIETY OF JAPAN VOL. 41 1158—1164 (1968)

A Kinetic Study of the Metal Ion-catalyzed Glycolysis of Benzonitrile

Takashi IKEDA, Michitoshi KITABATAKE, Masatomo ITO and Yoshitaka NOGUCHI

The Central Research Laboratory, Showa Denko K.K., Tamagawa, Ohta-ku, Tokyo

(Received August 3, 1967)

The kinetics of the lead ion-catalyzed glycolysis of benzonitrile were studied in the presence of water. The experimental results indicated that the rate of the formation of ammonia followed the first-order rate law with respect to the concentrations of benzonitrile and of water. For the concentration of the catalyst, the rate found was of a 0.44 order. It was observed that the product, β-hydroxyethyl benzoate, exhibited an inhibiting effect on the glycolysis. The effects of substituents on benzonitrile were found to fit the Hammett rule. The reaction was remarkably influenced by the type of glycol used. The reaction also proceeded through the hydrolysis of benzonitrile, followed by the glycolysis of the benzamide thus formed. The rate of the glycolysis of benzamide was about one-third that of benzonitrile, which is the main reaction in the system. The reaction of imidate formation possessed a small equilibrium constant at a high temperature, but it had a high reaction rate. The proposed mechanism for these glycolysis reactions is as follows: the addition of glycol to benzonitrile yields imidate, which then forms a chelate compound with a metal ion. The imidate activated by the formation of the chelate is easily hydrolyzed by water to form ester and ammonia. This ester tends to chelate to the metal ion and so inhibits the reaction.

The effectiveness of the various kinds of metal compounds on the metal ion-catalyzed glycolysis of terephthalonitrile has been discussed in a previous paper.[1] The heavy metal ions, such as cupric, lead, and zinc ions, have been found to promote the glycolysis of terephthalonitriles. Their catalytic activities have been correlated with the coordination tendency of metal ions.

Kinetic studies of the metal ion-catalyzed glycolysis of benzonitrile are, therefore, important in order to gain a better understanding of the reaction mechanisms. However, no kinetic study of the glycolysis has been found in the literature.

We will attempt here to investigate the reaction kinetics and to propose a mechanism for the metal ion-catalyzed glycolysis of benzonitrile to yield β-hydroxyethyl benzoate.

Experimental

Kinetic Measurements for the Glycolysis of Nitriles and Amides. The experimental procedure and the methods of measurements for the glycolysis of nitriles and amides were similar to those described in a previous work.[1]

A typical set of reaction conditions used was as follows: a reaction mixture of 0.1 mol of nitrile or amide, 1.5 mol of glycol, 0.1 mol of water, and 0.001 mol of a catalyst was reacted at the reaction temperature of 170°C.

The rate of the formation of ammonia was determined by the titration of samples of the sulfuric acid solution taken from the ammonia-absorbing flask at given intervals. Further, the determination of the rate of the reaction of benzonitrile was carried out by analyzing the samples from the reaction mixture by gas-liquid chromatography at set intervals.

The analytical conditions used were as follows: the heated liquid product in the reaction state was quickly sampled with a micro-syringe (50 μl) and analyzed by gas-liquid chromatography on a 2 m × 6 mm stainless steel column of 25wt% Apiezon L on Chromosorb W at 205°C, using helium as a carrier gas and naphthalene as an internal-standard substance.

The formation of the ester, the main reaction product, was also examined by using gas-liquid chromatography and infrared spectroscopy.

1) T. Ikeda, M. Kitabatake, M. Ito and Y. Noguchi, This Bulletin, **41**, 1154 (1968).

Studies of Imidate Formation from Nitriles.[2] A reaction mixture of 1.85 g (0.0125 mol) of *m*-nitrobenzonitrile, 124 g (2 mol) of ethylene glycol, and 0.014 g (0.25×10^{-4} mol) of sodium metal was reacted at a given reaction temperature in a 100-m*l* flask immersed in an electrically-heated oil bath stirred by a magnetic apparatus.

Aliquots (5 cc) were withdrawn at intervals, added to a mixture of excess dilute hydrochloric acid and methanol (100 m*l*), and, after 30—45 min, backtitrated to the methyl-orange endpoint.

Materials. Isophthalonitrile and terephthalonitrile were prepared by the ammoxidation of *m*- and *p*-xylene respectively; they were purified by recrystallization from dioxane to melting points of 160—161°C and 222—224°C respectively.

The *p*-cyanoacetophenone (mp 54—56°C) was prepared according to the directions proposed by Mowry *et al.*[3]

p-Chlorobenzonitrile (mp 93—94°C) was prepared by the usual method from *p*-chloroaniline.

β-Hydroxyethyl *p*-cyanobenzoate (mp 58°C) was prepared by reacting ethylene chlorohydrine with *p*-cyanobenzoic acid sodium salt in a water solution and by recrystallization from water, evaporating under reduced pressure.

β-Hydroxyethyl benzoate was similarly prepared; bp 146—148°C at 10 mmHg.

m-Nitrobenzonitrile was a commercial product and was purified by recrystallization from methanol-chloroform; mp 148°C.

Lead acetate, a typical metal ion catalyst, was commercially available with a sufficient purity.

The other materials used in this study were the best commercial products available and were purified by distillation.

Results and Treatment of Data

Glycolysis of Benzonitrile. The conversion of benzonitrile in the presence of water and a catalyst is shown in Fig. 1 as a function of the reaction time. The rates of the formation of ammonia and *β*-hydroxyethyl benzoate are also given. These results indicate that, in the initial stage of the reaction, the rate of the consumption of benzonitrile is of nearly the same magnitude as the rates of the formation of ammonia and of *β*-hydroxyethyl benzoate.

In order to ascertain the mass-transfer effect of the rate of reaction, a few experiments were carried out at a faster gas flow rate of nitrogen, while the other conditions were kept constant. The rates of the formation of ammonia were not affected by the nitrogen gas flow rate. It was thus confirmed that the mass-transfer effect was insignificant in this system.

The first-order rate plots of the formation of ammonia observed at 170°C are shown in Fig. 2 for two initial concentrations of benzonitrile. The formation of ammonia and the consumption of benzonitrile are both first-order reactions at low conversions (up to 30% of benzonitrile). A higher conversions, however, the slope of the curve tends to decrease. The difference between the two first-order rate constants in Fig. 2 may be caused by the inhibiting effect of *β*-hydroxyethyl *p*-cyanobenzoate, which will be discussed later.

The first-order rate constants obtained from the initial rate of reaction for the glycolysis of benzonitrile

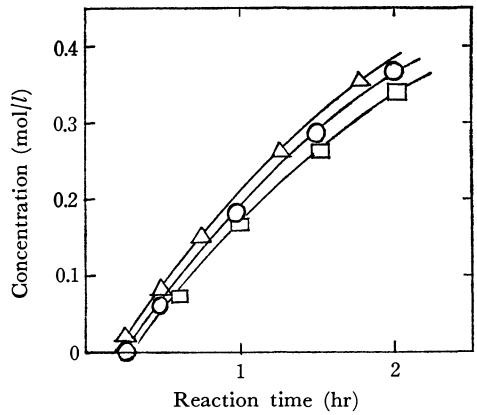

Fig. 1. The quantities of ammonia, ester formation and the reacted benzonitrile.
△: reacted benzonitrile
○: ammonia (formation)
□: ester (formation)
Reaction conditions: Benzonitrile 0.1 mol, E.G. 1.5 mol, H_2O 0.1 mol, $Pb(OAc)_2$ 0.001 mol, Temperature 170°C

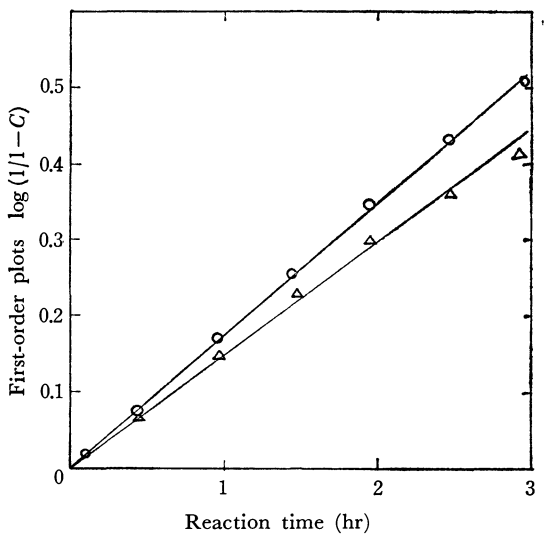

Fig. 2. The first-order formation of ammonia at different initial concentrations of benzonitrile.
○ 0.025 mol of benzonitrile
△ 0.1 mol of benzonitrile
Reaction conditions: E. G. 1.5 mol, H_2O 0.1 mol, Lead acetate 0.001 mol, Temperature 170°C

2) F. C. Schaefer and G. A. Peters, *J. Org. Chem.*, **26**, 412 (1961).
3) D. T. Mowry, M. Renoll and W. F. Huber, *J. Am. Chem. Soc.*, **68**, 1105 (1946).

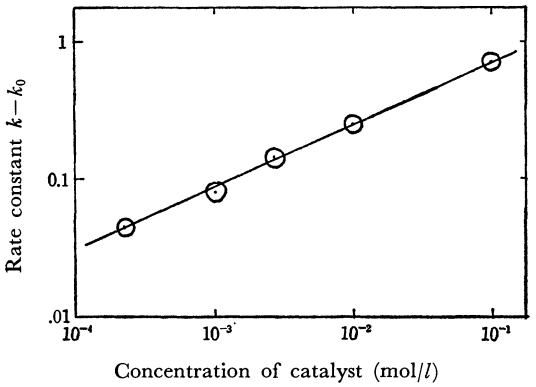

Fig. 3. The first-order rate constant in the glycolysis of benzonitrile *vs.* concentration of catalyst.
Reaction conditions: E.G. 1.5 mol, H_2O 0.1 mol, Temperature 170°C, Benzonitrile 0.1 mol
k_0: rate constant in the absence of catalyst

in the presence of various concentrations of lead acetate, a typical metal ion catalyst, are plotted in Fig. 3. It should be recalled here that the reaction proceeds slowly even in the absence of any catalyst.[1)]

In consideration of such complications, the first-order rate constants, k (hr^{-1}), in the glycolysis of benzonitrile can be represented by Eq. (1):

$$k = 0.046 + 4.75\ [\text{catalyst}]^{0.44} \qquad (1)$$

The rate of the formation of ammonia may be expressed by an identical equation.

The first-order rate constants in the glycolysis of benzonitrile obtained at 170°C and 150°C are plotted against the initial concentration of water in Fig. 4. The formation of ammonia was found to proceed considerably even in the absence of water. However, the first-order rate of the formation of ammonia increased remarkably with an increase in the concentration of water at the optimum reaction temperature, 170°C. Since the reaction mixture starts refluxing at a concentration of water higher than

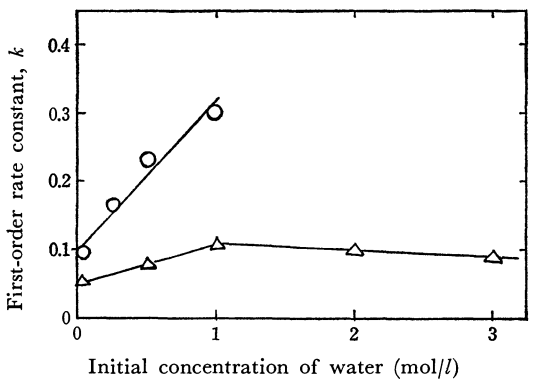

Fig. 4. The influence of the initial concentration of water in the glycolysis of benzonitrile.
○ Reaction temperature 170°C
△ Reaction temperature 150°C

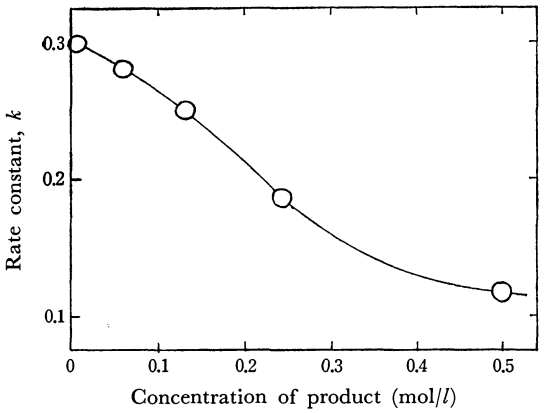

Fig. 5. The effect of the product in the glycolysis of benzonitrile.

1 mol/l, the reaction could not be carried out at the above-mentioned temperature, 170°C. The aforementioned first-order rate constant increased gradually up to the concentration of water of 1 mol/l at a lower temperature, 150°C. The effect of water when its concentration is higher than 1 mol/l will be reported in the succeeding paper, as well as the mechanism in the absence of any water in the glycolysis. The chemical equivalent volume of water to benzonitrile is 1 mol/l in the reaction system.

In order to ascertain the inhibiting effect exerted by the product, β-hydroxyethyl benzoate, the glycolysis of benzonitrile was carried out in the presence of extra β-hydroxyethyl benzoate at 170°C. The results obtained are shown in Fig. 5. The initial rate constant decreases from 0.3 to 0.12 as the concentration of β-hydroxyethyl benzoate varies over the range from 0 to 0.5 mol/l. It is evident here that the product tends to inhibit the glycolysis reaction

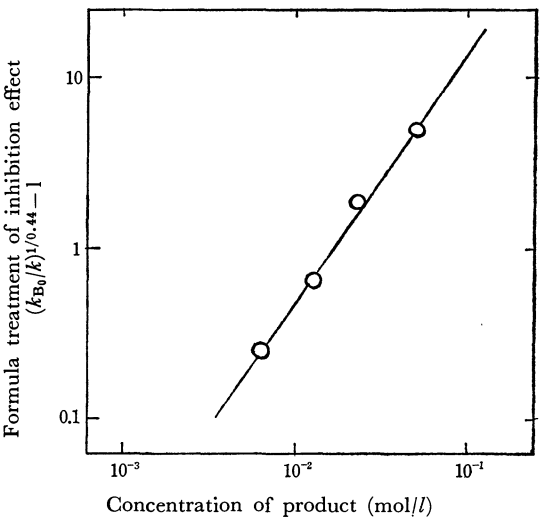

Fig. 6. The graphical analysis of the inhibiting effect of the product in the glycolysis of benzonitrile.

The rate of the formation of ammonia can be presented as follows:

$$k = k_{B_0}/(1 + C[\text{product}]^n)^{0.44} \quad (2)$$

where k_{B_0} represents the rate constant when no product is added, and where C and n are the constants.

Moreover, by treating the rate data as shown in Fig. 6, the inhibiting effect of the product in the glycolysis of benzonitrile is found to fit the above formula and may be represented as Eq. (2') for the rate of the formation of ammonia:

$$k = k_{B_0}/(1 + 330[\text{product}]^{1.50})^{0.44} \quad (2')$$

where k_{B_0} represents the above-described rate constant.

The Arrhenius plots of the first-order rate constant in the glycolysis of benzonitrile at a given concentration of the reactant are shown in Fig. 7. The apparent activation energy for the formation of ammonia in the temperature range of 150—170°C was 18.0 kcal/mol.

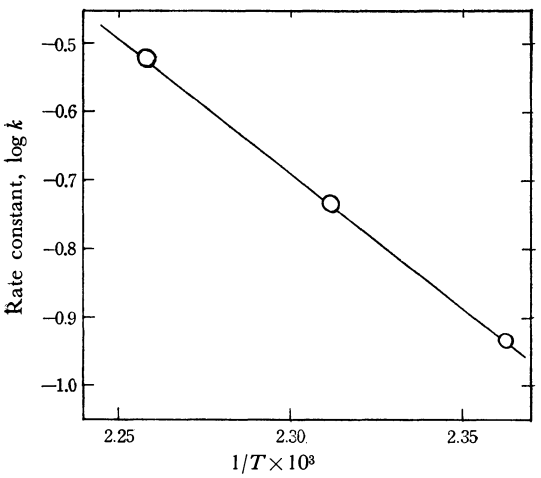

Fig. 7. Arrhenius plot of the first-order rate constant in the glycolysis of benzonitrile.

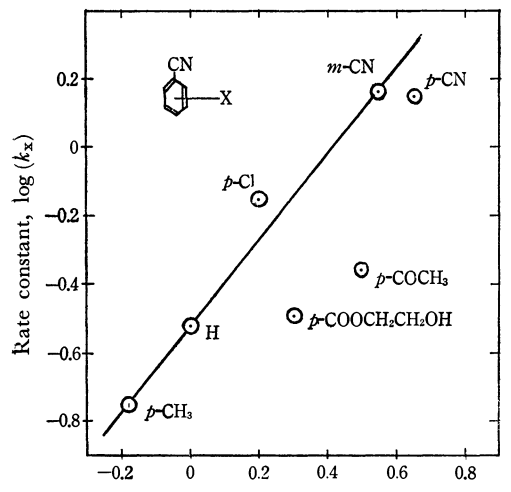

Fig. 8. Hammett correlation of $\log k_x$ *vs.* σ in the glycolysis of substituted benzonitrile.

The glycolysis reactions were also carried out with various substituted benzonitriles. The reaction rate constant is plotted against the Hammett constant, σ,[4] in Fig. 8.

The Hammett correlation gives a straight line except for substituted benzonitriles with the carbonyl group, such as β-hydroxyethyl *p*-cyanobenzoate and *p*-cyanoacetophenone. The Hammett reaction constant, ρ, calculated from the slope in Fig. 8 is 1.2.

The effects of the types of glycol on the glycolysis of benzonitrile at 150°C may be seen in Table 1. Here the rate of reaction decreases rapidly with an increase in the number of the carbon atoms between the two hydroxy groups.[5] The rate also decreases as the order of hydroxy group involved becomes higher. Thus, primary>secondary>tertiary.

Glycolysis of Benzamide. In order to examine to what extent the reaction proceeds through another path where benzamide is known to participate as an intermediates, we studied the reaction of benzamide with glycols under catalytic conditions. Here the benzamide may be formed through the hydrolysis of benzonitrile. The apparent first-oder rate constants in the glycolysis of benzamide are listed in Table 2. With ethylene glycol, the rate of reaction in the glycolysis of benzamide is about one-third that observed in the glycolysis of benzonitrile. The rate of the reaction in the glycolysis of benzamide with tetramethylene glycol is, however, in the same range as that with ethylene glycol.

Thus, with tetramethylene glycol, the rate of reaction in the glycolysis of benzamide is much greater than that in the glycolysis of benzonitrile. These results suggest that the glycolysis of nitrile may be different in mechanism from that of amide.

Reaction of *m*-Nitrobenzonitrile with Glycols. Since the rate of the glycolysis of benzonitrile was found to be remarkably affected by the type of glycol used (Table 1), we studied the kinetics of the formation of imidate from nitrile and alcohol.

The results of the kinetic investigation of the formation of imidate from *m*-nitrobenzonitrile with ethylene glycol under various conditions are summarized in Table 3. The equilibrium constants for the reaction with a series of butanols are also indicated. The equilibrium constant, K, between benzonitrile and imidate in the presence of ethylene glycol under the reaction conditions described in the Experimental Section is not different from that for *n*-butanol. With secondary or tertiary butanol, however, the reaction to imidate hardly proceeded at all.

The temperature dependence of the equilibrium

4) H. H. Jaffé, *Chem. Revs.*, **53**, 191 (1953).
5) B. Robinson, *J. Chem. Soc.*, **1963**, 2417.

TABLE 1. THE EFFECTS OF THE VARIOUS TYPES OF GLYCOLS IN THE GLYCOLYSIS OF BENZONITRILE
Reaction conditions, glycols: 93 g each, benzonitrile: 10.4 g (0.1 mol), $Pb(OAc)_2 \cdot 3H_2O$: 0.38 g (0.001 mol), H_2O: 1.8 g (0.1 mol), reaction temperature: 150°C

Kind of glycol used	Structural formula of glycol	First-order rate constant k (hr^{-1})
Ethylene glycol	$HOCH_2CH_2OH$	0.101
Trimethylene glycol	$HOCH_2CH_2CH_2OH$	0.041
Tetramethylene glycol	$HOCH_2CH_2CH_2CH_2OH$	0.0048
Pentamethylene glycol	$HOCH_2CH_2CH_2CH_2CH_2OH$	0.0036
Propylene glycol	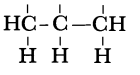	0.062
2,3-Butandiol	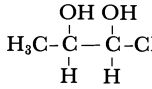	0.039
Pinacol	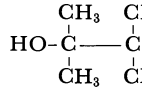	0.000

TABLE 2. THE FIRST-ORDER RATE CONSTANTS IN THE GLYCOLYSIS OF BENZAMIDE
Reaction conditions, benzamide: 12.1 g (0.1 mol), glycol: 93 g each, reaction temperature: 170°C

Glycol	Structural formula of glycol	$Pb(OAc)_2$ catalyst	First-order rate constant k (hr^{-1})
Ethylene glycol	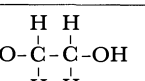	0.001 mol	0.088
Ethylene glycol	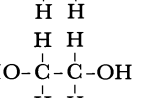	none	0.000
Tetramethylene glycol	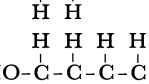	0.001 mol	0.067

TABLE 3. THE EFFECTS OF THE KIND OF ALCOHOLS IN THE IMIDATE FORMATION OF *m*-NITROBENZONITRILE AND ALCOHOLS AT VARIOUS REACTION TEMPERATURE
Reaction conditions, alcohol: 124 g each, sodium metal: 0.014 g (0.25×10^{-4} g atom), *m*-NBN: 0.0125 mol

Kind of alcohol	Additives	Reaction temperature	Time to reach equilibrium state	Equilibrium constant K (l/mol)
Ethylene glycol	—	25°C	24 hr	0.107
Ethylene glycol	—	60°C	1.5 hr	0.054
Ethylene glycol	—	100°C	15 min	0.024
Ethylene glycol	H_2O*1	100°C	10 min	0.025
Ethylene glycol	BHT*2	100°C	—	0.031
Ethylene glycol	$PbCl_2$*4	100°C	none*3	0
n-Butanol	—	60°C	1 hr	0.063
n-Butanol	—	100°C	10 min	0.030
sec-Butanol	—	60°C	—	0.000
t-Butanol	—	60°C	—	0.000

*1: 0.0125 mol *2: 0.0125 mol of bis-β-hydroxyethyl terephthalate
*3: none reaction *4: 6.25 mmol of $PbCl_2$ instead of Na

constant is presented in Fig. 9. The heat of reaction for the imidate formation was found to be −5.9 kcal/mol. By extrapolation from these results, the equilibrium constant for the imidate formation at 170°C was estimated to be *ca.* 0.01 $(mol/l)^{-1}$. The data listed in Table 3 also indicate that the rates of the

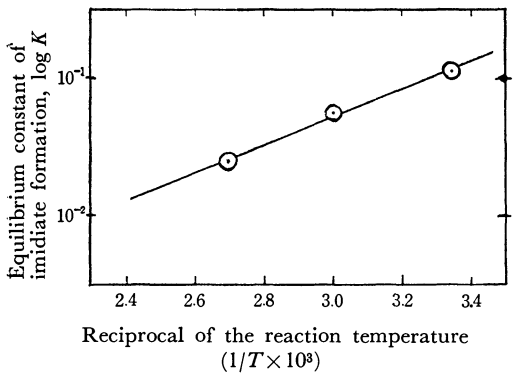

Fig. 9. Correlation of equilibrium constant log K *vs.* the reciprocal of reaction temperatures in the imidate formation reaction of benzonitrile. Reaction condition: *m*-NBN: 0.0125 mol, E.G: 2 mol, Na: 0.625 mg atom

formation of imidate in the presence of sodium metal are very fast at 170°C.

The data of Tabe 3 suggest that the formation of imidate can not be catalyzed by lead chloride, though it is known to promote the reaction of glycolysis.[1] The formation of imidate is not influenced by the presence of water or of bis-β-hydroxyethyl terephthalate, which inhibited the glycolysis reaction. The rates of the lead-ion catalyzed glycolysis of benzonitrile at 170°C were not affected by the addition of sodium metal (2.5×10^{-4} g atom) and were about five times faster than that of the sodium-catalyzed glycolysis of benzonitrile (2.5×10^{-4} g atom sodium).

Discussion

The experimental results presented above suggest that the rate-controlling step in the glycolysis reaction is the chemical reaction in the reaction mixture, while the rates of the desorption of ammonia are rapid. An analysis of the reaction rate data suggests that the formation of β-hydroxyethyl benzoate is accompanied by the formation of ammonia and that the rates of reaction may be inhibited by the presence of the product, β-hydroxyethyl benzoate. These may be the reasons why the rate of ammonia formation tends to deviate from the first-order reaction scheme at higher conversions and at different initial concentrations of benzonitrile, as is shown in Fig. 2. From the fact that *p*-cyanoacetophenone also inhibits the reaction, as is shown in Fig. 8, the inhibiting effect may be ascribed to the carbonyl group. Since the reaction was promoted by the metal ions, such as cupric, lead, and zinc ions, with a coordination tendency, as has been presented in the previous report,[1] the inhibition by the ester might be caused by the coordination of the carbonyl groups of the product to the lead ion, thus forming a more stable complex than the reaction intermediates. The deviation at the Hammett plots illustrated at Fig. 8 may be caused by the same factor.

The Hammett reaction constant for the glycolysis of variously substituted benzonitriles ($\rho=1.2$) is of the same magnitude as those for the alkaline hydrolysis of substituted benzonitriles ($\rho=1.5$) and of benzamides[6] ($\rho=1.75$) and that for the formation of imidate from benzonitrile[2] ($\rho=1.9$). This may suggest that the nucleophilic attack on benzonitrile is involved in the reaction mechanism.

From the results of the glycolysis of benzamide, the reaction route through the formation of benzamide from nitrile with water seems insignificant.

The addition of nitrile to glycols, the imidate formation, may be suggested to be involved in the reaction mechanism, since the rate of the reaction of glycols with a secondary or tertiary hydroxy group is smaller than that of ethylene glycol, and this tendency is similar to that in imidate formation. The presence of excess glycols, the effect of the type of glycol, and the effect of the substituted group of benzonitrile are other reasons to support the formation of imidate.

The reaction of the imidate formation of benzonitrile with glycol could not be promoted in the presence of a lead catalyst. The lead ion - catalyzed glycolysis of benzonitrile was found not to be promoted especially by the co-presence of alkaline metal and to be considerably faster than that of the sodium ion - catalyzed glycolysis of benzonitrile. Therefore, it seems likely that the reaction of imidate formation proceeds quickly under the given conditions.

Contrary to the lead ion-catalyzed trans-esterification of dimethyl terephthalate, in which the rate of the reaction with ethylene glycol is of a magnitude similar to that with tetramethylene glycol, the effect of the methylene sequence length of the two hydroxy groups is remarkable in the glycolysis of benzonitrile. Taking account of the effect of the neighboring hydroxy group's assistance in the alkaline hydrolysis of the ester,[7] the reaction mechanism may be considered to involve the internal solvation of the critical transition state by the neighboring hydroxy group.

In the basence of water, the rate of ammonia formation was slow and the amount of β-hydroxyethyl benzoate formed was very little in the glycolysis reaction, while in the presence of water the rate of ammonia formation was remarkably promoted and there was a sizable formation of β-hydroxyethyl benzoate. These facts obviously suggest the participation of water in the rate-determining step in the ester formation.

In view of the above facts, the following reaction mechanism may be proposed for the lead ion-catalyzed glycolysis of benzonitrile :

6) L. A. Cohen and W. M. Jones, *J. Am. Chem. Soc.*, **84**, 1625 (1962).

7) 1) T. C. Bruice and T. H. Fife, *ibid.*, **84**, 1973 (1962). b) T. C. Bruice and S. J. Benkovic, "Bioorganic Mechanism" Vol. 1, W. A. Benjamines Inc., New York, N.Y. (1966), p. 146. c) T. Yamanaka, A. Ichihara, K. Tabe and T. Matsumoto, *Shokubai* (*Catalysis*), **6**, 304 (1964).

(BN) (EG)

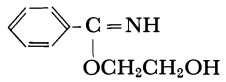

(I) (3)

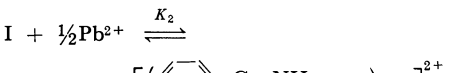

(II) (4)

(III) (5)

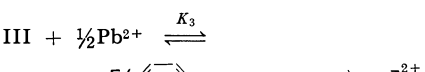

(IV) (6)

Here we consider that Eq. (5) represents the rate-determining step, in which the internal solvation of the critical transition state by the neighboring hydroxy group is involved. The above mechanism leads to Eqs. (7)—(11) for the rate of ammonia formation in the lead ion-catalyzed glycolysis of benzonitrile:

$$\frac{d[NH_3]}{dt} = k[II]^{1/2}[H_2O] \quad (7)$$

$$[II]^{1/2} = K_2[I][Pb^{2+}]^{1/2} \quad (8)$$

$$[I] = K_1[BN][EG] \quad (9)$$

$$[IV]^{1/2} = K_3[III][Pb^{2+}]^{1/2} \quad (10)$$

$$[Pb^{2+}] = [Pb^{2+}]_0 - [II] - [IV] \quad (11)$$

As the electronegativity of oxygen is larger than that of nitrogen, it is presumed that $K_3 > K_2$. In addition, as the concentration of [II] is very small under the given reaction conditions, in consideration of the mass balance, Eq. (11) may be simplified to Eq. (12):

$$[Pb^{2+}] \fallingdotseq [Pb^{2+}]_0 - [IV] \quad (12)$$

where $[Pb^{2+}]_0$ is the initial concentration of lead ions.

By combining Eq. (10) with Eq. (12), we have Eq. (13):

$$[Pb^{2+}] = \frac{[Pb^{2+}]_0}{1 + K_3^2[III]^2} \quad (13)$$

Thus, Eq. (7), replaced by Eqs. (8), (9), and (13), can be formulated as follows:

$$\frac{d[NH_3]}{dt} = kK_1K_2[BN][EG][H_2O]\left\{\frac{[Pb^{2+}]_0}{1 + K_3^2[III]^2}\right\}^{1/2} \quad (14)$$

Therefore, the initial rate of the formation of ammonia in the presence of excess ethylene glycol can be presented as follows:

$$\frac{d[NH_3]}{dt} = k'K_1K_2[BN][H_2O]\left\{\frac{[Pb^{2+}]_0}{1 + K_3^2[III]^2}\right\}^{1/2} \quad (15)$$

On the other hand, the observed initial rate of the lead ion-catalyzed glycolysis of benzonitrile, neglecting the reaction in the absence of any catalyst and of water, may be presented as in Eq. (16):

$$\frac{d[NH_3]}{dt} = k''[BN][H_2O]\left\{\frac{[Pb^{2+}]_0}{1 + 330[III]^{1.5}}\right\}^{0.44} \quad (16)$$

This equation agrees satisfactorily with Eq. (15).

Thus, the kinetic studies obviously support the afore-mentioned reaction mechanisms for the metal ion-catalyzed glycolysis of benzonitrile.

The reaction of non-catalytic glycolysis and that in the absence of water occured simultaneously in the above glycolysis of benzonitrile. These reactions are presumed to have more complicated reaction routes than that of the above-mentioned glycolysis; they will be discussed in the succeeding paper.

BULLETIN OF THE CHEMICAL SOCIETY OF JAPAN VOL. 41 1165—1169 (1968)

The Kinetics of the Metal Ion-catalyzed Glycolysis of Terephthalonitrile

Takashi IKEDA, Michitoshi KITABATAKE, Masatomo ITO and Ryoji ISHIOKA

The Central Research Laboratory, Showa Denko K.K., Tamagawa, Ohta-ku, Tokyo

(Received September 14, 1967)

The kinetics of the lead ion-catalyzed glycolysis of terephthalonitrile have been studied in the absence of and in the presence of water. In the absence of water, scarcely any formation of β-hydroxyethyl *p*-cyanobenzoate is observed, but some orthoesters are formed. The reaction rate data obtained in the absence of water are found to fit a reversible consecutive reaction scheme in which some basic compounds are involved as the intermediates. In proportion to the increase in the concentration of water, such intermediates as the orthoesters and basic compounds are hydrolyzed more rapidly to form β-hydroxyethyl *p*-cyanobenzoate, but simultaneously the hydrolysis of terephthalonitrile and the basic intermediates also takes place in the reaction mixture, thus yielding amide.

The effectiveness of the various kinds of metal compounds on the metal ion-catalyzed glycolysis of terephthalonitrile[1] and the kinetics of the metal ion-catalyzed glycolysis of benzonitrile[2] have been discussed in previous papers.

The heavy metal ions, such as cupric, lead, and zinc ions, have been found to promote the glycolysis of nitriles. Their catalytic activities have been correlated with the coordinating tendency of metal ions.

Benzonitrile first affords imidate upon the addition of glycol, and then two moles of the thus-derived imidates are chelated to a metal ion. The imidates activated by forming the chelate can be easily hydrolyzed by water to form esters and ammonia. However, these esters tend to chelate to the metal ions thus inhibiting the reaction.

The kinetic study of the metal ion-catalyzed glycolysis of terephthalonitrile is, therefore, important in order to have a better understanding of the reaction mechanisms and various reaction routes. No kinetic study of the glycolysis has been found in the literature.

We will attempt here to clarify the reaction routes and mechanisms of the metal ion-catalyzed glycolysis of terephthalonitrile in the absence of and in the presence of water.

Experimental

Kinetic Measurements. The procedure and measurements for the glycolysis of terephthalonitrile were similar to those employed in previous works.[1,2]

A typical set of reaction conditions employed is as follows: A reaction mixture of 0.05 mol of terephthalonitrile (T.P.N.), 1.5 mol of ethylene glycol (E. G.), 0.1 mol of water, and 0.00025 mol of a catalyst was reacted at the reaction temperature of 170°C. The reaction was carried out under a nitrogen atmosphere, nitrogen being bubbled into the mixture at the rate of 40 m*l*/min.

A 100-m*l* three-necked glass flask equipped with a reflux condenser, a thermometer, and a nitrogen gas inlet was used as the reaction vessel. The reaction mixture in the flask was immersed in an electrically-heated oil bath stirred by a magnetic apparatus. The ammonia formed during the reaction was absorbed in a dilute sulfuric acid solution stirred by a magnetic stirrer set in the flask.

The rate of the formation of ammonia was determined by the titration of samples of the sulfuric acid solution taken from the ammonia-absorbing flask at given intervals. The rate of the conversion of terephthalonitrile was determined at given intervals by using gas-liquid chromatography. The rates of the formation of both β-hydroxyethyl *p*-cyanobenzoate (H.C.B.) and bis-β-hydroxyethyl terephthalate (B.H.T.) were examined by using gas-liquid chromatography and ultraviolet spectroscopy.

The heated liquid product in the reaction state was quickly sampled with a micro-syringe (50 μ*l*) and analyzed by gas-liquid chromatography on a 2 m×6 mm stainless steel column of 25% Apiezon L on Chromosorb W at 190°C, using helium as a carrier gas and α-naphthol as an internal-standard substance.

The reaction of the glycolysis of terephthalonitrile proceeds as in the following sequence:

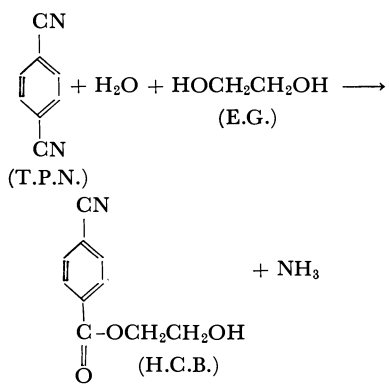

(1)

1) T. Ikeda, M. Kitabatake, M. Ito and Y. Noguchi, This Bulletin, **41**, 1154 (1968).

2) T. Ikeda, M. Kitabatake, M. Ito and Y. Noguchi, *ibid.*, **41**, 1158 (1968).

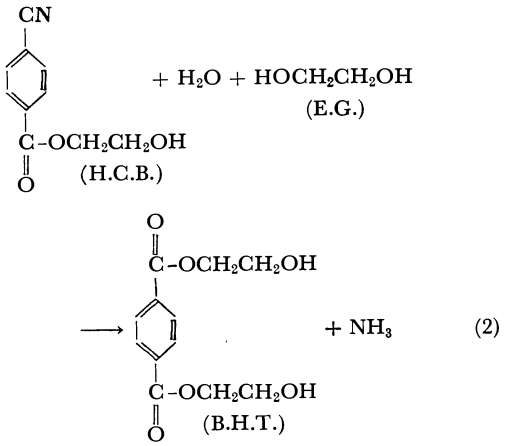

The reaction routes and the mechanism of the glycolysis of terephthalonitrile discussed here are limited to the first stage of the overall reaction.

Materials. Terephthalonitrile (mp 224°C) was prepared by the ammoxidation of *p*-xylene and was purified by recrystallization from dioxane.

Ethylene glycol (bp 197.2°C) and dipropylene glycol (bp 231.8°C) used were of reagent grades.

Lead acetate, a typical metal compound catalyst, was commercially available with a sufficient purity.

Results and Discussion

The influence of the concentration of water on the conversion rate of terephthalonitrile was investigated.

Data on the conversion of terephthalonitrile and on the formation of ammonia and β-hydroxyethyl *p*-cyanobenzoate for each concentration of water are shown in Figs. 1 and 2 in relation to the reaction time. The reactions were carried out under the standard reaction conditions described above except for the amount of water. These figures indicate that the conversion rate of terephthalonitrile increases with an increase in the amount of water below a 2-molar ratio of water to terephthalonitrile. The rate of the formation of β-hydroxyethyl *p*-cyanobenzoate has the same tendency, but scarcely any β-hydroxyethyl *p*-cyanobenzoate is formed in the absence of water, though the formation of ammonia is recognized.

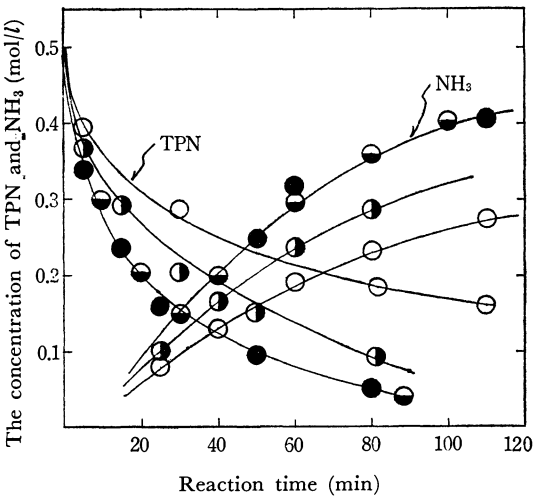

Fig. 1. The influence of concentration of water on the conversion of the concentration of terephthalonitrile and ammonia.
-○-: 0 initial molar ratio of H_2O to TPN
-◑-: 1 initial molar ratio of H_2O to TPN
-◒-: 2 initial molar ratio of H_2O to TPN
-●-: 3 initial molar ratio of H_2O to TPN
Reaction conditions: E.G./TPN=30, $Pb(OAc)_2$/TPN=1/200 at 170°C

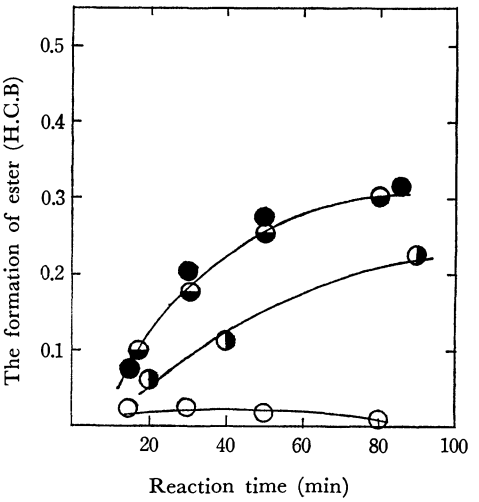

Fig. 2. The influence of the concentration of water on the formation of β-hydroxyethyl *p*-cyanobenzoate (H.C.B.).
-○-: 0 initial molar ratio of water to terephthalonitrile
-◑-: 1 initial molar ratio of water to terephthalonitrile
-◒-: 2 initial molar ratio of water to terephthalonitrile
-●-: 3 initial molar ratio of water to terephthalonitrile
Reaction conditions: E.G./TPN=30, $Pb(OAc)_2$/TPN=1/200 at 170°C

The rate of the conversion of terephthalonitrile is usually greater than that of the formation of ammonia. This fact indicates that nitrogen compounds may be present as intermediates in the routes from nitrile to the ester and/or that a side reaction such as the hydrolysis of nitrile to amide may exist.

The basic compounds which react with sulfuric acid were actually observed in the reaction mixture, as shown in Fig. 3. Since the desorption of ammonia from the reaction mixture was rapid under the given conditions, the amount of ammonia in the reaction mixture was insignificant. These basic compounds in the reaction mixture had a tendency to decrease with an increase in the concentration of water. Besides, at high concentrations of water,

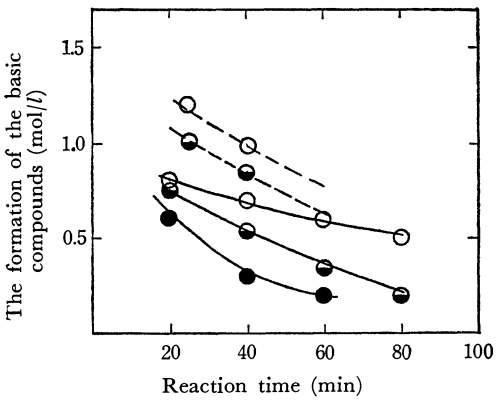

Fig. 3. The influence of the concentration of water and reaction temperature on the formation of basic compounds.
-○-: 0 initial molar ratio of water to terephthalonitrile
-◒-: 2 initial molar ratio of water to terephthalonitrile
-●-: 3 initial molar ratio of water to terephthalonitrile
——: 170°C
- - -: 145°C
Reaction conditions: E.G./TPN=30, $Pb(OAc)_2$/TPN=1/200

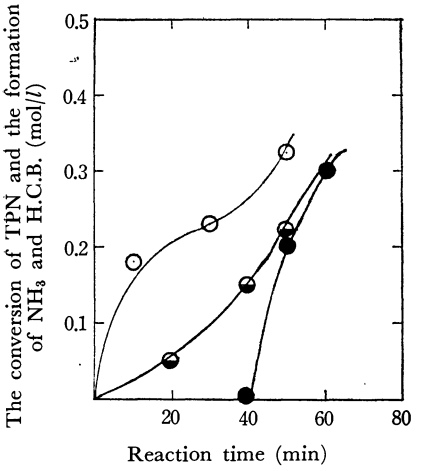

Fig. 4. The conversion of TPN and the formation of ammonia and ester (H.C.B.) by the addition of water to the non-aqueous reaction mixture at the reaction time of 40 min.
-○-: concentration of TPN reacted
-◒-: formation of NH_3
-●-: formation of ester (H.C.B.)
Reaction conditions: E.G/TPN=30, $Pb(OAc)_2$/TPN=1/200 at 170°C

there were quite large differences between the amount of the conversion of terephthalonitrile and that of both β-hydroxyethyl *p*-cyanobenzoate and the basic compounds, suggesting the formation of amide.

It is shown in Fig. 2 that scarcely any β-hydroxyethyl *p*-cyanobenzoate is formed in the absence of water, though the amounts of terephthalonitrile reacted and of ammonia formed increase considerably. However, the ester was observed to be formed, as shown in Fig. 4, when water was added to this non-aqueous reaction mixture in the course of the reaction. This fact indicates that the compounds other than the ester are formed in the absence of water and are susceptible to being hydrolyzed to the ester.

In Fig. 5 the experimental data on the concentration of unchanged terephthalonitrile, the amounts of the basic compounds titrated by sulfuric acid in the reaction mixture, and the formation of orthoester-type compounds are plotted against the reaction time at 170°C in the absence of water.

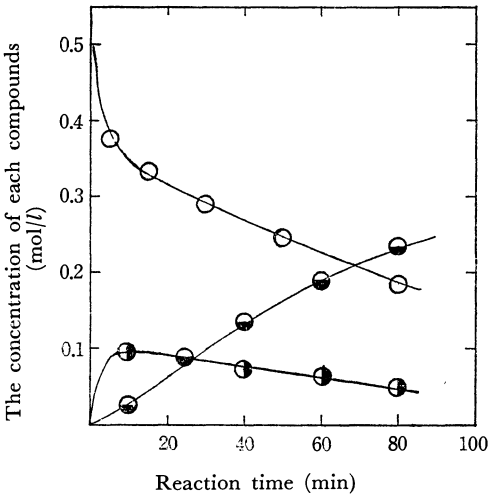

Fig. 5. The experimental data of the concentration of terephthalonitrile, orthoester and basic compound represented by marks and the calculated results with analog computer represented by real curved lines in the absence of water.
-○-: the concentration of terephthalonitrile unchanged
-◒-: the formation of orthoester (ammonia)
-◑-: the formation of basic intermediate compounds
Reaction conditions: E.G/TPN=30, $Pb(OAc)_2$/TPN=1/200, H_2O=0 at 170°C

The total amounts of ammonia formed and of the basic compounds in the reaction mixture in the absence of water correspond to the amounts of terephthalonitrile reacted. On the other hand, the rate of the reaction of terephthalonitrile was found to be first-order for the concentration of terephthalonitrile at a low conversion rate of terephthalonitrile.[1)]

In view of the above facts, the following rate expressions for the reaction scheme (Eq. (3)) were chosen:

$$\text{T.P.N.} \underset{k_2,\ HOCH_2CH_2OH}{\overset{k_1}{\rightleftarrows}} \text{B} \xrightarrow[HOCH_2CH_2OH]{k_3} \text{C} + NH_3 \quad (3)$$

B: basic compounds
C: orthoester-type compounds

The curves calculated by an analog computer according to Eqs. (4), (5) and (6) are presented in Fig. 5 by real curved lines, which are more agreeable to the experimental data.

$$d[TPN]/dt = k_2[B] - k_1[TPN] \quad (4)$$

$$d[B]/dt = k_1[TPN] - k_2[B] - k_3[B] \quad (5)$$

$$d[C]/dt = k_3[B] \quad (6)$$

The rate constants of the three reaction paths, k_1, k_2, and k_3, were 0.129 min^{-1}, 0.343 min^{-1}, and 0.033 min^{-1} respectively.

In order to get information about the C intermediate, initial reaction rates of the terephthalonitrile at different initial concentrations of ethylene glycol were investigated in an inert solvent such as dipropylene glycol; the following rate expression were chosen:

$$r_0 = k_1[TPN]_0[EG]_0^n \quad (7)$$

r_0: initial reaction rate of terephthalonitrile

Plots of k_1 in relation to the initial concentration of ethylene glycol give a straight line, as shown in Fig. 6, and the reaction order of ethylene glycol is nearly equal to 2. This fact suggests that two moles of ethylene glycol participate in the formation of the intermediate, B, or the product, C.

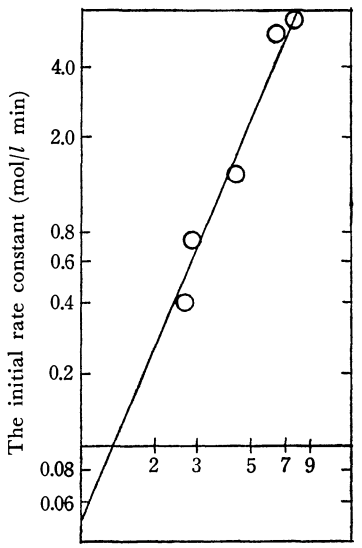

Fig. 6. The correlation between the initial rate constants and the initial concentration of ethylene glycol.
Reaction condition: $Pb(OAc)_2$/TPN=1/200 at 170°C

The reaction intermediate, B, is, in the absence of water, a substance which reacts with sulfuric acid. It may, therefore, be expected to have the following structures:

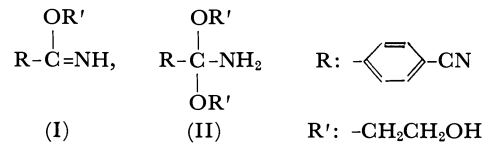

(I) (II)

The product, C, is presumed to be a orthoester-type compound:

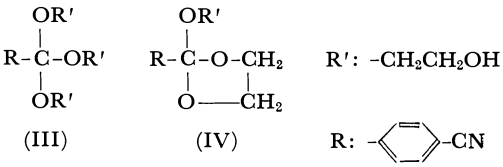

(III) (IV)

In Fig. 6 the straight line intercepts the vertical axis at the value of 0.0055. Using the values of 0.0055 and the initial concentration of terephthalonitrile of 0.448 mol/l, the rate constant, k_1, is calculated to have the value of 0.123 min^{-1}, a value which is almost equal to the above calculated value, k_1= 0.129 min^{-1}. These results indicate that the proposed reaction scheme and kinetics are consistent with all the experimental observations.

Even in the presence of water, the reaction to form B from the nitrile and that to give C from B may take place successively. Water is considered to participate in the reaction steps to form the ester and the amide.

Thus the following reaction scheme and rate equations may be considered for the first step of the glycolysis reaction:

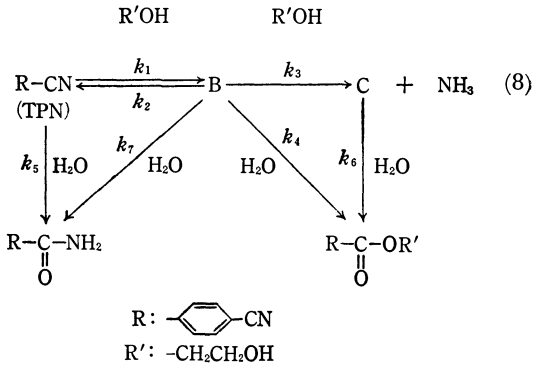

$$\frac{d[TPN]}{dt} = k_2[B] - k_1[TPN] - k_5[TPN][H_2O] \quad (9)$$

$$\frac{d[B]}{dt} = k_1[TPN] - k_2[B] - k_3[B] - k_4[B][H_2O] - k_7[B][B_2O] \quad (10)$$

$$\frac{d[C]}{dt} = k_3[B] - k_6[C][H_2O] \quad (11)$$

$$\frac{d[RCOOR']}{dt} = k_4[B][H_2O] + k_6[C][H_2O] \quad (12)$$

$$\frac{-d[H_2O]}{dt} = k_5[TPN][H_2O] + k_4[B][H_2O] + k_6[C][H_2O] + k_7[B][H_2O] \quad (13)$$

$$\frac{d[NH_3]}{dt} = k_3[B] + k_4[B][H_2O] \quad (14)$$

In Fig. 7 the experimental data of the concentration of unchanged terephthalonitrile, the amounts of basic compounds titrated by sulfuric acid in the reaction mixture, and that of the formation of ammonia and β-hydroxyethyl *p*-cyanobenzoate are plotted against the reaction time at 170°C in the presence of water.

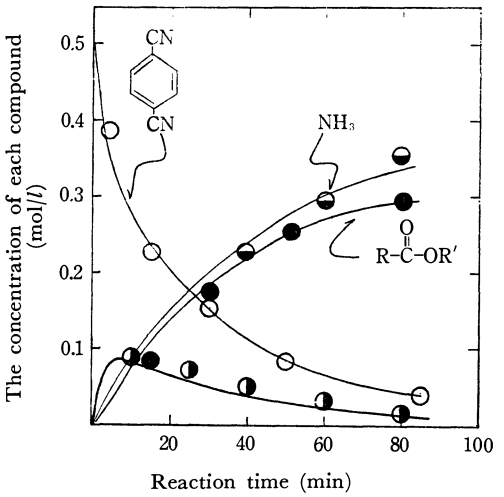

Fig. 7. The experimental data of the concentration of terephthalonitrile, ammonia, basic intermediate compounds and ester (H.C.B.) represented by marks and the calculated results with analog computer represented by real curved lines in the presence of water.
-○-: the concentration of TPN
-◒-: the formation of NH_3
-◑-: the formation of basic intermediate compound
-●-: the formation of ester (H.C.B.)
Reaction conditions: E.G./TPN=30, $Pb(OAc)_2$/TPN=1/200 H_2O/TPN=2, at 170°C

On the basis of the experimental data in Fig. 7, theoretical curves, as calculated by the analog computer, are shown in Fig. 7 by real curved lines using the above equations, (9), (10), (11), (12), (13), and (14). These rate constants at 170°C are obtained as follows:

$k_1 = 0.129\ min^{-1}$

$k_2 = 0.343\ min^{-1}$

$k_3 = 0.033\ min^{-1}$

$k_4 = 0.055\ min^{-1}\ mol^{-1}l$

$k_5 = 0.011\ min^{-1}\ mol^{-1}l$

$k_6 = 0.071\ min^{-1}\ mol^{-1}l$

$k_7 = 0.040\ min^{-1}\ mol^{-1}l$

The above results are also supported by the facts that scarcely any formation of the intermediate, C, is observed in the presence of water and that the rate constant of the direct hydrolysis of terephthalonitrile to amide in dipropylene glycol is very small, even in the presence of water.

It may, therefore, be considered that the glycolysis of terephthalonitrile to form β-hydroxyethyl*p*-cyanobenzoate may proceed *via* the hydrolysis of an ortho-ester-type compound, C, especially at a low concentration of water, and *via* an imidate- or amine-type intermediate, B, at a high concentration of water. Furthermore, at a higher concentration of water the formation of amide becomes a little more significant.

The authors wish to thank Messrs. Yoshitaka Noguchi and Ichiro Hashimoto for their valuable discussions. Thanks are also due to Mr. Katsumi Terayama for his technical assistance.

BULLETIN OF THE CHEMICAL SOCIETY OF JAPAN VOL. 41 1170—1174 (1968)

Intramolecular Hydrogen Bonding in Monoterpene Alcohols Containing π-Electronic System[1]

Tsuyoshi SHISHIBORI

Department of Chemistry, Faculty of Science, Hiroshima University, Hiroshima

(Received July 26, 1967)

The nature of intramolecular hydrogen bonding in diastereoisomeric pairs of 10-nor-8-oxomenthols (VIII and IX) and 10-nor-8-oxocarvomenthols (X and XI) has been studied by infrared spectroscopy. It was found that 10-nor-8-oxoneomenthol (IX) contains the OH···O type intramolecular hydrogen bond, while 10-nor-8-oxomenthol (VIII) contains the OH···π interaction in addition to the OH···O hydrogen bond. 10-Nor-8-oxocarvomenthols (X and XI) were internally unbonded. In addition, the extent and the limitation of the intramolecular OH···π interaction has been investigated for the diastereoisomeric pairs of a series of *p*-menth-8-enols: *p*-menth-8-en-4-ols (I and II), isopulegols (III and IV), dihydrocarveols (V and VI), and *trans*-β-terpineol (VII). Thus, the hydroxyl group in α- or β-unsaturated alcohols I, II, III and IV was found to be internally bonded to the π-electrons on the double bond; the other isomers are internally unbonded.

The facts that intramolecular hydrogen bonding depends on the configuration and the conformation of compounds containing a hydroxyl group are of great potential utility for the structure elucidation and the conformational analysis.[2,3] The relationship between the configuration and the infrared spectral parameter has been studied extensively for the open chain and the cyclic compounds.[3] However, little data are available on intramolecular hydrogen bonding in cyclohexanol derivatives bearing the hydrogen accepting group, such as an isopropenyl, an acetyl, or a hydroxyisopropyl group. For the cyclohexanol derivatives having one of these groups, the rotational conformations of the group are possible in addition to the chair-chair interconversion of the ring. It is expected that the conformation of the group can be suggested from the examination of intramolecular hydrogen bonding.

In this paper, the spectral parameters relating to the intramolecular hydrogen bond between the hydroxyl and carbonyl groups in a diastereoisomeric pair of 10-nor-8-oxomenthols (VIII and IX) were compared with the ones of the OH···O hydrogen bond and the OH···π interaction in the diastereoisomeric pairs of isopulegols (III and IV) and *p*-menthane-3,8-diols (XII and XIII). In addition, the extent and the limitation of the intramolecular interaction between the hydroxyl group and the π-electrons has been investigated for the diastereoisomeric pairs of a series of *p*-menth-8-enols: *p*-menth-8-en-4-ols (I and II), isopulegols (III and IV), dihydrocarveols (V and VI) and *trans*-β-terpineol (VII).

Results and Discussion

In Figs. 1 and 2 are shown the actual O–H stretching absorption curves of the monoterpene alcohols (III, IV, VIII and IX). An unresolved band was divided by graphical separation,[4] assuming that the band is an overlapping of the symmetric bands. The data of the hydroxyl bands divided are summarized in Table 1.

***trans*- and *cis*-*p*-Menth-8-en-4-ols (I and II).** The spectra of I and II exhibited the principal band 3606 and 3604 cm^{-1} with a weak shoulder at 3622 and 3621 cm^{-1} respectively. In both I and II, the strong band at the low frequency side is attributed to the hydroxyl group which interacts with the π-electrons of the isopropenyl group, and the weak, high-frequency band corresponds to the unbonded tertiary hydroxyl band, which has been reported[5-7] to appear at 3613—3619 cm^{-1}. The separation by 16 and 17 cm^{-1} between the free and bonded hydroxyl bands in I and II, respectively, agrees with 15.4 cm^{-1} of allyl alcohol.[8,9] It is possible to say roughly

1) This paper forms Paper IV[2] in the Hiroshima University series on Stereochemical Studies of Monoterpene Compounds, and was presented at 20th Annual Meeting of the Chemical Society of Japan, Tokyo, April 1967.

2) Paper III of this series: T. Suga, T. Shishibori and T. Matsuura, This Bulletin, **41**, 944 (1968).

3) M. Tichý, "Advances in Organic Chemistry," Vol. 5, Interscience Publishers and John Wiley & Sons, Inc., New York, N. Y. (1965), p. 115.

4) Examples of the graphical separation are shown in Figs. 1 and 2. N. Mori, S. Omura, N. Kobayashi and Y. Tsuzuki, This Bulletin, **38**, 2149 (1965).

5) L. P. Kuhn, *J. Am. Chem. Soc.*, **74**, 2492 (1952).

6) A. R. H. Cole, G. T. A. Müller, D. W. Thornton and R. L. S. Willix, *J. Chem. Soc.*, **1959**, 1218.

7) A. R. H. Cole, P. R. Jefferies and G. T. A. Müller, *ibid.*, **1959**, 1222.

8) M. Ōki and H. Iwamura, This Bulletin, **32**, 567 (1959).

9) P. von R. Schleyer, D. S. Trifan and R. Bacskai, *J. Am. Chem. Soc.*, **80**, 6691 (1958).

Table 1. Hydroxyl stretching absorptions of *p*-menth-8-enols, 10-nor-8-oxomenthols and *p*-menthane-3,8-diols

Compound	ν_{OH}^{free} cm^{-1}	ε	ν_{OH}^{bonded} cm^{-1}	ε	$\varepsilon b/\varepsilon f$
trans-p-Menth-8-en-4-ol (I)	3622[a]	14	3606	68	4.9
cis-p-Menth-8-en-4-ol (II)	3621[a]	6	3604	74	12.3
Isopulegol (III)	3625[a]	10	3593[a]	9	0.9
			3573	35	3.5
Neoisopulegol (IV)	3626	9	3575	43	4.8
Dihydrocarveol (V)	3630	50			
	3610[a]	25			
Neodihydrocarveol (VI)	3633	72			
trans-β-Terpineol (VII)	3617	58			
10-Nor-8-oxomenthol (VIII)	3625	20	3599	36	1.8
			3535[a]	9	0.5
10-Nor-8-oxoneomenthol (IX)	3626	12	3537	46	3.8
10-Nor-8-oxocarvomenthol (X)	3630	42			
	3608	26			
10-Nor-8-oxoneocarvomenthol (XI)	3634	81			
cis-p-Menthane-3,8-diol (XII)	3622[a]	62	3522	110	1.7
	3615	66			
trans-p-Menthane-3,8-diol (XIII)	3614	61	3509	120	2.0

a: shoulder

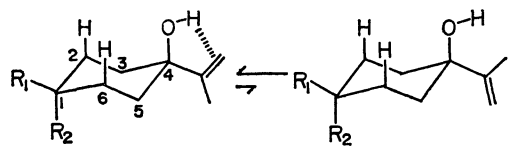

Ia (R_1=Me, R_2=H) Ib
IIa (R_1=H, R_2=Me) IIb

that the $\varepsilon b/\varepsilon f$ value reflects the relative population of the bonded and free species,[3] where εb is the molecular extinction coefficient of the bonded hydroxyl and εf is that of the free hydroxyl group. The $\varepsilon b/\varepsilon f$ values were 4.9 for I and 12.3 for II. Comparison of these values with the value (1.8) of allyl alcohol[10] reveals that the population of such an internally hydrogen-bonded molecules as Ia and IIa is larger in *p*-menth-8-en-4-ols (I and II) than in allyl alcohol. The reason for this appears to be that the axial hydrogens on C-2 and C-6 in Ib and IIb may sterically repel the hydrogen of the tertiary hydroxyl group, forcing to direct it to the outer side of the cyclohexane ring, and towards the double bond of the isopropenyl group, as in Ia and IIa, whereas such repulsion is absent in allyl alcohol.

Isopulegol (III) and Neoisopulegol (IV). Neoisopulegol (IV) showed two distinct bands at 3626 and 3575 cm^{-1}. This carbinol may take the intramolecularly hydrogen bonded conformation IVa and unbonded one IVb. The former band is ascribed to a free hydroxyl group in IVb, because a free axial secondary hydroxyl frequency has been reported[5-7] to appear at 3627 to 3632 cm^{-1}. The latter is assigned to the band due to such a hydroxyl group interacted with the π-electrons as in IVa. On the other hand, isopulegol (III) showed an unresolved band, which was divided into three by graphical separation as shown in Fig. 1. The peak at 3625 cm^{-1} may be attributed to the free equatorial secondary hydroxyl group, a peak of which is said[5-7] to appear at 3623 to 3630 cm^{-1}. The peak at 3578 cm^{-1} indicates the presence of the OH$\cdots\pi$ interaction. The third band, which appeared at 3593 cm^{-1} seems to be due to either a hydrogen bonded hydroxyl or a conformational heterogeneity about the C–OH bond. Menthol corresponding to the saturated compound of III showed an unsymmetric band at 3626 and 3608 cm^{-1} owing to the conformational heterogeneity. The wave number of the third band of III is different by 15 cm^{-1} from the low-frequency band of menthol. Hence, the third band of III must be due to an intramolecularly interacted hydroxyl group. Thus, isopulegol (III) is considered to possess two intramolecularly interacted forms as shown in IIIa and IIIb.

The $\varepsilon b/\varepsilon f$ values were 0.9 and 3.5 for III, and 4.8 for IV. Comparison of these values with the value (0.45) of 3-buten-1-ol[10] reveals that the population of the internally hydrogen bonded molecules, such as IIIa and IVa, is larger in isopulegols (III and IV) than in 3-buten-1-ol. This can be explained in the following way. For 3-buten-1-ol, there are three internal rotational degrees of freedom about the alpha and the beta carbon-carbon single bonds and the carbon-oxygen bond. Isopulegols (III and IV) have one less internal rotational degree of freedom, since the incorporation of the C_3–C_4 bond into the

10) This value was calculated from the data of allyl alcohol in Ref. 8.

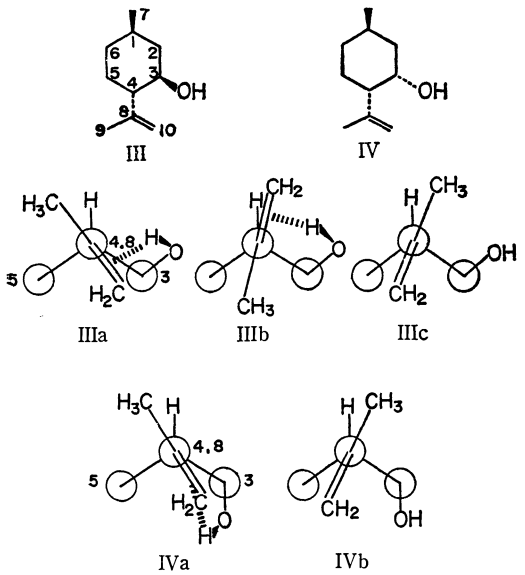

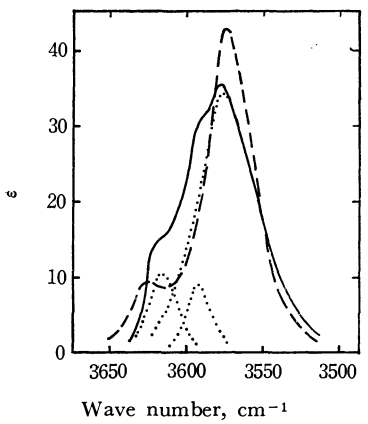

Fig. 1. IR spectra of isopulegol (III) (——; separated ·····) and neoisopulegol (IV) (- - -) in 0.005M CCl_4 solution.

cyclohexane ring restrains the rotation of this bond, and this restriction makes the hydroxyl group favorable towards the isopropenyl group. Hence, the opportunity of hydrogen bonding is larger in isopulegols than in 3-buten-1-ol.

Dihydrocarveol (V), Neodihydrocarveol (VI) and *trans*-β-Terpineol (VII). Dihydrocarveol (V) having an equatorial secondary hydroxyl group showed a peak at 3630 cm^{-1} with a shoulder at 3610 cm^{-1}. This unsymmetrical band is not attributable to the presence of the interaction between the hydroxyl group and the π-electrons, but rather to the presence of isomers (Va, Vb and Vc) due to the rotational conformations of the hydroxyl group about the C–O axis.[11] The corresponding saturated alcohol, carvomenthol, also revealed an unsymmetrical band at 3631 and 3612 cm^{-1}, whereas the epimeric alcohol, neocarvomenthol, showed a symmetrical one at 3633 cm^{-1}. Therefore, the band at 3630 or 3631 cm^{-1} observed in dihydrocarveol (V) and carvomenthol with an equatorial secondary hydroxyl group is attributable to the conformers Va and/or Vb, and the low-frequency bands at 3610 or 3612 cm^{-1} to the conformer Vc. On the other hand, neodihydrocarveol (VI) and *trans*-β-terpineol (VII) showed a symmetrical band at 3633 and at 3617 cm^{-1} respectively, which correspond to the free axial secondary hydroxyl and the free tertiary hydroxyl band.[5-7] Therefore, these alcohols are considered to be internally unbonded.

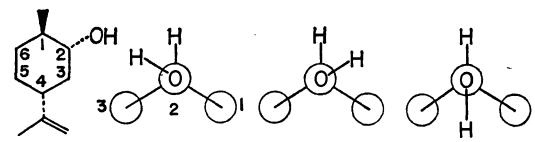

Thus, the intramolecular interaction between the hydroxyl group and the π-electrons on a double bond of *p*-menth-8-enols takes place only in the case of the hydroxyl group at the α- or β-position to the double bond. This kind of interaction can not be found in the case of hydroxyl group at farther than γ-position.

10-Nor-8-oxomenthol (VIII) and 10-Nor-8-oxoneomenthol (IX). The spectrum of VIII showed an unresolved band, which can be divided into three by graphical separation (Fig. 2). The peak at 3625 cm^{-1} is attributed to the free hydroxyl group and the peak at 3535 cm^{-1} to the OH···O intramolecularly hydrogen bonded hydroxyl group of the type of VIIIc, in which the hydroxyl group makes bonding to the lone pair electrons on the carbonyl oxygen atom. On the other hand, the intermediate band at 3599 cm^{-1} was separated only by 26 cm^{-1} from the free hydroxyl band. This small separation seems to indicate that the hydroxyl group interact with π-electrons on the carbonyl group,[12] as shown in VIIId and VIIIe. The spectrum of IX showed two peaks at 3626 and 3537 cm^{-1}, the former being attributed to the free hydroxyl group (IXc) and the latter to the intramolecularly hydrogen bonded hydroxyl group of the type IXd in which the hydroxyl group bonds to the lone pair electrons on the carbonyl oxygen atom.

The difference of interactions in VIII and IX was explained as follows: These keto alcohols may take two interconvertible chair-forms VIIIa and VIIIb, and IXa and IXb, respectively. However, the forms VIIIb and IXb containing three or two axial

11) M. Ōki and H. Iwamura, This Bulletin, **32**, 950 (1959).

12) M. Ōki and H. Iwamura, Preprints for the 20th Annual Meeting of the Chemical Society of Japan (April 1967), Part III, p. 128.

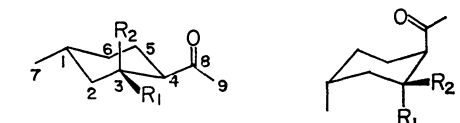

VIIIa (R_1=OH, R_2=H)
IXa (R_1=H, R_2=OH)

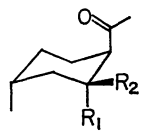

VIIIb
IXb

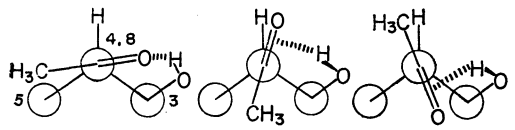

VIIIc VIIId VIIIe

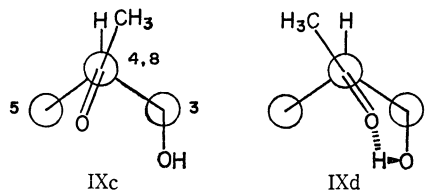

IXc IXd

groups are neglected on the basis of the consideration of the thermodynamic stability.[13] Furthermore, the internal rotation of the acetyl group must be considered to explain the difference of the interaction. Intramolecular hydrogen bonding between the axial hydroxyl group and the lone pair electrons on the carbonyl oxygen in IX is favorable in conformer IXd, in which the interaction between the 9-methyl group and the 5-methylene is not present. On the other hand, conformer VIIIc having the short OH···O distance is unfavorable, because the 9-methyl group eclipses the 5-methylene. Therefore, the compound VIII seems to take conformation VIIId or VIIIe, in which no such unfavorable interaction occurs. In these conformations VIIId and VIIIe, the angle made by the direction of the carbonyl n-orbital and the line connecting the hydroxyl hydrogen with the carbonyl oxygen atoms amounts to *ca.* 60°, and the hydroxyl group is thought to interact rather with the π-electrons than with the lone pair electrons of the carbonyl group.

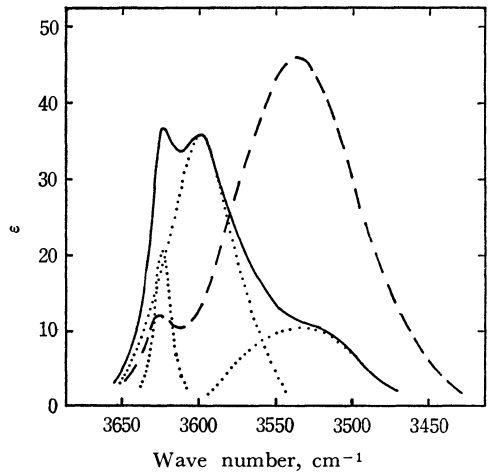

Fig. 2. IR spectra of 10-nor-8-oxomenthol (VIII) (——; separated ·····) and 10-nor-8-oxoneomenthol (IX) (- - -) in 0.005M CCl_4 solution.

10-Nor-8-oxocarvomenthol (X) and 10-Nor-8-oxoneocarvomenthol (XI). The spectrum of 10-nor-8-oxocarvomenthol (X) showed an unsymmetrical band at 3630 cm^{-1} with a weak shoulder at 3608 cm^{-1}. The shape of this band as well as the wave number of the peak and the shoulder are very similar to those of carvomenthol and dihydrocarveol (V). Hence, the unsymmetrical band of X must be due to the conformational heterogeneity about the C–OH bond. 10-Nor-8-oxoneocarvomenthol (XI) revealed a symmetrical band at 3634 cm^{-1} corresponding to the free axial secondary hydroxyl band. No intramolecular interaction between the hydroxyl and carbonyl groups was observed for γ-keto alcohols such as 10-nor-8-oxocarvomenthols (X and XI).

***cis*- and *trans*-*p*-Menthane-3,8-diols (XII and XIII).** The spectrum of XII gave two bands at 3615 and 3522 cm^{-1}; the higher frequency band has a shoulder at *ca.* 3622 cm^{-1}. Concerning the *cis*-diol XII with the secondary axial hydroxyl group, the band at 3615 cm^{-1} is attributed to the free tertiary hydroxyl group in XIIa, while the weak band at 3622 cm^{-1} is due to the free secondary hydroxyl group in XIIb. This is supported by the fact that these frequencies agree with those of the ordinary

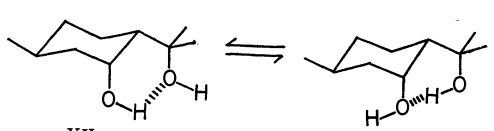

XIIa XIIb

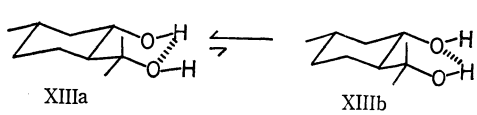

XIIIa XIIIb

13) The differences in free energy between the equatorial and axial forms of the hydroxyl and methyl groups are −0.7[14] and −1.7 kcal/mol respectively. The energy of 1,3-diaxial interaction between the 7-methyl and hydroxyl groups in conformer VIIIb is 1.9—2.4 kcal/mol.[14] As the difference has been unknown for the acetyl group, we assumed to be nearly equal to −1.8 kcal/mol[14] given for the ethyl group. The difference of the conformational energy for VIIIa—VIIIb and IXa—IXb was estimated as −5.2 and −2.8 kcal/mol,[15] respectively. These differences would give a room temperature equilibrium mixture containing >99% of VIIIa or IXa, and <1% of VIIIb or IXb.

14) E. L. Eliel, N. L. Allinger, S. J. Angyal and G. A. Morrison, "Conformational Analysis," Interscience Publishers, Inc. New York, N. Y. (1965), pp. 44 and 52.

15) Estimated approximately by adding the corresponding values for a hydroxyl, a methyl and an acetyl groups, and for the 1,3-diaxial interaction between the hydroxyl and methyl groups, since such summations have been said to be approximately correct in some cases.[16]

16) Ref. 14, p. 58.

free tertiary hydroxyl and secondary hydroxyl groups.[5-7] The strong band at 3522 cm^{-1} is attributable to both the bonded secondary and tertiary hydroxyl groups in XIIa and XIIb respectively. On the other hand, the spectrum of XIII showed two resolved peaks at 3614 and 3509 cm^{-1}. The band at 3614 cm^{-1} is assigned to the band due to the free tertiary hydroxyl group in XIIIa and the strong band at 3509 cm^{-1} is mainly due to the bonded secondary hydroxyl group in XIIIa, since the band corresponding to the free hydroxyl is absent. Therefore, the preferential formation of the hydrogen bond seems to be in the case, where the secondary hydroxyl group is bonded to the oxygen atom of the tertiary hydroxyl group.

Experimental

Infrared Measurements. The infrared absorption was measured with a Perkin-Elmer Model 621 Grating Infrared Spectrometer, the spectral slit width being 3.5 cm^{-1} in the region required. Spectro Grade carbon tetrachloride was used as a solvent. A salt absorption cell, 2 cm in length, was used and the concentration of the solution was 0.005 mol/*l* at which the association of the solute negligible. Measurements were made at 25°C.

***trans*- and *cis*-*p*-Menth-8-en-4-ols (I and II).** These *p*-menth-8-en-4-ols (I and II) kindly supplied by Dr. Klein were prepared from 4(8)-*p*-menthene by the photosensitized oxidation.[17]

(−)-Isopulegol (III) and (+)-Neoisopulegol (IV). These two alcohols were isolated by the partial esterification of an isopulegol mixture.[18] III showed the following properties: bp 65—66°C/3 mmHg, n_D^{25} 1.4684, d_4^{25} 0.9062, $[\alpha]_D^{25}$ −22.51° (homog.) (lit.,[18] n_D^{26} 1.4690, d_4^{26} 0.9062, $[\alpha]_D^{26}$ −23.6°), 3,5-dinitrobenzoate of III, mp 104—105°C (lit.[18] mp 104—104.5°C). IV showed the following properties: bp 81—81.2°C/9 mmHg, n_D^{25} 1.4695, d_4^{25} 0.9115, $[\alpha]_D^{25}$ +33.27° (homog.) (lit.,[18] n_D^{26} 1.4708, d_4^{26} 0.9121), 3,5-dinitrobenzoate of IV, mp 133—134°C (lit.,[18] 133—133.5°C).

(−)-Dihydrocarveol (V). This alcohol was prepared from (−)-carvone by the reduction with sodium-aqueous ammonia[19] and had following properties: bp 99—99.5°C/10 mmHg, n_D^{25} 1.4725, d_4^{25} 0.9162, $[\alpha]_D^{25}$ −34.15° (homog.) (lit.,[19] n_D^{23} 1.4748, d_{20}^{23} 0.9202, $[\alpha]_D^{23}$ −33.25°), 3,5-dinitrobenzoate of V, mp 122—123°C (lit.,[19] mp 121.5—122.5°C).

(+)-Neodihydrocarveol (VI) and *trans*-*β*-terpineol (VII). These alcohols were prepared from (+)-limonene monoxide by the reduction with lithium aluminum hydride.[20] The former VI was isolated from a reduction product by converting into the *p*-nitrobenzoate derivative followed by hydrolysis and showed the following properties: bp 107—107.9°C/19 mmHg, n_D^{25} 1.4763, d_4^{25} 0.9225, $[\alpha]_D^{25}$ +35.16° (homog.) (lit.,[20a] n_D^{20} 1.4798, d_4^{25} 0.9337, $[\alpha]_D^{25}$ +32.8°), *p*-nitrobenzoate of VI, mp 106—107°C (lit.,[20] 106°C).

The unesterified portion of the reduction product was fractionally distilled under a reduced pressure, and afforded *trans*-*β*-terpineol (VII): bp 100—100.5°C/17 mmHg, mp 30—31°C, n_D^{25} 1.4746, d_4^{25} 0.9230, $[\alpha]_D^{25}$ 0° (lit.,[20a] mp 31—31.5°C n_D^{20}, 1.4749, d_4^{25} 0.9235).

(−)-10-Nor-8-oxomenthol (VIII). A solution of 1.0 g of III was ozonized in glacial acetic acid. The reaction mixture was stirred with zinc powder (1.0 g), 20 m*l* of ether, and 15 m*l* of water for 2 hr. The usual work-up gave 0.56 g of VIII: mp 45—46°C, $[\alpha]_D^{25}$ −48.5° (*c* 0.34, methanol), 3,5-dinitrobenzoate of VIII, mp 152—153°C (Found: C, 54.68; H, 5.20%).

Found: C, 69.38; H, 10.52%. Calcd for $C_9H_{16}O_2$: C, 69.19; H, 10.32%.

(+)-10-Nor-8-oxoneomenthol (IX). (+)-Neoisopulegol (IV) (1.0 g) was ozonized in glacial acetic acid (20 m*l*). On treatment as in the case of VIII, the ozonized mixture gave 0.8 g of IX: mp 59—60°C, $[\alpha]_D^{25}$ +17.7° (*c* 0.37, methanol), 3,5-dinitrobenzoate, mp 93—94°C (Found: C, 54.96; H, 5.37%).

Found: C, 68.90; H, 10.48%. Calcd for $C_9H_{16}O_2$: C, 69.19; H, 10.32%.

(−)-10-Nor-8-oxocarvomenthol (X). When (−)-dihydrocarveol (V) (2.0 g) was ozonized in glacial acetic acid in the same way as in the case of VIII, it gave a crystalline mass (1.1 g) of X: mp 58—59°C, $[\alpha]_D^{25}$ −43.1° (*c* 0.21, methanol), 3,5-dinitrobenzoate, mp 126—126.5°C (Found: C, 54.77; H, 5.42%).

Found: C, 69.42; H, 10.50%. Calcd for $C_9H_{16}O_2$: C, 69.19; H, 10.32%.

(+)-10-Nor-8-oxoneocarvomenthol (XI). On ozonization in the same way as in the case of VIII, (+)-neodihydrocarveol (VI) (2.0 g) gave 1.2 g of XI as an oil: bp 107—108°C/2 mmHg, n_D^{25} 1.4732, d_4^{25} 1.0165, $[\alpha]_D^{25}$ +29.41° (homog.); 3,5-dinitrobenzoate, mp 136—137°C (Found: C, 54.58; H, 5.39%).

***cis*- and *trans*-*p*-Menthane-3,8-diols (XII and XIII).** These diols kindly supplied by Dr. Arai were prepared from (+)-citronellal by the acid-catalyzed cyclization[21]; XII, mp 73—74°C; XIII, mp 60—61°C.

The author wishes to express his hearty gratitude to Professor Tamon Matsuura and to Dr. Takayuki Suga for their guidance and encouragement, to Dr. E. Klein of DRAGOCO, Holzminden, for a gift of *p*-menth-8-en-4-ols, to Dr. Mannosuke Arai of Tohoku University, for *p*-menthane-3,8-diols, to Takasago Perfumery Co., Ltd., Tokyo, for spearmint oil and isopulegol, to Hasegawa Co., Ltd., Tokyo, for limonene. Microanalyses were performed at Faculty of Pharmacy of Kyoto University, Kyoto.

17) E. Klein and W. Rojahn, *Tetrahedron*, **21**, 2173 (1965).

18) H. Ueda and S. Shimizu, *Bull. Agri. Chem. Soc. Japan*, **24**, 402 (1960).

19) H. Ueda and S. Shimizu, *ibid.*, **23**, 524 (1959).

20) a) G. V. Pigulevskiĭ, S. A. Kozin and V. G. Kostenko, *Zhur. Obshchei. Khim.*, **28**, 1413 (1958); b) H. Kuczynski and K. Piatkowski, *Roczniki Chem.*, **33**, 299 (1959).

21) P. Barbier and G. Leser, *Compt. rend.*, **124**, 1308 (1897).

BULLETIN OF THE CHEMICAL SOCIETY OF JAPAN VOL. 41 1175—1179 (1968)

Stereochemical Studies of Monoterpene Compounds. V.[1] The Rotational Conformation of the Acetyl Group of 10-Nor-8-oxomenthols and 10-Nor-8-oxocarvomenthols[2]

Takayuki SUGA, Tsuyoshi SHISHIBORI and Tamon MATSUURA

Department of Chemistry, Faculty of Science, Hiroshima University, Hiroshima

(Received September 30, 1967)

The preferred rotational conformation of the acetyl group of (+)-10-nor-8-oxoneomenthol (I), (−)-10-nor-8-oxomenthol (II), (−)-10-nor-8-oxocarvomenthol (III), and (+)-10-nor-8-oxoneocarvomenthol (IV) has been examined by a combination of conformational analysis by *a priori* calculation and variable-temperature circular dichroism and infrared spectrum measurements. Compound I exhibited an inversion in the sign of the Cotton effect upon a change in the solvent. This phenomenon was interpreted as indicating the conformational change Ia⇄Ib. The cause of the change was ascribed to the formation and subsequent rupture of the intramolecular hydrogen bond. Compound II exhibited a solvent-depending circular dichroism curve similar to the curve of I; this was explained as indicating the existence of a conformational equilibrium between the free conformer, IIa, and the internally-hydrogen-bonded conformers, IIb, IIc, and IId. Furthermore, compounds III and IV were found to take preferentially the IIIa—IIIb and IVa—IVb conformations respectively.

In recent years, optical rotatory dispersion and circular dichroism (CD) measurements have been useful in assigning the rotational conformation of the 17-acetyl group of 20-ketosteroids[3] because of the peculiar sensitivity of this method to subtle conformational alterations. However, the conformation of the acetyl group of the cyclohexane derivatives has not yet been reported. 2- and 3- Acetylcyclohexanols seem to represent an interesting example of such a conformational alteration, since intramolecular hydrogen bonding can be expected in them, together with a rotational conformation of the acetyl group. For this paper the preferred rotational conformation of the acetyl group of (+)-10-nor-8-oxoneomenthol (I), (−)-10-nor-8-oxomenthol (II), (−)-10-nor-8-oxocarvomenthol (III) and (+)-10-nor-8-oxoneocarvomenthol (VI) has been examined by a combination of conformational analysis by *a priori* calculation and variable-temperature CD and infrared (IR) spectrum measurements.

Results and Discussion

Compounds I, II, III and IV were prepared from (+)-neoisopulegol, (−)-isopulegol, (−)-dihydrocarveol and (+)-neodihydrocarveol respectively by ozonolysis; the configurations are as shown in Fig. 1.

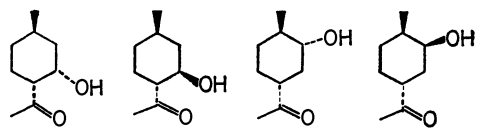

I II III IV

Fig. 1.

In the conformational analysis of compounds I, II, III and IV, the conformation of the cyclohexane ring will be assumed throughout the following discussion to take the 1,4-diequatorial chair-form.[1] We must next consider the problem of the rotational barrier about a bond joining a carbonyl group to a tetrahedral carbon in a molecule of the acetone type. As Fig. 2 shows, the conformational energies of the acetyl group of compounds III and IV were estimated by using the energy functions given by the conformational analysis of the acetyl-side chain of pregnan-20-one.[4]

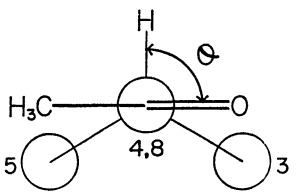

V

1) Paper IV of this series: T. Shishibori, This Bulletin, **41**, 1170 (1968).
2) Presented at the 20th Annual Meeting of the Chemical Society of Japan, Tokyo, April, 1967.
3) G. Snatzke and E. Schwinum, *Tetrahedron*, **22**, 761 (1966), and the references cited therein.
4) N. L. Allinger, P. Crabbé and G. Peréz, *Tetrahedron*, **22**, 1615 (1966).

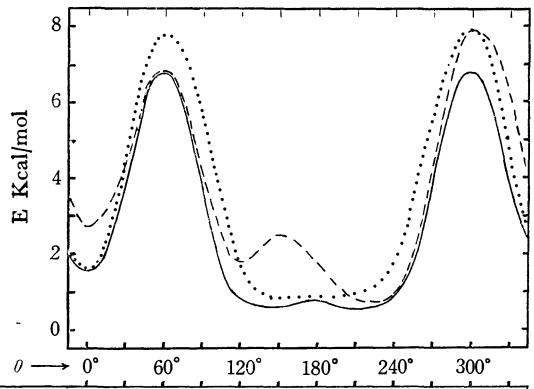

Compd.	The sign of cotton effect predicted											
I	±	+	+	+	+	+	−	−	−	−	−	−
II	+	+	+	+	+	+	−	−	−	−	−	+
III	+	+	+	+	+	±	−	−	−	−	−	±
IV	+	+	+	+	+	±	−	−	−	−	−	±

Fig. 2. Conformational energies calculated for the rotational conformation of the acetyl groups of I—IV as a function of θ: —— for III and IV, - - - for I, ····· for II. The signs of the Cotton effect predicted for each conformation were estimated from models as illustrated in Fig. 3.

With respect to compounds I and II, the functions of the van der Waals interaction between the C_3-hydroxyl and 9-methyl groups and between the C_3-hydroxyl group and the oxygen of the acetyl group must be superimposed upon the energy function for compound III or IV. The maximum of the former interaction in compound I should come around $\theta = 330°$, where θ corresponds to a dihedral angle of V, and should be similar to the 1,3-diaxial hydroxyl-methyl interaction, with a value of 2.1 kcal/mol.[5] Judging from the distance between the hydroxyl and methyl groups, this value should have fallen to less than 0.35 kcal[6] at $\theta = 270°$ and 30°, but to have a value of more than 0.35 kcal at $\theta = 300°$ and 360°. As the interaction between the C_3-hydroxyl group and oxygen of the acetyl group has been unknown, we assumed it to be nearly equal to the 1.9 kcal/mol[5] given for the 1,3-diaxial hydroxyl interaction. The maximum of this interaction should come around $\theta = 150°$. The rest of the curve is taken as proportional to the curve of the methyl-hydroxyl function, displaced appropriately. For compound II, the maximum of the interactions between the C_3-hydroxyl and 9-methyl groups and between the C_3-hydroxyl group and oxygen of the acetyl group are at $\theta = 270°$ and 90° respectively. The magnitudes of the interaction are equal to those of I.

5) E. L. Eliel, N. L. Allinger, S. J. Angyal and G. A. Morrison, "Conformational Analysis," Interscience Publishers, New York, N. Y. (1965), p. 52.

6) The energy of interaction and the distance between an equatorial methyl and an equatorial or axial hydroxyl groups on adjacent carbon atoms in cyclitols are 0.35 kcal/mol[7] and 2.8 Å respectively.

7) Ref. 5, p. 356.

If this function represents the relative energy of the conformations, the conformer with $\theta = 210°$ to 240° in compound I would be preferred over the conformer with $\theta = 120°$ by 1.0 kcal/mol. Concerning compound II, the conformer with $\theta = 150°$ to 210° would be preferred over the conformer with $\theta = 0°$ by 0.8 kcal/mol.

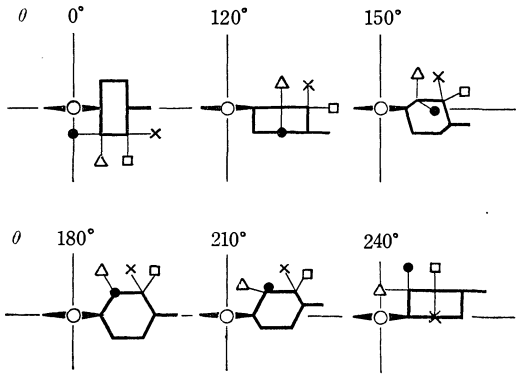

Fig. 3. Illustrations of the octant-rule projections used to predict the Cotton effect of the various rotational conformations of the acetyl group. Only the conformations eventually considered to be preferred are shown. Carbon skeleton is in heavy line; ○ for carbonyl oxygen; ● for OH of I; △ for OH of II; □ for OH of III; × for OH of IV.

Models[8] of each conformation were examined, and the signs of the Cotton effect were predicted according to the octant rules[9] (Fig. 3). As shown in Fig. 2, the results showed that the conformers with $\theta = 0°$ to 150° should exhibit a positive Cotton effect, and the conformers with $\theta = 180°$ to 300°, a negative one, in all compounds.

(+)-10-Nor-8-oxoneomenthol (I). As shown in Fig. 4, the CD curves of I exhibited a strong solvent-dependence, that is, a positive Cotton effect in isooctane and in carbon tetrachloride, but a negative one in methanol and in dimethyl sulfoxide. Such an inversion of the sign of the Cotton effect upon a change in solvent can be ascribed to the change in the equilibrium of the rotational conformation of the acetyl group; an inversion of the sign has been observed in α-hydroxycyclohexanone derivatives[10] and explained by the idea that intramolecular hydrogen bonds were present in carbon tetrachloride, but these bonds were ruptured, resulting in a conformational

8) "Dreiding Stereomodels," W. Büchi Manufacture of Glass Apparatus Flawil, Switzerland.

9) W. Moffitt, R. B. Woodward, A. Moscowitz, W. Klyne and C. Djerassi, *J. Am. Chem. Soc.*, **83**, 4013 (1961).

10) C. Djerassi, R. Records and B. Bach, *Chem. & Ind. (London)*, **1961**, 258; K. M. Wellman, W. S. Briggs and C. Djerassi, *J. Am. Chem. Soc.*, **87**, 73 (1965); T. Suga, T. Shishibori and T. Matsuura, *J. Org. Chem.*, **32**, 965 (1967).

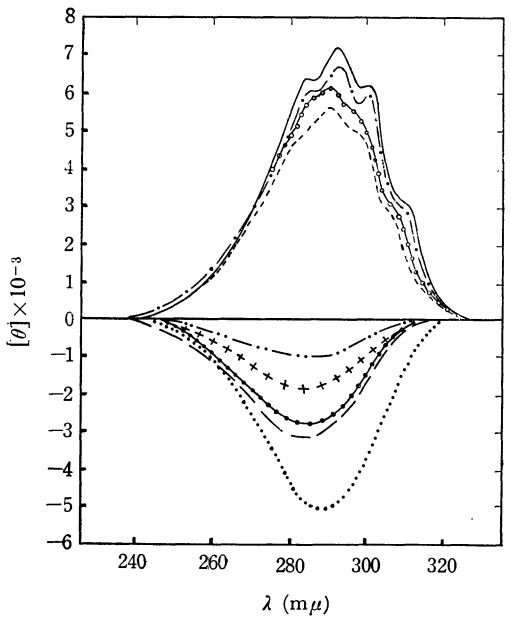

Fig. 4. CD curves of (+)-10-nor-8-oxoneomenthol (I) in selected solvents at 23°C: —— in isooctane; —·—· in CCl_4; - - - in $CHCl_3$; -o-o- in CH_2Cl_2; —··— in *t*-BuOH; + + in *i*-PrOH; -•-•-• in EtOH; — — in MeOH; ····· in $(CH_3)_2SO$.

change in the methanol. A similar change in hydrogen-bonding may occur in compound I.

The IR spectrum of I in a 0.005 M carbon tetrachloride solution showed a concentration-independent band at 3537 cm^{-1} (ε 46) resulting from the hydroxyl function, which is intramolecularly hydrogen bonded with the lone-pair electrons on the carbonyl oxygen atom. This OH···O hydrogen bond is favorable in the Ia conformation with $\theta = 150°$. On the other hand, the IR spectrum of I in dimethyl sulfoxide solution exhibited a broad band at 3330 cm^{-1} attributable to the formation of an intermolecular hydrogen bond between the hydroxyl group and the solvent. The CD and IR data, together with the results of conformational analysis (Fig. 2), suggest that the Ia conformer with $\theta = 150°$ is preferential in nonpolar solvents, whereas Ib conformer with $\theta = 120°$ is preferential in polar ones.

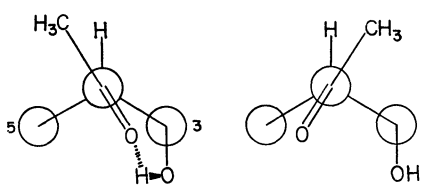

Ia Ib

This agrees with the expectation that the population of Ia will increase in a nonpolar solvents, because the destabilizing electrostatic interaction between the carbonyl and hydroxyl groups in Ib is overcome by the formation of an intramolecular hydrogen bond in Ia. On the other hand, methanol and dimethyl sulfoxide are solvents which would be expected to form an intermolecular hydrogen bond with the carbonyl and/or the hydroxyl groups, and the population of Ia decreases concomitantly in a polar solvent because the stabilizing intramolecular hydrogen bond is broken.

A correlation between the rotational strength, R_0^{25}, and Kosower's *Z* values[11] (an empirical index of solvent polarity) is shown in Fig. 5. An anomalous decrease in the rotational strength appears at *Z* values of from 65 to 70. This seems to signify that the intramolecular hydrogen bond of I is broken in solvents with the values of 65—70.

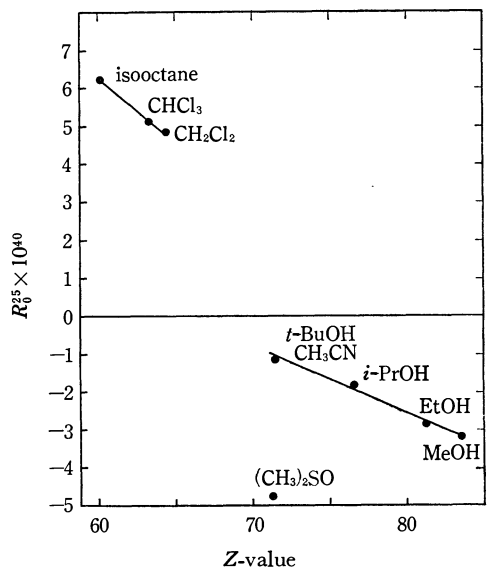

Fig. 5. Plot of rotational strength (R_0^{25}) of (+)-10-nor-8-oxoneomenthol (I) in various solvents *vs.* *Z*-value.

The variable-temperature CD curves of I in EPA[12] and in MI[13] are shown in Fig. 6. The CD curves in EPA exhibited a strong negative Cotton effect at −74°C, in contrast with the room-temperature CD curve. This signifies that the negatively rotating conformer, Ib, is energetically more favored at a low temperature in such a polar solvent. The CD curves in MI showed a positive Cotton effect and an increase in strength upon a lowering of the temperature. This implies that the positively-rotating, hydrogen-bonded conformer Ia is favored at a low temperature in a nonpolar solvent.

11) E. M. Kosower, *J. Am. Chem. Soc.*, **80**, 3254 (1958).
12) EPA solvent is composed of ether-isopentane-ethanol in the ratio 5 : 5 : 2 by volume.
13) MI solvent is composed of methylcyclohexane-isopentane in the ratio 1 : 3 by volume.

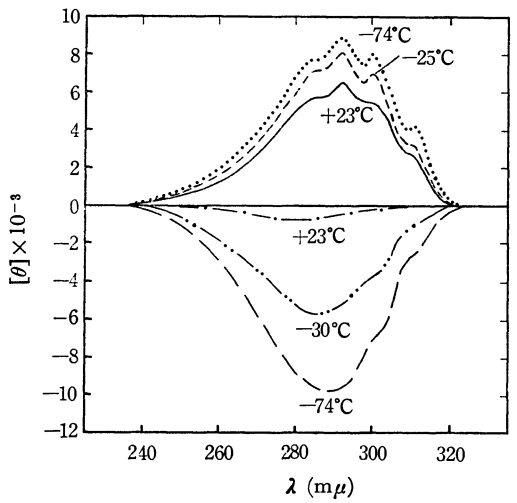

Fig. 6. CD curves of (+)-10-nor-8-oxoneomenthol (I) in EPA (—·—·, —··—, — —) and in MI (——, - - -, ····) at various temperatures.

(−)-10-Nor-8-oxomenthol (II). The IR spectrum of II showed two peaks, at 3625 (ε 20) and 3599 cm^{-1} (ε 35), and a shoulder at 3535 cm^{-1} (ε 9) in a 0.005 M carbon tetrachloride solution. The band at 3625 cm^{-1} was attributed to such a free hydroxyl group as in the IIa conformation with θ= 150°—210°, and the weak band at 3535 cm^{-1} to such an OH···O-type intramolecular hydrogen bond as in the IIb conformation with θ=90°. The band at 3599 cm^{-1} was also ascribed to an intramolecular, hydrogen-bonded hydroxyl group, and the small shift ($\Delta\nu$=26 cm^{-1}) of this band from the free hydroxyl band seems to indicate that the hydroxyl group interacts with the π-electrons on the carbonyl group,[14] as in IIc and/or IId. The IR spectrum in a dimethyl sulfoxide solution revealed the same results as in compound I.

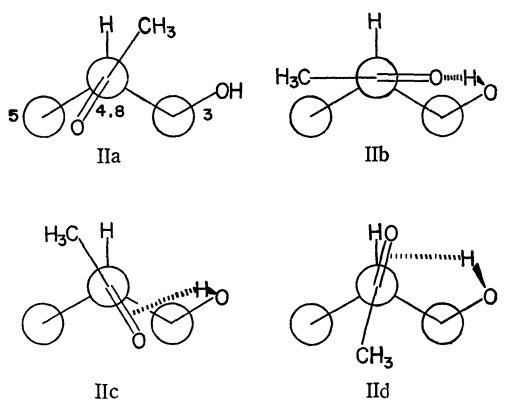

As Fig. 7 shows, the CD curves of II exhibited a solvent-dependence similar to those of I, but the negative curve was observed only in dimethyl sulfoxide. This phenomenon can be explained in terms of the conformational equilibrium, IIa⇄IIb, IIc and IId, resulting from the formation and the subsequent rupture of the intramolecular hydrogen bond, in view of the IR-spectra results described above. The acetyl group of II would preferentially exist in positively-rotating, internally-bonded conformations, IIb, IIc, and IId, in a nonpolar solvent. In a polar medium, the stabilizing intramolecular hydrogen bond is broken and the population of the IIb, IIc, and IId conformations decreases, in contrast to the increasing population of the negatively-rotating conformer, IIa, with θ=150—210°. Thus, a decrease in the rotational strength of the positive curve was observed upon changing from a nonpolar solvent to a polar one, and a negative curve appeared in dimethyl sulfoxide (Fig. 7). As shown in Fig. 8, the CD curves of II in EPA exhibited a weak positive Cotton effect at +23°C and a weak negative one at −74°C. This signifies that the nonbonded conformer, IIa, is energetically favorable at a low temperature in a polar medium.

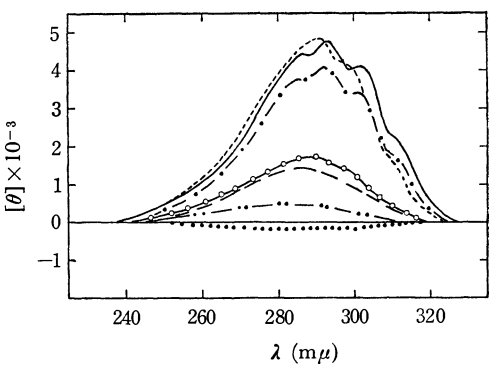

Fig. 7. CD curves of (−)-10-nor-8-oxomenthol (II) in selected solvents at 23°C: —— in isooctane; —·—· in CCl_4; - - - in $CHCl_3$; -o-o- in dioxane; —··— in *t*-BuOH; — — in MeOH; ···· in $(CH_3)_2SO$.

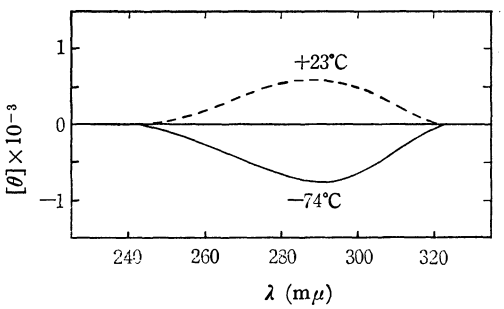

Fig. 8. CD curves of (−)-10-nor-8-oxomenthol (II) in EPA at +23°C and −74°C.

14) M. Ōki and H. Iwamura, Preprints for the 20th Annual Meeting of the Chemical Society of Japan, Tokyo (April, 1967), Part III, p. 128.

(−)-10-Nor-8-oxocarvomenthol (III) and (+)-10-Nor-8-oxoneocarvomenthol (IV). Furthermore, the rotational conformation of the acetyl group of III and IV has been examined. The IR spectra of III and IV in a 0.005 M carbon tetrachloride solution exhibited only a free hydroxyl band at 3630 (ε 42) and 3634 cm^{-1}(ε 80) respectively, showing the absence of a hydrogen bond between the carbonyl and hydroxyl groups. Thus, the rotational conformation of the acetyl group of III and IV is not affected by the hydrogen bond, and the acetyl group may be expected, from the conformational analysis (Fig. 2), to be situated near $\theta = 120$—$240°$ or $0°$.

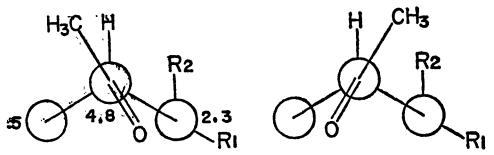

IIIa: R_1=OH, R_2=H IIIb
IVa: R_1=H, R_2=OH IVb

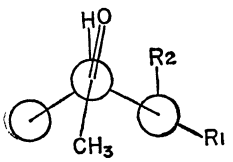

IIIc
IVc

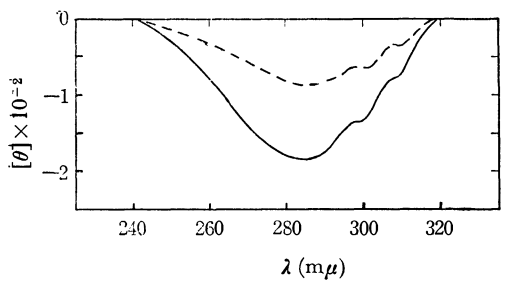

Fig. 9. CD curves of (−)-10-nor-8-oxocarvomenthol (III) in EPA at +23°C and −74°C.

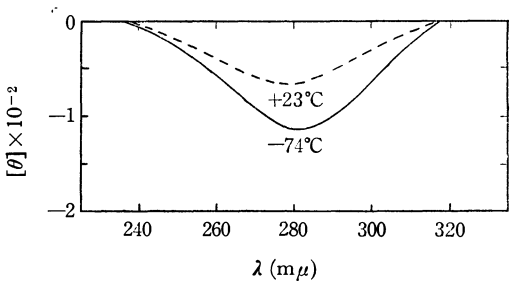

Fig. 10. CD curves of (+)-10-nor-8-oxoneocarvomenthol (IV) in EPA at +23°C and −74°C.

The CD curves of III in EPA showed a small increase in molecular ellipticity upon lowering of the temperature (Fig. 9). The CD curves of IV in EPA showed a similar tendency (Fig. 10). These results imply that the less stable, positively-rotating conformers, IIIc and IVc, with $\theta = 0°$, diminish, and that the stable ones, IIIa—IIIb and IVa—IVb, with θ = 120—240°, are favored at a low temperature.

Experimental

Materials. The (+)-10-nor-8-oxoneomenthol (I), (−)-10-nor-8-oxomenthol (II), (−)-10-nor-8-oxocarvomenthol (III), and (+)-10-nor-8-oxoneocarvomenthol (IV) were the same as were prepared in a preceding paper[1] of this series.

Spectral Measurements. The IR spectra in the hydroxyl-stretching region were measured with a Perkin-Elmer Model 621 Grating Infrared Spectrometer. A salt absorption cell, 20 mm long, was used, and the concentration of the solution was 0.005 mol/*l* at which value the association of the solute is negligible. The measurements were made at 25°C. The CD curves were obtained by a Japan Spectroscopic Co., Ltd., automatically-recording spectropolarimeter, Model ORD/UV-5, equipped with a circular dichroism attachment. The low-temperature CD curves were obtained by the same spectrometer, using a low-temperature CD cell[15] designed and constructed by the authors. These measurements were carried out using a cell 10 mm long and *c* 0.1.

15) T. Suga and T. Shishibori, JASCO Report (published by Japan Spectroscopic Co., Ltd., Tokyo), to be presented.

BULLETIN OF THE CHEMICAL SOCIETY OF JAPAN VOL. 41 1180—1184 (1968)

Stereochemical Studies of Monoterpene Compounds. VI.[1] The Stereochemistry of 2-Hydroxypinocamphone and Its Reduction Products[2]

Takayuki SUGA, Tsuyoshi SHISHIBORI, Toshifumi HIRATA and Tamon MATSUURA

Department of Chemistry, Faculty of Science, Hiroshima University, Hiroshima

(Received October 18, 1967)

The stereochemical structure of (+)-2-hydroxypinocamphone (II), which was obtained from (−)-α-pinene (I) by the permanganate oxidation, was examined by a combination of physico-chemical methods. It was thus found that the C-2 methyl group is trans with respect to the C-6 bridge and that the preferred conformation is V having an axial hydroxyl group. In addition, the preferred conformation of *cis*-α-pinene glycol (IX) and *trans*-α-pinene glycol (X), which were produced from II by the lithium aluminum hydride reduction, was found to be IXa and Xa respectively.

The configuration of C-2 in 2-hydroxypinocamphone (II) obtained by the potassium permanganate oxidation of α-pinene (I) is represented by IIa or IIb. Schmidt[3] has reported the configuration to be cis (IIb) on the basis of the fact that compound II gave isopinocampheol (III),[4] when reduced with sodium-ethanol. However, the assignment of this configuration seems not to be reliable, since the epimerization may occur at the 2-position during the sodium-ethanol reduction. In this paper the stereochemical structure of the hydroxyketone II was examined by a combination of such physico-chemical methods as ultraviolet, infrared and nuclear magnetic resonance spectra, optical rotatory dispersion, and circular dichroism measurements. In addition, an examination about the preferred conformation of a diastereoisomeric pair of α-pinene glycols (IX and X) was made, which were derived from II by the lithium aluminum hydride reduction.

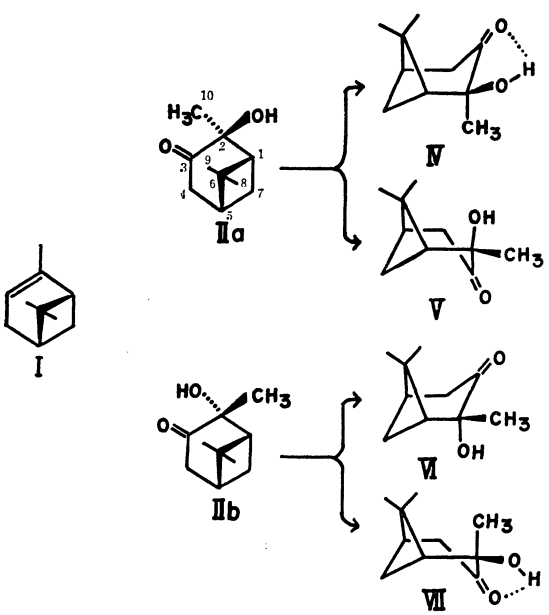

Results and Discussion

(+)-2-Hydroxypinocamphone (II) was prepared from (−)-α-pinene (I) in the same manner as in the case of Schmidt.[3] The lithium aluminum hydride reduction of II yielded a 63 : 37 mixture of α-pinene glycols, (IX) mp 55.5—56.0°C and (X) 160—161°C.

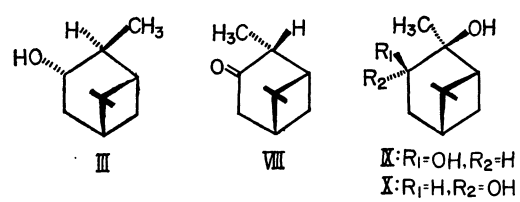

These glycols coincided with those reported by Schmidt[3] as cis- and trans-forms concerning the hydroxyl groups respectively. Both the diols were converted into the original ketone II by the potassium permanganate oxidation or by the chromium trioxide-pyridine complex oxidation.

Stereochemistry of 2-Hydroxypinocamphone (II). The compound II in question is formulated either by IIa or IIb, and each of these epimers may take interconvertible conformations IV and V, and VI and VII, respectively, as shown above. In the

1) Paper V of this series: T. Suga, T. Shishibori and T. Matsuura, This Bulletin, **41**, 1175 (1968).
2) Partly presented at the 9th Symposium on the Chemistry of Terpenes, Essential Oils and Aromatics of the Chemical Society of Japan, Kumamoto, October, 1965.
3) H. Schmidt, *Chem. Ber.*, **93**, 2485 (1960).
4) T. Kuwata, *J. Am. Chem. Soc.*, **59**, 2509 (1937).

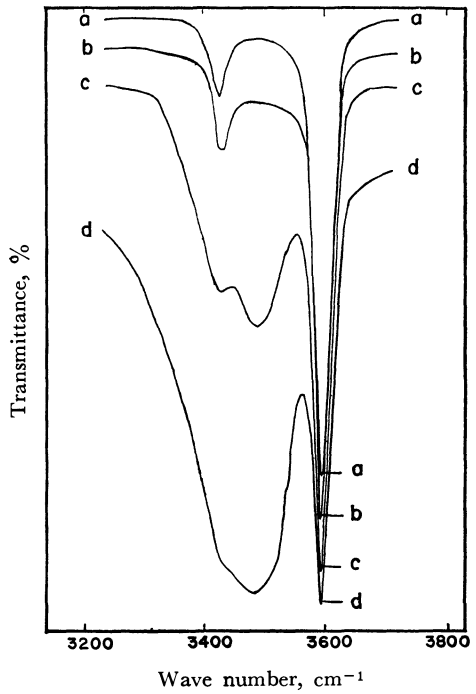

Fig. 1. Infrared spectra of 2-hydroxypinocamphone (II) in a carbon tetrachloride solution of various concentrations: a, 0.0025 M; b, 0.01 M; c, 0.05 M; d, 0.25 M.

first place, the preferred conformation of the hydroxyketone II was examined by IR, UV and NMR spectral measurements.

Intramolecular hydrogen bonding between the hydroxyl and carbonyl groups is possible in conformers IV and VII which have an equatorial hydroxyl group, whereas such bonding is impossible in V and VI having an axial one. The infrared spectra of II in the hydroxyl stretching region showed the concentration-depending bands at 3594 and 3474 cm^{-1} as shown in Fig. 1.*1 The nuclear magnetic resonance in a carbon tetrachloride solution exhibited a pronounced high-field shift of 1.36 ppm of the hydroxyl signal on dilution, and also this signal was shifted to the higher field by 0.67 ppm when the temperature was varied from 20°C to 60°C. These facts showed the hydroxyl group at the C-2 not to be intramolecularly bonded, and the group appeared to be axial.

This assignment of the hydroxyl group was confirmed by the fact that the carbonyl $n\rightarrow\pi^*$ band of II in the ultraviolet absorption spectrum (*cf.* Fig. 4) exhibited the bathochromic shift[5-7] by 13 mμ in methanol, as compared to the band of (−)-pinocamphone (VIII) lacking in the hydroxyl group. Furthermore, the axial orientation of the hydroxyl group of II was emphasized by the effect of benzene[8,9] on the C-2 methyl resonance in the nuclear magnetic resonance. When the nuclear magnetic resonance of II was measured on passing from deuteriochloroform to benzene solution, each of 8- and 9-methyl resonances suffered an upfield shift by 0.30 ppm, whereas the signal of the C-2 methyl group moved to the higher field by only 0.04 ppm as shown in Fig. 2. This fact indicates the C-2 methyl to be equatorial, and therefore the C-2 hydroxyl group must be axial. Thus, the preferred conformation of 2-hydroxypinocamphone (II) has been assigned as either V or VI, where the configuration of V is *S*-configuration[10] at C-2 and that of VI must be *R*-configuration.

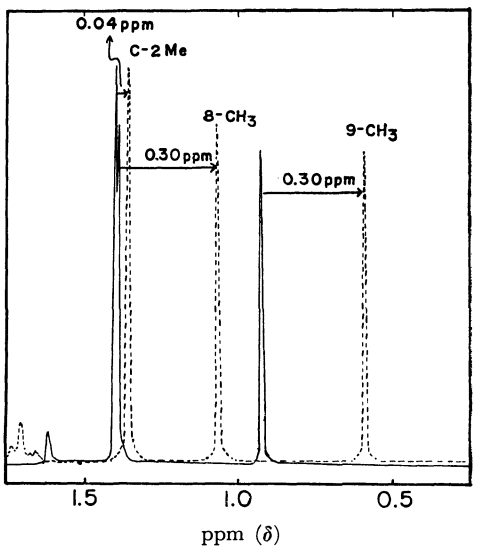

Fig. 2. The methyl resonances in the NMR spectra of 2-hydroxypinocamphone (II) in deuteriochloroform (the full line) and in benzene (the broken line).

In order to determine the configuration at the 2-position of II through ORD and CD measurements, models[11] were constructed for two conformers V and VI, the octant projection diagrams of which are shown in Fig. 3. The sign of the Cotton effect was predicted from this diagrams on assuming the octant

*1 A small peak at 3426 cm^{-1} is due to the overtone of the carbonyl stretching absorption.

5) C. Djerassi, "Optical Rotatory Dispersion: Applications to Organic Chemistry," Chapter 8, McGraw-Hill Book Co., Inc., New York, N. Y. (1960).

6) G. C. Cookson and S. H. Dandegaonker, *J. Chem. Soc.*, **1955**, 352.

7) G. Baumgartner and C. Tamm, *Helv. Chim. Acta*, **38**, 441 (1955).

8) N. S. Bhacca and D. H. Williams, "Applications of NMR Spectroscopy in Organic Chemistry," Holden-Day, Inc., San Francisco, Calif. (1965), p. 163.

9) N. S. Bhacca and D. H. Williams, *Tetrahedron Letters*, **42**, 3127 (1964).

10) R. S. Cahn, C. K. Ingold and V. Prelog, *Experientia*, **12**, 81 (1965).

11) "HGS Molecular Structure Model," Maruzen Co., Tokyo, was applied.

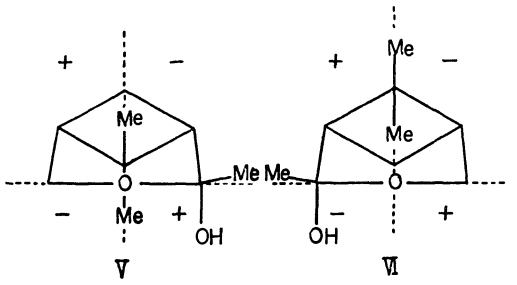

Fig. 3. The octant projections of conformers V and VI.

rule[12] to be applicable to the pinane skeleton. The conformer V was thus expected to exhibit a positive Cotton effect, whereas the conformer VI a negative one.

The ORD and CD curves of II in carbon tetrachloride showed the positive Cotton effect as shown in Fig. 4. The solvent-independent, positive ORD and CD curves were also observed in the other solvents, isooctane, dioxane, acetonitrile, dimethyl sulfoxide and methanol (see experimental section). These results imply that the C-2 methyl group is trans to the C-6 bridge, in contrast with Schmidt's report[8] in which the methyl group has been assigned

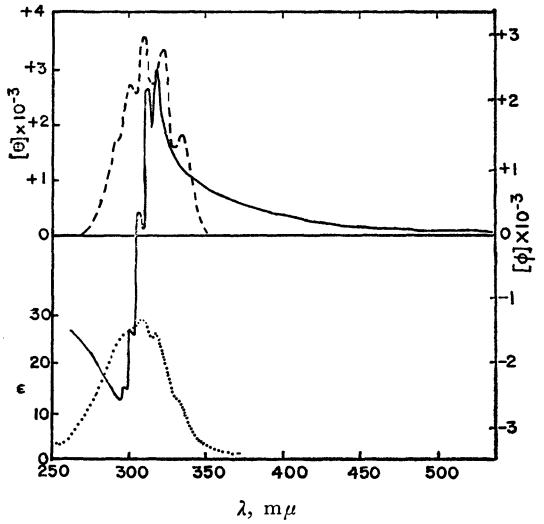

Fig. 4. Optical rotatory dispersion (the full line) and circular dichroism curves (the broken line) and ultraviolet spectrum (the dotted line) of (+)-2-hydroxypinocamphone (II) in carbon tetrachloride.

to be cis to the C-6 bridge. Consequently, it was confirmed that the stereochemical structure of (+)-2-hydroxypinocamphone (II) is V.

Conformation of *cis*- and *trans*-α-Pinene Glycols (IX and X). (−)-*cis*-α-Pinene glycol (IX)

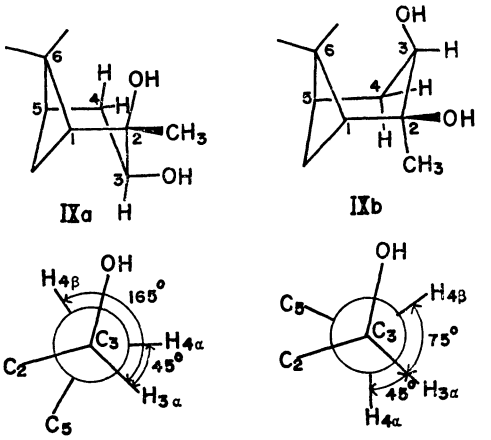

Fig. 5. The possible conformations for *cis*-α-pinene glycol (IX), and the dihedral angles between the C-3 proton and the C-4 protons in the conformers IXa and IXb.

may take two interconvertible forms IXa and IXb (Fig. 5). The hydroxyl stretching absorption in a dilute, carbon tetrachloride solution was found at 3614 and 3545 cm^{-1}. The former peak was attributed to a free hydroxyl group and the latter to an intramolecularly bonded one. In this case, the conformational preference between IXa and IXb cannot be determined only on the basis of $\Delta\nu$ in the infrared spectrum, because of the equality of the OH···O distance[11] (*ca.* 2.2 Å) in both IXa and IXb.

However, the NMR spectrum of the *cis*-diol IX afforded the reliable evidence for the conformational assignment. The C-3 proton of the *cis*-glycol IX exhibited a signal at 3.94 ppm (double doublets, $J=5.4$ and 9.3 cps). The coupling constants for the C-3 proton of the two possible conformations were calculated by the equation of Karplus.[13] The dihedral angles used in the calculation were estimated from the models[11] and are shown in Fig. 5. The calculated coupling constants for IXa were $J_{3\alpha,4\alpha}=3.9$ cps and $J_{3\alpha,4\beta}=8.5$ cps, and the constants for IXb were $J_{3\alpha,4\alpha}=3.9$ cps and $J_{3\alpha,4\beta}=0.1$ cps. The observed spectrum agrees nearly with the calculated coupling constants for IXa. Therefore, the preferred conformation of (−)-*cis*-α-pinene glycol (IX) was found to be IXa.

On the other hand, (−)-*trans*-α-pinene glycol (X) may take two interconvertible forms Xa and Xb.

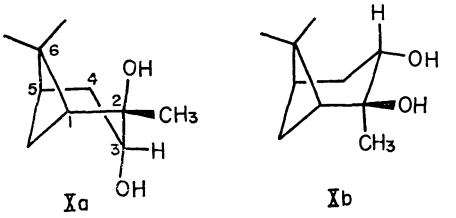

12) W. Moffitt, R. B. Woodward, A. Moscowitz, W. Klyne and C. Djerassi, *J. Am. Chem. Soc.*, **83**, 4013 (1961).

13) M. Karplus, *ibid.*, **85**, 2870 (1963).

Since the OH···O distances[11] are *ca.* 4.0 Å in Xa and *ca.* 2.5 Å in Xb, intramolecular hydrogen bonding is possible in conformer Xb having two equatorial hydroxyl groups, but such bonding is impossible in conformer Xa having two axial hydroxyl groups. The hydroxyl stretching absorption of *trans*-α-pinene glycol (X) in a dilute, carbon tetrachloride solution was found at 3610 and 3626 cm^{-1}, which would be attributed to the free, tertiary and secondary hydroxyl groups, respectively. It may be said *trans*-glycol X not to form the intramolecular hydrogen bond. Thus, the orientation of two hydroxyl group of glycol X was diaxial. As the C-2 configuration of the hydroxyketone II is retained in the lithium aluminum hydride reduction, it was seen that the conformation of (−)-*trans*-α-pinene glycol (X) is shown as Xa.

Experimental

The IR spectra were recorded by a Hilger H-800 Spectrophotometer (calcium fluoride prism) and a Perkin-Elmer Model 621 Grating Infrared Spectrometer. The ORD and CD spectra were measured at 25°C with a Japan Spectroscopic Co., Ltd. Model ORD/UV-5 Spectropolarimeter. The NMR spectra were recorded with a Hitachi Perkin-Elmer, R-20, and a Varian Associates, A-60, high-resolution spectrometers using tetramethylsilane as an internal standard. The variable-temperature NMR spectra were measured with a Japan Electron Optics Lab., JNM-C-60H. Microanalysis was done at the Microanalytical Center in the Faculty of Pharmacy of Kyoto University.

(+)-2-Hydroxypinocamphone (II). To a mixture of 579 g of (−)-α-pinene (I) (bp 71.0°C/51 mmHg, n_D^{25} 1.4626, d_4^{25} 0.8556, $[\alpha]_D^{25}$ −39.92°) and 5570 m*l* of 90% aqueous acetone was added 300 g of powdered potassium permanganate in small portions in a period of 8.5 hr at −5—5°C. The mixture was stirred for further 24 hr at 5°C. The filtrate free from manganese dioxide was treated as performed by Kuwata,[4] and gave 142 g of a neutral product boiling at 115—125°C/12.5 mmHg. This product solidified as a crystalline mass in a refrigerator. 2-Hydroxypinocamphone (II) was obtained by recrystallization from *n*-hexane and showed the following properties: mp 32.5—34.0°C (lit.[3] mp 34.5—35.3°C); $[\alpha]_D^{25}$ +21.1° (*c* 4.64, ethanol) (lit.[4] $[\alpha]_D^{25}$ −18.56° (*c* 14.44, ethanol), from (+)-α-pinene), $[\alpha]_D^{25}$ +38.1° (*c* 3.12, chloroform) (lit.[3] $[\alpha]_D$ −41.2° (chloroform), from (+)-α-pinene). UV: $\lambda_{max}^{CCl_4}$ 309 mμ (ε 29.6), $\lambda_{max}^{isooctane}$ 309 mμ (ε 24.6), $\lambda_{max}^{dioxane}$ 309 mμ(ε 27.8), $\lambda_{max}^{acetonitrile}$ 307 mμ (ε 26.1), $\lambda_{max}^{dimethyl\ sulfoxide}$ 309 mμ (ε 30.0), $\lambda_{max}^{methanol}$ 308 mμ (ε 28.0). ORD: $[\phi]_{336}^{CCl_4}$ +2410, $[\phi]_{288}$ −2501; $[\phi]_{338}^{isooctane}$ +2457, $[\phi]_{290}$ −2319; $[\phi]_{338}^{dioxane}$ +2227, $[\phi]_{289}$ −2014; $[\phi]_{337}^{acetonitrile}$ +2034, $[\phi]_{228}$ −1979; $[\phi]_{337}^{dimethyl\ sulfoxide}$ +2212, $[\phi]_{288}$ −2240; $[\phi]_{337}^{methanol}$ +1684, $[\phi]_{296}$ −1943. CD: $[\theta]_{310}^{CCl_4}$ +3793, $[\theta]_{310}^{isooctane}$ +3281, $[\theta]_{311}^{dioxane}$ +3281, $[\theta]_{310}^{acetonitrile}$ +3083, $[\theta]_{321}^{dimethyl\ sulfoxide}$ +3326, $[\theta]_{311}^{methanol}$ +2736.

The IR spectra in the hydroxyl stretching region were measured in 0.0025, 0.01, 0.05 and 0.25 M carbon tetrachloride solutions using salt absorption cells of 40.0, 10.0, 2.0 and 0.4 mm in length respectively.

The hydroxyl proton signal of the NMR spectrum appeared at δ 3.57 ppm in 20% carbon tetrachloride solution and at δ 2.21 ppm in 2.5% solution. This signal in 10% carbon tetrachloride solution was observed at δ 3.05 ppm at 20°C and at δ 2.38 ppm at 60°C. The methyl proton signal appeared at δ 0.88 ppm (C-9, 3H), 1.38 (C-8, 3H) and 1.39 (C-2 methyl, 3H) in 10% deuteriochloroform, and 0.58 (C-9, 3H), 1.08 (C-8, 3H) and 1.35 (C-2 methyl, 3H) in 10% benzene at 20°C.

(−)-*cis*- and (−)-*trans*-α-Pinene Glycols (IX and X). To 3.5 g of lithium aluminum hydride suspended in 200 m*l* of dry ether was added 22.0 g of II in a period of 3 hr at room temperature. Then, the reaction mixture was refluxed for 4 hr. After being left at room temperature for a day, the mixture gave 21.0 g of a crude diol, which was chromatographed on silica gel column with a mixture of ethyl acetate and *n*-hexane to separate into two components. The first eluate gave 9.6 g of a diol and the second eluate afforded 5.6 g of another diol. The homogeneity of these glycols separated was checked by chromatostrip analysis.

Properties of the First Eluate (cis-Glycol): mp 55.5—56.0°C (from petroleum benzine), $[\alpha]_D^{25}$ −0.89° (*c* 7.91, chloroform) (lit.[3] mp 55.5—56.0°C, $[\alpha]_D$ +3.3° (ethanol), from (−)-II).

The hydroxyl stretching absorption in 0.0021 M carbon tetrachloride solution was found at 3614 and 3545 cm^{-1}.

The NMR spectrum of the glycol was measured in 5 w/v% deuteriochloroform solution at 20°C.

The solution of 2.5 g of the glycol dissolved in 27 m*l* of 90% aqueous acetone was oxidized with 2.4 g of potassium permanganate for 12 hr at −5°C, and the original ketol II (1.7 g) was obtained, which was confirmed by comparison of the IR spectrum. Thus, the first eluate is *cis*-α-pinene glycol (IX).

Properties of the Second Eluate (trans-Glycol): mp 160—161°C (from ethanol), $[\alpha]_D^{25}$ −33.13° (*c* 4.8, ethanol) (lit.[3] mp 159—160°C, $[\alpha]_D^{25}$ +49° (ethanol), from (−)-II).

Found: C, 69.74; H, 10.68%. Calcd for $C_{10}H_{16}O_2$: C, 70.55; H, 10.66%.

The hydroxyl stretching absorption in 0.00079 M carbon tetrachloride solution appeared at 3626 and 3610 cm^{-1}.

A sample of 0.2 g of the second eluate was oxidized with a solution of 0.5 g of chromium trioxide in 5 m*l* of pyridine for 2 hr at room temperature, and 0.1 g of the original ketol II was obtained, which was confirmed by comparison of the IR spectrum. Thus, the second eluate is *trans*-α-pinene glycol (X).

(−)-Pinocamphone (VIII). Following the procedure reported,[14] 20 g of (+)-isopinocampheol (III) (mp 55—57°C, $[\alpha]_D^{25}$ +31.6° (*c* 10, benzene)), which was prepared from (−)-α-pinene (I) ($[\alpha]_D^{25}$ −39.32°) through hydroboration,[15] was oxidized with sodium dichromate to produce 17.8 g of (−)-isopinocamphone: bp 66°C/5 mmHg, n_D^{25} 1.4725, d_4^{25} 0.9618, $[\alpha]_D^{25}$ −9.77° (neat) (lit.[15] bp 54—56°C/1 mmHg, n_D^{25} 1.4745, α_D^{25} +10.3°, from (−)-III); 2,4-dinitrophenylhydrazone, mp 153°C (lit.[16] mp 151—152°C); semicarbazone, mp 227—228°C (lit.[4] mp 228°C).

14) H. C. Brown and C. P. Garg, *J. Am. Chem. Soc.*, **83**, 2952 (1961).
15) G. Zweifel and H. C. Brown, *ibid.*, **86**, 393 (1964).
16) A. Kergomard, *Bull. Soc. chim. France*, **1958**, 394.

Furthermore, following the method reported,[15] 0.50 g of (−)-isopinocamphone was added to the solution prepared by dissolving 0.12 g of metallic sodium in 25 m*l* of absolute ethanol, and then a mixture was stood for 24 hr at room temperature. The usual treatment of the mixture gave 0.35 g of the ketone VIII: $[\alpha]_D^{25}$ −18.56° (*c* 1.99, ethanol) (lit.[16] α_J −15°), λ_{max}^{MeOH} 295 mμ (ε 26.7).

The authors wish to express their hearty thanks to Takasago Perfumery Co., Ltd., Tokyo, for a gift of (−)-α-pinene, to Professor Shô Ito of Tohoku University, for measuring the NMR spectra by a Varian Associates, A-60, spectrometer, and to Japan Electron Optics Lab., Tokyo, for the variable-temperature NMR spectra measurement.

BULLETIN OF THE CHEMICAL SOCIETY OF JAPAN VOL. 41 1184—1187 (1968)

Preparation of Acetylene-Alcohol Dicobalt Hexacarbonyls and Their Reactivity towards Acid

Pu-Jun KIM and Nobue HAGIHARA

The Institute of Scientific and Industrial Research, Osaka University, Sakai, Osaka

(Received October 16, 1967)

A series of acetylene-alcohol dicobalt hexacarbonyls was prepared from acetylene-alcohols and dicobalt octacarbonyl. The reactivity towards aqueous sulfuric acid in boiling methanol was investigated. From the ethynyl carbinol complexes, $R^1R^2C(OH)C{\equiv}CH \cdot Co_2(CO)_6$, trinuclear cobalt complexes, $R^1R^2CHCH_2CCo_3(CO)_9$, were obtained accompanying the reduction of C–OH to a C–H moiety. On the other hand, from the butynediol complexes, $R^1R^2C(OH)C{\equiv}CC(OH)R^1R^2 \cdot Co_2(CO)_6$, binuclear cobalt complexes, $R^1R^2CHC{\equiv}CCHR^1R^2 \cdot Co_2(CO)_6$, or 1,1,4,4-tetraphenyl-1,3-butadiene were obtained. The structures of all these compounds have been confirmed by analytical measurements and by a study of their absorption spectra.

It is well known that acetylenes readily displace the two bridge carbonyl groups in dicobalt octacarbonyl to yield acetylenic dicobalt hexacarbonyls.[1,2] As a part of the study of the chemical behavior of these complexes, the reaction of acetylenic dicobalt hexacarbonyls, $RC{\equiv}CH \cdot Co_2(CO)_6$, (derived from terminal acetylenes) with aqueous mineral acids in boiling alcohol to yield trinuclear cobalt complexes, $RCH_2CCo_3(CO)_9$, has been reported on.[3]

In this paper, the preparation of various acetylene-alcohol dicobalt hexacarbonyls derived from the ethynyl carbinols and the butynediols, and the treatment of these complexes with aqueous sulfuric acid in boiling methanol will be reported.

Results and Discussion

Preparation of Acetylene-alcohol Dicobalt Hexacarbonyls. Various ethynyl carbinols and butynediols have now been treated with dicobalt octacarbonyl in diethyl ether or petroleum ether at room temperature under nitrogen for 2 hr to give red to reddish-brown acetylene-alcohol dicobalt hexacarbonyls. The properties of and analytical data on these complexes are summarized in Table 1. The spectra of each of the acetylene-alcohol dicobalt hexacarbonyls contain characteristic groups of three or four sharp bands in the range from 2000 to 2200 cm^{-1}; these bands are attributable to the terminal carbonyl groups. The band characteristic of the bridge carbonyl groups near 1800 cm^{-1} is absent. The band of the acetylenic C–H stretching at 3300 cm^{-1} in the starting materials was shifted by the complex formation to 3100 cm^{-1}, a characteristic olefinic C–H stretching frequency. The band characteristic of the carbon-carbon triple bond is absent. The PMR spectrum of ethynyl carbinol complexes shows a sharp singlet signal near τ 4.0 assignable to the coordinated terminal acetylenic proton.

Reactivity towards Aqueous Sulfuric Acid in Boiling Methanol. Ethynyl carbinol dicobalt hexacarbonyls have been treated with aqueous sulfuric acid in boiling methanol for 2 hr. Sublimable crystals, from dark purple to dark brown, were obtained. They were easily soluble in petroleum ether and were crystallized from methanol by deep cooling. The trinuclear structure for these compounds is supported by the results of the elemental analy se

1) H. W. Sternberg, H. Greenfield, R. A. Friedel, J. H. Wotiz, R. Markby and I. Wender, *J. Am. Chem. Soc.*, **76**, 1457 (1954).
2) H. Greenfield, H. W. Sternberg, R. A. Friedel, J. H. Wotiz, R. Markby and I. Wender, *ibid.*, **78**, 120 (1956).
3) R. Markby, I. Wender, R. A. Friedel, F. A. Cotton and H. W. Sternberg, *ibid.*, **80**, 6529 (1958).

Table 1. Acetylene-alcohol dicobalt hexacarbonyls

Compound	Description	Mp °C	Analyses, % Calcd C	Calcd H	Found C	Found H
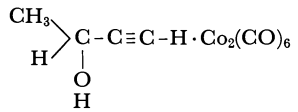	Red crystals	36—38	33.74	1.70	33.56	1.64
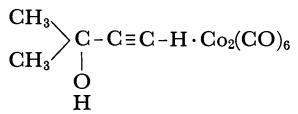	Red crystals	42—43.5	35.70	2.18	35.86	2.30
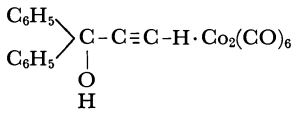	Red crystals	125 (dec.)	51.04	2.45	51.02	2.69
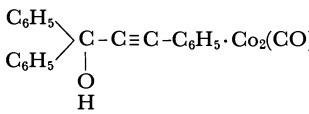	Reddish brown crystals	95 (dec.)	56.86	2.83	56.92	3.04
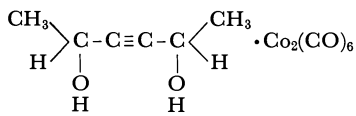	Red crystals	100 (dec.)	36.02	2.52	36.06	2.67
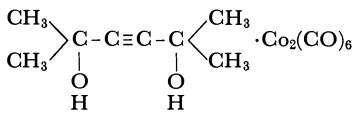	Reddish brown crystals	110 (dec.)	39.27	3.30	39.18	3.32
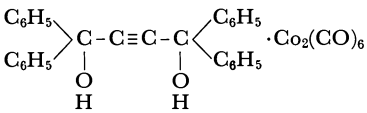	Reddish brown crystals	115 (dec.)	60.37	3.28	60.24	3.33

Table 2. Infrared spectra of $R^1R^2CHCH_2CCo_3(CO)_9$ in KBr disk (cm^{-1})

$CH_3CH_2CCo_3(CO)_9$	642	554,	532,	520	506	474
$CH_3CH_2CH_2CCo_3(CO)_9$	659	557,	543,	532	506	475
$(CH_3)_2CHCH_2CCo_3(CO)_9$	660	556,	542,	532	506	475
$(C_6H_5)_2CHCH_2CCo_3(CO)_9$	582	532,	526,	518	504	455
Suggested assignment*	RC-Co stretch			Co-CO stretch		

* Ref. 4

and of the molecular-weight determinations (cryoscopy in benzene), and by their absorption spectra. The infrared spectra of these compounds show the absence of a hydroxyl group and the presence of terminal carbonyl groups. The stretching frequency of the C–Co bond was observed to be as shown in Table 2. The band near 650 cm^{-1} is susceptible to the alkyl groups, while those in the 470—560 cm^{-1} region are almost independent of the alkyl groups.[4] The PMR spectra of these trinuclear cobalt complexes are summarized in Table 3. The spectra are in good agreement with the $R^1R^2CHCH_2$-$CCo_3(CO)_9$ structure. The chemical shift of the methylene proton neighboring the $CCo_3(CO)_9$ group is observed in the lower field, *e.g.*, near τ 6.3. This may be caused by the strong electron affinity of the $Co_3(CO)_9$ group.

4) W. T. Dent, L. A. Duncanson, R. G. Guy, H. W. B. Reed and B. L. Shaw, *Proc. Chem. Soc.*, **1961**, 169.

Table 3. Proton magnetic resonance data of $R^1R^2CHCH_2CCo_3(CO)_9$ complexes at 60 Mc/sec

Compound	Band position, τ	Relative intensity	Assignment	Coupling constant
$CH_3CH_2CCo_3(CO)_9$	8.46 (triplet)	3	CH_3	J=7.5 cps
	6.22 (quartet)	2	CH_2	J=7.5 cps
$CH_3CH_2CH_2CCo_3(CO)_9$	8.84 (triplet)	3	CH_3	J=7.0 cps
	8.09 (multiplet)	2	CH_2	
	6.35 (triplet)	2	CH_2	J=7.0 cps
$(CH_3)_2CHCH_2CCo_3(CO)_9$	8.81 (doublet)	6	CH_3	J=5.5 cps
	7.8—8.3 (multiplet)	1	CH	
	6.33 (doublet)	2	CH_2	J=5.5 cps

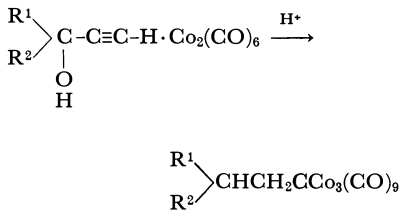

The $(CH_3)_2CHCH_2CCo_3(CO)_9$ complex was also formed from the ether complex $(CH_3)_2C(OCH_3)C{\equiv}CH\cdot Co_2(CO)_6$ under conditions analogous to those described above. The $CH_3CH_2CH_2CCo_3(CO)_9$ complex has also been obtained from vinylacetylene dicobalt hexacarbonyl $CH_2{=}CH{-}C{\equiv}CH\cdot Co_2(CO)_6$ by treatment with aqueous sulfuric acid in boiling methanol.[5]

Secondly, butynediol dicobalt hexacarbonyls have been treated with aqueous sulfuric acid in boiling methanol for 30 min. From tetramethylbutynediol dicobalt hexacarbonyl, brown crystals were obtained. The infrared spectra of this compound showed the absence of a hydroxyl group and the presence of terminal carbonyl groups. The PMR spectra in hexadeuterobenzene showed a doublet centered at τ 8.91*1 and a multiplet in the range from τ 6.9 to 7.6 with a relative intensity of 6 : 1. The analytical data of the elements were consistent with the composition in which two oxygen atoms were eliminated from the starting compound. Therefore, this compound seems to be di-isopropylacetylene dicobalt hexacarbonyl.*2 On the other hand, from tetraphenylbutynediol dicobalt hexacarbonyl, 1,1,4,4-tetraphenyl-1,3-butadiene was obtained.

In the well-known Meyer-Schuster Rearrangement free acetylenic carbinols are rearranged into unsaturated ketones or aldehydes by acidic reagents. In the present study, acetylenic carbinols coordinated to cobalt atoms were found not to take the Meyer-Schuster Rearrangement, but to be reduced and to form trinuclear cobalt complexes. As cobalt sulfate was recognized in an aqueous solution, the reduction of acetylene-alcohol may occur through the oxidation of Co^0 to Co^{2+} by the partial decomposition of the starting cobalt(0) complex. The hydrido cobalt carbonyl intermediate has been postulated for the formation of the trinuclear cobalt complex.[6] However, the reaction of $(CH_3)_2C(OH)C{\equiv}CH\cdot Co_2(CO)_6$ with $HCo(CO)_4$ in methanol was found to yield $(CH_3)_2CHC{\equiv}CH\cdot Co_2(CO)_6$*3 as the reduction product. The trinuclear cobalt complex $(CH_3)_2CHCH_2CCo_3(CO)_9$ was not formed. It remains to be proved how the reduction of C–OH to the C–H moiety occurs in the progress of the formation of the trinuclear cobalt complex.

Experimental

All melting points are uncorrected; they were measured by a micro melting point apparatus, Yanagimoto Model MP-S2. The infrared spectra were obtained by a Jasco Model DS-402 G grating spectrometer. The PMR spectra were recorded by a Varian Model A-60 instrument in carbon tetrachloride using tetramethylsilane as an internal standard. The molecular weights were measured by the cryoscopic method in benzene, using the vaporphase osmometer instrument developed by Dr.-Ing. Herbert Knauer.

Materials. The propargyl alcohol and 1-butyne-3-ol (35% in water) were of a Tokyo Kasei Reagent Grade. The 3-methyl-1-butyne-3-ol, 3-hexyne-2,5-diol, and 2,5-dimethyl-3-hexyne-2,5-diol were obtained from our laboratory. The ethynylbenzhydrol,[7] 3-phenylethynylbenzhydrol,[8] 1,1,4,4-tetraphenyl-2-butyne-1,4-diol,[9] and dicobalt octacarbonyl[10] were prepared by the methods described in the literature.

5) I. Kaneko and N. Hagihara, unpublished result.
6) G. Albanesi and E. Gavezzotti, *Chim e l'ind (Milan)*, **47**, 1322 (1965).
*1 The coupling constant was 7.0 cps.
*2 Added in Proof: From $(C_6H_5)_2C(OH)C{\equiv}CC_6H_5\cdot Co_2(CO)_6$, $(C_6H_5)_2CHC{\equiv}CC_6H_5\cdot Co_2(CO)_6$ was obtained by a method analogous to that described above. Reddish-brown crystals, mp 88—91°C. PMR : τ 2.60—3.00 (m) and 4.50 (s), with a relative intensity of 15 : 1 in CCl_4 at 60 Mc/sec.
*3 Satisfactory elemental analyses have been obtained. PMR spectra : τ 4.13 (s), 6.85—7.30 (m) and 8.72 (d) (J=7.0 cps), with a relative intensity of 1 : 1 : 6 in CCl_4 at 60 Mc/sec.
7) P. D. Landor and S. R. Landor, *J. Chem. Soc.*, **1963**, 2707.
8) K. Hess and W. Weltzien, *Ber.*, **54**, 2511 (1921).
9) A. Zweig and A. K. Hoffmann, *J. Am. Chem. Soc.*, **84**, 3278 (1962).
10) R. B. King, *Organometal. Syn.*, **1**, 99 (1965).

The Preparation of Acetylene-alcohol Dicobalt Hexacarbonyls. The ethynyl carbinols or butynediols and dicobalt octacarbonyl were allowed to react at room temperature for 2 hr in diethyl ether under a nitrogen atmosphere. Stoichiometric amounts or an excess of the acetylene-alcohols were used, depending upon the subsequent purification procedure. The reaction mixture was usually filtered to remove any insoluble impurities, and the filtrate was evaporated *in vacuo*. The residue was then purified by recrystallization from methanol on deep cooling or by molecular distillation.

A description of the compounds and the analytical data are given in Table 1. The preparation of $(CH_3)_2C(OH)C{\equiv}CH{\cdot}Co_2(CO)_6$ will be described in detail below: To a solution of 4.3 g (51 mmol) of $(CH_3)_2C(OH)C{\equiv}CH$ in 100 m*l* of diethyl ether, there were added 14 g (41 mmol) of dicobalt octacarbonyl under nitrogen. The mixture was stirred for 2 hr and then filtered. The filtrate was concentrated by a water aspirater and crystallized from methanol at −78°C. Red crystals, mp 42—43.5°C, were obtained (yield, 15 g, 98%).

The Preparation of 3-Methyl-3-methoxyl-1-butyne Dicobalt Hexacarbonyl, $(CH_3)_2C(OCH_3)C{\equiv}CH{\cdot}Co_2(CO)_6$. To a solution of 1.5 g (14.6 mmol) of 3-methyl-3-chloro-1-butyne[11] in 60 m*l* of diethyl ether, there were added 7.5 g (21.9 mmol) of dicobalt octacarbonyl under a nitrogen atmosphere. The mixture was stirred for 2 hr. Twenty milliliters of methanol were then added, after which the mixture was stirred for 45 min, washed with water, and extracted with diethyl ether. After drying over sodium sulfate and concentration, the residue was submitted to molecular distillation at 60—70°C/1 mmHg with a cold finger cooled by dry ice-acetone. 2.83 g of a deep red oil were obtained (yield, 50.5%). PMR: τ 8.50 (s) (CH_3), 6.77 (s) (OCH_3) and 3.99 (s) (CH) with a relative intensity of 6 : 3 : 1.

Found: C, 38.14; H, 2.61%. Calcd for $C_{12}H_{10}O_7Co_2$: C, 37.53; H, 2.62%.

The Formation of Trinuclear Cobalt Complexes $R^1R^2CHCH_2CCo_3(CO)_9$. $CH_3CH_2CCo_3(CO)_9$. Propargyl alcohol dicobalt hexacarbonyl (prepared from 2 g of propargyl alcohol and 5 g of dicobalt octacarbonyl) was dissolved in 60 m*l* of methanol. To this solution 10 m*l* of 10 N sulfuric acid were added, and the mixture was refluxed for 2 hr. After it had then been cooled to room temperature, the reaction mixture was diluted with 120 m*l* of water and extracted with petroleum ether. The organic layer was concentrated, and the residue was crystallized from methanol by cooling at −78°C. Violet crystals were obtained (yield, 560 mg).

Found: C, 30.46; H, 1.19%; mol wt, 477. Calcd for $C_{12}H_5O_9Co_3$: C, 30.67; H, 1.07%; mol wt, 470.

$CH_3CH_2CH_2CCo_3(CO)_9$. From $CH_3CH(OH)C{\equiv}CH{\cdot}Co_2(CO)_6$, dark violet crystals were obtained by a method analogous to that described above. Mp 110°C (dec.).

Found: C, 32.79; H, 1.49%. Calcd for $C_{13}H_7O_9Co_3$: C, 32.27; H, 1.48%.

$(CH_3)_2CHCH_2CCo_3(CO)_9$. *a) From the Alcohol Complex:* A mixture of $(CH_3)_2C(OH)C{\equiv}CH{\cdot}Co_2(CO)_6$ (2 g), methanol (40 m*l*), and 10 N sulfuric acid (8 m*l*) was refluxed for 2 hr. After it had then been worked up, reddish violet crystals were obtained. Mp 105°C (yield, 270 mg).

Found: C, 34.12; H, 1.96%; mol wt, 517. Calcd for $C_{14}H_9O_9Co_3$: C, 33.76; H, 1.82%; mol wt, 498.

b) From the Ether Complex: A mixture of $(CH_3)_2C(OCH_3)C{\equiv}CH{\cdot}Co_2(CO)_6$ (1.1 g), methanol (20 m*l*), and 10 N sulfuric acid (4 m*l*) was refluxed for 2 hr. After it had then been worked up, reddish violet crystals were obtained. The infrared spectra of this compound were consistent with those of that obtained in *a*).

$(C_6H_5)_2CHCH_2CCo_3(CO)_9$. From a mixture of $(C_6H_5)_2C(OH)C{\equiv}CH{\cdot}Co_2(CO)_6$ (2 g), methanol (40 m*l*), and 10 N sulfuric acid (8 m*l*), brown crystals were obtained after a 2-hr reaction. Mp 124°C (dec.). (Yield, 310 mg).

Found: C, 46.17; H, 2.00%; mol wt, 643. Calcd for $C_{24}H_{13}O_9Co_3$: C, 46.33; H, 2.11%; mol wt, 622.

Di-isopropylacetylene Dicobalt Hexacarbonyl. A mixture of $(CH_3)_2C(OH)C{\equiv}CC(OH)(CH_3)_2{\cdot}Co_2(CO)_6$ (2 g), methanol (20 m*l*), and 10 N sulfuric acid (8 m*l*) was refluxed for 30 min. After it had been cooled to room temperature, the reaction mixture was filtered and the precipitates were washed with water and dissolved in methanol. The filtrate was cooled by dry ice to give brown crystals, mp 95°C. (Yield, 370 mg).

Found: C, 42.19; H, 3.48%. Calcd for $C_{14}H_{14}O_6Co_2$: C, 42.45; H, 3.56%.

1,1,4,4-Tetraphenyl-1,3-butadiene. To a solution of 1 g of $(C_6H_5)_2C(OH)C{\equiv}CC(OH)(C_6H_5)_2{\cdot}Co_2(CO)_6$ in 20 m*l* of methanol, 4 m*l* of 10 N sulfuric acid were added. The reaction mixture was then refluxed for 30 min. Yellow crystals were thus precipitated. These were filtered, washed with water, and dried. Recrystallization from benzene gave pale yellow prisms with a pale green fluorescence, mp 192(sinter)—204°C. (Yield, 162 mg). Recrystallization from ethanol gave pale yellow needles with a pale green fluorescence, mp 197—198°C.

Found: C, 93.72; H, 5.99%. Calcd for $C_{28}H_{22}$: C, 93.81; H, 6.19%.

11) G. F. Hennion and K. W. Nelson, *J. Am. Chem. Soc.* **79**, 2142 (1957).

BULLETIN OF THE CHEMICAL SOCIETY OF JAPAN VOL. 41 1188—1191 (1968)

Polymerization Catalyst of the Triethylaluminum-Chloral Hydrate System. I. Triethylaluminum-Chloral Hydrate Reaction and Catalyst Activity in Cationic Polymerization

Takeo SAEGUSA, Hiroyasu FUJII, Takashi UESHIMA and Katsumi TANAKA*1

Department of Synthetic Chemistry, Kyoto University, Sakyo-ku, Kyoto

(Received October 28, 1967)

In reaction of $AlEt_3$ with chloral hydrate has been investigated. The reaction system was examined by means of infrared and NMR spectra and by the vapor-phase chromatographic analysis of the acidolysis product of this system. The gas evolved during the reaction was also analyzed. The $AlEt_3$-chloral hydrate system was proved to contain the linkages of $>AlOCH_2CCl_3$, $>AlOCH(CCl_3)OAl<$, $>AlOCH(Et)CCl_3$, $>AlOAl<$, $>Al-Et$ and $>Al-Cl$. This system showed a very high catalytic activity for the cationic polymerization of *i*-butyl vinyl ether. Tetrahydrofuran, 3,3-bis(chloromethyl)oxacyclobutane, α-methylstyrene, and styrene were also polymerized by this catalytic system. The acid strength of the $AlEt_3$-chloral hydrate system was examined by two methods, the Hammett indicator method and shift of the infrared carbonyl band of xanthone caused by coordination to Lewis acid. It has been shown that the acid strength of this system is as strong as $AlEt_3$-H_2O (1 : 0.8) and Et_2AlCl. The relation between the strong acid character of the $AlEt_3$-chloral hydrate system and its structure was discussed.

We have studied the polymerizations of aldehydes and cyclic oxides by the catalyst systems derived from aluminum alkyls.[1-10] Additives, such as water and alcohol, improve or markedly change the catalyst properties of the parent aluminum alkyl. In cationic polymerization, it is quite interesting that when $AlEt_3$ is treated with a controlled amount of water (about an equimolar amount), the acid strength is increased and, hence, the catalyst activity is much enhanced.[2]

In the present study, we have examined the reaction of $AlEt_3$ with chloral hydrate and the catalyst activity of the reaction product.

Experimental

Reagents. *$AlEt_3$.* A commercial reagent was rectified under a reduced nitrogen atmosphere, bp 83—84°C/4 mmHg.

Chloral Hydrate. A commercial reagent was dried over phosphoric anhydride.

The monomers and solvents were dried and purified by the usual methods.

Reaction of $AlEt_3$ with Chloral Hydrate. A typical example was as follows. A solution of 5 mmol of chloral hydrate in 100 m*l* of toluene was added, drop by drop, into 100 m*l* of a toluene solution containing 10 mmol of $AlEt_3$ with stirring at −50——60°C. The mixture was gradually warmed to room temperature over a 2-hr period, and then kept at 40°C for additional 2 hr. The reaction systems were homogeneous unless the molar ratios of chloral hydrate to $AlEt_3$ exceeded 1.5.

Analyses of Reaction Products. *Acidolysis.* The volatile matters were distilled off under reduced pressure (2—3 mmHg) at temperatures from room temperature to 40°C, and the residue was decomposed with an excess of glacial acetic acid. The acid decomposition product was analyzed by vapor-phase chromatography.

Vapor-phase Chromatography (VPC) Analysis. An apparatus, Model 2C, of the Shimadzu Co. (Japan) was used. In the analysis of the acid-decomposition mixture, a silicon column (3 m) was used (column temperature: 125°C; carrier gas: hydrogen; gas speed: 40 m*l*/min). Ethane and ethylene gases were analyzed by using a column of silica gel (3 m) at 40°C, with hydrogen as the carrier gas (flow rate: 60 m*l*/min).

Analysis of Inorganic Chlorine. The aluminum-chlorine linkage was formed in the chloral hydrate-$AlEt_3$ reaction. This inorganic chlorine was determined by the silver

*1 Present address: Central Research Institute, Mitsui Petrochemical Industries, Ltd., Waki-mura, Kuga-gun, Yamaguchi.

1) J. Furukawa, T. Saegusa and H. Fujii, *Makromol. Chem.*, **44/46**, 398 (1960).
2) T. Saegusa, H. Imai, S. Hirai and J. Furukawa, *ibid.*, **53**, 203 (1962).
3) T. Saegusa, Y. Fujii, H. Fujii and J. Furukawa, *ibid.*, **55**, 232 (1962).
4) T. Saegusa, H. Imai and J. Furukawa, *ibid.*, **56**, 55 (1962).
5) T. Saegusa, H. Imai and J. Furukawa, *ibid.*, **65**, 60 (1963).
6) T. Saegusa, H. Imai and J. Furukawa, *ibid.*, **79**, 207 (1964).
7) T. Saegusa, H. Imai and J. Furukawa, *ibid.*, **81**, 92 (1965).
8) H. Imai, T. Saegusa and J. Furukawa, *ibid.*, **81**, 92 (1965).
9) H. Fujii, I. Tsukuma, T. Saegusa and J. Furukawa, *ibid.*, **82**, 32 (1965).
10) T. Iwata, T. Saegusa, H. Fujii and J. Furukawa, *ibid.*, **97**, 49 (1966).

nitrate method after the reaction product had been decomposed by nitric acid.

Nuclear Magnetic Resonance (NMR) Measurements. The NMR spectra were taken with a Varian 60 MC spectrometer; the peak positions were determined by using tetramethylsilane as the internal reference.

Measurement of Acid Strength. *Indicator Method.* The acid strength of the catalytic system was measured by a method similar to that described in a previous paper.[8]

Xanthone Method. The shift of the carbonyl band in the infrared spectrum of xanthone coordinating onto the catalytic systems was examined by the method of Cook.[11] Solutions of the catalyst system and xanthone, both in a concentration of 0.5 mol/*l*, were mixed at room temperature, and the difference between the free and the shifted carbonyl bands was determined.

Results and Discussion

Reaction of $AlEt_3$ with Chloral Hydrate. Chloral hydrate exists in the following equilibrium:

$$Cl_3CCH\begin{matrix}OH\\OH\end{matrix} \rightleftarrows Cl_3CCHO + H_2O \quad (1)$$

Therefore, five possible ways of reaction may be postulated:

$$>Al\text{-}Et + H_2O \rightarrow$$

$$>Al\text{-}OH + EtH \xrightarrow{>AlEt} \underset{I}{\underline{>Al\text{-}O\text{-}Al<}} + EtH \quad (2)$$

$$>Al\text{-}Et + Cl_3CCHO \rightarrow$$

$$\underset{II}{\underline{>Al\text{-}OCH_2CCl_3}} + CH_2{=}CH_2 \quad (3)$$

$$>Al\text{-}Et + Cl_3CCHO \rightarrow \underset{III}{\underline{>Al\text{-}O\overset{Et}{\overset{|}{C}}HCCl_3}} \quad (4)$$

$$>Al\text{-}Et + Cl_3CCH\begin{matrix}OH\\OH\end{matrix} \rightarrow$$

$$>Al\text{-}OCHOH \xrightarrow{>Al\text{-}Et} \underset{IV}{\underline{>Al\text{-}O\overset{CCl_3}{\overset{|}{C}}HO\text{-}Al<}} \quad (5)$$

$$\begin{matrix}|\\CCl_3\\+\ EtH\end{matrix} \qquad \begin{matrix}\\\\+\ EtH\end{matrix}$$

The linkage (IV) has not yet been known; it is a special aluminum alkoxide.

The reaction mixture of $AlEt_3$ with chloral hydrate was decomposed by glacial acetic acid and analyzed by VPC. The results are shown in Table 1.

In the reaction in both ether and toluene, the linkage (II) derived from the reduction of chloral with the Al-Et linkage by Eq. (3) was mainly produced. The linkage (III) was formed very little in ether, but it was formed to a considerable extent in toluene. The regeneration of chloral by the acidolysis suggests the presence of the linkage (IV), because, before the acidolysis, the reaction mixture did not exhibit the absorption bands characteristic of OH and >C=O groups. The amount of linkage (I) was taken to be equal to be the sum of the linkages (II) and (III), because the reaction mixture did not show any indication of the presence of OH (water) or >C=O (free chloral).

Table 1. Analysis of acid decomposition mixture of $AlEt_3$-chloral hydrate (2 : 1) reaction system

Product	Mol% in ether	Mol% in toluene
Cl_3CCHO	22	32
Cl_3CCH_2OH	72 (70)[a]	44
$Cl_3CCH(Et)OH$	trace	4
$Cl^{\ominus}$	2	20

a) The value in the parenthesis was calculated from volume of ethylene gas evolved in the course of the reaction.

The formation of a considerable amount of inorganic chloride, especially in the reaction in a toluene solvent, is due to the reaction between the trichloromethyl group and the Al–Et group. This reaction seems very complicated. No dichloroacetaldehyde, monochloroacetaldehyde, or acetaldehyde, or any of their derivatives were detected by the VPC analyses of the acidolysis mixture.

The volume of the gas evolved in the course of the reaction was then measured using a gas burette. By VPC analysis, the gas was shown to be a mixture of ethane and ethylene. From the volume of ethylene, the amount of linkage (II) was calculated (see Table 1). The two values, the one from the ethylene and the other from the Cl_3CCH_2OH in the acidolysis mixture, agreed with each other.

Further support was given by the NMR spectra of this system. Chemical shifts of 5.6—5.7 τ and 4.4—4.6 τ were observed in the spectra of this system; these shifts were assigned to the protons of >Al–OCH_2CCl_3 and >Al–$OCH(CCl_3)$O–Al< respectively. The area ratios of the two peaks (>AlO-CH_2CCl_3/>Al–$OCH(CCl_3)$O–Al<) were 6.5 (in ether) and 2.8 (in toluene); these values are in fairly good agreement with the values calculated from Cl_3CCH_2OH and Cl_3CCHO in the acidolysis mixture (*cf.* Table 1).

Catalyst Behavior in Cationic Polymerization. The reaction mixture of $AlEt_3$ and chloral hydrate showed a high catalytic activity in the cationic polymerizations of isobutyl vinyl ether and tetrahydrofuran (Tables 2 and 3). Isobutyl vinyl ether was polymerized especially rapidly by this catalytic system.

The results shown in Table 2 indicate that the $AlEt_3$-chloral hydrate system is fairly active in initiating cationic polymerizations. The activating effect of the treatment with chloral hydrate has been well

11) D. Cook, *Can. J. Chem.*, **41**, 526 (1963).

demonstrated. No additional cocatalyst is required. It may be assumed that a part of the hydroxy group of chloral hydrate remains unreacted, thus affording the initiator proton. Even at low catalyst concentrations (0.2 mol% to monomer), the $AlEt_3$-chloral hydrate system induced the vinyl ether polymerization at a fairly high rate. The product polymers contained no methyl ethyl ketone-insoluble (crystalline) part. The lack of stereospecificity in the polymer produced by the $AlEt_3$-chloral hydrate system is unlike the case with the $AlEt_3$-water system, which gives the crystalline polymer of isobutyl vinyl ether.[6,7]

The polymerization of tetrahydrofuran by the $AlEt_3$-chloral hydrate-epichlorohydrin system is illustrated in Table 3.

The $AlEt_3$-chloral hydrate system also induced the

TABLE 2. POLYMERIZATION OF ISOBUTYL VINYL ETHER

Catalyst	mol ratio	mmol	Polymer yield (%)	$[\eta]_{30°C}^{benzene}$	$CH_3COC_2H_5$-insoluble part (%)
$Cl_3CCHO \cdot H_2O/AlEt_3$	0	1	0	—	—
	0.5	1	21.3	0.51	0
	1.0	1[b]	25.4	—	0
	1.0	1	71.2	—	0
	1.0	0.1	97.5	0.62	0
	1.5	1	100	0.22	0
	2.0	1	27.2	0.16	0
$H_2O/AlEt_3$	0.8	1[c]	28.0	1.35	5.3
	0.8	1	0	—	—
Et_2AlCl		1[c]	62.0	0.87	0
$AlEt_3$-H_2O-EtOH (1 : 0.8 : 0.4)		3[d]	0	—	—

a) Insoluble part deposited from a hot solution of 1 g of polymer in 100 m*l* of methyl ethyl ketone was kept standing at room temperature.
b) Polymerization was carried out in ether solvent (20 m*l*).
c) Equimolar amount of *t*-butyl chloride (to Et_2AlCl) was added as cocatalyst.
d) Equimolar amount of acetyl chloride (to $AlEt_3$) was added as cocatalyst.

TABLE 3. POLYMERIZATION OF TETRAHYDROFURAN
(Monomer: 0.1 mol; Catalyst: 2 mmol; Epichlorohydrin: 2.5 mmol; Polymn.: 0°C, 3.5 hr)

Catalyst	mol ratio	Polymer yield (%)	$[\eta]_{30°C}^{CH_3COOEt}$
$Cl_3CCHO \cdot H_2O/AlEt_3$	1/3	43.7	0.20
	1/2	44.4	0.26
	1/1	36.5	0.19
	1/5	4.5	0.33
	1/2[a]	100	—
$H_2O/AlEt_3$	0.8/1	29.0	0.48
Et_2AlCl		8.1	0.08

a) Polymerization in ether solvent for 1 day.

TABLE 4. POLYMERIZATION OF SOME MONOMERS
$AlEt_3$-$Cl_3CCHO \cdot H_2O$ (2 : 1): 1.5 mmol; Cocatalyst: 1 mmol

Monomer (mol)	Cocatalyst	Solvent (m*l*)	Temp. (°C)	Time (hr)	Yield (%)
BCMO (0.05)	CH_3COCl	Toluene (20)	0	24	93.4
	—	Toluene (20)	0	24	82.0
	ECH[a]	Ether (10)	0	24	82.8
St (0.05)	*t*-C_4H_9Cl	Toluene (20)	−78	24	47.5
	—	Toluene (20)	−78	24	0
α-MeSt (0.025)	*t*-C_4H_9Cl	Toluene (20)	−78	15 min	trace
	—[b]	Toluene (20)	−78	15 min	91.2

a) ECH: epichlorohydrin. b) $AlEt_3$-$Cl_3CCHO \cdot H_2O$ (1 : 1): 1 mmol.

TABLE 5. ACID STRENGTH OF ORGANOALUMINUM COMPOUNDS

Catalyst	mol ratio	Indicator[a] I	II	III	IV	V	VI	$\Delta\nu_{C=O}$ by xanthone method (cm^{-1})
$Cl_3CCHO \cdot H_2O/AlEt_3$	1/3	A	A	A	A	A	B	88
	1/2	A	A	A	A	A	B	104
	1/1			—[b]				100
Et_2AlCl		A	A	A	A	A	A	104
$H_2O/AlEt_3$	0.8/1	A	A	A	A	A	?	100
$AlEt_3$		A	A	A	A	B	B	83
$AlEt_3$-H_2O-EtOH (1 : 0.8 : 0.4)		B	B	B	B	B	B	0
$Al(OCH_2CCl_3)_3$		—	A	A	A	A	B	90

a) Indicators
I : Phenylazonaphthylamine; II : Butter yellow;
III: Benzeneazodiphenylamine; IV: Dicinnamalacetone;
V : Benzalacetophenone; VI: Anthraquinone
A : Acidic B : Basic

b) It was impossible to notice the color change because of the coloration of the system.

polymerizations of 3,3-bis(chloromethyl)oxacyclobutane (BCMO), α-methylstyrene (α-MeST), and styrene (St) (Table 4).

It has been established that, in many cases, a Lewis acid alone does not cause the cationic polymerization of vinyl monomers or four- and five-membered cyclic ethers. Therefore, a cocatalyst or a promoter[5,12] was used in the present study.

From one observations in the polymerizations of several monomers (Tables 2, 3, and 4), it is certain that the $AlEt_3$-chloral hydrate system is a cationic polymerization catalyst. Therefore, the acid strength of this system was examined by the Hammett indicator method and by the extent of the shift of the infrared carbonyl band ($\Delta\nu_{C=O}$) by the xanthone method[11] (Table 5).

Table 5 shows that the $AlEt_3$-chloral hydrate systems are strong acids, much stronger than $AlEt_3$ itself. The systems of $AlEt_3$/chloral hydrate = 1.0 and 2.0 are as strong as $AlEt_3/H_2O$ (1/0.8) and Et_2AlCl.

It is interesting to compare the strong acid character of the $AlEt_3$-chloral hydrate system with the acid nature of the $AlEt_3$-H_2O-EtOH (1 : 0.8 : 0.4) system. It has previously been reported by us[7] that the systems containing aluminum alkoxide linkages are generally weaker acids. $AlEt_3$-H_2O-EtOH is a weaker acid (Table 5) and does not induce the cationic polymerization of vinyl ether. Although the $AlEt_3$-chloral hydrate system contains considerable amount of aluminum alkoxide linkages (Eqs. (2) to (5)), it is a strong acid.

Such a characteristic behavior of this system may be attributed to the electron-withdrawing effect of the trichloromethyl group of the alkoxyl groups in the $AlEt_3$-chloral hydrate system. In fact, aluminum trichloroethoxide prepared by the reaction of $AlEt_3$ with trichloroethanol shows great acid strength[13] and high catalytic activities in cationic polymerizations.[13]

12) T. Saegusa, S. Matsumoto and T. Ueshima, *Makromol. Chem.*, **105**, 132 (1967).

13) T. Saegusa and T. Ueshima, *Inorg. Chem.*, **6**, 1679 (1967).

BULLETIN OF THE CHEMICAL SOCIETY OF JAPAN VOL. 41 1192—1194 (1968)

Polymerization Catalyst of the Triethylaluminum-Chloral Hydrate System. II. Copolymerization of Acetaldehyde with Chloral

Takeo SAEGUSA, Hiroyasu FUJII and Katsumi Tanaka*1

Department of Synthetic Chemistry, Kyoto University, Sakyo-ku, Kyoto

(Received October 28, 1967)

It has been found that the $AlEt_3$-chloral hydrate system induces the random copolymerization of acetaldehyde with chloral. The homogeneity of the product polymer was confirmed by a study of the infrared spectra and by turbidimetric titration. The thermal stability of the copolymer was much better than that of homopolyacetaldehyde. The copolymer was soluble in chloroform, and films were cast from chloroform solutions.

In our previous paper,[1] we reported the reaction of $AlEt_3$ with chloral hydrate and the cationic polymerizations of several monomers using the reactions mixture as the catalyst. In the present paper, we wish to report on the characteristic catalyst behavior of the $AlEt_3$-chloral hydrate system in the copolymerization of acetaldehyde with chloral.

The copolymerization between acetaldehyde and chloral was once performed using $AlEt_3$ as the catalyst; the product polymer was always 1 : 1 alternating copolymer.[2] Several aluminum alkoxides, such as $Et_2AlOC_4H_9$-*s*, $Et_2AlOCH_2CCl_3$, $Et_2AlOCH(Et)$-CCl_3, and some aluminum trialkoxides have been applied to the polymerization system of an acetaldehyde-chloral mixture. None of these aluminum alkoxides, however, caused any copolymerization; they gave only acetaldehyde homopolymers with low molecular weights.[2] The difference in catalytic behavior between $AlEt_3$ and aluminum alkoxides has been explained in terms of the mechanism of coordinate anionic polymerization.

The $AlEt_3$-chloral hydrate system of the present study is distinguished by its catalyst activity inducing random copolymerization between acetaldehyde and chloral.

Experimental

Reagents. *Acetaldehyde.* Acetaldehyde was prepared and purified by a method similar to that of the previous paper.[2]

The other reagents were purified by a method similar to that of another preceding paper.[1]

Preparation of Catalyst System. Catalytic systems were prepared similarly as has already been described in the preceding paper.[1]

Copolymerization. The monomer mixture and the solvent were placed in a glass tube under a nitrogen atmosphere and cooled to −78°C. After a catalyst solution had been added, drop by drop, to this cold mixture, the polymerization mixture was kept standing at −78°C for a definite reaction time. Then the polymerization was stopped by adding methanol. The copolymers were fractionated to methanol-soluble and chloroform-soluble (methanol-insoluble) fractions. The compositions of the copolymers were calculated from the

TABLE 1. COPOLYMERIZATION OF ACETALDEHYDE WITH CHLORAL. EFFECT OF SOLVENT

$AlEt_3$-$Cl_3CCHO \cdot H_2O$ (2/1): 2 mmol; Cl_3CCHO: 0.1 mol; CH_3CHO: 0.1 mol; polymn.: at −78°C

Solvent (ml)		Polymn. time (day)	Polymer (%)		
			Total yield	Methanol-soluble part[a]	Chloroform-soluble part[a]
Ether	(40)	16	22	6(27)	16(73)
Toluene	(45)	3	17	12(69)	5(31)
Toluene	(40)	11	18	8(43)	10(57)[b]
Methylene chloride	(45)	3	16	10(64)	6(36)
Dioxane	(45)	5	18	16(87)	2(13)

a) The values in parentheses indicate the relative percentages to total yield.
b) $[\eta]=1.55$ in chloroform at 30.0°C.

*1 Present address: Central Research Institute, Mitsui Petrochemical Industries, Ltd., Waki-mura, Kuga-gun, Yamaguchi.

1) Part I: T. Saegusa, H. Fujii, T. Ueshima and K. Tanaka, This Bulletin, **41**, 1188 (1968).
2) T. Iwata, T. Saegusa, H. Fujii and J. Furukawa, *Makromol. Chem.*, **97**, 49 (1966).

chlorine and carbon contents determined by elemental analyses.

Turbidimetric Titration. Turbidimetric titration was carried out using a photo-electric turbidimeter of the Shimadzu Co. (Kyoto, Japan). The copolymer sample was a chloroform-soluble (methanol-insoluble) fraction composed of CH_3CHO and Cl_3CCHO units in the ratio of 72/28; this fraction had been prepared using the $AlEt_3$-chloral hydrate (2/1) system. In 100 m*l* of chloroform, 20 mg or 40 mg of the sample were dissolved, and methanol was added to the mixture at a rate of 1.6 m*l*/min at 16°C. The light scattered was measured at an angle of 90°.

Table 2. Copolymerization of acetaldehyde with chloral, effect of monomer ratio

$AlEt_3$-$Cl_3CCHO \cdot H_2O$ (2/1): 2mmol; total monomer: 0.2mol; Polymn.: 3days; at −78°C

CH_3CHO/Cl_3CCHO (mmol) (mmol)	Polymer yield (%)	CH_3CHO unit in copolymer (mol%)
160 / 40	13	73
100 / 100	16	65
40 / 160	6	56

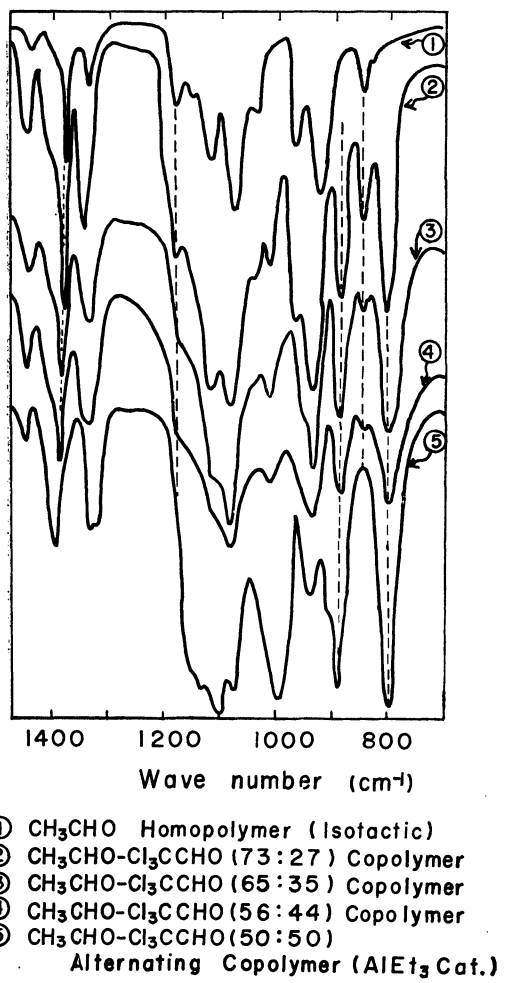

Fig. 1. Infrared spectra of the copolymer by $AlEt_3$-$Cl_3CCHO \cdot H_2O$ system compared with those of other aldehyde.

Results and Discussion

Copolymerization of Acetaldehyde with Chloral. In the copolymerization between acetaldehyde and chloral, the 1 : 1 alternating copolymerization by the $AlEt_3$ catalyst[2] was the sole example up to the present study. Several aluminum alkoxides have brought about the formation of the acetaldehyde homopolymer.

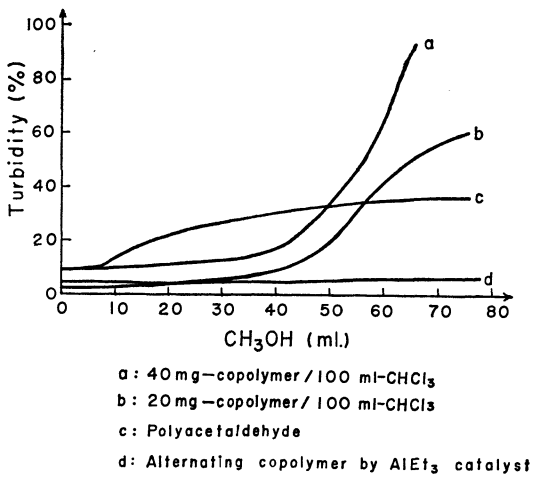

Fig. 2. Turbidimetric titration of the copolymer of acetaldehyde with chloral.

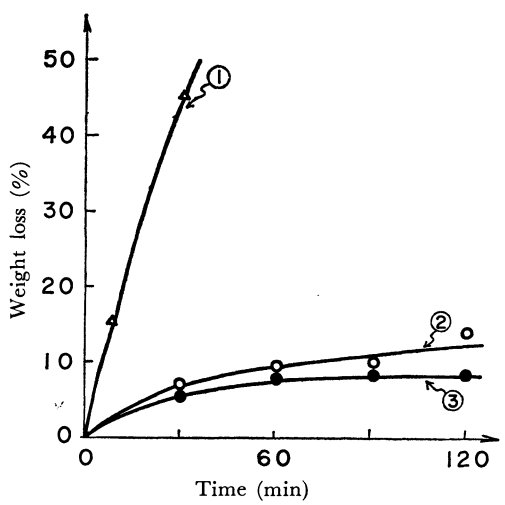

Fig. 3. Thermal decompositions of polyaldehydes at 105°C under nitrogen atmosphere.

①△: Polyacetaldehyde
②○: CH_3CHO-Cl_3CCHO (63 : 37) Copolymer [$AlEt_3$-$Cl_3CCHO \cdot H_2O$ catalyst)
③●: Alternating copolymer ($AlEt_3$ catalyst)

The results of the copolymerization by the $AlEt_3$-chloral hydrate system are illustrated in Tables 1 and 2.

As shown in Table 1, the product polymers can be fractionated into methanol-soluble and chloroform-soluble (methanol-insoluble) fractions. However, no difference was observed in the infrared spectra of these two fractions; only the difference in the molecular weights of the copolymers induced the fractionation.

The infrared spectra of the product copolymers of various compositions in Table 2 are shown in Fig. 1, where they are compared with those of the acetaldehyde homopolymer and the alternating copolymer prepared by the $AlEt_3$ catalyst. As shown in Fig. 1, the spectra of the copolymers gradually vary with the change in composition. The absorption bands at 1187, 973, and 845 cm^{-1} observed in homopolyacetaldehyde decrease with the increase of chloral units in the copolymer and vanish in the alternating copolymer, whereas the bands at 995 and 895 cm^{-1}, which are not observed in homopolyacetaldehyde, appear and gradually increase in the copolymers. These observations suggest that the copolymer produced by the $AlEt_3$-chloral hydrate system is a real random copolymer and not a mixture of homopolyacetaldehyde and the 1 : 1 alternating copolymer.

The homogeneity of the product copolymer was supported by turbidimetric titration. The results are shown in Fig. 2. It is there shown that the product copolymer is fairly homogeneous and does not contain homopolyacetaldehyde or the 1 : 1 alternating copolymer.

It is worthy of mention that copolymers prepared using the $AlEt_3$-chloral hydrate system are of fairly high molecular weights, as indicated by their intrinsic viscosity values in chloroform (*cf.* Table 1). The alternating copolymerization by $AlEt_3$ catalysts always gave polymers with lower intrinsic viscosities.[2)]

The thermal stability of the copolymer is much better than that of homopolyacetaldehyde (Fig. 3).

The copolymer is soluble in chloroform, and films can be cast from the chloroform solution. The copolymer, however, decomposes at 180 ± 5°C without melting.

BULLETIN OF THE CHEMICAL SOCIETY OF JAPAN VOL. 41 1194—1200 (1968)

Preparation and Properties of Aluminum and Zinc Haloalcoholates

Takashi UESHIMA, Shimpei TOMITA and Takeo SAEGUSA

Department of Synthetic Chemistry, Kyoto University, Sakyo-ku, Kyoto

(Received October 28, 1967)

Seven haloalcoholates of aluminum and zinc were prepared by the reactions of haloalcohols with metal alkyls in ethyl ether, and their properties were examined. The following differences have been observed between these haloalcoholates and the usual alcoholates, those with no halogen in the alkyl groups. (1) The metal haloalcoholates are unstable to heat and decompose at 90—220°C. Except for $Al(OCH_2CF_3)_3$, they are neither distilled nor sublimed even *in vacuo*. The usual aluminum alcoholates, such as ethoxide and isopropoxide, are easily distilled under reduced pressures. (2) The haloalcoholates are stronger Lewis acids than the usual alcoholates. The acid strength of some aluminum haloalcoholates is even higher than triethylaluminum. The strong acid nature of the aluminum haloalcoholate can be ascribed to the electron-withdrawing effect of halogen. (3) As expected from their strong acid strength, the haloalcoholates induce the cationic polymerizations of vinyl monomers and cyclic ethers, such as styrene, α-methylstyrene, isobutyl vinyl ether, 3,3-bis-(chloromethyl)oxacyclobutane, and tetrahydrofuran. The usual metal alcoholates are weaker acids and do not cause the polymerizations of these monomers. In the ethylene oxide polymerization, both the haloalcoholates and the usual alcoholates showed catalytic activity. However, these two types of alcoholates differ from each other in the catalysis mechanism. For the polymerization of ethylene oxide by the haloalcoholate catalyst, a cationic polymerization mechanism was assumed on the basis of the formation of dioxane as a by-product. The polymerization by the usual alcoholate catalysts is assumed to be of a coordinate anionic mechanism.

In the course of studies upon the polymerization catalyst behavior of metal alkyls and alcoholates, we have shown that aluminum and zinc alcoholates of unsubstituted alcohols are weak Lewis acids which do not induce the cationic polymerizations of vinyl monomers and cyclic ethers, but which do cause the

coordinate anionic polymerizations of alkylene oxides and acetaldehyde.[1,2] Recently, we reported the preparation of aluminum trichloroethoxide, $Al(OCH_2CCl_3)_3$, and showed its peculiar properties as compared with those of the usual aluminum alcoholates, such as aluminum isopropoxide and *t*-butoxide.[3] The dissociation of $Al(OCH_2CCl_3)_3$ to the monomeric form (I) in the presence of donor molecules (for example, dioxane, tetrahydrofuran, and pyridine) has been observed; this is in sharp contrast to the strong association tendency of the usual aluminum alcoholates even in the presence of the above donors.

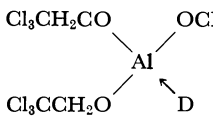

(I) (D: donor molecule)

It has also been found, from the results of the acid-strength measurements by the IR method[4,5] using xanthone as the reference base, that $Al(OCH_2CCl_3)_3$ is a fairly strong acid; it is as strong as $AlEt_3$ and much stronger than the usual aluminum alcoholates.

In the present experiments, several haloalcoholates of aluminum and zinc have been prepared and their properties, especially as polymerization catalysts, have been examined.

Experimental

Reagents. Commercially-available materials were purified carefully by the usual procedures. 1,1,1-Trifluoroethanol,[6] 1,1,1-trichloroethanol,[7] 1,1,1-tribromoethanol,[7] and 1,1-dichloroethanol[8] were prepared by the procedures described in the literatures and were purified by distillation. Tribromoethanol was further purified by recrystallization from a mixture of *n*-pentane and ethyl ether.

Preparation of Haloalcoholates. A typical procedure was as follows. $AlEt_3$ (0.1 mol) in ethyl ether (20 m*l*) was added, drop by drop, with vigorous stirring into a mixture of a haloalcohol (0.3 mol) and ethyl ether (60 m*l*) at −78°C. After the addition was complete, the reaction system was allowed to warm gradually to room temperature and finally heated to reflux for 2 hr. In the cases of $Al(OCH_2CCl_3)_3$ and $Al(OCH_2CBr_3)_3$, products separated from the reaction solutions; these

Table 1. Preparations and decomposition temperatures of haloalcoholates

Alcoholate	Methods of purification	Decomposition temperature[f]	Analysis: Al or Zn (%) Calcd	Analysis: Al or Zn (%) Found	Analysis: RO/Al[b] or RO/Zn[c] (mol ratio)
$Al(OCH_2CF_3)_3$[a]	Sublimation[a] (80°C/0.18 mmHg)	110	8.33	9.05	3.09
$Al(OCH_2CCl_3)_3$	Recrystallization from benzene	145	5.74	5.71	2.97
$Al(OCH_2CBr_3)_3$	Washing with ethyl ether[e]	155	3.09	3.07	2.98
$Al(OCH_2CHCl_2)_3$	Recrystallization from ethyl ether	180	7.32	7.45	3.02
$Al[OCH(CH_2Cl)_2]_3$	Recrystallization from ethyl ether	130	6.57	6.50	3.00
$Al(OCH_2CH_2Cl)_3$	Reprecipitation from *n*-heptane	220 (mp 180°C)	10.16	10.23	3.14
$Zn(OCH_2CCl_3)_2$	Reprecipitation from a mixture of *n*-heptane and pyridine	115	18.02	18.08	1.94[c]
$EtZnOCH_2CCl_3$	Washing with ethyl ether[e]	90	26.92	26.38	1.00[c,d]

a) Very hygroscopic.
b) The calculated value for each aluminum alcoholate is 3.00, relative error = ±5%.
c) Cl_3CCH_2O/Zn (mol ratio).
d) Et/Zn ratio was found to be 1.01 by gasometry.
e) Further purification was not possible, because no suitable solvent for recrystallization was found.
f) Decomposition temperature was measured under reduced pressure.
Metal haloalcoholates except $Al(OCH_2CF_3)_3$ and $Al(OH_2CH_2Cl)_3$ were decomposed without melting and subliming.

1) H. Imai, T. Saegusa and J. Furukawa, *Makromol. Chem.*, **81**, 92 (1965).
2) J. Furukawa, T. Saegusa and H. Fujii, *ibid.*, **44/46**, 398 (1960).
3) T. Saegusa and T. Ueshima, *Inorg. Chem.*, **6**, 1679 (1967).
4) D. Cook, *Can. J. Chem.*, **41**, 526 (1963).
5) T. Saegusa, S. Matsumoto and H. Imai, *J. Polymer Sci.*, **A-1**, in press.
6) K. N. Campbell, J. O. Knoblock and B. K. Campbell, *J. Am. Chem. Soc.*, **72**, 4380 (1950).
7) H. Meerwein, G. Hinz and H. Majert, *J. Prakt. Chem.*, **147**, 236 (1936).
8) C. E. Sroog, C. M. Chih, F. A. Short and H. M. Woodburn, *J. Am. Chem. Soc.*, **71**, 1710 (1949).

products were isolated, washed with cold ethyl ether, and dried *in vacuo*. In other cases ethyl ether was removed from the reaction mixture under reduced pressure to give a white solid. The haloalcoholates were isolated and purified by the procedures presented in Table 1.

The products were usually analyzed as follows: a weighed sample was decomposed by excess 1 N hydrochloric acid. The alcohol thus produced was then extracted with ethyl ether and analyzed by vapor-phase chromatography (v.p.c.). In the case of $Al(OCH_2CF_3)_3$, a sample was treated with excess acetic acid, while CF_3CH_2OH was analyzed directly by v.p.c. without the procedure of extraction. The results of the analyses are also shown in Table 1.

$EtZnOCH_2CCl_3$ and $Zn(OCH_2CCl_3)_2$ were prepared by the same procedure, using diethylzinc.

Polymerization Procedures and After-treatments. Ethylene oxide and a catalyst were placed in a sealed tube, and the tube was heated for 24 hr. Then the reaction mixture was poured into a large amount of *n*-pentane in order to isolate the product polymer as a white precipitate, which was then dried and extracted with benzene to remove the catalyst residue. In the pentane layer, dioxane, the dimer of ethylene oxide, was searched for and its quantity, if it was present, was determined by v.p.c.

The other polymerization procedures and after-treatments were performed as described before.[2,9,10]

Spectroscopic Measurements. All the samples were prepared under a nitrogen atmosphere. The NMR spectra were measured at room temperature with a Varian A-60 spectrometer, with tetramethylsilane used as the internal standard. The infrared spectra measurements were carried out with a model 402G (Japan Spectroscopic Company), using a KBr liquid cell.

Results and Discussion

Aluminum and zinc haloalcoholates were first prepared in our series of studies by means of the reactions of metal alkyls with halogen-substituted alcohols carried out in ethyl ether. It is important to employ ethyl ether as the reaction solvent in order to suppress the side reactions between the halogen-carbon bond and metal alkyls. The product of a metal haloalcoholate is sometimes insoluble in ether and separates from the reaction mixture. The reaction in ethyl ether is thus recommended.

The following differences have been observed between haloalcoholates and the usual alcoholates:

(1) **Heat-stability.** The usual aluminum alcoholates, such as aluminum ethoxide, isopropoxide, and amyloxides, are known to be distillable under reduced pressure at considerably high temperatures (160°C—250°C). Even unstable aluminum *t*-butoxide can be sublimed *in vacuo*. On the contrary, most aluminum haloalcoholates decompose without melting. Most of them can not be sublimed even under reduced pressures, as is shown in Table 1. Only $Al(OCH_2CF_3)_3$ can be sublimed at 80°C (0.18 mmHg). $Al(OCH_2CH_2Cl)_3$, which carries the minimum number of chlorine atoms, melts at 180°C, however, it is not distilled without decomposition.

(2) **Acid Strength (Interaction with Donor Molecules).** Acid-strength measurements of various haloalcoholates as well as of the usual alcoholates were done using infrared techniques and an indicator method.[1] From the magnitude of the $\Delta\nu_{C=N}$ of pyridine (the shift to a higher wavelength) and the $\Delta\nu_{C=O}$ of xanthone (the shift to a lower wavelength) caused by the coordination of these donor molecules to aluminum alcoholates, the following order of acid strength (acceptor powers of metal atoms) was found;

$Al(OCH\langle^{CH_2Cl}_{CH_2Cl})_3 \rangle Al(OCH_2CF_3)_3 \gtrsim Al(OCH_2CCl_3)_3 \gtrsim Al(OCH_2CBr_3)_3 > Al(OCH_2CHCl_2)_3 > Zn(OCH_2CCl_3)_2 > EtZnOCH_2CCl_3 > Al(OCH_2CH_2Cl)_3$, $Al(OR)_3$ (R: Et, *i*-Pr, *t*-Bu, *etc.*), EtZnOEt, and $Zn(OEt)_2$. The usual alcoholates and $Al(OCH_2CH_2Cl)_3$ did not cause any shift of $\nu_{C=N}$ and $\nu_{C=O}$ at all.

The weak acid strength of usual aluminum alcoholates has been explained in two ways. First, because of the contribution of the resonance structure (II), the electron-acceptor power of aluminum is lower than that to be expected from the electronegativities of aluminum and oxygen in the $\overset{\delta+}{Al}\text{–}\overset{\delta-}{O}$ bond. Secondly, the electron-acceptor power (strong acidic nature) of aluminum is neutralized by

$$\rangle Al\text{–}OR \longleftrightarrow \rangle \overset{\ominus}{Al}\text{=}\overset{\oplus}{O}R \quad (II)$$

the coordination of the oxygen atom of the neighboring aluminum-alkoxy linkage to make the coordination number of aluminum four or more than four (III); therefore, aluminum alcoholates do not act as strong electron acceptors.

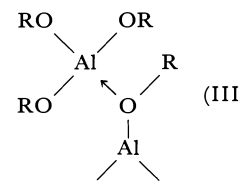

(III)

The examination of highly acidic aluminum haloalcoholates in the present study has an important bearing on this problem. The first explanation leads to the assumption that the electron-withdrawing effect of halogen is extended to aluminum through oxygen, thus increasing the acceptor power of the aluminum atom. In this case, a donor molecule coordinates to aluminum with an expansion of the coordination number of aluminum, as is illustrated by structure IV. According to the alternative explanation, the electron-withdrawing effect of a halogen atom decreases the basic strength of the oxygen of an alkoxy group. The association of the aluminum haloalcoholates is easily broken by a donor molecule, thus forming the acid-base complex of a

9) T. Saegusa, H. Imai and J. Furukawa, *Makromol. Chem.*, **65**, 60 (1963).
10) T. Saegusa, H. Imai and J. Furukawa, *ibid.*, **79**, 221 (1964).

TABLE 2. RELATION BETWEEN ACID STRENGTH AND NMR SPECTRA OF VARIOUS ALCOHOLATES

Alcoholate	$\Delta\nu_{C=N}$ of pyridine (cm^{-1})	$\Delta\nu_{C=O}$ of xanthone (cm^{-1})	NMR spectra[a] A	B	C
$Al(OCH_2CF_3)_3$	31	91	—	A quartet centered at 5.77 (in CH_2Cl_2)	—
$Al(OCH_2CCl_3)_3$	30	90	Two singlets: 5.68(a) 5.28(b). Integration ratio a/b=2.0 (in CH_2Cl_2)	A singlet at 5.75 (in CH_2Cl_2)	A singlet at 5.70 (in CH_2Cl_2)
$Al(OCH_2CBr_3)_3$	29	89	Insoluble	A singlet at 5.52 (in benzene)	A singlet at 5.70[b] (in benzene)
$Al[OCH(CH_2Cl)_2]_3$	39	91	Complexed (in benzene)	A doublet at 6.40(c) and a multiplet at 5.94(d) ratio c/d=4 (in benzene)	A doublet at 6.27(c') and a multiplet at 5.78(d') (in benzene)
$Al(OCH_2CHCl_2)_3$	26	0	Two doublets at 6.18(e) and 5.49(f), two triplets at 4.71(g) and 3.90(h). e/f/g/h= 4.0/2.0/2.0/1.0 (in benzene)	A doblet at 6.10(i), a triplet at 4.26(j) ratio i/j=2 (in benzene)	Essentially the same as A with slight broadening of peaks. e 6.15, f 5.42 g 4.66, h 3.88 (in benzene)
$Al(OCH_2CH_2Cl)_3$	0	0	Complexed. Signals appeared at the region of 6.9—5.5 (in benzene)	Complexed. Very broad singlet in the region of 6.9—5.5 (in benzene)[c]	Essentially the same as A with slight broadening of peaks. (in benzene)
$Al(OR)_3$ (R: *i*-Pr, *t*-Bu)	0	0	Two singlets at 8.80(k) and 8.55(l) (in CH_2Cl_2)[d]	The same as A 8.59 (k') 8.50(l') (in benzene)[d]	The same as A k''=8.80, l''=8.55 (in CH_2Cl_2)[d]
$Zn(OCH_2CCl_3)_2$	24	0			
$EtZnOCH_2CCl_3$	20	0	—	—	—
EtZnOEt, $Zn(OEt)_2$	0	0			

a) Chemical shifts are expressed in τ-value. A: NMR spectra in a non-donating solvent, B: in the presence of excess pyridine, C: in the presence of excess xanthone.

b) A small broad singlet was observed at 5.18 ppm and its peak area increased when the ratio (xanthone/$Al(OCH_2CBr_3)_3$) was decreased. In this case, some dissociation may occur. ($Al(OCH_2CBr_3)_3$ xanthone $\rightleftarrows$ $Al(OCH_2CBr_3)_3$ + xanthone).

c) From this NMR spectrum, considerable interaction between $Al(OCH_2CH_2Cl)_3$ and pyridine may be assumed although no shift of $\nu_{C=N}$ is observed.

d) NMR spectra of $Al(OC(CH_3)_3)_3$.

TABLE 3. ACID STRENGTH MEASUREMENT BY INDICATOR METHOD[a]

Alcoholate	Indicators: Neutral red (+6.8)[b]	Methyl red (+4.8)[b]	Benzeneazonaphtylamine (+4.0)[b]
$Al(OCH_2CH_2Cl)_3$	A	A	B
$Al(OR)_3$ (R: Et, *i*-Pr and *t*-Bu)	B	B	B

A: acidic color B: basic color

a) Measurements were carried out as described before.[1]

b) pK_a values of indicators.

monomeric structure (I), where the coordination number of aluminum is four.

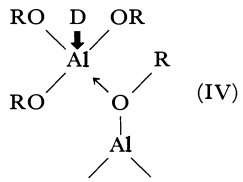

(IV)

As has been described in our previous paper[3] and in V. J. Shiner's work,[11] associated aluminum alcoholates carry more than two kinds of alkoxy groups, which are indicated by signals at different positions in the NMR spectra. In the NMR spectrum of the monomeric aluminum alcoholate - donor complex (structure I), only one type of alkoxy group is observed. In view of these considerations, the NMR spectra of the aluminum haloalcoholates were examined (see Table 2), and the following results obtained: (1) When a shift of the $\nu_{C=O}$ of xanthone or the $\nu_{C=N}$ of pyridine is observed, the three alkoxy groups in the NMR spectra are always equivalent in the donor-acceptor complexes. (2) When the IR shift is not caused by the alcoholate, the three alkoxy groups in the NMR spectrum are not equivalent in the alcoholate-donor mixture, as has been observed in such non-donating solvents as benzene.*1 From these findings, the strong acid nature of some aluminum haloalcoholates may be ascribed to the weak association tendency, which facilitates the formation of the monomeric donor-acceptor complex (structure I). The dissociation tendency is attributable to the decrease in the nucleophilicity of the oxygen atom in the alkoxy group by the electron-withdrawing effect of halogens.

It has also been realized, by comparing the magnitudes of $\Delta\nu_{C=N}$ and $\Delta\nu_{C=O}$, that the accepting power of aluminum alcoholates in the complexes (I) is affected to some extent by the kind and number of halogens in the haloalkoxy group. Thus, it is obvious that the electron-withdrawing effect of halogens directly influences the acceptor power of aluminum. The order of acid strength is as expected from the number and the electronegativities of halogen atoms, with the exception of $Al(OCH\langle^{CH_2Cl}_{CH_2Cl})_3$, whose alkoxy group has a structure very different from those of others. Although the acceptor powers of the aluminum haloalcoholates in the associated form were not measured by the above method, their order was supposed to be the same as that of the dissociated aluminum alcoholates if the coordination number of aluminum atoms is the same, which seems likely.

No difference in acid strength between $Al(OCH_2CH_2Cl)_3$ and the usual aluminum alcoholates was observed by the IR procedures. However, the indicator method[1] revealed that $Al(OCH_2CH_2Cl)_3$ was a stronger acid (see Table 3).

Nearly the same discussion is applicable to zinc haloalcoholates. Detailed studies of zinc haloalcoholates will be published elsewhere.[12]

TABLE 4. POLYMERIZATION OF TETRAHYDROFURAN BY ALUMINUM HALOALCOHOLATES*
Monomer 0.1 mol; catalyst and epichlorohydrin, each 0.00125 mol; CH_2Cl_2 2.5 m*l*; polymerizations, 48 hr, 0°C

Catalyst	Yield (%)	$[\eta]$
$Al(OCH_2CF_3)_3$	75.3	0.330
$Al(OCH_2CCl_3)_3$	29.5	0.360
$Al(OCH_2CBr_3)_3$	29.8	0.115
$Al[OCH(CH_2Cl)_2]_3$	70.5	0.440
$Al(OCH_2CHCl_2)_3$	73.9	0.260
$Al(OCH_2CH_2Cl)_3$	20.8	0.300
$Al[OCH(CH_3)_2]_3$, $Al[OC(CH_3)_3]_3$	0	—
$Al[OCH(CH_2Cl)_2]_3$	16.6[a]	1.37
	88.3 (3.183 g)[b]	0.356
	37.7 (3.974 g)[c]	0.445

* $EtZnOCH_2CCl_3$ and $Zn(OCH_2CCl_3)_2$ did not produce any polymer.
a) Bulk polymerization, catalyst and epichlorohydrin 0.1 mol% for monomer, 7 days, 0°C.
b) Monomer, 0.1 mol; catalyst and epichlorohydrin each 0.001 mol; CH_2Cl_2, 1 m*l*; 2 days, 0°C.
c) After two days' polymerization (condition (b)), 0.2 mol of tetrahydrofuran was added and polymerization was continued for 5 days.

11) V. J. Shiner, Jr., D. Whittaker and V. J. Fernandez, *J. Am. Chem. Soc.*, **85**, 2318 (1963).

*1 $Al(OCH_2CH_2Cl)_3$ is the only exception. There the shift of $\Delta\nu_{C=N}$ is not observed. However, in the NMR spectrum of $Al(OCH_2CH_2Cl)_3$-pyridine the signals due to the $ClCH_2CH_2O$-group are not the same as those in benzene.

12) T. Saegusa and T. Ueshima, This Bulletin, in press.

Table 5. Cationic polymerization by haloalcoholates

Monomer 0.1 mol, haloalcoholate and CH_3OCH_2Cl, each 2.5 mol% for monomer

Catalyst	Yield (%)	$[\eta]$[b]
CH_2=CHO-*i*-Bu[a] (in toluene, 30 m*l*; at −78°C, 24 hr)		
$Al(OCH_2CF_3)_3$	12.6	0.10
$Al(OCH_2CCl_3)_3$	71.1	0.10
$Al(OCH_2CBr_3)_3$	trace	—
$Al(OCH_2CHCl_2)_3$	16.9	0.12
$Al[OCH(CH_2Cl)_2]_3$	42.1	0.21
$Al(OCH_2CH_2Cl)_3$	0	—
$Zn(OCH_2CCl_3)_3$	3.0	0.09
$EtZnOCH_2CCl_3$	43.2	0.35
$Al(OR)_3$ (R: Et or *i*-Pr) $EtZnOEt$, $Zn(OEt)_2$	0	—
α-Methylstyrene (in CH_2Cl_2, 20 m*l*; at 0°C for 48 hr)		
$Al(OCH_2CCl_3)_3$	89.7	white powder
3,3-Bis(chloromethyl)oxacyclobutane[c] (in CH_2Cl_2, 20 m*l*; at 0°C for 72 hr)		
$Al(OCH_2CCl_3)_3$	34.9	white powder

a) All the polymers were amorphous (soluble in methyl ethyl ketone).
b) In benzene at 30°C.
c) Epichlorohydrin was used as a promoter.

Table 6. Polymerization of alkylene oxides

Monomer 0.1 mol

Catalyst	Yield of polymer (%)	$[\eta]$[f]	Yield of dioxane (%)
Ethylene oxide (catalyst 1.25 mol%; in 2.5 m*l* CH_2Cl_2; at 50°C for 24 hr)			
$Al(OCH_2CF_3)_3$	32.1[b]	0.425	3.0
$Al(OCH_2CCl_3)_3$	15.9[c]	0.031	2.4
$Al(OCH_2CBr_3)_3$	29.2[d]	—	3.3
$Al(OCH_2CHCl_2)_3$	21.8[d]	—	1.3
$Al[OCH(CH_2Cl)_2]_3$	23.4[c]	0.037	5.9
$Al(OCH_2CH_2Cl)_3$	9.6[d]	—	1.6
$Al[OCH(CH_3)_2]_3$	9.6[e]	0.345	0
$Al(OCH_2CH_3)_3$[a]	0.8[e]	—	0
$EtZnOCH_2CCl_3$	15.9[d]	—	1.2
$Zn(OCH_2CCl_3)_2$	100[b]	0.037	0
$EtZnOCH_2CH_3$	34.5[e]	0.638	0
$Zn(OCH_2CH_3)_2$	100[e]	0.380	0
Propylene oxide (2.5 mol% of catalyst; in 10 m*l* CH_2Cl_2, at 50—60°C for 8 hr)			
$Al(OCH_2CCl_3)_3$	59.7	—	—
Epichlorohydrin (2.5 mol% of catalyst; in 10 m*l* CH_2Cl_2, at 0°C for 72 hr)			
$Al(OCH_2CCl_3)_3$	46.2	—	—

a) time, 12 hr b) waxy c) tacky semi-solid d) oily
e) resineous solid f) in benzene 30°C

(3) Behavior as Polymerization Catalysts. It has already been established that the usual alcoholates of aluminum and zinc do not cause the cationic polymerizations of vinyl monomers and cyclic ethers, such as isobutyl vinyl ether, styrene, α-methylstyrene, 3,3-bis(chloromethyl)oxacyclobutane, and tetrahydrofuran.[1] On the contrary, the haloalcoholates in the present study induced the

cationic polymerizations of the above monomers, as was expected from the stronger Lewis acid character of the haloalcoholates. The polymerizations by haloalcoholate catalysts are illustrated in Tables 4 and 5. In the tetrahydrofuran polymerization, solid polymers with quite high molecular weights were produced in high yields by the catalysts of all aluminum haloalcoholates. Polytetrahydrofuran with $[\eta]$ values above 1 could be prepared at low catalyst concentrations. When a new tetrahydrofuran monomer was added to a system in which polymerization had proceeded nearly completely, the yield as well as the intrinsic viscosity of the polymer were increased (compare b and c in Table 4). In the second stage, however, the polymerization did not proceed beyond 10% of the added monomer, even after 5 days' reaction. This observation suggests slow termination.

Heterogeneous polymerization of isobutyl vinyl ether with haloalcoholate catalysts in toluene produced only amorphous polymers (Table 5).

The results of the polymerizations of alkylene oxides are summarized in Table 6. Polymerizations of these monomers by the usual alcoholates are known to proceed through the coordinate anionic mechanism. The polymerizations by haloalcoholates are different in some respects from those by the usual alcoholates: (1) The ethylene oxide polymerization is caused both by haloalcoholates and the usual alcoholates. However, only in the polymerization by the haloalcoholates, dioxane, a dimer of ethylene oxide, is formed as a by-product. Our previous work[13] has shown that dioxane is formed only by a cationic mechanism (Eq. (1)), not by a so-called coordinate anionic mechanism.

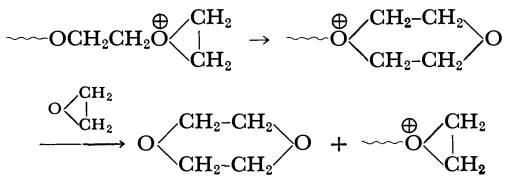

(1)

Therefore, it may be assumed that the haloalcoholates induce the cationic polymerization of ethylene oxide, whereas the usual alcoholates induce the coordinate anionic polymerization. (2) This assumption is consistent with the molecular weight of the product polymer. Polymers prepared using the haloalcoholates are oily or waxy (low molecular weights), whereas those prepared using the usual alcoholates were solid polymers with higher molecular weights. In the polymerizations of propylene oxide and epichlorohydrin, a similar tendency was observed.

13) T. Saegusa, T. Ueshima and S. Tomita, *Makromol. Chem.*, **107**, 131 (1967).

BULLETIN OF THE CHEMICAL SOCIETY OF JAPAN VOL. 41 1201—1208 (1968)

The Synthesis of 4-Hydroxyfuro[2′,3′:7, 8]coumarins and 5*H*-Benzofuro[3,2-*c*]furo[2,3-*h*][1]benzopyran-5-one*[1]

Yoshiyuki KAWASE, Mutsumu NANBU and Hirokazu YANAGIHARA

Department of Chemistry, Faculty of Literature and Science, Toyama University, Gofuku, Toyama

(Received November 1, 1967)

4-Hydroxyfuro[2′,3′:7,8]coumarin (16) and its 3-phenyl (10) and 3-(2-methoxyphenyl) (11) derivatives were prepared from the corresponding 4-hydroxy-5-benzofuranyl ketones (15, 8a and 8b) by the action of ethyl carbonate and sodium. The furocoumarin 11 thus obtained was converted to 5*H*-benzofuro[3,2-*c*]furo[2,3-*h*][1]benzopyran-5-one (18), a compound having a new pentacyclic ring system, by the demethyl-cyclization with pyridine hydrochloride, hydroiodic acid or aluminum chloride. The attempted preparation of these compounds through their dihydro compounds is also described; 2,3-dihydro-4-hydroxybenzofuran (1) was acylated with phenylacetic acid, with 2-methoxyphenylacetic acid or with 2,4,5-trimethoxyphenylacetic acid by the action of polyphosphoric acid to give a mixture of the 5- and 7-acylated compounds (3 and 2), and the formers were converted to the corresponding 4″,5″-dihydrofuro[2″,3″:7,8]isoflavones (6), 4″,5″-dihydro-2-methylfuro-[2″,3″:7,8]isoflavones (4) and 4′,5′-dihydro-4-hydroxyfuro[2′,3′:7,8]coumarins (7). The 2,3-dihydro-4-hydroxy-5-benzofuranyl benzyl ketone (3a) and the dihydrofuroisoflavones (4a and 4b) were also obtained by the catalytic reduction of the corresponding furo-compounds.

In previous papers, one of the authors and others reported the synthesis of furo[2″,3″ : 7,8]isoflavones,[1] 4-hydroxycoumarins,[2] and benzofuro[3′,2′:3,4]coumarins.[3] Now in this paper, the preparation of closely related 4-hydroxyfuro[2′,3′:7,8]coumarins (10, 11, 16, 17 and 19) and 5*H*-benzofuro[3,2-*c*]-furo[2,3-*h*][1]benzopyran-5-one (18) and the attempted preparation of them through their dihydro compounds will be reported. The synthesis of isomeric 4-hydroxyfuro[3′,2′ :6,7]coumarins[4] and 6*H*-benzofuro[3,2-*c*]furo[3,2-*g*][1]-benzopyran-6-one derivative (erosnin),[4b] having linearly fused furan ring, has recently been reported by Fukui and Nakayama and others, and that of dimethylfuro-derivatives of 4-hydroxy-3-phenylcoumarin by the thermal condensation of dimethylhydroxybenzofurans with ethyl phenylmalonate has been reported by Royer *et al.*[5]

In the case of isomeric compounds, 2,3-dihydro-6-hydroxybenzofuran was acylated to give the 5-acyl compounds,[6] which were converted to the corresponding dihydrofuro-4-hydroxycoumarins[4,7] and -isoflavones[8] which were further dehydrogenated to the furo-compounds, as the direct acylation of hydroxybenzofurans to give the *o*-hydroxyketones, the convenient starting materials for 4-hydroxycoumarins and isoflavones, was not successful although the acetylation of 2-substituted[9] or 2,3-dimethyl[10] 6-hydroxy- or 6-methoxy-benzofurans gave the 5-acyl compounds. But the dehydrogenation to give 4-hydroxyfurocoumarins was accomplished only in some cases with difficulty or indirectly.[4] Accordingly, the furocoumarins were also prepared[4a,b] by the pyrone ring formation on hydroxybenzofuranyl ketones which were obtained by alkaline degradation of furoisoflavones or by hydrolysis followed by

*1 A part of this was presented at the 20th Annual Meeting of the Chemical Society of Japan, Tokyo, March, 1967.

1) T. Matsumoto, Y. Kawase, M. Nanbu and K. Fukui, This Bulletin, **31**, 688 (1958); K. Fukui and Y. Kawase, *ibid.*, **31**, 693 (1958); Y. Kawase, K. Ogawa, S. Miyoshi and K. Fukui, *ibid.*, **33**, 1240 (1960).

2) Y. Kawase, *Experientia*, **14**, 435 (1958); This Bulletin, **31**, 440 (1958); **32**, 9, 11 (1959); **35**, 1869 (1962).

3) Y. Kawase, *ibid.*, **32**, 690 (1959); **35**, 573 (1962).

4) a) K. Fukui and M. Nakayama, *Nippon Kagaku Zasshi* (*J. Chem. Soc. Japan, Pure Chem. Sect.*), **85**, 444 (1964).
b) K. Fukui and M. Nakayama, *Tetrahedron Letters*, **1965**, 2559. c) A. Vialard-Goudon and N. Blanchecatte, *Compt. Rend.*, **263**, 255 (1966).

5) J.-P. Lechartier, P. Demerseman, A. Cheutin and R. Royer, *Bull. Soc. Chim. France*, **1966**, 1716.

6) J. S. H. Davies, P. A. McCrea, W. L. Norris and G. R. Ramage, *J. Chem. Soc.*, **1950**, 3206.

7) E. C. Horning and D. B. Reisner, *J. Am. Chem. Soc.*, **72**, 1514 (1950).

8) S. K. Pavanaram, L. R. Row and T. R. Seshadri, *J. Sci. Ind. Res.* (*India*), **15B**, 495 (1956); S. K. Pavanaram and L. R. Row, *Current Science* (*India*), **26**, 145 (1957); K. Fukui and M. Nakayama, *Experientia*, **19**, 621 (1963); **20**, 668 (1964); K. Fukui, M. Nakayama, A. Tanaka and S. Sasatani, This Bulletin, **38**, 845 (1965); A. S. R. Anjaneyulu, C. S. Krishna and L. R. Row, *Tetrahedron*, **21**, 2677 (1965).

9) P. K. Ramachandran, A. T. Tefteller, G. O. Paulson, T. Cheng, C. T. Lin and W. J. Horton, *J. Org. Chem.*, **28**, 398 (1963); J. Oda H. Fukami and M. Nakajima, *Agr. Biol. Chem.*, **30**, 59 (1966).

10) R. Royer, E. Bisagni, A.-M. Laval-Jeantet and J.-P. Marquet, *Bull. Soc. Chim. France*, **1965**, 2607.

Chart

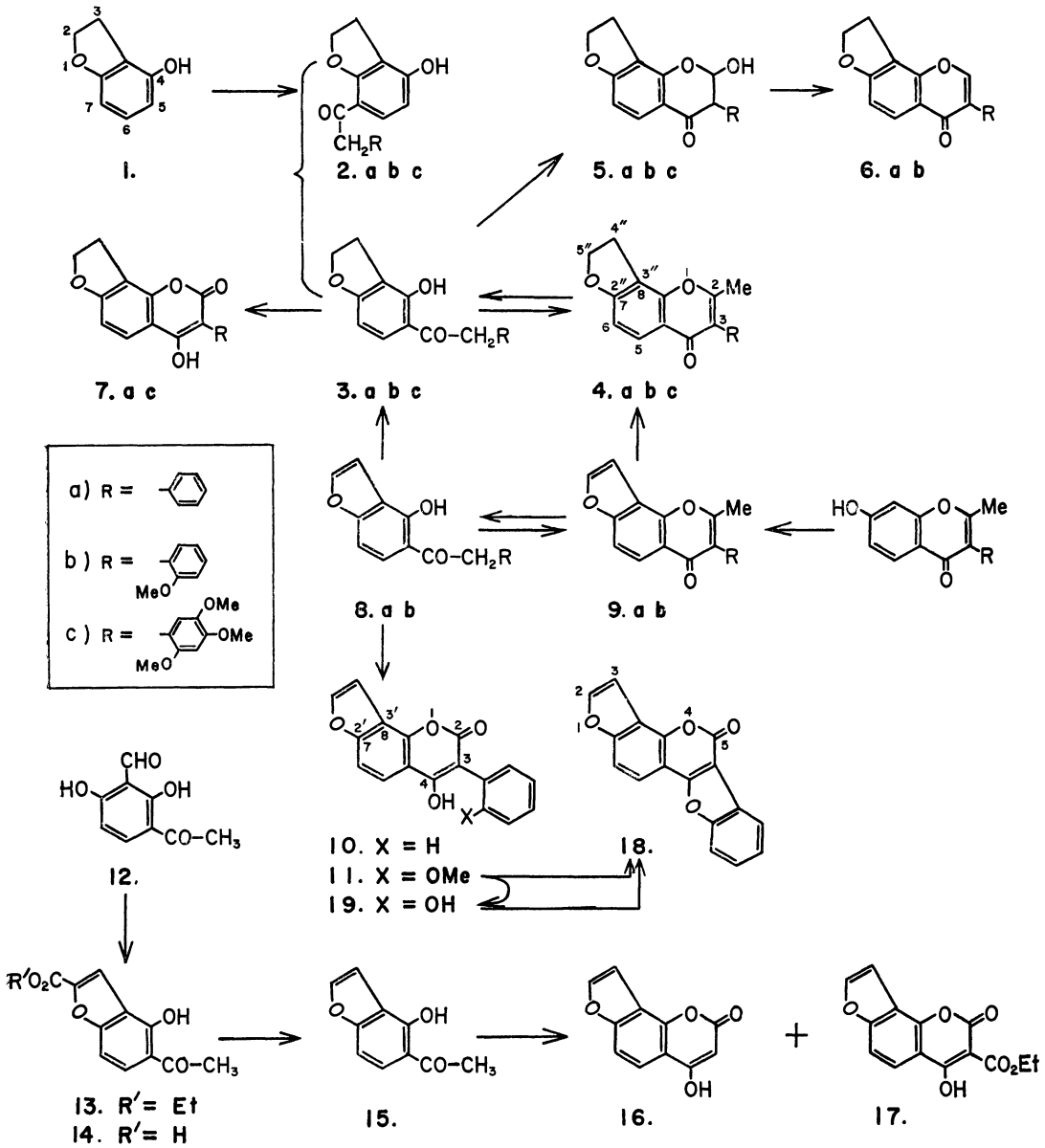

decarboxylation of acetyl-methoxybenzofuran-2-carboxylate.

Concerning the acylation of 2,3-dihydro-4-hydroxybenzofuran, Seetharamiah[11] reported the acylation of it according to the Hoesch reaction to give the 7-acyl compound while Miyano and Matsui[12] reported the analogous reaction of 2-alkyl compounds to give a mixture of the 5- and 7-acyl compounds, and Dyke *et al.*[13] reported the analogous reaction of 2-isopropyl derivative and the further convertion to the furoisoflavone through its dihydro-compound. On the other hand, Seshadri *et al.*[14] prepared 4″,5″-dihydro-4″-methylfuro[2″,3″ : 7,8]-isoflavone through another route and converted it to the furoisoflavone.

First, in the present experiments the acylation of

11) A. Seetharamiah, *J. Chem. Soc.*, **1948**, 894.
12) M. Miyano and M. Matsui, *Proc. Japan Acad.*, **35**, 175 (1959); *Chem. Ber.*, **92**, 2487 (1959); **93**, 54 (1960); M. Miyano, A. Kobayashi and M. Matsui, *Bull. Agr. Chem. Soc. Japan*, **24**, 540 (1960).
13) S. F. Dyke, W. D. Ollis and M. Sainsburg, *J. Chem. Soc. (c)*, **1966**, 748.
14) P. S. Sarin, J. M. Sehgal and T. R. Seshadri, *J. Sci. Ind. Res. (India)*, **16B**, 61, 206 (1957).

2,3-dihydro-4-hydroxybenzofuran (1) and the convertion of the products to dihydrofuro and then to furo derivatives of 4-hydroxycoumarins and isoflavones were studied. The acylation of 1 with phenylacetic acid, with 2-methoxyphenylacetic acid or with 2,4,5-trimethoxyphenylacetic acid by the action of polyphosphoric acid (PPA) furnished a mixture of the 5- and 7-acylated compounds (3a, b, c and 2a, b, c). The acylation by the Hoesch reaction with phenylacetonitrile furnished as well the ketones 2a and 3a, but with 2-methoxyphenylacetonitrile in poorer yield.

The 5-acyl compounds (3a, b, c), separated from the alkali-soluble isomeric 7-acyl compounds (2a,b,c), were converted to the corresponding 4″,5″-dihydro-2-methylfuro[2″,3″7,8]isoflavones (4a, b, c) by the action of acetic anhydride and sodium acetate, and the alkaline degradation of 4a furnished the starting ketone 3a. The ketone 3a and the dihydrofuroisoflavones 4a and 4b were also obtained by the catalytic reduction of the corresponding benzofuranyl ketone[1] (8) and furoisoflavones[1] (9a, b), respectively.

These experiments, their analyses, their infrared and ultraviolet spectra and the analogous acylation described before furnished the proof for the structures of the ketones (2a, b, c and 3a, b, c) and the isoflavones (4a, b, c).

The ketones (3a, b, c) were also converted to 4″,-5″-dihydro-2-hydroxyfuro [2″, 3″ : 7,8] isoflavanones (5a, b, c) by the action of ethyl formate and sodium, two (5a and 5b) among which were readily dehydrated to dihydrofuroisoflavones (6a and 6b). 4′,5′-Dihydro-4-hydroxyfuro[2′,3′:7,8]coumarins (7a and 7c) were also prepared from the ketones by the general method utilizing ethyl chlorocarbonate.

The attempts to dehydrogenate these compounds to the corresponding furo-compounds were unsuccessful.

Then, the 4-hydroxy-5-benzofuranyl ketones (8a and 8b) were prepared through another route by the alkaline degradation of the corresponding furoisoflavones[1] (9a and 9b), and 4-hydroxyfuro[2′,3′:7,8]-coumarins (10 and 11) were synthesized from these ketones by the general method utilizing ethyl carbonate and sodium. 4-Hydroxy-5-benzofuranyl methyl ketone[15] (15) was prepared, in the present experiments, from 2,4-dihydroxy-3-formylphenyl methyl ketone[16] (12) by the action of ethyl bromomalonate and potassium carbonate followed by the hydrolysis of the produced ester (13) and the decarboxylation of the acid (14). The action of ethyl carbonate and sodium on this ketone (15) furnished analogously 4-hydroxyfuro[2′,3′;7,8]coumarin (16) accompanied by a small amount of its 3-ethoxycarbonyl derivative (17); the formation of the latter seems to be the result of double ethoxycarbonylation of the ketone. The structures of these compounds were considered from their analyses and their infrared and ultraviolet spectra.

The 4-hydroxy-3-(2-methoxyphenyl)furocoumarin (11) thus obtained was converted to benzofuro-furobenzopyranone. The reported methods for the synthesis of 6*H*-benzofuro[3,2-c][1]benzopyran-6-ones are (a) by the demethyl-cyclization of 4-hydroxy-3-(2-methoxyphenyl)coumarins,[17] (b) by the hydrolytic cyclization of methoxy derivatives of α-benzoylacetonitrile,[3,18] (c) by the oxidative coupling of 4-hydroxycoumarins with catechol[19] and (d) by the oxidation of flavylium salts.[20] The isomeric 6*H*-benzofuro[3,2-*c*]furo[3,2-*g*][1]benzopyran-6-one derivative (erosnin) was synthesized by the method (c)[4] and the dihydrofuro analogues of it were synthesized by the methods (a),[21] (b),[22] and (c).[21]

In the present experiments, the method (a) was applied to the hydroxyfurocoumarin 11; the action of pyridine hydrochloride or hydroiodic acid on 11 furnished 5*H*-benzofuro[3,2-*c*]furo[2,3-*h*][1]benzopyran-5-one (18), a compound having a new pentacyclic ring system, and the action of aluminum chloride in nitrobenzene caused only the demethylation of the methoxy group to give 4-hydroxy-3-(2-hydroxyphenyl)furocoumarin (19), which was further converted to 18 by heating it with methanolic hydrogen chloride. The structures of these compounds were verified from their analyses and their infrared and ultraviolet spectra.

In the infrared spectra, the dihydrofuroisoflavones (4a, b, c and 6a, b) have their ν_{CO} at 1650—1635 cm^{-1}, characteristic for chromones, while dihydrofuro- (7a and 7c) and furocoumarins (10, 11, 16, 17 and 19) have their broad ν_{OH} at 3100—2950 cm^{-1} and their ν_{CO} at 1710—1660 cm^{-1}, characteristic for hydroxy-coumarins. Benzofuro-furobenzopyranone (18) has its ν_{CO} at somewhat higher wave number region, 1760 cm^{-1}. These data are comparable to those of the isomeric compounds having linearly fused furan ring.[4]

The ultraviolet absorption spectra were measured in ethanol and it proved that the dihydrofuroisoflavones (4a and 6a) have almost similar shape of absorption curves with that of the furo-compounds,[1] having high peaks at 245—250 mμ and low peaks at 305 mμ (Fig. 1), and the 3-(methoxyphenyl)

15) C. B. Rao, G. Subramayam and V. Venkateswarlu, *J. Org. Chem.*, **24**, 683 (1959).
16) K. Nakazawa, *J. Pharm. Soc. Japan*, **59**, 297 (1939).
17) W. J. Bowyer, A. Robertson and W. Whalley, *J. Chem. Soc.*, **1957**, 542; T. R. Govindachari, K. Nagarajan and P. C. Parthasarathy, *ibid.*, **1957**, 548; O. H. Emerson and E. M. Bickoff, *J. Am. Chem. Soc.*, **80**, 4381 (1958).
18) J. N. Chatterjea and S. K. Roy, *J. Indian Chem. Soc.*, **34**, 98 (1957); J. N. Chatterjea, *ibid.*, **36**, 256 (1959).
19) H. Wanzlick, R. Gritzky and H. Heidepriem, *Chem. Ber.*, **96**, 305 (1963).
20) L. Jurd, *Tetrahedron Letters*, **1963**, 1151; *J. Org. Chem.*, **29**, 3036 (1964).
21) K. Fukui *et al.*, Symposium on the Chemistry of Natural Products, Kyoto, Oct., 1965.
22) J. N. Chatterjea and N. Prasad, *Chem. Ber.*, **97**, 1252 (1964).

analogues (4b and 4c) have broader absorption at 220—240 mμ and higher peaks of the 300 mμ region (Fig. 2). Furocoumarins (16 and 17) have high peaks at about 235 mμ and lower ones at 290—300 mμ, and the 3-aryl derivatives (10, 11 and 19) have additional peaks at 217 mμ and broader absorption at 280—330 mμ, while the dihydrofurocoumarins (7a and 7c) have no peaks in the 210—270 mμ region and have higher peaks at about 320 mμ (Figs. 3 and 4). The benzofuro-furobenzopyranone (18) has high peak at 238 mμ and broader absorption at 280—345 mμ having four peaks (Fig. 4). These relations of the ultraviolet spectra are

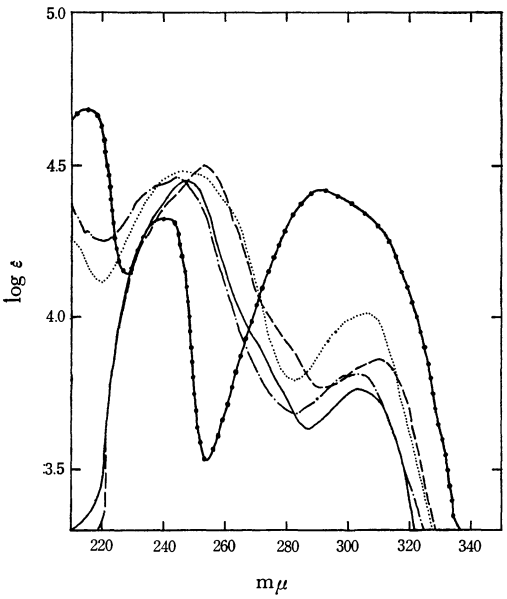

Fig. 1. The UV spectra of furo- and dihydrofuroisoflavones and dihydro-2-hydroxyfuroisoflavanone:
—— 9a*, ---- furoisoflavone* ·—· 4a, ····· 6a, •—• 5a (* from Ref. 1)

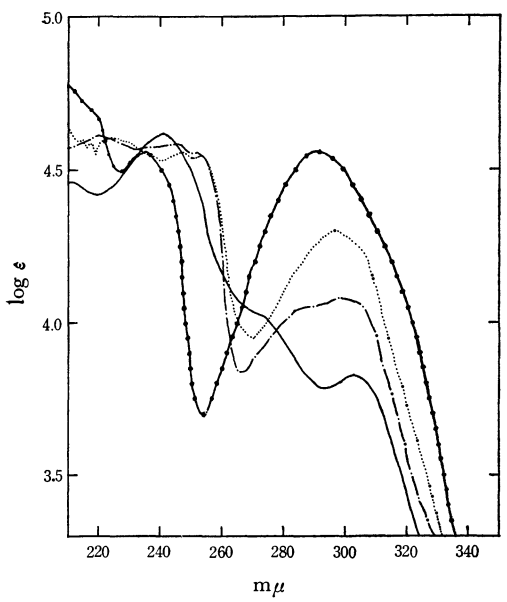

Fig. 2. The UV spectra of furo- and dihydrofuroisoflavones and dihydro-2-hydroxyfuroisoflavanone:
—— 9b, ·—· 4b, ····· 4c, •—• 5c

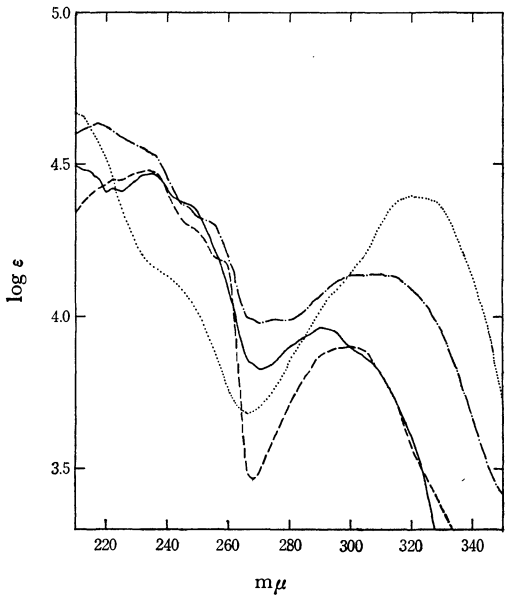

Fig. 3. The UV spectra of furo- and dihydrofurocoumarins:
—— 16, ---- 17, ·—· 10, ····· 7a

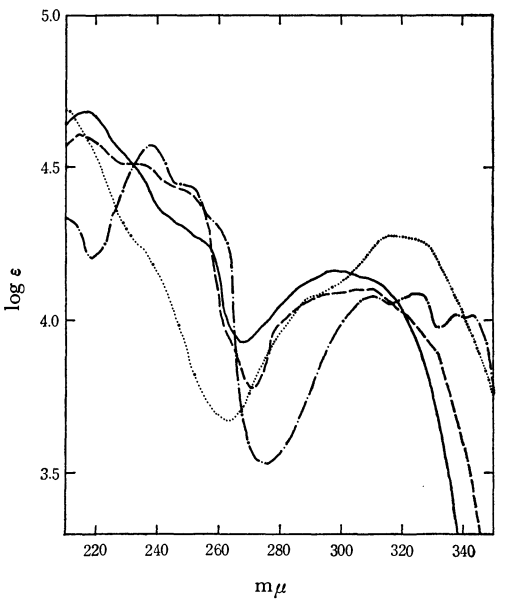

Fig. 4. The UV spectra of furo- and dihydrofurocoumarins and benzofuro-furobenzopyranone:
—— 11, ---- 19, ····· 7c, ·—· 18

Table 1. The acid-catalized acylation of compound 1

Compd.	Acylating agent	Procedure[a], temp.×time	Product composition yield, % 2	3
a	Phenylacetic acid	A, 100°×30′	22	25
a	Phenylacetonitrile	B	24	31
b	2-Methoxyphenylacetic acid	A, 80°×30′	34	28.5
c	2,4,5-Trimethoxyphenylacetic acid	A, 80°×30′	31	28

a) A: PPA, B: Hoesch procedure.

comparable to those of the isomers,[4] except that the absorption band in the 300 mμ region of the isomers appears at the wave length longer by 20 mμ than that of the others.

In conclusion, it seems that the influence of furan ring appears fairly clearly in the absorption of 230—270 mμ region in the case of furocoumarins, but not so clearly in the case of furoisoflavones, probably as coumarins have not or have only weak absorption in that region[23] while isoflavones themselves have already strong absorption in that region,[24] which and that due to furan ring overlap each other.

Experimental*2

Materials. The compound 1 was prepared[11] by the catalytic reduction of the furo-compound and the ketone 8a and furoisoflavones 9a and 9b were prepared according to the Ref. 1. The compound 12 was prepared[16] by the formylation of ethyl resorcylate.

The Preparation of 2,3-Dihydro-4-hydroxy-5-benzofuranyl Ketones and Isomers. *a) By the Acylation of 2,3-Dihydro-4-hydroxybenzofuran* (1) *by Means of Carboxylic Acid and Polyphosphoric Acid (PPA)* (*Table 1*). A mixture of 1 (1 g), phenylacetic acid (1 g, 1 mol equivalent) and PPA (n=1.5, 25 g) was heated at 100°C for 30 min with stirring. The cooled mixture was poured into ice-water and was extracted with ether. The ethereal solution was washed with aqueous sodium bicarbonate, and then was extracted with 5% aqueous sodium hydroxide. The product obtained from the ethereal layer was crystallized from ethanol to give 2,3-dihydro-4-hydroxy-5-benzofuranyl benzyl ketone (3a), having a positive ferric chloride color reaction in ethanol.

The alkaline extract was acidified and extracted with ether. The product obtained from the ethereal solution was crystallized from methanol to give the isomeric 2,3-dihydro-4-hydroxy-7-benzofuranyl benzyl ketone (2a), having a negative ferric chloride color reaction in ethanol.

Similarly, 2,3-dihydro-4-hydroxy-5-benzofuranyl 2-methoxybenzyl ketone (3b) and 2,3-dihydroxy-4-hydroxy-5-benzofuranyl 2,4,5-trimethoxybenzyl ketone (3c) and the isomeric 2,3-dihydro-4-hydroxy-7-benzofuranyl 2-methoxybenzyl ketone (2b) and 2,3-dihydro-4-hydroxy-7-benzofuranyl 2,4,5-trimethoxybenzyl ketone (2c) were also obtained by this method.

b) By the Acylation of 1 by Means of the Hoesch Reaction. (*Table 1.*) Anhydrous powdered zinc chloride (2.5 g) was added to a solution of 1 (1 g) and phenylacetonitrile (1 g, 1 mol equivalent) in anhydrous ether (30 ml), and the mixture was saturated with dry hydrogen chloride with stirring and cooling, and then was left 2 days. The upper ethereal layer was decanted off and the residual viscous lower layer was heated on a water-bath for 1 hr with the addition of dilute hydrochloric acid. The cooled mixture was extracted with ether and the ethereal solution was treated similarly as described in the procedure a) to give the ketones 3a and 2a.

c) By the Hydrogenation of Benzofuranyl Ketone (8a). A mixture of 4-hydroxy-5-benzofuranyl benzyl ketone(8a)[11] (0.5 g), palladium carbon (25%, 0.5 g) and ethyl acetate (100 ml) was shaken with hydrogen at atmospheric pressure and room temperature until one mole equivalent

Table 2. The synthesis of dihydrofuro-isoflavones, -isoflavanones, -coumarins and furo-coumarins

Compd.	Starting compd. (g)	Procedure[a]	Yield %
4a	3a (0.3)	A	61
4a	9a (0.5)	B	80
4b	3b (0.7)	A	26
4b	9b (0.5)	B	20
4c	3c (0.5)	A	b)
5a	3a (0.6)	C	30
5c[c]	3c (1)	C	28.5
6a	5a (0.5)	D	66
6b[d]	3b (0.3)	C	16
7a	3a (0.3)	E	60.5
7c	3c (0.4)	E	49
10	8a (0.9)	F	80.5
11	8b (1)	F	64
16[e]	15 (2.6)	F	59

a) A: Acetic anhydride and sodium acetate, B: Hydrogenation of furo-compounds, C: Ethyl formate and sodium, D: Reflux in acetic acid, E: Ethyl chlorocarbonate and potassium carbonate, F: Ethyl carbonate and sodium.
b) A small amount.
c) This was not dehydrated by the procedure D.
d) This was obtained directly from 3b.
e) A small amount of 17 was also obtained.

23) J. F. Garden, H. F. Hayes and R. H. Thomson, *J. Chem. Soc.*, **1956**, 3315; C. Mentzer and P. Vercier, *Monatsh.*, **88**, 264 (1957); K. Fukui and M. Nakayama, *Nippon Kagaku Zasshi* (*J. Chem. Soc. Japan, Pure Chem. Sect.*), **85**, 790 (1964).

24) L. Jurd, "The Chemistry of Flavonoid Compounds," ed. by T. A. Geissman, MacMillan, New York, N.Y. (1962), p. 147.

*2 All melting points are uncorrected, infrared spectra were measured by the KBr method and ultraviolet spectra were measured in ethanol. The detailed data are summarized in the tables and figures.

TABLE 3. THE PHYSICAL CONSTANTS AND ANALYSIS OF NEW COMPOUNDS

Compd.	Mp, °C (solvent)[a]	ν_{OH}^{KBr} cm^{-1}	ν_{CO}^{KBr} cm^{-1}	Formula	Found C%	Found H%	Calcd C%	Calcd H%
Dihydrobenzofuranyl Ketones								
2a	170—171 (M)	3150	1635—1575	$C_{16}H_{14}O_3$	75.38	5.39	75.57	5.55
2b	215—216 (E)	3375	1640—1590	$C_{17}H_{16}O_4$	72.03	5.72	71.82	5.63
2c	173—174 (M)	3360	1660	$C_{19}H_{20}O_6$	66.02	6.02	66.27	5.85
3a	81.5— 82.5 (E)		1640	$C_{16}H_{14}O_3$	75.63	5.38	75.57	5.55
3b	110—110.5 (P)		1635	$C_{17}H_{16}O_4$	72.57	5.53	71.82	5.63
3c	142—143 (E)		1640	$C_{19}H_{20}O_6$	66.09	5.85	66.27	5.85
Benzofuranyl Ketones								
8b	120—120.5 (E)		1630—1605	$C_{17}H_{14}O_4$	72.44	5.23	72.33	5.00
14	272—273 (D)	3100	1705, 1620	$C_{11}H_8O_5$	59.75	3.44	60.00	3.66
Dihydrofuroisoflavones								
4a	196—197 (E)		1635	$C_{18}H_{14}O_3$	77.82	4.52	77.68	5.07
4b	158—158.5 (E)		1635	$C_{19}H_{16}O_4$	74.12	5.25	74.01	5.23
4c	238—239 (E)		1635	$C_{21}H_{20}O_6$	68.25	5.68	68.47	5.47
6a	135—135.5 (E)		1640	$C_{17}H_{12}O_3$	77.26	4.58	77.19	4.73
6b	165.5—166.5 (E)		1650	$C_{18}H_{14}O_4$	73.51	5.16	73.46	4.80
Dihydrofuroisoflavanones								
5a	159—160 (dec) (A)	3150	1650	$C_{17}H_{14}O_4$	72.63	5.11	72.33	5.00
5c	181—182 (E)	3450	1670	$C_{20}H_{20}O_7$	64.18	5.56	64.51	5.41
Dihydrofurocoumarins								
7a	233.5—235 (E)	3100	1660	$C_{17}H_{12}O_4$	72.27	4.30	72.85	4.32
7c	263—265 (E)	3100	1680	$C_{20}H_{18}O_7$	64.84	4.97	64.86	4.90
Furocoumarins								
10	268—269 (E)	3000	1663	$C_{17}H_{10}O_4$	73.11	3.61	73.38	3.62
11	185—186.5 (E)	3250	1705	$C_{18}H_{12}O_5$	70.17	4.07	70.13	3.92
16	268—269[b] (M)	2950	1710	$C_{11}H_6O_4 \cdot H_2O$	60.60	3.18	60.00	3.66
17	163—164 (E)	3350	1735	$C_{14}H_{10}O_6$	61.70	3.33	61.32	3.68
19	274—276 (dec) (E)	3070	1675	$C_{17}H_{10}O_5$	69.21	3.52	69.39	3.43
Benzofuro-furocoumarin								
18	264—265 (E)		1762	$C_{17}H_8O_4$	73.56	3.11	73.91	2.92

a) A: Ethyl acetate, D: Dilute ethanol, E: Ethanol, M: Methanol, P: Petroleum ether.
b) The anhydride: mp 273—274°C. Found C, 65.05; H, 3.10%. Calcd for $C_{11}H_6O_4$: C, 65.35; H, 2.99%.

TABLE 4. THE UV SPECTRA OF DIHYDROFURO-ISOFLAVONES, -ISOFLAVANONES, -COUMARINS, FUROCOUMARINS AND BENZOFURO-FUROCOUMARIN

Compd.	λ_{max}^{EtOH} mμ[a] (log ε)
4a	244(4.96), 304(3.81)
4b	220(4.61), 245(4.58), 254[s](4.55), 285[s](4.04), 298(4.08)
4c	215(4.60), 218(4.59), 225(4.60), 248(4.56), 254(4.54), 298(4.30)
5a	215(4.39), 240(4.03), 292(4.12)
5c	235(4.27), 290(4.26)
6a	246(4.48), 306(4.01)
7a	243[s](4.10), 321(4.39)
7c	290[s](4.07), 318(4.28)
10	217(4.68), 235[s](4.53), 256[s](4.30), 300[s](4.14), 310(4.14)
11	217(4.68), 255[s](4.26), 298(4.16), 310[s](4.13)
16	235(4.47), 248[s](4.36), 290(3.97)
17	222[s](4.45), 234(4.78), 259[s](4.18), 290[s](3.87), 300(3.90)
18	238(4.57), 250[s](4.44), 311(4.08), 326(4.09), 335(4.02), 342(4.02)
19	215(4.61), 235[s](4.51), 250[s](4.44), 278[s](3.97), 295[s](4.08), 310(4.10)

a) s: Shoulder

of hydrogen was absorped (about 8 hr). Then, the catalyst was filtered and the solvent was distilled off, and the residual product was crystallized to give the ketone 3a, 0.4 g.

d) By the Alkaline Degradation of Dihydrofuroisoflavone (4a). A mixture of dihydrofuroisoflavone 4a (0.5 g) and ethanolic (not methanolic) potassium hydroxide (1 g in 30 m*l* ethanol) was refluxed for 3 hr, then was diluted with water and acidified. The crystalline product formed was collected and recrystallized to give the ketone 3a, 0.3 g.

The Preparation of Dihydrofuroisoflavones (Table 2). *a) By the Action of Acetic Anhydride and Sodium Acetate on the Ketones (3).* A mixture of the ketone 3a (0.3 g), anhydrous sodium acetate (0.3 g) and acetic anhydride (10 m*l*) was refluxed for 12 hr and the cooled mixture was poured into ice-water and left overnight. The crystalline product formed was collected and recrystallized from ethanol to give 4″,5″-dihydro-2-methylfuro[2″, 3″: 7,8]isoflavone (4a).

Similarly, 4″,5″-dihydro-2′-methoxy-2-methylfuro-[2″,3″:7,8]isoflavone (4b) and 4″,5″-dihydro-2-methyl-2′,4′,5′-trimethoxyfuro[2″,3″: 7,8]isoflavone (4c) were also obtained by this method.

b) By the Hydrogenation of Furoisoflavones (9). A mixture of 2-methylfuroisoflavone 9a (0.5 g), palladium carbon (25%, 0.5 g) and ethyl acetate (30 m*l*) was shaken with hydrogen and was treated similarly as described for the ketone 8a to give the dihydrofuroisoflavone 4a.

Similarly, 4b was also obtained by this method through purification by chromatography with alumina and ethyl acetate as a solvent.

c) By the Action of Ethyl Formate and Sodium on the Ketones (3) through Dihydrofuroisoflavanone (5). Small pieces of metallic sodium (0.7 g) were added to cooled (−10°C) ethyl formate (10 m*l*), and to this suspension was added a solution of 3a (0.6 g) in ethyl formate (10 m*l*) with stirring and cooling at 0—2°C over a period of 40 min, then the mixture was stirred for 3 hr at room temperature and left overnight. Methanol was added to destroy the excess sodium, ice-water was added and the excess ethyl formate was removed under diminished pressure. The residual solution was acidified and extracted with ether, and the product obtained from the ethereal solution was crystallized from ethyl acetate to give 4″,5″-dihydro-2-hydroxyfuro[2″,3″:7,8]isoflavanone (5a). The shape of UV spectrum is quite different from that of isoflavones.

Similarly, 4″,5″-dihydro-2-hydroxy-2′,4′,5′-trimethoxyfuro[2″,3″:7,8]isoflavanone (5c) was also obtained by this method from the ketone 3c. In the case of the ketone 3b, the crude product obtained seemed from its spectrum to be a mixture of the hydroxyisoflavanone and isoflavone, therefore, it was purified by chromatography with alumina and ethyl acetate as a solvent to give the pure 4″,5″-dihydro-2′-methoxyfuro[2″,3″:7,8]-isoflavone (6b), but the corresponding hydroxyisoflavanone (5b) was not obtained in a pure form.

To convert the hydroxyisoflavanone (5a) to the isoflavone, 0.5 g of it was heated with acetic acid (30 m*l*) on a water-bath for 1 hr. The cooled mixture was diluted with water and the crystalline product formed was collected and recrystallized from ethanol to give 4″,5″-dihydrofuro[2″,3″:7,8]isoflavone (6a). The hydroxyisoflavanone 5c was not dehydrated by this procedure.

The Preparation of Benzofuranyl Ketones. *4-Hydroxy-5-benzofuranyl 2-Methoxybenzyl Ketone (8b).* A mixture of furoisoflavone 9b (1.7 g), aqueous potassium hydroxide (50%, 8 g) and ethanol (100 m*l*) was refluxed for 4 hr, then most of the ethanol was distilled off. The residual solution was diluted with water and acidified to give the crystalline product. Recrystallization from ethanol furnished 8b, 1.2 g (77%).

5-Acetyl-4-hydroxybenzofuran-2-carboxylic Acid (14). A mixture of 2,4-dihydroxy-3-formylphenyl methyl ketone[16] (12) (27 g), ethyl bromomalonate (28 m*l*), anhydrous potassium carbonate (80 g) and methyl ethyl ketone (1.2 *l*) was refluxed for 8 hr. The cooled mixture was filtered and the solvent was distilled off and then the residual product was crystallized from dilute acetone to give crude ethyl 5-acetyl-4-hydroxy-benzofuran-2-carboxylate (13), mp 134.5—136°C, ν_{max} cm^{-1}: 1710, 1625 (CO). This ester 13 was heated with aqueous potassium hydroxide (10%, 150 m*l*) on a water-bath for 1 hr. The cooled solution was filtered and acidified to give the crystalline acid. Recrystallization from dilute ethanol gave pure 14, 11.5 g (37% from 12).

4-Hydroxy-5-benzofuranyl Methyl Ketone (15). A mixture of the acid 14 (13.5 g), copper powder (13.5 g) and quinoline (380 m*l*) was refluxed gently for 1 hr under a stream of nitrogen. The cooled mixture was filtered and acidified with dilute hydrochloric acid and then extracted with ether. The ethereal solution was washed with aqueous sodium bicarbonate and then extracted with aqueous sodium hydroxide. The product obtained by acidifying the alkaline solution was crystallized from petroleum benzine to give the ketone 15, mp 84—85°C (lit[15] mp 86—87°C), yield 5.6 g (47%), ν_{max} cm^{-1}: 1630 (CO). (Found: C, 68.44; H, 4.27%).

The Preparation of Dihydrofuro- and Furocoumarins (Table 2). *a) By the Action of Ethyl Chlorocarbonate and Potassium Carbonate on the Ketones (3).* A mixture of the ketone 3a (0.3 g), ethyl chlorocarbonate (0.9 g), anhydrous potassium carbonate (2.5 g) and acetone (30 m*l*) was refluxed for 4 hr. The cooled mixture was diluted with water and acidified. The precipitates formed were collected and heated with aqueous sodium hydroxide (1 N, 50 m*l*) for 1 hr on a water-bath. The resulting solution was diluted with water and acidified to give the crystalline product. Recrystallization from ethanol gave 4′,5′-dihydro-4-hydroxy-3-phenylfuro [2′,3′,: 7,8]coumarin (7a).

Similarly,4′,5′-dihydro-4-hydroxy-3-(2,4,5-trimethoxyphenyl)furo[2′,3′:7,8]coumarin (7c) was also obtained by this procedure.

b) By the Action of Ethyl Carbonate and Sodium on the Ketones (8 and 15). Small pieces of metallic sodium (1.1 g) were added to a solution of the ketone 8a (0.9 g) in ethyl carbonate (25 m*l*), and the mixture was heated gradually to 100°C. The mixture was heated at that temperature for 1 hr, then methanol was added to the cooled mixture to destroy the excess sodium. The resulting mixture was diluted with water, washed with ether and then was acidified to give the crystalline product. Recrystallization from ethanol gave 4-hydroxy-3-phenylfuro[2′,3′: 7,8]coumarin (10).

Similarly, 4-hydroxy-3-(2-methoxyphenyl)furo[2′,3′: 7,8]coumarin (11) was also prepared by this procedure.

In the case of the ketone 15, the crude product was recrystallized from methanol or ethanol to give 4-hydroxyfuro[2′,3′: 7,8]coumarin (16), mp 268—269°C, having one molecule of water of crystallization. The water of crystallization was removed by drying over phosphorus

pentoxide at 120—130°C in vacuum. From the mother solution of crystallization, a small amount of ethyl 4-hydroxyfuro[2′,3′:7,8]coumarin-3-carboxylate (17) was obtained.

The Preparation of 5*H*-Benzofuro[3,2-*c*]furo-[2,3-*h*][1]benzopyran-5-one (18). *a) By the Action of Pyridine Hydrochloride on 11.* A mixture of 11 (0.35 g) and anhydrous pyridine hydrochloride (2 g) was refluxed gently for 40 min. The cooled mixture was acidified with dilute hydrochloric acid, and the crystalline product formed was collected and recrystallized from ethyl acetate and then from ethanol. Yield 0.08 g.

b) By the Action of Hydroiodic Acid on 11. The furocoumarin 11 (0.4 g) was added to a mixture of hydroiodic acid (10 m*l*), acetic acid (5 m*l*) and acetic anhydride (4 m*l*), and the mixture was refluxed gently under a stream of nitrogen for about 15 min. The cooled mixture was poured into ice-water (100 m*l*) containing a small amount of sodium bisulfite. The crystalline product formed was collected and recrystallized from ethanol then from acetone to give a small amount of 18.

c) By the Action of Aluminum Chloride on 11 through 4-Hydroxy-3-(2-hydroxyphenyl)furo[2′,3′:7,8]coumarin (19). Powdered anhydrous aluminum chloride (0.9 g) was added to a solution of the furocumarin 11 (0.6 g) in nitrobenzene (50 m*l*), and the mixture was heated on a water-bath for 1 hr. The cooled mixture was poured into ice-water containing a small amount of hydrochloric acid, the nitrobenzene was removed by steam-distillation, and the residual mixture was extracted with ethyl acetate. The ethyl acetate solution was extracted with 5% aqueous sodium hydroxide. The product obtained by acidifying the alkaline solution was crystallized from ethanol to give 19, 0.3 g.

A mixture of this furocoumarin 19 (25 mg) and methanol (100 m*l*) saturated with hydrogen chloride was refluxed for 7 hr, then the methanol was distilled off and the residue was diluted with water. The crystalline product formed was collected and recrystallized to give 18, 12 mg.

The authors are grateful to Messrs. N. Takamatsu, M. Kuramoto, M. Uchida, S. Yamaguchi, T. Kishi, N. Shimizu and F. Miyoshi for their assistance and to the Members of the Laboratory of Analysis, Faculty of Pharmacology of this University for microanalyses. The authors' thanks are also due to the Ministry of Education for its grant-in-aid.

BULLETIN OF THE CHEMICAL SOCIETY OF JAPAN VOL. 41 1208—1220 (1968)

Acid-Catalyzed Isomerization of 1,3,4,5-Tetra-*O*-acetyl-2-deoxy-L-sorbopyranos-2,3-ene[1]

Mitsuru KATSUHARA, Shigeru WAKAHARA and Kanji TOKUYAMA

Shionogi Research Laboratory, Shionogi & Co., Ltd., Fukushima-ku, Osaka

(Received November 18, 1967)

An acid-catalyzed reaction in acetic anhydride was found to isomerize 1,3,4,5-tetra-*O*-acetyl-2-deoxyl-L-sorbopyranos-2,3-ene (V) to four new unsaturated compounds. When the reaction was allowed to continue for a longer period, they underwent polymerization, but did not afford 2-hydroxyacetylfuran acetate (XXVIb). The reaction in acetic acid containing water was shown to mainly convert V into XXVIb. This reaction pathway was thought to be different from the above.

Dehydrochlorination of 1,3,4,5-tetra-*O*-acetyl-α-L-sorbopyranosyl chloride (IV),[2,3] derived from L-sorbose (I), through the agency of mercuric cyanide,[4,5] yields 1,3,4,5-tetra-*O*-acetyl-2-deoxy-L-sorbopyranos-2,3-ene (V). This communication is concerned with isomerizations of this unsaturated compound.

The isomerizations and other reactions of acylated aldo-1-enoses have recently received considerable attention.[6,7] The facile dissociation of the C_3-substituent in these compounds is readily understood as resulting from activation of the C_3-position toward carbonium ion formation by the allylic double bond.[8] The activation is especially strong for 1-enose structures since the ring oxygen can participate in charge

1) Sorboses. Part XI. For Part X, see T. Maeda, K. Tori, M. Ohtsuru and K. Tokuyama, This Bulletin, **41**, 191 (1968).
2) K. Tokuyama and M. Katsuhara, This Bulletin, **39**, 2728 (1966).
3) H. H. Schlubach and G. Graefe, *Ann.*, **532**, 211 (1937).
4) R. U. Lemieux and D. R. Linback, *Can. J. Chem.*, **43**, 94 (1965).
5) B. Coxon, *Tetrahedron*, **22**, 228 (1966).
6) B. Helferic, *Adv. Carbohydrate Chem.*, **7**, 209 (1952).
7) J. Stanék, M. Cerný, J. Kocourek and J. Pacâk, "The Monosaccharides," Academic Press Inc., New York (1963), p. 384.
8) H. S. Isbell, *J. Res. Natl. Bur. Stand.*, **A32**, 45 (1944).

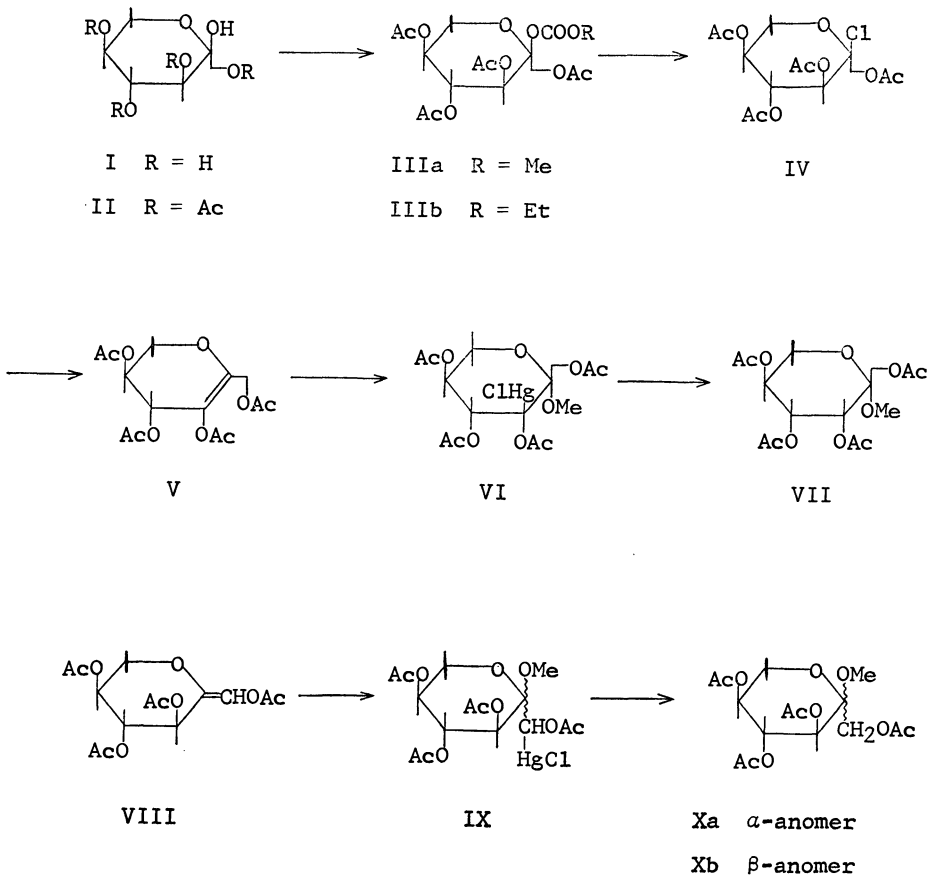

Chart 1.

delocalization.[9-13] It was anticipated that V would undergo similar isomerization, which pathway may provide interesting information regarding the acid-catalyzed degradation of ketohexose to 2-hydroxyacetylfuran (XXVIa)[14,15] through 2,3-enolization with the elimination of the hydroxyl group at the allylic C_4-position.[16,17]

The structure of V was confirmed by methoxymercuration[18] and NMR spectroscopy. NMR data obtained by 1st-order approximation are reported in Tables 1 and 2. The methoxymercuration of V gave a mercurichloride (VI). Reductive demercuration of VI with sodium borohydride in the presence of pyridine was accompanied by deacetylation, and yielded a methyl glycoside, which was isolated as a tetraacetate (VII).[19] Despite its large positive value of optical rotation, VII was not identical with methyl 1,3,4,5-tetra-*O*-acetyl-β-L-sorbopyranoside (Xb).[3] Thus, VII was concluded to be methyl 1,3,4,5-tetra-*O*-acetyl-β-L-tagatopyranoside.[20,21] The formation of the tagatopyranoside (VII) supports the structure of V, because another possible isomer VIII from the dehydrochlorination of IV should yield X *via* IX.

The NMR spectrum of V in chloroform-d (Fig. 1a) showed four singlets at about τ 7.9 due to acetoxyls, a somewhat broad singlet at τ5.39 due to H_1 (see also Fig. 1h) and signals due to H_6, $H_{6'}$, H_5, and H_4 as an ABXY pattern. This assignment

9) R. J. Ferrier and G. H. Sankey, *J. Chem. Soc.* (*C*), **1966**, 2339, 2345.
10) R. J. Ferrier, *ibid.*, **1964**, 5443.
11) D. M. Cement and R. J. Ferrier, *ibid.*, **1966**, 2830.
12) R. U. Lemieux, D. R. Linback, M. L. Wolfrom, F. B. Moody, E. G. Wallace and F. Komitsky, Jr., *J. Org. Chem.*, **30**, 1092 (1965).
13) R. K. Ness and H. G. Fletcher, Jr., *ibid.*, **28**, 435 (1963).
14) C. J. Moye, *Australian J. Chem.*, **19**, 2317 (1966)
15) R. E. Miller and S. M. Cantor, *J. Am. Chem. Soc.*, **74**, 5236 (1956).
16) E. F. L. J. Anet, *Chem. & Ind.*, **1962**, 262.
17) E. F. L. J. Anet, *Adv. Carbohydrate Chem.*, **19**, 181 (1964).
18) K. Tokuyama, E. Tsujino and M. Kiyokawa, This Bulletin, **38**, 1344 (1965).
19) G. R. Inglis, J. C. P. S. Schwartz and L. McLaren, *J. Chem. Soc.*, **1962**, 1014.
20) The evidence of NMR indicates that the favorable conformation of VII in chloroform-d is the Cl chair form. See Ref. 21.
21) C. V. Holland, D. Horton and J. S. Jewell, *J. Org. Chem.*, **32**, 1818 (1967).

TABLE 1. CHEMICAL SHIFTS (τ)[a]

Compound	H_6	$H_{6'}$	H_5	H_4	H_3	H_1 and $H_{1'}$	CH_3COO	Other signal
IIIa	6.00	6.29	4.88	4.46	4.73	5.32, 5.43	7.93, 7.96(2) 8.00	$COOCH_3$ 6.19
IIIb	5.93	6.38	4.90	4.46	4.74	5.32, 5.45	7.93, 7.96(2) 8.00	$COOCH_2CH_3$ 5.70 $COOCH_2CH_3$ 8.66
IV	5.88	6.08	4.92	4.44	4.72	5.57, 5.77		
V	5.72	5.97	5.04	4.61	—	5.39	7.89, 7.91 7.95(2)	
VI	5.92	6.22	5.08	4.41	—	5.46, 6.16	7.77, 7.80 7.92(2)	OCH_3 6.59
VII	5.89	6.23	5.09	4.70	4.59	5.76, 5.82	7.87, 7.92 7.91, 7.94	OCH_3 6.65
XII[b]	6.00	6.24	4.85	4.17	—	2.67[c]	8.27, 8.31 8.33	
XIV	5.67	5.95	5.04	4.55	—	2.55[c]	7.86, 7.90(2) 7.91, 7.94	
XV	5.23	5.38	2.88	3.70	—	2.92[c]	7.88, 7.93 7.95	
XX[b]	~5.51 ~6.14		2.94 3.92	3.89 4.12	— —	5.56 5.39	7.94 8.32	OCH_3 6.58 OCH_3 6.94
XXI	6.07	6.56	4.78	5.50	4.52	5.90	7.86, 7.91 7.95	OCH_3 6.71
XXII	5.80	6.23	4.83	5.58	4.65	5.79	7.85(2) 7.88	OCH_3 6.63
XXIV	5.61	5.94	4.96	4.79	4.06	0.74[c,d]	7.91, 7.94	

a) In chloroform-d (unless otherwise stated). b) In benzene-d_6. c) One proton.
d) Aldehyde proton.

TABLE 2. COUPLING CONSTANTS (cps)[a]

Compound	$J_{6,6'}$	$J_{5,6}$	$J_{5,6'}$	$J_{4,6}$	$J_{4,6'}$	$J_{4,5}$	$J_{3,5}$	$J_{3,4}$	$J_{1,4}$	$J_{1,1'}$
IIIa	11.2	5.8	11.2	—	—	9.7	1.5	8.4	—	11.8
IIIb[c]	10.4	5.7	10.4	—	—	10.1	1.0	8.3	—	11.5
IV	10.6	5.3	10.6	—	—	9.0	1.0	9.0	—	12.3
V	12.3	2.4	1.5	1.3	—	2.7	—	—	0.5	0
VI	13.2	2.4	1.3	—	1.3	3.7	—	—	—	12.0
VII	13.1	2.1	1.3	—	1.3	3.8	—	3.8	—	11.8
XII[b]	12.1	2.2	2.8	0.7	—	6.2	—	—	0.7	—
XIV	12.5	2.7	1.8	1.5	—	2.7	—	—	—	—
XV	18.4	2.4	3.6	2.4	1.8	11.0	—	—	—	—
XX	d)	2.4	3.4	2.0	2.0	10.5	—	—	—	d)
XXI	10.3	5.7	10.3	—	—	10.8	—	3.1	—	d)
XXII	13.2	3.0	1.6	—	1.6	3.0	—	4.4	—	d)
XXIV	12.4	3.0	2.0	1.7	—	3.0	1.4	5.0	—	—

a) In chloroform-d unless otherwise stated. b) In benzene-d_6. c) $COOCH_2CH_3$: $J_{CH_2,\ CH_3}$=7.0.
d) Obscured.

was confirmed by decoupling experiments (Fig. 1b—1g). Double irradiation at the center of resonance frequencies of H_6 and $H_{6'}$ (Fig. 1b) changed the 8-line multiplet of H_5 into a doublet ($J_{4,5}$ 2.7 cps) and the 8-line multiplet of H_4 into a somewhat broad doublet. By double irradiation on $H_{6'}$, the H_5 signal collapsed to a doublet-doublet ($J_{5,6}$ 2.4 cps), but no changes in the H_4 signal were observed (Fig. 1c). By double irradiation on H_6, the H_5 signal collapsed to a doublet-doublet and the H_4 signal to a somewhat broad doublet (Fig. 1d). Conversely, decouplings of H_4 (Fig. 1f) and H_5 (Fig. 1g) resulted in changes of the signals of H_5 and H_6 ($J_{5,6'}$ 1.5 cps) and of those of H_4, H_6 and $H_{6'}$ ($J_{6,6'}$ 12.3 cps and $J_{4,6}$ 1.3 cps), respectively. Decoupling of H_1 (Fig. 1e) made the broad signal

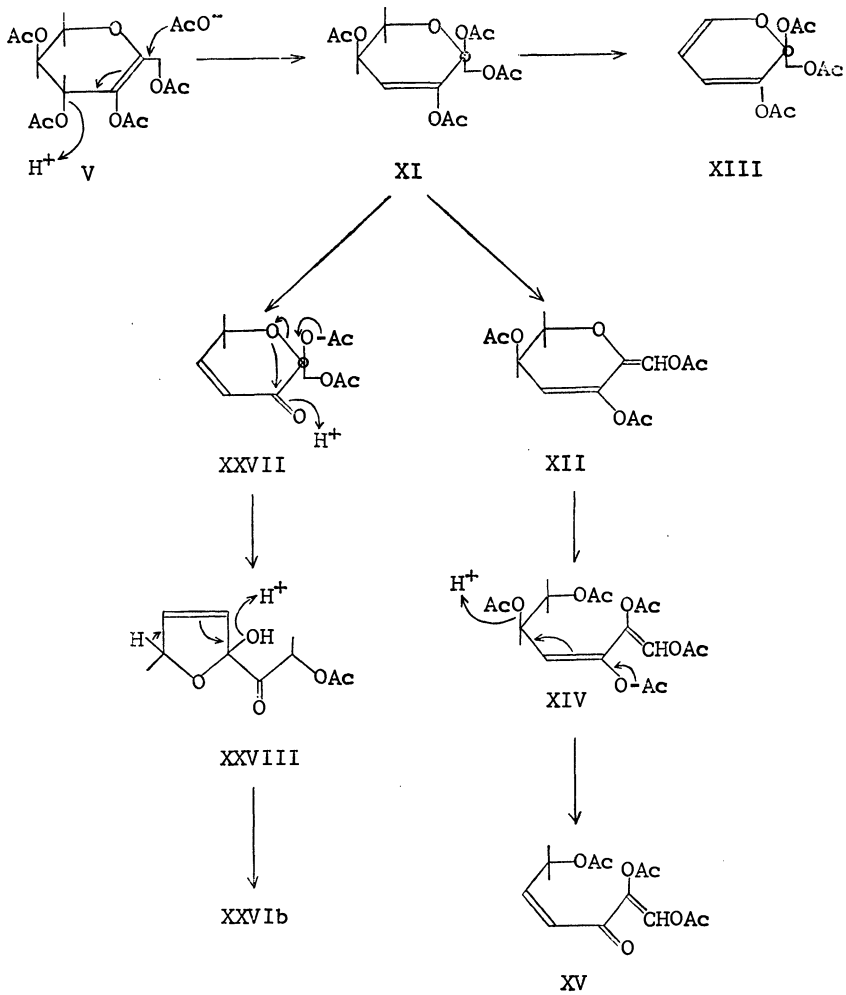

Chart 2.

of H_4 relatively sharper, showing the presence of homoallylic coupling between C_4 and C_1 protons. These observations provided evidence for the structure of V. Applying the Karplus correlation[22] for the coupling constants obtained and the "W-letter" rule[23] for the long-range spin coupling between H_4 and H_6, we reached the conclusion that V should exist in H_1 conformation.[24]

It was found that the treatment of V in acetic anhydride containing *p*-toluenesulfonic acid (TsOH) resulted in rapid formation of a mixture of at least four products (A, B, C, and D) in the thin-layer chromatograms. When the reaction was interrupted at the initial stages, the product A was mainly isolated. On the other hand, when the reaction was allowed to proceed for 48 hr, products B and C were detected as major products. These products could be resolved by preparative thin-layer chromatography using several solvent systems. The structures established for the new compounds described above were confirmed by the application of NMR spectroscopy with the use of spin decoupling to assign the origins of the signals. The assignment was also based on the chemical shifts with reference to those of V.

As it is expected that the reaction of V under acidic conditions undergoes allylic displacement of the C_4-ester grouping and the formation of a 3,4-unsaturated compound (XI),[8-13] the structure of compound A was thought to be XI or its derivative. The analytical data and the integration of an NMR spectrum determined it as a triacetate $C_{12}H_{14}O_7$, which was thought to be derived from XI by the elimination of one mole of acetic acid. The elimination may occur at the 1,2- or 5,6-position. Thus, the

22) M. Karplus, *J. Chem. Phys.*, **30**, 11(1959); *J. Am. Chem. Soc.*, **85**, 2870 (1963).
23) N. S. Bhacca and D. H. Williams, "Application of NMR Spectroscopy in Organic Chemistry," Holden-Day Inc., San Francisco (1964), p. 115.
24) R. J. Ferrier and W. G. Overend, *Quart. Rev.*, **13**, 265 (1959).

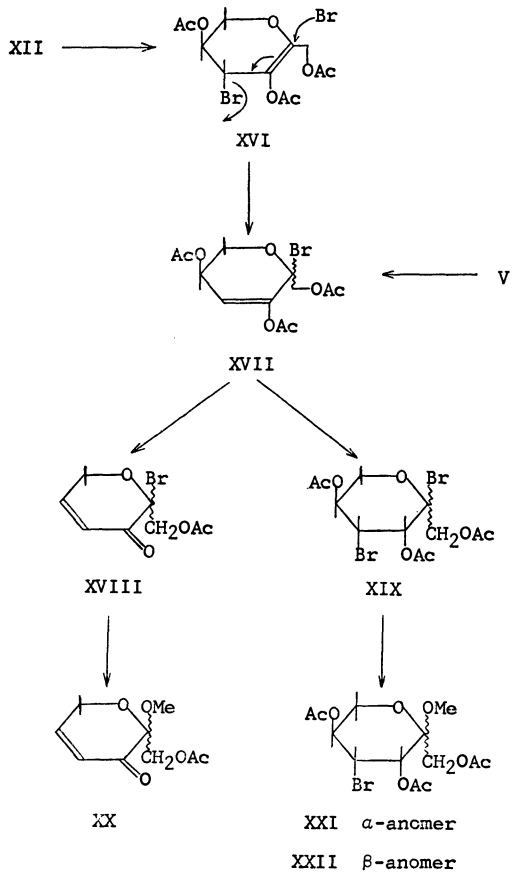

Chart 3.

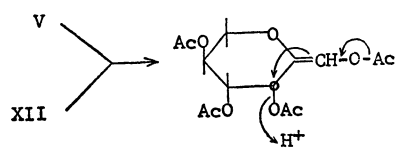

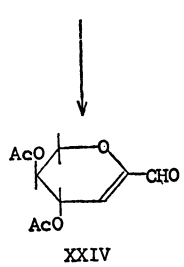

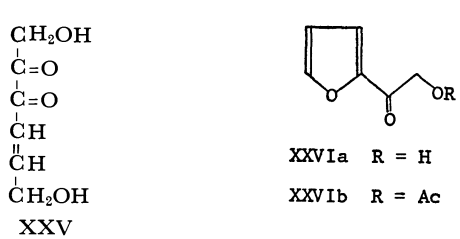

Chart 4.

structure is proposed to be XII or XIII. The UV and IR spectra showed the characteristic bands due to a conjugated diene and the NMR spectrum (Fig. 2) revealed the presence of C_6-methylene protons and an olefinic C_1-proton. The results clearly support the structure of XII. Figure 2a shows the assignment of the NMR spectrum in benzene-d_6. The rough, 1-proton singlet at τ2.67 should arise from the olefinic H_1. Its lower chemical shift is understandable in view of acetoxy substituent on the ethylenic group. The signals of the other protons (H_6, $H_{6'}$, H_5 and H_4) appear as the pattern of ABXY system, an AB quartet at τ6.00 (H_6) and 6.24 ($H_{6'}$), an 8-line multiplet (X part) at τ4.85 (H_5) and a 6-line multiplet (Y part) at τ4.17 (H_4). On double irradiation at the C_6-methylene position, the H_5 multiplet collapsed to a sharp doublet ($J_{4,5}$ 6.2 cps) and the H_4 multiplet to a doublet-doublet (Fig. 2b), showing the presence of long-range coupling between H_1 and H_4 ($J_{1,4}$ 0.7 cps). Double irradiation at the H_6 position caused the H_4 multiplet to collapse to a doublet-doublet (Fig. 2c), but double irradiation at the $H_{6'}$ position did not cause any changes of the H_4 signal (Fig. 2d). These decoupling experiments confirmed the above-described assignment (Fig. 2a), which is consistent with structure **XII.**

The reaction of XII with hydrogen bromide in benzene followed by glycosidation with methanol gave three pyranosides XX, XXI and XXII as major products. XX gave analytical data corresponding to methyl glycoside monoacetate, $C_9H_{12}O_5$, and its IR and UV spectra revealed bands due to an α,β-unsaturated ketone. The NMR spectrum in chloroform-d (Fig. 3) showed two singlets at τ7.94 due to one acetyl methyl and at τ6.58 due to one methoxy methyl, 2-proton singlet at τ5.56 due to C_1-protons and an AB type quartet of ABXY system due to C_6-protons at about τ5.5. The above-described data established the structure XX. The remaining two 1-proton multiplets at τ2.94 and 3.89 due to olefinic protons were assignable to H_5 and H_4, which are coupled to each other (J 10.5 cps), and the latter showed allylic coupling with C_6-methylene protons. These observations provided further proof for the structure XX. Evidence bearing on the anomeric configuration of XX was not obtained.

Analytical data and optical rotation showed that XXI was a methyl bromo-tri-*O*-acetyl-α-L-glycoside, $C_{13}H_{19}O_8Br$. The NMR spectrum showed a 2-proton singlet at τ5.90 due to C_1-protons, an AB type quartet of ABX system at τ6.07 (H_6) and 6.56 ($H_{6'}$) due to C_6-protons, an 8-line multiplet at τ4.78 due to H_5, a doublet-doublet at τ5.50 due to H_4 and a doublet at τ4.52 due to H_3. The relatively lower chemical shifts of H_3 and H_5 than H_4 determined the position of the bromine to be at the C_4-position. The coupling constants ($J_{3,4}$ 3.1 cps and $J_{4,5}$ 10.8 cps) suggest that the relationship of H_3 and H_4 should be *cis* (equatorial-axial) and that of H_4 and H_5 be trans

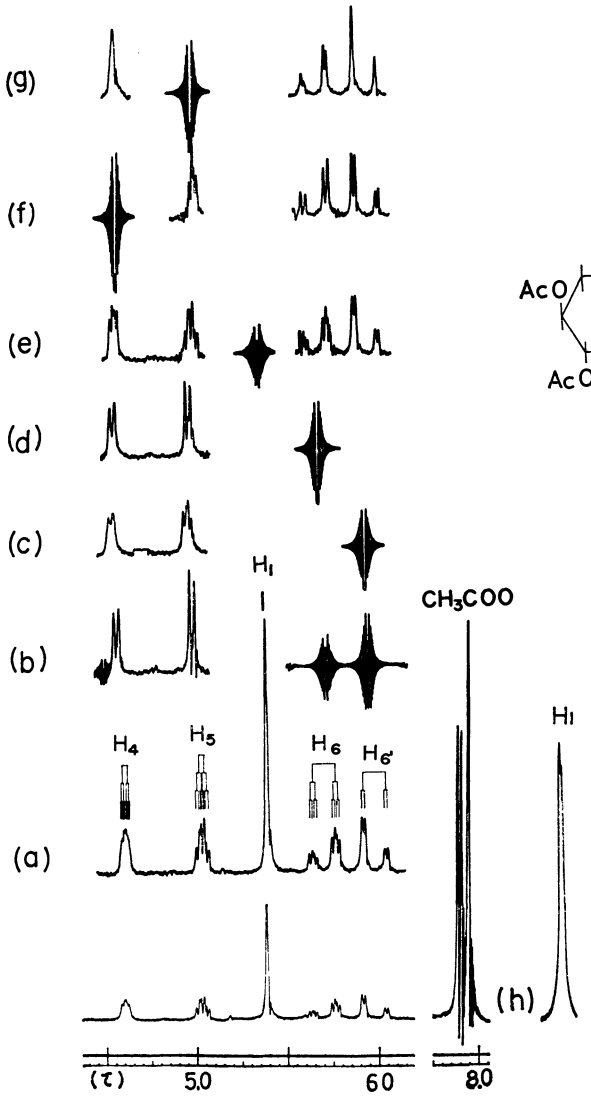

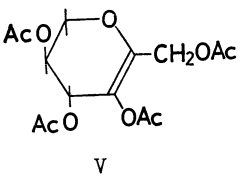

V

Fig. 1. NMR spectra of V in chloroform-d at 100 Mc.

(axial-axial).[25] Therefore, the structure of XXI was clearly determined as methyl 1,3,5-tri-*O*-acetyl-4-bromo-4-deoxy-α-L-tagatopyranoside.[26,27]

Treatment of XXII with hydrogen chloride in benzene followed by glycosidation with methanol gave XXI. Thus, it was determined to be the β-anomer of XXI.

The reaction process of the formation of these pyranosides is considered as shown in Chart 3. The 1,4-addition of hydrogen bromide to XII afforded XVI, which was then converted into XVII by an allylic displacement reaction with hydrogen bromide. Two reaction pathways can exist for the further reaction of XVII. The first is the addition of hydrogen bromide to the 3,4-double bond yielding XIX which is transformed to glycosides XXI and XXII. The preferable formation of tagatopyranosides is thought to be caused by the anchimeric effect of the acetoxy group at the C_5-position.[28,29] The second is the formation of XVIII, which may be formulated

25) R. H. Bible, " Interpretation of NMR Spectra," Plenum Press, New York (1965), p. 35.

26) The evidence of NMR indicates that the favored conformation of XXI is the 1C chair form. See, Ref. 27.

27) F. W. Lichtenthaler and H. K. Yahya, *Tetrahedron Letters*, **1965**, 1805.

28) Formation of 4,5-acetonium ion[29] may be thought on the protonation of XVII. In this ion form, the C_3-acetoxy group might be expected to predominantly be trans to 4,5-acetonium group.

29) H. Paulsen, W. P. Trautwein, F. G. Espinosa and K. Heynes, *Tetrahedron Letters*, **1966**, 4131.

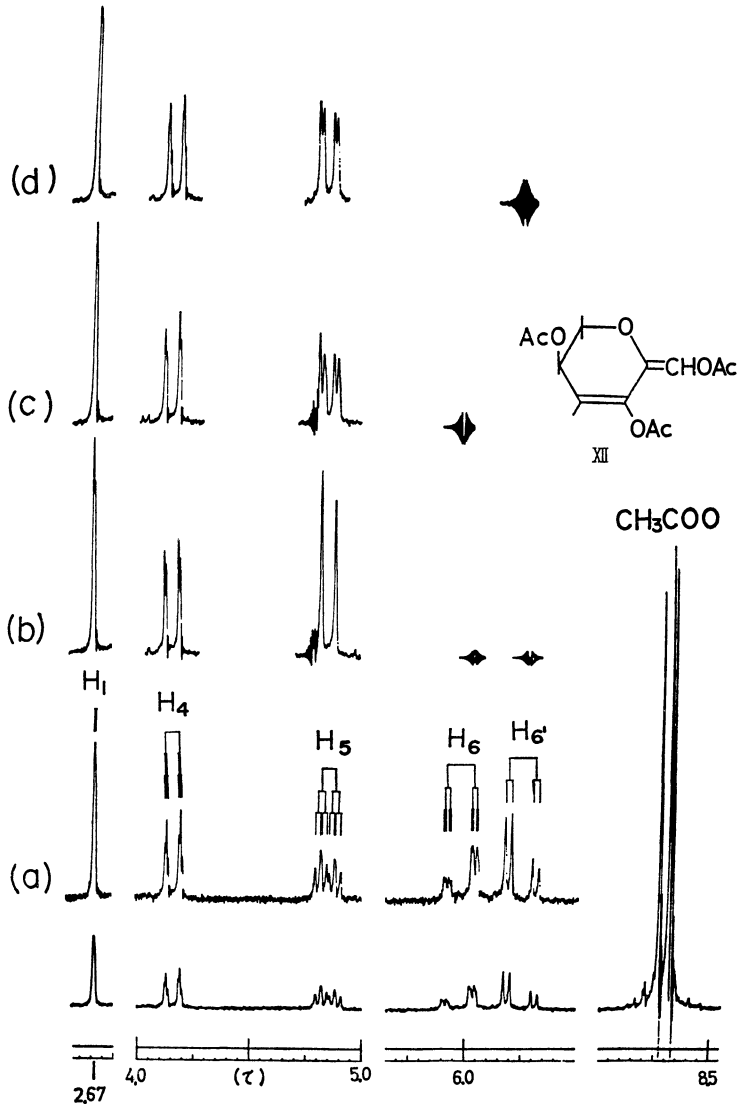

Fig. 2. NMR spectra of XII in benzene-d_6 at 100Mc.

as an elimination of the acetoxy group of the C_5-position to form an allylic cation, followed by loss of a C_3-acetyl cation. XVIII is converted into XX by methanolysis.

The same results were obtained in the treatment of V under the same reaction conditions, in which the formation of XVII is very probable. Therefore, the above pathway and, consequently, the structure XII were confirmed.

The compound B had the correct analysis for XII plus one mole of acetic anhydride and had a conjugate diene absorption in the infrared. It was also derived from the acid treatment of XII in acetic anhydride. Therefore, its structure should be XIV, which is the ring-open form of XII. The fact that the NMR data in chloroform-d are quite similar to those of XII supported this structure. The spectrum (Fig. 4a) contained singlets at about τ7.9 due to five acetoxyls, a noisy singlet at τ2.55 due to olefinic H_1, an AB type quartet of ABXY system at τ5.67 (H_6) and 5.95 ($H_{6'}$) due to C_6-protons, a 6-line multiplet at τ5.04 due to H_5 (X part) and a doublet-doublet at τ4.55 due to H_4 (Y part). Double irradiation at the H_4 position (Fig. 4b) caused the collapse of the H_5 and H_6 signals to doublet-doublets ($J_{5,6'}$ 1.8 and $J_{5,6}$ 2.7 cps), while double irradiation at the H_5 position caused the collapse of the H_4, H_6 and $H_{6'}$ signals to a somewhat broad doublet, a doublet-doublet ($J_{4,6}$ 1.5 cps) and a doublet ($J_{6,6'}$ 12.5 cps), respectively (Fig. 4c). The somewhat broad signals of H_4 and H_1 imply the presence of weak long-range spin coupling between them. Thus, the structure XIV was established.

The combined data of chemical analysis, the UV

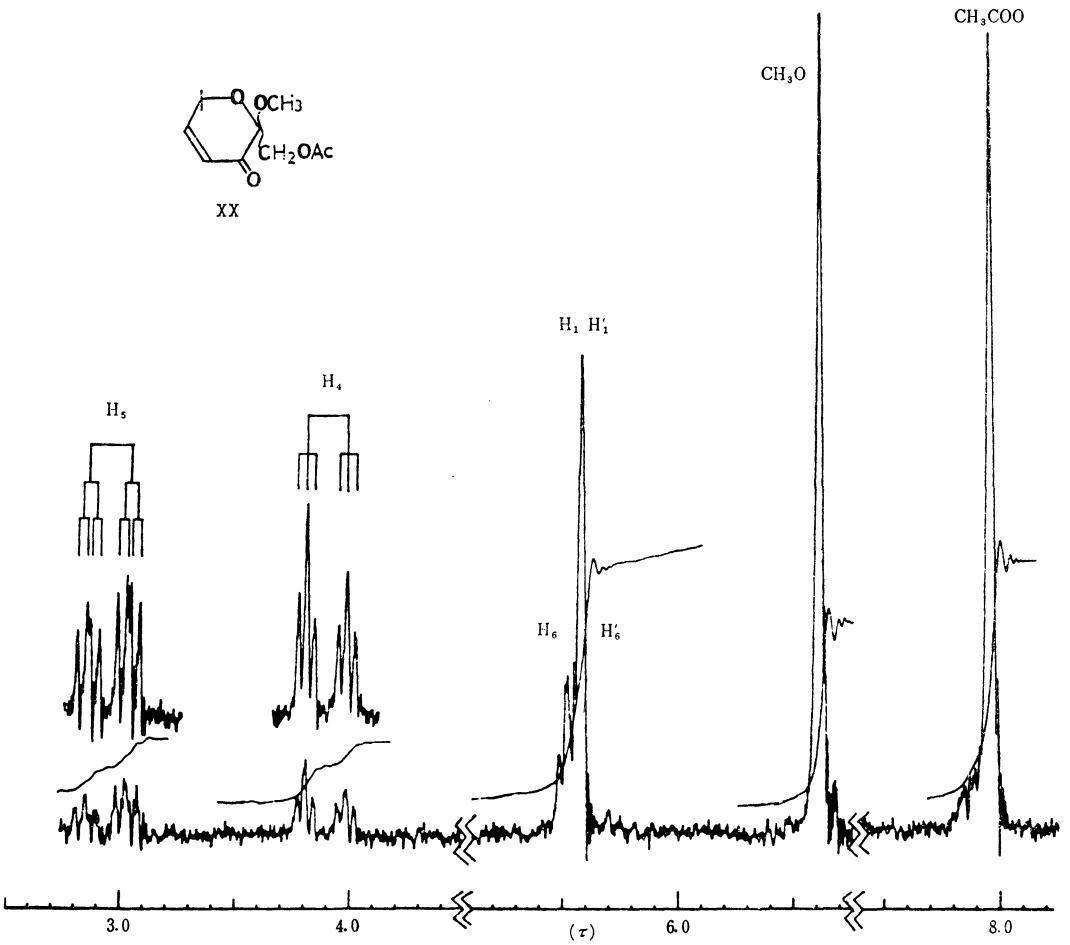

Fig. 3. NMR spectrum of XX in chloroform-d at 60Mc.

and IR spectra established that compound C was a conjugate ketone compound with an elementary composition corresponding to that of XIV minus one mole of acetic anhydride. It was also derived from the acid-treatment of XIV. As elimination of the acetoxy group at allylic C_5-position and an acetyl group at the C_6-position of XIV are reasonably expected,[30,31] its structure was concluded to be XV. In chloroform-d, XV displayed a well-resolved spectrum (Fig. 5) with three acetoxyl singlets at about τ7.9, a singlet at τ2.92 due to H_1 and an ABXY pattern of a 8-line multiplet at τ3.70 (Y part), an 8-line multiplet at τ2.88 (X part) and an AB quartet at τ5.23 and 5.38 due respective to olefinic H_4 and H_5, which are coupled to each other, and to methylene H_6 and $H_{6'}$. The double irradiation at the center of resonance of H_5 (Fig. 5b) changed the signals of H_4, H_6 and $H_{6'}$ into doublet-doublet. On double irradiation on C_6 protons (Fig. 5c), the signals of H_4 and H_5 collapsed into doublets ($J_{4,5}$ 11.0 cps), showing the presence of allylic coupling between C_4 and C_6 protons. These irradiation experiments supported the structure XV.

The formation of the compound D was also observed at the initial stage of the reaction of V as a minor product. The analytical data corresponded to a diacetate, $C_{10}H_{12}O_6$, showing IR bands due to an α,β-unsaturated aldehyde. Thus, this was tentatively assigned to XXIV. The NMR spectrum (Fig. 6a) showed unequivocally the presence of an aldehyde at τ0.74. An AB quartet due to C_6-methylene at τ5.61 and 5.94, multiplet at τ4.96 due to H_5 and at τ4.79 due to H_4 and a doublet-doublet at τ4.06 due to H_3 are also easily analyzed as an ABXY pattern. The chemical shifts show that H_3 should be an olefinic proton and acetoxy groups should be at the C_4- and C_5-positions. Therefore, the structure of compound D was determined to be XXIV. Double irradiation at H_3 (Fig. 6b), giving a pattern similar to that of V (Fig. 1), also supported the structure.

30) E. F. L. J. Anet, *Chem. & Ind.*, **1963**, 1035.
31) E. F. L. J. Anet, see Ref. 14, p. 195.

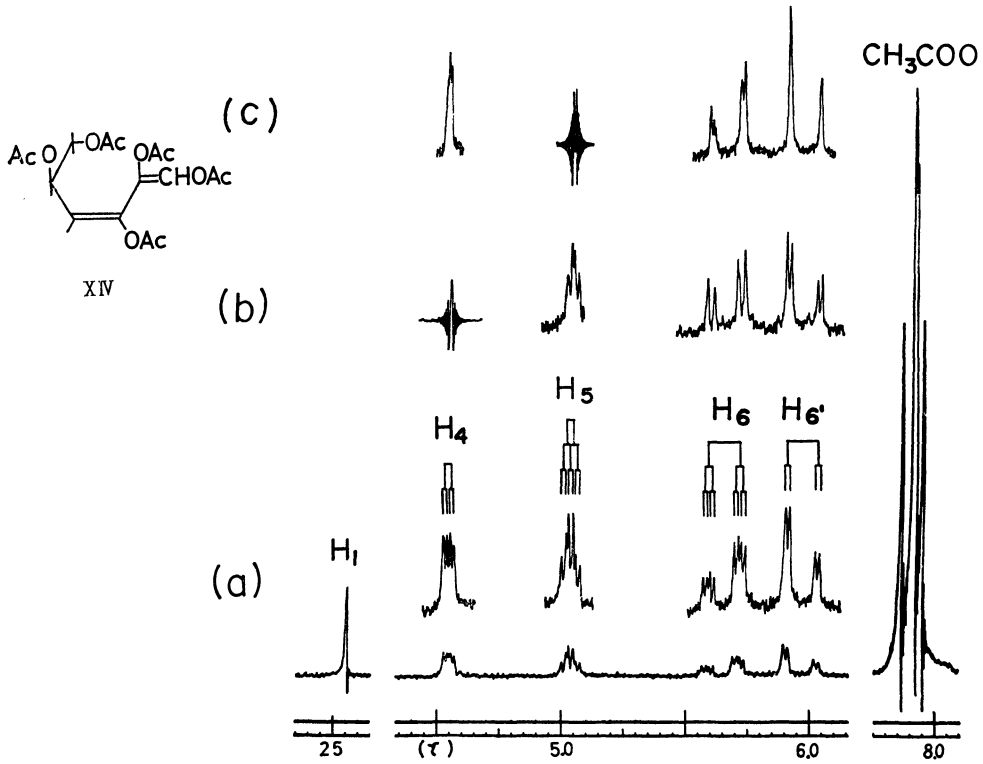

Fig. 4. NMR spectra of XIV in chloroform-d at 100Mc.

Thin-layer chromatographic studies on the above-described degradation of V in acetic anhydride showed that the initial products were primarily XII and a minor amount of XXIV. When the reaction was allowed to continue for longer periods of time, the amounts of XIV and XV increased at the expense of XII. Under similar acidic conditions, the conversion of XIV into XV was also observed, however, the reverse reactions XV→XIV and XIV→XII were not observed. Consequently, the reaction process of the degradation of V is concluded to proceed *via* a pathway of V→(XI)→XII→XIV→XV as shown in Chart 2.[32] No isolation of XI must be caused by its instability.[33]

It is quite natural to consider that the precursor of XXIV should be a 1,2-ene derivative, VIII or its epimer XXIII. The elimination of a protonated C_3 acetoxy group of VIII or XXIII, followed by the loss of C_1 acetyl cation yielded XXIV. For the formation of VIII or XXIII, two possible pathways can be proposed. One is the 3,4 addition of acetic acid to XII and the other is the rearrangement of the 2,3-double bond of V into 1,2-position; however, the latter is favorable, since thin-layer chromatographic data elucidated no formation of XXIV by acid-treatment of XII in acetic anhydride or in acetic acid.

Anet's mechanism for the acid-catalyzed degradation of hexose to furans proposed that a key intermediate is an unsaturated osone such as XXV which may be converted into XXVIa. As the deacetylated form of XV is quite similar to XXV, it is expected that XV may also be converted into XXVI. However, the possibility of the above-described intermediates XII, XIV and XV being the precursor of furans is excluded, since heating them in an acetic anhydride medium only gave polymeric substances.

The treatment of V in acetic anhydride also did not afford furans even under stronger conditions, however, treatment in acetic acid yielded XXVIb. Since the UV absorption spectrum of XXVIb gave an absorption maximum at 272 mμ, it was felt that furan formation could be followed by observing the appearance of this peak. Solutions were made of V (1%) in acetic acid containing different concentrations of water and the absorbance of each solution at 272 mμ was recorded after heating at 95°C for 4.5 hr. The results, as shown in Fig. 7, revealed that the formation of XXVIb tended to increase with increasing addition of water. Although XII was detected at the initial stages of these reactions, it yielded

32) This pathway *via* XI was thought to be more favorable than a pathway of V→XII→XIV→XV, since the formation of XX (XVII) was observed in the reaction of V with hydrogen bromide.

33) It was supposed that the two large substituents, of the C_2 position, OAc and CH_2OAc, make the molecule unstable.

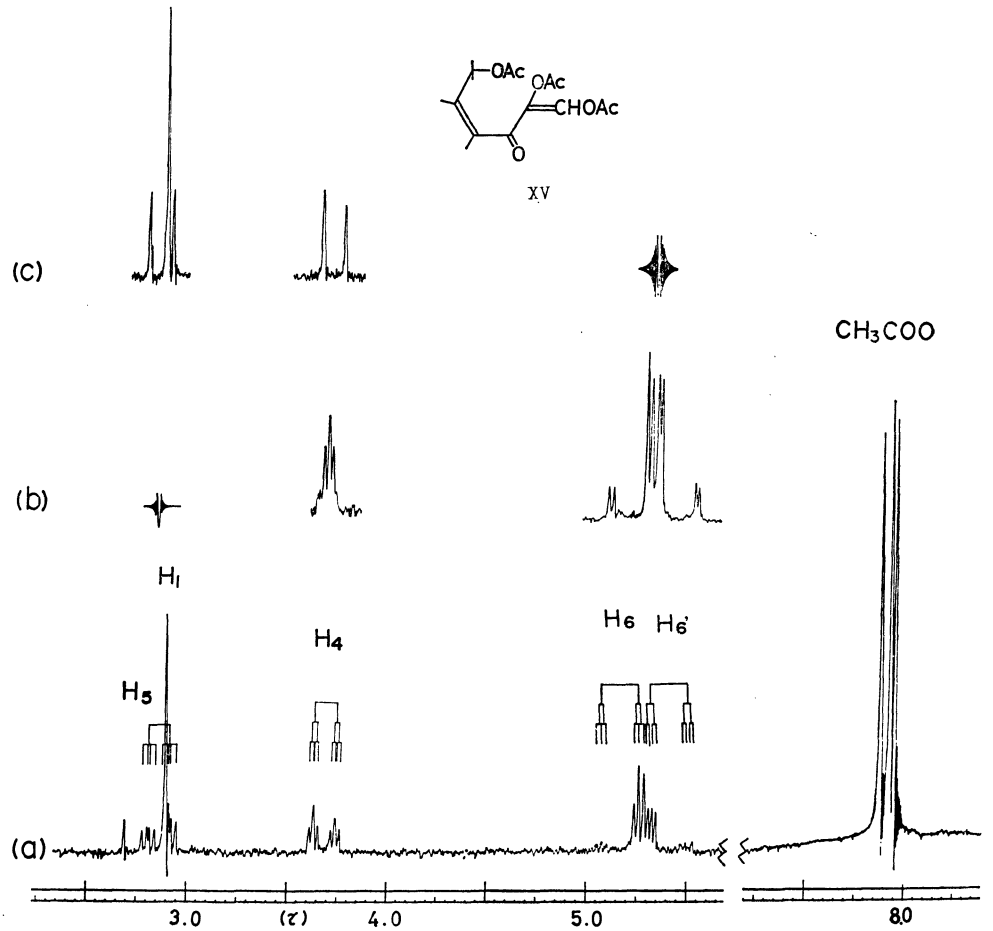

Fig. 5. NMR spectra of XV in chloroform-d at 100 Mc.

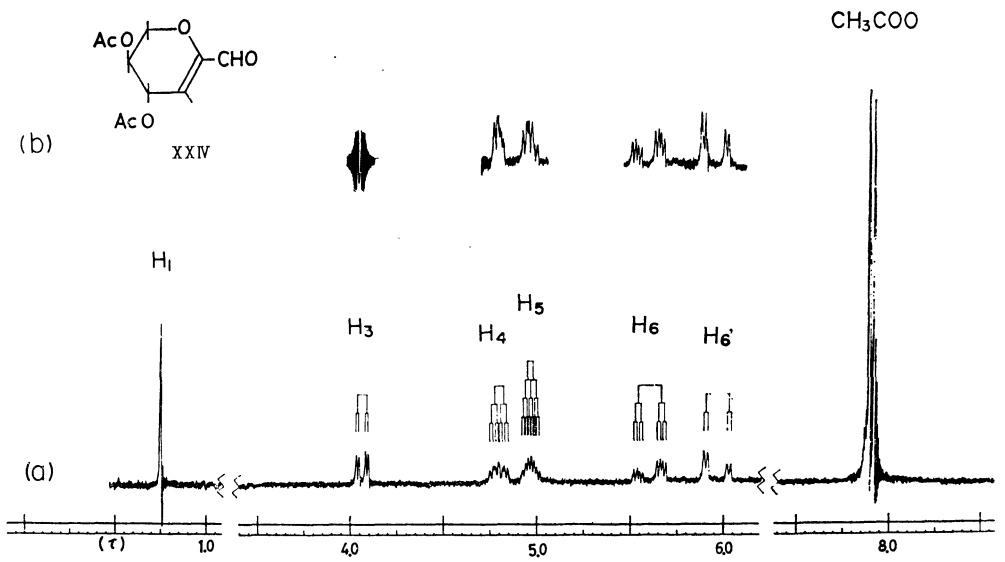

Fig. 6. NMR spectra of XXIV in chloroform-d at 100 Mc.

only traces of XXVIb under the same reaction conditions. Intermediates XIV and XV were hardly detected in the reaction mixtures and did not afford XXVIb in acetic acid-water. On the other hand, heating of another type of osone, XX, easily gave XXVIb. Therefore, the reaction process of the degradation of V to XXVIb is assumed to be as follows: V→XI→XXVII→XXVIII→XXVIb (see Chart 2). Attempts were made to isolate unknown osone XXVII from an acetic acid solution of V, but a complex mixture of products were isolated. By preparative thin-layer chromatography of the mixture, a compound showing IR and UV bands due to conjugate ketone and a quite similar pattern of NMR spectrum to XX was isolated, and was easily converted into XXVIb. Therefore, this thought to be XXVII, however, an adequate amount for determination of its correct structure was not obtained.[34-36]

It was somewhat surprising that the presence of water is very important for the degradation of V; it degradates to form polymeric substances under anhydrous conditions and to form furan XXVIb by aqueous treatment.

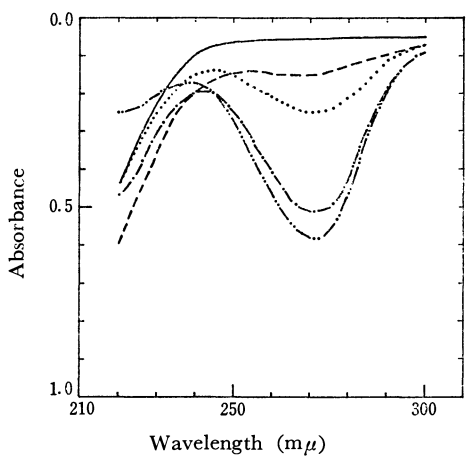

Fig. 7. The formation of XXVIb from V (at 95°C for 4.5hr).

a) acetic acid only (without V) ——
b) in acetic acid — — —
c) in acetic acid containing 10% of water - - - -
d) in acetic acid containing 50% of water —·—·
e) in acetic acid containing 90% of water —··—

Experimental

Melting points were determined on a Kofler block. The NMR spectra were measured on a Varian A-60 spectrometer at 60 Mc at room temperature using tetramethylsilane (TMS) as internal reference. Spectra at 100 Mc were obtained at room temperature from Varian HA-100 instrument internally locked on TMS in the frequency-sweep mode of operation. NMR data obtained by 1st-order approximation were summarized in Tables 1 and 2.

Thin-layer chromatography was performed on a silica gel plate. The solvent-systems used were ether-petroleum ether (3: 1, v/v, solvent A, 2: 1, v/v, solvent B and 1: 2, v/v, solvent C), benzene-ether (3: 1, v/v, solvent D), chloroform-acetone (60: 1, v/v, solvent E) and ethyl acetate-petroleum ether (2: 3, v/v, solvent F). The separated materials were developed with either iodine vapor or 0.2% resorcinol in 10% ethanolic phosphoric acid, and then heated in an oven.[37] In the cases of preparative thin-layer chromatography, the developed zones were extracted with acetone unless otherwise stated. The evaporation of the acetone under reduced pressure gave the materials.

The optical rotations were determined in a 10cm microtube in chloroform containing 1% of ethanol, and concentrations were recorded in percentage. The UV spectra were measured in ethanol.

1,3,4,5-Tetra-*O*-acetyl-2-*O*-carbomethoxy-α-L-sorbopyranose (IIIa). A mixture of II (10 g),[38] dimethyl pyrocarbonate (8 m*l*)[39,40] and potassium carbonate (0.1 g) was warmed at 50—60°C for 1.5 hr with stirring. The reaction mixture was filtered and washed with ether. The washings and the filtrate were combined and then evaporated under reduced pressure. The residue was recrystallized from ether to give colorless columns (6.9 g), mp 117—117.5°C, $[\alpha]_D^{22}$ −63.2° (*c* 1.038).

Found: C, 47.59; H, 5.58%. Calcd for $C_{16}H_{22}O_{12}$: C, 47.29; H, 5.46%.

1,3,4,5-Tetra-*O*-acetyl-2-*O*-carboethoxy-α-L-sorbopyranose (IIIb). A mixture of II (30 g), diethyl pyrocarbonate (23 m*l*) and potassium carbonate (0.3 g) was warmed at 50—55°C for 0.5 hr with stirring. IIIb (38.9 g) was obtained in a manner similar to IIIa. IIIb had mp 96—97°C, $[\alpha]_D^{22}$ −69.7° (*c* 1.116).

Found: C, 48.73; H, 5.92%. Calcd for $C_{17}H_{24}O_{12}$: C, 48.57; H, 5.76%.

1,3,4,5-Tetra-*O*-acetyl-α-L-sorbopyranosyl Chloride (IV). A solution of IIIb (30 g) in acetic acid (600 m*l*) saturated with anhydrous hydrogen chloride was kept at 0—5°C for 3.5 hr. The solution was added to chloroform (500 m*l*) and washed with ice-water, saturated aqueous sodium bicarbonate and ice-water,

34) Another new compound was isolated, which gave analytical data corresponding to $C_{12}H_{14}O_7$. Its NMR spectrum in chloroform-d at 60 Mc revealed three 3-proton singlets at τ 7.73, 7.92 and 7.94 due to acetoxyls, one 1-proton singlet at τ 3.51 and two 2-proton singlets at τ 4.99 and 5.01. Therefore, the structure was tentatively assigned to be 2,5-diacetoxymethyl-3-acetoxyfuran. Although further evidence seems to be required, a related experiment that D-glucal smoothly yielded 2-methoxymethyl-5-hydroxymethylfuran with methanolic hydrochloric acid seems support this structure (see Refs. 35 and 36).

35) F. Shafizadeh and M. Stacey, *J. Chem. Soc.*, **1952**, 3608.

36) D. Horton and T. Tsuchiya, *Carbohydrate Res.*, **2**, 349 (1966); *ibid.*, **3**, 257 (1966).

37) A. Anno and N. Seno, "Jikken Kagaku Kōza," Bd. 23, ed. by Chem. Soc. Japan, Maruzen, Tokyo (1957), p. 374.

38) Y. Khounine and G. Arragon, *Bull. Soc. Chim. France*, **1938**, 1404.

39) Kindly supplied by Dr. Shinzaburo Sumimoto of this Laboratory. S. Sumimoto, Japanese Pat. 42-19818 (1967).

40) M. Fujimoto, Japanese Pat. 42-12272 (1967).

and dired. Removal of the solvent gave a crude chloride (24.5 g) which was purified by silica gel chromatography with benzene. From 1.55 g of the crude syrup, using 30 g of silica gel, a colorless syrup (0.36 g) was obtained. The recrystallization of the syrup from ether and petroleum ether gave pure IV (0.15 g), mp 67.5—69.5°C, which was identical with an authentic sample.[2,3] IV was also prepared from IIIa in a similar way.

1,3,4,5-Tetra-*O*-acetyl-2-deoxy-L-sorbopyranos-2,3-ene (V). To a suspension of mercuric cyanide (19.9 g) in dry benzene (400 m*l*), a dry benzene solution (100 m*l*) of crude IV (24.5 g) was added. Traces of water were removed by azeotropic distillation with benzene (*ca.* 20 m*l*). After it had been refluxed for 8 hr with stirring, the reaction mixture was filtered and the filtrate was evaporated. The residue was extracted with chloroform (500 m*l*) and the chloroform was washed with 30% potassium iodide solution and then water and dried. Removal of the chloroform gave a dark brown syrup (18 g). The purification of the syrup on alumina column chromatography (135 g of alumina was used) with benzene gave V as a colorless syrup (13.7 g), $[\alpha]_D^{22}$ +217.6° (*c.* 1.032).

Found: C, 50.95; H, 5.51%. Calcd for $C_{14}H_{18}O_9$: C, 50.91; H, 5.49%. UV_{max} 209 mμ (ε 8800).

Methyl 1,3,4,5-Tetra-*O*-acetyl-3-*C*-chloromercuri-β-L-tagatopyranoside (VI). To a solution of mercuric acetate (1.05 g) in absolute methanol (20 m*l*), V (1.0 g) was added. After the mixture had stood overnight at room temperature, the solvent was removed and extracted with chloroform. The chloroform solution was shaken with saturated aqueous sodium chloride (100 m*l* ×2), washed with saturated aqueous sodium bicarbonate and water, dried and the solvent removed. The syrup (1.07 g) which was obtained was purified by preparative thin-layer chromatography (solvent A, R_f, 0.20). The purified syrup (0.21 g) was recrystallized from ethanol to give colorless columns (0.12 g), mp 184—189°C, $[\alpha]_D^{23}$ +71.1° (*c* 1.017).

Found: C, 30.72; H, 3.62; Hg, 32.96%; mol wt, 588. Calcd for $C_{15}H_{21}O_{10}HgCl$: C, 30.16; H, 3.54; Hg, 33.58%; mol wt, 597.385.

Methyl 1,3,4,5-Tetra-*O*-acetyl-β-L-tagatopyranoside (VII). Sodium borohydride (50 mg) was added as a solid in five portions, at intervals, to a pyridine solution (5 m*l*) of VI (0.7 g). After being kept at room temperature for 2.5 hr, the reaction mixture was filtered and washed with pyridine (5 m*l*). Acetic anhydride (10 m*l*) was added to a combined solution of the filtrate and the washings. The solution was allowed to stand overnight at room temperature, and then poured onto ice, made alkaline with sodium carbonate, and extracted with chloroform. The extract was washed with 5% sulfuric acid, water and dried, after which the solvent was removed under reduced pressure. The purification of the residue by preparative thin-layer chromatography (solvent A, R_f 0.38, extracted with chloroform) gave crude crystals (205 mg). Recrystallization of the crystals from ether and petroleum ether gave colorless columns (83 mg), mp 87—87.5°C, $[\alpha]_D^{22}$ +104.2° (*c* 0.947).

Found: C, 49.67; H, 6.12%. Calcd for $C_{15}H_{22}O_{10}$: C, 49.72; H, 6.12%.

Acid-catalyzed Isomerization of V in Acetic Anhydride.[41] A solution of V (6.68 g) in acetic anhydride (67 m*l*) containing 1% of TsOH was kept at 30°C for 24—48 hr (for 24 hr to obtain XII as a major product and for 48 hr to obtain XIV and XV as major products). The solution was then poured into ice-water (800 m*l*) under vigorous stirring, made alkaline with sodium bicarbonate and extracted with chloroform. The extract was washed with 5% aqueous sodium bicarbonate and water. The syrup (5.8 g) obtained on solvent removal from the dried extract was fractionated by preparative thin-layer chromatography. (i) From the syrup (3.6 g) obtained from the reaction for 24 hr, XII (0.40 g) was isolated as a syrup in a pure state by repeated preparative thin-layer chromatography (solvent D, R_f 0.65, extracted with ether). (ii) From the syrup obtained from the reaction for 48 hr, XIV, XV and XXIV were fractionated by thin-layer chromatography (solvent F, R_f 0.29 (XIV), 0.22 (XV), 0.4—0.7 (XXIV)). From the syrup (14.29 g), these were obtained in a crude state in the ratio of XIV (0.36 g), XV (0.46 g), and XXIV (0.94 g). XIV was recrystallized from ether (yield, 51 mg), and XV from ethanol (yield, 71 mg). XXIV was purified by repeated thin-layer chromatography (solvent E, R_f 0.61) (yield, 65.5 mg).

XII: Syrup $[\alpha]_D^{24}$ −88.0° (*c* 0.980). Found: C, 53.72; H, 5.73%; mol wt, 281. Calcd for $C_{12}H_{14}O_7$: C, 53.33; H, 5.22%; mol wt, 270.23. UV_{max} 261 mμ (ε 16100). IR_{film} 1635 cm^{-1} (conj. C=C).

XIV: Colorless columns, mp 110—111.5°C, $[\alpha]_D^{22}$ +198.8° (*c* 0.997). Found: C, 49,44; H, 5.23%; mol wt, 387. Calcd for $C_{16}H_{20}O_{10}\cdot H_2O$: C, 49.23; H, 5.68%; mol wt, 390.34. UV_{max} 213 mμ (ε 8970).

XV: Colorless columns, mp 111.5—113°C. Found: C, 51.43; H, 5.16%; mol wt, 298. Calcd for $C_{12}H_{14}O_7\cdot \frac{1}{2}H_2O$: C, 51.61; H, 5.41%; mol wt, 279.24. UV_{max} 230 mμ (ε 7280). IR_{CHCl_3} 1630, 1700 cm^{-1}(C=C-C=O).

XXIV: Syrup, $[\alpha]_D^{22}$ +236.8° (*c* 0.641). Found: C, 52.53; H, 5.55%. Calcd for $C_{10}H_{12}O_6$: C, 52.63; H, 5.30%. UV_{max} 253 mμ (ε 6390). IR_{film} 1640, 1705 cm^{-1} (C=C-C=O).

Reaction of XII with Hydrogen Bromide in Dry Benzene. A solution of XII (1.15 g) in dry benzene (21 m*l*) containing hydrogen bromide (2.34 g) was kept at 0—5°C for 1.5 hr. Evaporation of benzene under reduced pressure gave a dark red syrup, which was dissolved in methanol (8.4 m*l*) containing silver carbonate (1.53 g) and kept overnight at room temperature. The solution was filtered and evaporation of the filtrate gave a brown syrup. From the syrup, XX, XXI and XXII were isolated by preparative thin-layer chromatography (solvent B, R_f, 0.71 (XX), 0.93 (XXI), 0.85 (XXII), extracted with chloroform). Isolated materials were further purified by recrystallization or by preparative thin-layer chromatography.

XX: Syrup (purified by repeated preparative thin-layer chromatography, solvent D, R_f 0.50, yield, 0.1 g), $[\alpha]_D^{22}$ +66.6° (*c* 0.695). Found: C, 52.90; H, 5.97%. Calcd for $C_9H_{12}O_5$: C, 53.99; H, 6.04%. UV_{max} 226 mμ (ε 6800). IR_{film} 1635, 1690 cm^{-1} (C=C-C=O).

XXI: Colorless columns, mp 136—138°C (recrystallized from ether and petroleum ether, yield, 10 mg), $[\alpha]_D^{22}$ −30.9° (*c* 1.045). Found: C, 40.88; H, 5.01; Br, 20.93%. Calcd for $C_{13}H_{19}O_8$ Br: C, 40.74; H, 5.00; Br, 20.86%.

41) Products isolated from the reaction were rather unstable and should be stored in a refrigerator under strictly anhydrous conditions.

XXII:[42] Syrup (purified by repeated preparative thin-layer chromatography, solvent B, R_f 0.85, yield, 0.03 g), $[\alpha]_D^{23}$ +51.3° (*c* 0.825). Found: C, 41.42; H, 5.10; Br, 20.82%. Calcd for $C_{13}H_{19}O_8$ Br: C, 40.74; H, 5.00; Br, 20.86%.

Reaction of V with Hydrogen Bromide in Dry Benzene. When the above reaction was carried out by using V as the starting material, the same result was obtained.

Conversion of XXII into XXI. When the above reaction was carried out by using XXII as the starting material (instead of hydrogen bromide, hydrogen chloride was used), the formation of XXI was confirmed by thin-layer chromatography.

Acid-catalyzed Isomerization of XII. A solution of XII (0.25 g) in acetic anhydride (3 m*l*) containing 1% of TsOH was kept at 40—50°C for 7 hr. When the solution was worked up in a way similar to the acid-catalyzed isomerization of V, a crude syrup (0.18 g) was obtained from which XIV (38 mg) and XV (15 mg) were obtainable.

Acid-catalyzed Isomerization of XIV. A solution of XIV (15 mg) in acetic anhydride (0.3 m*l*) containing 1% of TsOH was kept at 50°C for 8 hr. The formation of XV was confirmed by thin-layer chromatography (solvent F, R_f 0.40).

Isomerization of V in Acetic Acid. (i) A solution of V (2.0 g) in acetic acid-water (1: 1, v/v) was kept at 95°C for 4.5 hr. The syrup obtained on solvent removal under reduced pressure was purified by repeated preparative thin-layer chromatography (solvent D, R_f 0.70). XXVIb (0.36 g) was obtained and was identical to an authentic sample.[43] (ii) A solution of V (0.54 g) in acetic acid was kept at 95°C for 6 hr. The solution was worked up in a way similar to the above. XXVIb (0.07 g) was obtained. 2,4-Dinitrophenylhydrazone of XXVIb was prepared in a usual way as red needles, mp 142.5—147°C (recrystallized from ethanol). Found: C, 48.42; H, 3.57; N, 15.89%, mol wt, 357. Calcd for $C_{14}H_{17}O_7N_4$: C, 48.28; H, 3.47; N, 16.09%; mol wt, 348.27.

Isomerization of XII in Acetic Acid. A solution of XII (0.13 g) in acetic acid-water (1: 1, v/v) (2 m*l*) was kept at 95°C for 2 hr. A syrup was obtained on solvent removal under reduced pressure. From the syrup, traces of XXVIb were isolated by repeated thin-layer chromatography (solvent D, R_f 0.70 and solvent C, R_f 0.28).

Isomerization of XX in Acetic Acid. A solution of XX (40 mg) in acetic acid-water (1: 1, v/v) (1.5 m*l*) was kept at 95°C for 6 hr. Evaporation of the solvent gave a syrup (20 mg), the thin-layer chromatography of which indicated XXVIb as a major component and XX as a minor one (the ratio was about 2: 1).

The authors wish to express their deep gratitude to Dr. Ken'ichi Takeda, Director of this Laboratory, for his encouragement.

42) The NMR data show that the favorable conformation of XXII is Cl chair form.

43) Synthesized by Schubert's method. H. Schubert, E. Hagen and G. Lehrmann, *J. Prakt.*, **17**, 173 (1962).

BULLETIN OF THE CHEMICAL SOCIETY OF JAPAN VOL. 41 1221—1224 (1968)

Oxygen Exchange and Racemization Reactions of Sulfoxides in Acetic and Chloroacetic Acid[1)]

Shigeru OAE, Mikihiko YOKOYAMA and Masahiro KISE

Department of Applied Chemistry, Faculty of Engineering, Osaka City University, Sugimoto-cho, Sumiyoshi-ku, Osaka

(Received November 22, 1967)

Oxygen exchange reaction of sulfoxides has been performed mainly in mineral acids such as sulfuric acid, aqueous hydrochloric and hydrobromic acids. We have found that concurrent oxygen exchange and racemization reactions take place also in carboxylic acids such as acetic, mono- and poly-chloroacetic acids. The pseudo first order reaction rates of both oxygen exchange and racemization reactions of *p*-tolyl phenyl sulfoxide have been determined using both optically active and ^{18}O-labeled *p*-tolyl phenyl sulfoxides in these acids. This reaction is found to be mainly dependent on the strengths of the acids; namely, the reaction velocity is faster in an acid of smaller pK_a value. Together with the fact that k(rac.)/k(exch.) is unity and the substituent effect is small, the reaction is suggested to proceed through an unimolecular type S–O bond cleavage, probably involving radical cation intermediate (II).

Sulfoxide, unlike sulfones, have been known to undergo concurrent oxygen exchange and racemizations in various acidic media, such as in concentrated sulfuric acid,[2,3)] hydrochloric acid in aqueous dioxane,[4)] hydrobromic acid in acetic acid,[5)] dinitrogen tetroxide,[6)] diluted nitric acid[7)] and acetic anhydride.[8)] In the course of our further extension of these concurrent oxygen exchange and racemization reactions of sulfoxides, we have recently found that sulfoxides undergo concurrent oxygen exchange and racemization reactions even in weak organic acids, such as acetic, monochloro-, dichloro- and trichloroacetic acids.

This paper will describe the detailed account of our kinetic and stereochemical investigations of various sulfoxides and their implications for the interpretation of the mechanism of the reaction.

Results and Discussion

Oxygen Exchange Reactions of Dimethyl-, Dibenzyl- and Diphenyl Sulfoxides. At the initial stage of this study, oxygen exchange reactions of sulfoxide were carried out in aqueous acetic acid. Namely, when ^{18}O-labeled diphenyl-, dibenzyl-, di-(*n*-butyl-) and dimethyl sulfoxides were treated separately in boiling 5 : 1 (w/w) glacial acetic acid-water mixture for three hours, a noticeable ^{18}O-exchange (13%) was observed only with dimethyl sulfoxide. However, under a prolonged heating at a somewhat higher temperature, the other sulfoxides were also found to undergo the oxygen exchange reaction. The Table 1 illustrates the amounts of oxygen-exchange of diphenyl-, dibenzyl- and dimethyl

TABLE 1. OXYGEN EXCHANGE REACTION OF ^{18}O-LABELED SULFOXIDES IN AQUEOUS ACETIC OR ACETIC ACIDS AT 130°C, FOR 24 HR

Sulfoxide	^{18}O-concentration of starting sulfoxide (atom%)	^{18}O-concentration of recovered sulfoxide (atom%)	
		in excess aq. acetic acid	in excess acetic acid
$PhCH_2-S(^{18}O)-CH_2-Ph$	0.77	0.59	0.59
$Ph-S(^{18}O)-Ph$	0.62	0.60	0.56
$CH_3-S(^{18}O)-CH_3$	1.67	0.24	—

1) Paper XXII on Sulfoxide, Paper XXI; S. Oae, and N. Kunieda, This Bulletin, **41**, 1025 (1968).
2) a) S. Oae, T. Kitao and Y. Kitaoka, *Chem. & Ind.*, **1961**, 291. b) S. Oae, T. Kitao and Y. Kitaoka, This Bulletin, **38**, 543 (1965). c) S. Oae, T. Kitao, S. Kawamura and Y. Kitaoka, *ibid.*, **38**, 546 (1965). d) S. Oae and N. Kunieda, *ibid.*, **41**, 696 (1968).
3) H. J. Shine and D. R. Tompson, *Tetrahedron Letters*, **1966**, 1591.
4) K. Mislow, T. Simmons, J. T. Mellello and A. L. Ternay, Jr., *J. Am. Chem. Soc.*, **86**, 1452 (1964).
5) W. Tagaki, K. Kikukawa, N. Kunieda and S. Oae, This Bulletin, **39**, 614 (1966).
6) a) S. Oae, N. Kunieda and W. Tagaki, *Chem. & Ind.*, **1965**, 1790. b) C. R. Johnson and D. McCants, Jr., *J. Am. Chem. Soc.*, **87**, 1109 (1965).
7) N. Kunieda and K. Sakai, Unpublished work from these laboratories.
8) S. Oae and M. Kise, *Tetrahedron Letters*, **1967**, 1409.

Table 2. Kinetic data on oxygen exchange and racemization reaction in acetic, monochloro-, dichloro- and trichloroacetic acids at 120°C

R in R- 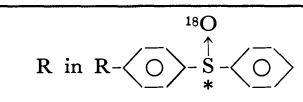	Acid used	k(rac.)$\times 10^5$ (sec^{-1})	k(exch.)$\times 10^5$ (sec^{-1})
CH_3	CH_3COOH	0.0129±0.0006	
	$ClCH_2COOH$	0.153±0.007	
	$Cl_2CHCOOH$	0.790±0.023	
	Cl_3CCOOH	2.39±0.23	2.41±0.28
	$Cl_2CHCOOH$*	0.750±0.041	
Cl	Cl_3CCOOH		1.47±0.12
H	Cl_3CCOOH		2.17±0.12

* $LiClO_4$, 0.001 mol, was added in 30 ml of dioxane containing 0.25 mol of dichloroacetic acid.

sulfoxides after heating each sample in both glacial and aqueous acetic acids for 24 hr at 130°C. Dimethyl sulfoxide was quite reactive as was expected, however, decomposed under the prolonged heating with glacial acetic acid. Apparently it underwent the Punmerer type rearrangement forming methyl mercaptomethyl acetate, which upon quenching with water hydrolyzed spontaneously to give acetic acid, methylmercaptan and formaldehyde. In fact, we isolated methylmercaptan by converting it to mercuric methylmercaptide.

The other sulfoxides could be nicely recovered even after a prolonged heating with glacial acetic acids. The order of the reactivities of the three sulfoxides, *i.e.*, dimethyl>dibenzyl>diphenyl, follows apparently that of the basicities of the sulfoxides,[9] suggesting that the reaction may be acid-catalyzed.

Oxygen Exchange and Racemization Reactions of *p*-Substituted Diphenyl Sulfoxides. In order to shed further light on the nature of the oxygen exchange reaction and also to examine the possible concurrent racemization, both optically active and ^{18}O-labeled *p*-tolyl phenyl sulfoxides were prepared and subjected to the oxygen exchange and racemization reactions in four different acids of varying acid strength, namely, acetic, monochloro-, dichloro- and trichloroacetic acids. Pseudo first order rate constants of oxygen exchange and racemization reactions along with the activation parameters of these reactions were obtained from the usual kinetic determinations. In addition, the rates of the oxygen exchange reactions, of *p*-chlorophenyl phenyl and diphenyl sulfoxides were determined in trichloroacetic acid under the same condition, in order to compare the effects of polar substituents. The results were summarized in Tables 2 and 3. When the log$k$(s) were plotted against the pK_a(S) of these acids, a straight line, though rough, can be drawn as shown in Fig. 1, clearly depicting that the oxygen exchange reaction is dependent on the Brönsted acidity, as was expected; namely smaller the pK_a of acid used, faster was the reaction rate. This observation is well accord with our earlier assumption that dimethyl sulfoxide, being most basic is extremely reactive while the least basic diphenyl sulfoxide is the least reactive as was shown in Table 1. The nearly identical rates of both racemization and oxygen exchange suggest that the reaction proceed through a rate-determining unimolecular S–O bond cleavage process. This is quite different from the similar oxygen exchange reaction with acetic anhydride in which the rate of racemization of *p*-tolyl phenyl sulfoxide was twice of that of the oxygen exchange, while the rate of racemization with acetic anhydride is estimated to be about 770 times faster than that with glacial acetic acid at 120°C. Therefore S_N2 type mechanism, suggested for the similar oxygen exchange reactions with acetic anhydride can not be applied for the reactions in carboxylic acids. One notices in Table 3, however, that the entropies of activation for these reactions were of large negative values. This would imply that the protonated sulfoxide was considerably solvated by carboxylic acid in the transition state.

Table 3. Activation parameter for racemization reaction of *p*-tolyl phenyl sulfoxide (120—140°C)

Acid	E_a (kcal/mol)	$\Delta S^{\neq}$(eu) 120°C
$CH_2ClCOOH$	24.4	−23.4
$CHCl_2COOH$	19.6	−32.8
CCl_3COOH	18.6	−32.9

There are two different mechanisms that can fit in these observations; the one is the heterolysis of the S–O bond that involves the rate determining formation of the doubly charged " sulfidonium ion " intermediate (I) and the other is the homolysis to form radical cation intermediate (II).

The first process, involving the double-positive charged intermediate (I) would be highly energy consuming and is expected to be strongly accelerated by an electron-releasing substituent while retarded remarkable by the substitution of an electron-withdrawing group, when the geometry of the activated complex is similar to that of the carbonium ion forming

9) K. K. Anderson, W. H. Edmonds, J. B. Biasotti and R. A. Strecker, *J. Org. Chem.*, **31**, 2859 (1966).

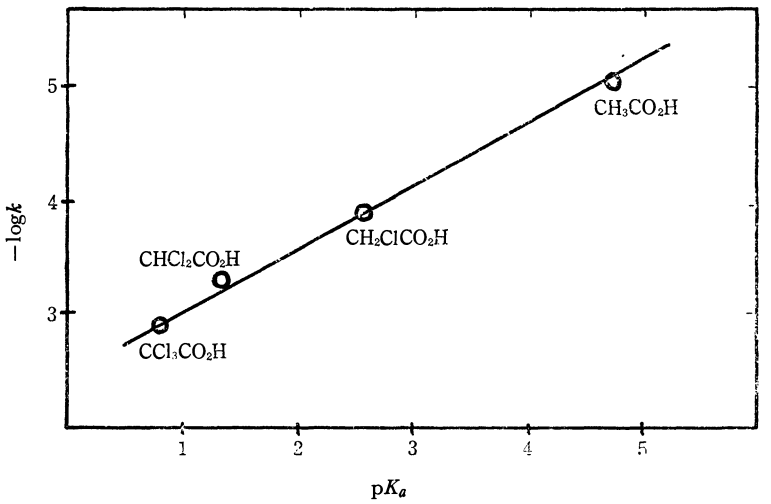

Fig. 1. The relation between the pK_a(s) of acids and the rates of racemization of optically active *p*-tolyl phenyl sulfoxide.

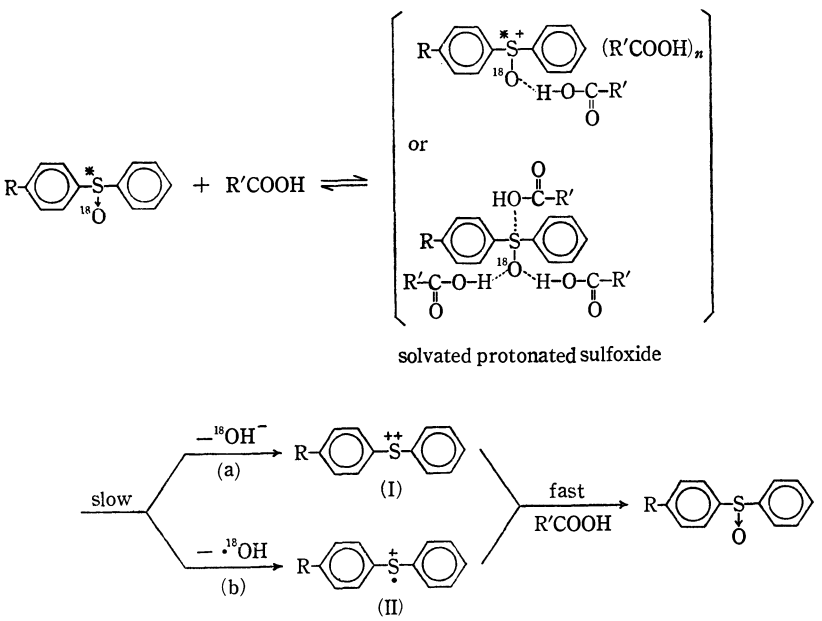

reaction (S_N1). The effect of the substituents would be similar to those observed in the solvolytic reaction of substituted benzhydryl compounds and correlated with the σ^+ values rather than the σ values. If, however, the hydroxy group of the sulfoxide would cleave without perturbing the original geometry of the molecular arrangement, the vacant *p*-orbitals of the leaving bond would overlap much less effectively with those π-molecular orbitals of the two aromatic ring due to the angular arrangement of the bonds around the sulfur atom and hence the effect of *p*-substituent would be rather small. Unfortunately very scant kinetic data or well-defined S_N1 (or A-1) type reaction on sulfur atom are available for comparison, especially the one forming any intermediate that bears double positive charges. However, this process, being unassisted by resonance, would be very highly energy-consuming and unlikely. The second path would be less energy consuming and not be effected markedly by the polar nature of the substituent, since there is not net charge variation before and after the reaction. The small effect of the substituents in this reaction ($\rho = -0.47$) and the rather facile nature of the reaction seem to suggest that the reaction follows

the homolytic cleavage process (b) of the protonated sulfoxide, as in other oxygen exchange and racemization reactions in mineral acids.

Experimental

Materials. *Optically Active p-Tolyl Phenyl Sulfoxide.* This sulfoxide was prepared by the method of Anderson[10] in which (−)menthyl (−)*p*-toluenesulfinate was reacted with phenylmagnesium bromide in ether. (Mp 91—93°C, $[\alpha]_D = +26.9$ in EtOH)

^{18}O-Labeled p-Tolyl Phenyl Sulfoxide. The corresponding sulfide was oxidized with bromine in the presence of pyridine in acetic acid-$H_2{}^{18}O$, according to our usual procedure.[11] (Mp 69.8—71°C ^{18}O-content 1.09 atom %)

Dioxane, obtained commercially, was purified according to the usual method, finally dried with sodium and ditilled (bp 101.5°C).

Acetic Acid, obtained commercially was treated with chromic anhydride and after refluxing for several hours, it was distilled (bp 117.5—118°C).

Monochloroacetic Acid, Dichloroacetic Acid and Trichloroacetic Acid. These acids, obtained commercially, were distilled under reduced pressure in a dry atmosphere. Contact with a moisture was intercepted very carefully.

Reaction of Dimethyl Sulfoxide with Acetic Acid. The mixture consisting of 1 g of dimethyl sulfoxide and 5 g of glacial acetic acid was refluxed under nitrogen stream, which was bubbled into methanol solution of mercuric chloride. White crystalline material was precipitated slowly. After the reaction, white crystalline material was collected by filteration and identified from the melting point and infrared spectrum by comparing with that of the authentic sample of dimethyl sulfide - $HgCl_2$ complex.

Kinetic Procedure. Oxygen exchange and racemization reaction was carried out at 120±0.03°C in sealed tubes while the molar ratio of sulfoxide to an acid was kept at 1 : 50. Namely, the mixture of sulfoxide (1/200 mol), acid (1/4 mol) and 30 m*l* of dioxane was divided in several sealed tubes and reacted. From time to time a sealed tube was drawn out from the paraffin bath and the content was poured into an excess water then neutralized with sodium hydroxide solution. The sulfoxide, separated out was extracted with carbon tetrachloride and dried with anhydrous magnesium sulfate. Carbon tetrachloride was distilled off and the resulting sulfoxide was recovered. The recovered sulfoxide was dried thoroughly and subjected to the measurement of both specific rotation and ^{18}O-analysis. The specific rotation was measured in ethanol at *c*: 3.00. While ^{18}O-analysis of the sulfoxide-oxygen was done as usual according to the modified Rittenberg-Porticorbo method.

10) K. K. Anderson, *Tetrahedron Letters*, **No. 3**, 93 (1962).

11) S. Oae, Y. Ohnishi, S. Kozuka and W. Tagaki, This Bulletin, **39**, 364 (1966).

BULLETIN OF THE CHEMICAL SOCIETY OF JAPAN VOL. 41 1224—1228 (1968)

Synthetic Studies of α-Tocopherol. I. Synthesis of α-Tocopheryl Acetate

Takehiko ICHIKAWA and Tetsuya KATO

Central Research Laboratories, Ajinomoto Co., Inc., Kawasaki

(Received December 4, 1967)

Geraniol (III) was reacted with trimethylhydroquinone (II) in the presence of boron trifluoride in benzene. The product was then acetylated to give a mixture of 2,5,7,8-tetramethyl-2-(4-methyl-3-penten-1-yl)-6-acetyloxychromane (VI) and 2,5,7,8-tetramethyl-2,3-(4,4-dimethylbutano)-6-acetyloxychromane (Vb). The VI was ozonized and decomposed with zinc and acetic acid to give 2,5,7,8-tetramethyl-2-(2-formylethyl)-6-acetyloxychromane (VII). Pseudoionone (VIII) was reduced with sodium borohydride to give pseudoionol (IX), but in certain cases the dehydration of IX occurred during the distillation. VII was condensed with IX by a Wittig reaction to give 2,5,7,8-tetramethyl-2-(4,8,12-trimethyl-3,5,7,11-tridecatetraen-1-yl)-6-acetyloxychromane (X), which was then hydrogenated to give α-tocopheryl acetate (I).

Tocopherols have long been known as a fertile factor, but only recently have its widespread physiological activities been discovered; now the importance of α-tocopherol is increasingly being recognized.[1] Many methods of synthesizing α-tocopherol have already been established,[2] but an attempt has now been undertaken to synthesize α-tocopheryl acetate (I) in short stages, as is illustrated in Scheme 1.

The condensation of geraniol (III) and trimethylhydroquinone (II) in the presence of zinc chloride

1) S. Kijima, *Yuki Gosei Kagaku Kyokaishi* (*J. Soc. Org. Synth. Chem. Japan*), **24**, 92, 200 (1966), review.

2) K. Sato and Y. Kurihara, *ibid.*, **20**, 824 (1962), review.

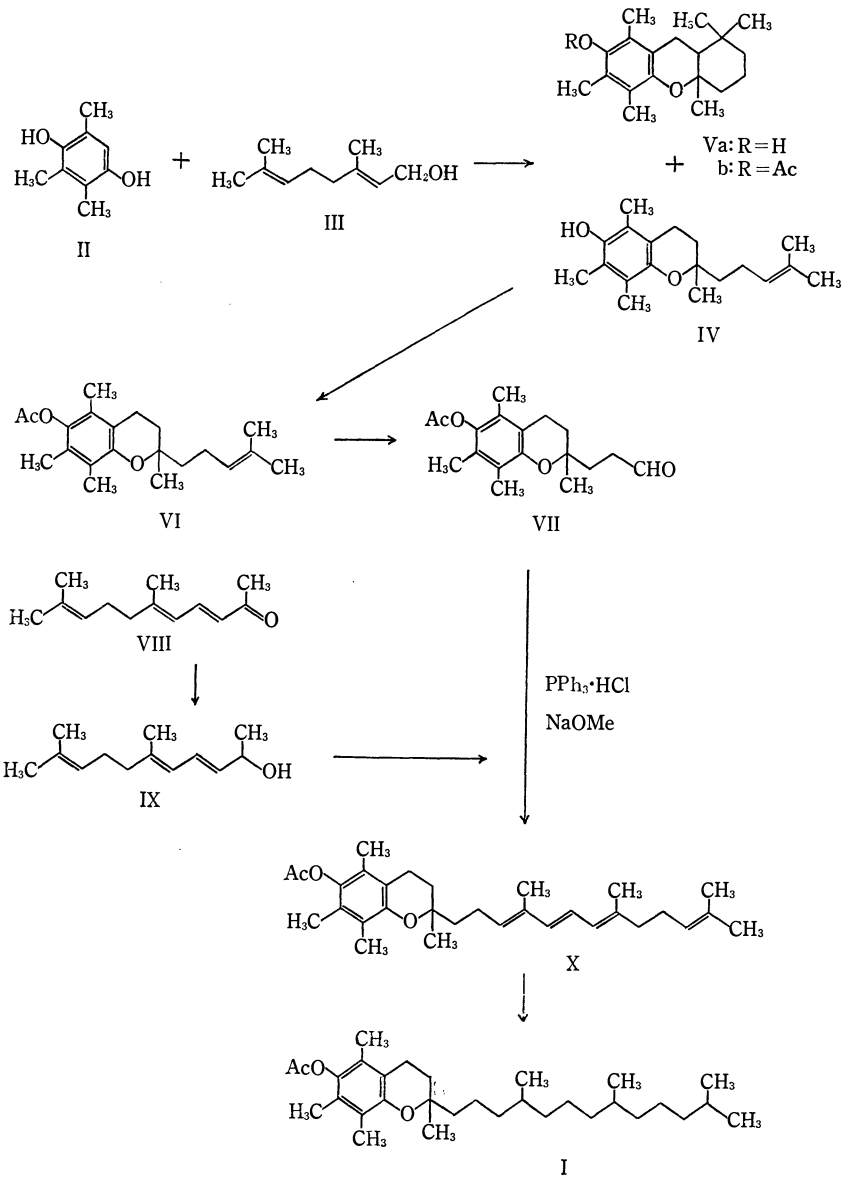

Scheme 1

was reported by Smith *et al.*,[3] but the structure of his product was ambiguous. Green *et al.* later obtained 2,5,7,8-tetramethyl-2-(4-methyl-3-penten-1-yl)-6-hydroxychromane (IV) by the condensation of II and III in dioxane with the aid of boron trifluoride.[4] In the present study, the condensation was achieved in benzene with boron trifluoride etherate. A fair yield of chromanol (λ_{max}^{EtOH} 294 mμ) was obtained; the results of the elementary analysis of this chromanol were consistent with the IV structure. Two moles of III to one mole of II were necessary; 0.1—0.2 mol of boron trifluoride to one mole of II were appropriate to obtain a good yield. The condensation did not proceed at all in dioxane in the presence of 0.1—0.2 mol of boron trifluoride. The acetylation of the product gave the corresponding acetate; a part of it crystallized to give white crystals melting at 137—138°C. A gas chromatogram*1 of the acetylated product showed a major peak (R_t 10.5 min) and two minor peaks (R_t 6.6 min and 12 min), and the crystalline compound corresponded to one of the

3) L. I. Smith, H. E. Ungnade, J. R. Stevens and C. C. Christman, *J. Am. Chem. Soc.*, **61**, 2615 (1939).

4) J. G. Green and D. McHale, British Pat. 949715 (1964); *Chem. Abstr.*, **60**, 13227d (1964).

*1 Column: SE-30 on Diasolid H, 4 mm×3 m; carrier gas: helium; flow rate: 46 ml/min; temp.: 205°C.

minor components (R_t 12 min). The results of the elementary analysis of the crystals were consistent with the experimental formula of $C_{21}H_{30}O_3$; hence, they may be considered to be isomers of 2,5,7,8-tetramethyl-2-(4-methyl-3-penten-1-yl)-6-acetyloxychromane (VI). The NMR spectrum in tetrachloromethane showed signals at δ 0.90 (singlet, 3H, $\underline{CH_3}$C–), 1.00 (singlet, 3H, $\underline{CH_3}$–C–), 1.16 (singlet, 3H, $\underline{CH_3}$C–O–), 2.35—2.6 (multiplet, 2H, Ar–$\underline{CH_2}$–); 1.3—1.8 (multiplet, 6H, –$\underline{CH_2}$–); 2.23 (singlet, 3H, $\underline{CH_3}$COO–), 2.05 (singlet, 3H, $\underline{CH_3}$–Ar), and 1.95 (6H, $\underline{CH_3}$–Ar), with no signal of the olefinic proton. The UV absorption was identical with that of α-tocopheryl acetate. These facts show the structure to be 2,5,7,8-tetramethyl-2,3-(4,4-dimethylbutano)-6-acetyloxychromane (Vb). The NMR spectrum of the original mixture of the acetate showed signals at δ 2.22 (singlet, 3H, $\underline{CH_3}$COO–); 2.06, 1.94, 1.90(singlets, 9H, $\underline{CH_3}$–Ar); 1.22 (singlet, 3H, $\underline{CH_3}$C–O–); 1.62, 1.56 (6H, $\underline{CH_3}$–$\underline{CH}$(CH$_3$)–$\underline{CH}$–); 2.4—2.7 (multiplet, Ar–$\underline{CH_2}$–) and 5.10 (1H, –$\underline{CH}$=C–), along with the small peaks of Vb. The signals of the other methylene protons (δ 1.3—2.3) were covered by other signals. Its IR spectrum ($\nu_{C=C}$ 1780 cm^{-1}) and the UV spectrum were also consistent with the VI structure.

The hydroboration of VI for the purpose of obtaining a ω-hydroxychromane derivative gave only a hydroborated product in a poor yield. The yield could not be improved, presumably because of the steric hindrance of the double bond.

The ozonolysis of VI in methylene chloride, followed by reductive decomposition by zinc and acetic acid, gave 2,5,7,8-tetramethyl-2-(2-formylethyl)-6-acetyloxychromane (VII). Its IR spectrum (1755 cm^{-1}, CH_3COO–; 1720 cm^{-1}, –CHO), its NMR spectrum (δ 9.61, triplet, 1H, –$\underline{CHO}$; 2.21, singlet, 3H, $\underline{CH_3}$COO–; 2.03, 1.95 and 1.95, singlets, 9H, $\underline{CH_3}$–Ar; 1.14, singlet, $\underline{CH_3}$–C–O), and the results of elementary analysis were all consistent with the VII structure.

The oxidation of VII with potassium permanganate gave its corresponding carboxylic acid, 2,5,7,8-tetramethyl-2-(2-carboxyethyl)-6-acetyloxychromane.*2

Pseudoionone (VIII) was reduced with sodium borohydride in ethanol, treated with an aqueous solution of sodium hydroxide, and distilled. The oil thus obtained was consistent with pseudoionol (IX) (IR: ν_{OH} 3300 cm^{-1}, NMR in carbon tetrachloride: δ 1.19, doublet, J=6 cps, 3H, $\underline{CH_3}$–CH–OH; 1.72, 1.66 and 1.58, singlets, 9H, $\underline{CH_3}$–CH=C–; 2.12, 2.06 and 2.02, 4H, –$\underline{CH_2}$–CH=C; 3.26, 1H, singlet, –$\underline{OH}$; 4.30, 1H, multiplet, $CH_3\underline{CH}$(OH)–; 4.8—6.6, 4H, multiplet, –$\underline{CH}$=C–). When the reaction product was not treated with aqueous alkali, the product obtained by distillation occasionally had no hydroxyl group (judging from the IR spectrum), and its absorption maximum (λ_{max}^{EtOH} 270 mμ, ε 48000) was longer than that of VIII (λ_{max}^{EtOH} 241 mμ, ε 24000). Accordingly, the product may be deduced to be the dehydrated product of IX, namely, 2,6-dimethylundeca-2,5,7,9-tetraene XI. As its NMR spectrum is accompanied by a small signal at δ 0.88 (doublet, CH_3–C–H, J=6 cps), the isomerized conjugated tetraene (XII) might be present in the product.

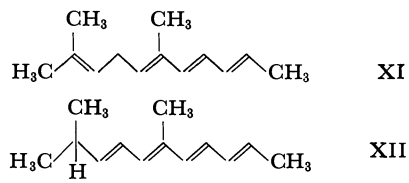

As the product before distillation always exhibits an absorption maximum at 241 mμ, the dehydration apparently takes place during distillation by the boric acid produced from the borohydride. However, the similar reduction of mesityl oxide, as an example of α,β-unsaturated ketone, always gave 4-methylpent-3-en-2-ol as a normal product and dehydration never occurred.

A simplified method of Wittig reaction proposed by Pommer *et al.*[5] has been applied to the condensation of VII and IX. Triphenylphosphine hydrochloride was reacted with IX in acetonitrile to yield the corresponding phosphonium salt. After the solvent had been substituted by dimethylformamide, VII was added and ylid was formed by the gradual addition of sodium methoxide and reacted *in situ* with VII. The product had an absorption maximum at 280 mμ, which was close to the expected value (278 mμ) of all *trans*-2,5,7,8-tetramethyl-2-(4,-8,12-trimethyl-3,5,7,11-tridecatetraen-1-yl)-6-acetyloxychromane (X). It can not be purified by distillation because it is very unstable to heat. Its IR spectrum showed the presence of the ester group ($\nu_{C=O}$ 1760 cm^{-1}), but no aldehyde group around 1720 cm^{-1}. The NMR spectrum showed signals at δ 1.22 ($\underline{CH_3}$–C–O–); 2.22 ($\underline{CH_3}$COO–); 2.05, 1.94 and 1.90 ($\underline{CH_3}$–Ar); 1.5—1.58 (CH_3–C=C–); 4.5—6.5 (–$\underline{CH}$=C–), supporting the idea of the X structure.

The hydrogenation of crude X with Raney Nickel was not feasible, presumably due to the presence of triphenylphosphine remaining in the product, so repeated treatment with Raney Nickel was necessary

*2 Green *et al.*[4] reported a melting point of 154°C.

5) H. Pommer, *Ang. Chem.*, **72**, 816 (1960).

to remove the catalyst poison in advance of the reduction. Heating during the reduction must be avoided since the isomerization of the side chain has been found to occur very easily. Reduction at room temperature with high-pressure hydrogen gave α-tocopheryl acetate (I), the structure of which was confirmed by a comparison of its IR, UV, and NMR spectra with those of an authentic sample.

Experimental

2,5,7,8-Tetramethyl-2-(4-methyl-3-penten-1-yl)-6-hydroxychromane (IV). To a solution of 50 g of trimethylhydroquinone (II) and 4.16 m*l* of boron trifluoride etherate in 1300 m*l* of anhydrous benzene, there were added, drop by drop, 101.2 g of geraniol (III) under stirring and refluxing. After it had then been heated to reflux for 3 hr, the benzene solution was washed with water, a sodium bicarbonate solution, and water, dried with anhydrous magnesium sulfate, and distilled; bp 130—156°C/0.01 mmHg, 81 g. A gas liquid chromatogram of the acetylated product showed the IV content to be 73%. Accordingly, the yield of IV from II was 62%. Rectification gave a pale yellow oil; bp 154—154.5°C/0.01 mmHg, λ_{max}^{EtOH} 294 mμ.

Found: C, 79.44; H, 9.92%. Calcd for $C_{19}H_{28}O_2$: C, 79.12; H, 9.79%.

2,5,7,8-Tetramethyl-2-(4-methyl-3-penten-1-yl)-6-acetyloxychromane (VI) and 2,5,7,8-Tetramethyl-2,3-(4,4-dimethylbutano)-6-acetyloxychromane (Vb). A mixture of 54 g of IV (73% pure) and 52 m*l* of acetic anhydride was refluxed for 3 hr. Fractional distillation then gave an oil; bp 143—158°C/0.02 mmHg, 54 g. For analysis, a part of it was redistilled; bp 133—134°C/0.04 mmHg, λ_{max}^{EtOH} 285 mμ (ε 1920).

Found: C, 76.58; H, 9.40%. Calcd for $C_{21}H_{30}O_3$: C, 76.32; H, 9.15%.

A part of the product crystallized to give white crystals, which were then triturated with methanol and filtered. Recrystallization from methanol gave white needles of Vb; mp 138—139°C, λ_{max}^{EtOH} 285 mμ (ε 1970).

Found: C, 76.53; H, 9.27%. Calcd for $C_{21}H_{30}O_3$: C, 76.32; H, 9.15%.

2,5,7,8-Tetramethyl-2-(2-formylethyl)-6-acetyloxychromane (VII). A solution of 16.5 g of VI (70% pure) was dissolved in 200 m*l* of methylne chloride and then cooled to −50°C. Oxygen containing 2.7% of ozone was introduced into the solution for 1 hr (the total amount thus corresponded to 1.2 g of ozone). The reaction mixture was immediately stirred, drop by drop, into a mixture of 4.3 g of zinc dust and 170 m*l* of 50% aqueous acetic acid. After the addition, the mixture was stirred for an hour; then the methylene chloride was distilled out, and the remaining mixture was heated at 100°C for 1 hr. After cooling, the mixture was extracted three times with 80 m*l* portions of ether, and the ether extract was washed with water, a sodium carbonate solution, and water to remove acetic acid. The ether layer was dried and concentrated. The residue was shaken vigorously with a solution of 10 g of sodium bisulfite in 15 m*l* of water, and the white precipitate was filtered and washed with petroleum ether. The precipitate was dissolved in 400 m*l* of water, an aqueous solution of 11 g of sodium carbonate was added, and the mixture was extracted with ether. The ether extract was washed with water, dried, and concentrated. The residue was almost pure VII (7.0 g, 66%). Distillation *in vacuo* gave an oil, bp 145—146°C/0.005 mmHg; which crystallized on standing; mp 48—49°C, λ_{max}^{EtOH} 285 mμ (ε 1880).

Found: C, 70.92; H, 8.02%. Calcd for $C_{18}H_{24}O_4$: C, 71.02; H, 7.95%.

2,5,7,8-Tetramethyl-2-(2-carboxyethyl)-6-acetyloxychromane. To a solution of 3.04 g of VII in 30 m*l* of acetone, there was added, drop by drop, 0.53 g of potassium permanganate in 20 m*l* of acetone at 0—2°C. The mixture was then stirred at the same temperature for 1 hr and poured into 200 m*l* of water. The precipitate was filtered and washed with ether. The filtrate was acidified with hydrochloric acid and extracted with ether. The combined ether solution was washed with water, dried with magnesium sulfate, and concentrated. The residue was triturated with petroleum ether and filtered to give white crystals; 1.0 g, mp 159.5—160.5°C (recrystallized from ethyl acetate).

Found: C, 67.34; H, 7.68%. Calcd for $C_{18}H_{24}O_5$: C, 67.48; H, 7.55%.

Pseudoionol (IX). A solution of 9.6 g of pseudoionone (VIII) was dissolved in 100 m*l* of 95% ethanol; after 0.68 g of sodium borohydride in ethanol had been added at room temperature, the mixture was stirred for 2 hr and then left standing overnight. The mixture was added to a solution of 2 g of sodium hydroxide in 500 m*l* of water. The mixture was extracted with ether, and the ether extract was washed with water, dried, and concentrated. The distillation of the residual oil *in vacuo* gave a colorless oil; bp 112—120°C/5 mmHg, 7.7 g (80%).

Found: C, 80.03; H, 11.36%. Calcd for $C_{13}H_{22}O$: C, 80.35; H, 11.41%.

2,6-Dimethyl-2,5,7,9-undecatetraene (XI). A solution of 29 g of VIII was dissolved in 100 m*l* of 99.5% ethanol, 2.1 g of sodium borohydride in ethanol were added at room temperature, and the mixture was stirred for 2 hr and then left standing overnight. The mixture was added to 500 m*l* of water and extracted with ether. The ether layer was washed with water, dried, and concentrated. Distillation *in vacuo* gave an oil; bp 89—103°C/2.5 mmHg, 23.4 g. The IR spectrum showed that a small quantity of a hydroxyl group was present. A part of the distillate was treated overnight with *p*-nitrobenzoyl chloride in pyridine; the mixture was then poured into water and extracted with ether, and the ether extract was washed with water, dried, and concentrated. The residue was dissolved in petroleum ether and passed through an alumina column to remove *p*-nitrobenzoic acid and its ester. The concentration and distillation of the petroleum ether solution gave an oil, bp 93—94°C/4 mmHg, which showed no hydroxyl group upon IR analysis; n_D^{15} 1.5328, λ_{max}^{EtOH} 270 mμ (ε 48000).

Found: C, 88.25; H, 11.26%. Calcd for $C_{13}H_{20}$: C, 88.56; H, 11.44%.

2,5,7,8-Tetramethyl-2-(4,8,12-trimethyl-3,5,7,11-tridecatetraen-1-yl)-6-acetyloxychromane (X) and α-Tocopheryl Acetate (I). To a solution of 2.97 g of IX in 10 m*l* of acetonitrile, there were added, under stirring and while the temperature was kept below 30°C, 4.53 g of triphenylphosphine hydrochloride which had been obtained by passing dry hydrogen chloride into a solution of triphenylphosphine in dry ether. After the mixture had then been left standing overnight at room

temperature, the acetonitrile was removed under reduced pressure below 50°C. To the residue there were added 4.2 g of VII in 15 m*l* of dimethylformamide, and the mixture was stirred. When a clear solution was obtained, sodium methoxide prepared from 0.352 g of sodium and 7 m*l* of anhydrous methanol was stirred in, drop by drop, below 15°C. The reaction mixture was turned red by the ylid formed. After the addition was complete, stirring was continued for 30 min at 10°C; then the mixture was gradually heated to 80°C, when the red color disappeared. The product was poured into 200 m*l* of 50% aqueous methanol and extracted with petroleum ether. The petroleum ether extract was washed three times with 50% methanol, dried, and concentrated *in vacuo*. The residual oil was dissolved in 20 m*l* of ether, and an ethereal solution of mercuric chloride was added until no more precipitate formed. When the precipitate was filtered and the filtrate was washed with water, dried, and concentrated, 4.7 g of a yellow oil were obtained (λ_{max}^{EtOH} 280 mμ). The oil solidified at about 120°C *in vacuo*, which made distillation impossible. To a solution of 3.0 g of the above oil in 50 m*l* of ethanol, 2 g of Raney Nickel were added, and the mixture was shaken under 22 atm of hydrogen at room temperature. The catalyst was renewed 3 times, whereby the calculated amount of hydrogen had been absorbed. The catalyst was filtered, and the filtrate was concentrated and distilled *in vacuo* to give an oil; bp 180—185°C/0.05 mmHg, 2.0 g. Its IR and UV spectra were identical with those of an authentic sample of α-tocopheryl acetate. A part of it was hydrolyzed by methanolic potassium hydroxide and converted into allophanate; mp 165—166°C (recrystallized from methanol).

Found: C, 72.15; H, 10.01; N, 5.32%. Calcd for $C_{31}H_{52}N_2O_4$: C, 72.05; H, 10.14; N, 5.42%.

The authors wish to express their thanks to Professor Masanao Matsui of the University of Tokyo and Dr. Tadao Takenishi of the Ajinomoto Co., Inc., for their valuable suggestions and encouragement.

BULLETIN OF THE CHEMICAL SOCIETY OF JAPAN VOL. 41 1228—1232 (1968)

Synthetic Studies of α-Tocopherol. II.*1 Synthesis of Trimethylbenzoquinone

Takehiko ICHIKAWA, Hiroko OWATARI and Tetsuya KATO

Central Research Laboratories, Ajinomoto Co., Inc., Kawasaki

(Received December 4, 1967)

Trimethylbenzoquinone (XII), a raw material for the synthesis of trimethylhydroquinone (XIII), was synthesized from trimethylcyclohexenones and trimethylcyclohexene by oxidation. Ethyl α-propionylpropionate (II) prepared from ethyl propionate was condensed with methyl vinyl ketone to yield 4-methyl-4-ethoxycarbonylocta-3,7-dione (IV), which was then dehydrated with beryllium chloride to give 2,3,6-trimethyl-6-ethoxycarbonyl-2-cyclohexen-1-one (V). The product (V) was heated with alkali to give 2,3,6-trimethyl-2-cyclohexen-1-one (VI). The refluxing of a solution of IV in a mixture of acetic acid and hydrochloric acid also gave rise to VI. When II was condensed with crotonaldehyde, 2,5,6-trimethyl-2-cyclohexen-1-one (VIII) was obtained in a single step. 1,4(or 1,5)-Dimethyl-5-(or 4)-formyl-1-cyclohexene (IX), obtained by the Diels-Alder reaction of crotonaldehyde with isoprene, was reduced by hydrazine hydrate to give 1,4,5-trimethyl-1-cyclohexene (X). X was oxidized with *t*-butyl chromate and acetic anhydride to give 3,5,6-trimethyl-2-cyclohexen-1-one (XI). VI, VIII, XI, and X were oxidized with *t*-butyl chromate and acetic anhydride to give XII in 53, 52, 22, and 12% yields respectively. The oxidation of VIII by selenium dioxide gave XII in a 23% yield, but only a trace of XII was formed by the similar oxidation of X.

Numerous syntheses of trimethylhydroquinone (XIII), an indispensable raw material for the synthesis of α-tocopherol, have hitherto been reported, but the starting materials have been restricted to such aromatic compounds as pseudocumene, hydroquinone, *m*-xylenol[1]; no report of synthesis from trimethylcyclohexene nor trimethylcyclohexenones is known.

Oppenauer *et al.* have found that *t*-butyl chromate has oxidizing ability enough to convert 2-cyclohexen-1-one into benzoquinone.[2] This oxidation has now been applied to trimethylcyclohexene and

*1 Part I: T. Ichikawa and T. Kato, This Bulletin, **41**, 1224 (1968).

1) K. Sato and Y. Kurihara, *Yuki Gosei Kagaku Kyokaishi* (*J. Soc. Org. Synth. Chem. Japan*), **20**, 824 (1962), review.

2) R. V. Oppenauer and H. Oberrauch, *Anales. asoc. quim. argentina*, **37**, 246 (1949); *Chem. Abstr.*, **44**, 3871 (1950).

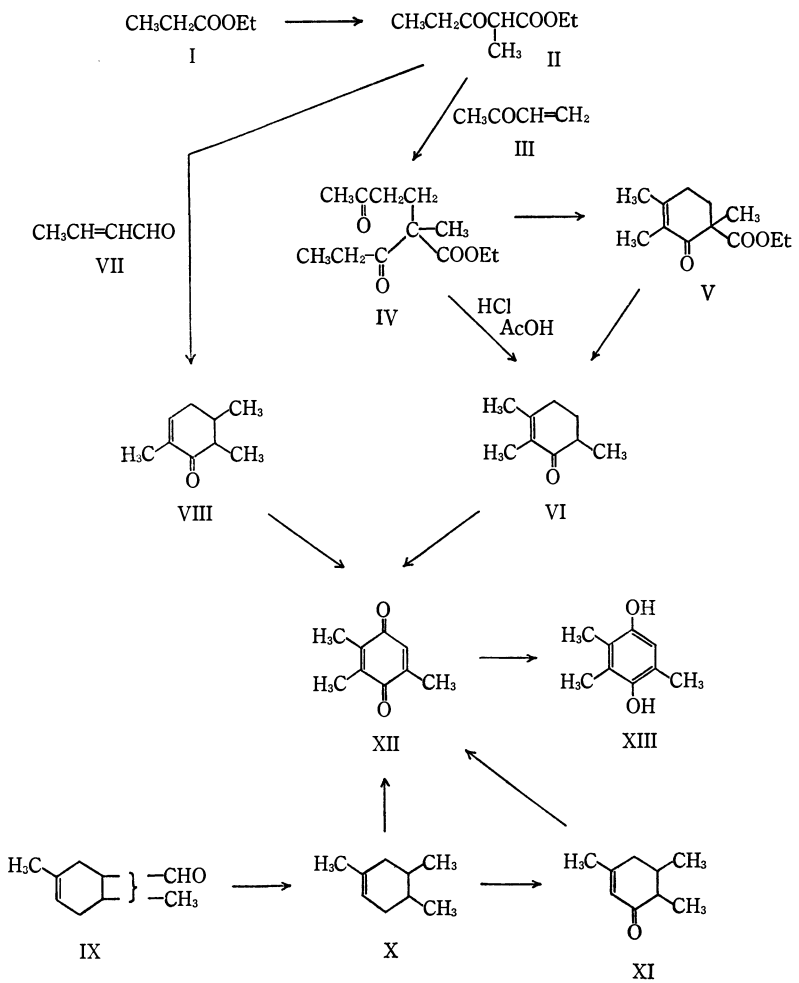

Scheme 1

trimethylcyclohexenones to obtain trimethylbenzoquinone (XII), which can then be easily reduced to give XIII. Three kinds of cyclohexenones and a cyclohexene were prepared, as shown in Scheme 1. Ethyl α-propionylpropionate (II)[3] prepared from ethyl propionate (I) was subjected to Michael condensation with methyl vinyl ketone (III) to yield 4-methyl-4-ethoxycarbonyloctane-3,7-dione (IV) (IR: $\nu_{C=O}$; 1715, 1725 (shoulder), and 1740 cm^{-1} (shoulder); NMR: δ 2.06, singlet, 3H, $\underline{CH_3}CO$; 1.25, singlet, 3H, $\underline{CH_3}$–C–; 4.15, quartet, $J=7$ cps, 2H, $CH_3\underline{CH_2}O$–). The dehydration of IV with beryllium chloride gave 2,3,6-trimethyl-6-ethoxycarbonyl-2-cyclohexen-1-one (V) (IR: $\nu_{C=O}$; 1733, 1665 and 1640 cm^{-1}; NMR: δ 1.25, singlet, 3H, $\underline{CH_3}$–C–COO–; 1.20, triplet, $J=7$ cps, 3H, $\underline{CH_3}$-CH_2O–; 1.71, 3H, $\underline{CH_3}C$=C–; 1.89, 3H, $\underline{CH_3}C$=C; 4.08, 2H, quartet, $CH_3\underline{CH_2}O$–), which was then converted to 2,3,6-trimethyl-2-cyclohexen-1-one(VI) by aqueous alkali. The refluxing of IV with hydrochloric acid and acetic acid gave VI directly. The absorption maximum of VI (244 mμ, ε 12400; 305 mμ, ε 90) is in good agreement with the expected value (242±5 mμ); the IR spectrum showed the presence of α,β-unsaturated ketone ($\nu_{C=O}$; 1670 cm^{-1}), while the NMR spectrum exhibited peaks at δ 1.68, 1.88 (singlets, 6H, $\underline{CH_3}$–C=C) and 1.05 (doublet, $\underline{CH_3}$–CH–, $J=7$ cps). All these facts sustain the VI structure.

When ethyl α-propionylpropionate (II) was condensed with crotonaldehyde (VII) in aqueous alkali, Michael addition, dehydration, saponification, and decarboxylation took place in succession to give directly 2,5,6-trimethyl-2-cyclohexen-1-one (VIII) (IR: $\nu_{C=O}$; 1680 cm^{-1}). The UV absorption maximum of VIII at 235 mμ ($\pi\rightarrow\pi^*$, ε 8900) was shorter than that of VI by 9 mμ, and the absorption

3) S. M. McElvain, *J. Am. Chem. Soc.*, **51**, 3124 (1929).

maximum at 318 mμ ($n\rightarrow\pi^*$, ε 80) was longer by 13 mμ (305 mμ); these facts are consistent with the idea of VIII being short of one olefin methyl group compared with VI.

An attempt to obtain 1,4,5-trimethyl-1-cyclohexene (X) by the direct Diels-Alder reaction between isoprene and 2-butene was a failure; the main product was the isoprene dimer, for it was identical with the product from isoprene alone under the same conditions. Therefore, 1,4(or 1,5)-dimethyl-5(or 4)-formyl-1-cyclohexene (IX), obtained by the Diels-Alder reaction of crotonaldehyde with isoprene,[4] was subjected to a Huang-Minlon reduction to give X. The IR spectrum showed a weak band at 1670 cm^{-1} ($\nu_{C=C-}$). The structure was further confirmed by ozonolysis and by converting the keto-aldehyde obtained into its disemicarbazone. When X was oxidized with *t*-butylchromate, an unsaturated ketone ($\nu_{C=O}$; 1670 cm^{-1}) with a small amount of trimethylbenzoquinone was obtained. The elementary analysis of its 2,4-dinitrophenylhydrazone is consistent with its being a trimethylcyclohexenone. The IR spectrum was quite different from the spectra of either VI or VIII, and the absorption maxima at 234 mμ (ε 12900) and 322 mμ (ε 70) coincided well with the expected value of 3,5,6-trimethyl-2-cyclohexen-1-one (XI). Each cyclohexenone can be distinguished from the others by gas liquid chromatography*2 and was gas chromatographically pure.

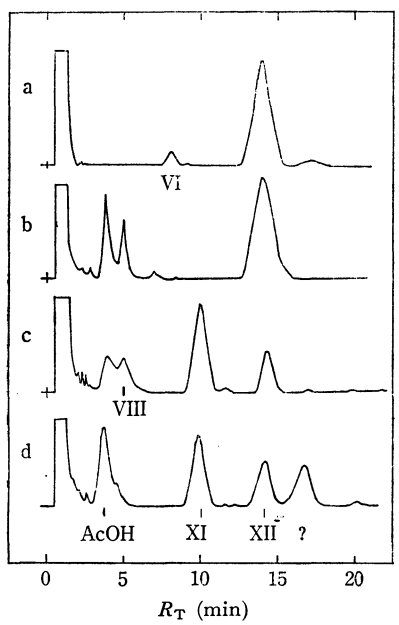

Fig. 1. Gas liquid chromatograms of oxidation products of VI(a), VIII(b), X(c) and XI(d) by *t*-butyl chromate.
Column: 5% PEG 6000 on Diasolid M, 4 mm ×3 m; carrier gas: helium; flow rate: 86 m*l*/min; temp: 205°C.

4) O. Diels and K. Alder, *Ann.*, **470**, 62 (1929).

It is reasonable that the less-hindered methylene group of X was selectively oxidized; the fact that the oxidation to XII can not proceed further easily is presumably due to the separation of the chromate complex during the reaction.

The three cyclohexenones (VI, VIII, XI) and one cyclohexene (X) thus obtained were then oxidized with *t*-butyl chromate in the presence of acetic anhydride. The chromatogram of the oxidation product of VI (Fig. 1a) showed the formation of benzoquinone (XII), accompanied by a small amount of the unreacted VI. Ten moles of the chromate to one mole of VI and refluxing for 12 hr in benzene were necessary to obtain the best yield of XII (53%). On long refluxing (24 hr), the yield of XII decreased to 38%. A similar oxidation of VIII gave 52% of XII (*t*-butyl chromate: 10 mol; refluxing time: 20 hr). The results (see Fig. 1b) were very similar to the case of VI, perhaps because of a similar steric hindrance at the C-4 positions. When XI was oxidized under similar conditions, an unknown side product (see Fig. 1d) was formed along with XII. The yield of XII was 22% (*t*-butyl chromate: 10 mol; refluxing time: 25 hr), which was rather low compared with those in the former cases. As the side product (R_t: 17 min, Fig. 1d) was not reduced by hydrosulfite, the olefinic methyl group might be oxidized in place of the sterically-hindered C-4 of XI.

As has been stated before, the oxidation of X gave XI as a major product, but small amounts of VIII and XII were also formed (see Fig. 1c). The employment of a small excess of the oxidizing agent and a long refluxing time gave a fair yield of XI, but that of XII did not exceed 12% even when an oxidizing agent was employed in a large excess (40 mol), under

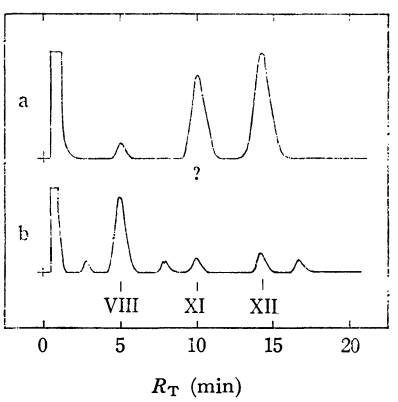

Fig. 2. Gas liquid chromatograms of oxidation products of VIII(a) and X(b) by selenium dioxide.
Column: 5% PEG 6000 on Diasolid M, 4 mm × 3 m; carrier gas: helium; flow rate: 86 m*l*/min; temp: 205°C.

*2 Column: PEG 6000, 5% on Diasolid M, 4 mm ×3 m; carrier gas: helium; flow rate: 86 m*l*/min; temp.: 134°C.

which conditions cyclohexenones completely vanished.

When VIII (1 mol) was oxidized with selenium dioxide (1.1 mol) in glacial acetic acid, XII was obtained in a 23% yield; this yield is considerably inferior to that obtained by the chromate oxidation. As can be seen from Fig. 2a, a side product was formed. This is probably an oxidized product of VIII at the olefinic methyl group. When one mole of X was oxidized with 1.5—2.0 mol of selenium dioxide, the major product was found to be VIII (5% from X), plus a trace of benzoquinone (see Fig. 2b). The yield of VIII was low, but it is interesting that this oxidation seems to have taken place at the more sterically-hindered methylene group.

When these oxidized products were reduced by sodium hydrosulfite, trimethylhydroquinone (XIII) was obtained in a quantitative yield.

Experimental

4-Methyl-4-ethoxycarbonyloctane-3,7-dione (IV). To 40 g of ethyl α-propionylpropionate (II) there was added a solution of sodium ethoxide prepared from 0.32 g of sodium and 20 m*l* of ethanol, with the temperature kept below 10°C. Freshly-distilled methyl vinyl ketone (19.6 g) was added, drop by drop, to the above solution under stirring at the same temperature. The reaction mixture was then stirred for 1 hr and left standing overnight at room temperature. The mixture was poured into 200 m*l* of water containing 1 m*l* of acetic acid, and then extracted with ether. The ether extract was washed with water, dried, and evaporated, and the residue was distilled under reduced pressure; bp 151—167°C/4 mmHg, 45 g (75%). Redistillation gave a colorless oil boiling at 123—124°C/3.5 mmHg.

Found: C, 63.32; H, 8.92%. Calcd for $C_{12}H_{20}O_4$: C, 63.13; H, 8.83%.

2,3,6-Trimethyl-6-ethoxycarbonyl-2-cyclohexen-1-one (V). A solution of IV (8.3 g) and beryllium chloride (2.9 g) in benzene (30 m*l*) was refluxed for 4 hr in a flask equipped with a calcium chloride tube. The reaction mixture was then poured into a mixture of 50 m*l* of 1 N hydrochloric acid and ice, extracted three times with benzene; the benzene extract was washed with a sodium bicarbonate solution and then with water, dried over calcium chloride, and distilled; bp 105—107°C/17 mmHg, 4.9 g (65%).

Found: C, 63.27; H, 8.41%. Calcd for $C_{12}H_{18}O_3$: C, 68.54; H, 8.63%.

2,3,6-Trimethyl-2-cyclohexen-1-one (VI). a) To a solution of potassium hydroxide (7 g) in 30 m*l* of water 3 g of V were added, and the mixture was refluxed for 2 hr. After cooling, the mixture was extracted with ether, and the ether extract was washed with water, dried, and distilled; bp 92—96°C/16 mmHg, 1.6 g (80%).

b) To 33.5 g of IV there were added 35 m*l* of concentrated hydrochloric acid and 70 m*l* of acetic acid, after which the mixture was refluxed for 6 hr. The mixture was concentrated under diminished pressure. The residue was added to water, neutralized with sodium bicarbonate, and extracted with ether. The ether extract was washed with water, dried, and distilled; bp 93—96°C/16 mmHg, 13.5 g (67%). The IR spectrum was identical with that of the product obtained by a).

Found: C, 78.48; H, 10.23%. Calcd for $C_9H_{14}O$: C, 78.21; H, 10.21%.

2,5,6-Trimethyl-2-cyclohexen-1-one (VIII). Into 21.3 g of ethyl α-propionylpropionate (II) there was stirred a solution of 0.3 g of sodium hydroxide in 50 m*l* of ethanol at 5—10°C. Crotonaldehyde (11.7 g) was stirred into the reaction mixture at the same temperature, and the solution was left standing overnight. It was then refluxed for 2 hr with a solution of 15 g of potassium hydroxide in 75 m*l* of water, poured into 300 m*l* of water, and neutralized with diluted hydrochloric acid. The mixture was extracted with ether, and the ether extract was washed with a 10% sodium bicarbonate solution and water, dried, and distilled; bp 92—100°C/24 mmHg, 8.9 g (48%). Semicarbazone; mp 230—231 °C.

Found: C, 61.01; H, 8.71; N, 22.00%. Calcd for $C_{10}H_{17}ON_3$: C, 61.51; H, 8.78; N, 21.52%.

1,4,5-Trimethyl-1-cyclohexene (X). A mixture of aldehydes prepared by the Diels-Alder reaction of isoprene and crotonaldehyde (IX, 40 g) and potassium hydroxide (50 g) was dissolved in 200 m*l* of diethylene glycol. Hydrazine hydrate (80%, 40.2 m*l*) was then added to the reaction mixture. On stirring, an exothermic reaction took place and the temperature of the reaction mixture rose to 80°C. The mixture was refluxed for 1 hr and then steam-distilled. The distillate was extracted with ether, and the ether extract was washed with water, dried, and distilled; bp 143—155°C, 22.5 g (63%). For analysis, a part was ozonized and reduced with zinc and acetic acid, and the product was precipitated as disemicarbazone, mp 176.5—178.5°C (decomp.).

Found: C, 49.34; H, 8.34; N, 30.83%. Calcd for $C_{11}H_{22}O_2N_6$: C, 48.87; H, 8.20; N, 31.09%.

3,5,6-Trimethyl-2-cyclohexen-1-one (XI). Fifteen grams of X were added to a mixture of 244 m*l* of the solution of *t*-butyl chromate (prepared from 185 g of chromic anhydride and 470 m*l* of *t*-butyl alcohol, diluted to 1.3 *l* with benzene, dried, and concentrated to 1 *l*) and 23 m*l* of acetic anhydride. The mixture was then refluxed for 22 hr under stirring and then steam-distilled. The distillate was extracted with ether, and the ether extract was washed with water, dried over magnesium sulfate, and distilled; bp 99—113°C/24 mmHg, 6.3 g (38%). Redistillation gave an oil; bp 104.5—106.5°C/21.5 mmHg. 2,4-Dinitrophenylhydrazone; mp 177—178°C (decomp.).

Found: C, 56.78; H, 5.93; N, 17.40%. Calcd for $C_{15}H_{18}O_4N_4$: C, 56.59; H, 5.70; N, 17.60%.

Oxidation by *t*-Butyl Chromate (General Procedure). To a trimethylcyclohexene or a cyclohexenone (1 g) dissolved in 10 m*l* of benzene, a solution of *t*-butyl chromate in benzene and acetic anhydride equimolar to the chromate were added and the mixture was heated to reflux under stirring. The reaction product was poured into water and steam-distilled until the distillate was no longer yellow. The distillate was then extracted with ether; the ether extract was washed with water, dried over sodium sulfate and concentrated to 10 m*l*, and the sample was submitted to gas chromatographic analysis.

Oxidation by Selenium Dioxide. To a trimethylcyclohexene or a cyclohexenone (2.8 g), 3 m*l* of glacial acetic acid were added. Selenium dioxide was then

stirred in, portion by portion. After the addition was complete, the temperature of the reaction mixture was gradually elevated until the mixture was finally heated to reflux. The product was steam-distilled as long as the distillate was yellow. The distillate was then extracted with ether, and the ether extract was washed with water, dried over sodium sulfate, concentrated to 20 m*l*, and submitted to gas chromatography.

Trimethyl Hydroquinone. The ethereal solution of trimethylbenzoquinone (XII) obtained by the oxidation described above was treated with an aqueous solution of sodium hydrosulfite until the yellow color vanished. The ether layer was then washed with water, dried, and concentrated. The residue was triturated with petroleum ether, and white crystals of trimethylhydroquinone were obtained. When the substance was recrystallized from water, its mp was 169—170°C; this mp was not depressed when it was admixed with an authentic sample, and its IR spectrum was identical with that of the authentic sample.

The authors wish to express their thanks to Professor Masanao Matsui of the University of Tokyo and to Dr. Tadao Takenishi of the Ajinomoto Co., Inc., for their valuable suggestions and encouragement.

BULLETIN OF THE CHEMICAL SOCIETY OF JAPAN VOL. 41 1232—1236 (1968)

Synthetic Studies of α-Tocopherol. III.*1 Synthesis of Phytone

Takehiko ICHIKAWA and Tetsuya KATO

Central Research Laboratories, Ajinomoto Co., Inc., Kawasaki

(Received December 4, 1967)

Phytone (XI), an important intermediate in the preparation of α-tocopherol, was synthesized by a selective Wittig reaction between geranyltriphenylphosphonium halide (VII) and the aldehyde group of 2-methyl-6-oxoheptanal (VIII), followed by the hydrogenation of the product. VIII was prepared from 1,3-dimethyl-1-cyclohexene (V) by ozonolysis and reductive decomposition. V could not be obtained in a pure state by the dehydration of 2,6-dimethylcyclohexan-1-ol (II), presumably because of the isomerization of the intermediate carbonium ion. The pyrolysis of the acetate of II (III) was found to give pure V. That the hardly-pyrolizable stereoisomer of III was *cis,cis*-2,6-dimethylcyclohexyl-1-acetate (VI) is consistent with the *cis*-elimination mechanism.

Recent advances in biological study have revealed numerous biological activities of tocopherols, and their physiological significance has come to be increasingly recognized.[1] Phytone (XI), namely, 6,10,14-trimethyl-2-pentadecanone, serves as an important intermediate for the synthesis of α-tocopherol, and a large number of methods of synthesizing it have been described.[2] However, we have now attempted to develop the new, simple method of synthesis as indicated in Scheme 1.

2,6-Xylenol (I) was hydrogenated in the presence of Raney Nickel and sodium salt of 2,6-xylenol[3] to yield 2,6-dimethyl-1-cyclohexanol (II) in a nearly quantitative yield. The description of how Ruzicka *et al.*[4] obtained 1,3-dimethylcyclohexene (V) by the dehydration of II with potassium hydrogen sulfate has been found to be erroneous, for the NMR spectrum of the dehydrated product showed two olefinic protons of about the same intensities (δ 5.2 and 5.3), while that of the ketoaldehyde obtained by its ozonolysis and reductive decomposition showed two pairs of doublets of methyl groups of about equal intensities (δ 0.88 and 1.07, $C\underline{H}_3CH$–, doublets, $J=7$ cps) and two kinds of aldehyde groups (δ 9.55, –CH–C$\underline{H}$O, doublet, $J=2$ cps; 9.70, –$CH_2C\underline{H}O$, triplet, $J=2$ cps) (Fig. 1a). These results show that the dehydrated product is a 1 : 1 mixture of V and 2,4-dimethylcyclohexene (IV), and that the ketoaldehyde is a mixture of 2-methyl-6-oxoheptanal (VIII) and 4-methyl-6-ketoheptanal. Neither the 85% phosphoric acid[5] nor the aluminum oxide[6] employed in the dehydration has been found to be effective in obtaining V in a pure state, as can be seen from Figs. 1b and 1c, the isomerization of the carbon skelton has apparently occurred in the latter case. The bromination and dehydrobromination of II gave a very pure 1 : 1 mixture of V and IV (see Fig.

*1 Part II: T. Ichikawa, H. Owatari and T. Kato, This Bulletin, **41**, 1228 (1968).

1) S. Kijima, *Yuki Gosei Kagaku Kyokaishi* (*J. Soc. Org. Synth. Chem. Japan*), **24**, 92, 200 (1966), review.

2) K. Sato and Y. Kurihara, *ibid.*, **20**, 824 (1962), review.

3) H. E. Ungnade and A. D. McLaren, *J. Am. Chem. Soc.*, **66**, 118 (1944); H. E. Ungnade and D. V. Nightingale, *ibid.*, **66**, 1218 (1944); R. B. Carlin, *J. Am. Chem. Soc.*, **67**, 931 (1945).

4) L. Ruzicka, D. R. Koolhaas and A. H. Wind, *Helv. Chim. Acta*, **14**, 1155, 1166 (1931).

5) B. B. Corson and V. N. Ipatieff, "Organic Syntheses," Coll. Vo. II, p. 152 (1950).

6) H. Pines, *J. Am. Chem. Soc.*, **55**, 3892 (1933).

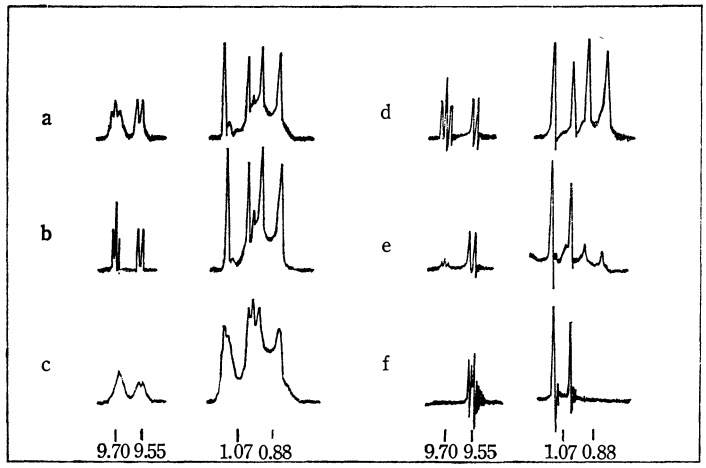

Fig. 1. NMR spectra of aldehyde and methyl groups of ketoaldehydes obtained from dehydrated products of 2,6-dimethylcyclohexan-1-ol (II) with potassium bisulfate (a), phosphoric acid (b), alumina (c), bromination and dehydrobromination (d), boric acid (e) and acetylation followed by pyrolysis (f), (in CCl_4).

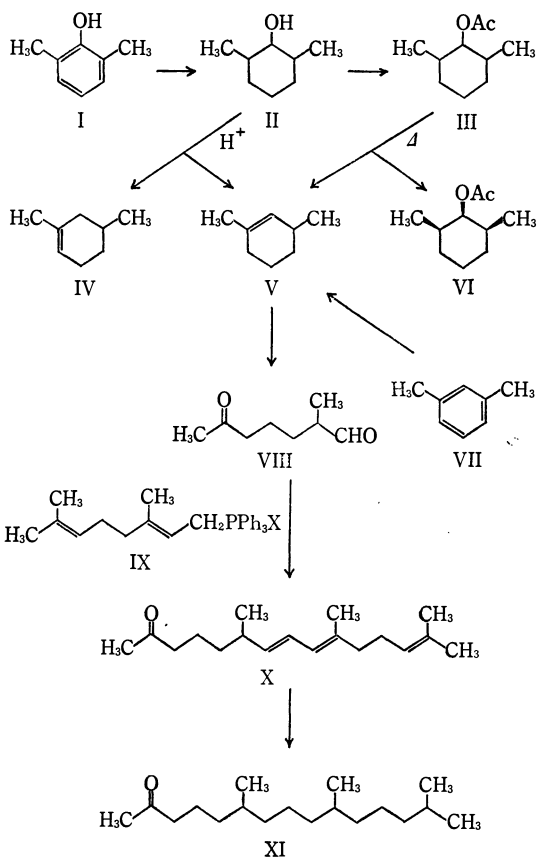

Scheme 1

ld). These results seem to suggest that the secondary cation (XII) formed by the protonation of II rapidly isomerizes to the more stable tertiary cation (XIII), and that the subsequent abstraction of the proton from XIII gives rise to a 1 : 1 mixture of V and IV.

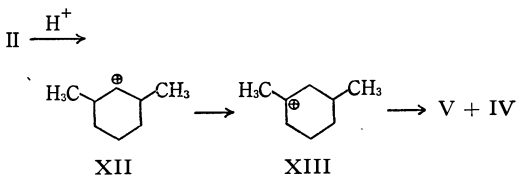

As no dehydrating process seems to serve in the present purpose, the pyrolysis of borate and acetate of II has been attempted. Boric acid and II were first reacted under mild conditions to give the borate of II; its following pyrolysis gave V as the major product (see Fig. 1e), but it was not free of IV. The dehydration of II seems to have taken place in part. The acetylation of II with acetic anhydride gave 2,6-dimethyl-1-cyclohexylacetate (III) in a quantitative yield. The pyrolysis of III was found to give pure V (δ 0.90, 3H, C<u>H</u>$_3$–CH–, doublet, J=7 cps; 1.60, 3H, C<u>H</u>$_3$–C=C, broad singlet, line width=4 cps; 5.21, 1H, <u>H</u>–C=C, broad singlet, line width=6 cps), and the ketoaldehyde obtained from it was naturally pure VIII (see Fig. 1f). The pyrolysis of the acetate (III) was achieved by passing vaporized III through a heated quartz column at 500—550°C, along with a flow of nitrogen. Considerable amounts of side products were formed at temperatures above 550°C, whereas the yields of V were low below 500°C. The yield was only slightly influenced by the flow rate of III at 500°C, but it decreased considerably when the velocity was decreased to below 0.4 g/min at 580°C. The highest yield (71%) was obtained at

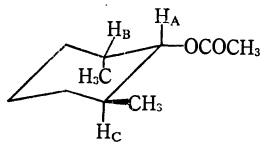

XIV

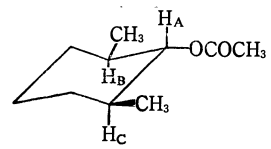

XV

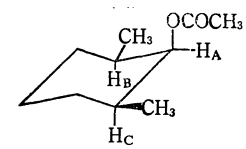

VI

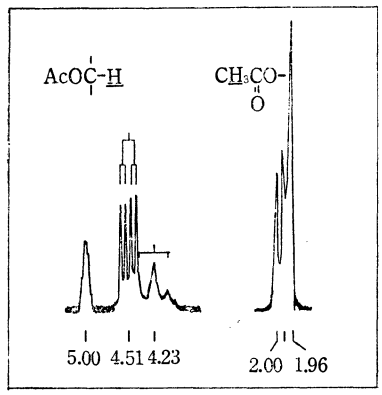

Fig. 2. NMR spectrum of 2,6-dimethylcyclohexyl-1-acetate (in CCl_4).

550°C with the flow rate of 1.5 g per minute. Although the recovered unreacted acetate was pyrolyzed under the same conditions, the yield of V amounted to only a few percent. A gas liquid chromatogram of III showed the presence of three stereoisomers (R_t: 11.6 (minor), 12.7 (minor), 13.8 (major) min); their ratio was slightly influenced by unknown factors during the hydrogenation of I. The recovered acetate was found to correspond to a minor component (R_t: 11.6 min). The NMR spectrum of III showed the presence of three kinds of -CH-OAc groups (δ 5.00, broad singlet, line width = 5 cps, 4.51, quartet, and 4.23, triplet) and three kinds of acetyloxy groups (δ 1.96, 1.97 and 2.00) (see Fig. 2), whereas the spectrum of the recovered acetate showed one -CH-OAc group, at δ 5.00, and one acetyloxy group, at δ 2.00. The possible conformations of V are XIV, XV, and VI. As J_{AB} ($\phi = 60°$) and J_{AC} ($\phi = 180°$) of XIV are expected to be about 2 cps and 9 cps respectively from the Karplus equation, the spectra of XIV, XV, and VI correspond to the signals at δ 4.51 and 1.96, at 4.23 and 1.97, and at 5.00 and 2.00 respectively. The pyrolysis of acetate is believed to feature intramolecular cis-elimination,[7] as is shown in XVI.

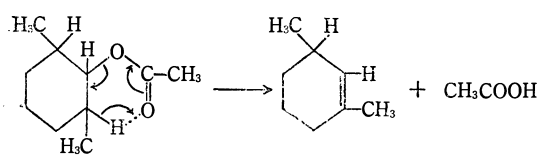

XVI

That VI is hard to pyrolyze is comprehensible from the fact that a conformation of sterically-hindered 1,3-diaxial methyl groups is inevitable when a cyclic transition state XVI is formed.

A recent method patented by Amagasa *et al.*[8] claims to be able to obtain V from *m*-xylene (VII) by reduction with sodium-water in liquid ammonia; this may offer a simpler way of obtaining V.

Geranyl triphenylphosphonium bromide (IX, X = Br) was prepared by the method of Isler *et al.*[9] from linalool or geraniol. The corresponding phosphonium chloride (IX, X = Cl) was prepared in a similar manner, but the yield was not satisfactory. The ylid from geranyl triphenylphosphonium halide has been prepared at first with phenyl lithium in ether, and the ketoaldehyde was added to the solutions of the ylid. The infrared spectra of the product showed an absorption band at 1715 cm^{-1}, while no absorption band of the unsaturated carbonyl group was found to be present, so the aldol condensation

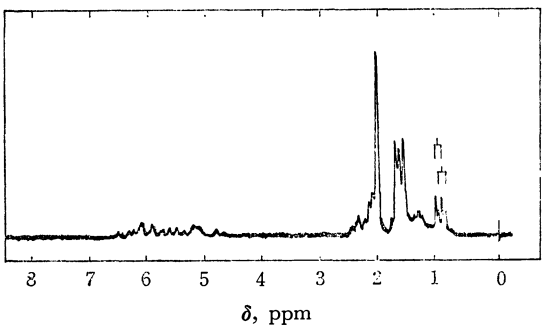

Fig. 3. NMR spectrum of 6,10,14-trimethylpentadeca-7,9,13-trien-2-one (X), (in CCl_4).

of aldehyde group seems not to have taken place. The Wittig reaction has been simplified in order to make it proceed in a better yield by adding sodium methoxide to a mixture of VIII and IX in an oxygen-containing solvent, such as ether, dioxane, tetrahydrofuran, dimethylformamide, or ethyl acetate. The yield was poor in a non-oxygen-containing solvent, such as chloroform or liquid ammonia. The NMR spectrum of the product shows an acetyl group (δ 2.00, 3H), three olefinic methyl groups (δ 1.58,

7) D. Y. Curtin and D. B. Kellom, *J. Am. Chem. Soc.*, **75**, 6011 (1953).
8) M. Amagasa and T. Yamaguchi, Japanese Pat. 40-11378 (1965).
9) O. Isler, H. Gutman, H. Lindler, M. Montavon, R. Ruegg, G. Ryser and P. Zeller, *Helv. Chim. Acta*, **39**, 463 (1956).

1.66, 1.70, 9H), and two kinds of methyl groups (δ 0.92, doublet, 3H, $J=7$ cps; 0.96, doublet, 3H, $J=7$ cps) and supports the expected structure, 6,10,14-trimethyl-7,9,13-pentadecatrien-2-one (X) (see Fig. 3). That the two kinds of secondary methyl group are present shows that the product is a mixture of 7-*cis*- and 7-*trans*-isomers, one of which, presumably *trans*-, predominates. For the hydrogenation of X, it was necessary to treat X with Raney Nickel or with cationic exchange resin, for example, Amberlist 15 (H^+), to remove the catalyst poison, which is presumably a trace of triphenylphosphine. Palladium (5%) on active carbon was satisfactory for hydrogenating the double bonds of X selectively, yielding phytone (XI) in a nearly quantitative yield. Its IR spectrum ($\nu_{C=O}$, 1720 cm^{-1}) showed the presence of ketone and no hydroxyl group; its NMR spectrum (δ 2.01, singlet, $C\underline{H}_3CO-$; 1.23, $-C\underline{H}_2-$; 0.88, doublet, $C\underline{H}_3-CH-$, $J=6$ cps; 2.32, triplet, $-CH_2-C\underline{H}_2-CO-$) is consistent with XI, and the shapes of the signals of methyl and methylene groups resemble those of authentic phytol.

Experimental

2,6-Dimethylcyclohexan-1-ol (II). To 2.5 g of xylenol (I), 0.5 g of sodium metal was added, after which the mixture was heated at 100°C for 30 min. After cooling, absolute benzene was added and the reddish white mass was crushed and filtered to afford a green precipitate of phenolate of I.

The hydrogenation of I (52 g) with Raney Nickel in the presence of 0.2 g of the phenolate[3] gave 50.4 g (93%) of II; bp 77—82°C/21 mmHg. For analysis a part of it was refractionated; bp 66.5°C/5 mmHg. $n_D^{16.8}$ 1.4660.

Found: C, 74.80; H, 12.44%. Calcd for $C_8H_{16}O$: C, 74.94; H, 12.58%.

2,6-Dimethylcyclohexyl-1-acetate (III). To a mixture of 106 g of cyclohexanol (II) and 101 m*l* of acetic anhydride, three drops of concentrated sulfuric acid were added, and the mixture was shaken in a flask equipped with a calcium chloride tube. The temperature of the mixture was maintained below 100°C by cooling it with running water. After the vigorous reaction had subsided, the mixture was further heated at 100°C for 2 hr. The mixture was then poured into 300 m*l* of water, salt was added, and the mixture was shaken thoroughly. The aqueous layer was extracted with ether, and the extract was combined with an organic layer, washed with water, saturated sodium bicarbonate, and water, dried with anhydrous magnesium sulfate, and distilled; bp 87—92°C/24 mmHg, 130.6 g (93%). For analysis, a part of it was refractionated; n_D^{18} 1.4422, bp 72°C/4 mmHg.

Found: C, 70.62; H, 10.51%. Calcd for $C_{10}H_{18}O_2$: C, 70.54; H, 10.66%.

Dehydration of 2,6-Dimethyl-1-cyclohexanol (II).

a) Dehydration by Potassium Bisulfate.[2] A mixture of 12.8 g of II and 25.6 g of potassium bisulfate was heated in an oil bath kept at 180—190°C. The distillate was then freed from water and distilled; bp 115—130°C, 4.8 g (44%). Ozonolysis and reductive decomposition gave a mixture of ketoaldehydes (see Fig. 2a).

b) Dehydration with 85% Phosphoric Acid.[3] To 2 g of 85% phosphoric acid heated at 165—170°C in an oil bath, 12.8 g of II were added, drop by drop, and the distillate was dried, redistilled, and converted into a mixture of ketoaldehydes (see Fig. 2b).

c) Dehydration by Alumina. Through a 2 cm × 25 cm column packed with 10-mesh active alumina and heated at 360—380°C, there were passed 10 g of II in 20 min. The pyrolysate was dried, redistilled, and converted into a mixture of ketoaldehydes by ozonolysis (see Fig. 2c).

d) Bromination and Dehydrobromination. To a solution of 19 g of II in 20 m*l* of tetrachloromethane, there was added, drop by drop, 17.6 g of phosphorous tribromide in 17 m*l* of tetrachloromethane. The mixture was then stirred for 1 hr at room temperature, poured into water, and extracted with ether; the ether extract was washed, dried, and distilled; bp 82—83°C/25 mmHg, 20.5 g. Five grams of the oil thus obtained were added, drop by drop, to a solution of 4.5 g of potassium hydroxide in 9 m*l* of methanol at 100—105°C. The mixture was then heated further 30 min, poured into water, and extracted with ether; the ether extract was washed, dried, distilled, and converted into ketoaldehydes (see Fig. 2d).

e) Dehydration by Boric Acid. To a solution of 6 g of II in 20 m*l* of 1,2-dichloroethane, 2.9 g of boric acid were added; the mixture was then distilled slowly through 1 cm × 20 cm Vigreux column. Distillation was continued, with dichloroethane supplied occasionally, until water no longer distilled out and a clean solution was finally obtained. The supply of dichloroethane was then stopped, and distillation was continued further. When the temperature of the solution reached 240°C, decomposition began and the distillate was dried with magnesium sulfate and fractionated. Yield; 3.8 g (73%). The product was ozonolysed to give mainly 2-methyl-6-ketoheptanal (see Fig. 1e).

f) Pyrolysis of III, 1,3-Dimethyl-1-cyclohexene (V). 370 grams of acetate (III) were evaporated in a preheater (1 g/min) and passed through a quartz column (30 mm × 300 mm) heated at 550°C under a nitrogen stream of 60 m*l*/min. When the pyrolysate was then condensed with an efficient cooler, 306 g of the pyrolysate were recovered (97%). Water (800 m*l*) was added, and the mixture was neutralized carefully with 320 m*l* of 5 N sodium hydroxide (74% of acetic acid was assumed to be formed). The oily layer was separated and fractionated through a Widmer column; bp 119—125°C, 170 g (71%). n_D^{17} 1.4520.

Found: C, 87.41; H, 12.80%. Calcd for C_8H_{14}: C, 87.19; H, 12.81%.

The residue (89 g, 24%) was fractionated under a vacuum; bp 73—79°C/13 mmHg, 8.4 g. It was found to be *cis,cis*-2,6-dimethylcyclohexyl-1-acetate (VI), which gave only 5% of the cyclohexene under the above pyrolytic conditions.

Found: C, 70.62; H, 10.49%. Calcd for $C_{10}H_{18}O$: C, 70.54; H, 10.66%.

2-Methyl-6-ketoheptanal (VIII). A solution of 22 g of V in 200 m*l* of dichloromethane was cooled to −50—−60°C, and then oxygen gas (350 m*l*/min) containing ozone was introduced for 7 hr (0.03 mol/hr). The solution was immediately added, drop by drop, to a mixture of 15 g of zinc dust and 140 m*l* of 70% acetic acid. After the addition was complete, the mixture was refluxed for 2 hr and neutralized to pH 6 with sodium hydroxide. Care was taken to keep the pH of the solution below 6 and the temperature below 20°C. The mixture

was extracted with ether, dried, and distilled; bp 49—57°C/0.3 mmHg, 20.3 g (71%). A part of it was fractionated with efficient column for analysis; bp 67°C/0.5 mmHg, n_D^{14} 1.4376.

Found: C, 67.51; 9.80%. Calcd for $C_8H_{14}O_2$: C, 67.57; H, 9.93%.

Geranyltriphenylphosphonium Bromide (IX, X=Br). Geraniol (10 g) purified through a calcium chloride complex was converted into the phosphonium bromide IX (X=Br; 23 g) in a 73% yield by Isler's method[9]; mp 178—183°C. The product was used in the subsequent reaction without further purification. Geraniol can be successfully replaced by linalool.

6,10,14-Trimethyl-7,9,13-pentadecatriene-2-one (X). To 60 m*l* of anhydrous dioxane there were added 2 g of ketoaldehyde (VIII) and 6.6 g of IX (X=Br), and the mixture was stirred under an atmosphere of dry nitrogen. A methanolic solution of 2 N sodium methoxide (7 m*l*) was added, drop by drop, to the above mixture at 25°C over a 30-min period. After the addition was over, the mixture was heated at 55°C for 30 min under stirring. Then the mixture was poured into 50% aqueous methanol and extracted with petroleum ether. The petroleum ether extract was washed twice with 50% methanol and water, dried with anhydrous magnesium sulfate, and distilled; bp 113—119°C/0.1 mmHg, 2.44 g (66%). Redistillation for analysis gave an oil; bp 121—123°C/0.17 mmHg, n_D^{21} 1.4960. λ_{max}^{EtOH} 242 mμ (ε 2.98 $\times 10^4$).

Found: C, 82.18: H, 11.42%. Calcd for $C_{18}H_{30}O$: C, 82.38; H, 11.52%.

When geranyltriphenylphosphonium chloride was used in place of the bromide, the yield was 64%. When the reactions were carried out in methanol, X was not obtained.

Phytone (XI). To 38 g of X 4 m*l* of methanol and 4 g of Raney Nickel were added and the mixture was heated to reflux for 1 hr. The treatment with Raney Nickel can successfully be replaced by a treatment with a cationic resin such as Amberlist 15 (H^+) at room temperature. The catalyst was filtered off, 2 g of palladium charcoal (5%) were added, and the mixture was shaken at room temperature in an autoclave under the initial hydrogen pressure of 125 kg/cm^2. After the calculated amount of hydrogen had been absorbed, the catalyst was filtered and the filtrate was fractionated; bp 114—117°C/0.2—03 mmHg, 35. 3 g (91%). For analysis, a part of it was refractionated; bp 115°C/0.2 mmHg.

Found; C, 80.57; H, 13.51%. Calcd for $C_{18}H_{36}O$: C, 80.52; H, 13.52%.

The authors wish to express their heartfelt thanks to Professor Masanao Matsui of the University of Tokyo and to Dr. Tadao Takenishi of the Ajinomoto Co., Inc., for their valuable suggestions and encouragement.

BULLETIN OF THE CHEMICAL SOCIETY OF JAPAN VOL. 41 1237—1240 (1968)

Synthesis of 4,5-Di- and 1,4,5-Trisubstituted Imidazole Derivatives from 4,5-Dicyanoimidazole

Yoshitaka YAMADA, Izumi KUMASHIRO and Tadao TAKENISHI

Central Research Laboratories Ajinomoto Co., Inc., Kawasaki

(Received December 13, 1967)

The chemical reactivities and the synthesis of various derivatives of 4,5-dicyanoimidazole formed by heating a solution of hydrogen cyanide in liquid ammonia were studied, as were the partial hydrolysis, hydrogenation, and addition reaction of cyano groups and the alkylation, cyanoethylation, and vinylation of the imidazole ring. From these experiments, a few new compounds were synthesized, which had been expected as intermediates of polymers containing imidazole rings.

In a previous paper,[1] the present authors have reported that adenine and 4,5-dicyanoimidazole were formed simultaneously by heating a solution of hydrogen cyanide in excess liquid ammonia. Though 4,5-dicyanoimidazole (I) has been already described in the literature,[2,3] the chemical properties of the compound have not yet been adequately described. This substance was recently found to be a valuable intermediate for the synthesis of various useful derivatives of imidazole and purine, *e.g.*, 4-amino-5-imidazolecarboxamide.[4] Furthermore, I may be expected to be a valuable intermediate for various polymers containing imidazole rings.

The present investigation was undertaken in order to clarify the reactivities of two cyano groups and one imino group of I and to prepare various imidazole derivatives.

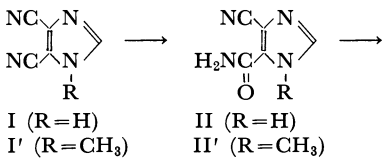

I (R=H) I′ (R=CH_3) II (R=H) II′ (R=CH_3)

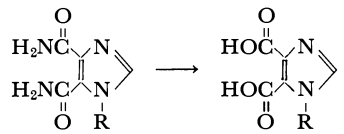

III (R=H) III′ (R=CH_3) IV (R=H) IV′ (R=CH_3)

The partial hydrolysis[4] of I to 4-cyano-5-imidazolecarboxamide (II) had been achieved in a 90% yield by treatment with a 1 N sodium hydroxide solution. Under more drastic conditions, however, the hydrolysis of I could not be stopped at the diamide (III) stage, and 4,5-imidazoledicarboxylic acid (IV) was obtained in a 88% yield. In contrast with these findings, the hydrolysis of 1-methyl-4,5-dicyanoimidazole (I′) was found to occur hundreds of times faster than that of I. Consequently, whereas 1-methyl-4,5-imidazoledicarboxamide (III′) was obtained in a 80% yield, it was difficult to isolate 1-methyl-4-cyano-5-imidazolecarboxamide (II′) in a high yield. Besides, far more reduction of cyano groups of I′ was achieved than in the case of the reduction of I by lithium aluminium hydride or by catalytic hydrogenation (Raney Cobalt). The increased reactivities of the cyano groups of I′ may be due to the electron-releasing effect of the methyl group in the position 1. Attempts to prepare amidine and orthoester derivatives *via* iminoether[3] of I were unsuccessful. These data on the addition reactions indicate that the cyano groups of I are extremely different from those of malononitrile and benzonitrile. Hydrogen sulfide, however, reacted

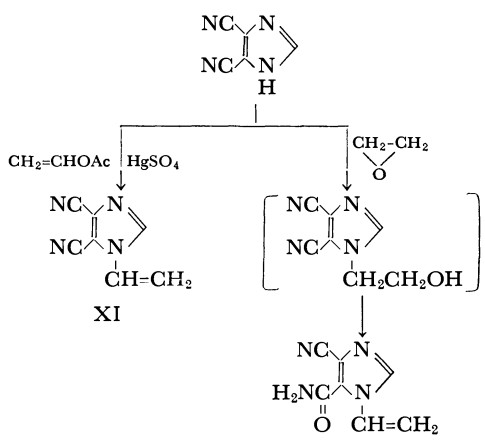

XI XII

1) H. Wakamatsu, Y. Yamada, T. Saito, I. Kumashiro and T. Takenishi, *J. Org. Chem.*, **31**, 2035 (1966).
2) D. W. Woodward, U.S. Pat. 2534331 (1950).
3) H. Bredereck and G. Schmötzer, *Ann.*, **600**, 95 (1956).
4) Y. Yamada, I. Kumashiro and T. Takenishi, This Bulletin, **41**, 241 (1968).

TABLE 1. IMIDAZOLE DERIVATIVES

No.	Substituents			Yield %	Solv. of recrystn[a]	Mp °C (Bp)	Empirical formula
	R_1	R_2	R_3				
III	H	$CONH_2$	$CONH_2$	54	A	>300 d	$C_5H_6N_4O_2$
IV	H	CO_2H	CO_2H	88	A	280 — 282 d	$C_5H_4N_2O_4$
I′	CH_3	CN	CN	95[c]	B	89 — 89.5	$C_6H_4N_4$
II′	CH_3	CN	$CONH_2$	19	D	212 — 212.5	$C_6H_6N_4O$
III′	CH_3	$CONH_2$	$CONH_2$	80	B	268	$C_6H_8N_4O_2$
IV′	CH_3	CO_2H	CO_2H	70	B	253.5— 254 d	$C_6H_6N_2O_4$
V	H	CH_2NH_2	CH_2NH_2	40[b]	C	285 — 290 d	$C_5H_{10}N_4\cdot 3HCl$
V	H	CH_2NH_2	CH_2NH_2	20[c]	C		
V	H	CH_2NH_2	CH_2NH_2	12[d]	C		
VI	CH_3	CH_2NH_2	CH_2NH_2	51[d]	C	265 — 268 d	$C_6H_{12}N_4\cdot 3HCl$
VII	$C_6H_5CH_2$	CH_2NH_2	CH_2NH_2	45[d]	C	260 — 262 d	$C_{12}H_{16}N_4\cdot 3HCl$
VIII	H	$CSNH_2$	$CSNH_2$	75	B	232 — 234 d	$C_5H_6N_4S_2$
IX	$CH_2CH=CH_2$	CN	CN	82	—	(148/1.5mmHg)	$C_9H_6N_4$
X	CH_2CH_2CN	CN	CN	90	D	95 — 96.5	$C_8H_5N_5$
XI	$CH=CH_2$	CN	CN	33	E	93.5— 94	$C_7H_4N_4$
XII	$CH=CH_2$	CN	$CONH_2$	60	B	191 — 191.5	$C_7H_6N_4O$
XIII	$COCH_3$	CN	CN	94	F	145 — 147.5	$C_7H_4N_4O$
XIV	$CH_2CH=CH_2$	CO_2H	CO_2H	70	B	204 — 205	$C_8H_8N_2O_4\cdot\frac{1}{4}H_2O$

a) Solvents of recrystallization; A, dissolved in alkali and precipitated with hydrochloric acid; B, b) Method A. c) Method B. d) Catalytic hydrogenation.

with I vigorously to form 4,5-imidazoledithiocarboxamide in a high yeild. I is a weakly acidic substance,[5] exhibiting different chemical reactivities than imidazole. Therefore, the imino group of I did not react with alkyl halide and dimethylsulfate, unless the basic substance was already present. The labile hydrogen atom of I was, however, readily added to acrylonitrile. In a similar fashion, I was converted to 1-vinyl-4-cyano-5-imidazolecarboxamide (XII) by the addition of ethylene oxide in the presence of sodium hydroxide as a catalyst. The imino group of I reacted with vinyl acetate in the presence of mercuric sulfate to form 1-vinyl-4,5-dicyanoimidazole (IX), though sodium salt of I did not react with vinyl halide in a nonaqueous solvent.

Experimental[6]

1-Methyl-4,5-dicyanoimidazole (I′). A) Into a solution of I (2.36 g, 20 mmol) in 0.2 N sodium hydroxide (100 m*l*), a 1 N silver nitrate solution (20 m*l*) was vigorously stirred. The precipitates were filtered, washed with water, and dried, and then treated with a solution of methyl iodide (1.25 m*l*, 20 mmol) in ether (50 m*l*) at 110°C for 2 hr in a sealed vessel. Silver iodide was then filtered out, and the clear etheral solution was evaporated to dryness. Crude I (1.68 g) was thus obtained. For further purification, the compound was recrystallized from hot water to give colorless crystals.

B) To a mixture of I (11.8 g, 0.1 mol) and sodium hydrogen carbonate (14.3 g, 0.17 mol) in 100 m*l* of water, dimethyl sulfate (14.3 m*l*, 0.15 mol) was added, drop by drop, over a 30-min period at 50—60°C. After the reaction mixture had been stirred at the same temperature for an additional hour, the product was extracted from the solution by ethyl acetate. The extract was washed with dilute aqueous sodium carbonate and water, and dried. The evaporation of the extract gave 12.5 g of I′.

1-Methyl-4-cyano-5-imidazolecarboxamide (II′). A solution of I′ (92 g) in 1.84 *l* of 0.5 N sodium hydroxide (as 50 v/v% aqueous ethanol) was allowed to stand at 24—25°C for 30 min. The solution was then neutralized with hydrochloric acid, and evaporated to 500 m*l*. The crystals formed were filtered off and washed with cold water. About five recrystallizations from ethanol gave an analytical sample of II′ (20 g).

4,5-Imidazoledicarboxamide (II). To a solution o I (2.36 g, 20 mmol) in 1.1 N sodium hydroxide (18 m*l*), 30% aqueous hydrogen peroxide (9.1 m*l*) was added, drop by drop, at 50—60°C over a 2-hr period. The solution was then neutralized with dilute hydrochloric acid, filtered, and the precipitates were washed with water and dried to give 1.66 g.

1-Methyl-4,5-imidazoledicarboxylic Acid (IV′). I′ (1.32 g, 10 mmol) was heated with a 6 N sodium

5) pK*a* 5.2 at 18°C.
6) The detailed data are listed in the table, in which the melting points and boiling point are uncorrected.

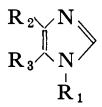

Ultraviolet absorption pH 1 λ_{max} mμ	ε	Ultraviolet absorption pH 13 λ_{max} mμ	ε	Carbon % Calcd	Carbon % Found	Hydrogen % Calcd	Hydrogen % Found	Nitrogen % Calcd	Nitrogen % Found
		286		38.96	39.02	3.92	3.75	36.35	36.10
235,	8500	250,	5500	38.47	38.25	2.58	2.86	17.95	18.10
250,	10000	252,	7100	54.54	54.60	3.05	3.24	42.41	42.62
248,	7400	250.5,	7500	48.00	48.10	4.03	4.16	37.32	37.24
		257,	7200	42.85	42.65	4.80	4.95	33.32	33.51
227,	8600	237,	4400	42.36	42.26	3.56	3.57	16.47	16.31
				25.49	25.52	5.56	5.94	23.78	23.31
				28.87	29.23	6.06	6.09	22.45	22.36
				44.25	43.99	5.88	5.91	17.21	17.03
312,	11100	285,	9500	32.24	32.84	3.25	3.75	30.08	29.87
		333,	10800						
249.5,	9700	250,	8300	60.74	60.56	3.82	3.77	35.43	35.43
248.5,	11400	251,	7300	56.13	56.13	2.94	3.24	40.92	41.21
251,	13200	255.5,	9300	58.33	58.34	2.80	2.91	38.87	39.05
252		263.5		51.85	52.12	3.73	3.88	34.56	34.50
247.5,	14200	(at pH 7)		52.50	52.69	2.52	2.56	34.99	35.54
250		280		47.88	47.72	4.27	4.09	13.96	14.11

water; C, dilute hydrochloric acid; D, ethanol; E, methanol; F, dioxane.

hydroxide solution (10 m*l*) under refluxing for 1 hr and then neutralized with 3 N hydrochloric acid. The solution was cooled in an ice box. The precipitates were filtered, washed with cold water, and dried to give 1.19 g of the product.

4,5-Bis(aminomethyl)imidazole (V). A) To a suspension of lithium aluminum hydride (4.55 g, 0.12 mol) in tetrahydrofuran (400 m*l*), a solution of I (4.72 g, 40 mmol) in tetrahydrofuran (50 m*l*) was added, drop by drop, at 25—30°C. The mixture was stirred at 35—40°C for an additional 2 hr, and then water was added to the reaction mixture under cooling. Aluminum hydroxide was filtered out, and the filtrate was evaporated under reduced pressure. The brown residue was dissolved in water, and the aqueous solution was passed through a column of Amberite IR-120 (H^+ form). After washing with water, elution was effected with dilute aqueous ammonia. The eluate was evaporated to dryness under reduced pressure, and the residue was acidified with hydrochloric acid and decolorized. The solution was again evaporated to give crude 4,5-(bisaminomethyl)imidazole trihydrochloride (3.8 g), which showed a violet-red color when treated with ninhydrin.

B) To a solution of I (1.18 g, 10 mmol) in isoamyl alcohol (150 m*l*), sodium (11 g, 0.48 g atom) was added a little at a time under refluxing. When the metallic sodium had been dissolved completely, the solution was evaporated to dryness under reduced pressure. The isolation of V (0.47 g) was achieved in the way described in A.

C) A solution of I (0.5 g, 4.25 mmol) in methanol (20 m*l*) saturated with ammonia at 0°C was hydrogenated in the presence of Raney cobalt (0.7 g as alloy) under an initial hydrogen pressure of 110 kg/cm² and at a temperature in the range from 100 to 110°C. After the catalyst had been removed from the reaction mixture, the solution was evaporated to dryness under reduced pressure. V (0.12 g) was isolated in the way described in A.

4,5-Imidazoledithiocarboxamide (VIII). I (2.36 g, 20 mmol) and powdered sodium hydroxide as a catalyst (2 g) were added to liquid hydrogen sulfide (50 m*l* at −75°C), and the reaction mixture was heated at 70°C for 3 hr in a pressure vessel. The solution was then cooled and evaporated to dryness. Water (30 m*l*) was added and the pH adjusted to 2—3 with hydrochloric acid. A crude yellow product (2.79 g) was filtered out, washed, and recrystallized from hot water.

1-Allyl-4,5-dicyanoimidazole (IX). To a mixture of allyl bromide (18 g, 0.15 mol) and I (11.8 g, 0.1 mol) in 100 m*l* of water, sodium hydrogen carbonate (14.3 g, 0.17 mol) was added. The mixture was then heated at 80°C for 2 hr, and the cooled mixture was extracted with ether. The etheral solution was washed with dilute aqueous sodium carbonate and water, and then dried. After the evaporation of the etheral solution, the residual oil was distilled to give 13 g of IX.

1-(β-Cyanoethyl)-4,5-dicyanoimidazole (X). A mixture of I (1.18 g, 10 mmol) and powdered potassium hydroxide (100 mg) as a catalyst in acrylonitrile (20 m*l*) was heated at 120°C for 5 hr in a sealed tube, and then the solution was evaporated to dryness. Water (20 m*l*)

was added and the pH adjusted to 7 with hydrochloric acid. The cooled solution gave 1.53 g of the product.

1-Vinyl-4,5-dicyanoimidazole (XI). To a solution of I (35.4 g, 0.3 mol) and mercuric acetate (12 g) in vinyl acetate (618 g, 7.2 mol), concentrated sulfuric acid (1.5 m*l*) was added. After the solution had been heated at 40—45°C for 48 hr, the precipitates were filtered and the excess vinyl acetate was removed under reduced pressure. The recrystallization of the residue from methanol gave 14.3 g of the product (IX).

1-Vinyl-4-cyano-5-imidazolecarboxamide (XII). A mixture of I (2.36 g, 20 mmol) and sodium hydroxide (0.4 g) as a catalyst in liquid ethylene oxide (10 m*l*) was carefully heated at 100°C for 3 hr in a pressure vessel. After the evaporation of the excess ethylene oxide, 1.95 g of XII were obtained by the recrystallization of the residue from hot water. The infrared spectrum (KBr) showed strong absorptions at 3025 (vinyl hydrogen), 2275 (cyano group), and 1670 cm^{-1} (amido group).

1-Acetyl-4,5-dicyanoimidazole (XIII).[7] To a solution of I (2.36 g, 20 mmol) and sodium hydrogen carbonate (0.42 g, 5 mmol) in 0.5 N sodium hydroxide (20 m*l*), acetic anhydride (2.04 g, 20 mmol) was added at 0—5°C. After 5 min, the resulting white precipitates (3.0 g) were filtered and recrystallized from dioxane. The infrared absorption spectrum (KBr) showed strong absorptions at 2270 (cyano group) and 1775 cm^{-1} (acetyl group).

The authors wish to express their deep thanks to Mr. Shinichi Motozaki, Director of the Central Research Laboratories, for his kind encouragement. The assistance of Mr. Takashi Zama throughout this work is also gratefully acknowledged.

7) The authors wish to thank Dr. Yoshioki Komachiya for his helpful suggestions regarding the synthesis of XIII.

BULLETIN OF THE CHEMICAL SOCIETY OF JAPAN VOL. 41 1240—1245 (1968)

Reaction of Oxymercurials. Synthesis of 6,6-Dimethyl-spiro[2,5]octan-4,8-dione*1

Katsuhiko ICHIKAWA, Osamu ITOH and Takahisa KAWAMURA

Department of Hydrocarbon Chemistry, Kyoto University, Yoshida, Kyoto

(Received December 14, 1967)

The reaction of oxymercurial of ethylene with dimedone in acetic acid containing perchloric acid, followed by treatment with sodium chloride, gave 2-(β-chloromercuriethyl)-5,5-dimethylcyclohexan-1,3-dione. Upon treating this mercurial with an equimolar amount of aqueous potassium hydroxide, 6,6-dimethyl-spiro[2,5]octan-4,8-dione was obtained. Oxymercurial of propylene reacted with dimedone to form a mixture of 4-oxo-2,6,6-trimethyl-2,3,4,5,6,7-hexahydrobenzofuran and 4-oxo-3,6,6-trimethyl-2,3,4,5,6,7-hexahydrobenzofuran under simultaneous demercuration; the mercurial corresponding to that in the case of ethylene could not be isolated.

In a previous paper,[1] it has been demonstrated that alkyl groups containing mercury can be introduced into active methylene by the reaction of acyclic β-diketones with oxymercurials of olefins. This paper will report that the same reaction takes place between dimedone (a cyclic β-diketone) and the oxymercurial of ethylene, and that the resulting mercurial, which is isolated as a chloromercury derivative, reacts with aqueous potassium hydroxide at room temperature to form 6,6-dimethyl-spiro[2,5]-octan-4,8-dione, which might be an interesting compound for UV absorption and NMR spectroscopy. The same attempt will also be applied to the oxymercurial of propylene.

Into a solution of β-acetoxyethylmercuric acetate (1,8 molar) which had been prepared by introducing ethylene to acetic acid containing mercuric acetate, perchloric acid (1 molar) and dimedone (a slight excess over the oxymercurial) were added.

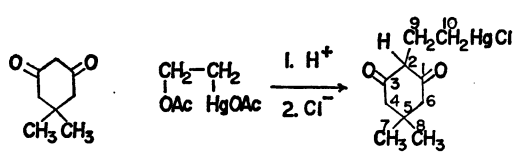

(I)

The reaction product was isolated as a crystalline chloromercury derivative for experimental convenience. After a reaction at 10—20°C for one day, 2-(β-chloromercuriethyl)-5,5-dimethylcycohexane-1,3-dione (I), mp 199—201°C, was obtained in a 25%

*1 A part of this paper was presented at the 19th Annual Meeting of the Chemical Society of Japan, Yokohama, April, 1966.

1) K. Ichikawa, O. Itoh, T. Kawamura, M. Fujiwara and T. Ueno, *J. Org. Chem.*, **31**, 447 (1966).

yield. By prolonging the reaction time to 7 days, the yield was increased to 35%. At temperatures above 25°C, metallic mercury was formed and the yield of I decreased. For example, the yields of I were 22% (accompanied by 11% demercuration) and 18% (accompanied by 22% demercuration) in the reactions at 25—30°C for 2 days and at 40°C for 5 hr respectively.

The results of the experiments with purified β-acetoxyethylmercuric acetate, which had been isolated and recrystallized, were the same as those with the oxymercurials prepared *in situ*.

The structure of I was assigned by analogy with the results obtained with acyclic β-diketones and on the basis of the spectral data. The UV spectra (λ_{max} 262 mμ, $\varepsilon=3600$ in chloroform and λ_{max} 269 mμ, $\varepsilon=12200$ with a shoulder at λ_{max} 300 mμ, $\varepsilon=5800$ in ethanol) showed the presence of an enolizable β-diketo group. The IR spectrum also supported this structure, since absorptions observed at 2300—2700 (w, broad), 1730 (w), 1700 (s), and 1630 (w) cm^{-1} can be assigned to $\nu_{O-H\cdots O=C}$, $\nu_{C=O}$, $\nu_{C=O}$, and $\nu_{C=C}$ respectively. The NMR spectrum obtained at 60 Mc, using tetramethylsilane as an internal standard, in pyridine can be explained reasonably in terms of the enol form of I. The signals observed at τ −1.43 (singlet), 6.84 (triplet), 7.57 (singlet) 7.75 (triplet), and 9.00 (singlet), with relative intensities of 1 : 2 : 4 : 2 : 6, can be assigned to those due to the protons at O, C_9, C_4 and C_6, C_{10}, and C_7 and C_8 respectively (Fig. 1).

When I was treated with an equimolar amount of potassium hydroxide (10% aqueous) at 40°C for 3 hr, demercuration proceeded and 6,6-dimethyl-spiro-[2,5]octan-4,8-dione (II), bp 86.2—86.5°C/3 mmHg, n_D^{25} 1.4808, was obtained in a 90% yield on the basis of demercuration (75%). The mechanism is considered to be the same as that of 1,1-diacetylcyclopropane formation from 3,3-diacetylpropylmercuric chloride,[1] since the reaction conditions and scheme are the same. In the latter case, it has been suggested that the demercuration was assisted by the chelation of the β-diketo group with mercury. However, this cannot be applied to the present case, since the diketo group of dimedone cannot form a chelate compound. This demercuration mechanism, however, appears to require further investigation, because the purification of the mercurials is a necessary condition for the demercuration. Unknown impurities appear to inhibit the reaction.

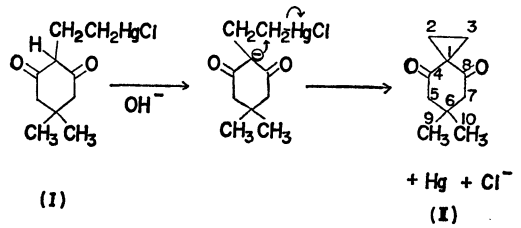

(I) (II)

The structure of II was identified on the basis of the results of elementary analysis and the spectral data. Analysis showed that II has a formula of $C_{10}H_{14}O_2$ (Found: C, 72.53; H, 8.74%. Calcd for $C_{10}H_{14}O_2$: C, 72.26; H, 8.49%). The IR spectrum showed absorptions at 1705 and 1678 cm^{-1} due to $\nu_{C=O}$, and at 3020 cm^{-1} due to the ν_{C-H} of the cyclopropane ring.

The NMR spectrum clearly proved that the assigned structure is correct. In deuterochloroform, using tetramethylsilane as an internal standard, signals were observed at τ 7.44, 8.25, and 8.87, with relative intensities of 4 : 4 : 6; these signals can be assigned to those due to the protons at C_5 and C_7, C_2 and C_3, and C_9 and C_{10} respectively (Fig. 2).

As further evidence, when II was hydrogenated over Pd-$BaSO_4$ catalyst in methanol at room temperature, the product was crystalline ethyldimedone.

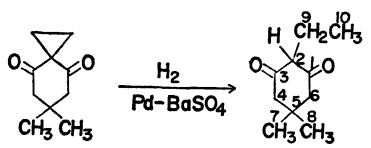

Since this product is unstable, it was identified by means of the NMR spectrum. In a pyridine solvent, signals were observed at τ 7.18 (quartet, $J=$ 7.3 cps), 7.63 (singlet), 8.73 (triplet, $J=7.3$ cps) and 8.98 (singlet), with relative intensities of 2 : 4 : 3 : 6. These signals may be assigned to the protons at C_9, C_4 and C_6, C_{10}, and C_7 and C_8 (Fig. 3).

When the reaction mixture of oxymercurial of ethylene and dimedone mentioned above was kept at the higher temperature of 40°C for 10 hr, the formation of metallic mercury (29% of the total amount) was observed. A work-up of the mixture gave 0.7 g of a liquid product, bp 109—113°C/4 mmHg. Gas chromatographical analysis showed that this product consisted of II (2%) and another product (96%). Spectral data disclosed that the latter was 4-oxo-6,6-dimethyl-2,3,4,5,6,7-hexahydrobenzofuran (III). The infrared spectrum showd a characteristic absorption of the 3-acetyl-4,5-dihydrofuran skeleton at 1635 cm^{-1}.[2-4]

The NMR spectrum is also consistent with this structure. Two singlets at τ 8.90 and 7.75 and three triplets at 7.70 ($J=1.5$ cps), 7.15 (broad, $J=9.2$ cps), and 5.39 ($J=9.2$ cps), with relative intensities of 6 : 2 : 2 : 2 : 2, can be assigned to the protons at C_{10} and C_{11}, C_5, C_7, C_3, and C_2 respectively.[2,5] The broading of the triplet at τ 7.15 is due to a long-range

2) F. H. Greenberg, *J. Org. Chem.*, **30**, 1251 (1965).
3) K. Ichikawa, S. Uemura and T. Sugita, *Tetrahedron*, **22**, 407 (1966).
4) K. Ichikawa and S. Uemura, *J. Org. Chem.*, **32**, 493 (1967).
5) O. H. Mattson and C. A. Wachtmeister, *Tetrahedron Letters*, **1967**, 1855.

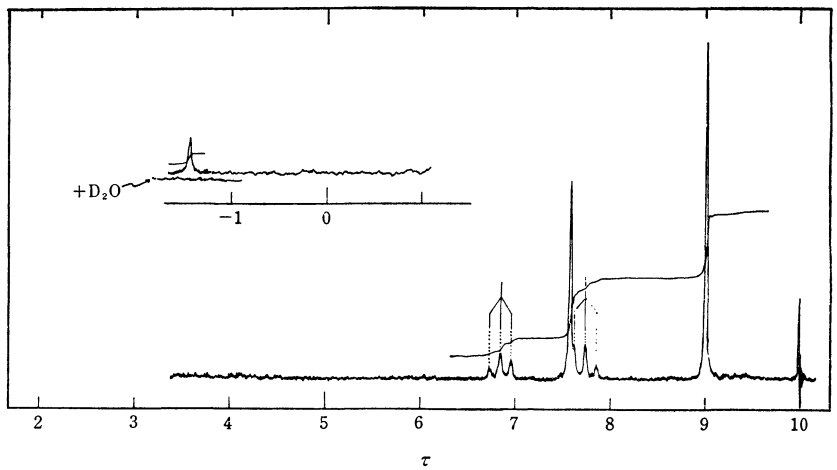

Fig. 1. NMR spectrum of β-chloromercuriethyldimedone (I) in $CDCl_3$ (60 Mc).

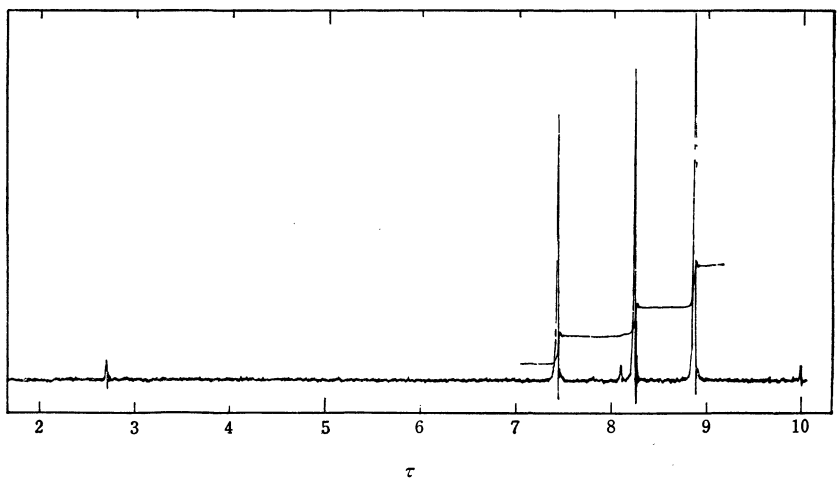

Fig. 2. NMR spectrum of 6,6-dimethyl-spiro[2,5]octan-4,8-dione in $CDCl_3$ (60 Mc).

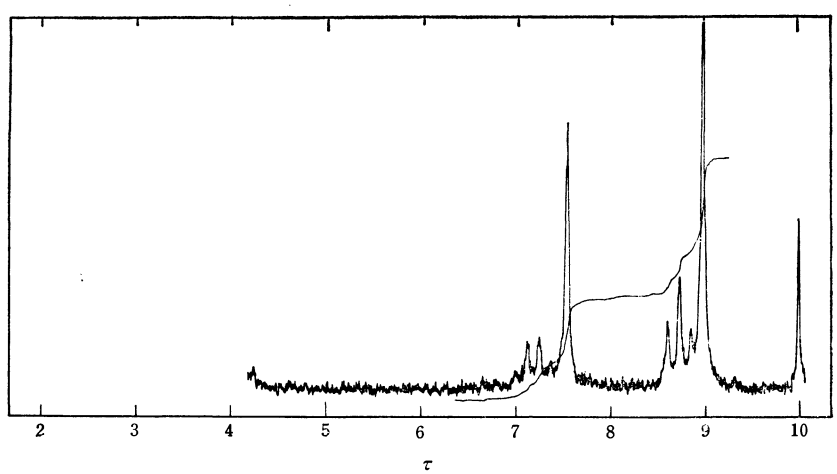

Fig. 3. NMR spectrum of ethyldimedone in pyridine (60 Mc).

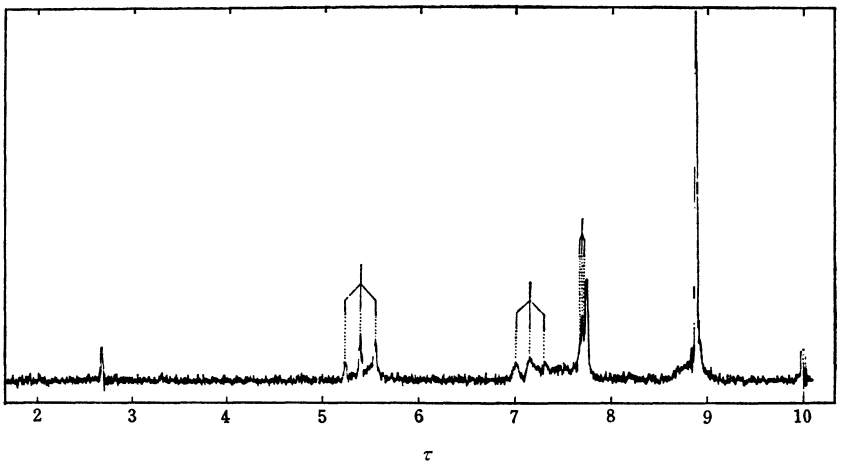

Fig. 4. NMR spectrum 4-oxo-6,6-dimethyl-2,3,4,5,6,7-hexahydrobenzofuran (III) in $CDCl_3$ (60 Mc).

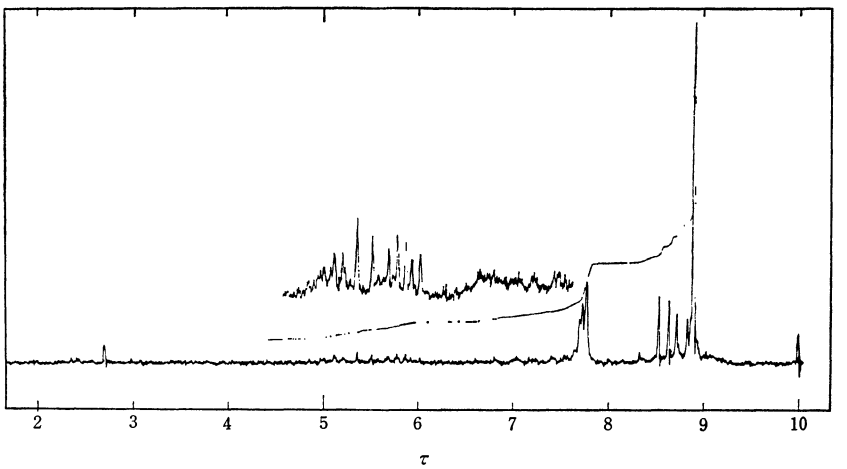

Fig. 5. NMR spectrum of a mixture of 4-oxo-2,6,6-trimethyl- (IV) and 4-oxo-3,6,6-trimethyl-2,3,4,5,6,7-hexahydrobenzofuran (V) in $CDCl_3$ (60 Mc).

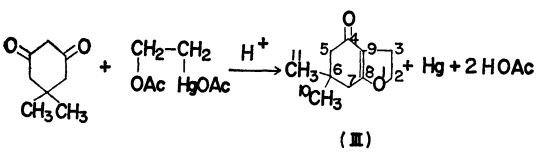

(III)

coupling ($J = 1.5$ cps) between 7-methylene and 3-methylene protons, this coupling is generally observed in this system and will be discussed in a separate paper.

This result of dihydrofuran formation is similar to those of the reactions between the oxythallate[3] and oxyplumbate[4] of ethylene and acetylacetone, and the mechanism also appears to be similar. However, the possibility of the formation of the same product through the isomerization of the cyclopropane (II) by acid cannot be excluded, because an attempt to obtain dinitrophenylhydrazone of II in ethanol containing sulfuric acid gave the hydrazone of III instead of II, and the same type of isomerization has been demonstrated to proceed in concentrated sulfuric acid.[6]

In the case of oxymercurial of propylene, 2-acetoxypropylmercuric acetate, the reaction with dimedone was slower than that of ethylene. Even after a reaction at 5—15°C for 5 days, the presence of unreacted oxymercurial was detected, and the formation of metallic mercury was also observed. The expected mercurial appears to be unstable and to be subject to demercuration under these conditions. Several attempts to isolate the mercurial corresponding to I in an earlier stage of the reaction were unsuccessful. After a reaction at 5—15°C for 5 days, 58% of the total mercury in the reaction mixture precipitated as metal.

Gas chromatographical analysis of the organic products showed that the main product (more than

6) O. Itoh, T. Kawamura and K. Ichikawa, *Bull. Inst. Chem. Res., Kyoto Univ.*, **44**, 207 (1966).

96%) is a mixture of two compounds (55 : 45), with close retention times. Because of the difficulty of purification and separation, the structures were estimated on the basis of the spectral data and the results of analogous reactions.[3,4]

The NMR spectrum was explained reasonably by assuming that the product is a mixture of 4-oxo-2,6,6-trimethyl-2,3,4,5,6,7-hexahydrobenzofuran (IV) and 4-oxo-3,6,6-trimethyl-2,3,4,5,6,7-hexahydrobenzofuran (V). The signals observed at τ 8.90 (singlet), 7.77 (singlet) and 7.71 (triplet), with relative intensities of 6 : 2 : 2, can be assigned to those due to the protons of the C_{10} and C_{11}, C_5, and C_7 of both IV and V. The broad complicated signals observed at τ 6.4—7.6 and 4.8—6.1, with relative intensities of *ca.* 1.5 : 1.5, are those due to protons of the C_2 and C_3 of IV and V respectively. The two doublets centered at τ 8.59 (J=6.2 cps) and 8.77 (J=6.8 cps) can be reasonably assigned to the protons of methyl groups attached to the C_2 of IV and the C_3 of V on the basis of the results observed in the NMR spectra of 3-acetyl-2,5-dimethyl-4,5-dihydrofuran[6] and 3-acetyl-2,4-dimethyl-4,5-dihydrofuran.[7]

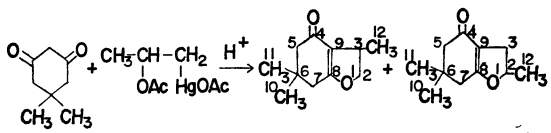

(V) (IV)

Experimental

2-(β-Chloromercuriethyl)-5,5-dimethylcyclohexan-1,3-dione (I). The following is an example of a typical experimental procedure. Into an acetic acid solution of β-acetoxyethylmercuric acetate which had been prepared by introducing ethylene into a mixture of mercuric acetate (0.6 mol) and acetic acid (180 g), dimedone (100 g, 0.6 mol) was added. The reaction mixture (heterogeneous) was kept at 0°C, and then 70% perchloric acid (48 g) was slowly added. Throughout the procedure, the mixture was stirred mechanically; it became homogeneous after the addition of the acid. After the mixture had stood at 5—15°C for 24 hr, a grey slurry was formed. This reaction mixture was then added to an aqueous sodium chloride solution to precipitate white crystals, which were dried and recrystallized from ethanol. Seventy-three g of I (18% yield), mp 199—201°C, were thus obtained. The results of mercury content analysis (49.3%)[8] agreed with the calculated value (49.7%). IR (KBr): 3300 (w), 2930 (m), 2700—2300 (broad, w), 1730 (m), 1700 (m), 1630 (w). 1570 (m), 1547 (s), 1415 (m), 1377 (sh., w), 1366 (s), 1355 (s), 1311 (m), 1246 (s), 1136 (s), 1015 (w), 820 (w), 800 (w), 690 (w), 645 (w), 595 (m), 575 (w), 490 (w), 455 (w) cm^{-1}.

6,6-Dimethyl-spiro [2,5] octan-4,8-dione (II). Into 50 m*l* of a 10% aqueous solution of potassium hydroxide, 40.3 g of I was added, and the mixture was stirred at room temperature (15—20°C) for 3 hr. When the reaction temperature was raised to 25—30°C, the formation of metallic mercury was observed. After a reaction at 25—30°C for 3 hr, the metallic mercury (14 g, 70% of the theoretical amount) was removed, and the mixture was acidified with 1 m*l* of 1 N hydrochloric acid and extracted twice with 100 m*l* portions of ether. By evaporating the solvent, 11.5 g of II (90% yield, on the basis of demercuration) was obtained. Gas chromatographical analysis showed that the product consisted only of II, bp 86.2—86.5°C/3 mmHg, n_D^{25} 1.4804. UV: $\lambda_{max}^{n\text{-Hexane}}$ 196 mμ (ε=4700) and 267 mμ (ε=35); λ_{max}^{EtOH} 203 mμ (broad, ε=4050) and 276 mμ (ε=60). IR (liquid film): 3020 (w), 2960 (m), 2880 (w), 1705 (s), 1678 (s), 1465 (m), 1405 (m), 1390 (w), 1370 (m), 1335 (s), 1320 (s), 1290 (m), 1265 (w), 1175 (m), 1140 (m), 1120 (w), 1080 (m), 1035 (w), 1015 (w), 985 (m), 915 (m), 610 (w), 585 (w) cm^{-1}.

Found: C, 72.53; H, 8.74%. Calcd for $C_{10}H_{14}O_2$: C, 72.26; H, 8.49%.

II was added to an excess 2,4-dinitrophenylhydrazine solution (ethanol-sulfuric acid) to prepare the hydrazone in the usual way.[9] The red crystals thus obtained were recrystallized from ethanol, mp 165—168°C. This hydrazone was not of II, but of III. A mixed melting point determination with that of III showed no depression.

Found: C, 54.68; H, 5.20%. Calcd for $C_{16}H_{18}N_4O_5$; C, 55.48; H, 5.24%.

This shows that II was converted to III during the preparation of hydrazone.

Hydrogenation of II to Ethyldimedone. With a palladium-barium sulfate catalyst (1.0 g), II (0.213 g, 1.05 mmol) was hydrogenated in methanol (30 m*l*) at room temperature. In 5 min, 23 m*l* of hydrogen were absorbed. After filtering off the catalyst, the solvent was distilled to give crystalline ethyldimedone. The IR spectrum disclosed the presence of two carbonyls (1690 and 1665 cm^{-1}), a carbon-carbon double bond (1620 cm^{-1}) and intermolecular hydrogen-bonded carbonyl (1550 cm^{-1}).

4-Oxo-6,6-dimethyl-2,3,4,5,6,7-hexahydrobenzofuran (III). To an acetic acid (15 g) solution of β-acetoxyethylmercuric acetate prepared from 0.05 mol of mercuric acetate and ethylene, dimedone (0.05 mol) and then 70% perchloric acid (4 g) were added. The reaction was continued at 40°C for 10 hr under stirring. After the metallic mercury formed (2.9 g, 29%) had been removed, the reaction mixture was added to an aqueous sodium chloride solution. The crystals formed (3 g, 15% yield) were filtered off and the remaining solution was extracted three times with 100-m*l* portions of ether. The ether extract was washed with a 5% sodium bicarbonate solution and then with water. After drying over sodium sulfate, the solvent was distilled off. Distillation gave 0.7 g of III (29% yield on the basis of demercuration), bp 109—113°C/4 mmHg. 2,4-Dinitrophenylhydrazone melted at 167—169°C.

Found: C, 55.55; H, 5.40%. Calcd for $C_{16}H_{18}N_4O_5$: C, 55.48; H, 5.40%.

7) S. Uemura, T. Nakano and K. Ichikawa, *Nippon Kagaku Zasshi* (*J. Chem. Soc. Japan, Pure Chem. Sect.*), **89**, 203 (1968).

8) I. A. Koten and R. Adams, *J. Am. Chem. Soc.*, **46**, 2764 (1924).

9) R. L. Shriner, R. C. Fuson and D. Y. Curtin, "The Systematic Identification of Organic Compounds," Wiley, New York (1956), p. 219.

4-Oxo-2,6,6-trimethyl-2,3,4,5,6,7-hexahydrobenzofuran (IV) and 4-Oxo-3,6,6-trimethyl-2,3,4,5,6,7-hexahydrobenzofuran (V). By the same method as has been described in the case of I, a reaction mixture of β-acetoxypropylmercuric acetate (0.5 mol), dimedone (0.68 mol), and perchloric acid (70%, 45 g) in acetic acid (150 g) was prepared. By a reaction at 5—15°C for 5 days, 58% of the total mercury was precipitated as metal. The reaction mixture was then filtered, water (twice the volume) was added, neutralized with a sodium hydroxide solution, and extracted with ether. After the ether had been removed, 80 g of an oily product were obtained. This contained unidentified mercury compounds, the oil was extracted with petroleum ether repeatedly (10 times with 100 m*l* portions). After the oil had been dried over anhydrous sodium sulfate and the solvent removed, a liquid product (15 g), bp 110—115°C/6 mmHg, was obtained. Gas chromatographic analysis showed that the main product (more than 96%) was a mixture of two components with close retention times. The two components could not be separated into pure components either by distillation or by column chromatography. IR (liquid film): 2950 (s), 2875 (s), 1718 (m), 1625 (s), 1460 (m), 1445 (m), 1398 (s), 1365 (m), 1335 (w), 1285 (w), 1240 (m), 1215 (s), 1165 (m), 1140 (m), 1100 (m), 1010 (m), 945 (m), 890 (m), 820 (w), 610 (m) cm^{-1}. UV: λ_{max}^{Hexane} 262 mμ ($\varepsilon=12500$), $\lambda_{max}^{Ethanol}$ 272 mμ ($\varepsilon=13300$).

Spectral Measurements. IR, UV, and NMR spectra were recorded by JASCO IR-S, Hitachi EPS 2, and Varian 60A apparatuses respectively.

Reagents. The commercial ethylene and propylene were used without further purification. The dimedone was also a commercial one, mp 144—146°C. All the other reagents were commercial products of an analytical grade.

BULLETIN OF THE CHEMICAL SOCIETY OF JAPAN VOL. 41 1245—1248 (1968)

Effect of Coexisting Minerals on Graphitization of Carbon. I. Heat Treatments of Carbon under 3 kbar in the Presence of Limestone

Tokiti NODA,*1 Michio INAGAKI, Shin-ichi HIRANO and Kiyoshi AMANUMA

Faculty of Engineering, Nagoya University, Nagoya

(Received November 24, 1967)

The effect of the presence of limestone on the graphitization of carbon was investigated by the heat treatments of the carbon sample under the quasi-hydrostatic pressure of 3.2 kbar. The carbon sample used was a coke (PV-7) prepared by carbonization of polyvinylchloride up to 680°C. It was placed between two disks of limestone so as to make a sandwich-type specimen. The heat treatments were performed in a simple piston-cylinder type vessel at various temperatures of 800—1300°C for 20—240 min. Above 1000°C, the carbon specimens were obtained as caked tablets. The profiles of (002) diffraction line of these carbon tablets were found to be composite, consisting of a sharp component profile at 26.5° and a broad one at lower angle than 26.2°. The component G_M corresponding to the sharp component profile seemed to have the graphite structure. The content of the component G_M increased very rapidly with the increase in heat treatment temperatures above 1000°C. Phenomenally, the developement of the graphite structure seemed to be closely related to the recrystallization and the melting of coexisting limestone, but some chemical effects should not be excluded.

In the nature, a good quality of graphite crystals has been found in beds of metamorphic rocks, such as limestone. The temperature-pressure condition of the graphite formation was estimated geologically as the temperature of several hundreds degrees and the pressure of several kilobars. On the other hand, it has been found in a laboratory that the carbon is graphitized very rapidly at around 1500°C under the pressure of 10 kbar[1] and even under 5 and 3 kbar.[2] However, any indication of the presence of graphite structure could not be found by X-ray diffraction at temperatures lower than 1300°C. Therefore, the limestone might have some effect on graphitization, like the pressure and the temperature have.

The purpose of the present work is to see the effect of the presence of limestone on the graphitization of carbon under the pressure.

Experimental and Results

The carbon sample used was a coke (PV-7) prepared by carbonization of polyvinylchloride and consequently heated up to 680°C. The grain size of the sample was limited in the range between 0.1 and

*1 Present address: Mie University, Tsu, Mie-ken.

1) T. Noda and H. Kato, *Carbon*, **3**, 289 (1965).

2) T. Noda, K. Kamiya and M. Inagaki, This Bulletin, **41**, 485 (1968).

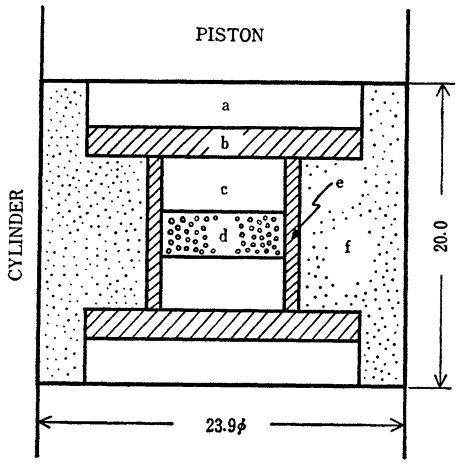

Fig. 1. Arrangement of the pressure cell used for heat treatments of carbon in the presence of limestone.

a: steel disk, b: graphite disk, c: limestone, d: carbon specimen, e: graphite tube heater, f: pyrophyllite

0.4 mm. Limestone disks of 3.5 mm thick and 8.0 mm in diameter were cut out from Fusulina limestone from Akasaka, Gifu-ken, Japan. The carbon sample of 180 mg was placed between two disks of limestone so as to make a sandwich-type specimen as shown in Fig. 1. A high pressure apparatus used was a simple piston-cylinder type one, which was made from a tool steel. The bore and outer diameter were 24 and 50 mm, respectively, and the cylinder was protected by a soft steel guard ring. The heat treatments were performed at various temperatures between 800 and 1300°C for 20—240 min under the quasi-hydrostatic pressure of 3.2 kbar. The heat treatment temperature (HTT) was estimated from input power using the relation between temperature and input power, which was determined beforehand using a chromel-alumel thermocouple inserted in the carbon specimen arranged in the same way as in the heat treatments. The temperature was controlled by adjusting the input power. The pressure was calibrated by using KNO_3 and AgI.[3]

In comparison, the carbon sample was heat-treated under the same pressure without limestone, replacing limestone disks (in Fig. 1) by glassy carbon plates and pyrophyllite disks. Glassy carbon plates were used to prevent the direct contact of carbon specimen with pyrophyllite disks.

Profiles of (002) diffraction line of the heat-treated specimens were measured by a recording X-ray diffractometer using Ni-filtered Cu$K\alpha$ radiation. Specimens for X-ray diffraction were taken from the central part of heat-treated carbon tablets.

3) M. Inagaki, S. Hirano and H. Saito, to be published.

Above 1000°C, the carbon specimens heat-treated with limestone were obtained as caked tablets. In the tablets, appreciable amounts of calcium carbonate were detected by X-ray diffraction method and the amounts increased with HTT. Limestone disks themselves were found to have recrystallized above 1000°C. The thickness of recrystallized part of limestone increased with the increase in HTT and residence time. Grains of recrystallized limestone grew along the axial direction of the heater (Fig. 2), to which the temperature gradient was parallel. Limestone was found to have melted above 1250°C.

Higher temperature

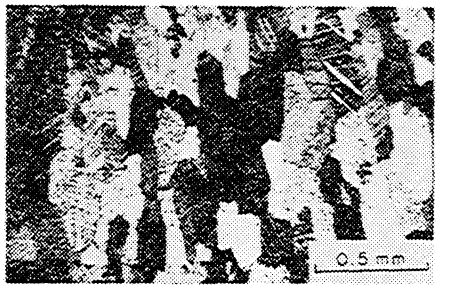

Lower temperature side

Fig. 2. Growth of grain of recrystallized calcite in contact with carbon sample treated at 1120°C for 60 min under 3.2 kbar (under polarized light).

Profiles of (002) diffraction line of the carbon samples heat-treated with linestone above 1000°C were found to be composite, consisting of a relatively sharp profile at 26.5° in 2θ (6.72 Å in the c_0-spacing) overlapping on a broad profile at an angle lower than 26.2°. With the increase in HTT and residence time, the sharp profile at 26.5° became stronger and narrower, while the broad profile shifted to higher angles. The profile of (002) diffraction line of the carbon sample heat-treated without limestone had only a hump at about 26.5° above 1300°C. The representative changes of the profiles with HTT are shown in Fig. 3 a) and b).

The composite profiles were graphically separated into two component profiles. The schema of the separation is shown in Fig. 4: After the observed composite profile (1) is corrected for the Lorentz-polarization, atomic scattering and absorption factors by conventional methods[4] (the profile (2)), the high angle side of the sharp profile is folded to the low angle side and the profile (3) is obtained. Subtracting the profile (3) from the composite profile (2), the balance profile (4) is obtained. Since the profile (4) is not symmetrical usually, however, the profile (5) for the broad component is obtained by folding the low angle side of the profile (4) at the angle of the maximum intensity. Finally, the profile (6) for the sharp component is obtained by subtracting the profile (5) from the profile (2). Some trial and error

4) W. R. Ruston, *Fuel*, **32**, 53 (1953).

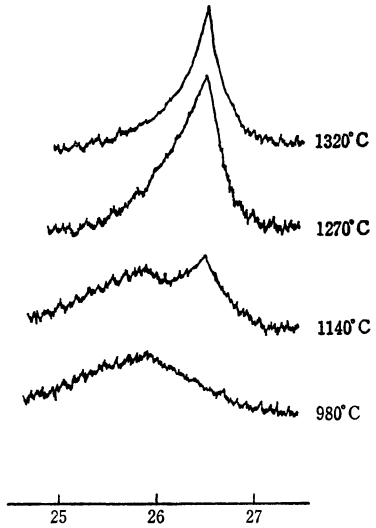

Fig. 3 (a).

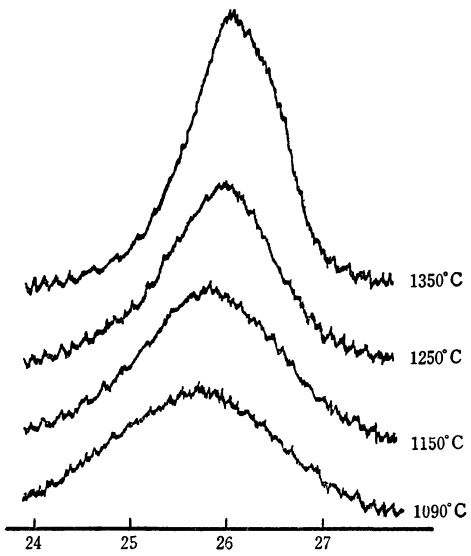

Fig. 3 (b).

Fig. 3. Changes of profiles of (002) diffraction line with HTT for 60 min.
a) treated in the presence of limestone
b) treated without any minerals

adjustments are needed in order to obtain the symmetrical component profiles and to fit the profile composed from the component profiles satisfactorily well with the original composite profile. The components which correspond to the sharp and broad component profiles are designated as G_M and A_M, respectively.*2

The c_0-spacing of the two components was measured from the separated profiles (5) and (6), and

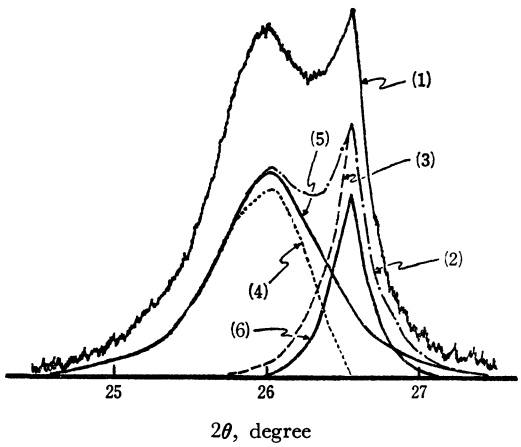

Fig. 4. Schema of separation of the composite profile.

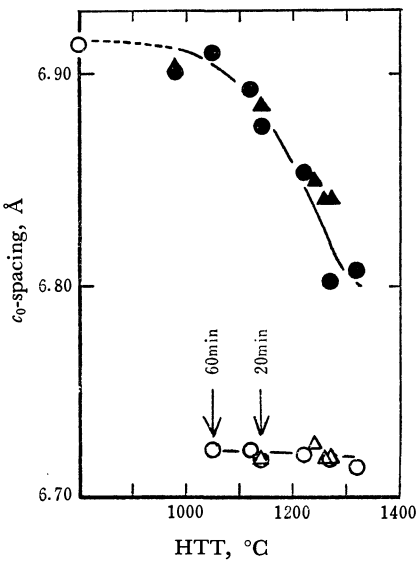

Fig. 5. Variation of c_0-spacing of two components, G_M and A_M, with HTT.
Above the temperature marked by the arrow, the component G_M could be observed on the diffraction profile.
G_M A_M
△ ▲: 20 min
○ ●: 60 min

the result is shown in Fig. 5. The c_0-spacing of the component G_M is almost constant and around 6.72 Å, while the c_0-spacing of the component A_M decreased

*2 For the soft and hard carbons heat-treated under pressure without any minerals, the composite profiles were observed and separated into two components G_S and A_S, and G_H and A_H, respectively. In the present work, the suffix " M " was used for each component in order to distinguish from the components reported previously.[2,5]

5) M. Inagaki, K. Kamiya, M. Mizutani and T. Noda, to be published.

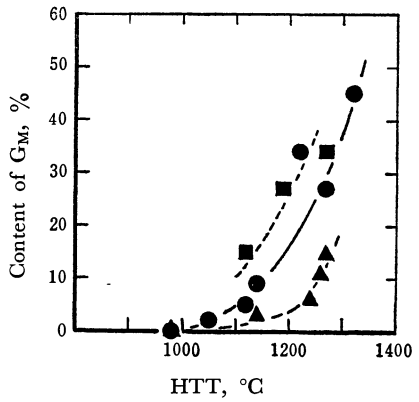

Fig. 6. Variation of content of the component G_M with HTT.
▲, 20 min ●, 60 min ■, 240 min

gradually from 6.91 to 6.80 Å. It is reasonable to take the component G_M as the graphitic component, because the component G_S having the c_0-spacing of 6.72 Å was reported to have the graphite structure.[2,6] Therefore, the content of the component G_M was used as a measure of graphitization of the sample. The content of the component G_M was obtained from the ratio of the area under the profile of the component G_M to the total area under the composite profile. The ratio of areas was corrected for the preferred orientation of crystallite in the specimens for X-ray diffraction, when the ratio was converted to the content of the component G_M. Changes of the content of the component G_M with HTT are shown in Fig. 6 for several residence times.

6) M. Inagaki, K. Kamiya and T. Noda, *Kogyo Kagaku Zasshi* (*J. Chem. Soc. Japan, Ind.Chem. Sect.*), **71**, 652, 812 (1968).

Discussion and Summary

The graphitization of carbon under pressure is evidently accelerated by limestone. Under 3 kbar in the presence of limestone, the component G_M, which seems to have the graphite structure, begins to appear just above 1000°C. This temperature is much lower than that in the case of the heat treatment of the same sample PV-7 under the same pressure without limestone.

The content of the component G_M increased very rapidly with the increase in HTT. The content was about 45% with the heat treatment at 1300°C for 60 min. However, with a longer treatment as 240 min, only a small increase in the content was observed.

Phenomenally, the developement of the graphite structure seems to be closely related to the recrystallization and the melting of the coexisting limestone, but some chemical effects should not be excluded. In order to know the mechanism of the effect of limestone on the graphitization of carbon under pressure, more precise experiments are needed.

The authors wish to thank Mr. Kan-ichi Kamiya in our laboratory for his kind coorperation and assistance, and also Tokai Electrode Mfg. Co. for supplying the graphite materials used.

NOTES

Photochemical Reduction of Nitrobenzene and Its Reduction Intermediates. III.[1] The Photochemical Reduction of Nitrobenzene*[1]

Shizunobu HASHIMOTO, Junzo SUNAMOTO,*[2] Hironori FUJII and Koji KANO

Department of Applied Chemistry, Doshisha University, Karasuma-imadegawa, Kamikyo-ku, Kyoto

(Received July 5, 1967)

Several studies of the photochemical reaction of nitrobenzene have been reported,[2-8] but no investigation of the photoreduction of nitrobenzene to anilines has been published.

Recently, Hurley and Testa[9] reported that the photoreduction of nitrobenzene in isopropyl alcohol gives phenylhydroxylamine as an initial product; this product is immediately oxidized by air to nitrosobenzene and coupled with the latter to give azoxybenzene. On the other hand, Kaneko and his co-workers[10] have shown that 4-nitropyridine-*N*-oxide undergoes a quantitative photoreduction to the corresponding hydroxylamino compound in ethanol.

In the present paper, the photoreductions of nitrobenzene to aniline in an isopropanoic hydrochloric acid solution with or without a photosensitizer will be described. In addition, the photoreduction of nitrosobenzene, phenylhydroxylamine, and azoxybenzene have been carried out in order to make the reduction process clear.

Experimental

Materials. Nitrobenzene and isopropyl alcohol commercially obtained were further purified by distillation prior to use. Nitrosobenzene,[11] phenylhydroxylamine,[11] and azoxybenzene[12] were prepared and recrystallized according to the procedures described in the literature. Disodium 2,6-anthraquinone disulfonate (=AQ) was prepared by the usual disulfonation of anthraquinone and was purified by recrystallization from methanol.

Photochemical Reduction Procedures. A typical method of photochemical reduction was as follows. A mixture of 5×10^{-4} mol of nitrobenzene (nitrosobenzene, phenylhydroxylamine, or azoxybenzene), 5 m*l* of concentrated hydrochloric acid, and 10 mg of AQ was placed in a 250 m*l* volumetric flask and diluted to exactly 250 m*l* by isopropyl alcohol. This isopropanolic solution was then placed in an inside-irradiation-type reaction flask equipped with a 130 W-pressure mercury lamp. The reaction was commenced by irradiation under a nitrogen atmosphere at the boiling point of the solvent used.

Rate Measurements. Nitrobenzene, nitrosobenzene, and phenylhydroxylamine were determined by polarography. The ionic strength and pH were adjusted by using a potassium biphthalate - sodium hydroxide buffer solution (pH=6.0) or a sodium boronate - sodium hydroxide buffer solution (pH=12.0); for nitrobenzene, pH=6.0 and μ=0.12; for nitrosobenzene and phenylhydroxylamine, pH=12.0 and μ=0.21.

The aniline produced during the course of the reaction was followed by the following method. Samples drawn out of the reaction flask at appropriate time intervals were diazotized and coupled with NW acid (1-naphthol-4-sulfonate) by the usual method. The resulting azo dye solution was paper chromatographed by a 2% aqueous ammonium solution, and then the dye spot corresponding to the aniline dye was separated and extracted by a 20% aqueous pyridine solution. The absorbance of the extract was measured at 490 mμ on a Shimadzu Bausch & Lomb Spectronic 20 photometer.

Identification of Products. In our present experiments, aminophenols, *p*-chloroaniline, benzidine, and diphenyline were produced simultaneously with aniline, as shown in Table 1. They were, therefore, identified

*1 Presented in part at the 20th Annual Meeting of the Chemical Society of Japan, Tokyo, April, 1967.

*2 Present address: Department of Organic Synthesis, Faculty of Engineering, Kyushu University, Hakozaki, Fukuoka.

1) Part II: S. Hashimoto, J. Sunamoto and H. Fujii, *Kogyo Kagaku Zasshi* (*J. Chem. Soc. Japan, Ind. Chem. Sect.*), **70**, 699 (1967).

2) E. Bamberger, *Ber.*, **35**, 1606 (1902).

3) L. Vecchiotti and G. Zanetti, *Gazz. chim. ital.*, **60**, 479 (1930).

4) L. Vecchiotti and C. Piccinini, *ibid.*, **61**, 626 (1931).

5) O. N. Shelegova, *J. Exp. Theoret. Phys. U.S.S.R.*, **9**, 1527 (1939).

6) S. H. Hasting and F. A. Matsen, *J. Am. Chem. Soc.*, **70**, 3514 (1948).

7) F. Kaluza and G. W. Perold, *J. S. African Chem. Inst.*, **13**, 89 (1960).

8) R. L. Letsinger and G. G. Wubbels, *J. Am. Chem. Soc.*, **88**, 5041 (1966).

9) R. Hurley and A. C. Testa, *ibid.*, **88**, 4330 (1966).

10) C. Kaneko, S. Yamada and I. Yokoe, *Tetrahedron Letters*, **1966**, 4729.

11) G. H. Coleman, C. M. McClosky and F. A. Stuart, "Organic Syntheses," Coll. Vol. III, p. 668 (1955).

12) H. E. Bigelow and A. Palmer, *ibid.*, Coll. Vol. II, p. 57 (1943).

Table 1. Experimental conditions and results obtained[a]

Paper: Toyo Filter Paper No. 50 Solvent: *n*-BuOH : conc. HCl = 4 : 1
Detection: Diazotizing and coupling with NW acid

No.	Starting material	HCl, m*l*	AQ, mg	Product (R_f value)
1	Nitrobenzene	5.0	10	*p*-Aminophenol (0.52), Aniline (0.68),[b] *p*-Chloroaniline (0.84), Unknown (0.76)
2	Nitrobenzene	5.0	—	Aniline (0.70),[c] *p*-Chloroaniline (0.85)
3	Nitrobenzene	—	10	Phenylhydroxylamine
4	Nitrobenzene	—	—	Phenylhydroxylamine
5	Nitrosobenzene	5.0	10	Benzidine (0.20), Diphenyline (0.25), *o*-Aminophenol (0.59), Aniline (0.66),[d] Unknown (0.84)
6	Phenylhydroxylamine	5.0	10	*p*-Aminophenol (0.59), Aniline (0.70),[e] *p*-Chloroaniline (0.84), Unknown (0.76)
7	Azoxybenzene	5.0	10	Benzidine (0.20), Diphenyline (0.27), *o*-Aminophenol (0.59), Aniline (0.68),[f] Unknown (0.36, 0.48)

a) Concentration of the starting materials was 2×10^{-3} mol/*l* in isopropyl alcohol. (at boiling point of isopropyl alcohol under nitrogen atmosphere)
Maximum yields of aniline were b) 36%, c) 25%, d) 23%, e) 38% and f) 65% respectively.

with authentic samples by paper chromatography (solvent: 4 : 1 = *n*-butanol : concentrated hydrochloric acid, cyclohexane, or a 2% aqueous hydrochloric acid solution; detection : diazotization and coupling with NW acid, or Schiff base formation with *p*-dimethylaminobenzaldehyde). Furthermore, all of the dyes separated from paper chromatograms were independently extracted by suitable solvents and their visible absorption spectra were examined.

The other photoreduction products were identified by spectrophotometry and/or polarography. The acetone generated during the course of the reaction was derived to 2,4-dinitrophenylhydrazone and identified by means of its melting point.

Results and Discussion

The disappearance of nitrobenzene and the formation of aniline are shown in Fig. 1. Much as in the case of Hurley and Testa,[9] in our photochemical reduction of nitrobenzene the formation of phenylhydroxylamine was obviously detected on the polarogram and by means of the UV spectra upon the disappearance of nitrobenzene. When hydrochloric acid was added to this system, the rate of the disappearance of nitrobenzene became fast and the phenylhydroxylamine intermediately produced was immediately changed to aniline, *p*-chloroaniline, and *p*-aminophenol. Figure 2 shows that, when hydrochloric acid is present, phenylhydroxylamine converts to the primary amines even in the dark.

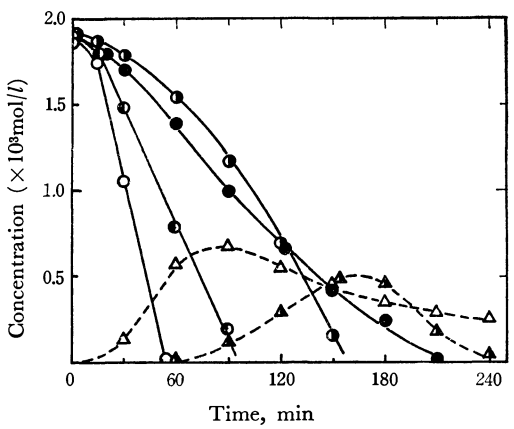

Fig. 1. Photochemical reduction of nitrobenzene.
—— Disappearance of nitrobenzene
○ No. 1, ◑ No. 2, ◐ No. 3, ● No. 4
--- Formation of aniline
△ No. 1, ◭ No. 2

In Bamberger's well-known reaction,[13] phenylhydroxylamine converts to *p*-anisidine, *p*-chloroaniline, and *p*-aminophenol in an acidic methanol solution. However, in our experiment aniline was given in a rather good yield (*ca.* 40%), and no alkoxyaniline was detected.

On the other hand, when AQ was added to this reaction system, the rate of the disappearance of nitrobenzene also became fast. Dependent upon the disappearance of nitrobenzene, the phosphorescence of excited AQ decreased in intensity. When the photoreduction of nitrobenzene was carried out in the presence of hydrochloric acid and AQ under an oxygen atmosphere, the same kinds of amines were produced as those under a nitrogen atmosphere.

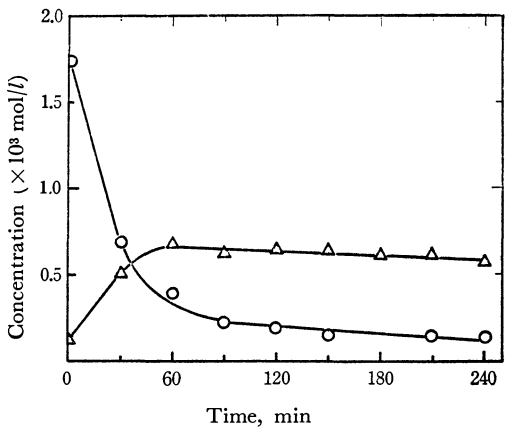

Fig. 2. Redution of phenylhydroxylamine in isopropyl alcohol in the dark; under nitrogen atmosphere, boiling point of isopropyl alcohol, conc. HCl=5 m*l*, AQ=10mg.

○ Phenylhydroxylamine, △ Aniline

However, the rate of the disappearance of nitrobenzene and the yields of amines became less than those under a nitrogen atmosphere. Comparing with AQ, benzophenone was not a useful catalyst in these photoreductions. From these results obtained above, it seems that the AQ used in the present photoreduction is useful as a reducing agent as well as a photosensitizer, because AQ can be easily photoreduced to give the semiquinone radical or the hydroquinone in a hydrogen-donating solvent.[14]

The light of 330—340 mμ, which are effective for the n–π^* transition of nitrobenzene, are also absorbed by phenylhydroxylamine. Therefore, it may be reasonable to suppose that the reaction rate of nitrobenzene will become slower if hydrochloric acid is absent, because of the inner-filter effect of the phenylhydroxylamine produced.

It was clarified that, in the photoreduction of nitrobenzene in the presence of hydrochloric acid, the primary product was phenylhydroxylamine, not nitrosobenzene; that the final products were aniline, *p*-aminophenol, and *p*-chloroaniline, and that hydrochloric acid and AQ were effective as the catalysts for this photoreduction. On the other hand, in the photochemical reduction of nitrosobenzene in the presence of hydrochloric acid and AQ, the detectable primary product was azoxybenzene, and the final reduction products were aniline, *o*-aminophenol, benzidine, and diphenyline. From these results obtained, it may be most reasonable to assume that the corresponding hydrazo compound may be produced as an intermediate in the photoreduction of nitrosobenzene, unlike as in that of nitrobenzene. Bamberger[15] and Cumming and Ferrier[16] have suggested that azoxybenzene and nitrobenzene are produced in the photodisproportionation of nitrosobenzene. In our present experiment, however, no nitrobenzene could be detected in the photoreduction of nitrosobenzene.

In the oxidation of phenylhydroxylamine to nitrosobenzene by *t*-butylhydroperoxide, $C_6H_5\dot{N}OH$ has been detected by ESR spectroscopy.[17] Therefore, it may be reasonable to assume that this radical will be produced as an intermediate of the photochemical reduction of nitrosobenzene to phenylhydroxylamine, which may then couple immediately with nitrosobenzene to form azoxybenzene.[18]

13) E. Bamberger, *Ber.*, **27**, 1347 (1894).

14) C. F. Wells, *Trans. Faraday Soc.*, **57**, 1703 (1961).

15) E. Bamberger, *Ber.*, **35**, 1610 (1902).

16) W. M. Cumming and G. S. Ferrier, *J. Chem. Soc.*, **127**, 2374 (1925).

17) K. Maruyama and T. Otsuki, 19th Discussion Meeting on Mechanisms of Organic Chemistry, Kyoto, October, 1967.

18) Y. Ogata, M. Tsuchida and Y. Takagi, *J. Am. Chem. Soc.*, **79**, 3397 (1957).

A Modified Wittig Synthesis of 6,10-Dimethyl-3,9-undecadien-2-one, Ethyl 5,9-Dimethyl-2,8-decadienonate, and Their α-Alkyl Homologs: Stereochemistry of the Reaction and Conformation of the Products

Kazuhiro SASAKI

Ichikawa Works, Kobayashi Perfumery Co., Ltd., Ichikawa, Chiba

(Received October 16, 1967)

In previous papers,[1-3] the modified Wittig reaction of citrals with diethyl 2-oxophosphonates was described. When the substituent on the α-carbon atom of the phosphonate was methyl group or hydrogen, the resultant C=C double bond of the condensation product had only *trans* configuration.

On the other hand, when the substituent was ethyl group, the formation of small amounts of *cis* isomers was observed together with the major formation of *trans* isomers.

It was of interest to investigate whether the saturation of the α,β-unsaturated linkage to the aldehydic group in citrals affects the stereochemistry of the reaction. I the present report, β-citronellal (I) was condensed with various diethyl 1-alkyl-2-oxoalkylphosphonates (II) or diethyl 1-ethoxycarbonylalkylphosphonates (III) under usual reaction conditions.

$$(EtO)_2P(O)\underset{\displaystyle R}{\underset{|}{C}}HCOR' \xrightarrow[\beta\text{-Citronellal (I)}]{NaNH_2}$$

II: R′=Alkyl
III: R′=OEt

$$CH_3\underset{\displaystyle CH_3}{\underset{|}{C}}=CHCH_2CH_2\underset{\displaystyle CH_3}{\underset{|}{C}}HCH_2CH=\underset{\displaystyle R}{\underset{|}{C}}COR'$$

IV:	R=H, R′=CH_3	VIII:	R=H, R′=OEt
V:	R=CH_3	IX:	R=CH_3
VI:	R=C_2H_5	X:	R=C_2H_5
VII:	R=H, R′=C_2H_5		

The results are summarized in Table 1. From these data the following points were notable: i) The relative amounts of the *cis* isomers in the products augmented with increasing size of the alkyl substituent on the α-carbon atom of the phosphonates. ii) The ethoxycarbonyl group on the α-carbon atom of a phosphonate was advantageous over the alkyl group in increasing the *cis-trans* ratio of the resulted olefins. iii) Saturation of the α,β-unsaturated linkage in citrals increased the proportion of a *cis* isomer in the product, although the dominance of a *trans* isomer over a *cis* isomer was unchanged.

The infrared and ultraviolet absorption data of the products are given in Table 2. It is well known that the α,β-unsaturated carbonyl compounds may exist in two possible conformations, *i.e.*, *s-trans-* and *s-cis-*forms. In the case of 3-*trans*-V and 3-*trans*-VI, the difference of wave numbers between the C=O and the C=C stretching vibration is less than 30 cm^{-1} and the intensity of the K-band at 232—233 mμ is very strong. These spectral properties are probably ascribed to the *s-trans* conformation. On the other hand, 3-*cis*-V and 3-*cis*-VI appear to have the *s-cis* conformation, since the difference of the wave numbers between the C=O and the C=C stretching vibration is more than 60 cm^{-1} and the K-band is rather shifted bathochromically and is remarkably weakened in intensity.*1 The splitting of the C=O stretching infrared absorption bands of 3-*trans*-IV and 4-*trans*-VII may be ascribed to an equilibrium between the *s-trans-* and *s-cis-*conformations as demonstrated in the case of *trans*-3-penten-2-one and its analogs.[1,5] The ascription seems to be supported by the fact that each of the splitting carbonyl bands of 3-*trans*-IV and 4-*trans*-VII apparently corresponds in its position to the carbonyl bands of 3-*trans*-V and 3-*trans*-VI, and 3-*cis*-V and 3-*cis*-VI, respectively.

Examination of scale models reveals that 3-*trans*-IV and 4-*trans*-VII can exist as two hindrance-free conformers. In the case of 3-*trans*-V and 3-*trans*-VI, the *s-trans* conformation is less-hindered, while the steric hindrance of 3-*cis*-V and 3-*cis*-VI is apparently stronger in the *s-trans*-conformation than in the *s-cis*-. These considerations also substantiate the above conclusions.

Analogous considerations with scale models of the α,β-unsaturated carboxylates disclosed that either of the two possible conformations is substantially hindrance-free and therefore energetically more favored *s-trans* form is the preferred conformation.

In summary, apparent difference in a steric hindrance between an α,β-unsaturated ketone and the relevant carboxylate is probably one of the cause for the different *cis-trans* ratio in these compounds obtained by means of the modified Wittig reaction.

1) K. Sasaki, This Bulletin, **39**, 2703 (1966).
2) K. Sasaki *ibid.*, **40**, 2967 (1967).
3) K. Sasaki, *ibid.*, **40**, 2968 (1967).
4) W. L. Walton and R. B. Hughes, *J. Am. Chem. Soc.*, **79**, 3985 (1957).

*1 Analogous spectroscopic ascription has been reported for the conformations of 3-methyl-, 3-ethyl-*trans*-3-penten-2-one, and 3-methyl-*cis*-3-penten-2-one by Mecke and Noack.[5]

5) R. Mecke and K. Noack, *Chem. Ber.*, **93**, 210 (1960); *cf.* E. A. Braude and C. J. Timmons, *J. Chem. Soc.*, **1955**, 3766.

TABLE 1. YIELDS AND COMPOSITIONS OF PRODUCTS

Attempted compound	Method[a]	Bp °C/mmHg	Yield %	Composition of the product[b] *cis*	*trans*	Formula	Analysis C, % Found	C, % Calcd	H, % Found	H, % Calcd
IV[c]	A	74—76/0.15	84	0	100	$C_{13}H_{22}O$	77.71	80.35	11.37	11.41
VII	A	83—85/0.18	83	0	100	$C_{14}H_{24}O$	80.14	80.71	11.49	11.61
V	A	74.5—78/0.15	82	5.5	94.5	$C_{14}H_{24}O$	80.62	80.71	11.49	11.61
VI	B	82—88/0.3	47	19.3	80.7					
VIII	A	88—94/0.35	75	6.5	93.5	$C_{14}H_{24}O_2$	74.93	74.95	11.04	10.78
IX	A	90—95/0.3	58	20.1	79.9	$C_{15}H_{26}O_2$	75.87	75.58	10.94	10.99
IX	B	87—94/0.3	18	17.9	82.1					
X	A	93—100/0.3	67	43.9	56.1	$C_{16}H_{28}O_2$	75.93	76.14	11.08	11.18

a) See Experimental.
b) Yields and compositions of the products were determined by gas chromatography.
c) The discrepancy between the found and the calculated values may be attributable partly to the decomposition during the distillation and partly to the contamination with a small amount of phosphorus compounds: 2,4-Dinitrophenylhydrazone of IV (mp 78.5—79.0°C) gave satisfactory results for the expected empirical formula. Found: C, 61.29; H, 6.97; N, 15.24%. Calcd for $C_{19}H_{26}N_4O_4$: C, 60.95; H, 7.00; N, 14.96%.

TABLE 2. INFRARED AND ULTRAVIOLET ABSORPTION DATA

Compound	Infrared absorption (liquid film) cm^{-1}[a] $\nu_{C=O}$	$\nu_{C=C}$	δ_{C-H}	Family band[d]	$\nu_{C=O}-\nu_{C=C}$	Ultraviolet absorption λ_{max}^{EtOH}	ε_{max}
3-*trans*-IV	1678 (vs), 1689 (s)[c]	1630 (s)	979 (s)			223.5	14900
4-*trans*-VII	1676 (vs), 1696 (s)[c]	1632 (vs)	979 (s)			225	14700
3-*trans*-V[b]	1670 (vs)	1641 (m)			29	232	13800
3-*cis*-V[b]	1689 (s)	1626 (m)			63	237	3500
3-*trans*-VI[b]	1666 (vs)	1638 (m)			28	233	15300
3-*cis*-VI[b]	1691 (s)	1629 (m)			63	238.5	4100
2-*trans*-VIII	1724 (vs)	1655 (m)	982 (m)	739 (w)		210	16100
2-*cis*-VIII[b]	1719 (vs)	1640 (m)					
2-*trans*-IX[b]	1715 (vs)	1654 (m)		741 (m)		219	13600
2-*cis*-IX[b]	1721 (vs)	1649 (m)				217.5	11600
2-*trans*-X[b]	1718 (vs)	1650 (m)		753 (m)		219	14300
2-*cis*-X[b]	1717 (vs)	1646 (w)				217.5	9400

a) Infrared spectra were measured through the kindness of Dr. Yoshitaka Matsuoka and Mr. Kenya Sakaguchi of Eisai Research Laboratories and Dr. Hisatake Ono and Dr. Asashi Kondo of Fuji Photo Film Co., Ltd.
b) These compounds were isolated by gas chromatography, the facilities of which were given by Mr. Kozo Takashima and Mr. Hiroo Miyazaki of Ohkura Rikagaku Kenkyusho Co., Ltd.
c) Splitting carbonyl bands.
d) A band characteristic of a *trans*-α,β-unsaturated carboxylate.[3,4]

Experimental

β-Citronellal (I). Commercial citronellal*[2] was purified by conversion to its sodium hydrogen sulfite-adduct followed by decomposing the adduct with sodium carbonate to yield the free aldehyde, which was gas chromatographically pure. Bp 78—79°C/8 mmHg.

2,4-Dinitrophenylhydrazone: Mp 78.5—79°C (lit.[6] mp 78°C).

*[2] This is of natural origin and the natural aldehyde is now known to be the β-form. P. Z. Bedoukian, "Perfumery and Flavoring Synthetics," 2nd ed., Elsvier Publ. Co., Amsterdam (1967), pp. 113, 168.

6) C. F. H. Allen, *J. Am. Chem. Soc.*, **52**, 2955 (1930).

Diethyl 2-Oxoalkyl- and 1-Ethoxycarbonylalkylphosphonates. These phosphonates were prepared from triethylphosphite and appropriate α-bromocarbonyl compounds by means of Michaelis-Arbuzov reaction.[1,3]

3,6,10-Trimethyl-3,9-undecadien-2-ones (V). (*A typical Example of the General Procedure*). *Method A.* To a suspension of 1.56 g (0.04 mol) of sodium amide in 30 m*l* of dry dimethylformamide (DMF), there was added a solution of 8.33 g (0.04 mol) of diethyl 1-methyl-2-oxopropylphosphonate in 20 m*l* of dry DMF with stirring and cooling in an ice-salt bath. Stirring and cooling were continued and dry nitrogen gas was passed into the mixture until the evolution of ammonia had ceased. The resultant solution was cooled below −10°C and

treated dropwise with 6.17 g (0.04 mol) of β-citronellal in 20 m*l* of dry DMF. After the solution had stood overnight, the solvent was removed under vacuum and the residue was poured into water and extracted with ether. The ethereal extract was washed with water and dried over sodium sulfate. The solvent being evaporated, the residue was distilled under reduced pressure to yield V as a colorless oil.

Method B. To the carbanion of diethyl 2-oxopropylphosphonate, prepared from 7.77 g (0.04 mol) of the phosphonate in a manner similar to the Method A, there was added dropwise 5.96 g (0.042 mol) of methyl iodide with stirring and cooling in an ice-water bath and the mixture was allowed to stand overnight. After the mixture was cooled below −10°C, 1.56 g (0.04 mol) of sodium amide was added all at once and the mixture was stirred under a slow stream of dry nitrogen gas. The resultant carbanion of diethyl 1-methyl-2-oxopropylphosphonate was treated with β-citronellal in an analogous manner to the Method A to give V as a colorless oil.

Procedures similar to those described above gave the ketones IV, VI, and VII. A minor modification of the condensation conditions was required for the preparation of the carboxylates VIII, IX, and X; at 75°C for 3 hr (for the preparation of X, Method A) to 24 hr (for the preparation of IX, Method A).

The author is indebted to Professor Masaki Ohta and Assistant Professor Rokuro Sudo of the Tokyo Institute of Technology for their encouragement and support; to Mr. Kenjiro Kobayashi, President of Kobayashi Perfumery Co., Ltd., and Mr. Mitsuhiro Takahashi, Director of the same company, for their permission to publish this paper.

Determination of Complex Species by the Method of Continuous Variation Using Infrared Spectroscopy

Keikichi NAKAMURA

National Research Institute For Metals, 2-3-12, Naka-meguro, Meguro-ku, Tokyo

(Received August 19, 1967)

The method of continuous variations has been widely used to determine the composition of complex species using such intensive properties of the systems as visible and ultraviolet absorption[1,2] and conductivity.[3] Few studies, however, have used infrared absorption as a basis for this method, apart from those studies where hydrogen bonded systems arise,[4] in which case large shifts are usually found.

In the case of lanthanide salts-TBP(tributyl phosphate) systems, the stoichiometry of the solvates formed have thus far been determined only by liquid-liquid partition methods and solubility methods.[5,6]

Since the organic diluents employed in the above studies dissolve the lanthanide thiocyanates only sparingly or not at all, the method of continuous variations could not be employed. However, such diluents as acetonitrile appear to be compatible with the use of the continuous variation method, provided that an absorption change due to complex formation takes place.

This paper will report the results obtained by the method of continuous variations from an infrared spectroscopic study of the $Ln(SCN)_3$-TBP and -TPPO(triphenyl phosphine oxide) systems using acetonitrile as the diluent.

Experimental

The lanthanide thiocyanates were prepared by dissolving the appropriate oxides in warm, freshly prepared hydrogen thiocyanate and the free water was removed by vacuum evaporation. The TBP was purified by the method of Alcock *et al.*[7] The acetonitrile was purified by distilling it several times from P_2O_5. The TPPO was prepared by the Grignard reaction between phenylmagnesium bromide and phosphorous oxychloride. The resulting product was recrystallized several times from a mixture of ethanol and water. The infrared spectroscopic data were recorded as previously described. Procedure: 0.1 M (0.02 M) of TBP (TPPO) and equimolar lanthanide thiocyanate solutions were equilibrated in varying proportions according to the expression:

$$x = \frac{[\mathrm{Ln}]}{[\mathrm{Ln}] + [\mathrm{TBP(TPPO)}]}$$

Thus, the total concentration was kept at 0.1 M (0.02 M). It was assumed that no appreciable volume change took place on the equilibration.

Results and Discussion

The effect on the infrared spectra of representative lanthanide thiocyanate-TBP(TPPO)-acetonitrile solutions by varying the x parameter is shown in Fig. 1.

1) P. Job, *Ann. Chem. Phys.*, **9**, 113 (1928).
2) W. C. Vosburgh and G. R. Cooper, *J. Am. Chem. Soc.*, **63**, 437 (1941).
3) R. Longhi and R. S. Drago, *Inorg. Chem.*, **2**, 85 (1963).
4) R. A. Zingaro and C. F. Coleman, *J. Inorg. Nucl. Chem.*, **29**, 1287 (1967).
5) T. Healy and H. A. Mckay, *Trans. Faraday Soc.*, **52**, 633 (1955).
6) T. Sekine, This Bulletin, **38**, 1972 (1963).
7) K. Alcock, S. S. Grmley, T. V. Healy, J. Kenedy and H. A. McKay, *Trans. Faraday Soc.*, **52**, 39 (1956).

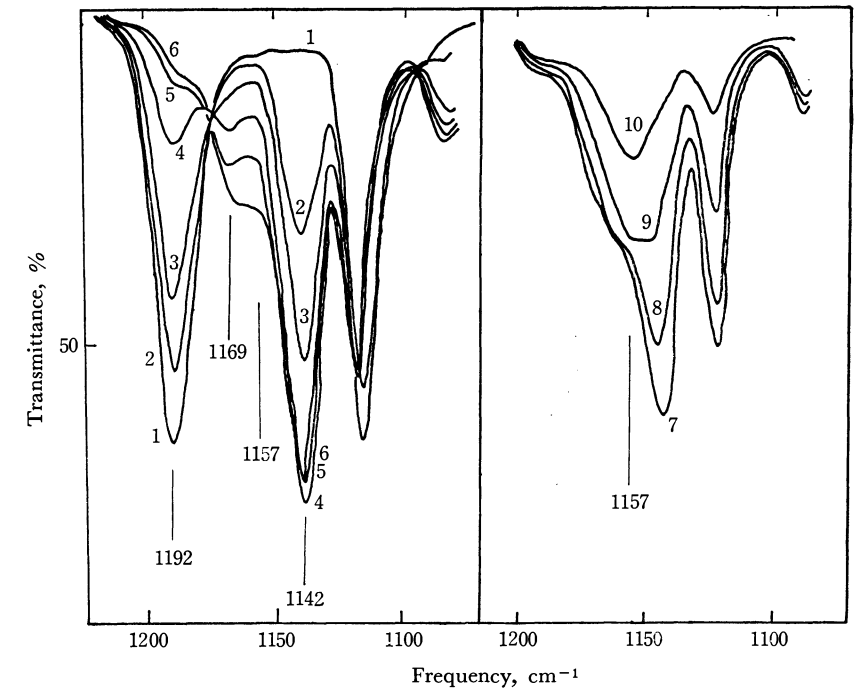

Fig. 1(a). $Er(SCN)_3$-TPPO-CH_3CN

	x
1	0.00
2	0.05
3	0.10
4	0.20
5	0.25
6	0.30
7	0.40
8	0.50
9	0.70
10	0.90

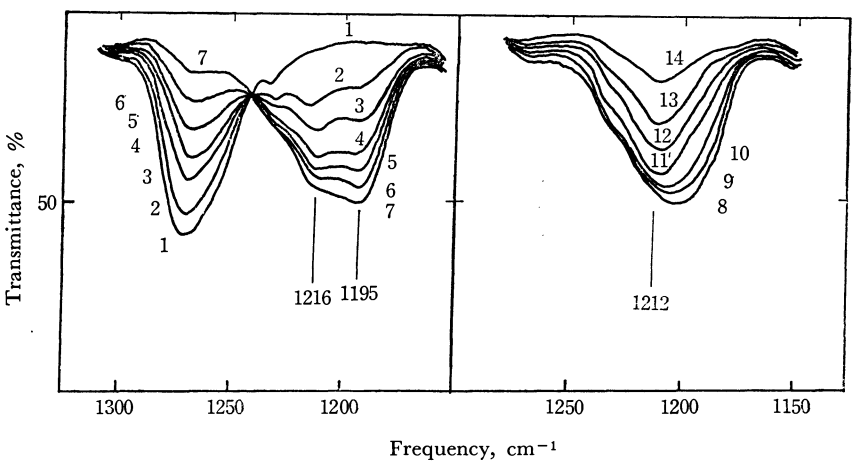

Fig. 1(b). $Dy(SCN)_3$-TBP-CH_3CN

	x
1	0.00
2	0.05
3	0.10
4	0.15
5	0.20
6	0.25
7	0.30
8	0.35
9	0.40
10	0.50
11	0.60
12	0.70
13	0.80
14	0.90

Fig. 1. Infrared spectra of acetonitrile solutions of $Er(SCN)_3$-TPPO and $Dy(SCN)_3$-TBP in the various proportions.

In the erbium thiocyanate-TPPO-acetonitrile system, as x increased, the free TPPO absorption band at 1192 cm^{-1} became increasingly weaker, while new absorption bands, which appeared at lower frequencies, became increasingly stronger. The examination of these new bands suggested that at least three species were present, represented by the absorption bands at 1142 cm^{-1}, 1157 cm^{-1} and 1169 cm^{-1}. A continuous variation analysis of these bands, shown in Fig. 2, indicates that the band at 1142 cm^{-1} represents the tri-solvated species, while the bands at 1157 cm^{-1} and 1169 cm^{-1} may be assigned to the mono- and di-solvated species respectively. The same assignment was found to be applicable for the yttrium and dysprosium systems as well.

In the case of the lighter lanthanide thiocyanate-TPPO complexes (*i.e.*, La and Ce), no distinct absorption bands could be distinguished, indicating that with them complex formation did not occur in distinct steps. For the lighter lanthanide thiocyanates, therefore, the strongest absorption, that at 1140 cm^{-1}, may be attributed to a tri- or tetra-solvated species.

As for the dysprosium thiocyanate-TBP-acetonitrile system, Fig. 1(b) will show that two distinct absorption bands appeared, one at 1216 cm^{-1} and the other at 1195 cm^{-1}, under the experi-

mental conditions of $0.05 \leqq x \leqq 0.15$. This result indicates the coexistence of two species, with the species absorbing at 1216 cm^{-1} predominantly. Under the conditions of $0.20 \leqq x \leqq 0.35$, the band at 1195 cm^{-1} became increasingly stronger, and when $x \geqq 4$, an absorption band appeared at 1212 cm^{-1} and increased in intensity as x increased. Thus, the results demonstrate the formation of at least three species, whose solvation number increases with respect to the observed absorption wavelength in the order: 1216 cm^{-1} > 1195 cm^{-1} > 1212 cm^{-1}.

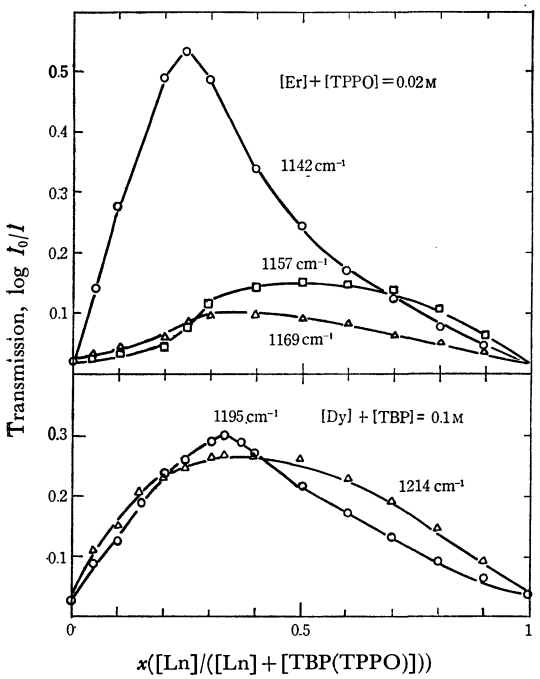

Fig. 2. Continuous variations for acetonitrile solutions of $Er(SCN)_3$-TPPO and $Dy(SCN)_3$-TBP.

A continuous variation analysis in this spectral region is shown in Fig. 2. An examination of Fig. 2 will show that the band at 1195 cm^{-1} may be assigned to the di-solvated species. The band at 1216 cm^{-1} and 1212 cm^{-1} overlap, which makes resolution very difficult. However, in view of the experimental conditions under which these two bands appeared, it is reasonable to assign the band at 1216 cm^{-1} to the tri- or tetra-solvated species, and the band at 1212 cm^{-1} to the mono-solvated species.

This study has revealed many difficulties in connection with the use of infrared spectroscopy on such systems. These difficulties may be listed as below:

1) The absorption shift due to complex formation is small.

2) Because of the strong absorption of the diluents the absorption frequency range for the detection of complex formation and the concentration range available are severely restricted.

3) The NaCl and KCl cells tend to dissolve slightly in polar diluents, and trace amounts of water cause frosting of the optical surface of the cell.

In spite of the above difficulties, however, infrared spectroscopy can be used for the determination of complex species provided that, with the above qualifications in mind, a suitable choice is made of the diluent, the material of construction of the cell, and the range of absorption frequency used for detection.

The author wishes to express his thanks to Dr. Kazutaka Kawamura and Dr. Akira Kawase for their encouragement and discussions. He also wishes to express his thanks to Dr. D. S. Flett of the Warren Spring Laboratory for his helpful discussions.

Comparison of Metal Bath Techniques in Vacuum Fusion Analysis by an Isotope Dilution Method

Hitoshi KAMADA and Keiichi FURUYA

Department of Industrial Chemistry, Faculty of Engineering, The University of Tokyo, Bunkyo-ku, Tokyo

(Received September 19, 1967)

Many applications of metal bath techniques to vacuum fusion analysis have been reported. In these reports, metal bath techniques are used to promote a reaction between carbon and oxygen in a flux and/or to eliminate a gettering action by the adsorptive elements evaporated from the samples. Beach and Guldner[1] measured the effect of evaporated films of carbon, nickel, iron, germanium, platinum, aluminum, manganese and titanium on the recovery of carbon monoxide, nitrogen and hydrogen at a crucible temperature of 1650°C.

Sloman[2] pointed out that carbon in the iron bath is very reactive, and the iron metal depresses the vaporization of adsorptive elements. McDonald,[3] and Smith,[4] on the other hand, showed that carbon

1) A. L. Beach and W. G. Guldner, *Anal. Chem.*, **31**, 1722 (1959).

2) H. A. Sloman, *J. Inst. Metals*, **71**, 391 (1945).

3) R. S. McDonald, J. E. Fagel and E. W. Balis, *Anal. Chem.*, **27**, 1632 (1955).

4) W. H. Smith, *ibid.*, **27**, 1636 (1955).

becomes easily oversaturated in an iron flux at high temperature and the bath becomes very viscous, which gives erroneous low results. Smiley,[5] and Gregory[6] used platinum metal as a metal bath for the determination of oxygen in titanium, and Ogahara[7] used it for oxygen analysis in stainless steels. Platinum metal has a low vapor pressure, which minimizes the amount of metal evaporating to the furnace walls, and does not become viscous. Wilkins[8] reported that the platinum bath does not adsorb the extracted gases. Tin has been used by many investigators as a metal bath in order to eliminate the adsorption of the extracted carbon monoxide by manganese evaporated from a flux. Guldner[9] pointed out that the function of the tin in the case of addition of both iron and tin to the crucible is two-fold: first, to increase the fluidity of the bath, and second, to act as a mechanical stirrer.

A method of isotope dilution employed in the determination of gases in metals has been reported by Kirshenbaum and Grosse,[10] Pearce,[11] and Burden.[12]

An isotope dilution method using ^{18}O-labelled carbon monoxide was employed in the present paper for the determination of oxygen in a high manganese steel without the bath technique, and with iron, platinum and tin bath techniques. When isotopic equilibrium is established only in the gas phase, this method gives results in which gas adsorption errors have been eliminated.

Experimental

The apparatus used is identical to that reported previously.[13,14]

NBS standard steel 1041 containing 1.2% manganese was used as a sample. Specimens for each metal bath were neighboring sections cut out parallel to the aixs in order to avoid the effect of sedimentation. They were then polished with carborundum paper, rinsed in petroleum benzene, and dried in air.

^{18}O-labeled carbon monoxide was prepared from $Hg^{18}O$ (about 90 atom%^{18}O), produced by the BIO-RAD Laboratory, Richmond, California, U.S.A.

Carbon Monoxide Adsorption Curves. After outgassing the graphite crucible, 10 g of the bath metal listed above was added and fused to be degassed at 1850°C, while metal vapor deposited continuously on the surface of the walls. A measured quantity of carbon monoxide was admitted from a storage bottle and circulated in the system. The recovery of carbon monoxide was measured. Figure 1 shows the carbon monoxide adsorption curves.

When 5 g of the sample was added to the fused metal, the carbon monoxide adsorption rate increased in platinum and in iron, while it did not change in tin. These phenomena may be related to the magnitude of the chemical affinity between the metal and carbon monoxide.

Determination of Oxygen in NBS 1041. The methods of isotope dilution and vacuum fusion were applied to the determination of oxygen in a sample of NBS standard steel 1041 using the above mentioned metal baths. The procedures employed were identical to those reported previously.[14]

In Table 1 are summarized these data, which are the arithmetic means of three or four determinations from outer portions of every sample rod.

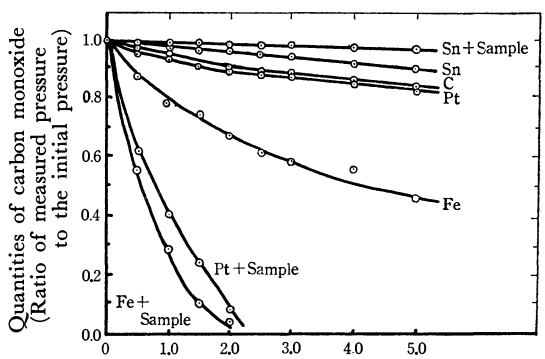

Fig. 1. Carbon monoxide adsorption curve.

Table 1. Analytical results of oxygen in NBS 1041

Bath metal	—	Pt	Sn	Fe
Vacuum fusion method	—	150	150	113
Isotope dilution method	163	214	159	223
Argon fusion method	160			
Adsorption of carbon monoxide	very large	small	no	medium
^{18}O content in the residual gas		close to the sample gas	diluted with ^{16}O	close to the sample gas

Sample: NBS 1041 Data are mean values of those from outer portions. (ppm)

5) W. G. Smiley, *ibid.*, **27**, 1098 (1955).
6) J. N. Gregory and D. Mapper, *Analyst*, **80**, 230 (1955).
7) I. Ogahara, W. Sekimoto and H. Matsumoto, *J. Iron & Steel Inst. Japan*, **47**, 300 (1961).
8) D. H. Wilkins and J. F. Fleisher, *Anal. Chim. Acta*, **15**, 334 (1956).
9) W. G. Guldner, *Talanta*, **8**, 191 (1961).
10) A. D. Kirshenbaum and A. V. Grosse, *Trans. Am. Soc. Metals*, **45**, 758 (1953).
11) M. L. Pearce and C. R. Masson, *Iron & Steel Inst., Spect. Rept. No.* 68, 121 (1960).
12) J. P. Burden and C. R. Masson, *J. Iron & Steel Inst.*, **202**, 28 (1964).
13) T. Somiya, S. Hirano, H. Kamada and I. Ogahara, *Talanta*, **11**, 581 (1964).
14) K. Furuya and H. Kamada, *Japan Analyst*, **15**, 1227 (1966).

When no metal bath was used, the oxygen content of the initial six specimens could not be determined owing to the large adsorption of carbon monoxide in the furnace. During 3 min of gas circulation, carbon monoxide in the system was completely adsorbed, so their isotope concentrations could not be measured. However, in the case of the final three specimens, the gas adsorption became rather small, and the isotope concentrations could be measured.

In the platinum bath method, the isotope concentration of residual gas extracted from the furnace after gas circulation was close to that of the collected gas sample. This indicates that almost all of the oxygen in the sample was already extracted from the crucible. However, there were marked differences between the results of the isotope dilution method and the vacuum fusion method caused by gas adsorption in the furnace.

In the iron bath method, the results were close to those in the case of the platinum bath in the isotope dilution method, while the results in the vacuum fusion method were lower than those in the platinum bath method. This is related both to the gas adsorption property of iron, and to the fatigue of bath action caused by carbonization viscousness. The isotope concentration of the residual gas was close to that of the collected gas sample.

In the tin bath method there were no differences between results of the isotope dilution and the vacuum fusion method. This shows that there is no gas adsorption lowering the vacuum fusion results in the tin bath method. The isotope concentration in a small quantity of the residual gas was about 90 atom% ^{16}O, and this shows that the oxygen in the sample was incompletely decomposed and remained in the crucible.

In argon fusion analysis using no metal bath,[15] the results agreed well with those obtained by the isotope dilution method with the tin bath.

The results of the isotope dilution method and the data obtained for the ^{18}O concentration of the residual gas indicate that the platinum and iron baths can promote reaction between carbon and oxygen in a melt. That these metal baths can partly suppress carbon monoxide adsorption is shown by a comparison of their data with the data in which no metal bath was used. The tin bath can effectively prevent the adsorption of carbon monoxide in the furnace, and does not promote the reaction in a flux.

From this consideration, though the vacuum fusion results for the platinum and tin baths are apparently in agreement, the processes of the extraction of oxygen were different from each other. In the platinum bath, part of the extracted carbon monoxide, after the promotion of the reaction by platinum, was adsorbed by the adsorptive elements such as manganese, while in the tin bath all of the incompletely extracted carbon monoxide was collected. When the metal bath technique was not used, extraction of oxygen was also incomplete.

According to the above consideration, it is desirable to use a combination bath, one containing a metal which promotes reaction in the flux, and also a metal which prevents the adsorption of carbon monoxide in the furnace. From this point of view, the mechanism of the iron-tin bath method, and the platinum-tin bath method can both be well explained.

15) H. Goto, S. Ikeda and A. Onuma, Rept. of Committee for the study of gaseous elements in nuclear metallic materials, No. 32, the Japan Soc. for Anal. Chem. (1963).

Studies on Heteroaromaticity. XIV.[1] Ring-opening Reaction of *N*-[β-(5-Nitro-2-furyl)vinyl]- and *N*-(2-Furyl)-*N'*-ethyleneurea

Tadashi SASAKI and Yoshiyuki YOSHIOKA

Institute of Applied Organic Chemistry, Faculty of Engineering, Nagoya University, Chikusa-ku, Nagoya

(Received October 25, 1967)

In the previous paper[2] we reported the ring-opening reaction of β-(5-nitro-2-furyl)acryloyl- and furoyl aziridine. In this paper the similar ring-opening reaction and nucleophilic rearrangement reaction of *N*-[β-(5-nitro-2-furyl)vinyl]- and *N*-(2-furyl)-*N'*-ethyleneurea will be described.

N-[β-(5-Nitro-2-furyl)vinyl]-*N'*-ethyleneurea (I) was easily prepared in 90% yield by the Curtius rearrangement of β-(5-nitro-2-furyl)acryloyl azide[3] in boiling benzene, followed by treatment with aziridine. β-(5-Nitro-2-furyl)vinyl isocyanate (II), the Curtius rearrangement product, could be isolated in quantitative yield by removing benzene prior to addition of aziridine in the former reaction. Compound I was treated with *p*-toluidine or *p*-phenetidine at room temperature for one month to give the corresponding ring-opened compounds, III or IV, in yields of 18% or 12% respectively. Compound I was refluxed in acetone or acetonitrile in the presence of sodium iodide to afford the rearranged imidazolidine-2-one (V) in 85% or 90% yield. The structure of V was confirmed by the following spectral data: the IR spectrum showed characteristic absorptions at 3420 (ν_{NH}) and 1730 cm^{-1} (ν_{CO} of five-membered ureide[3]), the UV spectrum showed λ_{max}^{DMSO} 440 mμ ($\varepsilon = 13800$), somewhat shifted bathochromically

1) Part XIII of this series: T. Sasaki and K. Shoji, *Yuki Gosei Kagaku Kyokai-shi* (*J. Soc. Org. Synth. Chem. Japan.*), **26**, 432 (1968).
2) T. Sasaki and T. Yoshioka, *ibid.*, **25**, 658 (1967).
3) A. Sugihara and M. Ito, *Yakugaku Zasshi* (*J. Pharm. Soc. Japan*), **86**, 269 (1966).

compared with that of I, and the NMR spectrum in DMSO-d_6 showed singals at 6.04 τ (multiplet, 4 H, methylene protons) and at 2.20 and 4.31 τ (each doublet, 1 H, $J=14.5$ cps, methine protons in a trans-configuration) and at 2.40 τ (broad, 1 H, N*H*, disappeared by deuteration) besides those due to furan ring protons.

Similarly, *N*-furyl-*N'*-ethyleneurea (VI) was prepared in 60% yield from furoyl azide.[4] This somewhat lower yield compared with that of I may be explained by the different stability of the intermediate isocyanates.[4] Compound VI was refluxed in acetone with sodium iodide to give 1-(2'-furyl)imidazolidine-2-one (VII) in 50% yield.

The mechanism of these rearrangements of I and VI to the corresponding imidazolidine-2-ones, V and VII, will be explained by Heine's theory about the rearrangement of the corresponding phenyl derivatives.[5] All attempts to isomerize I or VI with hydrochloric acid, hydrobromic acid and acetic acid failed and resulted in the formation of intractable tars.

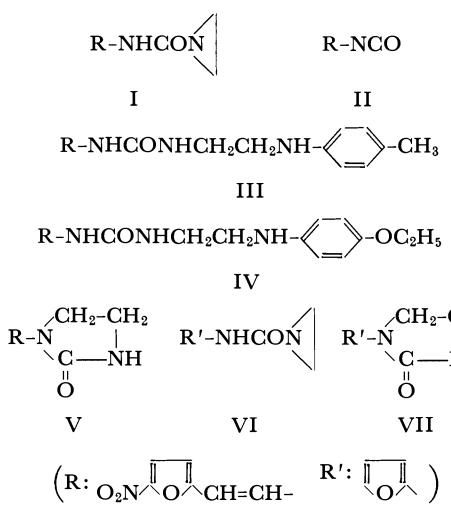

Experimental

***N*-[β-(5-Nitro-2-furyl)vinyl]-*N'*-ethyleneurea (I).** A solution of 5.0 g (0.025 mol) of β-(5-nitro-2-furyl) acryloyl azide[3] in 40 m*l* of dry benzene was refluxed in an oil bath at 105°C for 7 hr until the evolution of nitrogen had perfectly ceased. After filtering off a small amount of an insoluble material, the filtrate was cooled to 10°C and a solution of 2.0 m*l* of aziridine in 10 m*l* of dry benzene was added dropwise to the cooled solution and the resulting reaction mixture was stirred at 10°C for 1 hr and then, at room temperature for 1 day. Precipitated crystals were collected and washed with a small amount of benzene to afford I as red crystals, mp 181—182°C (EtOH–C_6H_6).

Found: C, 48.06; H, 3.96; N, 18.66%. Calcd for $C_9H_9O_4N_3$: C, 48.43; H, 4.06; N, 18.85%.

UV: λ_{max}^{DMF} mμ (ε) 421 (17900). IR: (KBr) cm^{-1} 3350 (ν_{NH}), 1678 (ν_{CO}).

β-(5-Nitro-2-furyl)vinyl Isocyanate (II). The above experiment was repeated and after filtering off a small amount of an insoluble material, benzene used as a solvent was removed under reduced pressure at room temperature and the residual yellow crystals were recrystallized from a small amount of benzene to give II of mp 88—89°C, indicating a characteristic IR absorption at 2260 cm^{-1} (ν_{NCO}).

Found: C, 46.58; H, 2.19; N, 15.63%. Calcd for $C_7H_4O_4N_2$: C, 46.67; H, 2.24; N, 15.55%.

Reaction of I with *p*-Toluidine. I, 0.5 g (0.002 mol), was melted with 0.5 g (0.004 mol) of *p*-toluidine at 50°C and the mixture was kept standing at room temperature for 1 month. Solidified masses were dissolved in chloroform and chromatographed on a silica gel column, using chloroform as an eluent. From the first and second fractions of the chromatography there obtained a small amount of intractable red oils, which were not further investigated and discarded; from the third fraction there obtained 0.15 g of purple-red crystals of mp 179—180°C (EtOH), the structure of which was confirmed as III by the following spectral data: IR spectrum (KBr disk), 3380 (ν_{NH}), 1687 (ν_{CO}) cm^{-1} and UV spectrum, λ_{max}^{EtOH} 412 ($\varepsilon=13400$) and 253 ($\varepsilon=17200$) mμ, shifting hypsochromically compared with **I**.

Found: C, 58.38; H, 5.39%. Calcd for $C_{16}H_{18}O_4N_4$: C, 58.17; H, 5.49%.

Reaction of I with *p*-Phenetidine. Similarly, red crystals of mp 194—195°C were obtained in 12% yield. The structure was confirmed as IV, considering from the similar spectral patterns as III.

Found: C, 56.34; H, 5.73%. Calcd for $C_{17}H_{20}O_5N_4$: C, 56.66; H, 5.59%.

1-(5'-Nitro-2'-furyl)vinylimidazolidine-2-one (V). I, 0.38 g (0.0015 mol), was dissolved in 20 m*l* of acetone and 0.22 g (0.0014 mol) of sodium iodide was added to this solution. The mixture was refluxed for 17 hr. During this period of time a crystalline substance was separated. After cooling, it was collected and recrystallized from a mixture of DMF and EtOH to give V as red crystals, mp 237—239°C (decomp).

Found: 48.41; H, 4.22; N, 18.58%. Calcd for $C_9H_9O_4N_3$: C, 48.43; H, 4.06; N, 18.83%.

***N*-Furyl-*N'*-ethyleneurea (VI).** Similarly as for the preparation of I, from furyl isocyanate, which was prepared in 70% yield from furoyl azide by the known procedure,[4] bp 111°C, and aziridine there obtained VI as white needles (petroleum ether + benzene), mp 98—99°C.

Found: C, 55.26; H, 5.16; N, 18.00%. Calcd for $C_7H_8O_2N_2$: C, 55.25; H, 5.30; N, 18.41%.

UV: λ_{max}^{EtOH} mμ (ε) 250 (13300). IR: (KBr) cm^{-1} 3200 (ν_{NH}), 1700 (ν_{CO}).

1-(2'-Furyl)imidazolidine-2-one (VII). VI, 0.4 g (0.0034 mol), was dissolved in 20 m*l* of dry acetone and 0.32 g (0.002 mol) of sodium iodide was added to this solution. After refluxing the reaction mixture for 11 hr, the solvent was removed under reduced pressure, 50 m*l* of water was added to the residue and the solution was extracted with ether. The ether extract was dried over anhydrous sodium sulfate and the ether was removed. The residue was recrystallized from benzene - petroleum ether to give VII as colorless crystals, mp 124—126°C.

4) H. M. Singleton and W. R. Edwards, Jr., *J. Am. Chem. Soc.*, **60**, 540 (1938).
5) H. W. Heine, *Angew. Chem.*, **60**, 540 (1962).

Found: C, 55.08; H, 4.96; N, 18.20%. Calcd for $C_7H_8O_2N_2$: C, 55.25; H, 5.30; N, 18.41%.

UV: λ_{max}^{EtOH} mμ (ε) 253 (13500). IR: (KBr) cm^{-1} 3230 (ν_{NH}), 1710 (ν_{CO}).

The authors wish to thank Mr. Akiho Ishihara at their laboratories for microanalyses and the Ueno Pharmaceutical Co. for kind supply of some starting materials. For the NMR spectral measurements the authors are much indebted to the Dainippon Pharmaceutical Co.

The Dipole Moment and Polarizability in the Excited State of *p*-Nitroaniline from Spectral Solvent Shifts

Takehiro ABE

College of General Education, Tohoku University, Kawauchi, Sendai

(Received November 2, 1967)

The absorption spectrum of *p*-nitroaniline in vapor has not yet been reported on, although there have been many data on the solvent effects. This paper will aim to estimate the dipole moment and polarizability in the π-π^* excited state of *p*-nitroaniline by a method similar to that used in previous papers[1,2] without a spectral datum on the absorption transition of *p*-nitroaniline in vapor.

Considering an unperturbed solute molecule and the solvent molecules already interacting with one another in the zeroth-order approximation, one may write an absorption frequency in cm^{-1} in a transition from the ground state to the *i*th excited state of the solute molecule in the solution as follows by the same procedure as was used in Ref. 1 :

$$\begin{aligned}\nu_{i0} = {} & \nu_{i0}^0 - 1.007\times10^{65}(\mathrm{erg^{-1}cm^{-1}})\times(d^v/M^v)^{2/3} \\ & \times[\{(M^u/d^u)^{1/3}+(M^v/d^v)^{1/3}\}^{-4}+\{(M^u/d^u)^{1/3} \\ & +3(M^v/d^v)^{1/3}\}^{-4}+\{(M^u/d^u)^{1/3} \\ & +5(M^v/d^v)^{1/3}\}^{-4}]\times[(2/3\boldsymbol{kT}) \\ & \times(\mu_1^v)^2\{(\mu_i^u)^2-(\mu_0^u)^2\}+3.963\times10^{-25} \\ & \times(M^v/d^v)\times\{(n^v)^2-1\}/\{(n^v)^2+2\} \\ & \times\{(\mu_i^u)^2-(\mu_0^u)^2\}+(\mu_1^v)^2\{(\alpha_i^u)-(\alpha_0^u)\} \\ & +5.945\times10^{-25}\times(M^v/d^v) \\ & \times\{(n^v)^2-1\}/\{(n^v)^2+2\}\times I_0^v \\ & \times\{(I_0^u-\boldsymbol{hc}\nu_{i0}^0)/(I_0^v+I_0^u-\boldsymbol{hc}\nu_{i0}^0)\times(\alpha_i^u) \\ & -I_0^u/(I_0^v+I_0^u)\times(\alpha_0^u)\}] \qquad (1)\end{aligned}$$

where M is the molecular weight, d is the liquid density, n is the refractive index, I is the ionization potential, μ is the permanent dipole moment, α is the isotropic polarizability, and $\boldsymbol{k}$, $\boldsymbol{c}$, and T have the usual meanings. Here ν_{i0}^0 is the frequency in the vapor, and μ_1 is the liquid dipole moment. The notations u and v refer to the solute and the solvent respectively. The subscript zero indicates the ground electronic state.

The procedure of calculation is as follows : Taking the value of $(I_0^u-\boldsymbol{hc}\nu_{i0}^0)$ which has been calculated with an arbitrary value for ν_{i0}^0, one applies Eq. (1) to the observed frequencies for various solvents and estimates the values of ν_{i0}^0, μ_i^u, and α_i^u by the least-squares method. Next, using the new value of ν_{i0}^0 estimated above, one recalculates the value of $(I_0^u-\boldsymbol{hc}\nu_{i0}^0)$ and continues the iterative process until the value of ν_{i0}^0 no longer changes.

In applying Eq. (1), the temperature was assumed to be 20°C. The values of d and n were taken from tables.[3,4] The value of 6.13 *D*[5] was used for μ_0^u (gas). The value of α_0^u was calculated as 157×10^{-25} cm^3 from a combination of the bond refractions and the value[5] observed for a deformation polarization of nitrobenzene. Neglecting α_0^u and α_i^u in Eq. (1), the author preliminarily obtained 33420 cm^{-1} and 20.9 *D* for ν_{i0}^0 and μ_i^u respcctively. Starting with these values, the author has finally estimated as follows; $\nu_{i0}^0=33740$ cm^{-1}, $\mu_i^u=10.26$ *D*, and $\alpha_i^u=729.8\times10^{-25}$ cm^3. By putting the above values into Eq. (1), the author has calculated the frequencies for the solutions listed in Table 1.

The ν_{i0}^0 value of 33740cm^{-1} is larger than the value of 32300 cm^{-1} calculated by Tanaka.[7] According to Tanaka,[7] the absorption band is a charge-transfer one and is polarized along the two-fold symmetry axis of the molecule. The large dipole moment in the excited state may be due to the charge transfer. The μ_i^u value of 10.26 *D* is smaller than

1) T. Abe, This Bulletin, **38**, 1314 (1965).
2) T. Abe, *ibid.*, **39**, 936 (1966).
3) Chem. Soc. Japan, " Kagaku-Binran (Chemical Table)," Elementary Sec. I and II, Maruzen, Tokyo (1966).
4) N. A. Lange, " Handbook of Chemistry," 10th Ed., McGraw-Hill, New York (1961).
5) Landolt-Börnstein, " Physikalisch-chemische Tabellen," Vol. 1, Part 3, 6th Ed., Springer, Berlin (1951), pp. 463, 517.
6) A. D. Buckingham and R. J. W. Le Fèvre, *J. Chem. Soc.*, **1952**, 1932.
7) J. Tanaka, This Bulletin, **36**, 833 (1963).

TABLE 1. SOLVENT EFFECTS ON ABSORPTION SPECTRUM OF *p*-NITROANILINE

Solvent	$\nu_{i0,\text{obs.}}$ cm^{-1}	$\nu_{i0,\text{calc.}}$ cm^{-1}	I_0, eV[3]	μ_1^v, *D*
(*p*-Nitroaniline)	—	—	(8.85)	—
n-Hexane	31200	31180	10.46	0
n-Heptane	31130	31220	10.41	0
Cyclohexane	30690	30630	10.79	0
Methylcyclohexane	30990	30940	10.19	0
Carbon tetrachloride	30380	30240	11.47	0
Chloroform	28670	29080	11.42	0.975[6]
Methylene chloride	28300	28080	11.35	1.145[6]

the value of 14 *D* obtained by Czekalla and Wick[8] from the measurement of dichroism under a high electric field.

8) J. Czekalla and G. Wick, *Z. Elektrochem.*, **65**, 727 (1961).

Experimental

p-Nitroaniline was recrystallized twice from water. All the solvents used were of a spectroscopic grade. The absorption spectra were obtained at room temperature by means of a Hitachi 139 spectrophotometer.

The Estimation of Free Ion Life Time by Pulse Electrical Conductivity Measurement

Kanae HAYASHI, Torao TAKAGAKI, Kiyoshi TAKADA, Koichiro HAYASHI and Seizo OKAMURA

Osaka Laboratories for Radiation Chemistry, Japan Atomic Energy Research Institute, 508 Mii, Neyagawa, Osaka

(Received November 13, 1967)

Hitherto the electrical conductivity measurements of liquid under the ionizing radiation have been reported in many compounds[1-5] to investigate the mechanism of free ion generation, however less attention had been paid for their life times.[2a,4] Nevertheless, the determination of free ion life time seems to be required in relation to active species of radiation-induced ionic reaction, especially polymerization.[6]

The life time of free ion, τ, was proved to be given by following equation,

$$\tau = \frac{\varepsilon}{4\pi\sigma} = 2.8\times10^{-13}\frac{\varepsilon}{\pi\sigma} \qquad (1)$$

and to depend only on the steady state specific conductance, σ,[4] where ε represents a dielectric constant. The measured life times are known to be fairly long for radiation-induced intermediates at room temperatures,[2a,4] for instance in *n*-hexane, 120 msec at the dose rate of 10^{14} eVcm^{-3}sec^{-1} or 2.6 R sec^{-1},[5] though such a long life time may be understood in terms of extremely diluted steady state concentration of free ions (in above instance, roughly 10^{-11} M). In order to confirm the previously reported free ion life times,an estimation was made by a completely different method from the steady state conductance method using Eq. (1).

When reaction intermediates generated by photoillumination disappear through bimolecular reaction, it is widely known that its steady state life time is estimated by the method of "intermittent illumination" or "rotating sector."[7] On the other hand, in our systems under investigation, a bimolecular decay of charged species through a neutralization between positive and negative ions has been established by the square root dependence of specific

1) a) A. O. Allen and A. Hummel, *Discussions Faraday Soc.*, **36**, 95 (1964); b) *J. Chem. Phys.*, **44**, 3426 (1966); c) *ibid.*, **44**, 3431 (1966).
2) a) G. R. Freeman, *ibid.*, **39**, 988 (1963); b) G. R. Freeman and J. M. Fayadh, *ibid.*, **43**, 86 (1965).
3) R. W. Ahrens, B. Suryanarayana and J. E. Willard, *J. Phys. Chem.*, **68**, 2947 (1964).
4) K. Hayashi, Y. Yamazawa, T. Takagaki, F. Williams, K. Hayashi and S. Okamura, *Trans. Faraday Soc.*, **63**, 1489 (1967).
5) K. Hayashi T. Takagaki, K. Takada, K. Hayashi and S. Okamura, *Ann. Repts. Japanese Assoc. Rad. Res. on Polymers*, **8**, 79 (1966-67).
6) F. Williams, K. Hayashi, K. Ueno, K. Hayashi and S. Okamura, *Trans. Faraday Soc.*, **63**, 1501 (1967).
7) H. W. Melville and G. M. Burnett, "Technique of Organic Chemistry," Vol. VIII: Investigation of Rates and Mechanisms of Reactions, ed. by S. L. Friess and A. Weissberger, Interscience Publishers, New York, N. Y. (1953), p. 113.

conductance on dose rate[1a,1b,2a,4,5] and decay behavior of cell current after an interruption of irradiation.[1a,1b,4] So as to apply the "intermittent illumination" method into the life time determination of free ion, Van de Graaf electron accerelator was modified for a repeated pulse irradiation and measurements of time-averaged ion currents were carried out.

Experimental

Distilled cyclohexane (Merk, spectrograde) was degassed in a vacuum line and dried through repeated contacts with sodium-potassium alloy. Then it was vacuum-distilled into a glass cell with stainless steel parallel plate electrodes of 30 mm diameter situated in a distance of 5 or 9 mm and sealed off under 10^{-5} mmHg. The details of electrical conductivity measurement were described elsewhere.[4] For the direct reading of average iron current under pulse irradiation, digital electrometer was connected to the output of vibrating reed electrometer. Measurements were carried out at room temperatures (15 ± 1°C).

Van de Graaf electron accerelator(High Voltage Corp.) was modified for the pulse irradiation applying pulsed negative voltage to a plate which is located just outside of filament. Only four kinds of pulses were available. Their repetition times are 10, 31, 120 and 250 msec. Synchroscopic traces of each pulse pattern were shown in Fig. 1. Except for superimposed a.c. signals on each top of pulses, which seems to give no influence on ion current on average, they all are consisted of rectangular wave. Irradiation ratio, a ratio of an irradiation interval of one pulse to the pulse repetition time, β, was maintained in all pulses to be 0.42, which is determined by the limitation of pulser.

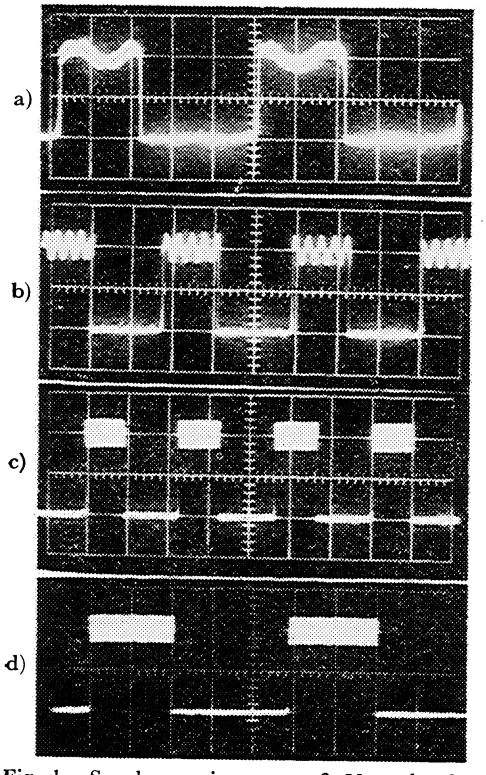

Fig. 1. Synchroscopic traces of Van de Graaf electron pulses ($\beta=0.42$).
Repetition times are; a) 10 msec (2 msec/div.), b) 31 msec (10 msec/div.), c) 120 msec (50 msec/div.), d) 250 msec (50 msec/div.).

Results

Cell current ratios, $i/\sqrt{\beta i_s}$, are shown in Fig. 2 for four kinds of pulses keeping the dose rate of each series invariable. Here, i and i_s represent an average cell current under pulse irradiation and that under the steady irradiation operated to have the same peak beam current as the corresponding pulses, respectively. It is valid that the cell current ratios gradually decrease at longer pulse repetition time and the three curves corresponding to the different dose rates are similar in their shape; at lower dose rate, the curve moves to the direction of slower pulse. These results qualitatively agree with the expected consequence from the ordinary kinetics of intermittent illumination,[7] indicating a bimolecular disappearence of charge carriers.

However, at the pulses of 120 and 250 msec, all the experimental curves show negative deviations from the kinetically calculated curve for $\beta=0.42$, given with a broken line in Fig. 2, and consequently considerable amounts of errors on the free ion life times are introduced since life times are determined through appropriate overlapping of experimental curves onto the kinetically calculated one. Such a negative deviation was always observed irrespective to the electrode distance, applied voltage or the effect of electrodes irradiation.

With no regard for such deviations, the free ion life times are roughly estimated at several dose rates and at various field strengths as shown in Fig. 3. Vertical lines above and below the each point show a

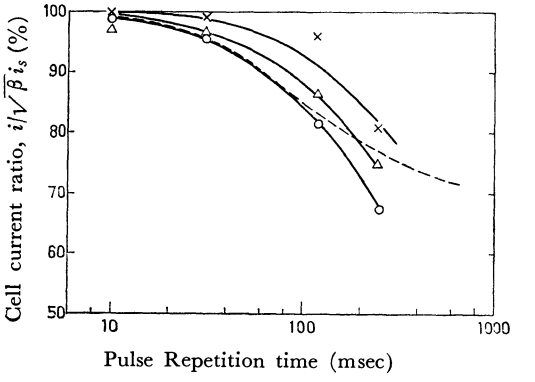

Fig. 2. Pulse repetition time *vs.* cell current ratio in cyclohexane at several dose rates; ○ 3.7×10^{14}, △ 1.5×10^{14}, × 3.7×10^{13}, eV cm^{-3} sec^{-1}. Applied voltage; 400 V. The distance between electrodes, 0.89 ± 0.05 cm. Broken line denotes the theoretical curve for $\beta=0.42$ drawn to fit lowest experimental curve.

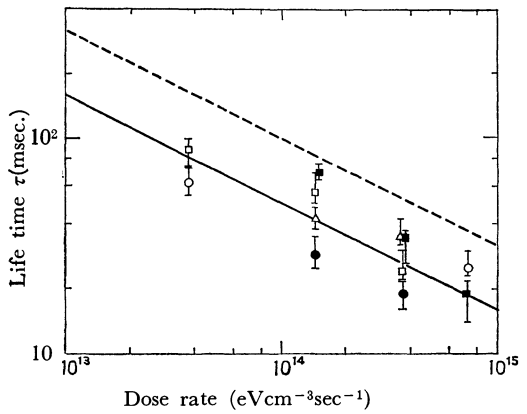

Fig. 3. Dose rate *vs.* estimated life time in cyclohexane at various field strength; ○; 800; ●; 440, □; 400, ■; 165, △; 40 Vcm^{-1}. Broken line denotes the life time calculated by steady state conductivity.

probable limit of error which may be introduced by the overlapping procedure of curves. Though the estimated life times scatter so much at a fixed dose rate, no systematic variation due to the field strength can be recognized. Thus estimated life time, as shown with solid line in Fig. 3 agreed with the calculated one by steady state conductance, dotted line, within a factor of two. The difference between the life times obtained through two independent methods may be attributed to the incompletion of both methods as the life time determination method. Even in steady state conductance measurements, the results from three independent experiments do not show so good agreements each other.[1a,2b,5]

Discussion

As reasons for the deviation of experimental curves from the kinetically calculated one, at first a deformity of pulse shape, an inhomogenity of ionic concentration to the direction perpendicular to the electric field attributed to an insufficient penetration of radiation and a competitive unimolecular decay of ions due to discharge at the electrodes are considered. However, corrections to the ordinary kinetics of intermittent illumination[7] indicate that such effects cannot account for the negative deviation at long repetition time pulses. If there were to be a distribution in the free ion life time, the observed deviation would be positive. Another possibility is an inhomogenity of ionic concentration to the direction of the electric field, which arises from a translational motion of ions along the field.

In the dark period between the pulses, there appear space-charge regions where positive or negative ions are exclusively present in neighborhood of anode and cathode respectively, since ions move toward the oppositely charged electrode all the time when a diffusional motion of charges is disregarded. Namely, the influence of the space-charge region on an average cell current should be considered from the both points of view *i.e.* the decrease of the space-averaged ionic concentration and the decrease of field strength in bulk region. A modified kinetics of intermittent illumination taking account of the space-charge regions under the assumption of the uniform field strength along the electrode distance[8] indicates that the deviation from the ordinary kinetics in cell current ratio-repetition time curve is negative and is proportional to the dark period or repetition time. Moreover, in the dark time, the observed cell current is expected to become smaller because of the decreasing field strength of bulk regions with time. In consequence, the deviation from the ordinary kinetics is negative and proportional to several powers of the pulse repetition time, which is consistent with our results; negative deviation at longer repetition time pulses, especially at the longest repetition time pulse.

At all events, pulse irradiation effect on cell current ratio was observed at the repetition time between 10 and 250 msec, the same range as the free ion life times estimated by steady state conductivity measurement. It confirms the validity of the free ion life time estimation method by steady state conductivity measurement.

8) K. Hayashi, T. Takagaki, K. Takada, K. Hayashi and S. Okamura, *Ann. Repts. Japanese Assoc. Rad. Res. on Polymers*, **8**, 89 (1966–67).

Correction of the Absolute Configuration of Nuphar Alkaloids

Ichiro KAWASAKI, Isao KUSUMOTO and Takeo KANEKO

Department of Chemistry, Faculty of Science, Osaka University, Toyonaka, Osaka

(Received December 5, 1967)

Previously, we reported the determination of the absolute configuration of *Nuphar* alkaloids[1] on the basis of (−)-α-methyladipic acid (VII), an oxidation product from anhydrodihydrodes-*N*-methyldeoxynupharidine (V), having the S-configuration. This configurational assignment of (−)-α-methyladipic acid was derived from the basis of its synthesis from (−)-α-methyl-γ-butyrolactone which was correlated with S(−)-methylsuccinic acid.[2],*1

Recently Turner *et al.* obtained R(−)-α-methylglutaric acid, R(+)-β-methyladipic acid and (−)-α-methyladipic acid from the oxidation of cytochalasins A and B,[3] metabolites of *Helminthosporium dematioideum*, and they suggested that (−)-α-methyladipic acid is shown to have the R-configuration.[4]

Now we reinvestigated the oxidation of the second Hofmann degradation product of deoxynupharidine (I) and found that the oxidation of anhydrodes-*N*-methyldeoxynupharidine (III) gave R(+)-methylsuccinic acid (VI).

Therefore (−)-α-methyladipic acid should have R-confuguration as was suggested by Turner and the stereostructures of nuphar alkaloids are shown to have the antipodal configuration of the previously presented formulae[5-7] (*e.g.* formula I is given to the stereostructure of the main alkaloid deoxynupharidine.).

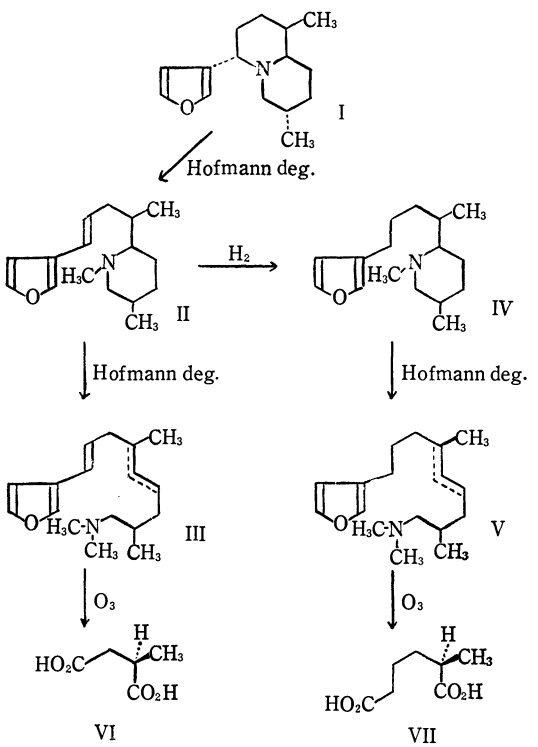

Experimental

Anhydrodes-*N*-methyldeoxynupharidine (III). Deoxynupharidine (I) methoiodide (40 g) was dissolved in methanol (300 m*l*) and shaken with silver oxide (prepared from 50 g of silver nitrate) for 1 hr and then filtered. The filtrate was evaporated and heated on the water bath for 2 hr. The reaction mixture was extracted with ether and the ethereal solution was washed with water. The solvent was evaporated and the residue was distilled at 113—115°C/10^{-3} mmHg to give 20.5 g of des-*N*-methyldeoxynupharidine.

To the above oil (20.5 g) was added methyl iodide (25 g) and then the methoiodide obtained was subjected to Hofmann degradation in the same manner mentioned above to give 14.6 g of anhydro base, bp 125°C/10^{-3} mmHg.

Oxidation of the Anhydro Base. The above anhydro base was dissolved in chloroform (200 m*l*) and treated with a stream of oxygen containing ozone under ice-salt cooling. To the reaction mixture was added water (600 m*l*) and heated on the water bath under removing the chloroform by evaporation, then 30% hydrogen peroxide (600 m*l*) was added to the solution and heated for an additional 4 hr. The resulting mixture was extracted continuously with ether for 36 hr and water was added to the ether extract, then the solvent removed. The residual aqueous solution, after decomposition of a remaining hydrogen peroxide by the addition of sodium bisulfite, was reextracted with ether and the dried ether extract was methylated with ethereal diazomethane. The obtained methyl esters were separated by fractional distillation. An ester distilled at 100—103°C/21 mmHg gave dimethyl methylsuccinate which was identical with an authentic specimen in IR spectra. The ester was boiled

1) M. Kotake, I. Kawasaki, T. Okamoto, S. Matsutani, S. Kusumoto and T. Kaneko, This Bulletin, **35**, 1335 (1962).

2) T. Kaneko, K. Wakabayashi and H. Katsura, *ibid.*, **35**, 1149 (1962).

*1 This conclusion was uncertain, owing to the very small optical rotation of α-methyladipic acid. Experiments on the confirmation of this acid by an unequivocal process are now in progress.

3) D. C. Aldridge, J. J. Armstrong, R. N. Speake and W. B. Turner, *Chem. Commn.*, **1967**, 26.

4) W. B. Turner's personal communication and D. C. Aldridge, J. J. Armstrong, R. N. Speake and W. B. Turner, *J. Chem. Soc.*, (*C*), **1967**, 1667.

5) I. Kawasaki, S. Matsutani and T. Kaneko, This Bulletin, **36**, 1474 (1963).

6) Y. Arata, *Chem. Pharm. Bull.*, **13**, 907 (1965).

7) Y. Arata and T. Ohashi, *ibid.*, **13**, 1247 (1965).

for 3 hr with 6 N hydrochloric acid and then evaporated to dryness. The residue was recrystallized three times from benzene to give 400 mg of methylsuccinic acid, mp 106—108°C, $[\alpha]_D^{16}$ +7.74 (*c* 20, abs. ethanol).

Found: C, 45.57; H, 6.10%. Calcd for $C_5H_8O_4$: C, 45.45; H, 6.10%.

TLC on silica gel G afforde done spot at R_f, 0.30. (EtOH: H_2O: NH_4OH, 51 : 6 : 7).

Additive Chlorination of 1-Iodonaphth-2-ol

Hitomi SUZUKI

Department of Chemistry, Faculty of Science, Kyoto University, Sakyo-ku, Kyoto

(Received December 9, 1967)

Naphth-2-ols with a substituent at the 1-position usually react with chlorine in an additive way to yield, depending on the amount of chlorine consumed, derivatives of either 2-keto-1,2-dihydronaphthalene or 2-keto-1,2,3,4-tetrahydronaphthalene.[1] An exception is 1-iodonaphth-2-ol. The conventional procedure involving chlorination in acetic acid has been found to result in the displacement of the iodine atom by chlorine, giving 2-keto-1, 1, 3, 4-tetrachloro-1, 2, 3, 4-tetrahydronaphthalene (mp 100—102°C)[1] as the final product. It had strong infrared absorptions in Nujol at 722, 760, 847, 1153, and 1751 cm^{-1}. Its PMR spectrum in carbon tetrachloride at 60 Mc/sec showed two doublets, due to aliphatic protons, at 4.67 and 5.11 τ (J—4.8 cps) and two aromatic multiplets, at 1.70—1.95 and 2.20—2.65 τ. The formation of remarkable amounts of polymeric substances accompanied the reaction. The use of an aprotic solvent such as chloroform, however, showed another mode of chlorine addition to the naphth-2-ol system. The saturation of the solution with chlorine also led to a considerable formation of resinous by-products, and the removal of the solvent together with the iodine liberated gave a light brown syrup which, on standing, slowly separated pale yellow fine needles (mp 149—150°C after recrystallization from hot ligroin (bp 80—100°C)). Analysis showed this substance to fit the formula $C_{10}H_6Cl_6O$ (Found: C, 33.99; H, 1.72; Cl, 59.88; O, 4.72%. Calcd for $C_{10}H_6Cl_6O$: C, 33.84; H, 1.70; Cl, 59.94; O, 4.53%), and its infrared spectrum in Nujol had prominent peaks due to the -C-OH group at 1192, 1416 and 3460 cm^{-1}, but no carbonyl absorption. Its PMR spectrum run in deuterochloroform at 60 Mc/sec revealed the presence of four aliphatic protons (two doublets at 4.60 τ (H^1) and 4.38 τ (H^4), two quartets at 5.57 τ (H^2) and 4.84 τ (H^3); $J_{1,2}=3.1$ cps, $J_{2,3}=10.1$ cps, and $J_{3,4}=4.4$ cps), one aromatic proton (singlet at 2.43 τ), and a hydroxylic proton (somewhat broad) at 3.6 τ. Therefore, this adduct is a tetrachloride of a dichloronaphth-2-ol, in which two chlorine atoms belong to an aromatic ring and four to an aliphatic ring. The high value of the coupling constant, $J_{2,3}$, shows that the 2,3-pair of C–H bonds are trans-diaxially disposed; the low values of $J_{1,2}$ and $J_{3,4}$ shows, then, that the 1- and 2-hydrogen atoms are *cis*, and that the 3- and 4-hydrogen atoms are *cis* to each other. The sharp appearance of the OH stretching absorption indicates that the hydroxyl group is blocked on both sides by chlorine atoms and is prevented from polymeric association. Thus, the α-hydrogen atom with signals in the low field is probably at the 4-position, near the chlorine atom. By analogy with the well-established α-naphthalene tetrachloride,[2] the stereochemistry may be formulated as below;

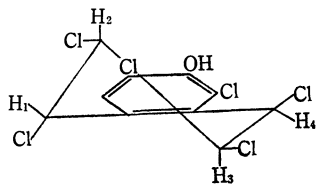

Considering the great tendency of naphth-2-ols to undergo additive chlorination to form ketopolychlorides, this is an unusual result. One possible explanation for such an anomaly may be that chlorine first reacts with the iodine substituent to form an unstable naphthyliododichloride, and that the strong electron-withdrawing effect of the dichloroiodo group directs further chlorine addition in the opposite ring. Decomposition of the tetrachloride thus formed would lead to the above addition product. A similar case has earlier been reported in the spontaneous decomposition of naphth-1-yliododichloride to 1,1,2,3,4-pentachloro-1,2,3,4,-tetrahydronaphthalene and 1-chloro-4-iodonaphthalene.[3]

The author wishes to thank Dr. M. D. Johnson for determining the PMR spectra and Dr. A. Bernhardt for his analysis.

1) Th. Zincke, *Ber.*, **21**, 3378, 3540 (1888); *ibid.*, **22**, 1024 (1889); P. M. James and D. Woodcock, *J. Chem., Soc.*, **1951**, 1931.

2) P. B. D. de la Mare, M. D. Johnson, J. S. Lomas and V. Sanchez del Olmo, *ibid.* (*B*), **1966**, 827.

3) C. Willgerodt and P. Schlösser, *Ber.*, **33**, 692 (1900).

Synthesis of DL-α-Aminosuberic Acid and Its Optical Resolution

Satoe HASE, Reiko KIYOI and Shumpei SAKAKIBARA

Peptide Center, Institute for Protein Research, Osaka University, Kita-ku, Osaka

(Received December 14, 1967)

α-Aminosuberic acid is a key substance in synthesizing an analogue of deamino-oxytocin which has an ethylene linkage in place of the disulfide bond of oxytocin. DL-α-Aminosuberic acid (I) was first synthesized in 1956 by the hydrogenation of α-oximinosuberic acid, but the procedure was not practical and the optical resolution of the racemate has not yet been achieved.[1] Farkašová and Rudinger[2] derived L-α-aminosuberic acid from L-glutamic acid by the step-by-step addition of methylene groups to the side chain.

In the present study, the racemic compound I was synthesized by the acetaminomalonate procedure using ethyl ε-bromocaproate. The latter had been obtained from cyclohexanone following the procedure of Brown and Partridge.[3] The optical resolution of

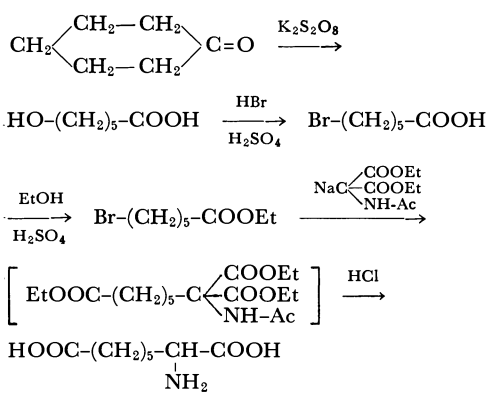

the racemate was carried out by two different procedures. One route was the enzymic digestion of *N*-chloroacetyl-DL-α-aminosuberic acid (II) at pH 7.2 with Taka-acylase. The other route was the fractional crystallization of *N*-carbobenzoxy-DL-α-aminosuberic acid (III) with D-tyrosine hydrazide according to the procedure of Vogler *et al.*[4] In the former case, it took about ten days at 37°C to complete the digestion, and L-α-aminosuberic acid (IV) was obtained in about an 80% yield; the all-around efficiency was found to be lower than in the latter method. The fractional crystallization procedure afforded carbobenzoxy-L-α-aminosuberic acid (V) in a good yield, and this was immediately available for the synthesis of its peptides; the recovery of the D-form from the mother liquor was also easy in this case. The same optical rotation value was obtained for the free L-amino acids prepared by the two methods, and this value was identical with that reported previously.[2]

Experimental

Materials. Ethyl ε-bromocaproate (bp 116—120°C/14 mmHg) was synthesized following the procedure of Brown and Partridge.[3] DL-Tyrosine was prepared from L-tyrosine by racemization with acetic anhydride.[5] DL-Tyrosine was converted to the ethyl ester and then to the hydrazide as has been described in the literature;[6,7] the over-all yield from L-tyrosine was 57%, mp 171—173°C. The optical resolution of DL-tyrosine hydrazide was carried out with carbobenzoxy-L-proline as has been described by Vogler and Lanz.[4] The Takadiastase was obtained from the Sankyo Co., Ltd.*1

DL-α-Aminosuberic Acid (I). Ethyl acetaminomalonate (183 g, 0.84 mol) was added to a solution of sodium ethoxide in absolute ethanol (18.4 g sodium in 800 m*l* of ethanol), and the mixture was refluxed gently. Ethyl ε-bromocaproate (183 g, 0.82 mol) was then stirred slowly in over a period of 80 min; refluxing and stirring were continued for a further 7.5 hr, and then the whole mixture was kept overnight at room temperature. The precipitate formed was removed, the ethanol solution was concentrated under reduced pressure, and the residual oil was taken up in ether. The ether solution was washed with water, and the solvent was removed by evaporation. The oily residue was refluxed with conc. hydrochloric acid (1.2 *l*) for 6 hr, and then concentrated to dryness. The final residue was dissolved in water (350 m*l*), the pH of the solution was adjusted to 3 with aqueous ammonia, and the mixture was kept overnight in a refrigerator. The crystals which appeared were collected by filtration, washed with water and with methanol, and dried in a desiccator over sulfuric acid; crude yield, 133 g (80%). The crude product was dissolved in boiling water, and the solution was decolorized with active charcoal; on cooling compound I crystallized as the monohydrate; yeild, 127 g (77%), mp 240—241°C (decomp.). Reported, mp 233°C (decomp.).[1] For analysis, this material was dried over phosphorus pentoxide *in vacuo* for 10 hr at 90°C.

Found: C, 50.67; H, 8.04; N, 7.41%. Calcd for $C_8H_{15}O_4N$: C, 50.78; H, 7.99; N, 7.40%.

1) W. Treibs and H. Reinheckel, *Chem. Ber.*, **89**, 51 (1956).
2) H. Farkašová and J. Rudinger, *Coll. Czech. Chem. Commn.*, **30**, 3117 (1965).
3) G. B. Brown and C. W. H. Partridge, *J. Am. Chem. Soc.*, **66**, 839 (1944).
4) K. Vogler and P. Lanz, *Helv. Chim. Acta*, **49**, 1348 (1966).
5) R. R. Sealock, "Biochemical Preparations," Vol. I, ed. by H. E. Carter, John Wiley and Sons, New York (1949), p. 71.
6) R. W. Chambers and F. H. Carpenter, *J. Am. Chem. Soc.*, **77**, 1522 (1955).
7) T. Curtius, *J. prakt. Chem.*, [2] **95**, 349 (1917).
*1 Ginza 2-1, Chuo-ku, Tokyo.

***N*-Chloroacetyl-DL-α-aminosuberic Acid (II).** Compound II was obtained from I (151 g, 0.73 mol as the monohydrate) by a normal Schotten-Baumann reaction with chloroacetyl chloride (100 g, 0.88 mol) and 4N sodium hydroxide. The crude product was recrystallized from ethyl acetate and petroleum ether; yield, 149 g (77%), mp 116—118°C.

Found: C, 44.97; H, 6.02; N, 5.22; Cl, 13.61%. Calcd for $C_{10}H_{16}O_5NCl$: C, 45.20; H, 6.07; N, 5.27; Cl, 13.34%.

***N*-Carbobenzoxy-DL-α-aminosuberic Acid (III).** Compound I (41.5 g, 0.2 mol as monohydrate) was treated with carbobenzoxy chloride (40.8 g, 0.24 mol) and with 2N sodium hydroxide under the normal conditions of a Schotten-Baumann reaction; crude yield, 58.5 g (90%), mp 123—125°C. Recrystallization from ethyl acetate afforded needles; yield, 54.3 g (84%), mp 124—125°C.

Found: C, 59.50; H, 6.52; N, 4.31%. Calcd for $C_{16}H_{21}O_6N$: C, 59.43; H, 6.55; N, 4.33%.

Isolation of L-α-Aminosuberic Acid (IV) and of Its D-Isomer by Enzymic Digestion of II. A solution of Takadiastase (250 g) made by extraction with ice water (1.8 *l*) was added to a mixture of II (266 g, 1 mol) and cobaltous chloride (460 mg) in 4N sodium hydroxide; the pH of the solution was adjusted to 7.2 with acetic acid and with sodium hydroxide before and after the addition of the enzyme solution respectively. During the incubation at 37°C the solution was frequently adjusted to pH 7.2 with 4N sodium hydroxide. After 8 days the mixture was boiled for 10 min to precipitate proteins, which were then removed by filtration with Hyflo Supercel. The unchanged chloroacetyl derivative (mainly the D-form) was extracted with ethyl acetate at pH 1.7, and then the water layer was adjusted to pH 3 and stored overnight in a refrigerator. The crude IV was collected by filtration and recrystallized from hot water after decolorization with active charcoal; yeild, 80 g (84%), mp 243—245°C (decomp.), $[\alpha]_D^{17}$ +20.1° (*c* 1.9, 5N hydrochloric acid), $[\alpha]_D^{26}$ +19.6° (*c* 1.4, 6N hydrochloric acid). Reported, $[\alpha]_D^{25}$ +20.2° (*c* 0.1, 5N hydrochloric acid).[2)]

Found: C, 50.73; H, 8.35; N, 7.64%. Calcd for $C_8H_{15}O_4N$: C, 50.78; H, 7.99; N, 7.40%.

The ethyl acetate extract, which was rich in the D-form, was dried over sodium sulfate and concentrated *in vacuo*. The oily residue was refluxed with concentrated hydrochloric acid for 5 hr, and then the solution was concentrated to dryness. The residue was dissolved in water, the pH of the solution was adjusted to 3, and the D-α-aminosuberic acid which precipitated was collected by filtration. The crude crystals were recrystallized from hot water, as in the case of the L-form; yield, 42.5 g (45%), mp 243—245°C (decomp.), $[\alpha]_D^{15}$ −19.9° (*c* 2.1, 6N hydrochloric acid).

***N*-Carbobenzoxy-L-α-aminosuberic Acid (V).** D-Tyrosine hydrazide (29.3 g, 0.15 mol) and III (32.3 g, 0.1 mol) were dissolved in boiling methanol (600 m*l*), and a small amount of an insoluble material was filtered off. The resulting clear solution was concentrated to about 300 m*l*, and V was precipitated as the salt of D-tyrosine hydrazide by the careful addition of ethyl acetate (about 350 m*l*). When oily material appeared during the precipitation procedure, the addition of ethyl acetate was stopped and the oil was rubbed vigorously with a glass rod until it changed to crystals. After the solution had stood overnight at room temperature, the crystals were collected by filtration, washed with a mixture of methanol and ethyl acetat , and dried; yeild, 32.3 g (90%), mp 151—153°C. (The mother liquor was used later for the isolation of VI.). This material, which represented the salt of D-tyrosine hydrazide and V (2: 1 mol/mol), was recrystallized from ethanol (800 m*l*) for purification; yeild, 25.8 g (72%), mp 153—154°C, $[\alpha]_D^{24}$ −56.0° (*c* 1.8, water). A second crop of crystals was recovered from the mother liquor; weight, 2.7 g (7.4%), mp 153—154°C, $[\alpha]_D^{25}$ −56.1° (*c* 2, water).

Found: C, 57.20; H, 6.94; N, 13.66%. Calcd for $C_{34}H_{47}O_{10}N_7$: C, 57.21; H, 6.64; N, 13.73%. This salt (25.6 g, 0.036 mol) was suspended in ethyl acetate (120 m*l*), and the mixture was shaken with 4N hydrochloric acid (30 m*l*). The ethyl acetate layer was separated, washed with water, dried over sodium sulfate, and concentrated to a residue, which was then recrystallized from ethyl acetate and petroleum ether; yield of V, 10.8 g (93%), mp 119—121°C, $[\alpha]_D^{26}$ −3.3° (*c* 7.7, acetic acid), $[\alpha]_D^{25}$ −9.1° (*c* 4, dimethylformamide).

Found: C, 59.39; H, 6.56; N, 4.29%. Calcd for $C_{16}H_{21}O_6N$: C, 59.43; H, 6.55; N, 4.33%. The optical purity of this compound was confirmed after the removal of the protective group by catalytic hydrogenolysis; the compound IV thus obtained showed a mp of 246—248°C (decomp.), $[\alpha]_D^{28}$ +20.0° (*c* 2, 5N hydrochloric acid).

***N*-Carbobenzoxy-D-α-aminosuberic Acid (VI).** The mother liquor mentioned above was concentrated, and crude VI was extracted from the residue with ethyl acetate in the presence of hydrochloric acid. On the concentration of the extract, a residue of crystals was obtained; yield, 17.3 g, $[\alpha]_D^{25}$ +6.3° (*c* 4, dimethylformamide). A part of this material (3.23 g, 0.01 mol) was dissolved in boiling methanol, together with L-tyrosine hydrazide (3.90 g, 0.02 mol), and the mixture was treated as in the case of V. The yield of the salt of L-tyrosine hydrazide and VI was 4.86 g (73%); mp 153—154°C, $[\alpha]_D^{27}$ +56.1° (*c* 2, water). Compound VI was isolated from the salt as has been described previously; yield, 97%, mp 119—121°C, $[\alpha]_D^{28}$ +9.1°(*c* 4, dimethylformamide). D-α-Aminosuberic acid was obtained from VI by the removal of the protecting group; mp 246—248°C (decomp.), $[\alpha]_D^{28}$ −20.1° (*c* 2, 5N hydrochloric acid).

Investigations on Polymolybdates of Rare Earths. Electrometric Studies on the Compositions of Samarium Polymolybdate

C. M. GUPTA and M. P. JOSHI

Department of Chemistry, Universty of Rajasthan, Jaipur, India

(Received March 24, 1967)

A survey of the literature reveals that the composition of samarium molybdate, which may be of great significance in the geochemistry of both elements, has not been studied so far by electrometric techniques. The only available reference is that of Cleve,[1] who has thrown some light on the composition of samarium molybdate by adopting analytical means. His results, however, could not be confirmed later. The present investigation has, therefore, been initiated with a view to study the reaction equilibria between $Sm(NO_3)_3$ and various molybdate polyanions by means of amperometic and conductometric titrations. The results have also been substantiated by gravimetric analysis of the compounds formed. These interesting results are a continuation of our similar type of studies.[2,3]

Appratus and Procedure

Anal. R. (B. D. H.) reagents sodium molybdate Na_2MoO_4, lithium chloride LiCl, samarium nitrate $Sm(NO_3)_3$ (Atomic Energy Establishment, Trombay) and gelatine were used. A manual polarograph with a spot galvanometer was used for polarographic and amperometric work. A dropping mercury electrode with the characteristics $m^{2/3}t^{1/6}=4.58$ mg$^{2/3}$ sec$^{-1/2}$, where m is the weight of mercury in a closed circuit= 7.166 mg/sec, and t is the drop time of the capillary at -1.0 V (*vs.* SCE)$=3.50$ sec, in Na_2MoO_4 solution, was used in conjunction with SCE and the proportionality of i_d with respect to concentration was observed. Conductance was measured with the help of a Tesla conductivity bridge, and the procedure adopted was the same as described earlier.[4] Amperometric titrations were carried out between $Sm(NO_3)_3$ and various alkali di, para, tri and meta molybdates at an applied potential of -1.7 V (*vs.* SCE) in the presence of 0.1 M LiCl as supporting electrolyte, and 0.005% gelatine as maxima supressor. The end points were located graphically with plots of diffusion current values and conductance drawn as a function of milliliters of titrant added.

Discussion

The addition of acid to alkalimolybdate causes the formation of various polyanions with regard to the changes occurring in H^+ ion concentration. It was considered of importance to ascertain electrometrically whether similar samarium salts can be obtained as a result of reaction between samarium nitrate and various alkali molybdates solutions.

Normal Molybdate Titration. Using different concentrations of $Sm(NO_3)_3$ and Na_2MoO_4, a series of amperometric titrations were carried out and the well defined breaks in curves (a) and (b) (Fig. 1) at the end points suggested the formation and precipitation of normal samarium molybdate $Sm_2O_3\cdot 3MoO_3$ at a pH range of 5.5—6.0 where the atomic ratio of Sm : Mo is 2 : 3. The reaction proceeds as follows:

$$2Sm(NO_3)_3 + 3Na_2O\cdot MoO_3 \rightarrow Sm_2O_3\cdot 3MoO_3 + 6NaNO_3.$$

Conductometric titration using similar solutions substantiated the formation of the above compound.

Para-Molybdate Titrations. The solution of sodium para-molybdate was prepared by adding 1.14 mol of HCl per mole of normal molybdate (Na_2MoO_4) at 100°C, and its reaction with $Sm(NO_3)_3$ was studied amperometrically and conductometrically. The well defined breaks obtained in the titration curves (Fig. 2) reveal the formation and precipitation of smarium para-molybdate with the molecular composition $Sm_2O_3\cdot 7MoO_3$ in the pH range 3.5—4.5. The formation can be described as follows:

$$7\,Na_2O\cdot MoO_3 + 8\,HCl \rightarrow 3\,(Na_2O\cdot 2.33\,MoO_3) + 8\,NaCl + 4\,H_2O$$

$$2\,Sm(NO_3)_3 + 3\,(Na_2O\cdot 2.33\,MoO_3) \rightarrow Sm_2O_3\cdot 7\,MoO_3 + 6\,NaNO_3.$$

Similar titrations were also performed with a view to study the reaction between Sm^{3+} and tri and meta alkali molybdates but they could not throw any light on the formation of tri and meta molybdates of samarium. The compositions of the compounds formed were also checked by analyzing the precipitate obtained at the end point gravimetrically, whose results were found to confirm those obtained by electrometric techniques.

ΔH for the formation of normal and para-molybdates of samrium has also been determined

1) A. Cleve, Oefners, *Akad. Forth*, **58**, 573 (1902).
2) C. M. Gupta, This Bulletin, **38**, 1401 (1965).
3) C. M. Gupta, *ibid.*, **39**, 837 (1966).
4) C. M. Gupta and R. S. Saxena, *J. Inorg. Nucl. Chem.*, **14**, 297 (1960).

TABLE 1. SUMMARY OF THE RESULTS OF AMPEROMETRIC AND CONDUCTOMETRIC TITRATIONS

Concentrations		Equivalence points		
$Sm(NO_3)_3$	Na_2MoO_4	Calcd, m*l*	Obsd, m*l*	
Amperometric titrations				
Normal molybdate		Direct titration		
M/40	M/200	2.66	2.80	Fig. 1 (a)
M/400	M/1200	4.44	4.55	
		(Reverse titration)		
M/200	M/20	3.00	3.00	Fig. 1 (b)
M/800	M/100	3.75	3.70	
Para molybdate		$Na_2O \cdot 2.33\ MoO_3$		
M/10	M/46.6	2.88	2.65	Fig. 2 (a)
M/20	M/116.5	2.28	2.20	Fig. 2 (b)
M/40	M/163.1	3.28	3.20	
Conductometric titrations				
Normal molybdate				
M/200	M/800	3.75	3.65	
M/40	M/400	1.33	1.30	
M/160	M/400	5.33	5.25	
Para molybdate				
M/160	M/699	3.05	3.00	
M/400	M/1175	4.54	4.50	
M/400	M/2330	2.30	2.20	

TABLE 2. COMPOSITION OF THE PRECIPITATES ANALYSED

Amount of Sm present, g	Amount of Mo present, g	Ratio Sm : Mo	Corresponding compound suggested
0.0380	0.058	2 : 3.05	$Sm_2O_3 \cdot 3\ MoO_3$
0.0380	0.0585	2 : 3.07	
0.0480	0.1690	2 : 7.04	$Sm_2O_3 \cdot 7\ MoO_3$
0.0480	1.1685	2 : 7.03	

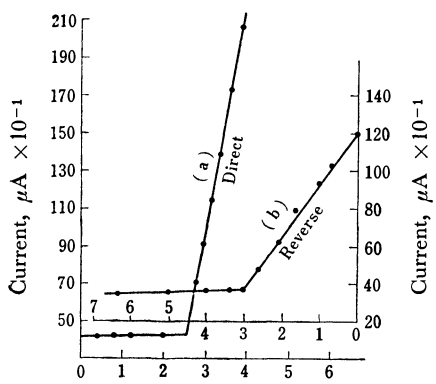

Fig. 1

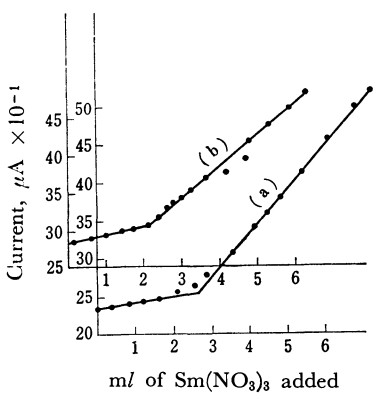

Fig. 2

by the procedure as mentioned by Findlay.[5]

ΔH for normal compound = −188.8 cal/g mol

ΔH for para-compound = −183.0 cal/g mol

The present investigation thus confirms the formation and precipitation of normal and para-molybdate of samarium with the molar compositions $Sm_2O_3 \cdot 3MoO_3$ and $Sm_2O_3 \cdot 7MoO_3$ at pH ranges of 5.5—6.0 and 3.5—4.5, respectively, and the heat of formation of the compounds are found to be −188.8 cal/g mol and −183.0 cal/g mol, respectively.

Thanks are due to Professor R. C. Mehrotra, D. Sc., F. N. I., Head of the Chemistry Department, University of Rajasthan, Jaipur for providing necessary facilities and also to C. S. I. R. for award of fellowship to one of the authors (M. P. Joshi).

5) "Practical Physical Chemistry" by A. Findlay, pp. 188—190.

SHORT COMMUNICATIONS

A Coordination Compound between Vanadium Oxytrichloride and Triphenyl Phosphine

Kimio TARAMA, Satohiro YOSHIDA, Hiroyoshi KANAI and Shozo OSAKA

Faculty of Engineering, Kyoto University, Sakyo-ku, Kyoto

(Received March 19, 1968)

While various kinds of coordination compounds of vanadium oxytrichloride ($VOCl_3$) have been reported,[1] any compound between $VOCl_3$ and triphenyl phosphine (Pph_3) has not been synthesised. The authors found the formation of this compound in the course of a study on the catalytic action of $VOCl_3$.[2] When $VOCl_3$ was added to petroleum ether solution of Pph_3, red brown powders precipitated at room temperature. The elemental analysis of this precipitate after purification showed that the composition of this compound was VOC_3lPph_3 (Found: V, 11.81; Cl, 23.66; C, 49.75; H, 4.24%. Calcd: V, 11.91; Cl, 24.43; C, 49.52; H, 3.45%).

This compound melts with partial decomposition at a temperature higher than 210°C. At room temperature it is decomposed by moisture, but is stable in dry oxygen. It is soluble in tetrahydrofuran, but is insoluble in carbon tetrachloride and *n*-hexane.

Infrared spectrum of $VOCl_3$ has a sharp absorption at 1035 cm^{-1} due to the stretching vibration of $(V{=}O)^{3+}$ [3] and the center of this peak shifts to 1000 cm^{-1} in the case of $VOCl_3Pph_3$ as shown in Fig. 1. This red shift reveals that an increase of electron density on vanadium ion is caused by coordination of Pph_3. This increase of electron density on vanadium ion is ascertained also by the ESR measurement.

Vanadium oxytrichloride does not show any ESR signal, but $VOCl_3Pph_3$ shows an ESR spectrum with h.f.s. similar to that of $(V{=}O)^{2+}$ in vanadium oxysulfate supported on γ-alumina[4] (Fig. 2). When triphenylphosphine was added to $VOCl_3Pph_3$ suspended in carbon tetrachloride at 10—25°C, oxygen was rapidly absorbed and triphenyl phosphine oxide was catalytically produced. Further kinetic studies for this oxidation reaction are in progress.

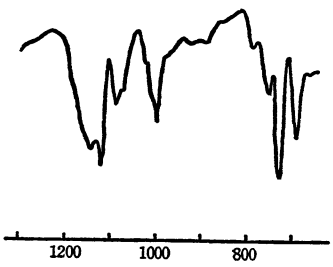

Wave number, cm^{-1}

Fig. 1. Infrared spectrum of $VOCl_3Pph_3$ (Nujol).

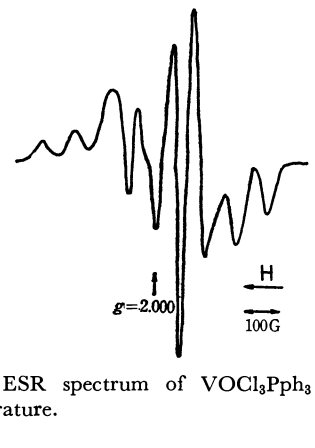

Fig. 2. ESR spectrum of $VOCl_3Pph_3$ at room temperature.

1) V. Funk, W. Weiss, M. Zeising, *Z. anorg. u. allgem. Chem.*, **296**, 36 (1958); H. L. Krauss, G. Gantz, *Chem. Ber.*, **95**, 1032 (1962); R. K. Mittal, R. C. Methrotra, *Z. anorg. u. allgem. Chem.*, **332**, 189 (1964).

2) K. Tarama, S. Yoshida, H. Kanai and S. Osaka, Proc. the 17th Disc. of Chem. of Coordination Comp. (Hiroshima) (1967), p. 75.

3) K. Tarama, S. Teranichi and S. Yoshida, *Shokubai (Catalyst)*, **6**, 299 (1964); L. Frederickson and D. Hausen, *Anal. Chem.*, **35**, 818 (1963).

4) K. Tarama, S. Teranishi, S. Yoshida, N. Tamura and S. Ishida, *Kogyo Kagaku Zasshi (J. Chem. Soc. Japan, Ind. Chem. Sect.)*, **68**, 1499 (1965); *Shokubai (Catalyst)*, **3**, 187 (1961).

δ-Bonded 2-Phenylpyridine Palladium Complex

Akira KASAHARA

Department of Chemistry, Faculty of Liberal Arts and Science, Yamagata University, Yamagata

(Received January 16, 1968)

In general, heterocyclic amines such as pyridine react with palladium(II) dichloride to give a square-planar complex such as $Pd(pyridine)_2Cl_2$. However, the observation[1] that azobenzenes and *N,N*-dimethylbenzylamine react with palladium(II) halides and platinum(II) halides in alcoholic solutions to give complexes (1) and (2) with carbon-metal σ-bonds has led to an examination of a similar reaction between palladium(II) dichloride and heterocyclic amines. We have found that, in alcoholic media, 2-phenylpyridine undergoes a similar unusual reaction with sodium chloropalladate.

2-Phenylpyridine and sodium chloropalladate were dissolved in alcohol and allowed to stand at room temperature for two days. A pale yellow material believed to have the structure (3) was isolated in about a 70% yield. The compound (3) is insoluble in all common organic solvents and does not melt before decomposition, which occurs at about 270°C. The structure of the complex (3) was established by the results of the elementary analysis (Found: C, 44.38; H, 2.56; N, 4.57%. Calcd for $C_{22}H_{16}N_2Pd_2Cl_2$: C, 44.82; H, 2.72; N, 4.14%) and the following data.

In the infrared spectrum of the compound (3), the characteristic C–H out-of-plane deformation modes of a mono-substituted benzene at 770—730 and 690 cm^{-1} are absent and are replaced by one at 737 cm^{-1}, which can be assigned to a C–H deformation mode of an ortho-disubstituted benzene.[2] The lithium aluminum hydride reduction of the compound (3) gave 2-phenylpyridine (4a), whose mass spectrum, picrate, and hydrochloride were identical with those of an authentic sample. On the other hand, the lithium aluminum deuteride reduction of the compound (3) gave 2-phenylpyridine-d_1 (4b). The position of the deuterium and, therefore, the site of the carbon-to-palladium σ-bond, were established by a comparison of the mass spectrum of (4b) with that of the undeuterated (4a). The compound (4a) gave peaks at *m/e* 155 (100%, parent ion), 128 (12%, loss of HCN), and 52 (21%, loss of PhCN). The mass spectrum of the compound (4b) showed peaks at *m/e* 156 (100%, parent ion), 129 (13%, loss of HCN), and 52 (21%, loss of PhCN-d_1).

2-Phenylquinoline also reacted with sodium chloropalladate in alcohol to give a yellow compound believed to have the structure (5) (dec. p. 270°C; Found: C, 51.72 H, 2.68; N, 3.87%. Calcd for $C_{30}H_{20}N_2Pd_2Cl_2$: C, 52.05; H, 2.91; N, 4.04%). In the infrared spectrum of the compound (5), the characteristic C–H deformation mode of a mono-substituted benzene is absent, but an intense band at 738 cm^{-1} can be assigned to the C–H deformation mode of an ortho-disubstituted benzene. This behavior is analogous to that of the spectra of the 2-phenylpyridine palladium complex (3). The presence of a bond between the metal atom and a carbon atom of the phenyl group in the 2-phenylquinoline molecule was also established by mass spectrometric analysis. The compound (5) was reduced with lithium aluminum hydride to 2-phenylquinoline (6a), whereas with lithium aluminum deuteride it was reduced to 2-phenylquinoline-d_1 (6b). The mass spectrum of the compound (6a) gave peaks at *m/e* 205 (100%, parent ion) and 102 (13%, loss of PhCN). The mass spectrum of 6b showed peaks at *m/e* 206 (100%, parent ion) and 102 (12%, loss of PhCN-d_1).

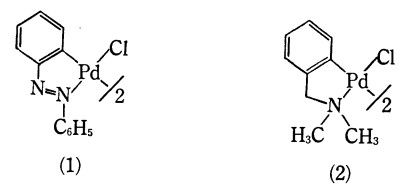

(1)

(2)

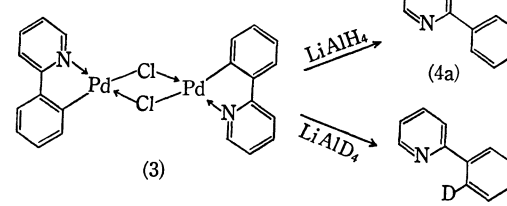

(3) (4a) (4b)

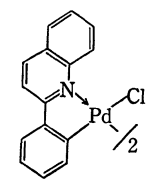

(5)

1) A. C. Cope and R. W. Sieman, *J. Am. Chem. Soc.*, **87**, 3272 (1965); A. C. Cope, J. M. Kliegman and E. C. Friedrich, *ibid.*, **89**, 287 (1967).

2) L. J. Bellamy, "The Infrared Spectra of Complex Molecules," 2nd ed., Methuen, London (1958), p. 77.

Synthesis of Poly-(L-prolyl-L-prolylglycyl) of Defined Molecular Weights

Shumpei SAKAKIBARA, Yasuo KISHIDA, Yasuo KIKUCHI, Rume SAKAI and Kinji KAKIUCHI

Institute for Protein Research, Osaka University, Kita-ku, Osaka

(Received February 3, 1968)

A major problem in polypeptide synthesis is the formation of products with a wide range of molecular weights. As a step toward the total synthesis of natural protein, an attempt was made to synthesize a sequential polypeptide with a defined molecular weight. Thus, poly-(L-prolyl-L-prolylglycyl) with ten or twenty repeating units was synthesized by the step-by-step addition of AOC-L-prolyl-L-prolylglycine (I)[1] using the solid-phase procedure.[2] The synthesis was started from glycine-anchored polystyrene (100—200 mesh, copolymerized with 2% divinylbenzene; 14 g, 0.1 mmol/g), to which AOC-L-prolyl-L-proline (1.4 g)[1] was coupled in methylene chloride with dicyclohexylcarbodiimide. The AOC-group was then removed with 2N hydrogen chloride in acetic acid, and the tripeptide-cycle was extended with I (1.7 g per cycle) and dicyclohexylcarbodiimide (0.9 g per cycle); each coupling reaction was carried out in methylene chloride for 3 hr at room temperature. After nine reaction cycles, when ten repeating units were expected to have been formed, a part of the resin was dried (wt 7 g) and placed in an HF-reaction cylinder;[3] anisole (7 ml) was added, and then anhydrous hydrogen fluoride (HF, 60—70 ml) was introduced over the resin by means of the HF-reaction apparatus.[3] After one hour at 0°C, the excess HF was removed, and the peptide liberated was extracted with water. The water extract was treated with IR-45 (OH^- form), and then dialyzed against distilled water for 3 days. The final solution was lyophilized (II, wt 0.74 g). Found: C, 53.49; H, 6.96; N, 15.54%. Calcd for $(C_{12}H_{17}O_3N_3)_{10}\cdot 10H_2O$: C, 53.52; H, 7.11; N, 15.60%.

The polypeptide-resin, which was expected to include the eicosamer (wt 6g), was also synthesized from the rest of the decamer-resin by ten more reaction cycles, and the resin was treated as has been described above. The lyophilizate (III, wt 0.67 g) thus obtained dissolved poorly in water, in contrast to the reported findings of Engel *et al.*,[4] but it was soluble in dilute aqueous acetic acid or 50% ethanol. Found: C, 53.40; H, 7.01; N, 15.62%. Calcd for $(C_{12}H_{17}O_3N_3)_{20}\cdot 20H_2O$: C, 53.52; H, 7.11; N, 15.60%.

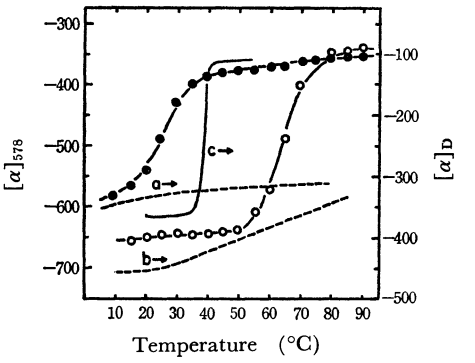

Fig. 1. Temperature dependence of specific optical rotation of (Pro-Pro-Gly)$_n$; (—●—), II, $n=10$, $c=0.187$ in 0.1 M NaCl solution; (—○—), III, $n=20$, $c=0.183$ in 10% acetic acid solution. The broken lines are cited from the data published by Engel *et al.*[4] for (Pro-Gly-Pro)$_n$, which were plotted by corrected data; a, mol wt 2950; b, mol wt 6900. The continuous line (c) is cited from the data published by Sakai *et al.*[5] for natural collagen.

The weight-average molecular weight of each polymer was determined by the sedimentation-equilibrium technique in the presence of 5M guanidine hydrochloride (0.73 was assumed for the partial specific volume). Found: 2300 (calcd for II: 2531). Found: 5300 (calcd for III: 5044). In these cases, plots for the logarithm of the concentration of the solute against the square of the radial distance, which was measured from the axis of the rotor, were completely linear. This indicates that the distribution of molecular weights was practically monodispersed in each case. The temperature-dependence of the optical rotation change was measured with the samples II and III. As is shown in Fig. 1, the behavior was much more similar to that of natural collagen[5] than those of the same type of polypeptides with a random molecular weight, (L-prolylglycyl-L-prolyl)$_n$.[4] Furthermore, it was found that the two regular polypeptides, II and III, each showed a different transition temperature, depending on their molecular weight.

Thus, a new route for the synthesis of regular polypeptides has been developed.

1) S. Sakakibara and N. Inukai, This Bulletin, **39**, 1967 (1567). AOC=*t*-Amyloxycarbonyl.
2) R. B. Merrifield, *J. Am. Chem Soc.*, **85**, 2149 (1963); *Science*, **150**, 178 (1965).
3) S. Sakakibara, Y. Shimonishi, Y. Kishida, M. Okada and H. Sugihara, This Bulletin, **40**, 2164 (1967); S. Sakakibara, Y. Kishida, R. Nishizawa and Y. Shimonishi, *ibid.*, **41**, 438 (1968).
4) J. Engel, J. Kurtz, E. Katchalski and A. Berger, *J. Mol. Biol.*, **17**, 255 (1966).
5) R. Sakai, S. Ikeda and T. Isemura, This Bulletin, **40**, 2890 (1967).

Triplet-Triplet Absorption Spectrum of *N,N*-Dimethylaniline (DMA) measured by the Flash Photolysis Technique

Katsumi KIMURA*[1], Satoshi ARIMITSU, Naoto YAMAMOTO and Hiroshi TSUBOMURA

Department of Chemistry, Faculty of Engineering Science, Osaka University, Toyonaka, Osaka

(Received February 19, 1968)

Land and Porter[1] have studied the photolysis of DMA in liquid paraffin at room temperature by the flash-photolysis technique, and assigned a transient absorption spectrum whose maxima are at 3140 and 4000 Å tentatively to the anilino radical ($C_6H_5\dot{N}CH_3$). In our previous work,[2] the flash photolysis of TMPD[3] in solution has been studied in detail and it has been shown that a transient spectrum obtained in liquid paraffin, which is similar to the absorption of $TMPD^+$, is due to the triplet-triplet (T-T) absorption. Except TMPD, so far, no T-T absorption spectra have been reported for benzene derivatives having electron donating groups such as the amino group.

A liquid-paraffin solution of DMA (about 10^{-4} mol/*l*) was deoxygenated by purging with dry nitrogen. The electronic absorption spectra of transient species formed by the flash illumination at room temperature were measured for various delay times by using the flash-photolysis apparatus in our laboratory.[2] The transient spectrum obtained with a delay time of 5 μsec, as shown in Fig. 1, consists of a fairly sharp band whose maximum is at 3400 Å and a broad band whose maximum is at 4800 Å. It was also found that the absorption at 4800 Å decays with a half-decay time of about 100 μsec. The spectrum shown in Fig. 1 may be assigned to the T-T transitions of DMA from the following reasons:

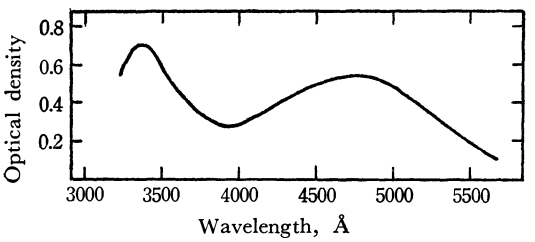

Fig. 1. A transient absorption spectrum obtained with a delay time of 5 μsec by the flash photolysis of DMA in liquid paraffin at room temperature.

1) The life time of the absorption measured at 4800 Å is comparable to that reported for the T-T spectrum of TMPD.[2]

2) In the present work, in order to confirm that the spectrum shown in Fig. 1 is attributable to T-T transitions, we also employed the steady-cross-illumination method with an EPA rigid glass of DMA at 77°K, and it was found that almost the same absorption spectrum is obtained as that by the flash illumination and its decay time is almost identical to that of the phosphorescence.[4]

3) The energy levels of triplet states of DMA have recently been calculated theoretically, by taking into account the configurational interactions between the locally-excited triplet configurations of benzene and the intramolecular charge-transfer (CT) configurations.[5] One of the present authors recalculated the triplet energy levels of DMA by selecting energy values of the CT configurations so as to reproduce the energy of the lowest triplet level estimated from the phosphorescence spectrum.[6] From this calculation, it has been confirmed that the band at about 4800 Å (2.58 eV) is due to a transition to the intramolecular CT state, its calculated energy being 3.10 eV ($f_{calc.}=0.05$), and the band at 3400 Å is concluded to correspond to a transition to one of the split states of $^3E_{2g}{}^+$ states of benzene ($f_{calc.}=0.03$), and furthermore a weak absorption ($f_{calc.}=0.01$) should exist at around 5500 Å due to a transition characteristic of one of the split states of the $^3E_{2g}{}^-$ states of benzene. It may be considered that the observed broad band probably includes this weak absorption in the longer wavelength side.

4) From our recent studies of the low temperature photolysis of DMA,[7] it has been found that the spectrum shown in Fig. 1 does not coincide with that of DMA^+ nor the anilino radical.

---

* Present address: Chemistry Laboratory, Institute of Applied Electricity, Hokkaido University, Sapporo.

1) E. J. Land and G. Porter, *Trans. Faraday Soc.*, **59**, 2027 (1963).

2) N. Yamamoto, Y. Nakato and H. Tsubomura, This Bulletin, **39**, 2603 (1966).

3) *N,N,N',N'*-Tetramethyl *p*-phenylenediamine.

4) Very recently, one of the present authors (H. T.) learned from Dr. K. D. Cadogan that he and A. C. Albrecht have measured the T-T absorption spectrum of DMA by cross-illumination technique.

5) K. Kimura and H. Tsubomura, *Mol. Phys.*, **11**, 349 (1966).

6) K. Kimura, Preprints for The 20th Annual Meeting of Chemical Society of Japan (Tokyo, April, 1967).

7) S. Arimitsu, K. Kimura and H. Tsubomura, Preprints for The 20th Annual Meeting of Chemical Society of Japan (Tokyo, April, 1967).

Absorption Spectra of Erbium TTA-TOPO Complexes Extracted from Aqueous Perchlorate Solutions

Tomitsugu TAKETATSU and Nobuyo TORIUMI

College of General Education, Kyushu University, Fukuoka

(Received March 2, 1968)

It has been reported that the absorption spectra of neodymium, holmium and erbium complexes extracted into toluene containing 2-thenoyltrifluoroacetone (TTA) and tri-*n*-octyl phosphine oxide (TOPO) from an aqueous acetate solution had a strong band in the visible region with a maximum of 584, 452 and 520 mμ, respectively, and the formulae of these complexes were estimated to be $Ln(TTA)_3 2TOPO$.[1]

In the present paper, we will describe the preliminary results of a spectrophotometric study of erbium TTA-TOPO complexes extracted into organic solvents with a series of various dielectric constants (ε) from aqueous solutions containing various amounts of perchlorate ions.

Figure 1 shows the absorption spectra for erbium complexes extracted into cyclohexane (ε: 2.02), isopropyl ether (ε: 3.88), chlorobenzene (ε: 5.62), dichloromethane (ε: 9.08) and 1,2-dichloroethane (ε: 10.36) from aqueous solutions containing a slight excess of perchlorate ion with respect to erbium ion. With increase in the dielectric constant of the organic solvents, a new sharp band appeared and grew regularly at 518 mμ. Moreover, even in the case of cyclohexane, a similar variation of the absorption band at 518 mμ was observed with increase in the concentration of perchlorate ion in an aqueous solution. The intensity at 518 mμ almost linearly increased with increase in $[ClO^-_4/Er^{3+}]_{org}$, which represented the mole ratio of perchlorate and erbium ions extracted into various organic solvents, and became constant in the region above a 1 : 1 ratio of $[ClO^-_4/Er^{3+}]_{org}$. When the intensity at 518 mμ was studied using 1,2-dichloroethane as a function of the mole ratio of TTA to erbium in the presence of excess TOPO, the break occurred at a mole ratio of TTA : Er = 2 : 1. On the other hand, in the case of mixtures containing excess TTA and various amounts of TOPO, the break was observed at a mole ratio of TOPO : Er = 5 : 1. Both intensities were almost constant with concentration of TTA and TOPO above these breaks. From these results and considering the coordination number of heavy lanthanide, it is felt that the complex in 1,2-dichloroethane prefers the formula $[Er(TTA)_2 5TOPO]^+ClO^-_4$ to $[Er(TTA)_2ClO_4 5TOPO]$.

Since the absorption spectrum obtained using cyclohexane coincides with that of the $Er(TTA)_3$-2TOPO complex in a previous paper,[1] it is supposed that the following equilibria may exist as a function of dielectric constant of the organic solvents and concentration of perchlorate ion in an aqueous solution.

$$Er^{3+} + 2HTTA_{(o)} + 5TOPO_{(o)} + ClO_4^- \rightleftarrows [Er(TTA)_2 5TOPO]^+ClO_4^-{}_{(o)} + 2H^+$$

An investigation using other lanthanide is in progress. Further discussion of the results and details of this study will be published later.

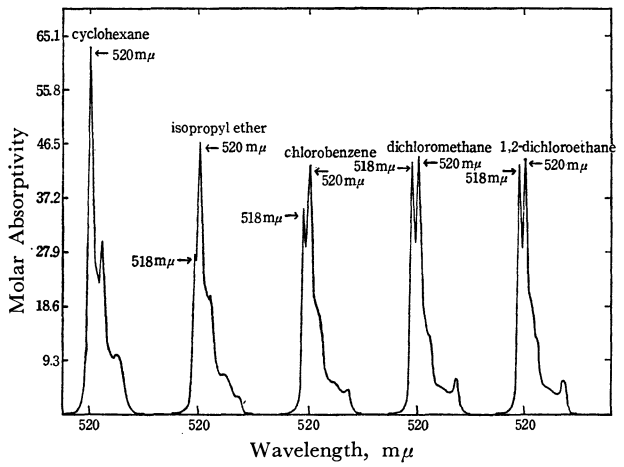

Fig. 1. Absorption spectra of erbium TTA-TOPO complexes in various organic solvents.

1) T. Taketatsu and C. V. Banks, *Anal. Chem.*, **38**, 1524 (1966).

On the Yield of Hydrogen Atoms in the Vapor Phase Radiolysis of Ammonia

Masaru NISHIKAWA, Kazufumi KURODA and Niro MATSUURA

Department of Pure and Applied Sciences, The University of Tokyo, Komaba, Meguro-ku, Tokyo

(Received March 4, 1968)

Recently, two different values were reported for the yield of hydrogen atoms in the radiolysis of ammonia vapor ; $G_H = 12.5 \pm 1$ by Jones and Sworski from their study on NH_3+D_2 and $NH_3+N_2H_4$ system,[1] and $G_H \gtrsim 7.2$ by Johnson and Simic on $NH_3+C_3H_8$ system.[2] In this communication, we wish to report some of the results of our study on the γ-radiolysis of $NH_3 + C_3H_8$ system which indicate still lower G_H from ammonia.

Purification of ammonia (99.9%, Matheson) and propane (>99.8%) and the method of irradiation were described.[3] Gas chromatographic analysis of propane indicated that no organic impurities were present at levels exceeding 10^{-3} mol%. The amount of energy absorbed in ammonia fraction (E_a) and in propane fraction (E_p) were calculated from that in a nitrous oxide dosimeter, assuming $G(N_2) = 10.0$,[4] for the runs at near-atmospheric pressure, and a Fricke dosimeter at higher densities, using the relative stopping powers obtained by Meisels.[5] The non-condensable products H_2 and N_2 were analyzed by combustion in a cupric oxide furnace.

The total hydrogen yield calculated for energy absorbed in ammonia fraction increased from $G(H_2) = 4.1$ to 7.8 at the propane concentration of 8.6 mol% in agreement with Johnson's value.[2] However, in contrast to their observation, no plateau was reached up to this concentration, suggesting hydrogen formation from the direct radiolysis of propane fraction. Therefore, in order to estimate the contribution of propane fraction for the observed yield of hydrogen, G-values of total hydrogen yields (G_t) were calculated for the total energy absorbed by the system ($E_t = E_a + E_p$) and are plotted against the fraction of energy absorbed in propane ($f_p = E_p/E_t$) in Fig. 1. A good straight-line relationship is demonstrated for f_p below 0.13 regardless of density and/or temperature and extrapolation to $f_p = 0$ yields $G(H_2)^\circ = 5.84$.

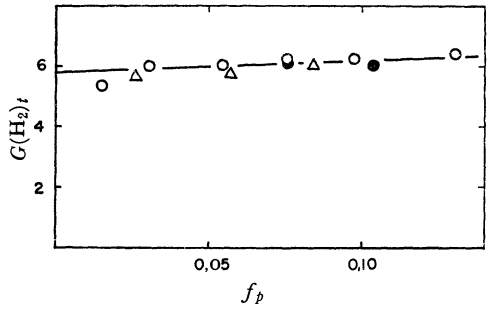

Fig. 1. Dependence of $G(H_2)_t$ on the fraction of energy absorbed by C_3H_8.
○, d~5.0×10^{-4} g/cc, 22°C
△, d~0.065 g/cc, 140°C
●, d~0.13 g/cc, 140°C

Hydrogen atoms react with propane by $H+C_3H_8 \rightarrow H_2+C_3H_7$. The yield of hydrogen at $f_p = 0$, $G(H_2)^\circ = 5.84$, is therefore a measure of the total yield of hydrogen atoms and the molecular hydrogen from the radiolysis of ammonia vapor. The latter has been determined to be 0.74,[3] hence $G_H = 5.84 - 0.74 = 5.10$.

The value of G_H thus obtained is significantly lower than those reported by Jones and Sworski[1] and by Johnson and Simic.[2] The disagreement with Johnson's value may be probably due to their neglect of hydrogen produced from propane radiolysis. It seems inconceivable in view of the large value of the relative stopping power of propane, $s_p/s_a = 2.65$,[5] that no hydrogen is produced from propane, for example, at 6 mol% where they observed the plateau in $G(H_2)$. The more serious disagreement with Sworski's value might be inherent in the system they used. For NH_3+D_2 system, they also noted that G_H as high as 90 ± 66 was obtained from their proposed mechanism at the total pressure of 600 mmHg, suggesting some kind of chain mechanism is operating. For $NH_3+N_2H_4$ system, their mechanism does not include reactions such as $NH_2+N_2H_3 \rightarrow NH_3+N_2+H_2$ ($\Delta H = -99$ kcal/mol) proposed by Dainton *et al.*,[6] the inclusion of which should lower the estimate of G_H. The use of $NH_3+C_3H_8$ system with proper corrections for hydrogen produced from propane appears more straight-forward and less ambiguous for the estimate of G_H from ammonia radiolysis.

1) F. T. Jones and T. J. Sworski, *Trans. Faraday Soc.*, **63**, 2411 (1967).
2) G. R. A. Johnson and M. Simic, *Nature*, **216**, 479 (1967).
3) M. Nishikawa and N. Shinohara, *Radiation Res.*, **33**, 194 (1968).
4) F. T. Jones and T. J. Sworski, *J. Phys. Chem.*, **70**, 1546 (1966).
5) G. G. Meisels, *J. Chem. Phys.*, **41**, 51 (1964).
6) F. S. Dainton, T. Skwarski, D. Smithies and E. Wezranowski, *Trans. Faraday Soc.*, **60**, 1068 (1964).

The Synthesis of 3-Carboxyalkyl-salicylaldehyde Derivatives and Application of Their Chelate Forming Properties to the Analysis of Copper and Nickel[1]

Tsuguo TANAKA

Department of Science and Technology, Saga University, Honjo, Saga

(Received March 7, 1968)

In connection with the previous report on the ethylenediamine conjugate of bis-*O*-carboxymethyl-salicylaldehyde-alkylenediimine-copper,[2] Reimer-Tiemann synthesis of the following three 3-carboxy-alkylsalicylaldehydes IIa, b, c and the synthesis of their derivatives were made with hydroxyacid Ia, b, c as the starting material.

Ia (mp 151°C, Found: C, 41.62; H, 3.19%. Calcd for $C_8H_7O_3Br$: C, 42.01; H, 3.05%) was prepared by the bromination of 2-hydroxyphenyl-acetic acid[3] in carbon disulfide solution. IIIa, b, c were obtained by the reaction of two moles of IIa,b,c, with one mole of ethylenediamine in ethanolic solutions and IVa, b were obtained by the reduction of IIIa, b with sodium borohydride in methanolic solutions.[4] The results are summarised in Table 1.

TABLE 1

Starting material	React. prod.		Yield %	Mp °C	Found (Calcd) C	H	N
Ia	IIa	PY	12.30	204	42.01 (41.72)	3.00 (2.72)	
Ib	IIb	PY	0.65	95	63.71 (63.45)	5.84 (5.81)	
Ic	IIc	Y	6.30	118	52.70 (52.53)	4.02 (3.97)	
IIa	IIIa	Y	92.23	242	44.69 (44.30)	3.16 (3.35)	4.94 (5.17)
IIb	IIIb	Y	83.63	195	64.19 (65.44)	6.46 (6.41)	7.09 (6.36)
IIc	IIIc	Y	46.98	204	54.89 (54.74)	4.61 (5.03)	5.82 (5.55)
IIIa	IVa	G	50.32	300*	43.37 (43.98)	4.32 (4.06)	5.41 (5.13)
IIIb	IVb-$2H_2O$	W	51.53	285	59.54 (59.98)	7.23 (7.55)	5.99 (5.83)

P=pale, Y=yellow, G=gray, W=white; * decomposition

Disodium salt of IVb works as a hexadentate ligand and forms a green copper(II) chelate but does not form any stable nickel chelate in aqueous solutions of pH 10 (it does not reveal any purple color of Murexide when added into an aqueous solution of nickel-Murexide complex), and was satisfactorily used in the spectrophotometric determination of copper(II) ions out of the mixed solutions of copper(II) and nickel(II) ions as illustrated in Fig. 2 and Table 2.

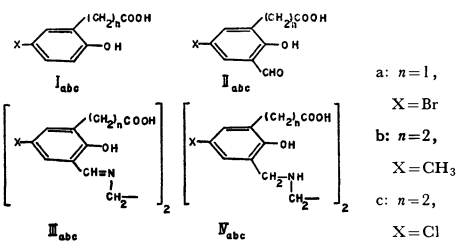

Fig. 1.

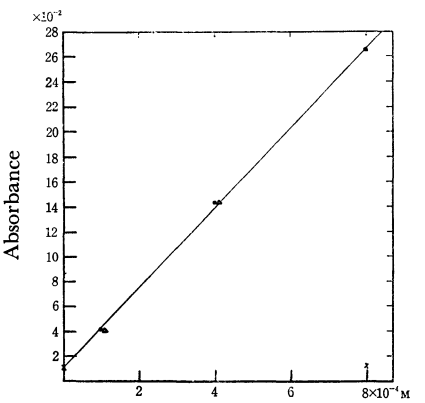

Fig. 2. Measurements were made of 5 m*l* of aqueous solutions containing 0.5 m*l* of 1/100 mol solution of disodium salt of IVb, 0.1 m*l* of pH 10 buffer solution[6] and; ○, moles of copper (II) acetate; ×, moles of nickel acetate; △, each moles of copper (II) acetate and nickel acetate, respectively. Cell depth 1 cm and pure water as reference.

TABLE 2

Sample		Found (as Cu)	Sample		Found (as Cu)
Cu	0.798 mg	0.798 mg	Cu	0.399 mg	0.411 mg
Ni	0.780 mg	0.001 mg	Cu	0.099 mg	0.094 mg
Cu	{0.399 mg}	0.411 mg	Cu	{0.099 mg}	0.091 mg
Ni	{0.390 mg}		Ni	{0.097 mg}	

In aqueous solutions of pH 10 containing Murexide indicator, IVa (Ni taken 1.76 mg, found 1.87 mg) and IVb (Cu taken 0.636 mg, found 0.699 mg) can be used as the reagent of chelatometric titration of nickel and copper respectively in place of EDTA.[5]

1) Part IX of "Some Addition Compounds of Salicylaldehyde-ethylenediimine-copper."
2) T. Tanaka, This Bulletin, **39**, 2558 (1966).
3) J. Levine, T. E. Eble and H. Fischbach, *J. Am. Chem. Soc.*, **60**, 1930 (1948).
4) I. L. Finar and K. Utling, *J. Chem. Soc.*, **1959**, 4015.
5) H. A. Flaschka, "EDTA Titrations," Pergamon Press., New York (1964), p. 82.
6) H. A. Flaschka, *ibid.*, p. 72.

The Behavior of Hydrogen Chemisorbed over the Electron Donor-Acceptor Complexes of Aromatic Hydrocarbons with Sodium in the Hydrogen Exchange and Hydrogenation Reactions

Sadao TANAKA, Masaru ICHIKAWA, Shuichi NAITO, Mitsuyuki SOMA, Takaharu ONISHI and Kenzi TAMARU

Department of Chemistry, The University of Tokyo, Hongo, Bunkyo-ku, Tokyo

(Received March 22, 1968)

In a previous paper[1] it was demonstrated that the hydrogen molecule is activated at room temperature over the electron donor-acceptor (EDA) complexes of various organic compounds with metals such as sodium, whereas no activations took place over the organic molecules or over such metals alone.

In this experiment anthracene-Na (1 : 1 and 1 : 2) films were prepared over the glass wall of a reaction vessel in an ordinary manner.[2] The reactions were carried out over the films after evacuation had been carried out for several hours at 100°C.

When 15 cmHg of D_2 gas was introduced onto the 1 : 1 and 1 : 2 complex films in the temperature range between 25 and 90°C, a considerable amount of HD was formed reversibly; the apparent activation energies for the reactions were approximately 16 and 12 kcal/mol respectively. The film of the anthracene-Na (1 : 2) complex was approximately ten times as active as that of the 1 : 1 complex for the hydrogen exchange. The rates of the H_2–D_2 (1 : 1) exchange reaction were of the same order of the magnitude as those of the D_2–HZ exchange reaction under similar conditions, where HZ represents the EDA complexes.

After the exchangeable hydrogens in these complexes had been replaced with deuterium to a considerable extent by treating the complexes with deuterium gas at 80°C, the deuterated positions in these complexes were studied by means of the ESR and NMR techniques, which revealed that the hydrogen at the 9 or 10 position of and 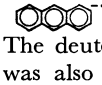 was only exchanged with deuterium. The deuterated position of similar EDA complexes was also studied in a similar manner. It was consequently found that the exchange reaction took place at the following positions:

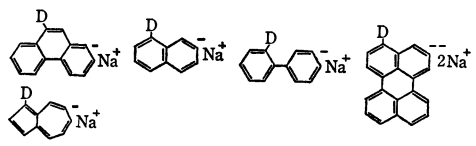

The positions where the exchange reaction took place were those with the lowest localization energy in the mononegative or dinegative ions, except for the case of azulene.

By admitting the hydrogen gas onto the thin films of 1 : 1 and 1 : 2 anthracene-Na complexes, which had been prepared on the wall of a quartz cell, a new peak appeared at 432 mμ, while the peaks due to the dinegative anion and to the mononegative radical anthracene in the complexes decreased correspondingly. The new peak is seemingly due to the 9-monohydroanthracenium anion; it disappeared after evacuation had been carried out at 100° C for several hours. The ESR measurements of the complexes indicated that the total spin concentration of the 1 : 1 complex film diminished considerably upon the introduction of hydrogen onto the complex. The free spins were restored almost completely by evacuation at 100°C. When 1 : 2 complex films were treated with hydrogen gas at 90°C and were then dissolved in THF at 25°C, the resulting solutions showed a new NMR signal, at $\tau = 8.73$, corresponding to H–Na.*1 The results suggest that the hydrogen molecule attacks the 9-position of the anthracene-dinegative anion and is dissociated heterolytically in the following manner:

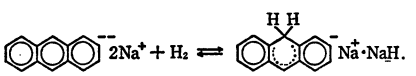

In this case the ambient hydrogen gas was replaced by deuterium, and the formation of hydrogen deuteride was followed with the time. It was accordingly found that almost all the hydrogens chemisorbed over the complex films participate in the exchange reaction with the ambient deuterium molecules, and the exchange rate was proportional to the amount of hydrogen adsorbed.

Monodeuteroanthracene of the 1 : 2 complex was prepared by treating the film with excess D_2 at 90°C for 2 days; subsequently the ambient hydrogen gas was replaced with dimethylacetylene, butadiene, or methylacetylene. As a consequence, a small amount of deuterated 2-butenes was selectively produced, while the peak at 432 mμ of 9-monohydroanthracene slowly decreased.

*1 The signal was the same as that of a THF solution of sodium hydride.

1) M. Ichikawa, M. Soma, T. Onishi and K. Tamaru, *Trans. Faraday Soc.*, **63**, 1215, 2015, 2528 (1967).

2) G. J. Hoijtink and P. J. Zandstra, *Mol. Phys.*, **3**, 371 (1960).

BULLETIN OF THE CHEMICAL SOCIETY OF JAPAN VOL. 41 1279—1284 (1968)

Measurement of Adsorbed Amount of Sodium Dodecylsulfate at Gas-Solution Interface by Radiotracer Method Using Tritium-Labeled Compounds

Mitsuo MURAMATSU, Kazuo TAJIMA and Tsunetaka SASAKI

Department of Chemistry, Faculty of Science, Tokyo Metropolitan University, Setagaya-ku, Tokyo

(Received September 13, 1967)

Sodium dodecyl-2,3-^{3}H,^{3}Hsulfate (SDS) was synthesized from non-radioactive dodecanol, and the adsorbed amount of SDS at the gas-water interface, Γ, was directly measured by the radiotracer method with the use of 2π gas-flow windowless counter and humidified propane as a flow-gas. Because of a very soft nature of tritium β-rays, surface radioactivity is exclusively due to the solute adsorption compared with the large contribution from the bulk of the solution as in the case of ^{14}C or ^{35}S labeled detergents. Therefore the use of ^{3}H labeled compounds enables the determination of the amount of adsorption in high accuracy, even in the region of high concentration beyond the critical micelle concentration (CMC) of SDS solution. However, no reliable reports have appeared as yet on the studies of adsorption of surfactant at gas-solution interface using ^{3}H labeled compounds. Our measurement was carried out under exactly specified conditions, namely using chemically and radiochemically pure sample and under the condition free from evaporation. It was confirmed that Γ increased with the increase of SDS concentration and approached the saturation value of 5.9×10^{-10} mol/cm^2 or 28.2 Å^2/molecule at the concentration higher than 6×10^{-3} mol/1000 g solution and beyond CMC. Furthermore, Γ proved to be independent of the acidity of solution above pH 4, while it increased with increasing acidity below pH 4. The phenomenon is explained by the presence of hydrolytically formed dodecylsulfuric acid whose surface activity is higher than that of SDS.

Recently, much experiment has been carried out in an effort of determining the adsorbed amounts of surface-active substances at gas-solution interfaces by the radiotracer technique using soft β-emitters, such as ^{35}S[1-3] or ^{14}C.[3,4] Though these isotopes enable us to make a direct and hitherto difficult measurement of adsorption for compact aqueous surfaces, the results obtained are not satisfactory in the accuracy especially in the region of concentrated solution and in the case of weak adsorption. In this connection, it is particularly recommended to use a compound labeled with tritium which emits an extremely soft β-radiation. This is best explained by the following equation:

$$\frac{A_1-A_2}{A_1}=\frac{1}{1+C/(1000\Gamma\mu)}, \qquad (1)$$

where A_1 denotes the total radioactivity in cpm measured over the solution surface and A_2 that due to the bulk of the solution, C the concentration (mol/1000 g solution), Γ the adsorbed amount (mol/cm^2) and μ the mass-absorption coefficient (cm^2/g) for β-rays in the solution. The higher accuracy can thus be expected either for small value of C/Γ, or for large μ value. The value for C/Γ, however, is inherent to the surfactant chosen as a sample. Therefore, in order to obtain a high accuracy for a relatively large value of C/Γ as in the case of SDS, a radioisotope of sufficiently small μ is required to use as a tracer. For this reason, ^{14}C or ^{35}S is not satisfactory, and the use of ^{3}H is recommended since μ value of ^{3}H is about 50 times as large as that of ^{14}C or ^{35}S. Also, the use of ^{3}H is favorable because hydrogen is a common constituent of organic compounds.

However, no reliable reports have appeared as yet on the studies of adsorption of surfactant at gas-solution interface using ^{3}H labeled compounds. It appears that the tentative experiments by Nilsson[5] on adsorption of tritiated sodium dodecylsulfate (TSDS) have involved some uncertainty as to his synthetic processes leading to the tritiated sample, as pointed out previously.[6]

1) G. Aniansson and O. Lamm, *Nature*, **165**, 357 (1950); D. J. Salley, A. J. Weith, Jr., A. A. Argyle and J. K. Dixon, *Proc. Roy. Soc.*, **A203**, 42 (1950); *etc.*

2) R. Matuura, H. Kimizuka, S. Miyamoto and D. Shimozawa, This Bulletin, **31**, 532 (1958).

3) K. Shinoda and K. Mashio, *J. Phys. Chem.*, **64**, 54 (1960); K. Shinoda and K. Kinoshita, *J. Colloid Sci.*, **18**, 174 (1963).

4) C. P. Roe and P. D. Brass, *J. Am. Chem. Soc.*, **76**, 4703 (1954); S. N. Flengas and E. Rideal, *Trans. Faraday Soc.*, **55**, 306 (1959); *etc.*

5) G. Nilsson, *J. Phys. Chem.*, **61**, 1135 (1957).

6) M. Muramatsu and K. Tajima, *J. Labelled Compounds*, **2**, 304 (1966).

We have obtained the radiochemically and surface-chemically pure surfactants,[6,7] and developed the 2π windowless gas-flow counting for determining tritium radioactivity over solution surfaces.[8] In the present paper an attempt is made to determine the adsorbed amount of TSDS at gas-solution interface by means of 2π windowless counter under the flow of humidified propane.

Experimental

Reagents. TSDS was prepared by the method formerly reported,[6] the process of which is shown as follows:

$$C_{12}H_{25}OH\ (I) \rightarrow C_{11}H_{23}COOH\ (II) \rightarrow$$
$$C_{10}H_{21}CHBrCOOH\ (III) \rightarrow$$
$$C_9H_{19}CH{=}CHCOOH\ (IV) \rightarrow$$
$$C_9H_{19}CH^3HCH^3HCOOH\ (V) \rightarrow$$
$$C_9H_{19}CH^3HCH^3HCH_2OH\ (TDOH) \rightarrow$$
$$C_9H_{19}CH^3HCH^3HCH_2OSO_3Na\ (TSDS).$$

Normal-dodecanol-1 (I) purified by fractional distillation (bp 141—142°C/11 mmHg) was oxidized by sulfuric acid and potassium dichromate mixture to II. For the bromination of the compound II it was mixed with phosphorus trichloride and bromine was added to the mixture gradually at 85—90°C. The compound III thus obtained was dehydrogenated by potassium iodide and potassium hydroxide. A resulting compound IV was tritiated to V with tritium gas using Urushibara nickel (U-N-A)[9] as a catalyst. The reduction of V to TDOH was carried out using lithium aluminum hydride with good yield. TDOH thus obtained was carefully purified by means of preparative gas chromatography to remove homologue impurities. TDOH thus purified was treated with chlorosulfonic acid to obtain TSDS. Purification of TSDS was performed in a usual manner.[10] In addition to the usual chemical purification, a radiochemical purification was worked out to remove radioactive TDOH by the isotopic dilution method, that is, by repeating the addition of non-radioactive dodecanol to the alcoholic solution of TSDS and subsequent precipitation of TSDS from the solution. TSDS was finally purified by the Soxhlet extraction using ether followed by a recrystallization from ethanol. The TSDS thus obtained was sufficiently pure both chemically and radiochemically showing neither minimum in surface tension *versus* concentration curve nor the trace of volatile radioactive impurities presumably due to TDOH. Specific activity was 720 mCi/mol both for TDOH and TSDS.

Other reagents used in the present experiment were purified thoroughly by pertinent procedures. Samples of propane (98—99% pure) and methane (99.6%) used as flow gases were kindly supplied from Toa Nenryo Kogyo K. K.

Apparatus. Figure 1 illustrates schematically the apparatus which consists of the flow-gas preheater C, humidifier D, and the counting probe F of 2π windowless gas-flow counter (Aloka DC-1001). A solution of TSDS or TDOH for counting was contained in the planchette G, covered with the concentric mask H, which eliminates radioactivity from the periphery of G. The planchette and the mask made of stainless steel were polished and cleaned electrolytically with 1.2 A/cm² d. c. current in a solution of phosphoric acid prior to the experiments. The whole system was thermostatted to 20±0.5°C.

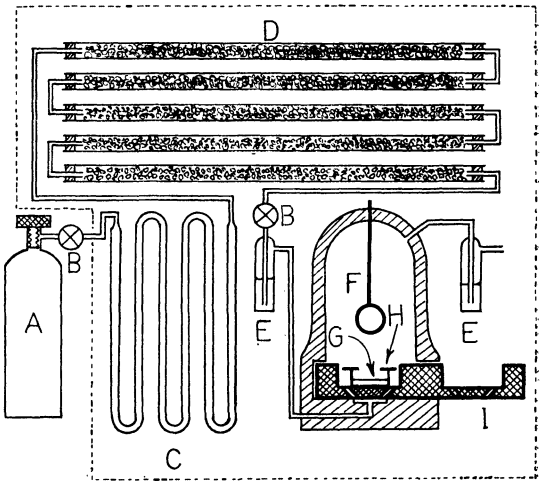

Fig. 1. Experimental apparatus.

A	Propane gas tank	B	Control valve
C	Preheater tube	D	Humidifying tubes
E	Bubbler	F	Counting probe
G	Planchette	H	Cover mask
I	Turn table		

It has been pointed out in the previous paper[8] that the flow gas for counting the radioactivity over a solution surface should be moistened moderately to keep humidity neither so high as to permit multiple discharge, nor so low to enhance evaporation, since evaporation sometimes causes the concentration of solute at gas-solution interface. The optimum conditions for the least evaporation without multiple discharge were examined by changing the type of flow gas, its humidity and flow rate. The humidity was controlled by changing the length of preheater C, and the number of humidifier tubes D (2.0 cm diameter and 55 cm length each), which were packed with pieces of filter paper soaked with distilled water. The best condition was found to use propane of 82.6% humidity and 9.7 ml/min gas flow rate, and a voltage from 4600 to 4900 V applied to the counter. Under this condition, the rate of water evaporation from SDS solution in the planchette G, was less than 0.10 mg/cm²/hr. This amount corresponds approximately to a surface deposition of SDS of 6×10^{-10} mol/cm²/hr at the surface of 6×10^{-3} mol/1000 g solution, if we assume the deposit to remain undisturbed. However, the surface cooling involved in the actual system causes a convection current which results in a retardation of surface enrichment

7) M. Muramatsu, O. Fujii and T. Sasaki, *Radioisotopes*, **10**, 100 (1961).
8) M. Muramatsu and T. Sasaki, "Proc. 3rd Japan Conference on Radioisotopes," Japan Atomic Energy Ind. Forum, Tokyo (1959), p. 453.
9) K. Hata, S. Taira and I. Motoyama, This Bulletin, **31**, 776 (1958); *ibid.*, **34**, 261 (1961); *etc.*
10) E. E. Dreger, C. L. Keim, G. D. Miles, L. Shedlovsky and J. Ross, *Ind. Eng. Chem.*, **36**, 610 (1944).

of solute.[11] Therefore, it seems possible that the surface enrichment of the actual system is much less than the above value, as has been suggested in the experiments using $^{35}SO_4^{2-}$ in aqueous solution under the flow of dry nitrogen.[12]

Procedures. A portion of 0.80 m*l* of TSDS solution which had been aged in the thermostat for more than 15 min was brought by a syringe into the planchette G. The turn table, I, was revolved to get it into the counting chamber, in which humidified propane had been flowed previously for 5 hr to make its humidity and temperature constant. Surface radioactivity, A_1, of the solution was then determined as a function of time which elapsed from the revolving of the table.

The bulk radioactivity, A_2, of aqueous TSDS solution was estimated by converting the radioactivity (bulk) A_2', obtained with TDOH solution of the same radioactive concentration in non-radioactive dodecanol under the same geometrical conditions in the flow counter. For the same radioactive concentration C_r (dpm/g solution), these quantities are expressed by

$$A_2 = G\eta C_r \frac{f}{\mu}(1 - e^{-\mu R}), \quad (2)$$

$$A_2' = G\eta C_r \frac{f'}{\mu'}(1 - e^{-\mu' R'}), \quad (3)$$

where G is the geometrical factor, η the counting efficiency, f the back- and self-scattering factor, and R the maximum range (g/cm^2) of medium for β-particles. The prime denotes the TDOH-dodecanol system. Combining the Eqs. (2) and (3), we have

$$A_2 = \frac{f}{f'}\frac{\mu'}{\mu}\frac{1 - e^{-\mu R}}{1 - e^{-\mu' R'}} A_2' = kA_2'. \quad (4)$$

The proportionality factor, k, was determined by evaluating the individual terms in Eq. (4).

The adsorption amount of surfactant Γ (mol/cm^2) was calculated by the following equation,

$$\Gamma = \frac{A_1 - A_2}{S\sigma D}, \quad (5)$$

where S denotes the surface area (cm^2), σ the specific activity of the radioisotope used (dpm/mol) and D the detection coefficient (cpm/dpm). The term $S\sigma D$ was determined separately by the method to be described in the following section.

Radioactivity was measured under the condition that the counting rate lies within a 1—1.5% standard deviation. The background radioactivity was about 30 cpm throughout the experiments.

Results and Discussion

Determination of A_1 and A_2. In Fig. 2 are shown the values of surface radioactivity of TSDS solutions as a function of time elapsed from revolving the turn table. Neither acid nor alkali was added to these solutions. Therefore pH values were in a range of 5.8 to 6.1, depending on concentration. It can be seen in this figure that the

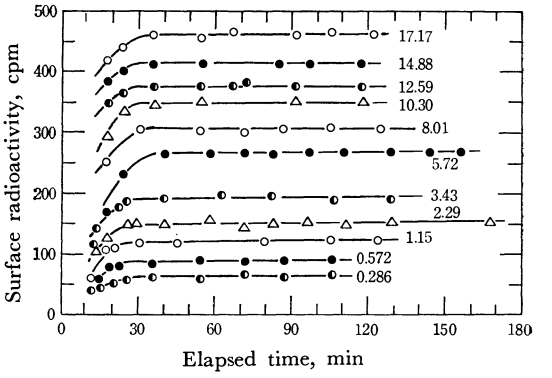

Fig. 2. Surface radioactivity for various TSDS solutions as a function of elapsed time.
The figures by the curves indicate concentration of the solutions in 10^{-3} mol/1000 g.

radioactivity increases with time and reaches a constant value in 30—40 min, depending on concentration. The initial increase with rather steep slope seems to indicate the dynamic processes of adsorption and the removal from flow gas of air which has been mixed by revolving the turn table. In fact, *ca.* 15 min was required for obtaining the stationary value of counting rate for a sample of stearic-9,10-^{3}H,^{3}H acid[7] spread over the same planchette. Thus, in Fig. 2, the linear portion of the curve after at least 40 min was extrapolated to time zero and the corresponding surface radioactivity was taken as A_1, for each solution.

Similar experiments were carried out for determining the radioactivity, A_2', over the surfaces of TDOH solutions in non-radioactive dodecanol-1 at 30—60 min after the initial revolving. To convert A_2' into A_2, reasonable approximations have been made for the propotionality factors in Eq. (4). First, the ratio, f/f' is estimated to be approximately unity, because the scattering power of aqueous TSDS solution is not much different from that of dodecanol-1. It is well known[13] that the scattering power for β-rays can be expressed as a function of the average atomic number

$$Z_{av} = \sum x_i m_i Z_i / \sum x_i m_i, \quad (6)$$

where x_i is fractional number of ith constituent atom of mass number m_i and atomic number Z_i. In the second line of Table 1 are shown the Z_{av} values calculated for the solutions of SDS in water and of TDOH in dodecanol-1. Putting these values into the empirical relationship between Z_{av} and the scattering factor[14] gives f/f'. Secondly, the mass-absorption coefficient, μ or μ', of a medium for given β-particles is determined by the

11) N. L. Jarvis and R. R. Kagarise, *J. Colloid Sci.*, **17**, 501 (1962); N. L. Jarvis, *ibid.*, **17**, 512 (1962).
12) T. Seimita and T. Sasaki, *J. Colloid Interface Sci.*, **21**, 229 (1966).
13) H. A. Bethe and J. Ashkin, "Experimental Nuclear Physics," Vol. 1, ed. by E. Segré, John Wiley and Sons, Inc., New York (1953), p. 166.
14) For example, K. Siegbahn, "Beta and Gamma Ray Spectroscopy," North-Holland Publ. Co., Amsterdam (1955), p. 7.

TABLE 1. FACTORS INVOLVED IN THE PROPORTIONALITY CONSTANT IN EQS. (5)—(8)

Medium	(0—2)×10⁻² mol/1000 g SDS solution	Dodecanol-1
Z_{av}	7.2	5.5
$(Z/m)_{av}$	0.833	0.833
Mass absorption coefficient, μ or μ'	19.4 cm²/mg	19.0 cm²/mg

average ratio of atomic number to mass number,

$$(Z/m)_{av} = \sum x_i Z_i/m_i \,. \tag{7}$$

As a first approximation,

$$\mu = \alpha(Z/m)_{av}, \tag{8}$$

where α denotes the proportionality constant, which depends only on the energy of β-particles. Equation (8) which has been verified with rather hard β-rays[15] seems to be applicable to the tritium β-rays, as shown in Table 2 from which one obtains 23.3 cm²/mg for average α value. Combining the value with individual $(Z/m)_{av}$ values, which are given in the third line of Table 1, one can estimate the mass-absorption coefficient, values

TABLE 2. μ, $(Z/m)_{av}$, AND α FOR TRITIUM β-RAYS IN GASEOUS ABSORBER

Absorber	μ cm²/mg	$(Z/m)_{av}$	α cm²/mg	Observer
Hydrogen	22	1.008	22	Dorfman[16]
Helium	11.4	0.500	22.8	Dorfman[16]
Air	12.5	0.500	25.0	Muramatsu *et al.*[17]
			Av. 23.3	

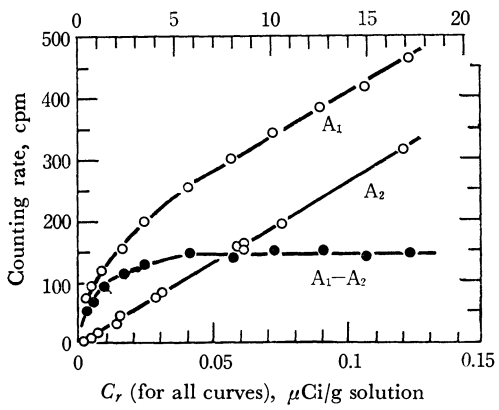

Fig. 3. A_1, A_2 and A_1-A_2 as a function of C_r or C (for A_1 and A_1-A_2).

15) G. Friedlander and J. W. Kennedy, "Nuclear and Radiochemistry," John Wiley and Sons, Inc., New York (1955), p. 198; C. Feldman, *Phys. Rev.*, **117**, 455 (1960).
16) L. M. Dorfman, *Phys. Rev.*, **95**, 393 (1954).
17) M. Muramatsu, N. Tokunaga and A. Koyano, *Nucl. Instr. Methods*, **52**, 148 (1967).

of which are shown in fourth line of Table 1. Thirdly, $R=R'=0.55$ mg/cm² was obtained by interpolation of the energy-range relationship for various β-particles.[18] Putting these values into Eq. (4), we have

$$A_2 = \frac{19.4}{19.4} \cdot \frac{1-\exp(-19.4\times 0.55)}{1-\exp(-19.0\times 0.55)} A_2' = 1.00\, A_2' \,. \tag{9}$$

The amounts of A_1, A_2 and A_1-A_2 thus obtained are plotted in Fig. 3 against the radioactive concentration, C_r, for each solution.

Determination of $S\sigma D$. The value of $S\sigma D$ in Eq. (5) was determined by counting the surface radioactivity for known amounts of TSDS film spread over the nearly saturated solution of ammonium sulfate. A mixture of ethanol and benzene (1 : 40 in volume) containing TSDS was applied to the surface of 0.80 m*l* of the solution in planchette G in Fig. 1 and, after evaporating the solvent, turn table I was revolved to count the surface radioactivity. Exactly same conditions on S, σ and D were employed in the experiments as in determination of A_1 for aqueous TSDS solution. Also, it has been assumed tacitly in the experiments that the value of D and so the back- and self-scattering factor of nearly saturated solution (75.4 g/100 g solvent) of ammonium sulfate is the same as that of TSDS solutions. The assumption seems to be valied, as Z_{av} values are 7.4 for the former and 7.2 for the latter throughout the concentration range from 0 to 2×10^{-2} mol/1000 g solution. The difference in back- and self-scattering factor between the above two solutions could thus be much less than 1%.[14] Consequently, the value of $S\sigma D$ measured on saturated solution of ammonium sulfate can be used for the calculation of Γ using Eq. (5).

Figure 4 shows the dependence of surface radioactivity upon the amount of TSDS, assuming

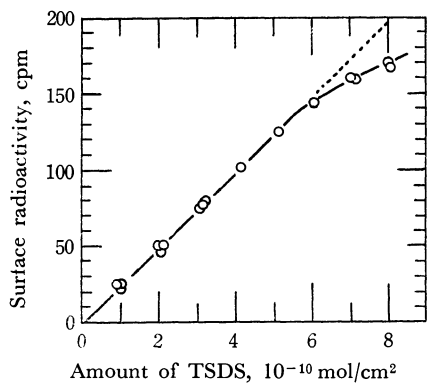

Fig. 4. Surface radioactivity as a function of TSDS applied to the surface of saturated solution of ammonium sulfate.

18) G. Friedlander and J. W. Kennedy, *loc. cit.*, p. 202.

that the molecules are all retained in the surface under the present experimental condition.[19] It can be seen in Fig. 4 that the radioactivity increases proportionally to the amount of TSDS up to *ca.* 5.5×10^{-10} mol/cm^2 or 30 Å^2/molecule; the value agreeing approximately with the limiting area of docosanylsulfate in insoluble monolayer at air-water interface.[20] Beyond this value, the curve tends to decrease in its slope, showing possible dissolution of the surfactant molecules into subphase. Similar phenomenon was observed by Brady[21] who employed surface tension and microtome methods for determining the nature of SDS films spread on various salt solutions. Therefore, the inclination of the linear portion in Fig. 4 is considered to give the value of $S\sigma D$ and we have empirically

$$\Gamma = 4.03\times10^{-12}(A_1-A_2) \qquad (10)$$

with A_1 and A_2 in cpm and Γ in mol/cm^2.

Adsorption Isotherm of SDS at about pH 6. Inserting the A_1-A_2 values shown in Fig. 3 into Eq. (10), we obtain Γ values as a function of TSDS concentration. The results are shown as the open circles in Fig. 5. The adsorbed amount increases with the increase of C and gives the saturation value of 5.9×10^{-10} mol/cm^2 or 28.2 Å^2/molecule beyond the concentration of 6×10^{-3} mol/1000 g solution, the value being in good accord with the value for alkylsulfates in the state of insoluble monolayers at air-water interfaces.[20,21]

In Fig. 5 the semi-closed and closed circles are those reproduced from the papers by Matuura *et al.*[2] and Nilsson,[5] respectively. These data are not in accord with our results. The former investigators used SDS-^{35}S which suffers from an inevitable errors, especially in large concentration; while in the study of the latter author, tritiated SDS contains surface-active impurities whose specific activity might be much high in comparison with that of the main component, as has been pointed out previously.[6] In fact, Nilsson's synthetic product, according to experience, was much complicated in its chemical and radiochemical composition, since he paid no attention to the separation of undesirable impurities in the intermediate and final products formed in his synthetic procedure.

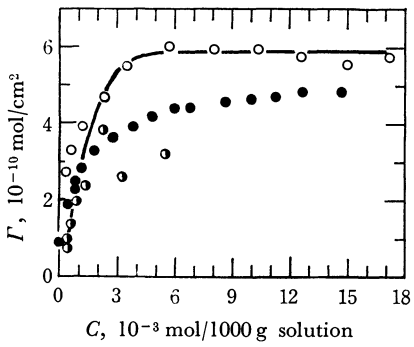

Fig. 5. Adsorption isotherm of SDS solution.
-○-, our results using ^{3}H as a tracer, pH 5.8—6.1;
●, by Nilsson,[5] using ^{3}H as a tracer;
◑, Matuura *et al.*,[2] ^{35}S as a tracer.

pH Dependence of Γ. Similar experiments were carried out with TSDS solutions below and above CMC at various pH values. It can be seen in Fig. 6 that Γ is almost constant throughout the range of pH beyond 4, while it increases markedly with decreasing pH below 4. This suggests at least the enhanced formation of dodecylsulfuric acid which might correspond with the lowering of surface tension at pH lower than 4.[22] The total increase of dodecylsulfate radicals as shown in Fig. 6 may be explained by taking account of the decrease in electrostatic repulsion between charged radicals in adsorbed layer, caused by introduction of free acid.

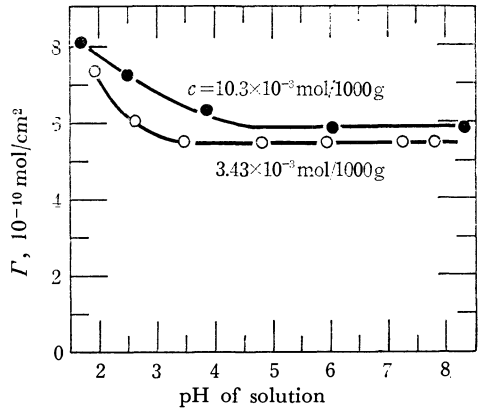

Fig. 6. Effect of solution pH upon the adsorbed amounts of SDS solution below (○) and above (●) CMC.

It might seem evident that the measured value of Γ, especially in acid region, is mainly attributable to TDOH formed by the hydrolytic reaction,

$$C_9H_{19}CH^3H\cdot CH^3H\cdot CH_2O\cdot SO_3^- + H_2O \rightarrow$$
$$C_9H_{19}CH^3H\cdot CH^3H\cdot CH_2OH + HSO_4^-,$$

which is more enhanced in acidic medium. However, a recent radiotracer study on the reaction rate[23] suggests that the dodecanol formation is too small to explain the enhanced adsorption. For 3.43×10^{-3} mol/1000 g SDS solution at 20°C,

19) B. A. Pethica, *Trans. Faraday Soc.*, **50**, 413 (1954).
20) E. Stenhagen, *ibid.*, **36**, 496 (1940).
21) A. P. Brady, *J. Colloid Sci.*, **4**, 417 (1949).
22) J. W. James and B. A. Pethica, "Proc. 3rd Int. Congr. Surface Activity," Vol. 1, Butterworths, London (1961), p. 227.
23) M. Muramatsu, M. Inoue and T. Sasaki, "Proc. 7th Japan Conf. on Radioisotopes," Japan Atomic Energy Ind. Forum, Tokyo (1966), p. 240.

as an example, the reaction rate was estimated to be 3.7×10^{-6} and 1.5×10^{-8} mol dodecanol/1000 g solution/day at pH 1 and 5, respectively. The figures correspond to at most 6.1×10^{-11} and 2.5×10^{-13} mol dodecanol/cm^2 respectively, for the "surface density" of dodecanol, even though we assume the exhaustive adsorption of dodecanol molecules from the bulk phase of 0.8 m*l* solution which has been contained in the planchette of 2.5 cm in diameter for 2 hr. Therefore, it is considered that the pH dependence observed may be mainly explained by the bulk and surface hydrolysis resulting in dodecylsulfuric acid which is more surface active than dodecylsulfate ion. Further studies along this line are desired.

Remarks on the Present Method. In general, 2π windowless gas-flow counting is one of the easiest, simplest and inexpensive methods for determining the radioactivity of tritiated specimen. It has been pointed out previously[8] that the method involves the advantage that the counting rate is not much influenced by the geometric position of the specimen, so far as it is contained in the metallic planchette. Thus, the method seems to be suited for counting the surface radioactivity of relatively small amount of solution containing tritiated specimen.

On the other hand, the windowless gas-flow counting inevitably encounters difficulties arising from the fact that the solution surface is always exposed to flowing gas, which should be humidified moderately so as to minimize the surface enrichment of solute due to the evaporation of the solvent, as mentioned in the former section. In the present experiment, the above mentioned rate and humidity of flowing gas proved to be sufficient to eliminate such a disturbance, since we could hardly detect the additional surface enrichment due to the evaporation. This results can reasonably be expected from the result of a similar evaporation experiment for $^{35}SO_4^{2-}$ solution in which even a flowing of dried nitrogen did not cause a measurable amount of a change in surface concentration.[8]

It must be noted that the results hereby obtained are concerned with the adsorption at the interface between "*humidified propane*" and SDS solution saturated with propane. Such an interface might be different in its nature from SDS solution-air interface, which would best be studied by an end-window counter specially designed for tritium radioactivity measurements.

This work was financially supported by the Scientific Research Expenditure Grant of the Ministry of Education.

BULLETIN OF THE CHEMICAL SOCIETY OF JAPAN VOL. 41 1284—1288 (1968)

Radiolysis of Co^{III}-EDTA in Aqueous Solution; The Effect of pH

Niro MATSUURA, Nobuyoshi SHINOHARA and Masaru NISHIKAWA

Department of Pure and Applied Sciences, College of General Education, The University of Tokyo, Komaba, Meguro-ku, Tokyo

and Masao TAKIZAWA

Radiation Chemistry Laboratory, Institute of Physical and Chemical Research, Bunkyo-ku, Tokyo

(Received October 13, 1967)

The hydrogen and hydrogen peroxide produced in the radiolysis of Co^{III}-EDTA ($Co^{III}Y^-$) in various pH's have been measured. $G_\infty(H_2)$ in the deaerated system sharply dropped from the value of 3.2 at pH$<$1 to the value of 0.8 at pH$>$4 where G_∞ denotes a limiting value which is reached with increasing solute concentration. $G_\infty(H_2O_2)$ in the aerated system was found to be 2.5—2.0. $G_\infty(-Co^{III}Y^-)$ ($=4.4$) was not affected by the addition of N_2O. $G_\infty(N_2)$ and $G_\infty(H_2)$ were found to be 2.6 and 0.8 respectively. From the results, it is concluded that H atoms and OH radicals reduce Co(III) to Co(II) through the dehydrogenation from the ligand, while e_{aq}^- reduce the complex without any degradation of the ligand.

In the previous papers of the series of study on the radiolysis of Co^{III}-EDTA, we reported that OH radicals and H atoms abstract hydrogen from α-carbon position of EDTA molecule of the complex and that the free radical $Co^{III}Y\cdot^-$ formed by hydrogen abstraction is reduced to $Co^{II}Y'$ by

intramolecular electron transfer from ligand to central cobalt(III) ion where Y′ denotes a degraded EDTA.[1-4]

In this paper the study of radiolysis of Co^{III}-EDTA in dilute solution was extended to higher pH region where hydrated electrons are the predominant reducing species.[5,6] We are particularly interested to see whether hydrated electrons react with Co^{III}-EDTA in a similar way as H atoms do in the acidic medium. Following reactions (1) and (2) are conceivable for e_{aq}^- and Co^{III}-EDTA.

$$Co^{III}Y^- + e_{aq}^- \xrightarrow{H_2O} Co^{III}Y^{\cdot -} + H_2 + OH^- \quad (1)$$

$$Co^{III}Y^- + e_{aq}^- \longrightarrow Co^{III}Y^{2-} \quad (2)$$

By the determination of the hydrogen yields, one can select one of the alternatives as the plausible reaction for e_{aq}^-. Some of the experiment was carried out in the presence of N_2O as the electron scavenger.[7]

Experimental

Material. Triply distilled water was used throughout the study. Ethylenediaminetetraacetatocobaltate(III) salt (KCo^{III}-EDTA·$2H_2O$) was prepared by the method, described previously[1] and then twice recrystallized. The other material used were of reagent grade.

Preparation of Samples and Their Irradiation. Sample solutions were prepared by dissolving the complex salt in 0.4 M sulfate solutions whose pH has been adjusted by adding the required amounts of sulfuric acid and potassium sulfate. The experiment was carried out in the range of pH 0.4—5.0. The irradiation vessel used was the same as that reported previously.[1] Deaerated solutions were prepared by bubbling nitrogen washed with alkaline pyrogarol solution or by thoroughly degassing by repeated freezing-pumping-thawing. The irradiation vessel for solution containing N_2O was cylindrical one of the capacity of 45 m*l*. The vessel containing 15 m*l* of the solution was thoroughly degassed and N_2O was introduced to various pressure. After being sealed off, the vessel was shaken and then irradiated with ^{60}Co γ-rays at the dose rate of 7.2×10^{18}—8.1×10^{18} eV·ml^{-1}hr^{-1} determined by the Fricke dosimeter, taking $G(Fe^{3+})=15.5$.

Analysis of Products. Hydrogen peroxide was determined polarographically.[4] The gases produced by irradiation were pumped from the solution by the freeze-thaw technique, passed thorugh traps at −196°C in order to condense N_2O, and collected in a gas burette. The amount of hydrogen was determined either by passing the gases over heated cupric oxide, or by the gas chromatographic method described previously[4]; these results agreed within experimental error.

Results

Hydrogen Peroxide. Hydrogen peroxide from irradiated solution of Co^{III}-EDTA in the presence of oxygen were determined at various values of pH. The yields of hydrogen peroxide were found to depend on the dose absorved but little on the solute concentration and initial pH of the solution. The good straight lines were obtained between the yield and the dose absorbed up to 4×10^{18} eV·ml^{-1}. Figure 1 shows the hydrogen peroxide yields as the function of solute concentration at a given pH, which shows that the yield is virtually constant except in the lower concentration region. The curve in Fig. 1 approaches to a limiting G value $G_\infty(H_2O_2)$ with increasing solute concentration. By the inverse plot method described in previous paper[1,3] the limiting G value can be calculated and plotted as function of pH in Fig. 2.

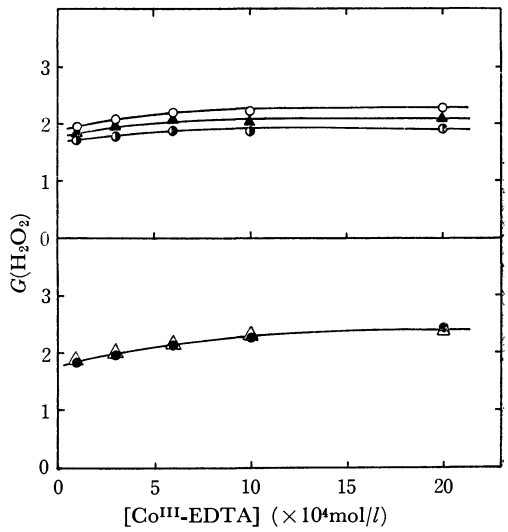

Fig. 1. Hydrogen peroxide yields in aerated Co^{III}-EDTA solution at various pH's.
Initial pH: ● 1.0, △ 2.0, ○ 3.0, ▲ 4.0, ◑ 5.0

Hydrogen peroxide could not be detected from the irradiated Co^{III}-EDTA solution, if oxygen is removed.

Hydrogen Yields. Hydrogen formed in the irradiated solution of Co^{III}-EDTA in the presence and absence of oxygen was measured. The amount depends both on the dose absorbed and initial pH of the irradiated solution. Straight lines were obtained between the yield and the dose absorbed

1) N. Matsuura, N. Shinohara and M. Takizawa, *Nippon Kagaku Zasshi (J. Chem. Soc. Japan, Pure Chem. Sect.)*, **85**, 897 (1964).
2) N. Matsuura, N. Shinohara and M. Takizawa, Scientific Papers of the College General Education of University of Tokyo, **13**, 179 (1964).
3) N. Matsuura, N. Shinohara and M. Takizawa, *Nippon Kagaku Zasshi (J. Chem. Soc. Japan, Pure Chem. Sect.)*, **86**, 590 (1965).
4) N. Matsuura, N. Shinohara and M. Takizawa, This Bulletin, **40**, 2042 (1967).
5) G. Czapski and H. A. Schwarz, *J. Phys. Chem.*, **66**, 471 (1962).
6) E. J. Hart and J. W. Boag, *J. Am. Chem. Soc.*, **84**, 4090 (1962).
7) F. S. Dainton and D. B. Peterson, *Proc. Roy. Soc.*, **A267**, 443 (1962).

(below 4×10^{18} eV·ml^{-1}). Figure 3 shows $G(H_2)$ in the deaerated system as function of solute concentration of various pH's. Each curve in Fig. 3 approaches to a limiting G value with increasing solute concentration. By the inverse plot method each limiting G value in deaerated solution was calculated and plotted as function of pH in Fig. 4 (black circle). $G(H_2)$ in aerated solution was 0.4 independent of the solute concentration and the initial pH; the results were shown as open circle in Fig. 4.

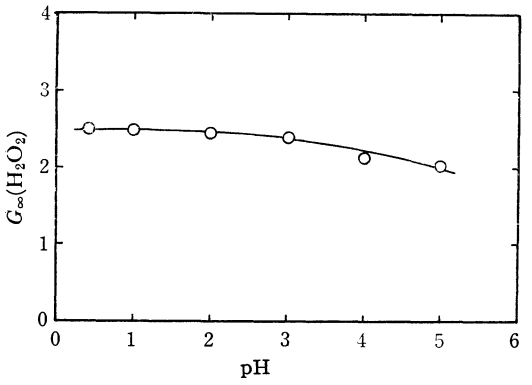

Fig. 2. Hydrogen peroxide yields in aerated Co^{III}-EDTA solution as a function of pH.

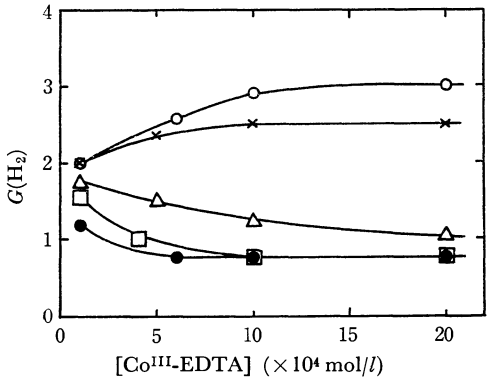

Fig. 3. Hydrogen yields in deaerated Co^{III}-EDTA solution at various pH's.
Initial pH: ○ 1.0, × 2.0, △ 3.0, □ 4.0, ● 5.0

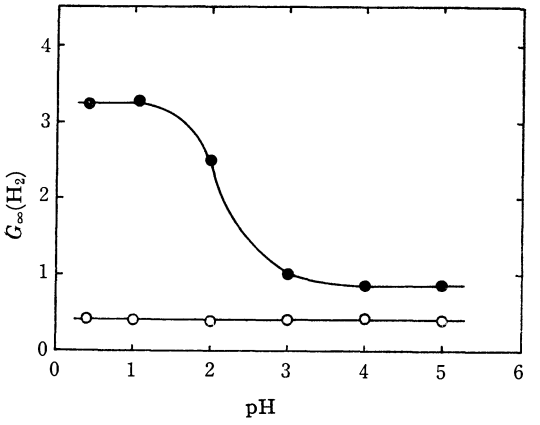

Fig. 4. Hydrogen yields in deaerated Co^{III}-EDTA solution as a function of pH.
● deaeraed, ○ aerated

Effect of N_2O. Figure 5 illustrates the effect of N_2O on $G(H_2)$ together with $G(N_2)$ at the fixed concentration of Co^{III}-EDTA 10^{-3} mol/l (pH= 4.0) in the absence of oxygen. $G(H_2)$ decreases and $G(N_2)$ increases with N_2O concentration until they reach constant values of 2.6 and 0.8 at the concentration of $\sim10^{-2}$ mol/l, indicating the complete scavenging of e_{aq}^-. Effect of variation of Co^{III}-EDTA concentration upon $G(H_2)$ and $G(N_2)$ in deaerated Co^{III}-EDTA solution containing N_2O in sufficiently high concentration to scavenge e_{aq}^- (2.5×10^{-2} mol/l) is shown in Fig. 6. It is readily seen that both $G(N_2)$ and $G(H_2)$ depend on Co^{III}-EDTA concentration up to $\sim10^{-3}$ mol/l, beyond which $G(N_2)$ and $G(H_2)$ were 2.6 and 0.8, respectively.

$G(-Co^{III}Y^-)$ in the presence of 2.5×10^{-2} mol/l of N_2O increases with Co^{III}-EDTA concentration,

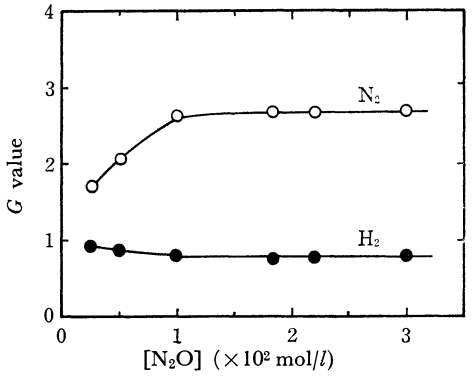

Fig. 5. Yields of nitrogen and hydrogen in the solution of N_2O and 1.0×10^{-3} mol/l Co^{III}-EDTA.

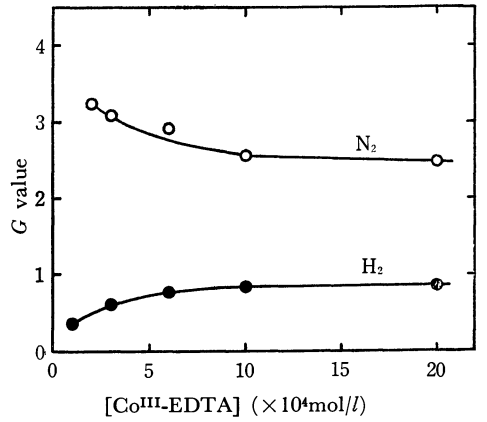

Fig. 6. Yields of nitrogen and hydrogen in the solution of 2.4×10^{-2} mol/l N_2O and Co^{III}-EDTA.

Table 1. Observed maximum G values

	pH	Co^{III}-EDTA + O_2	pH	Co^{III}-EDTA	pH	Co^{III}-EDTA+N_2O
$G(-Co^{III}Y^-)$*	0.4—2	2.5—2.8	0.4—5	5.0—4.5	4	4.4
	2—3	decrease				
	3—5	1.8				
$G(H_2)$	0.4—5	0.4	0.4—2	3.2	4	0.8
			2—3	decrease		
			3—5	0.8		
$G(H_2O_2)$	0.4—5	2.5—2.0	0.4—5	0		
$G(N_2)$					4	2.6

* These G values have been reported in the previous paper.[3]

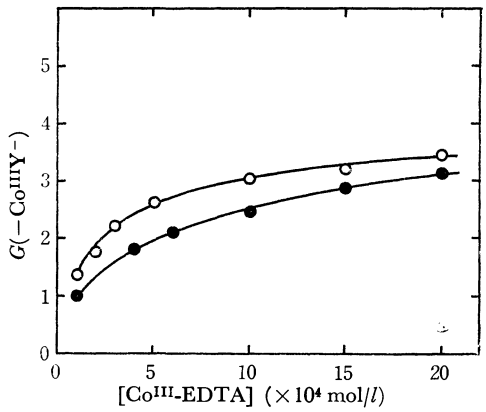

Fig. 7. $G(-Co^{III}Y^-)$ as a function of Co^{III}-EDTA concentration.
○ Co^{III}-EDTA
● Co^{III}-EDTA+2.4×10^{-2}mol/l N_2O

as shown in Fig. 7 together with the result of the system in the absence of N_2O. Each curve in Fig. 7 approaches to a limiting G value with increasing Co^{III}-EDTA concentration. By the inverse plot method, $G_\infty(-Co^{III}Y^-)$ was determined to be 4.5 for Co^{III}-EDTA system and 4.4 for Co^{III}-EDTA-N_2O system. The various limiting G values obtained were summarized in Table 1.

Discussion

Decomposition Mechanism in Deaerated System. Co^{III}-EDTA is reduced to Co(II) state in aqueous medium under the effect of irradiation and the decomposition mechanism of Co^{III}-EDTA in the 0.8 N sulfuric acid solution was explained in terms of a series of the processes of (3), (4), (5), (6), (7) and (8) as described in the previous papers,[1,2,4] where Y and Y′ denoted EDTA and a degraded form of EDTA, respectively.*1

$$Co^{III}Y^- + H \longrightarrow Co^{III}Y\cdot^- + H_2 \quad (3)$$

$$Co^{III}Y\cdot^- \longrightarrow Co^{II}Y' + H^+ \quad (4)$$

*1 Concievable forms of the species of Y· and Y′ were shown in Ref. 4.

$$Co^{III}Y^- + OH \longrightarrow Co^{III}Y\cdot^- + H_2O \quad (5)$$

$$H + O_2 \longrightarrow HO_2 \quad (6)$$

$$HO_2 + HO_2 \longrightarrow H_2O_2 + O_2 \quad (7)$$

$$H + H_2O_2 \longrightarrow OH + H_2O \quad (8)$$

In the present discussion we attempt to explain stoichiometrically the G values observed in higher pH solution. It seems reasonable to assume that oxidizing radicals OH, whose $pK_a=11.2$,[8] react as such with Co^{III}-EDTA by reaction (5) also at pH$\simeq$5 as in 0.8 N sulfuric acid, while it is expected that reactions of the reducing radicals in higher pH range are different. In the radiolysis of deaerated Co^{III}-EDTA solution, $G_\infty(H_2)$ sharply dropped from the value of 3.2 in the acidic medium to the value of 0.8 at pH=4 as shown in Fig. 4. $G(H_2)=0.8$ in the deaerated system is larger than the primary hydrogen yield $G_{H_2}=0.4$ from water. This suggests that H atoms ($G_H=0.55$)[9] are produced in higher pH region besides hydrated electrons, and it is only H atom that abstracts hydrogen from ligand EDTA of the complex by reaction (3) as in 0.8 N sulfuric acid medium. The facts that $G(H_2)\fallingdotseq G_H+G_{H_2}$ appears to indicate the absence of the reaction (1).

We found that the reduction yield of the complex was almost independent of pH as shown in Table 1. This may be interpreted as the result of the direct attack of e_{aq}^- to the central cobalt(III) ion of the complex *via* reaction (2).

$$Co^{III}Y^- + e_{aq}^- \longrightarrow Co^{II}Y^{2-} \quad (2)$$

The evidence for the participation of the hydrated electrons in the reduction of the complex is provided by $G_\infty(N_2)$ and $G_\infty(-Co^{III}Y^-)$ from the irradiated Co^{III}-EDTA in deaerated solution at pH=4 in the presence of N_2O which is believed to convert the hydrated electron to radical OH by reaction (9).

$$N_2O + e_{aq}^- \xrightarrow{H_2O} N_2 + OH + OH^- \quad (9)$$

8) J. Rabani and M. S. Matheson, *J. Am. Chem. Soc.*, **86**, 3175 (1964).
9) S. Gordon, E. J. Hart, M. S. Matheson, J. Rabani and J. K. Thomas, *ibid.*, **85**, 1375 (1963).

TABLE 2. COMPARISON BETWEEN THE OBSERVED G VALUES AND THE CALCULATED G VALUES FROM POSTULATED MECHANISM AT pH=4.0

System	$G(-Co^{III}Y^-)$	$G(H_2)$
Co^{III}-EDTA	$G_{e_{aq}^-} + G_H + G_{OH} = 5.10$ (4.5)	$G_H + G_{H_2} = 1.00$ (0.8)
Co^{III}-EDTA + O_2	$G_{OH} = 2.25$ (1.8)	$G_{H_2} = 0.45$ (0.4)
Co^{III}-EDTA + N_2O	$G_{e_{aq}^-} + G_H + G_{OH} = 5.10$ (4.4)	$G_H + G_{H_2} = 1.00$ (0.8)

System	$G(H_2O_2)$	$G(N_2)$
Co^{III}-DTA	(0)	—
Co^{III}-EDTA + O_2	$G_{OH} + (G_{e_{aq}^-} + G_H)/2 = 2.14$ (2.1)	—
Co^{III}-EDTA + N_2O	—	$G_{e_{aq}^-} = 2.3$ (2.6)

( ) denotes the observed G values.

As shown in Table 1 $G_\infty(N_2)$ and $G_\infty(-Co^{III}Y^-)$ were 2.6 and 4.4, respectively and $G(-Co^{III}Y^-)$ was almost the same value regardless of the presence or absence of N_2O. This observation may be explained by the reduction of $Co^{III}Y^-$ to $Co^{II}Y'$ *via* reactions (5) and (4) by OH radicals from reaction (9), which supplements the decreases of the reaction (2).

In the radiolysis of Co^{III}-EDTA in deaerated 0.8 N sulfuric acid solution, hydrogen peroxide was not detected, probably because it is destroyed by H atoms through reaction (8).[4] The fact that hydrogen peroxide can neither be detected in higher pH region may be explained by invoking a similar reaction of hydrated electron with hydrogen peroxide (reaction (10)).[9,10]

$$H_2O_2 + e_{aq}^- \longrightarrow OH + OH^- \qquad (10)$$

If H atoms react quantitatively with hydrogen peroxide (reaction (8)) $G(H_2)$ observed should be equal to the primary hydrogen yield ($G_{H_2}=0.45$) from water.

From the above consideration, it may be concluded that all the reacting species (H, e_{aq}^- and OH) from water radiolysis contribute to the reduction of the complex. H atoms and OH radicals reduce the complex through the hydrogen abstraction from the ligand, while e_{aq}^- reduced the complex by direct attack of the central cobalt(III) ion.

Decomposition Mechanism in Aerated System. As seen in the radiolysis in the 0.8 N sulfuric acid medium not only H atoms but also hydrated electrons are scavenged by oxygen to form anion O_2^- by the reaction (11).

$$e_{aq}^- + H^+ + O_2 \longrightarrow HO_2 \rightleftarrows H^+ + O_2^- \qquad (11)$$

The anion O_2^- does not usually participate in the reduction of complex, because the radiolysis of the aerated solution gives much smaller $G_\infty(-Co^{III}Y^-)$ than in the deaerated one as shown in Table 1. The $G_\infty(H_2O_2)$ in the aerated solution is 2.1 as shown in Fig. 2, which may be explained if we assume one equivalent of O_2^- is consumed for producing half equivalent of hydrogen peroxide by reaction (12) without any reaction with Co^{III}-EDTA.[1]

$$O_2^- + O_2^- \longrightarrow H_2O_2 + 2OH^- \qquad (12)$$

It implies that in the aerated system only OH radicals decompose the complex by reactions (5) and (4) as in 0.8 N sulfuric acid.

The decomposition mechanism of Co^{III}-EDTA invoking the reactions described above are consistent with the obtained results in that it satisfies the stoichiometric relationship between observed G values and the primary radical and molecular yields (taking $G_H=0.55$, $G_{e_{aq}^-}=2.30$, $G_{OH}=2.25$, $G_{H_2O_2}=0.71$, $G_{H_2}=0.45$).[11] As shown in Table 2, our observed G value can be explained quantitatively using the primary radical and molecular yields from water, except $G(-Co^{III}Y^-)$ where small discrepancy between calculated G values from the mechanism and observed G values exists. Nevertheless the discrepancy would not affect greatly the essential part of the decomposition mechanism.

The authors express thanks to Professor Y. Yoshino and his co-workers for many useful discussions.

10) J. P. Keene, *Rad. Res.*, **22**, 1 (1964).
11) E. Hayon, *Trans. Faraday Soc.*, **61**, 723 (1965).

BULLETIN OF THE CHEMICAL SOCIETY OF JAPAN VOL. 41 1289—1295 (1968)

The Electronic and Vibrational Spectra of Oxalyl Bromide*[1]

Hiroko SHIMADA, Ryoichi SHIMADA and Yoshiya KANDA

Department of Chemistry, Faculty of Science, Kyushu University, Fukuoka

(Received December 15, 1967)

The infrared and Raman spectra of oxalyl bromide have been observed. The spectral features suggest that this molecule is planar and *trans* at room temperature. An assignment has been given for all the fundamental vibrational frequencies. The ultraviolet absorption spectrum of oxalyl bromide has been studied in cyclohexane and in the vapor. The spectrum consists of four absorption systems. These were ascribed to a $^3A_u(n, \pi^*)\leftarrow{}^1A_g$, a $^1A_u(n, \pi^*)\leftarrow{}^1A_g$, the second $^1A_u(n, \pi^*)\leftarrow{}^1A_g$ and a $^1B_u(\pi, \pi^*)\leftarrow{}^1A_g$ transitions, respectively. Vibrational analyses have been made for the $^3A_u(n, \pi^*)\leftarrow{}^1A_g$ and the first $^1A_u(n, \pi^*)\leftarrow{}^1A_g$ systems.

The infrared and Raman spectra of oxalyl chloride have been investigated by several workers.[1-4] Recently, Hencher and King[5] have shown that only the *trans*-form contributes to the observed spectra and given assignments for all the fundamental vibrational frequencies.

Saksena and Kagarise[6] have studied the near ultraviolet absorption spectrum of oxalyl chloride and found two $n\rightarrow\pi^*$ absorption systems in the 3800—2400 Å region. Sidman,[7] and Saksena and Jauhri[8] have also observed the absorption spectrum of the oxalyl chloride vapor and carried out a vibrational analysis for the first $n\rightarrow\pi^*$ system. Shimada and Kanda[9] have studied the T–S emission and absorption spectra of oxalyl chloride and ascribed these spectra to a $^3A_u(n, \pi^*)$–^1A_g transition.

Very few spectroscopic works have been reported for oxalyl bromide, although its molecular stucture is quite similar to that of oxalyl chloride. A weak absorption spectrum of oxalyl bromide in the 4300 Å region has been observed by Shimada and Kanda and it was ascribed to a $T(n, \pi^*)\leftarrow S$ transition.[10] This assigmnent was confirmed by Borkman and Kearns.[11] In the present investigation, the electronic and vibrational spectra of this molecule have been studied in continuation of a previous work.

Experimental

Oxalyl bromide was synthesized with oxalyl chloride and gaseous HBr, which was produced by dropping bromine on a mixture of red phosphorus, sand and water. The crude product was distilled and a fraction which boiled at 103°C was collected. The collected distillate, which still contained free bromine, was shaken with a small quantity of mercury. After the red color of bromine disappeared, the transparent liquid was decanted and fractionally distilled repeatedly. The purified oxalyl bromide was stored in an evacuated cell. The sample was prepared in a dry room just before the measurement, because oxalyl bromide reacts quite easily with water and decomposes into CO, CO_2 and HBr.[12]

The Raman spectrum of oxalyl bromide was studied at 20°C, 77°K and 4.2°K with a two-prism spectrograph described previously.[13] An aqueous solution of $K_2Cr_2O_7$ was used as a filter in order to eliminate exciting light shorter in wavelength than 5460 Å (Hg-c line). Concentration of the filter solution was 0.2% and the optical path was 1 cm. Exposure time ranged from 12 to 48 hr with a slit-width of 50μ and Eastman Kodak 103a-F plates. The slit was widened up to 300 μ for the low temperature measurement. The liquid sample was replaced with new one for every three hours, since prolonged strong irradiation decomposes oxalyl bromide[12] and turns the sample reddish brown. A Wollaston prism was used for the study of the depolarization factor.

The infrared spectrum of oxalyl bromide was studied in the crystal at 77°K, in the liquid at 20°C, in CCl_4 and CS_2 solutions at 20°C and in the vapor at various temperatures ranging from 20 to 200°C without

*1 Preliminary part of this paper was presented at the Proc. Intern. Symp. Mol. Struct. Spectry., Tokyo (1962).

1) B. D. Saksena and R. E. Kagarise, *J. Chem. Phys.*, **19**, 987 (1951).
2) R. E. Kagarise, *ibid.*, **21**, 1615 (1953).
3) J. S. Ziomek, A. G. Meister, F. F. Cleveland and C. E. Decker, *ibid.*, **21**, 90 (1953).
4) B. D. Saksena, R. E. Kagarise and D. H. Rank, *ibid.*, **21**, 1613 (1953).
5) J. L. Hencher and G. W. King, *J. Mol. Spectry.*, **16**, 158 (1965).
6) B. D. Saksena and R. E. Kagarise, *J. Chem. Phys.*, **19**, 999 (1951).
7) J. W. Sidman, *J. Am. Chem. Soc.*, **78**, 1527 (1956).
8) B. D. Saksena and G. S. Jauhri, *J. Chem. Phys.*, **36**, 2233 (1962).
9) H. Shimada, R. Shimada and Y. Kanda, *Spectrochim. Acta*, **23A**, 2821 (1967).
10) Y. Kanda, R. Shimada, H. Shimada, H. Kaseda and T. Matsumura, Proc. Intern. Symp. Mol. Struct. Spectry., Tokyo (1962).
11) R. F. Borkman and D. R. Kearns, *J. Chem. Phys.*, **46**, 2333 (1967).
12) H. Staudinger and E. Anthes, *Ber.*, **46**, 1426 (1913).
13) M. Ito, *J. Chem. Phys.*, **41**, 1255 (1964).

altering the total number of molecules in the vapor cell with a Hitachi Infrared Spectrophotometer, type EPI-2. Since oxalyl bromide is not stable at high temperature,[12] the vapor cell was heated rapidly up to an appropriate temperature and the spectrum was scanned very quickly. The sample was replaced with new one for every run. The cell thickness was 10 cm for the vapor and 0.1 cm for solutions. A thin layer sample was used for studying the liquid phase. The spectrum of the crystal at 77°K was observed in the same way as described previously.[14]

The ultraviolet absorption spectrum was observed in cyclohexane solution at 20°C with a Hitachi Recording Spectrophotometer, type EPS-3, and in the vapor with a Shimadzu Large Quartz Spectrograph, type QL-170. Vapor pressure of oxalyl bromide in a vapor cell of 40 cm in length was controlled by changing the temperature of the cell from −20 to 50°C. A 1 m vapor cell was used for the observation of the T←S absorption. The vapor spectrum was also studied at various temperatures ranging from 20 to 200°C with keeping the total number of molecules constant in the cell. The same care was taken to prevent the sample from decomposition by heating as that taken for the infrared spectrum.

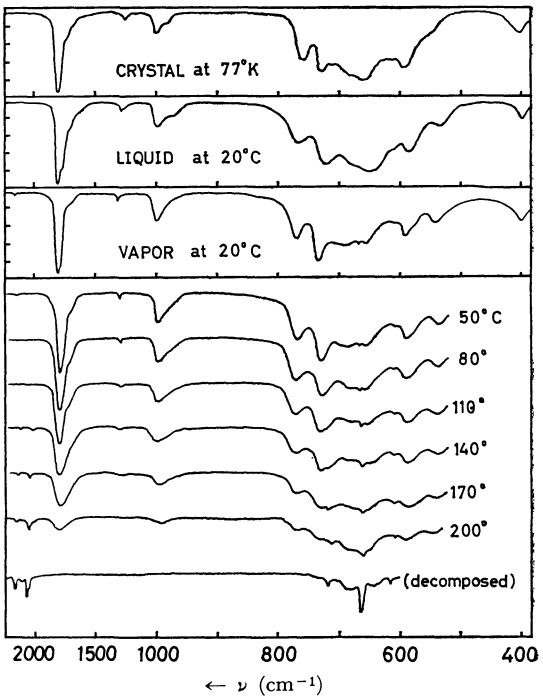

Fig. 1. Infrared spectrum of oxalyl bromide.
Upper half: in various phases.
Lower half: at various temperatures in the vapor phase.

Results and Discussion

Rotational Isomerism. Since oxalyl bromide contains two CoBr groups connected with a C–C bond, one can expect the existence of rotational isomers, that is, *trans*-, *cis*- and *staggered*-isomers. Among them, the first isomer is expected to be most stable, because (1) the resonance energy of π-electrons is greater in the *trans*- and *cis*-isomers than in the *staggered*-isomer, (2) the electrostatic potential is lower in the *trans*-isomer than in the *cis*-isomer, and

Table 1. Vibrational analysis of the infrared spectrum of oxalyl bromide

Crystal (77°K) ν, cm⁻¹	Liquid (20°C) ν, cm⁻¹	Solution (20°C) ν, cm⁻¹	Vapor (20°C) ν, cm⁻¹	Assignment
405 w	405 w	405 w	405 w	ν_{11} (b_u) COBr scissoring
	540 w	535 w	545 w	$\nu_{10}-\nu_5$
594 m	592 m	588 m	595 m	$\nu_5+\nu_{11}$
664 s br	660 s br	656 s br	661 m	$\nu_4+\nu_6$
			670 m	CO_2
685 m br	690 m br	690 m br	690 m br	$\nu_5+\nu_7+\nu_8$ or $\nu_7+\nu_{11}+\nu_{12}$
714 vw				CO_2
729 s	728 s	728 s	731 s	ν_{10} (b_u) C-Br stretching
762 m	772 m	770 m	773 m	$\nu_3+\nu_{12}$
980 vw sh	975 vw sh	972 vw sh		$\nu_3+\nu_8$
1013 m	1004 m	1002 m	1007 m	$\nu_3+\nu_{11}$
1290 w	1295 w	1302 w	1324 w	$\nu_3+\nu_{10}$
1720 vw	1723 vw	1725 vw	1733 vw	$\nu_3+\nu_4+\nu_{10}$
	1780 w sh	1785 m sh		$\nu_2+\nu_{10}$?
1815 vs	1807 vs	1807 vs	1818 vs	ν_9 (b_u) C=O stretching

s: strong, m: medium, w: weak, v: very, sh: shoulder, br: broad

14) T. Omori and Y. Kanda, *Mem. Fac. Sci. Kyushu Univ. Ser. C*, **6**, 29 (1967).

(3) the steric repulsion between the Br and O atoms is smaller than that between the two Br atoms.

In order to seek the possible evidences for the existence of rotational isomers in oxalyl bromide, we studied the temperature dependences of the Raman, infrared and ultraviolet absorption spectra of this molecule. The infrared spectra observed in various phases and at various temperatures are shown in Fig. 1 and the spectral data are given in Table 1. The Raman spectral datum observed in the liquid is given in Table 2. The observation of the Raman spectrum of the oxalyl bromide crystal was unsuccessful owing to quite weak scattering from the crystal and only a few bands were obtained. These are given in Table 2. The temperature dependence of the ultraviolet absorption spectrum is shown in the upper right of Fig. 3. It can be seen from these figures and tables that:

(1) Each band in the infrared spectrum observed in the vapor becomes broader with increasing temperature but the essential spectral structure remains unchanged except for a few bands which increase in intensity at high temperature and become quite prominent in the spectrum at 200°C. The infrared spectrum of the "oxalyl bromide"

Table 2. Vibrational analysis of the Raman spectrum of oxalyl bromide

Liquid (20°C)			Crystal (77°K)	Crystal (4.2°K)	Assignment
ν, cm^{-1}	Rel. int.	Pol.	ν, cm^{-1}	ν, cm^{-1}	
137	2				$\nu_8-2\nu_7$?
191	8	p	193		ν_5 (a_g) COBr rocking
246	1				$2\nu_7$ (ν_7: COBr twisting)
342	2 (sh)				$2\nu_{12}$ (ν_{12} : COBr rocking)
376	6	dp	364	363	ν_8 (b_g) COBr wagging
415	4	p			ν_4 (a_g) COBr scissoring
494	1				$2\nu_6$ (ν_6 : COBr wagging)
600	7	p	586	587	ν_3 (a_g) C-Br stretching
808	3	p ?			$2\nu_{11}$
870	3				$2\nu_6+\nu_8$?
1032	4	p			ν_2 (a_g) C-C stretching
1784	10	p	1754	1752	ν_1 (a_g) C=O stretching

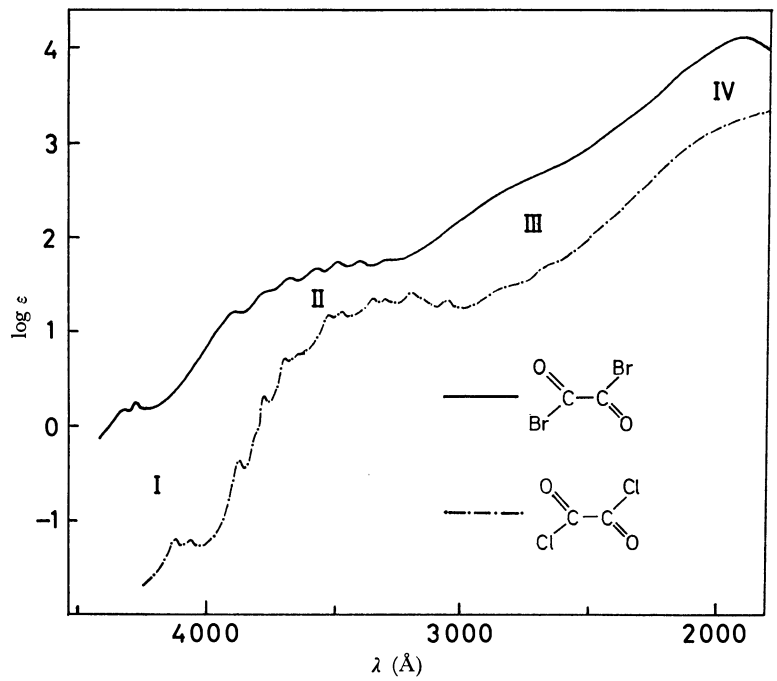

Fig. 2. Ultraviolet absorption spectra of oxalyl bromide and chloride in cyclohexane at room temperature.

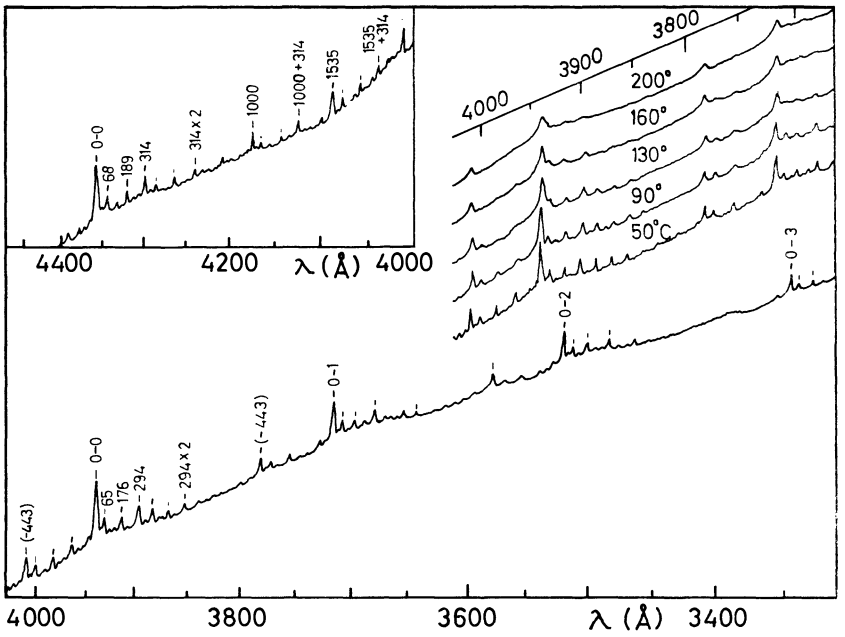

Fig. 3. Near ultraviolet absorption spectrum of the oxalyl bromide vapor.

vapor which was kept at about 220°C for about one hour and then cooled at room temperature is given in the bottom of Fig. 1. This spectrum consists of a few bands which coincide with the unusual bands observed in the high temperature spectrum. These frequencies are 2350, 2155, 2080, 720, 668 and 616 cm^{-1}. The 2155 cm^{-1} band is ascribed to the CO gas[15] and the others to the CO_2 gas.[16]

(2) There are no essential structural differences in the infrared spectra observed in various phases except for the bands at about 540, 660, 714, 975 and 1780 cm^{-1}. The 540 cm^{-1} band is assigned to a difference band and this must be diminished at low temperature. The 660 cm^{-1} band, whose intensity is fairly strong in the condensed phases, is ascribed to an unresolved band of 662 and 667 cm^{-1}. The 667 cm^{-1} band and the 714 cm^{-1} band, which is observed in the crystal, are ascribed to CO_2, because slight bubbling of oxalyl bromide was inevitable during the preparation of the sample. The weak 975 cm^{-1} band, which is not observed in the vapor, is assigned to an infrared inactive band which appears in the spectrum through perturbation by the medium.

(3) A mutual exclusion relationship is found between the infrared and Raman spectra except for the strongest Raman band at 1784 cm^{-1}. The same vibrational frequency was also observed in the infrared spectrum as a shoulder of the strongest band at 1807 cm^{-1} in the liquid and solutions, but this was not observed in the crystal nor in the vapor even at high temperature. This band is assigned to an infrared active band and will be discussed in the next section.

(4) The behavior of the temperature dependence of the ultraviolet absorption spectrum of the oxalyl bromide vapor is the same as that observed in the oxalyl chloride vapor by Sidman.[7] Although the spectral structure remains unchanged, the absorption bands, which are very sharp at room temperature, become broader and decrease in intensity with increasing temperature. At higher temperature, the discrete bands are superimposed on a continuous background and this background increases in intensity with increasing temperature. This phenomenon is reversible if heating does not exceed 130°C. Heating of the oxalyl bromide vapor above 130°C does not change the spectral structure when the sample is cooled at room temperature again, but the absorption decreases in intensity owing to the decomposition of the sample.

These experimental facts indicate that only one isomer contributes to the observed discrete spectral bands and thus it can immediately be concluded that the discrete band spectra are due to the *trans*-isomer of oxalyl bromide. A careful observation of the ultraviolet absorption spectrum of the oxalyl bromide vapor showed that the continuous background, which was assigned to the *cis*-form by Sidman,[7] was hardly detectable at room temperature. This indicates that the oxalyl bromide molecule is planar and *trans* at room temperature.

15) G. Herzberg, "Molecular Spectra and Molecular Structure. I. Spectra of Diatomic Molecules," D. Van Nostrand Company, New York (1950), p. 62.
16) G. Herzberg, "Molecular Spectra and Molecular Structure. II. Infrared and Raman Spectra of Polyatomic Molecules," D. Van Nostrand Company, New York (1949), p. 272.

Vibrational Spectrum and Assignments. For the *trans*-form of oxalyl bromide (C_{2h} point group), the twelve fundamental vibrations are classified into four symmetry species, that is, 5 vibrations into a_g species, 1 into b_g, 2 into a_u and 4 into b_u. The first six fundamentals are Raman active and the last six are infrared active.

The observed strong and polarized Raman bands of 191, 415, 600, 1032 and 1784 cm^{-1}*2 are straightforwardly assigned to totally symmetric COBr rocking ν_5, COBr scissoring ν_4, C–Br stretching ν_3, C–C stretching ν_2 and C=O stretching ν_1 vibrations, respectively and the strong and depolarized Raman band of 376 cm^{-1} to a COBr wagging vibration ν_8 of b_g species.

The strong infrared bands of 728 and 1807 cm^{-1} are assigned to a C–Br stretching vibration ν_{10} and a C=O stretching vibration ν_9, both are of b_u species, respectively. A weak infrared band around 405 cm^{-1}, whose intensity could not precisely be measured because of poor reliability of our spectrophotometer in this region, can be assigned to a COBr scissoring vibration ν_{11} of b_u species. The medium strong Raman band of 808 cm^{-1}, which seems to be polarized, and the medium infrared bands of 592 and 1004 cm^{-1} can be interpreted as an overtone vibration of ν_{11} and combination vibrations of $\nu_5+\nu_{11}$ and $\nu_3+\nu_{11}$, respectively.

The remaining three fundamentals, that is, a COBr rocking vibration ν_{12} of b_u species, a COBr wagging vibration ν_6 of a_u species and a COBr twisting vibration ν_7 of a_u species are expected to appear in the lower frequency region than 400 cm^{-1}, which is the limit of measurement with our spectrophotometer. The weak Raman bands of 246, 342 and 494 cm^{-1} were presumed to be assigned to overtone vibrations of ν_7, ν_{12}, and ν_6, respectively. The medium infrared bands of 662 (a component of the unresolved 660 cm^{-1} band), 690 and 772 cm^{-1} could be interpreted as combination vibrations of $\nu_4+\nu_6$, $\nu_5+\nu_7+\nu_8$ (or $\nu_7+\nu_{11}+\nu_{12}$) and $\nu_3+\nu_{12}$, respectively.

The weak but distinct infrared band of 1780 cm^{-1} is rather puzzling. This band was assigned to a combination vibration of $\nu_2+\nu_{10}$, but it cannot be understood why this band is not observed in the crystal nor in the vapor. Detailed analyses of the infrared and Raman spectra are given in Tables 1 and 2.

Ultraviolet Absorption Spectrum. *Assignment of the Electronic Transitions.* The ultraviolet absorption spectrum of oxalyl bromide in cyclohexane is given in Fig. 2 together with that of oxalyl chloride. The spectrum consists of four absorption systems, which will be called here system I, II, III and IV.

The system I appears in the longest wavelength region and its absorption maximum is located at 4276 Å with $\varepsilon=2.0$ in cyclohexane. We observed the corresponding absorption system of oxalyl chloride in the 4100 Å region with $\varepsilon_{max}=0.07$ and ascribed it to a $^3A_u(n, \pi^*)\leftarrow{}^1A_g$ transition on the basis of a vibrational analysis and the lifetime of the corresponding emission spectrum.[9] Comparing these two absorption spectra with one another, the system I has to be assigned to the same T←S transition as that of oxalyl chloride. A vibrational analysis of this system in the vapor spectrum, which will be described later, indicates that the transition has an allowed $n\rightarrow\pi^*$ character. This fact also supports the $^3A_u\leftarrow{}^1A_g$ assignment given to this system.

We tried to observe the T→S emission of oxalyl bromide but it was too weak to be measured in any solvent. Recently, Borkman and Kearns[11] studied the phosphorescence excitation spectrum of oxalyl bromide in rigid glass solutions containing naphthalene or phenanthrene and confirmed this assignment.

The $f_{T\leftarrow S}$-value observed in cyclohexane solution is 3.0×10^{-6}. This is unusually large for a multiplicity forbidden transition.[17]

The system II which appears in the 4000—3200 Å region with $\varepsilon_{max}=50$ is ascribed to a $^1A_u(n, \pi^*)\leftarrow{}^1A_g$ transition on the analogy of the corresponding absorption system of oxalyl chloride.[6] We observed the rotational spectrum of the 0–0 band of this system under high resolution condition and found that this band has a typical parallel type structure. This fact indicates that the transition moment of the 0–0 band is perpendicular to the molecular plane and this definitely confirms the above assignment. A detailed report on the rotational spectrum will be given elsewhere. The f-value observed in cyclohexane is 7×10^{-4}.

The system III which appears in the 3000—2500 Å region with $\varepsilon\approx500$ is very diffuse and was attributed to the second $^1A_u(n, \pi^*)\leftarrow{}^1A_g$ transition by analogy with the assignment given for the corresponding absorption system of oxalyl chloride.[6]

The onset of the system IV overlaps on a tail of the system III and a broad absorption appears to the shorter wavelengths with increasing intensity. Although the exact absorption maximum was not determined because of poor reliability of our spectrophotometer in this region, the apparent maximum is located around 1900 Å with $\varepsilon\approx10^4$. Sidman[18] calculated the energy of the first $^1B_u(\pi, \pi^*)\leftarrow{}^1A_g$ transition in glyoxal and obtained 7.4 eV for this energy, which corresponds to about 1680 Å. From the very strong intensity of this system and the general prediction that a bromine substitution causes a red shift for a $\pi\rightarrow\pi^*$ transition, we ascribed this system to a $^1B_u(\pi, \pi^*)\leftarrow{}^1A_g$

*2 The Raman and infrared frequencies observed in the liquid at room temperature are used in this discussion.

17) H. Shimada and Y. Kanda, This Bulletin, **40**, 2742 (1967).

18) J. W. Sidman, *J. Chem. Phys.*, **27**, 429 (1957).

TABLE 3. VIBRATIONAL ANALYSIS OF THE ULTRAVIOLET ABSORPTION SPECTRUM OF THE OXALYL BROMIDE VAPOR

ν, cm^{-1}	Assignment	ν, cm^{-1}	Assignment
22760 w	A−183	25615 m	
22828 w		25667 s	B+294
22916 vw		25735 m	B+294+65
22943 m	0-0 of the T←S(A)	25796 w	
22975 vw		25847 m	B+294+176
23011 w	A+68	25963 m	B+294×2
23074 vw	A+314−183	25994 w	
23132 w	A+189	26190 w	
23193 w		26433 w	
23226 w		26465 s	B+1537−443
23257 m	A+314	26498 w	
23297 vw		26532 m	B+1537−443+65
23320 vw	A+314+68	26568 w	
23414 vw		26640 m	B+1537−443+176
23440 w	A+314+189	26725 w	B+1537−180
23505 vw		26840 w	
23545 vw		26910 vs	B+1537
23573 w	A+314×2	26940 w	
23606 vw		26975 s	B+1537+65
23650 vw	A+314×2+68	27014 w	
23670 vw		27081 m	B+1537+176
23760 vw	A+1000−183	27146 w	
23792 vw		27206 s	B+1537+294
23825 vw		27274 w	B+1537+294+65
23943 w	A+1000	27377 m	B+1537+294+176
23970 vw		27856 w	
24010 vw	A+1000+68	27970 m	B+1537×2−443
24042 vw		27980 w	
24208 vw		28234 w	B+1537×2−180
24258 w	A+1000+314	28353 w	
24295 vw	A+1535−183	28410 s	B+1537×2
24325 vw		28445 w	
24452 vw		28473 m	B+1537×2+65
24478 m	A+1535	28587 m	B+1537×2+176
24512 vw		28655 w	
24608 vw		28714 m	B+1537×2+294
24664 vw	A+1535+189	28780 w	B+1537×2+294+65
24790 vw	A+1535+314	28888 w	B+1537×2+294+176
24857 vw		28960 vw	
24930 s	B−443	29013 w	B+1537×2+294×2
24995 m	B−443+65	29838 w	
25096 w		29890 s	B+1537×3
25113 w	B−443+176	29925 vw	
25135 w		29955 m	B+1537×3+65
25193 w	B−180	30069 m	B+1537×3+176
25227 m	B−443+294	30112 w	
25325 vw		30136 w	
25373 vs	0-0 of the S'←S(B)	30191 m	B+1537×3+294
25408 w		30257 vw	
25438 s	B+65	31347 m	B+1537×4
25470 w		31537 vw	
25549 m	B+176		

s : strong, m : medium, w : weak, v : very

transition.

Vibrational Analysis of the Absorption Spectrum. The absorption spectrum of the oxalyl bormide vapor due to the first $^1A_u(n, \pi^*) \leftarrow {}^1A_g$ transition consists of a number of sharp bands and its spectral structure quite resembles to that of oxalyl chloride.[7] The spectrum and the spectral data for this system are shown in Fig. 3 and Table 3, respectively.

The strongest band at 25373 cm^{-1} was taken as the 0–0 band of this system. The prominent feature of the spectrum is the interval of 1537 cm^{-1}, which produces a main progression starting from the 0–0 band. This frequency can be assigned to the totally symmetric C–O stretching vibration ν_1 in the excited state.

The next prominent feature is the interval of 443 cm^{-1} which appears in the longer wavelength side of the individual bands of the main progression. Temperature dependence of the 24930 cm^{-1} band, which is separated by 443 cm^{-1} from the 0–0 band, clearly shows a characteristic behavior of a hot band (see Fig. 3). We therefore, assigned the interval of 443 cm^{-1} to the ground state frequency of ν_4. The corresponding Raman frequency observed in the liquid is 415 cm^{-1}. The discrepancy between two frequencies is fairly large. The similar frequency shifts were also observed in the Raman spectrum by changing the phase from the liquid to the crystal (see Table 2). These observations may suggest that the modes of these vibrations are sensitive to a change of the phase in this molecule. The band at 26,465 cm^{-1} is separated by 445 cm^{-1} from the 0–1 band and by 1092 cm^{-1} from the 0–0 band. Although the interval of 1092 cm^{-1} might be assigned to the excited state frequency of the totally symmetric C–C stretching vibration ν_2, the behavior of the temperature dependence of the 26465 cm^{-1} band is the same as that of the 24930 cm^{-1} band. This fact denies the ν_2 assignment.

There are another prominent interval of 294 cm^{-1} which appears in the shorter wavelength side of the individual bands of the main progression. This interval very probably corresponds to the excited state frequency of ν_4, because the band structure of the 294 cm^{-1} band resembles to that of the 443 cm^{-1} band and the overtone of this frequency is also observed in the spectrum. Other intervals of 65 and 176 cm^{-1} are also quite prominent. All strong bands mentioned above are accompanied by these two subbands in their shorter wavelength side.

The absorption spectrum of the oxalyl bromide vapor due to the $^3A_u(n, \pi^*) \leftarrow {}^1A_g$ transition consists of a number of sharp bands. A microphotometer tracing of the spectrum and the spectral data are presented in the upper left of Fig. 3 and Table 3, respectively. The spectral structure is quite similar to that of the $^1A_u(n, \pi^*) \leftarrow {}^1A_g$ absorption system.

The strongest band at 22943 cm^{-1} was taken as the 0–0 band of this system. The totally symmetric C–O stretching vibration seems to constitute a main progression, but the tail of this system overlaps on the onset of the strong S′←S absorption system and, therefore, only one quantum of this vibration could be observed. A strong band at 24478 cm^{-1}, which is separated by 1535 cm^{-1} from the 0–0 band, is the first member of this progression. There is a sharp and distinct band at 23943 cm^{-1}, which is separated by 1000 cm^{-1} from the 0–0 band and by 535 cm^{-1} from the 0–1 band. The interval of 1000 cm^{-1} was assigned to the triplet state frequency of the C–C stretching vibration ν_2, because the interval of 535 cm^{-1} is too large to be assigned to the ground state frequency of ν_4. There are prominent intervals of 68, 189 and 314 cm^{-1} which appear in the shorter wavelength side of three strong bands mentioned above. The interval of 314 cm^{-1} very probably corresponds to the triplet state frequency of ν_4.

The fact that the spectral structure of this system quite resembles to that of the first $^1A_u(n, \pi^*) \leftarrow {}^1A_g$ absorption system (see Fig. 3) suggests that the system I is caused by an $n \rightarrow \pi^*$ promotion. The allowed $n \rightarrow \pi^*$ character of this transition definitely indicates that the triplet state involved in this transition is a $^3A_u(n, \pi^*)$ state.

Detailed vibrational analyses of both the systems I and II are given in Table 3.

The authors indebted to the Ministry of Education for grants-in-aid out of the Scientific Research Expenditure.

BULLETIN OF THE CHEMICAL SOCIETY OF JAPAN VOL. 41 1296—1301 (1968)

Studies of Poly-2-vinylpyridine. VI. Thermodynamic Data on Solutions of Poly-2-vinylpyridine in Various Solvents

Shizuo ARICHI

Department of Chemistry, Faculty of Science, Kumamoto University, Kurokami-machi, Kumamoto

and Yoshio TANIMOTO and Hiromu MURATA

Department of Chemistry, Faculty of Science, Hiroshima University, Higashisenda-machi, Hiroshima

(Received December 18, 1967)

The viscosities of dilute solutions of several fractions of poly-2-vinylpyridine have been measured in methanol, isopropanol, chloroform, benzene, dioxane, and methyl ethyl ketone at different temperatures, ranging from 15 to 65°C. The osmotic pressures of dilute solutions of fractions of the polymer have been measured in dioxane at 10, 25, 40, and 65°C. The data have then been analysed using the theories of Flory and Fox and of Kurata and Stockmayer. The results obtained are as follows: (1) the entropy parameters, ψ_1, for the solutions of poly-2-vinylpyridine in methanol and isopropanol are negative, while the critical miscibility temperatures, θ, are positive and extraordinary high; (2) ψ_1 is positive and θ is negative in chloroform; (3) These parameters behave regularly in benzene and dioxane. Qualitatively the same results have also been obtained with the poly-4-vinylpyridine fraction in several solvents, including methanol and chloroform. These results show that in alcohols and chloroform the temperature coefficient of the solubility of polyvinylpyridines is negative, and indicate the presence of strong interaction between segments and solvents, probably due to hydrogen-bond formation.

In the preceding paper[1] some properties of poly-2-vinylpyridine solution in ethanol have been described: the entropy parameter, ψ_1, from the viscosity data is negative; the critical consolute temperature, θ, from the same data is extraordinary high, and both the heat and the entropy of dilution obtained from the data of osmotic pressure are negative. It has been concluded that these peculiarities may be the result of the strong interaction between the segment and solvent itself, probably because of the hydrogen-bond formation between the nitrogen atom in the pyridine ring and the hydroxyl group in the solvent molecule.

The same results have been reported for the poly-4-vinylpyridine-*t*-butanol-benzene system[2] and the polyacrylic acid - dioxane system.[3] The negative value of ψ_1 has also been reported for the polymethacrylonitril - methyl ethyl ketone system.[4] However, the reports on such peculiar properties are very limited, and it is considered to be important to confirm the conclusions of the preceding paper by performing similar experiments in other acidic solvents which are capable of hydrogen-bond formation, and also in neutral or basic solvents which are not. In this report, thermodynamic data on poly-2-vinylpyridine solutions in methanol, isopropanol, and chloroform, and on such solutions in benzene, dioxane and methyl ethyl ketone as slovents of the latter category are presented. The results of complementary experiments on poly-4-vinylpyridine in several solvents will also be described.

Experimental

The fractions of poly-2-vinylpyridine, E-2, K-2, and C-1, were the same as those used in a previous study.[5] The unfractionated poly-2-vinylpyridine, $2U_0$, was obtained by block polymerization in a sealed tube at 60°C, and was purified by repeated precipitations in methyl ethyl ketone by addition of ligroin.

Poly-4-vinylpyridine was prepared by the suspension method.[6] Thirty-five grams of the polymer were fractionated into 8 fractions by the column-elusion method. The fourth fraction, 4F-4, was used in this study.

The intrinsic viscosity and osmotic pressure were measured by the methods described in a previous paper.[1] The solvents were dried and fractionally distilled according to usual methods.[7]

1) S. Arichi, This Bulletin, **41**, 548 (1968).
2) A. G. Boyes and U. P. Strauss, *J. Polymer Sci.*, **22**, 463 (1956).
3) S. Newman, W. R. Krigbaum, C. Laugier and P. J. Flory, *ibid.*, **14**, 451 (1954).
4) H. Morawetz, "Macromolecules in Solution," Interscience Publishers, Inc., New York (1965).
5) S. Arichi, This Bulletin, **39**, 439 (1966).
6) J. B. Berkowitz, M. Yamin and R. M. Fuoss, *J. Polymer Sci.*, **28**, 69 (1958).
7) A. Weissberger, E. S. Proskauer, J. A. Riddick and E. E. Toops, Jr., "Organic Solvents," Interscience Publishers, Inc., New York (1955).

Results

Temperature Variation of the Intrinsic Viscosity. The intrinsic viscosities of the solutions of the poly-2-vinylpyridine fraction, E-2, in methanol, isopropanol, and chloroform; those of the K-2 fraction in benzene, dioxane, and methyl ethyl ketone, and those of $2U_0$ in methanol at various temperatures are shown in Table 1. The experimental results for the poly-4-vinylpyridine fraction, 4F-4, in methanol, isopropanol, chloroform, and pyridine are summarized in Table 2.

The relations between the intrinsic viscosities and the temperature for poly-2-vinylpyridine fractions in various solvents are shown in Fig. 1, and those for the poly-4-vinylpyridine fractions, in Fig. 2.

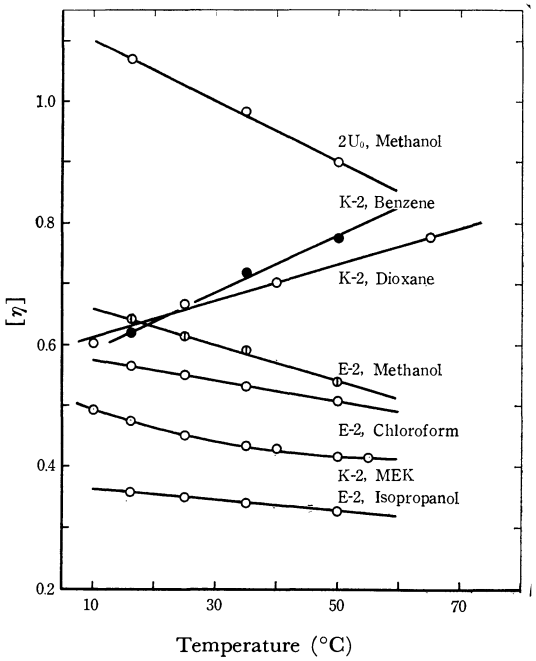

Fig. 1. Plots of the intrinsic viscosities of poly-2-vinylpyridine fractions in various solvents *vs.* temperature.

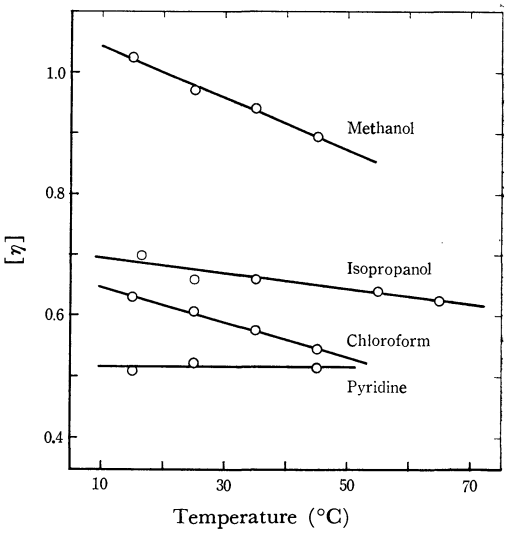

Fig. 2. Plots of the intrinsic viscosities of poly-4-vinylpyridine fractions *vs.* temperature.

Table 1. The intrinsic viscosities of poly-2-vinylpyridine fractions in various solvents at different temperatures

Fraction	Solvent	[η] Temperature (°C)						
		10	16.2	25	35	40	50	65
E-2	Methanol		0.640	0.614	0.583		0.540	
$2U_0$	Methanol		1.068		0.982		0.901	
E-2	Chloroform		0.566	0.549	0.531		0.510	
E-2	Isopropanol		0.358	0.349	0.344		0.328	
K-2	Benzene		0.620		0.719		0.775	
K-2	Dioxane	0.601		0.668		0.701		0.701
K-2	MEK	0.495	0.479	0.452	0.434	0.430	0.415	

Table 2. The intrinsic viscosities of poly-4-vinylpyridine fractions in various solvents at different temperatures

Fraction	Solvent	[η] Temperature (°C)						
		15	16.5	25	35	45	50	65
4F-4	Methanol	1.025		0.970	0.942	0.895		
4F-4	Chloroform	0.630		0.606	0.575	0.545		
4F-4	Isopropanol		0.700	0.660	0.660		0.640	0.625
4F-4	Pyridine	0.510		0.522		0.515		

As may be seen in these figures, the temperature coefficients of the intrinsic viscosities of both poly-2-vinylpyridine and poly-4-vinylpyridine fractions in methanol, isopropanol and chloroform are negative, as are those of poly-2-vinylpyridine[1] and poly-4-vinylpyridine[6] in ethanol. On the contrary, the coefficients are positive or almost zero in the case of neutral or basic solvents, such as benzene and pyridine, as is usual in a nonpolar polymer - nonpolar solvent system. Methyl ethyl ketone is a typical basic solvent,[8] but the temperature coefficient for the system of poly-2-vinylpyridine-methyl ethyl ketone is rather negative.

Although the results shown in Figs. 1 and 2 seem to support our previous conclusion[1,8] that, for polyvinylpyridine, acidic solvents are good solvents and neutral or basic solvents, poor solvents, further examinations were made by analysing the data using the Flory-Fox[9] and Kurata-Stockmayer[10] theories.

As is well known, the thermodynamic interactions between polymer segments and solvent molecules are represented by the following equations, (1) and (2), given by Flory and Fox[9] and by Kurata and Stockmayer[10] respectively:

$$(K_T/K_0)(\alpha_\eta^5-\alpha_\eta^3)/M^{1/2} = 2C_M\psi_1(1-\theta/T) \quad (1)$$

$$(K_T/K_0)(1-\alpha_\eta^{-2})(\alpha_\eta^2+1/3)^{3/2}/M^{1/2} = (3^5/2^3)1.10C_M\psi_1(1-\theta/T) \quad (2)$$

where the symbols are the same as those used in the previous paper.[1]

It has been reported[1] that the value of the Flory constant, K, for poly-2-vinylpyridine, as estimated from the intrinsic viscosity data in ethanol, is considerably larger than those in the neutral or basic solvents. Now, let us suppose that the values of the Flory constant, K_i, for the samples of poly-2-vinylpyridine with a homogeneous molecular weight in methanol and chloroform are the same as those in ethanol at a certain temperature,[1] and that those in neutral or basic solvents are all equal to the value[11] of 8.2×10^{-4}, regardless of the temperature and the kind of solvent. As for isopropanol, it has already been pointed out that, because of the steric hindrance, the interaction between this solvent and the nitrogen atom in the pyridine ring of poly-2-vinylpyridine is relatively small compared with that in other primary alcohols.[8] In fact, the values of the intrinsic viscosity in isopropanol in this study are very small. Consequently, it was supposed that the value of K_i for this solvent is nearly equal to that of the neutral solvent: 8.2×10^{-4}.

Using the following equations,[10] the values of K_w were calculated, assuming that the molecular-weight distribution for each polymer fraction is represented by the exponential-type molecular-weight distribution function:[12]

$$K_w = K_i q_w \quad (3)$$

$$q_w = \Gamma(h+1.5)/(h+1)^{1/2}\Gamma(h+1) \quad (4)$$

where h is the parameter of the molecular-weight inhomogeneity and is defined by the following equation:

$$M_w/M_n = (h+1)/h \quad (5)$$

The values of K_w thus calculated are shown in Table 3.

TABLE 3. THE VALUES OF K USED FOR CALCULATION OF EQS. (1) AND (2)

Fraction	$M_w\times10^{-4}$	$M_n\times10^{-4}$	M_w/M_n	q_w
E-2	12.01	7.42	1.62	0.955
K-2	52.06	18.07	2.88	0.924

For methanol and chloroform solutions

Temp. (°C)	$K_i\times10^4$ a)	$K_w\times10^4$	
		E-2	K-2
10	13.7	13.1	12.7
25	13.0	12.4	12.0
40	12.2	11.7	11.3
65	11.5	11.0	10.6

For benzene, dioxane, methyl ethyl ketone and isopropanol solutions

Temp. (°C)	$K_i\times10^4$ b)	$K_w\times10^4$	
		E-2	K-2
10—65	8.20	7.83	7.58

a) The values from Ref. 1.
b) The value from Ref. 2.

The values of α_η were calculated by inserting the values of $[\eta]$, K_w, and M_w into the following equation:[9]

$$\alpha_\eta^3 = [\eta]/K_w M_w^{1/2} \quad (6)$$

Plots of the left-hand side of Eq. (1) for data of the intrinsic viscosity of poly-2-vinylpyridine in various solvents against the reciprocal temperature, $1/T$, are shown in Fig. 3, and those for Eq. (2) are shown in Fig. 4. These figures show the relation to be linear for all the solvents used. The slopes of the lines for benzene and dioxane are normal, while those for the other solvents are negative, in contrast to the case with ordinary polymer-solvent systems.

8) S. Arichi, H. Matsuura, Y. Tanimoto and H. Murata, This Bulletin, **39**, 434 (1966).
9) P. J. Flory and T. G. Fox, *J. Am. Chem. Soc.*, **73**, 1904 (1951).
10) M. Kurata and W. H. Stockmayer, *Fortschr. Hochpolymer. Forsch.*, **3**, 196 (1963).
11) S. Arichi, *J. Sci. Hiroshima Univ., Ser.* **A-II**, **29**, 97 (1965).
12) S. Arichi, S. Mitsuta, N. Sakamoto and H. Murata, This Bulletin, **39**, 428 (1966).

Table 4. Thermodynamic data, ψ_1 and θ, estimated from the data of temperature variation of the intrinsic viscosity and the osmotic second virial coefficient, A_2

Solvent	θ (°K)			ψ_1		
	From A_2	From $[\eta]$		From A_2	From $[\eta]$	
		Eq. (1)	Eq. (2)		Eq. (1)	Eq. (2)
Methanol		482.8	450.0		−0.03	−0.02
Chloroform		−297.4	−173.9		0.01	0.01
Isopropanol		443.2	412.6		−0.03	−0.02
Benzene		275.4	278.8		0.07	0.04
Dioxane	268.9	267.6	272.5	0.28	0.05	0.03
MEK		258.9	249.3		−0.04	−0.01

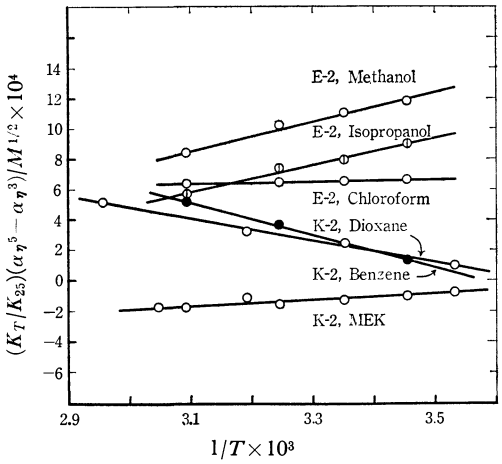

Fig. 3. Plots of the left hand side of Flory-Fox equation, Eq. (1), *vs.* the reciprocal temperature.

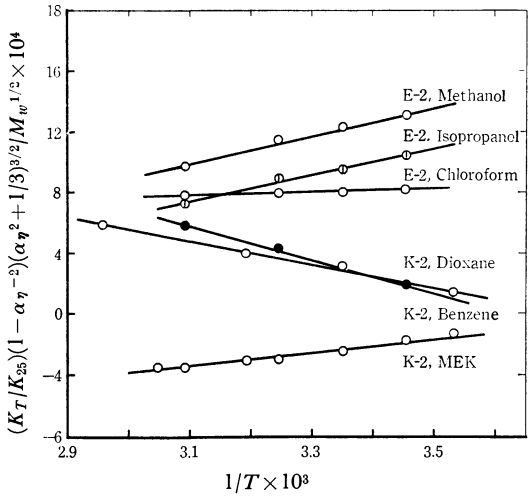

Fig. 4. Plots of the left hand side of Kurata-Stockmayer equation, Eq. (2), *vs.* the reciprocal temperature.

The equations of the linear lines in Figs. 3 and 4 were obtained by the least-square method; the values of the thermodynamic parameters, ψ_1 and θ, were calculated to be as shown in Table 4.

Thermodynamic Interaction Parameters Obtained from the Temperature Dependence of the Osmotic Pressure. The thermodynamic interaction parameters were estimated from the measurement of the temperature variation of the osmotic second virial coefficient, A_2. According to the Flory theory,[13] the relation between A_2 and T is shown by the following equation:

$$A_2 = (\bar{v}^2/V_1)\psi_1(1-\theta/T)F(X) \qquad (7)$$

where $\bar{v}$ is the specific volume of the polymer, and V_1, the molar volume of the solvent; $F(X)$ depends mainly on the thermodynamic interaction parameters but also partly on the molecular weight of the polymer and on the temperature, but at the temperature of θ, $F(X)$ takes a definite value of 1.

In order to compare the data on the intrinsic viscosity with those on osmotic pressure, measurements were carried out for solutions of the C-1 fraction in methanol, chloroform, and dioxane and for a solution of the F-2-3 fraction in methyl ethyl ketone. Unfortunately, the experiments succeeded only in the dioxane solution. In the other solutions the temperature variations of the second virial coefficient were very small, and, in addition, the leak of solute molecules from the membrane at relatively high temperatures could not be avoided. Thus, experimental accuracy was not good enough for the data to serve as the basis of further discussion.

Plots of the reduced osmotic pressure, π/c, against the concentration, c, at each temperature are shown in Fig. 5 for the solution of the poly-2-vinylpyridine fraction, C-1, in dioxane. As may be seen in this figure, the points lie on linear lines, so the osmotic third virial coefficient was neglected. In Fig. 6 the values of A_2 obtained by the least-square method are plotted against T. These plots are also represented by a linear line, whose equation was calculated by the least-square method; the value of θ was determined to be 268.9°K. This value of θ was then inserted into Eq. (7). Plots of $\psi_1 F(X)$ against T are shown in Fig. 7,

13) P. J. Flory and W. R. Krigbaum, *J. Chem. Phys.*, **18**, 1086 (1950).

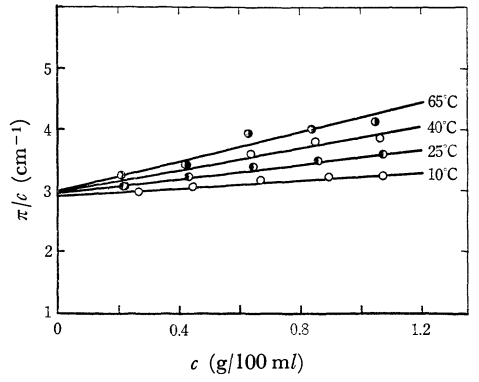

Fig. 5. Plots of the reduced osmotic pressure *vs.* the concentration of poly-2-vinylpyridine fraction, C-1, in dioxane at various temperatures.

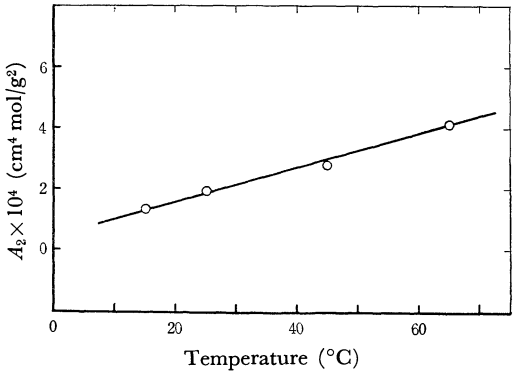

Fig. 6. Plots of the second virial coefficient *vs.* temperatures for the solution of poly-2-vinylpyridine fraction, C-1, in dioxane.

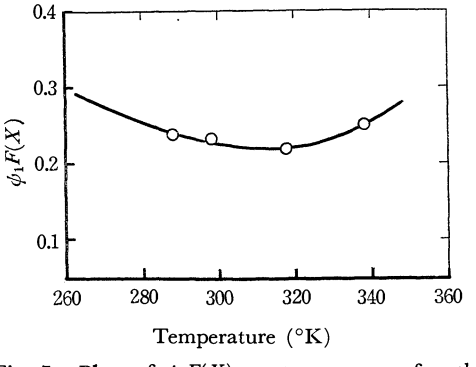

Fig. 7. Plots of $\psi_1 F(X)$ *vs.* temperature for the solution of poly-2-vinylpyridine fraction, C-1, in dioxane.

from which the value of ψ_1 is obtained as 0.28 for the system of poly-2-vinylpyridine - dioxane.

Discussion

As may be seen in Table 4, the estimated values of θ for benzene, dioxane, and methyl ethyl ketone are somewhat lower than room temperature and seem probable. The value of θ for chloroform is negative, while those for methanol and isopropanol are positive and extraordinary high. On the other hand, the value of ψ_1 for chloroform is positive, while those for methanol and isopropanol are negative. The heat of dilution for chloroform is, therefore, negative, indicating that chloroform is a very good solvent for this polymer. For the solutions of methanol and iospropanol, both the heat and the entropy of dilution are negative, as in the results for the poly-2-vinylpyridine - ethanol system.[1]

The hydrogen-bond formation, as described in a previous paper,[1] is considered to be the main reason for the peculiar findings on the thermodynamic interaction parameters in poly-2-vinylpyridine solutions in alcohols and chloroform. Nevertheless, it seemed useful to confirm that the peculiarity is not due to the presence of some impurities in the polymer. With this object, measurements of the temperature variation of the intrinsic viscosity in methanol with the $2U_0$ polymer and those of several solvents for poly-4-vinylpyridine were carried out; the results are shown in Table 1 and Fig. 1 for the former, and in Table 2 and Fig. 2 for the latter respectively. In order to avoid any possibility of contamination, the poly-2-vinylpyridine sample, $2U_0$, was thermally polymerized in a sealed tube without any initiator or solvent, and was carefully purified by reprecipitation. As may be seen in Fig. 1, the behavior of the intrinsic viscosity of $2U_0$ in methanol is just the same as that of K-2 in the same solvent. The behavior of the intrinsic viscosity of poly-4-vinylpyridine, fraction 4F-4, in pyridine is not so peculiar, while those in alcohols and chloroform are just the same as those of poly-2-vinylpyridine in the same solvents. From these results, it may be concluded that the peculiar behavior of the intrinsic viscosity is not due merely to the presence of some impurities in the samples.

The value of θ for the solution of poly-2-vinylpyridine in a neutral solvent, benzene, as estimated from the data on the intrinsic viscosity, seems appropriate, though the value is rather lower than the value obtained from the dependence of the consolute temperature on the polymer-chain length.[5]

The value of θ for the solution of poly-2-vinylpyridine in dioxane agrees well with that obtained from the osmotic second virial coefficient. It is noteworthy that the value of ψ_1 obtained from the osmotic pressure data is larger than that obtained from the intrinsic viscosity data.

As for the solution of poly-2-vinylpyridine in methyl ethyl ketone, various parameters which indicate that the θ temperatures lie near room temperature were described in a previous paper.[11] For example, at 25°C the long-range interaction

parameter, B, obtained from Fixman's plots is negative; the osmotic second virial coefficient, A_2, is negative, and the exponent, ν, in the Mark-Houwink-Sakurada equation is smaller than 0.5, which is theoretically the smallest value.[10]

The values of α_η obtained from the viscosity data in methyl ethyl ketone in this study are again smaller than 1 in the temperature range of 10—45°C. The osmotic second virial coefficients, A_2, were almost zero throughout the 10—40°C temperature range measured in steps of 5°C. The application of the viscoisity data to Eq. (2) gives 249.3°K and -0.01 for θ and ψ_1 respectively. In fact, the phaseseparation experiments showed that the critical temperature for the poly-2-vinylpyridine fraction, H-3 ($M_w = 14.9 \times 10^4$), is about 247°K.

These results show that the dilution of the solution is exothermic and that methyl ethyl ketone brings poly-2-vinylpyridine to the suspected θ state over a very wide range of temperature. Similar results have been reported by Fujita and others[14] for the polychloroprene - methyl ethyl ketone system. It is not yet clear what kind of chemical interaction is the source of the solution properties in the poly-2-vinylpyridine - methyl ethyl ketone system, but it is possible that the alcoholic –OH group produced by keto-enol tautomerism in methyl ethyl ketone[15] plays some role.

One of the authors (S. A.) wishes to thank Professor Masaji Miura of Hiroshima University and Professor Daisei Yamamoto of Kumamoto University for their kind encouragement and helpful discussions.

14) K. Hanafusa, A. Teramoto and H. Fujita, *J. Phys. Chem.*, **70**, 4004 (1966).
15) A. Gero, *J. Org. Chem.*, **19**, 1960 (1954); **26**, 3156 (1961).

BULLETIN OF THE CHEMICAL SOCIETY OF JAPAN VOL. 41 1301—1307 (1968)

The H/D Isotope Effect in the Conversion of the Electron into a Hydrogen Atom in Aqueous Acid Solutions at 300 and 77°K[1]

Shin-ichi OHNO

Japan Atomic Energy Research Institute, Tokai-mura, Ibaraki

(Received December 18, 1967)

The isotope effect in the formation of hydrogen atoms as a result of the reaction of the photochemically-produced electron in an acidified solution of hexacyanoferrate(II) has been investigated in both the liquid and solid phases. The magnitude of the effect (H/D) in the liquid phase, determined by a mass-spectrometric analysis of the hydrogen gas evolved from CH_3OH-containing solution, ranges from 3 to 4, and it depends on the temperature. The corresponding H/D ratio in acidic ices (at 77°K), determined by comparing the relative intensities of the ESR signals of the H and D atoms, is rather low (~1.5). Possible mechanisms by which the electron is converted into a hydrogen atom in aqueous acid solutions in both phases are discussed.

Electrons which are generated either by the ionization of water molecules (in radiation chemistry) or by photo-detachment from the solute (in photochemistry) have been shown to react with a variety of substances.[2,3] Many of these reactions in an aqueous solution are diffusion-controlled and may, therefore, be expected to occur even at low temperatures, provided that the reactants can encounter each other. The reaction:

$$e_{aq}^- + H_3O^+ \rightarrow H + H_2O \qquad (1)$$

is one such fast reaction.

The H/D isotope effect in the formation of hydrogen atoms as a result of the reaction of the photochemically-produced electron in an acidified solution of $[Fe(CN)_6]^{4-}$ by way of Reaction (1) has previously been reported;[4] the magnitude of the effect depends slightly on the temperature. Although, these experiments might be helpful in the understanding of the above reaction, no

1) Presented at the 10th Symposium of Radiation Chemistry, Hiroshima, October, 1967.

2) a) "Solvated Electron," *Advances in Chemistry Series*, No. 50, American Chemical Society, Washington, D. C., 1965. b) E. J. Hart, The Hydrated Electron, in "Actions Chimiques et Biologiques des Radiations," ed. by M. Haissinsky, Masson and Cie., Paris, 1966, Series 10, Chap. 1.

3) S. Ohno, This Bulletin **38**, 2018 (1965).

4) S. Ohno, *ibid.*, **39**, 2560 (1966).

details of the experimental results were given, nor was there any detailed discussion of them. The present author has since measured the ratio of the H/D atoms produced in UV-irradiated acidic ices (at 77°K) containing $[Fe(CN)_6]^{4-}$ by comparing the relative intensities of the ESR signals of the H and D atoms. The H/D ratio observed in an equi-molar mixture of H_2O-D_2O ice is rather low ($\sim$1.5) as compared with the corresponding value ($\sim$3.5) in the fluid phase. This paper will present these results and will consider the reaction mechanism of the electron in both phases.

Experimental

A low-pressure mercury lamp of the spiral type was used as the light source.[5] The light of wavelengths below 2000 Å was eliminated using a 0.1 M NaCl solution as a filter. Solutions were prepared from laboratory-distilled water. The heavy water (99.7%) was from Showa Denko Co., Ltd. The other chemicals used were of the purest grade available.

Liquid-phase Experiments. Irradiations were carried out in a quartz cylindrical vessel 3 cm in diameter employing 30 or 50 m*l* of the solution. The vessel immersed in a thermostat was connected to a vacuum system. The solution was evacuated as has been previously described.[5] The solution was irradiated for 30 min, during which period it was stirred by a magnetic stirrer. After irradiation, the evolved gas ($\sim$0.7 cm^3) was analysed by a CEC 103 mass spectrometer after having passed through a trap cooled to −196°C. The peak heights were determined in the order of *m/e*: 2, 3, 2, in order to take into account pressure changes in the mass spectrometer. The D_2 (*m/e*=4) was not observed at any time during the experiment. No correction for the fractionation in the mass spectrometer was made, as this is identical for all the samples and was found to be small (an absolute error <10%).[6]

Solid-phase Experiments (ESR Measurements). The electron spin resonance spectra were obtained with a JEP-1 spectrometer operating at 9.4 kMc and with 100 kc/s field modulation. The spectra recorded, after phase-sensitive detection, form the first derivative of the absorption curves.

Sample solutions, after having been flushed with argon, were rapidly frozen in 0.4-cm-diam. quartz tubes in liquid nitrogen. All the frozen samples appeared opaque, except for the 10 N NaOH-solutions, which appeared glassy. The samples weighed about 0.1 g; freezing was complete in about 10 sec. The quartz tube was then placed inside a quartz Dewar flask filled with liquid nitrogen and positioned in the center of the spiral lamp. After irradiation the specimens were transferred, without having been allowed to warm up, into liquid nitrogen in a quartz tipped-Dewar flask, which fits into the ESR cavity. A stream of nirogen gas was passed through the cavity in order to prevent condensation of moisture on the tip of the dewar.

Results

H/D Isotope Effects in the Liquid Phase. When an aqueous acidic solution of potassium hexacyanoferrate(II) containing 1 M CH_3OH is irradiated by light with a wavelength of 2537 Å, the following reactions occur:[5]

$$[Fe(CN)_6]^{4-} + h\nu \rightarrow [Fe(CN)_6]^{3-} + e_{aq}^- \quad (2)$$

$$e_{aq}^- + H_3O^+ \rightarrow H + H_2O \quad (1)$$

$$H + CH_3OH \rightarrow H_2 + CH_2OH \quad (3)$$

$$CH_2OH + [Fe(CN)_6]^{3-} \rightarrow H^+ + HCHO + [Fe(CN)_6]^{4-} \quad (4)$$

In an H_2O-D_2O mixture where the hydrogen ion exists as H_3O^+, H_2DO^+, HD_2O^+ and D_3O^+, both H and D atoms are formed in Reaction (1). Its isotope effect may be measured from the evolved H_2/HD ratio, as the hydrogen atoms thus produced, H and D, react with CH_3OH by Reaction (3) to yield H_2 and HD respectively. The results obtained at a constant temperature (*ca.* 27°C) using various sulfuric acid concentrations are presented in Table 1. In this table, $(H/D)_{water}$ means the H *vs.* D atom ratio in the solution; $(H/D)_{atom}$ means that of the hydrogen atom produced, which is measured as the observed H_2/HD ratio; *S* is the $(H/D)_{atom}/(H/D)_{water}$ ratio, and is commonly called the separation factor.[7] Table 2 presents the results obtained at $[H_2SO_4]$=0.1 N and $(H/D)_{water}$ =1.1, but at various temperatures of irradiation.

It should be noted that the interaction of H and D atoms with the solvent does not contribute to the isotope effect in the present case, since the exchange reaction:

$$D + H_2O \rightarrow H + HDO \quad (5)$$

was found to be slow (k=2 sec^{-1} at pH 2).[8] Formaldehyde, which is produced by Reaction (4),

TABLE 1. H/D ISOTOPE EFFECTS AS A FUNCTION OF SULFURIC ACID CONCENTRATION AT CONSTANT TEMPERATURE (*ca.* 27°C)

$[H_2SO_4]$, N	$(H/D)_{water}$	$(H/D)_{atom}$	*S*
1.2	1.94	6.78	3.5
0.6	1.92	6.90	3.6
0.35	1.11	3.49	3.1
0.12	1.90	6.85	3.6
0.07	1.11	3.52	3.2
0.05	1.12	4.3	3.9
0.01	1.11	3.16	2.9
0.001	1.11	1.88	1.7

5) S. Ohno, *ibid.*, **40**, 1770 (1967).

6) This was checked using the standard hydrogen gas sample prepared by Zn-decomposed water mixtures (H_2O-D_2O). The author wishes to thank Dr. Takuji Komori, Analytical Division, Japan Atomic Energy Research Institute, for his kindly offering the samples.

7) J. Jortner and G. Stein, *Intern. J. Appl. Radiation Isotopes*, **7**, 198 (1960).

8) H. L. Friedman and A. H. Zeltman, *J. Chem. Phys.*, **28**, 878 (1958).

Table 2. H/D isotope effects as a function of the temperature, observed at $[H_2SO_4]=0.1$ N and $(H/D)_{water}=1.1$

Temp., °C	L	$K(=L^{1/6})$	S	$S_{ion}(=S/K)$
2.0	9.43	1.45	4.35	3.00
10.4	8.94	1.44	4.16	2.89
21.6	8.36	1.42	3.80	2.68
25	8.20	1.42	—	—
30.2	7.97	1.41	3.64	2.58
40.8	7.54	1.40	3.61	2.58

shows a rather low reactivity toward e_{aq}^- and H atoms.[9]

In a solvent composed of light and heavy water, the isotopic composition of the hydrogen ion differs from that of the solvent.[10-12] These two quantities are related by the equilibrium constant;

$$K = (H/D)_{\text{hydrogen ion}}/(H/D)_{\text{water}} \quad (6)$$

which determines the fractionation effect. The K constant corresponds[13] to $L^{1/6}$, L being the equilibrium constant for the reaction:

$$2\,D_3O^+ + 3\,H_2O = 2\,H_3O^+ + 3\,D_2O,\ L \quad (7)$$

if one assumes that the proton is solvated in the H_3O^+ form.[14] The value of L has been evaluated by different methods; these have been reviewed and discussed by Heinzinger and Weston[10] and by Schaleger, Salomaa and Long.[11] Following these authors, here we take the value of 8.2 for L at 25°C. The values at other temperatures can be calculated using an approximate value of -1000 cal mol^{-1} for ΔH[10] for Reaction (7). The results of these calculations are included in Table 2. Fortunately, the uncertainty of this temperature coefficient is not at all serious when $K(=L^{1/6})$ is considered. The last coulmn of Table 2 refers to the isotopic fractionation (S_{ion}) due to the production of hydrogen atoms from the hydrogen ion (in Reaction (1)), calculated from the relation:

$$S = (H/D)_{atom}/(H/D)_{water} = \left[\frac{(H/D)_{atom}}{(H/D)_{\text{hydrogen ion}}}\right] \times \left[\frac{(H/D)_{\text{hydrogen ion}}}{(H/D)_{water}}\right] = S_{ion} \times K \quad (8)$$

ESR Measurements of Frozen Alkaline and Neutral Solutions. The irradiation of the $[Fe(CN)_6]^{4-}$ ions (10^{-2}—10^{-3} M) in 10 N NaOH at 77°K with a light with a wavelength of 2537 Å gave an intense blue-violet color and an ESR signal consisting of a single narrow line at $g=2.00$ and with a maximum slope-linewidth of 17 gauss (Fig. 1, (a)). On exposure to visible light, both the blue-violet color and the ESR signal are lost (Fig. 1, (a), dotted curve); this ESR line is identical with the well-known signal of the trapped electron, e_t^-.[15-19]

The same solution, however, if irradiated with light of 3660 Å, gave no blue-violet color and no ESR signal attributable to e_t^-. Instead, there appeared an unidentified signal (Fig. 1, (b));

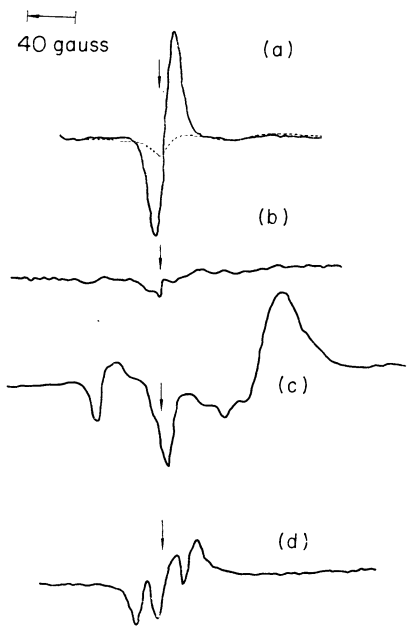

Fig. 1. ESR spectra of UV-irradiated frozen solutions of 10^{-2} M $[Fe(CN)_6]^{4-}$ at 77°K. Arrows show the field value of the DPPH signal. (a) 2537 Å, 10 N NaOH; (b) 3660 Å, 10 N NaOH; (c) 2537 Å, 10 N NaOH containing 10^{-2} M NO_3^-; (d) 2537 Å, neutral ice containing 10^{-2} M $ClCH_2COOH$

9) M. Anbar and P. Neta, *Intern. J. Appl. Radiation Isotopes*, **18**, 493 (1967).
10) K. Heinzinger and R. E. Weston, *J. Phys. Chem.*, **68**, 744 (1964).
11) L. L. Schaleger, P. Salomaa and F. A. Long, in "Chemical Physics of Ionic Solutions," ed. by B. E. Conway and R. G. Barradas, John Wiley and Sons, Inc., New York (1966), p. 237.
12) A. J. Kresge and A. L. Allered, *J. Am. Chem. Soc.*, **85**, 1541 (1963); V. Gold, *Proc. Chem. Soc.*, **1963**, 141.
13) This simplification results from the assumption of the rule of the geometric mean as applied to the isotopically homologous series H_3O^+, H_2DO^+, HD_2O^+, and D_3O^+, as well as to the series H_2O, HDO, and D_2O. See, for example, Ref. 10 or 11.
14) It has been shown that the various estimates of L are compatible with the results of proton magnetic resonance experiments (Ref. 12) only if the proton is formulated as H_3O^+. This by no means excludes the model for the hydrogen ion in which a hydronium ion is further solvated by three water molecules, *i. e.*, $H_9O_4^+$. See Refs. 10 and 11.
15) D. Schulte-Frohlinde and K. Eiben, *Z. Naturforsch.*, **17a**, 445 (1962); *ibid.*, **18a**, 99 (1963).
16) T. Henriksen, *Radiation Res.*, **23**, 63 (1964).
17) P. N. Moorthy and J. J. Weiss, *Phil. Mag.*, **10**, 659 (1964).
18) P. B. Ayscough, R. G. Collins and F. S. Dainton, *Nature*, **205**, 965 (1965).
19) M. J. Blandamer, L. Shields and M. C. R. Symons, *J. Chem. Soc.*, **1964**, 4352.

this is a strong confirmation of the previous findings that the d-d excitation of $[Fe(CN)_6]^{4-}$ does not lead to an electron-detachment,[5,20] while the charge-transfer excitation results in an electron release.

It should be noted that the presence of 10^{-2} M NO_3^- in an UV(2537 Å)-irradiated 10 N NaOH solution of $[Fe(CN)_6]^{4-}$ reduced completely the signal due to the e_t^-; instead, there appeared a more complex signal (Fig. 1, (c)), with the specimen turning yellow. The presence of 10^{-2} M N_2O in the same system, on the other hand, caused no significant change.

Moreover, in an UV(2537 Å)-irradiated neutral ice containing 10^{-2}—10^{-3} M $[Fe(CN)_6]^{4-}$ and $ClCH_2COOH$, the signal attributable to the radical, CH_2COOH,[18] is observed (Fig. 1, (d)):

$$e + ClCH_2COOH \rightarrow Cl^- + CH_2COOH \quad (9)$$

H/D Isotope Effects in Frozen Solutions. The electron is converted to the hydrogen atom in frozen aqueous acid solutions.[16,21-23] Figure 2 shows the ESR signals of the H and D atoms thus produced in an H_2O—D_2O mixture at 77°K. A doublet of 509 gauss and a triplet of 153 gauss (end-to-end) are due to the H and D atoms respectively. The origin of the small signal in the center portion of the spectrum is not known. In both the H and D atom spectra, the low-field lines are somewhat more intense than the high-field lines.

The relative concentrations of H and D atoms can be determined by calculating the sums of the hw^2 values of the H and D lines respectively, where h is the height of the line and w, its width at a maximum slope of the first derivative curve. In effect, the signal intensities were calculated simply from the heights of the lines, as the linewidths and shapes for the H and D lines in the H_2O-D_2O (50% D) system were nearly identical (the linewidth: about 4 gauss). The satellite lines appeared in some cases (Fig. 3), as is often observed in γ-irradiated ice,[16,23b,24] but this, too, was identical in both the H and D spectra.

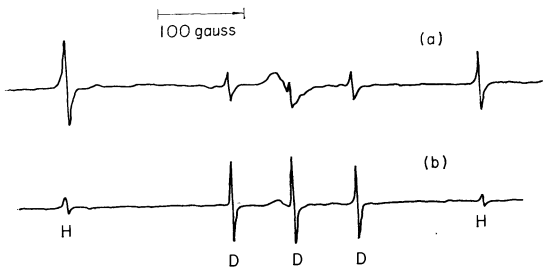

Fig. 2. ESR spectra of UV(2537 Å)-irradiated acid solutions (H_2O-D_2O) of 10^{-3} M $[Fe(CN)_6]^{4-}$ at 77°K.
(a) $[H_2SO_4]=0.01$ N, $(H/D)_{water}=1$
(b) $[H_2SO_4]=0.6$ N, $(H/D)_{water}=0.05$

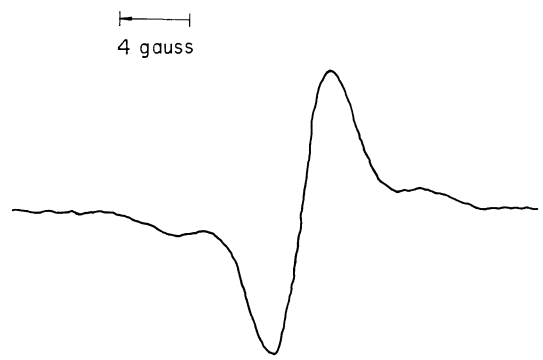

Fig. 3. The high field atomic D line in a frozen solution ($(H/D)_{water}=1$) of 1 N H_2SO_4 showing weak satellites.

Because of the well-known phenomenon of the microwave power saturation of the H atom signal,[16,25] it was necessary to check the saturation modes of both the H and D signals. Both of them

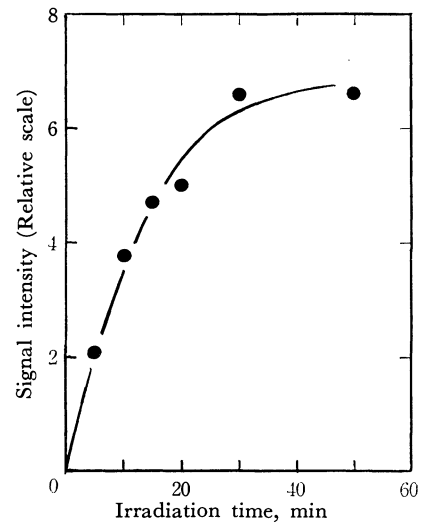

Fig. 4. Signal intensity of H-atoms as a function of irradiation time; Irradiation at 2537 Å and 77°K of a 10^{-3} M $[Fe(CN)_6]^{4-}$ solution containing 1 N H_2SO_4.

20) S. Ohno and G. Tsuchihashi, This Bulletin, **38**, 1052 (1965).
21) J. J. Weiss, *Nature*, **186**, 751 (1960); L. Kevan, P. N. Moorthy and J. J. Weiss, *ibid.*, **199**, 698 (1963).
22) F. S. Dainton and F. T. Jones, *Trans. Faraday Soc.*, **61**, 1681 (1965).
23) a) R. Livingston and A. J. Weinberger, *J. Chem. Phys.*, **33**, 499 (1960). b) R. Livingston, H. Zeldes and E. H. Taylor, *Discussions Faraday Soc.*, **19**, 166 (1955).
24) H. N. Rexroad and W. Gordy, *Phys. Rev.*, **125**, 242 (1962).
25) S. Siegel, J. M. Flournoy and L. H. Baum, *J. Chem. Phys.*, **34**, 1782 (1961); H. S. Jueikis, J. M. Flournoy and S. Siegel, *ibid.*, **37**, 2272 (1962).

were found to be nearly in the region of power saturation, even at the lowest crystal current employed. However, the signal heights for the H and D lines relative to each other are constant within the limits of experimental error at crystal currents below 0.2 mA. The actual measurements were made within this range.

No decay in the H and D signals was seen over a period of several days at the temperature of liquid nitrogen.

In all the systems examined, the signal intensities increased with the irradiation time, reaching a more or less steady value upon prolonged irradiation (Fig. 4). The signal intensities, resulting from irradiation for 15 min, on the linear part of the yield-time curve were used to calculate the relative yields of H and D atoms.

The results obtained with photolysed H_2O-D_2O mixtures containing 10^{-3} M $[Fe(CN)_6]^{4-}$ and varying amounts of sulfuric or perchloric acid are shown in Table 3. The error included may be small (±10%), as the conditions under which the spectra were obtained were exactly identical with those for the H and D atoms in each measurement.

Table 3. H/D Isotope effect in the formation of the hydrogen atoms originating from the reaction of the electron in acid ices at 77°K
Obtained at $(H/D)_{water} = 1.0$ and $[Fe(CN)_6^{4-}] 10^{-3}$ M

	Acid concn., N	S, (H/D)
H_2SO_4	1	1.33
H_2SO_4	0.5	1.46
H_2SO_4	0.1	1.42
H_2SO_4	0.05	~2.2*
$HClO_4$	1	1.86
$HClO_4$	0.1	1.56

* Hydrogen atom yields are low by a factor of ten.

Discussion

Possible Mechanisms for Observed Isotopic Effects in the Liquid Phase. In a previous communication,[4] the relative rates of O–H and O–D breakages, k_H/k_D, from the isotopic hydronium ion were computed on the simple assumptions that the $H_nD_{3-n}O^+$ species ($n=0$, 1, 2, or 3) gives the H or D atom in the $H/D = nk_H/(3-n)k_D$ ratio, and that the reactivity of $H_nD_{3-n}O^+$ with e_{aq}^- does not depend on the value of n. There, however, the implausibly high k_H/k_D value of 4—5 was obtained, in comparison with the low value observed ($S=1.2$)[26] for the isotope effects in the vapor-phase radiolysis of water, where monomolecular decompositions of the excited H_2O or the neutralization of the H_3O^+ ion are probably involved,[26,27] according to the following reactions:

$$H_2O^* \rightarrow H + OH \quad (10)$$

$$H_2O \rightarrow H_2O^+ + e \quad (11)$$

$$H_2O^+ + H_2O \rightarrow H_3O^+ + OH \quad (12)$$

$$H_3O^+ + e \rightarrow H + H_2O \quad (13)$$

In the condensed medium, where interaction with another water molecule can easily occur, the mode of H-atom production may be very complex.

The rate constant of Reaction (1)[28,29] is 2—2.3 $\times 10^{10}$ $M^{-1}sec^{-1}$; its activation energy is 3.2 kcal/mol.[30] This latter value is nearly identical with that of the diffusion-controlled neutralization reaction (14), namely, 3.5 kcal/mol:[31]

$$H_3O^+_{aq} + OH^-_{aq} \rightarrow 2\,H_2O \quad (14)$$

Yet Reaction (1) proceeds 6—7 times less rapidly than Reaction (14) ($k_{14} = 1.4 \times 10^{11}$ $M^{-1}sec^{-1}$ [32]). The most rapidly diffusing species in both of these reactions is likely to be $H_3O^+_{aq}$ presumably by a mechanism of H transfer along the chain of hydrogen-bonded waters,[33] since the diffusion coefficient of the e_{aq}^- (4.7×10^{-5} cm^2sec^{-1} at 25°C[34]) is rather low compared with that of $H_3O^+_{aq}$ (9.5×10^{-5} cm^2sec^{-1}).

It may be speculated that the proton interacting with the negative charge due to the e_{aq}^- forms an intermediate complex, *i. e.*, $(H_3O^+ \cdot e^-)_{aq}$, which then decomposes either to give the H atom or to regenerate e_{aq}^-:[35]

$$H_3O^+_{aq} + e_{aq}^- \rightarrow (H_3O^+ \cdot e^-)_{aq} \quad (1a)$$

$$(H_3O^+ \cdot e^-)_{aq} \rightarrow e_{aq}^- + H_3O^+ \quad (1b)$$

$$\searrow\ H + H_2O \quad (1c)$$

26) J. Y. Yang and I. Marcus, *J. Am. Chem. Soc.*, **88**, 1625 (1966).

27) J. H. Baxendale and G. P. Gilbert, *Discussions Faraday Soc.*, **36**, 186 (1963); F. Fiquet-Fayard, *J. Chim. Phys.*, **57**, 453 (1960); G. R. A. Johnson and M. Simic, *J. Phys. Chem.*, **71**, 1118 (1967); I. Santar and J. Bednar, *Collection Czechoslov. Chem. Commun.*, **32**, 953 (1967).

28) J. P. Keene, *Radiation Res.*, **22**, 1 (1964).

29) S. Gordon, E. J. Hart, M. S. Matheson, J. Rabani and J. K. Thomas, *J. Am. Chem. Soc.*, **85**, 1375 (1963).

30) J. K. Thomas, S. Gordon and E. J. Hart, *J. Phys. Chem.*, **68**, 1524 (1964).

31) M. S. Matheson in Ref. 2a; G. Ertl and H. Gerisher, *Z. Elektrochem.*, **66**, 560 (1962).

32) M. Eigen and L. DeMaeyer, *ibid.*, **59**, 986 (1955).

33) R. A. Horne and E. H. Axelrod, *J. Chem. Phys.*, **40**, 1518 (1964).

34) K. H. Schmidt and W. L. Buck, *Science*, **151**, 70 (1966).

35) Melton and Joy has recently reported the existence of H_3O in the gas phase evidenced by a mass-spectrometric study. If such a species exists in an aqueous solution, then one might consider the H_3O in place of $(H_3O^+ \cdot e^-)_{aq}$ in the present argument. See C. E. Melton and H. W. Joy, *J. Chem. Phys.*, **46**, 4275 (1967). The theoretical calculation of Bishop does not predict the existence of H_3O, however; D. M. Bishop, *J. Chem. Phys.*, **45**, 2474 (1966).

Reaction (1a) is expected to proceed at a diffusion-controlled rate (the same as Reaction (14); thus, $k_{1a}=1.4\times10^{11}$ M^{-1}sec^{-1}).[36] In this scheme, the observed rate of Reaction (1), k_1, is expressed by:

$$k_1 = \frac{k_{1a}k_{1c}}{k_{1b}+k_{1c}} \qquad (15)$$

Using the reported value for k_1[28,29] and the assumed value for k_{1a} as above, one gets $k_{1b}/k_{1c}=5$. The value of k_{1b}/k_{1c} might be different for each isotopic hydronium ion, $H_nD_{3-n}O^+$, where $n=0$—3, thus causing some part of the isotopic effects observed.

The results shown in Table 2 would indicate that the isotope effect for H-atom *vs.* D-atom production by way of Reaction (1c) ranges from 2.6 to 3, and that it depends slightly on the temperature. Even if the highest possible value for the ΔH of Reaction (7), namely, $\Delta H=-2000$ cal/mol,[10] is adopted, this causes only slight changes (1% or less) in the value of K and, thus, in the value of S_{ion}. Other systematic errors in obtaining S_{ion} are all identical for all the results. One may thus conclude that decreasing the temperature results in an enhancement of the isotope effect.

The isotope effect found here is too large to be attributed to a diffusion isotope effect. It can not be due to a difference in the vibrational frequencies of O–H and O–D bonds, either, since this would cause an isotope effect of only 1.4 or so and since this should be independent of the temperature. On the other hand, the large H/D isotope effect can be explained in terms of a difference in the activation energy for the O–H and O–D bond dissociations in the $(H_3O^+\cdot e^-)_{aq}$. As a result of the difference in zero-point energies,[37] more energy should be required to remove the D than the H. This would also account for the slight temperature dependence of the isotope effects seen in Table 2.

A similar intermediate, $(H_3O^+\cdot e^-)_{aq}$, has been considered by Hart[38] in a different connection. In the $(H_3O^+\cdot e^-)_{aq}$ complex, one of the water molecules in the hydration structure of the e^- may be incorporated in the outer shell of H_3O^+. This complex, which can be regarded as a closely-coupled unit, could either produce a hydrogen atom (Reaction (1c)) or decompose into H_3O^+ and e_{aq}^- (Reaction (1b)). These processes are caused by either a proton movement toward an adjacent hydrogen-bonded water molecule or rotations of the water molecules in the hydration sphere of the electron.

It should be emphasized here that, in the vapor-phase radiolysis, the H_3O-radical, if formed by the $(H_3O^+ + e^-)$ reaction, decomposes probably in the first vibration, and that, therefore, the relative probability of the dissociation of O–H and O–D bonds is closely related to the relative bond-stretching vibrational frequency, that is, 1.4.

Possible Reaction Mechanisms and Isotope Effects in the Solid State. The isotope separation factor which we have obtained for the frozen acid solution containing $[Fe(CN)_6]^{4-}$ and illuminated with ultraviolet light at 77°K (Table 3) is much smaller than the corresponding values of 3—4 obtained in the liquid phase. The present author considers this to be evidence that different mechanisms of the production of hydrogen atoms are operative for the two phases.

Dainton and Jones[22] have reported that the photo-detached electron, though differring from the radiolytically-formed electron in having much less kinetic energy, becomes a mobile electron in a frozen system. In a rigid medium, where the relaxation time for the orientation of the water dipoles is much longer than in a fluid medium, the electron could not easily polarize the surrounding medium; this would cause the electron to move larger distances from its point of origin. Moreover, the Coulombic repulsion between the ejected electron and the remaining species in the present case, namely $[Fe(CN)_6]^{3-}$, may be more effective than in a liquid phase, since the Coulomb interactions in a frozen solution at 77°K are, in an extreme case, mainly governed, not by the static dielectric constant (~80), but by the optical dielectric constant (~1.7).

The mobile electron moves through the medium until it finds a suitable site at which to be trapped (*e. g.*, a hydroxide anion vacancy[19,39]) or a species with which to react. The reaction of the electron in γ-irradiated frozen solutions has been studied in many works.[19,21,22,40,41] The trend in the rate-constant ratios at 77°K of the solutes, NO_3^-, NO_2^-, and acetone, with respect to $H_2PO_4^-$ was found to be the same as in an aqueous solution at 300°K.[40,41] More recently, the quantitative correlation of the rates in both phases for the electron reaction with Cd^{2+}, Cu^{2+}, CrO_4^{3-}, Zn^{2+}, and $ClCH_2COO^-$ ions has been verified further.[42] Unfortunately, no data on the H_3O^+ as well as on O_2 and N_2O have yet been given.

From the known values of the rate constants at *ca.* 25°C of Reactions (1) and (9), namely, $k_1=2.3\times10^{10}$ and $k_9=6.5\times10^9$ M^{-1}sec^{-1},[7] one may

36) Schwarz estimated the value of k_{1a} as 10.4×10^{10} M^{-1} sec^{-1} on the basis of a simple model of the diffusion-controlled reaction developed by Debye; H. A. Schwarz, *Radiation Res. Suppl.*, **4**, 89 (1964).

37) The difference in zero-point energy between O–H and O–D bonds in the $(H_3O^+\cdot e^-)_{aq}$ complex may not be largely different from that in the hydronium ion, namely 1.2 kcal/mol (see Ref. 4); a value of this order of magnitude is responsable to the temperature dependence shown in Table 2.

38) E. J. Hart in Ref. 2b, p. 32. See also E. J. Hart, *Science*, **146**, 19 (1964).

39) L. Kevan, *J. Am. Chem. Soc.*, **87**, 1481 (1965).

40) P. N. Moorthy and J. J. Weiss, in Ref. 2a.

41) L. Kevan, P. N. Moorthy and J. J. Weiss, *J. Am. Chem. Soc.*, **86**, 771 (1964).

42) L. Kevan, *ibid.*, **89**, 4238 (1967).

expect that, in a frozen solution containing equal amounts of $ClCH_2COOH$ and H_3O^+, Reaction (1) occurs predominantly over Reaction (9). However, the results shown in Table 4 indicate

Table 4. Competition between H_2SO_4 and $ClCH_2COOH$ for the electron

a. $[Fe(CN)_6^{4-}] = 10^{-2}$ M, $[ClCH_2COOH] = 10^{-2}$ M

H_2SO_4, N	H	CH_2COOH
0.1	−	+
0.5	+	±
1	+	−

b. $[Fe(CN)_6^{4-}] = 10^{-3}$ M, $[ClCH_2COOH] = 10^{-3}$ M

H_2SO_4, N	H	CH_2COOH
10^{-2}	±	+
0.1	+	±
1	+	−

+ Signals appeared; − Signals not appeared;
± Signals appeared slightly.

that considerably high concentrations of the sulfuric acid are needed to suppress Reaction (9). An apparent unreactivity of the hydrogen ion toward the electron in an ice has been previously reported by Weiss *et al.*[40,41] In order to explain the marked differences in the H atom yields in 1 M solutions of $HClO_4$, H_2SO_4, H_3PO_4, and HCl, these authors suggested[41] that Reaction (1) is rather insignificant compared with the reactions of the electron with the anions (HX^-) and with the undissociated acid molecules (H_2X):

$$e^- + HX^- \rightarrow H + H_2O + X^{2-} \quad (16)$$

$$e^- + H_2X \rightarrow H + H_2O + HX \quad (17)$$

The isotope effect of the production of H atoms *vs.* D atoms in this model must be governed by the isotopic fractionation between the solvent and the reacting species, HSO_4^-, H_2SO_4, or $HClO_4$. However, the reason for the relative insignificance of Reaction (1) compared with Reactions (16) and (17) at 77°K is not clear.

An alternative model for the production of hydrogen atoms as a result of the reaction of electrons in an acidic ice may be as follows: the electron reacts with the hydrogen ion, but in the hydrogen-bonded network, through which the hydrogen atom is transferred according to:

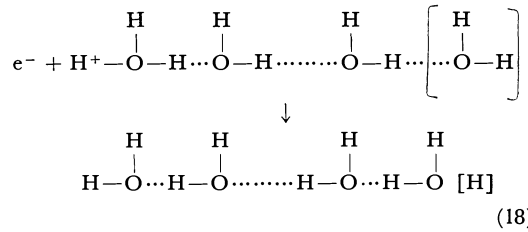

(18)

in which [ ] represents the site in the solid which can stabilize the hydrogen atom. The thermal vibrations of the lattice may be sufficient for such an H-atom transfer.[43] The hydrogen isotope separation factor by this model would be governed by the isotopic effect in the formation of the H atom from a water molecule at the trapping site. It is, thus, not surprising that a marked difference in the magnitude of the isotope effect is found between the solid and liquid phases.

Morevoer, it may be possible, by the mechanism of Eq. (18), for an electron transfer to a solute to take place easily if the solute is involved in the same hydrogen-bonded chain as the hydrogen ion initially reacting the electron:

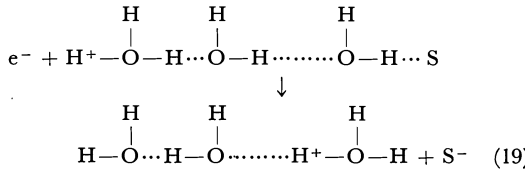

(19)

where S denotes the solute. Reactions (18) and (19) would compete with each other. Thus, one might expect that, in an acidic ice ($H_3O^+ >$ 1 M), competition between the solute and the H-atom-trapping site for the electron (or the H-atom moving by the above mechanism) occurs. This mechanism would predict the relative ineffectiveness as an electron scavenger of the solute which does not couple with the H-bonded unit. Such electron scavengers as O_2 or N_2O might be such cases.

The author is greatly indebted to Professor Shizuo Fujiwara, the University of Tokyo, for his useful suggestions and kind guidance throughout this work. The stimulating discussions of Dr. Kenji Ishida are also acknowledged.

43) A similar mechanism of H-transfer was suggested in Ref. 40 for a possibility that two hydrogen atoms form a molecule of hydrogen in an ice at 77°K without the diffusion of the two H-atoms.

BULLETIN OF THE CHEMICAL SOCIETY OF JAPAN VOL. 41 1308—1313 (1968)

An X-Ray Determination of the Structure of Motiol Iodoacetate*1

Yoriko NISHI, Tamaichi ASHIDA, Yoshio SASADA*2 and Masao KAKUDO

Institute for Protein Research, Osaka University, Joancho, Kita-ku, Osaka

(Received December 22, 1967)

The molecular configuration of motiol has been determined by the X-ray crystal analysis. The crystal of motiol iodoacetate, $C_{32}H_{52}O_2I$, is monoclinic with two molecules in a unit cell of dimensions; $a=17.37$, $b=6.78$, $c=13.04$ Å and $\beta=99.6°$, the space group being $P2_1$. The crystal structure was solved by the heavy atom method. The atomic coordinates and anisotropic temperature factors were refined by block-diagonal matrix least-squares method. The structure determined is, in general, compatible with that derived chemically. The rings A and D are of a chair form, and the rings B and C are of a semi-chair. The molecule bends at the rings B and C to make a bow as a whole. All but one of the methyl groups are in axial junction.

In 1965 Nakamura, Yamada, Wada, Inoue, Goto and Hirata have determined the stuctures of motiol, $C_{30}H_{50}O$, and four related compounds.[1] These triterpene alcohols are obtained from a viscous substance of *Rhododendoron Linearifolium*, from which motiol itself has been isolated by Kariyone, Hashimoto and Tobinaga early in 1952.[2]

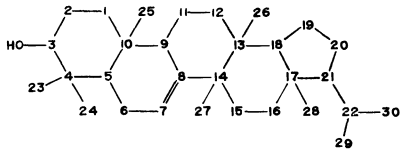

Before completing chemical studies, Professors Hirata and Goto of Nagoya University supplied us the crystals of motiol iodoacetate for an X-ray analysis. The present paper describes the three-dimensional structure determination of motiol iodoacetate.

Experimental

The crystals of motiol iodoacetate, $C_{32}H_{52}O_2I$, are colourless and of mica-like form. Cleavage is observed along the (001) plane.

Unit cell dimensions were obtained by the photographic method; the values of a and c were derived from the ($h0l$) Weissenberg photographs on which aluminum powder diffraction lines were superposed for calibration, while that of b was determined from the ($hk0$) and ($0kl$) precession photographs.

Equi-inclination Weissenberg photographs were taken up to the 5th layer along the b axis using multiple-film technique. With Cu$K\alpha$ radiation of 30 kV and 18 exposure time was about 70 hr for each layer. The size of crystal used was about $0.1\times0.3\times1.5$ mm. After X-ray exposure of about 200 hr the crystal was coloured brown and the shape of the diffraction spots became blurred foggy. Therefore, two crystals of about the same size were needed for collection of the complete intensity data.

Intensities of 2511 reflexions were measured by visual comparison with a standard intensity scale, the relative intensity being ranged between 23000 and 1. Some reflexions which were not accessible by the b axis Weissenberg photographs were supplemented from the precession photographs.

Corrections for Lorentz and polarization factors were made in the usual way, while that for absorption was neglected.

Crystallographic Data

Crystallographic and physical data obtained are: Motiol iodoacetate, $C_{32}H_{52}O_2I$. Monoclinic,

$a=17.37\pm0.04$, $b=6.78\pm0.02$, $c=13.04\pm0.03$ Å,

$\beta=99.6\pm0.5°$.

Volume of the unit cell, 1514.2 Å.

Systematic absence, ($0k0$) when k is odd. Space group, $P2_1$. Two molecules per unit cell. Density observed (by floatation), 1.32 g·cm^{-3}. Density calculated, 1.30 g·cm^{-3}. Total number of electrons per unit cell, $F(000)=626$. Linear abosrption coefficient for Cu$K\alpha$ radiation, $\mu=93.87$ cm^{-1}.

Structure Determination

Patterson projection on (010) showed clearly a peak corresponding to the iodine-iodine interaction, which gave the coordinates of the iodine as

*1 Read before the 19th Annual Meeting of the Chemical Society of Japan, April, 1966, Yokohama.

*2 Present address: Laboratory of Chemistry for Natural Products, Faculty of Science, Tokyo Institute of Technology, Ookayama, Meguro-ku, Tokyo.

1) S. Nakamura, T. Yamada, H. Wada, Y. Inoue, T. Goto and Y. Hirata, *Tetrahedron Letters*, **24**, 2017 (1965).

2) T. Kariyone, Y. Hashimoto and S. Tobinaga, *Pharm. Bull.* (Japan), **5**, 367 (1957).

$x=-0.025$ and $z=0.195$. On the other hand, the y coordinate of the iodine may be assigned arbitrarily as -0.25 in this space group.

A Fourier synthesis was carried out using phases based on the coordinates of the iodine atom. It was very easy to find a general lay-out of the molecule from the resulting electron density distribution; in the section $y=0.25$ where the equivalent iodine atom appeared, there were twelve high peaks which built up major part of the rings A, D and E. The atoms in iodoacetyl group and those in the rings B and C were also recognized as resolved peaks, although there is a pseudo mirror plane at $y=0.25$. Therefore, it was possible to construct two models of the main skeleton; in one model iodoacetyl group and the rings B and C are on the same side of the pseudo mirror plane and in another they are on the opposite. In the former model, the conformation of the cyclohexane ring A is of a boat form, while in the latter it is of a chair.

Since chemical studies supported the latter model, we proceeded at first the refinement of the structure based on it. Even if the general conformation of the molecule had been selected, it was still difficult to decide to which side the y coordinates deviate from the mirror if the deviations are small. For such atoms we gave appropriate y coordinates by inspection. Fourier synthesis was evaluated with phases based on all the atoms. In the resulting electron density distribution, all the peaks corresponding to the light atoms showed very reasonable height and there were found only a few ghost peaks whose heights were not over a half of those of the carbon.

Three cycles of a least-squares refinement were carried out with isotropic temperature factors, initial B being 5.2 Å. The iodine atom was treated as anisotropic (two cycles) and then all the atoms were taken as anisotropic (two cycles). The R factor decreased to 0.177.

In these processes, the y coordinate of C(7) moved from 0.24 to 0.285 across the pseudo mirror plane, and that of C(6) decreased from 0.22 to 0.194 and then increased gradually. Their standard deviations were larger than those of the others. Since it seemed likely that the anomaly should be due to the mislocation of C(6), its y coordinate was changed artificially to be 0.28 across the pseudo mirror. Two cycles of the refinement were conducted so that the R factor dropped from 0.178 to 0.172 and the standard deviations of all the atoms did not differ to much extent.

It is known that the effect of anomalous dispersion of the iodine could not be neglected. Two enantiomorphous structures with the parameters at this stage were examined for 165 sampled reflections. Difference between these enantiomorphs was not quite definite, but one of them seemed to be more favourable. With this model, the least-squares refinement including anomalous dispersion effect was made (one cycle). It gave a slightly lower R factor of 0.169 ($R=0.148$ for non-zero reflexions) and better bond lengths.

Table 1. The final atomic coordinates

Atom	x	y	z
I	−0.0262	−0.2500	0.1848
C(1)	0.3167	0.2839	0.0688
C(2)	0.2219	0.2439	0.0516
C(3)	0.2056	0.1334	0.1368
C(4)	0.2220	0.2120	0.2462
C(5)	0.3172	0.2702	0.2596
C(6)	0.3509	0.3124	0.3700
C(7)	0.4444	0.2918	0.3890
C(8)	0.4740	0.3250	0.2916
C(9)	0.4401	0.3703	0.1978
C(10)	0.3446	0.3777	0.1754
C(11)	0.4744	0.4144	0.1025
C(12)	0.5696	0.4223	0.1239
C(13)	0.5965	0.2782	0.2096
C(14)	0.5697	0.3545	0.3130
C(15)	0.6112	0.2194	0.4063
C(16)	0.7021	0.2588	0.4249
C(17)	0.7342	0.1949	0.3250
C(18)	0.6910	0.3115	0.2348
C(19)	0.7363	0.2630	0.1419
C(20)	0.8252	0.2629	0.2011
C(21)	0.8187	0.2901	0.3203
C(22)	0.8956	0.1840	0.3937
C(23)	0.1784	0.4206	0.2670
C(24)	0.2102	0.0589	0.3250
C(25)	0.3238	0.5978	0.1757
C(26)	0.5748	0.0640	0.1808
C(27)	0.5799	0.5691	0.3320
C(28)	0.7415	−0.0188	0.3189
C(29)	0.8914	0.1950	0.5069
C(30)	0.9667	0.2491	0.3581
C(31)	0.0852	−0.0504	0.0719
C(32)	−0.0034	−0.1083	0.0668
O(1)	0.1154	0.1091	0.1216
O(2)	0.1205	−0.1888	0.0342

The final atomic coordinates and anisotropic temperature factors are listed in Tables 1 and 2 respectively. The composite diagram of the final electron density distribution viewed along the b axis is shown in Fig. 1.

Throughout the refinement process, 2051 reflexions with $\sin\theta/\lambda$ less than 0.550 were used and the atomic scattering factors were taken from the International Tables for X-ray Crystallography. Programme for the least-squares method was written by one of us (T. A.) with block-diagonal matrix approximation. The weights in the least-squares were 1.0 for $F_o>1.0$ and 0.5 for $F_o\leqslant 1.0$, and fudge factors were 0.7 for the scale and positional parameters and 0.5 for the thermal parameters.

TABLE 2. THE FINAL TEMPERATURE FACTORS
in the form of
$\exp\{-(B_{11}h^2+B_{22}k^2+B_{33}l^2+B_{12}hk+B_{31}lh+B_{23}kl)\}$

Atom	B_{11}	B_{22}	B_{33}	B_{12}	B_{31}	B_{23}
I	0.0043	0.0439	0.0128	−0.0019	0.0017	0.0065
C (1)	0.0029	0.0347	0.0085	0.0082	0.0008	0.0070
C (2)	0.0025	0.0490	0.0099	−0.0009	−0.0010	0.0024
C (3)	0.0009	0.0416	0.0107	0.0023	−0.0023	0.0013
C (4)	0.0026	0.0273	0.0079	0.0153	0.0026	0.0076
C (5)	0.0028	0.0284	0.0075	0.0064	0.0017	0.0030
C (6)	0.0029	0.1088	0.0074	−0.0045	−0.0005	−0.0158
C (7)	0.0029	0.0594	0.0065	0.0039	0.0015	0.0122
C (8)	0.0027	0.0266	0.0065	−0.0053	0.0017	−0.0018
C (9)	0.0036	0.0256	0.0062	−0.0018	0.0004	0.0043
C (10)	0.0033	0.0166	0.0071	0.0029	0.0000	0.0034
C (11)	0.0034	0.0435	0.0097	−0.0010	0.0005	0.0113
C (12)	0.0023	0.0400	0.0082	−0.0013	−0.0013	0.0139
C (13)	0.0029	0.0555	0.0076	−0.0211	0.0013	−0.0169
C (14)	0.0029	0.0282	0.0071	−0.0062	0.0017	−0.0091
C (15)	0.0040	0.0330	0.0065	−0.0052	0.0004	0.0125
C (16)	0.0028	0.0546	0.0067	−0.0101	0.0009	−0.0064
C (17)	0.0045	0.0152	0.0086	−0.0048	0.0010	0.0077
C (18)	0.0026	0.0314	0.0059	−0.0072	0.0006	0.0093
C (19)	0.0029	0.0790	0.0088	−0.0197	0.0022	−0.0023
C (20)	0.0028	0.0552	0.0101	0.0015	0.0018	0.0155
C (21)	0.0021	0.0238	0.0096	−0.0005	0.0005	0.0056
C (22)	0.0026	0.0503	0.0097	−0.0032	−0.0010	−0.0020
C (23)	0.0030	0.0328	0.0128	−0.0010	0.0021	−0.0087
C (24)	0.0027	0.0407	0.0114	0.0000	−0.0005	0.0055
C (25)	0.0044	0.0668	0.0170	0.0100	0.0004	0.0019
C (26)	0.0039	0.0389	0.0130	−0.0068	0.0023	−0.0144
C (27)	0.0038	0.0356	0.0149	0.0018	−0.0015	−0.0065
C (28)	0.0030	0.0306	0.0188	0.0025	0.0002	0.0088
C (29)	0.0027	0.0717	0.0114	0.0125	0.0018	0.0123
C (30)	0.0034	0.0648	0.0153	−0.0057	0.0030	−0.0247
C (31)	0.0057	0.0200	0.0067	−0.0034	0.0001	−0.0000
C (32)	0.0015	0.1243	0.0110	0.0337	−0.0022	0.0151
O (1)	0.0038	0.0342	0.0119	0.0090	−0.0008	−0.0037
O (2)	0.0032	0.0411	0.0137	−0.0014	0.0009	−0.0206

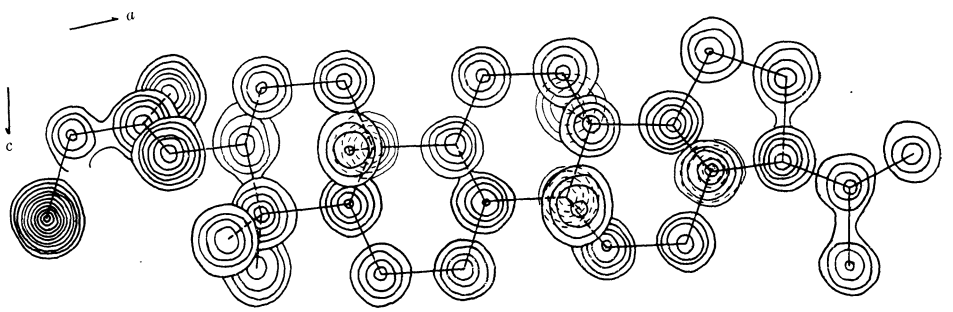

Fig. 1. A composite drawing of the final electron distribution viewed along the *b* axis.
For carbon and oxygen atoms, contours are drawn at intervals of 1 e.Å^{-3}, beginning with 1 e.Å^{-3}.
For iodine atom, contours are drawn at intervals of 5 e.Å^{-3}, beginning with 5 e.Å^{-3}.

Examination of the Alternative Structure

From the crystallographic point of view, the other model in which the ring A has a boat form was also possible as stated in the previous paragraph. This alternative model was subjected to the Fourier and least-squares refinement. Several abnormal figures were obtained in the course of refinement; for example, the bond length C(18)–C(19) became too longe, 1.99 Å, C(19)–C(20)rem arkably short, 1.19 Å and the isotropic temperature factor of C(19) was very large, 16.4 Å^2. The R factor did not go down less than 0.227. Therefore, it was concluded that this structure is not correct.

Some Remarks on Reliability of the Analysis

As mentioned in the previous paragraph, we changed artificially the y coordinate of C(6) at a certain stage. It may be of some interest whether this atom moves to the correct position in the other side of the pseudo mirror plane by continuing the least-squares process. We examined this, and found that it needed eight cycles to get the final result from the stage just before the artificial change. One of the reasons why the rate of convergence is so slow is that almost all the atoms in the principal skeleton of the molecule lie near the special plane and that since intensity data were collected from Weissenberg photographs about the b axis only the largest k reached to about a half of the possible maximum k within the copper sphere.

This crystal analysis met another serious difficulty. The crystal sufferred heavy degradation during the X-ray exposure. It was naturally supposed that reflexions on each layer might correspond to different stages of degradation. To examine this possibility the parameters except those related to the y direction were refined by the least-squares using several sets of the intensity data which were sampled from the individual layers. Intensity data of ($h0l$) and ($h3l$) were supposed to be those of rather fresh crystal. Corresponding bond lengths derived from the refinement of each layer are in good agreement, considering the fact that limited number of data makes standard deviations large; mean deviation being 0.054 Å and the maximum 0.17 Å. On the other hand ($h2l$) and ($h5l$) were taken from the heavily sufferred crystal. Corresponding lengths from these layer data fluctuated to much extent; mean deviation being 0.17 Å and the maximum 0.48 Å. Difference in bond lengths between the new and damaged crystals averages 0.08 Å. Therefore, it may be concluded that the error of the bond lengths due to such a systematic error in intensity data is about 0.1 Å, which is of about the same magnitude as the standard deviation derived formally from the least-squares calculation.

Description of the Structure and Discussion

The structure determined here is compatible, in general, with that derived from chemical studies. The rings A and D have a chair form. Owing to the existence of the double bond, the rings B and C have a half-chair form. All the neighboring rings are trans-fused. The molecule bends at the rings B and C, so that it is bow as a whole. Configurations of O(1) and seven methyl groups (C(22) to C(28)) are also in agreement with chemical argument. Figure 2 shows the perpendicular displacements of the atoms from the mean plane of each ring.

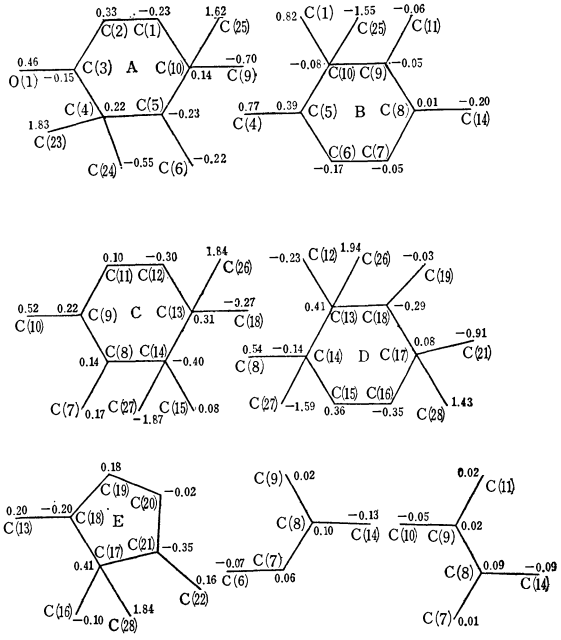

Fig. 2. The deviations of the atoms from the mean plane of each ring.

The bond lengths and angles are given in Fig. 3. Several interesting features are observed in the molecular dimensions, although their physical significance could not be insisted from the view of rather large errors.

(1) While the average bond length of all the C–C is 1.56 Å, the average of C–C bonds which are nearly parallel to the a axis is 1.62 Å. As the long axis of the molecule lies in the direction nearly parallel to the a axis, this elongation of the C–C may be interpreted as a result of long range intramolecular steric hindrance. The related nonbonded intramolecular distances are listed in Table 3.

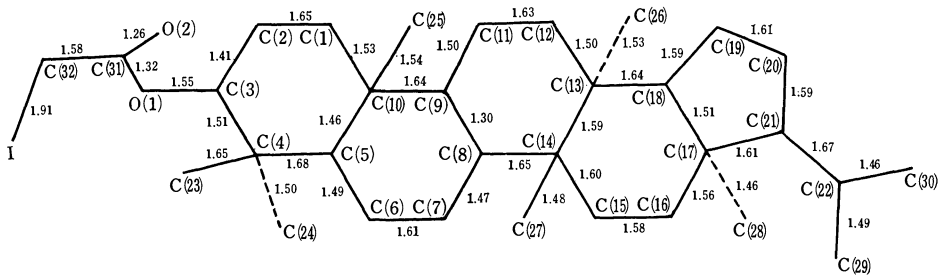

(a)

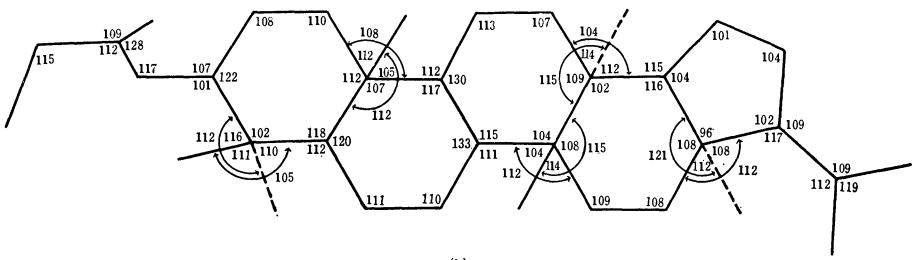

(b)

Fig. 3. (a) Bond longths (Å) and (b) bond angles (°) in the molecule of motiol iodoacetate.

TABLE 3. NON-BONDED DISTANCES IN THE MOLECULE (Å)

C(1) -C(11)	2.84	C(27)-C(12)	2.87
C(23)-C(6)	3.16	C(27)-C(16)	3.09
C(23)-C(25)	3.20	C(27)-C(18)	3.03
C(24)-C(6)	2.97	C(28)-C(15)	3.15
C(25)-C(11)	3.18	C(28)-C(19)	2.99
C(26)-C(8)	3.02	C(28)-C(20)	2.98
C(26)-C(9)	3.16	C(28)-C(22)	3.02
C(26)-C(28)	3.20	C(30)-C(20)	2.93
C(27)-C(7)	3.20		

(2) Chemical studies assigned C(7)–C(8) as a double bond. In the present analysis, the average deviation from the mean plane consisting of C(6), C(7), C(8), C(9) and C(14) is 0.079 Å, while that of the mean plane of C(7), C(8), C(9), C(10), C(11) and C(14) is 0.057 Å (Fig. 2). The difference might not be significant, however,

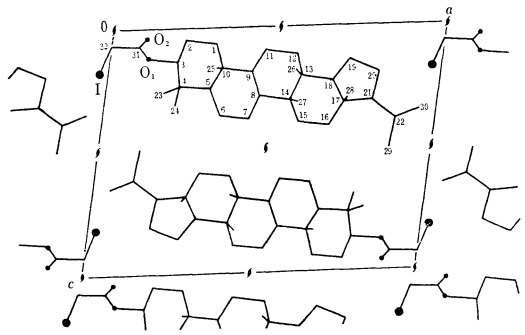

Fig. 4. Arrangement of molecules in the crystal viewed along the *b* axis.

TABLE 4. INTERMOLECULAR DISTANCES ($\leq$ 4.0Å)

From atom at x, y, z	To atom	In molecule	Distance (Å)
C(6)	C(15)	I	3.99
C(16)	C(24)	I	3.93
C(23)	C(29)	I	3.85
C(29)	C(24)	I	3.91
C(11)	C(26)	II	3.79
C(19)	O(2)	II	3.67
C(20)	O(2)	II	3.37
C(25)	O(2)	III	3.97
C(27)	C(26)	III	3.89
C(27)	C(28)	III	3.99
C(2)	C(32)	IV	3.98
C(31)	C(32)	IV	3.66
C(31)	I	IV	3.91
C(32)	C(32)	IV	3.82
C(32)	C(2)	IV	3.62
O(1)	C(32)	IV	3.45

Molecule	I	$1-x$,	$\frac{1}{2}+y$,	$1-z$
	II	$1-x$,	$\frac{1}{2}+y$,	$-z$
	III	x,	$1+y$,	z
	IV	$-x$,	$\frac{1}{2}+y$,	$-z$

C(7)–C(8) is 1.47 Å, while C(8)–C(9) is 1.30 Å. From these figures, it seems likely that the double bond is C(8)–C(9). According to Hirata, there is a possibility of the transfer of the double bond of C(7)–C(8) to C(8)–C(9) at the reaction of iodoacetylation of motiol.[5] If C(8)–C(9) is the double bond, the compound may be called as iso-motiol iodoacetate.

(3) There are observed very similar aspects of

molecular structures to those in the related compounds such as epilimonol iodoacetate[3] and methyl melaleucate iodoacetate.[4]

The arrangement of the molecules in the crystal is shown in Fig. 4. All the intermolecular distances shorter than 4.0 Å are listed in Table 4, which are equal or longer than the normal van der Waals contacts.

The authors would like to express their deep thanks to Professors Yoshimasa Hirata and Toshio Goto of Nagoya University for supplying the material and valuable discussions. All numerical computation were done on the NEAC 2101 of this Institute, NEAC 2206 of the Computing Centre of Osaka University and HITAC 5020 of the University of Tokyo.

3) S. Arnott, A. W. Davie, J. M. Robertson, G. A. Sim and D. G. Watson, *J. Chem. Soc.*, **1961**, 4183.
4) S. R. Hall and E. N. Maslen, *Acta Cryst.*, **18**, 265 (1965).
5) Y. Hirata, private communication (1967).

BULLETIN OF THE CHEMICAL SOCIETY OF JAPAN VOL. 41 1313—1319 (1968)

Thermodynamic Properties of Solutions of *m*-Terphenyl in Benzene. I. The Vapor Pressures and the Related Thermodynamic Functions at 30 and 50°C*[1]

Sadao TAKAGI, the late Katsuya FURUKAWA and Ryoichi FUJISHIRO

Department of Chemistry, Faculty of Science, Osaka City University, Sumiyoshi-ku, Osaka

(Received December 31, 1967)

Vapor pressures of solutions of *m*-terphenyl in benzene were measured for the concentration less than 0.23 in mole fraction x of terphenyl at 30 and 50°C. Vapor pressures P mmHg obtained are represented by $\log_{10} P(30°)=2.076970-0.4343x-0.06569x^2-0.4340x^3$ and $\log_{10} P(50°)=2.432100-0.4343x-0.14654x^2-0.3412x^3$. Chemical potentials observed were reproduced by the quasi-lattice theory for mixtures of molecules of different sizes. The Miller-Guggenheim expression ($r=3$, $z=6$—8) gives $w/\boldsymbol{k}=100\pm5°$, and the Flory-Huggins expression (r=molecular volume ratio) gives $\chi=0.272\pm0.004$ (30°) and $\chi=0.243\pm0.006$(50°). Partial molar heats of mixing are rather fitted by the regular solution theory similarly to the case for benzene+biphenyl, and the Flory-Huggins expression gives a concentration-dependent enthalpy parameter, $\chi_H=(0.77_2+1.7_{16}\phi)\times10^2/T$, where ϕ means a volume fraction of terphenyl. The average value of χ_H, 0.39 agreed with a theoretical estimate from solubility parameters.

It is well known that the thermodynamic study of the monomer+oligomer solutions is quite significant for the investigation of the molecular size effect in the solutions of small molecules as well as in the polymer solutions. In these monomer+oligomer mixtures, the monomer+dimer mixtures have been thermodynamically studied by many authors. Of those the benzene+biphenyl system has been most extensively studied, and has shown that the results of both vapor-pressure and heat of dilution measurements behave like those predicted for mixtures of molecules of different sizes.[1-6] Kortüm, *et al.* have shown, however, that the heats of mixing over the whole range of compositions at 71.6°C can not be fitted by the quasi-lattice model[7] for mixtures of molecules of different sizes but can only be fitted using the model for mixtures of molecules of the same size, and that the experimental values of the excess partial molar entropy of mixing are strongly temperature-dependent and cannot be fitted by the formulae for athermal mixtures of molecules of

*1 Presented at the 15th Annual Meeting of the Society of Polymer Science, Japan, Nagoya, May, 1966, and the preliminary work was presented at the 14th Annual Meeting, Tokyo, May, 1965.

1) J. H. Baxendale, B. V. Enüstün and J. Stern, *Phil. Trans. Roy. Soc.*, **A243**, 169 (1951).

2) D. H. Everett and M. F. Penney, *Proc. Roy. Soc. (London)*, **A212**, 164 (1952).

3) D. H. Everett and M. L. McGlashan, Published in Ref. 1, p. 234.

4) a) H. Tompa, *J. Chem. Phys.*, **16**, 292 (1948); b) "Polymer Solutions," Butterworths Scientific Publications, London (1956), p. 127.

5) A. Bellemans and C. Colin-Naar, *J. Polymer Sci.*, **15**, 121 (1955).

6) I. Prigogine, "The Molecular Theory of Solutions," North-Holland Publishing Company, Amsterdam (1957), p. 368.

7) E. A. Guggenhiem, "Mixtures," Oxford at the Clarendon Press (1952).

different sizes.[8,9] In order to obtain further information about size effect, thermodynamic properties of benzene+terphenyl system were begun to measure.

Experimental

Materials. Commercial *m*-terphenyl (chemical grade, Tokyo Kasei Kogyo K. K.) was purified carefully by repeating fractional recrystallizations from the solutions first with trichlorobenzene and thereafter with ethanol.[10] The *m*-terphenyl obtained was further purified by chromatography on silica gel (for chromatography, E. Merck) with benzene as an elutant. Finally occluded benzene was removed by vacuum sublimation. Mp 86.5°C.*2 An ultraviolet absorption spectrum of the purified *m*-terphenyl in alcohol showed no trace of the isomeric impurities.

Benzene was purified by an ordinary method with concentrated sulfuric acid, and then fractionally distilled twice over phosphorus pentoxide through a 1-m column packed with helices of stainless steel. After having been passed through silica gel, benzene was fractionally distilled once again, and finally submitted to repeated fractional crystallization. The boiling point sample used was 80.1°C.

Apparatus. The measurements of vapor pressures were carried out by using a liquid-vapor equilibrium still of recirculation type which was appropriate for small sample size.*3 Auxiliary equipments for the control and measurement of pressure were essentially the same as those described by Scatchard *et al.*,[11] and dry nitrogen was used as confining gas. The heights of mercury in a precision manometer which was immersed in a water thermostat were read to 0.05 mm by means of a 1-m cathetometer. Equilibrium temperatures were measured with a Beckmann thermometer which was calibrated against a standard thermometer certified by National Research Laboratory of Metrology, Tokyo. The error in the temperature measurements was within 0.003°C relatively, and within 0.03°C absolutely.

Procedures. The vapor pressures of the *m*-terphenyl solutions were measured over the concentration range less than 0.23 in mole fraction of terphenyl at 30 and 50°C. After about three or four hour's recirculation, both the equilibrium pressure and temperature were measured thrice. In order to obtain the equilibrium pressure at the precisely definite temperature as a function of composition, the interpolation of the points of three sets of measurements were carried out. The interpolation was made by first plotting the values of $\log P$ against reciprocals of temperature, and next reading a value from the smoothed curve at a desired temperature. This procedure is illustrated in Fig. 1. As the differences in temperatures were very small, each equilibrium composition was thought to be unchanged. An equilibrium liquid sample was withdrawn into a weighing bottle from the liquid trap of the still. The weight of this solution and that of *m*-terphenyl crystal which was produced by slow evaporation*4 of benzene from this solution were measured. The composition of the solution was determined by these weights. In the range of dilute concentration, *i. e.*, less than 0.1 in mole fraction, the composition was also determined by the measurement

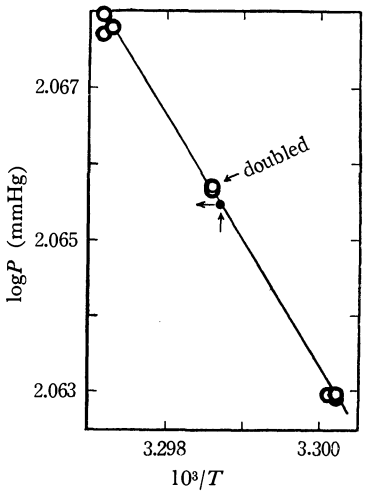

Fig. 1. Example of the determination of vapor pressure at 30.0°C. (x=0.0249)

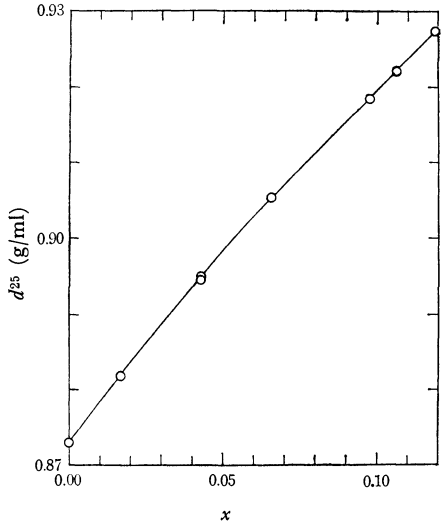

Fig. 2. Densities of dilute solutions of *m*-terphenyl in benzene at 25°C.

8) G. Kortüm, G. Dreesen and H.-J. Freier, *Z. Naturforsch.*, **8a**, 546 (1953).
9) D. S. Adcock and M. L. McGlashan, *Proc. Roy. Soc. (London)*, **A226**, 266 (1954).
10) S. Kato and H. Hashimoto, *Kogyo Kagaku Zassi (J. Chem. Soc. Japan, Ind. Chem. Sect.)*, **61**, 1265 (1958).
*2 The melting point was determined by the capillary method by us and was also kindly measured by Mr. M. Matsumoto by using a Cobble Automatic Thermoanalyzer, Type 201. Both results agreed each other.
*3 A detailed description of the design and the method of operation of the still will be published in this Bulletin in near future.
11) G. Scatchard, C. L. Raymond and H. H. Gilmann, *J. Am. Chem. Soc.*, **60**, 1275 (1938).
*4 Evaporation of benzene from the solution was carefully carried out in a hot atmosphere at the temperature not higher than 55°C.

of the density with the aid of a calibration curve shown in Fig. 2. The values of the composition obtained by both methods agreed within the experimental error.

Experimental Results

The values of vapor pressures obtained are summarized in Table 1 where P is in standard mm of mercury and x is the mole fraction of terphenyl in the solution. The vapor pressure of pure *m*-terphenyl melt has been measured by Mandel *et al.*[12] in the high temperature range. These data are represented by the following expression*5

$$\log_{10}P(\text{mmHg}) = 7.68211 - 2814.37/(207.79 + t) \quad (1)$$

where t is temperature expressed in degree Celcius. By assuming that this expression holds at temperature below the melting point, the values of the vapor pressure of the super-cooled pure *m*-terphenyl melt at 30 and 50°C are estimated to be 7.0×10^{-5} and 5.8×10^{-4} mmHg, respectively. The partial pressures of terphenyl in the solutions investigated were thus quite negligible, compared with the values of the vapor pressures of benzene over the solutions.*5

Usually, for a solution composed of a solvent and a non-volatile solute whose molecular sizes are not so different each other, the vapor pressure of the solvent can be expressed as

$$P=P^\circ(1-x)\exp(\alpha x^2+\beta x^3+\cdots)$$

or

$$\log_{10}P=\log_{10}P^\circ-0.4343x+cx^2+dx^3+\cdots \quad (2)$$

where x is the mole fraction of the solute, P° the vapor pressure of the pure solvent at the same temperature with the solution, and $\alpha, \beta, \cdots$, or $c, d, \cdots$, adjustable parameters. A least-squares treatment of our data according to Eq. (2), neglecting higher terms than the fourth power of x, gave

Table 1. Compositions of liquid phase, equilibrium vapor pressures, and deviations from the least-squares calculation at 30 and 50°C

(A) At 30°C

x	P mmHg	$P-P_{calc}$ mmHg
0.000_0	119.3_9	—
0.002_6	119.0_9	$+0.0_1$
0.024_9	116.2_7	-0.1_8
0.033_6	115.2_9	-0.1_3
0.042_1	114.3_3	-0.1_0
0.047_3	113.8_4	$+0.0_1$
0.074_4	110.4_3	-0.2_7
0.100_1	107.7_0	-0.0_4
0.122_4	104.9_8	-0.2_2
0.132_8	103.8_3	-0.1_9
0.140_5	103.4_4	$+0.3_1$
0.148_3	102.2_9	$+0.0_3$
0.155_8	101.5_0	$+0.0_9$
0.193_6	97.6_1	$+0.5_2$
0.205_6	95.3_6	-0.3_9
0.216_4	94.4_6	-0.0_6

(B) At 50°C

x	P mmHg	$P-P_{calc}$ mmHg
0.000_0	270.4_6	—
0.018_7	265.4_4	$+0.0_2$
0.046_1	257.9_2	-0.1_5
0.082_0	248.6_3	$+0.1_4$
0.108_1	241.3_1	-0.2_4
0.132_6	235.3_2	$+0.2_8$
0.140_0	233.0_7	0.0_0
0.188_6	219.9_3	-0.2_0
0.205_6	215.6_8	$+0.0_8$
0.226_5	210.0_4	$+0.0_2$

Table 2. Values of the second virial coefficients of benzene, molar volumes of the liquids, and volume ratio of the components

t °C	B [a] cm^3mol^{-1}	V_1° [b] $ml\,mol^{-1}$	V_2° [c] $ml\,mol^{-1}$	$r=V_2^\circ/V_1^\circ$
25	—	89.44	213.94	2.39_2
30	−1366	89.99	214.35	2.38_2
40	—	91.12	215.26	2.36_2
50	−1194	92.28	215.17	3.33_2

a Calculated with the expression: $B=70-13.2\times10^7/T^2[cm^3mol^{-1}]$.[13]
b Molar volume of benzene: calculated with Eq. (5).[14]
c Molar volume of super-cooled *m*-terphenyl; estimated from the data reported by Opdycke *et al.*[15] by extrapolation below the melting point.

*5 Constants in Eq. (1) were determined by a least-squares analysis of the smoothed values reported.[12] A plot of $\log P$ *vs.* $1/T$ showed significant deviation of lowest two values from others, so that these two values were omitted. If all values were used, Eq. (1) would be replaced by

$$\log_{10}P = 8.42379 - 3908.11/(326.8 + t),$$

from which the vapor pressures at 30 and 50°C were computed at 0.003 and 0.011 mmHg, respectively. We can safely regard the observed pressures over the dilute solutions as the vapor pressures of benzene.

12) H. Mandel, F. Silvey and K. Koda, *U. S. At. Energy Comm.*, **NAA-SR-5128**, 25 (1964).
13) P. W. Allen, D. H. Everett and M. F. Penney, *Proc. Roy. Soc. (London)*, **A212**, 149 (1952).
14) "International Critical Tables," Vol. 3, p. 29 (1928).
15) J. Opdycke, J. P. Dawson, R. K. Clark, M. Dutton, J. J. Ewing and H. H. Schmidt, *J. Phys. Chem.*, **68**, 2385 (1964).

TABLE 3. SMOOTHED VALUES OF VAPOR PRESSURE P, EXCESS CHEMICAL POTENTIAL DIVIDED BY RT, $\log_{10}\gamma_1=\mu_1^E/2.3026RT$, PARTIAL MOLAR EXCESS ENTROPY $\overline{S}_1^E$, AND PARTIAL MOLAR EXCESS HEAT $\overline{H}_1^E$ OF BENZENE IN SOLUTION AT 30 AND 50°C

x	30°C			30—50°C	50°C		
	P mmHg	$10^5 \log\gamma_1$	$\overline{S}_1^E$ e. u.	$\overline{H}_1^E$ cal/mol	P mmHg	$10^5 \log\gamma_1$	$\overline{S}_1^E$ e. u.
0.06	112.3_5	$73._4$	0.009_6	$3._9$	254.3_5	55.8	0.009_7
0.09	108.9_0	137.7	0.013_9	6.1	246.3_6	110.4	0.014_0
0.12	105.4_8	217.3	0.033_1	$13._0$	238.3_9	159.1	0.033_1
0.15	102.0_7	307.2	0.058_0	$21._8$	230.4_1	$209._7$	0.058_0
0.18	98.6_6	$404._7$	0.088_2	$32._3$	222.4_3	$260._4$	0.088_2
0.21	95.2_5	$506._4$	0.12_2	$44._0$	214.4_2	$310._1$	0.12_2

TABLE 4. $\log_{10}\gamma_1$ FOR THE MIXTURES AND TERMS WHICH MAKE UP $\log_{10}\gamma_1$ AT 30 AND 50°C

x	$\log_{10}\frac{P}{P^\circ(1-x)}$	$-\frac{B(P^\circ-P)}{2.3026RT}$	$\frac{V_1^\circ(P^\circ-P)}{2.3026RT}$	$\log_{10}\gamma_1$
	30°C			
0.06	0.0004987_3	0.00022_1	0.0000145_5	0.00073_4
0.09	0.001026_3	0.000329_1	0.0000216_8	0.001377_1
0.12	0.001707_8	0.000436_6	0.0000287_6	0.002173_1
0.15	0.002492_2	0.000543_6	0.0000358_1	0.003071_7
0.18	0.00335_4	0.000650_5	0.0000428_5	0.00404_8
0.21	0.00425_7	0.000757_6	0.0000499_0	0.00506_4
	50°C			
0.06	0.0001118_9	0.000414_3	0.0000320_3	0.000558_3
0.09	0.0004358_2	0.000619_9	0.0000479_2	0.001103_7
0.12	0.0007021_2	0.000825_2	0.0000637_2	0.001591_1
0.15	0.0009869_0	0.00103_0	0.0000796_5	0.00209_7
0.18	0.001272_8	0.00123_6	0.0000955_3	0.00260_4
0.21	0.001548_1	0.00144_2	0.000111_5	0.00310_1

$$\log_{10}P = 2.076970 - 0.4343x - 0.06569x^2 - 0.4340x^3 \text{ at } 30^\circ\text{C}$$

and

$$\log_{10}P = 2.432100 - 0.4343x - 0.14654x^2 - 0.3412x^3 \text{ at } 50^\circ\text{C} \quad (3)$$

The calculated values of vapor pressure by using Eq. (3) are seen to be in good agreement with the observed ones, as shown in the last column of Table 1, suggesting that Eqs. (3) are adequate expressions for representing the vapor pressure of the benzene solutions of *m*-terphenyl at both temperatures.

Then the activity coefficients of the solvent were obtained at every 3 mol per cent for each temperature by making use of Eq. (3) and the following equation including the correction due to the gas imperfection,

$$\log_{10}\gamma_1 = \log_{10}\frac{P}{P^\circ(1-x)} - \frac{B(P^\circ-P)}{2.3026RT} + \frac{V_1^\circ(P^\circ-P)}{2.3026RT} \quad (4)$$

where B is the second virial coefficient of pure benzene in the gaseous state and V_1° the molar volume of pure benzene. Values used for B's are evaluated from the expression given by Allen *et al.*,[13] which are tabulated in Table 2 as well as the values of V_1° used. The molar volume of benzene at t°C are calculated from the density,[14]

$$d = 0.90005 - 1.0636\times10^{-3}t - 0.0376\times10^{-6}t^2 - 2.213\times10^{-9}t^3, \quad (\pm2\times10^{-4}). \quad (5)$$

Numerical values of $\log_{10}\gamma_1$ thus obtained are listed in Table 3. The deviations from the ideal solutions are positive. The relative contribution of each of the terms in Eq. (4) to the total $\log_{10}\gamma_1$ is illustrated in Table 4 which shows the importance of the term involving the second virial coefficient B.

From $\log_{10}\gamma_1$'s, the excess partial molar enthalpy and entropy of benzene are derived by the following thermodynamic relationships;

$$\overline{H}_1^E = \partial(\overline{G}_1^E/T)/\partial(1/T) = 2.3026R[\Delta\log_{10}\gamma_1/\Delta(1/T)] \quad (6)$$

$$\bar{S}_1^E = \bar{H}_1^E/T - 2.3026\boldsymbol{R}\log_{10}\gamma_1 \quad (7)$$

and are also summarized in Table 3.

Discussion

For a solution which consists of N_1 monomers and N_2 r-mers, Guggenheim[16] has derived the theoretical formula, according to which the activity coefficient of solvent (monomer) is written in the zeroth approximation as follows:

$$\log_{10}\gamma_1 = -\log_{10}(1-x) + \log_{10}[N_1/(N_1+rN_2)] + (z/2)\log_{10}[(N_1+rN_2)/(N_1+qN_2)] + (1/2.3026)[qN_2/(N_1+qN_2)]^2 w/\boldsymbol{k}T \quad (8)$$

where z is the co-ordination number, $zq(=rz-2r+2)$ is the number of the nearest neighbor contacts around a r-mer molecule, w is the free energy parameter of interaction between monomer and r-mer molecules, and $\boldsymbol{k}$ is the Boltzmann constant. Assuming that terphenyl is a trimer of benzene ($r=3$), and z lies between 6 and 8,*6 one can calculate the values of $w/\boldsymbol{k}$ by substitution of the observed values of $\log_{10}\gamma_1$ into the Miller-Guggenheim expression, Eq. (8), as shown in Table 5.

Table 5. Values of interaction parameter obtained with the zeroth approximation of Guggenheim

x	$10^{-2}w/\boldsymbol{k}$,[deg^{-1}]			
	$z=8$		$z=6$	
	30°C	50°C	30°C	50°C
0.06	1.0_3	1.03	0.97	0.96
0.09	1.02	1.03	0.98	0.99
0.12	1.02	1.02	0.99	0.98
0.15	1.03	1.02	1.00	0.98
0.18	1.04	1.02	1.01	0.99
0.21	1.05	1.02	1.02	0.99

The constancy in the values of $w/\boldsymbol{k}$ irrespective of the mole fraction of terphenyl in the solution seems to suggest that Eq. (8) is adequate to the system such as benzene+*m*-terphenyl solution. The constant value of about 100° for $w/\boldsymbol{k}$ may be reasonable, compared with 76° or 77° found for the benzene solution of biphenyl which is regarded as a dimer ($z=6$).[3,4b]

It is well known that the Miller-Guggenheim formula becomes the Flory-Huggins expression when the co-ordination number z reaches infinity. The Flory-Huggins expression for activity coefficient of a solvent (monomer) is

$$\log_{10}\gamma_1 = \log_{10}[(1-\phi)/(1-x)] + (1/2.3026)(1-1/r) + (1/2.3026)\chi\phi^2 \quad (9)$$

where ϕ is the volume fraction of solute (r-mer), r the volume ratio of r-mer to monomer, and χ the free energy parameter of interaction between solvent and solute. By using Eq. (9), the free energy parameters χ were evaluated and values obtained are summarized in Table 6 where the

Table 6. Flory-Huggins free-energy and enthalpy parameters

Benzene + *m*-Terphenyl mixture				
x	χ		χ_H	
	30°C	50°C	30°C	50°C
0.06	0.274_5	0.248_3	0.38	0.37
0.09	0.269_1	0.248_7	0.28	0.27
0.12	0.269_3	0.242_9	0.36	0.35
0.15	0.271_2	0.240_7	0.41	0.40
0.18	0.273_7	0.240_1	0.46	0.44
0.21	0.276_3	0.237_7	0.49	0.47
mean	0.272_3	0.243_1	0.40	0.38
Benzene + Biphenyl mixture[a]				
χ(65°C)=0.185,		χ_H(25°C)=0.194		
		χ_H(50°C)=0.158		

a Cited from Ref. 4b.

corresponding value for the case of benzene+biphenyl is cited from the literature for comparison, and are plotted in Fig. 3. The numerical values of volume ratios r used are shown in Table 2. Figure 3 shows a slight tendency of the concentration-dependence of the parameters, which decrease with the volume fraction of terphenyl at 50°C and increase with the concentration at 30°C. The reasons for these behaviors, however, have not been discussed here, because there is no information about the excess volumes at those temperatures. The average values of χ at 30 and 50°C, $\chi=0.272_3$ and 0.243_1, correspond to $w/\boldsymbol{k}=83$ and 79°, respectively when r is chosen to be the volume ratio. The corresponding value for benzene+biphenyl mixture is $w/\boldsymbol{k}=63°$. Figure 4 shows that the Flory-Huggins expression, as well as the Miller-Guggenheim expression, represents the experimental values of free energy of mixing.

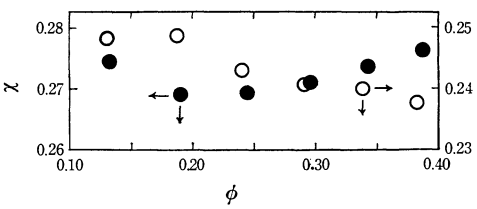

Fig. 3. Concentration-dependence of free energy parameters at 30°C (filled circles) and 50°C (open circles).

16) E. A. Guggenheim, "Mixtures," *l. c.*,[7] Chapt. XI.

*6 For the sake of comparison with the case of benzene+biphenyl, 6 and 8 are used as z after Everett and McGlashan.[3] If $z=10$ are used, a little larger values of $w/\boldsymbol{k}$ will be obtained.

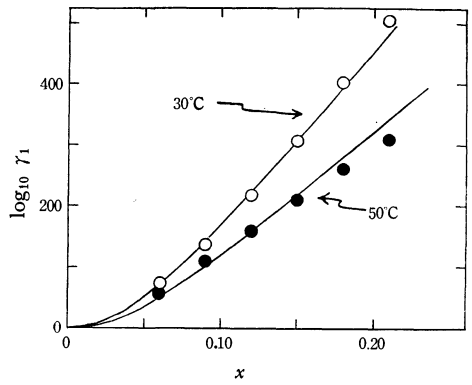

Fig. 4. $\log_{10}\gamma_1$ as a function of x.
○ or ● Experimental
—— Thpeoretical curves calculated by the Flory-Huggins expression by using $\chi = 0.272_3$ (at 30°C) and 0.243_1 (at 50°C).

The enthalpy parameter χ_H calculated through Eq. (10) at each temperature are also given in

$$\chi_H = H_1^E/\boldsymbol{R}T\phi^2 \tag{10}$$

Table 6. Their composition dependence at 30 and 50°C is given as a linear function of the volume fraction of terphenyl, Eq. (11), by a least-squares calculation.

$$10^{-2}T\chi_H = 0.77_2 + 1.7_{16}\phi \tag{11}$$

In the case of benzene+biphenyl mixtures heat of dilution measured are compatible to both the quasi-lattice theory for mixtures of molecules of different sizes and the regular solution theory with the same degree of accuracy within the experimental error,[4b,9] and the heat of mixing of benzene and molten biphenyl can not be expressed by other than the regular solution theory.[8] In our case of *m*-terphenyl also the regular solution theory can reproduce the partial molar heats of mixing of benzene as shown in Fig. 5. Figure 6 shows the systematic deviation of the experimental

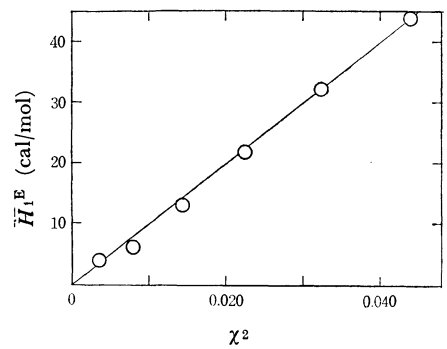

Fig. 5. Regular solution plot of the partial molar heat of mixing of benzene at 40°C.
○ Experimental

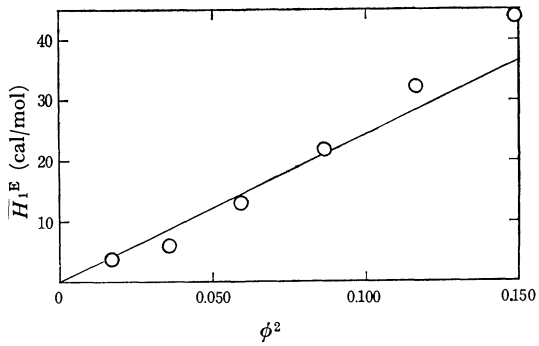

Fig. 6. Flory-Huggins plot of the partial molar heat of mixing of benzene at 40°C.
○ Experimental
—— $\boldsymbol{R}T\chi_H\phi^2$ when $\chi_H=0.39$.

points from the Flory-Huggins equation. If the Flory-Huggins equation holds, the experimental points would lie on a straight line through the origin. The quasi-lattice theory which contains the molecular size effect reproduces the experimental values only when the composition dependence of the parameter χ_H is considered. The average value of the parameter is $\chi_H=0.39$ (at 40°) which corresponds to $zu/\boldsymbol{k}=122°$ and $\boldsymbol{N}zu=242._7$ cal/mol, on the other hand those reported[4b] for benzene+biphenyl mixture are $zu/\boldsymbol{k}=58°$ and $\boldsymbol{N}zu=114._9$ cal/mol at 25°C and $zu/\boldsymbol{k}=51°$ and $\boldsymbol{N}zu=101._5$ cal/mol at 50°C.

The χ_H parameter can be estimated by using Eq. (12) based on the zeroth approximation of mixtures of molecules of different sizes,

$$\chi_H = (\bar{V}_1/\boldsymbol{R}T)(\delta_1 - \delta_2)^2 \tag{12}$$

where $\bar{V}_1$ is the partial molar volume of benzene and δ's are the solubility parameters which are defined by

$$\delta^2 = (\Delta H^v - \boldsymbol{R}T)/V \tag{13}$$

$$= n^{-1}(\partial E/\partial V)_T \tag{14}$$

where ΔH^v is the heat of vaporization, V the molar volume, $(\partial E/\partial V)_T$ the internal pressure, and n the parameter which is slightly greater than 1.0 for non-polar liquids.[17] The internal pressure can be computed directly from the thermal pressure coefficient or from the coefficient of expansion α and the isothermal compressibility β_T. The external pressure P is negligibly small, compared to the thermal pressure term in a condensed phase under atmospheric pressure.

$$(\partial E/\partial V)_T = T(\partial P/\partial T)_V - P$$
$$\simeq T(\partial P/\partial T)_V = T(\alpha/\beta_T) = T\gamma \tag{15}$$

17) J. H. Hildebrand and R. L. Scott, "The Solubility of Noneletrolytes," 3rd Edition, Dover Publications, Inc., New York, N. Y. (1964), p. 97.

Since there is the experimental evidence of constancy of the quantity $TV^2\gamma$ over a range of temperature,[18-20] once it is known at an appropriate temperature it is possible to deduce the internal pressure at any desired temperature by using only the knowledge of the molar volume at that temperature.

The internal pressures of benzene were calculated from the data given by Stavely *et al.*[18] The comparison with the cohesive energy density[21] gave 1.06 as a numerical value of n at 25°C which agreed very well with the value obtained at 20°C ($n=1.06$).[22] Thus, $n=1.06$ has been used for both components at 30 and 50°C. The internal pressures of *m*-terphenyl were estimated from the solubility parameter at 90°C given by Clark and Schmidt,[23] under the assumption that $TV^2\gamma$ is constant over the range of temperature. The solubility parameters obtained are given in Table 7. The values of χ_H calculated through Eq. (12) are 0.3_9 and 0.3_2 at 50 and 30°C, respectively, on the assumption that the partial molar volume of benzene is approximately equal to the molar volume in pure state, $V_1°$. Taking account of the assumptions made in the calculation, agreement between the values of χ_H obtained by the experiment and those calculated by using Eq. (12) is satisfactory as shown in Table 7. After the present measurements had been completed, the studies of this system by gas-liquid partition chromatography were presented by Clark and Schmidt.[23] They reported that the heat of solution at infinite dilution for benzene in *m*-terphenyl ($x\rightarrow 1$) at 90°C is 180±50 cal/mol. It corresponds to 0.25±0.07 as χ_H which is consistent with the present experimental values obtained at 50 and 30°C.

Table 7. Prediction of χ_H from the solubility parameters

t °C	δ_1	δ_2	χ_H Eq. (12)	χ_H Expt.
50	8.8_5	10.5_0	0.3_9	0.38
30	9.0_8	10.5_4	0.3_2	0.40

The partial molar excess entropies of mixing of benzene are described by the Flory-Huggins formula as follows,

$$\overline{S}_1^E = \overline{S}_1^E(\mathrm{I}) + \overline{S}_1^E(\mathrm{II}) \quad (16)$$

$$\overline{S}_1^E(\mathrm{I}) = -R\{\ln[(1-\phi)/(1-x)] + (1-1/r)\phi\} \quad (17)$$

$$\overline{S}_1^E(\mathrm{II}) = -R\chi_S\phi^2 \quad (18)$$

where $\chi_S=\chi-\chi_H$. In Fig. 7 the experimental partial molar excess entropies and the athermal contributions for those, given by Eq. (17), are plotted against the volume fraction of terphenyl, where the curves have been drawn by hand through the origin of the co-ordinate. Figure 7 shows that the contribution for the excess entropy from the non-athermal term, Eq. (18), seems to be significant,*7 although the detailed studies on the physical meanings of the χ_S must be postponed until the excess volumes and compressibilities at the temperatures where present experiments were undertaken become available.

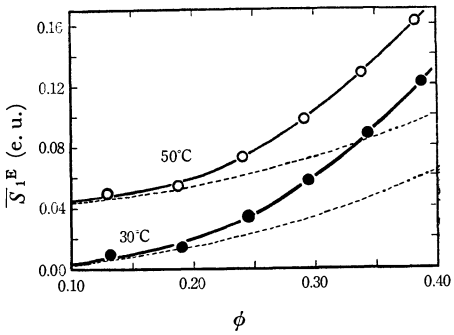

Fig. 7. Excess partial molar entropies of benzene (plots for 50°C is shifted upwards by 0.04 in e. u.).
——: $\overline{S}_1^E$, Experimental
- - -: $\overline{S}_1^E(\mathrm{I})$, Calculated

Since calculations of the excess thermodynamic functions in terms of the average potential, corresponding states theory of polymer mixtures extended by Prigogine implicitly, include the effects of volume changes on mixing,[24] the experimental results have been compared with the predictions by this theory. Explicit expression derived for excess Gibbs energy of mixing at vanishing pressure agreed with that given by Clark *et al.*[23] In this case, however, it was not able to predict the thermodynamic properties obtained by the measurements.

Finally we conclude that the thermodynamic behavior of benzene+*m*-terphenyl solution is similar to that of benzene+biphenyl solution.

We thank Mr. M. Matsumoto, of Kayagaki Irikakikai-Kogyo K. K. for the measurement of mp of *m*-terphenyl.

18) L. A. K. Staveley, W. I. Tupman and K. R. Hart, *Trans. Faraday Soc.*, **51**, 323 (1955).
19) J. H. Hildebrand and J. M. Carter, *J. Am. Chem. Soc.*, **54**, 3592 (1932).
20) W. Westwater, H. W. Frantz and J. H. Hildebrand, *Phys. Rev.*, **31**, 135 (1928).
21) G. M. Bristow and W. F. Watson, *Trans. Faraday Soc.*, **54**, 1731 (1958).
22) G. Allen, G. Gee and G. J. Wilson, *Polymer*, **1**, 456 (1960).
23) R. K. Clark and H. H. Schmidt, *J. Phys. Chem.*, **69**, 3682 (1965).

*7 If we evaluate $\overline{S}_1^E(\mathrm{I})$ by using the Miller-Guggenheim formula, difference of $\overline{S}_1^E$ and $\overline{S}_1^E(\mathrm{I})$ becomes larger, because the Flory-Huggins formula ($z=\infty$) gives the largest athermal entropy of mixing.
24) I. Prigogine, Chapt. XVII of Ref. 6.

BULLETIN OF THE CHEMICAL SOCIETY OF JAPAN VOL. 41 1320—1323 (1968)

Electron Spin Resonance Study of the Radiolysis of Monocarboxylic Acids Adsorbed on Silica Gel

Masaji MIURA, Akinori HASEGAWA and Yoshio YAMADA

Department of Chemistry, Faculty of Science, Hiroshima University, Higashisenda-machi, Hiroshima

(Received January 12, 1968)

Electron spin resonance measurements were carried out on γ-irradiated monocarboxylic acids (formic, acetic, and propionic acids) adsorbed on silica gel. In the case of formic acid, the spectrum assigned to the CO_2^- radical was mainly observed, but also observed was the signal caused by the defects of γ-irradiated silica gel, whereas for the acetic acid a quartet due to the methyl radical was obtained. These spectra, however, were not found in the frozen acids alone. As regards propionic acid, ethyl radicals were produced in both the adsorbed and frozen states. It was concluded from these results that the characteristic radiolysis of monocarboxylic acids on the adsorbed state is to be attributed to interaction between the acids adsorbed on silica gel as monomers and the surface. On the basis of these spectra, the adsorbed state of the acids and the stability of the radicals have been discussed.

The investigation of radicals adsorbed on solid surfaces seems to be of interest not only in the field of catalysis, but also in connection with the behavior of radicals on the surfaces.[1-4] Recent studies of the radiolysis of substances adsorbed on insulators with high surface areas have indicated that the radiolysis yield is higher on the adsorbed state than on the homogeneous state as a result of the energy migration from the solid surface to the adsorbate.[5-7] The behavior of hydrogen atoms and of methyl and ethyl radicals on silica gel has been studied by the ESR technique by Kazanskii *et al.*[8] They have determined the state of the adsorbed radicals by an analysis of the hyperfine structure and the coupling constant; they have found that these radicals are much stabilized on silica gel in comparison with those in a solid matrix.

In connection with their reports, we have attempted a study of the radicals formed by the radiolysis of monocarboxylic acids adsorbed on silica gel. For the adsorbate which interacts with the surface by means of the hydrogen bond, the characteristic radiolysis due to the change in the electronic state can be expected, among other things, when the coverage is less than unity. For this purpose, the ESR technique was used to obtain information on the radicals of the adsorbed state and on the nature of their thermal motion.

Experimental

The silica gel was prepared from water glass and sulfuric acid. It was purified by washing and electrodialysis, and was then calcinated in the air for 10 hr at about 450°C. Its surface area was measured by the BET method (S=790 m^2/g). The formic, acetic, and propionic acids used as adsorbates were dehydrated and distilled by the ordinary method.

The silica gel was outgassed in a vacuum of 10^{-5} mmHg for 5 hr at 450°C. The adsorption isotherms of these three acids on the silica gel were then measured by using a thermo-balance. The amounts of these acids adsorbed in a complete monolayer film were determined from these isotherms. The gel in a sample tube was exposed to the vapor of acid in a vacuum. When the desired coverage was attained, the tube was sealed off. In such a way samples with various coverages were obtained. The γ-irradiation was carried out by exposure to a ^{60}Co source at −196°C. The sample tubes used here were of quartz glass for acid on silica gel and of spectrosil for acid alone. The ESR spectra were obtained by using a Japan Electron Optics Laboratory JES-3BS-X type ESR spectrometer. The magnetic field was modulated at 100 kc/sec, and the g-value was determined by comparison with the value for DPPH.

Results and Discussion

γ-Irradiated Silica Gel. The spectra of the silica gel irradiated at −196°C and at room temperature are illustrated in Figs. 1a and 1b respectively. The spectrum shown in Fig. 1a

1) V. B. Kazanskii, G. B. Pariiskii and V. V. Voevodskii, *Discussions Faraday Soc.*, **31**, 203 (1961).
2) R. J. Kokes, *J. Phys. Chem.*, **66**, 99 (1962).
3) J. H. Lunsford and J. P. Jayne, *ibid.*, **69**, 2182 (1965).
4) C. L. Gardner, *J. Chem. Phys.*, **46**, 2991 (1967).
5) R. R. Hentz, *J. Phys. Chem.*, **68**, 2889 (1964).
6) J. G. Rabe, Birget Rabe and A. O. Allen, *ibid.*, **70**, 1098 (1966).
7) Yu. A. Sorokin, A. G. Kotov and S. Ya Pshezhetskii, *Zhur. Fiz. Khim.*, **40**, 2277 (1966).
8) V. B. Kazanskii, G. B. Pariiskii, I. V. Aleksandrov and G. M. Zhidomirov, *Fiz. Tverdogo Tela (USSR)*, **5**, 649 (1963).

consists of a doublet with the coupling constant of 506.5 gauss and broad lines. This is in good agreement with the spectrum reported by Kazanskii *et al.*[1] The doublet is due to hydrogen atoms formed by the cleavage of hydroxyl groups on the surface, while the broad lines are caused by residual oxygen radicals and by radiation defects in the irradiated silica gel.[9] The hydrogen atoms and residual oxygen radicals gradually decreased with a rise in the temperature and disappeared at a high temperature, while the defects were still present at room temperature. When the silica gel was irradiated at room temperature, only one singlet spectrum coincident with that of the defects appeared at $g=2.0009$, as is seen in Fig. 1b.

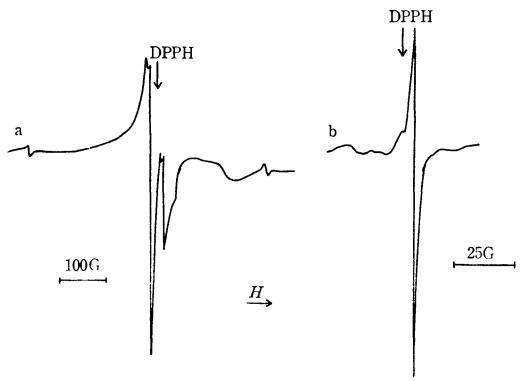

Fig. 1. ESR spectra of γ-irradiated silica gel (a) at liquid nitrogen temperature and (b) at room temperature.

γ-Irradiated Formic Acid Adsorbed on Silica Gel. The spectrum of the radicals which are produced by the radiolysis of the formic acid adsorbed on silica gel is different from that of formic acid alone (Fig. 2a, 2b). It has been reported regarding the X-irradiated formic acid that the radical, $H-\dot{C}(\diagup OH\cdots)(\diagdown O^-\cdots)$ or $H-\dot{C}(\diagup OH\cdots)(\diagdown OH\cdots)$, is formed by the radiation-induced reaction of the formic acid dimer.[10] The dotted lines indicate the hydrogen bond with the other molecule. From the close similarity of the spectrum obtained here to that previously reported, the spectrum shown in Fig. 2a can be assigned to the radical described above.

In the case of the adsorbed state, besides the defects of the γ-irradiated silica gel, another radical was formed, as is seen in Fig. 2b. In addition to these signal, a weak signal due to the radical, $H-\dot{C}(\diagup OH\cdots)(\diagdown O^-\cdots)$ or $H-\dot{C}(\diagup OH\cdots)(\diagdown OH\cdots)$, also appeared; this became still weaker with a decrease in the coverage.

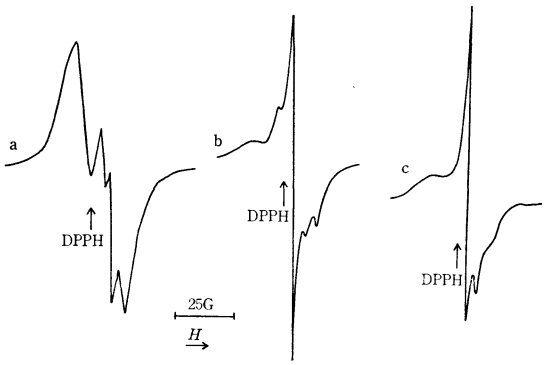

Fig. 2. (a) Spectrum of γ-irradiated formic acid, (b) spectra of γ-irradiated formic acid on silica gel at -196°C and (c) at -140°C.

The new signal became distinct at elevated temperatures as is seen in Fig. 2c. This radical may be assigned to the CO_2^- by a comparison of its g-value with the literature values.[3,11] The formation of carbon dioxide from the decomposition of formic acid was confirmed by gas chromatography. In view of the strong interaction of the formic acid monomer with the surface by means of the hydrogen bond,[12] it may be said that both the C–H bond and the O–H bond of the adsorbed acid were ruptured by γ-irradiation.

The formation of the CO_2^- radical was further studied as follows. Carbon dioxide was introduced to γ-irradiated silica gel. The ESR measurement was done while the sample was being irradiated with UV light.*1 The spectrum was in complete agreement with that shown in Fig. 2c. Our results on the g-value for CO_2^- radical are summarized in Table 1, along with those obtained by other authors.[3,11]

Table 1. Summary of g-values for CO_2^- radical

	g_x	g_y	g_z
CO_2^- on MgO[a]	2.0029	1.9974	2.0017
CO_2^- in NaCOOH[b]	2.0032	1.9975	2.0014
CO_2^- on SiO_2	2.0024	1.9978	2.0024

a) Ref. 3 b) Ref. 11

γ-Irradiated Acetic Acid on Silica Gel. Acetic acid irradiated at -196°C gave a doublet with splitting of *ca.* 30 gauss (Fig. 3a). As the temperature was raised from -196°C, this doublet gradually changed into a quartet (Fig. 3b). The coupling constant of the quartet was *ca.* 15 gauss. These results are in good agreement with those reported by Miyagawa *et al.*[10] The doublet has

9) H. W. Kohn, *J. Chem. Phys.*, **33**, 1588 (1960).
10) I. Miyagawa and W. Gordy, *J. Am. Chem. Soc.*, **83**, 1036 (1961).
11) D. W. Ovenall and D. H. Whiffen, *Mol. Phys.*, **4**, 135 (1961).
12) B. Imelik, J. Francois-Rassetti and P. Sigli, *J. Chim. Phys.*, **56**, 1048 (1959).
*1 The details of this study will be reported later.

been assigned by them to the radical, $CH_3\dot{C}(OH\cdots)(OH\cdots)$ or $CH_3\dot{C}(OH\cdots)(O^-\cdots)$. The change in the spectrum may be due to the rotational motion of the methyl group of the radical at higher temperatures.

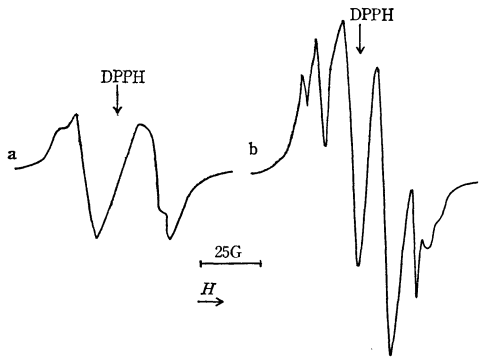

Fig. 3. Spectra of γ-irradiated acetic acid (a) at -196°C and (b) at -160°C.

The spectrum of the irradiated acetic acid on silica gel (Fig. 4a) consists of a quartet superimposed on a broad doublet. Since the quartet has the coupling constant of *ca.* 23 gauss, it is assigned to the methyl radical. The formation of the methyl radical indicates that the cleavage of the C–C bond occurred on the adsorbed acetic acid. The intensity ratio of the methyl radical spectrum at the coverage $\theta=1$ was 1 : 4.3 : 4.7 : 1.3, where θ is the fraction of the surface covered by the adsorbate. In comparison with the usual binominal coefficient ratio, the intensities of the central two components are too large. The central two components became sharp with a decrease in the coverage (Fig. 4b). The intensity ratios were 1 : 5.1 : 5.9 : 1.7 at $\theta=0.15$ and 1 : 6.0 : 6.2 : 2.0 at $\theta=0.04$. The abnormality in the intensity ratio suggests that the methyl radical interacts with the silica gel surface.

In addition to the quartet and doublet, a signal due to the defects in the silica gel begins to appear with a decrease in the coverage. The spectrum of the ·COOH radical was not observed. The difference between the spectra in the frozen and adsorbed states might be explained as follows. It is well-known that acetic acid forms a dimer by means of the hydrogen bond. However, when the acetic acid was adsorbed on silica gel, the three hydrogens of the methyl group as well as the carboxylic hydrogen may interact considerably with the surface.[13] According to this view, the transfer of the electron from the carboxyl group to the surface and the reduction of the inductive effect of the methyl group due to the interaction with the surface would lead to the weakness of the C–C bond. If this effect is taken into account, the breakage of the C–C bond can be understood. The appearance of the quartet and doublet shows that the acetic acid adsorbed on the silica gel decomposes through the following two simultaneous processes:

Fig. 4. Spectra of γ-irradiated acetic acid on silica gel (a) at $\theta=1$ and (b) at $\theta=0.15$.

$$CH_3COOH \rightarrow \cdot CH_3 + \cdot COOH \quad (1)$$

$$CH_3COOH \rightarrow CH_3\dot{C}(OH\cdots)(OH\cdots) \text{ or } CH_3\dot{C}(OH\cdots)(O^-\cdots) \quad (2)$$

The process (2) is considered to arise from the acetic acid, which interacts weakly with the surface.

In order to investigate the stability of the methyl radical, ESR measurements were made at various temperature. As the temperature was raised from -196°C, the intensity ratio of the quartet approached the binominal ratio. The radical continued to be present up to about -60°C. From these results it can be concluded that the methyl radical is initially fairly-well stabilized on the surface of silica gel but becomes mobile with a rise in the temperature.

γ-Irradiated Propionic Acid on Silica Gel. In the spectrum observed from the γ-irradiated

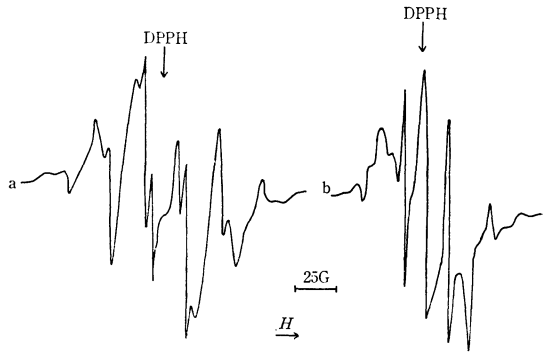

Fig. 5. (a) Spectrum of γ-irradiated propionic acid, (b) spectrum of γ-irradiated propionic acid on silica gel.

13) M. Shimizu and I. Higuchi, *Nippon Kagaku Zasshi (J. Chem. Soc. Japan, Pure Chem. Sect.)*, **81**, 1501 (1960).

propionic acid on silica gel (Fig. 5b), the singlet signal in the center seems to be due to the defects. With the exception of this singlet, this spectrum has a close resemblance to that of γ-irradiated propionic acid alone (Fig. 5a). The formation of the ethyl radical on the adsorbed state may be explained in the same way as in the case of acetic acid. However, because of the disappearance of the outer two components of the spectrum due to the ethyl radical on silica gel and the superposition of other radicals, it is impossible to discuss the adsorbed state of the ethyl radical.

The authors wish to express their hearty thanks to Assistant Professor Keiji Kuwata of Osaka University for his valuable discussions. Special thanks are also extended to Professor Satoru Tsuda, Mr. Akira Yokohata, and Mr. Osamu Yamamoto of Hiroshima University for kindly offering facilities for the γ-irradiation.

BULLETIN OF THE CHEMICAL SOCIETY OF JAPAN VOL. 41 1323—1325 (1968)

Microwave Spectrum of Cyclohexanone*[1]

Yoshitake OHNISHI and Kunio KOZIMA

Laboratory of Chemical Spectroscopy, Tokyo Institute of Technology, Ookayama, Meguro-ku, Tokyo

(Received January 16, 1968)

The microwave spectrum of cyclohexanone has been investigated in the frequency region from 7.7 to 23.4 Gc/sec. The R- and Q-branches for both the a- and the c-type have been assigned for the vibrationally ground state. The rotational constants obtained are $A=4195.30$ Mc/sec, $B=2502.57$ Mc/sec, and $C=1754.49$ Mc/sec. From these values it can be concluded that the molecules have the chair form. The value of the component of the dipole moment $|\mu_a|$ is 2.74 ± 0.03 D, and that of $|\mu_c|$ is 0.86 ± 0.03 D. The value of the total dipole moment is 2.87 ± 0.04 D, a value which is in agreement with that obtained by Debye's method. For the structural parameters Romers' data obtained by the electron diffraction seems to be nearly correct.

An electron diffraction investigation of cyclohexanone has been reported by Romers.[1] By assuming the chair form for this molecule, the structural parameters obtained in his investigation were as follows: the bond distances were 1.54 ± 0.01 Å, 1.24 ± 0.02 Å, and 1.09 ± 0.02 Å for C–C, C=O, and C–H respectively, and all the carbon bond angles were $109.5°\pm2.5°$, with the exception of the valency angle of the carbonyl carbon atom, which was $117°\pm3°$ for the C–C–C angle. By the study of the microwave spectrum of acetone,[2] the ∠C–C–C valency angle has been estimated to be $117°12'\pm20'$. This value is essentially the same as that obtained by Romers. However, no structural investigation of cyclohexanone by microwave spectroscopy has yet been reported. The present work has been carried out in the hope of determining the special ring structure of this molecule.

Experimental

The spectrum was measured over the frequency range from 7700 to 23400 Mc/sec with a conventional Stark modulation microwave spectrometer, employing 100 kc/sec square-wave or sine-wave modulation. All the measurements were made at about −15°C. The frequencies were measured by the method reported in a previous paper.[3]

The sample of cyclohexanone, obtained from a commercial source, was distilled twice before use.

Results and Discussion

Microwave Spectrum and Rotational Constants. To obtain an idea of how the spectrum would appear, preliminary rotational constants were calculated by use of the structural parameters obtained by Romers[1] for three possible structures, *i. e.*, the chair form, the boat form, and the skew-boat form, as shown in Fig. 1.

It was difficult to assign the spectrum because of its richness, but almost all of the low J transitions for the a-type and some of the low J, c-type transitions were identified by their characteristic Stark effects; these assignments were confirmed by fitting them with rigid-rotor rotational constants. The measured frequencies and the transitions for both a- and c-type are listed in Table 1, together with the rotational constants obtained. In view

*1 Presented at the Symposium on Structural Chemistry held by The Chemical Society of Japan, Sapporo, Oct., 1967.

1) C. Romers, *Rec. trav. chim.*, **75**, 956 (1956).

2) R. Nelson and L. Pierce, *J. Mol. Spectry.*, **18**, 344 (1965).

3) A. Hatta, C. Hirose and K. Kozima, This Bulletin, **41**, 1088 (1968).

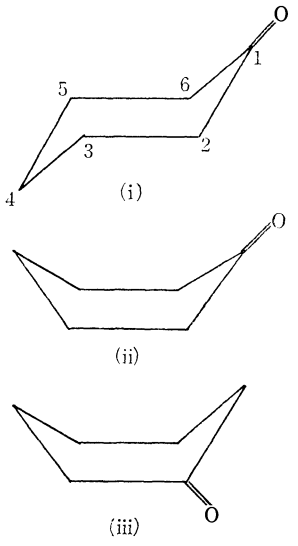

Fig. 1. Possible structures for cyclohexanone ring. (i) chair form, (ii) boat form, and (iii) skew-boat form.

TABLE 1. GROUND-STATE ROTATIONAL TRANSITIONS OF CYCLOHEXANONE

Transitions		Observed* in Mc/sec	$\nu_{obs}-\nu_{calc}$
a-type	$1_{11} \rightarrow 2_{12}$	7766.4	+0.4
	$1_{01} \rightarrow 2_{02}$	8316.0	+0.2
	$1_{10} \rightarrow 2_{11}$	9261.9	−0.3
	$2_{12} \rightarrow 3_{13}$	11537.9	−0.1
	$2_{02} \rightarrow 3_{03}$	12055.6	+0.4
	$2_{21} \rightarrow 3_{22}$	12771.7	+0.5
	$2_{20} \rightarrow 3_{21}$	13487.3	+0.2
	$2_{11} \rightarrow 3_{12}$	13748.5	+0.6
	$3_{13} \rightarrow 4_{14}$	15217.1	−0.3
	$3_{03} \rightarrow 4_{04}$	15553.8	−0.5
	$3_{22} \rightarrow 4_{23}$	16871.0	−0.3
	$3_{31} \rightarrow 4_{32}$	17343.2	+0.3
	$3_{30} \rightarrow 4_{31}$	17537.4	−0.8
	$3_{12} \rightarrow 4_{13}$	18014.5	+0.1
	$3_{21} \rightarrow 4_{22}$	18340.3	0.0
	$5_{15} \rightarrow 5_{14}$	10381.3	−0.7
c-type	$1_{01} \rightarrow 2_{11}$	11702.9	−0.2
	$1_{10} \rightarrow 2_{20}$	14539.0**	+0.3
	$1_{11} \rightarrow 2_{21}$	15088.6	+0.1
	$2_{02} \rightarrow 3_{12}$	17135.5	+0.4
	$2_{11} \rightarrow 3_{21}$	18764.2**	+0.5
	$2_{12} \rightarrow 3_{22}$	20093.6	0.0
	$2_{21} \rightarrow 3_{31}$	23215.8	−0.3
	$4_{22} \rightarrow 4_{32}$	8532.4	−0.9
Rotational constants:		$A=4195.30$ Mc/sec	
		$B=2502.57$ Mc/sec	
		$C=1754.49$ Mc/sec	

* Maximum uncertainty of the observed values is ±0.2 Mc/sec.

** Uncertainty of the observed value is ±0.5 Mc/sec, because of an overlap with other line.

of the relative intensities of the spectrum, it is sure that the frequencies listed in Table 1 are those for the vibrationally ground state. No b-type transitions could be found.

Because the rotational constants thus obtained almost agreed with the preliminary constants of the chair form and differed markedly from the preliminary constants of both the boat and skew-boat forms, it can be concluded that the molecules of cyclohexanone have the chair form, with C_h symmetry.

Dipole Moment. The Stark displacements of the $M=1$ component of the $1_{11} \rightarrow 2_{12}$ transition and of the $M=2$ and M=3 components of the $3_{13} \rightarrow 4_{14}$ transition were measured in order to determine the a and c components, μ_a and μ_c, of the electric dipole moment. These lines were nicely fitted to quadratic Stark displacements. The absorption cell was calibrated using the $J=0 \rightarrow 1$ transition of OCS, taking the dipole moment of OCS as 0.7124 D.[4] The observed and calculated Stark coefficients are given in Table 2.

TABLE 2. STARK COEFFICIENTS AND DIPOLE MOMENT

		$\Delta\nu/E^2$ (Mc/sec)/(kV/cm)^2	
Transition,	M	Obsd	Calcd
$1_{11} \rightarrow 2_{12}$	1	645 ±10	640.3
$3_{13} \rightarrow 4_{14}$	2	42.3± 1.0	42.4
	3	96.2± 2.5	98.6
$\lvert\mu_a\rvert=2.74\pm0.03$ D			
$\lvert\mu_c\rvert=0.86\pm0.03$ D			
$\mu=2.87\pm0.04$ D			

The subscripts a and c refer to principal inertial axes of cyclohexanone.

An analysis of these data yields $\lvert\mu_a\rvert=2.74\pm0.03$ D, $\lvert\mu_c\rvert=0.86\pm0.03$ D, and a total dipole moment of 2.87±0.04 D. This value agrees with that of 2.90 D[5] obtained in a 1,4-dioxane solution by Debye's method.

By taking into account the fact that the vector of the dipole moment should be nearly parallel to the C=O bond, the directions of the vectors of μ_a and μ_c can be determined; from this, the angle, α, made by the vector of the total dipole moment and the a axis can then be determined to be 17.5°±1°.

Structural Calculations. Since the experimental results provide only three moments of inertia and the orientation of the dipole moment vector, a number of assumptions are required in order to extract any structural information. It may be assumed that (i) all C–H bonds are of equal length; (ii) the oxygen atom is coplanar with the three

4) S. A. Marshall and J. Weber, *Phys. Rev.*, **105**, 1502 (1957).

5) I. F. Halverstadt and W. D. Kumler, *J. Am. Chem. Soc.*, **64**, 1982 (1942).

carbon atoms of C_6, C_1, and C_2; (iii) the internuclear distance, r_{2-3}, between C_2 and C_3 is equal to that, r_{3-4}, between C_3 and C_4; (iv) the HC_iH angle bisector is located along the $C_{i-1}C_iC_{i+1}$ angle bisector; (v) the HC_iH plane is perpendicular to the $C_{i-1}C_iC_{i+1}$ plane, and (vi) all of the HCH angles are the same. We then find that there are still nine undetermined structural parameters: r_{1-2}, r_{2-3}, r_{C-H}, $r_{C=O}$, $\angle C_1C_2C_3$, $\angle C_2C_3C_4$, $\angle C_3C_4C_5$, $\angle C_6C_1C_2$, and $\angle HCH$, where the numbers denote the positions of the carbon atoms in the ring, as shown in Fig. 1, and where r denotes the internuclear distance between the atoms shown in the subscripts. Therefore, we have to make six additional assumptions.

In our calculations the four internuclear distances and the two angles of $\angle C_6C_1C_2$ and $\angle HCH$ were assumed, and the remaining three angles were determined so as to get agreement between the observed and the calculated rotational constants. For the set I of the structural parameters, the assumed values are those[1] obtained by the electron diffraction. For the set II, the assumed values are those found in the microwave studies of acetone[2] and propane,[6] except that $\angle HCH$ is assumed to be a tetrahedral angle. The values of $r_{C=O}$, r_{1-2}, and $\angle C_6C_1C_2$ are those of acetone, and the values of r_{2-3} and r_{C-H} are those of propane. The angles of the ring obtained are listed in Table 3. Since, for the set II, the angle, β, made by the C=O bond and the a axis is considerably larger than the value of α, the set II seems to be inadequate. With an increase in the values of r_{2-3} or r_{1-2}, or with a decrease in the value of $C_6C_1C_2$, the value of β decreases. By the use of these facts, the sets III and IV, shown in Table 3, are tentatively calculated.

The agreement between the angle of α and that of β is satisfactory in the case of the set I; this favors Romers' data.

Table 3. Structural parameters of cyclohexanone

	Set I	Set II	Set III	Set IV
r_{1-2}*	1.54	1.507	1.507	1.516 Å
r_{2-3}*	1.54	1.526	1.535	1.535 Å
r_{C-H}*	1.09	1.096	1.096	1.096 Å
$r_{C=O}$*	1.24	1.222	1.222	1.222 Å
$\angle C_6C_1C_2$*	117°	117°12′	117°12′	116°12′
$\angle HCH$*	109°30′	109°28′	109°28′	109°28′
$\angle C_1C_2C_3$	109°35′	109°25′	109°31′	110°27′
$\angle C_2C_3C_4$	107°48′	119°31′	116°34′	114°39′
$\angle C_3C_4C_5$	106°34′	110°19′	109°40′	110°41′
β	17°05′	23°33′	22°28′	21°55′

β: The angle between the C=O bond and the a axis.

* These values were assumed for each set.

6) D. R. Lide, Jr., *J. Chem. Phys.*, **33**, 1514 (1960).

BULLETIN OF THE CHEMICAL SOCIETY OF JAPAN VOL. 41 1325—1329 (1968)

Anticatalytic Effect of Mn(II) in the Silver Catalyzed Oxidations by Peroxydisulphate

H. G. S. SENGAR and Y. K. GUPTA

Department of Chemistry, University of Rajasthan, Jaipur, India

(Received July 25, 1967)

Mn(II) has been found to be an anticatalyst in the silver catalyzed oxidations of oxalate, citrate, tartrate, malonate and arsenious acid and the limiting value of the rate constants in each case is about 0.4 *l*/mol·min at 35°C which is very much comparable to the rate constant for the separate silver catalyzed oxidation of Mn(II), H_2O, Ce(III), N_2H_4 and vanadyl ion. A mechanism has been proposed in which the simultaneous oxidation of Mn(II) and the organic substrate or arsenious acid takes place and when sufficiently large concentration of Mn(II) is present, the latter oxidation is almost completely suppressed. The oxidations of citrate and tartrate are consecutive reactions. The first faster reaction is followed by the second slower reaction.

Mn(II) has been reported to be an anticatalyst in the silver catalyzed oxidations of As(III)[1] and oxalate[2] by peroxydisulphate, but no mechanism to explain its action has been proposed so far. We have made a systematic relevant study in the oxidations of arsenious, malonic, oxalic, tartaric,

1) Y. K. Gupta and D. D. Mishra, This Bulletin, **32**, 1306 (1959).

2) E. Ben-zvi and T. L. Allen, *J. Am. Chem. Soc.*, **83**, 4352 (1961).

citric, acetic and formic acids. The kinetics have been followed by estimating peroxydisulphate iodometrically by the method of Szabo, Csanyi and Galiba.[3] The detailed kinetic study of the oxidation of malonic, tartaric and citric acids has not been made in the past and nor we intend to report such results in the present paper. We have considered their oxidations only with reference to the effect of Mn(II).

Experimental

All chemicals used were either B. D. H. Analar or E. Merck G. R. quality. Manganous sulphate was used for Mn(II). Water used was doubly distilled in pyrex glass vessels. Potassium peroxydisulphate was freshly prepared by direct weighing and its concentration checked by any known method.

Calculated quantities of perchloric acid, substrate (arsenious, malonic, citric, tartaric, acetic, oxalic or formic acid), silver nitrate, manganous sulphate and water were taken in the reaction vessel placed in a thermostat at 35°C. Peroxydisulphate solution was separately thermostated. Calculated quantity of peroxydisulphate was then added to the reaction vessel to initiate the reaction. Total reaction mixture was 100 m*l*. After suitable intervals 5 m*l* of the reaction mixture was pipetted out and determined for peroxydisulphate.[4] For this aliquots were transferred to a beaker containing 2.5 m*l* of 60% KI (added in the last), 2.5 m*l* of conc. HCl, 5 m*l* of water and 1 m*l* of the catalyst. The catalyst was prepared by dissolving 2.59 g of ferrous ammonium sulphate and 9.52 g of copper sulphate in 500 m*l* of water. A drop or two of conc. H_2SO_4 was added to make the solution clear.

The liberated iodine was titrated against a standard solution of thiosulphate from a burette using starch as indicator. A blank was also run with the catalyst and all other reactants except the peroxydisulphate and this was subtracted from all observed readings of the burette.

The results of experiments referred to Fig. 1 were also obtained in a similar way. The fortunate circumstance is that in any run Mn(II) and the substrate are not oxidized simultaneously, at least apparently. In case of oxalate, citrate, tartarate, malonate, As(III), *etc.*, these are first oxidized and no Mn(III) or MnO_2 is seen or found in the system. Mn(III) or MnO_2 could be found only when the substrate was completely oxidized. In case of acetate Mn(II) is first oxidized to MnO_2, and when this is complete, only then acetate is oxidized. It was possible to make a check on this conclusion in case of acetate. MnO_2 formed was separated by centrifuging the reaction mixture, and the precipitate and the liquid were separately analyzed for MnO_2 and peroxydisulphate respectively iodometrically. It was found that the decrease in peroxydisulphate was exactly equal to MnO_2 formed and hence it was concluded that acetate was not oxidized till there was any Mn(II) in the system. In other cases (oxalic, citric acid, *etc.*) there appeared no MnO_2 in the system till there was any substrate. The reduction of peroxydisulphate, therefore, takes palce in two parts with two different rates as shown in Fig. 1.

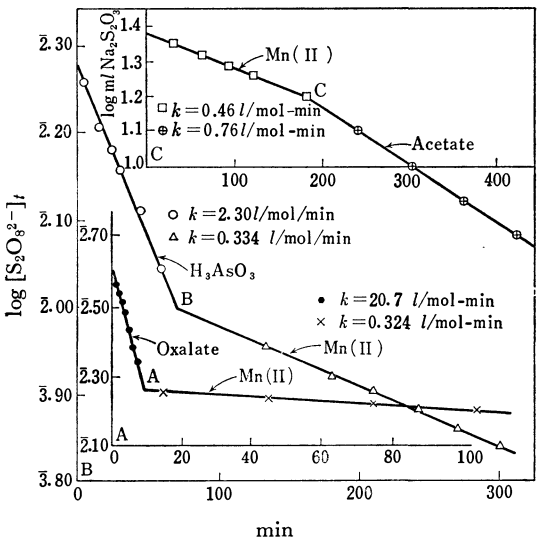

Fig. 1. First order plots showing the oxidation of Mn(II) only when that of oxalate or arsenious acid is complete, or before the oxidation of acetate starts.

A: $[S_2O_8^{2-}]=0.0199$ M; $[Na_2C_2O_4]=0.01$ M
B: $[S_2O_8^{2-}]=0.0093$ M; $[H_3AsO_3]=0.005$ M
C: $[S_2O_8^{2-}]=0.05$ M; $[CH_3COONa]=0.10$ M
$[HClO_4]=0.182$ M, $[Mn(II)]=0.01$ M, $[Ag^+]=0.005$ M

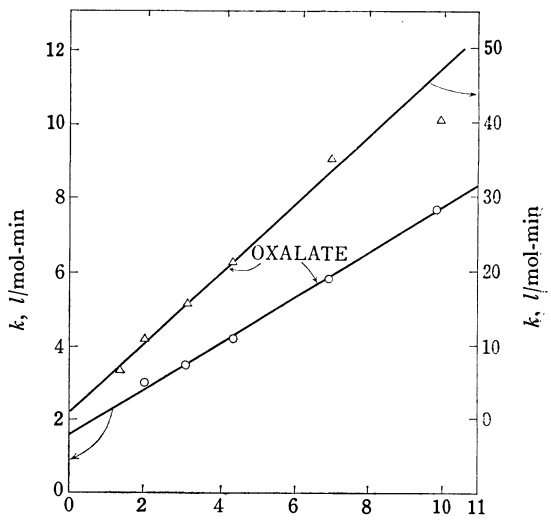

Fig. 2. Effect of manganous ion on the oxidation of oxalate by peroxydisulphate.
$[S_2O_8]=0.02$ M;
○: [oxalate]=0.10 M, $[AgNO_3]=0.0005$ M
$[HClO_4]=0.91$ M;
△: [oxalate]=0.01 M, $[AgNO_3]=0.002$ M
$[HClO_4]=0.182$ M

3) Z. G. Szabo, L. Csanyi and H. Galiba, *Z. anal. Chem.*, **135**, 269 (1952).
4) Y. K. Gupta and S. Ghosh, *J. Inorg. Nucl. Chem.*, **11**, 320 (1959).

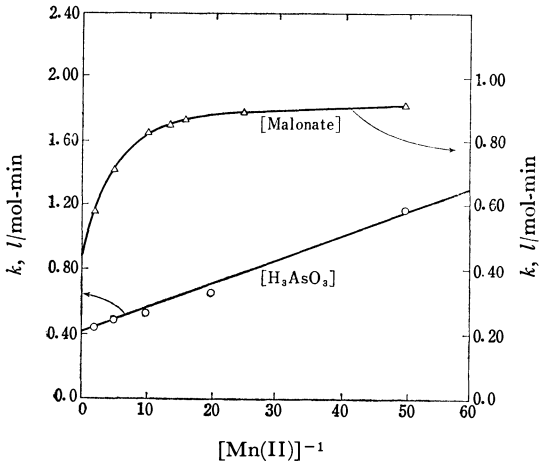

Fig. 3. Effect of manganous sulphate on the oxidation of arsenious and malonic acids by peroxydisulphate.
$[S_2O_8^{2-}]=0.02$ M; $[H_3AsO_3$ or $CH_2(COOH)_2]=0.02$ M; $[HClO_4]=0.182$ M; $[NaClO_4]=0.50$ M; $[AgNO_3]=0.002$ M

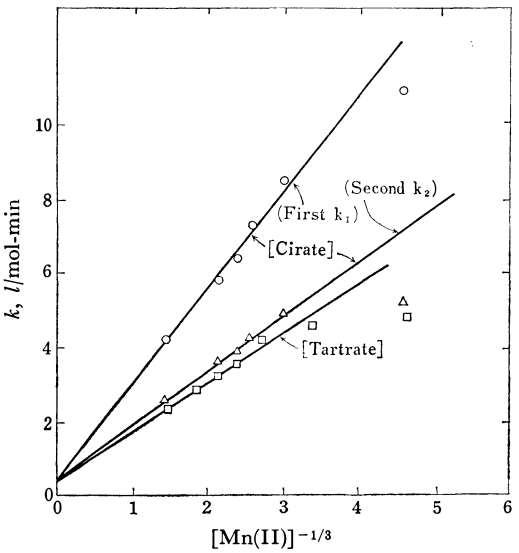

Fig. 4. Effect of manganous sulphate on the oxidation of citrate and tartrate by peroxydisulphate.
$[S_2O_8^{2-}]=0.02$ M; [citraie or tartrate]$=0.02$ M; $[HClO_4]=0.182$ M; $[NaClO_4]=1.0$ M; $[AgNO_3]=0.002$ M.

Results and Discussion

All the reactions are first order with respect to peroxydisulphate and the first order catalytic constants, k were calculated[5] from the following equation:

$$k = \frac{2.303 \times \text{slope}}{[Ag^+]}$$

where the slope refers to that of the straight line obtained by plotting the logarithm of the concentration of peroxydisulphate at different intervals of time, against time. The effect of Mn(II) on all these acids is shown in Figs. 2, 3 and 4 and a comparison of the rate for one concentration of Mn(II) has been made in Table 1.

A particular function of the concentration of

Table 1
$[S_2O_8^{2-}]=0.02$ M; $[Ag^+]=0.002$ M; $[HClO_4]=0.182$ M

Reducing substance	k, l/mol-min: In absence of Mn(II)	k, l/mol-min: In presence of 0.1 M Mn(II)	Limiting value of k	Other conditions
Oxalate, 0.01 M	153.5	16.16	1.5	Induction period
0.1 M	35.44	3.57	1.6	Induction period
As(III),* 0.02 M	23.03	0.55	0.42	$HClO_4=0.91$ M
Malonic acid, 0.02 M	0.98	0.83	0.41—0.43	
Citric acid, 0.02 M				
First reaction	12.25	5.87	0.45	1 M $NaClO_4$
Second reaction	3.90	3.65	0.40	
Tartaric acid, 0.02 M				
First reaction	17.42	3.70	0.40	1 M $NaClO_4$
Second reaction	3.83	4.65	—	
Acetic acid, 0.02 M	1.36	0.44	—	0.5 M $NaClO_4$

* Arsenious acid solution was prepared by boiling arsenious oxide with water as detailed in an earlier paper.[6]

5) H. G. S. Sengar and Y. K. Gupta, *J. Indian Chem. Soc.*, **43**, 223 (1966).

6) Y. K. Gupta and S. Ghosh, *J. Inorg. Nucl. Chem.*, **11**, 62 (1959).

Mn(II) has been selected for a graphical plot to obtain a limiting value of k in presence of infinite amount of Mn(II). The dependency of the pseudo-first order rate constants upon Mn(II) concentration is of varying nature in different cases. Only complete kinetic studies of the oxidation of organic acids by Mn(III) can give an explanation for this curious behaviour. However, we are concerned here only with the mechanism of the reduction of peroxydisulphate in presence of Mn(II) and the limiting value of the rate constant and not with the mechanism of the oxidation of the organic acids by Mn(III) or MnO_2. Nevertheless, this curious dependency on Mn(II) appears to be connected in some way with the complex formation of Mn(III) with the organic acids.

A look at the figures of Table 1 will indicate that in all cases except one, the limiting value of k is about 0.4—0.5 l/mol-min which is the same as for the oxidations of Mn(II),[7,8] Tl(I),[5] Ce(III),[9] H_2O,[10] *etc.* These results can be explained on the basis of the following general mechanism which has already been advanced by the previous workers.

$$S_2O_8^{2-} \rightleftharpoons 2SO_4^- \qquad \text{(i)}$$

$$2SO_4^- + Ag^+ \rightarrow 2SO_4^{2-} + Ag^{3+} \qquad \text{(ii)}$$

(1)

$$Ag^{3+} + IS \rightarrow \text{Products}$$

$$Ag^{3+} + Mn(II) \rightarrow Ag^+ + Mn(III) \text{ or } MnO_2 \qquad \text{(iiia)}$$

(2)

$$Ag^{3+} + S \rightarrow Ag^+ + R_1 \qquad \text{(iiib)}$$

$$S_2O_8^{2-} + R_1 \rightarrow SO_4^- + SO_4^{2-} + \text{products}$$

$$SO_4^- + R_1 \rightarrow SO_4^{=} + \text{products}$$

$$2R_1 \rightarrow \text{products}$$

Steps (iiia) and (iiib) are faster than (ii). Mechanism (I) refers to the oxidation of inorganic substrate (IS) and hence, is independent of the concentration of the latter giving overall catalytic rate constant of 0.4—0.5 l/mol-min (or the observed rate constant of $8—10\times10^{-4}$/min). Mechanism (2) involving the organic substrate is a chain mechanism. This mechanism and hence the overall rate constant would slightly change (the chain breaking step in particular) depending on the species being oxidized.

It appears that in presence of Mn(II), both mechanisms (I) and (2) occur simultaneously. Mn(II) competes with S in reaction with Ag^{3+}. Mn(II) is oxidized to Mn(III) or MnO_2 and the latter in acid medium quickly reacts with S. In previous studies of oxidations of tartarate,[11] citrate,[12] malonate[13] and oxalate[14] by MnO_2, the first order rate constants were found to be of the order of $5\times10^{-2}—1\times10^{-1}$/min which are about a hundred times higher than the observed rate constant of the present study. Hence the reaction of MnO_2 with S is fast, but this process may not be an efficient chain mechanism. Although S is oxidized by both mechanisms, the chain process becomes less significant in competition with the reaction with MnO_2 and the rate decreases. In the limit when sufficient Mn(II) is present, the chain mechanism (2) may not work at all and S is oxidized only through mechanism (1). The rate, therefore, falls to the limiting value of 0.4—0.5 l/mol-min. The limiting value in case of oxalate is slightly higher, but is by no means very different than 0.5. The probable reason for this higher value is that the reaction of Mn(III) with oxalate itself is a free radical reaction involving chains as reported by Taube[15] and Alder and Noyes[16].

The results with acetate are a little different. The catalytic rate constant was found to be about 1.1 to 1.5 l/mol-min depending on the ionic strength, and in absence of Mn(II). In presence of any concentration of Mn(II), the rate constant was 0.44 l/mol-min. Mn(II) is oxidized to MnO_2, but the latter does not react with acetate and hence accumulates in the system. (The peroxydisulphate was estimated after separating MnO_2 by centrifuging the reaction mixture.) Acetate, however, was not oxidized by the independent path (mechanism (2)) also and it was oxidized only when the oxidation of Mn(II) was complete. There are two distinct oxidations as is apparent from Fig. 1. This was proved by the fact that the rate of decrease of peroxydisulphate was exactly equal to the rate of formation of MnO_2, and acetate had absolutely no effect, *i. e.*, it was neither oxidized nor it affected the oxidation of Mn(II). This may indicate that the step (iiib) is too slow as compared to step (iiia), although the former is quite fast as compared to step (i) or step (ii). The situation is similar to the oxidation of water[10] in absence of any reducing substance, which takes place at the same rate at which Mn(II), if present, is oxidized and in that case water is not at all oxidized so long any Mn(II) is present. Another point of mechanistic interest

7) Y. K. Gupta and S. Ghosh, *ibid.*, **9**, 178 (1959).
8) A. O. Dekker, H. A. Levy and D. M. Yost, *J. Am. Chem. Soc.*, **59**, 2129 (1937).
9) W. H. Cone, *ibid.*, **67**, 78 (1945).
10) H. C. S. Sengar and Y. K. Gupta, *J. Indian Chem. Soc.*, **44**, 769 (1967).
11) Y. K. Gupta and S. Ghosh, *Proc. Natl. Acad. Sci., India*, **28A**, 214 (1959).
12) Y. K. Gupta and S. Ghosh, *ibid.*, **29A**, 331 (1960).
13) Y. K. Gupta and R. Dutta, *Bull. Acad. polon. Sci.*, **7**, 821 (1959).
14) Y. K. Gupta and S. Ghosh, *Z. physik. Chem.*, **208**, 368 (1957).
15) H. Taube, *J. Am. Chem. Soc.*, **70**, 1216 (1948).
16) S. J. Alder and R. M. Noyes, *ibid.*, **77**, 2036 (1955).

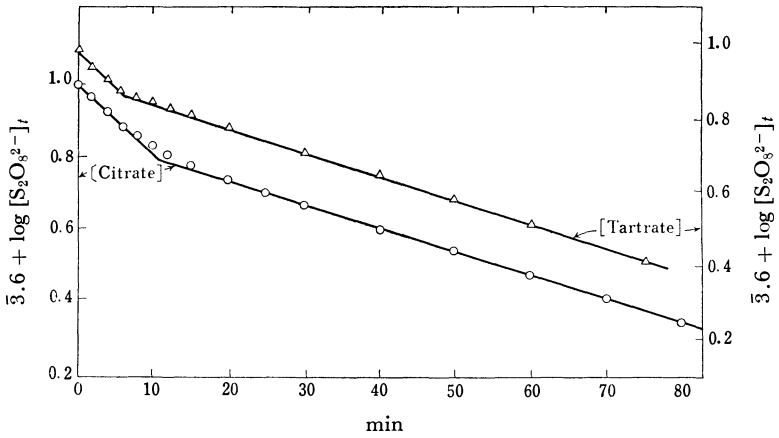

Fig. 5. First order plots for the oxidation of citrate and tartrate by peroxydisulphate, each one of them showing two reactions, one after the other.
$[S_2O_8^{2-}]=0.02$ M; [citrate]=[tartrate]$=0.02$ M; $[Ag^+]=0.005$ M; $[HClO_4]=0.182$ M; $[NaClO_4]=0.50$ M

found was that the rate of decrease of peroxydisulphate or the rate of oxidation of acetate (in absence of Mn(II)) was always about three times that of the oxidation of Mn(II).

A reverse behaviour is seen with the pair oxalate-Mn(II) or As(III)-Mn(II). So long any oxalate or arsenious acid is present in the system, Mn(II) is apparently not oxidized, and MnO_2 begins to form only after the oxidation of oxalate or arsenious acid is complete. Figure 1 shows these results. In fact Mn(II) is definitely oxidized as stated earlier, but Mn(III) formed reacts with oxalate or arsenious acid. The reaction is almost instantaneous in high acid medium.

In the oxidation of formic acid in presence of Mn(II), MnO_2 is formed as in the case of acetate, but the results show that the formic acid is also oxidized because the rate of decrease of peroxydisulphate is more than the rate of formation of MnO_2. In fact the rate of formation of MnO_2 is less than even the value of 0.4—0.5. A plot of log[MnO_2] *vs.* time also does not give a straight line. It appears that MnO_2 is further oxidized to permanganate which then slowly reacts with the formic acid. In this process more of peroxydisulphate is used up and some quantity of MnO_2 is also consumed. The overall observed first order rate constant, therefore, is more (0.51) than 0.4 (for Mn(II) alone). However, this constant is much less than the rate constant for the oxidation of formic acid alone in absence of Mn(II) which was found[17] to be 8—10 *l*/mol-min. The reaction mixtures were found to turn pink, obviously due to the formation of permanganate which subsequently slowly reacted with the formic acid forming back Mn(II). Mn(II), therefore, is never completely oxidized to MnO_2 in such a case till any formic acid is present. However, in case of acetate, permanganate even if formed does not react with the acetate.

We thus find that Mn(II) retards the rate in the silver catalyzed peroxydisulphate oxidations which go by a chain mechanism and this it does by reacting with the chain propagating free radical in competition with the substance being oxidized.

Oxidation studies of citrate and tartrate revealed another interesting fact though not relevant to the present paper. Both reactions seem to involve two consecutive reactions and that the first faster reaction is followed by the second slower reaction almost after when the former is complete (Fig. 5). First and second of Fig. 4 refer to these first and second reactions. In case of tartarate the first reaction is retarded and the second accelerated in presence of Mn(II). A detailed study of this reaction is being made to explain such behaviour of Mn(II). In case of citrate both the reactions are retarded in presence of Mn(II) and the limiting value in each case is 0.4 *l*/mol-min.

17) R. K. Nigam and Y. K. Gupta, *J. Indian Chem. Soc.*, **37**, 125 (1960).

BULLETIN OF THE CHEMICAL SOCIETY OF JAPAN VOL. 41 1330—1333 (1968)

Stability Constants of Some Uranyl Complexes

S. RAMAMOORTHY and M. SANTAPPA

Department of Physical Chemistry, University of Madras, Madras-25, India

(Received August 1, 1967)

Complexes of uranyl ion with benzoic, phenylacetic, phenoxy-acetic, thiomalic and itaconic acids were studied by pH titration method at 31 ±0.1°C. A 1 : 1 complex is formed in all the cases in the pH range 2.5—3.5 and their stability constants are reported.

In a potentiometric study of chelates of Uranyl nitrate with hydroxy, mercapto and amino acids, Cefola and coworkers[1] reported the first and second formation constants of uranyl-thiomalate complex in the pH range 2—4, neglecting the hydrolysis of uranyl ion till pH 4.00. Later, Mathur, Nigam and Srivastava[2] in a spectrophotometric study (Job's method) of the uranyl-thiomalic acid system reported the formation constants of the 1 : 1 complex in the pH range 3—7, neglecting again the hydrolysis of uranyl ions. It may be mentioned here that extensive investigations by Sutton,[3] Ahrland[4] and recently by Sommer[5] revealed that hydrolytic species of the type $U_2O_5^{2+}$, $U_3O_8^{2+}$, $U_3O_8(OH)$, $(UO_2)_2(OH)_2$, $(UO_2)_2OH$, *etc.*, at pH >3.5 were present. As a part of our studies on complexes, systems of uranyl ion with benzoic, phenyl acetic, phenoxy acetic, thiomalic and itaconic acids were studied by pH titration method at 31 ±0.1°C with a view to determine the composition(s) and formation constant(s) of the complex(es) and to detect possible formation of polymeric species especially in the systems of uranyl ion with thiomalic and itaconic acids in the pH range 1.5—3.5 in which hydrolysis of uranyl ion may be completely neglected.

From the results of our studies, it is concluded that a 1 : 1 complex is formed in all the systems. The stability constants of all the complexes were evaluated at 31±0.1°C.

Experimental

Materials. The uranyl perchlorate prepared from uranyl nitrate (BDH, AnalaR) by the standard procedure[6] was assayed by the Jone's reductor method[7] for uranyl content and by cation resin exchange method[8] for free acid. A stock solution (0.26 M in uranyl and 0.09 M in hydrogen ion) was prepared. Carbonate free sodium hydroxide (1.0 M) was used in all the titrations, the former after dilution to ten times was standardized against potassium hydrogen phthalate (0.1 M). The ligand acids (A. R.; all correct M. ps) were standardized with sodium hydroxide solution (0.2 M). Deionised water free from carbonate was used in all the titrations. Sodium perchlorate (2.008 M) prepared from perchloric acid (60% G. R., E. Merck) and AnalaR sodium hydroxide was used for constancy of ionic strength at 0.1.

Procedure. A pH meter (Cat. No. 7666, Leeds and Northrup) with glass and calomel electrodes standardized with potassium hydrogen phthalate buffer (0.05 M; pH 4.01 at 31°C) was used for measurements of pH during titrations of the system, ligand - perchloric acid - sodium perchlorate with or without uranyl perchlorate against standard alkali (1.0 M). All titrations were carried out in a double walled glass titration vessel provided with inlet and outlet tubes for circulating water at constant temperature (31°C or 45°C). The cell was covered with black cloth during titrations. Nitrogen freed from carbon dioxide was continually passed through the system under study in the titration cell. After each addition of the alkali titrant (0.05 m*l*), solutions were allowed to stand for 10—15 min for attainment of equilibrium. The titrations were carried out from an initial pH 1.5 to 11.0 and for ratios of [Ligand/Uranyl]≡1 to 10.

Results and Discussion

pH Titrations. Acid dissociation constants of the ligand acids were determined by titrating systems of ligand - perchloric acid - sodium perchlorate against standard sodium hydroxide solution (1.0 M). The initial volume of the solution was 100 m*l* and the ionic strength was kept at 0.1. pHs of the solution were recorded after each addition of

1) M. Cefola, R. C. Taylor, P. S. Gentile and A. V. Celiano, *J. Phys. Chem.*, **66**, 790 (1962).
2) V. K. Mathur, H. L. Nigam and S. C. Srivastava, This Bulletin, **36**, 1658 (1963).
3) J. Sutton, *J. Chem. Soc.*, **1949**, (Suppl) 2, S-275.
4) A. Ahrland, S. Hietanen and L. G. Sillen, *Acta Chem. Scand.*, **8**, 1907 (1954); S. Hietanen and L. G. Sillen, *ibid.*, **13**, 1828 (1959).
5) M. Bartusek and L. Sommer, *Z. Phys. Chem. (Leipzig)*, **226**, 309 (1964).
6) J. Heidt and A. Moon, *J. Am. Chem. Soc.*, **75**, 5803 (1953).
7) A. I. Vogel, "Text Book of Quantitative Inorganic Analysis," Longmans Green & Co., Ltd., (1962), p. 333.
8) D. W. Bhatnagar, *J. Sci. Ind. Res. (India)*, **B16**, 23 (1957).

0.05 m*l* of sodium hydroxide solution. Acid dissociation constants of benzoic, phenyl acetic and phenoxy acetic acids were calculated by the algebraic method and those of thiomalic and itaconic acids (first, K_1 and second, K_2) were determined conveniently by the method of slope and intercept due to Irving and Rossotti[9] because the two inflexions in the titration curves overlapped to give single inflexion points in the latter two cases. The following equation[9] due to Irving and Rossotti was used:

$$\frac{\bar{n}_H}{(1-\bar{n}_H)\,[H]} = \frac{1}{K_2} + \frac{1}{K_1K_2}\,\frac{(2-\bar{n}_H)\,[H]}{(1-\bar{n}_H)} \qquad (1)$$

$$K_1=[HA][H]/[H_2A] \text{ and } K_2=[H][A]/[HA]$$

$\bar{n}_H$, the average number of hydrogen ions bound to a ligand anion and corresponds to the Bjerrum's formation function[10]; charged species H^+ are written as H for simplicity. The pK_1 and pK_2 values for all acids are given in Table 1. A value of 0.83 for activity coefficient for H^+ (0.1 N) was used[11] for computing the concentration of the latter. p*K* values for various acids with those reported in literature[12-14] are given (Table 1).

TABLE 1.

Temperature 31°C $\mu=0.1$ ($NaClO_4$)

Ligand	p*K*(Authors)		p*K*(Lit.)		log K_{ML}*
	pK_1	pK_2	pK_1	pK_2	
1. Benzoic acid	4.01	—	4.01[14a]		2.59
2. Phenyl acetic acid	4.20	—	4.557[14b]		3.25
3. Phenoxy acetic acid	2.96	—	2.93[12]		2.41
4. Thiomalic acid	3.01	4.51	3.22	4.69[13]	3.75
5. Itaconic acid	3.61	5.08	3.68	5.14[14a]	4.85**

* Concentration constants
** Temperature: 28°C

Stability Constants K_{ML}. A known concentration, C_L, of the ligand was titrated without and with a known concentration, C_M, or uranyl ion, so that $[C_L/C_M]=1$ or 2 to facilitate formation of complexes 1 : 1 (ML_1) and 1 : 2 (ML_2) respectively. Titrations were also carried out for $[C_L/C_M]=10$ to allow the formation of higher complexes, if any. The degrees of formation of the metal complexes, $\bar{n}$, were calculated from the titration curves by Irving and Rossotti's difference method.[15] Values for the log of free ligand concentration, p*L* were obtained from the equation:

$$pL = \log_{10}\frac{\{1+([H]/K_2)+([H]^2/K_1K_2)\}}{(C_L-\bar{n}C_M)} \qquad (2)$$

Values of $\bar{n}$ and p*L* were used to draw the formation curves for the systems and $\log K_{ML}$ of the complex was evaluated from the value of p*L* at $\bar{n}=0.5$ (Fig. 1a). The stability constants were also determined graphically using Eq. (3), also due to Irving and Rossotti.[9]

$$\frac{\bar{n}}{(1-\bar{n})[L]} = K_{ML} + K_{ML}K_{ML_2}\frac{(2-\bar{n})[L]}{(1-\bar{n})} + \sum_{n=3}^{N} K_{ML}K_{ML_2}\cdots K_{ML_n}\frac{(n-\bar{n})[L]^{n-1}}{(1-\bar{n})} \qquad (3)$$

K_{ML}, $K_{ML_2},\cdots,K_{ML_n}$=successive formation constants and [L]=free ligand concentration. The formation of only 1 : 1 complex was also obvious from the plots $\bar{n}/(1-\bar{n})[L]$ *vs.* $(2-\bar{n})[L]/(1-\bar{n})$ being parallel to the abscissa (Fig. 1b). The stability constants calculated from $\bar{n}$ *vs.* p*L* curve agreed very well with those calculated from Eq. (3). It may be mentioned that $\bar{n}$ did not go beyond unity even when $[C_L/C_M]\geqq 1$ up to 10. From the order of stability constants (Table 1) for phenoxy acetic acid and benzoic acid being similar it appears that a chelate ring involving phenoxy oxygen atom is not formed for UO_2^{2+}-phenoxy acetic acid complex. The difference in the stability constant values between phenyl acetic acid and phenoxy acetic acids may be due to the respective p*K* values being different and therefore affecting considerably the stabilities of the complexes formed.[16,17] No data for stability constants for UO_2^{2+}-monobasic acid complexes (studied by us) are available in literature for comparison.

Thiomalic and Itaconic Acids. The formation curves of these systems showed the formation of only 1 : 1 complex in the pH range (1.5—3.5) (Fig. 1a and 1b). In order to detect the possible polymerization of the UO_2^{2+}-thiomalate and UO_2^{2+}-itaconate complexes, the pH titrations of the 1 : 1 uranyl-thiomalate and uranyl-itaconate systems were carried out for $[UO_2^{2+}]=[\text{Ligand}]=0.02$ M, 0.008 M, 0.005 M, 0.0025 M and 0.001 M for the former and 0.02 M, 0.0032 M, and 0.0016 M for the latter system which amounts to variation in

9) H. Irving and H. S. Rossotti, *J. Chem. Soc.*, **1953**, 3397; F. J. C. Rossotti and H. S. Rossotti, *Acta Chem. Scand.*, **9**, 1166 (1955).
10) J. Bjerrum, "Metal Ammine Formation in Aqueous Solution," Hasse, Copenhagen (1941).
11) J. Kielland, *J. Am. Chem. Soc.*, **59**, 1675 (1937).
12) K. Suzuki and K. Yamasaki, *J. Inorg. Nucl. Chem.*, **24**, 1093 (1962).
13) E. R. Clark, *ibid.*, **25**, 353 (1963).
14) a) M. Yasuda, K. Yamasaki and H. Okutaki, This Bulletin, **33**, 1067 (1960). b) "Stability Constants," 2nd Ed., ed. by L. G. Sillen and A. E. Martell, The Chemical Society, London (1964), p. 567.
15) H. M. Irving and H. S. Rossotti, *J. Chem. Soc.*, **1954**, 2904.
16) M. Yasuda, K. Suzuki and K. Yamasaki, *J. Phys. Chem.*, **61**, 229 (1957).
17) H. Irving and H. Rossotti, *Acta Chem. Scand.*, **10**, 72 (1956).

Fig. 1a Fig. 1b

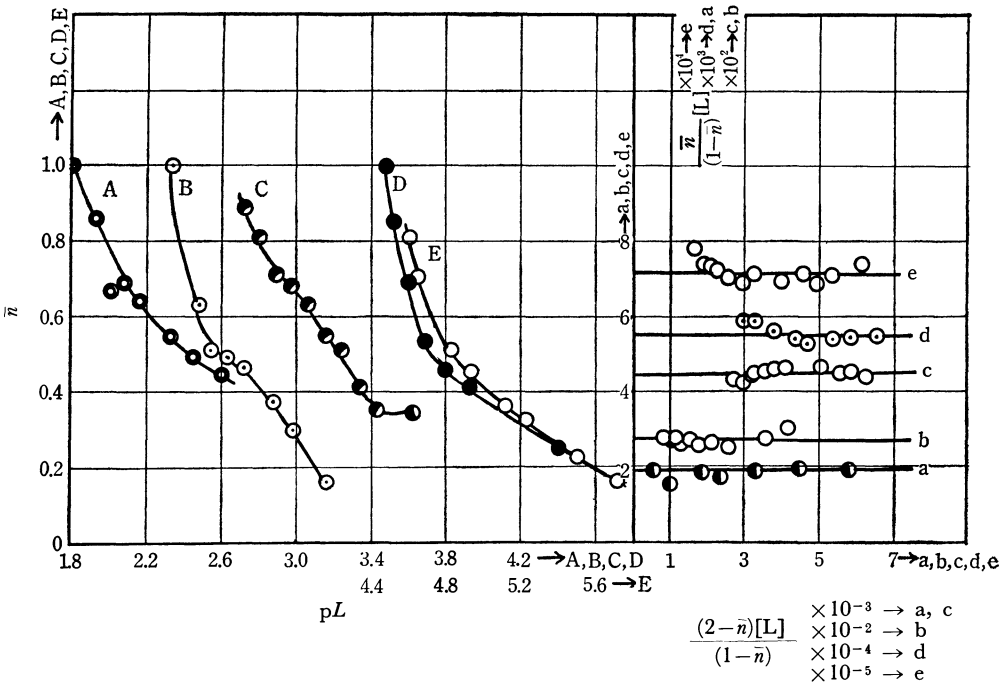

Fig. 1a. Formation curves ($\bar{n}$ *vs.* pL) of the systems of UO_2^{2+} with
(A) Phenoxy acetic acid, (B) Benzoic acid, (C) Phenyl acetic acid,
(D) Thiomalic acid, (E) Itaconic acid.

Fig. 1b. Plots of $\frac{\bar{n}}{(1-\bar{n})\,[L]}$ *vs.* $\frac{(2-\bar{n})\,[L]}{(1-\bar{n})}$ of UO_2^{2+} with
(a) Phenyl acetic acid, (b) Phenoxy acetic acid, (c) Benzoic acid,
(d) Thiomalic acid, (e) Itaconic.

TABLE 2

Ionic strength=0.1 ($NaClO_4$)
Acid dissociation constants
Thiomalic acid pK_1=3.01; pK_2=4.51 (31°C)
pK_1=2.95; pK_2=4.45 (45°C)
Itaconic acid pK_1=3.61; pK_2=5.08 (28°C)

T_M= T_L(M)×10³	log K_{ML} 31°C	log K_{ML} (av.). 31°C	log K_{ML}(av.) 45°C
UO_2^{2+}-Thiomalate			
20	3.75		
8	3.89	3.82±0.08	3.91±0.08
5	4.01		
2.5	4.00		
UO_2^{2+}-Itaconate			
20	4.85		
3.2	4.58	4.72±0.13	
1.6	4.73		

the total ligand and total metal concentrations by factors of 20 and 12 respectively. The data (Table 2) show that the log K_{ML} values for the uranyl-thiomalate and uranyl-itaconate systems increase slightly with decreasing concentration of the metal chelates and therefore polymeric complexes may be assumed to be absent in these systems.[18] We restricted our studies to pH<3.5 so that hydrolytic equilibria did not interfere with the systems under consideration.

pH titrations of the thiomalic acid against sodium hydroxide with and without uranyl ion were also carried out by us at 45°C. The stability constants for uranyl - thiomalic acid system at 31°C and 45°C (Table 2) did not vary very much within the limits of experimental errors and therefore calculation of thermodynamic parameters ΔH and ΔS under these circumstances would be futile according to Rossotti[19] and therefore no attempts for calculation of these parameters were made by us. Values of stability constants for uranyl-itaconic acid complex are not available in literature for comparison. Our value for the stability constant for UO_2^{2+}-thiomalic acid complex has been calculated under conditions of negligible hydrolysis and least complexing medium and therefore represents an improvement over the values already reported.[1,2]

18) K. S. Rajan and A. E. Martell, *J. Inorg. Nucl. Chem.*, **26**, 789 (1964); **26**, 1927 (1964).
19) F. J. C. Rossotti, "Modern Coordination Chemistry, Principles and Methods," Interscience Publishers, New York (1960), p. 18.

Conclusion

From our results, it is evident that uranyl ion forms a 1 : 1 complex with all the ligands under study in the pH range, (1.5—3.5). This is the case even when the ratio [Ligand/Uranyl] = 1 to 10.

It is probable that itaconic acid may coordinate through two COO^- groups to uranyl ion, forming a chelate ring. But in the case of thiomalic acid, a consideration of magnetic susceptibility data of uranyl-thiomalate complex by Mathur *et al.*,[2] and comparison of the log K_{ML} (3.75) for the latter with that for uranyl-malate complex (log K_{ML} = 1.66)[18] under more or less identical conditions indicate the possible involvement of neutral sulfur atom in coordination to uranyl forming a chelate ring, similar to coordination of neutral oxygen in hydroxy acids to metal ions.[20,21] The possibility of coordination of S^- to UO_2^{2+} cannot be discounted. The coordination of –SH group to metal ion even in the acidic region resulting in the deprotonation of the former is possible; however, we were unable to detect the release of the third proton in the pH range 2.0 to 5.0 of our studies. (Absence of inflexion corresponding to the release of third proton in our plots of pH *vs.* "moles of base"/"mole of ligand" added.)

20) D. I. Ryabehikov, I. N. Marao, A. N. Ernakao and V. K. Belyaeva, *J. Inorg. Nucl. Chem.*, **26**, 965 (1964).
21) R. C. Olberg and M. Stammler, *ibid.*, **26**, 565 (1964).

BULLETIN OF THE CHEMICAL SOCIETY OF JAPAN VOL. 41 1333—1339 (1968)

Kinetics of Multidentate Ligand Substitution Reactions. II. Substitution Reactions of BT with Nitrilotriacetato Nickelate(II) Chelate and with Ethylenediaminetetraacetato Nickelate(II) Chelate

Mutsuo KODAMA, Chifumi SASAKI and Mitsuko MURATA

Department of Chemistry, Ibaraki University, Mito, Ibaraki

(Received October 4, 1967)

This paper reports a spectrophotometric study of the solution equilibria and the kinetics of the substitution reaction of Eriochrom Black T (BT) with nickel(II)-NTA and with nickel(II)-EDTA chelates. In solutions of pH 8.50—9.50 containing a large excess of uncomplexed NTA over BT and nickel(II)-NTA chelate, BT forms only 1-to-1 normal chelate, NiD^-, with the nickel(II) ion, the stability constant of which is $10^{20.8}$ ($\mu=0.30$). Kinetically, the ligand-exchange reaction of BT with the nickel(II)-NTA chelate was found to proceed through the following two simultaneous reaction paths and to be much faster than that with the nickel(II)-EDTA chelate,

i) $NiX^- + HD^{2-} \rightleftharpoons NiD^- + HX^{2-}$ (rapid $\updownarrow$ NiX_2^{4-})

ii) $HD^{2-} \overset{\text{rapid}}{\rightleftharpoons} D^{3-} + H^+$; $NiX^- + D^{3-} \rightleftharpoons NiD^- + X^{3-}$ (rapid $\updownarrow$ NiX_2^{4-}) rate-determining step

where NiX^-, NiX_2^{4-}, HD^{2-}, and D^{3-} represent Ni(II)-NTA chelate of 1-to-1 composition, Ni(II)-NTA chelate of 1-to-2 composition, doubly deprotonated BT anion and completely deprotonated BT anion, respectively. The substitution reaction of BT with nickel(II)-EDTA chelate was found to proceed mainly through the following reaction path,

$$HD^{2-} \overset{\text{rapid}}{\rightleftharpoons} D^{3-} + H^+ \qquad NiY^{2-} + D^{3-} \rightleftharpoons NiD^- + Y^{4-}$$

rate-determining step

and the contribution of the following reaction to the whole reaction is negligible at pH 9.00—10.50.

$$NiY^{2-} + HD^{2-} \rightleftharpoons NiD^- + HY^{3-}$$

In a previous paper,[1] the kinetics of the substitution reaction of Eriochrom Black T (BT, H_3D) and ethylenediaminetetraacetato cobaltate(II) were studied spectrophotometrically. The substitution

1) M. Kodama, This Bulletin, **40**, 2575 (1967).

reaction was found to proceed through doubly dissociated and completely dissociated BT ions, but contribution of the reaction path where the dissociation of Co(II)-EDTA chelate is rate-determining is negligible.

In this paper, we report the kinetics of the substitution reactions of BT with nitrilotriacetato nickelate(II) chelate (Ni(II)-NTA) and with ethylenediaminetetraacetato nickelate (II) chelate (Ni-(II)-EDTA).

Experimental

Reagents. NTA and EDTA were recrystallized as free acids, and their solutions were standardized by the methods described previously.[1,2] Nickel(II) perchlorate solution was prepared by the following procedure. A known amount of metallic nickel of 99.99% purity was dissolved in dilute HNO_3 solution (1+1), and the nickel(II) was precipitated as hydroxide. The nickel(II) hydroxide was washed thoroughly with redistilled water and dissolved in diluted perchloric acid solution (0.25 M). The concentration of nickel(II) perchlorate solution was standardized against a standard EDTA solution using Murexide as indicator.[3] The purification of BT and the test of its purity are also described in an earlier paper.[2]

Apparatus and Procedure. The apparatus and the experimental procedures were the same as described previously.[1] In this study no buffer reagent was used because uncomplexed EDTA and NTA are considered to have enough buffer capacity to maintain pH values constnat.

Results and Discussion

The Substitution Reaction of BT with Nickel(II)-NTA Chelate. First, the composition and the stability constant of nickel(II)-BT chelate were determined by the same method as in the equilibrium study of the BT-cobalt(II)-EDTA system.[1] As shown in Fig. 1, the concentration ratio between uncomplexed BT and nickel(II)-BT chelate can be determined successfully by measuring the absorbance at 640 mμ. Under the experimental conditions where free NTA is present in a large excess over BT and nickel(II)-NTA chelate, by the analogy to the equilibrium between BT and zinc(II)-NTA chelate,[2] the following relation can be derived when only 1-to-1 chelate, NiD^-, is formed between BT and the nickel(II) ion.

$$\log \frac{A_D-A}{A-A_{NiD}} \cdot \frac{1}{m-\dfrac{A_D-A}{A_D-A_{NiD}}} \cdot [BT]_0 = \log \frac{K_{NiD}}{K_{NiX}} \frac{(\alpha_H)_x}{(\alpha_H)_{BT}} + \log \frac{1}{[X]_f \cdot \left\{1+\dfrac{K_{NiX_2}\cdot[X]_f}{(\alpha_H)_x}\right\}} \quad (1)$$

where symbols, A_D, A, $(\alpha_H)_{BT}$ and $[X]_f$, have the same meanings as were used in the previous paper[2] and other notation definitions used are as follows. A_{NiD}: Absorbance of the solution where all the BT ions are considered to form complex with nickel(II) ion, m: The ratio of the total concentration of nickel(II) to that of BT, $[BT]_0$: The total concentration of BT, K_{NiX}: Stability constant of Ni(II)-NTA chelate of 1-to-1 composition, K_{NiX_2}: Equilibrium constant defined as $K_{NiX_2}=[NiX_2^{4-}]/[NiX^-]\cdot[X^{3-}]$, K_{NiD}: Stability constant of Ni(II)-BT chelate, $(\alpha_H)_x$: (α_H) value of NTA.

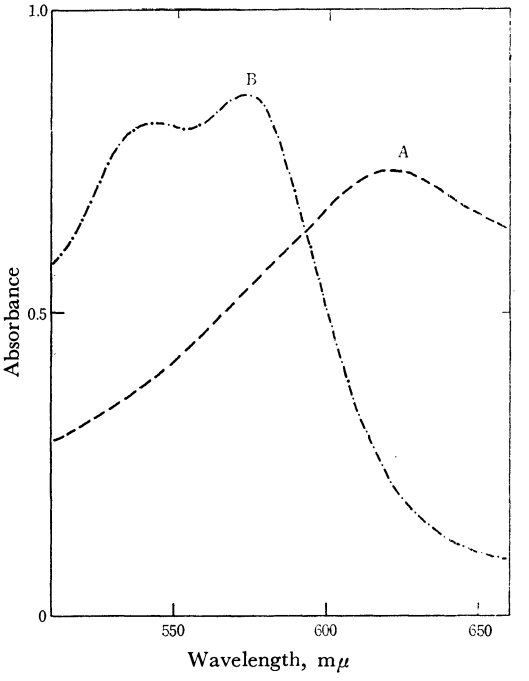

Fig. 1. Absorption curves.
$\mu=0.30$, pH=9.45
The concentration of uncomplexed NTA=27.0 mM
The concentration of BT=2.26×10^{-5} M
A. No nickel(II)-NTA chelate
B. 9.0 mM nickel(II)-NTA chelate

The ratio of the total concentration of nickel-(II) to that of BT m, was made 1.50 and all measurements were conducted in solutions at constant pH 9.54. A straight line with a slope of unity was obtained by plotting

$$\log \frac{A_D-A}{A-A_{NiD}} \cdot \frac{1}{m-\dfrac{A_D-A}{A_D-A_{NiD}}} \cdot [BT]_0 \text{ vs. } \log \frac{1}{[X]_f \cdot \left\{1+\dfrac{K_{NiX_2}\cdot[X]_f}{(\alpha_H)_x}\right\}}$$

2) M. Kodama and H. Ebine, *ibid.*, **40**, 1857 (1967).
3) H. Flaschka and H. Abdie, *Chemist-Analyst*, **44**, 30 (1955).

showing a confirmatory evidence that under the present experimental conditions only normal chelate NiD^- is formed (Fig. 2). From the intercept, K_{NiX} value[4] and pK values[5] in Table 1, the K_{NiD} value was determined to be $10^{20.8}$ (μ= 0.30, 25°C). This value can satisfactorily account for the well-known interference of nickel(II) ions in the EDTA titration of Mg(II) using BT as indicator.

As described previously,[2] the numerical values used in the above calculation were estimated from the related stability and the dissociation constants.[4] The concentration of free NTA $[X]_f$ was calculated by using the following relation.

$$[X]_f = \frac{-\left\{1-\frac{K_{NiX_2}}{(\alpha_H)_x}([X]_t-2[Ni(II)]_t)\right\}+\sqrt{1+\frac{2\cdot K_{NiX_2}\cdot[X]_t}{(\alpha_H)_x}+\frac{K^2_{NiX_2}}{(\alpha_H)_x{}^2}([X]_t-2\cdot[Ni(II)]_t)^2}}{\frac{2\cdot K_{NiX_2}}{(\alpha_H)_x}} \quad (2)$$

where $[X]_t$ and $[Ni(II)]_t$ refer to the total concentrations of NTA and nickel(II), respectively.

The kinetics of the substitution reaction of BT with Ni(II)-NTA chelates was studied at 16°C in the presence of a large excess of NTA and its nickel(II) chelate at a pH range 8.50—9.50. Therefore, the reaction can be treated as a pseudo first-order reaction, and simplified to,

$$\left\{\begin{array}{l} HD^{2-} \\ \uparrow\downarrow \\ D^{3-} \end{array}\right. \overset{\overset{k^+}{\rightleftharpoons}}{\underset{k^-}{}} NiD^- \quad (3)$$

The reaction gave invariably the linear relation between $\log(A_D/(A-A_{NiD}))$ and time, t, with the intercept identical with $\log(\varepsilon_{BT}/(\varepsilon_{BT}-\varepsilon_{NiD}))$

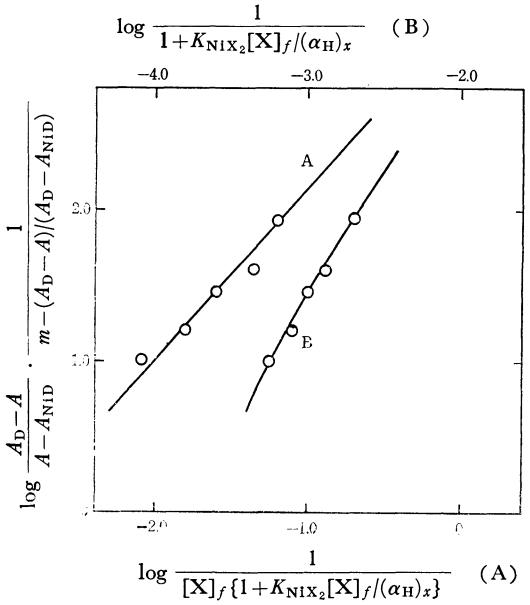

Fig. 2. The plot of $\log[X]_f(1+K_{NiX_2}[X]_f/(\alpha_H)_x)$ against $\log\frac{A_D-A}{A-A_{NiD}}\cdot\frac{1}{m-\frac{A_D-A}{A_D-A_{NiD}}}$.
μ=0.30, pH=9.54, λ=640 mμ
Initial concentration of BT=2.89×10^{-5} M
The concentration of uncomplexed NTA, $[X]_f$, ranged from 10 mM to 50 mM.

Table 1. Equilibrium constants (μ=0.30)*

i) Stability constants of Ni(II)-NTA chelates
K_{NiX}[4]$=10^{11.09}$ K_{NiX_2}[7]$=10^{4.47}$

ii) Dissociation constants of NTA[5]
pK_1=1.86 pK_2=2.38 pK_3=9.54

iii) Dissociation constants of BT[9]
pK_1=6.80 pK_2=11.31

* These values were calculated from the related dissociation constants and the stability constants in the solution of ionic strength 0.10 at 20°C and the activity constants of the ions calculated by means of Davis equation in the same way as was described previously.[2]

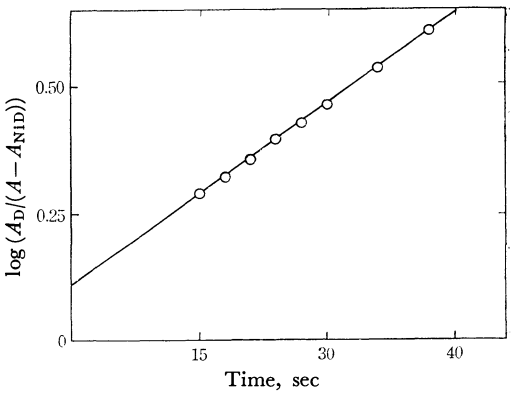

Fig. 3. The plot of $\log A_D/(A-A_{NiD})$ against t.
μ=0.30, pH=9.40, λ=630 mμ
Initial concentration of BT=2.00×10^{-5} M
The concentration of uncomplexed NTA=12.0 mM
The concentration of Ni(II)-NTA chelate=9.10 mM

(Fig. 3). Where ε_{BT} and ε_{NiD} represent the apparent extinction coefficient of uncomplexed BT and the true extinction coefficient of nickel(II)-BT chelate, respectively. The apparent extinction coefficient of uncomplexed BT, ε_{BT}, is constant

4) G. Schwarzenbach, G. Anderegg, W. Schneider and H. Senn, *Helv. Chim. Acta*, **38**, 1147 (1955).
5) G. Schwarzenbach and R. Gut, *ibid.*, **39**, 1589 (1956).

when the pH value of the solution is kept constant, because it can be thermodynamically equated as $(\varepsilon_{H_2D}[H^+]^2/k_1 \cdot k_2 + \varepsilon_{HD} \cdot [H^+]/k_2 + \varepsilon_D)/(\alpha_H)_{BT}$. Therefore, in this study, ε_{BT} value observed at the pH, where the kinetic measurement was conducted, was used in the analysis of experimental data. Here, ε_{H_2D}, ε_{HD} and ε_D mean true molar extinction coefficients of singly deprotonated, doubly deprotonated and completely deprotonated BT anion respectively, and k's are dissociation constants of BT.[9] Strictly k_1 should refer to the dissociation of sulfonic acid, but Schwarzenbach's notation was followed here, k_1 and k_2 referring to the dissociation of the phenolic hydrogen atoms. Considering that the stability constants of Ni(II)-BT chelate is much greater than that of nickel(II)-NTA chelate, under the present experimental conditions where the concentration of free NTA (the sum of concentrations of free singly deprotonated, doubly deprotonated and completely deprotonated NTA anions and of free NTA) is comparable with that of nickel(II)-NTA chelate, the concentration of free BT (the sum of concentrations of free singly deprotonated, doubly deprotonated and completely deprotonated BT anion and of free BT) at equilibrium, $[BT]_e$, is negligibly small as compared with its initial concentration, $[BT]_0$, and the free BT concentration at t, [BT], at an early stage of the reaction. Therefore, the slope of the linear relation between $\log(A_D/(A-A_{NID}))$ and t should correspond to the apparent rate constant, k^+, of the reaction (3) as was discussed in the substitution reaction of BT with cobalt(II)-EDTA chelate.[1]

The following facts were also found in the preliminary experiments where free NTA ranged from 10 mM to 40 mM and nickel(II)-NTA chelate, from 2.0 mM to 9.0 mM.

i) The slope of the linear relation between $\log(A_D/(A-A_{NID}))$ and t was independent of the initial concentration of BT, $[BT]_0$, in solutions of a given pH, a given concentration of free NTA and a given total concentration of nickel(II)-NTA chelate (Table 2).

TABLE 2. DEPENDENCE OF THE SLOPE ON THE INITIAL CONCENTRATION OF BT

pH=9.25, μ=0.30
Concentration of uncomplexed NTA=27.0 mM
Total concentration of Ni(II)-NTA chelate=6.50 mM

Concentration of BT, 10^{-5} M	Slope, sec^{-1}
0.90	3.33×10^{-3}
1.50	3.47×10^{-3}
2.00	3.50×10^{-3}
3.00	3.40×10^{-3}

ii) In solutions of a given pH and given initial concentrations of BT and of uncomplexed NTA, the slope of the above linear relation was proportional to the total concentration of Ni(II)-NTA chelate, $[NiX]_t$ (Table 3).

TABLE 3. DEPENDENCE OF THE SLOPE ON THE TOTAL CONCENTRATION OF Ni(II)-NTA CHELATES

pH=9.40, μ=0.30
Initial concentration of BT=2.00×10^{-5} M
Concentration of uncomplexed NTA=12.0 mM

Concentration of Ni(II)-NTA chelate, mM	Concentration ratio	Slope, sec^{-1}	Slope ratio
2.60	1.00	3.33×10^{-3}	1.00
3.90	1.50	5.20×10^{-3}	1.56
6.50	2.50	8.66×10^{-3}	2.60
9.10	3.50	1.18×10^{-2}	3.53

iii) In solutions of a given pH, a given initial concentration of BT and a given total concentration of Ni(II)-NTA chelate, the slope of the linear relation was inversely proportional to $1+K_{NiX_2}\cdot[X]_f/(\alpha_H)_x$ value (Table 4).

TABLE 4. DEPENDENCE OF THE SLOPE ON THE CONCENTRATION OF UNCOMPLEXED NTA

pH=9.25, μ=0.30
Initial concentration of BT=2.00×10^{-5} M
Total concentration of Ni(II)-NTA chelate=6.50 mM

Concentration of uncomplexed NTA, mM	$1+\frac{K_{NiX_2}\cdot[X]_f}{(\alpha_H)_x}$ (A)	Slope sec^{-1}	$A\times$slope
12.0	121	8.00×10^{-3}	9.70×10^{-1}
17.0	171	5.73×10^{-3}	9.80×10^{-1}
27.0	271	3.50×10^{-3}	9.50×10^{-1}

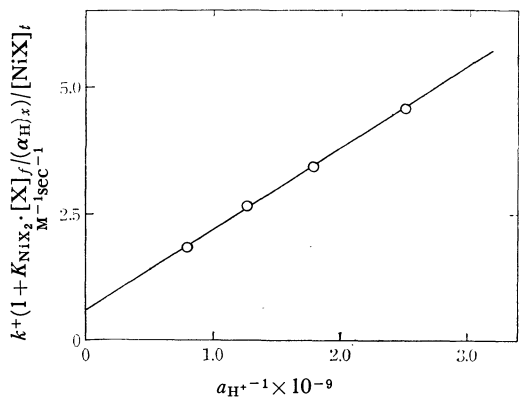

Fig. 4. Relation between $k^+(1+K_{NiX_2}\cdot[X]_f/(\alpha_H)_x)/[NiX]_t$ and the concentration of hydrogen ion.
μ=0.30
Initial concentration of BT=2.00×10^{-5} M
The concentration of uncomplexed NTA=12.0 mM
The concentration of Ni(II)-NTA chelate=6.50 mM

iv) In solutions of a given initial concentration of BT and given concentrations of free NTA and Ni(II)-NTA chelates, the slope of the linear relation was a linear function of the reciprocal of the hydrogen ion concentration and given by the Eq. (4) (Fig. 4).

$$\text{slope} = k_a + k_b/[H^+] \quad (4)$$

The nickel(II) ion can form chelates of 1-to-1 as well as 1-to-2 composition and the concentration of the former is given by $[NiX]_t/(1+K_{NiX_2}\cdot[X]_f/(\alpha_H)_x)$. Thus, the above experimental results clearly suggest that the substitution reaction of BT and nickel(II)-NTA chelates has the following reaction mechanism.

$$\text{i}_a)\quad NiX^- + HD^{2-} \underset{k_1^-}{\overset{k_1^+}{\rightleftharpoons}} NiD^- + HD^{2-}$$

$$\text{rapid}\ \uparrow\downarrow$$

$$NiX_2^{4-}$$

$$\text{ii}_a)\quad HD^{2-} \overset{\text{rapid}}{\rightleftharpoons} H^+ + D^{3-}$$

$$NiX^- + D^{3-} \underset{k_2^-}{\overset{k_2^+}{\rightleftharpoons}} NiD^+ + D^{3+}$$

$$\text{rapid}\ \uparrow\downarrow$$

$$NiX_2^{4-}$$

(rate-determining step)

The following relation can be derived, as was proposed for the substitution reaction of BT and Co(II)-EDTA chelate.[1]

$$\text{slope} = (k_1^+ + k_2^+\cdot k_2^{0})/[H^+])\ \frac{[NiX]_t}{1+\dfrac{K_{NiX_2}\cdot[X]_f}{(\alpha_H)_x}} \quad (5)$$

From the linear relation between the slope $\times(1+K_{NiX_2}\cdot[X]_f/(\alpha_H)_x)/[NiX]_t$ and $1/[H^+]$ (Fig. 4), k_1^+ and k_2^+ were determined to be 5.8×10^1 $M^{-1}\,sec^{-1}$ and 3.27×10^4 $M^{-1}\,sec^{-1}$, respectively.

Similar results were also obtained in the experiments at 24.5°C and 30°C and given in Table 5 along with the results at 16°C. Linear relation was found between $\log k^+$ and $1/T$ for those two elementary reactions, which made it possible to calculate the heat and the entropy of activation. The results for k_2^+ are shown in Table 5. Values for the elementary reaction (i_a) are considered less accurate as compared with the other data and not given here.

Table 5. Rate constants, k_2^+, for BT reaction with Ni(II)-NTA at various temperatures, and heat of activation and entropy of activation for reaction (iia)

Temperature °C	Rate constant $M^{-1}\,sec^{-1}$	$\Delta H^{\neq}$ kcal/mol	$\Delta S^{\neq}$ e.u.
16	3.27×10^4		
24.5	1.15×10^5	11.5	37.6
30	2.51×10^5		

During the course of the exchange reaction, BT is considered to hold its planar configuration. Therefore, less conformational freedom would be lost in the substitution reaction. On the basis of this fact, as far as the conformational freedom is concerned, the great gain in the conformational freedom in the leaving NTA or EDTA ion may contribute to the positive entropy of activation. This expectation was satisfied by the results listed in Table 5.

The Substitution Reaction of BT with Nickel(II)-EDTA Chelate. The substitution reaction of BT with Ni(II)-EDTA chelate was also studied in the presence of a large excess of free EDTA and its nickel(II) chelate ions over BT in the pH range 9.00—10.50 at 15°C. The reaction gave the linear relation between $\log(A_D/(A-A_{NiD}))$ and time, t, whose intercept was identical with $\log(\varepsilon_{BT}/(\varepsilon_{BT}-\varepsilon_{NiD}))$ (Fig. 5). An analogous relation among $[BT]_0$, $[BT]$ and $[BT]_e$ also holds for the present system, and this fact clearly indicates that the slope of the linear relation can exactly correspond to the apparent rate constant, k^+, of the pseudo first-order reaction (3).

In addition to the above fact, the following experimental facts were also found under the present experimental conditions (free EDTA ranged from

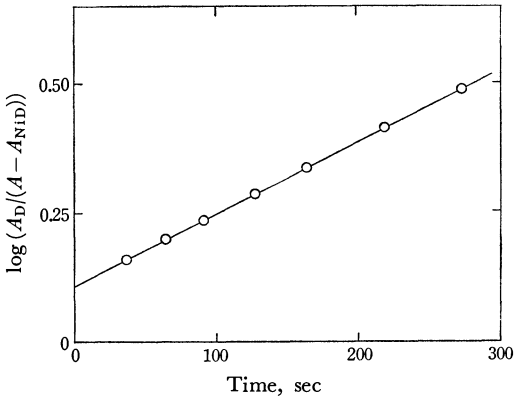

Fig. 5. The plot of $\log(A_D/(A-A_{NiD}))$ against t.
$\mu=0.30$, pH=10.25, $\lambda=630$ mμ
Initial concentration of BT=2.25×10^{-5} M
The concentration of uncomplexed EDTA=10.0 mM
The concentration of Ni(II)-EDTA=16.51 mM

Table 6. Dependence of the slope on the concentration of uncomplexed EDTA
pH=10.0, $\mu=0.30$
Initial concentration of BT=2.25×10^{-5} M
Concentration of Ni(II)-EDTA=8.25_5 mM

Concentration of uncomplexed EDTA, mM	Slope, sec^{-1}
10	3.20×10^{-4}
15	3.22×10^{-4}
25	3.18×10^{-4}

10 to 40 mM and Ni(II)-EDTA, from 8.0 mM to 25.0 mM).

i) The slope of the plot of $\log(A_D/(A-A_{NID}))$ against t was independent of the concentration of uncomplexed EDTA in solutions of a given pH and the given concentrations of BT, $[BT]_0$, and nickel(II)-EDTA chelate (Table 6).

ii) The slope of the plot of $\log(A_D/(A-A_{NID}))$ against t was independent of the initial concentration of BT in solutions of a given pH and given concentrations of free EDTA and its nickel(II) chelate (Table 7).

TABLE 7. DEPENDENCE OF THE SLOPE ON THE INITIAL CONCENTRATION OF BT

pH=10.0, μ=0.30
Concentration of uncomplexed EDTA=10.0 mM
Concentration of Ni(II)-EDTA=8.25_5 mM

Concentration of BT, 10^{-5} M	Slope, sec^{-1}
1.61	3.18×10^{-4}
2.25	3.20×10^{-4}
3.21	3.15×10^{-4}

iii) The slope of the above linear relation was proportional to the concentration of nickel(II)-EDTA chelate, [NiY], in solutions of a given pH and the given concentrations of BT, $[BT]_0$ and of free EDTA (Table 8).

TABLE 8. DEPENDENCE OF THE SLOPE ON THE CONCENTRATION OF Ni(II)-EDTA CHELATE

pH=10.25, μ=0.30
Concentration of uncomplexed EDTA=10.0 mM
Initial concentration of BT=2.25×10^{-5} M

Concentration of Ni(II)-EDTA, mM	Concentration ratio	Slope, sec^{-1}	Slope ratio
8.25_5	1.00	5.62×10^{-4}	1.00
16.51	2.00	1.12×10^{-3}	2.00
24.77	3.00	1.70×10^{-3}	3.03

iv) The slope for the linear relation was found to be a linear function of the reciprocal of the hydrogen ion concentration and given by Eq. (6) (Fig. 6).

$$\text{slope} = k_I + k_{II}/[H^+] \qquad (6)$$

where k_i is almost zero.

Since Ni(II)-EDTA chelate behaves in an identical manner with Co(II)-EDTA chelate, it can be concluded that the substitution reaction of BT with Ni(II)-EDTA chelate proceeds mainly through the reaction path (ii_b), and the percentage of the contribution of the reaction path (i_b) is practically zero.

$$i_b) \quad HD^{2-} + NiY^{2-} \underset{k_1^-}{\overset{k_1^+}{\rightleftharpoons}} NiD^- + HY^{3-}$$

$$ii_b) \quad HD^{2-} \overset{\text{rapid}}{\rightleftharpoons} H^+ + D^{3-}$$

$$D^{3-} + NiY^{2-} \underset{k_2^-}{\overset{k_2^+}{\rightleftharpoons}} NiD^- + Y^{4-}$$

(rate-determining step)

where NiY^{2-}, HY^{3-} and Y^{4-} mean Ni(II)-EDTA chelate, triply deprotonated EDTA anion and completely deprotonated EDTA anion, respectively.

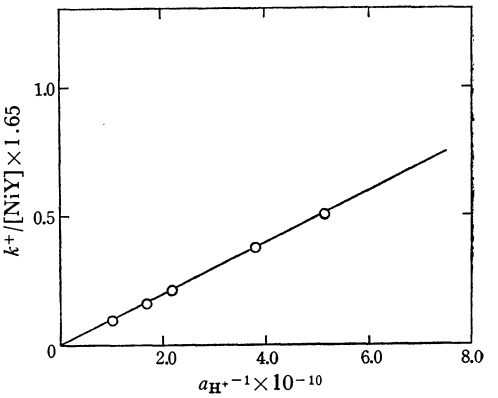

Fig. 6. Relation between $k^+/[NiY]$ and the concentration of hydrogen ion.
μ=0.30
Initial concentration of BT=2.25×10^{-5} M
The concentration of uncomplexed EDTA=10.0 mM
The concentration of Ni(II)-EDTA chelate=8.25_5 mM

On these assumptions, the following relation can be obtained.

$$k^+ = \frac{k_2^+ \cdot k_2^{9)}}{[H^+]} \cdot [NiY^{2-}] \qquad (7)$$

From the linear relationship between $k^+/[NiY]$ and $1/[H^+]$ (Fig. 6), k_2^+ value was determined to be 1.25 $M^{-1}\,sec^{-1}$.

The above reaction mechanism proposed for the substitution reactions of BT clearly involves the formation of mixed ligand intermediate complexes between BT and nickel(II) chelate of NTA or EDTA. By forming coordinate bonds with a nickel(II) ion prior to the complete dissociation to give X^{3-} or Y^{4-} from the nickel(II) ion, BT is considered to block the reformation of the nickel-(II)-NTA or nickel(II)-EDTA bonds and to help the dissociation of NTA or EDTA anion. Thus, rate constants of the substitution reactions of metal-(II)-NTA and EDTA chelates with BT are expected to be much greater than those of the dissociation of metal(II)-NTA and -EDTA chelates. A comparison of the rate constant of the dissociation reaction of cobalt(II)-EDTA chelate reported by Tanaka *et al.*[6] with that of the substitution reaction of BT

6) N. Tanaka, H. Osawa and M. Kamada, This Bulletin, **36**, 68 (1963).

with cobalt(II)-EDTA chelate[1] clearly confirms this explanation. Since the protonation of chelate is responsible to the rapid dissociation of metal chelate, the finding that k_2^+ value for the reaction of BT with nickel(II)-EDTA chelate is much greater than the rate constant for the dissociation of protonated nickel(II)-EDTA chelate, $NiHY^-$ [10],*1 is also an evidence for the above expectation. As in the case of the exchange reaction of EDTA with nickel(II)-polyamine,[8] the protonation of the incoming ligand (Strictly, in the substitution reaction of BT, incompletely dissociation of BT, HD^{2-}) tends to slow the reaction (k_2^+ is much greater than k_1^+).

Generally, for the reaction mechanism involving the formation of mixed ligand intermdiate complexes, the reaction rate is expected to be sensitive to the steric effect. The kinetic studies of the substitution reaction of BT with cobalt(II) and nickel(II) chelates of other chelons (EDTA-OH, GEDTA, CyDTA and DTPA) are now in progress. The importance of the steric effect on the rate of the substitution reaction of BT and the assignment of the reaction mechanism will be discussed in some detail in the subsequent paper.

7) G. Schwarzenbach and W. Biedermann, *Helv. Chim. Acta*, **31**, 331 (1948).
8) D. B. Rorabacher and D. W. Margerum, *Inorg. Chem.*, **3**, 382 (1963).
9) G. Schwarzenbach and W. Biedermann, *Helv. Chim. Acta*, **31**, 678 (1948).
10) N. Tanaka and Y. Sakuma, This Bulletin, **32**, 578 (1959).
*1 The rate constant was calculated from the reverse rate constant and appropriate stability constant to be 2.8×10^{-6} M^{-1} sec^{-1}.

BULLETIN OF THE CHEMICAL SOCIETY OF JAPAN VOL. 41 1339—1343 (1968)

Studies on Photo-polarography. I. Polarographic Behavior of Trioxalatoferrate(III) Ion under Ultraviolet Irradiation

Kazuo YAMASHITA and Hideo IMAI

Department of Chemistry, Faculty of General Education, Hiroshima University, Hiroshima

(Received December 2, 1967)

The polarographic behavior of trioxalatoferrate(III) ion under irradiation of ultraviolet light was studied. Trioxalatoferrate(III) was photo-chemically reduced in the bulk and the polarographic reduction current changed into the oxidation one, which showed a highly kinetic characteristic. The current-time curve during one drop growth of the dropping mercury electrode under irradiation was analyzed, and the rate constant of the photo-chemical reaction (k_ν) was evaluated. The apparent value given as $k_\nu' = I_0 \varepsilon k_\nu$ was 0.35 cm^{-1}, where I_0 being the intensity of the incident light and ε the extinction coefficient. The time dependence of the photopotential was elucidated on the basis of the Nernst equation. The possible photonometric determination of dissolved oxygen was suggested from the effect of dissolved oxygen on the half-life of the photo-chemical reaction.

The redox behavior of ferri- and ferro-oxalate complexes has been studied by von Stackelberg and von Freyhold,[1] Lingane,[2] and Randles and Somerton.[3] In their early work, the chemical constitution of ferrooxalate complex, which depends on the concentration of excess oxalate, was determined.

On the other hand, Rao and Aravamudan[4] have shown that iron(III) is photo-chemically reduced in the presence of excess citric acid, and that it can then be titrated with a standard solution of sodium vanadate. Thus, they proposed a photonometric determination of oxalic acid in the presence of excess ferric sulfate. Bricker and Schonberg[5] reported a new photonometric method for the separatory determination of vanadium and chromium by using the photo-chemical reduction of ferrioxalate.

Recently, Berg and his coworkers have investigated the effect of continuous or flash irradiation on the current-potential characteristics of ketyl radicals,[6] hydroquinones,[7,8] benzophenone,[6] and

1) M. von Stackelberg and H. von Freyhold, *Z. Elektrochem.*, **46**, 120 (1940).
2) J. J. Lingane, *Chem. Revs.*, **29**, 1 (1941).
3) J. E. B. Randles and K. W. Somerton, *Trans. Faraday Soc.*, **48**, 937 (1952).
4) G. G. Rao and G. Aravamudan, *Anal. Chim. Acta*, **13**, 328, 415 (1955).
5) C. E. Bricker and S. S. Schonberg, *Anal. Chem.*, **30**, 923 (1958).
6) H. Berg and H. Schweiss, *Naturwiss.*, **47**, 513 (1960); *Nature*, **191**, 1270 (1961).
7) H. Berg, *ibid.*, **47**, 320 (1960); *Z. Chem.* (Leipzig), **2**, 237 (1962).
8) H. Berg, *Rev. of Polarog.* (Japan), **11**, 29 (1963).

other organic compounds.[6] As a result of their studies they have suggested four groups of photopolarographic reaction.

The present authors have investigated the photopolarographic behavior of trioxalatoferrate(III) ion in 0.5 M potassium oxalate with the continuous ultraviolet irradiation. The results and the apparent rate constant of the photo-chemical reaction evaluated are presented in this paper.

Experimental

Apparatus. The current-voltage curves were recorded with Yanagimoto Polarograph Model PA-102 and Shimadzu Polarograph Model RP-2.

The characteristics of the dropping mercury electrode (DME) were as follows: $m=1.30$ mg/sec, $t=4.5$ sec with the open circuit in an air-free 0.5 M potassium oxalate solution. A hammer with 4.0 sec interval was used to give the constant life-time of the DME.

For recording the current-time curve during one drop of the DME under a given voltage, Iwasaki Model 5155 cathode-ray oscilloscope with a plug-in amplifier Model SP-30H-A were used. The constant applied voltage was supplied from Yokogawa Model P-1 precision potentiometer through series 1 kΩ resistor, which is used to give the current signal.

The experimental arrangement is shown in Fig. 1. The light beam was emitted from Ushio Type UXL 500 DV xenon lamp (A in Fig. 1). The light was passed through a focusing lens, B, and was focused on a side of the DME. A quartz cell, C, (a conventional 10 mm quartz cell for the UV spectrophotometer) was used and the optical path of the incident light through the solution to the DME was about 3 mm. The geometry was kept constant throughout the measurements.

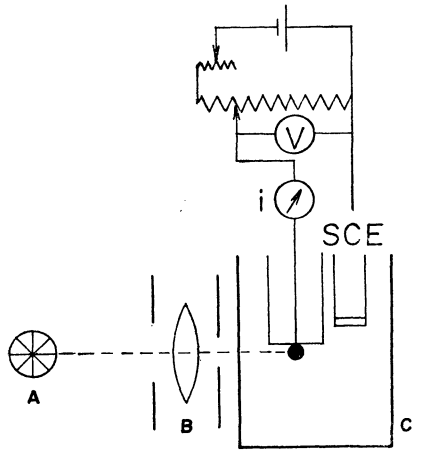

Fig. 1. The irradiation system.

The variation of the room temperature was about ±2°C. The temperature rise by the continuous irradiation is shown in Fig. 2. It is concluded that the temperature rise of the solution by the continuous irradiation during 5 min is as small as 1.8°C.

Reagents. The trioxalatoferrate(III) solution was prepared by dissolving metallic iron in dilute sulfuric acid, evaporating the excess acid, and then diluting to be 1.0×10^{-2} M in its concentration (pH=9.5) with aqueous 0.5 M potassium oxalate solution. Purified nitrogen was used to remove dissolved oxygen in the solutions.

All other chemicals were of analytical reagent grade, and they were purified by the conventional methods.

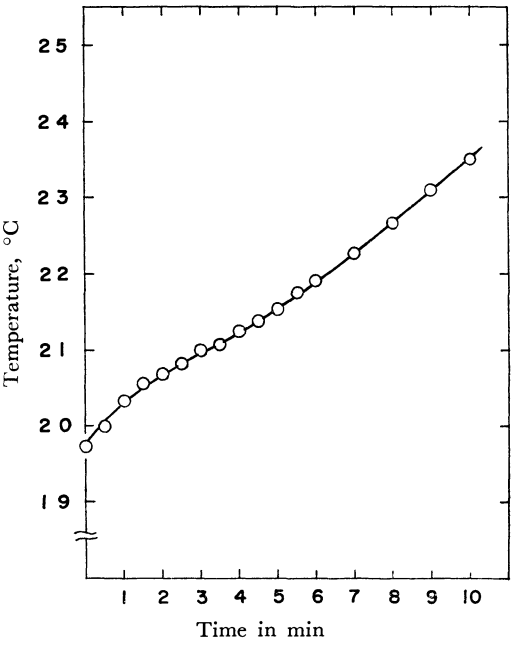

Fig. 2. Variation of temperature with the irradiation time in 0.5 M potassium oxalate solution.

Results and Discussion

D. C. Polarography. Trioxalatoferrate(III) developed a well-defined polarographic reduction wave, of which the half-wave potential was −0.26

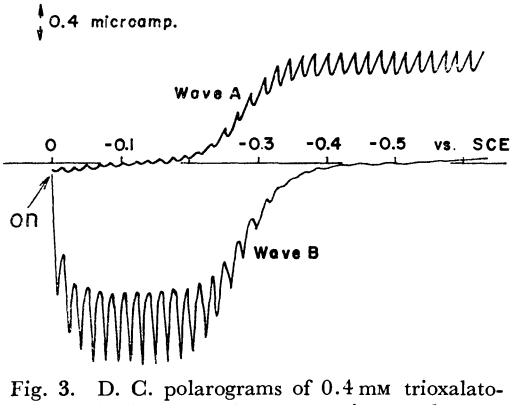

Fig. 3. D. C. polarograms of 0.4 mM trioxalatoferrate(III) ion in 0.5 M potassium oxalate solution.
Wave A: the reduction wave of trioxalatoferrate(III).
Wave B: the anodic wave appeared by the irradiation.

V *vs.* SCE (Wave A in Fig. 3). During the ultraviolet irradiation, the cathodic wave disappeared rapidly and a new anodic wave (Wave B in Fig. 3) appeared at almost the same potential as the cathodic wave. It is noteworthy that the anodic limiting current was about 1.6 times greater than the cathodic limiting current.

The dependence of the photo-polarographic limiting current at −0.15 V (the potential to give the limiting anodic current) on the height of mercury reservoir was examined. The result is shown in Fig. 4. It is seen in Fig. 4 that the photo-polarographic limiting current is actually unchanged by the mercury head, while the cathodic current without irradiation shows a trend to increase with increase of the mercury head.

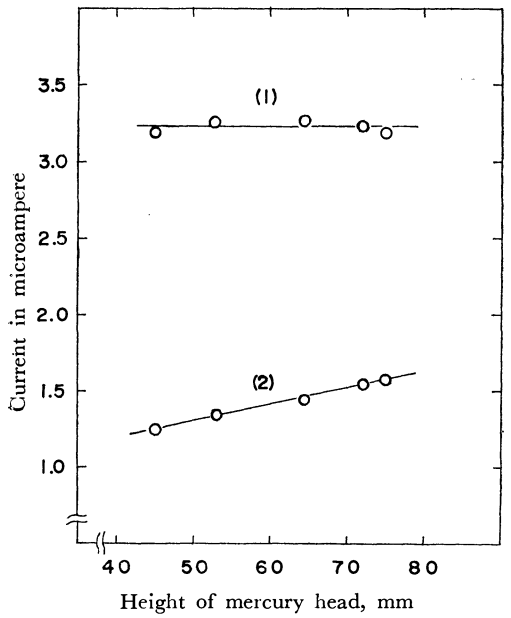

Fig. 4. Dependence of limiting current of (1) wave B and (2) wave A on the height of mercury head.

Figure 5 shows the plot of log *i versus* log *t* during one drop growth of the DME at −0.15 V after the continuous irradiation for 200 sec. From the inclination of the plot it was found that the photo-polarographic current varied with time to the power of 0.59. This result coupled with the above mentioned result in relation to the effect of the mercury head suggests the kinetically controlled feature of the photo-polarographic current. Thus, the following scheme of the parallel reactions is assumed at −0.15 V under continuous irradiation.

$$\text{Electrode Reaction:} \quad R - e = O \qquad (1')$$

$$\text{Photo-chemical Reaction:} \quad O + h\nu = R \qquad (2')$$

The reaction scheme shown in Eqs. (1') and (2') involves the regeneration of the reductant at the vicinity of the electrode surface by the photo-chemical reaction. Thus, the flux of the reductant toward the electrode surface is increased by the ultraviolet irradiation. This seems to elucidate the above-mentioned fact that the anodic limiting current under irradiation is about 1.6 times greater than the cathodic limiting current, which is observed without irradiation.

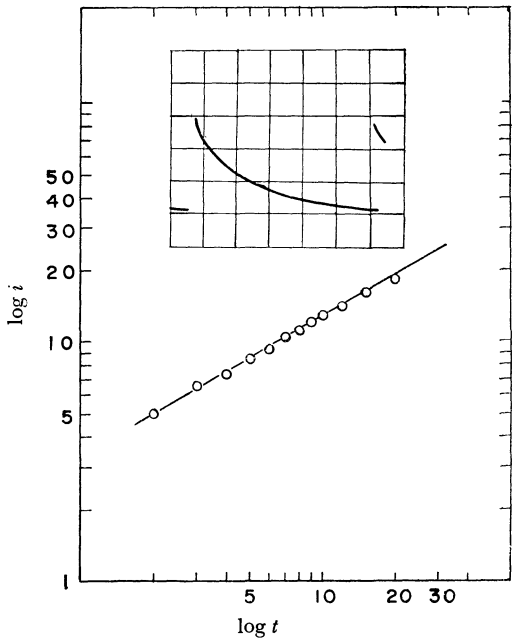

Fig. 5. log *i* - log *t* plots for the curve shown above, which was recorded during one drop growth of the DME after irradiation for 200 sec at −0.15 V.

Polarographic Current-Time Curve during One Drop Growth of DME. The parallel reactions occurring at −0.5 V and in the bulk are expressed as Eqs. (1) and (2), *i. e.*,

$$Fe(ox)_3^{3-} + e^- \rightleftarrows Fe(ox)_3^{4-} \qquad (1)$$

$$Fe(ox)_3^{3-} + \tfrac{1}{2}C_2O_4^{2-} + h\nu \rightleftarrows Fe(ox)_3^{4-} + CO_2 \qquad (2)$$

The variation of the concentration of the trioxalatoferrate(III) ion by the reaction given in Eqs. (1) and (2) is expressed by the following differential equation, *i. e.*,

$$\frac{\partial C}{\partial t} = D\left(\frac{\partial^2 C}{\partial x^2}\right) + \left(\frac{2x}{3t}\right)\left(\frac{\partial C}{\partial x}\right) - k_\nu\left(\frac{I_0}{l}\right)\left(1 - e^{-\varepsilon lC}\right) \qquad (3)$$

In the right hand side of Eq. (3) the first term represents Fick's 2nd. law, the second term represents the convection due to the growth of the mercury drop, and the third term represents the effect of the coupled photo-chemical reaction, where the absorption of the incident light is obeyed by Beer's law.

The magnitude of the photo-kinetic current for Eq. (3) can then be evaluated for the initial and boundary conditions given as follows:

$$\left.\begin{array}{lll} C=C_i^* & \text{for } x\geqq 0, & t=0 \\ C=0 & \text{for } x=0, & t>0 \\ C=C_i^* e^{-k_\nu' t} & \text{for } x\to\infty, & t\geqq 0 \\ \text{with } k_\nu'=k_\nu \varepsilon I_0 & & \end{array}\right\} \quad (4)$$

where C_i^* is the initial bulk concentration of the trioxalatoferrate(III) ion, and t the reaction time from the irradiation.

Reinert derived an explicit equation for this boundary value problem,[9] and Berg and Schwiess applied the Reinert's equation to a similar problem.[7,8] The explicit equation for the photopolarographic current (i_{rd}) during the growth of one mercury drop is then expressed as,

$$i_{rd} = KC_i^* e^{-k_\nu'(t+t'-u\tau)\bar{\alpha}} \quad (5)$$

where t is the reaction time from the irradiation, t' the time difference between the start of the drop growth of the DME and the start of the reaction, τ the life-time of the DME, $u=0, 1, 2, \cdots$ for the first, second, third, — drop, $\bar{\alpha}$ the average exponent for i_d-t curve, K the Ilkovic constant, I_0 the intensity of the incident light, ε the extinction coefficient, and l the length of the layer.

In Eq. (5) the plot of $\log(i_{rd}/(t+t'-u\tau)^{\bar{\alpha}})$ *versus* t yields a straight line and the value of k_ν' can be computed from the inclination. On the other hand, Eq. (6) can be derived from Koutecky's theory,[10] *i. e.*,

$$i_{rd}/i_d = F(y_t) \quad \text{with } y_t = k_\nu \varepsilon I_0 t = k_\nu' t \quad (6)$$

where $F(y_t)$ is an exponential function of y_t.[9] From Eq. (6) the plot of $\log(i_{rd}/i_d)$ *versus* t also yields a straight line, of which the inclination gives the value of k_ν'. These two plots are shown in Fig. 6, and the value of k_ν' is computed to be 0.35 cm^{-1} from the slopes of two plots, the slopes being agreed well with each other as is seen in Fig. 6. This value of k_ν' is the apparent rate constant of the photo-chemical reaction, and it involves the terms, the intensity of the incident light (I_0), the extinction coefficient (ε), and the net rate constant of the photo-chemical reaction (k_ν). Among these terms the absolute intensity of the incident light was difficult to measure at this stage, so that only the total dosage of light was determined under the same geometry. The experiment was carried out for 0.6 mM trioxalatoferrate(III) solution by irradiation during 150—200 sec, followed by stirring of the solution and polarographic determination of the concentration of trioxalatoferrate(III) remaining unreduced in the solution. The total dosage evaluated was 1.8×10^{15} molecules/sec. Only this rather relative datum is available at this stage. Since the photo-chemical reaction proceeds in the bulk of the solution, but only the reaction proceeded in the reaction zone at the vicinity of the electrode surface pertains to the electrode reaction, it seems to be very complicated to confer an absolute physical significance on the apparent value of k_ν', and further investigation is required before the physical meaning of k_ν' will be embodied.

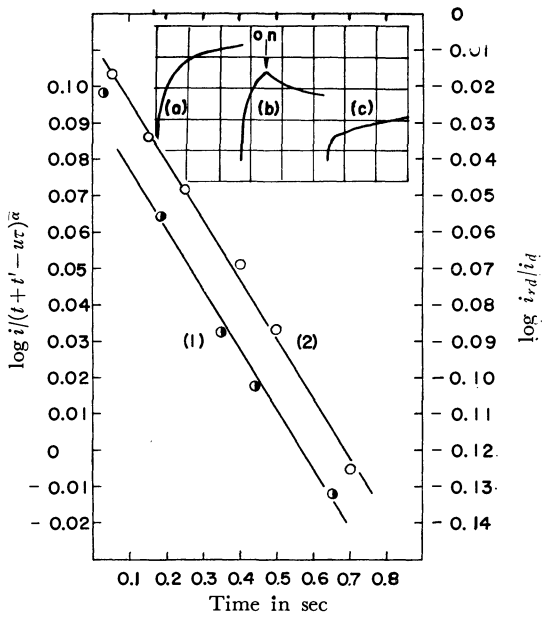

Fig. 6. log-plots plotted from the current-time curve (b) which shows the current during the drop growth of the DME. In curve (b) the continuous irradiation was started on the way of the second drop and the time of irradiation is denoted by ↓.

Photopotential. A typical photopotential-time curve for ferri-oxalate/ferro-oxalate system is shown in Fig. 7. It is evident that the potential rapidly shifts toward more negative potentials during irradiation and finally it attains to a plateau. When the irradiation was extinguished, the electrode potential slowly returned to the value near the initial potential. Similar trend has been observed for a variety of organic compounds,[11-13] and this trend can be attributed to the mixing of the irradiated part and unirradiated part of the solutions. The shift of the electrode potential by irradiation can simply by elucidated by the Nernst equation, *i. e.*,

$$E = E^\circ + \left(\frac{RT}{nF}\right)\ln\frac{[Fe(ox)_3^{3-}]}{[Fe(ox)_3^{4-}]} \quad (7)$$

9) K. E. Reinert, *Z. Electrochem.*, **66**, 379 (1962).
10) J. Koutecky, *Collection Czechoslov. Chem. Commun.*, **18**, 311 (1953).
11) I. Levin and C. E. White, *J. Chem. Phys.*, **18**, 417 (1950); **19**, 1079 (1951).
12) I. Levin, J. R. Wiebush, M. B. Bush and C. E. White, *ibid.*, **21**, 1654 (1953).
13) J. J. Surash and D. M. Hercules, *Z. Electrochem.*, **66**, 1602 (1962).

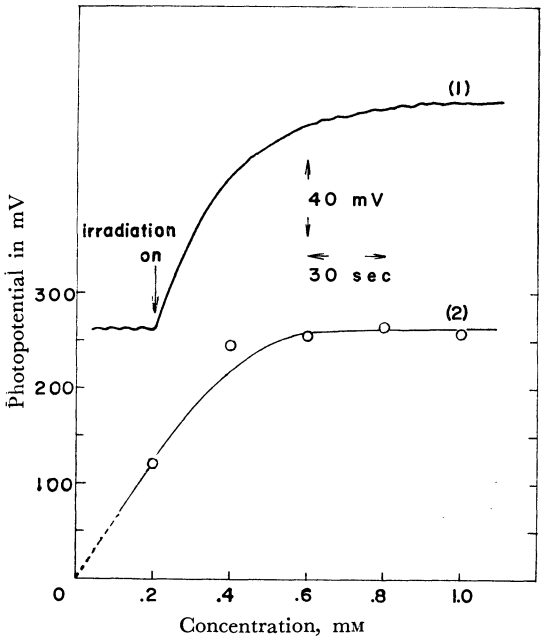

Fig. 7. (1) Photopotential-time curve of 0.2 mM trioxalatoferrate(III) in 0.5 M potassium oxalate solution.
(2) Dependence of photopotential on the concentration of trioxalatoferrate(III).

During the course of irradiation $Fe(ox)_3^{3-}$ is gradually converted into $Fe(ox)_3^{4-}$, and then the ratio of $Fe(ox)_3^{3-}/Fe(ox)_3^{4-}$ becomes smaller as a function of time. Such a behavior will tend to produce a negative-going potential according to Eq. (7). After the sufficient irradiation a steady state of the ferro-oxalate concentration is reached at the electrode surface, and a plateau is observed as is seen in curve (1) of Fig. 7. The photo-potential at the concentrations higher than 0.6 mM trioxalatoferrate (III) was evaluated as great as 258 mV.

Effect of Oxygen. Figure 8 shows the dependence of half-life time, which means the time required to attain the half-wave height of the anodic wave since the time of irradiation, on the concentration of dissolved oxygen. The measurement was carried out at the constant applied voltage of +0.05 V *vs.* SCE, where trioxalatoferrate(III) and oxygen are not electrolytically reduced.

When oxygen is present in the solution containing trioxalatoferrate(III), the decay time of trioxalatoferrate(III) by irradiation is elongated by the regeneration of the oxidant due to the chemical reaction of oxygen with the reductant formed during the course of irradiation. The reaction scheme will be expressed as follows;

$$\begin{aligned} &Fe(ox)_3^{3-} + (1/2)C_2O_4^{2-} + h\nu \rightleftarrows Fe(ox)_3^{4-} + CO_2 \\ &Fe(ox)_3^{4-} + O_2 \rightleftarrows Fe(ox)_3^{3-} + O_2^- \\ &Fe(ox)_3^{4-} \rightleftarrows Fe(ox)_3^{3-} + e^- \\ &\cdots\cdots\cdots\cdots\cdots\cdots \end{aligned} \quad (8)$$

In Fig. 8 an induction period is seen at the very low concentration of dissolved oxygen. This effect can often be seen in the usual redox reactions. Then, the variation of the half-life is apparently linear with increase of the oxygen concentrations covered in this experiment. This effect can be used for the photonometrical determination of dissolved oxygen.[14]

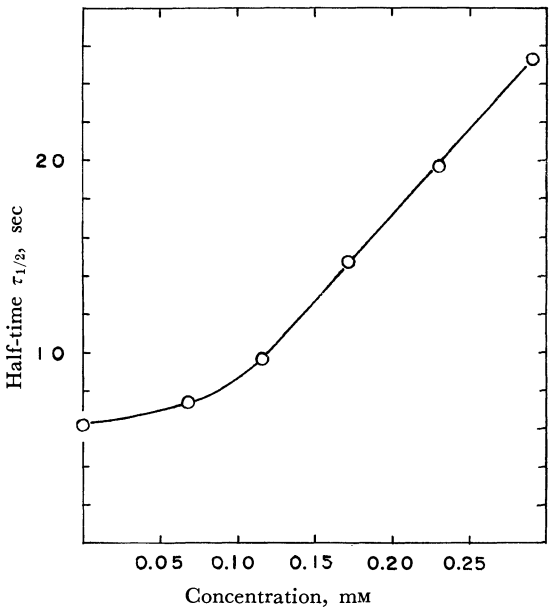

Fig. 8. Dependence of half-life of the photochemical reaction on the concentration of dissolved oxygen in 0.5 M potassium oxalate solution containing 0.6 mM trioxalatoferrate(III) ion.

The authors wish to express their hearty gratitude to Professor Mutsuaki Shinagawa of Osaka University and Professor Niro Matsuura of University of Tokyo for their valuable suggestions, especially for their discussion on this investigation in relation to γ-ray dosimetry. The financial support by the Scientific Research Fund from the Ministry of Education is gladly acknowledged.

14) T. Kuwana, *Anal. Chem.*, **35**, 1398 (1963).

BULLETIN OF THE CHEMICAL SOCIETY OF JAPAN VOL. 41 1344—1352 (1968)

Synthesis of Chelating Agents. VI.*1 Chelating Behavior of 1,2,3-Triaminopropanehexaacetic Acid with Divalent Metal Ions*2

Yoshiki MORIGUCHI, Mitsumasa MIYAZAKI*3 and Keihei UENO

Department of Organic Synthesis, Faculty of Engineering, Kyushu University, Hakozaki, Fukuoka

(Received December 6, 1967)

The chelate stability constants of 1,2,3-triaminopropanehexaacetic acid (TAPHA) with alkaline earth metals, cobalt(II), nickel(II), copper(II), zinc(II) and cadmium(II) were determined at 25°C and an ionic strength of 0.1 (KNO_3). The stability constants of monoprotonated mono nuclear-, dinuclear- and mixed metal dinuclear chelates as well as normal mononuclear chelate were determined. The structure and chelating behavior of TAPHA in an aqueous solution were discussed by refering to those of the other complexanes of related structure. The crystalline metal chelates of TAPHA were also prepared and their structures were proposed on basis of the results of elementary analyses and infrared spectra.

1,2,3-Triaminopropane-*N,N,N',N',N'',N''*-hexaacetic acid (TAPHA) is a nonadentate ligand, having three nitrilodiacetic acid groups pending from each carbon atom of propane. As easily understood from the structure, these three nitrilodiacetate groups can not coordinate to a metal ion simultaneously. If the neighboring two nitrilodiacetate groups coordinate to a metal ion, leaving the remaining nitrilodiacetate group uncoordianted, then the coordinating structure of TAPHA resembles EDTA chelate. If the terminal two nitrilodiacetate groups coordinate to a metal ion, leaving the central nitrilodiacetate group uncoordinated, then the structure of TAPHA chelate resembles TMDTA (trimethylenediamine-*N,N,N',N'*-tetraacetic acid) chelate. It is of great interest to investigate the structure of TAPHA metal chelate from this standpoint of view.

Following to the previous paper,[1] in which the acid dissociation scheme of TAPHA was investigated, this paper is to report on the chelating behavior of TAPHA with divalent cations, such as magnesium(II), calcium(II), strontium(II), barium(II), cobalt(II), nickel(II), copper(II), zinc(II) and cadmium(II) in an aqueous solution as well as in a solid state.

The stability constants of normal mononuclear chelates, monoprotonated mononuclear chelates, diprotonated mononucelar chelates, dinuclear chelates and mixed dinuclear chelates have been determined. By comparing their values with those of other complexanes of related structure, a possible structure of TAPHA chelates in aqueous solution is proposed.

Experimental

The pH measurement was carried out at 25±0.1°C. in aqueous solution of ionic strength with $\mu=0.1$ by KNO_3. The same apparatus as described in our previous paper was employed.[2] The procedure for the determination of chelate stability constants with

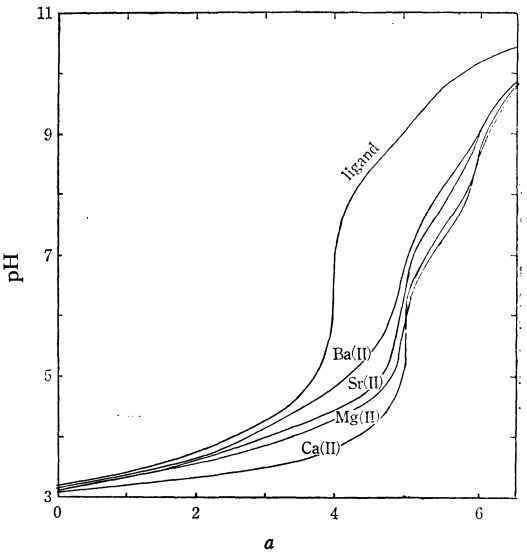

Fig. 1. Potentiometric titration curves of alkaline earth metals-TAPHA chelates at 25°C in 0.1 M KNO_3 with molar ratio of metal ion to ligand, 10 : 1.
Concentration of TAPHA: 4.66×10^{-4} M

*1 Paper V; M. Miyazaki, Y. Moriguchi and K. Ueno, This Bulletin, **41**, 838 (1968).

*2 Contribution No. 147 from the Department of Organic Synthesis, Kyushu University.

*3 Present address: Amagasaki Plant, Dainippon Ink Chem. Ind., Ltd., Amagasaki-shi.

1) M. Miyazaki, Y. Moriguchi and K. Ueno, This Bulletin, **41**, 838 (1968).

2) T. Ando, *ibid.*, **36**, 1593 (1963).

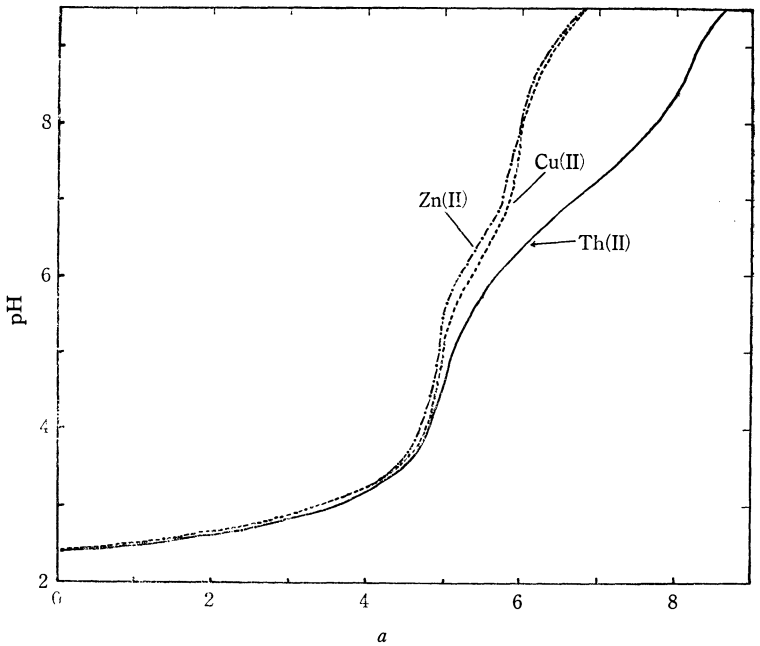

Fig. 2. Potentiometric titration curves of some heavy metals-TAPHA chelates at 25°C in 0.1 M KNO_3 with molar ratio of metal ion to ligand, 1 : 1. Concentration of TAPHA: 4.66×10^{-4} M

Table 1. Compositions of crystalline chelates of TAPHA

		C(%)	H(%)	N(%)	M(%)[a]	Na(%)[b]	H_2O(%)
$Na_4MgL\cdot3H_2O$	Found	30.13	4.50	6.87	3.98	15.2	8.82
	Calcd	29.95	3.85	6.98	4.04	15.3	8.98
$Na_4CaL\cdot3.5H_2O$	Found	29.90	4.34	6.49	6.35	14.4	9.20
	Calcd	28.76	3.86	6.71	6.40	14.7	10.1
$Na_4SrL\cdot3.5H_2O$	Found	27.64	3.98	6.21	12.7	13.6	8.75
	Calcd	26.73	3.59	6.23	13.0	13.6	9.36
$MgH_4L\cdot3H_2O$	Found	35.45	5.61	8.05	4.98		10.4
	Calcd	35.07	5.30	8.18	4.73		10.5
$CaH_4L\cdot2H_2O$	Found	34.86	4.99	7.89	7.85		6.45
	Calcd	35.23	4.93	8.22	7.84		7.04
$SrH_4L\cdot2H_2O$	Found	30.62	4.56	7.81	15.9		5.41
	Calcd	32.23	4.51	7.52	15.7		6.45
$CoH_4L\cdot2.5H_2O$	Found	33.69	5.27	7.86	10.7		8.00
	Calcd	33.41	4.86	7.79	10.9		8.35
$NiH_4L\cdot2.5H_2O$	Found	33.98	5.39	7.99	10.2		8.76
	Calcd	33.42	4.86	7.79	10.9		8.35
$CuH_4L\cdot1.5H_2O$	Found	34.45	4.94	8.10	11.7		5.20
	Calcd	34.24	4.60	8.01	12.2		5.34
$Mg_2H_2L\cdot4H_2O$	Found	32.62	5.19	7.50	8.51		12.8
	Calcd	32.52	4.91	7.58	8.78		13.0
$Ca_2H_2L\cdot3H_2O$	Found	31.79	4.84	7.31	13.6		8.90
	Calcd	31.75	4.44	7.40	14.1		9.52
$Cu_2H_2L\cdot4H_2O$	Found	28.35	4.53	6.81	20.0		11.6
	Calcd	28.49	4.30	6.64	20.1		11.4

a) Metal content was determined by EDTA titration after wet digestion of the metal chelate with nitric acid and hydrogen peroxide. Y. Tsuchitani, Y. Tomita and K. Ueno, *Talanta*, **9**, 1023 (1962).

b) Sodium was determined by precipitating as zinc sodium uranyl acetate from acid digested solution, followed by EDTA titration of zinc in the precipitate.

alkaline earth metals involved the direct pH titration of 200 m*l* of 5×10^{-4} M ligand solution in 1 : 1 and 10—24 : 1 molar ratios of metal nitrate to ligand. The typical pH titration curves are shown in Figs. 1 and 2.

As for transition metal ions, the chelate stability constants were determined by the competitive reaction using triaminotriethylamine (tren)*4 and calcium ion as an auxiliary ligand and a metal ion respectively.[3] The measurements were carried out on the five solutions containing equimolar amounts of TAPHA (4×10^{-4} M), tren and metal ion, ten fold excess of calcium ion to TAPHA and different amounts of 1×10^{-1} N potassium hydroxide solution. The pH values of each soluiotn were measured until constant readings were obtained. They were usually attained within a week.

The acid dissociation constants of monoprotonated mononuclear chelates and the stability constants of dinuclear chelates were determined by the direct pH titration method as described above in the presence of equimolar amounts of TAPHA and metal ion and in the presence of 10—24 fold excess of metal ion to TAPHA respectively. The pH meter used and the method of calibration were those reported previously.[2]

Preparation of Crystalline Metal Chelates. TAPHA chelates of selected divalent metal ions were prepared in crystalline form by the procedures described below. Of the possible compositions of the chelates from the nonadentate hexa-basic ligand (H_6L) and divalent cations (M), three types of the chelates, $Na_4ML\cdot xH_2O$, $H_4ML\cdot xH_2O$ and $H_2M_2L\cdot xH_2O$, were isolated as well difined crystalline materials. The compositions of the chelates were determined by elementary analyses (C, H and N) as well as metal determinations. Hydrated water was determined from the weight loss after drying the sample in vacuum over phosphorus pentoxide at 100°C until it became constant weight. The results are summarized in Table 1.

$Na_4M^{II}L\cdot xH_2O$. Two millimoles (911 mg) of TAPHA ($H_6L\cdot H_2O$) and equimolar amount of metal carbonate in 80 m*l* of hot water was heated on a water bath. After complete dissolution, twice equivalent amounts of sodium carbonate (424 mg) were added, and the total volume of the solution was concentrated to 15 m*l*, to which 200—250 m*l* of ethanol was added to precipitate the sirupy product. After washing the precipitate by decantation with ethanol for several times, the crude chelate was dissolved into a small amount of water, and reprecipitated by adding a large amount of ethanol. The chelate was dried in vacuum over silica gel overnight at room temperature.

$H_2M_2^{II}L\cdot xH_2O$. An equimolar mixture of TAPHA and metal carbonate in hot water was heated on a water bath in a same scale as described above, and the solution was concentrated to 10—15 m*l*. To this solution, ethanol was added until the solution became slightly cloudy, and the mixture was kept in a refrigerator to precipitate the chelate. The crude chelate was recrystallized several times from 70—80% aqueous ethanol. The chelate was dried by the same fashion as described above.

$H_2M_2^{II}L\cdot xH_2O$. The chelate was prepared by the similar procedure as in the case of 1 : 1 hydrogen chelates, but twice molar equivalent of metal carbonate was used.

Besides the chelates listed in Table 1, which were obtained as well defined crystalline product, the chelates of manganese (II), cadmium(II) and lead(II) were prepared. However, manganese gave a sirupy chelate and cadmium and lead gave no products with consistent analytical results, so that the further purifications of these chelates were given up.

Infrared Spectra. The measurements were made with a Nippon Bunko Model DS 301 double-beam infrared spectrophotometer equipped with sodium chloride optics. The spectra were studied in Nujol mull.

Calculation of Chelate Stability Constants

Equilibrium Constants Involving Alkaline Earth Metal Ions. Definitions of equilibrium constants discussed in this paper, are summarized in Table 2.

TABLE 2. DEFINITIONS OF EQUILIBRIUM CONSTANTS

1) Acid dissociation constants of TAPHA

$K_1=[H_5L^{1-}][H^+]/[H_6L]$

$K_2=[H_4L^{2-}][H^+]/[H_5L^{1-}]$

$K_3=[H_3L^{3-}][H^+]/[H_4L^{2-}]$

$K_4=[H_2L^{4-}][H^+]/[H_3L^{3-}]$

$K_5=[HL^{5-}][H^+]/[H_2L^{4-}]$

$K_6=[L^{6-}][H^+]/[HL^{5-}]$

2) Composite acid dissociation constants[4,5]

$K_4'=[H^+]([H_2L^{4-}]+[MH_2L^{2-}])/[H_3L^{3-}]$

$K_5'=[H^+]([HL^{5-}]+[MHL^{3-}])/([H_2L^{4-}]+[MH_2L^{2-}])$

$K_6'=[H^+]([L^{6-}]+[ML^{4-}]+[M_2L^{2-}])/([HL^{5-}]+[MHL^{3-}])$

3) Acid dissociation constants of triaminotriethylamine trihydrochloride (H_3 tren)

${}^tK_1=[H_2\ tren^{2+}][H^+]/[H_3\ tren^{3+}]$

${}^tK_2=[H\ tren^{1+}][H^+]/[H_2\ tren^{2+}]$

${}^tK_3=[tren][H^+]/[H\ tren^{1+}]$

4) Acid dissociation constant of monoprotonated mononuclear chelate

$K^H_{MHL}=[H^+][ML^{4-}]/[MHL^{3-}]$

5) Chelate stability constants of TAPHA

$K_{MH_2L}=[MH_2L^{2-}]/[M^{2+}][H_2L^{4-}]$

$K_{MHL}=[MHL^{3-}]/[M^{2+}][HL^{5-}]$

$K_{ML}=[ML^{4-}]/[M^{2+}][L^{6-}]$

$K^M_{M_2L}=[M_2L^{2-}]/[M^{2+}][ML^{4-}]$

$K^{M'}_{MM'L}=[MM'L^{2-}]/[M'^{2+}][ML^{4-}]$

6) Chelate stability constant of tren

$K_{Mtren}=[Mtren^{2+}]/[M^{2+}][tren]$

In the following discussion, however, the charges on the ions, such as those in Eqs. (5)—(12) and (14)—(19), were omitted for the purpose of simplicity. The procedure of Schwarzenbach modified by Grims[4]

*4 Triaminotriethylamine trihydrochloride was synthesized by Mr. Y. Toyota in our laboratory.

3) G. Schwarzenbach and E. Freitag, *Helv. Chim. Acta*, **34**, 1492, 1503 (1951).

4) J. H. Grimes, A. J. Huggard and S. P. Wilford, *J. Inorg. Nucl. Chem.*, **25**, 1225 (1963).

was followed to determine the chelate stability constants of alkaline earth metals. The outline of this procedure is as follows. By an analogus treatment to the determination of acid dissociation constants of the free ligand,[1] the composite acid dissociation constants, K'_4, K'_5, K'_6 are obtained by the direct pH titration method in the presence of excess metal ions to ligand.[5] Then, the stability constants of mono- and diprotonated mononuclear chelates, K_{MH_2L}, K_{MHL}, can be calculated from the composite and the simple acid dissociation constants with an aid of Eqs. (1) and (2).

The acid dissociation constants of monoprotonated mononuclear chelates, K^{H}_{MHL}, can be determined by the direct pH titration method in the presence of equimolar amounts of metal and ligand, in a similar manner to the determination of simple acid dissociation constants.

Now, the stability constants of mononuclear chelates, K_{ML} and that of dinuclear chelates, $K^{M}_{M_2L}$ can be obtained from Eqs. (3) and (4) respectively, as the equilibrium constants on the right hand side are known, and [M] can be approximated as M_t, a total concentration of the metal ion, if a large excess of metal ions to ligand is present.

$$K_{MH_2L} = \frac{K'_4}{K_4[M]} - \frac{1}{[M]} \tag{1}$$

$$K_{MHL} = \frac{K'_4K'_5}{K_4K_5[M]} - \frac{1}{[M]} \tag{2}$$

$$K_{ML} = \frac{K^{H}_{MHL}K_{MHL}}{K_6} \tag{3}$$

$$K^{M}_{M_2L} = \frac{1}{K_{ML}[M]}\left(\frac{K_4'K'_5K'_6}{[M]K_4K_5K_6} - \frac{1}{[M]} - K_{ML}\right) \tag{4}$$

Equilibrium Constants Involving Transition Metal Ions. The stability constants of mononuclear chelates of nickel(II), cobalt(II), copper(II), zinc(II) and cadmium(II) were determined by extending Schwarzenbach's procedure[3] using the competitive reaction with an auxiliary ligand (tren) and a metal ion (calcium). In the case of thorium(IV) ion, the stability constant K_{ML} could not be obtained because of the precipitate formation. The final equations for the transition metal chelates are as follows:

$$M_t = c = [ML]\cdot(1 + [H]/K^{H}_{MHL}) + [Mtren] \tag{5}$$

$$tren_t = c = [Mtren] + \beta[H_3tren] \tag{6}$$

$$L_t = c = [ML]\cdot(1 + [H]/K^{H}_{MHL}) + [CaL]\cdot(1 + [H]/K^{H}_{CaHL}) \tag{7}$$

$$9c - [KOH] = [H] - [OH] + [ML][H]/K^{H}_{MHL} + [CaL][H]/K^{H}_{CaHL} + \gamma[H_3tren] \tag{8}$$

$$\beta = 1 + \frac{{}^tK_1}{[H]} + \frac{{}^tK_1{}^tK_2}{[H]^2} + \frac{{}^tK_1{}^tK_2{}^tK_3}{[H]^3} \tag{9}$$

$$\gamma = 3 + \frac{2{}^tK_1}{[H]} + \frac{{}^tK_1{}^tK_2}{[H]^2} \tag{10}$$

$$K_{ML} = \frac{{}^tK_1{}^tK_2{}^tK_3K_{CaL}K_{Mtren}}{K_C} \tag{11}$$

$$K_C = \frac{[H]^3[CaL][Mtren]}{[ML][H_3tren][Ca]} \tag{12}$$

The acid dissociation constants, K^{H}_{MHL}, of monoprotonated mononuclear chelates of transition metals and thorium(IV) were determined according to Anderegg[6] by the direct pH titration in the presence of equimolar amounts of metal and ligand. Then, the stability constants of monoprotonated mononuclear chelates, K_{MHL}, can be calculated from the known values, K_6, K^{H}_{MHL} and K_{ML}*5.

Mixed Metal Dinuclear Chelates.[6] The formation of dinuclear chelate could be considered by the two step process. The first step is the formation of 1 : 1 mononuclear chelate. The second step is the formation of 1 : 2 dinuclear chelate from mononuclear chelate and the second metal ion. When the first and the second metal ions are same, a homo-dinuclear chelate is formed. When these two metal ions are different, and the stability constant with the first metal ion (K_{ML}) is considerablly larger than that with the second metal ($K_{M'L}$), the stability constants of the mixed metal dinuclear chelates ($K^{M'}_{MM'L}$) could be obtained from Eq. (14) by the direct pH titration in the presence of an equimolar amount of the first metal ion (M) to the ligand, and in the presence of large excess of the second metal ion (M') to the first metal ion.

$$MHL^{3-} + M'^{2+} \overset{K_m}{\rightleftharpoons} MM'L^{2-} + H^+ \tag{13}$$

$$K^{M'}_{MM'L} = \frac{[H][MM'L]}{[M'][MHL]}\cdot\frac{[MHL]}{[H][ML]} = \frac{K_m}{K^{H}_{MHL}} \tag{14}$$

$$[MHL] = p\cdot L_t \tag{15}$$

$$[MM'L] = L_t(1 - \alpha p) \tag{16}$$

$$[M'] = M_t' - L_t(2 - \alpha p) \tag{17}$$

$$\alpha = 1 + K^{H}_{MHL}/[H] \tag{18}$$

$$p = 6 - \frac{[KOH] - [H] - [OH]}{L_t} \tag{19}$$

In the treatment of the mixed metal dinuclear chelates, it is assumed that a mononuclear chelate with the first metal ion is formed in the first step ($a \leqq 5$), then it reacts with a second metal ion to form a mixed metal dinuclear chelate in the second step ($5 < a \leqq 6$).

In the case of alkaline earth meatl ions, the stability constants of homo-dinuclear chelates were obtained as described previously. However, in the cases where the second metal ions are transition metals, the stability constants of homo-dinuclear or mixed metal dinuclear chelates could not be obtained, because the formation of precipitate was observed even at the earlier stage of pH titration in the presence of excess amount of transition metal ion to the ligand.

However, the pH titration was carried out successfully when the transition metals and calcium were chosen as the first and the second metal ions respectively, and the stability constants for the transition metal-calcium TAPHA chelates (K^{Ca}_{MCaL}) were obtained from Eq. (14).

The various equilibrium constants thus obtained are summarized in Tables 3—8.

5) G. Schwarzenbach and H. Ackermann, *Helv. Chim. Acta*, **31**, 1029 (1948).

*5 $\log K_{MHL} = -pK_6 + \log K_{ML} + pK^{H}_{MHL}$.

6) G. Anderegg, P. Nägeli, F. Müller and G. Schwarzenbach, *Helv. Chim. Acta.*, **42**, 827 (1959).

Results and Discussion

Crystalline Chelates. The infrared spectra of alkaline earth metal chelates and some transition metal chelates are shown in Fig. 3. These spectra were interpreted with an aid of our knowledge on nitrilotriacetate chelates.[7] As for sodium salt of alkaline earth metal chelates ($Na_4ML \cdot xH_2O$), the absorption peak of -COOM and that of $\overset{+}{\rangle}NHCH_2COO^-$ appear in a similar region and become a single peak at around 1600 cm^{-1}. This peak shifts to lower frequency with the increase of ionic radius of metal ion. On the other hand, in the case of protonated chelate ($MH_4L \cdot xH_2O$), the two absorption peaks appear at around 1600 cm^{-1} and 1720 cm^{-1} respectively, and they are assigned to -COOM and -COOH groups respectively.[7] Therefore, if the ratio of -COOM to -COOH is estimated from the relative intensity of the two peaks, it is possible to presume the structure of $MH_4L \cdot xH_2O$. In order to make this estimation, the peak intensities were measured by the base-line method[8] and it is assumed that the values of molar extinction coefficient on EDTA chelates in aqueous solution can be adopted to TAPHA chelates, that is the molar extinction coefficient of -COOM is nearly equal to that of $-COO^-$, and the values for -COOH and -COOM are 240 and 705 $mol \cdot cm^{-1}$ respectively.[9] The latter assumption seems to be rather critical, since the absorption data in solution are employed in the interpretation of solid state spectra. However, the result may be still useful for the meaningful discussion of the structure, because the ratio of the band intensities of -COOM to -COOH will not differ appreciablly between the states in solid and in solution. The result shows that the ratio of -COOM to -COOH is approximately 1 : 1 in the case of protonated chelate ($MH_4L \cdot xH_2O$), and the structure of these chelates is presumed as shown in Fig. 4A or 4B.

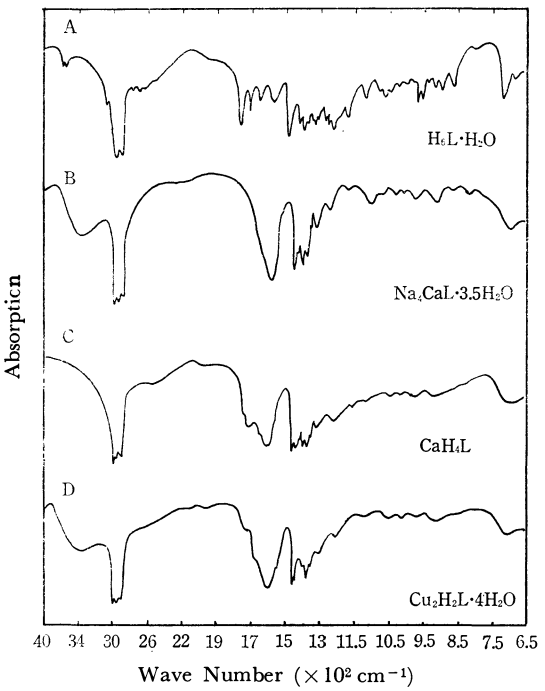

Fig. 3. Infrared spectra of crystalline TAPHA chelates in Nujol mull.

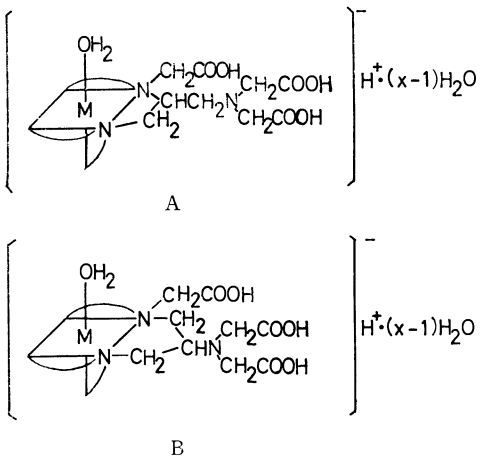

Fig. 4. Proposed structure of $MH_4L \cdot xH_2O$.

As for copper(II) dinuclear chelate ($Cu_2H_2L \cdot 4H_2O$), a peak at 1578 cm^{-1} and a shoulder at 1728 cm^{-1} are assigned to -COOM and -COOH groups respectively. The presence of two protons which is supported by the elementary analysis, suggests the existence of two uncoordinated carboxylic acid groups. Although the structures proposed in Fig. 5A or 5B may satisfy such requirment,

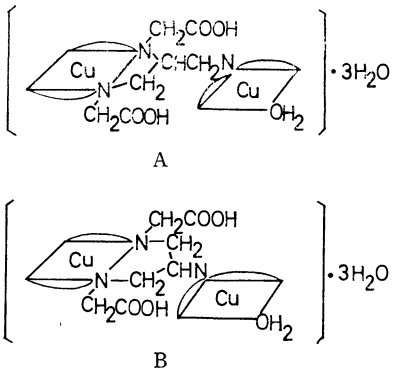

Fig. 5. Proposed structure of $Cu_2H_2L \cdot 4H_2O$.

7) Y. Tomita and K. Ueno, This Bulletin, **36**, 1069 (1963).
8) N. Wright, *Ind. Eng. Chem., Anal. Ed.*, **13**, 1 (1941). J. J. Heigl, M. F. Bell and J. U. White, *Anal. Chem.*, **19**, 293 (1947).
9) K. Nakamoto, Y. Morimoto and A. E. Martell, *J. Am. Chem. Soc.*, **85**, 309 (1963).

TABLE 3. STABILITY CONSTANTS ($\log K_{ML}$) OF MONONUCLEAR CHELATES OF TAPHA AND ITS RELATED COMPLEXANES

	Mg	Ca	Sr	Ba	Ref.	Co	Ni	Cu	Zn	Cd	Ref.
TAPHA	9.21 ±0.08	10.50 ±0.04	8.56 ±0.05	7.41 ±0.09		13.8 ±0.12	18.00 ±0.09	18.37 ±0.02	15.80 ±0.08	16.18 ±0.09	
EDTA*	8.9	10.7	8.7	7.9	10[a]	16.31	18.62	18.7	16.4	16.4	10[a]
TMDTA*	6.02	7.12	5.18	4.24	14[b]	15.55	18.15	18.92	15.26	13.90	11[b]
DTPA*	9.03	10.63	9.68	8.63	13[b]	19.27	20.22	21.53	18.55	19.31	6[b]
TTHA*	8.47	10.06	9.26	8.24	4[c]	20.6	18.8	20.3			12[a]

a) 25°C, $\mu=0.1$, b) 20°C, $\mu=0.1$, c) 30°C, $\mu=0.1$
* EDTA: ethylenediaminetetraacetic acid, TMDTA: trimethylenediaminetetraacetic acid
DTPA: diethylenetriaminepentaacetic acid, TTHA: triethylenetetraminehexaacetic acid

the relative absorption intensity of –COOH group against that of –COOM group is too weak to support the proposed structures, and more experimental results are needed to conclude the structure of this chelate.

Solution Equilibria. Mononuclear Chelates (ML). As shown in Table 3, the chelate stability order of TAPHA for alkaline earth and transition metal ions is same as that of other complexanes. In the case of alkaline earth metal chelates, it is noticed that the stability constants of TAPHA chelates are very close to those of EDTA chelates, but not to those of TMDTA chelates. This results may suggest that the ligand of mononuclear chelate (ML) will take a EDTA type coordination, but not a TMDTA type coordination, as far as the effect of uncoordinated nitrilodiacetate group on the chelate stability is assumed to be same order in either case.

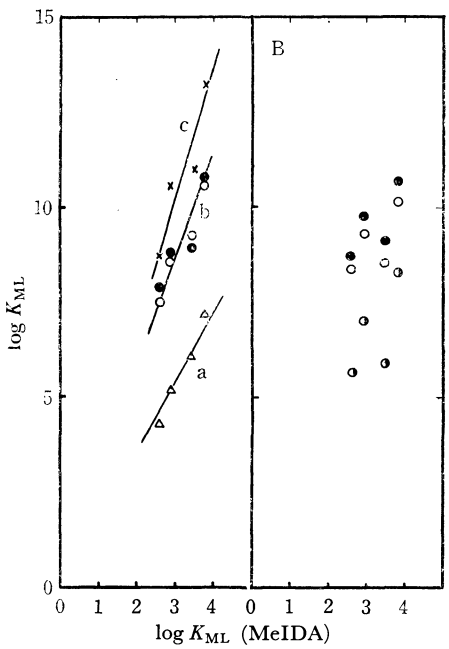

Fig. 6. Relationship between stability constant of alkaline earth metals - methyliminodiacetic acid chelates and stability constant of its related complexane chelates.
A ×: CyDTA, ○: EDTA, ●: TAPHA, △: TMDTA
B ●: DTPA, ⊙: TTHA, ◑: HEDTA

Now, if one looks into the structure of complexanes under consideration, the coordinating groups of these ligands can be divided into two classes, *i. e.*, *N*-methyliminodiacetic acid (MeIDA) and *N,N*-dimethylglycine. Figure 6 shows a plot of the chelate stability constants of various complexanes for alkaline earth metals versus those of *N*-methyliminodiacetic acid. The plots for TMDTA, EDTA, CyDTA and TAPHA give straight lines which pass through the origin (Fig. 6A), but those for HEDTA, DTPA and TTHA do not give straight lines (Fig. 6B). The complexanes of the first family have only *N*-methyliminodiacetic acid groups as coordinating group, but those of the second family have both *N*-methyliminodiacetic acid groups and *N,N*-dimethylglycine groups within a ligand molecule. The fact that the plots for TAPHA fit on the same line as those of EDTA, is indicative that the chelating behavior of TAPHA for alkaline earth metal ions is very similar to that of EDTA, since the slope of straight lines in Fig. 6A seems to be related with the nature and size of the chelate ring.

In the case of transition metal chelates, the stabilities of EDTA and TMDTA chelates are so close to those of TAPHA chelates that it is not so easy to discuss the coordinating structure of the chelates by comparing stability data of mononuclear chelate alone. In spite of the general concept that the chelate stability increases with increasing number of coordinating groups in the ligand, a nonadentate TAPHA chelate is less stable than an octadentate DTPA chelate. The result may be explained by the number of nitrogen

10) R. W. Schmid and C. N. Reilley, *ibid.*, **78**, 5513 (1956).
11) G. Anderegg, *Helv. Chim. Acta*, **47**, 1801 (1964).
12) T. A. Bohigian, Jr. and A. E. Martell, *J. Am. Chem. Soc.*, **89**, 832 (1967).
13) E. J. Durham and D. P. Rydkiewich, *ibid.*, **80**, 4812 (1958).
14) G. Schwarzenbach, R. Gut and G. Anderegg, *Helv. Chim. Acta*, **37**, 937 (1954).

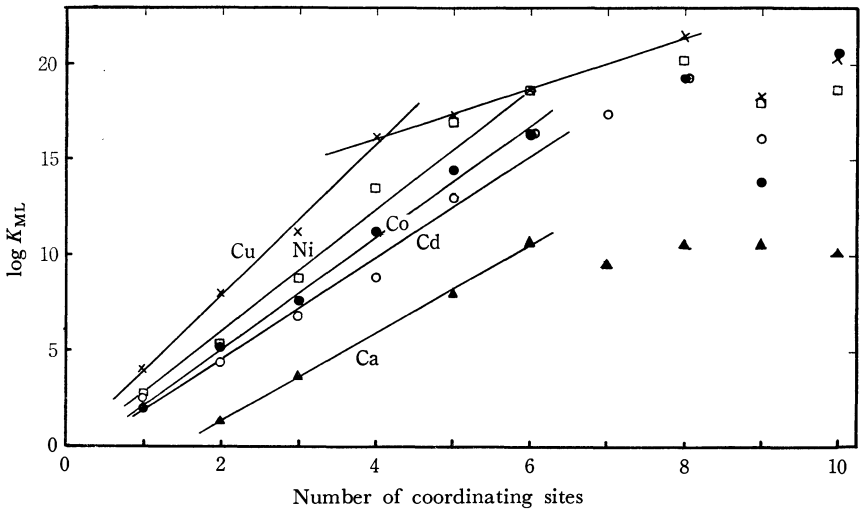

Fig. 7. Relationship between stability constant of complexanes chelates and number of coordinating sites.
Coordinating sites 1: NH_3, 2: *N*-methylglycine or glycine, 3: MeIDA or IDA, 4: EDDA, 5: HEDTA, 6: EDTA, 7: bis-[di(carboxylmethyl)aminoethyl]-methylamine, 8: DTPA, 9: TAPHA, 10: TTHA.
× Cu(II), □ Ni(II), ● Co(II), ○ Cd(II), ▲ Ca(II)

TABLE 4. STABILITY CONSTANTS ($\log K_{MHL}$) OF MONOPROTONATED MONONUCLEAR CHELATES OF TAPHA AND ITS RELATED COMPLEXANS

	Mg	Ca	Sr	Ba	Ref.	Co	Ni	Cu	Zn	Cd	Ref.
TAPHA	6.46 ±0.07	8.03 ±0.05	6.32 ±0.05	5.42 ±0.09		10.5 ±0.13	14.6 ±0.10	14.93 ±0.03	12.7 ±0.10	13.1 ±0.11	
EDTA	2.28	3.51	2.30	2.07	15[b]	9.15	11.56	11.54	9.0	9.1	11[b]
TMDTA	2.91	3.07	2.39	2.11	16[b]	7.4	9.9	10.7	7.3	6.5	11[b]
DTPA	5.59	6.17	4.78	3.77	13[b]	13.43	15.26	15.69	13.40	12.79	6[b]
TTHA	7.39	8.07	6.71	5.55	4[c]	18.4	17.7	18.1			

* $\log K_{MHL} = -pK_6 + \log K_{ML} + pK^{H}_{MHL}$
b) 20°C, $\mu=0.1$. c) 30°C, $\mu=0.1$

TABLE 5. STABILITY CONSTANTS ($\log K_{MH_2L}$) OF DIPROTONATED MONONUCLEAR CHELATES OF TAPHA AND TTHA

	Mg	Ca	Sr	Ba	Ref.
TAPHA	2.8	2.9	1.7	1.4	
TTHA	1.9	2.4	1.6	1.7	4[c]

c) 30°C, $\mu=0.1$

atoms which are involved in the coordination. In the case of DTPA chelate, all three nitrogens can coordinate to a metal ion, whereas, in the case of TAPHA, only two of three nitrogens can coordinate to a metal ion. Since the nitrogen atom has a larger affinity with transition metals than with alkaline earth metals, the number of coordinating nitrogens mainly affects the stability of transition metal chelates. Therefore, the values of the stability constant among EDTA, TMDTA and TAPHA chelates resemble each other.

An availability of only two nitrilodiacetate groups in the chelate formation of TAPHA, may also be proved by the following discussion. The dependence of the chelate stability of complexanes on the number of coordinating sites of the ligands can be clearly shown in Fig. 7, in which $\log K_{ML}$ values for selected metal ions are plotted against number of coordinating sites of the ligands form unidentate ammonia to multidentate complexanes.

15) G. Schwarzenbach and H. Ackermann, *Helv. Chim. Acta*, **30**, 1798 (1947).
16) G. Schwarzenbach and H. Ackermann, *ibid.*, **31**, 1029 (1948).

Table 6. Acid dissociation constants (pK^{H}_{MHL}) of monoprotonated mononuclear chelates of TAPHA and its related complexans

	Mg	Ca	Sr	Ba	Ref.	Co	Ni	Cu	Zn	Cd	Th	Ref.
TAPHA	7.13 ±0.03	7.40 ±0.02	7.64 ±0.02	7.89 ±0.03		6.52 ±0.01	6.45 ±0.01	6.44 ±0.01	6.75 ±0.02	6.81 ±0.02	5.99 ±0.09	
EDTA	3.9	3.1			11[b]	3.0	3.2	3.0	3.0	2.9		11[b]
TMDTA	7.3	6.34			11[b]	2.4	2.2	2.2	2.5	3.06		11[b]
DTPA	7.09	5.99	5.69	5.55	13[b]	4.81	5.59	4.79	5.46	4.09		13[b]
TTHA	9.25	8.34	7.78	7.66	4[c]	7.97	9.11	7.96				12[a]

a) 25°C, μ=0.1. b) 20°C, μ=0.1. c) 30°C, μ=0.1

It is noticed that the chelate stability increases linearly with increasing number of coordinating sites until the coordination number of metal ion is filled up. However, the values for the chelates of TAPHA which is a nonadentate ligand, is almost same as those of EDTA which is a sexadentate ligand. This result is indicative that only six of nine coordinating site of TAPHA, or in other word, two of three nitrilodiacetate groups, are involved in the formation of mononuclear chelate.

Protonated Chelates (MHL and MH_2L). As TAPHA is a hexabasic acid, protonated chelates are formed more easily than in the case of tetrabasic EDTA. The stability constants of monoprotonated mononuclear chelates (MHL) and diprotonated mononuclear chelates (MH_2L) of TAPHA are shown in Tables 4 and 5 along with the corresponding values of other complexanes of related structure. It is seen from Table 4 that, in the case of transition metal ions, the values of stability constant of TAPHA lie in between those of EDTA and of DTPA, while, in the case of alkaline earth metal ions, the values of stability constant of TAPHA are comparable with those of TTHA which is a decadentate hexabasic ligand. It is also noticed that the stability constants of diprotonated TAPHA chelates for alkaline earth metal ions are comparable with those of TTHA chelates.

The acid dissociation constants of monoprotonated TAPHA chelates were also determined and their values are listed in Table 6 along with the corresponding values of other complexanes. The acidity of protonated chelate is found to decrease with increasing the number of coordination sites in the ligands.

In contrast with the stability constants of normal chelates as well as protonated chelates which are very much dependent upon the kind of metal ions, the difference of acid dissociation constants of protonated chelates among alkaline earth metal ions as well as transition metal ions is very small in TAPHA chelates. The average value of pK^{H}_{MHL} is 7.52±0.25 for alkaline earth metal ions and 6.54±0.14 for transition metal ions. Thus, although the acidity of free monoprotonated ligand

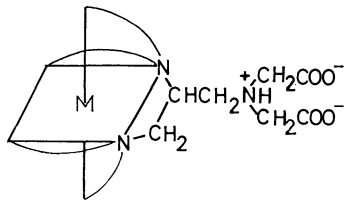

Fig. 8. Monohydrogen mononuclear chelate, MHL^{3-}.

(HL) is increased by metal chelation, the influence of the kind of metal ion on the acid dissociation constant of protonated chelate is found to be not so significant. The result may suggest that the bonding site of proton is so remote from the site of metal coordination, that the acidity is not so sensitive with the kind of metal ion within each group of metals. Therefore, the most reasonable structure for monoprotonated TAPHA chelate may be an EDTA type chelate in which a terminal uncoordinated group is protonated (Fig. 8). This coordination structure, in its deprotonated form, may also be true in the case of normal mononuclear chelate of transition metal ions, whose coordination structure was not concluded in the foregoing discussion.

Dinuclear Chelates (M_2L and $MM'L$). The formation of polynuclear chelates becomes easier when the number of coordination sites of the ligand is increased beyond the coordination number of the metal ion to be complexed. Thus, the formation of dinuclear chelates and di- and trinuclear chelates have been reported for DTPA and TTHA respectively.[6,12] The stability constants of polynuclear chelates have to be determined in the presence of large excess of metal ion. In the case of TAPHA, the formation of dinuclear chelate was observed for alkaline earth metals except magnesium. However, in the case of transition metals and magnesium, no satisfiable result could be obtained because of the formation of precipitation as the pH titration proceeded.

The stability constants of the dinuclear TAPHA chelate (M_2L) are shown in Table 7, together with those of TTHA. The values of $\log M^{M}_{M_2L}$ are

TABLE 7. STABILITY CONSTANTS ($\log K^{M}_{M_2L}$) OF ALKALINE EARTH METAL-DINUCLEAR CHELATES OF TAPHA AND TTHA

	Mg	Ca	Sr	Ba	Ref.
TAPHA		2.3	1.4	1.6	
TTHA	5.94	4.10	3.44	3.41	4c)

c) 30°C, $\mu=0.1$

considerably lower than those of $\log K_{ML}$ and are same order as those of 1 : 1 iminodiacetic acid chelates. This result suggests that the second metal ion may be chelated by the uncoordinated terminal nitrilodiacetate group of normal mononuclear TAPHA chelate. The structure of dinuclear chelate is proposed in Fig. 9.

It is also noticed that the values of the stability constant of dinuclear TAPHA chelate are apparently lower than those of TTHA. The magnitude of $\log K^{M}_{M_2L}$ for TTHA is comparable with those of quadridentate or quinquedentate complexanes, and this result can easily be understood if one consider the structure of mononuclear TTHA chelate, which can chelate the second metal ion by more coordination sites than does TAPHA.

As described in the experimental part, the stability

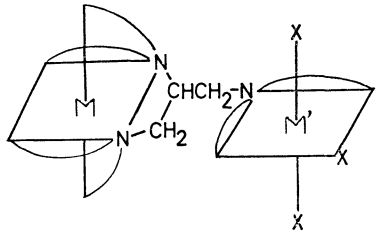

Fig. 9. Dinuclear chelate, $MM'L^{2-}$.

TABLE 8. STABILITY CONSTANTS ($\log K^{Ca}_{MCaL}$) OF MIXED METAL DINUCLEAR CHELATE OF TAPHA

Co	Ni	Cu	Zn	Cd
2.05 ±0.01	2.08 ±0.01	2.08 ±0.03	2.62 ±0.01	2.19 ±0.01

constants of mixed dinuclear chelate (MM'L) were also determined by choosing transition metals and calcium as the first and the second metal ions respectively. The values of $\log K^{Ca}_{MCaL}$ can be understood as the dinuclear chelate formation constants when calcium ion is bound by a mononuclear TAPHA chelate of transition metal. The observed values are listed in Table 8. It is seen from the table that the stability constants of MCaL chelates are same order as that of Ca_2L chelate and that the values of $\log K^{Ca}_{MCaL}$ are not sensitive to the kind of the first metal ions as in the case of pK^{H}_{MHL}. These results may also support the structure of dinuclear TAPHA chelate which is shown in Fig. 9.

Th(IV)-TAPHA System. Titration of TAPHA in the presence of excess of thorium to ligand could not be carried out because of the precipitate formation. Titration of 1 : 1 mixture was successful only in the lower pH region, where no precipitate was formed and no pH drift was observed. From the data of pH titration, the acid dissociation constant of monoprotonated chelate (ThHL) was calculated as shown in Table 6. In the higher pH region, however, the hydrolyses of aquo and chelated species as well as the polymerization through olation may take place to result in a complicated system.

Authors are grateful to the Ministry of Education, for the financial support to this work.

BULLETIN OF THE CHEMICAL SOCIETY OF JAPAN VOL. 41 1353—1355 (1968)

Studies on Hydroxy Amino Acids. I. A New Synthesis of Aziridine Derivative from β-Hydroxy α-Amino Acid

Kenji OKAWA, Teiji KINUTANI and Katsunobu SAKAI

Department of Chemistry, Faculty of Science, Kwansei-Gakuin University, Nishinomiya

(Received August 16, 1967)

N-Tosyl-3-methyl-2-aziridinecarboxylic acid anilide was obtained by the β-elimination reaction of *N,O*-ditosyl-L-threonine anilide. The ethyleneimine ring of this compound was readily cleaved by acetic acid in the presence of boron trifluoride and *N*-tosyl-*O*-acetyl-L-threonine anilide was obtained. Formaldehyde also reacted with this compound in the presence of the same catalyst and gave 1,3-oxazolidine and 1,3-oxazine derivatives.

We have been studying the synthesis of α,β-unsaturated α-amino acid derivatives by dehydration of β-hydroxy-α-amino acid derivatives and have observed the formation of *N*-acyl-α,β-unsaturated amino acid esters from the corresponding *N*-acyl-β-hydroxyamino acid esters as described by Photaki.[1]

However, in the case of *N,O*-ditosyl-L-threonine anilide, an unexpected product, *N*-tosyl-3-methyl-2-aziridinecarboxylic acid anilide, was obtained in good yield.

Among the reports concerning the synthesis of aziridinecarboxylic acid derivatives,[2-6] only Smrt[7] has reported findings similar to the above. In his study he asserted that the aziridinecarboxylic acid ester was produced when *N*-trityl-*O*-mesyl-serine methyl ester in the benzene solution was treated with *N*-ethyl-piperidine.

We have also found that the ethyleneimine ring of our aziridine derivative is readily cleaved by acetic acid or formaldehyde in the presence of boron trifluoride. Acetic acid gave *N*-tosyl-*O*-acetyl-L-threonine anilide and formaldehyde gave 3-tosyl-5-methyl-1,3-oxazolidine-4-carboxylic acid anilide (IVA) and 3- phenyl-4-oxo-5-tosylamino-6-methyl-1,3-tetrahydro-oxazine (IVB) as shown in Fig. 1.

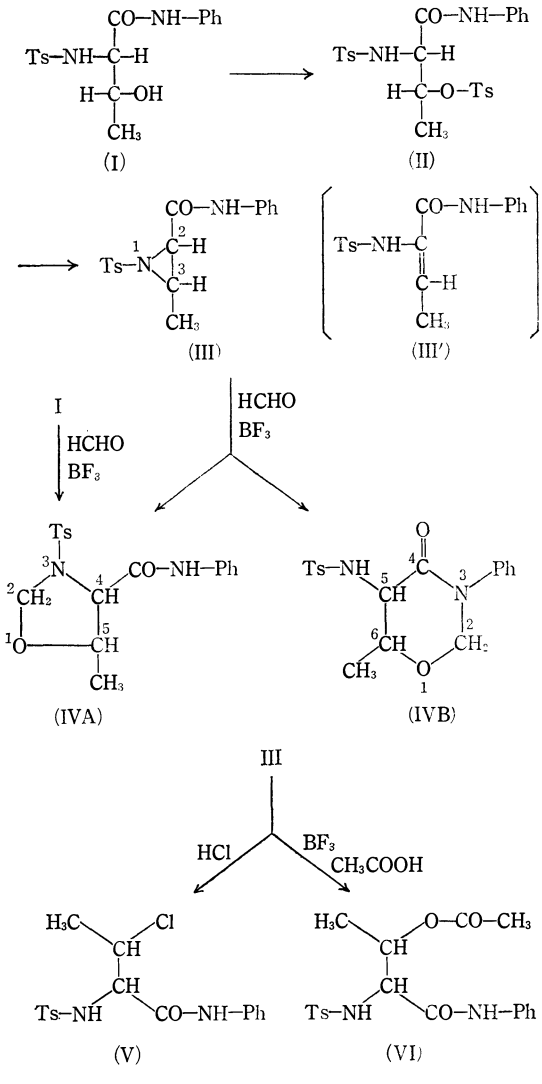

Fig. 1.

1) I. Photaki, *J. Am. Chem. Soc.*, **20**, 1123 (1963).
2) E. Kyburz, H. Els, St. Majnoni, G. Englert. C. von Pluta, A. Furst and Pl. A. Plattner, *Helv. Chim. Acta*, **49**, 359 (1966).
3) K. D. Gundermann and G. Holtmann, *Chem. Ber.*, **91**, 160 (1958).
4) Pl. A. Plattner, A. Boller, H. Frick, A. Furst, B. Hegedus, H. Kirchensteiner, St. Maunoni, R. Snlapfer and H. Spiegelberg, *Helv. Chim. Acta*, **40**, 1531 (1957).
5) M. A. Stolberg, J. J. O'Neill and Th. Wagner-Jauregg, *J. Am. Chem. Soc.*, **75**, 5045 (1953).
6) Y. Yukawa and S. Kimura, *Nippon Kagaku Zassi (J. Chem. Soc. Japan, Pure Chem. Sect.)*, **78**, 454 (1957).
7) J. Smrt, J. Beránek and J. Sicher, *Chem. Abstr.* **55**, 10468i U. S. 2958691 Nov. 1. 1960.

The compound II in dry tetrahydrofurane was treated with an equivalent amount of diethylamine to produce III. The elemental analysis and the molecular weight of III showed the molecular formula $C_{17}H_{18}O_3N_2S$. From this results, it was suggested that the compound is a dehydration product of I and has a structure of either III or III'. But III was confirmed by the spectral data.

The infrared spectrum indicated the presence of secondary amide bands at 1675 cm^{-1} and 1523 cm^{-1} respectively. But the characteristic absorption of a trisubstituted vinyl double bond was not detected. However, a new absorption band appeared at 885 cm^{-1}, this may be attributed to the aziridine ring deformation.

The NMR spectrum also supported the structure III. The vinyl proton and tosylated amide proton were not detected in the corresponding regions. The NMR spectrum of III showed one-proton octet at δ 3.12 ppm with J=7.7 cps for the C_3-proton, one-proton doublet at δ 3.47 ppm with J=7.7 cps for the C_2-proton, $J_{2,3}$=7.7 cps (*cis*-position).[8]

The ethyleneimine ring of III is readily cleaved by hydrochloric acid or toluenesulfonic acid, and V and II were obtained respectively. However, acetic acid cannot react with III but reacted with it in the presence of boron trifluoride - etherate and IV was obtained.

In the presence of the same catalyst, III also reacted with paraformaldehyde at 45°C and the products, IVA and IVB were separated by silica gel chromatography in the yield of 45% and 5% respectively. From the elemental analyses and the molecular weights, IVA and IVB were shown to have the same molecular formula of $C_{18}H_{20}O_4N_2S$ which indicated just one formaldehyde molecule combined with III.

Proof for the structure IVA was obtained by the spectral data and the direct synthesis of IVA from I and formaldehyde.

The infrared absorption spectrum of IVA shows secondary amide bands at 1685 cm^{-1} and 1525 cm^{-1} respectively and the characteristic strong bands of –N–C–O– group in a ring structure at 1155, 1110, 1087 and 1073 cm^{-1}.[9]

The NMR spectrum of IVA showed a three-proton doublet at δ 1.05 ppm with J=5.8 cps for the C_5-methyl protons, one-proton doublet at δ 3.64 ppm with J=6.8 cps for the C_4-proton, one-proton octet at δ 4.17 ppm with J=5.8 and 6.8 cps for the C_5-proton, two one-proton doublets at δ 4.62 and 5.34 ppm for the AB type C_2-methylene protons, and no tosylated amide proton was detected in the corresponding region.

The final structure IVB was determined by the spectral data.

The infrared absorption spectrum of IVB indicated the presence of a carbonyl group in tertiary amide bond at 1695 cm^{-1} and also showed a –N–C–O– group in a ring structure at 1145, 1112, 1087 and 1050 cm^{-1}.[9]

The NMR spectrum of IVB showed a three-proton doublet at δ 1.19 ppm with J=6.8 cps for the C_6-methyl protons, one-proton quartet at δ 4.20 ppm with J=2.0 and 3.3 cps for the C_5-proton, one proton octet at δ 3.86 ppm with J=3.3 and 6.8 cps for the C_6-proton, two-proton doublet at δ 5.39 ppm for the C_2-methylene protons and one proton doublet at δ 5.58 ppm with J=2.0 cps for the tosylated amide proton. The monosubstituted amide proton was not detected in the corresponding region.

Experimental

All melting points are uncorrected. NMR spectra were obtained with a Varian A-60 spectrometer in $CDCl_3$ solution and chemical shifts are given from TMS as an internal reference. Infrared spectra were recorded with a JASCO-DS-402G (Japan Spectroscopic Co., Ltd.).

***N*-Tosyl-L-threonine Anilide (I).** Dicyclohexylcarbodiimide (30.9 g, 0.15 mol) in methylene chloride (80 m*l*) was added drop by drop to the mixture of *N*-tosyl-L-threonine (30.9 g, 0.1 mol) and aniline (9.3 g, 0.1 mol) in methylene chloride (800 m*l*) with stirring at 0°C. After adding the solution, the stirring was continued for one hour at 0°C and the reaction mixture was allowed to stand at room temperature for 4 hr. The urea produced was filtered off and the filtrate was allowed to stand in a refrigerator. The separated crystals were collected and recrystallized from tetrahydrofuran - *n*-hexane. The total yield was 26.9 g (70%), mp 145—146°C; $[\alpha]_D^{24}$ −37.21° (*c* 1.13, dioxane).

Found: C, 58.48; H, 5.77; N, 8.10%. Calcd for $C_{17}H_{20}O_4N_2S$: C, 58.60; H, 5.79; N, 8.04%.

***N,O*-Ditosyl-L-threonine Anilide (II).** *p*-Toluenesulfonyl chloride (38.0 g, 0.2 mol) in pyridine (60 m*l*) was added drop by drop to a solution of I (38.4 g, 0.1 mol) in pyridine (200 m*l*) with stirring at 0°C. After stirring for thirty minutes, the reaction mixture was allowed to stand at room temperature for 4 hr.

Ice water was added to the reaction mixture until it became turbid and the mixture was kept in a refrigerator overnight. The separated crystals were filtered and washed with ethanol. Recrystallization from tetrahydrofuran - *n*-hexane gave fine crystals. The total yield was 29.6 g (65%), mp 186—188°C; $[\alpha]_D^{24}$ −16.11° (*c* 1.21, CH_2Cl_2).

Found: C, 57.70; H, 5.27; N, 5.63; S, 12.32%. Calcd for $C_{24}H_{26}O_6N_2S_2$: C, 57.35; H, 5.21; N, 5.57; S, 12.73%.

***N*-Tosyl-3-methyl-2-aziridinecarboxylic Acid Anilide (III).** Diethylamine (1.02 m*l*, 0.01 mol) was added to a solution of II (5.02 g, 0.01 mol) in tetrahydrofuran (50 m*l*). After incubation at 37°C for 5 hr, the reaction mixture was diluted with ether until it became turbid. The diethylamine *p*-toluenesulfonate produced was filtered off and from the filtrate solvent

8) G. Szeimies and R. Huisgen, *Chem. Ber.*, **99**, 491 (1966).

9) Z. Eckstein, P. Gluzinske and W. Hofman and T. Urbanski, *J. Chem. Soc.*, **1961**, 489.

was removed under reduced pressure. The resultant material was dissolved in ether under warming, insoluble material was filtered off and the filtrate was allowed to stand in a refrigerator. White needle crystals were obtained. The yield was 2.15 g (65%). The melting point was different depending upon the solvent of recrystallization: mp 50—56°C for ether, 90—91°C for ethanol-water. $[\alpha]_D^{20}$ −65.3° (*c* 1.08, EtOH), $\lambda_{max}^{MeOH\cdot H_2O}$ 246 mμ (ε=13000), ν_{max}^{KBr} 1675 (amide I), 1523 (amide II) and 885 cm^{-1} (aziridine ring).

Found: C, 61.97; H, 5.61; N, 8.21; S, 9.54%; mol wt (Rast), 315±15. Calcd for $C_{17}H_{18}O_3N_2S$: C, 61.80; H, 5.49; N, 8.48; S, 9.70%; mol wt, 330.4.

NMR: δ 1.33 ppm (3H (d), *J*=5.8 cps, C_3-methyl proton); 3.12 ppm (1H (d) *J*=5.8, *J*=7.7 cps, C_2-proton) 3.47 ppm (1H (d) *J*=7.7 cps, C_2-proton)

3-Tosyl-5-methyl-1,3-oxazolidine-4-carboxylic Acid Anilide (IVA).

3-Phenyl-4-oxo-5-tosylamino-6-methyl-1,3-tetrahydrooxazine (IVB). Paraformaldehyde (1.8 g, 0.02 mol) and ten drops of boron trifluoride etherate (47%) were added to the solution of III (6.60 g, 0.02 mol) in chloroform (50 m*l*) and stirred at 45°C for 50 hr.

Unreacted paraformaldehyde was filtered off and the solvent was removed. The oily residue (8.5 g) was chromatographed on silica gel (150 g) with benzene-ethyl acetate (10 : 1, v/v) to yield two reaction products.

From the fraction of R_f 0.74 on silica gel thin-layer chromatography with benzene - ethyl acetate (10 : 1, v/v) was obtained a product IVA yield 3.25 g (45%), mp 36—38°C from ether - petroleum ether; $[\alpha]_D^{20}$ −215.5° (*c* 1, EtOH), $\nu_{max}^{CCl_4}$ 1685 (amide I), 1525 (amide II), 1115, 1110, 1087 and 1073 cm^{-1} (–N–C–O– ring).

Found: C, 59.28; H. 5.79; N, 7.64; S, 9.27%; mol wt, 350±10,(Rast). Calcd for $C_{18}H_{20}O_4N_2S$: C, 59.98; H, 5.59; N, 7.77; S, 8.90%; mol wt, 360.

NMR: δ 1.05 ppm (3H (d) *J*=5.8 cps, C_5 methyl proton); 3.64 ppm (1H (d) *J*=6.8, C_4 proton); 4.17 ppm (1H (o) *J*=5.8, *J*=6.8, C_5 proton); 4.62, 5.34 ppm (2H (d) C_2 methylene proton)

From the fraction of R_f 0.44 (on the same silica gel thin-layer chromatography) was obtained a product IVB, 0.35 g (5%) mp 137—137.5°C (from ethyl acetate-ether); $[\alpha]_D^{20}$ +35.6° (*c* 1, EtOH), ν_{max}^{KBr} 1145, 1112, 1087 and 1060 (–N–C–O– ring), 3250 cm^{-1} (Tos-NH–).

Found: C, 60.04; H, 5.60; N, 7.71; S, 8.59%; mol wt, 355±10 (Rast). Calcd for $C_{18}H_{20}O_4N_2S$: C, 59.98; H, 5.59; N, 7.77 S, 8.90%; mol wt, 360.

NMR: 1.19 ppm (3H (d) *J*=6.8 cps, C_6 methyl proton); 3.86 ppm (1H (o) *J*=3.2, 6.8 cps, C_6 proton); 4.86 ppm (1H (q) *J*=2.0, 3.2 cps, C_5 proton); 5.39 ppm (2H (d) C_2 methylene proton); 5.58 ppm (1H (d) *J*=2.0 cps, tosylated amide proton)

From the fraction of R_f 0.66 on the same silica gel thin-layer chromatography 0.32 g of unreacted starting material was recovered.

3-Tosyl-5-methyl-1,3-oxazolidine-4-carboxylic Acid Anilide (IVA) from *N*-Tosyl-L-threonine Anilide (I). Five drops of boron trifluoride etherate (47%) were added to a mixture of I (1.74 g, 0.005 mol) and paraformaldehyde (0.9 g) in acetic acid (10 m*l*) and the mixture was stirred at 85°C for 20 min, and the solvent was evaporated under reduced pressure. The residual oily substance was dissolved in ether and was washed with 1 N sodium bicarbonate and water to remove a trace amount of acetic acid and aldehyde. The ether solution was dried over anhydrous sodium sulfate and the solvent was removed. Colorless oil (1.75 g) obtained gradually solidified to a glassy mass mp 36—38°C, R_f 0.74 (on silica gel thin-layer chromatography with benzene - ethyl acetate (10 : 1, v/v). This compound was identified with IVA by the IR spectrum and R_f value on silica gel thin-layer chromatography.

***N*-Tosyl-α-amino-β-chloro-*n*-butyric Acid Anilide (V).** Compound III (0.33 g, 1mmol) was warmed to be dissolved in 2 N hydrochloric acid (2 m*l*). The solution was kept at 40°C for 2 hr, and fine crystals gradually appeared during this period. The crystals were filtered and collected with theoretical yield. Recrystallization from methanol-water gave pure materials, mp 163—164°C, $[\alpha]_D^{24}$ −51.13° (*c* 1.02, MeOH).

Found: C, 55.70; H, 5.62; N, 7.63; S, 8.87; Cl, 9.66%. Calcd for $C_{17}H_{19}O_3N_2ClS$: C, 55.66; H, 5.22; N, 7.64; S, 8.74; Cl, 9.66%.

***N*-Tosyl-*O*-acetyl-L-threonine Anilide (VI).** A mixture of III (1.98 g, 0.006 mol), acetic acid (6 m*l*), and five drops of boron trifluoride etherate (47%) was stirred at 45°C for 4 hr. The reaction mixture was dissolved in ethyl acetate (100 m*l*) and was washed with 1 N sodium carbonate and then with 1 N sodium bicarbonate and water. The organic layer was dried over anhydrous sodium sulfate. After removal of the solvent, the crystalline residue was recrystallized from ethyl acetate - *n*-hexane to give a substance, mp 173—173.5°C in 88% yield. This substance was found to be identical with the authentic sample*1 (*N*-tosyl-*O*-acetyl-L-threonine anilide) by the IR spectrum and the mixed melting point test.

$[\alpha]_D^{20}$ −1.82° (*c* 1.92, dioxane), ν_{max}^{Nujol} 1736 (–OAc), 1661 (amide I) and 1534 cm^{-1} (amide II).

Found: C, 58.62; H, 5.78; N, 7.25; S, 8.23%. Calcd for $C_{19}H_{22}O_5N_2S$: C, 58.45; H, 5.68; N, 7.17; S, 8.21%.

The authors wish to express their hearty thanks to Fujisawa Pharmaceutical Company for the measurements of NMR spectra and for a grant-in-aid for fundamental scientific research.

*1 This sample was prepared from *N*-Tosyl-L-threonine anilide (I) and acetic anhydride in dry pyridine.

BULLETIN OF THE CHEMICAL SOCIETY OF JAPAN VOL. 41 1356—1360 (1968)

Studies of the Pinacol Rearrangement. IV.*[1] The Kinetics and Mechanism of the Rearrangement of *meso*- and *dl*-2,2'-Dimethoxybenzopinacol

Kiyoshi MATSUMOTO

Department of Chemistry, Faculty of Science, Kyoto University, Sakyo-ku, Kyoto

(Received October 6, 1967)

The first-order rate constants of the perchloric acid-catalyzed rearrangements of the *meso*- and *dl*-2,2'-dimethoxybenzopinacols were measured in anhydrous acetic acid. A linear correlation of the logarithm of the first-order rate constants ($\log k$) with Hammett acidity function (H_0) was obtained in each case. The large positive values of the entropy of activation support the A-1 mechanism, which is also supported by the linearities of $\log k$ with H_0, suggesting that the classical carbonium ion is an intermediate in these processes. The migration aptitude of the *meso*-isomer decreases with time, while that of *dl* increases. On the basis of this information, the mechanism of the rearrangement was discussed.

The pinacol rearrangement is one of the most classical reactions, therefore, a large amount of information about it and about related rearrangements has been reported.[1] Collins has reviewed the evidence on the mechanisms of the pinacol rearrangement and has concluded that it supports the general scheme:

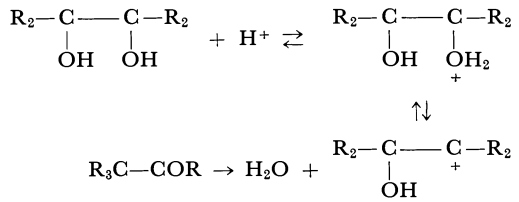

However, there are numerous detailed aspects of these reactions which have been inadequately investigated.[2] The kinetics of the reactions of the tetraarylpinacols have received particularly little attention except for the rearrangement of the benzopinacol.[3]

The present communication will present our findings on the kinetics of the rearrangements of the *meso*- and *dl*-2,2'-dimethoxybenzopinacols (I) to the 2-methoxybenzoyl-2-methoxyphenyldiphenylmethane (II) and benzoyldi-2-methoxyphenylphenylmethane (III) in anhydrous acetic acid, with perchloric acid as the catalyst.

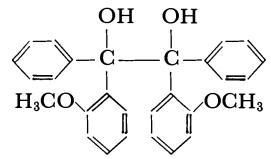

(I)

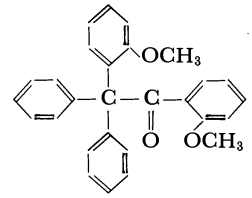

(II)

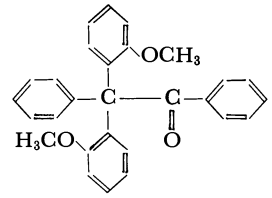

(III)

Experimental

Materials. *Anhydrous Acetic Acid.* Glacial acetic acid (commercial, extra pure) was refluxed with acetic anhydride and distilled through a 1-m column packed with glass tubes (1 cm long). The first 20% of the distillate was rejected, and the fraction of the 117.0—118.3°C boiling range was collected. This fraction was redistilled, after which the fraction of the 117.8—118.1°C boiling range was collected.

*1 Presented at the 20th Annual Meeting of the Chemical Society of Japan, Tokyo, April, 1967. Part III: K. Matsumoto, R. Goto, T. Asano and H. Wada, *Nippon Kagaku Zasshi (J. Chem. Soc. Japan, Pure Chem. Sect.)*, **88**, 92 (1967).

1) For an excellent review of the pinacol rearrangement, see C. J. Collins, *Quart. Rev.*, **14**, 357 (1960).

2) a) R. Goto, K. Matsumoto and A. Sera, *Nippon Kagaku Zasshi (J. Chem. Soc. Japan, Pure Chem. Sect.)*, **87**, 93 (1966). b) *Ibid.*, **87**, 1076 (1966). c) *Ibid.*, **88**, 92 (1967).

3) H. J. Gebhart and K. H. Adams, *J. Am. Chem. Soc.*, **76**, 3925 (1954).

The methods of preparing and purifying *meso*- and *dl*-2,2'-dimethoxybenzopinacol have already been reported.[2c]

A standard stock solution of perchloric acid was prepared by the addition of 1.00 m*l* of a 70—72% reagent grade commercial product to approximately 200 m*l* of anhydrous acetic acid containing a stoichiometric amount of the redistilled acetic anhydride required to react with the water of the aqueous perchloric acid. The solution was then standardized by titration with a standard solution (0.0500 N) of sodium acetate in glacial acetic acid, using bromophenol blue as an indicator.[4]

Analytical Method. Since the oxidation method with lead tetraacetate is not accurate for 2,2'-disubstituted benzopinacol,[2c] the optical densities of the pinacolones were measured and the concentration of the pinacol remaining was calculated.

Reaction-rate Measurements. A reaction flask containing about 0.01 M of a pinacol solution was immersed in a thermostated oil bath. After half an hour, a measured volume of the catalyst was added to this solution. At appropirate times, 1-m*l* samples were removed and put into test tubes containing 0.0010 m*l* of a concentrated solution of potassium acetate. Each sample (0.20 m*l*) was treated by thin-layer chromatography.[2b] Each pinacolone fraction was extracted with chloroform to a 10.0-m*l* solution. Measurements of the optical densities of these solutions gave the concentrations of the pinacol remaining.*2 A straight line correlating the concentrations of the pinacolone, (II) or (III), with the optical densities at 2820 or 2765 Å was used to obtain the concentrations of the pinacolones. The reaction-rate constants were evaluated by the graphical method.

Results and Discussion

Products. The *meso*- and *dl*-2,2'-dimethoxybenzopinacols rearranged to produce *o*-anisoylanisyldiphenylmethane (II) and benzoyldi-*o*-anisylphenylmethane (III), which have absorption maxima at 282 mμ and 276 mμ respectively in chloroform. The thin-layer chromatography showed that the *meso*-isomer isomerizes to the *dl*, while neither pinacol forms a stable epoxide intermediate.[3,5]

Kinetics. We have much evidence that the pinacol rearrangement shows first-order kinetics, as was observed in the present case (*cf.* Fig. 1). The *dl*-isomer is rearranged about three times as fast as the *meso*. In the case of the *meso*-isomer, a slight curvature was evident. This curvature corresponded to acceleration as the reaction proceeded. This deviation may be due to the contribution of the isomerization of the *meso*-isomer to the *dl*, which was observed in the thin-layer chromatography of the reaction products. A similar phenomenon was observed in the rearrangements of the *cis*- and *trans*-1,2-diphenylacenaphthene-1,2-diol.[6]

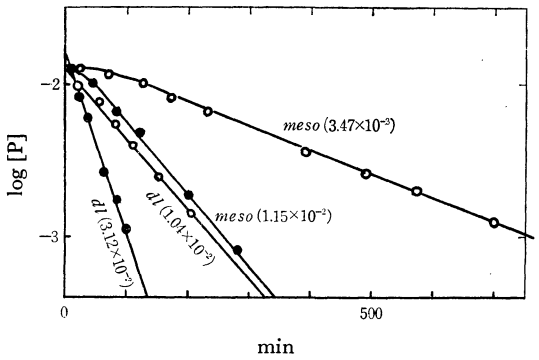

Fig. 1 First order plots of rearrangement of 2,2'-dimethoxybenzopinacol (1.36×10^{-1} mol $HClO_4$).
○ 62°C ● 72°C

Table 1. Summary of kinetic data for the perchloric acid-catalyzed rearrangement of 2,2'-dimethoxybenzopinacol in anhydrous acetic acid at 72°C

$HClO_4$ (mol×10⁴)	H_0	$k\times10^2$(min⁻¹)	log k	$k'\times10^{-2}$ (l/mol×min)
		(*meso*)		
0.518	−2.23	0.502	−2.30	0.969
0.857	−2.00	0.724	−2.14	0.845
1.36	−1.79	1.15	−1.96	0.846
2.60	−1.50	1.94	−1.72	0.746
3.98	−1.30	2.81	−1.55	0.706
		(*dl*)		
0.532	−2.22	1.38	−1.86	2.71
0.863	−2.00	1.99	−1.70	2.32
1.36	−1.79	3.12	−1.51	2.28
1.87	−1.65	4.14	−1.39	2.21
2.87	−1.45	6.03	−1.22	2.10

Table 1 summarizes the effects of the catalyst concentration upon the rate constant.[7] The plots of the Hammett acidity function values shown in Table 1 against log k are two straight lines with slopes of 0.90 and 0.85 for the *dl*- and *meso*-isomer respectively (Fig. 2). These correlations support the A-1 (acid-catalyzed first-order reaction) mechanism, according to the original form of the Zucker-Hammett hypothesis.[8]

The values of the experimental activation energy, E_a, and of the free energy, $\Delta F^{\neq}$, and entropy, $\Delta S^{\neq}$, of the activation were calculated from the specific rate constants, k' (Table 2).

4) S. Winstein, E. Grunwald and L. L. Ingraham, *J. Am. Chem. Soc.*, **70**, 821 (1939).

*2 The experimental errors of the analysis were *ca.* 3—5%. The *meso*-isomer formed the *dl*-isomer in addition to the ketones. The *dl* produced only the ketones.

5) K. Matsumoto, unpublished work.

6) P. D. Bartlett and R. F. Brown, *J. Am. Chem. Soc.*, **62**, 2927 (1940).

7) $k'=k/(HClO_4)$.

8) F. A. Long and M. A. Paul, *Chem. Revs.*, **57**, 935 (1957).

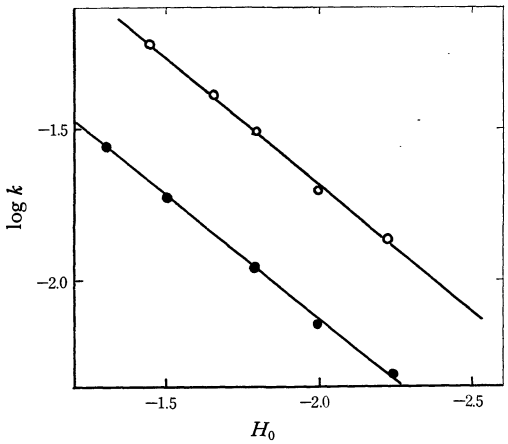

Fig. 2. Correlation of first order rate constant with the Hammett acidity function of the medium at 72°C.
○ *dl*-isomer ● *meso*-isomer

Table 2. Thermodynamics of activation for rearrangement of 2,2'-dimethoxybenzopinacol in 1.36×10^{-4} mol $HClO_4$ - acetic acid

	Temp. °C	Specific rate $10^{-2}\times$ (l/mol×min)	E_a kcal/mol	$\Delta S^{\neq}$ a) e. u.	$\Delta F^{\neq}$ a) kcal/mol
	82	6.72			
dl	72	2.29	26.2	15.7	19.4
	62	0.765			
	82	2.57			
meso	72	0.846	27.1	18.4	20.1
	62	0.249			

a) Computed from the equation
$k'=(e\boldsymbol{k}T/\boldsymbol{h})\exp(-\Delta F^{\neq}/\boldsymbol{R}T)$
$=(e\boldsymbol{k}T/\boldsymbol{h})\exp(-E_a/\boldsymbol{R}T)\exp(\Delta S^{\neq}/\boldsymbol{R})$.

Variation of Migration Aptitude with Time. Although the molecular rearrangements of tetraarylpinacols to pinacolones have been studied extensively with respect to the relative migration aptitudes of the aryl groups, most of the foregoing data were obtained without any knowledge of whether the configuration of the pinacols was *meso* or *dl*. In the rearrangement of *p,p'*-disubstituted benzopinacol, which probably rearranges *via* long-lived carbonium ion intermediates, the rate of the interconversion of the different rotational isomers is rapid in comparison with the rate of aryl-group migration, and a Hammett-type $\rho\sigma^+$ correlation is observed.[9] In the rearrangement of such sterically-condensed glycols as *o,o'*-disubstituted benzopinacols, however, the rate of the interconversion of the rotational isomers of the carbonium ions may be comparable with the rate of aryl-group migration. Thus, it is expected

9) J. E. Leffler and E. Grunwald, "Rate and Equilibria of Organic Reactions," John Wiley and Sons, New York and London (1963), p. 208.

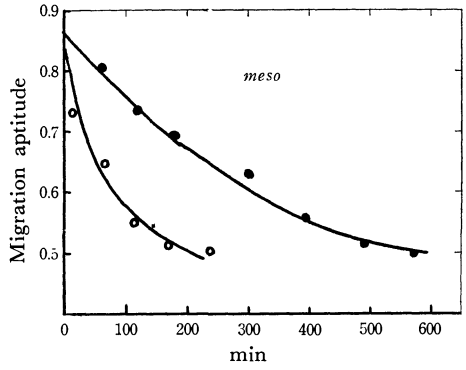

Fig. 3. Variation of migration aptitude with time (1.36×10^{-4} mol $HClO_4$).
● 62°C ○ 72°C

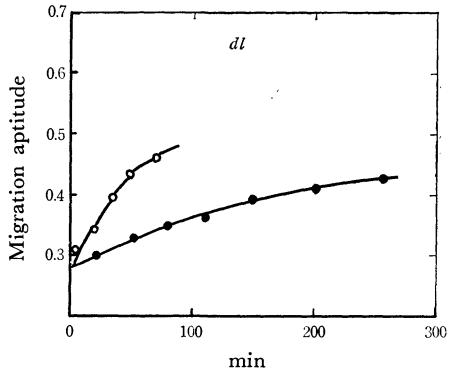

Fig. 3. Variation of migration aptitude with time (1.36×10^{-4} mol $HClO_4$).
● 62°C ○ 72°C

that the migration aptitude*3 would vary with time, as was observed in the present case (shown in Fig. 3). The implication of the variation of the migration aptitude of the *meso*-isomer with time is more complicated because of the isomerization of the *meso*-isomer to the *dl*. Figure 3 shows that the migration aptitude of the *meso*-isomer decreases with time, while that of the *dl* increases.

It seems that the isomerization of the *meso*-isomer to the *dl* and the change in the migration aptitude with time can reasonably be interpreted on the basis of the kinetic consideration, when the rate constants of the aryl-group migration are assumed to be roughly comparable with the rate constants, k_{-MI}, k_{MI}, k_{RI}, k_{-RI} and k'_{-2}, k_{-2} being much smaller in Scheme 1 (where $[R\cdots OH_2]^+_M$, $[R\cdots OH_2]^+_R$, and $[R]^+_O$ are two carbonium aggregate intermediates which retain *meso*(M) and *dl*(R) configurations, and an open carbonium ion (O) intermediate respectively). The decrease in the migration aptitude with time in the reaction of the *meso*-isomer may be interpreted by assuming the contribution of the aryl-group migration *via*

*3 Migration aptitude = Aryl/Phenyl.

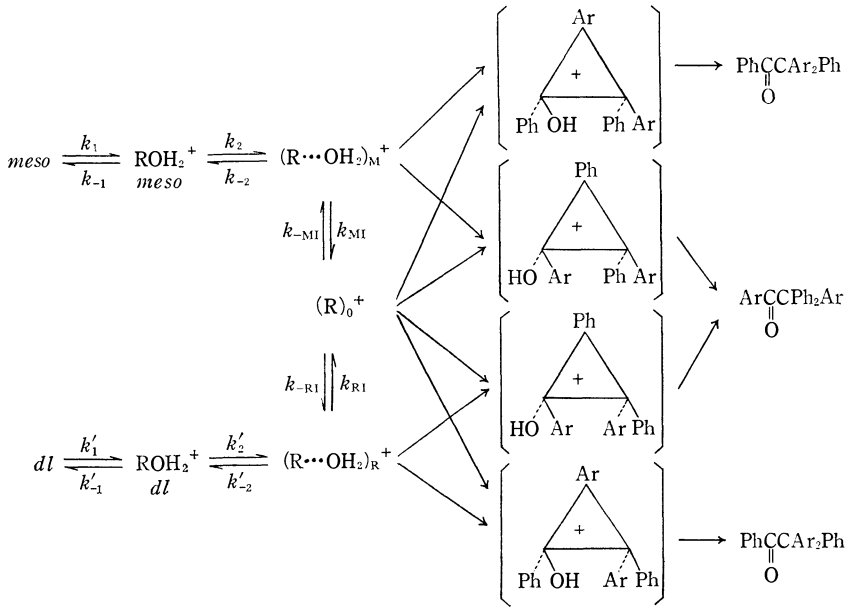

Scheme 1 { I ……Isomeisotion; R ……*dl*; M……*meso* }

intermediates without any configurational identities, such as $[R]^{+}_{O}$ and $[R\cdots OH_2]^{+}_{R}$, intervening through isomerization. The increase in the migration aptitude with time in the reaction of the *dl*-isomer can be explained in a similar way.

It is a sound assumption that the extrapolated value of the migration aptutude at time 0 (in Fig. 3) reflects the value of the intrinsic migration aptitude of $[R\cdots OH_2]^{+}_{M}$ or $[R\cdots OH_2]^{+}_{R}$. The difference between these two intrinsic migration aptitudes (0.3 and 0.85) may be explained in terms of the difference in the magnitude of the eclipsing effects in the transition states of the aryl-group migrations (see Scheme 1). An inspection of the model will reveal that the eclipsing effects in the transition states of the phenyl (*o*-anisyl)-group migration *via* the *dl*-aggregate intermediate, $[R\cdots OH_2]^{+}_{R}$ (*meso*-aggregate intermediate, $[R\cdots OH_2]^{+}_{M}$) is smaller in magnitude than that *via* the *meso*-aggregate intermediate, $[R\cdots OH_2]^{+}_{M}$ (*dl*-aggreagate intermediate, $[R\cdots OH_2]^{+}_{R}$), therefore, the phenyl-group migration *via* $[R\cdots OH_2]^{+}_{R}$ may be more probable than that *via* $[R\cdots OH_2]^{+}_{M}$. Thus, the diminished difference in the observed migration aptitudes of the *meso*- and *dl*-isomers may reasonably be interpreted in terms of the interconversion among the intermediates, $[R\cdots OH_2]^{+}_{M}$, $[R\cdots OH_2]^{+}_{R}$, and $[R]^{+}_{O}$.

Although the possibility of a contribution of the concerted mechanism and/or of the nonclassical carbonium ion mechanism*4 could not be excluded by the present results, the classical carbonium ion mechanism can be explained as follows:

(i) A considerable amount of the isomerization of the *meso*-isomer to the *dl* was observed.[2b] If $k_S > k_C$ (a rate enhancement is observed by neighboring-group participation) in the following chart,

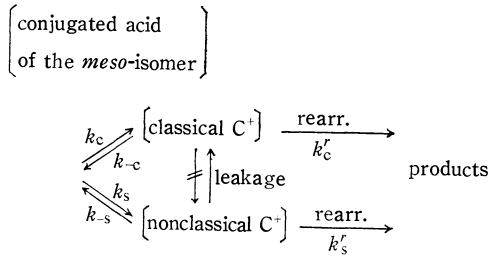

$k_{-S} > k_{-C}$ would be valid on the basis of the principle of the microscopic reversibility. Since it is liekly that $rate_S^{rearr}$ and $rate_C^{rearr}$ are not very different, the return of the *meso*-isomer to the *meso*-isomer may be effected to be much more predominant than the return of the *meso*-isomer to the *dl*-isomer in addition to the *meso*-isomer. This is not, however, in accord with the observed results. Therefore, the case $k_S < k_C$ would be valid, showing a smaller contribution of nonclassical carbonium ions.

(ii) The large positive values of the entropy of activation is in accord with the classical carbonium ions if the contribution of the entropy of desolvation in the transition state is assumed to be small (Table 2).

*4 The concerted mechanism implies a two-step mechanism, while the nonclassical carbonium ion mechanism implies a three-step mechanism, $P \rightleftarrows PH^{+} \rightleftarrows C^{+}_{N} \rightarrow K$.

(iii) It is known that, in general, the neighboring group participation tends to decrease with an increase in the phenyl substitution of the carbon atom at which heterolysis occurs.[10]

(iv) In such a sterically-condensed system as 2,2'-dimethoxybenzopinacol, a classical carbonium ion would give more chances for a decrease in the steric interaction than would a nonclassical carbonium ion, as an inspection of molecular models suggests.

(v) If one assumes that either the concerted or nonclassical mechanism is exclusively operative, the extrapolated migration aptitude at time 0 in Fig. 3 would be observed, since the transition states or intermediates are considered to have structures similar to those of the transition states of aryl-group migration described in Scheme 1. The observed change in migration aptitude with time, therefore, seems to suggest that the classical carbonium ions are more favored as intermediates.

In conclusion, again, the contribution of the concerted mechanism and/or the nonclassical carbonium ion mechanism would be small, if not entirely absent.

The slightly larger rate constant (*ca.* three times) of the *dl*-isomer compared with the *meso* may be considered to be due to the conformational predominance of the *meso*-pinacol with a *trans* arrangement of the hydroxyl groups, while the *dl* has a *cis*.[2c]

Although the low migration aptitude (<1) of the *o*-anisyl group is usually ascribed to steric hindrance,[2b] it has been suggested by Pocker[11] that it could be due to the interaction of the *o*-anisyl oxygen with a developing carbonium ion.[12] However, this suggestion is not in accord with the large positive values of the entropy of activation which follow if the degree of desolvation in the transition state is assumed to be small. The abnormally low migration aptitude of the *o*-anisyl group may instead be ascribed to steric hindrance by the solvated methoxy group.[13]

Though the epoxide intermediates were not detected by thin-layer chromatography, the by-passed mechanism *via* unstable epoxide intermediates can not be excluded.

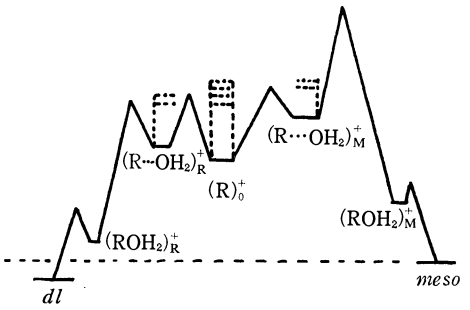

Fig. 4. Schematic energy diagram for interconversion of the diols (full line) and for formation of the products (broken line).

The conclusions as to the fates of the carbonium ions are summarized qualitatively in a plot of the free energy against the reaction co-ordinate (Fig. 4). From the evidence for the strong hydrogen bonding in the *dl*-isomer, it may be assumed that the *dl*-isomer is more stable than the *meso* in the ground state.[2c]

The author wishes to thank Professor Ryozo Goto for his helfpul discussions and encouragement, and Dr. Akira Sera and Dr. Jun'ichi Hayami for their kind and valuable advice and discussions.

10) S. Winstein and E. Grunwald, *J. Am. Chem. Soc.*, **70**, 828 (1948); S. Winstein, B. K. Morse, E. Grunwald, K. C. Schreiber and J. Corse, *ibid.*, **74**, 1113 (1952).
11) Y. Pocker in "Molecular Rearrangements," P. de Mayo ed., Interscience Pub., New York and London (1963), p. 22
12) S. Winstein, *Experientia*, Suppl. No. 2, 153 (1955).
13) For this problem, see R. Goto, T. Asano, K. Matsumoto and A. Sera, *The Review of Physical Chemistry of Japan*, **37**, 16 (1967).

BULLETIN OF THE CHEMICAL SOCIETY OF JAPAN VOL. 41 1361—1367 (1968)

Some Reactions of *N*-Haloamidines*[1]

Eiichi HARUKI, Toshihiro INAIKE*[2] and Eiji IMOTO

Department of Applied Chemistry, College of Engineering, University of Osaka Prefecture, Sakai, Osaka

(Received October 25, 1967)

The reactions of a variety of *N*-haloamidines with silver oxide, sodium ethoxide, thiourea derivatives, and phenols are described. In these reactions, *N*-phenyl-*N'*-chlorobenzamidine gave diphenylcarbodiimide, benzimidazole, *N*-amidinobenzamidine and 2,4-diphenylthiadiazole respectively, while the other *N*-haloamidines afforded the corresponding products. The mechanistic implications of these reactions are discussed.

Although *N*-haloamidines had been prepared by Bougault and Robin early in the 1920's from amidine hydrochlorides and sodium hypochlorite,[1] the chemistry of the compounds has not been widely studied. The representative reactions of *N*-haloamidines were the nucleophilic replacement of the halogen atom with the cyanide or isothiocyanate ion,[2] and the oxidation of the iodide ion.[1] Recently, Grenda *et al.*[3] and we[4] have reported that the reaction of *N*-chlorobenzamidine with sodium ethoxide leads to the formation of benzimidazole, probably *via* a nitrene intermediate. These results indicate that the halogen atom of *N*-haloamidines could react in two different ways. In the first type of reaction, the halogen atom of *N*-haloamidines leaves as a halide ion, this reaction can be realized by treating the compounds with such reagents as (a) the silver ion, which has a strong affinity towards the halogen atom, (b) strong nucleophiles, such as cyanide or isothiocyanate ions, which replace the halogen atom directly, and (c) strong bases, such as the ethoxide ion, which takes up first a proton from the amino- or imino group and subsequently eliminates the halide ion. In the second type of reaction, the halogen atom of *N*-haloamidines leaves as a halogen cation, *i.e.*, a positive halogen; this reaction can be realized by the reaction with such reagents as (d) phenols, which readily undergo electrophilic substitution with a positive halogen, and (e) thioamides, which are oxidized with a positive halogen.

This paper will summarize the results obtained so far in our laboratory as to the reaction of *N*-haloamidines with the various kinds of reagents mentioned above.

Results and Discussion

Halogenation of Amidines. Haloamidines have been prepared from amidines and sodium hypochlorite or hypobromite in water.[1] However, the yield of this reaction was not always good, mainly because of the instability of *N*-haloamidines. The process of the separation of haloamidines from the reaction mixture also caused a marked drop of the yield. In this investigation, therefore, the halogenation of amidines was carried out using *t*-butyl hypohalite as a halogenation agent in such organic solvents as chloroform, benzene, or a benzene-ethanol mixture, and the resulting *N*-haloamidines were used for the subsequent reactions without separation. The yields of *N*-haloamidines varied with the structures of the amidines. Aromatic amidines usually gave *N*-haloamidines in good yields, but aliphatic amidines resulted in poor yields. *N*-Substitution with alkyl or aryl group did not affect the yield of the *N*-halogenation, but *N,N'*-disubstitution with two alkyl or two aryl groups completely inhibited the *N*-halogenation.

Formation of Carbodiimide. If the chlorine atom of *N*-haloamidine is removed as a chloride ion by the silver cation, the resulting nitrenium cation may react subsequently according to the following scheme to form carbodiimide:

$$R\text{-}C\begin{matrix}\diagup NX \\ \diagdown NH\text{-}R'\end{matrix} \rightarrow R\text{-}C\begin{matrix}\diagup N^{+} \\ \diagdown NH\text{-}R'\end{matrix} \rightarrow$$

$$R\text{-}N{=}\overset{+}{C}\text{-}NH\text{-}R' \rightarrow R\text{-}N{=}C{=}N\text{-}R'$$

*1 This constitutes Part III of a series entitled "Studies of the Syntheses of Heterocyclic Compounds," by E. Imoto *et al.* It was presented at the 19th Annual Meeting of the Chemical Society of Japan, Yokohama, April, 1966. Part II: T. Takaya, H. Yoshimoto, E. Imoto, This Bulletin **40**, 2844 (1967).

*2 Present address: Research Institute, Ube Kosan Co., Ltd., Ube, Yamaguchi.

1) P. Robin, *Compt. rend.*, **173**, 1805 (1921); *ibid.*, **177**, 1304 (1923); J. Bougault and P. Robin, *Compt. rend.*, **171**, 38 (1920).

2) J. Goerdeler and D. Loevenich, *Chem. Ber.*, **86**, 890 (1953).

3) V. J. Grenda, R. E. Jones, G. Gale and M. Sletzinger, *J. Org. Chem.*, **30**, 259 (1965).

4) E. Haruki, T. Inaike and E. Imoto, This Bulletin, **38**, 1805 (1965).

Table 1. Formation of benzimidazole derivatives from *N*-haloamidine

Amidine	Reaction product	Yield %	Mp °C	Analysis C%	Analysis H%	Analysis N%
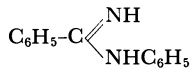	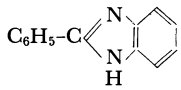	87	289—290	80.20 (90.38)	5.17 (5.19)	14.65 (14.24)
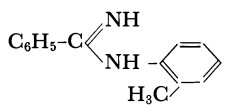	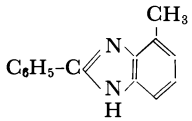	76	247—248	80.96 (80.74)	5.67 (5.81)	13.32 (13.45)
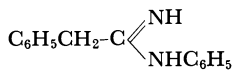	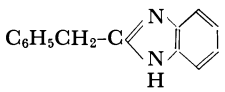	36	183—184	80.77 (80.74)	5.60 (5.81)	13.62 (13.45)
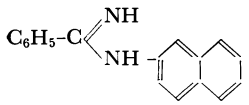	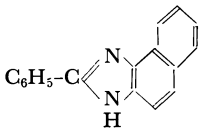	64	215—216	83.55 (83.58)	4.87 (4.95)	11.52 (11.47)
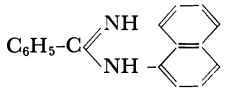	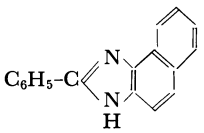	24	215—216	83.65 (83.58)	5.01 (4.95)	11.50 (11.47)
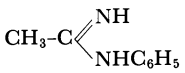	Polymeric product	—	—	—	—	—

The figures in parentheses are calculated values for the corresponding benzimidazoles.

In accordance with this expectation, the reaction of *N*-chlorobenzamidine with silver oxide gave the corresponding diphenyl carbodiimide.

Formation of Benzimidazoles.[3] *N*-Phenylhaloamidines may exist in an equilibrium of three tautomeric forms, A, B and C:

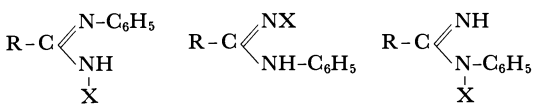

(A) (B) (C)

When R is an aryl, the most favorable strcture is presumed to be A because of the great conjugation ability between the aryl and phenyl groups across the carbon nitrogen double bond. When R is an alkyl, however, the most of favorable structure could not be determined analogously. Furthermore, the hydrogen atom attached to the chloroimino group of the A structure is supposed to be fairly acidic, and it could be removed readily by a strong base. The resulting anion may spontaneously release a chloride ion to form a nitrene. The nitrene thus produced probably attacks the adjacent benzene nucleus to give a benzimidazole ring, as is illustrated in the following scheme. The same mechanism has been suggested by Grenda

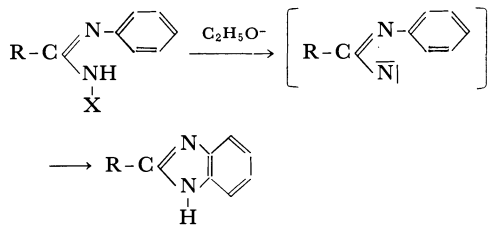

et al. in the benzimidazole formation from *N*-chloroamidines. Such a nitrene intermediate has also been proposed by Smith and Leon[5] in the pyrolysis of 1,5-diphenyltetrazole to give benzimidazole and *N,N'*-diphenylcarbodiimide.

When aromatic *N*-arylhaloamidines were treated with sodium ethoxide in ethanol, the expected benzimidazoles were obtained in good yields, as Table 1 shows. However, aliphatic *N*-arylhaloamidines such as *N*-phenyl-*N'*-chloroacetamidine did not form the expected 2-methylbenzimidazole, but only a resinous material.

The reaction of *N*-phenyl-*N*(or *N'*)-chlorophenylacetamidine with ethoxide ions was also investigated. If this haloamidine exists predominantly in the B structure, ethoxide ions may

5) P. A. S. Smith and E. Leon, *J. Am. Chem. Soc.*, **80**, 4647 (1958).

remove a proton from the α-methylene group rather than from the NH group. In such a case, an α-aminocarboxylic amide may be produced *via* the following processes, similar to the formation of the α-aminocarboxylic ester from imino ether[6]:

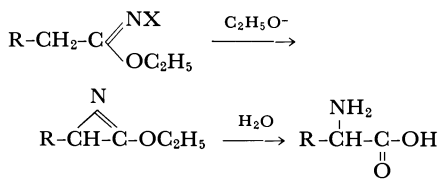

However, our expectation was pot realized; instead 2-benzylbenzimidazole was obtained in a 36% yield, as shown in Table 1. These results show that the hydrogen atom of the α-methylene group in *N*-phenyl-*N*(or *N'*)-chlorophenylacetamidine is not removed by ethoxide ions in ethanol; this amidine exists predominantly in the structure A.

Reaction of *N*-Bromobenzamidine with Phenol. *N*-Bromobenzamidine reacted with phenol in carbon tetrachloride to yield benzamidinium tribromophenolate. Similarly, *p*-hydroxybenzaldehyde yielded benzamidinium 2,6-dibromo-4-formylphenolate.

We also attempted a direct amination of phenol with *N*-haloamidines in the presence of aluminum chloride in nitrobenzene or carbon disulfide, and also in the presence of boron trifluoride etherate in ether. The direct amination of phenol was unsuccessful; only halophenol was obtained.

Reactions of Thioureas with Haloamidines. The reactions of *N*-haloamidines with thioureas are supposed to proceed though the following four processes. Routes A and B are a nucleophilic attack of the nitrogen or the sulfur atom of thioureas on the chloroamino (or chlorimino) group of haloamidines, followed by cyclization to give 1,2,4-thiadiazoles or 1,2,4-triazoles. On the other hand, routes C and D may result in the halogenation of the amino or sulfhydryl group of thiourea by the positive chlorine produced from *N*-haloamidines. Such halogenation has been proposed by Goerdeler *et al.*[7] as the first step in the formation of isothiazoles from β-iminothioamides and iodine in pyridine or in other solvents.

The experiments showed that the reaction of thiourea with *N*-chlorobenzamidine in ethanol or in water at room temperature affords *N*-amidinobenzamidine, which is then converted to *N*-cyanobenzamidine by treating it with sodium ethoxide in ethanol or to benzamide by refluxing it

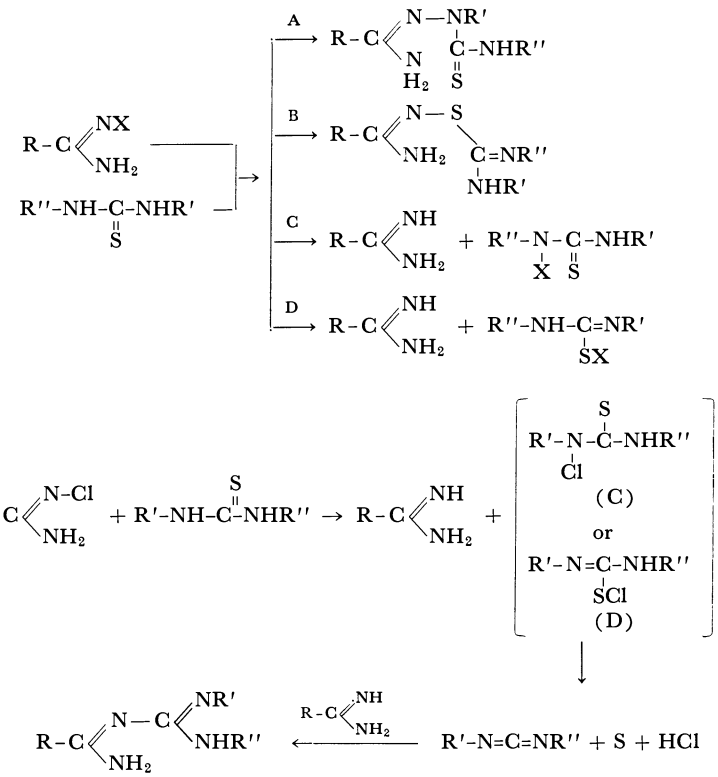

6) H. E. Baumgarten, J. E. Dirkes, J. M. Petersen and D. C. Wolf, *ibid.*, **82**, 4422 (1960); H. E. Baumgarten, J. E. Petersen and R. L. Zey, *J. Org. Chem.*, **31**, 3708 (1966).

7) J. Goerdeler and H. W. Phland, *Chem. Ber.*, **94**, 2950 (1961); *ibid.*, **96**, 596 (1963); J. Goerdeler and W. Miltler, *ibid.*, **96**, 944 (1963); J. Goerdeler and H. Horn, *ibid.*, **96**, 1551 (1963).

with sodium hydroxide in water for a long period of time. The *N*-cyanobenzamidine thus obtained was identical with that prepared from *N*-chlorobenzamidine and sodium cyanide in every respect. However, when the reaction between thiourea and *N*-chlorobenzamidine was carried out in the presence of sodium ethoxide in ethanol or of potassium hydroxide in water, *N*-cyanobenzamidine was obtained directly. These *N*-(*N'*-substituted amidine)benzamidines could not be converted to *N*-cyanobenzamidine by treating them with sodium ethoxide.

These results indicate that the process of the formation of *N*-amidinobenzamidines may proceed through the intermediate C or D, followed by the elimination of elemental sulfur and hydrogen chloride to form carbodiimide, to which the addition of amidine then takes place.

Formation of Thiadiazoles. The reaction of benzthioamide with *N*-chlorobenzamidine or *N*-chloro-*N'*-phenylbenzamidine in ethanol at room temperature for 5 hr afforded 3,5-diphenyl-1,2,4-thiadiazole, together with the amidine hydrochloride and elemental sulfur.

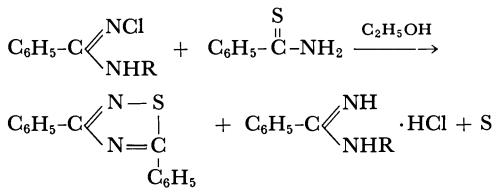

In this reaction *N*-haloamidines act as oxidizing agents on benzthioamide, as is shown in the following scheme. It is interesting to note that thiadiazoles have previously been obtained upon the oxidation of thioamides with halogen.[8]

Reaction of Carbon Disulfide with *N*-Haloamidines. The reaction of carbon disulfide with *N*-haloamidines was also investigated, although the structures of the products have not yet been completely determined. Carbon disulfide reacted with *N*-chlorobenzamidine in the presence of sodium ethoxide in an ethanol-benzene mixture at the reflux temperature to yield an oily material (bp 109—111°C/0.6 mmHg), while no reaction occurred in the absence of sodium ethoxide. The oily material obtained was assumed to be 3-phenyl-5-ethoxy-1,2,4-thiadiazole from the results of elemental analysis and from its absorption characteristics in the infrared spectrum (1520, 1430, 1330, 1300, and 1250 cm^{-1}). This compound may be formed from *N*-chlorobenzamidine and sodium ethyl xantate. That is, the reaction of *N*-chlorobenzamidine and sodium ethyl xantate may produce first an unstable intermediate, benzthioamidoxime ethyl thiocarbonate, and then this intermediate might cyclize, eliminating hydrogen sulfide, to produce the product. The eliminated hydrogen sulfide may be oxidized with *N*-chlorobenzamidine to sulfur. Carbon disulfide also reacted with *N*-chloro-*N'*-phenylbenzamidine to afford crystals with a mp of 146—156°C, the

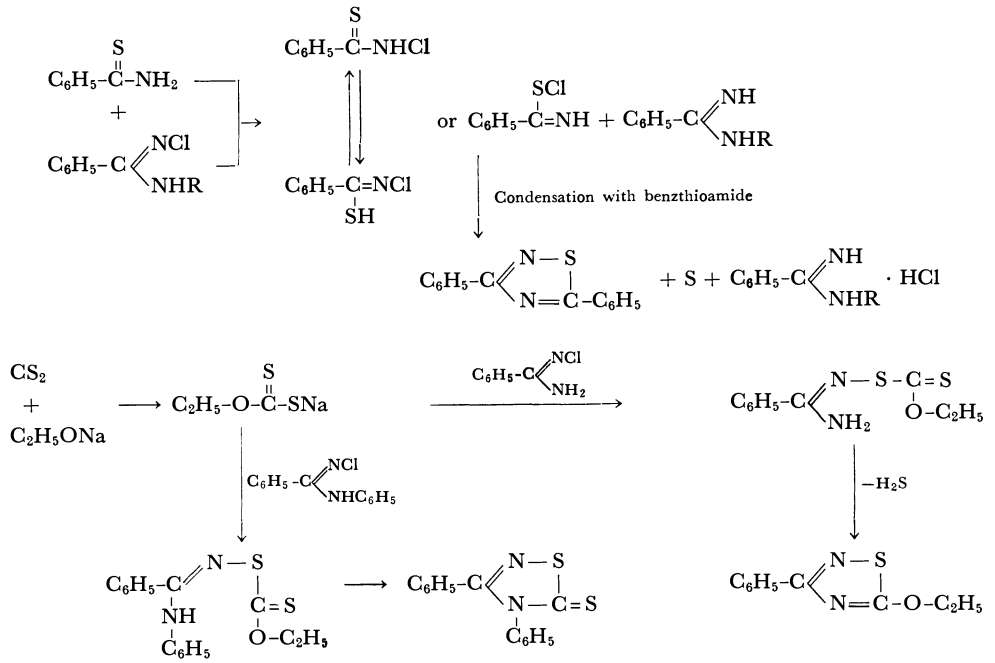

8) A. W. Hoffmann and S. Gabriel, *Ber.*, **25**, 1586 (1892); S. Ishikawa, *Chem. Abstr.*, **22**, 1581 (1928); **19**, 3087 (1925); G. C. Charkravarti, *J. Chem. Soc.*, **123**, 964 (1923).

structure of which seemed to be 3,4-diphenyldihydro-1,2,4-thiadiazole-5-thione. When sodium *N*,*N'*-diethyl dithiocarbamate was used in the above reaction instead of sodium ethyl xantate, the product obtained seemed to be 3-phenyl-5-diethylamino-1,2,4-thiadiazole.

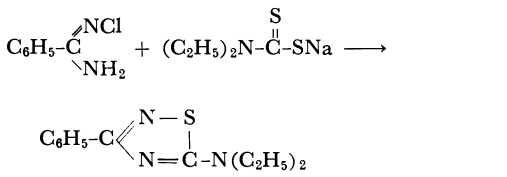

Reaction of *N*-Haloamidines with Acylating Agents. 1,2,4-Oxadiazoles have been prepared by the acylation of amidoxime, followed by a cyclization between the amino group and the ethoxycarbonyl carbon atom. Thus, it could be expected that 1,2,4-oxadiazole can also be produced from *N*-haloamidine and an acylating agent *via* the following processes.

However, even when a mixture of *N*-chlorobenzamidine and acetic anhydride was heated under reflux for 2 hr, the product was the unexpected 2-methyl-4,6-diphenyl-*s*-triazine, which was identified by a comparison of its mp and infrared spectrum with those of an authentic sample.[9] When a solution of *N*-chlorobenzamidine and benzoyl chloride in benzene was heated under reflux for 5 hr, the products were 2,4,6-triphenyl-*s*-triazine and *N*-benzoylbenzamide. In this case the expected 1,2,4-oxadiazole derivative was not obtained.

Experimental

Amidines. *N*-Phenylbenzamidine,[10] mp 110—112°C, *N*-phenylphenylacetamidine,[10] mp 137—139°C, *N*-(α-naphthyl)benzamidine,[11] mp 140—142°C, and *N*-(β-naphthyl)benzamidine,[12] mp 153—155°C, were prepared from the corresponding amine hydrochlorides and nitriles by a method similar to that described in the literature. *N*-Methyl-*N'*-phenylbenzamidine,[13] mp 126—130°C, was prepared from the *N*-phenylbenziminochloride and methyl amine hydrochloride. Benzamidine hydrochloride, mp 167—169°C, *N*-butylbenzamidine hydrochloride, mp 188—190°C, *N*, *N*-pentamethylenebenzamidine hydrochloride, mp 204—207°C, and *N*, *N*-pentamethylenephenylacetamidine hydrochloride, mp 218—220°C, were prepared from the corresponding iminoethers and amines by Pinner's method.[14]

Free amidines were obtained by extracting a solution of the respective amidine hydrochloride in 30% sodium hydroxide with chloroform and by then removing the solvent.

***N*-Haloamidines.** *N*-Bromobenzamidine was prepared from benzamidine hydrochloride and sodium hypobromite in water, according to the method reported in the literature;[15] it had a mp of 80—81°C after recrystallization from carbon tetrachloride.

N-Chloroamidines were prepared from amidines and *t*-butyl hypochlorite in organic solvents, such as chloroform, benzene, ligroin or a benzene-ethanol mixture, at 0—10°C. Among these solvents, chloroform gave the best results. The following is a typical experiment for the preparation of *N*-chloroamidines.

To a solution of *N*-phenylbenzamidine (78 g, 0.40 mol) in chloroform (300 ml) *t*-butyl hypochlorite (50 g, 0.46 mol) was added, drop by drop, at 0—10°C over

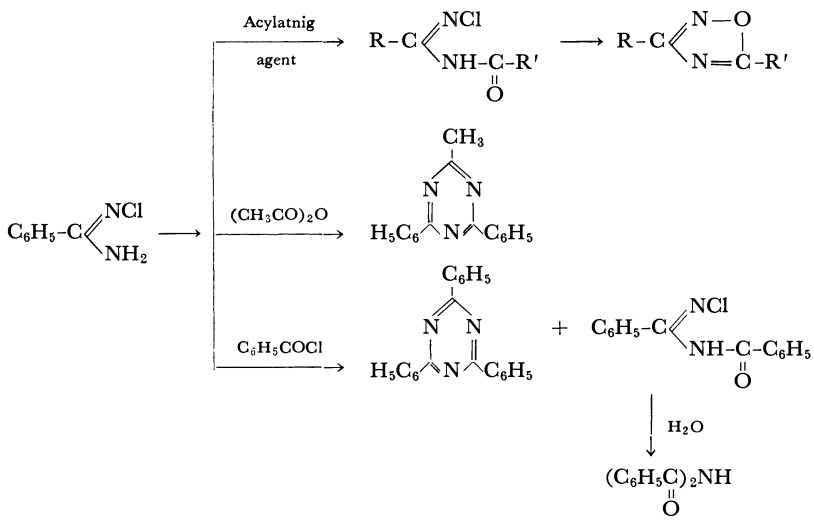

9) A. Pinner, *Ber.*, **17**, 2512 (1884); **25**, 1624 (1892).
10) A. Bernthsen, *Ann.*, **184**, 348 (1877).
11) A. Bernthsen and H. Trompetter, *Ber.*, **11**, 1756 (1878).
12) B. River and Ch. Shneider, *Helv. Chim. Acta*, **3**, 132 (1920).
13) C. Gerhsrt, *Ann.*, **108**, 219 (1858).
14) A. Pinner, "Organic Synthesis," Coll. I, John Wiley and Sons, New York, (1956), p. 5.
15) J. Goerdeller and D. Loevenich, *Chem. Ber.*, **86**, 890 (1953); J. Goerdeller and H. Haubrich, *ibid.*, **93**, 397 (1960).

30 min; then the mixture was stirred at the same temperature for 3 hr. The solvent was removed by distillation under reduced pressure at room temperature, and the residue, a brown solid, was recrystallized from ligroin, mp 126—128°C. The yield of *N*-chloro-*N'*-phenylbenzamidine was 46 g (50%).

Found: C, 67.37; H, 4.88; N, 12.08%. Calcd for $C_{13}H_{12}N_2Cl$: C, 67.68; H, 4.81; N, 12.14%.

The other *N*-haloamidines were prepared by a method similar to that described above and were used for the subsequent reactions without separation.

Preparation of Carbodiimide. Diphenylcarbodiimide. A suspension of *N*-chloro-*N*(or *N'*)-phenylbenzamidine (2.3 g, 0.01 mol) and silver oxide (5.0 g, 0.02 mol) in ligroin was heated at reflux for 2 hr. After the precipitate had been removed by filtration, the filtrate was distilled under reduced pressure to give a fraction with a bp of 140—144°C (14 mmHg) (1.6 g), which was identified as diphenylcarbodiimide by a comparison of its infrared spectrum with that of an authentic sample prepared from *N,N'*-diphenylthiourea. The distillate (1.9 g) was dissolved in methanol (10 m*l*), mixed with 10 m*l* of 6 N hydrochloric acid, and then boiled for 30 min. After cooling, the solid which was precipitated, *N,N'*-diphenylurea showed no depression of its melting point (229—230°C) upon a mixed-melting-point determination with an authentic *N,N'*-diphenylurea.

2-Substituted Benzimidazoles and 2-Phenylnaphtho[1',2'-*d*]imidazole. To 3.9 g (0.02 mol) of *N*-phenylbenzamidine in 15 m*l* of dry benzene and 15 m*l* of absolute ethanol, 2.3 g of *t*-butyl hypochlorite were added at −5—0°C. After the mixture had been stirred at the same temperature for 2 hr, sodium (0.9 g, 0.039 mol) in 10 m*l* of absolute ethanol was added, and then the mixture was refluxed for 3 hr. When the mixture was cooled and poured into ice water, brown precipitates were obtained. Recrystallization from aqueous ethanol gave 3.1 g (80%) of a pure product, mp 289—290°C. This compound was identified with 2-phenylbenzimidazole by means of infrared and ultraviolet spectroscopic measurements, and by a mixed-melting-point test with an authentic sample which had been prepared according to the method described in the literature.[16] By the same procedure, *N*-(*o*-tolyl)-benzamidine was converted to 4-methyl-2-phenylbenzimidazole in a 76% yield, and *N*-phenylphenylacetamidine, to 2-benzylbenzimidazole in a 35% yield. However, an attempt to convert *N*-phenylacetamidine to 2-methylbenzimidazole was unsuccessful. Both *N*-(α-naphthyl)benzamidine and *N*-(β-naphthyl)benzamidine afforded the same product, 2-phenylnaphtho-[1',2'-*d*]-imidazole, in 24% and 64% yields respecti-vely.

Reaction with Thiourea and Thiourea Derivatives. *N*-Amidinobenzamidine. Thiourea (1.5 g, 0.020 mol) was added, portion by portion, to a solution of *N*-chlorobenzamidine (3.1 g, 0.020 mol) in 20 m*l* of absolute ethanol. An exothermic reaction started immediately, and sulfur soon began to precipitate. The reaction mixture was then kept overnight at room temperature. After separating the precipitated sulfur (0.38 g, 0.012 mol) by filtration, the filtrate was concentrated by distillation. The residual viscous liquid crystallized upon the addition of a small amount of ether. The *N*-amidinobenzamidine hydrochloride thus obtained 3.2 g (81%) was very hygroscopic and was used for the subsequent reactions without further purification.

***N*-Cyanobenzamidine.** A mixture of *N*-amidinobenzamidine hydrochloride (2.5 g, 0.013 mol) and metallic sodium (0.4 g, 0.017 mol) in 10 m*l* of absolute ethanol was kept overnight at room temperature. After the ethanol had then been removed from the reaction mixture by distillation, the addition of a small amount of water to the residue gave crude *N*-cyanobenzamidine, which was recrystallized from an ethanol-benzene mixture (4 : 1). The yield was 0.92 g (50%); mp 142—143°C. The *N*-cyanobenzamidine thus obtained was identified by a comparison of its infrared spectrum and melting point with those of an authentic sample which had been prepared by the method described in the literature.[14] A mixed-melting-point test with the authentic sample showed no depression.

Direct Preparation of *N*-Cyanobenzamidine from Thiourea and *N*-Chlorobenzamidine. To a suspension of thiourea (1.5 g, 0.02 mol) in 10 m*l* of ethanol, there was added, drop by drop, a solution of sodium (1.5 g, 0.065 mol) in 15 m*l* of ethanol, and then a solution of *N*-chlorobenzamidine (3.1 g, 0.02 mol) in 20 m*l* of ethanol. The reaction mixture immediately became turbid and sodium chloride precipitated out. After being allowed to stand overnight at room temperature, the reaction mixture was filtered and the precipitate was washed with water to give 0.47 g of sulfur. The filtrate was distilled under reduced pressure to remove the solvent. The viscous residue solidified upon the addition of a small amount of water. Recrystallization from a benzene-ethanol mixture, gave 1.8 g of *N*-cyanobenzamidine mp 142—143°C.

***N*-(*N,N'*-Diphenylamidino)benzamidine and *N*-(*N*-Phenylamidino)benzamidine.** A solution of *N*-chlorobenzamidine (3.1 g, 0.02 mol) in 20 m*l* of ethanol was added, drop by drop, to a solution of sodium (0.5 g, 0.022 mol) and *N,N'*-diphenylthiourea (4.0 g, 0.02 mol) in 20 m*l* of ethanol, after which the mixture was heated at reflux for 5 min. After it had been filtrated while hot to remove the sodium chloride, the filtrate gave, on cooling, crude *N*-(*N,N'*-diphenylamidino)-benzamidine which was recrystallized from ligroin, mp 134—135°C. The yield was 3.8 g (60%).

Found: C, 76.21; H, 5.44; N, 18.05%. Calcd for $C_{20}H_{18}N_4$: C, 76.40; H, 5.77; N, 17.82%.

N-(*N*-Phenylamidino)benzamidine was prepared by the same procedure as that of *N*-(*N,N'*-diphenylamidino)benzamidine.

Found: C, 70.37; H, 5.87; N, 23.83%. Calcd for $C_{14}H_{14}N_4$: C, 70.56; H, 5.92; N, 23.51%.

3,5-Diphenyl-1,2,4-thiadiazole. *N*-Chlorobenzamidine (3.1 g, 0.02 mol) was added in one portion to a solution of benzthioamide (2.7 g, 0.02 mol) in 20 m*l* of ethanol. The reaction mixture soon became turbid. When the exothermic reaction ceased and the reaction mixture was cooled to room temperature, colorless needle crystals gradually precipitate out. After standing for 5 hr, the precipitate was collected by filtration and recrystallized three times from an ethanol-water (4 : 1) mixture, mp 89—90°C. The 3,5-diphenyl-1,2,4-thiadiazole obtained was identified by a comparison of its infrared spectrum and melting point with those of an

16) B. A. Porai-Koshits, O. F. Ginzburg and L. S. Eflos, *J. Gen. Chem. (U. S. S. R.)*, **17**, 1768 (1947).

authentic sample synthesized from benzthioamide and benzthioperimidic acid by the method described in the literature.[17] A mixed-melting-point determination of the compound with the authentic sample showed no depression. The filtrate was concentrated under reduced pressure and the residual solid was washed with ether to obtain crude hydrated benzamidine hydrochloride with a mp of 75—85°C. The reaction between benzthioamide and *N*-chloro-*N'*-phenylbenzamidine was carried out as described above to give 3,5-diphenyl-1,2,4-thiadiazole, mp 87—89°C, after recrystallization from an ethanol-water mixture. The yield was 78%.

Reaction of Carbon Disulfide with *N*-Chlorobenzamidine. To a solution of carbon disulfide (1.5 g, 0.02 mol) and *N*-chlorobenzamidine (3.1 g, 0.02 mol) in 15 m*l* of ethanol, there was added a solution of sodium ethoxide prepared from sodium (0.46 g, 0.02 mol) and 10 m*l* of ethanol. The reaction mixture was heated gradually. An exothermic reaction occurred suddenly and the temperature rose to 60°C and boiled spontaneously. After having been heated for 1 hr, the reddish-colored reaction mixture was cooled and the precipitated crystals of sodium chloride were collected by filtration. The filtrate was concentrated under reduced pressure to remove the solvent and then distilled to give two fractions: (1) bp 95—109°C/0.6 mmHg, (0.4 g, n_D^{23} 1.5830), and (2) bp 109—111°C/0.6 mmHg (1.2 g, n_D^{23} 1.6042). The second fraction, the main product, was soluble in ether, ethanol, and glacial acetic acid, but was insoluble in water, 2 N hydrochloric acid, and 2 N sodium hydroxide.

Found: C, 58.12; H, 4.71; N, 13.67%. Calcd for $C_{10}H_{10}ON_2S$: C, 58.23; H, 4.89; N, 13.58%.

The structure of this compound was assumed to be 3-phenyl-5-ethoxy-1,2,4-thiadiazole on the basis of its infrared spectrum (1580, 1520, 1335, and 1300 cm^{-1}).

Reaction with Acetic Anhydride. A solution of *N*-chlorobenzamidine (3.1 g, 0.02 mol) in acetic anhydride (6.1 g, 0.06 mol) was refluxed for 2 hr. After cooling, the precipitate was collected by filtration, washed with a small amount of cold 95% aqueous ethanol, and then recrystallized three times from ethanol to give 1.4 g of 2-methyl-4,6-diphenyl-*s*-triazine, mp 108.5—109.5°C, which had the same melting point and infrared spectrum as an authentic sample; the melting point showed no depression upon a mixed-melting-point determination with an authentic sample.[9]

Reaction with Benzoyl Chloride. A solution of *N*-chlorobenzamidine (3.1 g, 0.02 mol) and benzoyl chloride (2.8 g, 0.02 mol) in 20 m*l* of benzene was refluxed for 5 hr. After the solution had been cooled and a small amount of the precipitates by removed filtration, the filtrate was evaporated and the residual solid was recrystallized from ethanol. The needles obtained were 2,4,6-triphenyltriazine (0.30 g, mp 225—230°C). The precipitates obtained upon the addition of water to the mother liquor were recrystallized from ligroin. The needles obtained were *N*-benzoylbenzamide (1.7 g, mp 145—146°C).

Bromination of Phenols with *N*-Bromobenzamidine. A solution of phenol (0.4 g, 0.004 mol) and *N*-bromobenzamidine (2.6 g, 0.013 mol) in carbon tetrachloride was refluxed for 10 min. Upon the cooling of the mixture, crystals (0.90 g, mp 116—122°C) were obtained. The same compound, benzamidinium tribromophenolate, was obtained by the addition of tribromophenol to a solution of benzamidine in ethanol, followed by the removal of the ethanol and washing with chloroform. The benzamidinium tribromophenolate thus obtained (0.9 g, 0.0027 mol) was heated for a little while together with 7 m*l* of 2 N hydrochloric acid, and cooled to give tribromophenol (0.4 g, 0.0012 mol).

p-Oxybenzaldehyde reacted similarly with *N*-bromobenzamidine in carbon tetrachloride to produce benzamidinium 2,6-dibromo-4-formylphenolate, mp 143—144°C. The salt obtained was treated with an acidic solution of 2,4-dinitrophenylhydrazine to yield 2,4-dinitrophenylhydrazone of 3,5-dibromo-4-hydroxybenzaldehyde, which was identified by a comparison of its melting point and infrared spectrum with those of an authentic sample.

17) R. Kitamura, *Yakugaku Zasshi. (J. Pharm. Soc. Japan)*, **58**, 809 (1938).

BULLETIN OF THE CHEMICAL SOCIETY OF JAPAN VOL. 41 1368—1371 (1968)

Syntheses of Heterocyclic Compounds from Benzamidine, Aldehydes, and Hydrogen Cyanide*1,*2,*3

Eiichi HARUKI, Hiroshi IMANAKA and Eiji IMOTO

Department of Applied Chemistry, College of Engineering, University of Osaka Prefecture, Sakai, Osaka

(Received October 25, 1967)

The reactions of benzamidine with several aldehydes in the presence of hydrogen cyanide were studied, using an aqueous methanol as a solvent. When formaldehyde or acetaldehyde was used as an aldehyde component, α-hydroxyalkyldiphenyl-*s*-triazines were obtained, while when benzaldehyde, *p*-chlorobenzaldehyde, or furfural was used, the corresponding 4-arylmethylidenamino-2,5-diphenyloxazoles were obtained. However, under the same reaction conditions, *m*-nitrobenzaldehyde afforded dimethyl azoxybenzene-3,3'-dicarboxylate.

An α-aminonitrile, an intermediate of the Strecker synthesis of α-amino acid, can usually be prepared in a good yield from an aldehyde, hydrogen cyanide, and ammonia, though it is not obvious through which the following routes of the reaction proceeds:

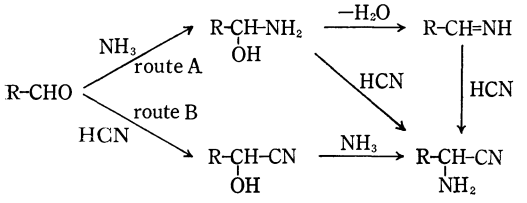

If an amidine behaves similarly to ammonia in this reaction, Compound I may be formed and I may cyclize further to an imidazole derivative. Contrary to this expectation, however, when an aromatic aldehyde was used as an aldehyde component, an oxazole derivative VI was obtained, and when an aliphatic aldehyde was used, a triazine derivative, VII, was obtained, as is shown in the following chart.

The structures of VI and VII were confirmed from the following experimental evidence. Compound VIa ($C_{22}H_{16}ON_2$, mp 156—157°C) had no absorption band in the N–H region in its infrared spectrum and gave an equimolar amount of benzaldehyde 2,4-dinitrophenylhydrazone when it was treated with a solution of 2,4-dinitrophenylhydrazine in 2 N hydrochloric acid at room temperature for 24 hr. Furthermore, the steam distillation of VIa in the presence of concentrated hydrochloric acid gave benzaldehyde, benzoic acid, and mandelic acid as a result of hydrolysis. These facts exclude any structures other than VIc. Compound XI, which is an isomer of VIa and which was synthesized by Lichtenberger,[1] has, accidentally, the same melting point as VIa. However, the Compound XI prepared by the method described in the literature was found to be surely different from Compound VIa, for a mixed-melting-point determination showed a depression and the features of the infrared spectra were different.

Since Compounds VIb and VIc have infrared and ultraviolet spectra similar to those of VIa, and since they gave one mole of 2,4-dinitrophenylhydrazone of *p*-chlorobenzaldehyde and of furfural respectively, they must also be oxazole derivatives. Compounds VIIa and VIIb, which were obtained by the reaction with formaldehyde and acetaldehyde respectively, had ultraviolet spectra similar to that of methyl diphenyl-*s*-triazine, and their oxidation with potassium permanganate yielded the known diphenyl-*s*-triazine carboxylic acid. Hence, the presence of a triazine ring having two phenyl groups in VIIa and VIIb was established. The presence of the O–H group in VIIa and VIIb was confirmed by the absorption band at 3480 cm^{-1} in their infrared spectra and by the formation of the acetyl derivative, IX, from VIIa and of the phenylcarbamate, X, from VIIb, respectively.

The question now arises of why aromatic and aliphatic aldehydes yielded different products. The formations of VI and VII might indicate that the addition reaction of hydrogen cyanide to an aliphatic or aromatic aldehyde predominates over the addition of benzamidine to the aldehyde, and that the hydroxyl group of the cyanhydrine formed

*1 Part IV of "Studies of the Syntheses of Heterocyclic Compounds."

*2 Part III: E. Haruki, T. Inaike and E. Imoto, This Bulletin, **41**, 1361 (1968).

*3 Presented at the 18th Annual Meeting of the Chemical Society of Japan, Osaka, April, 1965.

1) J. Lichtenberger, *Bull. Soc. Chim. France*, **1956**, 1184.

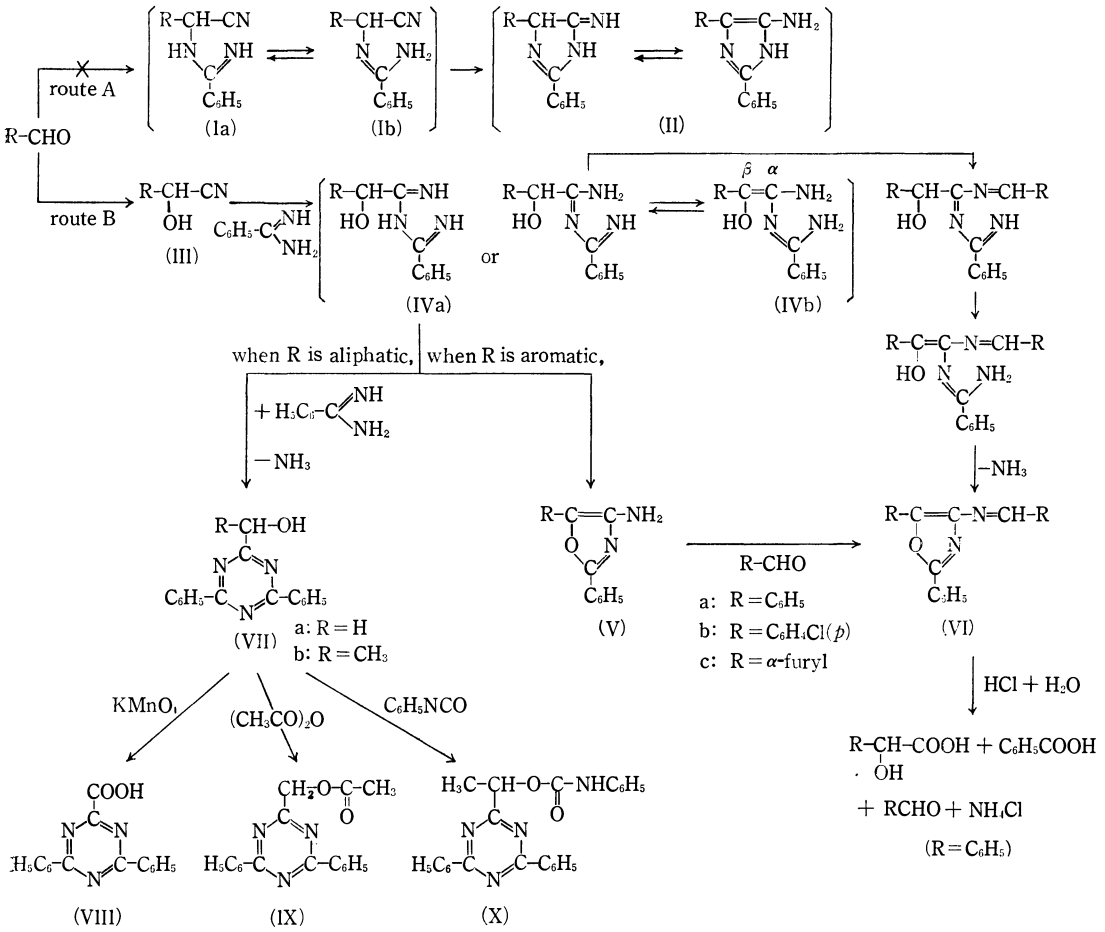

Chart 1.

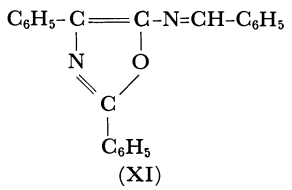

(XI)

was not replaced by the amino group of benzamidine, because of the lower nucleophilicity of benzamidine than that of ammonia. Under these conditions, benzamidine may be forced to react with the cyano group to form IVa. When R in IVa is aromatic, IVb would be more probable than IVa because of its larger degree of conjugation.

Since the carbon atom to which the hydroxyl group attaches in IV corresponds to the β-carbon atom of a vinylamine system, as in IVb, one of the tautomers of IV, this carbon atom may be attacked by a nucleophile only with great difficulty. For this reason, the nucleophilic attack of the hydroxyl group on the carbon atom of the amidino group would occur more easily to produce an oxazole ring. When R in IVa is aliphatic, the IVb tautomer is not always more favorable than IVa, and IVa may react with another molecule of benzamidine to form triazine derivatives, VIIa and VIIb.

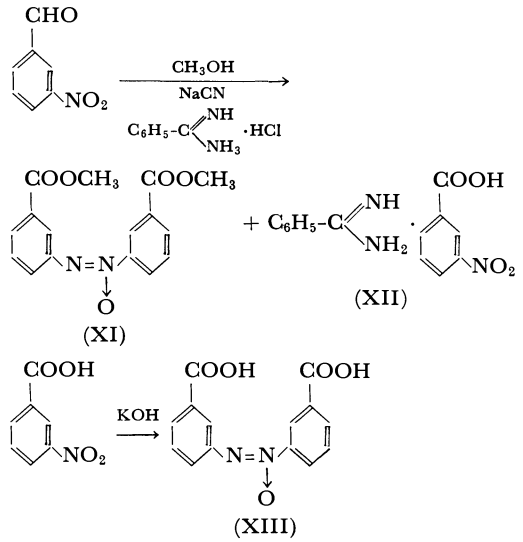

m-Nitrobenzaldehyde in aqueous methanol reacted with sodium cyanide in the presence of an equimolar amount of benzamidine hydrochloride in a manner completely different from that in the reactions described above. In this case, dimethyl azoxybenzene-3, 3'-dicarboxylate (XI) and benzamidinium nitrobenzoate (XII) were produced. However, in this reaction benzamidine seems to act only as a base, because *m*-nitrobenzaldehyde and sodium cyanide in methanol without benzamidine hydrochloride also reacted to yield the same compound, XI. Compound XI was hydrolysed to azoxybenzene-3,3'-carboxylic acid (XII), which was identified by comparison with an authentic sample prepared from *m*-nitrobenzoic acid and potassium hydroxide.

Though the reaction of nitrobenzaldehyde with sodium cyanide seems to be very interesting, the details of this reaction will be reported elsewhere, for this reaction has no relation with the subject reported on this paper.

Experimental

General Method for the Preparating of Oxazole Derivatives. A solution of an aldehyde (0.02—0.04 mol) in methanol (10 m*l*) and a solution of sodium cyanide (0.01 mol) in water (20 m*l*) were mixed with a solution of benzamidine hydrochloride (0.1 mol) in methanol under ice-cooling, after which the reaction mixture was allowed to stand for few days. After about one day a small amount of crystals precipitated. After standing for three days, the crystals precipitated were collected by filtration and recrystallized from the solvents shown in Table 1. The melting points, the yields, and the results of the elemental analyses of the products obtained are shown in Table 1.

Hydrolysis of the Oxazole Derivatives. *a) Under Mild Conditions.* A solution of VIa (103.2 mg) in 50 m*l* of 2 N hydrochloric acid and a small amount of methanol was mixed with a saturated solution of 2,4-dinitrophenylhydrazine in 2 N hydrochloric acid. After the mixture has stood for 24 hr at room temperature while being stirred, benzaldehyde 2,4-dinitrophenylhydrazone was collected by filtration and weighed (94.6 mg, yield, 95%) after drying.

b) Under Severe Conditions. The steam distillation of a mixture consisting of 3.3 g (0.01 mol) of VIa and 20 m*l* of concentrated hydrochloric acid gave at first about 0.7 g (0.007 mol) of benzaldehyde. After the complete distillation of the benzaldehyde, benzoic acid was distilled out gradually; the total amount was 1.1 g (0.009 mol). The residue of distillation was evaporated to dryness, and the residue was extracted with ether to give 1.1 g (0.007 mol) of mandelic acid. The benzoic acid and mandelic acid obtained above were identified by comparison with respective authentic samples, while the benzaldehyde obtained was identified as its 2,4-dinitrophenylhydrazone.

c) Hydrolyses of VIb and VIc under Mild Conditions. Hydrolyses of VIb and VIc were performed similarly to that of VIa. *p*-Chlorobenzaldehyde 2,4-dinitrophenylhydrazone was obtained from VIb in a yield of 92%, while furfural 2,4-dinitrophenylhydrazone was obtained from VIc in a yield of 71%.

A General Method for the Preparation of *α*-Hydroxyalkyldiphenyl-*s*-triazine (VII). A solution of 0.04 mol of sodium cyanide (1.6 g) in 10 m*l* of water was added, portion by portion and under ice-cooling, to a solution of 0.07 mol of an aliphatic aldehyde in 10 m*l* of methanol. Into this mixture there was then stirred, drop by drop, under ice-cooling, a

TABLE 1

	Yield (%)	Mp °C	Solvent for recrystallization	Analysis C%	Analysis H%	Analysis N%	λ_{max}^{EtOH} (mμ)	ε_{max}
VIa (R=C_6H_5)	32	156—157	Ethanol-Benzene	81.65 (81.46)	5.15 (4.97)	8.99 (8.64)	334	5.7×10^4
VIb (R=C_6H_4Cl*p*)	35	189—190	Ethanol-Benzene	67.26 (67.21)	3.43 (3.59)	6.90 (7.12)	337	2.6×10^4
VIc (R=)	28	133—134	Benzene	70.93 (71.04)	4.09 (3.98)	9.16 (9.21)	352	6.0×10^4

Values in parentheses are calculated for $C_{22}H_{16}ON$ (VIa), $C_{22}H_{14}ONCl_2$ (VIb) and $C_{18}H_{12}O_3N_2$ (VIc).

TABLE 2.

Product	Yield, g (%)	Mp, °C	Mol Wt	Analysis C%	Analysis H%	Analysis N%
VIIa (R=H)	1.5 (34)	122—124	250*	72.33 (72.98)	5.15 (4.98)	15.50 (15.50)
VIIb (R=CH_3)	1.4 (31)	114—115	280**	73.37 (73.63)	5.46 (5.45)	14.97 (15.15)

* This value was measured by the depression of melting point of nitrobenzene.

** This value was measured by the depression of the melting point of benzene. Analytical values in parentheses are calculated for $C_{16}H_{13}ON_3$ (VIIa) and $C_{17}H_{15}ON_3$ (VIIb).

solution of 5.0 g of benzamidine hydrochloride in 10 m*l* of methanol, and then 20 m*l* of water were added. The stirring was continued for 1 hr, after while the reaction mixture was allowed to stand at room temperature for three days. The crystals precipitated were collected by filtration. The concentration of the filtrate gave a further small amount of the same crystals. These crystals were combined and recrystallized from an ethanol-water.

Acetylation of VII. A solution of 1.0 g of VIIa in 10 m*l* of dry benzene was mixed with 5 m*l* of acetic anhydride and then refluxed for 3 hr. The evaporation of the solvents gave crystals, which were then recrystallized from ethanol; mp 112—114°C, yield 69%.

Found: C, 70.74; H, 4.86; N, 13.39%. Calcd for $C_{18}H_{15}O_2N_3$: C, 70.80; H, 4.95; N, 13.76%.

An attempt to prepare the acetyl derivative of VIIb was unsuccessful; only the starting material was recovered in a yield of 80%.

Preparation of Phenylurethane of VIIb. A mixture of VIIb (0.5 g), phenylisocyanate (0.3 m*l*), pyridine (one drop), and dioxane (5 m*l*) was warmed for 30 min. The solvent was evaporated to give colorless needles with a mp of 169—170°C. The yield was 0.5 g (70%).

Found: C, 72.46; H, 5.32; N, 14.02%. Calcd for $C_{24}H_{20}O_2N_4$: C, 72.71; H, 5.09; N, 14.13%.

Oxidation of VIIa and VIIb to VIII with Potassium Permanganate. A solution of potassium permanganate (0.5 g) and potassium hydroxide (0.5 g) in 20 m*l* of water was mixed with VIIa (0.1 g), and the resulting mixture was refluxed for 2 hr. The reaction mixture was filtered while hot. When the filtrate was cooled, potassium diphenyl-*s*-triazinecarboxylate was obtained as a precipitate. The acidification of the filtrate yielded a precipitate of diphenyl-*s*-triazinecarboxylic acid, which was identified by comparison with an authentic sample of this acid, which had been prepared by oxidation of methyldiphenyl-*s*-triazine[2] with potassium permanganate (which had in turn been prepared from benzamidine hydrochloride and acetic anhydride by the method described in the literature[2]).

Preparation of Dimethyl Azoxybenzene-3,3'-dicarboxylate (XI). *a) In the Presence of Benzamidine.* A solution of sodium cyanide (0.04 mol) in water (10 m*l*) was added, drop by drop, to a solution of *m*-nitrobenzaldehyde (4.53 g, 0.03 mol) in methanol (70 m*l*), and then to this mixture there was added a solution of benzamidine hydrochloride (5.0 g, 0.03 mol) in methanol (10 m*l*). The reaction mixture was stirred at 35—40°C for 4 hr. The crystals which precipitated on cooling were recrystallized from ethanol-benzene to produce 0.9 g of colorless needles with a mp of 132—133°C.

Found: C, 61.36; H, 4.47; N, 8.60%. Calcd for $C_{16}H_{14}O_5N_2$: C, 61.14; H, 4.49; N, 8.91%.

The filtrate was evaporated to dryness, and the solid obtained was recrystallized from ethanol to give benzamidinium *m*-nitrobenzoate with a mp of 237—239°C (yield 5.0 g, 60%).

Found: C, 58.54; H, 4.61; N, 14.85%. Calcd for $C_{14}H_{13}O_4N_3$: C, 58.53; H, 4.56; N, 14.63%.

b) In the Absence of Benzamidine. Sodium cyanide (1.0 g, 0.025 mol) was added to a solution of *m*-nitrobenzaldehyde (1.0 g, 0.007 mol) in methanol (20 m*l*). After the addition was complete, an exothermic reaction soon began to take place and a large amount of a pale yellow powder started to precipitate. After the heat evolution had ceased, the precipitates were collected by filtration, washed thoroughly with water, and recrystallized from an ethanol-benzene mixture to produce colorless needles with a mp of 132—133°C in a yield of 70%. The needles showed no depression upon a mixed-melting-point determination with Compound XI, obtained above. The aqueous solution which had been obtained by washing the precipitate was acidified with hydrochloric acid to give a small amount of *m*-nitrobenzoic acid (mp 140—141°C), which was identified by comparison with an authentic sample.

2) A. Pinner, *Ber.*, **17**, 2512 (1884); **25**, 1642 (1892).

BULLETIN OF THE CHEMICAL SOCIETY OF JAPAN VOL. 41 1372—1375 (1968)

Syntheses of Some Heterocyclic Compounds from α-Benzoyliminobenzyl Cyanide and Related Compounds*1,*2

Masahiro FUJIMORI, Eiichi HARUKI and Eiji IMOTO

Department of Applied Chemistry, College of Engineering, University of Osaka Prefecture, Sakai, Osaka

(Received October 25, 1967)

The reaction of α-benzamidobenzyl cyanide (I) with thionyl chloride and pyridine in benzene gave α-benzoyliminobenzyl cyanide (II) in a 52% yield. II is a novel compound which can react readily with nucleophilic reagents, such as alcohols, mercaptans and amines. The reaction of II with ethyl-mercaptan and with alcohols gave α-ethylthio-α-benzamidobenzyl cyanide and α-alkoxy-α-benzamidobenzyl cyanide respectively. Furthermore, II reacts with bifunctional nucleophilic reagents to form heterocyclic compounds. The reaction of II with hydrazine and with hydroxylamine afforded 3,5-diphenyl-1,2,4-triazole and 3,5-diphenyl-1,2,4-oxadiazole respectively.

During the course of investigations concerning the reactions of α-aminonitriles, we happened to find a novel method for the preparation of α-benzoyliminobenzyl cyanide (II) from α-benzamidobenzyl cyanide (I) and thionyl chloride in pyridine. The structure of II was confirmed by the following experimental evidence: (i) The infrared spectrum shows the presence of C=N and C≡N bonds at 1620 and 2250 cm^{-1}, but shows no N–H bond near 3200 cm^{-1}. (ii) An acid hydrolysis of II with hydrochloric acid gave benzoylformic acid (62.5 mol%), benzamide (9.7 mol%), and a small amount of ammonium chloride. (iii) An alkaline hydrolysis of II gave benzoic acid (105.3 mol%) and benzamide (42.6 mol%), along with a small amount of sodium cyanide, as is shown below:

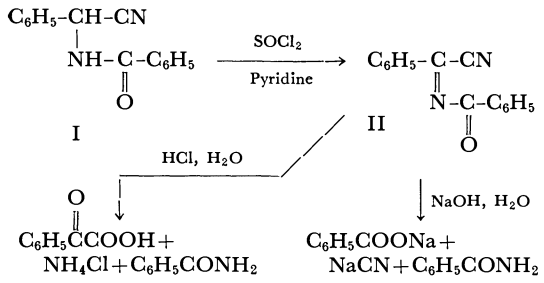

The formation of II is obviously due to the oxidation of I with thionyl chloride, even though the products derived from thionyl chloride could not be identified. Only a few reactions in which thionyl chloride acts as an oxidizing agent have been reported.[1-4] Hence, sulfuryl chloride, the oxidizing ability of which is usually stronger than that of thionyl chloride, was used for the above reaction instead of thionyl chloride. However, the yield of II was only 5%, and 70—75% of the starting material was recovered, as Table 1 shows. *N*-Bromosuccinimide (NBS) or *t*-butyl hypochlorite was also used as the oxidizing agent for the above reaction. As is shown in Table 1, *t*-butyl hypochlorite produced II in a yield of 51%, but NBS did not.

Table 1. Oxidation of α-benzamidobenzyl cyanide (I)

Oxidizing agent	Reaction temp (°C)	Yield of II (%)	I. Recovered (%)
Thionyl chloride	0—5	52	0
Thionyl chloride	Room temp.	2	0
Sulfuryl chloride	0—5	5	70
Sulfuryl chloride	Room temp.	5	70
Sulfuryl chloride	50—60	11	62
t-Butyl hypochlorite	Room temp.	51	0
NBS	Room temp.	0	55
NBS	50—60	0	52

It seems to be very strange that no α-acyliminobenzyl cyanide, represented by II, has ever been prepared in spite of the simplicity of its structure. Compound II has three carbon atoms, indicated by Gothic letters in Formula II, which a nucleophilic reagent may attack. We studied the reactions of II with several nucleophiles. The results

*1 Part VI of "Studies of the Syntheses of Heterocyclic Compounds."

*2 Part V: E. Haruki, Y. Hirai and E. Imoto, This Bulletin, **41**, 267 (1968).

1) H. Takimoto and L. Krbechek, *J. Org. Chem.*, **27**, 4688 (1962).
2) K. A. Pollart and H. J. Harwood, *ibid.*, **27**, 4444 (1962).
3) S. Patai and F. Bergmann, *J. Am. Chem. Soc.*, **72**, 1035 (1950).
4) W. B. Brownell and L. C. King, *ibid.*, **71**, 2926 (1949).

are shown in the following scheme:

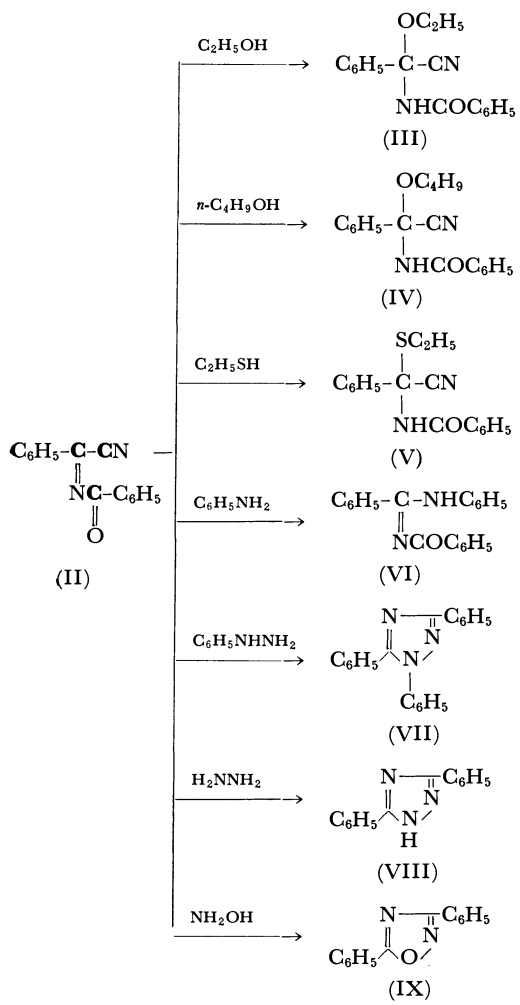

Alcohols and thioalcohols attacked the α-carbon atom of II and added to the C=N bond. Similarly, an amine attacked the cyano group, as aniline produced VI in a 65% yield as a result of the reaction with II. The bifunctional nucleophilic reagents, such as hydrazines and hydroxylamines, form 1,2,4-triazoles (VII) and (VIII) or oxadiazoles (IX) respectively. This reaction may be caused by a substitution of the cyano group with the amino group, followed by a cyclization between the carbonyl carbon and the amino or the hydroxyl group. All these cyclization reactions are, of course, novel reactions.

The structures of Compounds, VI, VII, VIII, and IX were confirmed by a comparison of their properties with those of authentic samples. The structures of Compounds, III, IV, and V were unknown. Hence, their structures were confirmed by elemental analyses, by a study of their infrared spectra, and by the results of the acid and alkaline hydrolysis described below:

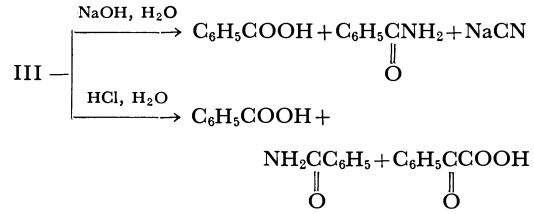

If the reaction between ethanol and II does not form Compound III, but forms another compound such as Compound X, which is formed by the addition of ethanol to the cyano group, Compound X, an imino ether, must be very unstable toward water and must be hydrolyzed quickly.

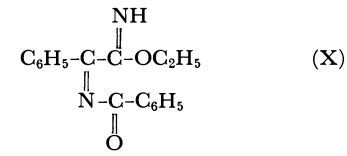

The actuality was opposite, in fact. The compound obtained from ethanol and II was not hydrolyzed at all but was recovered in a quantitative yield after having been treated with a water-ethanol mixture for 6 hr at 40—50°C. Therefore, Compound III does not have the structure of X. The structure of IV was also confirmed by methods similar to those used in the determination of III. The structure V was assumed on the basis of the data of elemental analyses, the presence of the N–H and C≡N groups in the infrared spectrum, and the similarity of the chemical behavior of thioalcohol to that of alcohol on a nucleophilic reaction.

The starting material for the above reaction, α-benzamidobenzyl cyanide, was prepared by the benzoylation[5] of α-aminobenzyl cyanide, which can be prepared easily from benzaldehyde, hydrogen cyanide, and ammonia. Another kind of α-(benzoylamino)-nitrile could be obtained by the *N*-benzoylation of the α-aminonitriles, when aldehydes other than benzaldehyde were used for the preparation of an α-aminonitrile. We tried to prepare α-benzamidopropionitrile from acetaldehyde, but this attempt failed.

Next, we prepared α-acetamidobenzyl cyanide and carried out its reaction with thionyl chloride in pyridine, but no crystalline product was obtained from the reaction mixture. Furthermore, we tried to react thionyl chloride with ethyl α-benzamidophenylacetate,[6] (XI), in which the cyano group is replaced by the ethoxycarbonyl group; we thus obtained ethyl α-benzoyliminophenyl acetate, (XII), in a yield of 18%, together with ethyl benzoylformate and benzamide. Ethyl benzoylformate and benzamide must be formed by the

5) R. Ruggeri and G. Rigoli, *Gazz. Chim. Ital.*, **54**, 555 (1924); *Chem. Abstr.*, **19**, 262 (1925).
6) A. Kossel, *Ber.*, **24**, 4151 (1901).

oxidation of XI with thionyl chloride, followed by the hydrolysis of the C=N bond:

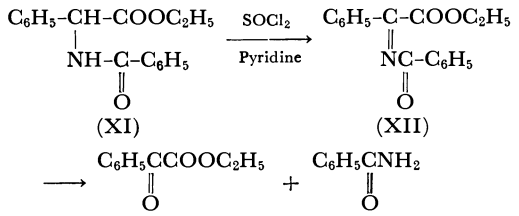

From the above observations, it may be concluded that the oxidation with thionyl chloride would be facilitated by the benzoyl group attached to the amino group, and also be favored by the aryl group attached to the α-carbon atom in II. Furthermore, among the compounds of the II type, II was the only one which was accessible. It is, therefore, unlikely, in view of these limitations, that the reaction is of general utility for the synthesis of α-acyliminonitriles from α-acylamidonitriles.

However, the reactions are still of considerable interest in that thionyl chloride acts as an oxidizing reagent for the conversion of the acylamino group into the acylimino group in α-acylaminonitriles. The mechanism of this oxidation reaction is not at all clear. One can postulate that the active hydrogen atom attached to the α-carbon of Compound II is responsible in some manner for this oxidation. This postulation prompted us to examine the reaction of the three compounds, ethyl benzamidoacetate, diethyl acetamidomalonate, and, *N*-benzoylbenzylamine, all of which have an active hydrogen atom, with thionyl chloride. However, in no case was the expected reaction product obtained.

Experimental

The melting points and boiling points were not corrected. The molecular weights were measured with Hitachi Perkin-Elmer 115 Molecular Weight Apparatus, using benzene as the solvent.

α-Benzoyliminobenzyl Cyanide (II). To a solution of α-benzamidobenzyl cyanide (I) (5.0 g, 0.021 mol) in dry benzene (40 m*l*), there was added dry pyridine (3 m*l*) and then thionyl chloride (3.0 g, 0.026 mol), drop by drop, at 0—5°C. The mixture was stirred at this temperature for 3 hr and then left to stand overnight at room temperature. The precipitate pyridinium hydrochloride, was collected by filtration and washed with a small amount of dry benzene. After the combined filtrate had been concentrated under reduced pressure at 30—40°C, the solid residue obtained was recrystallized from ligroin to give α-benzoyliminobenzyl cyanide (II) (2.6 g, 52%), mp 80—82°C (decomp.).

Found: C, 76.93; H, 4.27; N, 11.80%; mol wt, 248. Calcd for $C_{15}H_{10}ON_2$: C, 76.91; H, 4.30; N. 11.96%; mol wt, 234.

Acid Hydrolysis of α-Benzoyliminobenzyl Cyanide (II). α-Benzoyliminobenzyl cyanide (1 g, 0.0043 mol) was dissolved in a mixture of 15 m*l* of 6 N hydrochloric acid and 15 m*l* of dioxane, and the solution was stirred at 45—50°C for 6 hr. After the reaction mixture had been concentrated *in vacuo* at 30—40°C, the viscous residue was mixed with 30 m*l* of water and extracted with ether. The ethereal extract was evaporated and treated with a solution of 2,4-dinitrophenylhydrazine in a dilute hydrochloric acid; benzoylformic acid 2,4-dinitrophenylhydrazone (0.85 g, 0.0027 mol) was thus obtained. The 2,4-dinitrophenylhydrazone obtained was recrystallized from ethanol, mp 180—185°C (decomp.). Its mixed melting point with an authentic sample showed no depression and its infrared spectrum coincided with that of the authentic sample. The aqueous layer was evaporated *in vacuo*, and the residue obtained was washed with a small amount of benzene to obtain ammonium chloride (0.12 g, 0.0024 mol). The evaporation of the benzene gave benzamide (0.05 g, 0.0004 mol).

Alkaline Hydrolysis of α-Benzoyliminobenzyl Cyanide (II). α-Benzoyliminobenzyl cyanide (1 g, 0.0043 mol) and sodium hydroxide (1 g, 0.025 mol) were dissolved together in a mixture of 15 m*l* of water and 15 m*l* of dioxane, and the solution was stirred at 45—60°C for 6 hr. After the evaporation of the solvent from the reaction mixture *in vacuo*, the solid residue was washed with 20 m*l* of water and separated by filtration, thus giving benzamide (0.22 g, 0.0018 mol). The acidification of the filtrate with 10 m*l* of 6 N hydrochloric acid gave benzoic acid (0.55 g, 0.0045 mol).

Hydrolysis of α-Benzoyliminobenzyl Cyanide (II) in a Neutral Medium. α-Benzoyliminobenzyl cyanide (0.5 g, 0.0021 mol) was dissolved in a mixture of 5.0 m*l* of water and 15 m*l* of dioxane, and the solution was stirred at 45—50°C for 6 hr. The reaction mixture was evaporated *in vacuo*, and the residue obtained was washed with 10 m*l* of a 10% aqueous solution of sodium carbonate. The insoluble crystals, benzamide (0.22 g, 0.0018 mol), were collected by filtration. The acidification of the filtrate with 6 N hydrochloric acid gave benzoic acid (0.25 g, 0.0020 mol).

α-Ethoxy-α-benzamidobenzyl Cyanide (III). α-Benzoyliminobenzyl cyanide (1.0 g, 0.0043 mol) was dissolved in absolute ethanol (20 m*l*), and the solution was refluxed for 3 hr. After the reaction mixture had been cooled in an ice bath, the precipitates were collected by filtration and recrystallized from 99% ethanol. Needle crystals of α-ethoxy-α-benzamidobenzyl cyanide melting at 153—154°C (decomp.) were thus obtained. Yield, 92%.

Found: C, 72.76; H, 5.67; N, 9.73%; mol wt, 291. Calcd for $C_{17}H_{16}O_2N_2$: C, 72.84; H, 5.75; N, 9.99%; mol wt, 280.

Acid Hydrolysis of α-Ethoxy-α-benzamidobenzyl Cyanide. α-Ethoxy-α-benzamidobenzyl cyanide (1 g, 0.0036 mol) was dissolved in a mixture of 15 m*l* of 6 N hydrochloric acid and 15 m*l* of dioxane, and the solution was stirred at 45—50°C for 6 hr. Benzoylformic acid 2,4-dinitrophenylhydrazone was obtained by treating a small portion of the reaction mixture with an acidic solution of 2,4-dinitrophenylhydrazine. Another portion of the reaction mixture was evaporated, and the residue obtained was washed with 20 m*l* of benzene to give ammonium chloride (0.15 g, 0.0028 mol). The benzene extract was washed with 10 m*l* of a 10% aqueous solution of sodium carbonate. The concentration of the benzene extract gave benzoic acid (0.4 g, 0.0033 mol).

Alkaline Hydrolysis of α-Ethoxy-α-benzamidobenzyl Cyanide. α-Ethoxy-α-benzamidobenzyl cyanide (1 g, 0.0036 mol) and sodium hydroxide (1 g, 0.025 mol) were disolved in a mixture of 15 m*l* of water and 15 m*l* of dioxane, and the solution was stirred at 45—50°C for 6 hr. After the reaction mixture had been evaporated *in vacuo*, the residue obtained was washed with 20 m*l* of water to give benzamide (0.22 g, 0.0018 mol). The acidification of the aqueous filtrate with 10 m*l* of 6 N hydrochloric acid evolved hydrocyanic acid, which was recognized by its characteristic odor and which gave benzoic acid (0.55 g, 0.0045 mol).

α-*n*-Butoxy-α-benzamidobenzyl Cyanide (IV). α-Benzoyliminobenzyl cyanide (0.5 g, 0.0021 mol) was dissolved in a 20 m*l* of *n*-butyl alcohol, and the mixture was stirred at 80—90°C for 3 hr. After standing in an ice-bath for 6 hr, the reaction mixture gave a precipitate of α-*n*-butoxy-α-benzamidobenzyl cyanide (0.12 g). The concentration of the filtrate *in vacuo* gave an addition 0.47 g of the same product. The total yield was 0.59 g (0.0019 mol, 90%). Recrystallization from carbon tetrachloride gave colorless needle crystals with a mp of 125—127°C.

Found: C, 73.68; H, 6.61; N, 9.07%. Calcd for $C_{19}H_{20}O_2N_2$: C, 74.00; H, 6.54; N, 9.09%.

α-Ethylthio-α-benzamidobenzyl Cyanide (V). A solution of α-benzoyliminobenzyl cyanide (1 g, 0.0043 mol) and ethyl mercaptan (1 g, 0.016 mol) in dioxane (15 m*l*) was stirred at 50—60°C for one hour. The subsequent concentration of the reaction mixture gave colorless needle crystals of α-ethylthio-α-benzamidobenzyl cyanide. Mp 159—161°C after recrystallization from benzene.

Found: C, 68.91; H, 5.48; N, 9.71%. Calcd for $C_{17}H_{16}ON_2S$: C, 68.90; H, 5.44; N, 9.45%.

***N*-Benzoyl-*N'*-phenylbenzamidine (VI).** After a solution of α-benzoyliminobenzyl cyanide (0.5 g, 0.0021 mol) and aniline (1 g, 0.011 mol) in 15 m*l* of dioxane had been stirred at 80—90°C for 3 hr, the reaction mixture was concentrated *in vacuo*. The recrystallization of the residue from ethanol gave *N*-benzoyl-*N'*-phenylbenzamidine (0.42 g, 0.0014 mol, 65%), mp 140—141°C (lit.,[7] 141°C). Admixture with an authentic sample[7] showed no depression of the melting point, and the infrared spectrum coincided with that of the authentic sample.

Found: C, 79.78; H, 5.47; N, 9.28%. Calcd for $C_{20}H_{16}ON_2$: C, 79.98; H, 5.37; N, 9.33%.

1,3,5-Triphenyl-1,2,4-triazole (VII). After a solution of α-benzoyliminobenzyl cyanide (2 g, 0.008 mol) and phenylhydrazine (2.0 g, 0.019 mol) in dioxane (40 m*l*) had been stirred at 70—80°C for 2.5 hr, the reaction mixture was concentrated *in vacuo*; the viscous residue thus obtained was recrystallized from ethanol to give 1,3,5-triphenyl-1,2,4-triazole (2.1 g, 0.0072 mol, 83.9%). Mp 103—104°C (lit.,[8] 104°C). No depression of melting point was observed on admixture with an authentic specimen, and the infrared spectrum of the compound obtained was identical with that of the authentic specimen.

Found: C, 80.54; H, 5.06; N, 13.67%. Calcd for $C_{20}H_{15}N_3$: C, 80.78; H, 5.09; N, 14.13%.

3,5-Diphenyl-1,2,4-triazole (VII). After a solution of α-benzoyliminobenzyl cyanide (2.0 g, 0.0086 mol) and hydrazine (1.0 g, 0.031 mol) in 40 m*l* of 99% ethanol had been stirred at 70—80°C for 2.5 hr, the reaction mixture was concentrated *in vacuo* to give a viscous residue. The residue was recrystallized from chloroform to produce 3,5-diphenyl-1,2,4-triazole (1.78 g, 0.0084 mol, 97.2%), mp 189—190°C (lit.,[9] 192°C). Admixture with an authentic sample showed no depression of the melting point, and the infrared spectrum was identical with that of the authentic sample.

Found: C, 75.85; H, 5.01; N, 18.69%. Calcd for $C_{14}H_{11}N_3$: C, 75.99; H, 5.01; N, 18.99%.

3,5-Diphenyl-1,2,4-oxadiazole (IX). A solution of hydroxylamine hydrochloride (1 g, 0.014 mol) in methanol (15 m*l*) was neutralized by a solution of sodium methoxide in methanol which had been prepared from sodium (0.33 g, 0.0014 gram atoms) and methanol (10 m*l*). The sodium chloride which precipitated was removed by filtration, and the filtrate was mixed with α-benzoyliminobenzyl cyanide (1 g, 0.0043 mol). The mixture was stirred at 50—60°C for 2 hr and then cooled to give precipitates. The precipitates were collected by filtration and recrystallized from ethanol. Mp 106—107°C (Needle crystals). A mixed-melting-point determination with an authentic sample[10] showed no depression and the infrared spectra was identical with that of the authentic sample.

Found: C, 75.70; H, 4.41; N, 12.41%. Calcd for $C_{14}H_{10}ON_2$: C, 75.65; H, 4.54; N, 12.61%.

Ethyl α-Benzoyliminophenylacetate (XII). To a solution of ethyl α-benzamidophenylacetate (XI) (25 g, 0.088 mol) in dry benzene (200 m*l*), there was added pyridine (40 m*l*) and then thionyl chloride (30 g, 0.25 mol), drop by drop, at room temperature. The mixture was stirred at 70—80°C for 6 hr. After the removal of the pyridinium hydrochloride by filtration, the filtrate was evaporated to afford a viscous residue. The distillation of the residue under a reduced pressure gave two fractions. The first fraction (bp 90—100°C/1.0 mmHg) consisted of ethyl benzoylformate, which showed the same infrared spectrum as that of an authentic sample. The second fraction (bp 165—180°C/1.0 mmHg) was a yellow oil, which solidified partly upon standing overnight. The filtration of the oily solid gave benzamide (2.0 g, 0.0165 mol). The distillation of the filtrate gave 4.5 g of pure ethyl α-benzoylimidophenyl acetate (X), which was hydrolyzed very quickly by moisture in air to ethyl benzoylformate and benzamide. The elemental analyses were carried out immediately after the distillation.

Found: C, 72.80; H, 5.45; N, 4.80%. Calcd for $C_{17}H_{15}O_3N$: C, 72.58; H, 5.37; N, 4.98%.

7) H. L. Wheeler, T. B. Johnson and D. F. McFarland, *J. Am. Chem. Soc.*, **25**, 788 (1903).
8) O. Silberrad, *J. Chem. Soc.*, **77**, 1189 (1900).
9) R. Engelhart, *J. Prakt. Chem.*, [2] **54**, 153 (1896).
10) E. Tiemann and P. Kruger, *Ber.*, **17**, 1694 (1884).

BULLETIN OF THE CHEMICAL SOCIETY OF JAPAN VOL. 41 1376—1380 (1968)

The Reaction between Hydrocarbon and Hydrogen Cyanide in Silent Electrical Discharge. I. The Formation of Cyclohexyl Cyanide from Cyclohexane and Hydrogen Cyanide*1

Kazuaki KAWAMOTO,*2 Noboru SONODA and Shigeru TSUTSUMI

Department of Chemical Technology, Faculty of Engineering, Osaka University, Miyakojima-ku, Osaka

(Received November 13, 1967)

In order to examine the possibility of the direct introduction of a cyano radical into cyclohexane by means of silent discharge, a mixture of cyclohexane and hydrogen cyanide was discharged in an ozonizer under various conditions. As a result, cyclohexyl cyanide was obtained. The yield of cyclohexyl cyanide depended upon the voltage of discharge, the residence time in the discharge tube, the temperature of the discharge tube, and the structual characteristics of the apparatus. In the refluxing method the maximum yield of cyclohexyl cyanide was obtained when the discharge was carried out at a low temperature. Besides cyclohexyl cyanide, the reaction products were confirmed to consist of bicyclohexyl, cyclohexene, methylcyclohexane, ethylcyclohexane, 3-cyclohexylcyclohexene, methylenecyclohexane, 1-hexene, *n*-hexane, *n*-pentane, methylcyclopentane, a solid brown deposit, and cracked gas. The principal reactions can be interpreted as being the formation of cyclohexyl and cyano radicals and the combination of these radicals, their dehydrogenation, their isomerization, their polymerization, and their decomposition.

In recent years, the oxidation of hydrocarbons by silent electrical discharge has been studied by Sugino *et al.*[1] However, no detailed study of the interaction of hydrocarbons and hydrogen cyanide under silent discharge has yet been reported. The synthesis of the cyano-compounds formed by the direct combination of these compounds in the silent discharge seems to be interesting and important from both the practical and the theoretical points of view.

The direct synthesis of cyclohexyl cyanide from cyclohexane and cyano-compounds has been attempted by several chemists: It was found by Müller and Huber[2] that cyclohexyl cyanide was obtained by the reaction of cyclohexane with cyanogen chloride upon irradiation with ultraviolet light. McKusick *et al.*[3] found that the irradiation of a mixture of cyclohexane and hydrogen cyanide with high-energy electrons led to cyclohexylnitriles. Grof[4] found that the reaction of cyclohexane with cyanogen chloride in the presence of peroxide ($C_6H_{11}SO_3OAc$) gave cyclohexyl cyanide. It was found by one of the present authors[5] that, when the irradiation of a solution of ethyl cyanoformate in cyclohexane by a 600 W high-pressure mercury arc lamp was carried out at room temperature, the direct-introducing reaction of cyano and ethoxycarbonyl radicals took place.

The present study was undertaken to find out whether or not the direct formation of cyclohexyl cyanide results from the reaction between cyclohexane and hydrogen cyanide occurring in the silent discharge; to determine, if possible, the optimum conditions for the preparation of cyclohexyl cyanide, and at the same time to ascertain the mechanism of this reaction. In this research, the silent discharge was carried out by three methods (passing, bubbling, and refluxing methods; see Experimental section) in a Siemen ozonizer for 5 hr, using voltages from about 12 to 15

*1 The major part of these research results were presented at the 18th Annual Meeting of the Chemical Society of Japan, Osaka, April, 1965.

*2 Present address: Institute of Commodities, Faculty of Economics, Kagawa University, Takamatsu.

1) K. Sugino and E. Inoue, This Bulletin, **24**, 93 (1951); K. Sugino and E. Inoue, *Nippon Kagaku Zassi (J. Chem. Soc. Japan, Pure Chem. Sect.)*, **75**, 10, 617 (1954); E. Inoue, *J. Electrochem. Soc. Japan*, **22**, 668 (1954); E. Inoue, *ibid.*, **23**, 18, 76, 403, 452, 574, 648. (1955); E. Inoue and K. Sugino, *ibid.*, **24**, 33 (1956); K. Sugino, E. Inoue, K. Shirai, T. Koseki and T. Gomi, *Nippon Kagaku Zasshi (J. Chem. Soc. Japan, Pure Chem. Sect.)*, **86**, 114 (1965).

2) E. Müller and H. Huber, *Chem. Ber.*, **96**, 670 (1963).

3) B. C. McKusich, W. E. Mochel and F. W. Stracey, *J. Am. Chem. Soc.*, **82**, 723 (1960); C. S. Cleaver and B. C. McKusick, U. S. Pat. 2952597; *Chem. Abstr.*, **55**, 5428 (1961).

4) R. Grof, *Ann.*, **578**, 50 (1952).

5) T. Tominaga, Y. Odaira and S. Tsutsumi, This Bulletin, **37**, 596 (1964).

kilovolts and frequency of 60 cycles per second. Furthermore, the effect of the temperature of the discharge tube was investigated, and a large number of reaction products were examined in detail.

Experimental

Materials. The cyclohexane used in this experiment was purified according to the procedure of Ho and Freeman:[6] bp 80—81°C, n_D^{25} 1.4226, d_4^{25} 0.7666. The hydrogen cyanide was prepared according to the procedure of Brauer.[7] Purification was carried out by passing the substance over calcium chloride (E) and phosphorus pentoxide (F), as in Fig. 1. In each experiment, about a 2-mol portion of hydrogen cyanide was used.

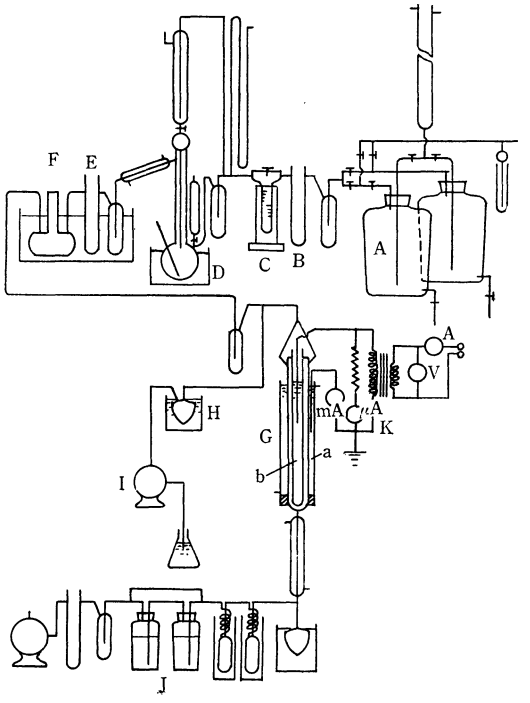

Fig. 1. Apparatus used in the passing method.

Apparatus. The apparatuses illustrated in Figs. 1, 2, and 3 were used. (1) Helium coming from a reservoir (A) was passed over calcium chloride (B), and the helium flow was measured by passing it through a calibrated flow meter (C). (2) The hydrogen cyanide was prepared in a flask (D) according to Brauer's method.[7] (3) The outside (a) of the discharge tube was filled with water, and the inner tube (b), with a 3% $CuSO_4$ solution. (4) In both the passing method and the refluxing method, the discharge tube (G) used was a Pyrex tube 40 cm in effective length, 4 cm in outside diameter, and with a space gap of 0.25 cm. In the case of the bubbling method, the central glass tube shown in Fig. 2 was 2.4 cm in diameter, and this tube was enclosed in a Pyrex tube 3.3 cm in diameter and 2 mm thick. A spiral glass stick was inserted in the space gap (0.25 cm). (5) Cyclohexane was vaporized through a vaporizer (H); the rate of the flow of the cyclohexane can be kept approximately constant by the use of a pump (I). (6) Unchanged hydrogen cyanide was absorbed in two bottles (J) (containing a mixture of NaOH and $Fe_2(SO_4)_3$). (7) The electrical energy was supplied by a 15-kV transformer (K).

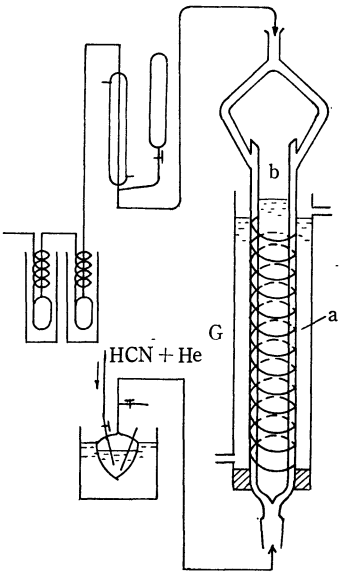

Fig. 2. Discharge tube used in the bubbling method.

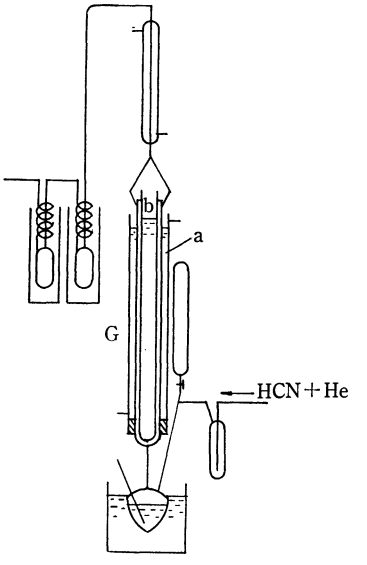

Fig. 3. Apparatus used in the refluxing method.

Procedure. In the passing method, helium, as the carrier gas, was passed through the discharge tube at a constant velocity, and the vaporizer (H) was heated at 150°C. The discharge tube was then heated to the

6) S. K. Ho and G. R. Freeman, *J. Phys. Chem.*, **68**, 2189 (1964).

7) G. Brauer, "Handbuch der Präparativen Anorganischen Chemie," Ferdinand Enke Verlag, Stuttgart (1954), p. 500.

operating temperature. Cyclohexane and hydrogen cyanide were passed through the tube at a regular velocity for the period of the reaction. A current of 60 cycles was then sent through a voltage regulator, and the voltage was stepped up by a transformer in order to give it the necessary value. The products coming out of the discharge tube were condensed by passing them through a condenser, then they were cooled by being passed through two traps to 7°C, thus catching almost all of the unreacted cyclohexane, together with the reaction product. The liquid products were analyzed by the method described below, while the noncondensable gas was analyzed by gas chromatography at intervals of 30 min. In the bubbling method, the discharge tube and a round flask attached to it were filled with cyclohexane. A gas mixture of hydrogen cyanide and helium was bubbled into cyclohexane at a constant rate of flow. In the refluxing method, cyclohexane was boiled in a round flask attached to discharge tube. A gas mixture of hydrogen cyanide and helium was then flowed into the cyclohexane flask at a constant velocity. The discharge was carried out as in the case of the passing method.

Analysis of the Products. The reaction products were identified by comparing their retention times on gas chromatography with those of authentic samples.*3 (Columns of tricresyl phosphate, PEG 6000, and silicone DC 550 were used.) In addition, the reaction products were dried with anhydrous sodium sulfate and then fractionally distilled, and the constituents of the cut were identified b means of the derivatives formed.

Cyclohexyl cyanide was obtained in a fraction boiling at 180—188°C. From this fraction, the *p*-bromophenacyl ester of cyclohexanecarboxylic acid,*4 mp 92—93°C, and cyclohexanecarboxamide,*5 mp 184—185°C, were obtained. They showed no depression of their melting points when mixed with authentic synthesized specimens. The infrared spectrum of this fraction agreed with that of authentic cyclohexyl cyanide.

The quantitative analysis of the reaction products in this experiment was performed by gas chromatography. The gaseous products were also analyzed by gas chromatography. (Columns of activated charcoal, tricresyl phosphate, Molecular Sieve 13 X, and dimethyl sulfolane were used.) In both the passing method and the refluxing method, a solid brown deposit was formed on the glass wall of the ozonizer. This deposit dissolved in acetone, but its constitution was not determined.

Results and Discussion

The influence of the discharge conditions on the reaction between cyclohexane and hydrogen cyanide was examined. When the experiments were carried out under the conditions listed in Table 1, a large number of compounds were obtained as well as cyclohexyl cyanide, the object substance. Those of these compounds which have been identified are summarized in Table 2. The percentage of the compound shown in this table does not necessarily represent the maximum yield, but is an average of three experiments under constant operating conditions. However, the fluctuation in the yield of these compounds obtained in repeated experiments was less than 1 per cent. Since this discharge does not occur in the high temperature zone, the thermal pyrolysis of cyclohexane can not occur in this experiment. When the liquid products obtained by both the passing method and the refluxing method absorbed oxygen from the air, they were transformed into the solid products. The gaseous products given by the reaction of cyclohexane and hydrogen cyanide or cyclohexane alone consisted of hydrogen, methane, ethane, ethylene, acetylene, propane, propylene, *n*-butane, 1-butene, and 1,3-butadiene. The gaseous products could not be determined quantitatively. These hydrocarbons were considered to be decomposition products of activated cyclohexane. It has been found that a mixture of cyclohexane and hydrogen cyanide decomposes more violently than does cyclohexane alone, and that a portion of the energy is consumed, resulting in a rise in the temperature of the discharge wall.

Influences of the Discharge Temperatures and Voltages on the Reaction between Cyclohexane and Hydrogen Cyanide by Using the Passing Method. By running cyclohexane with hydrogen cyanide only one time in the ozonizer under the conditions described in Experiment Nos. 1, 2 and 4 of Table 1, these reactants were slightly converted to cyclohexyl cyanide, as is shown in Table 2. The yield of cyclohexyl cyanide depends upon the voltage and the temperature at which the discharge is carried out. It has been found that increasing the voltage increases the yield of cyclohexyl cyanide, and that cylohexyl cyanide is obtained when the ozonizer is kept "cold," while this compound is not formed when

*3 The authentic samples were prepared as follows: (1) Cyclohexyl cyanide was prepared according to the procedure of Tilford *et al.* (C. H. Tilford, M. G. Van Campen, Jr., and R. S. Shelton, *J. Am. Chem. Soc.*, **69**, 2902 (1947)). (2) Bicyclohexyl and 3-cyclohexylcyclohexene were prepared by Hickinbottom's method (W. J. Hickinbottom, "Reactions of Organic Compounds," Longmans, Green and Co., 3rd Ed., (1957), p. 56, 544). (3) Cyclohexene was prepared according to the procedure of Coleman and Johnstone (G. H. Coleman and H. F. Johnstone, "Organic Syntheses," Coll. Vol. I, 2nd Ed., p. 183 (1956)). (4) Methylenecyclohexane (bp 102—103°C, n_D^{20} 1.4494, d_4^{20} 0.8032) was given by the pyrolysis of cyclohexylmethyl acetate (bp 94—98°C/22 mmHg) prepared by refluxing cyclohexylcarbinol and acetic anhydride. The cyclohexylcarbinol (bp 91—96°C/22 mmHg) was prepared by the action of formaldehyde on cyclohexylmagnesium bromide. (5) The other authentic reagents used for the identification were commercial materials.

*4 The *p*-bromophenacyl ester of cyclohexanecarboxylic acid was prepared according to the procedure of Shriner *et al.* (R. L. Shriner, R. C. Fuson and D. Y. Curtin, "The Systematic Identification of Organic Compounds," John Wiley & Sons, New York (1956), p. 200).

*5 Cyclohexanecarboxamide was prepared according to Radziszewski method (B. Radziszewski, *Ber.*, **18**, 355 (1885)).

TABLE 1. THE REACTION BETWEEN CYCLOHEXANE AND HYDROGEN CYANIDE IN SILENT ELECTRICAL DISCHARGE
(Experimental condition)

Method		Passing				Bubbling		Refluxing		
Experiment No.		1	2	3	4	5	6*	7	8	9*
Cyclohexane used	g	242.94	86.88	85.26	88.02	145.91	127.86	81.52	86.78	80.12
Velocity	g/hr	48.6	17.4	17.1	17.6	—	—	—	—	—
Flow rate of helium	*l*/hr	2.96	3.05	3.04	2.98	2.93	2.91	2.92	2.88	2.86
Discharge time	hr	5	5	5	5	5	5	5	5	5
Second. voltage	kV	12	12	12	15	15	15	12	12	11.5
Second. current	mA	2.1	2.1	2.1	2.3	1.4	1.4	1.9	1.9	1.7
Temp. of discharge tube										
Inside	°C	15—20	15—22	85—91	15—20	10—12	10	31—68	77—78	31—68
Outside	°C	15	15	85—93	15	10—12	10	31—68	80—81	31—68

* Cyclohexane alone was used.

TABLE 2. THE REACTION BETWEEN CYCLOHEXANE AND HYDROGEN CYANIDE IN SILENT ELECTRICAL DISCHARGE
(Experimental result)

Method		Passing				Bubbling		Refluxing		
Experiment No.		1	2	3	4	5	6	7	8	9
Product collected	g	254.76	81.26	26.95	80.07	128.46	121.14	84.94	89.14	75.81
Reaction product	g	3.41	5.55	11.42*3	6.74	2.05	1.43	8.18	8.79*3	2.58
Conversion efficiency*1	%	1.4	6.4	13.4	7.7	1.4	1.1	10.0	10.1	3.2
Composition of liquid reaction products*2										
Cyclohexyl cyanide	%	5.0	3.4	0	3.1	1.0	—	4.0	2.1	—
Bicyclohexyl	%	30.5	23.4	0	22.2	2.4	2.1	64.4	23.4	28.3
Cyclohexene	%	51.0	36.4	0.2	34.0	88.8	92.3	13.8	14.7	41.5
3-Cyclohexylcyclohexene	%	T	0.9	0	0.8	0	0	T	1.7	0
Methylcyclohexane	%	2.1	1.6	0	2.0	2.0	1.4	2.4	2.2	7.8
Ethylcyclohexane	%	3.8	2.9	0	3.2	2.9	2.1	3.2	2.3	8.5
Methylenecyclohexane	%	T	T	0	T	0	0	T	T	T
Methylcyclopentane	%	T	T	0	T	T	T	T	T	T
n-Hexane	%	T	T	0	T	T	T	T	T	T
1-Hexene	%	T	T	0	T	T	T	T	T	T
n-Pentane	%	T	T	0	T	T	T	T	T	T
Unidentified product	%	7.6*4	31.4*4	99.8*4	34.7*4	2.9	2.1	12.2*4	53.6*4	13.9*4

*1 The conversion efficiency was given by (grams of reaction product per grams of cyclohexane used)×100.
*2 The yields of each compound produced were given by (grams of each compound per grams of total reaction product)×100.
*3 The reaction product consisted mostly of a brown solid.
*4 The unidentified product contained a brown solid.
T Trace

the ozonizer is kept "warm." Further, the liquid product obtained at a high-temperature discharge absorbed oxygen from the air quite readily and it was polymerized upon standing at room temperature. When materials were passed through at a high flow rate in the discharge tube, only a very small quantity of a solid was deposited.

The Reaction between Cyclohexane and Hydrogen Cyanide by Using the Bubbling Method. In the passing method, the solid brown deposit was alway formed on the glass wall; this seems to be the main reason for the decrease in the conversion of cyclohexane to cyclohexyl cyanide. Therefore, the glass wall of the discharge tube was covered with liquid cyclohexane and a gas mixture of hydrogen cyanide and helium was bubbled at a constant rate of flow into the liquid cyclohexane. A spiral glass stick was inserted in order to extend the residence time of the hydrogen cyanide vapor. In this case, a small amount of cyclohexyl cyanide was obtained, while little or no solid was formed.

Influence of the Discharge Temperatures on the Reaction between Cyclohexane and Hydrogen Cyanide by Using the Refluxing Method. As may be seen from Experiment Nos. 7 and 8 in Table 2, when the refluxing method

was used the yield of solid product increased with the rise in the discharge temperature. Thus, it may be said that a low temperature favors the formation of cyclohexyl cyanide.

There are differences between the refluxing method and the passing method. For instance, in the refluxing method, when the discharge was carried out at a low temperature, the maximum yield of cyclohexyl cyanide was obtained.

From the facts described above, the important variables may be said to be the voltage and the temperature of discharge, the residence time in the discharge tube, and the structual characteristics of the apparatus. By controlling these variables, the yield and the composition of the reaction product can be controlled to some extent.

The Mechanism of the Formation of Cyclohexyl Cyanide. It has been reported by Egloff *et al.*[8] that there are essential differences between thermal activation and electronic activation: In thermal activation energy must be put into the entire aggregation of molecules, but in electronic activation the electron collides with the electron which forms a part of the chemical bond. Devins and Burton[9] found that, in the decomposition of ammonia in an electric discharge at a pressure of 0.6 to 11mm, hydrazine and nitrogen (as well as hydrogen) were produced. In this reaction, they reported that, relative to the number of chemically important excited entities, the number of ionized molecules was very low. The formation of cyclohexyl cyanide by the reaction of cyclohexane with hydrogen cyanide in a silent discharge may be described as follows. The most striking characteristic of the action of the silent discharge on a mixture of cyclohexane and hydrogen cyanide seems to be the attack of the electron on the C–H linkage of cyclohexane and hydrogen cyanide molecules; that is to say, the electron collides with these materials and the activated molecules thus formed change into a cyclohexyl radical and a cyano radical. Cyclohexyl cyanide may be formed by a combination of these radicals. In addition, when cyclohexane alone was passed through the discharge tube, as is shown in Experiment No. 9 of Table 1, bicyclohexyl was obtained in poor yields. Accordingly, a part of the cyclohexyl radical seems to be formed by hydrogen abstraction from cyclohexane with a cyano-radical.

It is assumed that the cyclohexyl radical is the major active particle formed in this discharge; the formations of cyclohexyl cyanide, bicyclohexyl, methylcyclohexane, and ethylcyclohexane seem to be due to the greater stability of this radical.

The Reaction Occurring in the Silent Discharge. Although the reaction between cyclohexane and hydrogen cyanide in an ozonizer is somewhat complicated by secondary reactions, the principal reactions seem to be as follows: (1) The formation of radicals to give cyclohexyl cyanide and bicyclohexyl. (2) The dehydrogenation of a portion of the cyclohexane to produce cyclohexene. (3) Decomposition to give methane, ethane, ethylene, acetylene, *etc.* (4) Polymerization to give a brown solid. (5) Isomerization to give methylcyclopentane and 1-hexene. Lind and Schultze[10] found that, when *n*-butane was treated in an ozonizer, isobutane was formed in the reaction products. In the present research, isomerization seems to occur. Further, a secondary reaction gave alicyclic hydrocarbons with a side chain, such as methylcyclohexane, ethylcyclohexane, and methylenecyclohexane. From the retention time of its gas chromatogram, vinylcyclohexane seems to be present in the unidentified products listed in Table 2.

Compared with olefines*6 (ethylene and propylene), cyclohexane is less reactive and therefore requires a more intense discharge to make it react at a usable rate. The reaction of cyclohexane alone in the silent discharge resembles the reaction by irradiation with ^{60}Co γ-rays.[6]

It is of interest that cyclohexyl cyanide can be prepared in one step from cyclohexane and hydrogen cyanide using the silent discharge at a low temperature.

8) C. L. Thomas, G. Egloff and J. C. Morell, *Chem. Revs.*, **28**, 1 (1941).

9) J. C. Devins and M. Burton, *J. Am. Chem. Soc.*, **76**, 2618 (1954).

10) S. C. Lind and G. R. Schultze, *J. Phys. Chem.*, **42**, 547 (1938).

*6 Presented at the 19th Annual Meeting of the Chemical Society of Japan, Yokohama, April, 1966.

BULLETIN OF THE CHEMICAL SOCIETY OF JAPAN VOL. 41 1381—1385 (1968)

Studies on Cow's Urine. IV.[1] Determination by Gas-liquid Chromatography of an Acidic Part Obtained from Cow's Urine*[1]

Rikisaku SUEMITSU, Shin-ichi FUJITA, Yasuo MISHIMA and Mitsuo YOSHIMURA

Department of Applied Chemistry, Faculty of Engineering, Doshisha University, Kamikyo-ku, Kyoto

(Received November 15, 1967)

An acidic part obtained from cow's urine was examined by gas-liquid chromatography. As the major components of the acidic part, benzoic acid, phenylacetic acid, β-phenylpropionic acid, and derivatives in which hydroxyl or methoxyl groups are attached to, respectively, *para*-, *ortho*-, and 3,4-positions of the aromatic ring were identified. It is conceivable that these compounds were mainly metabolic products of the phenylalanine, tyrosine, and 3,4-dihydroxyphenylalanine (DOPA). Moreover, a new metabolic pathway of phenylalanine and its derivatives was tentatively represented.

Urine contains a vast number of substances as intermediates and end-products in the metabolic pathways of both endogenous and exogenous compounds. Many of these compounds are of great interest in the metabolism of amino acids.

In previous papers,[1,2] the phenolic part obtained from Holstein urine has been examined. In this paper, an acidic part from the urine of Nihon-ushi (*Bos taurus* Linneaus) will be examined by gas-liquid chromatography.

Experimental

The gas-liquid chromatography were performed on a Yanagimoto type GCG-3 Gas Chromatograph, equipped with a thermal-conductivity detector. Column; Silicone SE-30 (25%) on 80—100 mesh Celite 545, 2 m×5

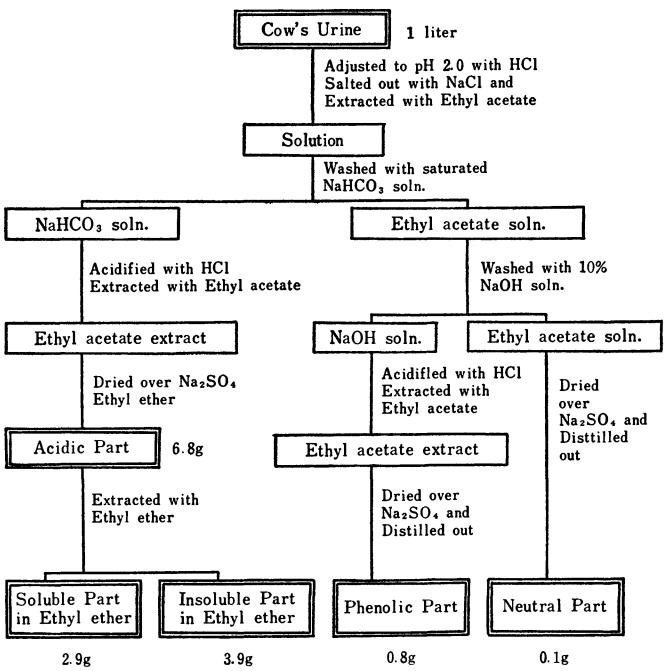

Fig. 1. Extraction process of the acidic, phenolic, and neutral parts obtained from cow's urine.

*1 Presented at the 20th Annual Meeting of the Chemical Society of Japan, Tokyo, April, 1967.

1) Part III. R. Suemitsu, S. Fujita and H. Matsubara, *Agr. Biol. Chem.*, **29**, 908 (1965).

2) R. Suemitsu and M. Hiura, *Nippon Nogei-kagaku Kaishi (J. Agr. Chem. Soc. Japan)*, **27**, 825 (1953).

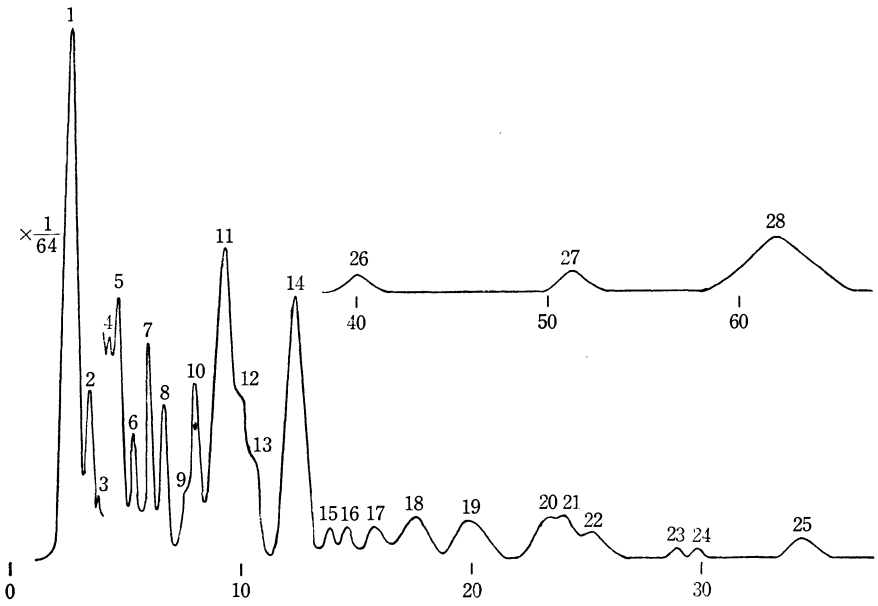

Fig. 2. Gas chromatogram of the methylesters of urinary acids (Method 1).

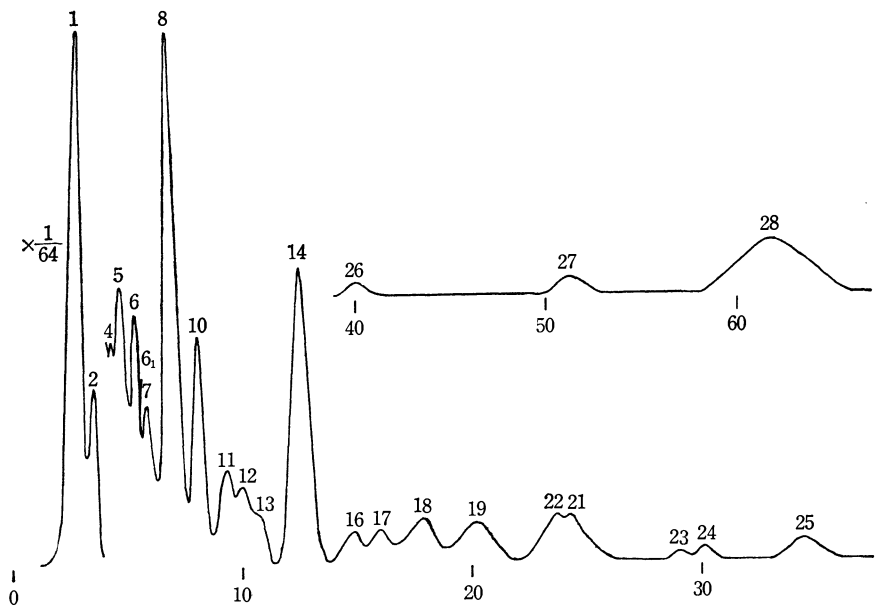

Fig. 3. Gas chromatogram of the methylesters of urinary acids (Method 2).

mmϕ: temperature 170°C; flow rate of hydrogen, 80 ml/min. The retention times were measured from the time of the injection to the initial emergence of the peaks.

Extraction of Urinary Compounds. Sodium chloride (200 g) was added to one liter of the fresh urine (pH 8.6) of a Nihon-ushi, and the pH was adjusted to 2.0 with 10% hydrochloric acid. The urine was extracted three times with 100 ml portions of ethyl acetate, and the extracts, containing acids, phenols, and neutral compounds, were washed three times with 100 ml portions of a saturated sodium bicarbonate solution. The sodium bicarbonate solution was then acidified with 10% hydrochloric acid and extracted with ethyl acetate. After drying over anhydrous sodium sulfate, the solution was evaporated to a brown solid with acidic compounds (6.8 g), which was then separated into an ethyl ether - soluble part (2.9 g) and

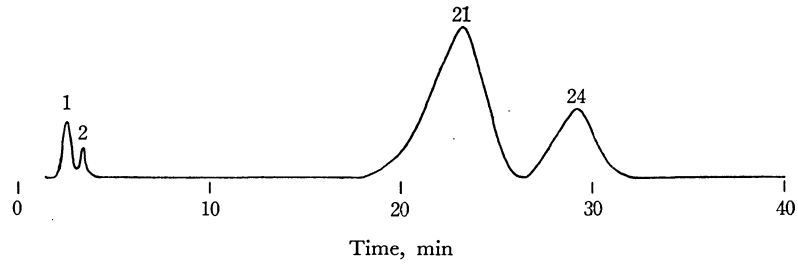

Fig. 4. Gas chromatogram of the methylesters of acidic part insoluble in ethyl ether.

an insoluble part (3.9 g). The fractionation of acidic, phenolic, and neutral part is shown in Fig. 1.

Determination of the Acidic Part Soluble in Ethyl Ether. The methylation of urinary carboxylic acids was carried out according to the following two methods: (1) The acidic part was refluxed with methanol in the presence of concentrated sulfulic acid, and (2) the acidic part was treated with ethereal diazomethane and methanol by the ordinary method. Both carboxylic groups and hydroxyl groups were also methylated by the latter method. Gas chromatograms of methylesters of the acidic part soluble in ethyl ether are presented in Fig. 2 (method 1) and Fig. 3 (method 2) respectively. The quantitative determination was carried out by measuring the peaks of Fig. 2 (triangulation method). When the peaks of Fig. 3 were compared with those of Fig. 2, it was found that there were clear differences between them. As is shown in Fig. 3, the 3, 9, 11, 13, 15, and 22 peaks decreased in area, while the 6, 6_1, 8, 10, 14, and 23 peaks increased; on the other hand, the 1, 2, 4, 5, 7, 12, 16, 17, 18, 19, 20, 21, 24, 25, 26, 27, and 28 peaks gave the same areas. These facts show that decreases in the areas in peaks are due to the presence of hydroxyl groups in urinary carboxylic acids.

The components were identified by comparing their retention times with those of authentic samples under the same conditions. The components of the acidic part obtained from cow's urine are shown in Table 1.

Determination of the Acidic Part Insoluble in Ethyl Ether. A gas chromatogram of the methyl esters of urinary acids insoluble in ethyl ether is shown in Fig. 4. The acidic part insoluble in ethyl ether was recrystallized from water, resulting in colorless needles with a mp of 186°C, and its infrared spectrum was perfectly identical with that of hippuric acid. Then the 21 peak was proved to be hippuric acid by comparing its gas chromatogram with that of an authentic sample.

On the hydrolysis of the same acidic part with 10% sodium hydroxide, followed by the identification of the components of the hydrolyzed products by the gas-liquid chromatographic method, benzoic acid and phenylacetic acid were proved to be the components. On the other hand, only glycine was proved to be present in the amino acid part by paper chromatography. Consequently, the 24 peak may be said to be due to phenacetyl glycine, which was proved to be another component of the acidic part.

Determination of the Phenolic Part Obtained from Cow's Urine. The determination of the phenolic part was carried out by means of a method previously reported.[1] The gas chromatogram and the components of the phenolic part are shown in Fig. 5 and Table 2 respectively.

Table 1. The components of acidic part obtained from cow's urine

Peak No.	Rt.	Component	%
1	2.1	Benzoic acid	68.4
2	2.8	Phenylacetic acid	17.4
3	3.2	*o*-Hydroxybenzoic acid	1.75
4	3.5	Unidentified	trace
5	3.8	*β*-Phenylpropionic acid	0.7
6	4.6	*o*-Methoxybenzoic acid	0.35
7	5.2	Unidentified	0.65
8	5.8	*p*-Methoxybenzoic acid	0.4
9	6.9	*m*-Hydroxybenzoic acid	trace
10	7.2	*p*-Methoxyphenylacetic acid	0.45
11	7.9	*p*-Hydroxybenzoic acid	3.5
12	8.6	Unidentified	trace
13	9.2	*p*-Hydroxyphenylacetic acid	0.95
14	11.0	*p*-Methoxyphenylpropionic acid	1.95
15	12.9	*p*-Hydroxyphenylpropionic acid	0.2
16	13.1	3,4-Dimethoxybenzoic acid	0.2
17	14.9	3,4-Dimethoxyphenylacetic acid	0.2
18	16.6	Unidentified	0.4
19	18.5	Unidentified	0.35
20	21.7	3,4-Dimethoxyphenylpropionic acid	0.55
21	22.5	Hippuric acid	trace
22	23.5	*o*-Hydroxyphenylpropionic acid	0.2
23	27.4	*o*-Methoxyphenylpropionic acid	trace
24	27.7	Phenacetylglycine	trace
25	32.4	Unidentified	0.15
26	38.7	3-Indoleacetic acid (?)	0.1
27	48.5	*β*-3-Indolepropionic acid (?)	0.15
28	57.6	Unidentified	0.95

Table 2. The components of phenolic part obtained from cow's urine

Peak No.	Rt.	Component	%
1	2.6	Guaiacol	0.9
2	4.0	Phenol	7.7
3	5.3	*p*-Cresol	85.2
4	8.4	*p*-Ethylphenol	1.4
5	12.9	Unidentified	4.8

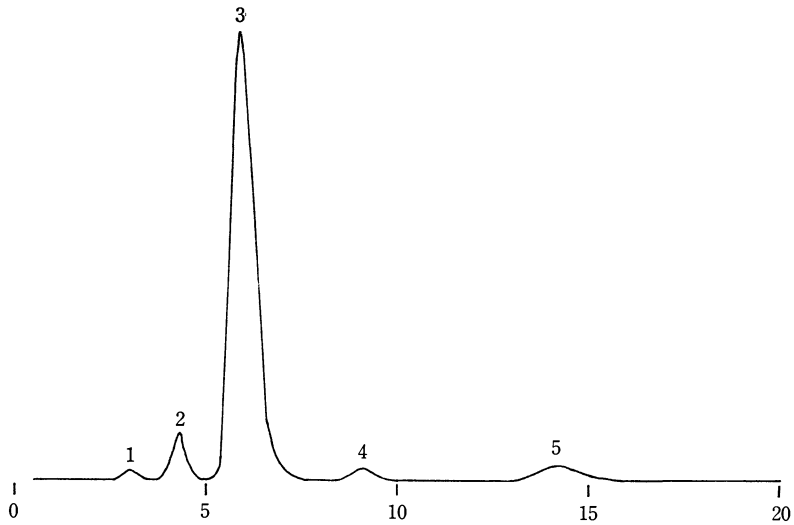

Fig. 5. Gas chromatogram of the phenolic part obtained from cow's urine. 2,4-Xylenyl phosphate (5%) 3 m×5 mmϕ, 165°C, 80 ml/min H_2.

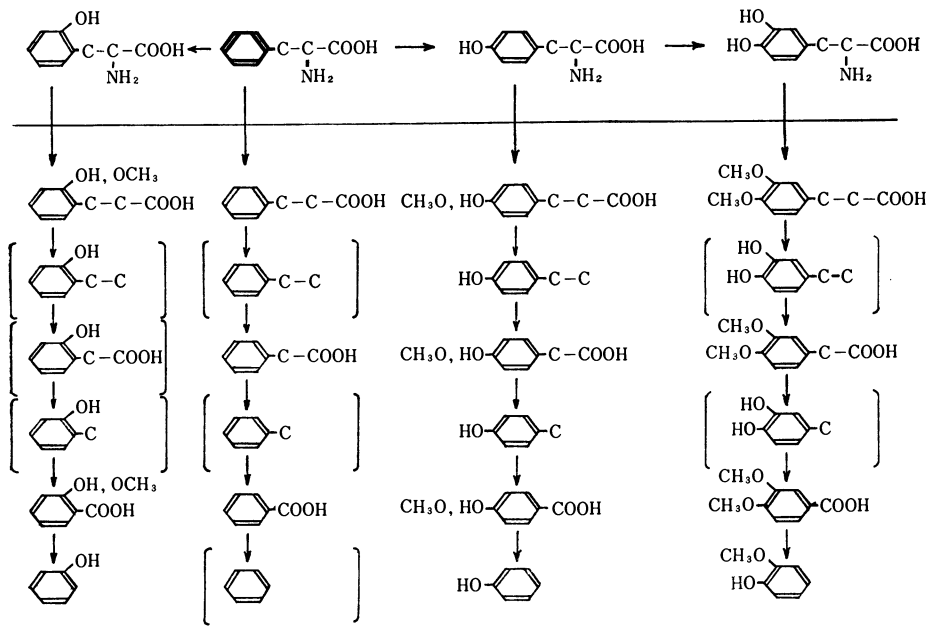

Fig. 6. Mode of formation of the metabolic products of phenylalanine.

Discussion

The following compounds were found in the acidic and phenolic parts of the cow's urine. The acidic components were benzoic acid, phenylacetic acid, β-phenylpropionic acid, *o*-hydroxybenzoic acid, *o*-methoxybenzoic acid, *p*-methoxybenzoic acid, *m*-methoxybenzoic acid, *p*-methoxyphenylacetic acid, *p*-hydroxybenzoic acid, *p*-hydroxyphenylacetic acid, *p*-methoxyphenylpropionic acid, *p*-hydroxyphenylpropionic acid, 3,4-dimethoxybenzoic acid, 3,4-dimethoxyphenylacetic acid, 3,4-dimethoxyphenylpropionic acid, *o*-hydroxyphenylpropionic acid, *o*-methoxyphenylpropionic acid, 3-indoleacetic acid (?), β-3-indolepropionic acid (?), hippuric acid, and phenacetyl glycine. As the phenolic components, we found phenol, guaiacol, *p*-cresol and *p*-ethylphenol.

It is well known that phenylalanine is easily converted to tyrosine, which is then further oxidized to 3,4-dihydroxy phenylalanine (DOPA); on the other hand, a part of the phenylalanine is

converted to *o*-hydroxyphenylalanine (*o*-tyrosine) *in vivo*.[3] It has also been reported that phenylalanine is converted metabolically to phenylacetic acid through phenylpyruvic acid.[4] However, the presence of the acidic and phenolic components mentioned above suggests the new metabolic pathways of phenylalanine, tyrosine, DOPA, and *o*-tyrosine shown in Fig. 6. As the pathways show, amino groups of the aromatic amino acids are deaminated to the corresponding phenylpropionic acids, which are then further converted to benzene or phenols by decarboxylation and ω-oxidation. Parentheses show the components which were not detected in this experiment, but which are very probably present. We are now trying to verify these routes; we will report on our studies in the near future.

The authors are grateful to Dr. R. Kawashima of Kyoto University for supplying the cow's urine. They wish also to thank Dr. K. A. Watanabe of the Sloan-Kettering Institute for his helpful suggestions regarding the preparation of this report.

3) M. D. Armstrong and K. N. F. Shaw, *J. Biol. Chem.*, **213**, 805 (1955).
4) A. Meister, "Biochemistry of The Amino Acids," Academic Press, New York (1957), p. 354.

BULLETIN OF THE CHEMICAL SOCIETY OF JAPAN VOL. 41 1385—1387 (1968)

Total Synthesis of Nepseudin*[1]

Kenji FUKUI and Mitsuru NAKAYAMA

Department of Chemistry, Faculty of Science, Hiroshima University, Higashi Sendamachi, Hiroshima

(Received December 1, 1967)

The Hoesch reaction of 6-hydroxy-2,3-dihydrobenzo[b]furan with 2,3,4-trimethoxyphenylacetonitrile yielded 6-hydroxy-5-(2,3,4-trimethoxyphenylacetyl)-2,3-dihydrobenzo[b]furan. The cyclization of the dihydrobenzofuran with ethyl orthoformate-pyridine-piperidine gave dihydrodehydronepseudin, an isoflavone. The dehydrogenation of the above isoflavone with N.B.S. or Pd-C yielded dehydronepseudin. Nepseudin was derived by the reduction of dehydronepseudin with sodium borohydride and by subsequent oxidation with the chromium trioxide-pyridine complex.

Nepseudin was isolated as colorless needles, along with neotenone, dolineone and pachyrrhizin, from the roots of *Neorautanenia pseudopachyrrhiza (Leguminosae)* by Crombie and Whiting.[1] On the basis of degradation experiments and spectral examinations, its structure was shown to be furano-(3'',2'' : 6,7)-2',3',4'-trimethoxyisoflavanone (I), which is very similar to that of neotenone (II).[1] However, the oxygenation pattern, 2',3',4', instead of the usual 2',4',5', is unique in the A ring of the isoflavonoid and rotenoid series. On dehydrogenation with manganese dioxide, I has been converted[1] into dehydronepseudin (III), a furanoisoflavone. In a previous paper,[2] the authors reported the synthesis of 7-hydroxy-2',3',4'-tritrimethoxyisoflavone (IV), which has the same oxygenation pattern as I and III. The present paper will describe the total synthesis of I *via* III, thus confirming the proposed structure.

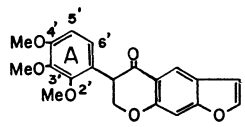

I

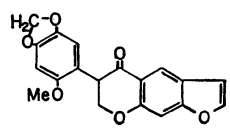

II

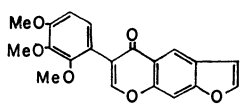

III

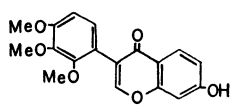

IV

The Hoesch reaction of 6-hydroxy-2,3-dihydrobenzo[b]furan (V)[3] with 2,3,4-trimethoxyphenylacetonitrile (VI)[2] yielded 6-hydroxy-5-(2,3,4-trimethoxyphenylacetyl)-2,3-dihydrobenzo[b]furan

*1 Parts of this work have been briefly communicated: K. Fukui and M. Nakayama, *Experientia*, **19**, 621 (1963); *Chem. Ind. (London)*, **1963**, 1843.

1) L. Crombie and D. A. Whiting, *Tetrahedron Letters*, **1962**, 801; *Chem. Ind. (London)*, **1962**, 1946; *J. Chem. Soc.*, **1963**, 1569.

2) K. Fukui, M. Nakayama and N. Eto, *Nippon Kagaku Zasshi (J. Chem. Soc. Japan, Pure Chem. Sect.)*, **84**, 752 (1963).

3) J. S. H. Davies, P. A. McCrea, W. L. Norris and G. R. Ramage, *J. Chem. Soc.*, **1950**, 3206.

(VII) (mp 129—130°C). The cyclization of dihydrobenzofuran VII with ethyl orthoformate-pyridine-piperidine gave dihydrodehydronepseudin (VIII) (mp 143—144°C). By dehydrogenation either with *N*-bromosuccinimide in carbon tetrachloride or with 10% palladium on a carbon catalyst in diphenyl ether, the dihydrocompound VIII was converted into dehydronepseudin (III) (mp 164—165°C). III was identical with the isoflavone obtained from natural nepseudin by Crombie and Whiting.[1] On alkaline hydrolysis, III gave 6-hydroxy-5-(2,3,4-trimethoxyphenylacetyl)benzo[b]-furan (IX) (mp 118°C). III was resynthesized from IX with ethyl orthoformate-pyridine-piperidine. The isoflavone III, when reduced with sodium borohydride, gave furano-(3'',2'' : 6,7)-2',3',4'-trimethoxyisoflavan-4-ol (X) (mp 161—

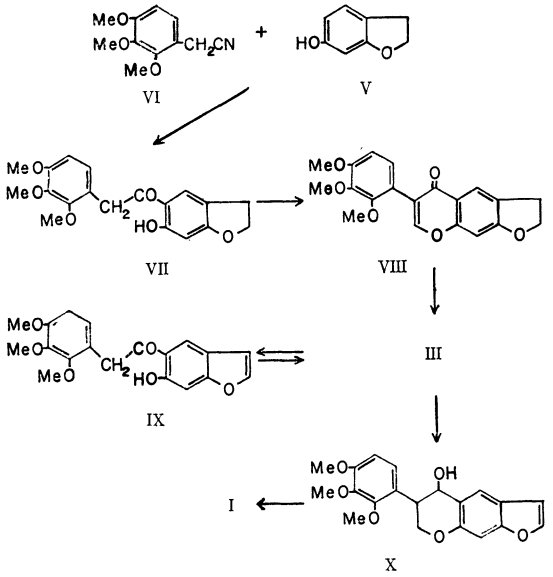

162°C), presumably a product of 1,4-addition to the γ-pyrone system, followed by further reduction.[1,4]

On oxidation with the chromium trioxide-pyridine complex, isoflavanol X gave the desired isoflavanone I (mp 114—115°C); its identity

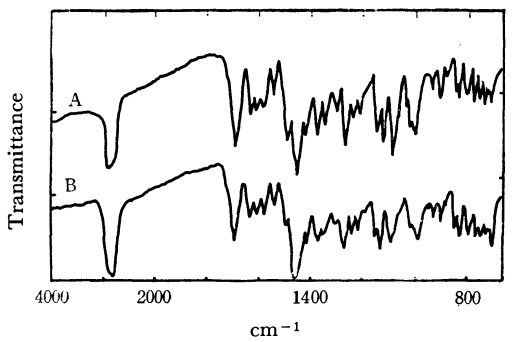

Fig. 1. IR spectra of synthetic (A) and natural (B) nepseudin in Nujol.

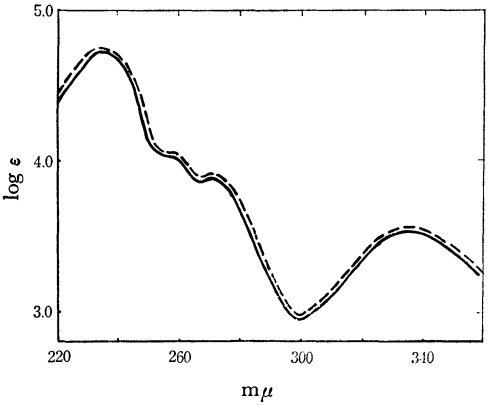

Fig. 2. UV spectra of synthetic (——) and natural (----) nepseudin in ethanol.

with natural nepseudin was confirmed by mixed-melting-point, infrared, and ultraviolet spectral comparisons (Figs. 1 and 2).

Experimental*2

6-Hydroxy-5-(2,3,4-trimethoxyphenylacetyl)-2,3-dihydrobenzo[b]furan (VII). A mixture of 6-hydroxy-2,3-dihydrobenzo[b]furan (V)[3] (5.0 g), 2,3,4-trimethoxyphenylacetonitrile (VI)[2] (5.0 g), and fused zinc chloride (4.0 g) in dry ether (150 m*l*) was saturated with dried hydrogen chloride for 4 hr at 0°C and then allowed to stand 2 days. The ethereal solution was decanted from the ketimine hydrochloride which had separated. The residue was washed twice with dry ether, and then heated on a steam bath with water (100 m*l*) for an hour. The resulting precipitates were collected and recrystallized from ethanol to give VII as colorless needles, mp 129—130°C, which gave a dark-brown ferric chloride reaction in ethanol; yield, 4.6 g (55%). IR: 1637 (C=O) cm^{-1}. UV: λ_{max} mμ (log ε); 281 (4.11), 330 (4.02).

Found: C, 66.37; H, 5.99%. Calcd for $C_{19}H_{20}O_6$: C, 66.27; H, 5.85%.

Dihydrodehydronepseudin (4'',5''-Dihydrofurano(3'',2'' : 6,7)-2',3',4'-trimethoxyisoflavone) (VIII). To a solution of VII (1.8 g) and ethyl orthoformate (8 m*l*) in pyridine (30 m*l*), piperidine (2 m*l*) was added; the mixture was then refluxed for 24 hr. The cooled reaction mixture was poured into ice-cooled dilute hydrochloric acid, and the resulting precipitates were colected. After being washed with water, the residue was recrystallized from ethanol to give VIII as colorless needles, mp 143—144°C; yield, 1.4 g (76%). IR: 1628 (γ-pyrone) cm^{-1}. UV: λ_{max} mμ (log ε); 240.5 (4.42), 310 (4.11).

Found: C, 67.87; H, 5.22%. Calcd for $C_{20}H_{18}O_6$: C, 67.79; H, 5.12%.

4) M. Miyano and M. Matsui, *Chem. Ber.*, **91**, 2044 (1958); H. Suginome and T. Iwadare, This Bulletin, **39**, 1536 (1966); K. Fukui, M. Nakayama, T. Harano and H. Tsuge, The Chemistry of Natural Products, Symposium Papers, **10**, Tokyo (1966), p. 145.

*2 All melting points are uncorrected; the infrared spectra were measured in Nujol, while the ultraviolet spectra were measured in an ethanol solution.

Dehydronepseudin (Furano(3'',2'' : 6,7)-2',3',4'-trimethoxyisoflavone) (III). *a) N. B. S.* A mixture of VIII (1.0 g), *N*-bromosuccinimide (500 mg), and benzoyl peroxide (50 mg) in dry carbon tetrachloride (60 m*l*) was refluxed gently for an hour. The precipitates which separated on cooling were filtered off. The resulting filtrate was washed with a 5% sodium bisulfite solution and dried with anhydrous calcium chloride. The evaporation of the solvent under reduced pressure left a light yellow residue. After the addition of acetic acid (30 m*l*) and potassium acetate (5.0 g), the mixture was refluxed for an hour and then poured into water (300 m*l*). The resulting precipitates were collected and recrystallized from methanol to give III as colorless prisms, mp 164—165°C; yield, 550 mg (55%) (lit.[1] mp 158—160°C). IR: 1649 (γ-pyrone) cm^{-1} (lit.[1] 1647). UV: λ_{max} mμ (log ε); 244 (4.59), 324 (3.86) (lit.[1] λ_{max} mμ (log ε); 245 (4.64), 325 (3.92)).

Found: C, 67.96; H, 4.61%. Calcd for $C_{20}H_{16}O_6$: C, 68.18; H, 4.58%.

b) 10% *Pd-C.* A mixture of VIII (1.0 g), 10% palladium on a carbon catalyst (700 mg), and diphenyl ether (20 m*l*) was refluxed for 10 hr. The catalyst was then filtered off, and the solvent removed by steam distillation. The resulting precipitates were collected and recrystallized from methanol to give III (mp 164—165°C), which was identical with the above sample; yield, 740 mg (74%).

6-Hydroxy-5-(2,3,4-trimethoxyphenylacetyl)benzo[b]furan (IX). A mixture of III (300 mg), a 5% aqueous sodium hydroxide solution (15 m*l*), and ethanol (20 m*l*) was refluxed for 3 hr on a steam bath. After the solvent had been evaporated, the residue was extracted with ethyl acetate. The resulting precipitates were recrystallized from methanol to give IX as pale yellow plates, mp 118°C, which gave a dark-green ferric chloride reaction; yield, 200 mg (69%) (lit.[1] mp 118—119°C). IR: 1639 (C=O) cm^{-1} (lit.[1] 1645). UV: λ_{max} mμ (log ε); 236 (4.76), 258.5 (4.07), 272.5 (3.97), 345 (3.71); (lit.[1] 235 (4.66), 258 (4.00), 270 (3.86), 345 (3.60)).

Found: C, 66.69; H, 5.40%. Calcd for $C_{19}H_{18}O_6$: C, 66.66; H, 5.30%.

The Cyclization of IX to III. By a reaction similar to that used for VII, III was prepared from IX (70 mg), ethyl orthoformate (3 m*l*), pyridine (10 m*l*), and piperidine (5 drops). Recrystallization from methanol gave III (mp 163—164°C), which was identical with the above sample; yield, 50 mg (69%).

Furano(3'',2'' : 6,7)-2',3',4'-trimethoxyisoflavan-4-ol (X). III (400 mg) in tetrahydrofuran (30 m*l*) was treated at 60°C for 90 min with sodium borohydride (300 mg) in 70% aqueous ethanol (30 m*l*) containing potassium hydroxide (30 mg). The mixture was kept at 20°C for 30 min and then diluted with a saturated ammonium chloride solution and extracted with ether. After the solvent had been evaporated, the residue was recrystallized from methanol to give X as colorless prisms, mp 161—162°C; yield, 200 mg (50%). IR: 3400 (broad) (OH) cm^{-1}.

Found: C, 67.23; H, 5.47%. Calcd for $C_{20}H_{20}O_6$: C, 67.40; H, 5.66%.

Nepseudin (I). Chromium trioxide (300 mg) was added to dry pyridine (3 m*l*); the mixture was swirled until it turned to an orange paste, and then X (100 mg) was added. The mixture was allowed to stand overnight at room temperature. After the addition of water, the resulting mixture was extracted with ether. The ether layer was washed with dilute hydrochloric acid, water, and a dilute sodium hydroxide solution, and finally dried over anhydrous potassium carbonate. After the solvent had been evaporated, the residue was recrystallized from methanol to give I as colorless prisms, mp 114—115°C; yield, 300 mg (75%) (lit. mp 115—116°C[1]; mp 115°C*[3]). IR: 1688, 1630, 1603, 1581, 1544, 1502 cm^{-1} (lit. 1686, 1631, 1605, 1585, 1541, 1490[1]; 1688, 1630, 1602, 1580, 1544, 1500*[3] cm^{-1}). UV: λ_{max} mμ (log ε); 235 (4.73), 257_i*[4] (4.03), 272.5 (3.88), 336 (3.56) (lit. 235 (4.74), 257_i (4.08), 272 (3.94), 335 (3.61)[1]; 235 (4.78), 257_i (4.06), 272.5 (3.91), 336 (3.60)*[3]). It was found, by mixed-melting-point measurement and by infrared and ultraviolet spectral comparisons, to be identical with the natural nepseudin supplied by Crombie.

Found: C, 67.94; H, 5.41%. Calcd for $C_{20}H_{18}O_6$: C, 67.79; H, 5.12%.

The authors are grateful to Professor L. Crombie, King's College, University of London, for his gift of natural nepseudin. Grateful acknowledgement is also made to Professor Tetsuo Mitsui, Kyoto University, for his microanalyses. This work was supported by a grant-in-aid from the Ministry of Education.

*3 The natural nepseudin kindly supplied by Professor Crombie was measured in this laboratory.

*4 i=Inflection point.

BULLETIN OF THE CHEMICAL SOCIETY OF JAPAN VOL. 41 1388—1394 (1968)

The Thermal Decompositions and Mass Spectral Studies of the Cyclic Anhydrides of Some β-Sulfocarboxylic Acids

Katsuhiko NISHITOMI, Toshikazu NAGAI and Niichiro TOKURA

Department of Applied Chemistry, Faculty of Engineering, Osaka University, Suita, Osaka

(Received December 5, 1967)

The thermal decompositions of the cyclic anhydrides of β-sulfopivalic acid (III) and β-sulfoisobutyric acid (IV) have been studied. The pyrolysis of III without a solvent gave pivalic acid, isobutene, isobutane, water, and a mixture of trimers of isobutene, while the pyrolysis of IV resulted in the formation of methacrylic acid and acetone. In the case of III, the evolution of sulfur dioxide and carbon dioxide occurred mainly. On the contrary, in the case of IV, the carboxylic acid derivative was the predominant product. These results might be interpreted in terms of a decomposition mechanism in which the compound (IV) having α-hydrogen to a carbonyl group undergoes thermal decomposition *via* a concerted mechanism. In the case of IV, it should be noted that acetone was formed. This paper will also be concerned with the mass spectra of III and IV and with the cyclic anhydride of β-sulfopropionic acid.

In a previous paper,[1] we reported the formation and decomposition mechanisms of cyclic anhydride of β-sulfopropionic acid (I); we found that acrylic acid (II) was formed intramolecularly in a 30.2% yield, and that the evolution of carbon dioxide was not detected, when I was heated at 180°C without a solvent.

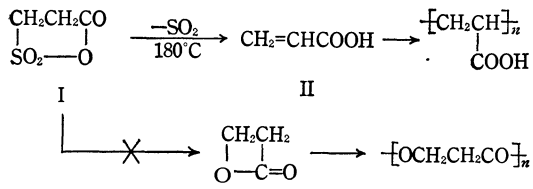

No such a sterically unfavorable, intramolecular 1,3 hydrogen shift to oxygen as is described above has yet been reported so far as we know, while the 1,5 hydrogen transfer to oxygen[2-4] and the 1,3 hydrogen shift to carbon[5-7] have been reported. Thus, it was inferred that such a cyclic anhydride as I, with α-hydrogens to a carbonyl group, should exhibit interesting behavior upon thermal decomposition. Moreover, there have not yet been any reports about the 1,3 methyl shifts to oxygen in pyrolyses of saturated hydrocarbon systems. Therefore, we have examined the behavior of compounds similar to I upon heating. In the present paper, we wish to report on the behavior in thermal decomposition of the cyclic anhydrides of β-sulfopivalic acid (III) and β-sulfoisobutyric acid (IV). In these two systems, no 1,3 methyl shifts to oxygen were observed, through hydrogen shifts did occur in the case of IV. It was also found that the reaction courses of the pyrolyses were considerably affected with presence of the α-hydrogen to the carbonyl group; a possible mechanisms for this will be presented.

We will then deal further with the mass spectra of these three cyclic anhydrides (I, III and IV) in connection with pyrolysis studies of them.

Results and Discussion

Thermal Decompositions. When cyclic anhydride of β-sulfopivalic acid (III) was heated at 230°C without a solvent, there were obtained pivalic acid (V, in a 1.4% yield*1), isobutene (VI, in a 17.7% yield), isobutane (VII, in a 20.0% yield), water (VIII, in a 69.0% yield), and some bad-smelling, dark yellow liquid (IX, in a 6.1% yield as isobutene trimer); at the same time, sulfur dioxide and carbon dioxide were evolved. The residue was a black and spongy material which was insoluble and non-melting.

The sulfur dioxide, isobutene, and isobutane were identified by comparing their retention times in vapor-phase chromatography with those of authentic samples. No *n*-butane or propylene was

1) T. Nagai, K. Nishitomi and N. Tokura, This Bulletin, **40**, 1183 (1967).
2) F. D. Greene, M. L. Savitz, H. H. Lau, F. D. Osterholtz, and W. N. Smith, *J. Am. Chem. Soc.*, **83**, 2196 (1961).
3) C. Walling and A. Padwa, *ibid.*, **83**, 2207 (1961).
4) M. Akhtar and D. H. R. Barton, *ibid.*, **83**, 2213 (1961).
5) J. A. Kerr and A. F. Trotman-Dickenson, *J. Chem. Soc.*, **1960**, 1602.
6) A. S. Gordon and J. R. McNesby, *J. Chem. Phys.*, **33**, 1882 (1960).
7) C. P. Quinn, *Trans. Faraday Soc.*, **59**, 2543 (1963).

*1 The yields described in this paper are in mole % based on the starting cyclic compounds used.

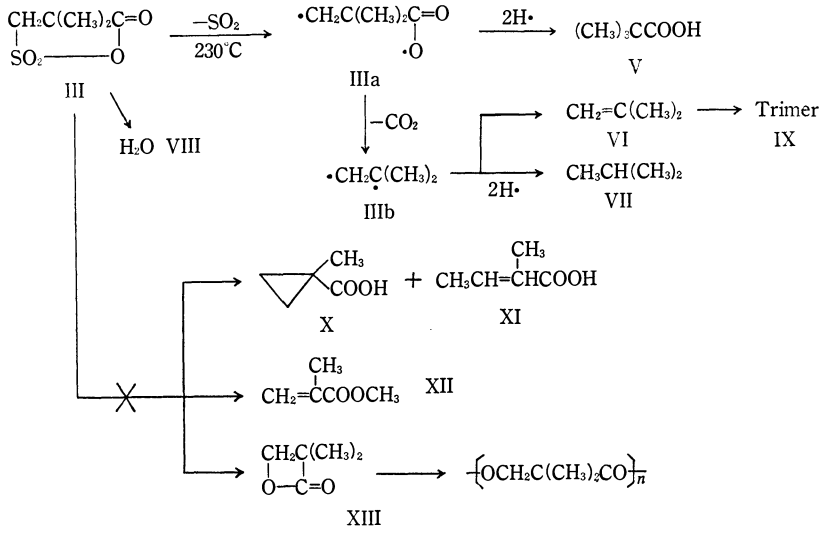

Scheme I

detected.

The pivalic acid (V) was identified by comparing its IR and NMR spectra with those of an authentic sample. The dark yellow liquid was confirmed to be a mixture of trimers of isobutene (IX) on the basis of the IR, UV, and NMR spectra, the boiling point, and chemical evidence. The IR spectrum showed absorptions at 2900 (methyl), 1365, 1380 (geminal dimethyl), and 800 cm^{-1}(C=C), among others. It also exhibited a moderate absorption at 1700 cm^{-1}, but this was not due to the carbonyl group, since authentic di-isobutylene showed a similar absorption at 1700 cm^{-1}. The NMR spectrum of IX showed multiplet peaks centered at τ 8.9, 7.9 and 3.4, the area ratio being 9 : 10 : 3. The UV spectrum of IX exhibited a very broad absorption at around 230 mμ ($\varepsilon = 3.0 \times 10^4$), with tailing up to 350 mμ. The multiplet at τ 3.4 and the broad absorption at near 230 mμ suggest the presence of a conjugated double bond in the IX molecule. The color of bromine in a carbon tetrachloride solution disappeared upon the addition of IX. The boiling point of IX was determined to be about 180°C. This boiling point coincided with that of the isobutene trimer which is obtainable from isobutene in the presence of sulfuric acid or by heating.[8] No further studies of the isomers or the structures of IX were carried out.

1-Methyl-1-carboxylcyclopropane (X) and its isomer, α-methylcrotonic acid (XI), were prepared by ordinary methods.[9] A comparison of their NMR spectra with that of the mixture of liquid products obtained in the present study showed that X and XI were not the products in the present case. Neither methyl methacrylate (XII), which should be formed if a 1,3 methyl shift to oxygen occurred, nor β-lactone (XIII), which might be obtained from IIIa, was detected in NMR analyses. From these results, it seems that the reaction products might be formed through a pathway such as that described in Scheme I. In this case, the fact that V and VII, which should be formed by intermolecular hydrogen abstraction, were obtained suggests that III undergoes thermal decomposition *via* a radical mechanism rather than *via* a concerted one.

Sulfur dioxide evolves first; the resulting diradical (IIIa) partly abstracts hydrogens intermolecularly to form V, and then mostly loses carbon dioxide to give another diradical (IIIb). Thus, IIIb, in one part, abstracts hydrogens intermolecularly to form VII and, in another part, converts to VI. Further, VI may be changed to IX. The formation of IX may be caused by heating under the experimental conditions or by the action of sulfuric acid, for the system evolves sulfur dioxide and water, and contains oxygen under an atmosphere. These results obviously indicate that no 1,4 hydrogen shift or 1,3 methyl shift occurs under these conditions. The formation of VIII should be noted, although the pathway to VIII is not clear.

Next, we examined the behavior of the cyclic anhydride of β-sulfoisobutyric acid (VI), with one α-hydrogen to a carbonyl group. When IV was heated at 220°C without a solvent, there were obtained methacrylic acid (XIV, in a 66.9% yield) and acetone (XV, in a 6.1% yield); at the same time sulfur dioxide and a small amount of carbon dioxide were evolved. In this case no gaseous compounds other than sulfur dioxide and carbon dioxide were detected by vapor-phase chromatography. The residue was a black and

8) S. W. Lebedew and G. G. Kobliansky, *Ber.*, **63**, 103 (1930).

9) S. Siegel and C. G. Bergstrom, *J. Am. Chem. Soc.*, **72**, 3815 (1950).

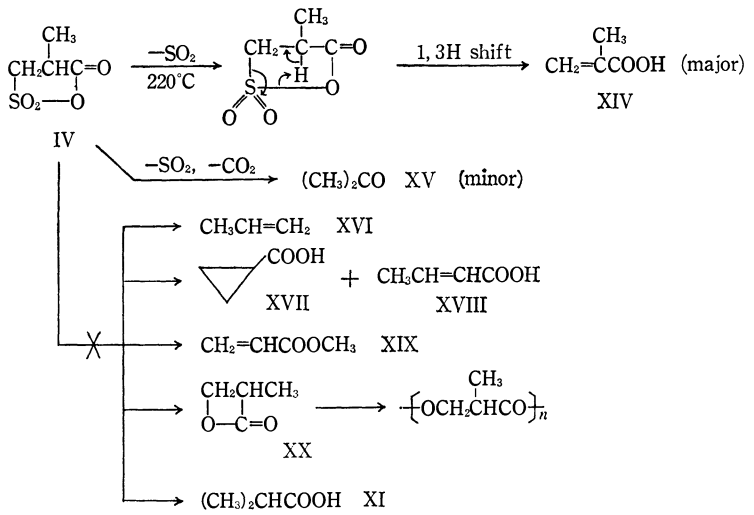

Scheme II

spongy material which was insoluble and non-melting.

Methacrylic acid (XIV) was identified by comparing its IR and NMR spectra with those of an authentic sample. Acetone (XV) was identified by comparing its NMR spectrum and the melting point of its 2,4-dinitrophenylhydrazone (mp 123.5—124°C) with those of an authentic sample. Propylene (XVI) was not detected by vapor-phase chromatography. There were none of the peaks at fields higher than 9.0 τ in the NMR spectrum which are characteristic of the methylene protons of 1-carboxylcyclopropane (XVII). Moreover, there were no peaks assignable to crotonic acid (XVIII), the isomer of XVII.[10] Neither methyl acrylate (XIX) nor β-lactone (XX) was detected in NMR analyses. Moreover, isobutyric acid (XXI), which should be formed by intermolecular hydrogen abstraction if the thermal decomposition proceeds, *via* such a radical mechanism as was observed in the case of III, was not detected in NMR analyses of the reaction mixture.

These results are presented in Scheme II. In this case, the fact that XXI, which should be formed by intermolecular hydrogen abstraction in a radical mechanism, was not obtained suggests that XIV is formed *via* a concerted mechanism rather than *via* a radical one. Moreover, no 1,4 hydrogen shift or 1,3 methyl shift occurred under these conditions, either.

It is very interesting that XV was formed in a 6.1% yield in this system, for the formation of XV involves the possibility of a 1,2 hydrogen shift in the thermal process, though there have hitherto been few examples of 1,2 hydrogen shifts in pyrolyses[11-15] (below 300°C). The fact that carbon dioxide was detected must be related to the formation of XV. In this case, it seems that XV is not formed *via* a free dimethylcarbene, for if this were the case, propylene (XVI) should be formed,[16] while XVI was not detected by vapor-phase chromatography. Also, it may be very difficult to consider the intermolecular hydrogen shift upon the formation of XV. Thus, Path B below may be more plausible than Path A, although the details of the process are obscure:

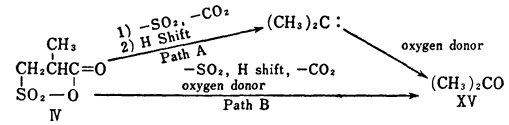

Sheme III

There exist two possibilities in this system as to the oxygen donor. One is atmospheric oxygen, and the other is sulfur dioxide. The former can be neglected from the fact that, in the experiment on the thermal decomposition of IV under a nitrogen stream, the yield of XV was essentially

10) Crotonic acid, $\begin{matrix} CH_3^a \\ \diagdown \\ H_b \end{matrix}\!\!>C=C<\!\!\begin{matrix} H^c \\ \diagup \\ COOH \end{matrix}$, exhibited peaks at τ 8.10 (a), 2.90 (b), and 4.17 (c), while methacrylic acid, $\begin{matrix} H^b \\ \diagdown \\ H_c \end{matrix}\!\!>C=C<\!\!\begin{matrix} CH_3^a \\ \diagup \\ COOH \end{matrix}$, showed peaks at τ 8.03 (a), 4.28 (b), and 3.70 (c).

11) D. Y. Curtin and M. J. Hurwitz, *J. Am. Chem. Soc.*, **74**, 5381 (1952).
12) M. S. Kharasch, F. L. Lambert and W. H. Urry, *J. Org. Chem.*, **10**, 298 (1945).
13) H. C. Brown and G. A. Russell, *J. Am. Chem. Soc.*, **74**, 3995 (1952).
14) L. H. Slaugh, *ibid.*, **81**, 2262 (1959).
15) N. Kornblum and H. E. De LaMare, *ibid.*, **74**, 3079 (1952).
16) W. Kirmse, "Carbene Chemistry," Academic Press, New York, N. Y. (1964), p. 47ff.

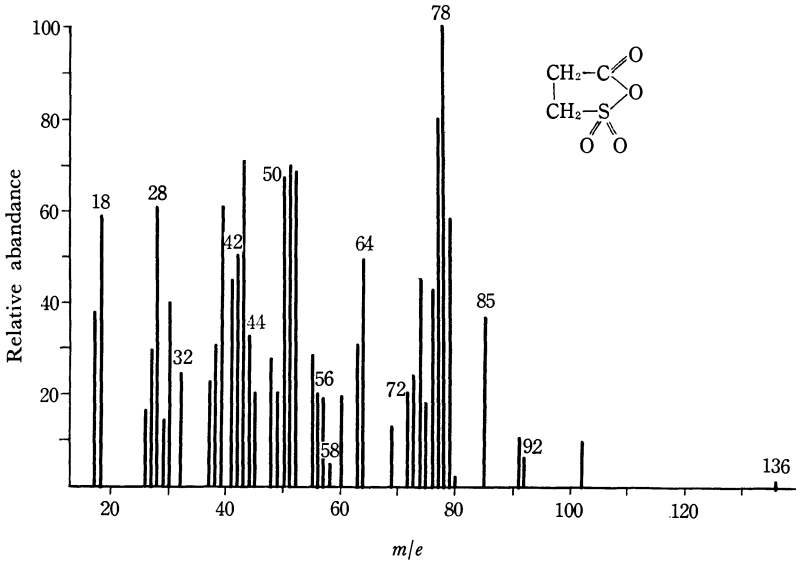

Fig. 1. Mass spectrum of cyclic anhydride of β-sulfopropionic acid (I). (Weaker peaks are omitted here.)

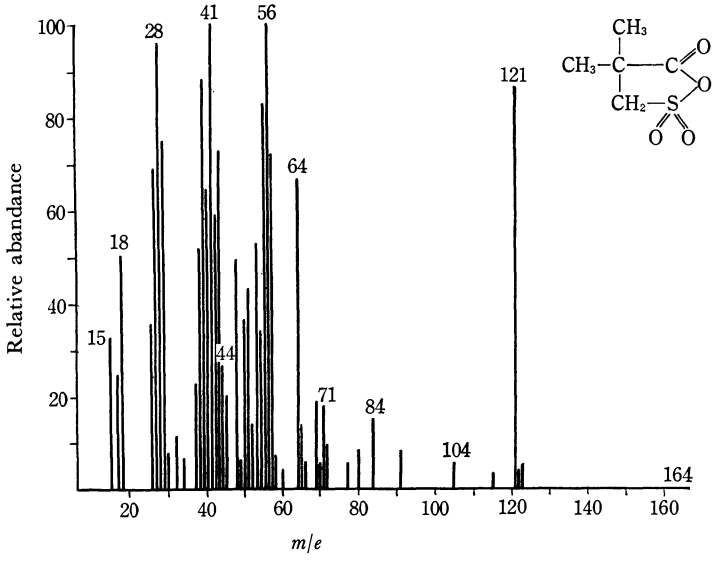

Fig. 2. Mass spectrum of cyclic anhydride of β-sulfopivalic acid (III). (Weaker peaks are omitted here.)

the same as that in the experiment under an atmosphere (see Experimental Section). Sulfur dioxide can be used as the source of oxygen at a high temperature,[17] so the oxygen donor to XXII seems to be sulfur dioxide.

Mass Spectral Studies. There have been no reports on mass spectral studies of such compounds as cyclic anhydrides of β-sulfocarboxylic acids (I, III and IV) except that by Meyerson *et al.*[18] about benzyne formation. In the present work, we are going to compare the behavior of the compounds under electron impact with those under thermal decomposition. The mass spectra of I, III, and IV are shown in Figs. 1, 2, and 3 respectively. They display different features, although the parent peaks are all very weak. The intense peak at *m/e* 78 in Fig. 1 may be assigned as $CH_2SO_2^+$. The other peaks may be understood

17) T. H. Strickland and A. Bell, *Ind. Eng. Chem.*, **53**, 7 (1961).
18) S. Meyerson and E. K. Fields, *Chem. Commun.*, **1966**, 275.

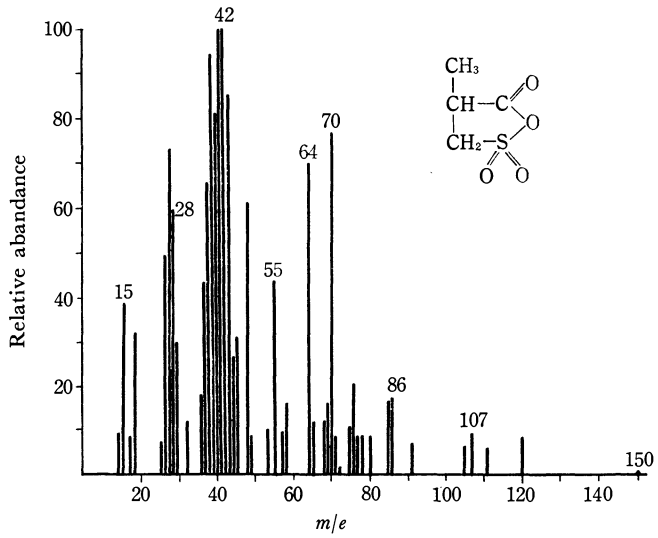

Fig. 3. Mass spectrum of cyclic anhydride of β-sulfoisobutyric acid (IV). (Weaker peaks are omitted here.)

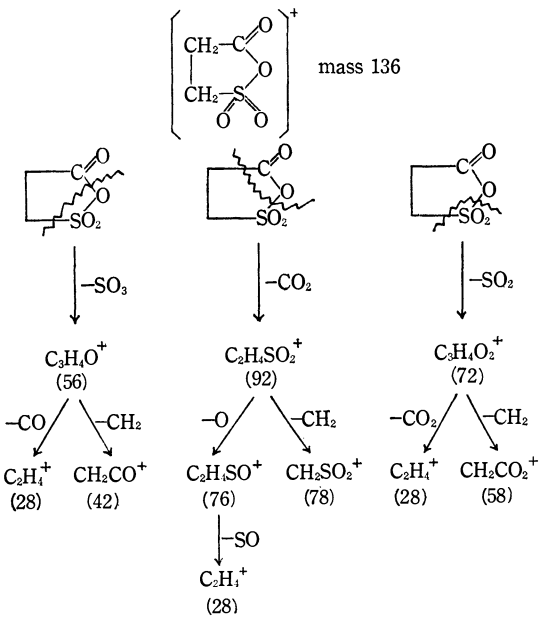

Scheme IV

in such a manner as in Scheme IV. The peak at *m/e* 28, which may be assigned to $C_2H_4^+$ (=I–SO_2–CO_2) and CO^+, is not so intense. This tendency is similar to that in thermal decomposition. The intense peaks at *m/e* 28, 41, 56 and 121 in Fig. 2 may be assigned to $C_2H_4^+$, $C_3H_5^+$, $C_4H_8^+$, and $C_4H_8SO_2^+ + 1$ (=III–CO_2+1) respectively. The other peaks may be understood in such a manner as in Scheme V. The intense peaks at *m/e* 28, 41, and 56 may correspond to olefins; this tendency is similar to that in thermal decomposition. The intense peaks at *m/e* 27, 42, and 70 in Fig. 3 may be assigned to $C_2H_3^+$, $C_3H_6^+$, and $C_4H_6^+$ (=IV–SO_3) respectively. The other peaks may be understood in such a manner as in Scheme VI. The intense peaks near *m/e* 42 may correspond to propylene or dimethylcarbene; this tendency is different from that in the thermal decomposition.

Experimental

Cyclic Anhydride of β-Sulfopivalic Acid (III). This was prepared by the photosulfonation of pivalic acid, which had been synthesized in the same manner as has been described in the literature,[19] with sulfuryl chloride in a manner similar to that described by Kharasch *et al.*[20] In this case, we added one or two drops of pyridine as a catalyst. The product was separated as a white solid. It was dried *in vacuo* in a desiccator containing phosphorus pentoxide and paraffin wax. The yield was about 17%. The melting point of this material (III) was 62—63°C (lit.[21,22] 62—64°C), which did not change upon crystallization from thionyl chloride. The NMR spectrum of III in water (10 wt%) showed two singlets at δ(ppm) 3.30 (β-methylene, 2H) and 1.40 (α-methyl, 6H), where water was used as the internal reference (its chemical shift relative to TMS was assumed to be δ=5.05 (ppm)).

Cyclic Anhydride of β-Sulfoisobutyric Acid (IV). This was prepared by the photosulfonation of isobutyric acid with sulfuryl chloride in the same manner as was described by Kharasch *et al.*[20] The boiling point of IV was 134—135°C/3 mmHg. The NMR spectrum

19) L. T. Sandborn and E. W. Bousquet, "Organic Syntheses," Coll. Vol. I, p. 526 (1948).
20) M. S. Kharasch, T. H. Chao and H. C. Brown, *J. Am. Chem. Soc.*, **62**, 2393 (1940).
21) J. L. Greene, Jr., and H. J. Hagemeyer, Jr., *ibid.*, **77**, 6065 (1955).
22) A. G. Schering, B. P. 1012325 (1965); *Chem. Abstr.*, **64**, 6503 (1966).

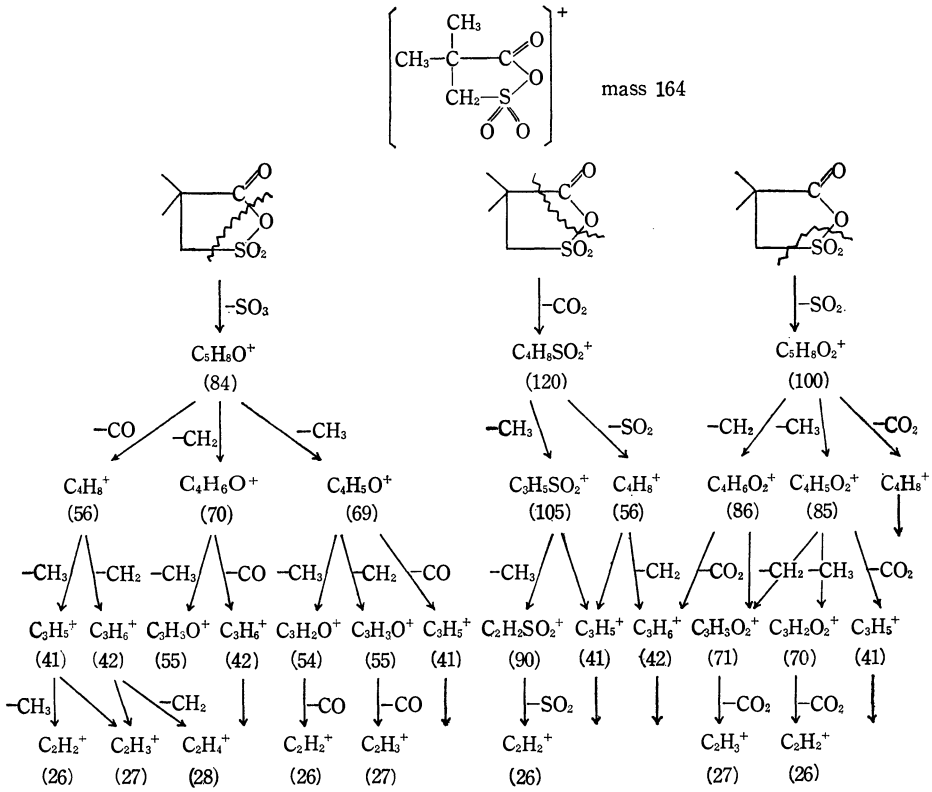

Scheme V

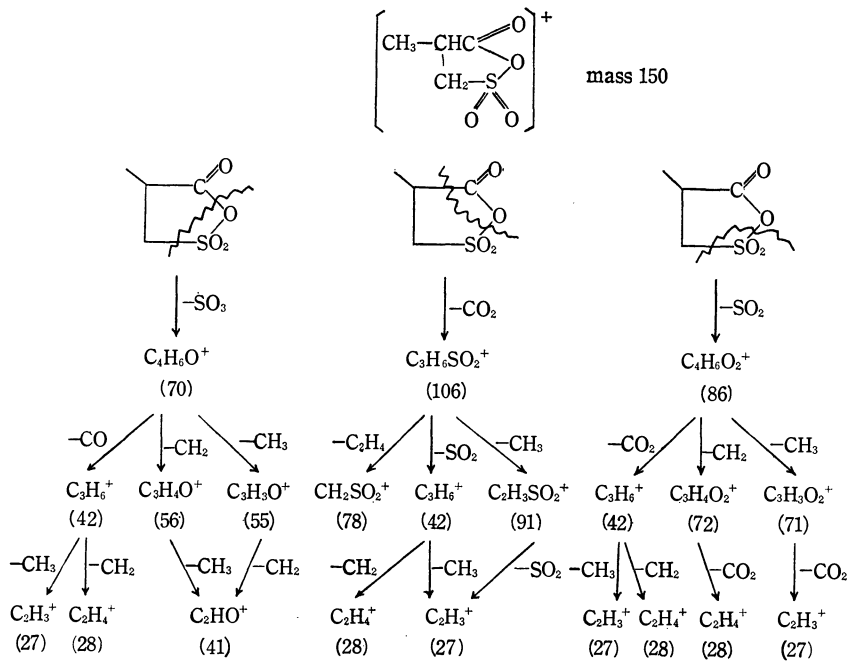

Scheme VI

of IV in water (11.76 wt%) showed a doublet at δ (ppm) 1.07 (α-methyl, 3H), and a doublet and a multiplet centered at δ 2.90 (β-methylene, 2H and α-methyne, 1H), where 1,4-dioxane was used as the internal reference (its chemical shift relative to TMS was assumed to be δ=3.57 (ppm)).

Thermal Decomposition of III. *A Typical Experiment.* In a 50 m*l*, round-bottomed flask fitted with an outlet tube leading to a cooler equipped with a receiving vessel and a calcium chloride tube, 10.6 g of III without a solvent were placed. The calcium chloride tube led to a trap dipped in dry ice and trichloroethylene bath equipped with a rubber tube. The trap further led to a 100 m*l* flask in which an aqueous calcium hydroxide solution was placed in order to remove carbon dioxide; the outlet gas was collected on the water. The round-bottomed flask was placed in an oil bath equipped with a thermometer, and heated gradually. When the temperature reached 65°C, the solid in the flask melted; upon further heating, to 220°C, sulfur dioxide gas evolved. The temperature was maintained at about 230°C for 3 hr, until the liquid in the flask changed to a black, spongy matter. During the heating, a mixture of a dark yellow liquid (IX) and a colorless liquid (VIII) was distilled out, and another mixture of sulfur dioxide and VI was trapped, while VII was collected on the water. Further calcium carbonate was also found to be deposited. The gaseous products were analysed by vapor-phase chromatography. As a result, VI and VII were identified by comparing their retention times with those of authentic samples. *n*-Butane and propylene were not detected.

The mixture of IX and VIII was treated as follows. It was mixed with anhydrous ether in a separate funnel, and the lower layer was removed. This lower layer was identified as water (0.802 g). The upper layer was further extracted with an alkali solution. The extract was acidified with hydrochloric acid and extracted with ether. The ether extract was dried over anhydrous sodium sulfate, and then the ether was distilled out. The resulting solid was identified as pivalic acid (V) by comparing its IR and NMR spectra with those of an authentic sample (0.124 g). The other ether extract, which was not extracted with the alkali solution, was dried over anhydrous sodium sulfate. Then the ether was distilled out. The resulting dark yellow liquid was confirmed to be isobutene trimer (0.591 g) by comparing its boiling point with that reported in the literature[8] and its IR spectrum with that of authentic di-isobutylene, and by considering the NMR spectrum and chemical evidence. The yield of VII was calculated from the volume of the collected gas by considering the dead volume. The yield of VII was 20.0%. The yield of VI was calculated from the weight of the mixture of sulfur dioxide and VI, and from their relative areas in vapor-phase chromatography. The yield of VI was 17.7%. The black, spongy residue was treated with anhydrous ether, and then the ether was distilled out from the ether extract. The resulting material was dissolved in chloroform, and the undissolved part was treated with aniline in a benzene solution. A white solid, which was supposed to be a monoaniline salt of β-sulfopivalic acid, was deposited, although it was only a trace. The dissolved part in chloroform was chromatographed over alumina. The resulting material (0.094 g) was identified as IX by its IR spectrum.

Thermal Decomposition of IV. *A Typical Experiment.* In a 50 m*l*, round-bottomed flask fitted with equipment in the same manner as has been described above in the case of III, 7.25 g of IV without a solvent were placed. The flask was placed in an oil bath equipped with a thermometer, and heated gradually. When the temperature reached 215—220°C, sulfur dioxide gas evolved. The temperature was maintained at about 220°C for 3 hr, by which time the liquid in the flask had changed to a black, spongy matter. During the heating, a colorless liquid (2.95 g) was distilled out. Most of it was identified as XIV by comparing its NMR and IR spectra with those of an authentic sample; the rest was identified as XV by comparing its NMR spectrum and the melting point of its 2,4-dinitrophenylhydrazone with those of an authentic sample. The yields of XIV and XV were caluclated from the total weight of the mixture and from their relative NMR areas. The yields were thus determined to be 66.9% (XIV) and 6.1% (XV). In this system no gaseous products except sulfur dioxide were detected by vapor-phase chromatography analyses. Calcium carbonate was also deposited, but its quantity was small. The black, spongy residue was treated in the same manner as has been described above in the case of III. The resulting liquid was identified as XIV (0.05 g) by means of its IR spectrum. In an experiment under a nitrogen stream, the yields of XIV and XV were 66.1% and 6.9% respectively.

IR Spectra. The infrared spectra were recorded on an EPI-S2-TYPE Hitachi spectrometer.

NMR Spectra. The proton resonance spectra were run on a Nihondenshi spectrometer at 60 Mc.

Vapor-phase Chromatography. Routine separations were carried out on a Yanagimoto Model GCS-100 gas chromatograph. A 3 m×0.25 in. stainless steel column packed with liquid paraffin (Column A) and a 4 m×0.25 in. stainless steel column packed with silicone hivac grease (Column B) were used. The column temperature was room temperature (31—33°C) for all fractions. Hydrogen (48 m*l*/min in Column A and 50 m*l*/min in Column B) was used as the carrier gas. The retention times in minutes were as follows: 1.4 (sulfur dioxide), 2.85 (VII), 3.45 (VI), 1.45 (propylene) and 3.75 (*n*-butane) in Column A; 3.0 (sulfur dioxide), 2.5 (VII), 3.15 (VI), 1.85 (propylene) and 3.2 (*n*-butane) in Column B.

Mass Spectra. The mass spectra were run on a VD-10001-A Hitachi spectrometer.

BULLETIN OF THE CHEMICAL SOCIETY OF JAPAN VOL. 41 1395—1400 (1968)

Reactions of Transition-Metal-Olefin Complexes. III. Kinetics of the Oxidation of Substituted Styrenes Catalyzed by Palladium Salts in an Aqueous Tetrahydrofuran Solution*[1]

Hiroyoshi OKADA, Takashi NOMA, Yoshihisa KATSUYAMA*[2] and Harukichi HASHIMOTO

Department of Synthetic Chemistry, The University of Tokyo, Hongo, Bunkyo-ku, Tokyo

(Received December 7, 1967)

The kinetics of the oxidation of ring-substituted styrenes catalyzed by palladium(II) salts in a homogeneous aqueous tetrahydrofuran solution containing *p*-benzoquinone have been investigated at 30°C under a nitrogen atmosphere. The rate equation was found to be identical with the one previously found for styrene, *i. e.*, $-d[olefin]/dt = (k_I+k_{II})[Pd^{2+}][olefin]$, where k_I is the rate constant for ketone-formation and k_{II} is the rate constant for aldehyde-formation. It was found that both the proton and the chloride ion affect the rate inhibition at high concentrations and the rate acceleration at low concentrations. The product ratio of the ketone to the aldehyde decreased monotonously with the increase in proton concentration and with the increase in chloride ion concentration. An increase in the ionic strength from 0.052 to 0.787 increased the rate constants, but the ratio of the products scarcely changed at all. The substituent effects for the sites of nucleophilic attack were specific; *i. e.*, the electron-releasing substituents facilitated the formation of substituted acetophenone and diminished the formation of substituted phenylacetaldehyde. The reverse trend was found for the electron-withdrawing substituents. From these results, there is proposed a mechanism in which two active species, $[ArCH{=}CH_2Pd(H_2O)(OH)Cl]$ and $[ArCH{=}CH_2Pd(H_2O)(OH)Cl_2]^-$, are involved and in which the rate-determining step is the decomposition of the σ-complexes with the hydride shift to the carbonyl products.

Since the report of the palladium(II) ion oxidation of olefins by Smidt *et al.*,[1] many kinetic studies of the oxidation of ethylene and some olefins by palladium salts in aqueous solutions have been reported.[2] However, few kinetic studies concerning the sites of nucleophilic attack in the above oxidation of substituted olefins have been reported.[3] This study was undertaken to clarify the influences of such factors as proton concentration, chloride ion concentration, ionic strength, and the substituents on the sites of nucleophilic attack in the oxidation of ring-substituted styrenes by palladium salts in a homogeneous aqueous tetrahydrofuran (THF) solution at 30°C.

Results and Discussion

The oxidations of the substituted styrenes proceeded as is shown by the following equation;

$$X\text{-}C_6H_4CH{=}CH_2 + H_2O + Q \xrightarrow[THF\text{-}H_2O]{Pd^{2+}} \underset{I}{X\text{-}C_6H_4COCH_3} + \underset{II}{X\text{-}C_6H_4CH_2CHO} + H_2Q \quad (1)$$

(X: *p*-CH_3, *p*-Cl, *m*-CH_3, *m*-Cl and H)

where Q indicates the *p*-benzoquinone used as an oxidizing agent for palladium in the system and where H_2Q indicates hydroquinone. The reaction rates were followed by the gas chromatography of the unreacted styrenes and of the produced substituted acetophenone (I) and substituted phenylacetaldehyde (II). The reaction was first order in styrene and in palladium salts, and the ratio of acetophenone to phenylacetaldehyde was almost constant throughout the reaction.[3] For substituted styrenes, the kinetic relationships were identical with that of styrene. Thus, the rate expression is:

*1 Reported at the 20th Annual Meeting of the Chemical Society of Japan, Tokyo, April, 1967; Part II of this series: H. Okada and H. Hashimoto, *Kogyo Kagaku Zasshi (J. Chem. Soc. Japan, Ind. Chem. Sect.)*, **70**, 2152 (1967).

*2 Present address: Central Research Laboratory, The Furukawa Electric Co., Ltd., Futabacho, Shinagawa-ku, Tokyo.

1) J. Smidt, W. Hafner, R. Jira, J. Sedlmeier and R. Sieber, *Angew. Chem.*, **71**, 176 (1959).

2) For example, K. Teramoto, T. Oga, S. Kikuchi and M. Ito, *Yuki Gosei Kagaku Kyokaishi (J. Soc. Org. Synth. Chem. Japan)*, **21**, 298 (1963); T. Dozono and T. Shiba, *Bull. Japan Petrol. Inst.*, **5**, 8 (1963); P. M. Henry, *J. Am. Chem. Soc.*, **86**, 3246 (1964); I. I. Moiseev, M. N. Vargaftik, S. V. Pestrikov, O. G. Levanda, T. N. Romanova and Ya. K. Syrkin, *Dokl. Akad. Nauk SSSR.*, **171**, 1365 (1966).

3) H. Okada and H. Hashimoto, *Kogyo Kagaku Zasshi (J. Chem. Soc. Japan, Ind. Chem. Sect.)*, **69**, 2137 (1966).

$$-\frac{d[olefin]}{dt} = \frac{d[I]}{dt} + \frac{d[II]}{dt}$$
$$= (k_I + k_{II})[Pd^{2+}][olefin] \quad (2)$$

where k_I and k_{II} are the second-order rate constants for substituted acetophenone (I) and substituted phenylacetaldehyde (II) respectively.

Table 1. The effect of proton concentration on the rate constants in the oxidation of *p*-chlorostyrene*

$[H^+]\times10^2$ (M)	$k_I\times10^2$ (l/M·sec)	$k_{II}\times10^2$ (l/M·sec)
3.01	1.80	2.40
3.83	2.06	2.89
8.63	1.94	5.53
9.73	1.58	4.56
25.6	0.55	1.65

* $[Pd^{2+}]=4.41\times10^{-3}$ M
$[p\text{-}ClC_6H_4CH{=}CH_2]_0=[Q]_0=5.34\times10^{-2}$ M
$[Cl^-]/[Pd^{2+}]=2.00$

When the perchloric acid concentration was changed from 0.03 M to 0.25 M in the oxidation of *p*-chlorostyrene by palladium chloride in THF-water (60 : 40 vol/vol) in the absence of added salts, the values of k_I and k_{II} reached their maxima, as shown in Table 1. The effect of the proton concentration on the rate constants in the oxidation of *m*-methylstyrene at a constant ionic strength of 0.44 and a constant chloride ion concentration (Cl/Pd=2) in the same solvent system is shown in Fig. 1. The rate constants, k_I and k_{II}, had their

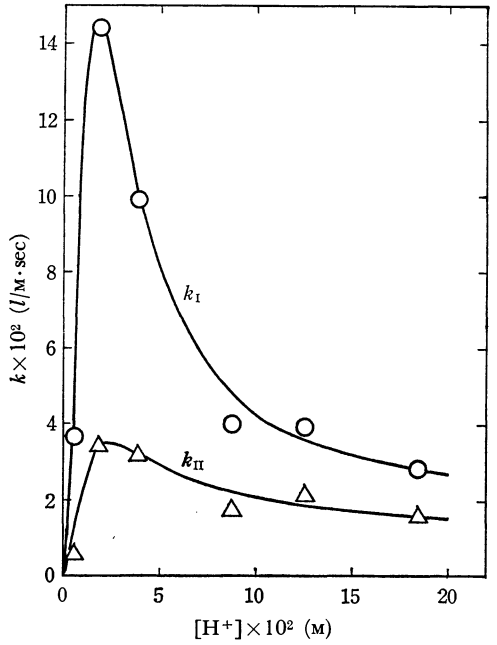

Fig. 1. The effects of proton concentration on the rate constants in the oxidation of *m*-methylstyrene.
$[m\text{-}CH_3C_6H_4CH{=}CH_2]_0=[Q]_0=5.34\times10^{-2}$ M; $[Pd^{2+}]=4.41\times10^{-3}$ M; $[Cl^-]/[Pd^{2+}]=2.00$; $\mu=0.44$
○: *m*-methylacetophenone
△: *m*-methylphenylacetaldehyde

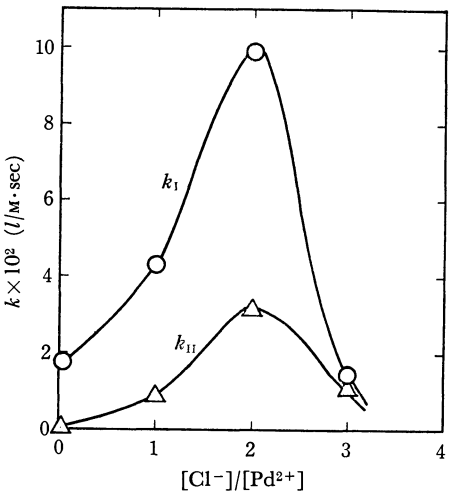

Fig. 2. The effects of chloride ion concentration on the rate constants in the oxidation of *m*-methylstyrene.
$[m\text{-}CH_3C_6H_4CH{=}CH_2]_0=[Q]_0=5.34\times10^{-2}$ M; $[H^+]=3.83\times10^{-2}$ M; $[Pd^{2+}]=4.41\times10^{-3}$ M; $\mu=0.44$
○: *m*-methylacetophenone
△: *m*-methylphenylacetaldehyde
The chloride ion concentration was varied by addition of NaCl.

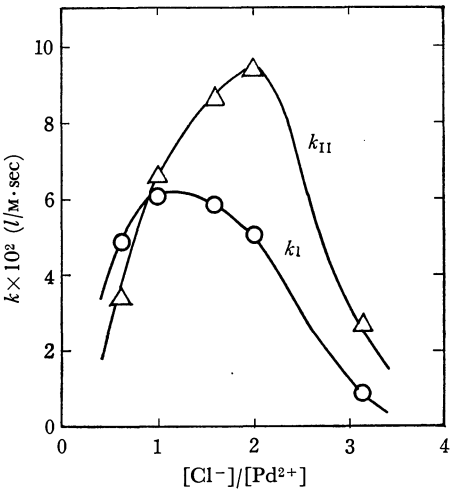

Fig. 3. The effects of chloride ion concentration on the rate constants in the oxidation of *m*-chlorostyrene.
$[m\text{-}ClC_6H_4CH{=}CH_2]_0=[Q]_0=5.34\times10^{-2}$ M; $[H^+]=0.74\times10^{-2}$ M; $[Pd^{2+}]=4.41\times10^{-3}$ M; $\mu=0.90$
○: *m*-chloroacetophenone
△: *m*-chlorophenylacetaldehyde

maximum values in a proton concentration of about 0.02 M. Therefore, it appears that k_I and k_{II} generally have their maximum values at low proton concentrations in these systems.

Figures 2 and 3 show the effect of the chloride ion concentration on the rate constants in the oxidation of *m*-methylstyrene and *m*-chlorostyrene at a constant ionic strength (μ=0.44 and 0.90 respectively) and at a constant proton concentration (0.038 M and 0.0074 M respectively). It is obvious that, in these cases, the maximum points appear in the curves of k_I and k_{II} at low chloride ion concentrations, when the ratio of chloride ions to palladium ions is 2 : 1 or less.

In the oxidations of ethylene and propylene by palladium chloride in aqueous solutions in the presence of excess chloride ions, the first-order proton inhibition and the second-order chloride inhibition have been established.[4] Also, in the oxidation of styrene by palladium chloride in aqueous tetrahydrofuran, the logarithm of the rate constants of acetophenone-formation is approximately proportional to the values of the acidity function, H_0, of the system in high proton concentrations,[3] showing a first-order proton inhibition similar to that of ethylene. However, Smidt *et al.*[5] has recently reported, regarding the aqueous palladium chloride oxidation of ethylene in the presence of *p*-benzoquinone, that the rate constants have maximum values both in low proton concentrations and in low chloride concentrations; they obtained the experimental rate expression of Eq. (3):

$$-\frac{d[CH_2=CH_2]}{dt}=\frac{a[H^+][Cl^-]}{b+[H^+]^2[Cl^-]^3} \qquad (3)$$

Although the influences of the acid concentration and the anion concentration on the rate were not independently analyzed, similar results were obtained in the oxidation of carbon monoxide by palladium chloride in aqueous dioxane in the presence of *p*-benzoquinone,[6] and in the acetoxylation of ethylene by palladium chloride or palladium acetate in acetic acid containing sodium acetate and *p*-benzoquinone.[7] Therefore, it may be concluded to be generally true in these reactions that protons and chloride ions have both effects of the rate inhibition and acceleration. These facts suggest that, under the conditions of low proton concentrations and of limited amounts of chloride ions, the mechanisms of these oxidation processes or the reaction species may differ from those proposed previously.[3,8]

In all the experiments, the ratio of the acetophenone (I) to the products, *i. e.*, $k_I/(k_I+k_{II})$, decreased monotonously with any increase in either the proton or chloride ion concentration, independently of the maximum values of k_I and k_{II}, for example, from 0.86 to 0.63 in Fig. 1, from 1.00 to 0.57 in Fig. 2, and from 0.59 to 0.25 in Fig. 3. With palladium perchlorate in the absence of chloride ions, no oxidation of styrenes occurred in very low proton concentrations. While higher proton concentrations generally caused side reactions to produce ring-substituted benzaldehydes (substituents: *p*-CH_3, *m*-CH_3, *p*-Cl and *m*-Cl)

Table 2. The influence of ionic strength on the rate constants in the oxidation of *m*-chlorostyrene*

μ	$k_I\times10^2$ (l/M·sec)	$k_{II}\times10^2$ (l/M·sec)	$k_I/(k_I+k_{II})$
0.052	2.53	3.33	0.431
0.393	4.21	5.16	0.450
0.787	7.49	9.69	0.436

* $[H^+]=3.84\times10^{-2}$ M
$[m\text{-}ClC_6H_4CH=CH_2]_0=[Q]_0=5.34\times10^{-2}$ M
$[Cl^-]/[Pd^{2+}]=2.00$

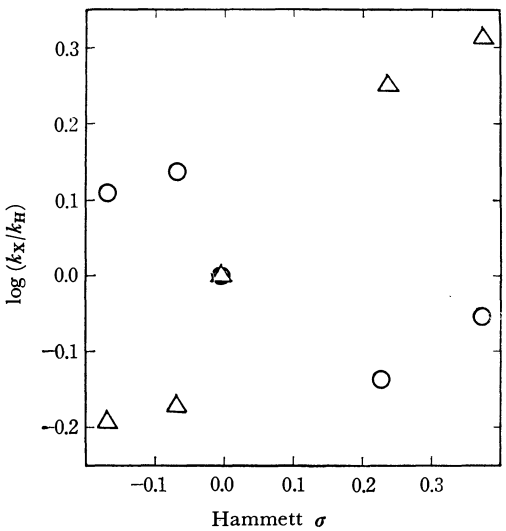

Fig. 4. The Hammett plots of the rate constants.
[substituted styrene]$_0$=[Q]$_0$=5.34×10^{-2} M; $[H^+]=3.83\times10^{-2}$ M; $[Pd^{2+}]=4.41\times10^{-3}$ M; $[Cl^-]/[Pd^{2+}]=2.00$; μ=0.052
○: substituted acetophenone
△: substituted phenylacetaldehyde

4) I. I. Moiseev, M. N. Vargaftik and Ya. K. Syrkin, *Dokl. Akad. Nauk SSSR.*, **153**, 140 (1963); P. M. Henry, *J. Am. Chem. Soc.*, **88**, 1595 (1966).
5) R. Jira, J. Sedlmeier and J. Smidt, *Liebigs Ann. Chem.*, **693**, 99 (1966).
6) A. B. Fasman, V. A. Golodov and D. V. Sokol'skii, *Zhur. Fiz. Khim.*, **38**, 1545 (1964).
7) R. Ninomiya, M. Sato and T. Shiba, *Bull. Japan Petrol. Inst.*, **7**, 31 (1965); A. P. Velov, I. I. Moiseev and N. G. Uvarova, *Izv. Akad. Nauk SSSR., Ser. Khim.*, **1966**, 1642; I. I. Moiseev, A. P. Velov, V. A. Igoshin and Ya. K. Syrkin, *Dokl. Akad. Nauk SSSR.*, **173**, 863 (1967).
8) J. P. Collman, in "Transition Metal Chemistry," Vol. II, ed. by R. L. Carlin, Marcel Dekker, New York (1966), p. 73.

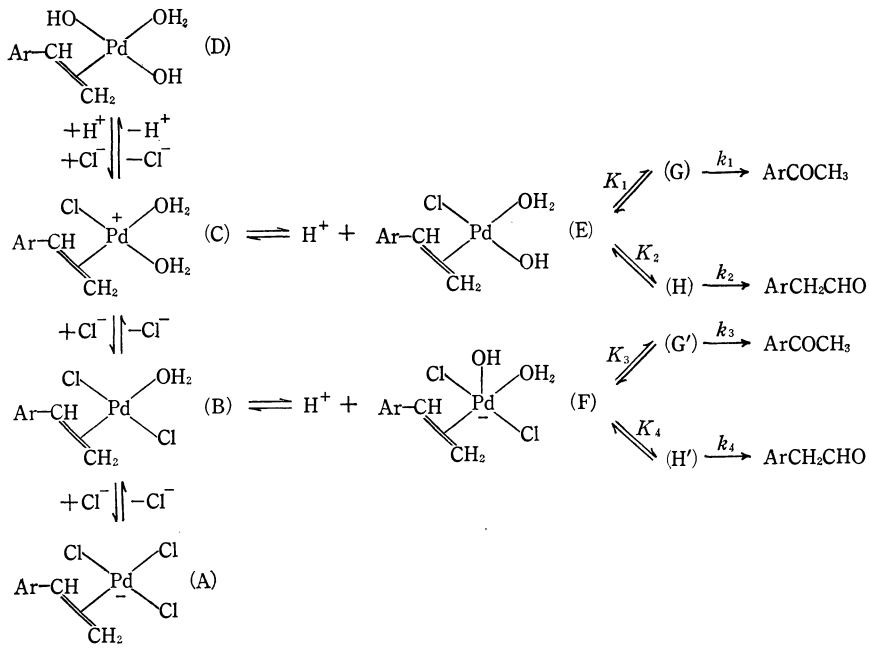

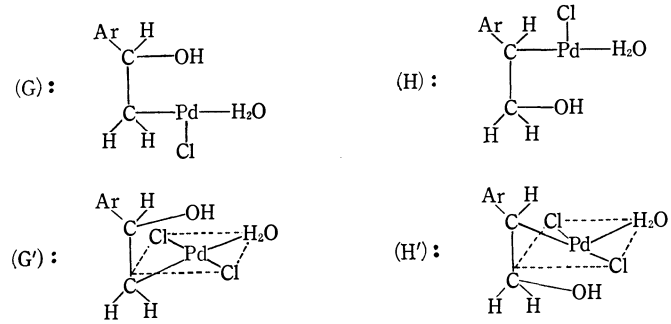

in the oxidation of the corresponding substituted styrenes, their amounts were no more than 5%.

Table 2 shows the effect of the ionic strength in the oxidation of *m*-chlorostyrene under comparable conditions. The results indicate that an increase in ionic strength considerably increases the values of both k_I and k_{II}, whereas it has little effect on the ratio of the products, that is to say, the value of $k_I/(k_I+k_{II})$.

In order to obtain further information regarding the mechanism of the reaction, we have investigated the effects of the ring-substituents on the oxidation rates. One example of the Hammett plots of the rate constants under typical experimental conditions is shown in Fig. 4. The rates roughly follow the Hammett $\rho\sigma$ equation. However, the sign of ρ is opposite for the α- and β-positions; that is, it is negative for the substituted acetophenone-formation and positive for the substituted phenylacetaldehyde-formation. This shows that electron-releasing substituents accelerate the reaction at the α-position and diminish the rate at the β-position. The reverse relationship holds for electron-withdrawing substituents. When the reaction conditions, especially the proton concentration and the chloride ion concentration were varied, the ρ-values changed somewhat, but the general tendency was the same. The reverse signs of ρ-values for the α- and β-positions have also been found in the hydroboration of substituted styrenes.[9,10]

The following reaction scheme is proposed to explain all of the results obtained: 1) the effects of both rate acceleration and retardation by protons and chloride ions; 2) the influence of the proton and chloride ion concentrations on the product ratio and 3) the opposite effects of the substituents on the reaction sites. In this scheme some assumptions are involved because of the complexity of the chemical species concerned.

In the above scheme, the A, B, C, D, E and F π-complexes are in a state of equilibrium. Both

9) J. Klein, E. Dunkelblum and M. A. Wolff, *J. Organometal. Chem.*, **7**, 377 (1967).
10) H. C. Brown and G. Zweifel, *J. Am. Chem. Soc.*, **82**, 4708 (1960).

the A and D complexes may be considered to be inactive species, for at a very high chloride ion concentration the reaction almost stopped, and in the complete absence of chloride ions, *i. e.*, in a palladium perchlorate or palladium hydroxide solution, the reaction scarcely proceeded at all. The specific effects of the protons and chloride ions on the rate and on the product distribution described above suggest that at least two active species participate in the reaction, because it is difficult to explain those effects in terms of only one reactive species. We propose that the E and F π-complexes are active species, with E more reactive than F. Although a five-coordinated species such as F could not be isolated, it seems reasonable to assume its existence, as has been proposed by Khan *et al.*[11] for the stereospecific hydrogenation of benzyl derivatives.*3 At lower proton and chloride ion concentrations, the reaction path through the E complex is predominant. The higher the chloride ion concentration, the more does the reaction proceed through the F complex. The net effects will result the maximum of the rate constant at a given proton concentration and at a given chloride ion concentration respectively.

From the observed substituent effects, it is reasonable to consider that the transformation of the π-complex to the σ-complex is probably a reversible step and that the decomposition of the σ-complex to carbonyl compounds, involving a hydride shift, is the rate-determining step. If the conversion of the π-complex to the σ-complex were rate-determining, the electron-withdrawing substituents would facilitate this transformation and the same sign of the ρ-value would be observed in the Hammett plots regardless of the reaction sites.

In the σ-complexes the effects of the ring-substituents may be stronger at the α-carbon than at the β-carbon. Thus, the electron-releasing groups increase the electron density at the α-carbon in the G and G' σ-complexes and facilitate the hydride transfer from the α-carbon to the β-carbon atom and interrupt the hydride transfer from the β-carbon to the α-carbon in the H and H' σ-complexes. The tendency is the reverse in the case of the electron-withdrawing groups.

The ratio of the ketone to the aldehyde produced is determined by the ratio of the product of the rate constant and the equilibrium constant, for example, k_1K_1 to k_2K_2 and k_3K_3 to k_4K_4. The monotonous decrease in the ratio of $k_I/(k_I+k_{II})$ with increases in both the proton and chloride ion concentrations means that, in the reaction path through the F π-complex, k_3K_3 may be considered to be nearly equal to k_4K_4. The reason for this may be as follows. When the coordinated substituted styrene molecule of E rotates from a position nearly vertical to the palladium coordination plane to a coplanar orientation,*4 the d_{xy} metal orbital is used for π-bonding in place of the d_{xz} metal orbital, and there arises an opportunity to rearrange to the G or H σ-complex. In the coplanar orientation, if the α-carbon atom lies near the *cis*-Cl ligand (III), the overlap between the d_{xy} metal orbital and the π-antibonding orbital of substituted styrene will be prevented by the steric hindrance resulting from the interaction between the aryl group and chloride ions. Moreover, since the β-carbon atom lies far from the *cis*-OH ligand,*5 the conversion from the E π-complex to the H σ-complex, which is preferable for aldehyde formation, would be difficult. On the contrary, if the β-carbon atom lies near the *cis*-Cl ligand (IV), the p_π*-d_{xy} overlap will not be prevented and then the α-carbon atom will lie near the *cis*-OH ligand.*5 Thus, transformation to the G σ-complex, which is preferable for ketone formation, would be predominant.

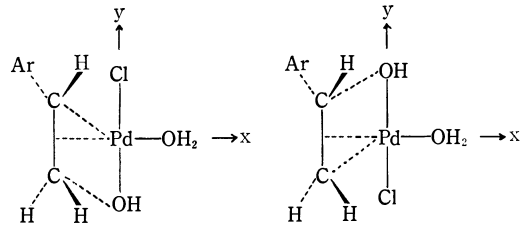

11) A. M. Khan, F. J. McQuillin and I. Jardine, *Tetrahedron Letters*, **1966**, 2649.

*3 A five-coordinated complex is well known for some group VIII metals; for example: $[Pt(SnCl_3)_5]^{3-}$ and $[HPt(SnCl_3)_4]^{3-}$,[12] $[CH_3(CH_2)_4CORhCl_2(PPh_3)_2]$,[13] $[RuCl_2(PPh_3)_3]$,[14] and so on.[15]

12) R. V. Lindsey, Jr., G. W. Parshall and U. G. Stolberg, *J. Am. Chem. Soc.*, **87**, 658 (1965); G. W. Parshall, *ibid.*, **88**, 704 (1966).

13) J. Tsuji and K. Ohno, *ibid.*, **88**, 3452 (1966).

14) S. J. L. Placa and J. A. Ibers, *Inorg. Chem.*, **4**, 782 (1965).

15) F. Basolo and R. G. Pearson, "Mechanisms of Inorganic Reactions," John Wiley and Sons, New York (1958), p. 186.

*4 It is supposed that the substituted styrene molecule rotates with the coordination bond as axis, as in the case of ethylene rotation in bis-ethylene-π-cyclopentadienyl rhodium(I).[16]

16) R. Cramer, *J. Am. Chem. Soc.*, **86**, 217 (1964).

*5 Although in $[C_2H_4PdCl_2]_2$ the axis of the ethylene molecule is perpendicular to the plane of the dimer and the center of the ethylene double bond lies on the plane of the dimer,[17] in $[C_6H_5CH{=}CH_2PdCl_2]_2$ the styrene molecule coordinates to palladium(II) not at the center of the double bond but at the point near β-carbon atom.[18] The NMR spectra of such assymmetrically-substituted ethylene complexes as $K[(C_6H_5CH{=}CH_2)PtCl_3]$[19] and $[CH_3CH{=}CH_2PtCl_2(C_5H_5NO)]$[20] suggest that the CH_2 groups are positioned nearer to the platinum atom and that the olefin molecules are slightly twisted out of the original ethylene plane, with the bulky group away from and the *trans*-hydrogen atom toward the platinum.

17) J. N. Dempsey and N. C. Baenziger, *ibid.*, **77**, 4984 (1955).

18) J. R. Holden and N. C. Baenziger, *ibid.*, **77**, 4987 (1955).

19) H. P. Fritz, K. E. Schwarzhans and D. Sellman, *J. Organometal. Chem.*, **6**, 551 (1966).

20) P. D. Kaplan and M. Orchin, *Inorg. Chem.*, **6**, 1096 (1967).

In a vertical orientation such as in the F complex, the overlap between the p_π* orbital of olefin and the d_{xz} palladium orbital is at a maximum and an interaction with a fifth hydroxide ligand above or below the square plane of the four-coordinated planar complex may be expected. Because of the rapid rotation of olefin and/or the two coordination sites for the hydroxide ligand, the probability of an attack of the hydroxide ion on either the α-position or the β-position will be nearly equal. This may decrease the selective formation of either carbonyl compound from F. The transformation of the E π-complex to the G or H σ-complex may involve a four-center-type transition state. The four-center-type transition state has also been proposed for the rearrangement of the hydrido-π-olefin complex to a σ-alkyl complex in the hydrogenation of fumaric acid by ruthenium(II) chloride.[21]

Experimental

Materials. In the oxidation of *p*-chlorostyrene, *p*-dibromobenzene was used as an internal reference in the gas chromatographic quantitative analysis. It was the same material as was employed in the oxidation of styrene.[3] Bromomesitylene was used as an internal reference in the oxidations of the other three substituted styrenes; it was prepared by the bromination of mesitylene,[22] bp: 136—137°C/50 mmHg. Ring-substituted styrenes were prepared by the dehydration of the alcohols which were formed by the action of the corresponding ring-substituted phenylmagnesium bromide and acetaldehyde[23]; *p*-methylstyrene, bp: 61.5—62.5°C/13 mmHg; *m*-methylstyrene, bp: 61.0—62.0°C/13 mmHg; *p*-chlorostyrene, bp: 90.5—91.3°C/30 mmHg; *m*-chlorostyrene, bp: 62.0—63.0°C/7—8 mmHg. All the substituted styrenes described above were confirmed to be pure by means of g.l.c. and by means of their NMR spectra.

Kinetic Runs. The unreacted styrenes and reaction products were analyzed by means of g.l.c., using a 3-m copper column packed with 20% silicon DC 550 on Diasolid, at a hydrogen gas flow rate of 80 ml/min at 130°C. The other experimental techniques used in this study have been described previously.[3]

Identification of the Products. The ring-substituted acetophenones, phenylacetaldehydes, and benzaldehydes were identified by means of g.l.c. and their IR and/or NMR spectra in comparison with those of the authentic samples synthesized by the methods cited below or by similar methods. The boiling points of the authentic samples are also given below. The IR spectra were taken on neat liquid or on KBr tablets. The NMR spectra were measured by a Japan Electron Optics C-60 chemical analyzer at 60 Mc in carbon tetrachloride, containing tetramethylsilane as an internal reference.

Compounds Obtained in the Oxidation of p-Methylstyrene.
p-Methylacetophenone.[24] bp: 225—226.5°C/760 mmHg. IR: 1184, 1285, 1385 and 1677 cm^{-1}.
p-Methylphenylacetaldehyde.[25] bp: 104—129°C/20 mmHg. IR: 810, 1725 and 2718 cm^{-1}.
p-Methylbenzaldehyde.[26] bp: 107.0—109.0°C/32 mmHg. IR: 1389, 1690, 2736 and 2816 cm^{-1}.

Compounds Obtained in the Oxidation of m-Methylstyrene.
m-Methylacetophenone.[27] bp: 107.0—107.5°C/18 mmHg. NMR: 7.60 τ (3H, singlet); 7.50 τ (3H, singlet); 2.10—2.70 τ (4H, multiplet).
m-Methylphenylacetaldehyde.[28] bp: 84.5—85.0°C/8 mmHg. IR: 703, 783, 1740 and 2710 cm^{-1}. NMR*[6]: 7.77 τ (3H, singlet); 6.62 τ (2H, doublet); 2.80—3.20 τ (4H, multiplet).
m-Methylbenzaldehyde.[26] bp: 93.0—94.0°C/17 mmHg. IR: 685, 780, 1700 and 2710 cm^{-1}. NMR: 7.55 τ (3H, singlet); 2.10—2.60 τ (4H, multiplet); −0.17 τ (1H, singlet).

Compounds Obtained in the Oxidation of p-Chlorostyrene.
p-Chloroacetophenone.[29] bp: 136.0—136.5°C/36 mmHg. IR: 1177, 1264, 1359 and 1690 cm^{-1}. NMR: 7.42 τ (3H, singlet); 2.10—2.55 τ (4H, multiplet).
p-Chlorophenylacetaldehyde.[28] bp: 134—136°C/29 mmHg. IR: 1721, 2740 and 2820 cm^{-1}.
p-Chlorobenzaldehyde. mp: 46.0—47.0°C, bp: 108.0—110.0°C/ 25 mmHg. IR: 769, 1325 and 1690 cm^{-1}. NMR: 2.10—2.70 τ (4H, multiplet); 0.03 τ (1H, singlet).

Compounds Obtained in the Oxidation of m-Chlorostyrene.
m-Chloroacetophenone.[27] bp: 109°C/12 mmHg. IR: 670, 800, 1280, 1360 and 1690 cm^{-1}. NMR: 7.55 τ (3H, singlet); 2.20—2.90 τ (4H, multiplet).
m-Chlorophenylacetaldehyde. NMR: 6.51 τ (2H, doublet); 2.70—3.10 τ (4H, multiplet); 0.45 τ (1H, triplet). All of the compounds listed above had the same retention time as the authentic samples in g.l.c.

21) J. Halpern, J. F. Harrod and B. R. James, *J. Am. Chem. Soc.*, **88**, 5150 (1966).
22) L. I. Smith, "Organic Syntheses," Coll. Vol. II, p. 95 (1948).
23) C. G. Overberger and J. H. Saunders, "Organic Syntheses," Coll. Vol. III, p. 204 (1955).
24) C. R. Noller and R. Adams, *J. Am. Chem. Soc.*, **46**, 1889 (1924).
25) H. Stephen, *J. Chem. Soc.*, **127**, 1874 (1925).
26) M. Sommelet, *Compt. rend.*, **157**, 852 (1913).
27) G. Lock and R. Schreckeneder, *Ber.*, **72**, 516 (1939).
28) C. E. Wood and M. A. Comley, *J. Soc. Chem. Ind.*, **42**, 432 T (1923).
*6 The aldehyde peak was not measured.
29) R. Adams and C. R. Noller, "Organic Syntheses," Coll. Vol. I, p. 109 (1956).

BULLETIN OF THE CHEMICAL SOCIETY OF JAPAN VOL. 41 1401—1404 (1968)

Cleavage Reactions of Alkoxy Radicals Produced by Anodic Oxidation of *t*-Alcohols

Kazuhiro MARUYAMA and Katsuya MURAKAMI*1

Department of Chemistry, Faculty of Science, Kyoto University, Sakyo-ku, Kyoto

(Received December 7, 1967)

The anodic oxidation of *t*-alcohols in water - dioxane - sodium hydroxide system has been examined. The possibility of production of *t*-alkoxy radicals by anodic oxidation of *t*-alcohols in the electrolytic system was found. The relative ease of bond scission of the intermediate *t*-alkoxy radical was determined by quantitative analysis of the mixture of ketones produced. The relative rates of cleavage decrease in the order: allyl>*sec*-butyl>isopropyl>ethyl>*n*-propyl>*n*-butyl>*n*-pentyl>isobutyl>methyl. The hyperconjugative effect of β-hydrogen and effect of double bond at β-position to the rate enhancement of cleavage reaction was confirmed.

The two typical reactions of *t*-alkoxy radicals are, in general, i) hydrogen abstraction to form alcohols and ii) fragmentation to ketone and alkyl radical.[1,2] The cleavage reaction of *t*-alkoxy radical to form ketone and alkyl radical has been extensively investigated.[3-9] There are three ways of bond scission for an *t*-alkoxy radical theoretically (Eq. (1)).

$$R_1R_2R_3CO\cdot \longrightarrow \left\{ \begin{array}{l} \rightarrow R_1\cdot + R_2COR_3 \\ \rightarrow R_2\cdot + R_1COR_3 \\ \rightarrow R_3\cdot + R_1COR_2 \end{array} \right\} \quad (1)$$

The relative rates of formation of alkyl radicals can be determined if one can estimate quantitatively the amount of ketones and of alkyl radicals which are produced from the fragmentation of *t*-alkoxy radical. By such an idea the relative ease of cleavage reactions has been determined from 1) the redox reaction between alkyl hydroperoxides and reducing metal ion,[4] 2) the thermolysis of dialkyl peroxides,[4] 3) the oxidation of alcohols with Co(III),[5] and 4) the photolytic decomposition of alkyl hypochlorites.[6,8,9]

In this study we examined the possibility of production of *t*-alkoxy radicals by anodic oxidation of *t*-alcohols and intended to obtain a quantitative measure of the relative ease of cleavage reaction in the absence of the oxidising metallic cation or halogen radical, especially at low temperature. Using platinum electrodes the electrolytic oxidation of *t*-alcohols were conducted in a solvent system: dioxane - water - sodium hydroxide.

Results and Discussion

The synthetic methods of *t*-alcohols: R_1R_2PhCOH (R_1, R_2=alkyl, Ph=phenyl) used in this study and their physical constants are described in experimental part (Table 4). The reaction mixture resulted from electrolysis of *t*-alcohols in the dioxane-water - sodium hydroxide system, was extracted by ether and analysed by g.l.p.c. technique. Since it was confirmed by preliminary experiments that the expected ketones were produced efficiently at anode by electrolysis of *t*-alcohols if one used the dioxane - water - sodium hydroxide system as a solvent (80—90% of theoretical yields for ketones in 10—15 hr) and no successive reaction of the ketones was observed in this electrolytic system, the further reactions were conducted as it was described in experimental part. The yields of ketones obtained from the anodic oxidations of *t*-alcohols are given in Table 1. The values given in Table 1 are average of the values obtained by several runs (3—5 times) for an *t*-alcohol. The probable error was lower than 5%. Gaseous products corresponding to the respective runs are given in Table 2.

*1 Present address: Kurashiki Rayon Co. LTD., Kurashiki-shi, Sakazu.

1) J. H. Raley, F. F. Rust and W. E. Vaughan, *J. Am. Chem. Soc.*, **70**, 88 (1948); F. F. Rust, F. H. Seubold and W. H. Vaughan, *ibid.*, **70**, 95 (1948); J. H. Raley, F. F. Rust and W. H. Vaughan, *ibid.*, **70**, 1336 (1948); E. R. Bell, F. F. Rust and W. E. Vaughan, *ibid.*, **72**, 337 (1950); M. G. Evans, *Discussions Faraday Soc.*, **10**, 1 (1951).

2) P. Gray and A. Williams, *Chem. Revs.*, **59**, 239 (1959); *Trans. Faraday Soc.*, **78**, 1190 (1956).

3) A. L. Williams, E. A. Oberright and J. W. Brooks, *J. Am. Chem. Soc.*, **78**, 1190 (1956).

4) J. K. Kochi, *ibid.*, **84**, 1193 (1962).

5) D. G. Hoare and W. A. Waters, *J. Chem. Soc.*, **1964**, 2552.

6) C. Walling and A. Padwa, *J. Am. Chem. Soc.*, **85**, 1593 (1963).

7) C. Walling and B. B. Jacknow, *ibid.*, **82**, 6108, 6113 (1960); **83**, 3877 (1961).

8) F. D. Greene, M. L. Savitz, F. D. Osterholz, H. H. Lau, W. N. Smith and P. M. Zanet, *J. Org. Chem.*, **28**, 55 (1963).

9) J. D. Bacha and J. K. Kochi, *ibid.*, **30**, 3272 (1965).

TABLE 1. ANODIC OXIDATION OF *t*-ALCOHOLS : R_1R_2PhCOH

Run	R_1	R_2	R_1COPh	R_2COPh	R_2/R_1
1	C_2H_5	*i*-C_3H_7	60%	~1%	~60
2	C_2H_5	*n*-C_3H_7	35	53	0.66
3	C_2H_5	*s*-C_4H_9	85	~1	~85
4	C_2H_5	*n*-C_4H_9	35	57	0.62
5	C_2H_5	*i*-C_4H_9	25	57	0.44
6	C_2H_5	*n*-C_5H_{11}	32	56	0.57
7	*i*-C_3H_7	*s*-C_4H_9	50	33	1.50
8	*n*-C_3H_7	*n*-C_4H_9	31	47	0.66
9	C_2H_5	CH_3	~1	67	~0.01
10	C_2H_5	$-CH_2CH=CH_2$	71	0	∞
11	*i*-C_3H_7	$-CH_2CH=CH_2$	58	6.3*	9.0

Solvent : dioxane : water = 10 : 4
* Contained 3.1% of *n*-propyl phenyl ketone

TABLE 2. COMPOSITIONS OF GASEOUS PRODUCTS

Run	R_1	R_2	Components of gaseous products
1	C_2H_5	*i*-C_3H_7	C_3H_6
2	C_2H_5	*n*-C_3H_7	C_2H_4, C_3H_6, *n*-C_4H_{10}, *n*-C_5H_{12}
3	C_2H_5	*s*-C_4H_9	C_2H_4, *n*-C_4H_{10}, 1-C_4H_8, 2-C_4H_8
4	C_2H_5	*n*-C_4H_9	C_2H_4, *n*-C_4H_{10}, 1-C_4H_8, 2-C_4H_8, *i*-C_4H_8
5	C_2H_5	*i*-C_4H_9	C_2H_4, *n*-C_4H_{10}, *i*-C_4H_8
9	C_2H_5	CH_3	C_2H_4, *n*-C_4H_{10}

TABLE 3. RELATIVE RATES OF CLEAVAGE OF ALKYL RADICALS FROM *t*-ALKOXY RADICALS AT 25—35°C

Radicals		$CH_2CH=CH_2$	*s*-C_4H_9	*i*-C_3H_7	C_2H_5	*n*-C_3H_7	*n*-C_4H_9	*n*-C_5H_{11}	*i*-C_4H_9	CH_3
Relative rates		~540[a]	~85 ~90[b]	~60 ~57[c]	1.0	0.66 0.93[d]	0.62 0.45[e]	0.57	0.44	~0.01
	Ref. *		64		1.0	0.63—0.74	0.59—0.72		0.47—0.57	0.005
	Ref. **				1.0	0.65	0.43			0.003
	Ref. ***				1.0	0.34	0.28		0.1	0.01

a) from runs 1 and 11, b) from runs 1 and 7, c) from runs 3 and 7, d) from runs 4 and 8, e) from runs 2 and 8.
* J. D. Bacha and J. K. Kochi, *J. Org. Chem.*, **30**, 3272 (1965).
** J. K. Kochi, *J. Am. Chem. Soc.*, **84**, 1193 (1962).
*** D. G. Hoare and W. A. Waters, *J. Chem. Soc.*, **1964**, 2552.

The components of gaseous products could be identified by g.l.p.c. technique, but the amounts of each component could not be determined quantitatively, because the gaseous products produced at electrodes contained a large amount of hydrogen and oxygen which were the invariable products of electrolysis in an aqueous solvent.

Although an ambiguity remains in the anodic oxidation of *t*-alcohols, generation of *t*-alkoxy radical at anode and consequently the ejection of an alkyl radical from *t*-alkoxy radical can be deduced from the results given in Table 1 and Table 2; the high yields of ketones and generation of dimerization product of the ejected alkyl radical are indicative for the generation of *t*-alkoxy radical at anode (Eq. (2)).*2

*2 There is a possibility of the anodic oxidation of *t*-alkoxy radical to *t*-alkoxy cation which produces ketone and alkyl cation. However, *t*-alkoxy cation which would be formed, should decompose to produce aliphatic ketone and phenol:

$$R_1R_2PhCO\cdot \xrightarrow{-e} R_1R_2PhCO^+ \xrightarrow[(H_2O)]{} R_1R_2CO + PhOH$$

because the alkoxy cation is a well established intermediate of the acid catalysed decomposition of aralkyl hydroperoxides. For example, α,α-dimethylbenzyl hydroperoxide decomposes to acetone and phenol (M. S. Kharasch, A. Fono and W. Nudenberg, *J. Org. Chem.*, **15**, 748 (1950)). Since none of phenolic product nor aliphatic ketone could be detected as the reaction product, such a possibility of the anoidic oxidation of *t*-alkoxy cation can be ignored.

$$\left.\begin{array}{l} R_1R_2PhCOH \xrightarrow{-e} R_1R_2PhCO\cdot + H^+ \\ R_1R_2PhCO\cdot \begin{cases} \xrightarrow{k_1} R_2COPh + R_1\cdot \\ \xrightarrow{k_2} R_1COPh + R_2\cdot \end{cases} \\ R_1\cdot + R_2\cdot \begin{cases} \longrightarrow R_1R_1 + R_2R_2 + R_1R_2 \\ \longrightarrow R_1H + R_2H + \text{olefins} \end{cases} \end{array}\right\} \quad (2)$$

Since the hydrogen abstraction from solvent by *t*-alkoxy radical which is another main reaction of it, produces the starting material in this reaction, such a way of stabilization of *t*-alkoxy radical can be neglected from the consideration. Assuming the relative amounts of ketones are equal to the relative ease of fragmentation of an alkyl moiety from *t*-alkoxy radical; $k_1/k_2 = R_2COPh/R_1COPh$, a trend of the relative ease of cleavage can be deduced, which is shown in Table 3 with the values obtained from the other reactions by several investigators. Thus, the trend of the relative ease of cleavage reaction deduced from the results of the anodic oxidation of *t*-alcohols coincides qualitatively with the results which are obtained from the other different type of reactions. It has been generally accepted that the predominant cleavage is that which forms the largest alkyl radical; qualitatively, the relative ease of ejection of an alkyl radical from *t*-alkoxy radical decreases in the order: *tertiary* > *secondary* > *primary*, but recently have presented the facts which are inconsistent with this conception from the study of dissociation energy of alkanes by electron impact[10] and from the study of photolytic decomposition of alkyl hypohalites.[9] Bacha and Kochi have shown that the relative rates of cleavage decreases in the order which is shown in Table 3; ethyl > γ,γ-dimethylbutyl > *n*-propyl, *n*-butyl > isobutyl > neopentyl ≫ methyl, from the study of photolytic decomposition of various *t*-alkyl hypochlorites, and have proposed that the most important factor which determines the relative rate of ejection of an alkyl radical from *t*-alkoxy radical is the hyperconjugative effect of β-hydrogen of a departing alkyl radical for the stabilization of transcient stage of bond scission.[9] Our results obtained from the anodic oxidation of *t*-alcohols seem to substantiate the conception presented by Bacha and Kochi. In order to examine further this problem, 1-phenyl-2-methyl-cyclohexanol which is considered to be relatively strain free compound, has electrolysed in the dioxane - water-sodium hydroxide system. If the bond scission occurred at (a), the number of β-hydrogen is two. If the bond scission occurred at (b), then the number of β-hydrogen is five. Actually, *n*-hexyl phenyl ketone which indicates the bond scission at (b), was the sole product as the ketonic product; this shows the importance of the hyperconjugative effect of β-hydrogen (Eq. (3)).

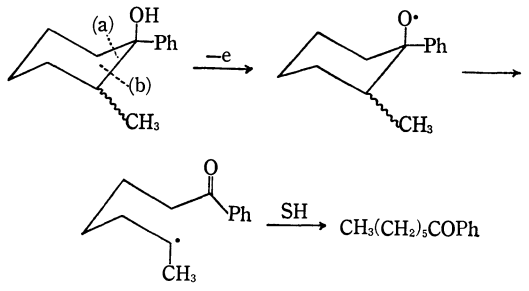

SH: solvent (3)

In addition to the effect of the number of β-hydrogen, a prominent rate enhancement for the bond scission by double bond at β-position can be found from the results of runs 10 and 11. Such an effect of double bond for the rate enhancement as well as the effect of β-hydrogen suggests that a stabilization of the polarized transcient stage for the bond scission is predominant factor (Eq. (4)).

$$R_2\text{-}\overset{\overset{R_1}{|}}{\underset{\underset{Ph}{|}}{C}}\text{-}O\cdot \rightarrow \left[R_2\cdot\overset{\overset{R_1}{|}}{\underset{\underset{Ph}{|}}{C}}{=}O \longleftrightarrow R_2{}^+\overset{\overset{R_1}{|}}{\underset{\underset{Ph}{|}}{C}}{=}O^- \right] \rightarrow R_2 + R_1COPh \quad (4)$$

The importance of the polarized transient stage has already pointed out by Bacha and Kochi as to the rate enhancement by β-hydrogen.[9] We can find ample evidences for such an importance of polar effects to the radical reactions.[11] Effects of ring size and ring strain are also shown to be a determining factor of the relative ease of ejection of an alkyl radical from the parent alkoxy radical.[8]

Experimental

Preparation of Alcohols. The tertiary alcohols were prepared by the Grignard procedure from phenyl bromide and corresponding ketones and were purified by vacuum distillation until to obtain materials giving a single spot *via* thin layer chromatography. Physical constants of *t*-alcohols found are shown in Table 4.

Anodic Oxidation and Quantitative Analysis of Reaction Mixtures. A typical anodic oxidation of *t*-alcohol was conducted as following; 1.00 g of an *t*-alcohol and 20 mg of sodium hydroxide were dissolved into a mixture of 10 m*l* of dioxane and 4 m*l* of water. The solution was electrolysed in a 100 cylindrical flask with two parallel platinum plates as electrodes (surface area: 2.0×1.5 cm^2, distance between electrodes: 0.2 cm, electric potential between electrodes: 10—20 V, current: 0.3—0.5 A). A violent evolution of gaseous product at anode could be observed. The temperature of the solution was held at 25—35°C by cooling with water. After electrolysis was continued for about ten

10) D. P. Stevenson, *Trans. Faraday Soc.*, **49**, 867 (1953).

11) G. A. Russel, *J. Org. Chem.*, **23**, 1407 (1958); C. Walling and B. Miller, *J. Am. Chem. Soc.*, **79**, 4181 (1957); M. M. Martin and G. J. Gleicher, *ibid.*, **86**, 242 (1964); W. A. Pryor, "Free Radicals," McGraw-Hill Book Company, New York (1966).

Table 4. Physical constants of *t*-alcohols: R_1R_2PhCOH

	R_1	R_2	Bp (°C)	Press (mmHg)
1	C_2H_5	*i*-C_3H_7	128—129	20
2	C_2H_5	*n*-C_3H_7	125—127	20
3	C_2H_5	*s*-C_4H_9	123—125	16
4	C_2H_5	*n*-C_4H_9	82—84	3
5	C_2H_5	*i*-C_4H_9	106—110	15
6	C_2H_5	*n*-C_5H_{11}	105—110	4
7	*i*-C_3H_7	*s*-C_4H_9	100—105	4
8	*n*-C_3H_7	*n*-C_4H_9	127	16
9	C_2H_5	CH_3	100—101	15
10	C_2H_5	$-CH_2CH=CH_2$	110	17
11	*i*-C_3H_7	$-CH_2CH=CH_2$	118—124	17

hours, the reaction mixture was treated with ether, dried with anhydrous sodium sulfate, and quantitatively analysed by g.l.p.c. techniques. Identifications of products were carried out by the comparison of the retention time of each component on chromatogram with authentic samples. The columns used for analyses of the ketones were calibrated with standard solutions at the same time under the same condition. Bromobenzene was used as an inner standard sample. From the ratio of peak areas (ketone to bromobenzene), the amount of each component could be determined. The gas chromatographic columns for the determination of ketonic components are following; (1) 200 cm Apiezon-L on Cerite (80—100 mesh), (2) 200 cm TG-3000 on Certie (80—100 mesh), (3) 300cm High Vacuum Grease on Cerite (80—100 mesh), Carrier gas: H_2 at 150—200°C. The gas chromatographic column for the identification of gaseous products was a 200 cm column of β,β'-oxydipropionitrile on Cerite, carrier gas: H_2 at 25°C.

BULLETIN OF THE CHEMICAL SOCIETY OF JAPAN VOL. 41 1404—1413 (1968)

Perchloro-compounds. IV. *anti*-Perchloro-(3,4,7,8-tetramethylenetricyclo-[4.2.0.0^{2,5}]octane), a Dimer of Perchloro-(3,4-dimethylenecyclobutene)

Koichi MANO, Kousuke KUSUDA and Akira FUJINO

Organic Chemistry Division, Research Institute for Atomic Energy, Osaka City University, Sumiyoshi-ku, Osaka

(Received December 16, 1967)

The structure of the first of the four thermolytic dimers of perchloro-(3,4-dimethylenecyclobutene) was characterized as *anti*-perchloro-(3,4,7,8-tetramethylenetricyclo[4.2.0.0^{2,5}]octane) (II). This structure elucidation was principally based on: (a) the permanganate oxidation of II to perchloro-(dimethylenesuccinic) acid; (b) the two-step reduction of II to 1,2,3',4',5,6,7',8'-octachloro-3,4,7,8-tetramethylenetricyclo[4.2.0.0^{2,5}]octane and 1,2,5,6-tetrachloro-3,4,7,8-tetramethyltricyclo[4.2.0.0^{2,5}]octa-3,7-diene (VII), and (c) the hydrogenation of the ozonized product from VII to two tetraacetylcyclobutanes (XVII and XVIII). The physical and chemical properties of II and of those substances derived from II and VII were discussed in detail. The stereochemical configurations of II and XVII were estimated to be *anti* and all-*trans* respectively.

It has already been briefly reported that the temperature-controlled thermolysis of perchloro-(3,4-dimethylenecyclobutene) (I)[1,2] affords, besides perchlorofulvene, perchloro-(4-methylenecyclopentene), and perchlorobenzene, at least four dimeric products, the first isomer of which is formed in the vicinity of 160°C and may be characterized as a cycloadduct, *anti*-perchloro-3,4,7,8-tetramethylenetricyclo[4.2.0.0^{2,5}]octane) (mp 266°C) (II).[3,4] The differential thermal analysis data suggest that the successive transformation of II takes place, step by step as the thermolysis temperature rises, to

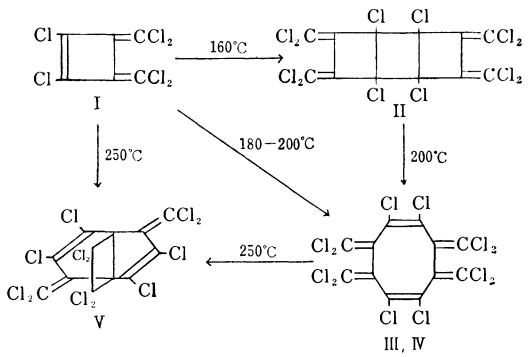

Chart 1

1) A. Roedig, F. Bischoff, B. Heinrich and G. Märkl, *Ann.*, **670**, 8 (1963).
2) A. Fujino, Y. Nagata and T. Sakan, This Bulletin, **38**, 295 (1965).
3) K. Mano, K. Kusuda, A. Fujino and T. Sakan, *Tetrahedron Letters*, **1966**, 489.
4) A. Furusaki, Y. Tomiie and I. Nitta, *ibid.*, **1966**, 493.

give the second isomer, labile perchloro-(3,4,7,8-tetramethylenecyclooctadiene) (mp 215°C) (III),[5] mixed with the third isomer (rigid form of III) (mp 262°C) (IV)[5] and the fourth isomer, perchloro-(4,8-dimethylenetricyclo[3.3.2.0^{1,5}]deca-2,6-diene) (mp 273°C) (V)[6] (Chart 1). The present paper will describe a detailed study of the structure elucidation of II as well as the physical and chemical properties of some related compounds obtained in the course of our investigation.

Results

The material necessary for the elucidation was best supplied by means of the ionic dimerization of I in dichloromethane with anhydrous aluminum chloride,[3] since the average yield of *ca.* 60% was much higher than that in thermolysis. It was observed that II is hardly soluble in ordinary nonpolar organic solvents (*e. g.*, approx. 2 g/1*l* carbon tetrachloride), is inert to acid or alkaline hydrolysis, and is stable against the UV-light irradiation in solution, in contrast to its remarkable thermal instability. The attempted chlorination of II in liquid chlorine or with chlorine gas in a heated solution was unsuccessful, only the unreacted substrate being recovered. The permanganate oxidation of II in acetone proceeded rapidly to give perchloro-(dimethylenesuccinic) acid in a yield as low as that in the similar oxidation of I.[1] The reduction of II with zinc in ethanol or acetic acid smoothly furnished 1,2,3′,4′,5,6,7′,8′-octachloro-3,4,7,8-tetramethylenetricyclo[4.2.2.0.0^{2,5}]octane (mp 223—225°C) (VI), which was then further hydrogenated over palladium charcoal at room temperature to give 1,2,5,6-tetrachloro-3,4,7,8-tetramethyltricyclo[4.2.2.0.0^{2,5}]octa-3,7-diene (mp 180°C, decomp.) (VII). The latter compound was also directly obtained in 77% yield from II by hydrogenation with the same catalyst. In this case there was isolated as a by-product a small amount of hydrocarbon (bp 80°C(bath)/20 mmHg) (VIII) to which the structure of 3,4,7,8-tetramethylbicyclo-

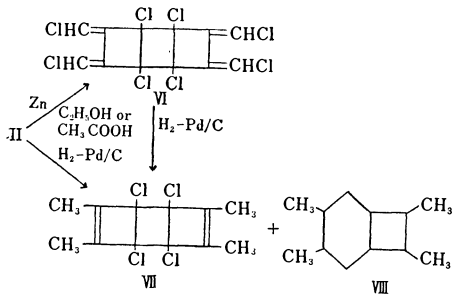

Chart 2

[4.2.0]octane was assigned. These reactions are illustrated in Chart 2.

The residual chlorine substituents in VII strongly resisted the attack of other reducing or basic reagents, such as lithium alanate-lithium hydride in ether, nickel carbonyl in benzene, Raney nickel in methanol, zinc-acetic acid, liquid ammonia, and alcoholic potassium hydroxide. So far as we have examined, only *n*-butyllithium in ether reacted with VII, but even if did so without any conclusive result. On the other hand, a variety of the ring-cleaved products were obtained when VII was subjected to ozonization. There was observed a marked dependence of the product on the solvent employed. Thus, in dichloromethane or carbon tetrachloride-chloroform at −20°C, VII was transformed by ozone to an unstable viscous oil which then gradually decomposes, liberating a gas with a phosgene-like odor. When this oil was treated with mineral acid, a crystalline compound, $C_{12}Cl_4H_{12}O_3$ (mp 125—127°C) (IX) was obtained. In ozonization in petroleum ether at room temperature, an isomer (mp 122—124°C) (X), possibly isoozonide of VII, and 5,6-diacetyl-1,4,5,6-tetrachloro-2,3-dimethylbicyclo[2.2.0]hexene-2 (mp 113—115°C) (XI) were the products, along with a small amount of IX. The low reactivity toward ozone of the remaining ring-double-bond in XI had already been briefly described.[3] Further careful work has revealed that the ozonization of VII in carbon tetrachloride-methanol at −20°C resulted in the production of a new crystalline isoozonide, $C_{12}Cl_4H_{12}O_5$ (mp 182°C, decomp.) (XII) (16% yield), in addition to X (4%) and XI (66%). A trend to form this extremely stable isoozonide was demonstrated in the experiment; the result of the ozonization of XI in ethyl acetate in the presence of tetracyanoethylene, a very effective oxygen-acceptor of ozonide,[7] was essentially the same as that in an experiment without such a special reagent. In a much higher yield (70—80%), XII was obtained by the ozonization of VII either in carbon tetrachloride or in acetic acid at room temperature, and later, quantitatively from XI under the same conditions.

Several attempts to synthesize a compound like XIIIa or XIIIb bearing a "Dewar-benzene" structure were made, since it appeared that the substituents on the ring were bulky enough to stabilize it rather than the benzene derivative.[8] However, the high cyclizing tendency between the vicinal acetyl groups in XI was a decisive disadvantage for any dechlorinating agent used; with zinc metal in ethanol or nickel carbonyl in benzene, the only product isolated was a ketol (XIV) (mp

5) K. Mano, K. Kusuda and A. Fujino, *ibid.*, **1968**, 1375.
6) a) A. Furusaki and I. Nitta, *ibid.*, **1966**, 6027. b) A. Furusaki, This Bulletin, **49**, 2518 (1967).
7) R. Criegee and P. Günther, *Chem. Ber.*, **96**, 1564 (1963).
8) E. E. van Tamelen and S. P. Pappas, *J. Am. Chem. Soc.*, **84**, 3789 (1962); **85**, 3297 (1963).

160°C, *ca.* a 50% yield in either case), while with a freshly-prepared nickel metal in benzene, the reaction again ended with the production of XIV (20% yield), along with the dehydrated dienone (mp 192—193°C) (XV). Contrary to our expectations, attempts at the degradation of XI by oxidation with sodium hypobromite or with nitric acid to dicarboxylic acid also resulted in cyclization to XIV or a lactol (mp 167—169°C) (XVI).

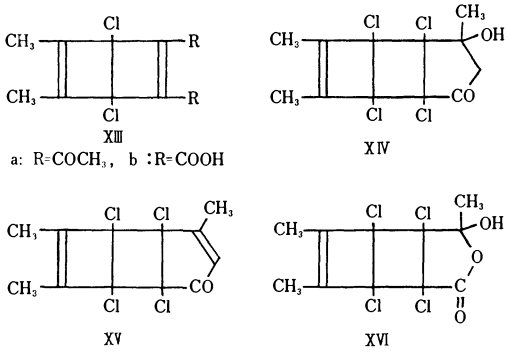

a: R=$COCH_3$, b: R=COOH

The isoozonide ring in XII was opened by catalytic hydrogenation over palladium charcoal in ethanol, giving all-*trans*-tetraacetylcyclobutane (mp 145°C) (XVII), identical with that reported by Griffin,[9] and the tetraketal (mp 282°C, decomp.) (XVIII) of its all-*cis*-isomer in a ratio of approximately 4 : 1. When a similar hydrogenation was carried out in the presence of sodium acetate, XVIII dominated XVII in the product yield. Chart 3 summarizes the results of the ozonization and hydrogenation of the compounds concerned.

Discussion

The reactivities of I toward various chemical reagents have been discussed in previous papers.[2,10,11] It can easily be inferred that II is a cycloaddition product, since the dimerization takes place in the thermal reaction at a high temperature, where the process is known to be essentially homolytic. The structural evidence for II and its degradation will be briefly discussed below.

Evidently, there is a close relationship between both the ultraviolet and the infrared spectral data of II and those of perchloro-(1,2-dimethylenecyclobutane) (XIX). The former gives rise to UV absorptions with the $\lambda_{max}^{n\text{-hexene}}$ of 287, 299, and 314 mμ (log ε 4.44, 4.65 and 4.43), which are, respectively, 8, 11 and 9 mμ shorter in their positions and 2—3 times more intense in their ε values than those described for the latter[1] (Fig. 1). The IR absorptions for the dichloromethylene groups of II ($\nu_{C=C}^{Nujol}$ 1610s, 1580s; $-C=CCl_2$ 910s[2] (cm^{-1})) consistently correspond to those (1605s, 1570s and 910s (cm^{-1}), Nujol mull) of XIX. The former compound resists chlorination under mild conditions, as, indeed, does the latter.

These data can reasonably be explained by assuming that II is composed of two units of the carbon skeleton of XIX. The permanganate oxidation of II to perchloro-(dimethylenesuccinic) acid has

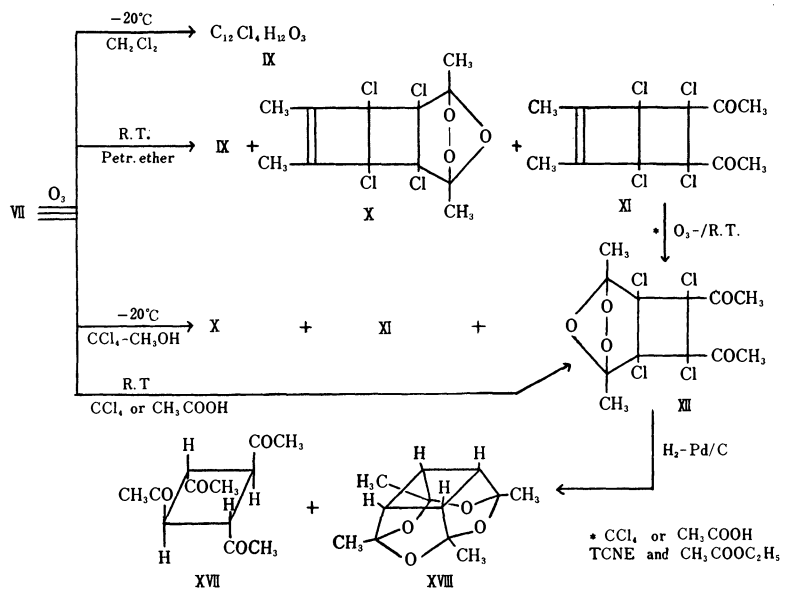

Chart 3

9) G. W. Griffin and R. B. Hager, *Rev. Chim. (Acad. Rep. Populaire Roumaine)*, **7**, 901 (1962).
10) A. Fujino, K. Kusuda and T. Sakan, This Bulletin, **39**, 160 (1966).
11) K. Mano, K. Kusuda, A. Fujino and T. Sakan, *ibid.*, **40**, 1188 (1967).

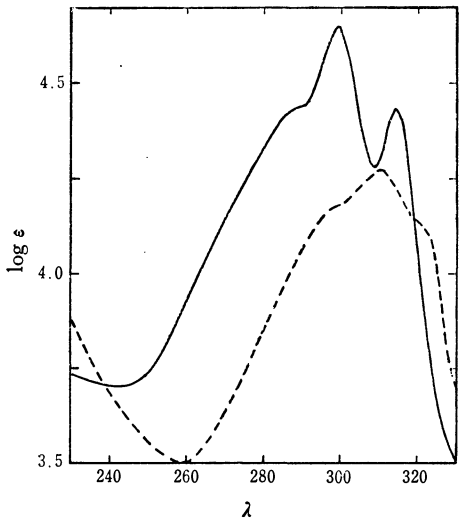

Fig. 1
—— Perchloro-(3,4,7,8-tetramethylenetricyclo-[4.2.0.0^{2,5}]octane) (II)
---- Perchloro-(1,2-dimethylenecyclobutane) (XIX)

proved the presence of at least one vicinal dichloromethylene pair in the molecule. As for the position where the new bonding results, no other possibility than C_1 and C_2 in I can be considered in view of the relative reactivity of the double bonds.[2] The $\Delta\lambda_{max}$ (*ca.* 10 mμ) between II and XIX may well be interpreted by evaluating the hyperconjugative effect[12] of allylic chlorine substituents on both and a double bond-central ring interaction for the former. If the λ_{max} of 246 mμ for 1,2-dimethylenecyclobutane[13] is taken as a reference value, the substitution of its four exomethylene hydrogens by chlorines should cause a bathochromic shift of 32—34 mμ.[14] This is a common factor in both. The further increment of *ca.* 30 mμ for XIX was discussed by assigning it to the hyperconjugative effect of four allylic chloro-substitutions on the ring (7.5 mμ/Cl).[2] However, a similar interaction does not seem so effective in II, where the increment of 20 mμ is to be ascribed only to the paired angular chloro-substitution. On the contrary, X-ray crystallographic analysis[15] suggests that in II the angle, for instance, between the C_1–Cl bond and the p_z orbital of C_2 is near 42°, which is significantly wider than is the corresponding one in XIX (*cf.* near 35° in perchlorocyclobutane[16]). This relationship holds also in solutions (less than 7.5 mμ/Cl in II). Therefore, it may be speculated that there exists some interaction between the double bonds and the central cyclobutane ring in II. White and Dunathan[17] observed similar spectral evidence in a tricyclo[4.2.0.0^{2,5}]octa-3,7-diene system. A few additional pieces of evidence supporting this interpretation have been obtained in the course of our study and will be published later.

The assignment of the VI structure to the tetrahydro-compound rests on the following observation: (a) VI is further smoothly reduced to VII suggesting that no hydrogen atom is attached to the angular carbons; (b) the appearance of some new characteristic IR-absorptions, $\nu_{=CH}^{Nujol}$ 3060 and 3050 and $\delta_{=CH}$ 810 vs (cm^{-1}); (c) the value calculated (282 mμ) for the λ_{max} of the UV-absorption based on the reference hydrocarbon[13] is in good accordance with the observed value (278 mμ) if the same bathochromic displacement factor (20 mμ) as above is again taken into account. Unfortunately, it was impossible to examine the stereochemical configuration of the four hydrogens by means of NMR spectrometry because of the extremely low solubility of the sample. However, an alternative structure, partly shown by VIa, may be ruled out since only one strong singlet absorption is observed in the frequency range 970—830 cm^{-1} in IR, where VIa should give rise to at least two strong, distinguishable bands, corresponding to dimethylene and dichloromethylene groups. The band at 810 cm^{-1}, the most intense band over the whole range, could be due to the deformations of the four –C(Cl)=CHCl groups. The observed doublet due to $\nu_{=CH}$ absorption appears to indicate the non-equivalence of the hydrogens like VIb in each paired chloromethylene group, although the data of measurement in solution are lacking.

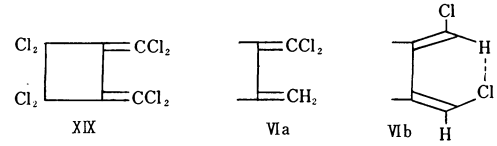

It is of interest to speculate on a possible course of the reduction of II to VI, in which the attack of the nascent hydrogen would first cause the replacement of one of the *endo*-chlorine atoms in each half of the molecule, resulting in some effective release of the Cl–Cl interaction. The distances in crystals[15] of Cl_2–$Cl_{3'(exo)}$ and $Cl_{4'(exo)}$–Cl_5 (both 3.32 Å), and of $Cl_{3'(endo)}$–$Cl_{4'(endo)}$ (3.28 Å), closer than twice the van der Waals radius of the chlorine atom, may reflect an interaction sufficient to make this stereospecificity possible.

12) E. A. Braude and E. S. Waight, "Progress in Stereochemistry," Vol. 1, ed. by W. Klyne, Butterworth Scientific Publication, London (1954), p. 154.
13) A. T. Blomquist and J. A. Verdol, *J. Am. Chem. Soc.*, **77**, 1806 (1955).
14) A. Roedig and E. Klappert, *Ann.*, **605**, 126 (1957).
15) A. Furusaki, This Bulletin, **40**, 758 (1967).
16) T. B. Owen and J. L. Hoard, *Acta Cryst.*, **4**, 172 (1951).
17) E. H. White and H. C. Dunathan, *J. Am. Chem. Soc.*, **86**, 453 (1964).

Nenitzescu *et al.*[18] reported obtaining *syn*- and *anti*-tricyclo[4.2.0.0^{2,5}]octa-3,7-diene (XXa and XXb) from 3,4-dichlorocyclobutene by dechlorination. A more analogous pair (XXc and XXd) was synthesized by, respectively, the dechlorination of the suitable cyclobutene derivative (XXIb)[19] and by the thermal decomposition of tetramethylcyclobutadienenickel chloride.[20] Mechanistically, the formations of *syn*-stereomer involving those with other substituents[17,21] have been classified as by way of true cyclobutadiene intermediates.[22] Table 1 lists some physical properties of VII and XXa—XXd, along with those for cyclobutene (XXIa) and its derivatives (XXIb—XXId). The difference (0.45) in τ values between VII and XXc and XXd seems too large even if some difference in the shielding effect of the β-positioned angular

TABLE 1. COMPARISON OF TETRAMETHYL-DERIVATIVE WITH RELATED COMPOUNDS

	IR $\nu_{C=C}$ (cm^{-1})	NMR =C-CH_3 (τ)	Dipole moment (D)
VII	1680[a]	8.12	0.46[b]
XXa	1545[c]		
XXb	1555[c]		
XXc	1684[a]	8.57[d]	0.64±0.19
XXd	1681[a]	8.57	
XXIa	1566[c,e]		
XXIb	1684[a,f]	8.35	2.38[g]
XXIc	1684[c,g]		
XXId		8.59[d]	

a) In carbon tetrachloride.
b) Measured with a dilute carbon tetrachloride solution.
c) Liquid film.
d) T. J. Katz and E. H. Gold, *J. Am. Chem. Soc.*, **86**, 1600 (1964).
e) R. C. Lord and K. W. Walker, *ibid.*, **76**, 2518 (1954).
f) Same value as with the *trans*-isomer.
g) R. Criegee and K. Noll, *Ann.*, **627**, 1 (1959).

substituents is considered. The unusually low τ value of VII might be explained by assuming an especially sterically-enhanced shielding of the γ-positioned chlorine atoms which are, in the *anti*-form, on the same side of the paired methyl groups with respect to the central ring. Inasmuch as a value higher by far than 2.38 D (for XXIb) may be expected as the dipole moment for the *syn*-form, the ring configuration in VII may be ascribed to the *anti*-form.

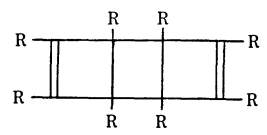

XX

a: R=H(*syn*)
b: R=H(*anti*)
c: R=CH_3(*syn*)
d: R=CH_3(*anti*)

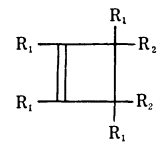

XXI

a: $R_1=R_2=H$
b: $R_1=CH_3$, R_2=Cl(*cie*)
c: $R_1=CH_3$, R=H
d: $R_1=R_2=CH_3$

The extreme low reactivity of bridge-head chlorine substituents in compounds having a fused ring has been reported in many cases.[23] The four angular chlorines in VII were also very inert to reducing or hydrolyzing agents, even when the most drastic conditions were used.

Supporting evidence for the VIII structure was obtained in the mass spectrometric analysis as well as in the UV (no chromophore above 210 mμ) and the IR (no C=C band) spectra. The observed spectrum contains main peaks of $m/e=166$ (molecular ion), M−15, M−29, M−42, 110, 95 (base peak), 81, 69, and 55, and one metastable ion peak of m* 59.65 (110→81). These data are in accord with the bicyclic structure and the following degradation pattern.

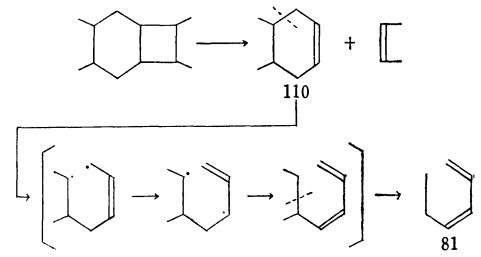

The NMR spectrum also indicates the presence of ten and twelve protons in the ranges of, respectively, 7.70—9.00 τ and 9.00—9.45 τ; this is consistent with the formula shown above.

In co-operation with us, Furusaki *et al.*[15] have made a detailed X-ray analysis of II as well as a two-dimensional X-ray analysis of VII and have confirmed, in agreement with our estimation,[24] that the *anti*-form is referred to both the compounds.

Although the composition of IX corresponds to the ozonide of VII, its structure has remained uncertain. The isomeric product, X, may be presumed to be a stable isoozonide of VII on the

18) M. Avram, I. G. Dinulescu, E. Marica, G. Mateescu, E. Sliam and C. D. Nenitzescu, *Chem. Ber.*, **97**, 382 (1964).
19) R. Criegee and G. Louis, *ibid.*, **90**, 417 (1957).
20) R. Criegee, G. Schröder, G. Maier and H. G. Fischer, *ibid.*, **93**, 1553 (1960).
21) a) H. H. Freedman and D. R. Petersen, *J. Am. Chem. Soc.*, **84**, 2837 (1962). b) Y. Kitahara, M. C. Caserio, F. Scardiglia and J. D. Roberts, *ibid.*, **82**, 3106 (1960).
22) M. P. Cava and M. J. Mitschell, "Cyclobutadiene and Related Compounds," Academic Press, New York and London (1967), Chapter 1 and 2.
23) E. L. Eliel, "Stereochemistry of Carbon Compounds," McGraw-Hill Book Company, Inc., New York (1962), Chapter 13.

basis of its behavior toward a potassium iodide-starch solution being similar to that of XII (to be described below), as well as on the basis of the spectral data ($\nu_{C=C}$ 1680 m (cm^{-1}), 8.13 τ for $C{=}CCH_3$ and 8.13 τ for $\rangle CCH_3$). Compare these values with those of the related compounds, VII (Table 1), XI ($\nu_{C=C}$ 1680 w (cm^{-1}); 8.15 τ for $C{=}CCH_3$ and 7.63 τ for $COCH_3$), and XII (8.10 τ for $\rangle CCH_3$ and 7.70 τ for $COCH_3$). In X there is no λ_{max} in the UV spectrum observable above 215 mμ, but there are signals in NMR for the vinylic methyl groups coinciding with those for the saturated C-methyl groups. As expected from the least-satisfactory peroxide detection, X does not suffer any hydrolysis with mineral acid, reduction with zinc - acetic acid, or oxidation with permanganate.

The spectral data (UV: no λ_{max} with an ε value higher than 10^3 above 210 mμ; IR: $\nu_{C=O}^{CCl_4}$ 1720s, doublet; $\nu_{C=C}$ 1680 w, δ_{CH_3} 1380 m, 1360s (cm^{-1}); NMR: as above; two singlets equal in intensity) of XI support the diketone structure.

The observation that there is a complicated solvent- and temperature-dependency of the products in the ozonization of VII is noteworthy. Attention should also be paid to the fact that the exhaustive ozonization of VII, or the successive ozonization of XI, at room temperature affords a unique product, isoozonide XII, in good yields regardless of the type of solvent used. In our interpretation, it seems most possible that the ozone-adduct (XXII) first formed from VII is normally converted to the methoxy hydroperoxide (XXIII) according to the Criegee mechanism for the low-temperature reaction in a polar solvent (containing methanol),[25] and that hence XI is obtained as a preponderant product. Although the isolation of XXIII as substantial evidence has been unsuccessful, the alternate process through the X isoozonide does not seem to fit, particularly when the solvent contains methanol. Evidently, the ozonization of XI in such a solvent as carbon tetrachloride-methanol or acetic acid does not afford an analogous hydroperoxide (XXVa or XXVb) which, if produced, could eventually be converted to the isolable tetraacetyl-compound (XXVI). The difference in the ozonization modes shown above may be accounted for by the difference in the ease of isoozonide formation from the corresponding intermediate zwitter ions, XXII and XXIV, the former of which is bicyclic and the latter, monocyclic. The ring strain unfavorable for isoozonide formation would be significantly higher in the former than in the latter. The unexpected results of the ozonization of XI, even in the presence of tetracyanoethylene, indicate that the transfer of an oxygen atom from XXIV to the acceptor can not compete with the very smooth formation of the isoozonide ring.

Proofs for the structures of XIV and XV are as follows: (a) For XIV: IR: ν_{OH}^{Nujol} 3570s, 3490m, $\nu_{C=O}$ 1760s, $\nu_{C=C}$ 1680m, lack of a band at 1360 (cm^{-1}); NMR: 8.15 (6H, singlet, vinylic methyls), 8.72 (3H, singlet, saturated C-methyl), 6.80 (OH), and 6.50 and 7.27 (doublet, J=15.5 cps, methylene) (τ); (b) For XV: UV: λ_{max}^{EtOH} 225 mμ (log ε 3.97); IR: $\nu_{CH}^{CHCl_3}$ 3020w, $\nu_{C=O}$ 1740s, $\nu_{C=C}$ 1690w, 1625m (cm^{-1}); NMR: 3.90 (1H, quartet), 7.70 (3H, doublet, J=3 cps), 8.12 (6H, singlet) (τ).

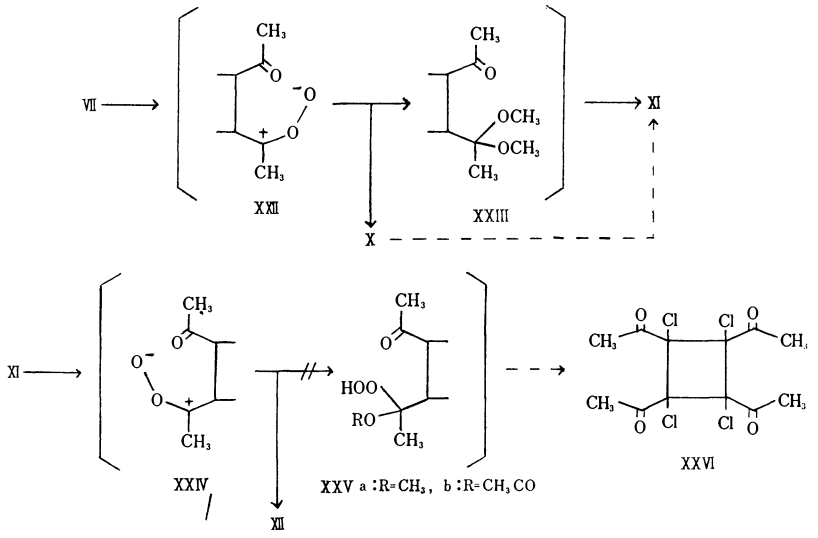

24) Criegee *et al.*[20] describes an ozonization product of XXc, which can not be formulated as *syn*-5,6-diacetyl-1,2,3,4,5,6-hexamethylbicyclo[2.2.0]hexene-2 and probably be an unsaturated ketoether formed by a transannular reaction between the carbonyl groups and the sterically neighboring ring double bond in the expected bicyclohexene-2. If the *syn*-type is given to VII, the ozonolyzed product would be an analogous ketoether and not be diketone XI as is our case.

25) P. S. Bailey, *Chem. Revs.*, **58**, 925 (1958).

The easy occurrence of the intramolecular aldol-type cyclization from XI to XIV, followed by the dehydration to dienone XV, has indeed been a high barrier to approaching the "Dewar benzene." It has also made unsuccessful the attempted oxidation of XI with hypobromite - methanol, which would lead to another potential compound for the especially interesting benzene isomer. Contrary to the reported case with a permethyl analog,[26] the undesired XIV was obtained almost quantitatively. Nitric acid (sp. gr. 1.38) oxidizes one of the acetyl groups of XI to the carboxyl, which is then lactonized with the residual keto-group to form XVI. The structural evidence for XVI is: IR: ν_{OH}^{Nujol} 3320s, $\nu_{C=O}$ 1780s, $\nu_{C=C}$ 1690m (cm^{-1}); NMR: 7.99 (1.4H, singlet, $COCH_3$ due to partial dissociation), 8.13 (6H, singlet), 8.34 (1.6H, singlet) (τ) (in $CDCl_3$).

Practically, the hydrogenation was the only way achieved to cleave the isoozonide ring of XII, which strongly resists conversion to XXVI. Thus, the products were two isomeric chlorine-free compounds, XVII and XVIII. The spectral data for XVII (UV: λ_{max}^{EtOH} 283 mμ log ε 2.08; IR: $\nu_{OH}^{CHCl_3}$ 3400w, ν_{CH_3} 3030m, 3005m, ν_{CH} 2910w, $\nu_{C=O}$ 1715vs, $\nu_{C=C}$ 1675w, δ_{CH_3} 1425m, 1360s (cm^{-1}); NMR: 6.39 and 7.79 (both singlets, intensity ratio 1 : 3) (τ)) do not contradict the structure of all-*trans*-1,2,3,4-tetraacetylcyclobutane. The identification has been established by an IR spectra comparison between XVII and an authentic sample kindly offered by Professor Griffin. With both samples, the spectra in the solid state indicate weak absorptions for hydroxyl group and the C=C double bond absorptions, which become much weaker still when measured in chloroform. No OH-signal can be noticed in the NMR spectrum taken in D-chloroform. These facts suggest that at least one of the four acetyl groups in XVII exists in an enol-form in the solid; the equilibrium in solution between keto- and enol-forms is by far in favor of the former (more than 90% in the saturated solution). The production of the all-*trans*-isomer further suggests the inversion of at least two of the carbon moieties attached to the cyclobutane ring of XII.

Product XVIII shows much lower solubilities in alcohol, acetone, chloroform, carbon tetrachloride, *etc.*, than those for XVII, which is easily isolated by the recrystallization of the mixture. The IR (no carbonyl) and the NMR (6.76 and 8.47 (τ)) spectral data accord with the suggested structure. An analogous compound with the intramolecular tetraketal type has been reported by Criegee *et al.*;[20] *i. e.*, XXc was converted to the tetraketal of all-*cis*-1,2,3,4-tetraacetyl-1,2,3,4-tetramethylcyclobutane. Although a certain similarity was observed between the mass spectral data of XVII and XVIII, a significant difference was found in their base peaks (*m/e* 43 for acetyl and 18 for H_2O respectively), a difference which can reasonably be explained in terms of the proposed structures.

26) R. Criegee, W. D. Wirth, W. Engel and H. A. Brune, *Chem. Ber.*, **96**, 2230 (1963).

Experimental[27]

***anti*-Perchloro - (3,4,7,8 - tetramethylenetricyclo-[4.2.0.0^{2,5}]octane (II) from Perchloro-(3,4-dimethylenecylobutene) (I).** *a) By Pyrolysis.* In a sublimation apparatus, I (10 g, 35 mmol) was carefully heated at 155—165°C (oil bath temperature) for 3 hr without water in the cold finger. When the pyrolysis was over, water running was allowed to enter and there was collected a small amount of unreacted I by vacuum sublimation at 130—140°C/3 mmHg. The residue was refluxed with ligroin (300 m*l*) to remove the tarry by-product, and the insoluble fraction was, after filtration, recrystallized from carbon tetrachloride to give II (2.8 g, 5 mmol). Yield: 28%. Mp 266°C.

Found: C, 25.77; H, 0.90; Cl, 75.04%. Calcd for $C_{12}Cl_{12}$: C, 25.30; H, 0.00; Cl, 74.70%.

b) With Anhydrous Aluminum Chloride. To crystals of I (2.5 g, 8.8 mmol) well-mixed with anhydrous aluminum chloride (2.5 g, 19 mmol), dichloromethane (3 m*l*) was added while the moisture was shut off. The mixture immediately turned green, evolving hydrogen chloride. It was then allowed to stand at room temperature overnight. The reaction mixture was poured onto ice water, shaken with carbon tetrachloride (10 m*l*), and an insoluble fraction was separated by the decantation of the aqueous layer. Crude crystals (1.6 g, 2.8 mmol) of II were thus obtained. Yield: 64%.

Oxidation of II with Potassium Permanganate. A suspension of II (570 mg, 1.0 mmol) in acetone (100 m*l*) was vigorously stirred under refluxing, and then powdered potassium permanganate (1.4 g, 7.8 mmol) was added, portion by portion. After the complete consumption of the oxidizing agent, manganese dioxide was filtered off and washed with hot water. The filtrate was evaporated under reduced pressure to give the residue, which was, after being dissolved in ether, separated into acidic and neutral parts by the ordinary procedure. From the acidic fraction there was obtained a crystalline product (50 mg) which was recrystallized from water to furnish a pure sample (mp 215°C, decomp.) identical in all respects with authentic perchloro-(dimethylenesuccinic) acid.[2] The neutral fraction gave recovered II (26 mg).

Reduction of II with Zinc in Ethanol, *anti*-1,2,3',4',5,6,7',8'-Octachloro-3,4,7,8-tetramethylenetricyclo[4.2.0.0^{2,5}]octane (VI). Zinc powder freshly treated with dilute hydrochloric acid was added to a suspension of II (2.60 g, 4.5 mmol) in ethanol (280 m*l*), and the mixture was then heated under refluxing for 1.3 hr. The reaction mixture was centrifuged to separate

27) The differential thermal analysis data will be described in the succeeding paper. All melting points are measured under microscope and not corrected. Ultraviolet spectra are taken with Hitachi Ultraviolet Spectrophotometer EPS-2U, infrared spectra with Perkin-Elmer Infrared Spectrophotometer Model 337, and NMR spectra with Nuclear Magnetic Resonance Spectrometer JNM-C-60.

the insoluble material. The mud thus obtained was extracted with a large amount of boiling benzene to give the crude VI (1.20 g, 2.8 mmol) in a 62% yield. Recrystallization from carbon tetrachloride afforded a pure sample, mp 223—225°C.

Found: C, 32.96; H, 1.25; Cl, 66.03%. Calcd for $C_{12}Cl_8H_4$: C, 33.38; H, 0.93; Cl, 65.74%. λ_{max}^{EtOH} 278 (4.26), λ_{sh} 290 (4.04) mμ (log ε). ν_{CH}^{Nujol} 3060m, 3050m, $\nu_{C=C}$ 1650w, 1620s; $\delta_{=CH}$ 810vs (cm^{-1}).

Similarly, the reduction of II (570 mg) with zinc powder (5.0 g) in acetic acid (35 m*l*) at room temperature for 1 hr resulted in the isolation of VI (99 mg). Yield: 23%.

***anti*-1,2,5,6-Tetrachloro-3,4,7,8-tetramethyltricyclo[4.2.0.0^{2,5}]octa-3,7-diene (VII).** *a) Catalytic Hydrogenation of II.* In an autoclave (500 cc), a suspension of II (5.70 g, 10 mmol) in ethanol (300 m*l*) was, after the addition of 5% palladium-charcoal (5.0 g) and sodium acetate (12.0 g), stirred at room temperature under a compressed hydrogen atmosphere for 50 hr, during this period the initial pressure (60 atm) dropped to 32 atm. The product solution was filtered, concentrated, and extracted with petroleum ether, from which solution crude crystals (2.3 g, 7.7 mmol) of VII were isolated with a slight contamination of an oily material. Recrystallization from ethanol and subsequent sublimation at 100°C/3 mmHg afforded a pure sample. Mp 180°C, decomp.

Found: C, 48.35; H, 4.06; Cl, 47.43%. Calcd for $C_{12}Cl_4H_{12}$: C, 48.32; H, 4.02; Cl, 47.65%. No absorption maximum above 210 mμ (ethanol solution).

b) Catalytic Hydrogenation of VI. In an autoclave (50 cc), VI (650 mg, 1.5 mmol), 5% palladium-charcoal (800 mg), and sodium acetate (1.50 g) were suspended in methanol (300 m*l*), after which the whole mixture was shaken with an initial hydrogen pressure of 60 atm at room temperature for 77 hr. The final pressure was 30 atm. The same subsequent treatment as above gave VII (100 mg, 34% yield).

3,4,7,8-Tetramethylbicyclo[4.2.0]octane (VIII). The oily fraction separated in the recrystallization of VII in a) was vacuum-distilled; bp 80—100°C (bath)/20 mmHg. The gas chromatographic analysis of the colorless distillate showed a purity of approx. 98%.[28] No chlorine appeared in a Beilstein test.

Found: C, 86.80; H, 13.20%. Calcd for $C_{12}H_{22}$: C, 86.74; H, 13.25%. No absorption maximum above 210 mμ (ethanol solution). IR: 2950s, 2920s, 2860s, 1470s, 1460s, 1380s, 1010w (cm^{-1}) (liquid film). NMR: 7.70—9.00 (10H), 9.00—9.45 (multiplet, 12H) (τ) (CCl_4).

Ozonization of VII under Various Conditions. *a) In Carbon Tetrachloride-Methanol at a Low Temperature.* A stream of oxygen-ozone was passed into a suspension of VII (3.00 g, 10 mmol) in a mixture of carbon tetrachloride (220 m*l*)) and methanol (300 m*l*) which had been cooled at −20°C until the suspension disappeared and the solution VII became completely clear. On the evaporation of the solvent under diminished pressure at 0°C, white crystals (3.11 g) were obtained. The crude product was dissolved in carbon tetrachloride and chromatographed on silica gel (Mallinckrodt Chem. Works, 100 mesh,[29] 40 g) with the same developing solvent. From the No. 1 fraction (20 m*l*) unreacted VII (230 mg) was obtained. The No. 4, 5, and 6 fractions furnished, on the evaporation of the solvent, colorless crystals (130 mg in total, 4.0% yield), which were then recrystallized from ethanol to give a pure sample (mp 122—124°C) of X.

Found: C, 42.03; H, 3.56; Cl, 40.64%. Calcd for $C_{12}Cl_4H_{12}O_3$: C, 41.62; H, 3.47; Cl, 41.04%. No absorption maximum above 215 mμ (ethanol solution). $\nu_{C=C}^{Nujol}$ 1680 cm^{-1}. 8.13 τ (singlet, CCl_4).

The adsorbed product was further developed with carbon tetrachloride - chloroform (1 : 1 by vol.). The eluted crystals (2.04 g, 66% yield) were recrystallized from ethanol. The pure XI melted at 113—115°C.

Found: C, 43.75; H, 3.68; Cl, 42.78%. Calcd for $C_{12}Cl_4H_{12}O_2$: C, 43.64; H, 3.64; Cl, 43.03%. $\nu_{C=C}^{CCl_4}$ 1720s, 1710s, $\nu_{C=C}$ 1680w, δ_{CH_3} 1380m, 1360s (cm^{-1}); 7.63 (singlet, 6H), 8.15 (singlet, 6H) (τ) (CCl_4).

Finally, an ether - chloroform mixture (1 : 1) eluted the third fraction (549 mg) of crystals, which were purified to XII by recrystallization from ethanol. Mp 182°C (decomp.). Yield: 16%. Positive to a potassium iodide-starch test.

Found: C, 38.41; H, 3.24; Cl, 38.17%. Calcd for $C_{12}Cl_4H_{12}O_5$: C, 38.10; H, 3.17; Cl, 37.57%. $\nu_{C=C}^{CCl_4}$ 1750s, 1730s, δ_{CH_3} 1380s, 1360s (cm^{-1}); 7.70 (singlet, 6H), 8.10 (6H) (τ) ($CDCl_3$).

b) In Dichloromethane or Carbon Tetrachloride - Chloroform at a Low Temperature. By essentially the same procedure as above, a viscous oil (800 mg) was obtained from a solution of VII (600 mg, 2 mmol) in dichloromethane (100 m*l*) by ozonization, followed by solvent evaporation. Nitric acid (sp. gr. 1.38, 2 g) was then added to the oil, and the mixture was heated at 100°C on a water bath for 1 hr, during this time some crystals were sublimated on the wall of the cooler. Ether extraction from the aqueous solution and the subsequent fractionation of the neutral part furnished a crystal sludge (300 mg). The chromatography of the benzene solution on aluminum oxide (Woelm, neutral, activation grade 1, 6 g) gave a fraction of IX (180 mg, 26% yield), which was then eluted with acetone and further purified by recrystallization from benzene or by vacuum sublimation (100°C (bath)/3 mmHg). Mp 125—127°C. 25 mg.

Found: C, 41.75; H, 3.56; Cl, 40.51%. Calcd for $C_{12}Cl_4H_{12}O_3$: C, 41.62; H, 3.47; Cl, 41.04%. No absorption maximum above 215 mμ (ethanol solution). Starting with the same amount of VII, ozonization in carbon tetrachloride - chloroform at −20°C afforded the identical oily product (720 mg), from which IX (155 mg, crude) was isolated.

c) In Petroleum Ether at Room Temperature. After the ozonization of VII (600 mg, 2 mmol) in petroleum ether (boiling below 45°C, 70 m*l*) at room temperature, a crystal sludge (600 mg) was obtained. It was dissolved again in petroleum ether and chromatographed on silica gel much as in a). 1) Petroleum ether - carbon tetrachloride eluted first a crystalline material (mp 122—124°C, 59 mg) identical with X. Yield:

28) Hitachi Perkin-Elmer Gas Chromatography Model F6D; Carrier gas: nitrogen; Column: 3 mmOD × 1 m packed with SE-30 Silicon Oil on Chromosorb W. Programmed from 50°C to 150°C.

29) The same silica gel will be used hereinafter.

8%. 2) The next crop, eluted with carbon tetrachloride alone, was the crude XI (107 mg, 16% yield), melting at 113—115°C after recrystallization from methanol. 3) Finally, crystals (40 mg) identical with IX were eluted with chloroform. Yield: 6%. Mp 125—127°C.

d) In Carbon Tetrachloride or Acetic Acid at Room Temperature. From VII (300 mg, 1 mmol) dissolved in carbon tetrachloride (10 ml) and water (1 ml), a crystalline product (220 mg) identical with XII was obtained; it was then recrystallized from carbon tetrachloride. Mp 182°C (decomp.). The runs with acetic acid as a solvent resulted in a comparable yield of XII.

Ozonization of 5,6-Diacetyl-1,4,5,6-tetrachloro-2,3-dimethylbicyclo[2.2.0]hexene-2 (XI). *a) In Acetic Acid or Carbon Tetrachloride at Room Temperature.* At room temperature, XI (900 mg, 2.7 mmol) dissolved in acetic acid (40 ml) and water (10 ml) was ozonized for 3 hr after which period some solid material crystallized out. The ozone-passing was stopped after an additional hour, and the solvent was evaporated. The residue consisted of colorless prisms of XII melting at 182°C (1.00 g). When carbon tetrachloride (15 ml) was used as the ozonization solvent, the yield of XII was 72% from XI (750 mg, 2.1 mmol).

b) In Ethyl Acetate at Room Temperature in the Presence of Tetracyanoethylene (TCNE). From XI (330 mg, 1 mmol) dissolved in ethyl acetate (20 ml), after working up ozonization in the presence of TCNE (160 mg, 1.25 mmol) afforded XII (230 mg, 61% yield).

Attempted Dechlorinations of XII to a Dewar Benzene (XIII). *a) With Zinc Powder-Ethanol or Nickel Carbonyl in Benzene; 1,2,5,6-Tetrachloro-7-hydroxy-3,4,9-trimethyl-7-oxotricyclo[4.3.0.0^{2,5}]nonene-3 (XIV).* After XI (400 mg, 1.2 mmol) had been refluxed with zinc powder (250 mg) in ethanol (10 ml) for 3 hr the soluble material was filtered off. The evaporation of the solvent of the filtrate furnished a crystalline product, which was then purified by chromatography on silica gel (5 g). The fraction eluted with chloroform afforded, on solvent evaporation, white crystals (206 mg) of XIV. Mp 150—156°C. Recrystallization from carbon tetrachloride gave a pure sample melting at 160°C. Yield: 52%.

Found: C, 43.91; H, 3.95; Cl, 42.86%. Calcd for $C_{12}Cl_4H_{12}O_2$: C, 43.64; H, 3.64; Cl, 43.03%.

The run with XI (300 mg, 1 mmol) and nickel carbonyl (27% benzene solution, 2 ml) also resulted in the production of XIV (150 mg, 0.5 mmol).

b) With Freshly-Prepared Nickel Metal; 1,2,5,6-Tetrachloro-3,4,9-trimethyl-7-oxotricyclo[4.3.0.0^{2,5}]nona-3,7-diene (XV). Nickel formate (10.6 g, 71 mmol) was pyrolyzed under reduced pressure at 245°C. After complete decarboxylation and spontaneous cooling, a solution of XI (580 mg, 1.75 mmol) in anhydrous benzene (20 ml) was added under a nitrogen atmosphere and the suspension was refluxed for 2 hr. The reaction mixture was then cooled and filtered, and the solid residue was washed with benzene. On the evaporation of the solvent of the filtrate, a crystalline product (crude XV, 470 mg) was obtained. Chromatographical purification on silica gel (10 g) afforded a fraction (200 mg, 0.64 mmol) eluted with carbon tetrachloride. Further recrystallization from the same solvent gave colorless prisms melting at 192—193°C.

Found: C, 46.24; H, 3.37; Cl, 45.68%. Calcd for $C_{12}Cl_4H_{10}O$: C, 46.15; H, 3.21; Cl, 45.51%.

A second crop (116 mg), isolated by subsequent elution with chloroform, was identical with the XIV obtained in a). Mp 160°C. Yield 21%.

Oxidation of XI with Sodium Hypobromite; Conversion to XIV. A methanol solution (20 ml) of XI (100 mg) was added to a 10% aqueous solution (30 ml) of sodium hydroxide and bromine (0.2 ml), whereupon an exothermal reaction occurred, turning the solution dark yellow. After the solution had been allowed to stand overnight, the product was isolated according to the ordinary procedure. From the neutral fraction XIV was obtained in an almost quantitative yield. Mp 160°C. No detectable amount of the acidic fraction was found.

Nitric Acid Oxidation of XI; Lactol (XVI). A mixture of the crude XI (900 mg, 2.7 mmol) and nitric acid (sp. gr. 1.38, 50 ml) was kept at 80°C for 2.5 hr. From the bicarbonate-soluble fraction, the product (200 mg) was precipitated on acidification. It was purified by chromatography on silica gel. The fraction eluted with chloroform consisted of colorless crystals, which were then further recrystallized from the same solvent to give a pure sample. Mp 167—169°C.

Found: C, 39.74; H, 3.12; Cl, 42.29%. Calcd for $C_{11}Cl_4H_{10}O_3$: C, 39.76; H, 3.01; Cl, 42.77%. No 1360 cm^{-1} band originally observed in XI was found.

Catalytic Hydrogenation of XII; all-*trans*-Tetraacetylcyclobutane (XVII) and Tetraketal of all-*cis*-Tetraacetylcyclobutane (XVIII). *a) Without Sodium Acetate.* The solution of XII (1.00 g, 2.65 mmol) in ethanol (100 ml) was subjected to hydrogenation at an ordinary pressure over 5% palladium-charcoal (1.0 g). The absorption of hydrogen ceased when a 5.42 equimolar amount had been consumed. The catalyst was then filtered and washed. The filterate was concentrated by evaporation at reduced pressure to approx. one-third the original volume. During this process, the solution gradually turned dark brown. Complete evaporation resulted in a mixture of white crystals and a brown oil, the latter of which was removed by being dissolved in water. White crystals (250 mg), when showed no chlorine contamination when submitted to a Beilstein test, were recrystallized from methanol to give pure needle crystals of XVIII (50 mg) melting at 282°C under decomposition. No carbonyl band was observed in the IR spectrum. Yield: *ca.* 8%.

Found: C, 64.20; H, 7.37%. Calcd for $C_{12}H_{16}O_4$: C, 64.28; H, 7.14%. IR: 3020m, 2980s, 2940m, 1460m, 1380s (hexachlorobutadiene mull); 1330s, 1300s, 1260s, 1200—1130 (broad), 1000—880 (5 bands), 805—800 (doublet), 650—635 (doublet), 530s (Nujol mull) (cm^{-1}) NMR: 6.76 (singlet, 4H), and 8.47 (singlet, 12H) (τ) ($CDCl_3$).

The filtrate of the recrystallization of XVIII furnished on the evaporation of the methanol, crystals (mp 133—134°C) slightly contaminated by XVIII. Recrystallization from acetone gave pure needle crystals of XVII (mp 145°C), identical with an authentic sample of all-*trans*-tetraacetylcyclobutane[9] (reported melting point: 139—140°C) in a comparison of the IR spectra.

Found: C, 64.05; H, 7.20%. Calcd for $C_{12}H_{16}O_4$: C, 64.28; H, 7.14%.

b) With Sodium Acetate. In ethanol (80 ml), XII

917 mg, 2.42 mmol) was hydrogenated at ordinary pressure over 5% palladium-charcoal with sodium acetate (1.62 g). In all 5.04 equimolar hydrogen was absorbed. Treatment similar to that in a) gave a mixture of colorless oil and crystals. The mixture was washed with dilute hydrochloric acid to remove the sodium acetate recovered and the sodium chloride formed. The crystals thus obtained were almost XVII-free. Vacuum sublimation at 100°C (bath)/3 mmHg afforded pure needle crystals (mp 282°C, decomp.). Yield: *ca.* 20%.

We wish to express our deep thanks to Professor G. W. Griffin, Louisiana State University, New Orleans, Louisiana, U. S. A., for his kind gift of the sample for identification, and to Professor I. Nitta and Dr. A. Furusaki, Kwansei Gakuin University, for their X-ray analyses. Thanks are also due to Mr. Goda, Osaka City University for his elemental analyses.

BULLETIN OF THE CHEMICAL SOCIETY OF JAPAN VOL. 41 1413—1417 (1968)

Synthetic Studies of the Flavone Derivatives. VII.*1 The Synthesis of Jaceidin

Kenji FUKUI, Takashi MATSUMOTO, Shigehiro NAKAMURA and Mitsuru NAKAYAMA

Department of Chemistry, Faculty of Science, Hiroshima University, Higashi-sendamachi, Hiroshima

and Tokunaru HORIE

Department of Applied Chemistry, Faculty of Engineering, University of Tokushima, Tokushima

(Received December 16, 1967)

The Hoesch reaction of iretol with methoxyacetonitrile yielded 2,4,6-trihydroxy-3,ω-dimethoxyacetophenone. According to the Allan-Robinson flavone synthesis with *O*-benzylvanillic anhydride, the acetophenone afforded 4'-benzyloxy-5,7-dihydroxy-3,3',6-trimethoxyflavone. The catalytic debenzylation of the flavone gave jaceidin, 4',5,7-trihydroxy-3,3',6-trimethoxyflavone, which had previously been isolated from Centaurea species. Its triethyl ether was prepared from 3,5-diethoxy-4-methoxyphenol *via* the corresponding acetophenone, followed by the above-mentioned flavone synthesis with *O*-ethylvanillic anhydride. The ultraviolet spectra of these flavones will also be reported.

Jaceidin (I) was isolated from the leaves and stems of *Centaurea jacea* L. by Farkas *et al.*[1] Their hydrolysis of I with hydrochloric acid afforded an aglycone, jaceidin. They established the structure of jaceidin to be 4',5,7-trihydroxy-3,3',6-trimethoxyflavone (II) on the basis of analytical data, the results of the degradation reaction, and a comparison of the triethyl ether (III) with a synthetic sample.

Recently, I and II have also been isolated from the Centaurea species by Bowie *et al.*[2] and by Bohlmann *et al.*[3]

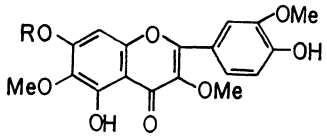

I R=Glycosyl
II R=H

The present paper deals with the total synthesis of jaceidin (II) and confirms the proposed structure. The Hoesch reaction of iretol (IV) with methoxyacetonitrile yielded 2,4,6-trihydroxy-3,ω-dimethoxyacetophenone (V). According to Allan-Robinson's flavone synthesis, the condensation of V with *O*-benzylvanillic anhydride (VI) in the presence of triethylamine, followed by treatment with alcoholic potassium hydroxide, affords a hydroxyflavone, which then gives a diacetate. Two structures (VII and VIII) may be expected for this hydroxyflavone. In order to elucidate the structure of the flavone, a diethyl derivative, which was easily obtained with diethyl sulfate and anhydrous potassium carbonate in dry acetone, was synthesized by the following unambiguous method.

3,5-Diethoxy-4-methoxyphenol (IX) was converted to 4,6-diethoxy-2-hydroxy-5,ω-dimethoxyacetophenone (X) by a Hoesch condensation with methoxyacetonitrile or by a Friedel-Crafts reaction with methoxyacetyl chloride. The ketone (X),

*1 This has been reported in a preliminary form: K. Fukui, T. Matsumoto, S. Nakamura, M. Nakayama and T. Horie, *Experientia*, **24**, 108 (1968).
Part VI of this series: T. Horie, M. Masumura, K. Fukui and M. Nakayama, This Bulletin, **41**, 1460 (1968).

1) L. Farkas, L. Hörhammer, H. Wagner, H. Rösler and R. Gurniak, *Chem. Ber.*, **97**, 610 (1964).

2) J. H. Bowie and D. W. Cameron, *J. Chem. Soc.*, **1965**, 5651.

3) F. Bohlmann and C. Zdero, *Tetrahedron Letters*, **No. 33**, 3239 (1967).

when subjected to the Allan-Robinson flavone synthesis using VI, gave 4'-benzyloxy-5,7-diethoxy-3,3',6-trimethoxyflavone (XI), which was identified by a direct comparison with the diethyl derivative obtained by the ethylation of the hydroxyflavone. Furthermore, the partial methylation of the hydroxyflavone with diazomethane gave the monomethyl ether (XII), which was then debenzylated to give 4',5-dihydroxy-3,3',6,7-tetramethoxyflavone (XIII). This was also identified by direct comparison with an authentic sample, prepared by the method of

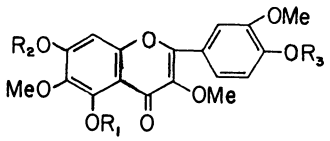

III $R_1=R_2=R_3=Et$
VII $R_1=R_2=H$, $R_3=Bz$
XI $R_1=R_2=Et$, $R_3=Bz$
XII $R_1=H$, $R_2=Me$, $R_3=Bz$
XIII $R_1=R_3=H$, $R_2=Me$
XIV $R_1=R_2=R_3=Ac$
XV $R_1=R_2=R_3=Me$
XVI $R_1=H$, $R_2=R_3=Me$

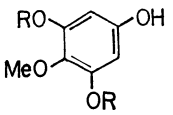

IV R=H
IX R=Et

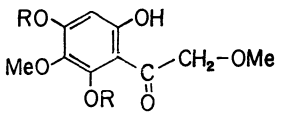

V R=H
X R=Et

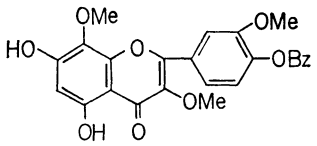

VIII

Bz=Benzyl

Hörhammer *et al.*[4] From these facts, the structure of the hydroxyflavone was established as 4'-benzyloxy-5,7-dihydroxy-3,3',6-trimethoxyflavone (VII).

The catalytic debenzylation of VII gave the desired flavone (II), which was shown to be identical with natural jaceidin by a mixed-melting-point determination, and by NMR, infrared, and ultraviolet spectral comparisons.

The infrared and ultraviolet spectra of synthetic and natural jaceidin are superimposable, as is shown in Figs. 1 and 2 and in Table 1. By the addition of fused sodium acetate,[5] the short-wavelength bands of jaceidin (II) and 4'-benzyl ether (VII) in ethanol undergo bathochromic shifts (18 mμ and 20.5 mμ), which show the presence of a free 7-hydroxyl group. The 5-hydroxyl group in II and VII is indicated by the bathochromic shifts (20 mμ and 19 mμ) of the

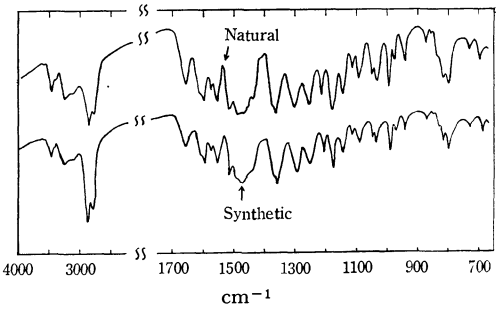

Fig. 1. Infrared spectra of natural and synthetic jaceidin in Nujol.

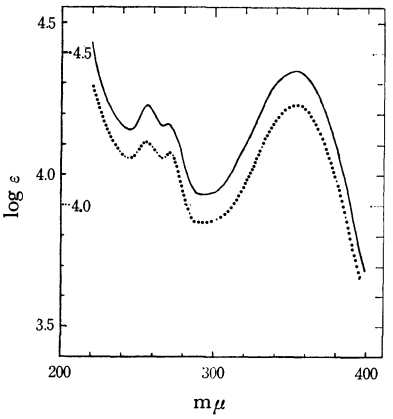

Fig. 2. Ultraviolet spectra of natural (·····) and synthetic jaceidin (——) in ethanol.

long-wavelength band in the presence of aluminum chloride.[6] The large bathochromic shift (64.5 mμ) of the long-wavelength band, without a decrease in its relative intensity, observed on making the ethanol solution of II alkaline indicates a 4'-hydroxyl group.[6] Both II and VII are stable in an alkaline solution, for when the alkaline solution is acidified, the spectra change to the parent respective spectrum in ethanol.

The synthetic jaceidin was converted to triacetate (XIV), trimethyl ether (XV), triethyl ether (III), and artemetin (XVI) by the usual method. The triethyl ether (III) was also synthesized by the

4) L. Hörhammer, H. Wagner, E. Graf and L. Farkas, *Chem. Ber.*, **98**, 548 (1965).

5) L. Jurd and R. M. Horowitz, *J. Org. Chem.*, **22**, 1618 (1957).

6) L. Jurd, "The Chemistry of Flavonoid Compounds," ed. by T. A. Geissman, Pergamon Press, Oxford (1962), Chap. 5.

Table 1. Ultraviolet spectra of natural and synthetic jaceidin (II) and its 4'-benzyl ether (VII)

	λ_{max}, mμ (log ε)				
	EtOH	NaOAc*3	$AlCl_3$*4	NaOH*4	NaOH-HCl*5
Synthetic jaceidin (II)	257 (4.23) 272.5(4.17) 353 (4.34)	275 (4.32) 323 (4.09) 373 (4.24)	265.5(4.21) 281.5(4.19) 373 (4.32)	273.5(4.33) 339 (4.15) 417.5(4.48)	257.5(4.21) 270*2 (4.14) 353 (4.30)
Natural jaceidin	257 (4.21) 272.5(4.16) 354 (4.33)	275 (4.31) 323 (4.08) 373 (4.23)	265.5(4.20) 281.5(4.18) 373 (4.31)		
VII	256 (4.21) 274 (4.20) 347 (4.31)	276.5(4.39) 315 (4.10) 381 (4.19)	262.5(4.21) 284.5(4.19) 366 (4.31)	277 (4.46) 314 (4.18) 382 (4.24)	256.5(4.22) 272.5(4.18) 346 (4.31)

Allan-Robinson reaction of the ketone (X) with *O*-ethylvanillic anhydride.

Experimental*6

2, 4, 6-Trihydroxy-3, ω-dimethoxyacetophenone (V). A mixture of iretol (IV)[7] (5.0 g), methoxyacetonitrile (3.0 g), and anhydrous zinc chloride (8.2 g) in anhydrous ether (500 m*l*) was saturated with dried hydrogen chloride in an ice bath and then allowed to stand overnight. After the ether layer had been decanted, the ketimine hydrochloride was washed with anhydrous ether and then hydrolyzed with water (200 m*l*) on a steam-bath for 30 min. The mixture was evaporated under a vacuum, and the residue (*ca.* 50 m*l*) was extracted with ethyl acetate. The extract was washed with water, dried, and evaporated. The residue was recrystallized from water to give colorless needles, mp 79—80°C.

Found: C, 45.49; H, 5.96%. Calcd for $C_{10}H_{12}O_6 \cdot 2H_2O$: C, 45.45; H, 6.10%.

These needles were recrystallized from dry toluene to give colorless needles, mp 157—158°C; yield 4.3 g. They gave a dark green ferric chloride reaction in ethanol.

Found: C, 52.94; H, 5.31%. Calcd for $C_{10}H_{12}O_6$: C, 52.63; H, 5.30%.

4'-Benzyloxy-5, 7-dihydroxy-3, 3', 6-trimethoxyflavone (VII). A mixture of the ketone (V) (1.0 g), *O*-benzylvanillic anhydride (8.7 g), and triethylamine (2.2 g) was heated at 170°C for 5 hr under a stream of nitrogen. The reaction mixture was then cooled, powdered, and refluxed with a solution of potassium hydroxide (9.5 g) in aqueous ethanol (70%; 100 m*l*) for 20 min. After the evaporation of the solvent under a vacuum, the residue was dissolved in water (150 m*l*) and saturated with carbon dioxide. The precipitate was collected, washed with water, and recrystallized from aqueous acetone to give yellow needles, mp 181.5—183°C, which gave a dark green ferric chloride reaction in ethanol; yield 670 mg.

Found: C, 66.86; H, 5.06%. Calcd for $C_{25}H_{22}O_8$: C, 66.66; H, 4.92%.

Diacetate of VII: hot acetic anhydride-pyridine method; mp 161.5—162.5°C (colorless needles from ethanol). It gave a negative ferric chloride reaction.

Found: C, 65.30; H, 4.84%. Calcd for $C_{29}H_{26}O_{10}$: C, 65.16; H, 4.90%.

4,6-Diethoxy-2-hydroxy-5,ω-dimethoxyacetophenone (X). *a) Friedel-Crafts Reaction.* With stirring and cooling at 10°C, methoxyacetyl chloride (8 g) was added, drop by drop, to a solution of anhydrous aluminum chloride (12.5 g), 3,5-diethoxy-4-methoxyphenol (IX)[8] (10 g) and anhydrous ether (50 m*l*). After stirring below 20°C for 3 hr, the mixture was poured into a mixture of ice and dilute hydrochloric acid, and extracted with ether. The ether extract was washed successively with water, aqueous sodium carbonate, and water. After drying over sodium sulfate, the solvent was evaporated; the residue was distilled under a vacuum to give the ketone (X) as a pale yellow oil, bp 145—146°C/0.2 mmHg; yield 9.7 g.

Found: C, 59.24; H, 7.37%. Calcd for $C_{14}H_{20}O_6$: C, 59.14; H, 7.09%.

b) Hoesch Condensation. A mixture of IX (10 g), methoxyacetonitrile (7.1 g), anhydrous ether (300 m*l*), and anhydrous zinc chloride (10 g) was treated by a method similar to that used for V. The crude product was distilled under a vacuum to give X, bp 145—146°C/0.2 mmHg, which was proved identical with the sample of a) by infrared spectral comparison; yield 1.0 g.

4'-Benzyloxy-5, 7-diethoxy-3, 3', 6-trimethoxyflavone (XI). *a) From VII.* A mixture of VII (130 mg), diethyl sulfate (1.0 g), anhydrous potassium carbonate (2.5 g), and dry acetone (25 m*l*) was refluxed for 24 hr, then the acetone was, after addition of water, evaporated. The precipitate was collected, washed with water, and recrystallized from aqueous ethanol to give the diethyl ether (XI) as colorless needles, mp 116—117°C, which gave a negative ferric chloride reaction; yield 115 mg. UV: λ_{max}^{EtOH} mμ (log ε); 336 (4.27).

Found: C, 69.03; H, 6.04%. Calcd for $C_{29}H_{30}O_8$: C, 68.76; H, 5.97%.

b) From X. A mixture of the ketone (X) (1.0 g), *O*-benzylvanillic anhydride (3.5 g), and triethylamine (1.7 g) was treated by a method similar to that used for

*2 Inflection.
*3 Saturated with anhydrous sodium acetate.
*4 0.002 mol/*l*.
*5 The alkaline solution was acidified with dilute hydrochloric acid.
*6 All melting points and boiling points are uncorrected.

7) R. E. Damschroder and R. L. Shringer, *J. Am. Chem. Soc.*, **59**, 931 (1937).

8) M. Krishnamuri and T. R. Seshadri, *Proc. Indian Acad. Sci.*, **39A**, 144 (1954).

VII. The crude product was recrystallized from ethanol to give XI; mp 117—118°C, which was undepressed on admixture with the sample of a); yield 400 mg.

Found: C, 68.50; H, 5.77%. Calcd for $C_{29}H_{30}O_8$: C, 68.76; H, 5.97%.

4'-Benzyloxy-5-hydroxy-3,3',6,7-tetramethoxyflavone (XII). To a solution of VII (1.2 g) in acetone (150 m*l*), an ethereal diazomethane solution was added, then the solution was allowed to stand at room temperature for 2 hr. After the evaporation of the solvent, the residue was recrystallized from ethyl acetate to give yellow needles, mp 167.5—168.5°C, which gave a dark green ferric chloride reaction in ethanol; yield 1.0 g.

Found: C, 67.23; H, 5.16%. Calcd for $C_{26}H_{24}O_8$: C, 67.23; H, 5.21%.

Monoacetate of XII: hot acetic anhydride - pyridine method; mp 222.5—223.5°C (almost colorless needles from ethyl acetate). It gave a negative ferric chloride reaction.

Found: C, 66.17; H, 5.11%. Calcd for $C_{28}H_{26}O_9$: C, 66.39; H, 5.17%.

4',5-Dihydroxy-3,3',6,7-tetramethoxyflavone (XIII). A solution of XII (750 mg) in ethyl acetate (250 m*l*) was submitted to catalytic reduction at room temperature in the presence of Pd-C (10%: 1.0 g). After the catalyst had been filtered, the filtrate was evaporated under a vacuum and the residue was recrystallized from methanol to give yellow needles, mp 181.5—182.5°C (reported[4] mp 181—182°C), which gave a dark green ferric chloride reaction in ethanol; yield 450 mg. The melting point was undepressed on admixture with a sample prepared by the method of Hörhammer *et al.*[4] UV: λ_{max}^{EtOH} mμ (log ε); 258.5 (4.33), 270*2 (4.28), 352 (4.42).

Found: C, 60.79; H, 4.80%. Calcd for $C_{19}H_{18}O_8$: C, 60.96; H, 4.85%.

Diacetate of XIII: hot acetic anhydride - pyridine method; mp 191—192°C (colorless needles from methanol), (reported[4] mp 191—192°C), undepressed on admixture with a sample prepared by the method of Hörhammer *et al.*[4] It gave a negative ferric chloride reaction.

Found: C, 60.11; H, 4.81%. Calcd for $C_{23}H_{22}O_{10}$: C, 60.26; H, 4.84%.

Jaceidin (4',5,7-Trihydroxy-3,3',6-trimethoxyflavone) (II). A mixture of VII (2.40 g,) Pd-C (10%: 2.0 g), and ethyl acetate (460 m*l*) was treated by the method described for XIII. The product was then recrystallized from aqueous methanol to give pale yellow needles, mp 130—135°C (reported[1,2] mp 127—133°C, 99—100°C, 111—112°C and 165—166°C),*7 which gave a green ferric chloride reaction in ethanol; yield 1.76 g. This was identified with natural jaceidin by a mixed-melting-point determination and by infrared and ultraviolet spectral comparisons. NMR*8 in $CDCl_3$: 3.88(s), 3.99(s), 4.06(s) (OMe), 6.03(s), 6.56(s) (C_7-OH, $C_{4'}$-OH), 6.61(s) (C_8-H), 7.09 (d: J_{ortho}=9.0 cps) ($C_{5'}$-H), 7.76 (dd: J_{ortho}=9.0 cps, J_{meta}=2.5 cps) ($C_{6'}$-H), 7.78 (d: J_{meta}=2.5 cps) ($C_{2'}$-H), 12.96(s) (C_5-OH). (Reported[2] NMR in $CDCl_3$: 3.86, 3.97, 4.04 (OMe), 6.59 (C_8-H), 7.05 ($C_{5'}$-H), 7.68 ($C_{6'}$-H), 7.70 ($C_{2'}$-H), 12.86 (C_5-OH); J_{ortho}=9.0 cps, J_{meta}=2.0 cps).

Found: C, 58.57; H, 4.82%. Calcd for $C_{18}H_{16}O_8 \cdot \frac{1}{2}H_2O$: C, 58.54; H, 4.61%.

After drying at 50—60°C/0.1 mmHg for 2 hr, it had a mp of 166—166.5°C (sintering at 127°C).

Found: C, 59.86; H, 4.48%. Calcd for $C_{18}H_{16}O_8$: C, 60.00; H, 4.48%.

Jaceidin Triacetate (XIV): hot acetic anhydride - pyridine method; mp 163—164°C (colorless needles from ethyl acetate) (reported[2] mp 159—160°C). It gave a negative ferric reaction. UV: λ_{max}^{EtOH} mμ (log ε); 248.5 (4.34), 326 (4.26) (reported[2] UV: λ_{max}^{EtOH} mμ (log ε); 248 (4.29), 325 (4.17)). NMR*8 in $CDCl_3$: 2.36(s), 2.38(s), 2.52(s) (OAc), 3.82(s), 3.89(s), 3.92(s) (OMe), 7.22 (d: J_{ortho}=9.0 cps) ($C_{5'}$-H), 7.30(s) (C_8-H), 7.72 (dd: J_{ortho}=9.0 cps, J_{meta}=2.5 cps) ($C_{6'}$-H), 7.78 (d: J_{meta}=2.5 cps) ($C_{2'}$-H). Reported[2] NMR in $CDCl_3$: 2.37, 2.39, 2.44 (OAc), 3.83, 3.89, 3.92 (OMe), 7.20 ($C_{5'}$-H), 7.29 (C_8-H), *ca.* 7.70 ($C_{2'}$-H, $C_{6'}$-H).

Found: C, 58.94; H, 4.42%. Calcd for $C_{24}H_{22}O_{11}$: C, 59.26; H, 4.56%.

Hydrolysis of Jaceidin Triacetate (XIV). A solution of XIV (400 mg) in ethanol (8 m*l*) was gently refluxed with aqueous potassium hydroxide (30%: 3 g) for 10 min. After the evaporation of the solvent under a vacuum, the residue was dissolved in water (20 m*l*) and filtered, and the filtrate was acidified. The precipitate was collected, washed with water, and recrystallized from ethanol to give yellow needles, mp 130—135°C, which gave a green ferric chloride reaction in ethanol; yield 250 mg. This yield was identical with that of natural jaceidin.

Jaceidin Triethyl Ether (4',5,7-Triethoxy-3,3',6-trimethoxyflavone) (III). *a) From Jaceidin (II).* A mixture of synthetic jaceidin (II) (150 mg), anhydrous potassium carbonate (4.0 g), diethyl sulfate (1.5 g), and dry acetone (15 m*l*) was treated by a usual method. The crude product was recrystallized from aqueous ethanol to give colorless needles, mp 118—119°C (reported[1] mp 118°C); yield 155 mg. UV: λ_{max}^{EtOH} mμ (log ε); 334 (4.31).

Found: C, 64.60; H, 6.32%. Calcd for $C_{24}H_{28}O_8$: C, 64.85; H, 6.35%.

b) From the Ketone (X). A mixture of X (1.0 g), *O*-ethylvanillic anhydride (2.7 g), and triethylamine (1.7 g) was treated by a method similar to that used for VII. The crude product was recrystallized from aqueous ethanol to give colorless needles, mp 118—119°C which was undepressed on admixture with the sample of a); yield 120 mg.

Found: C, 64.82; H, 6.27%. Calcd for $C_{24}H_{28}O_8$: C, 64.85; H, 6.35%.

Jaceidin Trimethyl Ether (3,3',4',5,6,7-Hexamethoxyflavone) (XV). A mixture of synthetic jaceidin (II) (500 mg), dimethyl sulfate (0.4 m*l*), anhydrous potassium carbonate (5.0 g) and dry acetone (50 m*l*) was treated by a method similar to that of Farkas *et al.*[1] The crude product was then recrystallized from aqueous ethanol to give colorless needles, mp 142—143°C (reported mp 142°C[1] and 142—

*7 Depend on the crystallization conditions. The same results were also obtained with a synthetic sample.

*8 The NMR spectra were taken on a Hitachi Model R-20 NMR spectrometer (60 Mc/sec), using tetramethylsilane as an internal standard; their chemical shifts are presented in terms of δ values; s: singlet, d: doublet, dd: double doublet.

143°C[2]), which gave a negative ferric chloride reaction; yield 490 mg. UV: λ_{max}^{EtOH} mμ (log ε); 335 (4.29).

Found: C, 62.52; H, 5.45%. Calcd for $C_{21}H_{22}O_8$: C, 62.68; H, 5.51%.

Jaceidin Dimethyl Ether (5-Hydroxy-3,3',4',6,7-pentamethoxyflavone) (XVI). Synthetic jaceidin (II) (380 mg) in acetone (70 m*l*) was partially methylated with diazomethane, and the product was recrystallized from methanol to give yellow needles, mp 161—162°C (reported mp 161—162°C[4] and 158—159°C[2,9]), which gave a dark green ferric chloride reaction in ethanol; yield 380 mg. UV: λ_{max}^{EtOH} mμ (log ε); 257 (4.38), 274 (4.34), 348 (4.45).

Found: C, 61.58; H, 5.05%. Calcd for $C_{20}H_{20}O_8$: C, 61.85; H, 5.19%.

Monoacetate of XVI: hot acetic anhydride - pyridine method; mp 163—163.5°C (colorless needles from ethanol) (reported[9] mp 160.5—161.5°C). It gave a negative ferric chloride reaction.

Found: C, 59.84; H, 5.22%. Calcd for $C_{22}H_{22}O_9 \cdot \frac{1}{2}H_2O$: C, 60.13; H, 5.24%.

9) W. Herz, *J. Org. Chem.*, **26**, 3014 (1961).

The authors are grateful to Professor H. Wagner, University of München, for his gifts of natural jacein and jaceidin. This work was supported by a grant-in-aid from the Ministry of Education.

BULLETIN OF THE CHEMICAL SOCIETY OF JAPAN VOL. 41 1417—1422 (1968)

The Benzylation and Phenylation Reactions of Unsaturated Compounds Using Organo Monohalides and Polynuclear Iron Carbonyl

Ilsong RHEE, Norio MIZUTA, Membo RYANG and Shigeru TSUTSUMI

Department of Chemical Technology, Faculty of Engineering, Osaka University, Miyakojima, Osaka

(Received December 23, 1967)

The reaction of iodobenzene and benzyl halides (Cl, Br and I) with $Fe_3(CO)_{12}$ (mole ratio; $Fe_3(CO)_{12}/R-X=1/3$) gave the corresponding symmetrical ketones (18—55.2%). The increasing order of the reactivity of the organo halides to $Fe_3(CO)_{12}$ was as follows: iodobenzene< benzyl chloride<benzyl bromide<benzyl iodide. In the reaction of benzyl chloride with $Fe_3(CO)_{12}$, when two-thirds of the $Fe_3(CO)_{12}$ had been used, or moles equal to benzyl chloride, the yields of the ketones were increased to 87% (total yield). The same reaction in the presence of olefin produced benzylation or phenylation products of the olefin; for example, the reaction of benzyl iodide with $Fe_3(CO)_{12}$ in the presence of acrylonitrile (in tetrahydrofuran) gave 4-phenylbutyronitrile (30.2%) and 4-cyano-6-phenylhexanonitrile (10.0%). When olefin with a higher coordinating ability to iron carbonyl was used, the yields of the benzylated adducts of the olefin decreased, while when the more reactive organo halide was used, the yields increassed. Thus, it was postulated that organo halide reacted with $Fe_3(CO)_{12}$ to form the σ-complex, benzyl(or phenyl)iron carbonyl halide, as an intermediate to the benzylation (or phenylation) products. The benzylation and phenylation reactions proceeded smoothly in a polar solvent (dimethylformamide or ethanol) to give high yields. The benzylation of phenylacetylene did not occur in benzene, but in a polar solvent it proceeded, giving 1,3-diphenylpropane and -propene. The mechanistic aspects of these reactions are discussed below.

In a previous paper,[1] we reported that organo monohalide (benzyl chloride and iodobenzene) reacted with polynuclear iron carbonyls, triiron dodecacarbonyl [$Fe_3(CO)_{12}$], and diiron nonacarbonyl [$Fe_2(CO)_9$], to form the σ-complex as an intermediate, from whose decomposition the corresponding symmetrical ketone was produced, while when olefin was present in the reaction, its benzylated adduct was obtained.

In this paper, we wish to report on our study of several factors which affect the above benzylation reaction; the reactivity of organo monohalide to $Fe_3(CO)_{12}$, the coordinating ability of olefin to $Fe_3(CO)_{12}$, the remarkable solvent effect, and the effect of the mole ratio between organo monohalide and $Fe_3(CO)_{12}$.

Results and Discussion

A) The Reaction of Organo Monohalide with $Fe_3(CO)_{12}$ in the Presence of Olefin. *The Effect of the Coordinating Ability of Olefin.* The reaction of iodobenzene (0.05 mol) with $Fe_3(CO)_{12}$

1) I. Rhee, M. Ryang and S. Tsutsumi, *J. Organometal. Chem.*, **9**, 361 (1967).

TABLE 1. REACTION OF ORGANO MONOHALIDE WITH $Fe_3(CO)_{12}$ (mole ratio 1 : 1/3)

R-X	Solvent	Temp. °C	Convn.[c] %	Products, %[a]		
				R-R	RCOR	$RCOCH_2C_6H_4$-R[b]
PhI	Toluene	110	30	Trace	20.0	—
$PhCH_2Cl$	THF	67	50	Trace	18.0	11.1
$PhCH_2Br$	THF	67	80	12.7	26.4	25.0
$PhCH_2I$	THF	40—45	100	37.6	55.2	—

a) Theoretical yield, based on organo halide used.
b) Crude yield.
c) Based on moles of organo halide used.

TABLE 2. REACTION OF ORGANO HALIDE WITH $Fe_3(CO)_{12}$ IN THE PRESENCE OF OLEFIN (mole ratio; R-X : $Fe_3(CO)_{12}$: CH_2=CHY = 0.05 : 0.015 : 0.05)

R-X	Solvent	Temp. °C	CH_2=CHY	Convn.[c] %	Products, %[a]	
					RCH_2CH_2Y and RCH=CHY	$RCH_2CH(Y)$-CH_2CH_2Y[b]
PhI	Toluene	110	CH_2=CHPh[d]	18	3.0	—
PhI	Toluene	110	CH_2=$CHCO_2Et$[e]	0	—	—
PhI	Toluene	110	CH_2=CHCN[e]	0	—	—
$PhCH_2Cl$	THF	67	CH_2=CHPh[d]	50	4.0	—
$PhCH_2Cl$	THF	67	CH_2=$CHCO_2Et$	35	20.0	6.8
$PhCH_2Cl$	THF	67	CH_2=CHCN	30	18.7	4.0
$PhCH_2Cl$	THF	67		0	—	—
$PhCH_2Br$	THF	67	CH_2=CHCN	50	24.0	8.5
$PhCH_2I$	THF	40—45	CH_2=CHCN	60	30.2	10.0
$PhCH_2I$	THF	40—45		30	9.6	—

a) Theoretical yield, based on organo halide used.
b) Crude yield.
c) Based on moles of organo halide used.
d) In this reaction, polymerization of styrene proceeded predominantly and dimer and ketone were also produced (see experimental section).
e) Even in THF as solvent, the reaction did not occur.

(0.015 mol) in refluxing toluene gave benzophenone in a 20% yield. In the presence of acrylonitrile, however, iodobenzene did not react with $Fe_3(CO)_{12}$ in refluxing toluene and all the iodobenzene was recovered. The results are extremely interesting in contrast with those in the case of benzyl chloride, which reacted with $Fe_3(CO)_{12}$ in the presence of acrylonitrile [in tetrahydrofuran (THF)] at 67°C to give benzylated adducts of the olefin in a 22.7% yield.*1 Furthermore, when styrene was used as an olefin, iodobenzene reacted with $Fe_3(CO)_{12}$ to give *trans*-stilbene in a low yield.

These results stimulated us to study the reactions of iodobenzene and benzyl halides (Cl, Br and I) with $Fe_3(CO)_{12}$ in the presence of some olefins (styrene, ethyl acrylate, acrylonitrile and maleic anhydride). The coordinating ability of the above olefins decreases in the following order: maleic anhydride > acrylonitrile > ethyl acrylate > styrene.*2

*1 All yields in this paper are theoretical yields based on the organo halide used.

*2 The order was assumed by considering the ease of formation and the stability of the olefin-iron carbonyl π-complex; for example, maleic anhydride - iron tetracarbonyl[2] is produced in a 78% yield by the reaction of maleic anhydride with $Fe_2(CO)_9$, and it is relatively stable in air. Acrylonitrile - iron tetracarbonyl[3] is obtained in a 3% yield from the reaction of acrylonitrile with $Fe_2(CO)_9$, decomposes at 60°C, and is unstable at room temperature. However, the unstable π-complexes of ethyl acrylate and styrene are first obtained by a reaction between the olefins and iron pentacarbonyl under UV irradiation.[4]

2) R. B. King, "Organometallic Syntheses," Vol. I, Academic Press, New York (1965), p. 130.
3) S. F. A. Kettle and L. E. Orgel, *Chem. Ind. (London)*, **1960**, 49; M. R. Tuter and A. R. Tturmoore, *Proc. Chem. Soc.*, **1961**, 466.
4) E. Koerner von Gustorf, M. C. Henry and C. D. Pietro, *Z. Naturforsch.*, **21** b, 42 (1966).

Table 3. Effect of mole ratio of $Fe_3(CO)_{12}$ to organo halide

R-X	$Fe_3(CO)_{12}$/R-X[c]	Products, %[a]		
		R-R	RCOR	$RCOCH_2C_6H_4$-R[b]
PhI	1/3	Trace	20.0	—
PhI	2/3	Trace	53.3	—
$PhCH_2Cl$	1/3	Trace	18.0	11.1
$PhCH_2Cl$	2/3	5.4	45.1	25.0
$PhCH_2Cl$	1	5.4	52.0	35.0

a) Theoretical yield, based on organo halide used.
b) Crude yield.
c) Mole ratio.

First, the results of the reactions of iodobenzene and benzyl halides with $Fe_3(CO)_{12}$ are summarized in Table 1.

The reactivity of organo halide to $Fe_3(CO)_{12}$ increased in the following order: iodobenzene< benzyl chloride< benzyl bromide< benzyl iodide.

The results of the same reaction in the presence of olefin are summarized in Table 2.

As may be seen in Table 2, the yields of benzyl adducts of olefins increase in parallel with the increasing order of reactivity of the halide. By comparing Table 1 with Table 2, it can easily be found that the addition of olefin to the reaction system between halide and $Fe_3(CO)_{12}$ markedly affected the reactivity of the halide to $Fe_3(CO)_{12}$; for example, iodobenzene, which reacted with $Fe_3(CO)_{12}$ to give benzophenone in a 20% yield, did not react at all with $Fe_3(CO)_{12}$ in the presence of acrylonitrile. When olefin was present, each conversion of organo halides decreased; furthermore, when the coordinating ability of olefin became stronger, the conversion of the halide was suppressed more (Tables 1 and 2).

The Effect of the Solvent. As has been mentioned, iodobenzene did not react with $Fe_3(CO)_{12}$ in the presence of acrylonitrile or ethyl acrylate in toluene or THF, but when dimethylformamide (DMF) was used as a solvent at 100°C, the reaction proceeded well, giving phenylated products of the olefins: in the case of acrylonitrile, hydrocinnamonitrile (18%) and cinnamonitrile (5%), and in the case of ethyl acrylate, ethyl hydrocinnamate (22%) and ethyl cinnamate (9%). These results indicate that, in this reaction, the solvent plays a very important role. A similar tendency was also observed in the reaction of benzyl chloride. That is, when DMF was used as the solvent instead of THF, the reaction of benzyl chloride (0.05 mol) with $Fe_3(CO)_{12}$ (0.015 mol) at 80°C gave the increased yields of the dibenzyl ketone (40%) and the benzyl *p*-benzylbenzyl ketone (crude yield, 12%). When acrylonitrile was present in the above reaction, benzylated adducts, 4-phenylbutyronitrile and 4-cyano-6-phenylhexanonitrile, were obtained in yields of 35.8 and 12.1% (in THF, 18.7 and 4.0%) respectively.

When refluxing ethanol was the solvent, the reaction of benzyl chloride (0.05 mol) with $Fe_3(CO)_{12}$ (0.015 mol) gave ethyl benzyl ether (20%), ethyl phenylacetate (3.3%), and dibenzyl (8%). The same reaction in the presence of acrylonitrile produced ethyl benzyl ether (7.8%), ethyl phenylacetate (3.6%), dibenzyl (6.6%), and 4-phenylbutyronitrile (44.8%). Thus, the yields of the benzylation and phenylation products of olefins were much increased by using a polar solvent.

The Effect of the Mole Ratio of Organo Halide-Iron Carbonyl. In the reaction described above, $Fe_3(CO)_{12}$ has been used in the ratio of one-third of a mole to one of the organo halide, on the basis of the assumption that the halide reacts with each iron atom of $Fe_3(CO)_{12}$. On the other hand, when the ratio is two-thirds of a mole to one or when $Fe_3(CO)_{12}$ and the halide are equal, the yields of the products were markedly increased (Table 3).

Therefore, it was expected that if olefin were added to this reaction system, the yields of the adducts would increase. In truth, the reaction of benzyl chloride (0.05 mol) with $Fe_3(CO)_{12}$ (0.033 mol) in the presence of acrylontirile (0.05 mol) in THF at 67°C for 30 hr gave increased yields of 4-phenylbutyronitrile (26.2%) and 4-cyano-6-phenylhexanonitrile (crude yield, 10%).

B) The Reaction of Benzyl Chloride with $Fe_3(CO)_{12}$ in the Presence of the Acetylenic Compound. It is well-known[5] that the metal-carbon σ-bonding complex undergoes insertion reactions readily with a large variety of acetylenes; also, the σ-complex, derived from the reaction between benzyl chloride and $Fe_3(CO)_{12}$, may be assumed to react with an acetylenic compound. Thus, the reaction of benzyl chloride (0.067 mol) with $Fe_3(CO)_{12}$ (0.023 mol) in the presence of diphenylacetylene (0.056 mol) was carried out in refluxing benzene under argon for 30 hr. From the residual oil obtained after the removal of the solvent under reduced pressure, the following

5) R. F. Heck, "Advances in Chemistry Series 49, Am. Chem. Soc." Washington D. C. (1965), pp. 194—201 and references cited therein.

products were given: diphenylmethane*3 (8%), dibenzyl (3.3)%, dibenzyl ketone (12.1%), $Fe_2(CO)_6(PhC{\equiv}CPh)_2$ (43.3%, based on the diphenylacetylene used), and $Fe(CO)_4(PhC{\equiv}CPh)_2$ (6.8%). However, the expected benzylation product of diphenylacetylene was not isolated. Similarly, from the same reaction using phenylacetylene, the benzylated adduct was not obtained. On the other hand, when ethanol was used as the solvent, the same reaction gave 1,3-diphenylpropane and -propene in low yields (total yield, 2%). Furthermore, when DMF was the solvent, the former and the latter were produced in yields of 5.4 and 3.6% respectively. Thus, the insertion reaction of an acetylenic compound into a carbon-metal bond is markedly affected by the solvent polarity, although the reason for this is not yet clear.

C) Mechanistic Aspects. We have proposed that organo halide reacts with $Fe_3(CO)_{12}$ to yield the σ-complex, benzyliron carbonyl halide, as an intermediate, whose decomposition then produces the dibenzyl ketone, while when olefin is present, the σ-complex reacts with the olefin to give the benzylated products of olefin. Herein, the formation of the σ-complex was postulated as preceding the benzylation.

However, although iodobenzene reacted with $Fe_3(CO)_{12}$ in toluene to give benzophenone (20%), which was assumed to be produced by the decomposition of the σ-complex, iodobenzene did not react with $Fe_3(CO)_{12}$ in the presence of acrylonitrile and all the iodobenzene was recovered. Furthermore, in the case of benzyl halide, the presence of an olefin which has a strong coordinating ability resulted in a decreased conversion of benzyl halide. These results indicate that the olefin acts as an inhibitor of the reaction of halide with $Fe_3(CO)_{12}$. This inhibiting action may be interpreted in terms of the formation of an olefin-iron carbonyl π-complex prior to the formation of the σ-complex.

It is well known that π-complexes between iron carbonyl and acrylonitrile or maleic anhydride are easily formed under our reaction conditions.[2,3] Thus, the formations of the π-complex and the σ-complex are competitive with each other, and therefore, if a more reactive halide or a olefin of a lower coordinating ability is used, the conversion of the halide should be increased, and *vice versa*. For example, benzyl chloride reacted with $Fe_3(CO)_{12}$ in the presence of acrylonitrile to give benzylated adducts, and in the same reaction using maleic anhydride instead of acrylonitrile, all the benzyl chloride was recovered, while benzyl iodide reacted with $Fe_3(CO)_{12}$ not only in the presence of acrylonitrile, but also in the presence of maleic anhydride, to give benzylated adducts of the olefins.

The information reported about the reaction of the π-complex with organo halide is as follows; the reaction of bis-acrylonitrile nickel with allyl halide results in the formation of bis-(1-cyano-4-pentenyl)nickel, $(CH_2{=}CHCH_2CH_2CHCN)_2Ni$, while benzyl chloride or iodobenzene reacts a little with bis-acrylonitrile nickel,[6] but the reaction of π-allylnickel bromide with alkyl (aryl) halide does not occur in benzene or THF.[7]

The reaction of π-olefin - metal carbonyl with organo halide, however, has not yet been reported, and it was assumed that the π-complex was unreactive to halide in nonpolar solvents (THF, toluene, and benzene). Supporting evidence for our assumption was provided by the results of the reaction of benzyl chloride with a maleic anhydride-iron tetracarbonyl complex,*4 for the reaction did not proceed and all the benzyl chloride was recovered.

In the presence of an acetylenic compound, no benzylation product was yielded in a nonpolar solvent, so the iron carbonyl reacted predominantly with an acetylenic compound with a very strong coordinating ability, thus forming several previously-known iron complexes.[8] However, when ethanol or DMF was the solvent, benzyl chloride reacted with $Fe_3(CO)_{12}$ in the presence of phenylacetylene to give its benzylated adducts, 1,3-diphenylpropane and -propene.

Similarly, aroylnickel carbonyl halide does not react with acetylenic compound in benzene or THF,[9] but when water is the solvent, it reacts with acetylene to yield the adduct with acetylene, 3-benzoylpropionic acid.[10]

A similar interesting solvent effect was observed in the reaction between organo halide and $Fe_3(CO)_{12}$ in the presence of an olefin. In toluene iodobenzene did not react with $Fe_3(CO)_{12}$ in the presence of acrylonitrile, but when DMF was used as the solvent, it reacted well with $Fe_3(CO)_{12}$ to give phenylated adducts of the olefin. Hence, the insertion reaction of an unsaturated compound into a carbon-metal σ-bond is markedly affected by the solvent polarity. During the course of our study, Corey and Semmelhack reported that the π-allylnickel bromide complex, which did not

*3 It has been assumed that diphenylmethane was produced from a Friedel-Crafts type reaction between benzyl chloride and benzene by the action of iron carbonyl chloride, although it has not yet been isolated.

6) M. Dubini and F. Montino, *J. Organometal. Chem.*, **6**, 188 (1966).

7) E. J. Corey and M. F. Semmelhack, *J. Am. Chem. Soc.*, **89**, 2755 (1967).

*4 This π-complex was synthesised by the reaction of maleic anhydride with $Fe_2(CO)_9$ and was purified by recrystallization from acetone.[2]

8) W. Hübel und E. H. Braye, *J. Inorg. Nucl. Chem.*, **10**, 250 (1959).

9) E. Yoshisato, M. Ryang and S. Tsutsumi, unpublished observation.

10) G. P. Chiusoli, S. Merzoni and G. Mondelli, *Tetrahedron Letters*, **1964**, 2777.

react with alkyl halide in benzene or THF, reacted smoothly in DMF to give coupling products in high yields.[7] As for the solvent effect of DMF, they suggested that dimeric π-allylnickel bromide became monomeric π-allylnickel bromide by the coordination of DMF, and that the latter reacted with alkyl halide. However, in our work, the olefin-iron carbonyl π-complex is monomeric.[2,3] Therefore, our results can evidently not be explained in terms of their explanation.

The solvent effect and the precise mechanism of these reactions are now under investigation; a detailed description of the mechanism and further applications of this reaction will be reported in due course.

Experimental

The Reaction of Organo Monohalide with $Fe_3(CO)_{12}$. The reaction and the identification of the product were carried out according to the method described in a previous paper.[1]

The Reaction of Organo Monohalide with $Fe_3(CO)_{12}$ in the Presence of Olefin. Most of these reactions were carried out in a method similar to that described in the previous paper. Only a typical reaction will be described here.

The reaction of iodobenzene (10.2 g, 0.05 mol) with $Fe_3(CO)_{12}$ (8.1 g, 0.015 mol) in the presence of styrene (5.2 g, 0.05 mol) was carried out in refluxing toluene for 30 hr under an atmosphere of argon. The resulting reaction mixture was filtered through magnesium sulfate under reduced pressure, and, after the removal of the solvent from the filtrate, the residual oil thus obtained was distilled to give a fraction (bp 45—172°C/0.7 mmHg, 0.7g) and a large quantity of a polymer. The fraction was then chromatographed on silica gel; the subsequent elution of the first band with petroleum ether gave white crystals after the removal of the solvent. This material was recrystallized from ethanol (mp 70.5°C) and confirmed to be biphenyl (3.5%) by a mixed-melting point determination with an authentic sample. The elution of the second band with petroleum ether gave *trans*-stilbene (3.0%) (mp 124°C, from petroleum ether). Elution with benzene showed the presence of a carbonyl group (ν_{CO} 1680 cm^{-1}); after the removal of the benzene, it was identified as benzophenone (8.4%) by a mixed-melting point determination of its 2,4-dinitrophenylhydrazone (mp 232°C, from ethyl acetate) with an authentic sample. The theoretical yields of the products were determined by vpc analysis. [Column, S.E. 30, 2.25 m; column temperature, 230°C; flow rate of carrier gas (helium), 7 m*l*/min; internal standard, dibenzyl; retention times, 2.8, 6.0 and 8.5 min respectively.] A large quantity of a polymeric material was assumed to be a polymer of styrene, but it was not examined.

The reaction of benzyl chloride (6.4 g, 0.05 mol) with $Fe_3(CO)_{12}$ (8.1 g, 0.015 mol) in the presence of styrene (5.2 g, 0.05 mol) was carried out at 67°C in THF (100 m*l*) for 30 hr. The residual oil obtained by a treatment similar to that described above was distilled under reduced pressure to give the following fractions: (1) bp 90—108°C/0.3 mmHg, 1.2 g, and (2) bp 150—190°C/0.3 mmHg, 0.8 g. The results of vpc analysis showed the fraction (1) to be a mixture of the following materials: dibenzyl (1.7%), 1,3-diphenylpropane (1.8%), 1, 3-diphenylpropene (2.2%), and dibenzyl ketone (17.0%) [Column, S. E. 30, 2.25 m; column temperature, 230°C; flow rate of carrier gas (helium), 7 m*l*/min; flame ionization detector; retention times, 4.8, 6.8, 8.2 and 9.7 min respectively]. The fraction (2) has not yet been identified.

The reaction of benzyl iodide (10.9 g, 0.05 mol) with $Fe_3(CO)_{12}$ (8.1 g, 0.015 mol) in the presence of maleic anhydride (4.7 g, 0.05 mol) was carried out at 40—45°C in THF for 30 hr. The residue after the removal of the THF *in vacuo* was dissolved in benzene and filtered through magnesium sulfate. The mother liquors were then chromatographed on silica gel after the benzene had been removed under reduced pressure. The product of elution with petroleum ether was confirmed by vpc to be unreacted benzyl iodide (7.6 g). The product of elution with benzene was hydrolyzed with 6 N hydrochloric acid and then extracted with benzene; the resulting free acid was recrystallized from water to give 1.0 g of white crystals (mp 161°C). This material was then assumed to be benzylsuccinic acid (9.6%). [Found: C, 62.97; H, 5.83%; mol wt (in the neutralization equivalent method), 209.8. Calcd for $C_{11}H_{12}O_4$: C, 63.10: H, 5.80%; mol wt, 208]. Therefore, the product of elution with benzene was mainly the anhydride of benzylsuccinic acid.

With DMF as the Solvent, the Reaction of Organo Halide with $Fe_3(CO)_{12}$ in the Presence of Olefin. The reaction of iodobenzene (9.6 g, 0.044 mol) with $Fe_3(CO)_{12}$ (7.4 g, 0.014 mol) in the presence of ethyl acrylate (5.0 g, 0.05 mol) was carried out at 100°C in DMF (100 m*l*). After the reaction had continued for 30 hr, the reaction mixture was hydrolyzed with 6 N hydrochloric acid and then extracted with diethyl ether. The residual oil obtained after the removal of the solvent was distilled under reduced pressure to give the following fractions: (1) bp 78—100°C/0.7 mmHg, 2.4 g, and (2) bp 150—220°C/0.6 mmHg, 1.9 g. The fraction (1) showed the presence of ester groups (1740, 1100—1300 cm^{-1}) and was found by vpc to be a mixture of ethyl hydrocinnamate (22%) and ethyl cinnamate (9%) [Column, S. E. 30 (5%), 2.25 m; column temperature, 180°C; flow rate of carrier gas (helium), 10 m*l*/min; flame ionization detector; retention times, 2.3 and 3.4 min]. The fraction (2) also showed the presence of an ester group, but has not yet been identified. The other reactions and the identification of the product were carried out according to the methods described above.

With Ethanol as the Solvent, the Reaction of Benzyl Chloride with $Fe_3(CO)_{12}$ in the Presence of Acrylonitrile. The reaction (at 80°C) and treatment were carried out by a method similar to that described in the case of DMF; the following fractions were thus obtained; (1) bp 60—70°C/25 mmHg, 1.2 g, and (2) bp 80—90°C/0.9 mmHg, 4.2 g. Vpc analysis showed 44% of the fraction (1) to be ethyl benzyl ether (7.8%), while the fraction (2) was found to be a mixture of ethyl phenylacetate (3.6%), dibenzyl (6.6%), and 4-phenylbutyronitrile (44.8%) [Column, S.E. 30 (5%); column temperature, 210°C; flow rate of carrier gas (helium), 10 m*l*/min; flame ionization detector; retention times, 1.6, 2.1, 4.2, and 3.0 min respectively].

The Reaction of Benzyl Chloride with $Fe_3(CO)_{12}$ in the Presence of an Acetylenic Compound. The reaction of benzyl chloride (8.6 g, 0.067 mol) with $Fe_3(CO)_{12}$ (11.6 g, 0.023 mol) in the presence of diphenylacetylene (10.0 g, 0.056 mol) was carried out for 30 hr in refluxing benzene. The residual oil obtained after the removal of the benzene *in vacuo* under an atmosphere of argon was dissolved in hot acetic acid (70 m*l*). The red crystals (6.7 g) crystallized from this solution were recrystallized from acetic acid (mp 197—199°C). This material was identified as a known π-complex, $Fe_2(CO)_6(PhC{\equiv}CPh)_2$ (IR: ν_{CO} 2020, 1993, 1969, 1950 and 1905 cm^{-1}; NMR: τ 3.2 ppm; Found: C, 63.85; H, 3.25%. Calcd for $Fe_2C_{34}H_{20}O_6$: C, 64.15; H, 3.14%), an identification which agreed with the data of Ref. 8 (43.2%). The residual oil remaining after the removal of acetic acid from the filtrate was chromatographed on silica gel. Orange crystals were obtained from elution with benzene; they were recrystallized from ethanol, mp 184—186°C (Found: C, 74.01; H, 3.59%. Calcd for $FeC_{32}H_{20}O_4$: C, 73.25; H, 3.81%). This material was identified as $Fe(CO)_4(PhC{\equiv}CPh)_2$ by the agreement with the data of Ref. 8 (6.8%). The products of all the other elutions were distilled together *in vacuo* under argon to give the following fractions: (1) bp 53—60°C/12 mmHg, 3.6 g, and (2) bp 100—130°C/3 mmHg, 4.0 g. The fraction (1) was confirmed to be unchanged benzyl chloride, while the fraction (2) was found by vpc to be a mixture of diphenylmethane (8%), dibenzyl (3.3%), and dibenzyl ketone (12.1%).

In the presence of phenylacetylene, the same reaction gave diphenylmethane (26%), dibenzyl (4.4%), dibenzyl ketone (5.5%), and $Fe_2(CO)_6(PhC{\equiv}CH)_2$, the data of all of which agreed with that in Ref. 8. The other complex was not examined.

With ethanol as the solvent, the same reaction was carried out and the residual oil obtained after the removal of the ethanol *in vacuo* was distilled under argon. From the fraction thus obtained, the following products were identified by vpc: ethyl benzyl ether (32.8%), ethyl phenylacetate (2%), dibenzyl (0.5%), ethyl cinnamate (6.6%, based on the phenylacetylene used), 1,3-diphenylpropane (1.5%), 1,3-diphenylpropene (0.5%), and the dibenzyl ketone (1%). [Column, S.E. 30; column temperature, 230°C; flow rate of carrier gas (helium), 5 m*l*/min; flame ionization detector; retention times, 4.1, 5.4, 11.5, 9.2, 16.5, 19.6 and 21.1 min]. No other complexes were examined.

From the same reaction with DMF as the solvent, dibenzyl (3.2%), 1,3-diphenylpropane (5.4%) and 1,3-diphenylpropene (3.6%) were obtained.

The Reaction of Benzyl Chloride with Maleic Anhydride-Iron Tetracarbonyl. The reaction of benzyl chloride (3.2 g, 0.025 mol) with maleic anhydride-iron tetracarbonyl (6.4 g, 0.025 mol), which had been obtained by the reaction[2] of maleic anhydride with $Fe_2(CO)_9$, was carried out for 30 hr in refluxing THF (60 m*l*). The resulting reaction mixture was filtered through magnesium sulfate *in vacuo*, and, after the removal of THF from the filtrate, unchanged benzyl chloride (2.9 g) was recovered by distillation under reduced pressure; the residue (6.0 g) was dried *in vacuo* and was confirmed from its IR to be the starting π-complex.

Authentic Samples. *Ethyl Cinnamate* was prepared from the reaction of cinnamic acid with ethanol, n_D^{20} 1.5597 (lit., n_D^{20} 1.55982).

Ethyl Hydrocinnamate was obtained from the reduction of ethyl cinnamate using a sodium amalgam, n_D^{20} 1.4955 (lit., n_D^{20} 1.49542).

1,3-Diphenylpropene was prepared by a Wittig reaction using benzyl iodide, triphenylphosphine, *n*-butyllithium, and phenylacetaldehyde (mp 56°C, from ethanol; lit., mp 57°C).

1,3-Diphenylpropane was afforded by the reduction of 1,3-diphenylpropene using palladium black, n_D^{20} 1.5697 (lit., n_D^{20} 1.5694).

Cinnamonitrile was prepared by the reaction of benzaldehyde with cyanoacetic acid in pyridine and piperidine (bp 89°C/1.8 mmHg).

Hydrocinnamonitrile was obtained by the reaction of β-phenethyl bromide with potassium cyanide (bp 114°C/8 mmHg).

BULLETIN OF THE CHEMICAL SOCIETY OF JAPAN VOL. 41 1423—1426 (1968)

Nitration of Thenyl Derivatives. II. Preparation of Three Isomeric Mononitro Derivatives of 2-Thenyl Chloride and 2-Thenyl Acetate*1

Tyo SONE*2 and Yasuo MATSUKI

The Chemical Research Institute of Non-Aqueous Solutions, Tohoku University, Katahira-cho, Sendai

(Received December 26, 1967)

In connection with the investigation of the products of the nitration of 2-thenyl chloride (I) and 2-thenyl acetate (II), three isomeric mononitro derivatives of I and II were prepared, and it was shown by NMR spectral study that, as in the case of I, the product obtained in the nitration of II by nitric acid in acetic anhydride consisted of all three isomeric mononitro derivatives. The isomer distribution of the mononitro derivatives of II, as determined by infrared spectroscopy, indicated 77% of the 5-, 9% of the 4-, and 14% of the 3-nitro isomer.

In the previous communication[1] it was shown by NMR study that, in the nitration of 2-thenyl chloride (1) by the nitric acid-acetic anhydride procedure, the product consisted of all three isomeric mononitro derivatives of I. This seems to have been the first observation of the formation of the 4-substituted isomer in the electrophilic substitution of thiophene derivatives with an *o*-, *p*-directing group in the 2-position, though it had long been recognized that the substitution occurred predominantly at the 5-position and occurred at the 3-position, if at all, to only a minor extent. However, several attempts at the isolation of the isomers from the total product were all unsuccessful.

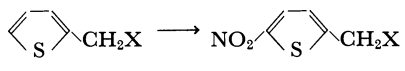

I: X=Cl III: X=Cl
II: X=OCOCH$_3$ VI: X=OCOCH$_3$

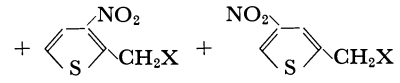

IV: X=Cl V: X=Cl
VII: X=OCOCH$_3$ VIII: X=OCOCH$_3$

The same is the case in the nitration of 2-thenyl acetate (II). Figure 1 shows the NMR spectrum of the nitration product[2] of II. The assignment of the peaks to each of the isomers is based on the ring-coupling constants[3] and on the coupling constants[4] between the methylene protons and the ring protons. The set of four strong peaks, two triplets at 5.59 ppm relative to cyclohexane as an internal standard and a doublet at 6.29 ppm (J= 4.0 cps, $J_{2CH_2\text{-ring H}}$=0.7 cps), is clearly due to 5-nitro-2-thenyl acetate (VI), while the two doublets at 5.81 ppm and 6.10 ppm (J=5.8 cps) are due to 3-nitro-2-thenyl acetate (VII). The doublet at the lowest field is due to the proton at the 5-position of 4-nitro-2-thenyl acetate (VIII), while the proton at the 3-position appears as a quintet with a relative intensity of 1 : 2 : 2 : 2 : 1 centered at 6.13 ppm; the proton at the 3-position is coupled with both the one at the 5-position and the methylene protons at the 2-position to form two triplets, the overlapping of which shows a quintet ($J_{3\text{-}5}$=1.6 cps, $J_{2CH_2\text{-}3}$=0.7 cps). Besides the peaks arising from the ring protons, there are four peaks in the higher field which are related to the methylene and the methyl protons, the shifts of these peaks being 4.16 ppm (VII CH_2), 3.76 ppm (VI CH_2, VIII CH_2), 0.72 ppm (VII CH_3), and 0.66 ppm (VI CH_3, VIII CH_3) respectively. The chemical shifts and the coupling constants are in accordance with those expected for the spectra of VI, VII, and VIII.

In order to confirm the facts shown by the NMR spectra, two sets of three isomeric mononitro derivatives of I and II were prepared.

VI was isolated as colorless needles, mp 36—37°C, from the nitration product of II. The acidic hydrolysis of VI gave the corresponding alcohol, IX, which was then converted into III, bp 112—114°C/4 mmHg, by being treated with a mixture of zinc chloride and hydrochloric acid.

*1 Presented at the Tohoku District Meeting of the Chemical Society of Japan, Yonezawa, June, 1965.

*2 Present address: Department of Applied Chemistry, Faculty of Engineering, Yamagata University, Yonezawa.

1) Part I of this series: T. Sone and Y. Matsuki, This Bulletin, **37**, 1235 (1964).

2) T. Sone, K. Takahashi and Y. Matsuki, *ibid.*, **35**, 1420 (1962).

3) S. Gronowitz, "Advances in Heterocyclic Chemistry," Vol. 1, ed. by A. R. Katritzky, Academic Press, New York (1963), p. 7.

4) K. Takahashi, T. Sone, Y. Matsuki and G. Hazato, This Bulletin, **36**, 108 (1963).

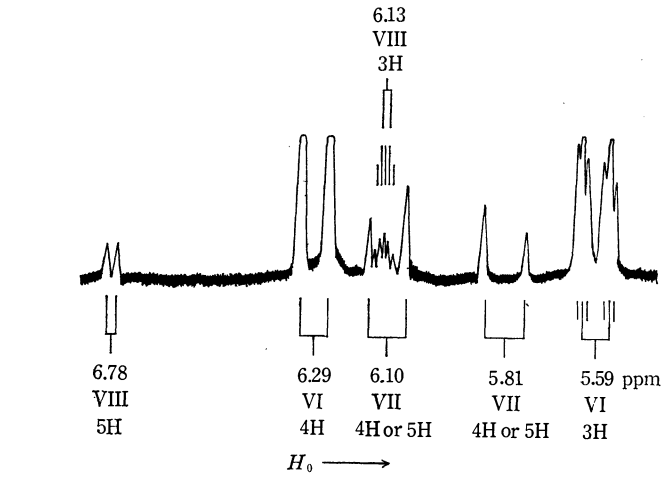

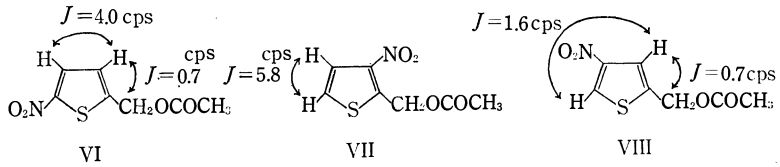

Fig. 1. NMR spectrum of the ring protons of the nitration product of 2-thenyl acetate (II) in carbon tetrachloride (60 Mc; Relative to cyclohexane as 0.00 ppm)

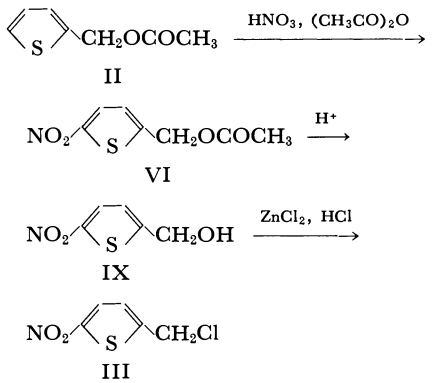

While 2-nitrothiophene, as well as nitrobenzene, is extremely difficult to be chloromethylated in the usual manner, 3-nitrothiophene is reactive enough for chloromethylation by a mixture of trioxane, hydrogen chloride, and zinc chloride; it gives V, bp 105—107°C/2 mmHg, which in turn is converted into VIII, mp 27—29°C.

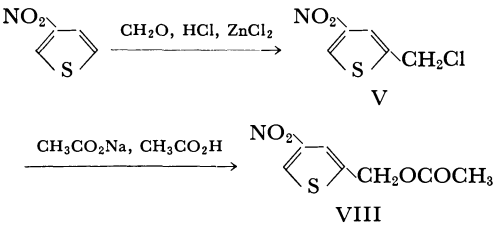

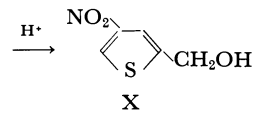

VII,[6] mp 60—61°C, was prepared by treating 3-nitro-2-thenyl bromide with sodium acetate in acetic anhydride. The hydrolysis of VII, followed by the chlorination of the resultant alcohol by phosphorus pentachloride, gave IV, mp 49—50°C.

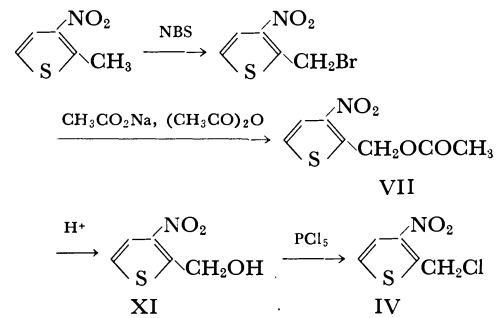

The signals in the NMR spectra of the nitration mixture of I and II correspond well with those of authentic samples.

The isomer distribution of the nitration product of II was determined by infrared spectroscopy using the absorption bands at 814 cm^{-1} for VI, at 1077 cm^{-1} for VIII, and at 705 cm^{-1} for VII, indicating 77% of VI, 9% of VIII, and 14% of VII

in the product. As the nitration was accompanied by the formation of a small amount of a resinous material, the results obtained by the determination of the isomer distribution should be considered with care, but they do clearly show that the 4-substitution occurs in a relatively higher proportion.

Experimental[5]

5-Nitro-2-thenyl Acetate (VI). 2-Thenyl acetate (31.2 g) was nitrated by nitric acid in acetic anhydride as has been described before[2] to give an oily mixture of nitro-2-thenyl acetates (25.2 g, 62.6%; bp 138—142°C/4 mmHg), a mixture which, on being left standing, partially solidified to colorless crystals. The crystals were collected by filtration and recrystallized from low-boiling petroleum ether to afford VI (9.0 g) as colorless needles, mp 36—37°C.

5-Nitro-2-thenyl Alcohol (IX). A mixture of VI (8.0 g) and 10% sulfuric acid (150 m*l*) was gently refluxed for 1 hr. The clear yellow solution was then cooled, and the resultant oily material was extracted with ether. The ether extract was dried (Na_2SO_4), and the ether was evaporated. The distillation of the residual oil gave IX (4.0 g, 63.0%) as a pale yellow oil, bp 148—150°C/3 mmHg, mp 20—21.5°C.

Found: C, 37.69; H, 2.71; N, 8.60%. Calcd for $C_5H_5NO_3S$: C, 37.73; H, 3.17; N, 8.80%.

5-Nitro-2-thenyl Chloride (III). A mixture of IX (5.0 g), zinc chloride (8.5 g), and hydrochloric acid (5.1 m*l*) was gently refluxed for 30 min, and then the reaction mixture was poured into water. The resultant oil was extracted with ether, and the ether extract was washed with water and dried (Na_2SO_4). After the evaporation of the solvent, the residue was distilled to give III (3.8 g, 68.2%) as a pale yellow oil, bp 112—114°C/4 mmHg, n_D^{20} 1.6213.

Found: C, 33.95; H, 2.08; N, 7.65%. Calcd for $C_5H_4ClNO_2S$: C, 33.81; H, 2.27; N, 7.88%.

3-Nitro-2-thenyl Alcohol (XI). A mixture of VII[6] (10 g) and 10% sulfuric acid (180 m*l*) was gently refluxed for 1 hr. The solution was then decolorized with charcoal and cooled to yield pale yellow needles (5.5 g, mp 71—72°C). Another crop of XI (1.6 g, mp 71—72°C) was obtained by extracting the filtrate by ether and by the subsequent evaporation of the solvent. The total yield of XI was 7.1 g (89.9%). The recrystallization of the crude XI from water gave pale yellow needles, mp 71—72°C.

Found: C, 37.73; H, 2.99; N, 8.56%. Calcd for $C_5H_5NO_3S$: C, 37.73; H, 3.17; N, 8.80%.

3-Nitro-2-thenyl Chloride (IV). To a mixture of XI (3.2 g) and chloroform (30 m*l*), phosphorus pentachloride (4.2 g) was added in small portions with shaking at room temperatre. After standing overnight, the reaction mixture was washed with water and dried ($CaCl_2$). The evaporation of the solvent and the recrystallization of the crude crystalline product from a mixture of ether and petroleum ether gave IV (2.1 g, 59.1%) as pale yellow prisms, mp 49—50°C.

Found: C, 33.81; H, 2.27; N, 7.88%. Calcd for $C_5H_4ClNO_2S$: C, 33.90; H, 2.30; N, 7.76%.

4-Nitro-2-thenyl Chloride (V). Into a mixture of 3-nitrothiophene (6.5 g), trioxane (2.4 g), zinc chloride (2.6 g), and carbon tetrachloride (50 m*l*), a stream of dry hydrogen chloride was stirred for 30 min. Then the mixture was gradually warmed to 50°C and stirred for 1 hr at that temperature, while the stream of hydrogen chloride continued to pass through. The resultant solution was poured into water, and the organic layer was separated, washed well with water, dilute sodium carbonate solution, and again with water, and dried. After the solvent had been removed, the residue was distilled under reduced pressure to yield V as a pale yellow oil, along with a small amount of a high-boiling material which was not examined further. Yield 4.1 g (46.1%). Bp 105—107°C/2 mmHg, n_D^{20} 1.6065, d_4^{20} 1.4825.

Found: C, 33.89; H, 2.02; N, 7.52%. Calcd for $C_5H_4ClNO_2S$: C, 33.81; H, 2.27; N, 7.88%.

4-Nitro-2-thenyl Acetate (VIII). A mixture of V (4.6 g), anhydrous sodium acetate (3.5 g) and acetic anhydride (20 m*l*) was heated for 6 hr at 60—70°C, and then gently refluxed for 4 hr. The mixture was cooled and poured into water. The resulting organic layer was extracted with ether, and the ether extract was washed with water and dried (Na_2SO_4). After the evaporation of the solvent, the residue was distilledunder reduced pressure to give crude VIII (3.3 g; bp 120—135°C/2—3 mmHg), which was found to contain a small amount of the starting chloride. The above distillate was then gently boiled for 5 hr with anhydrous sodium acetate (1 g) in acetic anhydride (5 m*l*), after which the reaction mixture was treated as before. The distillation of the product gave VIII (2.0 g, 38.4%) as a pale yellow oil, bp 129—131°C/3.5 mmHg, mp 27—29°C.

Found: C, 41.44; H, 3.42; N, 7.22%. Calcd for $C_7H_7NO_4S$: C, 41.78; H, 3.50; N, 6.90%.

4-Nitro-2-thenyl Alcohol (X). VIII (0.8 g) was treated with dilute sulfuric acid in the same way as has been described for VI. Crude alcohol (0.4 g, 63.4%; mp 52—54°C) was recrystallized from a mixture of ether and petroleum ether to yield colorless needles, mp 54—55°C.

Found: C, 37.81; H, 2.96; N, 8.47%. Calcd for $C_5H_5NO_3S$: C, 37.73; H, 3.17; N, 8.80%.

IR Spectrophotometric Determination of the Isomer Distribution of Nitro-2-thenyl Acetates. The quantitative analysis was carried out by a routine peak-intensity method based on the proportionality between the concentration and the absorption-peak height. The calibration spectra for the pure nitro-2-thenyl acetates were measured in a 0.5-mm cell in carbon disulfide solutions, the absorption bands chosen as key bands for the determination being 814 cm^{-1} for VI, 1077 cm^{-1} for VIII, and 705 cm^{-1} for VII. A linear relationship exists between the concentration of the isomers and the optical density within the concentration range examined. Known mixtures prepared from pure samples of each isomer were analyzed in order to determine the accuracy, and the results

5) All melting points and boiling points are uncorrected. The infrared spectra were recorded with a Hitachi EPI-2A spectrophotometer. The NMR spectra were recorded with a Varian Associates Model V-4300B or A-60 spectrophotometer at 60 Mc, using cyclohexane as an internal reference. The microanalyses were carried out by Miss Yoko Endo and Miss Noriko Matsukawa of this Institute, to whom the authors are indebted.

6) H. R. Snyder, L. A. Carpino, J. F. Zack, Jr., and J. F. Mills, *J. Am. Chem. Soc.*, **79**, 2556 (1957).

were examined by Youden's method[7] to reveal that the standard deviations were 0.80%, 0.67%, and 0.96% for VI, VIII, and VII respectively.

7) W. J. Youden, *Anal. Chem.*, **19**, 946 (1947).

The authors wish to thank Dr. Kensuke Takahashi for his NMR spectral measurements and Dr. Yusaku Ikegami for his useful advice on the measurement of the isomer distribution by IR spectroscopy.

BULLETIN OF THE CHEMICAL SOCIETY OF JAPAN VOL. 41 1426—1432 (1968)

Mechanism of Asymmetric Reactions. II.*[1] Kinetical Resolution of Racemic Primary Amines by Means of Sulfonylation with (+)-Camphor-10-sulfonyl Chloride—Preferential Conservation of an Absolute Configuration in the Asymmetric Sulfonylation of Racemic Amines

Kunio Okamoto, Etsuo Minami and Haruo Shingu

Department of Hydrocarbon Chemistry, Faculty of Engineering, Kyoto University, Sakyo-ku, Kyoto

(Received December 26, 1967)

α-Phenylethylamine (I), α,β-diphenylethylamine (II), α-(β-naphthyl)-ethylamine (III) α-(α-naphthyl)-benzylamine (IV), α-pipecoline (V), 2-aminobicyclo[2.2.2]octane (VI), and methylamine (VII) have been partially sulfonylated by (+)-camphor-10-sulfonyl chloride in benzene (or toluene); the optical rotations for the unsulfonylated amines, partially resolved, have been measured. Examination of absolute configurations for the amines indicates that the (R) enantiomers of these amines (I, II, V and VII, including neomenthylamine (VIII)[3] and isomenthylamine (IX)[3]) react faster than the respective (S) enantiomers, with exception of III. The rate for the sulfonylation of (−)-menthylamine with (+)-camphor-10-sulfonyl chloride have been determined in toluene at the temperatures ranging from −20 to −40°C; the rate ratio of the (+)-menthylamine to the (−)-amine has been estimated from the extent of the kinetical resolution of the (±)-menthylamine. Kinetical implication of the coincidence of the preferred absolute configurations has been discussed.

A number of studies[1] concerned with the kinetic method of resolution have been reported since the beginning of this century. However, relatively few data[2] are available for a systematic scrutiny of the correlation between the structural factors of the racemic substrate and the extents or the directions of the resolution.

One of the purposes of this study was to provide additional examples of the kinetical resolution in the partial sulfonylation of a series of racemic primary amines (heretofore only three isomers of menthylamines[3] had been examined) by means of (+)-camphor-10-sulfonyl chloride as an asymmetric reagent.

Another purpose was to scrutinize steric factors which characterize the extent and the direction of such kinetical resolutions, and to discuss its mechanistic implication.

Results

The Partial Sulfonylation of Several Racemic Amines with (+)-Camphor-10-sulfonyl Chloride. Equal molar quantities of racemic amine and (+)-camphorsulfonyl chloride were allowed to react in benzene (or toluene). Since the reaction proceeds following the stoichiometric relation shown below, after the completion of this reaction the half of the starting amine was recovered as the hydrochloride. The amounts of one enantiomer enriched in

*1 Presented at the 9th Annual Meeting of the Chemical Society of Japan, Kyoto, April, 1956; Part I. K. Okamoto, K. Takeuchi and H. Shingu, This Bulletin, **34**, 1137 (1961).

1) For a summary, see a) J. R. Partington, "An Advanced Treatise of Physical Chemistry," Vol. 4, Longmans, Green and Co., London (1953), pp. 298—300; b) E. L. Eliel, "Stereochemistry of Carbon Compounds," McGraw-Hill Book Co., New York (1962), pp. 67—75.

2) a) R. Wegler, *Liebigs Ann. Chem.*, **506**, 77 (1933); b) F. Hawthorne and D. J. Cram, *J. Am. Chem. Soc.*, **74**, 5859 (1952); c) G. Pracejus, *Liebigs Ann. Chem.*, **622**, 10 (1959); d) O. Cervinka and L. Hub, *Chem. Commun.*, **1966**, 761; e) F. Akiyama, K. Sugino and N. Tokura, This Bulletin, **40**, 359 (1967); f) H. Herlinger, H. Kleimann and I. Ugi, *Liebigs Ann. Chem.*, **706**, 37 (1967).

3) J. Read and R. A. Story, *J. Chem. Soc.*, **1930**, 2761.

Table 1. Optical rotations and the extents of kinetical resolution (α%) for unsulfonylated amines[a]

Amine	Temp. °C	$[\alpha]_D$ (c, solvent, temp.) for unsulfonylated amine or derivatives of the amine	α%[b]
α-Phenylethylamine (I)	27—30	−0.057°[c] (29.0, water, 32°C)	0.69%
α, β-Diphenylethylamine (II)	25—30	−1.83°[c] (0.87, water, 31°C)	2.61%
α-(β-Naphthyl)-ethylamine (III)	28—30	+2.04°[d] (1.5, ethanol, 30°C)	3.0%
α-(α-Naphthyl)-benzylamine (IV)	25	−0.94° (9.68, benzene, 22°C)	1.48%
α-Pipecoline (V)	23—25	+0.43° (13.3, benzene, 24°C)	1.44%
2-Aminobicyclo[2.2.2]octane (VI)	15	0.00° (3.0, benzene, 15°C) 0.00°[c] (5.0, water, 15°C)	0.00%
Menthylamine (VII)[f]	−6.0	+7.27°[c] (1.0, water, 25°C)	19.9%
Menthylamine (VII)[f]	−40.0	+10.73°[c] (1.0, water, 25°C)	29.3%
Menthylamine (VII)	room temp.	+10.7°[c,e] (water)	29.2%[e]

a) All reactions were conducted in benzene except when otherwise noted.
b) The rotations, $[\alpha]_D$, of the optically pure materials are taken to be −8.27° (c 31.45, water)[4] for the hydrochloride of I, 70° (c 0.7, water, 15°C)[5] for the hydrochloride of II, +67.9° (c 1.12, water, 17°C)[6] for carbamide of III, +63.6° (p 4.76, benzene, 15°C)[7] for IV, +30.0° (c 20, benzene, 15°C)[8] for V, +36.6° (water, 15°C)[9] for the hydrochloride of VII, respectively.
c) For the hydrochloride. d) For the carbamide.
e) Data given by Read and Story.[3] f) In toluene.

the unsulfonylated amine were determined by the measurement of the optical rotation of the recovered amine.

$$2RNH_2 + (+)\text{-}RSO_2Cl = RNH_2\cdot HCl + (+)\text{-}RSO_2NHR$$

The extents (α%) of the resolution for the unsulfonylated amines were estimated by the comparison of their rotations with those of the optically pure amines (or hydrochlorides).[4-9] The reaction conditions, the otpical rotations and the extents of the resolution (α%) are listed in Table 1. Among several amines examined, menthylamine (VII), which seems to be the most dissymmetric with regards to the reaction center, has been resolved in the greatest extent, and, in contrast, for 2-aminobicyclo[2.2.2]octane (VI), which is relatively symmetric because of its ball-like structure, there is no rate difference between the (R)- and the (S)-enantiomer.

Rate Measurements for the Sulfonylation of (−)-Menthylamine with (+)-Camphor-10-sulfonyl Chloride in Toluene. In order to compare the activation parameters for the sulfonylation of (+)- and (−)-menthylamine, first, the rates of the reaction of (−)-menthylamine with (+)-camphor-10-sulfonyl chloride were measured at the temperatures ranging from −20 to −40°C. The reaction was started by a rapid mixing of the toluene solutions (0.1 M for each) of the (−)-amine and the (+)-sulfonyl chloride; after an appropriate reaction time the reaction was stopped by adding a cold toluene solution of formic acid. The liberated chloride ion was extracted with

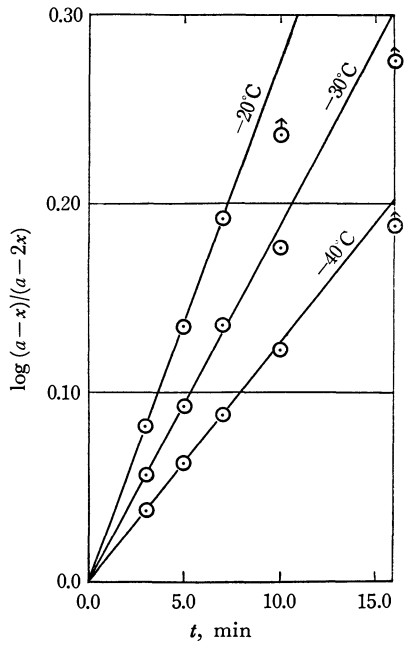

Fig. 1. Rates of the sulfonylation of (−)-menthylamine with (+)-camphor-10-sulfonyl chloride in toluene.

4) W. Marckwald and A. R. Meth, *Ber.*, **38**, 806 (1905).
5) R. Söderquist, *J. prakt. Chem.*, [2] **101**, 300 (1921).
6) E. Samuelsson, Thesis Univ. Lund, 1923, 75; *Chem. Abstr.*, **18**, 1833 (1924).
7) S. Berlingozzi, *Gazetta Chim. Ital.*, **50**, **II**, 57 (1920); *Chem. Zentr.*, **92**, **I**, 84 (1921).
8) W. Leithe, *Monatsh.*, **50**, 45 (1928).
9) J. Read, C. C. Steele and P. G. Carter, *J. Chem. Soc.*, **1929**, 28.

water and titrimetrically determined. Since the reaction was started with the equimolar quantities of the substrate and the reagent, we interpreted the rate data by a modified second-order kinetic equation (Eq. (1)), which was derived on the basis of the stoichiometry of this reaction:

$$k_2 = \frac{1}{at} \ln \frac{a-x}{a-2x} \quad (1)$$

where a is the initial concentration of the amine or the sulfonyl chloride, and x is the instantaneous concentration of the chloride ion at time t. The rate constants were calculated graphically by plotting $\log (a-x)/(a-2x)$ against time, and the results are illustrated in Fig. 1.

Secondly, the rate ratio of (+)- to (−)-menthylamine was estimated from the extent of the kinetical resolution of the racemic menthylamine with the (+)-sulfonyl chloride in toluene, as is described in the following.

The reaction of the racemic menthylamine and (+)-camphor-10-sulfonyl chloride is expressed as a competitive reaction of the (+)- and (−)-amine toward the sulfonyl chloride. So that, we obtain the following rate expression.

$$\frac{d[(+)\text{-RNHSO}_2\text{R}']}{dt} = k_{(+)\text{-Amine}}[\text{R}'\text{SO}_2\text{Cl}][(+)\text{-RNH}_2]$$

$$\frac{d[(-)\text{-RNHSO}_2\text{R}']}{dt} = k_{(-)\text{-Amine}}[\text{R}'\text{SO}_2\text{Cl}][(-)\text{-RNH}_2]$$

or when the reaction is conducted with the equal molar quantities of the racemic amine and the chloride,

$$\frac{dx}{dt} = k_{(+)\text{-Amine}}(a-x-y) \times \left\{0.5a - x - (x+y)\frac{(0.5a-x)}{(a-x-y)}\right\} \quad (2)$$

$$\frac{dy}{dt} = k_{(-)\text{-Amine}}(a-x-y) \times \left\{0.5a - y - (x+y)\frac{(0.5a-y)}{(a-x-y)}\right\} \quad (3)$$

where $x = [(+)\text{-RNHSO}_2\text{R}']$,

$y = [(-)\text{-RNHSO}_2\text{R}']$, $a = [\text{R}'\text{SO}_2\text{Cl}]_0$,

$0.5a = [(+)\text{-RNH}_2]_0 \equiv [(-)\text{-RNH}_2]_0$,

$(x+y) = \{[(+)\text{-RNH}_2\cdot\text{HCl}] + [(-)\text{-RNH}_2\cdot\text{HCl}]\} \equiv \{[(+)\text{-RNHSO}_2\text{R}'] + [(-)\text{-RNHSO}_2\text{R}']\}$,

$(a-x-y) = [\text{R}'\text{SO}_2\text{Cl}] \equiv \{[(+)\text{-RNH}_2]_0 + [(-)\text{-RNH}_2]_0\} - \{[(+)\text{-RNHSO}_2\text{R}'] + [(-)\text{-RNHSO}_2\text{R}']\}$,

$(0.5a-x) = \{[(+)\text{-RNH}_2]_0 - [(+)\text{-RNHSO}_2\text{R}']\}$, and

$(0.5a-y) = \{[(-)\text{-RNH}_2]_0 - [(-)\text{-RNHSO}_2\text{R}']\}$.

From Eqs. (2) and (3), dx/dy is expressed as:

$$dx/dy = k_{(+)\text{-Amine}}(0.5-x)/k_{(-)\text{-Amine}}(0.5a-y) \quad (4)$$

The integration of Eq. (4) gives:

$$k_{(+)\text{-Amine}}/k_{(-)\text{-Amine}} = \log\left(\frac{0.5a-x}{0.5a}\right)\Big/\log\left(\frac{0.5a-y}{0.5a}\right) \quad (5)$$

Since $x_{t=\infty} = [(-)\text{-RNH}_2\cdot\text{HCl}]_\infty$ and $y_{t=\infty} = [(+)\text{-RNH}_2\cdot\text{HCl}]_\infty$, the Eq. (5) is expressed as:

$$\frac{k_{(+)\text{-Amine}}}{k_{(-)\text{-Amine}}} = \frac{\log\left\{\dfrac{[(-)\text{-RNH}_2]_0 - [(-)\text{-RNH}_2\cdot\text{HCl}]_\infty}{[(-)\text{-RNH}_2]_0}\right\}}{\log\left\{\dfrac{[(+)\text{-RNH}_2]_0 - [(+)\text{-RNH}_2\cdot\text{HCl}]_\infty}{[(+)\text{-RNH}_2]_0}\right\}} \quad (6)$$

When $[(-)\text{-RNH}_2\cdot\text{HCl}]_\infty > [(+)\text{-RNH}_2\cdot\text{HCl}]_\infty$, the Eq. (6) can be expressed as the Eq. (7), which indicates the relation between $k_{(+)\text{-Amine}}/k_{(-)\text{-Amine}}$ and α% of the unsulfonylated menthylamine.

$$\frac{k_{(+)\text{-Amine}}}{k_{(+)\text{-Amine}}} = \log\left(\frac{100-\alpha}{200}\right)\Big/\log\left(\frac{100+\alpha}{200}\right) \quad (7)$$

Using the rate ratio (Eq. (7)) and the rate constant observed for the (−)-amine, the rate constant for the (+)-menthylamine can be estimated.

Table 2. Rates and activation parameters for the sulfonylation of (−)- and (+)-menthylamine by (+)-camphor-10-sulfonyl chloride in toluene

Temp. °C	(−)-Menthylamine[a] 10^2k_2 ($\text{sec}^{-1}\,\text{M}^{-1}$)	(+)-Menthylamine 10^2k_2, calcd.[c] ($\text{sec}^{-1}\,\text{M}^{-1}$)
−6.0	3.20[b]	2.50[d]
−20.0	2.07	—
−30.0	1.44	—
−40.0	0.965	0.656[d]
E_A (kcal/mol)	4.40	4.84
$\Delta S^\ddagger$ (e.u.) at −40°C	−50.2	−49.1

a) The initial concentrations of the amine and the sulfochloride was 0.0500 M for each run.
b) Extrapolated from the data at other temperatures.
c) Calculated from the k_2 for the (−)-amine and the rate ratio, $k_{(+)\text{-Amine}}/k_{(-)\text{-Amine}}$ (*cf.* Eq. (7)).
d) $k_{(+)\text{-Amine}}/k_{(-)\text{-Amine}} = 0.78$ (at −6.0°C) and 0.68 (at −40°C).

In Table 2, the rate constants for the (−)- and the (+)-menthylamine are tabulated along with the respective activation parameters. In view of the observation that the reaction does not obey good second-order kinetics (*vide infra*), obviously the values for $k_{(+)\text{-Amine}}$ should be condisered as approximate ones.

As is shown in Table 2, (−)-menthylamine is sulfonylated 1.3 to 1.5 times as fast as (+)-menthylamine in the temperature range −6 — −40°C. The slower rate for the (+)-amine is attributed to the higher activation energy for the (+)-amine sulfonylation.

Discussion

The Mechanism of the Sulfonylation of the Primary Amines. The kinetics of the sulfonylation of the various amines have been studied by Litvinenko and his collaborators;[10] the second-order kinetics of an arylsulfonylation of a primary amine in nitrobenzene[10a] was interpreted by a two-step mechanism, which was composed of a rapid reversible formation of an adduct and a subsequent slow splitting of the adduct into *N*-alkylarylsulfonamide and hydrogen chloride; this is shown as in the following.

$$RNH_2 + ArSO_2Cl \overset{\text{rapid}}{\rightleftharpoons}$$

$$ArSO_2Cl\cdot NH_2R \overset{\text{slow}}{\longrightarrow} HCl + ArSO_2NHR$$

In benzene, however, they found the reaction of *n*-butylamine (R=*n*-Bu) and 2,4-dinitrobenzenesulfonyl chloride (Ar=2,4-$(NO_2)_2C_6H_3$) to be the 2.6 order,[10b] and explained this order assuming the parallel paths. Namely, for both paths an adduct was formed rapidly and reversibly; the adduct then splits into HCl and $ArSO_2NHR$ by the second-order path as is in nitrobenzene, but this decomposition (*i. e.*, dehydrochlorination) is accelerated by a second RNH_2 in the third-order path.

$$RNH_2 + ArSO_2Cl \rightleftharpoons$$

$$ArSO_2Cl\cdot NH_2R \rightarrow HCl + ArSO_2NHR \quad \text{(2nd-order path)}$$

$$\overset{+RNH_2}{\longrightarrow} RNH_2HCl + ArSO_2NHR \quad \text{(3rd-order path)}$$

In a similar fashion, Ebel[11] proposed a two-step mechanism for the sulfonylation of aniline with *p*-toluenesulfonyl chloride in ether. However, in this case the reaction was found to obey the fifth-order kinetics, and this was attributed to the formation of an intermediate between one mole of the sulfonyl chloride and three moles of aniline at the first step of this reaction, this being shown as follows:

$$3C_6H_5NH_2 + ArSO_2Cl \rightleftharpoons$$

$$ArSO_2Cl\cdot 3C_6H_5NH_2 \overset{+C_6H_5NH_2}{\longrightarrow}$$

$$ArSO_2NHC_6H_5 + C_6H_5NH_2HCl + 2C_6H_5NH_2$$

Such association of amines has been proposed in the case of the Menschutkin reaction of alkyl halides with diethylamine in cyclohexane.[12]

In our experiments carried out in toluene, the sulfonylation of (−)-menthylamine obeyed fairly good second-order kinetics, as is shown in Fig. 1. However, in view of a downward drift of the linear plot, the incursion of the third-order process (proposed by Litvinenko[10b]) or of the association of the amines might be considerable at least after the completion of 60% or more.

For the amines other than menthylamine we have not carried out kinetic measurements. However, it seems reasonable to consider that the reactions of these amines proceed through an amine-adduct to the sulfonyl chloride, as is considered in the case of sulfonylation with arylsulfonyl chloride.[10,11]

The Absolute Configuration of the Unsulfonylated Amines. In Table 3 the absolute

Table 3. Absolute configurations of unsulfonylated amines in the partial sulfonylation by (+)-camphor-10-sulfonyl chloride[a]

Amines	Signs of rotation[b] and absolute configurations[c] for unsulfonylated amines
α-Phenylethylamine (I)	(−)-S
α,β-Diphenylethylamine (II)	(−)-S
α-(β-Naphthyl)-ethylamine (III)	(+)-R
α-(α-Naphthyl)-benzylamine (IV)	(−)-?[g]
α-Pipecoline (V)	(−)-S
Menthylamine (VII)	(+)-S[d,f]
Neomenthylamine (VIII)	(+)-S[e,f]
Isomenthylamine (IX)	(+)-S[e,f]

a) In benzene.
b) The optically active hydrochlorides or carbamides possess the same signs of rotation as those for the respective amines of the same absolute configurations.
c) For the absolute configuration of I, III, V and methylamines (VII, VIII and IX), confer the Refs. 13, 2f, 14 and 15, respectively. The absolute configuration of II was deduced from the configuration of phenylbenzylcarbinol.[16]
d) The amines with the same configuration were obtained in toluene and in benzene (see Table 1).
e) The results obtained by Read and Story.[3]
f) The absolute configuration of the asymmetric carbon atom attached to the amino group.
g) The absolute configuration is not known.

10) a) L. M. Litvinenko and V. A. Dadali, Reaktsionnaya Sposobnost Organicheskikh Soedineni (Organic Reactivity), Tartu, Vol. 4, No. 2, 258 (1967); b) L. M. Litvinenko and A. F. Popov, *Dokl. Akad. Nauk SSSR*, **160**, 1124 (1965); *Chem. Abstr.*, **63**, 452e (1965).
11) F. Ebel, *Ber.*, **60**, 2079 (1927).

Table 4. Absolute configurations of unacylated alcohols in the partial acylation of racemic alcohols in the presence of brucine or strychinine[a)]

R, R′CHOH		Unacylated alcohol (sign of rotation[2a)] and absolute configuration[16)])		
R	R′	Acetic anhydride + Brucine	Benzoyl chloride + Brucine	Benzoyl chloride + Strychinine
Me	Et	—	(−)-R	—
Me	*i*-Pr	—	(−)-R	(+)-S
Me	*n*-Bu	(−)-R	(−)-R	(−)-R
Me	Ph	(+)-R	(+)-R	(+)-R
Me	*cyclo*-Hex.	(−)-R	(−)-R	(−)-R
Me	Benzyl	(+)-S	(−)-R	(−)-R
t-Bu	Ph	(+)-?	(+)-?	(+)-?
n-Bu	Ph	—	(+)-R	(+)-R
n-Bu	*cyclo*-Hex.	—	(+)-?	(−)-?
Et	*n*-Pr	—	—	(−)-R
Et	*n*-Bu	—	—	(−)-R
Et	Ph	(+)-R	(+)-R	(+)-R
Et	*cyclo*-Hex.	—	(+)-R	(+)-R
Et	Benzyl	—	—	(−)-R
i-Pr	Benzyl	(+)-?	(−)-?	—
n-Bu	*i*-Pr	—	(−)-S	(−)-S

a) Data were taken from the experimental results of Wegler.[2a)]

configurations[2f,13-15)] of unsulfonylated amines are listed along with the observed signs of rotation; the signs of rotation for neomenthylamine (VIII) and isomenthylamine (IX) were cited from the data reported by Read and Story.[3)]

It is immediately obvious from Table 3 that the amine, with (R)-carbon atom attached to the amino-group, reacts faster than the (S)-enantiomer, with exception of III.

In a similar fashion, we can point out that in the benzoylation or the acetylation of various secondary alcohols, which were conducted in the presence of brucine or strychinine by Wegler,[2a)] the (S)-alcohols react faster than the (R)-alcohols, This is illustrated in Table 4; among 27 examples of the alcohols with known configurations,[16)] four examples seem to be the exceptions.

Recently, the similar coincidence of preferred absolute configurations has been disclosed for the kinetical resolution in some amidation reactions. For example, in amidation with (S)-(+)-2-methylamino-1-phenylpropane in the presence of dicyclohexylcarbodiimide,[2d)] six (R)-alkylphenylacetic acids, with excption of two, were found to react faster than respective (S)-enantiomers. Furthermore, the *N*-substituted amides of (−)-hydratropic acid were found to be formed in the presence of ethyl carbonate preferentially from (R)-primary amines (ten examples with exception of one), in comparison with the respective (S)-amines.[2f)]

In general, the enantiomeric rate ratio in these kinetical resolutions depends on the free-energy difference between the diastereomeric intermediates. Therefore, the simple coincidence of the preferred absolute configurations may suggest that the free-energy difference in these cases may be controlled phenomenally by the combinations (*e. g.*, dextro+dextro and levo+dextro) of the arrangements of three (large-, medium- and small-sized) groups attached to the respective asymmetric carbons of the diastereomeric intermediates. This coincidence seems to be a general trend in the kinetical resolution, so far as it has been explored. However, we should find more examples available in order to confirm its conclusive generality.

In connection with an interpretation of the preference in configuration, examination of the most preferred constellation in the diastereomeric intermediates seems to be successful for several examples[2b,2d,17)] on the basis of a "rigid" model, which was proposed in the case of asymmetric "synthesis" of carbonyl-addition type.[18,19)] However, in the present case of asymmetric sulfonylation with (+)-camphor-10-sulfonyl chloride, in a

12) R. F. Hudson and I. Stelzer, *J. Chem. Soc. (B)*, **1966**, 775.
13) H. E. Smith, S. L. Cook and E. Warren, Jr., *J. Org. Chem.*, **29**, 2270 (1964).
14) W. Leithe, *Ber.*, **65**, 929 (1932).
15) See J. L. Simmonsen, "The Terpenes," Vol. II, Cambridge Univ. Press, London (1949), p. 242.
16) K. Freudenberg, "Stereochemie," Vol. II, Franz Deuticke, Leipzig (1932), p. 696.
17) H. Falk and K. Schlögl, *Monatsh. Chem.*, **96**, 276 (1965).
18) D. J. Cram and F. A. A. Elhafez, *J. Am. Chem. Soc.*, **74**, 5828 (1952); see also Ref. 1b, p. 69.
19) V. Prelog, *Helv. Chim. Acta*, **36**, 308 (1953); see also Ref. 1b, p. 71.

supposed intermediate (see below) the two asymmetric groups lie so remote from each other that it seems difficult to apply a "rigid" model similar to the one proposed by Cram[18] or Prelog.[19] A reasonable elucidation of the preferred configuration in these sulfonylations should be postponed in the future study.

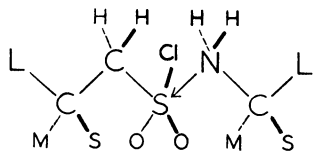

With respect to the extent of these kinetic resolution, we can point out the following factors which may affect the extent of resolution. First, the more tightness of the bonds between the substrate and the reagent in the supposed intermediate may cause the greater degree of inhibition of the free rotation of the respective asymmetric groups, and result in the more extent of resolution. Secondly, the greater degree of the polymolecular association of amines may require their more specific orientation[12] in the intermediate, and cause an enlarged difference in the free energies of diastereomeric intermediates. Thirdly, the multiplicity of the reaction step may enlarge the extent of resolution, since in the multi-step reaction the substrate is kinetically resolved at least twice, or more, until it is converted to the product. The exderimental verification of these factors will be a subject of the future study.

Experimental

Materials. (+)-Camphor-10-sulfonyl chloride was prepared according to Smiles and Hilditch[20] from thionyl chloride and (+)-camphor-10-sulfonic acid, and recrystallized twice from ether; mp 67.0—68.0°C, corr.; $[\alpha]_D^{29}$ +36.5° (*c* 7.72, chloroform). (±)-α-Phenylethylamine (bp 74.0°C/15 mmHg) and (±)-α-pipecoline (bp 128°C) were purified by fractional distillation. (±)-α,β-Diphenylethylamine (bp 165—170°C/15 mmHg), (±)-α-(β-naphthyl)-ethylamine (bp 160°C/13 mmHg; mp 198—199°C, uncorr., for the hydrochloride), and (±)-α-(β-naphthyl)-benzylamine (bp 200—206°C/5 mmHg, mp 119—120°C) were prepared from the respective ketones by the method described by Ingersoll.[21] (±)-Menthylamine (bp 70.0°C/7 mmHg) and (−)-menthylamine (bp 80°C/12 mmHg) were prepared from the respective menthone oximes according to the method of Wallach.[22] (±)-2-Aminobicyclo[2.2.2]octane (mp 138—140°C, decomp.) was prepared by the method described by Seka and Tramposch.[23]

The Recovery of Unsulfonylated Amines from the Products of the Sulfonylation (General Procedure). The sulfonylation was carried out by mixing the sulfonyl chloride with the equal molar quantity of the racemic amine in dry benzene (or toluene). After standing overnight at room temperature, the hydrochloride of the unchanged amine was filtered, and its optical rotation was measured in aqueous solution, or else it was measured in an appropriate solvent after isolation as a free amine or a carbamide. No characterization of the sulfonamide so produced was carried out. The details of the isolation procedures for the respective sulfonylations are cited below.

Isolation of Unsulfonylated α-Phenylethylamine (I). To a solution of (+)-camphor-10-sulfonyl chloride (40.0 g, 0.155 mol) in benzene (50 cc), 20.0 g (0.164 mol) of (±)-I in 50 cc of benzene was added. After standing overnight at 27—30°C, α-phenylethylamine hydrochloride (9.0 g, mp 155—159°C, 34.7% of the starting amine), which separated from the reaction mixture, was filtered; a part of the hydrochloride was dissolved into an appropriate amount of water for the measurement of the optical rotation; $[\alpha]_D^{32}$ of the hydrochloride, −0.038±0.004° (*c* 20.0, water); lit.[4] $[\alpha]_D$ for the optically pure hydrochloride, −6.20° (*c* 20.0, water).

In a duplicate run, 15.2 g (0.125 mol) of (±)-I and 31.4 g (0.125 mol) of (+)-camphor-10-sulfonyl chloride afforded 6.0 g (30.5% of the starting amine) of (−)-phenylethylamine hydrochloride (mp 156—159°C; $[\alpha]_D^{32}$ −0.057°±0.005° (*c* 29.0, water); lit.[4] $[\alpha]_D$ for the optically pure hydrochloride, −8.27° (*c* 31.45, water)).

Isolation of Unsulfonylated α,β-Diphenylethylamine (II). A mixture of (±)-II (10.5 g, 0.0537 mol) and (+)-camphor-10-sulfonyl chloride (13.5 g, 0.0538 mol) in 100 cc of dry benzene was allowed to react overnight at 25—30°C. The crystals (15.0 g, 42.2% yield) of α,β-diphenylethylamine hydrochloride (mp 220—230°C), which precipitated in the reaction mixture, was filtered, and washed with 20 cc of benzene; $[\alpha]_D^{31}$ −1.83±0.15° (*c* 0.87, water); lit.[4] $[\alpha]_D^{15}$ for the optically pure hydrochloride, −70° (*c* 0.7, water). After evaporation of a part of the filtrate, the second crop (1.0 g) of the hydrochloride (total yield 50.7%) was obtained. No characterization of the product from the mother liquors was undertaken.

Isolation of Unsulfonylated α-(β-Naphthyl)-ethylamine (III). A mixture of (±)-III (10.0 g, 0.0588 mol) and (+)-camphor-10-sulfonyl chloride (14.8 g, 0.0588 mol) in benzene (100 cc) was allowed to stand overnight at 28—30°C. The crystals of α-(β-naphthyl)-ethylamine hydrochloride (5.5 g, 45.4% of the starting amine, mp 200—210°C), which precipitated during the reaction, was filtered. A part (2.7 g) of the hydrochloride was converted to its carbamide (2.5 g) by mixing aqueous potassium cyanate with the chloride. The carbamide was recrystallized from 95% ethanol giving 2.3 g of pure carbamide (mp 197—198°C; $[\alpha]_D^{30}$ +2.04±0.03° (*c* 1.5, ethanol), +2.03° (*c* 0.96, ethanol); lit.[6] $[\alpha]_D^{17}$ for the optically pure carbamide, +67.9° (*c* 1.12, ethanol).

20) S. Smiles and T. P. Hilditch, *J. Chem. Soc.*, **91**, 522 (1907).
21) A. W. Ingersoll, "Organic Syntheses," Coll. Vol. 2, p. 503 (1943); see also M. L. Moore, "Leuckart Reaction," in "Organic Reactions," Vol. 5, p. 320 (1949).
22) O. Wallach, *Liebigs Ann. Chem.*, **276**, 300 (1893).
23) R. Seka and O. Tramposch, *Ber.*, **75**, 1379 (1942).

Isolation of Unsulfonylated α-(α-Naphthyl)-benzylamine (IV). A mixture of (±)-IV (4.45 g. 0.0192 mol) and (+)-camphor-10-sulfonyl chloride (4.80 g, 0.0191 mol) in 130 cc of benzene was allowed to stand overnight at 25°C. The crystals (2.50 g) of α-(α-naphthyl)-benzylamine hydrochloride, which separated from the reaction mixture, was filtered, and shaken with 30% aqueous sodium hydroxide and ether. From the ethereal solution 2.0 g (45.0% of the starting amine) of the amine (IV) (mp 116—118°C) was recovered; $[\alpha]_D^{22}$ −0.94±0.04° (*c* 9.68, benzene); lit.[7] $[\alpha]_D^{15}$ for the optically pure IV, +63.6° (*c* 4.8, benzene).

Isolation of Unsulfonylated α-Pipecoline (V). A mixture of (±)-V (4.6 g, 0.0464 mol) and (+)-camphor-10-sulfonyl chloride (12.0 g, 0.0478 mol) in 100 cc of benzene was kept overnight at 23—25°C. The hydrochloride (3.0 g) of α-pipecoline, separated as a slightly hygroscopic crystals, was shaken with 20% aqueous sodium hydroxide and ether. The ethereal solution was dried with potassium hydroxide, and fractionated to give α-pipecoline (2.0 g; 43.4% of the starting amine; bp 110—120°C; $[\alpha]_D^{24}$ +0.43±0.01° (*c* 13.3, benzene); lit.[8] $[\alpha]_D^{15}$ for the optically pure V, 30.0° (*c* 20, benzene).

Isolation of Unsulfonylated 2-Aminobicyclo-[2.2.2]octane (VI). A mixture of (±)-VI (6.0 g, 0.0480 mol) and (+)-camphor-10-sulfonyl chloride (12.0 g, 0.0478 mol) in 110 cc of benzene was allowed to react for two days at 15°C. The hydrochloride (3.5 g; 45.7% of the starting amine) of VI was filtered, and showed no optical rotation within the experimental error ($[\alpha]_D^{15}$ 0.00+0.01° (*c* 5.0, water) for the hydrochloride, $[\alpha]_D^{15}$ 0.00±0.05° (*c* 3.0, benzene) for the free amine).

Isolation of Unsulfonylated Menthylamine (VII). A solution of (+)-camphor-10-sulfonyl chloride in toluene was prepared by dissolving about 6 g of the chloride into 100 cc of toluene; the concentration (0.213 M) was determined by the analysis of chloride ion liberated after 2 hr refluxing of an aliquot (1 cc) with 15 cc of 0.05 N ethanolic potassium hydroxide. The (±)-VII solution (100 cc) was prepared by dissolving 3.30 g of the amine into dry toluene (100 cc). The toluene solutions (80 cc for each) of the chloride and the amine were cooled at −40.0°C, and mixed with each other in one portion. After standing for 5 hr at −40.0°C, the unsulfonylated menthylamine was isolated following the method described by Read and Story.[3] The reaction mixture was made slightly alkaline with 5% sodium hydroxide and shaken until no further reaction occured. The toluene solution was washed with two 100-cc portions of water and extracted with two 100-cc portions of 10% aqueous hydrochloric acid. The hydrochloric acid solution of the amine was evaporated to afford 1.1 g (34.1%) of menthylamine hydrochloride ($[\alpha]_D^{25}$ +10.73±0.18° (*c* 1.0, water); lit.[9] $[\alpha]_D^{15}$ +36.6° (water)).

In the succeeding run carried out for 5 hr at −6.0°C, from a 0.23 M solution (80 cc) of (+)-camphor-10-sulfonyl chloride and a 0.23 M solution (80 cc) of (±)-menthylamine 1.8 g of menthylamine hydrochloride ($[\alpha]_D^{25}$ +7.27±0.10° (*c* 1.0, water)) was obtained.

Kinetic Measurements. A solution (0.1 M, 2.0 cc for each) of (+)-camphor-10-sulfonyl chloride and of (−)-menthylamine in toluene were placed in a Y-shaped tube, and kept at an appropriate reaction temperature in a thermostatted ethanol bath, which was cooled in another carbon dioxide - ethanol bath kept at about −45°C. The two 0.1 M solutions (2 cc for each) were mixed in one portion under nitrogen atmosphere; after appropriate reaction time, the reaction was stopped by adding 1 cc of cold toluene, saturated with formic acid; the solution was extracted with 10 cc of water. From the aqueous extracts 5 cc of an aliquot was titrated by the Volhard method. The rate data were treated graphically by the plot described in text; the results are shown in Table 2 and Fig. 1. In each case the reaction was followed to at least 60% completion.

BULLETIN OF THE CHEMICAL SOCIETY OF JAPAN VOL. 41 1433—1440 (1968)

Kinetic Studies of Solvolysis. XV.*1 Racemization Caused by the Molecular-Complex Formation in the Acetolysis of Optically Active 2,4,7-Trinitro-9-fluorenyl (+)-Camphor-10-sulfonate

Kunio OKAMOTO, Issei NITTA and Haruo SHINGU

Department of Hydrocarbon Chemistry, Faculty of Enginering, Kyoto University, Sakyo-ku, Kyoto

(Received December 26, 1967)

Optically active 2,4,7-trinitro-9-fluorenyl (+)-camphor-10-sulfonate (II) has been synthesized by asymmetric attack of (+)-camphor-10-sulfonic acid to 9-diazo-2,4,7-trinitrofluorene. Acetolysis of II is accelerated by added phenanthrene, anthracene, and hexamethylbenzene at 116—120°C. This acceleration is attributed to molecular complex formation between II and these hydrocarbons. The complex formation has been examined by spectrophotometry or by the isolation of the crystalline complex of II. The acetolysis product, *i. e.*, optically active 2,4,7-trinitro-9-fluorenyl acetate (III), has been racemized in the greater degree in the presence of the more aromatic hydrocarbons. This racemization is ascribed to the prolonged life of the S_N1 ion-pair intermediate caused by the rapid equilibration between the uncomplexed and the complexed S_N1-intermediate; the kinetic nature of this interaction has been discussed.

In the previous papers of this series[1] we have reported on several examples of the solvolysis of α-phenylethyl chloride which proceeded with net retention of configuration. With regard to these retentive solvolyses, it was not clear whether the "back-side shielding"[2] of the S_N1 solvolysis intermediate by a molecule of such retentive solvents as phenol[1a-c] and acrylonitrile[1d] was responsible for those retentive courses or not. In connection with this problem, we undertook the examination of the steric course for the acetolysis of a molecular complex formed from an aromatic hydrocarbon and an optically active substrate, because this reaction might be a model solvolysis which proceeds with net retention of the configuration possibly due to "back-side" shielding of the S_N1 intermediate by such aromatic hydrocarbons.

As a solvolysis substrate which exhibits facile complexation with some aromatic hydrocarbons, we chose a 2,4,7-trinitro-9-fluorenyl system, since Colter and his collaborators[3] clearly established that 2,4,7-trinitro-9-fluorenyl *p*-toluenesulfonate (I) forms a molecular complex with such aromatic hydrocarbons as phenanthrene, anthracene and hexamethylbenzene, and that the rate of the acetolysis of I is enhanced by this molecular complexation.

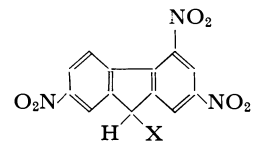

I : X = *p*-toluenesulfoxy
II : X = (+)-camphor-10-sulfoxy
III : X = acetoxy

The 2,4,7-trinitro-9-fluorenyl system with optical activity, caused by an asymmetric carbon at the 9-position, was prepared by an asymmetric attack of (+)-camphor-10-sulfonic acid to 9-diazo-2,4,7-trinitrofluorene; the complexation of 2,4,7-trinitro-9-fluorenyl (+)-camphorsulfonate (II) so synthesized was examined by spectrophotometry and by the isolation of the molecular complexes in the cases of phenanthrene and anthracene; then the kinetic measurements and the product analyses were attempted of II in the presence of those aromatic hydrocarbons.

It is the purpose of the present report to show that the acetolysis of II is accelerated in the presence of the aromatic hydrocarbons as it was found in the case of the acetolysis of I,[3] and that, contrary to our anticipation, the acetolysis involves inversion

*1 Presented at the 20th Annual Meeting of the Chemical Society of Japan, Tokyo, March 1967; Abstract III, p. 13. Part XIV of this series: Ref. 1c.

1) a) Part XI: K. Okamoto, H. Yamada, I. Nitta and H. Shingu, This Bulletin, **39**, 299 (1966); b) Part XIII: K. Okamoto, M. Hayashi, K. Komatsu and H. Shingu, *ibid.*, **40**, 624 (1967); c) Part XIV: K. Okamoto, K. Komatsu and H. Shingu, *ibid.*, **40**, 1677 (1967); d) K. Okamoto, K. Komatsu and H. Shingu, *ibid.*, **39**, 2785 (1966).

2) a) W. von E. Doering and H. H. Zeiss, *J. Am. Chem. Soc.*, **75**, 4733 (1953); b) A. Streitwieser, Jr., and W. D. Schaeffer, *ibid.*, **79**, 6233 (1957); c) A. Streitwieser, Jr., and S. Andreades, *ibid.*, **80**, 6553 (1958); d) H. Weiner and R. A. Sneen, *ibid.*, **87**, 287, 292 (1965); e) N. Kornblum and D. E. Hardies, *ibid.*, **88**, 1707 (1966).

3) a) A. K. Colter and S. S. Wang, *ibid.*, **85**, 114 (1963); b) A. K. Colter, S. S. Wang, G. H. Megerle and P. S. Ossip, *ibid.*, **86**., 3106 (1964).

of configuration, accompanied by predominant racemization, in the presence of those hydrocarbons; the mechanistic implications of the kinetic and the steric characteristics of these acetolyses have been discussed.

Results and Discussion

Optically Active 2,4,7-Trinitro-9-fluorenyl (+)-Camphor-10-sulfonate (II). A mixture of 9-diazo-2,4,7-trinitrofluorene[4] and (+)-camphor-10-sulfonic acid in nitromethane was allowed to react for 2 hr at 40°C. The desired 2,4,7-trinitro 9-fluorenyl (+)-camphor-10-sulfonate (II), $[\alpha]_D^{16}$ +24.45°, was obtained in a fair yield. The sulfonate II was converted to the optically-active 2,4,7-trinitro-9-fluorenyl acetate (III), $[\alpha]_D^{20}$ −6.21°, in good yields after 20 hr of reflux in acetic acid. This indicates that the attack of (+)-camphor-10-sulfonic acid to the 9-diazofluorene had been made asymmetrically, namely, that the optical activity of the sulfonate II was originated partly from a carbon atom at 9-position of 2,4,7-trinitro-9-fluorenyl group, besides from the original (+)-camphor-10-sulfonyl group.

Since under a basic condition, *e. g.*, in pyridine, the sulfonate II and the acetate III were led to highly colored materials from which neither pure starting materials nor identifiable products could be obtained, the usual optical resolution through the hydrogen phthalate of 2,4,7-trinitro-9-fluorenol was not undertaken. Furthermore, in the S_N2 reaction with sodium acetate in nitromethane, the sulfonate II did not afford the acetate III, but colored materials. This made difficult to confirm the relationships between the optical rotations and the configurations with respect to II and III (*vide infra*).

Formation of Crystalline Molecular Complexes of the Sulfonate II. The formation of crystalline molecular complexes involving some aromatic hydrocarbons and 2,4,7-trinitro-9-fluorenyl *p*-toluene-sulfonate (I) has been reported by Colter and Wang.[4] According to their methods, the complex forming properties of the sulfonate II were investigated briefly in the present work. The crystalline molecular complexes between II and phenanthrene (or anthracene), which formed from the benzene or nitromethane solution, are described in Table 1. The isolation of the complex between II and hexamethylbenzene, using benzene or nitromethane as the solvent, was unsuccessful.

Table 1. Complexes of aromatic hydrocarbons with 2,4,7-trinitro-9-fluorenyl (+)-camphor-10-sulfonate (II)

Aromatic hydrocarbon	Melting point °C, corr.	Color	Analysis N% Found	Calcd
Phenanthrene	145.0—146.0	Yellow	5.73	5.92
Anthracene	149.0—149.5	Red	5.25	5.92

Spectrophotometric Studies of the Formation of Molecular Complexes of the Sulfonate II. On the assumption of 1 : 1 complex-formation in the solution, the complex-formation between the sulfonate II and aromatic hydrocarbons was investigated spectrophotometrically in glacial acetic acid at 24°C. The procedure of Colter and his collaborators[3b] was followed; optical densities of four to five mixtures of II ($18.4-8.84\times10^{-4}$ M) and various aromatic hydrocarbons (*i. e.*, hexamethylbenzene ($1.55-2.65\times10^{-2}$ M), phenanthrene ($1.25-5.00\times10^{-2}$ M)), and anthracene ($0.828-1.375\times10^{-3}$ M) were measured at 400 and 410 mμ (or at 450 and 475 mμ for anthracene). The data were treated using Eq. (1),[5,6]

$$\frac{[A]_0}{E_\lambda-\varepsilon_\lambda^A[A]_0}=\frac{1}{\varepsilon^{D\cdot A}-\varepsilon_\lambda^A}+\frac{1}{K_T[D]_0(\varepsilon_\lambda^{D\cdot A}-\varepsilon_\lambda^A)} \quad (1)$$

$[A]_0$ and $[D]_0$ are the stoichiometric concentrations of II and an aromatic donor hydrocarbon; ε_λ^A and $\varepsilon_\lambda^{D\cdot A}$ are the molar extinction coefficients of the sulfonate II and the 1 : 1 complex; E_λ is the measured optical density of the mixture, and K_T is the equilibrium constant for the reaction $A + D \rightleftarrows A\cdot D$.

From the plots of $[A]_0/(E_\lambda-\varepsilon_\lambda^A A)$ *vs.* 1/[D], the K_T's and $\varepsilon_\lambda^{D\cdot A}$'s were estimated. The results are listed in Table 2.

Table 2. The K_T and $\varepsilon_\lambda^{D\cdot A}$ values for 1 : 1 complex formation between II and aromatic hydrocarbons in acetic acid at 24.0°C

Aromatic hydrocarbon	Wavelength mμ	$\varepsilon_\lambda^{D\cdot A}$ $M^{-1}cm^{-1}$	K_T[a] M^{-1}	
Hexamethyl-benzene	400	1100	2.4	Av. 2.6
	410	873	2.8	
Phenanthrene	400	2040	2.5	Av. 2.7
	410	1320	2.9	
Anthracene	450	425	4.6	Av. 4.1
	475	547	3.6	

a) Based on four measurements.

Rate Measurements and Product Analyses for Acetolyses of the Sulfonate II in the Presence of Aromatic Hydrocarbons. Acetolysis rates of the sulfonate II were measured at 116.3°C

4) A. K. Colter and S. S. Wang, *J. Org. Chem.*, **27**, 1517 (1962).

5) The Ketelaar modification of the Benesi-Hildebrand equation:[6] J. A. A. Ketelaar, C. Van de Stolpe, A. Goudsmit and W. Dzcubas, *Rec. trav. chim.*, **71**, 1104 (1952).

6) H. A. Benesi and J. H. Hildebrand, *J. Am. Chem. Soc.*, **71**, 2703 (1949).

Table 3. Rates of acetolysis of II in the presence of aromatic hydrocarbons at 116.3±0.5°C[a)]

Hexamethylbenzene		Phenancerene		Anthracene	
10^2[Hexa.][b)] M	$10^4 k_1$ sec^{-1}	10^2[Phena.] M	$10^4 k_1$ sec^{-1}	10^2[Anth.] M	$10^4 k_1$ sec^{-1}
0	0.75	0	0.75	0	0.75
5.11	1.42	4.10	1.34	2.06	5.04
7.49	1.74	5.46	1.54	3.00	6.40
8.56	1.82	7.55	1.79	4.05	8.16
9.22	1.92				

a) Initial concentrations of II were 2.75×10^{-5} M.
b) Concentrations were corrected for solvent expansion and referred to the temperature of the kinetic measurements.

Table 4. Results of analysis of kinetic data in the acetolysis of II in the presence of aromatic hydrocarbons

Aromatic hydrocarbon	$10^3 k_c$ sec^{-1} (116.3°C)	k_c/k_u[a)]	K_T M^{-1} (116.3°C)	K_T[b)] M^{-1} (24°C)
Hexamethylbenzene	1.5	20	1.0	2.6
Phenanthrene	1.3	18	1.2	2.7
Anthracene	2.9	39	8±4	4.1±3

a) $k_u = 7.5\times10^{-5}$ (sec^{-1}), at 116.3°C
b) Data from spectrophotometric measurements (see Table 2).

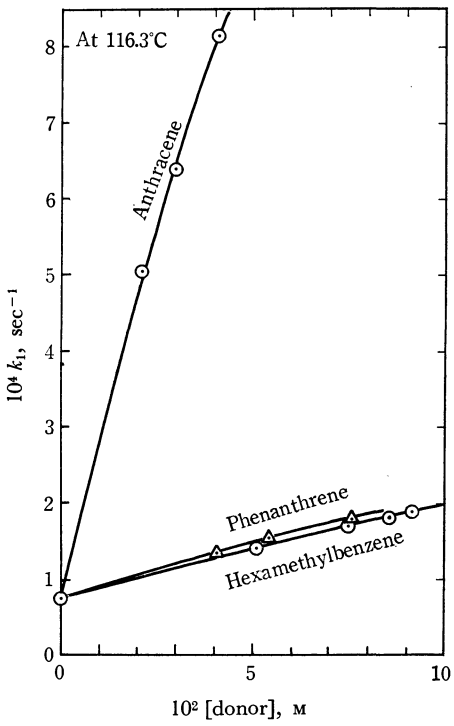

Fig. 1. Rates of acetolysis of II in the presence of aromatic hydrocarbons.

by following titrimetrically the liberated (+)-camphorsulfonic acid. The first-order rate constants, k_1's in the presence of the aromatic hydrocarbons are tabulated in Table 3 along with the rate constant in the absence of aromatic hydrocarbons. Plots of k_1 *vs.* the concentration of the added aromatic hydrocarbon are almost linear with gentle downward drift (see Fig. 1). This is a similar tendency to the observation made by Colter and Wang[3a)] on the acetolysis of the sulfonate I.

The product for the acetolysis of the sulfonate II, *i. e.*, the acetate III, was isolated in 85% yield after 20 hr of reflux of the reaction mixture. In the acetolyses in the presence of hexamethylbenzene, phenanthrene, or anthracene, were obtained some aromatic nitrohydrocarbons, along with the acetate III and unchanged aromatic hydrocarbons. Although the thorough characterization of these nitrohydrocarbons were not carried out, the hydrocarbons had rather high melting points and exhibited the infrared absorption bands characteristic for the nitro and the aromatic nucleus groups but no carbonyl absorption bands. From these facts the nitrohydrocarbons were assumed as the alkylated, *i. e.*, 2,4,7-trinitro-9-fluorenylated, products of the respective aromatic hydrocarbons.

The relation between the yields of the products and the initial concentrations of the added hydrocarbons is shown in Fig. 2 (see also Table 6). On the assumption mentioned above, the yields for nitrohydrocarbons were calculated as a monoalkylated product. The yields of the acetate III exhibit a decreasing tendency with increasing concentrations of added aromatic donor hydrocarbons, whereas the yields of monoalkylated aromatic hydrocarbons show an increasing tendency.

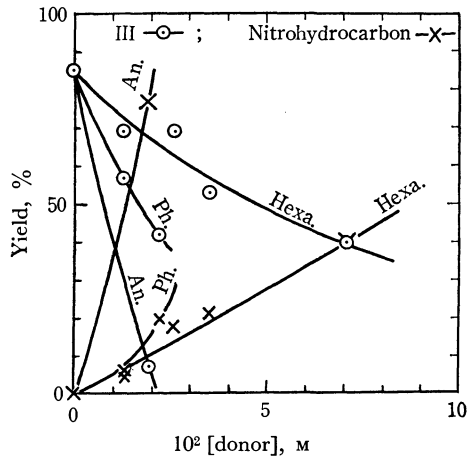

Fig. 2. Yields of III and nitrohydrocarbon in the acetolysis of II in the presence of aromatic hydrocarbons at a reflux temperature (Hexa. = hexamethylbenzene; Ph. = phenanthrene; An. = anthracene).

The latter tendency is enhanced in the case of the aromatic hydrocarbon with more facile complexing character (see the values of K_T's in Table 4).

Estimation of the Specific Rate for Complexed and Uncomplexed Sulfonate II. Among possible mechanisms for the rate enhancement by added hydrocarbons, as the simplest and the most probable one we chose the mechanism proposed by Colter and his collaborators.[3] According to the following reaction scheme A, in which a slight modification is introduced on the original mechanism[3] with respect to the nature of the reaction products,

$$\begin{array}{ccc} RX + D & \overset{K_T}{\rightleftharpoons} & RX\cdot D \\ {\scriptstyle HOAc}\downarrow{\scriptstyle k_u} & & {\scriptstyle HOAc}\downarrow{\scriptstyle k_c} \\ ROAc + D & \overset{K_A}{\rightleftharpoons} & ROAc\cdot D \\ + RD + HX & & + RD + HX \end{array}$$

Scheme A

(RX for II, ROAc for III, D for aromatic donor hydrocarbons, HX for (+)-camphorsulfonic acid, RD for alkylated hydrocarbons), the observed rate constant is given by the expression

$$k_{obsd} = k_u F_u + k_c F_c \qquad (2)$$

where F_u and F_c are fractions of II uncomplexed and complexed, respectively. Under experimental conditions where the hydrocarbon concentration $[D]_0$ is greater than the complex concentration $\{[RX\cdot D]+[ROAc\cdot D]\}$, we obtain the Colter's expression (Eq. (3)).

$$\frac{1}{(k_{obsd}-k_u)} = \frac{1}{(k_c-k_u)} + \frac{1}{K_T[D]_0(k_c-k_u)} \qquad (3)$$

A plot of $1/(k_{obsd}-k_u)$ *vs.* $1/[D]_0$ for the acetolysis in the presence of anthracene at 116.3°C is shown in Fig. 3, and the results of analysis of kinetic data for the respective aromatic hydrocarbons are tabulated in Table 4.

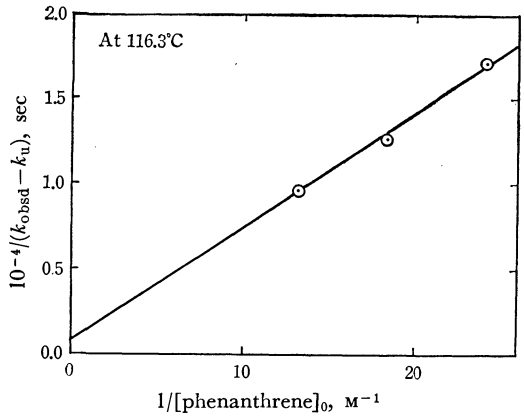

Fig. 3. Plot of $10^{-4}/(k_{obsd}-k_u)$ *vs.* 1/[phenanthrene].

Except the case of anthracene where only rough estimation of the K_T was made due to a large experimental error, the two sets of K_T's *i. e.*, K_T's from kinetic and spectrophotometric data, show a fair agreement with each other.

The values of the rate constant for the complexed substrate, k_c, are greater than those of the rate constant for the uncomplexed substrate, k_u (Table

Table 5. Estimation of the amounts of the products formed from the complexed and uncomplexed substrate in the acetolysis of II in the presence of hexamethylbenzene at 116.3°C[a]

10²[Hexa.] M	Equilibrium composition		Product[b] composition from	
	Complexed II	Uncomplexed II	Complexed II	Uncomplexed II
0.00	0.00%	100%	0.00%	100%
1.30	1.27	98.7	22.2	77.8
2.61	2.59	97.4	34.7	65.3
3.47	3.31	96.7	40.7	59.3
7.11	6.54	93.5	58.3	41.7

a) Initial concentration of II = 1.30×10^{-2} M; K_T = 1.0 (M^{-1}); k_c/k_u = 20.
b) III and nitrohydrocarbon (see text).

Table 6. Optical rotations of III and the yields of the products in the acetolysis of II in the presence of aromatic hydrocarbons at the reflux temperature (116—120°C)

Aromatic hydrocarbon	10^2 [Arom.] M	III		Nitrohydrocarbon % yield
		% yield	$[\alpha]_D$ in $MeNO_2$	
None	0.00	85	$-6.2\pm0.3°$	—
Hexamethylbenzene	1.30	69	$-1.6\pm0.3°$	6
	2.61	69	$-0.4\pm0.3°$	18
	3.47	53	$-0.8\pm0.7°$	21
	7.11	40	$-0.9\pm0.6°$	41
Phenathrene	1.30	57	$-4.4\pm0.5°$	4
	2.18	42	$-2.2\pm1.0°$	20
Anthracene	1.93	7	—	77

a) Initial concentration of II ($[\alpha]_D$ +24.45°) was 1.30×10^{-2} (M).
b) See text.

4); this rate increase for the complexed substrate is elucidated as due to the neutralization of the electron-withdrawing effect of the nitro substituents on the sulfonate II by complexation with the electron-donating aromatic hydrocarbon, since the nitro group on the substrate is known as a retarding substituent of the S_N1 solvolysis rate.

On the basis of the scheme A, we can calculate the respective amounts of the solvolysis products formed from the complexed substrate, RX·D, and the uncomplexed substrate, RX, using the estimated values for K_T, k_c and k_u. The results for the case of hexamethylbenzene are shown in Table 5, along with the equilibrium compositions for the complexed and uncomplexed substrate under the respective reaction conditions.

Optical Rotations of the Acetate III Obtained in the Presence of Aromatic Hydrocarbons. Figure 4 shows relationships between the optical rotations of the acetate III and the initial concentrations of aromatic hydrocarbons. The optical rotations of the acetate III decrease with an increase of the added hexamethylbenzene concentration; at the higher concentrations the optical rotations exhibit a tendency to a complete loss of the optical activity. In a similar fashion, optical rotations of the acetate III show a rapid decrease with an increase of the amounts of added phenanthrene (Fig. 4).

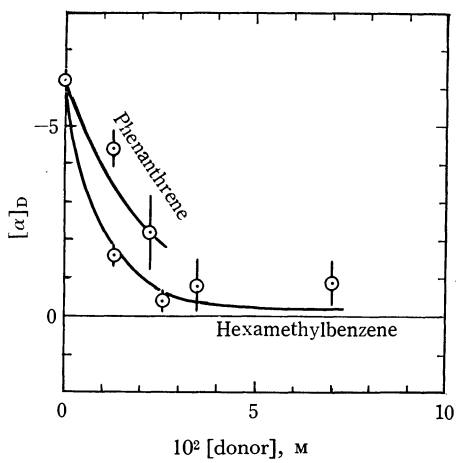

Fig. 4. Optical rotations of III formed in the acetolysis of II in the presence of aromatic hydrocarbons at reflux temperature.

As is mentioned above, an S_N2 reaction of the sulfonate II, which was carried out to determine the configurations of the sulfonate II or the acetate III, was unsuccessful owing to the unstability of II or III under the basic reaction condition. However, in acetolysis of a simple secondary alkyl substrate, the inversion of the configuration accompanying some racemization is usually observed, and this inversion is considered as a general character for the steric course of the solvolysis of simple alkyl compounds.[7] Accordingly, we may consider that the acetolysis of the sulfonate II also proceeds with net inversion of configuration.

If the greater S_N1 rate constant for the complexed substrate, as is compared with that for the uncomplexed sulfonate II, reflects on the prolonged life for the 2,4,7-trinitro-9-fluorenyl cation produced as the S_N1 intermediate, this longer life of the intermediate may cause the greater extent of racemization in the product III.

The Estimation of the Extents of Racemization of the Acetate III on the Basis of the Reaction Scheme A. In view of the complete racemization of III formed in the presence of added hexamethylbenzene, we may assume that the acetate III produced through the complexed substrate has no optical activity, and that, on the other hand, the uncomplexed substrate affords the acetate III with an optical rotation ($[\alpha]_D$ −6.2°) under the same reaction conditions.

On the basis of this assumption, the predicted values for the optical rotation of the acetate III can be calculated from the reaction scheme A, using the value for the product composition (*cf.*

7) See the footnote 1 of the Ref. 1b.

Table 7. Comparison of the optical rotations of III formed in the acetolysis of II in the presence of various amounts of hexamethylbenzene at the reflux temperature (116—120°C)[a]

10^2 [Hexa.]	$[\alpha]_D$ of III	
	Observed	Calculated, based on the reaction scheme A[b]
0.00	−6.2°	—
1.30	−1.6°	−4.8°
2.61	−0.4°	−4.0°
3.47	−0.8°	−3.7°
7.11	−0.9°	−2.6°

a) Initial concentration of II were 1.30×10^{-2} (M).
b) $[\alpha]_{D\,calcd} = -6.2°\times[\ \%$, Product from the uncomplexed II]/100.

Table 5). Since the actual products contain some nitrohydrocarbon, and since the S_N1 intermediate, which is formed from a complexed substrate, may afford much more nitrohydrocarbon than the uncomplexed intermediate, this prediction from the scheme A (Table 7) may be somewhat lower estimation.

Table 7 shows that the observed optical rotations for III are substantially lower than the values calculated on the basis of the scheme A. This gap clearly indicates that the aromatic hydrocarbon makes an additional contribution, other than the complexation of the substrate, to the loss of the optical activity of the acetate III. Therefore, we may add to the reaction scheme A an interconversion course between the complexed and uncomplexed S_N1 intermediate in order to explain this excess of racemization in the acetate. This is shown in the scheme B.

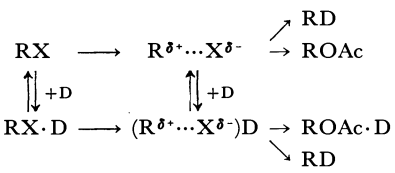

Scheme B

Kinetic Nature of the Interaction between the Aromatic Hydrocarbon and the S_N1 Intermediate. It may be difficult to find an unambiguous elucidation of the reason why the interconversion between the complexed and the uncomplexed intermediate causes the excess of the racemization for the acetate III. However, as one of the possible explanations, we may suggest the following mechanism.

The association and dissociation rates in the equilibrium between the complexed and the uncomplexed intermediate would be so frequent that the attack of the nucleophilies, *i. e.*, acetic acid or the acetate ion, would relatively be hindered. Consequently, the life of the ion-pair intermediate is prolonged and the cationic part of the intermediate rotates[8] more frequently until its asymmetric center is attacked by the nucleophile. This means that the intermediate would be racemized in greater extent in the presence of aromatic donor hydrocarbons.

Furthermore, the rate of the nucleophilic attack on the complexed intermediate would be lower than the rate for the uncomplexed intermediate, and accordingly the more acetate III (inverted) may be produced from uncomplexed intermediates than complexed ones. Thus, even if the nucleophilic attack on the complexed intermediate were made from the front-side, resulting in the retention of the configuration of the acetate, the predominance of the acetate produced from the inversive attack on the uncomplexed intermediate would lead to the over-all net inversion of configuration of the acetate. If this is the case in our experiments, it would be unable to verify whether the retentive attack is predominant for the complexed intermediate or not.

Experimental

Materials. Phenanthrene (mp 100.7—101.5°C, corr.) was purified according to the method of Phillips[9] by refluxing a mixture of phenanthrene, maleic anhydride, and xylene, and by succeeding recrystallization from ethanol; anthracene (mp 219.5—221.0°C, corr.) was recrystalized from acetic acid and then chromatographed over basic alumina, using benzene as an eluent. Hexamethylbenzene (mp 166.9—168.4°C, corr.) was used as received. Acetic acid (bp 118.0—118.5°C) was purified by refluxing with a small amount of acetic anhydride and by subsequent fractional distillation.

9-Diazo-2,4,7-trinitrofluorene (mp 204—205°C, decomp.) was prepared by the method described by Colter and Wang.[4] (+)-Camphor-10-sulfonic acid (mp 201°C, corr.; $[\alpha]_D^{20}$ +40.5° (*c* 3.16, ethanol)) was recrystallized from ethyl acetate.

The Asymmetric Synthesis of Optically Active 2,4,7-Trinitro-9-fluorenyl (+)-Camphor-10-sulfonate (II). A mixture of 9-diazo-2,4,7-trinitrofluorene (13.0 g, 0.0397 mol) and (+)-camphor-10-sulfonic acid (13.0 g, 0.0559 mol) in nitromethane (350 cc) was placed in a 500-cc three-necked flask equipped with a thermometer, a drying tube, and a magnetic stirrer. After 2 hr of stirring at 40°C, the reaction mixture was washed with two 100-cc portions of 10% aqueous sodium chloride and then with two 100-cc portions of water. Concentration of the nitromethane solution afforded bright yellow crystals (13.64 g). After recrystallization from 40 cc of nitromethane, 11.29 g (53.6%) of II (mp 192.0—193.0°C, decomp., corr.;

8) K. Okamoto, N. Uchida, S. Saitô and H. Shingu, This Bulletin, **39**, 307 (1966).
9) D. D. Phillips in "Organic Syntheses," Coll. Vol. IV, p. 313 (1963).

$[\alpha]_D^{16}$ $+24.45\pm0.4°$ (*c* 2.12, nitromethane)) was obtained.

Found: C, 51.78; H, 4.05%. Calcd for $C_{33}H_{21}O_{10}N_3S$: C, 51.98; H, 3.98%.

The Acetolysis of II in the Absence of Added Aromatic Hydrocarbons. A mixture of II (0.600 g, 0.00113 mol) and acetic acid (81 cc) was refluxed for 20 hr in a 200-cc round-bottomed flask equipped with a reflux condenser and a drying tube. After evaporation of acetic acid in vacuo, the residual yellow crystals were washed with water, ethanol, and ether, leaving 0.340 g (85%) of 2,4,7-trinitro-9-fluorenyl acetate (III) (mp 234—236°C, decomp. (lit.[4] mp 235°C, decomp.); $[\alpha]_D^{20}$ $-6.21\pm0.5°$ (*c* 2.13, nitromethane)).

The Acetolysis of II in the Presence of Added Aromatic Hydrocarbons. In a similar fashion to the acetolysis in the absence of added aromatic hydrocarbons, a mixture of II, an aromatic hydrocarbon and acetic acid was refluxed in a 200-cc three-necked flask equipped with a reflux condenser and a thermometer. After an appropriate reaction time, acetic acid was evaporated *in vacuo*, and the reaction products were isolated by extraction or by recrystallization. The details of the experimental procedures for some representative runs are cited below.

The Acetolysis of II in the Presence of Hexamethylbenzene. A mixture of II (1.00 g, 0.00188 mol), hexamethylbenzene (0.612 g, 0.0037 mol), and acetic acid (135 cc) was refluxed for 19 hr at 120°C. After evaporation of acetic acid *in vacuo* at 50—60°C, the residual yellow solid was washed with 80 cc of water and with 80 cc of ether to remove the remaining acetic acid and the unchanged hexamethylbenzene. The crude yellow crystals (0.551 g) was dissolved in 15 cc of hot nitromethane; after being kept at room temperature, the solution deposited bright yellow crystals (0.140 g; 18% yield, calculated as an alkylated hexamethylbenzene, *vide infra;* mp 279—280.5°C, decomp., corr.). After three recrystallizations of these crystals from nitromethane, 0.030 g of crystals (mp 293.7°C, decomp., corr.) were obtained (Found: C, 64.30; H, 4.98; N, 8.14%. Calcd for $C_{24}H_{21}O_6N_8$: C, 64.42; H, 4.73; N, 9.39%). These purified crystals exhibited infrared absorptions at 1520 and 1345 cm^{-1} (NO_2), at 2920 cm^{-1} (CH_3), at 3150 and 810 cm^{-1} (aromatic C–H). No carbonyl absorption was exhibited in the range 1650—1800 cm^{-1}. Although no further characterization was carried out, we assumed these crystals as an aromatic nitrohydrocarbon produced from hexamethylbenzene and II. The mother liquors obtained from the recrystallization of the above mentioned crude crystals were condensed to 5 cc, and 0.407 g (69%) of III (mp 231—234°C, uncorr.; the identical infrared spectrum with that of the authentic sample; $[\alpha]_D^{20}$ $-0.42\pm0.3°$ (*c* 1.79, nitromethane)) was obtained.

The Acetolysis of II in the Presence of Phenanthrene. A mixture of II (1.00 g, 0.00188 mol), phenanthrene (0.337 g, 0.001885 mol), and acetic acid (135 cc) was refluxed at 120°C for 17 hr. After evaporation of acetic acid *in vacuo* at 50—55°C, and washing with water, 0.739 g of yellow crystals were obtained. These crystals were refluxed with 15 cc of ether, leaving 0.49 g of a yellow solid; this was dissolved in 15 cc of nitromethane. After standing overnight in an ice-box, 0.033 g (4.2% yield, calculated as trinitrofluorenylphenanthrene, *vide infra*) of bright yellow crystals (mp 273.5—275.0°C, uncorr.) were obtained. Four recrystallizations of these crystals from nitromethane afforded 0.010 g of bright yellow needles (mp 297.5—298.5°C), which infrared spectra had characteristic bands at 3100 and 740 cm^{-1} (aromatic C–H) and at 1525 and 1345 cm^{-1} (NO_2). No carbonyl bands was found in the spectra (Found: C, 62.49; H, 3.29; N, 9.55%. Calcd for $C_{27}H_{15}O_6N_3$: C, 67.92; H, 3.17; N, 8.80%). Although results of elemental analysis were not satisfactory, we considered these crystals as trinitrofluorenylphenanthrene from the high melting point and the characteristic bands of the infrared spectra. After being condensed to 5 cc, the filtrate from the nitromethane solution of the crude reaction products afforded 0.399 g (57.2%) of III (mp 227—229°C, uncorr.; $[\alpha]_D^{22}$ $-4.37\pm0.44°$ (*c* 1.71, nitromethane); the same infrared spectrum as the authentic sample).

The Acetolysis of II in the Presence of Anthracene. A mixture of II (0.500 g, 0.000943 mol), anthracene (0.250 g, 0.00140 mol), and acetic acid (62.5 cc) was refluxed for 10.3 hr. After evaporation of acetic acid *in vacuo* at 50—60°C, the residual red-brown solid was washed with water. The dried solid was dissolved in 10 cc of acetone, leaving 0.240 g (53.4% yield, calculated as trinitrofluorenylanthracene) of insoluble crystals. After five recrystallizations from nitromethane, 0.050 g of orange needles (mp 294.0—294.5°C, uncorr.; Found: C, 67.09; H, 3.14; N, 8.19%. Calcd for $C_{27}H_{15}O_6N_3$: C, 67.92; H, 3.17; N, 8.80%). The infrared spectra had characteristic bands at 3110 and 730 cm^{-1} (aromatic C–H), 1520 and 1340 cm^{-1} (NO_2); No carbonyl bands were found. After condensation of the filtrate from the 10 cc of acetone solution, 0.105 g (23.4% yield, calculated as trinitrofluorenylanthracene) of the second crop (mp 305°C, corr., red-orange needle after four recrystallizations; the same infrared spectrum as the first crop) was obtained. From the mother liquors 0.165 g of a mixture of anthracene and III was obtained; the composition was determined by elution chromatography over acidic alumina. Anthracene (0.067 g) was eluted with benzene, and 0.025 g (7%) of III (mp 208—216°C, uncorr.; the same infrared spectrum as the authentic sample) was obtained from the succeeding fractions using ether as an eluent.

Isolation of Crystalline Molecular Complexes of II. To the solution of II (0.176 g, 0.000331 mol) in benzene (6 cc) was added anthracene (0.067 g, 0.000376 mol), resulting in a deep red solution. After standing overnight at room temperature, the red needles were collected by filtration, washed with small portions of ether. The dried complexes melted at 149.0—149.5°C (corr.) and weighed 0.11 g (0.000155 mol).

Found: C, 63.81; H, 4.96; N, 5.25%. Calcd for $C_{37}H_{31}O_{10}N_3S$: C, 62.62; H, 4.40; N, 5.92%.

From a mixture of II (0.305 g, 0.000575 mol) and phenanthrene (0.102 g, 0.000573 mol) in 3 cc of nitromethane, 0.120 g (0.000169 mol) of bright yellow complexes (mp 145.0—146.0°C, corr.) were obtained after standing overnight at room temperature.

Found: C, 62.64; H, 4.11; N, 5.73%. Calcd for $C_{37}H_{31}O_{10}N_3S$: C, 62.62; H, 4.40; N, 5.92%.

A trial to obtain the complexes between hexamethylbenzene and II from the benzene or nitromethane solution of a mixture (1 : 1 mol) of these components was unsuccessful.

Kinetic Measurements. All kinetics were measured at 116.4±0.5°C. The reaction vessels were 50-cc measuring flasks, and about 40 cc of the reaction mixture was placed. The first aliquot (3 cc) was removed 10 min after setting the flask in a thermostat. The subsequent aliquots (3 cc for each) were removed at intervals, added into 1 cc of cooled sodium acetate solution (0.01 N) in acetic acid, and titrated with 0.01 N perchloric acid in acetic acid, using crystal violet as an indicator. All the data were treated graphically by a plot of log $a/(a-x)$ against the time. In each run the reaction was followed to at least 80% conversion, and a smooth linear relationship was obtained for each run.

Spectrophotometric Determination of K_T. Optical density measurements were carried out with a double set of thermospacers connected to a circulating constant temperature bath. The temperature of the cell compartment was held in this way at 24.0±0.2°C. The measurements were carried out at the range of 390 to 600 mμ, using quartz cells with a path length of 10 mm. The data were treated in the manner described in text.

BULLETIN OF THE CHEMICAL SOCIETY OF JAPAN VOL. 41 1440—1444 (1968)

Azirines. III. The Preparation of Azirine Derivatives by the Base-Catalyzed Rearrangement of Quaternary Hydrazones[1]

Shimao SATO

Kyorin Chemical Laboratory, Kyorin Pharmaceutical Co., Ltd., Ukima, Kita-ku, Tokyo

(Received December 27, 1967)

An attempt to prepare azirines by the base-catalyzed rearrangement of some quaternary hydrazones gave the corresponding azirine derivatives. Namely, 2-phenyl-3-methylazirine was obtained by the treatment of propiophenone dimethylhydrazone methiodide with potassium *t*-butoxide, but treatment with sodium isopropoxide gave 2,5-diphenyl-3,6-dimethylpyrazine or 2-phenyl-2-isopropoxy-3-methylaziridine, depending on the reaction conditions. 2-Phenyl-3,3-pentamethyleneazirine was obtained in a good yield by the treatment of cyclohexyl phenyl ketone dimethylhydrazone methiodide with sodium isopropoxide.

In 1957, Smith and Most[2] reported the rearrangement of quaternary hydrazones with a base to give aminoketones, but no intermediate azirine rings were isolated. Recently, Parcell[3] reported that 2-phenyl-3,3-dimethylazirine was isolated in a good yield by the treatment of isobutyrophenone dimethylhydrazone methiodide with sodium isopropoxide in isopropanol, but he did not describe the application of this reaction to other ketones or the effectiveness of other base-catalysts:

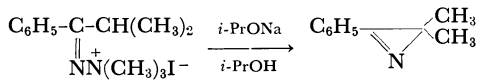

In a previous paper,[1] it was reported that 2,4-diphenylpyrrole, not 2-phenylazirine, was obtained by the treatment of acetophenone dimethylhydrazone methiodide (I) with methylsulfinyl carbanion as a base-catalyst:

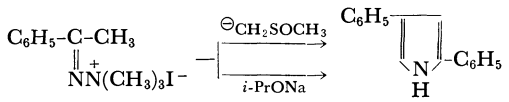

I II

These results suggest that this rearrangement does not proceed along the same pathway for all ketones, and that the reaction is dependent upon the structures of the ketones or on the properties of the base-catalysts. Therefore, the object of the present study has been to examine the relationship between the azirine formation and the structures of the ketones or the properties of the base-catalysts.

When **I** was treated with a slightly less than one equivalent amount of sodium isopropoxide in isopropanol, 2,4-diphenylpyrrole (II) was obtained in a 32% yield, but 2-phenylazirine or its hydrolyzed product could not be isolated.

When propiophenone dimethylhydrazone methiodide (III), which possesses a *sec*-carbon atom in the α-position to the C=N double bond, was treated with a slightly less than one equivalent amount of sodium isopropoxide in isopropanol, 2,5-diphenyl-3,6-dimethylpyrazine (IV) was obtained in a 33% yield. The mechanism of the formation of IV is not clear, but it might be possible to consider that the reaction proceeds through the initial formation of the intermediate 2-phenyl-3-methylazirine,

1) Part I and II: S. Sato, H. Kato and M. Ohta, This Bulletin, **40**, 2936, 2938 (1967).

2) P. A. S. Smith and E. E. Most, *J. Org. Chem.*, **22**, 358 (1957).

3) R. F. Parcell, *Chem. & Ind.*, **1963**, 1396.

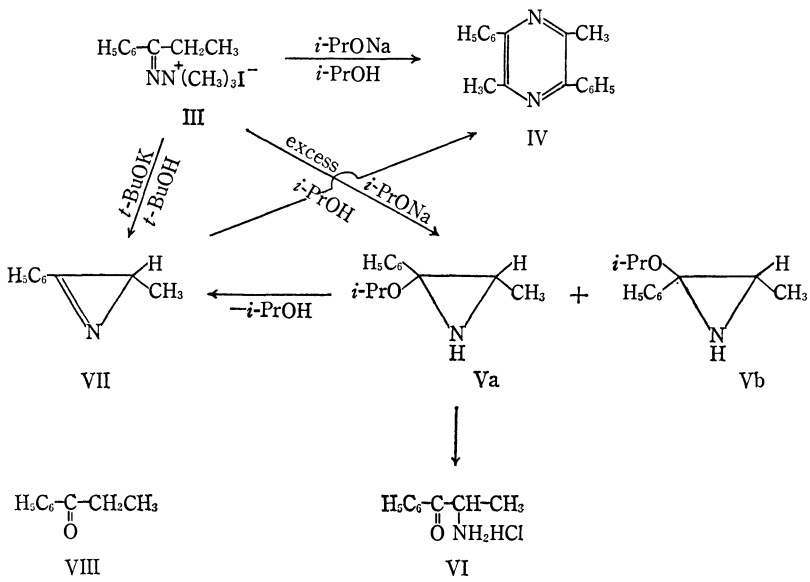

followed by dimerization to IV. Therefore, in order to clarify the above mechanism, the same reaction was attempted in the presence of an excess of sodium isopropoxide. In this case, if the reaction did proceed through an azirine, it might be expected to be trapped by the addition of isopropanol in the presence of a base-catalyst and so give a stable aziridine derivative. The reaction indeed gave 2-phenyl-2-isopropoxy-3-methylaziridine (V) in a 72% yield. This structure was supported by the results of elemental analysis; by the infrared absorptions at 3300 cm^{-1} for the NH group, at 1380 and 1370 cm^{-1} for the isopropyl group, and at 1120 cm^{-1} for the alkoxy group, and by the fact that hydrolysis by hydrochloric acid afforded α-aminopropiophenone. The vapor phase chromatography (vpc) analysis of this product suggested that it is a mixture of three components (A, B and C) in a ratio of 21 : 53 : 26.[4] Accordingly, its NMR spectrum was rather complex: it shows superimposed doublets at τ 8.85 (total of 9H, $J=7$ cps) for the methyl groups, a pair of singlets, at 8.18 and 8.08 (total of 1H), for the proton on the ring nitrogen and a pair of quartets centered at 7.04 and 6.65 (total of 1H, $J=7$ cps) and a pair of superimposed septets at 6.28 and 5.99 (total of 1H, $J=7$ cps) for the methine proton of the isopropyl group, besides a multiplet of the phenyl group at 2.5—2.9 (10H). The ratio of the *cis* and *trans* isomers was 2 : 1 judging from the vpc peak area ratio of 2.6 : 1 and by the NMR peak height ratio of the imine proton. These spectral data suggest that the product is a mixture of *cis* and *trans* isomers, Va and Vb.

Next, when the rearrangement of III was effected in the presence of an excess of potassium *t*-butoxide in place of sodium isopropoxide, an oily product boiling at 85—90°C/5 mmHg was obtained. Infrared spectrum of this product exhibits a band at 1740 cm^{-1} for the C=N bond of an azirine and one at 1690 cm^{-1} for the carbonyl, and the vpc peak shows the presence of two components (D and E) in a ratio of 55 : 45. The component E was found to have the same vpc retention time as an authentic specimen of propiophenone. The NMR spectrum of this product shows a double at τ 8.2 (3H) for the methyl group on the 3-position of the ring, a quartet at 7.8 (1H) for the hydrogen on the 3-position of the ring, a multiplet at 2—3 (10H) for the phenyl group and a triplet at 8.8 (3H) for the methyl group of propiophenone, and a quartet at 7.2 (2H) for the methylene group of propiophenone. These spectral data suggest that the component D is 2-phenyl-3-methylazirine (VII) and that the component E is propiophenone (VIII). The *t*-butanol addition product could not be isolated; this is probably because the addition of a bulky *t*-butyl group to the C=N double bond was more hindered than the addition of an isopropyl group.

Parcell reported that 2-phenyl-3,3-dimethylazirine was re-produced by the azeotropic distillation of isopropanol from a solution of the 2-phenyl-2-isopropoxy-3,3-dimethylaziridine in toluene in the presence of a catalytic amount of sodium isopropoxide.[3] Accordingly, compound V was treated by the same procedure in order to find out whether or not such a reaction can be used in the preparation of 3-monoalkylazirine. An oily product which boils at 75—82°C/1 mmHg was

4) Component A may be a decomposition product during the v.p.c. analysis, because the product gave a good elemental analysis and its spectrum did not show prominent peaks which may be assigned to the presence of an impurity.

obtained. The infrared spectrum of this product exhibits a band at 3300 cm^{-1} for the NH group, at 1740 cm^{-1} for the C=N double bond of an azirine and one at 1120 cm^{-1} for the alkoxy group. These infrared data suggest that this product is a mixture of azirine (VII) and aziridine (V); the vpc peak shows the presence of four components (F, G, H and I) in a ratio of 50 : 2 : 40 : 8. The components H and I had the same vpc retention times as the components B and C (azirdidine Va,b) described above, and the component F had the same retention time as that of the component D (azirine VII) described above, but the components F and G could not be separated because their retention times were very close to one another. However, the product partly solidified on standing in a refrigerator for one week; the melting point of this solid was undepressed on admixture with compound IV. Thus, it may be concluded that this product is a mixture of *cis*, *trans* aziridine Va, Vb and azirine VII.

When cyclohexyl phenyl ketone dimethylhydrazone methiodide (IX), which possesses a *t*-carbon on the α-position of the C=N bond, was treated with sodium isopropoxide in isopropanol, 2-phenyl-3,3-pentamethyleneazirine (X) was isolated in an 80% yield. This compound was identified by elemental analysis and by its showing an infrared absorption at 1740 cm^{-1} for the C=N double bond of azirine.

In order to examine the applicability of this method to a cyclic ketone,[5] cyclohexanone dimethylhydrazone methiodide (XI) was treated with sodium isopropoxide in isopropanol. In this case

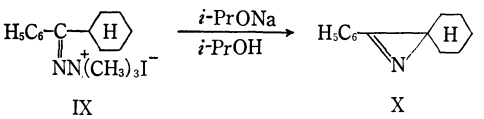

IX X

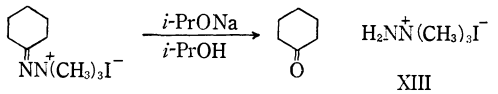

XI XII XIII

no ring formation occurred, but XI dissociated to cyclohexanone and trimethylhydrazinium iodide (XIII).

Compound XI probably dissociated because XI is a very unstable compound and is readily dissociated by isopropanol to XII and XIII; indeed, XIII was formed by an attempted recrystallization of XI from ethanol.

When this rearrangement was tried by means of methyl sulfinyl carbanion in DMSO, only an intractable red-brown resinous matter was formed. Similarly, an attempt to synthesize ethyl benzoylacetate dimethylhydrazone methiodide from ethyl benzoylacetate dimethylhydrazone and methyl iodide in ether gave only trimethylhydrazinium iodide.

In summary, it may be said that this method of preparing an azirine ring is affected by the activity of the hydrogen atom on the α-position of the C=N double bond, by the stability of the reaction product, and by the properties of catalyst and solvent. Namely, when the α-position was *t*-carbon, the reaction gave an azirine ring in a good yield, and when it was *sec*-carbon, it was attacked by the base to give unstable azirine, which was easily dimerized. When the α-position was primary carbon, the reaction gave a completely different product. Therefore, this method of preparation seems to be limited by the structure of the starting materials.

Experimental

The melting points were measured on a micro hot stage and are not corrected; all boiling points are uncorrected. The infrared spectra were taken on KBr tablets or neat liquid films. The vpc analysis was performed at a column temperature of 150°C, using a 150 cm column packed with 10% Apiezone Grease L on Diasolid A.

Propiophenone Dimethylhydrazone. A mixture of 25 g (0.18 mol) of propiophenone, 15 g (0.25 mol) of dimethylhydrazine, 2 g of anhydrous sodium acetate, and 2 drops of glacial acetic acid was heated, in a sealed tube, on an oil bath under reflux for 16 hr (bath temperature 120°C). After the two layers had been separated, the aqueous layer was extracted with ether, the combined organic layers were washed with water and dried over sodium sulfate, and the solvent was removed by distillation. The residual oil was distilled under reduced pressure to give 30 g (90%) of a pale yellow liquid boiling at 120—122°C/20 mmHg.

Found: C, 75.08; H, 8.92; N, 15.56%. Calcd for $C_{11}H_{16}N_2$: C, 74.95; H, 9.15; N, 15.96%.

Cyclohexyl Phenyl Ketone Dimethylhydrazone. A mixture of 10 g (0.053 mol) of cyclohexyl phenyl ketone,[6] 6 g (0.1 mol) of dimethylhydrazine, 1 g of anhydrous sodium acetate, and one drop of glacial acetic acid was treated in essentially the same manner to give 12 g of a pale yellow oil boiling at 115—118°C/1—2 mmHg.

5) Hassner and Fowler reported the synthesis of fused azirines by photolysis of the corresponding vinyl azides but the azirine fused to a six-membered ring could not be isolated probably because of a highly strained structure of the expected compound. In our experiment, however, if the desired fused azirine I was formed, it may readily add a molecule of isopropanol to give isolable stable fused aziridine II under the reaction conditions.

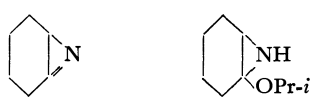

I II

A. Hassner and F. W. Fowler, *Tetrahedron Letters*, **1967**, 1545.

6) V. Meyer and W. Scharvin, *Ber.*, **30**, 1942 (1897).

Found: C, 77.98; H, 9.75; N, 11.98%. Calcd for $C_{15}H_{22}N_2$: C, 78.21; H, 9.63; N, 12.16%.

Ethyl Benzoylacetate Dimethylhydrazone. A mixture of 19.2 g (0.1 mol) of ethyl benzoylacetate, 12 g (0.2 mol) of dimethylhydrazine, 2 g of anhydrous sodium acetate, and 2 drops of glacial acetic acid was treated in the same manner to give 11 g (48%) of a pale yellow liquid boiling at 130—135°C/1 mmHg.

Found: C, 66.72; H, 7.47; N, 11.97%. Calcd for $C_{13}H_{18}O_2N_2$: C, 66.64; H, 7.74; N, 11.96%.

Propiophenone Dimethylhydrazone Methiodide (III). To a solution of 25 g of propiophenone dimethylhydrazone in 50 m*l* of absolute ethanol, there was added 80 g of methyl iodide, and then the mixture was refluxed for five hours. After cooling, the white crystals which separated out were collected, further crops being obtained by dilution with ether. Recrystallization from ethanol gave 31 g of white prisms melting at 157—159°C.

Found: C, 45.15; H, 5.78; N, 8.88%. Calcd for $C_{12}H_{19}N_2I$: C, 45.30; H, 6.02; N, 8.80%.

Cyclohexyl Phenyl Ketone Dimethylhydrazone Methiodide (IX). To a solution of 12 g of cyclohexyl phenyl ketone dimethyl hydrazone in 30 m*l* of dry ether, there was added 15 g of methyl iodide; the mixture was refluxed for one hour, and then allowed to stand overnight at room temperature. The crystals which separated out were collected and then washed with acetone to give 9.5 g of colorless prisms melting at 148—149°C.

Found: C, 50.66; H, 6.38; N, 7.10%. Calcd for $C_{16}H_{24}N_2I$: C, 50.18; H, 6.46; N, 7.52%.

Cyclohexanone Dimethylhydrazone Methiodide (XI). To a solution of 20 g of cyclohexanone dimethylhydrazone[2] in 30 m*l* of dry ether, 50 g of methyl iodide was added; the mixture was then treated in essentially the same manner as above to give 23 g of very hygroscopic white needles melting at 95—103°C.

Found: C, 36.92; H, 6.76%. Calcd for $C_9H_{19}N_2I$: C, 38.31; H, 6.78%.

2,4-Diphenylpyrrole (II). 15 g of I was added to a solution of 1.4 g (0.06 g-atom) of sodium in 150 m*l* of isopropanol at 40°C. Stirring was continued for one hour, after which the solvent was removed on a rotary evaporator. The residual oil solidified on cooling, and the solid was recrystallized from methanol-water to give 1.6 g of 2,4-diphenylpyrrole as pale yellow leaflets melting at 177—179°C. The IR spectrum was identical with that of an authentic sample.[1]

2,5-Diphenyl-3,6-dimethylpyrazine (IV). To a solution of 0.65 g (0.028 g-atom) of sodium in 60 m*l* of isopropanol, 10 g (0.031 mol) of III were added at 40°C; the mixture was then stirred for one hour at 40°C. The solvent was removed on a rotary evaporator. The residual paste was extracted with *n*-hexane, and the extracts were dried over sodium sulfate. The solvent was then removed by distillation under reduced pressure to give an oily residue. The residual oil which solidified on cooling was washed with *n*-hexane and was recrystallized from ethanol to give 1.2 g of colorless leaflets melting at 125—126°C (lit. 124—125°C).[7] (Found: C, 83.48; H, 6.12; N, 10.48%). Picrate, mp 153—154°C (lit. 153—154°C).[6]

2-Phenyl-2-isopropoxy-3-methylaziridine (V). To a solution of 0.9 g (0.034 g-atom) of sodium in 80 m*l* of isopropanol, 10 g (0.03 mol) of III were added at 40°C, after which the mixture was stirred for one hour. The solvent was removed on a rotary evaporator. The residual paste was extracted with *n*-hexane, and the extracts were dried over sodium sulfate. The solvent was then removed by distillation under reduced pressure, and the residual oil was distilled under reduced pressure, giving 4.3 g (72%) of V boiling at 105—108°C/8—9 mmHg. IR: 3350 (NH), 1380, 1370 (isopropyl) and 1120 cm^{-1} (alkoxy).

Found: C, 75.40; H, 8.86; N, 7.32%. Calcd for $C_{12}H_{17}ON$: C, 75.35; H, 8.96; N, 7.32%.

Hydrolysis of V. To a solution of 0.5 g of V in 20 m*l* of ether, 40 m*l* of 2 N hydrochloric acid was added, after which the mixture was stirred for 30 min. The reaction mixture was evaporated on a rotary evaporator at 50—60°C to a volume of 5—10 m*l*. The solid which separated out was collected by filtration, and then washed with ether and dried to give 0.3 g of white crystals melting at 187—189°C, while its picrate melted at 168—169°C. These melting points are identical with the literature values of α-aminopropiophenone hydrochloride and its picrate.[8]

Found: C, 47.83; H, 3.50; N, 15.16%. Calcd for $C_{15}H_{14}O_8N_4$: C, 47.62; H, 3.73; N, 14.81%.

2-Phenyl-3-methylazirine (VII). a) To a solution of 1.4 g (0.036 g-atom) of potassium in 150 m*l* of *t*-butanol, 10 g (0.03 mol) of III was added at 50°C, after which the mixture was stirred for 1.5 hr at 50—55°C. The solvent was removed on a rotary evaporator, the residual paste was extracted with *n*-hexane, and the extracts were dried over sodium sulfate and distilled to give 1.2 g of a pale brown liquid boiling at 85—90°C/5 mmHg. IR: 1740 (C=N) and 1690 cm^{-1} (C=O).

b) To a solution of 0.1 g of sodium in 10 m*l* of isopropanol, 2 g of V and 15 m*l* of dry toluene were added. The mixture was slowly distilled through a short column on an oil bath until the toluene distilled off; the residual oil was then distilled under reduced pressure to give 1 g of a product boiling at 75—82°C/1—2 mmHg. IR: 3350 (NH), 1740 (C=N), 1380, 1370 (isopropyl) and 1120 cm^{-1} (alkoxy).

2-Phenyl-3,3-pentamethyleneazirine (X). To a solution of 0.46 g (0.02 g-atom) of sodium in 60 m*l* of isopropanol, 9.0 g (0.025 mol) of IX was added at 40°C, after which the mixture was stirred for one hour at 40°C. The solvent was then removed on a rotary evaporator. The residual paste was extracted with ether, the extracts were dried over sodium sulfate, and the solvent was removed by distillation under reduced pressure. The residual oil was distilled under reduced pressure, giving 3.5 g (80%) of X boiling at 110—111°C/1—2 mmHg.

Found: C, 84.07; H, 7.80; N, 7.45%. Calcd for $C_{13}H_{15}N$: C, 84.28; H, 8.16; N, 7.56%. IR: 1740 cm^{-1} (C=N).

Rearrangement of XI. To a solution of 1.2 g (0.05 g-atom) of sodium in 150 m*l* of isopropanol, 10 g (0.035 mol) of XI were added at 45—50°C, after which the mixture was stirred for one hour at 50°C. After cooling, the solid which separated out was collected by filtration; then it was washed with ether, dried, and recrystallized from ethanol to give 2.5 g of white

7) A. Kolb, *Ann.*, **291**, 267 (1898).

8) S. Gabriel, *Ber.*, **41**, 1152 (1908).

prisms of trimethylhydrazinium iodide, mp 239°C (dec.).[2] The filtrate was treated with a 2,4-dinitrophenylhydrazine reagent. There was thus obtained cyclohexanone 2,4-dinitrophenylhydrazone, mp 159°C.

The author wishes to express his deep gratitude to Professor M. Ohta and Dr. H. Kato, Tokyo Institute of Technology, for their advice and guidance on this study. Thanks are also due to Dr. S. Ogihara, President of the Kyorin Pharmaceutical Co., Ltd., and to Dr. T. Irikura, Director of the Kyorin Chemical Laboratory, for their permission to publish this work.

NOTES

The Potassium Fluoride-Catalyzed Reaction. V. Aldol Condensation of Nitroalkanes and Aliphatic Aldehydes

Satoshi KAMBE

Oyama College of Technology, Oyama, Tochigi

and Heinosuke YASUDA

Laboratory of Chemistry, Utsunomiya University, Utsunomiya

(Received August 26, 1967)

Midorikawa and his collaborators first reported base-catalyzed reactions by potassium fluoride.[1a-f] This apparent basic property of the fluoride was recently illustrated by Rand *et al.*[2a-d] and by LeGoff.[3] In extension of our own previous studies,[4,5] the action of nitroalkanes on aliphatic aldehydes under the catalytic influence of the fluoride has now been investigated. In general, most aldehydes, especially paraformaldehyde, react conventionally with nitroalkanes in the presence of bases, giving the next higher homologs, or mixtures of them and non-distillable materials.[6,7] The condensation of paraformaldehyde and nitromethane, for example, readily afforded the final tris-product, nitroisobutylglycerol, along with a very poor yield of 2-nitroethanol (I). More recently, Namba and Yamashita[8] reported a convenient method for the preparation of the alcohol (I) using ethanolic potash, but the yield was only 25%. The nitroalcohol (I), on the other hand, can be obtained from ethylene and fuming nitric acid[9] or liquid nitrogen peroxide on direct nitration, although, these procedures have not generally been utilized in synthesis.

In the present base-catalyzed reaction of nitromethane with paraformaldehyde, it is noted that the yield of I is very high (73%) and is dependent upon the concentration of potassium fluoride used. The use of 0.05 mol of the fluoride per mol of paraformaldehyde appreciably alters the yield of I. Furthermore, the nature of the solvent has a remarkable effect on the rate of the reaction and on the product yield; thus, as is shown in Table 1, the 2-nitroethanol formation in isopropanol consistently gives higher yields than those in other solvents. The polymer formation may be avoided completely at temperatures below 50°C. It is difficult to isolate pure di- or tri-hydric derivatives in any case.

A systematic study of the aldol condensation of

1) a) H. Baba, H. Midorikawa and S. Aoyama, *J. Sci. Res. Inst.*, **52**, 99 (1958); b) M. Igarashi, H. Midorikawa and S. Aoyama, *ibid.*, **52**, 105 (1958); c) A. Sakurai, H. Midorikawa and S. Aoyama, *ibid.*, **52**, 112 (1958); d) A. Sakurai, *ibid.*, **53**, 250 (1959); e) H. Yasuda, H. Midorikawa and S. Aoyama, *Sci. Papers Inst. Phys. Chem. Res.*, **53**, 19 (1959); f) S. Kambe, H. Yasuda and H. Midorikawa, *ibid.*, **58**, 118 (1964).

2) a) L. Rand and M. J. Albinak, *J. Org. Chem.*, **25**, 1837 (1960); b) L. Rand, W. Wagner, P. O. Warner and L. R. Kovac, *ibid.*, **27**, 1034 (1962); c) L. Rand, J. V. Swisher and C. J. Cronis, *ibid.*, **27**, 3505 (1962); d) L. Rand, D. Haidukewych and R. J. Dolinski, *ibid.*, **31**, 1272 (1966).

3) E. LeGoff, *J. Am. Chem. Soc.*, **84**, 3975 (1962).

4) S. Kambe and H. Yasuda, *Sci. Papers Inst. Phys. Chem. Res.*, **58**, 148 (1964).

5) S. Kambe and H. Yasuda, This Bulletin, **39**, 2549 (1966).

6) M. M. Hollemann, *Rec. trav. chim.*, **23**, 298 (1904).

7) B. M. Vanderbilt and H. B. Hass, *Ind. Eng. Chem.*, **32**, 34 (1940).

8) K. Namba and T. Yamashita, *Kogyo Kayaku*, **12**, 31 (1951).

9) N. Levy, C. W. Scaife and A. E. W. Smith, *J. Chem. Soc.*, **1946**, 1096.

Table 1. Comparative yield[a] of 2-nitroethanol (I) obtained from nitromethane and paraformaldehyde in various solvents and in various concentrations of potassium fluoride

Methanol		Ethanol		*n*-Propanol		Isopropanol		*n*-Butanol		Isobutanol	
KF (mol)	Yield (%)	KF (mol)	Yield (%)	KF (mol)	Yield (%)	KF (mol)	Yield (%)	KF (mol)	Yield (%)	KF (mol)	Yield (%)
0.01	20	0.01	25	0.01	28	0.01	29	0.01	10	0.01	7
0.05	35	0.05	37	0.05	57	0.05	73	0.05	15	0.05	7
0.1	32	0.1	35	0.1	40	0.1	59	0.1	9	0.1	6

a) Reaction of 2 mol of nitromethane and 1 mol of paraformaldehyde at 30—35°C for 6 hr; Overall yield from the aldehyde used.

Table 2. Physical constants of nitroalcohols obtained

Nitroalcohol	Prepared from		Bp °C/mmHg	Lit., bp °C/mmHg	Reac. time (hr)	Yield (%)
	Nitroalkane	Aldehyde				
2-Nitro-1-propanol (II)	Nitroethane	Paraformaldehyde	80—81/3	99/10[a]	6	62
2-Nitro-1-butanol (III)	1-Nitropropane	Paraformaldehyde	93—94/5	105/10[a]	6	74
2-Nitro-2-methyl-1-propanol (IV)	2-Nitropropane	Paraformaldehyde	90—91*	90*[a]	6	65
3-Nitro-2-propanol (V)	Nitromethane	Acetaldehyde	77—79/4	89/8[b]	6	44
3-Nitro-2-butanol (VI)	Nitroethane	Acetaldehyde	72—74/2	92/10[a]	6	67
3-Nitro-2-pentanol (VII)	1-Nitropropane	Acetaldehyde	75—77/2	100/10[a]	6	68
3-Nitro-3-methyl-2-butanol (VIII)	2-Nitropropane	Acetaldehyde	82—84/5	90/10[a]	7	70
4-Nitro-3-butanol (IX)	Nitromethane	Propionaldehyde	75—76/5	99/9[b]	7	86
4-Nitro-3-pentanol (X)	Nitroethane	Propionaldehyde	82—84/5	96/8[b]	7	82
4-Nitro-3-hexanol (XI)	1-Nitropropane	Propionaldehyde	87—88/4	89/2[c]	7	73
4-Nitro-4-methyl-3-pentanol (XII)	2-Nitrpropane	Propionaldehyde	78—79/5	75/4[c]	10	56
1-Nitro-2-pentanol (XIII)	Nitromethane	*n*-Butyraldehyde	93—94/3	85/2[c]	10	75
2-Nitro-3-hexanol (XIV)	Nitroethane	*n*-Butyraldehyde	89—90/3	100/10[a]	10	55
3-Nitro-4-heptanol (XV)	1-Nitropropane	*n*-Butyraldehyde	88—89/3	115/10[a]	10	44
2-Nitro-2-methyl-3-hexanol (XVI)	2-Nitropropane	*n*-Butyraldehyde	81—82/4	109/10[a]	10	37
1-Nitro-3-methyl-2-butanol (XVII)	Nitromethane	Isobutyraldehyde	91—92/6	66/1[c]	15	57
2-Nitro-4-methyl-3-pentanol (XVIII)	Nitroethane	Isobutyraldehyde	88—89/2	89/2[c]	15	48
4-Nitro-2-methyl-3-hexanol (XIX)	1-Nitropropane	Isobutyraldehyde	90—91/3	78/2[c]	15	36

* Melting point.

a) B. M. Vanderbilt and H. B. Hass, *Ind. Eng. Chem.*, **32**, 34 (1940).
b) C. D. Hurd and M. E. Nilson, *J. Org. Chem.*, **20**, 927 (1955).
c) D. Nightingale and J. R. Janes, *J. Am. Chem. Soc.*, **66**, 352 (1944).

various nitroalkanes with aliphatic aldehydes was attempted (see Table 2). The solvent employed was isopropanol. In the condensation of paraformaldehyde with a primary nitroalkanes, such as nitroethane or 1-nitropropane, a di-hydric compound can be isolated in a low yield.

There are great differences in reactivity between the aldehydes used; *i. e.*, the yield decreases in the following order:

$$CH_3CHO \approx C_2H_5CHO > n\text{-}C_3H_7CHO > i\text{-}C_3H_7CHO$$

This suggests that the substitution of the methyl group at the α-position of the aldehyde would offer a steric hindrance to nitroalkane addition. The results obtained are shown in Table 2.

Experimental*1

Preparation of 2-Nitroethanol (I) (in Isopropanol as a Recommended Solvent). Paraformaldehyde (30 g, 1 mol) was stirred into isopropanol (300 ml)

*1 All boiling and metling points are uncorrected.

containing potassium fluoride (2.9 g, 0.05 mol), and the stirring was continued until the aldehyde had completely dissolved. To a stirred alcoholic solution then was added, drop by drop, nitromethane (120 g, 2 mol) at 30—35°C within 2 hr. After this addition stirring was continued for 4 more hours, and then the catalyst was removed by filtration. The residue, on the removal of the solvent, was poured into water, and the residual oily matter was extracted with ether. After the ethereal extract had then been dried over anhydrous sodium sulfate, the solvent was removed. The desired reaction product was distilled at 86—87°C/4 mmHg was collected (*cf.* Table 1).

Preparation of Other Nitroalcohols. To a mechanically stirred solution of 0.05 mol of potassium fluoride and 1 mol of the appropriate aldehyde in 150 m*l* of isopropanol, then was added, drop by drop, 1 mol of the appropriate nitroalkane below 40°C; the stirring was continued for a suitable period. After the catalyst had then been removed, the residual oily matter was treated by the procedure described above. The results are listed in Table 2.

The authors wish to express their gratitude to Dr. Hiroshi Midorikawa of the Institute of Physical and Chemical Research for his continued encouragement.

Rotational Isomers of *n*-Pentane

Atsushi TOMONAGA and Takehiko SHIMANOUCHI

Department of Chemistry, Faculty of Science, The University of Tokyo, Hongo, Tokyo

(Received September 19, 1967)

The *n*-pentane molecule has three possible rotational isomers, TT (trans-trans), TG (trans-gauche) and GG(gauche-gauche). It was reported by Mizushima *et al.*[1] and Sheppard *et al.*[2] that in the solid state only the TT form exists and in the liquid state the TT and TG forms coexists. Theoretical considerations[1,3,4] forecast the stability of the GG form. However, no experimental evidence has been reported as yet. We have recently measured the far infrared spectra of *n*-pentane in the liquid and solid states and succeeded in finding a band due to the GG form.

In Fig. 1 the spectra in the region 500—100 cm^{-1} are shown. The solid state spectrum shows only the

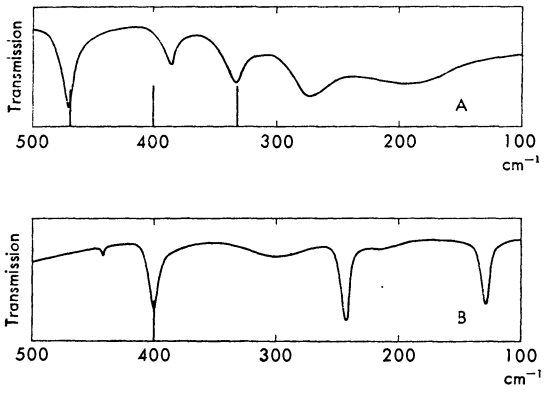

Fig. 1. Infrared spectra of *n*-pentane.
Curve A: liquid at room temperature, thickness 4 mm.
Curve B: solid at liquid nitrogen temperature.
The spectra were measured by a Hitachi FIS-1 spectrometer.
The vertical lines show the frequencies of Raman lines.

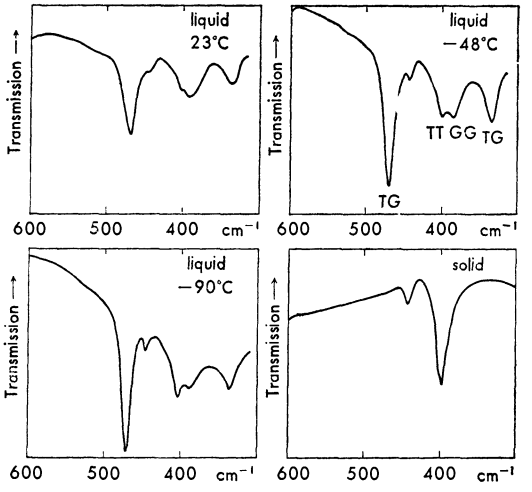

Fig. 2. Infrared spectra of *n*-pentane at various temperatures.
The measurements were made by a Hitachi EPI-L spectrometer.

1) T. Shimanouchi and S. Mizushima, *Sci. Papers Inst. Phys. Chem. Research*, **40**, 467 (1943); S. Mizushima and H. Okazaki, *J. Am. Chem. Soc.*, **71**, 3411 (1949); S. Mizushima, "Structure of Molecule and Internal Rotation," Academic Press Inc., N. Y. (1954).
2) N. Sheppard and G. J. Szasz *J. Chem. Phys.*, **17**, 86 (1949).
3) A. Abe, R. L. Jernigen and P. J. Flory, *J. Am. Chem. Soc.*, **88**, 631 (1966).
4) R. A. Scott and H. A. Scherraga, *J. Chem. Phys.*, **44**, 3054 (1966).

TABLE 1. OBSERVED AND CALCULATED FREQUENCIES OF *n*-PENTANE IN cm^{-1}

Observed				Calculated		
Liquid IR	Liquid Raman	Solid IR	Solid Raman	TT form	TG form	GG form
470	467				456	
444*		444*		416		439
400	400	400	399	392		
386						395
334	333				350	
276		246		223	283	321
		131		221	250	318
				184	215	249
				121	130	153
				112	101	104

* This band is weak and the frequency somewhat deviates from what calculated for the TT form. This band may be ascribed to the impurity band.

bands of the TT form. In the liquid state new bands appear. The details of the spectra in the region 600—300 cm^{-1} are shown in Fig. 2. In the liquid state at −90°C the bands at 470, 386 and 334 cm^{-1} appear in addition to the 400 cm^{-1} band of the TT form. The 470 and 334 cm^{-1} bands are assigned to the TG form, since they are in agreement with the frequencies of the TG form calculated from the force constants of propane (see Table 1).[5] The TG form does not have any calculated frequencies near 386 cm^{-1}. The intensity of the 386 cm^{-1} band increases far more largely than the 470 and 334 cm^{-1} bands at higher temperatures as shown in Fig. 2 Furthermore, the observed frequency, 386 cm^{-1}, corresponds very well to the value, 395 cm^{-1}, calculated for the GG form. Accordingly, this band is assigned to the GG form. The intensity increase in the absorption of the 386 cm^{-1} GG band at higher temperature shows that the GG form is less stable than the TG form. The energy difference between the two forms could not be accurately obtained, since the 386 cm^{-1} band has a shoulder due to the TT band at 400 cm^{-1}. All the observed bands shown in Fig. 2 are assigned to the TT, TG, and GG forms as shown in Table 1. The bands due to the GG′ form could not be found.

After this work was finished Snyder[6] proved existence of the GG form from the CH_2 wagging vibrations. The conclusion is in agreement with ours.

5) A. Tomonaga and T. Shimanouchi, to be published.

6) R. G. Snyder, private communication.

A Consideration of the Micelle Formation of an Ionic-Nonionic Surfactant through Its Ionization Energy

Fumikatsu TOKIWA and Kenji OHKI

Research Laboratories, Kao Soap Company, Minato-Yakushubata, Wakayama-shi

(Received September 21, 1967)

It is a widely-accepted concept that the micelle formation of ionic surfactants in aqueous solutions is governed by two factors, the cohesive energy among the hydrocarbon chains and the repulsive electrical energy among the charged heads.[1-3] In previous papers,[3,4] we have discussed the micelle formation of surfactants, such as dimethyldodecylamine oxide[3] and sodium decylbenzene sulfonate,[4] by means of these two factors. With a surfactant whose electrical state depends on the pH of the solution, however, there is yet another way to discuss its micelle formation—through the ionization energies of the micellar and monodispersed species. In the present paper an attempt is made to treat micelle formation in terms of the ionization energy of an ionic-nonionic surfactant. The surfactant studied is dimethyldodecylamine oxide, which can exist in either nonionic or cationic form, depending upon the pH of the solution. These two forms are related by the equation:

$$C_{12}H_{25}N(CH_3)_2O + H^+ \rightleftarrows C_{12}H_{25}N^+(CH_3)_2OH$$

Figure 1 sets out the relationship between micellization equilibria at $\beta=0$ and $\beta=p$, where β is the degree of ionization of the surfactant. The process 1 represents the micellization in the nonionic form at $\beta=0$. The standard free energy change

1) K. Shinoda, "Colloidal Surfactants," Academic Press, New York, N. Y. (1963).
2) M. F. Emerson and A. Holtzer, *J. Phys. Chem.*, **69**, 3718 (1965).
3) F. Tokiwa and K. Ohki, *J. Colloid Interface Sci*, **23**, 456 (1967).
4) F. Tokiwa and K. Ohki, This Bulletin, **41**, 253 (1968).

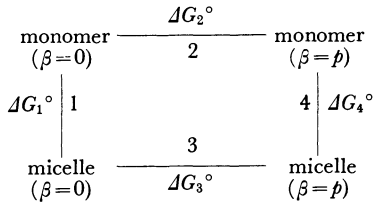

Fig. 1. The diagram of micellization and ionization equilibria.

in micellization per mole, ΔG_1°, is given[5,6] by:

$$\Delta G_1^\circ = \boldsymbol{R}T \ln \mathrm{CMC}_{\beta=0} \quad (1)$$

The process 4 represents the micellization in the cationic form at $\beta=p$, whose free energy change, ΔG_4°, is given by:

$$\Delta G_4^\circ = \boldsymbol{R}T \ln \mathrm{CMC}_{\beta=p} \quad (2)$$

when one assumes that the system is ideal in the presence of excess added salt.[7,8] The processes 2 and 3 represent the ionization of the monomer and micelle, respectively, from $\beta=0$ to $\beta=p$. In the process 2 the free energy change in ionization, ΔG_2°, may be written by:

$$\Delta G_2^\circ = \boldsymbol{R}T\int_{\beta=0}^{\beta=p} \ln K_\mathrm{m}(\beta)\mathrm{d}\beta = -2.3\boldsymbol{R}T\int_{\beta=0}^{\beta=p} \mathrm{p}K_\mathrm{m}(\beta)\mathrm{d}\beta \quad (3)$$

where K_m is the ionization constant of the monomer, which, in the present case, is constant independently of β, as may be seen in Fig. 2.[9] Therefore, the right-hand side of Eq. (3) may be reduced to $-2.3\,p\cdot\boldsymbol{R}T\cdot\mathrm{p}K_\mathrm{m}$. In the process 3, the free energy change in ionization, ΔG_3°, may be written by:

$$\Delta G_3^\circ = \boldsymbol{R}T\chi\int_{\beta=0}^{\beta=p} \ln K_\mathrm{M}(\beta)\mathrm{d}\beta = -2.3\boldsymbol{R}T\chi\int_{\beta=0}^{\beta=p} \mathrm{p}K_\mathrm{M}(\beta)\mathrm{d}\beta \quad (4)$$

where K_M is the ionization constant of the micelle, which depends on β as is shown in Fig. 2.[9] The χ in Eq. (4) is a correction factor for the ionization energy of the micelle, which may have some relation, for example, with the number of gegenions around the micelle and with the change in micellar-aggregation number with β. In the diagram under consideration, the following energy balance should hold:

$$\Delta G_1^\circ + \Delta G_3^\circ = \Delta G_2^\circ + \Delta G_4^\circ \quad (5)$$

Therefore:

$$\Delta G_4^\circ = \Delta G_1^\circ - \Delta G_2^\circ + \Delta G_3^\circ \quad (6)$$

Table 1 gives the values of χ, which were calculated to satisfy Eq. (6) from the observed values of CMC at different pH values in the presence of 0.10 M NaCl. (The addition of excess salt is required if one is to use Eq. (2) and also obtain a constant value of χ at a constant ionic strength.) The correction factor, χ, is nearly equal to 0.86 and is independent of the pH (or β) value except at a low pH. Thus, the CMC value at a certain degree of ionization, p, may be estimated by the equation:

$$\log \mathrm{CMC}_{\beta=p} = \log \mathrm{CMC}_{\beta=0} + p\cdot\mathrm{p}K_\mathrm{m} - 0.86\int_{\beta=0}^{\beta=p} \mathrm{p}K_\mathrm{M}(\beta)\mathrm{d}\beta \quad (7)$$

In Fig. 3 the CMC values obtained from Eq. (7) are plotted against pH in comparison with those experimentally obtained in the presence of 0.10 M NaCl. The similar plots in the absence of added

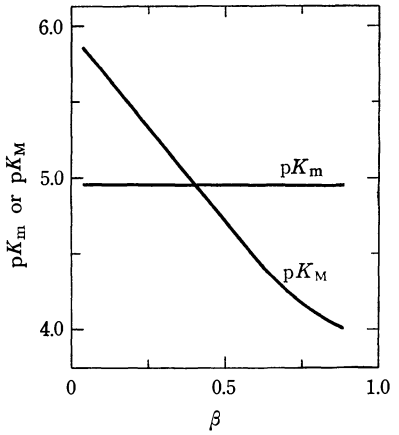

Fig. 2. Values of $\mathrm{p}K_\mathrm{m}$ and $\mathrm{p}K_\mathrm{M}$ as a function of β.

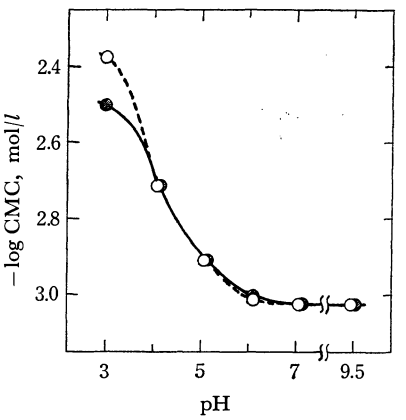

Fig. 3. The CMC *vs.* pH plots obtained from Eq. (7) (○) and from the experiment (▨) in the presence of 0.10 M NaCl.

5) J. N. Phillips, *Trans. Faraday Soc.*, **51**, 561 (1955).
6) K. W. Herrmann, *J. Phys. Chem.*, **66**, 295 (1962).
7) L. Benjamin, *J. Phys. Chem.*, **68**, 3575 (1964).
8) E. Matijevic and B. A. Pethica, *Trans. Faraday Soc.*, **54**, 587 (1958).
9) F. Tokiwa and K. Ohki, *J. Phys. Chem.*, **70**, 3437 (1966).

TABLE 1. VARIATIONS OF CMC_{obs}, $\Delta G_4°$, $(\Delta G_1° - \Delta G_2° + \Delta G_3°)$ AND χ WITH pH

pH	β	CMC_{obs} mol/$l \times 10^3$	$-\Delta G_4°$ kcal/mol	$-(\Delta G_1° - \Delta G_2° + \Delta G_3°)$ kcal/mol	χ
3.0	0.91	3.16	5.77	$0.36+6.02\chi$	0.89
4.1	0.65	1.94	6.06	$2.13+4.54\chi$	0.86
5.1	0.41	1.24	6.33	$3.73+3.03\chi$	0.86
6.1	0.19	1.00	6.45	$5.18+1.50\chi$	0.85
7.1	0.052	0.95	6.48	$6.13+0.41\chi$	0.86
9.5	0.00	0.95	6.48	$6.48+0.00$	—

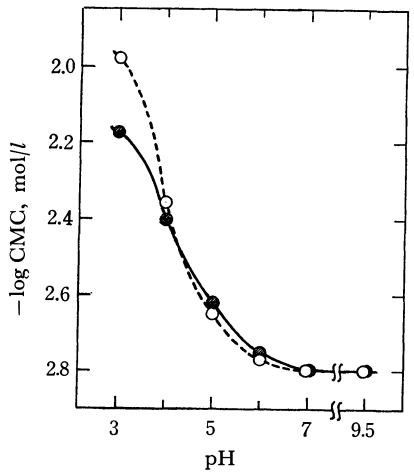

Fig. 4. The CMC *vs.* pH plots obtained from Eq. (7) (○) and from the experiment (◍) in the absence of added salt.

salt, obtained by Eq. (7), are shown in Fig. 4. The discrepancy in the calculated CMC values from the observed values at low pH values in the absence of added salt is somewhat larger than that in the presence of excess added salt. Probably, the assumption described in Eq. (2) is no longer reasonable in the absence of added salt, especially in the lower pH region.

From the preceding considerations, it can be said, in conclusion, that the CMC of a surfactant whose ionized state depends on the pH of the solution can be estimated by using the ionization constants of the monomer and micelle of the surfactant. At any degree of ionization, p, the CMC can be expressed by Eq. (7) as long as Eq. (2) is valid.

Experimental

The CMC values at different pH values were determined by the solubilization method using an oil soluble dye, Yellow-OB, as a solubilizate.[9,10] The ionization constants of the monomer and micelle were obtained from the potentiometric titration of the surfactant, the details of which have been presented in a previous paper.[9]

10) F. Tokiwa, This Bulletin, **36**, 222 (1963).

The Substituent Effects on the Chemical Shifts for Substituted Benzyl Acetates

Satoshi ARAKAWA and Masahisa HASHIMOTO

Research Laboratory, Dainippon Pharmaceutical Co., Ltd., Fukushima-ku, Osaka

(Received October 24, 1967)

A number of studies of the NMR spectra of substituted benzene derivatives, with particular attention paid to substituent effects, have been reported in the literature.[1-6] The relative chemical shifts arising from substituent effects have been known to be affected primarily by changes in the local electron-charge-density distribution caused by the substituents. The substituent effects have been discussed in terms of electronic transmission for the system of $X-C_6H_4-Y-H$, where X = the substituent,

1) H. Spieseke and W. G. Schneider, *J. Chem. Phys.*, **35**, 731 (1961).
2) R. W. Taft. Jr., S. Eherenson, I. C. Lewis and R. E. Glick, *J. Am. Chem. Soc.*, **81**, 5352 (1959).
3) Y. Yukawa, M. Sakai and K. Kabazawa, *Memories of Sci. & Ind. Research Osaka Univ.*, **17**, 185 (1960).
4) C. Heathcock, *Can. J. Chem.*, **40**, 1865 (1962).
5) K. I. Williamson, N. C. Jacobus and K. T. Soucy, *J. Am. Chem. Soc.*, **86**, 4021 (1964).
6) S. H. Marcus, W. F. Reynolds and S. I. Miller, *J. Org. Chem.*, **31**, 1872 (1966).

C_6H_4-Y=the transmitting group, and H=the terminal proton in the side chain.[6,7] However, there has been no report on the molecules where the terminal proton is separated from the aromatic ring by four atoms.

This study will deal with substituted benzyl acetates ($Y=CH_2OCCH_2$), which were originally
O
studied as model compounds for side chains of poly-β-(p-substituted)-benzyl-L-aspartates.[8]

The insertion of the -OC- group between two
O
methylene groups of ethylbenzene ($Y=CH_2CH_2$) was found to attenuate the electronic transmission to a lesser extent.

Experimental

Materials. The substituted benzyl acetates were prepared by the reaction of benzyl chlorides with potassium acetate. They were purified by distillation or recrystallization, and were checked by elementary analyses and by a study of their IR and NMR spectra.

Measurements. The NMR spectra were recorded on a Varian A-60 spectrometer. The magnet-gap temperature was 31°C. The chemical shifts were determined by the side-band technique relative to tetramethylsilane (TMS) as the internal standard. The concentrations were in the 0.2—0.15 mol/l range in a carbon tetrachloride solution; the dilution shifts were examined for in four compounds, but were not found. The data shown are the mean values of five measurements and are precise to ± 0.2 cps.

Results and Discussion

The chemical shifts of the acetyl protons and the benzylic methylene protons of substituted benzyl acetates in a carbon tetrachloride solution are shown in Table 1. Figure 1 shows the plots of the relative

Table 1. Chemical shifts for methyl and methylene protons of benzyl acetates in carbon tetrachloride

Substituent X	$-\nu_{CH_3}$ (in cps)	$-\nu_{CH_2}$ (in cps)	σ_p or σ_m
p-OCH_3	119.4	296.5	−0.268
p-CH_3	120.2	298.2	−0.170
p-Cl	121.6	299.5	+0.227
p-Br	121.8	298.6	+0.232
m-Cl	123.3	300.4	+0.373
H	121.8	301.5	0.000
p-CN	124.4	305.5	+0.628
p-NO_2	125.2	308.0	+0.778
m-NO_2	125.7	308.5	+0.710

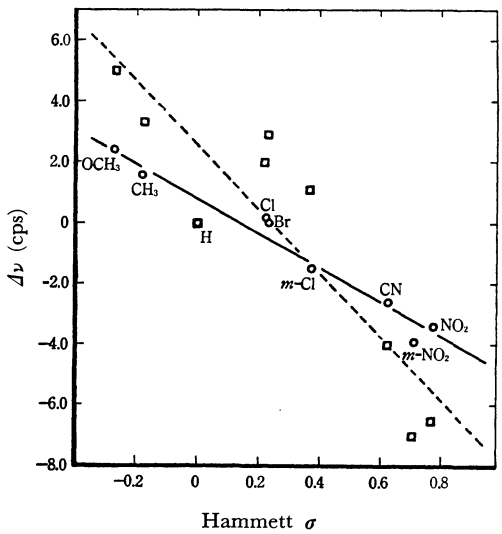

Fig. 1. Plots of the relative chemical shifts in substituted benzyl acetates against Hammett σ.
—○—: Acetyl methyl protons
---□---: Benzylic methylene protons

chemical shifts against the Hammett σ constants. The relative chemical shifts have been correlated with several substituent constants, such as σ^0, σ^+, σ^-, σ_I, and σ_R. In the present study, however, the plottings against these constants do not improve greatly and lead to such correlations as are shown in Fig. 1.

In the present study the substituent effects are examined in the form of the Hammett equation, $\Delta\nu=\rho\sigma+\Delta\nu_0$,[6] in order to make possible the comparison of the present data with those published for related series of compounds. The constants in this equation were obtained by the least-squares method. Table 2 lists the constants thus obtained, together with some of the published data. The ρ values in Table 2 represent a measure of the transmission of electronic effects of the substituent, X, through the side chain, Y, in the X-C_6H_4-Y-H type.

The ρ values for methylene and methyl protons of benzyl acetates are −10.45 and −5.63 respectively. This may indicate that substituent effects are decreased to about a half by the side-chain, $-OCCH_2-$,
O
group. On the other hand, the ρ value for methyl protons of ethylbenzene is about a half of that for toluene (ρ-ethylbenzene/ρ-toluene=0.53), as shown in Table 2. This means that the methylene group in the side chain transmits about a half of the electronic effects. For the carbonyl group, the transmission of electronic effects may be estimated to be 0.65 from the ρ values for the methyl protons of acetophenones and toluenes. On the other hand, the insertion of an oxygen atom into toluene, that is, anisole, increases the electronic effects (ρ-anisole/ρ-toluene=1.26). The oxygen atom is known to be a superconducting

7) N. Inamoto and S. Masuda, "16th Symposium on Organic-reaction Mechanism," Toyama, Japan (1965).
8) M. Hashimoto and S. Arakawa, This Bulletin, **40**, 1698 (1967).

TABLE 2. ρ VALUES OBTAINED FROM HAMMETT EQUATION FOR NMR CHEMICL SHIFTS

X-C_6H_4-Y-H	Number of atoms in Y	$-\rho$[a]	$\Delta\nu_0$[b]	r[c]	S[d]	Ref.
Y=CH_2	1	12.8	2.0	0.884	2.56	6
CH_2CH_2	2	6.76	0.6	0.967	0.789	5
OCH_2	2	16.2	−0.61	0.891	0.044	4
$\overset{\overset{O}{\|}}{C}CH_2$	2	8.34	1.5	0.975	0.895	6
$CH_2O\overset{\overset{O}{\|}}{C}CH_2$	4	5.63	0.77	0.974	0.531	
(X-C_6H_4-$\underline{CH_2O\overset{\overset{O}{\|}}{C}CH_3}$)	—	10.45	2.56	0.898	2.133	

a) ρ Values are given in the units of cycle per second per Hammett σ unit.
b) The intercept. c) The correlation coefficient. d) The standard deviation.

group.[6] For the methyl protons of substituted benzyl acetates, the ρ value is found to be similar to that reported for the methyl protons of substituted ethylbenzenes, even though benzyl acetate corresponds to the insertion of an ester group (-$O\overset{\overset{O}{\|}}{C}$-) between the methylene and methyl groups of ethylbenzene. If the ester group can be regarded simply as a combination of oxygen and the carbonyl group in relation to the transmission of electronic effects, the ester group may somewhat decrease the electronic transmission ($1.26\times0.65=0.82$). The ρ value of benzyl acetates can, then, be estimated as about -5.54 ($=0.82\times\rho$-ethylbenzene). This value is very close to the ρ value of -5.63 observed for benzyl acetates.

The methylene group of the side chain attenuates about a half for the transmission of the electronic effects of substituents, while the ester group does so slightly. The latter can be accounted for by a combination of the transmission properties of the oxygen atom and the carbonyl group.[9] The present study shows that the substituent effects on the chemical shifts of the terminal proton in the side chain of benzyl acetates can be estimated, if only roughly, by a simple combination of the transmission property of each group involved in the side chain.

Anomalous behavior in halogen substituents, deviating from the correlation line, has been established.[10] As is evident from Fig. 1, considerable deviations were found for the methylene protons, whereas slighter deviations were found for the methyl protons. The deviations observed for the latter are decreased more than was to be expected from the decrease in the ρ value. Slighter deviations similar to these can be estimated for the methyl protons of acetophenones.[3,6] These facts suggest that the deviation of halogen substituents is primarily due to anisotropy and to field effects, which are consistent with the following finding. It should be noted that good linear correlation-lines, even including halogen substituents, were found among the chemical shifts of three series of benzylic protons: toluenes *vs.* ethylbenzenes ($\Delta\nu_{CH_2\text{-ethylbenzene}}=+1.08\Delta\nu_{CH_3\text{-toluene}}-1.08$, $S=0.605$, $r=0.995$), toluenes *vs.* benzyl acetate ($\Delta\nu_{CH_2\text{-benzyl acetate}}=+0.84\Delta\nu_{CH_3\text{-toluene}}+0.61$, $S=0.156$, $r=0.996$). This finding indicates that the anomalous effects of halogen substituents are almost identical among the protons attached to the α-carbon atoms, even in different side-chains.[10]

The authors wish to express their gratitude to Drs. Shinsuke Ose, Hideji Takamatsu and Kiyoshi Nakamura of this laboratory for their encouragement.

9) This is consistent with the kinetic results that similar σ values have been found for the saponifications both of substituted benzyl benzoates ($\sigma=0.990$) and of substituted ethyl phenylacetates ($\sigma=0.978$); Y. Yukawa, Y. Tsuno and M. Sawada, *ibid.*, **39**, 2274 (1966).

10) In private discussion, Dr. Yuho Tsuno suggested that he and his coworkers have found similar evidences for other series of compounds.

Investigation of Copper(II) Chelate with Chromotropic Acid

Ryousuke WAKE,*1 Haruo MIYATA and Kyoji TÔEI

Department of Chemistry, Faculty of Science, Okayama University, Tsushima, Okayama

(Received November 9, 1967)

Copper(II)-chelate with chromotropic acid was investigated by potentiometric titration. The measurements have been carried out at 25.0±0.1°C and $\mu=0.10$ (with KNO_3). The acid dissociation constant of chromotropic acid, the formation constant of the 1 : 1 chelate (the molar ratio of ligand to copper(II) ion) and the hydrolysis constant of this chelate were determined.

Experimental

Reagents. Chromotropic acid disodium salt (1,8-dihydroxynaphthalene-3,6-disulfonic acid disodium salt) was supplied by Dojindo Co., Ltd., and was used without further purification. The concentration of the acid was determined by potentiometric titration with standard potassium hydroxide solution. Analytical grade cupric nitrate was used. The solution of Copper(II) ion was standardized by chelatometric titration.

Potentiometric Measurements. The same apparatus and procedures as in a preceding paper[1] were used for the potentiometric titrations.

Results and Discussion

The corrected potentiometric titration curves of chromotropic acid with and without copper(II) ion are shown in Fig. 1. Two sulfonic acid groups in chromotropic acid are completely dissociated even at a very low $-\log[H^+]$ range. The third dissociation constant pK_{H_2L} is 5.30±0.1. Schwarzenbach *et al.*,[2] Zollinger *et al.*[3] and Tôei *et al.*[4] have reported that pK_{H_2L} is 5.36, 5.53 and 5.44, respectively, at ≃20°C. The fourth dissociation is very weak because of the hydrogen bridge between two naphtholic hydroxyl groups and thus the fourth dissociation constant, pK_{HL}, can not be determined by usual potentiometric titration. Therefore, $pK_{HL}=15.6$, which was reported by Schwarzenbach *et al.*,[2] was used for the calculation of the formation constant and the hydrolysis constant of the copper(II) chelate. When the concentration of chromotropic acid is 1.0×10^{-3} M, the concentration of copper(II) ion should be less than 1.0×10^{-3} M, otherwise, copper hydroxide precipitates above $-\log[H^+]$ 7.

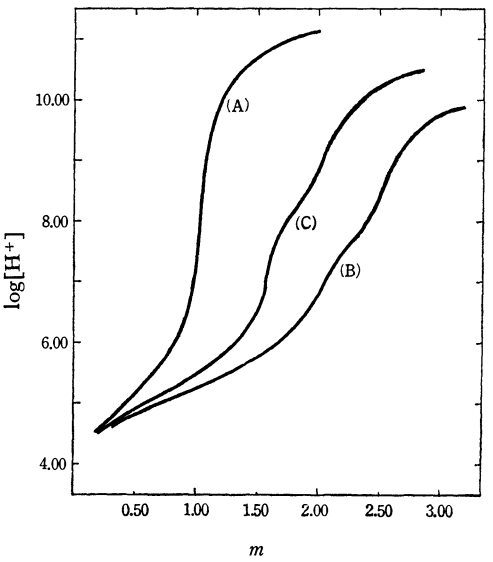

Fig. 1. Potentiometric titration curves with and without cupric ion. (A) Chromotropic acid alone; (B) and (C) are the curves of 1 : 1 and 2 : 1 (the ratio of ligand to cupric ion).
m=moles of base added per mole of ligand.
$T_L=1\times10^{-3}$ M

The formation constant of the copper(II)-chelate was calculated through the following equations:

$$H_2L^{2-} \rightleftharpoons H^+ + HL^{3-}$$

$$K_{H_2L^{2-}} = \frac{[H^+]\cdot[HL^{3-}]}{[H_2L^{2-}]} \quad (1)$$

$$HL^{3-} \rightleftharpoons H^+ + L^{4-}$$

$$K_{HL^{3-}} = \frac{[H^+]\cdot[L^{4-}]}{[HL^{3-}]} \quad (2)$$

$$Cu^{2+} + L^{4-} \rightleftharpoons CuL^{2-}$$

$$K_{CuL} = \frac{[CuL^{2-}]}{[Cu^{2+}]\cdot[L^{4-}]} \quad (3)$$

From the relationships among the electroneutrality, the total copper(II) concentration and the total ligand concentration, Eq. (4) is derived:

$$K_{CuL}=\frac{\left(T_{OH}+[H^+]-[OH^-]-T_L\right)-[L^{4-}]+[H_2L^{2-}]}{\left(\{T_{Cu}+T_L+[OH^-]-T_{OH}-[H^+]+[L^{4-}]-[H_2L^{2-}]\}[L^{4-}]\right)} \quad (4)$$

T_L, T_{Cu} and T_{OH} represent the total concentration of the ligand, copper and potassium hydroxide

*1 Present address: Institute for Chemical Research, Kyoto University, Sakyo-ku, Kyoto.

1) S. Nakashima, H. Miyata and K. Tôei, This Bulletin, **40**, 870 (1967).
2) L. Heller and G. Schwarzenbach, *Helv. Chim. Acta*, **34**, 1876 (1951).
3) H. Zollinger and W. Buchler, *ibid.*, **34**, 591 (1951).
4) M. Sakaguchi, A. Mizote, H. Miyata and K. Tôei, This Bulletin, **36**, 886 (1963).

added, respectively. Data obtained from B and C in Fig. 1 were employed in this calculation, and the results obtained are identical up to $-\log[H^+]=7.0$ for both titrations (Table 1).

The titration curves also indicate that 1 : 1 (ligand to metal ion) chelate is predominant in the low $-\log[H^+]$ region. Jantti[5] has considered species of copper(II)-L and copper(II)-HL, and has evaluated the equilibrium constants of these complexes (Table 1). However, Eq. (4) was fairly well satisfied by the data up to $-\log[H^+]=7.0$, and the existence of the copper(II) chromotropate chelate was verified, but copper(II)-HL was not observed in this experiment. The existence of the 2 : 1 chelate (copper(II)-L_2) could not be determined from the calculations and titration curves.

The second inflection on the titration curves, which is striking in the 2 : 1 titration, indicated more complicated reactions, such as hydrolysis, olation of the chelate or precipitation of $Cu(OH)_2$. As described above, the equations were not satisfied above $-\log[H^+]$ 7.5 at all, and the formation of $Cu(OH)_2$ and $Cu_2(OH)_2^{2+}$ did not improve the situation. Then, assuming that the hydrolysis of the chelate occurs according to the following equation

$$CuL^{2-}(H_2O)_2 \rightleftharpoons CuL(OH)(H_2O)^{3-} + H^+,$$

the authors tried to determine the hydrolysis constant.

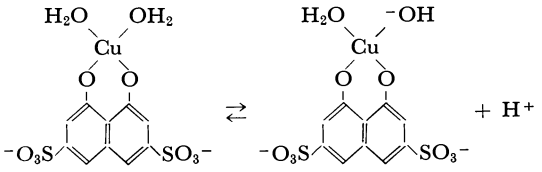

$$K_{CuL(OH)} = \frac{[CuL(OH)^{3-}]\cdot[H^+]}{[CuL^{2-}]} \qquad (5)$$

From the relationship concerning electroneutrality, the total copper(II) content and the amount of hydroxide, Eq. (6) is derived.

$$K_{CuL(OH)} = \frac{\left(\begin{array}{l}\{T_{OH}-2T_L+[H^+]-[OH^-]\\ +2[H_2L^{2-}]+[HL^{3-}]\}[H^+]\end{array}\right)}{\left(\begin{array}{l}3T_L-T_{OH}-[H^+]+[OH^-]\\ -3[H_2L^{2-}]-2[HL^{3-}]-[L^{4-}]\end{array}\right)} \qquad (6)$$

In this calculation, it is difficult to consider all four equations (1), (2), (3) and (5) at once, so $\log K_{CuL}=13.45$, which was determined at a low $-\log[H^+]$ range, was employed. The result is shown in Table 1. In a high $-\log[H^+]$ range, these equations did not explain the system, for the titration curves are unexpectedly low above $-\log[H^+]$ 9.5. It may be due to the olation of the chelate, the pecipitation of $Cu(OH)_2$ and so on. It is too complicated to study this system quantitatively above $-\log[H^+]$ 9.5.

Jantti[5] studied copper(II) chelate potentiometrically at a low pH range and Rahman[6] investigated the chelate spectrophotometrically; however they treated chromotropic acid as a monobasic acid in their calculations. The results are shown in Table 1 and they are very different from each other, the present authors' result being far apart from their values.

A similar potentiometric titration was carried out for solutions of a 1 : 1 molar ratio of chromotropic acid to other bivalent transition metal ions, such as manganese, cobalt, nickel and zinc. However, depression of the hydrogen ion concentration was not observed in any of these cases. This fact indicates that copper(II) forms the most stable chelate with chromotropic acid among the metals of the Irving-Williams stability series.

Table 1

The authors	$\log K_{CuL}=13.45\pm0.1$	$-\log K_{CuL(OH)}=8.3$
O. Jantti[5]	pK_h*$=2.68$	pK_1**$=7.4$
S. M. F. Rahman[6]	$\log K=5.54$	

* $H_2L^{2-} + Cu^{2+} = CuHL^- + H^+$

$$K_h=\frac{[CuHL^-]\cdot[H^+]}{[H_2L^{2-}]\cdot[Cu^{2+}]}$$

** $H_2L^{2-} + Cu^{2+} = CuL^{2-} + 2H^+$

$$K_1=\frac{[CuL^{2-}]\cdot[H^+]^2}{[HL^{3-}]\cdot[Cu^{2+}]}$$

The authors wish to gratefully acknowledge Dr. A. E. Martell, who checked the derivation of equations and gave some suggestions, and Dr. Olävi Jantti for his kind suggestions.

5) O. Jantti, *Suomen Kem.*, **30**, B, 136 (1957).
6) S. M. F. Rahman, *J. Inorg. Nucl. Chem.*, **26**, 385 (1964).

An Improved Photometric Method for the Determination of Sulfite with Pararosaniline and Formaldehyde

Yoshiko ARIKAWA,*1 Takejiro OZAWA and Iwaji IWASAKI

Laboratory of Analytical Chemistry and Geochemistry, Tokyo Institute of Technology, Ookayama, Tokyo

(Received November 14, 1967)

Many investigations have been made on the determination of sulfur dioxide based on the reaction of rosaniline and/or *p*-rosaniline with formaldehyde.[1-10] West and Gaeke[4] developed a method which involved the process of absorbing sulfur dioxide into a solution of sodium tetrachloromercurate, followed by the addition of the *p*-rosaniline hydrochloride and the formaldehyde to form a purple-colored sulfonic acid derivative of *p*-rosaniline. Present authors tried to apply the method to the analysis of sulfur in igneous rocks. The reproducible results, however, were not obtained

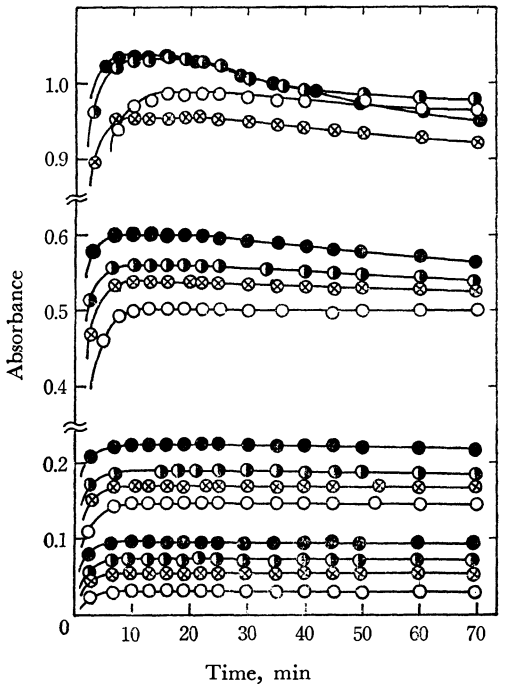

Fig. 1. Effects of temperature and concentration of sulfite on color development. Sulfite was dissolved in redistilled water.
—●— 40.0, 21.5, 5.4 μg of sulfur and reagent blank at 30°C.
—◑— 41.3, 20.9, 5.0 μg of sulfur and reagent blank at 25°C.
—⊗— 38.7, 20.9, 5.0 μg of sulfur and reagent blank at 20°C.
—○— 41.4, 20.7, 5.3 μg of sulfur and reagent blank at 10°C.

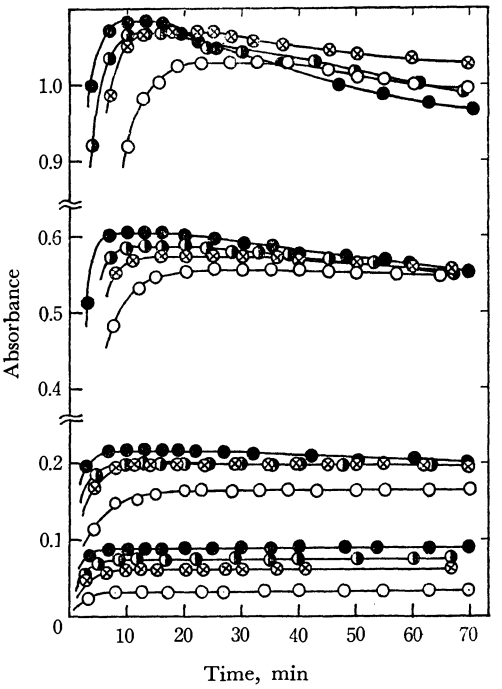

Fig. 2. Effects of temperature and concentration of sulfite on color development. Sulfite was dissolved in a 0.1 M sodium tetrachloromercurate solution.
—●— 40.5, 19.8, 4.7 μg of sulfur and reagent blank at 30°C.
—◑— 40.5, 19.7, 4.8 μg of sulfur and reagent blank at 25°C.
—⊗— 41.5, 19.8, 5.3 μg of sulfur and reagent blank at 20°C.
—○— 41.0, 20.5, 5.1 μg of sulfur and reagent blank at 10°C.

*1 Present address: Chemistry Department, Japan Women's University, Mejiro, Tokyo.

1) A. Steigman, *J. Soc. Chem. Ind.*, **61**, 18 (1942).
2) S. Atkin, *Anal. Chem.*, **22**, 947 (1950).
3) P. F. Urone, and W. E. Boggs, *ibid.*, **23**, 1517 (1951).
4) P. W. West, and G. C. Gaeke, *ibid.*, **28**, 1816 (1956).
5) C. Broomfield, *Analyst*, **87**, 586 (1962).
6) J. B. Pate, J. P. Lodge, Jr., and A. F. Wartburg, *Anal. Chem.*, **34**, 1660 (1962).
7) S. Barabas and J. Kaminski, *ibid.*, **35**, 1702 (1963).
8) J. G. Sen Gupta, *ibid.*, **35**, 1971 (1963).
9) H. A. Huitt and J. P. Lodge, Jr., *ibid.*, **36**, 1305 (1964).
10) L. Acs and S. Barabas, *ibid.*, **36**, 1825 (1964).

under such experimental conditions,[4,7,8,10] because the color development depended on both the temperature and concentration of sulfite. Previous studies[3,4,7,10] on the effect of temperature on the color development were not satisfactory to the determination of sulfite at the various concentrations and temperatures.

Preparation of 0.04% *p*-Rosaniline Hydrochlolic Acid Solution. Exactly weighed 0.2 g of *p*-rosaniline hydrochloride was added in a small volume of redistilled water containing 15 m*l* of concentrated hydrochloric acid and then mixed well. After *p*-rosaniline dissolved completely, 15 m*l* of concentrated hydrochloric acid was added into the mixture, which was diluted exactly to 500 m*l* with the redistilled water. The color of this solution faded gradually from red to pale yellow. Reagent prepared by this method always showed constant absorbance and was stable for at least three months and also stable against light. No significant difference was observed in experimental results with the use of three *p*-rosaniline reagents from different sources.

Effects of Temperature and Concentration of Sulfite on Color Development. The effect of temperature on color development was examined for the solutions containing about 0, 5, 20 and 40 μg of sulfur as sulfite in 50 m*l*, respectively. A series of temperatures was chosen : 10, 20, 25 and 30°C. All the reagents and the redistilled water freshly boiled and cooled were kept in a thermostat adjusted at a desired temperature. Five milliliters each of the 0.04% *p*-rosaniline hydrochloric acid solution and the 0.2% formaldehyde solution were added to the sodium sulfite standard solution in the 50 m*l* volumetric flask. Then the contents were mixed well and diluted to the mark with the redistilled water or a 0.1 M sodium tetrachloromercurate solution. Flasks were kept in the thermostat. The absorbance of the colored solution was measured every several minutes at the wavelength of 562 mμ using the redistilled water as a reference. Results for sulfite in the redistilled water and for sulfite in the 0.1 M sodium tetrachloromercurate solution were shown in Figs. 1 and 2, respectively. As can be seen in Figs. 1 and 2, each colored solution had a time range in which the absorbance remained maximum. The length of these ranges depended on both the temperature and the concentration of sulfite. In order to obtain the reproducible results, the measurement of

Table 1. Time ranges of constant absorbance

Temperature °C	Time range (min)	
	A	B
10	14—34	21—40
20	8—25	14—25
25	8—22	9—17
30	7—15	8—15

A: Sulfite was dissolved in redistilled water.
B: Sulfite was dissolved in a 0.1 M sodium tetrachloromercurate solution.

Table 2. Effects of diverse ions

Ion	Added as	Concn. mg/50 m*l*	Absorbance	
			Reagent blank	SO_3^{2-} 20 μg(as sulfur)
None		0	0.056±0.001	0.516±0.008
Na^+	$NaNO_3$	50	0.053	0.510
Ca^{2+}	$Ca(NO_3)_2 \cdot 4H_2O$	50	0.048	0.504
Mg^{2+}	$Mg(NO_3)_2 \cdot 6H_2O$	50	0.047	0.487
Al^{3+}	$Al(NO_3)_3 \cdot 9H_2O$	5	0.056	0.522
Fe^{3+}	$Fe(NO_3)_3 \cdot 9H_2O$	5	0.058	0.060
Fe^{2+}	$FeSO_4 \cdot 7H_2O$	5	0.055	0.456
F^-	NaF	5	0.061	0.515
Cl^-	NaCl	250	0.044	0.484
		5	0.056	0.513
Br^-	KBr	5	0.056	0.517
I^-	KI	5	0.056	0.509
SO_4^{2-}	Na_2SO_4	250	0.064	0.519
$S_2O_3^{2-}$	$Na_2S_2O_3 \cdot 5H_2O$	5	>1.200	>1.200
$S_4O_6^{2-}$	$K_2S_4O_6$	0.5	0.061	0.521
$S_5O_6^{2-}$	$K_2S_5O_6 \cdot 1.5H_2O$	0.5	0.059	0.512
$S_6O_6^{2-}$	$K_2S_6O_6$	0.5	0.059	0.512
S^{2-}	$Na_2S \cdot 9H_2O$	5	0.795	0.860
NO_2^-	$NaNO_2$	5	0	0
NO_3^-	KNO_3	50	0.055	0.512
PO_4^{3-}	NaH_2PO_4	5	0.059	0.512
AsO_4^{3-}	$Na_2HAsO_4 \cdot 7H_2O$	5	0.057	0.513

absorbance must be made within these time ranges of constant absorbance. The optimum ranges for the determination of sulfite up to the concentration of 40 μg of sulfur were decided referring to Figs. 1 and 2. These were shown in Table 1.

Calibration Curves. Using sodium sulfite standard solution, calibration curves were obtained by measuring the absorbance within the time ranges shown in Table 1 at each temperature. The calibration curve for sulfite in the redistilled water was straight and that for sulfite in the 0.1 M sodium tetrachloromercurate solution was somewhat curved. In both cases the calibration curves at each temperature were parallel with each other.

Effects of Diverse Ions. To examine the effects of diverse ions on this method, some experiments were made in the presence of 20 μg of sulfite sulfur and its absence at 20°C. The results were shown in Table 2.

Reactions of Nitrogen Atom with Methane and with Ethylene

Shozo MIYAZAKI and Saku TAKAHASHI

Department of Chemistry, Defense Academy, Yokosuka

(Received November 18, 1967)

Recent works on the reactions of nitrogen atom with methane and with ethylene have shown that these can not be discussed adequately by the simple mechanisms.[1] However, the appearent over-all rate constants of these reactions can be defined respectively as follows[2];

$$N + CH_4 \xrightarrow{k_1} HCN + \tfrac{3}{2}H_2\,, \qquad (1)$$

$$N + \tfrac{1}{2}\,C_2H_4 \xrightarrow{k_2} HCN + \tfrac{1}{2}H_2\,. \qquad (2)$$

In this paper, we evaluate the values of k_1 and k_2 at room temperature from the measurements of decay rate of afterglow intensity in the mixture of nitrogen atom and a reactant.

Experimental

The investigations were made with conventional flow techniques.[3] The afterglow was monitored by an RCA 6217 photomultiplier tube. The nitrogen was activated by a microwave discharge. Only a few percent of nitrogen molecules were decomposed into nitrogen atoms. The reactant was introduced between the discharge and entry of the quartz observation tube. The afterglow intensity was observed at a selected level. The observed lights were in the regions of 1st and 2nd positive bands of the nitrogen molecule.

In order to take a picture of the decay rate of afterglow intensity a single sweep from a synchroscope was used.

The concentration of nitrogen atom at the observation level was determined by nitric oxide titration.

Results and Discussion

Rate of Recombination of Nitrogen Atom. For the reaction

$$N + N + N_2 \xrightarrow{k_3} N_2 + N_2 + h\nu\,, \qquad (3)$$

the differential form of the rate equation is

$$-\frac{d[N]}{dt} = k_3[N]^2[N_2]\,.$$

It may be considered that the concentration of nitrogen keeps an approximately constant value through the reaction. In this case, if the concentration of nitrogen atom is equal to the half of its initial concentration, $a/2$, after time τ, the following equation is obtained:

$$k_3 = 1/[N_2]\tau a^2\,. \qquad (4)$$

Table 1 lists values of [N] or a, τ, $[N_2]$, flow rate and evaluated value of k_3.

Rate Constant of Reaction of Nitrogen Atom with Methane. At room temperature, a few percent of methane reacts with nitrogen atom.[4] Hydrogen cyanide is the only product of the reaction obtained in measurable quantities.

For competitive reaction

$$N + N + N_2 \xrightarrow{k_3} N_2 + N_2 + h\nu\,, \qquad (3)$$

$$N + CH_4 \xrightarrow{k_1} HCN + \tfrac{3}{2}H_2\,, \qquad (1)$$

the differential form of the rate equation is

$$-\frac{d(a-x)}{dt} = k_3[N_2](a-x)^2 + k_1[CH_4](a-x).$$

Since the concentrations of methane and nitrogen may be considered to keep an approximately constant values through the reaction, when t is τ, x is equal to $a/2$, the following equation is obtained;

1) P. A. Gartaganis and C. A. Winkler, *Can. J. Chem.*, **34**, 1457 (1956); J. T. Herron, *J. Phys. Chem.*, **69**, 2736 (1965).

2) D. A. Armstrong and V. A. Winkler, *Can. J. Chem.*, **33**, 1649 (1955).

3) M. A. A. Clyne and D. H. Stedman, *Trans. Faraday Soc.*, **62**, 2164 (1966).

Table 1. Rate data for the evaluation of rate constant k_3

Flow rate cm/sec	$[N_2]\times10^{-17}$ molecule/cc	$[N]\times10^{-15}$ atom/cc	$\tau\times10$ sec	$k_3\times10^{32}$ cc²/molecule² sec
		1 st positive band		
42	1.41	4.33	1.20	1.37
38	1.41	4.16	1.22	1.40
35	1.41	3.82	1.25	1.49
32	1.41	3.62	1.30	1.51
27	1.41	3.72	1.35	1.41
		2 nd positive band		
45	1.41	4.31	1.13	1.46
45	1.41	4.31	1.12	1.47
39	1.41	3.79	1.21	1.57
35	1.41	3.46	1.30	1.58
26	1.41	3.06	1.51	1.54

Table 2. Rate data for the evaluation of rate constant k_1

Flow rate cm/sec	$[N_2]\times10^{-17}$ molecule/cc	$[CH_4]\times10^{-17}$ molecule/cc	$[N]\times10^{-15}$ atom/cc	$\tau\times10$ sec	$k_1\times10^{16}$ cc/molecule sec
		1 st positive band			
51	1.04	0.37	1.77	1.08	1.07
47	1.12	0.29	2.16	1.10	1.21
40	1.09	0.32	2.00	1.17	1.05
33	1.04	0.37	1.92	1.30	0.84
29	1.18	0.23	2.32	1.35	1.09
		2 nd positive band			
47	1.11	0.29	3.02	0.56	2.72
42	1.25	0.15	3.62	0.78	2.95
38	1.16	0.24	3.02	0.76	2.12
33	1.04	0.37	2.60	0.75	1.54
27	1.24	0.17	3.15	1.09	1.79

Table 3. Rate data for the evaluation of rate constant k_2

Flow rate cm/sec	$[N]\times10^{-15}$ atom/cc	$[C_2H_4]\times10^{-15}$ molecule/cc	$\tau\times10^{2}$ sec	$k_2\times10^{14}$ cc/molecule sec
		1 st positive band		
39	0.96	6.06	2.09	0.58
38	1.85	3.52	2.58	0.82
33	0.60	7.05	2.08	0.47
26	0.45	7.75	2.08	0.43
25	1.50	3.52	3.07	0.68
		2 nd positive band		
37	1.59	1.74	1.00	4.58
33	0.97	2.37	0.70	4.47
32	3.57	1.50	1.94	3.81
25	0.90	3.02	0.78	3.09
24	4.74	1.55	2.77	3.31

$$1+\frac{k_1[CH_4]}{a\,k_3([N_2]+[CH_4])}=\frac{1}{2(0.6723-k_1[CH_4]\tau)}. \quad (5)$$

Inserting the observed values into Eq. (5), the rate constant k_1 is evaluated. The results are listed in Table 2.

Rate Constant of Reaction of Nitrogen Atom with Ethylene. In the reaction of nitrogen atom with ethylene, it is found that the reaction proceeds rapidly with a low activation energy and hydrogen cyanide is the only gas product.[4]

4) C. A. Winkler and H. I. Schiff, "The reactivity of free radical" General discussion of Faraday Society, 63 (1953).

TABLE 4. RATE CONSTANTS FOR SOME REACTIONS OF NITROGEN ATOM

Reaction	Rate constant	Reference
$N + N + N_2 \rightarrow N_2 + N_2$	1.5×10^{-32} cc^2/molecule^2 sec	5
	2.2×10^{-32} cc^2/molecule^2 sec	6
	$1.4-1.5\times10^{-32}$ cc^2/molecule^2 sec	This paper
$N + 1/2C_2H_4 \rightarrow HCN + 1/2H_2$	1.6×10^{-13} cc/molecule sec	7
	9.7×10^{-14} cc/molecule sec	8
	$2.4-0.8\times10^{-14}$ cc/molecule sec	9
	$3.8-0.6\times10^{-14}$ cc/molecule sec	This paper
$N + CH_4 \rightarrow HCN + 3/2H_2$	$1.0-2.2\times10^{-16}$ cc/molecule sec	This paper

For competitive reactions

$$N + N + N_2 \xrightarrow{k_3} N_2 + N_2 + h\nu\,,$$

$$N + \tfrac{1}{2}C_2H_4 \xrightarrow{k_2} HCN + \tfrac{1}{2}H_2\,,$$

it is quite plausible to assume that the rate of recombination of nitrogen atom is negligible, compared to the rate of reaction of nitrogen atom with ethylene. In this case, the following differential form of the rate equation is obtained;

$$-\frac{d(a-x)}{dt} = k_2(a-x)(b-x/2)$$

where b is the initial concentration of ethylene and $(b-x/2)$ is the concentration of ethylene at time t. From this equation, when t is τ, x is equal to $a/2$, the following equation is derived;

$$\frac{2}{(2b-a)}\ln\frac{4b-a}{2b} = k_2\tau\,. \qquad (6)$$

Table 3 lists the observed values and the evaluated value of k_2.

Our measured values of rate constants are listed in Table 4 along with the values measured by other workers. It is known that the results obtained in this paper are in agreement with them.

5) P. Harteck, R. R. Reeves and G. G. Manella, *J. Chem. Phys.*, **29**, 608 (1958).
6) K. M. Evenson and D. S. Burch, *ibid.*, **45**, 2450 (1966).
7) E. R. V. Milton and H. B. Dunford, *ibid.*, **34**, 51 (1961).
8) H. G. V. Evan, G. R. Freeman and C. A. Winkler, *Can. J. Chem.*, **34**, 1271 (1956).
9) J. Herron, *J. Phys. Chem.*, **70**, 2803 (1966).

Solvent-Extraction Behavior of Carrier-Free Rhodium

Tomitaro ISHIMORI, Yoshii KOBAYASHI and Yoshie USUBA

Japan Atomic Energy Research Institute, Tokai, Ibaraki

(Received November 21, 1967)

Distribution of carrier-free rhodium in the 21 extraction system given in Table 1 was studied with aids of Rh-105.

Distribution ratio, K_d, was obtained in a similar manner to that previously reported.[1] Namely, 2 m*l* each of the pre-equilibrated organic and aqueous phases were shaken in a 5 m*l* glass-stoppered cylinder for 2 min. After the separation of the two phases, aliquots of each phase were taken into two glass tubes respectively for radioassay. The K_d value was determined as the total activity of the organic phase divided by that of the aqueous phase. All procedures were carried out at the room temperature.

The 35.5 h-^{105}Rh tracer was prepared in a hydrochloric acid solution according to Kobayashi's procedure.[2] The solution was evaporated to dryness, then the tracer was taken up into hydrochloric, nitric or sulfuric acid solution and used without any further treatment.

Results obtained are summarized in Fig. 1, where K_d values in logarithmic scale are shown as the function of the acidity of the aqueous phase for the respective extraction system. In Fig. 1, average values of several measurements are represented by dots with their standard deviations, while values obtained by a single measurement as only dots. Figures given here can be compared with those for many other elements of the corresponding systems in the previous works of the present authors.[3]

1) T. Ishimori, K. Watanabe and E. Nakamura, This Bulletin, **33**, 637 (1960); K. Kimura, *ibid.*, **33**, 1038 (1960).

2) Y. Kobayashi, *J. Inorg. Nucl. Chem.*, **29**, 1374 (1967).

3) T. Ishimori *et al.*, JAERI Report 1047 (1963); 1062 (1964); 1106 (1966).

TABLE 1. EXTRACTION SYSTEMS STUDIED

Organic phase	Aqueous phase
100% TBP (Tri-butyl phosphate)	HCl or HNO_3
50, 25 or 10% TBP in toluene	HCl or HNO_3
25% TBP in CCl_4	HNO_3
10% TIOA (Tri-isooctyl amine) in xylene	H_2SO_4
5% TIOA in xylene	H_2SO_4, HCl or HNO_3
0.1% TIOA in xylene	H_2SO_4
100% Isopropyl ether	HCl
10% Amberlite LA-1 in xylene	HCl or HNO_3
5% TOPO (Tri-octyl phosphine oxide) in xylene	HCl or HNO_3
10% Primene JM-T in xylene	HCl
DIPK (Di-isopropyl ketone)	HCl

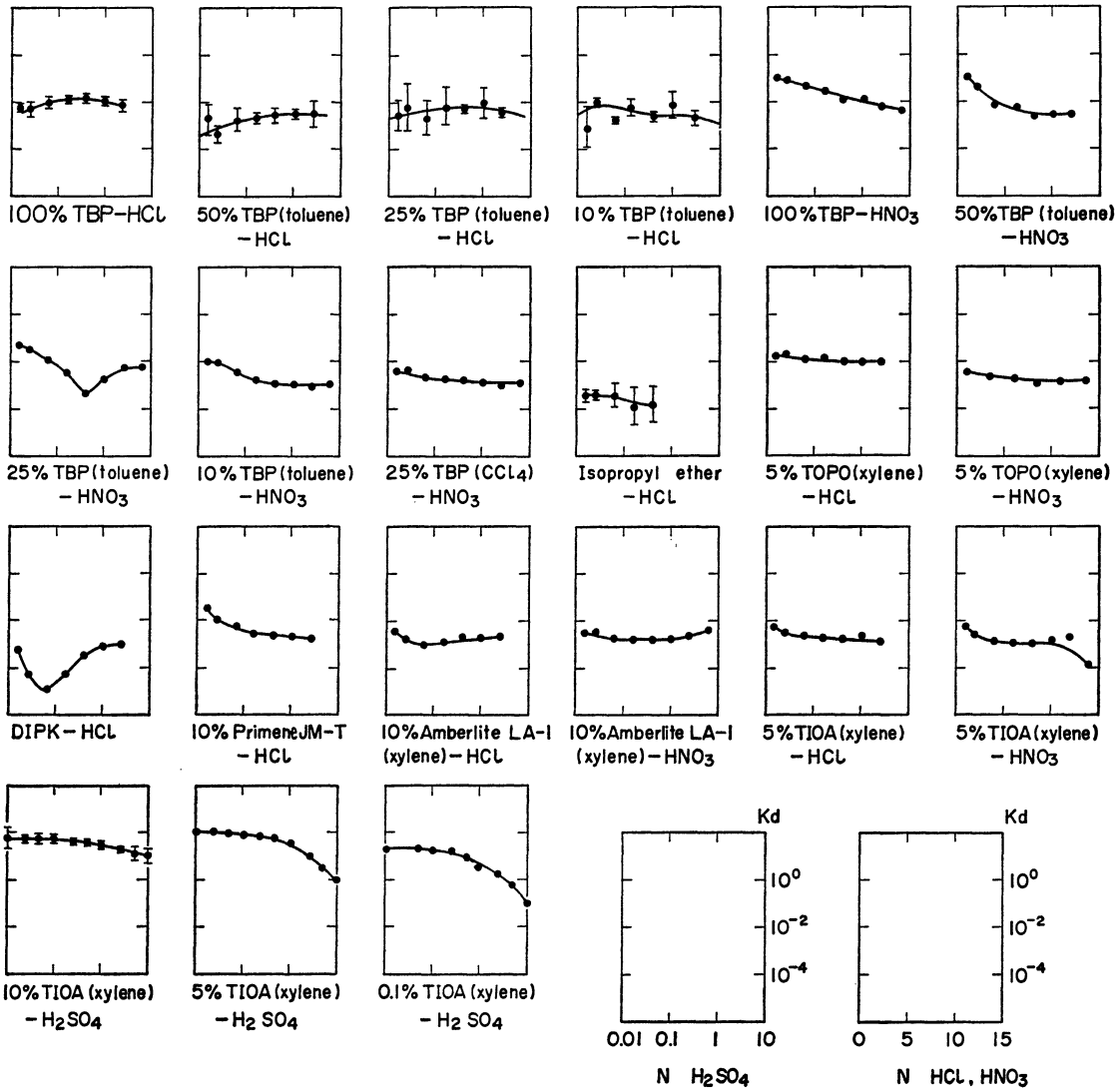

Fig. 1. Extraction behavior of Rh.

Synthetic Studies of the Flavone Derivatives. VI.*1 The Synthesis of 3′,6-Dimethoxy-4′,5,7-triethoxyflavone

Tokunaru HORIE and Mitsuo MASUMURA

Department Applied of Chemistry, Faculty of Engineering, University of Tokushima, Tokushima

and Kenji FUKUI and Mitsuru NAKAYAMA

Department of Chemistry, Faculty of Science, Hiroshima University, Higashi Sendamachi, Hiroshima

(Received November 27, 1967)

In 1963, a flavonoid pigment was isolated from *Digitalis lanata* L. by Whalley *et al.*[1] They established that the pigment was 3′,6-dimethoxy-4′,5,7-trihydroxyflavone (I) on the basis of degradative studies of its trimethyl ether (II) and triethyl ether (III). In this paper, we wish to report the synthesis of 3,6′-dimethoxy-4′,5,7-triethoxyflavone (III), which confirms the proposed structure (I) of the pigment by an unambiguous method.

The esterification of 4,6-diethoxy-2-hydroxy-5-methoxyacetophenone (IV)[2] with 4-ethoxy-5-methoxybenzoyl chloride in the presence of anhydrous pyridine yielded 4,6-diethoxy-2-(4′-ethoxy-3′-methoxybenzoyloxy)-5-methoxyacetophenone (V) (mp 102—103°C). According to the Baker-Venkataraman rearrangement,[3] the subsequent reaction of the acetophenone (V) with sodium amide gave 3′,5-dimethoxy-2-hydroxy-4,4′,6-triethoxy-dibenzoylmethane (VI) (mp 124.5—125.5°C). The cyclization of the dibenzoylmethane (VI) with concentrated sulfuric acid afforded the desired flavone (III) (mp 172—173°C) (lit.[1] mp 165—168°C). The structure of this compound was confirmed by a study of its infrared, ultraviolet, and NMR spectra.

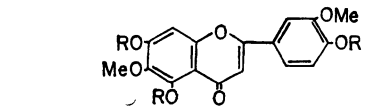

I R=H
II R=Me
III R=Et

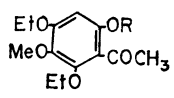

IV R=H

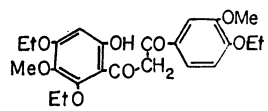

VI

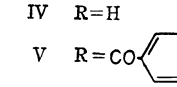

V R=CO-

Experimental*3

4,6-Diethoxy-2-hydroxy-5-methoxyacetophenone (IV). This acetophenone was prepared from 3,5-diethoxy-4-methoxyphenol[4] in the manner described by Farkas *et al.*[2]; bp 135—137°C/1.5 mmHg (62%).

Found: C, 61.69; H, 7.17%. Calcd for $C_{13}H_{18}O_5$: C, 61.40; H, 7.14%.

4,6-Diethoxy-2-(4′-ethoxy-3′-methoxybenzoyloxy)-5-methoxyacetophenone (V). A mixture of IV (2.5 g), 4-ethoxy-3-methoxybenzoyl chloride (2.5 g), and anhydrous pyridine (4.0 m*l*) was heated in an oil bath at 120°C for 1.5 hr. After having then been cooled, the reaction mixture was poured into ice-cold dilute hydrochloric acid and extracted with ether. The ether solution was washed with dilute hydrochloric acid, with an aqueous sodium carbonate solution, and finally with water. The resulting solution being dried over sodium sulfate and evaporated, the residual product was recrystallized from methanol to give V in the form of colorless needles, mp 102—103°C; yield 2.2 g (52%).

Found: C, 64.18; H, 6.57%. Calcd for $C_{23}H_{28}O_8$: C, 63.88; H, 6.53%.

3′,5-Dimethoxy-2-hydroxy-4,4′,6-triethoxy-dibenzoylmethane (VI). The acetophenone (V) (1.9 g) was heated with finely-powdered sodium amide (1.9 g) in anhydrous xylene (15 m*l*) at 110°C for 1 hr. After the excess sodium amide had been completely decomposed with ice water, the resulting solution was saturated with carbon dioxide. The precipitate was collected, washed with water, and recrystallized from ethanol to give VI in the form of golden yellow prisms, mp 124.5—125.5°C; yield 760 mg (40%). This substance gave a green ferric reaction in ethanol.

Found: C, 63.86; H, 6.50%. Calcd for $C_{23}H_{28}O_8$: C, 63.88; H, 6.53%.

3′,6-Dimethoxy-4′,5,7-triethoxyflavone (III). To a solution of VI (360 mg) in glacial acetic acid (8.0 m*l*), concentrated sulfuric acid (1 m*l*) was added; the mixture

*1 Part V: K. Fukui and T. Matsumoto, *Nippon Kagaku Zasshi (J. Chem. Soc. Japan, Pure Chem. Sect.)*, **86**, 1079 (1965).

*2 Presented in part at the Okayama Meeting of the Chemical Society of Japan, Okayama, October, 1967.

1) J. W. ApSimon, N. B. Haynes, K. Y. Sim and W. B. Whalley, *J. Chem. Soc.*, **1963**, 3780.

2) L. Farkas, L. Hörhammer, H. Wagner, H. Rösler and R. Gurniak, *Chem. Ber.*, **97**, 610 (1964).

3) W. Baker, *J. Chem. Soc.*, **1933**, 1381; H. S. Mahal and K. Venkataraman, *ibid.*, **1934**, 1767.

*3 All melting points are uncorrected.

4) M. Krishnamuri and T. R. Seshadri, *Proc. Indian Acad. Sci.*, **39A**, 144 (1954).

was heated at 70°C for 5 min. Then, it was cooled and treated with water. The resulting mixture was boiled until a crystalline solid separated. The precipitate was collected, washed with water, and recrystallized from ethanol to give III in the form of colorless prisms, mp 172—173°C (lit.[1] mp 165—168°C); yield 310 mg (90%). This substance gave a yellow solution when treated with concentrated sulfuric acid. IR: ν_{max}^{Nujol} cm^{-1}; 1635 (γ-pyrone). UV: λ_{max}^{EtOH} mμ (log ε); 215.5 (4.67), 240.5 (4.36), 266 (4.17), 328 (4.45). NMR[*4] ppm; 6.59_s (H-3), 6.81_s (H-8), 7.36_d (J=2.5 Hz) (H-2′), 6.99_d (J=9 Hz) (H-5′), 7.53_q (J=9, 2.5 Hz) (H-6′).

Found: C, 66.89; H, 6.26%. Calcd for $C_{23}H_{26}O_7$: C, 66.65; H, 6.32%.

[*4] The NMR spectrum was measured with Hitachi Model R-20 NMR Spectrometer (60 Mc) for $CDCl_3$ solution containing tetramethylsilane as internal reference.

Preparation and Properties of Polyhexamethyleneguanidine*1,*2

Rokuro KITAWAKI, Kozo SHIRAI*3 and Kiichiro SUGINO

Department of Applied Electrochemistry, Tokyo Institute of Technology, Ookayama, Meguro-ku, Tokyo

(Received November 28, 1967)

In previous studies,[1,2] we prepared alkylenedicyanamide in a pure state for the first time and studied its polymerization, which yielded a transparent, insoluble-infusible polymer. In the first paper,[1] it was also pointed out that alkylenedicyanamide reacted with alkylenediamine to give an anion exchange resin which might have the structure of polyalkyleneguanidine.

This is the first report on polyalkyleneguanidine and its properties. In regard to this problem, one previous patent[3] had indeed been granted. However, the polyhexamethyleneguanidine described in the patent was questionable because of the erroneous method used for the preparation of hexamethylenedicyanamide.

Preparation of Polyhexamethyleneguanidine. A methanolic or aqueous methanolic (or ethanolic) solution of a mixture of hexamethylenedicyanamide (I) and hexamethylenediamine dihydrochloride (II) was refluxed until no crystal was separated by cooling. The condensation was accelerated by adding a small amount of hexamethylenediamine. The removal of the solvent at a reduced pressure left a colorless, transparent gel which was in turn solidified by simple heating. The solubility of the resulting polymers in water varied with the molar ratio of the starting materials, as is shown in Table 1.

TABLE 1. SOLUBILITY OF THE POLYMERS IN WATER

Starting materials I mole	Starting materials II mole	Solubility
1	1	soluble
1	0.9	soluble
1	0.8	insoluble
1	0.7	insoluble
1	0.6	insoluble
1	0.5	insoluble

As is clear from the table, water-insoluble polymers could be obtained when 1 mol of I was reacted with less than 0.8 mol of II. The product obtained was a colorless, transparent glassy mass which was infusible and insoluble (in the case of water-insoluble polymers) in all common solvents.

Structure of the Polymer. The reaction of I with II may be supposed to proceed as follows:

$$n\,\mathrm{NCHN(CH_2)_6NHCN} + n\,\mathrm{ClH\cdot H_2N(CH_2)_6NH_2\cdot HCl} \rightarrow \cdots(\mathrm{CH_2})_6\mathrm{NH\cdot C(NH\cdot HCl)\cdot NH(CH_2)_6NH\cdot C(NH\cdot HCl)\cdot NH(CH_2)_6}\text{-}\mathrm{NH\cdot C(NH\cdot HCl)\cdot NH(CH_2)_6}\cdots$$

That is, the result expected is a polymer having guanidine linkage. It is also supposed that the product obtained using a mixture of I and II in a molar ratio of 1 : 1 will have a simple polyguanidine structure, but that when a mixture of the

*1 Presented at the 14th Annual Meeting of the Chemical Society of Japan, Tokyo, April, 1961.

*2 Cyanamide Derivatives. LXXVI, Preceding papers of this series: LXXV. K. Sugino and T. Tanaka, "The Reactions of Acrylates and Acrylonitrile with Guanidine in DMF", submitted to *J. Org. Chem.* LXXIV: H. Nagasaka, E. Ichikawa and K. Odo, *Yuki Gosei Kagaku Kyokai Shi (J. Soc. Synth. Org. Chem. Japan)*, **25**, 1048 (1967).

*3 Present address: Department of Chemistry, Faculty of Science, Tokai University, Kitakaname, Hiratsuka-shi, Kanagawa-ken.

1) K. Sugino, K. Shirai and R. Kitawaki, *J. Org. Chem.*, **26**, 4122 (1961).

2) R. Kitawaki, K. Shirai and K. Sugino, *Kogyo Kagaku Zasshi (J. Chem. Soc. Japan, Ind. Chem. Sect.)*, **67**, 1485 (1964).

3) E. K. Bolton *et al.* (Du Pont), U. S. Pat. 2325586 (1943).

same compounds in a molar ratio of 1 : less than 0.8 is reacted, the polymerization of I itself occurs simultaneously, resulting in the formation of insoluble polymers.

One piece of evidence for the presence of guanidine linkage in the polymer molecule is that when the resin was decomposed by digesting it with hot concentrated hydrochloric acid, the resulting solution gave a distinctly positive Sakaguchi test.

Another piece of evidence for the polyguanidine structure of the polymer is its infrared spectrum. It is shown in Fig. 1, along with that of hexamethylenediguanidine dihydrochloride[4] for comparison.

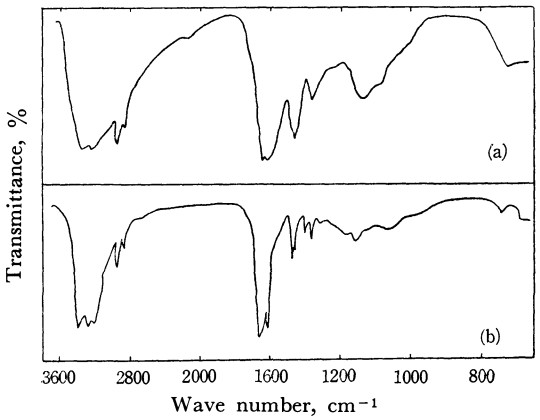

Fig. 1. Infrared spectra of the polymer and hexamethylenediguanidine 2HCl. (KBr pellet method)
(a) The polymer
(b) Hexamethylenediguanidine

The two spectra may be seen to be very similar to one other. Moreover, the spectrum of the polymer indicates the presence of methylene-group bands at 2920 cm^{-1}, 2860 cm^{-1}, and 1470 cm^{-1}, of imino-group bands at 3220—3240 cm^{-1}, and of C=N band at 1650 cm^{-1}.

Ion-exchange Property of the Polymer. When the polymer was pulverized into particles and treated with an aqueous solution of sodium hydroxide, it swelled and released the chloride ion into the solution. After it had been allowed to stand, it was collected, washed with water, and dried, resulting in a resin of the OH^- type. The resin thus obtained was found to have a strong anion-exchange property, as was expected from its guanidine structure. Figure 2 shows the rate of the adsorption of hydrochloric acid by the resin.

The exchange capacities of this resin were found to be 7.68 mmol/g and 3.34 mmol/g for Cl^- in a 0.5 N hydrochloric acid and in a 1 N sodium chloride solution respectively.

4) K. Odo and K. Sugino, *Nippon Kagaku Kaisi (J. Chem. Soc. Japan)*, **63**, 336 (1942); see also Ref. 2.

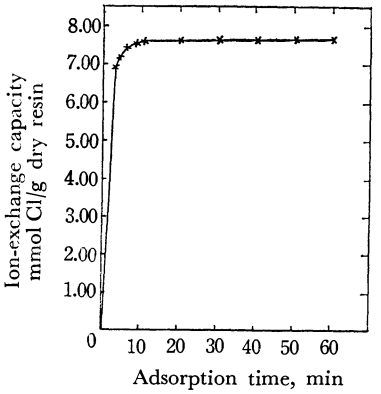

Fig. 2. The rate of adsorption of 0.5 N HCl by the resin.

Experimental

Hexamethylenedicyanamide (I). It was prepared by the procedure described earlier.[1,2] Mp 64—65°C.

Hexamethylenediamine Dihydrochloride (II). A commercially available reagent was used after recrystallization. Mp 248°C.

Preparation of Polyhexamethyleneguanidine Hydrochloride. *Water-soluble Polymer:* A mixture of 8.3 g of I, 8.5—9.6 g of II, and 0.2 g of hexamethylenediamine (III) was dissolved in 40 cc of 50% aqueous ethanol, and the solution was refluxed on a water bath for 2—5 hr. After the reaction, the ethanol and water were removed by distillation at reduced pressure, leaving a colorless, transparent gel-like mass. It was solidified by being heated at 100—110°C for 2—5 hr, resulting in a water-soluble resinous product.

Water-insoluble Polymer: A mixture of 16.6 g of I and 9.6 g of II was dissolved in 60 cc of methanol or 60 cc of 50% aqueous methanol, and the solution was refluxed on a water bath for 3 hr in the presence of III. After the reaction, the methanol (and the water) were removed by distillation at reduced pressure, leaving a colorless, transparent gel-like mass. It was solidified by being heated at 100—110°C for 2 hr, resulting in a water-insoluble resinous product.

Preparation of an Anion-exchange Resin. The water-insoluble polymer was softened with swelling by treating it with hot water at 80—90°C. Then it was pulverized, dried, and sieved into particles of 50—60 mesh. The resulting powdered resin was agitated with a 1 N sodium hydroxide solution for 2 hr. Then it was collected by filtration, thoroughly washed with water, and dried at 60—70°C.

Measurement of the Exchange Capacities of the Resin. 4.000 g of the OH^--type resin thus obtained, after being completely dried in an air bath, was placed in a flask containing 200 cc of 0.5 N hydrochloric acid, and the mixture was stirred by magnetic stirrer. The concentration of hydrochloric acid was determined by using a 5 cc sample every 10 min.

2.000 g of the same resin were placed in a flask contaiaing 200 cc of a 1 N sodium chloride solution, and the mixture was stirred by magnetic stirrer. The pH of the solution reached a constant value of 11.86 after 2 hr. The concentration of Cl^- in the solution was then determined.

This investigation was supported by a grant from Nippon (Japan) Carbide Industries, Inc., for which the authors wish to express their deep appreciation. The authors also wish to thank Dr. M. Takimoto and his staff in the Research Laboratory of the above company (at Uozu, Toyama Pref.) for the measurement of the infrared spectra.

The Mechanism of the Base Catalyzed Cleavage of Diphenyl Sulfide, Sulfone and Sulfonic Acid Ester[1]

Naomichi FURUKAWA, Hideoki TANAKA and Shigeru OAE

Department of Applied Chemistry, Faculty of Engineering, Osaka City University, Sugimoto-cho, Sumiyoshi-ku, Osaka

(Received December 4, 1967)

The cleavage reactions of diphenyl sulfide, sulfone and phenyl benzenesulfonate by strong bases have been known for many decades and studies on their product assay have been made by previous workers.[2] However, the mechanisms of these reactions have remained totally unclarified. Only recently the mechanism of the alkaline fusion of diphenyl sulfone has been rather extensively studied by the aid of ^{14}C and ^{18}O tracer techniques[3] and was suggested to involve the S_N2 type substitutions on both carbon and sulfur atoms.

Recently, Brotherton and Bunnett have demonstrated that diphenyl sulfone, sulfide and sodium benzenesulfonate react with sodium amide in boiling piperidine to give rise to *N*-phenylpiperidine and sulfinic acid or thiophenol in comparative yields.[4] They suggest that the reaction has proceeded by way of the initial attack of piperidide anion on the carbon atom bearing sulfonyl or sulfenyl group. In view of this particular reaction condition in which a very strong base is used, there remains a possibility that the reaction may proceed through the initial abstraction of *o*-hydrogen followed by the elimination of sulfone or sulfide group to form "benzyne" intermediate, to which piperidine adds to result the final product. Another possibility is that the reaction may proceed *via* the initial attack of the base on the sulfur atom as in the case of the alkaline fusion of diphenyl sulfone. These possible mechanisms are schematically illustrated as shown below.

1) Benzyne Mechanism

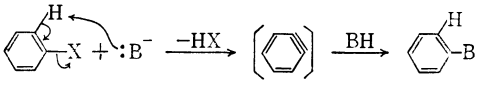

2) S_N2 Substitution on Carbon

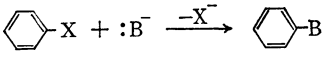

3) S_N2 Substitution on Sulfur

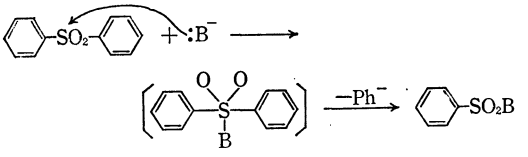

X=$-SO_2Ar$, $-SAr$; : B=a base

This paper will describe the detailed account of the mechanisms of the base cleavage reaction of diphenyl sulfide, sulfone and phenyl benzenesulfonate together with the corresponding *p*-methyl derivatives.

Results and Discussion

The reactants, bases used and the products obtained are shown in Table 1. The reactions were usually carried out in boiling piperidine in the presence of sodium amide or in hot DMSO containing potassium *t*-butoxide. The products were then carefully isolated by conventional distillation and recrystallization and identified by comparing their bp, mp, gas chromatograms and infrared absorption spectra with those of the authentic samples.

The results are summarized in Table 1.

Diphenyl Sulfide and Sulfone. Products isolated from the reaction of diphenyl sulfide were *N*-phenylpiperidine (I), thiophenol and diphenyl disulfide, while the reaction of diphenyl sulfone

1) Phenol and Phenolic Esters. XV.
2) W. E. Truce, D. P. Tate and D. N. Burdge, *J. Am. Chem. Soc.*, **82**, 2872 (1960); R. Otto, *Ber.*, **19**, 2425 (1886); C. K. Ingold and J. A. Jessop, *J. Chem. Soc.*, **1930**, 708; S. Oae and R. Kiritani, This Bulletin, **38**, 765 (1965); T. J. Broxton, Y. C. Mac, A. J. Parker and M. Ruane, *Aust. J. Chem.*, **19**, 521 (1966).
3) D. R. Christman and S. Oae, *Chem. & Ind.*, **1959**, 1251; S. Oae and N. Furukawa, This Bulletin, **39**, 2260 (1966).
4) T. K. Brotherton and J. F. Bunnett, *Chem. & Ind.*, **1957**, 80.

Table 1. Experimental conditions and products

Substrate	Reagent	Products (yields in %)	Recovered (%)
$C_6H_5SC_6H_5$	$NaNH_2$–$C_5H_{10}NH$	C_6H_5SH(54%), $C_6H_5NC_5H_{10}$(74%), $(C_6H_5)_2S_2$(trace)	12%
$C_6H_5SO_2C_6H_5$	$NaNH_2$–$C_5H_{10}NH$	$C_6H_5SO_2H$(17%), $C_6H_5NC_5H_{10}$(29%)	16%
$(p\text{-}MeC_6H_4)_2S$	$NaNH_2$–$C_5H_{10}NH$	$p\text{-}MeC_6H_4SH$(51%), $p\text{-}MeC_6H_4NC_5H_{10}$(37%)	29%
$(p\text{-}MeC_6H_4)_2SO_2$	$NaNH_2$–$C_5H_{10}NH$	$p\text{-}MeC_6H_4SO_2H$(12%), $p\text{-}MeC_6H_4NC_5H_{10}$(73%)	7%
$C_6H_5SO_3C_6H_5$	$NaNH_2$–$C_5H_{10}NH$	C_6H_5OH(76%), $C_6H_5SO_2NH_2$(17%), $C_6H_5NC5H_{10}$(13%)	—
$C_6H_5SO_3C_6H_4Me\text{-}p$	$NaNH_2$–$C_5H_{10}NH$	$p\text{-}MeC_6H_4OH$(85%), $C_6H_5SO_2NH_2$(39%), $p\text{-}MrC_6H_4NC_5H_{10}$(10%)	—
$C_6H_5SC_6H_5$	*t*-BuOK–DMSO	*t*-$BuOC_6H_5$	
$C_6H_5SO_2C_6H_5$	*t*-BuOK–DMSO	*t*-$BuOC_6H_5$	

gave *N*-phenylpiperidine (I) and benzenesulfinic acid. All these products are apparently formed by the initial attack on benzene carbon bearing sulfur atom (mechanism 2). In no case, we could detect the formation of any product which is formed by the initial attack of the amide ion on the sulfur atom (mechanism 3). In order to examine the other possible route (benzyne mechanism), di-(*p*-tolyl) sulfide and sulfone were subjected to the reaction, since the mechanism 1 would require the formation of both meta- and para-substituted *N*-tolylpiperidines. The identification of both meta- and para-*N*-tolylpiperidines can be readily done by the comparison of their characteristic infrared absorption bands (*m*-derivative 10.5 μ, 12.95 μ; *p*-derivative 12.32 μ)[5] and also gas chromatograms. When the reactions were actually performed, we obtained only the para-substituted compound and could not detect the presence of the meta-*N*-tolylpiperidine among the products. Now that the mechanism 1 is also eliminated, the best plausible route for these reactions is shown to be the one involving the aromatic S_N2 process (mechanism 2).

Phenyl Benzenesulfonate. The reaction of phenyl benzenesulfonate gave not only *N*-phenylpiperidine but also benzenesulfonyl amide and phenol. While *N*-phenylpiperidine is a product formed by the substitution at the aromatic carbon, the other two products are considered to form by the initial attack of amide ion on the sulfur atom. In this case, *N*-phenylpiperidine would be a product of aromatic S_N2 type reaction (mechanism 2), but there remains a route involving benzyne intermediate. In our case, however, *p*-cresyl benzenesulfonate gave only *p*-tolylpiperidine, suggesting that the reaction proceeds through the aromatic S_N2 reaction process (mechanism 2), similar to the nucleophilic substitution of *p*-nitrohalobenzenes.

The Reaction of *t*-Butoxide in DMSO. Potassium *t*-butoxide catalyzed reactions of diphenyl sulfide and sulfone gave several products among which were identified *t*-butyl phenyl ether and phenol and much of the starting sulfide and sulfone were recovered unchanged.

5) R. Huisgen and J. Sauer, *Chem. Ber.*, **91**, 1453 (1958).

Problem of Attacking Sites of Nucleophilic Reagents. All the above results indicate that the base cleavage reactions of diphenyl sulfide and sulfone proceed through the initial attack of the base on aromatic carbon atom bearing the functional group, while with the sulfonate, the main route is the initial attack of base on sulfonyl sulfur along with a side reaction involving the attack on the aromatic carbon atom similar to the case of the sulfide and sulfone. The reason of the difference between these two passways can easily be explained on the basis of the relative stabilities of the leaving groups. The initial attack of the sulfur atom of the sulfide or sulfone would have to give rise to the unstable phenyl anion as the leaving group, whereas the initial attack on the aromatic carbon atom bearing the sulfone or sulfide group should give either sulfinate or thiophenolate ion which would be a good leaving group. Thus the substitution on carbon atom will be more facile. While, in the case of the sulfonate, no matter which atom the nucleophile would attack, the leaving group is a very good one, namely, stable phenoxide ion in the case of sulfur attack, and benzenesulfonate ion in the case of the aromatic carbon attack. Therefore, both the sulfur and the carbon attack are expected to be quite facile and in fact it was found to be the case.

Experimental

Reagents. Diphenyl sulfide, sulfone, phenyl benzene-sulfonate, di-*p*-tolylsulfide, sulfone, *p*-tolyl benzenesulfonate were prepared by the standard procedures. Sodium amide commercially available was washed with anhydrous *n*-hexane before use. Potassium *t*-butoxide was prepared from *t*-butanol and potassium. Commercial piperidine was dried with sodium, bp 105—106°C. DMSO was distilled and dried over molecular sieve conventionally as usual.

Reaction and Product Isolation. A typical example of the experiments is as follows.

Diphenyl Sulfide with Sodium Amide in Piperidine. Sodium amide (2 g) was refluxed in 8 m*l* of piperidine for 30 min. To this solution was added 3 g of diphenyl sulfide and then the mixture was refluxed for 6 hr. After cooling, the solution was quenched with ice water to decompose sodium amide. The

aqueous solution was extracted with ether. The aqueous layer was acidified with concentrated hydrochloric acid and extracted again with ether. After evaporation of ether, thiophenol was obtained (0.964 g) (54%). The first ether layer was extracted with concentrated hydrochloric acid and the separated ether layer gave the unreacted sulfide. The aqueous acidic solution was made alkaline with aqueous sodium hydroxide and extracted with ether, from which 1.19 g of *N*-phenylpiperidine was obtained (74%). All the products isolated were identified by comparing those IR spectra and gas chromatograms with those of the authentic samples.

All other sulfides, sulfones and sulfonates were treated similarly to diphenyl sulfide.

Potassium *t*-Butoxide in DMSO with Diphenyl Sulfide. Diphenyl sulfide 1.0 g and potassium *t*-butoxide 1.5 g were dissolved into 10 m*l* of DMSO. The solution was sealed into a glass tube and heated for 3 hr at 150°C. After cooling, the sealed tube was broken and the products were detected by gas chromatograph. The products are summarized in Table 1.

Sesquiterpene Alcohols and a Phenol Ether of the Essential Oil of the Kusunoki (*Cinnamomum Camphora*, Sieb.)

Shûichi HAYASHI, Katsumi YANO, Nanao HAYASHI and Tamon MATSUURA

Department of Chemistry, Faculty of Science, Hiroshima University, Hiroshima

(Received December 7, 1967)

In connection with a previous report[1] on sesquiterpene hydrocarbons in camphor blue oil, which is a high-boiling fraction of the essential oil of the Kusunoki, the present work will deal with the sesquiterpene alcohol fraction of the blue oil. Five alcohols, elemol (6%), guaiol (10%), α-cadinol (13%), β-eudesmol (trace), and juniper camphor (2%), and a kind of phenol ether, myristicin (trace), have been identified.

The high-boiling fraction of camphor oil has been taken up by several workers as a subject of investigation, but no oxygen-containing constituents of this fraction have been identified up to the present time*1 except nerolidol.[2] In the present investigation, however, we could not detect nerolidol in spite of our great care.

Experimental

A sesquiterpene alcohol fraction, bp 120—160°C/4 mmHg, 456 g, which was separated from a camphor oil commercially supplied, was precisely fractionated through a packed-type distillation column under reduced pressure; it was divided into 19 fractions.

Myristicin. The first fraction, bp 115—116°C, $[\alpha]_D^{25}$ +11.31°C, was eluted on a silica gel-packed column with petroleum ether; an oily substance, n_D^{25} 1.5370, was thus isolated, a substance which showed only one peak, at t_R 12.6 min, in gas chromatography (DEGS-Diasolid-L, 125°C). Found: C, 68.93; H, 6.60%. Calcd for $C_{11}H_{12}O_3$: C, 68.73; H, 6.29%.

The IR spectrum of this substance coincided with that of myristicin,[3] and bromination in chloroform produced white needles, mp 129—130°C, of dibromomyristicin dibromide.[4] The NMR spectrum of the substance, consisting of signals at 2.30 (2H, d, J=6 cps), 3.80 (3H, s), 5.00 (2H, m), 5.80 (2H, s), 5.80 (1H, m), and 6.25 ppm (2H, s), had a strong resemblance with that of safrole,[5] and so the substance could easily be identified as myristicin on the basis of a comparison of the two spectra. The mass spectrum[6] also fit myristicin.

Elemol. A white crystalline mass was isolated from fraction 4, bp 122—124°C/4 mmHg, $[\alpha]_D^{25}$ −8.99°, by eluting it on an alumina (Grade II) column with petroleum ether. The substance showed an IR spectrum which agreed with that of elemol;[7] the gas chromatography (Thermol-1) also showed it to be elemol.

Guaiol. A white crystalline mass separated from fraction 5, bp 124—126°C/4 mmHg, $[\alpha]_D^{25}$ −9.31°C, by keepting it in a refrigerator was recrystallized from petroleum ether; white needles, mp 92.5°C, $[\alpha]_D^{25}$ −30.1° (c 1.5, ethanol), were thus obtained. The IR spectrum of the needles coincided with that of guaiol,[8] and the 3,5-dinitrobenzoate, mp 134.5—135.5°C, was established to be that of guaiol by a mixed melting point determination.

*1 Hikino *et al.* reported on the structure of the main sesquiterpene alcohols, kusunol and campherenol, of camphor oil at the 11th Symposium on the Chemistry of Terpenes, Essential Oils, and Aromatics, held in October, 1967, at Matsuyama.

1) S. Hayashi, N. Hayashi, K. Yano, M. Okano and T. Matsuura, This Bulletin, **41**, 234 (1968).
2) M. Hiroi, *ibid.*, **40**, 1003 (1967).
3) T. Biernacka, B. Kontnik, A. Paraczewski and J. Rajkoaski, *Diessetat. Pharm.*, **15**, 419 (1963).
4) E. Guenther, "The Essential Oils," Vol. II, D. Van Nostrand Company, New York (1949), p. 531.
5) N. S. Bhacca, L. F. Johnson and J. N. Shoolery, "NMR Spectra Catalog," Vol. I, Varian Associates (1962), No. 253.
6) S. Hayashi and H. Satô, *The Hitachi Scientific Instrument News*, **8**, 365 (1965).
7) J. Pliva, M. Horak, V. Herout and F. Šorm, "Die Terpen, Sammlung der Spectren und physikalischen Konstanten," Akademie-Verlag, Berlin (1960), p. 25.
8) *Ibid.*, p. 140.

α-Cadinol and β-Eudesmol. Two spot portions, of R_f 0.33 and 0.10, were gathered in the thin-layer chromatography of fraction 9, bp 132—134°C/4 mmHg, $[\alpha]_D^{25}$ +16.91°, with silica gel-G coating with silver nitrate; these portions were then extracted with ether to isolate two kinds of white crystalline matter. The IR spectra of these substances agreed with those of α-cadinol (R_f 0.33)[9] and β-eudesmol (R_f 0.10)[10] respectively.

Juniper Camphor. A crystalline mass which appeared in fraction 14, bp 142—144°C/4 mmHg, $[\alpha]_D^{25}$ +1.79°, when it was left standing at room temperature was separated, and then recrystallized repeatedly from ethanol. White crystals, mp 166.7°C, were thus obtained. This melting point and the IR spectrum agreed with those of juniper camphor.[11] Furthermore, the NMR spectrum, which had three methyl singlets, at 0.96 ppm (3H, a tertiary methyl group), 1.15 ppm (3H, a tertiary methyl attached to a carbon atom carrying a hydroxyl group), and 1.18 ppm (6H, two methyl groups in a isopropylidene), and the signals of the two methylene groups adjacent to a double bond at 2.14—2.80 ppm (4H), fit the structure of juniper camphor well.

The authors are indebted to Professor Shô Ito of Tohoku University for his kind measurement of the NMR spectra and to Dr. Hiroshi Satô of the Hitachi Co., Ltd., for his measurement of the mass spectra.

9) S. Hayashi, K. Yano and T. Matsuura, This Bulletin, **37**, 474 (1964).

10) F. J. Mc Quillin and J. D. Parrack, *J. Chem. Soc.*, **1956**, 2973.

11) V. Herout and F. Šorm, *Collection Czechoslov. Chem. Commn.*, **19**, 990 (1954).

Hydrogen Atom Abstraction by a Cumyloxy Radical

Etsuo NIKI, Yoshio KAMIYA and Nobuto OHTA

Department of Fuel Technology, Faculty of Engineering, The University of Tokyo, Hongo, Tokyo

(Received December 7, 1967)

It has been generally understood that the rates of hydrogen atom abstraction from liquid hydrocarbons increase in the sequence: primary, secondary, and tertiary. This order has been considered to be independent of the nature of the attacking species, and has been explained as being due to the strengths of the C–H bonds being broken. In the course of our investigation of the autoxidation of hydrocarbons in the liquid phase, the relative reactivities of a series of hydrocarbons toward cumyloxy radicals were measured in view of the fact that, although many data had been reported on the relative reactivities toward atoms and free radicals,[1] the reactivities of a series of hydrocarbons toward cumyloxy radicals had not yet been obtained. Another purpose is to compare the reactivities (and selectivities) of cumyloxy and cumylperoxy radicals,*1 since there are no definite data on the reactivities of two oxy radicals with the same alkyl group, the hydrocarbon portion in the radical.

Dicumyl peroxide was chosen as the source of the cumyloxy radicals since its thermal decomposition had been studied in detail by Kharasch and his co-workers,[2] and by Bailey and Godin.[3] These authors showed that dicumyl peroxide decomposed by a strictly first-order non-chain mechanism up to almost completion, the rate-determining step being the breakdown of the peroxide into free alkoxy radicals.[2,3] Kharasch and his co-workers[2] used cumene, *t*-butylbenzene, diisopropylcarbinol, and dodecane as solvents, and found the rates of decomposition to be nearly independent of the solvents.

The decomposition products were reported to be cumyl alcohol, acetophenone, methane, and the dimer of the solvent hydrocarbon.[2,3] In addition to these products, a small amount of α-methylstyrene was found to be formed. No ethane, acetone, or α,α-dimethylbenzyl methyl ether was detected.

The first step in the decomposition of dicumyl peroxide is the scission of the peroxidic bond to produce two cumyloxy radicals. This radical either abstracts a hydrogen atom from the solvent to form cumyl alcohol, or decomposes to acetophenone and a methyl radical. The absence of acetone in the product mixture shows that the fission of the cumyloxy radical occurs at the carbon-methyl bond and not at the carbon-phenyl bond; this is in agreement with thermochemical predictions[4] that the elimination of a methyl group requires an enthalpy increase of 0.3 kcal/mol, while that of a phenyl group would require 8.0

1) W. A. Pryor, "Free Radicals," McGraw-Hill Book Co., N. Y. (1966), p. 149.

*1 The investigation of the cumylperoxy radical is now in progress in our laboratory.

2) M. S. Kharasch, A. Fono and W. Nudenberg, *J. Org. Chem.*, **16**, 105 (1951).

3) H. C. Bailey and G. W. Godin, *Trans. Faraday Soc.*, **52**, 68 (1956).

4) P. Gray and A. Williams, *Chem. Revs.*, **59**, 239 (1959).

Table 1. The products of the thermal decomposition of dicumyl peroxide[a)]
(140°C, [peroxide] = 1.00×10^{-3} mol)

Solvent	Products in mol$\times10^3$			k_1/k_2	Relative k_1[b)]
	I+II	III	(I+II)/III		
Tetralin	1.58	0.295	5.35	0.728	1.9
Phenylcyclohexane	1.12	0.740	1.52	0.285	
p-Xylene	0.961	0.990	0.972	0.119	0.20
Ethylbenzene	0.833	0.990	0.843	0.103	0.51
Cumene	0.797	1.14	0.700[c)]	0.0972	1.00
Toluene	0.725	1.07	0.677	0.0721	0.24
Diphenylmethane	0.748	1.28	0.585	0.0922	0.48

a) All experiments were performed in duplicate.
b) Relative reactivities per active α-hydrogen relative to cumene.
c) The values of 0.71 and 0.74 are given in Refs. 2 and 3 respectively.

kcal/mol. The absence of both ethane and α,α-dimethylbenzyl methyl ether, and the formation of methane in an amount equimolar to acetophenone,[2,3)] show that most of the methyl radicals attack the solvent and abstract the hydrogen atom. α-Methylstyrene is expected to be produced by the dehydration of cumyl alcohol.[5,6)] The amount of α-methylstyrene formed was always less than 5% of the cumyl alcohol formed.

These observations lead to the following scheme for the decomposition of dicumyl peroxide in a hydrogen-donor solvent:

$$C_6H_5(CH_3)_2COOC(CH_3)_2C_6H_5 \rightarrow 2C_6H_5(CH_3)_2CO\cdot$$

$$C_6H_5(CH_3)_2CO\cdot + RH \xrightarrow{k_1} C_6H_5(CH_3)_2COH + R\cdot \quad (I)$$

$$C_6H_5(CH_3)_2COH \rightarrow C_6H_5(CH_3)C{=}CH_2 + H_2O \quad (II)$$

$$C_6H_5(CH_3)_2CO\cdot \xrightarrow{k_2} C_6H_5COCH_3 + CH_3\cdot \quad (III)$$

$$CH_3\cdot + RH \rightarrow CH_4 + R\cdot$$

$$R\cdot + R\cdot \rightarrow R\text{–}R$$

The rates of the formation of cumyl alcohol and acetophenone can be expressed as Eqs. (1) and (2) respectively:*2

$$\mathrm{d(cumyl\ alcohol)}/dt = k_1[C_6H_5(CH_3)_2CO\cdot][RH] \quad (1)$$

$$\mathrm{d(acetophenone)}/dt = k_2[C_6H_5(CH_3)_2CO\cdot] \quad (2)$$

Hence,

$$\mathrm{cumyl\ alcohol/acetophenone} = k_1[RH]/k_2 \quad (3)$$

Since k_2 may well be assumed to be constant in aromatic hydrocarbon solvents*3 and since [RH] is known, the relative k_1 value can be measured on the basis of the knowledge of the amounts of cumyl alcohol and acetophenone formed.

The products obtained in eight solvents are shown in Table 1.

More than 90% of the initial peroxide was accounted for. The relative reactivities of the hydrocarbons toward cumyloxy radicals are also shown in Table 1. As Table 1 shows, toward the cumyloxy radical, the normal order of hydrogen reactivity, namely, primary<secondary<tertiary, is followed in the series of *p*-xylene, toluene<ethylbenzene, diphenylmethane<cumene. However, the secondary hydrogen atom of tetralin is much more reactive than that of cumene. The steric effect may be one of the reasons why cumene is less reactive than tetralin, since the α-hydrogen of cumene is rather hindered by two methyl groups. Another possibility is that, although the β-hydrogens of tetralin are not benzylic and although the derived radical can not be stabilized by resonance, the β-hydrogen atoms as well as the β-hydrogens may also be abstracted by the cumyloxy radical, since the *t*-butoxy radical abstracts hydrogen from cyclohexane more readily than from toluene.[7,8)]

Phenylcyclohexane has one tertiary and ten secondary hydrogen atoms. For the same reason as has been given above, the secondary hydrogens must also be abstracted by the cumyloxy radical; all the more, then, is the tertiary hydrogen in

5) P. Gray and M. J. Pearson, *J. Chem. Soc.*, **1964**, 5725.
6) W. G. Lloyd, R. G. Zimmerman and A. J. Dietzler, *Ind. Eng. Chem., P. R. D.*, **5**, 326 (1966).
*2 In this paper, the amount of cumyl alcohol formed was taken as the sum of cumyl alcohol and α-methylstyrene found.
*3 It has been known that the reactions of alkoxy radicals, especially the k_2 values, are influenced by the solvents. (E. S. Huyser, "Advances in Free-Radical Chemistry," Vol. I, Logos Press, London (1965), p. 103.) However, in similar alkyl aromatic hydrocarbon media k_2 may well be assumed to be constant.
7) C. Walling and B. B. Jacknow, *J. Am. Chem. Soc.*, **82**, 6108 (1960).
8) P. Wagner and C. Walling, *ibid.*, **87**, 5179 (1965).

phenylcyclohexane hindered by phenyl and cyclohexyl groups.

Experimental

Dicumyl peroxide was obtained from the Nippon Oils and Fats Co. and had a purity of 99.3%. Tetralin, cumene, ethylbenzene, *p*-xylene, and toluene were shaken successively with sulfuric acid, water, sodium hydroxide, and water, dried with calcium chloride, and then distilled under a reduced pressure of nitrogen. Diphenylmethane and phenylcyclohexane were fractionally distilled. All the solvents were passed through an activated alumina column immediately before use.

Decompositions were carried out in a sealed flask equipped with a condenser, a sample inlet, and two side arms. An aliquot of the solution of dicumyl peroxide was introduced into the reaction vessel, the concentration of the peroxide being maintained at 0.200 mol/*l*. The reaction mixture was degassed under a vacuum through one side arm, while through the other nitrogen was introduced. This procedure was repeated four times. The vessel was then immersed to an oil bath thermostated at 140±0.5°C, and the reaction mixture was stirred by means of a magnetic stirrer.

Acetophenone, cumyl alcohol, and α-methylstyrene were determined by gas-liquid chromatography; Polyethylene Glycol 6000 column, at 170°C and with helium carrier gas. Methane and ethane were analyzed by glc; Molecular Sieve-13X, 30°C, He carrier gas. It was found that methane was the only gaseous product. The injection of an initial solution of dicumyl peroxide to glc gave peaks of both acetophenone and cumyl alcohol. In order to avoid this interference, dicumyl peroxide was decomposed almost completely. The injection of cumyl alcohol did not give any other peak, indicating that the decomposition of cumyl alcohol in the glc was negligible.

Lactone Carboxylic Acids. V.*[1] A Way of Preparing a Lignans Skeleton

Akira TAKEDA

Department of Synthetics Chemistry, Okayama University, Okayama

and Sigeru TORII

Department of Industrial Chemistry, Okayama University, Okayama

(Received December 20, 1967)

In a previous paper,[1] we described the benzylation of γ,γ-dialkyl-α,β-dicarbethoxybutyrolactones at the α-position of the lactone ring, which is reminiscent of a synthetic route to lignans derivatives.[2]

It is the aim of the present study to apply this method to the synthesis of compounds with a lignans skeleton (I) (see Scheme 2). The required materials, γ-aryl-α,β-dicarbethoxybutyrolactones (IIa, R=4-methoxy or 3,4-methylene dioxy), were prepared by the condensation of ethyl β-arylglycidates with sodiomalonate.[3] In order to elucidate the course of the fission of the epoxy ring on the glycidates, the products (IIa or IIb) were converted into well-known compounds (VI),[4] as is shown in Scheme 1.

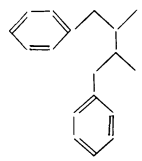

(I)

The hydrolysis of II was carried out with an 1 N aqueous alcoholic potassium hydroxide solution;[5] it gave *ca.* 70% yield of an acidic component

*1 Part II, III, and IV: *Memoirs of School of Engineering, Okayama Univ.*, **2**, 68, 74, 80 (1967).

1) A. Takeda and S. Torii, This Bulletin, **40**, 1261 (1967).

2) W. M. Hearon and W. S. MacGregor, *Chem. Revs.*, **55**, 957 (1955); F. M. Dean, "Naturally-occurring Oxygen Ring Compounds," Butterworths, London (1963), p. 29.

3) The reaction of ethyl β-phenylglycidate with sodiomalonate has previously been recorded; see G. V. Chelintsev and E. D. Osetrova, *J. Gen. Chem. USSR*, **7**, 2373 (1937).

4) a) A. B. Kulkarni, A. L. Pandit, H. D. Shroff, B. D. Hosangadi, M. N. Katrak, A. B. Diwadkar and B. C. Ginde, *Indian J. Chem.*, **2**, 443 (1964); *Chem. Abstr.*, **62**, 7616e (1965). b) N. A. Babiyan, V. A. Mnatsakanyan, R. G. Arutyunyan, N. E. Akopyan, and O. L. Mndzhoyan, *Izv. Akad. Nauk Arm. SSR, Khim. Nauki*, **17**, 549 (1964); *Chem. Abstr.*, **62**, 11732 (1965). c) J. W. Cornforth, G. K. Hughes, and F. Lions, *J. Proc. Roy. Soc. N. S. Wales*, **72**, 228 (1939).

5) In the case of the hydrolysis of γ,γ-dialkyl-α,β-dicarbethoxybutyrolactones, only acidic components, γ,γ-dialkyl-β-carbethoxy-α-carboxybutyrolactones, were isolated under these conditions; see A. Takeda and S. Torii, *Memoirs of School of Engineering, Okayama Univ.*, **1**, 44 (1966). On the other hand, the hydrolysis of α-benzylated γ,γ-dialkyl-α,β-dicarbethoxybutyrolactones gave exclusively neutral lactone derivatives, such as γ,γ-dialkyl-β-carbethoxy-α-benzylbutyrolactones.[1]

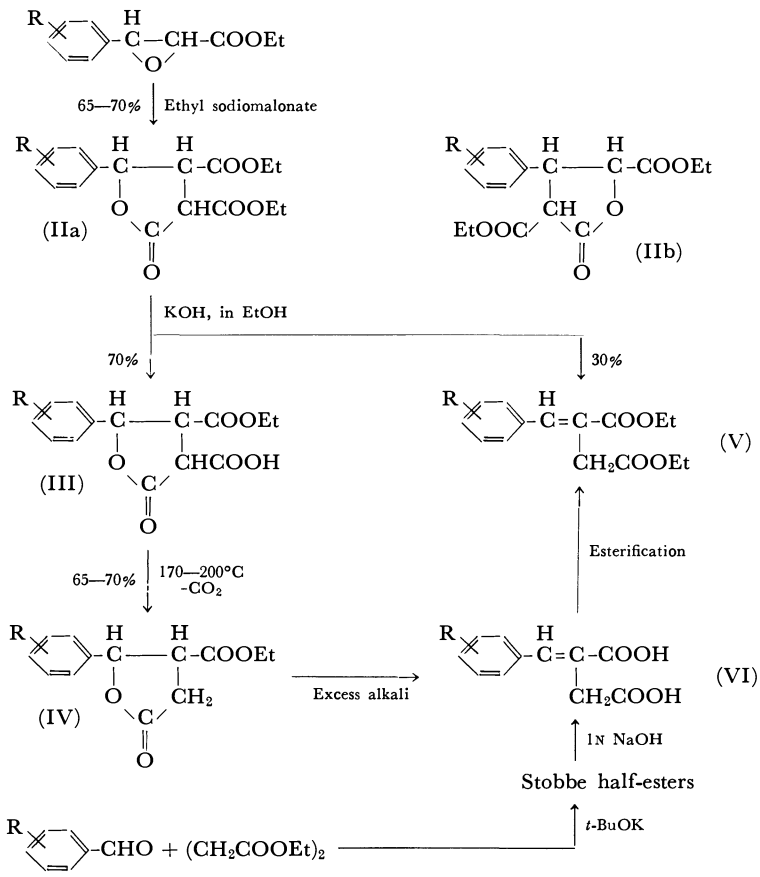

Scheme 1

(III), a viscous yellow oil, and *ca.* 30% yield of a neutral component (V).

The acidic materials (III), when heated to 170—200°C, were converted into ethyl γ-aryl-paraconates (IV), which were then further hydrolyzed with reflux in a 1 N aqueous sodium hydroxide solution to give dibasic acids (VI).[4] The authentic samples of VI were prepared by the Stobbe condensation[6] of aromatic aldehydes with diethyl succinate and by the subsequent hydrolysis of the Stobbe half-esters.[4a]

The structure of the neutral materials (V) was readily confirmed by means of these spectral data in comparison with those of an authentic sample prepared by the esterification of VI. These facts reveal that the attack of the carbanion of malonate occurs exclusively at the α-position of the β-aryl-glycidates.[7]

The benzylation of IIa (R=4-methoxy) was carried out with the use of an equimolar amount of 4-chlorobenzyl chloride, as a model compound, in the presence of sodium ethoxide in dry ethanol.[1] The structure of the condensation product (VII, R=4-methoxy and R'=4-chloro), which was not distillable but which was condensed at 170—180°C/1—2 mmHg, was supported by its infrared spectrum, which showed enhanced peaks at 1513, 1490, and 835 cm^{-1} assignable to the *p*-chlorobenzyl group.

Without being purified further, VII was subjected to hydrolysis in an 1 N alcoholic potassium hydroxide solution to afford a 65% yield of acidic materials (VIII) and a 35% yield of neutral materials (IX). The structure of VIII (R=4-methoxy and R'=4-chloro), a sticky oil, was indicated by its infrared spectrum, which exhibited peaks at 3500—2400, 1770, 1735, and 1700 cm^{-1}, consistent with carboxylic acid, lactone, and ester groups respectively. The neutral material (IX, R=4-methoxy and R'=4-chloro) was purified by distillation and showed the expected combustion analytical results. Further proof of the structure of IX (R=4-methoxy and R'=4-chloro)

6) W. S. Johnson and G. H. Daub, "Organic Reactions," Vol. VI, John Wiely and Sons, New York, N. Y. (1951), p. 1.

7) Detailed studies of the ring opening of the epoxide group upon the reaction of ethyl β-alkyl- and β,β-dialkylglycidates with sodiomalonate have been reported; see A. Takeda, Y. Kariya and S. Torii, *Memoirs of School of Engineering, Okayama Univ.*, **2**, 74 (1967); K. Sisido, S. Torii, and M. Kawanisi, *J. Org. Chem.*, **29**, 904 (1964).

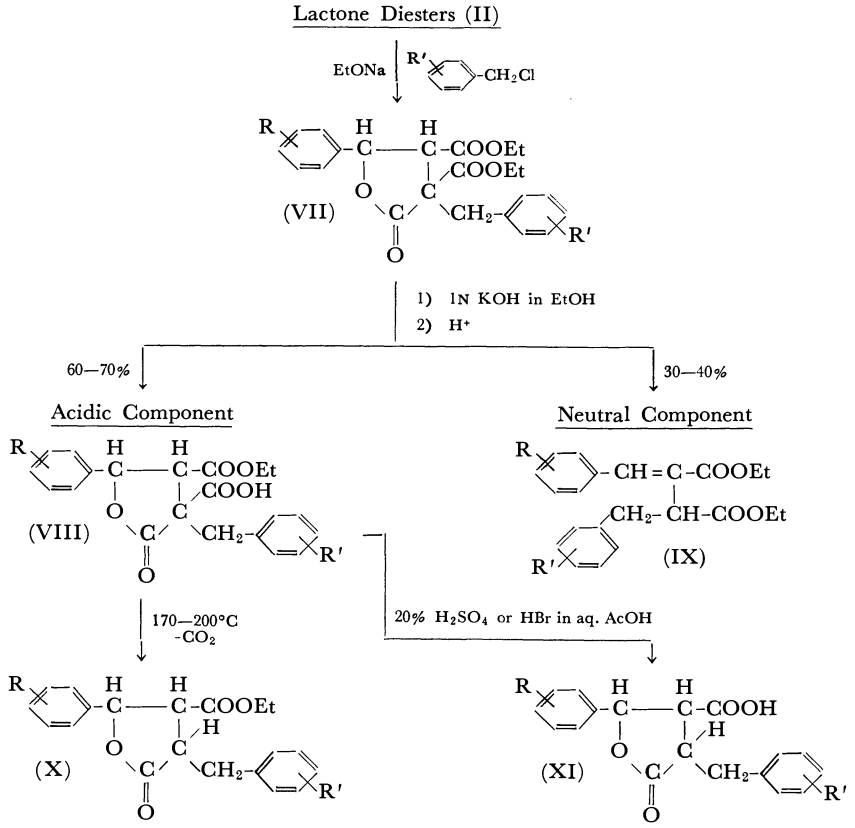

Scheme 2

was given by the following evidence. The absorption spectrum of IX (R=4-methoxy and R'=4-chloro), when carefully compared with that of V (R=4-methoxy), showed enhanced peaks at 1513 and 840—820 cm^{-1} due to the newly-introduced *p*-chlorobenzyl group. A Beilstein test was positive also.

Experimental

The microanalyses were performed by Miss Teruko Nisi of our department. All melting and boiling points are uncorrected.

Reaction of Ethyl β-(4-Methoxyphenyl)glycidate with Sodiomalonate. Following the method described in the previous paper,[1] to a mixture of 13.6 g (0.2 mol) of sodium ethoxide and 37.6 (0.25 mol) of diethyl malonate in 120 m*l* of anhydrous ethanol, 22.2 g (0.1 mol) of ethyl β-(4-methoxyphenyl)glycidate, bp 158°C/3 mmHg (lit.[8] bp 187—191°C/18 mmHg), were added. The mixture was refluxed for 25 hr with stirring, extracted with ether after the addition of ice water, and dried over anhydrous sodium sulfate. Upon the distillation of the residue *in vacuo*, there were obtained 22.5 g (67% based on the glycidate) of the γ-(4-methoxyphenyl)-α,β-dicarbethoxybutyrolactone (IIa, R=4-methoxy), bp 215—225°C/2 mmHg, ν_{max} (cm^{-1}) 1790 (lactone $\nu_{C=O}$) and 1735 (ester $\nu_{C=O}$). Found: C, 61.02; H, 6.04%. Calcd for $C_{17}H_{20}O_7$: C, 60.71; H, 5.99%.

Similarly, a 60% yield [based on ethyl β-(3,4-methylenedioxyphenyl)glycidate, bp 157—160°C/2.5 mmHg, lit.[8] bp 205—210°C/17 mmHg] of γ-(3,4-methylenedioxyphenyl)-α,β-dicarbethoxybutyrolactone, (IIa, R=3,4-methylenedioxy), bp 215°C/0.5 mmHg, ν_{max} (cm^{-1}) 1790 (lactone $\nu_{C=O}$) and 1730 (esters $\nu_{C=O}$) was obtained. Found: C, 58.45; H, 5.08%. Calcd for $C_{17}H_{18}O_8$: C, 58.29; H, 5.18%.

Hydrolysis of γ-(4-Methoxyphenyl)-α,β-dicarbethoxybutyrolactone (IIa, R=4-methoxy). A mixture of 2.8 g (0.05 mol) of potassium hydroxide with a trace of water and 4.5 g (0.013 mol) of IIa (R=4-methoxy) in 70 m*l* of ethanol was stirred for 2 days, neutralized to pH 6.5—7.0 with dilute sulfuric acid, and extracted with ether. The ethereal solution was then extracted several times with a saturated sodium bicarbonate solution, washed with water, dried over anhydrous magnesium sulfate, and evaporated. The distillation of the residual oil gave a *ca.* 30% yield of a neutral substance (V, R=4-methoxy), bp 183—186°C/0.5 mmHg (lit.[9] bp 285°C/4 mmHg), ν_{max} (cm^{-1}) 1730 and 1700 (esters $\nu_{C=O}$), which was identical with the authentic sample prepared by the esterification of the Stobbe half-ester.[4a]

8) K. W. Rosenmund and H. Dornsaft, *Ber.*, **52** 1734 (1919).

9) F. G. Baddar, L. S. El-Assal, N. A. Doss and A. H. Shehab, *J. Chem. Soc.*, **1959**, 1016.

The alkaline extracts were acidified with dilute sulfuric acid. The organic layer was taken up in ether, washed with a saturated sodium chloride solution, and dried over anhydrous sodium sulfate. The concentration of the ethereal solution gave a *ca.* 70% yield of III (R=4-methoxy), viscous oil, ν_{max} (cm^{-1}) 1785 (lactone $\nu_{C=O}$), 1730 (ester $\nu_{C=O}$), and 3500—2400, 1700 (COOH).

III (R=4-methoxy) was heated to 170—230°C for 30 min and then taken up in ether. The organic layer was washed with a saturated sodium bicarbonate solution and water, and dried over sodium sulfate. The distillation of the extract gave a 65—70% yield (based on III, R=4-methoxy) of ethyl γ-(4-methoxyphenyl)-paraconate, pale yellow oil, ν_{max} (cm^{-1}) 1785 (lactone $\nu_{C=O}$) and 1735 (ester $\nu_{C=O}$).

Found: C, 63.80; H, 6.25%. Calcd for $C_{14}H_{16}O_5$: C, 63.60; H, 6.19%.

In a similar manner, a 60—63% yield (based on III, R=3,4-methylenedioxy) of ethyl γ-(3,4-methylenedioxyphenyl)paraconate, bp 160°C/0.5 mmHg, ν_{max} (cm^{-1}) 1790 (lactone $\nu_{C=O}$) and 1730 (ester $\nu_{C=O}$) was obtained.

Found: C, 60.46; H, 5.37%. Calcd for $C_{14}H_{14}O_6$: C, 60.43; H, 5.07%.

By acidifying the alkaline extracts with dilute sulfuric acid, III (R=4-methoxy) was recovered unaffected.

Hydrolysis of Ethyl γ-(4-Methoxyphenyl)paraconate (IV, R=4-Methoxy). A mixture of 2.76 g (0.01 mol) of ethyl γ-(4-methoxyphenyl)paraconate (IV, R=4-methoxy) and 4.0 g (0.1 mol) of sodium hydroxide in 100 m*l* of water was refluxed for 10 hr. After it had then cooled to room temperature, the solution was neutralized with dilute sulfuric acid and extracted with ether. The organic layers were washed with a saturated sodium chloride solution and dried over anhydrous sodium sulfate. After the solvent had then been removed *in vacuo*, the residual solid was recrystallized to give VI (R=4-methoxy), mp 192°C (lit. mp 202.3°C[4a] and 187—188°C[4b]), whose infrared spectrum was identical with that of the specimen prepared by the hydrolysis of the corresponding Stobbe half-ester.[4a]

***p*-Chlorobenzylation of γ-(4-Methoxyphenyl)-α,β-dicarbethoxybutyrolactone (IIa, R=4-Methoxy).** Into a mixture of 6.72 g (0.02 mol) of γ-(4-methoxyphenyl) - α,β - dicarbethoxybutyrolactone (IIa, R=4-methoxy) and 1.34 g (0.02 mol) of sodium ethoxide in 10 m*l* of dry ethanol, 3.2 g (0.02 mol) of 4-chlorobenzyl chloride were stirred over a 14-hr period. The mixture was then neutralized with dilute sulfuric acid, extracted with ether, washed with water, and dried over anhydrous sodium sulfate. After the removal of the solvent, the residue was distilled. The forerun fraction which was distilled below 170°C/2 mmHg was removed. The residual high-boiling fraction, ν_{max} (cm^{-1}) 1790 (lactone $\nu_{C=O}$), 1735—1720 (esters $\nu_{C=O}$), with enhanced absorption bands at 1610, 1513, 1490, and 835 (4-chlorobenzyl group), which were decomposed as the distillation continued, was hydrolyzed with an excess 1 N alcoholic potassium hydroxide solution at 30—40°C for 20 hr and then neutralized to pH 6.5—7.0 with dilute sulfuric acid. The organic layer was taken up in ether, washed with a saturated sodium chloride solution, and extracted with a saturated sodium bicarbonate solution. The ethereal extract was washed with water and dried over anhydrous sodium sulfate. After the solvent had been removed *in vacuo*, the distillation of the residue gave 2.5 g (30% based on IIa) of diesters (IX, R=4-methoxy and R'=4-chloro), bp 170—175°C/0.05 mmHg, ν_{max} (cm^{-1}) 1730 (esters $\nu_{C=O}$), enhanced absorption bands at 1605, 1513, 840, and 820, due to the 4-chlorobenzyl group, in comparison with that of V (R=4-methoxy).

Found: C, 65.92; H, 6.52%. Calcd for $C_{23}H_{25}ClO_5$: C, 66.26; H, 6.04%.

The alkaline extracts were neutralized with dilute sulfuric acid to pH 6.5—7.0. The organic layer was taken up in ether, washed with a saturated sodium chloride solution and with water, and dried over anhydrous magnesium sulfate. Upon removing the solvent *in vacuo*, there was obtained 5.04 g of a viscous oil (VIII, R=4-methoxy and R'=4-chloro), ν_{max} (cm^{-1}) 1770 (lactone $\nu_{C=O}$), 1730 (ester $\nu_{C=O}$), 3400—2400, 1700, 930—900 (COOH).

The viscous oil (VIII), when heated to 170—220°C, gave a 30% yield of the lactone ester (X, R=4-methoxy and R'=4-chloro), bp 195—200°C/2 mmHg, ν_{max} (cm^{-1}) 1790 (lactone $\nu_{C=O}$) and 1735 (ester $\nu_{C=O}$).

Found: C, 64.90; H, 5.59%. Calcd for $C_{21}H_{21}ClO_5$: C, 64.83; H, 5.44%.

The viscous oil (VIII), when boiled with excess 20% sulfuric acid for 8 hr or with an excess 1 N sodium hydroxide solution for 4 days, gave a 45% yield of lactone acid (XI, R=4-methoxy and R'=4-chloro), mp 130°C, ν_{max} (cm^{-1}) 1770 (lactone $\nu_{C=O}$), and 1730 and 1705 (carboxylic acid $\nu_{C=O}$).

Found: C, 63.29; H, 4.94%. Calcd for $C_{19}H_{17}ClO_5$: C, 63.24; H, 4.76%.

Synthesis of 5-Deoxy-1,2-*O*-isopropylidene-3-*O*-methyl-α-D-xylofuranose-4-ene and Its Benzylmercaptan Adduct

Saburo INOKAWA, Hiroshi YOSHIDA, Chih-Cheng WANG and Roy L. WHISTLER

Department of Synthetic Chemistry, Faculty of Engineering, Shizuoka University, Johoku, Hamamatsu, and Department of Biochemistry, Purdue University, Lafayette, Indiana

(Received December 26, 1967)

The present report will describe the synthesis of a new unsaturated sugar, 5-deoxy-1,2-*O*-isopropylidene-3-*O*-methyl-α-D-xylofuranose-4-ene [4] from 1,2-*O*-isopropilydene-5-*O*-*p*-toluenesulfonyl-α-D-xylofuranose [1], and the photocatalyzed addition of benzylmercaptan to the unsaturated sugar [4], which gives 5-benzylthio-5-deoxy-1,2-*O*-isopropylidene-3-*O*-methyl-α-D-xylofuranose [5]

1,2-*O*-Isopropylidene-5-*O*-*p*-toluenesulfonyl-α-D-xylofuranose [1][1] was treated with methyl iodide and silver oxide in dimethylformamide (DMF)[2] to give, in a 72% yield, a white crystalline product analyzed as 1,2-*O*-isopropylidene-3-methyl-5-*O*-*p*-toluenesulfonyl-α-D-xylofuranose [2]. This [2] was heated with tetraethylammonium bromide in DMF to give, in a 73% yield, a colorless, oily product analyzed as 5-bromo-5-deoxy-1,2-*O*-isopropylidene-3-*O*-methyl-α-D-xylofuranose [3]. This [3] was then treated with silver fluoride[3] in pyridine to give, in a 60% yield, a colorless, oily product identified as 5-deoxy-1,2-*O*-isopropylidene-3-*O*-methyl-α-D-xylofuranose-4-ene [4] by infrared and NMR spectrum and by elementary analysis.

The infrared absorption spectrum of [4] shows absorption bands at about 800 cm^{-1} (s) (out-of-plane deformation vibration of the >C=CH_2 group), at about 1650 cm^{-1} (s) (C=C stretching vibration of >C=CH_2), and at about 3100 cm^{-1} (m) (C–H stretching vibration of the >C=CH_2 group). The NMR spectrum of [4] permits a straightforward analysis, as shown in Fig. 1.

The unsaturated sugar [4] was treated with benzylmercaptan, under ultraviolet light[4] to give, in a 85% yield, a white crystalline adduct analyzed as 5-benzylthio-5-deoxy-1,2-*O*-isopropylidene-3-*O*-methyl-α-D-xylofuranose [5]. The structure of this product was established by elementary analysis, by a study of its NMR spectrum (shown in Fig. 2), and by comparison with an authentic sample prepared by the treatment of [3] with sodium benzylmercaptanate in ethanol.

Experimental

General Methods. The infrared spectra were determined on a liquid film with a Perkin-Elmer 337 grating infrared spectrophotometer. The NMR spectra were measured at 60 Mc with a Hitachi Perkin-Elmer R-20 spectrometer. The ultraviolet illumination was from a Halos PIH-100 (100W) (a high-pressure mercury lamp).

Preparation of 1,2-*O*-Isopropylidene-3-*O*-methyl-5-*O*-*p*-toluenesulfonyl-α-D-xylofuranose [2]. [1] (12 g) was dissolved in 120 m*l* of dry DMF, 20 g of silver oxide and 15 m*l* methyl iodide were added, and then the whole was shaken at room temperature in the dark for 20 hr. The solution was filtered, and, after the addition of water, the filtrate was extracted four times with chloroform. The combined extracts were filtered again to remove white precipitates, washed thoroughly with water, and dried over sodium sulfate, and the chloroform was distilled *in vacuo*. The resulting crystalline residue was recrystallyzed from ethyl acetate-petroleum

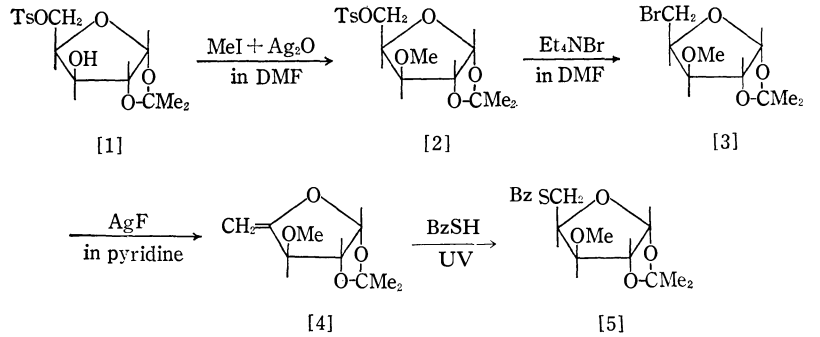

1) P. A. Levene and A. L. Raymond, *J. Biol. Chem.*, **102**, 317 (1933).
2) R. Kuhn, H. Trischmann and I. Löw, *Angew. Chem.*, **67**, 32 (1955).
3) B. Helferich and E. Himmen, *Ber.*, **61**, 1825 (1928).
4) J. Lehmann, *Carbohydrate Res.*, **2**, 1 (1966).

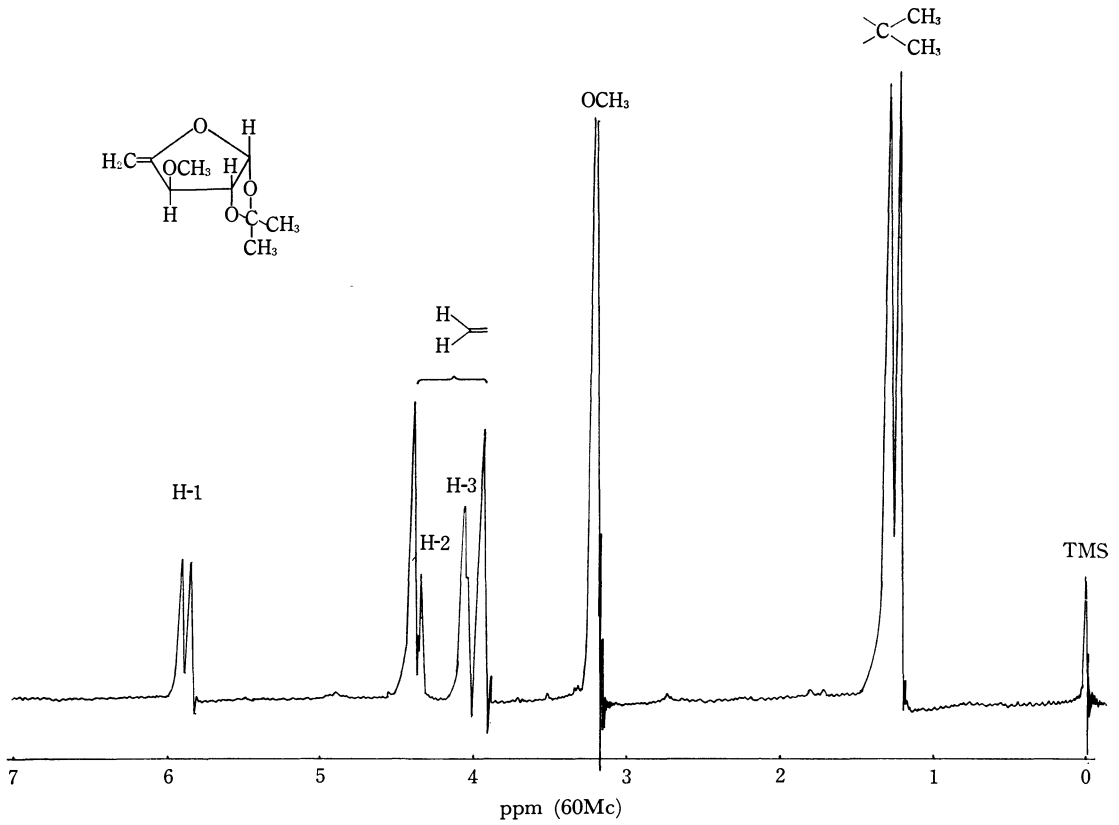

Fig. 1. NMR spectrum of 5-deoxy-1,2-*O*-isopropylidene-3-*O*-methyl-α-D-xylofuranose-4-ene (liq.).

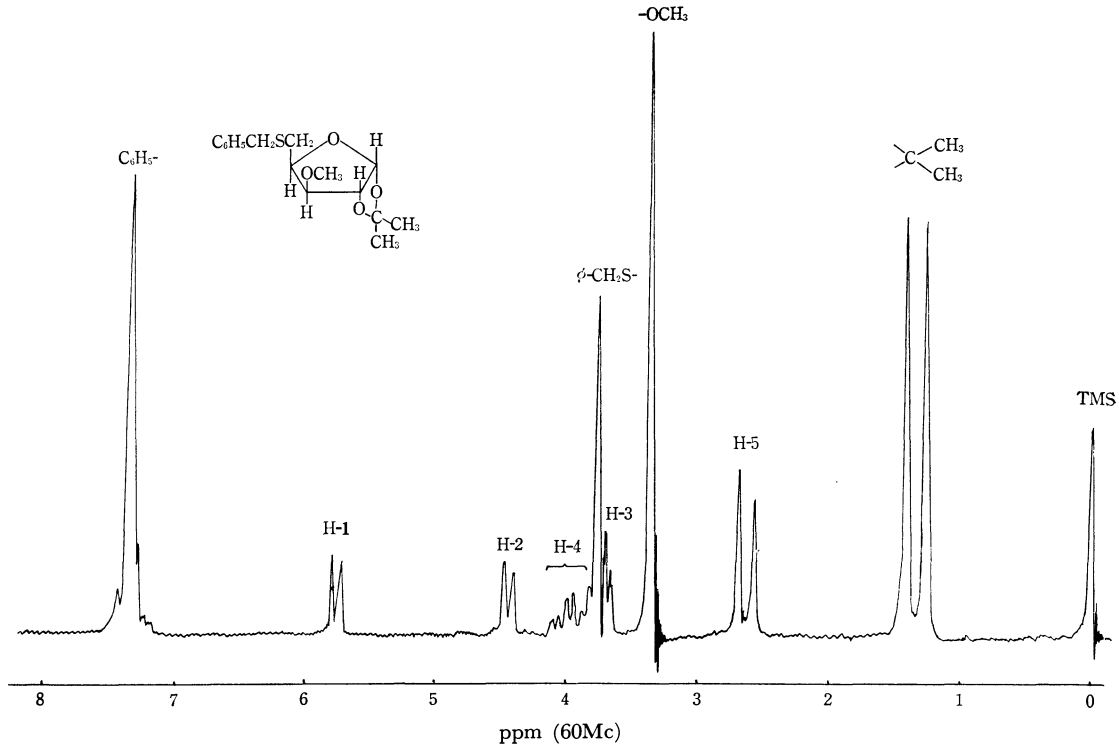

Fig. 2. NMR spectrum of 5-benzylthio-5-deoxy-1,2-*O*-isopropylidene-3-methyl-α-D-xylofuranose (in CCl_4).

benzine to give colorless prisms of [2] (9.1 g, 72% yield), mp 116—117°C.

5-Bromo-5-deoxy-1,2-*O*-isopropylidene-3-*O*-methyl-α-D-xylofuranose [3]. A solution of 5 g of [2] and 10 g of tetramethylammonium bromide in 100 m*l* of DMF was heated at 100°C for 14 hr and then concentrated *in vacuo*. After the subsequent addition of water, the solution was extracted with chloroform three times, and the combined extracts were washed thoroughly with water, dried over sodium sulfate, and concentrated *in vacuo* to give a sirup. The fractional vacuum distillation of the sirup gave, in a 73% yield (3.8 g), pure [3]. bp 67°C/0.2 mmHg, $[\alpha]_D^{18}$ −77.6° (*c* 10, chloroform).

Found: C, 40.1; H, 5.72%. Calcd for $C_9H_{15}O_4Br$: C, 40.5; H, 5.66%.

5-Deoxy-1,2-*O*-isopropylidene-3-*O*-methyl-α-D-xylofuranose-4-ene [4]. A mixture of 5 g of [3] and 7 g of silver fluoride in 40 m*l* of dry pyridine was warmed at 50°C for 30 hr. The product and the pyridine were separated from the inorganic salts by repeated extractions with ether. After filtration, the combined extracts were washed with an aqueous sodium carbonate solution and water, dried over sodium sulfate, and concentrated *in vacuo*. The fractional vacuum distillation of the resulting sirup gave, in a 60% yield (2.1 g), pure [4], bp 80°C/7 mmHg, $[\alpha]_D^{18}$ −66.0° (*c* 10, chloroform), NMR data (see Fig. 1).

Found: C, 57.8; H, 7.63%. Calcd for $C_9H_{14}O_4$: C, 58.2; H, 7.53%.

5-Benzylthio-5-deoxy-1,2-*O*-isopropylidene-3-*O*-methyl-α-D-xylofuranose [5]. i) A solution of 3 g of [4] in 5 m*l* of redistilled benzylmercaptan in a Vycor tube was irradiated for 1 hr with a high-pressure mercury ultraviolet lamp (100 W) under a nitrogen atmosphere. The solution was then concentrated *in vacuo*, and the residue was recrystallized from methanol to give, in a 82% yield (3.9 g), colorless needles of [5], mp 68°C, $[\alpha]_D^{18}$ +25.6 (*c* 5, chloroform), NMR data (see Fig. 2).

Found: C, 61.3; H, 7.20%. Calcd for $C_{16}H_{22}O_4S$: C, 61.9; H, 7.09%.

ii) To a solution of 0.1 g of metallic sodium in 2 m*l* of ethanol, 2 m*l* of redistilled benzylmercaptan and 1 g of [4] were added, and the whole was refluxed for 3 hr under a nitrogen atmosphere. The solution was then concentrated *in vacuo*, the residue was extracted with ether, and the extracts were washed with water, dried over sodium sulfate, and concentrated *in vacuo* to give crystals. Recrystallization from methanol yielded, in a 40% yield (0.6 g), colorless needles of [5], mp 68°C.

The authors are very grateful to Hashimoto Kaseikogyo, Ltd. for supplying them silver fluoride.

Preparation of Decamethyltetrasilane by Coupling of Pentamethylchlorodisilane with Lithium

Hideki SAKURAI, Hisayoshi YAMAMORI, Mineo YAMAGATA and Makoto KUMADA

Department of Synthetic Chemistry, Kyoto University, Sakyo-ku, Kyoto

(Received December 28, 1967)

In a previous paper,[1] we have described the preparation of (chloromethyl)pentamethyldisilane by coupling of chlorobromomethane and pentamethylchlorodisilane with lithium metal in tetrahydrofuran (THF). However, the yield was not reasonably good and among other products, a considerable amount of decamethyltetrasilane was obtained. This fact indicating the coupling of pentamethylchlorodisilane to decamethyltetrasilane seemed interesting to us, since usually trialkylchlorosilanes do not undergo the coupling easily in this reaction condition. Shackelford *et al.*[2] reported that triethylbromosilane did not afford hexaethyldisilane by the coupling with lithium metal in THF. Preparation of hexamethyldisilane by the coupling of trimethylchlorosilane requires usually drastic conditions.[3]

On the other hand, coupling reactions of halosilanes having at least one phenyl group on silicon are known to proceed quite smoothly.[3]

We are now reporting a facile coupling of pentamethylchlorodisilane with lithium metal in THF to give decamethyltetrasilane. Pentamethylchlorodisilane is by no means a *trialkylchlorosilane* but it is interesting to compare the present results with those of chloromonosilanes.

Pentamethylchlorodisilane underwent the coupling reaction very smoothly with lithium in THF to give decamethyltetrasilane in good yield (~84%).

$$2(CH_3)_3SiSi(CH_3)_2Cl + 2Li \xrightarrow{THF} CH_3[Si(CH_3)_2]_4CH_3 + 2LiCl$$

Coupling of pentamethylchlorodisilane with sodium-potassium alloy was reported to give tetrasilane in 27%[4] or in 50% yield[5], previously.

1) H. Sakurai, H. Yamamori and M. Kumada, *J. Org. Chem.*, **33**, 1527 (1968).
2) J. M. Shackelford, H. Deschmertzing, C. H. Henther and H. Podall, *ibid.*, **28**, 1700 (1963).
3) H. Gilman, W. H. Atwell and F. K. Cartledge, *Adv. Organometal. Chem.*, **4**, 1 (1966).
4) G. R. Wilson and A. G. Smith, *J. Org. Chem.*, **26**, 557 (1961).
5) M. Kumada and M. Ishikawa, *J. Organometal. Chem.*, **1**, 153 (1963).

The yield of the present reaction is therefore exceptionally high compared with these results. Accordingly, it provides a preferable route to decamethyltetrasilane.

Observations of such a smooth reaction prompted us to attempt isolating a possible intermediate of the reaction, pentamethyldisilanyllithium. Stolberg[6] has reported that the cleavage of decamethyltetrasilane by sodium-potassium alloy followed by coupling with trimethylchlorosilane gave a complicated mixture containing several lower homologs of methylpolysilanes. The result has been interpreted in terms of an intermediate pentamethyldisilanyl anion which would be stabilized by the charge distiribution over two silicon atoms.

$$(CH_3)_3Si\text{–}\overset{\ominus}{Si}(CH_3)_2 \longleftrightarrow (CH_3)_3\overset{\ominus}{Si}\text{=}Si(CH_3)_2$$

However, even in the presence of an excess amount of lithium metal, pentamethylchlorodisilane afforded no stable solution of pentamethyldisilanyllithium; quenching of the solution with trimethylchlorosilane gave only a trace amount of octamethyltrisilane. Therefore, it is concluded that pentamethyldisilanyllithium could be produced at first but it reacts very rapidly with pentamethylchlorodisilane. Cleavage of decamethyltetrasilane with lithium in THF is a very slow process contrary to cases of phenyl-substituted disilanes.[7]

$$(CH_3)_3SiSi(CH_3)_2Cl + 2Li \rightarrow (CH_3)_3SiSi(CH_3)_2Li + LiCl$$

$$(CH_3)_3SiSi(CH_3)_2Li + (CH_3)_3SiSi(CH_3)_2Cl \rightarrow CH_3[Si(CH_3)_2]_4CH_3$$

$$(CH_3)_3SiSi(CH_3)_2Li + (CH_3)_3SiCl \rightarrow CH_3[Si(CH_3)_2]_3CH_3$$

6) U. G. Stolberg, *Z. Naturforsch.*, **18b**, 765 (1963).
7) H. Sakurai, *Yukigosei Kagaku Kyokaishi (J. Soc. Org. Synth. Chem. Japan)*, **25**, 555 (1967).

Experimental

Materials. Pentamethylchlorodisilane was prepared from hexamethyldisilane by the procedure described before.[8] Trimethylchlorosilane, generously supplied by the Tokyo Shibaura Electric Co. Ltd., was distilled before use. Tetrahydrofuran was distilled from a stock solution containing lithium aluminum hydride.

Coupling of Pentamethylchlorodisilane with Lithium Metal. To a fine powdered lithium metal (2.5 g, 0.36 g atom) in 100 m*l* of THF, was added with stirring 15 g (0.090 mol) of pentamethylchlorodisilane dissolved in 20 m*l* of THF. The reaction mixture was heated to keep a gentle reflux during the addition. After addition was complete, the mixture was stirred and refluxed for 8 hr. After hydrolysis and work-up, 9.6 g (0.037 mol, 82% yield) of decamethyltetrasilane was obtained as a colorless liquid (homogeneous on vpc). Physical constants, IR spectra and retention times on vpc agreed with those of the authentic sample.[5]

An Attempt to Isolate Pentamethyldisilanyllithium. By the essentially same procedure, 17 g (0.1 mol) of pentamethylchlorodisilane in 100 m*l* of THF was allowed to react with 1.4 g (0.2 g atom) of lithium powder placed in 100 m*l* of THF. A grey solution was obtained but a considerable amount of lithium was remained unreacted. After filtering through an L-shaped sidearm packed with glass wool into a dropping funnel, this solution was added to 22 g (0.2 mol) of trimethylchlorosilane quickly. No appreciable heat evolution was observed. After refluxing 6 hr and standing overnight, solvent and then products were removed from the mixture under reduced pressure. Gas-chromatographic examination of the products showed existence of octamethyltrisilane only in a very small amount. Redistillation of the products gave 11 g (0.042 mol 84% yield) of decamethyltetrasilane, bp 109°C (16 mmHg), $n_D^{20}=1.4893$, $d_4^{20}=0.8126$, $MR_D=92.41$ (calcd 92.43).

8) H. Sakurai, K. Tominaga, T. Watanabe and M. Kumada, *Tetrahedron Letters*, **1966**, 5493.

Reaction of Propylene with a Mixture of Iodine and Iodosobenzene or Phenyl Iodine Diacetate*[1]

Keizo Aoki and Yoshiro Ogata

Department of Applied Chemistry, Faculty of Engineering, Nagoya University, Chikusa-ku, Nagoya

(Received December 28, 1967)

In our kinetic study of iodination by a mixture of iodine and peracetic acid, it has been postulated that acetyl hypoiodite, CH_3COOI, is a probable attacking species.[1] Recently, our further study has revealed that iodosobenzene or phenyl iodine diacetate is a more effective oxidizing agent than peracetic acid for iodinating aromatic compounds, but here again acetyl hypoiodite can be postulated as the attacking species[2]:

$$I_2 + PhI(OCOCH_3)_2 \rightarrow 2CH_3COOI + PhI \quad (1)$$

$$ArH + CH_3COOI \rightarrow ArI + CH_3COOH \quad (2)$$

The addition of the acetyl hypohalite formed by the reaction of silver acetate with elementary halogen to olefin has been called the "Prévost reaction."[3] Prévost products have also been observed in the reaction of cyclohexene[4] or propylene[5] with a mixture of iodine and peracetic acid, *e. g.*,

$$2CH_3CH{=}CH_2 + I_2 + CH_3CO_3H + CH_3CO_2H \rightarrow 2CH_3CH(OCOCH_3)CH_2I + H_2O \quad (3)$$

Therefore, we reacted olefin with a mixture of iodine and phenyl iodine diacetate or iodosobenzene.

The reaction of propylene with a mixture of iodine and phenyl iodine diacetate in a mixed solvent of acetic acid and ethyl ether at 21—27°C was found to give 1-iodo-2-acetoxypropane in a yield of 56%:

$$2CH_3CH{=}CH_2 + I_2 + PhI(OCOCH_3)_2 \rightarrow 2CH_3CH(OCOCH_3)CH_2I + PhI \quad (4)$$

Also, the reaction of propylene with a mixture of iodine and iodosobenzene in acetic acid-ethyl ether at 22—28°C was found to give a lower yield (37%) of 1-iodo-2-acetoxypropane:

$$2CH_3CH{=}CH_2 + I_2 + PhIO + 2CH_3CO_2H \rightarrow 2CH_3CH(OCOCH_3)CH_2I + PhI + H_2O \quad (5)$$

The reaction of propylene with a mixture of iodine and peracetic acid in a similar method gave 1-iodo-2-acetoxypropane in a 56% yield.

Although the reaction of phenyl iodine diacetate with olefin alone is known to give *vic*-diacetoxy alkane,[6] 1,2-diacetoxypropane was not detected in the present reaction products.

These results suggest that iodine is converted by phenyl iodine diacetate to acetyl hypoiodite, which then adds to propylene to give an iodoacetoxy compound.

Experimental

Materials. The iodobenzene was prepared by the reaction of benzene with a mixture of iodine and peracetic acid, bp 182—185°C.[1] The phenyl iodine diacetate was prepared by the peracetic acid oxidation of iodobenzene, mp 157—159°C (lit., mp 158°C[7] and 161.1—162.2°C[8]). The iodosobenzene was prepared from iodobenzene *via* iodobenzene dichloride.[9] Ethyl ether and iodine were reagent-grade. 99.5% acetic acid and 99.5% propylene were used. The peracetic acid solution was prepared by stirring acetic anhydride (407 g) drop by drop into a solution of 60% hydrogen peroxide (100 g) and concentrated sulfuric acid (1 m*l*) as a catalyst at 30—40°C over a period of 3 hr.[10] The 1,2-diacetoxypropane was prepared by the reaction of propylene and peracetic acid in a mixture of ether and acetic acid, bp 51—52°C/1.3 mmHg.[5]

Analysis of the Products. The infrared spectra were determined by a Perkin-Elmer Model 333 spectrophotometer. The products were analyzed by means of gas chromatography employing a Yanagimoto Model GCG 550 F apparatus equipped with a flame ionization detector operated with a 2 m×3 mm column packed with Apiezon grease L 15% on Celite 545 (80—100 mesh), using nitrogen as a carrier (18—12.5 m*l*/min) at 80—200°C (6°C/min); hydrogen flow rate 25 m*l*/min, injection temperature 255°C, detector temperature 250°C. The retention times of 1-iodo-2-acetoxypropane, iodobenzene, and 1,2-diacetoxypropane were 9.7, 12.5, and 7.1 min respectively.

Reaction of Propylene with a Mixture of Iodine and Phenyl Iodine Diacetate. Into a stirred ethereal solution (100 m*l*) of iodine (2.54 g, 0.01 mol), phenyl

*1 Contribution No. 108.

1) Y. Ogata and K. Nakajima, *Tetrahedron*, **20**, 43, 2751 (1964).

2) Y. Ogata and K. Aoki, *J. Am. Chem. Soc.*, **90**, in press (1968).

3) a) C. V. Wilson, "Organic Reactions," **9**, 350 (1957). b) R. G. Johnson and R. K. Ingham, *Chem. Revs.*, **56**, 219 (1956).

4) Y. Ogata, K. Aoki and Y. Furuya, *Chem. & Ind. (London)*, **1965**, 304.

5) Y. Ogata and K. Aoki, *J. Org. Chem.*, **31**, 1625 (1966).

6) R. Criegee and H. Beucker, *Ann.*, **541**, 218 (1939).

7) K. H. Pausacker, *J. Chem. Soc.*, **1953**, 107.

8) J. E. Leffler and L. J. Story, *J. Am. Chem. Soc.*, **89**, 2333 (1967).

9) H. J. Lucas, E. R. Kennedy and M. W. Formo, "Organic Syntheses," Coll. Vol. III, p. 483 (1955).

10) Y. Ogata and K. Aoki, *J. Org. Chem.*, **31**, 4181 (1966).

iodine diacetate (3.22 g, 0.01 mol) was added. Propylene was passed into the solution, but apparently no reaction occurred, because phenyl iodine diacetate is virtually insoluble in ether. Therefore, acetic acid (50 m*l*) was added to the solution to dissolve it, and propylene was passed into the solution at 21—27°C over a period of 35 min. The mixture was then kept standing for additional 1 hr. Finally, the solution became transparent. The mixture was transferred into a separatory funnel containing ether (50 m*l*) and water (100 m*l*). The ether layer was washed three times with a 5% sodium hydroxide solution (each 50 m*l*) to remove the acetic acid, and finally washed with 5% sodium thiosulfate (50 m*l*) and dried over anhydrous sodium sulfate. The ether was evaporated under reduced pressure (42 mmHg) at 17°C. The residual liquid (4.01 g) was analyzed by gas chromatography in order to estimate the yields of 1-iodo-2-acetoxypropane (56% on the basis of the iodine) and iodobenzene (72% on the basis of the phenyl iodine diacetate). The infrared spectrum of the liquid is consistent with a binary mixture of the corresponding authentic samples. The absorption bands at 2970, 1740, 1370, 1240, 1023, and 600 cm^{-1} are characteristic of 1-iodo-2-acetoxypropane, and while those at 3050, 1570, 1470, 1440, 730, 685, and 655 cm^{-1} are characteristic of iodobenzene. Gas chromatography shows that the products do not contain 1,2-diacetoxypropane.

Reaction of Propylene with a Mixture of Iodine and Iodosobenzene. Iodosobenzene (2.20 g, 0.01 mol) was added to a stirred ethereal solution (100 m*l*) of iodine (2.54 g, 0.01 mol). The iodosobenzene was insoluble in ether. Acetic acid (50 m*l*) was then added to the mixture, and propylene was passed into the solution at 22 −28°C over a period of 30 min, and the mixture was left standing overnight. The solution gradually turned pale yellow and transparent, and some unreacted iodosobenzene settled at the bottom of the flask. The reaction mixture was then worked up as above, giving a residual liquid (2.89 g). The yields of 1-iodo-2-acetoxypropane (37%) and iodobenzene (60%) were estimated by gas chromatography.

Reaction of Propylene with a Mixture of Iodine and Peracetic Acid. Into a stirred ethereal solution (100 m*l*) of iodine (2.54 g, 0.01 mol) there was added, drop by drop, an acetic acid solution of 1.79 M peracetic acid (30 m*l*, 0.0537 mol). Propylene was passed into the solution at 16—25°C over a period of 110 min. The product was worked up as above, giving 1-iodo-2-acetoxypropane (2.56 g, 56%), bp 33.5—35.5°C/0.7—0.8 mmHg.[5] This was used as the authentic sample for the infrared spectrum study and for the gas chromatography.

Use of Anhydrous Hydrogen Fluoride in Peptide Synthesis. III. Synthesis of Bradykinin

Shumpei SAKAKIBARA, Nobuhiro NAKAMIZO*1 Yasuo KISHIDA and Shoko YOSHIMURA

Peptide Center, Institute for Protein Research, Osaka University, Kita-ku, Osaka

(Received December 30, 1967)

During repeated synthesis of bradykinin following a recently published procedure,[1] the final stage of removal of the nitro group from the nitroarginine residue by catalytic hydrogenolysis was found to be unsatisfactory; that is, the biological activity of the final product varied within a range of 100 to 60%, with the quality of the palladium black catalyst used, even though the same protected nona-peptide was subjected to each reaction. This variance in the biological activity of the product was probably due to the formation of some side products during the reduction of the nitro group, as pointed out for general cases by Iselin.[2] Furthermore, removal of the nitro group from large arginine peptides by catalytic hydrogenolysis is known to be a time-consuming reaction. Recently,[3,4] anhydrous hydrogen fluoride (HF) has been shown to be useful for removal of various protective groups from peptides, and it was noted especially that a nitro group can be removed quickly from nitroarginine peptides in the presence of anisole.[3-5] This procedure was applied in the present study for removal of protecting groups from a nonapeptide, tricarbobenzoxy-L-arginyl-L-prolyl-L-prolylglycyl-L-phenylalanyl-L-seryl-L-prolyl-L-phenylalanyl-N^G-nitro-L-arginine benzyl ester (V). Synthesis of the starting material V was carried out following the original procedure[1] with several improvements as described in the experimental part of this paper. This material V was treated with HF at 0°C for 30 min in the

*1 Present address: Kyowa Hakko Kogyo Co., Ltd., Otemachi 1, Chiyoda-ku, Tokyo.

1) S. Sakakibara and N. Inukai, This Bulletin, **39**, 1567 (1966).

2) B. M. Iselin, "Peptides," Proc. 6th European Peptide Symp., ed. by L. Zervas, Pergamon Press, London (1966), p. 27.

3) S. Sakakibara, Y. Shimonishi, M. Okada and Y. Kishida, "Peptides," Proc. 8th European Peptide Symp., ed. by H. C. Beyermann *et al.*, North Holland Publishing Co., Amsterdam (1967), p. 44; S. Sakakibara, Y. Shimonishi, Y. Kishida, M. Okada and H. Sugihara, This Bulletin, **40**, 2164 (1967).

4) S. Sakakibara, Y. Kishida, R. Nishizawa and Y. Shimonishi, *ibid.*, **41**, 438 (1968).

5) J. Lenard, *J. Org. Chem.*, **32**, 250 (1967).

presence of anisole as described in a preceding paper.[4] The HF which contaminated the final reaction product was eliminated by passing the aqueous solution through a column of Dowex 1 (OH^- form). Then the HF free product was converted to the acetate form, and was lyophilized. If a faint pink color remained in the product, it will be removed easily by passing the aqueous solution through a short column of Sephadex G 10. The biological activities of three different batches of bradykinin acetate synthesized in this way were assayed by the contraction test with guinea-pig ileum,*2 and they were found to show essentially the same biological activity which was as strong as that of an available authentic sample.[6] The purity of bradykinin synthesized by the HF procedure was also compared with that of another sample which was synthesized by catalytic hydrogenolysis of the same protected nonapeptide V. Both samples were converted to the DNS-derivatives,[7] and were analyzed by thin-layer chromatography with Silica-gel H.*3 The chromatogram clearly indicated the great advantage of the HF method, as shown in Fig. 1. Thus, it was concluded that homogeneous bradykinin can be obtained easily by the present HF method without the use of any additional purification procedure, while catalytic hydrogenolysis of the nitroarginine peptide may result in contamination with undesirable compounds.

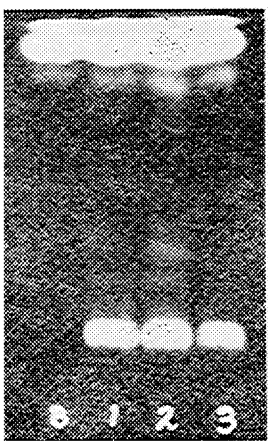

Fig. 1. Thin-layer chromatogram of DNS-bradykinin (10^{-8} mol) with Silica-gel H.
The solvent system was methyl acetate: isopropanol: 28% ammonia (9 : 7 : 4) containing mercaptoethanol (1%).
B: Control. 1: An available sample as the standard bradykinin. 2: Bradykinin synthesized by catalytic hydrogenolysis. 3: Bradykinin synthesized by the HF method.

Lenard and Robinson[8] have mentioned recently in a short communication that the HF method is also useful to release bradykinin from the Merrifield's polymer support. Although they reported the presence of four extra peaks in a distribution curve of their sample when it was analyzed by the counter current method, formation of such by-products did not occur on careful treatment of this peptide with HF.

Experimental

***t*-Amyloxycarbonyl-L-phenylalanyl-N^G-nitro-L-arginine Benzyl Ester (I).** This material was synthesized as described previously.[1] The melting point of the final product increased to 132—135°C on repeated recrystallization from ethyl acetate and petroleum ether; $[\alpha]_D^{24}$ −15.6° (*c* 3, ethanol), $[\alpha]_D^{26}$ −14,2° (*c* 1.6, pyridine). Cited values[1] were mp 120—124°C, $[\alpha]_D$ −15.8° (*c* 3, ethanol).

***p*-Methoxybenzyloxycarbonyl-L-prolyl-L-phenylalanyl-N^G-nitro-L-arginine Benzyl Ester (II).** The same procedure was followed for its synthesis as that described in the previous paper[1] for the preparation of *t*-amyloxycarbonyl-L-prolyl-L-phenylalanyl-N^G-nitro-L-arginine benzyl ester. *p*-Methoxybenzyloxycarbonyl-L-proline[9] was used instead of *t*-amyloxycarbonyl-L-proline. This *p*-methoxybenzyloxycarbonyl derivative was more easily crystallizable than the former *t*-amyloxycarbonyl compound. The yield of this compound after recrystallization from a mixture of methanol and chloroform by the addition of ether was 79%; mp 179—182°C, $[\alpha]_D^{26}$ −40.8° (*c* 1, dimethylformamide).

Found: C, 60.46; H, 6.30; N, 13.65%. Calcd for $C_{36}H_{43}O_9N_7$: C, 60.24; H, 6.04; N, 13.67%.

***t*-Amyloxycarbonyl-L-phenylalanyl-L-seryl-L-prolyl-L-phenylalanyl-N^G-nitro-L-arginine Benzyl Ester (III).** This material was prepared as described in the previous paper,[1] but compound II was used instead of the *t*-amyloxycarbonyl derivative. Although the compound was reported to be an amorphous powder, it was crystallized in this case from hot ethyl acetate or methanol by the addition of ether; yield 80%, mp 175—177°C, $[\alpha]_D^{24}$ −37.1° (*c* 1, dimethylformamide). Reported value[1] mp 100—115°C, $[\alpha]_D^{22}$ −38.2° (*c* 0.5, dimethylformamide).

***t*-Amyloxycarbonyl-L-prolyl-L-prolylglycine *p*-Nitrophenyl Ester (IV).** Although this material was used without purification in the previous case,[1] it was crystallized in the present study by trituration with ether; the yield of crude product was 85%. The crude crystals were recrystallized from ethyl acetate and petroleum ether; yield 80%, mp 191—192°C, $[\alpha]_D^{19}$ −92.7° (*c* 1, dimethylformamide).

*2 The biological tests were performed by Professor Tomoji Suzuki of Osaka University and his colleagues, to whom the authors are deeply grateful.

6) Obtained from Sandoz AG., Basel, Switzerland, (Batch No. 65226, BRS 640) as 0.1 mg/ml solution.

7) W. R. Gray and B. S. Hartley, *Biochem. J.*, **89**, 59p (1963); DNS-=1-Dimethylamino-naphthalene-5-sulfonyl-

*3 The authors wish to express their thanks to Professor Zenzo Tamura of the University of Tokyo for carrying out this procedure skillfully. *Cf.* Z. Tamura and T. Nakajima, *Protein, Nucleic Acid, Enzyme (Tampakushitsu, Kakusan, Kohso)*, **12**, 729 (1967).

8) J. Lenard and A. B. Robinson, *J. Am. Chem. Soc.*, **89**, 181 (1967).

9) F. Weygand and K. Hunger, *Chem. Ber.*, **95**, 1 (1962).

Found: C, 57.11; H, 6.34; N, 11.10%. Calcd for $C_{24}H_{32}O_8N_4$: C, 57.13; H, 6.39; N, 11.11%.

Bradykinin Triacetate. A protected nonapeptide V (402 mg, 0.25 mmol), which was synthesized by following a previously published procedure[1] with compound III and IV, was placed in an HF-reaction cylinder together with anisole (0.28 m*l*, 10 eq).[3] HF (5 m*l*) was added into the cylinder using an HF-reaction apparatus,[3] and the mixture was allowed to react at 0°C for 30 min with stirring. Excess HF was removed under reduced pressure at 0°C, and the residue was kept at reduced pressure (3 mmHg) for 5 hr at room temperature. The product was dissolved in water (10 m*l*), insoluble material was removed by filtration with Hyflo Supercel, and the clear solution thus obtained was passed through a column of Dowex 1 (X 2, OH^- form, 1 cm × 15 cm). The column was washed with distilled water (about 100 m*l*) until the pH of the washing became 7. The eluate and washing were collected together in a receiver which contained acetic acid (0.5 mol), and the solution was lyophilized. After drying in a desiccator over phosphorus pentoxide *in vacuo* for 24 hr, the yield of the product was 257 mg (77% as triacetate pentahydrate); mp 170—171°C; $[\alpha]_D^{13}$ −80.6° (*c* 0.28, water).*4

Found: C, 50.45; H, 7.30; N, 16.26%. Calcd for $C_{50}H_{73}O_{11}N_{15}\cdot 3CH_3COOH\cdot 5H_2O$: C, 50.57; H, 7.15; N, 15.80%.

After drying this compound at 110°C for 18 hr *in vacuo*, the anhydrous compound was obtained.

Found: C, 54.34; H, 7.10; N, 17.73%. Calcd for $C_{50}H_{73}O_{11}N_{15}\cdot 3CH_3COOH$: C, 54.22; H, 6.91; N, 16.94%.

*4 The concentration was calculated as dry bradykinin triacetate.

Empirical Estimations of the Taft σ^*

Isao MOCHIDA and Yukio YONEDA

Department of Synthetic Chemistry, Faculty of Engineering, The University of Tokyo, Hongo, Bunkyo-ku, Tokyo

(Received January 6, 1968)

In the previous paper,[1] the heats of formation of gaseous carbonium ions were well estimated by the group contribution method. In the present work, the estimation of the Taft σ^*[2] is tried by means of both group contribution method and quantum-chemical calculations with simple LCAO-MO. The Taft σ^* has been used as an empirical reactivity index to understand the reactivities in the heterogeneous catalysis,[3] as well as in liquid-phase organic reactions. The additivity of the σ^* was demonstrated by Taft,[4] and Leffler and Grunwald,[4a] hence the group contribution method should be applicable also for the extended estimation of the σ^*.

The reactivities of hydrocarbons have been extensively discussed with the simple LCAO-MO by Fukui.[5] On the other hand, many works have been reported concerning relations among σ, σ°, σ^+, and quantum chemical indexes.[6] In the present work, a correlation was also investigated between the Taft σ^* and $|C_r^N|$ determined by the simple LCAO-MO method for σ systems.[5]

Results and Discussion

Simple LCAO-MO Method. The absolute value of the coefficient, $|C_r^N|$, of a sp^3 hybridized orbital of an unpaired electron belonging to the non-bonding molecular orbital of an alkyl radical is reported to be correlated with the bond strength of R-H by Fukui *et al.*[7]: in their paper, the bond strength was given by $\Delta H_{C^+}(R_1)$, the enthalpy change in the hydride abstraction reaction from a paraffin, R_1H. The value of $\Delta H_{C^+}(R_1)$ has been suggested to have empirically a linear relation to σ^*.[3a] Thus, the value of σ^* may be correlated with the value of the above $|C_r^N|$ which is calculated by the simple LCAO-MO for σ electron systems.

The calculated values of $|C_r^N|$ are given in Table 1, where the values of Coulomb and resonance integrals were all taken from the paper by Fukui *et al.*,[7] and the calculation was carried out with a computation program named CHEMO-MO-2, which permits the chemical formula inputs.

1) I. Mochida and Y. Yoneda, This Bulletin, **40**, 2711 (1967).
2) R. W. Taft, in "Steric Effect in Organic Chemistry," ed. by M. S. Newman, Wiley, New York (1956), p. 591.
3) M. Kraus, *Advances in Catalysis*, **17**, 75 (1967). K. Kochloefl and V. Bazant, *J. Catalysis*, **8**, 386 (1967).
3a) I. Mochida and Y. Yoneda, *ibid.*, **7**, 386 (1967).
4) Ref. 2, p. 592.
4a) J. E. Leffler and E. Grunwald, "Rates and Equilibria of Organic Reactions," Wiley, New York (1964), p. 224; P. B. Wells, *Chem. Revs.*, **53**, 171 (1963).
5) K. Fukui, in "Molecular Orbitals in Chemistry, Physics, and Biology," ed. by Lowdin and Pullman, Academic Press, New York (1964), p. 513. in "Modern Quantum Chemistry," ed. by O. Shinanoglu, Academic Press, New York (1965), p. 49.
6) H. H. Jaffe, *J. Chem. Phys.*, **28**, 415 (1953); F. L. J. Sixma, *Rev. Trav. Chim.*, **72**, 673 (1953); M. J. S. Dewar and P. J. Griesdale, *J. Am. Chem. Soc.*, **84**, 3548 (1962); T. Fueno, T. Okuyama and J. Furukawa, This Bulletin, **39**, 569 (1966).
7) K. Fukui, H. Kato and T. Yonezawa, *ibid.*, **35**, 1475 (1962).

Table 1. Comparison of observed and calculated σ^*

		σ^* obs.[a]	σ^* calc.[b]	difference	$\lvert C_r^N \rvert$
1	CH_3	0	0[c]	—	0.8965
2	CH_3CH_2	−0.100	−0.098	−0.002	0.8789
3	n-C_3H_7	−0.115	−0.121	−0.006	0.8769
4	i-C_4H_9	−0.125	−0.143	0.018	0.8746
5	n-C_4H_9	−0.130	−0.130	0	0.8767
6	t-$C_4H_9CH_2$	−0.165	−0.166	0.001	0.8720
7	i-C_3H_7	−0.190	−0.196	0.006	0.8608
8	s-C_4H_9	−0.210	−0.218	0.008	0.8588
9	$(C_2H_5)_2CH$	−0.225	−0.241	0.016	0.8568
10	t-$C_4H_9(CH_3)CH$	−0.280	−0.264	−0.014	0.8539
11	t-C_4H_9	−0.300	−0.293	−0.007	0.8422
	n-C_5H_{11}				0.8766
	n-C_6H_{13}				0.8766
12	$(C_6H_5)_2CH$	0.405	0.400	0.005	0.8445
13	$C_6H_5CH_2$	0.215	0.200	0.015	0.8711
14	$C_6H_5(CH_3)CH$	0.110	0.102	0.008	0.8524
15	$C_6H_5(C_2H_5)CH$	0.04	0.079	−0.039	0.8504
16	$C_6H_5(OH)CH$	0.765	0.760	0.005	—
17	$(OH)CH_2$	0.555	0.560	−0.005	—

a) From Ref. 2. b) By the group contribution method. c) By definition.

The correlation is very fine for alkyl groups whose σ^* values are known, as shown in Fig. 1. Thus, σ^* is empirically given by Eq. (1),

$$\sigma^* = -5.16 + 5.75|C_r^N|. \quad (1)$$

However, the correlation with groups containing π-electrons or heteroatoms is poor, some examples of which are also given in Fig. 1.

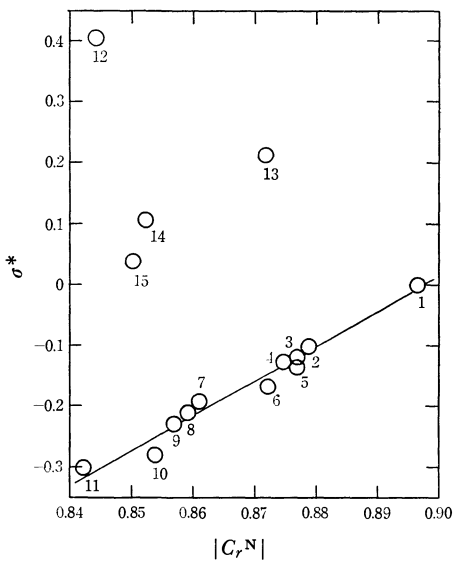

Fig. 1. A correlation between $|C_r^N|$ and σ^*. Numbers refer to Table 1.

Group Contribution Method. The principle of the group contribution method[1] for the calculation of σ^* is mathematically expressed by Eq. (2) with a methyl group as the base group,

$$\sigma^*(R) = \sigma^*(CH_3) + \sum n_i Z(X_i) \quad (2)$$

where $\sigma^*(R)$ is the Taft σ^* of a group R, $\sigma^*(CH_3)$ is that of a methyl group defined to be zero, $Z(X_i)$ is the group contribution of the part-structure to σ^*, and n_i is the number of the equivalent substitutions. The values of $Z(X_i)$ for three kinds of methyl substitutions are considered: primary,*1 next-adjacent secondary and two-next secondary.*2 These values together with those of primary phenyl and primary hydroxyl substitutions were obtained by the method of least-squares from seventeen σ^* values in Table 1. They are shown in Table 2, where primary phenyl and hydroxyl groups substitute the primary methyl group.

Table 2. Contribution of the substituting groups

	Contribution	St. error
CH_3		
Primary	−0.098	0.004
Next-adjacent secondary	−0.023	0.004
Two-next secondary[a]	−0.009	0.017
Primary phenyl[b]	0.297	0.007
Primary OH[b]	0.658	0.012

a) Calculated from $CH_3CH_2CH_2CH_2$ alone.
b) Substituting the primary methyl group.

*1 For the estimation of the heats of formation of carbonium ions (Ref. 1), primary methyl substitutions were classified into three kinds, however, here only a kind is considered for them.

*2 In C_4-C_3-C_2-C_1- of n-butyl group, C_1 is the base group, C_2 is primary, C_3 is next-adjacent secondary, and C_4 is two-next secondary.

The value for two-next secondary methyl group has a comparatively large standard error, which should be due to its estimation from only one value of $\sigma^*(CH_3CH_2CH_2CH_2)$. It may be, however, not so far from the true value, because the calculated σ^* of an isopentyl group agrees sufficiently with the one estimated in Fig. 1 from $|C_r^N|$ of an isopentyl radical.*3 The contribution of the farther than two-next should be zero, which is indicated by $|C_r^N|$ of *n*-pentyl and *n*-hexyl radicals.

The agreement of the calculated σ^* with the observed ones is satisfactory, except for $C_6H_5(CH_3CH_2)CH$. Thus, the σ^* values of homologous groups can be estimated by Eq. (2). The validity of the group contribution cannot be established for other part structures because σ^* was not observed upon many groups which have equivalent substitutions.

The attenuation of the inductive effect by methylene group has been discussed.[4,8] As regards σ^*, Taft gave 1/2.8 to methylene group as the attenuation factor for some functional groups.[4] In the present paper, it will be discussed on all available data, based on the group contribution concept. Because the σ^* values of the groups having fluorine, chlorine, phenyl, propenyl, and methoxyl substituents at the various locations are known, the contribution of the substituents can be calculated by using $Z(X_i)$ already obtained. An example of the calculation is shown by the case of $CF_3CH_2CH_2$,

$$\sigma^*(CF_3CH_2CH_2) = \sigma^*(CH_3) + Z(\text{primary } CH_3) + Z(\text{next-adjacent secondary } CH_3) + 3W(F)_3 \quad (3)$$

where the suffix 3 of $W(F)_3$ is the length of the carbon chain. Thus, the contribution of F attenuated by three methylenes, $W(F)_3$, can be calculated. The results of the calculations are shown in Fig. 2, where the abscissa is the carbon chain length, *m*. As for methyl groups, the *Z* values in Table 2 are used as the *W* values. In the cases of fluorine, chlorine, and methyl group, linear relations are obtained, which are formulated as following,

$$W(X_i)_m = W(X_i)_0 \exp(-2.3\, a(X_i) \cdot m) . \quad (4)$$

The slopes of these linear relations, $a(X_i)$, give the attenuation effects of the one carbon chain for each functional group. The slopes are all about 0.43. Thus, the contribution of the functional group is diminished to about 1/2.7 for each carbon chain. As for phenyl group, the value for unattenuated point is out of the line and the slope is distinctly different from the others.

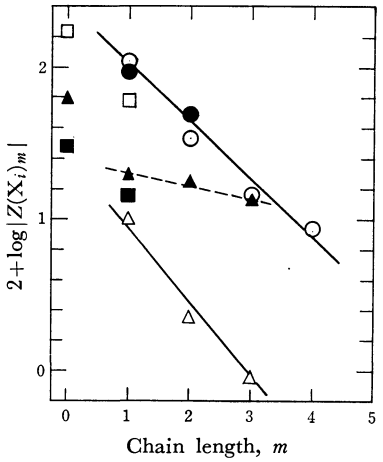

Fig. 2. The attenuation effect of methylene group for σ^*.
○: F, ●: Cl, ▲: Phenyl, △: Methyl
□: CH_3O, ■: $CH_3CH{=}CH$

TABLE 3. THE σ^* VALUES OF X_i CH=CH GROUPS

Group (X_i CH=CH)	σ^*[a]	$W(X_i)_0$ or $\sigma^*(X_i)$
trans-$O_2NCH{=}CH$	1.70	3.73[b]
trans-$Cl_3CCH{=}CH$	1.188	2.65
trans-$HOOCCH{=}CH$	1.012	2.84[c]
$ClCH{=}CH$	0.900	2.84[d]
trans-$Cl_2CHCH{=}CH$	0.882	1.94
$CH_2{=}CH$	0.653	0.490
$C_6H_5CH{=}CH$	0.420	0.600
$CH_3CH{=}CH$	0.360	0

a) From Ref. 2.
b) Calculated from $O_2NCH_2CH_2$.
c) Calculated from $HOOCCH_2$.
d) Calculated from $ClCH_2$.

An attenuation effect of the CH=CH group is studied on eight σ^* values shown in Table 3. The values of $W(X_i)_0$ are the observed or calculated $\sigma^*(X_i)$ by Eq. (4), of which $a(X_i)$ of the methylene group for various X_i is assumed to be 0.43. The calculation of the attenuation is made by the following equation,

$$\sigma^*(X_iCH{=}CH) = \text{const.} + a_{CH=CH}\ W(X_i)_0 \quad (5)$$

where the const. is the contribution of the CH=CH group and $a_{CH=CH}$ is its attenuation effect. The value of $a_{CH=CH}$ is statistically calculated as 0.29 ± 0.05. This figure means that the attenuation effect of CH=CH is smaller in comparison with that of two methylene groups.

If the attenuation effect is generally described, the application of the group contribution method for σ^* may be extended further.

*3 −0.132 from the $|C_r^N|$ value of 0.8764 and −0.139 by the group contribution method.

8) J. C. McGowan, *J. Appl. Chem.*, **10**, 312 (1960); K. Bowden, *Can. J. Chem.*, **41**, 2781 (1963); **43**, 3354 (1965).

Correlation of α-Asymmetric Carbon Atom of α-Methylglutaric Acid to Methyladipic Acid: a Correction

Ichiro KAWASAKI and Takeo KANEKO

Department of Chemistry, Faculty of Science, Osaka University, Toyonaka, Osaka

(Received January 11, 1968)

Previously, Kaneko *et al.* reported that (−)-α-methyladipic acid is considered to have the S-configuration on the basis of its synthesis from (−)-α-methyl-γ-butyrolactone, which configuration was correlated with S(−)-methylsuccinic acid.[1] Recently, however, Turner *et al.* showed that (−)-α-methyladipic acid must have the R-configuration because R(−)-α-methylglutaric acid, R(+)-β-methyladipic acid and (−)-α-methyladipic acid were isolated from the oxidation products of cytochalasin A and B, metabolites of *Helminthosporium dematioideum*.[2]

In order to confirm the configuration by an unequivocal process, the stereochemical relation between methyladipic acid and α-methylglutaric acid, absolute configuration of which was already known,[3] was established directly by the Arndt-Eistert synthesis of optically active α- and β-methyladipic acid from the ester chloride of α-methylglutaric acid. Treatment of S(+)-α-methylglutaric anhydride with methanol and then with thionyl chloride afforded the methyl ester chloride, which gave diazoketones with the treatment of ethereal diazomethane. The diazoketones were rearranged with silver benzoate as a catalyst in methanol to give a mixture of α- and β-methyladipic ester, which were separated into (+)-α- and S(−)-β-methyladipic ester[4] by vapor phase chromatography.

It is evident, therefore, (−)-α-methyladipic acid should have R-configuration as pointed out by Turner *et al.* The incorrect assignment presented in our previous paper was probably due to the very small optical rotation of α-methyladipic acid, decreased by the racemization occurred at the condensation of optical active ethyl γ-chloro-α-methylbutyrate with diethyl malonate.

Experimental

S(+)-α-Methylglutaric Acid. This compound was obtained by the resolution with the aid of strychnine,[5] mp 81°C; $[\alpha]_D^{15}$ +22.3° (*c*, 5.38 in abs EtOH).

S(+)-α-Methylglutaric Anhydride. (+)-α-Methylglutaric acid (4.3 g) afforded 3.4 g of the anhydride (93%), bp 112—114°C/2 mmHg, mp 56°C.[5]

Methyl Hydrogen α-Methylglutarate. To the above anhydride (3.4 g) was added methanol (0.9 g). The solution was heated on the water bath for 30 min and then distilled at 93—103°C/1 mmHg to give 4.1 g of the half ester (94%).

Methyl Ester Chloride of α-Methylglutaric Acid. A mixture of above half ester (4.1 g) and thionyl chloride (12 m*l*) was warmed at 50°C for 30 min and then distilled at 110—114°C/20 mmHg to give 3.6 g of the ester chloride (79%).

Dimethyl Methyladipate. The ester chloride (3.6 g) was converted into the diazoketone by means of diazomethane in ether solution. After standing for 3 hr, excess diazomethane and ether was removed. The residue was dissolved in absolute methanol (30 m*l*) and a mixture of silver benzoate (0.5 g) and trimethylamine (4.5 m*l*) was added to the solution with stirring. After a gentle evolution of gas a vigorous reaction occurred. The mixture was heated under reflux for 30 min. The catalyst was then filtered off, and the filtrate was evaporated. After the residue was dissolved in ether, the solution was washed with sodium carbonate solution and dried. The solvent was removed and the residual oil was distilled at 65—73°C/0.1 mmHg; yield, 2.95 g (79% from the ester chloride).

Separation of α- and β-Methyladipic Ester. The mixture of above ester was separated into dimethyl α- and β-methyladipate by vapor phase chromatography in a Varian Aerograph Model A-700 using a column (3/8 inch × 20 ft aluminum column) packed with 20% carbowax 20 M on chromosorb W with a helium as carrier gas at 200°C.

First fraction gave dimethyl (+)-α-methyladipate which was identical with authentic specimen in IR spectra; $[\alpha]_D^{23}$ +13.5° (*c*, 1.48 in EtOH), NMR; 1.12 ppm (doublet J=7 cps). From which (+)-α-methyladipic acid was obtained by acid hydrolysis and recrystallised from benzene, mp 81—83°C; $[\alpha]_D^{23}$ +13.8° (*c*, 1.91 in EtOH).

Found: C, 52.62; H, 7.57%. Calcd for $C_7H_{12}O_4$: C, 52.49; H, 7.55%.

Second fraction gave dimethyl (−)-β-methyladipate which was identical with authentic specimen in IR spectra; $[\alpha]_D^{23}$ −2.5° (*c*, 1.18 in EtOH), NMR; 0.95 ppm (doublet J=6 cps). From which (−)-β-methyladipic acid was obtained by acid hydrolysis and recrystallised from benzene, mp 86—87°C; $[\alpha]_D^{23}$ −3.4° (*c*, 2.75 in EtOH).

Found: C, 52.60; H, 7.51%.

1) T. Kaneko, K. Wakabayashi and H. Katsura, This Bulletin, **35**, 1149 (1962).
2) Dr. W. B. Turner's personal communication, and D. C. Aldridge, J. J. Armstrong, R. N. Speake and W. B. Turner, *J. Chem. Soc.*, (*C*), **1967**, 1667.
3) E. J. Eisenbraun and S. M. McElvain, *J. Am. Chem. Soc.*, **77**, 3383 (1955).
4) N. von Braun and E. J. Eisenbraun, *Ber.*, **59**, 1091 (1926).
5) E. Berner and R. Leonardsen, *Ann.*, **538**, 1 (1939).

Reaction of *cis*-1,4-Hexadiene with Iron Pentacarbonyl

Jitsuo KIJI*1 and Masao IWAMOTO

Central Research Lab., Toyo Rayon Company, Ltd., Sonoyama, Otsu

(Received January 13, 1967)

Nonconjugated dienes, such as 1,4-pentadiene and 1,5-hexadiene, react with iron pentacarbonyl ($Fe(CO)_5$) to give diene-iron tricarbonyl complexes, in which the ligand is an isomeric conjugated hydrocarbon.[1] Recently, *cis*-1,4-hexadiene has been easily obtainable by the reaction of butadiene with ethylene using a cobalt catalyst.[2] It is of interest now to study the migration of double bonds and to compare the structure of the ligand with that of free diene. The present paper is concerned with the reaction of *cis*-1,4-hexadiene with $Fe(CO)_5$.

The reaction of this hydrocarbon with $Fe(CO)_5$ affords the *trans*-1,3-hexadiene-iron tricarbonyl complex (I), plus a small amount of the *trans,trans*-2,4-hexadiene complex(II). The reactions were carried out in a stainless steel autoclave. The results are summarized in Table 1, in which the results obtained by the reactions of 1,3-hexadiene and 2,4-hexadiene are also included. The results of the elemental analysis of the complex obtained from 1,4-hexadiene were as follows; Found: C, 49.3; H, 4.8%. Calcd for $C_9H_{10}FeO_3$ ($(C_6H_{10})Fe(CO)_3$):

Table 1. Reactions of hexadiene with $Fe(CO)_5$

No.	$Fe(CO)_5$ mol	Hexadiene isomer (mol)	Temp. °C	Time hr	Product g	Composition of hexadiene (%)					
						The liganded diene		The recovered diene			
						1,3-	*trans,trans*-2,4-	1,3-	*cis*-1,4-	*trans,trans*-2,4-	*trans,cis*-2,4-
1	0.075	1.4—(0.13)	120	20	0.9	60	40	1.5	81.9	9.4	7.2
2	0.11	1.4—(0.13)	130	24	4.3[e]	70	30	5.2	2.0	59.0	33.8
3	0.11	2.4[a]—(0.13)	170	20	3.5[d]	n.d.			n.d.		
4	0.033	1.3[b]—(0.038)	150	24	2.7[e]	92	8	54.5	—	45.5	—

a) Prepared by isomerization of *cis*-1,4-hexadiene with $CoCl_2[(C_6H_5)_2PCH_2CH_2P(C_6H_5)_2]_2$-$(C_2H_5)_3Al$ catalyst; Composition of the isomers; *trans,trans*- 5%, *trans,cis*- 65%, *cis,cis*- 30%.
b) Prepared by the reaction of butadiene with ethylene using $Co(C_5H_7O_2)_3$-$(C_2H_5)_3Al$ catalyst and purified by a preparative chromatography. Purity 92%.
c) 67—70°C/6 mmHg. d) 73—74°C/7 mmHg. e) 80—82°C/8 mmHg.

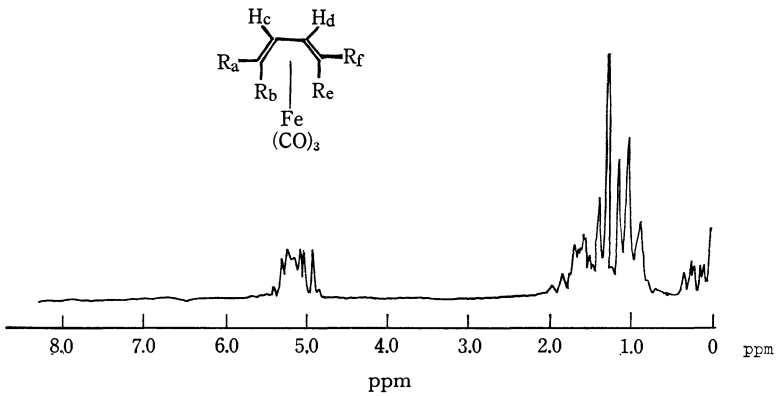

Fig. 1. NMR spectrum of the complex.
I: R_a, R_b, and R_e=H, R_f=C_2H_5. II: R_b and R_e=H, R_a and R_f=CH_3.

*1 Present address: Department of Synthetic Chemistry, Faculty of Engineering, Kyoto University, Kyoto.

1) R. West and F. G. A. Stone, ed., "Advances in Organometallic Chemistry." Vol. 1, Academic Press, New York (1964), p. 13.
2) M. Iwamoto and S. Yuguchi, This Bulletin, **41**, 150 (1968).

C, 48.6; H, 4.5%. The NMR spectrum is shown in Fig. 1. The multiplets centered at 5.1 and 0.2 ppm were assigned to the olefinic protons of I, and that at 5.0 ppm, to that of II.[3] The absence of the peaks in the 2—3 ppm range shows that the *cis*-1,3-hexadiene complex (III) and the *trans,cis*-2,4-hexadiene complex (IV) were not formed.

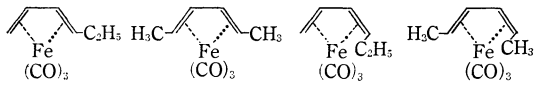

(I) (II) (III) (IV)

To examine the structure of the liganded dienes, an ethereal solution of the complex was treated with an excess 10% aqueous solution of ferric chloride at 0°C for 3 hr.[4] After it had been washed with water, the ethereal solution was gas-chromatographically analyzed. (Apiezon Grease L; column, 5 m; 100°C). *trans*-1,3-Hexadiene and *trans,trans*-2,4-hexadiene were detected (Table 1), with the former predominant. The reaction of $Fe(CO)_5$ with an isomeric mixture of 2,4-hexadiene (the *cis,trans*-isomer was predominant) gave II as the sole product.*2 The compositions of the hexadiene recovered as unreacted hydrocarbon are also shown in Table 1; it was indicative that 1,4-hexadiene was catalytically isomerized to the conjugated dienes with $Fe(CO)_5$. The fact that a considerable amount of *trans,trans*-2,4-hexadiene was found in both the unreacted dienes and the liganded dienes shows that *cis-trans* isomerization occurred during the reaction with $Fe(CO)_5$. The isomerization by $Fe(CO)_5$ proceeded so as to favor the end products lacking *cis*-substitutions, though the isomerization of *cis*-1,4-hexadiene with a carbanion (*e. g.*, $CH_3SOCH_2^-$ at 50°C) or a Ziegler catalyst (*e. g.*, $CoCl_2(DPE)_2$*3-Et_3Al, at 150°C) gave an isomeric mixture containing *trans, cis*-2,4-hexadiene as the main component.

3) G. F. Emerson, J. E. Mahler, R. Kochhar and R. Pettit, *J. Org. Chem.*, **29**, 3620 (1964).

4) H. W. Whitlock, Jr., and Y. N. Chuah, *Inorg. Chem.*, **4**, 424 (1965).

*2 It has been reported (*cf.* Ref. 3) that *cis,trans*-2,4-hexadiene reacts with $Fe(CO)_5$ at 110°C to yield *cis,trans*-2,4-hexadiene-iron tricarbonyl (yield, 6%).

*3 DPE: $(C_6H_5)_2PCH_2CH_2P(C_6H_5)_2$

SHORT COMMUNICATIONS

Transacylation from Acid Amides to Amines Catalyzed by Carbon Dioxide

Yoshio OTSUJI, Noboru MATSUMURA and Eiji IMOTO

Department of Applied Chemistry, Faculty of Engineering, University of Osaka Prefecture, Sakai-shi, Osaka

(Received January 18, 1968)

We wish to report our recent finding that certain acid amides undergo transacylation to amines when a mixture of the two compounds is simply heated in the presence of carbon dioxide.

A typical experiment for the transformylation from dimethylformamide (DMF) to amines was carried out as follows: a mixture of 10 g of *n*-butylamine in 50 m*l* of DMF was warmed at 60°C for 5 hr under a stream of dry carbon dioxide, and then the solvent, DMF, was evaporated under reduced pressure. The distillation of the residue gave 6.4 g (46%) of *N*-butylformamide, bp 107—109°C/3 mmHg. A similar transformylation from DMF was observed in *n*-tetradecylamine (66%), piperidine (48%), and morpholine (67%), giving the corresponding *N*-formyl derivatives in the yields indicated in the parentheses. These reactions did not occur in the absence of carbon dioxide. Aromatic amines such as aniline and tertiary amines such as pyridine were not formylated by this method.

Transacylation from acetamide or cyanoacetamide to amines was also attempted by heating a mixture of the amide and amine in dioxane under a stream of carbon dioxide. The transcyanoacetylation from cyanoacetamide took place in both *n*-hexadecylamine and *n*-hexylamine, giving *N*-*n*-hexadecylcyanoacetamide (63%) and *N*-*n*-hexylcyanoacetamide (37%) respectively. On the other hand, the transacetylation from acetamide took place only in *n*-hexadecylamine, giving *N*-*n*-hexadecylacetamide (6%).*1 The attempt at transacetylation from *N*,*N*-dimethylacetamide to amines was unsuccessful.

These results indicate that the reactivity of the amides for transacylation to amines decreases in the order: DMF>cyanoacetamide>acetamide>*N*,*N*-dimethylacetamide. This order of reactivity would seem to show that the ability of the amides to transacylate decreases with a decrease in the positive charge on the carbonyl carbon atom of the amides.

All of the results presented here might be explained in terms of the following mechanism:

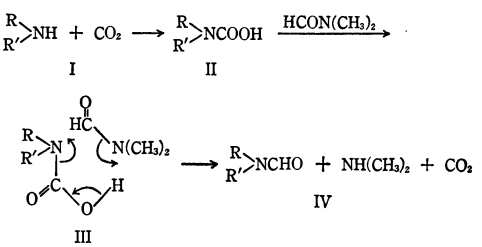

R: alkyl, R: alkyl or H

The amine (I) reacts with carbon dioxide to produce the corresponding carbamic acid (II), which itself subsequently reacts with DMF to form an intermediate (III). This intermediate III spontaneously collapses to the product (IV), ejecting carbon dioxide and dimethylamine. At this stage of the reaction the nucleophilic reactivity of the amine may be enhanced to some extent, because the temporary formation of an amide ion would be expected at the moment of the elimination of carbon dioxide and a proton which is taken up by the amino nitrogen of formamide.

A similar mechanism would operate in the other transacylation reactions. It is interesting to point out that carbon dioxide, which is an inert gas, might be able to play an important role in some chemical reactions such as those reported in this communication. In this connection, it is also noteworthy that carbon disulfide acts as an effective dehydrating reagent in the formation of pyrophosphates from phosphates.[2]

*1 The long-chain aliphatic amines such as *n*-hexadecylamine are known to react readily with carbon dioxide to form the stable carbamic acid.[1] This seems to be a reason for the relatively high reactivity for the transacylation from acid amides to *n*-hexadecylamine.

1) R. Goto, A. Watanabe, K. Hojo and M. Kosaka, *Nippon Kagaku Zasshi (J. Chem. Soc. Japan, Pure Chem. Sect.)*, **87**, 1220 (1966).

2) R. E. Atkinson and F. I. G. Cadogan, *J. Chem. Soc. (C)*, **1967**, 1356.

A Simple Electron Source for Impact Experiments

Kogoro MAEDA

Electrotechnical Laboratory, Tanashi P.O., Tokyo

(Received January 23, 1968)

A narrow energy width is necessary in the bombarding electron beam to derive useful information on the energy levels of a molecule from the ionization efficiency curve, and several techniques were proposed for the purpose. Amongst them the RPD method by Fox[1] and the electrostatic filter utilized first by Clarke[2] have been used widely in many laboratories. But the methods require some expensive and delicate devices, and they are sometimes not practical.

A hair-pin type filament is proposed for the purpose in the present note. A tungsten filament of 0.125 mm in dia. had a V shape with an angle about 60° and a tiny slice of the same metal was tipped at its point. The ion source was simply composed of the tungsten filament and a gold-plated cylindrical cage (8.5 mm dia. and 15 mm length) with an electron entrance aperture (1 mm dia.) and a trap at each side. No other electrode was used to narrow the energy spread it the electron beam. Ions produced by the beam were extracted through the system of electrodes of extractor and field adjuster around the cage, and then introduced to an analyzer after collimation by an intermediate electrode. Mass analysis of the ions was made by a quadrupole mass filter, which corresponds to no usage of auxiliary magnet for the bombarding electron collimation.

Samples used for the test were rare gases, Ne, Ar, Kr and Xe, and two hydrocarbons, CH_4 and C_2H_4. The sample was introduced at a pressure of $(3—6)\times10^{-5}$ Torr into the system, and intensity of the bombarding electron beam was set at about $(1—2)\times10^{-8}$ A. Ion current of the order of $10^{-12}—10^{-14}$ A was obtained at about 1V above the ionization potential with a multiplier in the mass filter system.

The results obtained in the efficiency curves are all in good agreement with those of the RPD or other methods. In the case of Kr, distinct changes in the slope of the curve are observed, which probably correspond to the states $^2P^\circ_{3/2}$ and $^2P^\circ_{1/2}$[3] (see Fig. 1). At least three breaks were also observed for CH_4^+ in the case of methane, at

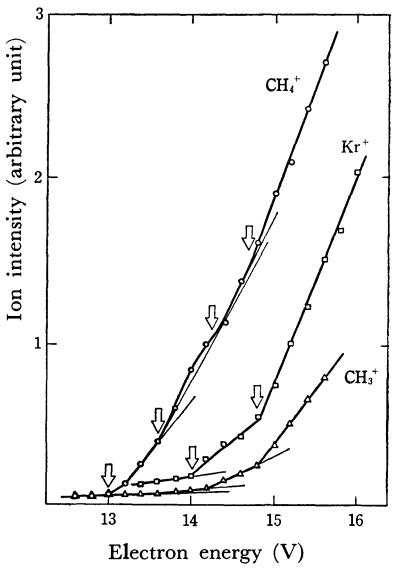

Fig. 1. Ionization efficiency curves for Kr^+ and for CH_4^+ and CH_3^+ from methane.
Sample pressure: $5—6\times10^{-5}$ Torr
Bombarding current: $1.5—2\times10^{-8}$ A.

0.6 V, 1.2 V, and 1.7 V above the ionization threshold. The result is also shown in Fig. 1, together with the results of CH_3^+. These features in the curves are almost the same with the results by the RPD method.[4] Ethylene also gave the same results with the RPD method, *i.e.*, breaks were found at 0.6 V, 1.2 V and 2.0 V above the ionization potential[4], and the difference of the appearance potentials of $C_2H_2^+$ and $C_2H_3^+$ was observed with a value about 0.4 V.

The obtained results show the present simple method is sufficiently good for obtaining the ionization efficiency curve with some structure. It might not be applicable for precise experiments, but practical enough compared with the RPD method because it requires no complicated electronic circuit and no delicate operation, nevertheless gives the adequate resolution. The width of the electron energy is now under measurement and details of the experiments will be presented in subsequent publications.

1) R. E. Fox, W. M. Hickam, T. Kjeldaas, Jr., and D. J. Grove, *Phys. Rev.*, **84**, 859 (1951).
2) E. M. Clarke, *Can. J. Phys.*, **32**, 764 (1954).
3) C. E. Brion, D. C. Frost and C. A. McDowell, *J. Chem. Phys.*, **44**, 1034 (1966).
4) C. E. Melton and W. H. Hamil, *J. Chem. Phys.*, **41**, 546, 1469 (1964).

Lateral Nitroxylation of Penta-alkylbenzenes

Hitomi SUZUKI, Kiyomi NAKAMURA and Kazuhiro MARUYAMA

Department of Chemistry, Faculty of Science, Kyoto University, Sakyo-ku, Kyoto

(Received January 25, 1968)

Nitrations of pentamethylbenzene have been reported to yield either nitropentamethylbenzene (I) or dinitroprehnitene (II).[1] However, the products were found not to be as simple as had generally been thought. Nitrations carried out at -10—$+5$°C by fuming nitric acid ($d=1.50$) in a variety of solvents, always gave, besides I, an appreciable amount of a non-crystallizable, syrupy substance, which, by careful chromatographic treatment on silica gel using light petroleum and benzene as eluants, could be separated into several side-chain substituted products. The main component (III) recrystallized from light petroleum melted at 45—46°C (Found: C, 63.06; H, 7.41; N, 6.69%. Calcd for $C_{11}H_{15}NO_3$: C, 63.14; H, 7.23; N, 6.69%) and showed strong infrared bands (in Nujol) at 1270 and 1636 cm^{-1} ($-ONO_2$); PMR peaks (in CCl_4) at 7.82 (2 CH_3), 7.77 (2 CH_3), 4.64 (CH_2) and 3.05 τ (aromatic H). The mixed acid converted III into II, so it was identified as 2,3,4,5-tetramethylbenzyl nitrate, the structure of which was further confirmed by synthesis from prehnitene through chloromethylation and by the subsequent treatment of the chloride with silver nitrate in acetonitrile. The other products were 2,3,4,5-tetramethylbenzyl alcohol, mp 81—82°C (Found: C, 79.76; H, 9.89%. Calcd for $C_{11}H_{16}O$: C, 80.44; H, 9.83%), probably formed by the hydrolysis of III; 6-nitro-2,3,4,5-tetramethylbenzyl nitrate, mp 100—101°C (Found: C, 52.03; H, 5.83; N, 10.94%. Calcd for $C_{11}H_{14}N_2O_5$: C, 51.96; H, 5.55; N, 11.02%), and 2,3,4,5-tetramethylbenzaldehyde (semicarbazone, mp 209—210 and 235—242°C*[1]; Found: C, 65.51; H, 7.88%. Calcd for $C_{12}H_{17}N_3O$: C, 65.72; H, 7.81%). The preferential attack by nitric acid on the side-chain rather than on the nuclear position becomes predominant with an increase in crowding around the ring. Thus, a similar treatment of pentaethylbenzene with fuming nitric acid gave a syrup, nearly half of which was found by means of a study of its PMR spectra to be composed of a nitrate. The chromatography of the syrup gave impure nitropentaethylbenzene (mp 86—90°C), a vinyltetraethylbenzene (IV), α-methyl-2,3,4,5-tetraethylbenzyl alcohol (mp 49—62°C), and a trace of a carbonyl compound. The last three compounds were doubtless the decomposition products of the unstable nitrate. The main product (IV), bp 103—104°C/2.5 mmHg (Found: C, 88.99; H, 11.22%. Calcd for $C_{16}H_{24}$: C, 88.82; H, 11.18%), had infrared bands at 888 (isolated ring H), 905, 989 and 1624 cm^{-1} ($-CH=CH_2$); PMR peaks at 8.69—9.02 (4 CH_3), 7.15—7.60 (4 CH_2), 4.83, 4.48 and 2.97 ($-CH=CH_2$; $J_{trans}=17.8$ cps; $J_{cis}=11.0$ cps; $J_{gem}=1.8$ cps), and 2.87 τ (aromatic H). Its structure was proved to be 2,3,4,5-tetraethylvinylbenzene by comparison with an authentic specimen prepared from 2,3,4,5-tetraethylacetophenone through the lithium aluminum hydride reduction and subsequent dehydration of the alcohol. This result differs from the earlier findings that the nitration of pentaethylbenzene mainly yielded *p*-dinitrotetraethylbenzene,[2] although the use of the mixed acid partly confirmed the latter results. The amounts of nitrous acid formed roughly paralleled the degree of side-chain substitution. Other mixed penta-alkylbenzenes were found to behave similarly.

The anomalous substitution may be explained by a process similar to that postulated for the side-chain chlorination of hexamethylbenzene;[3] *i. e.*, a process involving the initial attack of the nitronium ion on the open place of the ring, followed by the hyperconjugative release of a proton from the neighboring methyl group and the rearrangement of the unstable intermediate (V) to the benzyl nitrite, which may then further be transformed into the nitrate or decomposed into the aldehyde.[4]

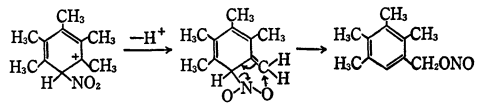

1) L. I. Smith and S. A. Harris, *J. Am. Chem. Soc.*, **57**, 1289 (1935); P. Kreienbuhl and H. Zollinger, *Tetrahedron Letters*, **1965**, 1739.

*1 The semicarbazone melted at 209—210°C to a liquid, which quickly solidified and remelted at 235—242°C with decomposition.

2) L. I. Smith and C. O. Guss, *J. Am. Chem. Soc.*, **62**, 2635 (1940).

3) E. Baciocchi, A. Ciana, G. Illuminati and C. Pasini, *ibid.*, **87**, 3953 (1965); also *cf.* P. B. D. de la Mare and H. Suzuki, *J. Chem. Soc. (C)*, **1967**, 1586.

4) R. G. Gillis, *J. Org. Chem.*, **21**, 805 (1956); also *cf.* D. H. R. Barton, G. C. Ramsay and D. Wege, *J. Chem. Soc. (C)*, **1967**, 1916.

On the Phase Transitions of 1,2-Dibromo-1,1,2,2-tetrachloroethane

Tsutomu KOIDE, Yoshihiko SAWAMURA and Tsutomu ODA

Laboratory of Physical Chemistry, the Osaka Kyoiku University, Tennoji, Osaka

(Received March 4, 1968)

The three solid phases of C_2Cl_6 have been well studied from the standpoint of crystal structure and molecular motion by the methods of X-ray diffraction,[1] heat capacity measurement,[2] nuclear quadrupole resonance,[3] *etc.* Similar studies have also been reported in the case of C_2Br_6.[4]

For the case of $BrCl_2C\text{-}CCl_2Br$, the interest is not only in the polymorphism[5] but in the isomerism between trans- and gauche-forms of the molecule in the solid state. From such standpoint, the polymorphism and the crystal structure are studied and the results will be described in this paper.

The material was prepared by bromination of tetrachloroethylene with bromine under the sun light.[6] Crude crystals were recrystallized three times from ethyl alcohol and sublimed twice at about 10^{-2} mmHg at about 50°C. The crystals melt at about 200°C in a sealed tube with decomposition.

A differential thermal analysis examination between about −190°C and about 230°C showed three phase transitions at 75, 101, and 108°C on heating. However, in the cooling direction transition occurred at 59, 99, and 105°C, indicating at large thermal hysteresis with regard to the lowest transition. The rate of temperature change was controlled to be at about 1/4 degree per minute.

The sample began to melt at about 200°C with decomposition, and the color of free bromine was observed.

The transition at 101°C was not reported by Gossner,[5] who described only two transitions at 80°C and at 108—109°C under a polarized microscope. Two transition temperatures, 75 and 108°C, agree with his optical results. Our reexamination of Gossner's experiment revealed that the transition at 101°C caused no detectable change in the optical properties, this explains the apparent discrepancy in the number of solid phase transitions reported. The solid phase above 108°C is optically isotropic.

The existence of these four solid phases was acertained also by X-ray diffraction method with powder samples.

The X-ray diffraction pattern of the phase above 108°C was consistent with a body-centered cubic lattice, the unit cell having a dimention of 7.7 Å at 130°C and containing two molecules (d_{cal}= 2.34 g/cc). This result suggests that the molecules undergo molecular rotation about the lattice points, taking the statistically high symmetry.

The lowest solid phase (IV), below 75°C, is orthorhombic with the crystal parameters a= 11.81, b=10.25, and c=6.51 Å, and these values are in accordance with the results given by Yardley.[7] The phase (III) in the temperature range of 75—101°C is of lower symmetry, possibly triclinic. The phase II between 101 and 108°C resembles the phase III but is different from the other three.

The crystal structure below 75°C will be studied in detail in future using single crystals.

1) C. D. West, *Z. Krist.*, **88**, 195 (1934); M. Atoji, T. Oda and T. Watanabè, *Acta Cryst.*, **6**, 868 (1953); Y. Sasada and M. Atoji, *J. Chem. Phys.*, **21**, 145 (1953).
2) K. J. Ivin and F. S. Dainton, *Trans. Faraday Soc.*, **43**, 32 (1947).
3) I. Tatsuzaki and Y. Yokozawa, *J. Phys. Soc. Japan*, **12**, 806 (1957).
4) G. J. Snaauw and E. H. Wiebenga, *Rec. trav. chim.*, **61**, 253 (1942).
5) B. Gossner, *Z. Krist.*, **38**, 151 (1904).
6) Nicodemus, *J. pract. Chem.* [2], **83**, 314 (1911).
7) K. Yardley, *Proc. Roy. Soc. London*, **A118**, 449 (1928).

An ESR Study of the Oxidation-Reduction Reaction of Piperidine with a Copper(II) Bis-dithiocabamate Complex

Hiroshi YOKOI and Taro ISOBE

The Chemical Research Institute of Non-Aqueous Solutions, Tohoku University, Katahira-cho, Sendai

(Received March 14, 1968)

Copper(II) ion, some copper(II) complexes and some copper proteins are known to undergo oxidation-reduction reactions with various organic compounds.[1] When piperidine is added to a solution of copper(II) bis-*N,N*-dialkyldithiocarbamate complex, the deep greenish-brown color of the complex in the solution disappears gradually. This is thought to bo due to the reduction of copper(II) ion to copper(I) ion in the complex by the strongly basic secondary amine, piperidine. The purpose of this work is to investigate the mechanism of the above oxidation-reduction reaction by detecting the unstable free radicals produced during reaction by an ESR technique. The ESR spectra were measured in solution below −70°C with a Hitachi K-band ESR spectrometer. The sample solution was a mixture of 1 vol of piperidine and 9 vol of 10^{-2}—10^{-3} M toluene solution of copper(II) bis-*N,N*-diethyldithiocarbamate complex. The ESR spectra obtained are shown in Figs. 1 and 2.

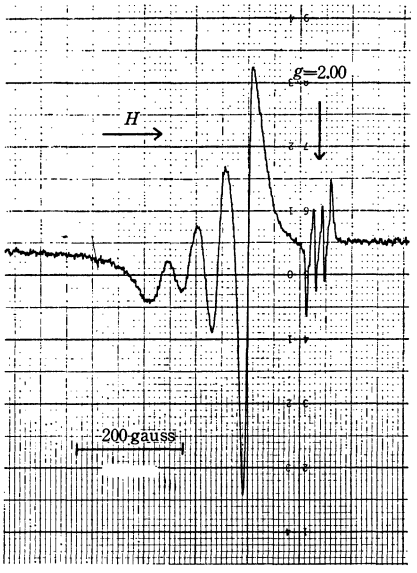

Fig. 1. The ESR spectrum (first derivative, 23808 Mc/s, at about −80°C) of the reaction mixture of piperidine and copper(II) bis-*N,N*-diethyldithiocarbamate in toluene.

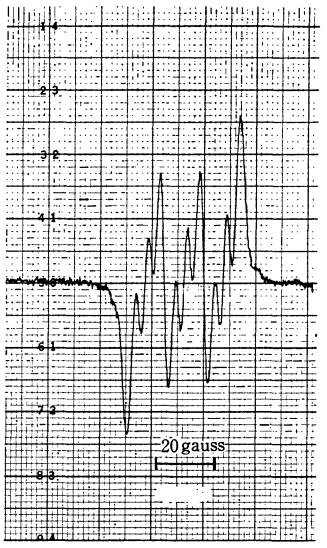

Fig. 2. The enlarged ESR spectrum of the free radical observed in the high field part of the spectrum in Fig. 1.

The ESR spectrum shown in Fig. 2 indicates that the spectrum was due to a free radical, and was composed of two triplets with intensity ratios of 1 : 1 : 1, whose hyperfine splitting constants were 17.6 gauss and 5.4 gauss. It is certain that the nitrogen of piperidine accounts for at least one of the triplets, and, therefore, that the initial step of the oxidation-reduction reaction is an electron transfer from the nitrogen lone pair of piperidine to the copper(II) complex. However, a definite conclusion on the structure of the free radical produced can not be safely drawn at this stage. The problem of investigating the mechanism of this type of oxidation-reduction reaction is very important from the standpoint of organic reactions, coordination chemistry and biochemistry. Interestingly, pyrrolidine and 2-methylpiperidine were also found to undergo a reaction similar to piperidine, but the ESR signals of their free radicals could not be so clearly detected.

Details, together with optical absorption spectral data, will be published elsewhere.

1) E. Frieden, "Horizons in Biochemistry," ed. by M. Kasha and B. Pullman, Academic Press, New York (1962), p. 461; T. E. King, H. S. Mason and M. Morrison (Editors), "Oxidases and Related Redox Systems," John Wiley & Sons, Inc., New York (1965), p. 207.

Red Chemiluminescence of Pyrene

Mizuka SANO and Fukuji EGUSA

Department of Chemistry, Faculty of Science, The University of Tokyo, Hongo, Tokyo

(Received March 26, 1968)

Light emission has been reported to occur by the reaction of aromatic hydrocarbon radical anions with various oxidants.[1,2] The emission thus produced has been interpreted as resulting from the formation of an excited singlet, since the spectrum of the emission corresponds to the normal fluorescence of the parent hydrocarbons. The electrical generation of a triplet has also been indicated for the explanation of a delayed electroluminescence in anthracene crystals,[3] and of a green emission from phenanthrene in solution.[4] We wish to report here the observation of a red emission, together with a blue emission during direct-current electrolysis of a solution of pyrene at room temperature.

Two platinum-wire electrodes separated from each other by about 1 cm were immersed into a 10^{-3} M solution of pyrene in anhydrous dimethylformamide, which included 10^{-3} M tetraethylammonium bromide as supporting electrolyte. When a direct-current voltage of about 7.5 V was switched on, a blue emission was detected on the electrode surface with negative polarity. The emission had extremely short duration, and then changed its color to red under the constant current passage. The blue emission was dim, but it was visually identified as the fluorescence of pyrene.

The red emission, on the other hand, was clearly visible in a dimly-lit room, and occurred continuously with a constant brightness as long as the constant current passed through. At the same time gas was evolved from a cathode, and the emitting species diffused upwards along streams of gas. When the applied voltage was turned off, the evolution of gas stopped immediately, but the emission continued to occur in a solution for more than 5 sec.

Pyrene is essential for the red emission because no red emission was observed at the same current when only supporting electrolyte and solvent were used, or when phenanthrene, perylene, *p*-quarterphenyl, 9,10-diphenylanthracene, or rubrene was used in place of pyrene. The possibility that the emission originated from a singlet state of dissolved oxygen was ruled out by the observation of the same emission from a carefully deoxygenated solution. The emission from oxygen, *e. g.*, the emission produced by the reaction of hydrogen peroxide with sodium hypochlorite in aqueous solution shows a different tint. The red emission was also observed by employing tetraethylammonium iodide or tetra-*n*-butylammonium bromide as supporting electrolyte. The applied voltage was far beyond the decomposition potentials of dimethylformamide and of supporting electrolyte, so that carbon monoxide would be evolved from a cathode,[5] and some kind of oxidant would be generated at an anode.

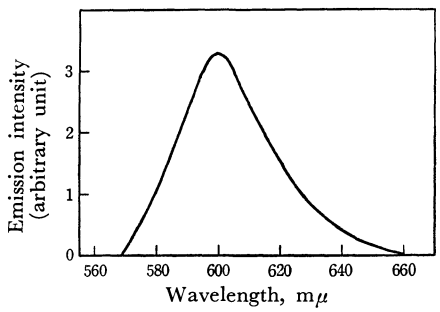

Fig. 1. Chemiluminescence spectrum of pyrene in dimethylformamide.

As shown in Fig. 1, the spectrum of the red emission recorded with a spectrophotometer was found to range from 570 to 660 mμ with a maximum around 600 mμ. This corresponds to the emission range of pyrene phosphorescence in rigid glass reported by Hochstrasser.[6]

From these observations, it is concluded that the red emission was derived from a pyrene molecule in a triplet state, resulting from the reaction of an electro-generated pyrene anion with an electrochemically generated oxidant.

1) E. A. Chandross and F. I. Sonntag, *J. Am. Chem. Soc.*, **86**, 3179 (1964); *ibid.*, **88**, 1089 (1966).
2) K. S. V. Santhanam and A. J. Bard, *ibid.*, **87**, 139 (1965).
3) M. Sano, M. Pope and H. Kallmann, *J. Chem. Phys.*, **43**, 2920 (1965).
4) A. Zweig, D. L. Maricle, J. S. Brinen and A. H. Maurer, *J. Am. Chem. Soc.*, **89**, 473 (1967).
5) S. Wawzonek, E. W. Blaha, R. Berkey and M. E. Runner, *J. Electrochem. Soc.*, **102**, 235 (1955).
6) R. M. Hochstrasser, *J. Chem. Phys.*, **40**, 1038 (1964).

Oxidation of Halomagnesium *sec*-Alkoxides to Ketones

Teruaki MUKAIYAMA, Katsuji TAKAHASHI and Isao KUWAJIMA

Laboratory of Organic Chemistry, Tokyo Institute of Technology, Ookayama, Meguro-ku, Tokyo

(Received April 1, 1968)

It is well known that alcohols are oxidized by carbonyl compounds such as acetone and cyclohexanone, in the presence of alminum alkoxide (Oppenauer Reaction).[1] It is expected from the above fact that aldehydes will be converted into ketones by oxidation of halomagnesium alkoxides, obtained from the reaction of aldehydes and Grignard reagents, with suitable dehydrogenating reagents.

This communication reports oxidation of halomagnesium alkoxides by the use of various dehydrogenating reagents such as *p*-quinone dibenzimide (I), *p*-quinone dibenzenesulfonimide (II), diethyl azodicarboxylate (III) and azodicarbonpiperidide (IV). When an equimolar amount of I in benzene was added dropwise to an ethereal solution of magnesium alkoxide, resulted by the reaction of phenylmagnesium bromide and benzaldehyde, at room temperature, bromomagnesium salt of *p*-phenylene dibenzamide deposited soon. The corresponding ketone, benzophenone, was produced in 58% yield after the reaction mixture was heated at 60—65°C for 1 hr. In a similar manner, bromomagnesium salts of 1-phenylpentanol and 1-phenyl-1-penten-3-ol, prepared by Grignard reaction, were converted into the corresponding aralkyl ketones. In the case of aliphatic alkoxide, however, the yield of the ketone was low and a large amount of tarry product resulted. For example, 3-octanone was produced in only 29% yield by treating the corresponding bromomagnesium alkoxide in benzene at 60—65°C for 3 hr.

Similar results were observed when bromomagnesium alkoxides were treated with II; the corresponding aromatic ketones were produced in fairly good yields, however, in the case of aliphatic ketone, the yield was comparatively low.

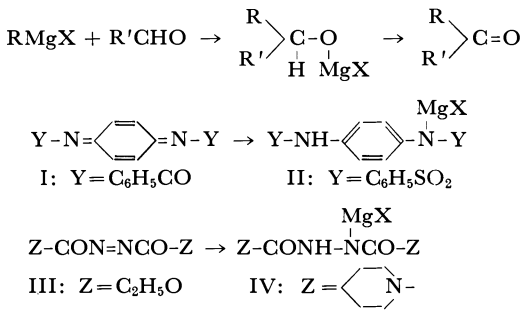

Next, it was found that aliphatic ketones were successfully prepared by treating the halomagnesium alkoxides with III, known to be a strong hydrogen abstracting reagent.[2] Treatment of butylmagnesium bromide with butyraldehyde, followed by the addition of diethyl azodicarboxylate under ice-cooling gave a brownish precipitate immediately. After keepting the reaction mixture to stand overnight at room temperature, 3-octanone was obtained in 66% yield. Similarly, 7-methyl-4-octanone, benzophenone and valerophenone were obtained in fairly good yields by treating the corresponding bromomagnesium alkoxide with the azo compound.

Furthermore, it was established that IV is also an effective dehydrogenating reagent in this type of reaction (see Table 1.)

Thus it can he noted that this procedure is a useful method for converting aldehydes to ketones *via* a Grignard route without isolating the intermediate alcohols.

TABLE I. THE REACTIONS OF HALOMAGNESIUM ALKOXIDES, PREPARED FROM GRIGNARD REAGENTS (RMgBr) AND ALDEHYDES (R'CHO), WITH OXIDANTS I—IV

Yields (%) of (a) ketones, RR'CO, and (b) the hydrogenated products of the oxidants

R	R'	I		II		III		IV	
		a	b	a	b	a	b	a	b
C_6H_5	C_6H_5	58	60	51	53	67	81	71	75
C_4H_9	C_6H_5	43	59	52	42	50	69	51	73
C_2H_5	$C_6H_5CH=CH$	45	52	62	75	66	87	35	73
C_4H_9	C_3H_7	29	52	15	21	66	82	53	64
i-C_5H_{11}	C_3H_7	—	—	—	—	65	71	67	81

1) C. Djerassi, "Organic Reactions," Vol. 6, John Wiley & Sons, Inc., New York, N. Y. (1951), p. 257.

2) F. Yoneda, K. Suzuki and Y. Nitta, *J. Org. Chem.*, **32**, 727 (1967).

Novel Dicyano Complexes of Cobalt(III)

Hiroaki NISHIKAWA, Kazuo KONYA and Muraji SHIBATA

Department of Chemistry, Faculty of Science, Kanazawa University, Marunouchi, Kanazawa

(Received April 8, 1968)

Mixed cyano complexes of cobalt(III) have been synthesized by the use of particular methods,[1] and it has been recognized that the reactions of familiar complexes of cobalt(III), such as those of the luteo or praseo type, with cyanides in an aqueous solution are usually unsuccessful when used for the synthesis of such mixed cyano complexes.

We have found a new method of preparing several mixed cyano complexes in which suitable complexes of cobalt(III) are treated with a suitable cyanide near 0°C in cold solvents containing activated charcoal. Here we wish to report the synthesis of $K[Co(CN)_2(acac)_2]$ (I) from tris(acetylacetonato)cobalt(III) in methanol by this new method, and also the synthesis of $[Co(CN)_2(acac)(P\phi_3)_2]$ (II) from (I) and $P\phi_3$. We have also studied the preparation of cobalt(III) complexes of cyanoammine or cyanodiamine series in an aqueous solution[2] by this method.

The treatment of a slurry of $Co(acac)_3$ in methanol with the calculated amount of powdered KCN in the presence of activated charcoal at −5—0°C for 4 hr gave a dark red solution. After the filtration and concentration of the reaction mixture at about 5°C, the concentrate was chromatographed on an alumina column in order to separate the (I) from the other substances. By the use of a methanol-ethanol mixture (2 : 1) as the eluant, several fractions were obtained.*1 From the third fraction, red crystals of (I) were obtained in a 20% yield; they were recrystallized from a solution of potassium acetylacetonate in a mixture of methanol and ethanol (3 : 1). Elemental analysis was undertaken after the substance had been dried for several hours in a vacuum at room temperature. Found: C, 41.09; H, 4.22; N, 7.76%. Calcd for $C_{12}H_{14}O_4N_2KCo$: C, 41.38; H, 4.05; N, 8.04%.

The complex I reacted readily with an excess of triphenylphosphine in boiling ethanol for one hour. After the evaporation of the solvent, the residue was extracted with small portions of boiling benzene and separated on an alumina column, using a mixture of benzene and acetone (5 : 1) as the eluant. From the second fraction*2 orange crystals of II were obtained. Found: C, 69.86; H, 5.45; N, 3.75%. Calcd for $C_{43}H_{37}O_2N_2P_2Co$: C, 70.30; H, 5.08; N, 3.81%.

The complexes I and II, having $Co(C)_2(O)_4$ and $Co(C)_2(O)_2(P)_2$ configurations respectively, are the first examples of compounds with such configurations. The IR spectra of I and II show sharp peaks at 2130 and 2100 cm^{-1} respectively, and strong peaks in the 1500—1600 cm^{-1} region, indicating the presences of the CN^- and the acetylacetonate groups. The PMR spectrum of (I) in CD_3OD shows that methyl protons of acetylacetone ions are not equivalent, exhibiting two sharp peaks (at 7.79 and 8.06 ppm) with the same intensity. This suggests the *cis*-configuration of the bisacetylacetonato complex.[3] The UV spectrum of (I) shows two absorption components at 57×10^{13} sec^{-1} ($\log\varepsilon$: 1.97) and *ca.* 70×10^{13} sec^{-1} ($\log\varepsilon$: *ca.* 2.45), while no component appears to be spin allowed in the longer-wavelength region. These features will be discussed in detail later. The PMR spectrum of II in $CDCl_3$ shows only one sharp peak of the CH_3 group, at 8.94 ppm. This suggests that the complex has the *trans*(C) or the *trans*-(P) configuration. The UV spectrum of II in dichloromethane shows a large absorption band with a distinct maximum in the visible region (at 63×10^{13} sec^{-1}, $\log\varepsilon$ 3.58, half width: 12×10^{13} sec^{-1}). No known triphenylphosphine complexes of cobalt(III) belonging to the Werner type have ever shown such a distinct maximum but only vague shoulders in the region of the ligand-field bands. The absorption data on II may be also useful for the determination of the position of the $P\phi_3$ molecule in the spectrochemical series. The complex I reacts readily with other phosphine derivatives; the detailed results will be reported elsewhere.

1) a) P. Ray and B. Sarma, *J. Indian Chem. Soc.*, **28**, 59 (1951). b) M. Shibata, M. Mori and E. Kyuno, *Inorg. Chem.*, **3**, 1573 (1964). c) H. Siebert, *Z. anorg. Chem.*, **327**, 63 (1964). d) K. Ohkawa, J. Fujita and Y. Shimura, This Bulletin, **38**, 66 (1965). e) H. Yoneda, T. Baba and M. Muto, *ibid.*, **40**, 1736 (1967).

2) Some results from the initial stage of the work of this series are in press. *Inorg. Chem.* (1968).

*1 The first fraction is green, while the second one is faintly violet.

*2 The first fraction, faintly grey, mainly contained $P\phi_3$.

3) R. D. Archer and B. P. Cotsoradis, *Inorg. Chem.*, **4**, 1583 (1965).

A New Bromoallene Alcohol. Its Isolation and Reaction

Fumio TODA, Takao KOMODA and Katsuhiko AKAGI

Department of Industrial Chemistry, Faculty of Engineering, Ehime University, Matsuyama

(Received April 15, 1968)

It has been postulated[1] that bromoallene alcohol II is an intermediate in the reaction of 1,1,4,4-tetraphenylbut-2-yne-1,4-diol (I) and phosphorus tribromide in acetic acid to give 2,2,5,5-tetraphenyl-3-bromodihydrofuran (IV) and 1,10,10-triphenylbenzofulvene (VI). We now wish to report the isolation and some reactions of a new bromoallene alcohol II.

The treatment of I with phosphorus tribromide in acetic acid at 0°C, followed by immediate decompostion with water, afforded 1,1,4,4-tetraphenyl-2-bromobuta-2,3-diene-1-ol (II) in a 35% yield, as colorless prisms (from ethyl acetate), mp 118.5—119.5°C. Found: C, 73.87; H, 4.37%; mol wt (Rast), 431. Calcd for $C_{28}H_{21}BrO$: C, 74.17; H, 4.64%; mol wt, 453. NMR: in $CDCl_3$, 2.75 (multiplet, 20 H) and 3.25 τ (singlet, 1H). UV: $\lambda_{max}^{dioxane}$, 290 mμ (ε, 27100). The UV spectrum was comparable to that of 1,1-diphenyl-3-bromopropadiene,[2] $\lambda_{max}^{dioxane}$, 280 mμ (ε, 21700). IR: 2.20×10^{-3} mol in 1 *l*. CCl_4, 3566 (νOH) and 1947 cm^{-1} (νC=C=C). The νOH band, at a lower frequencies than that of a usual *t*-alcohol, *ca.* 3620 cm^{-1},[3] shows the presence of intramolecular hydrogen-bonding, even though it is not clear whether allene or bromine is the electron-donating site.

The treatment of II in acetone with catalytic amounts of hydrobromic acid at room temperature for a few minutes gave IV[1] in a 53% yield. The reaction can be explained by the protonation of allene, followed by cyclization and deprotonation.

The action of equimolar amounts of phosphorus tribromide on II in acetic acid at room temperature for 30 min afforded IV and VI[1] in 14 and 80% yields respectively. Since the cyclization of tetraphenylbutatriene (V) to VI in acidic media has been well known,[4] the reaction leading to VI can be explained by assuming the formation of V as an intermediate. The transformation of II into V may be a similar reaction mode to that of I and phosphorus tribromide to give V.[5]

The treatment of II in acetone with catalytic amounts of conc. sulfuric acid at 50°C for a few minutes gave VIII in a quantitative yield, as red prisms, mp 160—161°C. Found: C, 77.20; H, 4.07%; mol wt (Rast), 420. Calcd for $C_{28}H_{19}Br$: C, 77.24; H, 4.37%; mol wt, 435. UV: $\lambda_{max}^{dioxane}$, 252 (24100), 295 (sh) (10600) and 368 mμ (ε, 14500). The UV spectrum was comparable to that of the chloro-analog of VIII.[6] The for mation of VIII may be explained by the intramolecular cyclization of the cation, VII, produced by the dehydroxylation of II.

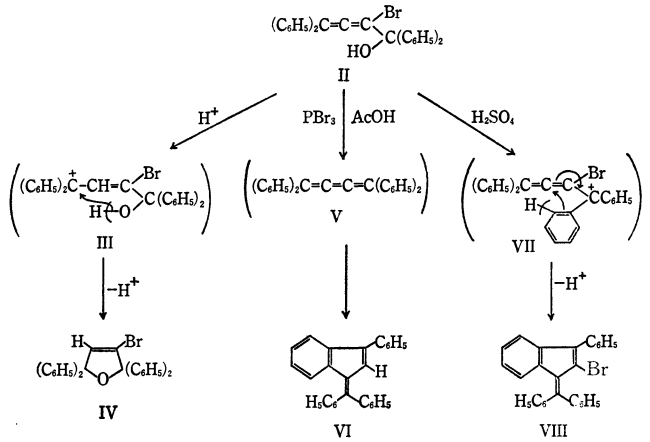

1) H. Tani and F. Toda, This Bulletin, **37**, 470 (1964).
2) P. Martinet and H. Doupeux, *Compt. rend.*, **261**, 2498 (1965).
3) K. Nakanishi, "Infrared Absorption Spectroscopy," Nankodo, Tokyo (1967), p. 36.
4) K. Brand and O. Horn, *Chem. Ber.*, **83**, 346 (1950).
5) J. Godineau, P. Cadiot and A. Willemart, *Compt. rend.*, **246**, 2499 (1958).
6) E. D. Bergmann, E. Fischer and J. H. Jaffe, *J. Am. Chem. Soc.*, **75**, 3230 (1953).

A New Route to Iodomethyl-substituted Methylpolysilanes[1]

Hideki SAKURAI, Mitsuo KIRA and Makoto KUMADA

Department of Synthetic Chemistry, Kyoto University, Sakyo-ku, Kyoto

(Received April 17, 1968)

In a previous communication,[2] we have described a new method of preparing methylthiomethyl-substituted silanes using a novel methylthiomethyl Grignard reagent. We wish to report the reaction of these methylthiomethylsilanes with methyl iodide leading to iodomethyl-substituted silanes.

(Methylthiomethyl)pentamethyldisilane (I) gave an expected sulfonium salt, $(Me_2S^+CH_2Si_2Me_5)\,I^-$, mp 98.5°C, when I was treated with methyl iodide in ether solution at room temperature. However, when I was refluxed in benzene with an excess amount of methyl iodide, (iodomethyl)-pentamethyl disilane, bp 79.5—80.0°C/17 mmHg, was obtained in 73.3% yield together with trimethylsulfonium iodide.

$$(CH_3)_3SiSi(CH_3)_2CH_2SCH_3 + CH_3I$$
$$\leftrightarrows [(CH_3)_3SiSi(CH_3)_2CH_2S^+(CH_3)_2]I^-$$
$$\rightleftarrows (CH_3)_3SiSi(CH_3)_2CH_2I + (CH_3)_2S$$
$$(CH_3)_2S + CH_3I \rightarrow [(CH_3)_3S^+]I^-$$

Many procedures for preparing carbon-functional silanes such as halogenations or other reactions with electrophiles[3] cannot be extended generally to higher polysilanes because of extensive silicon-silicon bond cleavage. Alternatively, nucleophilic substitutions on a silicon atom would be a preferred route to the carbon-functional organopolysilanes.[4] Therefore, the present procedure, methylthiomethylation of chlorosilanes followed by conversion to iodomethylsilanes, may be of value to open a new route to the iodomethyl-substituted silanes.

As another example was prepared 1,2-bis(iodomethyl)tetramethyldisilane, bp 113—116°C/8 mmHg, n_D^{20} 1.5820, d_4^{20} 1.7097. This compound has been once reported[5] but later disclosed to be a mixture of 1,2- and 1,1-bis(iodomethyl)tetramethyldisilane.[6]

Satisfactory analyses and NMR spectra were obtained for these compounds.

1) Presented in part at the 21st Annual Meeting of the Chemical Society of Japan, Osaka, Apr., 1968; Preprint, III, p. 1942.

2) H. Sakurai, M. Kira and M. Kumada, *Chem. Commun.*, **1967**, 889.

3) C. Eaborn, "Organosilicon Chemistry," Butterworths, London (1960), p. 377.

4) H. Sakurai, H. Yamamori and M. Kumada, *J. Org. Chem.*, **33**, 1527 (1968).

5) M. Kumada and M. Ishikawa, *J. Organometal. Chem.*, **1**, 411 (1964).

6) M. Kumada and M. Ishikawa, unpublished results.

The Substituent Effect on the Magnetic Interaction and d-d Bands in Dimeric Copper(II) Halide Complexes with Pyridine *N*-Oxides

Yoneichiro MUTO,* Michinobu KATO,** Hans B. JONASSEN*** and Koji KAKIUCHI*

* *Department of Chemistry, Saga University, Saga*
** *Aichi Prefectural University, Mizuho-ku, Nagoya*
*** *Department of Chemistry, Tulane University, New Orleans, La., U. S. A.*

(Received April 23, 1968)

In the previous papers,[1] we reported the correlation between the magnetic moments and d-d bands in dimeric copper(II) halide complexes with 3- or 4-substituted pyridine *N*-oxides. In these dimeric complexes, no correlation was observed between Hammett's constants and the magnetic moments or the d-d band positions. In order to elucidate why Hammett's rule is not obeyed in these complexes, we have now prepared copper(II) halide complexes with pyridine *N*-oxides with substituents in 2-, 3- and 4-positions on the pyridine ring and measured the magnetic susceptibilities and the reflectance spectra (*cf.* Table 1).

From the data in Table 1 the following conclusions about the substituent effect can be obtained: 1) For the same substituent group, the closer the site of substitution to the central metal ion is, the greater are the demagnetization and the blue shift of the d-d band. In the case of ethyl group, *e. g.*, these effects increase in the following order of substitution: 2->3->4-. It can also be seen that the difference between the λ_{max} of the d-d bands of 2- and 3-substituted complexes is fairly large, whereas the difference between those of 3- and 4-substituted complexes is small. 2) As for different substitutions at the same site (ethyl *vs.* methyl), the more bulky group has a greater demagnetization effect. This can also be observed in the greater demagnetization in the quinoline *N*-oxide complexes in comparison with pyridine *N*-oxide complexes.

These data seem to indicate that, in these dimeric complexes, the steric factor is more important in determining the extent of magnetic interaction or λ_{max} of d-d bands than the electronic effect.

The molecular framework model built up on the basis of the determined structure of the parent complex, $(CuCl_2 \cdot PyO)_2$,[2] indicates that, the ethyl groups attached in the 2 position of pyridine rings, which are almost perpendicular to the copper-oxygen plane, come above or below the plane to shield the fifth coordination sites of the copper ions. Such shielding of the coordination sites by chemically inert groups usually increases the tetragonality of complexes and the strength of the four coordinate bonds in the plane, as is seen in the unusual red color or the extremely large values of tetragonality ratio R of bis(*N*,*N*-dialkylethylenediamine)copper(II) complexes.[3] Therefore, it is very probable that, in the dimeric pyridine *N*-oxide complexes, the covalent bonding between the copper and the bridging oxygen atoms, through which the magnetic interaction occurs, is strengthened by the shielding effect of inert groups on the pyridine rings, and a much greater demagnetization or blue shift of d-d bands than expected from the electronic effect of the group is produced through it.

TABLE 1. MAGNETIC MOMENTS CORRECTED TO THOSE AT 25°C[a] AND d-d BANDS

Ligand	1 : 1 $CuCl_2$ Complex		1 : 1 $CuBr_2$ Complex	
	$\mu_{eff}^{25°C}$(B. M.)	λ_{max}(mμ)	$\mu_{eff}^{25°C}$(B. M.)	λ_{max}(mμ)
2-C_2H_5PyO[b]	0.32	763	0.31	765
3-C_2H_5PyO	0.46	810	0.37	812
4-C_2H_5PyO	0.59	820	0.41	820
2,4-$(CH_3)_2$PyO	0.37	765	0.35	760
QNO	0.33	733	0.33	735
4-CH_3QNO	0.40	750	0.33	745
i-QNO	0.51	810	0.43	807

a) *cf.* Ref. 1 b) PyO : Pyridine *N*-oxide c) QNO : quinoline *N*-oxide

1) Y. Muto, M. Kato, H. B. Jonassen and H. N. Ramaswamy, This Bulletin, **40**, 1535 (1967); M. Kato, Y. Muto and H. B. Jonassen, *ibid.*, **40**, 1738 (1967).
2) H. L. Schäfer, J. C. Morrow and H. M. Smith, *J. Chem. Phys.*, **42**, 504 (1965); R. S. Sager, R. J. Williams and W. H. Watson, *Inorg. Chem.*, **6**, 951 (1967).
3) S. Yamada and S. Miki, This Bulletin, **36**, 680 (1963); C. K. Jørgensen, "Biochemistry of Copper," ed. by J. Peisach, P. Aisen and W. E. Blumberg, Academic Press Inc., New York, N. Y. (1966), p. 1.

Studies of the Mechanism of the Isomerization of *n*-Butene over *p*-Toluene Sulfonic Acid by Means of Microwave Spectroscopy

Yuzo SAKURAI, Yoshihiro KANEDA, Shigeo KONDO, Eizi HIROTA
Takaharu ONISHI and Kenzi TAMARU

Department of Chemistry, The University of Tokyo, Hongo, Bunkyo-ku, Tokyo

(Received April 19, 1968)

Recently the microwave spectra of 1-butene, *cis*-2-butene and their deuterated species were successfully assigned. This presented a new powerful tool for studying the isomerization of butene, both *cis-trans* and double-bond migration over solid acids.

The monodeuterated species of 1-butene are designated as 1-d_1 ($CHD{=}CHCH_2CH_3$), 2-d_1 ($CH_2{=}CDCH_2CH_3$), 3-d_1 ($CH_2{=}CHCHDCH_3$), and 4-d_1 ($CH_2{=}CHCH_2CH_2D$), each of them giving different rotational spectra. As for *cis*-2-butene, however, there exist only two different monodeuterated species: 1-d_1 ($CH_2DCH{=}CHCH_3$) and 2-d_1 ($CH_3CD{=}CHCH_3$). The amounts and distribution of deuterium among each of the 1-butenes could be determined by measuring the relative intensities of the neighboring peaks of the species. In the case of *cis*-2-butene mass spectroscopy was also employed to determine the deuterium concentration, but the deuterium distribution or the relative amounts of 1-d_1 and 2-d_1 species could be determined only by means of microwave spectroscopy.

The isomerization of butene was carried out over *p*-toluene sulfonic acid (PTS) deposited on an equal amount of silica gel to get a greater surface area. The *p*-toluene sulfonic acid was pretreated with an amount of pure D_2O (99.8% or above) sufficient to deuterate its proton, and then it was evacuated at 50°C for 5 hr. This procedure was repeated three times to assure the complete deuteration of the PTS.

trans-2-Butene was isomerized over the deuterated PTS at room temperature for the purpose of studying both *cis-trans* isomerization and double-bond migration simultaneously.

The gas-chromatographic technique was employed to analyze the reaction mixture, and 1-butene and *cis*-2-butene were separated for microwave spectroscopic measurements in order to study the deuterium content and distribution. The results are summarized in the following tables.

Conversion to *cis*-2-butene from *trans*-2-butene	d_0	2-d_1	d_2
1.0%	51.3%	47.2%	1.5%
3.2	35.9	60.3	3.8
6.4	29.8	66.8	3.4
7.0	28.7	68.6	2.7
8.5	31.5	63.9	4.6
13.6	27.2	68.5	4.3
17.4	34.2	61.8	4.0

Conversion to 1-butene from *trans*-2-butene	3-d_1	2-d_1	d_0
0.20%	92.0%	6.0%	2.0%
0.58	85.5	7.5	7.0
0.75	78.4	13.1	8.5
1.00	75.3	14.7	10.0
2.86	67.1	20.9	12.0

The striking features of these results are as follows: 1) The amounts of the d_0 and 2-d_1 species of the *cis*-2-butene isomerized from *trans*-2-butene were approximately equal at the initial stage of the reaction. As the reaction proceeded, however, the 2-d_1 species predominated over the d_0 species, and the d_2 species, which was not detected at the initial stage, became appreciable, though its amount was not considerable at any time during the reaction. 2) The only 1-butene produced by the double-bond migration from *trans*-2-butene was the 3-d_1 species at the initial stage of the reaction; thereafter the relative concentration of the 3-d_1 species decreased continuously with the isomerization. The d_0 and 2-d_1 species, which could not be detected at the initial stage, appeared increasingly with the progress of the reaction.

The results thus obtained lead to the following reaction mechanism: the PTS behaves as a typical Brönsted acid, and the *cis-trans* isomerization of 2-butene over the PTS proceeds *via* the *s*-butyl carbonium ion, producing approximately equal amounts of the d_0 and 2-d_1 species of 2-butene, while the double-bond migration of 2-butene to 1-butene also takes place, taking a proton from the PTS at =CH– and giving it back to the PTS from the methyl group on the opposite side. The deuterated PTS acts as the reaction site, and the deuterium is replaced with a hydrogen on the reaction. These nondeuterated 1-butenes accordingly increase with the progress of the reaction; this is in accordance with the results obtained. Similarly, the 2-d_1 species of 1-butene produced may be interpreted to have been formed by the double-bond migration of the 2-d_1 of the *cis*-2-butene on the nondeuterated PTS.

The microwave spectroscopic measurements have thus been demonstrated to be capable of being use dsuccessfully in elucidating the reaction mechanism of the isomerization of *n*-butene.

BULLETIN OF THE CHEMICAL SOCIETY OF JAPAN VOL. 41 1497—1501 (1968)

Infrared Spectra and Stereochemistry of Bis-pyridine Complexes of Tin(IV)

Toshio TANAKA, Yoshio MATSUMURA and Rokuro OKAWARA

Department of Applied Chemistry, Osaka University, Suita, Osaka

and Yoshihiko MUSYA and Susumu KINUMAKI

Chemical Research Institute of Non-aqueous Solutions, Tohoku University, Katahira-cho, Sendai

(Received October 13, 1967)

Assignments are given for the infrared spectra of bis-pyridine complexes of SnX_4, $(CH_3)_2SnX_2$ (X=Cl, Br and I), and $(C_2H_5)_2SnCl_2$ in the 80—1610 cm^{-1} region. These complexes show the Sn-N stretching band near 200 cm^{-1}. Most pyridine vibrations shift to a higher or a lower frequency upon complex formation. Among these, the ν_{10}, in-plane ring deformation vibration is the most sensitive to the substituents on the tin atom as well as to the complex formation. Thus, the frequency may be a qualitative measure of the tin-pyridine coordination bond strength. The infrared spectra suggest a *cis*-configuration for the tin tetrahalide complexes and a distorted octahedral configuration for the dimethyltin diiodide complex. The remaining complexes may be assumed to have *trans*-alkyl and *cis*-halogen configurations.

It is well known that pyridine (Py) is a Lewis base which can coordinate to metal atoms or ions. For instance, it forms stable 2 : 1 adducts with SnX_4[1,2] and $(CH_3)_2SnX_2$[3] (X=Cl, Br and I), and a 1 : 1 adduct with $(CH_3)_3SnCl$.[4] Of these adducts, only $(CH_3)_3SnCl\cdot Py$ has been studied by X-ray crystallographic analysis; this analysis indicated that the adduct has a triangular bipyramidal structure, in which the pyridine molecule and the chlorine atom are located in the axial positions.[4] The infrared spectra of the tin(IV)-pyridine complexes have been described only for the CsBr region, in which tin-halogen and tin-carbon stretching vibrations are expected to be observed. For the $SnCl_4\cdot 2Py$ complex a *trans*-configuration has initially been assumed on the basis of the infrared study.[2] However, X-ray powder photographs showed that the complex is a crystal structure closely similar to that of $SnBr_4\cdot 2Py$, whose infrared spectrum, with three well-resolved Sn–Br stretching bands, indicates a *cis*-configuration.[3] On the other hand, the infrared spectra of $(CH_3)_2SnX_2\cdot 2Py$ (X=Cl, Br and I) have suggested *trans*-methyl and *cis*-halogen configurations.[3]

This paper will report on the assignments for the infrared spectra in the 80—1610 cm^{-1} region and the stereochemistry of bis-pyridine complexes of SnX_4, $(CH_3)_2SnX_2$ (X=Cl, Br and I) and $(C_2H_5)_2SnCl_2$; for the $(CH_3)_2SnI_2\cdot 2Py$ complex a distorted octahedral configuration is proposed; this is unlike that previously reported.[3]

Experimental

Preparation of Complexes. Bis-pyridine complexes of tin(IV) were prepared by reactions of the corresponding tin(IV) compounds with pyridine (mole ratio of about 1 : 2) in benzene, except for the case of the dimethyltin dibromide and diiodide complexes, which were synthesized in petroleum ether. Since the tin tetrahalide complexes are insoluble in common organic solvents, the precipitates resulting from the reactions were washed by petroleum ether until the pyridine smells had vanished. The dimethyltin dichloride complex was purified by sublimation under a reduced pressure, and the other three, by recrystallization from dichloromethane. The melting points and the analytical data are shown in Table 1.

Infrared Spectra. The spectra were recorded in Nujol and hexachlorobutadiene mulls using Hitachi EPI-2G (400—5000 cm^{-1}) and EPI-L (200—700 cm^{-1}) spectrophotometers, and in solid paraffin of a low melting point on a Hitachi FIS-1 vacuum spectrophotometer (80—500 cm^{-1}), all equipped with gratings. These spectrophotometers were calibrated with polystyrene film, CO_2 gas, and H_2O vapor.

Results and Discussion

Pyridine Vibrations. Assignments of the infrared spectra and a normal-coordinates analysis of pyridine and deuterated pyridines have been made by Long *et al.*[5,6] Using their results, the

1) I. R. Beattie, *Quart. Revs.*, **1963**, 382.
2) I. R. Beattie, G. P. McQuillan, L. Rule and M. Webster, *J. Chem. Soc.*, **1963**, 1514.
3) J. P. Clark and C. J. Wilkins, *ibid.*, **1966**, 871.
4) R. Hulme, *ibid.*, **1963**, 1524.
5) D. A. Long, F. S. Murfin and E. L. Thomas, *Trans. Faraday Soc.*, **59**, 12 (1963).
6) D. A. Long and E. L. Thomas, *ibid.*, **59**, 783 (1963).

TABLE 1. MELTING POINTS AND ANALYTICAL DATA OF BIS-PYRIDINE COMPLEXES OF TIN(IV)

Complex	Mp, °C	C% Anal. (Calcd)	H% Anal. (Calcd)	Sn% Anal. (Calcd)
$SnCl_4 \cdot 2Py$	300, decomp.	29.56 (28.66)	2.67 (2.38)	28.29 (28.34)
$SnBr_4 \cdot 2Py$	290, decomp.	20.36 (20.12)	1.85 (1.68)	19.70 (19.87)
$SnI_4 \cdot 2Py$	270, decomp.	15.72 (15.30)	1.77 (1.28)	14.64 (15.13)
$(CH_3)_2SnCl_2 \cdot 2Py$	162—163	38.40 (38.12)	4.22 (4.23)	
$(CH_3)_2SnBr_2 \cdot 2Py$	167.5—168	30.31 (30.88)	3.44 (3.46)	
$(CH_3)_2SnI_2 \cdot 2Py$	128, decomp.	25.90 (25.70)	2.99 (2.88)	
$(C_2H_5)_2SnCl_2 \cdot 2Py$	128—131	41.18 (41.40)	4.91 (4.92)	

infrared absorption bands related to the pyridine vibrations of bis-pyridine complexes of tin(IV) can easily be assigned, except for the ν_{17}, ν_{18}, and ν_{23} vibrations,*1 which are sometimes difficult to observe because of their weak intensities in the complexes. The observed frequencies of the pyridine vibrations and their probable assignments are given in Table 2.

As may be seen in Table 2, most pyridine vibrations shift to a higher or a lower frequency upon complex formation. It has already been indicated for the transition-metal complexes that the ν_{10} and ν_{27} vibrations undergo shifts to significantly higher frequencies upon the coordination of pyridine to metal,[7] and that the magnitude of these shifts depends on the stereochemistry of the complexes and on the metal atoms.[8] In the bis-pyridine complexes of tin(IV), the frequencies of ν_4, ν_9, ν_{10}, ν_{24}, and ν_{27} vibrations are sensitive to the substituents on the tin atom as well as to the complex formation; the most remarkable one is the ν_{10} vibration.

It has previously been described by the present authors, in reporting on the infrared spectra of $YZSn(acac)_2$*2 and $Y_2Z_2Sn \cdot 2DMSO$*2 (Y, Z= Cl, Br, I, alkyl and aryl), that the inductive effect of the substituents on the tin atom affects mainly the Sn–O coordination bond strength; the Sn–O stretching band shifts to a higher frequency with an increase in the electronegativity of the substituents on the tin atom.[9,10] This trend is not always clear in the Sn–N stretching frequency of the bis-pyridine complexes of tin(IV), probably because of its mixing with tin-halogen stretching vibrations, as will be described below. However, the ν_{10} vibration showed quite a similar tendency to the Sn–O vibrations of $YZSn(acac)_2$ and $Y_2Z_2Sn \cdot 2DMSO$, suggesting that the ν_{10} vibrational frequency may be used qualitatively as a measure of the bond strength of the tin-pyridine coordination bond. The ν_{27} vibration also shifted to a higher frequency with an increase in the electronegativity of the substituents on the tin atom, except for the diethyltin dichloride complex, which showed the band at an unexpected high frequency.

Skeletal Vibrations. Since the first-row transition metal-pyridine stretching vibration has been placed near 220 cm^{-1},[8] the tin-pyridine vibration might be expected to occur in a rather lower frequency region in view of mass considerations. Figures 1 and 2 show the far infrared

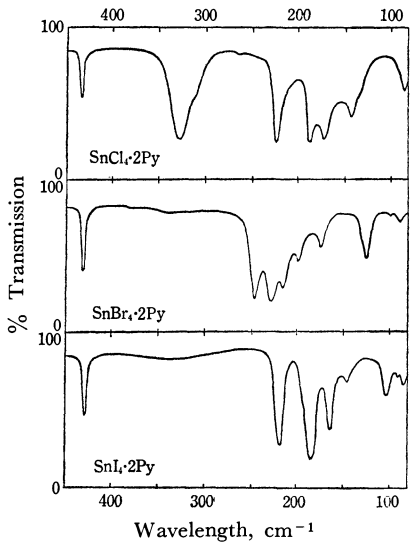

Fig. 1. Far infrared spectra of $SnX_4 \cdot 2Py$ (X= Cl, Br and I).

*1 The numbering of the vibrations follows that of Ref. 6.

7) N. S. Gill, R. H. Nuttall, D. E. Scaife and D. W. A. Sharp, *J. Inorg. and Nucl. Chem.*, **18**, 79 (1961).

8) R. J. H. Clark and C. S. Williams, *Inorg. Chem.*, **4**, 350 (1965).

9) Y. Kawasaki, T. Tanaka and R. Okawara, *Spectrochim. Acta*, **22**, 1571 (1966).

10) T. Tanaka, *Inorg. Chim. Acta*, **1**, 217 (1967).

*2 acac: Acetylacetonate; DMSO: Dimethylsulfoxide.

TABLE 2. OBSERVED FREQUENCIES AND ASSIGNMENTS FOR THE PYRIDINE VIBRATIONS OF BIS-PYRIDINE COMPLEXES OF TIN(IV), cm^{-1} a)

Assignments b)		Py c)	$SnCl_4 \cdot 2Py$	$SnBr_4 \cdot 2Py$	$SnI_4 \cdot 2Py$	$(CH_3)_2SnCl_2 \cdot 2Py$	$(CH_3)_2SnBr_2 \cdot 2Py$	$(CH_3)_2SnI_2 \cdot 2Py$	$(C_2H_5)_2SnCl_2 \cdot 2Py$
A_1	ν_4	1583 vs	1608 s	1605 s	1600 s	1602 s	1603 s	1603 s	1602 s
	ν_5	1482 s	1482m	1482m	1481m	1482m	1484m	1484m	1481m
	ν_6	1218 s	1208 s	1208 s	1208 s	1209 s	1210 s	1209 s	1209 s
	ν_7	1068 s	1062 s	1062 s	1061 s	1062 s	1062 s	1064 s	1063 s
	ν_8	1030 s	1042m	1038m	1034m	1036 s	1036 s	1037 s	1036 s
	ν_9	992 s	1018 s	1016 s	1011 s	1010 s	1010 s	1009 s	1006 s
	ν_{10}	605 s	644 s	641 s	634 s	627 vs	627 vs	626 vs	625 vs
B_1	ν_{13}	1572m	1571w	1570w	1570w	1572w	1572w	1573w	1570w
	ν_{14}	1439 vs	1449 vs	1447 vs	1444 vs	1448 vs	1446 s	1444 vs	1443 vs
	ν_{15}	1375w	1351 vw	1351 vw	1351 vw	1355 vw	1355 vw	1353 vw	?
	ν_{16}	1218 s	1208 s	1208 s	1208 s	1209 s	1210 s	1209 s	1209 s
	ν_{17}	1148 s	1155 vw (?)	1155 vw (?)	1153w	1154 vw (?)	1151w	1152m	1146m
	ν_{18}	1085 vw	1090 vw	1090 vw	1089 vw	?	1090 vw	1088 vw	?
	ν_{19}	652w	649 vw	648 vw	?	649 vw	648 vw	649 vw	649 vw
B_2	ν_{23}	942 vw	945w	942w	937w	?	946w (?)	939w	?
	ν_{24}	886 vw	863w	858w	858w	826 vw	875w (?)	?	886w (?)
	ν_{25}	749 vs	755 vs	753 vs	750 vs	756 vs 745 s	751 vs	751 vs	766 vs
	ν_{26}	700 vs	682 vs	682 vs	682 vs	698 vs 687 vs	692 vs	692 vs	707 vs 688 vs
	ν_{27}	405 s	432 s	431 s	428 s	423 s	423m	423m	427 s

a) vs: Very strong, s: Strong, m: Medium, w: Weak, vw: Very weak.
b) The ν_1, ν_2, ν_3, ν_{11}, and ν_{12} are C-H stretching modes and the ν_{20}—ν_{22} A_2 modes.
c) Ref. 6.

TABLE 3. OBSERVED FREQUENCIES FOR THE SKELETAL VIBRATIONS OF BIS-PYRIDINE COMPLEXES OF TIN(IV), cm^{-1} a)

$SnCl_4 \cdot 2Py$	$SnBr_4 \cdot 2Py$	$SnI_4 \cdot 2Py$	$(CH_3)_2SnCl_2 \cdot 2Py$	$(CH_3)_2SnBr_2 \cdot 2Py$	$(CH_3)_2SnI_2 \cdot 2Py$	$(C_2H_5)_2SnCl_2 \cdot 2Py$	Approximate descriptions
—	—	—	563m	560m	550m	531m	ν(Sn-C)
—	—	—	—	—	514 vw	480w	
324 vs	248 s	218m	245 s			218 s	ν(Sn-X)b) and ν(Sn-N)
305 sh	230 s	196 sh(?)	197m	193m	191m	206 s	
225 s	216m	183 s	173 s	160 s	147 s	180sh	
186 s	200m	163m					
168 s	174m	145w					
144m	123m	104m	146 s	135 s	133 s	131 sh	δ(skeletal)
136 sh	93w	82w	136 s	115 s	94m	126 s	
84m			98w	95w			

a) vs: Very strong, s: Strong, m: Medium, w: Weak, vw: Very weak, sh: Shoulder.
b) X: Halogen atoms.

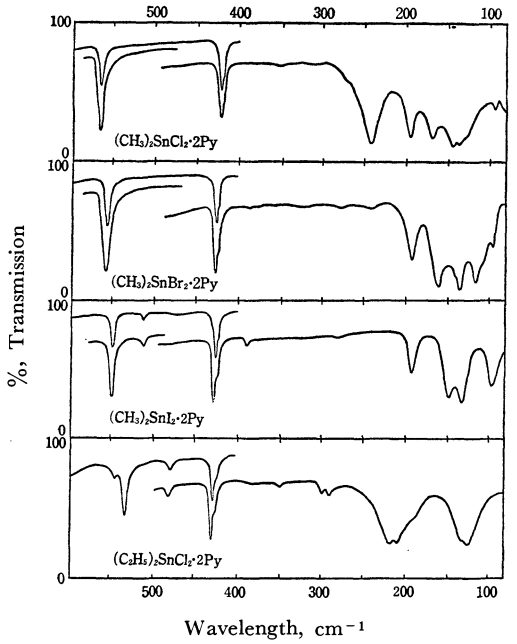

Fig. 2. Far infrared spectra of $(CH_3)_2SnX_2 \cdot 2Py$ (X=Cl, Br and I) and $(C_2H_5)_2SnCl_2 \cdot 2Py$.

spectra of bis-pyridine complexes of tin(IV). These complexes are considered to be non-ionic in the solid state.*3 Therefore except for the ν_{27} vibration of pyridine, the infrared spectra below 600 cm^{-1} may tentatively be assigned to skeletal vibrations around the hexa-coordinated tin atom, as is shown in Table 3. Among these, the bands of the dimethyltin and the diethyltin dihalide complexes in the 480—570 cm^{-1} range can undoubtedly be assigned to Sn–C stretching modes.

The three dimethyltin dihalide complexes showed a medium-intense band at 190—200 cm^{-1}. These frequencies decrease with a decrease in the electronegativity of the substituents on the tin atom, which is a similar trend to that of the Sn-O stretching frequencies of $YZSn(acac)_2$[9] and $Y_2Z_2Sn \cdot 2DMSO$.[10] The bands in this region may, therefore, be associated with the Sn-pyridine stretching mode. For the $(C_2H_5)_2SnCl_2 \cdot 2Py$ and $SnX_4 \cdot 2Py$ (X=Cl, Br and I) complexes, the assignment of the Sn–N vibration is not unambiguous, because these complexes give Sn-halogen stretching bands near 200 cm^{-1}, which could be mixed with the Sn–N stretching. This may spread the Sn–N stretching vibration over two or more frequencies.

It has previously been mentioned by one of the present authors that the Sn-halogen stretching bands of dimethyltin dichloride and dibromide shift to considerably lower frequencies upon the coordination of some donor molecules, such as DMSO[10] and dimethylselenoxide.[11] A similar shift of the Sn-halogen stretching bands might also be expected upon the coordination of pyridine. Thus, each strong band of the dimethyltin dihalide complexes at 245, 160, and 147 cm^{-1} may be associated with Sn-halogen stretching vibrations. The latter two frequencies may be contributed by the deformation vibrations around the tin atom, some of which may appear near these frequencies. The diethyltin dichloride complex showed split broad bands near 210 cm^{-1}. These are also assigned to Sn–Cl stretching vibrations, although they are probably mixed with Sn–N vibrations.

The far infrared spectrum of the tin tetrachloride complex (Fig. 1a) showed a fairly strong band due to the Sn–Cl stretching mode at 324 cm^{-1}, with a

*3 Although the electric conductance has not been measured for these complexes in solution, 2,2′-bipyridyl complexes of dimethyltin dichloride and dibromide gave non-conducting solutions in acetonitrile; T. Tanaka *et al.*, to be published.

11) T. Tanaka and T. Kamitani, *Inorg. Chim. Acta*, in press.

shoulder at 304 cm^{-1}; this finding is in agreement with that of the previous workers,[3] who also reported another weak shoulder at 327 cm^{-1}.*4 Another strong band, at 225 cm^{-1}, is more likely to be due to the ν(Sn–Cl) fundamental, in which there might be some contribution by the Sn–N stretching vibration.

The tin tetrabromide complex showed several absorption bands in the skeletal stretching region (Fig. 1b). The two highest frequencies are assigned to Sn–Br stretching modes because of their strong intensities. The remaining three may be associated with the Sn–Br and the Sn–N stretching vibrations, which are presumably coupled with each other. The four infrared bands of the tin tetraiodide complex, 218, 183, 163, and 145 cm^{-1} (Fig. 1c), are comparable with those of the corresponding bis(pyridine-*N*-oxide) complex, 210, 184, 157, and 140 cm^{-1}.[12] Therefore, these four bands of the $SnI_4 \cdot 2Py$ are likely to be associated with Sn–I stretching modes, although the Sn–N stretching may also contribute to these frequencies.

Stereochemistry. We shall assume the presence of discrete hexa-coordinated species for the solid bis-pyridine complexes of tin(IV). There is some disagreement on the stereochemistry of the $SnCl_4 \cdot 2Py$ complex. Beattie *et al.* initially considered, on the basis of the infrared spectrum, that the complex was more likely to be the *trans* than the *cis*-configuration.[2] On the contrary, Clark and Wilkins concluded it to have the *cis*-configuration after comparing an X-ray powder photograph with one of $SnBr_4 \cdot 2Py$ and after considering the infrared spectrum.[3] In the present infrared study, at least two strong bands (324 and 225 cm^{-1}) have been assigned to ν(Sn-Cl) fundamentals; therefore, it is reasonable to assume the *cis*-configuration for the $SnCl_4 \cdot 2Py$ complex. The tin tetrabromide and tetraiodide complexes showed several infrared bands associated with tin-halogen stretching modes, indicating the *cis*-configuration for these complexes also.

The dimethyltin dichloride and dibromide complexes showed only the asymmetric Sn–C stretching band in their infrared spectra, no symmetric ones (Fig. 2a and 2b), suggesting a linear geometry of the $(CH_3)_2Sn$ moieties.[10] The Sn–Cl stretching frequency of the former complex is close to those of $(CH_3)_2SnCl_2 \cdot 2DMSO$ and $(CH_3)_2SnCl_2 \cdot$bipyridyl, whose chlorine atoms are in *cis*-positions.[10] On the other hand, this frequency is quite a bit lower than that of $Cl_2Sn(acac)_2$ (345 cm^{-1}),[9] which has a *trans*-configuration,[13] as well as dimethyltin dichloride (361 and 356 cm^{-1}).*5 The Sn–Br stretching frequency of the $(CH_3)_2SnBr_2 \cdot 2Py$ complex is also markedly lower than those of dimethyltin dibromide (252 and 241 cm^{-1}).*5 These results would indicate the *trans*-methyl and *cis*-halogen configuration for the $(CH_3)_2SnCl_2 \cdot 2Py$ and $(CH_3)_2SnBr_2 \cdot 2Py$ complexes, which is in agreement with the findings of previous workers.[3]

On the other hand, the dimethyltin diiodide complex gave the symmetric Sn–C stretching band with less intensity as well as the asymmetric one (Fig. 2c), although the former had not been observed by the previous workers.[3] This is suggestive of a non-linear geometry of the C–Sn–C linkage. Thus, it is reasonable to assume a distorted octahedral configuration for the $(CH_3)_2SnI_2 \cdot 2Py$ complex, as is shown in Fig. 3. This configuration

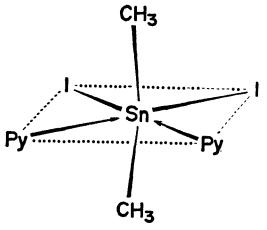

Fig. 3. Distorted octahedral configuration of $(CH_3)_2SnI_2 \cdot 2Py$.

is comparable with those of dimethyltin diacetate[14] and dimethyltin bis(kojate).[15]

The diethyltin dichloride complex also showed two Sn–C stretching bands. The considerable intensity of the symmetric one may be due to coupling with the inner vibrations of ethyl groups, as has been mentioned in the cases of bis-DMSO[10] and bis-dimethylselenoxide[11] complexes of diethyltin dichloride. The $(C_2H_5)_2SnCl_2 \cdot 2Py$ complex is, therefore, assumed to have a similar around the tin atom geometry to that of the dimethyltin dichloride complex, although a more or less distorted configuration can not be ruled out.

*4 This shoulder is not unambiguous in the present study.

12) Y. Kawasaki, M. Hori and K. Uenaka, This Bulletin, **40**, 2463 (1967).

13) Y. Kawasaki and T. Tanaka, *Inorg. and Nucl. Chem. Letters*, **3**, 15 (1967).

*5 The wave numbers in cyclohexane solution; F. K. Butcher *et al.*, *J. Organometal. Chem.*, **1**, 431 (1964).

14) Y. Maeda and R. Okawara, *J. Organometal. Chem.*, **10**, 247 (1967).

15) J. Otera, Y. Kawasaki and T. Tanaka, *Inorg. Chim. Acta*, **1**, 294 (1967).

BULLETIN OF THE CHEMICAL SOCIETY OF JAPAN VOL. 41 1502—1512 (1968)

Electron Spin Resonance of Anion Radicals of Aromatic Esters. IV. The Anion Radicals of Some Substituted Methyl Benzoates*[1]

Masatoshi HIRAYAMA and Taro ISOBE

The Chemical Research Institute of Non-Aqueous Solutions, Tohoku University, Katahira-cho, Sendai

(Received November 22, 1967)

ESR spectra are observed for the anion radicals of methyl *p*-, *m*- and *o*-nitrobenzoates, methyl ester of *p*-phthalaldehydic acid, and methyl and ethyl *p*-cyanobenzoates. Both the electrolytic and alkali-metal reduction methods are used for the radical generation. The spin densities calculated by McLachlan's procedure only with the adjustment of the resonance-integral parameter for the ester group-ring bond are in good agreement with those obtained experimentally for most of the substituted positions in these radicals. The result for the methyl *o*-nitrobenzoate anion suggests that the ester group is twisted considerably by the large steric hindrance between the ester and nitro groups. The ring-proton splittings of three *p*-substituted methyl benzoate anions show that the known order of electron-withdrawing effects of the substituents, $NO_2>CHO>COCH_3>COOCH_3>CN$, holds also for these anions. And it is suggested that the electron-withdrawing power of a XM^+ group produced on the alkali-metal reduction increases in the order of free NO_2, NO_2Cs^+, NO_2K^+, NO_2Na^+ and NO_2Li^+, and that the groups $CHONa^+$ and $CHOK^+$ are more electron-withdrawing than a free CHO group. The ring-proton splittings obtained from the VB-superposition calculations for all the anions except for the *o*-derivative are in satisfactory agreement with those from the MO calculations. Structural models of ion complexes are proposed for the *p*- and *m*-nitro derivatives and methyl ester of *p*-phthalaldehydic acid with the assistance of MO calculations.

A series of the anion radicals of aromatic esters has been studied by one of the present authors.[1-3] The present paper reports the ESR spectra of the anion radicals of methyl *p*-, *m*- and *o*-nitrobenzoates, methyl ester of *p*-phthalaldehydic acid, and *p*-cyano methyl and ethyl benzoates.

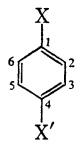

The di-*p*-substituted benzene anions with electron-withdrawing groups prepared by electrolysis are known to show some interesting correlations between the relative electron-withdrawing effect of X to that of X', and the ring proton splittings;[4] in the case of $X'=NO_2$, $a_2+a_3=-2.3$ gauss, irrespective of X,[5] and in the case of $X=X'$, the larger is the electron-withdrawing effect of X, the smaller is $|a_2|$,[2,4-6] and furthermore, when the electron-withdrawing effect of X is larger than that of X', $|a_2|>|a_3|$.[4-6] All these experimental results have been discussed by using the following relation to electron-withdrawing effects

$$NO_2>CHO>COCH_3>COOCH_3>CN$$

which was determined from the ESR measurements[1,6-8] and from the theoretical consideration of monosubstituted benzene anions.[9] This order is in accord with that predicted from the valence-bond superposition model proposed by Karplus and collaborators.[10]

In the present experiments on the *p*-substituted methyl benzoate anions, the measured values of ring-proton splittings are expected to satisfy the above mentioned relations. An alkali metal cation can be considered to interact with the group having a larger electron-withdrawing effect in the unsymmetrical di-*p*-substituted benzene anion. The effect of alkali metal cation on the splittings

*1 The experimental part was presented at the 17th Annual Meeting of the Chemical Society of Japan, Tokyo, April, 1964.

1) M. Hirayama, This Bulletin, **40**, 1822 (1967).
2) M. Hirayama, *ibid.*, **40**, 2234 (1967).
3) M. Hirayama, *ibid.*, **40**, 2530 (1967).
4) P. H. Rieger and G. K. Fraenkel, *J. Chem. Phys.*, **37**, 2811 (1962).
5) A. H. Maki and D. H. Geske, *J. Am. Chem. Soc.*, **83**, 1852 (1961).
6) P. H. Rieger, I. Bernal, W. H. Reinmuth and G. K. Fraenkel, *ibid.*, **85**, 683 (1963).
7) D. H. Geske and A. H. Maki, *ibid.*, **82**, 2671 (1960).
8) N. Steinberger and G. K. Fraenkel, *J. Chem. Phys.*, **40**, 723 (1964).
9) P. H. Rieger and G. K. Fraenkel, *ibid.*, **37**, 2795 (1962).
10) J. C. Shug, T. H. Brown and M. Karplus, *ibid.*, **37**, 330 (1962).

of protons and nitrogen is discussed by the MO calculation of spin densities.

Experimental

The anion radicals studied in this work were prepared by the electrolytic reduction mainly in acetonitrile (ACN) using tetra-*n*-propylammonium perchlorate as the supporting electrolyte, and by the alkali-metal reduction mainly in dimethoxyethane (DME) and tetrahydrofuran (THF) using, sodium, potassium and cesium metals and lithium amalgam. The ESR spectra were measured with a Hitachi X-band ESR spectrometer, model MPU-3B, using a field modulation of 100 kc/s. The experimental techniques were detailed elsewhere.[1]

Methyl *p*-, *m*- and *o*-nitrobenzoates and methyl ester of *p*-phthalaldehydic acid obtained commercially were used without further purification. Methyl *p*-cyanobenzoate was prepared from silver salt of *p*-cyanobenzoic acid and methyl iodide, while ethyl ester was synthesized by the Sandmeyer method after the esterification of *p*-aminobenzoic acid.

Results

The measured splitting constants are listed in Table 1.

Methyl *p*-Nitrobenzoate. A red-purple solution was obtained by both reduction methods of this compound, except for a purple solution obtained with cesium metal in THF. Dimethylformamide (DMF) was used as the solvent for electrolysis so that the spectrum could be precisely compared with those of the other *p*-substituted nitrobenzene anions measured already. The magnitude of each splitting constant observed by the electrolysis in DMF was slightly different from that measured in ACN by Maki and Geske.[5] All the radicals prepared were very stable at room temperature. The spectra observed at room temperature are shown in Fig. 1.

Methyl *m*-Nitrobenzoate. This compound yielded a green-brown solution on the electrolysis in ACN and on the reduction with lithium amalgam

Table 1. Hyperfine coupling constants

Anion		Coupling constants (in gauss)					
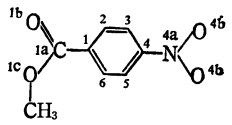		a_2	a_3	a_{CH_3}	a^N	a^M	
	Electrolysis	0.64	2.99	0.32	6.50		
	Li	0.96	3.22	0.28	9.08	<0.09	
	Na	0.96	3.20	0.32	8.06	0.32	
	K	0.88	3.12	0.32	7.92	<0.12	
	Cs	0.75	3.12	0.30	7.65	2.55	
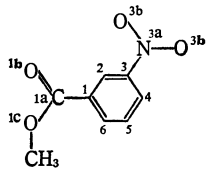		a_2	a_4	a_5	a_6	a^N	a^M
	Electrolysis	3.04	3.46	1.10	4.10	9.09	
	Li	3.48	3.73	1.13	4.15	11.13	<0.25
	Na	3.27	3.60	1.12	4.12	10.50	0.30
	K	3.29	3.69	1.12	4.35	10.18	0.22
	Cs	3.09	3.53	1.08	4.15	10.15	2.87
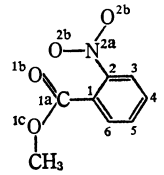		a_3	a_4	a_5	a_6	a_{CH_3}	a^N
	Electrolysis	3.18	1.11	4.02	1.11	<0.20	9.01
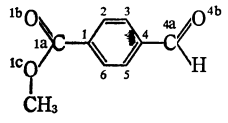		a_2	a_3	a_5	a_6	a_{CH_3}	a_{CHO}	a^M
	Electrolysis	1.02	2.01	2.61	0.15	0.67	5.04	
	K(Na)	0.88	2.41	3.12	<0.16	0.56	6.40	<0.16
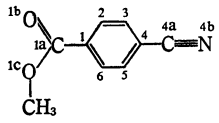			a_2	a_3	a_α	a^N	
	Electrolysis	$R=CH_3$	2.73	1.07	0.84	1.07	
		$R=C_2H_5$	2.70	1.05	0.80	1.05	

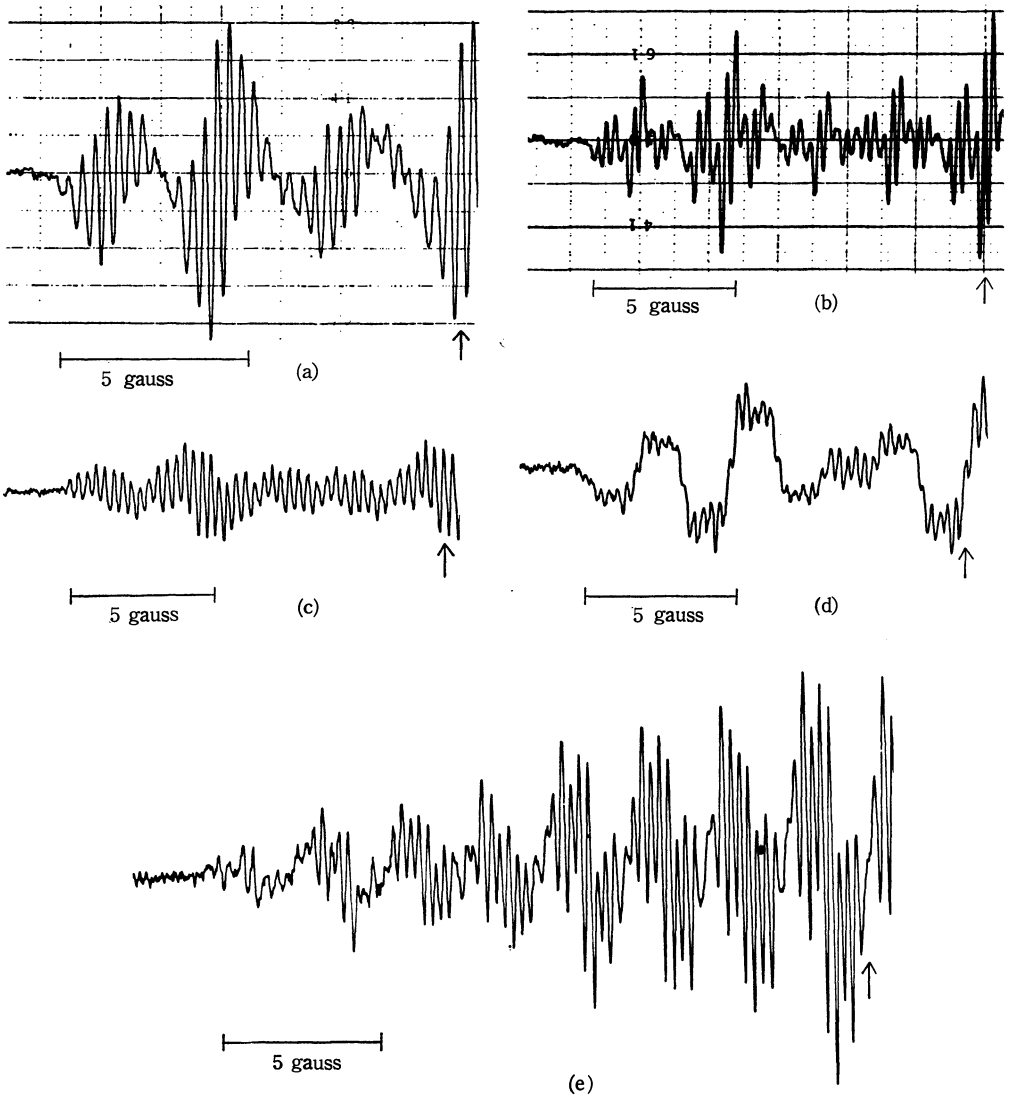

Fig. 1. Halves of ESR spectra of the methyl *p*-nitrobenzoate anions.

(a) Free anion in DMF, (b) Li-Complex in THF, (c) Na-Complex in DME, (d) K-Complex in DME, and (e) Cs-Complex in DME.
(The arrow shows the center of each spectrum.)

and potassium metal in THF, and a yellow solution with cesium metal in THF. The radicals were very stable at room temperature. The observed spectra are shown in Fig. 2.

Methyl *o*-Nitrobenzoate. A yellow-brown solution was obtained by the electrolysis of this compound in ACN. The radical prepared was comparatively stable at room temperature. The spectrum is shown in Fig. 3. No ESR signals could be observed by the reduction with sodium metal in THF.

Methyl Ester of *p*-Phthalaldehydic Acid. The electrolytic reduction of this compound in DMF gave a purple-red solution, which yielded a spectrum shown in Fig. 4(a). Although the spectrum was poorly resolved, because of instability of this radical at room temperature, the analysis was performed with reference to the result of analysis for the spectrum obtained with potassium metal (Fig. 5(b)). The result led the five doublets arising from an aldehyde proton and four unequivalent ring protons, and a quartet assignable to the three equivalent methyl protons. Since a number of lines occurred within the narrow total-width, a resolution of lines was very poor. Consequently, the reconstruction based on the coupling constants listed in Table 1 did not agree exactly with the measured spectrum, as is shown in Fig.

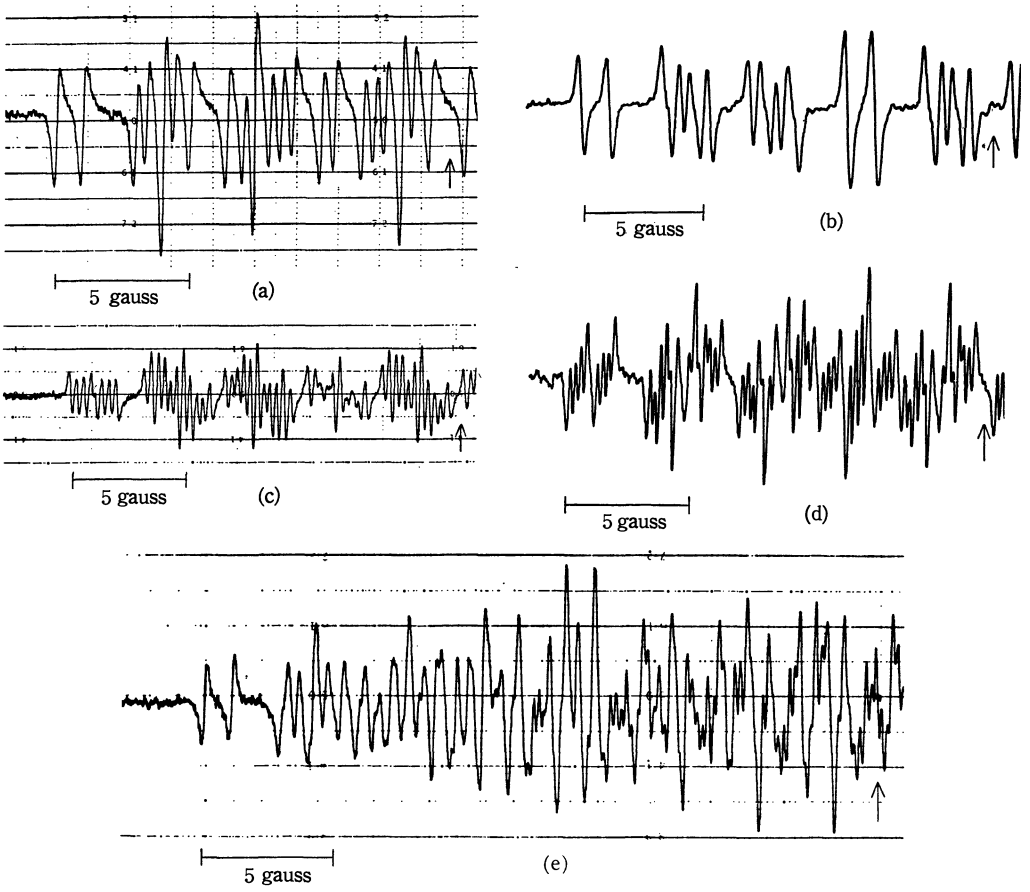

Fig. 2. Halves of ESR spectra of the methyl *m*-nitrobenzoate anions.
(a) Free anion in ACN, (b) Li-Complex in THF, (c) Na-Complex in THF, (d) K-Complex in THF, and (e) Cs-Complex in THF.
(The arrow shows the center of each spectrum.)

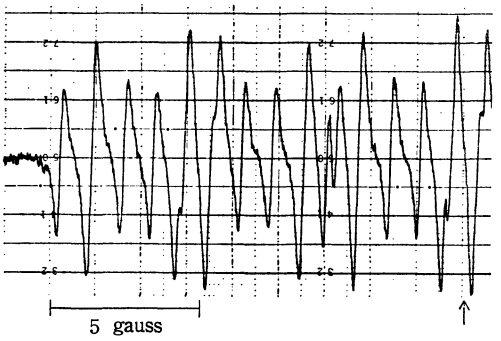

Fig. 3. Half of ESR spectrum of the methyl *o*-nitrobenzoate anion prepared by the electrolysis in ACN.
(The arrow shows the center of spectrum.)

4(b). The solution obtained by the electrolysis in ACN was liable to turn into brown from purple-red. The brown solution displayed a quite different spectrum from that measured in DMF. This spectrum has not yet been analyzed.

The spectrum obtained by the reduction with potassium metal in DME, shown in Fig. 5(a), was completely identical with that obtained with sodium metal in DME, except that the average line-width was slightly narrower than that of the latter. This spectrum was composed of four doublets and a quartet (Fig. 5(b)). A small doublet arising from the fourth ring proton may be covered within the line-width.

Methyl *p*-Cyanobenzoate. The electrolysis of this compound in ACN yielded a purple-red solution, the radical produced being not very stable at room temperature. The spectrum observed is shown in Fig. 6(a). Since 108 lines might occur within the narrow total width (about 12 gauss), they were anticipated to superpose extremely one another. The intensity of each line in the reconstruction based on the coupling constants listed in Table 1 did not agree well with that of the measured spectrum. Then, it was assumed that there was a small difference, though not measurable, between the splittings of two

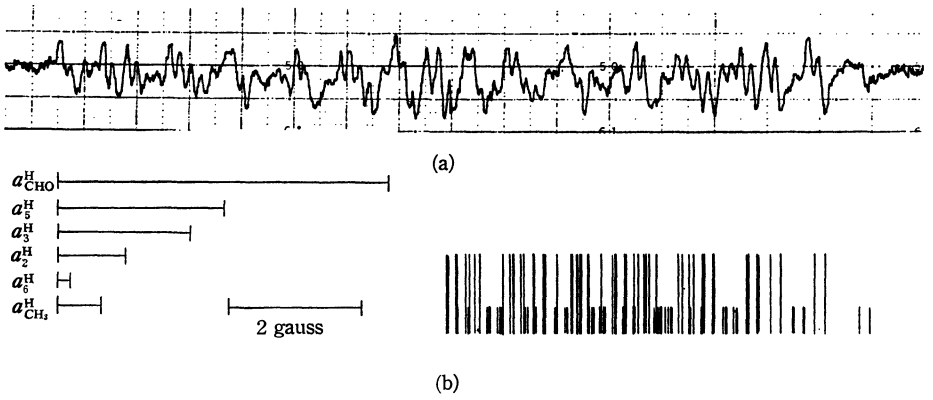

Fig. 4. ESR spectrum of the anion of methyl ester of *p*-phthalaldehydic acid prepared by the electrolysis in DMF (a) and half of its reconstruction (b).

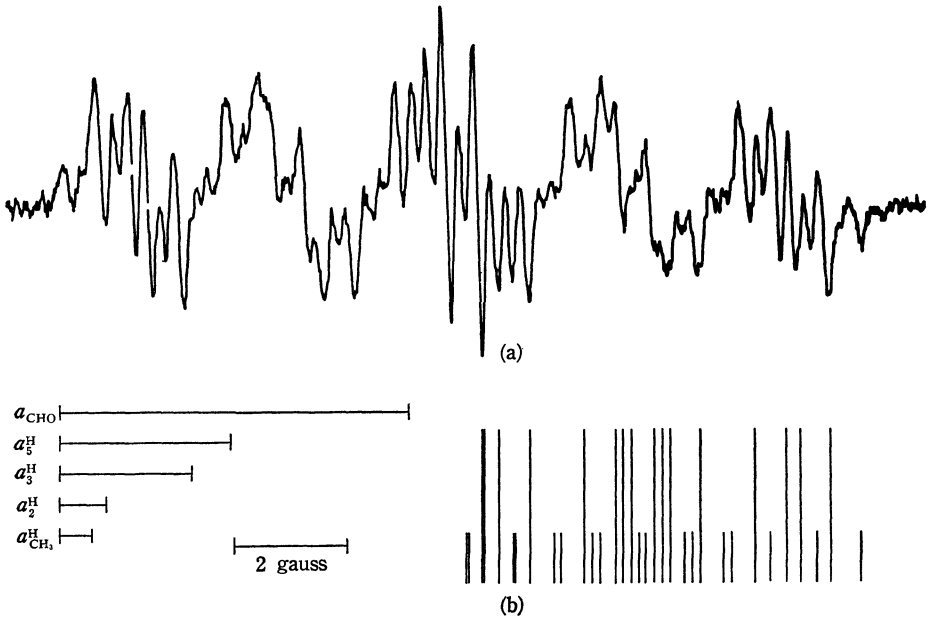

Fig. 5. ESR spectrum of the anion of methyl ester of *p*-phthalaldehydic acid prepared by the reduction with potassium metal in DME (a) and half of its reconstruction (b).

ring-protons in ortho position to the ester group, and consequently that the center line of this triplet was much broader and the peak-to-peak height of its first derivative was much smaller than in the case of a complete equivalence of these two ortho-protons. Thus, the spectrum was again reconstructed; the result is shown in Fig. 6(b), where the dotted lines show these lines of small height. As is seen from Fig. 6(b), the spectrum could be well explained by these coupling constants. This inequivalence of two protons in ortho position to the ester group may not be surprising, because in such anions having the comparatively large splittings of ring protons in ortho position to the ester group, a difference between the α-effects of two oxygen atoms in the ester group is considered to be effective to a difference between the two ortho-proton splittings.[2] In order to confirm the validity of this analysis, the spectrum of ethyl *p*-cyanobenzoate anion was measured and analyzed. Figure 7 shows that each of the splitting constants measured is equal to that of the methyl ester anion, and further that the above-mentioned technique is required for the analysis.

Also by the alkali-metal reductions of these two esters, purple-red solutions were obtained. The measured patterns of spectra were different from that obtained by electrolysis, though the total width was about 12 gauss. However, since they were further poorly-resolved, probably because of the existence of some alkali metal splittings, analyses of them were very difficult. On the

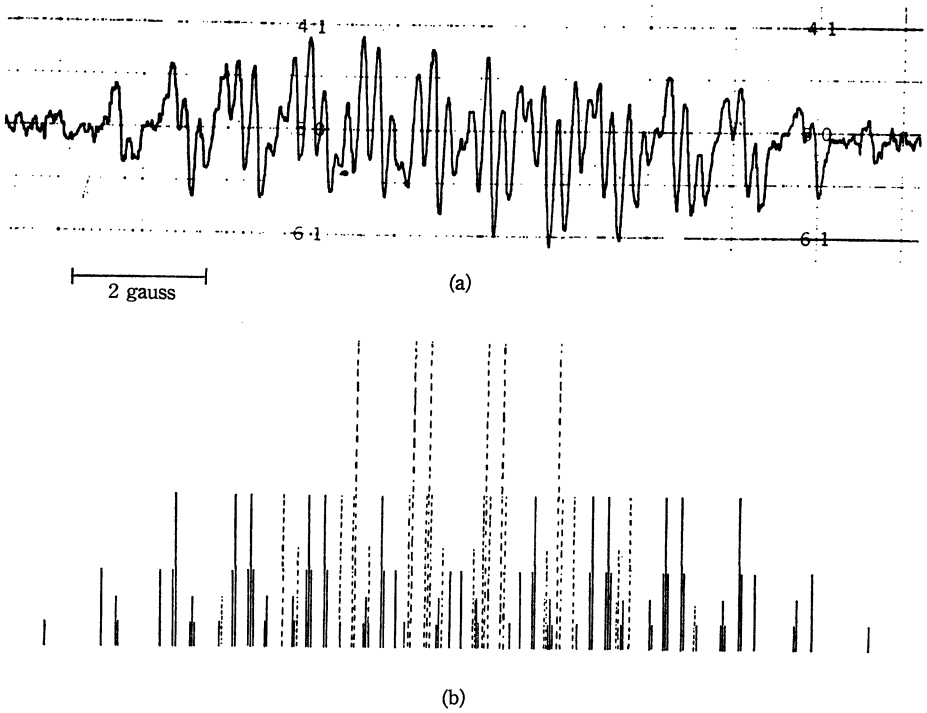

Fig. 6. ESR spectrum of the methyl *p*-cyanobenzoate anion prepared by the electrolysis in ACN (a) and its reconstruction (b).

other hand, the spectrum, measured at −45°C, of methyl ester anion prepared with sodium metal in THF was resolved better than that measured at room temperature, and was similar to that obtained by the electrolysis in ACN. This fact suggests that this ion-pair complex dissociates into a free anion and a cation under such condition.

Discussion

Molecular-Orbital Calculations of Spin Densities. Hückel molecular-orbital calculations with the approximate configuration interaction corrections of McLachlan[11] were performed for the anion radicals studied here in order to estimate the spin density distribution and to assist in the assignment of proton splittings. The values of parameters used here for the ester group, except for γ_{1-1a}, are those which have been determined to have the best fit of the calculated spin densities to the experimental ones for the methyl benzoate anion,[1] while those for the nitro, cyano, and aldehyde groups were taken from the works of Fraenkel *et al.*[8,9,12] These values of parameters are summarized in Table 2; the parameter $\lambda=1.2\beta$ was used in the correction terms. The results of calculations are given in Table 3. In the methyl

Table 2. The values of MO parameters

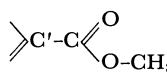	$\delta_{O(C=O)}=1.5$ $\delta_{O(C-O)}=2.0$ $\gamma_{CO(C=O)}=1.6$ $\gamma_{CO(C-O)}=1.2$
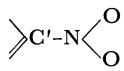	$\delta_N=2.2$ $\delta_O=1.4$ $\gamma_{NO}=1.67$ $\gamma_{NC'}=1.2$
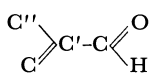	$\delta_O=1.5$ $\gamma_{CO}=1.6$ $\gamma_{CC'}=0.9$ $\delta_{C''}=-0.15$
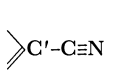	$\delta_N=1.0$ $\gamma_{CN}=2.0$ $\gamma_{CC'}=0.9$

$\delta_X=(\alpha_X-\alpha_C)/\beta_{CC}$, $\gamma_{XY}=\beta_{XY}/\beta_{CC}$

p-cyanobenzoate anion, the value of $\gamma_{1-1a}=1.2$ gave a relatively good fit to the experimental spin density at the position 2, but not at the position 3. In the anion of methyl ester of *p*-phthalaldehydic acid, the calculated result with $\gamma_{1-1a}=0.85$ was in good agreement with the experimental data, while in the methyl *p*- and *m*-nitrobenzoate anions, the values of 0.75 and 0.6 for γ_{1-1a} gave the best

11) A. D. McLachlan, *Mol. Phys.*, **3**, 233 (1960).
12) P. H. Rieger and G. K. Fraenkel, *J. Chem. Phys.*, **39**, 609 (1963).

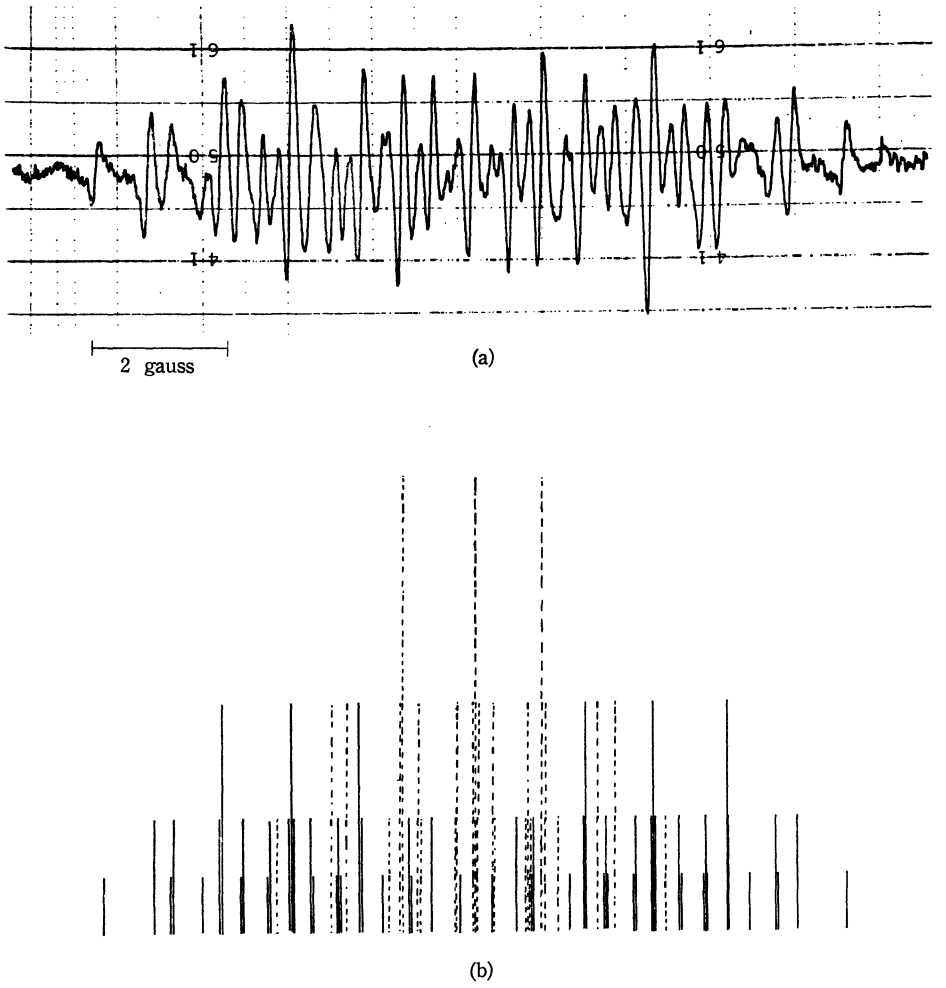

Fig. 7. ESR spectrum of the ethyl *p*-cyanobenzoate anion prepared by the electrolysis in ACN (a) and its reconstruction (b).

fits, respectively. In the methyl *o*-nitrobenzoate anion, a large steric hindrance between the ester and nitro groups may be considered to affect the spin-density distribution on the ring. Figure 8 shows that the normal value of $\gamma_{1-1a}=1.0$ does not give the fit to the experimental spin densities, and that the best fit, also for the nitrogen splitting, is obtained with $\gamma_{1-1a}=0.2$. This calculated result seems to show a structure with the ester group twisted considerably by the steric effect.

Electron-Withdrawing Effects. As is indicated in the section of introduction, the ester group has been experimentally determined to be more electron-withdrawing than the cyano group and less electron-withdrawing than the acetyl group. This has been also verified by the fact that the ring-proton splitting of dimethyl terephthalate anion in ACN, -1.56 gauss,[2] is situated between those of the terephthalonitrile and *p*-diacetylbenzene anions, *i. e.*, between -1.59[6] and -1.33 gauss.[4]*2

In a series of the *p*-substituted methyl benzoate anions, the ring-proton splittings in ortho position to the ester group, $|a_O|$, increase in the order of NO_2, CHO, $COOCH_3$ and CN derivatives, while conversely, those in meta position to the ester group, $|a_m|$, decrease in the same order, and furthermore, the methyl proton splittings increase according to this order. All these data imply that the order in the electron-withdrawing effect of the substitutents described in the introduction holds also for the anions studied here, and moreover, these data are consistent with the results from the superposition model of the valence-bond method described later. Similarly, the correlations among the ring proton splittings of each of *p*-substituted methyl benzoate anions and those of the other *p*-disubstituted benzene anions already measured[2,4-6] are approximately satisfactory in view of this order.

*2 The average value of the four ring-proton splittings in the cis and trans isomers.

TABLE 3. THEORETICAL AND EXPERIMENTAL SPIN DENSITIES

Anion	Position*1	Spin density: Theoretical: Hückel	Spin density: Theoretical: McLachlan	Spin density: Experimental*2
	1	0.1228*3	0.1600*3	
	2	0.0150	−0.0276	0.027
Methyl	3	0.0943	0.1195	0.125
p-nitro-	4	0.0534	0.0316	
benzoate	1a	0.0258	0.0269	
anion	1b	0.0192	0.0187	
	1c	0.0067	0.0050	
	4a	0.1968	0.2062	
	4b	0.1784	0.1840	
	1	0.0057*4	−0.0450*4	
	2	0.0978	0.1288	0.127
	3	0.0399	0.0068	
Methyl	4	0.1113	0.1501	0.144
m-nitro-	5	0.0045	−0.0495	0.046
benzoate	6	0.1298	0.1777	0.171
anion	1a	0.0009	−0.0002	
	1b	0.0006	−0.0019	
	1c	0.0002	−0.0006	
	3a	0.2233	0.2368	
	3b	0.1929	0.1984	
	1	0.1063*5	0.1411*5	
	2	0.0407	0.0084	
	3	0.1038	0.1370	0.133
Methyl	4	0.0055	−0.0463	0.046
o-nitro-	5	0.1236	0.1671	0.168
benzoate	6	0.0042	−0.0485	0.046
anion	1a	0.0018	0.0018	
	1b	0.0013	0.0012	
	1c	0.0004	0.0003	
	2a	0.2243	0.2379	
	2b	0.1941	0.2000	
	1	0.1671*6	0.2097*6	
	2	0.0611	0.0367	0.043
Anion of	3	0.0766	0.0745	0.084
methyl	4	0.1250	0.1320	
ester of	5	0.0947	0.1049	0.109
p-phthal-	6	0.0358	−0.0016	0.006
aldehydic	1a	0.0689	0.0749	
acid	1b	0.0426	0.0398	
	1c	0.0155	0.0110	
	4a	0.1931	0.2143	0.210
	4b	0.1195	0.1037	
	1	0.1512*7	0.1584*7	
	2	0.1074	0.1223	0.113
Methyl	3	0.0438	−0.0012	0.043
p-cyano-	4	0.1957	0.2533	
benzoate	1a	0.1357	0.1477	
anion	1b	0.0828	0.0754	
	1c	0.0301	0.0207	
	4a	0.0383	0.0300	
	4b	0.0639	0.0722	

*1 See Table 1 for numbering of the positions.
*2 The spin densities using the relation, $a_i^H = Q_{CH}^H \rho_i^\pi$, where $Q_{CH}^H = -24.0$ gauss.
*3 Calculated with $\gamma_{1-1a}=0.75$.
*4 Calculated with $\gamma_{1-1a}=0.6$.
*5 Calculated with $\gamma_{1-1a}=0.2$.
*6 Calculated with $\gamma_{1-1a}=0.83$
*7 Calculated with $\gamma_{1-1a}=1.2$.

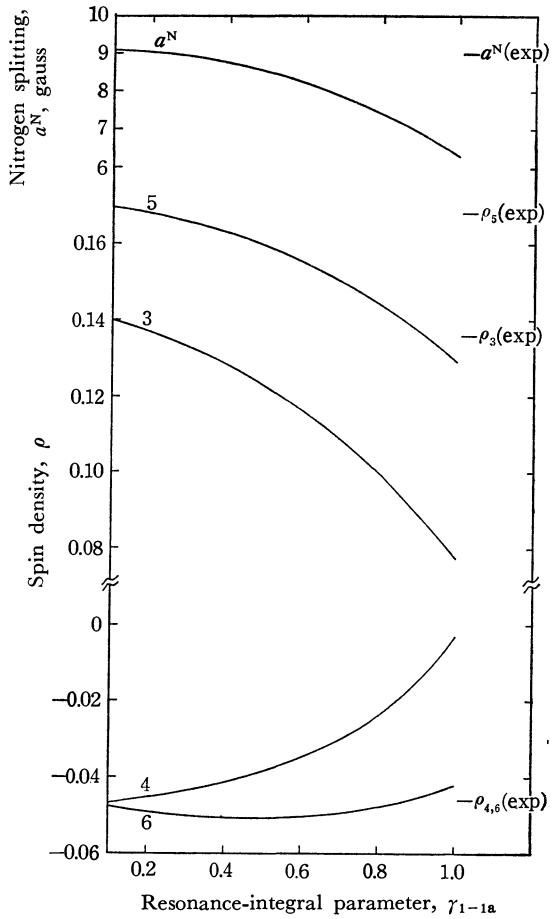

Fig. 8. Spin densities ρ and nitrogen splitting constant a^N calculated by the McLachlan modification of MO theory for the methyl *o*-nitrobenzoate anion as a function of the resonance-integral parameter for the 1-1a bond, γ_{1-1a}, and those obtained by the experiments.
The numbers on the curves indicate the positions in the radical.
The experimental values are shown in the right column.

It is reasonable to consider that the group having the larger electron-withdrawing effect in an unsymmetrical di-*p*-substituted benzene anion may interact with an alkali metal cation. Thus, regarding a group XM^+ produced on alkali-metal reduction as a new electron-withdrawing group, one may predict the effect of this group relative to the cation-free group X or to the other groups by comparing each ring proton splitting with the others. In the methyl *p*-nitrobenzoate-alkali metal ion pairs, a series of the values of a_2 and a^N in Table 1 indicates obviously that the order in the electron-withdrawing effects is $NO_2Li^+ > NO_2Na^+ > NO_2K^+ > NO_2Cs^+ >$ Free NO_2, and furthermore, the values of a_3 and a_{CH_3} seem to show that this order is reasonable within the experimental errors.

Also in the case of the methyl *m*-nitrobenzoate anion, it may be seen from a series of the values of a^N that there exists the same order of electron-withdrawing powers.

Similarly, since an aldehyde group has been decided to be more electron-withdrawing than a ester group, the aldehyde group (probably the oxygen atom) may interact with an alkali metal cation in the anion of methyl ester of *p*-phthalaldehydic acid. Thus, the $CHOK^+(Na^+)$ is compared with the free aldehyde group or the others in Table 1. One may recognize from the increment of a_{CHO} and of the splittings of ring protons in ortho position to the aldehyde group,*3 and further from the decrement of a_{CH_3}, that this group is more electron-withdrawing than the free aldehyde group. Furthermore, it may be suggested that the group $CHONa^+(K^+)$ is still slightly weaker than the free nitro group, and is strong as much as the $COOCH_3Li^+$ group[2] in the electron-withdrawing power. In the case of the methyl *p*-cyanobenzoate anion, although the spectrum of the ion pair complex could not be analyzed, the splittings in ortho position to a group $COOCH_3M^+$, may be expected to be larger than those in ortho position to the free ester group.

Valence-Bond Superposition Model. Karplus and collaborators[10] have developed an approximate valence-bond superposition theory which is applicable to the benzene anion radicals with strongly electron-withdrawing substituents; if $\rho_N(X)$ and $\rho_N(X')$ are spin densities for the monosubstituted species ϕX and $\phi X'$, respectively, the spin density ρ_N in the disubstituted anion can be written

$$\rho_N = \{k(X)\}^2\rho_N(X) + \{k(X')\}^2\rho_N(X'),$$

where $\{k(X)\}^2$ and $\{k(X')\}^2$ represent the contributions made by the ϕX and $\phi X'$ structures to the ground state of the system. By using this procedure, one of the present authors has predicted the ring proton splitting, -1.63 gauss, for the dimethyl terephthalate anion from the *m*-, and *o*-ring proton splittings of the methyl benzoate anion observed by the electrolysis in acetonitrile; this value has been in good agreement with the experimental value of -1.56 gauss.[2]

This theory has also given satisfactory results to most of the unsymmetrical di-*p*-substituted benzene anions, though inconclusive. Then, the model will be testified for the three *p*-substituted methyl benzoate anions studied here and further for the methyl *m*-nitrobenzoate anion.

At first, the relative weight of the methyl benzoate anion structure, $\{k(X)\}^2$, of each *p*-substituted methyl benzoate anion, was calculated by using the largest ring proton splitting. The calculated results are 9.2% for *p*-nitro, 36.8% for *p*-aldehyde, and 66.9% for *p*-cyano derivatives, respectively. The correlations between these values and those for the other *p*-disubstituted benzene anions having been already measured, are satisfactory in view of the order of the electron-withdrawing effects of these substituents. The predicted values of the remaining ring-proton splittings were then calculated by using the corresponding splittings of the monosubstituted benzene anions, the results being shown in Fig. 9 with those obtained from the MO calculations. These predicted values are in comparatively good agreement with the experimental values, except for the value of a_6 in the anion of methyl ester of *p*-phthalaldehydic acid and the value of a_3 in the methyl *p*-cyanobenzoate anion. These assignments are in accord with those made by the MO calculations.

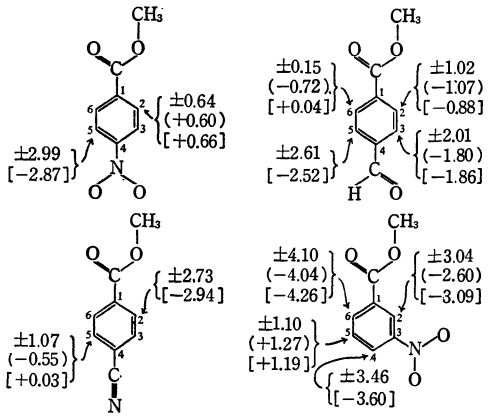

Fig. 9. Comparison of the valence-bond superposition and the molecular-orbital calculations for the ring proton splittings (gauss). Numbers not in parentheses or brackets are the experimental splittings using the MO assignments. Those in parentheses are from the valence-bond superposition procedure and those in brackets are from the MO calculation.

The spectrum of the methyl *m*-nitrobenzoate anion can be fitted comparatively well by the superposition model if the largest splitting of 4.10 gauss is assigned to the position 4. The weight of the methyl benzoate anion structure in the superposition is then 16.7%, a value of which is found to be reasonable from the comparison with the value of 22.0% predicted for the weight of the acetophenone anion structure in the *m*-nitroacetophenone anion.[4] The predicted splittings are shown in Fig. 9. However, the assignments required by the superposition model at the positions 4 and 6 are the opposite of those predicted by the MO calculations. Such the different assignments have occurred for the other meta isomers with electron-withdrawing groups.[9,12]

Interpretation of the Ion Complexes by MO Calculations. Assuming that the alkali metal cation may exist between two oxygen atoms of

*3 The average value of the splittings at the positions 3 and 5.

the nitro group, MO calculations of spin densities were performed with the modification that a small increase in the Coulomb-integral parameter of the oxygen atoms of a nitro group, $\delta_{O(NO_2)}$, was introduced. The dependence of spin density at each position on the Coulomb-integral parameter of oxygen atom is shown in Figs. 10 and 11 for methyl *p*- and *m*-nitrobenzoate anions, respectively. As is illustrated in Fig. 10, in the methyl *p*-nitrobenzoate anion, ρ_3 and $|\rho_2|$ increase with an increment of $\delta_{O(NO_2)}$ from 1.4, while conversely,

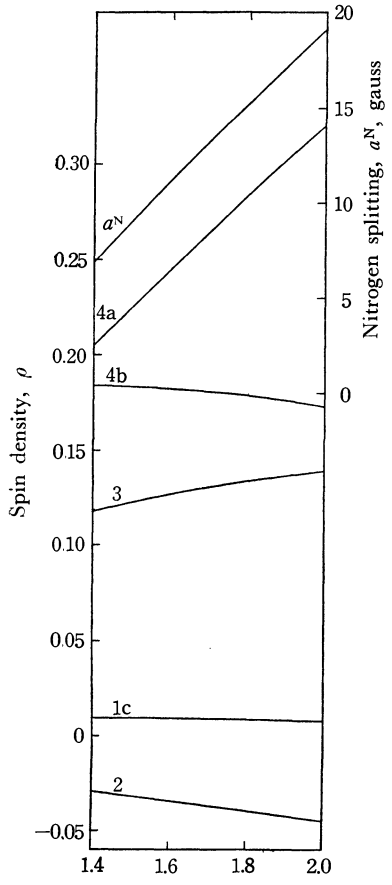

Fig. 10. Spin densities ρ and nitrogen splitting constant a^N calculated by McLachlan modification of MO theory for the methyl *p*-nitrobenzoate anion as a function of the Coulomb-integral parameter for the oxygen atom of nitro group, $\delta_{O(NO_2)}$. The numbers on the curves indicate the positions in the radical.

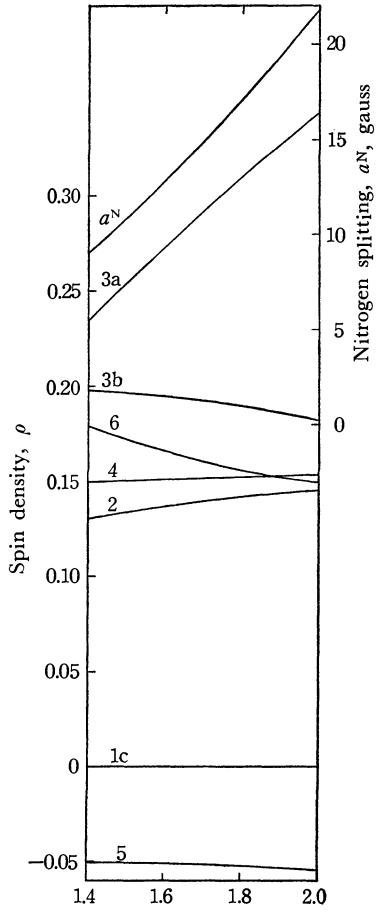

Fig. 11. Spin densities ρ and nitrogen splitting constant a^N calculated by McLachlan modification of MO theory for the methyl *m*-nitrobenzoate anion as a function of the Columb-integral parameter for the oxygen atom of nitro group, $\delta_{O(NO_2)}$. The numbers on the curves indicate the positions in the radical.

Table 4. The spin densities at the metal nuclei

	Li	Na	K	Cs
Q^M	143.3	316.2	82.38	820.08
$a^M(p)$	<0.09	0.32	<0.12	2.55
$a^M(m)$	<0.25	0.30	0.22	2.87
$a^M/Q^M(p)$	$<6.28\times10^{-4}$	1.01×10^{-3}	$<1.46\times10^{-3}$	3.11×10^{-3}
$a^M/Q^M(m)$	$<1.75\times10^{-3}$	9.48×10^{-4}	2.67×10^{-3}	3.50×10^{-3}

a^M: The splitting constant of metal nucleus.
Q^M: The splitting constans of free metal nucleus.
a^M/Q^M: The spin density at the metal nucleus.

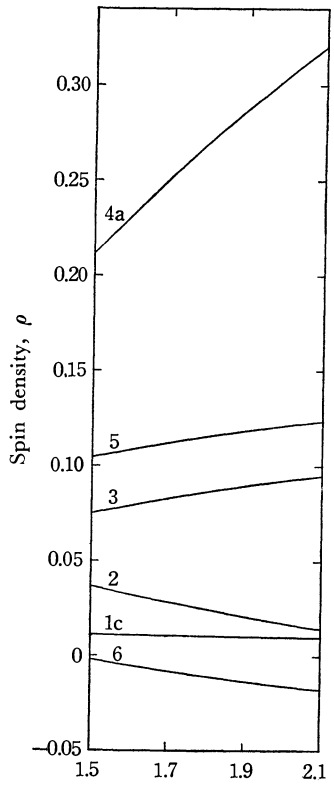

Fig. 12. Spin densities ρ calculated by McLachlan modification of MO theory for the anion of methyl ester of *p*-phthalaldehydic acid as a function of the Coulomb-integral parameter for the oxygen atom of aldehyde group, $\delta_{O(CHO)}$. The numbers on the curves indicate the positions in the radical.

ρ_{1c} decreases gradually. Furthermore, the value of a^N calculated from the values of ρ_{4a} and ρ_{4b} by using the equation proposed by Fraenkel *et al.*,[12] increases also with an increment of $\delta_{O(NO)_2}$. These results are consistent with the tendency of change of any splitting constant of the free anion to that of the ion complex listed in Table 1. Similarly, it is seen from Fig. 11 that in the methyl *m*-nitrobenzoate anion, the dependence of the values of ρ_2, ρ_4, ρ_5 and a^N on the value of $\delta_{O(NO_2)}$ is in accord with those to be expected from the experimental data, but ρ_6 is inconsistent with the experimental splitting constants.

Thus, the above-mentioned assumption on the position of the metal cation may be theoretically confirmed. Furthermore, one may determine that the smaller is the cationic radius, the stronger is the interaction between the alkali metal cation and the oxygen atoms.

On the other hand, the magnitude of spin density at the metal nucleus, a^M/Q^M,[13] increases in the order of increasing ionic radius, that is, Li<Na<K<Cs, as is shown in Table 4; this order is in contrast with that in the *o*-phthalate-alkali metal ion complexes.[2]

It seems to be plausible to consider that in the anion of methyl ester of *p*-phthalaldehydic acid the alkali metal cation may exist near the carbonyl oxygen atom. Then, a small increase in the Coulomb-integral parameter of carbonyl oxygen atom was introduced, the calculated result being shown in Fig. 12. In Fig. 12, ρ_3, ρ_5, ρ_{4a} and $|\rho_6|$ increase with an increment of $\delta_{O(CHO)}$ from 1.5, while ρ_2 decreases, and ρ_{1c} decreases gradually. These results explain very well the change in each splitting constant of the free anion to that of the ion complex, except for ρ_6. Thus, a model in which the alkali metal cation may interact with the carbonyl oxygen atom in the aldehyde group, may be supported by the theroetical consideration.

The numerical calculations were carried out on the NEAC 2230 at the Computation Center, Tohoku University.

The authors wish to thank Professor Masamoto Iwaizumi for his helpful discussions and encouragement through the course of this work. They are also indebted to Mrs. Masako Azumi for the synthesis of some of the samples.

13) P. Kusch and H. Taub, *Phys. Rev.*, **75**, 1477 (1949).

BULLETIN OF THE CHEMICAL SOCIETY OF JAPAN VOL. 41 1513—1518 (1968)

Intramolecular Energy Transfer in Europium Chelates Due to Excitation of the Triplet State

Yoshihisa MATSUDA,*1 Shoji MAKISHIMA and Shigeo SHIONOYA

The Institute for Solid State Physics, The University of Tokyo, Roppongi, Minato-ku, Tokyo

(Received November 25, 1967)

The purpose of this paper is to clarify whether intramolecular energy transfer in europium chelates occurs *via* the triplet state of the ligand. It is attempted to excite the triplet state of europium dibenzoylmethide (EuD) by utilizing intermolecular triplet-triplet energy transfer from lanthanum dibenzoylmethide (LaD). In mixed solutions of EuD and LaD, the intensity and decay time of the ligand phosphorescence of LaD decreases with increasing molar fraction of EuD at liquid nitrogen temperature. Nearly in proportion to this, the intensity of the europium emission of EuD is enhanced, veryfying the occurrence of energy transfer from LaD to EuD. This fact is taken as clear evidence that intramolecular energy transfer takes place *via* the triplet state.

Chelates of trivalent europium and some other rare earth ions emit luminescence of line spectrum characteristic of central rare earth ions due to f–f transitions. This luminescence is mainly caused by absorption by the ligand accompanied by subsequent intramolecular energy transfer to the central ions. Recently, these chelates have attracted great attention, since several investigators have suggested[1,2] the possibility of their use as laser materials, and succeeded[3-5] in achieving laser action with europium(III) β-diketonates. As for laser materials, one has to find chelates in which intramoecular energy transfer occurs efficiently. It is important, for this purpose, to clarify the mechanism of this intramolecular energy transfer.

Crosby *et al.*[6] investigated intramolecular energy transfer in chelates of various trivalent rare earth ions. They found that if the lowest triplet level of the ligand is located below the emitting levels of the chelated rare earth ions, luminescence attributed to the rare earth ions is not observed even if the singlet excited level of the ligand is located above them. Based on this fact, they suggested that intramolecular energy transfer takes place *via* the lowest triplet state of the ligand. El-Sayed and Bhaumik[7] reported that it is possible to enhance the luminescence of the chelated europium ion by intermolecular triplet-triplet energy transfer from benzophenone as energy donor. In this case, however, it is considered that the energy donor is further coordinated to the hexa-coordinated europium ion studied by them. If it is the case, the enhancement of the europium emission due to the addition of the energy donor would be attributed to the direct intramolecular energy transfer from the energy donor. Furthermore, Bhaumik and El-Sayed[8] showed that some aromatic compounds whose triplet levels are located between the emitting level of europium ion and the triplet level of the ligand of europium chelates quench the emission due to the europium ion. We have also showed[9] that the emission intensity of the chelated rare earth ion decreases if the triplet state of the ligand is quenched by the heavy-atom effect.

These observations all suggest that intramolecular energy transfer takes place *via* the triplet state of the ligand. However, clear evidence has not yet been reported, since it is difficult to excite the chelates directly from the ground state to the triplet state by optical absorption because of the very small probability of the singlet-triplet transition.

The purpose of this paper is to clarify whether energy transfer from the ligand to the europium ion takes place *via* the triplet state of the ligand. In this work, excitation of europium chelate to the triplet state is attempted by utilizing a phenomenon

*1 Presently at Department of Organic Synthesis, Faculty of Engineering, Kyushu University, Fukuoka.

1) R. E. Whan and G. A. Crosby, *J. Mol. Spectry,* **8**, 315 (1962).

2) E. J. Shimitschek and E. G. K. Schwarz, *Nature,* **196**, 832 (1962).

3) A. Lempicki and H. Samelson, *Phys. Letters,* **4**, 133 (1963).

4) N. E. Wolff and R. J. Pressley, *Appl. Phys. Letters,* **2**, 152 (1963).

5) E. J. Shimitschek, *ibid.,* **3**, 177 (1963).

6) G. A. Crosby, R. E. Whan and R. M. Alire, *J. Chem. Phys.,* **34**, 743 (1961).

7) M. A. El-Sayed and M. L. Bhaumik, *ibid.,* **39**, 2391 (1963).

8) M. L. Bhaumik and M. A. El-Sayed, *ibid.,* **42**, 787 (1965).

9) S. Shionoya, Y. Matsuda, M. Morita and S. Makishima, a contributed paper at Internatl. Conf. Luminescence, Budapest, 1966, p. 9—84, in press in Proc.

of intermolecular triplet-triplet energy transfer.

Europium dibenzoylmethide (EuD) was used as energy acceptor, because it shows intramolecular energy transfer of relatively high efficiency. Also, it is easily prepared and purified.[1] As energy donor, lanthanum dibenzoylmethide (LaD) was chosen, and the effect of its addition on the intensity of the europium emission of EuD investigated. Dibenzoylmethides of lanthanum, gadolinium, lutetium and samarium exhibit phosphorescence attributed to the transition from the ligand triplet state to the ground state. There is no significant differences in their phosphorescence.[1] This suggests that the energy level of the triplet state is independent of the species of coordinated rare earth ion. It is expected that if EuD is mixed with some other rare earth dibenzoylmethide showing ligand phosphorescence, intermolecular energy transfer takes place from the triplet state of the latter chelate to the triplet state of the former, since there is sufficient energy mathcing between the triplet states of the two chelates. We found that LaD has the longest lifetime of ligand phosphorescence among the various rare earth dibenzoylmethides. Therefore, LaD was chosen as energy donor.

Experimental Methods

Samples. EuD and LaD were prepared by the ordinary piperidine method at first, and then kept in vacuum at 150°C for 24—30 hr. In the optical measurements, these chelates were dissolved in either ethanol or ethanol-methanol (3 : 1). These solutions become rigid glasses when cooled to liquid nitrogen temperature.

Emission Spectra. A high pressure mercury arc lamp connected with a Bausch & Lomb grating monochromator was used as the exciting light source. A Kipp & Zonen double monochromator with flint prisms was used for spectral measurement. Emission spectra were obtained for the alcohol solutions of LaD and EuD of concentrations 10^{-4}—10^{-3} M.

Excitation Spectra. A 500 W xenon arc lamp and a 500W tungsten lamp combined with the Kipp & Zonen double monochromator with quartz and flint prisms, respectively, were used for the excitation sources. Emission from the samples was filtered by color and interference filters. For EuD, measurement was made for the strongest emission line of 612 mμ, due to the transition $^5D_0 \rightarrow {}^7F_2$ of the trivalent europium ion. For LaD, the excitation spectrum was measured for ligand phosphorescence at a wavelength of 490 mμ, and ligand fluorescence at 425 mμ.

Emission Lifetime. An Edgerton FX-3 1 joule and a Miyata 20 joule xenon flash lamp with durations of 2μ sec and 20μ sec, respectively, were used as excitation sources with ultraviolet pass glass filters and a 365 mμ interference filter. The output of the photomultiplier, RCA 931A, was fed to a synchroscope, and the decay curve photographed. The concentrations of the solutions were 10^{-3}—10^{-5} M for the pure solutions of EuD and LaD, and 2×10^{-4} M for the mixed solutions of LaD and EuD.

Time-Resolved Emission Spectra. An Edgerton FX-3 xenon flash lamp was used as the exciting light source with ultraviolet pass filters and a 365 mμ interference filter. This lamp was operated at a frequency of 10 cps. High pulse voltage with a 2 μ sec width was applied to the photomultiplier tube, RCA 931 A, with the delay time changing from zero to 1 msec for the light flash.

Results and Discussion

The emission spectra of LaD and EuD in ethanol solution at liquid nitrogen temperature are given in Fig. 1. EuD exhibits only sharp emission lines due to the f–f transition of trivalent europium ion. The strongest line is the one for the transition $^5D_0$

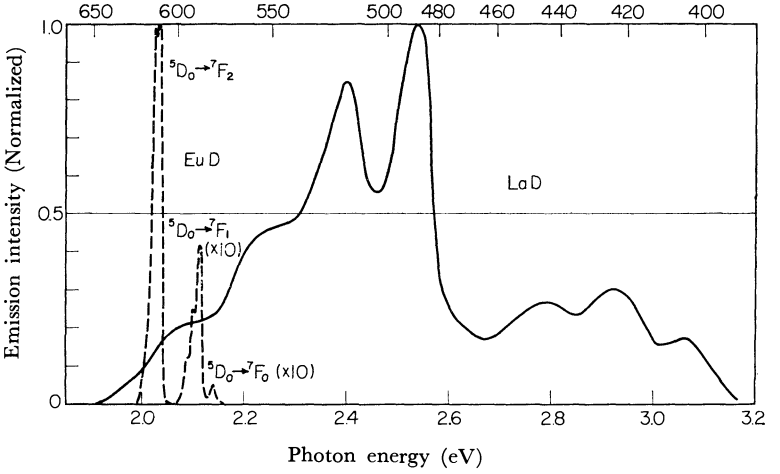

Fig. 1. Emission spectra of EuD and LaD in alcohol solutions at liquid nitrogen temperature. The intensities of EuD emission lines due to the transitions of $^5D_0 \rightarrow {}^7F_0$ and $^5D_0 \rightarrow {}^7F_1$ are magnified ten times.

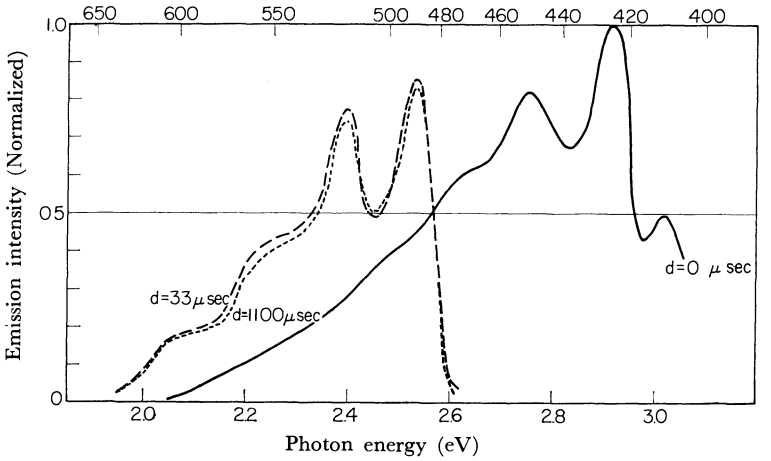

Fig. 2. Time-resolved emission spectra of LaD in alcohol solution at liquid nitrogen temperature. The delay time after the flash of exciting light is given by d. The relative intensities of emission bands for $d=33$ and 1100 μsec are magnified ten times.

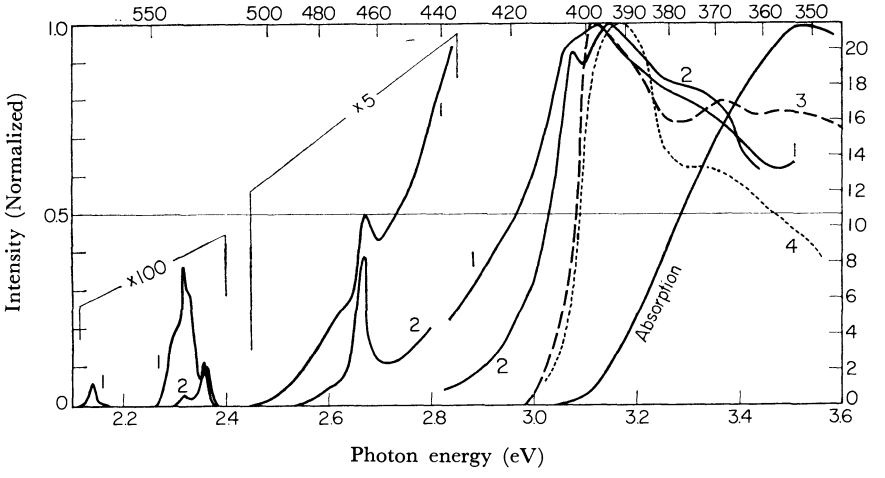

Fig. 3. Excitation spectra of EuD and LaD solutions at room and liquid nitrogen temperatures. No. 1: for europium emission of EuD at room temperature. 2: for europium emission at liquid nitrogen temperature. 3: for ligand phosphorescence of LaD at liquid nitrogen temperature. 4: for ligand fluorescence of LaD at liquid nitrogen temperature. The intensities of excitation bands in the region of 2.4—2.8 eV and 2.1—2.4 eV are magnified five and one hundred times, respectively. The absorption spectrum of EuD at room temperature is given for reference.

$\rightarrow {}^7F_2$. The emission spectrum of LaD consists of broad emission bands attributed to fluorescence and phosphorescence of the ligand. LaD exhibits no emission at room temperature. This is thought to be due to the collision of molecules in solution. At liquid nitrogen temperature, on the other hand, the sample is a rigid glass and no collisions take place; thus phosphorescence appears. EuD shows the emission both at room and liquid nitrogen temperatures although the emission intensity is much weaker at room temperature than at liquid nitrogen temperature.

The time-resolved emission spectra of LaD in ethanol solution at liquid nitrogen temperature are shown in Fig. 2. The higher energy bands in the spectra at 2.6 to 3.0 eV show very rapid decay, while the lower energy bands at 2.0 to 2.6 eV decay slowly. Thus the former is regarded as fluorescence due to the singlet-singlet transition and the later as phosphorescence due to the triplet-singlet transition.

The excitation spectra for europium emission due to the transition ${}^5D_0 \rightarrow {}^7F_2$ in EuD and also those for the ligand fluorescence and phosphorescence of LaD are shown in Fig. 3. The low energy edge of the excitation bands for the fluorescence and phosphorescence of LaD are located at nearly the same wavelength, 410 mμ. Comparing Fig. 3

with Figs. 1 and 2, it is obvious that the probability of excitation of the triplet state of the ligand due to direct optical absorption from the ground state is extremely small. As for europium emission, narrow excitation bands are found at 402 mμ, 464 mμ, 530 mμ and 580 mμ, in addition to the excitation band due to absorption by the ligand. These bands are attributed to transitions in the chelated europium ion, $^7F_{0,1}\rightarrow{}^5D_3$, $^7F_{0,1}\rightarrow{}^5D_2$, $^7F_{0,1}\rightarrow{}^5D_1$ and $^7F_{0,1}\rightarrow{}^5D_0$, respectively.

The decay curves of europium emission from EuD and of phosphorescence from LaD were measured at liquid nitrogen temperature. The decay time of the fluorescence from LaD could not be measured. The decay of the europium emission was exponential with a decay time of 0.394 msec. The phosphorescence from LaD also showed exponential decay with a decay time of 31.9 msec. This was found to be the longest decay time found among the various rare earth dibenzoylmethides.

The phosphorescence lifetime of LaD was measured in mixed solutions of LaD and EuD at liquid nitrogen temperature, in order to investigate whether energy transfer takes place from LaD to EuD. The total concentration, $C_{LaD}+C_{EuD}$, was kept at 2×10^{-4} M, while the ratio of C_{LaD} to C_{EuD} was changed. The result is shown in Fig. 4 as a function of the molar fraction of EuD (X_{EuD}). The lifetime is nearly constant in the region of X_{EuD} from 0 to 0.5, but in the region of X_{EuD} greater than 0.5, it decreases rapidly, becoming one fourth of the initial value at $X_{EuD}=0.9$. This fact indicates that the triplet state of LaD is quenched by the existence of EuD in the mixed solution.

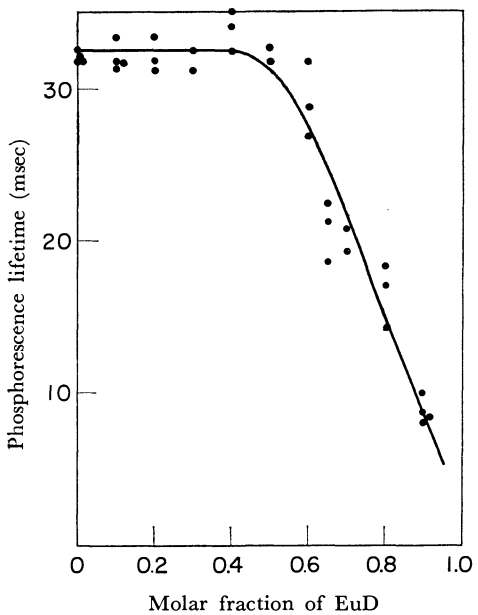

Fig. 4. The phosphorescence lifetime of LaD in mixed solutions of EuD and LaD at liquid nitrogen temperature.

The relative change of the europium emission intensity with the EuD molar fraction in the series of mixed solutions of EuD and LaD was measured with 546 mμ light excitation through the absorption of europium ion, and also with 365 mμ light excitation through the absorption by the ligand. The results at room temperature are given in Fig. 5. The intensities are normalized to unity at $X_{EuD}=1$ for both cases. It is seen that the europium emission intensity is exactly proportional to the EuD molar fraction.

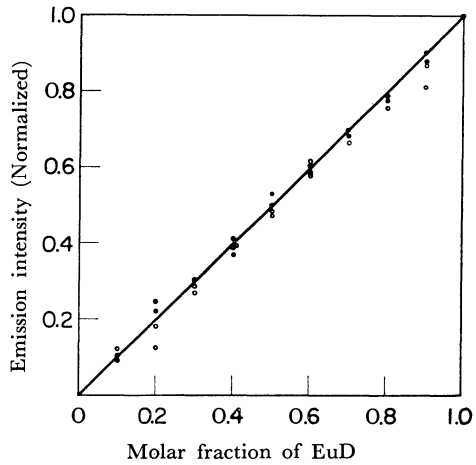

Fig. 5. The relative emission intensities of EuD in mixed solutions of EuD and LaD at room temperature. The mark ○ denotes the intensity obtained with direct excitation of europium ion (546 mμ), and ● indicates the intensity obtained with excitation of the ligand (365 mμ).

The absorbance of 546 mμ light by EuD is very small, and the optical density for a 1 cm thick layer of the solution with an EuD concentration of nearly 5×10^{-1} M is much smaller than 0.1. Therefore, the number of photons absorbed by the sample solution, n, is proportional to C_{EuD}, since

$$n = aI_0\{\exp(-\alpha C_{EuD}d)^{-1}\} \simeq a'I_0C_{EuD},$$

where I_0 is the intensity of light, α the absorption coefficient, and a and a' constants. If quenching of the emission from the chelated europium ion due to direct interaction between the europium ions does not occur, its emission intensity with 546 mμ excitation in the mixed solution, denoted by $I_{Eu}(546)$, should be

$$I_{Eu}(546) = \eta n = \eta a'IC_{EuD},$$

where η is the efficiency of the inner transition of europium ion. Figure 5 shows that this is actually the case.

For excitation with 365 mμ light, the absorption coefficient, α, of the ligand of EuD and LaD is nearly 2.0×10^4 l/mol cm. Therefore, light is

absorbed mostly in the vicinity of the front surface of the sample solution in the case of a concentration of $C_{LaD}+C_{EuD}=5\times10^{-3}$ M. The number of photons absorbed by EuD, n', is given by

$$n' = n_0 X_{EuD} = a' I_0' X_{EuD},$$

where n_0 is the number of photons absorbed by the mixed solution sample and I_0' the intensity of light. If intermolecular energy transfer from LaD to EuD is negligible, the europium emission intensity should be

$$I_{Eu}(365) = \eta' n' = \eta' a' I_0' X_{EuD},$$

where η' is the product of the efficiency of the intramolecular energy transfer and that of the emitting tansition of EuD. This agrees well with the experimental result given in Fig. 5. At room temperature, the phosphorescence of LaD, even in a solution of LaD only, is perfectly quenched, as mentioned above, because of the collision of molecules. This indicates that the lifetime of the triplet state of LaD is very short. Therefore, energy transfer from LaD to EuD at room temperature might be resonably neglected.

At liquid nitrogen temperature, since LaD shows phosphorescence, intermolecular energy transfer from LaD to EuD is expected to occur. In this case, it was difficult to measure directly the relative change of the europium emission intensity with EuD molar fraction in the mixed solutions. For this reason, the relative intensity was estimated from the excitation spectra in the following way. As mentioned above, at room temperature the concentration quenching of the europium emission due to interaction between chelated europium ions does not take place at the concentrations studied. This would also be the case at liquid nitrogen temperature. Then the relative change of the europium emission intensity with EuD molar fraction under 365 mμ light excitation, I_{Eu} (365), can be estimated by comparing the intensity of the excitation band due to ligand absorption with that of the excitation band due to europium absorption in the excitation spectrum for europium esmission. Namely,

$$I_{Eu}(365) = X_{EuD}\frac{J_{Eu}(365)}{J_{Eu}(568)\{\text{or } J_{Eu}(464)\}},$$

where $J_{Eu}(456)$ and $J_{Eu}(528)$ are the areas of the excitation bands at 456 and 528 mμ due to europium absorption, respectively, and $J_{Eu}(365)$ is the area of the excitation band due to ligand absorption between 360 and 380 mμ. The result is given in Fig. 6(a). The values are normalized to unity at $X_{EuD}=1.0$. If intermolecular energy transfer from LaD to EuD does not occur, $I_{Eu}(365)$ should be proportional to X_{EuD}. In the figure, it is seen that the curve of the intensity of the europium emission is located above the 45° line. This fact indicates that intermolecular energy transfer takes place from LaD to EuD, thus giving rise to an enhancement of the europium emission.

The relative change of the intensity of phosphorescence from LaD with EuD molar fraction in the mixed solutions was measured in a way similar to the case of europium emission. The relative intensity of the phosphorescence with 365 mμ excitation, $I_{ph}(365)$, is given by

$$I_{ph}(365) = X_{EuD}\frac{J_{ph}(365)}{J_{Eu}(464 \text{ or } 528)},$$

where $J_{ph}(365)$ is the area of the excitation band from 360 to 380 mμ for ligand phosphorescence. The result is given in Fig. 6(b). The values are normalized to 0.9 at $X_{EuD}=0.1$. If intermolecular energy transfer does not occur, $I_{ph}(365)$ should be proportional to the molar fraction of LaD. It is seen that the curve of phosphorescence intensity is located below the 45° line. As shown in Fig. 4,

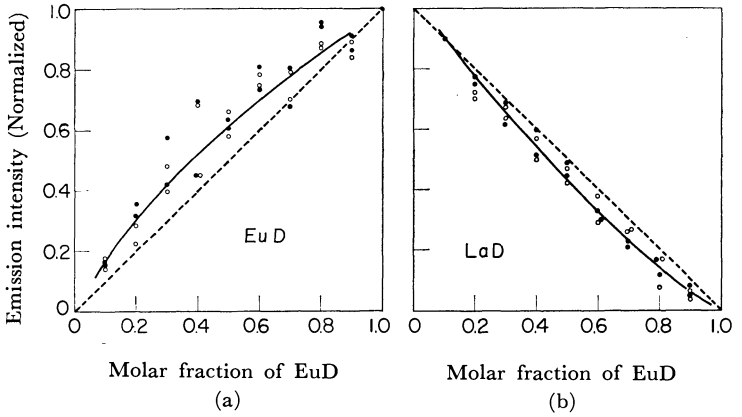

Fig. 6. The relative intensities of (a) europium emission of EuD and (b) ligand phosphorescence of LaD in mixed solutions of EuD and LaD with excitation of the ligand at liquid nitrogen temperature. The mark ● and ○ denote, respectively, that in the measurement the area of the excitation band at 528 and 464 mμ due to europium absorption is referred to.

the decay time of the phosphorescence of LaD is decreased in mixed solutions with higher EuD concentrations. These facts clearly indicate that ligand phosphorescence is quenched by the existence of EuD in solutions because of energy transfer at liquid nitrogen temperature.

Comparing Fig. 6(a) and 6(b), it is seen that enhancement of the europium emission is nearly proportional to the quenching of the phosphorescence of LaD. Therefore, it is quite obvious that intermolecular energy transfer occurs efficiently from the triplet state of LaD to the chelated europium ion in EuD. The possibility that this energy transfer occurs directly from the triplet state of LaD to the excited state of the europium ion in EuD can be rejected, since it was confirmed that in the mixed ethanol solution of europium free ion and free ligand, *i. e.*, dibenzoylmethane, energy transfer from the latter to the former is not observed.

It is, therefore, undoubted that energy transfer takes place from the triplet state of LaD to the triplet state of EuD, and further to the chelated europium ion. Then, in final conclusion, one can say that this fact is clear evidence that intramolecular energy transfer in europium chelates occurs *via* the triplet state of the ligand.

The authors wish to thank Mr. M. Morita in this laboratory for his discussion.

BULLETIN OF THE CHEMICAL SOCIETY OF JAPAN VOL. 41 1518—1524 (1968)

Group Interactions in Polyelectrolytes. I. Amination Kinetics of Chloromethylated Polystyrene

Hiroshi KAWABE and Masaya YANAGITA

The Institute of Physical and Chemical Research, Yamato-machi, Saitama

(Received December 2, 1967)

Chloromethylated polystyrene is quantitatively aminated by *n*-butylamine or *n*-dibutylamine in dioxane, but the plot of the logarithmic term in the simple second-order rate equation against the time is not represented by a single straight line, but is divided into two lines which intersect nearly at the half-amination point. These results are interpreted in terms of the step-by-step amination resulting from the steric effect of the already-aminated neighbors which have bulky alkyl groups. By assuming two distinct reactivities of chloromethyl groups according to their neighboring environment, rate equations for two separate steps are derived; these equations give k_1, the rate constant in the first step, and k_2, that in the second step. In the presence of a large excess of amine, the over-all kinetics can be expressed by:

$$dx/dt = [ab/(2k_1 - k_2)][2k_1(k_1 - k_2)e^{-2k_1at} + k_1k_2e^{-k_2at}],$$

where x is the concentration of chloride ions at time t; a is the initial concentration of amine, and b, that of the chloromethyl group. The equation is found to be substantially valid for the values of k_1 and k_2 computed by the equations for the individual steps.

The kinetics of the reaction of chloromethylated polystyrene with triethylamine in dimethylformamide was studied by Noda and Kagawa,[1] who found that the rate conforms to the simple second-order equation. In dioxiane, however, they could measure only the rate at the initial stage, because the quaternized polymer precipitated in the solvent. Fouss *et al.*[2] observed that, in the quaternization of poly-4-vinylpyridine by *n*-butyl bromide in tetramethylene sulfone or in propylene carbonate, the rate becomes less than that corresponding to the simple second-order kinetics as the quaternization proceeds, rapidly beyond half-quaternization; they ascribed this to the charge being built up on the polymer.

The present authors have carried out the amination of chloromethylated polystyrene with *n*-butylamine or di-*n*-butylamine in dioxane and have found that the reaction proceeds quantitatively and that the apparent second-order rate constant decreases markedly beyond the half-amination point. Analysis of the experimental results suggests that the amination proceeds in two steps due to the steric effect of the already-aminated neighboring groups on the polymer, to which bulkyl alkyl groups are introduced by amination. The purpose

1) I. Noda and I. Kagawa, *Kogyo Kagaku Zasshi (J. Chem. Soc. Japan, Ind. Chem. Sect.)*, **66**, 857 (1963).
2) R. M. Fuoss, M. Watanabe and R. D. Coleman, *J. Polymer Sci.*, **48**, 5 (1960).

of the present study is to derive rate equations for the step-by-step reaction and to evaluate the kinetics data by means of those equations.

Experimental

Materials. The chloromethylated polystyrene was prepared as follows. Styrene, which had been distilled under a reduced pressure (69.5°C/60 mmHg), was polymerized by the suspension-polymerization procedure.[3] Styrene containing 1% benzoyl peroxide was stirred at 90°C for seven hours in a solution of polyvinyl alcohol. The process of polymerization was followed by occasional measurements of the specific gravity of the polymer beads; it reached a constant value of 1.05 after three hours. The chloromethylation of polystyrene was carried out by the procedure reported by Pepper *et al.*[4] Two samples of different degrees of chloromethylation were prepared; they are shown in Table 1. The anhydrous amines, benzyl chloride, and ethylene bromide were distilled before use. All the other chemicals were of a reagent grade, while de-ionized, de-carbonized water was used throughout.

Table 1. Chloromethylation of polystyrene

Code	Content of Cl	Degree of chloromethylation
SC-1	19.79%	0.85
SC-2	12.88%	0.55

Amination of Chloromethylated Polystyrene. Jones[5] found that the amination of chloromethylated polystyrene with ammonia or amines other than tertiary amines brought about cross-linking. Since this cross-linking is to be ascribed to a side-reaction of chloromethyl groups with amino groups formed on the polymer, it can be prevented by avoiding the contact of polymer molecules, by lowering the rate of the side-reaction, and by enhancing the principal reaction. This can be done under the following conditions: (i) a low concentration of the polymer, (ii) a large molar ratio of the amines to the chloromethyl group, and (iii) the use of an amine with a bulky alkyl group. Preliminary experiments carried out to examine these conditions showed that the precipitation of the polymer or the separation of the dissolved phase took place in amination with ammonia or monomethylamine. An experiment with a large excess of *n*-butyl amine proved that the amination proceeded to completion without any precipitation of the polymer or any separation of the dissolved phase. The polymer was also quantitatively aminated by di-*n*-butylamine without any separation of the polymer phase, though a few crystals of the amine hydrochloride precipitated.

Kinetic Measurements. One gram of chloromethylated polystyrene was dissolved in 50 m*l* of a dioxane and thoroughly mixed with 100 m*l* of a dioxane solution containing a large excess of an amine. The molar ratio of the amine to the chloromethyl group was about 20. The temperature of the reaction mixture was maintained within ±0.5°C by means of a thermostat. At appropriate intervals, portions of the solution, which were taken out by a pipet from the reaction vessel or which had previously been distributed in tubes dipped in the thermostat, were poured into aqueous solutions containing an amount of nitric acid sufficient to neutralize the amine. The precipitate of the polymer was then filtered off and washed with water, and the filtrate was potentiometrically titrated with 0.1 N silver nitrate by the use of Beckman's Model G pH meter to determine the chloride ions. The error caused by the titration was less than ±0.3%. The volume concentration of the amine and the chloromethyl group in a reaction mixture were calculated by considering the coefficient of the expansion of dioxane. The experimental conditions are listed in Table 2, where *a* denotes the initial concentration of the amine, and *b* the initial concentration of the chloromethyl group.

Table 2. Amination of chloromethylated polystyrene

Code	Temp. °C	Polymer	*b* mol/*l*	Amine	*a* mol/*l*	*a*/*b*
A	30	SC-1	0.0367	*n*-Butyl	0.661	18
B	45	SC-1	0.0361	*n*-Butyl	0.657	18
C	60	SC-1	0.0356	*n*-Butyl	0.646	18
D	50	SC-1	0.0359	Di-*n*-butyl	0.723	20
E	60	SC-1	0.0356	Di-*n*-butyl	0.715	20
F	70	SC-1	0.0352	Di-*n*-butyl	0.708	20
G	60	SC-2	0.0232	*n*-Butyl	0.464	20

Amination Kinetics of Ethylene Dibromide and Benzyl Chloride. The amination of ethylene dibromide or benzyl chloride in dioxane was examined kinetically in the same way as the amination of chloromethylated polystyrene. The experimental conditions are shown in Table 3.

Table 3. Amination of ethylene bromide and benzyl chloride

Code	Temp. °C	Halide	*b* mol/*l*	Amine	*a* mol/*l*	*a*/*b*
H	50	Ethylene bromide	0.0687	*n*-Butyl	1.374	20
I	60	Ethylene bromide	0.0680	Di-*n*-butyl	1.360	20
J	30	Benzyl chloride	0.0561	*n*-Butyl	1.123	20
K	40	Benzyl chloride	0.0514	*n*-Butyl	1.029	20
L	50	Benzyl chloride	0.0512	*n*-Butyl	1.395	27
M	60	Benzyl chloride	0.0522	*n*-Butyl	1.423	27

***N*-Methylation of Ethylenediamine.** In a vessel protected from light, there was placed a 300 m*l* portion of an aqueous solution of methyl iodide (0.1 mol/*l*), and then 5 m*l* of an aqueous solution of ethylenediamine

3) H. Kawabe and M. Yanagita, *Kogyo Kagaku Zasshi (J. Chem. Soc. Japan, Ind. Chem. Sect.)*, **61**, 137 (1958); *J. Sci. Res. Inst.*, **51**, 182 (1957).
4) K. W. Pepper, H. M. Raislay and M. A. Young, *J. Chem. Soc.*, **1953**, 4097.
5) G. D. Jones, *Ind. Eng. Chem.*, **44**, 2686 (1952).

(1 mol/l) were added. The temperature of the system was maintained at 30±0.5°C during the course of the reaction. The initial concentrations of methyl iodide and ethylenediamine were 0.0984 mol/l and 0.0160 mol/l respectively. At time intervals aliquots were withdrawn; each was poured into diluted nitric acid and titrated potentiometrically with 0.1 N silver nitrate. An amount of iodide ions nearly equivalent to the quantitative methylation of both amino groups was produced within 48 hr; this amount remained substantially constant even after 100 hr. A blank test for the hydrolysis of methyl iodide in pure water showed that the error caused in amination by the hydrolysis would not exceed 0.8% after six hours, 1.4% after 24 hr, and 2.4% after 48 hr. The *N*-methylation of ethylenediamine was found to be fully inhibited by the presence of excess nitric acid; this was shown by the fact that no production of iodide ions was observed, even after six hours, when ethylenediamine had previously been neutralized with an excess of nitric acid.

Results

Since benzyl chloride is quantitatively aminated in dioxane by *n*-butylamine, its rate can be fully given by the simple second-order equation:

$$dx/dt = k(a - x)(b - x) \quad (1)$$

where x is the concentration of chloride ions at time t; a is the initial concentration of the amine, and b, that of benzyl chloride. Upon integration, Eq. (1) yields:

$$k = \frac{1}{(a-b)t}\ln\frac{b(a-x)}{a(b-x)} = \frac{2.303}{(a-b)t}\log\frac{1-\alpha}{1-\beta} \quad (2)$$

where $\alpha(=x/a)$ is the fraction of converted amine, and $\beta(=x/b)$, that of benzyl chloride. As may be seen in Fig. 1, where the logarithmic term in Eq. (2) is plotted against the time, the linearity of the plots indicates that the amination proceeds normally; a single value of k is obtained from the slope for each temperature. Table 4 summarizes the values of k computed by Eq. (2); the activation energy, E, obtained from a plot of $\log k$ against $1/T$, and the frequency factor, A, computed by the relation $k=A\cdot\exp(-E/RT)$. A value of k at any given temperature may be obtained by:

$$k = (7.88\times10^5)\cdot e^{-12500/RT}\ l/\text{mol min}$$

TABLE 4. AMINATION OF BENZYL CHLORIDE BY *n*-BUTYLAMINE

Code	Temp. °C	$k\times10^3$ l/mol min	$A\times10^{-5}$ l/mol min	E kcal/mol
J	30	0.777	7.98	12.5±0.2
K	40	1.42	7.57	
L	50	2.73	7.76	
M	60	5.03	8.20	

The amination of a chloromethylated polystyrene, SC-1, in dioxane has been carried out in the presence of a large excess of *n*-butylamine or *n*-dibutylamine. The polymer, as well as benzyl chloride, is quantitatively aminated by the amines without separating polymer phase. This fact suggests that cross-linking can hardly take place. This effective inhibition of the cross-linking may be ascribed to the steric effect of bulky alkylamino groups, which hinder the access of halide groups.

The rate constant for the polymer computed by Eq. (2), in contrast to the case of benzyl chloride, decreases with β, markedly beyond $\beta=0.5$ Figures 2 and 3 show plots of the logarithmic term in Eq. (2) against the time. Each plot seems to consist of two straight lines which intersect near $\beta=0.5$; this implies that the amination proceeds in two steps. This results may be explained by postulating that the amination of chloromethyl groups proceeds normally at the initial stage, but that after the half-amination point it is obstructed by both nearest neighbors, which are already aminated.

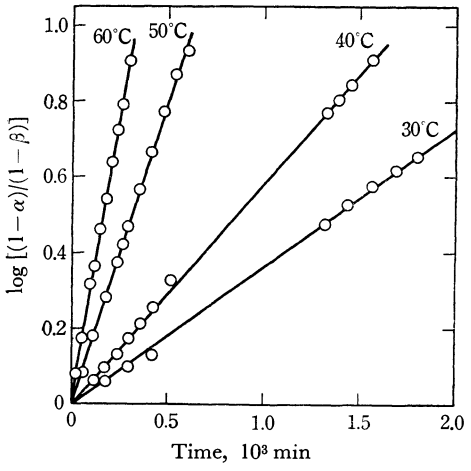

Fig. 1. Amination of benzyl chloride by *n*-butylamine.

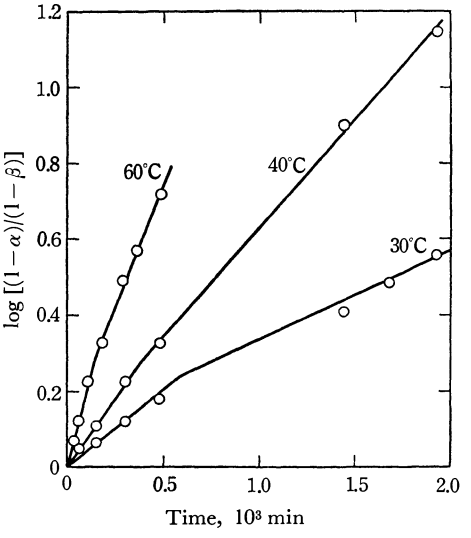

Fig. 2. Amination of SC-1 by *n*-butylamine.

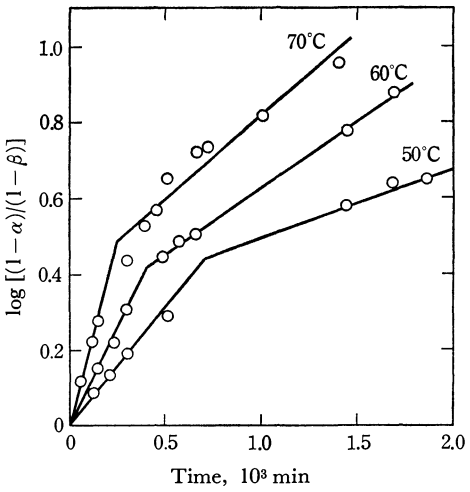

Fig. 3. Amination of SC-1 by di-*n*-butylamine.

The possible effect of this obstruction may be (i) electrostatic and/or (ii) steric. The electrostatic effect is less possible here, since amino groups formed on the polymer may not ionize because of a large excess of amine in the system and because of the rather non-polar property of dioxane as a solvent. The steric effect is more likely, since the amine molecules are presumably hindered from access to a reacting point by its nearest neighbors, which have bulky alkyl groups.

These assumptions have been examined by the aminations of a half-chloromethylated polystyrene, SC-2, and of ethylene dibromide, both of which are shown in Fig. 4. Since the plots are linear, the rates of these reactions are given fully by Eq. (1). The results support the second assumption

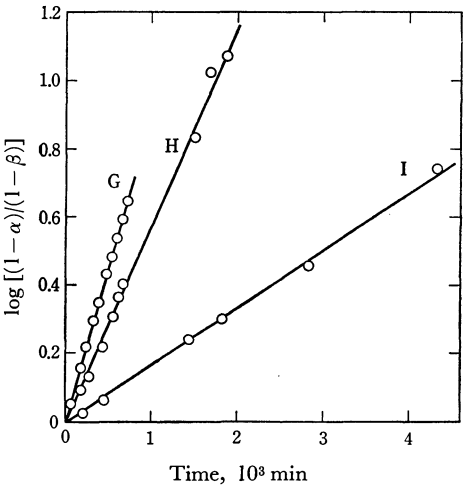

Fig. 4. Amination of half-chloromethylated polystyrene (SC-2) and ethylene bromide.

G: SC-2, *n*-butylamine, 60°C
H: Ethylene bromide, *n*-butylamine, 50°C
I: Ethylene bromide, di-*n*-butylamine, 60°C

(ii). If the effect of charged or polar groups is a dominant factor, the plots will not be linear, especially for ethylene dibromide. The linearity of the plot for SC-2 suggests, moreover, that the spacing of the groups can control the access of amine molecules. The value of k for SC-2, as computed by Eq. (2), is 4.61×10^{-3} l/mol min, which is comparable to that for benzyl chloride at the same temperature, 5.03×10^{-3} l/mol min.

Rate Equations

Derivation of the Rate Equations. In the reaction of chloromethylated polystyrene with the amines, two kinds of reactivity are assumed for chloromethyl groups, which are classified into the isolated ones which have a normal reactivity and the ones under the steric effect, both of whose nearest neighbors are already aminated. If each reaction is bimolecular and takes place separately, the rate constant for each reaction will be given by:

$$k = \frac{2.303}{(a-b)} \cdot \frac{\mathrm{d} \log[(1-\alpha)/(1-\beta)]}{\mathrm{d}t} \qquad (3)$$

In the actual course of reaction, however, the two kinds of reaction may overlap. This situation is illustrated by Fig. 5, where the broken lines represent the assumed separated courses of reaction and the full line, the actual course of reaction. When the isolated chloromethyl groups are almost consumed at point P, only the groups under the steric effect remain and the actual curve lies essentially on the assumed one for the second step. Since the actual curve (full line) in the initial

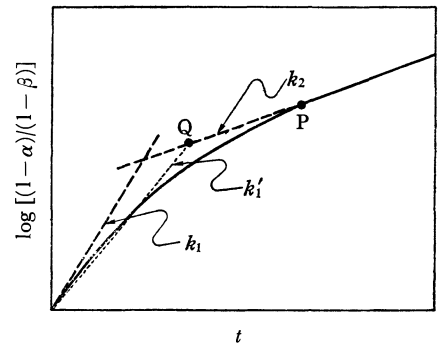

Fig. 5. Illustration of stepwise amination.

stage of reaction can be expressed approximately by the dotted line, the over-all course of the reaction may apparently be expressed by two straight lines intersecting at point Q. The experimental results summarized in Figs. 2 and 3 can be explained by this illustration based on the two-step-reaction concept.

A polymer reaction of this kind may thus be reduced to a reaction between a low molecular compound with two reactive groups and a reagent,

a reaction which is illustrated by the following figure:

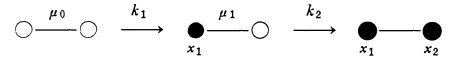

where white circles represent unchanged groups and black circles, changed ones. The relationships among the concentrations are:

$$\mu_0 = M - x_1 = (b/2) - x_1 \quad (4)$$

$$\mu_1 = x_1 - x_2 = 2x_1 - x \quad (5)$$

where M is the initial concentration of the compound; μ_0 and μ_1 are the concentration of the unchanged and the partially-changed compound, respectively, at time t; b is the initial concentration of the reactive group; x is the change in the concentration of a reagent or the concentration of the changed group at time t, and x_1 and x_2 are concentrations of the first and second changed groups in the compound, respectively, at that time.

The over-all rate of the above reaction with the rate constants of k_1 and k_2 is given by :

$$\begin{aligned} dx/dt &= (a-x)(2k_1\mu_0 + k_2\mu_1) \\ &= (a-x)[k_1 b - 2(k_1-k_2)x_1 - k_2 x] \end{aligned} \quad (6)$$

where a is the initial concentration of a reagent.

On the assumption that $x \simeq x_1$ in the initial stage of reaction ($\beta < 0.5$) and $x_1 \simeq b/2$ in the final stage of reaction ($\beta > 0.5$), the integration of Eq. (6) yields:

$$k_1 = \frac{1}{[(2-k_2/k_1)a-b]t} \ln \frac{1-\alpha}{1-(2-k_2/k_1)\beta} \quad (7)$$

$$k_2 = \frac{1}{(a-b)(t-\tau)} \left(\ln \frac{1-\alpha}{1-\beta} - \ln \frac{1-\chi/a}{1-\chi/b} \right) \quad (8)$$

where τ is a time and χ is a value of x at a point, where $x_1 \simeq b/2$. An approximate value of k_1 may be obtained by Eq. (9), as is illustrated in Fig. 5:

$$k_1' = \frac{1}{(a-b)t} \ln \frac{1-\alpha}{1-\beta} \quad (9)$$

A value of k_1 can be determined from a value of k_2/k_1' by the use of Eq. (7).

When a large excess of a reagent is used, $(a-x)$ in Eq. (6) is replaced by a and x_1 is given by:

$$x_1 = (b/2)(1 - e^{-2k_1 at}) \quad (10)$$

Thus, Eq. (6) integrates to:

$$x = b\left[1 - \frac{k_1-k_2}{2k_1-k_2} e^{-2k_1 at} - \frac{k_1}{2k_1-k_2} e^{-k_2 at}\right] \quad (11)$$

and the over-all rate is given by:

$$dx/dt = \frac{ab}{2k_1-k_2}[2k_1(k_1-k_2)e^{-2k_1 at} + k_1 k_2 e^{-k_2 at}] \quad (12)$$

Examination of the Equations by the *N*-Methylation of Ethylenediamine. The rate equation should first be tested on a low-molecular compound of two reactive groups as a model of the amination of chloromethylated polystyrene, where steric hindrance is a predominant factor. Since it was difficult to find such a compound, however, the equation have been examined by the *N*-methylation of ethylenediamine. Ethylenediamine is quantitatively *N*-methylated with an excess of methyl iodide in water, but the reaction is inhibited in the presence of excess acid. This fact means that the higher substitution of an amino group is inhibited, probably by the electrical charge formed on the methylated group. When one amino group of ethylenediamine is methylated, the charge of the group may also electrostatically hinder the methylation of another group on the same molecule. Thus, the reaction will proceed in two steps and the rate is given by Eq. (6), where a and b are the initial concentrations of methyl iodide and the amino group respectively. Figure 6, where α and β are fractional conversions of methyl iodide and the amino group respectively, shows that the reaction proceeds in two distinct steps. The value of k_2 is 1.30×10^{-2} l/mol min, a value which is obtained from the slope in the second step according to Eq. (8). An appropriate value for k_1', estimated according to Eq. (9), is 4.79×10^{-2} l/mol min. The values of k_1 obtained from repeated computations by Eq. (7) are 5.97×10^{-2} l/mol min for the first computation, 6.10×10^{-2} for the second, and 6.12×10^{-2} for the third.

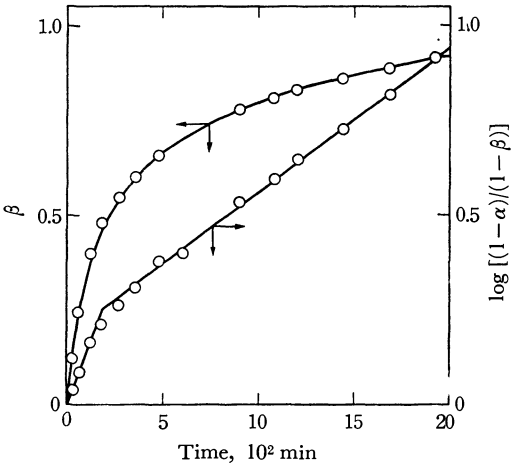

Fig. 6. *N*-Methylation of ethylenediamine in water at 30°C.

Discussion

The rate equations presented in the previous section were applied to the amination of chloromethylated polystyrene; the results of these calculations are summarized in Table 5.

Since a large excess of amine is used for the amination, the over-all course of reaction may be described by Eq. (11), using the values of k_1 and k_2 listed in Table 5. The values are compared in

TABLE 5. RATE CONSTANTS OF AMINATION OF SC-1

(a) *n*-Butylamine

Code	Temp. °C	Rate constants $\times 10^3$, *l*/mol min k_2 Eq. (8)	k_1' Eq. (9)	k_1 Eq. (7)	k_2/k_1
A	30	0.922	1.39	1.54	0.60
B	45	2.09	2.82	2.88	0.73
C	60	4.84	7.54	8.17	0.59

(b) Di-*n*-butylamine

Code	Temp. °C	Rate constants $\times 10^3$, *l*/mol min k_2 Eq. (8)	k_1' Eq. (9)	k_1 Eq. (7)	k_2/k_1
D	50	0.598	2.12	2.67	0.22
E	60	1.14	3.56	4.22	0.27
F	70	1.50	6.52	7.95	0.19

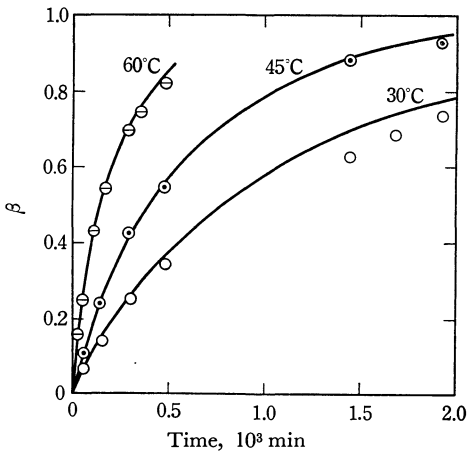

Fig. 7. Amination of SC-1 by *n*-butylamine.
○: 30°C ⊙: 45°C ⊖: 60°C

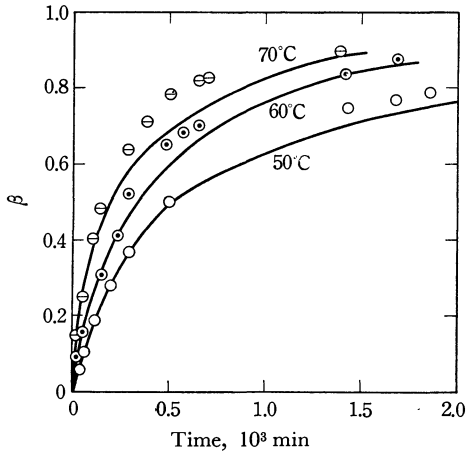

Fig. 8. Amination of SC-1 by di-*n*-butylamine.
○: 50°C ⊙: 60°C ⊖: 70°C

Figs. 7 and 8, where the full lines have been calculated by the use of Eq. (11) and where the circles represent the observed values. The reasonable agreement between the two values justifies the application of the rate equations to the polymer reaction. In Fig. 9, two runs, with *n*-butylamine and with di-*n*-butylamine, are compared; they have almost the same value of k_1. In the figure, β is divided into two components, *viz.* $\beta_1(=x_1/b)$ and $\beta_2(=x_2/b)$, by virtue of Eq. (10); the components apparently illustrate how overall rate is modified by the value of k_2, and also support the validity of the assumptions that $x \simeq x_1$ for the initial stage of reaction and that $x_1 \simeq b/2$ for the final stage.

The rate constants are plotted against $1/T$ in Fig. 10, while the values of E, the activation energy, as calculated by the least-squares method, are

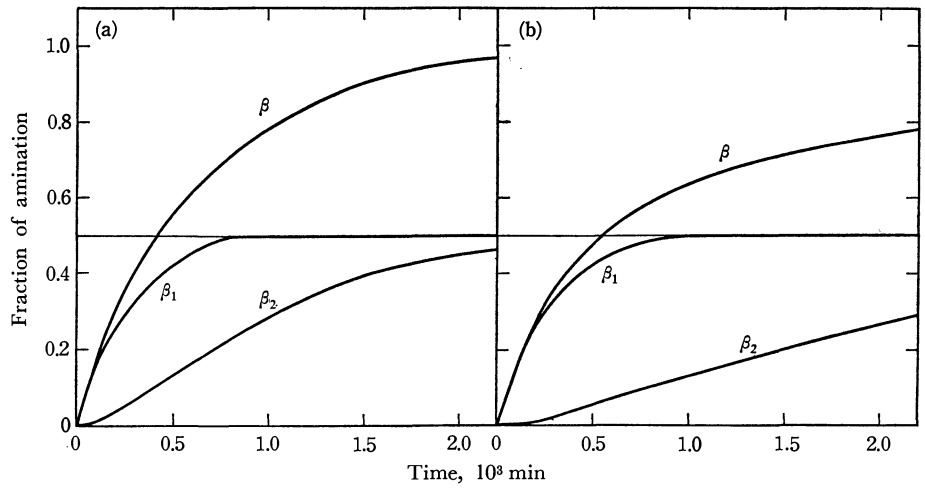

Fig. 9. Dependence of amination kinetics on the group interaction.
(a) Code B, *n*-butylamine, $k_1=2.88\ 10^{-3}$ *l*/mol min, $k_2=2.09\ 10^{-3}$ *l*/mol min
(b) Code D, di-*n*-butylamine, $k_1=2.67\ 10^{-3}$ *l*/mol min, $k_2=5.98\ 10^{-4}$ *l*/mol min

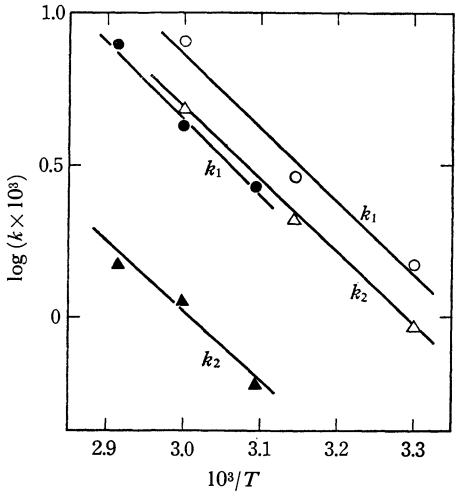

Fig. 10. Dependence of rate constants on temperature.

○, △: *n*-Butylamine
●, ▲: *n*-Dibutylamine

listed in Table 6, as are the mean values of A, the frequency factor, computed by means of:

Table 6. Activation energies and frequency factors of amination of SC-1

Amine		E kcal/mol	$A\times10^{-4}$ l/mol min
n-Butyl	k_1	11.1±1.3	14.5
	k_2	11.1±0.5	9.14
n-Dibutyl	k_1	12.0±0.9	8.69
	k_2	10.2±1.5	1.96

$$k = A\cdot e^{-11100/RT}\ l/\text{mol min}$$

The values of E thus obtained are fairly constant, being comparable to that of the monomeric one. On the other hand, the A value for k_2 is lower than that for k_1, and the difference is significantly larger in *n*-dibutylamine than in *n*-butylamine. These facts also suggest that the abnormal decrease in the rate in the course of amination is due to the steric effect of the neighbors.

The authors wish to express their thanks to Mr. A. Oohata for his helpful assistance in preparing the polymers and in carrying out the measurements.

BULLETIN OF THE CHEMICAL SOCIETY OF JAPAN VOL. 41 1524—1532 (1968)

Deuteron Magnetic Resonance of $NiSiF_6 \cdot 6D_2O$ and $NiSnCl_6 \cdot 6D_2O$

Takehiko CHIBA*1 and Gen SODA*2

The Institute for Solid State Physics, The University of Tokyo, Roppongi, Minato-ku, Tokyo

(Received December 15, 1967)

Deuteron magnetic resonance study was made on single crystals of $NiSiF_6 \cdot 6D_2O$ and $NiSnCl_6 \cdot 6D_2O$. Deuteron quadrupole coupling tensors were determined at various temperatures. In $NiSiF_6 \cdot 6D_2O$, the quadrupole coupling at -116°C is that of stationary D_2O, at 23°C and at 70°C that of D_2O under rapid 180°-flip motion and at 150°C that of rapid $Ni(D_2O)_6^{2+}$ reorientation. The eqQ/h values at -116°C, 238.3 ± 1.3 kc and 235.7 ± 1.9 kc do not appear to show marked effect of strong coordination. In $NiSnCl_6 \cdot 6D_2O$, the quadrupole coupling corresponding to D_2O under 180°-flip motion is observed at -53°C, at 25°C, and at 55°C. Spectra corresponding to a stationary D_2O are not observed even at 77°K. From the orientation of quadrupole tensors probable crystal structures of these compounds are proposed. Line width transitions were observed from which the reorientation rate was derived. The estimated activation energies of the 180°-flip motion of D_2O are 7.6 and 4.3 kcal/mol in the fluosilicate and chlorostannate, respectively, and that of $Ni(D_2O)_6^{2+}$ reorientation in the fluosilicate is 19 kcal/mol. Additional measurements of ^{19}F and ^1H resonances indicate the setting in of the SiF_6^{2-} reorientation at -110°—-120°C in $NiSiF_6 \cdot 6H_2O$, and that of the $Ni(H_2O)_6^{2+}$ reorientation in the chlorostannate at approximately the same temperature as the fluosilicate.

It has been shown in recent studies that the deuteron magnetic resonance (DMR) can provide useful informations about the structure and the motion of hydration water in crystals.[1,2] DMR of some O–D···O systems revealed strong dependence

*1 Present address: Department of Chemistry, Nihon University, Sakurajosui, Setagaya-ku, Tokyo.

*2 Present address: Department of Physical Chemistry, Faculty of Science, Osaka University, Toyonaka.

1) T. Chiba, *J. Chem. Phys.*, **39**, 947 (1963).

2) T. Tsang and D. E. O'Reilly, *ibid.*, **43**, 4234 (1965).

of the deuteron quadrupole coupling on the hydrogen bond strength.[3] Temperature dependence of the line-width was used to determine the barrier to the motion of water molecule in crystals.[1-3]

When the position of a water molecule is fixed by hydrogen bondings of X···H–O–H···Y, the activation energy to reorientation may be considered to be the work required to break these hydrogen bondings. Then the activation energy would be a good measure of the strength of the hydrogen bond.

The purpose of the present study is (1) to see the effect of strong coordination of a water molecule to a metal ion on the deuteron quadrupole coupling, and (2) to study the motion of a water molecule where hydrogen bond is to atoms other than oxygen, for instance, to chlorine where hydrogen bond is supposed to be weak, and also to study other possible motions such as an over-all rotation of a cluster ion.

It may be noted that frequently used technique for the study of motions in crystals is the measurement of temperature dependence of the spin-lattice relaxation time T_1, which in the present case is inapplicable, because of the strong relaxation due to the presence of paramagnetic ions.

The compounds studied here are $NiSiF_6 \cdot 6D_2O$ and $NiSnCl_6 \cdot 6D_2O$. The crystal structures of these compounds are isomorphous, consisting of $Ni(H_2O)_6^{2+}$ and $(SiF_6)^{2-}$ or $(SnCl_6)^{2-}$ group ions. According to Pauling's early X-ray analysis,[4] the crystal is trigonal of space group $R\bar{3}$, assuming distorted CsCl-like structure. One formula unit is contained in a unit cell. All the water molecules are in equivalent positions.

Experimental

Preparation of the Crystals. A single crystal of $NiSiF_6 \cdot 6D_2O$ (which had been grown from a solution of this compound synthesized from $BaSiF_6$ and $NiSO_4$ in heavy water) was kindly supplied by K. Kume. The crystal exhibits {110} and {1$\bar{1}$0} faces.

$NiSnCl_6 \cdot 6D_2O$. A solution of this compound was prepared by adding an equivalent amount of $NiCl_2$ into heavy water solution of $SnCl_4$. A single crystal was grown by slowly lowering the temperature of the saturated solution. The crystal exhibits dominant {100} faces.

Measurement of DMR. The apparatus and the method of the measurement of DMR have been described elsewhere.[5] Spectra of quadrupole-split lines are measured at various angles of rotation of the probe perpendicular to the static magnetic field H_0(rotation pattern). Orientation of the crystal on the mounting head of the probe is determined using a reflection goniometer. Measurement of the DMR was made at H_0 of 16600 G.

3) T. Chiba, *ibid.*, **41**, 1352 (1964).
4) L. Pauling, *Z. Kristallogr.*, **72**, 482 (1930).
5) T. Chiba, *J. Chem. Phys.*, **36**, 1122 (1962).

Results

Deuteron Quadrupole Coupling Tensor. $NiSiF_6 \cdot 6D_2O$. The appearance of the spectral lines is fairly broad throughout the temperature range studied indicating the rapid relaxation due to the presence of paramagnetic ions. Spectra with fairly good signal-to-noise ratio were obtained, however, since high rf level operation was possible.

The crystal structure is such that quadrupole coupling tensors can be transformed to one another by three-fold rotations about the [111] direction; therefore, it is sufficient for the determination of quadrupole coupling tensors to measure the rotation pattern for only one crystal setting provided that the axis of rotation does not coincide with the [111] direction.

A crystal-fixed coordinate (X_C, Y_C, Z_C) is defined here as,

X_C parallel to [1$\bar{1}$0],

Y_C parallel to [11$\bar{2}$],

Z_C parallel to [111].

The laboratory-fixed coordinate (X_L, Y_L, Z_L) is such that H_0 is in the plane of X_LY_L, and θ, the angle of rotation of H_0 is measured from X_L. For the crystal setting in this experiment the transformation matrix $\boldsymbol{U}$ from the crystal-fixed system to the laboratory-fixed system was determined optically as:

	X_C	Y_C	Z_C
X_L	0.4759	−0.8644	0.1624
Y_L	0.7805	0.3300	−0.5309
Z_L	0.4054	0.3794	0.8317

Figure 1(a) shows the rotation pattern of the spectra at −116°C. The paramagnetism of the crystal produces a small shift of central frequency, thus distorting the symmetry of the rotation pattern of high and low frequency satellites as seen in the figure. The effect of paramagnetic ions on the measurement of the quadrupole splitting will now be considered.

The bulk susceptibility of a nonspherical sample can produce a local field component perpendicular to the external field at the nucleus. If this field is large, correct angular dependence of quadrupole splitting may not be obtained. From a crude estimation, however, the shape effect in the present experiment is found to be negligible.

The internal field due to contact and dipolar interactions can give rise to a paramagnetic shift. This shift is small, however, as seen in the figure in the present study, less than 20 kc/sec. Therefore, the nucleus-electron spin interaction can be treated as a first-order perturbation, just like the quadrupole interaction. The effect is only to shift the Larmor frequency, and the correct rotation pattern of

quadrupole splitting can be obtained from the frequency difference between the upper and lower satellites just as in the absence of paramagnetic ions. The situation is analysed in more rigorous manner in the forthcoming paper on $CuSO_4 \cdot 5D_2O$.[6] Paramagnetic shifts in ^1H and ^{19}F resonances of $NiSiF_6 \cdot 6H_2O$ have been studied in detail at the liquid helium temperature by Kume and Sugawara.[7] In this study the paramagnetic shift is not analysed.

The rotation pattern of quadrupole splitting is obtained at -116°C, 23°C, 70°C, and at 150°C. At -116°C, six pairs of lines are obtained corresponding to two nonequivalent deuterons (D_1 and D_2) of D_2O. At room temperature and at 70°C, only three pairs are observed which means that the field gradient tensors (q-tensors) of D_1 and D_2 are averaged to give a single q-tensor by a rapid 180°-flip of D_2O (Fig. 1(b)). At 150°C only one pair is observed (Fig. 1(c)). This shows an additional averaging of q-tensors, corresponding to a setting in of rapid motion which interchanges D_2O at different sites. These motions will be discussed in a later section.

The determination of quadrupole coupling tensors is made as follows. First, the spectra at room temperature and at 70°C will be analysed. The curves A, B and C of rotation pattern of quadrupole splitting are formed as differences between A_+ and A_-, B_+ and B_- and C_+ and C_- of Fig. 1(b). Assume that curve A corresponds to a particular one of the three equivalent q-tensors, $q^{(1)}$, then curve B corresponds to a rotation pattern of $q^{(1)}$ in a crystal setting defined by the transformation matrix UC_3 or UC_3^{-1}, where

$$C_3 = \begin{pmatrix} \frac{1}{2} & -\frac{\sqrt{3}}{2} & 0 \\ \frac{\sqrt{3}}{2} & \frac{1}{2} & 0 \\ 0 & 0 & 1 \end{pmatrix}.$$

Similarly, curve C corresponds to a crystal setting of UC_3^{-1} or UC_3. Relative sign of the curves A, B and C can be readily found from the fact that the sum of A, B and C should give a rotation pattern of a quadrupole coupling tensor which is axially symmetric about Z_C axis. For the two alternative cases,

$$\left.\begin{array}{l} \text{Curve A}\cdots U \\ \text{Curve B}\cdots UC_3 \\ \text{Curve C}\cdots UC_3^{-1} \end{array}\right\} \text{ and } \left\{\begin{array}{l} U \\ UC_3^{-1} \\ UC_3 \end{array}\right\},$$

$q^{(1)}$ can be determined in the crystal-fixed coordinate system by the procedure described elsewhere.[6] The wrong set gives unrealistic result with large standard deviations and can easily be eliminated.

The low temperature pattern is analysed as follows. Here the assignment of the lines is made by comparison with the estimated rotation pattern from the room temperature data. Since the obtained room temperature quadrupole tensor is a typical of D_2O under rapid 180° flip motion approximate orientation of water molecule can be estimated and the predicted rotation pattern can be drawn by assuming 1) q_{zz} of D_1 and D_2 making an angle of 110° to each other, 2) $\eta = 0.1$, and 3) q_{yy} perpendicular to the molecular plane.[1,3] Here q_{zz} *etc.* are the principal components of q-tensor defined such that $|q_{xx}| \leq |q_{yy}| \leq |q_{zz}|$. The agreement of estimated pattern with the experimental one at -116°C is sufficient for the assignment of each curve of rotation pattern to be readily made. The low temperature rotation pattern is then analyzed in the same way as before and the quadrupole coupling tensors for the D_1 and D_2 are determined.

At 150°C the rotation pattern corresponds to the average of the room temperature pattern and is axially symmetric about Z_C axis. eqQ, η and the principal axis directions are given in Table 1.

$NiSnCl_6 \cdot 6D_2O$. General appearance of the spectra is similar to that of the fluosilicate. In this case three pairs of lines were observed at room temperature as in the fluosilicate indicating the averaging of field gradient tensors by a 180°-flip motion of water molecules. It is found that the line broadening due to this motion takes place at considerably lower temperatures than in the fluosilicate. The rotation pattern of the quadrupole splitting for the flipping water molecule is measured at -53°C, 23°C and at 55°C, and the quadrupole coupling tensor is determined in the same way as in the fluosilicate as shown in Table 1. Line broadening is observed in the temperature range of -85——125°C but spectra corresponding to the stationary deuterons are not observed even at the temperature of liquid nitrogen. Therefore, we were unable to determine quadrupole coupling for each deuteron.

Temperature Dependence of the Linewidth—Motional Effect. $NiSiF_6 \cdot 6D_2O$. As mentioned above, two different motions are observed by DMR, one is a 180°-flip motion of water molecules and the other is a motion which interchanges water molecules at different sites. Fortunately, broadening of spectral lines by these two motions occur in stepwise at different temperature ranges so that separate analysis of the motions can be made.

Temperature dependence of the linewidth at the fast and slow exchange limits of these two motions is observed at various temperatures and at various values of frequency splitting. To reduce the complexity of motional broadening due to dipolar structure the measurements are made at directions where original linewidth is small. These

6) G. Soda and T. Chiba, *J. Chem. Phys.*, to be published.
7) K. Kume and T. Sugawara, *J. Phys. Soc. Japan*, **19**, 688 (1964).

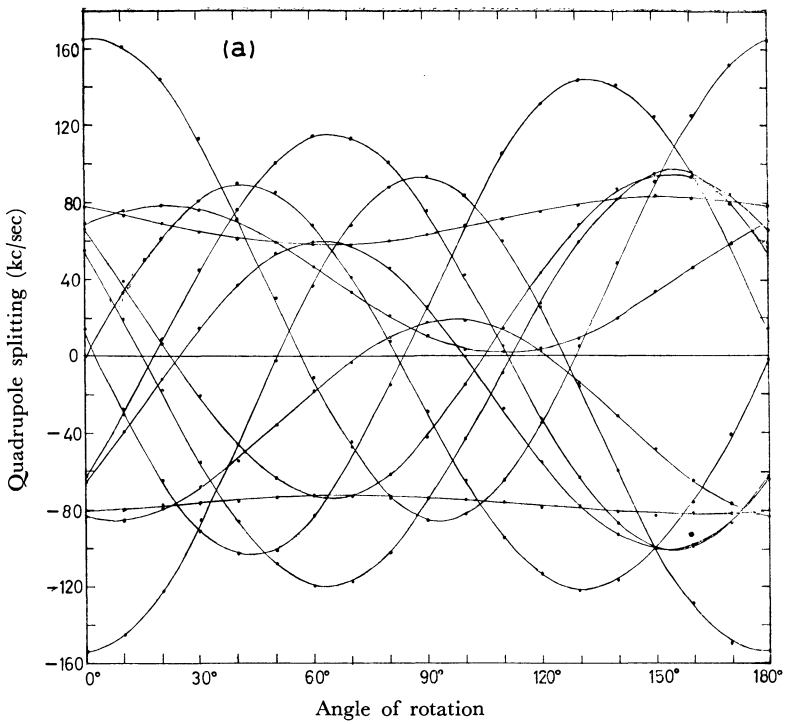

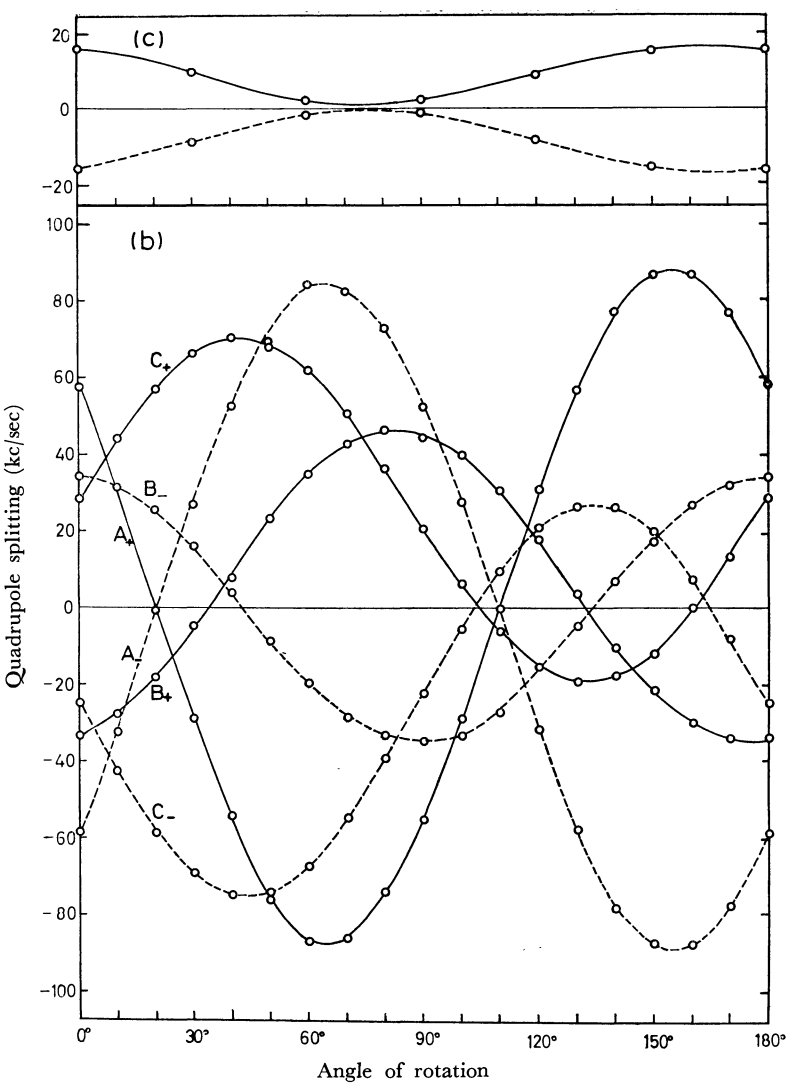

Fig. 1. Rotation pattern of deuteron resonance in $NiSiF_6 \cdot 6D_2O$ in the crystal orientation given in the text.
(a) at −116°C, (b) at 23°C and (c) at 150°C. Note thet a different frequency scale is used in drawing (a).

TABLE 1. DEUTERON QUADRUPOLE COUPLING eqQ/h, ASYMMETRY PARAMETER η AND THE PRINCIPAL AXIS DIRECTIONS* OF FIELD GRADIENT TENSOR IN $NiSiF_6 \cdot 6D_2O$ AND IN $NiSnCl_6 \cdot 6D_2O$ CRYSTALS

$NiSiF_6 \cdot D_2O$					
−116°C			X_C	Y_C	Z_C
D_1 eqQ/h	238.3±1.3 kc	q_{xx}	0.690	0.679	0.250
η	0.100±0.005	q_{yy}	0.721	−0.676	−0.154
		q_{zz}	−0.064	−0.287	0.956
D_2 eqQ/h	235.7±1.9 kc	q_{xx}	0.196	−0.055	0.979
η	0.110±0.005	q_{yy}	0.777	−0.600	−0.189
		q_{zz}	0.598	0.798	−0.075
23°C					
eqQ/h	120.7±0.6 kc	q_{xx}	0.509	0.421	0.751
η	0.950±0.007	q_{yy}	0.443	0.620	−0.648
		q_{zz}	0.738	−0.662	−0.129
70°C					
eqQ/h	115.1±0.5 kc	Same as above within experimental errors.			
η	0.963±0.006				
150°C					
eqQ/h	44.5±0.7 kc	q_{zz} parallel to Z_C.			
η	0				
$NiSnCl_6 \cdot 6DO$					
−53°C			X_C	Y_C	Z_C
eqQ/h	129.5±1.2 kc	Same as below within experimental errors.			
η	0.880±0.024				
25°C					
eqQ/h	121.1±0.8 kc	q_{xx}	0.498	0.431	0.752
η	0.906±0.012	q_{yy}	0.390	0.664	−0.638
		q_{zz}	0.775	−0.611	−0.162
55°C					
eqQ/h	118.4±1.1 kc	Same as above within experimental errors.			
η	0.906±0.025				

* The other two sets of principal axis directions which can be obtained from the one listed here by three-fold rotations about Z_C are omitted.

are used to determine the reorientation rate at various temperatures by the procedure used previously.[1,8] For the 180°-flip motion of water molecules the reorientation rate is determined as shown in Fig. 2. Assuming Arrhenius equation for this motion an activation energy of 7.6 kcal/mol with a pre-exponential factor of about 10^{14} sec^{-1} is obtained.

Three quadrupole coupling tensors of room temperature are averaged by a motion at high temperatures. We assume that this motion is a random reorientation of hydrated Ni ion among three equivalent sites in the equilibrium configuration. If the rate of jump from a site to another is denoted by Ω, we get from a theory,[9] for the slow exchange limit,

$$\Omega = \pi \Delta\nu_M, \tag{1}$$

and for the fast exchange limit,

$$\Omega = \frac{2\pi}{9} \frac{(\nu_1^2+\nu_2^2+\nu_3^2)}{\Delta\nu_M}, \tag{2}$$

where $\Delta\nu_M$ is the width due to the motion, ν_1 is the frequency difference at site 1, *etc.*, from the center of gravity of the spectra (*i.e.*, $\nu_1+\nu_2+\nu_3=0$). $\Delta\nu_M$ is determined from the line width change as before and the reorientation rates from the above equations are shown in Fig. 2.*3 An activation energy of 19 kcal/mol is obtained.

$NiSnCl_6 \cdot 6D_2O$. The line broadening at the fast exchange limit was observed as in the case of the fluosilicate. To estimate the activation energy of reorientation it is necessary to know the frequency difference between the two deuterons of a water molecule at the orientation of the crystal where

8) T. Chiba and Y. Kakiuchi, This Bulletin, **41**, 828 (1968).
9) P. W. Anderson, *J. Phys. Soc. Japan*, **9**, 316 (1954).

*3 For the fast exchange limit $\Delta\nu_M$ is derived from the width between maximum slopes ($\Delta\nu_{msl}$) as $\Delta\nu_M = \frac{\sqrt{3}}{2}\Delta\nu_{msl}$, neglecting dipolar width.

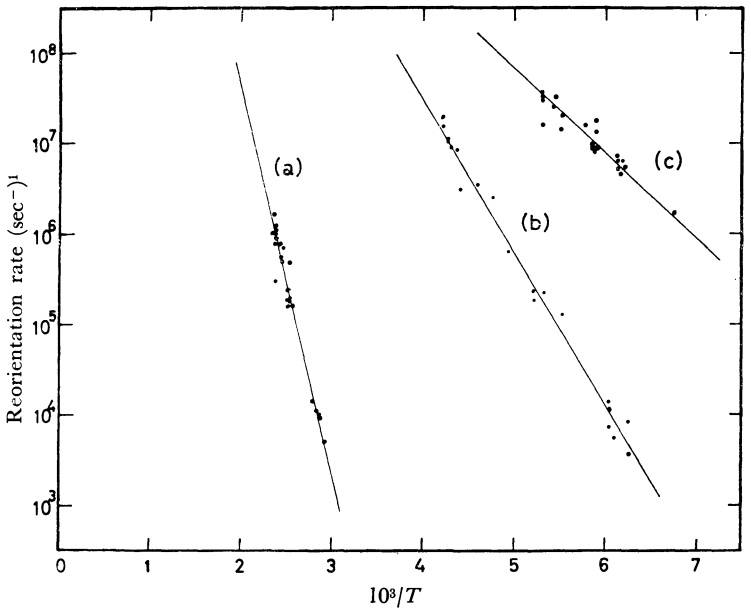

Fig. 2. Temperature dependence of reorientation rates determined from the line width change of DMR.

(a) $Ni(D_2O)_6^{2+}$ reorientation in $NiSiF_6 \cdot 6D_2O$.
(b) 180° flip motion of D_2O in $NiSiF_6 \cdot 6D_2O$.
(c) 180° flip motion of D_2O in $NiSnCl_6 \cdot 6D_2O$.

linewidth is measured. Since the spectra of stationary state were not measured this is estimated from the high temperature quadrupole coupling tensor. It is assumed that the two deuterons of a water molecule have the same quadrupole coupling tensor nearly axially symmetric about each OD bond making an angle of 110° with each other. With this assumption using the quadrupole coupling data at room temperature it is possible to estimate frequency difference between the lines of two deuterons at a given orientation of the crystal. The result is shown in Fig. 2. The activation energy for reorientation is then estimated to be 4.3 kcal/mol.

Discussion

Quadrupole Coupling Tensor. The value of eqQ and η are nearly the same as those observed in other water of crystallization. There appears to be no marked effect of coordination on eqQ of deuteron.

Crystal structure has not been known for $NiSiF_6 \cdot 6H_2O$ except the lattice constant and space group ($a=6.255$ Å, $\alpha=96°6'$, space group $R3$).[4] A neutron diffraction study has recently been done on $FeSiF_6 \cdot 6H_2O$[10] which was believed to be isomorphous with $NiSiF_6 \cdot 6H_2O$. It was concluded that ferrous fluosilicate has space group $R\bar{3}m$ instead of $R\bar{3}$, presumably due to statistical distribution of two slightly differently oriented structures. If it were also the case in the nickel salts, it could be easily detected as doubling of the number of satellite pairs*4 and/or from the symmetry of observed field gradient tensor. Since no such effects are indicated in nickel fluosilicate and chlorostannate, the crystal symmetry is not $R\bar{3}m$.

It has been known that to a good approximation the q_{zz} direction is in the bond direction and q_{yy} direction perpendicular to D_1OD_2 plane.[3] In the case of $NiSiF_6 \cdot 6D_2O$ the angle between the direction of q_{zz} of D_1 and that of D_2 is 109.8°, and the deviations of the q_{yy} directions of D_1 and D_2 from the normal to the plane defined by the q_{zz} directions of D_1 and D_2 are 5.9° and 3.8° respectively.

The approximate orientation of water molecule can be determined from the present result. If the dispositions of ions in nickel fluosilicate are assumed to be the same as one of the two mirror image structures of the ferrous salt it is found that the q_{zz} directions do not agree with the OH bond directions (deviation being 13° and 26°). Now, the crystal structure of this salt will be considered under the following assumptions.

1) D-O directions are in the q_{zz} directions.

10) W. C. Hamilton, *Acta Cryst.*, **15**, 353 (1962).

*4 If a sufficient rapid exchange motion between the mirror image structures is present the number of satellite pairs will not be doubled, however, in that case one of the principal axes of the q-tensor should be perpendicular to [111], which is readily detectable.

2) Dimension of SiF_6^{2-} ion is the same as that in $FeSiF_6 \cdot 6H_2O$, a regular octahedron with an Si–F distance of 1.71 Å.[10,11]

3) NiO_6 octahedron is regular with an Ni–O distance of 2.07 Å.[11]

4) Ni–O direction must not deviate greatly from the bisector of D_2O*5.

Rotation angles of both positive and negative group ions about the [111] axis are adjusted so as to give reasonable hydrogen-bond distances and angles.

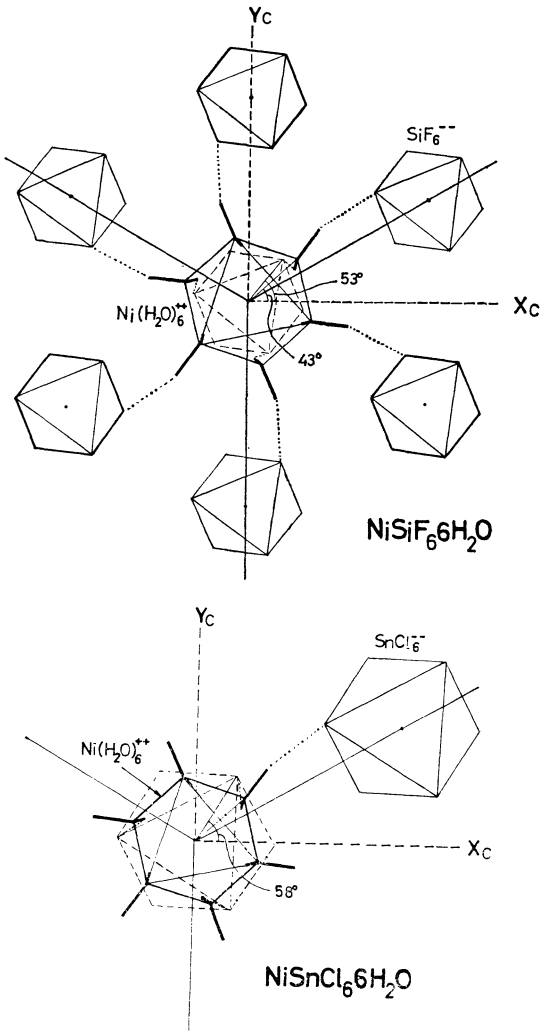

Fig. 3. Proposed crystal structures of $NiSiF_6 \cdot 6H_2O$ and $NiSnCl_6 \cdot 6H_2O$. [111] projection. Hydrogen bonds are indicated by dotted lines. Only one of the six $SnCl_6^{2-}$ ions surrounding $Ni(H_2O)_6^{2+}$ is shown for brevity.

The proposed structure is shown in Fig. 3. The D···F distances are 1.72 Å (D_1···F) and 1.77 Å (D_2···F) with corresponding O–D···F angles of 154° and 156°, respectively. Further improvement of the D···F distances and O–D···F angles may be possible but is hardly meaningful in the present approximations. The hydrogen-bond network in the suggested structure is essentially the same as that of ferrous silicate, one hydrogen-bond being approximately parallel to [111] and the other approximately perpendicular to it.

For $NiSnCl_6 \cdot 6D_2O$, though we were not able to determine eqQ for each deuteron of a water molecule, quadrupole coupling tensors and their orientations of D_1 and D_2 are probably nearly the same as those in the fluosilicate as seen from the close agreement of the room temperature values in Table 1.*6 Pauling gives atomic coordinates for the heavy atoms. However, difficulty is encountered when we try to fit our data of directions of quadrupole coupling tensor to his structure.*7 Trial structure as shown in Fig. 3 is proposed assuming $SnCl_6^{2-}$ as regular octahedron with Sn–Cl=2.45 Å[11] and treated in the same way as above. D···Cl distances are 2.02 Å with O–D···Cl angles of 158° and 139°.

It is hoped that more refined structure analysis of these compounds will be made. We were unable to detect NQR spectra of ^{35}Cl in this compound and the attempt to determine Cl–Sn direction by the Zeeman effect of NQR was unsuccessful.

Reorientational Motions. The barrier to reorientation of water molecules is considerably smaller in the chlorostannate than in the fluosilicate, which is well understood from the difference in hydrogen-bond strength in the two crystals.

A reorientational motion of $M(H_2O)_6^{2+}$ group ions similar to the one observed in $NiSiF_6 \cdot 6D_2O$ at high temperature has been detected by the line-shape transition of the proton resonance in the isomorphous zinc and magnesium fluosilicates by Dereppe *et al.*[12] They conclude that motion is excited in both $SiFe_6^{2-}$ and $M(H_2O)_6^{2+}$ groups in these crystals, the activation energies being 6.6 and 11.6 kcal/mol, respectively, for the magnesium salt.

In nickel fluosilicate the barrier to the $M(H_2O)_6^{2+}$ motion is considerably higher. Since the Z_C component of field gradient is preserved it can be concluded that the motion is not a free rotational one, but is a reorientation among equilibrium sites and even the rotational motion of water molecules is not a free motion. A reorientation about any axis which interchanges adjacent three

11) R. W. G. Wyckoff, "Crystal Structure" (2nd Ed.), Vol. 3, Chapter X, Interscience Publishers, New York (1965).

*5 In $FeSiF_6 \cdot 6H_2O$, Fe–O and the bisector of H_2O are linear within 8.1° (Ref. 10).

*6 At room temperature, q_{xx}, q_{yy} and q_{zz} directions of $NiSiF_6 \cdot 6D_2O$ are in agreement with the corresponding ones of $NiSnCl_6 \cdot 6D_2O$ within 1°, 4°, and 4°, respectively.

*7 An Ni–O distance of 2.40 Å in Pauling's structure is too large compared to the average Ni–O distance of 2.07±0.04 Å of various nickel salts (Ref. 11).

12) J. M. Dereppe, P. W. Lobo and M. V. Meersche, *J. Chim. Phys.*, **61**, 1076 (1964).

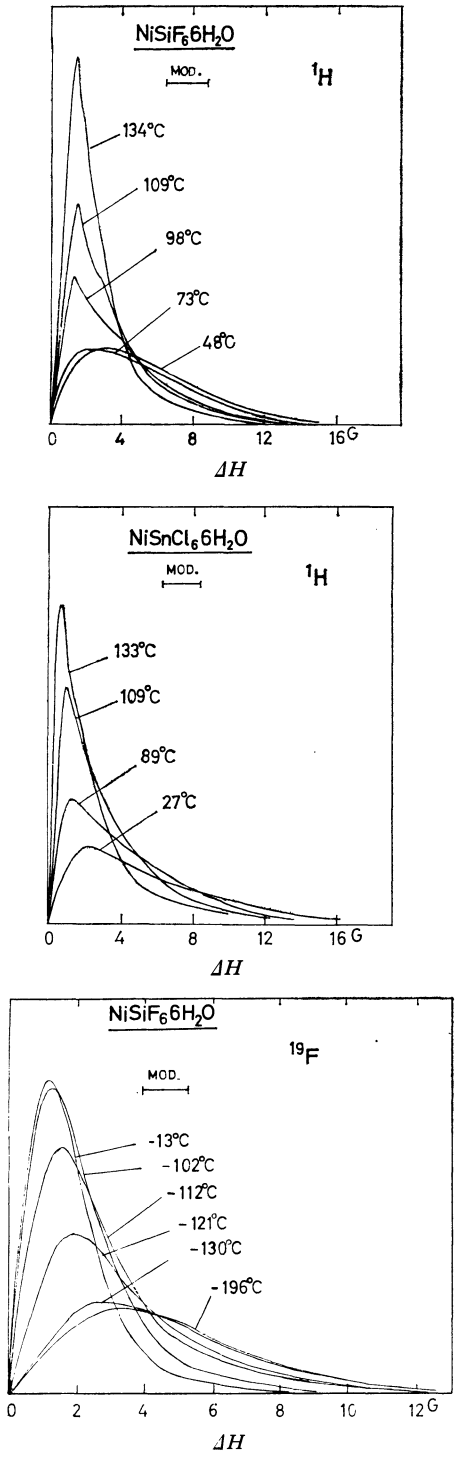

Fig. 4. ^1H and ^{19}F resonance line shapes (a half of the derivative curve) at various temperatures.

water molecules can produce the observed effect. There are four three-fold reorientational modes,*8 one of which is about the [111] axis, and other three four-fold reorientational modes about the O–Ni–O axes. (All these modes except the one about [111] are not pure rotational modes in a rigorous sense because the $Ni(H_2O)_6^{2+}$ ion is not a regular octahedron.) It is not possible to determine which of the two types of motions is operative in the observed averaging process. However, if one considers the number of hydrogen bonds to be broken in the course of reorientation the four-fold motion seems more probable.

For $NiSnCl_6 \cdot 6D_2O$ no measurement of $Ni(D_2O)_6^{2+}$ cluster motion was made on a single crystal. Attempt to observe powder pattern of reorienting $Ni(D_2O)_6^{2+}$ was made on chlorostannate up to 140°C but was unsuccessful (the crystal decomposes at the higher temperatures).

The line shape transition of ^1H resonance on $NiSnCl_6 \cdot 6H_2O$ powder was compared with that of $NiSiF_6 \cdot 6H_2O$ as shown in Fig. 4. Both has similar temperature dependence. The activation energy of $Ni(D_2O)_6^{2+}$ motion in chlorostannate is, therefore, probably nearly the same as that in the fluosilicate.

The line shape transition of ^{19}F resonance of nickel fluosilicate was also measured as shown in Fig. 4. Line width transition centered at -110—-120°C is observed. The temperature of transition is considerably lower than that of magnesium fluosilicate, and the activation energy of SiF_6^{2-} reorientation in the nickel salt is likely to be less than 6.6 kcal/mol. As Dereppe *et al.*[12] point out, the activation energies of reorientation of $M(H_2O)_6^{2+}$ and SiF_6^{2-} should be nearly the same if only the interactions between ions of opposite sign are considered. Their explanation of large difference in activation energies between $Mg(H_2O)_6^{2+}$ and SiF_6^{2-} reorientations is based on the assumption of the same crystal structure for this salt as the ferrous salt. It is clear that such an explanation is not applicable to the nickel salt where no mirror symmetry is observed. Yet the difference in the activation energy of cation and anion reorientation is much larger in the latter case than in the former. There is also another question. For the 180°-flip of a water molecule the observed activation energy is generally reasonable value considered as the energy required to break two hydrogen bonds of the water molecule. Now, if one simply takes hydrogen-bonding energy alone, both the reorientations of $Ni(H_2O)_6^{2+}$ and SiF_6^{2-} should require at least four times the activation energy of 180°-flip of D_2O or 30 kcal/mol, because hydrogen-bonds of four water molecules are broken in the course of the four-fold reorientation. Same order of the observed activation energy for the $Ni(H_2O)_6^{2+}$ reorientation in the chlorostannate as in the fluosilicate is also difficult to understand.

*8 In the three-fold reorientation the motion should be that all the six water molecules move together and not that three move independent of three others, since the latter means the breakage of coordination bonds.

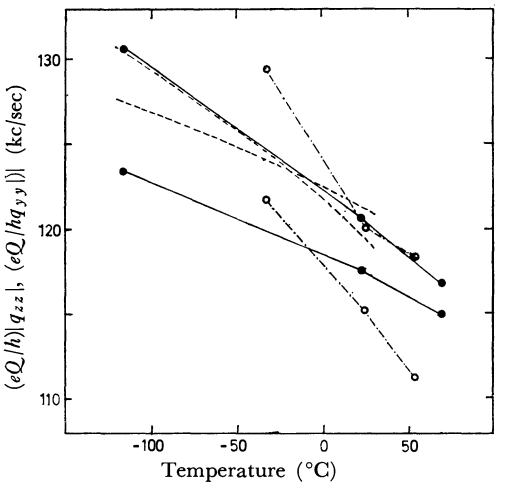

Fig. 5. Temperature dependence of z and y components of averaged quadrupole coupling tensor in D_2O.
—— $NiSiF_6 \cdot 6D_2O$, -·-· $NiSnCl_6 \cdot 6D_2O$,
- - - $Ba(ClO_3)_2 \cdot D_2O$ (Ref. 1).

The experimental results in disagreement with the expectation from such a simple picture indicate that various factors, such as electrostatic energy other than hydrogen-bonding energy, steric effect and nonrigidity of the structure, of cluster ions, are the important factors determining the activation energy of reorientation of a large group of atoms. Although no satisfactory explanation of molecular motions in crystals are available at present, nickel fluosilicate presents as interesting example that three types of reorientational motion, that is, the motion of D_2O, $Ni(D_2O)_6^{2+}$ and SiF_6^{2-} are observed in a single compound.

Torsional Oscillations. $(eQ/h)|q_{zz}|$ and $(eQ/h)|q_{yy}|$ of the quadrupole coupling of D_1OD_2 under 180° flip motion, that is, the quadrupole coupling tensor averaged for D_1 and D_2, are plotted in Fig. 5. (The z direction is perpendicular to the plane of water molecule and the y direction parallel to the direction of D_1–D_2). As discussed in Ref. 1 the temperature dependence of these values can be explained from Bayer's theory[13] in terms of torsional motions of a water molecule. For nickel fluosilicate the temperature dependence of q_{zz} and q_{yy} resembles that of $Ba(ClO_3)_2 \cdot D_2O$ previously obtained.[1] Trend of smaller temperature dependence of q_{yy} compared to q_{zz} is also seen in the present case. This is due to the effect of torsional motion about the D–D axis which only decreases the q_{yy} component. The torsional motions in both cases are probably similar since the activation energy for the two cases is nearly the same (7 kcal/mol for $Ba(ClO_3)_2 \cdot D_2O$).[1,8] Therefore, approximately the same torsional frequencies as obtained in $Ba(ClO_3)_2 \cdot D_2O$ are expected. However, since the oscillation may be more complex and coupling among the modes may be stronger in the present case, no detailed analysis of the torsional frequencies are made. The effect of the torsional motion of $Ni(D_2O)_6^{2+}$ cluster on the temperature dependence of quadrupole coupling is estimated assuming a three-fold cosine type potential of barrier height 19 kcal/mol about the [111] direction. It is found that the change in quadrupole coupling is less than one percent over the temperature range of observation and may be negligible.*9

In the chlorostannate the observed large temperature dependence can be readily expected from the small hindering potential to 180°-flip motion of water molecules. An approximate calculation assuming a cosine-type potential of 4.3 kcal/mol shows for the temperature range of observations (−53°C to 55°C), about 5% of the observed 9% decrease can be explained by the torsional motion about the bisector of D_2O.

We would like to thank Professor Yoshinobu Kakiuchi for helpful dicussions and comments. We are also grateful to Assistant Professor Kiyoshi Kume of Tokyo Metropolitan University for supplying us with a sample of deuterated nickel fluosilicate single crystal and for discussions.

13) H. Bayer, *Z. Physik*, **130**, 227 (1951).
*9 The effect is even less when the four-fold reorientation is assumed.

BULLETIN OF THE CHEMICAL SOCIETY OF JAPAN VOL. 41 1533—1537 (1968)

Desorbability of Chemisorbed Water on Metal Oxide Surfaces. I. Desorption Temperature of Chemisorbed Water on Hematite, Rutile and Zinc Oxide

Tetsuo MORIMOTO, Mahiko NAGAO and Fujiko TOKUDA

Department of Chemistry, Faculty of Science, Okayama University, Tsushima, Okayama

(Received December 19, 1967)

The desorbability of water molecules chemisorbed on the surfaces of metal oxides has been investigated in the cases of α-Fe_2O_3, TiO_2 (rutile) and ZnO. Water vapor adsorption isotherms were determined on the samples treated at various temperatures in a vacuum of 10^{-5} Torr. The BET V_m-values of water adsorption were plotted against the temperature of the pretreatment. The curves obtained show a sharp increase at a moderate temperature which is varied by the nature of solid substance. This fact makes us conclude that, at this temperature, the chemisorbed water on oxide surfaces starts to be removed. The variation in the desorption temperature due to the nature of metal oxide is considered to come from the magnitudes of the bonding force of the surface hydroxyl groups to the surface metal atoms on each solid.

It has become clear that the surface of metal oxide is usually covered by hydroxyl groups in the atmosphere, which have serious effects on such surface properties as selective adsorbability, hydrophilicity, catalytic activity, and surface charge. Their existence and behavior have been investigated by various methods: specific chemical reactions,[1] infrared absorption spectroscopy,[2-6] water-content measurements,[7,8] and nuclear magnetic resonance study.[9,10] However, we still have no exact knowledge of the temperature at which the desorption of chemisorbed water on oxide surfaces starts. The primary purpose of this investigation is to determine this temperature experimentally. Since the bonding force of surface hydroxyl groups to surface metal atoms should vary with the nature of the metal oxide,[11] the desorption temperature may be expected to be characteristic for each substance. The results of this study, therefore, can indicate the extent of the removal of hydroxyl groups on solid surfaces and, accordingly, give a criterion for powder conditioning.

Experimental

Materials. The samples used in this research were hematite (α-Fe_2O_3), rutile (TiO_2), and zinc oxide (ZnO). The hematite, presented by the Nippon Bengara Kogyo Co., had been produced by the calcination of ferrous sulfate. The rutile, presented by the Teikoku Kako Co., had been made by calcining titanium hydroxide formed by the hydrolysis of titanium sulfate. The zinc oxide, presented by the Sakai Chemical Co., had been produced by oxidizing zinc vapor in the atmosphere at a high temperature. The former two samples were repeatedly treated with 0.1 N nitric acid in order to remove basic impurities, carefully treated with 0.1 N ammonia water in order to remove acidic impurities, thoroughly washed with distilled water, and dried at 110°C in the atmosphere.

Measurement of Surface Area. The surface areas of the samples were determined by the BET method using nitrogen, assuming the area of a nitrogen molecule to be 16.2 Å^2. The specific surface areas obtained for α-Fe_2O_3, TiO_2, and ZnO were found to be 13.8, 9.43, and 4.31 m^2/g respectively.

Measurement of Water Vapor Adsorption. The principle of the present investigation was to repeat the measurement of the water vapor adsorption on the same sample, while varying the conditions of the pretreatment. The volumetric method was used to determine the adsorption isotherms of water vapor, and an oil manometer was used to read the equilibrium pressure of the vapor. A sample of about 10 m^2 in total area was taken for every adsorption measurement. Prior to the first measurement of water vapor adsorption, the sample was treated at a high temperature (600°C for α-Fe_2O_3 and TiO_2, 450°C for ZnO) in a vacuum of 10^{-5} Torr in order to remove all the physically-adsorbed water and most of the chemisorbed

1) H. P. Boehm, *Angew. Chem. Internat. Ed.*, **5**, 533 (1966).
2) D. J. C. Yates, *J. Phys. Chem.*, **65**, 746 (1961).
3) G. Blyholder and E. A. Richardson, *ibid.*, **66**, 2597 (1962).
4) K. E. Lewis and G. D. Parfitt, *Trans. Faraday Soc.*, **62**, 204 (1966).
5) J. H. Taylor and C. H. Amberg, *Can. J. Chem.*, **39**, 535 (1961).
6) G. J. Young, *J. Colloid Sci.*, **13**, 67 (1958).
7) G. J. Young and T. P. Bursh, *ibid.*, **15**, 361 (1960).
8) T. Morimoto, K. Shiomi and H. Tanaka, This Bulletin, **37**, 392 (1964).
9) J. R. Zimmerman and J. A. Lasater, *J. Phys. Chem.*, **62**, 1157 (1958).
10) D. E. O'Reilly, *Advan. Catalysis*, **12**, 31 (1960).
11) T. Morimoto, M. Nagao and F. Tokuda, This Bulletin, **40**, 2723 (1967).

water. Then the adsorption experiment of water vapor was carried out at a room temperature (10°C for α-Fe_2O_3, 18°C for TiO_2 and ZnO). Thus, we obtained the first adsorption isotherm. Subsequently, this sample was degassed at 30°C for 4 hr in a vacuum of 10^{-5} Torr in order to desorb water molecules. The preliminary tests showed that the desorption equilibrium can be attained within 4 hr in this process. Again the adsorption isotherm of water vapor was determined at the same temperature as before. After the completion of the second adsorption measurement, the same sample was again evacuated at a higher temperature (*e. g.*, 50°C) than 30°C. In the successive experiments the temperature of the pretreatment was raised step by step. By repeating the adsorption measurements and the desorption treatments alternately, we obtained a series of adsorption isotherms of water vapor.

Measurement of Water Content. The water content of the samples was determined volumetrically by using the same equipment as was used to measure the water-vapor adsorption. The same initial pretreatment as was given to the sample for the adsorption measurement was given to the original sample (600°C for α-Fe_2O_3 and TiO_2, 450°C for ZnO), and then the sample was exposed to saturated water vapor. This sample was degassed at 30°C for 4 hr in a vacuum of 10^{-5} Torr. By keeping the vacuum system closed, the water molecules adsorbed were evaporated at a given higher temperature (*e. g.*, 50°C) for 4 hr and trapped in a vessel kept at the temperature of liquid nitrogen. The amount of the condensed water was determined volumetrically at room temperature after reevaporation. This procedure was repeated on the same sample at various evaporation temperatures up to 1000°C. Since the number of water molecules remaining on the surface at 1000°C was found to be negligibly small, we calculated the water contents at various temperatures by assuming the water content at 1000°C to be zero.

Infrared Absorption Spectrum. The technique of absorption spectroscopy[2] was applied to the surface species of the samples described above. The infrared spectra were measured with an apparatus of the Japan Spectroscopic Co. (IR-G). A small disk of the sample was prepared for infrared spectroscopic measurement at every step of the treatment.

Results and Discussion

The water contents of α-Fe_2O_3, TiO_2 and ZnO are shown in Fig. 1 as a function of the pretreatment temperature. The numerical value of the amount is expressed by the number of surface hydroxyl groups on an area of 100 Å^2, assuming that the water molecules released have been chemisorbed as hydroxyl groups on the surface. It may be seen in Fig. 1 that all the samples lose adsorbed water greatly until 400°C, and then gradually until 800°C. At 1000°C almost all the water molecules have been removed from the surface. The water molecules released at higher temperatures are, of course, those chemisorbed on the surface, while those found at lower temperatures should have been adsorbed both physically and chemically. From the curves of the water content, however, the

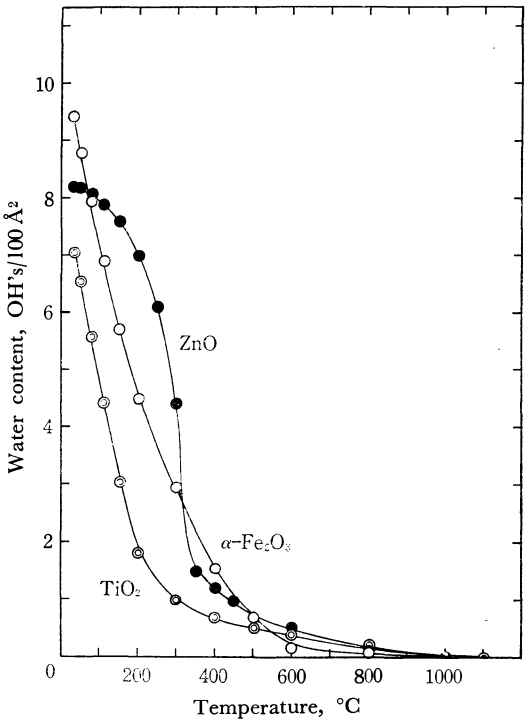

Fig. 1. Water content of α-Fe_2O_3, TiO_2, and ZnO at various temperatures.

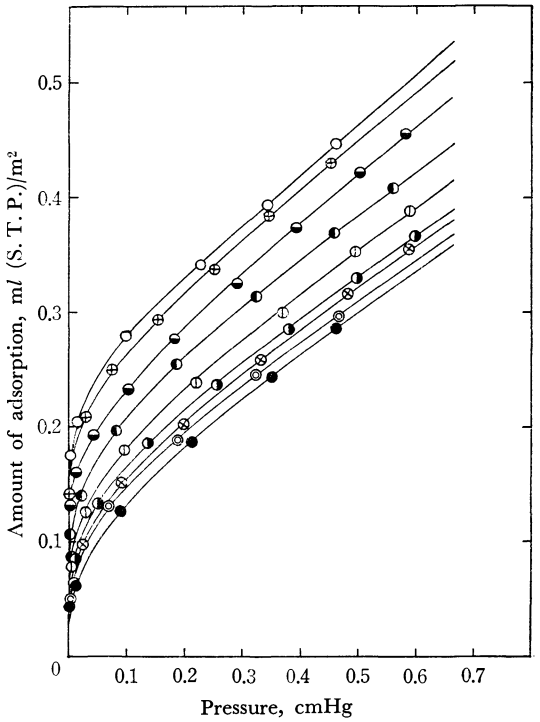

Fig. 2. Adsorption isotherms of water vapor on α-Fe_2O_3 pretreated at various temperatures; degassing temp. ○ 600, ● 30, ◎ 50, ⊗ 80, ◑ 110, ⓘ 150, ◐ 200, ◒ 300, ⊕ 400°C.

temperature at which the removal of chemisorbed water starts can not be recognized.

Figure 2 shows the adsorption isotherms of water on α-Fe_2O_3. The ordinate represents the amount of water adsorbed on the unit surface area of the sample in ml/m^2, which is then converted into the standard temperature and pressure. The first adsorption isotherm which was obtained after degassing at 600°C is much higher than the second one, which was obtained after degassing at 30°C. The amount adsorbed increases gradually with the rise in the pretreatment temperature and closely approaches the value of the original isotherm. All the isotherms are almost the same in shape, except that the amount adsorbed at zero pressure differs slightly from sample to sample.

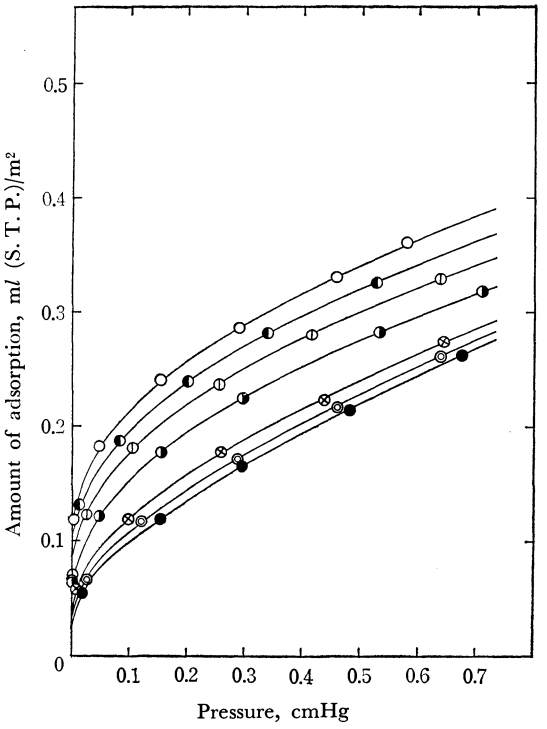

Fig. 3. Adsorption isotherms of water vapor on TiO_2 pretreated at various temperatures; degassing temp. ○ 600, ● 30, ◎ 50, ⊗ 80, ◑ 110, ◫ 150, ◐ 200°C.

Figure 3 shows the adsorption isotherms of water on TiO_2. Although at first sight the characteristics seem to be the same as in the case of α-Fe_2O_3, the isotherms on TiO_2, after degassing at 30°C to 110°C, are close to each other and that of the 200°-degassed sample closely approaches the first adsorption isotherm.

The adsorption isotherms of water on ZnO are given in Fig. 4. The shapes of these curves are quite different from those on TiO_2 and Fe_2O_3, representing a sharp increase in the amount adsorbed at a moderate pressure of the vapor. The

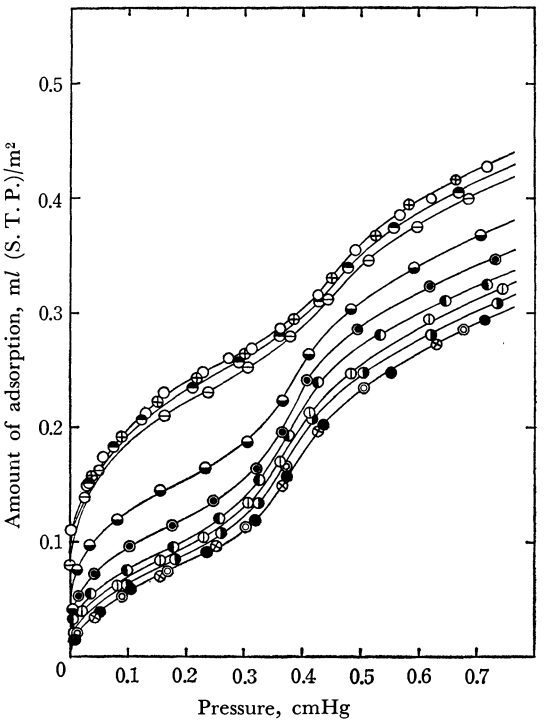

Fig. 4. Adsorption isotherms of water vapor on ZnO pretreated at various temperatures; degassing temp. ○ 450, ● 30, ◎ 50, ⊗ 80, ◑ 110, ◫ 150, ◐ 200, ⊙ 250, ◒ 300, ⊖ 325, ◓ 350, ⊕ 400°C.

appearance of such humps in the adsorption isotherm has been reported in other systems: carbon and adsorbates such as argon,[12] C_2H_5Cl, $CHCl_3$ and $CFCl_3$,[13] and cadmium bromide or sodium bromide and argon.[14] In the former systems, the surface of carbon was rather uniform and the hump appeared at the boundary between the first and second monolayers of an adsorbate. In the latter cases, the hump has been explained in terms of the interaction between adsorbate molecules and surface hydroxyl groups. In the case of metal oxide, we have no literature reporting the appearance of the hump on the adsorption isotherm. Detailed investigations of this phenomenon in the present system are now in progress. In any case, in the case of ZnO, the adsorption isotherms obtained on the sample treated above 300°C are extremely close to the first adsorption isotherm.

By applying the BET method[15] to the above data, the amount of the monolayer capacity of water on the unit surface, V_m, can be calculated.

12) W. R. Smith and D. G. Ford, *J. Phys. Chem.*, **69**, 3587 (1965).
13) B. W. Davis and C. Pierce, *ibid.*, **70**, 1051 (1966).
14) S. Ross, J. P. Oliver and J. J. Hinchen, *Advan. Chem. Ser.*, **33**, 317 (1961).
15) S. Brunauer, P. H. Emmett and E. Teller, *J. Am. Chem. Soc.*, **60**, 309 (1938).

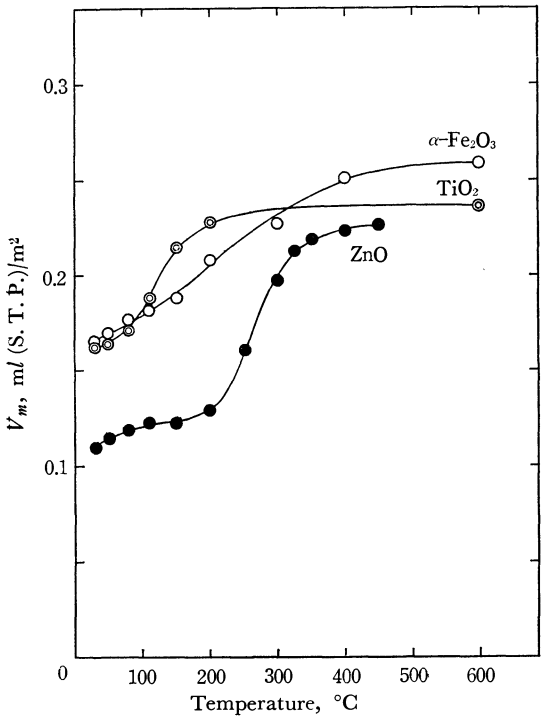

Fig. 5. Relation between V_m-value and pretreatment temperature.

BET plots were satisfactorily linear in the range of relative pressures from 0.05 to 0.35 in the cases of Fe_2O_3 and TiO_2, and from 0.05 to 0.20 in the case of ZnO. In Fig. 5 the V_m-values of the water adsorption are plotted against the temperature of the pretreatment. It may be seen from Fig. 5 that the V_m-values on TiO_2 and ZnO start to increase steeply at 110 and 200°C respectively, while in the case of Fe_2O_3 the value shows only a slow increase.

Even when a series of adsorption measurements were made in order from higher to lower pretreatment temperatures, the results obtained were quite reproducible. The reproducibility of the present experiments is satisfactory in this sense. This implies that the number of sites accepting water molecules is determined by the pretreatment conditions. The solid surface will be hydrated thoroughly after every adsorption measurement. Therefore, after treatments at moderate temperatures sites for both the physical and the chemical adsorption of water will be formed, the latter increasing in number with a rise in the pretreatment temperature.

It has been found that the rate of surface hydration on metal oxide is so fast that it seriously affects the value of immersional heat.[16] The V_m-value obtained, therefore, will contain both physical adsorption and chemisorption. Accordingly, the starting point of the sharp increase in V_m-values that is shown in Fig. 5 will correspond to the commencement of chemisorption in addition to the physical adsorption of water. Jurinak[17] assumed that only physical adsorption would occur on the samples of TiO_2 (anatase), α-Fe_2O_3, and α-FeOOH which were treated at 30°C in a vacuum of 10^{-6} Torr. Hollabaugh and Chessick[18] also considered that all the physically-adsorbed water might be removed near room temperature in a vacuum of 10^{-6} Torr. The present results substantiate the assumptions of these authors. From Fig. 5 we can find the temperature of pretreatment above which the reversible chemisorption sites for water abruptly increase. Moreover, this temperature is found to vary with the nature of the metal oxide, indicating that the surface hydroxyl groups bond to the surface metal atoms with a certain strength characteristic of each substance.

The desorption temperature of chemisorbed

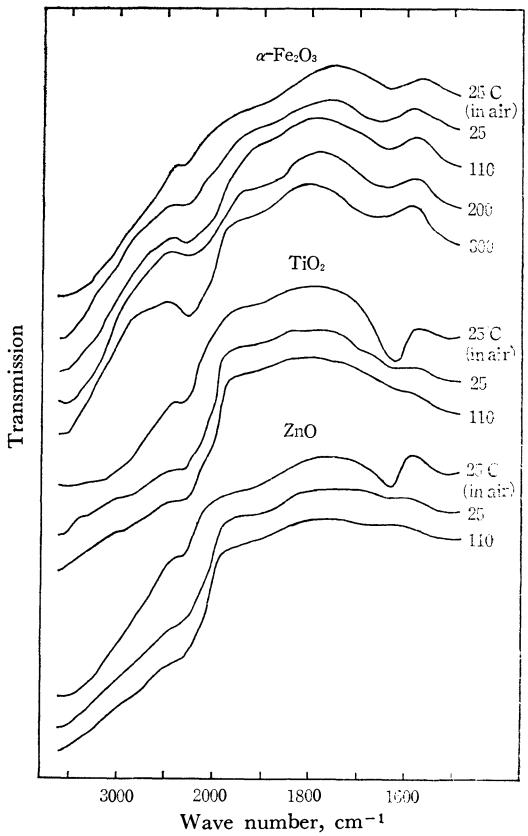

Fig. 6. Infrared absorption spectra of α-Fe_2O_3, TiO_2, and ZnO under various conditions of treatment.

16) T. Morimoto, M. Nagao and M. Hirata, *Kolloid-Z. u. Z. Polymere*, in press.

17) J. J. Jurinak, *J. Colloid Sci.*, **19**, 477 (1964).

18) C. M. Hollabaugh and J. J. Chessick, *J. Phys. Chem.*, **65**, 109 (1961).

water is much higher in the case of ZnO than in the case of TiO_2. This means that the bonding force of hydroxyl groups to surface metal atoms on ZnO is much stronger than that on TiO_2. The reason for the difference between the two bonding forces may be explained by the structural or coordination factors of the solid substances concerned, but it is not clear at present. In the case of Fe_2O_3, there is no sharp increase in V_m-value. The desorption of chemisorbed water on Fe_2O_3 may start at such a low temperature that the removal of physically-adsorbed water can occur, and continue over a wide range of temperature. The heat of hydration, which was calculated by combining the data of immersional heat and of the water content of the powder, has been found to be 12.1 kcal/mol for Fe_2O_3,[19] and 23 kcal/mol for TiO_2 (rutile)[19] and ZnO.[16] These data have been interpreted in the following way: in the case of Fe_2O_3, the removal of chemisorbed water starts at a relatively low temperature, while on the other hand, the physically-adsorbed water remains until relatively high temperatures. This interpretation seems to be useful in the present case also.

19) to be published.

Figure 6 shows the results of the infrared absorption spectroscopy of the three samples. The absorption band due to physically-adsorbed water appears near 1600 cm^{-1} on all the samples tested at room temperature in the atmosphere; it is extinguished by degassing in a vacuum of 10^{-5} Torr at room temperature in the cases of TiO_2 and ZnO, but it still remains in the case of Fe_2O_3 even after evacuating at higher temperatures. The difficulty of the desorption of chemisorbed water from Fe_2O_3 probably arises from the fact that water molecules have been adsorbed on the inner surface of Fe_2O_3. Healey *et al.*[20] suggested that the desorption of water vapor took place from the inner surface of ferric oxide powder. The X-ray data observed in connection with the present sample of Fe_2O_3 proved the crystallinity to be inferior to that of the other two samples. The behavior of adsorbed water on Fe_2O_3 suggests the existence of an inner surface on which nitrogen molecules can not be adsorbed at the temperature of liquid nitrogen.

20) F. H. Healey, J. J. Chessick and A. V. Fraioli, *J. Phys. Chem.*, **60**, 1001 (1956).

BULLETIN OF THE CHEMICAL SOCIETY OF JAPAN VOL. 41 1537—1539 (1968)

The Termination Processes of the Autoxidations of Benzene, Toluene and Ethylbenzene in the Aqueous Phase as Studied by Oxygen-18*1,*2

Hiroshi HOTTA and Nobutake SUZUKI

Japan Atomic Energy Research Institute, Takasaki, Gunma

(Received December 22, 1967)

The autoxidations of benzene, toluene and ethylbenzene were investigated at 70°C by using the oxygen-18 enriched Fenton's reagent. The oxygen-18 atom percentage in the products suggests that all the oxygen of benzaldehyde from toluene and of acetophenone from ethylbenzene is donated by molecular oxygen dissolved in the aqueous phase, while the oxygen of the hydroxylation products, namely, phenol from benzene, benzyl alcohol from toluene and methyl phenyl carbinol from ethylbenzene, is donated partly from water and partly from molecular oxygen. From the latter finding, the rate of the carbonium cation formation from the intermediate radicals without their oxidation to the peroxide is in the order of phenyl > α-methyl-benzyl > benzyl.

The autoxidations of benzene[1,2] and toluene[3], catalyzed by metal ions in the aqueous phase have been studied by using a stainless-steel reactor between 100°C and 200°C. Although this oxidation procedure is very suitable to obtain the main product due to the high selectivity, the oxygen-18 enriched Fenton's reagent was used at 70°C for the confirmation of the termination processes,

*1 The Autoxidation of Aromatic Hydrocarbons in Aqueous Solutions. XI. This series succeeds "Thermal and Radiation Oxidations of Benzene to Phenol in Aqueous Solutions Containing Metal Ions at Elevated Temperatures."

*2 Partly presented at the 5th Symposium on Stable Isotopes, Leipzig (GDR), October, 1967.

1) N. Suzuki and H. Hotta, This Bulletin, **37**, 244 (1964).

2) H. Hotta, N. Suzuki and T. Abe, *ibid.*, **39**, 417 (1966).

3) N. Suzuki and H. Hotta, *ibid.*, **40**, 1361 (1967).

because this method gives other products in addition to the main one. Since the accuracy in the previous study of toluene[3] was not so good due to the rather carelessness of the sampling method, the present study was carried out by the revised method for benzene, toluene and ethylbenzene.

Experimental

As in the previous study,[3] an oxygen-18 enriched aqueous solution of 1.5% hydrogen peroxide (10 cc) was added drop by drop, over a period of about 90 sec, in the oxygen-18 enriched 0.4 N sulfuric acid solution of 0.01 M ferrous sulfate (100 cc) at 70°C in a 300 cc flask opened to the air, in which 1 cc of aromatic hydrocarbons was suspended by a magnetic stirrer. Acetone (10 cc) was added except the case of benzene to increase the solubility of aromatic hydrocarbons. Such solutions seemed to be homogeneous at 70°C. The aqueous solutions were prepared by using the 1.64_5 ^{18}O-atom-% water.

For reference, the natural compounds (*ca.* 0.2 cc) corresponding to the products were treated for 10 min by the same conditions without hydrogen peroxide and aromatic hydrocarbons.

After the mixture had been stirred magnetically for 10 min from the beginning of dropping and then cooled, the products were extracted in ether and separated by gas chromatography at 165°C using a column of PEG 6000. The procedure after that was revised. That is, the fractions (*ca.* 100 mg) were converted to carbon dioxide by heating them for 12 hr at 500°C with mercuric chloride (100 mg) and mercuric cyanide (100 mg). The oxygen-18 atom percentage in the carbon dioxide was determined by mass spectrometry. Phenol was transformed to tribromophenol[2] in advance.

Results and Discussion

The observed values of the oxygen-18 atom percentage for the oxidation products (x) and the treated compounds for reference (x_0) are shown in Table 1 respectively. The values shown by an asterisk are for phenol produced from benzene at 150°C and 180°C in the ferrous sulfate solution by using a high-pressure reactor in the previous study.[2] As described in the experimental section, the values of x and x_0 for phenol were obtained without addition of acetone. The values of x_0 in the acetonic aqueous solution agreed within experimental error with those in the aqueous solution except benzaldehyde.

When it is assumed that the oxygen exchange reaction with water is of first order, this rate constant, k_e, can be estimated by equation

$$\frac{x_0-0.20_4}{1.64_5-0.20_4} = 1-e^{-k_e t} \qquad \text{(i)}$$

where t is the exchange time, and 0.20_4 is the natural abundance of oxygen-18 in atom%. Since it takes some time for cooling, it is difficult to determine the effective exchange time. The k_e's in Table 1 are estimated on putting $t=10$ min. These values indicate that, as reviewed by Samuel and Silver,[4] aldehyde and ketone exchange oxygen rapidly with water, and methyl phenyl carbinol also does so considerably. On the other hand, phenol, benzyl alcohol and β-phenyl ethyl alcohol do not so practically.

For benzaldehyde and acetophenone, x is smaller than x_0. It is because, at the oxidation process, the product is accumulated gradually and may be partly lost by some secondary reaction during the oxidation time, while, at the reference treatment, all the reactant is present from the beginning and not lost by some secondary reaction. The smaller value of x suggests that oxygen-18 of these products is not enriched during their formation process, but done due to the oxygen exchange with water after their formation.

According to the previous studies,[2,3] the following reaction scheme can be assumed as the propagation processes of the present autoxidation after the formation of hydroxyl radicals:

$$RH + \cdot OH + O_2 \rightarrow R'OO\cdot \qquad (1)$$

TABLE 1

Reactant	Product	^{18}O atom-% x	^{18}O atom-% x_0	k_e min^{-1}	F_w	Temp. °C
Benzene	Phenol	1.17_4	0.21_8	0.0010	0.67	70
		0.48*	—	—	0.18	150*
		0.90*	0.20_8	0.0003	0.47	180*
Toluene	Benzaldehyde	0.53_7	1.34_3	0.20	0	70
	Benzyl alcohol	0.37_7	0.21_1	0.0005	0.12	70
Ethylbenzene	Acetophenone	0.73_9	1.10_0	0.097	0	70
	Methyl phenyl carbinol	1.03_2	0.46_6	0.020	0.48	70
	Unknown	0.38_0	—	—	—	70
	β-Phenyl ethyl alcohol	—	0.21_3	0.0006	—	70

* See Ref. 2.

4) D. Samuel and B. L. Silver, *Advances in Phys. Org. Chem.*, **3**, 123 (1965).

$$RH + R'OO\cdot \rightarrow R\cdot + R'OOH \quad (2)$$

$$R\cdot + O_2 \rightarrow ROO\cdot \quad (3)$$

$$RH + ROO\cdot \rightarrow ROOH + R\cdot \quad (4)$$

$$ROOH + Fe^{2+} \rightarrow RO\cdot + OH^- + Fe^{3+} \quad (5)$$

$$ROOH + Fe^{3+} \rightarrow ROO\cdot + H^+ + Fe^{2+} \quad (6)$$

$$ROO\cdot + ROO\cdot \rightarrow ROOR + O_2 \rightarrow 2\,RO\cdot \quad (7)$$

where R· represents phenyl, benzyl or α-methyl benzyl radical. Reaction (1) represents that hydroxyl radicals give some peroxide in the presence of oxygen as the result of either the hydrogen abstraction from RH or the addition to RH.

From the above findings, the following process independent of the water oxygen is assumed for the formation of benzaldehyde and acetophenone, that is, the elimination process of proton from the oxyradical catalyzed by ferric ion;

$$C_6H_5CH_2O\cdot + Fe^{3+} \rightarrow C_6H_5CHO + H^+ + Fe^{2+} \quad (8)$$

and

$$C_6H_5\dot{C}HOCH_3 + Fe^{3+} \rightarrow C_6H_5COCH_3 + H^+ + Fe^{2+} \quad (9)$$

This is supported by the fact that the content of ferrous ion in the iron ion increases with the production of these products.[3]

For the hydroxylation compounds, *i. e.*, phenol, benzyl alcohol and methyl phenyl carbinol, their oxygen-18 atom percentages in Table 1 are

$$1.64_5 > x > x_0$$

This means that the oxygen of these products is donated partly by water and partly by molecular oxygen dissolved. The fraction of the product, to which oxygen is donated by water, is estimated as F_w in Table 1 by equation

$$F_w = \frac{x' - 0.20_4}{1.64_5 - 0.20_4} \quad \text{(ii)}$$

$$x' = x - \alpha(x_0 - 0.20_4) \quad \text{(iii)}$$

where the oxygen exchange with water after the product formation is corrected by α, which is put tentatively as 0.5.

The reaction

$$RO\cdot + H^+ + Fe^{2+} \rightarrow ROH + Fe^{3+} \quad (10)$$

is assumed as the process by which molecular oxygen is donated to the product after reactions (5) and (7). On the other hand, the reaction

$$R\cdot + OH^- + Fe^{3+} \rightarrow ROH + Fe^{2+} \quad (11)$$

is assumed as the transfer process for the oxygen of water. Reaction (11) is consistent with the reduction of iron ion at the oxidation of benzene to phenol. Reaction (11), which is competitive with reaction (3), postulates the formation of carbonium cation as the intermediate from the radical without oxidation to the peroxide. Such probability is in the order of

$$\text{phenyl} > \alpha\text{-methyl benzyl} > \text{benzyl} \quad (12)$$

from the value of F_w in Table 1. α-Methyl benzyl cation is assumed as the intermediate for the oxygen exchange of methyl phenyl carbinol with water in the acidic solution in comparing the rate with the rate of the racemization.[5] It is acceptable that α-methyl benzyl carbonium cation is more probable than benzyl one. The highest ionization probability of phenyl radical to the carbonium cation without oxidation to phenyl peroxide gives a new subject for us. The less reactivity of phenyl radical towards oxygen is suggested by some investigators.[6,7] The electron affinity of phenyl radical is larger than that of benzyl radical.[8]

The unknown product from ethylbenzene in Table 1 could not be identified. This product has a retention time of gas chromatography close to that of β-phenyl ethyl alcohol, and gives the same highest mass number of the mass spectrum with this alcohol, but the NMR spectrum is quite different from this alcohol.

For phenol in Table 1, the present values, obtained in the 0.4 N acidic solution at 70°C, is higher than the previous value, obtained in the 0.01 N acidic solution at 150°C and 180°C.[2] If the value of F_w increases with an increase of temperature as seen between 150°C and 180°C, the high value of F_w at 70°C suggests the promotion of the carbonium cation formation by hydrogen ions.

The authors wish to express their appreciation to Dr. Toshio Sugiura, for his cooperation in the mass spectrometry, and to Mr. Naohiro Hayakawa, for the measurement of NMR.

5) E. Grunwald, A. Heller and F. S. Klein, *J. Chem. Soc.*, **1957**, 2604.
6) G. A. Russell and R. F. Bridger, *J. Am. Chem. Soc.*, **85**, 3765 (1963).
7) D. F. DeTar, *ibid.*, **89**, 4058 (1967).
8) A. F. Gaines and F. M. Page, *Trans. Faraday Soc.*, **59**, 1266 (1963).

BULLETIN OF THE CHEMICAL SOCIETY OF JAPAN VOL. 41 1540—1545 (1968)

Heats of Mixing for Binary Mixtures. V

Sachio MURAKAMI, Mituo KOYAMA and Ryoichi FUJISHIRO

Department of Chemistry, Faculty of Science, Osaka City University, Sumiyoshi-ku, Osaka

(Received January 6, 1968)

The heats of mixing were measured at 25.0°C for binary mixtures of chloroform+tetrahydrofuran,+ furan, and +2-methyl furan systems and for cyclohexane+chloroform, +tetrahydrofuran, +furan, and +2-methyl furan systems. Using these data and the treatment described in a previous paper [*Bull. Chem. Soc. Japan*, **37**, 1776 (1964)], the intermolecular hydrogen bond energies between chloroform and cyclic ethers were estimated to be $\Delta H=-12$ kJ for the chloroform-tetrahydrofuran-cyclohexane system, $\Delta H=-4$ kJ for the chloroform -2-methyl furan-cyclohexane system, and $\Delta H=-3$ kJ for the chloroform-furan-cyclohexane system. From these results, two types of intermolecular hydrogen bonds between chloroform and cyclic ethers are discussed.

In recent years, extensive studies have been made of the relative strengths of hydrogen bonds formed between alcohols, haloform, and oxygen- and nitrogen-containing Lewis bases. Using a number of techniques, such as infrared spectra,[1] NMR spectra,[2] refractive indices[3] and heats of solution,[4] the equilibrium constants and enthalpies for these complexes have been determined.

We estimated the enthalpy of OH-π type hydrogen bonds from our measurements of the heats of mixing for aromatic alcohol (including *m*-cresol)-aromatic hydrocarbon and aromatic alcohol-cyclohexane.[5] This paper is a continuation of our previous work.[5] The enthalpies of intermolecular hydrogen bonds between chloroform and cyclic ether will be estimated by a method similar to that described in another previous paper.[6]

Experimental

The calorimeter used in this study was a model CM-502 microcalorimeter (Applied Electric Lab. Ltd., Tokyo).[5,7] For the present work, two metal solution cells supported from the lids of an aluminum block by a framework were removed and replaced by copper mixing-cell holders with glass-mixing cells. The shape of the mixing cell was similar to that used by Larkin and McGlashan;[8] it is shown schematically in Fig. 1. Initially, the two components to be mixed were separated by a longitudinal partition and by mercury. The mixing was performed by rotating the calorimeter assembly back and forth through a 180° arc, as has been described in a previous paper.[5]

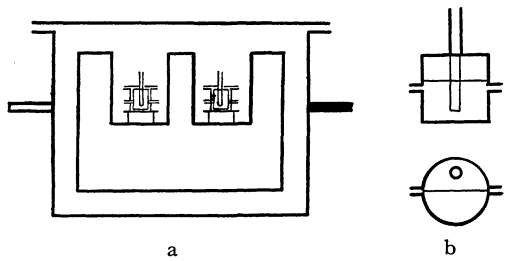

Fig. 1. a. Calorimeter. b. Cross section and upper side view of mixing cell.

The chloroform was washed with concentrated sulfuric acid and a dilute sodium hydroxide solution. Then it was dried over potassium carbonate and distilled before use. Tetrahydrofuran, furan, and 2-methyl furan were supplied by the Kaō Soap Co., Ltd.; all these materials were fractionally distilled before use. The cyclohexane was purified by the method described previously.[5] The purity of all the materials was examined by gas chromatography. The results showed only a single peak.

The physical constants of these materials are given in Table 8.

Results and Discussion

The results of the experimental measurement of the heats of mixing for the seven systems at 25.0°C are given in Tables 1—7, where x_1 is the mole fraction of the component 1; w_i ($i=1$ or 2) is the mass of the component i; Q is the quantity of heat produced during the mixing process, and $\Delta H^{M}_{x_1}$ and ΔH^{M} are the heats of mixing per mole of the

1) Z. Yoshida and E. Ōsawa, *J. Am. Chem. Soc.*, **88**, 4019 (1966); M. R. Busila, E. L. Sair and L. R. Cousins, *ibid.*, **87**, 1665 (1965).
2) F. J. Cioffi and S. T. Zenchelsky, *J. Phys. Chem.*, **67**, 357 (1963).
3) Z. Yoshida and E. Ōsawa, This Bulletin, **38**, 140 (1965).
4) M. Tamres, *J. Am. Chem. Soc.*, **74**, 3375 (1952).
5) S. Murakami and R. Fujishiro, This Bulletin, **40**, 1784 (1967).
6) S. Murakami, K. Amaya and R. Fujishiro, This Bulletin, **37**, 1776 (1964).
7) K. Amaya and S. Hagihara, the first Japanese Calorimetry Meeting, Osaka, 1965.
8) J. A. Larkin and M. L. McGlashan, *J. Chem. Soc.*, **1961**, 3425.

component 1 and per mole of the mixture respectively.

A comparison of our data with those recorded in the literature is only possible for the chloroform-tetrahydrofuran and chloroform-cyclohexane systems. In the former case, our value for ΔH^M at an equimolar mixture agrees with that of Tamres, 677 cal at 25°C.[9] On the other hand, in the latter case, our data agree with those of Baud[10] over the whole concentration range except for around $x_1=0.7$, although his data were measured between 15 to 20°C.

The experimental data for $\Delta H^M_{x_1}$ have been plotted against the mole fraction, x_1, in Figs. 2 and 3. By smoothing and extrapolating the curve to an infinite dilution ($x_1 \to 0$) for each system,

Table 1. Heat of mixing of chloroform (1) and tetrahydrofuran (2) at 25.0°C

w_1 (g)	w_2 (g)	x_1	Q (J)	$-\Delta H^M_{x_1}$ (kJ/mol)	$-\Delta H^M$ (J/mol)
3.1976	0.0923	0.9544	12.84	0.4795	457.7
1.5688	0.0955	0.9085	12.89	0.9811	893.7
1.5885	0.0938	0.9109	12.70	0.9623	869.9
1.5414	0.1520	0.8597	19.69	1.525	1310
0.7067	0.1477	0.7430	18.02	3.047	2262
1.4944	0.4005	0.6927	43.76	3.495	2429
0.9703	0.4045	0.5917	37.26	4.582	2713
0.6587	0.3945	0.5021	30.87	5.594	2809
0.6464	0.6314	0.3821	36.46	6.732	2573
0.5987	1.4388	0.2009	40.46	8.079	1624
0.1874	0.9848	0.1032	12.61	8.030	828.9
0.2265	0.9595	0.0653	16.05	8.456	554.8

Table 2. Heat of mixing of chloroform (1) and furan (2) at 25.0°C

w_1 (g)	w_2 (g)	x_1	Q (J)	$-\Delta H^M_{x_1}$ (kJ/mol)	$-\Delta H^M$ (J/mol)
1.7009	0.0471	0.9535	0.702	0.049	46.9
3.0837	0.1293	0.9315	1.989	0.077	71.5
1.5962	0.1191	0.8843	1.518	0.113	100.4
1.6199	0.1410	0.8695	1.944	0.143	124.3
1.3313	0.2544	0.7490	2.721	0.244	182.8
0.8686	0.2840	0.6356	2.409	0.331	210.4
0.9787	0.4407	0.5557	3.098	0.382	212.5
0.4545	0.8744	0.5232	2.892	0.395	206.7
0.6600	0.6057	0.3864	2.627	0.469	181.1
0.4107	0.7876	0.2290	1.819	0.528	121.3
0.2047	1.1137	0.0949	0.938	0.547	51.9
0.1273	1.1235	0.0607	0.551	0.515	31.4

Table 3. Heat of mixing of chloroform (1) and 2-methyl furan (2) at 25.0°C

w_1 (g)	w_2 (g)	x_1	Q (J)	$-\Delta H^M_{x_1}$ (kJ/mol)	$-\Delta H^M$ (J/mol)
0.1665	0.8220	0.1223	1.993	1.428	174.7
0.2378	0.6763	0.1947	2.565	1.288	250.8
0.5642	0.8126	0.3232	5.513	1.166	377.0
0.6162	0.6075	0.4109	5.255	1.018	418.4
0.8779	0.4488	0.5736	5.634	0.766	439.5
1.2416	0.3675	0.6991	5.927	0.570	398.5
1.2731	0.1153	0.8837	2.309	0.217	192.1

9) M. Tamres, *J. Am. Chem. Soc.*, **73**, 3704 (1951).

10) E. Baud, *Bull. Soc. Chim. France*, **17**, 329 (1915).

TABLE 4. HEAT OF MIXING OF CHLOROFORM (1) AND CYCLOHEXANE (2) AT 25.0°C

w_1 (g)	w_2 (g)	x_1	Q (J)	$-\Delta H^M_{x_1}$ (kJ/mol)	ΔH^M (J/mol)
1.1833	0.0986	0.8939	2.732	0.273	146.4
1.0467	0.2240	0.7671	5.109	0.582	446.9
0.8337	0.2846	0.6722	5.874	0.841	565.7
0.7483	0.4237	0.5545	6.912	1.103	611.7
0.5457	0.5253	0.4227	6.816	1.491	630.5
0.6962	0.9819	0.3332	9.937	1.705	567.8
0.4729	0.6861	0.3270	7.079	1.787	584.5
0.3277	0.6584	0.2597	5.389	1.963	510.0
0.2048	1.1957	0.1077	4.163	2.427	261.5
0.1839	1.6153	0.0738	3.724	2.417	179.5
0.1011	1.9255	0.0357	2.081	2.453	87.4

TABLE 5. HEAT OF MIXING OF TETRAHYDROFURAN (1) AND CYCLOHEXANE (2) AT 25.0°C

w_1 (g)	w_2 (g)	x_1	Q (J)	$\Delta H^M_{x_1}$ (kJ/mol)	ΔH^M (J/mol)
0.8603	0.0967	0.9068	2.974	0.266	241.2
0.8209	0.2055	0.8234	5.747	0.505	415.7
0.4930	0.3198	0.6427	7.274	1.064	683.8
0.4316	0.3458	0.5929	7.136	1.192	706.9
0.3576	0.4867	0.4546	7.899	1.639	745.0
0.2635	0.6788	0.3118	7.492	2.051	639.3
0.2039	0.6171	0.2781	6.280	2.224	618.3
0.2559	1.7158	0.1433	8.944	2.623	375.9
0.0829	1.9460	0.0474	3.385	2.946	139.7

TABLE 6. HEAT OF MIXING OF FURAN (1) AND CYCLOHEXANE (2) AT 25.0°C

w_1 (g)	w_2 (g)	x_1	Q (J)	$\Delta H^M_{x_1}$ (kJ/mol)	ΔH^M (J/mol)
0.9315	0.2019	0.8546	9.774	0.693	592.3
0.4863	0.3153	0.6627	11.431	1.552	1029.9
0.4122	0.4619	0.5319	13.336	2.137	1136.8
0.3866	0.4863	0.5031	13.516	2.310	1162.0
0.2113	0.5274	0.3379	9.405	2.941	993.3
0.1428	0.7019	0.2058	7.861	3.638	748.4
0.1047	1.1349	0.1051	6.343	4.005	504.7
0.0864	1.5444	0.0665	5.428	4.153	296.2
0.0748	1.5288	0.0587	4.782	4.224	247.9

shown in Figs. 2 and 3, we can obtain the heats of mixing at an infinite dilution ($\lim_{x_1 \to 0} \Delta H^M_{x_1}$). They are as follows: 2.70 kJ for the chloroform(1)+cyclohexane(2) system; 3.15 kJ for the tetrahydrofuran(1)+cyclohexane(2) system; 4.20 kJ for the 2-methyl furan(1)+cyclohexane(2) system; 4.50 kJ for the furan(1)+cyclohexane(2) system, −9.20 kJ for the chloroform(1)+tetrahydrofuran(2) system; −1.56 kJ for the chloroform(1)+2-methyl furan(2) system; and −0.57 kJ for the chloroform(1)+furan(2) system.

The values of $\lim_{x_1 \to 0} \Delta H^M_{x_1}$ in the cyclohexane series provide energies sufficient to break up all the interactions existing between molecules in the pure state, that is, dipole-dipole interaction in chloroform and tetrahydrofuran, and dipole-dipole and π-π interactions in 2-methyl furan and furan.

In a previous paper,[6] we estimated the energies of dipole-dipole interaction in *n*-ether, ketones, and tertiary amine as the difference in the dipolar stabilization energy of the dipole arising from the reaction field with different media in Onsager's

TABLE 7. HEAT OF MIXING OF 2-METHYL FURAN (1) AND CYCLOHEXANE (2) AT 25.0°C

w_1 (g)	w_2 (g)	x_1	Q (J)	$\Delta H^M_{x_1}$ (kJ/mol)	ΔH^M (J/mol)
0.7752	0.1380	0.8521	5.339	0.566	481.8
0.6164	0.2031	0.7567	6.958	0.927	701.3
0.5816	0.2761	0.6815	8.205	1.158	791.6
0.5945	0.3281	0.6507	9.530	1.315	856.5
0.4207	0.4143	0.5101	9.435	1.841	939.0
0.3854	0.5303	0.4269	10.429	2.222	948.6
0.2694	0.5901	0.3188	8.534	2.601	829.1
0.2126	0.7271	0.2306	7.962	3.075	709.1
0.1446	0.7446	0.1660	5.776	3.280	544.5
0.0800	0.8111	0.0918	3.481	3.572	328.0
0.1000	1.0529	0.0885	4.574	3.768	333.3
0.0777	1.0220	0.0717	3.578	3.781	271.2

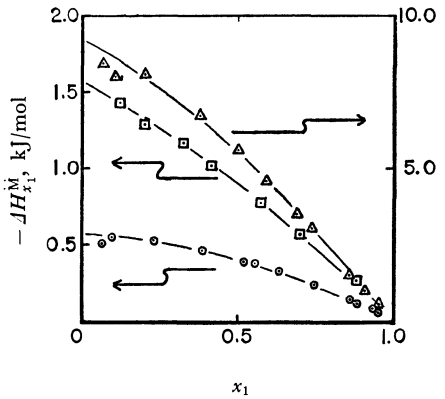

Fig. 2. Heats of mixing of $CHCl_3$+cyclic ether systems: ⊙, furan; ⊡, 2-methylfuran; △, tetrahydrofuran.

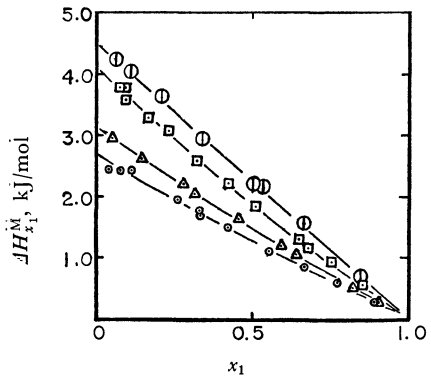

Fig. 3. Heats of mixing of polar liquid+cyclohexane systems: ⊙, $CHCl_3$; △, tetrahydrofuran; ⊡, 2-methylfuran; ⓘ, furan.

treatment of polar liquids. The calculated results seem to agree with the $\lim_{x_1\to 0} \Delta H^M_{x_1}$ values for the polar liquid-nonpolar solvent systems. However, in the 2-methyl furan- and furan-cyclohexane systems of the present investigation, the $\lim_{x_1\to 0} \Delta H^M_{x_1}$ values differ from the results calculated by the above-described method (0.28 kJ for the furan+cyclohexane system and 0.14 kJ for the 2-methyl furan+cyclohexane system). Therefore, the furan derivatives seem to have another interaction, such as a π-π interaction due to a π-electron of the furan nucleus. The energies of such π-π interaction in furan derivatives can not be estimated directly. However, it seems reasonable to regard the value evaluated by subtracting the dipole-dipole interaction energy from the $\lim_{x_1\to 0} \Delta H^M_{x_1}$ value as the energy of π-π interaction—that is, 4.22 kJ (4.50—0.28) for the furan+cyclohexane system and 4.06 kJ (4.20—0.14) for the 2-methyl furan+cyclohexane system.

On the other hand, the values of $\lim_{x_1\to 0} \Delta H^M_{x_1}$ in the chloroform series represent the energies of transfer from the pure chloroform state to one in which each chloroform molecule make a hydrogen bond with an ether molecule, and in which such associated complex molecules are surrounded by a large amount of the ether medium.

Although there are various methods for estimating the energy of the intermolecular interaction, we can estimate the energies of intermolecular hydrogen bonds between chloroform and cyclic ethers in the same way as has been described in a previous paper.[6]

Of the enthalpy cycle shown in Fig. 7 of Ref. 6, ΔH_1, ΔH_2, and ΔH_3 are also measured in the present work, while ΔH_4 in Process 4 is estimated by the same treatment as has been described previously.[6] In the tetrahydrofuran case, two energy changes will contribute to ΔH_4. One, the heat of the mixing of $(x-1)$ mol of tetrahydrofuran with a large quantity of cyclohexane, is equal to $(x-1)\,\Delta H_2$, and the other is ΔH^d_4, due to the enthalpy change from the state in which the associated complex molecules are surrounded by the ether medium to

TABLE 8. PHYSICAL CONSTANTS OF SUBSTANCES NECESSARY FOR THE CALCULATION OF DIPOLAR ENERGIES

	t°C	n_D	d	ε	μ	μ_{12}
Chloroform	20	1.4456	1.4892	4.791	1.22D	
	25	1.4429	(1.4809)	4.724		
	30	1.4339	1.4706	4.653		
Tetrahydrofuran	20	1.4071	0.8892	7.521	1.77D[c]	2.53D[c]
	25	1.4041	0.8823	7.402		
	30	1.4020	0.8773	7.252		
Furan	20	1.4215	0.937[a]	2.954[b]	0.67D[d]	(1.39D)
	25	1.4181	0.913	2.932		
	30	1.4152	(0.899)	2.910		
2-Methylfuran	20	1.4320	0.91365	2.742	0.70D[d]	(1.41D)
	25	1.4295	0.90779	2.716		
	30	1.4265	0.90202	2.693		

a) J. A. Riddick and E. E. Toops, Jr., "Organic solvents," second edition, Interscience Publishers, N. Y. (1955).
b) P. Smyth *et al.*, *J. Phys. Chem.*, **59**, 1088 (1955).
c) A. Weisbecker, *J. Chim. Phys.*, **62**, 1170 (1966).
d) A. L. McClellan, "Tables of Experimental Dipole Moments," W. H. Freeman and Co., San Francisco (1964).

that in which they are surrounded by the cyclohexane medium. On the other hand, in furan derivatives, another contribution to ΔH_4 comes from the π-π interaction of the associated complex molecules. As this contribution can not be estimated, we shall assume it to be equal to the energies of the π-π interaction in the furan derivative. The contribution due to $\Delta H_4{}^d$ may be calculated by the previously-described method. The physical constants necessary for this calculation are summarized in Table 8, where d, ε, n_D, and μ are the density, dielectric constant, refractive indices, and dipole moment respectively. μ_{12} is the dipole moment of the associated complex molecule. Its value for the tetrahydrofuran system was derived by Weisbecker.[11] He determined it by assuming that a hydrogen atom of chloroform forms a hydrogen bond with an oxygen atom of tetrahydrofuran. On the other hand, the μ_{12} values for the furan derivative systems were calculated by assuming that a chloroform molecule combines on the nucleus of furan and by the vector addition of the dipoles of two component molecules. The reasons for this assumption will be given later.

The $\Delta H_4{}^d$ values thus obtained are as follows: 3.08 kJ for the chloroform-tetrahydrofuran complex; 0.38 kJ for the chloroform-furan complex; 0.35 kJ for the chloroform-2-methyl furan complex; 0.28 kJ for the furan-cyclohexane system, and 0.14 kJ for the 2-methyl furan-cyclohexane system.

By using the $\Delta H_4{}^d$ values calculated above and the other measured values, the intermolecular hydrogen bond energies between chloroform and cyclic ethers, ΔH_5, are found to be:
for the chloroform-tetrahydrofuran-cyclohexane system:

$$\begin{aligned}\Delta H_5 &= -\Delta H_1 - x\Delta H_2 + \Delta H_3 + \Delta H_4 \\ &= -\Delta H_1 - x\Delta H_2 + \Delta H_3 + (x-1)\Delta H_2 \\ &\quad + \Delta H_4{}^d \\ &= -2.70 - 3.15x - 9.20 + 3.15(x-1) \\ &\quad + 3.08 \\ &= -11.97\ \text{kJ};\end{aligned}$$

for the chloroform-furan-cyclohexane system:

$$\begin{aligned}\Delta H_5 &= -\Delta H_1 - x\Delta H_2 + \Delta H_3 + \Delta H_4 \\ &= -\Delta H_1 - x\Delta H_2 + \Delta H_3 + (x-1)\Delta H_2 \\ &\quad + \Delta H_{\pi-\pi} + \Delta H_4{}^d \\ &= -2.70 - 4.50x - 0.57 + 4.50(x-1) \\ &\quad + 4.22 + 0.38 \\ &= -3.17\ \text{kJ, and}\end{aligned}$$

for the chloroform-2-methyl furan-cyclohexane system:

$$\begin{aligned}\Delta H_5 &= -2.70 - 4.20x - 1.56 + 4.20\,(x-1) \\ &\quad + 4.06 + 0.35 \\ &= -3.99\ \text{kJ}.\end{aligned}$$

As may be seen in the above calculations, the energies of the intermolecular hydrogen bonds between chloroform and cyclic ethers are in the order: tetrahydrofuran > 2-methyl furan > furan.

Let us now consider this order. In furan derivatives, π-electron is present, but not in tetrahydrofuran. Therefore, furan has a negative net charge on the ring carbon and a positive net charge on the oxygen atom, as is shown in Fig. 4.[12] The hydrogen-bond forming power of furan with chloroform will be weakened. On the other hand, it is known that the tetrahydrofuran molecule makes

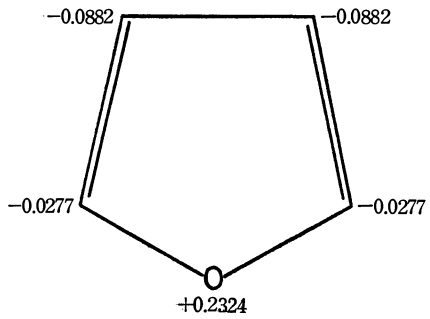

Fig. 4. Net charge on the atoms of furan molecule.

a CH-O type intermolecular hydrogen bond with chloroform.[11] Generally, the hydrogen bond strength is stronger in the H-O type than in the H-π type.[13] As the introduction of a methyl group to the furan ring causes an increase in basicity, the hydrogen bond energy for the 2-methyl furan system increases in comparison with that for the furan system. Furthermore, it is known from the spectroscopic study that the shift in the frequency of the O-H band, $\Delta\nu$, of alcohol is correlated with the hydrogen-bond energy. The frequency shifts, $\Delta\nu$, of phenol due to hydrogen bonding with some heteroaromatics were measured in carbon tetrachloride.[1] The results were arranged in the order of: tetrahydrofuran>2-methyl furan> furan; this order is consistent with that one which we have estimated on the basis of the thermochemical measurements.

11) A. Weisbecker, *J. Chim. Phys.*, **62**, 1170 (1966).
12) K. Nishimoto, private communication.
13) G. C. Pimentel and A. L. McClellan, "The Hydrogen Bond," W. H. Freeman and Co., San Francisco (1960); R. West, International Symposium on Molecular Structure and Spectroscopy, Tokyo, 1962.

The authors wish to thank Professor Zenichi Yoshida, Faculty of Engineering, Kyoto University, for his helpful advice. The authors are also grateful to Dr. Kichisuke Nishimoto for his valuable discussions. Thanks are also due to the Kaō Soap Co., Ltd., Wakayama, for supplying the tetrahydrofuran and furan derivatives, and to the Applied Electric Lab., Ltd., for freely allowing the use of a model CM-502 microcalorimeter. The expenses of this work have been partly defrayed by a grant from the Ministry of Education.

BULLETIN OF THE CHEMICAL SOCIETY OF JAPAN VOL. 41 1545—1551 (1968)

Studies on the Delayed Fluorescence by Means of a Flash Technique*[1]

Koichi KIKUCHI, Hiroshi KOKUBUN and Masao KOIZUMI

Department of Chemistry, Faculty of Science, Tohoku University, Katahira-cho, Sendai

(Received January 16, 1968)

It has been shown that the delayed and normal fluorescence can be measured accurately by a usual flash apparatus. Such measurements, combined with that of T–T absorption, have enlarged the potentiality of a flash technique to a large extent. As an example, a simple method of differentiation between E-type and P-type delayed fluorescence has been presented. Detailed studies have been made on the T–T annihilation process of anthracene (A) and the probability for Process $A^T+A^T \rightarrow A+A^*$, has been decided. The value obtained is 0.077 ± 0.005. E-Type delayed fluorescence of eosine and proflavine have been studied and the value of $k_t \cdot \phi_{ST}$ (k_t, the rate constant of Process, $T \rightarrow S^*$; ϕ_{ST}, the probability of the intersystem crossing) have been evaluated, to be 3.3_6 and 2.7_8 sec^{-1} respectively. Some advantages of the present method over the sector method have been discussed.

A flash photolytic technique is now extensively used for studying the behavior of intermediates produced in the photochemical reaction of organic substances. The method, however, usually relies upon the measurement of the UV absorption spectra of transient species.

If the measurement is extended to the emission phenomena such as the normal and delayed fluorescence, the potentiality of the flash technique will largely be enlarged. Such attempts have been made by Zahlan *et al.*[1] and by Powell[2] to determine the intersystem-crossing probability of some hydrocarbons in the gaseous state. Wild *et al.*[3] also measured the delayed fluorescence of

*1 A preliminary report was published in *Photochem. and Photobiol.*, **7**, 499 (1968).

1) A. B. Zahlan, S. Z. Weisz, R. C. Jarnagin and M. Silver, *J. Chem. Phys.*, **42**, 4244 (1965).
2) G. L. Powell, *ibid.*, **47**, 95 (1967).
3) U. Wild and Hs. H. Günthard, *Helv. Chim. Acta*, **48**, 1843 (1965).

anthrancene in glycerol in the temperature range from −20 to 90°C. In spite of these reports, it does not seem that the methodology has been fully established and that its availability has been duly recognized. We believe that various kinds of process such as delayed fluorescence, quenching of fluorescence, T-T energy transfer and other elementary processes in the excited states can be attacked by combining the measurement of the emission-time relation with that of the T-T absorption.

The objective of the present paper is to report firstly, how the time dependence of the delayed fluorescence and of the normal fluorescence (during flash irradiation) can be accurately measured with an ordinary flash apparatus now generally used, and secondly how the method can be applied, as an example, to the investigation of the mechanisms of the delayed fluorescence.

Delayed fluorescence has been studied extensively by Parker and his coworkers[4]; and now it has been well established that there are two types of delayed fluorescence, *i. e.*, E-type and P-type. Choosing anthracene of which the elementary processes in the excited state have been studied in detail, we would like to show how the present method is used for studying the P-type delayed fluorescence, with some advantages over the sector method. For this purpose, the delayed fluorescence of anthracene as well as the sensitized one, using eosine, erythrosine and proflavine as sensitizers, have been studied. E-Type delayed fluorescence of proflavine and eosine have also been studied and the results have been compared with those obtained by other methods.

Experimental

A great advantage of the present method is that the time dependence of the delayed fluorescence and the triplet decay can be compared in the similar experimental condition with the same apparatus. In order to do this, it is, of course, necessary to keep the geometry of the entire apparatus rigorously fixed. It is also required that the intensity of the flash and its time dependence can be controlled reproducibly. These requirements could be achieved with some satisfaction.

In order to investigate the mechanism of the delayed fluorescence, measurement has to be performed of A) the triplet decay and the intensity of the delayed fluorescence as a function of time both in the same condition, and besides, of B) the normal fluorescence intensity (during a flash) and the yield of the triplet state under the same condition which is, however, different from A).

To make an accurate measrement of the time dependence of the delayed fluorescence, it is necessary to remove the effect of the scattered light during a flash and to make the duration of a flash as short as possible. Use of some suitable sensitizers with appropriate filters is very effective for removing the scattered light and accordingly for separating the normal and delayed fluorescence satisfactorily.

Decay of T-T absorption and the change of delayed fluorescence with time, were measured at fixed wavelengths by means of a Nalumi-RM 23 monochromator. Photomultipliers employed, were Hamamatsu TV R106 and R132. A Iwasaki-Tsushinki SS-5004 synchroscope was used. Cells were the standard ones *i. e.*, quartz cells 10 mm in diameter, 100 mm in length or SB glass tubes 10 mm in diameter with two quartz plates pasted on both ends. Energy input to the flash lamp was selected in the region from 10 to 120 joules.

For the measurement of normal fluorescence, which is quite strong, neutral filters were inserted in between the monochromator and the cell. Measurement of the normal fluorescence from an aerated solution was of great help to examine the degree of superposition of the normal and delayed fluorescence. Because the aerated solution gives no delayed fluorescence and the profile of the emission is closely related with that of the flash.[5]

Anthracene, β-acetonaphthone, eosine, proflavine, erythrosine and ethanol were purified by the standard methods.

Method of Analysis and Results

Typical Examples for the Time Dependence of the Normal and Delayed Fluorescence. The intensity of the delayed fluorescence, I_{DF} and the second order decay constant of T-T absorption were measured at the same high energy input to the flash lamp. Figures 1 and 2 give respectively the I_{DF} *vs.* t plots for the case of direct excitation of anthracene and for the eosine-sensitized excitation. The dotted line in Fig. 1 represents the normal fluorescence from the aerated solution. It is evident that the shaded area can be used as the quantity of the delayed fluorescence during the time interval from a to b. A small peak existing

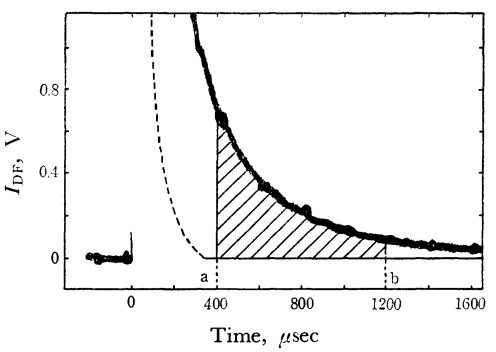

Fig. 1. Delayed fluorescence (solid line) and normal fluorescence (dotted line) of anthracene at 400 nm by direct excitation.
[Anthracene] = 1.0×10^{-4} M.

4) C. A. Parker, "Advances in Photochemistry," Vol. II, ed. by W. A. Noyes, G. S. Hammond and J. N. Pitts, Interscience Publishers, New York, N. Y. (1964). p. 305.

5) A. Kira and S. Kato, *Sci. Rep. of Tohoku Univ., Ser. I*, **48**, 142 (1965).

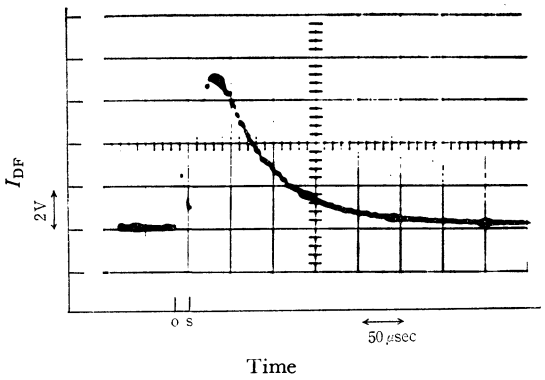

Fig. 2. Delayed fluorescence of anthracene at 400 nm sensitized by eosine.
[Anthracene] = 3.6×10^{-5} M
[Eosine] = 2.0×10^{-5} M

between o and s in Fig. 2 is due to the scattered light during a flash. The area after s gives the quantity of the delayed fluorescence. It is evident that in the case of the sensitized emission, rise and fall of the delayed fluorescence can be measured with enough accuracy. As will be reported elsewhere, the analysis of the rising portion of the curve enables us to evaluate the rate constant for the process of T–T energy transfer. Figure 3 gives the spectrum of the delayed fluorescence of anthracene sensitized by eosine. This was obtained by measuring the decay curves such as shown in Fig. 2, at various wavelengths, and by plotting the intensities at the peak positions against the wavelength. The spectrum agrees satisfactorily with that of the normal fluorescence; this ensures the reliability of the intensity measurement.

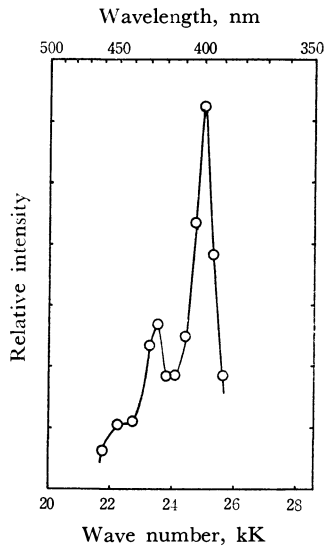

Fig. 3. Delayed fluorescene spectrum of anthacene sensitized by eosine.
[Anthracene] = 3.6×10^{-5} M
[Eosine] = 2.0×10^{-5} M

Normal fluorescence was measured at a low energy input to the flash lamp. Under such a condition, the yield of triplet state could be determined precisely because the decay was practically first order. Figure 4 is an example of the profile of the normal fluorescence of anthracene in the aerated solution. Since this reflects the profile of the flash, the reproducibility of flashing can be checked by making such measurements from time to time. It was found that the reproducibility was quite excellent. The optical density of T–T absorption corresponding to the yield of triplet state, $(D_T)_0$, was decided by extrapolation of the decay curve of T–T absorption to the time-point S'. This is somewhat conventional but was found to be most satisfactory.

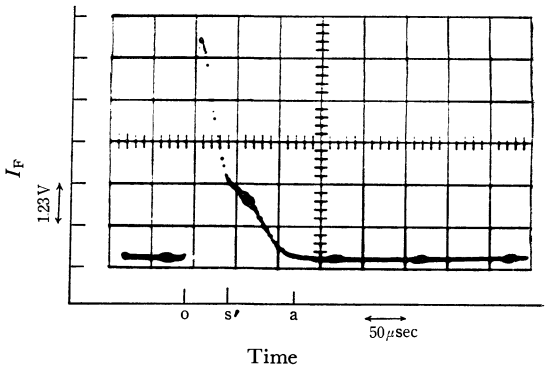

Fig. 4. Normal fluorescence of anthracene during a flash.
[Anthracene] = 1.0×10^{-4} M
Flash energy 80 joule

In the case of E-type delayed fluorescence, the intensity was so weak that it was very difficult to distinguish the delayed fluorescence from the normal one. This was almost impossible in the case of direct excitation. An example of the

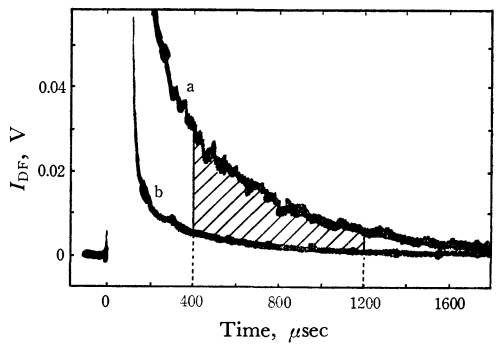

Fig. 5. Delayed fluorescence of eosine sensitized by β-acetonaphthone.
[Eosine] = 6.8×10^{-6} M
[β-Acetonaphthone] = 5.0×10^{-4} M
Curve a, deaerated soln.; b, aerated soln.

delayed fluorescence of eosine in the case of sensitized emission, by β-acetonaphthone, is shown in Fig. 5. Curve a in Fig. 5 is a plot of emission intensity from the deaerated solution and curve *b*, from the aerated solution. Since the latter is due mainly to the scattered light, the shaded area can be used as a measure of the delayed fluorescence. The accuracy is rather poor in this case.

Differentiation between P-Type and E-Type Delayed Fluorescence. It is well known that the delayed fluorescence of aromatic hydrocarbons occurs through the T–T annihilation, $T+T \xrightarrow{k_1} S^*+S$. The details of other processes simultaneously occurring, however, still remain to be studied in future. Here the following scheme is conventionally assumed.

$$T + T \begin{cases} \xrightarrow{k_1} S^* + S \\ \xrightarrow{k_2} T + S \end{cases} \qquad k_{TT} = k_1 + k_2$$

Putting $p=(k_1/k_{TT})$, the intensity of the delayed fluorescence can be written as follows,

$$I_{DF} = \alpha\phi_F p k_{TT}[T]^2 = \alpha\phi_F p k_{TT}[D_T/\varepsilon_T d]^2 \qquad (1)$$

where α is a constant depending upon the apparatus and upon the entire experimental conditions, where ϕ_F is a quantum yield of the fluorescence and where D_T, ε_T and d are respectively the optical density for T–T absorption, molar absorbance for it and the light path of a cell (100 mm in the present case).

Taking logarithm of Eq. (1), one obtains

$$\log I_{DF} = 2\log D_T + \log(\alpha\phi_F p k_{TT}/(\varepsilon_T)^2 d^2) \qquad (2)$$

Eq. (2) requires that the plot of $\log I_{DF}$ *vs.* $\log D_T$ should have a slope of 2. Figure 6 shows that this relation really holds very satisfactorily. This is perhaps the simplest method for verifying the P-type delayed fluorescence. It is somewhat disappointing that the four lines do not coincide. This is, of course, due to the fluctuation in α-values. The smallest value for proflavine may perhaps be attributed to a large value of its molar absorbance at 400 nm, which reaches 8.5×10^3 M^{-1} cm^{-1}. For the other three cases the deviation of α from the average is within ±40%.

E-Type delayed fluorescence was more difficult to study because of its very weak intensity. Moreover, since both eosine and proflavine have more or less absorption in the entire UV region, the dye concentrations should be less than $\sim10^{-5}$ M in order to reduce the perturbing effect of the normal fluorescence.

It is therefore necessary to examine how the energy transfer from β-acetonaphthone to a dye occurs at such a low concentration. Figure 7 shows the decay of T–T absorption of β-acetonaphthone in the presence and in the absence of eosine.

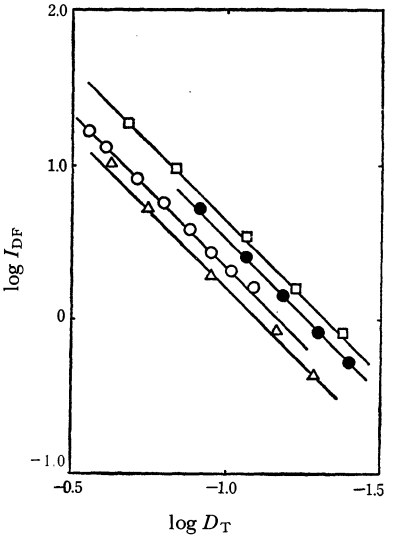

Fig. 6. Confirmation of Eq. (2).
[Anthracene] = 1.0×10^{-4} M
● Direct excitation
□ [Eosine] = 5.0×10^{-6} M
△ [Proflavine] = 1.2×10^{-5} M
○ [Anthracene] = 8.0×10^{-5} M
[Erythrosine] = 8.0×10^{-6} M

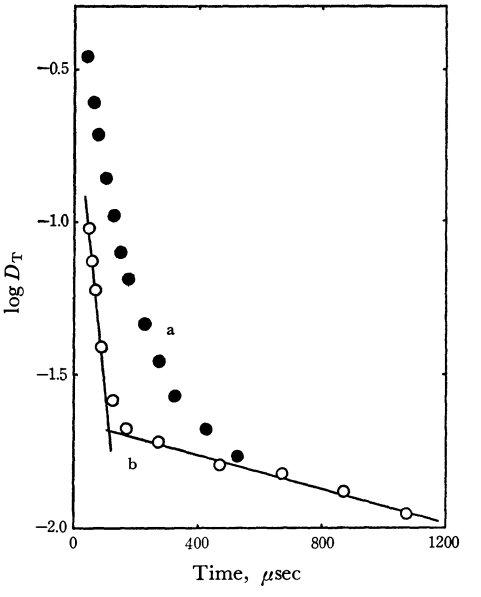

Fig. 7. Decay of T–T absorption of β-acetonaphthone at 430 nm.
● [Eosine] = 0 M
○ [Eosine] = 6.0×10^{-6} M
[β-Acetonaphthone] = 5×10^{-4} M

One can say that the energy transfer is practically complete in 200 μsec. Thus in the present system, the experimental data after 200 μsec should be used. The slow decay in the later stage of curve b, is related with another intermediate produced

by the reaction of the eosine triplet state with ethanol.[5]

It is well-known that the process T→S* for the E-type delayed fluorescence, is a monomolecular thermal activation. Thus I_{DF} is given by the following relation,

$$I_{DF} = \alpha\phi_F k_t[T] = \alpha\phi_F k_t \frac{D_T}{\varepsilon_T d} \qquad (3)$$

where k_t is the rate constant of the T→S* process. Figure 8 gives the plots of $\log D$ and $\log I_{DF}$ against time for the case of eosine, and Fig. 9 gives the similar plots for proflavine. As seen from these figures, the delayed fluorescence and the T-T absorption decay with essentially the same rate constant. This verifies that the delayed fluorescence of these dyes is mainly of E-type. However, there is a tendency, in the case of eosine, that the decay of the T-T absorption is appreciably smaller in the later stage. This is due to the existence of the absorption of another transient intermediate which is produced in the reaction between T and ethanol.[5] In the case of proflavine, the slopes for the $\log D_T$ and $\log I_{DF}$ plots agree quite well in the later stage. In both eosine and proflavine, the slopes of $\log I_{DF}$ at the early stage are somewhat larger. This suggests

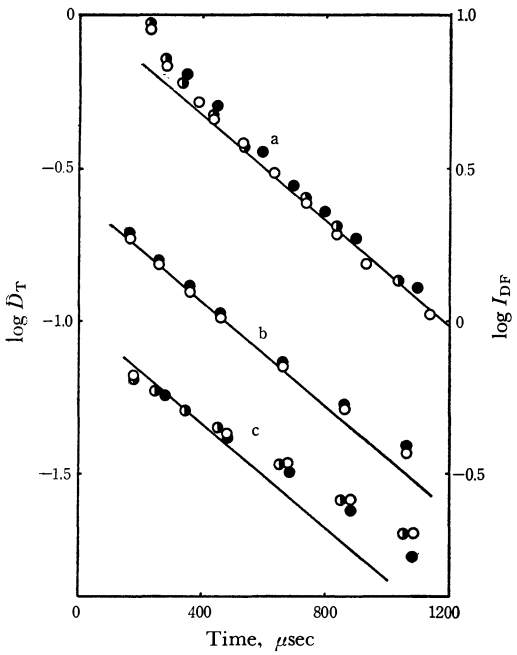

Fig. 8. Decay of T-T absorption at 580 nm and delayed fluorescence at 570 nm of eosine. a) Delayed fluorescence sensitized by β-acetonaphthone, b) T-T absorption by direct excitation, c) T-T absorption sensitized by β-acetonaphthone.
[Eosine] = 6.0×10^{-6} M
[β-Acetonaphthone] = 5.0×10^{-4}

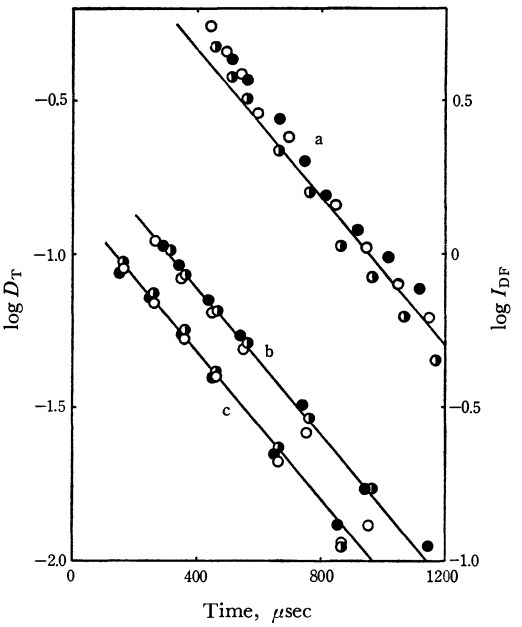

Fig. 9. Decay of T-T absorption at 550 nm and delayed fluorescence at 500 nm of proflavine. a) Delayed fluorescence sensitized by β-acetonaphthone, b) T-T absorption by direct excitation, c) T-T absorption sensitized by β-acetonaphthone.
[Proflavine] = 1.66×10^{-5} M
[β-Acetonaphthone] = 5.0×10^{-4} M

the occurrence of P-type delayed fluorescence, as has been established by Parker *et al.*[6]

Experimental Verification of the Relation between the Normal Fluorescence and the Triplet Yield. The intensity of the normal fluorescence is proportional to the absorption of light (per unit time) and can be written as follows,

$$I_F = \alpha\phi_F I_{ab} \qquad (4)$$

Integrating Eq. (4),

$$\int I_F dt = \alpha\phi_F \int I_{ab}\, dt \qquad (5)$$

The yield of the triplet state, on the other hand, can be given by the following equation,

$$[T_0] = \frac{[D_T]_0}{\varepsilon_T d} = \phi_{ST} \int I_{ab}\, dt \qquad (6)$$

where $[T]_0$ and $[D_T]_0$ are respectively the concentration of T and the corresponding optical density immediately after flashing and where ϕ_{ST} is the probability of the intersystem crossing. It is to be noted that this equation holds only when the decay of the triplet state is negligible during a flash. When the flash intensity is set rather weak,

6) C. A. Parker, C. G. Hatchard and T. A. Joyce, *Nature*, **205**, 1282 (1965); *J. Mol. Spectry.*, **14**, 311 (1964).

this holds practically and furthermore, the extrapolation of the triplet decay is easy. From Eqs. (5) and (6), one gets

$$[D_T]_0 = \frac{\varepsilon_T d\phi_{ST}}{\alpha\phi_F}\int I_F\,dt \qquad (7)$$

Figure 10 shows that this relation really holds in the case of anthracene. This is considered to be one of the most fundamental relations in the present method. If, ε_T, ϕ_{ST} and ϕ_F are all known, the value of α can be decided from the slope of the plot in Fig. 10.

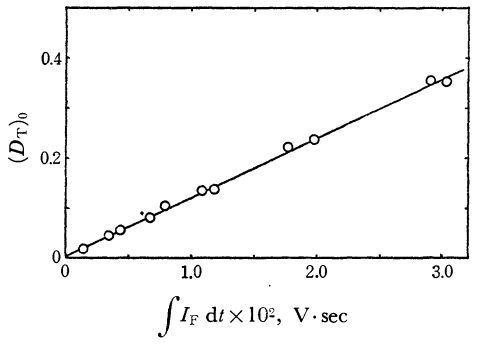

Fig. 10. Confirmation of Eq. (7).
[Anthracene] = 1.0×10^{-4} M

Putting $\varepsilon_T = 6.2\times10^4$ M^{-1} cm^{-1},[7] $\phi_{ST}=0.7$,[8] $\phi_F=0.27$,[9,10] one obtains a value of α to be 1.36×10^5 (at 400 nm). The value of α perhaps depends only on the wavelength when all the other experimental conditions are kept constant. It is most desirable to decide the reliable α-values at various wavelengths.

Analysis of the P-Type Delayed Fluorescence. Integration of Eq. (1) gives

$$\int I_{DF}\,dt = \frac{\alpha\phi_F p k_{TT}}{(\varepsilon_T d)^2}\cdot\int (D_T)^2\,dt \qquad (8)$$

Elimination of α from Eqs. (7) and (8) gives the following relation,

$$\frac{\int I_{DF}\,dt}{\int I_F\,dt} = \phi_{ST} p\,\frac{k_{TT}}{\varepsilon_T d}\,\frac{\int (D_T)^2\,dt}{(D_T)_0} \qquad (9)$$

In this equation, the values of $\int I_{DF}\,dt$, $\int (D_T)^2\,dt$, $\int I_F\,dt$ and $(D_T)_0$ can be obtained experimentally. It is to be noted that the upper and lower limit of the first and the second integrals should respectively be set equal. The k_{TT}/ε value can be obtained by analysing the decay curve of T–T absorption. There is no need to know the value of ε_T. Thus the value of the product $p\cdot\phi_{ST}$ can be evaluated from the data obtained in the flash experiments. The value of ϕ_{ST} is 0.70 according to Medinger and Wilkinson.[8] The values of $p\cdot\phi_{ST}$ and p thus obtained from five different sets of experiments are given in Table 1 along with Parker's value of p.[6] The agreement is satisfactory. We believe that our value is more reliable since it is based only on the experimental data whereas Parker's value was evaluated by using as the k_{TT} value, the diffusion controlled rate constant theoretically calculated.

It is to be added that when the value of α is known (as in the present case), simple insertion of its value into Eq. (2) or into the intercepts of the plots in Fig. 6, gives the value of p. Of course, the same equation can be used to decide the α value if p is a known quantity.

Analysis of the E-Type Delayed Fluorescence. Integration of Eq. (3) gives

$$\int I_{DF}\,dt = \frac{\alpha\phi_F k_t}{\varepsilon_T d}\int D_T\,dt \qquad (10)$$

By eliminating α from Eqs. (7) and (10), one gets

$$\frac{\int I_{DF}\,dt}{\int I_F\,dt} = k_t\phi_{ST}\,\frac{\int D_T\,dt}{(D_{OT})_0} \qquad (11)$$

The upper and lower limits of the integrals $\int I_F\,dt$ and $\int D_T\,dt$ were suitably chosen by taking the perturbing effect of the scattered light into consideration. Thus the value of the product $k_t\cdot\phi_{ST}$ can be obtained in this case; for eosine 3.36 sec^{-1} and for proflavine 2.78 sec^{-1}. The values of the first order triplet decay constant for eosine and proflavine are respectively 1.98×10^3 sec^{-1} and 5.64×10^3 sec^{-1}. The value of ϕ_{ST} for eosine is 0.71 according to Porter.[11] Our recent experiment has given a value of 0.4.[12] Thus the value of k_t for eosine is 8.4 sec^{-1} (at room temperature). This value is compared with 3.77 sec^{-1} at 288°K calculated from the following relation reported by Parker.[9]

$$k_t = 7.4\times10^7\exp\left(-\frac{9.6\text{ kcal}}{RT}\right)$$

7) G. Porter and M. W. Windsor, *Discussions Faraday Soc.*, **17**, 178 (1954).
8) T. Medinger and F. Wilkinson, *Trans. Faraday Soc.*, **61**, 620 (1965).
9) C. A. Parker and C. G. Hatchard, *ibid.*, **57**, 1894 (1961).
10) E. J. Bowen and J. Sahu, *J. Phys. Chem.*, **63**, 4 (1959); G. Weber and F. Teale, *Trans. Faraday Soc.*, **53**, 646 (1957); W. H. Melhuish, *J. Phys. Chem.*, **65**, 229 (1961).
11) P. G. Bowers and G. Porter, *Proc. Roy. Soc. London*, **A296**, 435 (1967).
12) To be published.

TABLE 1. P-TYPE DELAYED FLUORESCENCE OF ANTHRACENE

Sensitizer			Proflavine 1.2×10^{-5} M	Eosine 5.0×10^{-6} M	Erythrosine 8.0×10^{-6} M
Anthracene	1.0×10^{-4} M	1.0×10^{-4} M	1.0×10^{-4} M	1.0×10^{-4} M	8.0×10^{-5} M
$(D_T)_0$	0.080	0.289	0.151	0.203	0.347
$\int I_F\,dt$	6.7×10^{-3}	6.3×10^{-2}	2.3×10^{-2}	4.9×10^{-2}	4.8×10^{-2}
$\int (D_T)^2 dt$	1.4×10^{-4}	7.9×10^{-6}	1.4×10^{-5}	1.5×10^{-5}	5.3×10^{-5}
$\int I_{DF}\,dt$	3.7×10^{-4}	5.2×10^{-4}	7.2×10^{-4}	1.1×10^{-3}	2.5×10^{-3}
$k_{TT}/\varepsilon_T d$ (sec^{-1})		6.0×10^{3}			
$p\cdot\phi_{ST}$	5.4	5.1	5.5	5.0	5.8
ϕ_{ST}[a]		0.70			
$p\times10^2$	7.7	7.3	7.9	7.1	8.3
p (average)		0.07			
p (Parker)[b]		0.09			

a) Ref. 8 b) Ref. 6

TABLE 2. E-TYPE DELAYED FLUORESCENCE OF EOSINE AND PROFLAVINE

Sensitizer / Acceptor	5.0×10^{-4} M β-acetonaphthone	
	Eosine 6.8×10^{-6} M	Proflavine 1.66×10^{-5} M
$(D_T)_0$	0.248	0.227
$\int I_F\,dt$	9.6×10^{-2}	1.7×10^{-1}
$\int (D_T)\,dt$	1.3×10^{-5}	3.6×10^{-6}
$\int (I_{DF})\,dt$	1.5×10^{-5}	7.5×10^{-6}
$k_t\phi_{ST}$ (sec^{-1})	3.36	2.78
k_t (sec^{-1})	8.4	
ϕ_{ST}[a]	0.4	
k_{total} (sec^{-1})	1.98×10^{3}	5.64×10^{3}

a) Ref. 12)

Concluding Remarks

In the present paper it has been shown that in suitable systems both the normal and delayed fluorescence can be accurately measured by a flash apparatus. E-Type and P-type delayed fluorescence have been studied to demonstrate the availability of the present method. In particular, the value of p for anthracene (P-type) and the values of $k_t\cdot\phi_{ST}$ for eosine and proflavine (E-type) have been decided. Although there are reliable values for ϕ_{ST} and k_{TT} of anthracene reported in the literature, Parker's p-value for anthracene is the only one ever reported.

A brief description will be added on some advantages of the present method over the sector method.

1) It is possible to compare the triplet decay and the time dependence of the delayed fluorescence, with the same one apparatus and accordingly under quite the similar condition.

2) Since the triplet yield is very high in the flash experiment it is rather easy to make the intensity of the delayed fluorescence large enough to be measureable.

3) P-Type and E-type can be distinguished rather easily by examining the applicability of Eqs. (2) and (3). In the sector method on the other hand, the decay constant of the delayed fluorescence, becomes twice that of the triplet decay, only when the triplet concentration is low enough.

4) In evaluating the $p\cdot\phi_{ST}$ values of the P-type delayed fluorescence, it is unnecessary to know the absolute value of the second order rate constant of the triplet state decay. The knowledge of the apparent second order decay constant of the T-T absorption is enough for this purpose.

There will be no need to say that the present method can be used to investigate other elementary processes pertaining to the excited state. In particular, studies on the mixed T–T annihilation are expected to afford detailed information. Medinger's method for determining ϕ_{ST}[8] also will be easily modified for the present method. Lastly the application of Eq. (7) seems to be very promising, provided the dependence of α upon wavelength is systematically investigated. Studies upon these problems are now in progress.

BULLETIN OF THE CHEMICAL SOCIETY OF JAPAN VOL. 41 1552—1557 (1968)

Anomalous Effect of the Concentration of Metal-salt Catalysts in the Liquid-phase Oxidation of *p*-Xylene and Toluene

Kanekichi KAGAMI

Government Chemical Industrial Research Institute, Tokyo, Shibuya-ku, Tokyo

(Received January 20, 1968)

By studying the relation between the concentration and the oxidation activity of various metal catalysts, mostly naphthenates, oleates, linoleates, and caprates of manganese, cobalt, and nickel salts, as well as mixed catalysts of two kinds, it has been established that, in general, there is an anomalous effect of the catalyst concentration-namely, the catalytic activity disappears above a certain point in the concentration of the catalyst. The anomalous concentration effect of a catalyst is observed in the oxidation of toluene and *p*-xylene with all the catalysts, but chromium naphthenate is a lone exception in the oxidation of *p*-xylene. It has been shown that the anomalous effect is due to the association of the catalyst in the hydrocarbon solvent to be oxidised, and that the associated catalyst does not act to promote oxidation. The association is reversible, being dependent on the concentration of the catalyst, so the anomalous concentration effect of a catalyst disappears on dilution.

While numerous papers and reviews[1] have been published on the liquid-phase oxidation of hydrocarbons in the presence of metal-salt catalysts, little is known of the relation between the concentration and the activity of metal-salt catalysts. George *et al.*[2] and Kamiya[3] have reported on the relation between the concentration of a catalyst and the progress of the reaction in the oxidation of tetralin and ethylbenzene. Shigeyasu *et al.*[4] studied the oxidation of alkylbenzenes in a similar way. In the course of their study of the oxidation of *p*-xylene, Ohta *et al.* found a certain limit of concentration above which the catalytic activity is lost with catalysts of copper salts[5] as well as with a mixed catalyst[6] of the salt of manganese and cobalt. Brook *et al.*[7] observed in the oxidation of lubricating oils, using salts of copper and iron as catalysts, that the oxidation rate reaches a maximum and then gradually falls upon an increase in the concentration of the catalysts. They attributed this phenomenon to the formation of an inactive micelle structure at higher concentrations of Cu and Fe salt catalysts.

Since then there has been, as far as we know, no paper treating the variation in catalytic activity with the variation in the concentration of metal-salt catalysts.

In view of the fact that the concentration of a catalyst has an unexpectedly large influence on the velocity of the liquid-phase oxidation of *p*-xylene and toluene in the presence of metal-salt catalysts, the present author has studied how the catalytic activity varies with the concentration of the catalyst, using such catalysts as Mn, Co, and Ni salts of naphthenic, oleic, linoleic, and capric acids, as well as mixed catalysts of two kinds of these salts. He has found that the catalytic activity diminishes above a certain limit of concentration of the catalyst, and is entirely lost at higher concentrations. In view of this rather peculiar phenomenon, which may be called an anomalous effect of the catalyst concentration, the author has determined the molecular weight of the catalysts at the critical concentration in the medium of the hydrocarbons to be oxidised, and has already published in Japanese all the essential results obtained in connection with the catalytic activity in oxidation. This paper is a brief summary dealing with the author's reports[8-12] on the anomalous effect of the

1) Y. Kamiya, *Yukagaku (J. Japan Oil Chem. Soc.)*, **14**, 539 (1965); Y. Takegami, *Yuki Gosei Kagaku (J. Synth. Org. Chem. Japan)*, **21**, 858 (1963).
2) P. George and A. Robertson, *Trans. Faraday Soc.*, **42**, 217 (1946).
3) Y. Kamiya, *Can. J. Chem.*, **41**, 2029, 2034 (1963); **42**, 1027, 2424 (1964); *Kogyo Kagaku Zasshi (J. Chem. Soc. Japan, Ind. Chem. Sect.)*, **69**, 897 (1966).
4) M. Shigeyasu, *Kogyo Kagaku Zasshi (J. Chem. Soc. Japan, Ind. Chem. Sect.)*, **67**, 1396 (1964); **68**, 304 (1965); **70**, 1150, 1155, 1259, 1375 (1967).
5) N. Ohta, *Tokyo Kogyo Shikensho Houkoku (Report of Government Chem. Ind. Research Institute, Tokyo)*, **51**, 215 (1965).
6) N. Ohta, *Kogyo Kagaku Zasshi (J. Chem. Soc. Japan, Ind. Chem. Sect.)*, **63**, 768 (1960).
7) J. H. T. Brook, J. B. Matthews, *Discussions Faraday Soc.*, **10**, 298 (1951).
8) K. Kagami, *Yuki Gosei Kagaku (J. Synth. Org. Chem. Japan)*, **20**, 282 (1962).
9) K. Kagami, *Kogyo Kagaku Zasshi (J. Chem. Soc. Japan, Ind. Chem. Sect.)*, **70**, 162 (1967).
10) K. Kagami, *ibid.*, **70**, 166 (1967).
11) K. Kagami, *ibid.*, **70**, 906 (1967).
12) K. Kagami, *ibid.*, **70**, 1683 (1967).

catalyst concentration (abbreviated as the AC-effect).

Experimental

The oxidation of *p*-xylene was carried out under the normal pressure of oxygen in a 200 m*l* flask. Temperature of oxidation: 136—137°C; quantity of *p*-xylene: 0.5 mol; duration of oxidation: 4 hr; rate of flow of oxygen: 6 *l*/hr; rate of stirring: 700—1000 rpm.

The oxidation of toluene was effected under compressed air in a 200 m*l* stainless-steel autoclave. Temperature of oxidation: 178±2°C; quantity of toluene: 0.7 mol; duration of oxidation: 4 hr; rate of flow of air: 30 *l*/hr; pressure of reaction: 10 atm; velocity of stirring: 800—1000 rpm.

The catalyst was prepared in the following way: the metal salt, obtained by double decomposition between the sodium salt of the organic acid and the metal nitrate, was washed and dried. The quantity of the metal in the catalyst was determined, and the concentration of the catalyst was expressed in terms of the metal gram atoms per mole of *p*-xylene or toluene times 10^5. For brevity, the metal-salt catalysts will be indicated by the following notations: metal-naphthenates: Me-N; metal-oleate: Me-O; metal-linoleate: Me-L; metal-caprate: Me-; metal-stearate: Me-S.

The separation and analysis of the reaction products was carried out as follows:

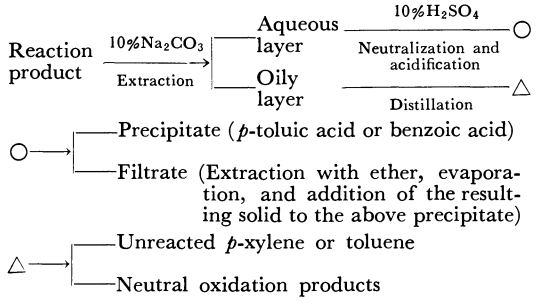

The molecular weights of the metal-salt catalysts in the reaction fluids were determined at 37°C in advance of the oxidation reaction in a VPO vessel, model 301, of the Mechrolab Co. by means of studying the vapor-pressure depression. For the preparation of corrected curves, benzil was used as the standard substance. Since the induction period in the oxidation of either *p*-xylene or toluene was nearly constant, irrespective of the concentration of the catalyst (except for the oxidation of *p*-xylene under the catalytic influence of Mn-L), the activated rates of oxidation were expressed in the following manner; the activation of oxidation effected by the metal-salt catalyst in the oxidation of *p*-xylene was estimated by the ratio (in wt%) of the *p*-toluic acid produced or of the sum of the *p*-toluic acid and the neutral oxidation products *vs.* the initial quantity of *p*-xylene measured after 4 hr oxidation.

The rate of oxidation was expressed by the rate of the formation of water, since the two rates were found to be in a nearly parallel relation with the same catalyst.

Similarly, the catalytic activity in the oxidation of toluene was expressed by the rate of the formation (in wt%) of benzoic acid or by the sum of benzoic acid and neutral oxidation products *vs.* the initial quantity of toluene, measured after 4 hr reaction. Furthermore, the rate of the absorption of oxygen in the oxidation of toluene was obtained by determining the quantities of oxygen and carbon dioxide in the waste gas.

Results and Discussion

Figure 1 shous how the catalytic activity in the oxidation of *p*-xylene is related to the concentration of various metal naphthenates (Mn, Co, Ni, Cr and Cu salts).

The AC-effect was observed in all cases except that of the Cr-N catalyst; the effect was particularly remarkable with the Mn-N and Cu-N catalysts. Besides, the AC-effect was observed in all the cases using the following metal-salt catalysts[8-10]: such singl catalysts as Mn-O, Co-O, Ni-O, Mn-L, Co-L, Ni-L, Mn-C, Co-C, Ni-C, and Mn-S, and such mixed catalysts as (Ni-N)+(Co-N), (Cr-N)+(Co-N), (Mn-N)+(Co-N), (Cu-N)+(Ni-N), (Mn-N)+(Ni-N), (Mn-N)+(Cu-N), (Cu-N)+(Co-N), (Cu-N)+(Cr-N), (Mn-O)+(Ni-O), (Mn-L)+(Ni-L), and (Mn-C)+(Ni-C). With the mixed catalysts, however, the AC-effect was observed at lower concentration than with single catalysts.

It has been reported[5,13] that, in liquid-phase oxidation, metal atom of higher valencies (*e. g.*, Mn^{3+}, Co^{3+}) exist in the active state of the metal-salt catalyst. In the oxidation of *p*-xylene with a Mn-N catalyst, the appearance of the reacting solution changed from the light pink color of Mn^{2+} to the dark brown of Mn^{3+} 10—15 min after the introduction of oxygen, as long as the catalyst concentration remaind within the limits, no AC-effect was exhibited, and soon afterwards oxidation set in. Similar color changes were observed, however, even when the oxidation reaction did not start readily in spite of the introduction of oxygen as a result of too high a catalyst concentration (Experiment on the Mn-N catalyst in a concentration of 100 in Fig. 1), but eventually the reaction took place (after 40—50 min). On the other hand, the author has established that the metal ion Mn^{2+} is oxidised to the Mn^{3+} state, even when oxidation does not occur, because of the AC-effect observed; he did this in an oxidation experiment with *p*-xylene and the Mn-N catalyst in a concentration of 100.

Figure 2 gives the relation between the concentration and the rate of oxidation by the Co-N catalyst.

In Fig. 3 is shown the rate of the oxidation of *p*-xylene carried out with a catalyst with a Mn-N concentration of 50 by adding a further quantity (conc. 25) of the Co-N catalyst after an oxidation period of 150 min.

13) C. E. H. Bawn, A. A. Pennington, C. F. H. Tipper, *Discussions Faraday Soc.*, **10**, 282 (1951).

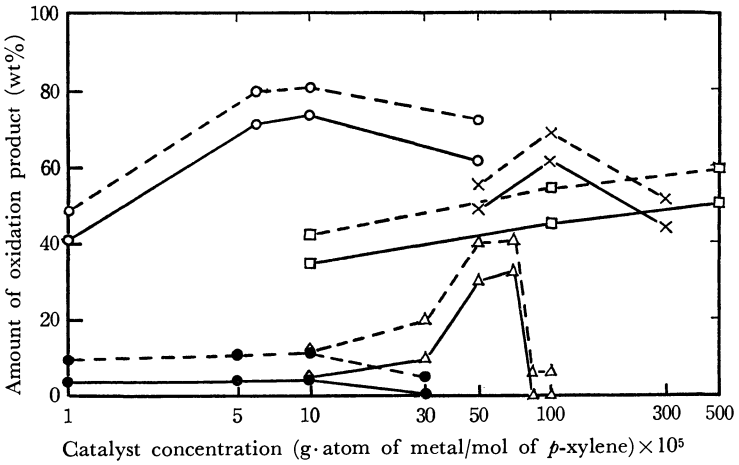

Fig. 1. Effect of concentration of metal-naphthenate catalyst in the oxidation of *p*-xylene.
Amount of oxidation product: wt% of *p*-toluic acid and wt% of *p*-toluic acid and neutral product based on *p*-xylene used.
—— : *p*-Toluic acid formed
---- : *p*-Toluic acid + neutral product
○ : Co-naphthenate □ : Cr-naphthenate
△ : Mn-naphthenate ● : Cu-naphthenate
× : Ni-naphthenate

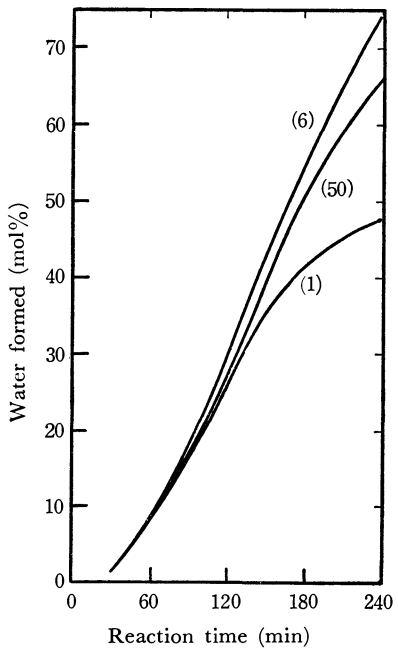

Fig. 2. Relation between rate of water formation and concentration of Co-naphthenate catalyst in the oxidation of *p*-xylene.
The arabic numerals show the concentration of Co-naphthenate [(g·atom of Co/mol of *p*-xylene)×10⁵] Water formed: mol% of water formed based upon *p*-xylene used.

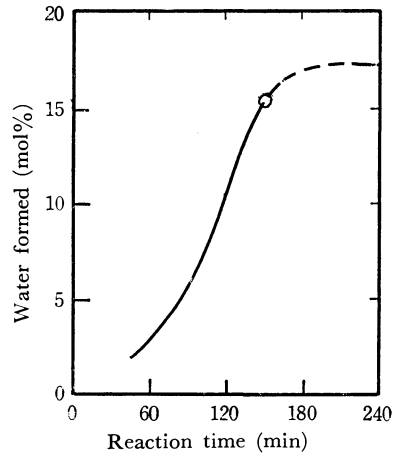

Fig. 3. Effect of the addition of Co-naphthenate to Mn-naphthenate catalyst in the course of oxidation.
○: Co-naphthenate was added at this point.
——: Oxidation in the presence of Mn-naphthenate catalyst [50×10^{-5} g·atom of Mn/mol of *p*-xylene]
----: Oxidation in the presence of Mn-naphthenate [50×10^{-5} g·atom of Mn/mol of *p*-xylene] and Co-naphthenate [25×10^{-5} g·atom of Co/mol of *p*-xylene]

The oxidation of *p*-xylene was not initiated in 4 hr with an Mn-N catalyst in a concentration of 100, as in the case shown in Fig. 1. However, after 0.5 mol of *p*-xylene had been, added, when the concentration of Mn-N became 50 the reaction of oxidation started and proceeded smoothly, *p*-toluic acid and a neutral oxidation product were formed in quanitities of 23.2% and 4.2% respectively, and 65.2% of *p*-xylene was recovered.

The AC-effect appeared during the propagation period in the oxidation of *p*-xylene and was observed as a phenomenon reducing the rate of oxidation. However, when an intense AC-effect appeared, it was recognized as a phenomenon incapable of initiating oxidation.

It was already observed that no reaction is initiated by too high a concentration of a catalyst in the oxidation of *p*-xylene using Cu salts[5] or a mixed catalyst[6] of Mn and Co salts. In view of similar phenomena occurring with a larger number of other catalysts, they may be regarded as quite general with metal-salt catalysts.

The AC-effect of a catalyst is not due to the poisoning phenomenon of the catalyst, but is a reversible phenomenon controlled by the catalyst concentration in the reaction system.

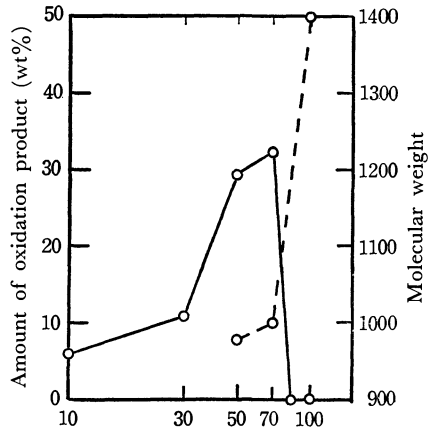

Fig. 4. Relation between concentration of catalyst of Mn-naphthenate and oxidation activity and molecular weight.
Amount of oxidation product: wt% of *p*-toluic acid based on *p*-xylene used
——: *p*-Toluic acid formed
----: Molecular weight of Mn-naphthenate

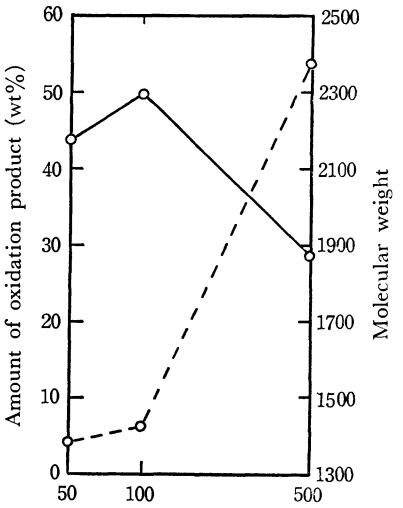

Fig. 5. Relation between concentration of catalyst of Ni-linoleate and oxidation activity and molecular weight.
Amount of oxidation product: wt% of *p*-toluic acid based on *p*-xylene used
——: *p*-Toluic acid formed
----: Molecular weight of Ni-linoleate

Figures 4 and 5 and Table 1 show the relation between the molecular weight of the metal-salt catalyst in *p*-xylene and its catalytic activity in the oxidation of *p*-xylene.

The molecular weight of the metal-salt catalyst rapidly increased in the region in which the catalytic activity rapidly decreased with an increase in the catalyst concentration, although in the region where the activity increased with an increase in the catalyst concentration the molecular weight

TABLE 1. RELATION BETWEEN CONCENTRATION OF SALT CATALYST AND ACTIVITY FOR OXIDATION OF *p*-XYLENE AND MOLECULAR WEIGHT

Catalyst	Catalyst concn.	30×10⁻⁵	50×10⁻⁵	70×10⁻⁵	75×10⁻⁵	100×10⁻⁵	200×10⁻⁵	300×10⁻⁵	500×10⁻⁵	700×10⁻⁵
Mn-C	activity		28.5		30.0	1.0	0			
	MW		700		600	1060				
Mn-L	activity	20.9	24.7	22.0		19.0	10.9			
	MW	870		940		1070	1540			
Mn-S	activity	15.3	31.0	23.8		0				
	MW	670	590	730		930				
Ni-N	activity					10.7	21.7	1.0	0	
	MW					390	380	1700	1800	
(Ni-N) (Co-N)	activity					56.4			12.1	
	MW*					420			1400	1600

Catalyst concn.: g of metal/mol of *p*-xylene
Activity: wt% of *p*-toluic acid based on *p*-xylene used
MW: Molecular weight of metal salt catalyst
*: Quantity determined by a cryoscopic method

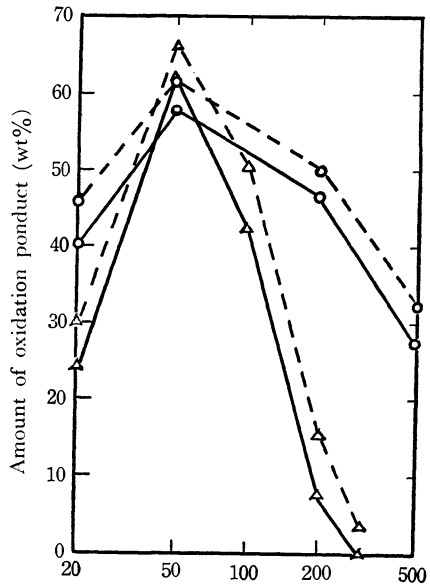

Fig. 6. Effect of concentration of Co-linoleate and Mn-caprate catalyst in the oxidation of toluene.
Amount of oxidation products: wt% of benzoic acid and wt% of benzonic acid and neutral product based on toluene used
——: Benzoic acid
----: Benzoic acid+neutral product
○: Co-linoleate
△: Mn-caprate

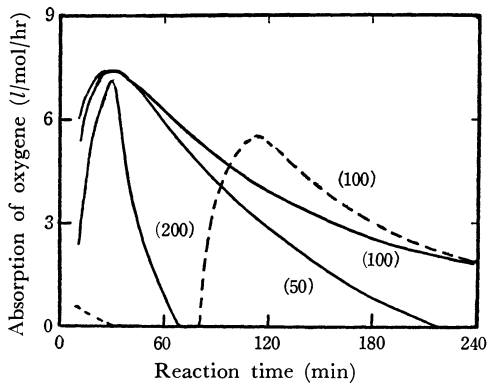

Fig. 7. Relation between concentration of Mn-caprate catalyst and absorption velocity of oxygen in the oxidation of toluene.
Arabic numerals show concentration of the catalyst [(g·atom of Mn/mol of toluene)×10⁵]
----: Absorption rate of oxygene in the oxidation of the solution which was obtained by diluting the reaction mixture with toluene to the concentration of 100 after the oxidation had been carried out for 120 min at the Mn salt concentration of 200.

of the metal-salt catalyst increased only slightly with an increase in the concentration.

Figure 6 shows the relation between the concentration of the Co-L and Mn-O catalysts and the catalytic activity in the oxidation of toluene. Furthermore,[11] in the oxidation of toluene with single catalysts, such as Co-N, Mn-N, Ni-N, Cu-N, Cr-N, Co-O, Mn-L, Mn-C, and Co-C, or with mixed catalysts, such as (Co-N)+(Mn-N), (Co-N)+(Ni-N), (Mn-N)+(Ni-N), (Co-O)+(Mn-O), (Co-O)+(Ni-O), (Mn-O)+(Ni-O), (Mn-L)+(Co-L), and (Mn-C)+(Co-C), the relation between the activity and the concentration of the catalyst was studied; the AC-effect was observed without exception with single as well as with mixed catalysts.

Figure 7 shows the absorption of oxygen during the oxidation reaction of toluene in the presence of Mn-C in concentrations 50, 100, and 200; the dotted line represents the progress of the absorption of oxygen when the catalysts present in a concentration of 200—though this concentration was reduced to 100 by adding toluene after 120 min reaction. Furthermore,[10] a similar tendency was recognized also in the cases of Mn-L and Mn-O.

It was observed[14] with the oxidation of toluene that oxidation rapidly terminated when the catalyst concentration was too small. However, the reaction also terminates at higher concentrations of catalyst above a certain limit (Fig. 7); furthermore,

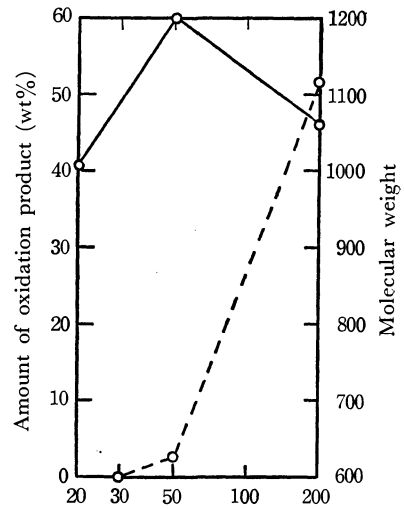

Fig. 8. Relation between concentration of catalyst of Co-linoleate and oxidation activity and molecular weight.
Amount of oxidation product: wt% of benzoic acid based on toluene used
——: Benzoic acid formed
----: Melecular weight of Co-linoleate

14) N. Ohta and T. Tezuka, *Kogyo Kagaku Zasshi (J. Chem. Soc. Japan, Ind. Chem. Sect.)*, **59**, 71 (1956).

at a much higher concentration oxidation is not even initiated (Fig. 6). These two new phenomena have led to the discovery of the AC-effect.

Figure 8 exhibits the relation between the catalytic activity and the molecular weight of the Co-L catalyst in toluene; the AC-effect appears at the point of rapidly-increasing molecular weight. A similar phenomenon occurred with the Mn-O[12] catalyst.

The experiments described above suggest that metal-salt catalysts for the oxidation of *p*-xylene and toluene associate in the region where the AC-effect is observed, and that the associated catalyst plays no part in promoing the oxidation.

The author cordially thanks Professor Nobuto Ohta and Dr. Yasuo Takami for their guidance throughout the work. Thanks are also due to Professor Yojiro Tsuzuki for his interest and encouragement.

BULLETIN OF THE CHEMICAL SOCIETY OF JAPAN VOL. 41 1557—1563 (1968)

The Crystal and Molecular Structure of 1,1′-Bis(pentamethyldisilanyl)-ferrocene, (π-$C_5H_4Si(CH_3)_2Si(CH_3)_3)_2Fe$

Ken HIROTSU, Taiichi HIGUCHI and Akira SHIMADA

Department of Chemistry, Faculty of Science, Osaka City University, Sumiyoshi-ku, Osaka

(Received January 22, 1968)

Crystals of 1,1′-bis(pentamethyldisilanyl)ferrocene, (π-$C_5H_4Si(CH_3)_2Si(CH_3)_3)_2Fe$, are monoclinic, with $a=6.84$, $b=30.87$, $c=12.67$ Å and $\beta=96.80°$. The space group is $P2_1/n$ and there are four molecules in a unit cell. The structure was solved by Patterson and minimum functions, and further refined by Fourier and difference syntheses, and finally by a least-squares method. The final R value is 14.4% for 883 observed reflections. The two cyclopentadienyl rings are planar, approximately parallel to each other, separated by 3.28 Å and deviated by about 6° from the fully *eclipsed* configuration. The molecular configuration is *gauche* with respect to the two side-chains. The mean values of the bond distances are found to be Fe-C(cyclopentadienyl rings)= 2.05, C-C=1.45, C(cyclopentadienyl rings)-Si=1.87, C(methyl groups)-Si=1.90 and Si-Si= 2.34 Å. All intermolecular separations correspond to the normal van der Waals interactions.

Since the molecular structure of ferrocene had been determined, several of its derivatives have also been studied by means of X-rays to elucidate the spacial configurations of the two cyclopentadienyl rings in the molecules. It was found that in some of the molecules the *staggered* configurations of rings are maintained, while in others, intermediate configurations, between *staggered* and *eclipsed*, are preferred. The differences in these ring configurations might be very interesting.

1,1′-Bis(pentamethyldisilanyl)ferrocene was investigated in order to determine which ring configuration it takes in the crystalline state. Moreover, the present molecule has one substituent (pentamethyldisilanyl group) on each ring, and therefore the configuration of the substituents in the molecule and their arrangement in the crystal would be another interest.

Experimental

The crystals were kindly prepared and supplied by Professor Makoto Kumada of Kyoto University.[1] The specimens, which are suitable for X-ray work, were crystallized from ethanol solution in the form of ferrocene-like orange-yellow plates, elongated along the a axis, with the (010) plane developed. The crystals sublime gradually in air. Multiple Weissenberg intensity data were collected with Ni-filtered Cu$K\alpha$ radiation on the b and the c axes for zero layers, and on the a axis for zero and first layers. 1285 reflections were observed; 402 were too weak to be measured. Intensities were estimated visually with calibrated intensity scales. No correction was applied to absorption and extinction. All intensity data exhibit a high background due to strong fluorescence by the iron atoms. Atomic scattering factors for iron were used after being corrected for the effect of dispersion. After the Lorentz

TABLE 1. CRYSTAL DATA (λ, Cu$K\alpha$=1.5418 Å)

1,1′-bis(pentamethyldisilanyl)ferrocene
$C_{20}H_{38}Si_4Fe$; MW=446.7 mp=58—59°C
Monoclinic
$a=6.84$, $b=30.87$, $c=12.67$ Å $\beta=96.80°$
$Dm=1.01$ g·cm^{-3}, Dc(with $Z=4$)=1.02 g·cm^{-3}
$\mu=64.2$ cm^{-1} (Cu$K\alpha$)
Space group is $P2_1/n$.

1) M. Kumada, K. Mimura, M. Ishikawa and K. Shiina, *Tetrahedron Letters*, **1965**, 83.

and the polarization corrections were made, intensities were placed on a common relative scale. The crystal data are given in Table 1.

Structure Determination

At first, the structure projected along the *a* axis was sought by means of the Patterson and minimum functions. The iron atom and two silicon atoms directly bonded to the cyclopentadienyl rings were easily located. The first Fourier synthesis based on these three atoms revealed the iron and all the four silicon atoms clearly, while the positions of carbon atoms were not resolved. They were found and refined by a combination of successive Fourier and difference syntheses, molecular geometry being taken into consideration. The analysis of the *c* axis projection was also done in a similar way to the *a* axis projection.

Refinements were carried out by means of a least-squares method, using all the reflection data. The function minimized was $\sum w(|F_o| - |F_c|)^2$, where w (weights) were set equal to unity for all reflections. After four cycles of the refinement, the discrepancy index R was 14.4% for the observed reflections only.

Table 2 gives the final positional and isotropic thermal parameters, and their e. s.d.'s obtained from the last cycle of the least-squares refinement.

TABLE 2. ATOMIC PARAMETERS

Atomic parameters and estimated standard deviations

	x $10^4\sigma(x)$	y $10^4\sigma(y)$	z $10^4\sigma(z)$	B $10^2\sigma(B)$
Fe	0.1886(10)	0.1481(1)	0.1938(3)	3.72(12)
Si(1)	0.0321(19)	0.0480(2)	0.2933(6)	4.11(20)
Si(2)	0.1080(19)	0.2570(2)	0.1180(6)	3.86(19)
Si(3)	−0.0836(20)	−0.0173(2)	0.2147(6)	4.33(20)
Si(4)	0.1810(19)	0.3241(2)	0.1965(6)	4.25(20)
C(1)	0.0779(56)	0.0857(7)	0.1852(18)	3.37(58)
C(2)	0.2667(57)	0.0897(7)	0.1384(18)	3.77(59)
C(3)	0.2427(62)	0.1233(8)	0.0512(20)	5.46(69)
C(4)	0.0393(61)	0.1364(8)	0.0466(20)	4.99(69)
C(5)	−0.0617(60)	0.1158(8)	0.1250(20)	4.74(66)
C(6)	0.1970(61)	0.2140(8)	0.2167(20)	5.20(69)
C(7)	0.3870(60)	0.1962(8)	0.2242(21)	5.69(68)
C(8)	0.3967(61)	0.1660(8)	0.3130(21)	5.05(67)
C(9)	0.1959(60)	0.1645(8)	0.3495(20)	5.62(69)
C(10)	0.0840(59)	0.1950(8)	0.2880(20)	4.80(66)
C(11)	−0.1645(60)	0.0727(8)	0.3742(21)	6.07(69)
C(12)	0.2741(62)	0.0357(8)	0.3808(21)	6.45(69)
C(13)	−0.1567(60)	−0.0547(8)	0.3236(20)	5.26(69)
C(14)	0.1192(59)	−0.0454(8)	0.1413(20)	5.45(68)
C(15)	−0.2917(62)	−0.0055(8)	0.1179(21)	7.25(68)
C(16)	−0.1653(61)	0.2536(8)	0.0754(21)	5.84(68)
C(17)	0.2382(64)	0.2513(8)	−0.0068(20)	4.87(69)
C(18)	0.0900(58)	0.3699(8)	0.1017(20)	4.71(65)
C(19)	0.4485(59)	0.3264(8)	0.2394(20)	6.40(69)
C(20)	0.0217(61)	0.3303(8)	0.3157(20)	6.11(69)

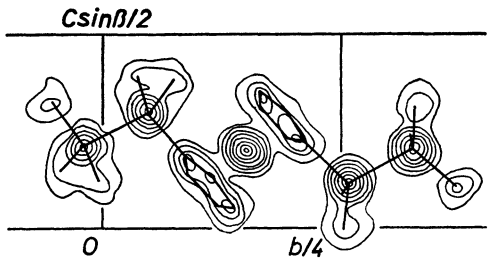

Fig. 1. Electron density projected along the *c* axis, contours are drawn in an arbitrary scale.

The observed and calculated structure factors are listed in Table 7.*1 Figure 1 shows the electron-density map along the *a* axis.

Discussion

The views of the molecule perpendicular to and parallel to the cyclopentadienyl rings are given in Fig. 2. The best planes through the cyclopentadienyl rings are given in Table 4, together with the deviations of the atoms from these planes. These two planes are nearly parallel (the angle between them is 1.02°) to each other and the spacing between them is 3.28 Å, which may be compared with 3.32, 3.32 and 3.30 Å found in ferrocene,[2] biferrocenyl[3] and diferrocenyl ketone,[4] respectively. Si(1) and Si(2) lies 0.05 Å above and below each of the best planes of the cyclopentadienyl rings to which they are attached, with respect to the Fe atom. The angle between plane 1 (see Fig. 2B) and the plane through Si(1), Si(3) and C(1) is 88.7°, while plane 2 and the plane through Si(2), Si(4) and C(6) makes an angle of 92.0°. Therefore, Si(3) lies on the plane which is normal to plane 1 and passes through C(1) and Si(1). This relation also holds for Si(4). Figure 3 shows one half of a molecule viewed along the Si(1)-Si(3) bond and the other half of the molecule viewed along the Si(2)-Si(4) bond. The conformation around the Si(1)-Si(3) and Si(2)-Si(4) bonds is *staggered*, though the dihedral angles seem to be a little different. From the above results, this molecule has roughly a twofold axis through the Fe atom, parallel to both cyclopentadienyl rings.

Ferrocene derivatives with one substituent on each ring have three possible configurations (*cis*, *trans* or *gauche*). It is well shown in Fig. 2A that

*1 The complete data of the $F_o - F_c$ table are kept as Document No. 6802 at the office of the Bulletin of the Chemical Society of Japan. A copy may be secured by citing the document number and by remitting, in advance, ¥ 600 for photoprints. Pay by check or money order, payable to: Chemical Society of Japan.

2) J. D. Dunitz, L. E. Orgel and A. Rich, *Acta Cryst.*, **9**, 373 (1956).
3) A. C. MacDonald and J. Trotter, *ibid.*, **17**, 872 (1964).
4) J. Trotter and A. C. MacDonald, *ibid.*, **21**, 359 (1966).

TABLE 3. BOND DISTANCES, BOND ANGLES AND NON-BONDED INTERATOMIC DISTANCES IN A MOLECULE
e. s. d. values in parenthesis

Bond distances		Å
Fe-C(1)	2.07	(0.02)
Fe-C(2)	2.03	(0.02)
Fe-C(3)	2.04	(0.03)
Fe-C(4)	2.05	(0.03)
Fe-C(5)	2.08	(0.04)
Fe-C(6)	2.06	(0.02)
Fe-C(7)	2.02	(0.03)
Fe-C(8)	2.03	(0.04)
Fe-C(9)	2.03	(0.03)
Fe-C(10)	2.06	(0.03)
C(1)-C(2)	1.49	(0.05)
C(2)-C(3)	1.51	(0.03)
C(3)-C(4)	1.44	(0.06)
C(4)-C(5)	1.42	(0.04)
C(5)-C(1)	1.48	(0.05)
C(6)-C(7)	1.40	(0.06)
C(7)-C(8)	1.46	(0.04)
C(8)-C(9)	1.50	(0.05)
C(9)-C(10)	1.39	(0.04)
C(10)-C(6)	1.39	(0.04)
Si(1)-Si(3)	2.34	(0.01)
Si(2)-Si(4)	2.33	(0.01)
Si(1)-C(1)	1.85	(0.02)
Si(2)-C(6)	1.88	(0.03)
Si(1)-C(11)	1.94	(0.03)
Si(1)-C(12)	1.92	(0.04)
Si(3)-C(13)	1.91	(0.03)
Si(3)-C(14)	1.96	(0.03)
Si(3)-C(15)	1.80	(0.04)
Si(2)-C(16)	1.89	(0.04)
Si(2)-C(17)	1.91	(0.03)
Si(4)-C(18)	1.91	(0.03)
Si(4)-C(19)	1.85	(0.04)
Si(4)-C(20)	1.97	(0.03)

Bond angles		(°)
C(1)-Fe-C(2)	42.6	(1.1)
C(2)-Fe-C(3)	43.6	(1.2)
C(3)-Fe-C(4)	41.4	(1.3)
C(4)-Fe-C(5)	40.4	(1.2)
C(5)-Fe-C(1)	41.7	(1.2)
C(6)-Fe-C(7)	40.3	(1.3)
C(7)-Fe-C(8)	42.2	(1.3)
C(8)-Fe-C(9)	43.4	(1.3)
C(9)-Fe-C(10)	39.8	(1.2)
C(10)-Fe-C(6)	39.4	(1.2)

Bond angles		(°)
C(1)-C(2)-C(3)	108.9	(2.4)
C(2)-C(3)-C(4)	104.1	(2.6)
C(3)-C(4)-C(5)	113.0	(2.8)
C(4)-C(5)-C(1)	107.7	(2.6)
C(5)-C(1)-C(2)	106.2	(2.4)
C(6)-C(7)-C(8)	105.1	(2.7)
C(7)-C(8)-C(9)	107.4	(2.6)
C(8)-C(9)-C(10)	105.6	(2.6)
C(9)-C(10)-C(6)	109.8	(2.8)
C(10)-C(6)-C(7)	111.9	(2.8)
C(2)-C(1)-Si(1)	125.3	(2.1)
C(5)-C(1)-Si(1)	128.4	(2.2)
C(1)-Si(1)-C(11)	109.4	(1.4)
C(1)-Si(1)-C(12)	110.0	(1.4)
C(1)-Si(1)-Si(3)	107.7	(1.0)
C(11)-Si(1)-C(12)	112.1	(1.4)
C(11)-Si(1)-Si(3)	110.0	(1.0)
Si(3)-Si(1)-C(12)	107.5	(1.1)
Si(1)-Si(3)-C(15)	108.3	(1.1)
Si(1)-Si(3)-C(13)	108.5	(1.1)
Si(1)-Si(3)-C(14)	111.1	(1.0)
C(15)-Si(3)-C(13)	111.2	(1.5)
C(15)-Si(3)-C(14)	108.2	(1.4)
C(13)-Si(3)-C(14)	109.6	(1.4)
C(10)-C(6)-Si(2)	124.9	(2.4)
C(7)-C(6)-Si(2)	123.2	(2.4)
C(6)-Si(2)-C(17)	109.9	(1.4)
C(6)-Si(2)-C(16)	112.6	(1.4)
C(6)-Si(2)-Si(4)	108.0	(1.1)
C(17)-Si(2)-Si(4)	109.8	(1.1)
C(17)-Si(2)-C(16)	107.5	(1.4)
Si(4)-Si(2)-C(16)	109.1	(1.1)
Si(2)-Si(4)-C(20)	107.7	(1.0)
Si(2)-Si(4)-C(18)	110.7	(1.0)
Si(2)-Si(4)-C(19)	108.4	(1.1)
C(18)-Si(4)-C(20)	104.0	(1.4)
C(19)-Si(4)-C(20)	112.8	(1.4)
C(18)-Si(4)-C(19)	113.2	(1.4)

Non-bonded interatomic distances		Å
C(1)-C(9)	3.24	(0.04)
C(2)-C(8)	3.28	(0.04)
C(3)-C(7)	3.21	(0.04)
C(4)-C(6)	3.32	(0.04)
C(5)-C(10)	3.28	(0.04)
Fe-Si(1)	3.55	(0.01)
Fe-Si(2)	3.52	(0.01)

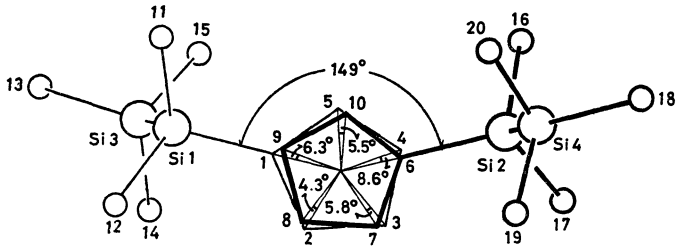

Fig. 2A. View of the molecule along the normal to the mean plane of the rings.

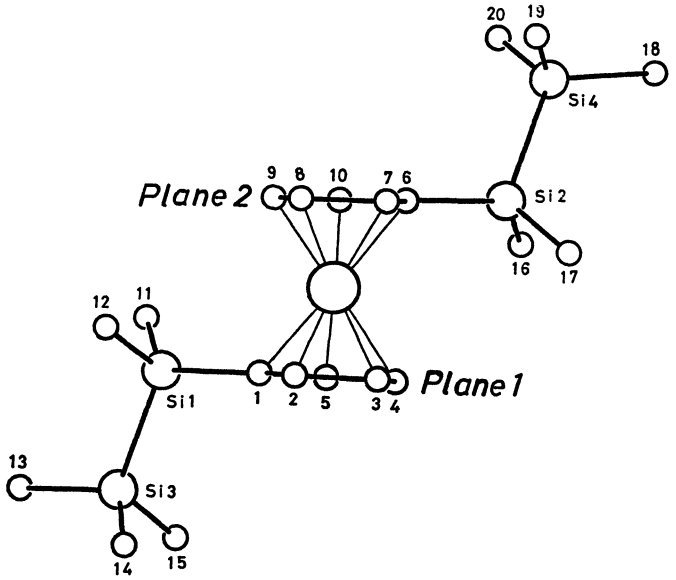

Fig. 2B. View of the molecule along the plane 1.

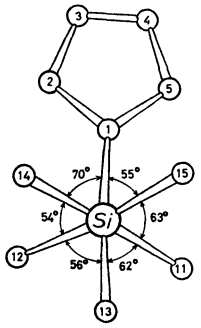

Fig. 3A. View of one half of the molecule along the Si(1)-Si(3) bond without Fe atom.

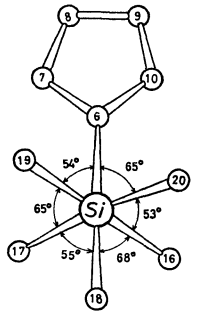

Fig. 3B. View of the other half of the molecule along the Si(2)-Si(4) bond without Fe atom.

TABLE 4. LEAST SQUARES PLANES OF THE RINGS

Plane 1 defined by C(1), C(2), C(3), C(4), C(5): $0.3878X + Y + 0.8626Z = -4.8146$		Plane 2 defined by C(6), C(7), C(8), C(9), C(10): $0.4135X + Y + 0.8788Z = -9.4048$	
Deviations of atoms from plane 1		Deviations of atoms from plane 2	
C(1)	0.005	C(6)	0.020
C(2)	−0.012	C(7)	−0.029
C(3)	0.015	C(8)	0.027
C(4)	−0.013	C(9)	−0.017
C(5)	0.005	C(10)	−0.001
*Si(1)	−0.047	*Si(2)	0.050

Atoms with * were not included in calculation of the plane.

TABLE 5. CONFIGURATIONS OF CYCLOPENTADIENYL RINGS IN SOME OF FERROCENE DERIVATIVES

Compound	Ring configuration	Reference
Ferrocene	*Staggered*	Dunitz, Orgel & Rich (1956)
Ferrocenedisulfonyl chloride	*Staggered*	Starovskii & Struchkov (1963)[5]
Biferrocenyl	$\varphi^* = 17°$	MacDonald & Trotter (1964)
Diethyldiferrocenyl	$\varphi = 4°$	Kaluski & Struchkov (1964)[6]
Diferrocenyl ketone	$\varphi = 5°$	Trotter & MacDonald (1966)
α-Keto-1,5-tetramethylene ferrocene	$\varepsilon^{**} = 8.9°$	Fleischer & Hawkinson (1967)[7]
1,1′-Bis(pentamethyldisilanyl)ferrocene	$\varphi = 6°$	This paper

* The angle φ was defined as the angle between the projection of the Fe-C bonds on the mean plane of a cyclopentadienyl rings.

** The angle ε was defined as the angle between the lines passing through the nearly superimposed atoms and the midpoint of the opposite sides of the rings.

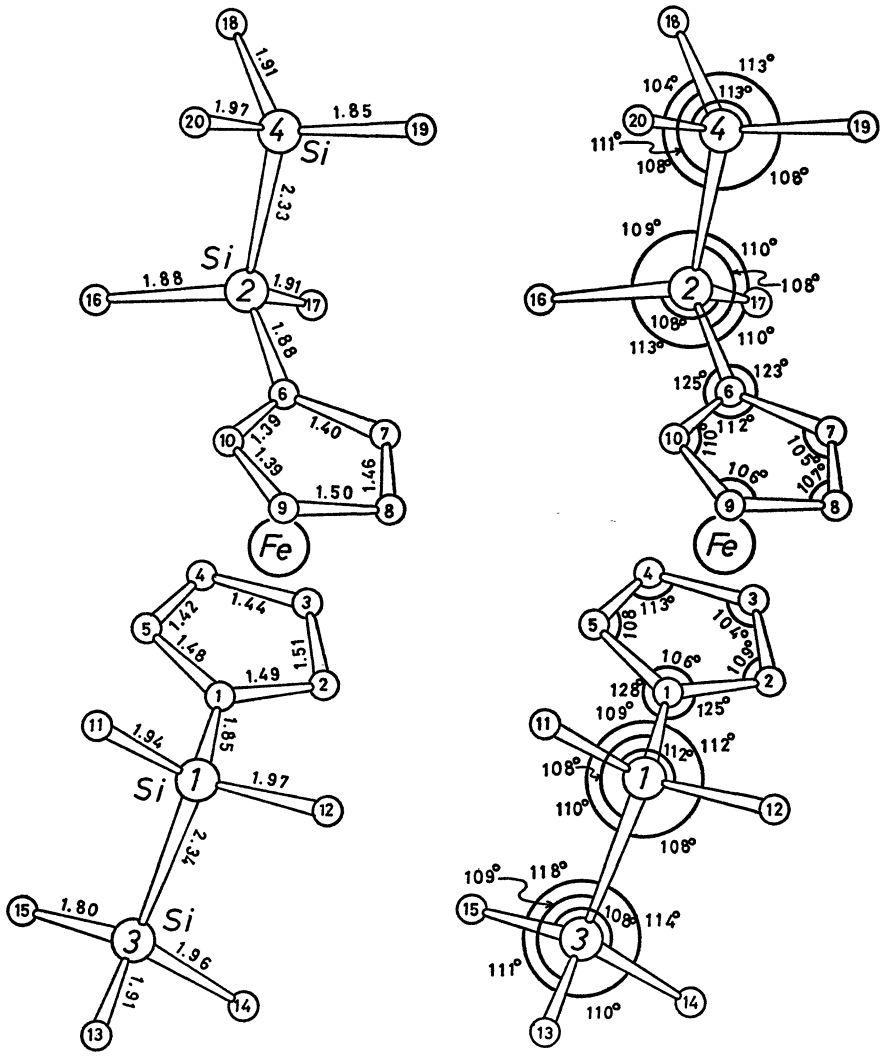

Fig. 4. Bond distances and angles in a molecule.

5) O. V. Starovskii and Yu. T. Struchkov, *Zh. Strukt. Khim.*, **5** (2), 257 (1963).
6) Z. L. Kaluski and Yu. T. Struchkov, *ibid.*, **5**, 743 (1964).
7) E. B. Fleischer and S. W. Hawkinson, *Acta Cryst.*, **22**, 376 (1967).

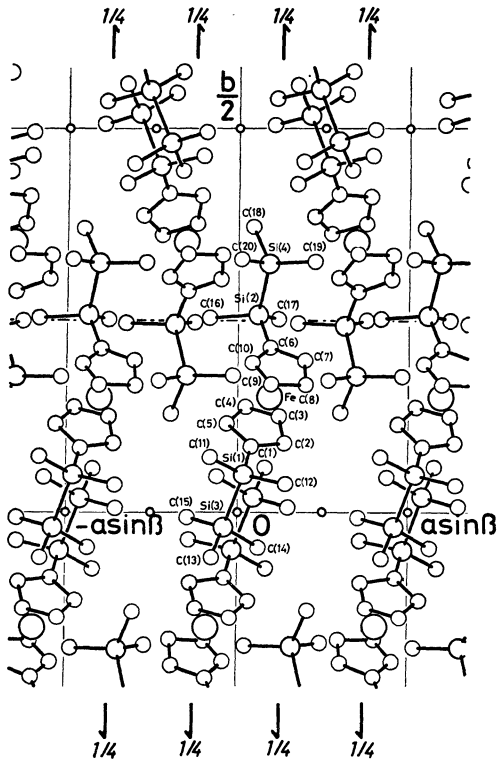

Fig. 5. Arrangement of the molecules along the *c* axis.

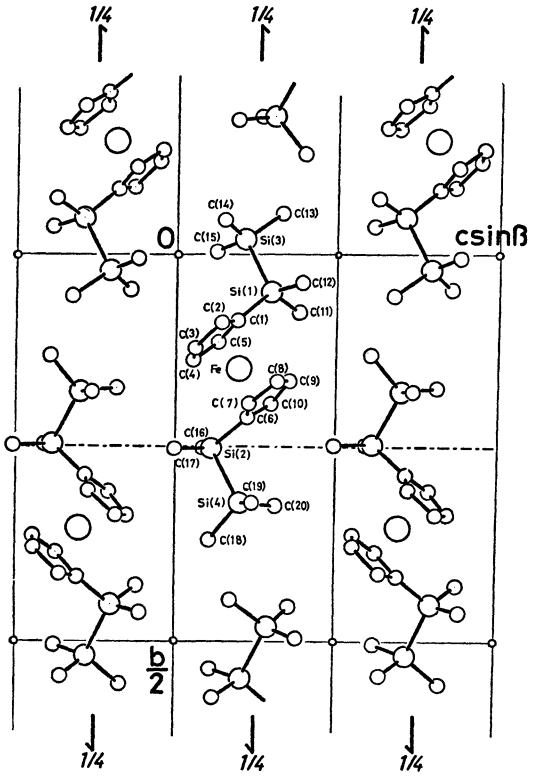

Fig. 6. Arrangement of the molecules along the *a* axis.

the present molecule has the *gauche* form. The angle between the projection of C(1)-Si(1) bond and that of C(6)-Si(2) on the mean plane of five-membered rings is 149°.

The angles φ between the Fe-C bonds projected on the mean plane of the rings are:

C(1)-Fe-C(9)	6.3°
C(2)-Fe-C(8)	4.3°
C(3)-Fe-C(7)	5.8°
C(4)-Fe-C(6)	8.6°
C(5)-Fe-C(10)	5.5°

The average value 6.1° shows that the configuration is almost the *eclipsed* one. Table 5 shows the ring configurations of ferrocene and its derivatives. These results may indicate that in ferrocene and its derivatves the *staggered* position is preferred owing to a small *inter-ring* separation, but this orientation will be easily rotated by stronger intermolecular forces until the *inter-ring* repulsion and intermolecular forces become comparable. In this compound, the substituent on each ring occupies the larger portion of the molecule and the ring configuration will be greatly affected by the arrangement of the substituents. Consequently, a stronger

TABLE 6. INTERMOLECULAR DISTANCES LESS THAN 4.2 Å

The reference molecule 1 lies at x, y, z.

from Atom	to Atom	in molecule at	d
(molecule 1)			
C(20)	C(19)	2	3.95 Å
C(7)	C(11)	3	4.17
C(12)	C(11)	3	4.09
C(14)	C(11)	3	4.19
C(14)	C(15)	3	3.93
C(17)	C(16)	3	4.01
C(20)	C(20)	4	3.89
C(17)	C(18)	5	3.97
C(3)	C(15)	6	3.99
C(12)	C(15)	6	4.02
C(11)	C(9)	7	3.85
C(11)	C(10)	7	4.15
C(13)	C(8)	7	3.90
C(13)	C(9)	7	4.07
C(10)	C(12)	8	4.07
C(14)	C(4)	9	4.04

Molecule 1 at	x,	y,	z
2 at	$-x$,	$-y$,	$-z$
3 at	$1+x$,	y,	z
4 at	$-1-x$,	$-y$,	$-z$
5 at	$-x$,	$-y$,	$1-z$
6 at	$1/2+x$,	$1/2-y$,	$-1/2+z$
7 at	$-1/2+x$,	$1/2-y$,	$-1/2+z$
8 at	$-1/2+x$,	$1/2-y$,	$1/2+z$
9 at	$1/2+x$,	$1/2-y$,	$1/2+z$

intermolecular force than the *inter-ring* repulsion may force such an arrangement as $\varphi = 6.1°$.

The bond distances and angles are listed in Table 3 and shown in Fig. 4. The average C(Cp*[2])-C(Cp) bond distances is 1.45 Å (the average e.s.d. value is 0.05 Å), which is comparable to the values observed in the many ferrocene derivatives. The mean bond angle in the five-membered rings is 108.0±2.6°. The distortion in some bond angles from 108° is not significant. The mean Fe-C (Cp) distance, 2.05±0.03 Å, is consistent with those found in ferrocene derivatives. The average bond angle of C(Cp)-C(Cp)-Si is 125.4±2.3°. The average Si-C(Cp) distance, 1.87±0.03 Å is quite consistent with that of phenylsilane,[8] 1.84±0.005 Å. The Si-Si bond distances (2.34 and 2.33 Å) are normal values. The average value of Si-C (methyl group) bonds is 1.90±0.03 Å, which is normal. The average angle around Si atoms is 109.5°, equal to the tetrahedral angle.

The average isotropic temperature factor of carbon atoms is 5.35 Å^2, which is relatively high in view of the fact that the absorption effect might be expected to reduce the temperature factors a little. This shows, together with the comparatively small density (*Dm* is 1.02 g·cm^{-3}), that thermal vibration in this molecule is considerable. The average isotropic temperature factor of Cp-carbons is 4.87 Å^2, and that of methyl carbons 5.84 Å^2. It may be significant that the difference between them is fairly large.

The mode of packing of the molecules in the crystal can be seen in Figs. 5 and 6. Molecules are packed with their long axes arranged along the *b* axis. Sets of molecules related by a twofold screw axis have approximately hexagonal packing. Most of the closest contacts are either of the CH_3---CH_3 or CH_3---CH(Cp) type. All shorter intermolecular distances (<4.2 Å) are given in Table 6.

The authors wish to express their appreciation to Professor Makoto Kumada and Dr. Mitsuo Ishikawa of Kyoto University for kindly supplying the samples for this study, to Dr. Kazumi Nakatsu of our laboratory and Dr. Noritake Yasuoka of Osaka University for their electronic computer programs, and to the Oki Electric Industry Co., Ltd., and the Japan Information Processing Service Co., Ltd., for the use of electronic computers. The present study was partly supported by a Scientific Reserch Grant from the Ministry of Education.

*2 Cp is cyclopentadienyl.

BULLETIN OF THE CHEMICAL SOCIETY OF JAPAN VOL. 41 1563—1568 (1968)

An Experimental Study on the Faradaic Impedance of an Electrode Process with a Preceding Chemical Reaction

Kiyoshi MATSUDA and Reita TAMAMUSHI

The Institute of Physical and Chemical Research, Yamato-machi, Kita-adachi-gun, Saitama

(Received January 22, 1968)

The frequency dependence of the faradaic impedance and its phase angle of an electrode process with a preceding chemical reaction was studied with the Cd(II)-EDTA system. The experimental results were analyzed by means of Smith's equation, and the rate constant of the reaction, $Cd^{2+}+HY^{3-}\rightarrow CdY^{2-}+H^{+}$, was estimated to be equal to $2.3\times10^{9}\ l\ mol^{-1}\ sec^{-1}$ at the ionic strength of 0.5 and at 25°C. In connection with this study, the faradaic impedance behavior of simple electrode processes was re-examined with the Cd(II)-, Pb(II)-, and Zn(II)-KCl systems.

The measurement of the faradaic impedance provides a useful method of analyzing the mechanism of electrode reactions. The frequency dependence of the faradaic impedance at reversible electrode potentials was applied by Randles and Somerton[1] and by Gerischer[2] to the determination of exchange currents of relatively simple electrode reactions. Sluyters *et al.* examined the frequency dependence of the faradaic impedance by using the complex impedance plane.[3] The relation between the peak currents on alternating current (a.c.) polarograms and the frequency of the superimposed alternating voltage was studied first

1) J. E. B. Randles, *Discussions Faraday Soc.*, **1**, 11 (1947); J. E. B. Randles and K. W. Somerton, *Trans. Faraday Soc.*, **48**, 937 (1952).

2) H. Gerischer, *Z. physik. Chem.*, **202**, 302 (1953).

3) M. Sluyters-Rehbach, D. J. Kooijman and J. H. Sluyters, "Polarography 1964," (Graham J. Hills, ed.), Vol. I, MacMillan, London (1966), p. 135.

by Breyer, Bauer and Hacobian[4] and later by Bauer and Elving.[5] The faradaic impedance of the polarographic reduction processes of cadmium, zinc, and thallium ions was investigated by Tamamushi and Tanaka as a function of the electrode potential;[6] they also reported that, in the case of cadmium ions, the faradaic impedances measured at 500, 1000, and 2000 cps were inversely proportional to the square root of the frequency.

The effect of preceding chemical reactions to the faradaic impedance was studied first by Gerischer in the absence of a direct current (d. c.) polarization.[7] Recently, theoretical equations were proposed by Smith describing the a. c. polarographic phase angle behavior for electrode processes with coupled chemical reactions,[8] and the equation was applied to the catalytic reduction of titanium(IV) ions in the presence of chlorate ions.[9] The behavior of a. c. polarographic peak currents was applied by Aylward and Hayes to the determination of the rate constant of a coupled following reaction.[10] To authors' knowledge, however, experimental studies on the phase angle-frequency behavior of polarographic electrode processes with preceding reactions have not been reported previously.

This paper presents some experimental results on the faradaic impedance behavior of the polarographic reduction process of cadmium ions in acetate buffer solutions containing ethylenediaminetetraacetate (EDTA) and an excess of calcium chloride; the results are discussed in terms of Smith's equations.[8] In connection with this study, the faradaic impedance-frequency relationship of some simple electrode processes was re-examined in a wider frequency range.

Experimental

The electrolytic cell subjected to the impedance measurement is represented by the scheme,

DME	solution	MPE

where DME means a dropping mercury electrode and MPE a mercury pool electrode of a large surface area.

In the frequency range of 200—4000 cps, the resistance and capacitance components of the equivalent impedance of the cell were measured by an a. c. bridge similar to that described in a previous paper.[11] At lower frequencies (30—200 cps), however, the cell admittance and its phase angle were measured by a potentiostatic a. c. polarograph.[12] The DME was negatively polarized by a d. c. potentiometer against the MPE in the solution. The amplitude of the superimposed alternating voltage was less than 5 mV in the bridge measurement and about 10 mV in the a. c. polarographic measurement, respectively. The faradaic impedance and phase angle reported in this paper are the values for the given constant surface area (0.035 cm^2) of the DME at the end of the life of a mercury drop (drop time, 9 sec).

Vacuum-distilled mercury was used for the DME and the MPE. All solutions were prepared from analytical reagent grade chemicals and redistilled water. In each system except the Cd-EDTA a small amount of polyoxyethylene lauryl ether (LEO) was used as a maximum suppressor. The dissolved oxygen was expelled from the solution by bubbling nitrogen through the solution. All measurements were carried out in a water-thermostat of 25.0±0.1°C.

Results

Cd(II)-, Pb(II)-, and Zn(II)-KCl Systems. In the polarographic reduction of cadmium, lead, and zinc ions in 1 M potassium chloride solutions, both the resistance and the capacitance readings, R_m and C_m, of the bridge gave a peak at the summit potential, E_s, characteristic to the given electrode reaction. The series resistance, R_F, and the series capacitance, C_F, of the faradaic impedance, Z_F, were determined by the vector calculation from the R_m- and C_m-values under the assumption that the R_m- and C_m-values of the supporting electrolyte solution are equal to the resistance of the solution and the double layer capacity, respectively. The frequency dependence of Z_F, R_F, $1/(\omega C_F)$, and $\cot\phi(=\omega C_F R_F)$ of the Cd(II)-, Pb(II)-, and Zn(II)-KCl systems is shown in Fig. 1, where these quantities are plotted as a function of $1/\sqrt{\omega}$ (ω, the angular frequency).

Cd(II)-EDTA System. The polarographic reduction of a cadmium ion (8 mM $Cd(NO_3)_2$) in an acetate buffer solution (pH=3.7; ionic strength, μ, adjusted to be 0.5 by potassium nitrate) containing 1.119×10^{-2} M EDTA and 0.1 M calcium chloride gives a kinetic current due to the dissociation reaction,

$$CdY^{2-} + H^+ \underset{k_2}{\overset{k_1}{\rightleftharpoons}} Cd^{2+} + HY^{3-} \qquad (1)$$

where Y^{-4} means that tetravalent anion of EDTA; the aquo-cadmium and chloro- and acetato-complexes of cadmium then contribute to the charge-transfer process.[13,14] This reduction process

4) B. Breyer, H. H. Bauer and S. Hacobian, *Australian J. Chem.*, **8**, 322 (1955).
5) H. H. Bauer and P. J. Elving, *Anal. Chem.*, **30**, 334 (1958); H. H. Bauer, D. L. Smith and P. J. Elving, *J. Am. Chem. Soc.*, **82**, 2094 (1960).
6) R. Tamamushi and N. Tanaka, *Z. physik. Chem., Neue Folge*, **21**, 89 (1959); *ibid.*, **28**, 158 (1961).
7) H. Gerischer, *Z. Elektrochem.*, **55**, 98 (1951).
8) D. E. Smith, *Anal. Chem.*, **35**, 602 (1963).
9) D. E. Smith, *ibid.*, **35**, 610 (1963).
10) G. H. Aylward and J. W. Hayes, *ibid.*, **37**, 195 (1965).
11) R. Tamamushi and K. Matsuda, *J. Electroanal. Chem.*, **12**, 436 (1966).
12) R. Tamamushi and K. Matsuda, This Bulletin, **41**, 1568 (1968).
13) N. Tanaka, R. Tamamushi and M. Kodama, *Z. physik. Chem., Neue Folge*, **14**, 141 (1958).
14) T. Fujisawa and N. Tanaka, *Nippon Kagaku Zasshi (J. Chem. Soc. Japan, Pure Chem. Sect.)*, **87**, 965 (1966).

gave an a. c. polarogram and a phase angle change as shown in Fig. 2.

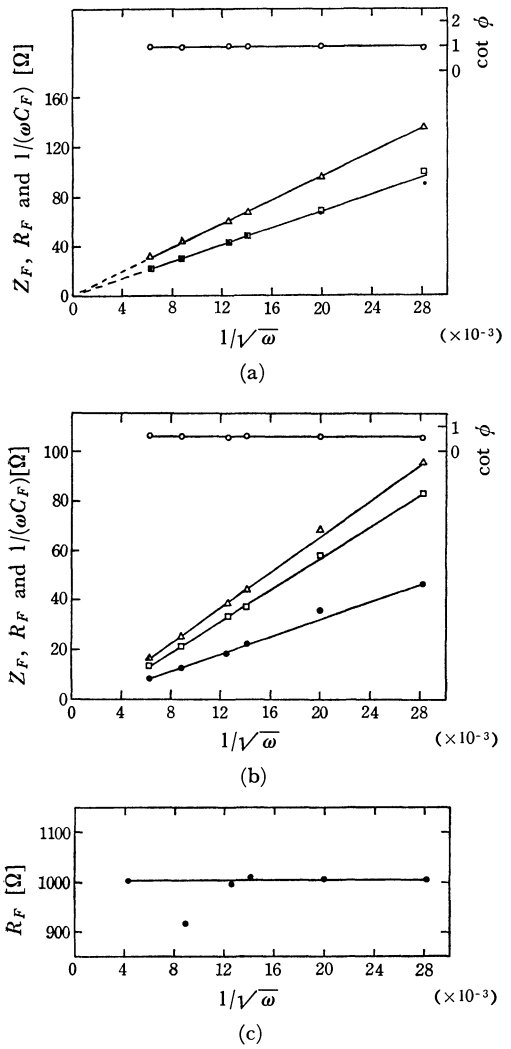

Fig. 1. Frequency dependence of Z_F (-△-), R_F (-●-), $1/(\omega C_F)$ (-□-) and cot ϕ(-○-) at the summit potential: (a), DME/0.5mM $CdSO_4$, 1M KCl, 2×10^{-6}M LEO/MPE; (b), DME/0.5 mM $Pb(NO_3)_2$, 1M KCl, 0.01N HCl, 5×10^{-6}M LEO/MPE; (c), DME/1 mM $Zn(NO_3)_2$, 1M KCl, 2×10^{-6} M LEO/MPE.

An example of the potential dependence of R_m and C_m at higher frequencies is reproduced in Fig. 3. The summit potential, being approximately independent of frequency, was −0.72——0.73 V *vs.* MPE.

The C_m-values of the Cd(II)-EDTA system in the potential region outside the impedance peak did not coincide with the C_m-values of the supporting electrolyte solution (Fig. 3); this is probably due to the effect of the concentration of free EDTA anions on the double layer capacity. Therefore,

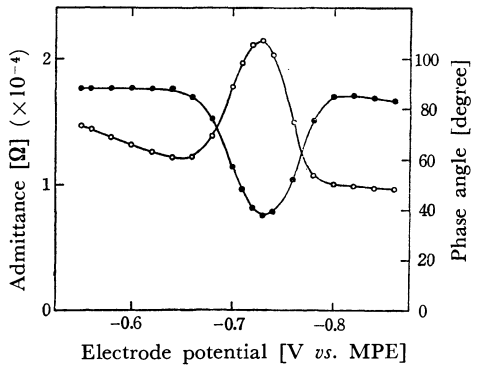

Fig. 2. A. c. polarogram (-○-) and phase angle change (-●-) at 30 cps of 8 mM $Cd(NO_3)_2$ in an acetate buffer solution (pH=3.7, μ=0.5) containing 1.119×10^{-2} M EDTA and 0.1 M $CaCl_2$.

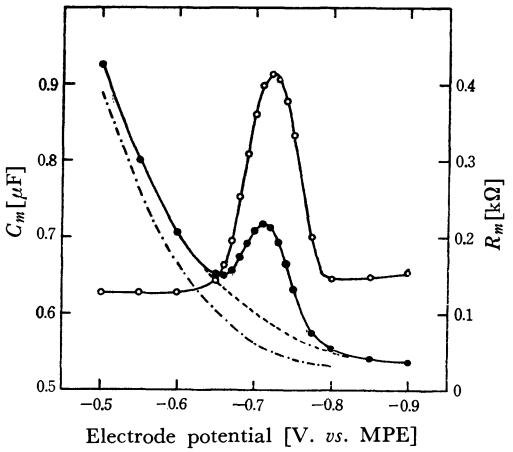

Fig. 3. Potential dependence of R_m(-○-) and C_m(-●-) of the DME/8 mM $Cd(NO_3)_2$, 1.119×10^{-2}M EDTA, 0.1 M $CaCl_2$, acetate buffer (pH=3.7, μ=0.5)/MPE system at 200 cps. (-·-: C_m-values of the supporting electrolyte solution (acetate buffer solution of pH=3.7 and μ=0.5 containing 1.119×10^{-2} M EDTA and 0.1 M $CaCl_2$)).

the double layer capacity of the present system was estimated by the method of interpolation as shown by the dotted line in Fig. 3. In Fig. 4 the values of R_F, $1/(\omega C_F)$, and Z_F of the Cd(II)-EDTA system at the summit potential are plotted as a function of $1/\sqrt{\omega}$.

Discussion

The faradaic impedance of the electrode process is given by a series combination of the charge-transfer resistance which is independent of frequency, and the impedances due to the accompanying processes such as preceding and following chemical reactions, adsorption-desorption process, mass-transfer of reacting species, *etc.* According to the theory of a. c. polarization, these impedances have different

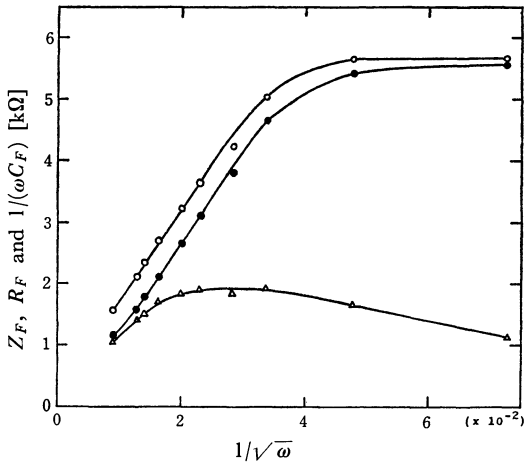

Fig. 4. Frequency dependence of Z_F (-○-), R_F (-●-) and $1/(\omega C_F)$ (-△-) at the summit potential of the DME/8 mM $Cd(NO_3)_2$, 1.119×10^{-2} M EDTA, 0.1 M $CaCl_2$, acetate buffer (pH=3.7, μ =0.5)/MPE system.

frequency dependence; for example, the Warburg impedance due to the diffusion process is expected to be proportional to $1/\sqrt{\omega}$, while the reaction impedance is a more complicated function of frequency.[15]

Cd(II)-, Pb(II)-, and Zn(II)-KCl Systems. The faradaic impedance of a simple electrode reaction mainly consists of the charge-transfer resistance, θ, and the Warburg impedance, Z_W; the faradaic impedance and its components are expected to be linear functions of $1/\sqrt{\omega}$.[15,16] This expectation is supported by the experimental results of Cd(II), Pb(II), and Zn(II) ions in 1 M potassium chloride solutions (Fig. 1).

The polarographic reduction of zinc ions in 1 M potassium chloride solutions is a well-known example of the quasi-reversible electrode reaction with the standard rate constant of the order of 10^{-3} cm/sec.[17] In such a quasi-reversible system, the charge-transfer resistance, θ, at the summit potential is expected to be much larger than the Warburg impedance, Z_W, even at low frequencies, and the resistance component, R_F, of the faradaic impedance at the summit potential will be approximately equal to θ and independent of frequency as shown in Fig. 1 (c).

The theory also suggests that the phase angle, ϕ, of a simple electrode process should be equal to $\pi/4$, being independent of frequency, for a totally reversible system, and it decreases with the decrease in the reversibility. The cot ϕ values of the reversible reduction of cadmium ions in potassium chloride solutions, as given in Fig. 1 (a), are in good agreement with the theory. In the Pb(II)-KCl system, however, the cotϕ value at each frequency studied was smaller than unity inspite of the high reversibility of the system (Fig. 1 (b)); this anomaly in the faradaic impedance may be attributed to the adsorption of the reacting species on the electrode surface.[18,19]

Cd(II)-EDTA System. In the polarographic reduction of the Cd(II)-EDTA system, the plots of Z_F, R_F, and $1/(\omega C_F)$ against $1/\sqrt{\omega}$ gave significant deviations from the linearity at lower frequencies (Fig. 4). These deviations can be explained in terms of the contribution of the reaction impedance due to the preceding chemical reaction (1).

According to Smith's treatment,[8] the cotϕ of the electrode reaction,

$$Y \underset{k_b}{\overset{k_f}{\rightleftharpoons}} O \tag{2}$$

$$O + ne \rightleftharpoons R \tag{3}$$

is given by the equation,

$$\cot\phi = \frac{\frac{\sqrt{2\omega}}{\lambda} + \frac{1}{(1+e^j)}\left\{\frac{1}{1+K}\left[\frac{(1+g^2)^{1/2}+g}{1+g^2}\right]^{1/2} + \frac{K}{1+K} + e^j\right\}}{\frac{1}{(1+e^j)}\left\{\frac{1}{1+K}\left[\frac{(1+g^2)^{1/2}-g}{1+g^2}\right]^{1/2} + \frac{K}{1+K} + e^j\right\}} \tag{4}$$

where

$K = k_f/k_b$, $g = l/\omega$, $l = k_f + k_b$,

$\lambda = k_s f_O^{\alpha} f_R^{\beta} (D_O^{-\beta} D_R^{-\alpha})^{1/2} (e^{-\alpha j} + e^{+\beta j})$,

$\alpha + \beta = 1$, $j = nF(E-E^r_{1/2})/(RT)$

k_f, k_b: forward and backward rate constants, respectively, of reaction (2)

k_s: standard rate constant of reaction (3)

f_O, f_R: activity coefficients of O and R, respectively

D_O, D_R: diffusion coefficients of O and R, respectively

α, β: transfer coefficients

E: electrode potential

$E^r_{1/2}$: reversible half wave potential of reaction (3)

The impedance behavior of the Cd(II)-KCl

15) P. Delahay, "Advances in Electrochemistry and Electrochemical Engineering," Vol. I, Chap. 5, Interscience Publishers, New York (1961); K. J. Vetter, "Elektrochemische Kinetik," Springer-Verlag, Berlin (1961).
16) H. Matsuda, *Z. Elektrochem.*, **62**, 977 (1958).
17) N. Tanaka and R. Tamamushi, *Electrochim. Acta*, **9**, 963 (1964).
18) M. Senda and P. Delahay, *J. Phys. Chem.*, **65**, 1580 (1961).
19) M. Sluyters-Rehbach, B. Timmer and J. H. Sluyters, *J. Electroanal. Chem.*, **15**, 151 (1967).

Table 1. Rate constants of the formation reaction of cadmium-EDTA, $Cd^{2+}+HY^{3-} \rightarrow CdY^{2-}+H^+$, in acetate buffer solutions at 25°C

Ionic strength	Rate const. $l\,mol^{-1}\,sec^{-1}$	Method[b]	Reference
0.1	8.5×10^8	$E_{1/2}$	Koryta, Zábranský[20]
0.1	6.4×10^9	$E_{1/2}$	Aylward, Hayes[10]
0.5	4.0×10^9	$E_{1/2}$	Aylward, Hayes[10]
0.5[a]	5.3×10^8	$E_{1/2}$	Aylward, Hayes[10]
0.5[a]	6.1×10^8	f. a.	Aylward, Hayes[10]
0.5[a]	2.3×10^9	k. c.	Fujisawa, Tanaka[14]
0.5[a]	$2._3\times10^9$	ϕ	This study

a) Containing calcium ions.
b) $E_{1/2}$ refers to the analysis of the half wave potential, f. a., to the faradaic admittance measurement, k. c., to the kinetic current behavior, and ϕ, to the phase angle behavior, respectively.

system suggests that the value of $(\sqrt{2\omega}/\lambda)$ of the present system can safely be neglected against the following term in the numerator of Eq. (4); this is also supported by the behavior of R_F and $1/(\omega C_F)$ of the Cd(II)-EDTA system at higher frequencies as shown in Fig. 4. Therefore, the cot ϕ is represented by a simplified equation:

$$\cot\phi = \frac{\left[\frac{(1+g^2)^{1/2}+g}{1+g^2}\right]^{1/2} + K + (1+K)e^j}{\left[\frac{(1+g^2)^{1/2}-g}{1+g^2}\right]^{1/2} + K + (1+K)e^j} \quad (5)$$

Figure 5 presents the frequency dependence of cot ϕ at the summit potential ($E_s=-0.72$ V *vs.* MPE for 70—2000 cps, and $E_s=-0.73$ V *vs.* MPE for 30 cps), and the theoretical curves for $l=500$, 1000, and 2000 calculated by Eq. (5) with $K=[Cd]/[CdY^{2-}]=10^{-3.67}$ ([Cd], the total concentration of the electroactive cadmium species) and $E^r_{1/2}=-0.678$ V *vs.* MPE. The K-value was determined by using the equilibrium constants of EDTA, EDTA-complexes of cadmium and calcium ions, and chloro- and acetato-complexes of cadmium as given in the literature,[14] and $E^r_{1/2}$ was assumed to be equal to the half wave potential of Cd(II) in an acetate buffer solution (pH=3.7, $\mu=0.5$ adjusted by potassium nitrate) containing 0.1 M calcium chloride.

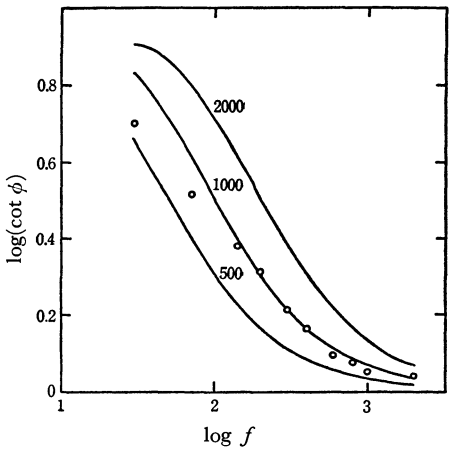

Fig. 5. Relation between log (cot ϕ) and log f (f, frequency) at the summit potential of the Cd-EDTA system; the circles represent the experimental values, and the solid lines correspond to the theoretical curves calculated by Eq. (5) with the l-values given on each curve.

This result shows that the best fit between the experimental and theoretical curves is obtained with $l=1000$. Because of the very small value of K of the present system, the l-value is practically equal to the pseudo first-order rate constant of the formation reaction of CdY^{2-} from the electroactive cadmium species and HY^{3-}, *i. e.*, $l=k'_2[HY^{3-}]=1000$, from which the value of k'_2 is estimated to be $2._4\times10^8\ l\ mol^{-1}\ sec^{-1}$. The rate constant, k'_2, thus determined should be regarded as the overall rate constant of the formation reaction related to the total concentration of the electroactive cadmium species (Cd^{2+}, $CdCl^+$, $CdCl_2$, and $CdOAc^+$). It is generally assumed, however, that only the aquo-cadmium ions react with HY^{3-} to form CdY^{2-}. If this simplified assumption is accepted, the k'_2-value must be multiplied by the factor of $(1+\beta_{CdCl}[Cl^-]+\beta_{CdCl_2}[Cl^-]^2+\beta_{CdOAc}[OAc^-])$, where β_i represents the overall formation constant of the i-species, in order to obtain the rate constant, k_2, corrected for chloro- and acetato-complexes of cadmium; the corrected k_2-value was thus determined to be $2._3\times10^9\ l\ mol^{-1}\ sec^{-1}$.

The rate constants for the formation of cadmium-EDTA have been reported by several authors; some examples of the k_2-values are listed in Table 1. Koryta and Zábranský determined the k_2-value by analyzing the d. c. polarograms of the anodic dissolution of cadmium amalgam in acetate buffer solutions containing EDTA.[20] The same

20) J. Koryta and Z. Zábranský, *Collection Czechoslov. Chem. Commun.*, **25**, 3153 (1960).

method of analysis was examined by Aylward and Hayes;[10] they also applied the faradaic admittance measurement of the anodic dissolution of cadmium amalgam followed by the formation reaction of cadmium-EDTA to the determination of the k_2-values. On the other hand, Tanaka *et al.* studied the kinetic current behavior of cadmium-EDTA at a DME in acetate buffer solutions containing calcium ions;[13,14] they determined the rate constant, k_1, of the dissociation reaction of CdY^{2-}, and then calculated the k_2-value by using the equilibrium constant of reaction (1). A survey of Table 1 shows that our figure is in good agreement with that of Fujisawa and Tanaka.[14]

Finally, the a. c. polarographic studies with the phase angle measurement is concluded to help in analyzing electrochemical mechanisms and in the determination of the rate constant of a coupled preceding reaction.

The authors wish to thank Professor N. Tanaka of Tohoku University and Dr. T. Fujisawa of Yamagata Technical College for valuable discussion.

BULLETIN OF THE CHEMICAL SOCIETY OF JAPAN VOL. 41 1568—1572 (1968)

Alternating Current Polarography of Peroxodisulfate and Ferricyanide Ions in the Absence of Supporting Electrolytes

Reita TAMAMUSHI and Kiyoshi MATSUDA

The Institute of Physical and Chemical Research, Yamato-machi, Kita-adachi-gun, Saitama

(Received January 22, 1968)

The admittance and its phase angle of the polarographic reduction of peroxodisulfate and ferricyanide ions in solutions containing no supporting electrolytes were measured at very low frequencies. The series resistance components, measured at 30 cps, of these systems gave anomalously small values at the electrode potentials where the falling-off of the cathodic current was observed on the direct current polarograms. This anomaly in the alternating current polarization behavior was attributed to the negative charge-transfer resistance due to the double layer effect on the charge-transfer process.

The electrochemical reduction behavior of peroxodisulfate and ferricyanide ions has been studied extensively by Frumkin and his coworkers.[1,2] They reported that the cathodic current of these ions in solutions of very low ionic strength shows a remarkable decrease at the electrode potentials more negative than the point of zero-charge; they attributed this anomaly to the double layer effect.

A similar decrease in the cathodic current was observed by the polarographic reduction of In(III)-SCN^-, Ni(II)-SCN^-, and In(III)-Br^- systems in solutions of moderate ionic strength, but in these cases the falling-off of the cathodic current appears at the potentials where the adsorption of the anions on the electrode surface begins to decrease.[3,4] On alternating current (a. c.) polargorams of these systems an anomalous admittance is observed in the potential region where the cathodic current decreases with the increase in the negative polarization.[5] From the measurement of faradaic impedance, the anomalous behavior of the a. c. polarograms was confirmed to be due to the negative charge-transfer resistance.[3,4]

In the absence of supporting electrolytes, the reduction process of peroxodisulfate and ferricyanide ions at a dropping mercury electrode is expected to give a negative charge-transfer resistance because of the large double layer effect. This study deals with the a. c. polarization behavior of peroxodisulfate and ferricyanide ions at very low frequencies; the results are discussed in terms of the double layer effect.

Experimental

The electrolytic cell used is represented by the scheme,

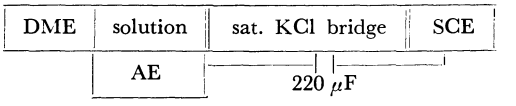

1) A. Frumkin, *Z. Elektrochem.*, **59**, 807 (1955).
2) A. N. Frumkin, *Trans. Faraday Soc.*, **55**, 156 (1959).
3) N. Tanaka and R. Tamamushi, "Proceedings 1st Australian Conference on Electrochemistry 1963," Pergamon Press, Oxford (1965), p. 248; N. Tanaka, T. Takeuchi and R. Tamamushi, This Bulletin, **37**, 1435 (1964).
4) R. Tamamushi and K. Matsuda, *J. Electroanal. Chem.*, **12**, 436 (1966).
5) H. Shirai, *Nippon Kagaku Zasshi (J. Chem. Soc. Japan, Pure Chem. Sect.)*, **81**, 1248 (1960).

where DME is a dropping mercury electrode, and AE, an auxiliary electrode of a platinum spiral surrounding the tip of the DME; the terminals of AE and SCE were connected by a 220 μF tantalum condenser in order to reduce the impedance between the DME and SCE. The drop time and the flow rate of mercury of the DME used were 8.1 sec and 0.88 mg/sec, respectively, in a 1 M potassium chloride solution at open circuit.

The direct current (d. c.) polarograms were recorded by a potentiostatic polarograph similar to that of Durst, Ross and Hume.[6] The d. c. polarograms of peroxodisulfate and ferricyanide ions have large maxima of the first kind, the appearance of which is affected by the scanning direction of the electrode potential. In this study, the electrode potential of the DME was scanned from the negative to the positive side; by this scanning direction a more well-defined limiting current plateau was obtained at the potentials less negative than the point of zero-charge.

The admittance and its phase angle of the system were measured by a potentiostatic a. c. polarograph as shown in Fig. 1. The electrode potential of the DME, both the d. c. and a. c. components, was controlled against the SCE by means of a stabilized operational amplifier, C, and the alternating current flowing through the cell was amplified by a current amplifier, CA (stabilized operational amplifier), and a tuned amplifier, TA (Model 4403A, Yokogawa-Hewlett-Packard), the output of which was then introduced to a rectifier circuit or to a phase meter, PM (Model PHM-8, Ando Electric Co.,

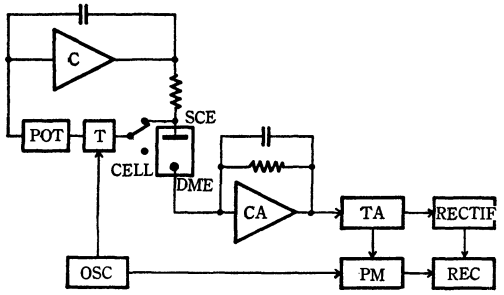

Fig. 1. Potentiostatic a. c. polarograph: C, controller (stabilized operational amplifier); CA, current amplifier (stabilized operational amplifier); TA, tuned amplifier; RECTIF, rectifier; PM, phase meter; REC, recorder; OSC, audio-frequency oscillator; T, transformer; POT, potentiometer (mechanical voltage scanner).

Ltd.). The d. c. component of the electrode potential was applied to the DME by a mechanical voltage scanner, POT, with the scanning rate of about 45 mV/min. The superimposed sinusoidal voltage, whose amplitude was approximately 10 mV and kept constant during each measurement, was supplied by an audio-frequency oscillator, OSC (Model VP-702B, Matsushita Communication Industrial Co., Ltd.). The admittance and phase angle readings were calibrated by using known resistors and capacitors as a dummy cell, and the values measured at the maximum size of a mercury drop of the DME were reported in this paper.

The square-wave polarization behavior was measured by essentially the same circuit as shown in Fig. 1. The square-wave voltage of 50 cps, whose amplitude was about 15 mV, was superimposed to the d. c. electrode potential, and the corresponding current flowing through the cell was observed by a cathode-ray oscilloscope (Tektronix Type 564) at the output of the current amplifier, CA.

The solutions were prepared from the analytical reagent grade chemicals and redistilled water, and vacuum-distilled mercury was used for the DME. The dissolved oxygen in the solution was expelled by bubbling nitrogen through the solution. Peroxodisulfate and ferricyanide ions are subjected to some redox reaction in aqueous solutions; an appreciable change in the solution was observed in a relatively short period of time, especially when the solution was kept in contact with mercury. Therefore, each measurement was carried out with fresh solutions, and the DME and the tip of SCE were introduced into the solution after the deaeration. All measurements were made in a water-thermostat of 25.0±0.1°C.

Results

The d. c. polarograms of 1 mM potassium peroxodisulfate and 1 mN potassium ferricyanide in aqueous solutions containing no supporting electrolytes are shown in Fig. 2, and their a. c. polarograms with the phase angle change at 30 cps in Figs. 3 and 4. In the ferricyanide system, the current decrease on d. c. polarograms was very much sensitive to the concentration of ferricyanide ions; a large decrease appeared in a 1 mN solution, while only a very small one was observed in a 1 mM solution.

From the measured values of admittance and phase angle, the series resistance and capacitance components, R_s and C_s, of the equivalent cell impedance were determined as given in Figs. 5 and 6.

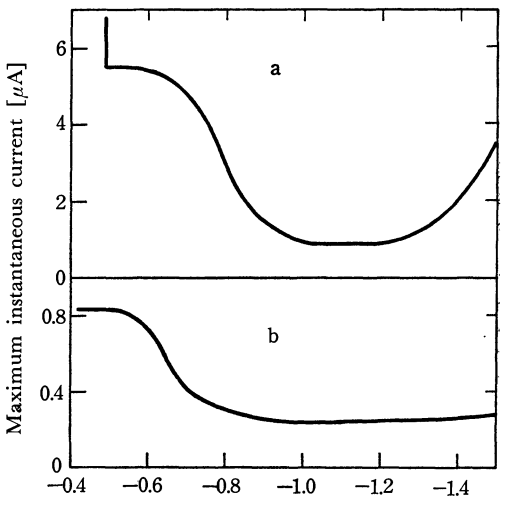

Fig. 2. D. c. polarograms of (a) 1 mM $K_2S_2O_8$ and (b) 1 mN $K_3[Fe(CN)_6]$ in aqueous solutions containing no supporting electrolytes.

6) R. A. Durst, J. W. Ross and D. N. Hume, *J. Electroanal. Chem.*, **7**, 245 (1964).

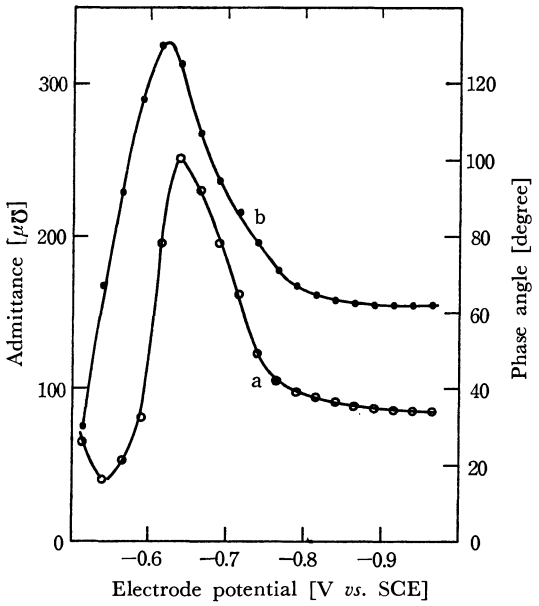

Fig. 3. A. c. polarogram and phase angle change of 1 mM $K_2S_2O_8$ at 30 cps: (a) admittance, and (b) phase angle.

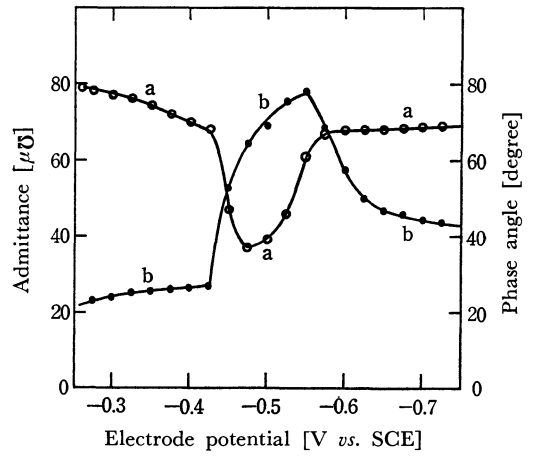

Fig. 4. A. c. polarogram and phase angle change of 1 mN $K_3[Fe(CN)_6]$ at 30 cps: (a) admittance, and (b) phase angle.

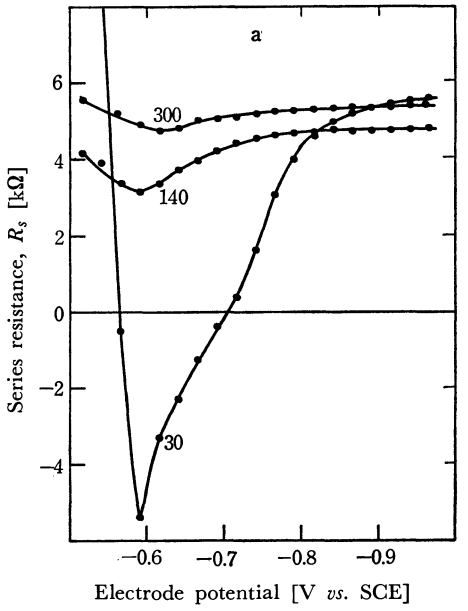

(a)

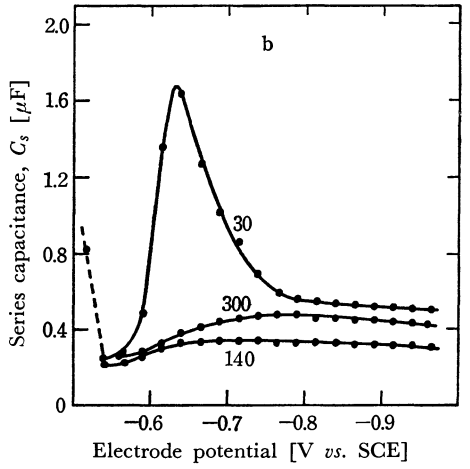

(b)

Fig. 5. Series resistance and capacitance components, R_s and C_s, of the DME/1 mM $K_2S_2O_8$ system: (a) resistance, and (b) capacitance. Figures on each curve represent the frequency of the superimposed sinusoidal voltage.

An example of the square-wave polarization behavior of peroxodisulfate ions is reproduced in Fig. 7; curve (a) represents the output current observed at the electrode potential on the limiting current plateau, and curve (b), the output current at the electrode potential where the cathodic current begins to decrease with increasing negative polarization. Similar results were obtained with the reduction process of ferricyanide ions.

Discussion

The a. c. polarographic behavior of peroxodisulfate and ferricyanide ions at 30 cps shows an anomalously large phase angle at the electrode potentials in the vicinity of the zero-charge point of mercury (Figs. 3 and 4). This anomaly in the phase angle results in a remarkable decrease in the series resistance component, R_s, as shown in Figs. 5 and 6. The R_s-values at 300 cps are assumed to be approximately equal to the resistance of the solution, but the values at 30 cps are very much smaller than the resistance of the solution, even negative in the case of peroxodisulfate ions, at the electrode potentials where the cathodic currents fall off.

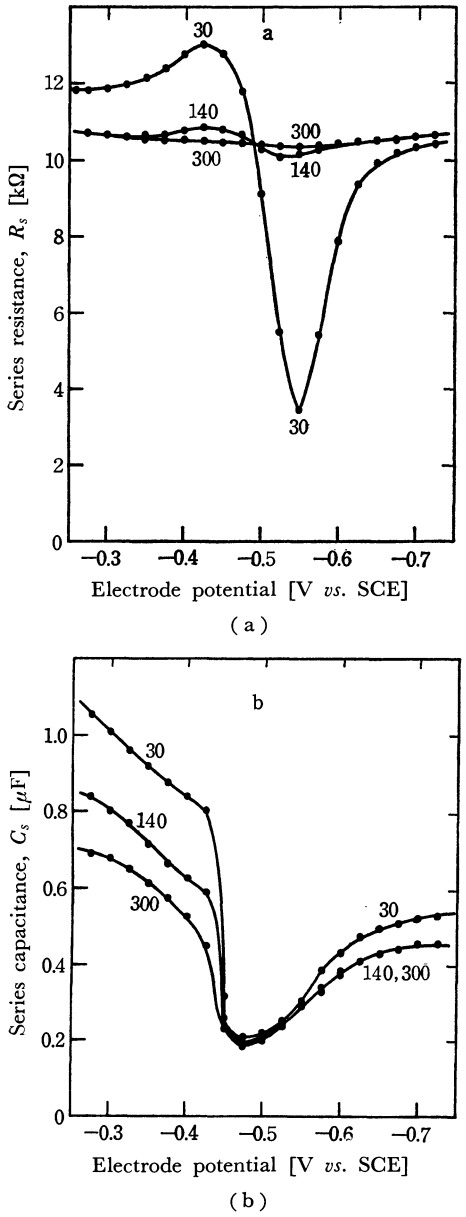

Fig. 6. Series resistance and capacitance components, R_s and C_s, of the DME/1 mN $K_3[Fe(CN)_6]$ system: (a) resistance, and (b) capacitance. Figures on each curve represent the frequency of the superimposed sinusoidal voltage.

The series capacitances, C_s, of the ferricyanide system at the potentials more negative than −0.5 V *vs.* SCE were not very much affected by the frequency, and they may be assumed to be nearly equal to the double layer capacity. On the other hand, the C_s-values of the peroxodisulfate system at 30 cps gave a peak at about −0.63 V *vs.* SCE, which suggests some complication in the electrode process. The details of the capacitance behavior, however, will not be discussed in this paper.

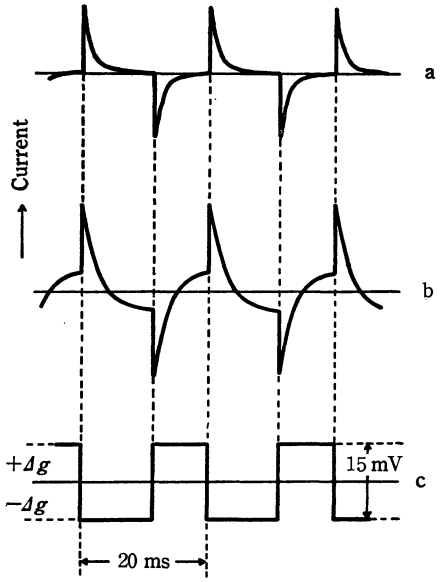

Fig. 7. Square-wave polarization behavior of the DME/1 mM $K_2S_2O_8$ system: (a) $g=-0.50$ V *vs.* SCE; (b) $g=-0.60$ V *vs.* SCE; (c) superimposed square-wave signal. The photographs were taken at the moment just prior to the detachment of a mercury drop from the tip of the DME.

The square-wave polarization behavior of the peroxodisulfate system at −0.60 V *vs.* SCE (Fig. 7, curve (b)) shows that the cathodic faradaic current in the period when the DME is more negatively polarized is smaller than that in the period when the DME is less negatively polarized. This result clearly indicates the decrease in the rate of overall reduction process with increasing negative polarization.

In analogy to the impedance behavior of the polarographic reduction of indium(III) ions in thiocyanate solutions,[3,4] the anomalous decrease in the series resistance component may be attributed to the negative charge-transfer resistance. The negative charge-transfer resistance of the peroxodisulfate and ferricyanide systems can be explained in terms of the double layer effect.

The charge-transfer resistance, θ, of the electrode reaction,

$$O + ne \rightleftharpoons R$$

is given by the equation,

$$\frac{1}{\theta} = \frac{n^2F^2}{RT} k^\circ \left\{ \alpha_+ c_R \exp\left[\frac{\alpha_+ nF}{RT}(g-g^\circ)\right] + \alpha_- c_0 \exp\left[\frac{-\alpha_- nF}{RT}(g-g^\circ)\right]\right\} \quad (1)$$

where k° is the standard rate constant, g, the d. c. component of the electrode potential, g°, the standard electrode potential, c, the d. c. component of the concentration at the plane just outside the

diffuse double layer, and α_+ and α_- are the apparent transfer coefficients for the anodic and cathodic directions, respectively.[7]

At the electrode potentials where the dip in cathodic currents appears, the condition $g<g^\circ$ can be satisfied, and Eq. (1) is simplified as

$$\frac{1}{\theta} = \frac{n^2F^2}{RT} k^\circ \alpha_- c_0 \exp\left[\frac{-\alpha_- nF}{RT}(g-g^\circ)\right] \quad (2)$$

This relation indicates that the sign of θ is determined by that of the apparent transfer coefficient, α_-, for the cathodic direction; θ should be positive when $\alpha_->0$, and should be negative when $\alpha_-<0$.

By assuming the simple Boltzmann-type distribution of reacting species in the diffuse double layer and that the charge-transfer process proceeds at the outer Helmholtz plane, the apparent transfer coefficient, α_-, is represented by Eq. (3) as a function of the electrode potential,

$$\alpha_- = (1-\beta) + \frac{1}{ng}[z_0 - n(1-\beta)](\phi_2-\phi^s) \quad (3)$$

where β $(1>\beta>0)$ is a symmetry factor, z_0, the charge of O with sign, and ϕ_2 and ϕ^s are the inner potentials of the outer Helmholtz plane and the bulk of solution, respectively.[7]

Equation (3) suggests that by the reduction of polyvalent anions in solutions of low ionic strength the apparent transfer coefficient, α_-, may assume negative values especially at the electrode potentials. in the vicinity of the point of zero-charge. No data is available for the double layer behavior of the mercury electrode in peroxodisulfate and ferricyanide solutions, and thus the quantitative estimation of $(\phi_2-\phi^s)$ is not feasible. The double layer effect, however, can reasonably be assumed to be large enough to give negative α_--values for the polarographic reduction of peroxodisulfate and ferricyanide ions in aqueous solutions of very low ionic strength. Peroxodisulfate and ferricyanide ions are supposed to be subjected to a specific adsorption at the DME, the effect of which was ignored in the present discussion. The specific adsorption of these species, if any, will increase the double layer effect.

Frumkin suggested the possibility that the rate determining step of the reduction of ferricyanide ions may be the penetration of the anion through the electric field of the diffuse double layer and not the charge-transfer process.[2] According to Matsuda[8] and Senda and Delahay,[9] the repulsion of the discharged species due to the electric field of the diffuse double layer results in an additional resistance in series with the Warburg impedance in the equivalent circuit of the faradaic impedance. This additional resistance is then expected to increase the resistance component, R_s, and therefore, the remarkable decrease in R_s of the ferricyanide system as shown in Fig. 6 (a) could not be explained without considering the effect of the double layer on the apparent transfer coefficient of the charge-transfer process.

In conclusion, the qualitative behavior of the a. c. polarization of the peroxodisulfate and ferricyanide systems can be explained satisfactorily by assuming the double layer effect on the charge-transfer process. The a. c. polarography with the phase angle measurement, particularly at very low frequencies, was proved to be a useful method of analyzing the mechanism of electrode reactions.

7) R. Tamamushi, "Denki Kagaku (Electrochemistry)," Tokyo Kagaku Dōzin, Tokyo (1967), Chap. 5.

8) H. Matsuda, *J. Phys. Chem.*, **64**, 339 (1960).

9) M. Senda and P. Delahay, *ibid.*, **65**, 1580 (1961).

BULLETIN OF THE CHEMICAL SOCIETY OF JAPAN VOL. 41 1573—1577 (1968)

The Diffusion of Gases at High Pressures. II. The Diffusion of $^{14}CO_2$ in the $^{12}CO_2$-Ar System

Shinji TAKAHASHI

Chemical Research Institute of Non-Aqueous Solutions, Tohoku University, Katahira-cho, Sendai

(Received January 24, 1968)

The diffusion coefficients of $^{14}CO_2$ in argon and in binary mixtures of normal carbon dioxide and argon were measured at the temperatures of 25, 50 and 75°C in the 15—250 atm pressure range. The measurements were made through a plug of porous bronze in the diffusion cell using the radioactive tracer technique. The products of the binary diffusion coefficient of $^{14}CO_2$ in argon and the density increase with an increase in the density. This tendency is not predicted by Enskog-Thorne's mixed dense gas theory, which requires that the products decrease with an increase in the density. The products of the diffusion coefficient of $^{14}CO_2$ in the mixtures and the density increase slightly with an increase in the density in the region of lower density at each temperature. However, in the region of higher density they decrease slightly at 25 and 50°C and are nearly constant at 75°C. The values extrapolated to 1 atm agree fairly well with the experimental findings of Holsen *et al.* and those predicted by kinetic theory.

Kinetic theory precicts[1,2] that, at low pressures, the effective diffusion coefficient, D, of a trace component, i, in a gas mixture will be given by the equation:

$$1/D = \sum_{j \neq i} x_j/D_{ij} \qquad (1)$$

where x_j is the mole fractions and D_{ij}, the binary diffusion coefficients. This equation has been confirmed by several recent experimental investigations.[3] At high pressures, however, much less is known about the diffusion in a multicomponent system either theoretically or experimentally. Recently, though, a few studies of high-pressure diffusion with ternary systems, $^{14}CO_2$-$^{12}CO_2$-CH_4,[4] $^{14}CO_2$-$^{12}CO_2$-H_2,[5] and $^{14}CO_2$-$^{12}CO_2$-C_3H_8,[5] have been made.

In the present paper the diffusion coefficients of $^{14}CO_2$ in argon and in binary mixtures of normal carbon dioxide and argon at the temperatures of 25, 50, and 75°C in the 15—250 atm pressure range are reported on.

Experimental

The experimental apparatus and procedure have been described in detail in a previous paper.[6] Exactly the same procedure was followed. In the present investigation a type-II porous plug with a grain size of ϕ 60—70 μ was used; the apparatus constant, K_{II}, determined at 25°C is shown in Table 1. K_{II}'s at 50 and 75°C were determined in the previous paper.[6] The proportionality between the ionization current and the concentration of $^{14}CO_2$, essential for the quantitative treatment of diffusion data, was confirmed experimentally for pure argon and for each mixture at a constant temperature and pressure. For example, the results at 50°C are shown in Figs. 1 and 2.

TABLE 1. DETERMINATION OF APPARATUS CONSTANT, K_{II} AT 25°C

P atm	$K_{II}D_{22}P \times 10^6$ * atm/sec	$D_{22} \times 10^3$ ** cm²/sec	$K_{II} \times 10^3$ 1/cm²
10	826	11.2	7.38
20	783	5.30	7.39
30	732	3.26	7.48
40	669	2.25	7.43
50	587	1.62	7.25
		Average	7.39

* The smoothed values of $K_{II}D_{22}P$ obtained experimentally.

** The self-diffusion coefficients of normal carbon dioxide obtained in the previous paper.[6]

1) J. O. Hirschfelder, C. F. Curtiss and R. B. Bird, "Molecular Theory of Gases and Liquids," John Wiley & Sons, Inc., New York (1954).

2) C. R. Wilke, *Chem. Eng. Progr.*, **46**, 95 (1950).

3) D. F. Fairbanks and C. R. Wilke, *Ind. Eng. Chem.*, **42**, 471 (1950); H. Wise, *J. Chem. Phys.*, **31**, 1414 (1959); R. E. Walker, N. De Haas and A. A. Westenberg, *ibid.*, **32**, 1314 (1960); B. N. Srivastava and R. Paul, *Physica*, **28**, 646 (1962); L. Miller and P. C. Carman, *Trans. Faraday Soc.*, **57**, 2143 (1961); **60**, 33 (1964); T. A. Pakurar and J. R. Ferron, *Ind. Eng. Chem. Fundamentals*, **5**, 553 (1966); A. Saran and Y. Singh, *Can. J. Chem.*, **44**, 2222 (1966); H. Watts, *Trans. Faraday Soc.*, **60**, 1745 (1964); *Can. J. Chem.*, **43**, 431 (1965); **45**, 1825 (1967).

4) Q. R. Jeffries and H. G. Drickamer, *J. Chem. Phys.*, **22**, 436 (1954).

5) C. Chou and J. J. Martin, *Ind. Eng. Chem.*, **49**, 758 (1957).

6) S. Takahashi and H. Iwasaki, This Bulletin, **39**, 2105 (1966).

TABLE 2. EXPERIMENTAL RESULTS

P atm	ρ mol/l	$D\times10^3$ cm^2/sec	$D\rho\times10^3$ cm^2·mol/sec·l
25°C			
x_3 (mole fraction of argon)=1.000			
10.57	0.4343	14.1	6.12
20.6	0.8515	7.46	6.35
20.8	0.8602	7.35	6.32
20.9	0.8647	7.24	6.26
30.9	1.286	4.95	6.37
40.7	1.702	3.76	6.40
51.6	2.170	2.97	6.44
60.8	2.569	2.48	6.37
97.6	4.178	1.56	6.52
151.6	6.543	1.01	6.61
204.8	8.780	0.793	6.96
249.8	10.53	0.666	7.01
x_3=0.719			
14.61	0.6096	9.40	5.73
20.4	0.8607	6.54	5.63
60.3	2.679	2.17	5.81
102.6	4.777	1.26	6.02
151.6	7.341	0.804	5.90
200.4	9.837	0.621	6.11
201.5	9.893	0.601	5.95
247.5	11.90	0.495	5.89
x_3=0.497			
14.48	0.6130	8.77	5.38
20.3	0.8717	6.09	5.31
61.9	2.966	1.84	5.46
90.9	4.710	1.14	5.37
102.7	5.467	1.00	5.47
146.3	8.467	0.650	5.50
150.1	8.733	0.626	5.47
199.7	11.98	0.447	5.36
x_3=0.245			
20.7	0.9150	5.48	5.01
30.9	1.440	3.54	5.10
31.3	1.457	3.43	5.10
51.1	2.606	1.91	4.98
51.2	2.616	1.97	5.15
70.2	4.050	1.24	5.02
101.0	7.724	0.652	5.04
120.1	10.62	0.447	4.75
148.4	13.99	0.334	4.67
50°C			
x_3=1.000			
14.50	0.5520	11.7	6.46
14.96	0.5671	11.6	6.58
15.35	0.5820	11.2	6.52
64.2	2.470	2.69	6.64
69.0	2.658	2.47	6.57
102.2	3.958	1.68	6.65
114.1	4.470	1.50	6.71
147.6	5.721	1.21	6.92
151.9	5.885	1.15	6.77
171.4	6.623	1.03	6.82
209.5	8.028	0.869	6.98
220.7	8.429	0.834	7.03
249.8	9.444	0.741	7.00
x_3=0.719			
14.51	0.5550	10.7	5.94
15.02	0.5746	10.5	6.03
15.31	0.5859	10.1	5.92
51.3	2.032	3.00	6.10
52.2	2.069	2.95	6.10
52.7	2.089	2.91	6.08
75.6	3.056	2.00	6.11
86.6	3.531	1.75	6.18
96.2	3.952	1.56	6.17
101.2	4.171	1.47	6.13
103.2	4.259	1.45	6.18
110.2	4.570	1.34	6.12
135.7	5.705	1.10	6.28
150.4	6.361	0.963	6.13
200.4	8.516	0.710	6.05
205.5	8.724	0.685	5.98
248.5	10.41	0.583	6.07
252.9	10.57	0.566	5.98
x_3=0.497			
14.44	0.5583	9.88	5.52
14.44	0.5583	9.80	5.47
14.45	0.5588	9.81	5.48
54.4	2.254	2.51	5.66
103.8	4.678	1.24	5.80
104.2	4.699	1.22	5.73
151.3	7.235	0.789	5.71
200.5	9.846	0.584	5.75
245.5	11.95	0.475	5.68
x_3=0.245			
14.36	0.5641	9.09	5.13
14.39	0.5650	9.03	5.10
14.49	0.5690	9.17	5.22
51.4	2.274	2.37	5.39
54.6	2.445	2.20	5.38
105.9	5.811	0.933	5.42
150.3	9.475	0.567	5.37
191.4	12.56	0.424	5.33
75°C			
x_3=1.000			
13.99	0.4910	13.9	6.82
50.6	1.787	3.90	6.97
50.9	1.797	3.94	7.08
98.5	3.489	2.04	7.12
104.5	3.701	1.92	7.11
157.6	5.555	1.28	7.11
202.5	7.066	1.03	7.28

TABLE 2 (Continued)

P atm	ρ mol/l	$D\times10^3$ cm^2/sec	$D\rho\times10^3$ cm^2·mol/sec·l
239.4	8.252	0.872	7.20
	$x_3=0.719$		
13.83	0.4890	13.0	6.36
45.4	1.642	3.88	6.37
52.9	1.923	3.40	6.54
112.5	4.220	1.53	6.46
151.1	5.733	1.16	6.65
196.5	7.470	0.878	6.56
247.1	9.286	0.701	6.51
	$x_3=0.497$		
14.44	0.5140	11.7	6.01
52.1	1.945	3.14	6.11
52.1	1.945	3.16	6.15
101.0	3.981	1.57	6.25
153.3	6.341	0.980	6.21
200.4	8.467	0.738	6.25
	$x_3=0.245$		
14.42	0.5206	11.0	5.73
14.43	0.5210	11.0	5.73
51.3	2.019	2.90	5.85
51.6	2.031	2.92	5.93
101.5	4.517	1.31	5.92
156.2	7.713	0.771	5.95

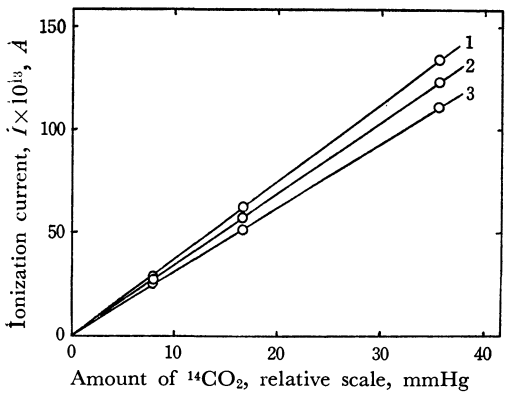

Fig. 1. Relations between the amount of $^{14}CO_2$ and ionization current in argon at 50°C.
1: 15 atm 2: 100 atm 3: 250 atm

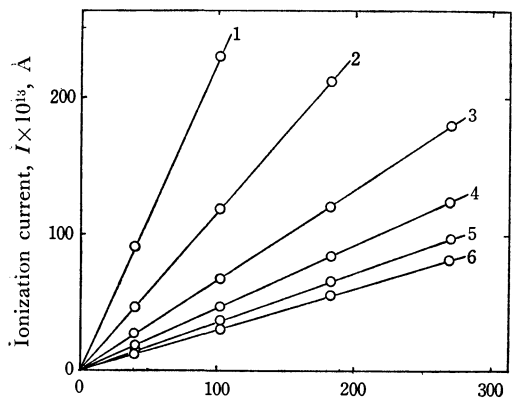

Fig. 2. Relations between the amount of $^{14}CO_2$ and ionization current in the mixture of $x_3=0.497$ at 50°C.
1: 15 atm 2: 50 atm 3: 100 atm
4: 150 atm 5: 200 atm 6: 250 atm

The nonradioactive mixtures were prepared from carbon dioxide and argon, certified to be 99.9 and 99.99% pure, respectively. Except for drying with silica gel, no further purification was attempted. Before measuring the diffusion, bulk mixtures of normal carbon dioxide-argon were prepared in storage cylinders. Their exact compositions were determined by bubbling samples through a potassium hydroxide solution. For this investigation the mixtures are not in the liquid state.[7]

Results and Discussion

The experimental results are given in Table 2. The densities, ρ (mol/l), for argon were calculated from the compressibility factors obtained by Michels *et al.*[8] The densities for carbon dioxide-argon mixtures were calculated by using the compressibility chart*1 with the pseudo critical temperature, T_c, and pressure, P_c, obtained by the following relations:

$$T_c = x_2(T_c)_2 + x_3(T_c)_3 \quad (2)$$

$$P_c = x_2(P_c)_2 + x_3(P_c)_3 \quad (3)$$

where the subscripts 2 and 3 denote normal carbon dioxide and argon. The compressibility calculated above agrees within 2.1% with Abraham's data,[10] which range from 50 to 1000 atm at 50°C. It may be noted that the maximum deviation of the values calculated from Abraham's data by using Weber's chart is 4.6%.

In Fig. 3 the diffusion coefficient-density products, $D\rho$, are plotted against the densities.

The values of $D\rho$ at a unit mole fraction of argon

7) G. Kaminishi, Private communication.
8) A. Michels, Hub. Wijker and HK Wijker, *Physica*, **15**, 627 (1949).
*1 This chart was prepared from the compressibility data with carbon dioxide and argon using the same method as was used for Weber's generalized compressibility chart.[9]
9) H. C. Weber, "Thermodynamics for Chemical Engineers," John Wiley & Sons, Inc., New York (1939).
10) W. H. Abraham and C. O. Bennett, *A. I. Ch. E. Journal*, **6**, 257 (1960).

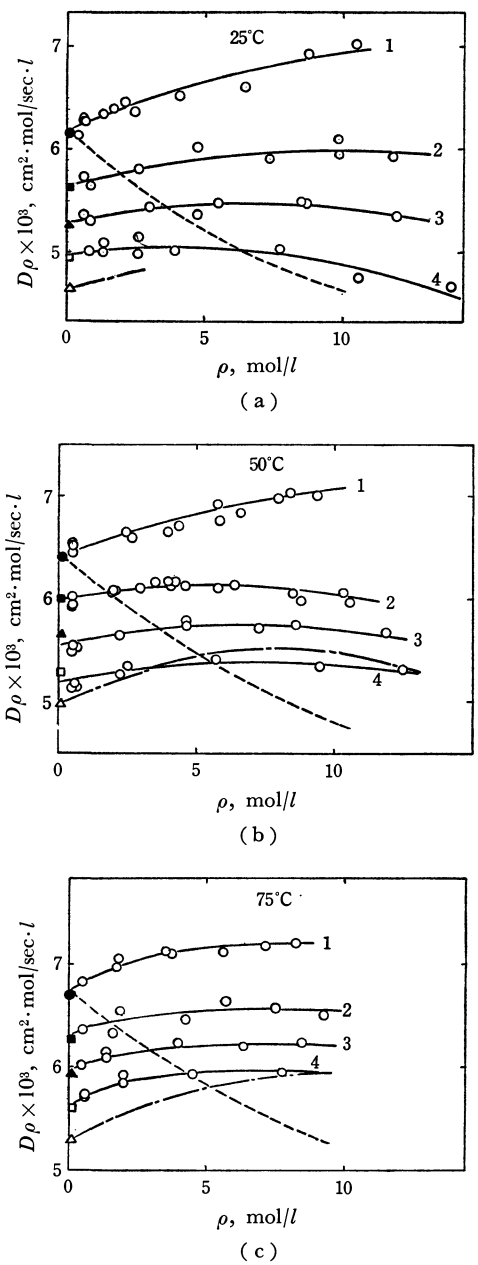

Fig. 3. Experimental results.
○: Present work, ——: Smoothed curves for experimental values, 1: $x_3=1.000$, 2: $x_3=0.719$, 3: $x_3=0.497$, 4: $x_3=0.245$. —·—: Smoothed curves for $D_{12}\rho$ obtained in the previous paper.[6] ----: Theoretical curves. ●: Calculated at 1 atm by the formula of Holsen for D_{13}. ■, ▲ and □: Calculated at 1 atm by using Eq. (6) for the mixtures of $x_3=0.719$, 0.497 and 0.245, respectively. △: Calculated at 1 atm from the experimental values for D_{12}.[14]

are equivalent to the binary diffusion coefficients of the $^{14}CO_2$-Ar system. These products at each temperature show a tendency to increase consistently with an increase in the density. The extrapolation of these products to 1 atm provides a basis for comparison with the low-pressure experimental results reported by other investigators. The formula of the experimental binary diffusion coefficients for the carbon dioxide-argon system published by Holsen *et al.*[11] yields values which are in agreement with the extrapolated values of this investigation.

The effect of the density (or the pressure) on the binary diffusion coefficient may be predicted by Enskog-Thorne's mixed dense gas theory,[12] which

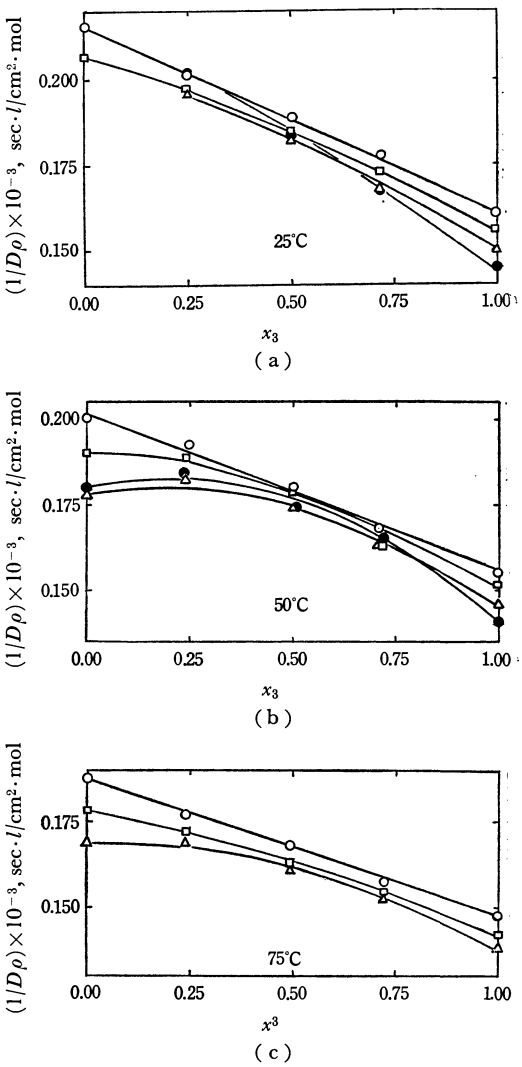

Fig. 4. Relations between $(1/D\rho)$ and x_3.
○: 1 atm, □, △ and ●: 2, 6 and 10 mol/l, respectively.

11) J. N. Holsen and M. R. Strunk, *Ind. Eng. Chem. Fundamentals*, **3**, 143 (1964).
12) S. Chapman and T. G. Cowling, "The Mathematical Theory of Non-Uniform Gases," Cambridge University Press, London (1960).

is the only theoretical treatment offering any practical application. It is expressed as follows:

$$D_{13}\rho = (D_{13})^\circ \rho/\chi_{13} \quad (4)$$

$$\chi_{13} = 1 + 0.2618 n_3 \sigma_3^3 (8 - 3\sigma_3/\sigma_{13}) \quad (5)$$

where the subscript 1 denotes radioactive carbon dioxide. D_{13} is the first approximation to the diffusion coefficient for dense gases, and $(D_{13})^\circ$ is the first approximation to the diffusion coefficient for dilute gases. The n is the number of molecules per unit of volume, and σ is the effective collision diameter. The empirical combining law, $\sigma_{13} = (\sigma_1+\sigma_3)/2 \fallingdotseq (\sigma_2+\sigma_3)/2$, was employed in the calculation. The collision diameters, $\sigma_2 = 3.996$ Å and $\sigma_3 = 3.418$ Å, were taken from Ref. 1 and are those determined from the viscosity measurements for the Lennard-Jones model. $(D_{13})^\circ$ was calculated by using the formula published by Holsen *et al.*,[11] with a mass correction. As is shown in Fig. 3 by dashed lines, the theory requires the $D_{13}\rho$ products to decrease with an increase in the density. The calculated products are lower by 28% at a density of about 8 moles per liter at each temperature. This poor agreement is in accordance with most of the other high-pressure-diffusion results.[13]

According to Eq. (1), the effective diffusion coefficient, D, of a trace component (radioactive carbon dioxide) in a gas mixture of normal carbon dioxide and argon is given by the equation:

$$1/D = x_2/D_{12} + x_3/D_{13} \quad (6)$$

where D_{12} and D_{13} are the binary diffusion coefficients of radioactive carbon dioxide in normal carbon dioxide and in argon respectively. The values of D_{12} and D_{13} at 1 atm were obtained by applying the mass corrections to the reported values of the self-diffusion coefficient of normal carbon dioxide, D_{22}[14], and to that of the binary diffusion coefficient between normal carbon dioxide and argon, D_{23}.[11] The calculated values of $D\rho$ at 1 atm thus obtained for intermediate concentrations are shown in Fig. 3. These calculated values are in agreement with the extrapolated values.

The Enskog theory has not yet been extended to ternary systems at high pressures. Therefore, the applicability of Eq. (1) to the high-pressure-diffusion coefficient was tested in the form:

$$1/D\rho = x_2/D_{12}\rho + x_3/D_{13}\rho \quad (7)$$

$$x_2 + x_3 \fallingdotseq 1$$

where D, D_{12}, and D_{13} are the values at density, ρ. Equation (7) indicates that $1/D\rho$ may vary linearly with either x_2 or x_3, that $D = D_{12}$ at $x_2 = 1$, and that $D = D_{13}$ at $x_3 = 1$. The values of $D\rho$ were read from the smoothed curves in Fig. 3, while the values of $1/D\rho$ are plotted against the mole fraction of argon, x_3, at 1 atm and $\rho = 2$, 6, and 10 mol/l in Fig. 4. The plots are straight lines at 1 atm. However, they are not straight lines but convex curves at densities above 2 moles per liter.

Conclusion

At high pressures the binary diffusion coefficient of $^{14}CO_2$ in argon can not be predicted by Enskog-Thorne's theory, and the effect of the composition on the diffusion coefficient of $^{14}CO_2$ in $^{12}CO_2$-Ar mixtures does not follow Eq. (1). These facts are understandable, for the above-mentioned theory has been derived for rigid spherical molecules, while Eq. (1) is only for ideal gases.

The author wishes to express his deep gratitude to Professor Hiroji Iwasaki for his kind direction and encouragement throughout this work.

13) E. W. Becker, W. Vogell and F. Zigan, *Z. Naturforschg.*, **8a**, 686 (1953); H. A. O'Hern, Jr., and J. J. Martin, *Ind. Eng. Chem.*, **47**, 2081 (1955); V. J. Berry, Jr., and R. C. Koeller, *A. I. Ch. E. Journal*, **6**, 274(1960); L. Durbin and R. Kobayashi, *J. Chem. Phys.*, **37**, 1643 (1962).

14) I. Amdur, J. W. Irvine, Jr., E. A. Mason and J. Ross, *J. Chem. Phys.*, **20**, 436 (1952).

BULLETIN OF THE CHEMICAL SOCIETY OF JAPAN VOL. 41 1578—1582 (1968)

The Polarographic Behavior of Aliphatic Aldehydes in Buffer Solutions Containing *o*-Phenylenediamine

Tamotsu WASA and Sôichirô MUSHA

Department of Applied Chemistry, College of Engineering, University of Osaka Prefecture, Sakai

(Received August 16, 1967)

Formaldehyde (I), acetaldehyde (II), propionaldehyde (III), *n*-butyraldehyde (IV), *n*-caproaldehyde (V), and *n*-octaldehyde (VI) condense with *o*-phenylenediamine (OPD) to yield products, each of which gives a single, irreversible but well-defined oxidation wave ($E_{1/2}$ *vs.* SCE at pH 8.0: −0.240 V for I, −0.242 V for II, −0.263 V for III, −0.290 V for IV, −0.316 V for V, and −0.338 V for VI). From these findings, it has been deduced that the condensation products of aldehydes with OPD would be benzimidazoline derivatives, which would be oxidized to benzimidazole derivatives at the dropping mercury electrode. Linear relations between the limiting currents of the condensation products with OPD and the concentrations of aldehydes [(1—20) × 10^{-4} M], except for I, were obtained under the following conditions: pH, 6—8 ($pH_{i\ max}$); the concentration of OPD, 2×10^{-2} M; the temperature, 25°C; and the condensation time, 15—60 min. The method was then applied practically in the determination of the purity of a commercial product of II and the quantity of II in the presence of glyoxal.

It has well been known that most aliphatic aldehydes show single reduction waves at the dropping mercury electrode in neutral and alkaline solutions containing lithium or tetraalkylammonium salt as the supporting electrolyte in the range of voltage between −1.6 V and −1.8 V *vs.* SCE, and that these waves can be used in the determination of aliphatic aldehydes.[1-4] However, the limiting current is markedly influenced by the pH and the temperature of the electrolytic solution,[5,6] and also decreases with time in the alkaline region because of the instability of these aldehydes.[7] For analytical use, in order to obtain the wave height proportional to the aldehyde concentration, the experimental conditions must be strictly controlled. To avoid this shortcoming, indirect polarographic methods which involve the chemical reactions of aldehyde with carbonyl reagents have been reported.[8-10]

The authors have previously reported on the oxidation waves of the condensation products of hydroxyaldehydes with *o*-phenylenediamine (OPD) in various buffer solutions, and on the polarographic determination of glycolaldehyde and glyceraldehyde.[11]

The present paper will describe the polarographic behavior of aliphatic aldehydes, *i. e.*, formaldehyde (I), acetaldehyde (II), propionaldehyde (III), *n*-butyraldehyde (IV), *n*-caproaldehyde (V), and *n*-octaldehyde (VI), in various buffer solutions containing an excess of OPD, and will present a method for determining such aldehydes by using this oxidation wave.

Experimental

Formaldehyde was a commercial product (Formalin, about 37%) from Wako Pure Chemical Industries, Ltd.; it was used without further purification. II was prepared from paraldehyde by distillation in the presence of a 1 vol% of concentrated sulfuric acid.[12] All the other aldehydes (III, IV, V, and VI) used were purified by the distillation of their commercial products. Aqueous or ethanolic stock solutions of the aldehydes were prepared at about 10^{-2} M; these concentrations were checked by the titration method.[13] All the other chemicals were the same as those used in previous

1) I. Tachi, ed., "Polarography," Iwanami, Tokyo (1954), p. 357.
2) I. M. Kolthoff and J. J. Lingane, "Polarography," 2nd Ed., Interscience, New York (1952), p. 652.
3) M. Brezina and P. Zuman, "Polarography in Medicine, Biochemistry, and Pharmacy," Revised English Ed., Interscience, New York (1958), p. 231.
4) D. J. Pietrzyk, *Anal. Chem.*, **38**, 278R (1966).
5) K. Vesely and R. Brýdička, *Collection Czech. Chem. Communs.*, **12**, 313 (1947).
6) R. Bieber and F. Trümpler, *Helv. Chim. Acta*, **30**, 706, 971, 1109, 1286, 1534, 2000 (1947); **31**, 5 (1948).
7) W. Dirscherl and Hans-Ulrich Bergmeyer, *Ber.*, **82**, 291 (1949).
8) P. Zuman, "Organic Polarographic Analysis," Pergamon, Oxford (1964), p. 120.
9) M. Masui and C. Yijima, *Bunseki Kagaku (Japan Analyst)*, **15**, 1350 (1966).
10) B. Fleet, *Anal. Chim. Acta*, **36**, 304 (1966).
11) T. Wasa and S. Musha, This Bulletin, **40**, 1624 (1967).
12) L. F. Burroughs and A. H. Sparks, *Analyst*, **86**, 381 (1961).
13) Sidney Siggia, "Quantitative Organic Analysis *via* Functional Groups," Wiley, New York (1963), p. 74.

works.[11,14,15] As for the buffer solutions, Britton-Robinson buffers (BR) were mainly employed except for examining the effect of the components of the buffer solution. No maximum suppressor was added, since no maximum was observed under the present polarographic conditions.

The apparatus and the experimental procedures were the same as those reported in previous papers.[11,14,15] To minimize the loss of aldehydes, the dissolved oxygen was removed by bubbling nitrogen which had previously been passed through a solution of the same composition. Reference electrode: SCE. Characteristics of capillary: m=1.143 mg/sec, t=4.00 sec/drop in the buffer solution at 0 V *vs.* SCE. The accuracy of the temperature control was ±0.1 °C.

Results and Discussion

Oxidation Waves of the Condensation Products of Aliphatic Aldehydes with OPD. All the aliphatic aldehydes (I—VI) examined show an ill-defined and unstable reduction wave in alkaline media, as may be seen in Fig. 1(a). In buffer solution containing an excess of OPD, however, they give a well-defined oxidation wave (Fig. 1(b)) corresponding to the condensation products, which are probably benzimidazoline derivatives, as has been previously reported for hydroxyaldehydes.[11]

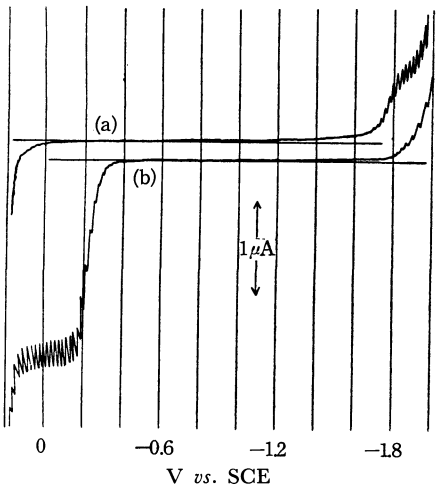

Fig. 1. Polarograms of acetaldehyde with or without OPD at 25°C.
(a) 2×10^{-3} M II in BR buffer (pH, 8.0)
(b) 6.5×10^{-4} M II in BR buffer (pH, 8.0) containing 2×10^{-2} M OPD; Condensation: 60 min

The Effect of pH. When the concentrations of aldehydes and OPD were kept constant and when polarograms were recorded 60 min after the addition of OPD at 25°C, the relationships between the limiting currents of the condensation products and the pH were as shown in Fig. 2. All the aldehydes examined, with the exception of I, exhibit almost the same polarographic behavior: the limiting currents reach their maximum values in the pH range between 6 and 8 and then decrease beyond this pH region. It seems that the decrease in the height of the oxidation waves with an increase in the pH on the alkaline side is related to the decrease in the rate of the condensation reaction, while the other decrease, on the acidic side, is due to some conversion of OPD involving protonation and also to the instability of the condensation products. The limiting current for I, with an increase in the pH, reaches its maximum value at a pH value of about 5.8; then it decreases markedly with a further increase in the pH, while, at the same time, the electrolytic solution becomes turbid. The optimum pH ranges, $pH_{i\ max}$, in which the oxidation wave corresponding to each of the aldehydes shows its maximum value, are presented in Table 1, together with the equilibrium constants (K'). At the $pH_{i\ max}$ the reaction of aldehyde with OPD reached its equilibrium state within 5—10 min after the addition of OPD and the condensation products were comparatively stable. The oxidation wave of the condensation products was diffusion-controlled; there is a proportionality between the limiting currents and the square root of the heights of mercury reservoir.

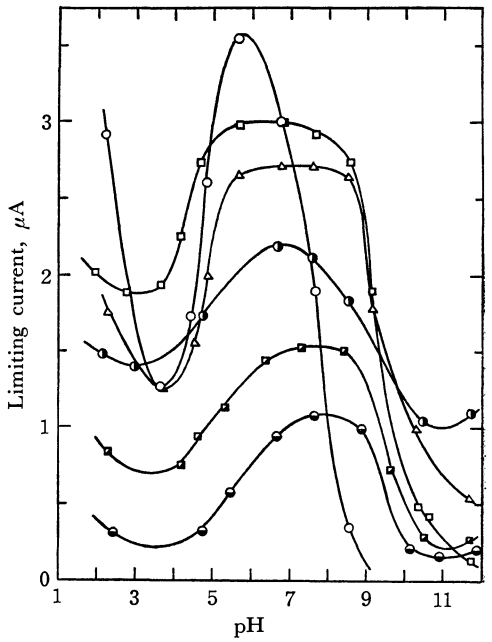

Fig. 2. Effect of pH on the oxidation waves of the aldehydes (1×10^{-3} M) in BR buffer containing 2×10^{-2} M OPD at 25°C.
Condensation: 60 min; ○—I, □—II, △—III, ◑—IV, ◪—V, and ◒—VI

The changes in the half-wave potentials with the

14) S. Musha, T. Wasa and T. Naito, This Bulletin, **39**, 1902 (1966).
15) T. Wasa and S. Musha, *ibid.*, **40**, 1617 (1967).

TABLE 1. OPTIMUM pH ($pH_{i\ max}$) AND EQUILIBRIUM CONSTANT (K') FOR THE CONDENSATION REACTION
Aldehyde: 1×10^{-3} M, OPD: 2×10^{-2} M; Condensation: 60 min, 25°C, BR buffer

Aldehyde	I	II	III	IV	V	VI
$pH_{i\ max}$	5.8	5.5—8	6—8	6—7.5	6.5—8.5	7—9
K', l/mol	474	176	138	117	73	60

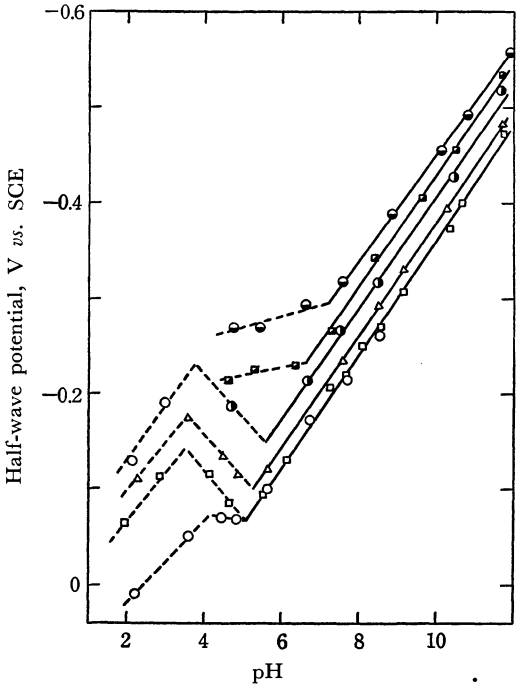

Fig. 3. pH-dependence of the half-wave potentials at 25°C.
Aldehyde: 1×10^{-3} M, OPD: 2×10^{-2} M; Condensation: 60 min, BR buffer; ○—I, □—II, △—III, ◑—IV, ◪—V, and ◒—VI

pH value are shown in Fig. 3. At pH values higher than $pH_{i\ max}$, the half-wave potential of the oxidation wave corresponding to each aldehyde showed a linear relation with the pH value (inclination; −60 mV/pH); this relation shifted to a more negative potential with an increase in the number of carbon atoms in the aldehydes used. At pH values of 4—6, it was also observed that the wave became less steep and that the half-wave potential shifted discontinuously.

The Effect of Concentration of OPD. The relationships between the limiting currents of the condensation products measured 60 min after the addition of OPD at 25°C and the concentration of OPD are shown in Fig. 4, when the concentration of aldehydes was kept constant at the $pH_{i\ max}$ value corresponding to each of the aldehydes. From the data of Fig. 4 and the fact the half-wave potential shifts to a more negative potential with an increase in the concentration of OPD, it may be deduced that the condensation reaction attains

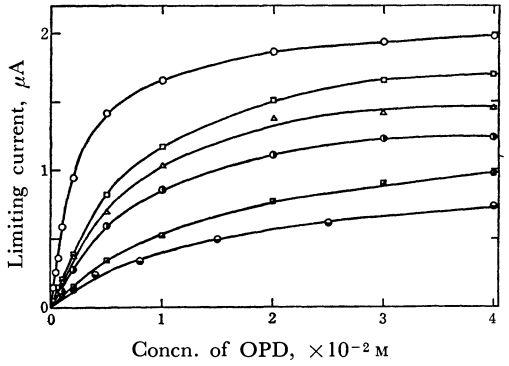

Fig. 4. Relationship between the limiting currents and the concentrations of OPD at 25°C.
Aldehyde: 5×10^{-4} M; Condensation: 60 min in BR buffer with $pH_{i\ max}$; ○—I, □—II, △—III, ◑—IV, ◪—V, and ◒—VI

an equilibrium state.[11] The reaction may be written as follows:

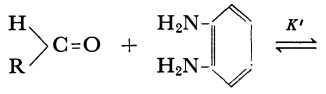

Aldehyde OPD

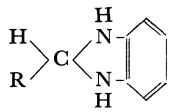

+ H_2O (1)

Benzimidazoline derivative

$R=C_nH_{2n+1}$; n=0, 1, 2, 3, 5, and 7

The equilibrium constants obtained in a manner similar to that previously reported for glyceraldehyde[11] are given in Table 1. Since the equilibrium constants for all the aldehydes are relatively small, for analytical purposes the concentration of OPD in the reaction mixture should be kept in a large excess and should be kept constant.

From the facts that no a. c. polarogram was obtained, except for a small peak which seems to be due to the adsorption, and that no reduction wave was obtained with the oxidation product by means of a controlled-potential electrolysis, the electrode reaction of the condensation products may be concluded to be an irreversible one. Moreover, because the UV-absorption spectra of the electro-oxidation products were in accordance with that of benzimidazole, the electrode process may be expressed as follows:

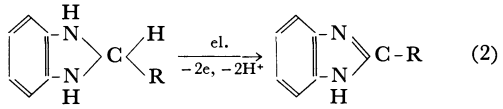

(2)

The discontinuous change in the half-wave potentials at pH values between 4 and 6, as seen in Fig. 3, seems to be due to the change in the electrode process resulting from the protonation of benzimidazoline derivatives.

The Effect of Bubbling Nitrogen. As a result of the volatility of all the aliphatic aldehydes examined, we desired to ascertain the effect of the deoxygenating time on the constancy of the wave heights of the condensation products by bubbling nitrogen. For that reason, a series of measurements were conducted to check the possible effects due to different bubbling times; the results obtained are summarized in Table 2. No remarkable decrease resulting from the volatility of aldehydes by bubbling nitrogen was observed when a large excess of OPD was present in the reaction mixture. However, a discrepancy apparently due to the oxidation of the condensation product by dissolving oxygen was observed. For analytical purposes, therefore, it is necessary to remove the dissolving oxygen by bubbling nitrogen immediately after the preparation of the electrolytic solution.

TABLE 2. INFLUENCE OF BUBBLING NITROGEN ON THE LIMITING CURRENT OF THE CONDENSATION PRODUCT

Acetaldehyde: *ca.* 1.5×10^{-3} M; Condensation: 2×10^{-2} M OPD, 60 min, 25°C, pH 8.2

Time, min		5	10	15	20	30
i, μA	early stage	4.62	4.62	4.58	4.71	4.65
	final stage	4.08	4.14	4.16	4.28	4.35

The Effect of the Temperature. The time required for the condensation shortened upon a rise in the temperature, but at temperatures higher than 30°C it was also observed that the anodic limting current, after attaining its maximum value, decreased with the time. The changes in the wave heights of the condensation products with the temperature at a pH value of 7.5 are shown in Fig. 5. The smaller temperature coefficients than those observed for the diffusion-controlled currents may indicate that the equilibrium of Eq. (1) is shifted more in the dissociation direction with the temperature.

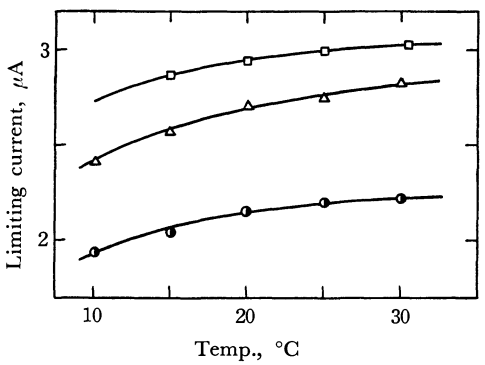

Fig. 5. Effect of the temperature on the limiting currents of the condensation products.
Aldehyde: *ca.* 1×10^{-3} M; Condensation: 2×10^{-2} M OPD, BR buffer (pH, 7.5), 2% ethanol; □—II, △—III, and ◑—IV

Application to the Determination of Aliphatic Aldehyde. On the basis of the experimental facts described above, the following conditions can be recommended for the determination of aliphatic aldehydes by using the oxidation wave of the condensation products with OPD: $pH_{i\ max}$ for pH, 2×10^{-2} M for the concentration of OPD, 25°C for the temperature, and 15—60 min for the condensation time. These recommended conditions are almost the same as those recommended for hydroxyaldehydes in a previous paper.[11] To obtain a better reproducibility, the dissolving oxygen must be removed by bubbling nitrogen for 10 min as soon as possible after the preparation of the electrolytic solution because of the oxidizable property of the condensation product. Under these conditions, linear relations are obtained between the concentrations of all the aldehydes except for

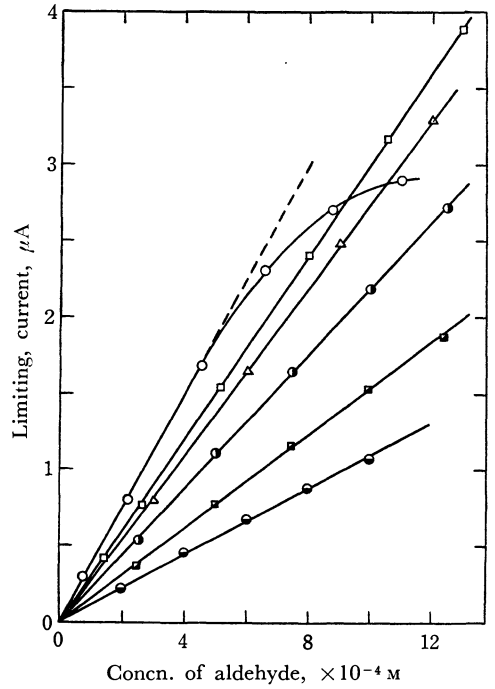

Fig. 6. Relation between the limiting currents of the condensation products and the concentrations of aldehydes in BR buffer at 25°C.
Condensation: 2×10^{-2} M OPD, 30 min;
○—I, □—II, △—III, ◑—IV, ◪—V, and ◒—VI.

I and the limiting currents of their condensation products in the range of $(1—20)\times10^{-4}$ M, as Fig. 6 shows.

The purity of a commercial aqueous solution (about 80%) of II was determined by means of the standard addition method[11] after the proper preliminary dilution of the sample with distilled water free from oxygen, utilizing the optimum conditions previously specified. The results obtained are shown in Table 3, along with those obtained by a modification of Siggia's method.[16] The results obtained by the two methods are in good agreement with each other.

The determination of II in an artificial sample containing II and glyoxal was also carried out; the results of this analysis are listed in Table 4. The presence of glyoxal does not seriously interfere with the determination of II by the polarographic OPD method, but it interferes strongly with the determination of II by the titration method.

The presence of alcohols, carboxylic acids, and esters in the sample does not interfere with the determination of any of the aldehydes examined, since these substances do not show the oxidation wave under the present experimental conditions. Though acetone does show an anodic wave under the present experimental conditions, it does not cause any interference at concentrations of less than 3×10^{-2} M. Sulfite ion strongly interfered with the determination of aliphatic aldehydes. Since the condensation products of all the aliphatic aldehydes and hydroxyaldehydes[11] with OPD behave similarly at the dropping mercury electrode, these aldehydes interfere with the determination of one other.

The present polarographic method is particularly well suited for the determination of aliphatic aldehydes in the presence of some other compounds which are polarographically reducible and not distinguishable by using reduction waves.

TABLE 3. RESULTS OF THE DETERMINATION OF ACETALDEHYDE IN COMMERCIAL PRODUCT

Condensation: 2×10^{-2} M OPD, 25°C, 60 min in BR buffer (pH 8.0)

Exp. No.	Acetaldehyde contents, %	
	Polarographic	Titrimetric*
1	75.5	75.2
2	75.9	76.0
3	75.3	76.0
4	75.6	75.7
5	76.7	76.5
Average	75.8_0	75.8_8

* The modified Siggia's method[16]

TABLE 4. ANALYSIS OF ACETALDEHYDE IN AQUEOUS SOLUTION CONTAINING ACETALDEHYDE AND GLYOXAL

Condensation: 2×10^{-2} M OPD, 25°C, 60 min BR buffer (pH 8.0)

Concn. of carbonyl compds., M		Acetaldehyde found M	
Acetaldehyde	Glyoxal	Polarographic	Titrimetric*
0.134_6	—	0.133	0.134
—	0.0420_8	0	0.0686
0.134_6	0.0420_8	0.135	0.207
0.0269_1	0.0420_8	0.0264	0.101
0.0672_8	0.0841_6	0.0673	0.214
0.0672_8	0.00841_6	0.0668	0.0783

* The modified Siggia's method[16]

Authors are indebted to Mr. Mitsutoshi Ochi for his assistance in the experimental work. Thanks are also due to the Shiono Koryo Kaisha Ltd., for supplying some of the aldehydes used.

16) Sidney Siggia and W. Maxcy, *Ind. Eng. Chem., Anal. Ed.*, **19**, 1023 (1947).

BULLETIN OF THE CHEMICAL SOCIETY OF JAPAN VOL. 41 1583—1587 (1968)

Liquidus Curve Measurements in the ZrO_2-MgO System with the Solar Furnace

Tetsuo NOGUCHI and Masao MIZUNO

Government Industrial Research Institute, Nagoya, Hirate-machi, Kita-ku, Nagoya

(Received October 25, 1967)

A liquidus curve in the system ZrO_2-MgO was investigated by the use of a heliostat type solar furnace. The cooling curves of a composition were obtained by the specular reflection method with a brightness pyrometer. Quenched specimens from the melt were examined with an X-ray technique and a petrographic microscope. Newly found anomalies on the liquidus curve were 7.5, 12.5 and 17.5 mol% MgO compositions. The composition of 12.5 mol% MgO quenched from the melt showed the new cubic-like phase of which optic angle of $2V$ equals to $-74°$ and decomposed easily into monoclinic and tetragonal forms by reheating at 1300°C.

Many papers have been published on the phase study of the ZrO_2-MgO system up to present, and the earlier works on the system were surveyed by Dietzel and Tober[1] in 1953. The melting diagram was first studied by von Wartenberg and Werth[2] in 1928 who proposed two eutectic points with 10 and 48 wt% MgO at about 1630 and 1600°C respectively, and with a maximum point with the composition of ZrO_2·MgO at about 2120°C. Ebert and Cohn[3] claimed that an eutectic point with 50 mol% MgO at 2100°C in 1933, and the same result was also estimated by Zirnowa[4] at 2070°C in 1939. Later the subliquidus phase of the system in ZrO_2 side below 2000°C was investigated by Dietzel and Tober, and also Duwez *et al.*[5] in 1952. Recently the phase boundary of the cubic ZrO_2 solid solution above 2000°C was reported by Hinz and Dietzel[6] in 1962, and by Viechnicki and Stubican[7] in 1965 respectively.

However, the data on the liquidus curve on the system with sufficient accuracy have not been published yet. The authors reported on the high temperature phase in ZrO_2-CaO system using a heliostat type solar furnace previously[8] and anomalies on the liquidus curve were found in ZrO_2 rich side region. This paper relates to the liquidus curve measurement on the ZrO_2-MgO system, in which the behaviors of magnesia are similar to those of calcia in the stabilization of zirconia refractory.

Equipment and Materials

The temperature and emissivity measurements were performed with the brightness pyrometer at 0.65 μ by the specular reflection method as reported by the author previously.[9] The standard deviation derived in the transmission measurement of the grey filter in the pyrometer was 1.7% and therefore the recorded value was estimated to be reliable within the error of about 2% as an amount of radiant energy. This corresponds to 10° at 3000°K and 15° at 4000°K calculating from Planck's equation respectively. These values were verified by the calibration with the tungsten filament standard lamp at the focal plane of the solar furnace, and the accuracy of the brightness pyrometer at 3237°K was within $\pm 7°$.[10] The accuracy of derived temperatures in this experiment was thus estimated to be within $\pm 20°$ at 3000°K and $\pm 15°$ at 2000°K including the reading errors of oscillograms. The heliostat type solar furnace used was the combination of the paraboloid of 1.5 m in diameter and 64 cm of focal length, and the heliostat plane mirror of 2.4×2.4 m with sixteen segments of front coated glass. The optical axis of the paraboloidal mirror was fixed horizontally.

Materials used were ZrO_2 of 99.8% purity from the Yokozawa Chemicals Co., Tokyo (including about 1.8% of HfO_2, and ignition loss, 0.05; Cl, 0.04; SO_4, 0.008; Fe, 0.001%) and MgO of 99.7% from the Kanto Chemicals Co., Ltd., Tokyo (ignition loss, 0.11; Cl, 0.002; heavy metal, 0.002; Fe, 0.0004; Zn, 0.002; Ba, 0.0025; Ca, 0.102%). The starting materials were carefully mixed in an agate mortar, calcined in an electric resistance furnace at 1700°C for 6 hr by two heating and grinding cycles, and pressed into $6 \times 6 \times 35$ mm bar under 4000 kg/cm^2 without any lubricant or binder.

1) A. von Dietzel and H. Tober, *Ber. Dtsch. Keram. Ges.*, **30**, 47 (1953).
2) H. von Wartenberg and H. Werth, *Z. anorg. u. allgem. Chem.*, **190**, 178 (1930).
3) F. Ebert and E. Cohn, *ibid.*, **213**, 321 (1933).
4) N. Zirnowa, *Zhur. Priklad. Khim.*, **12**, 1278 (1939).
5) P. Duwez, F. Odell and F. H. Brown, Jr., *J. Am. Ceram. Soc.*, **35**, 107 (1952).
6) I. Hinz and A. Dietzel, *Ber. Dtsch. Keram. Ges.*, **39**, 530 (1962).
7) D. Viechnicki and V. S. Stubican, *J. Am. Ceram. Soc.*, **48**, 292 (1965).
8) T. Noguchi, M. Mizuno and W. M. Conn, *J. Solar Energy*, **11**, 136 (1967).
9) T. Noguchi and T. Kozuka, *ibid.*, **10**, 125 (1966).
10) S. Takada, H. Ito, T. Noguchi and T. Kozuka, *Report Nat. Res. Lab. Metrology*, **16**, 206 (1967).

Eleven specimens in 10 mol% MgO increments and nine specimens in 2.5 mol% increments from 2.5 to 30 mol% were prepared by the heat treatment as referred to the previous study on ZrO_2-CaO system. Four specimens in 5 mol% MgO increments from 30 to 70 mol% were also added to confirm the eutectic points.

Results and Discussion

Freezing Point Measurement. On the sun's image of 6 mm in diameter on the specimen surface, the variation of the brightness temperature in the area of 0.25 mm ϕ was measured with the brightness pyrometer. The cooling curves of the specimen were obtained with the dual-beam cathode-ray oscilloscope (Multiscope VP 541 A) attached with the Polaroid camera and were shown schematically in Fig. 1. The freezing and melting temperatures of the specimen were also confirmed by the visual observation through the ocular lens of the pyrometer and by the data from the automatic voltage recorder. The cooling rate of the specimens was estimated from 1800 to 2300 deg/sec. The exothermic peak observed after the freezing point might be ascribed to the phase transformation in solid state.

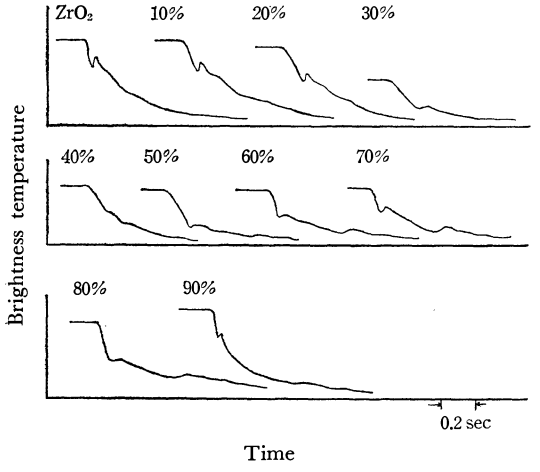

Fig. 1. Cooling curves of the composition in ZrO_2-MgO system.

ZrO_2 showed two weak exothermic peaks accompanied with the crystallization and the similar phenomenon was observed up to 25 mol% MgO composition. In the fusion of MgO specimen vigorous vaporization was observed and failed to give the emissivity data. Only the brightness temperature of the freezing point was hardly obtained and it was difficult to hold the specular reflection surface because of the deposition of vaporized magnesia on the specimen surface. No correction for transmission of magnesia vapor was also possible.

Figure 2 represents the freezing point data obtained in the ZrO_2-MgO system. The freezing point is indicated as the true temperature and both of the 2nd and the 3rd exothermic peaks observed in solid state are indicated by the brightness temperature. The mean value of forty to fifty individual readings on the freezing point is listed in Table 1 with the spectral emissivity data at 0.65 μ. Only the freezing point of MgO was cited from the

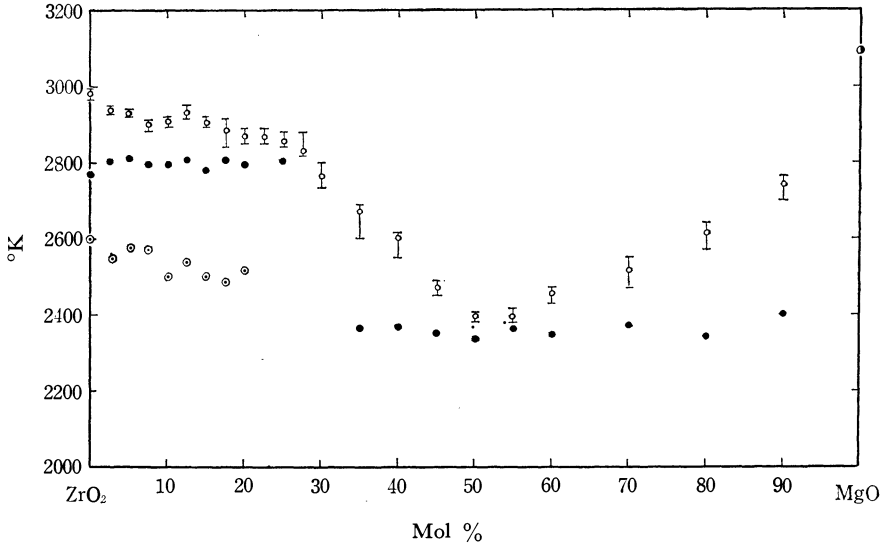

Fig. 2. Freezing point data in the ZrO_2-MgO system.

- ● The 2nd exothermic peak in solid state
- ○ Freezing point
- ⊙ The 3rd exothermic peak in solid state
- ◑ Cited from McNally *et al.*

TABLE 1. FREEZING POINT DATA OF ZrO_2-MgO SYSTEM

Composition ZrO_2 (mol%)	MgO (mol%)	Freezing point (±20°C)	Spectral emissivity at 0.65 μ	Temperature* of exothermic peaks in solid state (°C)	
97.5	2.5	2660	0.89	2528	2270
95	5	2647	0.90	2525	2295
92.5	7.5	2622	0.92	2512	2296
90	10	2632	0.95	2513	2224
87.5	12.5	2650	0.86	2531	2259
85	15	2633	0.94	2501	2217
82.5	17.5	2598	0.88	2518	2212
80	20	2594	0.90	2517	2235
77.5	22.5	2589	0.94	2532	
75	25	2576	0.91	2530	
72.5	27.5	2547	0.90		
70	30	2486	0.93		
65	35	2403	0.87	2078	
60	40	2329	0.90	2090	
55	45	2196	0.93	2073	
50	50	2121	0.90	2080	
45	55	2113	0.93	2054	
40	60	2171	0.96	2064	
30	70	2230	0.95	2087	
20	80	2332	0.96	2054	
10	90	2458	0.93	2116	

* These values were calculated as brightness temperature.

literature[11] because of the difficulty in obtaining the emissivity data and accordingly the true temperature. Anomalies not reported in the liquidus curve previously were found to be at 7.5, 12.5 and 17.5 mol% MgO compositions, showing the maximum point at 12.5 mol%. The tendency of this type was similar to those in ZrO_2-CaO system in ZrO_2 side region, though the maximum point shifted to 7 mol% CaO composition.

It should be noted that the solid state reaction observed in some of these cooling curves in the ZrO_2 rich side region could not be suppressed by the quenching rate as in this study. Since the specimen is heated from its surface at the focus of the solar furnace, the liquid phase formed at the solar image is surrounded by the solid even if the thermal equilibrium is obtained. Therefore, the solid crystal under the liquid layer might become the nuclei on crystallization and accelerate the growth of crystals in the cooling process.

Stoichiometry. The specimen for chemical analysis was prepared with the solar furnace in such a way that a test bar was fused at about 100°C higher than the respective melting temperature for 3 min before quenching. Since the necessary time for each measurement of cooling curve was within 10 sec and repeated measurements across the sun's image were made on five different points in three times, simulation for the heat treatment of a specimen might be considered satisfactory.

The weighed sample of about 50 mg in a platinum crucible was fused with the addition of tenfold sodium pyrosulfate. The extraction with dil. H_2SO_4 (5%) was neutralized with NH_4OH by the addition of NH_4Cl. The pH of the filtrate was then adjusted to 10 and the sample solution was titrated with EDTA solution by the aid of KCN and BT indicator. The results obtained are shown in Table 2 and the deviation of MgO component is clearly observed. These data differ from those claimed by Hinz and Dietzel who applied the argon plasma torch because of the estimated heating temperature of more than 5000°K.

TABLE 2. CHEMICAL ANALYSIS OF QUENCHED SPECIMENS FROM THE MELT BY CHELATE TITRATION IN THE ZrO_2-MgO SYSTEM

Sample	MgO content (Theoretical) wt%	MgO content (Determined) wt%	MgO content (Determined) mol%	Difference mol%
M 10	3.51	3.00	8.64	−1.36
M 30	12.29	9.65	24.61	−5.39
M 40	17.91	14.57	34.26	−5.74
M 50	24.66	21.27	45.22	−4.78
M 60	32.92	29.58	56.21	−3.79
M 70	43.29	36.56	63.78	−6.22
M 90	74.65	62.79	83.76	−6.24

The vaporization rates at melting temperatures for ZrO_2, 50 mol% MgO composition and MgO specimens which were prepared by sintering at 1700°C for 3 hr are 5.3×10^{-4}, 2.3×10^{-3}, and 9.0×10^{-3} g/cm^2 min respectively. These values were obtained by heating the specimen of about 1.5 g and were estimated from the weight decrease in 10 min. Even for the short heating duration as in the experiment, the vaporization of MgO can not be suppressed in air because of the high vapor pressure near the melting point.

X-Ray Analysis of Quenched Specimens from the Melt. The quenched specimens were examined by X-ray technique using a diffractometer of the Shimadzu Diffraction Unit GX-3 and nickel filtered Cu$K\alpha$ radiation. High temperature diffraction patterns were obtained using the Shimadzu HX-II model whose hot stage consists of a platinum-rhodium wound heating element encased in an alumina refractory sleeve. The temperature measurement was made with a platinum *versus* platinum-10% rhodium thermocouple. The results of the powder diffraction patterns of the quenched specimens are shown in Table 3, and sufficient explanation on the anomalies in the liquidus curve was not obtained.

In ZrO_2 rich side region up to 15 mol% MgO composition, the diffraction patterns showed broadening and were not identified as cubic form.

11) R. N. McNally, F. I. Peters and P. H. Ribbe, *J. Am. Ceram. Soc.*, **44**, 491 (1961).

Table 3. X-ray diffraction data of quenched specimens in ZrO_2-MgO system

Composition MgO mol%	Phase present after quenching		
2.5	M(s)		
5.0	M(m)	C*(m)	
7.5	M(vw)	C*(s)	
10.0	M(vvw)	C*(s)	
12.5		C*(s)	
15.0		C (s)	
17.5		C (s)	
20.0		C (s)	
25.0		C (s)	
30		C (s)	MgO(vw)
35		C (s)	MgO(vw)
40		C (s)	MgO(m)
50		C (s)	MgO(m)
60		C (s)	MgO(m)
70		C (s)	MgO(s)
80		C (s)	MgO(s)
90		C (m)	MgO(s)

M: Monoclinic ZrO_2 solid solution,
C: Cubic ZrO_2 solid solution,
C*: Cubic not resolved.

The slow scan pattern of 12.5 mol% MgO composition at 2θ 1/8° min gave no extra reflection up to 2θ 160°, as compared with that of 7 mol% CaO composition. Cubic zirconia was widely observed in the system except the ZrO_2 rich side region. Periclase coexisted from 30 mol% MgO composition through MgO side.

The lattice parameters of cubic zirconia solid solution were obtained from diffraction lines with $2\theta > 85°$ on 12.5 to 70 mol% MgO compositions and the boundary for the cubic zirconia solid solution in the quenched specimen from the melt was located at about 25.5 mol% MgO as shown in Fig. 3, almost identical to the results claimed by Duwez *et al.* at 2000°C. It might be assumed that the solid solution boundary for cubic zirconia above 2000°C up to melting temperature was vertical.

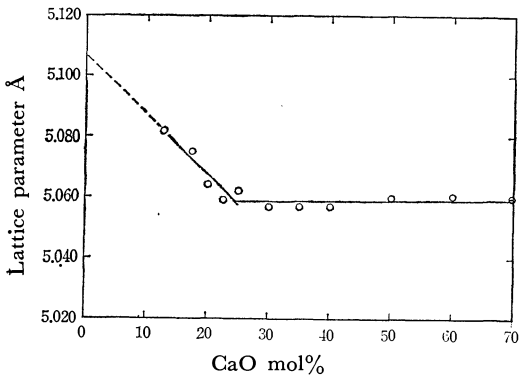

Fig. 3. Lattice parameters of cubic ZrO_2 solid solution.

The lattice parameters of magnesia from 40 to 100 mol% MgO were measured with diffraction lines with $2\theta > 95°$ and were constant at 4.211 Å. Very narrow region for the tetragonal zirconia solid solution *i. e.* the solid solution boundary between tetragonal zirconia and tetragonal zirconia plus magnesia might be assumed at less than 5% of MgO from the results in Table 3.

High temperature X-ray diffraction patterns on the quenched specimens of 5, 10, 12.5, 17.5 and 30 mol% MgO compositions were obtained on 2θ 20—45° and with heating and cooling rates of 20°C/min from 500 to 1300°C. No remarkable change was observed at the heating process and the tetragonal form was not found even at 1250°C except 5 mol% composition. However, in the specimens of 5, 10, 12.5 and 17.5 mol% MgO compositions the monoclinic form appeared at 900—850°C on cooling, and a decomposition of the 12.5 mol% MgO composition into tetragonal and monoclinic forms was observed as in the case of 7 mol% CaO composition.

Microscopic Observation on the Quenched Specimens. The thin section of the quenched specimens in ZrO_2 rich side region from the melt was examined by the petrographic microscope. The analytical data are shown in Table 4.

Table 4. Microscopic data on zirconia modifications in the quenched specimens in ZrO_2-MgO system

Composition MgO mol%	Monoclinic	Tetragonal	Biaxial negative $2V=-74°$	Isotropic cubic
2.5	+++++			
3	+++	++		
4	++	+++		
6		+++	+++	±
8		+	++++	±
10			+++++	
12.5			+++++	
15			++	++−

The biaxial negative crystals were found besides the monoclinic, tetragonal and cubic forms. The optic angle of the crystals was $2V=-74°$ and different to that of the monoclinic form of $-30°$. The single phase of this modification is limited at about 12.5 mol% MgO composition and Fig. 4 shows the photomicrographs of 3, 12.5 and 15 mol% MgO compositions quenched from the melt. Thus the new cubic like phase might be assumed to be rhombic modification rather than the distorted cubic lattice, though the verification of the presence of this form was not possible by the X-ray diffraction data.

Liquidus Curve in the ZrO_2-MgO System. The liquidus curve obtained by the freezing point measurements was corrected in relation to the

a) 3 mol% MgO composition

b) 12.5 mol% MgO composition

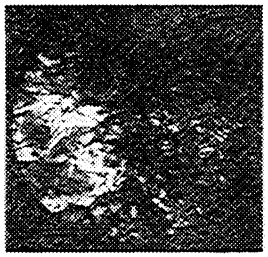

c) 15 mol% MgO composition ×180 Crossed nicols.

Fig. 4. Photomicrographs of the thin section of zirconia modifications in the specimens quenched from the melt.

chemical analysis of the quenched specimens from the melt and is shown in Fig. 5 with that of the ZrO_2-CaO system. The characteristic anomaly in ZrO_2 rich side region shifts to about 10 mol% MgO. The behaviors of MgO in this region at higher temperatures were not understood sufficiently because of the lack of knowledge on the crystal modification above 2300°C to present the complete phase diagram on the system. However, the maximum point observed in ZrO_2 rich side region might indicate the existence of a new cubic like phase, which decomposed easily after reheating into monoclinic and tetragonal forms. The anomalies in this

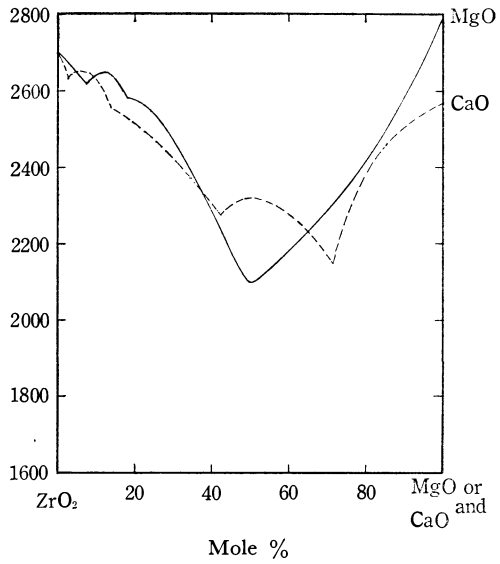

Fig. 5. Liquidus curve in the system ZrO_2-MgO.

experiment were not reported by the previous investigators. Ebert and Cohn[3] have assumed an peritectic point in this region without experimental evidences, however, the accuracy of temperature measurement by them was not described clearly, and it might be estimated within ±50°C at more than about 2500°C by a visual observation method. The eutectic point was found at 50 mol% MgO at 2113 ±15°C. And the other compound such as $Mg_2Zr_3O_8$ or $MgZr_3O_7$ reported in the earlier literatures[1] were not confirmed from this experiment. It is noted that the phase study in ZrO_2 rich side region above 2300°C should be further developed.

The authors wish to express their appreciation to Dr. H. Hayashi for his support in the chemical analysis and microscopic work.

BULLETIN OF THE CHEMICAL SOCIETY OF JAPAN VOL. 41 1588—1600 (1968)

An Experimental Study on the Role of Water Vapor in the Distribution of Fluorine and Chlorine in Volcanic Rocks

Tsutomu SUGIURA*1

Department of Earth Sciences, Nagoya University, Chikusa, Nagoya

(Received December 2, 1967)

Fluorine and chlorine contents of volcanic rocks were examined with respect to the characteristics of the rocks. Fluorine showed rather linear relationships with some chemical components of the rocks and also with stages in the differentiation of magmas. But any universal relationship covering all the rock types was not found. The cause of this fact is expected to be the loss of halogens from rocks resulted from the interaction between rocks and water vapor, which is believed to be ubiquitous in magma and is gradually emanated from it during or after the formation of rocks. So, in order to make clear the role of water vapor in the distribution of halogens in rocks, the author has distilled fluorine and chlorine from rock samples with water vapor at elevated temperatures and studied following relations; (1) the relationship between the amount of distilled halogens and the fluorine and chlorine contents of the rocks, and (2) the relationship between the amount of distilled halogens and the characteristics of the rocks. In distillation of fluorine and chlorine with water vapor, almost all fluorine remained in each rock specimen at low temperatures below 300°C, and at temperatures above 700°C the ratio of the amount of distilled fluorine to the initial amount of fluorine in rocks fluctuated among specimens. However, there was no relation between patterns of the distilled fluorine and the fluorine content of the rocks, and also the characteristics of the rocks. Meanwhile, distillation curve of chlorine showed various patterns without having any relation to chlorine content of the rocks, and indicated that chlorine was retained more in basic rocks than in acidic rocks at higher temperatures, although no relation was observed between the chlorine content of the rocks and the characteristics of the rocks. Generally the ratio of distilled fluorine to initial fluorine in rocks is smaller than the ratio of distilled chlorine to initial chlorine in rocks at low temperatures. The results of the distillation experiments suggest that the distillation process of halogens with water vapor controlls the distribution of halogens in volcanic rocks more than does the chemical and mineralogical nature of the rocks.

Fluorine and chlorine contents of volcanic rocks are known to vary in wide range from nearly zero to a few thousand ppm. The cause of the variation is not yet exactly known. Many investigators have attempted to find relationships between the halogen contents and the characteristics of the rocks. The relationship between chlorine and silica in rocks is controversial. According to Goldschmidt,[1] Simonen,[2] Behne[3] and others, chlorine is generally more abundant in acidic rocks than in basic rocks. Kuroda and Sandell,[4] Iwasaki *et al.*[5] Correns[6] and others, however, reported no marked association of chlorine with silica in rocks. From the mineralogical point of view, all the fluorine seemed to be fixed in apatite in the case of basaltic rocks.[7] Neverthless, Koritnig,[8] Iwasaki *et al.*[9,10] reported that the concentrations of fluorine and chlorine in rocks could not be explained from their amounts in apatite. Iwasaki and Katsura[11] experimentally concluded that the solubility of hydrogen chloride in volcanic rock melts was reciprocal to the silica content of the melts. The analytical results in Miyakejima leva flow, however, were inconsistent with the experiments mentioned above[12]; that is, the

*1 Present address: Department of Chemistry, Aichi Kyoiku University, Higashi, Nagoya, Japan.

1) V. M. Goldschmidt, "Geochemistry," Clarendon Press, Oxford (1954).
2) A. Simonen, *Bull. Comm. Geol. Finlande,* **143**, 1 (1948).
3) W. Behne, *Geochim. et Cosmochim. Acta,* **3**, 186 (1953).
4) P. K. Kuroda and E. B. Sandell, *Bull. Geol. Soc. Am.,* **64**, 879 (1953).
5) I. Iwasaki, K. Katsura, N. Sakato and K. Hirayama, *Nippon Kagaku Zasshi (J. Chem. Soc. Japan, Pure Chem. Sect.),* **78**, 164 (1957).
6) C. W. Correns, "The Physics and Chemistry of the Earth," Vol. 1, Pergamon Press, London (1956).
7) T. Barth, *J. Geol.,* **55**, 420 (1947).
8) S. Koritnig, *Geochim. et Cosmochim. Acta,* **1**, 89 (1951).
9) B. Iwasaki, This Bulletin, **38**, 992 (1965).
10) B. Iwasaki and T. Katsura, *ibid.,* **37**, 1827 (1964).
11) B. Iwasaki and T. Katsura, *ibid.,* **40**, 554 (1967).
12) B. Iwasaki, Read at the Meeting of the Geochemical Society of Japan, October, 1967.

chlorine concentration in the lava flow is generally higher in acidic rocks than in basic rocks. According to Yoshida *et al.*,[13] the variation in halogen contents of rocks placed in volcanic gases containing much halogens is independent of rock types. Anyway, essential factor affecting halogen contents of volcanic rocks is not decided so far.

Possible factors controlling halogen contents of volcanic rocks may be roughly classified into two groups. One group consists of factors concerning the characteristics of rocks, such as chemical, physical and petrological nature of rocks. The other comprises physico-chemical conditions of environments during or after the formation of rocks.

In the present research, it is aimed to make clear experimentally whether or not the former, the characteristics of the rocks, actually affect the halogen contents of rocks, even in the case where water vapor contained in magma emanates from rocks during or after the formation of rocks. First of all in this study, the distribution of fluorine and chlorine in rocks has been examined with relation to the characteristics of the rocks, such as magma types, rock types, solidification index of rocks and so on. The distribution of halogens in rocks was, thereby, supposed to be more affected by water vapor than the characteristics of the rocks. So, to ascertain the role of water vapor in the distribution of halogens in rocks, the author has heated the rocks in the presence of water vapor at temperatures from 100 to 900°C, and examined the mutual relationships among the amounts of halogens distilled from the rocks with water vapor at elevated temperatures and their concentrations in the rocks and the characteristics of the rocks. For this study, a systematic investigation has necessarily been made for series of rocks differentiated from the same magma; alkaline rocks collected at Okinoshima, Ehime Prefecture, hypersthenic and pigeonitic rocks sampled at Hakone, Kanagawa Prefecture and Oshima, Tokyo Metropolitan, which were already studied chemically and petrologically by Uchimizu[14] and Kuno.*2

Nagashima[15] reported that fluorine was more enriched in hypersthenic rocks than in pigeonitic rocks. Kokubu,[16] on the contrary, mentioned that there is no marked difference in fluorine content of rocks between them. The ranges of fluorine content*3 of rocks studied in the present study were from 40 to 200 ppm for pigeonitic rocks, from 150 to 240 ppm for hypersthenic rocks and from 70 to 980 ppm for alkaline rocks. From these figures, it may be concluded that there is no significant difference in fluorine content between pigeonitic rocks and hypersthenic rocks. Meanwhile, most alkaline rocks contain far much amount of fluorine as compared with other rocks. Chlorine content*4 ranges from 30 to 170 ppm in pigeonitic rocks, from 70 to 180 ppm in hypersthenic rocks and from 10 to 380 ppm in alkaline rocks. The value of 380 ppm chlorine in an alkaline rock is exceedingly larger than the values in other alkaline rocks, and most of the chlorine in this specimen is in water-soluble state. Excluding this value, the range of chlorine in alkaline rocks is from 10 to 175 ppm, which is nearly the same as those in rocks of other types. Although fluorine and chlorine are volatile constituents in rock melts and are expected to behave similarly, no relationship is observed between fluorine and chlorine contents, as shown in Table 1. They are also independent of the values of (+) H_2O and (−) H_2O in rocks. As mentioned above, some authors have claimed that fluorine and chlorine are generally concentrated in acidic rocks rather than in basic rocks. The total chlorine analyzed here, however, has no relation to silica content for any

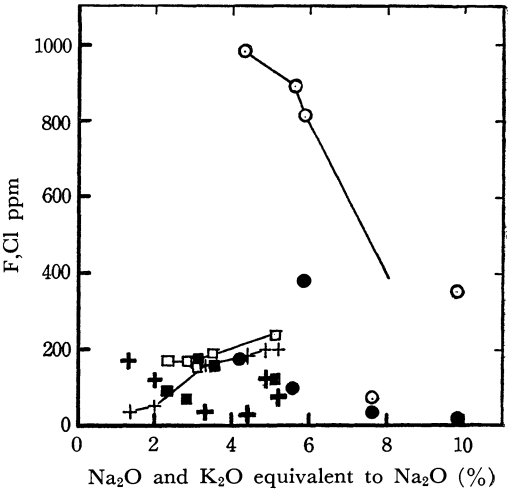

Fig. 1. Relationship between the fluorine and chlorine contents of rocks and alkaline elements (Na and K).

A.R.S. {-○-: F, -●-: Cl} P.R.S. {-+-: F, -+-: Cl}

H.R.S. {-□-: F, -■-: Cl}

13) M. Yoshida, T. Ozawa and J. Ossaka, Read at the Meeting of the Geochemical Society of Japan, October, 1967.

14) M. Uchimizu, *J. Fac. Sci. Tokyo Univ.*, **16**, 85 (1966).

15) K. Nagashima, *Bull. Fac. Agr., Tokyo Univ. of Agriculture and Technology*, **1**, No. 2, 1 (1953).

16) N. Kokubu, *Memoirs of the Faculty Sci. Ser. C. Chemistry, Kyushu Univ.*, **2**, No. 3, 96 (1956).

*2 References are given in remarks attached to Table 1.

*3 Fluorine was separated from other chemical elements by distillation, and determined colorimetrically by the method of Grimaldi *et al.*[20]

*4 Total chlorine and water soluble chlorine were determined by the method reported in a previous paper.[21]

TABLE 1. CHEMICAL AND NORMATIVE COMPOSITIONS OF

Specimen number Rock type	A. R. S. 1 basalt	A. R. S. 2 mugearite	A. R. S. 3 andesite	A. R. S. 4 trachyte	A. R. S. 5 rhyolite	P. R. S. 1 basalt	P. R. S. 2 basalt
Chemical composition (%)							
SiO_2	48.90	50.54	60.32	61.57	71.87	51.02	51.25
Al_2O_3	16.73	14.44	15.65	17.95	13.33	14.39	14.73
Fe_2O_3	2.30	3.58	3.79	3.19	1.30	3.17	3.82
FeO	8.26	8.24	2.51	2.39	0.99	9.98	10.22
MgO	7.49	3.08	1.96	0.07	0.05	7.48	5.47
CaO	8.22	6.98	4.82	0.87	0.31	11.35	11.73
Na_2O	3.23	3.75	3.52	6.25	4.03	1.29	1.85
K_2O	1.81	2.91	3.38	5.35	5.44	0.15	0.26
H_2O (+)	0.52	2.38	1.05	1.20	2.00	0.32	0.11
H_2O (−)	0.25	1.15	1.15	0.75	0.30	0.25	0.02
TiO_2	2.54	2.64	1.05	0.37	0.22	0.79	0.81
P_2O_5	0.10	0.34	0.51	0.06	0.06	0.07	0.13
MnO	0.16	0.21	0.10	0.15	0.03	0.23	0.28
SrO	—	—	—	—	—	—	—
Norme (%)							
Q	—	—	16.08	2.28	24.47	5.87	18.36
C	—	—	—	0.41	0.11	—	—
Or	10.62	17.38	19.35	31.58	30.52	0.89	7.23
Ab	25.57	31.70	29.19	52.58	38.88	10.91	25.15
An	25.80	13.98	19.15	4.03	—	33.04	23.35
Ne	0.40	—	—	—	—	—	—
Wo	6.01	7.68	1.10	—	—	9.53	3.60
En	3.75	6.26	4.09	0.17	—	18.62	8.30
Fs	1.89	6.77	—	1.43	1.56	14.81	7.13
Fo	10.39	0.97	—	—	—	—	—
Fa	5.79	1.12	—	—	—	—	—
Mt	3.34	5.20	3.97	4.64	1.79	4.61	4.87
Hm	—	—	1.41	—	—	—	—
Il	4.83	5.02	2.05	0.70	0.43	1.51	1.98
Ap	0.26	0.79	1.18	0.15	1.86	0.17	0.34
Halogen contents (ppm)							
F	980	890	810	350	70	40	50
Cl (total)	175	100	380	10	40	170	120
Cl (soluble)	35	15	295	10	40	155	40
Cl (insoluble)	140	85	85	0	0	15	80
F/Cl (total)	5.6	8.9	2.1	35	2.8	0.2	0.4
F/Cl (insoluble)	7.0	10.5	9.5	—	—	2.7	0.6

A. R. S. 1=no. 10, *J. Fac. Sci., Univ. Tokyo*, **16**, 60 (1966) (by Uchimizu).
A. R. S. 2=no. 11, *ibid.*, 61.
A. R. S. 3=no. 15, *ibid.*, 61.
A. R. S. 4=no. 18, *ibid.*, 61.
A. R. S. 5=no. 30, *ibid.*, 62.
P. R. S. 1=HK 36092301b, *J. Petrol.*, **6**, 304 (1965) (by Kuno).
P. R. S. 2=d, *Bull. Geol. Soc., Am.*, **61**, 1005 (1950) (by Kuno).
P. R. S. 3=21, *ibid.*, 1004.
P. R. S. 4=23, *ibid.*, 1004.

magma type. Meanwhile, fluorine content generally increases with increasing silica in both pigeonitic and hypersthenic rocks; but the trend is reverse in alkaline rocks; namely, fluorine obviously decreases with increasing silica.

Kogaruko and Gulyayeva[17] reported that alkaline elements in rocks make it difficult for halogens to diffuse from rocks. As shown in Fig. 1, the relation between alkali (Na and K) and chlorine

17) L. N. Kogaruko and L. A. Gulyayeva, *Geokhimiya*, 1011 (1965).

ROCKS, AND FLUORINE AND CHLORINE CONSTENTS OF ROCKS

P. R. S. 3 andesite	P. R. S. 4 andesite	P. R. S. 5 andesite	P. R. S. 6 tuff br.	H. R. S. 1 basalt	H. R. S. 2 andesite	H. R. S. 3 andesite	H. R. S. 4 andesite	H. R. S. 5 dacite
56.54	65.54	67.37	75.85	49.08	55.62	57.07	62.25	76.05
15.49	15.33	15.28	11.45	17.68	16.91	17.53	15.85	12.79
4.58	1.69	1.13	1.40	2.33	2.02	2.59	2.06	1.47
7.09	4.51	3.86	1.26	8.00	6.24	5.44	5.19	0.31
3.00	1.45	1.20	0.50	8.02	5.87	3.87	2.79	0.08
7.33	4.75	4.46	2.42	10.26	8.63	8.77	7.21	1.60
2.98	3.89	4.67	4.11	2.02	2.98	2.80	2.20	3.89
0.55	0.84	0.92	1.39	0.35	0.72	0.52	0.97	1.82
0.35	0.68	0.14	0.53	—	0.35	0.27	0.21	0.74
0.72	0.50	0.09	0.07	—	0.05	0.12	0.31	0.52
0.96	0.89	0.72	0.46	0.90	0.86	0.77	1.14	0.19
0.08	0.21	0.18	0.19	n. d	0.24	0.08	0.06	tr.
0.22	0.19	0.15	0.11	0.25	0.14	0.14	0.18	0.05
—	—	—	0.26	n. d	—	—	0.09	—
15.45	25.56	24.06	41.52	—	7.32	13.68	24.72	42.96
—	—	—	—	—	—	—	—	—
3.34	5.00	5.56	8.34	2.22	4.23	2.78	5.56	10.56
25.15	33.01	39.30	34.58	16.77	25.22	23.85	18.34	33.01
27.24	21.68	18.07	8.62	38.36	30.66	33.92	30.68	8.06
—	—	—	—	—	—	—	—	—
3.48	0.46	1.39	1.04	5.22	4.48	3.60	2.20	1.43
7.50	3.60	3.00	1.20	18.70	14.62	9.70	6.90	0.20
8.06	5.81	5.28	0.40	11.09	8.62	6.73	6.30	0.00
—	—	—	—	0.98	—	—	—	—
—	—	—	—	0.61	—	—	—	—
6.73	2.55	1.62	2.09	3.25	2.92	3.71	3.02	0.46
—	—	—	—	—	—	—	—	—
1.82	1.67	1.37	0.91	1.67	1.64	1.52	2.13	0.46
0.34	0.11	0.34	0.11	—	0.57	—	—	1.12
160	180	200	200	170	190	150	170	240
30	30	80	125	90	155	180	70	120
20	20	30	60	50	65	30	10	50
10	10	50	65	40	90	150	60	70
5.3	6.0	2.5	1.6	1.9	1.2	0.8	2.4	2.0
16.0	18.0	4.0	3.0	4.2	2.1	1.0	2.8	3.4

P. R. S. 5=banded lava of Hakone volcano, high way between Ashinoyu and Gannosuyama, Hakone, Kanagawa Pref.
P. R. S. 6=11, Catalogue of the Active Volcanoes of the World, Part XI, p. 77 (by Kuno).
H. R. S. 1=2, *J. Fac. Sci. Univ. Tokyo*, **9**, 258 (1955) (by Kuno).
H. R. S. 2=HK 62090502, *J. Petrol.*, **6**, 308 (1965) (by Kuno).
H. R. S. 3=14, *Bull. Geol. Soc. Am.*, **61**, 1000 (1950) (by Kuno).
H. R. S. 4=lava-flow of Hakone volcano, west-side slope of north road of Hatajyuku, Hakone, Kanagawa Pref.
H. R. S. 5=18, *Bull. Geol. Soc. Am.*, **61**, 1001 (1950) (by Kuno).

is not clear for any magma type: On the other hand, fluorine increases with the concentration of the alkaline elements in pigeonitic and hypersthenic rocks, and decreases in alkaline rocks, just like the relationship between fluorine and silica in rocks.

Fluorite is the most stable among simple fluorine compounds and is often found in volcanic rocks. A positive relationship between fluorine and calcium contents, however, is observed only in alkaline rocks.

Mica, amphibole and apatite are generally

considered to be important halogen containing minerals in volcanic rocks. Halogens are easily incorporated in their crystal lattices. Unfortunately, the amount of these minerals in the samples used here were not quantitatively measured except for the calculation of normative apatite. The fluorine and chlorine contents were plotted against the phosphate content of rocks in Fig. 2. A line drawn in the figure shows the relationship between fluorine content and the amount of apatite, assuming that all of phosphate exists as apatite. The relationship between apatite and fluorine is not generally observed, although the relation seemingly exists in pigeonitic rocks. Moreover, no correlation is seen between the amount of apatite and chlorine in rocks. Although the halogen contents of mica and amphibole were not determined

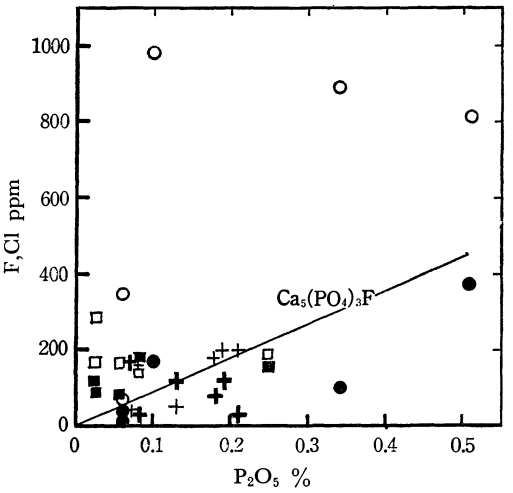

Fig. 2. Relationship between fluorine, chlorine contents and P_2O_5 content of rocks.

A. R. S. {-○-: F, -●-: Cl} P. R. S. {-+-: F, -+-: Cl}

H. R. S. {-□-: F, -■-: Cl}

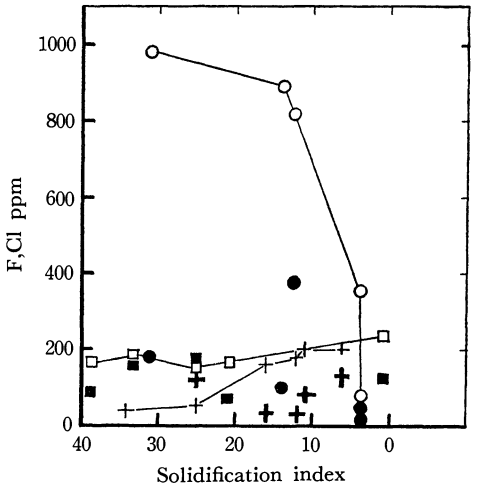

Fig. 3. Relationship between the fluorine and chlorine contents and solidification index of rocks (solidification index=MgO×100/MgO+FeO+Fe_2O_3+Na_2O+K_2O).

A. R. S. {-○-: F, -●-: Cl} P. R. S. {-+-: F, -+-: Cl}

H. R. S. {-□-: F, -■-: Cl}

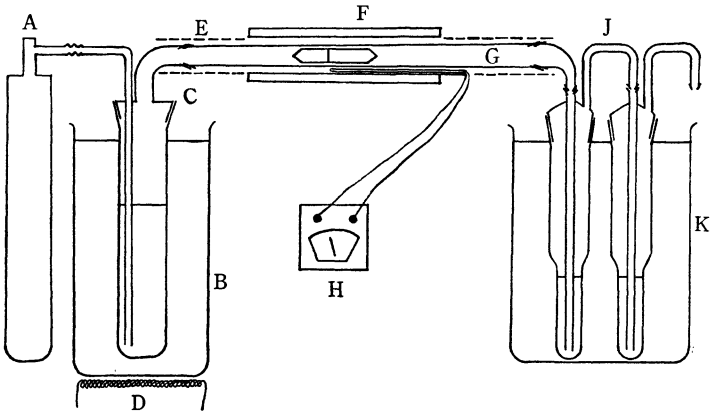

Fig. 4. Apparatus to distill halogens in rocks.

A: Commercial nitrogen gas tank.
B: 1 *l* beaker filled with water boiled with heater D.
C: Glass-vessel containing distilled water.
D: Heater.
E: Glass-heater.
G: Silica-glass-tubing (60 cm in length, 2 cm in inside diameter).
H: Thermocouple.
I: Silica-glass-boat (10 cm in length, 1.4 cm in inside diameter).
J: Absorption vessel.
K: 1 *l* beaker filled with cold water.

TABLE 2. REPRODUCIBILITY OF THE DISTILLATION METHOD
(sample: A. R. S.)

Temp. °C	Experiment 1		Experiment 2		Experiment 3	
	F ppm	Cl ppm	F ppm	Cl ppm	F ppm	Cl ppm
100	0	10	0	10	0	10
200	0	10	0	10	0	10
300	0	10	0	10	5	10
400	27	10	16	10	26	10
500	10	10	20	10	30	10
600	13	10	16	10	24	10
700	22	10	20	10	38	10
800	100	150	60	115	40	105
900	70	30	80	35	30	40
	232	180	212	150	193	145

TABLE 3. THE AMOUNT OF DISTILLED HALOGENS FROM A FEW COMPOUNDS CONTAINING HALOGENS WHEN DISTILLED WITH WATER VAPOR

Temp. °C	KF (0.59 g) and KCl (0.5 g)		CaF_2 (0.59 g) and $CaCl_2$ (0.5 g)		Biotite (1.0 g)	
	F (mg)	Cl (mg)	F (mg)	Cl (mg)	F (mg)	Cl (mg)
100	—	—	—	—	—	—
200	—	—	—	—	—	—
300	40	20	—	—	—	—
400	100	180	10	50	—	—
500	10	100	80	190	—	—
600	5	10	120	70	0.5	0.7
700	—	—	20	—	0.9	0.4
800	—	—	—	—	0.1	—

TABLE 4. THE AMOUNT OF DISTILLED CHLORINE AT HIGH TEMPERATURES ABOVE 500°C
(μg chlorine/1 g of sample)

	500°C	600°C	700°C	800°C	900°C	undistilled*
A. R. S. 1	—	—	—	105	40	30
A. R. S. 2	—	15	—	35	—	50
A. R. S. 3	50	38	—	—	—	−13
A. R. S. 4	—	—	—	—	—	0
A. R. S. 5	—	—	—	—	—	0
P. R. S. 1	22	25	—	10	—	62
P. R. S. 2	11	18	12	23	23	−4
P. R. S. 3	—	—	—	—	—	28
P. R. S. 4	—	—	—	—	—	30
P. R. S. 5	—	—	—	—	—	13
P. R. S. 6	15	10	—	—	—	−15
H. R. S. 1	—	—	—	—	—	70
H. R. S. 2	20	10	40	15	30	0
H. R. S. 3	10	40	70	40	—	−15
H. R. S. 4	—	—	20	—	—	5
H. R. S. 5	10	20	—	—	—	25

* Error can be accumulated to 20 ppm.

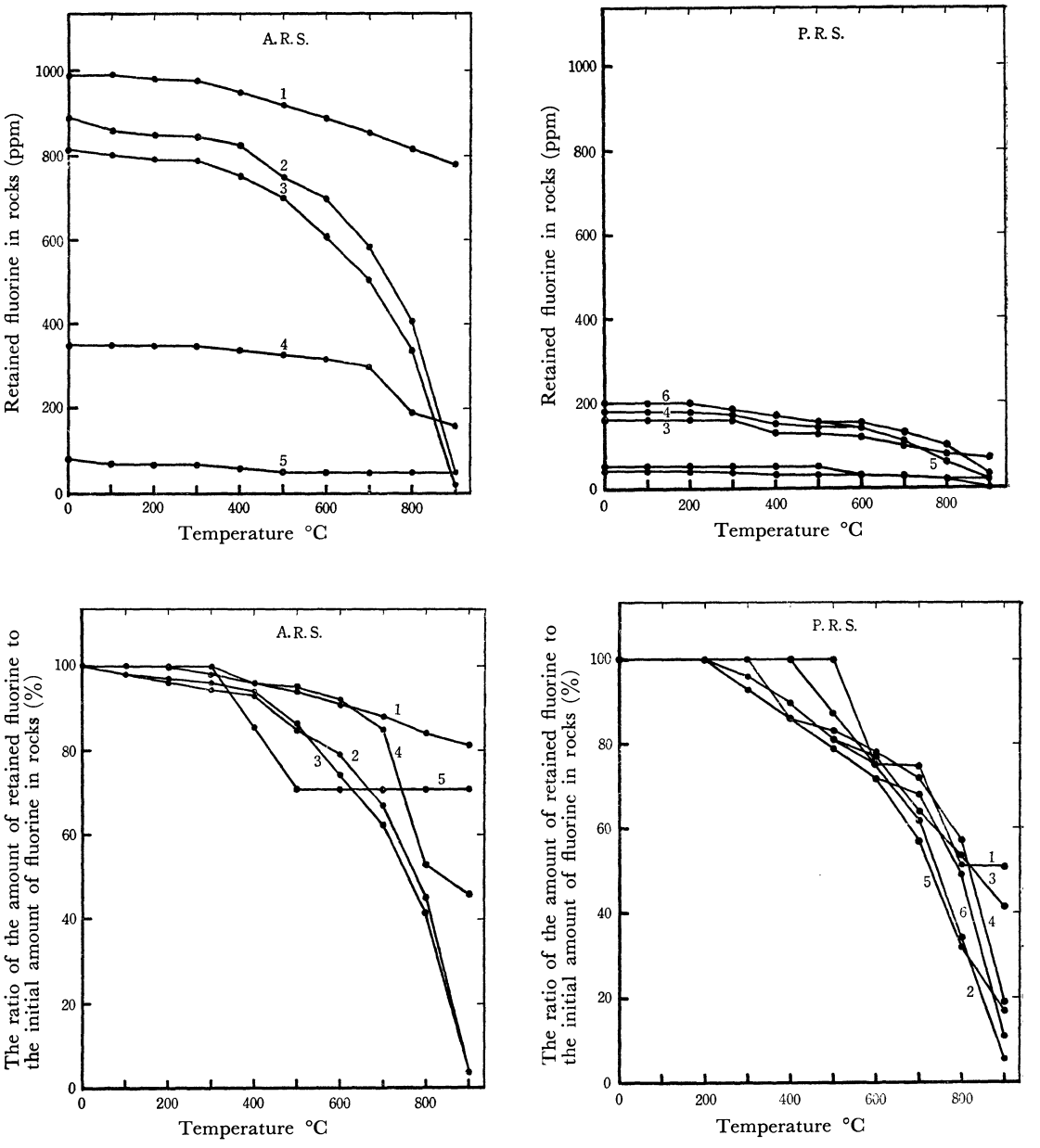

Fig. 5. The relationship between the retained fluorine and

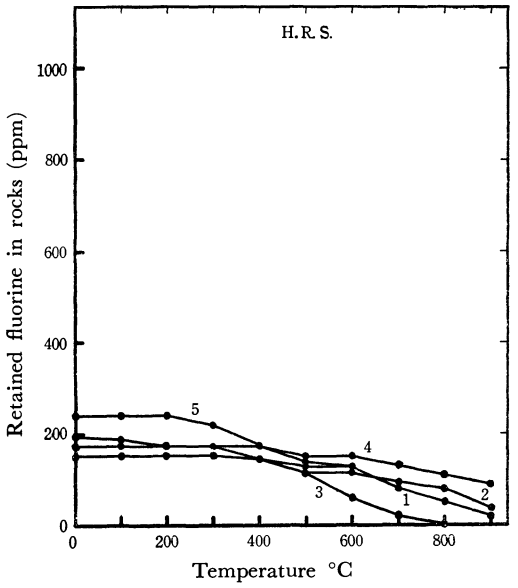

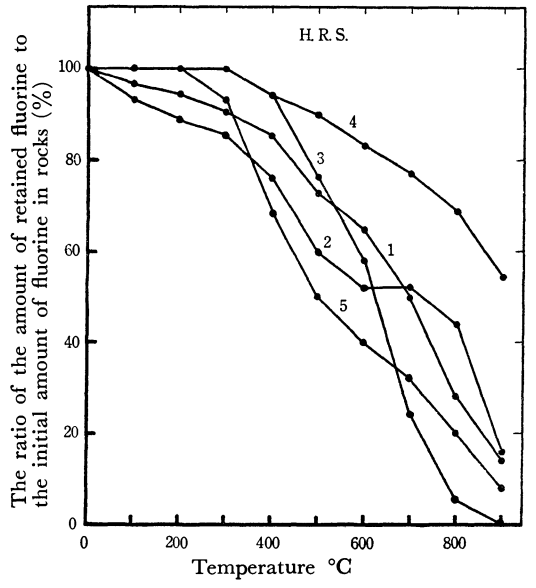

the distillation temperature.

in this study, chlorine in mica is considered to be a small portion of the total amount of chlorine in the rocks.[10]

As to a series of rocks differentiated from the same magma, Greenland and Lovering[18] reported that chlorine is generally more concentrated in differentiates of the later stage than in the earlier one. Figure 3 shows the variations of fluorine and chlorine in each stages expressed in terms of the solidification index given by Kuno *et al.*[19] No regularity is seen for chlorine variation. Fluorine is apparently enriched in later stage pigeonitic and hypersthenic rocks; on the contrary, it decreases in later stage alkaline rocks.

Thus, the variations of fluorine in alkaline rocks are always entirely different from those in other rocks: From the petrological point of view, alkaline rocks are clearly distinguished from others; nevertheless, any petrological evidence for the difference in fluorine content is not found.

From the above results concerning the relationship between the halogen contents of rocks and the chemical, mineralogical and petrological nature of the rocks, it is safely said that halogen contents of rocks are not decidedly controlled by the nature of the rocks considered above. The author considered that halogen contents of rocks would be controlled by water vapor rather than by the characteristics of the rocks. Water is ubiquitous in magma and evaporates from rocks reacting with rocks during or after the formation of the rocks. So, he made following experiments to find out the role of water vapor in the distribution of halogens in volcanic rocks.

Experimental

One gram of a rock sample ground finer than 200 mesh is placed in a boat of silica-glass (I), whch is put into a silica-glass-tubing (G) as shown in Fig. 4. Distilled water is heated to boiling in a distillation vessel (C). A mixture of water vapor from the vessel (C) and nitrogen gas, which is bubbled into the vessel (C) from tank (A) at a flow rate of 30 *l*/hr, is passed through the silica-glass-tubing heated in a furnace (F) at fixed temperatures. The distillate is collected in an absorption vessel (J) containing 5 m*l* of 1 N NaOH solution. About 50 m*l* is collected at each temperature. Fluorine and chlorine in distillates are determined by the methods mentioned above. Reproducibility of the determination is presented in Table 2.

Results and Discussion

Before a rock sample was tested, the possibility of distillation of halogens with water vapor had

18) L. Greenland and J. F. Lovering, *Geochim. et Cosmochim. Acta*, **30**, 963 (1966).
19) H. Kuno, K. Yamasaki, C. Iida and K. Nagashima, *J. Geol. Soc. Japan*, **28**, 179 (1957).
20) F. S. Grimaldi, B. Ingram and F. Cuttita, *Anal. Chem.*, **27**, 918 (1955).
21) T. Sugiura, in press.

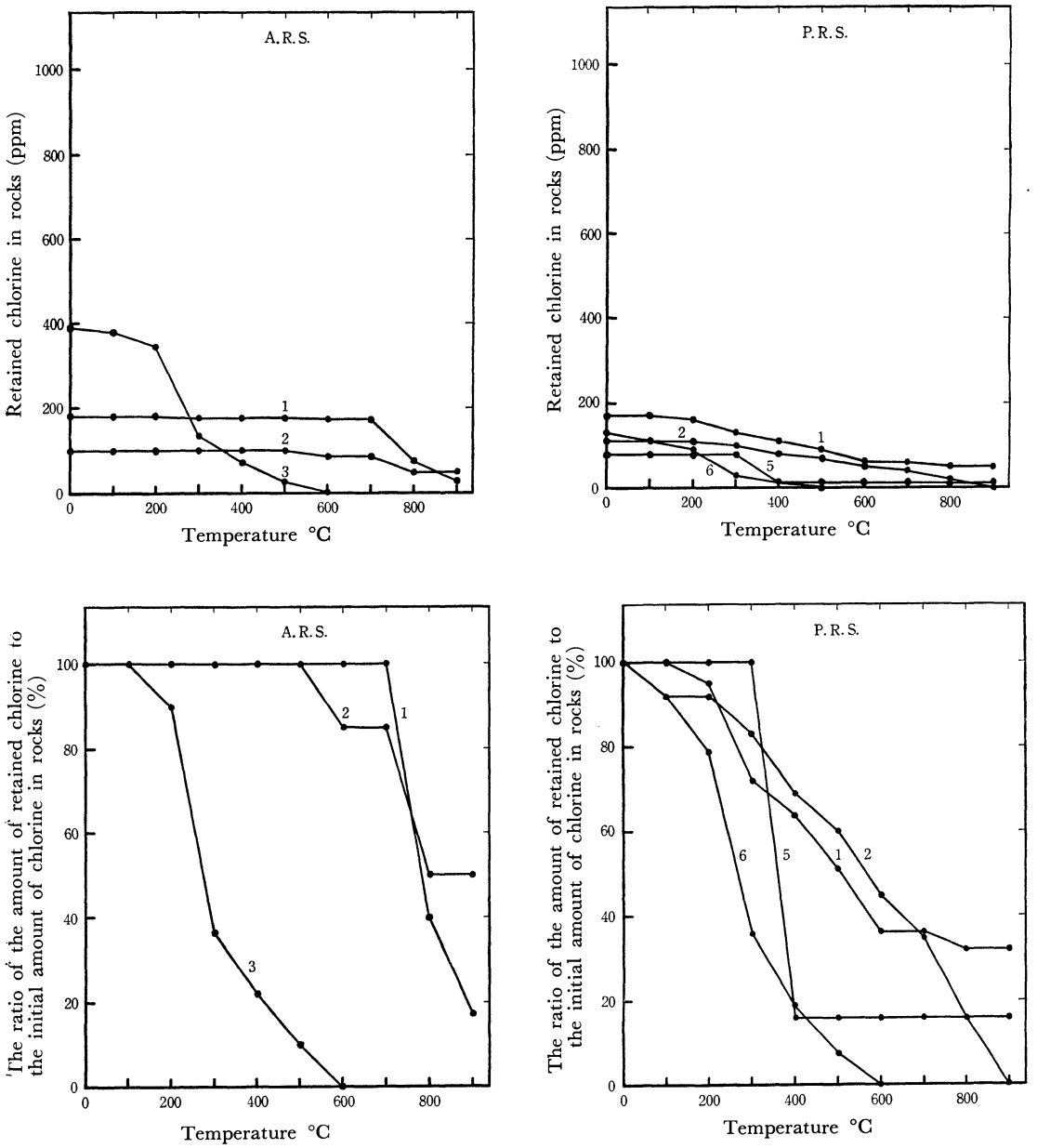

Fig. 6. The relationship between the retained chlorine and

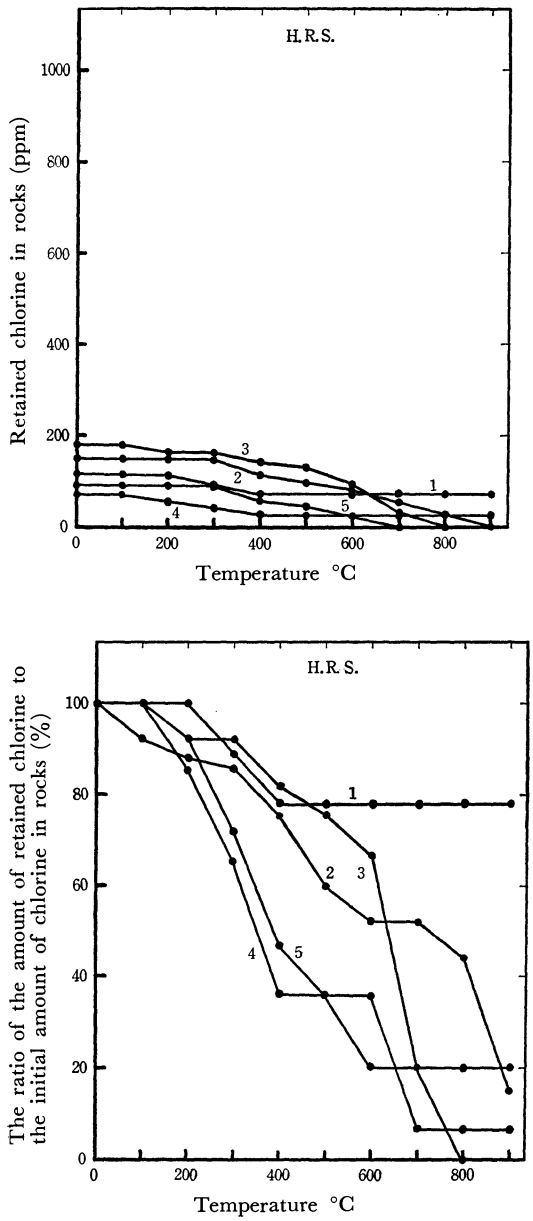

distillation temperature.

been verified for simple compounds containing fluorine or chlorine.

Different patterns of distillation were observed for various compounds containing halogens, as given in Table 3. The initial temperatures at which determinable amount of halogens appeared in distillate were 300°C, 400°C and 600°C for potassium halogenides, calcium halogenides and biotite, respectively. From a mixture of potassium fluoride and potassium chloride, fluorine was more easily distilled than chlorine; in the other materials, the relation was reverse.

The experimental results for rock samples are as follows. The amounts of residual fluorine in rocks at various distillation temperatures are graphically shown in Fig. 5. Almost all fluorine remained in each rock specimen at low temperatures below 300°C, and the lowest temperature at which detectable amount of fluorine appeared was around 400°C. The ratio of the amount of retained fluorine to the initial amount of fluorine in rocks fluctuated among specimens in the temperature range above 700°C. About 70% of fluorine in H. R. S. 1, H. R. S. 3 and H. S. R. 5 was distilled up to 800°C, while most fluorine in A. R. S. 1, A. R. S. 4 and H. R. S. 4 remained in rocks at the temperature. There seemed to be no relation between the pattern of fluorine distillation and rock types. The difficulty of the fluorine distillation was in the order of A. R. S. 1 > A. S. R. 4 > A. R. S. 2 ≈ A. R. S. 3 for alkaline rocks and H. R. S. 4 > H. R. S. 1 ≈ H. R. S. 2 > H. R. S. 3 ≈ H. R. S. 5 for hypersthenic rocks, and is not related to silica content of rocks. The smaller the specimen-number, the more basic the rock. The order of the difficulty of distillation was not clearly observed in pigeonitic rocks. The distillation pattern of fluorine was not related to the fluorine content even in rocks differentiated from a given magma; that is, the order of fluorine content in alkaline rocks was A. R. S. 1 > A. R. S. 2 > A. R. S. 3 > A. R. S. 4, and the difficulty of the fluorine distillation was in the order of A. R. S. 1 > A. R. S. 4 > A. R. S. 2 ≈ A. R. S. 3. The distillation pattern in alkaline rocks containing much fluorine was not essentially different from the patterns in pigeonitic and hypersthenic rocks with low concentration of fluorine.

On the other hand, the distillation pattern of chlorine considerably varied according to specimens as shown in Fig. 6. Chlorine in some specimens was mostly distilled in a lower temperature range, and in some others chlorine was gradually distilled in a higher temperature range. Water-soluble chlorine was naturally expected to be distilled at relatively low temperatures. Nevertheless, there was not a distinct relationship between distillation patterns and the amount of water-soluble chlorine. For instance, A. R. S. 3 contains 295 μg of water-soluble chlorine in one gram of the rock

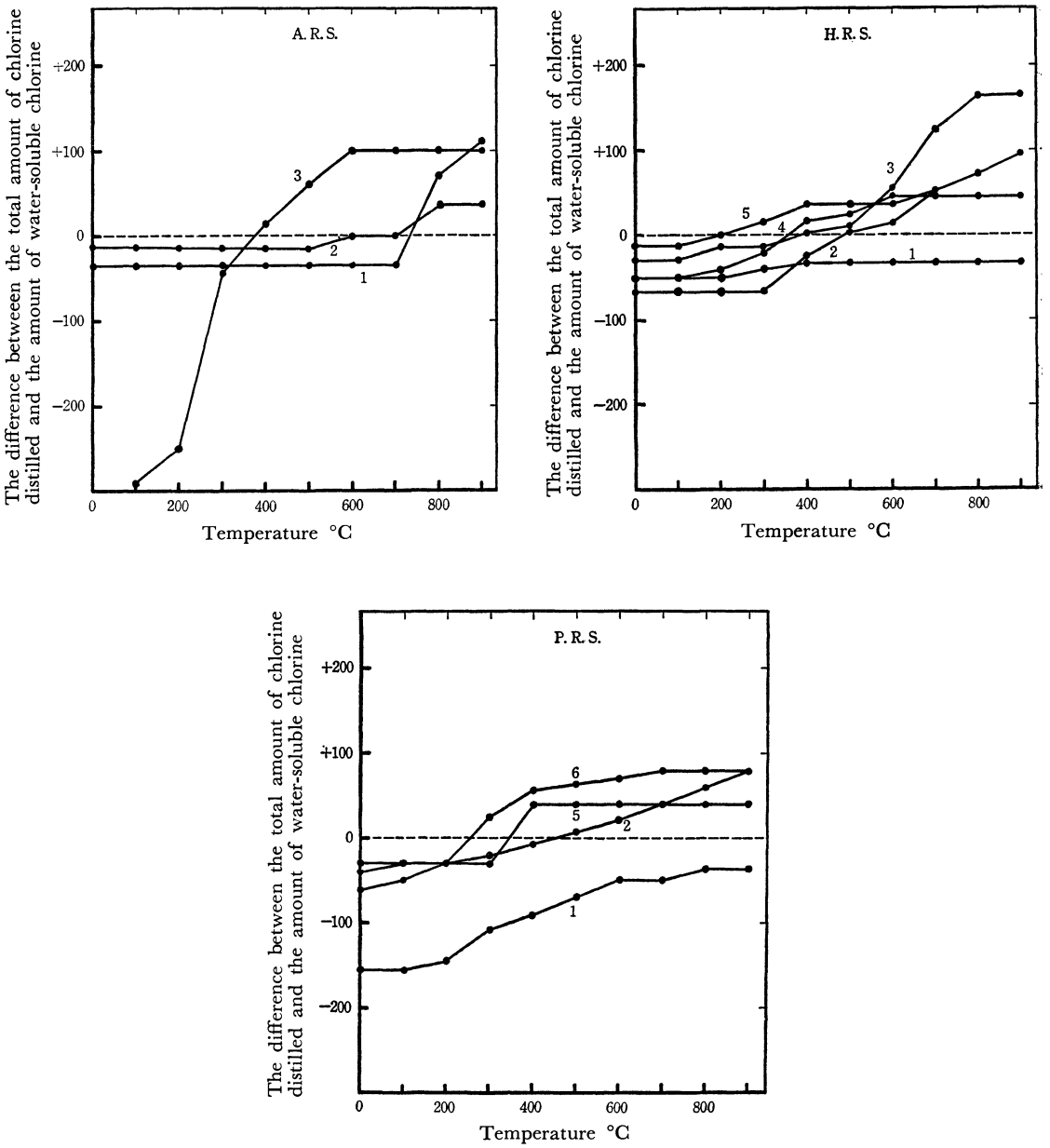

Fig. 7. The difference between the total amount of chlorine distilled and the amount of water-soluble chlorine.

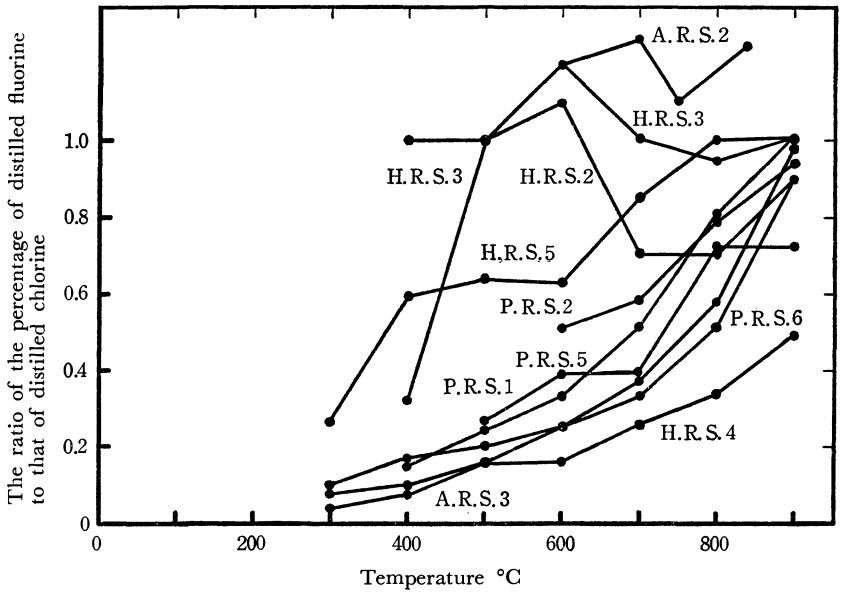

Fig. 8. The ratio of the percentage of distilled fluorine to that of distilled chlorine.

and the amount of chlorine distilled up to 400°C was 305 μg; similarly, from P. R. S. 6 with 60 μg of water-soluble chlorine, 90 μg was distilled, and from H. R. S. 5 with 50 μg, 65 μg was distilled. On the contrary, from P. R. S. 1 with 155 μg of water-soluble chlorine, only 61 μg was distilled up to 400°C; in H. R. S. 1, water-soluble chlorine was 50 μg and distilled chlorine was 20 μg.

The amount of chlorine distilled at temperatures above 500°C and the amount of chlorine remained at 900°C are listed in Table 4. These experiments show that chlorine distilled only at high temperatures and/or remained in rocks at 900°C obviously exists in basic rocks and does not exist in acidic rocks.

The difference between the total amount of chlorine distilled and the amount of water-soluble chlorine was plotted against distillation temperatures as shown in Fig. 7. Negative values in the figure indicate water-soluble chlorine which remains undistilled; the number of the line in the figure corresponds to the order of silica content of rocks. These results suggest that chlorine in basic rocks is generally more resistant to water vapor than in acidic rocks. Although this fact can not be explained reasonably, the chemical nature of rocks might be responsible for this result because it coincides with the experimental result of the chlorine solubility in rock melts reported by Iwasaki *et al.*[11]

The ratio of the distilled percentage of fluorine to that of chlorine at various temperatures is graphically shown in Fig. 8: Generally chlorine is distilled more easily than fluorine at low temperatures. The different behaviors of these elements in water vapor are very important for consideration of fluorine and chlorine contents of volcanic rocks. If rocks are placed in water vapor at a high temperature for a long time, both fluorine and chlorine would diffuse out from rocks at an approximately same rate, but at a low temperature, about 300°C, chlorine would diffuse out from rocks more rapidly than fluorine.

This experimental result also could have a geochemical significance to the origin of halogens in volcanic gases; the halogens in volcanic rocks are easily distilled with water vapor and the ratio of fluorine to chlorine increases with temperature. On the other hand, the ratio of fluorine to chlorine in volcanic gases from some volcanoes is known to be smaller for low temperature fumaroles and larger for high temperature fumaroles.[22,23]

Summary and Conclusion

There have been various interpretations on the effect of the characteristics of rocks on the abundance of fluorine and chlorine in volcanic rocks. This study has revealed that the chlorine content of rocks does not show any relation to the characteristics of rocks of any magma type, and fluorine content decreases in later stage of magmatic differentiation for alkaline rocks and slightly increases for pigeonitic and hypersthenic rocks. Meanwhile, when fluorine in rocks was distilled with water vapor, the pattern of distilled fluorine fluctuated considerably. The pattern, however, seemed to depend on neither the characteristics of the rocks nor fluorine content of rocks.

22) Y. Mizutani, *J. Earth Sci. Nagoya Univ.*, **10**, 125 (1962).
23) T. Sugiura, Y. Mizutani and S. Oana, *ibid.*, **11**, 272 (1963).

Accordingly, fluorine content of rocks can not be explained by the difference in chemical and mineralogical characteristics of rocks, but should be explained by the cooling histry of magma during the formation of rocks.

Chlorine is often reported to be concentrated rather in acidic rocks than in basic rocks. The present study, however, shows that chlorine concontent is independent of rock types. In the experiments, chlorine in basic rocks is more stable than in acidic rocks. From these evidences, it can be concluded that chlorine content of rocks is also controlled mainly by environmental conditions even if the characteristics of rocks might affect the behavior of chlorine in rocks.

In natural environments, water is much emanated from magma during its cooling, and probably carries out halogens with it as shown in the present experiments. The distillation process can be essentially responsible for halogen contents of rocks.

The distillation experiment with water vapor described here is important in considering the origin of halogens in volcanic gases. In order to study the behavior of halogens in volcanic emanation, Yoshida *et al.*[24,25] analyzed halogen compounds driven from rocks heated in nitrogen gas without water vapor. However, water plays essentially an important role in magmatic emanation. Accordingly, the present experiment with water vapor reproduces more closely natural conditions.

The author wishes to express his hearty thanks to Prof. S. Oana, Department of Earth Sciences, Nagoya University who gave him guidance throughout this study. He is also indebted to Dr. N. Nakai, Department of Earth Sciences, Nagoya University for his constant and valuable advice. Thanks are due to Dr. R. Sugisaki, Department of Earth Sciences, Nagoya University who gave him many useful suggestions and Dr. H. Kuno, Department of Geology, the University of Tokyo who supplied him with excellent samples.

24) M. Yoshida, This Bulletin, **36**, 773 (1963).
25) M. Yoshida, I. Makino, N. Yonehara and I. Iwasaki, *ibid.*, **38**, 1936 (1965).

BULLETIN OF THE CHEMICAL SOCIETY OF JAPAN VOL. 41 1600—1605 (1968)

Ion-exchange Properties of Anion-exchanger Containing Cobalticinium Cations

Takuji Ito

Department of Chemistry, Tokyo Institute of Technology, Ookayama, Meguro-ku, Tokyo

and Tadao Kenjo

Graduate School of Science and Engineering, Tokyo Institute of Technology, Ookayama, Meguro-ku, Tokyo

(Received December 12, 1967)

Selectivity coefficients of various anions *vs.* chloride or nitrate and water uptake at a saturated vapor pressure with polymeric pentamethylene cobalticinium exchanger were calculated from the experimental data and compared with those of anion-exchange resins. The selectivity coefficient sequence was nearly identical with that for quaternary ammonium type anion-exchangers, and the position of hydroxide ion indicated that the cobalticinium type anion-exchanger was a strong base type. Inspection of selectivity coefficients data revealed that strong base anion-exchangers were more selective than weak base anion-exchangers. The cobalticinium type anion-exchanger was found to have a high selectivity coefficient of iodide *vs.* bromide, even in comparison with strong base anion-exchange resins. Column separation of bromide and iodide using the cobalticinium type anion-exchanger was easily accomplished. The separation factor was three times that of the quaternary ammonium type anion-exchanger. The water uptake at a saturation vapor pressure by the cobalticinium type anion-exchanger in a given form increased with decreasing selectivity coefficient for the same anion. These trends were similar to those for quaternary ammonium type anion-exchanger. The relation between selectivity coefficient sequence of various anions *vs.* a common anion, and solubilities of the salt whose cation was the ionogenic group and anion adsorbed ion was discussed.

One of the weakest points of quaternary base anion-exchange resins is their instability toward heat. In order to exploit possible thermostable anion-exchangers, we synthesized polymeric olygo-

methylene cobalticinium anion-exchangers and investigated their properties (stability toward reagents and heat).[1]

In this paper, the ion-exchange properties of the anion-exchanger are investigated and compared with those of anion-exchange resins.

Experimental

Preparations and Conditionings of Anion-exchangers. The method of synthesis and procedure for conditioning cobalticinium type anion-exchanger were identical with those of a previous paper.[1] Among the series of olygomethylene compounds, pentamethylene compounds (Cl form) were used, being most stable against reagents. Anion-exchange resins (Dowex 1 X-1, Dowex 1 X-8, Amberlite IR-45 and Amberlite IR-4B) were obtained commercially and conditioned in the same manner. Anion-exchangers were converted to the desired salt forms with column operations.

Measurement of Selectivity Coefficients and Distribution Coefficients. The selectivity coefficient K_c is defined in the system of ion-exchange toward uni-valent ions as follows:

$$K_c = K_B^A = \left(\frac{m_A}{m_B}\right)_r \Big/ \left(\frac{m_A}{m_B}\right)_w$$

where K_B^A is the selectivity coefficient in the case of the displacement of anion B in the exchanger by anion A in the solution, r refers to the concentration of anion in the exchanger phase and ω the concentration of anion in the solution phase. The mole fraction of a particular anionic state of the exchanger is designated $X_A^B(=(m_A/(m_A+m_B))_r)$.

Selectivity coefficients were determined by the batch equilibrium method at 25.00±0.01°C using 0.250 g of exchanger. After shaking for 24 hr, concentrations of halogenide ions in the solution were determined with the potentiometric titration method using a solution of 0.1 N silver nitrate and a silver electrode. The anion-exchange systems were arranged in such a way that selectivity coefficients could be obtained by determining the concentration of halogenide ions. Other ions could be calculated by subtracting the amount of halogenide ions from the total amount of anion-exchange capacity.

The distribution coefficient of solute A (a trace constituent) is defined as the total amount of solute A per gram of dry exchanger divided by the total amount of solute A in one milliliter of external solution. Distribution coefficients for perchlorate, thiocyanate, iodide, bromide and chloride ions (trace constituents) against hydroxide ion were measured by the batch method at room temperature. The concentration of trace constituents was 10^{-3} M and that of hydroxide varied from 0.04 M to 2 M. Column operation was used for iodate, bromate, chloride, bromide and iodide ions against nitrate ion, and for iodide and thiocyanate ions against perchlorate ion. Distribution coefficients were calculated according to the following formula for column operation:[2]

$$V = I + mK_d$$

where V is the peak elution volume (ml), I the void space of the column (ml), m the mass of the dry exchanger (g) and K_d the distribution coefficient (ml/g). Determination of micro-amounts of anions was carried out by the colorimetric method[3] after a large excess of hydroxide ion was removed with Dowex 50W (H form) columns.

Measurements of the Amount of Water Adsorbed on the Cobalticinium Type Anion-exchanger in Various Anion Forms. After the cobalticinium type anion-exchanger in various forms were dried over silica gel to constant weight, they were equilibrated with saturated water vapor at room temperature. Then the amount of water adsorbed was calculated.

Solubilities of Cobalticinium and Tetramethylammonium Salts. Cobalticinium salts were obtained by converting the picrate into the desired salt form with Amberlite IRA-410 columns. Tetramethylammonium halogenides were obtained commercially. The halogenate was obtained by converting the chloride in the same manner as cobalticinium salts. The solubility was measured at 0°C and halogenide ions were determined by potentiometric titration with 0.1 N silver nitrate solution using a silver electrode. Halogenate ions were determined as chloride ion after converting them to chloride with Amberlite IRA-410 columns (Cl form).

Results and Discussion

Selectivity coefficients obtained are shown in Table 1. The selectivity coefficient sequence for the cobalticinium type anion-exchanger resembles that for strong base type anion-exchange resins,[4-6] particularly with respect to the position of hydroxide

Table 1. Selectivity coefficients of various anions *vs.* bromide with polymeric pentamethylene cobalticinium exchanger

Ion	X_A^{Br}	K_{Br}^A
BF_4^-	0.987	9.67
NO_3^-	0.926	1.45
Benzoate	0.925	1.44
ClO_3^-	0.924	1.41
NO_2^-	0.847	0.581
BrO_3^-	0.746	0.270
HCO_3^-	0.687	0.184
OH^-	0.672	0.158
HSO_4^-	0.653	0.147
CH_3COO^-	0.519	0.0664
$H_2PO_4^-$	0.444	0.0417
F^-	0.357	0.0237

1) T. Ito and T. Kenjo, This Bulletin, **41**, 614 (1968).
2) E. Glueckauf, *Trans. Faraday Soc.*, **51**, 34 (1955).
3) David F. Boltz (Ed.), "Colorimetric determination of nonmetals," Interscience Pub. Inc., New York (1958).
4) R. M. Wheaton and W. C. Bauman, *Ind. Eng. Chem.*, **41**, 1265 (1949).
5) M. Kikindal, *Compt. rend.*, **237**, 250 (1953).
6) H. P. Gregor, J. Belle and R. M. Marcus, *J. Am. Chem. Soc.*, **77**, 2713 (1955).

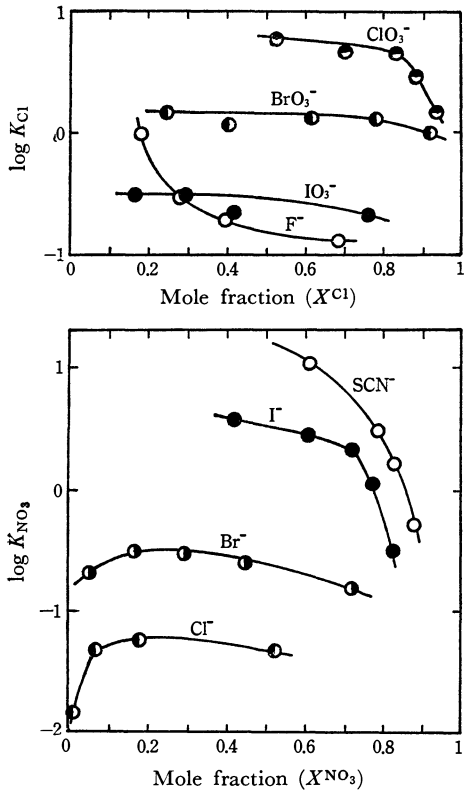

Fig. 1. Selectivity coefficients of various anions *vs.* chloride and nitrate with polymeric pentamethylene cobalticinium exchanger.
upper: fluoride (○) iodate (●) bromate (◐) chlorate (◓)
lower: chloride (◐) bromide (◑) iodide (●) thiocyanate (○)

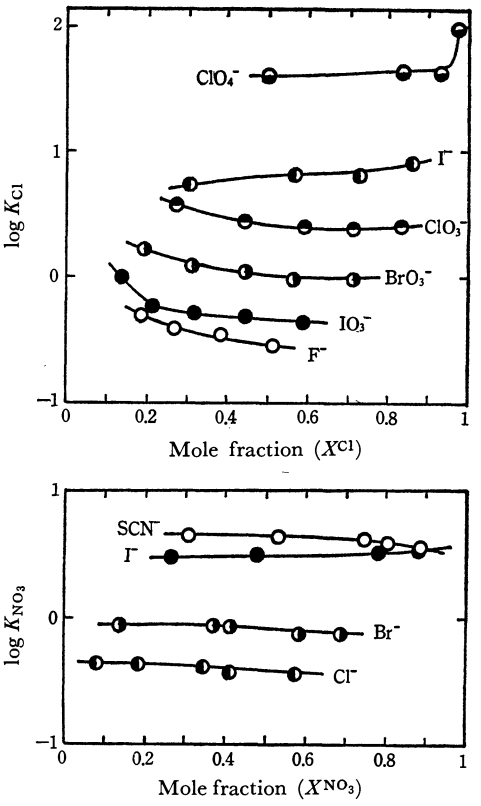

Fig. 2. Selectivity coefficients of various anions *vs.* chloride and nitrate with Dowex 1 X-1.
upper: fluoride (○) iodate (●) bromate (◑) chlorate (◓) iodide (◐) perchlorate (◒)
lower: chloride (◐), bromide (◑) iodide (●) thiocyanate (○)

ion. This fact indicates that cobalticinium type anion-exchanger is a strong base type, which is consistent with an observation that cobalticinium cations form a strong base.[7]

Respective selectivity coefficients on the polymeric pentamethylene cobalticinium exchanger, Dowex 1 X-1, Dowex 1 X-8, Amberlite IR-45 and Amberlite IR-4B are given in Figs. 1 to 5. Great differences in selectivity coefficients with strong base anion-exchangers (cobalticinium, Dowex 1) compared with those with weak base anion-exchangers (Amberlite IR-45 and Amberlite IR-4B) suggest that strong base anion-exchangers are more selective than weak base anion-exchangers. As regards selectivity coefficients for halide ions, cobalticinium type anion-exchanger is more selective than Dowex 1, particularly with respect to the difference between bromide ion and iodide ion. Figure 6 also indicates there is a large difference between bromide and iodide ion in the distribution coefficient, and ion-exchange ideality*1 is evidenced by straight lines with negative unit slopes. Distribution coefficients for various anions are summarized in Table 2. These values are consistent with the tendency seen in selectivity coefficients. The separation of bromide and iodide ion with a column using cobalticinium ion-exchanger was effected more readily than with

7) G. Wilkinson and F. A. Cotton, "Progress in Inorganic Chemistry," Vol 1, ed. by F. A. Cotton, International Pub., New York, N. Y. (1959), p. 13.

*1 The selectivity coefficient for uni-valent anion-exchange is defined by the equation written in the experimental section. If one of the adsorbed ions (A) is in trace concentration, and if ion-exchange reactions occur ideally, the composition of the exchanger is essentially independent of the concentration of the adsorbed trace ion. Then the equation simplifies to

$$K_{d(A)} m_{B(w)} = \text{constant}$$

where $K_{d(A)}$ is the distribution coefficient for A and $m_{B(w)}$ the concentration of B in external solution; $m_{B(w)}$ is equal to the concentration of hydroxide ion in this case. According to the equation, a plot of $\log K_{d(A)}$ *vs.* $\log m_{B(w)}$ should be a straight line with a negative unit slope. This relation has been taken to show ion-exchange ideality.[8]

8) K. A. Kraus, H. O. Phillips, T. A. Carlson and J. S. Johnson, Paper P/1832 Intern. Conference on Peaceful Uses of Atomic Energy, 2nd, Cof. (1958).

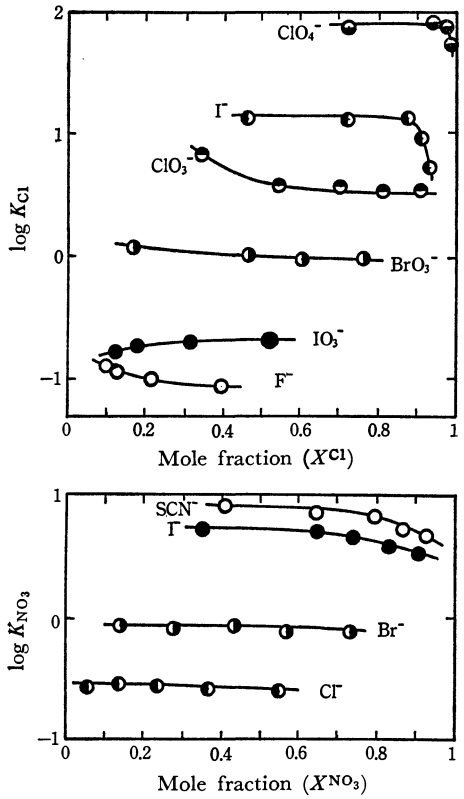

Fig. 3. Selectivity coefficients of various anions *vs.* chloride and nitrate with Dowex 1 X-8.
upper: fluoride (○) iodate (●) bromate (◑) chlorate (◓) iodide (◐) perchlorate (◒)
lower: chloride (◐) bromide (◑) iodide (●) thiocyanate (○)

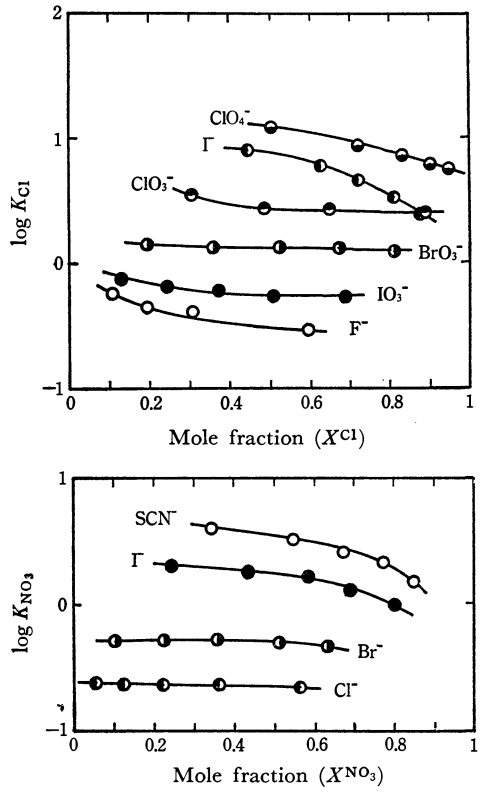

Fig. 4. Selectivity coefficients of various anions *vs.* chloride and nitrate with Amberlite IR-45.
upper: fluoride (○) iodate (●) bromate (◑) chlorate (◓) iodide (◐) perchlorate (◒)
lower: chloride (◐) bromide (◑) iodide (●) thiocyanate (○)

Table 2. Distribution coefficients for anions on polymeric pentamethylene cobalticinium exchanger (PPC) and anion-exchange resins

Ion	PPC (ml/g) (OH form)	Amberlite IRA-410 (ml/g) (OH form)	Amberlite IR-45 (normalized to the value for IO_3^-) (NO_3 form)
IO_3^-	15.4	9.80	1.0
Cl^-	26.8	33.5	1.45
BrO_3^-	26.8	33.5	1.67
Br^-	54.2	111	2.97
I^-	575	644	10.8
SCN^-	990	1290	28.1
ClO_4^-	2000	—	—

Table 3. The water uptake of polymeric pentamethylene cobalticinium exchanger in various salt forms
(mmol H_2O/meq. exchanger)

IO_3^-	11.31	Cl^-	11.78
BrO_3^-	9.28	Br^-	9.80
ClO_3^-	9.25	I^-	7.40
ClO_4^-	7.30	SCN^-	6.40
		OH^-	13.44

ion-exchange resins (Fig. 7). The separation factor calculated by dividing the distribution coefficient of iodide ion by that of bromide ion was about 10, from Fig. 7, which agrees well with the value of Table 2, and is three times that of strong base anion-exchangers.[9]

It may be seen from Table 3 that the water uptake at a saturated vapor pressure by cobalticinium type anion-exchanger in various forms increases with decreasing selectivity coefficient of anions *vs.* nitrate or chloride ion. These tendencies are analogous to that of a quaternary ammonium type exchanger.[10] The results can be understood if the selectivity is assumed caused by the difference in the two different anions adsorbed in their affinity to ionogenic groups. One of the most typical theories, suggesting an interaction

9) W. Rieman III, S. Lindenbaum, *Anal. Chem.*, **24**, 1199 (1952).

10) G. E. Boyd and B. A. Soldano, *Z. Elektrochem.*, **57**, 162 (1953).

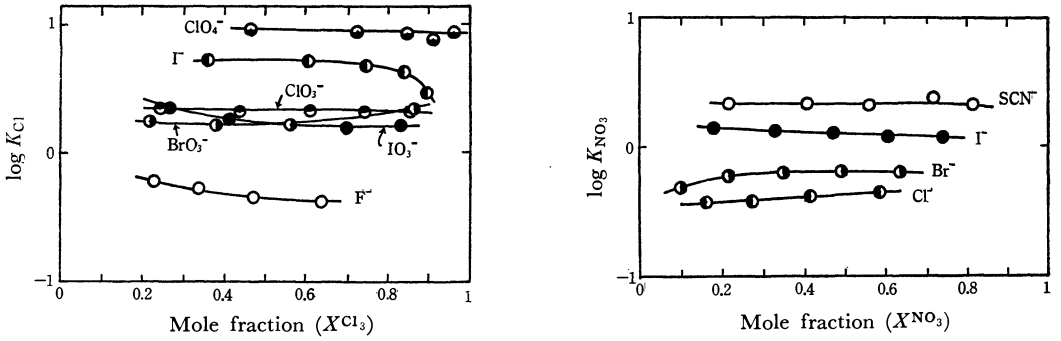

Fig. 5. Selectivity coefficients of various anions *vs.* chloride and nitrate with Amberlite IR-4B.
upper: fluoride (○) iodate (●) bromate (◑) chlorate (◓) iodide (◐) perchlorate (◒)
lower: chloride (◐) bromide (◑) iodide (●) thiocyanate (○)

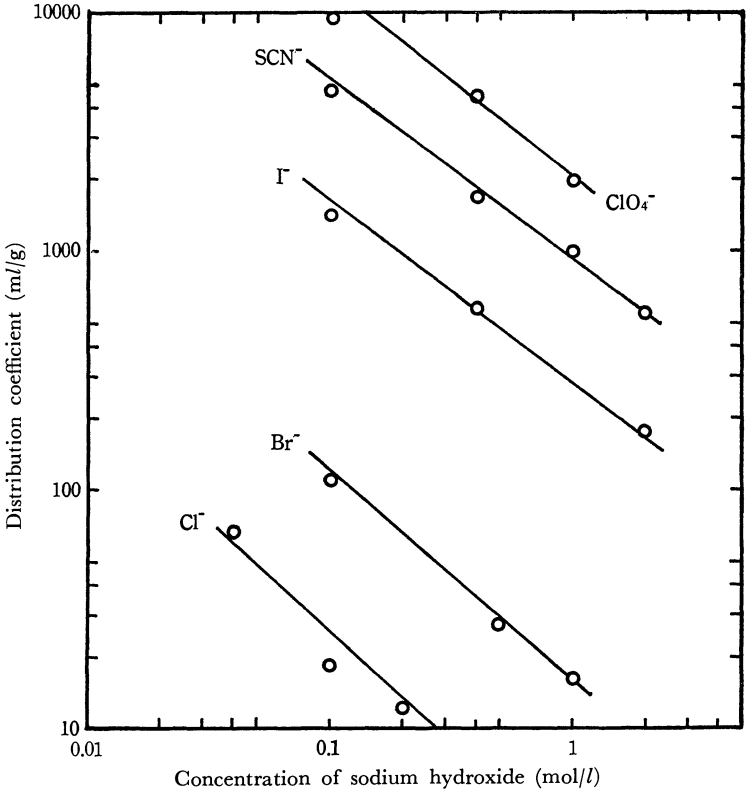

Fig. 6. Distribution coefficients for several anions on polymeric pentamethylene cobalticinium exchanger as a function of sodium hydroxide concentration.

between an ionogenic group and a counter ion was proposed by Gregor.[11] He assumed a dissociation equilibrium between ionogenic groups and adsorbed ions as follows;

$$RA \rightleftarrows R^+ + A^-$$
$$RB \rightleftarrows R^+ + B^-$$

where R's refer to the ionogenic group and A and B to adsorbed ions. The dissociation constants for A (D_A) and B (D_B) are given by

$$D_A = \frac{[R^+][A^-]}{[RA]}, \qquad D_B = \frac{[R^+][B^-]}{[RB]}$$

where the brackets refer to the molality of each species. Neglecting strain energy effects, the molality of unpaired ions in the exchanger phase is related to that of these ions in the external solution according to the Donnan equilibrium condition, or $[A^-]_r/[B^-]_r=[A^-]_w/[B^-]_w$, where the *r*'s refer

11) H. P. Gregor, J. Belle and R. A. Marcus, *J. Am. Chem. Soc.*, **77**, 2713 (1955).

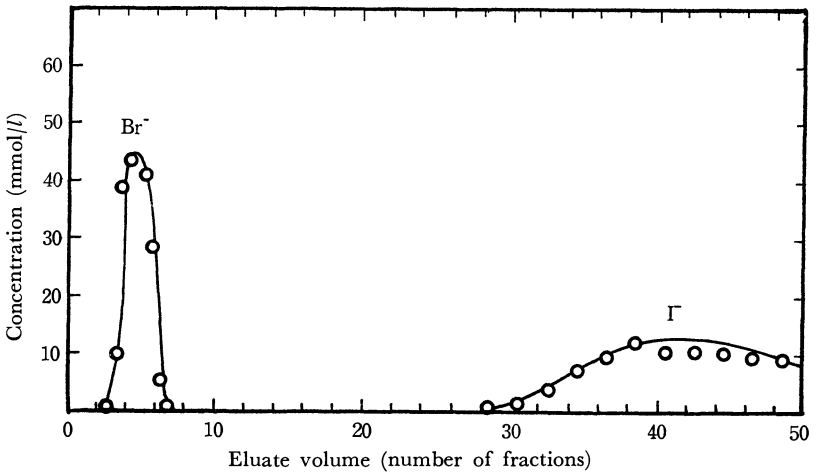

Fig. 7. Separation of bromide from iodide by polymeric pentamethylene cobalticinium exchanger with 0.25 M nitric acid.
Column: 10×111 mm; Flow rate: 0.64 ml/min
Volume of fraction: 4.8 ml

to the exchanger phase and w's to the external solution phase. Then the selectivity coefficient of A *vs.* B (K_A^B) can be related to the dissociation constants as follows:

$$K_A^B = \frac{[A^-]_w D_A + [A^-]_w (D_B - D_A)x}{[A^-]_w D_B - [B^-]_w (D_B - D_A)x}$$

where $$x = \frac{-D_A + \sqrt{D_A^2 + 4[A^-]_w D_A + \frac{4D_A^2[B^-]}{D_B}}}{2\left(1 + \frac{[B^-]_w D_A}{[A^-]_w D_B}\right)}$$

and $[A^-]_w$ and $[B^-]_w$ refer to the molality of anions A and B in the external solution phase, respectively. The above equation indicates that the selectivity coefficient of B *vs.* A increases with decreasing D_B/D_A at a given molality of A or B in the external solution phase. Accordingly, the relation between the water uptake and the selectivity coefficient may be interpreted as the hydration of unpaired ions in the exchanger phase, because unpaired ions may adsorb a greater amount of water than paired ions. These relations between the ionogenic group and the adsorbed ion can be compared to those between the solid phase and solution phase of the salt whose cation is the ionogenic group and anion the adsorbed ion. As shown in Table 4, the solubilities of halogenide salts decrease in the order $Cl^- > Br^- > I^-$, while selectivity coefficients of halogenide ions *vs.* common anion increase in the order $Cl^- < Br^- < I^-$. These results may show the validity of the above mentioned prediction. The solubilities of both cobalticinium and tetramethylammonium halogenates, however, decrease in the order $ClO_3^- > BrO_3^- > IO_3^-$, while the selectivity coefficients of halogenate ions *vs.* a common anion decreased in the order $ClO_3^- > BrO_3^- > IO_3^-$. Considering the Coulomb force, it is expected that the affinities to ionogenic groups decrease in the order $ClO_3^- > BrO_3^- > IO_3^-$ if the structures of the ions in water are the same as that in a crystalline state. These opposite tendencies, presumably, suggest some differences in the nature of interaction (*e. g.*, direction or distance) between the anion-exchangers and the corresponding salts in the crystalline state.

Table 4. Solubilities of cobalticinium and tetramethylammonium salts in water (0°C)

	Cobalticinium (mol/l)	Tetramethylammonium (mol/l)
Cl^-	3.76	6.67
Br^-	3.44	3.04
I^-	1.41	0.104
IO_3^-	3.01	1.00
BrO_3^-	3.60	2.14
ClO_3^-	4.77	2.64

BULLETIN OF THE CHEMICAL SOCIETY OF JAPAN VOL. 41 1606—1610 (1968)

Short-Lived Nuclides Formed by (γ, n) Reactions with 20 MeV Bremsstrahlung

Yoshinaga OKA, Toyoaki KATO and Akira YAMADERA

Department of Chemistry, Faculty of Science, Tohoku University, Katahira-cho, Sendai

(Received December 25, 1967)

The most prominent (γ, n) reaction products with half-lives from 10 sec to about 1 min formed by irradiation of some 7 elements with 20 MeV bremsstrahlung have been determined in order to study the applicability of these products to photoactivation analyses. Irradiation was carried out for 1 min with 20 MeV bremsstrahlung radiation with a dose rate of 10^7 R/min. The reactions investigated are $^{24}Mg(\gamma, n)^{23}Mg$, $^{76}Ge(\gamma, n)^{75m}Ge$, $^{78}Se(\gamma, n)^{77m}Se$, $^{92}Mo(\gamma, n)^{91m}Mo$, $^{140}Ce(\gamma, n)^{139m}Ce$, $^{142}Nd(\gamma, n)^{141m}Nd$ and $^{159}Tb(\gamma, n)^{158m}Tb$. The yields of these reactions have also been obtained through the absolute measurement of resultant activities. The isomeric yield ratios have been discussed on the basis of the nuclear properties of the residual nuclides. The observed ratios generally favor the isomer whose spin is closer to that of the target nucleus. For the elements studied, the lower limits of detection averaged about 1 μg under present experimental conditions.

As pointed out in previous reports,[1] the use of high-energy gamma-rays in activation analysis sometimes offers several advantages over the neutron activation method with respect to selectivity and specificity. A number of radioactive species with moderate half-lives (longer than 2 min) arising from photonuclear processes on many elements irradiated with 20 MeV bremsstrahlung have been investigated with respect to yield, and the applicability to activation analysis of those elements.[2]

On the other hand, short-lived nuclides can be obtained selectively with a short-irradiation period, suppressing longer-lived components in the gamma-ray spectra of the activated specimen, and can thereby be used as a rapid, sensitive and non-destructive method of analysis of the relevant element. Until recently, these problems have been investigated exclusively by means of thermal neutron activation, and a number of tabulations or catalogs on gamma-ray spectra of (n, γ) reaction products have been compiled by many workers.[3-8]

The purpose of the present report is to determine gamma-ray spectrometrically most important short-lived (γ, n) reaction products with half-lives from 10 sec to about 1 min, formed in the irradiation of some 7 elements with 20 MeV bremsstrahlung, and to discuss the reaction yields on the basis of the nuclear properties of those nuclides.

Experimental

Samples and Irradiation. Irradiation was carried out with bremsstrahlung radiattion, converted from a 20 MeV electron beam[9] generated from the linear electron accelerator of the Japan Atomic Energy Research Institute. The chemical forms of the sample materials used in these experiments were the elements of magnesium, germanium, selenium and molybdenum, and the oxides of cerium, neodymium and terbium. A definite amount of each sample (5—40 mg) was wrapped in thin aluminum foil and made into a small disk of diameter 5 mm and with a thickness of 1 mm.[10] The bremsstrahlung flux was monitored using a thin sheet of gold (10 μ thick, 5 mm dia.) adjacent to the samples. Each sample with gold monitor was encapsulated in a cylindrical aluminum rabbit[11] together with polyethylene foam to hold the sample tightly. The sample in the rabbit was transferred to the irradiation point immediately behind the photon-producing converter[12] by a pneumatic tube. All irradiations were for one minutes.

The dose rate of the bremsstrahlung photons at the target position was determined by the method of activating a manganese specimen as reported previously.[13] It was estimated at 10^7R/min. Following irradiation, the rabbit was brought back by a reversed air stream,

1) Y. Oka, T. Kato and M. Sasaki, *Nippon Kagaku Zasshi (J. Chem. Soc. Japan, Pure Chem. Sect.)*, **84**, 588 (1963), and other reports.
2) Y. Oka, T. Kato, K. Nomura and T. Saito, *J. Nucl. Sci. Technol.*, **4**, 364 (1967).
3) M. Okada, *Nucleonics*, **22**, No. 8, 110 (1964).
4) M. Okada, This Bulletin, **39**, 1340 (1966).
5) M. Okada, *Nucleonics*, **19**, No. 9, 79 (1961).
6) M. Okada, *ibid.*, **20**, No. 12, 61 (1962).
7) Y. Kamemoto, K. Shiba, H. Handa and M. Okada, JAERI-4019 (1961).
8) O. U. Anders, NP-14469 (1964).
9) Average current: 40 μA.
10) This was aimed at producing an optimum specific activity in the irradiation in a collimated bremsstrahlung beam.
11) 10 mm i. d., 40 mm long.
12) 2 mm thick platinum plate.
13) Y. Oka, T. Kato and I. Nagai, *J. Nucl. Sci. Technol.*, **4**, 300 (1967).

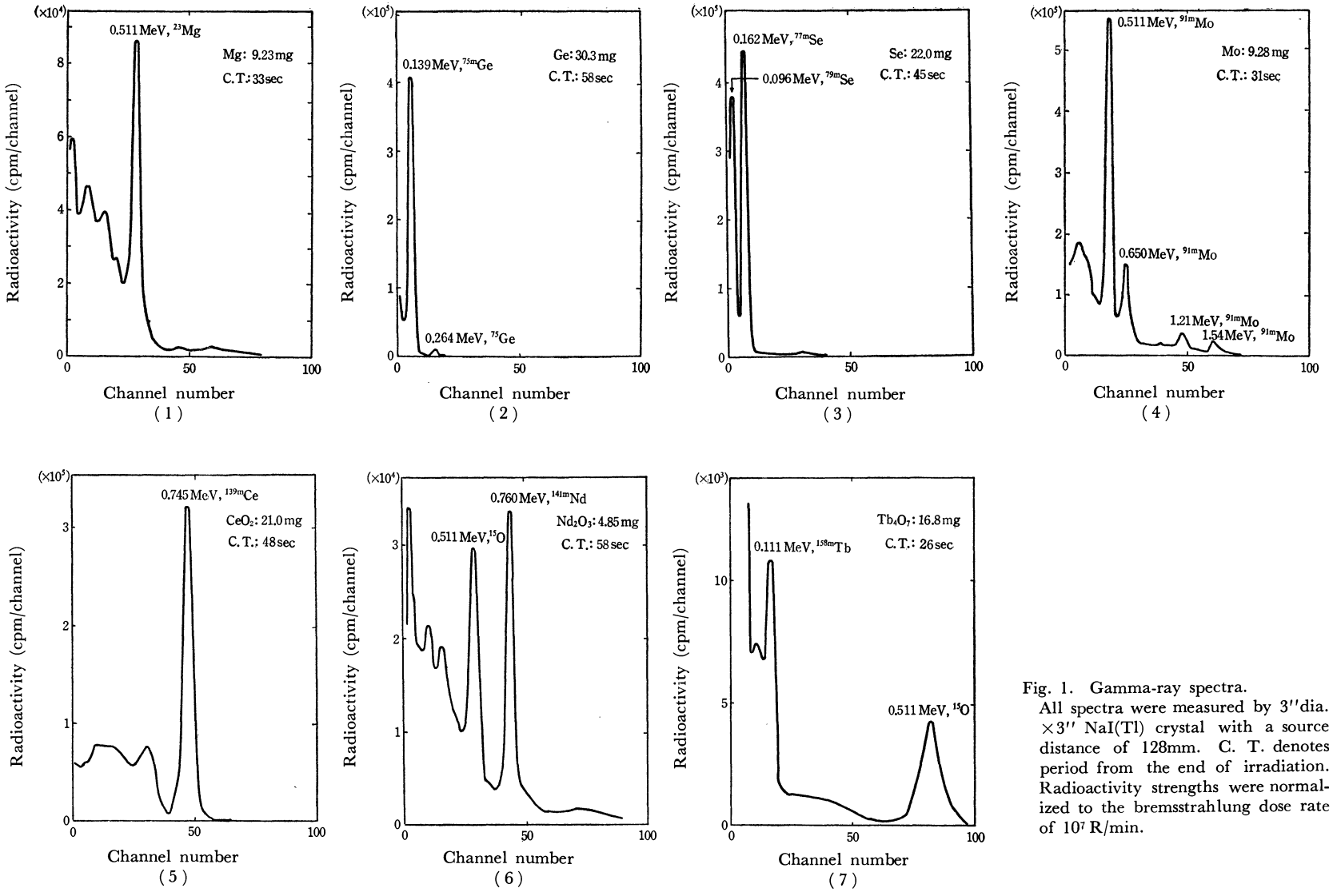

Fig. 1. Gamma-ray spectra.
All spectra were measured by 3″dia. ×3″ NaI(Tl) crystal with a source distance of 128mm. C. T. denotes period from the end of irradiation. Radioactivity strengths were normalized to the bremsstrahlung dose rate of 10^7 R/min.

and the sample disk removed. The travel time of the rabbit was 2 sec.

Radioactivity Measurement. Immediately after the removal of the sample from the rabbit, its gamma-ray spectrum was measured with a 3'' dia. $\times$3'' NaI(Tl) detector coupled to a TMC 400-channel pulse-height analyzer. The memory of the analyzer was subgrouped into 4$\times$100 channels, and a spectrum collected in each subgroup. This method was most efficient for activities with the half-life range from 10 sec to about 1 min.

Data Treatment. The radioactivity of the desired product was evaluated for the spectrum from the gamma-ray photopeak area by drawing a straight line across the bottom of the photopeak and summing up the counts above this line. These data were corrected both for decay during the time of each count and for the dead time of the analyzer. Further normalizations were applied to the activity data for the decay time, the dose rate, sample weight and counting geometry of the detector. Decay curve analyses were performed to separate out the undesired activities.

Nuclide identification was obtained from a knowledge of the target nuclide, the gamma-ray spectra, decay data, and data in the literature for the nuclides.[14,15]

The yield was measured for each (γ, n) reaction through the absolute determination of the resultant radioactivity. To obtain the disintegration rate from the counting rate of the relevant gamma-ray photopeak, appropriate corrections were made for the variation of photopeak efficiency with gamma-ray energy. The decay schemes used were those listed in the Nuclear Data Sheets.[14] The table of internal conversion coefficients[16] was also used.

Results

Induced Radioactivity. As reported earlier,[2] the prominent photoactivation products found in the energy region of 20 MeV bremsstrahlung are those from (γ, n) and (γ, p) reactions. A preliminary experimental investigation of the short-lived photoactivation properties of some 18 elements have indicated the usefulness of the present method for the determination of magnesium, germanium, selenium, molybdenum, cerium, neodymium and terbium.

With these elements, it was possible to let the activities of short-lived products be much larger than those of longer ones produced from irradiation for one minute.[17] The gamma-ray spectra obtained from 7 elements are given in Fig. 1 (1)—(7). Seven nuclides including ^{23}Mg, ^{75m}Ge, ^{77m}Se, ^{91m}Mo, ^{139m}Ce, ^{141m}Nd and ^{158m}Tb were found to be the most prominent species.

Table 1 lists particulars on the products and the data obtained in this experiment. Of the present results, the half-life of ^{23}Mg was determined as 9.9 sec, which is shorter than that listed in the Nuclear Data Sheets (12 sec).[14]

Limit of Detection. The limit of detection was calculated on the basis of the minimum detectable photopeak area. All activity strengths have been expressed in counts per milligram of the element at the end of one-minute irradiation with a counting geometry of 20% using a 3''dia.$\times$3'' NaI(Tl) detector, and have been normalized to a bremsstrahlung dose rate of 10^7 R/min. Because of the short-lives of the products to be determined, the limits of detection were assumed to be the quantities needed to give 1000 cpm under the above condition. These limits of detection are given in the seventh column of Table 1. It is seen that, on the average, these elements can be detected easily down to about 1 μg per sample by the proposed method.

TABLE 1. THE PARTICULARS OF THE (γ,n) REACTION PRODUCTS AND THE DATA OBTAINED WITH 20 MeV BREMSSTRAHLUNG

Nuclide		Half-life of product (sec)	Gamma-ray determined			Limit of detection (μg)	Yield ($mol^{-1}\cdot R^{-1}$)
Parent (Natural abundance, %)	Residual		Energy (MeV)	Branching ratio (%)	Photopeak activity (cpm/mg)[a]		
^{24}Mg(78.60)	^{23}Mg	9.9	0.511	200	2.04×10^6	0.49	8.1×10^4
^{76}Ge(7.67)	^{75m}Ge	48	0.139	100	6.37×10^5	1.6	1.1×10^4
^{78}Se(23.52)	^{77m}Se	17	0.162	100	1.82×10^6	0.55	1.2×10^6
^{92}Mo(15.86)	^{91m}Mo	65	0.650	57	2.22×10^5	4.5	2.7×10^6
^{140}Ce(88.48)	^{139m}Ce	58	0.745	100	1.06×10^6	0.95	1.3×10^6
^{142}Nd(27.13)	^{141m}Nd	64	0.760	100	3.19×10^5	3.1	1.4×10^6
^{159}Tb(100)	^{158m}Tb	11	0.111	100	2.56×10^5	3.8	2.2×10^6

a) The value corrected at the end of one-minute irradiation with the dose rate of 10^7 R/min; Counting geometry is 20% with a 3''dia.$\times$3''NaI(Tl) detector.

14) Nuclear Data Sheets, Natl. Academy of Science-Natl. Research Council, Washington, D. C. (1961).
15) B. S. Dzhelepov and L. K. Peker, "Decay Schemes of Radioactive Nuclei," Pergamon Press., New York (1961).
16) M. E. Rose, "Internal Conversion Coefficient," North-Holland Publ. Co., Amsterdam (1958).
17) The extraneous activities were due to the reactions, ^{27}Al(γ, n)^{26m}Al (6.6 sec, β^+ emitter) and ^{16}O(γ, n)^{15}O (124 sec, β^+ emitter).

Reaction Yield. The yield ($Y_{(E)}$) was obtained by the absolute measurement of the resultant activity through the following equation.

$$Y_{(E)} = \frac{D_o}{IM(1-e^{-\lambda t})}$$

where D_o is the disintegration rate at the end of irradiation, I the radiation dose rate, M the amount of target nucleus expressed in moles, and λ the decay constant. The data obtained are shown in the last column of Table 1. These values can be taken as the numbers of (γ, n) processes which occurred during the irradiation.

Discussion

It has been pointed out that the photon absorption cross section for a nucleus is an increasing function of Z.[18] In our measurements, through the residual activity method,[19] the yield of radioactive nuclides increases regularly with atomic number from 10^3 to 10^7 orders of magnitude. Of the yields given in Table 1, that for the reaction $^{24}Mg(\gamma, n)^{23}Mg$ is in excellent agreement in absolute magnitude with those expected from the yield curve above. However, the yields for other 6 nuclides, of metastable states, were obtained as $(1—3)\times 10^6$/mol·R, and do not vary significantly with Z values. This implies that the relative yield for the formation of a residual nuclide in its metastable state to that in the ground state should fall for heavier nuclei.

The relative probability of forming each member of a pair of nuclear isomeric states as a result of photonuclear process in the energy region above a giant resonance has been studied by several workers in order to obtain quantitative information about the spin distribution of the excited states.[20-28]

Table 2 shows the results of the isomeric yield ratios obtained for 5 isomeric pairs together with the spins of both the parent nuclei and the residual isomeric states.[29] The isomeric yield ratio has been expressed as a ratio of the yield for the metastable state to the sum of those for both states. Literature values are also included in Table 2.[30]

It has been noted that the formation of both isomeric states follows the steps: formation of the compound state upon electric dipole photon absorption; neutron decay of the compound states to form excited states of the residual nucleus; and gamma-ray cascades from these excited states to the two isomeric levels. In many cases in which an excited state of the residual nucleus can decay to either of the isomers, through intermediate states in gamma-cascades, the gamma-transitions of low multipolarity are accorded preference over those of high multipolarity. Thus the spins of each state of the isomers, as well as the spin differences between states, are the most important factors determining the isomeric yield ratio. Since the absorption of 20 MeV bremsstrahlung by a nucleus can be regarded as $E1$ absorption, the spins of the excited states may not differ remarkably from that of the parent nucleus. The observed ratios generally favor the isomer whose spin is closer to that of

Table 2. The yield ratio of some isomeric pairs

Parent		Residual				Type of multipole transition	Isomeric yield ratio, $Y_m/(Y_m+Y_g)$	
		Ground state		Metastable state				
Target nucleus	Spin	Spin	Half-life	Spin	Half-life		This work	Literature value
^{45}Sc	$7/2^-$	^{44}Sc 2^+	3.9 hr	6^+	2.4 d	$E4$	0.084	0.16[28] a)
^{76}Ge	0^+	^{75}Ge $1/2^-$	82 min	$7/2^+$	48 sec	$E3$	0.38	0.48[26] b)
^{85}Rb	$5/2^-$	^{84}Rb 2^-	33 d	6^+	20 min	$M4$	0.24	—
^{90}Zr	0^+	^{89}Zr $9/2^+$	79 hr	$1/2^-$	4.3 min	$M4$	0.33	0.49[26] b)
^{140}Ce	0^+	^{139}Ce $3/2^+$	140 d	$11/2^-$	58 sec	$M4$	0.091	0.087[26] b)

a) The value obtained with 24 MeV bremsstrahlung.
b) The value obtained with 30 MeV bremsstrahlung.

18) R. Montalbetti, L. Katz and J. Goldenberg, *Phys. Rev.*, **91**, 659 (1953).
19) Y. Oka, T. Kato, K. Nomura and T. Saito, This Bulletin, **40**, 575 (1967).
20) J. R. Huizenga and R. Vandenbosch, *Phys. Rev.*, **120**, 1305 (1960).
21) L. Katz, L. Pease and H. Moody, *Can. J. Phys.*, **30**, 476 (1952).
22) L. Katz, R. G. Baker and R. Montalbetti, *ibid.*, **31**, 250 (1953).
23) J. Goldenberg and L. Katz, *ibid.*, **90**, 308 (1953).
24) P. Axel and J. D. Fox, *ibid.*, **102**, 400 (1956).
25) J. H. Caver, G. E. Coote and T. R. Sherwood, *Nucl. Phys.*, **37**, 449 (1962).
26) S. Costa, F. Ferrero, S. Ferroni and L. Pasqualini, *ibid.*, **72**, 158 (1965).
27) J. R. Tatarczuk and H. A. Medicus, *Phys. Rev.*, **143**, 818 (1966).
28) W. B. Walters and J. P. Hummel, *ibid.*, **150**, 867 (1966).
29) The yields for the $^{45}Sc(\gamma, n)$, $^{86}Rb(\gamma, n)$ and $^{90}Zr(\gamma, n)$ reactions are taken from data reported previously.[19]
30) Although experiments were carried out with different excitation energies, there are no significant variations in the observed isomeric yield ratios with change in the bremsstrahlung maximum energy above a giant resonance region.[26]

the target nucleus. The yield of isomers with very high spins, including ^{44m}Sc, ^{75m}Ge, ^{84m}Rb and ^{139m}Ce, as well as ^{77m}Se, ^{141m}Nd and ^{158m}Tb, are found to be low. The result for ^{89}Zr isomers is unusual, and it is planned to investigate the reasons responsible for this behavior in the near future.

For analytical purposes, the lower limit of detection under the present experimental conditions is 1 μg on the average. As discussed above, the yield of short-lived metastable isomers is not as high as expected from the general behavior of the (γ, n) reaction yield curve. In addition, high multipolarity gamma-transitions with large internal conversion coefficients are inherent in the decay of these isomers. Despite these unfavorable properties, the use of short-lived activities in photoactivation analysis should enhance the efficacy of the method because of rapidity, selectivity and specificity.

BULLETIN OF THE CHEMICAL SOCIETY OF JAPAN VOL. 41 1610—1614 (1968)

The Coprecipitation and the Spectrophotometric Determination of Uranium as Dibenzoylmethane Chelate

Tsunenobu SHIGEMATSU, Masayuki TABUSHI, Masakazu MATSUI and Megumu MUNAKATA

Institute for Chemical Research, Kyoto University, Sakyo-ku, Kyoto

(Received December 30, 1967)

The coprecipitation and direct-photometric method was applied to the uranium β-diketonate system; uranyl ion was coprecipitated as dibenzoylmethanate with *o*-phenylphenol and determined spectrophotometrically after the precipitate was dissolved in butyl acetate. The effect of ligand concentration on the per cent coprecipitation-pH curve was studied and the curve was not affected by the ligand concentration in the range from 2×10^{-2} to 4×10^{-4} M. Over the 200 mg of *o*-phenylphenol, an almost quantitative coprecipitation was obtained, though the absorbance slightly decreased with the increase in the coprecipitant amount (about 2% per 1g *o*-phenylphenol). As many diverse ions interfered with the determination of uranium, the solution of calcium-EDTA chelate was used as a masking agent. When a small amount of alkylamine was added, the recovery of uranium became more complete. The effect of alkylamine was probably caused by the adduct formation of uranium chelate with alkylamine.

It has been considered that the coprecipitation of metal chelates with organic compounds is a very attractive problem in the sense of the theoretical treatment[1] and especially of the practical technique. The authors have been much interested in this subject and already reported the coprecipitation of ferric oxinate with some organic compounds and proposed a method for the photometric determination of ferric iron in very dilute solution.[2] The general procedure consists of three steps: Metal ions are allowed to react with a chelating reagent; the metal chelate formed is collected with an adequate organic coprecipitant; and the precipitate separated is then dissolved in a suitable organic solvent, followed by the absorbancy measurements. By this procedure, the metal ion present in much low concentration can be easily concentrated and determined, and the method is suitable, if the chelate-forming reaction is selective to the metal ion to be analysed, or if the absorbance of the metal chelate is not affected by the presence of diverse ions.

In the present research, the coprecipitation and the direct-photometric determination of uranium was investigated by using β-diketone and *o*-phenylphenol (OPP) as a chelating reagent and organic coprecipitant, respectively. Beta-diketones have been widely utilized for the solvent extraction of metal ions,[3] and is recognized to be a very useful reagent for the separation and the photometric determination of uranium, because uranium can

1) W. P. Tappmeyer and E. E. Pickett, *Anal. Chem.*, **39**, 1709 (1962).

2) T. Shigematsu, M. Matsui, M. Munakata and T. Sumida, This Bulletin, **41**, 609 (1968). b) M. Matsui, M. Munakata and T. Shigematsu, *Bull. Inst. Chem. Res., Kyoto Univ.*, **45**, 273 (1967).

3) See, for example, a) J. Stary, "The Solvent Extraction of Metal Chelates," Pergamon Press, London (1964). b) G. H. Morisson and H. Freiser, "Solvent Extraction in Analytical Chemistry, "John Wiley & Sons, New York (1957).

be selectively extracted by masking diverse ions with EDTA-calcium.[4,5] However, most of β-diketones show comparatively high absorption near the absorption maximum of the uranium chelates, and therefore the concentration of the reagent must be kept excactly constant, or the low concentration is desirable. In the coprecipitation method, the almost quantitative recovery was attained even in the low concentration (4×10^{-4} M) of the reagent and when the larger volume of sample solution was handled, the addition of a Lewis base such as *n*-butylamine *etc.* prevented the decrease of the recovery, and accordingly, the determination of uranium was not essentially influenced by the reagent blank. As previously described, OPP is one of the most suitable coprecipitants for such a methal chelate as oxinates.[2]

Experimental

Apparatus. Spectrophotometric measurements were made with a Hitachi Perkin-Elmer 139 UV-VIS spectrophotometer using 1.00 cm transmission cells. A Hitachi-Horiba glass electrode pH meter, model M3 was used for the pH measurements.

Materials. β-Diketones were obtained from the Dozindo Co., Ltd., Research Laboratories. A stock solution of uranium was prepared by dissolving $UO_2(NO_3)_2\cdot6H_2O$ in water; the concentration was determined gravimetrically as U_3O_8. *o*-Phenylphenol (OPP) was purified by the distillation under the pressure of 8—10 mmHg in the nitrogen atmosphere. Butyl acetate was purified by washing with water, followed by distillation. All the other reagents used were the reagent-grade materials and used without further purification.

Procedure. For investigating the effect of various factors, the following procedure was designed: An aliquot of the uranium stock solution, 5 m*l* of 0.2 M EDTA-calcium solution and 1 m*l* of 1 M acetic acid solution are taken in a 100 m*l* Erlenmeyer flask. The solution is diluted to 50 m*l*, and the pH of the solution is adjusted to a desired value with a dilute sodium hydroxide or hydrochloric acid solution. One-half milliliter of a β-diketone-acetone solution ($0.4—8\times10^{-3}$ M) and a suitable amount of *o*-phenylphenol which is previously smashed into fine pieces are added. After shaken with a mechanical shaker, the mixture is filtrated through a glass filter No. 3 and the precipitate is then dissolved in butyl acetate. The organic solution is made clear by filtering through a filter paper, transferred to a 10 m*l* measuring flask and the absorbance is obtained.

Results and Discussion

Because the adding method of the organic coprecipitant in an organic coprecipitation technique is an important factor, its effect on the coprecipitation behavior of uranium was studied by using the uranium-dibenzoylmethane (DBM)-OPP system. The following procedures were examined[4]: (A) OPP, which was freshly precipitated from alkaline solution with an acid, was added to a sample solution. (B) OPP dissolved in an alkaline solution was added to a buffered sample solution. (C) OPP, which was smashed in a mortar, was added to a sample solution. (D) OPP dissolved in acetone was added to a sample solution. As shown in Fig. 1, (A) and (B) were excellent, (C) was fairly effective, but (D) was not so effective. In the subsequent experiment, the procedure (C) was employed, because in the procedure (A) or (B), the pH value of the sample solution must be adjusted again after the addition of OPP. Effect of the concentration of the chelating agent was studied over the range 2×10^{-2} to 4×10^{-4} M, and the per cent coprecipitation-pH curve of uranium is shown in Fig. 2. The curve of uranyl dibenzoylmethanate is not affected by the reagent concentration in the range studied: This indicates that the system is not in a equilibrium state in the concentration over the solubility of DBM. The curve of uranyl thenoyltrifluoroacetone (TTA) complex, on the other hand, shifted to the lower pH value as the TTA concentration was increased. The same tendency was observed in the case of benzoyltrifluoroacetone or benzoylacetone. This difference in the behavior may be caused by the solubility of

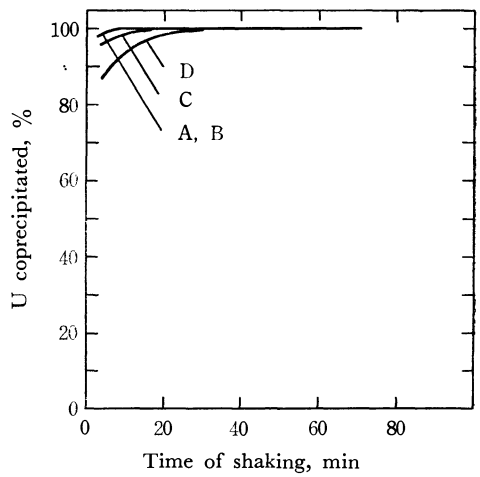

Fig. 1. Effect of adding methods of the coprecipitant on coprecipitation.

UO_2^{2+}: 8×10^{-6} M, DBM: 4×10^{-4} M, OPP: 500 mg, aqueous phase: 50 m*l*, organic phase: 10 m*l* of butyl acetate.
A: fresh precipitation from alkaline solution with an acid.
B: precipitation in a buffered sample solution from alkaline solution.
C: smashed in a mortar.
D: dissolution in acetone.

4) T. Shigematsu, M. Tabushi and M. Matsui, This Bulletin, **37**, 1333 (1964).
5) T. Shigematsu and M. Tabushi, *Nippon Kagaku Zasshi (J. Chem. Soc. Japan, Pure. Chem. Sect.)*, **81**, 265 (1960).

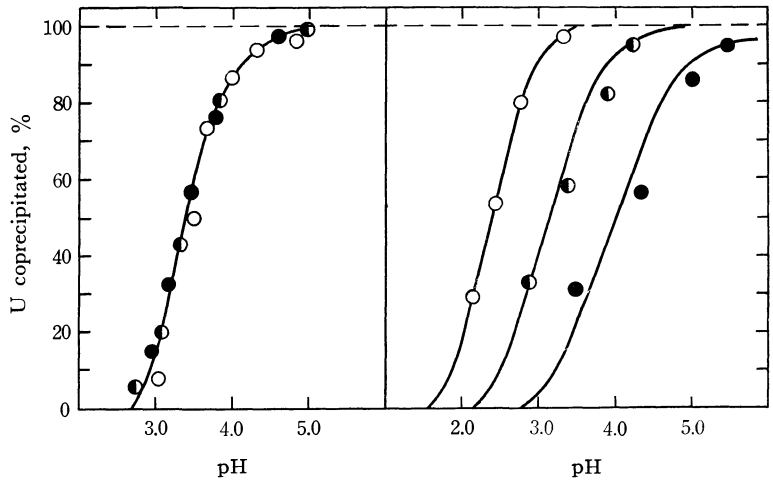

Fig. 2. Effect of β-diketone concentration on the coprecipitation of uranyl chelate.
Left: DBM ○ 2×10^{-2} M, ◐ 4×10^{-3} M, ● 4×10^{-4} M.
Right: TTA ○ 2×10^{-2} M, ◐ 4×10^{-3} M, ● 4×10^{-4} M.
Shaking for 30 min, others are the same as in Fig. 1.

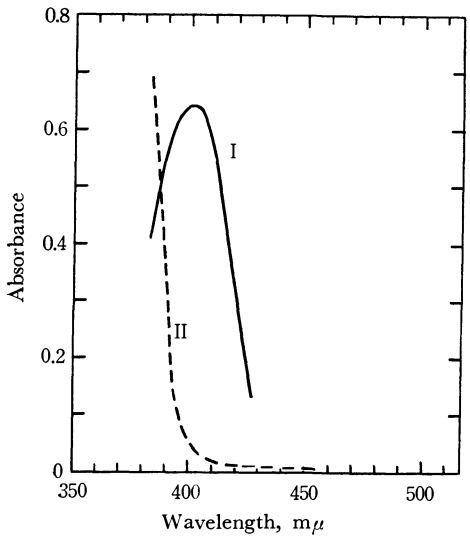

Fig. 3. Absorption spectra of uranyl DBM chelate.
I: UO_2^{2+} 4×10^{-5} M, DBM 2×10^{-2} M, pH 6.0, shaking for 30 min.
II: reagent blank.

β-diketone in water. The curve shifts to lower pH with the increase in the reagent concentration, until it probably arrives at the solubility of the reagent. The phenomenon that uranium acetylacetonate can not be coprecipitated well, may be due to the larger solubility of acetylacetone in comparison with that of other β-diketones. Because the photometric determination of uranium is influenced by the reagent blank (Fig. 3), it is desirable that the amount of the reagent contained in the precipitate is as small as possible. Since β-diketone is coprecipitated together with uranyl β-diketone chelate even when the reagent concentration does not exceed its solubility, the β-diketone which possessed the larger solubility did not always show lower reagent blank than the one which possessed the smaller solubility did. In the proceeding experiments, DBM was used as a chelating reagent, from the consideration described just above and other reasons, that is, uranium could be effectively and almost quantitatively coprecipitated in the relatively low concentration of the reagent, and the extinction coefficient of the uranyl chelate was larger than that of other uranyl β-diketone chelates.

A polar solvent was used for dissolving the precipitate, because the absorbance of uranyl-DBM chelate decreased in the nonpolar solvent (*e. g.*,

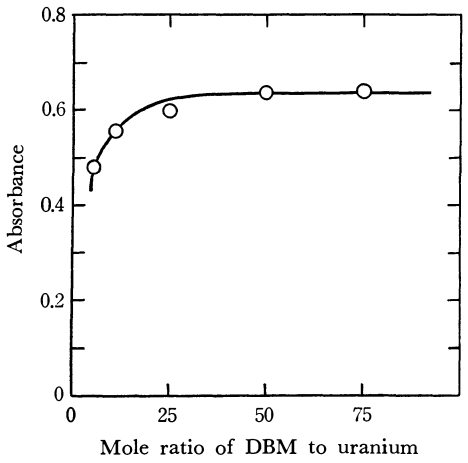

Fig. 4. Effect of reagent concentration.
UO_2^{2+} 4×10^{-5} M, pH 6.0, shaking for 30 min, others are the same as in Fig. 1.

benzene) with the lapse of time.[5] Normal-butyl acetate was an excellent solvent, because of its good separating property from water and of the larger extinction coefficient in comparison with other polar solvents (*e. g.*, *n*-hexyl alcohol, cyclohexanone).

The effect of the mole ratio of DMB to uranium is shown in Fig. 4: The constant absorbance can be obtained when the mole ratio is larger than fifty, while below fifty the absorbance decreases with the decrease of DBM concentration, and this is owing to the incomplete coprecipitation of uranium and to the decomposition of the chelate in the solvent: The decomposition may be caused by OPP.

The effect of the amount of coprecipitant, OPP, is indicated in Fig. 5. The absorbance rapidly diminishes when OPP amount is less than 200 mg. The reason for this low absorbance is attributed to

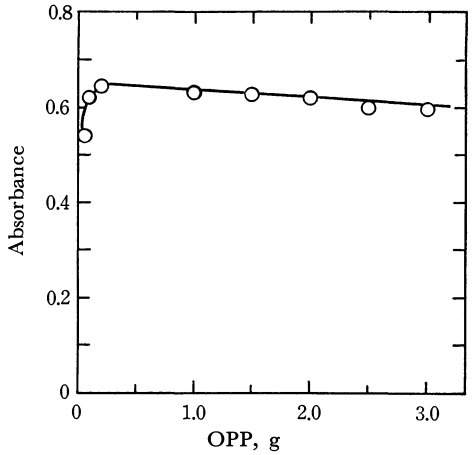

Fig. 5. Effect of coprecipitant, OPP.
UO_2^{2+} 4×10^{-5} M.

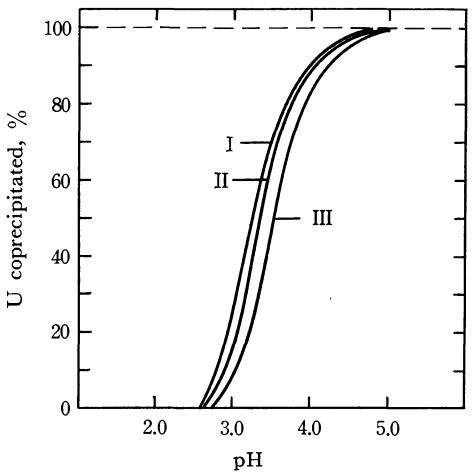

Fig. 6. Effect of OPP amount on per cent coprecipitation *vs.* pH curve.
OPP: I 30 g, II 1 g, III 300 mg

both the loss by the filtration of the precipitate and the decrease in the coprecipitation recovery, because OPP becomes a liquid state in such a small amount. Above 200 mg, the absorbance slightly decreases with the increase in OPP amount (about 2% per 1 g OPP). This unexpected phenomenon is probably resulted from the adduct formation of the chelate with OPP, but not from the coprecipitation yield. Figure 6 indicates the evidence of the adduct formation: The per cent coprecipitation-pH curve shifts somewhat to lower pH as the OPP amount increases, just like in the case of the adduct formation in the solvent extraction of metal chelates.[6]

Determination of uranium may be interfered by many diverse ions, and therefore, an available masking agent must be used. When 5 m*l* of 0.2 M EDTA solution and calcium chloride equivalent to EDTA (0.02 M Ca-EDTA in the final concentration) were added as a masking agent, the per cent coprecipitation-pH curve of uranyl bis-dibenzoylmethane chelate shifts about one pH unit to alkali side, but the extraction coefficient is the same with that obtained in the absence of EDTA in the pH region above 6.0[4] (Fig. 7).

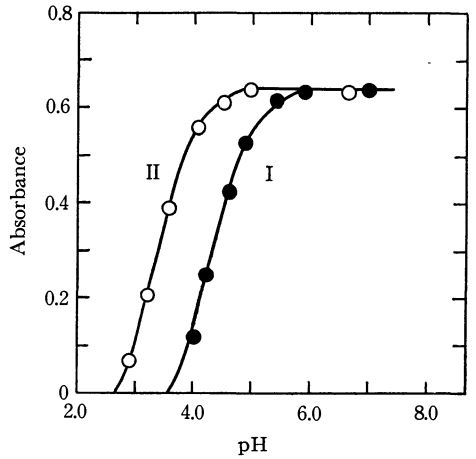

Fig. 7. Effect of masking agent, calcium-EDTA chelate.
I. 0.02 M of Ca-EDTA, II. no masking agent.

From the above experimental results, the conditions for the coprecipitation and the direct-photometric determination of uranium was controlled as follows. The concentration of DBM, acetic acid and EDTA-calcium are 8×10^{-4} M, 0.02 M and 0.02 M, respectively; pH, 6.0; and the volume, about 50 m*l*. One gram of OPP is added and the precipitate was dissolved and diluted to 10 m*l* with butyl acetate.

6) a) H. M. N. H. Irving and D. N. Edington, *J. Inorg. Nucl. Chem.*, **27**, 1359 (1965). b) T. Shigematsu, M. Tabushi, M. Matsui and T. Honjyo, This Bulletin, **39**, 165 (1966).

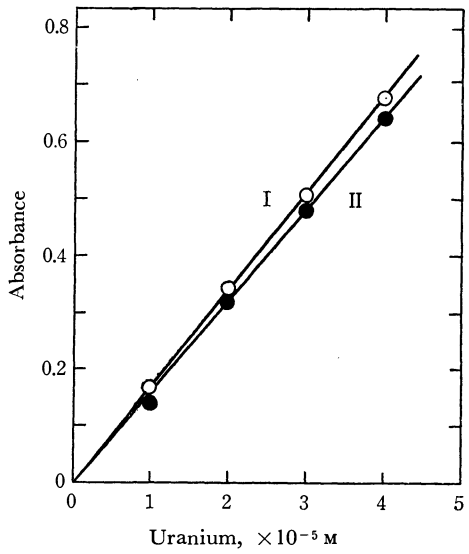

Fig. 8. Calibration curve of uranium.
I. extraction method, II. coprecipitation method

In Fig. 8, calibration curves for uranium are presented. One is obtained by this coprecipitation method and the other is obtained by extracting uranium with 10 m*l* of butyl acetate containing 1 g of OPP, from about 10 m*l* of aqueous solution including 4×10^{-3} M DBM, 0.02 M acetic acid and 0.02 M EDTA-calcium. Beer's law is obeyed up to 10 ppm, and the molar extinction coefficients at 400 mμ are 16100 (this method) and 16800 (liquid-liquid extraction), respectively. This difference may be due to the fact that the coprecipitation recovery of uranium is not precisely quantitative, but about 96 per cent. When a small amount (0.1 m*l*) of *n*-butylamine or *n*-hexylamine was added to the coprecipitation system, the recovery became complete, and two analytical curves quite well agreed. The effect of amines will be described later in this paper.

To investigate the influence of several metal ions, the measurements were made on a solution containing a proper amount of foreign cations with 94 μg of uranium. The results are summarized in Table 1. Aluminum, titanium, silver, tin(IV) and bismuth(III) interfer because of the formation of hydroxide.

Table 1. Influence of diverse ions
U present: 94 μg; DBM: 8×10^{-3} M; pH: 6.50

Ion	Present (mg)	U found (μg)	Ion	Present (mg)	U found (μg)
Mg^{2+}	2	93.0	Mo^{6+}	5	94.0
V^{5+}	1	94.3	Cd^{2+}	5	96.3
Cr^{6+}	1	96.0	Ba^{2+}	5	93.5
Mn^{2+}	1	94.7	Pb^{2+}	10	92.3
Fe^{3+}	1	93.0	Th^{4+}	1	95.2
Co^{2+}	1	94.5	Al^{3+}	2	*
Ni^{2+}	5	92.4	Ti^{4+}	1	*
Cu^{2+}	1	95.2	Ag^{+}	1	*
Zn^{2+}	5	93.4	Sn^{4+}	1	*
Sr^{2+}	5	94.5	Bi^{3+}	5	*

* Hydroxide or oxide of coexisting ion was precipitated.

Table 2. Recovery of uranyl ion from 500 m*l* of sample solution
U: 8×10^{-7} M, DBM: 8×10^{-5} M, pH: 6.5, OPP: 2.0 g

Organic solvent	Volume (m*l*)	U pptd. (%)
Acetone	0.5	42.3
	1.0	49.1
	5.0	72.3
	10.0	97.1
	12.0	*
n-Butylamine	1.0	99.8
	2.0	99.7
n-Hexylamine	1.0	99.6
	2.0	100.0
Pyridine	0.5	*
Tri-butyl phosphate	0.5	*

* Precipitate became liquid.

Recovery of uranium decreased with the increase in volume of sample solution. Although the element may be quantitatively recovered by rising the DBM amount, then the influence of the reagent blank appears. In order to remove the difficutly, a Lewis base was added to the sample solution. The results are presented in Table 2. Uranium was almost completely recovered from 500 m*l* of sample solution by adding *n*-butylamine or *n*-hexylamine. Pyridine or tri-*n*-butyl phosphate could not be employed, because the precipitate became a liquid state. This effect of Lewis bases on coprecipitation of uranium is probably caused by the adduct formation, and is the same phenomenom as the "synergistic effect" in the solvent extraction of metal chelates.[7-10] By increasing the DBM amount, uranium can be essentially quantitatively collected from larger volume: For example, the use of 4×10^{-5} M DBM and 5 m*l* of *n*-butylamine gave satisfactory yield on 2 *l* of sample.

7) A. E. Comyns, B. M. Gatehause and E. Wait *J. Chem. Soc.*, **1958**, 4655.
8) L. Sacconi, G. Carroti and Paoletti, *ibid.*, **1958** 4257.
9) W. W. Wendlandt, J. L. Bear and G. R. Horton, *J. Phys. Chem.*, **64**, 1289 (1960).
10) H. M. N. H. Irving and D. N. Edgington, *J. Inorg. Nucl. Chem.*, **15**, 158 (1960).

BULLETIN OF THE CHEMICAL SOCIETY OF JAPAN VOL. 41 1615—1618 (1968)

Kinetics of the Aquation of Pentammine Amino Acid Cobalt(III) Complexes

Kazuko OGINO, Tasuku MURAKAMI and Kazuo SAITO

Department of Chemistry, Faculty of Science, Tohoku University, Katahira-cho, Sendai

(Received January 22, 1968)

The rate of aquation of pentamminecobalt(III) complexes of the general formula $[Co(NH_3)_5amH]^{3+}$ (amH stands for an amino acid molecule with proton on the nitrogen atom), containing unidentate glycine, β-alanine, sarcosine and betaine, has been measured at 55°C, and ionic strength 0.1 and 1.0 in the acid concentration range up to 0.5 M. The kinetic term is expressed by

$$\text{Rate} = [\text{complex}](k_{H_2O}+k_{H^+}[H^+])$$

The k_{H_2O} and k_{H^+} values for glycine, β-alanine, sarcosine and betaine complex are respectively as follows (at $\mu=1.0$): k_{H_2O}, 0.40×10^{-6}, $\lesssim0.2\times10^{-6}$, 0.25×10^{-6}, and 0.44×10^{-6} sec^{-1}; k_{H^+}, 2.0×10^{-6}, 26×10^{-6}, 1.8×10^{-5}, and 1.0×10^{-6} M^{-1} sec^{-1}. The k_{H^+} values increase with increase in pK_a values of the amino acids, but are smaller than those for the aquation of carboxylatopentamminecobalt(III) complexes. This difference seems to be due to the electrostatic shielding of the carboxylate group by the protonated amino group.

An amino acid usually coordinates to a metal with its amino and carboxylate group to form a chelate ring. Recently, complexes were also prepared in which the amino acid coordinates as a unidentate ligand only with its carboxylate end, to form pentamminecobalt(III) complex.[1,2] Such a complex is similar to a carboxylatopentamminecobalt(III) complex, in the context that the ligands coordinate to the cobalt(III) ion with the carboxylate end. The reaction kinetics of acid hydrolysis of carboxylatopentamminecobalt(III) complexes was studied by Monacelli, Basolo and Pearson and the mechanism disucssed with special reference to the acid catalysis.[3] It seems interesting to carry out similar kinetic studies with pentammine amino acid cobalt(III) complexes, in which the protonated amino group can be linked with the carboxylate *via* hydrogen bonding. We have measured the rate of acid hydrolysis of the following complexes in aqueous solution,

$$[Co(NH_3)_5amH]^{3+} + H_2O \rightarrow [Co(NH_3)_5H_2O]^{3+} + amH \quad (1)$$

where "am" expresses amino acid anion, and compared the results with those of carboxylatopentammine complexes.

Experimental

Materials. Three complexes of the general formula $[Co(NH_3)_5amH](ClO_4)_3$ were prepared with glycine, β-alanine and betaine as described in the literature[1] and identified by elemental analyses of carbon, hydrogen and nitrogen, and absorption spectra. The sarcosine complex, a new compound, was also prepared by a similar method.

Found: C, 6.97; H, 4.72; N, 15.42; H_2O, 3.46%. Calcd for $[Co(NH_3)_5OOCCH_2NH_2(CH_3)](ClO_4)_3\cdot H_2O$: C, 6.56; H, 4.40; N, 15.32; H_2O, 3.28%.

The ionic strength was adjusted with sodium perchlorate, which was prepared from sodium carbonate and perchloric acid of guaranteed grade. Other reagents were all of guaranteed grade and used without further purification.

Experimental Procedure. A weighed amount of the complex ($\simeq10^{-4}$ mol) was added into an aqueous solution (100 ml) of a given ionic strength (0.1 or 1.0) and acid concentration (0.01—0.5 M) at a given temperature. The complex dissolved rapidly. Aliquots were withdrawn at appropriate intervals, cooled and the absorbances measured, or the amount of liberated amino acid determined with ninhydrin.

Spectrophotometric Method. The progress of reaction was best chased by measuring the change in extinction at 275 mμ, regardless of the kind of coordinated amino acid. The values of ε_{275} for glycine, sarcosine, betaine, β-alanine and aquo complex are 190, 206, 255, 400 and 3.1, respectively. The withdrawn aliquot was placed in a 10 mm quartz cell and the extinction measured at room temperature with a HITACHI EPU-IIA spectrophotometer. The reaction rate was slow enough, so that neither the time taken for the measurement nor the temperature change during the measurement does not affect the result. The pseudo first order rate constant k_{obs} was obtained by plotting

1) J. Fujita, T. Yasui and Y. Shimura, This Bulletin, **38**, 654 (1965).
2) R. T. M. Fraser, *Inorg. Chem.*, **3**, 1561 (1964).
3) F. Monacelli, F. Basolo and R. G. Pearson, *J. Inorg. Nucl. Chem.*, **24**, 1241 (1962).

$\log(\varepsilon-\varepsilon_a)$ *vs. t*, where ε is the apparent molar extinction coefficient of reaction mixture at time t and ε_a that of the aquopentammine complex.

Ninhydrin Method. This method was used only for the glycine complex. Free glycine should be separated from the aquopentammine and the glcyinepentammine complex. A 5 m*l* portion of the reaction mixture was passed through a column (10 mm in diameter, 10 cm in length) of the cation exchanger Amberlite CG-50 (Type 1, H-form) and the column washed with a citrate buffer of pH 5 (total effluent 50 m*l*). The complexes were completely captured by the resin, whereas the free amino acid was quantitatively recovered in the effluent and determined spectrophotometrically at 565 mμ by the Yemm-Cocking's method with ninhydrin.[4] The rate constant k_{obs} is given by plotting $\log(a-x)$ *vs. t*, where a is the initial concentration of the complex and x the concentration of isolated glycine.

Results

The plots of $\log(\varepsilon-\varepsilon_a)$ *vs. t* and $\log(a-x)$ *vs. t* were all linear under the experimental conditions

Table 1. The rate constant at varying initial concentrations of the glycine complex (55°C, $\mu=0.1$, by the ninhydrin method)

a mM	$k_{obs}\times10^6$ sec^{-1}
1.0	0.74
2.0	0.73
3.0	0.73

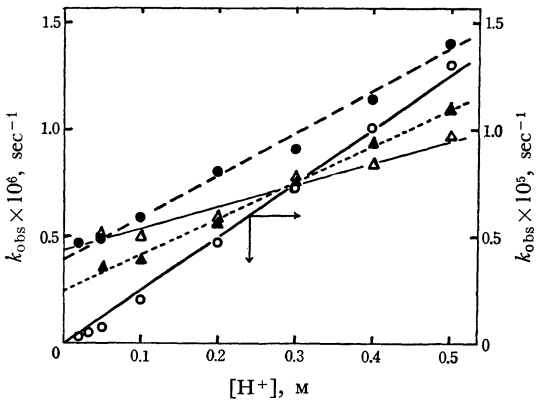

Fig. 1. Relationship between the observed rate constant k_{obs} and the hydrogen ion concentration, at 55°C and $\mu=1.0$.
--●-- $[Co(NH_3)_5OOCCH_2NH_3]^{3+}$ (glycine)
—○— $[Co(NH_3)_5OOCCH_2CH_2NH_3]^{3+}$ (β-alanine)[a]
---▲--- $[Co(NH_3)_5OOCCH_2NH_2(CH_3)]^{3+}$ (sarcosine)
—△— $[Co(NH_3)_5OOCCH_2N(CH_3)_3]^{3+}$ (betaine)
a) The scale of the ordinate for this complex is 10-fold of that for other complexes.

4) E. W. Yemm and E. C. Cocking, *Analyst*, **80**, 209 (1955).

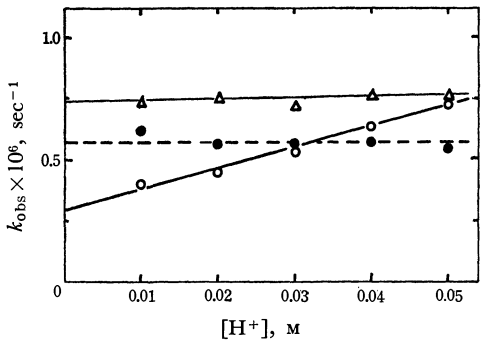

Fig. 2. Relationship between the observed rate constant k_{obs} and the hydrogen ion concentration, at 55°C and $\mu=0.1$.
—△— $[Co(NH_3)_5OOCCH_2NH_3]^{3+}$ (glycine)[a]
--●-- $[Co(NH_3)_5OOCCH_2NH_3]^{3+}$ (glycine)
—○— $[Co(NH_3)_5OOCCH_2CH_2NH_3]^{3+}$ (β-alanine)
a) By the ninhydrin method.

and the rate constant was independent of the initial concentration of the complex as exemplified in Table 1. Figure 1 shows the relationship between the rate constant k_{obs} and the hydrogen ion concentration for the glycine, the sarcosine, the betaine and the β-alanine complex in aqueous solutions of ionic strength 1.0, and Fig. 2 those for the glycine and the β-alanine complex in solutions of ionic strength 0.1. The results are those obtained by the spectrophotometric method unless otherwise stated. All of these plots are regarded to be linear. Therefore, the observed pseudo first order rate constant k_{obs} can be expressed by Eq. (2), as a linear function of the hydrogen ion concentration.

$$k_{obs} = k_{H_2O} + k_{H^+}[H^+] \quad (2)$$

The uncatalysed rate constant k_{H_2O} and the acid catalysed rate constant k_{H^+} are calculated from the diagrams and shown in Table 2, together with the pK_a values of the amino acids.

It has been known that some pentamminecobalt-(III) complexes tend to liberate ammonia as shown in Eqs. (3) and (4). (X, univalent anion)

$$[CoX(NH_3)_5]^{2+} + H_2O \rightarrow [CoX(NH_3)_4(H_2O)]^{2+} + NH_3 \quad (3)$$

$$[Co(NH_3)_5H_2O]^{3+} + H_2O \rightarrow [Co(NH_3)_4(H_2O)_2]^{3+} + NH_3 \quad (4)$$

The products can further undergo hydrolysis to liberate more ammonia.[5,6] Whenever a spectrophotometric method is used for a slow reaction, contribution of such side reactions should be taken into consideration.

Ammonium ions pass through the exchanger

5) F. Basolo, J. G. Bergmann and R. G. Pearson, *J. Phys. Chem.*, **56**, 22 (1952).
6) A. B. Lamb and J. W. Marden, *J. Am. Chem. Soc.*, **33**, 1873 (1911).

TABLE 2. RATE CONSTANTS OF AQUATION OF $[Co(NH_3)_5amH]^{3+}$ AND $[Co(NH_3)_5L]^{2+}$, AT 55°C AND $\mu=0.1$ AND 1.0

Ligand	pK_a [a]	μ	$k_{H_2O}\times10^6$ sec^{-1}	$k_{H^+}\times10^6$ $M^{-1}\,sec^{-1}$
Glycine ($H_3^+NCH_2COO^-$)	2.35	0.1	0.73[b]	$\lesssim1$[b]
		0.1	0.57	$\lesssim1$
		0.1	1.8[e]	$\lesssim1$[e]
		0.1	7.6[f]	$\lesssim1$[f]
β-Alanine ($H_3^+NCH_2CH_2COO^-$)	3·55	0.1	0.30	8.6
Acetate (CH_3COO^-)[c]	4.76	0.1	1.4	170
Trifluoroacetate (CF_3COO^-)[c]	0.3	0.1	~6[d]	~1[d]
Glycine ($H_3^+NCH_2COO^-$)	2.35	1.0	0.40	2.0
		1.0	1.1[e]	7.4[e]
		1.0	1.9[f]	27[f]
Sarcosine ($(CH_3)^+NH_2CH_2COO^-$)	2.35	1.0	0.25	1.8
Betaine ($(CH_3)_3^+NCH_2COO^-$)	1.84	1.0	0.44	1.0
β-Alanine ($H_3^+NCH_2CH_2COO^-$)	3.55	1.0	$\lesssim0.2$	26

a) Values for the acids at 25°C and $\mu=0$.
b) By the ninhydrin method.
c) Results from Ref. 3.
d) Extrapolated values from the data at 60, 70 and 79°C (Ref. 3).
e) Values at 65°C.
f) Values at 75°C.

column under the given condition and react with ninhydrin to give a similar coloration to that with glycine. Hence the ninhydrin method can easily overestimate the amount of glycine to give apparently greater rate constants. The presence of ammonium ions was confirmed with Nessler's reagent in the reaction mixtures kept at 55°C for more than 50 hr. The rate constant obtained by the ninhydrin method (k_{H_2O}, 0.73×10^{-6} sec^{-1} at 55°C, $\mu=0.1$) is slightly larger than that by the spectrophotometric method (k_{H_2O}, 0.57×10^{-6} sec^{-1}). However the difference is small especially when the rate is calculated from the kinetic data obtained at earlier stages of reaction, as in most cases by the spectrophotometric method. Hence it is quite certain that this method really gives the rate of reaction (1).

TABLE 3. THE ACTIVATION PARAMETERS FOR THE UNCATALYSED AQUATION OF PENTAMMINECOBALT(III) COMPLEXES, AT $\mu=0.1$

Ligand	$\Delta H^{\neq}$ kcal mol^{-1}	$\Delta S^{\neq}$ cal $mol^{-1}\,deg^{-1}$	Ref.
Glycine	29	+1	This work
Acetate	25	−8	3
Trifluoroacetate	26	−2	3

TABLE 4. THE ACTIVATION PARAMETERS FOR AQUATION OF THE GLYCINE COMPLEX, AT $\mu=1.0$

	$\Delta H^{\neq}$ kcal mol^{-1}	$\Delta S^{\neq}$ cal $mol^{-1}\,deg^{-1}$
k_{H_2O}	22	−20
k_{H^+}	29	+ 3

Activation parameters for the glycine complex were obtained by the measurements at 55, 65, and 75°C and ionic strength 0.1 and 1.0. The results are listed in Tables 3 and 4 together with those of related compounds.

Discussion

Equation (2) suggests that two reaction paths are involved in these aquations as exemplified in Eqs. (5) to (7).

$$[(NH_3)_5Co\text{-}O\overset{O}{\overset{\|}{C}}CH_2NH_3]^{3+} + H_2O \xrightarrow{k_{H_2O}} [(NH_3)_5CoH_2O]^{3+} + {}^-OOCCH_2NH_3^+ \quad (5)$$

$$[(NH_3)_5Co\text{-}O\overset{O}{\overset{\|}{C}}CH_2NH_3]^{3+} + H^+ \overset{K}{\rightleftharpoons} [(NH_3)_5Co\text{-}O\overset{H^+O}{\overset{\|}{C}}CH_2NH_3]^{3+} \quad (6)$$

$$[(NH_3)_5Co\text{-}O\overset{H^+O}{\overset{\|}{C}}CH_2NH_3]^{3+} + H_2O \xrightarrow{k'} [(NH_3)_5CoH_2O]^{3+} + {}^-OOCCH_2NH_3^+ + H^+ \quad (7)$$

The reaction (5) is the path independent of the hydrogen ion concentration and its rate constant is k_{H_2O}. The reactions (6) and (7) correspond to the path catalysed by acids and its rate constant k_{H^+} is expressed by Eq. (8).

$$k_{H^+} = k'K \quad (8)$$

Discussion

Equation (2) suggests that two reaction paths are involved in these aquations as exemplified in Eqs. (5) to (7).

$$[(NH_3)_5Co\text{-}O\overset{O}{\overset{\|}{C}}CH_2NH_3]^{3+} + H_2O \xrightarrow{k_{H_2O}} [(NH_3)_5CoH_2O]^{3+} + {}^-OOCCH_2NH_3^+ \quad (5)$$

$$[(NH_3)_5Co\text{-}O\overset{O}{\overset{\|}{C}}CH_2NH_3]^{3+} + H^+ \overset{K}{\rightleftharpoons} [(NH_3)_5Co\text{-}O\overset{H^+O}{\overset{\|}{C}}CH_2NH_3]^{3+} \quad (6)$$

$$[(NH_3)_5Co\text{-}O\overset{H^+O}{\overset{\|}{C}}CH_2NH_3]^{3+} + H_2O \xrightarrow{k'} [(NH_3)_5CoH_2O]^{3+} + {}^-OOCCH_2NH_3^+ + H^+ \quad (7)$$

The reaction (5) is the path independent of the hydrogen ion concentration and its rate constant is k_{H_2O}. The reactions (6) and (7) correspond to the path catalysed by acids and its rate constant k_{H^+} is expressed by Eq. (8).

$$k_{H^+} = k'K \quad (8)$$

The uncatalysed rate constants (k_{H_2O}) tend to decrease slightly with the increase in ionic strength (Table 2), whereas the acid catalysed rate constants (k_{H^+}) are significantly greater in solutions of $\mu=1.0$ than in $\mu=0.1$. The equilibrium constant K between cations such as that expressed by Eq. (6), generally increases with increase in ionic strength. Therefore, the increase in k_{H^+} values with the increase in ionic strength could be ascribed to the increase in K.

Basolo *et al.* reported that the aquations of carboxylatopentamminecobalt(III) complexes, Eq. (9), proceed by similar mechanisms to Eqs. (5) to (7).[3]

$$[Co(NH_3)_5OOCR]^{2+} + H_2O \rightarrow [Co(NH_3)_5H_2O]^{3+} + {}^-OOCR \qquad (9)$$

The rate constants, k_{H_2O} and k_{H^+}, for the acetato and the trifluoroacetato complex are also shown in Table 2 for comparison. The values for the trifluoroacetato complex were obtained by extrapolating their results to 55°C. The aquation of the amino acid complexes is considerably slower than that of the carboxylato complexes. The k_{H_2O} values in solutions of ionic strength 0.1 decrease in the order, trifluoroacetato, acetato, glycine and β-alanine complex. Basolo *et al.* stated that the k_{H_2O} values of carboxylato complexes tend to decrease with increase in pK_a values of the acids. However, the results in Table 2 do not indicate that such a relation fits the amino acid complexes. On the other hand, the k_{H^+} values for the carboxylato and the amino acid complexes increase with increase in pK_a values within each of these two groups of acid. The pK_a values affect the equilibrium constant K of Eq. (6), and hence the k_{H^+} values.

The k_{H^+} values of the amino acid complexes are much smaller than expected from the relationship between pK_a values and k_{H^+} values for carboxylato complexes. Concerning the glycine and the sarcosine complex, the hydrogen bonding between carboxylate and ammonium group could impede the protonation given by Eq. (6) to decrease the k_{H^+} values. The k_{H^+} value of the betaine complex, which cannot form such a hydrogen bond, is, however, still smaller than those of the two amino acid complexes. Therefore the retardation of protonation should rather be ascribed to an electrostatic effect due to the ammonium group present in the neighborhood of the carboxylate group. Thus the carboxylate end is "shielded" from the approach of a hydrogen ion by both the central cation and the ammonium group, to give a smaller K value.

A similar electrostatic effect is also seen in the hydrolysis of organic esters. Walker and Owens measured the rate of acid-catalysed hydrolysis of chloride of cyclohexyl betainate and found that the rate is *ca.* 1/80 of that of cyclohexyl acetate.[7] The retardation is understood as due to the influence of an electron-attracting group (*e.g.*, $-N^+(CH_3)_3$), rather than to that of steric hindrance or salt effect.[8]

The β-alanine complex has a considerably greater k_{H^+} value than α-amino acid complexes. Its ammonium group would shield the coordinated carboxylate group to a less extent than an α-amino acid does. Such a small influence of $-NH_3^+$ group upon the carboxylate seems to be also reflected in the large pK_a value of β-alanine.

The entropy of activation of the glycine complex is more positive than that of the acetato complex (Table 3). Such a difference might suggest that the local orientation of solvent water around the leaving group at the activated state would be less for the glycine complex, in which the negative charge of the carboxylate group is partly compensated by the influence of the ammonium group.

Bunton and Llewellyn disclosed that the aquation of acetatopentamminecobalt(III) complex takes place through the break of Co–O bond on the basis of a tracer study with oxygen-18.[9] On the other hand, the similar aquation of carbonatopentamminecobalt(III) complex proceeds *via* the cleavage of C–O bond,[10] and has an enthalpy of activation 17.1 kcal mol^{-1}.[11] The enthalpy of activation of the glycine complex is nearer to that of the acetato complex than to that of the carbonato complex, so that the break of Co-O bond appears to be more plausible on the aquation of the glycine complex.

7) H. G. Walker, Jr., and H. S. Owens, *J. Am. Chem. Soc.*, **74**, 2547 (1952).
8) R. P. Bell and F. J. Lindars, *J. Chem. Soc.*, **1954**, 4601.
9) C. A. Bunton and D. R. Llewellyn, *ibid.*, **1953**, 1692.
10) J. P. Hunt, A. C. Rutenberg and H. Taube, *J. Am. Chem. Soc.*, **74**, 268 (1952).
11) D. J. Francis and R. B. Jordan, *ibid.*, **89**, 5591 (1967).

BULLETIN OF THE CHEMICAL SOCIETY OF JAPAN VOL. 41 1619—1621 (1968)

Spectrophotometric Determination of Cyanide Ion with Mercury(II)-Methylthymolblue Complex

Toshiaki NOMURA

Department of Chemistry, Faculty of Science, Shinshu University, Asahi, Matsumoto

(Received January 24, 1968)

Cyanide ion reacted with mercury(II)-methylthymolblue (Hg-MTB) complex to form a mixed ligand complex. Since the resulting mixed ligand complex had a considerable absorption at 615 mμ, the spectrophotometric determination of cyanide ion was performed by measuring the increase in absorption of mercury(II)-methylthymolblue complex caused by formation of this mixed ligand complex. After excess MTB methanol and mercury(II) nitrate solutions were added to a cyanide sample solution which was adjusted to a definite pH value between pH 7.3 and 7.6 with phosphate buffer solution, it was diluted to exactly 50 m*l* with water. After standing for about 25 min, the absorbance of this solution was measured at 615 mμ against the reagent blank solution. Beer's law was obeyed in the concentration range of cyanide ion from 5 to 80 μg per 50 m*l*, and the molar extinction coefficient was found to be about 5100. Taking 55.0 μg of cyanide ion, the standard deviation and variation coefficient of absorbances in the mean value of 10 runs were 0.0019 and 0.90%, respectively. The molar ratio of cyanide ion to Hg-MTB in the mixed ligand complex was found to be 1 : 1.

Mercury(II) reacts with organic reagents having two diacetic amino groups to form mercury(II) complexes which further react with anions such as SCN^-, CN^-, I^- and Br^-, *etc.*, to form mixed ligand complexes. Nomura *et al.*, reported that ethylenediaminetetraacetate (EDTA),[1] cyclohexanediaminetetraacetate (CyDTA),[2] and cresolphthalein complexone (PC),[3] *etc.*, have the above property among organic reagents. Also, Hashitani[4] reported that alizarin complexone reacts with cerium or lanthanum to form a complex which reacts with fluoride ion to form the same mixed ligand complex.

Methylthymolblue (MTB), having two diacetic amino groups, reacts with mercury(II) to form a mercury(II)-methylthymolblue complex (Hg-MTB or $HgMe^{4-}$),[5] having a considerable absorption at 620 mμ, and the molar ratio of MTB to mercury(II) in this complex is 1 : 1. It was found that cyanide ion also reacted similarly with Hg-MTB to form a mixed ligand complex as thiocyanate ion.[6] Therefore, making use of this fact, the author has developed a rapid method for spectrophotometrically determinating small amounts of cyanide ion by measuring the absorbance of this cyano mixed ligand complex.

Experimental

Reagents. All analytical grade reagents were used without further purification.

Standard Cyanide Solution. The exact concentration of the stock solution of cyanide ion, prepared by dissolving potassium cyanide in water, was obtained through indirect chelatometric titration with $[HgY(CN)]^{3-}$ [7] before use. The working standard solutions were prepared by diluting this stock solution to the concentrations required for experiment.

Methylthymolblue (MTB) Methanol Solution. The MTB methanol solution of 1×10^{-3} M was prepared by dissolving 390 mg of Dotite MTB in a small amount of water, followed by the addition 250 m*l* of methanol, and dilution to exactly 500 m*l* with water. This solution, stored in a brown glass bottle, was stable at least for about three months.

Mercury(II) Solution. The stock solution mercury(II) was prepared by dissolving mercury(II) nitrate in a small amount of concentrated nitric acid and water, and diluting to exactly 1 *l* with water. The exact concentration of this solution was obtained through titration with 0.01 M standard EDTA solution using Cu-PAN as indicator. The working solution of 1×10^{-3} M (F=0.983) was prepared by dilution with water.

Buffer Solution. Buffer solutions having a definite pH were prepared by properly mixing 0.2 M potassium dihydrogen phosphate and 0.2 M disodium hydrogen phosphate solutions.

1) S. Komatsu and T. Nomura, *Nippon Kagaku Zasshi (J. Chem. Soc. Japan, Pure Chem. Sect.)*, **87**, 841 (1966); **87**, 845 (1966); **88**, 63 (1967).
2) T. Nomura, *ibid.*, **88**, 199 (1967).
3) T. Nomura, *ibid.*, **88**, 635 (1967).
4) H. Hashitani, *Dotite News Letter*, **13**, 3 (1965).
5) N. Iritani and T. Miyahara, *Bunseki Kagaku (Japan Analyst)*, **12**, 1183 (1963).
6) T. Nomura, *Nippon Kagaku Zasshi (J. Chem. Soc. Japan, Pure Chem. Sect.)*, **88**, 961 (1967).
7) S. Komatsu and T. Nomura, *ibid.*, **87**, 1060 (1966).

Apparatus. Spectrophotometric measurements were made with a Hitachi Perkin Elmer 139 type spectrophotometer with 10.0 mm glass cells. The pH measurements were made with a Hitachi-Horiba 4 type pH meter.

Procedure. The sample solution containing from 5 to 80 μg of cyanide ion was adjusted to a definite pH value between pH 7.3 and 7.6 with 10 m*l* of buffer solution, to each of which 5 m*l* of 1×10^{-3} M MTB methanol solution and aqueous mercury(II) solution were added and the total volume adjusted to 50 m*l* with water. After standing for about 25 min, the absorbance of this solution was measured at 615 mμ against a reagent blank solution which was prepared similarly without the addition of cyanide solution.

Results and Discussion

Absorption Spectra of Hg-MTB and Cyano Mixed Ligand Complex. Spectra are shown in Fig. 1. The maximum absorbances of Hg-MTB were found at 420 mμ and 610 mμ, respectively. However, the absorbance decreased at 420 mμ and increased at 610 mμ when cyanide ion was added to this complex solution. Then, the measurement of increase in the absorbance at 610 mμ caused by the formation of a cyano mixed ligand complex could be made to determine cyanide ion. The wavelength of 615 mμ, at which the cyanide mixed ligand complex had a maximum absorbance, was used practically in all subsequent measurements, because the difference in absorbance between Hg-MTB and the mixed ligand complex was greater at 615 mμ than at 610 mμ, as shown in Fig. 1.

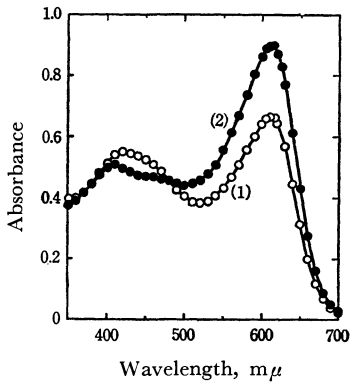

Fig. 1. Absorption spectra of Hg-MTB and cyano mixed ligand complex.
(1) Hg-MTB complex containing each 5 m*l* of 1×10^{-3} M MTB methanol and mercury(II) solutions at pH 7.4.
(2) Cyano mixed ligand complex containing above solutions and 66.0 μg of cyanide ion at pH 7.4.

Effect of pH. This complex was stable between pH 7.3 and 7.6, as shown in Fig. 2. Since the absorbance of Hg-MTB increased with pH,[6] the pH in a practical procedure should be adjusted to a definite value between pH 7.3 and 7.6.

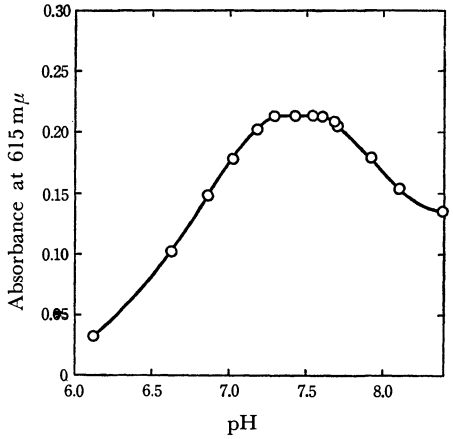

Fig. 2. Effect of pH.
The every absorbances of the mixed solution containing each 5 m*l* of 1×10^{-3} M·MTB methanol and mercury(II) solutions and 55.0 μg of cyanide ion were measured against a reagent blank solution after adjusting to the pH needed with phosphate buffer solution.

Effect of Standing Times. The time required for the complete formation of this mixed ligand complex (blue color) was about 20 min, and the color of this complex showed no change for at least three hours. The procedure for color development was carried out at room temperatures.

Molar Ratio of Hg-MTB to Cyanide Ion. The results are shown in Fig. 3. When Hg-MTB reacted with cyanide ion to form the mixed ligand complex, the molar ratio of Hg-MTB to cyanide ion was found to be 1 : 1. But, above the equivalent point, the mixed ligand complex reacted subsequently with cyanide ion in the same way as the cyano mixed liquid complex $[HgY(CN)]^{3-}$

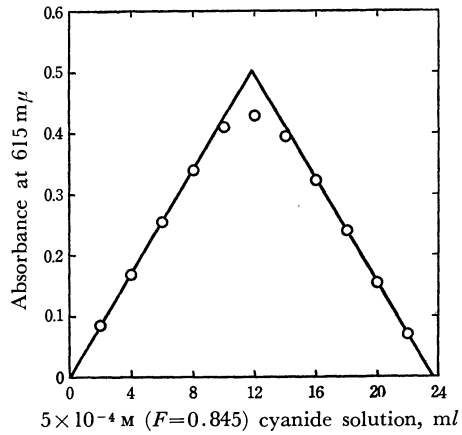

Fig. 3. Molar ratio of Hg-MTB to cyanide ion.
The every absorbances of the mixed solution containing each 5 m*l* of 1×10^{-3} M·MTB methanol and mercury(II) solutions were measured against a reagent blank solution after adding cyanide solution at pH 7.5.

(abbreviated Hg-EDTA as HgY^{2-}) reacted with cyanide ion to form mercury(II) cyanide and EDTA.[7]

$$[HgMe(CN)]^{5-} + CN^- + 2H^+ \rightarrow Hg(CN)_2 + H_2Me^{4-}$$

Hence, the absorbances of this mixed ligand complex solution decreased when an excess amount of cyanide ion (compared with Hg-MTB, in molar ratio) was added. The absorbances of the solutions which were prepared by the addition of different amounts of cyanide sample solution should be measured in order to avoid erroneous measurements, which may be made above the equivalent point.

Calibration Curve. The relationship between cyanide ion content and the absorbance was linear from 5 μg up to 80 μg cyanide ion content per 50 m*l*, as shown in Fig. 4. The molar extinction

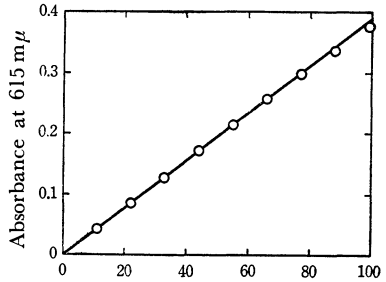

Fig. 4. Calibration curve for cyanide ions. pH 7.4

coefficient was found to be about 5100. Taking 55.0 μg of cyanide ion, the standard deviation and variation coefficient for the mean absorbances of 10 analyses were 0.0019 and 0.90%, respectively.

Effect of Diverse Ions. Results are given in Table 1. Taking 55.0 μg of cyanide ion, the absorbances were measured according to the above procedure in the co-existence of a number of various foreign ions. Measurements that differed from the expected absorbance by more than $\pm 2\%$ were taken as criterion for interference.

Anions such as SCN^-, S^{2-}, I^- and Br^- interfered in this method, because S^{2-} reacted with mercury(II) to form mercuric sulfide, and SCN^-, I^- and Br^- reacted with Hg-MTB to form mixed ligand complexes, as did cyanide ion. Cations, such as Mn^{2+}, Cd^{2+}, Zn^{2+}, Co^{2+}, Bi^{3+}, Ni^{2+} and NH_4^+, interfered since these cations, except NH_4^+, reacted with MTB to form metal-MTB complexes. These interfering ions should be separated or masked properly for the determination of cyanide ion. A method of separation has been reported by Okutani *et al.*[8]

Table 1. Effect of diverse ions

Ion	Added as	Tolerance limit	
SCN^-	KSCN	1.2 μg	+
Br^-	KBr	2.5 μg	+
I^-	KI	3.5 μg	+
S^{2-}	$Na_2S \cdot 9H_2O$	10 μg	−
Cl^-	NaCl	20 μg	+
F^-	NaF	>10 mg	
NO_3^-	KNO_3	>10 mg	
SO_4^{2-}	K_2SO_4	>10 mg	
ClO_4^-	$NaClO_4$	>10 mg	
Ni^{2+}	$NiSO_4 \cdot 7H_2O$	1.0 μg	+
Co^{2+}	$CoSO_4 \cdot 7H_2O$	1.2 μg	+
Mn^{2+}	$MnSO_4$	4 μg	+
NH_4^+	$(NH_4)_2SO_4$	4 μg	+
Bi^{3+}	$Bi(NO_3)_3$	5 μg	−
Cd^{2+}	$CdSO_4$	6 μg	+
Zn^{2+}	$ZnSO_4 \cdot 7H_2O$	9 μg	−
Pb^{2+}	$Pb(NO_3)_2$	18 μg	−
Fe^{3+}	$Fe(NO_3)_3 \cdot 9H_2O$	50 μg	−
Al^{3+}	$Al_2(SO_4)_3$	50 μg	−
Ag^+	$AgNO_3$	50 μg	+
Mg^{2+}	$MgSO_4$	120 μg	+
Cu^{2+}	$CuSO_4 \cdot 5H_2O$	120 μg	+
Ca^{2+}	$Ca(NO_3)_2$	350 μg	+
Hg^{2+}	$Hg(NO_3)_2$	350 μg	+
Th^{4+}	$Th(NO_3)_4$	900 μg	−
Sr^{2+}	$Sr(NO_3)_2$	>2 mg	
Ba^{2+}	$Ba(NO_3)_2$	>2 mg	

(+): positive error (−): negative error

The author wishes to thank Professor S. Komatsu for many helpful discussions and suggestions during this work.

8) T. Okutani and S. Utsumi, *Nippon Kagaku Zasshi (J. Chem. Soc. Japan, Pure Chem. Sect.)*, **87**, 444 (1966).

BULLETIN OF THE CHEMICAL SOCIETY OF JAPAN VOL. 41 1622—1628 (1968)

Kinetics of Electron-transfer Reactions Involving Ethylenediaminetetraacetatochromate(II) Ions as Reductants. I. Reactions with Some Isothiocyanatoammine Complexes of Chromium(III)*[1]

Hiroshi OGINO and Nobuyuki TANAKA

Department of Chemistry, Faculty of Science, Tohoku University, Katahira-cho, Sendai

(Received February 3, 1968)

Kinetics of electron-transfer reactions of ethylenediaminetetraacetatochromate(II) ions with some isothiocyanatoammine complexes of chromium(III), $Cr(NCS)_n(NH_3)_{6-n}^{(3-n)+}$ (n=0, 1, 4 and 6), have been studied. The former ions are present in the forms of both $Cr^{II}(H_2O)edta^{2-}$ and $Cr^{II}(H_2O)Hedta^-$, but the reaction of $Cr^{II}(H_2O)Hedta^-$ with $Cr(NCS)_n(NH_3)_{6-n}^{(3-n)+}$ is not significant in the pH range from 3.6 to 5.3. Second-order rate constants (l mol^{-1}sec^{-1}) of the reactions between $Cr^{II}(H_2O)edta^{2-}$ and $Cr(NCS)_n(NH_3)_{6-n}^{(3-n)+}$ at ionic strength 1.0 and 25°C are $<10^{-2}$ for $Cr(NH_3)_6^{3+}$, 0.2 for $CrNCS(NH_3)_5^{2+}$, 2.3 for $Cr(NCS)_4(NH_3)_2^-$, and 28.2 for $Cr(NCS)_6^{3-}$.

The electron-transfer reactions between chromium(II) ions and various oxidants have been investigated extensively. For example, it is known that the reactions of chromium(II) ions with various cobalt(III) complexes proceed through inner-sphere mechanisms, except haxaammine and tris(ethylenediamine)cobalt(III) complex ions.[1,2] The reactions between chromium(II) ions and acidopentaamminechromium(III) also proceed through inner-sphere mechanisms.[3] On the other hand, the electron-transfer reactions of tris(bipyridine)chromium(II) ions with various cobalt(III) complexes proceed through outer-sphere mechanisms.[2,4] The striking change in these electron-transfer reactions is brought by the complex formation of chromium(II) ions with bipyridine. Therefore, it seems worth while to investigate the electron-transfer reactions involving various chromium(II) complexes as reductants.

Stability constants of chromium(II) and chromium(III) complexes with ethylenediaminetetraacetate (EDTA) have been determined by Pecsok *et al.*[5] Recently, the rate constants of the complex-forming reactions between chromium(II) ions and EDTA have been determined in this laboratory.[6,7] These results have facilitated to investigate the electron-transfer reactions between chromium(II)-EDTA and various oxidants.

In this paper, kinetics of electron-transfer reactions between chromium(II)-EDTA and some isothiocyanatoammine complexes of chromium(III) ions, $Cr(NCS)_n(NH_3)_{6-n}^{(3-n)+}$ (n=0, 1, 4 and 6), are presented. Although Hunt and Earley[8] reported on the semiquantitative experiments of electron-transfer reactions between chromium(II) and hexaaquochromium(III) ions in the presence of number of ligands, rate laws of these reactions were not presented.

Experimental

Materials. Aquohydrogenethylenediaminetetraacetatochromium(III), $[Cr(H_2O)Hedta]$, was prepared by the method of Hamm.[9] The crude material was purified by the following procedures: 24 g of $[Cr(H_2O)Hedta]$ in 25 m*l* of water was dissolved with 10 g of sodium acetate trihydrate. After filtration, 20 m*l* of concentrated nitric acid was added. Crystals were obtained upon heating the solution on the water-bath. The crystals were washed with warm water, ethanol and ether. Infrared spectra of the compound gave two peaks at 1739 and 1639 cm^{-1} in the carbonyl region, which essentially agree with the results reported by Dwyer and Garvan.[10] The peak at 1739 cm^{-1} which could be assigned to the free carboxylic acid group was less intense than the other at 1639 cm^{-1}. The relative intensities of these peaks support EDTA in chromium(III)-EDTA complex functioning as a pentadentate ligand.

*1 Presented at the Tenth International Conference on Coordination Chemistry, Nikko, Japan, September, 1967.

1) H. Taube, "Advances in Inorganic Chemistry and Radiochemistry," Vol. 1, p. 1, Academic Press, New York (1959).
2) J. P. Candlin, J. Halpern and D. L. Trimm, *J. Am. Chem. Soc.*, **86**, 1019 (1964).
3) A. E. Ogard and H. Taube, *ibid.*, **80**, 1084 (1958).
4) A. M. Zwickel and H. Taube, *Discussions Faraday Soc.*, **29**, 42 (1960).
5) R. L. Pecsok, L. D. Shields and W. P. Schaefer, *Inorg. Chem.*, **3**, 114 (1964).
6) K. Ogino and N. Tanaka, This Bulletin, **39**, 2672 (1966).
7) N. Tanaka and A. Yamada, *Rev. Polarog.* (Kyoto), **14**, 234 (1967).
8) J. B. Hunt and J. E. Earley, *J. Am. Chem. Soc.*, **82**, 5312 (1960).
9) R. E. Hamm, *ibid.*, **75**, 5670 (1953).
10) F. P. Dwyer and F. L. Garvan, *ibid.*, **82**, 4823 (1960).

Complexes, $[Cr(NH_3)_6]Cl_3$,[11] $[CrNCS(NH_3)_5](SCN)_2$,[12] and $K_3[Cr(NCS)_6]\cdot 4H_2O$,[13] were prepared by the procedures described in literatures. $[CrNCS(NH_3)_5](SCN)_2$ was converted to perchlorate by recrystallization from aqueous perchloric acid. The solution of $(NH_4)_3[Cr(NCS)_6]\cdot 4H_2O$ was obtained by passing the solution of $K_3[Cr(NCS)_6]\cdot 4H_2O$ through Dowex 50W-X8 cation exchange resins in the ammonium form. Then, the solution was evaporated to dryness. The compound $(NH_4)_3[Cr(NCS)_6]\cdot 4H_2O$ thus obtained was purified by recrystallization from 95% ethanol. $NH_4[Cr(NCS)_4(NH_3)_2]\cdot 2/3\ H_2O$ of reagent grade was purchased from Nakarai Chemicals, Ltd.

The results of the chemical analysis of the chromium(III) complexes used in this paper are given in Table 1.

Table 1. Analysis of the chromium(III) complexes

Complex	Cr, %		N, %	
	Found	Calcd	Found	Calcd
$[Cr(H_2O)Hedta]$	14.22	14.47	7.80	7.80
$[Cr(NH_3)_6]Cl_3$	19.92	19.96	31.95	32.26
$[CrNCS(NH_3)_5](ClO_4)_2$	13.31	13.19	21.56	21.32
$NH_4[Cr(NCS)_4(NH_3)_2]\cdot 2/3H_2O$	14.28	14.92	28.25	28.14
$(NH_4)_3[Cr(NCS)_6]\cdot 4H_2O$	9.71	9.87	23.78	23.94

The acidic solution of hexaaquochromium(III) perchlorate was prepared by the reduction of sodium dichromate in perchloric acid with hydrogen peroxide. Solutions of chromium(II) perchlorate were obtained by the reduction of hexaaquochromium(III) perchlorate with zinc amalgam. Chromium(II) chloride solutions were prepared by dissolving chromium metal into hydrochloric acid.

All other chemicals used were of reagent grade.

Procedures. As chromium(II) solutions were air-sensitive, the experiments were carried out in an oxygen-free nitrogen atmosphere. A trace of oxygen was removed from nitrogen gas by passing the gas through a series of acidic chromium(II) solutions.

Total chromium concentration in a given solution was determined spectrophotometrically as CrO_4^{2-} after oxidation with alkaline peroxide.[14]

Chromium(II)-EDTA solutions were prepared by injecting chromium(II) solutions into excess EDTA solutions. The following two methods were used for the determination of the concentration of chromium(II)-EDTA: In the first method, the concentration of chromium(II)-EDTA was taken as equal to that of a known amount of chromium(II) ions. Chromium(II) content was determined by the method reported in the literature.[15] Chromium(II) solutions contained chromium(III) ions as impurity. The chromium(III) ions in the original solution may be $Cr(H_2O)_6^{3+}$ and/or $[CrOH(H_2O)_4]_2^{4+}$, the latter of which is known to be a product upon the air-oxidation of chromium(II) ions.[16,17] The contamination of chromium(III) ions was greater in the more dilute chromium(II) solutions. It was found spectrophotometrically that, when a chromium(II) solution which was contaminated by chromium(III) ions was injected into an excess EDTA solution, the same amount of chromium(III)-EDTA as that of chromium(III) in the original solution was formed within the time of mixing. The absorption spectra of chromium(II)-EDTA and chromium(III)-EDTA complexes which were obtained in this work are as mentioned later (see Fig. 1). In the second method, the following procedure was used: Absorbancy of the chromium(II)-EDTA solution containing chromium(III)-EDTA was measured at a proper wave length. The concentrations of both chromium(II)-EDTA and chromium(III)-EDTA were calculated from the total chromium concentration, the value of absorbancy and the extinction coefficients of both chromium(II)-EDTA and chromium(III)-EDTA. In most cases, this procedure was used, because this was simpler than the first one.

The determination of hydrogen ion concentrations in chromium(II) solutions and acidic hexaaquochromium(III) perchlorate solutions was carried out by the method reported in the literatures.[18,19] Concentrations of zinc(II) ions in the chromium(II) perchlorate solutions were determined polarographically.

Ionic strength of the solution was adjusted to be 1.0 with sodium perchlorate or sodium chloride. The pH of the solutions was regulated by using acetate buffer which was prepared from acetic acid and primary standard sodium carbonate. A Hitachi F-5 pH meter with accuracy of ± 0.01 pH unit was used for the measurement of the pH of the solutions.

The reaction vessels were quartz spectrophotometer cells of 1 cm in length of light path. Kinetic runs were made by recording the change of absorbancy at a given wave length as a function of time, using a Hitachi EPS-3 pen-recording spectrophotometer. In most of kinetic runs, the solutions containing a given amount of chromium(III) complex ions, EDTA, acetate buffer and indifferent salt were added to the cell which was then sealed with a serum cap. After the solution was purged with nitrogen gas for at least ten minutes, chromium(II) solution was added by a calibrated syringe. The mixing of the solutions was performed by passage of a rapid stream of nitrogen gas. In some experiments, the chromium(II) solution was added to the deoxygenated solution containing EDTA, acetate buffer and indifferent salt in a serum capped cell by a syringe and then the solution of chromium(III) complex ions was added as the last reagent by a syringe. In both manners, the first absorbancy reading was obtained within 5 sec.

Temperature of optical cells was controlled to be 25.0 ± 0.1°C by circulating water through cell holder. The deoxygenated solution of chromium(II) or chromium(III) ions in a syringe was also equilibrated at 25°C in the thermostated-bath before mixing.

11) M. Mori, *Nippon Kagaku Zassi (J. Chem. Soc. Japan, Pure Chem. Sect.)*, **74**, 253 (1953).
12) A. Werner and J. von Halben, *Ber.*, **39**, 2668 (1906).
13) J. Roesler, *Ann.*, **141**, 185 (1867).
14) G. W. Haupt, *J. Res. Natl. Bur. Std.*, **48**, 414 (1952).
15) E. S. Gould and H. Taube, *J. Am. Chem. Soc.*, **86**, 1318 (1964).
16) M. Ardon and R. A. Plane, *ibid.*, **81**, 3197 (1959).
17) R. W. Kolaczkowski and R. A. Plane, *Inorg. Chem.*, **3**, 322 (1964).
18) E. L. King and J. A. Neptune, *J. Am. Chem. Soc.*, **77**, 3186 (1955).
19) K. D. Kopple and R. R. Miller, *Inorg. Chem.*, **2**, 1204 (1963).

Results and Discussion

Absorption Spectra of Chromium(II)-EDTA and Chromium(III)-EDTA Complexes. A pentadentate structure of EDTA in chromium(II)-EDTA complex has been proposed by Pecsok *et al.*[5] Therefore, the formula $Cr^{II}(H_2O)edta^{2-}$ will be used in this paper for chromium(II)-EDTA complex.

Schwarzenbach and Biedermann[20] showed that chromium(III)-EDTA complex contains one water molecule in the first coordination sphere. And, Hoard *et al.*[21] reported that in an intermediate pH range from 5 to 9, both $Cr^{III}(H_2O)edta^-$ and $Cr^{III}(OH)edta^{2-}$ are probably converted, though perhaps slowly, into the hexadentate $Cr^{III}edta^-$. In addition, they isolated the hexadentate complex in the solid state. In the present paper, the formula $Cr^{III}(H_2O)edta^-$ is assigned tentatively to chromium(III)-EDTA complex in the solution by the following observations: (a) Infrared spectra of chromium(III)-EDTA complex in solid state supported a pentadentate structure of EDTA as mentioned in the experimental section. (b) Visible and ultraviolet spectra of $[Cr(H_2O)Hedta]$ dissolved in distilled water were essentially identical with those in acetate buffer solution. (c) In this work, the pH of the solutions was restricted within the range from 3.6 to 5.3 by using acetate buffer solutions. No spectral changes in visible and ultraviolet regions were observed by the change of the pH of the solutions.

The spectra of $Cr^{II}(H_2O)edta^{2-}$ and $Cr^{III}(H_2O)edta^-$ at ionic strength 1.0 ($NaClO_4$) in acetate buffer solutions are given in Fig. 1. The concentration of acetate in the buffer was varied from 0.24 to 0.75 M. For comparison, the spectrum of chromium(II) ions in perchloric acid is also given in Fig. 1. The molar extinction coefficients of maximum absorption of $Cr^{III}(H_2O)edta^-$ at 393 mμ and 545 mμ were 112 and 206, respectively, which essentially agree with the results reported by Hamm.[9]

The shape of spectrum of $Cr^{II}(H_2O)edta^{2-}$ resembles that of Cr^{2+} ions, so that the color of a $Cr^{II}(H_2O)edta^{2-}$ solution is sky blue similar to that of a chromium(II) solution. The molar extinction coefficients of maximum absorptions of $Cr^{II}(H_2O)edta^{2-}$ at 715 and 1060 mμ were 18 and 10, respectively. The extinction coefficient of $Cr^{II}(H_2O)edta^{2-}$ is the same with that of $Cr^{III}(H_2O)edta^-$ at 365 and 673 mμ, respectively, as indicated with arrows in Fig. 1.

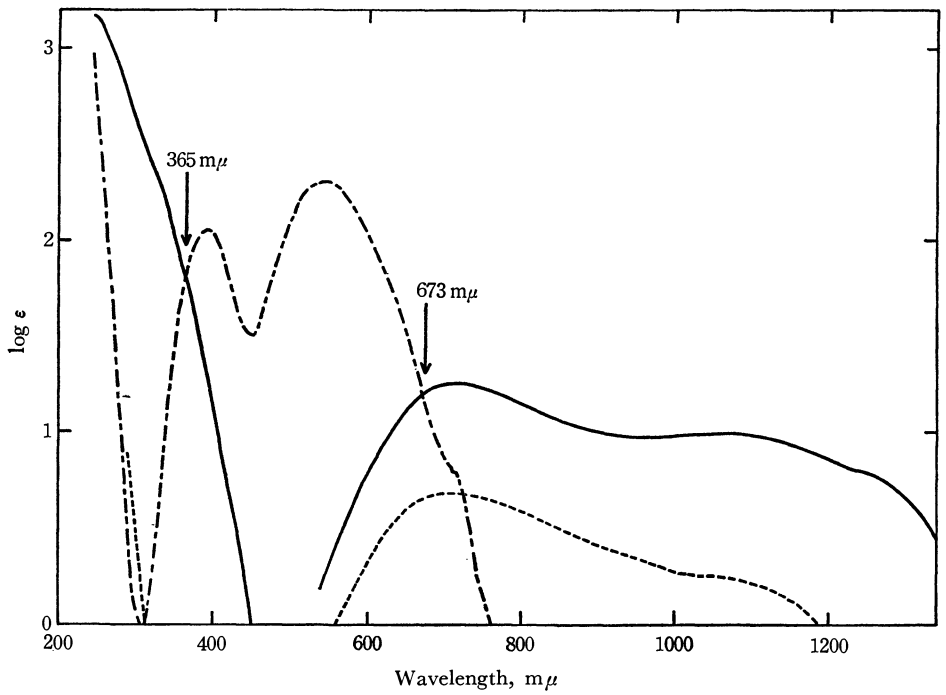

Fig. 1. Absorption spectra of $Cr^{II}(H_2O)edta^{2-}$ in sodium acetate-sodium perchlorate media (——), $Cr^{III}(H_2O)edta^-$ in sodium acetate-sodium perchlorate media (-·-·-) and Cr^{2+} in $HClO_4$ (----).

20) G. Schwarzenbach and W. Biedermann, *Helv. Chim. Acta*, **31**, 459 (1948).
21) J. L. Hoard, G. S. Smith and M. Lind, "Advances in the Chemistry of the Coordination Compounds" (S. Kirschner, ed.), Macmillan, New York (1961), p. 296.

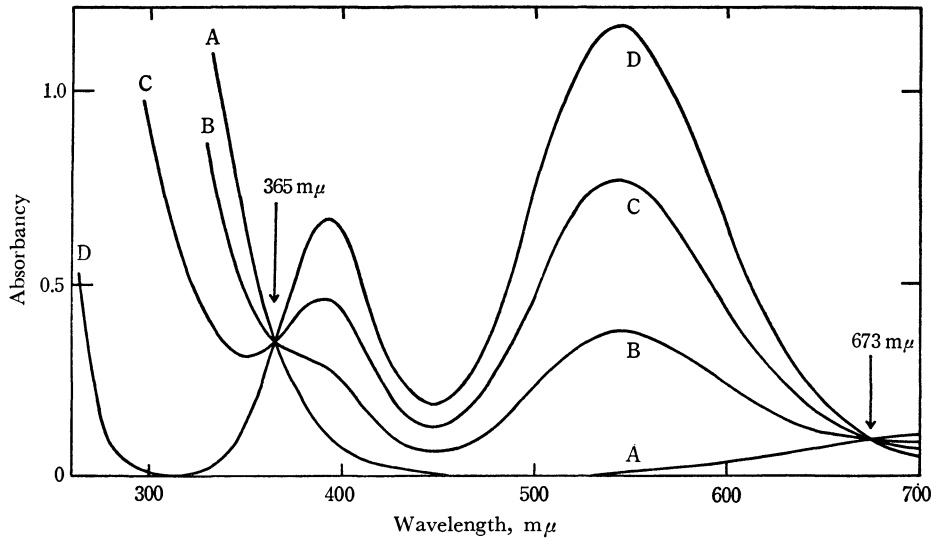

Fig. 2. Spectral change of $Cr^{II}(H_2O)edta^{2-}$ solution in sodium acetate-sodium perchlorate media of ionic strength 1.0: (A) 5.89 mM $Cr^{II}(H_2O)edta^{2-}$; (B and C) Partly oxidized with air; and (D) Completely oxidized with air. The concentration of acetate is 0.24 M.

Figure 2 shows the spectral change of $Cr^{II}(H_2O)edta^{2-}$ solution which occurred when air was bubbled through the solution. Two isosbestic points were observed at 365 and 673 mμ by the addition of appropriate amounts of oxygen. The spectrum obtained after the solution was saturated with air is shown by curve D in Fig. 2. This spectrum is in a satisfactory agreement with that of 5.89 mM $Cr^{III}(H_2O)edta^{-}$. These observations revealed that there was no indication of the formation of intermediates such as dimeric species. Therefore, the spectral change in Fig. 2 can be expressed reasonably with the following equation:

$$2Cr^{II}(H_2O)edta^{2-} + \frac{1}{2}O_2 + 2H^+ \rightarrow 2Cr^{III}(H_2O)edta^{-} + H_2O \quad (1)$$

Kinetics of the Electron-transfer Reactions between $Cr^{II}(H_2O)edta^{2-}$ and $Cr(NCS)_n(NH_3)_{6-n}^{(3-n)+}$. Figure 3 gives a typical example of the spectral change of the $Cr(NCS)_6^{3-}$ solution containing excess EDTA upon the addition of chromium(II) perchlorate solution (spectra A to D). The same spectral change was observed, when a $Cr(NCS)_6^{3-}$ solution was injected into a chromium(II) solution containing excess EDTA. The reaction seemed to be complete within 600 sec, since no change was observed in the spectrum after the measurement of spectrum D in Fig. 3. The shape of spectrum D is in a satisfactory agreement with that of $Cr^{III}(H_2O)edta^{-}$. Therefore, the overall reaction is expressed reasonably as follows:

$$Cr(NCS)_6^{3-} + H_jedta^{(4-j)-} + H_2O \rightarrow Cr^{III}(H_2O)edta^{-} + 6NCS^{-} + jH^+ \quad (2)$$

In Fig. 3, there are three isosbestic points at 380, 404 and 466 mμ. This is also consistent with Eq. (2). The rate of reaction (2) observed in the absence of chromium(II) ions was much slower than the rate of the reaction observed in the presence of chromium(II) ions. It was also found that the rate of the reaction between chromium(II) ions and $Cr(NCS)_6^{3-}$ complexes in sodium chloride-hydrochloric acid media was extremely slow.*2

After the completion of the reaction, the solution was exposed to air, the spectrum of which is shown by curve E in Fig. 3. This spectrum also coincides with that of $Cr^{III}(H_2O)edta^{-}$. The concentration of $Cr^{III}(H_2O)edta^{-}$ which corresponds to the difference in absorbancy in the spectra D and E was found to be equal to the concentration of chromium(II) ions which was initially added. That is, the concentration of chromium(II)-EDTA remained constant during the reaction. As shown in Fig. 1, the absorption of $Cr^{II}(H_2O)edta^{2-}$ is negligible over the range of wave length in Fig. 3 under the experimental condition.

By considering these results, the following mechanism can be deduced for reaction (2):

$$Cr^{2+} + H_jedta^{(4-j)-} + H_2O \rightleftharpoons Cr^{II}(H_2O)edta^{2-} + jH^+ \quad (3)$$

$$Cr^{II}(H_2O)edta^{2-} + Cr(NCS)_6^{3-} \xrightarrow{k} Cr^{III}(H_2O)edta^{-} + Cr^{2+} + 6NCS^{-} \quad (4)$$

*2 The reaction between chromium(II) ions and $Cr(NCS)_6^{3-}$ complexes may be the chromium(II)-catalyzed dissociation reaction of $Cr(NCS)_6^{3-}$ complexes, but, no systematic investigation either on the stoichiometry or on the kinetics of the reaction has been made.

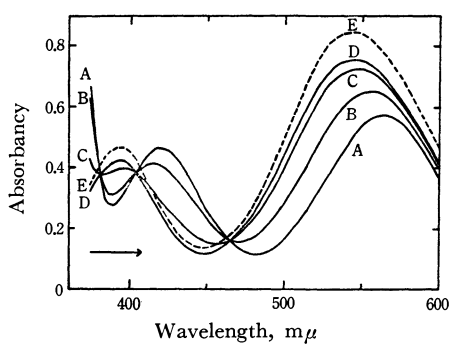

Fig. 3. Spectral change of the $Cr(NCS)_6^{3-}$ solution containing EDTA in sodium acetate-sodium perchlorate media upon the addition of chromium(II) ions: $[Cr(NCS)_6^{3-}]_{t=0}=3.56$ mM, $[Cr(II)]_{t=0}=0.47_2$ mM, $[EDTA]_{t=0}=12.5$ mM, 25°C, $\mu=1.0$, pH 3.71, Scanning speed=3.42 mμ/sec. (A) Spectrum at $t=0$ over the range of all wave length. (B) 10 sec (C) 120 sec and (D) 600 sec after the addition of chromium(II). Times given are for start of scan at 374 mμ. (E) Spectrum of the solution which was exposed to air after spectrum D was measured.

where reaction (4) is the electron-transfer reaction between $Cr^{II}(H_2O)edta^{2-}$ and $Cr(NCS)_6^{3-}$. In this mechanism, reaction (4) is a rate-determining step because the complex-forming reaction (reaction 3) of chromium(II) ions is considered to be very fast.[6,7] The rate law for reaction (2) is expressed as

$$-\frac{d[Cr(NCS)_6^{3-}]}{dt}=\frac{d[Cr^{III}(H_2O)edta^-]}{dt}$$
$$=k[Cr^{II}(H_2O)edta^{2-}][Cr(NCS)_6^{3-}] \quad (5)$$

Since the concentration of $Cr^{II}(H_2O)edta^{2-}$ remains constant during the reaction, the integration of Eq. (5) leads to

$$\ln|D_t-D_\infty| = -k[Cr^{II}(H_2O)edta^{2-}]t+\ln|D_0-D_\infty| \quad (6)$$

where D_0, D_t and D_∞ are absorbancies at time 0, t and infinite, respectively.

An example of the kinetic run of the reaction between chromium(II)-EDTA and $Cr(NCS)_6^{3-}$ ions is shown in Fig. 4. Excellent first-order plots were obtained as expected from Eq. (6).

Table 2 gives the results obtained on the rate of the reaction between chromium(II)-EDTA and $Cr(NCS)_6^{3-}$ ions. The rate constants were independent of the initial concentrations of both

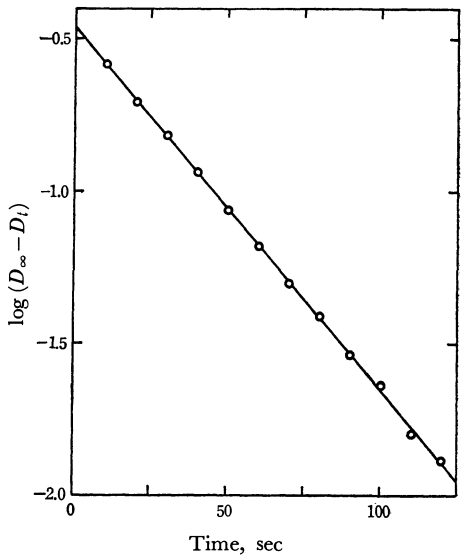

Fig. 4. A typical kinetic run of the reaction between $Cr^{II}(H_2O)edta^{2-}$ and $Cr(NCS)_6^{3-}$ in the presence of EDTA at 510 mμ: $[Cr^{II}(H_2O)edta^{2-}]=0.994$ mM, $[Cr(NCS)_6^{3-}]_{t=0}=3.47$ mM, $[EDTA]_{t=0}=12.5$ mM, pH 5.25.

Table 2. Rate constants of the reaction between chromium(II)-EDTA and $Cr(NCS)_6^{3-}$ at $\mu=1.0$ ($NaClO_4$) and 25°C

pH	$[Cr(NCS)_6^{3-}]_{t=0}$ mM	$[Cr^{II}(H_2O)edta^{2-}]$ mM	k $l\,mol^{-1}\,sec^{-1}$	Wavelength for measurement, mμ
5.25	3.47	0.994	27.6	510
4.93	2.86	1.06	29.5	510
4.92	3.37	1.03	29.3	510
4.87	2.78	2.78	28.4	510
4.81	2.96	5.73	27.7	510
4.80	0.949	1.06	28.8	510
4.74	3.93	1.06	30.0	545
4.73	5.62	1.06	29.0	422
4.60	3.23	0.964	27.2	510
4.48	3.03	0.457	29.2	510
4.28	3.01	0.964	27.8	422
4.17	2.92	2.78	26.7	510
4.11	3.33	5.78	24.5	510
4.00	3.24	0.964	25.3	510
3.81	3.48	0.964	24.6	510

chromium(II)-EDTA and $Cr(NCS)_6^{3-}$. Therefore, the reaction is strictly of second-order. Rate constants obtained at different wave length are in a good agreement. A rigorous treatment of the pH dependence of rates was made, because it is known that $Cr^{II}(H_2O)edta^{2-}$ forms protonated species, $Cr^{II}(H_2O)Hedta^-$, at lower pH's. If the presence of $Cr^{II}(H_2O)Hedta^-$ is considered, the electron-transfer reaction may proceed through the following two simultaneous reaction paths:

$$Cr^{II}(H_2O)edta^{2-} + Cr(NCS)_6^{3-} \xrightarrow{k_1} Cr^{III}(H_2O)edta^- + Cr^{2+} + 6NCS^- \quad (7)$$

$$Cr^{II}(H_2O)Hedta^- + Cr(NCS)_6^{3-} \xrightarrow{k_2} Cr^{III}(H_2O)Hedta + Cr^{2+} + 6NCS^- \quad (8)^{*3}$$

Then, the observed rate constant k can be expressed as

$$k = \frac{k_1/[H^+] + k_2K^H}{1/[H^+] + K^H} \quad (9)$$

where

$$K^H = \frac{[Cr^{II}(H_2O)Hedta^-]}{[Cr^{II}(H_2O)edta^{2-}][H^+]} \quad (10)$$

The value of K^H has been determined to be $10^{3.00}$ at ionic strength 0.1 and 20°C by Pecsok *et al.*[5] Equation (9) is rewritten as

$$k\alpha = \frac{k_1}{[H^+]} + k_2K^H \quad (11)$$

where

$$\alpha = \frac{1}{[H^+]} + K^H \quad (12)$$

Figure 5 shows the plots of $k\alpha$ vs. reciprocal hydrogen ion concentrations in the reaction of chromium(II)-EDTA with $Cr(NCS)_6^{3-}$. The value of k_1 obtained from the slope is equal to 28.2 l mol^{-1} sec^{-1}. The value of the intercept is approximately zero. It could be deduced from standard deviations of the plots that k_2 is less than 50 l mol^{-1}sec^{-1}.

Similar kinetic behaviors were found for the reactions involving other chromium(III) complexes.

Second-order rate constants of the reaction between $Cr^{II}(H_2O)edta^{2-}$ and $Cr(NCS)_n(NH_3)_{6-n}^{(3-n)+}$ are given in Table 3. Although $Cr(NH_3)_6^{3+}$ ions were found to react with chromium(II)-EDTA, only an upper limit of rate constant was obtained, because of extremely slow rate of the reaction. Since $Cr(NH_3)_6^{3+}$ complex has no electron-pair exposed, the mechanism of this electron-transfer reaction is probably of outer-sphere type.

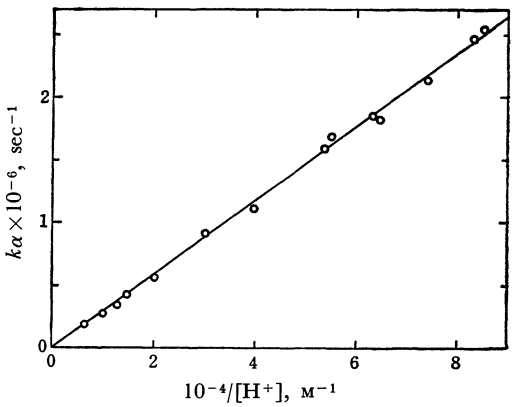

Fig. 5. The values of left hand side of Eq. (11) as a function of reciprocal hydrogen ion concentrations in the reaction between chromium(II)-EDTA and $Cr(NCS)_6^{3-}$.

Table 3. Rate constants of electron-transfer reactions between $Cr^{II}(H_2O)edta^{2-}$ and $Cr(NCS)_n(NH_3)_{6-n}^{(3-n)+}$ at μ=1.0 and 25°C

Complex	Rate constant l mol^{-1} sec^{-1}	Medium	Absorption maxima of ligand field bands $\bar{\nu}\times10^{-3}$, cm^{-1} 1 st band	2 nd band
$Cr(NH_3)_6^{3+}$	$<10^{-2}$	NaCl	21.46	28.41
$CrNCS(NH_3)_5^{2+}$	0.2	NaCl	20.49	27.32
$Cr(NCS)_4(NH_3)_2^-$	2.3	$NaClO_4$	19.08	25.38
$Cr(NCS)_6^{3-}$	28.2	$NaClO_4$	17.67	23.70

The rate constants of $Cr(NCS)_n(NH_3)_{6-n}^{(3-n)+}$ shown in Table 3 increase with the number of thiocyanate anions coordinated, in spite of the increase of electrostatic repulsion between reactants. If these reactions occur *via* activated complexes which involve thiocyanate anions as a bridge between chromium(II)-EDTA and $Cr(NCS)_n(NH_3)_{6-n}^{(3-n)+}$, it may be expected that the rate of electron-transfer reactions increases with the number of groups coordinated to chromium(III) which are able to mediate an electron. However, the increase of the rate constants given in Table 3 is much larger than expected from the statistical factor mentioned above. This suggests a large contribution of the free energy change of the reactions in question.

King and Ball[23] reported that the electron-transfer reaction of chromium(II) ions with $CrNCS(H_2O)_5^{2+}$ ions proceeds through an activated complex which involves a coordinated thiocyanate anion as a bridge between the chromium(II) and chromium(III). Haim and Sutin[24] reported

*3 It should be noted that chromium(III)-EDTA ions are present in the forms of both $Cr^{III}(H_2O)edta^-$ and $Cr^{III}(H_2O)Hedta$ at lower pH's. The pK value for the reaction

$$Cr^{III}(H_2O)edta^- + H^+ \rightleftharpoons Cr^{III}(H_2O)Hedta$$

has been determined to be 3.19[20] or 2.27.[22]

22) C. Furlani, G. Morpurgo and G. Sartori, *Z. anorg. u. allgem. Chem.*, **303**, 1 (1960).

23) D. L. King and E. L. Ball, *J. Am. Chem. Soc.*, **80**, 1091 (1958).

24) A. Haim and N. Sutin, *ibid.*, **88**, 434 (1966).

that chromium(II) ions react with $FeNCS^{2+}$ and various isothiocyanatocobalt(III) complexes to produce both $CrSCN^{2+}$ and $CrNCS^{2+}$. It was shown spectrophotometrically that the chromium(III)-EDTA of the products obtained in this work contained no thiocyanate anion in the first coordination sphere. This was also verified from the behavior of the product on the ion-exchange resins. However, this does not necessarily preclude inner-sphere mechanisms of the reactions investigated in this work. It is considered that the reactions of $Cr^{II}(H_2O)edta^{2-}$ with $CrNCS(NH_3)_5^{2+}$, $Cr(NCS)_4(NH_3)_2^-$ and $Cr(NCS)_6^{3-}$ proceed through an inner-sphere mechanism.[25]

The absorption maxima of the ligand field band of $Cr(NCS)_n(NH_3)_{6-n}^{(3-n)+}$ are also given in Table 3. It is of interest that there is a correlation between the rate constants and the wave numbers of the absorption maxima of $Cr(NCS)_n(NH_3)_{6-n}^{(3-n)+}$.

The authors wish to thank the Ministry of Education for the financial support granted for this research.

25) H. Ogino and N. Tanaka, This Bulletin, in press.

BULLETIN OF THE CHEMICAL SOCIETY OF JAPAN VOL. 41 1628—1633 (1968)

Behavior of Methyl Iodide in the Reaction of Acetic Acid Synthesis from Methanol and Carbon Monoxide

Tsutomu MIZOROKI and Mikitake NAKAYAMA

Government Chemical Industrial Research Institute, Tokyo, Meguro-ku, Tokyo

(Received September 2, 1967)

The reaction of methyl iodide with carbon monoxide in the presence of cobalt(II) iodide as the catalyst has been investigated to know the effect of methyl iodide on the acetic acid synthesis from methanol and carbon monoxide catalyzed by the same catalyst. The reaction, $CH_3I+CO+H_2O \rightarrow CH_3COOH+HI$, does not take place before the methyl iodide used has been hydrolyzed completely into methanol and sodium iodide by adding enough amount of sodium acetate ($CH_3I+CH_3COONa+H_2O \rightarrow CH_3OH+NaI+CH_3COOH$). Methyl iodide also strongly inhibits the reaction of methanol with carbon monoxide catalyzed by cobalt(II) ion or dicobalt octacarbonyl, although iodide ion promotes the reaction effectively. The promotion effect of iodide ion has been discussed by considering the effect of an additive on carbonylation reactions in terms of a labilizing ligand and a non-labilizing ligand and a possible reaction scheme of methanol with carbon monoxide catalyzed by cobalt(II) iodide has been proposed.

In the reaction of acetic acid synthesis from methanol and carbon monoxide in the presence of cobalt(II) iodide as the catalyst, hydrocobalt tetracarbonyl and methyl iodide were estimated to be formed in the course of the reaction as follows[1]: $2CoI_2+11CO+3H_2O \rightarrow 2HCo(CO)_4+4HI+3CO_2$, $HI+CH_3OH \rightarrow CH_3I+H_2O$. One may anticipate that the reaction of methyl iodide with carbon monoxide must be catalyzed more effectively by hydrocobalt tetracarbonyl to form acetic acid: $CH_3I+CO+H_2O \xrightarrow{HCo(CO)_4} CH_3COOH+HI$. This reaction, however, practically does not take place under the same conditions as those of the reaction with methanol. In our preceding papers dealing with the absorption spectrum of cobalt(II) ion in the course of the reaction of methanol with carbon monoxide, it was shown that most of cobalt(II) ion does not form dicobalt octacarbonyl, but tetrahedral iodo-cobalt(II) complex, $[Co(CH_3COO)_{4-n}I_n]^{2-}$,[2] and that the reaction is accelerated by adding a small amount of potassium acetate in spite that the presence of such a salt is unfavorable for the formation of methyl iodide from methanol and hydroiodic acid.[3] The addition of potassium acetate, in fact, effectively decomposes methyl iodide into methanol and potassium iodide through the reaction of $CH_3I+CH_3COOK+H_2O \rightarrow CH_3OH+CH_3COOH+KI$. It should be abandoned to discuss these facts in terms of the hydrocobalt tetracarbonyl and methyl iodide as the catalyst.

1) N. von Kutepow, W. Himmele and H. Hohenschutz, *Chem. Ingr. Tech.*, **37**, 383 (1965).

2) T. Mizoroki and M. Nakayama, This Bulletin, **38**, 1876 (1965).

3) T. Mizoroki and M. Nakayama, This Bulletin, **39**, 1477 (1966).

This work was undertaken to investigate the effect of methyl iodide on the reaction of methanol with carbon monoxide catalyzed by cobalt(II) iodide and to fully discuss the catalytic action of iodide ion and the course of the reaction.

Experimental

The apparatus and materials used in carrying out the reactions were the same as those described earlier.[3] The amounts of methanol, methyl acetate, dimethyl ether, methyl iodide and water were determined by the same gas chromatographic procedure described in the same paper. When the amount of methyl iodide contained in a liquid product was more than 0.1 mol% based on the methanol used (25% based on the cobalt-(II) ion used), it was quantitatively determined by this gas chromatographic procedure.

Results

The Reaction of Methyl Iodide with Carbon Monoxide. Methyl iodide (0.40 mol), water (6.0 mol) and cobalt(II) iodide (0.004 mol) were placed in the autoclave (300 ml in vol) and carbon monoxide (40—50 kg/cm^2) was introduced at a room temperature. It had been heated up to 215°C and kept the temperature constant for about one hour before the carbon monoxide was introduced again up to 350 kg/cm^2. The reaction was carried out at the constant pressure for 2 hr. Under these conditions, practically no carbon monoxide was absorbed and the reaction of $CH_3I+CO+H_2O\rightarrow CH_3COOH+HI$ did not take place. After the reaction, 0.23 mol (58%) of methyl iodide used was hydrolyzed into methanol and hydroiodic acid. While a nearly calculated amount of carbon monoxide was absorbed on adding sodium acetate more than the equimolar amount of methyl iodide used ($CH_3COONa/CH_3I\geqq 1$) and 100% of methyl iodide used reacted with carbon monoxide to form

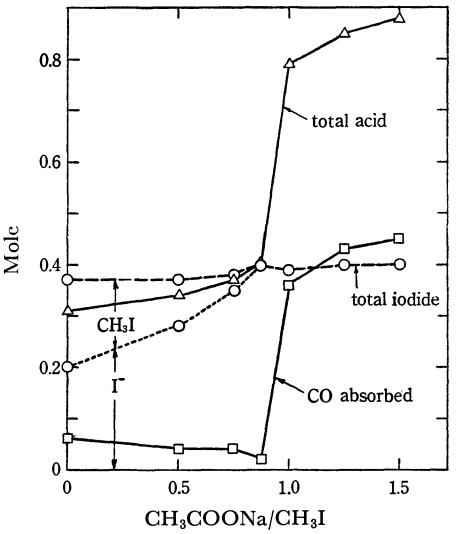

Fig. 1. Plots of the total acid formed and the carbon monoxide absorbed against the amounts of sodium acetate added.

acetic acid. The results are represented in Fig. 1 and Table 1. No carbon monoxide was absorbed as long as the amount of sodium acetate added was less than 0.40 mol ($CH_3COONa/CH_3I<1$). The hydrolysis of methyl iodide was checked by heating the solutions used in the experiments 3 and 6 without introducing any carbon monoxide. As shown in B3 and B6 of Table 1, 0.05 mol (13%) of methyl iodide used remained unchanged in the experiment B3 ($CH_3COONa/CH_3I=0.75$), no methyl iodide, however, was detected in B6 ($CH_3COONa/CH_3I=1.25$). These results show that the absorption of carbon monoxide takes place only when sodium acetate is added enough to hydrolyze the methyl iodide used completely and that the reaction can be represented as

Table 1. Effect of acetate on the reaction of methyl iodide with carbon monoxide

Exp. No.	CH_3COONa/CH_3I	Acid (mol)			I^- (mol)		
		Acid	CH_3COOCH_3	Total	CH_3I	I^-	Total
1	0.0	0.31	—	0.31**	0.17	0.20**	0.37
2	0.50	0.34	—	0.34	0.09	0.28	0.37
3	0.75	0.29	0.08	0.37	0.03	0.35	0.38
4	0.88	0.33	0.08	0.41	0.0	0.40	0.40
5	1.00	0.79	0.0	0.79	0.0	0.39	0.39
6	1.25	0.85	0.0	0.85	0.0	0.40	0.40
7	1.50	0.88	0.0	0.88	0.0	0.40	0.40
B3	0.75	0.27	0.08	0.35	0.05	0.34	0.39
B6	1.25	0.30	0.11	0.41	0.0	0.40	0.40
B*6′	1.25	0.83	0.0	0.83	0.0	0.40	0.40

* CH_3OH 0.4 mol, H_2O 5.6 mol, CH_3COOH 0.4 mol, CH_3COONa 0.1 mol, NaI 0.4 mol and CoI_2 0.004 mol.

** The difference in the amounts between total acid (0.31) and I^- (0.20) is probably caused by the formation of formic acid.

follows:

$$CH_3I + H_2O \rightarrow CH_3OH + HI \quad (a)$$

$$HI + CH_3COONa \rightarrow CH_3COOH + NaI \quad (b)$$

$$+ \quad CH_3OH + CO \rightarrow CH_3COOH \quad (c)$$

$$CH_3I + CH_3COONa + CO + H_2O \rightarrow 2CH_3COOH + NaI \quad (d)$$

The acids formed in the experiments 1—4 are the sum of the hydroiodic acid from (a) and the acetic acid from (b), they, however, do not contain the acetic acid formed from (c), because no carbon monoxide is absorbed. The experiment B6′ shown in Table 1 is the result obtained from the reaction of methanol with carbon monoxide under the same condition as that of the experiment 6 except that no methyl iodide was added to the starting materials. The absorption rates of carbon monoxide in the experiments 6 and B6′ are shown in Fig. 2. The amount of carbon monoxide absorbed in the experiment B6′ was nearly the same as that in the experiment 6 and negligibly small amounts of dimethyl ether and acetaldehyde were present in the product, but neither methanol, methyl acetate nor methyl iodide were detected. That the amount of the total acid is more than the calculated one (0.80 mol) is caused by the formation of a small amount of formic acid, because water was added enough to dissolve lots of sodium acetate or sodium iodide completely.

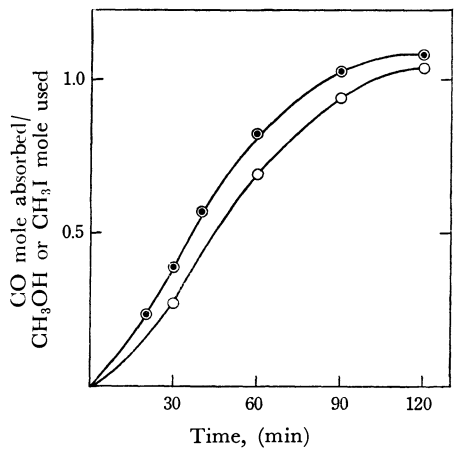

Fig. 2. Absorption rates of carbon monoxide.
⊙ the reaction with methyl iodide (No. 6)
○ the reaction with methanol (No. B6′)

Inhibition of Methyl Iodide in the Reaction of Methanol with Carbon Monoxide. Methanol (1.80 mol), acetic acid (0.20 mol), water (1.33 mol), cobalt(II) iodide (0.008 mol) and methyl iodide (0.016 mol, $CH_3I/CoI_2=2$ or 0.040 mol, $CH_3I/CoI_2=5$) were placed in the autoclave and the reaction with carbon monoxide was carried out for 2.5 hr under the constant pressure, 350 kg/cm² at the temperature, 215°C. Methyl iodide strongly inhibited the absorption rate of carbon monoxide and practically no acetic acid was formed especially when methyl iodide (0.040 mol) was added to the starting materials. While the inhibition was removed again by adding potassium acetate with which methyl iodide was hydrolyzed into methanol and potassium iodide. The result is shown in Fig. 3. The gas chromatographies of the liquid products obtained in the case of adding methyl iodide (0.016 mol) to the starting materials, showed that 0.003 mol of methyl iodide was contained in the product when the amount of potassium acetate added was 0.008 mol ($CH_3COOK/CH_3I=0.5$), while no methyl iodide was detected when it was more than 0.016 mole ($CH_3COOK/CH_3I \geqq 1$). For the purpose of investigating the effect of methyl iodide in the case of using dicobalt octacarbonyl as the catalyst, the following experiment was undertaken. Methanol (1.35 mol), acetic acid (0.15 mol), water (1.00 mol) and cobalt(II) acetate (0.006 mol) were placed in an autoclave (200 m*l*) equipped with another small high pressure vessel (25 m*l* in vol). Carbon monoxide was introduced up to the pressure, 300 kg/cm² at the temperature, 215°C and they were kept constant for about one hour to convert cobalt(II) acetate into dicobalt octacarbonyl,*1 within which period no carbon monoxide was absorbed by the reaction with methanol. Then methyl iodide (0.003—0.024 mol in tetrahydrofuran) which had been

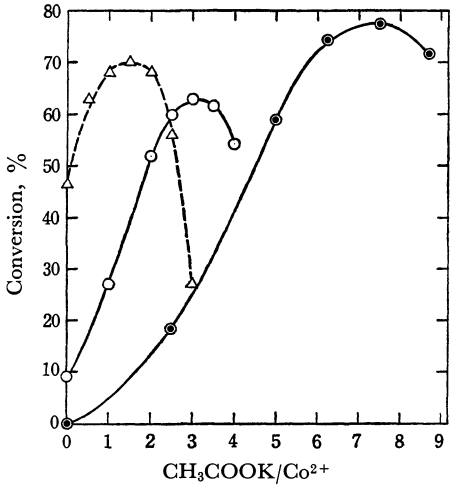

Fig. 3. Effect of methyl iodide on the reaction of methanol with carbon monoxide.
○ CH_3I 0.016 mol ⊙ CH_3I 0.040 mol
△ NaI 0.016 mol

*1 To formation of $Co_2(CO)_8$ was checked by taking the absorption spectrum of cobalt(II) ion under the same condition. The visible absorption spectrum (from 450 to 700 mμ) of cobalt(II) ion disappears completely when it is converted into $Co_2(CO)_8$ or $[Co(CO)_4]^-$.

Table 2. Mass balance of the liquid product

Catalyst: Inserted iodide: Iodide	Catalyst: Inserted iodide: mmol	Catalyst: I/Co	Mass balance of methanol: Total CH_3COOH: mol	Total CH_3COOH: %	Residual CH_3OH: mol	Residual CH_3OH: %	$(CH_3)_2O$: mol	$(CH_3)_2O$: %	Others %	Detected CH_3I mmol
CH_3I	3.0	0.50	0.50	37	0.56	41	0.21	16	6.1	0
	4.5	0.75	0.68	50	0.56	42	0.07	5.0	3.1	0
	6.0	1.00	0.63	47	0.49	36	0.12	9.2	8.0	0
	7.5	1.25	0.63	47	0.46	34	0.18	14	5.3	0
	12.0	2.00	0.52	38	0.46	34	0.23	17	10.4	3.8
	18.0	3.00	0.47	35	0.47	35	0.30	22	9.9	6.8
	24.0	4.00	0.28	21	0.44	32	0.35	26	21.1	8.3
HI	6.0	1.00	0.71	53	0.44	32	0.09	6.4	8.7	0
	18.0	3.00	0.50	37	0.40	29	0.24	18	15	3.8
NaI	6.0	1.0	0.48	36	0.82	61	0.01	1.0	2.1	0
	24.0	4.0	0.79	59	0.52	38	0.02	1.8	1.2	0
	36.0	6.0	0.91	67	0.37	27	0.03	2.5	2.9	0
	60.0	10.0	0.97	72	0.33	25	0.03	2.1	1.3	0

CH_3OH 1.35 mol, CH_3COOH 0.15 mol, H_2O 1.00 mol, $Co(CH_3COO)_2 \cdot 4H_2O$ 6.0 mmol.

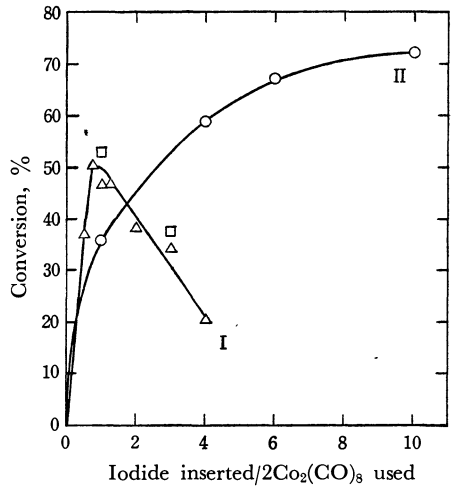

Fig. 4. Effect of iodide on the reaction of methanol with carbon monoxide in the presence of $Co_2(CO)_8$ as the catalyst.
△ CH_3I □ HI ○ NaI

charged in the small vessel was introduced into the autoclave by using a higher pressure of carbon monoxide and the reaction was carried out under the constant pressure, 350 kg/cm² for 2.5 hr. Mass balances of the liquid products are shown in Table 2 and methanol conversion (%) into total acetic acid (free acetic acid+methyl acetate) are plotted against the amount of methyl iodide introduced ($CH_3I/2Co_2(CO)_8$) in Fig. 4 (curve I). When the amount of methyl iodide introduced is 0.0045 mol ($CH_3I/2Co_2(CO)_8 \fallingdotseq 0.8$), methanol conversion becomes maximum and no methyl iodide was detected in the liquid product, the conversion, however, decreases sharply with increasing the amount of methyl iodide and that of dimethyl ether contained in the liquid products gradually increases. The same result is obtained on introducing hydroiodic acid*2 aqueous solution in place of methyl iodide. But it is very different from these results that the methanol conversion increases with increasing the amount of sodium iodide aqueous solution*2 introduced as shown by the curve II in Fig. 4.

Discussion

The following facts are, no doubt, inconsistent with the reaction scheme proposed by Reppe.[1] (i) When sodium iodide is used in place of methyl iodide or hydroiodic acid, the reaction rate of methanol with carbon monoxide increases with increasing the amount of sodium iodide added. (ii) No methyl iodide is detected in the liquid product when the reaction rate is large enough. (iii) In the course of the reaction, most of cobalt-(II) ion does not form dicobalt octacarbonyl, but tetrahedral iodocobalt complex $[Co(CH_3COO)_{4-n}I_n]^{2-}$. The addition of sodium iodide or an acetate is unfavorable for the formation of methyl iodide, because the equilibrium constant of Eq. (e) is much smaller than that of Eq. (f).*3

*2 The total amount of water added was constant in this experimental run (1.00 mol).

*3 The equilibrium constants, $\log K_p$ at 200°C, calculated from $\log K_p = -\Delta H^\circ_{298}/4.575T + \Delta S^\circ_{298}/4.575$ are −0.67 in Eq. (e) and 5.07 in Eq. (f), in which the entropy of CH_3COONa (39.2 cal/mol·°K) is obtained from assuming no change in the entropy of the reaction $CH_3COOH(g) + NaOH(s) \rightarrow CH_3COONa(s) + H_2O(g)$.

$$CH_3OH(g) + NaI(s) + CH_3COOH(g) \rightleftarrows CH_3I(g) + CH_3COONa(s) + H_2O(g) + 0.56\ kcal/mol \quad (e)$$

$$CH_3OH(g) + HI(g) \rightleftarrows CH_3I(g) + H_2O(g) + 11.0\ kcal/mol \quad (f)$$

The reaction rate, therefore, would not be increased by adding sodium iodide in place of methyl iodide or hydroiodic acid, if the formation of methyl iodide were necessary in the course of the reaction. If no detection of methyl iodide in the liquid product were caused by that the formation of methyl iodide were the rate determining step, the rate of the reaction with carbon monoxide would not depend on the pressure of carbon monoxide, nor the amount of cobalt(II) ion added. But, in fact, the higher the reaction pressure, the larger the reaction rate.[3,4]

Promotion Effect of Iodide Ion. Before the catalytic action of iodide ion will be discussed, it must be noticed that in a hydroformylation or a hydroesterification reaction catalyzed by $Co_2(CO)_8$ or $Rh_2(CO)_8$, its reaction rate is increased by adding an organic base such as pyridine[5-7] or *N*-ethylpyrolidine,[6] it is, however, rather strongly inhibited by carbon monoxide[5] or phosphorous compounds[6] such as $P(C_6H_5)_3$ or $P(OC_2H_5)_3$. In his recent paper,[8] Matsuda explained that in the hydroesterification of propylene or acrylonitrile pyridine (Py) would accelerate the insertion step of carbon monoxide to form acylcobalt tricarbonyl represented by $C_3H_7Co(CO)_4 + Py \rightarrow C_3H_7COCo(CO)_3Py$ or $NCC_2H_4Co(CO)_4 + Py \rightarrow NCC_2H_4COCo(CO)_3Py$. Such insertion reactions are well known also in the reactions of $RCo(CO)_4$ with carbon monoxide or phosphorous compounds[9] and of $CH_3Mn(CO)_5$ with carbon monoxide,[10] phosphorous compounds, amines[11] or iodide ion.[12] The question is why neither phosphorous compounds nor carbon monoxide accelerate the carbonylation reactions. According to the classification of ligands defined recently by Angelici,[13] halogen ions amines are labilizing ligands (hard base*[4]), while carbon monoxide and phosphorous compounds are non-labilizing ligands (soft base*[4]). This classification may provide a possible explanation on the effect of an additive on the carbonylation reactions catalyzed by a cobalt carbonyl. The following reaction scheme has been reported as a reasonable one of an oxo-reaction.[9] Although kinetic data have not been found enough, the rate determining step is probably the reaction (iii) in a hydroformilation reaction, while in a hydroesterification reaction it would be the reaction (ii).

$$RCHCH_2 + HCo(CO)_4 \rightleftarrows RC_2H_4Co(CO)_4 \quad (i)$$

$$RC_2H_4Co(CO)_4 \rightleftarrows RC_2H_4COCo(CO)_3 \overset{+CO}{\underset{-CO}{\rightleftarrows}} RC_2H_4COCo(CO)_4 \quad (ii)$$

$$RC_2H_4COCo(CO)_3 + HR \rightleftarrows RC_2H_4COR + HCo(CO)_3 \quad (iii)$$

$$HCo(CO)_3 + CO \rightleftarrows HCo(CO)_4 \quad (iv)$$

$$(R=H \text{ or } OCH_3)$$

The effect of an additive in this scheme, can be explained by considering Eq. (ii'). When L is one of labilizing ligands (Py, halide ion, some solvent), acylcobalt tricarbonyl will become sufficiently reactive, the rate determining step, then, will be the reaction (ii'). On the other hand, when L is one of non-labilizing ligands (carbon monoxide or phosphorous compounds), acylcobalt tricarbonyl will become unreactive, the rate determining step, then, will be the reaction (iii).

$$RC_2H_4Co(CO)_4 + L \rightleftarrows RC_2H_4COCo(CO)_3L \quad (ii')$$

In the reaction of methanol with carbon monoxide, authors postulated $[Co(CO)I_n(CH_3COO)_{4-n}]^{2-}$ and $[Co(OCCH_3)I_n(CH_3COO)_{4-n}]^{2-}$ $(n=1—4)$ as its intermediates.[3] Booth and Chatt[14] reported that $[CoX_2(PEt_3)_2]$ $(Et=C_2H_5,\ X=Cl^-,\ Br^-$ or $I^-)$ reacts with carbon monoxide at a room temperature under an atmospheric pressure to form penta-coordinating and paramagnetic carbonyl complexes $[CoX_2(CO)(PEt_3)_2]$. The order of their stabilities is $I^->Br^->Cl^-$. It would be explained from π-bonding theory that the coordination of carbon monoxide to cobalt(II) ion is facilitated by adding a good donors, as iodide ion, capable of coordinating to the metal ion. They also isolated the acyl complexes, *trans*-$[MX(COR)(PEt_3)_2]$ $(M=Pd$ or Pt, R=alkyl or aryl) from

4) T. Mizoroki, M. Nakayama, Y. Ando and M. Furumi, *Kogyo Kagaku Zasshi (J. Chem. Soc. Japan, Ind. Chem. Sect.)*, **65**, 1049 (1962).
5) I. Wender, H. W. Sternberg and M. Orchin, "Catalysis," Vol. V, ed. by P. H. Emmett, Reinhold Pub. Co., New York (1957), p. 110.
6) J. Falbe and N. Huppes, *Brenn. Chem.*, **48**, 46 (1967).
7) A. Matsuda and H. Uchida, This Bulletin, **38**, 710 (1965).
8) A. Matsuda, *ibid.*, **40**, 135 (1967).
9) R. F. Heck, "Advan. Organomet. Chem.," Vol. IV, ed. by F. G. Stone and R. West, Academic Press, New York (1966), p. 242.
10) F. Calderazzo and F. A. Cotton, *Inorg. Chem.*, **1**, 30 (1962).
11) R. J. Mawby, F. Basolo and R. Pearson, *J. Am. Chem. Soc.*, **80**, 3994 (1964).
12) F. Calderazzo and K. Noack, *J. Organomet. Chem.*, **4**, 250 (1965).
13) R. J. Angelici and J. R. Graham, *Inorg. Chem.*, **6**, 988 (1967).

*4 It can be said, labilizing ligands have no empty π orbital and they are good σ donors, while non-labilizing ligands have empty π orbitals (good $d\pi$ acceptor), although this classification can not be understood in terms of π-bonding theory.
14) G. Booth and J. Chatt, *J. Chem. Soc.*, **1962**, 2099.

trans-$[MXR(PEt_3)_2]$ and carbon monoxide[15] and estimated that such complexes would be intermediates in carbonylation reactions, although such cobalt or nickel complexes were too unstable to be isolated.

Inhibition Effect of Hydroiodic Acid. It can not be understood well why both methyl iodide and hydroiodic acid inhibit the reaction of methanol with carbon monoxide. The following facts, however, may provide an explanation on their inhibition effects. The addition of a salts of weak acid (acetate, benzoate, borax *etc*) is very effective for the formation of dicobalt octacarbonyl from cobalt(II) iodide, although it is easily formed under a milder condition without adding any additive when a cobalt(II) salt of weak acid (acetate or carbonate) is used as the starting material. Weak acids salts are good acceptors of hydroiodic acid formed, which results in decreasing the hydrogen ion concentration, because hydroiodic acid is a much stronger acid. This suggests that proton, which is an acceptor of electron, probably inhibits the coordination of carbon monoxide to cobalt(II) ion. On the other hand, Wakamatsu confirmed that the treatment of $RMn(CO)_5$ ($R=CH_3-$, C_6H_5- or $C_6H_5CH_2-$) with hydroiodic acid resulted in forming nearly stoichiometric amounts of RH and $IMn(CO)_5$ against his expectation that RI and $HMn(CO)_5$ would have been formed.[16] The similar reaction would take place between $CH_3Co(CO)_4$ and HI.

A Possible Reaction Scheme. From the above discussion, the course of the reaction of methanol with carbon monoxide catalyzed by cobalt(II) iodide can be represented as follows:

$$Co(II) + CO \underset{k_2}{\overset{k_1}{\rightleftharpoons}} Co(II)\text{-}CO \qquad (v)$$

$$H_2O \overset{K_1}{\rightleftharpoons} H^+ + OH^-,$$

$$CH_3OH + H^+ \overset{K_2}{\rightleftharpoons} CH_3OH_2^+ \qquad (vi)$$

$$CH_3OH_2^+ + Co(II)\text{-}CO \overset{K_3}{\rightleftharpoons} CH_3\text{-}Co(II)\text{-}CO + H_2O \qquad (vii)$$

$$CH_3\text{-}Co(II)\text{-}CO + I^- \xrightarrow{k_3} CH_3CO\text{-}Co(II)\text{-}I \qquad (viii)$$

$$CH_3CO\text{-}Co(II)\text{-}I + HR \xrightarrow{\text{fast}} CH_3COR + Co(II) + H^+ + I^- \qquad (ix)$$

(where R is H, OH or OCH_3 and Co(II) represents $[Co(CH_3COO)_{4-n}I_n]^{2-}$)

The formation of carbonium ion from methanol (Eq. (vi)) is generally accepted in the course of the esterification or dehydration of methanol catalyzed by hydrogen ion. In this scheme, it is postulated that the breaking of the bond between carbon and oxygen of methanol is assisted by hydrogen ion and that the formation of an acyl complex is promoted by iodide ion (Eq. (viii)). On the assumption that the reactions (vi) and (vii) become equilibrium and that the concentration of Co(II)–CO is nearly constant during the reaction, one can derive the following equations, which is qualitatively consistent with the reported results[3,4] obtained from the absorption rate of carbon monoxide.

$$r = k_3[CH_3Co(II)CO][I^-] = \frac{k_1k_3K_1K_2K_3[Co(II)][I^-][p_{CO}][CH_3OH]}{k_2[OH^-]+k_3K_1K_2K_3[CH_3OH][I^-]}$$

$$k_2 \gg k_3K_1K_2K_3$$

$$r = \frac{k_1k_3K_1K_2K_3}{k_2[OH^-]}[Co(II)][p_{CO}][I^-][CH_3OH] = \frac{k_1k_3K_2K_3}{k_2[H_2O]}[Co(II)][I^-][p_{CO}][H^+][CH_3OH]$$

From this reaction scheme, the effect of acetate shown in Fig. 3 can be also explained: the addition of potassium acetate will decrease the concentration of $[H^+]$ which would inhibit the coordination of carbon monoxide to cobalt(II) ion, so k_2 will become smaller and r increases, while the decrease in $[H^+]$ must be unfavorable for the equilibrium concentration of $[CH_3OH_2^+]$, r is, then, decreased again by adding excess amounts of acetate.

The authors wish to express their thanks to Professor Dr. Yukio Yoneda and Dr. Yasukazu Saito, Faculty of Engineering, The University of Tokyo, for their helpful discussions.

15) G. Booth and J. Chatt, *Proc. Chem. Soc.*, **1961**, 67.

16) H. Wakamatsu and K. Sakamaki, Preprints for the 20th Annual Meeting of the Chemical Society of Japan, (April, 1967), Part III, p. 587.

BULLETIN OF THE CHEMICAL SOCIETY OF JAPAN VOL. 41 1634—1638 (1968)

A Study of Unnatural Amino Acids and Their Peptides. III. The Syntheses of DL-β-(2-Pyridyl)-α-alanine and Its Peptides*1

Hiroshi WATANABE, Shigeru KUWATA, Kenzo NAOE*2 and Yoshiteru NISHIDA*3

Laboratory of Chemistry, Faculty of Science, Kōnan University, Okamoto Higashinada, Kobe

(Received October 5, 1967)

DL-β-(2-Pyridyl)-α-alanine has been synthesized in a good yield by the condensation of α-picolyl chloride and diethyl acetamidomalonate and by the subsequent hydrolysis of the product. The *N*-carbobenzoxy derivative of this amino acid, quite different from 3-pyridylalanine reported by Griffith and Harwood, could easily be prepared in a good yield. Only the carbodiimide method and the *N*-bromosuccinimide method proved to be successful in bringing the *N*-carbobenzoxylated amino acid into a peptide-coupling reaction with an amine component. Other methods, *i. e.*, the mixed anhydride method, the azide method and the *p*-nitrophenyl ester method, were unsuccessful. It is noteworthy that, in the former cases, the activation of the carboxyl group occurs *in situ* in the presence of an amine component. No difficulties were encountered in the coupling reaction of the alkyl ester of this amino acid with usual *N*-protected amino acids. The alkaline hydrolysis of the protected dipeptide ester afforded the *N*-protected peptide in a good yield. The catalytic hydrogenation could be used to remove the benzyl ester group as well as the carbobenzoxy group without any damage to the pyridine ring. Decarbobenzoxylation also proceeded smoothly with hydrogen bromide in acetic acid.

In connection with the previous reports[1] of this series, the syntheses of DL-β-(2-pyridyl)-α-alanine and its peptides will be reported in this paper. This amino acid had already been synthesized in several ways.[2-5] In this experiment it was prepared by the condensation of diethyl acetamidomalonate and α-picolyl chloride, easily obtainable from α-picoline, and by the subsequent hydrolysis of the condensation product. Both the condensation and the hydrolysis proceeded smoothly, and the hydrochloride of the amino acid was obtained in a good yield (Scheme I). By treating the hydrochloride with an ion exchange resin, there was obtained free amino acid, which gave a characteristic yellow-brown color in a ninhydrin test on paper.

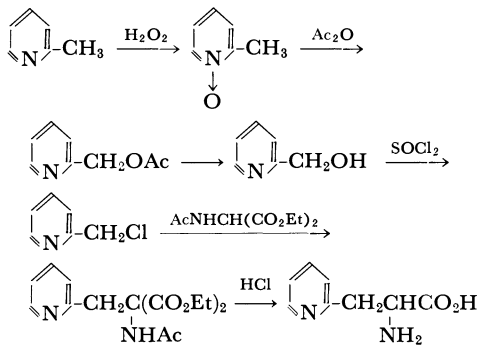

Scheme I

The carbobenzoxylation of this free amino acid with carbobenzoxy chloride proceeded smoothly in water, with sodium hydroxide as the base, and gave the expected carbobenzoxy derivative in a 77% yield. According to Griffith and Harwood,[6] 3-pyridylalanine is carbobenzoxylated only in a low yield (34%) by usual methods; they attributed this low yield to "the ability of carbobenzoxy-3-pyridylalanine, once formed, to rapidly promote the destruction of unreacted carbobenzoxy chloride." They also examined the carbobenzoxylation of phenylalanine in the presence of an equivalent of pyridine or a one-third equivalent of carbobenzoxy-3-pyridylalanine and observed that "the yield of carbobenzoxyphenylalanine fell essentially to zero." They concluded from these facts that organic soluble pyridine derivatives facilitate the decomposition of carbobenzoxy chloride in aqueous alkali. Therefore, we attempted the carbobenzoxylation of phenylalanine under similar conditions, using 2-pyridylalanine instead of 3-pyridylalanine, with

*1 This work was presented at the 15 th (April, 1962) and 17 th (April, 1964) Annual Meetings of the Chemical Society of Japan.

*2 Present address: Kansai Oil Co., Inc., 16, 3-Cho, Shinmachi, Chikko, Sakai.

*3 Present address: Res. and Dev. Center, Nippon Rayon Co., Ltd., Uji, Kyoto.

1) Part II: This Bulletin, **39**, 2473 (1966).
2) J. Overhoff, J. Boeke and A. Gorter, *Rec. trav. chim.*, **55**, 293 (1936).
3) C. Niemann, R. N. Lewis and J. T. Hays, *J. Am. Chem. Soc.*, **64**, 1678 (1942).
4) F. Zymalkowsky, *Arch. Pharm.*, **291**, 436 (1958).
5) S. J. Norton, C. G. Skinner and W. Shive, *J. Org. Chem.*, **26**, 1495 (1961).
6) R. K. Griffith and H. J. Harwood, *ibid.*, **29**, 2658 (1964).

a view to finding if there were any characteristics similar to those claimed for the latter amino acid derivative. The reaction, however, proceeded normally, and carbobenzoxyphenylalanine was isolated from the reaction mixture in a 90% yield; no unfavorable effect of this amino acid was observed during the carbobenzoxylation. A similar carbobenzoxylation of phenylalanine in the presence of picolinic acid afforded carbobenzoxyphenylalanine in a 78% yield. In the presence of an equivalent of pyridine, the yield of carbobenzoxyphenylalanine dropped to 42% (raw yield), but not to zero, in spite of the description of Griffith and Harwood.

The esterification of this amino acid proceeded smoothly in the presence of *p*-toluenesulfonic acid, giving 2-pyridylalanine benzyl ester in a 83% yield as *p*-toluenesulfonate.

To examine the applicability of common peptide synthetic methods to this amino acid, the coupling of carbobenzoxy-2-pyridylalanine and glycine benzyl ester was tried by the following four methods: mixed anhydride method, dicyclohexylcarbodiimide method, azide method, and *p*-nitrophenyl ester method.

(1) The mixed anhydride method: When ethyl chloroformate was added, drop by drop, to a dichloromethane solution of carbobenzoxy-2-pyridylalanine and an equivalent triethylamine, intense coloration (dark brown) occurred, even under strong cooling, and after the addition of the glycine ester, no expected dipeptide could be isolated from the reaction mixture. The replacement of triethylamine with a weaker base, *N*-ethylmorpholine, reduced the coloration of the reaction mixture, but the dipeptide could not be isolated in this case either.

(2) The dicyclohexylcarbodiimide method: When dicyclohexylcarbodiimide was stirred into a dichloromethane solution of carbobenzoxy-2-pyridylalanine, glycine benzyl ester *p*-toluenesulfonate, and an equivalent of triethylamine under ice-cooling, dicyclohexylurea soon began to be separated. When the reaction was carried out at room temperature, a strong coloration was observed, as in the preceding method, but under good cooling the color of the reaction mixture remained a pale yellow. After the usual treatment, the expected carbobenzoxy-dipeptide benzyl ester was isolated in a 75% yield.

(3) The azide method: Carbobenzoxy-2-pyridylalanylhydrazide could be obtained in a good yield from carbobenzoxy-2-pyridylalanine through its ester in a usual way. Into a solution of the hydrazide in hydrochloric acid, covered with ethyl acetate, there was stirred, drop by drop and under sufficient cooling, a cold concentrated solution of sodium nitrite and, after a few minutes, a 50% potassium carbonate solution. At this stage, a large quantity of an amorphous material, soluble in neither ethyl acetate nor an aquoeus alkaline solution, was separated out. When the ethyl acetate extract was made to react on the glycine ester, with or without this amorphous material, no expected dipeptide could be isolated. The amorphous material, obtained here during the preparation of the azide, melted at about 120°C. It afforded 2-pyridylalanine by hydrolysis, and its molecular weight was found to be 318; thus it was assumed to be carbobenzoxy-2-pyridylalanine amide, formed by the decomposition of carbobenzoxy-2-pyridylalanyl azide.

(4) The *p*-nitrophenyl ester method: To synthesize carbobenzoxy-2-pyridylalanine *p*-nitrophenyl ester, dicyclohexylcarbodiimide was added to a dichloromethane solution of carbobenzoxy-2-pyridylalanine and *p*-nitrophenol. After the removal of the precipitated dicyclohexylurea, the filtrate was, with or without purification, made to react on glycine benzyl ester, but no expected dipeptide could be isolated. This result can be attributed to the lack of success in the active ester synthesis rather than to that in the coupling reaction, because the attempts to obtain carbobenzoxy-2-pyridylalanine *p*-nitrophenyl ester in a crystalline state were all unsuccessful. Another attempt to prepare the *p*-nitrophenyl ester by the reaction of carbobenzoxy-2-pyridylalanine and *p*-nitrophenylsulfite in pyridine at 50°C afforded only a black, tarry material.

From these experiments, we concluded that, in the case of 2-pyridylalanine, it is very difficult to obtain the pyridylalanyl peptide by such methods as the previous activation of the carboxyl group of this amino acid and the subsequent addition of an amine component. On the contrary, only the activation of the acid component *in situ* in the presence of an amine component seems to give the desired peptide, as is the case with the dicyclohexylcarbodiimide method. To confirm these assumptions, another coupling method, the *N*-bromosuccinimide method, was attempted; this method permits the activation of an acid component in the presence of an amine component. According to the instructions of Wolman and his coworkers[7] *N*-bromosuccinimide was added in small portions to a mixture of carbobenzoxy-2-pyridylalanine, glycine benzyl ester *p*-toluenesulfonate, and three equivalents of triethylamine in tetrahydrofuran. From the reaction mixture, the desired dipeptide could be isolated, though the yield was very poor (about 6%).

When pyridylalanine was used as an amine component, no difficulty was encountered in coupling reactions with other ordinary *N*-protected amino acids. As an example, tritylglycine was

7) Y. Wolman, P. M. Gallop and A. Patchornik, *J. Am. Chem. Soc.*, **83**, 1263 (1961); Y. Wolman, P. M. Gallop, A. Patchornik and A. Berger, *ibid.*, **84**, 1889 (1962).

coupled with 2-pyridylalanine benzyl ester by the mixed anhydride method; tritylglycyl-2-pyridylalanine benzyl ester was thus obtained in a 48% yield.

The alkaline hydrolysis of dipeptide esters proceeds smoothly, on whichever side the pyridylalanine residue may be situated, thus enabling carbobenzoxy-pyridylalanylglycine or tritylglycyl-2-pyridylalanine to be obtained from its esters in a good yield.

In the case of peptide synthesis with this amino acid, another problem remains to be clarified: the stability of the pyridine ring during hydrogenation. In order to study this problem, tritylglycyl-2-pyridylalanine benzyl ester was hydrogenated in a quantitative hydrogenation apparatus, using palladium black as a catalyst. One mole equivalent of hydrogen was absorbed very quickly, but then the rate of hydrogenation decreased markedly; even after ten hours, the total volume of the absorbed hydrogen did not amount to two mole equivalents. When the incompletely hydrogenated contents were treated with hot aqueous acetic acid triphenylcarbinol was released, and from the filtrate glycylpyridylalanine was isolated in a chromatographycally-pure state. When carbobenzoxy-2-pyridylalanine was hydrogenated in the presence of sodium hydroxide in the same manner as has previously been reported,[1] one mole equivalent of hydrogen was absorbed very quickly, but then the rate of hydrogenation dropped markedly and only a small quantity of hydrogen was absorbed even after a longer period. All these facts show that the carbobenzoxy- and the benzyl ester-groups can be removed very easily by hydrogenolysis, but that the hydrogenolytic removal of the trityl group proceeds with difficulty, while the pyridine ring is preserved under these conditions. In fact, the simultaneous hydrogenolytic removal of the protecting groups from carbobenzoxy-2-pyridylalanylglycine benzyl ester proved to produce a good yield, accompanied by no reduction of the pyridine ring.

The removal of the carbobenzoxy group with hydrogen bromide in acetic acid proceeded smoothly, without any recognizable side reactions.

Experimental

2-Picolyl Chloride (I). According to the method of Itai and Ogura,[8] 2-pyridylmethanol,[9] obtained from α-picoline through its *N*-oxide and acetate of 2-pyridylmethanol, was converted into 2-picolyl chloride (I) by thionyl chloride. Bp 85—90°C/15 mmHg (lit.[8] bp 70—80°C/5 mmHg). Strongly-irritating pink liquid. Because of its strong resinifying tendency, it was used for the next step immediately after distillation.

Diethyl (2-Pyridylmethyl)-acetamidomalonate (II). To a solution of acetamidomalonate (50 g) and metallic sodium (5 g) in ethanol (300 m*l*), the above chloride (I) (28 g) was added, and then the mixture was stirred for 6 hr under reflux. After the removal of the precipitated sodium chloride by filtration, the filtrate was concentrated and water was added. The crystals separated were recrystallized from ethanol or acetone. Yield, 91%. Mp 92.5—93°C (lit.[4] 90—91°C).

DL-β-(2-Pyridyl)-α-alanine (III). The above malonate (II) (20 g) was boiled with 6 N hydrochloric acid for 8 hr. The solution was concentrated to dryness, and the residue was dissolved in water and treated with Amberlite CG-120 to obtain the free amino acid. Yield, 70%. Mp 200—208°C (lit.[4] 200—210°C). R_f*4= 0.30 (free amino acid); 0.21 (hydrochloride).

Found: C, 57.58; H, 6.06; N, 17.27%. Calcd for $C_8H_{10}O_2N_2$: C, 57.82; H, 6.07; N, 16.86%.

Carbobenzoxy-DL-β-(2-pyridyl)-α-alanine (IV). To a solution of (III) (16.6 g) and sodium hydroxide (4 g) in water (50 m*l*), carbobenzoxy chloride (19 g) and sodium hydroxide solution (sodium hydroxide 4 g; water 20 m*l*) were added under ice-cooling. When the reaction had finished, the mixture was adjusted to pH 4 with acetic acid. A white precipitate was collected by filtration, washed with water thoroughly, and recrystallized from aqueous alcohol to give colorless needles. Yield, 77%. Mp 145—147°C.

Found: C, 64.25; H, 5.45; N, 9.13%. Calcd for $C_{16}H_{16}O_4N_2$: C, 63.99; H, 5.37; N, 9.33%.

DL-β-(2-Pyridyl)-α-alanine Benzyl Ester Di-*p*-toluenesulfonate (V). A mixture of pyridylalanine (III) (16.6 g), *p*-toluenesulfonic acid monohydrate (45 g), benzyl alcohol (20 g), and benzene (200 m*l*) was boiled with occasional shaking and the continuous azeotropical removal of water. After 8.5 hr the solution was cooled, whereupon the crystals which had separated out were collected by filtration, washed thoroughly with ether, and recrystallized from alcohol-petroleum ether. Yield, 83%. Mp 158—159°C.

Found: C, 57.65; H, 5.27; N, 4.60%. Calcd for $C_{29}H_{32}O_8N_2S_2$: C, 57.98; H, 5.37; N, 4.66%.

Carbobenzoxy-DL-β-(2-pyridyl)-α-alanylhydrazide (VI). According to the method of Izumiya and his co-workers,[10] IV (40 g) was converted into the ethyl ester (yield 38.5 g); it was obtained as a yellow syrup and did not crystallize even after having been stored for a long time. To a methanol (120 m*l*) solution of the ester, 90% hydrazine hydrate (10 g) was added and the mixture was allowed to stand for 2 days at room temperature. When the clear solution had been cooled well and triturated, voluminous crystals were formed. Yield, 32.3 g (77.1% from IV). After recrystallization from ethyl acetate, it melted at 131—132°C into a turbid liquid, which became clear at 137°C.

Found: C, 61.14; H, 6.00; N, 17.78%. Calcd for $C_{16}H_{18}O_3N_4$: C, 61.13; H, 5.77; N, 17.83%.

8) T. Itai and H. Ogura, *Yakugaku Zasshi (J. Pharm. Soc. Japan)*, **75**, 296 (1955).

9) G. Kobayashi and S. Furukawa, *Chem. Pharm. Bull. Japan*, **1**, 347 (1953); V. Boekelheide and W. J. Linn, *J. Am. Chem. Soc.*, **76**, 1286 (1954).

*4 Circular paper chromatography. Solvent, *n*-BuOH : AcOH : H_2O=4 : 5 : 1.

10) T. Kato, K. Makisumi, M. Ono and N. Izumiya, *Nippon Kagaku Zasshi (J. Chem. Soc. Japan, Pure Chem. Sect.)*, **83**, 1151 (1962).

Carbobenzoxy-DL-β-(2-pyridyl)-α-alanyl-glycine Benzyl Ester (VII). *a) The Dicyclohexylcarbodiimide Method.* Into a cold solution of IV (3 g), glycine benzyl ester *p*-toluenesulfonate (3.8 g), and triethylamine (1.5 m*l*) in dichloromethane (80 m*l*), a solution of dicyclohexylcarbodiimide (2.1 g) in dichloromethane (2 m*l*) was stirred, drop by drop. After 2 hrs' stirring under ice-cooling, the mixture was allowed to stand overnight at room temperature. The dicyclohexylurea was then filtered off and washed with dichloromethane. The pale yellow filtrate and the washings were combined and washed successively with 0.5 N hydrochloric acid, N sodium hydroxide, and water, and dried over sodium sulfate. After the removal of the dicyclohexylurea which had separated during the evaporation of the solvent by filtration, the solution was concentrated to dryness. The viscous syrup which remained soon solidified completely. Yield, 3.2 g (72%). Mp 105—107°C (from ethanol).

Found: C, 67.01; H, 5.70; N, 9.26%. Calcd for $C_{25}H_{25}O_5N_3$: C, 67.10; H, 5.63; N, 9.39%.

b) The N-Bromosuccinimide Method. Carbobenzoxy-pyridylalanylhydrazide (1.6 g), glycine benzyl ester *p*-toluenesulfonate (1.7 g), and triethylamine (1.5 g) were dissolved in 30 m*l* of tetrahydrofuran. Into the cold solution solid *N*-bromosuccinimide (1.8 g) was then stirred in small portions. A remarkable evolution of gas was observed, and the color of the reaction mixture gradually changed to yellow brown. After the addition, the mixture was stirred for an additional 20 min, then diluted with water and extracted with ethyl acetate. The extract was washed successively with water, hydrochloric acid, a potassium carbonate solution, and water, and then dried over sodium sulfate and concentrated. The residual red-brown syrup (0.74 g) was dissolved in alcohol, from which mixture crystals were separated by letting it stand in a refrigerator overnight. Yield, 0.17 g (7.6%). Mp 105—107°C (from alcohol). The crystals showed no depression of the melting point when mixed with the preceding specimen.

c) An Attempted Coupling Reaction by the Azide Method. A solution of VI (942 mg) in 1 N hydrochloric acid (9 m*l*) was covered with ethyl acetate (12 m*l*), and then into the mixture there was stirred a solution of sodium nitrite (210 mg) in water (2 m*l*) at 0°C. After 2 min a 50% potassium carbonate solution (3.6 m*l*) was added, and the organic layer was separated. The aqueous layer was extracted with ether. At this stage a large amount of a solid material soluble in neither ethyl acetate and ether nor water was separated. This solid, insoluble also in aqueous alkali, melted at about 120°C. A paper chromatogram of the hydrolysate with hydrochloric acid showed one spot identical with that of an authentic sample of the hydrochloride of pyridylalanine. The molecular weight was determined to be 318 by a cryoscopic method, using 2,4,6-tribromophenol as the solvent. From these evidences, this substance was assumed to be carbobenzoxy-DL-β-(2-pyridyl)-α-alanine amide (molecular weight 299). To the organic layer mentioned above, after it had been dried over sodium sulfate, there was added an ether solution of the glycine benzyl ester (obtained from 1.18 g of glycine benzyl ester *p*-toluenesulfonate), but from the mixture no dipeptide derivative could be obtained.

Carbobenzoxy-DL-β-(2-pyridyl)-α-alanyl-glycine (VIII). VII (2.3 g) was dissolved in methanol (60 m*l* and hydrolyzed with N sodium hydroxide (6 m*l*) for 1 hr at room temperature. The solution was then diluted with water and treated with active charcoal. The clear solution was acidified with acetic acid and allowed to stand overnight in a refrigerator. The crystals which thus separated were collected and washed with water. Yield, 1.3 g (72%). Mp 178—179°C.

Found: C, 60.36; H, 5.35; N, 11.62%. Calcd for $C_{18}H_{19}O_5N_3$: C, 60.49; H, 5.36; N, 11.76%.

DL-β-(2-Pyridyl)-α-alanyl-glycine (IX). *a) By the Hydrogenolysis of VII.* Hydrogen gas was allowed to bubble through a solution of VII (4.0 g) in methanol (150 m*l*) for 4 hr in the presence of a Pd-catalyst (0.4 g). The catalyst was then filtered off, and a large amount of water was added to the filtrate. After treatment with active charcoal, the clear solution was concentrated *in vacuo* to a small volume, and then ethanol was added. The hydrated dipeptide was separated as needles (sintered at about 80°C), which became anhydrous upon being dried at 110°C *in vacuo*. Yield, 1.5 g (75%). Mp 179—180°C. A paper chromatogram showed only one spot (R_f*[4]=0.55).

Found: C, 53.23; H, 5.88; N, 18.78%. Calcd for $C_{10}H_{13}O_3N_3$: C, 53.80; H, 5.87; N, 18.83%

b) By the Action of Hydrogen Bromide in Acetic Acid on VIII. A mixture of VIII (0.36 g) and 20% hydrogen bromide in an acetic acid solution (*ca.* 2 m*l*) was kept for 5 min at about 25°C. Ether was then added, and the crystals were collected and washed several times with ether. Yield, 0.42 g (quantitative). Mp 169—171°C (decomp.). A paper chromatogram showed only one spot. The free dipeptide obtained by the passage of the hydrobromide through the column of an ion exchange resin showed a chromatogram identical with that of the sample obtained by the method *a*. The hydrobromide of the dipeptide obtained by the method *a* melted at 165—167°C (decomp.) and showed no depression of melting point when mixed with the hydrobromide obtained by the method *b*.

Tritylglycyl-DL-β-(2-pyridyl)-α-alanine Benzyl Ester (X). To a stirred solution of tritylglycine (4.7 g) and triethylamine (2.1 m*l*) in dichloromethane (100 m*l*), ethyl chlorocarbonate (1.43 m*l*) was added, drop by drop, under strong cooling. To this mixture, after an additional 30 mins' stirring, there was added a solution of V (9 g) and triethylamine (4.2 m*l*) in dichloromethane (400 m*l*). The solution was left to stand overnight at room temperature, then washed with an aqueous citric acid, an aqueous sodium carbonate, and water, and dried over sodium sulfate. When the solvent was evaporated off, there remained a viscous syrup (6 g) which crystallized when triturated with ethyl acetate and petroleum ether. Yield, 4 g (48%). Mp 119—121°C (large cubes from ethyl acetate).

Found: C, 77.75; H, 6.32; N, 7.22%. Calcd for $C_{36}H_{33}O_3N_3$: C, 77.81; H, 5.99; N, 7.56%.

Tritylglycyl-DL-β-(2-pyridyl)-α-alanine (XI). X (666 mg) was hydrolyzed with N sodium hydroxide (1.5 m*l*) in methanol (20 m*l*) for about 2 hr at room temperature and then treated as usual. Amorphous powder. Yield, 97%. Mp 93—95°C.

Found: C, 74.47; H, 5.69; N, 8.47%. Calcd for $C_{29}H_{27}O_3N_3$: C, 74.82; H, 5.85; N, 9.03%.

Glycyl-DL-β-(2-pyridyl)-α-alanine (XII). *a) From X.* X (2.23 g) was hydrogenated in aqueous

methanol (methanol 100 m*l*; water 20 m*l*) in the presence of a Pd-catalyst (0.2 g) with a quantitative hydrogenating apparatus. In about 50 min 97 m*l* of hydrogen was absorbed, but thereafter the rate of the absorption became so slow that even after 4 hr the volume of hydrogen absorbed amounted only to 34 m*l*. The solution, freed from the catalyst, was evaporated under reduced pressure. The residue was treated with 50% acetic acid on a boiling-water bath for 2 min; water was then added, and the triphenylcarbinol thus separated was filtered off. The filtrate decolorized with active charcoal was concentrated to dryness under reduced pressure. Yield, 0.33 g (37%). Mp 196—200°C (from water - ethanol). A paper chromatogram showed only one spot, R_f*[4]=0.43.

Found: C, 49.51; H, 6.31; N, 17.56%. Calcd for $C_{10}H_{13}O_3N_3 \cdot H_2O$: C, 49.78; H, 6.27; N, 17.42%.

b) From XI. XI (200 mg) was dissolved in 70% acetic acid (5 m*l*) and warmed to about 70°C for 10 min. Water was then added to the reaction mixture, and it was treated as above. Yield, 82 mg (58%). A paper chromatogram afforded an R_f value identical with that of the preceding specimen.

BULLETIN OF THE CHEMICAL SOCIETY OF JAPAN VOL. 41 1638—1642 (1968)

Synthetic Reactions by Complex Catalysts. IX. Reaction of Thiol with Isocyanide

Takeo SAEGUSA, Shiro KOBAYASHI, Kiwami HIROTA, Yoshiharu OKUMURA and Yoshihiko ITO

Department of Synthetic Chemistry, Faculty of Engineering, Kyoto University, Sakyo-ku, Kyoto

(Received October 19, 1967)

The reaction of a thiol with an isocyanide proceeds in two directions. In the first reaction (course a), the carbon atom of isocyanide with lone-pair electrons is inserted into the sulfur-hydrogen bond of thiol to produce thioformimidate (I). In the second reaction (course b), isothiocyanate (II) and the alkane (III) from the alkyl group of thiol are formed. The proportion of the participation of two reactions depends upon the alkyl group of thiol and upon the reaction conditions including whether or not a catalyst is employed. Primary thiol prefers course a to course b, whereas tertiary thiol prefers course b. In the reactions at 15°C, the Group IB and IIB metal compounds, *e. g.*, copper compounds, catalyzed the course a reaction preferably. At higher temperatures, *e. g.*, at 100°C, thiol reacts with isocyanide quite rapidly, even in the absence of a catalyst. However, the catalyst effect favoring course a is seen even in the high-temperature reactions. The mechanism of the reaction, especially course b, has been discussed. *Syn-anti* structures of thioformimidate were also studied by NMR.

We have reported a series of insertion reactions of isocyanide into the nitrogen-hydrogen bond of amine,[1] the oxygen-hydrogen bond of alcohol[2,3] and the silicon-hydrogen bond of silane.[4]

$$RN{\cong}C: + HNR'R'' \longrightarrow RN{=}CHNR'R'' \quad (1)$$

$$RN{\cong}C: + HOR' \longrightarrow RN{=}CHOR' \quad (2)$$

$$RN{\cong}C: + HSiR'_3 \longrightarrow RN{=}CHSiR'_3 \quad (3)$$

These reactions are all catalyzed by copper compounds to produce the corresponding derivatives of *N*-alkylformimidic acid. This paper will describe our studies of the reaction of thiol with isocyanide. The structure of thioformimidate will also be examined by NMR.

1) T. Saegusa, Y. Ito, S. Kobayashi, K. Hirota and H. Yoshioka, *Tetrahedron Letters*, **1966**, 6121.
2) T. Saegusa, Y. Ito, S. Kobayashi and K. Hirota, *ibid.*, **1967**, 521.
3) T. Saegusa, Y. Ito, S. Kobayashi, N. Takeda and K. Hirota, *ibid.*, **1967**, 1273.
4) T. Saegusa, Y. Ito, S. Kobayashi and K. Hirota, *J. Am. Chem. Soc.*, **89**, 2240 (1967).

Results and Discussion

Reaction of Thiol with Isocyanide. The reaction of a thiol with an isocyanide proceeds in the following two directions:

$$RN{\cong}C: + HSR' \begin{cases} \xrightarrow{\text{Course a}} RN{=}CHSR' \quad (I) & (4) \\ \xrightarrow{\text{Course b}} RN{=}C{=}S + R'H \quad (II)\ (III) & (5) \end{cases}$$

In the first reaction (course a, Eq. (4)), the carbon atom of isocyanide with lone-pair electrons is inserted into the sulfur-hydrogen bond of thiol to produce thioformimidate (I). In the second reaction (course

b, Eq. (5)), isothiocyanate (II) and alkane (III) from the alkyl group of thiol are formed by a process including the transfer of the sulfur atom from thiol to isocyanide. As will be discussed later, these reactions do not proceed consecutively, but they occur separately.

The proportion of the participation of the two reactions depends on the alkyl group of thiol and on the reaction conditions, including whether or not a catalyst is employed.

The results of the reactions of thiol with cyclohexyl isocyanide are shown in Tables 1 and 2, where the effects of the thiol alkyl group and of the reaction conditions are illustrated. In the reactions at 15°C, the catalyst activities of the Group IB and IIB metal compounds have been clearly demonstrated. However, at higher temperatures, *e. g.*, at 100°C, the reaction proceeds rapidly even without any added catalyst.

The alkyl group of thiol controls the relative participations of the two reactions. Primary thiols, *e. g.*, IV and VI in Tables 1 and 2, prefer course a to course b. On the other hand, tertiary thiols,

Table 1. Reactions of thiols with cyclohexyl isocyanide[a] (part 1)

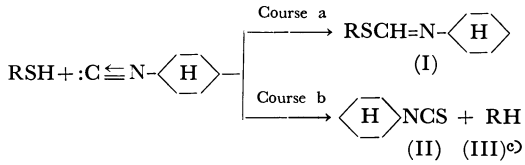

RSH	Catalyst	Yield[g] (%) I	II
C_2H_5SH (IV)	None	trace	3
	$Cu(acac)_2$[d]	86	1
	CuO	76	3
	$CuCl_2$	32	2
	$Cd(OAc)_2$[e]	67	4
i-C_3H_7SH (V)	None	1	16
	Cu_2O	78	3
	$ZnCl_2$	45	10
	$Hg(OAc)_2$[f]	41	14
n-C_4H_9SH[b] (VI)	Cu_2O	73	7
	Cu	81	4
t-C_4H_9SH (VII)	None	0	26
	$Cd(OAc)_2$[e]	13	68
	CuCN	8	54
	CuO	4	38
C_6H_5SH[b] (VIII)	None	89	0
	Cu_2O	42	0

a) The reactions were carried out at 15°C, for 3 hr, unless otherwise indicated.
b) Reaction conditions; at 20°C for 15 hr.
c) The yield of III was not determined.
d) Copper acetylacetonate.
e) Cadmium acetate.
f) Mercuric acetate.
g) The yield of each product is based on the amount of cyclohexyl isocyanide.

Table 2. Reactions of thiols with cyclohexyl isocyanide[a] (part 2)

RSH	Catalyst	Reaction time (hr)	Yield[b] (%) I	II	III
C_2H_5SH (IV)	None	3	85	8	n. d.[c]
	Cu_2O	3	93	1	n. d.
i-C_3H_7SH (V)	None	1.5	23	64	60
	Cu_2O	3	86	5	n. d.
t-C_4H_9SH (VII)	None	1.5	1	92	81

a) The reactions were carried out at 100°C.
b) The structures of the products are indicated in Table 1. The yield of each product is based on cyclohexyl isocyanide.
c) n. d.; not determined.

e. g., VII, prefer course b. 2-Methyl-2-heptanethiol also takes course b preferably.

Propane and isobutane are, respectively, the alkane products of the course b reactions of 2-propanethiol and 2-methyl-2-propanethiol with isocyanide. No olefinic hydrocarbon was detected in the products of these reactions by NMR analysis.

The Group IB and IIB metal compounds catalyze the thiol-isocyanide reaction and also increase the relative participation of the course a reaction. The effect of the catalyst upon the relative participations of two reactions is well demonstrated in the reaction of cyclohexyl isocyanide with 2-propanethiol. The uncatalyzed reaction is inclined towards course b, producing isothiocyante, whereas the catalyzed reaction preferably proceeds through course a. A similar tendency is seen in the reactions of isocyanide with other thiols. Copper compounds, such as cuprous and cupric oxides and copper acetylacetonate, dissolve in the thiol-isocyanide mixture at room temperature to form a homogeneous system. The compounds of cadmium, zinc, and mercury also accelerate the course a reaction in preference to the course b reaction. Catalyzed reactions (course a) proceeded at fairly high rates. For example, the yield of ethyl *N*-cyclohexylthioformimidate in the reaction of ethanethiol-cyclohexyl isocyanide with copper acetylacetonate at 15°C was 30% at 20 min, 55% at 40 min, 65% at 1 hr, and 86% at 3 hr.

Aromatic thiol also reacts with isocyanide through course a. The reaction of benzenethiol (VIII) with cyclohexyl isocyanide, with or without a catalyst, gave phenyl *N*-cyclohexylthioformimidate exclusively.

Aromatic isocyanides react with thiols to produce the corresponding thioformimidates. For example, *n*-butyl *N*-phenylthioformimidate was produced in a yield of 90% by the reaction of phenyl isocyanide with *n*-butanethiol.

The reactions of the two courses occur separately, but not consecutively. In other words, isothiocyanate (II) and alkane (III) are not formed

by the decomposition of thioformimidate. The reaction between 2-methyl-2-propanethiol and cyclohexyl isocyanide occurs preferably along course b, producing cyclohexyl isothiocyanate and isobutane. However, these products are not formed by the decomposition of *t*-butyl *N*-cyclohexylthioformimidate. It was observed that *t*-butyl *N*-cyclohexylthioformimidate, which was prepared by the thiol interchange between isopropyl *N*-cyclohexylthioformimidate and 2-methyl-2-propanethiol, remained unchanged under the same reaction conditions in the presence of a catalyst.

A mechanism involving a free radical may be considered to explain the over-all results of the reactions without any added catalyst.

$$\mathrm{RSH} \xrightarrow{\mathrm{R'\cdot}} \mathrm{RS\cdot} \xrightarrow{\mathrm{R''\text{-}N\rightleftarrows C}} \mathrm{RS\text{-}\dot{C}(H)\text{-}N\text{-}R''} \xrightarrow{\mathrm{RSH}} \mathrm{RSCH{=}NR''} + \mathrm{RS\cdot}$$

$$\mathrm{RS\text{-}\dot{C}(H)\text{-}N\text{-}R''} \xrightarrow[\beta\text{-scission}]{} \mathrm{R''\text{-}N{=}C{=}S} + \mathrm{R\cdot} \xrightarrow[\mathrm{RSH}]{} \mathrm{RH} + \mathrm{RS\cdot}$$

As to the above scheme of a free radical mechanism, it has been observed that the addition of a radical inhibitor such as hydroquinone does not affect the reaction between thiol and isocyanide. Further work is now in progress to elucidate the reaction mechanism, especially the function of the metal catalyst.

***Syn-anti* Structures of Thioformimidate.** For thioformimidate, the *syn* (IX) and *anti* (X) forms are expected as a result of the restricted rotation of the >C=N-bond.

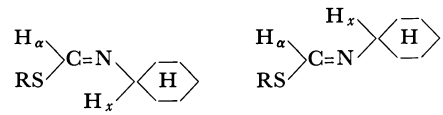

syn (IX) *anti* (X)

In the NMR spectra of thioformimidates in deuteriochloroform and benzene, two signals were obtained in the region of τ 1.7—2.1; both signals were assigned to H_α of IX and X (Table 3).

In Fig. 1, the NMR spectrum of ethyl *N*-cyclohexylthioformimidate is shown as an example. The two signals of H_α have been ascribed to *syn-anti* isomerism on the basis of the solvent effect on the NMR spectrum.[5,6]

Karabatsos *et al.*[5,6] have presented a method for assigning the *syn* and *anti* structures of hydrazone, semicarbazone, and related compounds with this general formula:

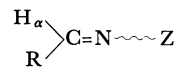

This method has been applied to thioformimidate in the present study. Because of the repulsion between the lone-pair electrons of the nitrogen of thioformimidate and the π-electrons of the benzene ring of the solvent, the shielding effect of the benzene ring upon *trans* H_α (*syn* form) is less than that upon *cis* H_α (*anti* form). In Table 3, the two signals of H_α hydrogen have been assigned on the basis of the above consideration. From the peak areas

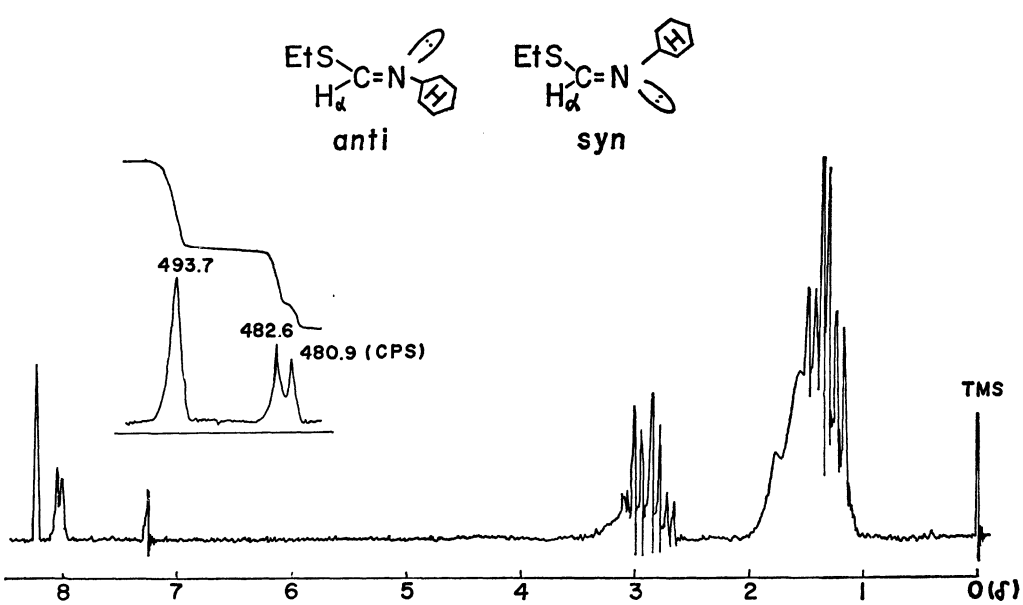

Fig. 1. NMR spectrum of ethyl *N*-cyclohexylthioformimidate (XI) (in deuteriochloroform).

5) G. J. Karabatsos, R. A. Taller and F. M. Vane, *ibid.*, **85**, 2326 (1963).

6) G. J. Karabatsos and R. A. Taller, *ibid.*, **85**, 3624 (1963).

TABLE 3. NMR DATA OF $-SCH_\alpha=N-$ OF THIOFORMIMIDATES[a]

Thioformimidate	Solvent		H_α cps	$J_{H\alpha Hx}$ cps	Ratio[b] (%)
$C_2H_5SCH_\alpha=N-$ 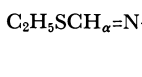	$CDCl_3$	*syn*	480.9, 482.6	1.7	47
		anti	493.7	0.0	53
(XI)	C_6H_6	*syn*	471.2, 472.9	1.7	—
		anti	476.7	0.0	—
i-C_3H_7-$SCH_\alpha=N-$ 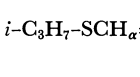	$CDCl_3$	*syn*	485.9, 487.5	1.6	56
		anti	495.1	0.0	44
(XII)	C_6H_6	*syn*	480.2, 481.8	1.6	—
		anti	477.6	0.0	—
t-C_4H_9-$SCH_\alpha=N-$ 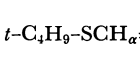	$CDCl_3$	*syn*	496.5, 498.2	1.7	73
		anti	506.7	0.0	27
(XIII)	C_6H_6	*syn*	496.3, 498.0	1.7	—
		anti	487.0	0.0	—
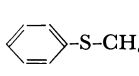	$CDCl_3$	*syn*	480.7, 482.6	1.9	72
		anti	500.4	0.0	28
(XIV)	C_6H_6	*syn*	481.0, 482.6	1.6	—
		anti	486.6	0.0	—
n-C_4H_9-S-$CH_\alpha=N-$ 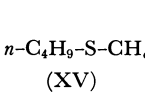	$CDCl_3$	*syn*	487.8	—	8
(XV)		*anti*	492.0	—	92

a) All spectra were recorded at 60 Mc/sec on a modified JEOL JNM-3H-60 spectrometer for 10—15% $CDCl_3$ or C_6H_6 solutions at 23°C. Chemical shifts values are in cps from TMS as an internal standard.

b) No reliable value is obtained in benzene, because the signals of H_α and benzene protons overlap each other.

TABLE 4. SOLVENT EFFECTS ON THE CHEMICAL SHIFTS OF PROTONS (H_α)

Thioformimidate		$\Delta\nu_{cps}$ value ($\nu_{\text{in } CDCl_3} - \nu_{\text{in } C_6H_6}$)
XI	*syn*	9.7
	anti	17.0
XII	*syn*	5.7
	anti	17.5
XIII	*syn*	0.2
	anti	19.7
XIV	*syn*	~0.0
	anti	13.8

of the two H_α signals, the *syn*/*anti* ratio has been calculated. As is indicated in Table 3, *syn* H_α gives a doublet, whereas *anti* H_α gives a singlet. The coupling of *syn* H_α with the α-hydrogen (H_x) of the cyclohexane ring is more pronounced than that of *anti* H_α. This observation corresponds to the fact that the coupling constant between *trans* hydrogens in olefin is larger than that between *cis* hydrogens. Table 4 summarizes the $\Delta\nu$ values ($\Delta\nu = \nu_{\text{in } CDCl_3} - \nu_{\text{in } C_6H_6}$) of four thioformimidates.

Experimental

Reaction of IV with Cyclohexyl Isocyanide. A mixture of 6.2 g (0.1 mol) of IV and 8.8 g (0.08 mol) of cyclohexyl isocyanide was stirred, with or without a catalyst (2 mmol), at the indicated reaction temperature. Then the reaction mixture was subjected to glpc, whereby ethyl *N*-cyclohexylthioformimidate (XI) and cyclohexyl isothiocyanate were identified and quantitatively analyzed. XI was isolated from the reaction mixture by distillation, bp 110—112°C/20 mmHg.

Found: C, 63.02; H, 10.05%. Calcd for $C_9H_{17}NS$: C, 63.10; H, 10.01%.

The structure of XI was established by means of NMR (Fig. 1) and infrared spectroscopy ($\nu_{C=N}$ at 1590 cm^{-1}). The authentic sample of cyclohexyl isothiocyanate was prepared by the reaction of cyclohexyl isocyanide with sulfur.[7]

Reaction of V with Cyclohexyl Isocyanide. The reaction of V with cyclohexyl isocyanide was carried out in the same manner as the above. By glpc analysis, isopropyl *N*-cyclohexylthioformimidate (XII) and cyclohexyl isothiocyanate were identified and quantitatively analyzed. XII was isolated by the distillation of the reaction mixture, bp 135—136°C/20 mmHg.

Found: C, 64.67; H, 10.23; N, 7.62%. Calcd for $C_{10}H_{19}NS$: C, 64.81; H, 10.33; N, 7.56%.

The structure of XII was further established by infrared ($\nu_{C=N}$ 1590 cm^{-1}) and NMR spectra studies. In some experiments, the gas evolved during the reaction was collected in a gas burette and quantitatively analyzed. The evolved gas was identified as propane by glpc and NMR.

7) A. J. Weith, *Ber.*, **6**, 210 (1873).

Reaction of VII with Cyclohexyl Isocyanide. The procedure of the preceding two reactions was adopted. In the glpc analysis of the reaction mixture, *t*-butyl *N*-cyclohexylthioformimidate (XIII) and cyclohexyl isothiocyanate were identified and quantitatively analyzed. The gas evolved from the reaction system was identified as isobutane by glpc and NMR. XIII was isolated by the distillation of the reaction mixture, bp 122—125°C/3 mmHg, mp 56—58°C.

Found: C, 65.98; H, 10.63; N, 7.05; S, 15.53%. Calcd for $C_{11}H_{21}NS$: C, 66.27; H, 10.62; N, 7.03; S, 16.08%.

The structure of XIII was further established by infrared ($\nu_{C=N}$ 1590 cm^{-1}) and NMR spectra studies.

Reaction of Other Thiols with Cyclohexyl Isocyanide. Similarly, VI and VIII were treated with cyclohexyl isocyanide to give *n*-butyl *N*-cyclohexylthioformimidate (bp 129—131°C/3 mmHg) (XVI) and phenyl *N*-cyclohexylthioformimidate (bp 120—122°C/0.1 mmHg) (XIV) respectively. XVI and XIV were identified by means of their infrared and NMR spectra as well as by elemental analysis.

Reaction of VI with Phenyl Isocyanide. Following the procedure described above, a mixture of 9.0 g (0.1 mol) of VI, 8.3 g (0.08 mol) of phenyl isocyanide, and 0.28 g (2 mmol) of cuprous oxide was stirred at 20°C. Then the mixture was distilled to yield *n*-butyl *N*-phenylthioformimidate (XV) (14 g, 90%), bp 151—152°C/20 mmHg.

Found: C, 68.18; H, 7.59; N, 7.11; S, 16.20%. Calcd for $C_{11}H_{15}NS$: C, 68.35; H, 7.82; N, 7.25; S, 16.59%.

The structure of XV was further established by a study of its NMR spectrum.

Exchange of Alkylthio Group of Thioformimidate. A mixture of 5.5 g (0.03 mol) of XII and 9.0 g (0.1 mol) of VII was stirred at 15°C for 1 hr. It was shown by glpc analysis that XII was converted quantitatively into XIII.

BULLETIN OF THE CHEMICAL SOCIETY OF JAPAN VOL. 41 1642—1647 (1968)

Hot Atom Chemistry of Phosphorus Compounds. II.[1] Chemical Effects of Neutron Irradiation on Phosphoric Esters of Hexoses*1

Yoshiyuki KISO, Mitsue KOBAYASHI, Yoshinori KITAOKA
Keizo KAWAMOTO and Jitsuya TAKADA

Research Reactor Institute, Kyoto University, Kumatori-cho, Sennan-gun, Osaka

(Received November 4, 1967)

Phosphoric esters of hexoses were subjected to neutrons and the resulting ^{32}P-labeled recoil products were separated by paper chromatography and paper electrophoresis. The main recoil products were phosphorous and phosphoric acids, independent of the chemical form of the target material and the kind of its salt. A small amount of inorganic acids containing a P–P or P–O–P bond was also found. The yield of the retention product was less than a few percents. The presence of organic diphosphorus compound was supposed by paper electrophoretic analysis. An addition of a small amount of water to the target material before irradiation favored formation of ^{32}P-labeled phosphorus oxyacids in lower oxidation state. The results from irradiation of aqueous solution gave an unexpected chromatographic behavior owing to some unstable complex of recoil ^{32}P atom with water molecule.

Although the elucidation of the chemical effects of neutron irradiation on biologically important compounds will give a clue to that on cells or tissues in a living body, little is known about the effects on such compounds except a few compounds.[2] The neutron irradiation of ATP (Adenosine Tri-Phosphate) has been reported.[3] However, the separation of the recoil products was not so good. The same attempt on DNA (Deoxyribonucleic Acid) have been reported by Halmann who studied on the recoil products and on the physical change due to radiolytic damage.[4] In this case, about one half of ^{32}P-labeled products was found in inorganic phosphorus compounds.

Recently, Yagi and coworkers[5] attempted a phosphorylation of glycerol by irradiating a mixture

1) Part I of this series: Y. Kiso *et al.*, This Bulletin, **40**, 2779 (1967).

*1 Presented at the 11th Symposium on Radiochemistry, Tokyo, October, 1967.

2) M. Halmann, *Chem. Revs.*, **64**, 686 (1964).

3) a) H. G. Mautner, B. Donnelly, C. M. Lee and G. W. Leddicotte, *J. Am. Chem. Soc.*, **84**, 2021 (1962). b) H. G. Mautner, C. M. Lee and M. H. Krackov, *ibid.*, **85**, 245 (1963).

4) M. Halmann and I. R. Miller, *Biochim. Biophys. Acta*, **72**, 483 (1963).

5) T. Yagi, S. A. El-Kinawy and A. A. Benson, *J. Am. Chem. Soc.*, **85**, 3462 (1963).

of glycerol and phosphoric acid. Almost all radioactivities in recoil products identified by paper chromatography were found in inorganic phosphorus oxyacids. The yield of ^{32}P-labeled organic phosphorus compounds was less than that of inorganic phosphorus compounds.

Thus, systematic study on organic compounds have not yet been made.

As the chemical effects on aromatic phosphorus compounds by bombardment with neutrons have been discussed in the previous paper,[1] we now should like to report the irradiation effects with neutrons on phosphoric esters of hexoses which play an important role in glycolysis. Salts of hexose phosphates chosen were as follows; glucose-1-phosphate dipotassium salt (G-1-P(K)), glucose-6-phosphate barium, potassium and sodium (G-6-P-(Ba, K or Na)), galactose-6-phosphate barium (Ga-6-P(Ba)), fructose-1-phosphate barium (F-1-P(Ba)), fructose-6-phosphate sodium (F-6-P(Na)), and fructose-1,6-diphosphate barium (F-1,6-P(Ba)). After these compounds were irradiated in a reactor, recoil products formed by the ^{31}P $(n,\gamma)^{32}P$ reaction were analyzed by paper chromatography and paper electrophoresis. The effect due to the chemical structure of target material on the production of recoil compounds, and influence by the presence of metallic elements such as barium, sodium and potassium on the recoil reactions are discussed on the basis of the yield of radioactive recoil products, as well as the dilution effcet of the target materials with water on the reaction.

Experimental

Materials. 50% aqueous solution of H_3PO_2 was purchased from Nakarai Chemicals Ltd. and stored in a refrigerator. Crystal H_3PO_3 (95.3%) was used without further purification. Guaranteed grade of H_3PO_4 was used. G-1-P(K) and F-1,6-P(Ba) purchased from Nakarai Chemicals Ltd. and other phosphoric esters of hexoses from Sigma Chemicals were used without further purification. The purity of each sample was checked by activation of chromatographed paper. For preparing phosphoric ester of glucose without containing metallic element, G-6-P(Na) was treated with Dowex 50 ion-exchanger.

Neutron Irradiation of Solid Materials. The sample was sealed into a polyethylene tube and put into a larger polyethylene capsule. The capsule was irradiated for 30—60 min in a pneumatic tube of KUR.*2

Neutron Irradiation of Diluted Solution. G-6-P(Na) (0.157 g) was dissolved in 1.643 g of water free from any cation. Solutions of 1/3, 1/9, 1/27 and 1/81 for the initial concentration were prepared by diluting with water. An aliquot (about 0.5 m*l*) of each solution was sealed in a quartz tube (dia. 5×50 mm). About twenty quartz tubes were put in a larger polyethylene capsule (dia. 10×15 cm) and irradiated for 10 hr in the slant exposual tube of KUR. The flux of thermal neutron in the slant was 2.5×10^{11} n/cm^2 sec, cadmium ratio 7.0 and γ-rays 5.0×10^6 R/hr.

Paper Chromatographic Separation of Recoil Products. After cooling for a week, the irradiated sample was dissolved in water and developed on Toyoroshi No. 50 (2×40 cm) by an assending method for 15 hr, using propanol-ammonia-water (6 : 3 : 1 in volume) as a combined solvent.[6] Radioactive distribution on the chromatographed strip was examined by autoradiography using Fuji Medical X-ray Film (27.9×35.6 cm) or by an autoradioscanner (Aloka, Model JPC-102). The R_f value of known nonradioactive compound was determined by activation of the chromatographed strip. This values was used for identification of the recoil products.

Paper Electrophoretic Separation of Recoil Products. The migration apparatus with multi-compartment cells was used.[7] Background buffer electrolytes of different pH value were adjusted by mixing 0.1 M HCl, 0.1 M citric acid and 0.1 M NH_4OH (ionic strength $\mu=0.1$ over a range of pH=1.0—11). After a paper strip was uniformly dipped in the background electrolyte solution and then the excess of the solution was removed with another filter paper, about 5 μl of a solution (0.05 M) containing irradiated sample was placed on a filter paper (Toyoroshi No. 50, 2×40 cm). The substance was migrated for 1—1.5 hr under a potential gradient of 500 V/34 cm, keeping the temperature of the migration box at 25°C. The strip was taken out, dried by an infrared lamp and followed with autoradioscanning or autoradiography. The mobility of known nonradioactive compound was determined by activation method.

Neutron Activation of the Chromatographed Paper. The chromatographed paper strip was enveloped in a polyethylene envelope and rolled to put into a polyethylene capsule. The capsule containing the rolled papers was irradiated for 30 min in the pneumatic tube. After cooling for a week to reduce radioactivities due to impurities, the radioactivities of phosphorus-32 on the strip were located by autoradiography.

Results and Discussion

Percentage of the radioactivities of recoil products on chromatographed strips are shown in Fig. 1. In general, the yield of hypophosphorous acid in recoil products was small, by taking the fact that the R_f values of H_3PO_4, H_3PO_3 and H_3PO_2 were 0, 0.30 and 0.67, respectively. On the other hand, large amounts of H_3PO_3 and H_3PO_4 were obtained. Although recoil products from G-6-P(Ba) or Ga-6-P(Ba) deposited mostly at the starting position of the filter paper, all of the activities is not considered to be due to phosphoric acid because the activity of phosphoric acid identified by using electrophoresis is not so much. The inconsistency among results obtained by the paper chromatography and the paper electrophoresis was often found when the target material was insoluble in

*2 Kyoto University Reactor (see Ref. 1).

6) T. Weil, *Helv. Chim. Acta*, **38**, 1274 (1955).
7) Y. Kiso, *J. Sci. Hiroshima Univ. Ser. A-II*, **27**, 24 (1963).

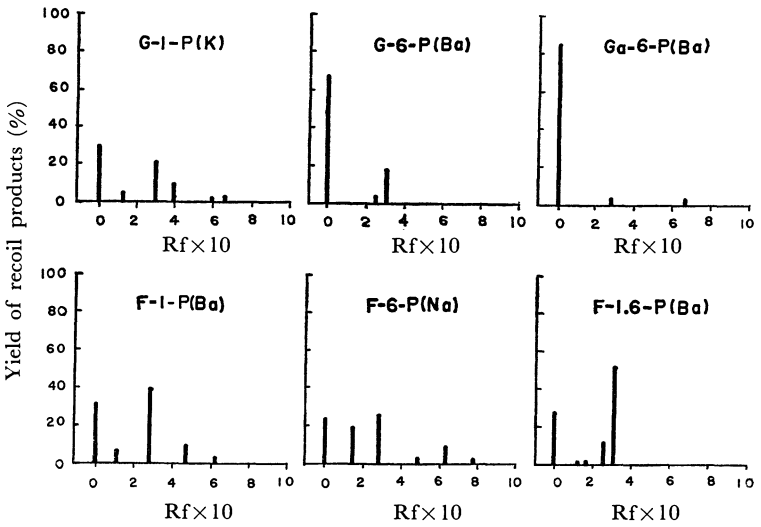

Fig. 1. Distribution of radioactive recoil products separated by paper chromatography.

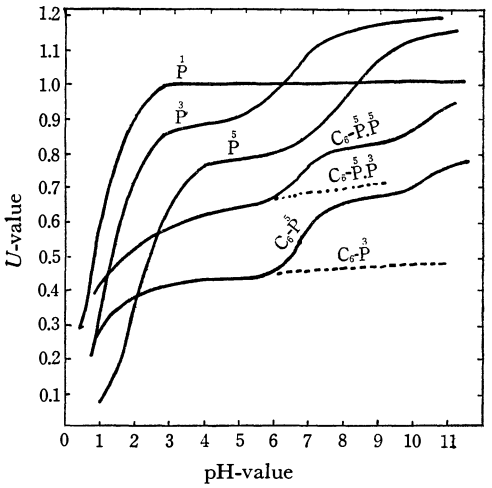

Fig. 2. *U*-pH curves of standard compounds.

$\overset{1}{P}$: H_3PO_2, $\overset{3}{P}$: H_3PO_3, $\overset{5}{P}$: H_3PO_4, $C_6\text{-}\overset{5}{P},\overset{5}{P}$: hexose containing two phosphate groups, $C_6\text{-}\overset{5}{P},\overset{3}{P}$: hexose containing one phoshate and one phosphite groups, $C_6\text{-}\overset{5}{P}$: hexose containing one phosphate group, $C_6\text{-}\overset{3}{P}$: hexose containing one phosphite group.

water. In these cases of barium salts, it is considered that the radioactive recoil product formed with recoil atom in a target material was not completely developed with the solvent, but remained in target materials. Thus, paper chromatography was used for only an aid of paper electrophoresis, especially in recognition of recoil products formed from barium salts. The chromatogram patterns by electrophoresis are shown in Figs. 2 and 3.

The *U* value shows the mobility of the compound relative to that of hypophosphorous anion. The curves in figures show the change of the *U* values as a function of pH. The pH values at inflection points in the curves correspond to consecutive dissociation constants of a given compound, respectively.[8] Thus, the curve of phosphoric acid has three points of inflection, phosphorus acid two and hypophosphorous acid only one. Hexose esters of phosphoric acids have two points which agree with those determined by a titration method.[9]

Another feature of electrophoresis is the fact that the equivalent mobility (mobility/charge number) of the compound is reversely proportional to squear root of the molecular weight,[10] providing that the shape and hydration of molecule are similar.*3 Then, analysis of mobility*U*-pH curve of electrophoresis is useful for identification of the recoil products and to determine the structure of unknown products.[11] Almost all inorganic phosphorus compounds show high *U*-values at a range of high pH-values while organic phosphorus compounds do not show high *U* value because of their higher molecular weight. Qualitative distinction between organic and inorganic phosphorus compounds can be easily made at the high pH region unless the organic compound is unstable. The electrophoretic behavior of the standard compounds is shown in Fig. 2. The mobility of the nonradioactive compound was determined by

8) D. Waldron-Edward, *J. Chromatog.*, **20**, 556 (1965).
9) C. A. Bunton and H. Chaimovich, *J. Am. Chem. Soc.*, **88**, 4082 (1966).
10) V. Jokl, *J. Chromatog.*, **14**, 71 (1964).
11) J. T. Edward and D. Waldron-Edward, *J. Chromatog.*, **20**, 563 (1965).
*3 Detailed study on the relationship between mobility and chemical form will be reported in *J. Chromatog.*, **36**, 215 (1968).

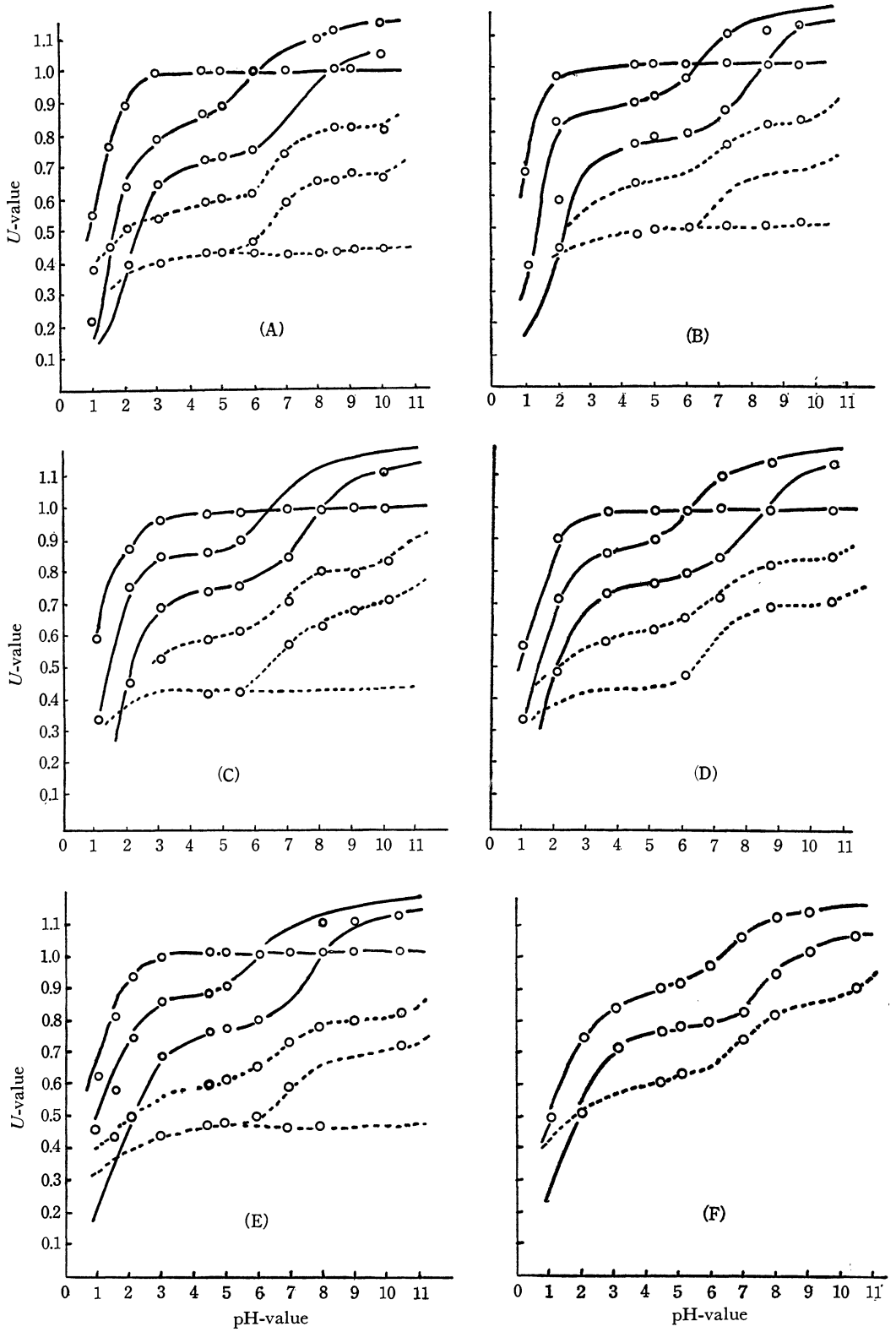

Fig. 3. Distribution of recoil products separated by paper electrophoresis.
A: G-1-P (K), B: G-6-P (Na), C: Ga-6-P (Ba),
D: F-1-P (Ba), E: F-6-P (Na), F: F-1,6-P (Ba).

activating the chromatographed paper with neutrons. The dotted line shows the *U*-pH curve speculated on the basis of the number of dissociable hydrogen in a molecule. The *U*-pH curves of recoil products in irradiated samples are shown in Figs. 3A—F, respectively for the target materials. Main recoil products or products clearly separated without overlapping of different fractions are qualitatively shown in Fig. 3. The dotted lines show the recoil products detected only in autoradiography. The results of quantitative analysis are shown in Fig. 4.

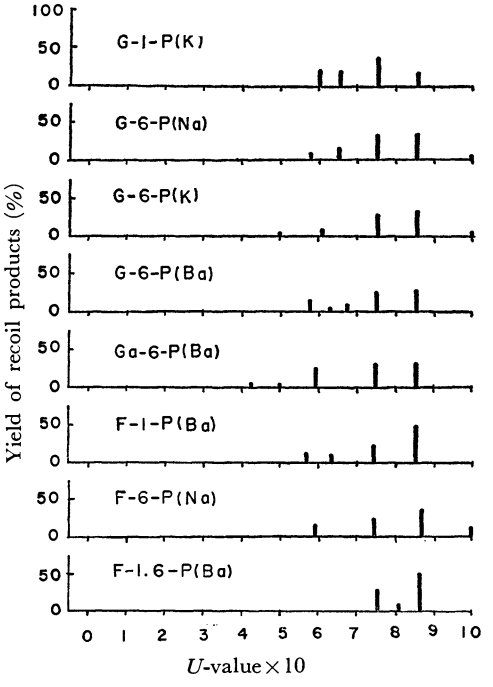

Fig. 4. Distribution of radioactive recoil products separated by electrophoresis at pH=5.

The distribution of activities on the chromatographed strip was obtained by scanning the filter paper migrated at pH=5.0 of background buffer solution. A similar procedure was carried out at pH=3.0, too.

Irradiation of C_1-ester (=G-1-P(K)) in which aldehyde group is blocked by phosphate group gave larger amounts of phosphoric acid (U=0.75) than that of phosphorous acid (U=0.85). On the other hand, irradiation of G-6-P yielded more phosphorous acid than phosphoric acid, independent of the kind of the salts. The tendency found in the case of G-6-P was also observed in irradiation of F-1-P(Ba), F-6-P(Na) or F-1,6-P(Ba). In any case, the yield of hypophosphorous acid was lower, comparing with that of other two inorganic oxyacids. It was concluded from the analysis of the distribution patterns that the yield of hypophosphorous acid is slightly larger in the case of sodium salts than in the case of potassium or barium. In irradiation of F-1,6-P(Ba), hypophosphorous acid was not found even in the autoradiogram.

It was found that P-P or P-O-P bond is included in other inorganic phosphorus compounds formed. As the P-O-P bond is easily formed by heating salts of phosphate,[12] the compounds mentioned above can be expected to be formed also by heat evolved in the nuclear reactions of phosphorus or another metals such as sodium, barium or potassium.[13] The yield of pyrophosphate (R_f= 0.05) estimated from a paper chromatogram was less than a few percents. On the contrary to pyrophosphate, the P-P compound was not formed by heating. When we used the background buffer solution described in Experimental section, the migration zone of $\overset{4}{P}$–$\overset{4}{P}$ compound overlapped with that of phosphorous or/and pyrophosphoric acids in a range of pH=4—5. Thus, in the case of identification of P-P compounds, a background buffer solution containing 0.05 M zinc acetate was specially prepared. Since Fenger[14] has determined the relative mobiliteis of $\overset{2}{P}$–$\overset{4}{P}$ and $\overset{4}{P}$–$\overset{4}{P}$ compounds to be 0.55 and 0.45 at pH=4.2, respectively, the radioactive species located in ranges of 0.4 and 0.5 may be considered compounds including a P-P bond.

The relative mobility of target material itself was smaller at electromigration using usual background buffer solution (0.45 in the case of monoester and 0.60 in diester). Although retention product which is ^{32}P-labeled target material was clearly found in autoradiography, the activities corresponding to that was less than a few percents, which was in agreement with the values theoretically calculated.[2] Irradiating monoester, we always obtained a compound which behaved electrophoretically in a manner similar to F-1,6-P. This seems to be an organic diphosphorus compound which resulted from an attack of recoil phosphorous atom on the target materials. From the facts that isomerization of hexose by γ-rays or neutrons was not found and that the dihalogenide was obtained by neutron irradiation of monohalogenide,[15,16] we can safely suppose the formation of diphosphorus compound in which the positions of phosphorus-32 will be probably statistically distributed. Branching of *U*-pH curves of irradiated materials shows the formation of phosphorous esters of hexoses. The characteristic results obtained from irradiated F-1,6-P(Ba) was the

12) S. Ohashi, "Topics in Phosphorus Chemistry," Vol. 1, John Wiley, New York (1964), p. 113.
13) T. R. Sato and H. H. Strain, *J. Inorg. Nucl. Chem.*, **18**, 24 (1964).
14) J. Fenger, *Risö Report* (Denmark), No. 95 (1964).
15) J. C. W. Chien and J. E. Willard, *J. Am. Chem. Soc.*, **79**, 4872 (1957).
16) T. E. Gilroy, G. Miller and D. F. P. Shaw, *ibid.*, **86**, 5033 (1964).

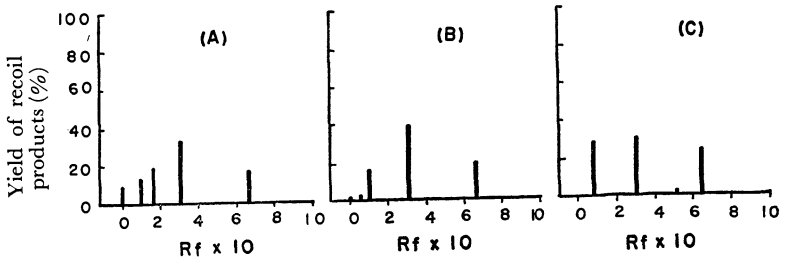

Fig. 5. Effect of water on recoil products.
(A) : glucose-6-phosphate, (B) : glucose-6-phosphate(20 mg) + H_2O(0.5m*l*)
(C) : glucose-6-phosphate sodium salt(17mg)+H_2O(0.1m*l*).

absence of ^{32}P-labeled monophosphoric ester of hexose. Generally speaking, the ^{32}P-labeled organic compounds containing the same number of phosphorus as target material or more than one are formed in the recoil event of phosphorus, and the oxidation state and the position of phosphorus in a molecule depend on chemical form of target materials.

The results of irradiated phosphate ester which is free from metallic element was shown in Fig. 5A.

In this case, lower oxidation products of phosphorus were obtained in abundance. An addition of a small amount of water to a target material also showed similar tendency as shown in Figs. 5B and C. Although the addition of water into the sample to be irradiated favored formation of hypophosphorous acid, the addition of excess of water, that is, dilution with water, lowerd.

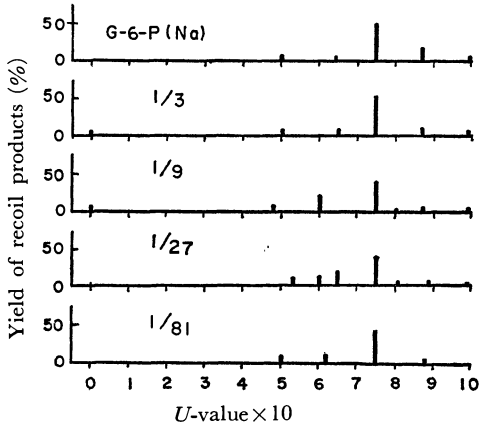

Fig. 6. Distribution of recoil products formed from glucose-6-phosphate sodium salt in diluted solution.

The effects of dilution with water on recoil products are shown in Fig. 6.

As the irradiation position in the reactor and the phase of target material were different from those of the irradiation without water, we can not strictly compare the results shown in Fig. 6 with that shown in Fig. 5, but we can say that the working of water molecule at the recoil event are not simple. Although it was said in early days that the presence of crystal water or of ammonium group in the irradiation sample favors formation of compounds in lower oxidation state, this experimental rule can be applied only within a limited range.

In the case of very diluted solution, the main product was phosphoric acid and the yields of phosphorous and hypophosphorous acids were very small. In addition to the characteristics mentioned above, an abnormal tailing in paper chromatogarm increased with increasing dilution. Such phenomenon was also observed in the irradiation of aqueous solution of phosphorus oxyacids.*4 The abnormal tailing may be due to the formation of an unstable complex by the recoil phosphorus atom with water molecules. A more detailed study on the dilution effect is in progress and will be reported in a near furure.

The authers are grateful to Professor S. Ohashi of Kyushu University for the generous gift of hypophosphoric acid.

*4 The results of phosphorus oxyacids were presented at the 11th Symposium on Radiochemistry, Tokyo, October, 1967.

BULLETIN OF THE CHEMICAL SOCIETY OF JAPAN VOL. 41 1648—1653 (1968)

Polymerizations by 1,3-Dipolar Cycloaddition Reactions. V. The 1,3-Dipolar Polycycloadditions of Dinitrile *N*-Oxides with Diolefins

Yoshio IWAKURA, Shinsaku SHIRAISHI,*1 Masayasu AKIYAMA*2 and Masahiro YUYAMA

Department of Synthetic Chemistry, Faculty of Engineering, The University of Tokyo, Hongo, Tokyo

(Received December 19, 1967)

Terephthalonitrile di-*N*-oxide and isophthalonitrile di-*N*-oxide were synthesized from the corresponding hydroxamic chlorides by dehydrochlorination with triethylamine. Their chemical properties and the polycycloadditions with diolefins were examined. The polymers obtained were amorphous and their molecular weights were not so high. The thermal gravimetric analyses of them showed that the polymers were stable up to 300—350°C in air.

Since Werner and Buss[1] reported the formation of benzonitrile *N*-oxide in 1894, the reaction of nitrile *N*-oxides, particularly those involving benzonitrile *N*-oxide, have been thoroughly investigated and it is well known that almost all types of olefins react with nitrile *N*-oxides to form 2-isoxazolines.[2,3] It is also known that, in cycloadditions of nitrile *N*-oxides to mono- or 1,1-disubstituted olefins, the substituents exclusively appear in the 5-position of the 2-isoxazolines.[4]

We have already reported the isolation of terephthalonitrile di-*N*-oxide by the action of triethylamine on terephthalohydroxamic dichloride in the earlier communication[5] and it was the first example of the isolation of dinitrile di-*N*-oxide. By the same procedure, isophthalonitrile di-*N*-oxide was also isolated and its diagnostic investigation in the polycycloaddition has also been reported.[6] In this paper, we wish to present further investigation in the reaction of those nitrile *N*-oxides and their polycycloadditions with diolefins.

Terephthalonitrile di-*N*-oxide (Ia) is rather stable and it can be stored almost unchanged for a few days, while isophthalonitrile di-*N*-oxide (Ib) is less stable and spontaneously changes into yellowish mass which is considered to be polyphenylenefuroxan on the basis of its infrared spectrum.[7,8]

These nitrile *N*-oxides gave the corresponding hydroxamic chlorides reversely by the reactions with hydrogen chloride. The treatment of them with triethyl phosphite afforded terephthalonitrile and isophthalonitrile respectively by deoxygenation in almost quantitative yields.

The 1,3-dipolar cycloadditions of Ia and Ib were carried out with various dipolarophiles to give the corresponding addition products as shown in Tables 1 and 2. When α,β-unsaturated carbonyl compounds were used as dipolarophiles, the reaction proceeded almost quantitatively. In the case of the reactions with olefins, the reaction products, 3,3'-phenylene bis(2-isoxazoline)s, have one asymmetric carbon at 5-position of each isoxazoline ring, where the substituents appear. Therefore, two isomeric products, *dl* and *meso*, should be formed in the each reaction. In fact, we have obtained the two isomers in the case of the reactions with methyl methacrylate, methyl acrylate and vinyl acetate. The NMR spectrum (60 Mc, in CH_3CN) of one of the two isomers obtained from Ib and methyl acrylate, having a lower melting point, has a methine triplet centered at 4.72 τ and a methylene doublet, overlapped with OCH_3 singlet (6.21 τ) centered at 6.30 τ ($J_{CH-CH_2}=9.3$ cps). That of the other, having a higher melting point, has a methine triplet centered at 4.77 τ and a methylene doublet, also overlapped with OCH_3 signal (6.24 τ), centered at 6.32 τ ($J_{CH-CH_2}=9.6$ cps). Methyl 3-phenyl-2-isoxazoline-5-carboxylate of known and unequivocal structure,[9] prepared

*1 Present address: Institute of Industrial Science, The University of Tokyo, Roppongi, Minato-ku, Tokyo.
*2 Present address: Tokyo Institute of Technology. Ookayama, Meguro-ku, Tokyo.

1) A. Werner and H. Buss, *Ber.*, **27**, 2193 (1894).
2) A. Quilico, G. S. D'Alcontres and P. Grünanger, *Nature*, **166**, 226 (1950); *Gazz. chim. ital.*, **80**, 479 (1950).
3) G. S. D'Alcontres and P. Grünanger, *ibid.*, **80**, 831 (1950); P. Grünanger, *ibid.*, **84**, 359 (1954); A. Quilico, P. Grünanger and R. Mazzini, *ibid.*, **82**, 349 (1952); G. S. D'Alcontres and G. L. Vecchio, *ibid.*, **90**, 1239 (1960).
4) R. Huisgen, *Angew. Chem.*, **75**, 742 (1963).
5) Y. Iwakura, M. Akiyama and K. Nagakubo, This Bulletin, **37**, 767 (1964).
6) Y. Iwakura, M. Akiyama and S. Shiraishi, *ibid.*, **38**, 335 (1965).
7) N. E. Boyer, G. M. Czerniak, H. S. Gutowsky and H. R. Synder, *J. Am. Chem. Soc.*, **77**, 4238 (1955).
8) Y. Imai, M. Akiyama, K. Uno and Y. Iwakura, *Makromol. Chem.*, **95**, 275 (1966).
9) G. Bianchi and P. Grünanger, *Tetrahedron*, **21**, 817 (1965).

Table 1. 1,3-Dipolar cycloaddition compounds of terephthalonitrile di-*N*-oxide

Product	Dipolarophile	Mp, °C	Recryst. solvent	Anal., % Found (Calcd) C	H	N
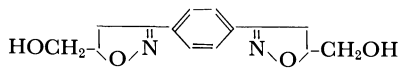	CH_2=$CHCH_2OH$	227—228	Aq. MeOH	60.44 (60.86	5.87 5.84	10.16 10.14)
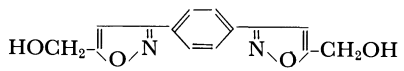	CH≡CCH_2OH	225—226	Aq. MeOH	61.52 (61.76	4.43 4.44	10.30 10.29
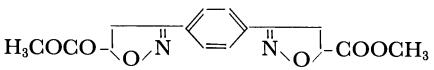 (*meso*, *dl*)	CH_2=$COOCH_3$	133—136 182—184	MeOH AcOEt	57.75 58.15 (57.83	4.97 5.16 4.85	8.42 8.47 8.43)
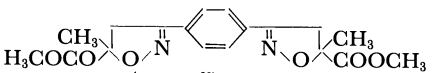 (*meso*, *dl*)	CH_2=$C(CH_3)COOCH_3$	172—173* 176—178*	MeOH AcOEt	60.16 60.03 (59.99	5.48 5.92 5.59	8.03 7.67 7.77)
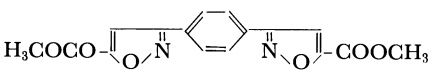	CH≡$CCOOCH_3$	250—251	Dioxane	58.68 (58.54	3.76 3.68	8.76 8.53)
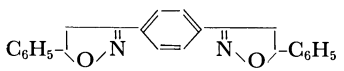	CH_2=CHC_6H_5	248—250	Benzene	78.29 (78.24	5.49 5.47)	
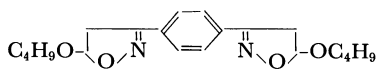	CH_2=$CHOC_4H_9$(*n*-)	83.5—84.5	*n*-Hexane	66.64 (66.75	7.83 7.77	7.77 7.98)
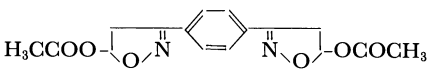 (*meso*, *dl*)	CH_2=$CHOCOCH_3$	185—187 145—150	MeOH Aq. MeOH	58.05 (57.83	4.68 4.85	8.68 8.43)
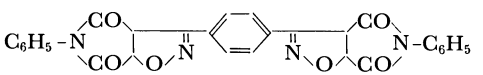	*N*-Phenylmaleimide	>300				

* Admixture of the two melted at 144—163°C.

Table 2. 1,3-Dipolar cycloaddition compounds of isophthalonitrile di-*N*-oxide

Product	Dipolarophile	Mp, °C	Recryst. solvent	Anal., % Found (Calcd)		
				C	H	N
	$CH_2=CHCH_2OH$	127—135	Aq. MeOH	60.51 (60.86	5.91 5.84	10.12 10.14)
	$CH\equiv CCH_2OH$	154—155	Aq. MeOH	61.60 (61.76	4.53 4.44	10.36 10.29)
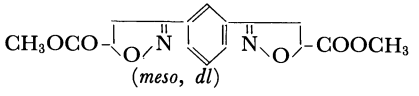 (*meso*, *dl*)	$CH_2=CHCOOCH_3$	(Viscous liq. 130—132	AcOEt	58.46 (57.83	5.24 4.85	8.56 8.43)
	$CH\equiv CCOOCH_3$	190—193	MeOH	58.52 (58.54	3.86 3.68	8.64 8.53)
	$CH_2=CHCONH_2$	195—210 (Decomp.)	Water	54.51 (55.62	5.18 4.67	18.54 18.54)
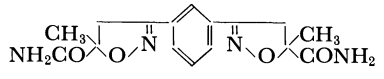	$CH_2=C(CH_3)CONH_2$	228—232 (Decomp.)	Water	58.15 (58.17	5.21 5.49	16.83 16.96)
	N-Phenylmaleimide	Gradual decomp. >220	*1	65.55 (66.40	4.74 3.58	10.72 11.06)

*1 Reprecipitated from a methanolic solution with water.

from benzohydroxamic chloride and methyl acrylate with use of triethylamine as a hydrogen chloride acceptor, has a methine triplet centered at 4.66 τ and a methylene doublet centered at 6.27 τ (J_{CH-CH_2} = 9.6 cps), one peak of which is overlapped with OCH_3 peak at 6.17 τ. These NMR data indicate the two products are diastereomeric isomers of 3,3'-*m*-phenylene bis-(5-carbomethoxy-2-isoxazoline). The orientation of the cycloaddition may be considered to be the same for the other examples of the reaction summarized in Tables 1 and 2. Similar aspects were reported in the reaction of cyanogen di-*N*-oxide with olefins by Grundmann and his coworkers[10] and also in the reaction of Ia with styrene and with cyclopentadiene by Overberger and Fujimoto.[11] The adducts obtained by the both reactions of Ib with vinyl acetate and with methyl methacrylate have a low crystallinity and therefore the separation of the two isomers was unsuccessful. The reaction products, however, were confirmed to be the corresponding isoxazoline derivatives from their infrared absorption spectra.

The 1,3-dipolar polycycloadditions were conducted with *p*- and *m*-phenylenedimaleimide (IIa and IIb) and with ethylenedimethacrylate (III) as difunctional dipolarophiles. Polymerization proceeded by the repetition of the 1,3-dipolar cycloaddition, in which cyclic shift of electrons accompanied, forming 2-isoxazoline rings along the growing polymer main chains as shown below.

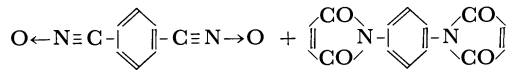

I a) *p*-, b) *m*- II a) *p*-, b) *m*-

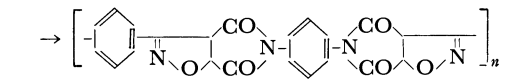

A B

	A	B
PI	*p*-	*p*-
PII	*p*-	*m*-
PIII	*m*-	*p*-
PIV	*m*-	*m*-

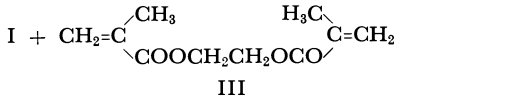

III

PV: *p*-, PVI: *m*-

The rate of polycycloaddition was considerably fast. Polycycloaddition of Ib with IIb was carried out in an Ubbelohde's viscometer at the concentration of 0.5 mmol of each Ib and IIb in 25 m*l* of dimethylformamide at 30°C and 60°C. After 30 min, no more increase of viscosity of the reaction mixture was observed in either case as seen in Fig. 1.

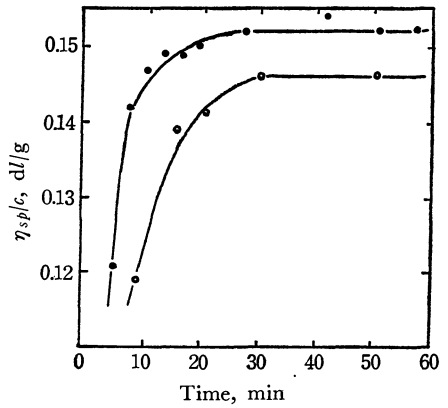

Fig. 1. Viscosity increase *versus* reaction time.
—●— 60°C —○— 30°C
0.5 mmol of each Ib and IIb in 25 m*l* of dimethylformamide.

The polymerization conditions and the results are summarized in Tables 3 and 4. The degree of polymerization was rather low, even in the case of homogeneous polymerization using a polar solvent as a reaction medium. The polymers derived from II are insoluble in benzene, tetrahydrofuran and anisole, and therefore, when such a solvent was used as the reaction medium, precipitation of polymer occurred before a high degree of polymerization was attained. In the case of polymerization of Ia with IIa, the polymer formed precipitated as the reaction proceeded even when a polar solvent was used as the reaction medium. The polymer (PI) was only soluble in concentrated sulfuric acid among the solvents tested.

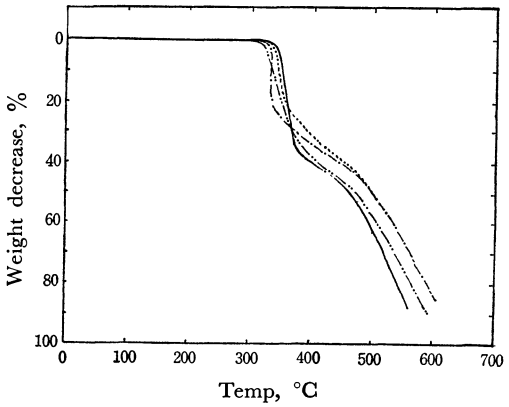

Fig. 2. Thermogravimetric analysis curves for polyphenylene-Δ^2-isoxazolinopyrrolidinediones.
—— PI ····· PII —·—· PIII —··—·· PIV
(2.5°C/min, in air)

10) C. Grundmann, V. Mini, J. M. Dean and H-D. Frommeld, *Ann.*, **687**, 191 (1965).
11) C. G. Overberger and S. Fujimoto, *Polymer Letters*, **B3**, 735 (1965).

TABLE 3. 1,3-DIPOLAR POLYCYCLOADDITION OF TEREPHTHALONITRILE DI-*N*-OXIDE

Exp. No.	Diolefin	Solvent mmol/m*l*	React. temp. °C	React. time hr	η_{sp}/c*1	PMT*2 °C	N anal., % Found	N anal., % Calcd
PI-1	IIa	DMF (1.25/5)[a]	R. t.[c]	20	0.19[d]	Gradual decomp. >310		
2		DMF (1.25/5)	R. t.	20	0.29[d]		11.96	13.08
3		DMAc (2.5/10)	55	1	—			
PII-1	IIb	DMF (2.5/10)	R. t.	20	0.11	Gradual decomp. >320	12.40	13.08
2		DMF (2.5/10)[a]	R. t.	20	0.09		12.34	13.08
3		DMAc (2/10)	R. t.	12	0.11			
4		DMAc (2/10)[b]	R. t.	24	0.11			
5		Anisole (2.5/10)	50	1	0.10			
PV-1	III	Benzene (2.85/5)	R. t.	1	0.30	147—152	8.43	7.82

*1 0.2 g/100 m*l* DMF, 30°C.
*2 Measured by using a capillary tube.
a) 3% of LiCl was added.
b) IIIb was 5 mol% less than equivalent amount.
c) R. t. means that the reaction mixture was not heated. As the polymerization reaction was exothermal, the temperature of the reaction mixture rose up to 50°C or higher at the beginning.
d) 0.2 g/100 m*l* 95%-H_2SO_4, 30°C.

TABLE 4. 1,3-DIPOLAR POLYCYCLOADDITION OF ISOPHTHALONITRILE DI-*N*-OXIDE

Exp. No.	Diolefin	Solvent mmol/m*l*	React. temp. °C	React. time hr	η_{sp}/c*1	PMT*2 °C	N anal., % Found	N anal., % Calcd
PIII-1	IIa	DMF (2/5)	R. t.	1	0.21	Gradual decomp. <310	12.42	13.08
2		DMF (2/5)[a]	R. t.	1	0.21			
PIV-1	IIb	DMF (2/4)	R. t.	2.5	(0.19)	Gradual decomp. >310	12.09	13.08
2		DMF (2/4)	75	2.5	(0.26)			
3		DMF (3.2/5)	R. t.	1	0.13			
4		DMAc (2/5)	R. t.	20	0.08		12.53	13.08
PVI-1	III	Dioxane (2/2.6)	R. t.	24	(0.21)		8.09	7.82
2		Benzene (4/5)	R. t.	1	0.20	121—130		

*1 0.2 g/100 m*l* DMF, at 30°C except the parenthesized which were measured at the concentration of 0.5 g/100 m*l* DMF.
*2 Measured by using a capillary tube.
a) Ten mol% less than equivalent amount of isophthalonitrile di-*N*-oxide was allowed to react with IIIa for 15 min, and then the shortage of the nitrile oxide was supplied to attain the equivalency.

The structures of the polymers obtained were verified by means of the comparison of their infrared spectra with those of the model compounds described above. Absorption bands at around 905 and 1180 cm^{-1} of medium intensity were characteristic of the isoxazoline polymers. Besides them, characteristic absorptions of imide carbonyl were observed at 1725 (strong) and at 1790 cm^{-1} (weak) in PI, PII, PIII and PIV. Whereas strong absorption of ester carbonyl was at 1740 cm^{-1} in the case of PV and PVI.

The X-ray diffraction diagrams of the polyphenyleneisoxazolinopyrrolidinediones measured by powder method with use of nickel-filtered Cu$K\alpha$ radiation indicated that PII, PIII and PIV were amorphous and that PI, in which all of phenylene groups were linked at *p*-position, was only slightly crystalline. Such poor crystallinity of them, in spite of their rigid structure, resulted presumably from the random distribution of asymmetric carbons, *i. e.* random ordination of *dl* and *meso* configuration units of the isoxazoline linkages along the polymer chains.

The thermal analyses of PI, PII, PIII and PIV showed that the oxidative degradation occurred at the temperatures above 300°C. The thermal stability of them decreased in the order of PI>PII>PIII>PIV, but even PI showed an abrupt weight loss at 350°C. Figure 2 shows the thermal gravimetric analysis curves of them. The curves may indicate that partial aromatization, besides the oxidative degradation, occurred as shown by the

equation below and consequently the thermal stability was retained temporarily in each case.

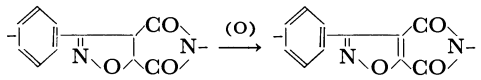

Experimental

Terephthalonitrile Di-*N*-oxide (Ia) and Isophthalonitrile Di-*N*-oxide (Ib). To a stirred solution of the corresponding hydroxamic chloride in methanol, a methanolic solution containing an equivalent amount of triethylamine was added dropwise at a temperature below −10°C. The nitrile oxide soon precipitated out of the mixture as colorless powder, which was filtered and washed thoroughly with methanol. The yield was higher than 70% of the theoretical. Ia decomposed explosively when it was put into a bath heated at a temperature above 150°C, and Ib also decomposed abruptly at a temperature above 90°C. When they were heated slowly, only gradual discoloration was observed without melting up to 300°C.

The Reaction of Ia and Ib with Hydrogen Chloride. Hydrogen chloride gas was introduced into a suspension of the corresponding nitrile oxide in methanol with occasional shaking until the suspension turned into a clear solution by exothermal reaction. Then, the reaction mixture was let stand for ten minutes. After that, the mixture was poured into water to give a white precipitate which was identified with the corresponding hydroxamic chloride by melting point and IR spectrum.

The Reaction of Ia and Ib with Triethylphosphite. To a stirred suspension of the corresponding nitrile oxide in methanol, a methanolic solution of triethylphosphite was added gradually with ice-cooling. The reaction was exothermal and almost instantaneous. After the mixture was let stand for an additional hour, methanol and excess triethylphosphite were distilled off under reduced pressure and the residue was recrystallized from aqueous methanol. The products from Ia and Ib were identified with terephthalonitrile and isophthalonitrile respectively.

1,3-Dipolar Cycloadditions of Ia and Ib. A typical example is described below. Ia was added portionwise into a tetrahydrofuran solution of 50 mol% excess of methyl acrylate with stirring. As the reaction proceeded exothermally, Ia dissolved into the solution. A few minutes later than the solution became clear, colorless crystals began to precipitate. The reaction mixture was let stand for an hour and then the precipitate was gathered by filtration and recrystallized twice from ethyl acetate, giving crystals; mp 182—184°C. The mother liquor of the tetrahydrofuran solution was evaporated under reduced pressure. The residual mass was recrystallized twice from methanol, giving colorless crystals; mp 133—136°C. The yield of the sum of those two substances was higher than 70% of the theoretical.

The analytical data and the other reaction products are summarized in Tables 1 and 2.

1,3-Dipolar Polycycloadditions: Materials and Solvent. *p*- (IIa) and *m*-Phenylenedimaleimide (IIb) were prepared in the usual way by the conversion of the phenylenediamines into the maleamic acids, followed by dehydration cyclization with acetic anhydride. IIa melted at 300—303°C when it was inserted into a bath preheated at the temperature, but it did not melt at the temperatures above 380°C, when heated gradually (lit.[12] mp 346—350°C). The melting point of IIb was 198—199°C (lit.[12] 202°C).

Ethylenedimethacrylate was obtained commercially and purified by distillation.

The solvents used were purified by usual way.

Polymerization Procedures. A typical example is as follows: Into a solution of 0.402 g (0.002 mol) of IIb in 4.0 m*l* of dimethylformamide, 0.320 g (0.002 mol) of Ib was added portionwise with stirring at room temperature. Then the mixture was let stand for an additional hour with stirring and poured into methanol. The polymer precipitated was gathered by filtration and washed thoroughly with hot methanol and dried under vacuum at 110°C to give an almost colorless powder.

12) P. Kovacic and R. W. Hein, *J. Am. Chem. Soc.*, **81**, 1187 (1959).

BULLETIN OF THE CHEMICAL SOCIETY OF JAPAN VOL. 41 1654—1657 (1968)

Polymerizations by 1,3-Dipolar Cycloaddition Reactions. VI. Syntheses of Polyurethans with Isoxazoline or Isoxazole Linkages

Yoshio IWAKURA, Shinsaku SHIRAISHI,*1 Zin ASAKAWA,*2 Masayasu AKIYAMA*3 and Nobuo TANAKA

Department of Synthetic Chemistry, Faculty of Engineering, University of Tokyo, Hongo, Tokyo

(Received December 19, 1967)

Polyurethans with isoxazoline or isoxazole linkages in the polymer main chains were prepared by polyadditions of diols with isoxazoline or isoxazole rings and diisocyanates. The diols were prepared by 1,3-dipolar cycloaddition reactions of tere- and iso-phthalonitrile di-*N*-oxides with allyl or propargyl alcohol. Polyurethans of the same structures were also prepared by 1,3-dipolar polycycloadditions of the nitrile oxides with bisallyl or bispropargyl carbamates.

The 1,3-dipolar cycloaddition reaction, first defined and extensively studied by Huisgen and his coworkers,[1] is an interesting method of synthesizing heterocyclic compounds. The high yields of the reaction products have prompted several recent investigations of the syntheses of the polymers with heterocyclic rings by this reaction. We ourselves have already reported[2] the preparation of new diols with heterocycles by the reactions of tere- and isophthalonitrile di-*N*-oxides with allyl or propargyl alcohol. The present paper is concerned with the preparation of new types of polyurethans with isoxazoline or isoxazole rings in their polymer main chains from those diols, and with the preparation of the polymers of the same structures by 1,3-dipolar polycycloadditions. The generalized reaction scheme and the structures of the polymers are shown below:

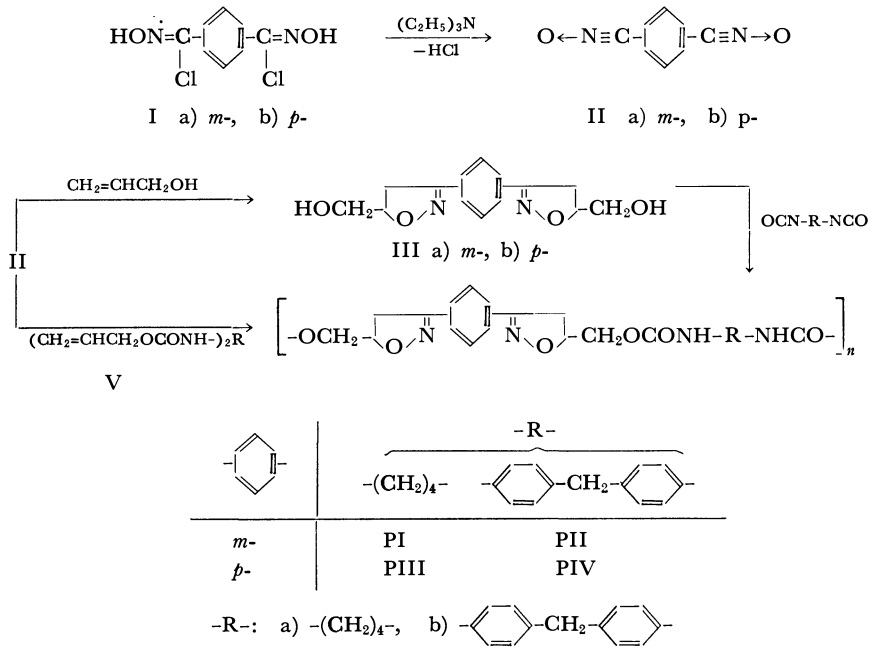

*1 Present address: Institute of Industrial Science, University of Tokyo, Roppongi, Minato-ku, Tokyo.

*2 Present address: Research and Development Center, Nippon Rayon Co., Ltd., Uji, Kyoto.

*3 Present address: Tokyo Institute of Technology, Ookayama, Meguro-ku, Tokyo.

1) R. Huisgen, *Angew. Chem.*, **75**, 604 (1963); R. Huisgen, R. Grashey and J. Sauer, in "The Chemistry of Alkenes," Interscience, New York (1963), p. 806.

2) Y. Iwakura, S. Shiraishi, M. Akiyama and M. Yuyama, This Bulletin, **41**, 1648 (1968).

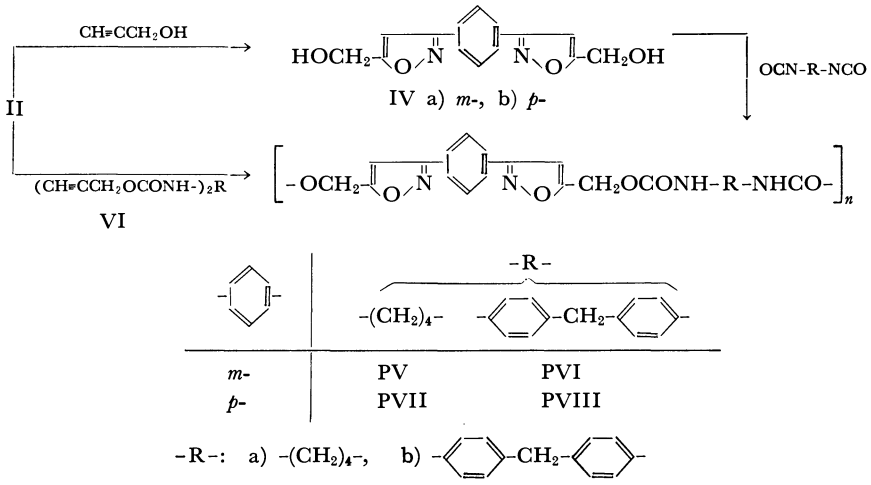

TABLE 1. DIOLS WITH ISOXAZOLINE OR ISOXAZOLE RINGS

Diol		Yield (%)	Mp (°C)	Anal. (%) C	H	N
HOCH2-(isoxazoline)-CH2OH	m-IIIa	72	127—135	60.51	5.91	10.12
	p-IIIb	74	227—228	60.44	5.87	10.16
	Calcd for $C_{14}H_{16}N_2O_4$:			60.86	5.84	10.14
HOCH2-(isoxazole)-CH2OH	m-IVa	40	154—155	61.60	4.53	10.36
	p-IVb	58	225—226	61.52	4.43	10.30
	Calcd for $C_{14}H_{12}N_2O_4$:			61.76	4.44	10.29

TABLE 2. POLYURETHANS PREPARED BY POLYADDITION REACTIONS

Polymer	Solvent (mmol/ml)	React. time (hr)	React. temp. (°C)	η_{inh}	PMT (°C)	N anal. (%) Found	Calcd
PI	Anisole(5/10)	2	Reflux	0.39[a]	180—198	13.42	13.46
PII	Anisole(5/10)	2	Reflux	0.50[a]	210—217	11.43	10.64
PIII	HMPA(5/10)	8	120	0.19[b]	260—267	14.06	13.46
PIV	HMPA(5/10)	30	80	0.22[b]	294—297	10.66	10.64
PV	Anisole(5/10)	2	Reflux	0.72[a]	194—207	13.77	13.58
PVI	Anisole(5/10)	4	Reflux	0.32[a]	200—228	10.60	10.72
PVII	DMAc(2.5/5)	22	120	0.11[b]	235—240	14.01	13.58
PVIII	DMAc(5/10)	28	100	0.17[b]	288—290	10.60	10.72

a) 0.5 g/100 ml of DMF, at 30°C. b) 0.5 g/100 ml of DMSO, at 30°C.

Diols with isoxazoline rings, 3,3'-(*m*- and *p*-phenylene)bis(5-hydroxymethyl-2-isoxazoline) (IIIa and IIIb), and those with isoxazole rings, 3,3'-(*m*- and *p*-phenylene)bis(5-hydroxymethylisoxazole) (IVa and IVb), were prepared by 1,3-dipolar cycloaddition reactions of iso- and tere-phthalonitrile di-*N*-oxides with allyl alcohol and with propargyl alcohol respectively in tetrahydrofuran (THF) solution at room temperature. They were also prepared from the corresponding hydroxamic chlorides and the alcohols mentioned above in THF, in the presence of triethylamines as a hydrogen chloride acceptor. IIIa and IIIb each have two asymmetric carbons to which a hydroxymethyl group attaches; therefore, they should each have two isomers, *meso* and *dl*. Indeed, the melting point of IIIa shows the broad range of 127—135°C, suggesting that it may be a mixture of the two isomers. However, attempts to separate the diastereomers have been unsuccessful. These diols are summarized in Table 1.

The polyaddition reactions of the diols described above were conducted with tetramethylene diisocyanate and with 4,4'-diisocyanatodiphenylmethane to give new types of polyurethans. The polyaddition conditions and the results are shown

TABLE 3. BISALLYL AND X-OCONH-R-

	Compound		Yield (%)	Recryst. solvent
	X	R		
Va	$CH_2=CHCH_2-$	$-(CH_2)_4-$	78.3	50%-CH_3OH
Vb	$CH_2=CHCH_2-$	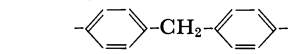	88.5	95%-CH_3OH
VIa	$CH\equiv CCH_2-$	$-(CH_2)_4-$	91.0	Benzene
VIb	$CH\equiv CCH_2-$	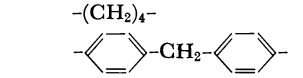	93.0	50%-CH_3OH

in Table 2. The diols with a *m*-phenylene link, IIIa and IVa, gave relatively-high-molecular-weight polymers with inherent viscosities of 0.3—0.7 (0.5 g/100 m*l* of DMF), while the diols with a *p*-phenylene link, IIIb and IVb, gave rather-lower-molecular-weight polymers with inherent viscosities of 0.11—0.22. The latter diols were less soluble in anisole; moreover, the polyurethans derived from them were also insoluble in the solvent. For that reason, the polymer formed precipitated from the reaction mixture before a high degree of polymerization was attained. Some other solvents, such as dimethylformamide (DMF), dimethylacetamide (DMAc), dimethylsulfoxide (DMSO), and hexamethylphosphoramide (HMPA) were also used as reaction media, but high-molecular-weight polymers were not obtained in such cases.

The polymers derived from IIIa and IVa are soluble in such polar solvents as DMF, DMAc, DMSO, and HMPA, but are insoluble in methanol, acetone, THF, anisole, and benzene. Those derived from IIIb and IVb are soluble in DMSO, but are only partly soluble in DMF and DMAc.

Polyurethans of the same structures were also obtained by 1,3-dipolar polycycloadditions of the nitrile oxides with a bisallyl carbamate or with a bispropargyl carbamate. These difunctional unsaturated carbamates were prepared by the reaction of the diisocyanates described above with allyl or propargyl alcohol. The carbamates are summarized in Table 3.

The 1,3-dipolar polycycloadditions were carried out in a THF solution by heating under reflux. When isolated nitrile oxides (II) were used, the molecular weights of the polymers obtained were rather low. The inherent viscosity of the polymers was not larger than 0.2 in any case. On the other hand, relatively-high-molecular-weight polymers were obtained when hydroxamic chlorides (I) were used in the presence of triethylamine as a hydrogen chloride acceptor. This indicates that the *in situ* addition of the nitrile oxide may be favorable to the polymerization reaction. Typical conditions and the results for the polymerization reactions of hydroxamic chlorides with difunctional dipolarophiles in THF are shown in Table 4. When anisole, *o*-dichlorobenzene, *m*-cresol, or DMSO was used as the reaction medium, the results were not better than those in Table 4.

TABLE 4. POLYURETHANS PREPARED BY 1,3-DIPOLAR POLYCYCLOADDITIONS

Polymer	Time (hr)	Yield (%)	η_{inh}	PMT (°C)
PI	0.5	48	0.47[a]	185—206
PII	1	34	0.58[a]	196—209
PIII	1	86	0.17[b]	242—256
PIV	2.5	88	0.23[b]	268—271
PV	1.5	64	0.25[a]	180—208
PVI	1	86	0.23[a]	195—217
PVII	2	70	0.22[b]	250—260
PVIII	2	95	0.23[b]	274—278

a) 0.5 g/100 m*l* of DMF, at 30°C.
b) 0.5 g/100 m*l* of DMSO, at 30°C.

The infrared spectra of the polymers obtained here coincided closely with the corresponding polymers obtained by the polyadditions described above. Their polymer melt temperatures (PMT) also exhibited similar values. As expected, the melting points of the polymers in this series are affected mostly by whether the heterocyclic units are linked by *m*-phenylene or *p*-phenylene groups. The melting points of PI, PII, PV, and PVI, all of which are *m*-phenylene-linked, are in the range of 180—210°C, whereas those of PIII, PIV, PVII, PVIII, which are *p*-phenylene-linked, are in the 250—280°C range.

Among the polymers prepared in this investigation, those with inherent viscosities above 0.3, which are exclusively *m*-phenylene-linked, can all be casted to a self-supporting film from a DMF solution. The film casted from the higher-molecular-weight polymer was tough and transparent.

Experimental

Preparation of the Diols. All of the diols were prepared by the reaction of the corresponding nitrile oxides with allyl alcohol and with propargyl alcohol in

BISPROPARGYL CARBAMATES
NHCOO-X

Mp (°C)	Anal. (%) Found C	H	N	Calcd C	H	N
76—77	56.33	7.84	11.00	56.23	7.87	10.93
123—124	68.70	6.23	7.92	68.83	6.05	7.65
84—85	57.00	6.56	11.13	57.13	6.39	11.11
163—164	69.74	5.22	7.73	69.60	5.00	7.73

a THF solution at room temperature. They were purified by recrystallization from aqueous methanol in all cases. The analytical data are shown in Table 1. A typical example is as follows: Into a stirred solution of 4 g (0.069 mol) of allyl alcohol in 75 m*l* of THF, there were added, portion by portion, 4.7 g (0.029 mol) of isophthalonitrile di-*N*-oxide (IIa). After the reaction mixture had been let stand overnight, the solvent was evaporated under reduced pressure. The residue was recrystallized twice from 50%-aqueous methanol to give 5.7 g (72% of the theoretical amount) of colorless crystals of IIIa, mp 127—135°C. Further recrystallization did not change the melting point.

Polyaddition of the Diols with the Diisocyanates. A typical example is as follows: 1.380 g (0.005 mol) of IIIa and 0.700 g (0.005 mol) of tetramethylene diisocyanate were placed in 10 m*l* of anisole, and the mixture was stirred and then gently heated to reflux. After the mixture became a clear solution, 15 mg (2.5×10^{-5} mol) of dibutyltin dilaurate was added to the solution as a catalyst. Stirring and heating were continued for 2 more hours. The resinous product separated from the solution and deposited at the bottom of the vessel. After the reaction mixture had cooled, the resinous product was separated and dissolved in DMF. The DMF solution was filtered with a glass funnel and poured into methanol to precipitate the polymer, PI. It was gathered by filtration, washed methanol, and dried at 60°C *in vacuo*. The analytical sample was obtained by treating the polymer with boiling methanol to remove the DMF occuluded in it.

The other polymers were prepared by a similar procedure.

Preparation of the Bisallyl Carbamates and Bispropargyl Carbamates. Bisallyl carbamates were prepared by the reaction of allyl alcohol with the corresponding diisocyanate in petroleum ether, and bispropargyl carbamates were prepared from propargyl alcohol and the diisocyanates in benzene. As the reaction proceeded, in each case the carbamate formed precipitated out of the reaction mixture. When tetrahydrofuran was used as the reaction medium, the solvent was evaporated to obtain the product as a solid. A typical example is as follows: Eight grams of tetramethylene diisocyanate (0.057 mol) and 7 g (0.12 mol) of propargyl alcohol were placed in 20 m*l* of THF, and the mixture was left to stand overnight. The subsequent evaporation of the solvent left a solid. It was recrystallized from benzene to give 12.8 g (91%) of colorless needles of VIa, mp 84—85°C.

The analytical data and the solvents of recrystallization are summarized in Table 3.

Procedures of the 1,3-Dipolar Polycycloadditions. A solution of a dihydroxamic chloride (I) (0.0025 mol) and a bisallyl or bispropargyl carbamate (V or VI) (0.0025 mol) in 5 m*l* of THF was heated under reflux with stirring. To the solution there was then added, drop by drop, 0.006 mole of triethylamine in 5 m*l* of THF. A white precipitate thereupon began to be deposited. The precipitate formed at the earlier stage of the reaction was triethylammonium chloride. The mixture was stirred for an hour, and then the solid deposited was gathered by filtration and dissolved in DMSO. The DMSO solution was filtered with a glass funnel and poured into methanol to precipitate the polymer. It was collected by filtration, washed with methanol, and dried under vacuum.

When other solvents were used as the reaction media, the reaction temperature was kept at a temperature in the range between room temperature and 70°C. The other procedures were similar to those mentioned above.

The polymerization procedures in which isolated nitrile di-*N*-oxides (II) were used as the starting components were the same as those described in a previous paper.[2]

BULLETIN OF THE CHEMICAL SOCIETY OF JAPAN VOL. 41 1658—1664 (1968)

Studies of Heteroaromaticity. IX.[1] Stability and Reactivity of 5-Nitro-2-furyl Diazo Compounds

Tadashi SASAKI, Shoji EGUCHI and Atsuyuki KOJIMA

Institute of Applied Organic Chemistry, Faculty of Engineering, Nagoya University, Furo-cho, Chikusa-ku, Nagoya

(Received December 23, 1967)

(5-Nitro-2-furyl)diazomethane (2), 3-(5-nitro-2-furyl)diazopropene (4), and 1-(5-nitro-2-furyl)diazoethane (6) were prepared by the oxidation of the corresponding hydrazones with active manganese dioxide. The relative stabilities of these diazo compounds were then compared with *p*-nitrophenyldiazomethane in their ethanolic solutions and in their solid states by measuring their decomposition rates spectroscopically; it was found that the stability decreased in the following order:

6 ≃ *p*-nitrophenyldiazomethane > 2 ≃ 4 in ethanol

p-nitrophenyldiazomethane > 2 > 4 > 6 in the solid state.

The reactivities of these diazo compounds were also investigated in the decomposition reactions; the thermal and photolytic decomposition of 2 afforded 1,2-di(5-nitro-2-furyl)ethylene (7) in a low yield, but 4 cyclized readily to 3-(5-nitro-2-furyl)pyrazole (8) in a good yield and 6, to an azine (9) even upon standing at room temperature. 2 was treated with benzoic acid in ether to give 5-nitro-2-furfuryl benzoate (10) in a quantitative yield, and with triphenylphosphine in the same solvent to afford the triphenylphosphazine (13) in a 75% yield; this last substance liberated nitrogen very easily in the presence of cuprous ions to give the phosphonium ylid (14), one of the Wittig reagents. 14 was then considered as a possible starting material for preparing (5-nitro-2-furyl)ethylenic compounds. Similarly, 3-(5-nitro-2-furyl)acrolein triphenylphosphazine (17) was prepared from 4 and triphenylphosphine.

Although the preparation[2] and chemical properties[3] of aromatic diazo compounds have been studied extensively, little is known about heterocyclic diazo compounds, among which 2-furyl-,[4] 2-thienyl-,[4b] phenyl-2-thienyl-[5] and di-2-thienyl diazomethane[5] have been reported.

In this paper we wish to describe the preparation of 5-nitro-2-furyldiazomethane (2), 3-(5-nitro-2-furyl)diazopropene (4), and 1-(5-nitro-2-furyl)-diazoethane (6), and some reaction thereof, from the viewpoint of their chemical reactivities and their antibacterial activity.[6]

Results and Discussion

Of the several methods for the preparation of aromatic diazo compounds, the best way is by the oxidation of the corresponding hydrazones; the choice of the oxidation reagent is known to play a very important role with respect to the yields of the diazo compounds.[2b,7]

5-Nitro-2-furfural hydrazone (1a) was oxidized with active manganese dioxide in ether at 0°C to afford a diazo compound 2 in over an 80% yield, though the oxidation with yellow mercuric oxide or lead tetraacetate, which is known to be very effective reagent for the preparation of dicyanodiazomethane from the corresponding hydrazone,[8] gave 2 in yields of less than 10%. The pyrolytic decomposition[2c] of the sodium salt of 5-nitro-2-furfural tosylhydrazone (1b) afforded 2 in around a 50% yield:

1a ⟶ 2 ⟵ 1b

The similar oxidation of the corresponding

1) Part VIII of this series: T. Sasaki and T. Yoshioka, This Bulletin, **40**, 2608 (1967).

2) a) A. Hantzsch and M. Lehmann, *Ber.*, **35**, 897 (1902); b) H. Staudinger and A. Gaule, *ibid.*, **49**, 1897 (1916); c) G. M. Kaufman, J. A. Smith, G. G. Van der Stouw and H. Shechter, *J. Am. Chem. Soc.*, **87**, 935 (1965), and the references cited therein.

3) a) C. D. Gutsche, G. L. Bachman and R. S. Coffey, *Tetrahedron*, **18**, 617 (1962); b) H. Nozaki, R. Noyori and K. Sisido, *ibid.*, **20**, 1125 (1964).

4) a) D. W. Adamson and J. Kenner, *J. Chem. Soc.*, **1935**, 286; b) J. B. F. N. Engerts, G. van Bruggen, J. String and H. Wynberg, *Rec. trav. chim.*, **84**, 1610 (1965).

5) H. Reimlinger, *Chem. Ber.*, **97**, 3493 (1964).

6) The pharmacological findings on the compounds in this paper will be published elsewhere.

7) W. Schroeder and L. Katz, *J. Org. Chem.*, **19**, 718 (1954).

8) E. Ciganek, *ibid.*, **30**, 4198 (1965).

TABLE 1. PROPERTIES OF NITROFURYL DIAZO COMPOUNDS: 2, 4 and 6

Compound	2			4			6		
Appearance	Red prisms			Reddish violet plates			Red plates		
Mp °C	86—88 dec. (from ether)			94—95 (from ether)			69—70 dec. (from ether)		
Formula	$C_5H_3O_3N_3$			$C_7H_5O_3N_3$			$C_6H_5O_3N_3$		
Anal. %	C	H	N	C	H	N	C	H	N
Calcd	38.66	1.98	27.45	46.93	2.81	23.46	43.12	3.02	25.15
Found	38.94	1.87	27.68	47.00	2.54	23.35	43.87	3.02	24.69[a]
Infrared data (KBr) cm^{-1}	2110(diazo), 1529 and 1357 (nitro), 1574, 1512, 1175, 1035 and 803(furyl)			2100(diazo), 1608(C=C), 1519 and 1358(nitro), 1560, 1500, 1193, 1036 and 807(furyl)			2070(diazo), 1519 and 1353(nitro), 1570, 1506, 1178, 1015 and 803(furyl)		
Ultraviolet data (EtOH)[b] $m\mu$ ($\varepsilon \times 10^{-2}$)	244(87.3), 300(104) and 406 (26.3)			220(110), 289(200) and 440 (248)			250(86.5), 292(109) and 423(111)		
NMR data ($CDCl_3$) τ, cps	2.64[c] (1 H, d, J=4.0), 3.83[c] (1 H, d, J=4.0) and 4.67(1 H, s)			2.70[c] (1 H, d, J=4.0), 3.78[c] (1 H, d, J=4.0), 4.07[d] (1 H, d, J=16), 3.13[e] (1 H, q, J=16 and 9.0) and 5.09[f] (1 H, d, J=9.0)					

a) Compound 6 was too unstable to obtain satisfactory values of the microanalysis, presumably by loosing nitrogen. b) See also Fig. 1. c) Nitrofuran ring protons signal. d) C-3-H signal. e) C-2-H signal. f) C-1-H signal.

hydrazones, 3 and 5, derived from 3-(5-nitro-2-furyl)acrolein and 5-nitro-2-furyl methyl ketone with active manganese dioxide afforded the corresponding diazo compounds, 4 and 6, in the good yields of 70 and 62% respectively:

$$3 \longrightarrow 4 \qquad 5 \longrightarrow 6$$

The structure of 2, 4, and 6 were confirmed by the analytical and spectral data which are summarized in Table 1. Judging from the data shown in this table ($J_{C-2-H,C-3-H}$=16 cps), 4 may be regarded as having a *trans*-configuration.

The relative stabilities of 2, 4, and 6 to *p*-nitrophenyldiazomethane[9] were measured in their ethanolic solutions from their ultraviolet spectra and in their solid states from their infrared spectra, both as a function of the time at 20°C. The half-lives and the rate constants of their decompositions are summarized in Table 2. From this table, it can be concluded that, in ethanol, 2 has nearly the same stability as 4, but only about a quarter that of 6 or of *p*-nitrophenyldiazomethane, while 2-furyldiazomethane has been reported to be a very unstable red oil.[4] In the solid state, the stability decreased in the following order: *p*-nitrophenyldiazomethane>2>4>6.

In both states, *p*-nitrophenyldiazomethane is the most stable except in the case of 6 in ethanol, where some solvent effects might be expected. This result is in good accordance with our expectations based on the resonance stability of each compound in the ground state. The facts that the final absorption maxima in ethanol were located at 300 $m\mu$ (from 406 $m\mu$) for 2, at 354 $m\mu$ (from 440 $m\mu$) for 4, and at 305 $m\mu$ (from 423 $m\mu$) for 6 showed that the final decomposition products of 2, 4, and 6 were 5-nitro-2-furfuryl ethyl ether (11), 3-(5-nitro-2-furyl)-pyrazole (8), and, presumably, α-(5-nitro-2-furyl)ethyl ethyl ether (12) respectively.

In order to attempt a carbenoid reaction, 2 was decomposed in carbenophilic cyclohexene in the presence of copper powder by heating it until nitrogen gas evolution had ceased; the products were then purified by column chromatography. The only crystalline product isolated was 1,2-di-(5-nitro-2-furyl)ethylene (7); neither insertion- nor addition-products to cyclohexene could be separated. The photolysis of 2 in the presence of a carbenophile, such as cyclohexene, styrene, or α-morpholinostyrene, led to the formation of 7 in a low yield, and in all cases a large amount of an intractable, dark brown mass was produced. These results indicate that 5-nitro-2-furylcarbene, even if produced from 2, is too stable to react further with those carbenophiles, but, rather, affords the dimer 7; consequently, 2 may be concluded to be an unsuitable precursor for the carbenoid reaction.

When 4 was heated over its melting point or was kept standing in ether in the presence of a catalytic amount of triethylamine, intramolecular cyclization occurred to give 8 in a good yield. The structure of 8 was confirmed from the following spectral data: the infrared spectrum showed no diazo-band, but it did show an NH-band at 3165 cm^{-1}, and the nmr spectrum in $CDCl_3$ had signals due to two protons of a pyrazole ring at 2.08 τ (1H, d, J=2.5 cps) and 3.17 τ (1H, d, J=2.5 cps), none of which disappeared on deuteration; a signal due to an NH proton of a pyrazole ring

9) T. Curtius and A. Lublin, *Ber.*, **33**, 2490 (1900).

Table 2. Relative stabilities of nitrofuryl diazocompounds and *p*-nitrophenyl diazomethane[a]

	Compound	2	4	6	O_2N-⟨⟩-CHN_2
In EtOH	Initial concentration (mmol)	0.536	0.0458	0.109	0.0459
	Rate constant, $k_1\times10^{-4}$ (sec^{-1})	1.72	2.27	0.494	0.520
	Half-life (min)	67	51	234	222
At Solid[b]	Rate constant, $k_1\times10^{-7}$ (sec^{-1})	1.34	6.70	22.9	0.803
	Half-life (day)	60	12	3.5	100

a) Measurements were carried out at 20°C. b) In potassium bromide pellet.

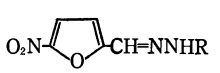

1a: R=H
b: R=Tosyl

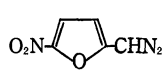

2

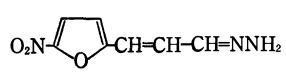

3

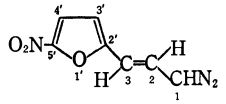

4

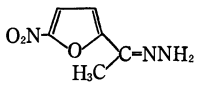

5

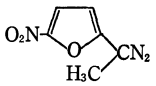

6

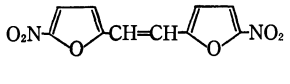

7

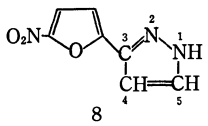

8

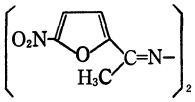

9

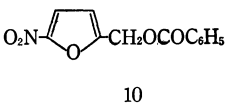

10

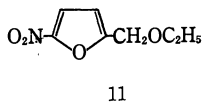

11

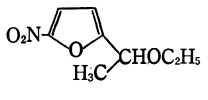

12

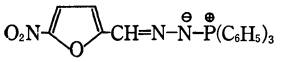

13

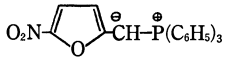

14

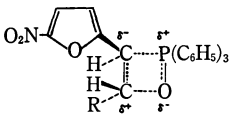

15

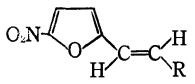

16a: R=$-C_6H_5$
b: R=$-CH=CH-C_6H_5$
c: R=$-C_4H_3O$

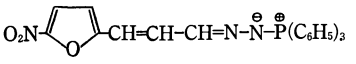

17

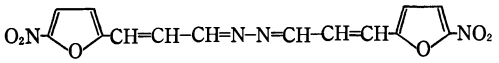

18

may be expected to be located in the lower field of around $-3.0\ \tau$,[10] besides those due to two protons of a nitrofuran ring at 2.21 τ (1 H, d, J= 3.8 cps) and at 2.87 τ (1 H, d, J=3.8 cps)[11] and the ultraviolet spectrum in ethanol had an absorption maximum at 354 mμ.[12] Such a facile intramolecular cyclization of unsaturated diazo compounds has also been reported with vinyldiazomethanes:[4a,13]

2 ⟶ 7 4 ⟶ 8

Compound 6 also decomposed very easily either in the solid state or as a benzene solution on only standing at room temperature; it gave an azine derivative 9 as the main product. A similar azine

10) C. L. Habraken, H. J. Munter and J. C. P. Westgest, *Rec. trav. chim.*, **86**, 56 (1967).
11) T. Sasaki and T. Yoshioka, This Bulletin, **40**, 2604 (1967).
12) Part XV of this series: T. Sasaki, S. Eguchi and A. Kojima, *J. Heterocyclic Chem.*, **5**, 243 (1968).
13) a) C. D. H. Hurd and S. C. Lui, *J. Am. Chem. Soc.*, **57**, 2656 (1935); b) A. Ledwith and D. Parry, *J. Chem. Soc., (B)*, **1967**, 41.

formation by the decomposition of diaryldiazomethane has also been reported.[14] This shows that nitrofurylcarbene, even if produced from 6, is a rather stable and unreactive species, similar to that produced from 2 described above:

$$6 \longrightarrow 9$$

By far the most common reactions of diazoalkanes are those in which they act as nucleophiles, the α-carbon being most often the nucleophilic center. It is generally believed[15] that the case of reaction decreases with a decrease in the basicity of the α-carbon and that it is affected by the steric effects as well, while the behavior of diazoalkanes as electrophiles is much less pronounced. As an example of a nucleophile, 2 was treated with benzoic acid in ether at room temperature; it afforded the corresponding benzoate, 10, in a quantitative yield. This reaction proceeded very slowly; it took about three days for 2 to be consumed completely even in the presence of an excess amount of benzoic acid, though 2-furyldiazomethane gives the corresponding benzoate in only 30 min.[4b] These results show that the presence of a nitro group in a furan ring causes an increase in the diazomethane stability because of the resonance stabilization and a lowering in the nucleophilicity of 2. Another example is given by the formation of 11 when 2 is left to stand in ethanol, as has been described above. As an example of 2 as an electrophile, 2 was treated in ether with triphenylphosphine at room temperature to afford 5-nitro-2-furfural triphenylphosphazine (13) in a 75% yield. 13 liberated nitrogen readily in the presence of cuprous ions to give 5-nitro-2-furfuryliidene triphenylphosphorane, a phosphonium ylid (14) and one of the Wittig reagents;[16] this provides a novel preparative method for (5-nitro-2-furfuryl)ethylenic compounds, for which the condensation of 5-nitro-2-furfural with active methylene and methyl compounds is the general procedure.[17] A Wittig reaction using 14 is interesting because the preparation of the Wittig reagent by the usual method from 5-nitro-2-furfuryl halides and triphenylphosphine, followed by base-treatment, was unsuccessful because of the facile furan-ring cleavage by a base, though the reaction of 5-nitro-2-furfural with the Wittig reagents has been reported.[18]

Thus, on the treatment of 2 with carbonyl compounds such as benzaldehyde, furfural, and cinnamaldehyde in the presence of triphenylphosphine and cuprous chloride, the corresponding (5-nitro-2-furyl)ethylenic compounds, 16a, b, and c, were obtained, but in low yields. A similar reaction with *p*-nitrobenzaldehyde 5-nitro-2-furfural resulted only in the formation of intractable masses, while that with acetophenone and acetone afforded small amounts of 7 and 5-nitro-2-furfural azine,[19a] with the ketones mostly recovered. The reactivity of the Wittig reaction is known to depend mainly on the charge on the α-carbon atom, and the most stable phosphinemethylenes are completely unreactive; thus, the *p*-nitrophenylmethine triphenylphosphonium ylid gives no olefins at all with benzaldehyde and cinnamaldehyde because of the resonance stabilization.[20]

The above results indicate that nitrofurfuryl phosphobetaine (15) is more basic—in other words, more reactive—than the corresponding *p*-nitrophenyl compound.

The diazo compound 4 reacted similarly with triphenylphosphine in ether to give the corresponding phosphazine (17), which was more labile than 13. Thus, 17 afforded the known β-(5-nitro-2-furyl)acrolein azine[19b] in a good yield upon only being warmed in acetone. Such a facile formation of an azine from phosphazine can be explained by the instability of 17; the decomposition of 17 may afford the corresponding phosphonium ylid, which will be attacked by 4 as an electrophile, this attack to be followed by the elimination of triphenylphosphine from the primary adduct to give an azine.

Experimental[21]

5-Nitro-2-furfural Tosylhydrazone (1b). This was prepared by the usual method from 5-nitrofurfural[22] and tosylhydrazine in a quantitative yield as yellow needles, mp 155—156°C (from methanol): λ_{max}^{EtOH} 352 mμ (ε 15000); ν(KBr) 3170, 1614, 1593, 1528, 1352, 1318 and 1168 cm^{-1}.

14) W. Kirmse, L. Horner and H. Hoffmann, *Liebigs Ann.*, **614**, 19 (1958).
15) C. G. Overberger, J-P. Anselme and J. G. Lombardino, "Organic Compounds with Nitrogen-Nitrogen Bonds," The Ronald Press Company, New York (1966), p. 51.
16) G. Wittig and M. Schlosser, *Tetrahedron*, **18**, 1023 (1962).
17) T. Sasaki, unpublished data.
18) H. Saikachi, private communication.
19) a) K. Miyake, *Yakugaku Zasshi (J. Pharm. Soc. Japan)*, **72**, 1162 (1952); b) H. Saikachi and H. Hoshida, *ibid.*, **71**, 982 (1951).
20) a) S. Fliszar, R. F. Hudson and G. Salvadori, *Helv. Chim. Acta*, **46**, 1580 (1963); b) F. Krohnke, *Chem. Ber.*, **83**, 291 (1950).
21) The microanalyses were carried out on a Yanagimoto C. H. N. Corder Model MT-1. All the melting-points were determined on a Yanagimoto micro-melting-point apparatus and have not been corrected. The ultraviolet spectra were run on a JASCO Model ORD/UV-5 spectrophotometer; the infrared spectra, on a JASCO Model IR-S infrared spectrophotometer, and the NMR spectra, on a Varian A-60 spectrometer, in which the chemical shifts are described in τ-values relative to tetramethylsilane as an internal standard and the singlet peaks are designated as s; the doublet, as d; the triplet, as t; the quartet, as q; and the multiplet, as m.
22) H. Gilman and G. F. Wright, *J. Am. Chem. Soc.*, **52**, 2550, 4165 (1930); *ibid.*, **53**, 1923 (1931).

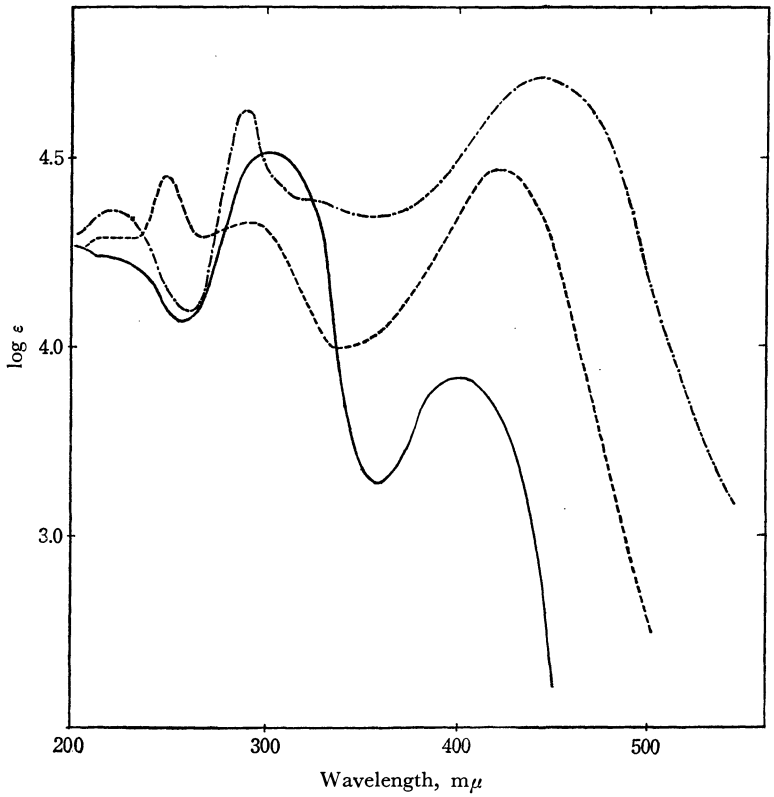

Fig. 1. Ultraviolet absorption spectra of nitrofuryldiazomethane, 2 (——), 4 (-·-·) and 6 (- - -) in ethanol.

Found: C, 46.60; H, 3.35; N, 13.36%. Calcd for $C_{12}H_{11}O_5N_3S$: C, 46.61; H, 3.59; N, 13.59%.

3-(5-Nitro-2-furyl)acroleinhydrazone (3). This was prepared similarly from 5-nitro-2-furylacrolein[23] and 80% hydrazine hydrate in a 52% yield as red needles, mp 150—151°C (from methanol): λ_{max}^{EtOH} 400 mμ (ε 17200): ν(KBr) 3375, 1609, 1572, 1555, 1490, 1356 and 807 cm^{-1}.

Found: C, 46.19; H, 3.95; N, 23.04. Calcd for $C_7H_7O_3N_3$: C, 46.41; H, 3.90; N, 23.20%.

5-Nitro-2-furyl Methyl Ketonehydrazone (5). This was prepared similarly from 5-nitro-2-furyl methyl ketone[24] and hydrazine hydrate in a 35% yield as red needles, mp 162—164°C (from methanol): λ_{max}^{EtOH} 384 mμ (ε 13600); ν(KBr) 3440, 3325, 3240, 1687, 1637, 1580, 1504, 1052 and 810 cm^{-1}; NMR ($CDCl_3$) τ 2.30 (1H, d, J=4.0 cps), 2.57 (2H, s, it disappeared on deuteration), 3.17 (1H, d, J=4.0 cps) and 8.00 (3H, s).

Found: C, 43.05; H, 3.62; N, 24.40%. Calcd for $C_6H_7O_3N_3$: C, 42.60; H, 4.17; N, 24.85%.

Preparation of 5-Nitro-2-furyl Diazo Compounds, 2, 4, and 6. *By Oxidation of the Hydrazones.* A mixture of 1.55 g (0.01 mol) of 1a, mp 162—164°C (dec.) (lit.[25] 164°C (dec.)), 6.20 g (0.07 mol) of active manganese dioxide,[26] and 3 g of anhydrous sodium sulfate in 40 m*l* of dry ether was stirred for 1 hr under ice cooling. The inorganic materials were then removed by filtration and washed with 100 m*l* of ether. The combined ethereal filtrate and washings were evaporated to dryness under reduced pressure to give 1.25 g (81.6%) of 2. The similar oxidation of 3 and 5 gave 4 in a 70% yield and 6 in a 62% yield. The appearance, melting point, and analytical and spectral data of these diazo compounds are summarized in Table 1, and their UV spectra, in Fig. 1.

By Pyrolysis of 1b. Sodium salt of 1b was pyrolyzed by the known procedure[2c] under the reduced pressure of 10^{-3} mmHg at 120—140°C to give 2 in a 50% yield from a sublimed portion.

Stability Measurement of 2, 4, and 6. The decreasing rates of the UV maximum absorption at 406 mμ for 2, at 440 mμ for 4, and 423 mμ for 6 in ethanol were followed as a function of the time at 20°; the half-life of the change and each rate constant were calculated, the results being as given in Table 2. Similarly, the decreasing rates of each diazo absorption band of these diazo compounds at 2110 for 2, at 2100 for 4, and at 2070 cm^{-1} for 6, together with that of *p*-nitrophenyldiazomethane at 2100 cm^{-1}, were followed to give each decomposition half-life in a KBr pellet and each rate constant (*cf.* Table 2).

Identification of the Final Products in Ethanol. After 2 had been kept standing in ethanol at room temperature for several hours, the ethanol was removed under reduced pressure; the residual red oil was identified as 11 spectroscopically (infrared and ultraviolet

23) H. Saikachi and H. Ogawa, *ibid.*, **80**, 3642 (1958).
24) I. J. Rinkes, *Rec. trav. chim.*, **50**, 834 (1931).
25) R. Hull, Brit. Pat. 816886 (1959); *Chem. Abstr.*, **55**, 24791 (1961).
26) J. Attenburrow, *J. Chem. Soc.*, **1952**, 1094.

spectra) by comparison with a specimen prepared by the known method.[27] Similarly, 4 was left in ethanol at room temperature for a while, and then, after the ethanol had been removed, the residual yellow solid, mp 199°C was identified as 8 by the comparison of the infrared spectra and by a mixed-melting-point determination. The similar treatment of 6 afforded a red oil, the amount of which was too small to be purified by distillation; in view of the similarity of the ultraviolet and infrared data to those of 11, we assumed this red oil to be 12.

Decomposition of 2 in Cyclohexene. *By Pyrolysis.* A mixture of 0.5 g (0.003 mol) of 2, and 0.2 g of copper powder in 16 m*l* of cyclohexene was heated at 70° for 40 min; during that time the nitrogen-gas evolution amounted to almost 100% of the theoretical yield. After the excess cyclohexene had been removed under reduced pressure, the oily residue, which showed two spots (R_f=0.50 and 0.01) on a silica-gel TLC*1 (benzene-methanol 95 : 5 vol% as the solvent and iodine as the developer), was chromatographed on a silica-gel (Mallinckrodt, 100 mesh) column, using benzene as the eluent, to give 22 mg (5.8%) of 7 as brownish yellow needles (mp 251—252°C (from benzene)), corresponding to the upper spot on TLC. λ_{max}^{EtOH} 242 mμ (ε 14300), 282 (7950), 406 (38000) and 424 (30400); ν(KBr) 1583, 1533, 1497, 1354, 1250, 1164, 960 and 820 cm^{-1}.

Found: C, 47.77; H, 2.34; N, 10.85%. Calcd for $C_{10}H_6O_6N_2$: C, 48.01; H, 2.42; N, 11.20%.

The fraction corresponding to the lower spot on TLC was eluted with methanol and a methanolic eluate was condensed to give a dark brown, intractable oil as the main product.

The decomposition of 2 in styrene, α-morpholinostyrene, tetrahydrofuran, and benzene as a carbenophile afforded only 7 in 4—6% yields after the purification of the products by silica-gel column chromatography; the main product was always an intractable, dark brown oil.

By Photolysis. A solution of 2 in cyclohexene or styrene was irradiated at room temperature through a Pyrex jacket with a 100-watt, high-pressure mercury lamp (UM-102, Ushio Denki Co., Tokyo, Japan) until nitrogen-gas evolution had ceased; when the products were then examined on TLC, they showed several spots, most of them seeming to originate from the decomposition products, including the nitrofuran-ring cleavage.

After the removal of the solvent, the crude product was purified by silica-gel column chromatography; this gave 7 in 3—5% yields.

3-(5-Nitro-2-furyl)pyrazole (8). A solution of 0.5 g (0.003 mol) of 4 and a few drops of triethylamine in 30 m*l* of ether was kept standing at room temperature for 18 hr. The yellow needles that were thus precipitated were filtered, washed with ether, and recrystallized from ethanol to give 0.26 g (51%) of 8 as faintly yellow needles, mp 199—200°C: λ_{max}^{EtOH} 354 mμ (ε 15300), 230 (11500); ν (KBr) 3165, 1604, 1538, 1500, 1348, 1020 and 810 cm^{-1}.

Found: C, 47.05; H, 3.17; N, 21.71%.[28] Calcd for $C_7H_5O_3N_3$: C, 46.93; H, 2.81; N, 23.46%.

5-Nitro-2-furyl Methyl Ketone Azine (9). A solution of 0.05 g (0.03 mol) of 6 in 20 m*l* of benzene was refluxed for 30 min. The precipitated crystals were filtered with cooling and recrystallized from acetone to give 25 mg (50%) of 9 as yellow needles, mp 189—190°C: λ_{max}^{EtOH} 223 mμ (ε 12000), 367 (32000); ν (KBr) 1610, 1568, 1514, 1473, 1350, 1035 and 812 cm^{-1}.

Found: C, 47.03; H, 3.27; N, 17.92%. Calcd for $C_{12}H_{10}O_6N_4$: C, 47.06; H, 3.29; N, 18.30%.

5-Nitro-2-furfuryl Benzoate (10). A solution of 0.26 g (0.002 mol) of 2 and 0.72 g (0.006 mol) of benzoic acid in 50 m*l* of ether was stirred at room temperature for 3 days, by which time 2 disappeared on TLC. The mixture was then evaporated to dryness to give yellow solids, which were recrystallized from ether to give 0.42 g (99%) of crude 10. Three recrystallizations from ether gave an analytical sample, mp 90—91°C: $\lambda_{max}^{Et_2O}$ 299 mμ (ε 8170); ν(KBr) 1719, 1597, 1533, 1348, 1242, 1021, 810, 749 and 710 cm^{-1}.

Found: C, 58.24; H, 3.50; N, 5.52%. Calcd for $C_{12}H_9O_5N$: C, 58.30; H, 3.67; N, 5.67%.

5-Nitro-2-furfural Triphenylphosphazine (13). To a solution of 0.015 g (0.001 mol) of 2 in 20 m*l* of ether, 0.29 g (0.001 mol) of triphenylphosphine in 10 m*l* of ether was added. After standing for 30 min at room temperature, the mixture was evaporated to dryness under reduced pressure, and the residue was recrystallized from an acetone - *n*-hexane mixture to give 0.31 g (75%) of 13 as deep red plates, mp 159—161°C: λ_{max}^{EtOH} 237 mμ (ε 11600) and 427 (21600); ν (KBr) 1598, 1542, 1500, 1368, 1062, 1026, 815, 736 and 700 cm^{-1}; NMR ($CDCl_3$) τ 1.77—2.52 (16 H, m, phenyl protons and –N=CH–), 2.69 (1H, d, J=3.8 cps, a furan-ring proton) and 3.49 (1 H, d, J=3.8 cps, a furan-ring proton).

Found: C, 65.02; H, 4.40; N, 9.85%. For an aged sample after one month: C, 63.91; H, 4.24; N, 9.57%. Calcd for $C_{23}H_{18}O_3N_3P$: C, 66.55; H, 4.38; N, 10.13%.

1-(5-Nitro-2-furyl)-2-phenylethylene (16a). A mixture of 0.5 g (0.003 mol) of 2, 0.35 g (0.0033 mol) of benzaldehyde, 0.86 g (0.0033 mol) of triphenylphosphine, and 15 mg of cuprous chloride in 30 m*l* of tetrahydrofuran was refluxed for 20 hr. The solvent was then removed under reduced pressure to give a brownish, sticky residue which was dissolved in benzene and chromatographed on a silica-gel column, using benzene as the eluent. The removal of the solvent from the eluate afforded yellow crystals, which were then recrystallized from ethanol to give 0.26 g (36%) of 16a as yellow needles, mp 109—110°C (lit.[29] 111—112°C): NMR ($CDCl_3$) τ 2.68 and 3.48 (each 1H, d, J=3.8 cps, nitrofuran-ring protons), 2.56—2.64 (5H, m, phenyl protons), 2.67 and 3.10 (each 1H, d, J=16.5 cps, olefinic protons).[30]

1-(5-Nitro-2-furyl)-4-phenylbutadiene (16b). A mixture of 0.538 g (0.0035 mol) of 2, 1.0 g (0.0076 mol) of cinnamaldehyde, 0.925 g (0.0035 mol) of

27) K. Kawabe, T. Suzuki and M. Iguchi, *Yakugaku Zasshi (J. Pharm. Soc. Japan)*, **80**, 62 (1960).

*1 Thin-layer Chromatography.

28) The smaller value of nitrogen analysis might be explained by the facile decomposition of 8, even at room temperature; the structural elucidation of this compound was done mainly on the basis of the spectral data.

29) I. Hirao and Y. Kitamura, *Nippon Kagaku Zasshi (J. Chem. Soc. Japan, Pure Chem. Sect.)*, **85**, 506 (1964).

30) This coupling constant shows a *trans*-configuration of the olefin protons for 16a, as expected from the four-centered transition state, keeping bulky phenyl and nitrofuran rings in a *trans*-configuration, as has been shown in 15.

triphenylphosphine, and 16 mg of cuprous chloride in 30 m*l* of tetrahydrofuran was refluxed for 40 hr. After the removal of the solvent, a brownish residue was chromatographed on a silica-gel column, using benzene as the eluent. The eluant was condensed to give yellowish-brown crystals, which were then recrystallized from ethanol to give 0.152 g (18%) of 16b as brownish-yellow needles, mp 137—139°C: λ_{max}^{EtOH} 228 mμ (ε 14100), 300 (24300) and 410 (29300); ν(KBr) 1612, 1593, 1560, 1517, 1506, 1390, 1355, 1246, 1174, 1070 and 809 cm^{-1}; NMR ($CDCl_3$) τ 2.39—3.39 (9H, m, phenyl protons and three olefinic protons), 3.52 (1 H, d, J=3.8 cps, C-3-H) and 3.60 (1 H, d, J=15 cps, C-1-H).

Found: C, 69.40; H, 4.42; N, 5.68%. Calcd for $C_{14}H_{11}O_3N$: C, 69.70; H, 4.59; N, 5.80%.

1-(5-Nitro-2-furyl)-2-furylethylene (16c). A mixture of 0.502 g (0.0033 mol) of 2, 0.312 g (0.0033 mol) of furfural, 0.86 g (0.0033 mol) of triphenylphosphine, and 20 mg of cuprous chloride in 30 m*l* of tetrahydrofuran was refluxed for 20 hr. The reaction mixture was then worked up as above to give 55 mg (10%) of 16 c as reddish-brown prisms, mp 94—96°C (from ethanol): λ_{max}^{EtOH} 208 mμ (ε 12300), 235 (8150), 294 (17600) and 409 (23400); ν(KBr) 1625, 1587, 1554, 1516, 1492, 1395, 1354, 1240, 1020 and 804 cm^{-1}.

Found: C, 58.37; H, 3.49; N, 6.39%. Calcd for $C_{10}H_7O_4N_2$: C, 58.54; H, 3.44; N, 6.83%.

3-(5 - Nitro - 2 - furyl) acrolein Triphenylphosphazine (17). To a solution of 0.22 g (0.00084 mol) of triphenylphosphine in 5 m*l* of ether, a solution of 0.156 g (0.00087 mol) of 4 in 20 m*l* of ether was added. After standing for 1 hr at room temperature, the mixture was concentrated to a volume of about 10 m*l*, thus giving red prisms which were collected to give 0.268 g (72.5%) of 17 with a mp of 144—146°C: λ_{max}^{EtOH} 219 mμ (ε 33500); 314 (19900), and 443 (24500); ν(KBr) 1610, 1592, 1562, 1537, 1504, 1487, 1350, 1254, 1024, 970, 812 and 721 cm^{-1}.

Found: C, 64.72; H, 4.29; N, 8.72%. Calcd for $C_{25}H_{22}O_4N_3P$: C, 65.30; H, 4.83; N, 9.14%.

3-(5-Nitro-2-furyl)acrolein Azine (18). A solution of 61 mg (0.00014 mol) of 17 in 10 m*l* of acetone was warmed at 50—60°C for several hours. After cooling, the precipitated solid was collected to give 12 mg (52%) of the azine as yellow powders, mp 226—228°C (dec.) (lit.[18b] mp 227—228°C (dec.)).

The authors wish to express their thanks to the Ueno Pharmaceutical Co. for kindly supplying the nitrofurfural and to the Dainippon Pharmaceutical Co. for the NMR measurements. The microanalyses were done by Mr. Akiho Ishihara at their laboratories; to him especially the authors are much obliged.

BULLETIN OF THE CHEMICAL SOCIETY OF JAPAN VOL. 41 1664—1668 (1968)

Photoreduction of Azoxybenzene to Azobenzene

Rikuhei TANIKAGA

Department of Chemistry, Faculty of Science, Kyoto University, Sakyo-ku, Kyoto

(Received December 26, 1967)

The photochemical reduction of azoxybenzene to azobenzene has been investigated. The direct irradiation of azoxybenzene leads to a rearrangement to 2-hydroxyazobenzene and to *cis-trans* isomerization, whereas the sensitized irradiation leads to a reduction to azobenzene in the presence of a sensitizer with a triplet excitation energy greater than *ca.* 62 kcal/mol. 2-Hydroxyazobenzene and *cis*-azoxybenzene seem to be formed from the excited singlet state of azoxybenzene, and azobenzene, from the excited triplet state. Even without a sensitizer, the irradiation of benzo[*c*]cinnoline *N*-oxide, which is incapable of undergoing rearrangement or isomerization, brings about a photochemical reduction, which is affected by a sensitizer or a quencher, and also by the hydrogen-donating ability of the solvent used (isopropanol>ethanol>cumene>toluene). Acetone is yielded when isopropanol is used as the solvent. On the basis of these results, a mechanism in which benzo[*c*]cinnoline is formed from the excited triplet state of benzo[*c*]cinnoline *N*-oxide, followed by hydrogen abstraction from a solvent, is proposed.

The photochemical rearrangement of azoxybenzene to 2-hydroxyazobenzene[1-4] is assumed to start from a $\pi \rightarrow \pi^*$ excitation, because the emission of the lines above 300 mμ in a mercury arc lamp causes the rearrangement, but it has not been established whether or not an excited triplet state

1) H. M. Knipscheer, *Rec. trav. chim.*, **22**, 14 (1903).
2) G. M. Badger and R. G. Buttery, *J. Chem. Soc.*, **1954**, 2243.
3) M. M. Shemyakin, V. J. Maimind and B. K. Vaichunaite, *Chem. Ind.*, **1958**, 755.
4) S. Oae, T. Fukumoto and M. Yamagami, This Bulletin, **34**, 1873 (1961).

intermediate is involved. In order to clarify this situation, we irradiated a solution of azoxybenzene in the presence of benzophenone, we thus found the reaction to take a completely different course, *i. e.*, azobenzene was formed as the major product.[5] This photoreduction seems to be similar to the deoxygenation from an excited triplet state of pyridine *N*-oxide or of picoline *N*-oxide in the gas-phase photolysis.[6]

A principal objective of this work is to discuss the photochemical reduction of azoxybenzene to azobenzene, and to give some suggestions regarding the photochemical oxygen migration and the *cis-trans* isomerization.

It is also interesting to note that the photochemical deoxygenation process of a compound containing a N→O bond may be involved in the photoreduction of nitrosobenzene to azoxybenzene.[7]

Results and Discussion

Photoreduction of Azoxybenzene (I) to Azobenzene (II). The irradiation of a degassed ethanolic solution of *trans*-azoxybenzene (I) in a quartz or Pyrex tube with a high-pressure mercury arc lamp afforded 2-hydroxyazobenzene (III) and *cis*-azoxybenzene (IV), but no azobenzene (II). On the other hand, II was obtained as the major product by the photolysis of a degassed solution of I, containing benzophenone as a sensitizer, in a quartz tube. The results of the irradiation of I in a quartz tube are given in Table 1.

Scarcely any II was formed in the presence of oxygen, presumably because the excited triplet state, T_1, of I was quenched by oxygen. Although it is desirable to use a $n\rightarrow\pi^*$ transition (λ_{max}^{EtOH} = 333 mμ, ε=160) of benzophenone in any discussion of its photosensitization, the $n\rightarrow\pi^*$ excitation is not expected to occur in the presence of I because of the strong absorption of I (λ_{max}^{EtOH}=323 mμ, ε=14700). In fact, the photosensitization did not occur when a Pyrex filter was used. Thus, the photosensitization of benzophenone shown in Table 1 may result from its $\pi\rightarrow\pi^*$ transition (λ_{max}^{EtOH} =253 mμ, ε=18000).[8] A possible mechanism for the formation of II with a wavelength of about 250 mμ is as follows:

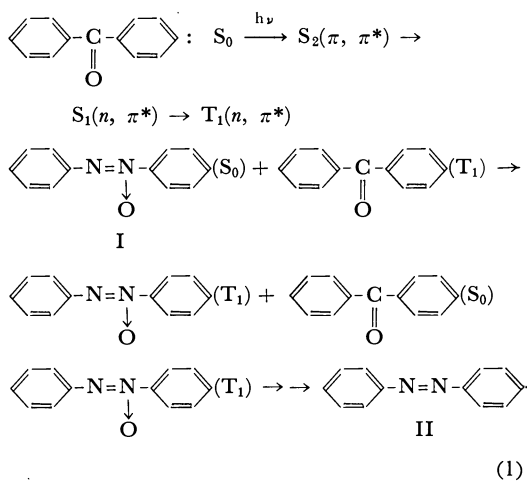

(1)

The irradiation of I without benzophenone never afforded II. This result indicates that III and IV may be formed directly from the excited singlet state, S_1, of I, but not through the excited triplet state, T_1.[9] The formation of III and IV even in the presence of benzophenone may be due to the direct photoreaction of I with a wavelength longer than 300 mμ, as is shown in Eq. (2):

$$I(S_0) \xrightarrow{h\nu} I(S_1(\pi, \pi^*)) \rightarrow\rightarrow III \qquad (2)$$

Table 1 shows that a side reaction took place from the sensitized photolysis. The by-products have not yet been identified, but hydrazobenzene and aniline derivatives may be formed by the reduction of II and III, because the azo bridge is able to abstract hydrogen atoms or free radicals upon

Table 1. Irradiation of azoxybenzene (10^{-2} M) at 25.0±0.1°C

Irradiation time (min)	30	30	30	30	120
Solvent	EtOH	EtOH	EtOH	EtOH	*n*-Hexane
Concentration of benzophenone (M)	0	10^{-3}	10^{-2}	10^{-2}	10^{-2}
Quencher	None*	None	None	O_2	None
Yields of products (%)					
Azoxybenzene (I, IV)	65	50	40	64	79
Azobenzene (II)	0	4	21	Trace	5
2-Hydroxyazobenzene (III)	24	19	9	23	15

* None means a degassed state.

5) R. Tanikaga, K. Maruyama, R. Goto and A. Kaji, *Tetrahedron Letters*, **1966**, 5925 .
6) N. Hata, This Bulletin, **34**, 1440, 1444 (1961); N. Hata and I. Tanaka, *J. Chem. Phys.*, **36**, 2070 (1962).
7) E. Bamberger, *Ber.*, **35**, 1606 (1902).
8) A process $S_2(\pi, \pi^*)\rightarrow S_1(n, \pi^*)$ of benzophenone is known to be efficient. N. J. Turro, "Molecular Photochemistry," W. A. Benjamin, Inc., New York (1965), p. 78.
9) A detailed account of this problem will be the subject of a forthcoming publication.

TABLE 2. IRRADIATION OF BENZO[*c*]CINNOLINE *N*-OXIDE (10^{-2} M) AT 25.0±0.1°C

Irradiation time (hr)	1	1	1	3	3
Filter	Q	Q	Q	P	P
Concentration of benzophenone (M)	0	0	10^{-2}	0	0
Quencher	None*	O_2	None	None	O_2
Yields of products (%)					
Benzo[*c*]cinnoline *N*-oxide (V)	63	97	27	25	93
Benzo[*c*]cinnoline (VI)	31	3	49	53	5

* None means a degassed state. P: Pyrex, Q: Quartz.

TABLE 3. IRRADIATION OF BENZO[*c*]CINNOLINE *N*-OXIDE (10^{-2} M) AT 25.0±0.1°C

Solvent	*iso*-PrOH	EtOH	Cumene	Toluene	Anisole	CCl_4
Yields of products (%)						
V	26	25	68	70	75	90
VI	63	53	30	14	18	0

irradiation.[10-12] At any rate, irradiation for many hours is not desirable for the investigation of the photoreduction of I to II.

I could be photochemically reduced to II with the ketones other than benzophenone. The following ketones were efficient photosensitizers: acetophenone (triplet excitation energy $E_{T_1}=74$ kcal/mol[13]), benzaldehyde (72), benzophenone (69), thioxanthone (65), phenylglyoxal (63), and anthraquinone (62). On the other hand, the following ketones were not efficient: flavone (62), Michler's ketone (61), 2-acetonaphthone (59), biacetyl (55), benzil (54), and fluorenone (53). From these results, the T_1 state of I is assumed to be about 62 kcal/mol.

In order to discuss the solvent effect on the photoreduction of I, ethanol and *n*-hexane were used as solvents transparent above 210 mμ. Since the sensitized photoreduction is derived from a $\pi\rightarrow\pi^*$ transition of benzophenone, it is essential to use such a solvent as ethanol or *n*-hexane without any absorption about 250 mμ. Reduction was easier in ethanol than in *n*-hexane, as is shown in Table 1, but it cannot be determined which stage of Eq. (1) is affected by a solvent. Therefore, for a more detailed discussion it was desirable to irradiate an azoxybenzene derivative with a high efficiency for intersystem crossing without a sensitizer. One possibility was to use an azoxybenzene derivative containing a keto group. Therefore, a degassed solution of 4,4'-diacetylazoxybenzene or 4,4'-dibenzoylazoxybenzene in ethanol was irradiated. However, no azobenzene derivative was obtained. A heavy-atom effect was also expected to promote intersystem crossing. The irradiation of a degassed solution of 4,4'-dichloroazoxybenzene or 4,4'-dibromoazoxybenzene never led to reduction. Azobenzene was not formed from the photolysis of I in such a solvent as methylene chloride or methylene bromide containing heavy atoms. Interestingly, I thus contrasts with pyridine *N*-oxide, which is reduced to pyridine through an excited triplet state in methylene chloride or *n*-propyl bromide as a result of a heavy-atom effect.[14]

When a solution of benzo[*c*]cinnoline *N*-oxide (V), incapable of undergoing *cis-trans* isomerization nor oxygen migration, was directly irradiated, V was found to lead to a photoreduction to benzo[*c*]cinnoline (VI). Therefore, V can be chosen as a model compound in consideration of the solvent effect on the photoreduction of I to II.

Photoreduction of Benzo[*c*]cinnoline *N*-Oxide (V) to Benzo[*c*]cinnoline (VI). The results of the photolysis of a solution of benzo[*c*]cinnoline *N*-oxide (V) in ethanol ($\lambda_{max}=332$ mμ, $\varepsilon=8700$) are given in Table 2.

The effect of oxygen and benzophenone can be explained if benzo[*c*]cinnoline (VI) is assumed to proceed *via* an excited triplet state of V. Moreover, the identification of the triplet state as a reactive intermediate is consistent with the quenching effect of 1-chloronaphthalene in the irradiation of an ethanolic solution of V with a wavelength longer than 350 mμ. A light longer than 300 mμ was efficient for photoreduction, but it cannot been determined what excitation is the first stage of the reaction, because no electronic spectrum of V has yet been assigned.

The results of the photolysis of degassed solutions of V in various solvents for 3 hr with a

10) J. K. S. Wan, L. D. Hess and J. N. Pitts, Jr., *J. Am. Chem. Soc.*, **86**, 2069 (1964).
11) S. Hashimoto, H. Fujii and J. Sunamoto, Preprints for the 18 th Annual Meeting of the Chemical Society of Japan (1965), p. 422; S. Hashimoto, J. Sunamoto and H. Fujii, *Kogyo Kagaku Zasshi (J. Chem. Soc. Japan, Ind. Chem. Sect.)*, **70**, 699 (1967).
12) D. C. Neckers, private communication.
13) The E_{T_1} values used here are according to a table in Ref. 8, p. 132.
14) N. Hata, Preprints for the 20 th Annual Meeting of the Chemical Society of Japan (1967), Vol. 1, p. 483.

Pyrex filter are given in Table 3.

Table 3 shows that the reduction of V was promoted and that a side reaction was suppressed in a solvent with a great hydrogen-donating ability. Besides, V was similar to benzophenone in its competitive hydrogen abstraction reaction, *i. e.*, isopropanol : cumene : toluene = 9.3 : 3.4 : 1.0.[15] The importance of hydrogen abstraction was implied by the fact that no VI was yielded upon the irradiation of V in carbon tetrachloride or in a solid phase; moreover, it was confirmed by the formation of acetone and water from the photolysis of V in isopropanol. Since the yields of acetone and water corresponded roughly with the amount of V reacted, VI may be produced by the following reaction sequence:

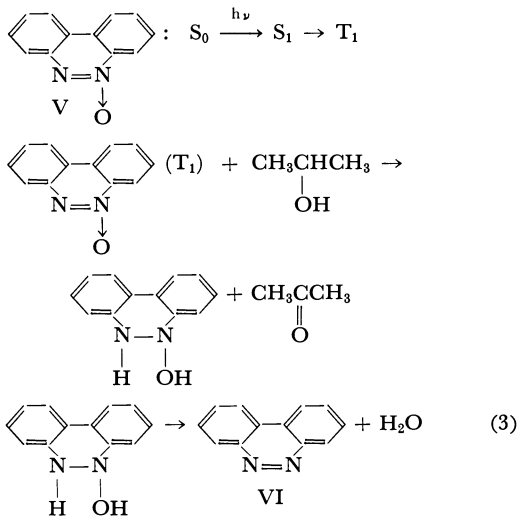

The hydrogen abstraction is a rate-determining process in the photoreduction of V to VI, although an intersystem-crossing process controls the reactivity of the photoreduction of pyridine *N*-oxide.[14] The mechanism shown in Eq. (3) is, interestingly, similar to that for I in reduction with an alkali metal:[16]

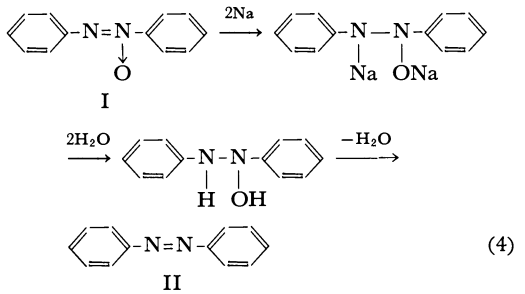

From these results, the reduction process from the excited triplet state of I to II may also be supposed to be followed by hydrogen abstraction.

The photochemical deoxygenation of a compound containing a N→O bond *via* an excited triplet state seems important in the photoreduction of dimeric nitrosobenzene to azoxybenzene.[7] This problem is currently being investigated.

Experimental

Materials. Azoxybenzene (I) was prepared by the reduction of nitrobenzene with sodium hydroxide in methanol, and was then recrystallized from methanol (mp 35.5°C).[17] Benzo[*c*]cinnoline *N*-oxide (V) was prepared by the reduction of 2,2'-dinitrodiphenyl with sodium sulfide in ethanol, and was then recrystallized from ethanol-water (mp 139.5°C).[18]

Photolysis of Azoxybenzene (I). The irradiation source was a 100 W, high-pressure mercury arc lamp fitted with a water-cooled immersion well (Eikosha Halos PIH 100). The degassed or oxygen-saturated solution (3 m*l*) of I was irradiated in a quartz tube (inner diameter 13 mm) directly attached to the lamp, and was thermostated at 25.0±0.1°C. The other reaction conditions, such as the solvent used, the irradiation time, and the concentration of benzophenone, were as shown in Table 1. After the irradiation, each component was separated by thin-layer chromatography (TLC) on silica gel (Merck silica gel G according to Stahl; an *n*-hexane - benzene mixture (2 : 1 in volume)) and was identified by the comparison of the infrared and ultraviolet spectral data, the melting point, and the R_f value with those of an authentic sample. The yield of the product was determined as follows. After the irradiation, the solution was left at *ca.* 40°C for one day to transform the *cis*-isomer into the more thermally-stable *trans*-isomer. 4,4'-Dichloro-2-hydroxyazobenzene (VII) was then added as an internal standard. Each component was then separated by TLC on silica gel and extracted with chloroform. The yield was determined from the intensity of the maximum absorption of the extract in an electronic spectrum, whose extinction coefficient had been previously determined by means of an authentic sample. The extinction coefficients used in this work were: I$\varepsilon_{326m\mu}$=14800, II$\varepsilon_{319m\mu}$=18500, III$\varepsilon_{325m\mu}$=18000 and VII$\varepsilon_{339m\mu}$=19500 (in chloroform).

Photolysis of Benzo[*c*]cinnoline *N*-Oxide (V). A solution (2 m*l*) of V was irradiated in a quartz or Pyrex tube (inner diameter : 13 mm) with a 100-W, high-pressure mercury lamp at 25.0±0.1°C. The other reaction conditions were as shown in Table 2 or 3. The products were separated by TLC (silica gel, chloroform), and their yields were determined as has been described above. 1-Benzeneazo-2-naphthol (VIII) was used as an internal standard. The extinction coefficients used in this work were: V$\varepsilon_{333m\mu}$= 8700, VI$\varepsilon_{309m\mu}$ = 8600 and VIII$\varepsilon_{317m\mu}$ = 7470 (in chloroform).

Photolysis of V in Isopropanol. A degassed solution (5 m*l*) of V (5×10^{-2} M) in isopropanol (purified by drying over magnsium ribbon and by fractional

15) C. Walling and M. J. Gibian, *J. Am. Chem. Soc.*, **86**, 3902 (1964).
16) T. Kauffmann, S. M. Hage and G. Ruckelshauss, *Chem. Ber.*, **100**, 1235 (1967).
17) A. Lachman, *J. Am. Chem. Soc.*, **24**, 1180 (1902).
18) F. Ullmann and P. Dieterle, *Ber.*, **37**, 24 (1904).

distillation) was irradiated in a Pyrex tube for 30 hr as has been described above. The yields of V and VI were then determined by TLC on silica gel, while that of acetone was determined by gas chromatography (Yanagimoto GCG-5DH, polyethylene glycol 20 M 4.5 m, 80°C, He). The presence of water was established by titration with a Karl-Fischer reagent (Mitsubishi Chemical Industries, Ltd.; Karl-Fischer Reagent SS). The yields of the products were as follows: V, 37%; VI, 56%; acetone, 70%, and water, 75—85%.

The author wishes to thank Professor Ryozo Goto for his helpful discussions and encouragement throughout the course of this work. He is also indebted to Professors Aritsune Kaji and Kazuhiro Maruyama for their valuable discussions.

BULLETIN OF THE CHEMICAL SOCIETY OF JAPAN VOL. 41 1668—1671 (1968)

Cationic Polymerization of Formaldehyde in Liquid Carbon Dioxide. III. Thermal Stabilization of the Resulting Polymer*1

Hisao YOKOTA*2 and Masatsune KONDO*2

Takarazuka Radiation Laboratory, Sumitomo Atomic Energy Industries Ltd., Takarazuka

and Tsutomu KAGIYA and Kenichi FUKUI

Faculty of Engineering, Kyoto University, Sakyo-ku, Kyoto

(Received December 27, 1967)

We investigated the acetylation of the endgroups of the polymer chain resulting from the polymerization of formaldehyde in liquid carbon dioxide in the presence of acetic anhydride. The thermal stability and the toughness of the resulting polymer were examined. All of the endgroups of polymer chains were satisfactorily acetylated by means of heating, between 140 and 150°C, the solid polymer, which was separated by discharging the unreacted monomer and carbon dioxide after polymerization. The acetic anhydride which was added in the beginning of the polymerization at a concentration of 5 mol% per monomer, was sufficient to stabilize the polymer thermally. On the acetylating of the polymer, the presence of air or acetic acid in the amount used to initiate the polymerization had no effect on the properties of the acetylated polymer. A simplified purification procedure for the acetylated polymer was presented.

Polyoxymethylene, ended with hemiformal groups, can be subjected to degradation by several processes; stepwise thermal depolymerization from the chain ends, autoxidative degradation leading to chain scission (observed at temperatures above 170°C), acidolytic scission of the acetal linkages of the main chain, and thermal chain scission at temperatures higher than 270°C.[1,2] In order to stabilize the polyoxymethylene by means of preventing the stepwise thermal depolymerization, acetylation,[3-5] etherification,[2,6,7] and other methods have been proposed. However, these stabilizing treatments must be carried out in separated processes. Wagner *et al.* have proposed a process of polymerizing formaldehyde in acetic anhydride as a solvent, followed with heating, *in situ*, the resulting polymer.[8] The acetic anhydride which is used in this process must, however, be drastically purified in order to remove the acid present in it.

The authors have previously reported on a cationic polymerization of formaldehyde in liquid carbon dioxide to produce high-molecular-weight polyoxymethylene.[9,10] The present work was

*1 This paper was first presented at the 15th Annual Meeting of the Society of Polymer Science, Japan, held in Nagoya, May, 1966.

*2 Present address; Takarazuka Laboratory, Sumitomo Chemical Co., Ltd., Takarazuka, Japan.

1) W. Kern and H. Cherdron, *Makromol. Chem.*, **40**, 101 (1960).

2) W. Kern, H. Cherdron and V. Jaacks, *Angew. Chem.*, **73**, 177 (1961).

3) H. Staudinger, R. Signer, H. Johner, M. Luthy, W. Kern, D. Russidis and O. Schweitzer, *Ann.*, **474**, 145 (1929).

4) C. E. Schweitzer, R. N. MacDonald and J. O. Punderson, *J. Appl. Polymer Sci.*, **1**, 158 (1959).

5) J. F. Walker, "Formaldehyde," 3rd. ed., Reinhold Publishing Co., New York (1964), pp. 188—189.

6) E. I. du Pont de Nemours Co., Brit. Pat. 770717 (1957).

7) E. Kuehn, G. Louis, E. Penning, R. Senninger and H. Wilhelm, Ger. Pat. 1091750 (1960).

8) K. Wagner and H. Kritzler, Ger. Pat. 1158709 (1963).

9) H. Yokota, M. Kondo, T. Kagiya and K. Fukui, *J. Polymer Sci., A-1*, **6**, 425 (1968).

10) H. Yokota, M. Kondo, T. Kagiya and K. Fukui, *ibid., A-1*, **6**, 435 (1968).

carried out in order to simplify the stabilization process by means of acetylating the polymer by acetic anhydride, which had already been added to the system at the beginning of the polymerization of formaldehyde in liquid carbon dioxide.

Experimental

Materials. The formaldehyde monomer was prepared as has been previously described.[9] The acetic anhydride was purified only by distillation at normal pressure, so that it usually contained acetic acid in a concentration slightly above 1 wt%. The amount of acetic acid used as a catalyst was, therefore, determined with due regard to this concentration. In the case of adding a large quantity of acetic anhydride, it was necessary to use extremely-purified acetic anhydride so that excess acetic acid did not mix in the polymerization system. The acetic anhydride was, therefore, purified from acetic acid by reacting it with carbodiimide, thus producing a non-volatile compound.[11] That is, acetic anhydride was mixed with dicyclohexylcarbodiimide, kept at 100°C for one hours and then distilled (bp 51.7°C/60 mmHg). The concentration of acetic acid in the acetic anhydride thus prepared was found to be less than 0.1 wt%.

Procedures for Polymerization and Stabilization. The polymerization was carried out in the same manner as has been described in the previous papers,[9,10] except that the reaction temperature was not carefully controlled.

After the unreacted monomer and carbon dioxide has been discharged, the resulting polymer was taken out from the the autoclave in an atmosphere of carbon dioxide or air, and transferred into a glass tube which was afterwards sealed. Then, the sample was held in an oil bath kept at a fixed temperature. The polymer which resulted from the polymerization or which was obtained after heat treatment was washed with cooled ethyl ether and with acetone, and dried *in vacuo*.

In the some experiments, the polymer was heated as it was in the autoclave after the inner pressure had been reduced. Then, the polymer was purified by removing the unreacted acetic anhydride and other compounds only by means of evacuating the autoclave under heating.

Measurements of the Properties of the Resulting Polymer. The degree of polymerization was determined by viscosity measurements in a manner which has previously been described.[9]

The thermal stability of the resulting polymer was determined by the continuous measurement of the thermal degradation in a nitrogen atmosphere, which was kept constant at 222°C in a vapor bath of boiling methyl salicylate; it was represented as a first-order reaction rate constant. When a plot of the log of the weight per cent under composed versus the time gave two straight lines, the rate constants, k_{222}, calculated from each straight line are listed together with the range of decomposition (noted in parentheses).

The acetyl and hydroxyl groups of the resulting polymer were determined by means of a study of the infrared spectrum, which was measured with a polymer film prepared by cold pressing. The degree of acetylation was calculated as the molar ratio of the acetyl endgroup to the total endgroup, which was estimated by the following equation;

$$\text{Degree of acetylation} = \frac{D_{C=O}}{\alpha D_{OH} + D_{C=O}} \quad (1)$$

Here, $D_{C=O}$ and D_{OH} are the absorption intensities of the carbonyl group at 1750 cm^{-1} and of the hydroxyl group at 3500 cm^{-1} respectively; they were measured on the infrared spectrum of a polymer film. An α factor, which is a ratio of the molar extinction coefficient of the two bands, was experimentally determined on six samples; it was 2.46 ± 0.05.

The degree of toughness was measured by the folding endurance test described below. The polymer, which was mixed with 1% portions of both 4,4'-butylidene-bis-(6-tertiary butyl metacresol) and polyamide, was heated under compression to mold a film 120 μ thick. The folding endurance test was carried out using an MIT folding endurance tester according to ASTM D 643—43. The number of creasing cycles until the film breaks off is referred to as the "degree of toughness." The value indicated in the table is the mean value for five runs.

Result and Discussion

Influence of Acetic Anhydride Concentration. In order to establish the effect of the acetic anhydride concentration on the acetylation of the resulting polymer in the stabilizing process, the monomer was polymerized in liquid carbon dioxide at 30°C, using acetic acid as the catalyst. After polymerization, a part of the unwashed resulting polymer was transferred into a sealed tube in an atmosphere of carbon dioxide and then heated at 140°C. The results are shown in Table 1.

It was found that the polymer yield in the polymerization was reduced by increasing the concentration of acetic anhydride, and that a part of the resulting polymer had already been acetylated. Acetic anhydride at a concentration above 5 mol% was also found to be sufficient to acetylate all of the endgroups of the polymer chain. Moreover, the film which was molded from the polymer mixed with the antioxidants exhibited satisfactory degree of toughness.

Influences of Heating Temperature and Time. The effects of the temperature and the time in the stabilization process on the properties of the polymer were studied by an experiment in which the polymer produced in the polymerization in the presence of acetic anhydride (5 mol%) was divided into sealed tubes in an atmosphere of carbon dioxide and then heated. The results are shown in Table 2. The heating temperature at 120°C was too low to perform sufficient acetylation, whereas the decomposition of the polymer was appreciable at 160°C. As a result, the optimum operation temperature in the stabilization process was in a range of 140 to 150°C, and a reacton time of more than 2 hr was not required.

11) N. S. Smart, G. T. Young and M. W. Williams, *J. Chem. Soc.*, **1960**, 3902.

TABLE 1. INFLUENCE OF ACETIC ANHYDRIDE CONCENTRATION ON ACETYLATION OF THE RESULTING POLYMER

I) Polymerization[a)]

Run No.	Acetic anhydride mol%/monomer	Polymer yield wt%	Degree of polym.	k_{222} %/min	Degree of acetylation mol%
1-1	0.5	76.8	1860	4.21	18
2	1.0	56.5	1680	5.2 (0—34%) 2.6 (34—%)	17
3	5.0	53.4	1580	4.99(0—27%) 1.48(27—%)	27
4	50.0	51.7	1520	6.60(0—39%) 0.86(39—%)	21

a) monomer, 6 g, 60 wt% in CO_2; acetic acid, 0.1 mol%/monomer; temp., 30°C.; time, 2 hr.

II) Acetylation[b)]

Run No.	Acetic anhydride per polymer end, mole ratio	Recovery yield wt%	Degree of polym.	k_{222} %/min	Degree of acetylation, mol%	Degree of toughness
1-1	6.0	97	1910	1.92(0—23%) 0.54(23—%)	77	—
2	14.9	96	1720	0.76(0—9%) 0.32(9—%)	95	—
3	74	97	1540	0.27	100	2.5×10^5
4	735	97	1580	0.21	100	2.0×10^5

b) heating temp., 150°C.; time, 1 hr.

TABLE 2. INFLUENCE OF TEMPERATURE AND REACTION TIME ON ACETYLATION OF THE RESULTING POLYMER[a)]

Run No.	Time hr	Recovery yield wt%	Degree of polym.	k_{222} %/min	Degree of acetylation, mol%
		Temperature, 120°C			
2-1	1	90	1680	3.2 (0—51%) 0.76(51—%)	71
2	2	88	1730	1.8 (0—16%) 0.55(16—%)	88
3	5	85	1650	0.52(0—11%) 0.36(11—%)	99
		Temperature, 140°C			
4	1	87	1700	0.51(0—6%) 0.30(6—%)	99
5	2	86	1670	0.28	99
6	5	82	1550	0.25	100
		Temperature, 160°C			
7	1	79	1650	0.27	99
8	2	75	1560	0.34	100
9	5	71	1450	0.26	100

a) Polymerization:
monomer, 6 g, 60 wt% in CO_2; acetic acid, 0.1 mol%/monomer; acetic anhydride, 5 mol %/monomer; temp., 30°C; time, 2 hr.
Result:
polymer yield, 56.5%; degree of polym., 1710; k_{222}, 3.1%/min; degree of acetylation, 23.8 mol%.
The resulting polymer was divided in the ampules of 30 ml.

TABLE 3. INFLUENCE OF THE ATMOSPHERE OF CARBON DIOXIDE AND AIR

I) Polymerization:
monomer; 6 g, 60 wt% in CO_2.
acetic anhydride; 5 mol%/monomer.
acetic acid; 0.1 mol%/monomer.
temperature; 30°C.
time; 2 hr.

Result:
polymer yield; 61.5 wt%.
degree of polym.; 1780.
k_{222}; 3.7 %/min.

II) Acetylation[a)]

Degree of polym.	k_{222} %/min	Degree of acetylation, mol%
	in carbon dioxide	
1740	0.51(0—6%) 0.32(6—%)	99
1560	0.32	100
	in air	
1550	0.55(0—5%) 0.30(5—%)	99
1730	0.76(0—11%) 0.32(11—%)	98

a) temp., 140°C; time, 2 hr.

Influence of Atmosphere. The crude polymer resulting from the polymerization was divided in an atmosphere of carbon dioxide or dry air into sealed tubes and heated 140°C for 1 hr. Table 3 shows these results. The presence of air caused the thermal stability of the resulting polymer to deteriorate somewhat, but this deterioration was not serious.

Influence of Acetic Acid. The polymerization of formaldehyde in liquid carbon dioxide is initiated by carboxylic acid as a catalyst, as has been described previously in this series. On the other hand, the acidolytic scission of acetal linkages of the main chain by carboxylic acid has been reported.[1] Therefore, the influence of acetic acid, as a sample of carboxylic acid, on the degree of polymerization and thermal stability of the resulting polymer in the stabilization process was investigated. The results are shown in Table 4. It was found that acetic acid reduced the thermal stability in a part of the resulting polymer, but 0.1 mol% per monomer, that is, the amount which was used as a catalyst, had no effect.

TABLE 4. INFLUENCE OF ACETIC ACID ON ACETYLATION

I) Polymerization[a]

Run No.	Acetic acid mol%/monomer	Polymer yield wt%	Degree of polym.	Degree of acetylation mol%
4-1	0.1	58.6	1210	27
2	0.1	57.8	1250	24
3	0.2	68.2	1070	21
4	1.0	74.1	640	26

a) monomer, 6 g, 60 wt% in CO_2; temp., 30°C; time, 2 hr; acetic anhydride, 5 mol%/monomer.

II) Acetylation[b]

Run No.	Recovery yield wt%	Degree of polym.	k_{222} %/min	Degree of acetylation mol%
4-1	89	1200	0.34	100
2	86	1140	0.25	100
3	83	1020	0.59(0—6%) 0.14(6—%)	99
4	62	660	1.53(0—13%) 0.35(13—%)	92

b) Crude polymer was divided in the atmosphere of carbon dioxide. temp., 140°C; time, 2 hr.

Procedure of Purifying the Resulting Polymer. After the unreacted monomer and carbon dioxide had been discharged, the polymer was a solid material and was wet with acetic anhydride. In addition to the polymer, the materials which exist in the stabilization process are acetic anhydride, carboxylic acid, carbon dioxide, and by-products which are volatile at the operating temperature. Therefore, these compounds can easily be removed by evacuating the reaction vessel under heating. The properties of the polymer purified by such a simple procedure were studied.

The polymerization was carried out under the condition shown in Table 5. After the autoclave had been heated at 150°C for 1 hour and then the inner pressure been reduced, the reaction vessel was evacuated under heating. The polymer, which was not washed or dried, exhibited satisfactory properties, as Table 5 shows. This result permitted the purification of the stabilized polymer to be simplified.

TABLE 5. EFFECT OF EVACUATION ON THE PURIFICATION OF THE RESULTING POLYMER

I) Polymerization
monomer, 6 g, 60 wt% in CO_2; acetic acid, 0.1 mol%/monomer; acetic anhydride, 5 mol%/monomer; temp., 30°C; time, 2 hr.

II) Acetylation
After purging out of the unreacted monomer and carbon dioxide, the polymer was heated at 150°C for 1 hr.

III) Results

Evacuation time at 150°C, min	Total polymer yield, wt%	Degree of polym.	k_{222} %/min	Degree of toughness
30	58.2	1680	0.31	24×10^4
60	57.4	1490	0.21	48

BULLETIN OF THE CHEMICAL SOCIETY OF JAPAN VOL. 41 1672—1679 (1968)

Cationic Polymerization of Formaldehyde in Liquid Carbon Dioxide. IV. A Kinetic Study of the Polymerization in the Presence of Acetic Anhydride*1

Hisao YOKOTA*2 and Masatsune KONDO*2

Takarazuka Radiation Laboratory, Sumitomo Atomic Energy Industries Ltd., Takarazuka

and Tsutomu KAGIYA and Kenichi FUKUI

Faculty of Engineering, Kyoto University, Sakyo-ku, Kyoto

(Received December 27, 1967)

The influence of acetic anhydride on the polymerization of formaldehyde, which was carried out by means of initiation with an acidic catalyst in liquid carbon dioxode, was studied at 20 to 40°C. Acetic anhydride decreased the polymer yield and the degree of polymerization of the polymer resulting from the polymerization with acetic acid. Moreover, the over-all rate of polymerization with acetic acid in the presence of acetic anhydride deviated from a first-order equation with respect to the monomer concentration. On the other hand, the polymerization which was initiated by dichloroacetic acid was not affected by the presence of acetic anhydride. On the basis of a kinetical consideration, it can be said that the termination which was proportional to the square of the concentration of the initiating species was caused by the presence of acetic anhydride in the polymerization with acetic acid. The rate constants and the activation energies of the elementary processes were estimated, and a rate equation satisfying the experimental results was presented.

As has been described in previous papers,[1,2] the present authors have already disclosed that formaldehyde monomer which is prepared by the thermal decomposition of α-polyoxymethylene without additional purification polymerizes in liquid carbon dioxide both with and without a carboxylic acid catalyst to give a polymer with a high molecular weight, and that this polymerization follows a cationic mechanism and belongs to a type of successive polymerization with rapid initiation and no termination.

It has also been reported by the present authors[3] that acetic anhydride, which has already been added to the reaction system at the beginning of polymerization, acetylates the endgroups of polyoxymethylene by heating the resulting polymer after discharging the unreacted monomer and carbon dioxide at the end of the polymerization.

The purpose of the present work is to determine quantitatively the effects of acetic anhydride on the elementary steps of the polymerization of formaldehyde in liquid carbon dioxide.

Experimental

The methods of preparing the monomer and the additives, such as acetic acid, and mono-, di- and trichloroacetic acids, and the experimental procedure for the polymerization were the same as have previously been described.[1,2] Acetic anhydride was carefully prepared to remove acetic acid, as has also previously been reported.[3] The acetic anhydride used contained less than 0.1 wt% acetic acid.

The concentration of formaldehyde in the monomer solution was 60 wt%, and the loading density, which was represented as a ratio of the amount of solution fed in to the volume of the reaction vessel used, was 10 g/30 m*l*.

Results and Discussion

Influence of the Addition of Acetic Anhydride on Polymerization with Various Acids. The influence of acetic anhydride on the polymerizations initiated by acetic and dichloroacetic acids studies, as is shown in Table 1. In polymerization with dichloroacetic acid, acetic anhydride had no effects on the polymerization. On the other hand, added acetic anhydride decreased both the polymer yield and the degree of polymerization of the resulting polymer in polymerization with acetic acid.

*1 This paper was first presented at 15th Annual Meeting of the Society of Polymer Science, Japan, held in Nagoya, May, 1966.

*2 Present address; Takarazuka Laboratory, Sumitomo Chemical Co., Ltd., Takarazuka.

1) Part I: H. Yokota, M. Kondo, T. Kagiya and K. Fukui, *J. Polymer Sci., A-1*, **6**, 425 (1968).

2) Part II: H. Yokota, M. Kondo, T. Kagiya and K. Fukui, *ibid., A-1*, **6**, 435 (1968).

3) H. Yokota, M. Kondo, T. Kagiya and K. Dukui, This Bulletin, **41**, 1668 (1968).

Table 1. Influence of the addition of acetic anhydride on the polymerization with various acids

Acid	Acetic anhydride	Polymer yield g	Polymer yield wt%	$\overline{P}_n$
Acetic acid	presence	1.734	28.9	1100
Acetic acid	absence	3.265	54.4	1750
Dichloroacetic acid	presence	4.032	67.2	1750
Dichloroacetic acid	absence	4.052	67.5	1800

monomer solution, 10 g ; $[M]_0 = 20$ mol/l ; $[CH_3COOH] = 0.02$ mol/l ; $[(CH_3CO)_2O] = 1.0$ mol/l ; temperature, 30°C ; time, 30 min ; reaction vessel, 30 ml.

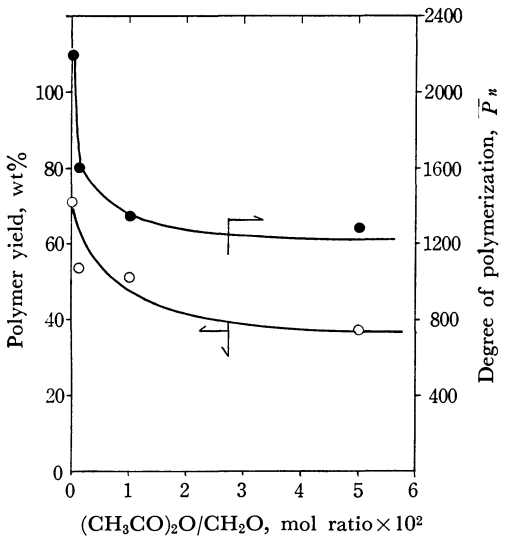

Fig. 1. Effect of acetic anhydride on the polymerization initiated by acetic acid.

Monomer solution, 10 g ; $[M]_0 = 20$ mol/l ; $[CH_3COOH] = 0.02$ mol/l ; temperature, 30°C ; time, 10 min ; reaction vessel, 30 ml.

In order to determine the effect of acetic anhydride, the influence of the amount of acetic anhydride on the polymerization with acetic acid was examined. As Fig. 1 shows, both the polymer yield and the degree of polymerization of the resulting polymer decreased rapidly with an increase in the concentration of acetic anhydride. Moreover, the number of moles of the polymer chain, which was calculated as a ratio of the polymer yield to the degree of polymerization, was almost constant. Because the amount of acetic anhydride added was less than 5 mol% that of the monomer, the results suggest that the decrease in the polymer yield with an increase in the concentration of acetic anhydride is not due to the decrease in the amount of the initiating species or of the monomer concentration, but to the increase in the termination reaction.

Influence of the Addition of Stronger Acids on Polymerization in the Presence of Acetic Anhydride. On polymerization in the absence of acetic anhydride, it has been established[1] that the polymer yield, the number of moles of the polymer chain, and the degree of polymerization of the resulting polymer all increase as the acidity of the acid used is increased. Analogously, the effects of acetic acid and mono-, di-, and tri-chloroacetic acids on polymerization in the presence of acetic anhydride were studied.

Table 2. Influence of various acidic catalyst on the polymerization in the presence of acetic anhydride

Catalyst	pK_a	Polymer yield g	Polymer yield wt%	$\overline{P}_n$	N_p mol ×10^5
Trichloroacetic acid	0.66	3.253	54.2	1200	9.0
Dichloroacetic acid	1.25	2.441	39.0	950	8.2
Monochloroacetic acid	2.87	1.512	25.2	900	5.6
Acetic acid	4.75	0.715	11.9	520	4.5

The experimental condition was the same as described in Table 1, except that the reaction time was 10 min.

The results are presented in Table 2. Here, pK_a and N_p represent the logarithmic value of the dissociation constant of the acid measured in water at 25°C, and the number of moles of the polymer chain (represented as a ratio of the polymer yield to the degree of polymerization), respectively. Results similar to those in the absence of acetic anhydride described previously[1] were obtained in the polymer yield, the degree of polymerization, and the number of moles of the polymer chain.

Using the results listed in Table 2, the logarithmic ratios of the polymer yield (log Y_0/Y) and of the number of moles of the polymer chain (log N_{p_0}/N_p) are plotted against the relative acidity of the catalyst (ΔpK_a) in Fig. 2. Here, Y_0/Y and N_{p_0}/N_p are calculated as the ratio of the polymer yield by trichloroacetic acid to that by another acid, and a similar ratio of the number of moles of the polymer chain, respectively, and ΔpK_a is the difference between the pK_a values of trichloroacetic acid and another acid. It was found that (log Y_0/Y) and (log N_{p_0}/N_p) were proportional to ΔpK_a, and that the ratio of the slopes of these straight lines was about 2. This value was just the same as that calculated in the polymerization in the absence of acetic anhydride which was previously reported.[1] In addition, the degree of polymerization of the resulting polymer also increased proportionally with a decrease in the pK_a value of the acid used. These results agree well with the behavior in the polymerization without acetic anhydride. Hence, it seems that the mechanisms of the initiation and propagation are the same whether acetic anhydride is present or not.

Polymerization with Dichloroacetic Acid. The finding that acetic anhydride did not affect the polymerization with dichloroacetic acid, a stronger acid than acetic acid, was quantitatively confirmed, as Fig. 3 shows. For comparison, the previously-reported date obtained in the polymerization without acetic anhydride[2] are also shown in the same figure.

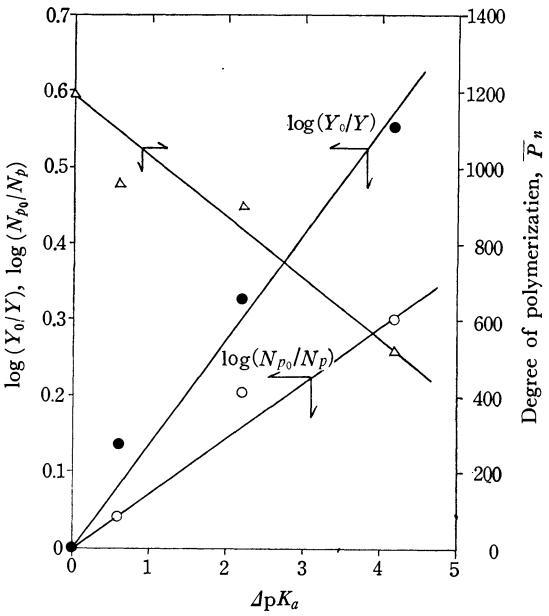

Fig. 2. Effect of acidity on the polymerization in the presence of acetic anhydride.

Monomer solution, 10 g ; $[M]_0=20$ mol/l ; [acid] $=0.02$ mol/l ; $[(CH_3CO)_2O]=1.0$ mol/l ; temperature, 30°C ; time, 10 min ; reaction vessel, 30 ml ; ●, $\log(Y_0/Y)$; ○, $\log(N_{p_0}/N_p)$; △, degree of polymerization.

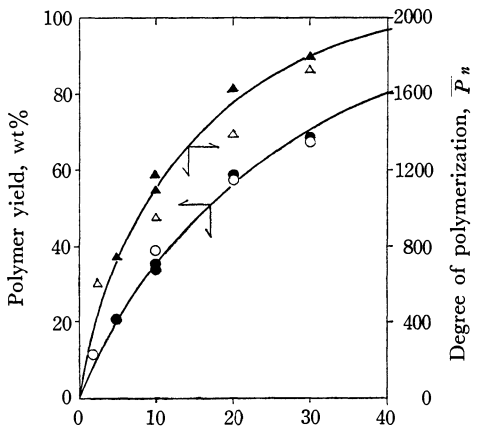

Fig. 3. Effect of the reaction time on the polymerization initiated by dichloroacetic acid.

Monomer solution, 10 g ; $[M]_0 = 20$ mol/l ; $[CHCl_2COOH]=0.02$ mol/l; temperature, 30°C; reaction vessel, 30 ml ; ○, △, in the presence of acetic anhydride of 1.0 mol/l ; ●, ▲, in the absence of acetic anhydride.

The behavior of the polymerization in this case was the same as that without acetic anhydride. It was, therefore, concluded that the polymerization by an acid stronger than acetic acid is not affected by acetic anhydride, and that the rate of polymerization follows a first-order equation with respect to the monomer concentration. Accordingly, the polymerization belongs to a type of successive polymerization with rapid initiation and no termination.

Polymerization with Acetic Acid. As has already been reported, the termination was apparently negligible in the polymerization in the absence of acetic anhydride, and also in the polymerization in the presence of acetic anhydride initiated by a stronger acid, such as dichloroacetic acid. On the other hand, termination was assumed in the polymerization with acetic acid in the presence of acetic anhydride, as has been described above. To determine quantitatively the effect of acetic anhydride on the polymerization with acetic acid, the influence of the reaction time and the temperature on the polymerization was also studied, as is shown in Table 3.

TABLE 3. EFFECT OF THE REACTION TIME AND TEMPERATURE ON THE POLYMERIZATION WITH ACETIC ACID IN THE PRESENCE OF ACETIC ANHYDRIDE

Time min	Polymer yield		$\overline{P}_n$
	g	wt%	
	Temperature, 20°C		
5	0.137	2.3	440
5	0.224	3.7	340
15	0.391	6.5	660
15	0.426	7.1	530
30	0.589	9.8	1000
30	0.756	12.6	1100
60	1.025	17.1	1600
60	0.934	15.6	1200
	Temperature, 30°C		
2	0.247	4.1	380
5	0.773	12.9	970
10	0.907	15.1	780
10	0.715	11.9	520
20	1.172	19.5	1050
30	1.734	28.9	1100
60	2.231	37.2	1300
	Temperature, 40°C		
2	0.977	16.3	320
5	1.483	24.7	820
10	2.186	36.4	1000
30	3.275	54.6	1200

Experimental conditions were the same as those in Table 1, except temperature and time.

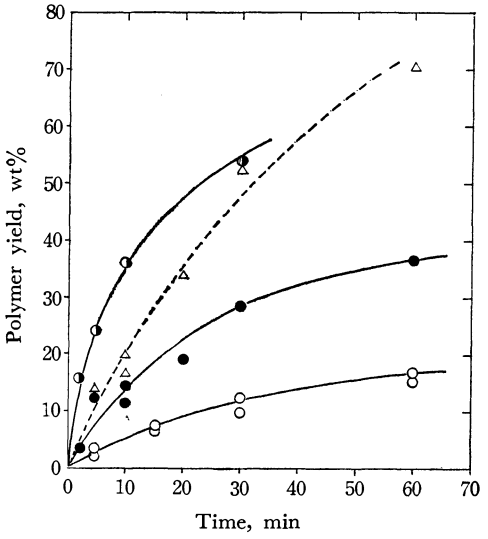

Fig. 4. Influence of reaction time and temperature on the rate of the polymerization in the presence of acetic anhydride.

Monomer solution, 10 g ; $[M]_0 = 20$ mol/l ; $[CH_3COOH] = 0.02$ mol/l ; $[(CH_3CO)_2O] = 1.0$ mol/l; reaction vessel, 30 ml; ○, 20°C; ●, 30°C; ◑, 40°C ; △, 30°C without acetic anhydride.

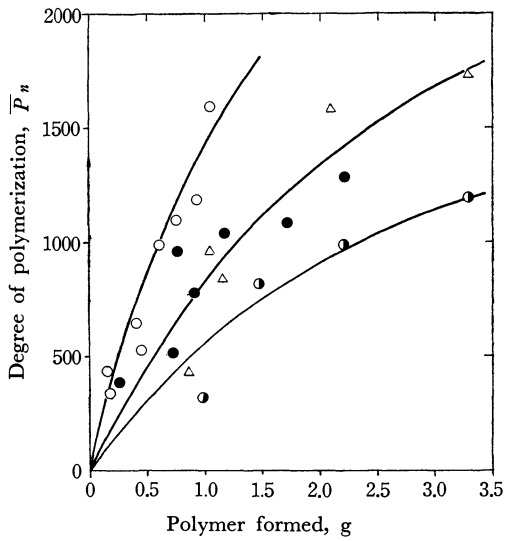

Fig. 5. Degree of polymerization *versus* polymer yield.

Reaction condition are the same as in Fig. 4.
with acetic anhydride : ○, 20°C ; ●, 30°C ; ◑, 40°C
without acetic anhydride : △, 30°C

Figure 4 is the plot of the polymer yield against the reaction time at each temperature, using the data listed in Table 3. The results[2] of the polymerization which was carried out at 30°C with acetic acid in the absence of acetic anhydride are also shown for the sake of comparison. The rate of polymerization in the early stages was almost the same as that without acetic anhydride. Two characteristics of the behavior of the polymerization with acetic anhydride were that the rate in the later stages decreased rapidly with the reaction time and that the polymer yield tended to reach a saturated value.

In Fig. 5, the degree of polymerization of the resulting polymer is plotted against the polymer yield, using the data listed in Table 3. It was found that the degree of polymerization increased with the polymer in the same way as in the polymerization without acetic anhydride. This indicates that the rate of chain transfer in this case is also considerably smaller than that of propagation.

Deviation from a First-order Rate Equation. In the polymerization with acetic acid in the presence of acetic anhydride, the rate of polymerization decreased rapidly with the progress of the polymerization, as has been described above. The following kinetical treatments of the polymerization were focused on the elucidation of this behavior.

As Fig. 6 shows, the over-all rate of polymerization, which was calculated by using the data in

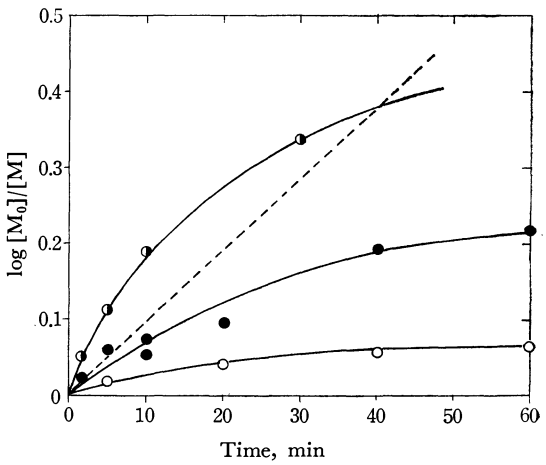

Fig. 6. Deviation of the polymerization rate from a first-order rate equation.

○, 20°C ; ●, 30°C ; ◑, 40°C ; Broken line is the same as in Fig. 4.

Table 3, deviated from the first-order equation with respect to the monomer concentration. The deviation from the first-order rate equation is a peculiarity observed only in the polymerization initiated by acetic acid in the presence of acetic anhydride. This characteristic fact let to the assumption that the decrease in the rate of polymerization may be attributed to a termination reaction between the growing polymer chain and a component which was originally present in the reaction system or which was produced as a by-product.

Kinetics in the Polymerization with Acetic Acid in the Presence of Acetic Anhydride. *Elementary Processes.* It may be concluded, in view of the characteristic behavior described above, that polymerization initiated with acetic acid in the presence of acetic anhydride belongs to the type of non-stationary successive polymerization, with rapid initiation.

In almost the same manner as in the polymerization without acetic anhydride, using the graphical method proposed by Kagiya *et al.*,[4] the elementary processes were postulated to be as follows:

Initiation:

$$C + M \xrightarrow{k_i} P^*, \qquad R_i = \text{rapid} \tag{1}$$

$$\int R_i dt = [P^*]_0 \tag{2}$$

Propagation:

$$P^* + M \xrightarrow{k_p} P_n^*, \quad R_p = k_p[P^*][M] \tag{3}$$

$$\int R_p dt = [M_p] \tag{4}$$

Chain Transfer:

$$P_n^* + Y \xrightarrow{k_{tr}} P_n + Y^*, \quad R_{tr} = k_{tr}[P^*][Y] \tag{5}$$

$$\int R_{tr} dt = \frac{k_{tr}[Y]}{k_p} \int \frac{R_p}{[M]} dt \tag{6}$$

Here R_i, R_p and R_{tr} are the rates of initiation, propagation, and chain transfer; k_p and k_{tr} are the rate constants of propagation and chain transfer; and $[P^*]_0$, $[P^*]$, $[M]$, $[M_p]$, and $[Y]$ are the concentrations of the initiating species, the monomer, the polymerized monomer, and the chain transfer agent respectively.

Termination:

$$P_n^* + Z \xrightarrow{k_d} P_n, \quad R_d = k_d[P^*][Z] \tag{7}$$

where R_d, k_d, and $[Z]$ are the rate of termination, the rate constant of termination, and the concentration of the terminator respectively. The experimental results could not be interpreted successfully on the assumption that $[Z]$ in Eq. (7) is constant during the course of polymerization. Hence, it was assumed that the concentration of the terminator is proportional to that of the growing polymer chain; then the following equation was derived from Eq. (7).

$$R_d = k_d'[P^*]^2 \tag{8}$$

Accordingly, the integration of R_d gives the following equation when Eq. (3) is substituted into Eq. (8):

$$\int R_d dt = \frac{k_d'}{k_p^2} \int \frac{R_p^2}{[M]^2} dt \tag{9}$$

Estimation of the Concentration of the Initiating Species and the Rate Constant of Chain Transfer. Because there is no termination caused by recombination between the growing polymer chains, the following equation for the degree of polymerization is given, in the same manner as has been reported in a previous paper[1]:

$$\frac{1}{\bar{P}_n} = \frac{\int R_i dt}{\int R_p dt} + \frac{\int R_{tr} dt}{\int R_p dt} \tag{10}$$

By substituting Eqs (2), (4), and (6) into Eq. (10), we derive:

$$\frac{[M_p]}{\bar{P}_n \int \frac{R_p}{[M]} dt} = \frac{[P^*]_0}{\int \frac{R_p}{[M]} dt} + \frac{k_{tr}[Y]}{k_p} \tag{11}$$

Here, $[M_p]$, $\bar{P}_n$, R_p, and $[M]$ are graphically determined by using the values in Figs. 4 and 5; of these, R_p was estimated from the tangent of the curve in Fig. 4. The estimated values are listed in Table 4. Here, the value of $\int \frac{R_p}{[M]} dt$ was calculated by a graphical integration.

In order to evaluate graphically the values of $[P^*]_0$ and $k_{tr}[Y]/k_p$, the relation between the values of $\frac{[M_p]}{\bar{P}_n \int \frac{R_p}{[M]} dt}$ and $\frac{1}{\int \frac{R_p}{[M]} dt}$ was plotted; it is shown in Fig. 7. The existence of linear relations in the same figure proves the validity of the assumption that the polymerization is rapidly initiated and that the reaction of chain transfer is quite slow.

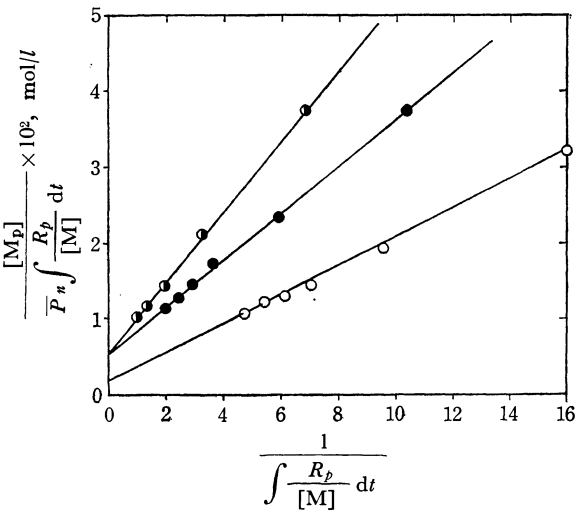

Fig. 7. Estimation of the concentration of initiating species and the rate constants of chain transfer.
○, 20°C; ●, 30°C; ◑, 40°C.

The $k_{tr}[Y]/k_p$ ratio, as shown in Table 5, was evaluated from all the intercepts on the ordinate, while the concentration of the initiator, $[P^*]_0$, was evaluated from the slopes of all the lines in

4) T. Kagiya, M. Izu and K. Fukui, This Bulletin, **40**, 1045 (1967).

TABLE 4. CALCULATED VALUES IN THE POLYMERIZATION WITH ACETIC ACID IN THE PRESENCE OF ACETIC ANHYDRIDE

Time	$[M_p]$	[M]	R_p	$\overline{P}_n$	$\frac{1}{\int \frac{R_p}{[M]}dt}$	$\frac{[M_p]}{\overline{P}_n \int \frac{R_p}{[M]}dt}$	$\frac{R_p}{[M]\int \frac{R_p^2}{[M]^2}dt}$	$\frac{[P^*]_0}{\int \frac{R_p^2}{[M]^2}dt}$
min	mol/l	mol/l	mol/l min			mol/l $\times 10^{-2}$		mol·min/l
Temperature, 20°C								
5	0.54	19.5	1.17	300	28.7	5.17	43.9	7.32
10	1.04	19.0	0.96	530	16.0	3.14	13.0	4.46
20	1.64	18.4	0.71	820	9.35	1.87	6.64	2.94
30	2.14	17.9	0.58	1050	6.98	1.42	4.44	2.43
40	2.56	17.4	0.45	1200	5.88	1.26	3.35	2.20
50	2.96	17.1	0.38	1330	5.18	1.15	2.66	2.04
60	3.16	16.8	0.33	1400	4.69	1.06	2.25	1.94
Temperature, 30°C								
5	1.72	18.3	2.89	470	10.2	3.78	8.83	1.82
10	2.96	17.0	2.09	750	5.82	2.31	4.88	1.17
20	4.56	15.5	1.32	970	3.59	1.70	2.26	0.853
30	5.66	14.3	0.93	1120	2.81	1.42	1.49	0.737
40	6.16	13.8	0.73	1180	2.39	1.25	1.11	0.675
50	7.10	12.9	0.57	1290	2.14	1.17	0.89	0.644
60	7.68	12.3	0.49	1340	1.96	1.12	0.78	0.622
Temperature, 40°C								
2	2.44	17.6	2.34	430	6.57	18.7	6.80	0.545
5	4.90	15.1	1.49	750	3.08	10.0	2.90	0.305
10	7.34	12.7	0.88	980	1.85	6.93	1.40	0.218
15	8.90	11.1	0.58	1100	1.45	5.87	0.995	0.187
20	9.96	10.0	0.43	1150	1.23	5.34	0.752	0.174
25	10.8	9.08	0.33	1180	1.10	5.05	0.605	0.166
30	11.5	8.55	0.27	1200	1.01	4.82	0.500	0.158

TABLE 5. CONCENTRATION OF INITIATING SPECIES AND RATE CONSTANTS OF ELEMENTARY REACTION IN THE POLYMERIZATION INITIATED BY ACETIC ACID

Temp. °C	$[P^*]_0$ mol/$l \times 10^{-3}$	k_p l/mol min	$k_{tr}[Y]$ $\min^{-1} \times 10^{-2}$	$k_{tr}[Y]/k_p$ mol/$l \times 10^{-3}$	k_d l/mol min
		In the presence of acetic anhydride			
20	1.7	4.0	1.0	2.5	22
30	3.2	7.1	3.6	5.0	25
40	5.0	15.0	6.7	4.5	30
		In the absence of acetic anhyride			
30	3.4	6.5	2.1	3.2	0

Fig. 7. The previously reported values[2] for the rate constants of the elementary processes are also listed in Table 5 for convenience in comparing the two polymerizations, initiated by acetic acid in the presence and absence of acetic anhydride.

Estimation of the Rate Constants of Propagation and Termination. The concentration of the growing polymer chain [P*] can be expressed by the following equation:

$$[P^*] = \int R_i dt - \int R_d dt \qquad (12)$$

By substituting Eqs. (2), (3), (4), and (9) into Eq. (12), it follows that:

$$\frac{R_p}{[M]\int \frac{R_p^2}{[M]^2}dt} = \frac{k_p[P^*]_0}{\int \frac{R_p^2}{[M]^2}dt} - \frac{k_d'}{k_p} \qquad (13)$$

The values of $\frac{R_p}{[M]\int \frac{R_p^2}{[M]^2}dt}$ and $\frac{[P^*]_0}{\int \frac{R_p^2}{[M]^2}dt}$, which were calculated in a way similar to that described above, are also listed in Table 4. The relation

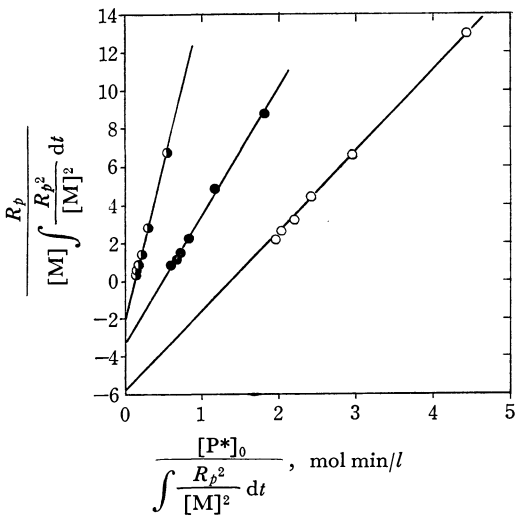

Fig. 8. Estimation of the rate constants of propagation and termination.
○, 20°C; ●, 30°C; ◑, 40°C.

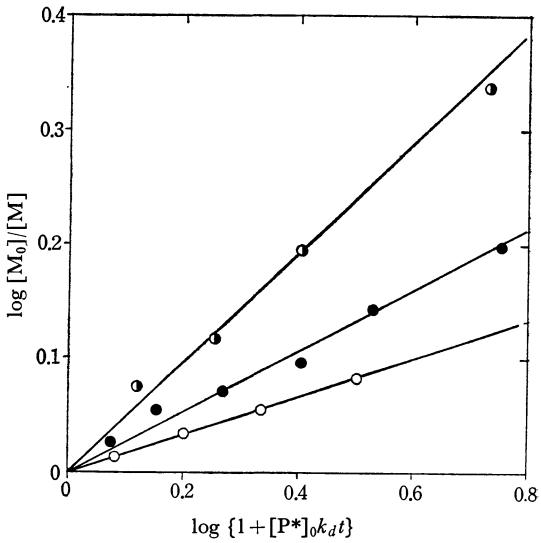

Fig. 9. Coincidence of the rate equation with the experimental results.
○, 20°C; ●, 30°C; ◑, 40°C

between the two values is plotted in Fig. 8. A distinct linear relation exists between them at each temperature. This fact indicates that the rate of termination is proportional to the square of the concentration of the growing polymer chain. The rate constants of propagation and termination were then estimated in the manner described above; they are listed in Table 5. Using the values of k_p, the $k_{tr}[Y]$ values were also estimated.

Over-all Rate Equation. It was concluded from the above considerations that the termination apparently ocurred according to a second-order equation with respect to the concentration of active species. Consequently, the concentration of the growing polymer chain may be represented as follows by integrating Equation 8:

$$[P^*] = [P^*]_0 \left\{ \frac{1}{1 + [P^*]_0 k_d t} \right\} \tag{14}$$

The rate of polymerization can, therefore, be expressed by the following equation by introducing Equation 14 into Eq. (3):

$$R_p = -\frac{d[M]}{dt} = k_p[M][P^*]_0 \left\{ \frac{1}{1+[P^*]_0 k_d t} \right\} \tag{15}$$

Hence;

$$\ln \frac{[M]_0}{[M]} = \frac{k_p}{k_d} \ln \{ 1 + [P^*]_0 k_d t \} \tag{16}$$

Figure 9 shows a plot of the logarithmic values of $[M]_0/[M]$, a plot which has been calculated by using the data in Table 3, against the value of $\log\{1+[P^*]_0 k_d t\}$, which was calculated by using the values of $[P^*]_0$ and k_d shown in Table 5. The linear relation observed proves the validity of Eq. (16).

In conclusion, the over-all rate of polymerization is proportional to the monomer concentration, and rate of termination is proportional to the square of the concentration of the intiating species.

Activation Energies of Each Elementary Process. By using the Arrhenius plot of the rate constants listed in Table 5, the activation energies for each elementary process were calculated to be as follows; 9.4, 12, 15 and 2.2 kcal/mol for initiation, propagation, chain transfer, and termination respectively. The activation energies in each process were larger in the polymerization with acetic anhydride than in that without acetic anhydride.

Comparison between the Kinetic Features of Polymerization both with and without Acetic Anhydride. The above-mentioned considerations and a previous paper[2] established that the polymerizations of formaldehyde in liquid carbon dioxide which were initiated by acetic acid in both the presence and absence of acetic anhydride were of the successive-polymerization type with a rapid initiation. The concentration of active species and the rate constant of propagation in the polymerization with acetic anhydride were almost the same as those in the polymerization without acetic anhydride at 30°C. Moreover, a small contribution of chain transfer was observed in both cases.

While the polymerization without acetic anhydride was a stationary successive polymerization, the polymerization with acetic anhydride was of the non-stationary successive polymerization type. The reaction of termination in the latter polymerization was attributable to the reaction of the growing polymer chain with a compound which was originally present in the reaction system or

which was produced as a by-product during the polymerization.

The increase in the rate constant upon the addition of acetic anhydride, which was observed in spite of the increase in the activation energy, may ascribed to the considerable increase in the entropy caused by the addition of acetic anhydride, and hence the decrease in the free energy as a whole.

The mechanism of the polymerization will be reported in a subsequent paper.

BULLETIN OF THE CHEMICAL SOCIETY OF JAPAN VOL. 41 1679—1681 (1968)

Studies of the *N*-Oxides of *N,N*-Dialkylamino Acids. I. The Syntheses of *N,N*-Dimethyl Neutral Amino Acids and Corresponding *N*-Oxides

Yoshikazu IKUTANI

Laboratory of Organic Chemistry, Osaka Kyoiku University, Tennoji-ku, Osaka

(Received December 30, 1967)

The *N,N*-dimethyl derivatives of neutral amino acids, such as glycine, L-alanine, DL-alanine, L-valine, DL-valine, L-leucine, L-phenylalanine, and L-tyrosine, were prepared by the catalytic reductive condensation of the corresponding amino acids with formaldehyde. The *N*-oxides were satisfactorily synthesized by the oxidation of the *N,N*-dimethyl derivatives with an aqueous mixture of hydrogen peroxide and acetic acid. The reaction conditions, the analytical data, and some properties of the products are presented.

As a part of an investigation of the syntheses and reactions of *N,N*-dialkylamino acids, the syntheses of *N,N*-dimethyl neutral amino acids and the corresponding *N*-oxides have been studied. Although several reagents, such as methyl iodide, dimethyl sulfate, and diazomethane, are available for the alkylation of the amino group, the most suitable method is the catalytic reductive condensation of amino acid with aldehyde.[1,2] In an earlier paper, Sweely and Horning reported the synthesis and ferric ion - catalyzed reactions of *N,N*-dimethylglycine *N*-oxide.[3] However, the melting point of the substance was indistinct, and the results of elementary analysis were not identical with the calculated value. The present author has prepared the various *N, N*-dimethyl neutral amino acids in good yields and has oxidised them to the corresponding *N*-oxides satisfactorily. The *N, N*-dimethylations were carried out at 50°C by the catalytic reductive condensation of an aqueous solution of neutral amino acid and formaldehyde in the presence of a silk-palladium catalyst, which showed no reductivity in responce to any aldehyde.[4] The period of the reduction depends on the solubility of the parent amino acid; for example, the *N,N*-dimethylation of L-tyrosine in an aqueous suspension proceeded very slowly. The reaction product was a mixture consisting of the *N, N*-dimethyl derivative and a trace of the unchanged parent amino acid. The *N*-monomethyl derivative has not been obtained in any case. The analytical data and some properties of the *N, N*-dimethyl derivatives are summarized in Table 1.

Generally the oxidation of aliphatic tertiary amine with aqueous hydrogen peroxide gives the corresponding *N*-oxide. However, in the case of *N,N*-dimethylamino acid, no reaction occurred at either room temperature or 60°C and the starting substance was recovered unchanged. Sweely and Horning prepared *N,N*-dimethylglycine *N*-oxide by the oxidation of *N,N*-dimethylglycine in an aqueous mixture of hydrogen peroxide and barium hydroxide. The present author oxidized the *N,N*-dimethylamino acids to the corresponding *N*-oxides using an aqueous mixture of hydrogen peroxide and acetic acid at 60°C. The most suitable oxidation conditions were detected by paper chromatographic studies of the reaction mixture. After the oxidation, the same volume of water was added to the reaction mixture and the solution was concentrated carefully below 40°C under reduced pressure. After this procedure had been repeated until the distillate gave a negative reaction in a potassium iodide starch test, the residue was dried up under reduced pressure. When the crude *N*-oxides were recrystallized from ethanol-acetone, the *N*-oxides obtained were of a high purity.

1) R. E. Bowman and H. H. Stroud, *J. Chem. Soc.*, **1950**, 1342.
2) K. Kanao, *Yakugaku Zasshi (J. Pharm. Soc. Japan)*, **66**, 4 (1946).
3) C. C. Sweely and E. C. Horning, *J. Am. Chem. Soc.*, **79**, 2620 (1957).
4) Y. Izumi, This Bulletin, **32**, 932 (1959).

TABLE 1. *N, N*-DIMETHYL NEUTRAL AMINO ACIDS

Parent amino acid	Reduction period (50°C) (hr)	Yield (%)	Mp (°C)	R_f Value[a]	C %		H %		N %	
					Found	Calcd	Found	Calcd	Found	Calcd
Gly	8	84	179	0.33	46.76	46.59	8.89	8.80	13.56	13.58
L-Ala	6	81	183	0.36	51.27	51.26	9.50	9.46	11.94	11.96
DL-Ala	7	92	182	0.36	51.18	51.26	9.45	9.46	12.02	11.96
L-Val	8.5	92	153	0.59	57.51	57.90	10.29	10.41	9.84	9.65
DL-Val	10	85	151	0.59	58.40	57.90	10.38	10.41	9.84	9.65
L-Leu	15	84	197	0.69	60.29	60.34	10.63	10.76	8.74	8.80
L-Phe	5	96	222	0.67	68.08	68.37	7.83	7.82	7.24	7.25
L-Tyr[b]	22	83	273	0.52	62.64	63.14	7.20	7.23	6.89	6.69
L-Tyr[c]	22	83	274	0.52	62.96	63.14	7.19	7.23	6.86	6.69

a) A *n*-butanol - acetic acid - water (60 : 15 : 25) solvent system was used. The location of the paper-chromatogram was carried out by spraying of alkaline aqueous ethanol solution of thymol blue.
b) This substance was obtained as filamentous needles.
c) This substance was obtained as short prisms.

TABLE 2. *N, N*-DIMETHYL NEUTRAL AMINO ACID *N*-OXIDES

Starting amino acid	Oxidation time (60°C) (hr)	Yield (%)	Mp (dec.) (°C)	R_f Value[a]	C %		H %		N %		ν_{N-O} cm^{-1}
					Found	Calcd	Found	Calcd	Found	Cacld	
Gly	7	83	136	0.44	40.70	40.33	7.72	7.62	11.84	11.76	972
L-Ala	6	74	120	0.50	45.22	45.10	8.25	8.33	10.40	10.52	963
L-Val	7	91	103	0.76	52.23	52.15	9.49	9.38	8.59	8.69	968
L-Leu	7	98	114	0.86	54.91	54.83	9.70	9.78	7.77	7.99	980
L-Phe	6	80	139	0.77	63.27	63.14	7.36	7.23	6.54	6.69	976
L-Tyr[b]	3	60	163	0.62	54.10	54.31	7.01	7.04	5.74	5.76	966
L-Tyr[c]	—	—	—	—	58.66	58.65	6.59	6.71	6.09	6.22	—

a) Same procedure was used as described in Table 1.
b) This substance was obtained as monohydrated crystal.
c) This substance was anhydrous powder.

N,N-Dimethyl-L-tyrosine *N*-oxide crystallized as monohydrate, and the crystal water was removed at 80°C under reduced pressure over an 8-hr period. The *N*-oxides show the infrared absorption band in the 960—980 cm^{-1} region, as does ordinary aliphatic tertiary amine *N*-oxide.[5] The basicity of the *N*-oxides are weaker than those of the corresponding *N,N*-dimethyl derivatives. The elementary analyses and some properties of the *N*-oxides are summarized in Table 2. The *N*-oxides were easily reduced to the parent *N,N*-dimethylamino acids by catalytic reduction.

Experimental

N,N-Dimethylglycine. A mixture of 19 g of glycine, 1.5 g of a silk-palladium catalyst, 80 m*l* of 37% aqueous formaldehyde, and 120 m*l* of water was placed in an autoclave, which was then filled with hydrogen. The mixture was shaken at 50°C for 7 hr, by which time the theroretical amount of hydrogen had been taken up. The catalyst was then filtered off, and the filtrate was evaporated under reduced pressure. A small amount of paraformaldehyde was present in the product; it was removed by re-evaporation with water. The residual syrup was dissolved in a small volume of ethanol, and the solution was dried up to remove a trace of water. After this procedure had been repeated three times, the crystalline product appeared. About 50 m*l* of acetone was added in small portions to the precipitates, and the crystallization was complete. The resulting crystalline precipitates were collected by filtration, washed with acetone several times, and then dried under reduced pressure. The yield of the crude product was almost equal to the theoretical yield. The crude product was dissolved in a minimum volume of hot ethanol, decolorized with a small amount of charcoal, and filtered. About 150 m*l* of acetone were added in small portions, and the mixture was stored in a refrigerator overnight. Fine crystals were then collected by filtration, washed with acetone, and dried under reduced pressure. The yield was 21.7 g (83%). This substance was very hygroscopic and deliquescent, and was soluble in ethanol and almost insoluble in acetone.

Other N,N-Dimethyl Derivatives of Neutral Amino Acids. *N,N*-Dimethyl derivatives of all the other neutral amino acids except L-tyrosine were

5) R. Mathis-Noel, R. Wolf and F. Gallais, *Compt. rend.*, **242**, 1873 (1956).

obtained by a similar method. *N,N*-Dimethyl-L-alanine and *N,N*-dimethyl-DL-alanine were very hygroscopic and deliquescent prisms. *N,N*-Dimethyl-L-valine and *N,N*-dimethyl-DL-valine were slightly hygroscopic. *N,N*-Dimethyl-L-leucine and *N,N*-dimethyl-L-phenylalanine were not hygroscopic. The *N,N*-dimethylation of 6.2 g of L-tyrosine in 20 m*l*-tyrosine 20 m*l* of 37% aqueous formaldehyde and 230 m*l* of water proceeded very slowly for about 22 hr. By a treatment similar to that described above, a crude product was obtained. The crude product was dissolved in a minimum volume of hot water, decolorized with charcoal, and filtered. To the filtrate, 50 m*l* of acetone were added, and the resulting mixture was rapidly cooled in a refrigerator. Fine filamentous needles were then collected by filtration, washed with acetone, and dried under reduced pressure. The yield was 6.0 g (83%). In another recrystallization, when a hot, saturated aqueous solution was allowed to cool slowly, short prisms were obtained. They showed almost the same properties, except that slight differences were observed in the infrared absorption spectra.

N,N-Dimethylglycine N-Oxide. A solution of 4 g of *N,N*-dimethylglycine, 20 m*l* of 30% aqueous hydrogen peroxide, and 40 m*l* of acetic acid was warmed at 60°C for 7 hr. To a reaction mixture, about 50 m*l* of water were added, after which the mixture was concentrated to about a half volume while being gently warmed below 40°C under reduced pressure. After this procedure had been repeated until the distillate gave a negative reaction to a potassium iodide starch test, the solution was evaporated to dryness under reduced pressure. The residual syrup was dissolved in a small volume of ethanol, and the solution was dried up under reduced pressure. This procedure was repeated twice, after which the residue was crystallized. The crude products were collected with acetone, washed with acetone, and dried under reduced pressure. The product thus obtained was recrystallized by a method similar to that described above. The yield of dimethylglycine *N*-oxide was 3.8 g (83%).

Other N,N-Dimethyl Neutral Amino Acid N-Oxides. The *N*-oxides of *N,N*-dimethyl-L-alanine, *N,N*-dimethyl-DL-alanine, *N,N*-dimethyl-L-valine, *N,N*-dimethyl-DL-valine, *N,N*-dimethyl-L-leucine, and *N,N*-dimethyl-L-phenylalanine were obtained in the same manner. However, *N,N*-dimethyl-L-tyrosine *N*-oxide was obtained as monohydrated crystals and the water was removed by heating at 80°C for 8 hr under reduced pressure.

The Reduction of N,N-Dimethylglycine N-Oxide to N,N-Dimethylglycine. A mixture of 2.4 g of *N,N*-dimethylglycine *N*-oxide, 1.5 g of a silk-palladium catalyst, and 150 m*l* of water was placed in an autoclave with hydrogen. The mixture was shaken at 40°C for 30 min. When the reaction mixture was then treated in the manner described above, 1.7 g of a product was obtained. The melting point of this sample was not depressed by admixture with authentic *N,N*-dimethylglycine, and the two substances had completely identical infrared absorption spectra. The recovery of *N,N*-dimethylglycine was 1.6 g (80%).

Found: C, 46.48; H, 8.98; N, 13.49%. Calcd for $C_4H_9O_2N$: C, 46.59; H, 8.80; N, 13.58%.

The author is indebted to Professor Eizo Matsumura for his constant guidance in the course of the work, and to Professor Yoshiharu Izumi of Osaka University for his valuable advice and encouragement.

BULLETIN OF THE CHEMICAL SOCIETY OF JAPAN VOL. 41 1682—1686 (1968)

Initiation and Propagation in the Copolymerization of *N*-Phenylethylenimine with β-Propiolactone

Tsutomu KAGIYA, Tomizo KONDO and Kenichi FUKUI

Faculty of Engineering, Kyoto University, Sakyo-ku, Kyoto

(Received December 30, 1967)

In the copolymerization of *N*-phenylethylenimine with β-propiolactone, the mechanisms of the initiation and propagation reactions were investigated. The rate of the copolymerization was markedly increased by the addition of propionic acid. When a mixture of triethylamine and propionic acid was used as additive, the rate decreased with an increase in the amount of triethylamine, while with an equimolar mixture the rate was almost equal to that without any catalyst. No polymer was obtained with an excess of triethylamine. With Brönsted acid, the composition of the copolymer was independent of the concentration of the catalyst, but it varied with the pK_a value. The monomer reactivity ratio of *N*-phenylethylenimine increased with a decrease in the pK_a value. While that of β-propiolactone decreased.

We have reported in a previous paper that *N*-phenylethylenimine and β-propiolactone copolymerized without any catalyst at 0°C in an acetonitrile solution, giving a powdery or a resinous polymer.[1] The copolymer had the ester structure of $-(-N(C_6H_5)-CH_2CH_2OC(=O)-CH_2CH_2-)_n-$ in the mainchain, and the monomer reactivity ratios of *N*-phenylethylenimine (r_I) and β-propiolactone (r_L) were estimated to be $r_I=7.5$ and $r_L=0.15$ respectively.

In this paper, the initiation mechanism of the copolymerization without any addition of the catalyst was first studied. Secondly, in order to elucidate the role of the catalyst in the propagation reaction, copolymerization by various acids was studied.

Experimental

Reagents. The method of the synthesis of *N*-phenylethylenimine, and that of the purification of β-propiolactone and acetonitrile, have been described in our previous paper.[1] Guaranteed reagents of acids and dimethylaniline were used without further purification. Triethylamine was purified by the usual method.

Copolymerization Procedure. Measured amounts of a catalyst and a solvent were placed into a glass ampule under a nitrogen atmosphere, β-propiolactone and *N*-phenylethylenimine were then added to this system at −78°C. The ampule was sealed and maintained at 0—1°C for the duration of the reaction. The products were then washed with chloroform and diethylether, separated by a centrifuge, and dried *in vacuo*.

Determination of the Composition of the Copolymer. The composition of the copolymer was determined by the method described in the previous paper.[1]

Results and Discussion

Initiation Mechanism in the Polymerization Without any Catalyst. The copolymerization was carried out in acetonitrile without any catalyst and at 0°C. The relation between the total conversion and the mole per cent of β-propiolactone in the monomer feed is shown in Fig. 1. The conversion of each monomer was obtained from the data of the total conversion and the composition of the copolymer. In Fig. 2 the rates of the consumption of the two monomers, defined as the ratio of the conversion of each monomer to the

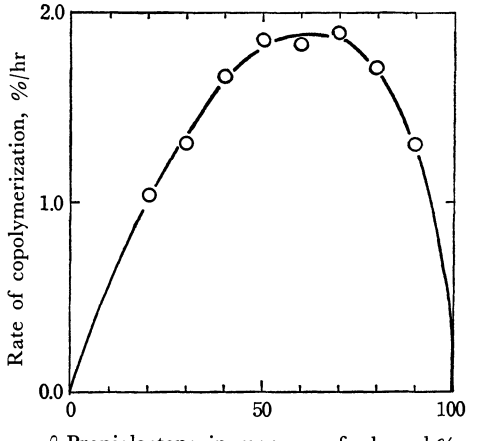

Fig. 1. Copolymerization of *N*-phenylethylenimine and β-propiolactone without any catalyst.

1) "Copolymerization of *N*-phenylethylenimine and β-propiolactone," T. Kagiya, T. Kondo, S. Narisawa and K. Fukui, This Bulletin, **41**, 172 (1968).

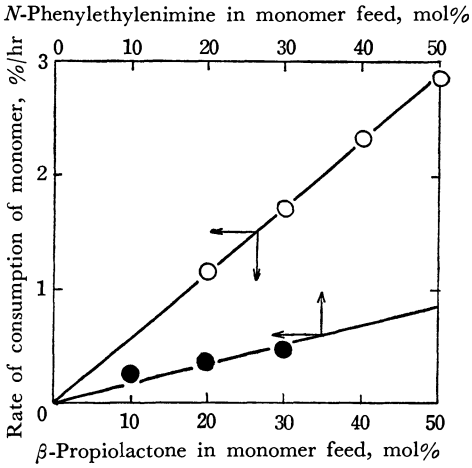

Fig. 2. Rates of the consumption of *N*-phenylethylenimine and β-propiolactone in the copolymerization.
○: *N*-phenylethylenimine ●: β-propiolactone

reaction time, are plotted against the amount of the comonomer in the monomer feed. The rate of the consumption of *N*-phenylethylenimine or β-propiolactone increased proportionately with an increase in the amount of the comonomer. Furthermore, Fig. 2 shows that the rate of the consumption of *N*-phenylethylenimine was about three times larger than that of β-propiolactone. From these results, it may be concluded that the effect of β-propiolactone on the polymerization of *N*-phenylethylenimine is greater than that of *N*-phenylethylenimine on the polymerization of β-propiolactone.

In order to elucidate the effect of the β-propiolactone on the polymerization of *N*-phenylethylenimine, and that of *N*-phenylethylenimine on the polymerization of β-propiolactone, the copolymerization was carried out using propionic acid or dimethylaniline respectively as substances analogous to the hydrolyzed compound of β-propiolactone and *N*-phenylethylenimine. The rate of the copolymerization was slightly increased by the addition of dimethylaniline, while the rate was remarkably increased by the addition of propionic acid (Fig. 3). The above facts suggest that the copolymerization without any catalyst was initiated by the acid present in β-propiolactone.

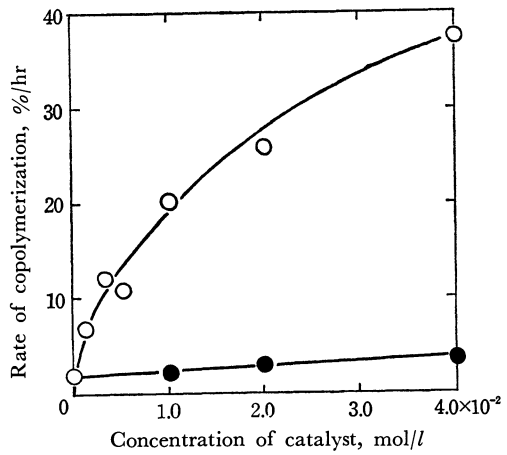

Fig. 3. Rates of copolymerization with propionic acid or dimethylaniline as additive.
○: propionic acid
●: dimethylaniline

Moreover, in order to study the role of the acid in the polymerization, the copolymerization was carried out using a mixture of triethylamine and propionic acid. As is shown in Fig. 4, the rate of the copolymerization markedly decreased with an increase in the amount of triethylamine, while in the case of an equimolar mixture of triethylamine and propionic acid the rate was almost equal to that without any catalyst. No polymer was obtained with an excess of triethylamine. This fact may be due to the neutralization of the acid present in β-propiolactone with triethylamine. These results are consistent with the initiation mechanism described above.

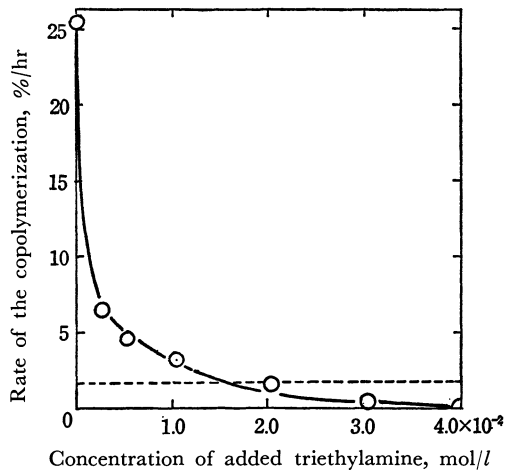

Fig. 4. Copolymerization with the mixture of propionic acid and triethylamine.
Concentration of propionic acid: 2.0×10^{-2} mol/*l*
----: Rate of copolymerization without any catalyst.

The Role of Various Brönsted Acids. Copolymerization was carried out by using various Brönsted acids as catalysts (pK_a=2.85—15.7). The relationship between the logarithm of the rate of copolymerization and the pK_a of the acids is shown in Fig. 5. Because the rate increased with a decrease in the pK_a of the catalyst, it has been concluded that the copolymerization was initiated by proton acids and that it proceeded by a cationic mechanism.

The relation between the rate of the consumption of *N*-phenylethylenimine (or β-propiolactone) and the pK_a of the acids is shown in Fig. 6. The rates

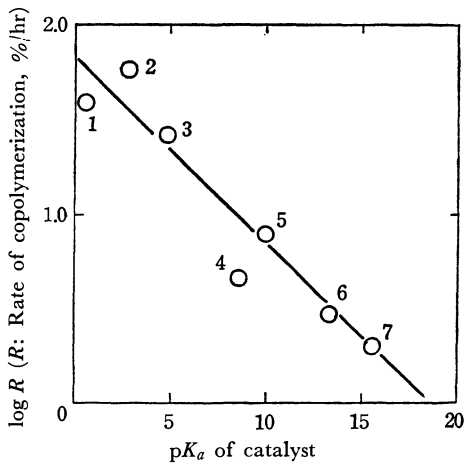

Fig. 5. Plots of rate of copolymerization against the pK_a of the catalyst.
Catalyst 1: Trichloroacetic acid, 2: Monochloroacetic acid, 3: Propionic acid, 4: Nitroethane, 5: Phenol, 6: Diethyl malonate, 7: Water

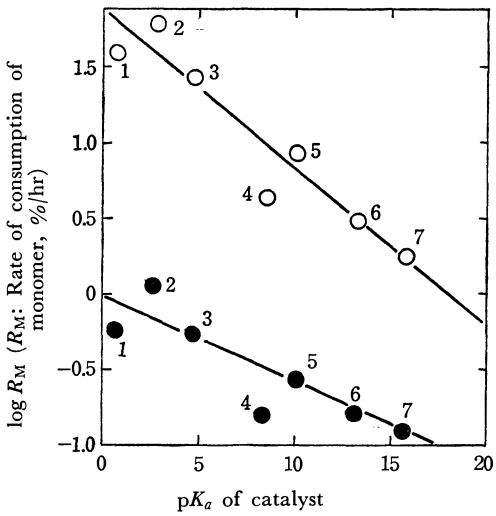

Fig. 6. Plots of rates of consumption of *N*-phenylethylenimine and β-propiolactone against pK_a of the catalyst in copolymerization.
○: *N*-phenylethylenimine
●: β-propiolactone
The number of the catalyst is the same as shown in Fig. 5.

of the consumption of both monomers decreased with an increase in the pK_a of the catalyst. The slopes of the lines in Fig. 6 show that the effect of the pK_a of the catalyst on the rate of the consumption of *N*-phenylethylenimine was greater than that of β-propiolactone. The cause of the lower dependency of the consumption rate of β-propiolactone than that of *N*-phenylethylenimine on the pK_a of the acid is not clear, but it may be that, as will be discussed below, the separation of the counter anion from the propagating oxonium ion is restricted by the electrophilic action of the carbonyl carbon of β-propiolactone on the counter anion.

The composition of the copolymer was independent of the concentration of the catalyst, but it varied with the pK_a of the acid, and the composition of *N*-phenylethylenimine in the copolymer decreased with an increase in its pK_a value (Fig. 7). This fact indicates that the rate of the propagation was influenced by the electronic nature of the counter anion.

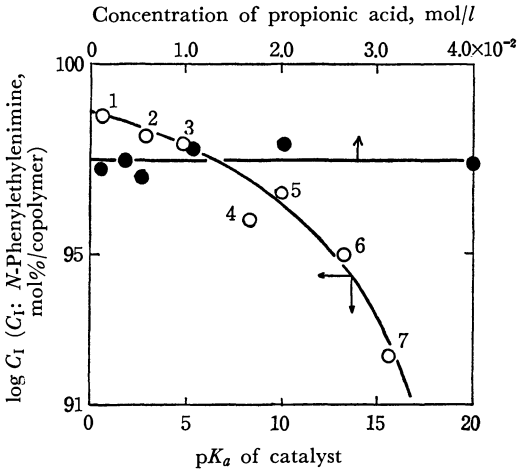

Fig. 7. Relation between composition of *N*-phenylethylenimine in copolymer and the pK_a of the catalyst or concentration of propionic acid.
The number of the catalyst is the same as shown in Fig. 5.

In order to investigate the role of the counter anion of the catalyst in the propagation reaction, the copolymerization was carried out using water, phenol, or propionic acid. The relation between the mole per cent of β-propiolactone in the copolymer and that in the monomer feed is shown in Fig. 8. The monomer reactivity ratios of *N*-phenylethylenimine (r_I) and β-propiolactone (r_L) were

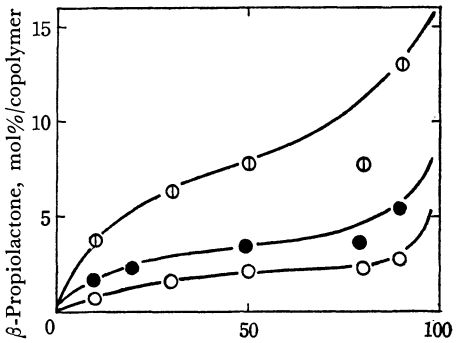

Fig. 8. Relation between the composition of β-propiolactone in the copolymer and in the monomer feed.
○: Propionic acid, ●: Phenol, ⊕: Water

Table 1. Monomer reactivity ratios of *N*-phenylethylenimine and β-propiolactone in the copolymerization with various Brönsted acid catalysts

Catalyst	pK_a	Monomer reactivity ratio	
		N-phenylethylenimine	β-propiolactone
Propionic acid	4.87	16.7	0.103
Phenol	9.98	9.10	0.106
Water	15.7	3.60	0.115

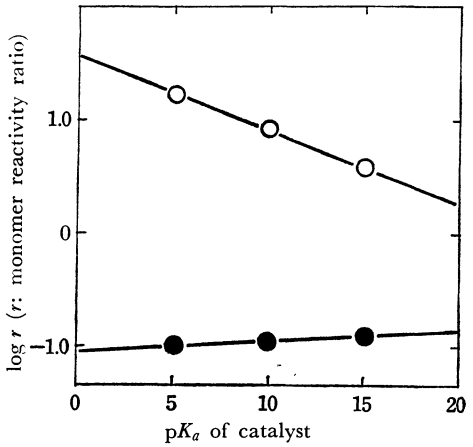

Fig. 9. Relation between monomer reactivity ratios and the pK_a of the catalyst.
○: *N*-phenylethylenimine
●: β-propiolactone

estimated from these curves by the method described in the previous paper[1] (Table 1). The relations between $\log r_I$ (or $\log r_L$) and the pK_a of the acid are plotted in Fig. 9. The monomer reactivity ratio of *N*-phenylethylenimine increased with a decrease in the pK_a of the catalyst, but, on the contrary, that of β-propiolactone decreased. The fact that the slope of the line for *N*-phenylethylenimine was larger than that for β-propiolactone shows that the effect of the pK_a of the acid on the monomer reactivity ratio of *N*-phenylethylenimine is much larger than that of β-propiolactone.

The Mechanism of the Copolymerization. From these experimental facts, the copolymerization mechanism was postulated to be as follows:

Initiation:

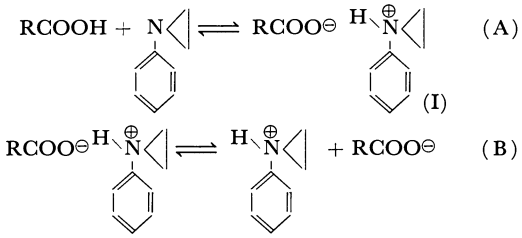

Propagation:

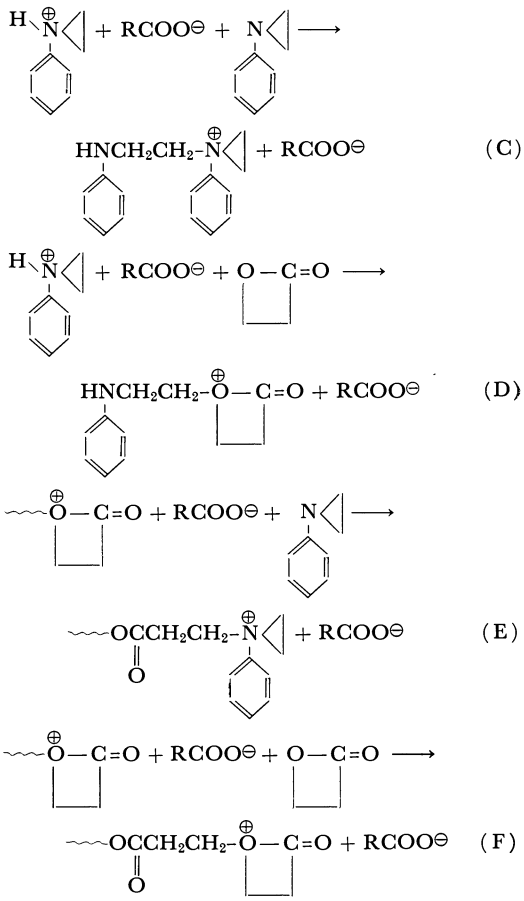

The initiation reaction is considered to be the reaction of the acid with *N*-phenylethylenimine to produce compound (I). The counter anion is separated from the immonium ion as shown in Eq. (B). It is considered that the equilibrium constant of the reaction (B) increases with a decrease in the pK_a of the catalyst, similar to the dissociation of the acid in water.

In the propagation, each monomer attacks a dissociated quarternary immonium ion or an oxonium ion. The rates of the consumption of the two monomers are expressed by the following equations:

$$-\frac{d[I]}{dt} = (k_{II}[I^{\oplus}] + k_{LI}[L^{\oplus}])[I] \quad (1)$$

$$-\frac{d[L]}{dt} = (k_{IL}[I^{\oplus}] + k_{LL}[L^{\oplus}])[L] \quad (2)$$

where [I], [L], [I⊕], and [L⊕] are the concentrations of *N*-phenylethylenimine, β-propiolactone, dissociated immonium ions, and oxonium ions respectively. The monomer reactivity ratios, r_I and r_L are given by Eqs. (3) and (4) respectively:

$$r_I = k_{II}/k_{IL} \quad (3)$$

$$r_L = k_{LL}/k_{LI} \quad (4)$$

Since r_I is larger, and r_L, smaller than unity, and since the immonium ion (three-membered ring) is more reactive than oxonium ion (four-membered ring), the rate constant in the propagation reaction is considered to decrease in the order:

$$k_{II} > k_{IL} > k_{LI} > k_{LL} \tag{5}$$

Furthermore, the propagating species is almost entirely the immonium ion, because the amount of β-propiolactone consumed is less than that of *N*-phenylethylenimine. Therefore, Eqs. (1) and (2) may be approximated as Eqs. (6) and (7) respectively:

$$-\frac{d[I]}{dt} \fallingdotseq k_{II}[I^{\oplus}][I] \tag{6}$$

$$-\frac{d[L]}{dt} \fallingdotseq k_{IL}[I^{\oplus}][L] \tag{7}$$

Taking the logarithm of Eqs. (6) and (7), and subtracting the latter from the former, Eq. (8) is derived:

$$\begin{aligned}\log r_I &= \log k_{II} - \log k_{IL} \\ &= \log(-d[I]/dt) - \log(-d[L]/dt) \\ &\quad + \log([I]/[L])\end{aligned} \tag{8}$$

From Fig. 6, the two empirical equations (9) and (10) are obtained:

$$\log(-d[I]/dt) = 1.7 - 0.102\, pK_a \tag{9}$$

$$\log(-d[L]/dt) = 0.04 - 0.042\, pK_a \tag{10}$$

substituting Eqs. (9) and (10) into Eq. (8), we obtain:

$$\log r_I = 1.66 - 0.06\, pK_a + \log([I]/[L]) \tag{11}$$

Considering that the concentration of *N*-phenylethylenimine is almost equal to that of β-propiolactone during the initial period of the copolymerization, Eq. (11) is approximately expressed by Eq. (12):

$$\log r_I \fallingdotseq 1.66 - 0.06\, pK_a \tag{12}$$

Equation (12) interprets the experimental finding that the monomer reactivity ratio of *N*-phenylethylenimine increases with a decrease in the pK_a value of the acid.

On the other hand, the empirical equation (13) is obtained from Fig. 9:

$$\log r_I = 1.51 - 0.06\, pK_a \tag{13}$$

The agreement of Eq. (13) with Eq. (12) indicates that the postulated mechanism of copolymerization and the method of approximation are suitable.

In the monomer reactivity ratio of β-propiolactone, the empirical equation (14) is obtained from Fig. 9:

$$\log r_L = -1.30 + 0.01\, pK_a \tag{14}$$

This result may be explained in the following way. If linear relations exist between $\log k_{LI}$ (and $\log k_{LL}$) and the pK_a of the acid as with k_{II} and k_{IL}, these relations may be expressed as:

$$\log k_{LI} = C_1 - C_2\, pK_a \tag{15}$$

$$\log k_{LL} = C_3 - C_4\, pK_a \tag{16}$$

where C_1, C_2, C_3, and C_4 are positive constants; C_2 is larger than C_4 since the effect of the pK_a value of the acid on the rate of the consumption of *N*-phenylethylenimine is greater than that of β-propiolactone. Subtracting Eq. (15) from Eq. (16), we obtain:

$$\begin{aligned}\log r_L &= \log k_{LL} - \log k_{LI} \\ &= (C_3 - C_1) + (C_2 - C_4)pK_a \\ &= C_5 + C_6\, pK_a \quad (C_6 > 0)\end{aligned} \tag{17}$$

where C_5 and C_6 are constants. Equation (17) interprets the fact that $\log r_L$ decreases with a decrease in the pK_a of the catalyst.

Further work on the effect of the solvent on the copolymerization will be reported in a subsequent paper.

BULLETIN OF THE CHEMICAL SOCIETY OF JAPAN VOL. 41 1687—1689 (1968)

Ring-opening Polymerization of the Macrocyclic Ester

Kentaro YODA and Kazuyuki KIMOTO

Katata Research Institute, Toyobo Co., Ltd., Honkatata-cho, Otsu

(Received January 10, 1968)

The ring-opening polymerization of cyclic bis(ethylene isophthalate) (I) was carried out in the presence of various metallic compounds as catalysts. Among the polycondensation catalysts for ethylene terephthalate, antimony and tin compounds were very effective in the ring-opening polymerization of I. On the other hand, titanium, zinc, calcium, and aluminum compounds did not show high catalytic activity. The polymerization of I proceeded even at temperatures below the melting point of I. As the melting point of the resulting poly(ethylene isophthalate) was much lower than the polymerization temperature, the reaction system gradually melted in consequence of the progress of the polymerization reaction.

With regard to the macrocyclic esters of aliphatic carboxylic acids, many investigations[1,2] have been carried out. Recently, the presence of families of macrocyclic oligoesters containing aromatic nuclei has been demonstrated in a number of technically important synthetic polyester resins.[3-6] On the other hand, it is well known that some cyclic esters with more than two ester groups, such as lactide, glycolide, and salicylide, can be polymerized to produce linear polyesters by the use of a metallic compound as the catalyst.[7-11]

Goodman and Nesbitt[5] obtained poly(ethylene terephthalate) by the ring-opening polymerization of macrocyclic oligo(ethylene terephthalates).

The present paper will be concerned with the ring-opening polymerization of cyclic bis(ethylene isophthalate)[4] (I) by various catalysts.

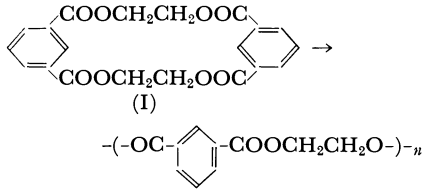

(I)

Experimental

The melting points were determined on a Yanagimoto electric micromelting-point apparatus. All the melting points are uncorrected. The infrared absorption spectra were obtained in a KBr disk using a Hitachi EPI-S2 infrared spectrophotometer. The NMR spectra were taken in trifluoroacetic acid, using tetramethylsilane as the external reference, on a Varian A-60 NMR spectrometer; their chemical shifts are presented in terms of δ values. All the solvents were purified and dried according to the ordinary methods.

Catalysts. Calcium acetate and zinc acetate, G. R. grade, were obtained from Nakarai Chemicals. Antimony trioxide, G. R. grade, was obtained from E. Merck AG. Di-*n*-butyltin oxide and di-*n*-butyltin dibenzoate were supplied by Yoshitomi Pharmaceutical Industries. Aluminum butoxide, triphenyl stibine, and titanium tetraglycoxide were prepared according to known procedures.[12-14]

Cyclic Bis(ethylene isophthalate) (I). The ring dimer of ethylene isophthalate was prepared by a procedure described in the literature[4] and was purified by vacuum sublimation, followed by recrystallization from dimethylformamide; mp 326—328°C (lit. 325—327°C).

Found: C, 62.75; H, 4.19%. Calcd for $C_{20}H_{16}O_8$: C, 62.50; H, 4.20%.

The infrared spectrum and the NMR spectrum of I are shown in Figs. 1 and 2 respectively. A fine powder (smaller than 200 mesh) of I was used as the starting material in the polymerization experiments.

The General Procedure for the Polymerization of I. A mixture of I and a catalyst was placed in a glass ampoule under a nitrogen atmosphere. Then the system was evacuated twice and sealed under a nitrogen flow. The polymerization was carried out

1) H. Mark and G. S. Whitby, "Collected Papers of W. H. Carothers on High Polymeric Substances," Interscience Publishers, Inc., New York (1940), pp. 141, 212, 221, 248, 259, 265.
2) J. Dale, *J. Chem. Soc.*, **1965**, 72.
3) S. D. Ross, E. R. Coburn, W. A. Leach and W. B. Robinson, *J. Polymer Sci.*, **13**, 406 (1954).
4) C. E. Berr, *ibid.*, **15**, 591 (1955).
5) I. Goodman and B. F. Nesbitt, *Polymer*, **1**, 384 (1960).
6) S. Hashimoto and J. Sakai, *Kobunshi Kagaku (Chem. High Polymers)*, **23**, 422 (1967).
7) C. E. Lowe, U. S. Pat. 2668162 (1954).
8) J. Kleine and H. H. Kleine, *Makromol. Chem.*, **30**, 23 (1959).
9) T. Turuta, K. Matsuura and S. Inoue, *ibid.*, **75**, 211 (1964).
10) K. Hirono, G. Wasai, T. Saegusa and J. Furukawa, *Kogyo Kagaku Zasshi (J. Chem. Soc. Japan, Ind. Chem. Sect.)*, **67**, 604 (1964).
11) A. K. Schneider, U. S. Pat. 2696481 (1954).
12) W. G. Young, W. H. Hartung and F. S. Crossley, *J. Am. Chem. Soc.*, **58**, 100 (1936).
13) G. S. Hiers, "Organic Syntheses," Coll. Vol. I, p. 550 (1956).
14) D. F. Herman, U. S. Pat. 2654770 (1953).

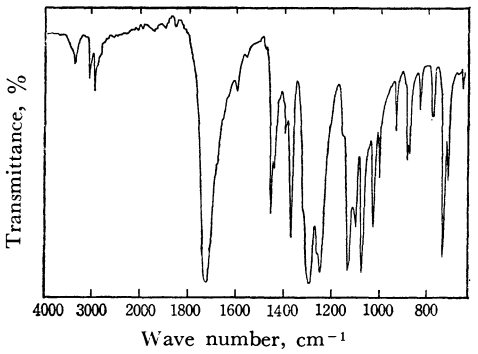

Fig. 1. Infrared spectrum of cyclic bis(ethylene isophthalate).

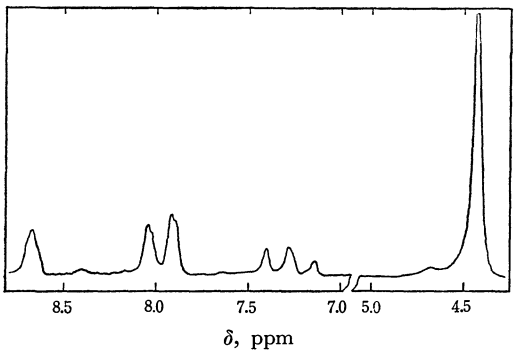

Fig. 2. NMR spectrum of cyclic bis(ethylene isophthalate).

at a given temperature for a definite period. The polymer produced was dissolved in chloroform, and the insoluble, unpolymerized I was filtered off. *n*-Heptane was added to the chloroform solution to precipitate the polymer. Then the separated polymer was dried under reduced pressure. The intrinsic viscosity of the polymer was measured by an Ubbelohde's viscometer in a mixed solvent composed of phenol and tetrachloroethane (6 : 4) at 30°C.

Results and Discussion

The experimental results are shown in Table 1. The polymerization of I proceeded even at temperatures below the melting point of I. However, no polymeric material was obtained by heating I at 265°C for 120 min.

Among the polycondensation catalysts[15,16] for ethylene terephthalate, antimony and tin compounds were very effective in the ring-opening polymerization of I. However, titanium, zinc, calcium, and aluminum compounds did not show any high catalytic activity.

When antimony trioxide was used as a catalyst, a white, powder-like polymer was obtained, while a slightly brownish polymer was obtained by the use of the di-*n*-butyltin oxide catalyst. These polymers were confirmed to be poly(ethylene isophthalate) by comparing their melting points, solubilities, infrared spectra, and NMR spectra with those of the poly(ethylene isophthalate) prepared by the melt polycondensation of bis-β-(hydroxyethyl isophthalate). The infrared spectrum and the NMR spectrum of the polymer are shown in Figs. 3 and

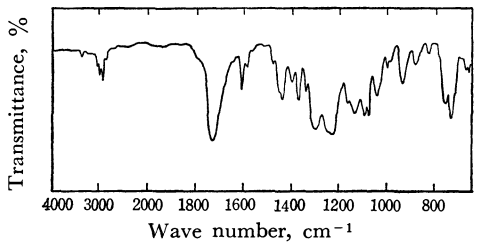

Fig. 3. Infrared spectrum of poly(ethylene isophthalate).

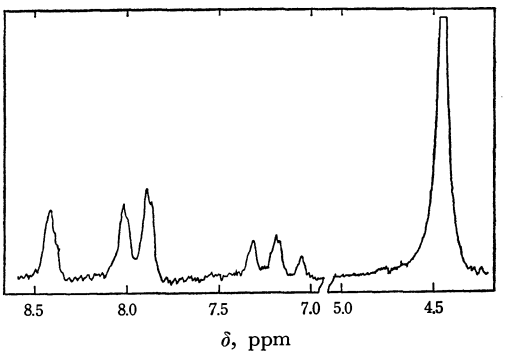

Fig. 4. NMR spectrum of poly(ethylene isophthalate).

4 respectively. In the NMR spectrum of poly(ethylene isophthalate), the complicated signals which appear at 8.42, 8.02, 7.88, 7.32, 7.20, and 7.06 ppm are due to the four protons attached to the benzene nucleus.[17] The singlet at 8.42 ppm may be due to the proton on C-2 surrounded by two ester groups. It should be noted that this singlet in the NMR spectrum of linear poly(ethylene isopthalate) shifts to 8.67 ppm in the spectrum of I (Fig. 2). The difference in the chemical shift of the proton on C-2 between linear and cyclic structures suggests that the structural conformation of a resonance system including two carbonyl groups and a benzene nucleus is different in poly(ethylene isophthalate) and in I, and that, therefore, the anisotropic effect of the resonance system is different in the linear polymer and in I.

As the melting point[18] of poly(ethylene isophthalate) was much lower than the polymerization temperature, the reaction system gradually

15) H. Zimmermann, *Faserforsch. u. Textiltechn.*, **13**, 481 (1962).
16) K. Yoda, *Kobunshi Kagaku (Chem. High Polymers)*, **24**, 472 (1967).
17) M. Murano, Y. Kaneishi and R. Yamadera, *J. Polymer Sci.*, **A3**, 2698 (1965).
18) R. Yamadera and C. Sonoda, *ibid.*, **B3**, 411 (1965)

TABLE 1. POLYMERIZATION OF CYCLIC BIS(ETHYLENE ISOPHTHALATE)

Cyclic bis(ethylene isophthalate): 1.3×10^{-3} mol
Catalyst: 1×10^{-5} mol (No. 1—23), 3×10^{-6} mol (No. 24)
2×10^{-5} mol (No. 25), 3×10^{-5} mol (No. 26)

No.	Catalyst	Temp. °C	Time min	Polymer yield, %	$[\eta]$	Mp °C
1	—	308	120	0	—	—
2	Sb_2O_3	308	120	94.5	0.50	140—143
3	Sb_2O_3	273	120	15.0	—	—
4	Sb_2O_3	265	120	trace	—	—
5	Sb_2O_3	292	20	16.2	0.21	129—131
6	Sb_2O_3	292	40	33.9	0.34	134—136
7	Sb_2O_3	292	60	86.1	0.37	133—135
8	Sb_2O_3	292	80	91.6	0.49	131—132
9	Sb_2O_3	292	120	93.0	0.50	133—135
10	Sb_2O_3	292	160	92.4	0.34	132—134
11	$SbPh_3$	308	120	78.6	0.33	118—120
12	$Ti(OC_2H_4OH)_4$	308	120	trace	—	—
13	$Al(OBu)_3$	308	120	trace	—	—
14	$Zn(OAc)_2$	308	120	trace	—	—
15	$Ca(OAc)_2$	308	120	trace	—	—
16	Bu_2SnO	265	120	trace	—	—
17	Bu_2SnO	293	120	74.6	0.21	—
18	Bu_2SnO	296	120	91.7	0.21	—
19	Bu_2SnO	321	120	84.4	0.22	—
20	Bu_2SnO	308	30	72.7	0.15	—
21	Bu_2SnO	308	60	81.3	0.26	—
22	Bu_2SnO	308	120	87.4	0.29	133—134
23	$Bu_2Sn(OBz)_2$	308	120	79.9	0.20	104—106
24	Sb_2O_3	292	40	19.8	0.21	—
25	Sb_2O_3	292	40	58.0	0.35	—
26	Sb_2O_3	292	40	62.5	0.41	135—137

melted in consequence of the progress of the polymerization reaction.

In the polymerization of I by antimony trioxide at 292°C, a high-molecular-weight polymer was obtained in spite of its low rate of conversion. Such a figure would indicate that the ring-opening polymerization of I is of a rather chain-reaction type; if so, the conversion should express the rate of polymerization. The polymerization proceeded heterogeneously, and the rate of polymerization of I was slow until the reaction time of 35 min had passed, as is shown in Fig. 5. After 35 min, the reaction system changed to a liquid and the polymerization reaction proceeded rapidly.

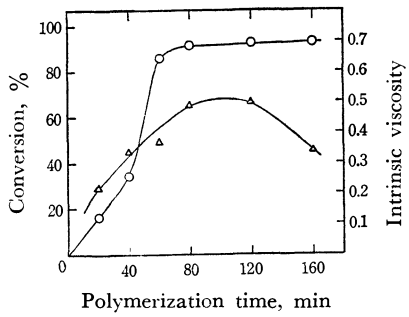

Fig. 5. Time dependences of conversion and intrinsic vicosity.
○ Conversion, △ Intrinsic viscosity
Polymerization temp. 292°C
Cyclic bis(ethylene isophthalate) 1.3×10^{-5} mol
Catalyst: Sb_2O_3 1.3×10^{-3} mol

The polymerization reaction proceeds in a heterogeneous state, and the rate of polymerization is affected by the particle size of the starting material and the degree of mixing with the catalyst. Therefore, the kinetic study is accompanied with some difficulty.

No polymeric substance was obtained by the solution polymerization of I in α-methylnaphthalene at 200°C for 600 min in the presence of diethylzinc, triethylaluminum, or triphenylstibine as a catalyst. Furthermore, an attempt at the radiation polymerization of I at room temperature by Co-60 γ-rays (total dose: 5.4×10^6R) failed.

The authors are much indebted to Mr. Murano of this Institute for the measurement of the NMR spectra.

BULLETIN OF THE CHEMICAL SOCIETY OF JAPAN VOL. 41 1690—1694 (1968)

Aminobutadienes. XIII. Anion-exchange Resins from Imidobutadiene Polymers[1]

Kenichi MURATA and Akira TERADA[2]

Government Industrial Research Institute, Osaka, Midorigaoka, Ikeda, Osaka

(Received January 18, 1968)

A method of preparing new-type anion-exchange resins from 1-phthalimido-, 1-succinimido-, and 2-phthalimido-1,3-butadiene polymers is shown. The procedure consists of two steps, the hydrolysis of the imido groups into free amine, followed by heating with hydrochloric acid to make the amino groups into the hydrochloride, and *N*-methylation by the Schotten-Baumann method. The anion-exchange resins obtained from the former two polymers show high exchange capacities, such as 5.85 and 7.21 meq/g of dry resin respectively. However, their salt-splitting capacities are not high. The mechanisms of their crosslinking on hydrolysis and of their heat-aging are also discussed.

During the studies of aminobutadiene chemistry which have been carried out in our laboratory, we attempted to prepare a new type of anion-exchange resin from the imidobutadiene polymers we had previously obtained. For the use of anion-exchange resin, a high exchange capacity per unit of volume is the chief requirement. From this point of view, it would be advantageous to use a monomer which had an amino group in a highly concentrated state per unit of weight. Since 2-phthalimido-1,3-butadiene (2-PB), on bulk polymerization by radical initiators, usually affords a tough resin as a homogeneous gel, as has already been reported,[3] we initially thought that the use of gelation agents such as divinylbenzene, divinylether, and divinylsulfide for the formation of crosslinkage in the 2-PB polymer could be unnecessary, and also that the gelation tendency of the 2-PB monomer itself was the most convenient way to introduce the exchange groups into the resin particles in a high concentration. On the other hand, in the case of 1-phthalimido-1,3-butadiene (1-PB) and 1-succinimido-1,3-butadiene (1-SB) polymers, it was usually possible to prepare soluble polymers.[4] However, insoluble gels were always afforded in the hydrolysis stage of their imido groups; this would also facilitate the preparation of the crosslinked polymers of anion-exchange-resin particles.

Although imido groups as those used here for the protection of the primary amino group can be altered into the corresponding primary amino group by a somewhat severe hydrolysis using either strong acid or alkali, hydrazinolysis by heating with hydrazine hydrate is a more effective and more moderate method for the same purpose. Several workers[5-7] have recommended the use of hydrazinolysis in preparing primary amino compounds from the corresponding phthalimides. The procedure usually consists of two cources. The first is hydrazinolysis, which gives primary amine and phthalhydrazide, commonly less soluble in solvents, while the second is treatment by hydrochloric acid, which changes the free amine into hydrochloride usually soluble in water. If a large excess of hydrazine is used, the formation of primary amine will be encouraged, as may be seen in Fig. 1.

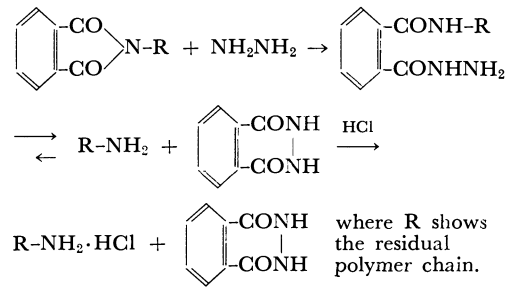

Fig. 1

A good example of this in a polymer reaction has been shown in the preparation of polyvinylamine

1) Partly reported in Japanese Patent 468683 (March 12, 1966).
2) Present address: Department of Industrial Chemistry, Kyushu Institute of Technology, Tobata-ku, Kita-kyushu.
3) K. Murata and A. Terada, *J. Polymer Sci., A-1*, **4**, 2989 (1966).
4) A. Terada and K. Murata, *ibid., A-1*, **5**, 2219 (1967).
5) G. D. Jones, J. Zomlefer and K. Hawkins, *J. Org. Chem.*, **9**, 500 (1944).
6) T. Yoshida and K. Naito, *Bull. Gov. Ind. Res. Inst., Osaka*, **1**, 144 (1950).
7) I. Skondak and A. F. Nikolaev, *Vysokomolekul Soedin*, **7**, 101 (1965); *Chem. Abstr.*, **62**, 13327 (1965).

from polyvinylphthalimide;[6] it was concluded that the reaction took place quantitatively.

The present paper deals with the hydrazinolysis of our imidobutadiene polymers and with the following quaternarization to make a new type of anion-exchange resin.

Experimental

Materials. Polymers of 1-PB, 1-SB, and 2-PB, and a copolymer of 2-PB with *N*-vinylphthalimide were prepared by radical polymerization, either in bulk or in solution process, according to the method previously reported (see also the footnotes of Table 1).[3,4]

Nitrogen Analysis. The nitrogen contents of the starting and the resulting polymers were determined by the usual Micro-Dumas method.

Hydrolysis of Imidobutadiene Polymer. On the hydrolysis of the imidobutadiene polymers, the following convenient type of procedure was usually carried out. For example, a mixture of 0.74 g of the 1-PB polymer and 16 m*l* of 80% hydrazine hydrate was refluxed for 15 hr. The mixture, which was a clear solution in the first stage of the reaction, coagulated after a while, and then a sponge-like mass separated. This cake was repeatedly washed with water to remove the excess hydrazine, and was then heated in 15 m*l* of 20% hydrochloric acid in a boiling-water bath for 6 hr to convert the free aminobutadiene polymer to the corresponding hydrochloride and to remove any phthalhydrazide formed. After the hydrochloride had been repeatedly washed with water, it was immersed in a large amount of 5% aqueous sodium hydroxide and gently heated for a while so as to generate free amine again; then it was repeatedly washed with hot water to remove any alkali and dried under a vacuum at room temperature. The yield was 0.23 g.

***N*-Methylation of Aminobutadiene Polymer.** A sample of 0.21 g of aminobutadiene resin, in a dried free-amine form, in 15 m*l* of ethanol was methylated with 5 g of methyl iodide by the Schotten-Baumann method in the presence of a small excess of 10% alcoholic potassium hydroxide. After the mixture had been refluxed for 10 hr, the resin was collected on a glass filter and washed with water. The resulting I-type resin was converted to the OH-type resin by treating it with 5% aqueous potassium hydroxide, and finally to the Cl-type resin by treating it with hydrochloric acid. This resin was then sufficiently washed with ethanol and dried under a vacuum at room temperature over potassium hydroxide pellets. The yield was 0.34 g.

Determination of Salt-splitting Capacity. A sample of dried Cl-type resin, exactly weighed and found to be from 100 to 200 mg, was immersed in 100 m*l* of 1 N sodium hydroxide for 24 hr at room temperature, and then repeatedly washed with water to remove the excess alkali. The resin was immersed in 100 m*l* of 1 N sodium chloride for 24 hr, gathered on a glass filter, and repeatedly washed with other portions of 1 N sodium chloride; the final volume of the filtrate with the gathered washings was then exactly adjusted to 200 m*l* using a volumetric flask. A 50 m*l* portion of the solution was titrated with 0.1 N hydrochloric acid in the presence of a methyl orange indicator to determine the amount of free alkali.

Determination of Total Anion-exchange Capacity. The sample used in the above salt-splitting-capacity determination was again immersed in 100 m*l* of 1 N hydrochloric acid for 24 hr, washed completely with methanol until the washings became neutral to remove the excess acid, and then immersed in 100 m*l* of 1 N sodium sulfate for 24 hr. The resin was repeatedly washed with other portions of 1 N sodium sulfate, after which the total volume of the filtrate and the washings was exactly adjusted to 200 m*l*. A 50 m*l* portion of the solution was titrated as usual with 0.1 N silver nitrate to determine the quantity of free chloride ions present.

Aging Test of the Cl-type Resin. The aging test of the *N*-methylated resin at room temperature and on heating under an atmospheric pressure was carried out using two different samples, which had been obtained from 1-PB and 1-SB polymers respectively. Both samples were successively heated at 60, 90 120, 150, and 180°C in that order for 24-hr periods; at the end of each heating step, the total anion-exchange and salt-splitting capacities were measured as mentioned.

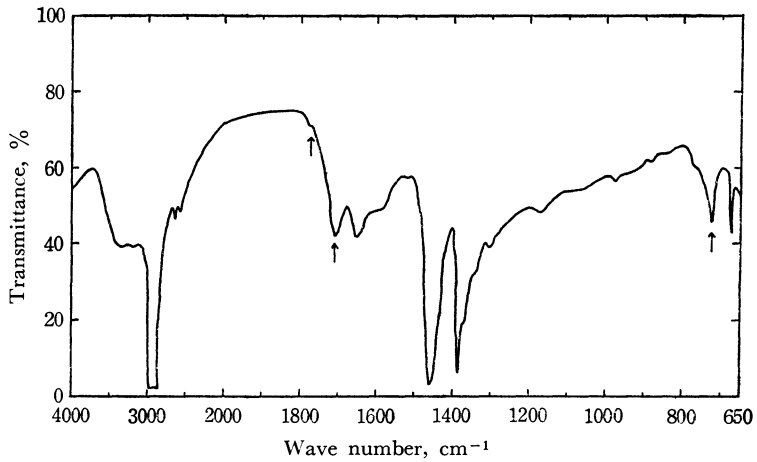

Fig. 2. Infrared spectrum of 2-aminobutadiene polymer (sample No. 6) in Nujol paste.

Results and Discussion

The hydrazinolysis and subsequent hydrochloric acid treatment of the 1-PB and 1-SB polymers gave crosslinked aminobutadiene polymers in good yields; they could be recognized as almost pure samples by their nitrogen contents. In the case of the 2-PB polymer, however, this treatment was unsatisfactory, giving a quite different result. The hydrolysis of the 2-PB polymer did not take place smoothly, and the resulting aminobutadiene polymer had less nitrogen content than in the other cases. Moreover, the yields were low, as Table 1 shows. This low yield seems to indicate a considerable loss of the used sample during the hydrolysis procedures.

Their low nitrogen contents may be considered to indicate a difficulty in the hydrolysis of the phthalimido group in the 2-PB polymer, because

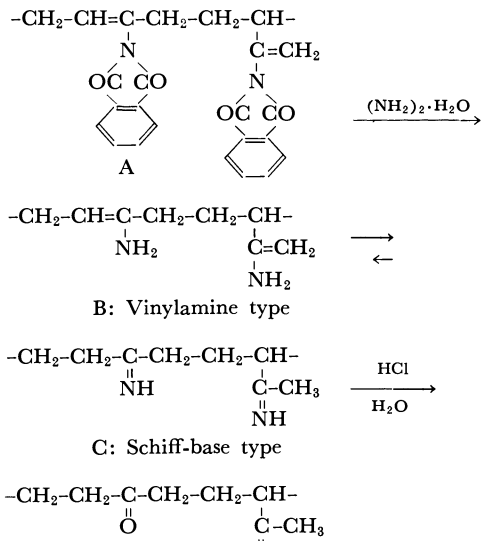

Fig. 3.

the infrared spectrum of the sample No. 6, for example, leaves phthalimido-carbonyl bands at 1770 (shoulder) and 1710 cm^{-1} and an *O*-disubstituted benzene band at 725 cm^{-1}, as is shown in Fig. 2. On the other hand, the 2-PB polymer, on hydrolysis, always gives a vinylamine structure in each of monomer unit, and this structure is generally in an equilibrium state with the ketimine structure—indeed, the latter form is usually preferable (Fig. 3, B and C).[8] This ketimine can be easily hydrolyzed partially with the concentrated hydrochloric acid of the post-treatment, and affords a ketone structure, which must reduced the nitrogen content of the resulting polymer less than the original one. On the direct hydrolysis of the 2-PB polymer with concentrated hydrochloric acid or 10% aqueous sodium hydroxide, the resulting polymers showed nitrogen contents of 1.92 and 2.62% respectively. This may show phthalimide elimination during hydrolysis, as is shown in Fig. 4, because of the phthalimido group attached to the carbon of the double bond.

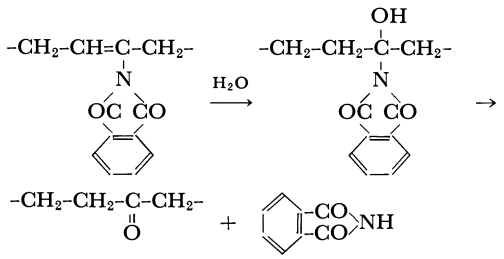

Fig. 4.

Also, both the 1-PB and 1-SB polymers contain approximately 80% of the 1,4-configuration and 20% of the 3,4-configuration.[4] On hydrolysis, the structure of the latter configuration should afford an aldmine structure analogous to that above. As to the crosslinking of these hydrolyzed polymers, some assumptions are possible. Some of these aldmine and ketimine will preferentially react with hydrazine to form their hydrazones

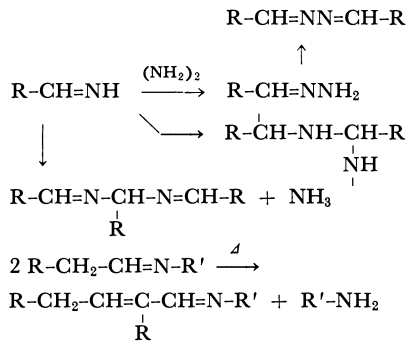

Fig. 5.

by exchange reactions,[9] and these ammonia- and hydrazine-derivatives of the carbonyl groups will partially react with each other to form intra- and inter-molecular crosslinking spontaneously,[10] as with the samples shown in Fig. 5. Carbon-carbon condensations of the aldol type often occur if there is an α-methylene group.[10]

The results of the *N*-methylation of the aminobutadiene polymers obtained from the above hydrolysis are shown in Table 2. Their total anion-exchange capacities were in the range between 2.6 and 7.2 meq/g of dry resin; however, their salt-splitting capacities were not high. For

8) For example, P. A. S. Smith, "The Chemistry of Open-chain Organic Nitrogen Compounds," Vol. I, W. A. Benjamin, New York (1965), p. 295.

9) Ref. 8, p. 301.

10) Ref. 8, p. 298.

Table 1. Hydrolysis of imidobutadiene polymers[a]

Sample No.	Polymer[b]	(g)	Hydrazine hydrate (ml)	Reaction time (hr)	Yield (g)	Nitrogen[h] content (%)	Yield as amino-butadiene polymer (%)
1	1-PB[c]	0.74	16	15	0.23	19.71	89
2	1-SB[d]	0.77	16	15	0.22	21.29 21.03	82
3	2-PB[e]	0.17	5	15	—	7.00 7.06	—
4	2-PB[e]	0.57	10	24	0.15	9.16 9.34	75
5	2-PB[f]	0.34	8	15	0.08	10.11	67
6	2-PB[f]	1.00	15	15	0.21	9.10 9.01	60
7	2-PB-VPI copolymer[g]	0.82	10	20	0.15	15.46 15.32	56[i]

a) The reactions were usually carried out under reflux, except in the case of No. 4. The reaction temperature for No. 4 was 180°C in a sealed tube. Each of sample numbers used from Table 1 through Table 3 indicate the same sample.
b) All the polymers were prepared by radical polymerization, using benzoyl peroxide as an initiator.
c) Obtained at 116°C in a bulk state, $\eta_{sp}/c=3.0$.
d) Obtained at 60°C in an acetylene tetrachloride solution, $\eta_{sp}/c=0.35$.
e) Obtained at 85°C in a bulk state.
f) Obtained at 60°C in an acetylene tetrahloride solution, $\eta_{sp}/c=1.0$.
g) Obtained by the copolymerization of 2-PB with *N*-vinylphthalimide at 60°C in an acetylene tetrachloride solution, N%; 7.22, 7.27%.
h) The theoretical nitrogen contents of phthalimidobobutadiene, succinimidobutadiene, and aminobutadiene polymers are 7.03, 9.27, and 20.27%, respectively.
i) Calculated on the assumption that this product is the homopolymer of 2-aminobutadiene.

Table 2. *N*-Methylation of aminobutadiene polymers[a] and their anion-exchange capacities

Sample No.	Weight (g)	Methyl iodide (g)	Ethanol (ml)	Reaction time (hr)	Yield[b] (g)	Nitrogen[c] content (%)	Total anion-exchange capacity (meq/g of dry resin)
1	0.21	10	15	10	0.28	11.87 11.46	5.85
2	0.21	5	15	10	0.34	11.28 11.54	7.21
4	0.11	5	8	10	0.12	7.37 7.85	3.22
5	0.07	5	7	10	0.09	6.87 7.14	2.62
6	0.13	5	10	14	0.20	8.57	3.52

a) The reactions were carried out under reflux.
b) The yields show those of the Cl-type resins.
c) As Cl-type resins vacuum-dried at room temperature.

Table 3. Heat-aging test of *N*-methylated resin hydrochlorides

Temperature (°C)	Sample No. 1		Sample No. 2	
	Salt-splitting capacity (meq/g of dry resin)	Total anion-exchange capacity (meq/g of dry resin)	Salt-splitting capacity (meq/g of dry resin)	Total anion-exchange capacity (meq/g of dry resin)
60	1.19	5.83	1.05	6.78
90	0.52	5.36	0.69	5.85
120	0.38	4.80	0.53	5.09
150	0.20	4.43	0.31	4.65
180	—	2.85	—	3.08

example, sample No. 1 showed a value of 0.84, while No. 2 showed 1.01 meq/g of dry resin.

The aging test of the *N*-methylated resin hydrochlorides showed that the usual keepting of them for two years under an atmospheric pressure and at room temperature was harmless to their total anion-exchange capacities. Table 3 shows the results of the heat-aging test.

The more rapid decrease in the rate of the salt-splitting capacity than in the rate of the total anion-exchange capacity indicates that there is a methyl chloride elimination[11] from a quaternary ammonium chloride group which reduces the salt-splitting capacity.

The authors wish to thank Professor Shizunobu Hashimoto of Doshisha University and Dr. Isao Shiihara of this Institute for their helpful suggestions during this work.

11) I. T. Millar and H. D. Springall, "Sidgwick's Organic Chemistry of Nitrogen," Clarendon Press, Oxford (1966), p. 114.

BULLETIN OF THE CHEMICAL SOCIETY OF JAPAN VOL. 41 1694—1696 (1968)

Aluminum Silanolates
Acid Strength and Polymerization Catalyst Activity

Takeo SAEGUSA, Takashi UESHIMA and Kunioki KATO

Department of Synthetic Chemistry, Kyoto University, Sakyo-ku, Kyoto

(Received January 24, 1968)

Two aluminum silanolates, diethyl(trimethylsiloxy)aluminum (I) and tris(trimethylsiloxy)-aluminum (II), were compared with the corresponding aluminum alcoholates in terms of their acid strength and in their catalyst behavior in the polymerizations of cyclic ethers and vinyl ether. The reference aluminum alcoholates were diethylaluminum *t*-butoxide (III) and aluminum *t*-butoxide (IV). The Lewis acid strength was examined by means of two methods, the Hammett indicator method and the shift of the IR carbonyl band ($\Delta\nu_{C=O}$) of *n*-butyraldehyde. Four aluminum compounds, I—IV, were weaker Lewis acids than triethylaluminum; *i. e.*, the replacement of the ethyl group of triethylaluminum with either a siloxy group or an alkoxy group brought about a decrease in the acid strength. The acid strength of I and II were demonstrated to be stronger than that of the reference alcoholates, III and IV. A difference in polymerization catalyst activity was also observed between aluminum silanolates and the reference alcoholates; it was reasonably explained by the difference in acid strength.

In a series of studies of metal alkyls and metal alcoholates as polymerization catalysts, we have reported that the triethylaluminum-trialkylsilanol system is an effective catalyst for the polymerizations of cyclic ethers such as tetrahydrofuran and epichlorohydrin, isobutyl vinyl ether and acetaldehyde.[1]

The purpose of the present study is to examine the acid characters and the polymerization catalyst activities of two aluminum silanolates, diethyl-(trimethylsiloxy)aluminum (I) and tris(trimethylsiloxy)aluminum (II), in comparison with those of two reference aluminum alcoholates, diethylaluminum *t*-butoxide (III) and aluminum *t*-butoxide (IV).

A difference between II and IV in their catalytic behavior in the Tishchenko reaction has previously been reported.[2]

Results and Discussion

Table 1 shows the results of the acid-strength measurements of aluminum silanolates and aluminum alcoholates as well as of triethylaluminum.

The acid strength was examined by two methods. The one was the Hammett indicator method,[3,4] while the other was based upon the magnitude of the shift of the ir carbonyl band of *n*-butyraldehyde, which was adapted as the reference base. The indicator method showed that both aluminum silanolates and aluminum alcoholates were weaker Lewis acids than triethylaluminum. This acid-strength difference was also demonstrated by the ir technics; *i. e.*, triethylaluminum caused a shift of the ir carbonyl band of xanthone ($\Delta\nu_{C=O}=83$

1) T. Saegusa, T. Ueshima, T. Nakajima and J. Furukawa, *Kogyo Kagaku Zasshi (J. Chem. Soc. Japan, Ind. Chem. Sect.)*, **68**, 2514 (1965).

2) T. Saegusa, S. Kitagawa and T. Ueshima, This Bulletin, **40**, 1960 (1967).

3) H. A. Benesi, *J. Am. Chem. Soc.*, **78**, 5490 (1956).

4) H. Imai, T. Saegusa and J. Furukawa, *Makromol. Chem.*, **81**, 92 (1965).

TABLE 1. ACID STRENGTH OF ALUMINUM SILANOLATES AND ALUMINUM ALCOHOLATES

	Indicators[a] (pK_a value)						$\Delta\nu_{C=O}$(cm^{-1}) of *n*-butyraldehyde[b]
	I (+6.8)	II (+4.8)	III (+4.0)	IV (+3.3)	V (−3.0)	VI (−5.6)	
$Al(C_2H_5)_3$	—	A	A	A	A	B	
$(C_2H_5)_2AlOSi(CH_3)_3$ (I)	A	A	B	B	B	B	156
$(C_2H_5)_2AlOC(CH_3)_3$ (III)	A	A	B	B	B	B	147
$Al(OSi(CH_3)_3)_3$ (II)	A	A	B	B	B	B	147
$Al(OC(CH_3)_3)_3$ (IV)	B	B	B	B	B	B	140

a) Indicators: I=Neutral red; II=Methyl red; III=Phenylazonaphthylamine; IV=Butter yellow V=Dicinnamalacetone; VI=Benzalacetophenone. A; acidic color; B: basic color.
b) Error=±3 cm^{-1}.

cm^{-1}), whereas two aluminum silanolates and two aluminum alcoholates did not. Thus, the replacement of the ethyl group of triethylaluminum by either a siloxy group or an alkoxy group decreased the acid strength. However, aluminum silanolates were stronger acids than the corresponding alcoholates. The magnitudes of the $\Delta\nu_{C=O}$ values of *n*-butyraldehyde caused by aluminum silanolates were higher than those caused by the reference aluminum alcoholates. This observation was partly supported by the indicator method; *i. e.*, II was acidic toward neutral red and methyl red, whereas IV was basic to these indicators. This acid-strength difference can not be explained by a simple consideration of electronegativity. From the electronegativities of carbon and silicon, the electron definciency of aluminum alcoholates is considered to be higher than that of aluminum silanolates. Hence, the former might be expected to be stronger acids. However, the reverse is true in the present case. The stronger acid character of aluminum silanolates in comparison with the reference aluminum alcoholates may be due, at least in part, to the electron-withdrawing effect of the silicon atom through the d_π—p_π bond of the silicon-oxygen linkage.[5]

The catalyst activities of these aluminum compounds in the polymerizations of cyclic ethers and vinyl ether were interpreted in terms of their acid strength. The data of the ethylene oxide polymerization are summarized in Table 2, in which the polymer yield and the yield of the dioxane byproduct, the cyclic dimer of ethylene oxide, are indicated. All four aluminum compounds induced the ethylene oxide polymerization. However, dioxane was formed only in the runs with aluminum silanolates catalysts. The dioxane formation is quite clear in the case of I, which implies the mechanism of cationic polymerization. In our mechanistic study[6] of the catalyst behavior of organoaluminum compound systems, we have established that the formation of dioxane as a byproduct in the ethylene oxide polymerization is an indication of cationic polymerization.

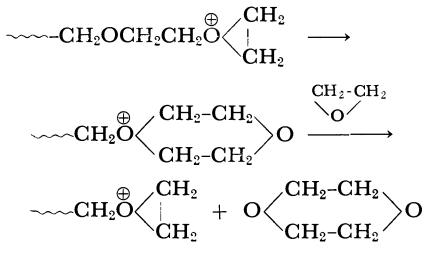

TABLE 2. POLYMERIZATION OF ETHYLENE OXIDE
(Monomer, 0.1 mol; catalyst, 2 mol%; bulk polymerization, at 55°C for 24 hr)

Catalyst	Polymer yield (%)	$[\eta]$[a]	Yield of dioxane (%)
$(C_2H_5)AlOSi(CH_3)_3$ (I)	13	0.62	5.8
$(C_2H_5)_2AlOC(CH_3)_3$ (III)	7	0.53	0
$Al(OSi(CH_3)_3)_3$ (II)	98	0.08	0.6
$Al(OC(CH_3)_3)_3$ (IV)	40	0.96	0

a) Measured in benzene at 30°C.
b) The limit of detection was 0.02%.

TABLE 3. POLYMERIZATIONS OF 3,3-BIS(CHLOROMETHYL)-OXACYCLOBUTANE (BCMO), TETRAHYDROFURAN (THF) AND ISOBUTYL VINYL ETHER (IBVE)
(Monomer, 0.1 mol; catalyst, 2 mol%; bulk polymerization, at 0°C for 24 hr)

Catalyst	Polymer yield		
	BCMO[a]	THF[a]	IBVE[b]
$(C_2H_5)_2AlOSi(CH_3)_3$ (I)	87	10	2
$(C_2H_5)_2AlOC(CH_3)_3$ (III)	2	0	0
$Al(OSi(CH_3)_3)_3$ (II)	—	3(7)[c]	77
$Al(OC(CH_3)_3)_3$ (IV)	—	0(0)	0

Cocatalyst: epichlorohydrin (2 mol%) for a)
$(CH_3)_3CCl$ (2 mol%) for b)
c) 40°C, 24 hr

5) R. West and R. H. Baney, *J. Am. Chem. Soc.*, **81**, 1645 (1959).

6) T. Saegusa, T. Ueshima and S. Tomita, *Makromol. Chem.*, **107**, 131 (1967).

Aluminum silanolates caused the polymerization of some cationically-polymerizable monomers, whereas the corresponding aluminum alcoholates did not do so (Table 3).

These cationic catalyst activities of aluminum silanolates correspond to their stronger Lewis-acid characters.

Experimental

All the experiments were conducted under a nitrogen atmosphere.

Reagents. *Monomers, Solvents and Cocatalysts.* All the reagents were carefully purified by the usual procedures.

Catalysts. I was prepared by a reaction between triethylaluminum and trimethylsilanol and was purified by fractional distillation; bp 103°C at 1.1 mmHg. II was synthesized according to the method reported in the literature.[7] III was prepared by the reaction of triethylaluminum with *t*-butanol which was sublimed at 90°C under reduced pressure (0.1 mmHg). IV was synthesized from *t*-butanol and aluminum foil and was purified, just prior to use, by being recrystallized from benzene five times. In the present study, it has been found that IV is not so stable and that it decomposed even at room temperature. The decomposition product, which was insoluble in hot benzene, was a stronger acid than IV. Therefore, it was necessary to purify IV by recrystallization just before use. Otherwise reliable results could not be obtained.

Others. Dioxane, methanol, and benzene were commercial reagents of a high purity and were used without further purification.

Acid-strength Measurements. The Hammett method was performed as has been described before.[4] The shifts of the carbonyl-stretching vibration of *n*-butyraldehyde were measured in Nujol.

Polymerization. Polymerization was performed in a sealed tube. The after-treatments of BCMO,[8] THF,[9] and IBVE[10] polymerization systems were the same as those described before.

In the ethylene oxide polymerization, the volatile matter was first evaporated from the reaction mixture at 80°C under reduced pressure (below 0.5 mmHg), and then analyzed by vpc for dioxane. A reference experiment showed that dioxane, if it was present in the polymerization mixture, could be detected and quantitatively analyzed by the above procedure. The evaporation residue was treated with a mixture of benzene and ammonia water and dried up. The polymer was then dissolved again in benzene. The catalyst precipitate was removed, and the polymer was recovered from the filtrate.

7) H. Schmidbaur, *Chem. Ber.*, **96**, 2696 (1963).

8) T. Saegusa, H. Imai and J. Furukawa, *Makromol. Chem.*, **65**, 224 (1963).

9) H. Imai, T. Saegusa, S. Matsumoto, T. Tadasa and J. Furukawa, *Makromol. Chem.*, **102**, 222 (1967).

10) T. Saegusa, H. Imai and J. Furukawa, *ibid.*, **79**, 221 (1964).

BULLETIN OF THE CHEMICAL SOCIETY OF JAPAN VOL. 41 1696—1700 (1968)

3d-Orbital Resonance in Divalent Sulfides. XIV. Free Radical Copolymerization of Ketene Diethylmercaptal with Styrene[1,2]

Waichiro TAGAKI, Tsutomu TADA,[3] Ryuichi NOMURA and Shigeru OAE

Department of Applied Chemistry, Faculty of Engineering, Osaka City University, Sugimoto-cho, Sumiyoshi-ku, Osaka

(Received January 24, 1968)

Free radical copolymerization reactions of ketene diethylmercaptal (I) and *p*-methylmercaptostyrene (III) with styrene have been carried out. The *Q*-values for I and III are found to be 2.7 and 3.3 respectively, and these and other related observations are discussed in terms of electron-sharing conjugation involving 3d-orbital of sulfur atom.

The ability of sulfur atom to stabilize carbanion has been well known for positively charged sulfur compounds.[4] The major factor for such stabilization is believed to be 3d orbital resonance of sulfur atom. As for divalent sulfides, we have also presented evidence for 3d orbital resonance in the base-catalyzed hydrogen exchange reactions of mercaptals.[5] Thus it seems to be clear that sulfur atom, regardless of its valence state, does stabilize carbanion, presumably by accepting negative charge into its vacant 3d orbital. This ability of

1) This work was generously supported by the Petroleum Research Fund, administered by the American Chemical Society.

2) This is a part of the works submitted to Osaka City University as the Master Thesis by T. Tada.

3) Present address, Toyo Rubber Co. Ltd.

4) C. C. Price and S. Oae, "Sulfur Bonding," Ronald Press, New York (1962).

5) a) S. Oae, W. Tagaki and A. Ohno, *Tetrahedron*, **20**, 417, 427 (1964). b) *Ibid.*, **20**, 437 (1964).

sulfur atom sharply contrasts with that of oxygen atom which does not have available d-orbital for such stabilization, and moreover α-oxygen group appears to destabilize carbanion.[5a,6]

Meanwhile, in carbonium ion reaction, electron donating conjugation becomes predominant, *i. e.*, nitrogen and oxygen compounds are generally more reactive than the corresponding sulfur analogs. In the free radical reaction, however, our present knowledge is not quantitative enough to predict satisfactorily the course of reaction or the extent of stabilization of an odd electron by sulfur atom. If a free radical center is electrophilic in nature, one might expect that electron-donating conjugation is more dominating over electron-accepting conjugation. In accord with this, the following resonance of the types of (1) and (2) has been suggested by Russell and his coworkers, which accounts for greater reactivity of nitrogen compound than that of the analogous sulfur compound toward the abstraction of α-hydrogen atom:[7]

$$\rangle\ddot{N}\text{-}\dot{C}H_2 \longleftrightarrow \rangle\dot{N}^+\text{-}\ddot{C}H_2^- \qquad (1)$$

$$\text{-}\ddot{S}\text{-}\dot{C}H_2 \longleftrightarrow \text{-}\dot{S}^+\text{-}\ddot{C}H_2^- \qquad (2)$$

On the other hand, another type of conjugation has been postulated by Price and Oae: electron-sharing conjugation of the type of (3) is conceivable for divalent sulfur compound where sulfur atom accepts odd electron by expanding its valence shell:[4]

$$\text{-}\ddot{S}\text{-}\dot{C}\text{-} \longleftrightarrow \text{-}\dot{S}^-\text{=}C\text{-} \qquad (3)$$

The importance of the latter type of 3d orbital resonance of the sulfur atom has been displayed in several radical reactions, *i. e.*, in free radical addition reaction to the double bond,[8] in peroxide decomposition,[9] and in radical copolymerization reaction,[10] etc. Unfortunately, most of these data are either qualitative or fragmental. Moreover the relative importance of the opposing effects of the type of (2) and (3) should depend on types of reaction, attacking radical and its acceptor.

In the free radical copolymerization reactions, Price and his coworkers found that vinyl sulfide and divinyl sulfide were much more reactive toward growing polystyryl radical than the corresponding oxygen analogs.[10] They treated the data by their *Q-e* scheme.[10c] Although this *Q-e* scheme is purely empirical, it has been shown in a number of cases that larger resonance stabilization of a growing radical seems to be associated with larger *Q* value, and it has been proved to be useful for quantitative estimation of resonance stabilization of a growing radical. For example, the *Q* value of vinyl sulfide is larger than that of vinyl ether, and this has been suggested to be due to the resonance stabilization of the growing radical according to the type of (3). One way to test this concept is to determine the *Q* value of ketene mercaptals, since, just as in the case of base catalyzed hydrogen exchange reactions of mercaptals, the substitution of one additional mercapto group in ketene mercaptal would increase *Q* value substantially over that of vinyl sufide, if *Q* value is a measure of such resonance.

As one of our broad interest in the nature of sulfur bonding, we have now carried out the copolymerization of ketne diethylmercaptal and *p*-methylmercaptostyrene with styrene and compared with those of the corresponding oxygen analogs.

Results and Discussion

All of the compounds, ketene diethylmercaptal (I), ketene diethylacetal (II) and *p*-methylmercaptostyrene (III), were prepared by the known methods as described in the experimental section. Their copolymerizations with styrene were conducted at 60°C with azoisobutyronitrile as the free radical initiator. The monomer, III, gave its copolymer in a satisfactory yield with each monomer ratio. The copolymerization of I was not entirely satisfactory, since, with higher proportion of I, we were unable to isolate any polymer. However, four mixtures (Table 4) gave enough copolymer for the *Q-e* analysis. Unfortunately, the monomer II did not give copolymer. Instead, the only polymer obtained was concluded to be polystyrene, leaving II unreacted (Table 6). This is not surprising in view of the expected increase of negative e-value, probably less than that of I, -2.1, and resulting in an increased difference between the e-values of styrene and the acetal. Perhaps a similar argument cannot be applied to the failure of obtaining copolymer of I in a higher monomer ratio, since, in this case, no polymer, not even polystyrene, could be isolated.

The *Q* and *e* values, thus obtained, are shown in Tables 1 and 2 together with those of the related compounds. Table 1 indicates: (1) The *Q* values of oxygen compounds are very small, especially for ketene diethylacetal (II) which underwent negligible copolymerization. (2) The *Q* values of the sulfone and the silicon compounds are also small. (3) In contrast, the divalent sulfur compounds have large *Q* values. (4) Substitution of one additional mercapto group for vinyl sulfide to ketene diethylmercaptal (I) results in a remarkable increase in *Q* values, much greater

6) J. Hine, L. G. Mahone and C. L. Liotta, *J. Am. Chem. Soc.*, **89**, 5911 (1967).
7) G. A. Russell and R. C. Williamson, Jr., *J. Am. Chem. Soc.*, **86**, 2357 (1964).
8) H. J. Alkema and J. F. Arens, *Rec. trav. chim.*, **79**, 1257 (1960).
9) W. G. Bentrude and J. C. Martin, *J. Am. Chem. Soc.*, **84**, 1561 (1962).
10) a) C. C. Price and J. Zomlefer, *ibid.*, **72**, 14 (1950). b) C. E. Scott and C. C. Price, *ibid.*, **81**, 2672 (1959). c) T. Alfrey and C. C. Price, *J. Polym. Sci.*, **2**, 101 (1947).

TABLE 1. THE Q-e VALUES FOR THE COPOLYMERIZATION OF KETENE DIETHYLMERCAPTAL (I) AND OF RELATED COMPOUNDS WITH STYRENE

Compound	Q	e	Ref.
$CH_2=CH-OC_2H_5$	0.02	−1.6	11
$CH_2=CH-SCH_3$	0.34	−1.5	10a
$(CH_2=CH)_2S$	0.68	−1.1	10b
$CH_2=C(OC_2H_5)_2$ (II)	—	—a)	12
$CH_2=C(SC_2H_5)_2$ (I)	2.70	−2.1	12
$CH_2=CHSO_2CH_3$	0.11	1.2	10a
$CH_2=CHSi(CH_3)_3$	0.03	−0.1	13

a) Only homopolymerization of styrene.

TABLE 2. THE Q-e VALUES FOR THE COPOLYMERIZATION OF p-METHYLMERCAPTOSTYRENE (III) AND OF RELATED COMPOUNDS WITH STYRENE

Compound	Q	e	Ref.
p-$CH_3S-C_6H_4-CH=CH_2$ (III)	3.29	−1.65	12
$C_6H_5-CH=CH_2$	1.0	−0.8	17
p-$CH_3O-C_6H_4-CH=CH_2$	1.0	−1.0	17
p-$NO_2-C_6H_4-CH=CH_2$	1.86	0.4	17
-$CH=CH_2$	3.0	−0.80	17

increase than that from vinyl sulfide to divinyl sulfide.

The smaller Q values of the oxygen compound compared with those of the sulfur compounds suggests that in this free radical addition reaction to the double bond the type (2) resonance is less important than the type (3) resonance. In an effort to extend the concept of the electron-sharing conjugation of the type (3), the hydrogen abstraction reaction with various compound substituted at α-carbon atom by heteroatom has been investigated. It was found, however, that the transition state of the hydrogen abstraction reaction by t-butoxy or even by phenyl radical is considered to assume a partial carbonium ion character when one judges from the substituent effect on the rates and the negative ρ-value. Thus the order of reactivity of the compounds substituted by hetero atom at α-position is in the order of nitrogen->oxygen-> unsubstituted compound.[14] However the situation is different with the mercapto-substituent whose rate-enhancing effect is somewhat larger than that of the corresponding oxygen substituent, despite of the less electron-releasing conjugative effect of mercapto group than that of the corresponding oxygen-compounds. This small anomaly has been suggested to be due to a small contribution of the electron-sharing conjugation of type (3). Meanwhile, ρ-values for the reactions of vinyl phenyl sulfides toward attacking polystyryl radical have been shown to be positive,[15] indicating that the transition state for this addition reaction resembles more carbanion rather than carbonium ion. Unusually low reactivity of the oxygen compounds is consistant with this view, since it has been shown in the carbanion forming reaction that α-alkoxy group even destabilizes the incipient carbanion.[5a,6] Importance of the type (3) resonance can be seen in the small Q-values of the sulfone and the silicon compounds which have no available lone electron pair for such conjugation. On the other hand, the abstraction of α-hydrogen atom from the sulfonyl compound has been noted to be extremely difficult.[14] Therefore the moderate Q value of methyl vinyl sulfone also seems to suggest the carbanion type transition state, for sulfonyl group is known to delocalize the charge very effectively.

Incidentally, as one can easily notice, the "electron-sharing" conjugation of the type (3) is possible only with groups bearing lone electron pair such as divalent sulfides that can expand the outer valence shell beyond octet to accomodate an odd electron from the adjacent carbon atom.

We believe that the observations, (3) and (4), together with (1) are good indications of the occurrence of such 3d orbital resonance. The large Q value of ketene diethylmercaptal (I) is in accord with the large rate enhancement in the base-catalyzed hydrogen exchange reaction in going from diethyl mercaptal to triethyl orthothioformate.[5a] The resonance stabilization of growing radical of I could be achieved by the contributions of the resonance structures shown in Ia-Ic, *i.e.*, the electron-sharing conjugation of the type (3).

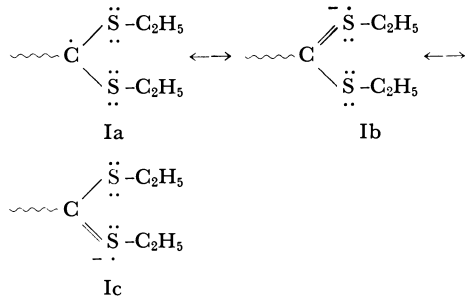

Ia Ib

Ic

The newly obtained Q value of p-methylmercaptostyrene (III) and those of the related compounds are shown in Table 2. Imoto, Kinoshita and their coworkers have developed a method to estimate resonance term in linear free energy relationship in

11) C. C. Price and T. C. Schwarm, *J. Polymer Sci.*, **16**, 577 (1955).
12) Present work.
13) C. E. Scott and C. C. Price, *J. Am. Chem. Soc.*, **81**, 2670 (1959).
14) K. Uneyama, Y. Nanba and S. Oae, *Yuki Radical Hanno Toronkai* (Symposium on Organic Radical Reaction, Nagoya, 1967, Unpublished work.
15) K. Tsuda, S. Kobayashi and T. Otsu, *J. Polymer Sci.*, submitted: T. Otsu, *Iokagobutsu Toronkai* (Symposium on Sulfur Compounds), Osaka, 1967.

the copolymerization of styrene.[16] Their method suggests the Q value of III to be unusually high. So is the value of 2-vinylthiophene. A likely explanation would be that while a hetero atom combined directly to vinyl double bond could destabilize growing radical by either inductive or lone electron-pair repulsion or by both, the removal of the hetero atom away from the reaction center, for example to the *p*-position of styrene, definitely reduces such effect, and hetero atom, in turn, would display more effective conjugation through phenyl ring, mobilizing an odd electron from its lone pair.

Table 3 shows the UV spectra of I together with those of the related compounds. The large red shift in divinyl sulfide than in vinyl sulfide has been suggested to be partly due to the "through conjugation".[4a] Although such through-conjugation is impossible, similar order of red shift is found in I. This would suggest a non-bonding interaction between the two sulfur atoms in I in the photo-excited state.[5b]

Table 3. Ultraviolet spectra of ketene diethylmercaptal and of the related sulfides

Compound	Solvent	λ_{max}, mμ	log ε	Ref.
CH_2=CH-SCH_3	EtOH (95%)	230	4.20	10a
		240	4.00	10a
$(CH_2$=CH-$)_2S$	Dioxane	240	3.90	10b
		255	3.90	10b
CH_2=C(S-$C_2H_5)_2$ (I)	EtOH	234	3.53	12
		249	3.60	12
C_2H_5-CH(S-$C_2H_5)_2$	EtOH	231	2.92	5b
C_2H_5-CH(S-CH_2)(CH_2-S-CH_2)	EtOH	231	2.71	5b
		250	2.79	5b

Experimental

Preparation of Materials. *Ketene Diethylmercaptal* (I)[18] was prepared by the acid catalyzed elimination of ethyl mercaptan from triethyl orthothioacetal (bp 121°C/10 mm), 80°C/15 mmHg., n_D^{20} 1.5304 (lit., 1.5306[18]).

Ketene Diethylacetal (II)[19] was prepared by the elimination reaction of triethyl β-bromoorthoacetate (bp 80°C/10 mmHg), with dispersed sodium metal in anhydrous benzene, bp 68°C/100 mmHg (lit., 68°C/100 mmHg[19]), n_D^{27} 1.4095 (lit., 1.4110[19]).

p-Methylmercaptostyrene was prepared starting from *p*-bromoacetanilide. *p*-Bromoacetanilide was converted to *p*-bromothioanisole by the diazotization, followed by the reaction with methyl mercaptan, bp 103—105°C/14 mmHg, mp 40°C (lit. mp 40°C[20]). *p*-Bromothioanisole was converted to Grignard reagent in tetrahydrofuran and reacted with acetaldehyde. The resulting alcohol was dehydrated with potassium hydrogen sulfate at 260°C under vacuum to give *p*-methylmercaptostyrene, bp 82°C/3 mmHg. (Lit. bp 83—85°C/3 mm[21]), identified by IR, and NMR spectra.

Table 4. Copolymerization of ketene diethylmercaptal (M_2) with styrene (M_1)[a]

M_2[b]	Reaction time, hr	Conversion, %[c]	S%[d]	C%	H%	m_2[e]
0.200	30	12.3	9.64	82.58	7.86	0.167
0.300	30	10.1	13.35	78.59	7.95	0.239
0.400	30	9.5	16.62	74.84	7.98	0.258
0.500	30	7.2	19.12	72.58	8.14	0.322
0.600	30	f				
0.700	30	f				
0.800	30	f				

r_1=1.046, r_2=0.1587, Q=2.79, e=−2.1[g]

a) The other two runs gave almost the same results.
b) Mole fraction in monomer mixture. Total 0.08—0.05 mol of monomer and 35 mg of azoisobutyronitrile.
c) Weight % of the dried copolymer precipitated from methanol.
d) Used for the estimation of Q and e.
e) Mole fraction of I in copolymer calculated from S %.
f) No polymer.
g) The other set of Q-e values were eliminated based on the fact that they did not accord with the reported value of k_{11}(=176 *l*/mol/sec, 60°C)[22] for styrene polymerization.

Table 5. Copolymerization of *p*-mercaptostyrene (M_2) with styrene (M_1)[a]

M_2	Reaction time, hr	Conversions, %	S%	m_2
0.250	0.75	5.67	8.56	0.317
0.333	0.75	5.43	10.32	0.393
0.500	0.75	7.13	13.16	0.527
0.667	0.75	7.58	16.48	0.700
0.750	0.75	8.12	17.32	0.749

r_1=0.596 r_2=0.812 Q=3.29 e=−1.65[b]

a) Apply the same foot notes of (a) to (e) in Table 4 to this table.
b) The other set was Q=0.85 and e=+0.05. The positive e value is unlikely for styrene derivative.

16) M. Imoto, M. Kinoshita and M. Nishigaki, *Makromol. Chem.*, **94**, 238 (1966).
17) C. C. Price, *J. Polym. Sci.*, **3**, 772 (1948).
18) L. C. Rinzew, J. Stoffelsma and J. F. Arens, *Rec. Trav. Chim.*, **78**, 355 (1959).
19) P. M. Walters and S. M. McElvain, *J. Am. Chem. Soc.*, **62**, 1482 (1940).
20) E. A. Nodiff, S. Lipschutz, P. N. Craig and M. Gordon, *J. Org. Chem.*, **25**, 60 (1960).
21) G. B. Bachman and C. L. Carlson, *J. Am. Chem. Soc.*, **73**, 2857 (1951).
22) M. S. Matheson, E. E. Auer, E. B. Bevilacque and E. J. Hart, *J. Am. Chem. Soc.*, **73**, 1700 (1951).

Table 6. Copolymerization of ketene diethylacetal (M_2) with styrene (M_1)

M_2[a]	Reaction time, hr	Conversion,	C%	H%	(C+H) %[b]
0.125	3	15.8	92.15	7.79	99.94
0.250	3	15.5	92.10	7.72	99.82
0.375	3	13.2	91.86	7.68	99.54
0.500	3	10.7	90.93	7.80	98.73
0.625	3	11.5	92.49	7.82	100.31
0.750	3	10.2	91.53	7.73	99.26
0.875	3	8.4	91.30	7.67	98.97

a) Each tube contained 35 mg of azoisobutyronitrile.
b) These values indicates that there was practically no copolymerization.

Copolymerization with Styrene. The reaction mixture was prepared by mixing styrene with each monomer and azoisobutyronitrile and sealed under high vacuum. The polymerization was carried out by shaking the sealed tubes in a constant temperature bath (60°C). Polymer was isolated by pouring the contents of the tube into 200 ml of cold methanol. The dried precipitate was dissolved in benzene again and reprecipitated in cold methanol. Dried pure sample, thus made was subjected to analysis and the results are listed in Tables, 4, 5 and 6.

From the data in Table 4 the copolymerization ratios, r_1 and r_2 were estimated by the intersection method using Eq. (4). The Q and e values were then calculated using Eqs. (5) and (6)[10c] and assuming the Q and e values for styrene as 1.00 and −0.8, respectively.[17]

$$r_2 = \frac{M_1}{M_2}\left[\frac{dM_2}{dM_1}\left(1+\frac{M_1}{M_2}r_1\right)-1\right] \quad (4)$$

$$r_1 = (Q_1/Q_2)e^{-e_1(e_1-e_2)} \quad (5)$$

$$r_2 = (Q_2/Q_1)e^{-e_2(e_2-e_1)} \quad (6)$$

The authors are indebted to the two Research Laboratories of Fujisawa Pharmaceutical Company and Shionogi Pharmaceutical Company for the elemental analyses. The authors are also indebted to Professor T. Otsu and his coworkers in Osaka City University for their discussions and some technical aids in carrying out this work.

BULLETIN OF THE CHEMICAL SOCIETY OF JAPAN VOL. 41 1700—1707 (1968)

The Wolff Rearrangement. IV. The Silver-salt Catalyzed Decomposition of α-Diazoacetophenones in Benzene Solution*[1]

Matsuji TAKEBAYASHI and Toshikazu IBATA

Department of Chemistry, College of General Education, Osaka University, Toyonaka, Osaka

(Received January 26, 1968)

The decomposition of α-diazoacetophenone (I) in benzene solution has been studied using a silver benzoate-triethylamine catalyst at 50°C in an atmosphere of nitrogen. The reaction gave 3-benzoyl-4-hydroxy-5-phenylpyrazole (II) and β-phenylpropiophenone (III). In the decomposition of the substituted compounds, such as *p*-methoxy-, *p*-methyl- and *p*-nitro-α-diazoacetophenones, the corresponding substituent products of II and III were also obtained. The formation of II and III is reasonably explained by assuming two kinds of reactions between phenylketene and I.

It has been recognized that the photochemical, thermal, and silver-salt catalyzed decompositions of diazoketones in protic solvents give carboxylic acids and their derivatives (Wolff Rearrangement).[1] Although these products have been interpreted in terms of ketene intermediates,[2] the high reactivity of normal ketenes does not allowed the isolation of them but leads to the carboxylic acids, esters, and amides, respectively, after reacting with water, alcohols, and amines existed in the reaction system.[3]

On the other hand, the decomposition of the diazoketones in aprotic solvents affords the β-lactam[4,5] and 1,2-diazacyaclobutane derivatives[6] in the presence of azomethine and azo compounds respectively.

Recently, one of the authors (T. I.) has made a

*1 Presented in part at the Symposium of Organic Radical Reactions, Osaka, September, 1964. For the preceding paper in this series, see; *Nippon Kagaku Zasshi (J. Chem. Soc. Japan, Pure Chem. Sect.)*, **88**, 1223 (1967).

1) W. E. Bachmann and W. S. Struve, "Organic Reaction," Vol I, John Wily & Sons Inc., New York (1942), p. 38.

2) L. Wolff, *Ann.*, **394**, 23 (1912).

3) P. Mayo, "Molecular Rearrangement Part I," Interscience Publishers, New York (1963), p. 528.

4) H. Staudinger, *Ann.*, **356**, 51 (1912).

5) L. Horner, *Chem. Ber.*, **89**, 2759 (1956).

6) L. Horner, *ibid.*, **89**, 2765 (1956).

kinetic study on the decomposition of substituted α-diazoacetophenones in various kinds of alcohols and in toluene solution,[7] using a solution of silver benzoate in triethylamine as a catalyst,[8] and has found that the substituent effect in alcohols is similar to that in toluene, and also has confirmed that the both reaction mechanisms are alike in the formation of ketene intermediates. In the experiments mentioned above, the evolution of nitrogen was almost quantitative and the corresponding phenylacetic esters were obtained in good yields in alcohols, while the evolution of nitrogen was not quantitative in toluene solution. A possible reason for the decrease in the evolution of nitrogen is given to the reaction between unreacted diazoketone and a ketene intermediate, when reactive substances with ketene are not present in the reaction medium. Therefore the investigation of the reaction products seems to be important. However, only a few studies of the decomposition of diazoketones in aprotic solvents, under the condition leading to rearranged products, have been published;*2 the photolysis of diazomethyl *t*-butyl ketone and of α-diazoacetophenone (I) in the absence of solvent has been reported by Wiberg,[11] and the thermal decomposition of napthalene-1,2-diazoxide in xylene and that of α-diazoacetophenone (I) in dodecane by Yates.[12,13]

The authors investigated the silver benzoate catalyzed decomposition of α-diazoacetophenones in benzene solution and obtained interesting results differed from those reported by Wiberg and Yates.

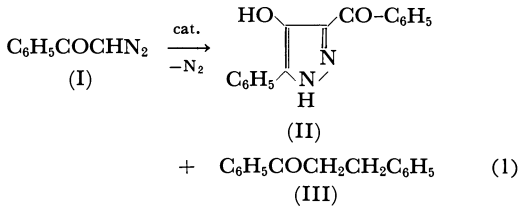

(I) (II) (III) (1)

Results

The decomposition of α-diazoacetophenone (I) in benzene solution was carried out in the presence of a 1/10 molar equivalent of silver benzoate, dissolved in a possibly smaller amount of triethylamine, at 50°C in an atmosphere of nitrogen. The reaction mixture turned to dark-brown color accompanied by the evolution of nitrogen gas. The evolution of nitrogen was ceased after about 60—70%*3 of its theoretical amount was generated (4—5 hr), and no evolution of nitrogen was recognized by further addition of the silver benzoate solution to the reaction mixture. After being left to stand at room temperature overnight, the reaction mixture was extracted several times with a saturated aqueous solution of sodium bicarbonate in succession with a 4 N solution of sodium hydroxide, and was separated in three fractions: (A) acidic fraction (soluble in sodium bicarbonate solution), (B) weak acidic fraction (soluble in sodium hydroxide solution), (C) neutral or basic fraction (soluble in benzene). Fraction (A) gave benzoic acid and a trace of phenylacetic acid. The benzoic acid is thought to be produced from silver benzoate, used as a catalyst, during the reaction or after treatment of reaction mixture, and the phenylacetic acid seems to be formed by the reaction of the phenylketene intermediate with a trace of water contained in the reaction medium.

On the acidification of fraction (B) by a concentrated hydrochloric acid under cooling with ice, followed by recrystallization from ethanol solution, 3-benzoyl-4-hydroxy-5-phenylpyrazole (II)[14] was obtained in the yield of 38%. However, 3-benzoyl-4-phenyl-5-hydroxypyrazole (IV),[14] the isomeric compound of II, and the ketene dimer (V)[15,16] were not detected in this fraction.

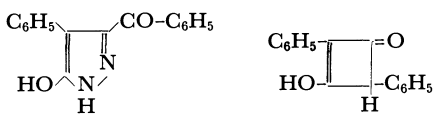

(IV) (V)

7) Y. Yukawa, Y. Tsuno and T. Ibata, This Bulletin, **40**, 2613, 2618 (1967).

8) M. S. Newman and P. F. Beal, *J. Am. Chem. Soc.*, **72**, 5163 (1950).

*2 Some works on the copper powder or copper-salt catalyzed decomposition of diazoketones to give ketocarbene intermediates have been reported.[9,10] In these works, the dimerization of ketocarbenes[9] and the intramolecular or intermolecular cyclo-addition of ketocarbenes to carbon-carbon double bonds[9] have been recoginized.

9) C. Grundmann and H. Trishmann, *Ann.*, **536**, 29 (1938).

10) W. Kirmse, "Carbene Chemistry," Academic Press, New York (1964).

11) K. B. Wiberg and J. W. Hutton, *J. Am. Chem. Soc.*, **76**, 5367 (1954).

12) P. Yates and E. W. Robb, *ibid.*, **79**, 5760 (1957).

13) P. Tates and T. J. Clark, *Tetrahedron Letters*, **1961**, 435.

*3 The yields of nitrogen vary as the concentration of the reaction mixture, making the change of the yields of II and III.

14) a) P. Yates and B. L. Shapiro, *J. Am. Chem. Soc.*, **81**, 212 (1959).
b) D. G. Farnum and P. Yates, *Chem. & Ind. (London)*, **1960**, 659.
c) D. G. Farnum and P. Yates, *Proc. Chem. Soc.*, **1960**, 224.
d) D. G. Farnum and P. Yates, *J. Am. Chem. Soc.*, **84**, 1399 (1962).
e) D. G. Farnum and P. Yates, *ibid.*, **85**, 2967 (1962).
f) D. G. Farnum and P. Yates, *J. Org. Chem.*, **27**, 2209 (1962).
g) D. G. Farnum and P. Yates, *Tetrahedron Letters*, **1960**, 22.

15) H. Staudinger, *Ber.*, **44**, 533 (1911).

16) J. E. Baldwin and J. D. Roberts, *J. Am. Chem. Soc.*, **85**, 2444 (1963).

On vacuum distillation of neutral fraction (C) after evaporating the solvent, β-phenylpropiophenone(III)[17-19] was obtained in 13% yield with very small amount of two kinds of compounds containing carbonyl groups. The structure of the ketone (III) was ascertained by the comparison of the IR and NMR spectra with those of authentic β-phenylpropiophenone, and still more ascertained

TABLE 1. THE EFFECT OF THE CONCENTRATION OF THE REACTION MEDIUM ON THE YIELDS OF II AND III

(Run)	(1)	(2)	(3)
$PhCOCHN_2$	5.0 g	10.0 g	15.0 g
PhCOOAg	0.5 g	1.0 g	2.0 g
$(C_2H_5)_3N$	5.0 m*l*	6.0 m*l*	20.0 m*l*
benzene	20 m*l*	200 m*l*	1000 m*l*
reaction temp.	50°C	40°C	40°C
(Products)			
PhCOOH	0.10 g	0.15 g	0.30 g
$PhCH_2COOH$	trace	trace	trace
II	1.70 g (38%)	2.10 g (23%)	0.50 g (3.7%)
III	0.34 g (12%)	0.93 g (13%)	3.05 g (38%)
unknown oil	0.47 g	1.0 g	1.5 g

TABLE 2. PRODUCTS OF THE DECOMPOSITION OF *p*-SUBSTITUTED α-DIAZOACETOPHENONES CATALYZED BY SILVER BENZOATE IN BENZENE[a]

Substituent	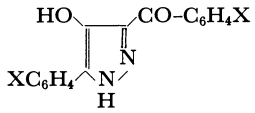		$XC_6H_4COCH_2CH_2C_6H_4X$	
	Mp (°C)	Yield (%)	Mp (°C)	Yield (%)
H	209.5—210.5	38	71.0—72.0	13
p-CH_3	251.0—252.0	26	64.5—65.5	12
p-CH_3O	207.0—208.0	12	84.0—85.0	9.1
p-NO_2	>300[b]	26		

a) Benzoic acid and a trace of the corresponding *p*-substituted phenylacetic acids were also obtained.
b) The melting point of this compound was not determined precisely because of its high degree.

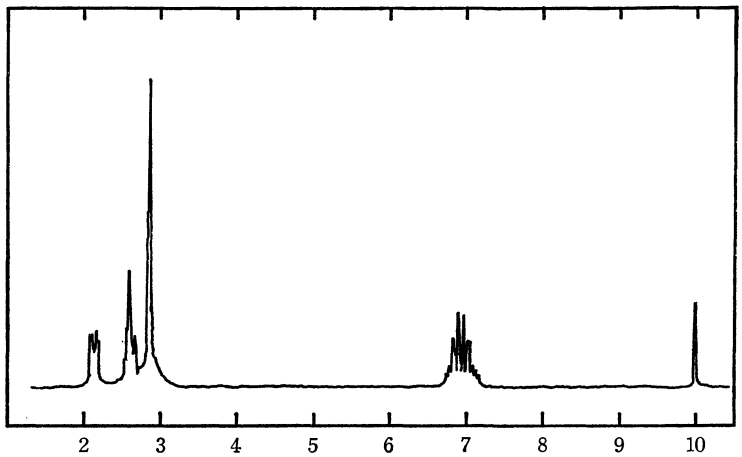

Fig. 1. The NMR spectrum of β-phenylpropiophenone (III).

17) H. H. Wasserman and N. E. Aubrey, *ibid.*, **77**, 590 (1955).
18) Yu. K. Yur'ev, Z. V. Belyakova and V. P. Volkov, *Zhur. Obshch. Khim.*, **28**, 2372 (1958) (*Chem. Abstr.*, **1959**, 3135e).
19) G. S. Fonken and W. S. Johnson, *J. Am. Chem. Soc.*, **74**, 831 (1952).

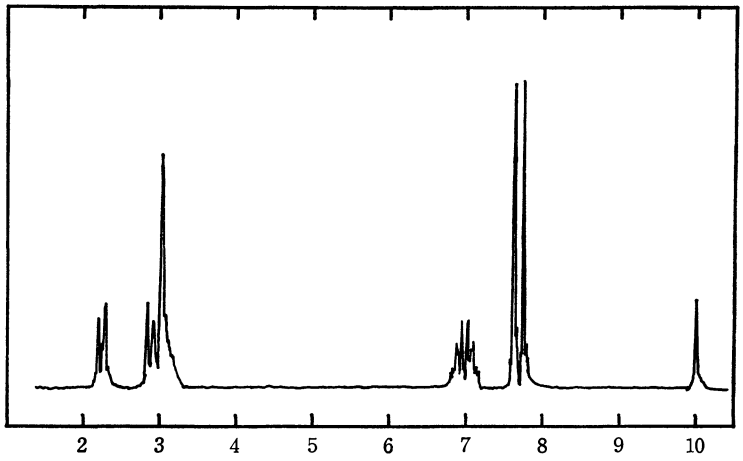

Fig. 2. The NMR spectrum of β-*p*-tolyl-*p*-methylpropiophenone.

by the Beckmann rearrangement of its oxime (VI) to α-chloro-β-phenylpropionanilide (VII) in the presence of phosphorus pentachloride.

$$\underset{\text{(III)}}{\text{PhCOCH}_2\text{CH}_2\text{Ph}} \xrightarrow{NH_2OH} \underset{\text{(VI)}}{\text{Ph-C(=N-OH)-CH}_2\text{CH}_2\text{Ph}} \xrightarrow{PCl_5} \underset{\text{(VII)}}{\text{PhNH-C(=O)-CHCl-CH}_2\text{Ph}}$$

$$\xrightarrow[OH^-]{\text{hydrolysis}} \text{PhCH=CHCOOH} + \text{HCl} \quad (2)$$

$$\xrightarrow[H^+]{} \text{PhNH}_2 \xrightarrow{\text{PhCOCl}} \underset{\text{(VIII)}}{\text{PhCONHPh}} + \text{HCl} \quad (3)$$

When the reaction mixture was diluted further with benzene, the evolution of nitrogen was increased with the increase of the ketone (III) to 38%, and the amount of pyrazole (II) was decreased to 4% as shown in Table 1.

The catalytic decomposition of *p*-methoxy-, *p*-methyl-, and *p*-nitro-α-diazoacetophenones also gave the corresponding derivatives of pyrazole and β-phenylpropiophenone. The results are listed in Table 2.

These results are quite different from those reported by Wiberg and Yates, and also from those obtained in the copper-salt catalyzed decomposition of α-diazoacetophenone in benzene, yielding 1,2-dibenzoylethylene.[9,20]

Discussion

Yates and his co-workers have obtained pyrazole derivatives (II) and (IV) besides benzoic acid, acetophenone and 3-benzoyl-5-phenyl pyrazole (IX) in the alkali catalyzed decomposition of α-diazoacetophenone.[14a,e,g] However, the mechanism of the formation of II in the reaction, which was carried out by Yates, will not be similar to that in our silver-salt catalyzed decomposition of α-diazoacetophenone, because both experimental conditions are quite different.*4

In the silver-salt catalyzed decomposition, the α-diazoacetophenone is converted, at first, to phenylketene (Eq.(4)) as has been reported previously.[7]

$$\underset{\text{(I)}}{\text{PhCOCHN}_2} \xrightarrow[-N_2]{\text{catalyst}} \underset{\text{(X)}}{\text{PhCH=C=O}} \quad (4)$$

The presence of ketene intermediate (X) is also confirmed by the isolation of a trace of phenylacetic acid, which is produced by the reaction between phenyketene (X) and water. The ketene will then add with its double bond to another molecule of α-diazoacetophenone (I). In general, the addition of diazoketones to the carbon-carbon double bond of unsaturated compounds takes place in two paths (A) and (B):

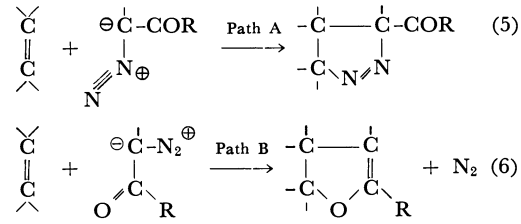

*4 As is shown in the Experimental section, consumption of the diazoketone in the reaction mixture was confirmed by the IR spectra before the alkaline extraction. Moreover, the shaking of a benzene solution of I with 4 N sodium hydroxide solution at room temperature in an extracting funnel gave yellowish color to the alkaline layer, but no II was obtained.

20) M. Takebayashi, T. Ibata and H. Kohara, unpublished.

For example, the formation of 3,4,5-tribenzoyl-2-pyrazoline (XI)[21] by the reaction of *trans*-1,2-dibenzoylethylene with α-diazoacetophenone and that of pyrazoline derivative (XII)[22] by the reaction of ethyl α-isopropylacrylate with diazoacetone have been recognized to proceed according to the path (A). However, the reaction between ketenes and diazoketones to give pyrazole derivatives has not been reported yet.

In the present decomposition, the reaction of phenylketene with the diazoketone takes place in a type of 1,3-dipolar cyclo-addition according to the path (A), followed by the enolization and proton shift, to give the product (II) as is shown in Eq. (7).*5

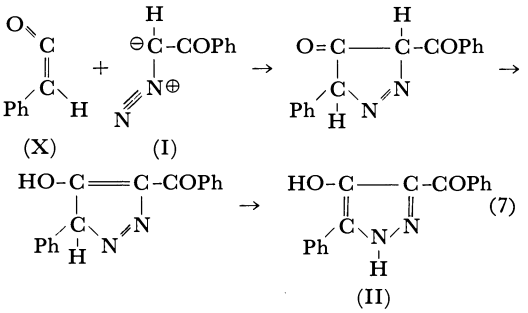

(X) (I)

(II) (7)

The absence of the isomer (IV) in the reaction products suggests that the direction of addition does not submited to the Eq. (8).

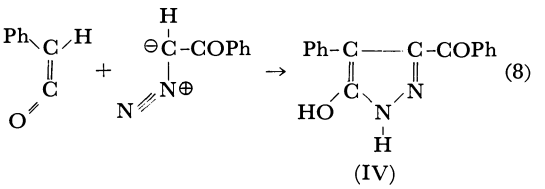

(IV) (8)

On the other hand, γ-enol-lactones, such as 3,5-di-*t*-butyl-1,2-dihydrofurane-2-one (XIII, R=*t*-Bu),[11] 3,5-diphenyl-1,2-dihydrofurane-2-one (XIII, R=Ph)[13] and 3,3-diphenyl-5-*p*-anisyl-1,2-dihydrofurane-2-one (XIV),[25,26] have been obtained by the photochemical decomposition of diazomethyl-*t*-butylketone, by the thermal decomposition of α-diazoacetophenone, and by the reaction of diazomethyl-*p*-methoxyphenylketone with diphenylketene, respectively.

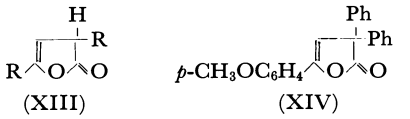

(XIII) (XIV)

The formation of these compounds is explained by the interaction of a ketene intermediate and another molecule of diazoketone according to the path (B).*6

Then, the formation of β-phenylpropiophenone (III) will be elucidated as follows: The phenylketene (X) adds to unreacted α-diazoacetophenone to give γ-enol-lactone (XVII) according to the path (B). When the enol-lactone (XVII) was hydrolyzed, the α-phenyl-β-benzoylpropionic acid (XVIII) produced will be converted to β-phenylpropiophenone (III) by decarboxylation.

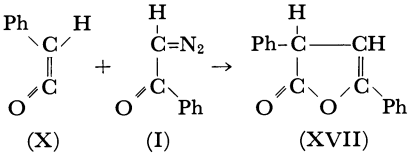

(X) (I) (XVII) (9)

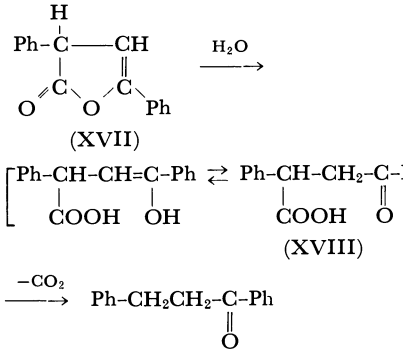

(XVIII)

(III) (10)

21) J. Clark and P. Yates, *J. Org. Chem.*, **27**, 286 (1962).

22) M. S. Muthanna and P. C. Guha, *Chem. Ber.*, **71**, 2665 (1938).

*5 The resonance structures of ketenes[23] and diazoketones[24] are shown as follows, respectively.

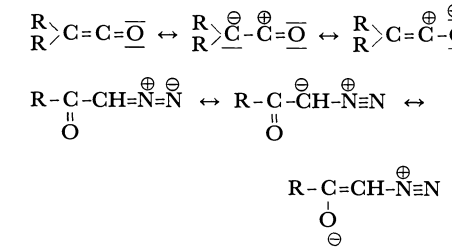

23) E. Müller, "Neuere Anschauungen der Organischen Chemie," (1941), p. 154.

24) D. J. Cram and G. S. Hammond, "Organic Chemistry," MacGraw-Hill, New York (1959) p. 496.

25) A. S. Kende, PhD. Thesis, Harvard, 1956.

26) A. S. Kende, *Chem. & Ind. (London)*, **1956**, 1053.

*6 Besides, the addition of diazoketones to the carbonyl double bond of ketenes also has been reported. For example, the thermal decomposition of *o*-naphthoquinonediazide[12] and the reaction of the quinonediazide with diphenylketene[12,27] afford XV and XVI, respectively.

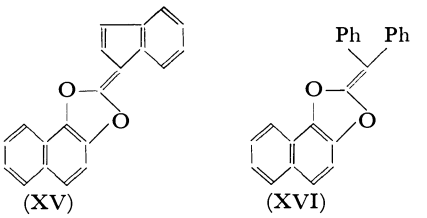

(XV) (XVI)

27) W. Ried and R. Rietrich, *Ann.*, **666**, 135 (1963).

If the formation of β-phenylpropiophenone (III) proceeds by the following free radical mechanism, acetophenone and carbon monoxide must be produced during the reaction.

$$\underset{\text{(I)}}{\text{PhCOCHN}_2} \xrightarrow{\text{cat.}} \underset{\text{(XIX)}}{\text{PhCOCH:}} + \text{N}_2 \quad (11)$$

$$\underset{\text{(XIX)}}{\text{PhCOCH:}} + \text{S-H} \rightarrow \text{PhCOCH}_2\cdot + \text{S}\cdot \quad (12)$$

$$\text{PhCOCH}_2\cdot + \text{S-H} \rightarrow \underset{\text{(XX)}}{\text{PhCOCH}_3} + \text{S}\cdot \quad (13)$$

$$\text{PhCOCH}_2\cdot + \text{PhCH=C=O} \rightarrow \text{PhCOCH}_2\dot{\text{C}}\text{HPh} + \text{CO} \quad (14)$$

$$\text{PhCOCH}_2\dot{\text{C}}\text{HPh} + \text{S-H} \rightarrow \underset{\text{(III)}}{\text{PhCOCH}_2\text{CH}_2\text{Ph}} + \text{S}\cdot \quad (15)$$

(S-H: benzene, triethylamine, *etc.*)

However, no acetophenone (XX) was obtained, and no peak of carbon monoxide was observed in the gas chromatogram of gaseous products. Moreover, *cis*- and *trans*-1,2-dibenzoylethylene, which should be produced in the reaction of benzoylcarbene (XIX) and diazoacetophenone (I), were not recognized in the reaction products. Therefore, the free radical mechanism is not suitable for the formation of β-phenylpropiophenone (III). The mechanism will be discussed in detail compared with that of photolysis of diazoketone.

Experimental*7

Materials. *The Substituted and Unsubstituted α-Diazoacetophenones* used in this investigation were prepared by the reaction of the corresponding acid chlorides with diazomethane according to the method of Newman and Beal.[28] An ether solution of benzoyl chloride was added dropwise to the ether solution of a small excess of diazomethane and an equivalent amount of triethylamine below 0°C with vigorous stirring. After the reaction mixture was allowed to stand overnight at room temperature, the precipitated triethylamine hydrochloride was filtered off. The filtrate was washed with water, saturated sodium bicarbonate, and water successively, and drived over anhydrous magnesium sulfate. The solvent was removed *in vacuo* and yellowish residue was collected. Several recrystallizations from ligroin or benzene gave pale yellow crystals. The melting points of diazoacetophenone were shown below:

unsubstituted: 47.5—48.0, *p*-CH_3: 52.0—52.8, *p*-CH_3O: 87.5—88.5, *p*-NO_2: 118.0—119.0°C

The diazoacetophenones obtained were stored in a dark place to prevent the decomposition by diffused light.

*7 All melting and boiling points are uncorrected. Infrared spectra were obtained with the Hitachi EPI-S2 model spectrophotometer. The NMR spectra were determined with the Varian Associates model A-60 instrument. Chemical shifts are given in τ units using tetramethylsilane as an internal standard. Gas chromatographic measurement was carried out using a Yanagimoto Gas Chromatograph model GCG-3DH.

28) M. S. Newman and P. F. Beal, *J. Am. Chem. Soc.*, **71**, 1506 (1949).

Benzene and Triethylamine were redistilled over metallic sodium to remove a trace of water dissolved in these materials.

The Silver Benzoate was prepared by the reaction between an equivalent molar amount of silver nitrate and sodium benzoate as has been reported previously.[7] The silver benzoate produced was collected on a hot-funnel, washed several times with hot water to remove sodium benzoate and benzoic acid, dried and stored in a dark place.

General Procedure. A solution of silver benzoate (0.5 g, 2.2 mmol) in 5 m*l* of triethylamine was added at a time to the solution of 5.0 g (33 mmol) of α-diazoacetophenone dissolved in 20 m*l* of benzene, which has already been deoxygenated by bubbling of nitrogen gas. The evolution of nitrogen began at once, and the mixture gradually turned to dark-brown. The reaction mixture was maintained at 50°C as long as the gas evolution was continued. After about 60—70% of theoretical amount of nitrogen was evolved, the silver-amine catalyst was added furthermore. However, no nitrogen was generated. The reaction mixture was allowed to stand overnight at room temperature, and the precipitated silver metal was filtered off. The IR spectra of the benzene solution have no characteric absorption band of diazoketone at 2120 cm^{-1} region. The precipitate was washeds everal times with each 10 m*l* of benzene. The combined benzene solution was further diluted with benzene up to 100 m*l*, and extracted twice with 20 m*l* of a saturated sodium bicarbonate solution. The benzene solution was furthermore extracted several times with 20 m*l* of 4 N sodium hydroxide solution until alkaline layer showed no reddish color. The sodium bicarbonate solution was acidified with 6 N hydrochloric acid. The precipitate produced was extracted with ether. On evaporation of ether, white crystals were obtained yielding 0.10 g. The IR spectra indicate that the crystalline product is a mixture of benzoic acid and a trace of phenylacetic acid. After several recrystallizations from petroleum benzine, the IR spectra and the melting point (122—123°C) were completely consistent with authentic benzoic acid.

The sodium hydroxide solution was acidified with concentrated hydrochloric acid with stirring in the presence of ice. A pale yellow powder was obtained, mp 209.5—210.5°C (from ethanol), yield 1.70 g (38%).

Found: C, 72.82; H; 4.79; N, 10.30%. Calcd for $C_{16}H_{12}N_2O_2$: C, 72.71; H, 4.58; N, 10.60%.

This compound showed wine-red color in aqueous solution of sodium hydroxide, decolorized alkaline solution of potassium permanganate, and converted an alcoholic solution of ferric chloride to dark-green. The chemical properties and the absorption spectrum data of IR (KBr disk, 3350 (m), 3250 (s), 1625 (s), 910 (s) cm^{-1}) and UV (λ_{max}^{EtOH} 276 mμ, log ε 4.51: 287 mμ, log ε 4.33) were in accord with those of 3-benzoyl-4-hydroxy-5-phenyl pyrazole (II) reported by Yates.[14]

The benzene layer was distilled under diminished pressure into two fractions (bp 130°C/1 mmHg, bp 130°C/2 mmHg). The low boiling fraction was found to be a mixture of two components containing carbonyl groups by means of gas chromatography,*8 but their structure

*8 The experimental conditions are as follows: carrier gas, H_2 65 m*l*/min at 200°C: 2 meter column packed with Apiezone Grease L; retention time, 46 min and 52 min.

was not determined because of their low yields. The high boiling fraction was crystallized after being left on standing in a refrigerator for several days. Several recrystallizations from petroleum ether (bp 55—60°C) gave white plates, $C_{15}H_{14}O$, 71.0—72.0°C, yield 13%. The IR absorption spectra (KBr, 1680 (s), 1595 (m) cm^{-1}) of this compound (III) showed the presence of carbonyl and phenyl groups. The NMR spectra of (III) in carbon tetrachloride solution showed absorption bands at 2.00—2.70 τ (multiplet, 5H, phenyl-H bonding to carbonyl group), at 2.83 τ (singlet, 5H, phenyl-H bonding to methylene), at 6.95 τ (A_2B_2type of quasi-quartet, 4H, $-CH_2CH_2CO-$). The melting points and the elemental analyses of the oxime (mp 83.0—84.0°C, lit. mp 83.5°C,[17] $C_{15}H_{15}NO$), the 2,4-dinitrophenylhydrozone (mp 179—181°C, lit. 182—183°C,[18] $C_{21}H_{18}N_4O_4$) and the semicarbazone (mp 144—145°C, lit. mp 144.0—144.8°C,[19] $C_{16}H_{17}N_3O$) derived from this compound are consistent with those of β-phenypropiophenone (III)[17-19]

The Beckmann Rearrangement of the Oxime (VI). The oxime (VI) (0.50 g) was treated with 2.0 g of phosphorus pentachloride in 50 m*l* of ether for 10 hr at room temperature. After quenched the reaction mixture with 10 m*l* of water, the ether solution was treated with 10 m*l* of saturated sodium bicarbonate solution, and the ether layer was dried over anhydrous magnesium sulfate. On evaporation of ether, white crystals were obtained, mp 124.5—125.0°C (from petroleum benzine), yield 0.45 g. This product showed positive Beilstein test. IR (KBr): 3240, 1660, 1605, 1550, 1325 cm^{-1}.

Found: C, 69.80; H, 6.18; N, 5.08; Cl, 13.74%. Calcd for $C_{15}H_{14}NOCl$: C, 69.36; H, 5.43; N, 5.39; Cl, 13.65%.

This product corresponds to α-chloro-β-phenylpropion anilide (VII), lit.[29] mp 125°C.

Alkali Catalyzed Hydrolysis of the Amide (VII). This amide (VII) (0.12 g) was hydrolyzed with an aqueous alcoholic solution of potassium hydroxide for 3 hr. After evaporating alcohol *in vacuo*, the reaction mixture was extracted twice with 10 m*l* of ether. On acidification of the alkaline solution, 0.04 g of white crystals were obtained, mp 134.5—135.0°C. The IR spectra of this product were closely agreed with those of authentic cinnamic acid, and the mixed-melting point test showed no depression. The ether layer and the acid layer gave no product besides resinous matter.

Acid Catalyzed Hydrolysis of the Amide (VII). The amide (VII) was hydrolyzed with an ethanol solution of hydrochloric acid (ethanol, 10 m*l*; c.HCl, 5 m*l*; H_2O, 5 m*l*) for 15 hr. The reaction mixture was turned violet *via* pink color. After evaporation of alcohol, 20 m*l* of water was added. The acidic and neutral substances in the reaction mixture were eliminated by the extraction with ether, and then the aqueous acidic solution was made basic with sodium hydroxide. The oily product produced was extracted three times with 20 m*l* of ether, and an excess of benzoyl chloride was added to the ether solution after drying with anhydrous magnesium sulfate. After being left on standing overnight at room temperature, the reaction mixture was washed with sodium bicarbonate solution to remove unreacted benzoyl chloride, and then dried. By evaporation of ether, 0.20 g of white crystals were obtained, mp 162°C (from ethanol and water). The IR spectra and melting point were closely consistent with authentic benzanilide. The IR and NMR spectra of the ketone-(III) were also superimposed completely with those of authentic β-phenylpropiophenone, which prepared by the reduction of benzalacetophenone by zinc powder and acetic acid.[30] The mixed melting point test also showed no depression.

Preparation of β-Phenylpropiophenone (III). An acetic acid (50 m*l*) solution of benzalacetophenone*[9] (10 g, 0.05 mol) was refluxed with 6.5 g (0.10 g atom) of zinc powder for 8 hr. After cooling, unreacted zinc was filtered off, and the solvent was distilled off *in vacuo* giving rise to β-phenylpropiophenone, bp 145°C/3 mmHg, mp 71.0—72.0°C.

Silver Benzoate-Catalyzed Decomposition of *p*-Methyl-α-diazoacetophenone in Benzene Solution. The reaction was carried out using 5.0 g of diazoketone, 0.60 g of silver benzoate, and 4.0 m*l* of triethylamine in 40 m*l* of benzene at 40°C, and the reaction mixture was treated with sodium bicarbonate and sodium hydroxide, successively. From the sodium bicarbonate solution, a small amount of benzoic acid was obtained, while *p*-methylphenylacetic acid was not detected by the measurement of the IR spectra. From the sodium hydroxide solution, 1.20 g (26%) of yellow crystals were obtained, mp 251.0—252.0°C. IR (KBr); 3350, 3260, 1605, 907 cm^{-1}.

Found: C, 73.89; H, 5.55; N, 9.53%. Calcd for $C_{18}H_{16}N_2O_2$: C, 73.95; H, 5.52; N, 9.58%.

These data and chemical properties suggest that the product is 3-*p*-toluyl-4-hydroxy-5-*p*-tolylpyrazole. From the benzene layer, 0.50 g (12%) of white needles were obtained, mp 64.5—65.5°C. IR (KBr), 1680, 1515, 1270, 1180, 800 cm^{-1}. NMR (in CCl_4), 2.25 τ and 2.87 τ (symmetric doublet, 4H, aromatic-H bonding to carbonyl group), 3.04 τ (singlet, 4H, aromatic-H bonding to methylene), 7.00 τ quasi-quartet of A_2B_2type, 4H, $-CH_2CH_2CO-$), 7.64 τ (singlet, 3H, *p*-CH_3) and 7.74 τ (singlet, 3H, *p*-CH_3). The data show that this product is β-*p*-tolyl-*p*-methylpropiophenone.

Silver Benzoate Catalyzed Decomposition of *p*-Methoxy-α-diazoacetophenone. The reaction was carried out using 5.0 g (0.029 mol) of diazoketone, 0.60 (0.0026 mol) of silver benzoate and 5.0 m*l* of triethylamine in 40 m*l* of benzene at 40°C. The reaction mixture was treated as described above. From sodium bicarbonate solution, 0.17 g of an yellow precipitate was obtained. The IR spectra showed that the precipitate was a mixture of benzoic acid and a trace of *p*-methoxyphenylacetic acid with undecided yellow compounds. Recrystallization of the precipitate gave benzoic acid. From the hydroxide solution, pale yellow crystals were obtained on acidification, mp 207.0—208.0°C (from ethanol), yield 0.55 g (12%). IR (KBr), 3350, 3250, 1620, 910 cm^{-1}.

Found: C, 66.61; H, 5.24; N, 8.73%. Calcd for $C_{18}H_{16}N_2O_4$: C, 66.66; H, 4.97; N, 8.64%.

29) A. N. Nesmeyanov, V. N. Kost, T. T. Vasil'eva and R. Kh. Freidlina, *Izvest. Akad. Nauk. SSSR., Otdel. Khim. Nauk.* **1958**, 152. (*Chem. Abstr.*, **1958**, 12756a).

30) N. C. Deno and J. D. Johnson, *J. Org. Chem.*, **17**, 1466 (1952).

*9 The benzalacetophenone was prepared by the alkali catalyzed reaction of benzaldehyde and acetophenone in ethanol. "Organic Syntheses," Coll. Vol I p. 78, (1948).

These results and the chemical properties show that this product is 3-*p*-anisoyl-4-hydroxy-5-*p*-anisylpyrazole. From the benzene layer, white needles were obtained, mp 84.0—85.0°C, yield 0.86 g (19%). IR (KBr), 1700, 1510, 1250, 1180, 820 cm^{-1}.

Found: C, 75.38; H, 6.73%. Calcd for $C_{17}H_{18}O_3$: C, 75.53; H, 6.71%.

From these results, this compound was assigned to β-*p*-anisyl-*p*-methoxypropiophenone. Another fraction of the benzene layer (bp 170°C/1 mmHg) (0.51 g) gave no detectable product.

Silver Benzoate Catalyzed Decomposition of *p*-Nitro-α-diazoacetophenone. The reaction was carried out using 5.0 g (0.029 mol) of diazoketone, 1.2 g (0.0052 mol) of silver benzoate and 5.0 m*l* of triethylamine in 80 m*l* of benzene at 50°C, and the reaction products were treated as described above. From the sodium bicarbonate solution, a small amount of benzoic acid and *p*-nitrophenylacetic acid were obtained. On acidification of the sodium hydroxide solution, 1.2 g (26%) of a yellow precipitate was obtained. This substance could not be purified by recrystallization because of its extremely low solubility in most organic solvents. mp>300°C. IR (KBr), 3350, 1730, 1515, 1350 cm^{-1}.

Found: C, 55.77; H, 3.56%. Calcd for $C_{16}H_{10}N_4O_6$; C, 54.24; H, 2.85%.

Although the analytical data do not agree with the calculated values, the chemical properties and the IR spectra resemble to those of (II). This product is also thought to be a *p*-NO_2-substituted pyrazole derivative of type (II).

The authors wish to express their hearty thanks to Mr. Y. Kawanishi for his experimental aid. This work has been supported in part by a grant-in-aid for Scientific Research from the Ministry of Eductation.

BULLETIN OF THE CHEMICAL SOCIETY OF JAPAN VOL. 41 1707—1711 (1968)

Photochemischer Zerfall von Benzoylphenylacetyl- und Benzoyl-*p*-chlorphenylacetyl-peroxyden in Toluol

Tadashi SUEHIRO, Shuji HIBINO und Tadashi SAITO

Chemisches Institut, Gakushuin Universität, Toshima-ku, Mejiro, Tokio

(Eingegangen am 2. Februar, 1968)

Benzoylphenylacetylperoxyd und Benzoyl-*p*-chlorphenylacetylperoxyd zerfallen photolytisch in Toluol bei −5——10°C in die Benzoyloxy und Benzyl bzw. *p*-Chlorbenzyl Radikale unter Bildung von Kohlendioxyd, Benzoesäure, Benzoesäure-benzyl- bzw. -*p*-chlorbenzyl-ester, Bibenzyle, Methyldiphenylmethane, Diphenylmethane und Methyldiphenyle. Eine Umlagerungsreaktion vom Peroxyd in den Benzylkohlensäurebenzoesäureanhydrid verläuft nebenbei und dieser Anhydrid liefert durch Einwirkung auf Benzoesäure, Kohlendioxyd, Benzylalkohol und Benzoesäureanhydrid. Die freie Radikale Reaktion und die Umlagerung in den Kohlensäureanhydrid vom Peroxyd finden im Verhältnis *ca.* 2 : 1 statt. Aus dem Lösungsmittel, Toluol, entsteht Benzyl Radikale während der Photolyse durch Einwirkung von Benzoyloxy Radikal, dies wurde durch das Vorkommen von Bibenzyl und *p*-Chlorbibenzyl bei der Photolyse von Benzoyl-*p*-chlorphenylacetylperoxyd in Toluol nachgewiesen.

Benzoylphenylacetylperoxyd zerfällt in Toluol bei Raumtemperatur heterolytisch in Benzyl Kation und Benzoat Anion unter Kohlendioxyd Abspaltung, das Benzyl Kation bei der Einwirkung auf Elektronen Donator Aromaten Diphenylmethanderivaten liefern kann, oder verwandelt sich das Peroxyd monomolekular in den Benzoesäurebenzylester und in den Benzylkohlensäurebenzoesäureanhydrid, und freie Radikale Reaktion vom Peroxyd konnten wir erst mittels Radikalabfängers in weniger als 10% Ausbeute erfassen.[1] Um die freie Radikale Reaktion vom Peroxyd genau zu ermitteln, haben wir die Photolyse von Benzoylphenylacetylperoxyd und Benzoyl-*p*-chlorphenylacetylperoxyd untersucht.

Ergebnisse und Diskussion

Benzoylphenylacetylperoxyd zerfällt bei der Photolyse in Toluol bei −5——10°C in freien Radikale ohne Begleitung von der thermischen Zersetzung vom Peroxyd. Wenn man das Peroxyd unter Stickstoff mit Nieder- oder Hoch-druck Brenner belichtet, bilden sich Kohlendioxyd, Carbonsäure, Bibenzyl, Benzoesäurebenzylester, Diphenylmethan, *o*-, *m*- und *p*-Methyldiphenyle, *p*-Methyldiphenylmethan und Benzylalkohol (Nr. 1 und 4 der Tabelle 1). Bibenzyl darunter ist der Beweis für das Auftreten

1) T. Suehiro, H. Tsuruta und S. Hibino, Dieses Bulletin, **40**, 674 (1967).

TABELLE 1. PRODUKTE DER PHOTOLYSE IN TOLUOL BEI −5——10°C (AUSBEUTE IN MOL% AUF DEM ANGESETZTEN PEROXYD)

Photolyse Nr.	1	2	3	4	5
Peroxyd	BPAP[a]	BPAP	BCPAP[b]	BPAP	BCPAP
Konz. $\times 10^3$ Mol/l	8.8	8.8	10	8.6	10
Atmosphäre	N_2	O_2	N_2	N_2	N_2
Hoch- od. Niederdruck Brenner	N	N	N	H	H
Belichtungsdauer Std.	8	8	8	6	8
CO_2	82	66	85(72)[c]	65	49
Carbonsäure PhCOOH	9.0	—	13(26)	10	9.2
$PhCO_2CH_2Ar$	33[d]	43[d]	30[e](16)	19[d]	23[e]
			2[d]		0.3[d]
$ArCH_2CH_2Ar'$	36[f]	2.7[f]	9[g]	10[f]	4.1[g]
			29[h]		31[h]
			5.6[f]		3.9[f]
$CH_3C_6H_4CH_2Ar$	3.3[i]	2.1[i]	—[j]	1.3[i]	—[j]
$PhCH_2Ar$	9.0[k]	14[k]	10[l]	2.4[k]	12[l]
$CH_3C_6H_4Ph$	6.0	3.0	2.0	1.9	1.2
$ArCH_2OH$	16[m]	—	14[n]	5.7[m]	6.9
$PhCOCOCH_2Ar$ (O O)	—	—	16[o](29)	—	8.0[o]
$(PhCO)_2O$	—	—	13	—	—
Peroxyd, zurückgebl.	9.0	21[p]	13	45	43
		36[q]			

a) Benzoylphenylacetylperoxyd, b) Benzoyl-*p*-chlorphenylacetylperoxyd, c) Ausbeute, berechnet. d) Benzoesäurebenzylester, e) Benzoesäure-*p*-chlorbenzylester, f) Bibenzyl, g) *p*,*p*'-Dichlorbibenzyl, h) *p*-Chlorbibenzyl, i) *p*-Methyldiphenylmethan, j) Spuren, nicht bestimmt., k) Diphenylmethan, l) *p*-Chlordiphenylmethan, m) Benzylalkohol, n) *p*-Chlorbenzylalkohol, o) *p*-Chlorbenzylkohlensäurebenzoesäureanhydrid, p) Ausg. Peroxyd, q) Peroxyd, das aus Kaliumjodid in verd. Essigsäure Jod frei machen kann.

der freien Radikale Reaktionen, weil dessen Ausbeute bei der Belichtung unter Sauerstoff (Nr. 2) stark unterdruckt wird und peroxydische Substanzen, die beim Versetzen mit Kaliumjodid in verdünnter Essigsäure Jod frei machen, d. h. anders als Benzoylphenylacetylperoxyd, werden in 36% Ausbeute gebildet. Dazu noch zu erwähnen ist, dass das Molverhältnis der entstandenen *o*-, *m*- und *p*-Methyldiphenyle 70 : 12 : 18 ist. Diese Werte sind etwas mehr in der *o*- und *p*- Isomeren als die berechneten aus der *partial rate factors* von Phenylierung Toluols mit *N*-Nitrosoacetanilid.[2] Diese Tatsache erklärt sich für die zugenommene Selektivität der Arylierung bei der tieferen Reaktionstemperatur. Diese Befunde sprechen für die Zwischenprodukte, Benzyl und Phenyl Radikale, bei der Photolyse. Dass Toluol allein unter den Reaktionsbedingungen kein Bibenzyl gibt, wurde experimentell festgestellt. Bemerkenswert sind die Ausbeuten von Benzoesäurebenzylester und Diphenylmethan, auf die kein Einfluss von Sauerstoff ausgeübt hat : diese Verbindungen können deshalb heterolytisch oder in "cage" homolytisch gebildet worden sein. Wir sind der Meinung lieber vom letzteren Mechanismus deswegen, weil unter Stickstoff (Nr. 1) in 36% Ausbeute eine Kombinationsreaktion freien Benzyl Radikals zu Bibenzyl ausserhalb "cage" auftritt, und für diese Benzyl Radikale mussen so und so viele Benzoyloxy Radikale auch gebildet werden. Es ist auch bekannt, dass die "cage" Reaktion in viskosen Lösungsmitteln öfter stattfindet als in den nicht viskosen.[3] Es kann also viel "cage" Reaktion in der Kälte verlaufen als in der Wärme. Weiter wurde es auch gezeigt, dass die Ausbeuten der Diphenylderivaten bei der thermischen Zersetzung von Benzoylperoxyd in Aromaten, wenn auch unter Sauerstoff, unverändert bleiben oder etwas zunehmen.[4] Von der hohen Ausbeute von Benzoesäurebenzylester aber werden wir nachher im Zusammenhang mit der des Benzylalkohols bei der Um-Umsetzung von Benzoyl-*p*-chlorphenylacetylperoxyd (Nr. 3) erwähnen.

2) R. Ito, T. Migita, N. Morikawa und O. Simamura, *Tetrahedron*, **21**, 955 (1965).

3) R. R. Hiatt und T. G. Traylor, *J. Am. Chem. Soc.*, **87**, 3766 (1965); T. Nakata, K. Tokumaru und O. Simamura, *Tetrahedron Letters*, **1967**, 3303.

4) M. Eberhard und E. L. Eliel, *J. Org. Chem.*, **27**, 2289 (1962); R. T. Morrison, J. Cazes, N. Samkoff und C. A. Howe, *J. Am. Chem. Soc.*, **84**, 4152 (1962); K. Tokumaru, K. Horie und O. Simamura, *Tetrahedron*, **21**, 4152 (1965).

Die Stoffbilanz der Benzyl Gruppe bei Nr. 1 bewährt nicht (142%).*1 Es besteht eine Möglichkeit der Mitwirkung vom Lösungsmittel Toluol in der Bilanz. Die Bilanz der Benzoyloxy Gruppe verliert auch enorm (66%).*1 Eine Ursache von dem letzten käme aus der Umwandlung vom Peroxyd über Benzylkohlensäurebenzoesäureanhydrid in den Benzoesäureanhydrid: wir konnten die Entstehung vom Kohlensäureanhydrid durch die IR-Bande bei 1800/cm von dem Reaktionsgemisch nach der Entfernung vom zurückgebliebenen Peroxyd festellen, leider war es uns nicht gelungen, die Menge vom Kohlensäureanhydrid zu bestimmen, wie bei der thermischen Zersetzung vom Peroxyd,[1] wegen der Schwierigkeit der Darstellung von 100% reiner authentischer Verbindung. Diese Probleme konnten wir durch Anwendung von Benzoyl-*p*-chlorphenylacetylperoxyd lösen.

Benzoyl-*p*-chlorphenylacetylperoxyd zerfällt in Toluol bei Raumtemperatur ziemlich rasch mit k_{ap} (20°C)$=8.24\times10^{-5}$ Sek^{-1} und $E_a=22.1$ Kcal, Mol.$^{-1}$ Das Verhalten ist sehr ähnlich wie von Benzoylphenylacetylperoxyd. Die Produkten der Photolyse von dem *p*-Chlorperoxyd (Nr. 3) sind mit denen von Nr. 1 zu vergleichen. Die Bildung von *p*-Chlorbibenzyl, Bibenzyl und sogar das klein aber deutliche Auftreten von Benzoesäurebenzylester, weisen ohne Zweifel auf das Benzyl Radical aus Toluol als Zwischenprodukt hin. Was das aus Toluol Wasserstoff Atom abziehende Radikal betrifft, ist es wahrscheinlich Benzoyloxy Radikal, wobei Benzoesäure sich bilden muss. Die Carbonsäure, die nach der Zersetzung vom zurückgebliebenen Peroxyd mit Natriumjodid-Aceton ausgezogen wurden, bestehen immer aus mehr Benzoesäure als Phenylessigsäure oder *p*-Chlorphenylessigsäure. Die Carbonsäure in der Tabelle wurden titrimetrisch nach der Zersetzung vom Peroxyd ermittelt und wir nehmen an die Carbonsäure als Benzoesäure auf Grund der grössere Beständigkeit von Benzoyloxy Radikal als die von Acetyloxy Radikal.[5]

Das Reaktionsgemisch von Nr. 3 zeigte nach der Entfernung vom Peroxyd die IR-Banden bei 1800 und 1745/cm von *p*-Chlorbenzylkohlensäurebenzoesäureanhydrid neben der 1725/cm Bande von Benzoesäure-*p*-chlorbenzylester, und die Bestimmung von dem Kohlensäureanhydrid nach IR-Methode gab 16% Ausbeute. *p*-Chlorbenzylkohlensäurebenzoesäureanhydrid zerfällt thermisch bei Gaschromatographie in 90% Ausbeute in Benzoesäure-*p*-chlorbenzylester und der Rest besteht aus Benzoesäure und Benzaldehyd, aber fast keinem *p*-Chlorbenzylalkohol (1).

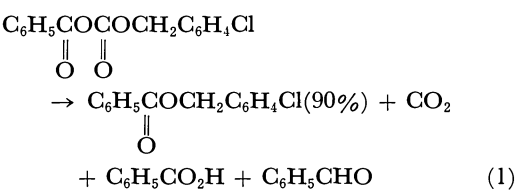

(1)

Die Ausbeute von Benzoesäurebenzylester in der Tabelle wird um so mehr, je mehr Kohlensäureanhydrid bei der Gaschromatographie da ist. Kohlensäureanhydrid ist weiter sehr empfindlich gegen Carbonsäure so stark wie Benzoesäure,[1,6] und er zerfällt schon bei Zimmertemperatur allmählich in Kohlendioxyd, Benzylalkohol und Benzoesäureanhydrid (2).

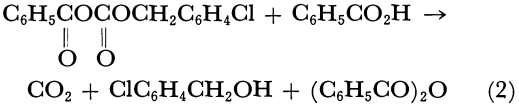

(2)

Wenn Benzoesäureanhydrid auch mal gebildet wird, kann man ihn leider nicht entfernen, ohne die anderen Produkte wie Estern oder Kohlensäureanhydrid zu beschädigen. Die IR-Bande von Benzoesäureanhydrid 1785/cm lagert sich sehr über die von 1800/cm von Kohlensäureanhydrid, wenn der letztere viel dabei ist. Wir haben deshalb versucht, das Reaktionsgemisch mit Äthylat bei 0° umzusetzen und die gebildeten Benzoat Anionen zur freien Benzoesäure zu überführen und sie nach der Methylierung mittels Diazomethans als Benzoesäuremethylester zu bestimmen. Die erhaltene Ausbeute von Benzoesäuremethylester bei Nr. 3, 38%, korrigiert man für Benzoesäureanhydrid nach den folgenden Blind-Reaktionen (3)—(8):

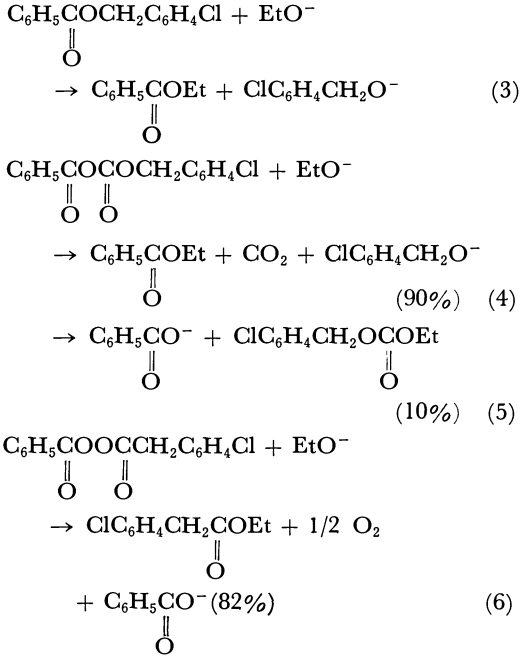

(3) (4) (5) (6)

*1 Berechnet auf Grund des angesetzten Peroxyds.

5) L. Jaffe und E. J. Prosen, *J. Chem. Phys.*, **27**, 416 (1957); A. Yamamoto, N. Inamoto, N. Morikawa und O. Simamura, 19. Jahrestagung der Chem. Gesellschaft, Japan, April 1966. Vordruck III, 113.

6) T. B. Windolz, *J. Org. Chem.*, **23**, 2044 (1958).

$$\rightarrow ClC_6H_4CH_2\overset{\overset{O}{\|}}{C}O^- + 1/2\ O_2$$

$$+ C_6H_5\overset{\overset{O}{\|}}{C}OEt(18\%) \qquad (7)$$

$$(C_6H_5CO)_2O + EtO^-$$

$$\rightarrow C_6H_5\overset{\overset{O}{\|}}{C}OEt + C_6H_5\overset{\overset{O}{\|}}{C}O^- \qquad (8)$$

Man erhält 12.7%*2.

Die berechnete Menge von Benzoesäureanhydrid stimmt gut mit der Ausbeute *p*-Chlorbenzylalkohols, 14%, überein, dieser Alkohol kann nach der Gleichung (2) entstehen.

Die Werte in der Tabelle, die direkt aus der Chromatographie usw. ermittelt wurden, muss man mit Rücksicht auf die Reaktionen (1) und (2) korrigieren, um die erste Stufe der Photolyse klar zu machen. Für Kohlendioxyd, z. B., erhält man 85−13=72% nach Gleichung (2), weil etwa 13% Kohlendioxyd in der zweiten Stufe der Reaktion entstanden ist. In der Weise errechnet man für *p*-Chlorbenzylkohlensäurebenzoesäureanhydrid 29% (=16+13 nach Gl. 2), für Benzoesäure-*p*-chlorbenzylester · 15.6%, und für Benzoesäure 26%. Auf Grund dieser korrigierten Werte kann man für die Photolyse Nr. 3 folgendes Schema mit einigen % Fehler zeichnen:

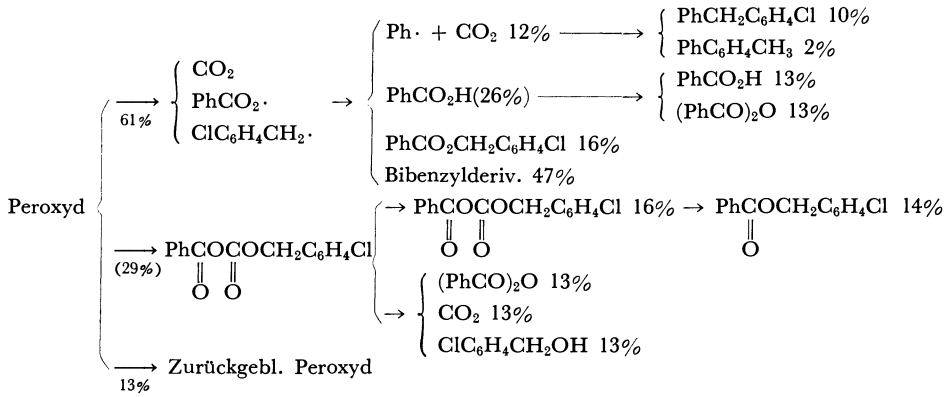

Kritischen Fehler findet man in der Bilanz der *p*-Chlorbenzyl Gruppe, *ca.* 15% zu viel. Die grösste Gründe dafür seien die fehlerhafte Bestimmung von Bibenzylderivaten, besonders der vom hohen Siedepunkt mit relativ flüchtigen inneren Standard bei Gaschromatographie.

Die Quantenausbeuten waren 0.49 bei Nr. 1 und 0.44 bei Nr. 3 und sie sind beide grösser als 0.25, die Walling und Gibian[7] bei der Benzophenon sensibilisierten Photolyse von Benzoylperoxyd erhielten.

Bei der Hochdruck Brenner Belichtung ist die Ergebnis fast genau so wie bei Niederdruck Brenner Belichtung und es ist noch zu früh den kleineren Unterschied der beiden Ergebnisse zu diskutieren.

Beschreibung der Versuche

Peroxyde. *Benzoylphenylacetylperoxyd* wurde nach der Angabe von Wieland und anderen[8] hergestellt. Schmp. 33.5—34°C, zers. Reinheit beträgt 95—97% nach Jodmetrie mit Natriumjodid-Aceton.

Benzoyl-p-chlorphenylacetylperoxyd wurde wie bei oben aus perbenzoesaurem Natrium und *p*-Chlorphenylacetylchlorid bei −5—−10°C in wässr. Aceton hergestellt und aus Toluol-*n*-Hexan umkristallisiert. Farblose Nadeln vom Schmp. 48—49°C, zers. Reinheit 93—95% nach Jodmetrie. Gef.: C, 61.94; H, 4.12%. Ber. für $C_{15}H_{11}O_4Cl$: C, 61.97; H, 3.81%. Zerfallsgeschwindigkeitskonstanten in Benzol, k_{ap}(20°C)=8.24×10^{-5} Sek^{-1} und k_{ap} (30°C)=2.92×10^{-4} Sek^{-1}. E_a=22.1 Kcal, Mol^{-1}, $\Delta S^{\neq}$=−4.2 cal, Grad^{-1}, Mol^{-1}. Versuche zur Darstellung von *Benzoyl-p-methoxyphenylacetylperoxyd* wurden wie bei oben durchgeführt. Man erhält eine peroxydische kristalline Substanz bei −50°C, sie wurde aber ein Öl bei −10°C unter Koholendioxyd Entwicklung. Aufarbeitung von einem Öl (Peroxyd Reinheit 16%) gab Benzoesäure-*p*-methoxybenzylester vom Schmp. 35—36°C. Er wurde durch Mischprobe mit der authentischen Verbindung[9] identifiziert.

***p*-Chlorbenzylkoholensäurebenzoesäureanhydrid.** Der Anhydride wurde nach der Methode von Tarbell und Longosz[10] aus Chlorameisensäure-*p*-chlorbenzylester und Benzoesäure in Gegenwart von Triäthylamin hergestellt. Farblose Nadeln vom Schmp. 40.5—41.5°C. Ausbeute 40%. Er hält länger bei 0°C. Gef.: C, 62.26; H, 4.22%. Ber. für $C_{15}H_{11}O_4Cl$: C, 61.97; H, 3.81%.

Belichtung. Ein Quecksilber Niederdruck Brenner von Rikosha, UVL-1000 Q von 160W wurde unter

*2 Man rechnet folgendermassen: 38—13 (freie Carbonsäure)−16×0.1 (Koholensäureanhydride)−13×0.82(zurückgebl. Peroxyd)=12.7

7) C. Walling und M. J. Gibian, *J. Am. Chem. Soc.*, **87**, 3413 (1965).

8) H. Wieland, T. Ploetz und H. Indest, *Ann.*, **532**, 166 (1937).

9) M. Tiffeneau und K. Fuhrer, *Bull. soc. chim. France*, [4] **15**, 170 (1914).

10) D. S. Tarbell und E. J. Longosz, *J. Org. Chem.*, **24**, 774 (1959).

Luft-Kühlung verwendet und die Peroxyd-Lösung wurde von aussen bis zum −5——10°C gekühlt. Bei der Belichtung mit dem Hochdruck Brenner, H-400P von 400W von Toshiba, wurde die Peroxyd Lösung in einem 100 ccm Quarz Kolben gestellt und den Kolben hält man in einem Pyrexglas Dewar Gefäss von −5—−10°C. Man Belichtet von aussen.

Aufarbeitung. Nach der Belichtung titriert man das zurückgebliebene Peroxyd jodmetrisch und zieht die Carbonsäure mit Carbonat Lösung aus. Die Carbonsäure methyliert man mit Diazomethane und bestimmt gaschromatographisch. Die Lösung von neutralen Produkten engt man unter vermindertem Druck ein und führt damit die IR- und gaschromatographische Bestimmungen. Zur Bestimmung von Carbonsäure titriert man das Reaktionsgemisch mit Bariumhydroxyd Lösung nach der Entfernung von zurückgebliebenem Peroxyd. Zur Bestimmung von Benzoesäureanhydrid versetzt man das Reaktionsgemisch mit Äthylat über Nacht bei 0°C und man verwandelt das gebildete Benzoat Anion über Benzoesäure in den Benzoesäuremethylester mittels Diazomethans, und untersucht den Methylester durch Gaschromatographie. Die Blindprobe des Versetzens von Äthylat mit *p*-Chlorbenzylkoholensäurebenzoesäureanhydride gab 10% Benzoesäuremethylester, mit Benzoyl-*p*-chlorphenylacetylperoxyd 82% Benzoesäuremethylester und 18% *p*-Chlorphenylessigsäuremethylester, und mit Benzoesäureanhydride 100% Benzoesäuremethylester. Die IR-Spektren wurden mit einem Gerät von Hitachi EPI-S Typ mit 0.5 mm Zell durchgeführt. Die molaren Extinktionskoeffizienten waren für Benzoesäure-*p*-chlorbenzylester 323 bei 1725/cm und für *p*-Chlorbenzylkohlensäurebenzoesäureanhydrid 371 bei 1745/cm, jede im Bereich von 10^{-2} Mol/*l*.

Gaschromatographie erfolgte mit einem Gerät von Hitachi KGL-2A Typ und die Kolonne Bedingungen waren wie folgenden: a) Silicon DC 200 bei 176°C, 3 m lang. He, 64.2 ccm/Min für Methylestern von Benzoesäure, Phenylessigsäure und *p*-Chlorphenylessigsäure, mit dem inneren Standard Essigsäurephenylester, b) Silicon DC 200 bei 206°C, 3 m lang. He, 85.6 ccm/Min für Diphenylmethan, *p*-Chlordiphenylmethan,[11] Benzoesäurebenzylester, Benzoesäure-*p*-chlorbenzylester vom Schmp. 56—57°C. Gef.: C, 68.01; H, 4.42%. Ber. für $C_{14}H_{11}O_2Cl$: C, 68.16; H, 4.49%, *p*-Chlorbibenzyl,[12] *p,p'*-Dichlorbibenzyl,[13] mit dem inneren Standard Dibenzyläther, c) Shimalite B-Apiezon L 25% bei 206°C, 7 m lang. He, 85.6 ccm/Min für Bibenzyl, *o*-, *m*- und *p*-Methyldiphenyle und *p*-Methyldiphenylmethan. Die Molverhältnisse von *o*-, *m*- und *p*-Methyldiphenyle waren 70 : 12 : 18. *p*-Methyldiphenylmethan kommt gleich nach dem grossen Signal von Bibenzyl und wir konnten die anderen isomeren Methyldiphenylmethane nicht bestimmen. Die Signale von Benzoesäurebenzylester und von *p*-Chlorbibenzyl stimmen vollkommen überein, so war es auch mit denen von Benzoesäure-*p*-chlorbenzylester und von *p,p'*-Dichlorbibenzyl. Folglich wurden die Mengen von Estern aus der Abnahme des Signales nach der Verseifung von Estern berechnet. Die oben erwähnten authentischen Verbindungen wurden nach den bekannten Methoden hergestellt.

Quantenausbeute: Die Ausbeute wurde nach der Methode von Parkar mit Kalium Eisen(III)trioxalat[14] bestimmt. Die Licht Intensität vom Niederdruck Brenner war 2.15×10^{19} Quanta/Min. Die Quantenausbeute der Photolyse Nr. 1 war 0.49 und die von Nr. 3 war 0.44.

---

11) J. B. Bernstein, J. S. Roth und W. T. Miller, Jr., *J. Am. Chem. Soc.*, **70**, 2312 (1948).
12) F. Bergmann, J. Weizman und D. Schapiro, *J. Org. Chem.*, **9**, 408 (1944).
13) R. Kade, *J. parakt. Chem.*, [2] **19**, 462 (1879).
14) C. A. Parkar, *Proc. Roy. Soc.*, **220A**, 104 (1953).

BULLETIN OF THE CHEMICAL SOCIETY OF JAPAN VOL. 41 1711—1716 (1968)

Reactions of Dimethylaniline with Some Resonance-stabilized Radicals

Renji OKAZAKI and Naoki INAMOTO

Department of Chemistry, Faculty of Science, The University of Tokyo, Hongo, Tokyo

(Received February 16, 1968)

Reactions of dimethylaniline with some resonance-stabilized radicals were studied. 2-Cyano-2-propyl radicals and 2-methoxycarbonyl-2-propyl radicals reacted to give *N*-methyl-*N*-(3,4-dicyano-3,4-dimethylpentyl)aniline and the corresponding 3,4-dimethoxycarbonyl derivative, respectively, while benzyl radicals and α-methoxycarbonylbenzyl radicals did not give reaction products with dimethylaniline. Mechanism of these reactions was proposed and it was pointed out that electron transfer from dimethylaniline to radicals was an important stage in these reactions.

Previously, one of the authors (N. I.) has studied the reaction of α,α'-azobisisobutyronitrile (AIBN) with some aromatic compounds and found that dimethylaniline reacts with 2-cyano-2-propyl radicals generated from AIBN.[1] We wish to report in this paper similar reactions of dimethylaniline with some resonance-stabilized radicals.

1) N. Inamoto, *Yuki Gosei Kagaku Kyokaishi (J. Soc. Org. Synth. Chem. Japan)*, **17**, 174 (1959).

generated by the thermal decomposition of azo compounds or organomercurials.

Results

Reaction with AIBN. The reaction of dimethylaniline with AIBN at water-bath temperature gave *N*-methyl-*N*-(3,4-dicyano-3,4-dimethylpentyl)-aniline (I)[2] in a 2.7% yield. The structure of I was determined by the NMR spectrum (Fig. 1) and the elemental analysis.

$$C_6H_5N(CH_3)_2 + (CH_3)_2C(CN)-N=N-C(CN)(CH_3)_2 \rightarrow$$

AIBN

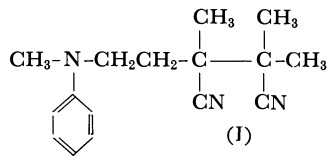

(I)

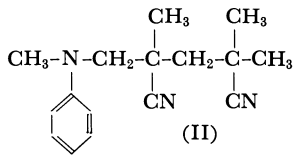

(II)

The NMR spectrum showed a singlet at τ 8.58 (9H, *C*-methyl protons), a multiplet between τ 7.8—8.5 (2H, methylene protons on C_β), a singlet at τ 7.13 (3H, *N*-methyl protons), a triplet at τ 6.55 (2H, J=7 cps, *N*-methylene protons), and a multiplet between τ 2.8—3.5 (5H, aromatic protons). That the structure of the product is not an isomeric one (II) was further confirmed by spin-spin decoupling technique. Thus, irradiation of the triplet at τ 6.55 caused the methylene multiplet between τ 7.8—8.5 to collapse to a typical AB type quartet. This fact shows that the methylene protons are on the carbon atom (C_β) adjacent to both the *N*-methylene group and the asymmetric center (C_γ).

Reaction with Dimethyl α,α'-Azobisisobutyrate (MAIB). The reaction of dimethylaniline with MAIB at *ca.* 100°C gave rise to *N*-methyl-*N*-(3,4-dimethoxycarbonyl-3,4-dimethylpentyl)aniline (III) in a 6% yield.

$$C_6H_5N(CH_3)_2 + (CH_3)_2C(CO_2CH_3)-N=N-C(CO_2CH_3)(CH_3)_2 \rightarrow$$

(MAIB)

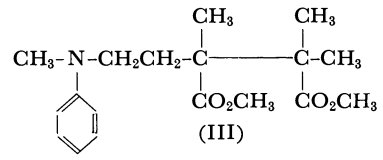

(III)

The compound (III) was identified by elemental analyses and NMR spectra of both III and its azo derivative. The compound (III) is very viscous but distillable oil. It did not give crystalline derivatives; the picrate, hydrazide, quaternary ammonium salt and *N*-oxide were oily products, all of which could not be purified. *p*-Nitrobenzenediazonium salt, however, reacted with III to give a reddish brown crystalline product, which was identified to be an azo-coupling product (IV) by the elemental analysis and the NMR spectrum.

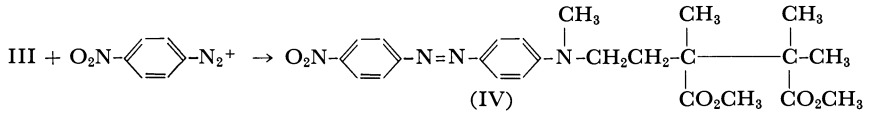

(IV)

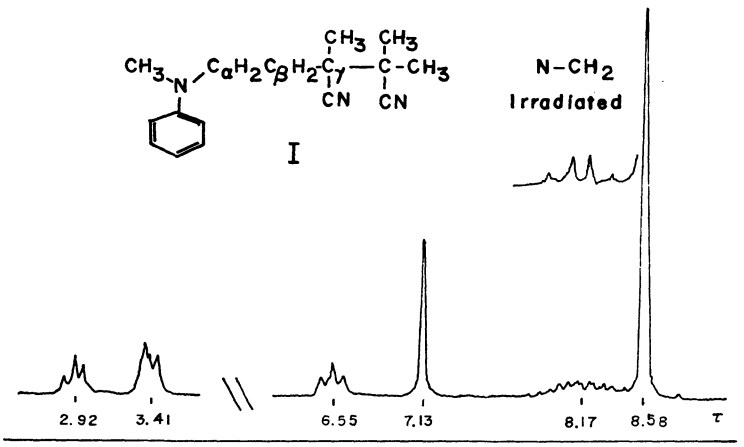

Fig. 1. NMR spectrum of the compound (I) in CCl_4 at 100 Mc.

2) The previously assumed structure[1] was found to be incorrect.

Reactions with Dibenzylmercury and Bis(α-methoxycarbonylbenzyl)mercury. The reaction of dimethylaniline with dibenzylmercury, which is known to generate benzyl radicals by heating,[3] was carried out at 120—160°C under nitrogen. The reaction products obtained were only those derived from the thermal decomposition of dibenzylmercury; mercury (99%), bibenzyl (75%), and toluene (4%), no reaction products between dimethylaniline and benzyl radicals being obtained.

The reaction of dimethylaniline with bis(α-methoxycarbonylbenzyl)mercury (V)[4] was performed at 120—180°C under nitrogen. In this case, again, products were those attributed to the thermal decomposition of V; mercury (95%), *meso* form of dimethyl diphenylsuccinate (71%), and methyl phenylacetate (15%). However, in addition to these products a trace of bis(4-*N*,*N*-dimethylaminophenyl)methane was obtained.

Discussion

It has been shown in the present study that dimethylaniline reacts with 2-cyano-2-propyl radicals and 2-methoxycarbonyl-2-propyl radicals, but not with benzyl radicals, the latter were expected to form such a substitution product as follows.

$$C_6H_5N(CH_3)_2 + 2C_6H_5CH_2\cdot \rightarrow$$

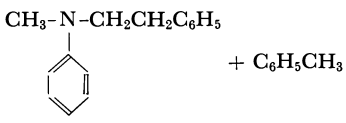

$$+ C_6H_5CH_3$$

This fact suggests that in these reactions electron transfer as shown in Eq. (1) is an important process, because the reaction occurred only with radicals having electronegative groups which make the radicals R· more electrophilic and the corresponding carbanion more stable.

$$C_6H_5\overset{\overset{CH_3}{|}}{\underset{+\cdot}{N}}-CH_3 + R\cdot \rightarrow C_6H_5\overset{\overset{CH_3}{|}}{\underset{+\cdot}{N}}-CH_3 + R^- \qquad (1)$$

It is known, indeed, that aromatic amines are readily subjected to one electron oxidation. Horner[5] and Imoto[6] have shown that the first stage in the reaction of dimethylaniline and benzoyl peroxide is electron transfer process from the former to the latter.

$$C_6H_5N(CH_3)_2 + (C_6H_5CO_2)_2 \rightarrow C_6H_5\overset{\overset{CH_3}{|}}{\underset{+\cdot}{N}}-CH_3 + C_6H_5COO\cdot + C_6H_5COO^- \qquad (2)$$

Franzen[7] has reported that *N*,*N*,*N'*,*N'*-tetramethyl-*p*-phenylenediamine is oxidized by various types of radicals, including 2-cyano-2-propyl radical, to give a stable cation radical, Wurster's salt.

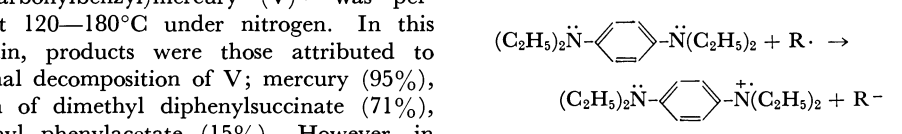

The conclusion that the more electrophilic the radicals R· are, the more readily the electron transfer occurs, has been drawn from the observation that, in radical polymerizations in the presence of dimethylaniline, the chain transfer for dimethylaniline becomes more effective when the end of a growing radical is more positive.[8]

On the basis of the facts described above, the mechanism of formation of I and III is considered as follows.

$$(CH_3)_2\dot{C}X + C_6H_5\ddot{N}(CH_3)_2 \rightarrow$$

(VI)

X=CN, $COOCH_3$

$$(CH_3)_2\bar{C}X + C_6H_5\overset{+\cdot}{N}(CH_3)_2 \qquad (4)$$

(VII) (VIII)

$$(CH_3)_2\bar{C}X + C_6H_5\overset{+\cdot}{N}(CH_3)_2 \rightarrow (CH_3)_2CHX + C_6H_5\overset{\overset{CH_3}{|}}{N}-CH_2\cdot \qquad (5)$$

(IX)

$$2(CH_3)_2\dot{C}X \rightarrow (CH_3)_2CHX + CH_2{=}C(CH_3)X \qquad (6)$$

$$C_6H_5\overset{\overset{CH_3}{|}}{N}-CH_2\cdot + CH_2{=}C(CH_3)X \rightarrow C_6H_5N(CH_3)CH_2CH_2\dot{C}(CH_3)X \qquad (7)$$

(X)

$$C_6H_5N(CH_3)CH_2CH_2\dot{C}(CH_3)X + (CH_3)_2\dot{C}X \rightarrow C_6H_5N(CH_3)CH_2CH_2-\overset{\overset{CH_3}{|}}{\underset{\underset{X}{|}}{C}}-\overset{\overset{CH_3}{|}}{\underset{\underset{X}{|}}{C}}-CH_3 \qquad (8)$$

(I or III)

3) A. G. Goble, A. G. Lidstone and P. J. S. Pauwels, *Chem. & Ind.*, **1959**, 1489.

4) Reutov and his coworkers have reported the synthesis of this mercurial compound (V) and described its melting point was 140—141°C. However, although we synthesized V by the same method as that of Reutov and identified by the elemental analysis and the NMR spectrum, the melting point of V prepared by us was 181—183°C (dec.). The reason for this discrepancy was not clear but it seems to be attributed to stereochemical isomerism due to asymmetric carbons. See experimental part.

5) L. Horner and E. Schenk, *Angew. Chem.*, **61**, 411 (1949).

6) M. Imoto and S. Choe, *J. Polymer Sci.*, **15**, 485 (1955).

7) V. Franzen, *Chem. Ber.*, **88**, 1697 (1955).

8) M. Imoto, T. Otsu, T. Ota, H. Takatsugi and M. Matsuda, *J. Polymer Sci.*, **22**, 137 (1956).

$$C_6H_5N(CH_3)CH_2\cdot + (CH_3)XC{=}CH_2 \rightarrow C_6H_5N(CH_3)CH_2\text{-}\underset{\underset{X}{|}}{\overset{\overset{CH_3}{|}}{C}}\text{-}CH_2\cdot \quad (7')$$

(XI)

$$C_6H_5N(CH_3)CH_2\text{-}\underset{\underset{X}{|}}{\overset{\overset{CH_3}{|}}{C}}\text{-}CH_2\cdot + (CH_3)_2\dot{C}X \rightarrow C_6H_5N(CH_3)CH_2\text{-}\underset{\underset{X}{|}}{\overset{\overset{CH_3}{|}}{C}}\text{-}CH_2\text{-}\underset{\underset{X}{|}}{\overset{\overset{CH_3}{|}}{C}}\text{-}CH_3 \quad (8')$$

(II) X=CN

A cation radical (VIII) formed by electron transfer is deprotonated by a carbanion (VII) yielding a radical (IX). This radical (IX) adds to an olefin formed by disproportionation of a radical (VI) to give a radical (X), which successively couples with the radical (VI) to form the final product (I or III). Since the radical (X) is more stable than an isomeric one (XI) owing the conjugation with methyl and X groups, the addition reaction like Eq. (7') and hence Eq. (8') are not considered to occur.

Although direct hydrogen abstraction like Eq. (9) may be possible, it can be ruled out by the facts that (1) the radical (VI) is a poor hydrogen abstractor and (2) that, if the reaction proceeds by direct hydrogen abstraction, reactions like Eqs. (10) and (11) should occur in the reaction with benzyl radicals.

$$C_6H_5N(CH_3)_2 + (CH_3)_2\dot{C}X \rightarrow C_6H_5N(CH_3)CH_2\cdot + (CH_3)_2CHX \quad (9)$$

$$C_6H_5N(CH_3)_2 + C_6H_5CH_2\cdot \rightarrow C_6H_5N(CH_3)CH_2\cdot + C_6H_5CH_3 \quad (10)$$

$$C_6H_5N(CH_3)CH_2\cdot + C_6H_5CH_2\cdot \rightarrow C_6H_5N(CH_3)CH_2CH_2C_6H_5 \quad (11)$$

The reason is not clear why the reaction between dimethyaniline and V (Eq. (12)) did not occur, because a radical (XII) generated from V is thought to be rather electrophilic like radicals VI.

$$C_6H_5N(CH_3)_2 + \underset{(V)}{[C_6H_5CH(COOCH_3)]_2Hg} \rightarrow C_6H_5N(CH_3)CH_2\text{-}\underset{\underset{H}{|}}{\overset{\overset{COOCH_3}{|}}{C}}\text{-}C_6H_5 \quad (12)$$

$C_6H_5\dot{C}HCOOCH_3$ (XII)

However, the formation of a trace amount of bis(4-*N*,*N*-dimethylaminophenyl)methane (XIII) may be considered to show that the reaction between dimethylaniline and the radical (XII) takes place at least to some extent, for the formation of the compound (XIII) can be explained reasonably by the reaction of dimethylaniline with formaldehyde (Eq. (13)) which is probably, though not conclusive, formed according to the following reactions.

$$C_6H_5\ddot{N}(CH_3)_2 + R\cdot \rightarrow C_6H_5\overset{+}{\ddot{N}}(CH_3)_2 + R^- \rightarrow \underset{(IX)}{C_6H_5N(CH_3)CH_2\cdot} + RH$$

$$IX + O_2 \rightarrow C_6H_5N(CH_3)CH_2OO\cdot \rightarrow C_6H_5N(CH_3)CH_2O\cdot \rightarrow C_6H_5\dot{N}CH_3 + CH_2O$$

$$2\,C_6H_5N(CH_3)_2 + CH_2O \rightarrow (CH_3)_2N\text{-}C_6H_4\text{-}CH_2\text{-}C_6H_4\text{-}N(CH_3)_2 \quad (13)$$

(XIII)

The oxidation of the radical (IX) is considered to be due to a small amount of oxygen dissolved in the reaction solution.

Experimental

Materials. α,α'-Azobisisobutyronitrile (AIBN) was used after recrystallization of commercial product from ether, mp 103—104°C. Dimethyl α,α'-azobisisobutyrate (MAIB) was prepared from AIBN[9] and recrystallized from petroleum ether, mp 29—31°C. Dibenzylmercury was prepared by the method of Jones and Werner,[10] mp 110—111°C.

Bis(α-methoxycarbonylbenzyl)mercury(V) was prepared according to the directions of Reutov.[11] However, there was a great difference between the description by Reutov and our observation. Reutov and his coworkers have reported that the shaking of methyl α-bromophenylacetate with mercury for 2 hr gave 80% of methyl α-bromomercuriphenylacetate, mp 92.5—94.0°C, which reacted with ammonia in the chloroform solution to give rise to V in a 74% yield, mp 140—141°C. On the other hand, we found that the reaction of 40 g (0.18 mol) of methyl α-bromophenylacetate with 201 g (1 g atom) of mercury at room temperature for 3 hr gave 44 g of very viscous oil, which reacted with ammonia in the chloroform solution to form only 7.3 g (10%) of a crude mercurial compound. The crude product was recrystallized from ethanol. The purified one mostly but not perfectly melted at 155—157°C to become grey and turbid liquid, which melted perfectly at 181—183°C. NMR (in $CDCl_3$): τ 6.24 (6H), 6.03(2H), and 2.58(10H).

Found: C, 43.22; H, 3.67%. Calcd for $C_{18}H_{18}O_4Hg$: C, 43.33; H, 3.63%.

Different products were formed under a slightly vigorous condition. Thus, the reaction of 60 g (0.27 mol) of methyl α-bromophenylacetate with 270 g (1.35 g atom) of mercury at room temperature for 3 hr and then at 60°C for one hour resulted in the formation of 21 g (55%) of *meso* form of dimethyl diphenylsuccinate, mp 217—219°C (lit.,[12] 219—220°C),

9) J. Thiele and K. Heuser, *Ann.*, **290**, 35 (1896).
10) L. W. Jones and L. Werner, *J. Am. Chem. Soc.*, **40**, 1266 (1918).
11) O. A. Reutov, I. P. Beletskaya and G. A. Artamkina, *Zhur. Obshchei Khim.*, **30**, 3220 (1960).
12) H. Wren and C. J. Still, *J. Chem. Soc.*, **111**, 1023 (1917).

3.5 g (9%) of racemic form of the same ester, mp 172—173°C (lit.,[13] 173—174°C) and a small amount of compound containing mercury, which was not identified.

Reaction with AIBN. a) The azonitrile (4.92 g, 0.030 mol) was added in small portions during one hour to dimethylaniline (18.15 g, 0.15 mol) heated on a steam bath, and the reaction solution was heated for additional few hours. The reaction solution was distilled under a current of steam in order to remove unchanged dimethylaniline and tetramethylsuccinodinitrile. The residue was extracted with ether, ether was evaporated, and 1 g of picric acid in alcohol was added. The precipitates thus obtained were recrystallized from ethanol to give 0.2 g (1.38%) of picrate, mp 150—151°C. When the reaction was carried out under the same condition as described above except further addition of 11.1 g of *n*-butanol to dimethylaniline, 0.35 g (2.4%) of the same picrate was obtained.

Found: C, 54.50; H, 5.24; N, 17.00%. Calcd for $C_{22}H_{24}N_6O_7$: C, 54.54; H, 4.99; N, 17.35%.

The picrate(0.3 g) was warmed with 20 m*l* of 28% aqueous ammonia to give a homogeneous solution. The reaction mixture was extracted with ether, the ethereal solution was dried with anhydrous potassium carbonate, ether was evaporated, and the residue was recrystallized from petroleum ether to give 100 mg (63.3%) of a compound, mp 72—73°C.

b) The same reaction was carried out using 90.8 g (0.75 mol) of dimethylaniline and 24.6 g (0.15 mol) of AIBN. After the reaction solution was distilled under atmospheric pressure to remove 2.1 g (10.1%) of isobutyronitrile, and then under reduced pressure to remove unchanged dimethylaniline and tetramethylsuccinodinitrile, the residue was extracted repeatedly with petroleum ether (bp 50—80°C). Condensation of the extract yielded crystals, which were recrystallized from petroleum ether to give 1.05 g (2.7%) of a compound of mp 72—73°C, which was the same as that obtained by the decomposition of the picrate in the procedure a).

Found: C, 75.25; H, 8.70; N, 16.39%. Calcd for $C_{16}H_{21}N_3$: C, 75.25; H, 8.29; N, 16.46%.

The IR spectrum of this compound (KBr disk) showed the presence of C≡N (2240 cm^{-1}) and N–CH_3 (2810 cm^{-1}). The NMR spectrum was shown in Fig. 1.

Reaction with MAIB. a) The reaction of 23 g (0.10 mol) of MAIB with 62 g (0.51 mol) of dimethylaniline was carried out by a similar procedure to that described in the reaction with AIBN. To the residue of steam distillation was added a saturated alcoholic solution of picric acid to give 0.29 g (1.9%) of crude picrate, which was brown viscous oil and could not be crystallized.

b) The azoester (69 g, 0.30 mol) was added in small portions to dimethylaniline (180 g, 1.50 mol) heated at 100—110°C and the reaction mixture was heated for 11 hr at this temperature. After methyl isobutyrate and dimethylaniline were distilled off, the residue was distilled under high vacuum in order to remove dimethyl tetramethylsuccinate, which distilled out up to 160°C (0.5 mmHg). The residue was 5.9 g of colorless and very viscous oil which distilled at 160—186°C (0.18 mmHg). The elemental analysis of the oil showed 3.8% of nitrogen content (calcd for $C_{18}H_{27}NO_4$: N, 4.36%), which indicated that it contained about 90% of the amine (III). The picrate of the crude amine was boiled with conc. aqueous ammonia to obtain free amine. Then it was twice purified by column chromatography on silica gel with benzene-ether (9 : 1) mixture as eluent.

Found: C, 67.21; H, 8.67; N, 4.51%. Calcd for $C_{18}H_{27}NO_4$: C, 67.26; H, 8.47; N, 4.36%.

The NMR spectrum of the purified amine in CCl_4 at 60 Mc: τ 8.90 and 8.85 (9H in total), 7.8—8.6 (multiplet, 2H), 7.17 (singlet, 3H), 6.76 (triplet, 2H, J=7 cps), 6.42 (singlet, 6H), and 2.7—3.7 (multiplet, 5H). Attempts to obtain crystalline derivatives were not successful except for a diazo-coupling product; the treatment of the crude amine with picric acid, hydrazine hydrate, methyl iodide, perbenzoic acid and conc. hydrochloric acid in order to obtain the corresponding picrate, hydrazide, ammonium salt, *N*-oxide, and free carboxylic acid, respectively, did not give crystalline products. The amine, however, underwent a diazo-coupling reaction with *p*-nitrobenzenediazonium chloride to yield reddish brown solid, which was recrystallized from carbon tetrachloride, mp 172—173°C. The NMR spectrum of the azo compound in $CDCl_3$ at 60 Mc: τ 8.76 (singlet, 9H), 7.5—8.5 (multiplet, 2H), 6.92 (singlet, 3H), 6.65 (triplet, 2H, J=7 cps), 6.25 (singlet, 3H), 6.33 (singlet, 3H), and 3.3—1.6 (multiplet, 8H).

Found: C, 60.85; H, 6.73; N, 12.18%. Calcd for $C_{24}H_{30}N_4O_6$: C, 61.16; H, 6.43; N, 11.91%.

Reaction with Dibenzylmercury. The solution of 15 g (0.04 mol) of dibenzylmercury in 24 g (0.2 mol) of dimethylaniline was heated under nitrogen at 120°C for one hour and at 160°C for half an hour. After mercury (7.94 g, 99%) was removed, the reaction mixture was distilled with steam. The distillate was extracted with ether and the ether solution was shaken with conc. hydrochloric acid. The aqueous layer was neutralized by aqueous solution of sodium carbonate, and extracted with ether. The ether solution was dried with anhydrous sodium sulfate and distilled to give only dimethylaniline. The ether layer was dried with anhydrous sodium sulfate, concentrated, and analyzed with glc using an apiezon grease column; 75% of bibenzyl and 4% of toluene were detected. The residue of the steam-distillation was extracted with ether, ether was evaporated, and then ethanol was added. Addition of picric acid to the ethanol solution gave only a trace amount of brown tarry compound, which was not identified.

Reaction with Bis(α-methoxycarbonylbenzyl)-mercury(V). The reaction between 13 g (0.11 mol) of dimethylaniline and 4.9 g (0.01 mol) of V was performed under nitrogen. Mercury began to deposit at about 120°C. The reaction temperature was gradually raised to 180°C during 30 min and kept at this temperature for 30 min. When the reaction solution was cooled, large quantities of white crystals precipitated. The precipitates were dissolved by adding of acetone and mercury isolated (1.87 g, 95%) was filtered off. To the acetone solution was added petroleum ether to give 2.1 g (71%) of white precipitates, which were identified by IR and mp (217—219°C) as *meso* form of dimethyl diphenylsuccinate. After distillation under reduced pressure in order to remove dimethylaniline, the filtrate was steam-distilled. The

13) H. Wren and C. J. Still, *ibid.*, **107**, 1453 (1915).

residue was extracted with methylene dichloride, the extract was dried, and methylene dichloride was evaporated to leave a small amount of purple oil. To the oil was added a saturated solution of picric acid in alcohol to form yellow precipitates. After ethanol was added enough to dissolve the yellow precipitates under reflux, the solution was cooled giving 0.29 g of crystals. Further recrystallization from ethanol gave yellow crystals of mp 180—181°C.

Found: C, 49.06; H, 3.69; N, 15.48%. Calcd for $C_{29}H_{28}N_8O_{14}$: C, 48.88; H, 3.69; N, 15.73%.

The picrate was decomposed by aqueous sodium hydroxide, the reaction solution was extracted with ether, and ether was evaporated leaving an almost white crystals. It was recrystallized from ethanol to give white crystals, mp 88—89°C. It was identified as bis(4-*N*,*N*-dimethylaminophenyl)methane (lit.,[14] mp 90°C). The NMR spectrum in CCl_4 at 60 Mc: τ 2.91 (12H), 3.71 (2H), 6.42, 6.63, 6.86, and 7.00 (8H, in total).

14) O. Doebner, *Ber.*, **12**, 810 (1879).

BULLETIN OF THE CHEMICAL SOCIETY OF JAPAN VOL. 41 1716—1723 (1968)

Magnesium Ammonium Phosphates, Related Salts and Their Behavior in Compound Fertilizers

Jumpei ANDO, Takashi AKIYAMA and Matsusaburo MORITA

Department of Industrial Chemistry, Faculty of Science and Engineering, Chuo University, Bunkyo-ku, Tokyo

(Received December 5, 1967)

Fluorine forms a previously unknown compound $MgNH_4HFPO_4$ (MAFP) when monoammonium phosphate made from wet-process phosphoric acid is treated with magnesium hydroxide above about 75°C in the presence of moisture. When treatment is conducted with a large quantity of water, fluorine forms a gelatinous material which resembles MAFP in chemical composition. Wet-process phosphoric acid ammoniated and reacted with magnesium hydroxide above about 75°C gives a very thick slurry, which almost solidifies due to the formation of gelatinous material, while the acid treated in the same way after being defluorinated gives a less viscous slurry in which most of the magnesium is present in the form of $MgNH_4PO_4 \cdot H_2O$ (MH). Fluorine shows less effect at lower temperature. When treated below about 60°C, most of the magnesium combines to form $MgNH_4PO_4 \cdot 6H_2O$ (M6H) and $Mg(NH_4)_2(HPO_4)_2 \cdot 4H_2O$ (M4H). M6H and M4H decompose during drying at about 100°C, losing ammonia and water of crystallization to form amorphous materials. The decomposition is promoted by the presence of potassium salts resulting in the formation of water-insoluble potassium. Another previously unknown compound, $MgKHFPO_4$ (MKFP), which is isomorphic with MAFP has also been identified. MKFP is less soluble in water while MAFP decomposes in water to precipitate amorphous material and M6H. Solid solutions of MAFP and MKFP are often present in commercial fertilizers, and provide a small amount of water-insoluble potassium. M4H decomposes rapidly in water to precipitate M6H. M6H and MH are less soluble in pure water but are considerably soluble in water which contains acidic salts, such as monoammonium phosphate.

Recently a large number of compound fertilizers containing magneisum with grades 12—26—10—5, 12—16—14—4, 11—11—11—4, *etc.* have been produced in Japan. The main source of magnesium is magnesium hydroxide precipitated from sea water, while serpentine and olivine are used in a few plants. It has been generally thought that most of the magnesium would combine to form $MgNH_4PO_4 \cdot H_2O$ (NH) and $MgNH_4PO_4 \cdot 6H_2O$ (M6H) in the fertilizers, both of which are less soluble in water and have good agronomic response as slow release fertilizers.

The present quantitative X-ray analysis on commercial products, however, showed that M6H is seldom present in the final products, and that although MH is often present, the yield is usually much lower than expected. Moreover, there are the following problems: (1) The products of reaction of magnesium hydroxide with ammonium phosphate and other materials are usually so sticky or viscous that cause much trouble in granulation.

(2) A considerable amount of potassium, up to 10% of the total, is sometimes changed into a water-insoluble form.

(3) Usually 30 to 35% of magnesium in the products is soluble in water when tested by the standard Japanese method.

The reasons for the above problems were not clear. The authors studied the forms and properties of magnesium compounds in compound fertilizers, and their behavior during production processes in order to clear up these problems.

Examples of Commercial Compound Fertilizers Tested

Ten examples of commercial compound fertilizers containing magnesium are shown in Table 1.

Sample No. 1 was produced with wet-process phosphoric acid, ammonia, amonium sulfate, urea, potassium chloride and magnesium hydroxide. Samples No. 2 and 3 were produced with ammonium chloride instead of the ammonium sulfate and urea of sample No. 1. Samples No. 4 and 5 were produced with potassium sulfate instead of the potassium chloride of sample No. 1. Samples No. 6 to 8 were made with powdered monoammonium phosphate made from wet-process phosphoric acid, ammonium sulfate, urea, potassium sulfate and magnesium hydroxide. Samples No. 9 and 10 were produced with wet-process phosphoric acid, sulfuric acid, olivine, ammonia and potassium chloride. Samples No. 6 to 8 were granulated at 50 to 60°C, others at 80 to 90°C. All of the granulated products were dried at about 100°C.

The water-solubility of the magnesium present in the samples ranged from 31 to 34%. The water-solubility of potassium ranged from 95 to 98% for samples No. 1 to 5 which were granulated at 80 to 90°C, and 90 to 92% for samples No. 6 to 8 which were granulated at 50 to 60°C.

Materials Used

For preparation tests in the laboratory, five samples of commercial ammonium phosphate made from wet-process phosphoric acid, and one sample each of wet-process phosphoric acid and magnesium hydroxide made from sea water were used. The chemical compositions of these samples are given in Table 2.

X-Ray tests of the ammonium phosphate samples showed that the water-soluble P_2O_5 of samples A, B, C and D was present as monoammonium phosphate, while that of sample E was present as

Table 1. Commercial compound fertilizers containing magnesium

No.	Grade	MgO, %			K_2O, %		
		T*	WS**	WS/T	T	WS	WS/T
1	14-18-14-6	7.4	2.3	31.1	15.2	14.8	97.4
2	12-16-14-4	4.5	1.5	33.3	15.4	14.9	96.8
3	12-16-14-4	4.5	1.1	31.1	15.6	14.9	95.5
4	12-26-10-5	5.8			10.6	10.4	98.1
5	12-26-10-5	5.0			10.8	10.5	97.3
6	12-26-10-5	6.0			12.1	10.9	90.1
7	12-26-10-5	6.0			11.4	10.4	91.2
8	12-26-10-5	6.1			11.6	10.7	92.2
9	10-14-12-4	5.0	1.7	34.0	12.9		
10	11-11-11-4	4.9	1.6	32.7	11.8		

* Total. ** Water-soluble.

Table 2. Chemical composition of materials used (%)

	Ammonium phosphate					Wet-process phosphoric acid	Magnesium hydroxide
	A	B	C	D	E		
N	12.3	12.3	11.7	10.9	13.4		
T-P_2O_5	50.9	48.3	51.2	49.7	53.2	28.0	
S-P_2O_5*	50.9	48.2	50.4	48.9	52.9		
WS-P_2O_5	47.7	44.4	45.1	41.4	47.4		
SO_3	5.5	7.3	4.4	6.0		4.9	1.2
R_2O_3	3.2	3.6	4.1	5.5		1.5	0.3
MgO	0.8	1.2	1.2	2.0	0.9	0.4	64.2
CaO	0.2	0.2	0.2	0.7		0.2	0.3
F_2	3.0	3.7	4.2	3.0	1.5	2.2	
pH**	3.9	4.1	4.0	4.0	5.7		

* Petermann's citrate-soluble. ** In 10% aqueous solution.

both monoammonium and diammonium phosphates. Considerable amounts of ammonium sulfate and a water-insoluble compound "S",[1] which is likely to have the formula $Al_3(NH_4)_5H_2 \cdot (PO_4)_4F_4$,[2] were present in all samples of ammonium phosphate.

Reagent grade monoammonium and diammonium phosphates, magnesium hydroxide, ammonium fluoride, hydrofluoric acid, ferric and aluminum phosphates, *etc.*, were also used for the tests.

Experimental and Results

Preparation of Standard Samples. Standard samples of $MgNH_4PO_4 \cdot H_2O$ (MH), $MgNH_4PO_4 \cdot 6H_2O$ (M6H) and $Mg(NH_4)_2(HPO_4)_2 \cdot 4H_2O$[3] (M4H) were prepared in the following way with reagent grade chemicals:

MH: In 500m*l* of phosphoric acid (30% P_2O_5), 100 g of magnesium hydroxide was dissolved. Concentrated aqueous ammonia was added to the solution at 95°C until the pH reached about 8. The precipitate was filtered, quickly washed with hot water and acetone, and dried at 50°C.

M6H: Concentrated aqueous ammonia was added to the magnesium phosphate solution below 50°C. The precipitate was filtered, washed with water and acetone, and dried at 50°C.

M4H: A mole of finely ground monoammonium phosphate and a half mole of magnesium hydroxide were mixed and allowed to react at about 50°C by the repeated addition of small amounts of water and mixing. The product was dried at 50°C.

Chemical and X-ray analyses of the products showed they were sufficiently pure for standard samples. All of the products consisted of small crystals of less than 5 microns, similar to those present in commercial and granulator products of compound fertilizers containing magnesium.

Quantitative X-Ray Analysis. The amounts of MH, M6H and M4H present in the commercial and laboratory products were determined by quantitative X-ray analysis using spinel as an internal standard.[4,5] Calibration curves for the determinations were obtained through tests with synthetic samples. The diffraction angle and height ratio of the peaks of each compound to that of spinel at a 2θ of 36.8° by Cu$K\alpha$ ray when each compound and spinel are present in equal amounts are shown in Table 3.

TABLE 3. DIFFRACTION ANGLE (2θ, Cu$K\alpha$) AND HEIGHT RATIO

Compound	2θ	Ratio
MH	31.8	0.78
MH	10.0	0.50*
M6H	15.7	0.33*
M6H	21.3	0.28
M6H	33.2	0.28
M4H	17.0	0.38

* Less reliable because the height varies considerably with crystal size and shape.

Magnesium Compounds in Commercial Products. A quantitative X-ray analysis of magneisum compounds was conducted on eight samples of commercial products.

Most of samples contained MH, while M6H and M4H were not detected in any of the samples. The amounts of MH present and the yields (MgO present as MH per cent of total MgO) are shown in Table 4.

TABLE 4. THE AMOUNT AND YIELD OF MH

Sample No.	1	2	3	6	7	8	9	10
MH, %	15	4	3	0	1	1	4	10
Yield, %	53	23	17	0	4	4	21	53

The yields were less than about 50%, and was especially low for samples No. 6 to 8, which were granulated at 50 to 60°C and dried at about 100°C. Unreacted magnesium hydroxide was detected only in small amounts in samples No. 1 to 3. Considerable amounts of an unknown compound were detected in samples No. 1 to 3. Other magnesium compounds were not detected.

These results indicate that a considerable portion of magnesium may be present as the unknown compound in samples No. 1 to 3, and as amorphous material in other samples.

Reaction Products of Reagent Grade Monoammonium Phosphate and Magnesium Hydroxide. Finely powdered reagent grade monoammonium phosphate and magnesium hydroxide were blended together in various ratios, and allowed to react at temperatures between 40 and 100°C for 30 min in water vapor. The products were checked by quantitative X-ray analysis. The relations among temperature, mole ratio P_2O_5/MgO and compound formed is shown in Fig. 1.

MH formed above 75°C, M6H below 65°C and the mixture between 65 and 75°C as were previously reported.[6] In addition, M4H formed below 65°C when the mole ratio was greater than 0.5. M4H did not form but M6H did in the presence of a large quantity of water, even when

1) J. Ando and T. Akiyama, *Kogyo Kagaku Zasshi (J. Chem. Soc. Japan, Ind. Chem. Sect.)*, **68**, 1056 (1965).
2) J. Ando, A. W. Frazier and J. R. Lehr (paper under preparation).
3) Crystallographic Properties of Fertilizer Compounds, *Chem. Eng. Bull.* No. 6, TVA, May 1967.
4) J. Ando and T. Akiyama, *Japan Analyst*, **13**, 717 (1964).
5) J. Ando, J. P. Smith, M. R. Siegel and J. E. Jordan, *J. Agr. Food. Chem.*, Vol. 13, No. 2, 186 (1965).
6) S. Iwata, *Kogyo Kagaku Zasshi (J. Chem. Soc. Japan, Ind. Chem. Sect.)*, **62**, 1668 (1959).

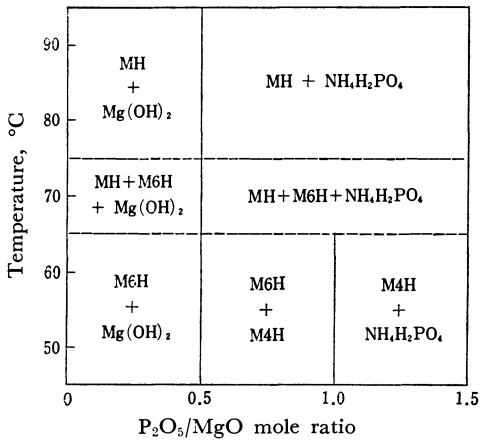

Fig. 1. Compounds present in the reaction products of reagent grade monoammonium phosphate and magnesium hydroxide.

(MH=$MgNH_4PO_4 \cdot H_2O$, M6H=$MgNH_4PO_4 \cdot 6H_2O$, M4H=$Mg(NH_4)_2(HPO_4)_2 \cdot 4H_2O$)

the mole ratio was greater than 0.5 and treatment was carried out below 65°C. In all of the tests, magnesium hydroxide reacted rapidly and quantitatively.

Reaction of Magnesium Hydroxide with Ammonium Phosphate made from Wet-process Phosphoric Acid. Similar tests were conducted with reagent grade magnesium hydroxide and the five samples of commercial ammonium phosphate made from wet-process phosphoric acid.

When the four samples of monoammonium phosphate A, B, C and D were treated above about 75°C in water vapor, only a part of the magnesium formed MH, and the yield of MH decreased linearly as the mole ratio P_2O_5/MgO increased (Fig. 2). During treatment, magnesium hydroxide reacted completely and an unknown compound,

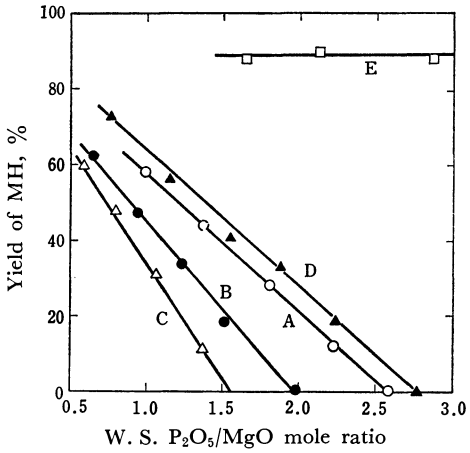

Fig. 2. Relation between the yield of $MgNH_4PO_4 \cdot H_2O$ and the mole ratio of water-soluble P_2O_5 of ammonium phosphate to MgO of magnesium hydroxide.

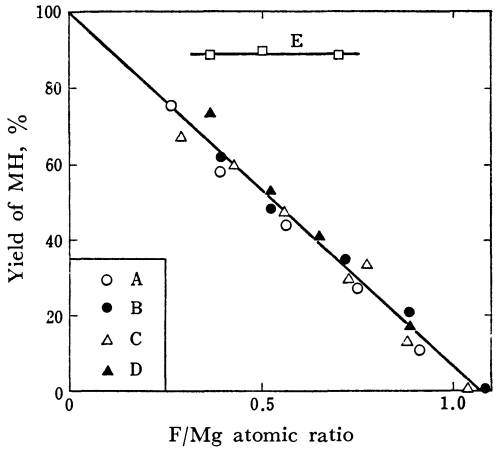

Fig. 3. Relation between the yield of $MgNH_4PO_4 \cdot H_2O$ and the F/Mg atomic ratio.

similar to that detected in commercial compound fertilizers No. 1 to 3, formed.

Through further tests it was found that fluorine in the samples of monoammonium phosphate was the cause of the formation of the unknown compound and the decrease in yield of MH. Figure 3 shows that for samples A, B, C and D, the yield decreases linearly on the same line as the atomic ratio F/Mg increases. Figure 3 also indicates that the unknown compound contains fluorine and magnesium in the atomic ratio of 1.

When sample E, which contained diammonium phosphate besides monoammonium phosphate, was used, magnesium hydroxide reacted very slowly releasing much ammonia; nearly 90% of the magnesium combined to form MH, regardless of the P_2O_5/MgO and F/Mg ratios (Figs. 2 and 3). The unknown compound formed in small amounts.

When samples A, B, C and D were allowed to react with magnesium hydroxide above about 75° in the presence of a large quantity of water or in a slurry state, the yield of MH decreased with increase in F/Mg ratio in the same manner as in the above tests, but the unknown compound was not detected in the products. An amorphous material formed instead of the unknown compound.

Fluorine showed less effect at lower temperature. Most of the magnesium combined to form M6H and M4H when the samples of ammonium phosphate were treated with magnesium hydroxide below about 60°C.

Tests were also conducted with magnesium hydroxide which was made from sea water and ground to minus 30 mesh. The results were similar to those obtained with reagent grade hydroxide, except that the hydroxide obtained from sea water reacted slowly because of the larger grain size.

Synthesis and Characterization of the Unknown Compound. The unknown compound was prepared in several ways using reagent

grade chemicals. The best sample was obtained by the following method:

One tenth mole of magnesium hydroxide was mixed with equimolecular ammonium fluoride. An amorphous material formed, losing ammonia. Two tenths mole of monoammonium phosphate was mixed with the above product and the result heated at 90 to 100°C for one hour in water vapor. The product was washed with 2% aqueous ammonium fluoride solution on a fritted glass filter with suction, and then washed with acetone and dried at room temperature. The chemical composition of the product is shown in Table 5.

Table 5. Chemical composition of the synthetic sample

	MgO	$(NH_4)_2O$	HF	P_2O_5
Composition (%)	22.49	16.50	11.58	41.83
Mole ratio	1.00	0.56	0.99	0.53

From chemical analysis, this compound was identified as $MgNH_4HFPO_4$, which should be called magnesium ammonium hydrogen filuroide phosphate and will be abbreviated to MAFP. Synthetic MAFP consisted of very small crystals of less than 0.1 μ in size. X-Ray diffraction data are shown in Table 6.

Table 5 shows that $(NH_4)_2O$ and P_2O_5 are present in slight excess. It is likely that a small amount of ammonium phosphate is absorbed by the fine crystals of MAFP. Excessive ammonium phosphate was used for preparation to promote the formation of MAFP. It was difficult to remove all of the remaining ammonium phosphate because the fine crystals of MAFP tend to decompose in washing.

Chemical analysis also shows that a considerable amount of water (about 8%) is contained in the product. By heating the product at 100°C in air, nearly all the water was removed, which resulted in considerable shrinkage of the crystal lattice as shown in Table 6. Shrinkage with heating hardly occurred when ammonium phosphate coexisted.

When the preparation of MAFP was conducted in a slurry by adding a large amount of water, an amorphous material or a mixture of MAFP with amorphous material was obtained. The amorphous material contained nearly equimolecular MgO and HF, similar to MAFP, but contained less $(NH_4)_2O$ and P_2O_5 than was contained in MAFP.

An amorphous material instead of MAFP formed also when preparation was conducted below about 60°C either with much or little water.

When preparation of MAFP was conducted at 90 to 100°C in the presence of a small amount of water using a mixture of monoammonium and diammonium phosphates, magnesium hydroxide reacted very slowly releasing ammonia; the product contained MH and less MAFP in the same manner as in the test with commercial ammonium phopshate E, indicating that only a part of the fluorine forms MAFP at high pH.

Another previously unknown compound, $MgKHFPO_4$ (MKFP), magnesium potassium hydrogen fluoride phosphate, was prepared in a similar way, treating one tenth mole each of potassium fluoride and magnesium hydroxide with one tenth mole of monopotassium phosphate at 90 to 100°C in water vapor, and washing with 2% aqueous potassium fluoride solution and acetone.

X-Ray diffraction data on MKFP are shown in Table 6. The synthetic MKFP also contained 5% water. Heating at 100°C removed the water and a slight shrinkage of the crystal lattice occurred. The synthetic MKFP consisted of small crystals less than 0.1 micron in size.

MKFP is isomorphic with MAFP and they form a continuous solid solution in each other. The unknown compound detected in the commercial products No. 1 to 3 was identified as a solid solution of MAFP and MKFP. The solid solution also consisted of small crystals less than 0.1 μ in size. X-Ray diffraction data on the solid solution obtained from sample No. 2 by removing water-soluble salts rapidly with small amount of water are also shown in Table 6. Considerable shrinkage of the crystal lattice was also observed to occur upon heating the solid solution at 100°C.

Table 6. X-Ray diffraction data on MAFP, MKFP and the solid solution

$MgNH_4HFPO_4$				$MgKHFPO_4$		Solid solution	
Synthetic		Heated at 100°C		Synthetic		Commercial product	
d (Å)	I	d (Å)	I	d (Å)	I	d (Å)	I
13.2	100	13.0	60	13.0	40	13.1	55
7.49	12	7.37	20			7.30	10
5.82	60	5.71	60	5.68	10	5.75	50
4.33	34	4.25	40	4.19	17	4.29	40
3.93	12	3.86	10				
3.45	10	3.42	20	3.35	14	3.40	12
3.23	32	3.17	50	3.14	30	3.18	12
3.07	80	3.00	100	2.96	100	3.01	100

Viscosity of the Slurry formed by Reaction of Magnesium Hydroxide with Ammonium Phosphate. The wet-process phosphoric acid (Table 2) was ammoniated with geseous ammonia to a pH of 4 to 5. Magnesium hydroxide obtained from sea water ground to minus 30 mesh was added to the amount to give equimolecular MgO to P_2O_5 and stirred at about 90°C. The viscosity of the slurry increased remarkably as the hydroxide reacted, and the slurry almost solidified in about 30 min. During the reaction, only a small portion of magnesium

formed MH and a larger portion formed a gelationous material which resembled MAFP in chemical composition, as was already mentioned.

A similar test was conducted with wet-process phosphoric acid from which about 90% of the fluorine had been removed by adding the correct amount of potassium chloride to form potassium fluorosilicate and removing the precipitate. In this test, nearly all of the magnesium formed MH, and the slurry was fluid with a viscosity of about 1 poise.

When potassium chloride was added to the acid and the mixture used without the separation of fluorosilicate, the fluorosilicate decomposed during ammoniation and fluorine reacted to depress the formation of MH and to increase the viscosity.

Tests with reagent grade phosphoric acid, hydrogen fluoride, potassium fluorosilicate, ammonia and magnesium hydroxide also showed the remarkable effect of fluorine on the viscosity.

In another series of tests, magnesium hydroxide was first added to wet-process phosphoric acid and then ammoniated to a pH of 4 to 6. In these tests, the slurry became quite viscous and almost solidified even when the acid had been defluorinated.

Water-Slolubility of Magnesium Compounds. A test with synthetic MAFP (Table 5) showed that 25% of Mg, 55% of N and 58% of P_2O_5 were water-soluble by the standard Japanese method, in which 5 g of sample is shaken for 30 min in 400 m*l* water, made up to 500 m*l* and then filtered. X-Ray analysis showed that essentially all MAFP decomposed during the standard treatment to precipitate an amorphous material and M6H. MKFP was less soluble; about 30% decomposed and 13% of magnesium was soluble in the standard method.

X-Ray tests were also conducted on commercial products No. 1 and 3 (Table 1) which contain a solid solution of MAFP and MKFP. It was found that about 90% and 60%, respectively, of the solid solution decomposed during the standard treatment. MAFP, MKFP and the solid solution are entirely soluble in 2% citric acid.

M4H decomposed rapidly in water to precipitate M6H; 18% of the magnesium was soluble in the standard method.

MH and M6H are less soluble; only 2% of magnesium dissolved in the standard method. In 100 m*l* water, 5.9 mg of MgO of MH and 4.0 mg of MgO of M6H dissolved.

Tests were made on the effect of the coexistence of several salts on the solubility of magnesium of MH and M6H. The synthetic sample (1 g each) was shaken for 30 min in 100 m*l* of 0.1, 0.5 and 2.5% aqueous solutions of monoammonium phosphate, ammonium sulfate, ammonium chloride, potassium chloride, diammonium phosphate and urea. The amounts of MgO (mg) which dissolved in 100 m*l* of the solutions of monoammonium phosphate, ammonium sulfate and ammonium chloride are shown in Table 7.

Table 7. MgO dissolved in 100 m*l* of the solutions (mg)

Salt	Form of magnesium compound	Concentration 0.1	0.5	2.5
$NH_4H_2PO_4$	MH	24.9	35.3	58.9
	M6H	11.5	—	40.1
$(NH_4)_2SO_4$	MH	12.6	14.7	16.5
	M6H	3.9	4.2	8.3
NH_4Cl	MH	12.1	13.1	15.4
	M6H	4.0	4.2	7.1

Table 7 shows that the water-solubility is increased remarkably by $NH_4H_2PO_4$, and significantly by $(NH_4)_2SO_4$ and NH_4Cl. Tests with the other compounds showed that potassium chloride and urea have little effect, and that diammonium phosphate reduced the solubility slightly. The solubility depends mainly upon the pH of the solutions.

Tests were also made on the solubility when a mixture of salts was present. When 15 parts of MH was blended with 15 parts of NH_4Cl, 20 parts of KCl, 40 parts of $(NH_4)_2SO_4$ and 10 parts of $NH_4H_2PO_4$ to give a 15-13-12-4 grade fertilizer and tested by the standard method, 44.3% of the magnesium present dissolved. When M6H, instead of MH, was used, 34.0% dissolved.

These results show that water-soluble magnesium in commercial fertilizers can be derived from the above magnesium compounds.

Thermal Changes. Thermal gravimetric analysis curves of the synthetic samples of MH, M4H, M6H and MAFP obtained during heating at a rate of 2°C/min are shown in Fig. 4.

Iwata[6] reported that M6H (crystals 20 to 120 μ in size) converted to MH at about 150°C. The

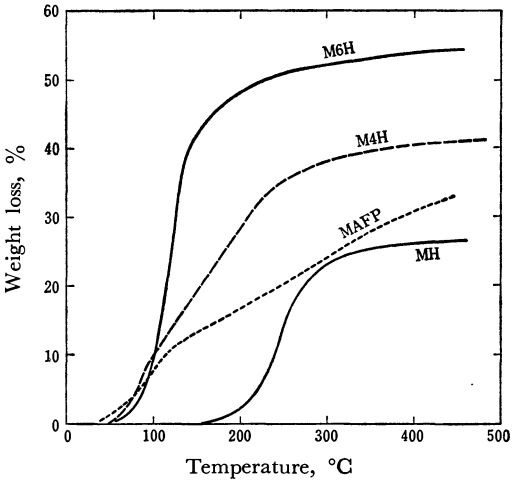

Fig. 4. Weight loss (%) during heating at a rate of 2°C/min.

present test showed that M6H began to decompose at about 60°C, losing water of crystallization and ammonia, and changed into an amorphous material at about 100°C; essentially no MH formed during heating to and above 150°C. Presumably the small crystal size (under 5 μ) is the reason for the instability.

M4H also started to decompose at about 60°C, losing water of crystallization and ammonia to form an amorphous material at about 100°C. M6H and M4H are sometimes present in the pre-mixer products and the granulator products of compound fertilizers containing magnesium. M6H and M4H in the products also consist of small crystals of less than 5 μ in size and undergo similar thermal decomposition (to be mentioned later). MH did not show any change below 150°C, and started to decompose above 160°C.

The synthetic MAFP lost about 8% water upon heating to 100°C, resulting in a considerable shrinkage of the crystal lattice, as previously mentioned. Above 100°C, MAFP started to lose ammonia, and slowly changed into an amorphous material.

A test on synthetic MKFP showed that no decomposition occurred with heating up to 150°C.

Formation of Water-insoluble Potassium. The water solubility of potassium present in compound fertilizers is apt to decrease when magnesium is present. The present tests have shown that one of the reasons for the decrease is the presence of a solid solution of MAFP and MKFP. The commercial fertilizers No. 1 to 3 (Table 1), the solubility of which ranges from 95 to 98%, contain the solid solution which partly remains undissolved in the standard treatment, as mentioned previously.

The potassium of samples No. 6 to 8 is less soluble (90 to 92%). Tests have shown that the decrease in water-solubility occurred during the drying of the granulated product at about 100°C. When magnesium hydroxide was mixed with monoammonium phosphate, ammonium and potassium sulfates and urea at 50 to 60°C for granulation, magnesium formed mainly M6H and M4H, and more than 98% of potassium was water-soluble. Both M6H and M4H decomposed into amorphous materials and the water-solubility of potassium decreased during the drying. Most of the fluorine present was in the form of potassium fluorosilicate before and after drying. The fluorosilicate was almost completely soluble in water in the standard method.

Laboratory tests have been conducted to study the relation between the decomposition of M6H and M4H and the decrease in solubility of potassium. Potassium chloride or sulfate ground to pass through a 150 mesh screen was mixed with synthetic M6H in a mole ratio MgO/K_2O of 1 : 1 and heated at temperatures between 80 and 120°C from 30 min to 7 hr. A remarkable decrease in the solubility of potassium occurred as shown in Fig. 5.

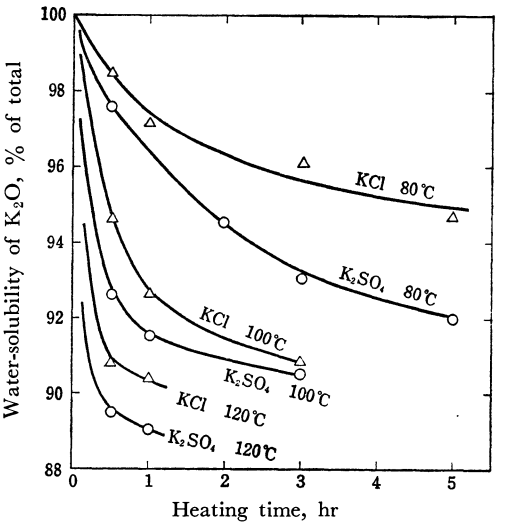

Fig. 5. Decrease of water-solubility of potassium during heating and $MgNH_4PO_4 \cdot 6H_2O$ (mole ratio $MgO/K_2O=1$).

Potassium salts were found to promote the thermal decomposition of M6H. For example, the loss of ammonia with heating at 100°C for an hour was 35% without potassium salts, 58% when potassium chloride was present, and 64% when potassium sulfate was present. Apparently, potassium combined with the amorphous material which formed by the decomposition of M6H and became insoluble in water.

An other series of tests with potassium sulfate showed that the per cent of insoluble K_2O of the total K_2O was nearly proportional to the mole ratio MgO/K_2O (Fig. 6).

Potassium nitrate gave a similar result as potassium chloride, while monopotassium phosphate showed a smaller decrease in water-solubility.

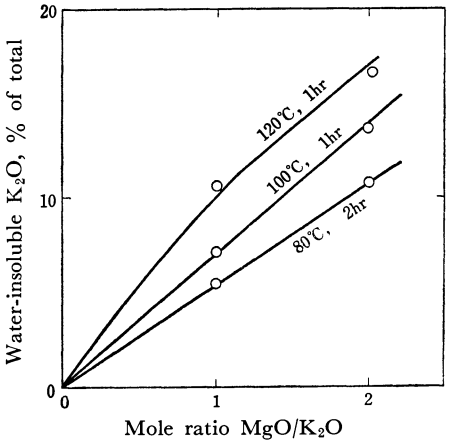

Fig. 6. Relation between mole ratio MgO/K_2O and insoluble K_2O formed by the reaction of $MgNH_4PO_4 \cdot 6H_2O$ and K_2SO_4.

For example, when mixtures of M6H and potassium salts ($MgO/K_2O=1$) were heated for an hour at 120°C, the water-solubility was 90.8% when potassium nitrate was used and 94.0% when monopotassium phosphate was used.

M4H also decomposed and combined with potassium salts during heating. The amount of insoluble potassium was roughly half that formed with M6H. For example, when a mixture of M4H and potassium sulfate ($MgO/K_2O=1$) was heated for an hour at 100°C, the water insoluble potassium was 4.1% while it was 8.6% with M6H.

MH was stable up to 150°C and did not react appreciably with potassium salts up to 130°C.

The potassium which combined with the amorphous material and became insoluble in the standard method was found to dissolve very slowly in water. For example, the water solubility of a smaple which was 89.7% by the official method increased to 92.5% when the sample was dipped in water for 5 days, and to 96.2% after 13 days.

Discussion

The present tests show that fluorine has remarkable effects on compound fertilizers containing magnesium when treated at relatively high temperatures. The weight ratio F/P_2O_5 of both wet-process phosphoric acid and ammonium phosphate made from the acid ranges from 0.05 to 0.1, and most of fluorine is usually present in fairly reactive forms. Consequently, by reaction above about 75°C, fluorine combines with 30 to 60% of the magnesium in fertilizers which have a P_2O_5/MgO weight ratio of about 3 (14-18-14-6, *etc.*), and with 50 to 100% of the magnesium in fertilizers which have a ratio about 5 (12-26-10-5, *etc.*). Fluorine thus forms MAFP, MKFP, the solid solution and a similar amorphous material, and depresses the formation of MH.

The high viscosity of the reaction products may be due to the above fluoride compounds, which consist of very small crystals under 0.1 μ in size, or a gel.

In order to eliminate the high viscosity which causes difficulties in plant operation, and to obtain products which contain most of their magnesium in the form of MH, a large portion of the fluorine should be removed or converted into a less reactive form.

Potassium fluorosilicate readily reacts with magnesium hydroxide and ammonium phosphate above about 75°C. There are indications that ammonium and sodium fluorosilicates are also fairly reactive. Those fluorosilicates should be removed from the system to eliminate the effects of fluorine. If fluorine can be converted into a less reactive form such as K_2NaAlF_6, the removal might not be necessary.

Another way to form a lot of MH in the presence of fluorine is to carry out treatment at high pH where a lot of ammonia is released. This treatment might not be favorable for plant operation because equipment for the recovery of ammonia would be necessary, the reaction of magnesium hydroxide would occur very slowly at the high pH, and moreover, the reaction products would still be fairly viscous.

The conversion of most of the magnesium into M6H and M4H when commercial monoammonium phosphate was treated with magnesium hydroxide below about 60°C is due to the poor reactivity of the fluoride compounds in the phosphate (such as $Al_3(NH_4)_5H_2(PO_4)_4$[2]) at low temperature; a test showed that fluorine, in the form of ammonium fluoride, depressed the formation of M6H and M4H below even 60°C.

M6H and M4H which forms in the pre-mixer and granulator at commercial scale plants usually consist of very small crystals less than 5μ in size and readily decompose during drying at about 100°C to form amorphous materials resulting in a remarkable decrease in the water-solubility of potassium. To prevent the great decrease in water-solubility, the drying temperature should be kept low, or magnesium hydroxide should be reacted above 75°C to prevent the formation of M6H and M4H.

By reaction at higher temperature, a solid solution of MAFP and MKFP is apt to form, giving a small amount of water-insoluble potassium. If the wet-process phosphoric acid was defluorinated or treated to convert fluorine into a less reactive form and reacted with ammonia and magnesium and potassium salts above 75°C, essentially all of the magnesium would form MH which is stable during drying, and essentially all of the potassium would be soluble in water.

Fluorine thus causes great trouble in the production of compound fertilizers containing magnesium. However, exploratory agronomic tests on barley have indicated that MAFP and the solid solution have good fertilizer value which might even be superior to MH. Further agronomic tests are in progress.

NOTES

An Acid-catalyzed Reaction of Methyl Ethers with Acetyl Fluoride. Syntheses of 1-Fluorobicyclo[2.2.2]octanes[1]

Zennosuke SUZUKI and Ken-ichi MORITA

The Basic Research Laboratories, Toyo Rayon Company, Ltd., Kamakura

(Received May 29, 1967)

We have previously reported convenient methods for the syntheses of 1-chloro-, 1-bromo-, and 1-iodobicyclo[2.2.2]octane by the reaction of 1-methoxybicyclo[2.2.2]octane with acetylhalides in the presence of an acid catalyst. The reaction has now been extended to the preparation of 1-fluorobicyclo[2.2.2]octane derivatives.[2-4]

It has been theorized that the reaction of ethers with acyl halides proceeds *via* acyl oxonium ions.[1] The synthetic utility of acyl oxonium ions as a carbonium ion generator has been confirmed. Diazonium ions,[4] isocarboxonium ions,[5] and carboxylium ions[6] have been established as carbonium ion sources.

The treatment of 1-methoxybicyclo[2.2.2]octane (1) with an excess of acetyl fluoride in the presence of a catalytic amount of anhydrous stannic chloride gave a mixture (*ca.* 1 : 1) of 1-fluoro- and 1-chlorobicyclo[2.2.2]octane in about an 80% yield. When the boron trifluoride-phosphoric acid complex was used as a catalyst, the reaction between 1 and acetyl fluoride afforded 1-fluorobicyclo-[2.2.2]octane (3), mp *ca.* 152°C (most of it sublimes without melting) in a 70% yield. Among the other catalysts examined were boron trifluoride etherate and zinc fluoride, in which cases 3 was also obtained.

An analogous treatment of 1-methoxy-4-methylbicyclo[2.2.2]octane (2) with acetyl fluoride in the presence of the boron trifluoride-phosphoric acid complex gave 1-fluoro-4-methylbicyclo[2.2.2]octane (4) in a 74% yield, bp 165—170°C, (760 mmHg), semi-solid, NMR τ 9.21 (CH_3) (in CCl_4). The reaction of methoxycyclohexane (5) with acetyl fluoride in the presence of the boron trifluoride-phosphoric acid complex furnished a mixture of fluorocyclohexane (6) (25%), cyclohexene (7) (6%), and acetoxycyclohexane (8) (18%).

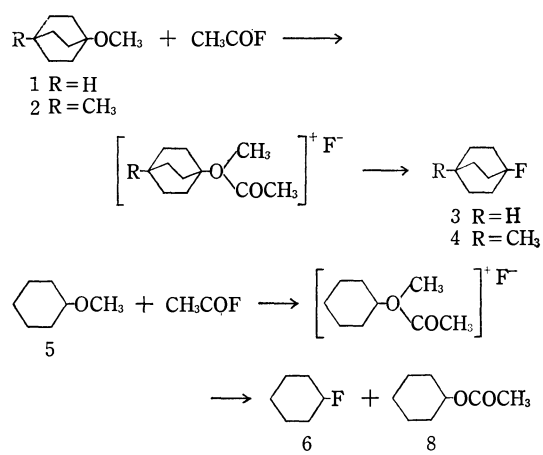

The formation of 1-acetoxybicyclo[2.2.2]octanes could not be detected when either 1 or 2 was reacted with acetyl fluoride in the presence of an acid catalyst. The formation of acetoxycyclohexane (8) in the case of 5 suggests that a 1-bicyclo[2.2.2]-octyl cation is more stable than a cyclohexyl cation. The mass spectra imply that a methyl carbonium ion is less stable than an ethyl carbonium ion[7]

1) Bridged Ring Compounds. IX. Paper VIII: Z. Suzuki and K. Morita, *J. Org. Chem.*, **32**, 31 (1967).

2) The following reagents has been used for the introduction of fluorine atom by the cleavage of carbon-oxygen bonds: a) Et_2NCF_2CHFCl: D. E. Ager, *Tetrahedron Letters*, **1962**, 1065; L. H. Knox, E. Velarde, S. Berger, D. Cuadriells and A. C. Cross, *J. Org. Chem.*, **29**, 2187 (1964); *Russ. Chem. Rev.*, **12**, 926 (1966). b) $Bu_4N^+F^-$: H. B. Henbest and W. R. Jackson, *J. Chem. Soc.*, **1962**, 954, c) HF: G. P. Mueller, *J. Org. Chem.*, **26**, 2403 (1961); C. W. Shoppee, *J. Chem. Soc.*, **1957**, 4813; C. G. Bergstrom, *J. Am. Chem. Soc.*, **82**, 3479 (1960).

3) It has been reported that the reaction of acetyl fluoride with boron trifluoride etherate furniches ethyl fluoride; [F. See], *Z. Anorg. Allgem. Chem.*, **250**, 331 (1943).

4) H. E. Zollinger, "Azo and Diazo Chemistry, Aliphatic and Aromatic Compounds," Interscience Publishers, New York, N. Y. (1961).

5) P. S. Skell and I. Starer, *J. Am. Chem. Soc.*, **81**, 4117 (1959); J. Landgrebe, *Tetrahedron Letters*, **1965**, 105.

6) P. Beak, R. J. Trancik, J. B. Mooberry and P. Y. Hohnson, *J. Am. Chem. Soc.*, **88**, 4288 (1966).

7) R. W. Taft, R. H. Mortin and F. W. Lampe, *J. Am. Chem. Soc.*, **87**, 2490 (1965).

and that the latter is in turn less stable than a 1-bicyclo[2.2.2]octyl ion.[8] No data concerning the stability of a cyclohexyl ion is available, however.

Experimental

1-Fluorobicyclo[2.2.2]octane (3). *A. The Boron Trifluoride-phosphoric Acid Complex as a Catalyst.* To a stirred mixture of 2.84 g (0.02 mol) of 1 and 3.10 g (0.05 mol) of acetyl fluoride,[9] twelve drops of the boron trifluoride-phosphoric acid complex were added with ice-bath cooling. After the mixture had been stirred for thirty minutes at 0°C, the reaction temperature was allowed to rise to 10—20°C, after which stirring was continued for 3 more hours. The reaction mixture was then poured onto cracked ice, and the mixture was stirred for 10 min and extracted three times with 25-m*l* portions of ether. The ether layers were then combined, washed with aqueous sodium bicarbonate and water, and dried over anhydrous calcium chloride. The ether was distilled off through a 10-in packed column, and the residue was sublimed to give 1.8 g (70%) of 3 mp *ca.* 152°C (most of it sublimes without melting).

Found: F, 14.7%. Calcd for $C_8H_{13}F$: F, 14.82%.

B. Boron Trifluoride Etherate as a Catalyst. An experiment similar to that described above was carried out using 0.5 m*l* of boron trifluoride etherate instead of twelve drops of the boron trifluoride-phosphoric acid complex; we thus obtained 1.6 g of 3.

C. Zinc Fluoride as a Catalyst. To a stirred suspension of 0.5 g (4.8 mmole) of zinc fluoride in 1.2 g (8.6 mmol) of 1, 2 m*l* of acetyl fluoride were added at 0°C over a 15-min period. The reaction temperature was then allowed to rise at room temperature (15—20°C), and stirring was continued for 24 hr. After the usual treatment (described for Procedure A), 1.0 g of an oil was obtained. Gas chromatographic analysis (PEG 6000 column at 180°C) showed that the product was about a 1-to-1.5 mixture of 3 and the starting material(1).

D. Stannic Chloride as a Catalyst. To a stirred mixture of 1.2 g (8.6 mmoles) of 3 and 2.1 g of acetyl fluoride 0.1 m*l* of stannic chloride was added with ice-bath cooling. An exothermic reaction was observed. The reaction mixture was then stirred for 4 hr at 4°C. After the usual treatment, the residue was crystallized from aqueous methanol to give 0.75 g of crystals with a mp of 112—123°C (in a sealed capillary tube). Gas chromatographic analysis (PEG 6000 column at 180°C) showed that the product was *ca.* a 1-to-1 mixture of 3 and 1-chlorobicyclo[2.2.2]octane.[10] The two materials were separated by preparative v.p.c. and identified.

1-Fluoro-4-methoxybicyclo[2.2.2]octane (4). To a stirred mixture of 3.12 g (0.02 mol) of 2 and 3.1 g (0.05 mol) of acetyl fluoride, fifteen drops of the boron trifluoride-phosphoric acid complex were added with ice-bath cooling. The mixture was then stirred for 3 hr at about 10°C. After the usual treatment, the product was collected by distillation (bp 165—170°C at 760 mmHg) to furnish 2.1 g (74%) of 4, n_D^{20} 1.4501, semi-solid, NMR τ 9.21[11] (in carbon tetrachloride).

Found: F, 13.3%. Calcd for $C_9H_{15}F$: F, 13.36%,

Fluorocyclohexane (6). To a stirred mixture of 4.56 g (0.04 mol) of methoxycyclohexane (5)[12] and 6.2 g (0.1 mol) of acetyl fluoride, twenty drops of the boron trifluoride-phosphoric acid complex were added with ice-bath cooling. After the mixture had been stirred for thirty minutes at 0°C, the reaction temperature was allowed to rise to 3—5°C and stirring was continued for two more hours. After the usual treatment, we obtained 2.83 g of an oil. The oil was separated by preparative vapor-phase chromatography (DC 550 column at 145°C) to give 1 g (25%) of fluorocyclohexane (6), n_D^{20} 1.4145 (lit.[13], n_D^{25} 1.4130), (Found: F, 18.25%. Calcd for $C_6H_{11}F$: F, 18.61%), 1 g (18%) of acetoxycyclohexane (8) and 0.2 (6%) of cyclohexene (7). The identity of 7 and 8 was established by a comparison of their infrared spectra and v.p.c. retention times with those of authentic samples.

8) J. L. Franklin, *J. Chem. Educ*, **40**, 28 (1963).
9) C. G. Swarin and C. B. Scott, *J. Am. Chem. Soc.*, **75**, 246 (1953).
10) The analysis of the NMR spectra of 1-fluorobicyclo[2.2.2]octanes (3 and 4) was presented at the 6th Meeting of the NMR symposium, Kyoto, October, 1967.
11) A. I. Vogel, *J. Chem. Soc.*, **1948**, 108.
12) S. M. McElvain J. W. Langston, *J. Am. Chem. Soc.*, **66**, 1759 (1944).

The Sulfonation of Crosslinked Polystyrene Copolymerized with Polar Vinyl Compounds

Yoichi UTSUNOMIYA and Hiroshi KUYAMA

Research Lab., Tokyo Organic Chemical Ind., Ltd., Toshima, Kita-ku, Tokyo

(Received October 24, 1967)

At present, most of strongly acidic cation-exchange resins are made by the sulfonation of crosslinked copolymers prepared from styrene and divinylbenzene. With a copolymer having a high degree of crosslinking, a long time is required for sulfonation because of its slow reaction rate. Although the reaction rate is increased by the addition of some catalyst[1] or solvent in order to swell the crosslinked copolymer,[2] no method has been reported to increase the rate of sulfonation by a modification of chemical composition of the crosslinked copolymer.

The present authors have found that the rate of sulfonation increases upon the introduction of small amounts of polar vinyl compounds, such as acrylonitrile, methyl acrylate and methylvinylketone, into crosslinked polystyrene as copolymerizable compounds.

Experimental

Copolymer beads (30—40 mesh) of styrene crosslinked with divinylbenzene (D. V. B.) were prepared by Pepper's method[3] in the presence of a 1.0% benzoyl peroxide initiator. In the copolymerization of styrene and D. V. B. with a polar vinyl monomer, some sodium chloride was added to the aqueous layer. The sulfonation of the crosslinked copolymer was carried out at different temperatures with a five-fold excess of 97.5% sulfuric acid under mechanical agitation.

To obtain a quantitative comparison of the sulfonation rate for each crosslinked copolymer, the increase in cation-exchange capacity was measured by the usual method,[4] this capacity was produced by the sulfonation of crosslinked polystyrene.

Results and Discussion

The crosslinked polystyrenes made by the copolymerization consisting of 92% of styrene, 8% (by weight) of D. V. B., and 0.02 mol% of acrylonitrile (AN), methyl acrylate (MA), methyl methacrylate (MMA) and methylvinylketone (MVK), were each sulfonated by sulfuric acid of a 36 normal solution at 110°C. The degree of sulfonation of these copolymers versus the reaction are shown in Fig. 1. These results indicate that the sulfonation rates of crosslinked polystyrenes made by the copolymerization of styrene, D. V. B., and polar vinyl compounds are much larger than that of styrene-D. V. B. copolymer, and that the use of acrylonitrile as the comonomer has a remarkable effect.

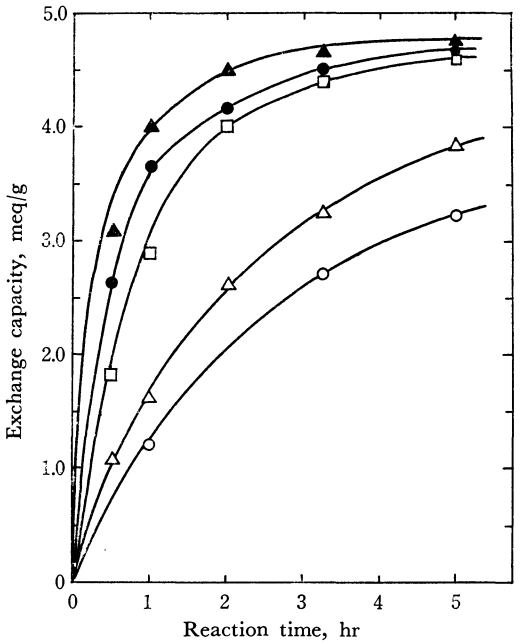

Fig. 1. Sulfonation of crosslinked polystyrene copolymerized with various vinyl compounds. (sulfonation temp. 110°C)
○ Homopolymer, copolymer with □ 1% AN, ● 1.7% MA, △ 2.0% MMA, ▲ 2.9% MVK

It has been described that, on the one hand, the rate of the sulfonation of crosslinked polystyrene is diffusion-controlled, since the reaction is entirely heterogeneous.[5] On the other hand, Reichenberg has reported that the difference in the sulfonation rates of crosslinked copolymers lies in the chemical rate, not in the diffusion.[6]

1) N. E. Topp and K. W. Pepper, *J. Chem. Soc.*, **1949**, 3299.
2) R. M. Wheaton and D. F. Harrington, *Ind. Eng. Chem.*, **44**, 1796 (1952).
3) K. W. Pepper, *J. Appl. Chem.*, **1**, 124 (1951).
4) S. Fischer and R. Kunin, "Analytical Chemistry of Polymers," ed. by G. M. Kline, Interscience Publishers, New York, N. Y. (1959), p. 521.
5) E. E. Gilbert, "Sulfonation and Related Reactions," Interscience Publishers, New York (1965), p. 77.
6) G. D. Jones, "Chemical Reactions of Polymers," ed. by E. M. Fettes, Interscience Publishers, New York (1964), p. 282.

Recently, Wiley and Venkatachalam[7] have shown that, as kinetic evidence for diffusion control in the sulfonation of crosslinked polystyrene-bead copolymers, a plot of the square of the capacity against the time would be linear.

The results of the applications of Wiley's theory to the sulfonation of the crosslinked polystyrene copolymer with 1%, with 3%, and with 5% acrylonitrile at different temperatures did not show any linear relationships except in the case of a much higher reaction rate. When the sulfonation of crosslinked polystyrene is assumed to be a first-order reaction with respect to the polystyrene molecule, the following Eq. (1) is obtained:

$$Ps\frac{dx}{dt} = kPs(1-x) \qquad \ln\frac{1}{1-x} = kt \qquad (1)$$

where x is the degree of sulfonation, P represents the concentration of polystyrene (mol/l), and k is the rate constant.

Applying Eq. (1) to the sulfonation of the above-described copolymers, the linear slopes shown in Fig. 2 could be obtained.

In view of the above facts, it seems reasonable to assume, as in Reichenberg's description, that the sulfonation process of crosslinked polystyrene is controlled by the reaction rate itself, not by the diffusion rate.

The rate constants of the sulfonation reaction calculated from the linear slopes of Fig. 2 and the activation energy values obtained from the individual rate constants are given in Table 1. From the results, it may be seen that the activation energy for sulfonation decreases with an increase in the acrylonitrile content in the copolymer.

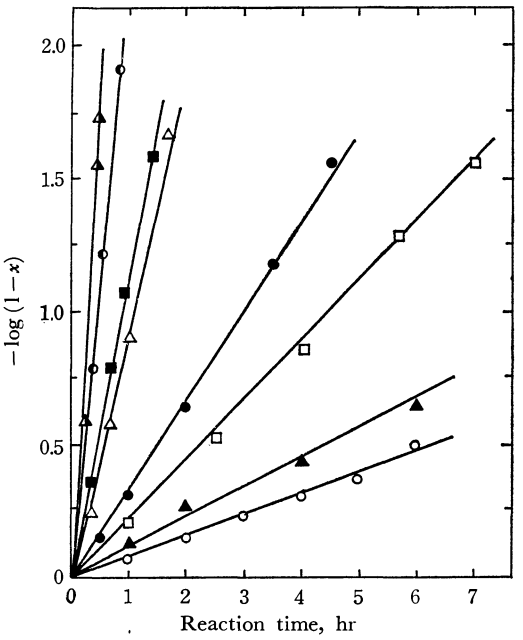

Fig. 2. First order plott of the sulfonation of crosslinked polystyrene copolymerized with acrylonitrile (AN).

	Copolymer with	Sulfonation temp., °C		Copolymer with	Sulfonation temp., °C
□	Homopolymer	110	△	Homopolymer	130
○	1%	100	△	1%	120
●	3%	100	◐	3%	120
▲	5%	80	■	5%	100

Table 1. Rate constant and activation energy

AN(%)	Rate constant k (hr^{-1}) at different sulfonation temperatures, (°C)					Activation energy E, (kcal/mol)
	80	100	110	120	130	
0	—	—	0.466	—	8.01	43.6
1.0	—	0.174	—	2.38	—	38.1
3.0	—	0.678	—	6.48	—	32.9
5.0	0.308	2.93	—	—	—	29.5

This decrease in activation energy is considered to be caused by the neighboring-group effect of such a polar vinyl monomer as acrylonitrile copolymerized in crosslinked polystyrene; this is a characteristic feature of a chemical reaction on the polymer.

The rate constant of a sulfonation reaction using very small copolymer beads (80—100 mesh) consisting of 1% acrylonitrile by 97.5% sulfuric acid was observed to be $k=2.84\ hr^{-1}$ at 80°C. On the contrary, no reaction was observed when the same sized copolymer beads but without acrylonitrile were used under the same conditions.

This fact seems to indicate that the sulfonation in the crosslinked polystyrene containing polar vinyl compounds is increased, but the precise mechanism remains to be investigated in the future.

7) R. H. Wiley and T. K. Venkatachalam, *Polymer Letters*, **4**, 981 (1966).

Spectrophotometric Study of the Complex of Hg(II)-X-Diphenylcarbazone [X: I, Br]*1

Tadao OKUTANI

Faculty of Science and Engineering, Nihon University, Chiyoda-Ku, Tokyo

(Received November 13, 1967)

Mercury(II) forms a reddish-violet complex with diphenylcarbazone which may be easily extracted by benzene.[1] Ions such as cyanide which react with mercury(II) decrease the color intensity.[2] However, in the presence of iodide or bromide ions, the color intensity increases slightly with an increase in the ions in the first step, while the color intensity decreases greatly above an equimolor concentration of mercury(II)[3] (see Fig. 1).

From these results, it is considered that a mercury-(II)-diphenylcarbazone complex containing iodide or bromide will be formed, although the composition of this complex has not yet been reported.

We have previously reported a spectrophotometric method for the determination of minute quantities of such anions as chloride,[4] thiosulfate,[5] sulfide,[6] cyanide,[7] sulfite,[8] iodide,[9] and bromide[9] ions by using a complex formed of mercury(II), iodide (or bromide), and diphenylcarbazone.

This paper will report the results of more detailed studies of the reaction of mercury(II), iodide (or bromide), and diphenylcarbazone, and of the composition of the complex.

Experimental Results and Discussion

Reagents and Apparatus. *So-Called Diphenylcarbazone (DC).* The reagent is a molecular compound of diphenylcarbazone and diphenylcarbazide, and its color is orange.[10]

$C_6H_5NHNHCONHNHC_6H_5 \cdot C_6H_5N=NCONHNHC_6H_5$ (mp 153°C).

Diphenylcarbazone (H_2DCN). Pure orange-yellow diphenylcarbazone was prepared by the removal of diphenylcarbazide from the so-called diphenylcarbazone using the method of Gerlach.[11]

$C_6H_5N=NCONHNHC_6H_5$ (mp 118—120°C).

Diphenylcarbazide (H_4DCD). White crystals were used.

$C_6H_5NHNHCONHNHC_6H_5$ (mp 170°C).

These solutions of various concentrations were prepared by dissolving the reagent in ethanol, and a 1 m*l* portions of the solution were used in all the experiments.

Mercuric Nitrate Solution. A mercuric nitrate solution was prepared by dissolving 8.5 g of mercuric nitrate in water containing 2 ml of concentrated nitric acid, and by then diluting it to 500 m*l* (about 0.05 mol/*l*). This solution was standardized by Volhards method, and then stored in a brown glass bottle. The working solutions were prepared by diluting the stock solution properly.

The other materials and apparatus used in this investigation were the same as those described in previous papers.[4-9]

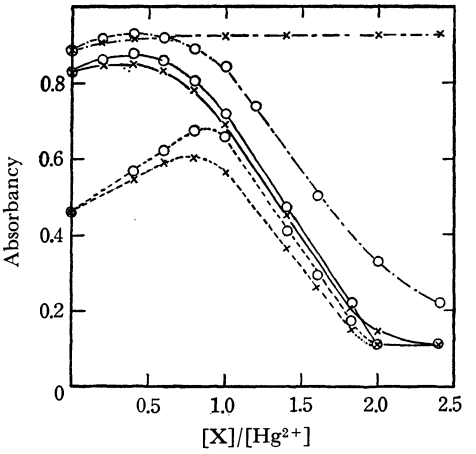

Fig. 1. The reactions between Hg(II)-diphenylcarbazone and iodide (or bromide) ion

Hg^{2+}; 1.5×10^{-5} mol/*l*
H_2DCN; 1.5×10^{-4} mol/*l*
Wavelength ; 562 mμ, at 25°C
X^-; ○ I^-, × Br^-,
pH; -·-· 7.0, —— 2.5, ---- 1.4

*1 Presented at the 16th Annual Meeting of the Japan Society for Analytical Chemistry, Chiba, October, 1967.

1) A. Tomonari, *Nippon Kagaku Zasshi (J. Chem. Soc. Japan, Pure Chem. Sect.)*, **82**, 864 (1961).
2) A. Tomonari, *ibid.*, **83**, 455 (1962).
3) A. Tomonari, *ibid.*, **83**, 459 (1962).
4) S. Utsumi and T. Okutani, *ibid.*, **85**, 543 (1964).
5) T. Okutani, S. Utsumi, K. Shibata and I. Iwasaki, *ibid.*, **86**, 831 (1965).
6) T. Okutani and S. Utsumi, *ibid.*, **86**, 1149 (1965).
7) T. Okutani and S. Utsumi, *ibid.*, **87**, 444 (1966).
8) T. Okutani and S. Utsumi, This Bulletin, **40**, 1386 (1967).
9) T. Okutani, *Nippon Kagaku Zasshi (J. Chem. Soc. Japan, Pure Chem. Sect.)* **88**, 737 (1967).
10) M. Uchida and M. Nakada, *Bulletin of the Faculty of Education, Chiba University*, **15**, 138 (1966).
11) J. L. Gerlach and R. G. Frazier, *Anal. Chem.*, **30**, 1142 (1958).

Formation of a Mercury(II)-Diphenylcarbazone Complex Containing Iodide or Bromide. Ten milliliters of a aqueous solution containing mercury(II), H_2DCN, and X^-(X^-; iodide or bromide ions) in which the pH was kept at 7, 2.5, or 1.4, and 10 m*l* of benzene were placed in a brown separatory funnel. Then the separatory funnel was shaken for about 1 min. The absorbance of benzene phase was measured at 562 mμ against pure water as a reference. The experimental results are plotted in Fig. 1. From Fig. 1 it may be considered that a complex of mercury(II)-diphenylcarbazone containing X^- is formed in the first step, and that then the color of all such complexes except one containing bromide at pH 7 fade as a result of the formation of HgX_2.

Therefore, mole ratio method was applied in order to clarify the relations of mercury(II) and X^- in the presence of H_2DCN (the molar concentration of H_2DCN was adjusted so as to be equal to that of X^-).

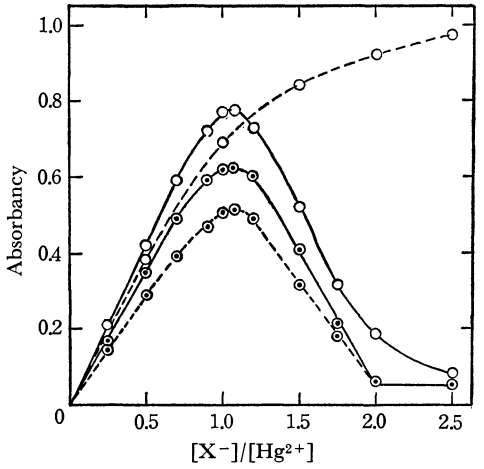

Fig. 2. Mole ratio method
Hg^{2+} ; 2.0×10^{-5} mol/*l* $[H_2DCN]=[X^-]$
Wavelength ; 562 mμ, at 25°C
—— I^-, - - - Br^-, ○ pH 7.0, ⊙ pH 2.5

As is shown in Fig. 2, all the curves except that of a complex containing bromide at pH 7 have a maximum absorbance in about an equimolar concentration of X^- and Hg^{2+}.

Similar experiments were carried out in which the molar concentration of H_2DCN was adjusted so as to be twice that of X^-. The maximum absorbance was also obtained in about an equimolar concentration of X^- and Hg^{2+}.

It may be considered that the diphenylcarbazone forms a complex with HgX^+ which is in a state of equilibrium as follows:

$$Hg^{2+}+X^- \rightleftharpoons HgX^+$$

These experiments (Figs. 1 and 2) were carried out using DC, and the experimental results were in agreement with the above results.

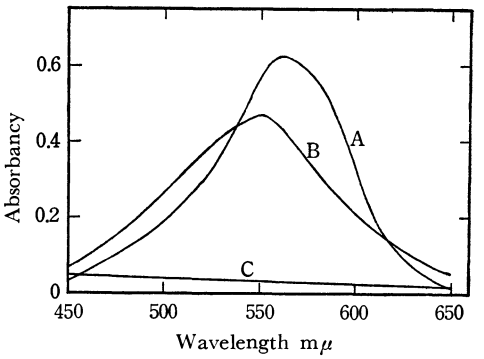

Fig. 3. Absorption spectra of Hg^{2+}-H_2DCN and HgI^+-H_2DCN complexes
Hg^{2+}(or HgI^+); 1.3×10^{-5} mol/*l*
H_2DCN; 2.6×10^{-5} mol/*l*
pH 7.0, at 25°C
A : HgI^+, B : Hg^{2+}, C : H_2DCN alone

Absorption Spectra. The absorption spectra of the benzene solution of the complex are shown in Fig. 3. The Hg^{2+}-H_2DCN complex has a maximum absorbance at 552 mμ, while the HgX^+-H_2CDN complex has its at 562 mμ, indicating that they are different.

Composition of the Complex. The compositions of the Hg^{2+}-H_2DCN and HgX^+-H_2DCN complexes were determined by the continuous-variation method. Mixed solutions of the Hg^{2+} (or HgX^+) and H_2DCN in various ratios were prepared, and the pH values of the solutions thus prepared were adjusted to 7.0, then the absorbances of the extracted benzene phase were measured at 562 mμ.

The results are shown in Fig. 4. The figure shows that either the Hg^{2+} or HgX^+ complex forms a 1-to-1 complex with H_2CDN. Moreover, the continuous-variation method was carried out using DC and H_4DCD. The mole ratio of DC and

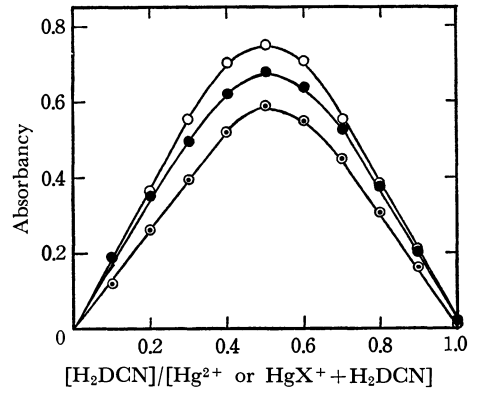

Fig. 4. Continious variation method
$[Hg^{2+}$ or $HgX^+] + [H_2DCN] = 4\times15^{-5}$ mol/*l*
Wavelength ; 562 mμ, at 25°C, pH 7.0
-○- HgI^+, -●- $HgBr^+$, -⊙- Hg^{2+}.

Hg^{2+}(or HgX^+) was also 1-to-1; on the other hand, H_4DCD did not form a complex at the concentration of 4×10^{-5} mol/*l*. The experimental results indicate that Hg^{2+} or HgX^+ forms a 1-to-1 complex with the H_2DCN which is present in the DC. These results were also conformed by further experiments using the mole-ratio method.

Gerlach *et al.*[11] have also reported a mole ratio of 1-to-1 between mercury(II) and diphenylcarbazone; on the other hand, a 1-to-2 complex has been reported by Feigl *et al.*[12]

If the so-called diphenylcarbazone(DC) is assumed to be a true diphenylcarbazone(H_2DCN), the mole ratio between mercury(II) and DC may become the 1-to-2 shown by Feigl *et al.*[12]

12) F. Feigl and F. L. Lendere, *Monatsh*, **45**, 115 (1924).

The reactions between mercury(II) or HgX^+ and H_2DCN may be expressed by the following equations;

$$Hg^{2+} + H_2DCN \rightleftharpoons HgDCN + 2H^+$$

$$HgX^+ + H_2DCN \rightleftharpoons HgXHDCN + H^+$$

As may be seen in Figs. 1 and 2, all the complexes are more stable at pH 7 than at pH 2.5. With regard to the effect of light, it has previously been reported[4] that the complex of HgXHDCN is more stable than that of HgDCN. The formation of the HgClHDCN complex is difficult under these conditions.[1]

The author wishes to express his gratitude to Professor Satori Utsumi of Nihon University for his kind guidance throughout this study.

Electrolytic Production of Lead Cyanamide

Kazuhide MIYAZAKI

Central Research Laboratory, Mitsui Mining & Smelting Co., Mitaka-shi, Tokyo

(Received November 20, 1967)

Lead cyanamide is an insoluble yellowish colored lead salt of cyanamide, designated as $PbCN_2$ or $Pb(HNCN)_2$ for its molar composition, and has been used fairly widely as anticorrosive pigment and is known to exhibit excellent protective performance, particularly in the field of marine applications.

However, production of the pigment seems to be relatively limited mainly because of its rather high production cost. The lead cyanamide has so far been synthesized through roundabout processing steps *via* intermediate soluble salts of lead such as acetate and nitrate[1] or insoluble lead compounds including litharge, PbO,[2] to provide the source of lead to combine cyanamide radical which usually comes from the leach of nitro-lime. Therefore, the production cost of lead cyanamide becomes substantially higher than those of many other anticorrosive lead pigments such as litharge which can be supplied in most cases *via* much fewer processing steps.

In this work an attempt has been made to establish a straightforward precipitation of lead cyanamide directly starting from metal lead as the source of lead to eliminate the need for the costly intermediate lead compounds, by applying the technique of soluble anode electrolytic process, and some of the important electrolytic variables are investigated to obtain the high grade lead cyanamide product.

Experimental

Materials. A commercial fertilizer grade nitro-lime whose cyanamide content as $CaCN_2$ was about 60% was leached with water and the leached solution was desulfurized by adding ferrous sulfate according to the conventional method. The concentration of $CaCN_2$ was controlled to from several to 10 g per liter of the purified leach. Sodium chlorate was then added as solubilyzer of lead anode in an amount of 10—80 g per liter and the final solution was provided as the electrolyte.

High purity lead of more than 99.9% Pb was cast into the form of electrodes with dimensions of 4 cm × 7 cm × 1 cm. The plate of anode was placed in between two plates of cathodes with anode-cathode distance of 5 cm.

Procedures. Electrolysis was carried out with a 2-liter experimental electrolytic cell with continuous circulation of electrolyte with fresh supply of cyanamide to maintain as homogeneous concentration as possible throughout the electrolytic run. The amperage was adjusted in the range of 1 to 3.5 A/dm^2, and the duration of electrolysis per each run was 8 hr.

Content of nitrogen as cyanamide form in the lead cyanamide precipitate was analyzed by the use of silver

1) *E. g.*, E. Blasiak and Z. S. Matsuszewski, Pol. Pat. 42862 (1960).
2) V. Koutnik and V. Novak, *Chem. Prumsi*, **9**, 18 (1959), *Chem. Abstr.*, **58**, 17445 (1959).

cyanamide precipitation method.[3-6] A quantity of 0.5 g of the lead cyanamide sample was dissolved with dilute nitric acid and the solution was passed through an ion exchange column which contained H^+-form Amberlite IR-120 resin to replace lead ion of the solution with hydrogen ion. Ammoniacal solution of silver nitrate was then added to the effluent to secure the cyanamide into the form of silver cyanamide, which was then dissolved with dilute nitric acid and the content of the cyanamide was determined by titrating the combined silver according to the Volhard method with a potassium thiocyanate solution using ferro-ammonium alum as indicator.

As for the alternative in expressing the composition of lead cyanamide, Costa and Bolis-Cannella[7] demonstrated that the analytical composition of their laboratoy-produced pigment was Pb 81.760, N 9.830, C 4.282, H 0.144, O and undetermined impurities of inorganic nature 3.984%, which was very near to $PbCN_2$ rather than $Pb(HNCN)_2$. The thermal work[8] on silver, copper, lead, and cadmium cyanamides exhibited that these compounds developed N, $(CN)_2$, CO_2 or CO when heated in air, and partially polymerized $(CN)_x$ when heated *in vacuo*,, respectively, with no decomposition product containing H. A recent work of Sole and Yoffe[9] to determine the nature of the bonds in the sodium, thallium, mercury, and lead cyanamides also showed that while sodium cyanamide was an ionic solid, silver and lead cyanamide salts were covalent ones. Accordingly, the composition of the product obtained in the present work was also expressed in terms of $PbCN_2$ basis instead of $Pb(HNCN)_2$.

Results and discussion

A series of experimentations have been carried out varying the composition of electrolyte and the current density, and the $PbCN_2$ content of the electrolytically obtained product is enlisted in Table 1. It is observed that the high grade lead cyanamide, the $PbCN_2$ content of which is more than 90%, has been obtained through one-step electrolytic process directly starting from the metal lead being attacked by the electrolyte composed of calcium cyanamide, supplier of CN_2^{-2} ion, and sodium chlorate, solubilyzer of the lead, with cell voltage of about 2—3 V.

It is seen that the increase in sodium chlorate concentration of the electrolyte increases the $PbCN_2$ content of the electrolytically precipitated product as illustrated in Fig. 1. The higher anodic current

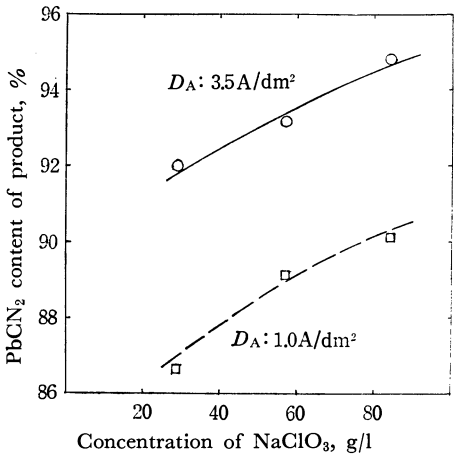

Fig. 1 Amount of $NaClO_3$ added to the electrolyte of 8 g $CaCN_2$/l *versus* grade of lead cyanamide obtained, in terms of applied current density.

Table 1. Electrolytic precipitation of lead cyanamide

Run No.	Composition of Electrolyte, g/l		Current Density D_A, A/dm²	Cell Voltage, v			$PbCN_2$ Content of Product, %
	$CaCN_2$	$NaClO_3$		Initial	Final	Average	
1	8.0	28.0	1.0	1.7	1.8	1.8	86.6
2	8.0	28.0	3.5	2.3	3.0	2.2	92.0
3	8.0	56.0	1.0	1.5	2.1	1.8	89.5
4	8.0	56.0	3.5	2.2	3.2	2.7	93.2
5	8.0	84.0	1.0	1.6	1.9	1.8	90.7
6	8.0	84.0	3.5	2.3	3.1	2.7	94.8
7	4.0	14.0	1.0	2.4	2.8	2.6	86.7
8	4.0	14.0	3.5	5.2	5.4	5.3	92.9
9	4.0	28.0	1.0	2.0	2.3	2.2	87.4
10	4.0	28.0	3.5	3.8	3.8	3.8	92.3
11	4.0	42.0	1.0	2.0	2.2	2.2	87.9
12	4.0	42.0	3.5	2.9	3.3	3.1	92.0

3) C. Brioux, *Ann. Chim. Anal.*, **15**, 341 (1911).
4) G. Grube and J. Krüger, *Z. Angew. Chem.*, **27**, 326 (1914).
5) L. A. Pinck, *Ind. Eng. Chem.*, **17**, 459 (1925).
6) H. Kittel, "Pigmente," Wiss. Verlagsg. m. b. H., Stuttgart (1960), p. 722.
7) D. Costa and C. Bolis-Cannella, *Ann. chim.*, **43**, 769 (1953).
8) C. Bolis-Cannella, *Ann. chim.*, **44**, 1064 (1954).
9) M. J. Sole and A. D. Yoffe, *Proc. Roy. Soc., Ser. A*, **277** (1371), 498 (1964).

density produces, the higher grade of lead cyanamide, *i. e.*, 92—95% of $PbCN_2$. The balance of the constituent is not yet definitely identified, however it may probably exist in the form of a basic oxide of lead. The values of $PbCN_2$ content in Table 1 is remarkably higher in comparison with those of the commercially available products marketed elsewhere including a sample from overseas which were found to be in the range of 82—84% $PbCN_2$ by the same analytical method.

It is to be noted, however, as is seen from Fig. 2, that when the original concentration of calcium cyanamide in the electrolyte is low, the increase of sodium chlorate will rather lower the grade of the pigment especially under higher current density. This is understood in such a way that the lead ion which is supplied from the anode in relatively excess amount over the cyanamide ion present in the electrolyte forms basic salts of lead to coprecipitate and dilute lead cyanamide content for the run.

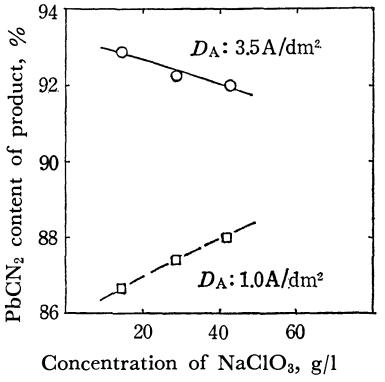

Fig. 2. Amount of $NaClO_3$ added to the electrolyte of 4 g $CaCN_2$/l versus grade of lead cyanamide obtained, in terms of applied current density.

The runs No. 1 through No. 6 and No. 7 through No. 12 in Table 1 divide total runs of experiment into two groups of $CaCN_2$ concentrations, *i. e.*, 8 and 4 g/*l*, while having same mixing ratios of $CaCN_2$ and $NaClO_3$ for the each adjacent runs respectively. It is interesting to note that the $PbCN_2$ content of a product obtained with a given $CaCN_2$-$NaClO_3$ combination will not depend solely on the mixing ratio of $CaCN_2$ and $NaClO_3$ even under a same anodic current density, but is largely determined by the concentration of the existing $CaCN_2$. It is seen that the higher concentration of $CaCN_2$ in the electrolyte gives rise to the higher grade of lead cyanamide.

It should be pointed out, therefore, that the proper choice of conditions is necessary to run favorable electrolysis of high quality lead cyanamide pigment. Continuation of electrolysis down to a too low concentration of $CaCN_2$ with high current density should cautiously be avoided.

Summary

Electrolytically precipitating process has been examined to obtain anti-corrosive lead cyanamide pigment, eliminating the need for the conventional intermediate lead compounds such as litharge. A soluble electrolysis of metallic lead anode has been carried out with calcium cyanamide electrolyte which contains a proper amount of sodium chlorate as a solubilyzer of anode. The electrolytically operated product was of a higher grade of lead cyanamide of 92—95% $PbCN_2$, in comparison with the conventionally available pigment of 82—84% $PbCN_2$. The $CaCN_2$-$NaClO_3$ ratio, $CaCN_2$ concentration and anodic current density have been found to be of major importance which primarily govern the quality of product.

Bakkenolide-E, a Minor Component of the Bud of *Petasites japonicus*, subsp *giganteus* Kitam.

Kunikatsu SHIRAHATA*, Nobuo ABE**, Tadahiro KATO* and Yoshio KITAHARA*,[1]

*Department of Chemistry, Faculty of Science, Tohoku University, Sendai

**Department of Chemistry, Akita University, Akita

(Received January 25, 1968)

Their investigations of the bitter principles of the bud of *Petasites japonicus*, subsp *giganteus* Kitam., (local name; BAKKE) were reported by the present authors in previous papers,[2,3] in which the isolation of four compounds, named Bakkenolide-A(I), -B(II), -C(III) and -D(IV), was described, as were their structures.

1) To whom all inquiries regarding this paper should be addressed.

2) N. Abe, R. Onoda, K. Shirahata, T. Kato, M. C. Woods and Y. Kitahara, *Tetrahedron Letters*, **1968**, 369.

3) N. Abe, R. Onoda, K. Shirahata, T. Kato, M. C. Woods, Y. Kitahara, K. Ro and T. Kurihara, *ibid.*, **1968**, 1993.

TABLE 1. NMR SPECTRA[a] OF II AND VII

	H_1	C_4-Me	C_5-Me	H_6[b]	H_9	H_{10}	H_{12}	H_{13}
II	*ca*5.2 (m)	0.91(d, J=5.9)	1.13(S)	2.10 (J=14.2)	5.75(d, J=11.2)	2.82(d,d J=11.2, 5.0)	4.67(t, J=2.0)	ca5.2 (m)
VII	*ca*5.1 (m)	0.91(d, J=5.3)	1.12(S)	2.10 (J=14.2)	5.78(d, J=11.2)	2.80(d,d J=11.2, 4.8)	4.65(t, J=2.1)	ca5.2 (m)

a) NMR data refer to $CDCl_3$ solution, with chemical shifts given in ppm down field from internal TMS (s=singlet, d=doublet, t=triplet, m=multiplet)
b) center of AB quartet,

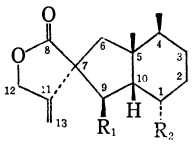

I R_1=H R_2=H

II R_1=OAc R_2=OCOC(=CHCH_3)CH_3

III R_1=OH R_2=OCOC(=CHCH_3)CH_3

IV R_1=OAc R_2=OCOC(=CHSCH_3)H

VII R_1=OAc R_2=OCOC(=CHCH_3)CH_3

VIII R_1=OH R_2=OH

These compounds belong to a new type of sesquiterpenoids and have the novel carbon skeleton (V), to which the authors propose to give the name "bakkane." Since many sesquiterpenoids with the eremophilane skeleton (VI) have been isolated[4,5] from the same genus, *Petasites*, the bakkane is biogenetically related with the eremophilane skeleton. The mode of the biogenesis of the bakkane might be bond fission at C_8 and C_9, with a concomitant bond formation at C_7 and C_9 of the eremophilane, but we can not yet define the direct precursor with the eremophilane skeleton and the oxidation stages at C_8, C_{11} and C_{12} of bakkenolide-A, from which the other bakkenolides might be biosynthetized. It is, therefore, desirable to make clear the components which might be expected to be biogenetically important intermediates so as to discuss the biogenesis of the bakkenolides of the plant.

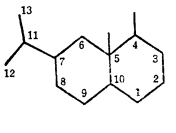

VI

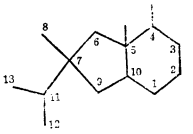

V

From this point of view, the minor components of the essential oil of the plant were investigated in detail.

The gas chromatograph of the oil shows the presence of at least nine components, in addition to compounds I—IV, from which the new compound, bakkenolide-E, was isolated.

Bakkenolide-E, (VII), mp 168°C (from ethanol) has the molecular formula of $C_{22}H_{30}O_6$ (found: C, 67.90; H, 8.00%). The IR spectrum (KBr) of VII suggests the presence of the following groups; γ-lactone at 1792 cm^{-1}, two different types of carboxylates at 1740 and 1700 cm^{-1} (acetate and tiglate), and exocyclic methylene at 1650 and 910 cm^{-1}.

VII, when hydrolysed with 25% potassium hydroxide in aqueous methanol, affords tiglic acid (identified by comparison with an authentic sample) and 1,9-dihydroxybakkenolide-A (VIII). The latter compound was also obtained from II, III, and IV by the same treatment, thus indicating that VII is a derivative of bakkenolide-A with tiglate and acetate (from IR and NMR) groups.

The similarities of the NMR spectra of bakkenolides-E and -B (Table 1) demonstrate that the acetate and tiglate groups of VII are located at C_9 and C_1 of bakkenolide-A respectively.

The other, minor components of the oil are now being investigated.

The authors wish to acknowledge their indebtedness to Messrs. S. Sakata, H. Kamata and M. Saga for their assistance with the collection and extraction of the plant material. One of the authors (N. A.) wishes also to thank Professor R. Onoda of Akita University for his kind encouragement.

4) For example, L. Novotny, V. Herout and F. Sorm, *Tetrahedron Letters*, **1961**, 697.
5) K. Naya, I. Takagi, M. Hayashi, S. Nakamura and M. Kobayashi, "Symposium Papers, The 11th Symposium on the Chemistry of Natural Products" (Kyoto, 1967), p. 88, and some references therein.

SHORT COMMUNICATIONS

Isotope Effects on the Hydrogen Formation Reaction in the Radiolysis of Cyclopentanone

Kinya UNOURA, Masayuki AIKAWA and Meiseki KATAYAMA[1]

Department of Chemistry, Faculty of Science, Hokkaido University, Sapporo

(Received April 12, 1968)

Hydrogen gas has been found to be one of the major products of the radiolysis of cyclopentanone in the liquid phase[2,3] but not in the photolysis,[4] while there are many common major reaction products in the two processes. The uniqueness of the hydrogen formation in this sense led us to study the reaction in detail in the hope of acquiring a knowledge of the excited species in the radiolysis different from the well-defined ones in the photolysis.[4,5]

Either a degassed sample, containing 0.5—1 m*l* each of cyclopentanone, cyclopentanone-d_8, and 2,2,5,5-cyclopentanone-d_4, or a mixture of cyclopentanone and cyclopentanone-d_8, was sealed into a reaction vessel and irradiated with γ-rays from a cobalt-60 source at a dose rate of 3.7×10^6 rad/hr. The amount of hydrogen formed was proportional to the absorbed dose, as has been reported previously.[2] The isotopic composition of the hydrogen gas was analyzed by means of a mass spectrometer.

The mechanism of the hydrogen formation may be summarized as:

$$\text{cyclopentanone} \xrightarrow{\Phi} (\text{cyclopentanone}^*)$$

$$\begin{cases}\rightarrow \text{hydrogen gas} + \text{residue} & (1)\\ \rightarrow \text{hydrogen atom} + \text{residue} & (2)\end{cases}$$

$$\text{hydrogen atom} + \text{cyclopentanone} \rightarrow \text{hydrogen gas} + \text{residue} \quad (3).$$

The yields of protium, $G(H_2)$, from cyclopentanone and of deuterium, $G(D_2)$, from cyclopentanone-d_8 were 0.60 ± 0.12 and 0.22 ± 0.04 respectively. The $G(H_2)/G(D_2)$ ratio was about 3, apparently indicating that such a rate constant as Φ is about three times larger in cyclopentanone than in cyclopentanone-d_8.

The $H_2 : D_2 : HD$ ratio in the hydrogen formed from the 1 : 1 mixture of cyclopentanone and cyclopentanone-d_8 was 5.6 : 1.0 : 3.6 It can readily be shown[6] that, in the mixture, if the isotope effects do not exist in such steps as (3), the ratio of $H_2 : D_2 : HD$ will range from approximately 3.0 : 1.0 : 2.0 to 3.0 : 1.0 : 0, depending on the magnitude of the molecular hydrogen contribution, *i. e.*, such second steps as are shown in reaction (1). The deviation of these values from the experimental value indicates the existence of such an isotope effect as well as the molecular hydrogen contribution. The ratio of $H_2 : D_2 : HD$ in the hydrogen formed from 2,2,5,5-cyclopentanone-d_4 was 1.5 : 1.0 : 2.9.*1 It can also be shown[6] that the ratio will be 1.0 : 1.0 : 2.0 if no such isotope effect, no molecular hydrogen formation, and no difference in the reactivities between hydrogens attached to α and β positions to the carbonyl group are assumed. The difference between the ratio found and that predicted in the partially-deuterated cyclopentanone suggests the existence of the isotope effect also or of different reactivities in addition to the isotope effect. Although the contribution of molecular hydrogen is indicated by the presence of 2-cyclopentenone among the radiolysis products[2b] as well as by the analytical results mentioned above, the contribution of "hot hydrogen" is also suggested by the fact that a relatively large amount of HD was found in the mixture of cyclopentanone and cyclopentanone-d_8, as well as by the fact that the amount of hydrogen reduced by the addition of such radical scavengers as DPPH was rather small.[2b]

1) Communications should be addressed to M. K.

2) a) M. Katayama, J. C. Whitmer and C. N. Trumbore, *J. Am. Chem. Soc.*, **84**, 4025 (1962). b) W. W. Bristowe, M. Katayama and C. N. Trumbore, *J. Phys. Chem.*, **69**, 807 (1965).

3) D. L. Dugle and G. R. Freeman, *Trans. Faraday Soc.*, **61**, 1161, 1174 (1965).

4) P. Dunion and C. N. Trumbore, *J. Am. Chem. Soc.*, **87**, 4211 (1965).

5) R. Srinivasan, *ibid.*, **83**, 4344, 4348 (1961).

6) K. Unoura, M. Aikawa and M. Katayama, to be published.

*1 This ratio is different from that (1 : 0.37 : 1.26) reported in Ref. 2b. The difference may be attributed to the greater degree of deuterium substitution in the present studies.

A Preparation Method of Dicyano-Cobalt(III) Complexes using Silver Cyanide

Nobufumi MAKI, Taihei HAMAZAKI and Shukichi SAKURABA

Department of Chemistry, Faculty of Engineering, Shizuoka University, Johoku, Hamamatsu

(Received March 13, 1968)

The CN^- ion is located at the end position of the spectrochemical series and has the strongest coordinating ability of cobalt(III) complexes of the Werner-type, while Cl^- ion is located above this. Such a difference in bonding character between them is the reason why direct substitution[1] is difficult. For example, the $[Co(CN)_2en_2]^+$ ion can be obtained only *via* the $[Co(S_2O_3)_2en_2]^-$ ion.[2]

In the present report, however, the substitution of Cl-ligands has been found possible even in water solution under the condition that CN^- ions are present in a very dilute concentration. For this purpose, we have adopted silver cyanide, the solubility of which in water is $2.2\cdot10^{-5}$ g/100 g water (20°C), and succeeded in obtaining directly dicyano-cobalt(III) complexes including new compounds, *cis*-$[Co(CN)_2dip_2]NO_3\cdot7H_2O$ and *cis*-$[Co(CN)_2phen_2]NO_3\cdot6H_2O$.[3]

Preparation of cis-$[Co(CN)_2en_2]NO_3$. To a suspension of *trans*-$[CoCl_2en_2]NO_3$(20 g) in 200 m*l* of water were added 20 g of AgCN powder. The paste-like mixture was further diluted with 500 m*l* of water after half an hour and heated on a water bath (90°C) for three hours. The solution was filtered, and the yellow filtrate obtained was concentrated on a water bath by evaporation and allowed to stand. On cooling, yellow crystals separated from solution. The crude product was recrystallized once from hot water. Found: Co, 19.77; C, 24.09; N, 33.59; H, 5.83%. Calcd for $[Co(CN)_2en_2]NO_3$: Co, 20.10; C, 24.58; N, 33.44; H, 5.50%.

The perchlorate was similarly prepared by using *trans*-$[CoCl_2en_2]ClO_4$ as the starting complex instead of the nitrate. Found: Co, 17.91; C, 21.63; N, 25.17; H, 4.90%. Calcd for $[Co(CN)_2en_2]ClO_4$: Co, 17.82; C, 21.80; N, 25.42; H, 4.88%.

Preparation of cis-$[Co(CN)_2dip_2]NO_3\cdot7H_2O$. Dicyanobis(2,2'-dipyridyl)cobalt(III) complex was prepared by the following method: Fifteen grams of *trans*-$[CoCl_2dip_2]NO_3$[4] were mixed with AgCN (10g) and a few milliliters of water. The paste-like mixture was allowed to stand for a while and further diluted with 500 m*l* of water. The mixture was heated on a water bath (70—80°C) for an hour and filtered. The residue was repeatedly extracted with hot water. The extracted solution and filtrate were added together and concentrated by evaporation. On cooling, lustrous needle-shaped yellow crystals deposited from solution, which were then filtered and washed with cold water, ethanol and ether. The product was recrystallized once from hot water. Found: Co, 11.98; C, 54.19; N, 19.95; H, 3.41%. Calcd for $[Co(CN)_2dip_2]NO_3$: Co, 12.14; C, 54.45; N, 20.20; H, 3.32%.

Preparation of cis-$[Co(CN)_2phen_2]NO_3\cdot6H_2O$. Twenty grams of *trans*-$[CoCl_2phen_2]NO_3$[5] were treated with 15 g of AgCN in 500 m*l* of water at 60—70°C for an hour. Silky yellow crystals deposited from the filtrate. Found: Co, 10.87; C, 58.31; N, 18.11; H, 3.38%. Calcd for $[Co(CN)_2phen_2]NO_3$: Co, 11.05; C, 58.55; N, 18.38; H, 3.02%. The NMR spectra in 99.75% D_2O indicated that the complexes were cis-isomers, as shown in Fig. 1.

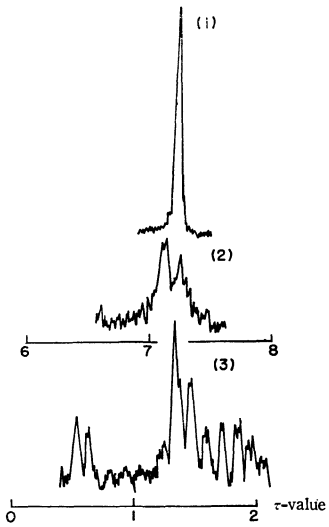

Fig. 1. The NMR spectra of dicyano-cobalt(III) complexes obtained in 99.75% D_2O; (1) *trans*-$[Co(CN)_2en_2]NO_3$, (2) *cis*-$[Co(CN)_2en_2]NO_3$, (3) *cis*-$[Co(CN)_2dip_2]NO_3\cdot7H_2O$.

1) H. Yoneda, T. Baba and M. Muto, This Bulletin, **40**, 1736 (1967).

2) P. R. Ray and B. Sarma, *J. Indian Chem. Soc.*, **28**, 59 (1951).

3) The complex, $[Co(CN)_2phen_2]OH\cdot7H_2O$, has been reported by Favini et al., but no description of the preparation has been found; G. Favini and E. Paglia, *J. Inorg. Nucl. Chem.*, **8**, 155 (1958): dip=2,2'-dipyridyl; phen=1,10-phenanthroline.

4) F. M. Jaeger and J. A. van Dijk, *Z. anorg. u. allgem. Chem.*, **227**, 273 (1936).

5) P. Pfeiffer and Br. Werdelmann, *ibid.*, **236**, 31 (1950).

On the ESR Studies of the Photoisomerization of Triethylphosphite

Kinichi TERAUCHI and Hiroshi SAKURAI

The Institute of Scientific and Industrial Research, Osaka University, Oaza-Yamada-Kami, Suita, Osaka

(Received March 26, 1968)

Although a number of inorganic phosphorus compounds have been studied by means of the ESR technique, a few reports have been published on the organic phosphorus compounds especially, UV-irradiated trialkylphosphite has never been subjected to ESR measurements. In this study, we wish to report the results obtained by the ESR measurements using the elevated-temperature method. We undertook those measurements in order to investigate the mechanism of the following photoisomerization reaction[1]:

$$P(OEt)_3 \xrightarrow{h\nu} EtP(O)(OEt)_2$$

This reaction has recently been reported on by LaCount *et al.*,[2] also but they have not suggested any mechanism for the photochemical formation of the phosphonate.

When a degassed sample of neat triethylphosphite (TEP) was irradiated at 77°K with a 400 Watt high-pressure mercury arc, two kinds of ESR signals were observed, as is shown in Fig. 1a. The (P_1) spectrum has an anisotropic doublet of 370—600 gauss separation and a high g value (2.02), while the other (spectrum C) contains an sixfold line of 25.6 gauss separation and a g value close to the free spin value. The P_1 spectrum showed a characteristic change upon the elevation of the temperature; when the temperature was raised to 100°K, the P_1 spectrum disappeared completely and a new ESR signal (P_2 spectrum) with an anisotropic doublet of 713—870 gauss separation and a g value of 2.03 appeared (Fig. 1b). The observed g and A values of P_1 and P_2 are summarized in Table 1. At 110°K, the P_2 signal vanished.

TABLE 1. LIST OF PHOSPHORUS-RELATED RADICALS FORMED IN IRRADIATED TEP

	$A_\perp$(G)	$A_\parallel$(G)	$\bar{g}$
P_1 Spectrum	596	369	2.021
P_2 Spectrum	860	713	2.032

On the other hand, the C spectrum did not show any significant change except for a great decrease in the intensity during the ESR measurements. The C spectrum as is shown in Fig. 1c, was identified as an ethyl radical. It is well known that the phosphorus atoms in trivalent phosphorus compounds take p^3-hybrid and partially sp^3 hybrid, while in tetravalent phosphate compounds the phosphorus atoms take stable sp^3 hybridization. There fore, the spectra with regard to phosphorus radicals obtained from the trivalent phosphorus compounds may be expected to have a large anisotropic character of a hyperfine structure. When we calculated the orbital spin density of an unpaired electron of these radicals from the isotropic and anisotropic parts of the hyperfine coupling tensor, it is estimated that P_1 has 12.3% 3s- and 73.9% 3p-character, while P_2 has 21.3% 3s- and 50.8% 3p-character. Thus, we may assign the P_1 radical to the $\rangle PO\cdot$-type radical with a p^3 hybrid and the P_2 radical to the $\rangle \dot{P}(O)$-type radical with a sp^3 hybrid. Therefore, the photochemical primary processes of TEP may be depicted as follows:

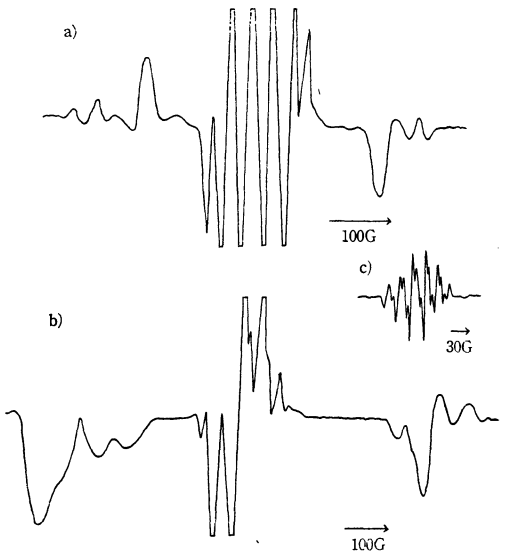

Fig. 1. ESR spectra of UV-irradiated TEP.
a) measured at 77°K.
b) measured at 100°K.
c) measured in the region of $g=2.00$, at 77°K

$$P(OEt)_3 \xrightarrow{h\nu} (EtO)_2PO\cdot + \cdot Et \quad (1)$$

$$\cdot OP(OEt)_2 \rightarrow \cdot P(OEt)_2 \quad (2)$$
$$\quad\quad\quad

An Estimation of the Propagation Rate Constant for the Radiation-Induced Polymerization of Gaseous Isobutene

Yasuyuki NORO, Kenji FUEKI and Zen-ichiro KURI

Department of Synthetic Chemistry, Faculty of Engineering Nagoya University, Chikusa-ku, Nagoya

(Received April 23, 1968)

In a previous paper,[1] we have shown that the cationic mechanism dominates in the radiation-induced polymerization of gaseous isobutene. Since it is well established by a number of studies in the field of radiation chemistry that ammonia is an efficient proton acceptor and neither a radical nor electron scavenger, ammonia may be used for an estimation of the propagation rate constant on the basis of the assumption that the mechanism of radiation-induced polymerization of gaseous isobutene is cationic.

In this communication, we report the propagation rate constant and the mean lifetime of the propagating ion estimated in a quantitative study of the effect of ammonia on this polymerization.

Figure 1 shows a plot of the G-value for monomer consumption *vs.* the mole ratio of isobutene to ammonia at 500 Torr and 20°C. In Fig. 1, a straight line can be drawn through the experimental points at low concentrations of ammonia. We put on this result an interpretation that the linear portion of the curve indicates the retardation by ammonia of the polymerization due to ions surviving as a result of diffusional loss of electrons on the vessel wall and the curved portion at higher concentrations of ammonia corresponds to that due to ions which undergo gas-phase recombination.

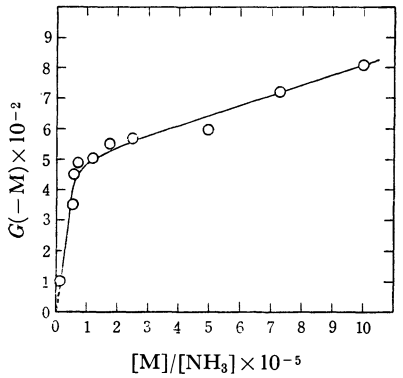

Fig. 1. The dependence of the polymerization yield on the mole ratio of isobutene to ammonia.

We apply the Klots-Anderson theory[2] to an estimation of the fraction of gas-phase recombination, f. A dimensionless parameter, κ, is defined by $\kappa^2=R^4I\alpha/D_+D_-$, where R is the radius of the vessel, I is the rate of ion-pair generation per unit volume, α is the bimolecular recombination coefficient, and D_+ and D_- are the diffusion coefficients for positive ions and electrons respectively. Taking $R=4$ cm, $I=2\times10^{11}$ ions $cm^{-3}sec^{-1}$, $\alpha=10^{-7}$ $cm^3ions^{-1}sec^{-1}$, $D_+=3\times10$ cm^2sec^{-1} and $D_-=2\times10^2$ cm^2sec^{-1}, we obtain $\kappa=920$. From Fig. 1 of Klots and Anderson, it can be estimated that this corresponds to 90% gas-phase recombination, $f=0.9$, and 10% loss by diffusion, $1-f=0.1$.

We can now evaluate the propagation rate constant, k_p, using the relation[3]

$$G(-M) = G_x \frac{k_p}{k_r} \frac{[M]}{[NH_3]} + G_c(-M), \qquad (1)$$

where k_r is the rate constant for termination by ammonia, which is of the order $10^{10\pm1}$ $M^{-1}sec^{-1}$, and $G_x=G_i\times(1-f)$, G_i is the ion-pair yield per 100 eV absorbed. From the slope of the linear portion in Fig. 1 and Eq. (1), we obtain $k_p=8.3\times10^{6\pm1}$ $M^{-1}sec^{-1}$.

The mean lifetime of a propagating ion during growth in the pure monomer is given by

$$\tau_p = G_0(-M)/G_xk_p[M]. \qquad (2)$$

Using the value $G_0(-M)=1000$ for pure isobutene and the previous values for G_x and k_p, we obtain $\tau_p=10^{-2\pm1}$ sec.

Since there is some ambiguity in the recombination coefficient and the diffusion coefficients in addition to the rate constant for termination by ammonia, the values for k_p and τ_p should be taken as representing the order of their magnitudes.

1) H. Okamoto, K. Fueki and Z. Kuri, *J. Phys. Chem.*, **71**, 3222 (1967).

2) C. E. Klots and V. E. Anderson, *ibid.*, **71**, 265 (1967).

3) M. A. Bonin, W. R. Busler and F. Williams, *J. Am. Chem. Soc.*, **87**, 199 (1965).

A New Synthesis of 3-Hydroxyfurans. The Reaction of Sulfonium Ylids with Ketene Dimer

Hisashi TAKEI, Moriaki HIGO, Kunio SAITO and Teruaki MUKAIYAMA

Laboratory of Organic Chemistry, Tokyo Institute of Technology, Ookayama, Meguro-ku, Tokyo

(Received April 25, 1968)

This communication reports a convenient method for the synthesis of 3-hydroxyfuran derivatives, structurally resemble to isomaltol which is obtained from lactose,[1] by the reactions of ketene dimer (I) and some stabilized ylids. A typical run was as follows; ketene dimer was added to a dry benzene solution of dimethylsulfonium *p*-bromophenacylid (IIa) at room temperature under nitrogen. When the solution was refluxed for a short time, evolution of dimethyl sulfide was observed by its characteristic odour. After removal of the solvent, a resulting yellow precipitate was purified by a silica gel column to afford slightly yellow crystals, 2-(*p*-bromo benzoyl)-3-hydroxy-5-methylfuran (IIIa).[2]

Similarly, 2-(*p*-substituted benzoyl)-, 2-acetyl-, 2-ethoxycarbonyl- and 2-diethylcarbamoyl-3-hydroxy-5-methylfurans were successfully synthesized by the reactions of the ylids, IIb-d, IIe, IIf and IIg, with ketene dimer in high yields. The results are summarized in Table 1.

The reaction can be considered to proceed through an initial formation of dimethylsulfonium acetoacetyl-(acyl)-methylid (IV) from II and I. The ylid IV, subsequently, is transformed into its tautomeric structure (V), which, on heating, decomposes to give III and dimethyl sulfide by an intramolecular nucleophilic displacement as shown below.

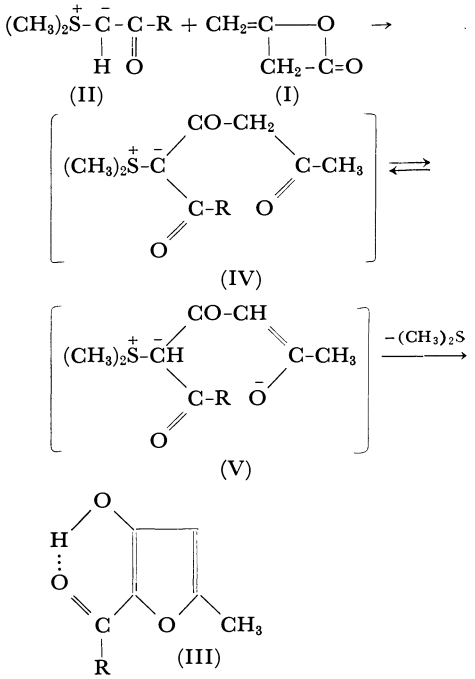

In conclusion, it is noted that this method enables to convert ketene dimer into 3-hydroxyfuran derivatives accompanied with ring expansion by the so-called methylene transfer.

TABLE 1. 3-HYDROXYFURANS BY THE REACTIONS OF STABILIZED SULFONIUM YLIDS WITH KETENE DIMER

Compd.	R in III	Method of ylid prepn.	Reaction time[a] min	Yield %	Mp °C	Anal % Found C	Found H	Found N	Calcd C	Calcd H	Calcd N
IIIa	-C_6H_4-Br(*p*)	A[b]	30	83	84—86	51.59	3.28		51.27	3.23	
IIIb	-C_6H_5	A	40	99	57—59	71.57	4.99		71.28	4.99	
IIIc	-C_6H_4-CH_3(*p*)	A[d]	20	87	49—52	71.93	5.33		72.21	5.59	
IIId	-C_6H_4-OCH_3(*p*)	B[c,d]	40	91	62.5—64	66.69	5.06		67.23	5.21	
IIIe	-CH_3	B[d]	45	81	93.5—95	60.08	6.04		59.99	5.75	
IIIf	-OC_2H_5	B	60	60	49—50	56.59	5.93		56.46	5.92	
IIIg	-$N(C_2H_5)_2$	B	20	47	52—54	61.05	7.51	7.08	60.89	7.67	7.10

a) All reactions were carried out in refluxing benzene.
b) Method A; ylids were prepared according to the method of Trost.[3]
c) Method B; ylids were prepared according to the method of Payne.[4]
d) These ylids were newly prepared from the corresponding sulfonium bromides.
Satisfactory elemental analyses were obtained.

1) B. E. Fisher and J. E. Hodge, *J. Org. Chem.*, **29**, 776 (1964), and references cited therein.
2) The structural assignment was made on the basis of analytical data, and IR and NMR spectrum.
3) B. M. Trost, *J. Am. Chem. Soc.*, **89**, 138 (1967).
4) G. B. Payne, *J. Org. Chem.*, **32**, 3351 (1967).

The Catalytic Activities and Electron Configuration of Poly-Negative Phthalocyanine Complex Films with Lithium

Masaru ICHIKAWA, Mitsuyuki SOMA, Takaharu ONISHI and Kenzi TAMARU

Department of Chemistry, The University of Tokyo, Hongo, Bunkyo-ku, Tokyo

(Received April 30, 1968)

It was previously reported that various phthalocyanines exhibit marked heterogeneous catalytic activities in many reaction systems, such as the H_2-D_2 exchange reaction, the hydrogenation of olefins, and the isomerization of butenes, at room temperature when they are exposed to a small amount of sodium or lithium.[1]

In this communication it will be demonstrated that such catalytic activities of the phthalocyanine electron donor-acceptor (EDA) complex films are not responsible for the reduced central metal ions of phthalocyanines, but for the poly-negatively-charged porphyrin ligands, where the excess electrons ($n=1$ to 4) are seemingly distributed in the π-systems.

Taube and other workers[2] have prepared many types of poly-negative ions of phthalocyanines, and their properties have been partly established by the iodine titration and measurements of the magnetic susceptibility of their stoichiometric salts with lithium.

In these experiments 50 mg portions of Fe-, Co-, Ni-, and Zn-phthalocyanines were reacted with lithium benzophenone ketyl, Li-naphthalene, Li, and Na in tetrahydrofuran at various stoichiometric ratios. The stoichiometric complex solutions exhibited their characteristic visible spectra. Various kinds of poly-negative ion complex films were prepared over silica wool (their surface areas were *ca.* 10 m^2) by the evaporation of the solvent from each complex solution. The results of the iodine titration of the complex films were in agreement with the expected stoichiometry. The reactions were carried out in the temperature range between 20 and 120°C over each complex film in a closed circulating system (the dead-volume was *ca.* 140 m*l*). The reaction product was analyzed by gas chromatography using an alumina column. Some typical results are summarized in the table, as are the relative activities for the hydrogen-exchange reaction between molecular hydrogen and the hydrogen in each of the complex films, the H_2-D_2 exchange reaction, the hydrogenation of propylene, and also the electron configuration of each poly-negative ion of the phthalocyanines,

TABLE

Complex	Electron configuration	D_2-HZ[a] $3+\log k$	H_2-D_2[b] $3+\log k$	$C_3+H_6+H_2$[c] % conversion
FePc	d_6	—	—	—
LiFePc	d_7	—	—	—
Li_2FePc	d_8	0.1	0.2	—
Li_3FePc	$d_8+\pi$	0.6	0.9	10
Li_4FePc	$d_8+\pi^2$	2.0	2.1	70
NiPc	d^8	—	—	—
LiNiPc	$d^8+\pi$	0.4	0.3	5
Li_2NiPc	$d^8+\pi^2$	1.3	1.3	28
Li_3NiPc	$d^8+\pi^3$	1.7	2.0	60
Li_4NiPc	$d^8+\pi^4$	2.1	2.5	82

a) HZ represents the EDA complexes. $k(hr^{-1})$ at 60°C, $P_{D_2}=12.5$ cmHg

b) $k(hr^{-1})$ at 60°C, $P_{H_2+D_2}=15$ cmHg, H_2:D_2=1:1

c) C_3H_6:H_2=1:2 at 60°C in 20 hr.

which were reported by Taube.

It is suggested in this table that the catalytic activities for the hydrogen exchange and hydrogen chemisorption are not observed even at higher temperatures over the $FePc^{-1}$, $FePc^{-2}$, and $CoPc^{-1}$ complex films with lithium cations, in which one or two electrons are localized in their bivalent central metal ions. However, the H_2-D_2 exchange reaction and the hydrogenation of propylene takes place at a considerable rate at room temperature over the $FePc^{-3}$, $FePc^{-4}$, $CoPc^{-2}$,…, $CoPc^{-5}$, $NiPc^{-1}$…, $NiPc^{-4}$, and $ZnPc^{-1}$, $ZnPc^{-4}$ complex films, in which excess electrons are delocalized in the π-system of the porphyrin ligands. In addition to this, such complex films of higher negative ions as $NiPc^{-4}$ and $NiPc^{-3}$, $CoPc^{-5}$, and $FePc^{-4}$ are much more active for the reactions than the complex films of a lower negativity under similar reaction conditions. As the number of delocalized electrons in the porphyrin ligand increases, the reactivities of the porphyrin are markedly enhanced. Upon contact with hydrogen gas, the absorption peaks of $FePc^{-4}$ (620 and 860 mμ) gradually decrease and new peaks appear in the regions of 570 mμ and 520 mμ; these peaks resemble those of $FePc^{-3}$ and $FePc^{-2}$. The spectra were restored completely to that of the $FePc^{-4}$ complex film by evacuation at 40°C for several hours.

1) M. Ichikawa, M. Soma, T. Onishi and K. Tamaru, *Trans. Faraday Soc.*, **63**, 1215 (1967).

2) R. Taube, *Z. Chem.*, **6**, 8 (1966); J. A. Elving and A. B. P. Lever, *J. Chem. Soc.*, **1961**, 1217; R. Taube and H. Munke, *Angew. Chem.*, **75**, 639 (1963).

A New Ion-exchange Method for the Determination of Polymerization Number of Metal Salt in Nonaqueous Solutions

Hirohiko WAKI and Nobuyuki UEMURA

Department of Applied Analytical Chemistry, Faculty of Engineering, Kyushu University, Hakozaki, Fukuoka

(Received April 23, 1968)

Although studies on ionic species present in solution with ion-exchange resins have been made by a number of workers, almost all of them have been on the determination of the ionic charge or stability constants of metal complexes, and polymerization equilibria have been left because of difficulties in theoretical treatment.

The polymerized molecule of a metal salt MA_a may be ionized in nonaqueous solvents of low dielectric constants in the following form:

$$2M_nA^0_{an} \rightleftarrows M_nA^+_{an-1} + M_nA^-_{an+1} \quad (1)$$

The equilibrium constant for Eq. (1) is written as

$$K_{ioniz} = \frac{[M_nA^-_{an+1}]^2}{[M_nA^0_{an}]^2} \quad (2)$$

In such a solvent most part of the salt may remain unionized as the neutral $M_nA^0_{an}$ and the ionic species of higher charges $|i| \geqq 2$ may hardly be produced. In an anion exchange resin phase these neutral and cationic complexes may be converted into the anionic form $M_nA^-_{an+1}$ to a large extent by combining with the resin counter ion A^-. Under these conditions, the distribution coefficient of M is given in the following form:

$$D \equiv \frac{[\sum M]_R}{[\sum M]} \approx \frac{[M_nA^-_{an+1}]_R}{[M_nA^0_{an}]+2[M_nA^-_{an+1}]}$$

$$= \frac{[M_nA^0_{an}]_R}{[M_nA^0_{an}]} \cdot \frac{\beta_R}{1+2\sqrt{K_{ioniz}}} \cdot [A^-]_R \quad (3)$$

where $\beta_R = [M_nA^-_{an+1}]_R/[M_nA^0_{an}]_R[A^-]_R$. Neglecting the neutral complexes of the metal salt present in the resin phase, uncomplexed $[A^-]_R$ is given as:

$$[A^-]_R = C - \frac{1}{n}[\sum M]_R \quad (4)$$

where C represents the exchange capacity of the anion exchange resin. Assuming that $[M_nA^0_{an}]_R/[M_nA^0_{an}]$, K_{ioniz} and β_R are effectively constant, the following equation can be derived from Eqs. (3) and (4).

$$\log D = \log(C - \frac{1}{n}[\sum M]_R) + K \quad (5)$$

where K is a constant. Hence by comparing the slope of experimental curve of log D vs $[\sum M]_R$ with those of theoretical curves obtained by inserting $n=1,2,\cdots$ into $\log(C-1/n[\sum M]_R)$ for corresponding $[\sum M]_R$, n can be presumed.

In case of $AlCl_3$-tetrahydrofuran (THF) solution, the following type of ionization is presumed from conductivity data.

$$2Al_nCl^0_{3n} = Al_nCl^+_{3n-1} + Al_nCl^-_{3n+1}$$

The experiment was carried out by passing $AlCl_3$-THF solutions of various concentrations through a small column containing 1 g of the resin Amberlyst

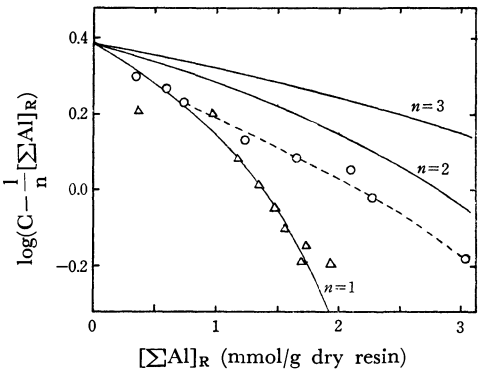

Fig. 1. The determination of the polymerization number "n" of $AlCl_3$ in THF by anion-exchange. ○: 24 hr △: 96 hr

A-27 Cl^- type of commercial particle size, followed by stripping the sorbed aluminum with diluted HNO_3 after equilibrium, and determining Al by EDTA titration. D was calculated in an ordinary way.

The experimental plots of log D *vs.* $[\sum Al]_R$ are compared with the theoretical lines of log $(C-1/n[\sum Al]_R)$ *vs.* $[\sum Al]_R$ in Fig. 1. It may be seen from the graph that the dimer species $Al_2Cl^{0\mp1}_{6\pm1}$ is predominant in THF solution for the Al concentration range larger than 0.2 mol/*l* in solution 24 hr after the preparation of $AlCl_3$-THF stock solution, and the monomeric $AlCl^{0\mp1}_{3\pm1}$ is predominant for the whole concentration range of Al at 96 hr after. These results may indicate that the dimer or higher Al-Cl complexes are produced immediately after the solution of $AlCl_3$ and the Cl-bridge in $\rangle Al\langle^{Cl}_{Cl}\rangle Al\langle$ gradually disappears by the attack of THF molecules.

The proposed method seemed to be valid in the system of low polymerization number like metal salts dissolved in nonaqueous solvents. Details of this work will be reported later.

The Formation of 3-Methyloctan-4-one and Polyketones by the Oxo Reaction of Butadiene

Masayuki DOKIYA and Ken-ichiro BANDO

Government Chemical Industrial Research Institute, Tokyo, Meguro-ku, Tokyo

(Received April 30, 1968)

It has previously been established that nonan-5-one, together with *n*- and isovaleraldehyde, is formed by the oxo reaction of butadiene catalysed by dicobalt octacarbonyl,[1,2] but neither branched-chain C_9-ketone nor polyketones.

We have found that 3-methyloctan-4-one (I) and polyketones ($C_4H_9\cdots(CC_4H_8)_n\cdots C_4H_9$, II, O) are also formed by the oxo reaction of butadiene.

The reaction of butadiene (8.1 g) with synthesis gas ($H_2/CO=1.3$: initial pressure, 230 kg/cm^2 at room temp.) was carried out at 165±5°C for 2 hr in a stainless-steel autoclave (100 m*l*) using cyclohexane (30 m*l*) as the solvent and dicobalt octacarbonyl (0.68 g) as the catalyst.

The gas chromatogram of the reaction products showed the presence of Compound I (0.77 g), which had a retention time near to that of nonan-5-one, and several compounds of a longer retention time in addition to the previously-known products (*n*-C_5-aldehyde: 1.34, iso-C_5-aldehyde: 0.75, *n*-C_5-alcohol: 0.33, iso-C_5-alcohol: 0.15, nonan-5-one: 1.48 g). A white, waxy material, II (4.6 g), was separated from the reaction products by the addition of aqueous methyl alcohol after the decobaltation.

The IR spectrum of I showed the existence of a carbonyl group (1715 cm^{-1}). The NMR spectrum, measured in $CDCl_3$, with tetramethylsilane used as the internal standard, showed bands at 9.1 (multiplet, $-C-CH_3$, 6H), 8.9 (doublet, $-\overset{\overset{O}{\|}}{C}-CH_3$, 3H), 8.6 (multiplet, $-C-CH_2-C-$, 6H) and 7.6 τ (multiplet, $C-\overset{\overset{O}{\|}}{C}H-C-$, 3H). Found: mol wt 142 (by mass spectrum). Calcd for $C_9H_{18}O$: mol wt 142. It was concluded from these results that I was 3-methyloctan-4-one.

The IR spectrum of II was essentially identical with that of I in the NaCl region. The NMR spectrum of II showed bands at 9.1 (broad, $-C-CH_3$, 22%H), 8.5 (broad, $-C-CH-C-$, 43%H) and 7.9 τ (broad, $-C-\overset{\overset{O}{\|}}{C}H-C-$, 35%H). Found: C, 72.60: H, 10.90%: mean mol wt 1180 (V.P.O. in benzene). Calcd for $(C_6H_{11}O)_n$: C, 72.8: H, 10.6%. The IR and NMR spectra showed no peaks characteristic of C=C, ester, aldehyde, or carboxylic acid. It was concluded from these results that II was mainly a mixture of polyketones, $C_4H_9\cdots(CC_4H_8)_n\cdots C_4H_9$, O, in which carbonyls were not always inserted regularly.

The yield of polyketones increased with the amount of charged butadiene under the same reaction conditions (Table 1).

Table 1. The yield of products (g)*1

Charged butadiene	5.4	8.1	10.8	13.5	16.2
C_5-aldehyde (*n*+iso)	1.81	2.09	2.40	1.94	0.41
Nonan-5-one	1.07	1.48	2.15	2.43	0.68
3-Methyl-octan-4-one	0.40	0.77	1.16	1.50	0.24
Polyketones	0.4	4.6	7.3	9.5	14.5

*1 The reaction conditions were similar to that described in the example.

The reaction scheme of the formation of polyketones may be represented as follows:

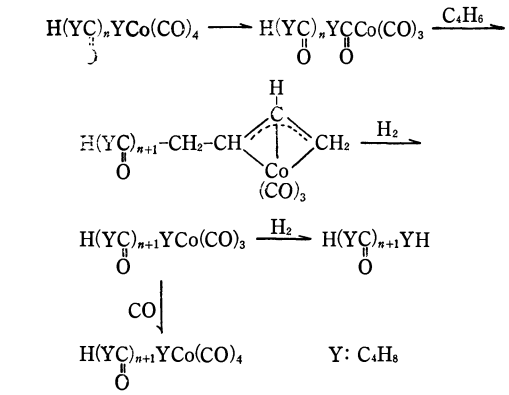

Detailed studies are now in progress.

1) H. Adkins and J. L. R. Williams, *J. Org. Chem.*, **17**, 980, (1952).
2) J. A. Bertrand, C. L. Aldridge, S. Husebye and H. B. Jonassen, *ibid.*, **29**, 790 (1964).

The Specific Hydrogen Bonding of Riboflavin Derivatives to an Adenine Compound

Yoshimasa KYOGOKU and Byung Sul YU

Faculty of Pharmaceutical Sciences, The University of Tokyo, Bunkyo-ku, Tokyo

(Received May 9, 1968)

Riboflavin-2',3',4',5'-tetraacetate was prepared by the reaction of riboflavin with acetic anhydride in pyridine. Yellow flaky crystals were obtained (mp 246°C). In the infrared spectrum of the 0.02 M solution (in $CDCl_3$) of riboflavin tetraacetate (R), a strong band due to the free imino group of the isoalloxazine ring is observed at 3380 cm^{-1} (Fig. 1 R), indicating that most of the riboflavin tetraacetate molecules are present as monomers. The infrared spectrum of 9-ethyladenine (A) shows two strong bands at 3527 and 3416 cm^{-1} which are due to the non-bonded amino group[1] (Fig. 1 A). When both solutions are mixed together, however, the association bands of the R-A complex appear at 3485, 3330, 3255 and 3200 cm^{-1} (Fig. 1 R+A). Using procedures described previously[1], the association constant for the formation of the R-A complex at 25°C was determined to be 130 (*l*/mol of dimer), as compared with the self dimerization constant of riboflavin tetraacetate (4.5) and of 9-ethyladenine (3.1).

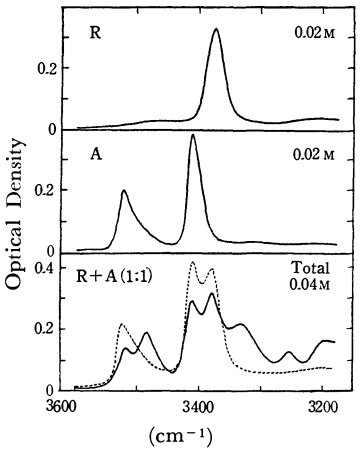

Fig. 1. Infrared spectra of the deuterochloroform solutions in a 1 mm quartz cell. Solid line: observed spectra. Dotted line: calculated sum of the upper two spectra.

From the mixing curve (the intensity of the association bands *vs.* mole fraction) and also from an analysis of the spectra in the carbonyl stretching region, the R-A complex was found to be the 1 : 1 cyclic dimer in which two hydrogen bonds are formed between the amino group of the ethyladenine molecule and one of the carbonyl oxygen atoms of the isoalloxazine ring and between the imino group of the riboflavin molecule and the nitrogen atom, probably, of the adenine ring. It has also been found that riboflavin tetraacetate does not associate with 1-cyclohexyluracil, 2',3'-benzylidine-5'-trityl-guanosine and -cytidine to any observable extent at 0.008 M. A similar experiment has been made with riboflavin tetrabutyrate.*1 The results were quite similar to those obtained for riboflavin tetraacetate.

Present results suggest the formation of the coplanar complex of the adenine and isoalloxazine rings in the flavin adenine dinucleotide (FAD) molecule, in contrast with the ring-stacking model proposed by Tsibris *et al.*[2]

Recently it has been shown that barbiturates form strong specific hydrogen bonds with the adenine residue.[3] The association constant for the formation of the phenobarbital-9-ethyladenine complex is 1200. Barbiturates are known to be inhibitors in the respiratory chain in mitochondria, where FAD serves as an electron carrier. It is suggested, therefore, that barbiturates inhibit respiration by disrupting the structure of FAD: it takes the adenine moiety from the intramolecular adenine-isolloxazine complex.

1) Y. Kyogoku, R. C. Lord and A. Rich, *J. Am. Chem. Soc.*, **89**, 496 (1967).

*1 Riboflavin tetrabutyrate was kindly provided to us by Prof. K. Yagi, Nagoya University and by Prof. J. Okuda, Meijo University.

2) J. C. M. Tsibris, D. E. McCormick and L. D. Wright, *Biochemistry*, **4**, 504 (1965).

3) Y. Kyogoku, R. C. Lord and A. Rich, *Nature*, **218**, 69 (1968).

Stable Free Radicals Derived from 4-Arylazo-2,6-di-*t*-butylphenols

Eiichiro MANDA

Government Chemical Industrial Research Institute, Tokyo, Honmachi, Shibuya-ku, Tokyo

(Received May 24, 1968)

It is well known that 2,6-di-*t*-butylphenol derivatives give stable phenoxy radicals (I) by oxidation.[1]

(I) X: *t*-butyl

In this study, 4-arylazo-2,6-di-*t*-butylphenols (II) were synthesized, and stable radicals were derived from them by KOH-$K_3Fe(CN)_6$ oxidation.

Seven derivatives of II were prepared from 2,6-di-*t*-butyl-*p*-benzoquinone and the corresponding arylhydrazine hydrochlorides by letting the aqueous-alcoholic reaction mixtures stand for five days at room temperature. The seven derivatives were as follows: R=4'-methoxy (II-A); R=4'-methyl (II-B); unsubstituted (II-C); R=4'-chloro (II-D); R=4'-nitro (II-E); R=2',4'-dinitro (II-F); R=2',4',6'-trinitro (II-G).

II-A, II-B, II-C, II-D, and II-E give a sharp OH absorption at 3670 cm^{-1}, but no NH absorption at 3300 cm^{-1} in benzene, and *vice versa* with II-F and II-G. Almost all the derivatives show two absorption maxima, near 360 mμ, and 450 mμ, in benzene (II-G shows only one peak, at 425 mμ), but their molecular coefficients vary with the substituents.

From the above data, it can be concluded that II-G exists exclusively in the hydrazone form, but the other six compounds show azo-hydrazone tautomerism in benzene.[2]

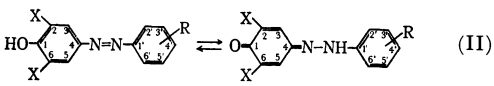

(II)

azo-form hydrazone-form

When the benzene solutions of II were treated with a large excess of an aqueous KOH-$K_3Fe(CN)_6$ solution, the benzene layers turned red immediately. After having been shaken for three minutes, the benzene layers were washed and degassed with cooling by dry ice and methanol, and then the ESR spectra were measured as soon as possible.

All the samples gave ESR signals, and the signals remained for a few days at room temperature in a sealed tube. The lifetimes of the radicals were three days (II-A, II-B, II-D, II-E), one day (II-C), and more than ten days (II-F, II-G).

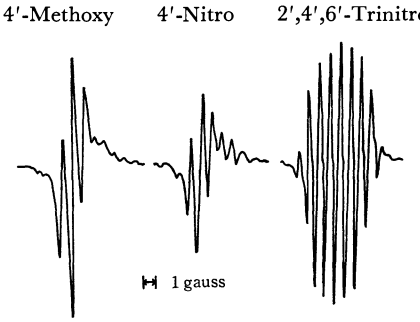

Fig. 1. Some ESR spectra of free radicals derived from II.

With the exception of II-G, the shapes of the ESR spectra suggest that two radical species exist in the sample solution. It is considered that the one species, which gives three lines, is derived from azo-tautomer, and the other, which gives nine lines, is derived from hydrazone-tautomer.

The details will be reported in the future.

1) E. A. Altwicker, *Chem. Revs.*, **67**, 475 (1967).

2) K. J. Morgan, *J. Chem. Soc.*, **1961**, 2151.

Butadiene Hydrogenation by Pentacyanocobaltate(II) in Glycerin Solvent

Kimio TARAMA and Takuzo FUNABIKI

Faculty of Engineering, Kyoto University, Sakyo-ku, Kyoto

(Received May 31, 1968)

Pentacyanocobaltate (II) has catalytic activity for the hydrogenation of conjugated dienes such as butadiene[1,2]. In the study of this complex, water has been used as a solvent exclusively. In the present communication, we report that the butadiene hydrogenation by pentacyanocobaltate in glycerin-methanol (MeOH) has very different characteristics from that in water, and that butadiene is hydrogenated without H_2 even in alcoholic solvent.

The reaction was carried out in closed system at 20°C. The reaction gas was circulated vigorously through the magnetically stirred solution of cyanocobaltate, which was prepared by mixing the glycerin-MeOH solution of KCN with the MeOH solution of $CoCl_2$ in N_2 atmosphere (Fig. 1) or in H_2 atmosphere (Fig. 2). Butadiene was supplied continuously to maintain atmospheric pressure, and the gas sample was analyzed by gaschromatography every 10 or 20 min. The reaction medium was always homogeneous.

As shown in Fig. 1, composition of the isomeric butenes produced in glycerin-MeOH solvent without H_2 changes very sharply with the ratio of CN/Co (=R). In the region of R<5.2, butenes are produced in the order of *trans*-2->>1->*cis*-2-butene as in water, but the order in the region of R>5.2 is *cis*-2>1->>*trans*-2-butene and this order markedly differs from that in water (1->>*trans*-2->*cis*-2-butene). When H_2 was absorbed (*cf.* Fig. 2) similar result was observed except 1->*cis*-2->>*trans*-2-butene at R>5.2.

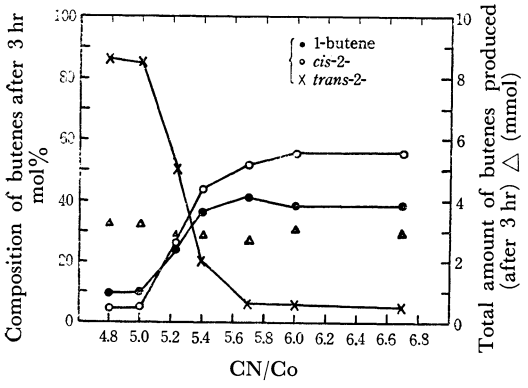

Fig. 1. Effect of CN/Co ratio.
$CoCl_2$=10 mmol
Solvent: glycerin 35 ml+MeOH 15 ml
without H_2 at 20°C

Because this hydrogenation was performed without H_2 in this solvent, hydrogen source should be alcoholic solvent.

Figure 2 shows the effect of some additives at R=5.7. When water was added in this solvent system, the formation of *cis*-2-butene was greatly suppressed and approached to the result in water. Addition of ethylenediamine increased the formation of *cis*-2-butene.

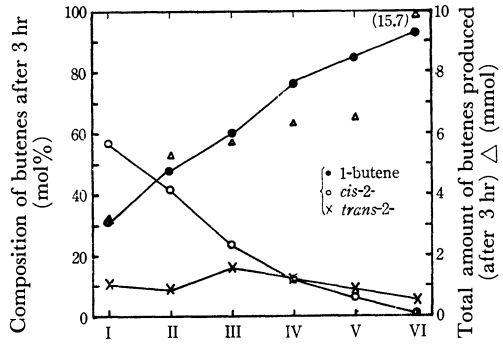

Fig. 2. Effect of additives.
$CoCl_2$=10 mmol
H_2 was absorbed for 2 hr before butadiene was added at 20°C.

I	Glycerin 35 ml+MeOH	10 ml+En	5 ml
II	Glycerin 35 ml+MeOH	15 ml	
III	Glycerin 35 ml+MeOH	10 ml+H_2O	5 ml
IV	Glycerin 35 ml+MeOH	5 ml+H_2O	10 ml
V	Glycerin 35 ml+MeOH	0 ml+H_2O	15 ml
VI	H_2O	50 ml	

(En=ethylenediamine)

It is noteworthy that *cis*-2-butene is very much producible at R>5.2 in glycerin-MeOH solvent. This result can not be explained by the π-allyl complex mechanism[1,2] acceptable in the case of water solvent. Detailed discussion of the mechanism of this reaction will be given in the forthcoming paper.

1) J. Kwiatek, K. L. Mador, and J. K. Seyler, *Adv. Chem. Ser.*, **37**, 201 (1963).
2) T. Suzuki and T. Kwan., *Nippon Kagaku Zasshi (J. Chem. Soc. Japan, Pure Chem. Sect.)*, **86**, 715 (1965).

Formation of α-Nitroso Carbonyl Compounds from Esters through β-Keto Sulfoxides

Yoshio OTSUJI, Hideo YABUNE and Eiji IMOTO

Department of Applied Chemistry, Faculty of Engineering, University of Osaka Prefecture, Sakai-shi, Osaka

(Received May, 31, 1968)

Aliphatic and aromatic carboxylic esters have been converted to β-keto sulfoxides by the reaction of the esters with methylsulfinyl carbanion.[1,2] Becker and Russell[3,4] have found that the treatment of dimethyl phthalate with methylsulfinyl carbanion and the acidification of the resulting mixture with hydrochloric acid give 2-chloro-2-methylmercapto-1,3-indanedione, which can then be readily converted to ninhydrin upon hydrolysis. This reaction has been supposed to proceed through 2-methylsulfinyl-1,3-indanedione as an intermediate.[3,4] We now wish to report a new reaction of esters, one which leads to α-nitroso carbonyl derivatives through β-keto sulfoxides.

A solution of methylsulfinyl carbanion in dimethyl sulfoxide (DMSO) was prepared by the method of Becker and Russell[2] from 2 g (0.05 g-atom) of potassium, 50 m*l* of *t*-butyl alcohol, and 40 m*l* of DMSO. To this mixture 3.8 g (0.025 mol) of ethyl benzoate in a stream of nitrogen were added at room temperature. The reaction mixture was agitated by a stream of nitrogen for 2 hr, and then most of the solvent was evaporated under reduced pressure. A solution of 5.2 g (0.075 mol) of sodium nitrite in 30 m*l* of water was added to the residue, and the mixture was extracted with 30 m*l* of ether. The aqueous layer was acidified with 40 m*l* of 6 N hydrochloric acid to give a yellow oil. The oil solidified on standing overnight. The recrystallization of the solid from chloroform gave 3.6 g (80%) of ω-chloro-ω-nitroso acetophenone (I), mp 132—133°C (lit.[5] 131—132°C).[6] The infrared spectrum (in KBr disk) showed that I exists predominantly in the form of hydroxamoyl chloride (Ia).

$$C_6H_5CO_2C_2H_5 + \bar{C}H_2SOCH_3 \rightarrow$$

$$C_6H_5\bar{C}OCHSOCH_3 \xrightarrow[2)\ HCl]{1)\ NaNO_2}$$

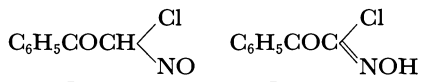

I Ia

In the second example, the similar treatment of dimethyl phthalate (II) afforded 2-nitroso-1,3-indanedione (III), mp 196—198°C, in a 37% yield. In this case methylsufinyl carbanion was prepared from DMSO and sodium methoxide[3,4]; the compound III thus obtained was identical in every respect with the authentic sample[7] prepared by the nitrosation of 1,3-indanedione.

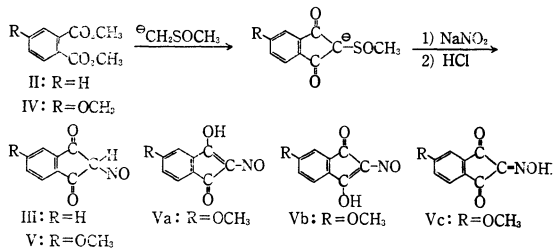

In the third example, when the reaction of dimethyl 4-methoxyphthalate (IV) with methylsulfinyl carbanion and sodium nitrite was carried out by a method similar to that described for ethyl benzoate, 5-methoxy-2-nitroso-1,3-indanedione (V), mp 204—206°C (decomp.), was obtained in a 66% yield. The infrared spectrum (in KBr disk) of V showed a hydroxyl absorption at 3500 cm^{-1} and carbonyl absorptions at 1730 and 1690 cm^{-1}. The hydroxyl absorption at 3500 cm^{-1} was sometimes missing, however; instead, a broad absorption appeared at 3150 cm^{-1}. The NMR spectrum (in DMSO-d_6) showed an acidic proton at τ 4.25 (1H, broad singlet), an aromatic proton at τ 2.02—2.15 (1H, broad doublet), two aromatic protons at τ 2.50—2.65 (2H, broad doublet), and a methoxy singlet at τ 6.00 (3H). These results suggest that V exists in an equilibrium among the Va, Vb, and Vc structures in polar solvents. In fact, V could be converted to the corresponding monoacetylated product, mp 185—189°C (decomp.), on acetylation with acetic anhydride in pyridine.

The scope and mechanism of these reactions are now being investigated and will be reported on in a subsequent paper.

1) E. J. Corey and M. Chaykovsky, *J. Am. Chem. Soc.*, **86**, 1639; *ibid.*, **87**, 1345 (1965).
2) H-D. Becker, G. J. Mikol and G. A. Russell, *ibid.*, **85**, 3410 (1963).
3) H-D. Becker and G. A. Russell, *J. Org. Chem.*, **28**, 1896 (1963).
4) H-D. Becker, *ibid.*, **29**, 1358 (1964).
5) H. Rheinbodt and O. S. Dumont, *Ann.*, **444**, 113 (1925).
6) Satisfactory elemental analyses were obtained for all compounds reported.
7) W. Wislicenus, *Ann.*, **246**, 347 (1888).

Fragmentation of *n*-Hexadecane by Electron Impact

Yoshio NIWA and Kozo HIROTA

Department of Chemistry, Faculty of Science, Osaka University, Toyonaka, Osaka

(Received June 8, 1968)

It has often been concluded[1] that the MO theory for mass spectra is completely inadequate to explain the mass spectra of normal paraffins obtained by electron impact, because it always predicts that bond-scission will occur at, or nearly at, the central bond of the C-C skeleton of higher paraffins; this is contrary to the ordinary mass spectra, where C_3 and C_4 fragments are the most abundant. In order to explain this discrepancy, secondary bond-scissions have been suggested by the present authors.[2,3] The purpose of this communication is to show that this suggestion is plausible.

Generally, fragmentation caused by electron impact is assumed to consist of two kinds of processes:[3] *i. e.*, the primary process, in which the superexcited species takes the main part, and the secondary process, in which the primary product undergoes slow further decomposition due to the localization of excess energy at a particular bond. The primary process is very fast and occurs before the localization of the excess energy, which becomes larger as the ionizing voltage and the temperature of the ionization chamber increase. Therefore, the fragmentation due to the primary process becomes independent of the ionizing conditions.

The MO-theory on mass spectra has to be applied to this primary process, and the statistical theory of Rosenstock *et al.*,[4] to the secondary processes, because the latter theory is applicable to those chemical processes which proceed *via* the activated complex.

Since the secondary processes are suppressed by a decrease in the ionizing voltage and in the temperature of the ionization chamber, one can confirm the above fragmentation scheme experimentally, if both effects on the bond-scission probability are investigated. Of course, the ionizing voltage may affect the secondary process much more than does the temperature. Therefore, the lower the ionizing voltage, the more evident becomes the effect of the temperature.

In order to confirm the above scheme, we investigated the mass spectra of *n*-hexadecane *n*-$C_{16}H_{34}$ in detail. The observed energy-dependence of its fragment distribution indicates that the abundant fragments shift to the C_9 and C_{10} fragments from the C_3 and C_4 fragments with a decrease in the electron energy. The fragment distribution at an ionizing voltage of 10 eV were measured at various temperatures of the ionization chamber. The C_8, C_9 and C_{10} fragments are the most abundant in the range from 100 to 200°C. With a rise in the temperature, the yields of these fragments decrease, while those of the lower fragments increase; C_5 and C_6 fragments come to be the most abundant at 285°C. The mass spectra, however, are practically independent of the temperature when the electron energy is above 15 eV.

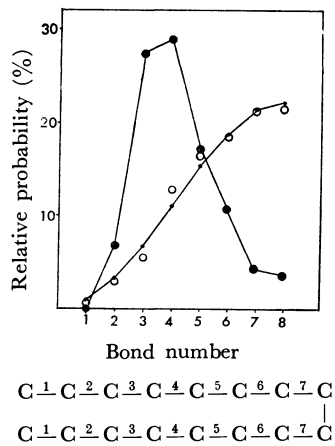

Fig. 1. Relative scission probability *vs.* number of skeletal bond.

—○— 10V, 90°C —•— Calculated
—●— 80V, 200°C

Some of the results are shown in Fig. 1, where the scission probability in % is plotted against the bond number, and where the calculated probability is obtained by the same procedure as was used in a previous study.[2] As expected, the observed values obtained at a low ionizing voltage (*ca.* 10 V) and at a low temperature of the ionization chamber (90°C) coincide well with the calculated values.

1) N. D. Coggeshall, *J. Chem. Phys.*, **30**, 595 (1959); Fairbairn, *Nature*, **186**, 152 (1960), *etc.*
2) K. Fueki and K. Hirota, *Nippon Kagaku Zasshi (J. Chem. Soc. Japan, Pure Chem. Sect.)*, **81**, 212 (1960).
3) K. Hirota and Y. Niwa, *J. Phys. Chem.*, **72**, 5 (1968).
4) H. M. Rosenstock, M. B. Wallenstein, A. L. Wahrhaftig and Henry Eyring, *Proc. Natl. Acad. Sci.*, **38**, 667 (1952).

BULLETIN OF THE CHEMICAL SOCIETY OF JAPAN VOL. 41 1747—1756 (1968)

Phase Transitions and Thermodynamic Properties of Rubidium and Cesium Cyanides*1

Masayasu SUGISAKI, Takasuke MATSUO, Hiroshi SUGA and Syûzô SEKI

Department of Chemistry, Faculty of Science, Osaka University, Toyonaka, Osaka

(Received December 21, 1967)

Heat-capacity measurements were performed for rubidium and cesium cyanide crystals between 15 and 300°K. It is found that each crystal has only one anomalous peak in its heat capacity curve, being located at 110.3°K and 193.1°K for rubidium and cesium cyanides, respectively. By the comparison of the present data with those for potassium and sodium cyanides, it was shown that these anomalous heat capacities can be interpreted in terms of the orientational ordering processes of cyanide ions in the crystals. It was suggested that there should exist the residual entropy due to the frozen-in state in their orientational configuration and they were estimated as $R \ln 4$ for rubidium cyanide and $R \ln 2$ for cesium cyanide.

In the two previous papers,[1,2] we have reported the results of our investigation on potassium and sodium cyanide crystals. In each salt we have found two kinds of phase transition which were interpreted as the orientational order-disorder phenomenon with respect to the distinction of carbon and nitrogen atoms in cyanide ion as well as to the random orientation of the carbon to nitrogen bonds. As a series of our study concerning the orientational motion of cyanide ion, we have studied the phase transition phenomenon of rubidium and cesium cyanides with paying special attention to the effect of the difference of their size of cation on the orientational motion of cyanide ion.

According to the X-ray analysis by Lely,[3] rubidium cyanide is of NaCl-type, while cesium cyanide is reported to have CsCl-type at room temperature. This is in contrast to the fact that both potassium and sodium salts have the same NaCl-type.

Thus, it seems interesting to study the effect of the difference of size of cation in rubidium salt and further of the difference in crystal structure for cesium cyanide on an appearance of phase transition.

We have measured heat capacity of these salts between 13 and 300°K and found only one anomalous peak of the heat capacity in each salt. This remarkable difference in the behavior of the temperature dependence of their heat capacities was attempted to interpret in connection with the thermal motion and ordering process of cyanide ion in the crystalline field.

Experimental

Samples. a) Rubidium Cyanide.[4] Commercial rubidium hydroxide (Nakarai Chemicals Co., Ltd.) was dissolved in the absolute ethyl alcohol and the insoluble substances supposed to be mainly of rubidium carbonate were removed by filtration. Liquid hydrogen cyanide was then poured slowly to the phase separated solution which consisted with liquid benzene over the ethanol solutions mentioned above. Rubidium cyanide crystal was first produced at the interfacial layer and then it was deposited to the bottom of the container with a solution of absolute methyl alcohol and absolute diethylether. After the product was filtrated, the sample was recrystallized twice from the solution of water and methyl alcohol. The final product thus obtained was dried *in vacuo* (about 10^{-3} mmHg) carefully for several hours at 120°C to remove the solvents completely.

b) Cesium Cyanide. The crystal was prepared by the same method as mentioned above. The cesium hydroxide used for preparation is the product of Nakarai Chemicals Co. Ltd.

By a spectroscopic analysis, all the impurity contents of carbonate ion were confirmed to be less than 0.1 mole percent, and the traces of metallic ions (Na^+, K^+, Si^{2+}, Mg^{2+}, and Ca^{2+}) were also found.

*1 Read before the 17th and the 18th Annual Meetings of the Chemical Society of Japan at Tokyo (1964) and at Osaka (1965).

1) H. Suga, T. Matsuo and S. Seki, This Bulletin, **38**, 1115 (1965).

2) T. Matsuo, H. Suga and S. Seki, *ibid.*, **41**, 583 (1968).

3) J. A. Lely, **1942**, *Dissertation*, Utrecht, pp. 84.

4) J. Meyer, *Z. anorg. Chem.*, **115**, 207 (1921).

Heat-Capacity Measurement. Measurements of heat capacities were made on the sample of 0.2899 mol of rubidium cyanide and 0.2357 mol of cesium cyanide, sealed in a gold calorimeter cell (18 K) with a small amount of helium gas. The low-temperature adiabatic type calorimeter, the details of which were described in the previous paper,[5] was used between 15°K and 300°K.

The reported values are based on a formula weight of 111.49 for rubidium cyanide and 158.92 for cesium cyanide, and also on the basic relations 0°C=273.15°K and 1 cal=4.1840 abs. joules. Temperature measurements were carried out with platinum resistance thermometer calibrated in terms of the International Temperature Scale between 90 and 500°K and the provisional scale of the National Bureau of Standards between 11 and 90°K.

Experimental Results

Heat Capacities. The heat capacities obtained from 15 to 300°K are listed in Table 1 for rubidium cyanide and in Table 2 for cesium cyanide. The heat-capacity curves are given in Figs. 1 and 2 for rubidium and cesium cyanides, each of which shows only one phase transition, respectively.

Thermodynamic Properties. Thermal data on phase transition are listed in Table 3, and the thermodynamic functions are given in Table 4 for rubidium cyanide and Table 5 for cesium cyanide. The values below 15°K are obtained by extrapolation on the assumption of the Debye T^3-law. As is shown in the previous paper,[5] the error in the values of the heat capacity is within $\pm 0.3\%$ above liquid nitrogen and $\pm 1\%$ in liquid hydrogen temperature regions, respectively.

TABLE 1. HEAT CAPACITIES OF RUBIDIUM CYANIDE

$T_{av.}$ °K	Approx. ΔT	$\Delta H/\Delta T$ cal/(mol degK)
	Series 1	
80.83	1.912	13.534
82.72	1.882	13.781
84.59	1.855	14.001
86.43	1.829	14.237
88.25	1.805	14.460
90.05	1.784	14.657
91.82	1.761	14.896
93.57	1.741	15.109
95.30	1.721	15.340
97.01	1.699	15.640
98.70	1.677	15.890
100.36	1.652	16.253
102.00	1.622	16.734
103.60	1.577	17.581
105.14	1.500	19.098
106.57	1.361	22.487
107.86	1.229	26.428
109.00	1.037	34.072
109.93	0.825	46.655
110.79	0.909	40.897
111.84	1.175	28.151
113.18	1.504	18.584
114.74	1.619	16.113
116.36	1.616	16.068
117.97	1.614	16.052
119.59	1.611	16.020
121.19	1.607	16.031
	Series 2	
22.09	2.510	3.059
24.41	2.098	3.630
26.66	2.364	4.204
28.89	2.077	4.765
31.05	2.215	5.321
33.31	2.284	5.873
35.50	2.090	6.405
37.61	2.109	6.882
39.81	2.280	7.307
42.03	2.143	7.718
44.11	2.029	8.120
46.25	2.257	8.485
48.45	2.151	8.853
50.55	2.058	9.222
52.75	2.338	9.598
55.04	2.248	9.974
57.25	1.085	10.340
59.39	2.101	10.686
61.46	2.042	11.031
	Series 3	
14.90	1.871	1.529
16.66	1.500	1.881
18.06	1.282	2.176
19.57	1.653	2.491
21.13	1.435	2.849
	Series 4	
62.10	2.213	11.154
64.26	2.100	11.459
66.34	2.050	11.732
68.36	2.006	11.985
70.35	1.965	12.243
72.30	1.929	12.471
74.21	1.895	12.708
76.09	1.862	12.950
78.03	1.833	13.153
79.75	1.804	13.398
	Series 5	
120.84	1.750	16.107
122.58	1.744	16.073
124.33	1.748	16.064
126.07	1.738	16.082
127.81	1.735	16.085
129.54	1.731	16.072
131.27	1.727	16.075

5) H. Suga and S. Seki, This Bulletin, **38**, 1000 (1965).

(Table 1 continued)

$T_{av.}$ °K	Approx. ΔT	$\Delta H/\Delta T$ cal/(mol degK)
133.00	1.722	16.082
134.72	1.719	16.075
136.54	1.929	16.066
138.49	1.926	16.058
140.39	1.921	16.081
142.31	1.917	16.070
144.23	1.925	16.083
146.15	1.910	16.092
148.08	1.907	16.088
149.96	1.904	16.078
151.86	1.904	16.042
157.73	1.901	16.054
	Series 6	
155.64	1.928	16.113
157.56	1.933	16.067
159.48	1.918	16.124
161.40	1.916	16.112
163.31	1.911	16.122
165.22	1.909	16.116
167.13	1.906	16.111
169.04	1.905	16.094
170.94	1.903	16.082
172.83	1.901	16.079
174.74	1.898	16.099
176.64	1.897	16.090
178.55	1.930	16.093
180.48	1.928	16.087
182.41	1.926	16.098
184.33	1.926	16.084
186.26	1.924	16.076
188.18	1.921	16.104
190.10	1.922	16.068
192.03	1.921	16.062
193.92	2.175	16.122
196.08	2.278	16.050
198.35	2.276	16.035
200.62	2.271	16.060
202.89	2.266	16.093
205.16	2.264	16.089
207.42	2.263	16.056
209.68	2.259	16.079
211.94	2.257	16.077
214.19	2.254	16.084
216.44	2.252	16.087
218.69	2.250	16.079
220.94	2.249	16.062
223.18	2.247	16.058
225.42	2.245	16.047
227.66	2.243	16.059
229.89	2.237	16.110
232.12	2.233	16.127
234.35	2.231	16.107
236.57	2.228	16.124
	Series 7	
238.44	2.223	16.048
240.65	2.217	16.115
242.86	2.212	16.144
245.07	2.209	16.150
247.27	2.205	16.174
249.47	2.206	16.117
251.67	2.204	16.124
253.87	2.202	16.115
256.07	2.200	16.111
258.27	2.197	16.132
260.46	2.195	16.132
262.65	2.192	16.146
264.84	2.190	16.151
267.04	2.186	16.152
269.21	2.184	16.156
271.40	2.178	16.215
237.57	2.177	16.191
275.75	2.178	16.146
	Series 8	
277.61	2.623	16.146
280.22	2.617	16.180
282.83	2.613	16.193
285.44	2.610	16.189
288.04	2.605	16.210
290.64	2.600	16.226
293.24	2.598	16.206
295.82	2.592	16.252
298.41	2.589	16.243
300.98	2.581	16.298
303.55	2.581	16.253

TABLE 2. HEAT CAPACITIES OF CESIUM CYANIDE

$T_{av.}$ °K	Approx. ΔT	$\Delta H/\Delta T$ cal/(mol degK)
	Series 1	
15.16	2.0484	1.473
17.09	1.7586	1.928
18.73	1.4853	2.235
20.42	1.8802	2.650
22.18	1.6196	3.062
	Series 2	
14.20	2.0124	1.213
16.23	1.9808	1.699
18.02	1.5974	2.103
19.50	1.3684	2.434
21.07	1.7785	2.792
22.73	1.5521	3.177
24.19	1.3927	3.525
26.90	1.9134	4.095
28.72	1.7335	4.497
30.50	1.8392	4.926
32.24	1.6986	5.306
33.85	1.5915	5.637
35.37	1.4969	5.977
36.81	1.4165	6.313
38.29	1.5535	6.572
39.80	1.4837	6.834

(Table 2 continued)

$T_{av.}$ °K	Approx. ΔT	$\Delta H/\Delta T$ cal/(mol degK)
41.24	1.4179	7.131
42.61	1.3530	7.520
43.92	1.3060	7.785
45.25	1.3808	8.022
46.60	1.3391	8.253
48.10	1.7014	8.493
49.76	1.6447	8.769
51.37	1.5939	9.044
53.06	1.8182	9.323
54.85	1.7711	9.526
56.58	1.7234	9.781
58.26	1.6789	10.040
59.91	1.6406	10.259
	Series 3	
60.02	1.8373	10.263
61.84	1.7944	10.493
63.61	1.7534	10.744
65.35	1.7164	10.991
67.15	1.8954	11.198
69.03	1.8612	11.394
70.87	1.8279	11.597
72.76	1.9691	11.758
74.71	1.9392	11.919
76.63	1.9045	12.152
78.51	1.8751	12.345
80.38	1.9606	12.467
82.33	1.9297	12.665
84.24	1.9027	12.840
86.13	1.8770	13.024
87.99	1.8543	13.196
89.83	1.8369	13.307
91.66	1.8175	13.458
93.47	1.8007	13.590
95.26	1.7857	13.703
97.11	1.9280	13.827
99.03	1.9120	13.959
100.90	1.8982	14.053
102.81	1.8849	14.144
104.68	1.8693	14.275
106.44	1.8556	14.370
108.38	1.8456	14.432
110.21	1.8325	14.548
112.03	1.8202	14.666
113.83	1.8060	14.818
115.62	1.7947	14.928
	Series 4	
115.71	1.7931	14.911
117.70	2.1834	15.048
119.87	2.1658	15.198
122.03	2.1514	15.319
124.17	2.1351	15.469
126.30	2.1185	15.626
128.41	2.1038	15.762
130.61	2.2949	15.844
132.89	2.2760	16.020
135.16	2.2588	16.181
137.41	2.2426	16.335
139.64	2.2282	16.475
141.86	2.2161	16.581
144.06	2.1981	16.765
146.25	2.1811	16.949
148.42	2.1691	17.066
150.58	2.1552	17.215
152.72	2.1398	17.392
154.84	2.1209	17.623
156.95	2.1050	17.821
	Series 5	
159.10	2.2396	18.007
161.33	2.2207	18.237
163.54	2.1997	18.503
165.73	2.1786	18.765
167.89	2.1591	19.044
170.04	2.1363	19.359
172.16	2.1120	19.711
174.26	2.0851	20.122
176.23	2.0590	20.522
178.37	2.0296	20.997
180.39	1.9961	21.564
182.37	1.9640	22.142
184.30	1.9224	22.892
186.19	1.8681	23.952
188.03	1.8066	25.237
189.79	1.7035	27.626
191.28	1.2847	38.347
192.18	0.5290	121.366
192.57	0.2516	271.700
192.78	0.1924	359.788
193.39	1.0437	54.074
195.08	2.3388	16.045
197.32	2.3397	16.038
199.76	2.3391	15.869
202.10	2.3401	15.924
204.44	2.3421	15.773
206.78	2.3397	15.881
209.12	2.3408	15.833
211.46	2.3403	15.808
213.80	2.3401	15.784
216.43	2.3414	15.799
218.78	2.3472	15.761
	Series 6	
216.10	2.3484	15.719
218.44	2.3429	15.728
220.78	2.3382	15.737
223.12	2.3356	15.729
225.45	2.3339	15.720
227.79	2.3319	15.732
230.11	2.3297	15.713
232.44	2.3265	15.726
234.77	2.3231	15.744
237.09	2.3219	15.732
239.41	2.3200	15.727
241.73	2.3207	15.687
244.05	2.3195	15.672
246.36	2.3167	15.678
248.67	2.3129	15.716
	Series 7	
251.01	2.4101	15.698
253.42	2.4072	15.706
255.82	2.4036	15.718

(Table 2 continued)

$T_{av.}$ °K	Approx. ΔT	$\Delta H/\Delta T$ cal/(mol degK)
258.23	2.4019	15.713
260.63	2.3985	15.763
263.02	2.3965	15.714
265.42	2.3911	15.754
267.81	2.3875	15.769
270.21	2.3894	15.710
	Series 8	
261.92	2.3830	15.676
264.30	2.3813	15.666
266.68	2.3780	15.681
269.06	2.3747	15.691
271.43	2.3736	15.681
273.80	2.3715	15.674
276.17	2.3674	15.700
278.54	2.3639	15.723
280.22	2.3625	15.673
282.12	2.3604	15.703
	Series 9	
285.52	2.3508	15.704
287.82	2.3503	15.682
290.22	2.3468	15.697
292.57	2.3443	15.700
294.91	2.3415	15.709
298.42	2.3367	15.725
300.75	2.3321	15.754
303.08	2.3799	15.771

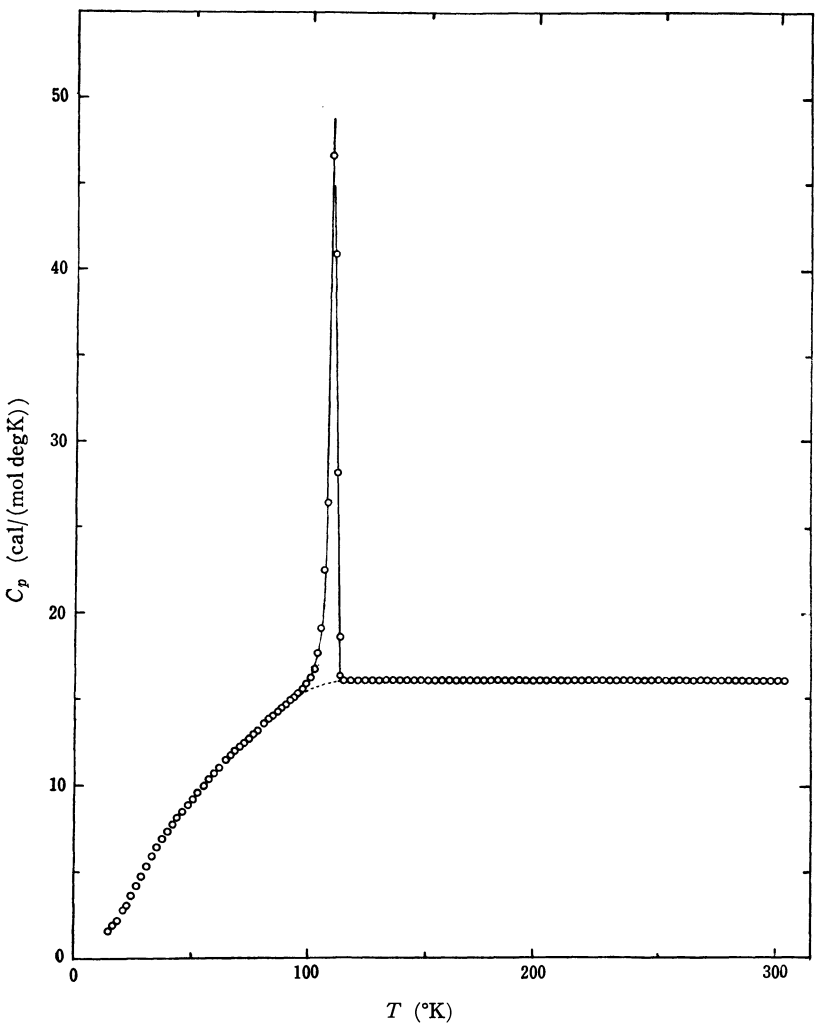

Fig. 1. Heat capacity curve of rubidium cyanide.

TABLE 3. THERMODYNAMIC PROPERTIES OF PHASE TRANSITIONS FOR RUBIDIUM AND CESIUM CYANIDES

	RbCN	CsCN
Transition temperature (degK)	110.3±0.1	193.1±0.1
Entropy change (cal/(mol degK))	1.38±0.04	2.60±0.05
Enthalpy change (cal/mol)	177±4	461±10

TABLE 4. THERMODYNAMIC PROPERTIES OF RUBIDIUM CYANIDE IN cal/(mol degK)

T (°K)	C_p°	S°	$(H^\circ-H_0^\circ)/T$	$-(G^\circ-H_0^\circ)/T$
10	(0.714)	(0.386)	(0.240)	(0.146)
15	1.555	0.830	0.533	0.297
20	2.595	1.421	0.916	0.505
30	5.048	2.926	1.875	1.051
40	7.362	4.709	2.968	1.741
50	9.108	6.542	4.030	2.512
60	10.807	8.354	5.013	3.341
70	12.200	10.130	5.946	4.184
80	13.408	11.838	6.803	5.035
90	14.655	13.492	7.608	5.884
100	16.166	15.106	8.380	6.726
110.3	Transition temperature			
120	16.100	19.079	10.613	8.466
130	16.080	20.364	11.034	9.330
140	16.080	21.555	11.394	10.161
150	16.080	22.665	11.707	10.958
160	16.080	23.702	11.980	11.722
170	16.080	24.677	12.221	12.456
180	16.080	25.597	12.435	13.162
190	16.080	26.467	12.627	13.840
200	16.080	27.292	12.800	14.492
210	16.080	28.076	12.956	15.120

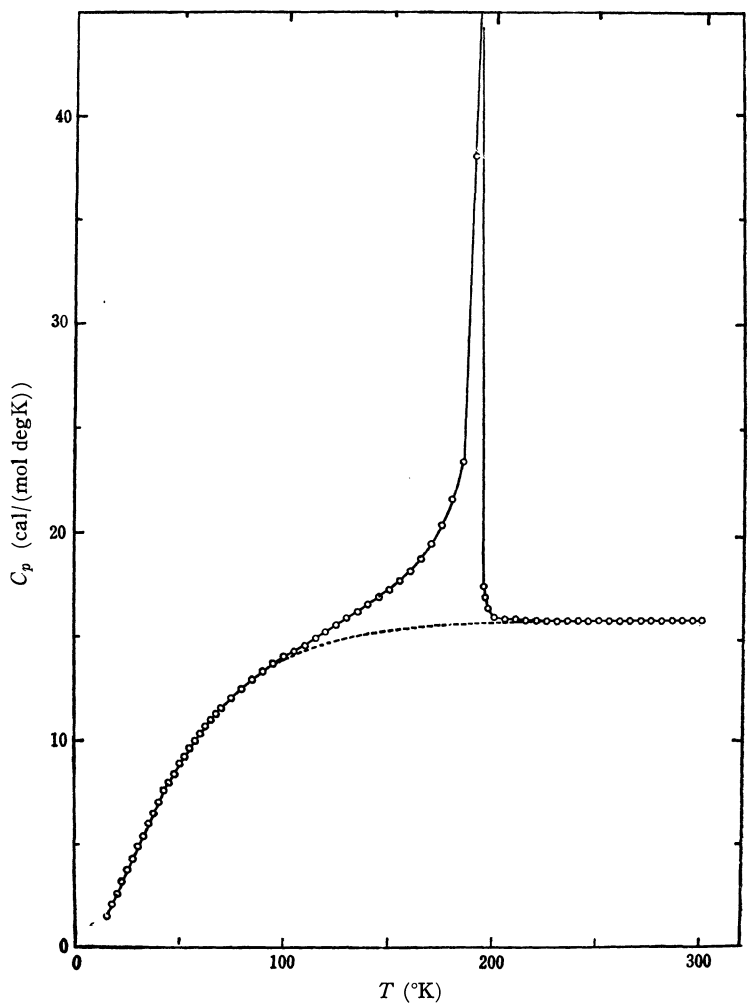

Fig. 2. Heat capacity curve of cesium cyanide.

(Table 4 continued)

T(°K)	C_p°	S°	$(H^\circ-H_0^\circ)/T$	$-(G^\circ-H_0^\circ)/T$	T(°K)	C_p°	S°	$(H^\circ-H_0^\circ)/T$	$-(G^\circ-H_0^\circ)/T$
220	16.080	28.824	13.098	15.726	270	16.160	32.127	13.659	18.468
230	16.100	29.540	13.228	16.312	280	16.180	32.715	13.749	18.966
240	16.130	30.226	13.348	16.878	290	16.200	33.284	13.834	19.450
250	16.130	30.885	13.460	17.425	298.15	16.200	33.673	13.949	19.724
260	16.150	31.517	13.563	17.945					

TABLE 5. THERMODYNAMIC PROPERTIES OF CESIUM CYANIDE IN cal/(mol degK)

T(°K)	C_p°	S°	$(H^\circ-H_0^\circ)/T$	$-(G^\circ-H_0^\circ)/T$	T(°K)	C_p°	S°	$(H^\circ-H_0^\circ)/T$	$-(G^\circ-H_0^\circ)/T$
10	(0.456)	(0.161)	(0.113)	(0.048)	150	17.231	20.219	10.390	9.829
15	1.425	0.509	0.373	0.136	160	18.121	21.358	10.844	10.514
20	2.554	1.074	0.772	0.302	170	19.371	22.036	11.306	10.730
30	4.812	2.538	1.742	0.796	180	21.452	23.650	11.805	11.845
40	6.954	4.220	2.782	1.438	193.1	Transition temperature			
50	8.803	5.976	3.808	2.168	200	15.940	27.117	13.925	13.192
60	10.280	7.716	4.768	2.948	210	15.822	27.893	14.019	13.874
70	11.501	9.398	5.646	3.752	220	15.743	28.627	14.099	14.528
80	12.467	10.998	6.440	4.558	230	15.728	29.326	14.170	15.156
90	13.338	12.518	7.160	5.358	240	15.715	30.636	14.294	16.342
100	14.010	13.960	7.813	6.147	260	15.713	31.253	14.348	16.905
110	14.563	15.321	8.401	6.920	270	15.712	31.846	14.399	17.447
120	15.210	16.616	8.941	7.675	280	15.710	32.417	14.446	17.971
130	15.852	17.858	9.448	8.410	290	15.704	32.968	14.489	18.479
140	16.496	19.056	9.928	9.128	298.15	15.701	33.404	14.523	18.881

Discussion

Behavior of Thermal Motion of Cyanide-groups. In order to investigate the mode of motion of the cyanide-group in these cyanide crystals, the torsional heat capacity was sorted out from the total heat capacity by following the same procedure taken in the previous papers.[1,2] By assuming the simple harmonic oscillation model for each cyanide group and also by making a flat portion in the Debye-temperature curve with suitable estimation of their oscillator frequencies, we have obtained the wave numbers of 185 cm^{-1} and 160 cm^{-1} for rubidium and cesium salts, respectively. Further, we have estimated the contributions of torsional motion of the cyanide-groups to the heat capacities which are given in Fig. 3. The potential barrier heights for the torsional motion at higher temperature, *i.e.* for the hindered rotational motion derived from these curves based on the Pitzer-Gwinn method[6] are 8.0 and 7.4 kcal/mol for the low temperature phases of rubidium and cesium cyanides, respectively. Finally this motion approaches the state of the free rotation where the heat capacity amounts to 2 cal/mol degK per two degrees of freedom. The fact that the heat capacity at room temperature is about 3 cal/mol degK in the range of relevant temperature

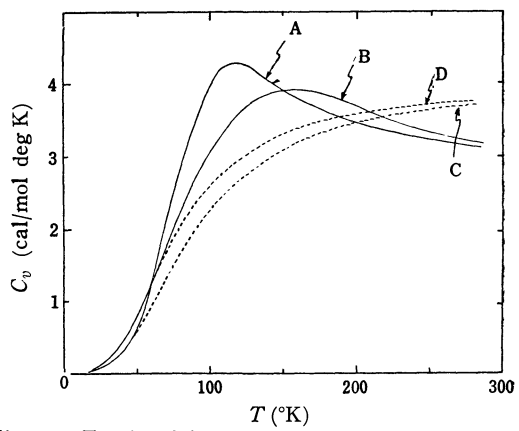

Fig. 3. Torsional heat capacity curves of cyanide-groups.
A: rubidium cyanide.
B: cesium cyanide.
C: assumed harmonic oscillator with its wave number $\omega=185\ cm^{-1}$.
D: assumed harmonic oscillator with its wave number $\omega=160\ cm^{-1}$.

shows that the rotation of the cyanide-group is still hindered considerably. The potential barrier heights of this hindered rotational motion are 1.7 and 1.1 kcal/mol for rubidium and cesium cyanides, respectively. It may be noted here that the potential barriers hindering the rotation of the cyanide-group estimated above are comparable with those for sodium and potassium cyanides.

6) K.S. Pitzer and W.D. Gwinn, *J. Chem. Phys.*, **10**, 428 (1942).

Possible Existence of the Residual Entropy. *a) Rubidium Cyanide.* In this compound we can observe only one peak of anomalous heat capacity at about 110°K. The value of entropy associated with amounts to be 1.38 e.u. which is corresponding to $R \ln 2$. This circumstance is markedly different from those of sodium and potassium cyanides in which two anomalous heat capacities are observed. They have been interpreted in terms of the stepwise cooperative phenomena concerning the reorientational motion of the cyanide-group in the crystalline phase. The cubic symmetry of the rubidium cyanide crystal at room temperature suggests that all cyanide-groups may orientate themselves equally at random in the directions of four body-diagonals of its unit cell as in the case of the highest temperature phases of sodium and patassium cyanides. In this case, the configurational entropy with respect to the possible orientations of the cyanide-groups comes out to be $R \ln 8$ if we can distinguish the individuality of carbon and nitrogen atoms. The amount of observed entropy change of $R \ln 2$ at the transition point leads us to expect that the configurational entropy in the low-temperature phase might be $R \ln (8/2) = R \ln 4$. As one of the explanation of such a value of entropy change as $R \ln 2$, we may refer to Parry's model[7] for the low temperature phase of rubidium cyanide. Based on the detailed X-ray analysis of the metastable monoclinic phase of potassium cyanide, he proposed that the crystal structure of the low temperature phase of rubidium cyanide is closely similar to the disordered structure of the metastable monoclinic phase of potassium cyanide. In this metastable phase, all cyanide-groups are at rest with their principal axis approximately parallel to the one direction of body-diagonals of the original cubic phase, the potassium ions being displaced alternately vertical to (110) plane by about 1/4 Å, as is shown in Fig. 4.

If the two kinds of y-parameter of the potassium ions are assumed te be zero and the new axis is taken as,

$$a = 1/2[a]_i, \quad c = 1/2[102]_i,$$

here, $[a]_i$ and $[102]_i$ represent the a-axis and direction of [102] of the original monoclinic cell, respectively. Then, the dimension of new unit cell becomes as follows;

$$a = 4.45, \quad b = 4.53, \quad c = 6.36 \text{ Å}, \quad \beta = 94.6°.$$

Comparing these dimensions with those of rubidium cyanide, the differences in the axial lenghts a, b and c of the two unit cells are found to be 0.28, 0.35 and 0.31 Å, respectively. Taking into account of the difference in ionic radii between the potassium and the rubidium ions, it gets clear that this unit cell seems to correspond to the unit cell of the low temperature phase of rubidium cyanide, its dimensions being $a = 4.78$, $b = 4.88$, $c = 6.67$ Å and $\beta = 94.5°$.

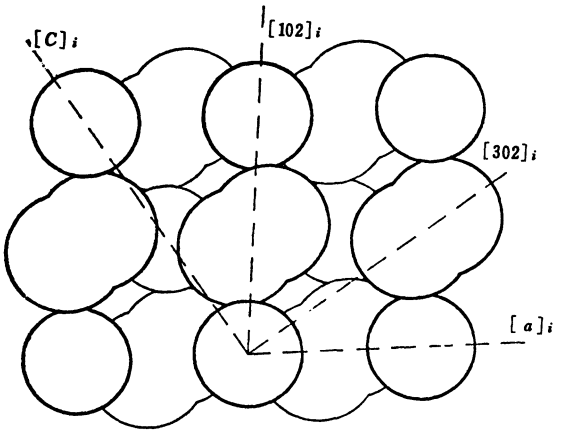

[G. S. Parry, *Acta Cryst.*, **15**, 601 (1962)]

Fig. 4. Proposed structure for the monoclinic low-temperature form of potassium cyanide projected on to $[010]_i$ which corresponds to [110] of the original cubic cell. The displacement $y(K^+)$ is perpendicular to the plane of this figure and has been established experimentally to be of the order of 1/4 Å. The orientation of the cyanide-group has not yet been experimentally confirmed, but is based on a self-consistent interpretation of the cell dimensions.[7]

Therefore it may not be so unreasonable to suppose that the cyanide ions are in the disordered state with two kinds of their orientation. If the carbon and the nitrogen atoms of the cyanide-groups are distinguished in this phase, the entropy change of $R \ln 2$ may be explained on this model.

Furthermore, the behavior of the rest of configurational entropy in low temperature region below 13°K will be an interesting problem. In our present measurement of the heat capacity from 13 to 320°K, no further anomalous heat capacity in addition to the anomaly at 110°K was observed. This implies that the degree of orientational freedom of the cyanide-group in low temperature phase will freeze and this frozen-in state will persist down to the lowest temperatures. Comparing the potential barrier (8 kcal/mol) hindering the rotation of the cyanide ions with the thermal excitation energy, it seems reasonable to suppose that there may persist the residual entropy of $R \ln 4$ at the absolute zero.

7) G. S. Parry, *Acta Cryst.*, **15**, 596, 601 (1962).

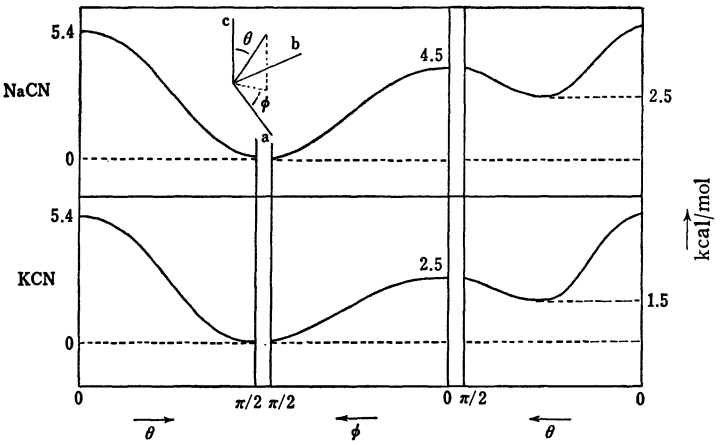

Fig. 5. The potential curves hindering the reorientation of cyanide groups of low temperature forms of potassium and sodium cyanide crystals.[8]

b) Cesium Cyanide. The entropy change of the phase transition of cesium cyanide at 193°K amounts to 2.6 e.u., nearly equal to $R \ln 4$, which is equivalent to those of the upper phase transitions of sodium and potassium cyanides at 288.1 and 168.3°K, respectively.

It is also shown that behavior of temperature dependence of torsional heat capacity of cesium cyanide is quite similar to those of both sodium and potassium salt, *i.e.*, in each case there appears hump of heat capacity near the phase transition. Thus, it is concluded that cyanide-groups are at rest along the three fold axis of the unit cell below the transition point, whereas they are in hindered rotational state above the transition point. This conclusion is consistent with the crystal structure determined by X-ray analysis.

The fact that the lower phase transitions of sodium and potassium cyanides are reasonably interpreted in terms of order-disorder phase transition with respect to the distinction of carbon and nitrogen atoms of cyanide-groups suggests that there is also the possibility of appearance of another phase transition of this kind for cesium cyanide. As a matter of fact, however, we can not find any further anomalous effect in its heat-capacity curve.

Consequently, the situation of cyanide-group in the low-teperature form of cesium cyanide crystal is such that the cyanide-groups are at rest along the three fold axis with no distinction of their heads and tails. This implies that a temperature region exists where the cyanide-groups are frozen in its fixed orientation and can no longer reorientate themselves.

The Appearance of the "Frozen-in" State and the Potential Barrier Hindering the Reorientation of Cyanide-groups. It is not definitely clear as to the reason why the cyanide-groups of rubidium and cesium cyanides behave differently from those of sodium and potassium cyanides in spite of the fact that they have nearly equal amount of potential barriers. It must be mentioned, however, that the potential barrier-height obtained from the analysis of the calorimetric data is such an averaged one over all possible directions, and it seems possible that a symmetry difference of the unit cell of potassium and sodium salts from the others may give rise to a somewhat lower barrier-height favourable to reorientation of cyanide-group in particular direction.

According to Nagamiya and Matsubara's calculation[8] for the case of the low temperature modification of sodium and potassium cyanides, the potential curve hindering the reorientation of cyanide-group has an anisotropy, *i.e.*, the potential barrier-height in the direction of c-axis is larger than that in the direction of a-axis. In the case of sodium cyanide this anisotropy is not so large, but in the case of potassium cyanide the anisotropy is so much larger that barrier-height along c-axis is larger by twice than that along a-axis (see Fig. 5). Moreover, it is characteristic to sodium or potassium cyanides that there exists a saddle point in the respective potential curves. Therefore, this saddle point provides a high transition probability concerning the reorientational motion of cyanide-group. Following the method used by Naga-

8) T. Matsuhara and T. Nagamiya, *Scientific Papers from the Osaka University*, **No. 14**, 17 (1949).

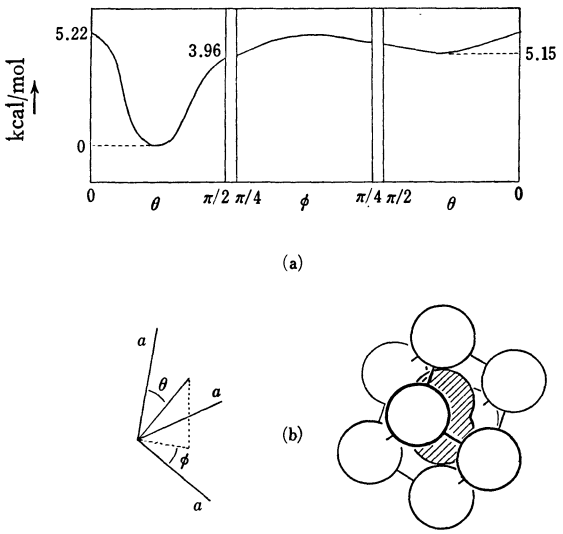

Fig. 6. (a) The potential curve hindering the reorientation of cyanide group of the low temperature form of cesium cyanide crystal.
(b) The unit cell of low temperature form of cesium cyanide crystal. This crystal structure is of a deformed *CsCl*-type. Hollow circles represent cesium ions, and a shaded deformed circle stands for cyanide group.

miya and Matsubara we have calculated the potential curve hindering the reorientation of cyanide-group of cesium cyanide. In this case the interaction due to a quadrupole effect will be neglected for approximate estimation of an anisotropy of the potential curve. The results obtained is given in Table 6. In the table W_{--} stands for the repulsive potential due to interaction between cyanide-groups, W_{+-} the repulsive potential for the interaction between cesium and cyanide-groups.

The potential form obtained is depicted in Fig. 6. As is seen there is no distinct anisotropy and the possibility of saddle point with appreciable low value is not expected.

TABLE 6. THE REPULSIVE LARTS OF THE HINDERING POTENTIAL FOR THE ROW-TEMPERATURE FORM OF CESIUM CYANIDE CRYSTAL (in kcal/mol)

(θ, ϕ)	W_{--}	W_{+-}	$W = W_{--} + W_{+-}$
$\pi/4$ $\pi/4$	1.47	7.43	8.90
0 0	5.04	8.91	13.95
$3\pi/4$ $\pi/4$	2.39	11.74	14.12
$\pi/4$ 0	1.79	11.07	12.86
$3\pi/4$ $3\pi/4$	2.82	11.56	14.39
0 $3\pi/4$	2.46	11.59	14.05

Accordingly it may be said that the realization of orientational frozen-in state of rubidium and cesium cyanides is closely related with the nonexistence of the appreciable anisotropy or a saddle point in their potential curves.

Finally, based on the same viewpoint we should like to infer the occurrence of a metastable phase of potassium cyanide. The saddle point of potassium cyanide is lower than that of sodium cyanide, so that the state probability on the saddle point, which corresponds to the [111] direction of the high temperature form, is larger for potassium cyande. In that case all cyanide-groups are frozen in the [111] direction of the original cubic form, and this structure is really corresponding to the monoclinic metastable phase. The corresponding one of sodium cyanide has not been found. This fact is certainly connected with the difference of the height of the saddle point in these two salts.

The authors should like to express their sincere thanks to Mr. Nobukatsu Fujino of Sumitomo Metal Industries, Ltd. for the spectroscopic analysis of metal ions in the specimens. They also wish to express their sincere thanks to the Toyo Rayon Co., Ltd. who defrayed a part of the financial support for the present investigation.

BULLETIN OF THE CHEMICAL SOCIETY OF JAPAN VOL. 41 1757—1760 (1968)

A Relation between Ion-exchange Selectivity Coefficient and Degree of Distribution for Model Compounds in Solvent Extraction

Tadao KENJO

Graduate School of Science and Engineering, Tokyo Institute of Technology, Ookayama, Meguro-ku, Tokyo

and Takuji ITO

Department of Chemistry, Tokyo Institute of Technology, Ookayama, Meguro-ku, Tokyo

(Received December 25, 1967)

An analogy of solvent extraction to ion-exchange was taken to explain anion affinities to anion-exchangers. Distributions of the model compound whose cation was the ionogenic group of an anion-exchanger and whose anion the counter ion, between water and an organic solvent, were investigated. The degree of distribution of the model compound for a solvent layer was expected to increase with increasing anion affinities to the corresponding anion-exchanger. Cobalticinium, benziltrimetylammonium and benzildimethylamine salts were employed as model compounds for the polymeric olygomethylene cobalticinium anion-exchanger, the strong base anion-exchange resin and the weak base anion-exchange resin, respectively. The distribution sequences in solvent extraction were essentially identical with the ion affinity series in anion-exchange. From these correlations, the selectivity coefficient for an anion was explained as the affinity of an anion to an ionogenic group with the use of an ion-pair concept. Some differences between ion-exchanges and solvent extractions were discussed.

In recent years, many attempts have been made to predict selectivity coefficients for ion-exchange systems. It has been thought that the activity coefficient in an ion-exchanger phase and the strain energy of the molecular network in an ion-exchange copolymer most seriously influence selectivities. The former was found to be dominant for ion-exchange resins[1,2] and the latter cannot be attributed to osmotic pressure but to the diffusion of network molecules because ion-exchangers are not bound by semipermeable membranes from the external solution. The strain energy effect seems to be difficult to estimate. This paper pays attention to the activity coefficient only.

The relation between the selectivity coefficient and the activity coefficient, or the evaluation of the latter from the former, has been studied by many workers.[3-6] However, the difference in activity coefficients for different anions has not been explained as affinities of adsorbed ion to ionogenic groups. According to thermodynamic considerations, a lower activity coefficient, or a higher selectivity coefficient, is interpreted as the higher sorbability to ion-exchangers. If the affinity of an anion to the same monomeric cation as the ionogenic group is similar to that in the corresponding exchanger, the salt whose cation is the ionogenic group and whose anion the counter ion may be suitable as a model compound for the ion-exchanger. The affinity should increase in organic solvents of low dielectric constant. From this point of view, cobalticinium (π-dicyclopentadienyl cobalt(III)), benziltrimethylammonium and benzildimethylamine salts were selected as model compounds for the polymeric pentamethylene cobalticinium anion-exchanger, the strong base anion-exchange resin and the weak base anion-exchange resin, respectively. Some interrelations between them were found.

1) G. E. Myers and G. E. Boyd, *J. Phys. Chem.*, **60**, 521 (1956).
2) G. E. Boyd, S. Lindenbaum and G. E. Myers, *ibid.*, **65**, 557 (1961).
3) F. Helfferich, "Ion-exchange," McGraw-Hill Book Co., Inc., New York, N. Y. (1962).
4) H. P. Gregor, *J. Am. Chem. Soc.*, **70**, 1293 (1948); **73**, 642 (1951).
5) H. P. Gregor, J. Belle and R. A. Marcus, *ibid.*, **77**, 2713 (1955).
6) J. A. Marinsky, *J. Phys. Chem.*, **71**, 1572 (1967).

Experimental

Preparation of Cobalticinium, Benziltrimethylammonium and Benzildimethylamine Salt Solutions. Cobalticinium picrate ($(C_5H_5)_2CoOC_6H_2(NO_2)_3$) was obtained by the method mentioned in a previous paper.[7] The desired form of the cobalticinium

salt was obtained by passing the picrate solution through Dowex 1 X-8 columns. The concentration of the resulting solution was 0.0444 M. The benzyltrimethylammonium salt ($C_6H_5CH_2N^+(CH_3)_3X^-$) was obtained commercially. It was converted to the perchlorate by adding 2 M sodium perchlorate solution, and the perchlorate was purified by recrystallization. The perchlorate solution was converted to the desired salt forms by the same procedure as for the cobalticinium salt. The concentration of the resulting solution was 0.0500 M. Benzildimethylamine ($C_6H_5CH_2N^+H(CH_2)_2X^-$) was obtained commercially. The procedure for preparing the solution was similar to that used for the benzyltrimethylammonium salt solution. The concentration of the solution was 0.0500 M.

The Solvent Extraction of Various Ions and Their Determination in the Organic Solvent Layer. *n*-Butanol, *n*-pentanol, *n*-hexanol, chloroform and benzene were used as organic solvents (obtained commercially). An aqueous solution of the salt (10 m*l*) and 10 m*l* of the solvent were shaken together for 10 min at room temperature. The solvent layer was separated and the concentration of salts determined colorimetrically using 1 cm quartz cells and a spectrophotometer (Hitachi EPU-2 A). The wavelength employed was 340 mμ for cobalticinium and 262 mμ for both benzyltrimethylammonium and benzildimethylamine. Calibrations were made by dissolving a known amount of perchlorate or picrate in a known amount of each solvent saturated with water.

Adsorption spectra in the UV region were measured on a Shimadzu multipurpose recording spectrophotometer.

Calculation of the Degree of Distribution. The degree of distribution of an anion A^- (K_A) was calculated according to the equation

$$K_A = \frac{[R^+]_w[A^-]_w}{[RA]_r},$$

where $[RA]_r$, $[R^+]_w$ and $[A^-]_w$ are the concentrations of RA in the solvent layer and cation R^+ and anion A^- in the aqueous layer, respectively. $[R^+]_w$ was always equal to $[A^-]_w$ in this experiment.

Results and Discussion

According to Bjerrum's theory,[8] the probability of an ion-pair formation increases with increasing concentration. Accordingly, ion-pair formation in ion-exchangers might be quite possible since the density of counter-ion arround an ionogenic group is very high. Further, many thermodynamic data for univalent cation exchanges[9-12] show that enthalpies decrease when entropies decrease in systems of decreasing free energy. This fact appears to support the assumption of ion-pair formation. One of the most typical theories of an ion-exchange equilibrium introducing the ion-pair concept has been proposed by Gregor.[5] He introduced a dissociation constant for ion-pair formation between an ionogenic group and a counter ion in an exchanger phase. For the processes of ion-pair formation,

$$RA \rightleftharpoons R^+ + A^- \quad \text{and} \quad RB \rightleftharpoons R^+ + B^-$$

dissociation constants D_A and D_B are given by

$$D_A = \frac{[R^+][A^-]}{[RA]}, \quad D_B = \frac{[R^+][B^-]}{[RB]},$$

where R's refer to ionogenic groups, A^- and B^- to exchange anions and brackets to the molality of each species. Neglecting strain energy effects, the molality of unpaired ions in the exchanger phase is related to that of these ions in the external solution according to the Donnan equilibrium condition and one obtains the equation

$$\frac{[A^-]_r}{[B^-]_r} = \frac{[A^-]_w}{[B^-]_w}$$

Then, selectivity coefficients K_A^B are given by

$$K_A^B = \frac{[B]_r}{[A]_r}\cdot\frac{[A^-]_w}{[B^-]_w} = \frac{[B^-]_r+[RB]}{[A^-]_r+[RA]}\cdot\frac{[A^-]_w}{[B^-]_w},$$

where A or B refers to the total amount of the species in the exchanger phase, subscript r and w to the exchanger and external solution phase, respectively. Additional conditions are

$$[R^+] = [A^-]_r + [B^-]_r$$
$$[RA] + [RB] + [R^+] = 1$$
$$[A^-]_w + [B^-]_w = 1$$

Then K_A^B is obtained as a function of $[A]_r$ or $[B]_r$ by a combination of the following equations:

$$K_A^B = \frac{D_A[A^-]_w + (D_B - D_A)x[A^-]_w}{D_B[A^-]_w - (D_B - D_A)x[B^-]_w}$$

and

$$\frac{[B]_r}{[A]_r} = \frac{D_A[B^-]_w + (D_B - D_A)x[B^-]_w}{D_B[A^-]_w - (D_B - D_A)x[B^-]_w},$$

where

$$x = \frac{-D_A + \sqrt{D_A^2 + 4D_A[A^-]_w + \dfrac{4D_A^2[B^-]_w}{D_B}}}{2\left(1 + \dfrac{D_A[B^-]_w}{D_B[A^-]_w}\right)}$$

7) T. Ito and T. Kenjo, This Bulletin, **41**, 614 (1968).
8) N. Bjerrum, *Kgl. Danske Selskab*, **7**, No. 9 (1926).
9) O. D. Bonnen and L. L. Smith, *J. Phys. Chem.*, **61**, 1614 (1957).
10) K. A. Kraus, R. J. Raridon and D. L. Holcomb, *J. Chromatog.*, **3**, 178 (1960).
11) F. Vaslow and G. E. Boyd, *J. Phys. Chem.*, **70**, 2507 (1966).
12) K. A. Kraus and R. J. Raridon, *ibid.*, **63**, 1901 (1959).

Figure 1 shows the selectivity coefficient-molality curves calculated from the above equation for various D_A and D_B values. The figure indicates that a larger selectivity coefficient for anion A^- than for anion B^- means a smaller dissociation constant for A^- than that for B^-.

Ion-pair formation between an ionogenic group and the counter-ion can be analogized to the Langmuir adsorption process; that is, the dissociation constant in an ion-exchange corresponds to the eqilibrium constant of the process

adsorbed molecules in a solid phase $\rightleftharpoons$ free molecules in a gas phase + vacant sites.

Therefore, the dissociation constant can be understood as an equilibrium constant for the process

paired ions $\rightleftharpoons$ unpaired ions + unpaired ionogenic groups.

This process can be compared to the distribution of the model compound between a solvent layer and an aqueous layer,

paired ions in solvent layer*1 $\rightleftharpoons$ cations in an aqueous layer + anions in an aqueous layer

From these analogies for ion-pair formation between an ion-exchanger and an organic solvent phase, it can be assumed that some correlation exists between selectivity coefficient sequences against a common anion and distribution sequences in solvent extraction for corresponding model compounds.

Tables 1, 2 and 3 give the degree of distribution for cobalticinium, benziltrimethylammonium and benzildimethylamine, respectively. From a comparison of selectivity coefficients in ion-exchange with the degree of distribution in solvent extraction, it is found that they are related to each other in sequences

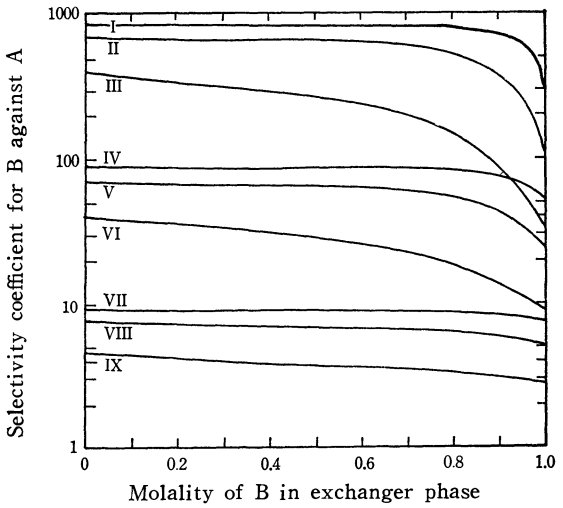

Fig. 1. Calculated curves for selectivity of anions A and B for the following sets of postulates;
I: $D_A=10^{-2}$ $D_B=10^{-5}$; II: $D_A=10^{-1}$ $D_B=10^{-4}$;
III: $D_A=1$ $D_B=10^{-3}$; IV: $D_A=10^{-2}$ $D_B=10^{-4}$;
V: $D_A=10^{-1}$ $D_B=10^{-3}$; VI: $D_A=1$ $D_B=10^{-2}$;
VII: $D_A=10^{-2}$ $D_B=10^{-3}$; VIII: $D_A=10^{-1}$ $D_B=10^{-2}$;
IX: $D_A=1$ $D_B=10^{-1}$

of values, except for the position of BrO_3^- and ClO_4^-.

A possible difference between ion-exchange and solvent extraction is the effect of freedom of rotation. In the case that A is a monoatomic anion and B a polyatomic anion, the effect of freedom of rotation between A and B would be greater in ion-exchange than in solvent extraction; that is the effect promotes the dissociation of polyatomic anions from ionogenic groups in ion-exchange more readily than in solvent extractions, because ionogenic groups are fixed to one another while the corresponding cation is moving freely in solvents. However, the trend mentioned above was not found to be very remarkable in the experimental results; the affinity of the poly-

TABLE 1. DEGREE OF DISTRIBUTION FOR COBALTICINIUM SALTS IN VARIOUS SOLVENT SYSTEMS AND SELECTIVITY COEFFICIENTS (K_c) OF POLYMERIC PENTAMETHYLENE COBALTICINIUM ION-EXCHANGER (PPC)

	K_c of PPC[14]	Chloroform (M)	*n*-Butanol (M)	*n*-Pentanol (M)	*n*-Hexanol (M)	Benzene (M)
IO_3^-	0.202	4.53	0.651	7.90	28.3	5.35
Cl^-	1	3.36	0.363	5.20	20.0	42.3
BrO_3^-	1.25	3.27	0.419	6.04	20.2	9.79
Br^-	3.58	3.09	0.298	4.73	14.6	29.6
ClO_3^-	4.46	2.74	0.258	4.45	14.3	19.1
I^-	25.3	2.49	0.174	2.96	8.58	22.0
SCN^-	36.4	2.42	0.124	1.91	5.84	35.5
ClO_4^-	73.5	1.49	0.159	2.61	7.81	15.6

*1 Almost all ions were found to form ion-pairs in a solvent witha very low dielectric constant.[13]

13) C. A. Kraus, *J. Phys. Chem.*, **60**, 129 (1956).

TABLE 2. DEGREE OF DISTRIBUTION FOR BENZILTRIMETHYLAMMONIUM SALTS IN VARIOUS SOLVENT SYSTEMS AND SELECTIVITY COEFFICIENTS (K_c) OF DOWEX 1X-8 (D1 X-8)

	K_c of D1 X-8[14]	Chloroform* (M)	*n*-Butanol (M)	*n*-Pentanol (M)	*n*-Hexanol* (M)
IO_3^-	0.198		0.648	7.34	
Cl^-	1		0.243	1.68	3.35
BrO_3^-	0.918		0.277	2.26	4.28
Br^-	3.14		0.137	0.856	1.71
ClO_3^-	3.35	96.0	0.0993	0.759	1.48
I^-	5.04	0.762	0.0439	0.243	0.137
SCN^-	6.89	8.35	0.0273	0.108	0.436
ClO_4^-	56.3	2.32	0.0311	0.166	0.606

* The salts of IO_3^-, Cl^-, BrO_3^-, and Br^- for chloroform and IO_3^- for *n*-butanol could not be detected in the solvent layer.

TABLE 3. DEGREE OF DISTRIBUTION FOR BENZILDIMETHYLAMMONIUM SALTS IN VARIOUS SOLVENT SYSTEMS AND SELECTIVITY COEFFICIENTS (K_c) OF AMBERLITE IR-45 (IR-45)

	K_c of IR-45[14]	Chloroform (M)	*n*-Butanol (M)	*n*-Pentanol (M)	*n*-Hexanol (M)
IO_3^-	0.528	21.6	0.446	3.88	2.89
Cl^-	1	19.0	0.175	1.01	1.75
BrO_3^-	1.21	10.6	0.190	1.35	2.19
Br^-	2.15	6.89	0.107	0.462	1.05
ClO_3^-	2.43	4.48	0.0850	0.397	0.942
I^-	2.38	0.622	0.0366	0.129	
SCN^-	3.61	0.868	0.0225	0.0579	0.257
ClO_4^-	5.46	4.07	0.0263	0.0998	0.433

atomic anion BrO_3^- was greater in the system of the cobalticinium type anion-exchanger and Amberlite IR-45 than in the corresponding solvent extraction systems. Accordingly, the effect of rotation of anions might be not very important.

Differences in interionic interactions between ion-exchange and solvent extraction can be mainly attributed to the difference in solvents. Possibly because of the effect of hydration, affinities of the counter ion to an ionogenic group in an aqueous layer are weaker than those of the same anion to the corresponding cation in solvents. The greater amount of water a solvent contains, the more similar to ion-exchange the solvent extraction system may be. In the system of benzene for cobalticinium halogenate (Table 1), the sequence is opposite to the affinity series for ion-exchange, and consistent with the order of solubilities.[14] This behaviour, perhaps, can be ascribed to the extremely low water content in the benzene layer. Because of the much lower dielectric constant of an organic solvent compared with that of water, an anion could approach a cation more closely in organic solvents than in water. Therefore, factors which are effective in a very short range *e.g.*, polarizability are more effective in an organic solvent than in water. Table 4 gives absorption peaks of UV spectra for benziltrimethylammonium in the *n*-butanol layer. It indicates that the absorption peak shifts to longer wavelength with increasing affinities. This result suggests some relation between the polarization of charge on ammonium cations and the interactive force between a cation and an anion.

TABLE 4. THE WAVELENGTH OF ABSORPTION PEAKS FOR BENZILTRIMETHYLAMMONIUM SALTS IN *n*-BUTANOL LAYER

	Wavelength (mμ)		Wavelength (mμ)
IO_3^-	215.3	ClO_3^-	219.8
Cl^-	218.4	SCN^-	226.0
BrO_3^-	218.6	ClO_4^-	220.2
Br^-	219.1		

Thus, these systems which consist of solvent extractions and model compounds have a possibility of being adequate models for ion-exchange although some differences can be pointed out.

14) T. Ito and T. Kenjo, This Bulletin, **41**, 1600 (1968).

BULLETIN OF THE CHEMICAL SOCIETY OF JAPAN VOL. 41 1761—1765 (1968)

Kinetic Studies of Ammonia Oxidation in Shock Waves. IV. Comparison of Induction Periods for the Ignition of NH_3-O_2-N_2 with Those for NH_3-O_2-Ar Mixtures

Hajime MIYAMA

Basic Research Loboratories, Toyo Rayon Company, Ltd., Tebiro, Kamakura, Kanagawa

(Received August 14, 1967)

Induction periods for ammonia oxidation in the NH_3-O_2-Ar and NH_3-O_2-N_2 mixtures were measured by monitoring an ultraviolet absorption of ammonia in reflected shock waves. For the NH_3-O_2-Ar mixtures, induction periods in the temperature range of 1450—2730°K were found to be expressed by

$$\log \tau_i[O_2]\,(\mathrm{mol}\cdot l^{-1}\mu\mathrm{sec}) = -(16.24\pm0.17) + (10080\pm320)/T$$

when oxygen content is in the range of 4—10%, and by

$$\log \tau_i(\mu\mathrm{sec}) = -(2.55\pm0.14) + (8810\pm220)/T$$

when the oxygen content is less than 1%. Values of induction periods for the 0.5% NH_3-0.5%O_2-99% N_2 and 1% NH_3-1% O_2-98% N_2 mixtures were also measured and compared with those for the NH_3-O_2 mixtures highly diluted with argon. Both results agreed well by taking into account vibrational relaxation of the reacting system if appropriate values of vibrational relaxation times for N_2 dilute in NH_3 is assumed. Therefore, possibility of coupling of vibrational relaxation of N_2 and oxidation reaction was considered to be small.

In the first paper of this series[1,2] we found a linear relationship between $\log \tau_i[O_2]$ and $1/T$ for the shock-heated NH_3-O_2-Ar mixtures where τ_i was induction period determined by the reaction between NH_2 and O_2. Thereafter, we[3] measured induction periods for the mixtures of 90% N_2-6% NH_3-4% O_2 and 90% N_2-4% NH_3-6% O_2, and made Arrhenius plots by assuming two possible cases; (a) nitrogen is relaxed translationally, rotationally and vibrationally, and (b) nitrogen is relaxed translationally and rotationally. Comparison of these plots with a plot for the NH_3-O_2-Ar mixtures showed that data calculated for the case (b) are very close to the plot for the NH_3-O_2-Ar mixtures at higher temperatures but those for the case (a) approach to the latter plot at lower temperatures. This phenomenon was attributed to the effect of vibrational relaxation of nitrogen which became comparable to the induction period of ammonia oxidation in certain temperature range. Also, it was considered that the coexistence of NH_3 and O_2 might shorten the vibrational relaxation time of N_2.

In order to minimize the effect of these additives and to examine the effect of vibrational relaxation of N_2 on the oxidation reaction, measurement of induction periods was performed for the NH_3-O_2 mixtures highly diluted with nitrogen and compared with those for the NH_3-O_2 mixtures highly diluted with argon.

Experimental

The experimental details have been described previously.[1-4] Induction periods were measured in reflected shock waves by monitoring the absorption of NH_3 at 2245 Å, 2300 Å or 2400 Å. One of these wavelengths was chosen depending on the NH_3 concentration because the extinction coefficient of NH_3 was higher at shorter wavelength. The mixtures used and experimental conditions were summarized in Table 1, where data for the mixtures VIII and X were taken from the previous report.[1]

Results and Discussion

The Induction Periods for NH_3-O_2-Ar Mixtures. Arrhenius plots of $\tau_i[O_2]$ for the mixtures I—XI are shown in Fig. 1. Here, data for the mixtures containing more than 4% oxygen are expressed by a straight line, a least-squares expressions of which is as follows:

$$\log \tau_i[O_2](\mathrm{mol}\cdot l^{-1}\cdot\mu\mathrm{sec}) = -(16.24\pm0.17) + (10080\pm320)/T \quad (1)$$

This indicates that the linear relation between

1) T. Takeyama and H. Miyama, This Bulletin, **39**, 2352 (1966).
2) T. Takeyama and H. Miyama, *ibid.*, **39**, 2609 (1966).
3) H. Miyama and R. Endoh, *J. Chem. Phys.*, **46**, 2011 (1967).
4) T. Takeyama and H. Miyama, *J. Chem. Phys.*, **42**, 3737 (1965); This Bulletin, **38**, 1670 (1965).

TABLE 1. EXPERIMENTAL CONDITIONS

Reaction mixture	Composition (%) NH_3%	O_2%	Ar%	N_2%	T_5 (°K)	P_5 (atm)	$[O_2]$ (10^{-3} mol/l)	τ_i (μsec)
I	0.5	0.5	99	0	1560—2230	2.61—7.41	0.0851—0.264	50—1250 (NH_3 2245 Å)
II	1	0.5	98.5	0	2160—2370	3.63—3.92	0.094 —0.111	16— 37 (NH_3 2245 Å)
III	0.5	1	98.5	0	2140—2320	3.64—3.97	0.196 —0.220	11— 38 (NH_3 2245 Å)
IV	1	1	98	0	1560—2730	1.89—7.48	0.113 —0.555	4—1230 (NH_3 2245 Å)
V	2	1	97	0	2100—2580	3.41—4.05	0.161 —0.229	7— 36 (NH_3 2245 Å)
VI	2	2	96	0	1580—2320	1.98—7.75	0.222 —1.12	13— 950 (NH_3 2245 Å or 2300 Å)
VII	3	3	94	0	1530—2130	4.74—8.33	0.814 —1.84	50—1280 (NH_3 2400 Å)
VIII	6	4	90	0	1600—2300	3.49—4.51	0.741 —1.32	28—1360 (OH 3067 Å)
IX	5	5	90	0	1490—2320	3.73—7.66	0.980 —2.81	12—1850 (NH_3 2400 Å)
X	4	6	90	0	1550—2110	3.54—5.52	1.23 —2.47	37—1026 (OH 3067 Å)
XI	10	10	80	0	1450—2120	3.62—7.31	2.08 —6.06	12—1400 (NH_3 2400 Å)
XII	0.5	0.5	0	99	1530—2190 (1670—2490)	1.52—4.75 (1.47—4.66)	0.0504—0.184 (0.0439—0.165)	17—1580 (NH_3 2245 Å)
XIII	1	1	0	98	1530—2300 (1660—2600)	1.49—4.55 (1.45—4.47)	0.0956—0.364 (0.0804—0.328)	6—1600 (NH_3 2245 Å)

Note : Shock parameters calculated for mixtures XII and XIII correspond to case (a), and those corresponding to case (b) are shown in parentheses. T_5 and P_5 are temperature and pressure behind reflected shock waves.

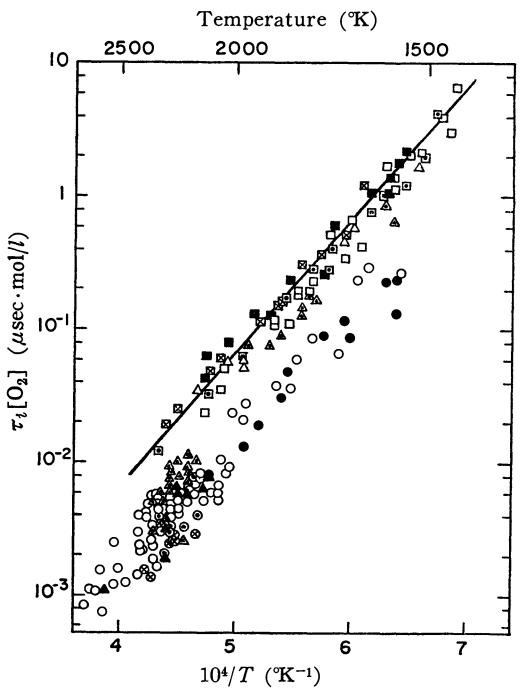

Fig. 1. Arrhenius plot for $\tau_i[O_2]$.

Marks ●, ⊗, ⊙, ○, ▲, ◬, △, ⊠, ⊡, ■, and □ refer to mixtures I, II, III, IV, V, VI, VII, VIII, IX, X, and XI respectively.

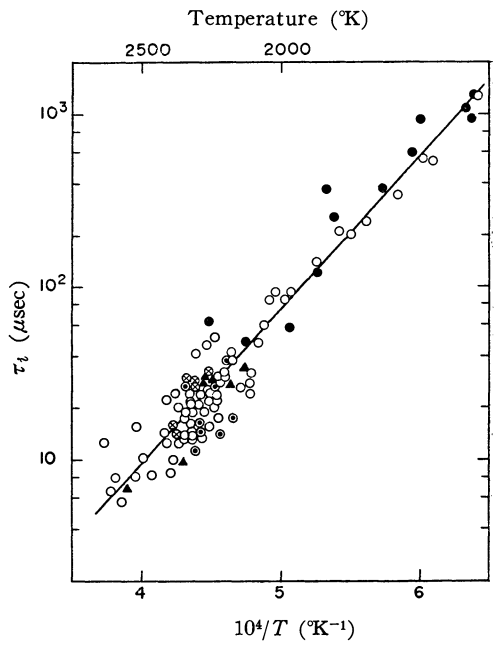

Fig. 2. Arrhenius plot for τ_i.
Marks are the same as in Fig. 1.

$\log \tau_i[O_2]$ and $1/T$ obtained previously[1] holds over a wide range of oxygen concentration (4—10%).

However, when the oxygen content is less than 3%, $\log \tau_i[O_2]$ decreases as the former decreases. Especially, when the oxygen content is less than 1%, the result is well expressed by a linear plot of $\log \tau_i$ *via* $1/T$ as shown in Fig. 2, where the solid line obtained by a least-squares calculation is expressed by :

$$\log \tau_i(\mu\text{sec}) = -(2.55\pm0.14) + (8810\pm220)/T \quad (2)$$

In order to explain this relationship from the viewpoint of chemical kinetics, available experimental data are not enough.

The Induction Periods for NH_3-O_2-N_2 Mixtures and Vibrational Relaxation of Nitrogen. According to the preliminary experiment, the dependence of τ_i on the oxygen content observed for NH_3-O_2-N_2 was similar in tendency to that for NH_3-O_2-Ar. In order to examine the effect of vibrational relaxation of nitrogen, it is desirable to use mixtures of small ammonia and oxygen contents. Therefore, detailed measurments were performed for the mixtures XII and XIII. The results are shown in Fig. 3, where a solid line is calculated by Eq. (2) and open and closed marks correspond to cases (a) and (b), respectively. These two cases were assumed to calculate reflected shock temperatures and oxygen concentrations from the initial pressures and incident shock velocities. As described previously,[4] nitrogen is considered to be relaxed translationally, rotationally, and vibrationally for (a), and to be relaxed translationally and rotationally for (b). In both cases, it was assumed that the internal degrees of freedom of ammonia and oxygen are completely relaxed. From the figure, it is obvious that data calculated for the case (b) agree with the plot for the NH_3-O_2-Ar mixtures at higher temperatures and those for the case (a) at lower temperatures.

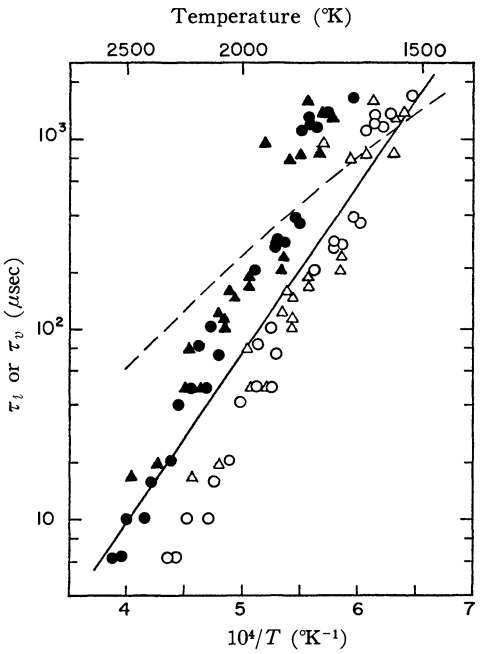

Fig. 3. Arrhenius plot for τ_i and $\tau_{N_2\text{-}N_2}$.
Triangles and circles refer to mixtures XII and XIII, respectively, open marks correspond to case (a) and closed marks to case (b), and a solid and a broken line were calculated from Eqs. (2) and (3).

Vibrational relaxation time of nitrogen, $\tau_{N_2\text{-}N_2}$, is given by the expression of Milliken and White[5] as follows.

$$\log P\tau_{N_2\text{-}N_2}(\text{atm}\cdot\text{sec}) = 102T^{-1/3} - 11.24 \quad (3)$$

Values of $\tau_{N_2\text{-}N_2}$ calculaletd by substituting $P=3.0$ atm, which is an average of pressures behind reflected shock waves for the mixtures XII and XIII, are also shown in Fig. 3 by a broken line. From the figure, it is seen that $\tau_{N_2\text{-}N_2}$ is equal to τ_i for the NH_3-O_2-Ar mixtures at 1570°K, and that $\tau_{N_2\text{-}N_2}<\tau_i$ below this temperature and $\tau_{N_2\text{-}N_2}>\tau_i$ above it. Therefore, it is expected that the case (a) is applicable at lower temperatures and (b) at higher temperatures. However, the crossover temperature from (a) to (b) in Fig. 3 is higher than that expected. This is considered to be due to the effect of NH_3 and O_2 in shortening the vibrational relaxation time.[3]

It is well known[6] that translational temperature of polyatomic gas behind the shock wave decreases exponentially with time t as follows.

$$\frac{T-T_a}{T_b-T_a} = \exp\left(-\frac{C_p t}{C_p'\tau_v}\right) \quad (4)$$

Here, T_a and T_b are shock wave temperatures corresponding to the cases (a) and (b), C_p is average specific heat at constant pressure, C_p' is C_p minus vibrational contribution, and τ_v is vibrational relaxation time. For the system diluted with argon, the temperature behind shock front is almost constant during the induction period. However, for the system diluted with nitrogen, the temperature decreases from T_b and approaches to T_a during the induction period according to Eq. (4). Therefore, instead of constant temperature in the case of argon dilution, average temperature must be adopted to define temperature of the system diluted with nitrogen. Thus, temperature T of the reaction system during the induction period τ_i is given as follows by using Eq. (4).

$$T=\frac{1}{\tau_i}\int_0^{\tau_i} T dt$$

5) R. C. Millikan and D. R. White, *J. Chem. Phys.*, **39**, 98 (1963).
6) T. L. Cottrell and J. C. McCoubrey, "Molecular Energy Transfer in Gases," Butterworths, London (1961), p. 54.

$$= \frac{\tau_v}{\tau_i}\cdot\frac{C_p'}{C_p}(T_b-T_a)\left\{1-\exp\left(-\frac{C_p\tau_i}{C_p'\tau_v}\right)\right\} + T_a \quad (5)$$

Therefore, if τ_v is known, it is possible to calculate temperature of the system from Eq. (5). According to the empirical expression of Millikan and White[7] (which is not correct theoretically but very useful) where only translation-to-vibration energy conversion was assumed, τ_v of the present system is expressed as follows.

$$(P\tau_v)^{-1} = \phi_{N_2}(P\tau_{N_2\text{-}N_2})^{-1} + \phi_{NH_3}(P\tau_{N_2\text{-}NH_3})^{-1} + \phi_{O_2}(P\tau_{N_2\text{-}O_2})^{-1} \quad (6)$$

Here, relaxation times with two subscripts refer to relaxation of the first species when it is present at high dilution in the second-named gas at a total pressure of P atm, and ϕ_s' are mole fractions of components. Although $\tau_{N_2\text{-}O_2}$ is not known, this can be estimated by using an empirical formula of Millikan and White[7] and was found to be comparable to $\tau_{N_2\text{-}N_2}$. Since $\phi_{N_2} \gg \phi_{O_2}$ in the present experimental conditions, the third term in Eq. (6) can be neglected. Therefore, Eq. (6) is expressed as follows.

$$(P\tau_v)^{-1} = \phi_{N_2}(P\tau_{N_2\text{-}N_2})^{-1} + \phi_{NH_3}(P\tau_{N_2\text{-}NH_3})^{-1} \quad (7)$$

Here, $\tau_{N_2\text{-}N_2}$ is given by Eq. (3), but no information about $\tau_{N_2\text{-}NH_3}$ is available. How-

TABLE 2. PARAMETERS USED FOR THE CALCULATION OF TEMPERATURES OF THE REACTION SYSTEM

Reaction mixture	T_a (°K)	T_b (°K)	P (atm)	C_p/C_p'	τ_i (μ sec)	T (°K)
XII	1550	1700	3.68	1.20	1320	1562
	1570	1720	4.71	1.20	1300	1579
	1590	1750	3.61	1.20	850	1608
	1640	1800	1.32	1.21	1580	1657
	1660	1830	4.66	1.21	800	1674
	1680	1860	3.13	1.22	790	1700
	1710	1890	3.57	1.22	240	1761
	1710	1890	1.93	1.22	210	1775
	1730	1920	1.78	1.22	970	1758
	1780	1980	2.86	1.22	170	1858
	1780	1980	3.50	1.22	190	1842
	1840	2050	1.50	1.22	160	1956
	1840	2050	2.75	1.23	105	1945
	1840	2050	4.30	1.23	110	1917
	1840	2050	3.31	1.23	170	1968
	1860	2080	3.15	1.23	130	1947
	1920	2160	2.65	1.23	50	2078
	1950	2190	3.07	1.23	50	2097
	1980	2230	2.51	1.24	80	2051
	2080	2350	2.41	1.25	20	2298
	2190	2490	2.29	1.25	17	2434
XIII	1550	1690	3.68	1.20	1600	1555
	1590	1740	3.61	1.20	1350	1596
	1610	1760	3.50	1.20	1200	1616
	1630	1790	1.62	1.21	1400	1642
	1630	1790	3.33	1.21	1250	1637
	1650	1820	3.11	1.21	1140	1658
	1650	1820	3.89	1.21	350	1670
	1680	1840	3.71	1.21	380	1698
	1700	1870	4.90	1.21	270	1719
	1730	1900	3.04	1.21	280	1758
	1730	1900	4.73	1.21	270	1749
	1780	1960	2.60	1.21	200	1823
	1780	1960	4.67	1.21	200	1805
	1890	2100	2.59	1.22	70	1987
	1910	2130	2.39	1.23	50	2034
	1910	2130	2.65	1.23	100	1987
	1940	2170	3.40	1.23	50	2045
	1940	2170	4.08	1.23	80	2006
	2010	2240	3.22	1.23	40	2127
	2040	2280	2.35	1.23	20	2218
	2110	2370	2.17	1.24	15	2315
	2140	2410	3.18	1.25	10	2352
	2220	2500	2.04	1.26	10	2454
	2260	2550	1.73	1.26	6	2523
	2300	2600	2.19	1.26	6	2564
	2300	2600	2.67	1.26	6	2557

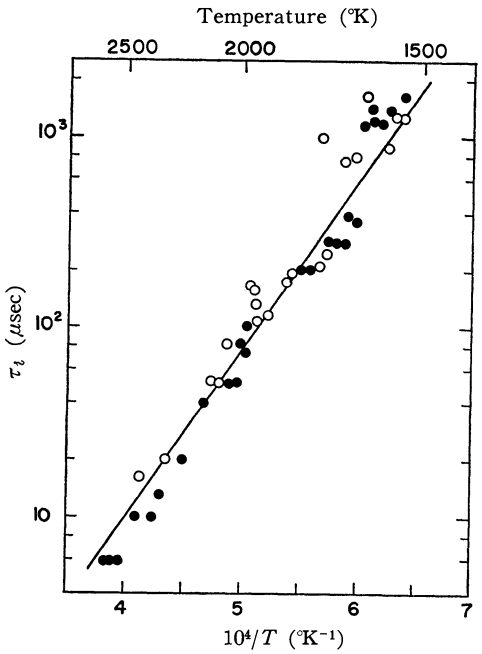

Fig. 4. Arrhenius plot for τ_i.
Marks ○ and ● refer to mixtures XII and XIII respectively and a solid line was calculated from Eqs. (2).

7) R.C. Millikan and D.R. White, *J. Chem. Phys.*, **39**, 3209 (1963).

ever, recently, White[8] found that $\tau_{N_2\text{-}He}$, $\tau_{N_2\text{-}C_2H_2}$, and $\tau_{N_2\text{-}CH_4}$ are approximately double, equal to, and 60% of $\tau_{N_2\text{-}H_2}$ in the range of 1600 to 2500°K. Since vibrational frequencies of NH_3 are not close to those of N_2, much more rapid vibration-to-vibration exchange between N_2 and NH_3 compared with that between N_2 and C_2H_2 or CH_4 is not expected and $\tau_{N_2\text{-}NH_3}$ may be comparable to $\tau_{N_2\text{-}C_2H_2}$ or $\tau_{N_2\text{-}CH_4}$, that is, to $\tau_{N_2\text{-}H_2}$. Therefore, as a rather reasonable approximation, let us assume

$$\tau_{N_2\text{-}NH_3} \fallingdotseq \tau_{N_2\text{-}H_2} \tag{8}$$

By using an expression for $\tau_{N_2\text{-}H_2}$ given by White,[9] $\tau_{N_2\text{-}NH_3}$ is expressed as follows.

$$\log P\tau_{N_2\text{-}NH_3} \fallingdotseq 35.0(T^{-1/3} - 0.0176) - 8.00 \tag{9}$$

From Eqs. (3), (5), (7), and (9), temperature of the present system can be calculated with a computor by using known values of T_a, T_b, P, C_p/C_p' and τ_i as shown in Table 2, where reflected shock pressure P is an average of those for (a) and (b) since difference between them is less than 0.5% at maximum. Also, calculated values of the temperature T are shown in the table. Thus, in Fig. 4, values of τ_i is plotted against newly obtained values of T. Here, excellent agreement between both polts for NH_3-O_2-N_2 and NH_3-O_2-Ar is observed. This agreement suggests that τ_i for the NH_3-O_2-N_2 is the same as that for NH_3-O_2-Ar and possibility of coupling of vibrational relaxation and oxidation reaction is small. However, we cannot say that it is conclusive unless $\tau_{N_2\text{-}NH_3} \fallingdotseq \tau_{N_2\text{-}H_2}$ is proved. It is a very challenging problem to measure vibrational relaxation times for N_2 dilute in NH_3 and to obtain more detailed informations about kinetics of NH_3–O_2–N_2 system.

The author wishes to express his thanks to Dr. Soji Tsuchiya for his helpful advice, to Mr. Kazutoshi Sugiyama for his help in the experiment, and to Mr. Takashi Suzuki for reviewing the manuscript.

8) D. R. White, *ibid.*, **48**, 525 (1968).
9) D. R. White, *ibid.*, **46**, 2016 (1967).

BULLETIN OF THE CHEMICAL SOCIETY OF JAPAN VOL. 41 1765—1769 (1968)

Studies of Photosensitive Resins. III. The Thermal Hardening of Polyvinyl Cinnamate

Kenichiro NAKAMURA, Toshifumi SAKATA and Shinichi KIKUCHI

The Institute of Industrial Science, The University of Tokyo, Roppongi, Minato-ku, Tokyo

(Received November 16, 1967)

The thermal hardening of polyvinyl cinnamate was investigated. The IR spectrum of the thermally-hardened polyvinyl cinnamate was measured, and the change of its structure by heat was studied. The results showed that the structure of the resin hardened by heat was the same as that of the illuminated resin. The kinetics of the crosslinking by heat was also evaluated; the activation energy for the crosslinking was estimated to be 25.4 kcal/mol. The critical hardening value of polyvinyl cinnamate was also measured and estimated to be about 1.3 crosslinking per polymer molecule.

It is well-known that polyvinyl cinnamate is crosslinked by ultraviolet light[1] and becomes insoluble to any solvent. However, its thermal character has not yet been made clear. Therefore, the mechanism and kinetics of thermal hardening were studied by measuring the IR spectra.

Inami and Morimoto[2] measured the IR spectra of polyvinyl cinnamate before and after light-irradiation, and concluded that the α,β double bond of the cinnamoyl group was broken to the single bond by light. Kirsh *et al.*[3] also measured its IR spectra and obtained the quantum yield and the critical hardening exposure. They estimated that the hardening ratio at the critical point was 0.02%. However, such a method may not be the best way of estimating the critical hardening value, for the resin is not hardened uniformly by light, but is, rather, hardened exponentially with

1) L.M. Minsk, J.Q. Smith, W.P. Van Deusen and J.F. Wright, *J. Appl. Pol. Sci.*, **2**, 302 (1959).

2) A. Inami and K. Morimoto, *Kogyo Kagaku Zasshi* (*J. Chem. Soc. Japan, Ind. Chem. Sect.*), **65**, 293 (1962).

3) Yu. E. Kirsh, K.S. Lyalikov and L. Kalnins. *Zh. Fiz. Khim.*, **39**, 1886 (1965).

the depth. On the other hand, the resin is hardened uniformly by heat. Therefore, the present authors also tried to ascertain the hardening ratio at the critical point.

In a previous paper,[4] the ESR spectrum of the irradiated polyvinyl cinnamate was investigated and it was established that two free radicals, the main-chain radical and the cinnamoyl radical, were produced by the irradiation of the resin. The photocrosslinking mechanism has been made fairly clear by such studies as have been described above, but its thermal hardening is still the subject of frequent discussion.

The sensitized polyvinyl cinnamate is sensitive to light in the ultraviolet and visible regions, while the nonsensitized one is sensitive only in the ultraviolet region. Tsuda[5] discussed the sensitization mechanism of the resin on the basis of the triplet-state mechanism. When a sensitizer is added to the resin, it is hardened by light in the region with longer wavelengths than intrinsic ones. The critical and activation energies for the hardening will be kinetically investigated. The thermal hardening of the photosensitive resin is important for the "afterhardening" process and for preservation in the dark. Therefore, the authors also intend to obtain data on such a process.

Experimental

Polyvinyl cinnamate was synthesized by the pyridine method.[1] The synthesized resin was dissolved into a cellosolve acetate solution, and coated on KBr tablet. The samples were heated at various temperatures, and their IR spectra were measured with a Nippon Bunko infrared spectrophotometer, DS-301. When the heated samples were introduced into water after IR measurements, the thin films of resin remained on the surface of the water. These films were put into the solvent, and their residual weights were measured in order to get information on their solubilities.

The authors estimated the hardening rate of the resin by measuring the concentration of the α,β double bond. The amount of the double bond was evaluated by means of the integrated area of the IR absorption signal at 1640 cm^{-1}. The calibration curve was obtained by means of the IR spectra of films with various depths. Beer's law could be applied to them fairly well.

Results and Discussion

The IR Spectrum of the Heated Polyvinyl Cinnamate. The IR spectra of polyvinyl cinnamate before and after illumination are shown in Fig. 1. The resin was exposed for 160 min with a 1000 W Xe lamp. The IR spectrum of the irradiated polyvinyl cinnamate has already been measured by Inami and Morimoto,[2] who reported that absorption band resulting from the double bond, $\nu_{C=C}$ (1640cm^{-1}), δ_{CH} (1315 cm^{-1}), and δ_{CH} (975 cm^{-1}), disappeared and the $\nu_{C=O}$ (171 8cm^{-1}) band shifted to a higher frequency band upon exposure. However, they could not detect any newly-appeared band becaus eof the photocrosslinking.

Figure 1 also shows evidence for the disappearance of the absorption bands resulting from the double bond and the shift of the $\nu_{C=O}$ band. The results agree with those

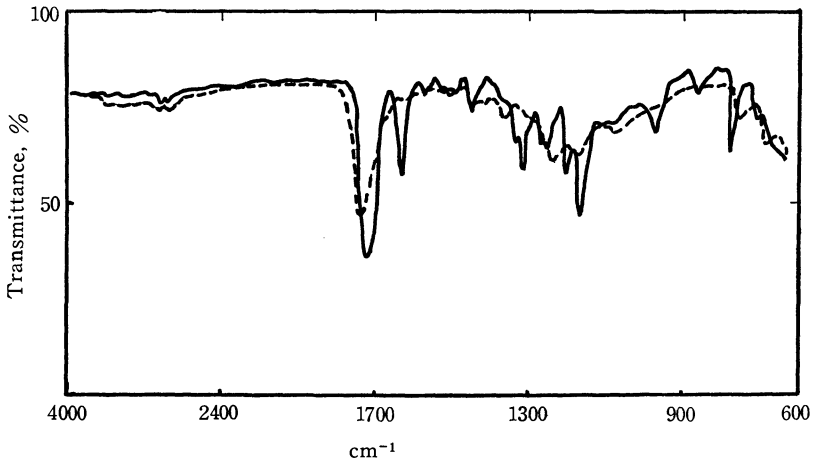

Fig. 1. IR spectra of polyvinyl cinnamate.
—— before illumination, ---- after illumination

4) K. Nakamura and S. Kikuchi, This Bulletin, **40**, 2684 (1967).

5) M. Tsuda, *J. Soc. Sci. Phot. Japan*, **28**, 7 (1965)

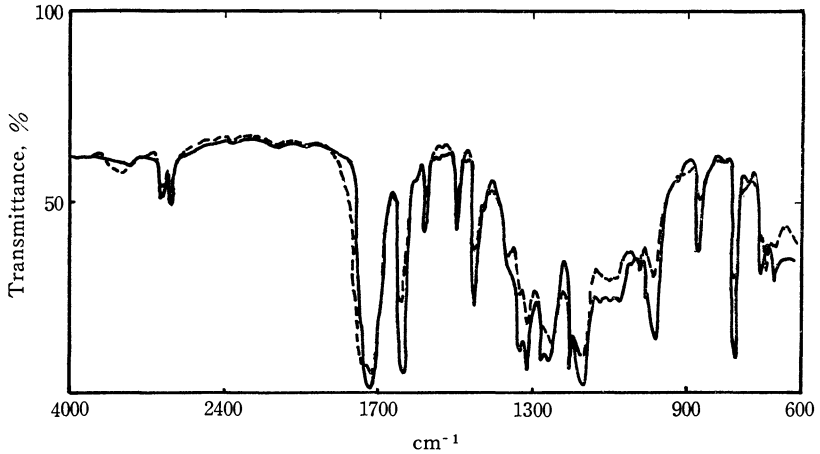

Fig. 2. IR spectra of polyvinyl cinnamate.
—— before heating, ---- after heating

obtained by Inami *et al.*, but Fig. 1 shows that the δ_{CH} band newly appears at 1375 cm^{-1} and that the absorption strengths of all the bands decrease upon exposure to light. It seems that the band is due to the bending vibrational absorption of the saturated CH, which is produced by light-irradiation. Kirsh *et al.*[3] reported that all the absorption bands decreased upon illumination, and concluded that this was caused by the change in electronic structure.

The IR spectrum of the heated polyvinyl cinnamate is shown in Fig. 2. The IR spectra after light-irradiation and after heating are the same. It may, therefore, be concluded that there is no difference between the thermal hardening and photo-hardening of polyvinyl cinnamate with regard to the crosslinking reaction. The disappearance of the $\nu_{C=C}$ (1640 cm^{-1}), and δ_{CH} (1315, 980 cm^{-1}) bands, the decrease of all absorption bands, and the appearance of a new absorption band (1375 cm^{-1}) may also be seen in Fig. 2.

Kinetics of the Thermal Hardening. The rate of the thermal hardening of polyvinyl cinnamate is estimated by measuring the IR spectra. The extent of the double bond was determined by means of the absorption of $\nu_{C=C}$ (1640 cm^{-1}). In the IR spectra of polyvinyl cinnamate, the absorption of the bands resulting from the double bond disappears upon heating, while all the other absorption bands decrease with illumination, as has been described previously. When the sensitized polyvinyl cinnamate was irradiated by a 350 $m\mu$ light, the same IR spectral results as with a non-sensitized one were obtained. The light may not be sufficient to decompose the resin, for its energy is only about 82 kcal/mol, while more than 100 kcal/mol may be necessary to decompose it. Therefore, it seems reasonable to assume that the decrease in the spectrum is not due to the decomposition of the resin, but is caused by the change in electronic

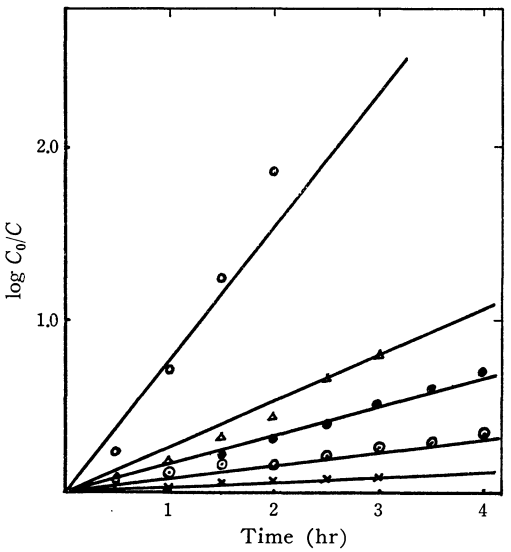

Fig. 3. Decay of cinnamoyl group.
× 182°C ◉ 195°C ● 200°C
△ 220°C ○ 235°C

TABLE 1. RATE CONSTANTS, α AT VARIOUS TEMPERATURES

T	log k
508 °K	0.254
493	−0.212
473	−0.416
455	−1.036

structure proposed by Kirsh.[3] The electronic structural change can be found only in the crosslinked group, and the non-crosslinked group is not affected by it. Therefore, the authors concluded that the IR-determining method of the double bond might be useful.

Relations between the heating times and the rates of the non-crosslinked cinnamoyl group at various temperatures are shown in Fig. 3 and Table 1.

The thermal hardening of polyvinyl cinnamate can be expressed by the formula:

$$\frac{dC}{dt} = -aC \qquad (1)$$

where a is a rate constant and C is the concentration of the non-crosslinked cinnamoyl group. Therefore, we obtained the following expression:

$$\log x = \log\frac{C_0}{C} = at \qquad (2)$$

where C_0 is the initial concentration of cinnamoyl groups. This formula shows that there is a linear relation between $\log x$ and t. In Fig. 3, the linear relation is satisfactory, so it may be concluded that, in the thermal-hardening process, the reaction can be expressed by the first order, as is shown in formula (1).

When polyvinyl cinnamate was heated to more than 250℃, the decomposition reaction took precedence over the crosslinking and the sample was colored, while the resin is rapidly hardened at more than 200℃. Therefore, in the "afterhardening process" it is better to keep the temperature at about 200℃. After the values at various temperature were estimated by means of formula (2), they were plotted against $1/T$. The relation is shown in Fig. 4. In Fig. 4 the good linear relation between them can be seen. The activation energy of the thermal crosslinking reaction can be obtained from the slope of the line: it is evaluated as 25.4 kcal/mol. About one hundred kcal per mole is necessary to harden polyvinyl cinnamate by light, but a much smaller energy is sufficient to harden it by heat. The energy level of the lowest triplet state of polyvinyl cinnamate was inferred to be 57.2 kcal/mol from the ground state by measuring the phosphorescence spectrum of cinnamic acid.[6] The activation energy is smaller than the triplet state energy. The critical energy of the sensitization should correspond to the triplet-state energy.[7] The above results suggest that the critical energy of sensitization can be diminished to 25.4 kcal/mol if the triplet-state energy is degraded by some methods such as introduction of substitutional groups to the benzene ring of the cinnamoyl group. The following expression can be derived from data in Table 1:

$$y = 1 - \exp(-at) \qquad (3)$$

where y is a hardening ratio and where:

$$a = a_0 \exp(-E/\boldsymbol{k}T)$$
$$a_0 = 4.22\times10^7 \text{ sec}^{-1}$$
$$E = 25.4 \text{ kcal/mol}$$

When the hardening ratio is very small, formula (3) can be expressed by:

$$y = at \qquad (4)$$

The solubilities of the thermally-hardened resin were investigated, thus making it clear that all the resins, which had been ascertained by IR measurements to be hardened, were insoluble in any solvent.

The critical hardening ratio of polyvinyl cinnamate was evaluated from formula (4). The resin become insoluble in the solvent when kept at 147℃ for 10 min. The average degree of polymerization of the resin was 2000, and the degree of esterification was estimated to be 76.5% by the method proposed by Tsuda.[8] The critical hardening ratio was

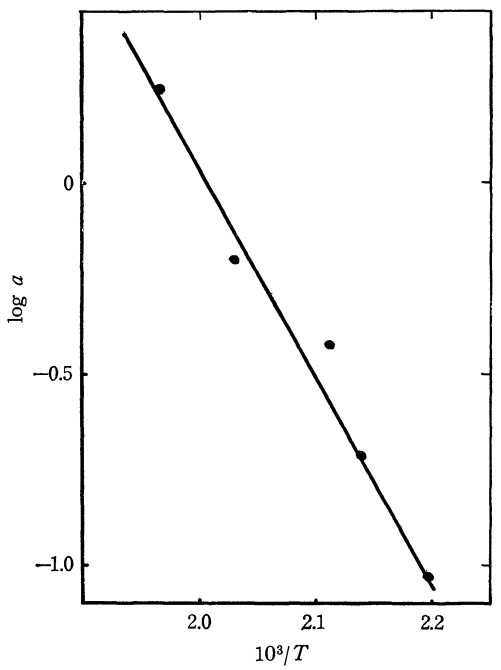

Fig. 4. Rate constants against $1/T$.

6) K. Nakamura and S. Kikuchi, This Bulletin, in press.
7) M. Tsuda, International Conference on Photographic Science, Tokyo, 1967.
8) M. Tsuda, *Kogyo Kagaku Zasshi* (*J. Chem. Soc. Japan, Ind. Chem. Sect.*), **66**, 1365 (1963).

calculated to be 7.68×10^{-4} by formula (4). Therefore, the number of crosslinked cinnamoyl groups per polymer molecule was computed to be 1.17. On the other hand, the critical value of the resin (the degree of polymerization was 1400, and the degree of esterification was 68.5 %) was found to be 15.36×10^{-4}, and the number of hardening groups was 1.47 groups per polymer molecule. Therefore, it seemed that the critical hardening value of polyvinyl cinnamate was about 1.3.

Formerly, the present authors showed that the minimum exposure time, t_{min}, for the photo-crosslinking of the resin could be expressed by[9]:

$$t_{min} = \frac{2\gamma_c Cd}{S_\phi \lambda} \qquad (5)$$

where γ_c is the critical hardening value, C is the concentration of the cinnamoyl group, d is the depth of the polymer layer, λ is average degree of polymerization, and S_ϕ is the quantum photosensitivity. The quantum photosensitivity can be evaluated by using the critical hardening value.

On the basis of above results, it was concluded that the most suitable temperature for the "afterhardening process" was about 200℃, that the activation energy for the thermal hardening was 25.4 kcal/mol, and that the critical hardening value was about 1.3 groups per polymer molecule.

9) K. Nakamura, S. Kikuchi, *Nippon Kagaku Zasshi* (*J. Chem. Soc. Japan, Pure Chem. Sect.*), **87**, 930 (1966).

BULLETIN OF THE CHEMICAL SOCIETY OF JAPAN VOL. 41 1769—1775 (1968)

The Primary Photochemical Process of 4-Nitropyridine *N*-Oxide

Norisuke HATA*[1]

Department of Applied Science, Tokyo Electrical Engineering College, Kanda Nishiki-chô, Chiyoda-ku, Tokyo

and Eiichi OKUTSU and Ikuzo TANAKA

Department of Chemistry, Tokyo Institute of Technology, Ookayama, Meguro-ku, Tokyo

(Received December 25, 1967)

In order to clarify the primary photochemical process of 4-nitropyridine *N*-oxide in solution, investigations by means of a steady-light irradiation and a flash spectroscopic method were carried out. 4-Nitropyridine *N*-oxide changes photochemically to 4-hydroxypyridine *N*-oxide nitrate (Process I) or 4-hydroxylaminopyridine *N*-oxide (Process II), depending on the reaction conditions. In either case, Process I and Process II, the photochemical reaction was found to proceed through the common intermediate species A. We concluded from the experimental results that Process I involves a bimolecular interaction between the intermediate A and the unexcited 4-nitropyridine *N*-oxide molecule, while Process II involves a hydrogen-abstracting reaction from a solvent molecule.

Recently, pyridine and quinoline-*N*-oxides and their several derivatives have been reported by various workers to cause a photochemical change in the N-O group when they are irradiated with ultraviolet light in either a solution or vapor.[1-4] The introduction of nitro group into the 4-position of pyridine *N*-oxide, has been found to cause a photochemical change completely different from those of pyridine- and 2-picoline-*N*-oxides in solution.[5,6] That is, 4-nitropyridine *N*-oxide in ethanol changes photochemically in two

*[1] Address after April 1, 1968: Department of Chemistry, College of Science and Technology, Aoyama Gakuin University, Megurisawa-chô, Setagaya-ku, Tokyo.

1) N. Hata and I. Tanaka, *J. Chem. Phys.*, **36**, 2072 (1962); N. Hata, This Bulletin, **34**, 1440, 1444 (1961).

2) J. Streith and C. Sigwalt, *Tetrahedron Letters*, **1966**, 1347.

3) O. Buchardt, *Acta. Chem. Scand.*, **17**, 1461 (1963); O. Buchardt, J. Becher and C. Lohse, *ibid.*, **19**, 1120 (1965); **20**, 2467 (1966); O. Buchardt, J. Becher, C. Lohse and J. Møller, *ibid.*, **20**, 262 (1966).

4) M. Ishikawa, S. Yamada and C. Kaneko, *Chem. Pharm. Bull.*, (*Tokyo*), **13**, 747 (1965); C. Kaneko and S. Yamada, *ibid.*, **14**, 555 (1966); C. Kaneko, S. Yamada and M. Ishikawa, *Tetrahedron Letters*, **1966**, 2145.

5) C. Kaneko, S. Yamada and I. Yokoe, Symposium on Photochemistry, Osaka, October, 1966.

6) C. Kaneko, S. Yamada, I. Yokoe, N. Hata and Y. Ubukata, *Tetrahedron Letters*, **1966**, 4729.

ways, depending on the reaction conditions, to give 4-hydroxypyridine *N*-oxide nitrate or 4-hydroxylaminopyridine *N*-oxide, while the N-O group remains unchanged.[5,6] Therefore, in order to clarify the primary process of such an interesting photochemical reaction of 4-nitropyridine *N*-oxide, we carried out investigations by means of a steady-light irradiation and also a flash spectroscopic method in solution.

Experimental

Materials. The 4-nitropyridine *N*-oxide used in this experiment was synthesized by Ochiai's method,[7] and the product was purified by several recrystallizations from acetone. Ethanol and glycerol were reagent-grade products of Wako Pure Chemical Industries, the spectro-grade ethanol was also used.

Steady-light Experiment. The light source employed was a Toshiba high-pressure mercury lamp (H-400 P), while for the 3130 Å irradiation a filter combination of a nickel sulfate solution with a UV-31 Toshiba filter was used. Sample solutions in various concentrations were added to the quartz cylindrical reaction cell and then placed in a thermostated box with two quartz windows, through which collimated light passed to irradiate the sample solutions. In order to determine the quantum yield of the 4-nitropyridine *N*-oxide disappearance, the light intensity was measured with a potassium ferrioxalate actinometer. The absorption spectra were taken with a Hitachi recording spectro-photometer, EPS-2 U.

Flash Spectroscopic Experiment. The photolysis flash lamp consisted of a quartz tube 200 mm in length and about 20 mm in diameter, filled with xenon gas to about 150 mmHg. By discharging a bank of a condenser with a capacity of 25 μF charged to 4 kV, 200 joules of energy were dissipated; the half-width of the discharge time was about 50 microseconds. The reaction cell, consisting of a quartz tube 70 mm in length and 20 mm in diameter, was set parallel to the photolysis lamp. The reaction cell and the photolysis lamp were surrounded by a reflection plate. The flash lamp for the spectrograph was constructed much like to the photolysis lamp, but the capacity was 8 μF charged to 3.2 kV, the energy was about 40 joules, and the half-width of the discharge time was about 20 microseconds.

Experimental Results

Before describing the experimental results, it will be usefull for understanding the primary photochemical process of 4-nitropyridine *N*-oxide to mention briefly the photochemical reaction in an ethanol solution. The absorption spectrum of 4-nitropyridine *N*-oxide (*ca.* 10^{-4}—10^{-3} mol l^{-1} in ethanol) decreases progressively in intensity, and a new absorption band with its maximum at 269 mμ appears, as the irradiation time increases. Figure 1 shows the results for the 5×10^{-5} mol l^{-1} ethanol solution. After concentrating the irradiated solution under reduced pressure, the oily residues (Prod. X) are gradually crystallized to afford 4-hydroxypyridine *N*-oxide nitrate.[7] This photochemical reaction is referred to as Process I. When the concentrated ethanol solution of 4-nitropyridne *N*-oxide (*ca.* 10^{-2} mol l^{-1}) is irradiated with a 3130 A light in a nitrogen atmosphere, however, the nitro group of the 4-position is photochemically reduced to yield 4-hydroxylaminopyridine *N*-oxide.[6] The progressive change in the absorption spectrum of 4-nitropyridine *N*-oxide at 3130 Å irradiation is shown in Fig. 2, where two isosbestic points are observed at 254 mμ and 308 mμ.[6] This photochemical reaction is referred to as Process II.

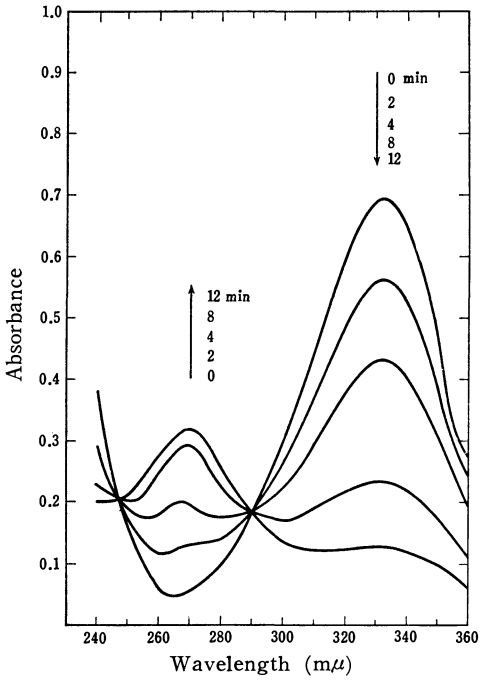

Fig. 1. The progressive spectral change of 4-nitropyridine *N*-oxide on 3130 Å irradiation in ethanol (5×10^{-5} mol l^{-1}). Numbers refer to irradiation time.

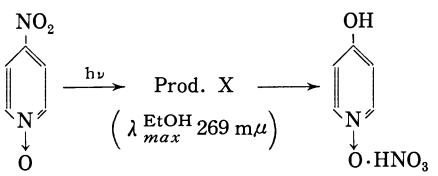

Process I

7) E. Ochiai, *J. Org. Chem.*, **18**, 535 (1953).

Process II

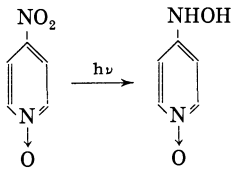

In order to examine the concentration dependency of the photochemical reaction, the 3130 Å irradiation was carried out in ethanol solutions with various concentrations of 4-nitropyridine *N*-oxide. Whether Process I or Process II was determined from the ultraviolet absorption spectrum of the irradiated solution, the results thus obtained are shown schematically in Fig. 3. As can be seen from Fig. 3, Process II proceeds both in a solution with an extremely low concentration (less than *ca.* 2×10^{-5} mol l^{-1}) and in a solution with a high concentration (over *ca.* 10^{-4} mol l^{-1}), whereas Process I proceeds strikingly in a solution with a medium concentration (*ca.* 10^{-4}—10^{-5} mol l^{-1}). The results obtained for the deaerated solution indicate that Process II can be facilitated by excluding any oxygen dissolved in the solution, and that Process I can proceed even in a deaerated solution.

Next, we examined the effect of the viscosity on the photochemical process and the effect of the concentration on the quantum yield of the 4-nitropyridine *N*-oxide disappearance. Figure 4 shows the progressive spectral change in 4-nitropyridine *N*-oxide when it is irradiated with 3130 Å light in glycerol and also in a glycerol solution mixed with various amounts of ethanol. Although Process II proceeded in a highly viscous solution, a lowering of the viscosity of the solution was observed to lead to a switch in the photochemical reaction from Process II to Process I. As is shown in Fig. 5, the quantum yield of 4-nitropyridine *N*-oxide disappearance in ethanol, where Process I takes

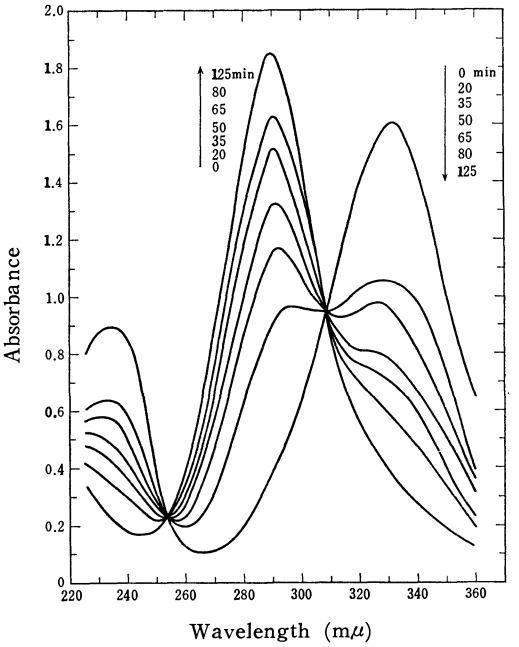

Fig. 2. The progressive spectral change of 4-nitropyridine *N*-oxide on 3130 A irradiation in ethanol (1.8×10^{-2} mol l^{-1}). Numbers refer to irradiation time.

place, increased markedly with an increase in the concentration, giving a maximum value (1.6—1.8) in the region of about 6×10^{-4} mol·l^{-1}. A further increase in the concentration caused a decrease in the quantum yield. On the other hand, the quantum yield in glycerol, where Process II takes place, was independent of the concentration and showed an average value of about 0.7. Figure 6 shows the temperature dependence of the quantum yield where the quantum yield of 4-nitropyridine *N*-oxide disappearance was observed to increase with a rise in the temperature. Although the quantum yield mentioned above was measured in a solution which had not

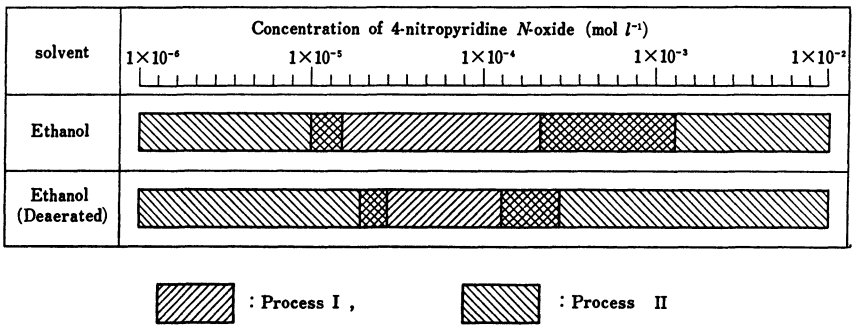

Fig. 3. Schematic representation of the photochemical processes of 4-nitropyridine *N*-oxide in ethanol.

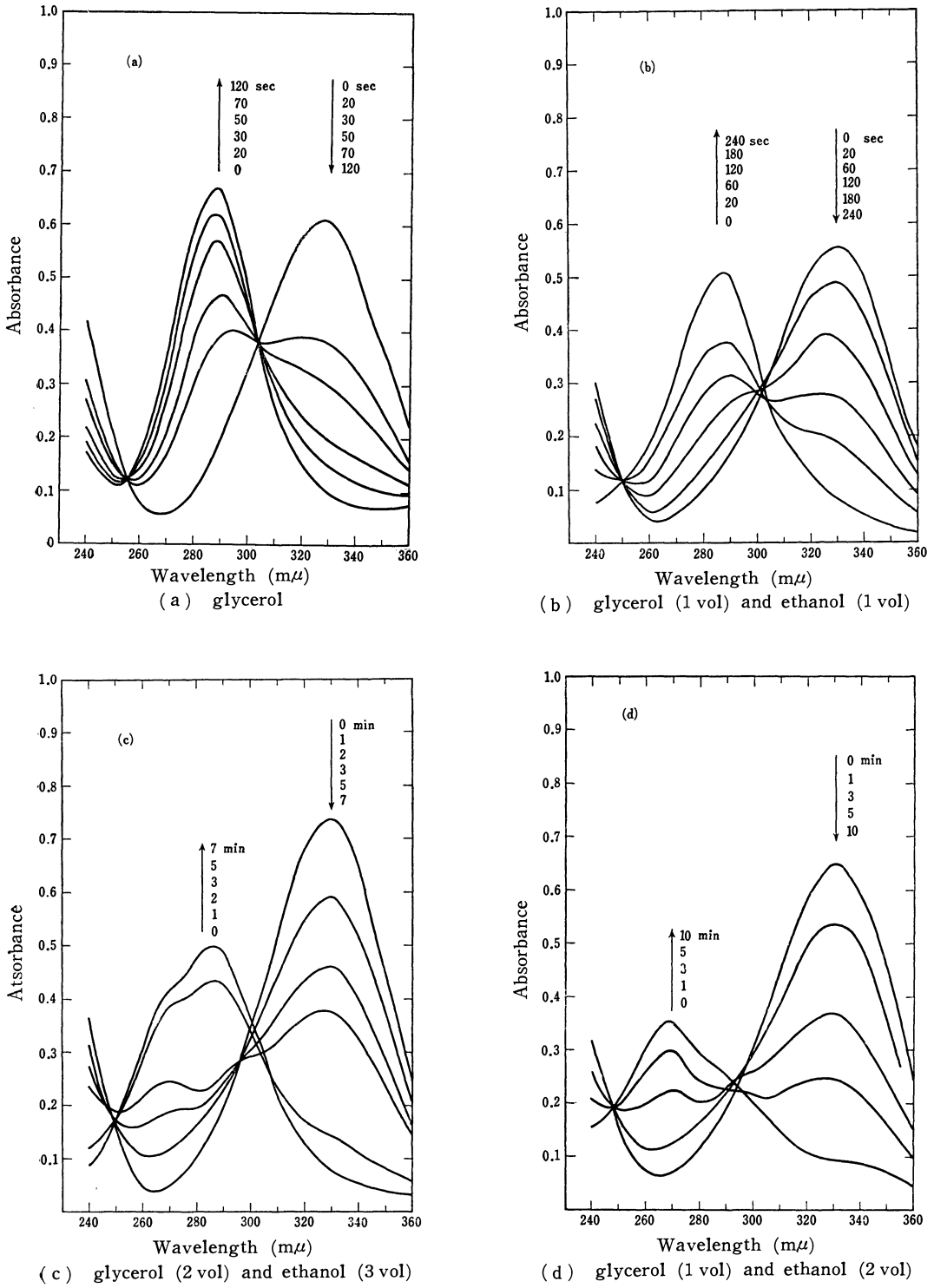

Fig. 4. The progressive spectral change of 4-nitropyridine *N*-oxide on 3130 Å irradiation in viscous solution (*ca.* 5×10^{-5} mol l^{-1}).
Numbers refer to irradiation time.

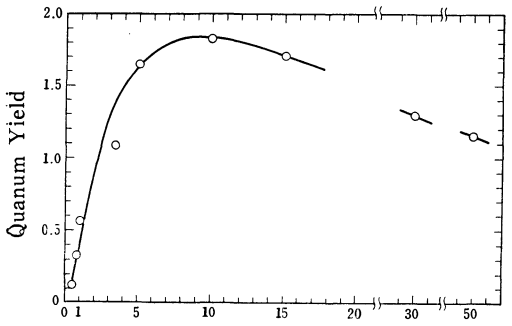

Fig. 5. Quantum yield (Φ) *versus* concentration of 4-nitropyridine *N*-oxide at 30°C in ethanol.

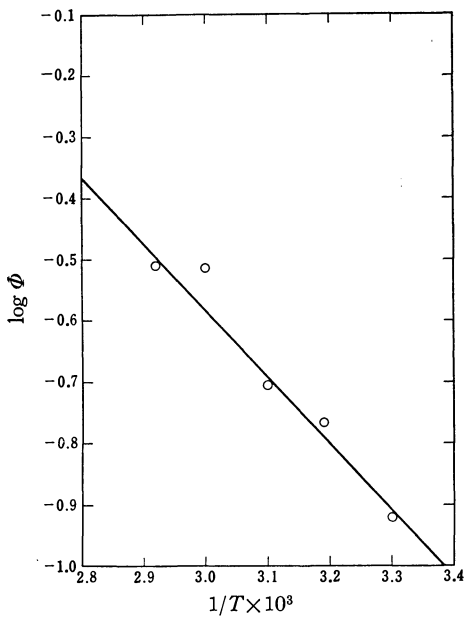

Fig. 6. Quantum yield (Φ) *versus* temperature in ethanol (5×10^{-5} mol l^{-1}).

been degassed, a comparison with the results for a solution degassed by flushing with nitrogen at 30°C indicated that there is possibly no effect of the oxygen dissolved in the solution on the quantum yield.

Finally, in order to get information on the photochemical intermediate which may be formed during the reaction, the flash spectroscopic examination was carried out in both ethanol and glycerol. In the case of a 5×10^{-5} mol l^{-1} ethanol solution (Fig. 7 (a)), transient absorptions were observed around 370 mμ and 570 mμ, but they disappeared within about 10^{-4} sec to give a shorter wavelength absorption (260 mμ—270 mμ) corresponding to the Prod. X being formed in Process I. In the case of a glycerol solution (4×10^{-5} mol l^{-1}), the same transient absorptions as in the case of an ethanol solution appeared around 370 mμ and 570 mμ, as is shown in Fig. 7 (b); these absorptions decayed within about 10^{-4} sec to give the absorption of 4-hydroxylaminopyridine *N*-oxide via Process II. Figure 7 (c) shows the results for the flash illumination in a very dilute ethanol solution (2×10^{-5} mol l^{-1}), which indicated the appearance of the same transient absorption, followed by Process I and Process II. In all these experiments, the transient absorption common to all three cases was independent of the presence or absence of oxygen in the solution.

Discussion

In the present paper, we propose the primary process shown schematically in Fig. 8 for the photochemical reaction of 4-nitropyridine *N*-oxide in solution, where S_0 and S_1 denote, respectively, the ground and the lowest excited singlet-state molecules, while both A and B represent intermediate species.

The following conclusions have been drawn from the flash spectroscopic experiments: 1) Both Process I and Process II proceed through the intermediate A. 2) The absorption spectrum of the intermediate A is always observed around 370 mμ and 570 mμ, regardless of the dissolved oxygen in solution, possibly meaning that the intermediate A is not a triplet state. 3) The intermediate A has a relatively long lifetime (*ca.* 10^{-4} sec), which suggests the possibility of a bimolecular interaction between the intermediate A and unexcited 4-nitropyridine *N*-oxide (S_0).

It is very difficult to bring the intermediate A together with an unexcited *N*-oxide molecule (S_0) in a glycerol solution because of the high viscosity of the solvent. As has been reported in a previous paper,[6] Process II involves a hydrogen atom-abstracting process from a solvent molecule, and thus an intermediate A probably abstracts a hydrogen atom from a glycerol molecule to form 4-hydroxylaminopyridine *N*-oxide finally. As to the hydrogen atom-abstracting species, however, it is not possible to say anything about whether it is an intermediate A or an intermediate B transformed further from an intermediate A. In any case, the intermediate A is responsible for Process II. Similarly, in a very dilute solution of 4-nitropyridine *N*-oxide the intermediate, either A or B, is considered to make an abstraction of a hydrogen atom from an ethanol molecule before colliding with an unexcited *N*-oxide molecule (S_0). In fact, the experimental results show that only Process II takes place in these solutions.

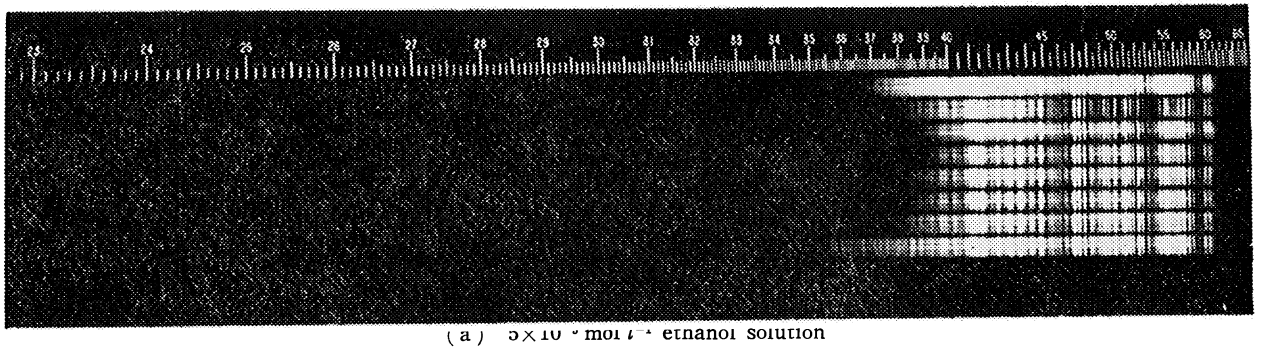

(a) 5×10^{-5} mol l^{-1} ethanol solution

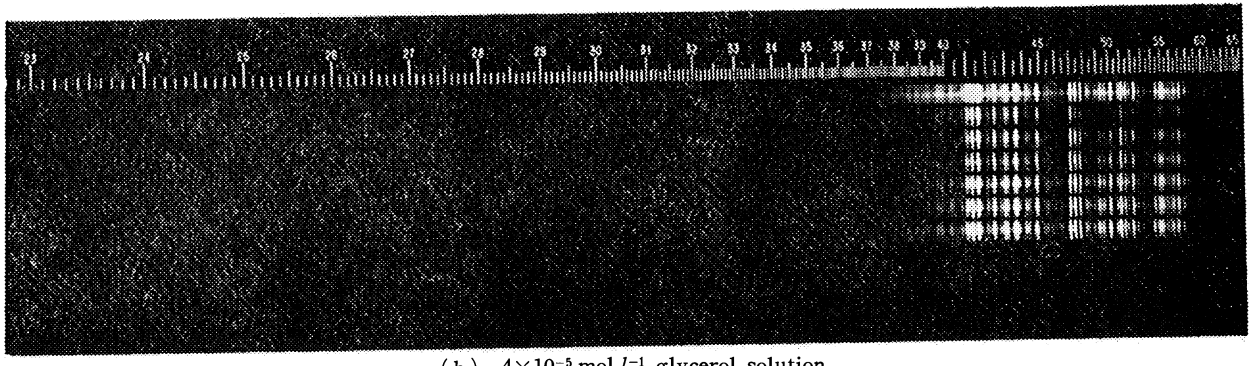

(b) 4×10^{-5} mol l^{-1} glycerol solution

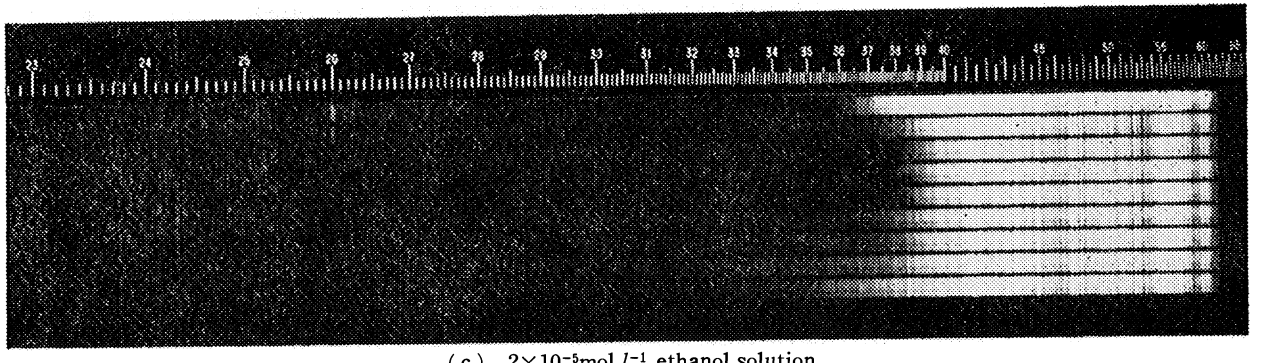

(c) 2×10^{-5}mol l^{-1} ethanol solution

Fig. 7. Flash photolysis of 4-nitropyridine *N*-oxide.

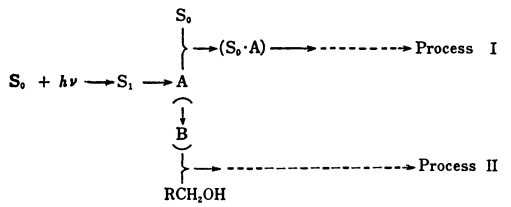

Fig. 8. The primary photochemical process of 4-nitropyridine *N*-oxide in solution.

On the other hand, as the concentration of 4-nitropyridine *N*-oxide in ethanol increases, the possibility of a collisional encounter of the intermediate A with an unexcited *N*-oxide molecule (S_0) becomes more likely; therefore, a bimolecular reaction between them can be expected to take place. This is confirmed by the experimental results on the concentration dependence of the photochemical reaction (Fig. 3) and on the quantum yield of 4-nitropyridine disappearance (Fig. 5). Moreover, further support for it is given by the following experimental results: 1) As the viscosity of the glycerol solution is lowered by adding various amounts of ethanol, the photochemical reaction is converted from Process II to Process I (Fig. 4). 2) The quantum yield of the 4-nitropyridine *N*-oxide disappearance in an ethanol solution increases gradually with a rise in the tempreature (Fig. 6), from which fact the activation energy is estimated to be about 5 kcal mol^{-1}, which is considered to correspond to the activation energy of diffusion.

However, the following experimental results are not clearly explained: 1) In a very concentrated ethanol solution Process I does not proceed; rather, Process II takes place. 2) In connection with 1), the quantum yield of the 4-nitropyridine *N*-oxide disappearance decreases with an increase in the concentration after reaching its maximum value. One possible explanation for these facts is to assume the formation of a transient weak complex between A and S_0. That is, with an increase in the concentration, most of the weak complex formed may be quenched by collision with an unexcited *N*-oxide molecule (S_0), thus reproducing S_0 and A, and the intermediate species, A, thus reproduced may be responsible for Process II. Further studies of these points, including the details of Process I and II and the nature of the intermediate A, are now in progress and will be reported on later.

In conclusion, the authors wish to express their hearty thanks to Professor S. Kato of Osaka University and Dr. Y. Mori of the Tokyo Institute of Technology for their valuable suggestions.

BULLETIN OF THE CHEMICAL SOCIETY OF JAPAN VOL. 41 1776—1783 (1968)

Studies of the Aggregation of Dyes. A Spectrophotometric Method of Determining the Aggregation Numbers of Dyes

Mitsuhiko HIDA

Faculty of Engineering, The University of Tokyo, Hongo, Tokyo

and Akihiko YABE, Hiroko MURAYAMA and Masako HAYASHI

Faculty of Home Economics, Ochanomizu University, Otsuka, Tokyo

(Received January 9, 1968)

The aggregation of dyes in an aqueous or alcoholic solution has been studied spectroscopically by a method named the "maximum slope method." The method can ascertain the molar absorptivity and formation constant of dye aggregate when a simple equilibrium model between a monomer and an *n*-mer is assumed to be operative, and when the absorptivity of monomer is given. Further, the molar absorptivities of the monomer and the polymers and the formation constants of the polymers are adjusted, in order to minimize the mean deviation, by an other method, named the "minimum deviation method." Using the latter method, the parameters of an equilibrium system including a monomer and several polymers can also be calculated. Aggregations of Benzopurprine 4 B and Sky Blue FF in aqueous salt solutions were studied by the above two methods. Aggregations of these dyes in aqueous alcoholic solutions were also discussed.

In resent years, the solvent-assisted dyeing of wool goods by acid dyes has been developed for the industrial use, and several fundamental discussions of the mechanism of solvent dyeing have been reported.[1,2]

Yabe and Hayashi[3,4] have already reported on the extraordinarily quick and high absorption of direct dyes on cellulose in the H_2O/*n*-BuOH dyebath system, and compared the absorption spectrum of the cellophane dyeings from normal and solvent-assisted systems.

A new way of determining the aggregation numbers of organic substances including dyes in solution has to be developed, as the physical state of direct dyes in solution is supposed to influence greatly on that of dyes on the substrates. This report may contribute to clarify the aggregation of dye molecules in solution.

When a dye aggregates in solution, the molar absorptivity (ε) changes with an increase in the dye concentration; it shall be given by a weighted mean of the molar absorptivities of each aggregate (Eq. (1)):

$$\varepsilon = \sum_{i=1}^{n} f_i \varepsilon_i, \qquad (1)$$

where ε_i is the molar absorptivity of the pure *i*-mer, and f_i, the corresponding molar fraction. Since the equilibrium constant, K_i and ε_i can not be determined from Eq. (1) alone, a simple equilibrium between the monomer and a polymer of only one distinct degree of aggregation is assumed*1; then:

$$\varepsilon = f_1\varepsilon_1 + f_n\varepsilon_n, \qquad (2)$$

$$1 = f_1 + nf_n. \qquad (3)$$

If the activity coefficients are assumed to be constant in the concentration range studied, we have:

$$f_n = K_n C_1{}^n C, \qquad (4)$$

where C_1 and C are the monomer and the total dye concentration respectively. By combining Eq. (2) with Eqs. (3) and (4), we get Eq. (5):

$$\log C(\varepsilon_1-\varepsilon) = n \log C(\varepsilon-\bar{\varepsilon}_n) + \log nK_n(\varepsilon_1-\bar{\varepsilon}_n)^{1-n}. \qquad (5)$$

In Eq. (5), ε_n/n is designated as $\bar{\varepsilon}_n$. Hence, if $\log C(\varepsilon_1-\varepsilon)$ is plotted against $\log C(\varepsilon-\bar{\varepsilon}_n)$, the points should lie on a straight line, the slope of which gives the degree of aggregation (n), and the equilibrium constant (K_n) can

1) L. Peters and C. B. Stevens, *J. Soc. Dyers & Colourists*, **72**, 241 (1956).
2) M. Korrholm and J. Lindberg, *Text. Res. J.*, **26**, 528 (1956).
3) M. Hayashi, Y. Matsumoto and A. Yabe, *Kogyo Kagaku Zasshi* (*J. Chem. Soc. Japan, Ind. Chem. Sect.*), **67**, 221 (1964).
4) M. Hayashi, K. Kawabata, Y. Matsumoto and A. Yabe, *ibid.*, **69**, 1176 (1966).

*1 This simplifying assumption of the monomer-*n*-mer equilibrium model has been accepted as being consistent in many dye aggregation systems.

be calculated from the intercept. By assuming suitable values for ε_1 and $\bar{\varepsilon}_n$, Kuhn[5] has shown that the association degree of sodium phthalocyaninetetrasulfonate is 2 and 4 in, respectively, lower and higher concentration ranges in aqueous solutions, while Zanker[6] and Mataga[7] suggested neglecting the $\bar{\varepsilon}_n$'s of basic dyes in the calculation of Eq. (5), as they are too small compared with ε and ε_1. However, the values of ε_1 and $\bar{\varepsilon}_n$ are not always determined accurately, or $\bar{\varepsilon}_n$ cannot be neglected, especially when the polymer band does not differ very much from the monomer band. In such cases, therefore, it seems difficult to obtain reliable results by the use of Eq. (5).

In an attempt to avoid these difficulties, Hosoya and Nagakura computed the ε_1, ε_2 and K_2 of benzoic acid in the dimerisation stage in an aqueous solution by means of least-squares calculation.[8] The method developed by them affords the most reliable results, but the computations must be carried out on a computer, since the least-squares calculation had to be repeated until the parameters converge to certain values.

The present authors have, therefore, developed a method, named the "maximum slope method,"*2 which involves a simpler computation and less supposition, and which still gives more reliable results.

Theoreticals

(1) **Maximum Slope Method.** Equation (6) is derived from Eq. (5):

$$\frac{1}{n-1}\log(\varepsilon_1-\varepsilon)-\frac{n}{n-1}\log(\varepsilon-\bar{\varepsilon}_n)=\log\alpha C,$$
$$\alpha=(nK_n)^{1/(n-1)}(\varepsilon_1-\bar{\varepsilon}_n). \qquad (6)$$

Taking $\log\alpha C=X$, Eq. (6) reads:

$$\frac{1}{n-1}\log(\varepsilon_1-\varepsilon)-\frac{n}{n-1}\log(\varepsilon-\bar{\varepsilon}_n)=X. \qquad (7)$$

The curve of ε *vs.* $\log C$ can be correlated with the curve of ε *vs.* X as follows.

(1) The two curves can be superposed on each other by sliding over the abscissa for some distance ($\log\alpha$); equilibrium constant (K_n) can thus be calculated.

(2) The maximum slope of the tangents of two curves ($\varepsilon-\log C$ and $\varepsilon-X$) are equal to each other; that is,

$$(\mathrm{d}\varepsilon/\mathrm{d}(\log C))_{\max}=(\mathrm{d}\varepsilon/\mathrm{d}X)_{\max}$$
$$=-2.3\left(\frac{\sqrt{n}-1}{\sqrt{n}+1}\right)(\varepsilon_1-\bar{\varepsilon}_n)$$

(3) The maximum slope is proportional to $(\varepsilon_1-\bar{\varepsilon}_n)$. The values of $\bar{\varepsilon}_n$, K_n and n are obtained by the following procedure on the basis of these three correlations:

(1) The maximum slope (m_0) of the tangent of the plotted curve ($\varepsilon-\log C$) is determined, and the absorptivity ε_1 is evaluated by extrapolating to an infinite dilution.

(2) On substituting a suitable value for $\bar{\varepsilon}_n$, and 2 for n, the X's corresponding to ε's are computed from Eq. (7).

(3) Then the maximum slope (m) of the tangent of the curve ($\varepsilon-X$) is determined. In general, m is not equal to m_0, because $\bar{\varepsilon}_n$ is not the true value. However, $\bar{\varepsilon}_n$ can easily be adjustable to its true value ($(\bar{\varepsilon}_n)_0$) by Eq. (9):

$$m_0/m=(\varepsilon_1-(\bar{\varepsilon}_n)_0)/(\varepsilon_1-\bar{\varepsilon}_n) \qquad (9)$$

(4) The curve ($\varepsilon-X$) is slided over the abscissa until the two tangential maximum-slope are superposed.

(5) These fitting processes are also carried out on $n=3$, 4, and so on.

(6) Then, we determine the theoretical n value which best fits the experimental curve.

Hosoya and Nagakura's results on the dimerisation of benzoic acid in an aqueous solution[8] have been analysed by this maximum slope method, and the final values of ε_1, ε_2 and K_2 and the accuracy were compared with those obtained by the repeated least-squares method by the above authors (Table

TABLE 1. DIMERISATION OF BENZOIC ACID

method	I[a]	II[b]	III[c]
$\varepsilon_1\times10^{-3}$	0.870	0.887	0.868
$\varepsilon_2\times10^{-3}$	3.300	3.274	3.240
$K\times10^{-3}$	0.659	0.661	0.795
Mean deviation (%)[d]	0.58	0.32	0.59

a) Maximum slope method
b) Minimum deviation method
c) Parameters given by Hosoya and Nagakura (Ref. 8)
d) Mean deviation $=N/100\sum|\varepsilon_{obs}-\varepsilon_{calc}|/\varepsilon_{obs}$, where ε_{obs} and ε_{calc} are apparent observed and calculated molar absorptivities, and N is number of data.

5) H. Kuhn, E. Schnabel and H. Nöther, "Recent Progress in the Chemistry of Natural and Synthetic Colour Matters and Related Field," ed. by T. S. Gore, Academic Press (1962), p. 561.
6) V. Zanker, *Z. Phys. Chem.*, **200**, 250 (1952).
7) N. Mataga, This Bulletin, **30**, 375 (1957).
8) H. Hosoya and S. Nagakura, *J. Mol. Spectroscopy*, **8**, 257 (1962).
*2 This method has been developed quite independently by the authors, but it has proved to be quite similar in idea to the one which had already been reported by Sanders and Hyne[9] for analyzing the NMR spectra of associated alcohols and phenol.
9) M. Sanders and J. B. Hyne, *J. Chem. Phys.*, **29**, 1319 (1958).

1). Table 1 shows that the accuracy of the maximum slope method is as good as that of the repeated least-squares method.

(2) The Minimum Deviation Method. In spite of its usefulness, the maximum slope method has the defect that one should assume a definite value of ε_1, for an error involved in the evaluation of ε_1 may result in some uncertainty in the $\bar{\varepsilon}_n$, K_n or even n value estimated. In this respect, the values, ε_1, $\bar{\varepsilon}_n$ and K_n obtained from the maximum slope method must be readjusted to minimize the possible errors by the minimum deviation method. The mathematical procedure is as follows:

The zero approximations, $(\varepsilon_1)_0$, $(\bar{\varepsilon}_n)_0$ and $(K_n)_0$, are chosen as the values obtained by the maximum slope method. The calculated absorptivities, ε_{calc}, are obtained from Eq. (2') using the monomer concentrations, C_1, obtained by solving Eq. (10):

$$\varepsilon_{calc} = (\varepsilon_1 C_1 + n\bar{\varepsilon}_n K_n C_1^n)/C \quad (2')$$

$$C = C_1 + nK_n C_1^n \quad (10)$$

A mean deviation (Δ) is given by Eq. (11):

$$\Delta = \frac{1}{N}\sum |\varepsilon_{calc} - \varepsilon_{obs}|/\varepsilon_{obs}$$

The effects (δ) of changing each parameter by 0.1% on the mean deviation are determined to be:

$$\left.\begin{aligned} \delta_1 &= \Delta(1.001\,\varepsilon_1, \bar{\varepsilon}_n, K_n) - \Delta(\varepsilon_1, \bar{\varepsilon}_n, K_n) \\ \delta_2 &= \Delta(\varepsilon_1, 1.001\,\bar{\varepsilon}_n, K_n) - \Delta(\varepsilon_1, \bar{\varepsilon}_n, K_n) \\ \delta_3 &= \Delta(\varepsilon_1, \bar{\varepsilon}_n, 1.001\,K_n) - \Delta(\varepsilon_1, \bar{\varepsilon}_n, K_n) \end{aligned}\right\} \quad (12)$$

Then, all the parameters are simultaneously changed in proportion to $\varepsilon_1\delta_1$, $\bar{\varepsilon}_n\delta_2$, and $K_n\delta_3$, respectively, until no further decrease in the mean deviation is found. Thus, the new parameters, the higher approximations, are obtained, and again their effects on the mean deviation are determined; the same fitting process continues until no further decrease in the mean deviation is possible.*3

The results refined by the minimum deviation method are compared with those obtained by the maximum slope method and those obtained by the least-squares method in Table 1. It can be seen that a combination of the maximum slope method with the minimum deviation method can give the best fit of the experimental curves of ε *vs.* $\log C$. Also, it is noticeable that the results obtained by the maximum slope method do not differ much from the best values.

When the mean deviations of several monomer-n-mer models are similar to one another, one should also consider models including all or some of those n-mers; that is,

$$mD \rightleftarrows D_{m_1} + D_{m_2} + \cdots + D_{m'} \quad (m = \sum m_i) \quad (13)$$

In this case the monomer concentration is obtained by solving Eq. (14), instead of Eq. (10), and ε_{calc} is computed by Eq. (15):

$$C = C_1 + m_1 K_{m_1} C_{1m_1} + \cdots + m' K_{m'} C_1^{m'} \quad (14)$$

$$\varepsilon_{calc} = (\varepsilon_1 C_1 + \varepsilon_{m_1} K_{m_1} C_{1m_1} + \cdots + \varepsilon_{m'} K_{m'} C_1^{m'})/C \quad (15)$$

The ε_i and K_i values of each polymer, as evaluated by the above-described procedure, were taken as the zero approximation and were treated by a process similar to the minimum deviation method.

Results and Discussions

(1) Benzopurprine 4B (C.I. Direct Red 2) in an Aqueous Salt Solution. Benzopurprine 4B did not aggregate in an aqueous solution; no change in absorptivity was observed in the concentration range between 10^{-7} and 10^{-4} mol/l.*4

On the other hand, upon the addition of

TABLE 2. THE AGGREGATION PARAMETERS OF BENZOPURPINE 4B AT SALT CONCENTRATION OF 20 mmol/l

Monomer-n-mer equilibrium model*

n	2	3	4
$\varepsilon_1\times10^{-5}$	0.5 (0.504)	0.5 (0.503)	0.5 (0.501)
$\varepsilon_n\times10^{-5}$	0.838 (0.822)	1.275 (1.265)	1.720 (1.695)
$K_n\times10^{-5(n-1)}$	1.62 (1.62)	5.92 (5.92)	18.76 (18.76)
Mean deviation (%)	1.44 (1.20)	1.37 (1.27)	1.61 (1.39)

Models including two or three polymers

Polymer included**	2+3	2+3+4
$\varepsilon_1\times10^{-5}$	0.511	0.510
$\varepsilon_2\times10^{-5}$	0.857	0.869
$\varepsilon_3\times10^{-5}$	1.260	1.318
$\varepsilon_4\times10^{-5}$	—	1.663
$K_2\times10^{-5}$	1.617	1.620
$K_3\times10^{-10}$	5.913	5.917
$K_4\times10^{-15}$	—	18.73
Mean deviation (%)	1.25	1.22

*The parameters computed by minimum deviation method are given in parenthesis.

**For example, 2+3 shows a model including dimer and trimer.

*3 In actuality the process was stopped when Δ increased with variations in ε_1, $\bar{\varepsilon}_n$, and K_n by $\varepsilon_1\delta_1$, $\bar{\varepsilon}_n\delta_2$, and $K_n\delta_3$ respectively.

*4 The constancy of molar absorptivity does not always preclude the existence of aggregates in solution. Much work has to be done in this connection.

salt (NaCl) the absorption spectrum shifted both hypso- and hypochromicaly; this shows the formation of dye aggregates in an aqueous salt solution. Table 2 shows the aggregation parameters at a salt concentration of 20 mmol/l and also the mean deviations of models, including monomer to tetramer; the latter appear to be similar to one another, although the deviation of the monomer-dimer system is the least. Unfortunately, we could not decide from the point of view of statistical analysis which model was preferable, because of the inevitable experimental errors.

The parameters at a salt concentration of 40 mmol/l are compared in Table 3. A statistical analysis showed that the monomer-dimer and monomer-dimer-trimer-tetramer models could be discarded, because of their large deviations. Thus, the monomer-dimer-trimer, monomer-trimer, and monomer-tetramer models are preferable in this case from the point of view of statistical analysis. On the other hand, Fig. 1 shows that the monomer-trimer model approximates the monomer-dimer-trimer model because of the negligible contribution of the dimer fraction in this case. If we assume that, in the aggregation stage of Benzopurprine 4B, several polymers exist together rather than a single polymer, and if the monomer - n-mer model can be considered as an approximation of the model including the monomer and all or some of the polymeres up to n-mer, the most preferable model among the models shown in Table 3 is the monomer-dimer-trimer model. Hence, the most preferable model at a salt concentration of 20 mmol/l may be determined to be among the monomer-dimer, monomer-trimer and monomer-dimer-trimer models. Figure 2 shows that the contribution of the dimer at a salt concentration of 20 mmol/l is larger than that at 40 mmol/l.

The deviations of the twenty models including all or a part of the monomer to heptamer at a salt concentration of 80 mmol/l are also compared. The monomer-tetramer-pentamer-hexamer-heptamer, the monomer-hexamer-heptamer, and the monomer-pentamer-hexamer-heptamer models may be preferable from the point of view of statistical analysis. The parameters of these models are also shown in Table 4.

TABLE 3. THE AGGREGATION PARAMETERS OF BENZOPURPRINE 4B AT SALT CONCENTRATION OF 40 mmol/l

Models including single polymer

n	2	3	4
$\varepsilon_1\times10^{-5}$	0.5 (0.506)	0.5 (0.504)	0.5 (0.509)
$\varepsilon_n\times10^{-5}$	0.712 (0.718)	1.242 (1.235)	1.760 (1.697)
$K_n\times10^{-5(n-1)}$	0.601 (0.599)	6.21 (6.21)	102.9 (102.9)
Mean deviation (%)	1.55 (1.09)	0.53 (0.46)	2.35 (0.55)

Models including several polymers

Model	2+3	2+3+4
$\varepsilon_1\times10^{-5}$	0.509	0.515
$\varepsilon_2\times10^{-5}$	0.715	0.714
$\varepsilon_3\times10^{-5}$	1.267	1.244
$\varepsilon_4\times10^{-5}$	—	1.718
$K_2\times10^{-5}$	0.600	0.600
$K_3\times10^{-10}$	6.21	6.21
$K_4\times10^{-15}$	—	102.8
Mean deviation (%)	0.49	0.74

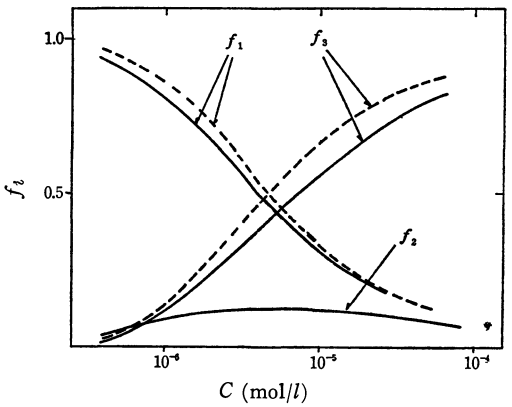

Fig. 1. Mole fractions of polymers *vs.* dye (Benzopuprine 4B) concentration (salt concentration ; 40 mmol/l). ($f_i=iC_i/C$)
—— monomer-dimer-trimer model
---- monomer-trimer model

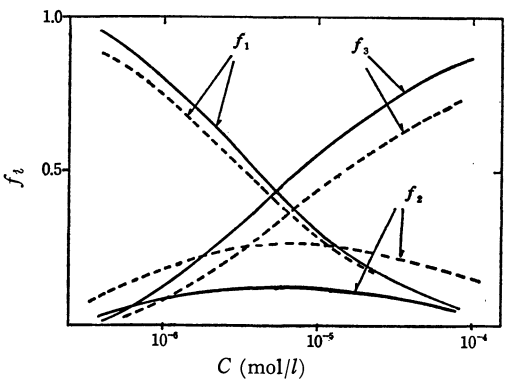

Fig. 2. Mole fractions of polymers *vs.* dye concentration (Benzopurprine 4B). ($f_i=iC_i/C$)
—— at salt concentration of 20 mmol/l
---- at salt concentration of 40 mmol/l

TABLE 4. THE AGGREGATION PARAMETERS OF BENZOPURPRINE 4B AT SALT CONCENTRATION OF 80 mmol/l

	1+5	1+6	1+7	1+2+3+4	1+2+3+4+5	1+2+3+4+5+6+7
$\varepsilon_1\times10^{-5}$	0.480	0.478	0.478	0.503	0.501	0.500
$\bar{\varepsilon}_2\times10^{-5}$	—	—	—	0.349	0.350	0.352
$\bar{\varepsilon}_3\times10^{-5}$	—	—	—	0.347	0.360	0.380
$\bar{\varepsilon}_4\times10^{-5}$	—	—	—	0.350	0.365	0.358
$\bar{\varepsilon}_5\times10^{-5}$	0.347	—	—	—	0.333	0.340
$\bar{\varepsilon}_6\times10^{-5}$	—	0.353	—	—	—	0.352
$\bar{\varepsilon}_7\times10^{-5}$	—	—	—	—	—	0.347
$K_2\times10^{-5}$	—	—	—	0.6	0.6	0.6
$K_3\times10^{-10}$	—	—	—	6.2	6.2	6.2
$K_4\times10^{-15}$	—	—	—	3.0	3.0	3.0
$K_5\times10^{-20}$	15.7	—	—	—	15.8	15.7
$K_6\times10^{-25}$	—	93.0	—	—	—	93.1
$K_7\times10^{-30}$	—	—	432.2	—	—	432.8
Mean deviation (%)	1.3	1.3	1.3	1.7	1.7	1.6

	1+4+5	1+4+5+6	1+4+5+6+7	1+5+6	1+5+6+7	1+6+7
$\varepsilon_1\times10^{-5}$	0.479	0.480	0.481	0.479	0.481	0.479
$\varepsilon_2\times10^{-5}$	—	—	—	—	—	—
$\varepsilon_3\times10^{-5}$	—	—	—	—	—	—
$\varepsilon_4\times10^{-5}$	0.363	0.360	0.360	—	—	—
$\varepsilon_5\times10^{-5}$	0.345	0.345	0.436	0.346	0.346	—
$\varepsilon_6\times10^{-5}$	—	0.360	0.364	0.360	0.363	0.362
$\varepsilon_7\times10^{-5}$	—	—	0.363	—	0.361	0.359
$K_2\times10^{-5}$	—	—	—	—	—	—
$K_3\times10^{-10}$	—	—	—	—	—	—
$K_4\times10^{-15}$	3.0	3.0	—	—	—	—
$K_5\times10^{-20}$	15.7	15.7	15.7	15.7	15.7	—
$K_6\times10^{-25}$	—	92.9	93.0	92.9	93.0	93.0
$K_7\times10^{-30}$	—	—	431.9	—	431.9	432.0
Mean deviation (%)	1.3	1.4	1.5	1.3	1.5	1.4

TABLE 5. THE EXTINCTION COEFFICIENTS PER MOLECULE OF AGGREGATE (Benzopurprine 4B)

	NaCl concentration		
$\bar{\varepsilon}_n$	20 mmol/l	40 mmol/l	80 mmol/l
ε_1	0.50	0.50	0.48
$\bar{\varepsilon}_2$	0.43	0.36	—
$\bar{\varepsilon}_3$	0.43	0.42	—
$\bar{\varepsilon}_4$	0.42	0.43	0.36
$\bar{\varepsilon}_5$	—	—	0.35
$\bar{\varepsilon}_6$	—	—	0.37
$\bar{\varepsilon}_7$	—	—	0.36

Thus, it may be concluded that Benzopurprine 4B tends to form higher aggregates in more concentrated salt solutions. Further, it is noteworthy that the extinction coefficients per molecule of aggregates are all approximately the same (Table 5), and that the logalism of K_n increases in arithmetical progression (Fig. 3); that is,

$$\log K_n = 5.3(n-1)^{*5}$$

*5 This may suggest the constancy of the molar free energy of aggregation; the subject will be discussed further elsewhere.

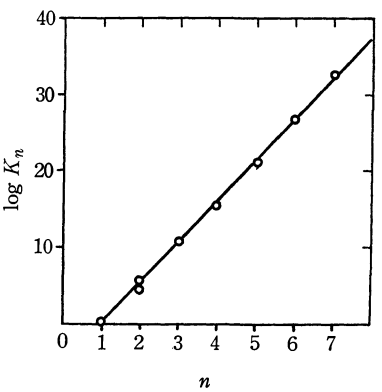

Fig. 3. Plot of $\log K_n$ *vs.* n (Benzopurprine 4B).

Alexander and Stacey observed the formation of the aggregation of Benzopurprine 4B by the light-scattering method; they estimated the degree of aggregation ($n>6$) in solutions of above 10^{-4} mol/l dye and above 10 mmol/l NaCl.[10] Table 6 shows that the dye did not scatter light below 10^{-4} mol/l dye and 20 mmol/l or 40mmol/l salt, but that it did scat-

TABLE 6. LIGHT SCATTERING DATA OF BENZOPURPRINE 4B

Concentration of the dye (mol/l)	Concentration of salt (mmol/l)				
	20	40	80		
	Scattering (τ)		Relative scattering* (τ/τ_0)×100		
				obs.	calc.
10^{-6}	0	0.1	0.2	0.4	0.2
10^{-5}	0.1	0.1	2.7	12	8
10^{-4}	0.1	1	44	100	100

*A value at dye concentration 10^{-4} mol/l are chosen as τ_0.

ter light markedly above 10^{-5} mol/l dye and 80 mmol/l salt.

It has been shown that the reduced scattering (C/τ) is in a linear relationship with the reciprocal of the molecular weight.[10] Thus:

$$\text{const. } n^2(dn/dC)^2(C/\tau) = \frac{1}{M} + B_c,$$

where $\tau = I_S/I_0$, and I_S denotes the intensity of the light scattered at a right angle to the incident beam. By supposing that each aggregate scatters light independently, that the interaction term (B_c) is negligible, and that the refractive index (n) may be taken to be nearly constant, the scattering may be approxmately represented by Eq. (15):

$$\tau = I_S/I_0 \propto (\sum i^2 f_i)CM_0, \qquad (15)$$

where the index, i, ranges over the polymers included, f_i is the molar fraction of the i-mer, and M_0 is the molecular weight of monomer. Then the relative scattering (τ/τ_0) can be written as:

$$\tau/\tau_0 = \frac{(\sum i^2 f_i)C}{(\sum i^2 f_i)_0 C_0}, \qquad (16)$$

where τ_0 denotes the scattering of the most concentrated solution. In the fifth and the sixth columns of Table 6, the observed relative scatterings are compared with that calculated by Eq. (16); the molar fractions of the aggregates were computed by the use of the parameters of the monomer-hexamer-hpetamer model.

(2) **Benzopurprine 4B in an Alcoholic Solution.** The plots of the absorptivities against the log C of Benzopurprine 4B in an alcoholic solution were not sigmoid, but in an L shape. This means that the aggregation numbers and or formation constants are very large. If n is taken to be very large, Eq. (6) can be rewritten as Eq. (6'):

10) P. Alexander and K. A. Stacey, *Proc. Roy. Soc. A*, **212**, 274 (1952).

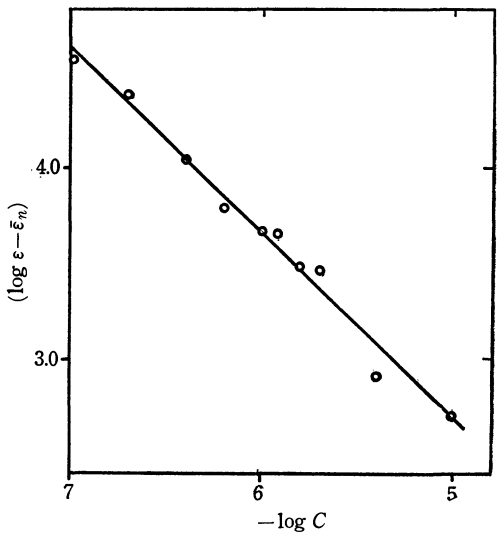

Fig. 4. Plot of log($\varepsilon-\bar{\varepsilon}_n$) *vs.* log C in 90% n-butanol aqueous solution (Benzopurprine 4B). ($\bar{\varepsilon}_n = 5.25\times10^4$)

$$\log(\varepsilon-\bar{\varepsilon}_n) = -\frac{n-1}{n}(\log C + \log\alpha) \qquad (6')$$

Thus, a plot of log($\varepsilon-\bar{\varepsilon}_n$) *vs.* log C gives a straight line with a slope of $-(n-1)/n$, near to -1, and an intercept of $[-(n-1)/n]\log\alpha$. As a typical example, Fig. 4 illustrates the aggregation in a 90% n-butanol aqueous solution in a high polymer ($n \doteqdot 30$). However, the equilibrium between the monomer and a single higher polymer may not be natural.

All from the monomer to the n-mer can be included, if it is assumed that all the absorptivities per molecule of n-mer's, except for the monomer, are identical, and that $K_n = K^{n-1}$. Then we have Eqs. (18) and (19):

$$C = \sum_i i k^{i-1} C_1{}^i \qquad (17)$$

$$C = \varepsilon_1 C_1 + \bar{\varepsilon}_n \sum_i i K^{i-1} C_1{}^i \qquad (18)$$

By combining Eq. (17) with Eq. (18), we obtain:

$$C_1/C = \frac{\varepsilon-\bar{\varepsilon}_n}{\varepsilon_1-\bar{\varepsilon}_n}. \qquad (19)$$

The sum of the progression in Eq. (17) may be calculated as:

$$C = \frac{C_1\{1-(n+1)(kC_1)^n + n(kC_1)^{n+1}\}}{(1-kC_1)^2} \qquad (20)$$

If kC_1 is taken to be much larger than unity, Eq. (20) can be written as follows:

$$kC \doteqdot n(kC_1)^n \qquad (21)$$

By substituting Eq. (19) into Eq. (21), we

get Eq. (22).

$$\log(\varepsilon-\bar{\varepsilon}_n) = -\frac{n-1}{n}(\log C+\log(\varepsilon_1-\bar{\varepsilon}_n)^n k^{1-n}/n) \quad (22)$$

when $(n-1)/n$ is near to unity, Eq. (22) is identical with Eq. (6′). Thus, Eq. (22) can give a physical meaning of Eq. (6′), derived by the monomer-n-mer model. The aggregation number in an n-butyl alcoholic aqueous solution (80%) is obtained as 30 by the linear plots of $\log(\varepsilon-\bar{\varepsilon}_n)$ *vs.* $\log C$. In this case kC_1 calculated by Eq. (23) is much larger than unity, since $\log k(\varepsilon_1-\bar{\varepsilon}_n)^{-1}$ is calculated as 5.3, and $\log C(\varepsilon-\bar{\varepsilon}_n)$ has values ranging between −2.4 and −2.3*6

$$kC_1 = k(\varepsilon_1-\bar{\varepsilon}_n)^{-1}C(\varepsilon-\bar{\varepsilon}_n) \quad (23)$$

(3) Sky Blue FF (C.I. Direct Blue 1) in Aqueous Salt and Alcoholic Solutions. Sky Blue FF aggregates in polymer form not more than in trimer form in an aqueous salt solution. The parameters are compared in Tables 7, 8 and 9.

TABLE 7. PARAMETERS OF SKY BLUE FF IN AQUEOUS SALT SOLUTION (20 mmol/l)

Polymers included	2	3	2+3
$\varepsilon_1\times10^{-5}$	0.85 (0.843)	0.85 (0.844)	0.850 (0.855)
$\varepsilon_2\times10^{-5}$	1.46 (1.454)	—	1.460 (1.483)
$\varepsilon_3\times10^{-5}$	—	2.31 (2.257)	2.31 (2.258)
$K_2\times10^{-5}$	0.658 (0.658)	—	0.658 (0.657)
$K_3\times10^{-10}$	—	4.07 (4.062)	4.07 (4.060)
Mean deviation (%)	1.04 (0.85)	1.63 (1.09)	1.27 (1.17)

TABLE 8. PARAMETERS OF SKY BLUE FF IN AQUEOUS SALT SOLUTION (40 mmol/l)

Polymers included	2	3	2+3
$\varepsilon_1\times10^{-5}$	0.83 (0.830)	0.83 (0.830)	0.83 (0.835)
$\varepsilon_2\times10^{-5}$	1.38 (1.380)	—	1.38 (1.380)
$\varepsilon_3\times10^{-5}$	—	2.22 (2.191)	2.22 (2.216)
$K_2\times10^{-5}$	0.32 (0.320)	—	0.32 (0.320)
$K_3\times10^{-10}$	—	1.03 (1.026)	1.03 (1.026)
Mean deviation (%)	0.47 (0.47)	0.86 (0.65)	0.66 (0.63)

TABLE 9. PARAMETERS OF SKY BLUE FF IN AQUEOUS SALT SOLUTION (80 mmol/l)

Polymers included	2	3	2+3
$\varepsilon_1\times10^{-5}$	0.82 (0.811)	0.82 (0.810)	0.82 (0.822)
$\varepsilon_2\times10^{-5}$	1.36 (1.361)	—	1.36 (1.370)
$\varepsilon_3\times10^{-5}$	—	2.19 (2.136)	2.19 (2.139)
$K_2\times10^{-5}$	0.24 (0.243)	—	0.24 (0.242)
$K_3\times10^{-10}$	—	0.54 (0.538)	0.54 (0.538)
Mean deviation (%)	1.21 (1.14)	1.68 (1.18)	1.53 (1.36)

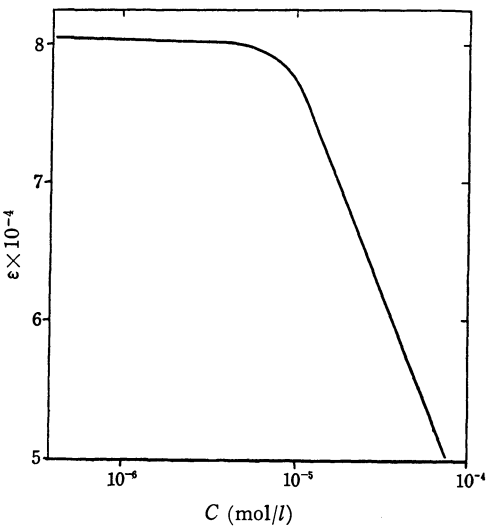

Fig. 5. Change of molar absorptivity of Sky Blue FF with the concentration in butanolic solution.

In aqueous ethanolic solutions the molar absorptivity did not change in a range of the dye concentrations between 10^{-6} and 10^{-4} mol/l. However, we cannot decide from the spectroscopic measurements alone whether Sky Blue FF in aqueous solutions is present in the monomeric or the polymeric state.

On the other hand, the dye in aqueous n-butanolic solutions aggregated suddenly into a very high polymer, or into particles, above 10^{-5} mol/l (Fig. 5). This fact might be connected with the dyeing behavior of the dye in this solvent, but more work is required in order to elucidate this connection.

Experimental

The dyes have been purified several times by the Robinson-Mill method, until no variation in the

*6 If $kC_1 \ll 1$, which is the case in an aqueous ethanolic solution, then :

$$\sqrt{\varepsilon-\bar{\varepsilon}_n} = \sqrt{\varepsilon_1-\bar{\varepsilon}_n} - \frac{k}{\sqrt{\varepsilon_1-\bar{\varepsilon}_n}}C(\varepsilon-\bar{\varepsilon}_n).$$

Hence, k and $(\varepsilon_1-\bar{\varepsilon}_n)$ can be obtained from a plot of $\sqrt{\varepsilon-\bar{\varepsilon}_n}$ *vs.* $C(\varepsilon-\bar{\varepsilon}_n)$.

absorption spectra was found. All the dye solutions were allowed to stand for 24 hr at 30°C after having been prepared, and their absorption spectra were measured at the same temperature.

Computations by the minimum deviation method were carried out on a HITAC 5020 E computer (the Tokyo University computation Center). The computation program used in these calculations was similar to that by Lepse.[11]

11) K. B. Wiberg, "Computer Programming for Chemists," Benjamin (1965), p. 185.

BULLETIN OF THE CHEMICAL SOCIETY OF JAPAN VOL. 41 1783—1787 (1968)

Dynamic Mechanical Behaviour of Organic Molecular Crystals. II. Elastic Constants of Single-Crystal Anthracene

Takaaki DANNO and Hiroo INOKUCHI

Department of Chemistry, Tokyo Gakugei University, Koganei, Tokyo, and The Institute for Solid State Physics, The University of Tokyo, Roppongi, Tokyo

(Received January 10, 1968)

The thirteen elastic constants, C_{ij}, and the elastic compliances, s_{ij}, of monoclinic single-crystal anthracene were determined from sound velocities measured by the ultrasonic pulse method at room temperture. The observed elastic constants were $C_{11}=8.92$, $C_{12}=4.63$, $C_{13}=4.49$, $C_{15}=-2.58$, $C_{22}=13.8$, $C_{23}=8.45$, $C_{25}=-2.59$, $C_{33}=17.0$, $C_{35}=-2.88$, $C_{44}=2.42$, $C_{46}=1.14$, $C_{55}=2.84$ and $C_{66}=3.16$ (in units of 10^{10} dyn/cm^2). The hydrostatic linear compressibilities, β, of the anthracene molecular crystal were then calculated from these elastic constants and compliances; the β along [100] was 12.7×10^{-12} cm^2/dyn, $\beta_{[010]}=4.41\times10^{-12}$ cm^2/dyn, and $\beta_{[001]}=3.59\times10^{-12}$ cm^2/dyn.

It is well known that the general forces of the cohesion, or van der Waals forces, between the polycyclic aromatic molecules play an important part in the building up of organic crystals. The dynamic mechanical properties of these organic molecular crystals provide a sensitive test of the forces, but those studies on this problem have scarcely been undertaken.[1]

In a preceding paper,[2] the dynamic elastic moduli and losses of organic crystals, perylene, anthracene, coronene, 1,2,3,4-dibenzanthracene, and their complexes with trinitrobenzene were observed by a forced-resonance vibration method. By this method, however, only information on the dynamical mechanical properties of the crystals along the longest axis, mainly the b-axis, was obtained.

Since the crystal structures of polycyclic aromatic crystals belong to the monoclinic or the triclinic system, thirteen elastic constants for the monoclinic system and twenty-one constants for the triclinic system must be measured if we are to ascertain all their dynamic mechanical properties exactly.

This paper will present experimental results of acoustic velocity measurements in monoclinic single-crystal anthracene, $C_{14}H_{10}$, by the ultrasonic pulse technique, and the thirteen elastic constants calculated from them.

Experimental Procedures

Sample Preparation. Anthracene, purified by means of zone-refining, was grown by the Bridgman method. The sample, a clump composed of a moderately large single crystal, 20 mm×20 mm×10 mm, was cut along the cleavage plane with a razor blade. The cleavage plane lies parallel to the ab crystalline axes. Further, the direction of the b-axis was decided on the cleavage plane by means of the double refraction method.[3]

Then, four parallelepipeds of anthracene crystals, about 5 mm×5 mm×5 mm, as shown in Fig. 1, were cut out and rubbed on benzene-soaked leather until the surface became clear. The ultrasonic pulse technique requires a pair of plane parallel faces for transmitter and receiver mounting. Therefore, two surfaces of the crystal specimen were polished on benzene-soaked deer leather. This procedure was repeated until the desired parallelism and smoothness of the end surfaces of the crystal were obtained.

The crystal structure of anthracene is of the monoclinic symmetry, with a $P2_1/a$ space group, and with $a=8.56$ Å, $b=6.04$ Å, $c=11.16$ Å, and

1) J. C. W. Heseltine, D. W. Elliott and E. B. Wilson, Jr., *J. Chem. Phys.*, **40**, 2584 (1964).
2) T. Danno, T. Kajiwara and H. Inokuchi, This Bulletin, **40**, 2793 (1967).
3) I. Nakada, "Organic Semiconductors," (H. Inokuchi, I. Nakada and M. Hatano ed.), Kyoritsu Publ., Tokyo (1966), p. 92.

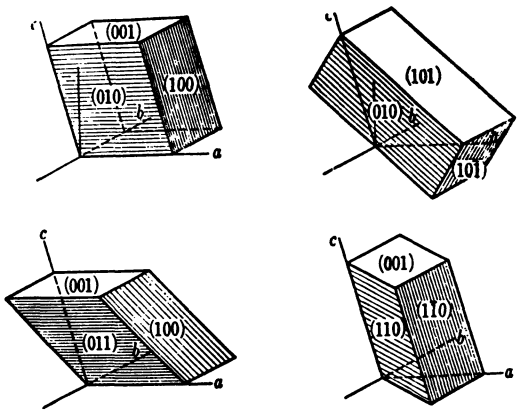

Fig. 1. Four parallelepipeds used for sound velocity measurement.

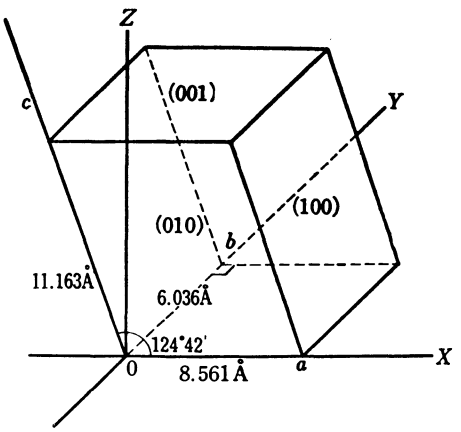

Fig. 2. The relation between XYZ orthogonal system and crystal axes.

$\beta=142°40'$.[4,5] The formulation of the strain-energy function for a monoclinic crystal results in thirteen independent elastic constants. The XYZ orthogonal system of coordinates was used for calculation in the following way: The Y-axis is the monoclinic b-axis of the crystal, the X-axis, the a-axis, and the Z-axis is perpendicular to the ab cleavage plane, as is shown in Fig. 2. The thirteen elastic constants may be shown, in accordance with Cady,[6] as:

$$\begin{vmatrix} C_{11} & C_{12} & C_{13} & 0 & C_{15} & 0 \\ C_{12} & C_{22} & C_{23} & 0 & C_{25} & 0 \\ C_{13} & C_{23} & C_{33} & 0 & C_{35} & 0 \\ 0 & 0 & 0 & C_{44} & 0 & C_{46} \\ C_{15} & C_{25} & C_{35} & 0 & C_{55} & 0 \\ 0 & 0 & 0 & C_{46} & 0 & C_{66} \end{vmatrix}. \quad (1)$$

Using the observed values of the velocities of longitudinal and transverse sound waves along the three principal axes, the three diagonal terms of elastic constants, that is C_{22}, C_{44}, and C_{66}, may be calculated easily; the results are shown in Table 1.

TABLE 1. THE WAVE DIRECTIONS USED AND THE VELOCITIES MEASURED FOR DETERMINING THREE DIAGONAL CONSTANTS

Direction of propagation	Direction of particle displacement	Measured velocity	Constants determined
[010]	[010]	v_{YY}	$C_{22}=\rho v_{YY}^2$
[100]	[010]	v_{XY}	$C_{66}=\rho v_{XY}^2$
[001]	[010]	v_{ZY}	$C_{44}=\rho v_{ZY}^2$

TABLE 2. THE WAVE DIRECTIONS USED AND THE VELOCITIES MEASURED FOR DETERMINING THE REMAINING THREE DIAGONAL AND SEVEN OFF-DIAGONAL CONSTANTS

Direction cosines of propagation direction l	m	n	Measured velocity	Related constants
0	1	0	$v_{YX}v_{YZ}$	$C_{44}C_{66}C_{46}$
1	0	0	$v_{XX}v_{XZ}$	$C_{11}C_{55}C_{15}$
0	0	1	$v_{ZZ}v_{ZX}$	$C_{33}C_{55}C_{35}$
0.254	0	0.852	v_{t_1}	$C_{44}C_{66}C_{46}$
			$v_{NN}v_{t_2}$	$C_{11}C_{33}C_{55}$ $C_{13}C_{15}C_{35}$
$1/\sqrt{2}$	$1/\sqrt{2}$	0	$v_1v_{t_1}v_{t_2}$	$C_{11}C_{22}C_{44}C_{55}$ $C_{66}C_{12}C_{15}C_{25}$ C_{46}
0	$1/\sqrt{2}$	$1/\sqrt{2}$	$v_1v_{t_1}v_{t_2}$	$C_{22}C_{33}C_{44}C_{55}$ $C_{66}C_{23}C_{25}C_{35}$ C_{46}

However, the calculation of the remaining three diagonal terms and the seven off-diagonals is somewhat complicated. In order to determine these diagonal and off-diagonal terms of C_{ij}, it is necessary to carry out the acoustic velocity measurements along other than the principal axes of the crystal. We chose to make velocity measurements along the following three directions: [110], [011] and [101]. Adopting the method of calculation which was used by Aleksandrov[7] for the monoclinic crystal, the remaining three diagonal constants and seven off-diagonal terms were obtained from the measurement of the transversal and longitudinal velocities along each direction, assuming that the density of anthracene $\rho=1.25$ g/cm^3.*1 Table 2 summarizes the wave directions and the velocities measured in determining these constants.

Velocity-measurement Apparatus. The ultrasonic pulse technique was used in this work; the pulse duration time was less than 1 μ sec. Figure 3 shows a schematic diagram of the ultrasonic pulse apparatus. The pulsed high-frequency generator was triggered by a negative pulser, which was similar to that described by Shimoda.[8] Further,

4) A. M. L. Mathieson, J. M. Robertson and V. C. Singlar, *Acta Cryst.*, **3**, 245 (1950).
5) J. M. Robertson, *Rev. Mod. Phys.*, **30**, 155 (1958).
6) W. G. Cady, "Piezoelectricity," McGraw-Hill Book Co., New York (1946).
7) K. S. Aleksandrov, *Soviet Phys. Cryst.*, **3**, 630 (1958).
*1 See Appendix 2.
8) K. Shimoda, *J. Appl. Phys. Japan*, **27**, 346 (1958).

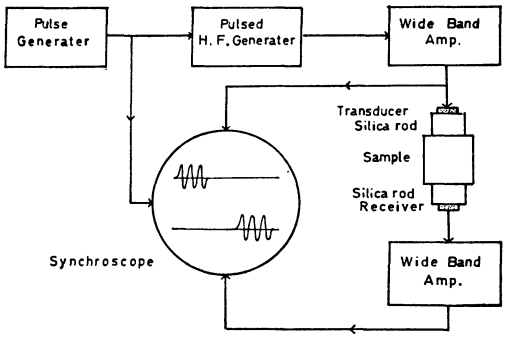

Fig. 3. The schematic diagram of the measurement of ultrasonic velocity across the anthracene crystal.

the synchroscope was triggered by a negative pulse simultaneously. Figure 4 shows the circuit of the high-frequency generator.

The anthracene specimen was sandwiched between two fused silica rods, 5 mm in diameter. A pair of Pb-Zr-titanate ceramics, 4 mm in diameter and 0.6 mm thick, having a fundamental resonance at 3 Mc/sec, were used as the transmitter and the receiver respectively. The transducers were cemented to the fused silica rods using silicone grease. After the transmitter and the receiver had been attached, the assembly was mounted in a holder which contained conductive rubber electrodes pressed against the transducers by a micrometer screw, as is shown in Fig. 5. The micrometer screw permitted a precise control of the acoustic path length.

The signal, transmitted through the specimen, was received by the ceramic receiver and was then amplified by a wide-band amplifier. After the signals from both the specimen and the delayed line had been led to a dual-beam synchroscope, the

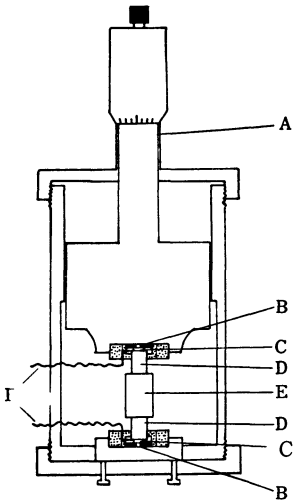

Fig. 5. The assembly for sound velocity measurement across organic crystal. A micrometer screw, B conductive rubber electrodes, C tansmitter, D fused silica rods, E sample, F lead wire and receiver.

sound velocity in the specimen was calculated.

Results and Discussion

The measured sound velocities along each direction of crystal are summarized in Table 3, while Table 4 shows the calculated elastic constants of the anthracene crystal.

The elastic compliances, s_{ij}, were calculated from the elastic constants, C_{ij}, by the following equation:

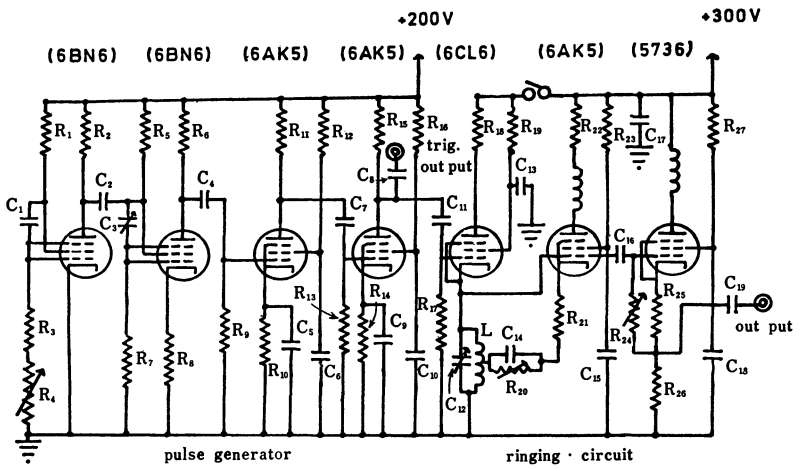

Fig. 4. The circuit of the pulsed high frequency generator, where R_1, R_5 30 kΩ; R_2, R_6 2 kΩ; R_3, R_{11}, R_{15} 1 kΩ; R_4, R_{24} 500 kΩ; R_7, R_{22}, R_{27} 20 kΩ; R_8 500 kΩ; $R_9, R_{12}, R_{13}, R_{16}$ 10 kΩ; R_{10}, R_{14} 180 Ω; R_7 250 kΩ; R_{18}, R_{26} 2 kΩ (20 W); R_{20} 5 kΩ; R_{21} 100 Ω; R_{23} 70 kΩ; R_{25} 150 Ω; C_1, C_{14} 50 pF; C_2 30 pF; C_3 100 pF; C_4, C_{16} 0.01 μF; C_5, C_9, C_{11}, C_{18} 0.1 μF; $C_6, C_{10}, C_{13}, C_{15}$ 0.5 μF; C_7, C_8, C_{16}, C_{19} 0.01 μF; C_{17} 5 μF and C_{12} 400 pF.

TABLE 3. SOUND VELOCITY IN ANTHRACENE CRYSTAL (in 10^5 cm/sec)

Direction of propagation of wave	Direction displacement in wave	Velocity of sound
[001]	[001]	3.75
	[100]	1.35
	[010]	1.39
[010]	[010]	3.32
	[001]	1.15
	[100]	1.75
[100]	[100]	2.81
	[010]	1.59
	[001]	1.32
[101]	[101]	2.91
	[010]	1.76
	[10$\bar{1}$]	1.32
[011]	[01$\bar{1}$]	2.99
	[011]	1.42
	[100]	1.53
[110]	[110]	3.33
	[1$\bar{1}$0]	1.49
	[001]	1.43

TABLE 4. ELASTIC CONSTANTS OF ANTHRACENE (in 10^{10} dyn/cm^2)

C_{11}	C_{12}	C_{13}	C_{15}	C_{22}	C_{23}	C_{25}
8.92	4.63	4.49	−2.58	13.8	8.44	−2.59
C_{33}	C_{35}	C_{44}	C_{46}	C_{55}	C_{66}	
17.0	−2.88	2.42	1.14	2.84	3.16	

TABLE 5. ELASTIC COMPLIANCES OF ANTHRACENE (in 10^{-12} cm^2/dyn)

s_{11}	s_{12}	s_{13}	s_{15}	s_{22}	s_{23}	s_{25}
16.5	−2.75	−1.05	11.4	11.6	−4.41	−3.58
s_{33}	s_{35}	s_{44}	s_{46}	s_{55}	s_{66}	
9.05	4.19	49.9	−18.0	53.1	38.2	

$$s_{ij}=\bar{D}_c\begin{pmatrix} i \\ j \end{pmatrix}\Big/D_c, \qquad (2)$$

The calculated elastic compliances are summarized in Table 5.

When a monoclinic crystal anthracence is compressed under hydrostatic pressure, the linear compressibility, β, is related to the elastic compliance and the direction cosine as follows:

$$\beta=(s_{11}+s_{12}+s_{13})l^2+(s_{21}+s_{22}+s_{23})m^2 + (s_{31}+s_{32}+s_{33})n^2+(s_{15}+s_{25}+s_{35})ln. \qquad (3)$$

Therefore, the linear compressibility along [100], [010] and [001] are calculated by means of Eq. (3); that is:

$$\beta_{[100]}=12.7\times10^{-12}\ \text{cm}^2/\text{dyn}$$
$$\beta_{[010]}=-4.41\times10^{-12}\ \text{cm}^2/\text{dyn}$$
$$\beta_{[001]}=3.59\times10^{-12}\ \text{cm}^2/\text{dyn}.$$

The elastic constants of anthracene are one-tenth or one-hundredth those of valence crystals, ionic crystals, or metals, because of the van der Waals coupling between molecules. The facts that the s_{11} elastic compliance, is the largest and s_{33} is the smallest seem reasonable in view of the packing of the molecules in the monoclinic anthracene crystal.

Further, the pressure-dependence of the electrical properties of the anthracene single crystal is consistent with the results of the compressibility reported here; the electron-drift mobility in the crystal along the direction perpendicular to the ab plane is approximately constant up to a pressure of 6.6 kbar, but the drift mobilities at 6.6 kbar along the a and b axes increase to 1.3 times the atmospheric pressure-value.[9]

In an X-ray investigation of some organic monoclinic molecular crystals, linear polyphenyls, the linear compression was reported to be a 5.4% contraction along the c axis under a pressure of 10 kbar.[10] Our results tend to support this.

Appendix

1) In general, when a plane wave propagates along a direction of which the direction cosine is (lmn), the velocity of this wave is given as the root of the next equation[11]:

$$\begin{vmatrix} \lambda_{11}-\rho v^2 & \lambda_{12} & \lambda_{13} \\ \lambda_{12} & \lambda_{22}-\rho v^2 & \lambda_{23} \\ \lambda_{13} & \lambda_{23} & \lambda_{33}-\rho v^2 \end{vmatrix}=0 \qquad (A\text{-}1)$$

where ρ is the density, and λ is the function of both the direction cosine (lmn) and the elastic constants, C_{ij}, as follows:

$$\begin{aligned}
\lambda_{11} &= l^2C_{11}+m^2C_{66}+n^2C_{55}+2mnC_{56} \\
&\quad +2nlC_{15}+2lmC_{16} \\
\lambda_{22} &= l^2C_{66}+m^2C_{22}+n^2C_{44}+2mnC_{24} \\
&\quad +2nlC_{46}+2lmC_{26} \\
\lambda_{33} &= l^2C_{55}+m^2C_{44}+n^2C_{33}+2mnC_{34} \\
&\quad +2nlC_{35}+2lmC_{45} \\
\lambda_{12} &= l^2C_{16}+m^2C_{26}+n^2C_{45}+mn(C_{25}+C_{46}) \\
&\quad +nl(C_{14}+C_{56})+lm(C_{12}+C_{66}) \\
\lambda_{13} &= l^2C_{15}+m^2C_{46}+n^2C_{35}+mn(C_{36}+C_{45}) \\
&\quad +nl(C_{36}+C_{55})+lm(C_{14}+C_{56}) \\
\lambda_{23} &= l^2C_{56}+m^2C_{24}+n^2C_{34}+mn(C_{23}+C_{44}) \\
&\quad +nl(C_{36}+C_{45})+lm(C_{25}+C_{46})
\end{aligned} \qquad (A\text{-}2)$$

2-a) Solving the above determinant (A-1), three equations related to wave propagation along the Y axis to the elastic constants are obtained:

$$C_{22}=\rho v_{\mathrm{Y}}^2{}_{\mathrm{Y}} \qquad (A\text{-}3)$$
$$C_{44}+C_{66}=\rho v_{\mathrm{Y}}^2{}_{\mathrm{X}}+\rho v_{\mathrm{Y}}^2{}_{\mathrm{Z}} \qquad (A\text{-}4)$$
$$C_{44}C_{66}-C_{46}^2=\rho^2 v_{\mathrm{Y}}^2{}_{\mathrm{X}} v_{\mathrm{Y}}^2{}_{\mathrm{Z}} \qquad (A\text{-}5)$$

9) T. Kajiwara, H. Inokuchi and S. Minomura, This Bulletin, **40**, 1055 (1967).
10) S. S. Kabalkina, *Soviet Phys. Solid State*, **4**, 2288 (1963).
11) M. J. P. Musgrave, *Proc. Roy. Soc.*, **A 226**, 339 (1954).

The six analogous equations are obtained from the wave propagations along the X and Z axes respectively:

$$C_{66} = \rho v_{XY}^2 \tag{A-6}$$
$$C_{11} + C_{55} = \rho v_{XX}^2 + \rho v_{XZ}^2 \tag{A-7}$$
$$C_{11}C_{55} - C_{15}^2 = \rho^2 v_{XX}^2 v_{XZ}^2 \tag{A-8}$$

and

$$C_{44} = \rho v_{ZY}^2 \tag{A-9}$$
$$C_{33} + C_{55} = \rho v_{ZZ}^2 + \rho v_{ZX}^2 \tag{A-10}$$
$$C_{33}C_{55} - C_{35}^2 = \rho^2 v_{ZZ}^2 v_{ZX}^2 \tag{A-11}$$

2-b) As for the propagation along the [101] direction, of which the direction cosine is $l=0.254$, $m=0$, and $n=0.852$, the following three equations are derived from Eqs. (A-1) and (A-2).

$$0.274\,C_{66} + 0.726\,C_{44} + 0.893\,C_{46} = \rho v_{t_1}^2 \tag{A-12}$$
$$0.274\,C_{11} + C_{55} + 0.726\,C_{33} + 0.893\,(C_{15} + C_{35}) = \rho v_{NN}^2 + \rho v_{t_2}^2 \tag{A-13}$$
$$\{0.274\,C_{15} + 0.726\,C_{35} + 0.446\,(C_{13} + C_{55})\}^2 - (0.274\,C_{11} + 0.726\,C_{55} + 0.893\,C_{15}) \times (0.274\,C_{55} + 0.726\,C_{33} + 0.893\,C_{35}) = \rho^2 v_{NN}^2 v_{t_2}^2 \tag{A-14}$$

where v_{NN}, v_{t_1}, and v_{t_2} are the velocities of one longitudinal and two transverse waves respectively.

2-c) As for the propagation along the [110] direction, the next determinant is obtained when the direction cosine is $l=1/\sqrt{2}$, $m=1/\sqrt{2}$ and $n=0$.

$$\begin{vmatrix} C_{11}+C_{66}-2\rho v^2 & C_{12}+C_{66} & C_{15}+C_{46} \\ C_{12}+C_{66} & C_{22}+C_{66}-2\rho v^2 & C_{25}+C_{46} \\ C_{15}+C_{46} & C_{25}+C_{46} & C_{55}+C_{44}-2\rho v^2 \end{vmatrix} = 0 \tag{A-15}$$

2-d) Analogously with the propagation along the [110] direction, the determinant for the propagation along the [011] direction is:

$$\begin{vmatrix} C_{66}+C_{55}-2\rho v^2 & C_{25}+C_{46} & C_{46}+C_{35} \\ C_{25}+C_{46} & C_{22}+C_{44}-2\rho v^2 & C_{23}+C_{44} \\ C_{46}+C_{35} & C_{23}+C_{44} & C_{44}+C_{33}-2\rho v^2 \end{vmatrix} = 0 \tag{A-16}$$

BULLETIN OF THE CHEMICAL SOCIETY OF JAPAN VOL. 41 1787—1792 (1968)

Analysis of Vapor Pressure of Some Molecular Crystals*1

Hideaki CHIHARA and Nobuo NAKAMURA

Department of Chemistry, Faculty of Science, Osaka University, Toyonaka, Osaka

(Received January 22, 1968)

Vapor pressure equations of the form $\log PT^{n/2}=a/T+b$ were derived, using high temperature Thirring expansion, which are applicable to crystals of polyatomic molecules. The exponent n is determined by the type of motion of molecules in the crystal, libration or rotation. If combined with the heat capacity data, the method of analysis may be used to derive such vibrational propoerties as static energy, zero point energy, geometric mean frequency, and molecular libration frequency. Examples of the analysis of existing vapor pressure data are given for solid iodine, iodine monochloride, and high temperature modifications of nitrogen, hydrogen chloride, and methane.

A vapor pressure equation for monatomic crystals was derived by Salter[1] using high temperature expansion for the Gibbs energy of the crystal. He was also able to show that the vapor pressures could 'see' the effect of vacancy formation near the triple point of solid argon. Salter's treatment was later extended to the case of alkali halides by Leadbetter and Newsham.[2]

The present paper is an extention of Salter's equation to molecular crystals in an attempt to extract information about molecular motion in crystalline solids from available vapor pressure data. The result turns out to be rather against our expectation but it will be shown that in certain cases some useful deductions can be made from vapor pressures if combined with other experimental information such as heat capacity and entropy.

Vapor Pressure Equations

What we are interested in is to incorporate the molecular rotational degrees of freedom in solid into Salter's formulation. It will be assumed that the temperature is sufficiently high so that Thirring expansion holds for the free energy of the crystal but not too high so that we can ignore anharmonic terms in the vibrations.

The molar Gibbs energy of a molecular crystal may be written as

*1 Presented before the 19th Annual Meeting of the Chemical Society of Japan, Yokohama, March 31, 1966; Abstract of Paper 1S005.

1) L. Salter, *Trans. Faraday Soc.*, **59**, 657 (1963).

2) A. J. Leadbetter and D. M. T. Newsham, *ibid.*, **61**, 1646 (1965).

$$G^c = G^c_{\text{trans}} + G^c_{\text{vib}} + G^c_{\text{rot}} + G^c_{\text{exp}} \quad (1)$$

Here the terms represent contributions from translational, vibrational (intramolecular), and rotational degrees of freedom and from thermal expansion. At high temperatures ($T > \Theta_D/6$), the translational part may be expanded into a series of the form[1]

$$G^c_{\text{trans}} = E_0' + 3\boldsymbol{N}\boldsymbol{k}T\Big[\ln(\boldsymbol{h}\nu_g/\boldsymbol{k}T) + \sum_{n=1}^{\infty}(-1)^{n-1}B_{2n}/2n(2n)! \times \eta_{2n}(\boldsymbol{h}/2\pi\boldsymbol{k}T)^{2n}\Big] \quad (2)$$

where E_0' is the pseudo-static lattice energy, $\boldsymbol{N}$ the Avogado's number, ν_g the geometric mean frequency for the translational lattice modes, B_{2n} the Bernoulli number, and η_{2n} the $2n$th moment of the translational part of the lattice frequency spectrum. The static lattice energy E_0 is related to E_0' by

$$E_0 = E_0' - E_{z,\text{lib}}$$

because '*translationally static*' lattice may still possess the zero-point kinetic energy $E_{z,\text{lib}}$ of molecular libration. For monatomic crystals or crystals in which all molecules are rotating, E'_0 is of course equal to E_0.

The vibrational part of the Gibbs enrgy is given by[3]

$$G^c_{\text{vib}} = \boldsymbol{N}\boldsymbol{k}T\sum_i[\ln(\boldsymbol{h}\nu_i^c/\boldsymbol{k}T) - \boldsymbol{h}\nu_i^c/2\boldsymbol{k}T + 1/24(\boldsymbol{h}\nu_i^c/\boldsymbol{k}T)^2 + \cdots] + \sum_i \boldsymbol{N}\boldsymbol{h}\nu_i^c/2 \quad (3)$$

where ν_i^c is the frequency for the ith intramolecular vibration mode, the last term being the vibrational zero point energy.

The rotational part of the free energy can not be treated in a general way since the Schrödinger equation for three-dimensional rotation of a molecule in a general periodic potential field can not be solved. We shall therefore be content with two extreme cases, *viz.* either librational motion or free rotation.

In the harmonic librational case, G^c_{rot} assumes exactly the same form as Eq. (3). In the case of free rotation it is given by[3]

$$G^c_{\text{rot}} = -\boldsymbol{N}\boldsymbol{k}T\sum_j \ln[(1/n_j)(8\pi^2 I_j \boldsymbol{k}T/\boldsymbol{h}^2)^{1/2}] \quad (4)$$

where I_j is the moment of inertia and n_j is the symmetry number of the rotational potential. Finally, the expansion part contributes

$$G^c_{\text{exp}} = \boldsymbol{N}pv_c \quad (5)$$

to the total Gibbs energy, p and v_c being the pressure and the volume per molecule.

The corresponding Gibbs energy of a mole of vapor is

$$G^v = G^v_{\text{trans}} + G^v_{\text{vib}} + G^v_{\text{rot}} + G^v_{\text{exp}} \quad (6)$$

and terms on the right-hand side are given in a standard textbook[3]:

$$G^v_{\text{trans}} = -\boldsymbol{N}\boldsymbol{k}T[\ln(2\pi m\boldsymbol{k}T/\boldsymbol{h}^2)^{3/2} + \ln v_v - B(T)/v_v + 1] \quad (7)$$

$$G^v_{\text{vib}} = \boldsymbol{N}\boldsymbol{k}T\sum_i[\ln(\boldsymbol{h}\nu_i^v/\boldsymbol{k}T) - \boldsymbol{h}\nu_i^v/2\boldsymbol{k}T + (1/24)(\boldsymbol{h}\nu_i^v/\boldsymbol{k}T)^2 + \cdots] + \sum_i \boldsymbol{N}\boldsymbol{h}\nu_i^v/2 \quad (8)$$

$$G^v_{\text{rot}} = -\boldsymbol{N}\boldsymbol{k}T[\sum_j \ln(8\pi^2 I_j \boldsymbol{k}T/\boldsymbol{h}^2)^{1/2} - \ln(\sigma/\pi^{1/2})] \quad (9)$$

$$G^v_{\text{exp}} = \boldsymbol{N}pv_v \quad (10)$$

where m is the mass of a molecule, $B(T)$ is the second virial coefficient, and v_v is the volume per molecule. v_v may be approximated by

$$v_v = \boldsymbol{k}T/p. \quad (11)$$

For a linear molecule, the symmetry number σ of the molecule in Eq. (9) is to be replaced by $\sqrt{\pi}\sigma'$, where σ' is 2 or 1 according as the molecule has the center of symmetry or not.

From the condition for vapor-solid equilibrium, we obtain the equation of the form

$$\ln P(T^{1/2})^n = a/T + b \quad (12)$$

The exponent n is determined by whether the molecule executes libration or rotation and a is given by

$$a = E'_0/\boldsymbol{N}\boldsymbol{k}, \quad (13)$$

and therefore a linear plot of $\ln(PT^{n/2})$ against $1/T$ gives the static lattice energy from its slope, and its intercept b should give the geometric mean frequency ν_g. Values of n and expressions of b are given in Table 1 for typical cases. Other cases can be evaluated easily. It is evident that Eq. (12) reduces to Salter's equation for monatomic case.[1] In deriving b, it has been assumed that

$$\boldsymbol{h}\nu_i/\boldsymbol{k}T < 1, \quad \boldsymbol{h}\eta_{2n}^{1/2n}/2\pi\boldsymbol{k}T \ll 1, \quad B(T)/v_v \ll 1. \quad (14)$$

The first of these assumptions may be justified only in the case of the low frequency librational modes in the solid state. While it may not be valid for intramolecular vibrations, the terms containing ν_i enter only as a difference between the gaseous and the crys-

3) J.E. Mayer and M.G. Mayer, "Statistical Mechanics," John Wiley, New York (1940); G.N. Lewis and M. Randall, "Thermodynamics," revised by K.S. Pitzer and L. Brewer, 2nd Ed., McGraw-Hill, New York (1961).

TABLE 1. THE VALUES OF n AND THE EXPRESSIONS OF b TO BE USED IN EQ. (12). APPROPRIATE FOR DIFFERENT MODELS OF MOLECULAR MOTION

Model	n	b
Linear molecule; librations about two axes	3	$\ln[8\pi^2(2\pi m/k)^{3/2}\cdot 1/\sigma'\cdot I_v\nu_g^3\cdot\nu_t^2\nu_c^{\text{intra}}/\nu_v^{\text{intra}}]$
Linear molecule; libration + rotation	2	$\ln[(8\pi^2)^{1/2}(2\pi m)^{3/2}\cdot 1/k\cdot n_c/\sigma'\cdot I_v/I_c^{1/2}\cdot\nu_g^3\nu_t\cdot\nu_c^{\text{intra}}/\nu_v^{\text{intra}}]$
Linear molecule; rotations about two axes	1	$\ln[(2\pi m)^{3/2}\cdot 1/k^{1/2}\cdot n_1n_2/\sigma'\cdot I_v/(I_{c1}I_{c2})^{1/2}\cdot\nu_g^3\cdot\nu_c^{\text{intra}}/\nu_v^{\text{intra}}]$
Non-linear molecule; librations about three axes	4	$\ln[8\pi^5m^{3/2}\cdot 1/k\cdot 1/\sigma(I_{v1}I_{v2}I_{v3})^{1/2}\cdot\nu_g^3\cdot\nu_{t1}\cdot\nu_{t2}\cdot\nu_{t3}\cdot\prod_i(\nu_{ci}/\nu_{vi})]$
Non-linear molecule; rotations about three axes	1	$\ln[(8\pi)^{1/2}m^{3/2}\cdot 1/k^{1/2}\cdot n_1n_2n_3/\sigma\cdot(I_{v1}I_{v2}I_{v3}/I_{c1}I_{c2}I_{c3})^{1/2}\cdot\prod_i(\nu_{ci}/\nu_{vi})]$

talline states and therefore the higher order terms of $h\nu_i^v/kT$ and $h\nu_i^c/kT$ would give only trivial effects on the results derived here.

We have ignored the effect of vacancy formation or any other type of defects but these can be taken into account if the energy and the combinatory factor associated with the defect formation can be evaluated. If the molecules in the vapor associate to form dimers or higher polymers, the effect has also to be and can be taken into accout provided that the molecular structures and concentrations of the associated species are known. Equation (12) is also applicable to such a case of NH_4Cl that dissociation is accompanied with vaporization.

Analysis of Experimental Vapor Pressures

All that one may anticipate to deduce from the application of Eq. (12) to experiment are, besides E_0 and ν_g, whether the molecules are librating at a certain frequency or rotating almost freely. Yet the application is not straightforward since the appropriate value of n is not known in advance. One obvious way is to decide n by trial-and-error procedure and see which value gives the best fit to Eq. (12). This is possible only when extremely accurate vapor pressure data are available over a reasonably wide temperature range. Usual situation is, as illustrated by the three equally well fitted straight lines in Fig. 3, that the exponent n can not be determined unambiguously. If the primary pressure and temperature values were sufficiently accurate, one should, in principle, be able to discriminate between different values of n. However in order for this to be practical, it appears that the accuracy of measurements will have to be improved by a factor of 10 or to within ± 0.005 Torr. Under these circumstaces, the analysis by use of Eq. (12) must be assisted by other information. Figure 1 is the diagram of cycles devised for this purpose. What is aimed at here is to use a and b of Eq. (12) for deriving other vibrational properties and at the same time examining the internal consistency of the calculation. It is noted that the derived properties all refer to a volume at some mean tem-

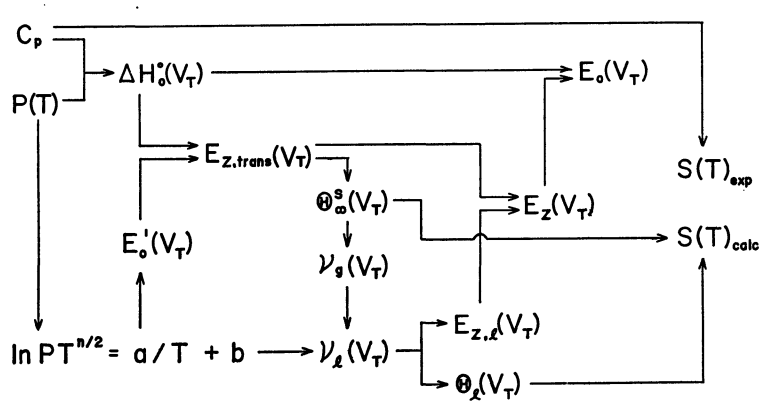

Fig. 1. Correlation diagram.

perature of the vapor pressure measurements.

Thus $\Delta H_0^\circ(V_T)$ is the heat of sublimation as 0°K corresponding to the crystal volume at temperature T; it is calculated from the relation

$$\Delta G^\circ/T = \boldsymbol{R}\ln(760/P) = \Delta(G^\circ - H^0)/T + \Delta H_0^\circ/T \qquad (15)$$

ΔG° is the standard Gibbs energy of sublimation at temperature T and $\Delta(G^\circ - H_0^\circ)$ may be obtained from heat capacity values. The translational zero point energy $E_{z,\mathrm{trans}}(V_T)$, obtained by

$$E_{z,\mathrm{trans}}(V_T) = -E_0'(V_T) - \Delta H_0^\circ(V_T),$$

is related to the limiting Debye temperature (from entropy) Θ_∞^S and the geometric mean frequency ν_g through[2,4]

$$E_{z,\mathrm{trans}} = \frac{9}{8}\boldsymbol{N}\boldsymbol{k}\Theta_\infty^S \doteqdot \frac{9}{8}e^{1/3}\boldsymbol{N}\boldsymbol{h}\nu_g$$

n the quasi-harmonic approximation. $\nu_l(V_T)$ is the molecular libration frequency and may be obtained as an average over the degrees of freedom (two or three) by inserting appropriate figures to the expression of b. The solid-state shift of the intramolecular frequencies is usually small so that it may be ignored if spectral frequencies in solid are not available. Knowledge of $\nu_l(V_T)$ may be directly compared with Raman or far-infrared spectral data on what is called '*lattice modes*' or with ν_l derived from temperature dependence of nuclear quadrupole resonance frequency. It also leads to the harmonic librational zero point energy $E_{z,\mathrm{lib}}(V_T)$ and Einstein temperature $\Theta_l(V_T)$; the former gives, together with $E_{z,\mathrm{trans}}(V_T)$, the total zero point energy $E_z(V_T)$ and the static lattice energy $E_0(V_T)$.

An overall check for internal consistency may be done by the help of entropy $S(T)$. Thus two characteristic temperatures Θ_∞ and Θ_l give an entropy for translational and librational modes to which intramolecular contributions are added. This $S(T)_{\mathrm{calc}}$ is then compared with the calorimetric entropy. Entropy may look a rather insensitive quantity for the purpose of consistency check. However the value of b is very sensitive to the choice of the exponent n in Eq. (12) and this outweighs the insensitivity of the entropy.

Results of Calculation

Results of calculations are displayed in Tables 2 and 3.

I_2 and ICl

The case of solid iodine probably serves best to illustrate how our analysis works. Molecules in solid iodine are undergoing librational motion (though perhaps not isotropic) in the orthorhombic crystal. Figure 2 shows the plot of $\log(PT^{3/2})$ *vs.* $1/T$, from which

TABLE 2. THE RESULT OF THE ANALYSIS OF THE VAPOR PRESSURE DATA

Substance	Model	T_M[a] (°K)	ΔH_0°[b] (cal/mol)	E_z (cal/mol)	$-E_0'$ (cal/mol)	$-E_0$ (cal/mol)	Θ^S (°K)	ν_g ($10^{12}\,\mathrm{sec}^{-1}$)	Θ_l (°K)	ν_l (cm^{-1})	Reference for $P(T)$
I_2	libration	321	15658	312	15800	15970	63.5	1.01	85.7	59.5	g)
ICl	libration	268	13273	428	13476	13701	89.5	1.43	113	78.6	h)
N_2	libration	59	1653	233	1823	1886	76.1	1.21	31.5	21.9	i)
N_2	rotation[c]	59	1653	153	1765	1806	50.1	0.80	41.4	28.8	i)
CH_4	libration	78	2237	521	2615	2758	169	2.69	47.8	33.2	j)
CH_4	rotation[d]	78	2237	150	2387	2387	67.1	1.07	——	——	j)
HCl	libration	146	4452	716	5059	5168	272	4.32	27.4	19.0	k)
HCl	rotation[e]	146	4452	571	4915	5023	207	3.30	54.4	37.8	k)
HCl	rotation[f]	146	4452	319	4771	4771	143	2.27	——	——	k)

a) Mean temperatures of vapor pressure measurement.
b) Computed from literature values for thermodynamic quantities (Landolt-Börnstein, "Zahlenwerte und Funktionen," II Band, 4 Teil, Springer, Berlin (1961).
c) Rotation about one axis; $n_c=6$ assumed.
d) Rotation about three axes; $n_1=n_2=n_3=4$ assumed.
e) Rotation about one axis; $n_c=1$ assumed. f) Rotation about two axes; $n_1=n_2=1$ assumed.
g) G.P. Haxter, C.H. Hickey and W.C. Holmes, *J. Am Chem. Soc.*, **29**, 127 (1907).
h) G.V. Calder and W.F. Giauque, *J. Phys. Chem.*, **69**, 2443 (1965).
i) W.F. Giauque and J.O. Clayton, *J. Am. Chem. Soc.*, **55**, 4875 (1933).
j) D.R. Stull, *Ind. Eng. Chem.*, **39**, 517 (1947).
k) W.F. Giauque and R. Wiebe, *J. Am. Chem. Soc.*, **50**, 101 (1928).

4) C. Domb and L. Salter, *Phil. Mag.*, **43**, 1083 (1952).

TABLE 3. CALCULATED AND OBSERVED ENTROPIES OF SOME MOLECULAR CRYSTALS

Substance	T (°K)	S_{exp} (e.u.)	S_{calc} (e.u.)	$\Delta S/S$ (%)	Reference for S_{exp}
I_2	298	27.76	28.20	1.6	a)
ICl	268	22.1	23.0	4.1	b)
N_2(lib.)	60	13.08	13.28	1.5	c)
N_2(rot.)	60	13.08	13.12	0.31	c)
CH_4(lib.)	80	12.26	13.29	8.4	c)
CH_4(rot.)	80	12.26	13.40	9.3	c)
HCl(lib.)	140	14.07	14.99	6.5	c)
HCl(lib.+rot.)	140	14.07	14.14	0.5	c)
HCl(rot.)	140	14.07	12.49	11.2	c)

a) D.A. Shirley and W.F. Giauque, *J. Am. Chem. Soc.*, **81**, 4778 (1959).
b) G.V. Calder and W.F. Giauque, *J. Phys. Chem.*, **69**, 2443 (1965).
c) Landolt-Börnstein, "Zahlenwerte und Funktionen," II Band, 2 Teil, Springer, Berlin (1960).

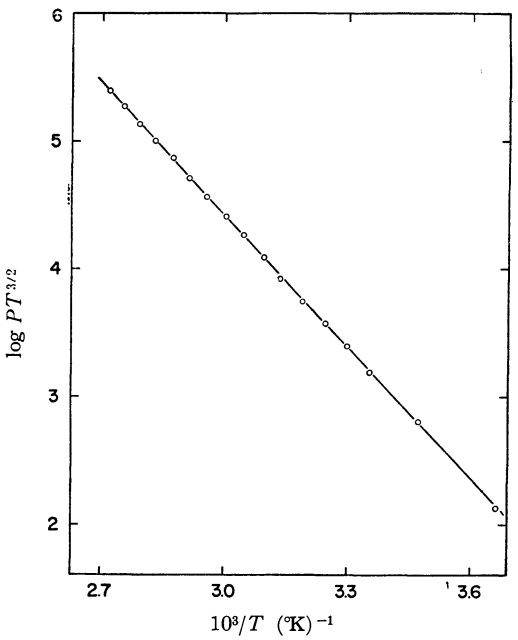

Fig. 2. The plot of $\ln PT^{3/2}$ against T^{-1} for solid iodine.

the static lattice energy 15970 cal/mol and the average libration frequency $\nu_l = 59.5\,cm^{-1}$ were obtained. These two values, combined with the heat of sublimation at 0°K obtained by the calorimetric method, give the librational zero point energy 170 cal/mol (2 degrees of freedom) and the translational zero point energy 142 cal/mol. The libration frequency of $59.5\,cm^{-1}$ compares favorably with $69.5\,cm^{-1}$ obtained from analysis of low temperature heat capacities[5] if one considers that the former corresponds to a larger volume of the crystal. Far infrared spectrum of solid iodine shows two translational lattice frequencies at $41\,cm^{-1}$ and $65\,cm^{-1}$ at 77°K.[6] An average of these two gives a Debye temperature of 74°K as compared with $\Theta^s_\infty = 63.5$°K given in Table 2. Also a Mössbauer study around 150°K led to $\Theta = 60$°K.[7] The entropy deviation is only 1.6%. Thus we believe that we have a fairly nice picture for solid iodine. The situation with respect to solid iodine monochloride is similar. The various quantities derived take values of reasonable magnitude in comparison with those of iodine although no other independent informations are available.

N_2

The high temperature phase of nitrogen was examined in two alternative models; *i.e.* the molecule undergoes libration about two axes ($n=3$) or rotates about one axis while doing libration about the other axis ($n=2$). Entropy consideration favors the one-axis rotation model slightly over the two-axes libration. The total zero point energy is then 153 cal/mol, of which 112 cal/mol comes from translational motion. Kohin estimated $E_{z,trans}$ theoretically to be 213 cal/mol.[8] Her estimate is based on the low temperature phase and therefore we see that the high temperature structure has a smaller zero point energy. Recent X-ray diffraction study suggested that the molecules precess about the c-axis of the high temperature hexagonal crystal.[9] They will of course be undergoing nutation also. This type of motion is consist-

5) H. Chihara and T. Shinoda, *J. Phys. Soc. Japan*, **17**, 1395 (1962).
6) S.H. Walmsley and A. Anderson, *Mol. Phys.*, **7**, 411 (1964).
7) M. Pasternak, A. Simopoulos and Y. Hazony, *Phys. Rev.*, **140**, A1892 (1965).
8) B.C. Kohin, *J. Chem. Phys.*, **33**, 882 (1960).
9) W.E. Streib, T.H. Jordan and W.N. Lipscomb, *ibid.*, **37**, 2962 (1962).

ent with nuclear quadrupole resonance results: We have made a rough estimate, using Scott's unpublished data,[10] that the molecular axis makes an angle of 54°17′ with the precession axis at a precession frequency greater than 4.10^6 Hz. We also calculated the low temperature libration frequency as 31.5 cm^{-1} at 35.6°K from the nuclear quadrupole frequencies[10] by the method described elsewhere.[11] This ν_l is to be compared with 28.8 cm^{-1} in Table 2.

CH_4

It has been shown that methane is in effectively free rotation in the highest temperature solid phase.[12] Our analysis of vapor pressure does not provide a clear-cut interpretation but leads to very large discrepancy of the entropies. This is probably due to in sufficient accuracy in the pressure determinations.

HCl

The structure and molecular motion in solid HCl have been extensively discussed elsewhere.[13] In short, neutron diffraction study on DCl favors a disordered orientation model above the transition point,[14] whereas nuclear magnetic and quadrupole studies point to a hindered rotation model.[13] The vapor pressure plots of Fig. 3 alone do not allow to differentiate one from the other possibilities in Table 2. The entropy considerations (Table 3) seem to clearly indicate that a combination of one-axis rotation and one-axis libration is by far appropriate than other models. This may be reconciled to nuclear resonance results if we consider that our treatment of vapor pressures here developed corresponds only to extreme cases of free molecular rotation or harmonic libration. What is actually happening is probably an intermediate, *i.e.* hindered rotation about two axes.

Attempts were also made to examine vapor pressures of solid chlorine, bromine, and the low temperature phases of hydrogen chloride and nitrogen. But these led either to very small E_z or to very large $\Delta S/S$. The failure

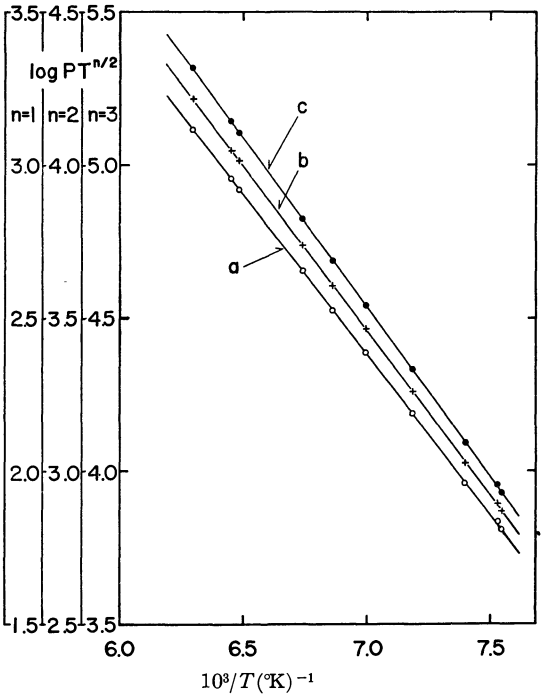

Fig. 3. The plot of $\ln PT^{n/2}$ against T^{-1} for the high temperature phase of solid hydrogen chloride. (a: $n=1$; b: $n=2$; c: $n=3$)

is perhaps due partly to poor accuracy in the vapor pressure determinations and partly to the breakdown of the high temperature approximation.

Conclusion

It has been demonstrated that accurate vapor pressure values of molecular crystals serve to provide useful informations about the lattice vibrational properties such as the static energy, the geometric mean frequency, the molecular libration frequency, and the zero point energy, in combination with heat capacity data. When the accuracy of the pressure allows, it is possible to detect molecular rotational states in solids. However, most of the presently available data are not accurate enough to deduce the information on higher order effect and the effect of vacancy formation.

The authors are grateful to Professor T. A. Scott of University of Florida for sending us his recent unpublished results on the nuclear quadrupole resonance of solid nitrogen.

10) T. A. Scott, private communication.
11) N. Nakamura and H. Chihara, *J. Phys. Soc. Japan*, **22**, 201 (1967).
12) H. Chihara and T. Shinoda, This Bulletin, **37**, 125 (1964).
13) H. Ōkuma, N. Nakamura and H. Chihara, *J. Phys. Soc. Japan*, **24**, 452 (1968).
14) E. Sándor and R. F. C. Farrow, *Nature*, **215**, 1265 (1967).

BULLETIN OF THE CHEMICAL SOCIETY OF JAPAN VOL. 41 1793—1968 (1968)

Ionization and Dissociation of Formic Acid, Acetic Acid, Propanoic Acid, and Butanoic Acid under Electron Impact

Yoko Ono, Tutomu Makita and Kumasaburo Kodera

Department of Chemistry, Faculty of Science, Kyoto University, Sakyo-ku, Kyoto

(Received January 29, 1968)

The mass spectra of DCOOD, DCOOH, CD_3COOD, CD_3COOH, CH_3COOD, C_2H_5COOD, and C_3H_7COOD are compared with spectra of the H-containing compounds. Besides, the ^{18}O-labeled acetic acid is measured. The labeling helps to determine the origin of a number of fragment ions. It is found that the two fragment ions $C_3H_5O_2^+$ and $C_4H_7O_2^+$ are produced by the removal of the hydrogen atom from the alkyl group and have the structures of $C_2H_4CO_2H^+$ and $C_3H_6CO_2H^+$ respectively. Neither $CH_2CO_2H^+$ nor $CH_3CO_2^+$ is produced. The rerrangement ion CH_3O^+ is found to have the structure of CH_2OH^+, one of whose hydrogen atoms comes from the carboxyl group. The origins of the hydrogen atom and the oxygen atom in the other rearrangement ions are also determined. The mechanisms for the fragmentation of the molecular ions are discussed.

Mass spectrometric studies of the ions from the carboxylic acids have been carried out by several investigators.[1-5] Melton[3] discussed the fragmentation of formic acid by a comparison of the mass spectra of an H-containing compound and a deutero-isomer. Other works have concerned themselves only with the appearance potentials. However, there have been no studies of either acetic acid or of the higher acids.

In this paper we will discuss the ionization and the ionic fragmentation of formic acid, acetic acid, propanoic acid, and butanoic acid molecules, each of which consists of an alkyl group and a carboxyl group. Emphasis has been placed in the atomic rearrangement during the fragmentation. For this purpose, it is useful to study the systems in some detail with the help of suitably-labeled compounds. In the present work the deuterium and the oxygen-18 labeling have been utilized particularly for the study of some rearrangement processes as well as for the identification of some fragment ions. Also, the presence of the metastable ions and the ion-molecule reactions have been utilized.

1) T. Mariner and W. Bleakney, *Phys. Rev.*, **72**, 792 (1947).
2) G. P. Happ and D. W. Stewart, *J. Am. Chem. Soc.*, **74**, 4404 (1952).
3) G. A. Ropp and C. E. Melton, *ibid.*, **80**, 3509 (1958).
4) K. Hirota, K. Nagoshi and M. Hatada, This Bulletin, **34**, 226 (1960).
5) "Catalog of Mass Spectral Data," Am. Pet. Inst. Res. Proj. Nat. Bur. Stds., Washington D. C., Serial No. 300.

Experimental

Materials. The purest commercial acids were used without purification. Three deuterated compounds, CD_3COOD, CDOOD, and D_2O, were obtained from Merck, Ltd., while the other deuterated compounds were synthesized as follows: CD_3COOH: the deuterium atom of the carboxyl group of CD_3COOD was replaced by a hydrogen atom by bubbling gaseous hydrogen chloride through the acid.

DCOOH: The deuterium atom of the carboxyl group of DCOOD was replaced by a hydrogen atom by the addition of H_2O.

CH_3COOD and n-C_3H_7COOD: The anhydride of each acid reacted with D_2O at room temperature or higher.

Apparatus. The mass spectra were taken with a CEC 21-401 Mass Spectrometer, modified in order to determine the appearance potentials of the ions. The standard conditions for analysis were as follows: electron-accelerating voltage, 70 V; ion-accelerating voltage, 210 V; total emission current, 10.0 μA; temperature of the ion source, 250±0.2°C. When necessary, the temperature of the ion source, the repeller voltage, and the electron energy were changed.

As the compounds are adsorbed strongly on the walls, precaution was taken against the effects of adsorption. In advance the sample inlet-system was sufficiently flashed with argon and then with the sample. The contamination of the sampling systems was examined by the measurement of the background of the mass spectra with a flow of argon. In order to avoid as much as possible the influence of the isotope exchange during the measurement, the mass spectra were taken as soon as

possible after the sample had been introduced.

Results and Discussion

Certain ions in the mass spectra of the H-containing and deuterated acids are given in Tables 1—4. The intensities are expressed as the intensities relative to those of the parent ions except in the cases of n-C_3H_7COOH and i-C_3H_7COOH. In these cases, the intensities are expressed as the percentages of total ionization. It was possible to give the structural formulas for the various ions by comparing the mass distribution of the normal compound with that of the deutero-isomer. These formulas are given in the third column of Table 1. When it is likely that more than one ion is associated with the intensity as the given mass, the measured intensity has been partitioned among the contributing ions. The assignments of the individual contributions were made somewhat arbitrarily, assuming that the loss of an H or D atom in the deutero-isomer occurred with the same probability as the loss of H in the H-containing compound. Similarly, the loss of a given group such as methyl was assumed to occur with the same probability in both isomers.

Fragment ions: $C_nH_{2n}CO_2H^+$ or $C_nH_{2n+1}CO_2^+$. It is of interest to determine whether the hydrogen atom is eliminated from the

TABLE 1. SOME IONS IN THE MASS SPECTRA OF FORMIC ACID AND DEUTEROFORMIC ACIDS

	HCOOH		DCOOH		DCOOD	
m/e	Intensity*	Ion	Intensity*	Ion	Intensity*	Ion
28	16.2	CO^+	15.5	CO^+	10.0	CO^+
29	76.6	COH^+	14.6	COH^+	0.54	
30	——	——	66.7	DCO^+	68.6	DCO^+
44	20.3	CO_2^+	15.6	CO_2^+	7.38	CO_2^+
45	73.9	CHO_2^+	35.7	CO_2H^+	——	——
46	**100**	HCO_2H^+	41.0	DCO_2^+	54.5	CDO_2^+
47			**100**	DCO_2H^+	0.6	
48					**100**	DCO_2D^+

* Relative intensity for ionizing voltage 70 V

TABLE 2. SOME IONS IN THE MASS SPECTRA OF ACETIC ACID-d AND DEUTEROACETIC ACIDS

	CH_3COOH		CH_3COOD		CD_3COOH		CD_3COOD	
m/e	Intensity*	Ion	Intensity*	Ion	Intensity*	Ion	Intensity*	Ion
14	12.3	CH_2^+	11.9	CH_2^+	2.48		2.12	
15	46.3	CH_3^+	41.5	CH_3^+	0.87		0.21	
16					6.70	CD_2^+	6.49	CD_2^+
17					5.82		1.44	
18					45.3	CD_3^+ CO^+	46.0	CD_3^+
28	8.81	CO^+	5.31	CO^+	6.82	$C_2D_2^+$	6.46	CO^+
29	11.8	CHO^+	7.78	HCO^+	3.17	COH^+	0.07	
30	0.54		5.53	COD^+	6.44	DCO^+	10.6	DCO^+
31	2.53	CH_2OH^+	0.89		0.29		0.11	
32	——	——	3.19	CH_2OD^+	0.13		0.44	
33	——	——	——	——	2.05	CD_2OH^+		
34	——	——	——	——	——	——	2.59	CD_2OD^+
43	118	CH_3CO^+	119	CH_3CO^+	0.78		0.39	
44	5.90		11.4		14.8		14.2	
45	112	$COOH^+$	6.90		107	$COOH^+$	1.35	
46	2.08		115	$COOD^+$	148	CD_3CO^+	270	CD_3CO^+ $COOD^+$
60	**100**	$CH_3CO_2H^+$			——	——	——	——
61	2.18		**100**	CH_3COOD^+	——	——	——	——
62	——	——	3.18		——	——	——	——
63	——	——	——	——	**100**	$CD_3CO_2H^+$	——	——
64	——	——	——	——	2.27		**100**	$CD_3CO_2D^+$
65	——	——	——	——	——	——	2.72	

* Relative intensity for ionizing voltage 70 V

TABLE 3. SOME IONS IN THE MASS SPECTRUM OF PROPANOIC ACID AND DEUTERO-PROPANOIC ACID

	C_2H_5COOH		C_2H_5COOD	
m/e	Intensity*	Ion	Intensity*	Ion
28	125	$C_2H_4^+$, CO^+	66.4	$C_2H_4^+$, CO^+
29	114	$C_2H_5^+$, HCO^+	145	$C_2H_5^+$, COH^+
30	17.5		24.0	COD^+
31	4.33	CH_2OH^+	13.5	
32	——	——	4.46	CH_2OD^+
45	68.9	$COOH^+$	0.08	
46	9.95		71.4	$COOD^+$
55	13.9	$C_2H_3CO^+$	13.6	$C_2H_3CO^+$
56	11.9	$C_2H_4CO^+$	9.05	$C_2H_4CO^+$
57	27.4	$C_2H_5CO^+$	29.2	$C_2H_5CO^+$
73	59.4	$C_2H_4CO_2H^+$	——	——
74	**100**	$C_2H_5CO_2H^+$	60.6	$C_2H_4COOD^+$
75			**100**	$C_2H_5COOD^+$

TABLE 4. SOME IONS IN THE MASS SPECTRA OF n-C_3H_7COOH and i-C_3H_7COOH

		n-C_3H_7COOH	i-C_3H_7COOH
m/e	Ion	Intensity %*	Intensity %*
14	CH_2^+	0.23	0.36
15	CH_3^+	0.63	2.51
26		0.86	0.96
27	$C_2H_3^+$	6.70	8.46
28	$C_2H_4^+$, CO^+	1.66	1.40
29	$C_2H_5^+$, HCO^+	3.90	1.98
30		0.08	0.07
31	CH_2OH^+	0.38	0.28
39		2.70	2.79
40		0.47	0.51
41	$C_3H_5^+$	5.91	11.9
42	$C_3H_6^+$	5.91	3.70
43	$C_3H_7^+$, $C_2H_3O^+$	6.06	39.5
44	CO_2^+	0.41	1.75
45	CO_2H^+	4.60	3.01
55		1 72	1.11
56		0.15	0.08
57		0.14	0.17
58		0.10	3.06
59		0.04	0.24
60	$C_2H_4O_2^+$	37.9	0.97
71	$C_3H_7CO^+$	1.02	0.60
72		0.08	0.04
73	$C_2H_4CO_2H^+$	10.8	8.62
74		0.54	0.43
87	$C_3H_6CO_2H^+$	0.66	0.28
88	$C_3H_7CO_2H^+$	**1.82**	**2.76**

* Ion abundance in % of total ionization

alkyl group or from the carboxyl group.

In the spectrum of HCOOH the relative intensity of the CHO_2^+ ion ($m/e=45$) is 73.9. In the spectrum of the deutero-isomer DCOOH, the intensities of CO_2H^+ ($m/e=45$) and DCO_2^+ ($m/e=46$) are 35.7 and 41.0 respectively. Therefore, the ions at the mass (M−1) in the spectrum of HCOOH must be HCO_2^+ and CO_2H^+, occurring in the same abundance.

In the spectrum of CH_3COOH the ion at the mass (M−1) was not observed. In the spectra of the other acids, $C_2H_3O_2^+$ ($m/e=59$) was never observed. This ion may be unstable, or the $C_2H_3O_2$ fragment may have the negative charge more stably.*1

In the mass spectrum of C_2H_5COOH the relative intensity of $C_3H_5O_2^+$ ($m/e=73$) is 59.4. The mass spectrum of the deutero-isomer C_2H_5COOD shows that the corresponding intensity has moved to mass 74. Therefore, $C_3H_5O_2^+$ must be $C_2H_4CO_2H^+$.

The ion of this type was found in the mass spectrum of C_3H_7COOH. The occurrence of the metastable ions provides further information concerning the process leading to this ion. In the mass spectra of both n-C_3H_7COOH and i-C_3H_7COOH the metastable ion peak of mass 60.6 was found. In the mass spectrum of the deuterated-compound n-C_3H_7COOD, this metastable ion peak shifted to mass 61.5. The transitions consistent with these masses are:

$$C_3H_7CO_2H^+(88) \longrightarrow C_2H_4CO_2H^+(73)+CH_3(15)$$
$$m^*=\frac{(73)^2}{88}=60.6,$$
$$C_3H_7CO_2D^+(89) \longrightarrow C_2H_4CO_2D(74)+CH_3(15)$$
$$m^*=\frac{(74)^2}{89}=61.5.$$

In the mass spectrum of C_3H_7COOH, the relative intensity of $C_4H_7O_2^+$ ($m/e=87$) is 36.2. In the mass spectrum C_3H_7COOD, the corresponding ion intensity moved to mass 88. In the same way as in C_2H_5COOH, the $C_4H_7O_2^+$ ion must have the structure of $C_3H_6CO_2H^+$.

From the above discussion, we are led to the conclusion that, except for HCOOH and CH_3CO_2H, the $C_{n+1}H_{2n+1}O_2^+$ ions in the mass spectrum of $C_nH_{2n+1}CO_2H$ have the C_nH_{2n}-CO_2H^+ structure.

Fragment Ion R-C≡O$^+$. It is well known that the carbonyl compounds produce very stable ions, R-C≡O^+, the oxygen atom of which has a triple bond.[6] In the spectra of the acids these ions occur in appreciable amounts. The H-C≡O^+ ion in the mass spectra of HCOOH will be discussed later.

Although, in the mass spectrum of CH_3-

*1 The ion at mass 59 has been measured appreciably on the background of the negative ion mass spectra. This ion is thought to come from the oil of the diffusion pumps. *Cf.* our unpublished data.

6) I. Kanomata, This Bulletin, **34**, 1964 (1961).

COOH, the CH_3–C≡O^+ ion peak is the highest of all, neither the C_2H_5–C≡O^+ from $C_2H_5CO_2H^+$ nor the C_3H_7–C≡O^+ from $C_3H_7CO_2H^+$ is so high as expected. This may be partly because C_2H_5–C≡O^+ and C_3H_7–C≡O^+ are not stable, further decomposing to $C_3H_7^+$, $C_2H_5^+$, CO^+, *etc.*

Rearrangement Ion CH_2OH^+. It is well known that, in the mass spectra of many esters,[7] the rearrangement ion CH_3O^+ (mass 31), with the CH_2OH^+ structure, occurs as the most abundant ion. In the spectrum of CH_3COOH, the relative intensity of the CH_3O^+ ion (mass 31) is 2.53. In view of the CH_3COOH structure, it seemed of interest to investigate closely the process responsible for the production of this ion.

The spectra of the three deutero-isomers CH_3COOD, CD_3COOH, and CD_3COOD show that the corresponding ion intensity has moved to masses 32, 33, and 34 respectively. These ions must be CH_2OD^+, CD_2OH^+, and CD_2OD^+ respectively. The appearance potentials of all these ions are the same within the limits of experimental error. These ions proved to be primary ions judging from the effect of the repeller voltage and the sample pressure on the intensities of these ions.

In order to obtain further information on the process producing this type of ion, measurements were made with ^{18}O. The oxygen-18-labeled acetic acid was synthesized by the reaction of $H_2{}^{18}O$ (oxygen-18 atomic % 7) with CH_3COCl.

In the spectrum of the oxygen-18-labeled isomer, half of the intensity of CH_2OH^+ ion has moved to mass 33. This shows that the oxygen atom in this ion may, with equal probability, be either of the two oxygen atoms in CH_3COOH. The reason for this may be either that the two oxygen atoms in the molecular ion are equivalent due to resonance, or that it is essentially impossible to replace the hydroxylic oxygen atom selectively with oxygen-18.

Also, in the spectra of C_2H_5COOH and *n*-C_3H_7COOH, the CH_3O^+ (mass 31) occurs in an appreciable abundance. A comparison of the mass spectra of C_2H_5COOH and *n*-C_3H_7-COOH with those of C_2H_5COOD and *n*-C_3H_7-COOD respectively shows that the CH_3O^+ ion must have the CH_2OH^+ structure.

To summarize, the CH_3O^+ ion (mass 31) must be CH_2OH^+, two of whose hydrogens come from the alkyl group and the rest, from the carboxyl group. The origin of the carbon and the oxygen atoms can not be determined. An experiment with ^{13}C is desirable.

Rearrangement Ion and Fragment Ion CHO^+. The spectrum of HCOOH shows that the CHO^+ ion (mass 29) occurs with the highest abundance except for the parent ion. This ion also occurs in the spectra of CH_3-COOH, C_2H_5COOH, and C_3H_7COOH. In order to determine the mechanism of producing this ion, the same method was used as for the CH_2OH^+ ion.

In the case of HCOOH, the spectra of HCOOD and DCOOH were compared with that of HCOOH. The relative intensity of the HCO^+ ion (mass 29) is 77 in the mass spectrum of HCOOH. In the spectrum of DCOOD, the corresponding ion, whose intensity is 68.6, has moved to mass 30. On the other hand, in DCOOH, two ions, COH^+ and DCO^+, occurred; their relative intensities were 14.6 and 66.7 respectively. The reason why the intensity of the COH^+ is weaker than that of DCO^+ may be that, while DCO^+ is formed by a one-bond fission, the formation of COH^+ requires the fission of two bonds. In addition, DCO^+ has a stable structure, D–C≡O^+, which is well known in carbonyl compounds. From these facts it may be supposed that two structures, H–C≡O^+ and C–OH^+, contribute to the mass 29.

Also, in the spectrum of CH_3COOH, the CHO^+ ion (mass 29) occurs with a relative intensity of 11.8. In the spectrum of CD_3-COOH the corresponding ion must be considered to be CDO^+ and CHO^+, whose intensities were 6.44 and 3.17 respectively. The deuterium of CDO^+ must have come from the methyl group of the acetic acid, so this ion is the rearrangement ion. In CH_3COOD, CDO^+ and CHO^+ were found also, indicating that rearrangement had occurred. Their intensities were 5.33 and 7.78 respectively. Of course, the appearance potentials of these ions were the same within the limits of experimental error, and the examination of the effect of the repeller voltage and the pressure shows that these ions are primary ions.

From the mass spectrum of acetic acid containing oxygen-18, the origin of the oxygen atom in this ion was not determined unequivocally, as in the case of CH_2OH^+.

We can conclude that, in the spectrum of CH_3COOH, CHO^+ (mass 29) consists of the simple fragment ion COH^+ and the rearrangement ion HCO^+. The hydrogen of the former comes from the carboxyl group, and that of the latter, from the methyl group. The abundance of the simple fragment ion is

7) E. W. Godbole and P. Kebarle, *Trans. Faraday Soc.*, **58**, 1897 (1962).

TABLE 5. THE RELATIVE INTENSITY* OF REARRANGEMENT IONS TO THE LOWER ACID

	M−CH_2		M−C_2H_4		M−C_3H_6	
	Ion	Intensity	Ion	Intensity	Ion	Intensity
CH_3COOH	$CH_2O_2^+$	0.4—0.5	——	——	——	——
C_2H_5COOH	$C_2H_4O_2^+$	0.32	$CH_2O_2^+$	9.0	——	——
n-C_3H_7COOH	$C_3H_6O_2^+$	11	$C_2H_4O_2^+$	2080	$CH_2O_2^+$	11.5
i-C_3H_7COOH	$C_3H_6O_3^+$	6	$C_2H_4O_2^+$	35	$CH_2O_2^+$	5.3

* The relative abundance with each parent ion peak being taken as 100%

equivalent to, or a little less than, that of the rearrangement ion. In the spectra of C_2H_5-$COOH$ and C_3H_7COOH, the mass-29 ion also occurs, but we could not determine the origin of this ion because of the presence of the $C_2H_5^+$ ion, which gives a strong peak at the same mass.

Rearrangement Ion $C_nH_{2n}O_2^+$. The spectrum of n-C_3H_7COOH shows that $C_2H_4O_2^+$ occurs very abundantly. This ion has the same mass as the acetic acid molecular ion, so it is considered to be a rearrangement ion. Other ions of the same type as this are also observed. The relative intensities of these ions; $CH_2O_2^+$, $C_2H_4O_2^+$, and $C_3H_6O_2^+$, are given in Table 5. Except in the case of CH_3COOH, many ions of this type produced in the acids. It is of interest to discuss the mechanism for producing these rearrangement ions. As for $C_2H_4O_2^+$, in the spectra of n-C_3H_7COOH a metastable ion peak of mass 40.9 was observed. The transition consistent with this mass is:

$$C_3H_7COOH^+(88) \longrightarrow C_2H_4O_2^+(60) + C_2H_4(28)$$

$$m^* = \frac{(60)^2}{(88)} = 40.9$$

The neutral fragment C_2H_4 has the stable structure[8] $CH_2{=}CH_2$. The high intensity of the $C_2H_4O_2^+$ ion may be due to this stability.

The mechanism for this rearrangement ion may be speculated to be as follows:

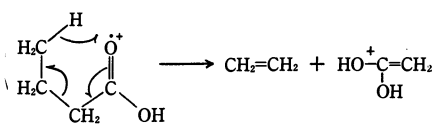

and for $CH_2O_2^+$

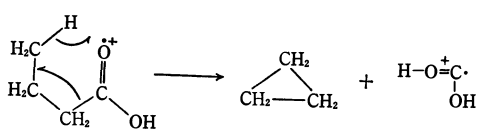

The ring-formation mechanisms shown above are well-known in the electron impact of organic compounds.

In the mass spectra of C_2H_5COOH and i-C_3H_7COOH, no such rearrangement mechanism can be expected in view of the orientation and steric hindrance. In spite of this, the mass spectra of C_2H_5COOH and i-C_3H_7COOH show that $CH_2O_2^+$ and $C_2H_4O_2^+$ occur in an appreciable abundance. Therefore, for these ions we must consider other mechanisms.

Ion-molecule Reaction "Protonated Molecular Ions" The mass spectra of acids show ions of appreciable intensities whose masses are larger than that of the molecular ion by one mass.

Sharkey[9] and Kebarle[7] have pointed out

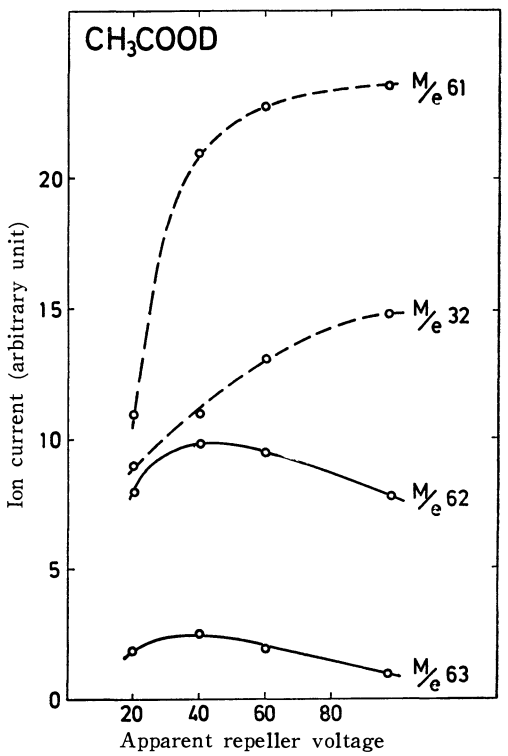

Fig. 1. The effect of the repeller voltage on the ion intensity

8) F. W. McLafferty "Mass Spectrometry of Organic Ions," Academic Press, New York and London (1963).

9) A.G. Sharkey, Jr., J.L. Shultz and R.A. Friedel, *Anal. Chem.*, **31**, 87 (1959).

that analogous ions occur as rearrangement ions in appreciable intensities in the mass spectra of most aliphatic esters.

The mass spectra of the deuterated acids show that some of the corresponding ions have moved to a mass larger than that of molecular ions by one mass or two—such as the ion of mass 50 in DCOOD(48), that of mass 66 in CD_3COOD, and those of mass 64 and mass 65 in CD_3COOH. Those ions were observed in appreciable amounts when the sample pressure in the ionization chamber was higher than 10^{-6} mmHg. The intensities of these ions were in proportion to the square of the sample pressure.

Generally, the intensity of the primary ion increases as the repeller voltage increases (*cf.* Fig. 1). However, the intensities of these protonated molecular ions decreased as the repeller voltage increased. These properties are those of secondary or higher-order ions. Therefore, these ions may be considered to be produced by the ion-molecule reaction.

Summary

The mass spectra of several carboxylic acids, *i.e.*, HCOOH, DCOOH, DCOOD, CH_3COOH, CH_3COOD, CD_3COOH, CD_3COOD, C_2H_5COOH, C_2H_5COOD, n-C_3H_7COOH, i-C_3H_7COOH, and n-C_3H_7COOD, were examined. The ions of the mass spectra were then classified into the simple fragment ions, the rearrangement ions, and the ion-molecule reaction ions.

The main fragment ions were R^+, RCO^+, and CO_2H^+. One of the most interesting fragment ions was $C_nH_{2n}CO_2H^+$ ($n \geqq 2$), which was found to occur upon the loss of one hydrogen atom from the alkyl group. $CH_2CO_2H^+$ was not observed in any case.

Among the rearrangement ions, CH_3O^+ ($m/e=31$) was of special interest; two of its hydrogen atoms were proved to come from the alkyl group, and the rest, from the carboxyl group. From this, we concluded the structure to be CH_2OH^+.

About half of CHO^+ ($m/e=29$) was also proved to be a fragment ion whose hydrogen atom came from the alkyl group, while the other half was the simple fragment ion COH^+.

In addition, we observed protonated molecular ions which had been produced by the ion-molecule reactions.

BULLETIN OF THE CHEMICAL SOCIETY OF JAPAN VOL. 41, 1798—1808 (1968)

Intrachain Force Field and Normal Vibrations of Polyethylene Glycol

Hiroatsu MATSUURA and Tatsuo MIYAZAWA

Institute for Protein Research, Osaka University, Kita-ku, Osaka

(Received January 29, 1968)

Normal vibrations of polyethylene glycol and the perdeuterated species were treated. Intrachain force field was expressed in terms of local-symmetry coordinates. Force constants were adjusted by the method of least squares, with reference to observed infrared and Raman frequencies. A set of force constants was obtained, which reproduces the observed frequencies with an r.m.s. deviation of 0.9%. The values of the force constants thus refined were discussed in comparison with corresponding values of related molecules. Vibrational assignments of the observed infrared absorption bands and Raman lines were revised on the basis of potential-energy distributions refined in the present treatment.

The chain vibrations of an isolated helical molecule are specified with the phase difference δ between the vibrational displacements of the corresponding atoms in neighboring repeat units. The selection rules for the infrared absorption and Raman scattering are related with the angle θ of rotation, per unit, about the helix axis. Thus, the infrared bands arise from the chain vibrations with $\delta=0$ or θ and the Raman lines arise from the vibrations with $\delta=0$, θ, or 2θ.[1,2] For the neutron scattering, there is no selection rule

1) P. Higgs, *Proc. Roy. Soc.* (*London*), **A 220**, 472 (1953).

2) T. Miyazawa, *J. Chem. Phys.*, **35**, 693 (1961); *Nippon Kagaku Zasshi* (*J. Chem. Soc. Japan, Pure Chem. Sect.*), **88**, 111 (1967); H. Sugeta and T. Miyazawa, *J. Chem. Phys.*, **47**, 2034 (1967).

and accordingly the frequency-distribution peaks give rise to inelastic scattering peaks.

The X-ray diffraction and infrared and Raman spectra of polyethylene glycol have been studied, and this polymer chain has been found to contain seven chemical units of CH_2CH_2O and two helical turns per fiber period.[3-6] The internal-rotation conformation about the O-CH_2, CH_2-CH_2, and CH_2-O bonds are trans, gauche, and trans, respectively. The vibrational frequencies calculated for the 7_2 helix conformation agree satisfactorily well with the observed frequencies of the far-infrared bands below 300 cm^{-1}.

For the polyethylene-glycol chain, the repeat unit contains seven atoms, and accordingly, there are twenty-one branches of the chain vibrations. In the region below 600 cm^{-1}, there are six branches associated with C-C-O and C-O-C angle-bending modes and internal-rotation modes about C-C and C-O bonds. From dispersion curves (frequency *versus* phase difference) for these branches, frequency distribution of the chain vibrations has been calculated,[7] in comparison with neutron inelastic scattering peaks.[8] Also, Young's modulus along the chain axis may be treated by the use of the intrachain force field. For the polyethylene-glycol chain, the calculated value[7] of 0.008 mdyn/Å^2 agrees closely with the experimental value[9] of 0.010 mydn/Å^2.

Thus, the infrared and Raman frequencies, frequency distribution and neutron inelastic scattering, and Young's modulus may be treated systematically on the basis of the intrachain force field. An extensive study on the force field of the polyethylene-glycol chain is also important for analyses of infrared and Raman spectra of model molecules[10] $RO(-CH_2CH_2O-)_pR$ [R: H, D or CH_3; p= 1−7] and of molten polyethylene glycol.[11]

In the present study, the intrachain force field of polyethylene glycol was refined, by the method of least squares, with reference to the observed infrared and Raman frequencies.[4,5] Nature of the infrared and/or Raman active vibrations was elucidated, referring to the calculated potential-energy distributions.

Normal Coordinate Treatment

For the 7_2 helix conformation of polyethylene glycol, the unit rotation about the axis is given as $\theta=4\pi/7$. Also, as confirmed by the analysis of the parallel infrared bands, the molecular chain has two twofold axes per repeat unit; one axis bisects the C-O-C bond-angle while the other axis intersects the C-C bond at right angle. Accordingly, the non-degenerate A vibrations (with $\delta=0$) are classified into the A_1 and A_2 vibrations which are symmetric and antisymmetric, respectively, with respect to the twofold axes.[12] The parallel infrared bands of polyethylene glycol are due to the A_2 vibrations with $\delta=0$ while the perpendicular bands are due to the E_1 vibrations with $\delta=4\pi/7$. The Raman lines are due to the A_1, E_1, or E_2 vibrations with $\delta=8\pi/7$.

In the present study, the A_1, A_2, and E_1 vibrations were treated for the normal species $(-CH_2CH_2O-)_p$ and the perdeuterated species $(-CD_2CD_2O-)_p$ of the polyethylene-glycol chain. The general method for treating the helical chain vibrations[2] was used. The stretching (Δr), angle-bending ($\Delta\phi$), and internal-rotation coordinates (Δt)[13] were denoted with the atom indices given previously[4] (see also Fig. 1). The internal coordinates

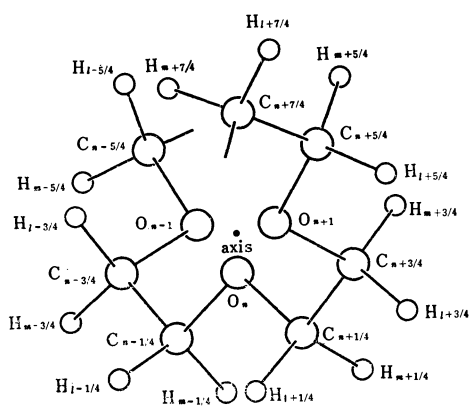

Fig. 1. Numbering of atoms of polyethylene glycol as used in the normal coordinate treatment.

3) T. Miyazawa, *J. Polymer Sci.*, **55**, 215 (1961), addendum.
4) T. Miyazawa, K. Fukushima and Y. Ideguchi, *J. Chem. Phys.*, **37**, 2764 (1962).
5) H. Tadokoro, Y. Chatani, T. Yoshihara, S. Tahara and S. Murahashi, *Makromol. Chem.*, **73**, 109 (1964).
6) T. Yoshihara, H. Tadokoro and S. Murahashi, *J. Chem. Phys.*, **41**, 2902 (1964).
7) H. Matsuura and T. Miyazawa, *Rept. Progr. Polymer Phys. Japan*, **9**, 179 (1966).
8) S. Trevino and H. Boutin, *J. Macromol. Sci.*, **A1**, 723 (1967).
9) I. Sakurada, T. Ito and K. Nakamae, *J. Polymer Sci.*, **C15**, 75 (1966).
10) H. Matsuura and T. Miyazawa, Symposium on Molecular Structure, Toyonaka, 1966; *Rept. Progr. Polymer Phys. Japan*, **10**, 187 (1967).
11) H. Matsuura and T. Miyazawa, Annual Meeting of the Chemical Society of Japan, Tokyo, 1967.
12) C. Y. Liang and S. Krimm, *J. Chem. Phys.*, **25**, 563 (1956).
13) T. Miyazawa and K. Fukushima, *J. Mol. Spectry.*, **15**, 308 (1965).

were then transformed into the local-symmetry coordinates ($\sigma's$),[14] namely σ_{ss} (CH_2 symmetric stretching), σ_{as} (CH_2 antisymmetric stretching), σ_{sc} (CH_2 scissoring), σ_{wa} (CH_2 wagging), σ_{tw} (CH_2 twisting), σ_{ro} (CH_2 rocking), σ_{CCst} (C-C stretching), σ_{COst} (C-Ostretching), σ_{CCO} (C-C-O bending), σ_{COC} (C-O-C bending), σ_{CCto} (C-C internal-rotation), and σ_{COto} (C-O internal-rotation). These coordinates were grouped into four vectors,

$$\boldsymbol{R}^s_n,\ \boldsymbol{R}_{n+1/4},\ \boldsymbol{R}^s_{n+1/2},\ \text{and}\ \boldsymbol{R}_{n+3/4}.$$

$$\begin{aligned}
\boldsymbol{R}^s_n:\quad & \sigma_{COC}=\Delta\phi(C_{n-1/4}\text{-}O_n\text{-}C_{n+1/4})\\
\boldsymbol{R}_{n+1/4}:\quad & \sigma_{ss}=[\Delta r(C_{n+1/4}\text{-}H_{m+1/4})+\Delta r(C_{n+1/4}\text{-}H_{l+1/4})]/2^{1/2}\\
& \sigma_{as}=[\Delta r(C_{n+1/4}\text{-}H_{m+1/4})-\Delta r(C_{n+1/4}\text{-}H_{l+1/4})]/2^{1/2}\\
& \sigma_{sc}=[4\Delta\phi(H_{m+1/4}\text{-}C_{n+1/4}\text{-}H_{l+1/4})-\Delta\phi(H_{m+1/4}\text{-}C_{n+1/4}\text{-}C_{n+3/4})\\
& \qquad -\Delta\phi(H_{m+1/4}\text{-}C_{n+1/4}\text{-}O_n)-\Delta\phi(H_{l+1/4}\text{-}C_{n+1/4}\text{-}C_{n+3/4})\\
& \qquad -\Delta\phi(H_{l+1/4}\text{-}C_{n+1/4}\text{-}O_n)]/20^{1/2}\\
& \sigma_{wa}=[\Delta\phi(H_{m+1/4}\text{-}C_{n+1/4}\text{-}C_{n+3/4})-\Delta\phi(H_{m+1/4}\text{-}C_{n+1/4}\text{-}O_n)\\
& \qquad +\Delta\phi(H_{l+1/4}\text{-}C_{n+1/4}\text{-}C_{n+3/4})-\Delta\phi(H_{l+1/4}\text{-}C_{n+1/4}\text{-}O_n)]/2\\
& \sigma_{tw}=[\Delta\phi(H_{m+1/4}\text{-}C_{n+1/4}\text{-}C_{n+3/4})-\Delta\phi(H_{m+1/4}\text{-}C_{n+1/4}\text{-}O_n)\\
& \qquad -\Delta\phi(H_{l+1/4}\text{-}C_{n+1/4}\text{-}C_{n+3/4})+\Delta\phi(H_{l+1/4}\text{-}C_{n+1/4}\text{-}O_n)]/2\\
& \sigma_{ro}=[\Delta\phi(H_{m+1/4}\text{-}C_{n+1/4}\text{-}C_{n+3/4})+\Delta\phi(H_{m+1/4}\text{-}C_{n+1/4}\text{-}O_n)\\
& \qquad -\Delta\phi(H_{l+1/4}\text{-}C_{n+1/4}\text{-}C_{n+3/4})-\Delta\phi(H_{l+1/4}\text{-}C_{n+1/4}\text{-}O_n)]/2\\
& \sigma_{COst}=\Delta r(C_{n+1/4}\text{-}O_n)\\
& \sigma_{CCO}=[5\Delta\phi(C_{n+3/4}\text{-}C_{n+1/4}\text{-}O_n)-\Delta\phi(H_{m+1/4}\text{-}C_{n+1/4}\text{-}H_{l+1/4})\\
& \qquad -\Delta\phi(H_{m+1/4}\text{-}C_{n+1/4}\text{-}C_{n+3/4})-\Delta\phi(H_{m+1/4}\text{-}C_{n+1/4}\text{-}O_n)\\
& \qquad -\Delta\phi(H_{l+1/4}\text{-}C_{n+1/4}\text{-}C_{n+3/4})-\Delta\phi(H_{l+1/4}\text{-}C_{n+1/4}\text{-}O_n)]/30^{1/2}\\
& \sigma_{COto}=\Delta t(C_{n+1/4}\text{-}O_n)\\
\boldsymbol{R}^s_{n+1/2}:\quad & \sigma_{CCst}=\Delta r(C_{n+1/4}\text{-}C_{n+3/4})\\
& \sigma_{CCto}=\Delta t(C_{n+1/4}\text{-}C_{n+3/4})
\end{aligned}\qquad (1)$$

The elements of the $\boldsymbol{R}_{n+3/4}$ vector may be derived from the $\boldsymbol{R}_{n+1/4}$ vector by interchanging the subscripts, $n \leftrightarrow n+1$, $n+1/4 \leftrightarrow n+3/4$, $l+1/4 \leftrightarrow m+3/4$, and $m+1/4 \leftrightarrow l+3/4$.

The inverse kinetic-energy matrix $\boldsymbol{G}$ or the potential-energy matrix $\boldsymbol{F}$ for the infinite helical chain may be factored into the matrices associated with the symmetry coordinate vectors for the phase difference δ. The symmetry coordinates for polyethylene glycol were constructed as follow,

$$\begin{aligned}
\boldsymbol{S}_1(\delta)&=(2/N)^{1/2}\sum_n \boldsymbol{R}^s_n\cos n\delta\\
\boldsymbol{S}_3(\delta)&=(2/N)^{1/2}\sum_n \boldsymbol{R}^s_{n+1/2}\cos(n+1/2)\delta\\
\boldsymbol{S}_5(\delta)&=(1/N)^{1/2}\sum_n[\boldsymbol{R}_{n+1/4}\cos(n+1/4)\delta+\boldsymbol{R}_{n+3/4}\cos(n+3/4)\delta]\\
\boldsymbol{S}_6(\delta)&=(1/N)^{1/2}\sum_n[\boldsymbol{R}_{n+1/4}\cos(n+1/4)(\delta+2\pi)+\boldsymbol{R}_{n+3/4}\cos(n+3/4)(\delta+2\pi)]
\end{aligned}$$

and

$$\begin{aligned}
\boldsymbol{S}_1'(\delta)&=-(2/N)^{1/2}\sum_n \boldsymbol{R}^s_n\sin n\delta\\
\boldsymbol{S}_3'(\delta)&=-(2/N)^{1/2}\sum_n \boldsymbol{R}^s_{n+1/2}\sin(n+1/2)\delta\\
\boldsymbol{S}_5'(\delta)&=-(1/N)^{1/2}\sum_n[\boldsymbol{R}_{n+1/4}\sin(n+1/4)\delta+\boldsymbol{R}_{n+3/4}\sin(n+3/4)\delta]\\
\boldsymbol{S}_6'(\delta)&=-(1/N)^{1/2}\sum_n[\boldsymbol{R}_{n+1/4}\sin(n+1/4)(\delta+2\pi)+\boldsymbol{R}_{n+3/4}\sin(n+3/4)(\delta+2\pi)]
\end{aligned}\qquad (2)$$

where $(2/N)^{1/2}$ or $(1/N)^{1/2}$ is the normalization factor. The symmetry coordinate $S(\delta)$ is symmetric with respect to the twofold axis passing through the zeroth oxygen atom, whereas $S'(\delta)$ is antisymmetric with respect to this axis. Accordingly, the inverse kinetic-energy matrix (or potential-energy matrix) for the phase difference δ is factored into the $\boldsymbol{G}(\delta)$ [or $\boldsymbol{F}(\delta)$] associated with $S(\delta)$'s and the other identical one associated with $S'(\delta)$'s.

For calculating $\boldsymbol{G}(\delta)$ matrices, the bond lengths of r(C-C)=1.54 A, r(C-O)=1.43 A, and r(C-H)=1.09 Å, and tetrahedral bond angles were used. From these bond lengths and angles and the fiber period[15] of 19.25 Å,

14) T. Shimanouchi, *Nippon Kagaku Zasshi* (*J. Chem. Soc. Japan, Pure Chem. Sect.*), **86**, 261, 768 (1965); Symposium on Molecular Structure, Tokyo, 1964; Toyonaka, 1966.

15) E. R. Walter and F. P. Reding, National Meeting of the American Chemical Society, San Francisco, 1958.

the internal-rotation angles about the C-C and C-O bonds were calculated as 63°55′ and 188°51′, respectively, by the use of equations for helical parameters.[3,16] The atomic masses of 12.01115 for carbon, 15.99940 for oxygen, 1.00797 for hydrogen, and 2.01410 for deuterium were used for calculating the $\boldsymbol{G}(\delta)$ matrix elements.

For degenerate vibrations, phase angles $\varepsilon(\delta)$ are useful for describing phase relations in normal modes. Setting $\varepsilon=0$ for internal coordinates $\boldsymbol{R}^s_n(\delta)$, the phase angle for $\boldsymbol{R}^s_{n+1/2}(\delta)$ is given as $\varepsilon=\delta/2$. The phase angles for $[\boldsymbol{R}_{n+1/4}(\delta)]_k$*1 and $[\boldsymbol{R}_{n+3/4}(\delta)]_k$ are given as $\varepsilon_k=\delta/2-\varepsilon'_k(\delta)$ and $\varepsilon_k=\delta/2+\varepsilon'_k(\delta)$, respectively, where the values of $\varepsilon'_k(\delta)$ may be calculated from the eigenvector components for the kth coordinates.[2] Then, the phase-angle difference between $[\boldsymbol{R}_{n+1/4}(\delta)]_k$ and $[\boldsymbol{R}_{n+3/4}(\delta)]_k$ is $\Delta\varepsilon_k(OCH_2\text{-}CH_2O)=2\varepsilon'_k(\delta)$. Vibrational modes with $\Delta\varepsilon_k(OCH_2\text{-}CH_2O)\sim0$ and $\sim\pm180°$ are quasi-symmetric and quasi-antisymmetric, respectively, with respect to the twofold axis that intersects the CH_2-CH_2 bond. The phase-angle difference between $[\boldsymbol{R}_{n-1/4}(\delta)]_k$ and $[\boldsymbol{R}_{n+1/4}(\delta)]_k$ is $\Delta\varepsilon_k(\text{C-O-C})=\delta-2\varepsilon'_k(\delta)$. Vibrational modes with $\Delta\varepsilon_k(\text{C-O-C})\sim0$ and $\sim\pm180°$ are quasi-symmetric and quasi-antisymmetric, respectively, with respect to the twofold axis that intersects the C-O-C angle. It may be remarked that the phase-angle differences for the A_1 and A_2 vibrations are $\Delta\varepsilon=0$ and 180°, respectively.

Numerical calculations in the present treatment of normal vibrations were carried out with a HITAC 5020 E computer (Hitachi, Limited) at the University of Tokyo and a NEAC 2200-500 computer (Nippon Electric Company, Limited) at Osaka University.

Potential Function

In a previous study,[4] the Urey-Bradley force field (UBFF)[17] with supplementary terms was used, and the potential constants were transferred from polyethylene, dimethyl ether, and propyl alcohol. In the present treatment, however, a more generalized potential function (local-symmetry force field)[14] was used. Accordingly, the infinite potential-energy matrix of the infinite polyethylene-glycol chain is expressed in terms of the local-symmetry coordinate vectors. Nonzero submatrices in the lower half columns associated with $\boldsymbol{R}^s_n$, $\boldsymbol{R}_{n+1/4}$, $\boldsymbol{R}^s_{n+1/2}$, and $\boldsymbol{R}_{n+3/4}$ are shown below:

	$\tilde{\boldsymbol{R}}^s_n$	$\tilde{\boldsymbol{R}}_{n+1/4}$	$\tilde{\boldsymbol{R}}^s_{n+1/2}$	$\tilde{\boldsymbol{R}}_{n+3/4}$
$\boldsymbol{R}^s_n$	$\boldsymbol{A}^a_0$			
$\boldsymbol{R}_{n+1/4}$	$\tilde{\boldsymbol{F}}^a_{1/4}\boldsymbol{C}_0$			
$\boldsymbol{R}^s_{n+1/2}$	0	$\boldsymbol{F}^b_{1/4}$	$\boldsymbol{A}^b_0$	
$\boldsymbol{R}_{n+3/4}$	0	$\boldsymbol{C}^b_{1/2}$	$\tilde{\boldsymbol{F}}^b_{1/4}$	$\boldsymbol{C}_0$
$\boldsymbol{R}^s_{n+1}$	0	0	0	$\boldsymbol{F}^a_{1/4}$
$\boldsymbol{R}_{n+5/4}$	0	0	0	$\boldsymbol{C}^a_{1/2}$
$\boldsymbol{R}^s_{n+3/2}$	0	0	0	0

where the matrices with tilde are the transposed matrices. The elements of the submatrices are given below:

$$\boldsymbol{A}^a_0=[f(\text{COC})]$$

$$\boldsymbol{A}^b_0=\begin{bmatrix} f(\text{CC st}) & 0 \\ 0 & f(\text{CC to}) \end{bmatrix}$$

$$\boldsymbol{C}_0=\begin{bmatrix}
f(\text{ss}) & & & & & & & & \\
0 & f(\text{as}) & & & & & & & \\
* & 0 & f(\text{sc}) & & & & & & \\
* & 0 & f\begin{pmatrix}\text{sc}\\ \text{wa}\end{pmatrix} & f(\text{wa}) & & & & & \\
0 & * & 0 & 0 & f(\text{tw}) & & & & \\
0 & * & 0 & 0 & f\begin{pmatrix}\text{tw}\\ \text{ro}\end{pmatrix} & f(\text{ro}) & & & \\
* & 0 & * & * & 0 & 0 & f(\text{CO st}) & & \\
* & 0 & f\begin{pmatrix}\text{sc}\\ \text{CCO}\end{pmatrix} & f\begin{pmatrix}\text{wa}\\ \text{CCO}\end{pmatrix} & 0 & 0 & f\begin{pmatrix}\text{CO st}\\ \text{CCO}\end{pmatrix} & f(\text{CCO}) & \\
0 & 0 & 0 & 0 & 0 & 0 & 0 & 0 & f(\text{CO to})
\end{bmatrix}$$

(symmetric)

16) H. Sugeta and T. Miyazawa, *Biopolymers*, **5**, 673 (1967).

*1 The subscript k indicates the kth component of internal-coordinate vectors.

17) T. Shimanouchi, *J. Chem. Phys.*, **17**, 245, 734, 848 (1949); *Pure Appl. Chem.*, **7**, 131 (1963).

$$\boldsymbol{C}^{a}_{1/2}=\begin{bmatrix} 0 & & & & & & & & \\ 0 & 0 & & & & & & & \\ 0 & 0 & 0 & & & \text{symmetric} & & & \\ 0 & 0 & 0 & 0 & & & & & \\ 0 & 0 & 0 & 0 & 0 & & & & \\ 0 & 0 & 0 & 0 & 0 & 0 & & & \\ 0 & 0 & 0 & 0 & 0 & 0 & f\binom{\text{CO st}}{\text{CO st}} & & \\ 0 & 0 & 0 & 0 & 0 & 0 & 0 & 0 & \\ 0 & 0 & 0 & 0 & 0 & 0 & 0 & 0 & 0 \end{bmatrix}$$

$$\boldsymbol{C}^{b}_{1/2}=\begin{bmatrix} 0 & & & & & & & & & \\ 0 & 0 & & & & & & & & \\ 0 & 0 & 0 & & & & \text{symmetric} & & & \\ 0 & 0 & 0 & f'\binom{\text{wa}}{\text{wa}} & & & & & & \\ 0 & 0 & 0 & 0 & f'\binom{\text{tw}}{\text{tw}} & & & & & \\ 0 & 0 & 0 & 0 & 0 & f'\binom{\text{ro}}{\text{ro}} & & & & \\ 0 & 0 & 0 & 0 & 0 & 0 & 0 & & & \\ 0 & 0 & 0 & 0 & 0 & f'\binom{\text{ro}}{\text{CCO}} & 0 & f'\binom{\text{CCO}}{\text{CCO}} & & \\ 0 & 0 & 0 & 0 & 0 & 0 & 0 & 0 & 0 & \end{bmatrix}$$

$$\boldsymbol{F}^{a}_{1/4}=\begin{bmatrix} 0 & 0 & 0 & 0 & 0 & 0 & f\binom{\text{CO st}}{\text{COC}} & f'\binom{\text{CCO}}{\text{COC}} & 0 \end{bmatrix}$$

$$\boldsymbol{F}^{b}_{1/4}=\begin{bmatrix} * & 0 & * & * & 0 & 0 & f\binom{\text{CC st}}{\text{CO st}} & f\binom{\text{CC st}}{\text{CCO}} & 0 \\ 0 & 0 & 0 & 0 & 0 & 0 & 0 & 0 & 0 \end{bmatrix}$$

where the elements denoted with asterisk are related with the UBFF's repulsion constants, F(HCO), F(HCC), and F(HCH).

The force constants f(ss), f(as), f(sc), f(wa), f(tw), f(ro), f(CC st), f(CO st), f(CCO), f(COC), f(CC to), and f(CO to) are diagonal elements associated with the local-symmetry coordinates shown in parentheses. The non-diagonal elements of UBFF, namely, f(sc, wa), f(sc, CCO), f(wa, CCO), f(tw, ro), f(CO st, CCO), f(CO st, CO st), f(CO st, COC), f(CC st, CO st), f(CC st, CCO), and F(HCO), F(HCC), and F(HCH) were taken as independent force constants. The potential constants denoted with primes f'(wa, wa), f'(tw, tw), f'(ro, ro), f'(CCO, CCO), f'(ro, CCO), and f'(COC, CCO) are not found in the simple UBFF. However, these constants were also taken into account as supplementary elements, which are associated with the vibrational interactions between the adjacent methylene groups or between the adjacent skeletal-bond angles.

In the beginning, the modified UBFF constants of the previous studies[4,7] were transformed into the constants of the local-symmetry force field (LSFF). The LSF Fforce constants were then adjusted by the method of least squares,[18] with reference to the infrared absorption frequencies of the normal and perdeuterated species of polyethylene glycol,[4,5] and the Raman frequencies of the normal species.[19,20] The observed frequencies[21] of *p*-dioxane and *p*-dioxane-d_8 were also used in the refinement, since these molecules consist of the same chemical units of CH_2CH_2O and CD_2CD_2O, respectively, as those of the normal and perdeuterated species of this polymer. The force constants thus obtained are shown in Table 1. The observed and calculated frequencies are listed in Table 2—5, together with the potential-energy distributions (P. E. D.)[22] defined as follows,

$$(P.E.D.)_{ia}=(F_{ii}L^{2}_{ia}/\lambda_a)\times 100 \qquad (3)$$

where F_{ii} is the ith diagonal element of the potential-energy matrix, L_{ia} is the ith element of the ath eigenvector, and λ_a is the

18) D. E. Mann, T. Shimanouchi, J. H. Meal and L. Fano, *J. Chem. Phys.*, **27**, 43 (1957).

19) Y. Matsui, T. Kubota, H. Tadokoro and T. Yoshihara, *J. Polymer Sci.*, **A3**, 2275 (1965).

20) R. F. Schaufele, *Trans. New York Acad. Sci.*, to be published.

21) H. Matsuura and T. Miyazawa, Symposium on Molecular Structure, Sapporo, 1967.

22) Y. Morino and K. Kuchitsu, *J. Chem. Phys.*, **20**, 1809 (1952); I. Nakagawa, *Nippon Kagaku Zasshi* (*J. Chem. Soc. Japan, Pure Chem. Sect.*), **74**, 243 (1953).

TABLE 1. INTRACHAIN POTENTIAL CONSTANTS OF POLYETHYLENE GLYCOL

f(ss)	4.711[a]	f(tw, ro)	−0.140[b]	f(CCO)	1.063[b]	f'(ro, ro)	0.026[b]
f(as)	4.694[a]	f(CC st, CO st)	0.395[a]	f(COC)	1.523[b]	f'(CCO, CCO)	−0.127[b]
f(sc)	0.577[b]	f(CO st, CO st)	0.340[a]	f(CC to)	0.113[b]	f'(ro, CCO)	0.178[b]
f(wa)	0.739[b]	f(CC st, CCO)	0.017[c]	f(CO to)	0.099[b]	f'(CCO, COC)	−0.029[b]
f(tw)	0.681[b]	f(CO st, CCO)	0.455[c]	f(sc, wa)	0.026[b]	F(HCO)	0.889[d]
f(ro)	0.778[b]	f(CO st, COC)	0.259[c]	f(sc, CCO)	0.028[b]	F(HCC)	0.317[d]
f(CC st)	4.208[a]	f'(wa, wa)	0.028[b]	f(wa, CCO)	−0.004[b]	F(HCH)	0.200[d]
f(CO st)	5.227[a]	f'(tw, tw)	0.017[b]				

a) In unit of mdyn·Å. b) In unit of mdyn·Å. c) In unit of mdyn.
d) Repulsion constants of Urey-Bradley force field in unit of mdyn/Å, F' is taken as $-F/10$.

TABLE 2. OBSERVED AND CALCULATED FREQUENCIES (cm^{-1}) AND POTENTIAL-ENERGY DISTRIBUTIONS FOR THE A_1 AND A_2 VIBRATIONS OF NORMAL POLYETHYLENE GLYCOL $(-CH_2CH_2O-)_p$

	Obs. freq.[a] Infrared[b]	Raman[c]	Calc. freq.	Potential-energy distributions
		2939 m	2940	CH_2 antisym stretch (101)
			2874	CH_2 sym stretch (101)
		1484 s	1479	CH_2 scissor (98)
		1398 w	1423	CH_2 wag (88), CC stretch (20)
		(1235)	1252	CH_2 twist (81)
A_1	inactive	1126 m	1137	CH_2 rock (36), CO stretch (18)
		(1064)	1073	CO stretch (47), CC stretch (46)
		861 m	866	CO stretch (50), CH_2 rock (46)
		279 w	274	CCO bend (24), CC internal-rotation (19), COC bend (17)
		216 w	218	COC bend (48), CO internal-rotation (22)
			2943	CH_2 antisym stretch (101)
	2890 s		2883	CH_2 sym stretch (100)
	1463, 1457 m		1470	CH_2 scissor (100)
	1345 s		1344	CH_2 wag (107)
A_2	1244 m	inactive	1264	CH_2 twist (81)
	1102 vs		1087	CO stretch (94)
	963 s		964	CH_2 rock (49), CH_2 twist (18)
	529, 508 w		533	CCO bend (89), CH_2 rock (33)
	107 w		105	CO internal-rotation (90)

a) Relative intensities are shown after the frequencies;
vs: very strong, s: strong, m: medium, w: weak, and sh: shoulder.
b) Ref. 4. c) Ref. 20.

ath eigenvalue (frequency parameter).

For E_1 vibrations listed in Tables 3 and 5, phase-angle differences $\Delta\varepsilon(OCH_2\text{–}CH_2O)$ are given for CH_2 (or CD_2) sym. and antisym. stretch., scissor., wag., twist., and rock. modes and CCO bend. mode, while $\Delta\varepsilon$(C-O-C) are given for CO stretch. and internal-rotation modes.

Potential Constants

The potential constants for the polyethylene-glycol chain are listed in Table 1. By the use of these constants, calculated frequencies agree closely with observed frequencies, with a root-mean-square deviation as small as 0.9%.

The potential constants of methylene groups of polyethylene glycol (Table 1) may be compared with those of hydrocarbons[14] and polyethylene.[23] For example, symmetric- [f(ss)] and antisymmetric-stretching [f(as)] and scissoring constants [f(sc)] are nearly the same for polyethylene glycol (4.71 and 4.69 mdyne/Å and 0.58 mdyn·Å) and for propane (4.74 and 4.66 mdyn·Å and 0.59 mdyn·Å). However, the wagging constant [f(wa)] of polyethylene glycol (0.74 mdyn·Å) is appreciably larger than those of propane (0.64 mdyn·Å), and polyethylene (0.67 mdyn·Å), possibly due

23) M. Tasumi, T. Shimanouchi and T. Miyazawa, *J. Mol. Spectry.*, **11**, 422 (1963).

TABLE 3. OBSERVED AND CALCULATED FREQUENCIES (cm^{-1}), POTENTIAL-ENERGY DISTRIBUTIONS AND PHASE-ANGLE DIFFERENCES FOR THE E_1 VIBRATIONS OF NORMAL POLYETHYLENE GLYCOL $(-CH_2CH_2O-)_p$

Obs. freq.[a] Infrared[b]	Raman[c]	Calc. freq.	Potential-energy distributions and phase-angle differences[d]
2950 m		2943 2940	CH_2 antisym stretch (101, −162°) CH_2 antisym stretch (101, 18°)
2885 s	2890 s	2883	CH_2 sym stretch (100, 175°)
		2873	CH_2 sym stretch (100, −5°)
1470 m		1476	CH_2 scissor (100, 48°)
1453 w	1449 w	1471	CH_2 scissor (100, −132°)
1415 w		1401	CH_2 wag (95, 53°)
1364 m	1364 w	1353	CH_2 wag (107, −129°)
1283 m	1282 s	1286	CH_2 twist (73, −40°)
1236 w	1235 m	1234	CH_2 twist (87, 146°)
1149 s	1143 s	1142	CO stretch (37, −27°), CH_2 rock (29, −66°)
1119 s		1112	CO stretch (81, 136°), CC stretch (21)
1062 m	1064 m	1060	CO stretch (36, −102°), CH_2 rock (35, 70°), CC stretch (17)
947 m		941	CH_2 rock (34, 42°), CC stretch (27), CO stretch (14, 167°)
844 s	846 s	847	CH_2 rock (58, −149°), CO stretch (39, −9°)
	537 w	524	CCO bend (49, −142°), COC bend (21), CH_2 rock (17, 152°)
363 w	363 w	366	CCO bend (42, −73°), COC bend (38)
216 w	216 w	216	CCO bend (48, 64°), CC internal-rotation (28), COC bend (16)
165 w	160 w	164	CC internal-rotation (42), CO internal-rotation (38, −161°), CCO bend (18, 16°)
		92	CO internal-rotation (77, 66°), CCO bend (21, −10°)

a, b, c) See a), b), c) of Table 2.
d) Phase-angle differences $\Delta\varepsilon(OCH_2\text{-}CH_2O)$ are shown for CH_2 sym. and antisym. stretch., scissor., wag., twist., and rock. modes and CCO bend. mode, while $\Delta\varepsilon$(C-O-C) are shown for CO stretch. and internal-rotation modes.

TABLE 4. OBSERVED AND CALCULATED FREQUENCIES (cm^{-1}) AND POTENTIAL-ENERGY DISTRIBUTIONS FOR THE A_1 AND A_2 VIBRATIONS OF PERDEUTERATED POLYETHYLENE GLYCOL $(-CD_2CD_2O-)_p$

	Obs. freq.[a] Infrared[b]	Raman[c]	Calc. freq.	Potential-energy distributions
			2172	CD_2 antisym stretch (102)
			2078	CD_2 sym stretch (101)
			1293	CC stretch (56), CD_2 wag (37)
			1092	CD_2 scissor (57), CO stretch (39)
			1031	CO stretch (47), CD_2 scissor (29)
A_1	inactive		919	CD_2 twist (36), CD_2 rock (21)
			865	CD_2 twist (44), CD_2 wag (24)
			721	CD_2 rock (53), CD_2 twist (20), CO stretch (19)
			245	COC bend (38), CC stretch (21)
			192	CO internal-rotation (34), COC bend (27), CC internal-rotation (21)
	2164 s		2173	CD_2 antisym stretch (102)
	2072 s		2088	CD_2 sym stretch (100)
	1117 vs		1144	CO stretch (84), CD_2 wag (52)
	1087 sh		1080	CD_2 scissor (92)
A_2	996 m	inactive	979	CD_2 twist (35), CD_2 rock (19)
	940 m		950	CD_2 wag (40), CO stretch (21)
	800 m		795	CD_2 twist (46), CCO bend (24), CD_2 rock (23)
	453 434 w		455	CCO bend (71), CD_2 rock (46)
	95 w		96	CO internal-rotation (88)

a) See a) of Table 2.
b) Ref. 6.
c) Not yet reported.

TABLE 5. OBSERVED AND CALCULATED FREQUENCIES (cm^{-1}), POTENTIAL-ENERGY DISTRIBUTIONS AND PHASE-ANGLE DIFFERENCES FOR THE E_1 VIBRATIONS OF PERDEUTERATED POLYETHYLENE GLYCOL $(-CD_2CD_2O-)_p$

Obs. freq.[a] Infrared[b]	Raman[c]	Calc. freq.	Potential-energy distributions and phase-angle differences[d]
2171 s		2173	CD_2 antisym stretch (103, −97°)
		2172	CD_2 antisym stretch (103, 83°)
2082 s		2089	CD_2 sym stretch (100, 172°)
		2077	CD_2 sym stretch (102, −7°)
1255 m		1252	CC stretch (57), CD_2 wag (41, 15°)
1145 s		1140	CO stretch (72, −158°), CD_2 wag (46, −164°)
1121 s		1116	CO stretch (54, 19°), CD_2 scissor (36, 122°)
1087 sh		1083	CD_2 scissor (76, −83°), CD_2 wag (22, 139°)
1050 w		1040	CD_2 scissor (51, 111°), CO stretch (22, 27°)
1016 s		1001	CD_2 wag (36, −92°), CO stretch (16, 145°), CD_2 twist (12, −45°), CD_2 rock (12, −12°)
942 m		959	CD_2 twist (37, −106°), CO stretch (16, −111°), CD_2 rock (15, −64°)
919 m		905	CD_2 twist (34, 166°), CD_2 rock (31, 86°)
885 w		869	CD_2 twist (61, 42°)
780 w		771	CD_2 rock (30, 46°), CD_2 wag (23, 8°), CD_2 twist (19, 62°)
703 m		699	CD_2 rock (46, −133°), CD_2 twist (33, −135°), CO stretch (21, 3°)
458 w		458	CCO bend (36, −148°), CD_2 rock (26, 155°), COC bend (26)
		320	CCO bend (46, −80°), COC bend (33)
183 w		182	CCO bend (59, 55°), COC bend (14), CO internal-rotation (14, 134°)
156 w		156	CC internal-rotation (62), CO internal-rotation (30, −147°)
		83	CO internal-rotation (78, 64°), CCO bend (20, −4°)

a, b, c) See a), b), c) of Table 4. d) See d of Table 3.

to the effect of nonbonded interaction between methylene-hydrogen atoms and oxygen or carbon atoms. Since the C-O bond length (~1.43 Å) is appreciably shorter than the C-C bond length (~1.54 Å), the repulsive interaction to the methylene-hydrogen atoms of [O-CH_2-C] is expected to be greater than for [C-CH_2-C]. In fact, the repulsion constant of F(HCO)=0.89 mdyn·Å (Table 1) is much larger than F(HCC)=0.32 mdyn/Å. Then, the repulsive interaction is expected to be even greater for polyoxymethylene $[-CH_2-O-]_p$, where a methylene group is bonded to two oxygen atoms. In fact, the wagging constant of polyoxymethylene[24] [f(wa)=0.83 mdyn·Å] is larger than for polyethylene glycol. In accordance with the variation of the wagging constant, the rocking [f(ro)] and twisting constants [f(tw)] increase for the series of polyethylene (0.69 and 0.64 mdyn·Å) or propane (0.73 and 0.66 mydn·Å), polyethylene glycol (0.78 and 0.68 mydn. Å), and polyoxymethylene (1.05 and 0.76 mdyn. Å).

Before comparing the present force field with the force field of earlier normal coordinate treatments, Urey-Bradley force constants of K(CC), K(CO), F(CCO), F(COC), F(HCO) and F(HCC) may be transformed into local-symmetry force constants. Thus, the C-C and C-O stretching constants of polyethylene glycol in earlier treatments[4,6] are derived as f(CC st)=4.72 or 5.11 mdyn/Å and f(CO st)=4.26 or 4.68 mdyn/Å. These values of f(CC st) are much larger than for propane (4.35 mdyn/Å) and polyethylene (4.24 mdyn/Å). On the other hand, the previous values of f(CO st) are much smaller than for dimethyl ether[14] (5.20 mdyn/Å). However, in the present study, the C-C and C-O stretching constants were refined by the method of least squares and now these constants of f(CCst) =4.21 mydn/Å and f(CO st)=5.23 mdyn/Å agree closely enough with the corresponding constants for propane, polyethylene or dimethyl ether. Accordingly, the present set of force constants is considered to be more reasonable than those of earlier treatments. Because of considerable refinements in the force field, vibrational assignments (potential-energy distributions) in the region 1200—800 cm^{-1} were revised as will be presented in the next section.

The internal-rotation constants about the C-C and C-O bonds of polyethylene glycol were refined as f(CC to)=0.113 mdyn·Å and f(CO to)=0.099 mdyn·Å. These values correspond to the internal-rotation potential $V=V_3(1-\cos 3t)/2$ with the barrier height of V_3=3.6 and 3.2 kcal/mol for the C-C and C-O

24) H. Sugeta and T. Miyazawa, Annual Meeting of the Chemical Society of Japan, Tokyo, 1967.

bonds, respectively. These values may be compared with the corresponding values of polyethylene [f(CC to)=0.107 mdy. Å and V_3=3.4 kcal/mol][23] and polyoxymethylene [f(CO to) =0.108 mdyn. Å and V_3=3.5 kcal/mol].[24]

Vibrational Assignments

For the helical chain of polyethylene glycol $[-CH_2-CH_2-O-]_p$, there are seven atoms per repeat unit, so are 10 A_1 and 9 A_2 vibrations, 20 pairs of E_1 and 21 pairs of E_2 vibrations. The A_1, E_1 and E_2 vibrations are Raman active while the A_2 and E_1 vibrations are infrared active giving rise to parallel and perpendicular bands, respectively.

Polarized infrared spectra of polyethylene glycol were measured by Miyazawa *et al.*[4] and Tadokoro *et al.*[5] The Raman effect with mercury-lamp excitation was recorded by Matsui *et al.*[19] Referring to selection rules for infrared and Raman spectra and to observed dichroism of infrared bands, observed frequencies were already assigned[4,6] reasonably to symmetry species of A_1, A_2 or E_1. Recently, Schaufele[20] observed the Raman effect with helium-neon laser excitation (6328 Å) and found a number of Raman lines in the region 3000—25 cm^{-1}. Almost all the A_1, A_2 and E_1 frequencies of the normal species and the A_2 and E_1 frequencies of the perdeuterated species have now been observed as infrared bands and/or Raman lines. These observed frequencies are listed in Tables 2—5, together with frequencies, potential-energy distributions and phase-angle differences calculated in the the present study. Revised vibrational assignments of observed frequencies will be discussed, in contrast to previous assignments.[4,6]

Polyethylene Glycol $(-CH_2CH_2O-)_p$. Infrared bands due to fundamental vibrations of polyethylene glycol in the region 3000—2800 cm^{-1} were identified, with reference to vibrational frequencies of related molecules. Thus, the parallel band at 2890 cm^{-1} and perpendicular band at 2885 cm^{-1} are assigned to the A_2 and E_1 CH_2 symmetric-stretching vibration.[4] The strong Raman line at 2890 cm^{-1} corresponds to the infrared band at 2885 cm^{-1}. The medium-intensity Raman line at 2939 cm^{-1} and the perpendicular infrared band at 2950 cm^{-1} are assigned to the A_1 and E_1 antisymmetric stretching modes, respectively.

The parallel infrared band (doublet at 1463 and 1457 cm^{-1}) and perpendicular bands at 1470 and 1453 cm^{-1} are assigned to the A_2 and E_1 CH_2 scissoring vibrations. The strong Raman line at 1484 cm^{-1} is assigned to the A_1 scissoring vibration while the weak line at 1449 cm^{-1} corresponds to the infrared band at 1453 cm^{-1}.

The Raman line at 1398 cm^{-1} (weak) and parallel infrared band at 1345 cm^{-1} (strong) are assigned to the symmetric (A_1) and antisymmetric (A_2) wagging modes of CH_2-CH_2 groups (Table 2). The two perpendicular bands at 1415 and 1364 cm^{-1} correspond to the CH_2 wagging frequencies of the E_1 species, calculated at 1401 cm^{-1} (with $\Delta\varepsilon$=53°) and at 1353 cm^{-1} (with $\Delta\varepsilon$=−129°), respectively (Table 3). The calculated values of $\Delta\varepsilon$ indicate that the higher-frequency vibration is associated with quasi-symmetric wagging mode of CH_2-CH_2 groups while the lower-frequncy vibration is associated with quasi-antisymmetric mode. The weak band at ~1410 cm^{-1} and strong band at ~1360 cm^{-1} have also been observed for higher oligomers $HO[-CH_2CH_2O-]_pH$ in the crystalline state.[25]

The parallel infrared band at 1244 cm^{-1} is due to the A_2 vibration associated with the antisymmetric twisting mode of CH_2-CH_2 groups. The perpendicular bands at 1283 (medium) and 1236 cm^{-1} (weak) are due to quasi-symmetric ($\Delta\varepsilon$=−40°) and quasi-antisymmetric twisting modes ($\Delta\varepsilon$=146°), respectively, of CH_2-CH_2 groups.*2 It may be remarked that the intensities of the infrared bands at 1244 and 1283 cm^{-1} compare with the intensities of the bands (at 1345 and 1364 cm^{-1}) due to CH_2 wagging modes (see Fig. 2 of Ref. 4). Strong absorption of twisting modes of C-CH_2-O groups has been discussed previously[4] in relation with dissimilarity of C-C and C-O bonds (as for polarity or conformation).

The Raman line observed at 1235 cm^{-1} appears to correspond to the perpendicular infrared band at 1236 cm^{-1} (E_1 species). The Raman line due to the A_1 vibration calculated at 1252 cm^{-1} is possibly overlapped by the Raman line at 1235 cm^{-1}.

Infrared bands and Raman lines in the region 1150—800 cm^{-1} are due to C-C and C-O stretching modes and CH_2 rocking mode. Two parallel infrared bands are assigned to A_2 vibrations (Table 2). The very strong band

25) H. Matsuura and T. Miyazawa, *Spectrochim. Acta*, **23A**, 2433 (1967).

*2 In a previous treatment[4] of potential-energy distributions, CH_2 wagging and twisting modes were considerably mixed for vibrations in the region 1430—1230 cm^{-1}. However, with the force field refined in the present study, vibrations calculated above 1340 cm^{-1} are almost purely associated with CH_2 wagging modes and vibrations below 1290 cm^{-1} are associated with twisting modes.

at 1102 cm^{-1} is associated almost exclusively with the C-O-C antisymmetric stretching mode while the strong band at 963 cm^{-1} is associated primarily with the antisymmetric rocking mode of CH_2-CH_2 groups.

The medium-intensity Raman lines at 1126 and 861 cm^{-1} are assigned to the A_1 vibrations calculated at 1137 and 866 cm^{-1}, respectively (Table 2). As for potential-energy distributions, these lines are due to hybridized vibrations of the CH_2-CH_2 symmetric rocking mode and C-O-C symmetric stretching mode. For the A_1 species, the C-C stretching mode is coupled with the C-O-C symmetric stretching mode, to yield the vibration calculated at 1073 cm^{-1}. However, a corresponding Raman line has not been identified, possibly because of overlap with the medium-intensity line at 1064 cm^{-1}.

The Raman line at 1143 (strong), 1064 (medium) and 846 cm^{-1} (strong) correspond to the perpendicular infrared bands (E_1 species) at 1149 (strong), 1062 (medium) and 844 cm^{-1} (strong). The vibration calculated at 1142 cm^{-1} is associated with quasi-symmetric C-O stretching mode and CH_2 rocking mode,*3 whereas the vibration calculated at 847 cm^{-1} is associated with quasi-antisymmetric ($\Delta\varepsilon=-149°$) CH_2 rocking mode and quasi-symmetric ($\Delta\varepsilon=-9°$) C-O stretching mode. The vibration calculated at 1060 cm^{-1} is also associated with the C-O stretching ($\Delta\varepsilon=-102°$) and CH_2 rocking mode ($\Delta\varepsilon=70°$).

The strong perpendicular band at 1119 cm^{-1} is primarily due to quasi-antisymmetric ($\Delta\varepsilon=136°$) C-O stretching mode as coupled with the C-C stretching mode. The medium-intensity band at 947 cm^{-1} is due largely to CH_2 quasi-symmetric ($\Delta\varepsilon=42°$) rocking mode and C-C stretching mode. This perpendicular band at 947 cm^{-1} together with the bands at 963 and 844 cm^{-1} have been discussed[26-29] in relation with the conformation of O-CH_2-CH_2-O groups. However, vibrational assignments of these bands are now established after the refined treatment of the present study.

A weak Raman line has been observed at 930 cm^{-1} by Matsui *et al.*[19] or at 936 cm^{-1} by Schaufele.[20] This line does not correspond to any calculated A_1 frequencies or to perpendicular infrared bands (E_1) in this region. As mentioned previously, E_2 vibrations are infrared inactive but they are active in the Raman effect. Accordingly, the Raman line at 936 cm^{-1} may be assigned to the E_2 vibration (with the phase difference of $\delta=2\theta$) calculated at 922 cm^{-1}. This E_2 vibration is associated with the C-C stretching and C-O stretching modes.

Chain vibrations of polyethylene glycol in the region below 600 cm^{-1} are associated with C-C-O and C-O-C bending modes and internal-rotation modes about C-C and C-O bonds. Raman lines have been observed at 537, 363, 279, 216 and 160 cm^{-1}, parallel infrared bands at 529, 508 and 107 cm^{-1}, and perpendicular bands at 216 and 165 cm^{-1}. In the present study, a weak band was found at 363 cm^{-1} for Carbowax 6000 (high molecular-weight polyethylene glycol from Carbide and Carbon Chemicals Corporation).

The parallel band (doublet at 529 and 508 cm^{-1}) corresponds to the A_2 vibration calculated at 533 cm^{-1}. This is the C-C-O bending vibration as coupled with the CH_2 rocking mode. The doublet splitting is either due to Fermi resonance with combination vibrations or to interchain ineractions in the crystalline lattice.[4] In the present study, therefore, the infrared absorption (600—400 cm^{-1}) was measured for solid solutions of Carbowax 6000 and *n*-octacosane ($C_{28}H_{58}$)*4 with the mixing weight-ratio of 1 : ~50. At this low concentration, any interchain effect is reduced negligible. However, the peak positions and relative intensities of the doublet in the solution are still the same as in the crystalline state. This observation indicates that the doublet splitting is possibly due to Fermi resonance rather than to interchain interactions. Therefore, the dispersion curves (frequency *versus* phase difference) of the polyethylene-glycol chain[30] were reviewed, for possibilities of Fermi resonance with the A_2 fundamental calculated at 533 cm^{-1}. In fact, the splitting may now be ascribed to the Fermi resonance between the A_2 fundamental

*3 In previous treatments[4,6] the potential energy for the A_1 vibration at 1126 cm^{-1} and the E_1 vibration at 1149 cm^{-1} was largely associated with the C-C stretching mode, because the C-C stretching constant was perphaps too large and the C-O stretching constant was too small.

*4 In the region 600—400 cm^{-1}, *n*-octacosane exhibits only aweak peak at 564 cm^{-1}.

26) W. H. T. Davison, *J. Chem. Soc.*, **1955**, 3270.
27) Y. Kuroda and M. Kubo, *J. Polymer Sci.*, **26**, 323 (1957); **36**, 453 (1959).
28) H. F. White and C. M. Lovell, *J. Polymer Sci.*, **41**, 369 (1959).
29) A. Miyake, *J. Am. Chem. Soc.*, **82**, 3040 (1960).
30) H. Sugeta, H. Matsuura and T. Miyazawa, International Symposium on Macromolecular Chemistry, Tokyo, 1966.

*5 Another resonance may also be expected between the A_2 fundamental and the binary combination of B_1 (calc. 196 cm^{-1}) and B_2 (calc. 289 cm^{-1}) vibrations. The symmetry species for overtones and combinations have been given.[12,31]

and the binary combination of the E_1 vibrations [363+165=528 cm^{-1}].*5

The Raman lines at 537 cm^{-1} (E_1) and 279 cm^{-1} (A_1), Raman line and infrared band (perpendicular) at 363 cm^{-1} (E_1) are assigned to the hybridized vibrations of C-O-C and C-C-O bending modes. The perpendicular band at 216 cm^{-1} is assigned to the E_1 vibration associated with the quasi-symmetric C-C-O bending mode and C-C internal-rotation mode. The weak Raman line at 216 cm^{-1} corresponds to this E_1 vibration and/or to the A_1 vibration (calculated at 218 cm^{-1}) which is associated with the C-O-C bending mode and symmetric internal-rotation mode about C-O bonds.

The perpendicular infrared band at 165 cm^{-1} (and corresponding Raman line at 160 cm^{-1}) is due to the hybridized vibration of the C-C internal-rotation mode and quasi-antisymmetric internal-rotation mode about C-O bonds. The parallel band at 107 cm^{-1} is due to the antisymmetric internal-rotation mode about C-O bonds.

A weak infrared band[2] is observed at 580 cm^{-1} and the corresponding Raman line[20] at 584 cm^{-1}. Accordingly, this vibration is assigned to the E_1 species. There is no E_1 fundamental calculated around this frequency. However, the observed vibration may be assigned reasonably to the combination (E_1 species) of the A_1 vibration at 216 cm^{-1} and the E_1 vibration at 363 cm^{-1}. Supporting this assignment, the corresponding band (shoulder) is observed[6] around 500 cm^{-1} for the perdeuterated species, just as expected for the combination of the A_1 and E_1 vibrations calculated at 192 and 320 cm^{-1}, respectively.

The Raman lines at 126 and 75 cm^{-1} can not be explained as due to chain vibrations of A_1, E_1 or E_2 species, and are possibly due largely to lattice modes. Intensities or positions of the bands due to lattice vibrations are sensitive to temperature changes. In fact, Schaufele[32] observed that, at lower temperature, the Raman lineat 126 cm^{-1} intensifies relative to the line at 75 cm^{-1}.

Polyethylene-d_4 Glycol $(-CD_2CD_2O-)_p$. The strong parallel band of polyethylene-d_4 glycol at 1117 cm^{-1} is due to the A_2 vibration associated with the antisymmetric C-O stretching and CD_2 wagging modes (Table 4). Similarly the strong perpendicular band at 1145 cm^{-1} is due to the E_1 vibration associated with quasi-antisymmetric C-O stretching ($\Delta\varepsilon=-158°$) and CD_2 wagging modes ($\Delta\varepsilon=164°$). On the other hand, the E_1 vibration at 1121 cm^{-1} is due to quasi-symmetric C-O stretching mode ($\Delta\varepsilon=19°$) as coupled with quasi-antisymmetric CD_2 scissoring mode ($\Delta\varepsilon=122°$) (Table 5). The infrared bands, at 1050 and 1087 cm^{-1}, primarily due to CD_2 scissoring modes are weak and not well-defined. The C-C streching mode is strongly coupled with quasi-symmetric CD_2 wagging mode, giving rise to the medium-intensity infrared band at 1255 cm^{-1} (E_1). Infrared bands in the region 1000—700 cm^{-1} are due to hybridized vibrations of CD_2 wagging, twisting and rocking modes and C-O stretching mode.

In the region below 500 cm^{-1}, infrared bands due to skeletal bending and internal-rotation modes are observed. Similar to the doublet bands (529 and 508 cm^{-1}) of the normal species, doublet bands with parallel dichroism are again observed at 453 and 434 cm^{-1} for the perdeuterated species. This doublet, in fact, corresponds to the A_2 vibration calculated at 455 cm^{-1}, which is associated with the CCO bending mode heavily coupled with the CD_2 rocking mode. The doublet splitting is reasonably ascribed to the Fermi resonance between the A_2 fundamental and the combination of E_1 vibrations [320+156=476].*6 The perpendicular bands at 458 and 183 cm^{-1} are largely due to quasi-antisymmetric and quasi-symmetric bending modes, respectively, of O-C-C-O groups. The infrared bands of the deuterated species at 95 cm^{-1} (parallel) and 156 cm^{-1} (perpendicular) correspond to the bands of the normal species at 107 and 165 cm^{-1}, respectively, and are assigned to internal-rotation modes about C-O and C-C bonds.

31) G. Herzberg, "Molecular Spectra and Molecular Structure," Vol. II, D. Van Nostrand Co., Inc., New York (1945), p. 123.

32) R. F. Schaufele, private communication.

*6 Another possibility is the resonance with the combination of the B_1 and B_2 vibrations calculated at 175 and 247 cm^{-1}, respectively.

BULLETIN OF THE CHEMICAL SOCIETY OF JAPAN VOL. 41 1809—1815 (1968)

Nuclear Quadrupole Resonance Study of Antimony Pentachloride and Its Phase Transition

Hideaki CHIHARA, Nobuo NAKAMURA, Hideo ŌKUMA and Syûuzô SEKI

Department of Chemistry, Faculty of Science, Osaka University, Toyonaka, Osaka

(Received February 16, 1968)

A phase transition was found in solid antimony pentachloride at 212°K by the nuclear quadrupole resonance and the differential thermal analysis. In the high temperature solid phase, five resonance lines were observed that were all assigned to antimony resonances and that were dependent on temperature only slightly. The quadrupole coupling constant of ^{121}Sb was 84.54±0.01 MHz (asymmetry $\eta=1.0\pm0.3\%$). Chlorine resonances were not detected above the transition point. In the low temperature phase, many resonance lines were observed due both to chlorine and antimony; the latter gave the coupling constant for ^{121}Sb 186.43±0.03 MHz ($\eta=79.54\pm0.02\%$) and 172.8±0.3 MHz ($\eta=79.2\pm0.3\%$). There are two nonequivalent sites for antimony. The structure in the two solid phases was suggested as being trigonal bipyramidal above 212°K and a dimerized Sb_2Cl_{10} bridged by two chlorine atoms with hexa-coordinated antimony atoms below 212°K.

Pentahalides of phosphorus and its homologues are an interesting group of compounds in that they may exist in ionic or molecular form or in both forms in the solid state.[1] Other compound such as $NbCl_5$ exists in a dimeric molecular structure.[2a]

Phosphorus pentachloride dealt with in our previous paper exists in an ionic structure $PCl_4^+ \cdot PCl_6^-$ though a molecular solid does form as a metastable modification.[3] On the other hand antimony pentachloride has been shown to assume the trigonal bipyramidal structure as shown in Fig. 1 by the X-ray diffraction study.[4] Since antimony is a quadrupolar nucleus, it was also hoped to detect antimony resonance by virtue of small distortion of the bipyramid. The result turned out that the solid exhibits an unusual phase transition by which molecules are dimerized at lower temperatures. The present paper describes the results of the nuclear quadrupole resonance (NQR) of chlorine and antimony in solid antimony pentachloride together with differential thermal study of the phase transition.

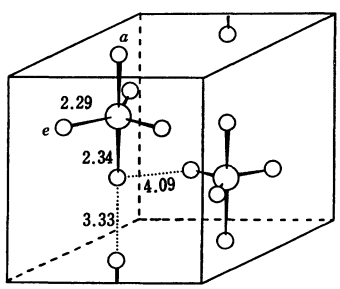

Fig. 1. Crystal structure of HTP at −30°C.[4] The numbers in the figure are internuclear distances in Å and *a* and *e* stand for axial and equatorial chlorine atoms.

In the rest of the present paper, we identify the chlorine atoms in the basal plane as 'equatorial' chlorines and the other two lying on the threefold axis of the molecule as 'axial' chlorines (see Fig. 1).

Experimental

Antimony pentachloride (Wakô Pure Chem. Ind., Ltd.) was distilled at 79°C under reduced pressure of 30 mmHg, condensed into the NQR cell and sealed off under reduced pressure. A small thermal anomaly caused by impurities, probably elementary chlorine, was observed at 170°K by the differential thermal analysis (DTA)[5] of the commercial speci-

1) R. R. Holmes, *J. Chem. Education*, **40**, 125 (1963).

2a) R. W. G. Wyckoff, "Crystal Structures," 2nd ed., Vol. 2, Interscience, New York, N. Y. (1964), p. 171. b) *Ibid.*, Vol. 3. c) *Ibid.*, Vol. 1, p. 331.

3) H. Chihara, N. Nakamura and S. Seki, This Bulletin, **40**, 50 (1967).

4) S. M. Ohlberg, *J. Am. Chem. Soc.*, **81**, 811 (1959).

5) H. Suga, H. Chihara and S. Seki, *Nippon Kagaku Zasshi* (*J. Chem. Soc. Japan, Pure Chem. Sect.*), **82**, 24 (1961).

men as obtained. Purification removed such a thermal anomaly and gave the melting point of 274.7±0.2°K. This is to be compared with 276.2°K found in the literature.[6] Both impure and purified specimens were used for NQR experiments for the reason to be described in the following section.

A Dean type super-regenerative spectrometer was used for measurements of chlorine and antimony resonances. The resonance was searched between 7.5 and 60 MHz, the maximum sensitivity of the spectrometer being in the range 25 to 45 MHz.

Digital frequency determinations and the cryostat have been described elsewhere.[3] The accuracy of the frequency determination was within 0.001 MHz.

Results and Discussion

General Features of Phase Transition. A thermal anomaly in solid phase was found at 211.8±0.4°K by the DTA as shown in Fig. 2. It is convenient to denote the phase below the transition as the low temperature phase (LTP) and that above as the high temperature phase (HTP).

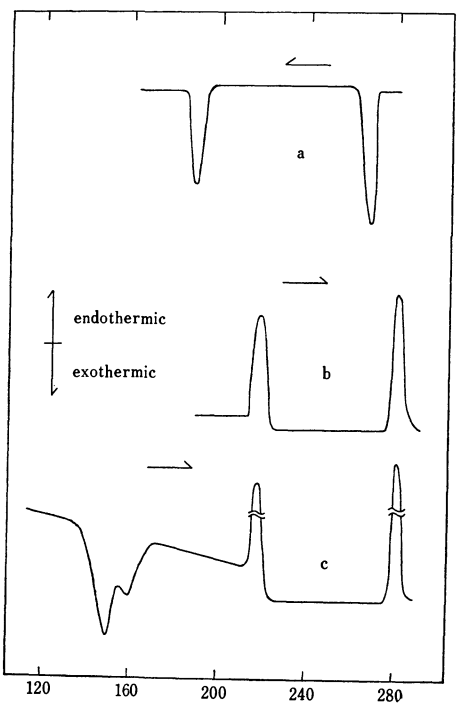

Fig. 2. The DTA curves of $SbCl_5$.
a : slow cooling curve
b : heating curve of slowly cooled sample
c : heating curve of rapidly cooled sample. The ordinate scale is enlarged 5 times of that for curve b. The transition and the melting point coincide with those of curve b.

A typical DTA curve in the cooling direction is shown in Fig. 2a, where the HTP is supercooled down to about 190°K for an impure sample, and to still lower temperature for a pure one. The LTP is superheated only by about 1°.

The area of the transition peak under the DTA curve b in Fig. 2 was about half of that of the melting peak where 2.4 kcal/mol is absorbed.[6] This phase transition is probably of the first order or of the isothermal type because there is a marked hysteresis in transition temperature[7] and also because NQR frequencies change abruptly at the transition as discussed later in this paper.

Figure 2c is the DTA curve (at the heating rate 10°/min) of $SbCl_5$ quenched by immersion of the liquid into liquid nitrogen (several minutes to reach 77°K); here exothermic peaks were observed before the phase transition took place. The exotherm occurred in two stages, one peak at 150°K and the other at 160°K. These peaks were displaced to lower temperatures by about 10° respectively at a slower rate of heating (1°/min) and the second peak became a shoulder of the first.

It is probable that $SbCl_5$ forms a glass by rapid cooling of the liquid to 77°K although a search for a glass transition was not successful. The exothermic peaks may be attributed to the crystallization of the glass into the LTP. This crystallization is likely to occur in the sequence

glass ⟶ HTP (supercooled) ⟶ LTP

in accordance with law of successive transformation.[8] In support of this view, the relative area under the exothermic peaks in Fig. 2c was found to be 1 : 2.1 in comparison with 1 : 2.3 for the ratio of the areas of transition and fusion. There is an indication that a quenched specimen also contains a certain amount of LTP because the exothermic peak area is much smaller than the endothermic peak area. A quantitative estimate of that amount, however, did not seem meaningful.

The phase transition appeared to be sluggish particularly in the cooling direction. Thus the resonance lines of LTP were broad and weak after first cooling through the transition point although the HTP resonances

6) F. D. Rossini, D. D. Wagman, W. H. Evans, S. Levine and I. Jaffe, "Selected Values of Chemical Thermodynamic Properties," circular of NBS 500, NBS, U. S. Government Printing, Washington (1952).

7) D. G. Thomas and L. A. K. Staveley, *J. Chem. Soc.*, **1951**, 2572.

8) See *e.g.* R. S. Bradley, *Quart. Revs.*, **5**, 315 (1951).

disappeared abruptly. It was therefore necessary to anneal the LTP, before the measurements on the LTP were started, by subjecting it to heating and cooling cycles across the transition point. Thus, the sample was first cooled to just below the transition temperature while watching for the disappearance of an HTP signal and then warmed up so that the signals from both phases could be seen. The temperature was then lowered slightly to aid in crystallization of LTP. Such cycle was repeated several times until the resonance lines of LTP were observed distinctly. This procedure enhanced the intensity of the chlorine resonances, but the antimony resonances were generally much broader and weaker than the chlorine resonances.

Although the resonance frequencies were independent of the purity of the sample, the line intensity of unpurified sample was stronger than that of pure one probably because the rate of the transition was faster. Annealing was more effective for an impure sample. Therefore, the frequencies were determined by use of unpurified specimen.

One outstanding feature of the transition is the large abrupt change in the antimony resonance frequencies at the transition point; in fact it is so large that it could hardly be accounted for merely by a change in the crystal structure.

All available evidences are consistent with a possibility that the transition is accompanied with a change in the valence state of the antimony atom. It is perhaps significant to note that one of the HTP resonance lines (ν_5') was observed in supercooled HTP, even at 180°K, about 30° below the transition point. Its frequency was practically independent of the temperature, remaining the same as that at the transition point (25.391 MHz). Similarly, the intensity did not change until the transition started. The intensity decrease was used to monitor the progress of phase transition.

High Temperature Phase. Five strong NQR lines were observed in HTP between 7.5 and 40 MHz as listed in Table 1a together with their assignments. The frequency values agree well with those reported by Schneider and DiLorenzo[9] within experimental errors. All of these lines were ascribed toantimony nuclei. The quadrupole coupling constants e^2Qq/h and asymmetry parameters η are calculated[10,11] and listed in Table 1b.

As expected from the trigonal bipyramidal molecular structure of the HTP (Fig. 1), the coupling constants of central atoms (antimony nuclei) are small but they do not vanish be-

TABLE 1a. RESONANCE FREQUENCIES IN HTP AND THEIR ASSIGNMENTS

Resonance line	Frequency (MHz) 215°K	274°K	Assignment
ν_1'	——	7.71*	$^{123}Sb(3/2\leftrightarrow1/2)$
ν_2'	——	12.682	$^{121}Sb(3/2\leftrightarrow1/2)$
ν_3'	15.415	15.396	$^{123}Sb(5/2\leftrightarrow3/2)$
ν_4'	23.130	23.096	$^{123}Sb(7/2\leftrightarrow5/2)$
ν_5'	25.389	25.361	$^{121}Sb(5/2\leftrightarrow3/2)$

* Accurate to within 0.01 MHz

TABLE 1b. QUADRUPOLE COUPLING CONSTANTS AND ASYMMETRY PARAMETER OF ANTIMONY IN HTP AT 274°K

	$\left\lvert\frac{e^2Qq}{h}\right\rvert$ (MHz)	$\eta(\%)$
^{121}Sb	84.54±0.01	1.0±0.3
^{123}Sb*	107.78±0.01	1.4±0.4

* Calculated from ν_3' and ν_4'. The calculated value of ν_1' lies at 7.704±0.004 MHz and agrees well with the observed value in Table 1a.

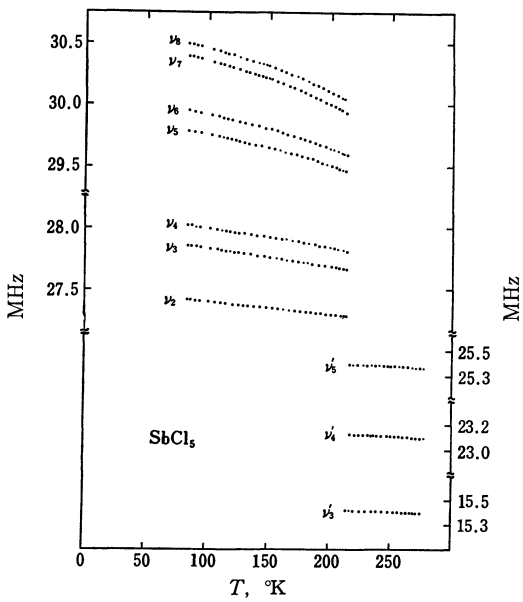

Fig. 3. Temperature dependence of the NQR frequency in both phase. The resonances of LTP are due to ^{35}Cl, and those of the HTP are due to ^{121}Sb and ^{123}Sb.

9) R.F. Schneider and J.V. DiLorenzo, *J. Chem. Phys.*, **47**, 2343 (1967).
10) R. Livingston and H. Zeldes, "Table of Eigenvalues for Pure Quadrupole Spectra, Spin 5/2," ORNL Report 1913, Oak Ridge National Laboratory, Oak Ridge, Tenn. (1955).
11) See the appendix of H. Chihara, N. Nakamura and H. Ōkuma, *J. Phys. Soc. Japan*, **24**, 306 (1968).

cause the bond lengths from antimony to equatorial chlorines are different from those to axial chlorines. Furthermore the field gradient is almost axially symmetric.

As is seen from Fig. 3, all the resonance frequencies are only slightly dependent on temperature in HTP (*e.g.* 0.5 kHz/deg for ν_5') in comparison with those of LTP. This behavior is rather extraordinary though there are examples of this sort (for instance ν_1 of ionic solid PCl_5[3]). If the molecules are undergoing librational motion, it should cause much greater decrease in frequency as the temperature is raised.[12]

Another experimental fact to be noted is that chlorine resonances are entirely missing in the range of 7.5 to 40 MHz*1 whereas antimony resonances are observable.

An off-hand approach to a plausible interpretation for these experimental results is to assume a reorientational motion about the threefold axis of the $SbCl_5$ molecule. X-ray diffraction study[4] shows a deformed chlorine electron density suggesting a large angular amplitude perpendicular to the molecular axis. Disappearance of resonance due to equatorial chlorine atoms may be explained by such reorientation. Similar situation has been found in the case of *trans*-1, 2-dichloroethane which undergoes reorientation about the Cl···Cl axis.[13] However, the disappearance of resonances of axial chlorine atoms must be due to some additional effect. Now, if one examines the molecular packing in the crystal, the intermolecular approach of axial chlorine atoms are found considerably shorter (3.33 A) than the sum of van der Waals radii (3.60 Å). Since it is difficult to imagine a special type of interaction between these chlorine atoms, we assume that the distance found is actually the one between the average positions of the chlorine atoms and that the molecule precesses about its figure axis. Nutation is very likely to be superposed upon the precession. Actual instantaneous separation between the intermolecular chlorines would then be longer than 3.33 Å and the field gradient at the axial chlorine nucleus would be disturbed severely to the extent that its resonance frequency falls below 7.5 MHz. The effect of the precession upon the resonance frequency may be evaluated by the formula[14]

$$\nu = \nu_Q(3\cos^2\theta - 1)/2,$$

where ν_Q is the resonance frequency corresponding to the static lattice and θ is the angle of precession. If the chlorine frequency is reduced greatly by precession, the same factor must apply to the antimony frequency.

Therefore, using the relation

$$\frac{\nu^{Cl}}{\nu^{Sb}} = \frac{\nu_Q{}^{Cl}}{\nu_Q{}^{Sb}}$$

and substituting $\nu_Q{}^{Cl} = 35$ MHz, $\nu^{Cl} \leq 10$ MHz, and $\nu^{Sb(121)} = 12.682$ MHz $(3/2 \leftrightarrow 1/2)$, we obtain $\nu_Q{}^{Sb} = 44.38$ MHz which corresponds to $|e^2Qq(^{121}Sb)/\boldsymbol{h}| = 295$ MHz. While this is not of unconceivable magnitude in comparison with the atomic $|e^2Qq(^{121}Sb)/\boldsymbol{h}| = 410$ MHz, we get more or less embarassed with a large angle of precession (43°) necessary to give rise to the reduction of the resonance frequency. In the present instance of $SbCl_5$, X-ray diffraction does not indicate a possibility of such a large angle of precession.

Very short relaxation time associated with chlorines can also explain the disappearance of their resonances by virtue of extremebroadening of the resonance lines as suggested by Schneider, *et al.* However the reason for shortening of chlorine relaxation time and not for antimony relaxation time is rather difficult to find.

Another possibility is to take account of a special intermolecular effect. Thus, if an axial chlorine atom forms a charge transfer bond to an equatorial chlorine atom on the neighboring molecule and if such bonds are switched owing to reorientation about the threefold axis, the effect would be seen not in antimony resonances but only in chlorine resonances. The effect could be so large as to cause a broadening of chlorine resonance by, say, 1 MHz. However, quantitative explanation based on this mechanism does not seem feasible with our present knowledge on the nature of Sb–Cl bond and the electronic structure of chlorine atom.

Low Temperature Phase. After the first cooling, a number of spurious signals appeared in addition to the LTP resonances and supercooled HTP resonances. The extraneous absorptions may have been due to a piezoelectric effect and could be sorted out by application of weak magnetic field to the specimen. Annealing did eliminate many of them but several lines persisted even after annealing. Altogether sixteen resonance absorption lines were observed at liquid nitrogen temperature and seven of them are shown in Fig. 3. They are also listed in Tables 2 and 3 indicating

12) H. Bayer, *Z. Phys.*, **130**, 227 (1951).

*1 This is in agreement with the results of Schneider and DiLorezo.[9]

13) J. L. Ragle and A. P. Caron, *J. Chem. Phys.*, **40**, 3497 (1964); T. Tokuhiro, *ibid.*, **41**, 438 (1964).

14) T. P. Das and E. L. Hahn, "Nuclear Quadrupole Resonance Spectroscopy," Academic Press, New York (1958).

our assignments. An independent study of this material by Schneider *et al.* was helpful in making these assignments.

Generally, antimony resonances were broader (width being 30—40 kHz) than chlorine resonances (2—3 kHz). It is seen that chlorine resonances appear in pairs (ν_3 and ν_4; ν_5 and ν_6; ν_7 and ν_8); ν_1 of ^{35}Cl also seems to have a doublet structure above 100°K though it was not made definite because the intensities were very weak and their separation was about twice the quench frequency of the spectrometer. The corresponding ^{37}Cl resonances were not obrerved in the frequency range covered. All the chlorine resonances observed are in agreement with the result by Schneider *et al.* With regard to antimony resonances, we did not detect two absorptions, which Schneider *et al.* reported at 27.93 and 54.22 MHz, but instead were able to observe absorptions at 47.3±0.1 (ν_{16}), 49.8±0.1 (ν_{17}), and 51.00±0.01 (ν_{18}) MHz. Extremely weak ν_{17} was not assigned; this may have been a spurious signal but the effect of magnetic field was not evident.

TABLE 2. RESONANCE FREQUENCIES OF ^{35}Cl IN LTP AT SELECTED TEMPERATURES AND THEIR ASSIGNMENTS BASED ON THE DIMER STRUCTURE

Resonance line	Frequency (MHz) 77°K	124.7°K	211.7°K	Assignment[a]
ν_1	18.718	18.646[b]	——	*b*
		18.700		
ν_2	27.417	27.370	27.283	*a*
ν_3	27.860	27.796	27.665	*a*
ν_4	28.013	27.958	27.815	*a*
ν_5	29.789	29.704	29.465	*t*
ν_6	29.953	29.860	29.599	*t*
ν_7	30.396	30.281	29.937	*t*
ν_8	30.494[c]	30.385	30.047[d]	*t*

a) *b*, *a* and *t* stand for bridging, axial, and terminal chlorines.
b) Doublet structure is dubious, see in text.
c) at 83.3°K.
d) at 210.4°K; this line faded out at 211.7°K.

TABLE 3a. RESONANCE FREQUENCIES, APPARENT INTENSITIES AND ASSIGNMENTS OF ANTIMONY IN LTP AT LIQUID NITROGEN TEMPERATURE

Resonance line	Frequency (MHz)	intensity[a]	assignment[b]
ν_{11}	28.71 ±0.05	W	$^{123}Sb'$ (5/2↔3/2)
ν_{12}	31.02 ±0.01	W	^{123}Sb (5/2↔3/2)
ν_{13}	38.42 ±0.01	M	^{123}Sb (3/2↔1/2)
ν_{14}	39.68 ±0.01	W	$^{121}Sb'$ (3/2↔1/2)
ν_{15}	42.893±0.001	S	^{121}Sb (3/2↔1/2)
ν_{16}	47.3 ±0.1	V.W	$^{121}Sb'$ (5/2↔3/2)
ν_{17}	49.8 ±0.1	V.W	——[c]
ν_{18}	51.00 ±0.01	M	^{121}Sb (5/2↔3/2)
ν_{19}[d]	35.6		$^{123}Sb'$ (3/2↔1/2)
ν_{20}[d]	44.1		$^{123}Sb'$ (7/2↔5/2)
ν_{21}[d]	47.6		^{123}Sb (7/2↔5/2)

a) V.W; very weak, W; weak, M; medium, S; strong.
b) Two sites for antimony are distinguished by the primed and the unprimed.
c) Unassignable.
d) ν_{19}, ν_{20} and ν_{21} are not observed but calculated values.

TABLE 3b. QUADRUPOLE COUPLING CONSTANTS AND ASYMMETRY PARAMETERS OF ^{121}Sb AND ^{123}Sb AT LIQUID NITROGEN TEMPERATURE

	$\lvert e^2Qq/h \rvert$ (MHz)	η(%)	calculated from
Site I			
^{121}Sb	186.43±0.03	79.54±0.02	ν_{15}, ν_{18}
^{123}Sb	238.22±0.08	79.26±0.04	ν_{12}, ν_{13}
Site II			
$^{121}Sb'$	172.8 ±0.3	79.2 ±0.3	ν_{14}, ν_{16}
$^{123}Sb'$*	221	79	——

* These values were derived by taking 1.278 times the coupling constant of ^{121}Sb's and assuming the same η as ^{121}Sb.

From the observed frequencies and the assignments given in Table 3a for antimony nuclei, the quadrupole coupling constants and the asymmetry parameters were calculated by help of the tables of eigenvalues for spins 5/2[10] and 7/2[11]. They are listed in Table 3b. ν_{19}, ν_{20}, and ν_{21} were not detected, either because the intensities were weak or because of the noise disturbance from external sources between 34 and 36 MHz.

There are two nonequivalent antimony sites, one having slightly lower coupling constant than the other and both having about 79% asymmetry. We ascribe the small difference in the coupling constant between the two sites to crystallographic nonequivalence.

Structure of the Low Temperature Phase. We shall now consider what structure of the low temperature phase would be consistent with the experimental results. A drastic change in the antimony resonances, particularly its asymmetry parameter, across the transition point strongly suggests that the transition is related to a change in molecular structure. There are several possibilities, ionic $SbCl_4^+ \cdot SbCl_6^-$ structure, dimerized structure Sb_2Cl_{10}, and tetramer or higher polymer structure. In the following these different structural models will be separately examined.

a) Ionic Structure, $SbCl_4^+ \cdot SbCl_6^-$. Since

phosphorus pentachloride exists in this structure in the stable solid phase, there is a good reason to assume this type of ionic units. We previously measured[3] the chlorine resonance frequencies in $PCl_4^+ \cdot SbCl_6^-$ to aid in the assignment for PCl_5 and found them at 24.03 and 24.96 MHz at 77°K. A comparison with the frequencies in Table 2 implies that $SbCl_6^-$ is not a likely species in LTP. Also large asymmetry in the electric field gradient at Sb is not compatible with the symmetric chlorine arrangements in $SbCl_4^+$ or $SbCl_6^-$.

b) Dimer Structure, Sb_2Cl_{10}, and Higher Polymars. Dimerized form of molecules are not rare although few compounds possess corresponding monomers as stable species. Ex-

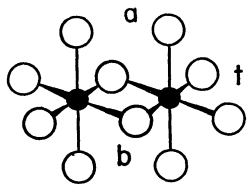

a. Dimer.

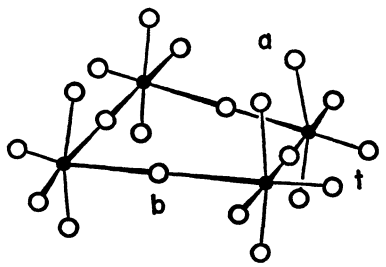

b. Tetramer.

Fig. 4. The suggested molecular structure in LTP. Filled circles are antimony and open circles are chlorine atoms; *a*, *b*, and *t* denote axial, bridging and terminal chlorines.

amples are $NbCl_5$, $NbBr_5$, $TaCl_5$, $MoCl_5$,[2a] $NbOCl_3$,[2b] UCl_5,[15] $AlBr_3$, $AuCl_3$, ICl_3[2a] and others. Some pentahalides take a molecular shape shown in Fig. 4a. It is interesting to note that the niobium resonance frequencies in $(NbCl_5)_2$ give a rather small coupling constant 78 MHz and a large asymmetry parameter 32%[16] as in the present case of $SbCl_5$.

Many investigators also observed bridging and terminal halogen resonances of dimerized trihalogen compounds as summerized in Fig. 5. The figure shows the frequency ratio of the terminal and bridge halogen *vs.* the electronegativity difference between the halogen

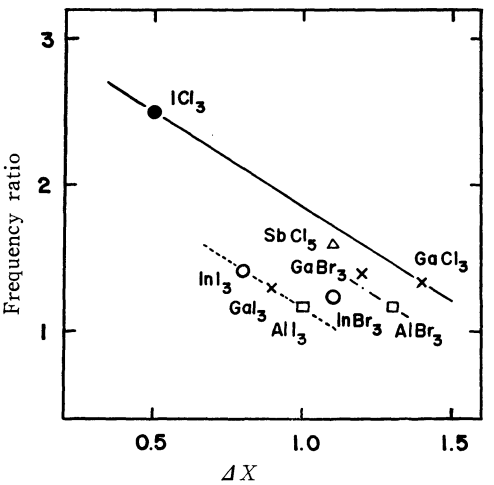

Fig. 5. Ratio of the resonance frequencies for terminal and bridging halogen atoms *vs.* electronegativity difference of central atom and halogen. The resonance frequencies were taken from É. I. Fedin and G. K. Semin, 'Use of Nuclear Quadrupole Resonance in Chemical Crystallography II', in 'The Mössbauer Effect and its Applications in Chemistry,' Consultants Bureau Enterprises, Inc., New York (1964).

and the central atom. It is seen that different ligands lead to different but parallel straight lines on each of which various central atoms are arranged according to their electronegativity. This empirical relationship may be useful in making assignments. Now, the four higher frequencies (ν_5 to ν_8 in Table 2) can be assigned to the terminal chlorines (identified with *t* in Fig. 4a), the three medium frequencies (ν_2 to ν_4) to the axial chlorines (*a* in Fig. 4a), and the remaining ν_1 to the bridge chlorine (*b* in Fig. 4a). The ratio of the average of ν_5 through ν_8 to ν_1 is then 1.6 and is included in Fig. 5; the point lies close to the chloride line. We agree with Schneider *et al.* on this assignment.

The differential thermal analysis experiments also support dimerization model or any type of polymerization model. Thus, the slow transition in the cooling direction can be explained by the difficulty in perfect pairing of monomers; annealing does help to grow dimer nuclei larger. The reverse reaction, the decomposition, can proceed quickly upon heating.

Tetramer structure as shown in Fig. 4b is known for $TaCl_4F$[17a] and $SbCl_4F$.[17b] However bridge atoms are not chlorine but fluorine.

15) G. S. Smith, Q. Johnson and R. E. Elson, *Acta Cryst.*, **22**, 300 (1967).
16) A. H. Reddoch, *J. Chem. Phys.*, **35**, 1085 (1961).
17 a) H. Preiss, *Z. Anorg. Allg. Chem.*, **346**, 272 (1966). b) H. Preiss, *Z. Chem.*, **6**, 350 (1966).

Similarly, polymer chains are known for $BeCl_2$.[2c] We consider that tetramer or higher polymers are rather unlikely for $SbCl_5$ for two reasons; (a) chlorine polyhedra usually share edges rather than corners or faces in forming polymer chains and if $SbCl_5$ should form a polymer chain, the six-coordinated polyhedra must share corners and (b) the number and distribution of chlorine resonances are not readily reconciled with such a polymer structure while keeping the number of nonequivalent antimony sites two.

We are inclined to think that the dimer structure is the most probable structure for the low temperature phase of antimony pentachloride. Crystal structure determination of the low temperature phase is very desirable in order to correlate the asymmetry parameter and the coupling constant of antimony with the geometry of the dimer. It would also be interesting to study kinetics and detailed mechanism of the phase transition since this is one of very few phase transitions which accompany a change in the valence state, perhaps to our knowledge the sole example for a molecular crystal.

When the measurements of the present study were completed, Professor R. F. Schneider of New York State University at Stony Brook drew our attention to that he and his colleague were also studying the same compound. We were benefited in making some of the assignments through his courtesy of showing us his results prior to publication for which we extend our gratitude.

BULLETIN OF THE CHEMICAL SOCIETY OF JAPAN VOL. 41 1815—1820 (1968)

The Crystal Structure of the 1 : 1 Complex of 1, 2, 4, 5-Tetracyanobenzene and Hexamethylbenzene

Nobuo NIIMURA, Yuji OHASHI and Yoshihiko SAITO

The Institute for Solid State Physics, The University of Tokyo, Roppongi, Tokyo

(Received February 19, 1968)

The crystal structure of the 1 : 1 complex formed between hexamethylbenzene and 1, 2, 4, 5-tetracyanobenzene has been determined by X-rays. The crystal is monoclinic, with two formula units of the complex in a cell of dimensions ; $a=15.07$, $b=8.92$, $c=7.41$ Å and $\beta=104.9°$. The space group is $P2_1/n$. The structure was deduced from a three-dimensional Patterson synthesis, and refined by block-diagonal least-squares method. The constituent molecules are stacked alternately in infinite columns along the c-axis. The relative configuration of the donor and acceptor molecules is consistent with the theoretical calculation.

The complex between 1, 2, 4, 5-tetracyanobenzene (TCNB) and hexamethylbenzene (HMB) is the third member of the series of charge transfer complexes containing TCNB as an electron acceptor, of which the crystal structures have been determined in this laboratory. The structure of the complex between

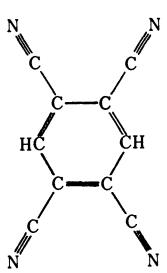

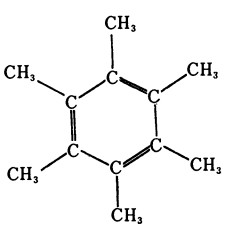

TCNB and N, N, N', N'-tetramethyl-p-phenylenediamine (TMPD)[1] indicated specific interaction localized between the nitrogen atoms of the donor and the cyano groups of the acceptor, whereas the structure of the TCNB-naphthalene complex[2] was found to exhibit π-π interaction between the donor and the acceptor, and was consistent with the result of the theoretical calculation and the electronic spectra.[3] It is expected that in the crystals of the complex between TCNB and typical π-donor such as benzene or hexa-

1) Y. Ohashi, H. Iwasaki and Y. Saito, *This Bulletin*, **40**, 1789 (1967).
2) S. Kumakura, F. Iwasaki and Y. Saito, *ibid.*, **40**, 1826 (1967).
3) S. Iwata, J. Tanaka and S. Nagakura, *J. Am. Chem. Soc.*, **89**, 2813 (1967).

methylbenzene, the relative arrangement of the donor and acceptor molecules may be consistent with the result of theoretical calculation involving the π-π interaction only. In the present paper, haxametylbenzene was selected as a donor. The relative configuration of the donor and the acceptor of this complex has been presumed theoretically.[4] It may be of interest to see whether this presumption is correct or not and to compare the crystal structure with those of the related molecular complexes.

Experimental

The molecular complex of TCNB and HMB crystallizes as yellow needles. They decompose easily when exposed to X-rays in the air. Specimens had to be sealed in thin-walled borosilicate glass capillaries. The crystals are monoclinic and the cell dimensions and the space group were determined from oscillation and Weissenberg photographs taken around the b- and c-axes using Cu$K\alpha$ radiation (λ=1.542 Å). They are listed in Table 1.

TABLE 1. CRYSTAL DATA

TCNB-HMB
Monoclinic
a=15.07±0.01 Å
b= 8.92±0.01 Å
c= 7.41±0.04 Å
β=104.9±0.4°
Z=2
$P2_1/n$
μ=5.6 cm^{-1} (Cu $K\alpha$)

Intensity data were recorded on the equi-inclination Weissenberg photographs taken around the b- and c-axis up to the fourth layer, respectively, using multiple film technique. The relative intensities, estimated visually with a set of standard scales, were corrected for Lorentz and polarization factors, and spot shape, and were put on a common scale. The absorption correction was neglected in view of the small size of the specimen and the small value of the linear absorption coefficient. 587 independent reflections were observed.

Structure Determination

From the systematic absences the space group was uniquely determined to be $P2_1/n$. Since there are only two pairs of component molecules in the unit cell, the centers of gravity of each molecule must lie on a set of special positions. In order to obtain familiar mixed stacks, the TCNB and HMB molecules must be centered at positions, (000), (1/2 1/2 1/2) and (0 0 1/2), (12/ 1/2 0) respectively.

The trial structure was readily deduced from the three-dimensional Patterson synthesis. The structure thus obtained was refined by difference syntheses projected along the b- and c-axes, and later by a three-dimensional block-diagonal least-squares method with HBLS program written by Ashida. After a few cycles of this refinemet, anisotropic temperature factors were introduced. A weighting scheme,

$$w=1 \quad \text{if} \quad F_o \geq 2.0$$
$$\text{otherwise} \quad w=0.2$$

was employed.

The final discrepancy factor, $R=\sum||F_o|-|F_c||/\sum|F_o|$ became 0.154 for all the observed reflections. Atomic scattering factors were taken from the International Tables for X-ray Crystallography.[5] Final atomic parame-

TABLE 2. ATOMIC PARAMETERS

The expression of the temperature factor is $\exp[-(h^2B_{11}+k^2B_{22}+l^2B_{33}+hkB_{12}+hlB_{13}+klB_{23})]$

Atom	$x\times10^4$	$y\times10^4$	$z\times10^4$	$\sigma(x)$ $\times10^4$	$\sigma(y)$ $\times10^4$	$\sigma(z)$ $\times10^4$	B_{11} $\times10^4$	B_{22} $\times10^4$	B_{33} $\times10^4$	B_{12} $\times10^4$	B_{13} $\times10^4$	B_{23} $\times10^4$
TCNB												
N 1	788	4064	−960	12	18	28	95	177	506	−47	132	144
N 2	1908	−2847	2645	10	20	22	59	263	356	87	19	1
C 1	547	2925	−734	11	22	25	45	233	294	−16	50	34
C 2	1349	−2055	1905	12	21	24	64	178	253	−22	69	−2
C 3	924	457	596	11	19	21	57	159	132	14	2	103
C 4	675	−984	949	11	20	25	35	176	323	20	39	22
C 5	255	1431	−396	12	19	22	71	146	158	0	81	58
HMB												
C 6	1062	2738	4706	16	24	35	110	171	692	−173	175	−36
C 7	1006	−2719	6672	17	23	33	132	128	571	142	29	214
C 8	2020	32	6394	13	36	34	28	543	602	16	2	−96
C 9	512	1298	4879	11	21	25	50	172	306	−31	45	−7
C 10	461	−1291	5787	13	21	24	81	160	226	53	36	38
C 11	953	1	5655	11	22	26	39	229	285	17	15	−7

4) S. Iwata, J. Tanaka and S. Nagakura, *ibid.*, 88, 894 (1966).
5) "International Tables for X-Ray Crystallography" Vol. III, Kynoch Press, Birmingham (1962), p. 202.

TABLE 3. OBSERVED AND CALCULATED STRUCTURE FACTORS

h	k	Fo	Fc
l=0			
2	0	83.1	86.4
4	0	-47.3	-45.3
6	0	-51.2	-46.2
8	0	-40.6	-34.6
10	0	8.6	6.2
12	0	-8.6	-7.1
1	1	90.2	72.8
2	1	-10.9	-2.2
3	1	5.2	0.9
4	1	-54.6	-46.2
6	1	-11.5	-8.9
7	1	-21.4	-16.7
0	2	-43.7	-33.9
1	2	10.0	5.6
2	2	-7.8	-2.2
3	2	35.0	32.8
4	2	12.1	10.2
5	2	12.9	11.8
6	2	-22.6	-18.4
7	2	-7.7	-7.2
8	2	-7.4	-6.5
9	2	-3.5	-4.7
10	2	11.9	11.3
11	2	-10.0	-9.9
12	2	8.4	7.9
13	2	-6.8	-6.8
1	3	11.6	5.2
2	3	-35.4	-26.9
3	3	-35.2	-29.3
4	3	10.4	9.3
5	3	-20.4	-15.4
6	3	5.4	3.1
7	3	-23.5	-20.9
8	3	5.6	6.8
9	3	7.2	8.3
11	3	15.8	17.1
12	3	-5.8	-6.8
0	4	3.6	3.3
2	4	-40.0	-30.9
3	4	-7.6	-6.9
4	4	-34.0	-26.5
5	4	9.4	6.1
6	4	-3.7	-1.3
7	4	8.8	9.1
8	4	9.9	10.0
9	4	-5.3	-6.1
10	4	16.9	17.6
1	5	-16.8	-14.2
2	5	-4.9	-1.1
3	5	-15.1	-10.5
4	5	-5.3	-4.5
5	5	-6.8	-4.6
6	5	6.3	6.2
7	5	11.5	11.0
8	5	4.9	5.0
9	5	12.3	11.4
10	5	5.7	2.9
0	6	-7.1	-6.9
4	6	6.9	8.7
6	6	7.8	7.4
9	6	8.7	9.7
1	7	17.9	17.8
3	7	8.3	6.8
4	7	-4.8	-4.3
7	7	-6.8	-8.7
0	8	5.6	6.9
1	8	-4.2	-3.6
2	8	5.0	4.2
3	8	-10.1	-9.7
5	8	-5.7	-4.7
l=1			
-5	0	-33.7	-35.5
-3	0	9.6	12.4
1	0	3.8	0.3
3	0	38.3	40.1
5	0	21.5	20.4
7	0	-5.3	-2.3
9	0	-8.7	-9.5
13	0	7.8	8.3
-8	1	13.2	11.8
-7	1	12.3	9.1
-6	1	-5.6	-3.6
-5	1	38.0	40.6
-4	1	22.0	22.1
-3	1	-8.6	-13.1
-2	1	8.6	7.2
-1	1	12.5	14.0
0	1	-25.8	-23.9
1	1	13.0	20.9
3	1	-26.3	-28.1
4	1	-30.3	-27.4
5	1	-4.4	-2.6
6	1	18.7	17.1
7	1	-13.2	-12.8
8	1	8.4	8.8
9	1	-5.5	-5.1
11	1	-4.5	-3.1
12	1	9.8	11.3
13	1	-4.4	-4.1
-14	2	9.2	9.4
-12	2	8.2	10.0
-10	2	9.3	9.1
-9	2	8.8	9.2
-8	2	14.0	15.3
-7	2	-7.8	-6.6
-6	2	-5.2	-5.2
-5	2	-9.0	-6.9
-4	2	-16.9	-15.6
-3	2	16.2	12.1
-2	2	-16.6	-17.4
-1	2	-20.3	-17.7
0	2	-9.7	-7.9
1	2	43.7	39.9
2	2	17.1	12.1
3	2	-23.2	-22.6
4	2	9.3	9.4
5	2	-29.3	-30.5
6	2	6.0	5.1
7	2	5.4	8.6
9	2	-3.9	-3.2
10	2	-9.0	-9.4
11	2	7.8	9.3
12	2	-7.8	-9.3
13	2	2.2	0.4
-13	3	8.3	10.7
-11	3	8.3	8.7
-10	3	-10.8	-13.7
-7	3	-14.9	-15.9
-6	3	3.7	3.2
-5	3	-24.2	-25.4
-3	3	25.2	26.6
-2	3	-4.0	-4.3
-1	3	18.6	15.8
0	3	-10.9	-9.5
1	3	-5.9	-6.1
2	3	21.7	19.9
4	3	11.9	11.5
5	3	-8.0	-6.5
6	3	-7.3	-8.5
7	3	5.5	4.9
8	3	-10.3	-11.6
10	3	-8.4	-9.3
12	3	-4.7	-5.0
-11	4	-7.0	-7.9
-9	4	-8.0	-9.1
-8	4	-8.1	-7.3
-7	4	3.2	4.4
-5	4	7.7	8.9
-4	4	7.0	7.7
-3	4	8.0	6.7
-2	4	-4.6	-4.6
-1	4	-8.5	-9.1
0	4	-8.9	-7.3
1	4	-13.0	-13.5
2	4	-11.9	-9.1
3	4	16.1	14.2
4	4	14.5	13.6
5	4	7.8	8.4
6	4	10.9	9.8
8	4	-6.4	-7.6
9	4	-11.3	-13.4
11	4	-9.8	-9.0
-11	5	-6.3	-7.4
-9	5	-9.4	-11.3
-8	5	6.4	6.7
-7	5	-6.9	-6.3
-6	5	-8.8	-10.3
-5	5	9.2	9.5
-3	5	7.4	5.3
0	5	3.7	6.5
2	5	7.2	5.8
4	5	-8.0	-7.2
5	5	2.7	5.1
6	5	2.0	2.9
8	5	-4.0	-3.6
9	5	4.9	2.8
10	5	-5.9	-5.5
-10	6	-6.9	-6.2
-8	6	-4.0	-4.0
-7	6	6.6	6.5
-6	6	-7.5	-6.6
-2	6	5.9	6.2
-1	6	-6.9	-7.1
0	6	5.4	2.4
1	6	-6.6	-5.6
3	6	-3.8	-3.1
4	6	-6.5	-8.6
5	6	7.1	6.7
7	6	8.5	10.0
8	6	11.1	12.0
-7	7	5.0	4.2
-6	7	4.9	7.7
-3	7	2.1	0.7
-2	7	-6.9	-8.7
0	7	-7.2	-8.5
1	7	-2.1	-1.7
2	7	4.9	6.2
3	7	-6.0	-5.5
4	7	11.8	14.1
6	7	4.5	4.9
7	7	2.2	4.7
-7	8	2.2	3.6
-6	8	6.0	5.4
-5	8	6.5	5.5
-4	8	10.3	9.7
-2	8	6.2	4.8
-1	8	-9.5	-9.9
1	8	-5.2	-2.7
2	8	-7.7	-7.8
l=2			
-10	0	-10.0	-7.1
-8	0	-21.7	-21.7
-6	0	-40.4	-43.6
-2	0	98.2	117.2
0	0	51.8	65.8
2	0	25.6	31.5
4	0	2.5	1.4
6	0	-20.1	-19.9
8	0	3.8	6.4
-10	1	-3.5	-5.4
-9	1	-20.4	-21.5
-8	1	-6.4	-5.2
-7	1	-12.5	-13.1
-6	1	-9.0	-12.1
-5	1	11.1	13.7
-3	1	45.2	53.9
-2	1	81.0	105.2
-1	1	68.4	81.8
0	1	56.2	64.3
1	1	-4.5	-6.3
2	1	-12.5	-17.0
3	1	-19.9	-24.0
4	1	-11.5	-13.6
5	1	-20.6	-21.4
6	1	-16.4	-16.9
7	1	-5.8	-4.1
8	1	-4.9	-6.9
9	1	11.3	12.3
10	1	-7.1	-8.3
12	1	-3.1	-4.8
-12	2	6.6	7.7
-9	2	6.2	5.4
-8	2	-11.2	-13.4
-7	2	8.1	8.6
-6	2	8.7	11.9
-5	2	11.2	13.0
-4	2	-10.7	-8.6
-3	2	11.0	15.3
-2	2	5.2	5.3
-1	2	4.7	3.0
0	2	24.2	24.1
1	2	6.1	8.0
2	2	-19.8	-23.0
3	2	4.8	6.5
4	2	-18.2	-19.2
5	2	7.5	9.1
6	2	-16.2	-17.0
8	2	4.9	6.2
9	2	-10.5	-12.6
10	2	10.7	12.5
11	2	-5.8	-7.8
-14	3	4.6	6.8
-13	3	10.8	9.8
-11	3	10.0	10.6
-10	3	-4.1	-4.5
-9	3	2.7	1.2
-8	3	-9.4	-11.1
-7	3	-6.0	-6.2
-5	3	-25.7	-27.8
-4	3	20.1	22.3
-3	3	-16.0	-17.6
-2	3	-2.6	-4.3
0	3	2.4	2.1
1	3	-9.4	-5.8
2	3	21.7	24.5
3	3	-10.1	-7.1
4	3	3.0	2.7
5	3	-18.3	-18.3
6	3	-2.6	-3.4
7	3	2.7	5.8
8	3	-8.5	-10.0
9	3	12.3	13.9
-13	4	2.9	3.6
-12	4	11.7	11.7
-10	4	7.3	8.2
-9	4	-13.9	-13.9
-7	4	-4.8	-5.8
-6	4	-13.2	-14.5
-5	4	2.2	1.9
-4	4	-15.1	-13.4
-3	4	8.7	8.7
-1	4	4.4	4.6
0	4	-17.2	-20.0
1	4	-5.7	-8.2
2	4	-17.8	-17.0
3	4	3.7	3.9
4	4	-8.2	-8.6
7	4	-3.8	-5.0
8	4	10.6	13.1
9	4	3.1	3.1
-11	5	10.7	13.4
-9	5	6.9	8.2
-8	5	-6.9	-7.5
-6	5	-7.9	-8.3
-5	5	-5.4	-4.4
-4	5	-5.9	-7.1
-3	5	-11.0	-12.6
-2	5	3.7	4.3
-1	5	-5.4	-6.8
0	5	-4.0	-4.8
1	5	-9.8	-8.7
2	5	-11.8	-15.0
4	5	-2.7	-3.8
5	5	7.8	8.6
6	5	2.9	5.5
8	5	8.1	9.5
-9	6	2.9	5.1
-5	6	-2.7	-2.9
-4	6	2.6	3.4
-3	6	-7.7	-9.6
-2	6	2.9	3.8
-1	6	-13.0	-14.7
1	6	-10.1	-10.3
3	6	-6.1	-6.3
4	6	2.9	3.6
5	6	6.1	9.0
7	6	10.6	12.2
-6	7	6.2	7.2
-4	7	2.9	5.1
-3	7	2.8	2.9
-2	7	-2.8	-4.3
-1	7	7.2	9.1
0	7	-6.7	-9.0
1	7	10.4	11.8
2	7	-4.6	-5.4
3	7	7.3	7.4
-5	8	3.0	3.5
-4	8	3.0	2.3
-3	8	4.9	7.6
-2	8	3.8	3.5
-1	8	3.9	6.8
0	8	4.0	4.0
l=3			
-7	0	-23.3	-24.6
-5	0	5.6	8.5
-3	0	-10.9	-5.9
-1	0	-29.1	-32.0
1	0	20.4	16.6
3	0	7.6	6.4
5	0	21.2	19.8
7	0	8.1	8.1
9	0	4.4	5.6

TABLE 3. (Continued)

h	k	Fo	Fc	h	k	Fo	Fc	h	k	Fo	Fc	h	k	Fo	Fc
11	0	11.3	11.3	-4	4	7.6	5.9	-3	1	34.1	32.3	3	4	-6.7	-7.0
-13	1	3.3	3.8	-3	4	4.4	4.5	-2	1	22.3	20.4	5	4	2.8	0.8
-12	1	-4.5	-6.3	0	4	-7.6	-8.6	-1	1	13.8	13.2	7	4	3.8	5.4
-9	1	5.9	3.5	1	4	9.8	9.0	0	1	14.0	14.1	-14	5	2.6	3.1
-8	1	-7.0	-5.0	2	4	7.1	7.4	1	1	-7.5	-6.2	-13	5	4.5	5.0
-6	1	3.9	1.9	7	4	-8.3	-8.3	2	1	10.2	10.3	-9	5	-2.6	-2.3
-5	1	-13.8	-8.8	9	4	-8.7	-8.0	3	1	-12.6	-13.5	-8	5	-5.8	-4.8
-4	1	18.1	16.6	10	4	-1.8	-4.3	5	1	-11.8	-10.4	-6	5	-7.5	-7.0
-3	1	14.7	13.0	-11	5	-7.6	-8.3	7	1	9.1	9.5	-4	5	-3.9	-3.8
-2	1	4.5	3.5	-10	5	1.9	3.5	8	1	-10.0	-11.4	-3	5	4.1	4.0
-1	1	-4.6	-3.5	-9	5	-8.2	-8.5	9	1	7.8	6.9	-2	5	-8.0	-9.6
0	1	2.1	3.4	-8	5	3.7	4.1	10	1	-7.1	-5.3	0	5	-10.1	-11.6
1	1	7.2	7.7	-6	5	5.4	5.4	-14	2	2.5	0.9	2	5	-5.8	-5.3
2	1	-14.7	-13.4	-5	5	2.1	2.1	-13	2	-3.6	-3.6	5	5	-4.9	-6.2
3	1	24.4	22.4	-3	5	1.4	4.0	-11	2	-6.5	-6.5	6	5	6.1	7.3
4	1	-2.1	-3.4	-2	5	-6.1	-5.9	-10	2	-4.2	-3.8	-12	6	3.1	2.9
6	1	3.3	3.4	-1	5	-2.9	-2.9	-9	2	-5.3	-4.7	-8	6	-6.1	-5.4
7	1	-2.0	-4.8	0	5	-3.0	-4.2	-7	2	9.6	10.1	-6	6	-5.0	-5.6
9	1	-6.5	-7.9	2	5	4.2	6.6	-6	2	-10.0	-10.8	-5	6	-2.7	-3.2
10	1	10.7	12.1	3	5	3.5	2.9	-5	2	26.2	25.1	-3	6	-8.7	-9.6
-14	2	3.5	4.4	4	5	8.9	8.9	-4	2	16.3	17.6	-2	6	7.1	7.3
-13	2	-3.9	-5.1	6	5	-4.3	-6.6	-3	2	26.8	29.6	-1	6	-13.0	-14.6
-12	2	4.8	5.0	8	5	-8.1	-8.2	-2	2	26.5	28.1	0	6	2.7	4.5
-10	2	7.4	6.3	9	5	-1.8	-2.4	-1	2	14.3	11.0	1	6	-10.8	-11.4
-9	2	5.6	5.1	-8	6	-3.8	-4.2	0	2	-11.8	-12.8	3	6	2.8	4.4
-7	2	16.2	15.9	-4	6	3.1	2.9	2	2	-16.1	-15.2	5	6	6.4	6.1
-6	2	7.2	6.8	-3	6	-1.5	-3.0	4	2	-14.8	-14.5	-2	7	-3.9	-3.9
-5	2	2.6	0.7	1	6	2.9	3.3	5	2	-4.4	-3.4	-1	7	2.5	2.1
-4	2	7.7	9.2	2	6	-10.0	-11.3	7	2	-8.2	-7.9	0	7	-4.6	-5.1
-3	2	-13.0	-10.2	3	6	7.2	7.1	8	2	7.3	8.3	5	7	5.1	4.8
-1	2	9.5	11.7	6	6	1.9	4.9	-15	3	3.3	2.7	-6	9	3.4	4.0
0	2	-8.8	-9.8	7	6	-3.1	-1.6	-13	3	6.3	6.2				
1	2	-7.0	-5.3	-6	7	-3.8	-3.7	-12	3	-4.2	-2.7	l=5			
2	2	-17.2	-18.1	-5	7	4.0	5.0	-11	3	6.5	7.4	-7	0	11.2	6.5
3	2	-10.7	-10.1	-4	7	-6.1	-7.3	-10	3	-6.1	-6.7	-3	0	-9.2	-7.0
5	2	-7.4	-1.6	-3	7	5.4	5.7	-8	3	4.4	4.2	1	0	-12.3	-11.7
6	2	7.7	9.2	-2	7	-7.8	-7.4	-7	3	-6.8	-5.1	7	0	12.9	9.9
7	2	-4.9	-5.2	1	7	-7.5	-7.7	-6	3	11.1	10.8	9	0	9.3	10.6
-15	3	3.9	4.5	2	7	6.0	7.1	-5	3	-7.6	-6.5	-3	1	-10.1	-8.8
-14	3	3.5	4.4	3	7	-1.8	-4.3	-4	3	2.0	2.4	1	1	8.1	7.3
-13	3	4.9	5.6	4	7	3.7	4.7	-2	3	9.6	8.8	3	1	7.7	8.0
-11	3	8.0	8.0	5	7	1.7	4.2	0	3	7.3	7.5				
-10	3	2.5	3.9	7	7	6.2	4.3	1	3	-11.3	-10.4	l=6			
-9	3	-2.1	-1.9	-1	9	-4.1	-2.8	2	3	2.3	2.8	0	0	-12.3	-10.2
-7	3	-11.6	-9.5					3	3	-10.2	-8.7	6	0	13.0	12.2
-6	3	-2.4	-2.5	l=4				4	3	-2.5	-1.7	8	0	8.5	8.4
-3	3	-3.5	-3.8	-10	0	-8.2	-9.4	5	3	2.6	3.8	-6	1	11.7	8.0
-2	3	-11.1	-8.6	-8	0	-8.0	-6.7	6	3	-7.9	-7.0	-8	2	-9.4	-7.3
-1	3	11.0	10.6	-6	0	10.9	10.4	7	3	4.8	6.2	-7	2	10.5	8.2
0	3	13.9	10.4	-4	0	1.7	2.3	-15	4	4.0	4.5	-6	2	9.5	5.6
2	3	5.3	1.5	0	0	2.2	2.0	-14	4	7.0	6.1	-5	2	16.2	14.7
3	3	-10.7	-9.2	6	0	5.6	8.5	-12	4	6.4	8.1	-4	2	14.1	11.0
4	3	-8.3	-8.1	8	0	10.1	10.5	-11	4	-8.2	-8.0	-3	2	13.5	9.5
8	3	-8.7	-8.5	-13	1	2.5	2.6	-10	4	5.8	2.9	-6	3	9.1	7.2
9	3	4.2	3.8	-12	1	-3.4	-3.5	-9	4	-6.7	-6.5	-5	3	12.5	7.2
10	3	-5.4	-5.7	-11	1	-7.6	-6.7	-8	4	-3.3	-4.1	-4	3	6.4	10.1
-13	4	3.4	3.3	-9	1	-12.9	-13.1	-7	4	-3.3	-3.8				
-12	4	-4.7	-6.0	-8	1	-11.4	-9.4	-6	4	-4.9	-3.3	l=8			
-10	4	-10.1	-11.0	-7	1	-9.0	-7.3	-5	4	3.3	3.0	-2	0	-8.2	-5.3
-7	4	-10.5	-9.9	-6	1	-2.6	-4.7	-4	4	-6.9	-4.5	0	0	-8.4	-6.6
-6	4	4.9	6.1	-5	1	8.1	5.7	-3	4	2.9	1.9				
-5	4	1.3	2.2	-4	1	34.9	31.1	-2	4	-5.5	-4.3				

ters and their standard deviations are listed in Table 2. The observed and calculated structure factors are tabulated in Table 3.

Description of the Structure and Discussion

The component molecules are stacked alternately in infinite columns along the *c*-axis. Both the TCNB and HMB molecules are planar within the experimental errors and the mean planes are expressed by:

$$-0.3747x + 0.3132y + 0.9400z = 0$$

and

$$-0.3221x + 0.2903y + 0.9538z = 3.5435$$

respectively, where x, y and z are coordinates (in Å) with respect to the crystal axes a, b and c.

Bond distances and angles in each molecule are listed in Table 4 and they are also shown in Fig. 1. The C(5)-C(4′) distance of 1.41 Å found in TCNB molecule is longer than the C(3)-C(4) distance of 1.38 Å or C(3)-C(5) distance of 1.39 Å. This deformation of the aromatic ring in the TCNB molecule is also found in the complex between TCNB and naphthalene, and is consistent with the result of theoretical calculation.[2)]

Intermolecular atomic distances less than 3.6 Å are indicated in Fig. 2 and listed in Table 5. These distances are of the same order as generally accepted van der Waals distances.

The nature of the anisotropic thermal motion is illustrated in Fig. 3. For HMB molecule, the motion appears to be simply

TABLE 4. BOND DISTANCES AND ANGLES AND THEIR STANDARD DEVIATIONS

TCNB					
N(1)-C(1)	1.11	(0.02) Å	N(2)-C(2)-C(4)	176.7	(1.9)°
C(1)-C(5)	1.44	(0.02)	C(2)-C(4)-C(5′)	118.5	(1.6)
C(5)-C(4′)	1.41	(0.02)	C(2)-C(4)-C(3)	121.2	(1.5)
C(5)-C(3)	1.39	(0.02)	C(3)-C(4)-C(5′)	120.3	(1.5)
C(3)-C(4)	1.38	(0.02)	C(4)-C(3)-C(5)	119.2	(1.5)
C(4)-C(2)	1.44	(0.02)	C(3)-C(5)-C(4′)	121.0	(1.5)
C(2)-N(2)	1.13	(0.02)	C(3)-C(5)-C(1)	117.3	(1.6)
			C(1)-C(5)-C(4′)	122.2	(1.5)
			N(1)-C(1)-C(5)	178.4	(2.1)
HMB					
C(6)-C(9)	1.55	(0.02) Å	C(6)-C(9)-C(10′)	120.0	(1.7)°
C(9)-C(11)	1.38	(0.02)	C(6)-C(9)-C(11)	121.1	(1.6)
C(11)-C(8)	1.56	(0.02)	C(10′)-C(9)-C(11)	118.8	(1.7)
C(11)-C(10)	1.39	(0.02)	C(9)-C(11)-C(8)	118.2	(1.6)
C(10)-C(7)	1.57	(0.02)	C(8)-C(11)-C(10)	120.7	(1.6)
C(10)-C(9′)	1.42	(0.02)	C(9)-C(11)-C(10)	121.1	(1.6)
			C(11)-C(10)-C(7)	118.2	(1.7)
			C(7)-C(10)-C(9′)	121.7	(1.6)
			C(11)-C(10)-C(9′)	120.1	(1.6)

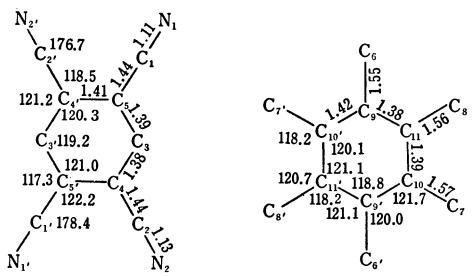

Fig. 1. Bond distances and angles.

rigid-body libration about the center of gravity, chiefly in the molecular plane. The thermal motion of the less rigid TCNB molecule is more complex and defies rigorous analysis. However, it is at least certain that the out-of-plane vibration of the cyano groups is appreciable.

The molecules overlap each other as shown in Fig. 4, with interplanar spacing of 3.54 Å. The molecular plane of TCNB makes an angle of about 2° with that of HMB. This spacing is about 0.11 Å larger than that found in TCNB-naphthalene complex.[2] This difference is clearly due to the difference in the thickness of the donor molecules.

Iwata, Tanaka and Nagakura[4] calculated the electronic structures of this molecular complex only by considering the interaction between π-electrons of the donor and the acceptor. They concluded that the center of the donor molecule should lie above the carbon atom or the C-C bond of the benzene ring of the acceptor molecule in the stable configuration. As shown in Fig. 4, their conclusion agrees well with the determined structure. It is particularly noteworthy that the relative arrangement of the donor and acceptor molecules in the crystal agrees with the result of the theoretical calculation based on the π-π interaction only. It is certain that the relative arrangement of the donor and the acceptor molecules will be affected by various interactions other than the charge tranfer interaction, such as van der Waals, repulsive interactions etc. Actually the packing of the molecular stacks along the *c*-axis seems to be determined mainly by van der Waals interactions. But, as for the relative arrangement of the component molecules, the following conditions seem to enable the theoretical conclusion to be consistent with the result of the structure analysis. Firstly both the acceptor and the donor molecules are planar. Especially, the donor molecule which is surrounded by six methyl groups is disc-shaped. The relative translation of one component molecule with respect to another does not result in any particular stable molecular packing. Secondly the donor molecules contain neither nitrogen nor oxygen atom having lone pair electrons. Consequently any localized interaction between the component molecules

TABLE 5. CLOSEST INTERMOLECULAR CONTACTS

C(7)-N(2′)	3.51 Å
N(1)-N(1′)	3.50
N(1)-C(7′)	3.49
N(1′)-C(6)	3.45
C(3)-N(1′)	3.53
C(6′)-N(2)	3.59
C(5)-C(10)	3.52
C(11)-C(3)	3.48

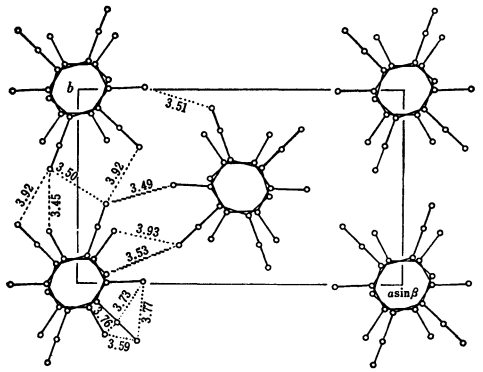

(a) viewed along [001]

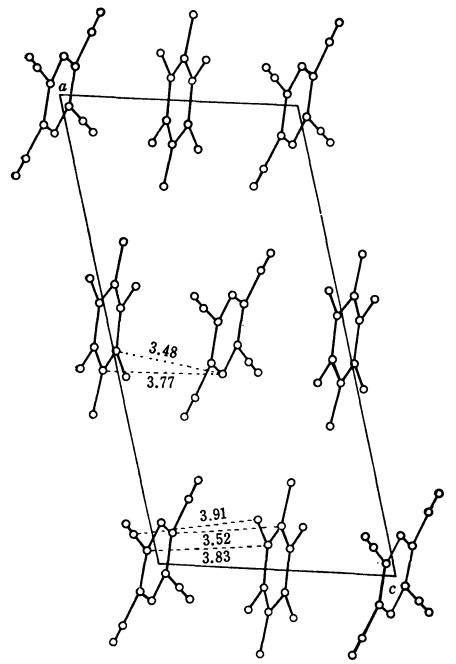

(b) viewed along [010]

Fig. 2. Closest intermolecular contacts between TCNB and HMB.

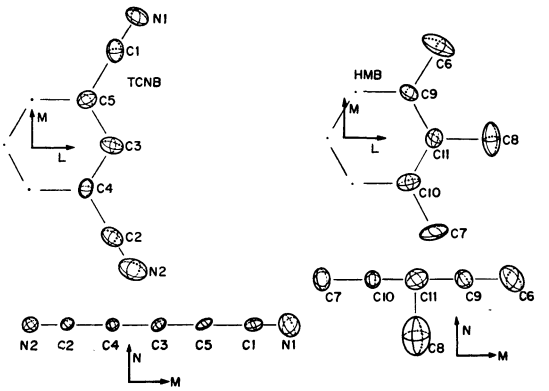

Fig. 3. The thermal motion ellipsoids.

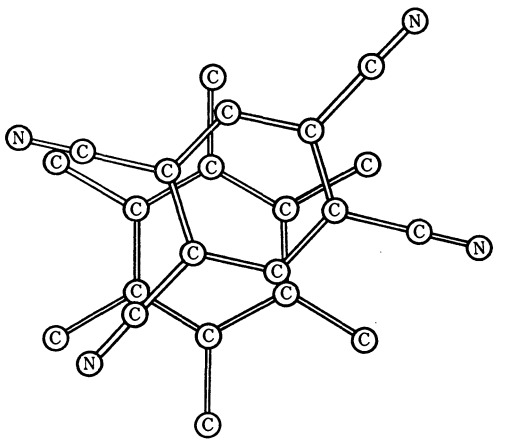

Fig. 4. Overlapping molecules, viewed approximately normal to their plane.

cannot be expected. Therefore the relative arrangement of the donor and the acceptor molecules in the molecular stack is mainly determined by the π-π interaction. The same situation will also be found in the case of the TCNB-naphthalene,[2] TCNE-naphthalene,[6,7] TCNE-pyrene[6,8] and TCNE-perylene[9] complexes.

Calculations were carried out on FACOM 202 computer at this institute and on HITAC 5020 at the Computer Center of the University.

The authors are grateful to Professor S. Nagakura and Dr. S. Iwata for kind supply of the specimens and valuable discussions. Part of the cost of the study was defrayed by a Scientific Research Grant of the Ministry of Education, to which the authors' thanks are due.

6) H. Kuroda, T. Amano, I. Ikemoto and H. Akamatu, *J. Am. Chem.* Soc., **89**, 6056 (1967).
7) R. M. Williams and S. C. Wallwork, *Acta Cryst.*, **22**, 899 (1967).
8) H. Kuroda, I. Ikemoto and H. Akamatu, *This Bulletin*, **39**, 547 (1966).
9) I. Ikemoto and H. Kuroda, *ibid.*, **40**, 2009 (1967).

BULLETIN OF THE CHEMICAL SOCIETY OF JAPAN VOL. 41 1821—1829 (1968)

Infrared Spectrum of Deoxyribonucleic Acid —— Effects of Base Composition and of ^{15}N-Substitution ——

Masamichi Tsuboi, Katsuichi Shuto and Shigesada Higuchi

Faculty of Pharmaceutical Sciences, University of Tokyo, Hongo, Bunkyo-ku, Tokyo

(Received February 22, 1968)

Infrared absorption spectra have been observed in the 4000—500 cm^{-1} region of deuterated and undeuterated films of deoxyribonucleic acids (DNA's) obtained from *Micrococcus lysodeikticus* (guanine plus cytosine content or GC content 72%), from *Bacille de Calmette-Guérin* (GC 65%), from *Pseudomonas aeruginosa* (GC 65%, ^{15}N-substituted), from calf thymus (GC 44%), and from *Cancer borealis* (GC 3%). Of the undeuterated DNA, 14 absorption bands have been assigned to the GC pair and 17 absorption bands to the adenine-thymine (AT) pair. Of the deuterated DNA, 19 absorption bands have been assigned to the GC pair and 16 to the AT pair. For 4 bands of undeuterated DNA and 13 bands of deuterated DNA, appreciable ^{15}N isotopic shifts have been observed. A discussion has been given of a few of these bands on the basis of the observed ^{15}N shift and some other data.

This work is a part of our attempt to establish a basis of an infrared base-analysis which should eventually give the amount of guanine-cytosine, adenine-thymine, and adenine-uracil base pairs and the amounts of unpaired guanine, cytosine, adenine, thymine, and uracil base residues in a given polynucleotide sample. In our present knowledge, every native deoxyribonucleic acid (DNA) obtained from a bacterium or a higher organism contains only the guanine-cytosine (GC) and adenine-thymine (AT) pairs, and practically no unpaired bases. Some of such DNA's have high GC contents and some very low. Therefore, infrared absorption bands assignable to the GC and AT pairs are considered to be found by comparing infrared absorption spectra of these DNA's. This has been the case as will be described below. In additon, the ^{15}N-substitution effect on the spectrum of a DNA with a GC content 65% has been examined. From the result in combination with data previously obtained, some nature of the normal vibration of each of the absorption bands has been clarified. A preliminary account of this work appeared already elsewhere.[1,2] It should also be mentioned here that Fritzsche[3] made independently an observation of the infrared spectra of a few deuterated DNA's with different GC contents.

Experimental

The DNA samples used are listed in Table 1.

DNA from *Micrococcus lysodeikticus* was prepared by ourselves. Mostly, the procedure described by Marmur[4] was followed. For dissociating the nucleic acid from protein, however, not only the

TABLE 1. DNA SAMPLES USED IN THE PRESENT WORK

Source	GC content	
Micrococcus lysodeikticus	72%[a]	
Bacille de Calmette-Guérin	65 [b]	
Pseudomonas aeruginosa	65 [a]	(^{15}N-substituted)
Calf thymus	44 [c]	
Cancer borealis	3 [d]	(light component)

a) N. Sueoka and T. Y. Cheng, *J. Mol. Biol.*, **4**, 161 (1962).

b) Determined by Professor T. Tsumita (by hydrolysis).

c) E. Chargaff, "The Nucleic Acids," E. Chargaff and J. N. Davidson, Eds., Vol. 1, Academic Press, Inc., New York (1955), p. 354.

d) N. Sueoka and T. Y. Cheng.[7]

Marmur's method but also the method described by Kay, Simmons, and Dounce[5] was adopted. The molecular weight of the product was estimated to be 3.2×10^6 from the sedimentation coefficient. DNA from *Bacille de Calmette-Guêrin* (B. C. G.) was pre-

1) M. Tsuboi and K. Shuto, *Chem. Pharm. Bull.*, **14**, 784 (1966).

2) M. Tsuboi and K. Shuto, Paper read at 5th Annual Meeting of Biophys. Soc. Japan, 17 p-C-4, Kyoto, Dec., 1966; M. Tsuboi, K. Shuto and S. Higuchi, Paper read at 7 th International Congress of Biochemistry, Tokyo, Aug., 1967 (Abstract B-38).

3) H. Fritzsche, *Studia biophysica, Berlin*, **1**, 273 (1966).

4) J. Marmur, *J. Mol. Biol.*, **3**, 208 (1961).

5) E. R. M. Kay, N. S. Simmons and A. L. Dounce, *J. Am. Chem. Soc.*, **74**, 1724 (1952).

pared by Professor Toru Tsumita in the Institute of Medical Science, University of Tokyo, and kindly placed at our disposal by him. ^{15}N-DNA from *Pseudomonas aeruginosa* was donated by Dr. Ts'ai-Ying Cheng, now at the Institute for Cancer Research, Fox Chase, Philadelphia, Pennsylvania, U. S. A. This was obtained by the Marmur's method[4] from *P. aeruginosa* grown for many generations in $^{15}NH_4Cl$ as the sole nitrogen source. In this DNA sample, practically all of the nitrogen atoms is considered to be ^{15}N, on the basis of the manner of preparation. Calf thymus DNA was purchased from Sigma Chemical Company. The "light DNA" from *Cancer borealis*, which contains 97 mol percent of deoxyadenylate and deoxythymidylate in predominantly alternating sequence,[6,7] was again a gift from Dr. Cheng.

For the infrared absorption measurements oriented or unoriented films were prepared on AgCl plates. The control of the humidity of the air over the sample and deuteration of the sample were made by the method described by Sutherland and Tsuboi.[8] The instruments used were a model DS-402 G double-beam grating spectrometer of Japan Spectroscopic Company, a Perkin-Elmer model 12C Spectrometer with CaF_2, NaCl, and KBr prisms, and a Perkin-Elmer model 221 Spectrometer. For obtaining polarized radiation an AgCl polarizer was used.

Absorption Bands Assignable to the GC and AT Base Pairs

Infrared absorption spectra of an oriented film of the "light DNA" from *Cancer borealis* observed with the polarized radiation are shown in Fig. 1. As may be seen in the figure, many details of the spectra of this DNA are different from what are observed of calf thymus DNA.[8,9] Some parts of the infrared absorption spectra of unoriented films of the five DNA's (see Table 1) observed with the ordinary radiation are given in Figs. 2—6. The spectral features are found to depend

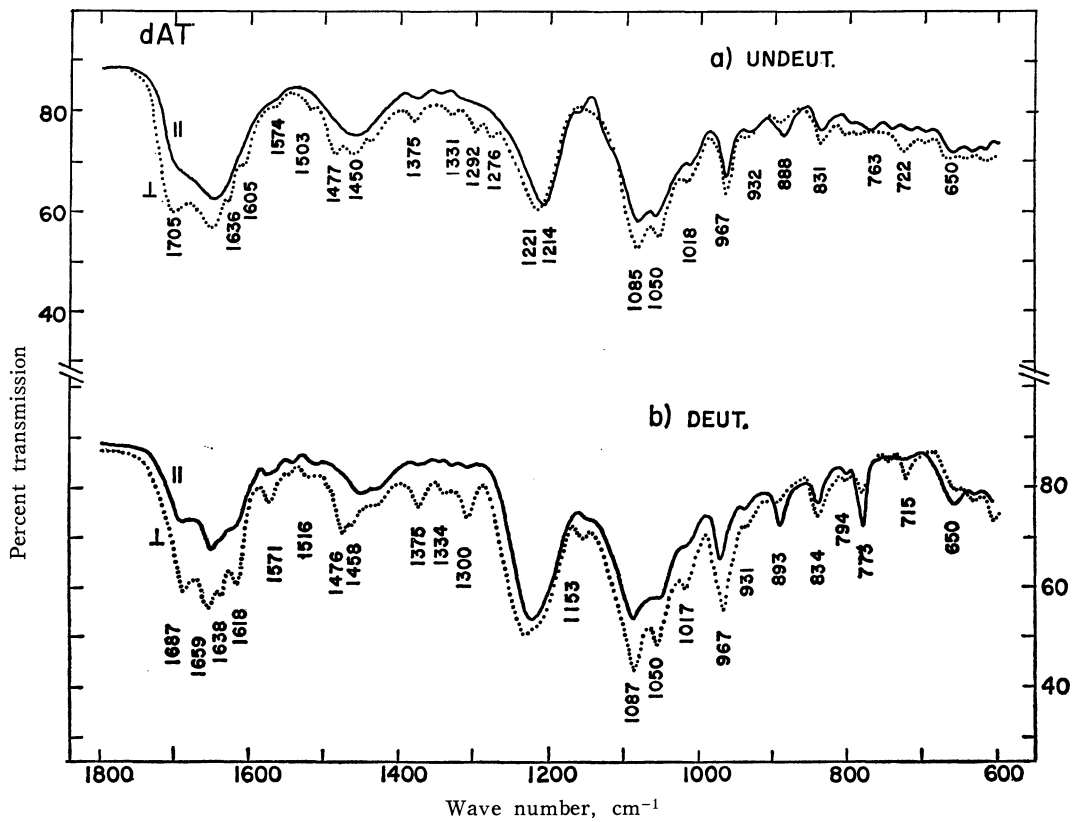

Fig. 1. Infrared absorption spectra of oriented films of the light DNA from *Cancer borealis* with GC 3%. (a) Undeuterated, at 92% relative humidity; (b) deuterated, at 92% relative humidity. Full line: electric vector of the incident radiation is parallel to the fiber axis. Broken line: electric vector the incident radiation is perpendicular to the fiber axis.

6) N. Sueoka, *J. Mol. Biol.*, **3**, 31 (1961).
7) N. Sueoka, and T. Y. Cheng, *Proc. Nat. Acad. Sci.* (*U. S. A.*), **48**, 1851 (1962).
8) G. B. B. M. Sutherland and M. Tsuboi, *Proc. Roy. Soc.*, **A 239**, 446 (1957).
9) E. M. Bradbury, W. C. Price and G. R. Wilkinson, *J. Mol. Biol.*, **3**, 301 (1961).

markedly upon the base compositions of the DNA samples. All of these spectra were observed at 92% relative humidity. At this humidity, the DNA fiber takes the B-form irrespective of the base compositions.[10,11] The geometrical structures of DNA's with different base compositions are so similar that practically no difference can be found in their X-ray diffraction patterns.[10,11] Therefore, the marked difference in their infrared spectra are to be ascribed solely to the difference in the normal vibrations of the structure with the GC pair and that with the AT pair. In most of the vibrational modes corresponding to the absorptions in the 4000—500 cm^{-1} region, the displacements of atoms are localized within relatively small atomic groups. In addition, the vibrational coupling between the adjacent two nucleotide residues would not be great. Therefore, most of the absorption bands of DNA in the spectral region now in question are expected to be classified into three groups: (i) bands assignable to some vibrations localized in the guanine-cytosine (GC) base pair, (ii) bands assignable to some vibrations localized in the adenine-thymine (AT) base pair, and (iii) bands assignable to some vibrations localized in the phosphate-deoxyribose main-chain. An examination of the spectra was made first with this expectation in mind.

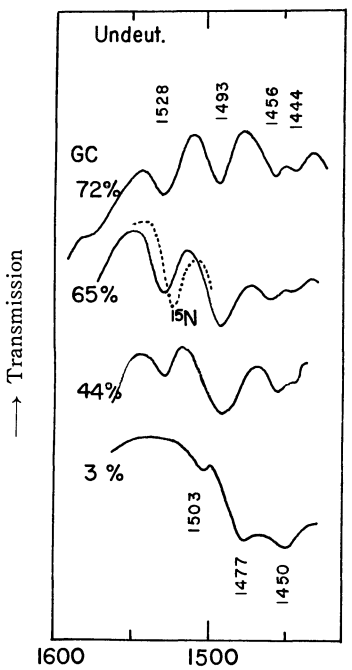

Fig. 2. Infrared absorption spectra in the 1560—1440 cm^{-1} region of undeuterated films of the five DNA's listed in Table 1. Observed at 92% relative humidity.

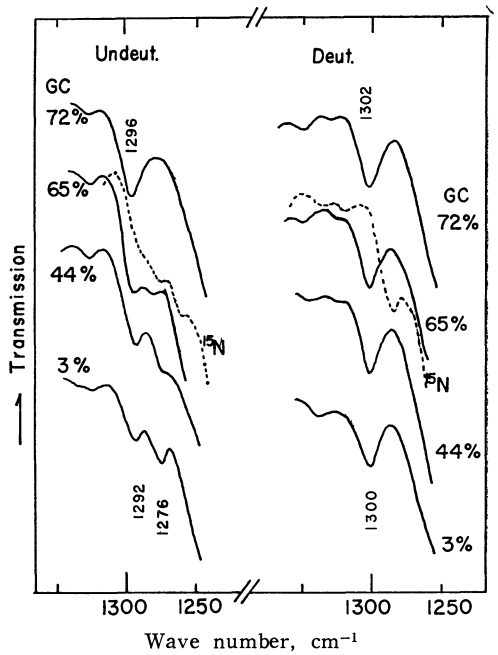

Fig. 3. Infrared absorption spectra in the 1340—1250 cm^{-1} region of undeuterated and deuterated films of the five DNA's listed in Table 1. Observed at 92% relative humidity.

In Fig. 2, an absorption band at 1528 cm^{-1} is found to become weaker with the GC content. Therefore, this band may be assigned to the GC base-pair. The weak band at 1503 cm^{-1} and another band at 1477 cm^{-1} of the light DNA of cancer are not observed in DNA's with higher GC contents. Therefore, these should be assigned to the AT pair. The occurrence of a broad band at about 1490 cm^{-1} of the calf thymus DNA may be interpreted as a result of a superposition of 1503, 1477, and the 1493 cm^{-1} bands. The last one is to be assigned to the GC pair.

As has been pointed out previously,[1] the 1276 cm^{-1} band is attributed solely to the AT pair (see Fig. 3). On the other hand, the absorptions around the 1292—1296 cm^{-1} region are caused by both of the AT and GC pairs. Here, however, the absorption bands due to the AT and GC pairs seem to be situated at

10) L. D. Hamilton, R. K. Barclay, M. H. F. Wilkins, G. L. Brown, H. R. Wilson, D. A. Marvin, H. Ephrussi-Taylor and N. S. Simmons, *J. Biophys. Biochem. Cytol.*, **5**, 397 (1959); R. Langridge, H. R. Wilson, C. W. Hooper M. H. F. Wilkins and L. D. Hamilton, *J. Mol. Biol.*, **2**, 19 (1960); R. Langridge, D. A. Marvin, W. E. Seeds, H. R. Wilson, C. W. Hooper, M. H. F. Wilkins and L. D. Hamilton, *ibid.*, **2**, 38 (1960).

11) D. R. Davies and R. L. Baldwin, *J. Mol. Biol.*, **6**, 251 (1963).

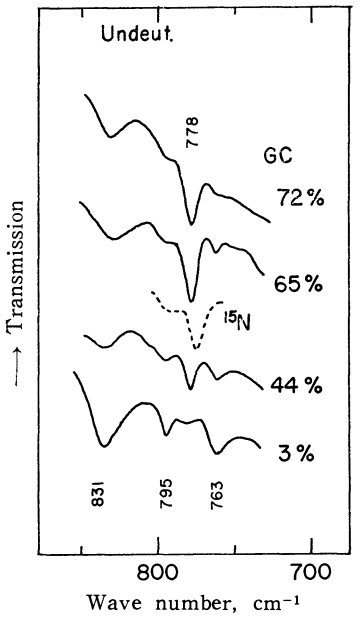

Fig. 4. Infrared absorption spectra in the 850—740 cm^{-1} region of undeuterated films of the five DNA's listed in Table 1. Observed at 92% relative humidity.

slightly different frequencies. On deteration, both of the 1296 and 1276 cm^{-1} bands disappear, and a slightly stronger band appears at about 1300 cm^{-1}. Both of the AT and GC pairs give a band here, but again at slightly different frequencies.

In a similar way, we may pick up the absorption band at 831, 795, and 763 cm^{-1} (see Fig. 4) as those assignable to the AT pair and the absorption band at 778 cm^{-1} as one assignable to the GC pair.

The absorption spectra of deuterated DNA's in the 1700—1450 cm^{-1} region are rather complicated (Fig. 5). As has been mentioned by Sutherland and Tsuboi,[8] almost all the absorption bands in this region are assignable to in-plance vibrations of bases. It was difficult, however, to proceed a further analysis by examining the calf thymus DNA only. It is now safely concluded that the absorptions at 1687, 1659, 1638, 1618, 1571, 1476, and 1458 cm^{-1} are due to the AT base pair, because at these frequencies the AT-DNA of cancer

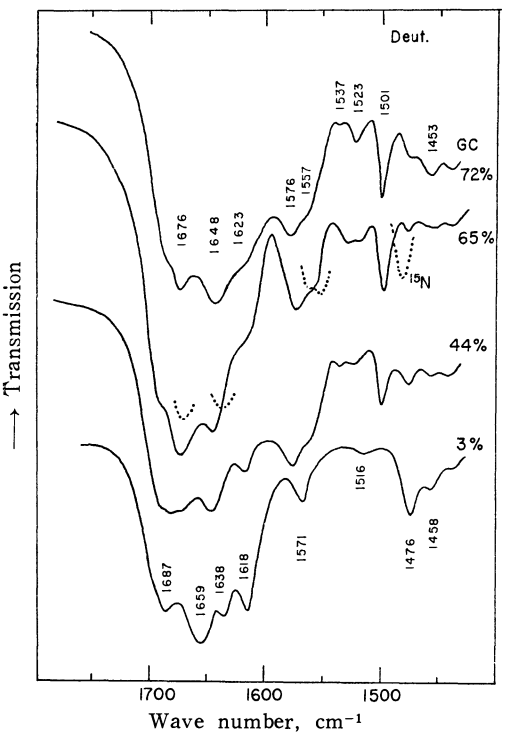

Fig. 5. Infrared adsorption spectra in the 1800—1430 cm^{-1} region of deuterated films of the five DNA's listed in Table 1. Observed at 92% relative humidity.

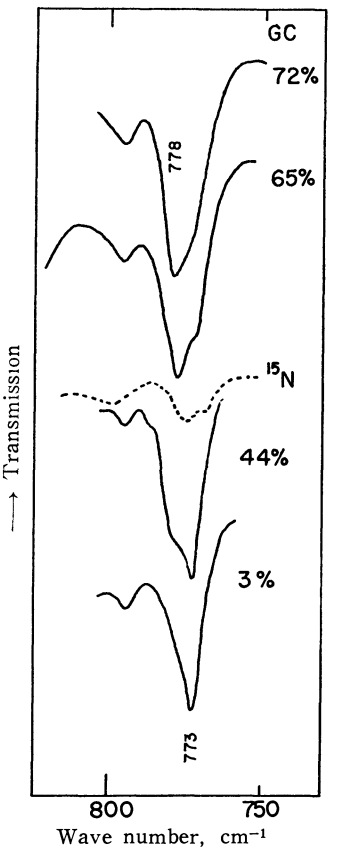

Fig. 6. Infrared absorption spectra in the 800—750 cm^{-1} region of deuterated films of the five DNA's listed in Table 1. Observed at 92% relative humidity.

gives absorption peaks (Figs. 1b and 5) but DNA's with higher GC contents do not (Fig. 5). The absorptions at 1676, 1648, 1576, 1523, 1501, and 1453 cm^{-1} are ascribed to the GC pair, because the Micrococcus DNA with GC 72% gives absorption peaks at these frequencies. The absorption curves of DNA's with the GC contents of 65% and 44% are interpreted in an approximation as proper superpositions of the absorption curves of DNA's with the GC contents 72% and 3% (Fig. 5).

As may be seen in Fig. 6, both of the GC and AT pairs give sharp peaks around 780 cm^{-1}. The former, however, gives a peak at a slightly higher frequency (778 cm^{-1}) then the latter (773 cm^{-1}). Therefore, the fact[8] that the calf thymus DNA gives a shoulder at 778 cm^{-1} besides the sharp peak at 773 cm^{-1} is now quite understandable on the basis of its base compositions.

Absorption bands at 1218, 1087, 1069, 1050, 1018, 967, and 650 cm^{-1} appear in every DNA and show almost no changes in their frequencies and intensities on deuteration. Therefore, they are assignable to some vibrations of atomic groups other than the bases.

As has been illustrated so far nearly all the absorption bands of DNA observed in the 1800—500 cm^{-1} region can be classified into the three groups, (i), (ii), and (iii), defined above, and a spectrum of any DNA appears, at least qualitatively, to be an assembly of the absorption bands of these groups with a proper set of intensities which depends upon the GC content of the DNA. The frequencies of the absorption bands belonging to these three groups are listed in Tables 2 and 3, with their intensities.

Most of the absorption bands assignable to the GC or AT base pair are found to be strongly polarized, if they are observed in the oriented films, either along the perpendicular direction to the fiber axis or along the parallel direction to it. This fact is understandable, because, in the B-form of DNA, base residues are arranged with their planes perpendicular to the fiber axis,[10] and because the normal vibrations localized in the base residues should take place with their transition moments either in their plane or perpendicular to the plane. Among the absorption bands of bases, what are strongly polarized along the perpendicular

TABLE 2. INFRARED ABSORPTION BANDS ASSIGNABLE TO THE GC BASE PAIR, AT BASE PAIR, AND OTHER PARTS OF THE UNDEUTERATED DNA MOLECULE

Bands due to GC				Bands due to AT			Others		
Frequency	Characterization[a]	^{15}N shift		Frequency	Characterization[a]	^{15}N shift	Frequency	Intensity	^{15}N shift
		Frequency shift	$\Delta\lambda/\lambda°$						
cm^{-1}		cm^{-1}		cm^{-1}			cm^{-1}		cm^{-1}
1705	s, *i*	−5*	−0.006*	1705	s, *i*				
							1220	s	0*
				1636	m, *i*		1087	s	0*
1609	m, *i*			1605	m, *i*				
1576	w, *i*			1574	w, *i*		1050	s	0*
1528	m, *i*	−8	−0.010	1503	w		1018	m	0*
1493	m, *i*			1477	m, *i*		967	s	0*
1456	w, *i*			1450	m, *i*		650	m	
1444	w, *i*			1375	w,				
1414	w, *i*			1331	w,				
				1292	w, *i*				
1380	m, *i*			1276	w, *i*				
1331	w, *i*			932	m, *i*				
1296	m, *i*	−20*	−0.031*	888	m, *o*				
893	m, *o*	0	0	831	m				
860	w, *o*			795	w				
				763	w, *o*				
				722	w,				
778	m, *o*	−3	−0.008						

a) s : strong, m : medium, w : weak, *i* : in-plane vibration, *o* : out-of-plane vibration,
* less accurate than others.

TABLE 3. INFRARED ABSORPTION BANDS ASSIGNABLE TO THE GC BASE PAIR, AT BASE PAIR, AND OTHER PARTS OF THE DEUTERATED DNA MOLECULE

Bands due to GC				Bands due to AT				Others		
Frequency	Characterization[a]	^{15}N shift		Frequency	Characterization[a]	^{15}N shift		Frequency	Intensity	^{15}N shift
		Frequency shift	$\Delta\lambda/\lambda$°			Frequency shift	$\Delta\lambda/\lambda$°			
cm^{-1}		cm^{-1}		cm^{-1}		cm^{-1}		cm^{-1}		cm^{-1}
1676	s, *i*	0	0	1687	s, *i*			1087	s	
1648	s, *i*	−6	−0.007	1659	s, *i*			1050	s	0
1623	m, *i*	−6	−0.007	1638	m, *i*			1017	m	0
1576	s, *i*	−17*	−0.021*	1618	s, *i*			967	s	0
1557	m, *i*									
1537	w, *i*	−20	−0.026	1571	m, *i*					
1523	w, *i*	−18	−0.023							
1501	m, *i*	−14	−0.019	1516	w, *i*					
1453	w, *i*			1476	m, *i*			650	m	
1439	w, *i*			1458	w, *i*					
1377	w, *i*	0	0	1375	w, *i*					
1350	w	−14	−0.021	1334	w, *i*					
1302	m, *i*	−17	−0.026	1300	w, *i*					
851	w,			1153	w, *i*					
831	m,			834	m					
797	w,	+3*	+0.008*	794	w,					
778	s, *o*	−3	−0.008	773	m, *o*	−3*	−0.008*			
727	w, *o*	−8	−0.022	715	w, *i*					
698	w, *o*	−5	−0.014							

a) s : strong, m : medium, w : weak, *i* : in-plane vibration, *o* : out-of-plane vibration.
* less accurate than others.

direction to the fiber axis are assigned to some in-plane (*i*) vibrations, and what are strongly polarized along the parallel direction to some out-of-plane (*o*) vibrations. These are also indicated in Tables 2 and 3.

^{15}N Isotope Shifts in the Vibrational Frequencies

The ^{15}N-DNA from *Pseudomonas aeruginosa* (GC 65%) shows an infrared absorption spectrum similar in its general feature to that of the DNA from *Bacille de Calmette-Guérin* (GC 65%). Many of the absorption maxima of the former DNA, however, are found to be shifted towards the lower frequencies from the corresponding maxima of the latter DNA (Figs. 2—7).

In principle, the ^{15}N isotope effect on an infrared spectrum of DNA should be found by comparing the ^{15}N-DNA and ^{14}N-DNA obtained from the same organism. Unfortunately, these were not available in our laboratory, and the ^{15}N-^{14}N comparison has been made between different species of bacteria having the same GC content as above. Practically, however, this is justified, because the DNA's from *Pseudomonas* and *B.C.G.* are expected to make no difference in their infrared spectra. These DNA's are different only in the sequence and arrangement in the GC and AT base pairs. The infrared spectrum in the spectral region now in question is not sensitive to the sequence and arrangement. Absorptions of a base residue might appreciably be different depending upon the neighbours. Such a difference, however, should disappear in an average, unless the nearest neighbour sequence frequencies of the two DNA's are greatly different; the nearest neighbour sequence frequencies have been found to be rather similar for natural DNA's from different sources but with almost equal GC contents.[12]

The significance of the observed shift may be judged, not only on the basis of the above consideration, but also by examining the experimental results given in Figs. 2—7. For example, the positions of relatively sharp bands at 1528 cm^{-1} (Fig. 2), at 1302 cm^{-1} (Fig.

12) J. Josse, A. D. Kaiser and A. Kornberg, *J. Biol. Chem.*, **236**, 864 (1961).

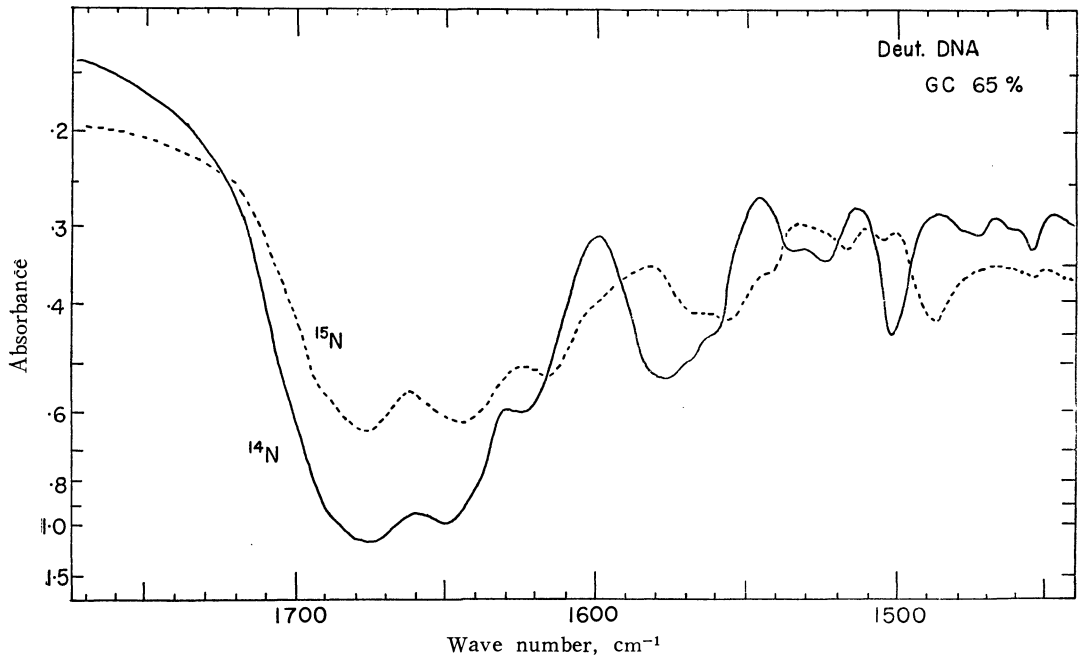

Fig. 7. An expanded recording of the infrared absorption spectra of deuterated films of DNA from *Bacille de Calmette-Guérin* (——) and of ^{15}N-DNA from *Pseudomonas aeruginosa* (·····). Observed at 92% relative humidity.

3), at 778 cm^{-1} (Fig. 4), at 1501 cm^{-1} (Fig. 5), and at 778 cm^{-1} (Fig. 6) are all found to remain constant within 2 cm^{-1} for ^{14}N-DNA's from Micrococcus, B. C. G., and calf thymus, while the corresponding bands are found at 3—17 cm^{-1} lower frequencies for the ^{15}N-DNA. This fact indicates that the frequencies of these bands are not sensitive to the origin of the DNA samples, and observed shifts are solely ascribed to the $^{14}N \rightarrow {}^{15}N$ substitution in the base residues.

The amount of the frequency shift was measured for each absorption band by repeating a recording of the ^{14}N and ^{15}N spectra alternately in a small spectral range with a low scan speed and with an expanded wavenumber scale (see Fig. 7, for example). The results of such measurements are given in Tables 2 and 3. For sharp and isolated absorption peaks, the amounts of shift were determined almost as accurately as those for simpler samples,[13] within 0.5 cm^{-1} or so. Sometimes, however, the measurement can be made only less accurately because the band in question is too broad or because the shifted absorption maximum is obscured by another absorption band. Such a case is indicated by * in Tables 2 and 3. The data of ^{15}N-isotope shifts are in general useful for judging the nature of the normal vibrations by which the absorption bands are caused. The judgement is often made through the amount:

$$\frac{\Delta\lambda}{\lambda^\circ} = \frac{\lambda(^{15}\mathrm{N}) - \lambda(^{14}\mathrm{N})}{\lambda(^{14}\mathrm{N})} \qquad (1)$$

rather than through the frequency shift $\Delta\nu$ itself. Here, $\lambda = 4\pi^2 c^2 \nu^2$, c being the velocity of light and ν the observed frequency (in reciprocal centimeters). This amount $\Delta\lambda/\lambda^\circ$ directly reflects how much movements of nitrogen atoms take place in the normal vibration now in question. Thus, on the basis of what Miyazawa[14] showed,

$$\frac{\Delta\lambda_k}{\lambda_k^\circ} = -\sum_N (L_{Nk})^2 \Delta m \qquad (2)$$

where, L_{Nk} is the amount of the displacement of each nitrogen atom relative to the center of gravity of the molecule, which is caused by the unit displacement (a deformation of the whole molecule) along the kth normal coordinate of the molecule. If the normal coordinate is expressed by the unit Å (atomic mass unit)$^{1/2}$ the unit of $(L_{Nk})^2$ should be (atomic mass unit)$^{-1}$. The isotopic mass change Δm is practically +1 in the atomic

13) M. Tsuboi, *Spectrochim. Acta*, **16**, 505 (1960); M. Tsuboi, T. Takenishi and A. Nakamura, *Spectrochim. Acta*, **17**, 634 (1961); M. Tsuboi, T. Takenishi and A. Nakamura, *ibid.*, **19**, 271 (1963).

14) T. Miyazawa, *J. Mol. Spectroscopy*, **13**, 321 (1964).

mass unit in the present case, and therefore this factor Δm can be ignored in the numerical calculation on Eq. (2). The summation is to be conducted for all the nitrogen atoms, on which the isotopic replacement has taken place.

In a less strict discussion of an infrared spectrum, the vibrational mode for each absorption band is often expressed in terms of the internal symmetry coordinate, such as NH_2 scissoring or NH out-of-plane deformation. Even in a complicated large molecule, a normal coordinate can sometimes be expressed approximately by an internal symmetry coordinate or by a linear combination of only a few internal symmetry coordinates. Therefore, it would be convenient to know the ^{15}N isotopic frequency shift for a hypothetical vibration along an internal symmetry coordinate t. This can be obtained by the formula,[13]

$$\frac{\Delta\lambda}{\lambda^\circ} = \frac{\Delta G_{tt}}{G_{tt}^\circ} \qquad (3)$$

where $\Delta \boldsymbol{G} = \boldsymbol{G} - \boldsymbol{G}^\circ$, $\boldsymbol{G}$ and $\boldsymbol{G}^\circ$ being the inverse kinetic energy matrices for the ^{15}N and ^{14}N species, respectively.

The $\Delta\lambda/\lambda^\circ$ values calculated by Eq. (1) from the observed frequencies are also given in Tables 2 and 3.

Discussion

The assignments of the infrared absorption bands of DNA were previously made on the basis of the deuteration effects, humidity effects, anisotropy of the absorptions, and the knowledge on the molecular vibrations of hypophosphites and other simple compounds. The effects of the base composition and of a ^{15}N-substitution are now obtained as new data. Based upon these new date, a few additional aspects of the nature of some of the absorption bands listed in Tables 2 and 3 are given below.

A strong band at 1705 cm^{-1} of undeuterated calf thymus DNA was found to be characteristic of its secondary structure.[15,16] It has now be shown that both of the GC and AT base pairs contribute to this band. The dipole oscillation takes place in the base plane in both base pairs. On the basis of the frequency and on the basis of the observed deuteration effect (see Fig. 1, for example), an NH_2 or NH in-plane deformation vibration is considered to take part in the normal vibration now in question. The observed amount of ^{15}N isotopic shift ($\Delta\lambda/\lambda_\circ = -0.006$) of the 1705 cm^{-1} band of the GC pair is almost equal to the calculated value ($\Delta\lambda/\lambda^\circ = -0.007$) for a pure (C-)$NH_2$ scissoring vibration and also to the calculated value ($\Delta\lambda/\lambda^\circ = -0.007$) for a pure NH in plane deformation vibration (on Eq. (3)). This, however, does not necessarily mean that the 1705 cm^{-1} band should be assigned to either an almost pure NH_2 scissoring or an almost pure NH in-plane deformation. It is possible, for example, that the actual mode of vibration is a combination of the NH_2 scissoring, NH deformation, C-N stretching and C=O stretching.

No normal coordinate treatment has yet been made of adenine, thymine, guanine, or cytosine. For cyanuric acid, however, which is somewhat similar structure to thymine, a normal coordinate treatment was made by Dr. Issei Harada (Master Thesis, 1963, and Doctor Thesis, 1966, University of Tokyo). His calculation was made of a hydrogen-bonded sheet in the cyanuric acid crystal. According to his calculation, there should be hree infrared-active vibrations at 1752, 1745, and 1696 cm^{-1} (There are actually three or four strong bands observed in the 1780—1715 cm^{-1} region). In all of these vibrations the C=O stretching motions are predominant but there are appreciable contributions from C-N stretching and NH in plane deformation vibrations. By applying Eq. (2) on the result of his calculation, it has been found that the three frequencies 1752, 1745, and 1696 cm^{-1} should give ^{15}N-shifts, $\Delta\lambda/\lambda^\circ = -0.015$, -0.013, and -0.003, respectively.

It is noteworthy that the band at 1705 cm^{-1} of base residues shifted towards lower frequency (but not towards higher) on breaking the base pairing. A possible explanation has been given elsewhere[15] on the basis of an assumption that the vibration in question involves the C=O and C=N stretching modes.

A strong absorption at 1680 cm^{-1} of deuterated calf thymus DNA was also found to be characteristic of its secondary structure.[15,16] This absorption is now found to be a superposition of the two bands: the 1676 cm^{-1} band of the GC pair and the 1687 cm^{-1} band of the AT pair (Fig. 5). The 1676 cm^{-1} band does not shift at all on ^{15}N substitution (Fig. 7). Therefore, this band is assignable to a vibration in which the main contribution comes from the carbonyl stretching motions in the GC base pair.

The 1576 cm^{-1} band of the deuterated DNA is due to the GC pair (Fig. 5). This is further assigned to the guanine moiety of the GC

15) Y. Kyogoku, M. Tsuboi, T. Shimanouchi and I. Watanabe, *Nature*, **189**, 120 (1961).
16) Y. Kyogoku, M. Tsuboi, T. Shimanouchi and I. Watanabe, *J. Mol. Biol.*, **3**, 741 (1961).

pair, because deuterated guanosine gives a very strong absorption band at 1570 cm^{-1} while deuterated cytidine does not.[17] Also, deuterated poly (G+C) gives a strong absorption band at 1577 cm^{-1} [18] while deuterated poly (I+C) does not.[19] On the basis of its frequency and on the basis of the observed amount of ^{15}N isotope shift ($\Delta\lambda/\lambda = -0.021$), this band is associated to a C-N stretching vibration in the guanine residue. According to the calculation made by Dr. Harada (mentioned above), cyanuric acid (undeuterated) should have vibrations at 1542, 1473, and 1459 cm^{-1}. In each of these vibrations, C-N stretching motions are predominant. If Eq. (2) is applied to the results of his calculation, it is concluded that the three frequencies should give ^{15}N-shift of the amounts $\Delta\lambda/\lambda^\circ = -0.040$, -0.021, and -0.021, respectively.

The 1501 cm^{-1} band of the deuterated DNA, which has been assigned to the GC pair, may further be assigned to the cytosine moiety. A strong absorption is found here in the spectra of deuterated cytidine,[17] and deuterated polyribocytidylic acid,[20] and deuterated poly (I+C)[19] whereas no strong absorption is found in the spectum of deuterated guanosine.[17] Because it is shifted greatly ($\Delta\lambda/\lambda^\circ = -0.019$) on ^{15}N-substitution, it is assigned to a C-N stretching vibration in the cytosine residue.

As was mentioned earlier,[8,20,21] the absorptions around 780 cm^{-1} of deuterated polynucleotides are noticeable ones. The fairly strong and sharp absorption peaks in this region are assigned to some out-of-plane vibrations in the base residues involved in wet polynuclotides. As has been mentioned above, it is now clear that the absorption peak at 773 cm^{-1} is due to the A-T base pair and that at 778 cm^{-1} to the G-C base pair. These absorption peaks appear only for deuterated DNA's and not for undeuterated ones. Therefore, the absorptions may be associated with the N-D and/or ND_2 groups. If the vibration for each of these bands were a pure N-D out-of-plane deformation vibration, however, the ^{15}N-isotope shift should be as high as $\Delta\lambda/\lambda^\circ = -0.028$ (Eq. (3)). If it were a pure ND_2 out-of-plane deformation vibration, the ^{15}N-isotope shift should be as high as $\Delta\lambda/\lambda^\circ = -0.023$. Actually observed ^{15}N-shift is only $\Delta\lambda/\lambda^\circ = -0.008$ for the 778 cm^{-1} band of the G-C base pair, and hence the normal vibration at 778 cm^{-1} would be a mixture of an N-D and/or ND_2 out-of-plane motion with some other out-of-plane modes of the G-C base-pair structure.

We wish to express our deep thanks to Dr. T. Cheng for the samples of ^{15}N-DNA from *Pseudomonas aeruginosa* and the "light DNA" from *Cancer borealis*, and to Professor T. Tsumita for the sample of DNA from *Baciile de Calmette-Guérin*. The work was supported partly by a grant from the Ministry of Education of Japan and partly by a grant from the U.S. Public Health Service (GM 10024-03).

Note : After the completion of the manuscript of this paper, a paper by H. Fritzsche (*Biopolymers*, **5**, 863 (1967)), which reports the infrared spectra of DNA's with different base compositions, has appeared. His assignments of the 1505 and 1573 cm^{-1} bands respectively to C and G are in agreement with ours.

17) M. Tsuboi, Y. Kyogoku and T. Shimanouchi, *Biochim. Biophys. Acta*, **55**, 1 (1962).

18) Poly (G+C) is a double helical complex of polyriboguanylic acid and polyribocytidylic acid. Its infrared spectrum was observed by S. Higuchi and M. Tsuboi (to be published).

19) Poly (I+C) is a double-helical complex of polyriboinosinic acid and polyribocytidylic acid. Its infrared spectrum was observed by M. Tsuboi, K. Matsuo, and S. Higuchi (*Biopolymers*, **6**, 123 (1968).

20) M. Tsuboi, *J. Poly. Sci.*, Part C, No. 7, 125 (1964).

21) M. Tsuboi, *Biopolymers*, Symposia No. 1, 527 (1964).

BULLETIN OF THE CHEMICAL SOCIETY OF JAPAN VOL. 41 1830—1834 (1968)

Rheological Properties of Hydrogels of Agar-agar. III. Stress Relaxation of Agarose Gels

Mineo WATASE and Kiyoshi ARAKAWA

The Department for Liberal Arts, Shizuoka University, Shizuoka and Research Institute of Applied Electricity, Hokkaido University, Sapporo

(Received February 26, 1968)

A stress relaxation experiment on hydrogels of agarose isolated from agar-agar was made by means of a chainomatic balance relaxometer for the purpose of investigating the mechanism of gelation. The measurements were made on the agarose gels of the concentration range from 1.2 to 2.0 wt%, and also on agar-agar gels for the comparison, at various temperatures from 25 to 55°C. The relaxation curves obtained were represented approximately by a mechanical model consisting of three Maxwell models in parallel. The apparent activation energy, ΔH, which was calculated from the temperature dependence of the longest relaxation time, τ_1, was about 5 kcal/mol for all gels treated in this study, which was nearly the same magnitude as that for agar-agar gels. It was observed in the curves obtained that the relaxation curves for agarose gels had quite similar characteristics to those for agar-agar gels of the same concentration and was observed that the total instantaneous modulus of the former gels amounted to about 80% of that of the latter gels. From these results it may be concluded that agarose is a main constituent in the network structure in agar-agar gels and that the hydrogen bonding plays a major role in the agar-agar gels as well as in the agarose gels.

In the preceding papers[1,2] the authors reported the results of stress relaxation experiments made for hydrogels of agar-agar. The hydrogels of agar-agar is well-known as a typical example of thermoreversible gels, and has long been the object of rheological and colloid-chemical studies. It is believed at present that a dominant factor governing the mechanism of gelation of agar-agar gels is the balance between the hydrophilic and the hydrophobic properties of the molecule of agar-agar, or the balance between the affinity to water and the tendency of formation of microcystalline structures in agar-agar molecules.[3-6] The detailed mechanism of gelation has not yet been cleared.

According to a series of studies made by Araki *et al.*[7] agar-agar is composed of two polysaccharides, agarose and agaropectin. Agarose is the major component. In the present paper, an attemt is made to measure the stress relaxation of the hydrogels of agarose isolated from agar-agar, and the results are compared with the data of agar-agar gels themselves.

Experimental

A sample used was the powder of agar-agar obtained from Nihon Kaiso Kogyo, Co., Ltd. The ash content of the sample is 0.95 wt%, and the intrinsic viscosity in the aqueous solution obtained with Ostwald viscometer,*1 $[\eta]_{25°C}$, is 15.6 (100 cc/g). The molecular weight of the sample calculated from the intrinsic viscosity was 4.2×10^4.[5]

Agarose was isolated from agar-agar as follows:[8] agar-ggar, 1% by weight, was dissolved into water, and then acrynol*2 was added to make the solution of 0.1 mol/*l*. Agarose was separated from the solution by centrifuge (6000 rpm). Agarose gel separated was heated to melt, mixed with ethyl alcohol,

1) K. Arakawa, This Bulletin, **34**, 1233 (1961).
2) M. Watase and K. Arakawa, *ibid.*, **40**, 472 (1967).
3) T. Nakagawa "Rheology," Iwanami Pub., Tokyo (1960), p. 68.
4) I. Kagawa, *Kagaku* (*Science*), **26**, 243 (1956).
5) N. Hirai and N. Nishimura, *Nippon Kagaku Zasshi* (*J. Chem. Soc. Japan, Pure Chem. Sect.*), **75**, 248 (1954).
6) M. Watase and K. Arakawa, *ibid.*, to be published.
7) C. Araki, This Bulletin, **29**, 543 (1950); C. Araki and K. Arai, *ibid.*, **30**, 287 (1957); S. Hirase, *ibid.*, **30**, 68, 70, 75 (1957).

*1 The flow time of pure water through the viscometer is 194.3 sec at 25°C.
8) T. Akabane and K. Katsuura, The 13th Annual Symposium on Polymers, Kobe, July 8, 1967.
*2

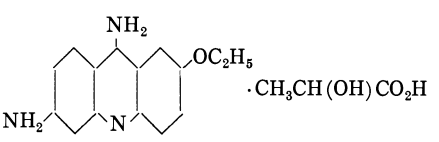

and centrifuged again to separate agarose. This purification with alcohol was repeated until the yellow color due to acrynol vanished. The intrinsic viscosity of purified agarose in aqueous solution is 15 (100 cc/g) at 25°C.

The test piece of agarose gels was prepared by the same procedure as that of agar-agar gels reported previously.[1] The concentrations of agarose gels prepared was 1.25, 1.43, 1.67 and 2.0 wt% respectively. The concentration of agar-agar gels was 2.0 wt%.

Stress relaxation curves up to 4 hr were obtained with a chainomatic balance relaxometer. The details of the apparatus and the experimental procedures were reported previously.[9] The measurements were made at temperatures from 25 to 55°C.

Results

Stress Relaxation Curves. The relaxation Young's modulus of hydrogels of agarose and agar-agar was obtained. The results are shown in Figs. 1 (a)—(e). These relaxation curves are approximately represented by a six-element mechanical model composed of three Maxwell models in parallel. In this model the relaxation Young's modulus, $E_r(t)$, is expressed as:

$$E_r(t) = \sum_{i=1}^{3} E_i \exp(-t/\tau_i) \qquad (1)$$

where E_i and $\tau_i(\tau_1 > \tau_2 > \tau_3)$ are the elastic constant and the relaxation time for the ith Maxwell element respectively, and t is the time. All relaxation curves obtained were fitted with Eq. (1), and the parameters in it are shown in Table 1.

Concentration Dependence of the Elastic

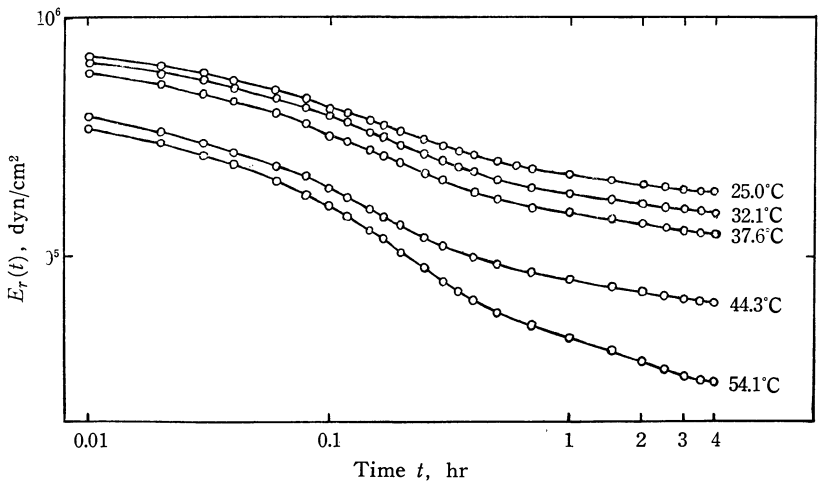

Fig. 1(a). Relaxation curves for agarose gels. 2.0 wt%

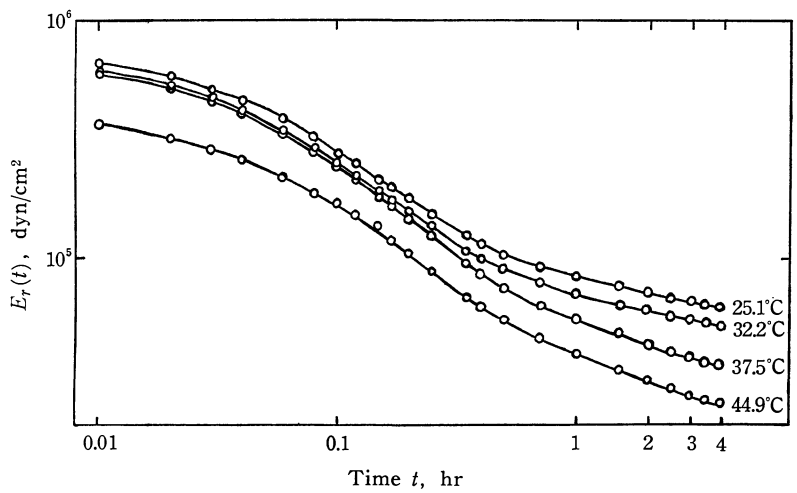

Fig. 1(b). Relaxation curves for agarose gels. 1.6$_7$ wt%

9) K. Arakawa, This Bulletin, **33**, 1568 (1960).

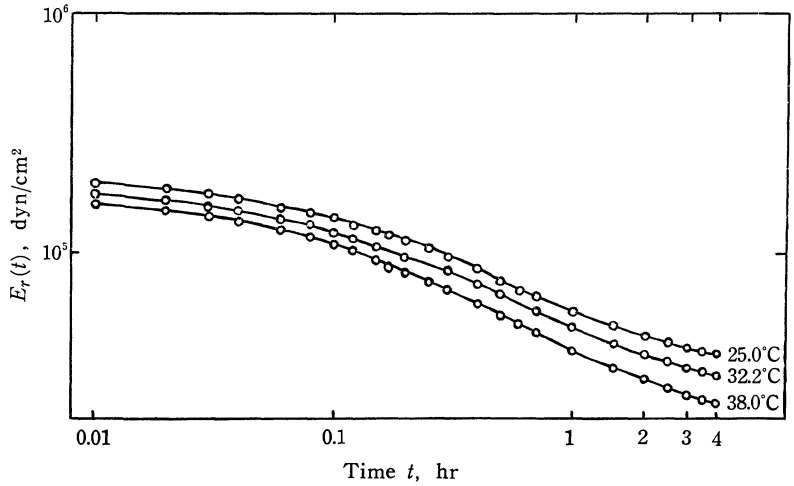

Fig. 1(c). Relaxation curves for agarose gels. 1.4_3 wt%

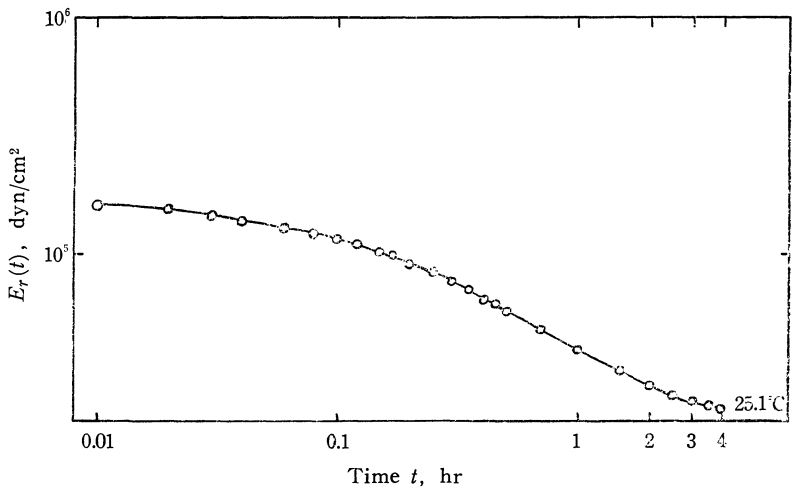

Fig. 1(d). Relaxation curves for agarose gels. 1.2_5 wt%

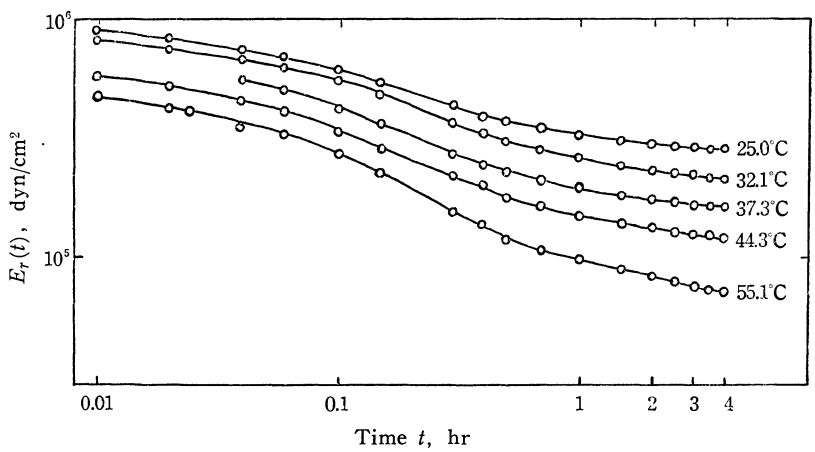

Fig. 1(e). Relaxation curves for agar-agar gels. 2.0_5 wt%

TABLE 1. CONSTANTS OF MECHANICAL MODEL

Temp. °C	E_1	E_2	E_3	E_0 (10^5 dyn/cm^2)	τ_1 hr	τ_2 min	τ_3 min
(a) Agarose gel, 2.0 wt%							
25.0	2.1	2.0	3.8	7.9	27.2	24	3.7
32.1	1.7_5	1.9	3.5_5	7.2	27.2	19_5	3.9
37.6	1.4_5	1.6	3.5_5	6.6	22.6	19	3.9
44.3	0.7_5	0.8_7	3.0	4.6	20.5	19	3.7
54.1	0.4	0.8	2.7	3.9	12.1	22	4.4
(b) Agarose gel, 1.6_7 wt%							
25.1	0.8	1.5_5	4.8	7.1_5	16.5	17_5	3.8
32.2	0.7	1.2	5.0	6.9	15.3	19_5	3.7_5
37.5	0.5	1.3_5	5.1_5	6.8_5	13.4	19	3.8
44.9	0.3_5	0.8_7	2.9	4.1	10.6	23_5	3.7_5
(c) Agarose gel, 1.4_3 wt%							
25.0	0.5	1.0	0.6_7	2.2	13.7	23	2.8
32.2	0.4_2	0.8_7	0.7_1	2.0	12.3	26	3.3
38.0	0.3_3	0.7_6	0.8	1.9	8.4	25	3.9
(d) Agarose gel, 1.25 wt%							
25.1	0.3_2	0.9_2	0.4_7	1.7	10.5	25	4.1
(e) Agar-agar gel, 2.0 wt%							
25.0	3.2	2.9	3.3	9.4	28.6	18	4.4
32.1	2.5	2.9	3.6	9.0	21.3	19	4.2
37.3	1.9	1.9	3.4	7.2	20.1	18_5	4.7
44.3	1.4	1.8_7	3.2_5	6.5	18.1	21	3.8
55.1	0.9_2	1.8	3.1	5.8	12.8	18	3.3

Constant, E_1. The values of E_1 at 25°C, thus obtained for agarose gels, are plotted against the concentrations in Fig. 2.

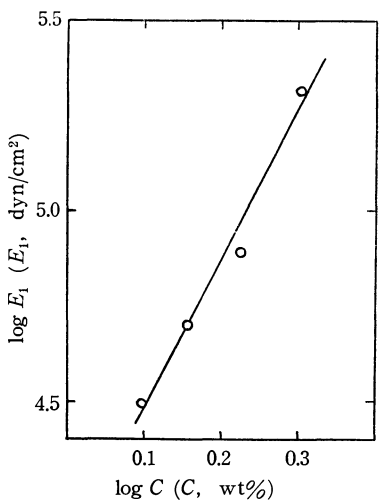

Fig. 2. Concentration dependence of the elastic constant, E_1, for agarose gels at 25°C.

The concentration dependence of E_1, which is the elastic constant of the Maxwell element with the longest relaxation time, τ_1, is approximately represented by an equation

$$E_1 = k_1 C^4 \qquad (2)$$

where k_1 is a constant and C the concentration. According to N. Hirai, who made similar studies on various kinds of gels,[10] the elastic modulus of gels, E_0, which corresponds to $\sum_{i=1}^{3} E_i$ in our case, was found to be proportional to about 4th power of concentration below a certain critical concentration, C_0, and to be proportional to about 2nd power above C_0. The critical concentration C_0 was found to be 0.85% for the hydrogels of agar-agar.[10] Our results are proportional to the 4 th power of concentration as is shown by Eq. (2), and therefore the critical concentration C_0 of agarose gels should be higher than that of agar-agar gels.

Relaxation Times and Activation Energy. The values of $\log \tau_1$ have been found

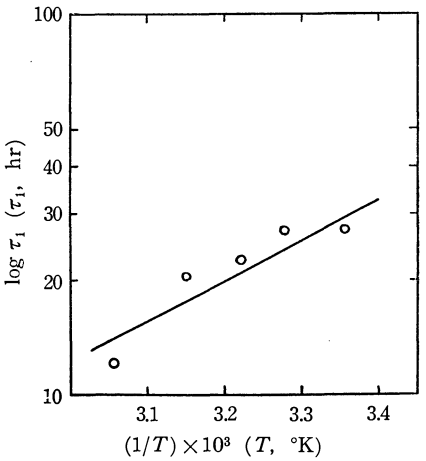

Fig. 3 (a). Temperature dependence of the relaxation time, τ_1, for the 2.0 wt% agarose gels.

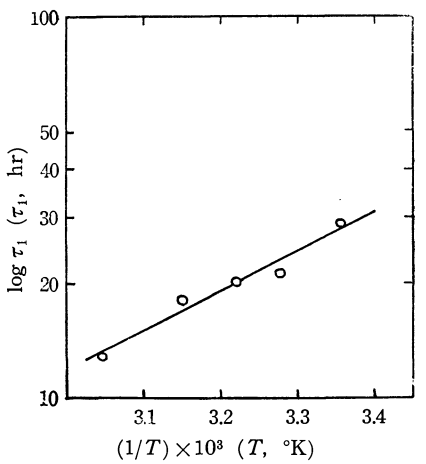

Fig. 3 (b). Temperature dependence of the relaxation time, τ_1, for the 2.0 wt% agar-agar gels.

10) N. Hirai, *Nippon Kagaku Zasshi* (*J. Chem. Soc. Japan, Pure Chem. Sect.*), **72**, 837 (1951).

TABLE 2. ACTIVATION ENERGY ΔH

Agarose gel	Concn. wt%	ΔH kcal/mol
	2.0	5.1
	1.6_7	4.5
	1.4_3	4.8
Agar-agar gel	2.0	5.0

to change approximately linearly with $1/T$. The $\log \tau_1$ is plotted against $1/T$ for the 2.0 wt% agarose gel and 2.0 wt% agar-agar gel in Fig. 3 (a) and (b) as illustrative examples. The apparent activation energy ΔH obtained from the plots is given in Table 2. The activation energy is about 5 kcal/mol for hydrogels of agarose, which is nearly equal to that of agar-agar gels reported in the preceding paper.[2]

Discussion

According to Araki and his coworkers[7] agar-agar is a mixture of agarose and agaropectin. Agarose, which is a major component of agar-agar, is composed of residues of β-D-galactopyranose and 3,6-anhydro-α-L-galactopyranose arrayed alternatively. The molecular constitution of agaropectin is not clear. The most of uronic acid and sulfuric acid ester in agar-agar are known to be contained in agaropectin as its components. The possible chemical structure of agarose proposed by Araki is shown in Fig. 4.

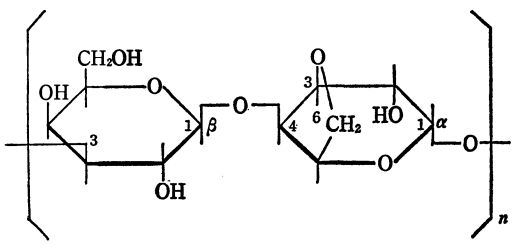

D-Galactose 3,6-Anhydro-L-Galactose

Fig. 4. Possible structure of agarose.[7]

The stress relaxation curves of 2 wt% agarose shown in Fig. 1 (a) are quite similar to those of agar-agar gels of the same concentration given in Fig. 1 (e). The similarity is also seen in the calculated values of relaxation times given in Table 1, where the relaxation times of agarose are nearly equal to that of agar-agar gels. The magnitude of ΔH of the main network structure in gels is about 5 kcal/mol for both gels. As is seen in Table 1, the magnitude of instantaneous elastic modulus, $E_0 = \sum_{i=1}^{3} E_i$ for agarose gels is about 80% of E_0 for the agar-agar gels of the same concentration. These facts show that agarose plays a major role in the gel formation of agar-agar gels.

In conclusion, the mechanical behavior of hydrogels of agarose is quite similar in its character to that of hydrogels of agar-agar, and agarose is a component of agar-agar gels which plays a major role in the gel formation.

As has been shown by Araki *et al.*, agarose contains only a small amount of ionic groups,[11] and in the gelation mechanism of aqueous solutions of agarose the electrostatic interaction is of little importance. The magnitude of ΔH for agarose gels obtained in this experiment is about 5 kcal/mol, which is of the order of magnitude of that for the breaking of hydrogen bond. From these facts as well as from the possible chemical structure of agarose shown in Fig. 4 it may be concluded that the hydrogen bonding plays a major role in the gelation mechanism of agarose gels, and also concluded that it is the case in agar-agar gels since agarose plays a major role in the gel formation of agar-agar gels.

The authors wish to express their heartiful thanks to Miss Yuko Endo for her cooperation in performing this study.

11) C. Araki, *ibid.*, **58**, 1338 (1937).

BULLETIN OF THE CHEMICAL SCCIETY OF JAPAN VOL. 41 1835—1844 (1968)

Infrared Studies of Transition-Metal Nitrosyl (^{14}NO and ^{15}NO) Complexes—Nitrosylruthenium(III),*1 Nitrosylchromium(II)*1 and Nitrosylcobalt(II)*1 Complexes

Eiichi MIKI

Department of Chemistry, College of Science, St. Paul's (Rikkyo) University, Nishi-Ikebukuro, Tokyo

(Received December 21, 1967)

For $K_2[RuX_5(NO)]$ (X=Cl and Br), $K_3[Cr(CN)_5(NO)]\cdot H_2O$, $[Cr(NH_3)_5(NO)]X_2$ (X=Cl and ClO_4) and black-$[Co(NH_3)_5(NO)]Cl_2$, it was attempted to determine the coordinating atom of the nitrosyl group to the metal atom and to assign the skeletal vibrations between the metal and the nitrosyl group by measuring the effect of the nitrogen isotope ^{15}N on infrared spectra. The isotopic shifts for the ^{15}NO-complex to the ^{14}NO-complex were calculated for two kinds of a linear three-body model, M-N-O and M-O-N (M=metal atom), and the calculated shifts were compared with the observed ones. For nitrosylruthenium and nitrosylchromium complexes, the M-N-O arrangement was found, and of the two absorption bands in the region 530—620 cm^{-1}, the higher wave number was assigned to the M-N stretching vibration and the lower one to the M-N-O bending vibration. For black-$[Co(NH_3)_5(NO)]Cl_2$, the Co-O-N arrangement was found.

It has been conventionally described that the nitrosyl group of the transition-metal nitrosyl compounds is bound to the metal atom through the nitrogen atom. There have been some studies on whether the nitrosyl group is coordinated to the metal atom through the nitrogen atom or through the oxygen atom. A neutron diffraction study of $Na_2[Ru(OH)(NO_2)_4(NO)]\cdot 2H_2O$[1] clearly showed that the nitrogen atom of the nitrosyl group is coordinated to the ruthenium atom, and that the Ru-N-O group is linear; infrared studies of black-$[Co(NH_3)_5(NO)]Cl_2$,[2] including an examination of its chemical properties, suggested the Co-N-O arrangement. On the other hand, visible-ultraviolet spectroscopic studies of the red-pentamminenitrosylcobalt(II) complex[3] have led to the Co-O-N arrangement. Moreover, an infrared study of $Co(NO)(CO)_3$ and its ^{15}NO-complex[4] determined the coordinating atom of the NO group to the cobalt atom, and led to the assignment of the absorption bands due to the Co-N stretching vibration and the Co-N-O bending vibration. The infrared study of $Na_2[Fe(CN)_5(NO)]\cdot 2H_2O$[5] in polarized light has enabled the assignment of the absorption bands due to the Fe-N stretching vibration and the Fe-N-O bending vibration.

This paper presents the determination of the coordinating atom of the NO group to the metal atom, and assignments of the skeletal vibrations between the metal and the NO group by measuring the effect of the nitrogen isotope ^{15}N on the infrared spectra for $K_2[RuX_5(NO)]$ (X=Cl and Br),[6] $K_3[Cr(CN)_5(NO)]\cdot H_2O$, $[Cr(NH_3)_5(NO)]X_2$ (X=Cl and ClO_4) and black-$[Co(NH_3)_5(NO)]Cl_2$.

Experimental

Preparations of Transition-metal Nitrosyl Compounds. ^{15}N enriched potassium nitrate, containing ^{15}N more than 92 atom %, used to prepare the ^{15}NO-complexes was obtained from the Institute of Physical and Chemical Research in Japan. The ^{15}NO-complexes were prepared on a semimicro scale. These preparations on a semimicro scale were thought to give the correct products because the prepared ^{14}NO-complex gave the same infrared spectrum as that prepared on an ordinary scale.

*1 The oxidation number is given according to Rule 7323 of IUPAC Nomenclature of Inorganic Chemistry, because the oxidation state of the metal bound to the nitrosyl group can not be determined from the sole criterion unequivocally.

1) S. H. Simonsen and M. H. Mueller, *J. Inorg. & Nucl. Chem.*, **27**, 309 (1965).
2) W. P. Griffith, J. Lewis and G. Wilkinson, *ibid.*, **7**, 38 (1958).
3) S. Yamada, H. Nishikawa and R. Tsuchida, *This Bulletin*, **33**, 930 (1960).
4) R. S. McDowell, W. D. Horrocks and J. Yates, *J. Chem. Phys.*, **34**, 530 (1961).
5) A. Sabatini, *Inorg. Chem.*, **6**, 4756 (1967).
6) E. Miki, T. Ishimori, H. Yamatera and H. Okuno, *Nippon Kagaku Zasshi (J. Chem. Soc. Japan, Pure Chem. Sect.)*, **87**, 703 (1966).

The infrared spectra of the ^{15}NO-complexes prepared showed that the NO group in the complexes retained almost the same ^{15}N-atom percentages as those of the starting ^{15}N-materials.

$K_2[RuX_5(NO)]$ (X=Cl and Br). Compounds with normal nitrogen isotopes were prepared by conventional methods.[7] The ^{15}N-labeled compound was prepared on a semimicro scale using a vacuum line. Nitrosylruthenium(III) solution could be prepared with a good yield by bringing an excess of ^{15}NO gas derived from 50—200 mg $K^{15}NO_3$ (^{15}N atom %= 92 and 96.9) in contact with ruthenium halide (10—30 mg ruthenium) in hydrohalogenic acid solution, and then closing off the reaction vessel and allowing it to stand for 1—2 days at room temperature. A small excess of potassium halide was added to the nitrosylruthenium(III) solution and the solution evaporated to obtain the ^{15}NO-complex. The separation of ruthenium (III and IV) and nitrosylruthenium (III)*2 showed that ruthenium ion was converted to nitrosylruthenium ion almost completely (more then 99.9%) in this semimicro scale preparation.

Found: K, 20.1; Ru, 25.7; N, 3.66%. Calcd for $K_2[RuCl_5(NO)]$: K, 20.23; Ru, 26.15; N, 3.62%. Found: K, 12.7; Ru, 16.3; N, 2.38%. Calcd for $K_2[RuBr_5(NO)]$: K, 12.85; Ru, 16.60; N, 2.30%.

$K_3[Cr(CN)_5(NO)]\cdot H_2O$ and $[Cr(NH_3)_5(NO)]X_2$ (X=Cl and ClO_4). The pentacyano- and pentammine-nitrosylchromium(II) compounds with normal nitrogen isotopes were prepared by the methods of Griffith[8] and Mori,[9] respectively. The ^{15}NO-complexes were prepared on a scale 1/10—1/20 that of ordinary methods. $K_3[Cr(CN)_5(^{15}NO)]\cdot H_2O$ was obtained with ^{15}N-substituted hydroxylamine hydrochloride prepared according to the method of Ogata and Hirono,[10] who used sodium nitrite instead of potassium nitrate. $[Cr(NH_3)_5(^{15}NO)]X_2$ was prepared by Mori's method[9] using nitrogen-15 enriched potassium nitrate (^{15}N atom %=97.6) instead of sodium nitrite.

Found: K, 33.1; Cr, 15.0; C, 17.46; N, 24.74%. Calcd for $K_3[Cr(CN)_5(NO)]\cdot H_2O$: K, 33.77; Cr, 14.97; C, 17.29; N, 24.19%. Found: Cr, 21.5; N, 34.22; H, 6.00; Cl, 29.6%. Calcd for $[Cr(NH_3)_5(NO)]Cl_2$: Cr, 21.84; N, 35.30; H, 6.36; Cl, 29.78%. Found: Cr, 14.2; N, 22.76; H, 3.95%. Calcd for $[Cr(NH_3)_5(NO)](ClO_4)_2$: Cr, 14.20; N, 22.96; H, 4.13%.

Black-$[Co(NH_3)_5(NO)]Cl_2$. The black chloride with normal nitrogen isotopes was made according to the method of Moeller and King[11] and of Odell *et al.*,[12] but external cooling was not necessary in the reaction of Co(II)-ammoniacal solution with NO gas. The ^{15}NO-complex was prepared on a semimicro scale using ^{15}NO gas derived from about 1 g $K^{15}NO_3$ (^{15}N atom %=99.3 and 99.8). By cooling with liquid nitrogen, a slight excess of ^{15}NO gas was trapped in a reaction vessel containing an aqueous ammoniacal solution of cobalt(II) chloride freshly prepared, the concentration of ammonia in the solution of cobalt(II) chloride being about 10 mol/*l*. The reaction vessel was shaken in running water for about 20 min until the frozen solution was molten and the black chloride was formed as gray powder. The black chloride prepared by this procedure gave the same infrared spectra as those reported by several workers.[13,14] In the preparation of deuterated black chloride, deuterated aqueous ammonia obtained from magnesium nitride and deuterium oxide was used.

Found: Co, 24.1; N, 33.55; H, 6.01; Cl, 28.9%. Calcd for $[Co(NH_3)_5(NO)]Cl_2$: Co, 24.05; N, 34.30; H, 6.17; Cl, 28.94%.

Infrared Spectra. Infrared spectra were measured over 200—4000 cm^{-1} in Nujol mull, hexachlorobutadiene mull and a potassium bromide disk. The spectra were recorded on JASCO DS-301 (700—4000 cm^{-1}), DS-402 G (400—4000 cm^{-1}), DS-401 G (300—700 cm^{1-}) and Hitachi EPI-L type (200—700 cm^{-1}) infrared spectrophotometers. Reproducibility was about ± 1 cm^{-1} in the region 200—3000 cm^{-1}, and ± 10 cm^{-1} in the region 3000—4000 cm^{-1}.

Results

Assignments of Infrared Spectra. The assignments of the N-O stretching and the skeletal vibrations between the metal and the NO group were based first on the observation of isotopic shifts. As for the skeletal vibrations, a set of two absorption peaks in the range 530—620 cm^{-1} was selected and the assignment of each absorption was then determined so as to obtain agreement between the calculated isotopic shifts and the observed ones.

The assignments of vibrations other than those mentioned above were in accordance with the following references:

Ref. 15 for the stretching vibrations of Ru-X (X=Cl and Br),

Ref. 16 for the skeletal vibrations between the metal and the CN group,

7) "Gmelins Handbuch," Ruthenium (1938), pp. 93, 99; J. M. Fletcher, I. L. Jenkins, F. M. Lever, F. S. Martin, A. R. Powell and R. Todd, *J. Inorg. & Nucl. Chem.*, **1**, 378 (1955).

*2 unpublished work.

8) W. P. Griffith, J. Lewis and G. Wilkinson, *J. Chem. Soc.*, **1959**, 872.

9) M. Mori, S. Ueshiba and S. Kawaguchi, This Bulletin, **36**, 796 (1963).

10) A. Ogata and S. Hirono, *Yakugaku Zasshi* (*J. Pharm. Soc. Japan*), **50**, 555 (1930).

11) T. Moeller and G. King, *Inorg. Syn.*, **4**, 168 (1953).

12) A. L. Odell, R. W. Olliff and A. A. Taggart, *J. Chem. Soc.*, **1965**, 6024.

13) E. P. Bertin, S. Mizushima, T. J. Lane and J. V. Quagliano, *J. Am. Chem. Soc.*, **81**, 3821 (1959).

14) J. B. Raynor, *J. Chem. Soc. Inorg. Phys. Theoret.*, **1966**, 997.

15) J. Hiraishi, I. Nakagawa and T. Shimanouchi, *Spectrochim. Acta*, **20**, 819 (1964).

16) I. Nakagawa and T. Shimanouchi, *ibid.*, **18**, 101 (1962).

TABLE 1. FREQUENCY (cm^{-1}) AND ASSIGNMENT OF INFRARED ABSORPTION BANDS IN $K_2[RuX_5(NO)]$ (X=Cl and Br)

$K_2[RuCl_5(NO)]$		$K_2[RuBr_5(NO)]$		Assignment
^{14}NO-complex	^{15}NO-complex	^{14}NO-complex	^{15}NO-complex	
1915 vs.	1874 vs.	1888 vs.	1850 vs.	NO str. (A_1)
1904 vs.	1865 vs.	1880 vs.	1843 vs.	
606 w.	600 w.	606 w.	605 w.	RuN str. (A_1)
588 s.	588 w.	573 s.	572 w.	RuNO bend. (E)
	572 s.		557 s.	
336 vs.		257 vs.		RuX str. (E)
327 vs.				
286 vs.		221 vs.		RuX str. (A_1)

Abbreviations: str.=stretching; bend.=bending; vs.=very strong; s.=strong; m.=medium; w.=weak; vw.=very weak; sh.=shoulder; b.=broad; deg.=degenerate; def.=deformation; sym.=symmetric; rock.=rocking.

Ref. 17 for the characteristic absorption bands on ammine complexes and
Ref. 18 for perchlorate ion.

The infrared bands and their assignments for $K_2[RuX_5(NO)]$ (X=Cl and Br) are shown in Table 1. The two very strong absorption peaks in the region 1840—1920 cm^{-1} correspond to the N-O stretching vibration reported by Lewis *et al.*[19] The two absorption bands in the region 550—610 cm^{-1} are thought to be skeletal vibrations between the ruthenium atom and the NO group as reported by Gans[20] and Cleare.[21] The weak absorption bands at 588 cm^{-1} for $K_2[RuCl_5(^{15}NO)]$ and at 572 cm^{-1} for $K_2[RuBr_5(^{15}NO)]$ are thought to be due to the presence of a small amount of the corresponding ^{14}NO-complex.

The assignment of the infrared spectra of $K_2[RuBr_5(NO)]$ can be carried out in a similar manner.

The absorption band of the N-O stretching vibration split into two peaks for $K_2[RuX_5(NO)]$, and the wave number of the stronger peak was used to calculate the isotopic shifts.

The infrared bands and their assignments for $K_3[Cr(CN)_5(NO)]\cdot H_2O$ are given in Table 2. The strong band of the ^{14}NO-complex at 1643 cm^{-1} was assigned to the N-O stretching vibration[8]; this band shifted to 1610 cm^{-1} for the ^{15}NO-complex. The absorption bands at 620 cm^{-1} and 610 cm^{-1} (shoulder) seem to correspond to skeletal vibrations between the chromium and the NO group[20]; these absorption shifted and appeared separately as two peaks at 617 and 600 cm^{-1} upon ^{15}NO-substitution.

TABLE 2. FREQUENCY (cm^{-1}) AND ASSIGNMENT OF INFRARED ABSORPTION BANDS IN $K_3[Cr(CN)_5(NO)]\cdot H_2O$

^{14}NO-complex	^{15}NO-complex	Assignment
3600–3200 w.	3600–3200 w.	H_2O
2121 vs.	2121 vs.	CN str.
2092 vw.	2092 vw.	
2078 vw.	2078 vw.	
1643 vs.	1610 vs.	NO str.
1635 sh.	1590 sh.	
620 s.	617 s.	Cr-NO str.
610 sh.	600 w.	Cr-N-O bend.
428 s.	426 s.	CrC str.
417 sh.	415 sh.	
398 s.	397 s.	
360 sh.	360 sh.	CrCN bend.
345 s.	345 s.	
330 sh.	330 sh.	
304 vw.	303 vw.	?
291 w.	290 w.	?

Table 3 shows the infrared bands and their assignments for $[Cr(NH_3)_5(NO)]X_2$ (X=Cl and ClO_4). For the chloride, the absorptions due to the N-O stretching and the skeletal vibrations were assigned according to Cleare and Griffith.[21] For the perchlorate, similar assignments could be made. The strong band at 626 cm^{-1} due to perchlorate ion[18] did not disturb the weak absorptions (577 cm^{-1} for ^{14}NO-complex and 574 cm^{-1} for ^{15}NO-complex) due to one of the skeletal vibrations.

Table 4 and Fig. 1 show the infrared bands and their assignments for black-$[Co(NH_3)_5(NO)]Cl_2$. Absorptions caused by impurities were found as reported by Bertin[13] and Raynor.[14] These impurities are discussed later. Griffith *et al.*[2] assigned the absorption

17) L. Sacconi, A. Sabatini and P. Gans, *Inorg. Chem.*, **3**, 1772 (1964); T. Shimanouchi and I. Nakagawa, *ibid.*, **3**, 1805 (1964).
18) H. Cohn, *J. Chem. Soc.*, **1952**, 4282.
19) J. Lewis, R. J. Irving and G. Wilkinson, *J. Inorg. & Nucl. Chem.*, **7**, 32 (1958).
20) P. Gans, A. Sabatini and L. Sacconi, *Inorg. Chem.*, **5**, 1877 (1966).
21) M. J. Cleare and W. P. Griffith, *J. Chem. Soc. Inorg. Phys. Theoret.*, **1967**, 1144.

TABLE 3. FREQUENCY (cm^{-1}) AND ASSIGNMENT OF INFRARED ABSORPTION BANDS IN $[Cr(NH_3)_5(NO)]X_2$ (X=Cl and ClO_4)

$[Cr(NH_3)_5(NO)]Cl_2$

^{14}NO-complex	^{15}NO-complex	Assignment
3290 vs.	3290 vs.	NH str.
3230 sh.	3230 sh.	
3170 sh.	3170 sh.	
1685 s.	1649 s.	NO str.
1612 m. b.	1615 m. b.	NH_3 deg. def.
1298 m. b.	1300 sh.	NH_3 sym. def.
1281 s.	1281 s.	
1244 w.	1244 w.	
791 sh.	786 sh.	NH_3 rock.
776 m. b.	774 m. b.	
734 m.	736 sh.	
573 s.	570 s.	Cr–NO str.
535 m.	526 m.	CrNO bend.
464 w.	464 w.	Cr–NH_3 str.
455 sh.	455 sh.	
440 vs.	438 vs.	
359 w.	359 w.	?
306 s.	306 s.	H_3N–Cr–NH_3 bend.
264 vs. b.	264 vs. b.	

$[Cr(NH_3)_5(NO)](ClO_4)_2$

^{14}NO-complex	^{15}NO-complex	Assignment
3360 vs.	3330 vs.	NH str.
3270 s.	3270 s.	
3200 sh.	3190 sh.	
1727 s.	1723 vw.	^{14}NO str.
	1692 s.	^{15}NO str.
1616 m. b.	1622 m. b.	NH_3 deg. def.
1299 s.	1300 s.	NH_3 sym. def.
1092 vs.	1092 vs.	ClO_4 str.
764 sh.	758 sh.	NH_3 rock.
732 m.	733 m.	
700 sh.		
626 vs.	626 vs.	ClO_4 bend.
577 vw.	574 vw.	Cr–NO str.
531 s.	521 s.	Cr–N–O bend.
462 m.	462 m.	Cr–NH_3 str.
421 s.	418 s.	
347 w.	350 w.	?
315 sh.	315 sh.	H_3N–Cr–NH_3 bend.
264 vs.	263 vs.	
255 vs.	256 vs.	
230 sh.	230 sh.	

at 1172 cm^{-1} to the N–O stretching vibration. However, the absorption bands at 1172 cm^{-1} for the ^{14}NO-complex and 1173 cm^{-1} for the ^{15}NO-complex were shifted by deuterium substitution to 899 cm^{-1} and 901 cm^{-1}, respectively, as shown in Table 5. On the other hand, Bertin[13] and Raynor[14] assigned the absorption band at *ca.* 1600 cm^{-1} to the N–O stretching vibration. Isotopic shift of the absorption at 1614 to 1589 cm^{-1} was observed upon ^{15}NO-substitution, as reported by Mercer *et al.*[22] The absorptions in the region 1630

22) E. E. Mercer, W. A. McAllister and J. R. Durig, *Inorg. Chem.*, **6**, 1816 (1967).

TABLE 4. FREQUENCY (cm^{-1}) AND ASSIGNMENT OF INFRARED ABSORPTION BANDS IN BLACK-$[Co(NH_3)_5(NO)]Cl_2$

^{14}NO-complex	^{15}NO-complex	Assignment
3260 vs.	3270 vs.	NH str.
3170 vs.	3170 vs.	
1614 vs.	1589 vs.	NO str.+NH_3 deg. def.
1425 vw.	1453 vw.	?
1362 vw.	1397 vw.	?
1293 vs.	1292 vs.	NH_3 sym. def.
	1257 w.	?
1172 vs.	1173 m.	NH_3 sym. def. of Co(II)-ammine complex
	1025 w.	?
	854 sh.	NH_3 rock.
818 vs.	820 s.	
638 vs.	640 vs.	NH_3 rock. of Co(II)-ammine complex
581 vs.	579 vs.	Co–ON bend. ?
564 vs.	558 vs.	Co–ON str. ?
	494 w.	?
470 w.	467 w.	Co–NH_3 str.
444 s.	445 s.	
403 w.	405 w.	?
	340 sh.	H_3N–Co–NH_3 bend.
295 s.	295 s.	
250 sh.	250 sh.	

TABLE 5. FREQUENCY (cm^{-1}) AND ASSIGNMENT OF INFRARED ABSORPTION BANDS IN BLACK-$[Co(ND_3)_5(NO)]Cl_2$

^{14}NO-complex	^{15}NO-complex	Assignment
2450 vs.	2460 vs.	ND str.
2360 s.		
2310 vs.	2310 vs.	
1613 vs.	1589 vs.	NO str.
1495 w.		
1427 w.	1451 m.	?
1344 w.	1393 vw.	
1302 w.		
1260 vw.	1278 w.	
1166 w. b.	1167 w. b.	ND_3 deg. def.
1068 w.	1070 w.	?
	1015 sh.	?
991 s.	996 m.	ND_3 sym. def.
899 m.	901 m.	ND_3 sym. def. of Co(II)-ammine complex
829 w.	820 w.	?
	785 w.	?
	669 m.	?
637 v.	637 v.	ND_3 rock.
572 m.	561 m.	Co–ON str. ?
	490 sh.	?
454 vs.	455 vs.	ND_3 rock. of Co(II)-ammine complex

—1700 cm^{-1} for the other nitrosylcobalt complexes have been assigned to the N–O stretch-

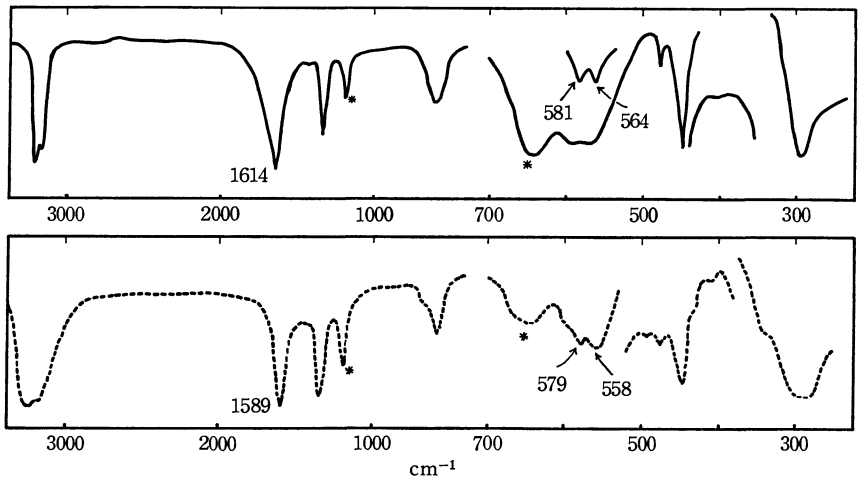

Fig. 1. Infrared spectra of black-$[Co(NH_3)_5(NO)]Cl_2$.
—— : ^{14}NO-complex.
- - - : ^{15}NO-complex (^{15}N atom %=99.3 and 99.8).
* : Co(II)-ammine impurities in black chloride.

ing vibrations.[23,24] Hence, the absorption of the ^{14}NO-complex at 1614 cm^{-1} was assigned to the N-O stretching vibration. The frequencies of the nitrosyl stretching vibration for the deuterated ^{14}NO- and ^{15}NO-complexes were also measured to eliminate interfering absorptions due to the NH_3 degenerate deformation in the 1600 cm^{-1} region. This degenerate deformation was found to have no effect on the observed frequency value for the N-O stretching vibration as shown in Table 5.

Mercer *et al.*[22] assigned the absorptions at 578 and 644 cm^{-1} to the Co-N-O bending and Co-N stretching vibrations, respectively. In the present measurement, no definite absorption peak was observed at 644 cm^{-1}, instead the peak at 578 cm^{-1} was quite definitely split into two peaks at 581 and 564 cm^{-1}, which were shifted to 579 and 558 cm^{-1}, respectively, for the ^{15}NO-complex (Table 4 and Fig. 1).

On the other hand, for the deuterated complexes only one absorption was found in the region 560—580 cm^{-1}; the absorption at 572 cm^{-1} for the ^{14}NO-complex shifted to 561 cm^{-1} for the ^{15}NO-complex as shown in Table 5 and Fig. 2.

To assign the observed peaks and calculate the isotopic shifts, the following cases are considered: Case-1. For the NH_3-complex, the two peaks in the region 560—580 cm^{-1} are due to skeletal vibrations, while for the ND_3-complex these two peaks happen to overlap. Case-2. One of the two peaks observed with

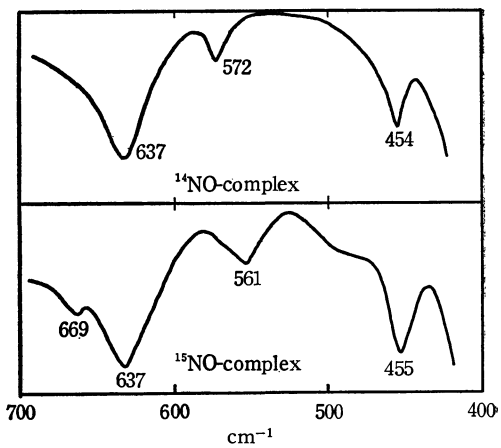

Fig. 2. Infrared spectra of black-$[Co(ND_3)_5(NO)]Cl_2$ in the region 400—700 cm^{-1}.

the NH_3-complex is due to an impurity. The absorption intensity of an other skeletal vibration is very weak, and this absorption is assumed to be in the 570 cm^{-1} region because two skeletal vibrations between the metal and the NO group are within the limited region observed for the nitrosyl complexes examined.

Impurities in Black-$[Co(NH_3)_5(NO)]Cl_2$. Bertin[13] and Raynor[14] reported that the absorption band at *ca.* 1170 cm^{-1} for the black chloride is due to the NH_3 symmetric deformation of hexamminecobalt(II) impurity in the black chloride. However, a recent magnetic study by Asumussen *et al.*[25] has shown that carefully prepared black chloride gives $\chi_g = +0.17 \times 10^{-6}$ cgs units at room tempera-

23) R. D. Feltham and R. S. Nyholm, *ibid.*, **4**, 1334 (1965).
24) T. B. Jackson, M. J. Baker, J. O. Edwards and D. Tutus, *ibid.*, **5**, 2046 (1966).
25) R. W. Asumussen, Ole Bostrup and J. P. Jensen, *Acta Chim. Scand.*, **12**, 24 (1958).

ture; that is, the black chloride is essentially diamagnetic. Examples of magnetic susceptibilities of black chlorides used in this study are $\chi_g = 1.25$ (288°K), 1.58 (237°K), 2.16 (173 °K) and 3.05×10^{-6} (115°K) cgs units. These show the temperature dependence, and also that the chloride is paramagnetic. So the black chloride may be contaminated by strong paramagnetic compounds (Co(II)-ammine complexes such as $[Co(NH_3)_6]Cl_2$). Magnetic data reveal the presence of as much as 25% $[Co(NH_3)_6]Cl_2$ in the black salt, assuming that the black chloride is essentially diamagnetic and the impurity is only $[Co(NH_3)_6]Cl_2$.

An infrared study has shown that the black salt contains cobalt atoms in the +3 oxidation state.[13] The wave numbers of the NH_3 rocking vibration in ammine complexes are characteristic of the oxidation state of the central atom.[26] Moreover, the wave numbers of the NH_3 symmetric deformation for cobalt-ammine complexes seem to be characteristic of the oxidation state of the cobalt atom. Infrared absorptions of $[Co(NH_3)_6]Cl_3$ and $[Co(NH_3)_6]Cl_2$ are listed in Table 6 as representative of cobalt(III)-ammine and cobalt(II)-ammine complexes, respectively. If most of the impurities are hexamminecobalt(II) or cobalt(II)-ammine complexes, assignment of infrared spectra for the black chloride can be reasonably made by comparing the infrared spectra for the black chloride (Tables 4 and 5) with those for hexamminecobalt(III) and hexamminecobalt(II) chlorides (Table 6). The absorption bands at 1166 and 1167 cm^{-1} for the deuterated ^{14}NO-complex and ^{15}NO-complex in Table 5 were assigned to the ND_3 degenerate deformation due to the deuterated black chloride and cobalt(II)-ammine complex impurities. The absorption bands at 1293 cm^{-1} for the ^{14}NO-complex and at 1292 cm^{-1} for the ^{15}NO-complex were shifted by deuterium substitution to 991 and 996 cm^{-1}, respectively, which were assigned to the NH_3 symmetric deformation of the black chloride; the absorptions at 1172 cm^{-1} for the ^{14}NO-complex and at 1173 cm^{-1} for the ^{15}NO-complex were shifted by deuterium substitution to 899 and 901 cm^{-1}, respectively. These bands were assigned to the NH_3 symmetric deformation of the cobalt(II)-ammine complex impurities in the black chloride. The absorption bands at *ca.* 820 cm^{-1} for the ^{14}NO- and ^{15}NO-complexes were shifted by deuterium substitution to 637 cm^{-1}. These bands are due to the NH_3 rocking vibration for the black chloride. The absorptions at *ca.* 640 cm^{-1} for the ^{14}NO- and ^{15}NO-complexes were shifted by deuterium substitution to *ca.* 455 cm^{-1}. These bands are due to the NH_3 rocking vibration of cobalt (II)-ammine complex in the black chloride. These magnetic and infrared data lead to the conclusion that the black chloride used in this study may be contaminated by cobalt(II)-ammine complexes.

TABLE 6. INFRARED SPECTRA OF HEXAMMINECOBALT(II) AND HEXAMMINECOBALT(III) CHLORIDE

Compound	$\delta(NH_3)_d$	$\delta(NH_3)_s$	$\delta(NH_3)_r$
$[Co(NH_3)_6]Cl_3$	1613	1330	830
$[Co(ND_3)_6]Cl_3$*	1155	1016	665
$[Co(NH_3)_6]Cl_2$	1598	1160	634
$[Co(ND_3)_6]Cl_2$ (calc.)	1170	884	464

$\delta(NH_3)_d$: NH_3 degenerate deformation.
$\delta(NH_3)_s$: NH_3 symmetric deformation.
$\delta(NH_3)_r$: NH_3 rocking vibration.
* From Ref. 17.

Calculation of Isotopic Shifts. Crystal X-ray studies of $K_2[RuCl_5(NO)]$,[27] $K_3[Cr(CN)_5(NO)]$,[28] black-$[Co(NH_3)_5(NO)]Cl_2$ [29] and electron spin resonance studies of $[Cr(NH_3)_5(NO)]^{2+}$ and $[Cr(CN)_5(NO)]^{3-}$ [30] have shown an approximately linear arrangement of the metal and the NO group, although crystallographic X-ray studies are not now thought to be able to distinguish nitrogen from oxygen. Hence, the two linear three-body models, M-N-O and M-O-N were used to calculate the isotopic shifts for all of the nitrosyl complexes examined here. For the skeletal vibrations between the metal and the NO group, two assignments are possible. Assignment 1 is that, of the two absorptions assumed due to skeletal vibrations, the higher wave number is assigned to the stretching vibration between the metal and the NO group, and the lower one to the bending vibration. Assignment 2 is the reverse of Assignment 1. Then, by the Valence Force Field method, the calculation of the isotopic shifts for absorptions due to the N-O stretching, the metal-nitrosyl stretching and the metal-nitrosyl bending vibrations was carried out for the four cases corresponding to the two models (M-N-O and M-O-N) and the two possible assignments (Assignment 1 and

26) S. Mizushima, I. Nakagawa and J. V. Quagliano, *J. Chem. Phys.*, **23**, 1367 (1955).
27) T. S. Khodashova and G. B. Bokii, *Zh. Struk. Khim.*, **5**, 144 (1964).
28) N. Vannerbeg, *Acta Chem. Scand.*, **20**, 1571 (1966).
29) D. Hall and A. A. Taggart, *J. Chem. Soc.*, **1965**, 1359; D. Dale and D. C. Hodgkin, *ibid.*, **1965**, 1364.
30) I. Bernel, *Chem. Commun.*, **1965**, 571.

TABLE 7. OBSERVED AND CALCULATED ISOTOPIC SHIFTS ($\Delta\nu_{obs.}$ AND $\Delta\nu_{calc.}$ IN cm^{-1}) OF $K_2[RuX_5(NO)]$ (X=Cl and Br), $K_3[Cr(CN)_5(NO)]\cdot H_2O$, $[Cr(NH_3)_5(NO)]X_2$ (X=Cl AND ClO_4) AND BLACK-$[Co(NH_3)_5(NO)]Cl_2$

$K_2[RuCl_5(NO)]$

^{14}NO-complex wave number (cm^{-1})	$\Delta\nu_{obs.}$	$\Delta\nu_{calc.}$ Assignment 1		Assignment 2	
		model RuNO	RuON	RuNO	RuON
1904 (νNO)	39	40	28	40	29
606	6	6	9	16	4
588	16	16	4	5	9

$K_2[RuBr_5(NO)]$

^{14}NO-complex wave number (cm^{-1})	$\Delta\nu_{obs.}$	$\Delta\nu_{calc.}$ Assignment 1		Assignment 2	
		model RuNO	RuON	RuNO	RuON
1880 (νNO)	37	40	27	39	28
606	1	5	10	16	4
573	16	16	4	5	9

$K_3[Cr(CN)_5(NO)]\cdot H_2O$

^{14}NO-complex wave number (cm^{-1})	$\Delta\nu_{obs.}$	$\Delta\nu_{calc.}$ Assignment 1		Assignment 2	
		model CrNO	CrON	CrNO	CrON
1643 (νNO)	33	36	23	36	23
620	3	4	9	16	4
610	10	16	4	4	8

$[Cr(NH_3)_5(NO)]Cl_2$

^{14}NO-complex wave number (cm^{-1})	$\Delta\nu_{obs.}$	$\Delta\nu_{calc.}$ Assignment 1		Assignment 2	
		model CrNO	CrON	CrNO	CrON
1685 (νNO)	36	36	25	35	26
573	3	4	8	15	4
535	9	14	4	4	7

$[Cr(NH_3)_5(NO)](ClO_4)_2$

^{14}NO-complex wave number (cm^{-1})	$\Delta\nu_{obs.}$	$\Delta\nu_{calc.}$ Assignment 1		Assignment 2	
		model CrNO	CrON	CrNO	CrON
1727 (νNO)	35	36	26	35	27
577	3	4	8	15	4
531	10	14	4	4	7

$[Co(NH_3)_5(NO)]Cl_2$

^{14}NO-complex wave number (cm^{-1})	$\Delta\nu_{obs.}$	$\Delta\nu_{calc.}$ Assignment 1		Assignment 2	
		model CoNO	CoON	CoNO	CoON
1614 (νNO)	25	35	23	35	23
581	2	4	8	15	4
564	6	15	4	4	8

Assignment 1: Of the two wave numbers in the region 530—620 cm^{-1}, the higher wave number is assigned to the stretching vibration between the metal and the NO group and the lower one to the bending virbation.

Assignment 2: The reverse of Assignment 1.

$\Delta\nu_{obs.}=\nu^{14}$NO-complex (obs.) $-\nu^{15}$NO-complex (obs.). $\Delta\nu_{calc.}=\nu^{14}$NO-complex (obs.) $-\nu^{15}$NO-complex (calc.).

(νNO): The N-O stretching vibration.

2). The secular equation for the calculation of isotopic shifts was set up in accordance with Wilson's procedure.[31] The calculated shifts were compared with the observed ones.

Table 7 shows the observed and calculated isotopic shifts for $K_2[RuX_5(NO)]$ (X=Cl and Br), $K_3[Cr(CN)_5(NO)]\cdot H_2O$, $[Cr(NH_3)_5(NO)]X_2$ (X=Cl and ClO_4) and black-$[Co(NH_3)_5(NO)]Cl_2$. For black-pentammine-nitrosylcobalt complex, the isotopic shifts for the NH_3-complex calculated by assuming Case-1 are compared with the observed isotopic shifts.

The calculated isotopic shifts in Table 7 were calculated neglecting off-diagonal interaction constants. Calculations were also performed with off-diagonal interaction constants of 0.4 mdyn/Å and 0.2 mdyn/Å for $K_2[RuCl_5(NO)]$ and $[Cr(NH_3)_5(NO)]Cl_2$, respectively. However, these latter calculated isotopic shifts differed only negligibly from those in Table 7.

The electron spin resonance study of $K_3[Cr(CN)_5(NO)]\cdot H_2O$ by McGarvey and Pealman[32] has shown that the Cr-N-O or Cr-O-N bond is bent slightly. Calculation of the isotopic shifts was made over a bond angle ranging from 170—180°. However, in this angle range, the range of shifts was very small.

Arrangement and Assignment. Comparison of observed isotopic shifts with calculated ones shows that the calculated isotopic shifts in the case of the M-N-O arrangement with Assignment 1 are in agreement with the observed ones for both the nitrosylruthenium(III) and nitrosylchromium(II) complexes. For black-$[Co(NH_3)_5(NO)]Cl_2$, the following conclusions were obtained. For the NH_3-complex is Case-1, the calculated isotopic shifts for the Co-O-N arrangement with Assignment 2 are in agreement with observed values. For the ND_3-complex in Case-1, the Co-O-N arrangement is found and only one absorption in the region 560—580 cm^{-1} is thought mainly attributable to the Co-O stretching vibration. In Case-2, the Co-O-N arrengement is also found but the distinction between skeletal vibrations cannot be made. However, the calculated isotopic shifts in all cases of possible assignments supported the Co-O-N arrangement for the black-pentam-minenitrosylcobalt complex.

Discussion

The agreement between the observed isotopic shifts and calculated ones is excellent for the nitrosylruthenium(III) complexes with the Ru-N-O arrangement and Assignment 1, but less so for the nitrosylchromium(II) complexes with the Cr-N-O arrangement and Assignment 1 and for black-$[Co(NH_3)_5(NO)]Cl_2$ with the Co-O-N arrangement. In the latter cases, however, the poorer agreement is attributable to the use of the three-body model in calculating the isotopic shifts.

The wave numbers of the normal vibrations calculated for the ^{15}NO-complexes from the observed wave numbers for the ^{14}NO-complexes by the three-body model are expected to

TABLE 8. OBSERVED AND CALCULATED ISOTOPIC SHIFTS ($\Delta\nu_{obs.}$ AND $\Delta\nu_{calc.}$ IN cm^{-1}) OF $K_2[RuCl_5(NO)]$ AND $Co(NO)(CO)_3$

$K_2[RuCl_5(NO)]$

Assignment	Observed			Calculated (1)[a]			Calculated (2)[b]		
	^{14}NO-complex	^{15}NO-complex	$\Delta\nu_{obs.}$	^{14}NO-complex	^{15}NO-complex	$\Delta\nu_{calc.}$	^{14}NO-complex	^{15}NO-complex	$\Delta\nu_{calc.}$
NO str.	1904	1865	39	1909	1869	40	1904	1864	40
RuN str.	606	600	6	607	602	5	606	600	6
RuNO bend.	588	572	16	589	574	15	588	572	16

$Co(NO)(CO)_3$

Assignment	Observed[c]			Calculated (1)[c]			Calculated (2)[b]		
	^{14}NO-complex	^{15}NO-complex	$\Delta\nu_{obs.}$	^{14}NO-complex	^{15}NO-complex	$\Delta\nu_{calc.}$	^{14}NO-complex	^{15}NO-complex	$\Delta\nu_{calc.}$
NO str.	1822	1786	36	1860	1822	38	1822	1784	38
CoN str.	594	591	3	588	585	3	594	589	5
CoNO bend.	565	555	10	600	591	9	565	550	15

a) Calculated by Dr. Jiro Hiraishi (Department of Chemistry, Faculty of Science, The University of Tokyo) using the eight-body model.
b) Calculated by the author using the three-body model.
c) Taken from Ref. 4.

31) E. S. Wilson, Jr., *J. Chem. Phys.*, **7**, 1047 (1939); **9**, 76 (1941).
32) B. R. McGarvey and J. Pearlman, *ibid.*, **46**, 4992 (1967).

be smaller than those calculated by a complete treatment because of interactions of vibrations neglected in the three-body model. Thus, the shifts calculated with the three-body model ($\nu_{obs.}$ (^{14}NO-complex) $-$ $\nu_{calc.}$ (^{15}NO-complex)) would be larger than the observed shifts.

In the case of $K_2[RuX_5(NO)]$ (X=Cl and Br), the central metal atom and ligands other than the NO group are much heavier than nitrogen and oxygen. The three-body model can be expected to be a good approximation, and good agreement is actually obtained between the calculated and observed shifts. In Table 8, the calculated isotopic shifts using the three-body model for $K_2[RuCl_5(NO)]$ are compared with those obtained using the eight-body model,*3 and good agreement is found also between these. However, for the Ru-N stretching and the Ru-N-O bending vibration the isotopic shifts obtained using the three-body model are slightly larger than those obtained with the eight-body model. Since the three-body model is a good approximation for pentachloronitrosylruthenium(III) ion, the results based on the three-body model for $K_2[RuX_5(NO)]$ lead to the conclusion that the complexes have a Ru-N-O arrangement and, of the two absorptions in the region 570 —610 cm^{-1}, the higher wave number is assigned to the Ru-N stretching vibration and the lower one to the Ru-N-O bending vibration.

On the other hand, the central metal atom and ligands other than the NO group in $K_3[Cr(CN)_5(NO)]\cdot H_2O$, $[Cr(NH_3)_5(NO)]X_2$ (X =Cl and ClO_4) and black-$[Co(NH_3)_5(NO)]Cl_2$ are lighter than ruthenium and halide ion in $K_2[RuX_5(NO)]$. So, for the chromium and the cobalt complexes examined, the difference between the calculated isotopic shifts obtained using the three-body model and the observed shifts can be expected to be greater than the difference for the ruthenium complexes.

McDowell *et al.*[4] have determined the Co-N-O arragement and assigned the skeletal vibrations between the cobalt and the NO group by comparing the calculated isotopic shifts using the nine-body model with the observed ones for $Co(NO)(CO)_3$ and its ^{15}N-substituted compound. In order to demonstrate the relation between the results obtained with the three-body model and a more complete model, the present author calculated the isotopic shifts with the three-body model using McDowell's data for $Co(NO)(CO)_3$. In Table 8, these calculated isotopic shifts are compared with the observed ones and with the calculated ones of McDowell. The calculated isotopic shifts of McDowell are nearly equal to the observed ones, and for the Co-N stretching and Co-N-O bending vibrations, are slightly smaller then the isotopic shifts calculated by the author. The N-O stretching vibration would be less affected by the other vibrations than the two skeletal vibrations between the metal and the NO group would be. Thus, the isotopic shifts calculated with the three-body model are greater than the observed ones, especially for the skeletal vibrations between the metal and the NO group. These considerations support the following conclusions: the nitrosylchromium(II) complexes examined in this study have a Cr-N-O arrangement and of their two absorptions in the region 530—620 cm^{-1}, the higher wave number is assigned to the Cr-NO stretching vibration and the lower one to the Cr-N-O bending vibration; black-$[Co(NH_3)_5(NO)]Cl_2$ has a Co-O-N arrangement.

For black-$[Co(NH_3)_5(NO)]Cl_2$, the very strong absorption at about 640 cm^{-1} due to hexamminecobalt(II) impurity interfered considerably with the skeletal vibrations between the cobalt and the NO group, as the absorption at 637 cm^{-1} due to the ND_3 rocking vibration of the deuterated complex did for black-$[Co(ND_3)_5(NO)]Cl_2$; there may be some uncertainty concerning values of the wave numbers for the skeletal vibrations. However, this uncertainty is not thought to be great enough to change the conclusion on arrangement.

The Ru-N-O arrangement found for pentahalogenonitrosylruthenium(III) complexes is in agreement with the result of a neutron diffraction study.[1] The Cr-N-O arrangement for the nitrosylchromium(II) complexes examined is very interesting when the great affinity of Cr(III) for oxygen is considered. The nitrosyl group of black-$[Co(NH_3)_5(NO)]Cl_2$ is found to coordinate to the cobalt atom through the oxygen atom. The Co-O-N arrangement is not in agreement with the assumption by Griffith[2] and Mercer *et al.*[22] The present result is the first to establish the Co-O-N arrangement for black-$[Co(NH_3)_5(NO)]Cl_2$.

The assignments of the skeletal vibrations between the metal and the NO group for the nitrosyl complexes examined have been reported by several workers.[20-22,33-35] However,

*3 The calculated isotopic shifts by the eight-body model were kindly provided by Dr. Jiro Hiraishi (Department of Chemistry, Faculty of Science, The University of Tokyo).

33) M. B. Fairey and R. J. Irving, *Spectrochim. Acta.*, **22**, 359 (1966).

their assignments have been tentative, or a distinction between the two skeletal vibrations has not been made. Clear assignments of the skeletal vibrations for the compounds examined, except for the black chloride, are established by this study.

For metal-nitrosyl complexes, calculation of the ^{15}N-isotopic shifts using the three-body model of the metal and nitrosyl group is a useful method for the determination of the coordinating atom of the NO group, and a clear assignment of the skeletal vibrations between the metal atom and the NO group.

The author would like to express his gratitude to Professor Yuzo Kakiuchi and Mr. Hiroshi Saito of St. Paul's (Rikkyo) University, and Assistant Professor Ichiro Nakagawa and Dr. Jiro Hiraishi of the University of Tokyo for their valuable suggestions concerning measurement of the infrared spectra and calculations of normal vibrations. Thanks are also due to Dr. Ryohei Nakane of the Institute of Physical and Chemical Research in Japan for making available the ^{15}N potassium nitrate.

34) J. R. Durin, W. A. McAllister, J. N. Willis, Jr., and E. E. Mercer, *ibid.*, **22**, 1091 (1966).
35) B. Jeżowska-Trzebiatoska and J. Ziołkoski, *Bull. Acad. Polon. Sci. Ser. Sci. Chim.*, **12**, 503 (1964).

BULLETIN OF THE CHEMICAL SOCIETY OF JAPAN VOL. 41 1844—1854 (1968)

Cationic Effect on the Polarographic Reduction of Nickel(II) in Acetonitrile

Shigero IKEDA and Eiki ITABASHI

Department of Chemistry, Faculty of Science, Osaka University, Toyonaka, Osaka

(Received December 27, 1967)

The polarographie behavior of nickel(II) acetate salts dissolved in acetonitrile solvent containing small quantities of acetic acid has been investigated in various natures and concentrations of supporting electrolytes. A single reduction wave is observed in the solutions of lithium perchlorate or sodium perchlorate. The limiting current has an intermediate nature of both diffusion- and kinetic controlled polarographic current. A double wave, on the other hand, is observed in the solutions of tetraalkylammonium perchlorate supporting electrolyte such as $(CH_3)_4NClO_4$, $(C_2H_5)_4NClO_4$ or $(n\text{-}C_4H_9)_4NClO_4$. The limiting current of the first step exhibits an intermediate nature of both diffusion and kinetic currents, and that of the second step is kinetic in nature. The effect of the nature and concentration of electrolyte on the visible absorption spectra of acetatonickel(II) complexes in acetonitrile containing small quantities of acetic acid are also discussed. On the basis of evidence, a mechanism which involves a substitution reaction of acetatonickel(II) complexes with the supporting electrolytes is proposed. The substitution reaction in tetraalkylammonium perchlorate solutions is thought to be the rate-determining step. The first step of a double wave is also thought to be due to the inhibition of charge transfer process by the weakly absorption of tetraalkylammonium cations of supporting electrolytes on the DME.

The supporting electrolyte effects in a non-aqueous electrochemistry have been reported by several investigators and, especially Murray and Kenneth Hiller[1] have done extensive works on the polarography of metal β-diketone chelate compounds.

The polarographic behaviors of nickel(II) ion in an acetonitrile solvent have been reported by several investigators. Kolthoff and Coetzee[2] observed a single reversible reduction wave with the half-wave potential of -0.33 V *vs.* SCE in an acetonitrile solution containing a 0.1 M sodium perchlorate. Popov and Geske,[3] on the other hand, obtained a double wave with the half-wave potentials of -0.69 V and -1.22 V *vs.* Ag-$AgNO_3$ electrode, in the same solvent containing 0.1 M

1) R. W. Murray and L. Kenneth Hiller, Jr., *Anal. Chem.*, **39**, 1221 (1967).

2) I. M. Kolthoff and J. F. Coetzee, *J. Am. Chem. Soc.*, **79**, 1852 (1957).

3) A. I. Popov and D. H. Geske, *ibid.*, **79**, 2074 (1957).

tetra-*n*-butylammonium perchlorate. Two-reduction steps for nickel(II) ion have also investigated in an acetonitrile[4] or a benzonitrile solvent[5] containing 0.1 M tetraethylammonium perchlorate. Iwamoto *et al.*[5] attributed the two-steps to the reduction of two kinds of nickel(II) species, and concluded that the second step involves the reduction of hydrated nickel(II) ions. The more easily reduced species, however, was not understood except the case of the presence of chloride ions. The first step in an acetonitrile solvent containing 0.1 M tetraethylammonium perchlorate and a small amount of chloride ions was involved the reduction of nickel(II)-chloride complex ions and the catalytic nature of the first wave has been established by Nelson and Iwamoto.[4]

The cationic effect of the supporting electrolyte for the polarographic reduction of nickel(II) ions has been carried out in an aqueous solvent[6,7] and an ethanol solvent,[8] respectively.

A distorated polarographic waves of nickel(II) ions in various kinds of natures and in various concentrations of supporting electrolyte solutions were initially reported by Gierst[6] and were later expanded by Dandoy and Gierst.[7] Dandoy and Gierst interpreted the polarographic behavior of nickel(II) ions in non-complexing media in terms of the dehydration kinetic current.

In the course of the studies for the reduction of acetatonickel(II) complexes in an acetonitrile solvent, the present authors observed a pronounced variation of the polarographic behaviors with the supporting electrolytes employed. Acetatonickel(II) complexes containing a small amount of acetic acid gave a single reduction wave in lithium perchlorate or sodium perchlorate supporting electrolytes, the two-reduction steps, on the other hand, were observed in the solutions of various tetraalkylammonium perchlorate supporting electrolytes.

The limiting current exhibited an intermediate nature of both diffusion and kinetically controlled polarographic currents, that of the second step in tetraalkylammonium perchlorate solutions, especially, was kinetic in nature.

The cationic effect is discussed on the basis of the chemical reaction of acetatonickel(II) complexes with cations of supporting electrolytes proceeding to the charge transfer process, and the inhibition of the charge transfer of nickel(II) ion, freeing of acetate ions from acetatonickel(II) complexes, by the weakly adsorption of tetraalkylammonium ions on the dropping mercury electrode.

Experimental

Reagents. Extra pure reagent acetonitrile purchased from Nakarai Chemicals Ltd. (Kyoto) was purified by a modified procedure of Forcier and Olver's method.[9] The purity was checked by the polarographic and spectrophotometric method.[10] The content of water was determined with Karl Fisher titration. Water content was approximately 2 to 5 mM.

Guaranteed reagent acetic acid and acetic anhydride were purified with the procedures given in the literature.[11]

Analytical reagent nickel(II) acetate salt ($Ni(CH_3COO)_2 \cdot (H_2O)_4$) was recrystallized three times from an aqueous solution containing 5 M acetic acid. The analysis of nickel(II) acetate salt gave the following result.

Found: C, 19.53; H, 5.79%. Calcd for $Ni(CH_3COO)_2(H_2O)_4$: C, 19.31; H, 5.67%.

Hexaaquonickel(II) perchlorate was prepared and recrystallized with the procedure given in the literature.[12] $Ni(H_2O)_6(ClO_4)_2$ was dried under a vacuum oven to constant weight at 110°C for 60 hr, and the formula $Ni(H_2O)_2(ClO_4)_2$ was obtained as reported by Hill and Nyholm.[13] The analysis of $Ni(H_2O)_2(ClO_4)_2$ gave the following results.

Found: Ni, 19.0±0.8, ClO_4, 65.8±1.4%. Calcd for $Ni(H_2O)_2(ClO_4)_2$: Ni, 19.99, ClO_4, 67.74%.

Lithium perchlorate was prepared by neutralizing the aqueous solution of lithium hydroxide, to pH about 5 with perchloric acid, evaporating and recrystallizing three times from water.

Anhydrous lithium perchlorate was obtained by drying in a vacuum oven at 150 to 160°C for 60 hr.

Anhydrous sodium perchlorate was obtained by drying sodium perchlorate monohydrate (B. D. H.) in a vacuum oven at 110 to 115°C for 40 hr.

Tetramethylammonium perchlorate was prepared by neutralizing a 10% tetramethylammonium hydroxide solution (Tokyo Kasei Kogyo Co., Ltd.) to pH 6 with 3 M perchloric acid. After evaporating at

4) I. V. Nelson and R. T. Iwamoto, *J. Electroanal. Chem.*, **6**, 234 (1963).
5) R. C. Larson and R. T. Iwamoto, *J. Am. Chem. Soc.*, **82**, 3239 (1960).
6) L. Gierst, "Transactions of the Symposium on Electrode Processes," ed. by W. Yeager, Wiley, New York (1961), pp. 106—138.
7) J. Dandoy and L. Gierst, *J. Electroanal. Chem.*, **2**, 116 (1961).
8) K. Tanaka and R. Tamamushi, *Rev. Polarog.*, **14**, 259 (1967).
9) G. A. Forcier and J. W. Olver, *Anal. Chem.*, **37**, 1447 (1965).
10) J. F. O'Donnell, J. T. Ayes and C. K. Mann, *ibid.*, **37**, 1161 (1965).
11) J. A. Riddick, E. E. Toops, Jr., "Organic Solvent," Interscience Publishers, New York (1955), p. 394.
12) A. E. Wickenden and R. A. Plane, *Inorg. Chem.*, **4**, 404 (1965).
13) N. S. Hill and R. S. Nyholm, *J. Chem. Soc.*, **1959**, 3997.

room temperature in a desicator containing calcium chloride under lower pressure, the salt was recrystallized three times from a purified acetonitrile solvent, and dried in a vacuum oven at 60 to 65°C for 40 hr. Tetraethylammonium perchlorate was prepared with the procedure in the literature,[4] recrystallized several times from water and subsequently three times from a purified acetonitrile, and dried in a vacuum oven at 60 to 65°C for 40 hr.

Tetra-*n*-butylammonium perchlorate was prepared by neutralizing a 40% tetra-*n*-butylammonium hydroxide solution (B. D. H) to pH 6 with perchloric acid. The salt was recrystallized several times from ethyl alcohol, and dried in a vacuum oven at 80°C for 40 hr.

Tetramethylammonium acetate ($(CH_3)_4NCH_3COO$) was prepared by a similar procedure with the one given in the literature,[14] and recrystallized three times from a purified acetonitrile and dried in a vacuum oven at 50 to 55°C for 30 hr. The analysis of tetramethylammonium acetate gave the following results.

Found: C, 54.01; H, 11.48; N, 10.49%. Calcd for $(CH_3)_4NCH_3COO$: C, 54.11; H, 11.35; N, 10.52%.

Procedures. Current-potential curves and current-time (*i-t*) curves during the life of a mercury drop at the constant potential were obtained with a Underkofler and Shain type potentiostat[15] based on operational amplifier K2-XA and stabilized amplifiers K2-P and K2-PA of Philibrick Researches Inc. (Boston). Polarograms were recorded with a Yokogawa X-Y Recorder, PRO-11A type. Current-time curves were recorded with a Riken Denshi SP-G2 type recorder.

In the following section, the word "current" denoted by means of the maximum current obseved just before the mercury drop. Measurements were made at 25±0.1°C unless otherwise stated. A beaker type cell was used. The test solution was connected to an aqueous saturated calomel electrode (SCE) through a pair of glass frit junctions arranged to prevent water contamination of the test solution. A platinum foil electrode served as the counter electrode was placed in the glass tube with a glass frit, the glass tube was contained with the test solution.

The dissolved oxygen in the solution was removed by bubbling a pure nitrogen gas through the solution. The two-type dropping mercury electrodes were used. The electrode A had an *m* value of 1.48_2 mg/sec and a drop time, t_d, of 5.02 sec in a deaerated 0.1 M sodium perchlorate acetonitrile solution at −0.70 V *vs.* SCE and at 50 cm mercury height. The electrode B and an *m* value of 1.33_4 mg/sec and a drop time, t_d of 4.98 sec in a deaerated 0.1 M lithium perchlorate acetonitrile solution at −0.8 V *vs.* SCE and at 60 cm mercury height.

The measurements of the visible and ultraviolet absorption spectra were carried out with a Hitachi EPS-3T spectrophotometer at a room temperature.

14) W. F. Luder, P. B. Kraus, C. A. Kraus and R. M. Fuoss, *J. Am. Chem. Soc.*, **58**, 255 (1936).
15) W. L. Underkofler and I. Shain, *Anal. Chem.*, **35**, 1778 (1963).

Results

The current-potential curves of acetatonickel(II) complexes were obtained in the acetonitrile solutions of various natures and concentrations of supporting electrolytes. The typical current-potential curves are given in Fig. 1.

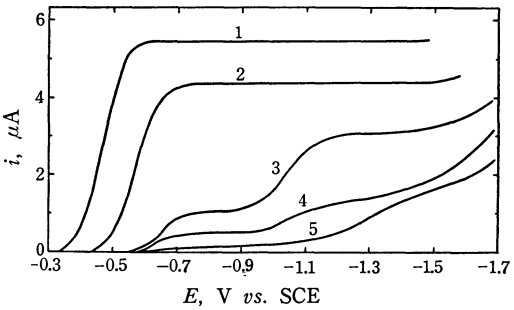

Fig. 1. Current-potential curves of 0.5 mM acetatonickel(II) complexes in various supporting electrolyte solutions containing 0.4% acetic acid and 0.2% acetic anhydride: (1), 0.05 M $LiClO_4$; (2), 0.05 M $NaClO_4$; (3), 0.05 M $(CH_3)_4NClO_4$; (4), 0.05 M $(C_2H_5)_4NClO_4$; (5), 0.05 M $(n\text{-}C_4H_9)_4NClO_4$. (Electrode A)

Figure 1 shows the current-potential curves in the solutions of various univalent electrolytes containing 0.4% acetic acid and 0.2% acetic anhydride in volume. The polarographic data of acetatonickel(II) omplexes in various supporting electrolyte solutions are summarized in Table 1.

TABLE 1. EFFECT OF SUPPORTING ELECTROLYTE ON THE REDUCTION OF ACETATONICKEL(II) CONPLEXES IN 0.05 M PERCHLORATE SOLUTIONS CONTAINING 0.4% ACETIC ACID AND 0.2% ACETIC ANHYDRIDE (Electrode A)

M^+	Concen. of Ni(II) mM	$E_{1/2}$ V *vs.* SCE	Reciprocal slope of log-plot mV	*x* value[a] at $i_l = kt^x$
Li^+	0.5	−0.47	82	0.29
Na^+	0.5	−0.58	80	0.33
$(CH_3)_4N^+$	1.0	−0.63[b]	78	0.54
		−1.05[c]	135	0.62
$(C_2H_5)_4N^+$	1.0	−0.60[b]	68	0.53
		−1.1 [c]	——[d]	0.64
$(n\text{-}C_4H_9)_4N^+$	4.0	−0.56[b]	70	0.63
	2.0	−1.2 [c]	——[d]	0.63

a) The slop of the plot of log *i* *vs* log *t* for the current-time curve during the life of a mercury drop at the potential region giving the limiting current.
b) 1st. reduction step.
c) 2nd. reduction step.
d) Not determined because of maximum.

A single irreversible reduction wave was obtained in the solution of lithium perchlorate or sodium perchlorate. In the tetraalkylammonium perchlorate electrolyte solutions, on the other hand, the wave was found to split into two-steps; the first step was observed at the potential range from −0.5 V to −1.1 V *vs.* SCE, and the second one at more negative potential regions than −1.1 V *vs.* SCE. The limiting current decreased with the increasing radius of cations of supporting electrolytes, and was found not to be purely diffusion controlled from the results of the measurements of current-time curves. In a solution of tetraalkylammonium perchlorate supporting electtrolyte, especially, the limiting current of the second reduction step was found to be kinetic in nature.

Effect of Acetic Acid, Acetic Anhydride and Water. The effects of the concentration of acetic acid, acetic anhydride and water on the current-potential curves were investigated. Table 2 presents the limiting currents, half-wave potentials and slopes of the log-plots which are obtained at 0.5 mM acetatonickel(II) complexes in a 0.1 M lithium perchlorate solution containing the various concentrations of acetic acid.

TABLE 2. EFFECT OF ACETIC ACID ON THE REDUCTION OF 0.5 mM ACETATONICKEL(II) COMPLEXES IN 0.1 M $LiClO_4$ SOLUTIONS (Electrode B)

Concen. CH_3COOH %	i_l μA	$E_{1/2}$ V *vs.* SCE	Reciprocal slope of log-plot mV
0.2	4.83	-0.47_0	82
0.4	4.79	-0.47_3	80
0.8	4.80	-0.47_5	82
2.0	4.74	-0.47_8	87
4.0	4.66	-0.48_2	107
10.9	4.43	-0.49_3	110

No appreciable change was observed in the half-wave potential with the change of the concentration of acetic acid. On the other hand, the decrease of the limiting currents and the increase of the slopes of the log-plots were found with the increasing concentrations of acetic acid.

The polarographic behavior of nickel(II) ions in acetic acid solvent has been investigated by Coulter and Iwamoto,[16] who reported that nickel(II) ions in an acetic acid solvent containing a 1.0 M lithium perchlorate gave a single irreversible reduction wave with the half-wave potential of −0.645 V *vs.* SCE and the slope of the log-plot of 127 mV.

In this experiment, the current-potential curves were drawn out in an acetonitrile solution containing the higher concentration of acetic acid than 10% in volume.

The limiting currents, half-wave potentials and slopes of the log-plots at 0.5 mM acetatonickel(II) complexes in a 0.1 M lithium perchlorate and 0.4% acetic acid solution containing various concentrations of acetic anhydride are represented in Table 3.

TABLE 3. EFFECT OF ACETIC ANHYDRIDE ON THE REDUCTION OF 0.5 mM ACETATONICKEL-(II) COMPLEXES IN 0.1 M $LiClO_4$ CONTAINING 0.4% ACETIC ACID (Electrode B)

Concen. of $(CH_3CO)_2O$ %	i_l μA	$E_{1/2}$ V *vs.* SCE	Reciprocal slope of log-plot mV
0	4.85	-0.47_2	82
0.1	4.86	-0.47_0	81
0.2	4.84	-0.47_8	81
0.4	4.80	-0.47_6	81
1.0	4.77	-0.48_1	83
4.0	4.71	-0.48_5	82
10.0	4.61	-0.48_3	83

No appreciable change was observed in the half-wave potentials and slopes of the log-plots, but the limiting currents decreased gradually with the increasing concentration of acetic anhydride.

In the solution of tetraalkylammonium perchlorate electrolytes in the absence of acetic anhydride, on the other hand, a maximum wave appeared at the second reduction step when the measurements were made at a higher concentration of acetatonickel(II) complexes than 1.5 mM, the maximum wave, however, was suppressed by addition of 0.2% acetic anhydride in volume.

In the following sections, acetic anhydride was not added unless otherwise stated, because the measurements were carried out at the concentration of 0.5 mM acetatonickel(II)

TABLE 4. EFFECT OF WATER ON THE REDUCTION OF 0.5 mM ACETATONICKEL(II) IN 0.1 M $LiClO_4$ SOLUTIONS CONTAINING 0.4% ACETIC ACID (Electrode B)

Concen. of water %	i_l μA	$E_{1/2}$ V *vs.* SCE	Reciprocal slop of log-plot mV
0.04	4.78	-0.47_2	79
0.2	4.73	-0.47_8	81
0.4	4.72	-0.48_2	80
0.8	4.70	-0.49_8	83
2.0	4.67	-0.53_5	83
4.0	4.61	-0.60_5	85

16) P.D.T. Coulter and R.T. Iwamoto, *J. Electroanal. Chem.*, **13**, 21 (1967).

complexes.

The effect of water content on the reduction wave in a 0.1 M lithium perchlorate solution was also investigated as shown in Table 4.

The half-wave potentials and slopes of the log-plots were not affected up to 0.4% water content. At higher concentrations than 2% water, the half-wave potentials shift to more negative potentials and the limiting currents decrease, with the increasing concentrations of water.

Effect of Concentration of Lithium Perchlorate. Appreciable variations were observed in the current-potential curves for the reduction of acetatonickel(II) complexes by changing the natures and concentrations of supporting electrolytes. The typical current-potential curves for the reduction of 0.5 mM acetatonickel(II) complexes containing 0.4% acetic acid and various concentrations of lithium perchlorate are reproduced in Fig. 2.

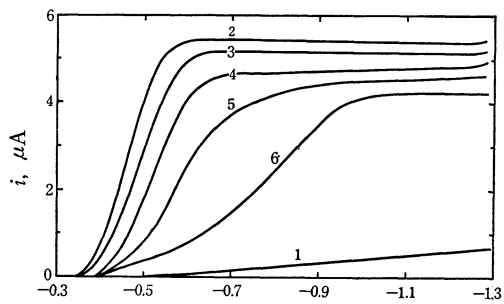

Fig. 2. Effect of concentration of lithium perchlorate on the current-potential curves of 0.5 mM acetatonickel(II) complexes containing 0.4% acetic acid: (1), 0 M; (2), 0.05 M; (3), 0.1 M; (4), 0.2 M; (5), 0.4 M; (6), 1.0 M $LiClO_4$. (Electrode A)

The limiting current decreases and the reduction potentials shifts to more negative potentials, with the increasing concentrations of limthium perchlorate. An ill-defined reduction wave was observed in the absence of supporting electrolyte.

Effect of Mixed Electrolytes. Stepwise addition of lithium perchlorate up to a concentration of about 10 mM to 0.5 mM acetatonickel(II) complexes in tetraalkylammonium perchlorate solution causes an increase in heights of the limiting currents and a shift of the reduction potential to less negative potentials.

A double wave obtained in a tetramethylammonium perchlorate solution changes gradually to a single one by the stepwise addition of lithium perchlorate up to a concentration of about 5 mM as presented in Fig. 3.

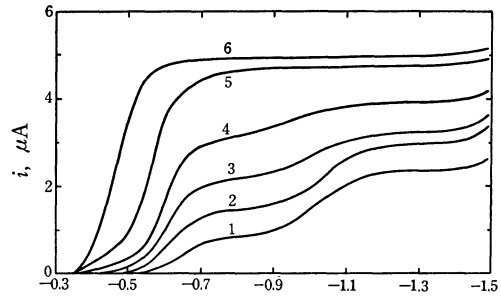

Fig. 3. Current-potential curves of 0.5 mM acetonickel(II) complexes in tetramethylammonium perchlorate solutions containing 0.4% acetic acid and various concentrations of lithium perchlorate at ionic strength 0.05: (1), 0 M; (2), 2×10^{-4} M; (3), 5×10^{-4} M; (4), 1×10^{-3} M; (5), 5×10^{-3} M; (6), 5×10^{-2} M $LiClO_4$. (Electrode B)

TABLE 5. EFFECT OF LITHIUM PERCHLORATE ON THE REDUCTION OF 0.5 mM ACETATONICKEL (II) COMPLEXES IN $(CH_3)_4NClO_4$ SOLUTIONS CONTAINING 0.4% ACETIC ACID AT IONIC STRENGTH 0.05 (Electrode B)

Concen. of $LiClO_4$ mM	1st wave i_l μA	1st wave x at $i_l=kt^x$	2nd wave i_l μA	2nd wave x at $i_l=kt^x$
0	0.85	0.52	2.35	0.62
0.1	1.20	0.46	2.72	0.56
0.2	1.50	0.43	2.98	0.56
0.5	2.22	0.41	3.20	0.53
1.0	3.20	0.39	3.88	0.46
3.0	4.18	0.38	4.43	0.46
5.0	4.70	0.35	4.75	0.42
50	4.96	0.31	5.02	0.30

At the potentials of −0.82 V and −1.30 V *vs.* SCE corresponding to the potentials to the first and the second reduction step, respectively, in a tetramethylammonium perchlorate solution, the measurements of current-time curves were made at various concentrations of lithium perchlorate. Table 5 shows the limiting currents and slopes of the plots for $\log i$ *vs.* $\log t$ which are obtained from the current-time curves of the first drop.[17] The currents increase and the slopes of the plots of $\log i$ *vs.* $\log t$ decrease with the increasing concentrations of lithium perchlorate at the constant ionic strength.

At more concentrations than 5 mM lithium perchlorate, no appreciable difference was observed in the currents and slopes of the plots

17) J. Kůta and I. Smoler, "Progress in Polarograhy," Vol. 1, ed. by P. Zumann and I. M. Kolthoff, Interscience Publishers, New York (1962), pp. 43—63.

of both the first and second steps.

Similar changes of the current-potential curves and the current-time curves by the stepwise addition of lithium perchlorate were observed in the solutions of tetraethylammonium perchlorate or tetra-*n*-butylammonium perchlorate supporting electrolytes.

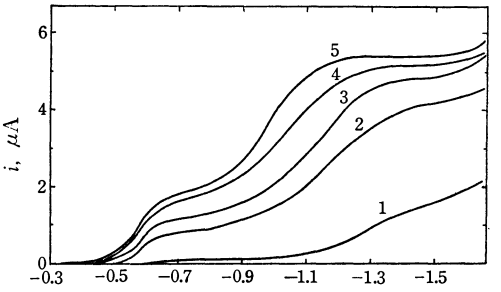

Fig. 4. Current-potential curves of 0.5 mM acetatonickel(II) complexes in tetra-*n*-butylammonium perchlorate solutions containing 0.4% acetic acid and various concentrations of lithium perchlorate at ionic strength 0.05: (1), 0 M; (2), 1×10^{-3} M; (3), 2×10^{-3} M; (4), 5×10^{-3} M; (5), 1×10^{-2} M $LiClO_4$. (Electrode A)

Figure 4 shows the current-potential curves obtained in a tetra-*n*-butylammonium perchlorate solution containing various concentrations of lithium perchlorate.

In this case, the limiting current of the second step increases with the increasing concentrations of lithium perchlorate up to about 10 mM. The limiting current of the second step obtained in a solution containing 40 mM tetra-*n*-butylammonium perchlorate and 10 mM lithium perchlorate becomes nearly equal to the limiting current obtained in a solution of 0.05 M lithium perchlorate alone. On the other hand, no appreciable enhancement of the limiting current of the first step by the stepwise addition of lithium perchlorate is observed as compared with the degree of the increase of that of the second step.

Spectral Studies. The measurement of the visible absorption spectrum of acetatonickel(II) complexes were carried out in the solutions of various kinds of electrolyte. Figure 5 shows the spectra of 50 mM nickel(II) acetate salts in various natures of electrolyte solutions at the constant concentration.

The absorption bands shifted to shorter wavelengths with the decreasing radius of cations of electrolyte. Similar shifts of the absorption bands were also obtained by the increasing concentrations of electrolyte. The

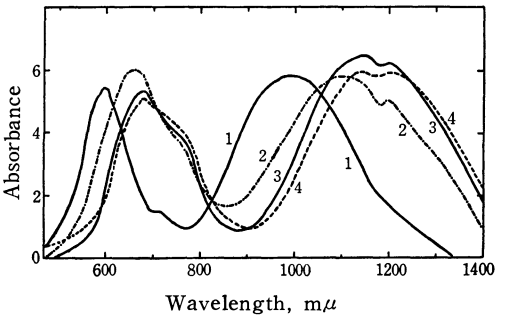

Fig. 5. Visible absorption spectra of 50 mM acetatonickel(II) complexes in various electrolyte solutions containing 1.6% acetic acid: (1), 0.01 M $HClO_4$; (2), 0.25 M $LiClO_4$; (3), 0.25 M $NaClO_4$; (4), 0.25 M $(C_2H_5)_4NClO_4$.

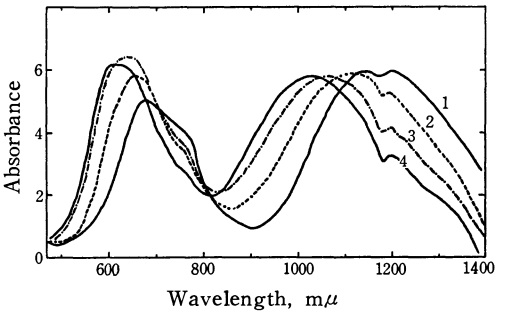

Fig. 6. Visible absorption spectra of 50 mM acetatonickel(II) complexes in various concentrations of lithium perchlorate solutions containing 1.6% acetic acid: (1), 0 M; (2), 0.1 M; (3), 0.5 M; (4), 1.0 M $LiClO_4$.

typical absorption spectra of acetatonickel(II) complexes in various concentrations of lithium perchlorate are reproduced in Fig. 6.

No appreciable change of the absorption bands in the case of tetraalkylammonium perchlorate electrolyte was observed.

Discussion

Spectrophotometric Studies. Nickel(II) acetate salt ($Ni(CH_3COO)_2(H_2O)_4$) does not dissolve in an acetonitrile solvent alone, but dissolves easily in the same solvent in the presence of a small amount of acetic acid or acetate salts such as tetramethylammonium acetate or tetra-*n*-butylammonium acetate which dissolve in an acetonitrile solvent alone.

The visible absorption spectrum of acetatonickel(II) complexes in an acetonitrile containing 1.6% acetic acid shows four bands and, the band positions are nearly equal to those of hexaaquo-nickel(II) ion in an aqueous solvent or the nickel(II) acetate salt dissolved in an aqueous solvent containing 20%

TABLE 6. ABSORPTION MAXIMA OF NICKEL(II) COMPLEXES IN AQUEOUS AND ACETONITRILE SOLVENTS

Compound	Solvent	Band position*				Ref.
$Ni(OAc)\cdot 4H_2O$	CH_3CN, 1.6% Acetic Acid	8.55(0.78)	13.33(0.66)	14.82(0.71)	25.13(1.46)	
$Ni(OAc)_2\cdot 4H_2O$	H_2O, 20% Acetic Acid	8.66(0.45)	13.89(0.41)	15.15(0.38)	25.25(0.79)	
$Ni(H_2O)_6(ClO_4)_2$	H_2O	8.70(0.32)	13.50(0.31)	15.40(0.23)	25.30(0.68)	18
$Ni(OAc)_2\cdot 4H_2O$	CH_3CN, $HClO_4$**	10.21(0.82)	13.92(0.16)	16.93(0.77)	27.23(0.92)	
$Ni(H_2O)_2\cdot 2H_2O$	CH_3CN	10.20(0.82)	13.9 (0.17)	16.95(0.76)	27.20(0.90)	
$Ni(CH_3CN)_6(ClO_4)_2$	CH_3CN	10.40(0.74)	13.90(0.15)	17.20(0.66)	27.20(0.80)	19
$Ni(CH_3CN)_6(BF_4)_2$	CH_3CN	10.53	13.94	17.09	27.56	20

* Band positions in $10^3\ cm^{-1}$; $\log\varepsilon$ in parentheses.

** Nickel(II) acetate salt was dissolved in acetonitrile containing 1.6% acetic acid, and then the solution was titrated with anhydrous perchloric acid dissolved in acetic anhydride.

acetic acid, as seen from Table 6.

The absorption spectra of a number of octahedral nickel(II) complexes have been listed in Table 6. The extinction coefficients of acetatonickel(II) complexes in an acetonitrile containing 1.6% acetic acid are larger than those of hexaaquonickel(II) ions in an aqueous solvent or nickel(II) acetate salts dissolved in the same solvent containing 20% acetic acid. In an aqueous solution, the intensity of the absorbance of nickel(II) ions is enhanced by the addition of acetate ions, because of the formation of the species, $Ni(OAc)_2$ or $Ni(OAc)^+$, as have been reported by Watelle-Morion.[21]

These results suggest that appreciable quantities of acetato complexes of nickel(II) are formed in an acetonitrile solvent containing a small amount of acetic acid and, that acetatonickel(II) complexes in the same solution is in an octahedral configuration coordinated with six oxygen atoms.

A potentiometric titration of acetatonickel(II) complexes in an acetonitrile solvent containing a small amount of acetic acid with an anhydrous perchloric acid shows that acetatonickel(II) complexes are quantitatively titrated in the same solvent, at a mole ratio of two of perchloric acid to one of nickel(II) acetate salt.[22] In addition to the potentiometric titrations, the color of the solution changes successively from green to blue with the increasing concentration of perchloric acid, the spectra of the solution at the equivalent point is similar to those of $Ni(H_2O)_2(ClO_4)_2$ salt dissolved in an acetonitrile as shown in Fig. 5 and Table 6.

Consequently, it is found that acetatonickel(II) complexes in an acetonitrile solvent containing a small amount of acetic acid is in an octahedral configuration coordinated with two acetate ions and four neutral acetic acid or water molecules.

Table 6 also indicates that appreciable quantities of $(Ni(CH_3CN)_6)^{2+}$ are present in the solution when acetatonickel(II) complexes were titrated with an anhydrous perchloric acid or, $Ni(H_2O)_2(ClO_4)_2$ salt was dissolved in an acetonitrile.

The fact that nickel(II) ion forms a complex ion with acetonitrile, thus freeing acetate ions for the reaction with the acid titrant, may be explained by the following reaction:

$$\{Ni(OAc)_2(HOAc)_x(H_2O)_{4-x}\} + 2HClO_4 + n\,CH_3CN \longrightarrow Ni(CH_3CN)_n^{2+} + 2ClO_4^- + (2+x)HOAc + (4-x)H_2O \quad (1)$$

where HOAc refers to acetic acid.

In the case of addition of lithium perchlorate to the acetonitrile solutions containing acetatonickel(II) complexes and a small amount of acetic acid, the spectrophotometric measurements shows that the spectra of acetatonickel(II) complexes shift to lower wavelengths with the stepwise addition of lithium perchlorate as seen from Fig. 6, the spectra, however, is not consisted with those of nickel(II) perchlorate in an acetonitrile solvent, at the mole ratio of twenty times of lithium perchlorate to nickel(II) acetate salt. Similar shifts of spectra of acetatonickel(II) complexes to shorter wavelengths were observed by addition of the other perchlorate salts. The magnitude of the shift to lower wavelengths decreases in the order of $LiClO_4$, $NaClO_4$, $(CH_3)_4NClO_4$, $(C_2H_5)_4NClO_4$ and $(n\text{-}C_4H_9)_4NClO_4$ at the constant concentration of perchlorate salts, and in the case of the addition

18) W. Manch and W. C. Fernelius, *J. Chem. Educ.*, **38**, 192 (1961).

19) A. E. Wickenden and R. A. Drause, *Inorg. Chem.*, **4**, 404 (1965).

20) B. J. Hathaway, D. G. Holan and A. E. Underhill, *J. Chem. Soc.*, **1962**, 2444.

21) G. Watelle-Morion, *Compt. rend.*, **246**, 3610 (1958).

22) S. Ikeda andE. Itabashi, unpublished results.

of tetraalkylammonium perchlorate the shift is very small.

A reasonable explanation of these results is possible by considering the substitution of acetate ions by acetonitrile in acetatonickel-(II) complexes which may be written by the following equation.

$$\{Ni(OAc)_2(HOAc)_x(H_2O)_{4-x}\} + 2\,MClO_4 + n\,CH_3CN \rightleftharpoons Ni(CH_3CN)_n^{2+} + 2\,ClO_4^- + 2\,MOAc + x\,HOAc + (4-x)H_2O \quad (2)$$

where M refers to the cation of electrolyte.

The above reaction is considered to proceed quantitatively on employing perchloric acid as an electrolyte, and to be in equibrium in the case of the other electrolytes such as alkali metal perchlorates or tetraalkylammonium perchlorates.

Polarographic Studies. On the polarographic studies, the limiting currents of acetatonickel(II) complexes in various supporting electrolytes at the constant concentration, decrease with the radius of cation of the supporting electrolyte present in the solution.

A single irreversible reduction wave is observed in the solutions of lithium perchlorate or sodium perchlorate, the limiting current shows an intermediate nature of both diffusion- and kinetic-controlled polarographic currents, which were found from the results of the measurement of current-time curves.

The two-reduction steps, on the other hand, are observed in the solution of tetraalkylammonium perchlorate, the limiting current of the second step is kinetic in nature, as seen from Table 1.

The character of the limiting current is also seen from the temperature coefficients of the limiting current. It has been stated that if the temperature coefficient is greater than +2% per degree, the current is probably not a diffusion-controlled.[23] The measurement of the limiting current for the reduction of nickel(II) perchlorate in an acetonitrile solvent containing 0.1 M lithium perchlorate as a supporting electrolyte were made at the temperature over range 0.3 to 35°C, indicating that the temperature coefficient was 1.9% per degree. The result of the measurement of the current-time curve also suggest that the limiting current for the reduction of nickel-(II) perchlorate in an acetonitrile containing 0.1 M lithium perchlorate is diffusion-controlled.

In the case of the reduction of acetatonickel-(II) complexes in the same solvent containing 0.4% acetic acid, the temperature coefficients in a 0.1 M lithium perchlorate solution are 2.3% per degree at lower temperatures and, 3.5% per degree at higher temperatures than 20°C. The temperature coefficients in a 0.05 M tetramethylammonium perchlorate solution, on the other hand, are 4.4% and 6.1% per degree for the first and the second step, respectively, at the temperature range over 0.3 to 35°C.

Consequently, the limiting currents for the reduction process of acetatonickel(II) complexes in an acetonitrile solvent containing 0.4% acetic acid and various supporting electrolyte are undoubtedly not entirely diffusion-controlled.

The authors assume that the chemical reaction expressed in Eq. (2) is a rate determining step and, $\{Ni(OAc)_2(HOAc)_x(H_2O)_{4-x}\}$ in Eq. (2) is an electro inactive and $Ni(CH_3CN)_n^{2+}$, produced by freeing of acetato ions from nickel(II) acetate, is electroactive polarographically.

This assumption may be suggested from the results of the spectrophotometric studies, the dependence of the limiting current on the nature of cation of the supporting electrolytes present in the solution and the enhancenment of the limiting current in a tetraalkylammonium perchlorate supporting electrolyte solution with the stepwise addition of lithium perchlorate.

The polarographic inactivity of $\{Ni(OAc)_2(HOAc)_x(H_2O)_{4-x}\}$ is ascertained from the following experiments. Nickel(II) acetate salt dissolved containing 0.4% acetic acid gives an ill-defined and little reduction wave in the absence of a supporting electrolyte as seen from Fig. 2. If acetatonickel(II) complexes are electroactive, a well-defined and apparent reduction wave with a migration current would be observed.

Nickel(II) acetate salt dissolved in an acetonitrile solvent in the presence of 1 mM tetramethylammonium acetate and 0.05 M tetramethylammonium perchlorate, on the other hand, undergoes two reduction steps with the half-wave potentials of −1.7 V and −2.25 V *vs.* SCE, respectively, as shown in Fig. 7.

In an acetonitrile solution containing acetic acid, the reduction wave of acetatonickel(II) complexes at more negative potentials than −1.8 V *vs.* SCE is not observed by discharge of hydrogen ion. For that reason, the measurements of current-potential curves of acetatonickel(II) complexes were carried out in the absence of acetic acid.

With a 1 mM tetramethylammonium acetate

23) L. Meites, "Polarographic Techniques," Interscience, New York (1955), pp. 78—82.

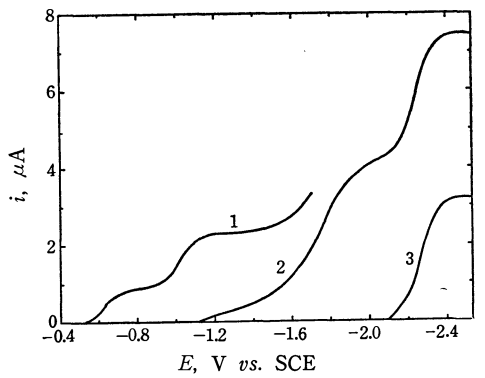

Fig. 7. Current-potential curves of 0.5 mM acetatonickel(II) complexes (curves 1 and 2), and 1 mM tetramethylammonium acetate (curve 3) in 0.05 M $(CH_3)_4NClO_4$ solutions.
(1) 0.5 mM $Ni(OAc)_2$, 0.4% acetic acid
(2) 0.5 mM $Ni(OAc)_2$, 1 mM $(CH_3)_4NOAc$
(3) 1 mM $(CH_3)_4NOAc$. (Electrode B)

and 0.05 M tetramethylammonium perchlorate solution in the absence of nickel(II) acetate salt, a single reduction step with the half-wave potential of −2.23 V *vs.* SCE is observed.

The second reduction step in the presence of nickel(II) acetate salts suggests that it involves the reduction of acetate ions.

The ill-defined first reduction step may be due to the reduction of nickel(II) ions, although it is uncertain whether nickel(II) ions are acetatonickel(II) complexes or nickel(II)-acetonitrile complexes, which are produced by freeing of acetate ions from acetatonickel(II) complexes. The limiting current of the first reduction step is not a pure diffusion-controlled, but shows an intermediate nature of both diffusion and kinetic controlled currents. Under these conditions, consequently, the reduction wave obtained in an acetonitrile solution dissolved nickel(II) acetate salts with a small amount of acetic acid is not thought to involve the polarographic reduction of nickel(II) ions coordinated with acetate ions could not proceed up to the potentials of −1.7 V *vs.* SCE.

The increase of the limiting current with the decreasing radius of the cation of supporting electrolyte present in the solutions, indicates the increase of the equilibrium concentrations of $Ni(CH_3CN)_n^{2+}$.

The addition of lithium perchlorate in the solutions of tetraalkylammonium perchlorate electrolytes causes an enhancement of the limiting current and also a decrease of the slopes of the plots of $\log i$ *vs.* $\log t$ during a life of mercury drop at the constant potential, as presented in Table 5 in the case of the results in tetramethylammonium perchlorate solutions, indicating that the equilibrium concentrations of $Ni(CH_3CH)_n^{2+}$ increase gradually with increasing concentrations of lithium perchlorate, and the rate-determining step change gradually from the chemical reaction (2) to the diffusion process of $Ni(CH_3CN)_n^{2+}$.

A similar enhancement of the limiting current in tetraalkylammonium perchlorate electrolyte solutions is also observed by addition of a small amount of sodium perchlorate instead of lithium perchlorate, lithium perchlorate being more efficient than sodium perchlorate for the enhancement of limiting current at the constant ionic strength.

The two reduction steps in a solution of tetramethylammonium perchlorate electrolyte changes to a single one at a less mole ratio of lithium perchlorate to nickel(II) acetate salts than ten.

On the other hand, a double wave in the solutions of tetraethylammonium perchlorate or tetra-*n*-butylammonium perchlorate electrolyte is also observed under the conditions that the enhanced limiting current of the second step becomes nearly equal to the limiting current obtained in the solution of lithium perchlorate electrolyte alone, as shown in Fig. 3.

These data indicate that the charge transfer reaction of nickel(II) ion is inhibited by the weakly absorption of tetraalkylammonim ions at the dropping mercury electrode.

The conclusion is also supported by the results presented in Fig. 8.

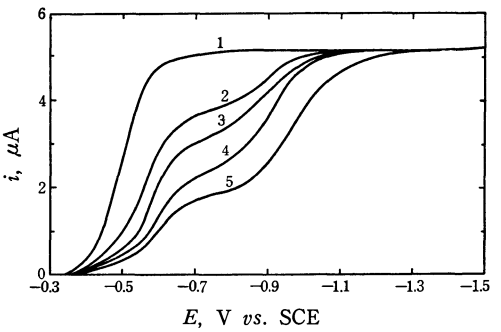

Fig. 8. Effect of tetra-*n*-butylammonium perchlorate on the current-potential curves of 0.5 mM acetatonickel(II) complexes in lithium perchlorate solutions containing 0.4% acetic acid at ionic strength 0.1: (1), 0 M; (2), 5×10^{-3} M; (3), 1×10^{-2} M; (4), 2.5×10^{-2} M; (5), 5×10^{-2} M $(n\text{-}C_4H_9)_4NClO_4$. (Electrode A)

A single wave obtained in the solution of lithium perchlorate supporting electrolyte is

found to split into the twosteps by the addition of tetra-*n*-butylammonium perchlorate. The limiting current at the potential over range −0.6 V to −1.0 V *vs.* SCE is not only suppressed but also becomes gradually independent on the heights of a mercury reservoir, with the increasing concentrations of tetra-*n*-butylammonium perchlorate, and reduction potentials shift to more negative potentials.

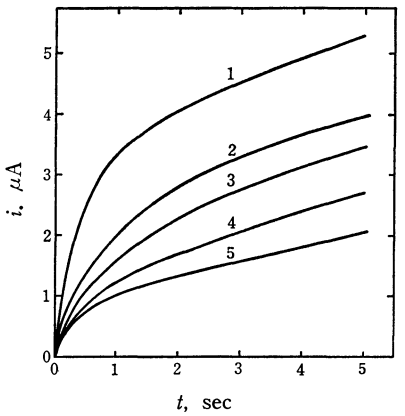

Fig. 9. Current-time curves of 0.5 mM acetatonickel(II) complexes measured at −0.75 V. *vs.* SCE in lithium perchlorate solutions containing 0.4% acetic acid and various concentrations of $(n\text{-}C_4H_9)_4NClO_4$ at ionic strength 0.1: (1), 0 M; (2), 5×10^{-3} M; (3), 1×10^{-2} M; (4), 2.5×10^{-2} M; (5), 5×10^{-2} M $(n\text{-}C_4H_9)_4NClO_4$ present. (Electrode A)

This unusual situation is also evident from the results of the measurements of the current-time curves given in Fig. 9. The stepwise addition of tetra-*n*-butylammonium perchlorate at the ionic strength 0.1 causes to decrease the maximum current observed just before the mercury drop and also to depress the current from the initial stage of the formation of a mercury brop. The current at the first step observed at −0.75 V *vs.* SCE, in the presence of a 50 mM tetra-*n*-butylammonium perchlorate shows the property of the kinetic current. At more negative potentials than −0.8 V *vs.* SCE, the reduction current rises again and reaches to a full height, and becomes almost independent on the presence of tetra-*n*-butylammonium perchlorate.

The profiles of the current-time curves changes successively from the curve 5 to 1 in Fig. 9 in the presence of 50 mM tetra-*n*-butylammonium perchlorate by means of the shift of the potential from −0.75 V to −1.3 V *vs.* SCE. A single wave obtained in the sulotion of lithium perchlorate supporting electrolyte also splits into a double one by the stepwise addition of the other tetraalkylammonium perchlorate instead of tetra-*n*-butylammonium perchlorate. But the suppressing action is found to decrease in the order of $(n\text{-}C_4H_9)_4N^+$, $(C_2H_5)_4N^+$ and $(CH_3)_4N^+$ at the definite concentration.

These phenomena may be explained by taking into consideration the weak absorption of tetraalkylammonium cations on the DME. It is well known theoretically[24] and experimentally[25] that the weakly surface-active substances with considerably higher concentrations make the limiting current decrease and also change successively the drop life dependence of the instantaneous current from a $t^{1/6}$ to a $t^{2/3}$.

Tetraalkylammonium ions in an aqueous solvent has been found to act as a relatively strong surface-active substances on DME.[26] In an acetonitrile solvent, however, they would act as a weakly surface-active substance.

In conclusion, with nickel(II) acetate salts dissolved in an acetonitrile solvent containing a small amount of acetic acid the nickel(II) ion is in an octahedral configuration coordinated with two acetate ions and four neutral acetic acid or water molecules.

The reaction mechanism of the polarographic reduction of acetatonickel(II) complexes can probably be represented by the following sequence:

$$\{Ni(OAc)_2(HOAc)_x(H_2O)_{4-x}\} + 2\,MClO_4 + n\,CH_3CN \overset{K_{eq}}{\rightleftharpoons} Ni(CH_3CN)_n^{2+} + 2\,ClO_4^- + 2\,MOAc + x\,HOAc + (4-x)H_2O \quad (2')$$

$$Ni(CH_3CN)_n^{2+} + 2\,e \longrightarrow Ni(Hg) + n\,CH_3CN \quad (3)$$

where HOAc refers to acetic acid, $MClO_4$ represents a supporting electrolyte, K_{eq} the effective equilibrium constant in the bulk solution, substance $\{Ni(OAc)_2(HOAc)_x(H_2O)_{4-x}\}$ is not reduced at the potential at which $Ni(CH_3CN)_n^{2+}$ is reduced under the experimental conditions.

The limiting current obtained in lithium perchlorate or sodium perchlorate supporting electrolyte solutions exhibits an intermediate nature of both diffusion and kinetic controlled currents. In tetraalkylammonium perchlorate supporting electrolyte solutions, the chemical reaction (2′) is a rate-determining step. The first step of a double-wave in a tetraalkyl-

24) H. Matsuda, *Rev. Polarogr.*, **14**, 87 (1967).
25) R. W. Schmid and C. N. Reilley, *J. Am. Chem. Soc.*, **80**, 2087 (1958).
26) P. Delahay, "Double Layer and Electrode Kinetics," Interscience Publishers, New York (1965), p. 228.

ammonium perchlorate solution is due to the inhibition of charge transfer of nickel(II) ion by the weak adsorption of tetraalkylammonium ions on the DME.

The authors wish to thank the Ministry of Education for the financial support granted for this research.

BULLETIN OF THE CHEMICAL SOCIETY OF JAPAN VOL. 41 1854—1858 (1968)

Distribution of Thenoyltrifluoroacetone and Its Scandium Chelate in Ketone Solvent System

Toshiki WAKABAYASHI, Katsuko TAKAIZUMI, Kunio SETO, Nobuo SUZUKI*1 and Ken-ichi AKIBA*1

The College of General Education, Tohoku University, Kawauchi, Sendai

(Received January 24, 1968)

The distribution equilibria of thenoyltrifluoroacetone (TTA) and its scandium chelate between aqueous solutions with an ionic strength of 0.1 and ketones at 25°C have been studied. The distribution of TTA was correlated with the solubility parameters of the ketones and the correlation between the distribution coefficients of TTA and those of scandium chelate was confirmed. The characteristic properties of ketones were discussed in comparison with those of other oxygen containing solvents.

The excellent properties of methyl-isobutyl ketone (hexone) as a solvent for solvent extraction, not only in ion association systems but also in chelate systems, have been shown by many authors. However, few systematic studies on ketone solvents are to be found.

In order to clarify the relation between some physico-chemical properties of solvents and the distribution coefficients of extractable species, the authors studied the partition equilibria of some β-diketones and those of scandium chelate in some solvent systems; *i.e.*, so called inert solvents,[1-3] alcohol solvents[4,5] and ester solvents.[6] As a further example, the distribution of oxine in inert solvent systems was also studied.[7] It was shown that solubility parametr theory provides a useful approach to the problem, and that the solubility parameters of solvents are more important factors than other parameters such as dielectric constants and dipole moments, which have often been used to explain the role of solvents, in the case where the specific interaction between solute and solvent is not significant.

The present authors will detemine the distribution coefficients of TTA and its scandium chelate in ketone solvent systems, demonstrate the relation between the distribution coefficients and the solubility parameters of the solvents and discuss the characteristic properties of ketone solvents in comparison with other solvents.

Experimental

Materials. Thenoyltrifluoroacetone was obtained from Dojindo Co., Ltd., and was purified by sublimation. Solvents were purified by distillation. Other chemicals were all GR grade. Scandium-46, obtained from the New England Nuclear Corp. (USA) as chloride in a hydrochloric acid solution, was used as a tracer after substituting perchlorate in a perchloric acid solution. The carrier solution of scandium was prepared from scandium oxide of 99.9% purity.

Determination of Distribution Ratio of TTA. A volume 5 m*l* of a ketone solution containing a known amount of TTA was equilibrated by shaking with an equal volume of aqueous solution with an ionic strength of 0.1 adjusted with sodium perchlorate and perchloric acid in an air thermostat at 25 °C. To minimize the error accompanied by volume

*1 Present address: Research Institute of Mineral Dressing and Metallurgy, Tohoku University, Nagamachi, Sendai.

1) T. Wakabayashi, T. Omori, S. Oki and N. Suzuki, *J. Inorg. Nucl. Chem.*, **26**, 2255 (1964).
2) T. Omori, T. Wakabayashi, S. Oki and N. Suzuki, *ibid.*, **26**, 2265 (1964).
3) S. Oki, T. Omori, T. Wakabayashi and N. Suzuki, *ibid.*, **27**, 1141 (1965).
4) N. Suzuki, K. Akiba, T. Kanno and T. Wakabayashi, to be published.
5) N. Suzuki, K. Akiba, T. Kanno, T. Wakabayashi and K. Takaizumi, to be published.
6) N. Suzuki, K. Akiba and T. Kanno, to be published.
7) T. Wakabayashi, This Bulletin, **40**, 2836 (1967).

change due to the mutual solubility, both phases were pre-saturated with each other previous to preparing the TTA solution. After centrifuging, the concentration of TTA in the aqueous phase was determined photometrically; an aliquot of the solution was transferred to a constant volume of 0.6 M phosphate buffer of about pH 6.5 and then the absorbance at 337 mμ resulting from the enolate ion of TTA was measured against a blank run at 25°C. It was confirmed by the preliminary experiment that under the conditions the optical density of the solution closely obeys Beer's law. The distribution ratios thus obtained in a pH region below 4 are equal to the distribution coefficients with an error of less than 1 per cent, as previously shown.[1]

Measurement of Absorption Spectra of TTA in Ketone Phase. The spectra of TTA in ketone phases equilibrated with aqueous phase were measured with a Hitachi EPS-3 recording spectrophotometer using a thin layer cell in order to cancel out strong absorption by the solvent in the UV region.

Determination of Enol Content in Ketone Phase. To determine the enol content of TTA, defined as the ratio of the concentration of enol form to the total concentration of TTA in organic phase, the NMR spectrum was measured with a Varian A-60 NMR Spectrometer. The concentration of TTA was about 0.5 M in all solvents. The enol content was determined from the area ratio of the spectrum for the vinyl type protons to that for protons in the thiophen ring.

Determination of Distribution Ratio of Sc. The procedure and experimental conditions were almost the same as TTA. After two phases were separated, γ-activities of each phase were measured by a well-type scintillation counter. The carrier concentration was 10^{-6} M throughout the experiment, except in the case of examining the influence of carrier concentration on the distribution ratio of scandium.

For almost all ketones, complete equilibrium was attained in several hours in a normal extaction; however, a shorter time of 2 hr was required in the back extraction. To confirm the equilibrium, the normal and back extractions were carried out for all solvents. In the case of back extraction, the concentration of TTA in the aqueous phase was determined in the manner described above. The pH of the aqueous phase at equilibrium was measured with a glass electrode pH meter. Although it should be taken into account that the the pH value obtained above for the aqueous solution containing organic solvent is only an apparent one, the value was adopted without any correction because the solubilities of the solvents in water are of the order of a per cent or less.

Results and Discussion

Distribution of TTA. As shown in Fig. 1, TTA is in a keto-enol equilibrium in the ketone phase, while in inert solvents it exists almost completely as the enol form. Taking into account the spectrum of the aqueous solution below pH 4, the peaks at 266 mμ and 292 mμ may be attributed to the ketohybrate.[8] In the case of petanone, the absorption due to the enol form near 320 mμ does not appear as a peak, while in the case of diisobutylketone containing more carbon atoms, the peak at 320 mμ is clearly seen. It was shown that the spectra are independent of hydrogen ion concentration over the pH range 1—4. In a pH region higher then 5, the absorption at 340 mμ in the organic phase increases with pH in the aqueous phase, which corresponds to the absorption at 337 mμ due to the enolate ion in the aqueous phase. At a higher temperature, the peak at 340 mμ becomes stronger.

TABLE 1. DISTRIBUTION RATIOS OF TTA AND ITS SCANDIUM(III) CHELATE IN KETONE-WATER SYSTEMS, 25°C, IONIC STRENGTH, 0.1 ($HClO_4$+$NaClO_4$)

No	Solvent	δ[a]	δ[b]	log D_{HA}	log D_M (pA=8.0)	r_e
1	Butanone	9.3	9.0	1.37	−2.10[c]	0.18
2	2-Pentanone		8.6_9	2.31	0.31	0.33
3	3-Pentanone	8.8	8.7_6	2.30	0.40	0.32
4	4-Methyl-2-pentanone	8.4	8.3_0	2.30	0,50	0.42
5	Cyclohexanone	9.9	10.0	2.30	0.50	0.23
6	5-Methyl-2-hexanone		8.3_8	2.26	0.25	0.44
7	2-Heptanone		8.4_4	2.28	0.22	0.43
8	3-Heptanone		8.4_4	2.18	0.16	0.50
9	4-Heptanone		8.3_4	2.16	−0.17	0.52
10	5-Methyl-3-heptanone		8.1_7	2.06	−0.40	0.59
11	2,6-Dimethyl-4-heptanone	7.8	7.8_0	1.90	−0.62	0.62
12	2-Octanone		8.3_8	2.20	0.66	0.46
13	2-Nonanone		8.2_6	2.03	−0.23	0.55

a) Found in literature (10).
b) Estimated value by Hildebrand rule.
c) Corrected value considering the contribution of ion associated complex.

8) E. L. King and W. H. Reas, *J. Am. Chem. Soc.*, **73**, 1806 (1950).

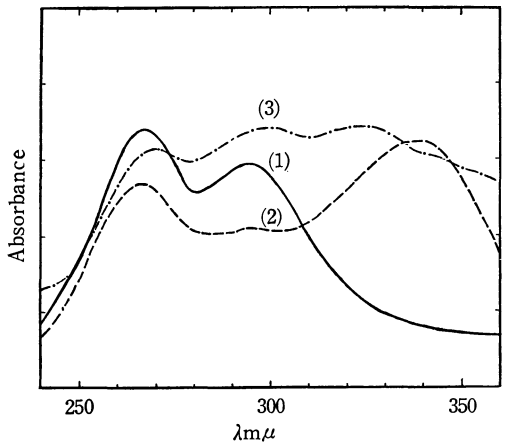

Fig. 1. Absorption spectra of TTA in ketone phase.
(1) 2-Pentanone (below pH 4 in aqueous phase)
(2) 2-Pentanone (pH 7 in aqueous phase)
(3) Diisobutylketone (below pH 4 in aqueous phase)

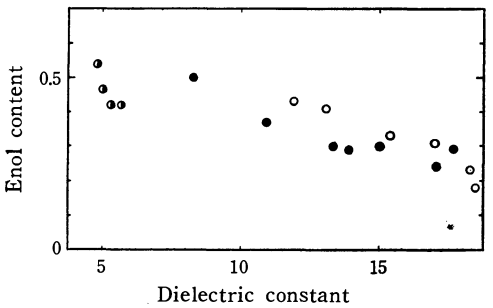

Fig. 2. Enol content of TTA in oxygen containing solvents equilibrated with aqueous solution with pH 2 as a function of dielectric constant of solvent.
● Alcohol, ○ Ketone, ◑ Ester

These facts are common to all the ketones examined. It is, therefore, thought that in the ketone phases, TTA is found as an enolate ion or a sodium salt in a higher pH region.

In the last column of Table 1, the enol contents, r_e, in ketone phases equilibrated with the aqueous phase in a pH range below 4 are summarized. In Fig. 2, the enol contents in oxygen containing solvents under the same conditions are plotted as a function of the dielectric constant of the solvent, though the dielectric constant for the solvent saturated with water should be referred to in order to discuss the influence of dielectric constant on the keto-enol equilibrium. On the whole, there is a trend that the enol content increases with the dielectric constant of solvent.

The distribution ratios of TTA for ketone solvents are shown in Table 1. These values are larger, on the whole, by two or three times than those found in the case of inert solvents, and it is true also in the case of esters.[6] The reason why the distribution coefficients of TTA in the former are larger than those in the latter is understood by considering the fact that in the inert solvents the enol form is almost the only species in the organic phases, while in the case of oxygen containing solvents the enol form is rather a minor species and it is in equilibrium with the keto-hydrate. In alcohol solvents,[4] the distribution ratios are comparable to values in the inert solvents in spite of the similar circumstances to other oxygen containing solvents with respect to the keto-enol equilibrium in the organic phase. In this case, the effect of hydrogen bonding among the solvent molecules should be considered; that is, it may act as if the mole fraction of the solvent were reduced.

As previously reported,[1] the following equation is derived for the distribution coefficient of the enol form of TTA defined as the ratio of the mole fractions in the two phases, P_e,

$$\frac{\log P_e}{\delta_{aq}-\delta_{solv}} = \frac{V_e}{2.30\,RT}(\delta_{aq}+\delta_{solv}-2\delta_e) \quad (1)$$

were δ stands for the solubility parameter for the species corresponding to the subscript. Solubility parameters for some ketones have not been reported. It is possible, however, to estimate the values from the boiling point of the solvent according to the Hildebrand rule.[9] In Table 1, the estimated parameters are listed together with the values found in the literature.[10] In order to apply Eq. (1), it is required to know the distribution coefficients of the enol form. The following relation is established between the distribution coefficient of the enol form and that of the overall forms, D_{HA},

$$P_e = D_e\frac{V_{solv}}{V_{H_2O}} \quad \text{and} \quad D_e = r_e\frac{K_e}{K_a}D_{HA} \quad (2)$$

where K_e, K_a and D_e stand for the dissociation constant of enol, the apparent dissociation constant of TTA and the distribution coefficient of enol form TTA in terms of molarity, respectively. The enol contents of Table 1 are regarded as approximate ones for the present purpose because the values are for a 0.5M TTA solution, and the values

9) J. H. Hildebrand and R. L. Scott, "Regular Solutions," Prentice-Hall, Inc., Englewood Cliffs, New Jersey (1962).
10) J. H. Morrison and H. Freiser, "Solvent Extraction in Analytical Chemistry," John Wiley and Sons Corp., New York (1957).

required are for more dilute solutions of the order of 10^{-2} M, and because there is considerable error in estimating the areas of NMR spectra. However, since no more accurate data are available, the distribution coefficients for the enol form were estimated using the enol contents of Table 1. An attempt to determine the enol ratios more accurately is now undertaken.

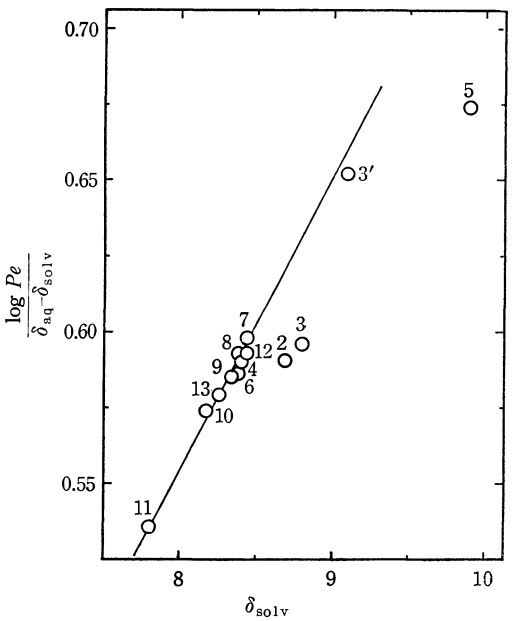

Fig. 3. A relation between distribution coefficients of TTA and solubility parameters of solvents.
Numbers refer to Table 1. 3′ is a corrected value of 3 by Eq. (3).

Since the solubility parameters for aqueous solution and for enol in Eq. (1) are considered constant in all present systems, there should be a linear relation between the left-hand side of the equation and the solubility parameters of the solvents, provided that the equation is valid in the present systems. The result is shown in Fig. 3. For some solvents, such as pentanones, cyclohexanone and butanone, are found considerable deviations from the straight line. The fact may be ascribed to the considerable mutual solubility of water and the solvents. If there are data available on the mutual solubility, it may be possible to correct the solubility parameters for the solvents with the following equation, as is the case of 3-pentanone;

$$\bar{\delta}_{solv} = \phi_{solv}\delta_{solv} + \phi_{H_2O}\delta_{H_2O} \qquad (3)$$

where $\bar{\delta}_{solv}$ and ϕ denote the corrected parameter and the volume fraction of each component in the organic phase, respectively. As the solubility parameter for water, the value of 16.3$_5$ which was obtained previously[1] was used also in the present work. The applicability of Eq. (1) is examined further by the slope of the line which should be related to the molar volume of the reagent. The slope of the line corresponds to a volume of near 140 cc, which is about 10 per cent less than in the previous case.

The reason that the application of the solubility parameter theory is approximately possible even in the present systems may be ascribed to the circumstance that the dispersion effect is dominant among the effects contributing to the cohesive energy, even in polar solvents such as ketones.[11]

Distribution of Scandium. As previously described,[2] the distribution of Sc(III) can be expressed as

$$D_M = \frac{D_{M,0}K_{i=3}[A^-]_{aq}^{\,3}\{1+\Sigma K_j[HA]_{org}^{\,j}\}}{1+\Sigma K_i[A^-]_{aq}^{\,i}}$$

and

$$pA = -\log[A^-]_{aq} = pK_a - pH - \log[HA]_{aq},$$

where K_i is the overall formation constant for $ScA_i^{+(3-i)}$, K_j the overall formation con-

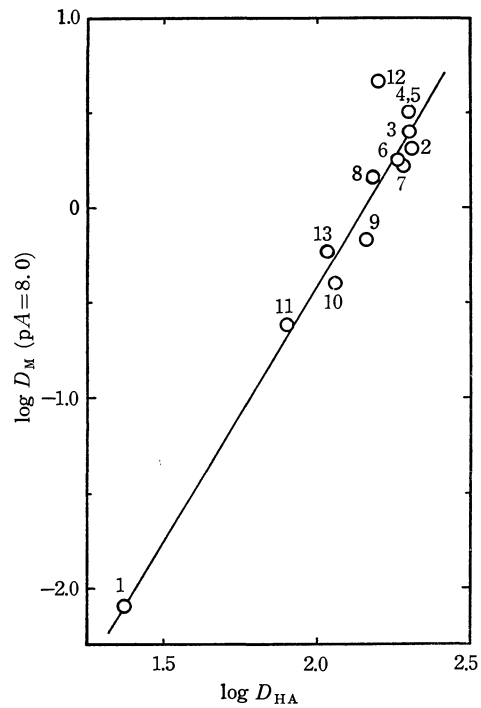

Fig. 4. A correlation between distribution ratios of TTA and those of its scandium chelate in ketone solvent systems.
Numbers refer to Table 1.

11) E. F. Meyer and R. F. Wagner, *J. Phys. Chem.*, **70**, 3162 (1966).

stant corresponding to additive compound formation in the organic phase and $[HA]_{aq}$ the total concentration of the reagent in the aqueous phase determined photometrically. For all ketones, the plotting of $\log D_M$ against pA 8. Considering the fact that, so long as the plotting was carried out against pA, the distribution curves for Sc(III) were common to the various runs under different conditions with respect to the concentration of TTA in the organic phase and pH, it is concluded that the extractable species is of the type ScA_3 alone, except in the case of 2-butanone, in which the ion associated complex with perchlorate ion was extracted. In Table 1, the distribution ratios of scandium at a constant pA of 8.0, which are proportional to the distribution coefficients in each solvent, are summarized.

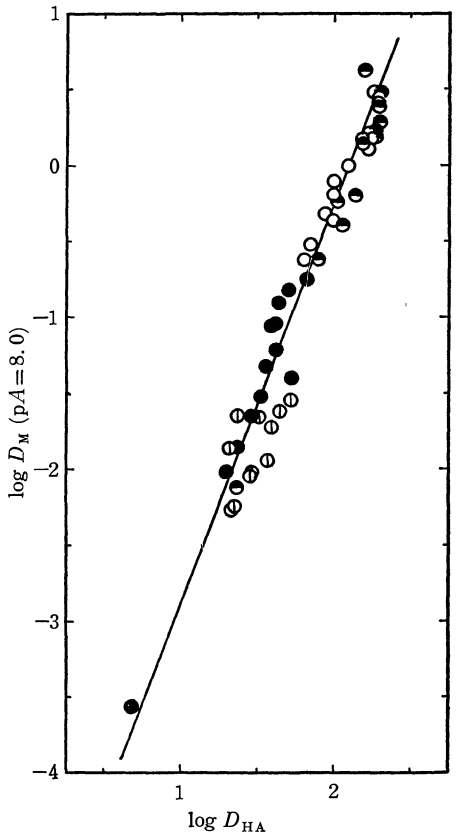

Fig. 5. A correlation between distribution ratios of TTA and those of its scandium chelate in various solvent systems.
● Inert solvent ◓ Ketone
ⓘ Alcohol ○ Ester

There is a distinct correlation between the distribution coefficients of the reagents and those of the chelate, as shown in Fig. 4. In Fig. 5, all of the data obtained until now are plotted similarly. Through all of the solvents, a common straight line can be drawn. Although the relation may be ascribed to the similarity, as already discussed,[2,3] of the interactions with solvent molecules in both cases of free TTA and of that bound to scandium, it should be noted that the abscissae in Figs. 4 and 5 express not the distribution coefficients for the enol form but the overall ones. It cannot be asserted that the enol form should be preferable to the other form of TTA in describing the relation, for the relation is only an approximate one and is not so strict that the difference in interactions between the two forms of TTA and solvent molecules can be considered.

BULLETIN OF THE CHEMICAL SOCIETY OF JAPAN VOL. 41 1859—1864 (1968)

The Bromination of Tris(3-phenyl-2,4-pentanediono)cobalt(III)*1

Yukito MURAKAMI and Katsuyuki NAKAMURA*2

Department of Organic Synthesis, Faculty of Engineering, Kyushu University, Hakozaki, Fukuoka

(Received January 30, 1968)

Tris(3-phenyl-2,4-pentanediono)cobalt(III) has been treated with three kinds of bromination reagents; bromine in the presence of pyridine, pyridine perbromide, and *N*-bromosuccinimide. Components of the product species have been detected by means of thin-layer chromatography and fractionated by liquid-chromatography. The characterization of bromination products has been performed by the aid of infrared and nuclear magnetic resonance spectroscopy. The bromination has taken place with the chelate ring remaining intact, and converted methyl groups in the coordinated ligands to bromomethyl. The cleavage of coordinate bonds, which has occurred afterward, has resulted in the formation of a metal-absent brominated ligand. Among various bromination products, the one with lowest bromination degree (monobrominated chelate) has been fully characterized in accordance with the experimental facts: elemental analysis, the appearance of a new infrared band at 1248 cm^{-1} which is attributable to CH_2 wagging vibration of the CH_2Br group, and two doublet NMR peaks at 3.55, 3.69, 3.94 and 4.09 in δ-value which are due to nonequivalent protons of the CH_2Br group. Reaction mechanism has been discussed in terms of electrophilic substitution process.

Much work has been carried out on the halogenation of metal chelate compounds of β-diketones in relation to the quasiaromatic nature of the chelate rings.[1-5] In order to extend the halogenation reaction to the metal complexes formed with 2,4-pentanediones which carry an aromatic substituent at the 3-position, tris(3-phenyl-2,4-pentanediono)-chromium(III)*3 has been treated in the previous study.[6] In pursuing this type of reaction with the same purpose, tris(3-phenyl-2,4-pentanediono)cobalt(III)*4 was brominated in this work and the resulting products were characterized by means of infrared and nuclear magnetic resonance spectroscopy. In addition, these results were compared with the reactivity of the chromium chelate.

Experimental

Bromination of $Co(PAA)_3$ with Bromine. (a) $Br_2/Co(PAA)_3=2$. A solution of bromine (0.96 g, 6 mmol) in 10 m*l* of chloroform was added dropwise, with stirring, to a solution of $Co(PAA)_3$ (1.75 g, 3 mmol) and pyridine (0.48 g, 6 mmol) in 150 m*l* of chloroform in 30 min at 25°C, and the stirring was continued for another 15 min. The resulting reaction mixture was evaporated under reduced pressure below 15°C, and extracted with benzene. The extraction residue of blue solid was identified as the pyridine-cobalt(III) complex. The benzene extract was evaporated to remove benzene (A), washed with water, and then dissolved in a small amount of methanol. The methanol solution was allowed to stand overnight in a refrigerator and the resulting green solid (B) was collected. The thin-layer chromatograms with a combination of Wakogel B-O (silica gel with no binder) and chloroform for materials A and B along with other related ones are shown in Fig. 1. The brominated material A was then fractionated into five components by means of liquid-chromatography with a combination of silica gel (60—80 mesh) and benzene. The solid materials recovered from the eluted fractions were recrystallized from chloroform-methanol. These products are (see Fig. 1): i) yellow liquid; ii) green crystals (bromination prod-

*1 Contribution No. 148 from the Department of Organic Synthesis, Faculty of Engineering, Kyushu University.

*2 Present address: Technical Research Laboratories, Asahi Chemical Industries, Ltd., Itabashi-ku, Tokyo.

1) R. W. Kluiber, *J. Am. Chem. Soc.*, **82**, 4839 (1960).

2) J. P. Collman, R. A. Moss, H. Maltz and C. C. Heindel, *ibid.*, **83**, 531 (1961).

3) Y. Nakamura and S. Kawaguchi, This Bulletin, **38**, 954 (1965).

4) Y. Nakamura and S. Kawaguchi, *ibid.*, **40**, 1179 (1967).

5) Y. Nakamura, M. Hirata and S. Kawaguchi, *ibid.* **40**, 2572 (1967).

*3 Abbreviated as $Cr(PAA)_3$ hereafter.

6) Y. Murakami and T. Wakabayashi, *ibid.*, **38**, 2207 (1965).

*4 Abbreviated as $Co(PAA)_3$ hereafter. Preparation of this chelate has been mentioned previously (K. Nakamura and Y. Murakami, *Tech. Reports Kyushu Univ.*, **38**, 329 (1965)).

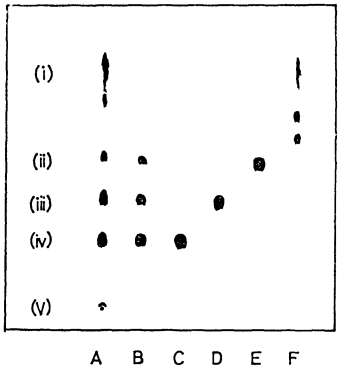

Fig. 1. Thin-layer chromatograms of various bromination products obtained with a combination of Wakogel B-O and chloroform: A, bromination product obtained from the reaction of $Co(PAA)_3$ with bromine at 1:2 molar ratio; B, green solid obtained from A; C, $Co(PAA)_3$; D, BRP-1; E, BRI-2; F, BRP-3.

uct 2*[5]), mp 140—140.5°C (dec.), yield a few mg, R_f 0.30; iii) green crystals (bromination product 1*[5]), mp 161—162.5°C (dec.), yield 100 mg, R_f 0.20; iv) green crystals (unreacted cobalt chelate), mp 183—184°C (dec.), 240 mg, R_f 0.15; v) greenish brown solid (unidentified).

Found for BRP-1: C, 59.83; H, 5.01%. Calcd for $C_{33}H_{32}O_6BrCo$ (monobromochelate): C, 59.74; H, 4.86%.

(b) $Br_2/Co(PAA)_3=6$. A solution of bromine (2.88 g, 18 mmol) in 10 m*l* of carbon tetrachloride was added, with stirring, to a solution of $Co(PAA)_3$ (1.75 g, 3 mmol) and pyridine (2.5 g) in 200 m*l* of carbon tetrachloride in 20 min at 9—11°C. The stirring was continued for another 10 min at 9°C, and the mixture was evaporated under reduced pressure at room temperature. The residue was extracted with benzene, washed with water and then dried over sodium sulfate. The thin-layer chromatogram for this benzene extract is shown in Fig. 1 (bromination product 3*[5]). However, the liquid-chromatographic separation of this extract into components was not successful.

Bromination of $Co(PAA)_3$ with Pyridine Perbromide. A solution of pyridine perbromide (0.72 g, 3 mmol) in 10 m*l* of chloroform was added dropwise, with stirring, to a solution of $Co(PAA)_3$ (1.75 g, 3 mmol) in 150 m*l* of chloroform in 90 min at 1°C, and the stirring of another 60 min was performed at the same temperature. The resulting bluish green solution was evaporated under reduced pressure to remove solvent, and the residue was washed several times with each small portion of water. Into this residue was added a small amount of methanol, and the mixture was allowed to stand overnight in a refrigerator to afford a green precipitate. This solid was then washed with cold methanol and petroleum ether successively; 0.89 g. Repeated liquid-chromatographic separation and purification of this green substance with a combination of silica gel (60—80 mesh) and benzene, followed by recrystallization from benzene, afforded green crystals; mp 161—162°C, yield 10 mg, identified as BRP-1. The unreacted cobalt chelate was also recovered; 0.71 g.

Bromination of $Co(PAA)_3$ with *N*-Bromosuccinimide. A 1.60 g (9 mmol) sample of *N*-bromosuccinimide was added to a solution of $Co(PAA)_3$ (1.75 g, 3 mmol) in 250 m*l* of carbon tetrachloride. Then, the mixture was placed in an oil-bath (85—90°C) and refluxed for 15 min with vigorous stirring. After being cooled down by the use of an ice-water bath, the reaction mixture was filtered off. The filtrate was then concentrated *in vacuo* to recover green solid (1.66 g). Liquid-chromatographic separation of the green material into components with the combination of silica gel (60—80 mesh) and benzene afforded BRP-1 (a few mg), BRP-2 (very small amount), and the unreacted cobalt chelate (1.6 g).

Bromination of $Cr(PAA)_3$ with Bromine. A solution of bromine (5.75 g, 36 mmol) in 30 m*l* of carbon tetrachloride was added dropwide, with stirring, to a solution of $Cr(PAA)_3$ (3.45 g, 6 mmol) and pyridine (2.85 g, 36 mmol) in 500 m*l* of carbon tetrachloride in 35 min at 15°C, and the stirring was continued for another 20 min. Then, the mixture was filtered off, and the filtrate was concentrated *in vacuo* and then extracted with benzene. The thin-layer chromatogram with a combination of Wakogel B-O and benzene for the benzene extract is shown in Fig. 2. The product was then fractionated into components by means of liquid-chromatography with a combination of silica gel (60—80 mesh) and benzene: i) yellow oily liquid, 530 mg; ii) green solid, 150 mg; iii) and iv) dark yellow solid, 220 mg; v) brownish violet solid, 430 mg; and vi) unreacted chromium chelate, 560 mg.

Spectral Measurements. The infrared spectra were obtained on a Koken Model DS-301 spectrophotometer equipped with sodium chloride optics.*[6]

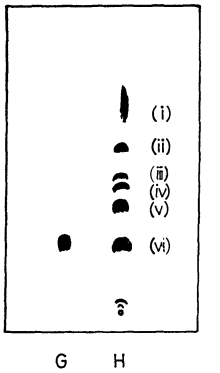

Fig. 2. Thin-layer chromatograms of Cr-$(PAA)_3$ (G) and its bromination product (H) obtained with a combination of Wakogel B-O and benzene.

*[5] Bromination products 1, 2 and 3 are designated as BRP-1, BRP-2, and BRP-3, respectively, throughout this paper.

*[6] Measurements were carried out by Miss Y. Tomita of this Department.

The NMR spectra were recorded on a Varian A-60 spectrophotometer*7 operating at 60 Mc. Chemical shifts are reported in ppm from internal tetramethylsilane (TMS) and data are good to 0.5 cps. The spectra were calibrated by the use of chloroform signal (436 cps from TMS) as the secondary reference. Chloroform used as solvent was purified by the standard method and was free from alcohol. Fractional distillation of this solvent was carried out just before use.

Characterization of Bromination Products

As described in the preceding section, the brominated material obtained from $Co(PAA)_3$ consists of various species of different bromination-degree. Among these reaction products, however, BRP-1 was obtained in the highest yield, relative to others, under mild conditions. BRP-1 was isolated in the form of green crystals and eluted from a chromatographic column before the unreacted chelate $Co(PAA)_3$. First of all in characterizing this material, elemental analysis confirms this undoubtedly to be a monobrominated chelate. Infrared spectra, which are illustrated in Fig. 3, provide the second information. Among various alteration of absorption peaks in the brominated product with reference to the starting chelate $Co(PAA)_3$, the appearance of a new peak at 1248 cm^{-1}, which can be assigned to CH_2 wagging vibration of the CH_2Br group,[6,7] is most significant and provides the decisive evidence for the characterization of the bromination product. In addition, the following changes in absorption bands are observed: absorption peaks due to asymmetric and symmetric deformation of CH_3 group in $Co(PAA)_3$, which appear at 1423 and 1349 cm^{-1} respectively, diminish their intensity in the bromination product. On the other hand, in the brominated material the 1433 cm^{-1} band assigned to CH_2 deformation is detected and the 1300—1400 cm^{-1} region, where the CH_3 symmetric deformations demonstrate their peaks, becomes more crowded by the appearance of other peaks at 1387 and 1368 cm^{-1}. Moreover, the CH_3 rocking vibration absorb-

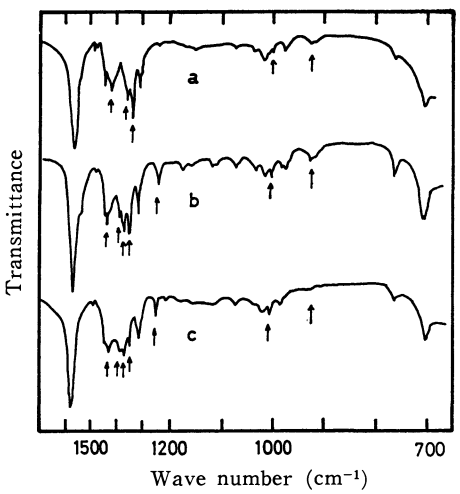

Fig. 3. IR spectra of cobalt(III) chelates (KBr disk method): a, $Co(TAA)_3$; b, BRP-1; c, BRP-2.

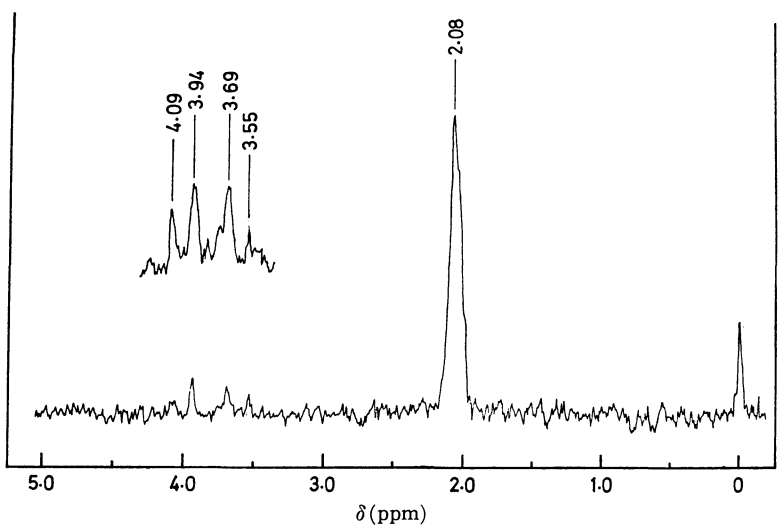

Fig. 4. NMR spectrum of the brominated cobalt(III) chelate (BRP-1) in chloroform (73 mg/0.8 ml); TMS as an internal reference.

*7 Measurements were carried out by Mr. Y. Nakayama and Mr. M. Fukumitsu of this Department.

7) N. B. Colthup, L. H. Daly and S. E. Wiberley, "Introduction to Infrared and Raman Spectroscopy," Academic Press, New York (1964), p. 317.

i ng at the 1000 cm^{-1} region increases its band-intensity as $Co(PAA)_3$ is converted to the brominated substance. The NMR spectrum is to be investigated in the third place. Figure 4 shows the NMR spectrum for the bromination product in part, where proton signals characteristic of CH_3 and CH_2X group can be observed. A NMR signal at δ 2.08 is attributed to CH_3 protons, while four signals at 3.55, 3.69, 3.94 and 4.09 in δ-value are due to protons of the CH_2Br group. Judging from the steric interaction of the CH_2Br group with the phenyl in the brominated chelate, it is reasonable to consider that the former is somehow fixed in space relative to the latter. This may provide a small chemical shift difference between two protons of the CH_2Br group (CH_aH_b type) and then produces two doublets as a result. In conformity with the above experimental evidence, structure I is now assigned to BRP-1, where only one methyl is brominated to bromomethyl (CH_2Br) among six methyl groups in the chelate.

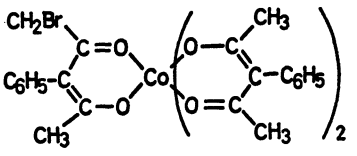

I

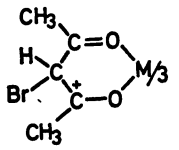

VI

BRP-2 was isolated as green crystals and eluted from chromatographic column faster than BRP-1. All the significant changes in infrared spectrum noticed for BRP-1 become more apparent in BRP-2, and in addition the 929 cm^{-1} band in the unbrominated chelate attributable to the coupling stretching vibration of C–CH_3 and CO[8] reduces its intensity

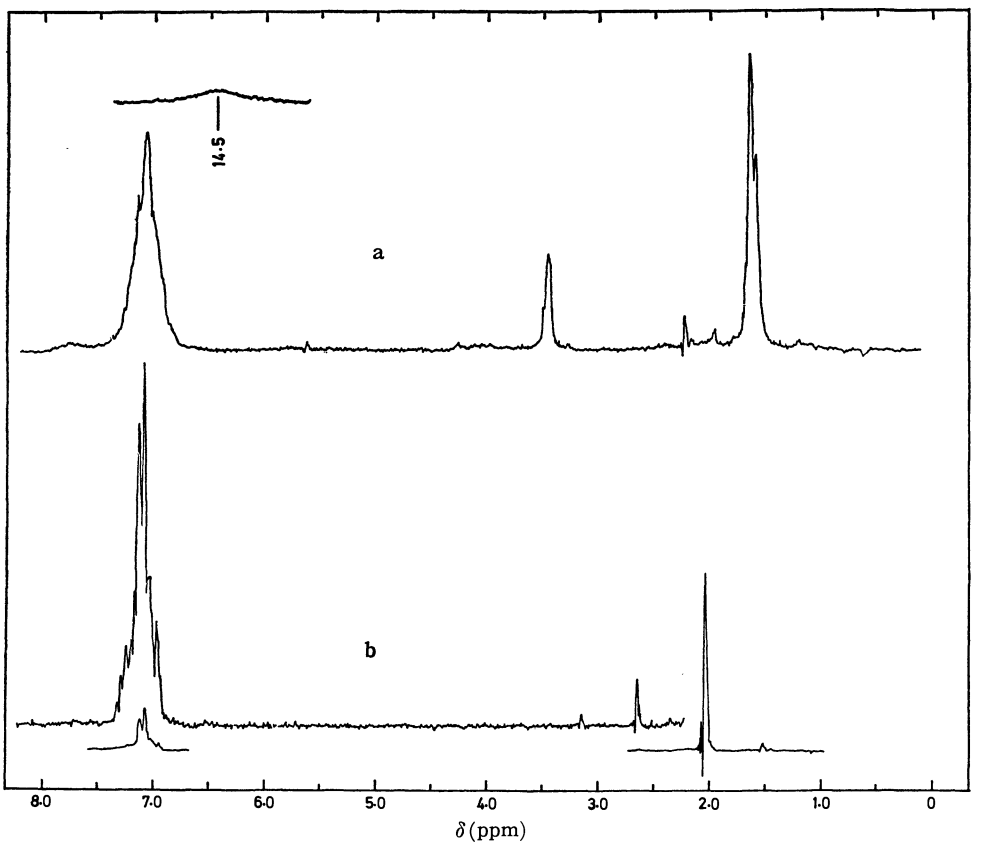

Fig. 5. NMR spectra of 2,4-pentanediones: a, yellow liquid (the metal-free bromination product of $Co(PAA)_3$); b, 3-bromo-3-phenyl-2,4-pentanedione.

8) K. Nakamoto, P. J. McCarthy, A. Ruby and A. E. Martell, *J. Am. Chem. Soc.*, **83**, 1066 (1961).

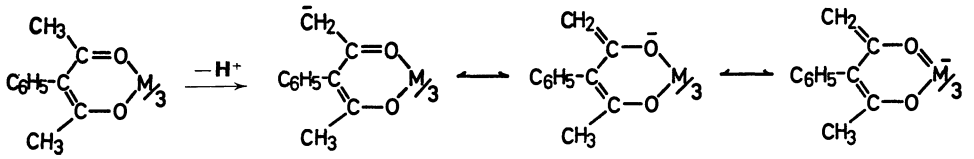

II III IV V

in this product. The above experimental facts suggest that the material is of higher bromination-degree with more bromomethyl groups relative to BRP-1.

It is evident that BRP-3 contains two kinds of cobalt complexes as thin-layer chromatogram indicates (Fig. 1). But characterization of these species was not performed since these cobalt complexes were not made completely free from yellow oily liquid. Nevertheless, investigation and comparison of chromatographic behavior and infrared spectra of bromination products of $Cr(PAA)_3$ with those of $Co(PAA)_3$ suggest that above brominated cobalt complexes contain more bromomethyl groups than BRP-2 does.

Yellow liquid which came off first from a chromatographic column was not stable in the air at room temperature, and turned brown by evolution of white acidic fumes upon overnight standing. Since this yellow substance freshly obtained from a chromatographic column reacted with copper acetate to yield the corresponding metal chelate species, it is evident that this yellow substance still hold the β-diketone moiety. The NMR spectrum for the yellow substance obtained when 2 mol of bromine reacted with 1 mol of $Co(PAA)_3$ is shown in Fig. 5. The NMR signals located at 1.64, 3.48, 7.13 and 14.5, which can be assigned to protons of CH_3, CH_2Br, C_6H_5, and OH respectively, demonstrate their intensity ratio to be approximately 4:1:5:1. Thus, the NMR evidence suggests that this yellow liquid consists of 3-phenyl-2,4-pentanedione and 1-bromo-3-phenyl-2,4-pentanedione at approximately equal ratio. Moreover, it is clear that no bromine has been introduced at the 3-position of 3-phenyl-2,4-pentanedione, as understood by comparison of the NMR spectrum for 3-bromo-3-phenyl-2,4-pentanedione with the above one (Fig. 5 a, b).

The comparison of the bromination products for $Cr(PAA)_3$ with those obtained previously in this laboratory[6] by means of spectroscopic and other physical and chemical methods confirms the bromination product ii stated in the preceding section to be the highly brominated chelate (with hexa or pentabromomethyl groups) in agreement with the previous results, while the later fractions from a chromatographic column (iii—v) were identified as less-brominated compounds.

Discussion

3-Phenyl-2,4-pentanedione undergoes substitution with bromine at the 3-position to yield 3-bromo-3-phenyl-2,4-pentanedione, while the metal-absent material (yellow liquid) obtained by the bromination of $Co(PAA)_3$ and $Cr(PAA)_3$ carries only a bromomethyl group. Thus, the bromination takes place undoubtedly with the chelate ring remaining intact, and the cleavage of coordinate bonds occurs afterward. In the halogenation reaction of metal complexes formed with the unsubstituted 2,4-pentanedione, the reagents employed for that purpose were considered to be electrophilic.[9] If the same situation can be applied to the present reaction, an activated complex, which is formed through deprotonation of methyl groups, may be represented by resonance structures III—V. In accordance with our previous spectroscopic studies on the metal complexes of 3-phenyl-2,4-pentanedione,[10,11] it became evident that the phenyl ring interacts electronically with the chelate ring and the π-electron delocalization in the chelate ring increases as a result relative to the corresponding metal complexes of the unsubstituted 2,4-pentanedione. This effect may help to stabilize the above-mentioned activated state and thus facilitate the reaction. Moreover, the effect of metal species on the reactivity was also noticed in this work. At 2:1 molar ratio of bromine to $Cr(PAA)_3$, no bromination product was detected, while various bromination products were obtained in the reaction of $Co(PAA)_3$ under comparable experimental conditions. Judging from this result, the cobalt chelate is more reactive than the corresponding chromium chelate. This may be ascribed to the greater π-electron delocalization in the chelate rings of $Co(PAA)_3$ than in those of $Cr(PAA)_3$ as became evident by spectroscopic studies.[10,11]

9) J. P. Collman, *Angew. Chem., Internat. Edit.*, **4**, 132 (1965).
10) Y. Murakami and K. Nakamura, This Bulletin, **39**, 901 (1966).

Meanwhile, Kluiber[1] has put forward an activated complex shown by VI for the bromination of 2,4-pentanedione complexes, where the chelate ring remains intact throughout the transformation. In the bromination of either $Co(PAA)_3$ or $Cr(PAA)_3$, however, a great steric hindrance of the phenyl group seems to be exerted against a bromine approaching to the 3-position, and this interaction prohibits the formation of an activated complex similar to VI. As a result, this effect fails to give any kind of the 3-brominated compounds.

In summary, the bromination of both $Co(PAA)_3$ and $Cr(PAA)_3$ proceeds with retention of coordinate bonds. The reactivity of 3-phenyl-2,4-pentanedione complexes suffers metal-dependency and $Co(PAA)_3$ is more reactive than $Cr(PAA)_3$. On the other hand, a bromomethyl group seems to destabilize the coordinate bonds in the brominated complexes and the metal-free brominated ligand was also produced as a result.

11) Y. Murakami, K. Nakamura, H. Uchida and Y. Kanaoka, *Inorg. Chim. Acta*, June (1968).

BULLETIN OF THE CHEMICAL SOCIETY OF JAPAN VOL. 41 1864—1870 (1968)

Magnetic Moments and d–d Bands of *N*-*n*-Propanol-salicylaldiminato-copper(II)*1

Michinobu KATO,* Yoneichiro MUTO,** Hans B. JONASSEN,***
Kyoko IMAI* and Akiko HARANO**

*Aichi Prefectural University, Mizuho-ku, Nagoya
**Department of Chemistry, Saga University, Saga
***Department of Chemistry, Tulane University, New Orleans, La., U. S. A.

(Received February 29, 1968)

The reaction of cupric acetate with the reaction mixture of γ-aminopropyl alcohol and substituted salicylaldehydes in ethanol gave dimeric copper(II) complexes. The postulated structure of these complexes makes it possible to test the substituent effect transmitted to the coordinating atoms which are not in the superexchange pathway between copper(II) ions in a pair. The magnetic moments observed at room temperature were corrected for the temperature variations to those at 25°C by graphic method based on Bleaney and Bowers' equation. The observed substituent effect on the relation between $\mu_{\text{eff}}^{25°C}$ and λ_{max} is different from that observed for dimeric cupric halides complexes of substituted pyridine *N*-oxides. In these complexes the substituent effect transmits to the bridging oxygen atom in the superexchange pathway. As compared with the parent complex (H), methyl, chloro and benzo groups weakened the magnetic interaction but nitro group strengthened it. An interpretation of the substituent effect is given based on the idea of the mutual influences on the coordinate bonds.

The correlation of the magnetic interaction between copper(II) ions in a pair in dimeric copper(II) complexes or of some other physicochemical properties of the complexes with their chemical structures has primarily been our interest.[1-3] Several papers of investigation along this line have recently been pub-

*1 A part of this study was presented a) by M. Kato, Y. Muto, K. Imai and H. B. Jonassen at the 20th Annual Meeting of the Chemical Society of Japan, Tokyo, April, 1967, Proceedings Vol. II, p. 75; b) by Y. Muto, M. Kato, H. B. Jonassen, H. N. Ramaswamy and K. Imai at the 10th International Conference on Coordination Chemistry, Nikko, September, 1967, Proceedings, p. 337; and c) by M. Kato, Y. Muto, H. B. Jonassen, K. Imai and A. Harano at the 17th Conference on Coordination Chemistry of the Chemical Society of Japan, Hiroshima, December, 1967, Proceedings, p. 196. d) The parent compound of this study and some related compounds were reported by S. Yamada, Y. Kuge, and K. Yamanouchi in *Inorg. Chim. Acta*, **1**, 139 (1967). e) A. Nakahara and his coworkers also reported the parent compound and its related compounds at the 17th Conference on Coordination Chemistry of the Chemical Society of Japan, Hiroshima, December, 1967, Proceedings, p. 29.

1) Y. Muto and H. B. Jonassen, This Bulletin, **39**, 58 (1966).

2) Y. Muto, M. Kato, H. B. Jonassen and H. N. Ramaswamy, *ibid.*, **40**, 1535 (1967).

3) M. Kato, Y. Muto and H. B. Jonassen, *ibid.*, **40**, 1738 (1967).

lished.[4-9] Unfortunately, however, the observed phenomena are often too complicated to give consistent, clear-cut interpretation throughout the whole studies. In the preceding communication,[3] we reported some empirical rules which were observed for dimeric complexes of cupric halides with pyridine *N*-oxide derivatives. In these complexes, the effect of substituents attached to the pyridine ring essentially propagates to the bridging oxygen atoms in the superexchange interaction pathway.[10,11]

This study reports observations in which the substituent effect transmits to the coordinate bonds not in the pathway of magnetic interaction. Such bonds are shown as (2) or

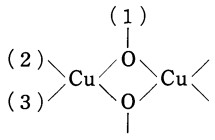

I

(3) in I. The most suitable compounds for the study of this problem are those with unidentate ligands at (2) or (3) because in such a case the pathway of transmission of the substituent effect is definitely established. However, very few stable dimeric copper(II) complexes with an unidentate ligand containing a variety of substituents have been reported.

For the present purpose, chelation between positions 2 and 3 should not as a first approximation, introduce any important complexity in the interpretation of obtained data. However, the coordinate bonds at (2) or (3) should be electronically insulated from that of (1). The postulated structure of the complexes reported here essentially satisfies the above structural conditions (*cf.* structure II): The mesomeric effect of substituent X is insulated by three methylene groups, between the π-electron system being attached to X and the bridging alcoholic oxygen atoms. The inductive effect of X can also be ignored at the bridging alcoholic oxygen atom owing to its rapid attenuation through the three methylene groups.

In addition to such structural characteristics, these compounds have the following advantages: 1) They are so stable that they do not decompose in boiling sodium hydroxide solution. 2) The bridging oxygen atoms do not have any vacant orbitals of π character capable of accepting the d-electrons of the metal. This makes the mutual influence of the coordinate bonds quite simple and the experimental results can be interpreted unambiguously.[12-19]

Experimental

Materials. Salicylaldehyde and its 5-chloro, 5-nitro and 5,6-benzo derivatives were obtained commercially. The 5-methyl derivative was prepared by the Reimer-Tiemann reaction of *p*-cresol with chloroform.[20]

The Preparation of the Copper(II) Complexes. The reaction mixture of a slight excess of γ-aminopropyl alcohol and salicylaldehyde or one of the derivatives in ethanol was added to the ethanol solution of cupric acetate monohydrate acidified with few drops of glacial acetic acid. Complete dissolution of cupric acetate monohydrate in ethanol

TABLE 1. ANALYTICAL DATA OF COMPLEXES

Substituent X		Analysis, % Cu	C	H	N
H	Found	26.39	49.88	4.60	5.81
	Calcd	26.14	49.92	4.64	5.91
5-CH_3	Found	24.94	51.86	5.14	5.49
	Calcd	25.11	52.09	5.24	5.81
5-Cl	Found	23.09	43.65	3.66	5.09
	Calcd	22.80	43.67	3.73	5.37
5,6-Benzo	Found	21.84	57.82	4.50	4.81
	Calcd	21.64	58.00	4.55	4.92
5-NO_2	Found	22.23	42.03	3.53	9.80
	Calcd	22.22	42.06	3.61	9.81

4) M. Kato, H. B. Jonassen and J. C. Fanning, *Chem. Revs.*, **64**, 99 (1964).
5) J. Lewis, Y. C. Lin, L. K. Royston and R. C. Thompson, *J. Chem. Soc.*, **1965**, 6464.
6) W. E. Hatfield and F. L. Bunger, *Inorg. Chem.*, **5**, 1161 (1966).
7) W. E. Hatfield and J. C. Morrison, *ibid.*, **5**, 1390 (1966).
8) W. E. Hatfield, C. S. Fountain and R. Whyman, *ibid.*, **5**, 1855 (1966).
9) L. Dubicki and R. L. Martin, *ibid.*, **5**, 2203 (1966).
10) H. L. Schäfer, J. C. Morrow and H. M. Smith, *J. Chem. Phys.*, **42**, 504 (1965).
11) R. S. Sager, R. J. Williams and W. H. Watson, *Inorg. Chem.*, **6**, 951 (1967).
12) F. Basolo and R. G. Pearson, "Progress in Inorganic Chemistry," Vol. IV, ed. by F. A. Cotton, Interscience Publishers, New York (1962), p. 381.
13) J. Chatt, L. A. Duncanson and L. M. Venanzi, *J. Chem. Soc.*, **1955**, 4456.
14) J. Chatt, L. A. Duncanson and L. M. Venanzi, *ibid.*, **1955**, 4461.
15) J. Chatt, L. A. Duncanson, B. L. Shaw and L. M. Venanzi, *Faraday Soc. Discussions*, No. 26, 131 (1958).
16) F. Basolo, J. Chatt, H. B. Gray, R. G. Pearson and B. L. Shaw, *J. Chem. Soc.*, **1961**, 2207.
17) D. M. Adams, J. Chatt, J. Gerratt and A. D. Westland, *ibid.*, **1964**, 734.
18) J. Chatt, N. P. Johnson and B. L. Shaw, *ibid.*, **1964**, 1662.
19) G. W. Parshall, *J. Am. Chem. Soc.*, **88**, 704 (1966).
20) F. Tiemann and C. Schotten, *Ber.*, **11**, 773 (1878).

TABLE 2. MAGNETIC DATA OF COMPLEXES

Substituent X	Susceptibility $\chi_g \cdot 10^6$ (cgs, emu.)	Temperature (°K)	μ_{eff} (B. M.)	$\mu_{eff}^{25°C}$ (B. M.)	Difference between the two values of $\mu_{eff}^{25°C}$ (B. M.)
H	−0.11	288	0.45_7	0.49_0	0.00_2
	−0.05	303	0.50_5	0.48_8	
5-CH_3	0.00	298	0.55_5	0.55_5	0.00_7
	−0.03	290	0.53_0	0.56_2	
5-Cl	-0.08_6	288	0.49_7	0.52_8	0.00_6
	−0.07	290	0.51_0	0.53_4	
5,6-Benzo	-0.08_4	287	0.54_9	0.58_6	0.01_0
	−0.04	302	0.58_8	0.57_6	
5-NO_2	-0.12_5	303	0.46_3	0.44_7	0.00_7
	-0.16_5	289	0.42_8	0.45_5	

is not required. The mixture was stirred at an elevated temperature for a while. The product precipitated and was filtered off on a glass filter, washed with ethanol and dried. The crude material was recrystallized from pyridine. To obtain a better yield, some ethanol or methanol can be added to the pyridine solution. The preparation was repeated at least twice for each type of compound. The analytical data are listed in Table 1.

Magnetic Susceptibility Determinations. These were obtained by the Gouy method at room temperature. The effective magnetic moment, μ_{eff}, per copper atom was calculated from the expression $\mu_{eff}=2.83\sqrt{\chi_M \cdot T}$ B. M., where χ_M is the molar susceptibility corrected using Pascal's constants[21,22] for the diamagnetism of all the atoms in the compounds. The temperature-independent paramagnetism associated with the copper ion was not included in the calculation of μ_{eff} throughout this work. The magnetic moments were corrected for minor room temperature variations to those at 25°C, $\mu_{eff}^{25°C}$, by using Bleaney and Bowers' equation[23] assuming $g=2.2$. The actual correction was made by a graphic method as described in the next section. The susceptibility measurements were made of two different preparations for each compound. The two corrected moment values for each compound coincided within 0.01 B. M. at maximum deviation. The magnetic data were given in Tables 2 and 3.

Graphic Method for Correction of Magnetic Moments for Room Temperature Variations. The Bleaney and Bowers' equation is rearranged as

$$\begin{aligned} J &= kT \ln\{3(g^2/\mu_{eff}^2-1)\} \\ &= 2.303\,kT\{0.4771+\log_{10}(g^2/\mu_{eff}^2-1)\} \\ &= 2.303\,kTX \end{aligned} \quad (1)$$

where

$$X = 0.4771 + \log_{10}(g^2/\mu_{eff}^2-1) \quad (2)$$

J is the energy difference between the singlet and triplet states, k, Boltzmann's constant, and g, the Landé splitting factor.

Taking advantage of the constancy of J, from (1) we obtain

$$T_1X_1 = T_2X_2 \quad (3)$$

Assuming $g=2.2$ in Eq. (2), a graph of the plot of X *versus* μ_{eff} (B. M.) is prepared (Fig. 1). X_1 corresponding the μ_{eff} observed at T_1 is read from the graph. From Eq. (3) one obtains the value of X_2 for T_2 to which the correction is to be made. The μ_{eff} corresponding to X_2 is obtained from the graph.

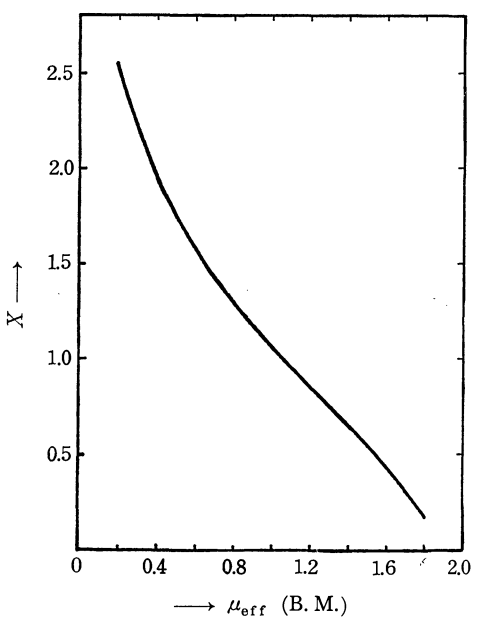

Fig. 1. Plot of X *versus* μ_{eff} (B. M.) in Eq. (2), where $g=2.2$ is assumed.

Diffuse Reflectance Spectra. The diffuse reflectance spectra of the complexes were measured in 400—1000 mμ region on a Shimadzu QR-50 spectrophotometer with a reflectance attachment. Magne-

21) G. Foëx, C. J. Gorter and L. J. Smits, "Constantes Sélectionnées, Diamagnétisme et Paramagnétisme, Relaxation Paramagnétique," Masson & Cie, Paris (1957), p. 222.
22) P. W. Selwood, "Magnetochemistry," Interscience Publishers, New York (1956), pp. 78, 91.
23) B. Bleaney and K. D. Bowers, *Proc. Roy. Soc.* (*London*), **A 214**, 451 (1952).

sium carbonate (heavy) was used as the standard of light reflectance and as the base material to dilute the complexes to obtain appropriate intensities in the reflected light. The preparation of the samples for the spectral measurements involves the following steps: A compound was first ground up in a small agate mortar and it was transferred into another agate mortar containing magnesium carbonate which was previously ground up well. The ground complexes and carbonate were mixed up in the mortar. The mortars and other tools for use were kept in a desiccator. The spectrophotometer was checked for wavelength before and after each measurement at 546.1 mμ by use of a mercury lamp. The temperature of the room should be kept as constant as possible during measurement to obtain a good accuracy in wavelength. Using this procedure the greatest variation in the wavelengths at the band maxima was ± 1 mμ. The band maxima, λ_{max}, are recorded in Table 3.

TABLE 3. DIFFUSE REFLECTANCE SPECTRAL AND MAGNETIC DATA

Substituent X	$\mu_{eff}^{25°C}$	λ_{max}(mμ)
H (Standard)	0.49	570
5-CH_3	0.56	567
5-Cl	0.53	566
5,6-Benzo	0.58	565
5-NO_2	0.45	566

Results and Discussion

Postulation of Structure. The dimeric nature of the parent compound has been established by molecular weight determinations by Yamada *et al.*[*1d] and Nakahara *et al.*[*1e] Two dimeric structures are possible for the complexes under study; one with bridging alcoholic oxygen atoms (II) and the other with bridging phenolic oxygen atoms (III): The data reported here are more in line with structure II and this structure is postulated throughout this study. It was also postulated by Nakahara and coworkers.[*1e] Various physicochemical studies of these complexes are presently in progress by our group and Nakahara's group.[*1e] The data reported here seem to indicate that structure II is the preferred one. Nakahara and coworkers also

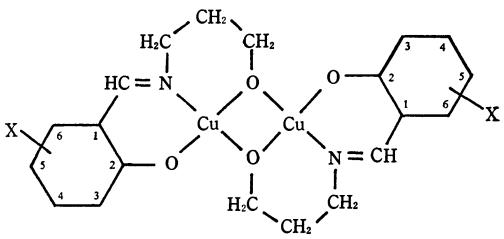

II

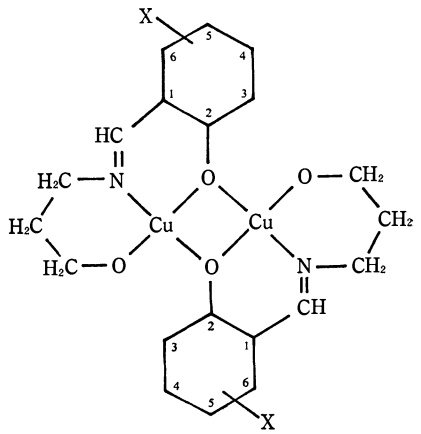

III

prefer this structure. Several experimental facts seem to point in this direction.

The first is related to the various synthetic efforts to make the complexes with the two ligands given in structure IV and V. The stability of the dimeric complexes should essentially be determined by the nature of the bridging groups and the electronic atmosphere of its neighbors in the chelate ring. If the phenolic oxygen atoms bridge between the two copper ions the stability of the two complexes represented in IV and V should be about the same since the electronic atmosphere in the chelating rings are the same (structure VI). On the other hand if the alcohol oxygens are the bridging atoms, the stabilities of the two complexes should be quite different. As structures VII and VIII show the sizes of the chelate rings involving the bridging oxygen are different in the two cases.

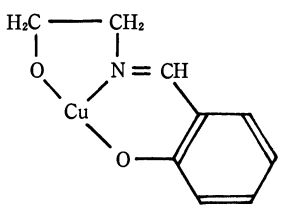

IV

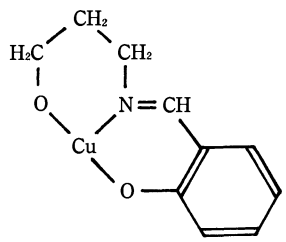

V

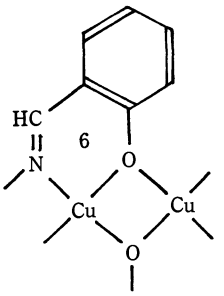

VI

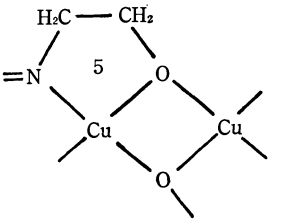

VII

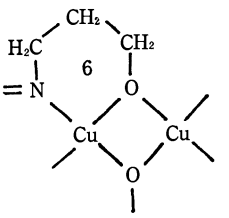

VIII

Nakahara and coworkers[24] have reported that they were able to prepare the monomeric complex of IV with a water molecule occupying the fourth coordination position. This complex could not be prepared for the ligand from V. On the other hand, the dimeric complex can be prepared with ligand V but not with ligand from IV. Such differences would be expected if the structural difference were large enough such as shown in VII and VIII. Nakahara and coworkers*[1e,24-26] are presently investigating the correlation between the stability of complexes with fused rings and the number of members in the fused ring.

The second experimental fact is related to magnetic studies. Comparative studies of magnetic studies of dimeric copper(II) complexes indicate that the magnetic moments of complexes with bridging phenolic oxygen atoms are usually greater than those of complexes with bridging alcoholic oxygen atoms.*[1a,b,27-29] The observed moments of about 0.5 B.M. for copper(II) ion for the complexes are much smaller than those complexes containing phenolic oxygen bridges.

Diffuse Reflectance Spectra. The five complexes investigated show essentially the same absorption characteristics and are very similar to that of the parent complex given in Fig. 2. The monomeric complexes of some

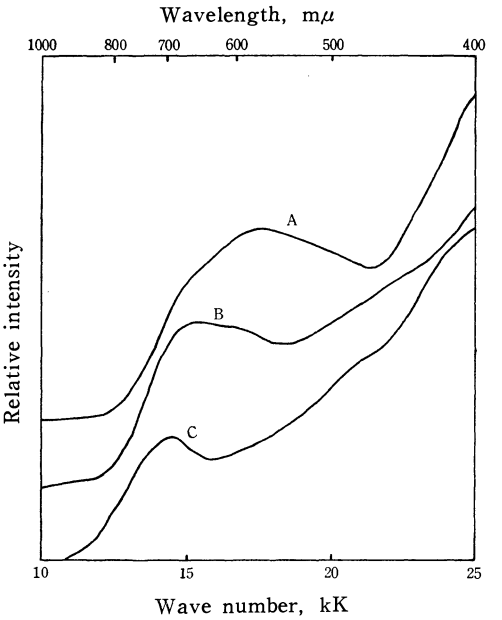

Fig. 2. Diffuse reflectance spectra of *N*-*n*-propanolsalicylaldiminato-copper(II) (A), bis (*N*-methylsalicyl-aldiminato)-copper(II) (B), and bis(*N*-phenylsalicylaldiminato)-copper(II) (C).

of these ligands have been studied by X-ray analysis and were found to be planar: [bis-(*N*-phenylsalicylaldiminato)-copper(II)[30] and bis(*N*-methylsalicylaldiminato)-copper(II)[31]]. For comparison, in Fig. 2, are given the reflectance spectra of these complexes. Their solution spectra have also been reported.*[1d,32,33] A comparative study of the spectra of the dimeric and monomeric complexes indicates that both types can be described as square coplanar.[34,35] Even though in the dimeric

24) A. Nakahara, H. Yamamoto and H. Matsumoto, *Sci. Rep., College of Gene. Edu., Osaka Univ.*, **12**, 11 (1963),

25) A. Nakahara, H. Yamamoto and H. Matsumoto, This Bulletin, **37**, 1137 (1964),

26) A. Nakahara and his coworkers, Paper presented at 20th Annual Meeting of the Chemical Society of Japan, Tokyo, April, 1967, Proceedings Vol. II, p. 9.

27) M. Kato, Y. Muto, H. N. Ramaswamy, H. B. Jonassen, K. Imai and K. Ito, Paper presented at the 19th Annual Meeting of the Chemical Society of Japan, Tokyo, April, 1966, Proceedings Vol. II, p. 135.

28) J. A. Bertrand and R. I. Kaplan, *Inorg. Chem.*, **4**, 1657 (1965).

29) E. Uhlig and K. Staiger, *Z. anorg. u. allgem. Chem.*, **346**, 21 (1966).

30) L. Wei, R. M. Stogsdill and E. C. Lingafelter, *Acta Cryst.*, **17**, 1058 (1964).

31) E. C. Lingafelter, G. L. Simmons, B. Morosin, C. Scheringer and C. Freiburg, *ibid.*, **14**, 1222 (1961).

32) Y. Muto, This Bulletin, **33**, 604 (1960).

33) S. Yamada and H. Nishikawa, *ibid.*, **36**, 755 (1963).

34) The present authors, unpublished data.

35) J. Ferguson, *J. Chem. Phys.* **35**, 1612 (1961).

complexes the ratio of the number of oxygen atoms to the number of nitrogen atoms is greater than in the monomeric complexes, the d-d bands of the dimers occur at shorter wavelengths than the monomers. This seems to indicate that the ligand fields of the alcoholic oxygen atoms are stronger than those of the imino nitrogen atoms.[36]

Sacconi and Ciampolini[37] determined the λ_{max} of a series of planar monomeric bis-salicylaldimine-copper(II) complexes with variation in substituent X. They found a maximum difference of 90 mμ in λ_{max} with variation in X.

Careful measurements of the dimeric complexes of the series reported have shown a maximum difference of only 5 mμ. Since the number of substituent X in dimeric complexes is one per one copper atom compared to two in the monomeric complexes, it would be expected that the monomeric complexes should show a larger substituent effect. However, this effect is very much larger (20 times) in the monomeric species. A study is under way to clarify this anomaly which cannot be explained at the present time.

Relation of Spectra and Magnetism. A linear relationship[3] between λ_{max} and $\mu_{eff}^{25°C}$ has recently been shown to exist for the dimeric complexes of copper(II) halides with substituted pyridine *N*-oxides. The parent complex (X=H) has a greater μ_{eff} and its λ_{max} is at longer wavelength than the X=CH_3, Cl, *etc.* In the complexes reported in this study, however, the parent complex (X=H) has a smaller μ_{eff} and a larger λ_{max} than those complexes in which X=Cl, CH_3, benzo. The nitro substituted complex again behaves normally just as found for the nitro-substituted pyridine *N*-oxide complex; As was observed in the previous study[3] a smaller value in $\mu_{eff}^{25°C}$ leads to a shorter wavelength for λ_{max}.

The mechanism which determines the relation between $\mu_{eff}^{25°C}$ and λ_{max} seems to be different for the dimeric copper(I) complexes of substituted pyridine *N*-oxides and the dimeric copper(II) complexes under investigation here. This must be due to the fact that the pathway for transmission of the substituent effect is different for the two types of complexes.

On first thought it might be argued that this observed difference might be due to differences in the structures of the two types of complexes. This, in turn, would then lead to differences in the superexchange pathway since in the pyridine *N*-oxide complexes this pathway is through bridging oxygen atoms slightly out of the plane, whereas in the salicylaldiminato-complexes, the superexchange occurs through bridging oxygen atoms in the plane. However, as Goodenough points out[38] as long as the Cu-O-Cu angle remains about 90° the superexchange pathway is not effected by the structural differences between the pyridine *N*-oxide and the salicylaldiminato dimeric complexes.

The substituent effect in the pyridine *N*-oxide dimers is directly transmitted to bridging oxygen atom in the superexchange pathway and changes in the copper-bridging oxygen distance will directly effect the μ_{eff} and the λ_{max}.

In the substituted salicylaldiminato-complexes, on the other hand, it is proposed that the alcohol oxygen bridges and is in the superexchange pathway. Under these conditions the substitution on the benzene ring effects primarily the phenolic oxygen or imino nitrogen *not* in the superexchange pathway. The effect on the alcoholic oxygen should only be secondary and opposite in divertion as shown below.

If a methyl group is substituted into the benzene ring of the parent compound the inductive character of this group would increase the σ electron donor capacities of the phenolic oxygen and the imino nitrogen atoms. This would enhance the ligand field around the copper(II) ion and shift the d-d band toward shorter wavelengths. However, simultaneously by the increase in σ electron density in the copper(II) orbitals would decrease its electron affinity. This in turn leads to a weakening of the σ bond of the bridging alcoholic oxygen atoms trans to the phenolic oxygen or the imino nitrogen bond. Such a decrease in the covalent bond character in the superexchange pathway will in turn result in a decrease in the superexchange itself. This should produce an increase in the magnetic moment which indeed was observed as shown in Table 3.

The chloro and benzo groups in this series seem to act in the same manner. The nitro group, on the other hand, being a strong electron withdrawing enhances markedly the π backbonding capacities of the aromatic π-electron system from the copper(II) ion. As a result, compared to the parent compound

36) H. Ojima and K. Sone, *Z. anorg. u. allgem. Chem.*, **309**, 110 (1961).

37) L. Sacconi and M. Ciampolini, *J. Chem. Soc.*, **1964**, 276.

38) J. B. Goodenough, "Magnetism and the Chemical Bond," Interscience Publishers, New York, London (1963), pp. 180—183.

(X=H), the splitting of the d-d levels of the nitro compound will be increased.[39] Such was indeed observed by Sacconi[37] who reported the greatest "blue shift" in λ_{max} for the monomeric nitro substituted salicylaldimine-copper(II) complexes.

The mechanism of the "blue shift" seems to be the same for these monomeric and dimeric complexes. Backbonding from the copper(II) d-orbitals into the aromatic π-electron system increases the electron affinity of the copper(II) ion. This will increase the covalency of the bond from the copper(II) ion to the alcoholic oxygen atom. This, in turn, will increase its superexchange capacity and will lower the value of μ_{eff}.

The data reported in this study indeed indicate that in these complexes the alcoholic oxygen atoms are the bridging atom rather than the phenolic oxygen attached to the benzene ring.

Fruitful discussions with Dr. L. C. Cusachs are gratefully acknowledged.

39) D. W. Herlocker, R. S. Drago and V. I. Meek, *Inorg. Chem.*, **5**, 2009 (1966).

BULLETIN OF THE CHEMICAL SOCIETY OF JAPAN VOL. 41 1871—1875 (1968)

Intramolecular Hydrogen Bonds. XII.[1] The Dipolar-field and the Hydrogen-bonding Effects of the Hydroxyl Group on the Carbonyl Frequencies of Aliphatic Hydroxy-carboxylates

Nobuo Mori, Yuzuru Asano and Yojiro Tsuzuki

Science University of Tokyo, Kagurazaka, Shinjuku-ku, Tokyo

(Received September 25, 1967)

The infrared carbonyl-stretching absorption bands of several methoxy- and hydroxy-alkanoates have been measured in dilute carbon tetrachloride solutions, and their frequency shifts from the normal bands of ethyl alkanoates have been explained in terms of the dipolar-field and the hydrogen-bonding effects of the substituents. Further, as regards the direction of hydrogen bonding, the spectral data of the hydroxy-esters lead to essentially the same conclusion as that based on their hydroxyl spectra. However, the magnitudes of the carbonyl-frequency shifts due to hydrogen bonding can not be related to those of the corresponding hydroxyl shifts.

In general, the hydrogen bonding of an alkoxycarbonyl group with a hydroxyl preferably involves the carbonyl group, rather than the alkoxy group, as the proton acceptor; the most striking spectral evidence for this is the lowering in carbonyl frequency which results from the formation of a hydrogen bond,[2,3] this lowering usually being of the order of about 10—20 cm^{-1}. In unusual cases where the alkoxy group participates in the hydrogen bonding, however, the carbonyl frequency rises about 10 cm^{-1} above the usual value.[4] This can be a criterion for deciding which of the two proton-acceptors is involved in the hydrogen bonding.

This spectroscopic method of determination has hitherto been used in elucidating similar problems in several intramolecularly hydrogen-bonded systems, such as alicyclic diol-monoacetates,[5] alicyclic hydroxy-carboxylates,[6] and pyrrole-carboxylates.[7] In their own previous papers[8-10] the present authors reported, on the basis of the hydroxyl spectra exclusively, that the intramolecular hydrogen bonding in aliphatic hydroxy-carboxylates involved predominantly the carbonyl group as the proton acceptor. In the cases of ethyl *d,l*-lactate and *d*-tartrate, the carbonyl frequencies were about 4 cm^{-1} lower in carbon tetrachloride than in ether.[8] However, the extent of frequency-lowering in the former solution did not provide any reliable evidence for the above type of hydrogen bonding. In order to elucidate this problem, the carbonyl spectra in dilute carbon tetrachloride solutions have now been measured, together with those of corresponding methylated-hydroxy compounds selected for purposes of comparison.

Experimental

Samples. All the esters examined were known compounds, some of them were commercial products and others, prepared by known methods. They were purified through several fractional distillations; their physical constants were equal or very close

1) Part XI: N. Mori, Y. Takahashi and Y. Tsuzuki, This Bulletin, **40**, 2720 (1967).

2) R. N. Jones, P. Humphries, F. Herling and K. Dobriner, *J. Am. Chem. Soc.*, **74**, 2820 (1952).

3) S. Searles, M. Tamres and G. M. Barrow, *ibid.*, **75**, 71 (1953).

4) H. B. Henbest and B. J. Lovell, *J. Chem. Soc.*, **1957**, 1965.

5) H. B. Henbest, G. D. Meakins and T. I. Wrigley, *ibid.*, **1958**, 2633; F. Dalton, J.I. McDougall and G. D. Meakins, *ibid.*, **1963**, 4063; R. West, J. J. Korst and W. S. Johnson, *J. Org. Chem.*, **25**, 1976 (1960); T. C. Bruice and T. H. Fife, *J. Am. Chem. Soc.*, **84**, 1973 (1962).

6) H. R. Cole and G.T.A. Müller, *J. Chem. Soc.*, **1959**, 1224; J. Castells and J. Palau, *ibid.*, **1964**, 4398.

7) R. Grigg, *ibid.*, **1965**, 5149.

8) N. Mori, Y. Tsuzuki and H. Tsubomura, *Nippon Kagaku Zassi (J. Chem. Soc. Japan, Pure Chem. Sect.)*, **77**, 459 (1956).

9) N. Mori, S. Omura, O. Yamamoto, T. Suzuki and Y. Tsuzuki, This Bulletin, **36**, 1401 (1963).

10) N. Mori, S. Omura, N. Kobayashi and Y. Tsuzuki, *ibid.*, **38**, 2149 (1965).

to the literature values. The carbon tetrachloride was fractionally distilled over phosphorus pentoxide.

Infrared Measurement. The carbonyl-stretching spectra were measured at *ca.* 25°C, using a Hitachi EPI-2 double-beam spectrophotometer equipped with a sodium chloride prism. The measurement was carried out both in the neat state and in solutions of such low concentrations (of about 1—2 mmol/*l*) that any intermolecular hydrogen bonding, as revealed by the hydroxyl spectra,[8-10] was negligible. For the solution measurement, both the reference- and the sample-cell used had a path length of 1.0 cm. The observed frequencies were calibrated against the spectrum of a standard polystyrene film.

Results and Discussion

For purposes of comparison, a series of alkyl alkanoates (1—8) also were examined under the same conditions, since there have been no descriptions of their carbonyl data being measured in concentrations as low as 1 mmol/*l*; the spectra in solutions were almost equal to those in the neat state and they were essentially symmetric with respect to the ordinate at the apparent maximum. The peak frequencies are equal to, or very close to, the

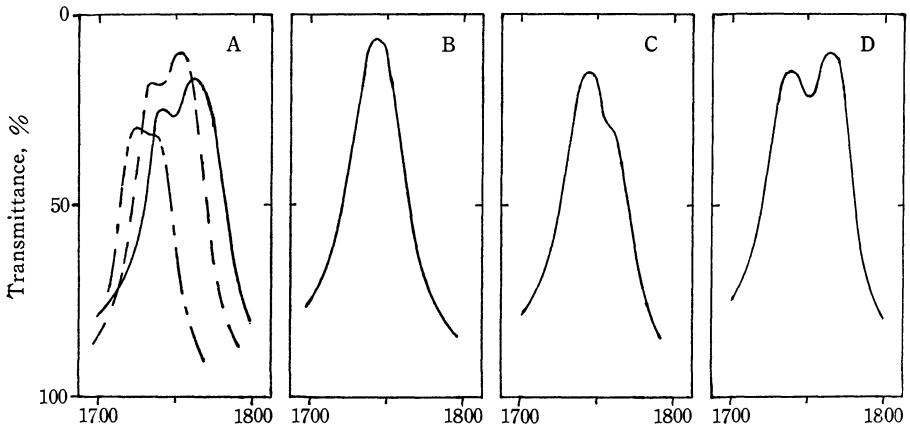

Fig. 1. Carbonyl spectra of methoxy-esters in solutions.
A: ethyl methoxyacetate (9) ——; ethyl α-methoxypropionate (10) — — —; ethyl α-methoxyisobutyrate (11) — - —
B: ethyl β-methoxypropionate (12)
C: dieteyl monomethoxysuccinate (13)
D: diethyl D-α,β-dimethoxysuccinate (14)

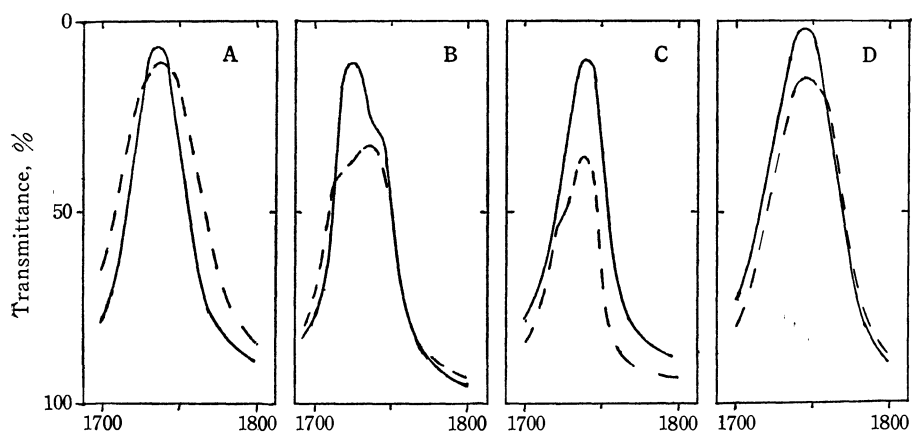

Fig. 2. Carbonyl spectra of hydroxy-esters in solutions —— and in the neat state — — —.
A: ethyl lactate (17); B: ethyl β-hydroxypropionate (20); C: ethyl ε-hydroxycaproate (22); D: diethyl D-tartrate (26)

TABLE 1. CARBONYL FREQUENCIES OF ALKANOATES*

No.	Compound	$\nu_{C=O}$ cm^{-1}	
		CCl_4 soln.	Neat
1	CH_3COOCH_3	1751	1748
2	$CH_3COOC_2H_5$	1745	1744
3	$CH_3COOi\text{-}C_3H_7$	1740	1741
4	$CH_3COOt\text{-}C_4H_9$	1740	1740
5	$C_2H_5COOC_2H_5$	1741	1739
6	$(CH_3)_2CHCOOC_2H_5$	1737	1736
7	$(CH_3)_3CCOOC_2H_5$	1731	1728
8	$(CH_2COOC_2H_5)_2$	1741	1736
9	$CH_2(OCH_3)COOC_2H_5$	1741, 1761	1736, 1754
10	$CH_3CH(OCH_3)COOC_2H_5$	1737, 1752	1739, 1751
11	$(CH_3)_2C(OCH_3)COOC_2H_5$	1733, 1742 sh	1736
12	$CH_2(OCH_3)CH_2COOC_2H_5$	1743	1741
13	$CH_3OCHCOOC_2H_5$ $CH_2COOC_2H_5$	1744, 1759 sh	1736, 1751 sh
14	$CH_3OCHCOOC_2H_5$ (D-form) $CH_3OCHCOOC_2H_5$	1739, 1765	1736, 1756

* Unless otherwise noted, the esters are of the racemic form.
sh = shoulder.

TABLE 2. CARBONYL AND HYDROXYL FREQUENCIES OF HYDROXY-ALKANOATES*[1]

No.	Compound	CCl_4 soln.					Neat	
		$\nu_{C=O}$*[3]		ν_{O-H}[9,10]*[2,3]			$\nu_{C=O}$	ν_{O-H}[9]
		I	III	I	II	III		
15	$CH_2(OH)COOC_2H_5$	1743		3550	3618 w		1745	3427
16	$CH_3CH(OH)COOCH_3$	1741		3549	3616 w		1740	
17	$CH_3CH(OH)COOC_2H_5$	1736		3543	3613 w		1738	3436
18	$CH_3CH(OH)COOi\text{-}C_3H_7$	1738		3544	3614 w		1735	
19	$(CH_3)_2C(OH)COOC_2H_5$	1732		3544	3606 w		1733, 1744 sh	3478
20	$CH_2(OH)CH_2COOC_2H_5$	1725	1744 sh	3584		3640 w	1723 sh, 1734	3426
21	$CH_3CH(OH)CH_2COOC_2H_5$	1725	1743 sh	3560		3626 w	1723 sh, 1738	3430
22	$HO(CH_2)_5COOC_2H_5$		1741	3542 w		3640	1738, 1718 sh	
23	$HO(CH_2)_6COOC_2H_5$		1738			3638	1738, 1720 sh	
24	$HO(CH_2)_8COOC_2H_5$		1738			3638	1739, 1721 sh	
25	$HOCHCOOC_2H_5$ $CH_2COOC_2H_5$	1743		3535	3590 sh		1742	3441
26	$HOCHCOOC_2H_5$ (D-form)	1746		3532	3588 w		1745	3454
27	$HOCHCOOC_2H_5$ (meso-form)	1745		3534	3584 sh			
28	$CH_3CH(OH)CH(OH)COOC_2H_5$ (Threo)	1738		3522	3585*[4]		1740	
29	$CH_3CH(OH)CH(OH)COOC_2H_5$ (Erythro)	1736		3533	3588*[4]		1738	

*[1] Unless otherwise noted, the esters are of the racemic form.
*[2] The frequencies are those of the apparent band-peaks described in the literature.
*[3] I, II and III denote the types of hydrogen bonding : I = C=O···HO; II = >O···HO; III = Unbonded. w = weak; sh = shoulder.
*[4] This is the bonded β-OH frequency to be associated with the OH(β)-to-OH(α) bonding.[11]

reported values, and they depend on both the type of the alcohol part and the type of the acid part, as is shown in Table 1. According to the generally-accepted explanation, this dependence can be attributed predominantly to the electronic effects, operating along the bonds, of both parts on the double-bond character of the carbonyl group. Therefore, the ethyl esters of methoxy- and hydroxy-alkanoic acids, which are the most popular, have been examined in the present study. Some typical spectra are shown in Figs. 1 and 2, while the carbonyl data are summarized, together with the hydroxyl data, in Tables 1 and 2.

Ethyl Methoxy-alkanoates. In solutions, each of the α-methoxy-esters (9—11) shows two bands; one of them appears at the normal frequency characteristic of the corresponding ester with a methyl group instead of a methoxy group, and the other, at a higher (by *ca.* 10—20 cm^{-1}) frequency. The appearance of such a boublet band has hitherto been observed in many α-halo-carbonyl compounds,[12-14] such as some α-halogenated ketones, alkanoates, aldehyds, acid halides, and amides, and, further, in several α-alkoxy-ketones[15] and in some phenoxy- and ethoxy-acetates.[13,16] The doublet has been attributed to the existence of rotational isomers showing two carbonyl frequencies, such as the forms I and II, which can be represented by Newman's projection along the C_1–C_2 bond:

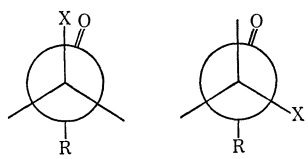

cis Form (I) gauche Form (II)

where X is a highly polar group or atom. The nature of the effects causing the frequency shift has been discussed by Bellamy and Williams,[14] who attributed it primarily to the dipolar field effect operating across the space. When the negatively-charged atom or group X is close in space to the readily polarisable, negatively-charged oxygen atom of the carbonyl group, as in the form I, such a geometry results in a mutual induction of opposite charges; consequently, the carbonyl group becomes less polar, and its vibrational frequency rises above the frequency of the carbonyl group, which is twisted away from X, as in the form II. This mechanism can conveniently explain the present case; the higher frequency band can be associated with the cis form, and the lower frequency band, with the gauche form. Further, the α-methoxy group in the gauche form does not lead to any appreciable carbonyl-frequency shift (*i. e.*, the lower frequency is almost equal to the normal carbonyl frequency of the corresponding ester with a methyl group instead of a methoxy group). This does not necessarily suggest, however, that all inductive effects are absent; rather, it could be due to the cancellation of the inductive effects by small residual field effects, which in that form would be expected to operate in the opposite direction. Such a cancellation has been suggested in accounting for a similar behavior of α-halogens observed in several carbonyl compounds.[14]

Ethyl β-methoxypropionate (12) shows a single band that is identical in both shape and frequency with that of ethyl propionate (5). This indicates that the methoxy group in the β-position, and probably also in a more separated position, has no influence on the carbonyl double-bond character.

Diethyl mono- and di-methoxysuccinate (13 and 14) each shows a doublet band the peak-frequency and relative intensity of which agree with that would be expected from their structures; the monomethoxy-ester shows the overlapped spectra of ethyl α- and β-methoxypropionates (10 and 12), while the dimethoxy-ester shows nearly the same spectrum as that of ethyl α-methoxypropionate.

Ethyl Hydroxy-alkanoates. The α-hydroxy-esters (15—19) show, in solutions, a single, almost symmetric band at nearly the same frequency as the lower-frequency band of the corresponding α-methoxy-esters. This suggests that the hydroxy-esters exist predominantly in an internally-bonded cis-geometry. If the carbonyl and the hydroxyl group (X) are in the cis-relationship, as in the form I,

11) N. Mori, S. Omura and Y. Tsuzuki, *ibid.*, **38**, 2199 (1965).

12) S. Mizushima, T. Shimanouchi, T. Miyasawa, I. Ichishima, K. Kuratani, I. Nakagawa and N. Shido, *J. Chem. Phys.*, **21**, 815 (1953); L. W. Daasch and R. E. Kagarise, *J. Am. Chem. Soc.*, **77**, 6156 (1955); L. J. Bellamy, L. C. Thomas and R. L. Williams, *J. Chem. Soc.*, **1956**, 3704; R. N. Jones and E. Spinner, *Can. J. Chem.*, **36**, 1020 (1958).

13) M. L. Josien and R. Calas, *Compt. rend.*, **240**, 1641 (1955).

14) L. J. Bellamy and R. L. Williams, *J. Chem. Soc.*, **1957**, 4294.

15) N. H. Cromwell, R. E. Bambury and J. L. Adelfang, *J. Am. Chem. Soc.*, **82**, 4241 (1960); N. H. Cromwell, F. H. Schumacher and J. L. Adelfang, *ibid.*, **83**, 974 (1961); J. L. Adelfand, P. H. Hess and N. H. Cromwell, *J. Org. Chem.*, **26**, 1402 (1961).

16) M. Ōki and M. Hirota, This Bulletin, **34**, 374 (1961); T. L. Brown, *J. Am. Chem. Soc.*, **80**, 3513 (1958).

the dipolar electrical forces operating across the space between the groups would raise the carbonyl frequency, much as in the case of the α-methoxy-esters, while the possible hydrogen bonding between them should have the effect of decreasing the carbonyl frequency. On the other hand, if the groups are situated as in the form II, the carbonyl frequency may be expected to be nearly equal to the lower frequency of the corresponding α-methoxy-esters, while the possible hydrogen bonding between the hydroxyl and the ethoxy group (R) should raise the carbonyl frequency. The observed frequencies indicate the preferential existence of the internally-bonded cis-form or the internally-unbonded gauche-form. In reality, however, the latter can not be considered. Nevertheless, this does not obviate the existence of the internally-bonded gauche-form, *i. e.*, another type of hydrogen bonding which involves the ethoxy group as a proton acceptor, because the resolution power of the instrument used is not strong enough to detect a weaker band which may appear at a slightly separated position. The above indication is in good agreement with the conclusion, previously reported on the basis of the hydroxyl spectra,[8-10] that the hydrogen bond is predominantly formed on to the carbonyl group, the ethoxy group being involved to only a minor extent.

In solutions, the β-hydroxy-esters (20 and 21) show, apart from the normal-frequency band appearing as a shoulder, a stronger band at a lower (by *ca.* 20 cm^{-1}) frequency. Since the β-hydroxyl group is expected to have no field and electronic effects, like the β-methoxy group, the strong band can reasonably be assigned to the bonded carbonyl group,*1 and the shoulder, to the free carbonyl group. This provides other striking evidence for the conclusion, previously deduced from their hydroxyl spectra,[10] that the hydrogen bonding in these esters involves the carbonyl group predominantly, while their unbonded molecules are much lower in proportion.

The other higher ω-hydroxy-esters (22—24) show no bonded-carbonyl band, although their hydroxyl spectra indicated that only one of them, ethyl ε-hydroxycaproate (22), was internally bonded to a very small extent.[10] Accordingly, a very weak band due to the bonded carbonyl group in the ester (22) probably overlaps the observed free-carbonyl band.

Diethyl malate (25) and tartrates (26 and 27) show a single band, whose frequency is close to the lower frequency of the corresponding mono- or di-methoxysuccinate (13 or 14). Therefore, the type of hydrogen bonding in these esters is essentially the same as in the α-hydroxy-esters, as was previously concluded on the basis of their hydroxyl spectra.[8,9] Similarly, ethyl α,β-dihydroxybutyrates (28 and 29) form a hydrogen bond between the α-hydroxyl and the carbonyl group, as is indicated by their having the same carbonyl data as the α-hydroxy-esters and as was previously conjectured on the basis of their hydroxyl spectra.[11]

In the neat state, the spectra of all the mono- and di-hydroxy-esters are interesting in comparison with their spectra in solutions. Although the hydroxyl bands in the neat state are very broad and shift greatly towards the lower-frequency side as compared with the spectral bands in solutions, the carbonyl bands, except for those of the β- and the higher ω-hydroxy-esters, remain nearly unchanged in both frequency and band shape. In the β-hydroxy-esters (20 and 21), the relative intensities of the higher-frequency bands to the lower ones are reversed, while in the higher ω-hydroxy-esters (22—24) a new band appears as a shoulder on the lower-frequency side. The authors can not give any decisive explanation for this observation, because more complex, unknown intermolecular interactions are probably involved in the liquid state.

The authors wish to thank Mr. Yutaka Kikuchi of this University for his infrared measurements. Their thanks are also due to the Ministry of Education for its grant-in-aid for Fundamental Scientific Research.

*1 Note Added in Proof : We have recently been informed by Professor P. von R. Schleyer of Princeton University of his study of intramolecular hydrogen bonding between the π-electrons on a carbonyl oxygen atom and a hydroxyl group in hydroxy-carbonyl compounds. He regards, exclusively on the basis of a comparison of $\Delta\nu_{OH}$'s and possible conformations, that the hydrogen bonding in β-hydroxy-ketones involves the π-electrons as the predominant proton acceptor, while in α-hydroxy-ketones the n-electrons on the oxygen atom is the proton acceptor. The same may be suggested in the cases of the α- and β-hydroxy-esters examined, since they have essentially the same $\Delta\nu_{OH}$ values and possible conformations as have the corresponding hydroxy-ketones.

BULLETIN OF THE CHEMICAL SOCIETY OF JAPAN VOL. 41 1876—1883 (1968)

The Cobalt Carbonyl-catalyzed Intramolecular Hydroesterification of Allyl Alcohol with Carbon Monoxide

Akio MATSUDA

Government Chemical Industrial Research Institute, Tokyo, Mita, Meguro-ku, Tokyo

(Received November 1, 1967)

The intramolecular hydroesterification of allyl alcohol with carbon monoxide to give γ-butyrolactone occurred in the presence of cobalt carbonyl under the pressure of carbon monoxide containing a small amount of hydrogen; propionaldehyde and isobutyraldehyde were produced as by-products. The selectivity toward γ-butyrolactone increased with the use of acetonitrile or its derivatives as the solvent. The addition of pyridine, in the absence of these solvents, was effective only in increasing the reaction rate, not in increasing the selectivity toward γ-butyrolactone. On the other hand, in the presence of acetonitrile as a solvent, the selectivity toward γ-butyrolactone increased together with the reaction rate when a catalytic amount of an organic base such as pyridine was added. The higher the reaction temperature, the higher the pressure necessary to attain a maximum selectivity toward γ-butyrolactone; the best yield of γ-butyrolactone was *ca.* 60%. The effect of the partial pressures of hydrogen and carbon monoxide on the initial rate of the formation of each product was made clear. The experimental results were explained by a mechanism involving two different paths for the formation of an alkylcobalt carbonyl-intermediate. The order of effectiveness of acetonitrile and its derivatives as solvents has been interpreted in terms of the HSAB principle by Pearson *et al.*

In a preceding paper on the cobalt carbonyl-catalyzed hydroesterification of acrylonitrile with carbon monoxide and methanol, it was reported that the reaction carried out in the presence of a small amount of hydrogen proceeded rapidly upon the addition of as little pyridine (Py) as 1—4 in terms of the Py/$Co_2(CO)_8$ mole ratio, and that the reaction resulted in a high yield of methyl cyanopropionate, while in the absence of Py the reaction proceeded very little.[1]

In the present study, the possibility of using this method for the synthesis of hydroxymethylbutyrate from allyl alcohol, carbon monoxide, and methanol was first tested. As a result, the intramolecular hydroesterification of allyl alcohol with carbon monoxide to give γ-butyrolactone, the isomerization of allyl alcohol to give propionaldehyde, and the hydroformylation of allyl alcohol with carbon monoxide and hydrogen to give β-hydroxyisobutyraldehyde, which can then be readily dehydrated and hydrogenated into isobutyraldehyde, were found to occur, but not the expected hydroesterification of allyl alcohol with carbon monoxide and methanol to give hydroxy-methylbutyraet.

Adkins and Kresk tested the hydroformylation of allyl alcohol with carbon monoxide and hydrogen and obtained γ-hydroxy-butyraldehyde.[2]

Goetz and Orchin studied the isomerization of allyl alcohol with cobalt hydrocarbonyl, which gave propionaldehyde.[3]

The report by Falbe concerning the ring-closure reactions with carbon monoxide describes the reaction between allyl alcohol and carbon monoxide in the presence of dicobalt octacarbonyl, but the yield of the resulting γ-butyrolactone is reported to be as little as 2%.[4]

The aim of the present investigation, in this connection, is directed at obtaining γ-butyrolactone in as good an yield as possible by the intramolecular hydroesterification of allyl alcohol with carbon monoxide. The synthesis of γ-butyrolactone from allyl alcohol and carbon monoxide may be interesting from

1) A. Matsuda, This Bulletin, **40**, 135 (1967).

2) H. Adkins and G. Kresk, *J. Am. Chem. Soc.*, **70**, 383 (1948).

3) R. W. Goetz and M. Orchin, *ibid.*, **85**, 1549 (1963).

4) J. Falbe, *Angew. Chem.*, **78**, 532 (1966).

an industrial point of view. Moreover, the present reaction may be convenient for determining the factors governing the rate of double-bond isomerization and the factors governing the rate of carbonylation, because, as was pointed out by Goetz *et al.*,[3] if the double-bond isomerization of allyl alcohol should occur, the isomerized product would tautomerize rapidly to propionaldehyde, so equilibrium reactions are unlikely.

Experimental

Such reagents as allyl alcohol, acetonitrile, and pyridine were obtained commercially and rectified before use, except for nicotine and nicotinic acid, which were used without rectification. The synthesis gas was prepared by mixing carbon monoxide with an appropriate amount of hydrogen so that the desired percentage of hydrogen could be obtained. Carbon monoxide and dicobalt octacarbonyl were prepared by the procedure described previously.[5]

The reactions were carried out in a 100-cc stainless-steel autoclave equipped with a magnetic up-and-down stirrer, using essentially the same procedure as was described previously.[1] The reaction temperature was controlled within a range of ±1°C. In the case of the constant-pressure experiment, the synthesis gas was automatically supplied by means of a pressure regulator from a pressure storage vessel in order to keep the total pressure constant throughout the reaction. The amount of gas supplied during the reaction was calculated from the pressure drop in the pressure storage. Experiments at pressures over 300 kg/cm² were carried out with another apparatus, one which had been designed for use at pressures of 1000 kg/cm², but the method of the experiments was essentially the same as in the case of experiments at pressures lower than 300 kg/cm², except that the pressure level in the pressure storage was recorded during the reaction by means of a Strain gauge for the sake of accuracy.

The product composition was quantitatively determined by the gas chromatographical method: the γ-butyrolactone was analyzed with a 3-m column of ethyleneglycol-adipic acid polyester by adding octylacetate, as an internal standard, to the reaction product at the temperature of 200°C, while lower-boiling components, such as propionaldehyde, isobutyraldehyde, and allylalcohol, were analyzed with a 3-m column of ethyleneglycol-adipic acid polyester plus a 2-m column of dioctylphthalate by adding toluene as an internal standard at the temperature of 100°C.

Results

The Effect of Solvents. Preliminary experiments carried out under conditions similar to those of Table 1 showed that the yield of γ-butyrolactone was larger in the absence of a solvent than in the presence of such a solvent as methanol and benzene; they thus suggested that a solvent might have some effect, whether positive or negative, on the selectivity of the reaction. Experiments were, therefore, carried out with various kinds of solvents in order to test their effects, the Py/$Co_2(CO)_8$ mole ratio being kept constant at the optimum value of 1. The results are summarized in Tables 1 and 2.

Solvents such as acetonitrile and its derivatives, as can be seen from Tables 1 and 2,

TABLE 1. THE EFFECT OF SOLVENT (I)

4 mmol $Co_2(CO)_8$, 4 mmol Py, 1/4 mol allyl alcohol; total pressure, 300(initial)—*ca.* 200 kg/cm²; reaction temperature, 100°C; hydrogen content of the gas used, 11%

Solvent	mol	Reaction time min	Conversion mol%	Selectivity toward each product (mol%)			
				$CH_2—CH_2$ / CH_2 $C=O$ / O	C_2H_5CHO	i-C_3H_7CHO	Residue
None	0	60	98	42	15	6.9	36
CH_3CN	0.04	60	97	45	13	7.9	34
CH_3CN	0.1	60	92	49	12	8.5	30
CH_3CN	0.2	60	88	56	11	8.0	25
CH_3CN	0.5	135	91	57	12	8.1	23
CH_3CH_2CN	0.07	60	95	52	15	9.7	23
$(CH_3)_2CHCN$	0.06	60	90	47	14	6.2	33
C_6H_5CN	0.1	60	94	38	12	8.4	42
n-C_3H_7CHO	0.1	60	93	41	21	4.8	33
C_6H_6	0.1	60	98	38	24	6.4	32
CH_3OH	0.2	60	91	38	27	7.8	27

5) A. Matsuda and H. Uchida, This Bulletin, **38**, 710 (1965).

TABLE 2. THE EFFECT OF SOLVENT (II)

4 mmol $Co_2(CO)_8$, 4 mmol Py, 1/4 mol allyl alcohol; total pressure, 100 kg/cm²; reaction temperature, 100°C; hydrogen content of the gas used, 14%

Solvent	mol	Reaction time	Initial rate×10³	Conversion	Selectivity toward each product (mol%)			
					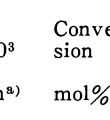	C_2H_5CHO	i-C_3H_7CHO	Residue
		min	mol/min[a]	mol%				
None	0	60	8.8	98	38	28	3.3	31
CH_3CN	1/8	45	7.0	97	49	23	3.0	25
CH_3CN	1/2	60	5.5	93	58	17	4.3	21
CH_3CH_2CN	1/8	55	6.4	98	47	20	3.6	29
CH_3CH_2CN	1/2	60	6.1	95	55	19	3.0	23
$(CH_3)_2CHCN$	1/8	55	6.9	98	51	22	3.9	23
$(CH_3)_2CHCN$	1/2	60	4.9	96	53	26	3.2	18
$NC(CH_2)_4CN$	1/8	120	4.3	98	50	15	3.0	32
CH_3OCH_2CN	1/8	60	3.3	92	50	20	3.1	27
$HOCH_2CN$	1/8	100	3.5	83	55	14	1.7	29
$C_6H_5CH_2CN$	1/8	100	3.9	98	49	21	3.9	26
$HCOOCH_3$	1/8	60	4.1	93	42	31	3.2	24
$(C_2H_5)_2O$	1/8	60	6.1	99	34	47	4.6	14
Dioxane	1/8	60	3.4	95	37	45	5.3	13

a) The amount of gas supplied during the initial 10 min is listed in Tables 2—6 as a rough measure of the initial rate.

are effective in increasing the selectivity toward γ-butyrolactone and in decreasing the selectivity toward propionaldehyde and the residue, but the reaction rate is decreased by these solvents; these effects are apt to be enhanced by the use of a larger amount of such a solvent. Benzonitrile, unlike acetonitrile or its derivatives, has no effect on the selectivity toward γ-butyrolactone.

The effectiveness of such acetonitrile derivatives as $HOCH_2CN$, CH_3OCH_2CN, and $C_6H_5CH_2CN$ in increasing the selectivity toward γ-butyrolactone decreases in the order $HOCH_2CN > CH_3OCH_2CN > C_6H_5CH_2CN$. When methyl-substituted acetonitriles are used as solvents, the above effectiveness decreases as the number of methyl-substitution increases, *i.e.*, in the order $CH_3CN > CH_3CH_2CN > (CH_3)_2CHCN$.

Aldehyde and formic esters as solvents have almost no effect on the selectivity toward γ-butyrolactone. Such ethers as diethyl ether and dioxane, however, when used as solvents increase the selectivity toward propionaldehyde and decrease the selectivity toward γ-butyrolactone. Methanol and benzene also increase the selectivity toward propionaldehyde and decrease the selectivity toward γ-butyrolactone, but their effects are smaller than those of ethers.

The Effect of Acetonitrile as a Solvent and the Effect of the Addition of Py and Other Organic Bases. The selectivity toward γ-butyrolactone has thus been found to increase remarkably with the use of acetonitrile as a solvent and with the use of an amount of Py equimolar to $Co_2(CO)_8$. Experiments were then carried out in the absence of both acetonitrile and Py, in the presence of acetonitrile and no Py, in the presence of Py and no acetonitrile, in the presence of acetonitrile with various amounts of Py, and in the presence of acetonitrile with various kinds of bases other than Py. The results are shown in Table 3.

Evidently, the addition of Py increases the reaction rate, it but does not by itself affect the selectivity, while acetonitrile, when used as a solvent, is, even in the absence of Py, effective in increasing the selectivity toward γ-butyrolactone and in decreasing the selectivity toward propionaldehyde and the residue. Clearly, acetonitrile is effective in increasing the selectivity toward γ-butyrolactone simply because it retards the formation of propionaldehyde and the residue, not because it accelerates the formation of γ-butyrolactone, for Tables 2 and 3 indicate that the reaction rate rather decreases upon the use of acetonitrile as a solvent. Both the reaction rate and the selectivity toward γ-butyrolactone, in the presence of acetonitrile as a solvent, increase as the amount of Py is increased, reach maxima when the $Py/Co_2(CO)_8$ mole ratio is

TABLE 3. THE EFFECT OF ACETONITRILE AS A SOLVENT AND THE ADDITION OF ORGANIC BASES

4 mmol $Co_2(CO)_8$, 1/4 mol allyl alcohol; total pressure 100 kg/cm²; reaction temperatue 100°C; reaction time 1.0 hr; hydrogen content of the gas used, 14%

CH_3CN mol	Organic base	mmol	Initial rate×10³ mol/min[a)]	Conversion mol%	Selectivity toward each product (mol%)			
					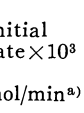	C_2H_5CHO	i-C_3H_7CHO	Residue
0	None	0	2.6	99	35	21	3.3	41
0	Py	4	8.8	98	38	28	3.3	31
0.5	None	0	3.2	78	49	17	2.2	32
0.5	Py	2	4.3	94	54	17	3.7	25
0.5	Py	4	5.5	93	58	17	4.3	21
0.5	Py	6	4.9	87	55	18	4.2	23
0.5	Quinoline	4	5.0	92	54	19	2.8	24
0.5	Nicotinic acid	4	4.8	93	54	18	6.5	21
0.5	Nicotine	2	5.0	93	56	18	2.9	23
0.5	Piperidine	2	4.8	93	55	17	2.2	26
0.5	Pyrrolidine	2	4.2	93	53	18	2.7	26
0.5	*N*, *N*-Dimethyl propionamide	2	3.2	86	51	16	1.6	31

a) *Cf.* Table 2.

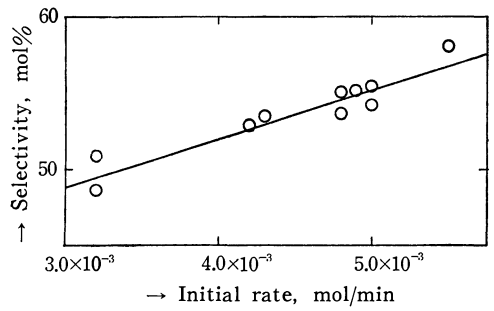

Fig. 1. The relation between the selectivity toward γ-butyrolactone and the initial rate.

1, and then decline. In fact, from the results of experiments carried out with acetonitrile as a solvent in the presence of various amounts of Py or other organic bases, an almost linear relation between the reaction rate and the selectivity toward γ-butyrolactone was obtained, as is shown in Fig. 1. This means that the intramolecular hydroesterification, in the presence of acetonitrile as a solvent, is fairly selectively accelerated by the addition of Py or other organic bases.

The Effect of Pressure and Temperature. The results of experiments which were carried out under various pressures at the constant temperatures of 100, 120, and 130°C are shown in Tables 4 and 5. Clearly the selectivity toward propionaldehyde decreases as the pressure increases, while that toward isobutyraldehye increases. The selectivity toward γ-butyrolactone reaches its maximum at a certain pressure, which increases along with the temperature; the pressure for the best selectivity is 100 kg/cm² at 100°C, 300 kg/cm² at 120°C, and 500 kg/cm² at 130°C.

The results of the experiments carried out under the constant pressures of 400, 600, and 800 kg/cm² at various temperatures are shown in Table 6. Clearly the selectivity toward propionaldehyde increases along with the temperature. The higher the pressure, the higher the optimum temperature for attaining the best selectivity toward γ-butyrolactone; it is 130°C under 400 kg/cm², 140°C under 600 kg/cm², and in the 150—160°C range under 800 kg/cm².

The Effects of the Partial Pressures of Hydrogen and Carbon Monoxide. In order to understand the effect of the total pressure on the rate of the formation of each product, the effects of the partial pressures of hydrogen and carbon monoxide must be examined.

Constant-pressure experiments were carried out at 120°C with 1/4 mol of allyl alcohol, 1/2 mol of acetonitrile, 2 mmol of $Co_2(CO)_8$, and 2 mmol of Py, the composition of the synthesis gas used and the total pressure being varied so that the desired initial partial pressures of hydrogen and carbon monoxide could be attained. Aliquots of the reacting solution were withdrawn from the autoclave at definite intervals of time from the beginning of the reaction and were analyzed in order to

TABLE 4. THE EFFECT OF TOTAL PRESSURE (I)

4 mmol $Co_2(CO)_8$, 4 mmol Py, 1/4 mol allyl alcohol, 1/2 mol acetonitrile; reaction time 1.0 hr; hydrogen content of the gas used, 14%

Total pressure kg/cm²	Reaction temp. °C	Initial rate×10³ mol/min[a)]	Conversion mol %	Selectivity toward each product (mol%)			
				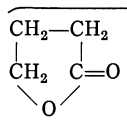	C_2H_5CHO	i-C_3H_7CHO	Residue
50	100	5.8	93	49	26	3.3	22
100	100	5.5	93	58	17	4.3	21
150	100	5.2	88	53	13	5.9	28
200	100	4.9	83	52	11	7.2	30
250	100	3.8	80	52	8.9	8.0	31
300	100	—	77	51	8.5	9.9	31
100	120	12.6	99	51	28	4.7	16
250	120	14.7	100	56	16	7.6	20
300	120	13.7	99	60	12	10	18
400	120	—	99	50	14	12	24

a) *Cf.* Table 2.

TABLE 5. THE EFFECT OF TOTAL PRESSURE (II)

2 mmol $Co_2(CO)_8$, 2 mmol Py, 1/4 mol allyl alcohol, 1/2 mol acetonitrile; reaction time 1.0 hr; hydrogen content of the gas used, 10%

Total pressure kg/cm²	Reaction temp. °C	Initial rate×10³ mol/min[a)]	Conversion mol %	Selectivity toward each product (mol%)			
				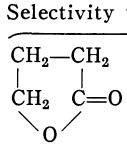	C_2H_5CHO	i-C_3H_7CHO	Residue
300	130	6.1	98	51	17	4.1	28
400	130	6.8	98	52	16	6.0	26
500	130	6.6	97	54	15	7.9	23
600	130	5.9	95	52	13	8.6	26

a) *Cf.* Table 2.

TABLE 6. THE EFFECT OF RECATION TEMPERATURE

1/4 mol allyl alcohol, 1/2 mol acetonitrile; Py/$Co_2(CO)_8$ 8 mole ratio, 1; hydrogen content of the gas used, 4%

Reaction temp. °C	Total press. kg/cm²	Py mmol	Reaction time min	Initial rate×10³ mol/min[a)]	Conversion mol %	Selectivity toward each product (mol%)			
						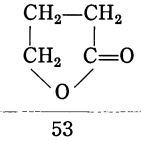	C_2H_5CHO	i-C_3H_7CHO	Residue
120	400	4	60	6.5	95	53	11	3.3	33
130	400	4	60	12.1	98	61	19	4.5	16
140	400	2	60	—	99	57	30	4.1	9
130	600	4	60	7.2	97	51	16	6.0	27
140	600	2	60	6.2	99	56	19	4.8	20
150	600	2	30	13.6	98	53	24	3.7	19
150	800	1	60	5.8	94	54	19	5.3	22
160	800	1	60	8.2	99	54	25	5.1	16
170	800	1	30	12.9	98	46	39	4.8	10

a) *Cf.* Table 2.

determine the individual products. Examples of the plot of the yields of individual products against the reaction time are shown in Fig. 2. In Table 7 are summarized the initial rates calculated on the basis of results of analyses of samples withdrawn at the reaction time of 20 min; the initial rates of the formation of γ-butyrolactone, propionaldehyde, and isobutyraldehyde are denoted by v_1, v_2, and v_3 respectively. The specific increments of the initial rates of the formation of individual products caused by a unit increase in the hydrogen partial pressure, $\Delta v_{1,2,3}/v_{2,2,3}\Delta P_{H_2}$, and those caused by a unit increase in the carbon monoxide partial pressure, $\Delta v_{1,2,3}/v_{1,2,3}\Delta P_{CO}$, were calculated from Table 7. Table 8 lists the specific increment of v caused by a 10 kg/cm² increase in $P_{H_2}(10\Delta v_{1,2,3}/v_{1,2,3}\cdot\Delta P_{H_2})$, and the specific increment of v caused by a 100 kg/cm² increase in P_{CO} $(100\Delta v_{1,2,3}/v_{1,2,3}\Delta P_{CO})$. It is clear from Table 8 that v_1, v_2, and v_3 all increase along with increases in the hydrogen partial pressure, v_3 increasing most conspicuously; that v_1 and v_2 decrease with increases in the carbon monoxide partial pressure, v_2 decreasing more than v_1, and that v_3 is essentially independent of the carbon monoxide partial pressure.

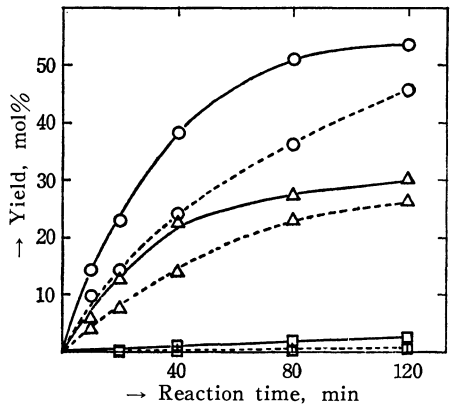

Fig. 2. The plot of the yields of individual products *vs.* the reaction time.
Full line: Expt. No. 2
Dotted line: Expt. No. 1
-○- : γ-Butyrolactone
-△- : Propionaldehyde
-□- : Isobutyraldehyde

Discussion

Since the rates of the formation of γ-butyrolactone, propionaldehyde, and isobutyraldehyde all increase with increases in the hydrogen partial pressure, cobalt hydrocarbonyl evidently plays a part in each of these formations. The cobalt hydrocarbonyl-catalyzed isomerization of allyl alcohol is assumed to take place through the hydrogen-shift in an intermediate π-complex, which is formed between coordinately-unsaturated cobalt hydrotricarbonyl and allyl alcohol, just as is usually assumed in the case of the metal carbonyl-catalyzed isomerization of olefins.[6,7]

Since the overall reaction rate in the present experiment decreases with an increase in the carbon monoxide partial pressure, the first step of the reaction would involve, at least partially, the formation of cobalt hydrotricarbonyl, as was proposed by Heck *et al.* to

TABLE 7. THE EFFECT OF THE RESPECTIVE PARTIAL PRESSURES OF HYDROGEN AND CARBON MONOXIDE ON THE INITIAL RATE OF FORMATION OF EACH PRODUCT

Expt. No.		1	2	3	4	5	6	7
H_2 content of the gas, %		6	10	6	10	6	10	6
Total pressure, kg/cm²		100	104	250	261	160	180	300
P_{H_2} (initial), kg/cm²		6	10	15	26	10	18	18
P_{CO} (initial), kg/cm²		94	94	235	235	150	162	282
Initial rate of formation, mmol/min	V_1	1.8	2.9	2.1	2.8	2.1	2.9	1.7
	$10\,V_2$	9.4	16	5.6	7.4	8.7	7.4	3.5
	$100\,V_3$	1.9	3.9	6.3	19	4.9	9.6	8.9

TABLE 8. SPECIFIC INCREMENTS CALCULATED FROM TABLE 7

P_{CO}, kg/cm²	$10\Delta V_1/V_1\Delta P_{H_2}$	$10\Delta V_2/V_2\Delta P_{H_2}$	$10\Delta V_3/V_3\Delta P_{H_2}$
94	1.5	1.8	2.6
235	0.30	0.29	1.8
P_{H_2}, kg/cm²	$100\Delta V_1/V_1\Delta P_{CO}$	$100\Delta V_2/V_2\Delta P_{CO}$	$100\Delta V_3/V_3\Delta P_{CO}$
10	−0.49	−0.81	+0.46
18	−0.34	−0.44	−0.061

6) T. A. Manuel, *J. Org. Chem.*, **27**, 3941 (1962).
7) F. Asinger, B. Fell and K. Schrage, *Chem. Ber.*, **98**, 372 (1965).

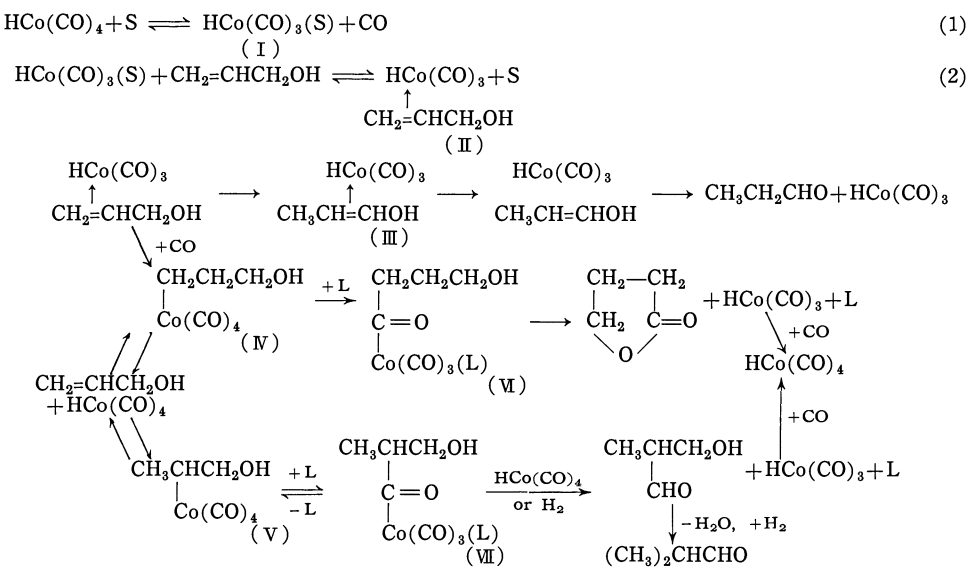

explain the inhibition by CO of the reaction of cobalt hydrotetracarbonyl with olefins.[8]

In a preceding paper on the hydroesterification of acrylonitrile,[1] two separate paths were proposed for the formation of alkylcobalt tetracarbonyl; one was the direct addition of $HCo(CO)_4$ to acrylonitrile, while the other was the path which goes through an acrylonitrile π-complex. In the present paper, also, the reaction mechanism will be discussed taking into account the possibility of the two separate above-mentioned paths.

The catalytic mechanism shown below can explain the experimental results; S denotes a solvent such as acetonitrile, while L denotes a basic ligand such as Py. The intermediate cobalt hydrotricarbonyl is assumed to form a complex with a solvent molecule before it reacts with allyl alcohol, since it is coordinately unsaturated and can, therefore, easily be attacked by surrounding molecules. A basic ligand such as Py (L) is assumed to take part in the reaction by forming complexes (VI) and (VII), since it was proved in a previous study that Py was necessary for the formation of acylcobalt carbonyls.[1]

Acetonitrile forms a complex with metal carbonyls, and, according to Cotton,[9] it possesses a small but real ability to accept π-electrons in competition with CO groups. Accordingly, the complex (I), when S is acetonitrile, will be comparatively stable as a result of π-bonding. The concentration of the complex (II) will, therefore, decrease with an increase in the concentration of acetonitrile as a solvent according to the equilibrium relation (2). Hence, the isomerization, which proceeds *via* the complex (II), will be retarded when acetonitrile is used as a solvent, and the selectivity toward the intramolecular hydroesterification, which can proceed *via* another path, will, relatively, increase; this is in good agreement with the results shown in Table 1. The residue of the analysis shown in Table 1—6, which is an aldolic polymer with a molecular weight of 290,[10] seems to be formed, at least in part, *via* the complex (II), since the selectivity toward the residue decreases together with the selectivity toward propionaldehyde as the amount of acetonitrile increases; however, the exact mechanism of its formation is not known.

The facts that, in the presence of acetonitrile as a solvent, the initial rate increases upon the addition of a small amount of pyridine or another organic base as a ligand (L), and that the selectivity toward γ-butyrolactone in this case increases in proportion to the initial rate (Fig. 2), can be understood by this scheme, for when the step (IV)→(VI) is accelerated by the addition of L, the extent of the isomerization and the polymerization, which are assumed to be independent of the concentration of L, will relatively decrease, and consequently the selectivity toward γ-butyrolactone

8) R. F. Heck and D. S. Breslow, *J. Am. Chem. Soc.*, **83**, 4023 (1961).

9) F. A. Cotton, *Inorg. Chem.*, **3**, 702 (1964).

10) The residue was isolated fom the other products for the determination of the molecular weight and the infrared absorption spectrum.
Molecular weight: 290
IR spectrum: -OH (alcohol), 3420 cm^{-1}
C=O (aldehyde), 1730 cm^{-1}

will increase. The retarding effect of Py on the overall reaction when the $Py/Co_2(CO)_8$ mole ratio exceeds 1 may be due to the formation of pyridinium salt of cobalt hydrocarbonyl, as was proposed in a previous study.[1)]

The fact that the selectivity toward isobutyraldehyde increases with an increase in the hydrogen partial pressure is reasonable, since the rate of the hydrogenolysis of VII by hydrogen or $HCo(CO)_4$ will increase with an increase in the hydrogen partial pressure.[11)] The hydrogenolysis of VII, therefore, should be the rate-determining step in the isobutyraldehyde formation; this well accounts for the other experimental fact that the rate of isobutyraldehyde formation is essentially independent of the carbon monoxide partial pressure.

Considering the two equilibrium relations, (1) and (2), it is clear that the larger the carbon monoxide partial pressure, the smaller the concentration of the complex (II) becomes. Hence, the rate of propionaldehyde formation *via* the complex (II) must decrease with an increase in the carbon monoxide partial pressure, while the rate of γ-butyrolactone formation, if it can proceed *via* another path, as is assumed in the scheme, must not be so much retarded by the increase in the carbon monoxide partial pressure. In fact, the results in Table 8 shows that the rate of propionaldehyde formation is retarded by the increase in the carbon monoxide partial pressure to a larger extent than that of γ-butyrolactone formation. Thus, the presence of the two different paths, assumed in the scheme is supported by this fact.

11) Neither γ-hydroxybutyraldehyde, which may be formed by the hydrogenolysis of VI, nor β-isobutyrolactone, which may be formed by the intramolecular alcoholysis of VII, could be detected in the reaction products; this may be because the intramolecular alcoholysis of VI is very fast, and that of VII, very slow.

Although it is conceivable that the more stable the complex (II) is made by the choice of the solvent (S), the larger the selectivity toward γ-butyrolactone becomes, no better solvent than acetonitrile has yet been found.

The fact that the effectiveness of solvents in increasing the selectivity toward γ-butyrolactone decreases in the order $CH_3CN > CH_3CH_2CN > (CH_3)_2CHCN > C_6H_5CN$ seems to be related to the concept of HSAB by Pearson *et al.*[12,13)] They pointed out that the hardness and, consequently, the electronegativity of the carbonium ion decreases in the order $C_6H_5^+ > (CH_3)_3C^+ > (CH_3)_2CH^+ > CH_3CH_2^+ > CH_3^+$.[13)] Accordingly, the softness of the above-mentioned solvents must decrease in the order $CH_3CN > CH_3CH_2CN > (CH_3)_2CHCN > C_6H_5CN$. Hence, according to the principle of HSAB, the complexing ability of these solvents with regard to zero-valent cobalt, which is classified as in the group of soft acids,[12)] must decrease in this order. Thus the ability of these solvents (S) to decrease the concentration of complex (II) by means of the equilibrium relation (2) shown in the above scheme and, therefore, their ability to increase the selectivity toward γ-butyrolactone by reducing the rate of isomerization, should decrease in that order also.

A similar effect of nitriles in reducing the isomerization was observed by Roos *et al.*, who studied the effect of nucleophiles on the stoichiometric hydroformylation of 1-pentene.[14)]

The author is indebted to Mr. Toshiro Minegishi for his aid in constructing the high-pressure apparatus and to Dr. Ken-ichiro Bando for his discussions.

12) R. G. Pearson, *J. Am. Chem. Soc.*, **85**, 3533 (1963).

13) R. G. Pearson and J. Songstad, *ibid.*, **89**, 1827 (1967).

14) L. Roos and M. Orchin, *J. Org. Chem.*, **31**, 3015 (1966).

BULLETIN OF THE CHEMICAL SOCIETY OF JAPAN VOL. 41 1884—1890 (1968)

Solvolysis of *cis* and *trans* 2-Cyclohexylcyclohexyl, 2-Phenylcyclohexyl and 2-*p*-Anisylcyclohexyl *p*-Toluenesulfonate

Shun-Ichi MURAHASHI and Ichiro MORITANI

Department of Chemistry, Faculty of Engineering Science, Osaka University, Machikaneyama, Toyonaka, Osaka

(Received December 21, 1967)

trans-2-*p*-Phenylcyclohexyl *p*-toluenesulfonate acetolyzes (75°C), at one-eighth of the rate of cyclohexyl *p*-toluenesulfonate, and one-sixteenth times smaller than that of the *cis* isomer. *trans*-2-*p*-Anisylcyclohexyl *p*-toluenesulfonate acetolyzes (75°C) much the same as cyclohexyl *p*-toluenesulfonate, and one-third times smaller than that of the *cis* isomer. Thus, the slow rate of the trans isomers cannot be interpreted in term of significant phenyl and *p*-anisylparticipation. This may be due to high cost in energy required to place the aryl group in the axial position where it would be in a favorable position to participate. However, it is noteworthy that the acetolysis of *trans*-2-*p*-anisylcyclohexyl *p*-toluenesulfonate gave *trans*-2-*p*-anisylcyclohexyl acetate in 70% yield, which had retention of configuration. The mechanism of this reaction is discussed. The greater reactivities of *cis* isomers are interpreted in terms of E_2 type elimination involving nucleophilic participation by the solvent as well as 2-alkylcyclohexyl *p*-toluenesulfonate.

On the cyclohexyl system the conformation of substituent might be consider to be fixed because the chair form is by far stable.[1] Thus it is very suitable to investigate the cyclohexyl system stereochemically or kinetically. Since the acceleration of rate or the stereochemistry of the reaction of aliphatic compounds is usually interpreted in terms of neighbouring participation or bridged nonclassical carbonium ion,[2] it is interesting to investigate these concepts in cyclohexyl system. The neighbouring participation of acetoxy,[3] halogen[4] and methoxy[5] groups are already investigated. In the acetolysis of *trans*-2-acetoxycyclohexyl *p*-toluenesulfonate the reactivity of *cis* isomer is 630 times greater than that of the *trans* one, and *trans* acetate which has retention of configuration is obtained. Furthermore, the acetate which is obtained from optically active *p*-toluenesulfonate is found to be racemic. These results are reasonably explained by assuming that symmetrical bridged ion is involved as an intermediate.[3]

We have investigated on behavior of the neighboring participation of cyclohexyl, phenyl and anisyl groups in cyclohexyl system.

Results

Preparation of Materials and Infrared Spectra. The *cis* and *trans* isomers of 2-cyclohexylcyclohexanol (Ia), (IIa) and 2-phenylcyclohexanol (IIIa), (IVa) were prepared with the usual manner.[6,7] *trans*-2-*p*-Anisylcyclohexanol (VIa) was prepared by the reduction of the corresponding ketone with lithium aluminum hydride or hydrogenation-oxidation of 1-*p*-anisylcyclohexene. The latter reaction is better than the former one. On the other hand the hydrogenation of 2-*p*-anisylcyclohexanone in the presence of platinum black catalyst gave the *cis* isomer (Va).

1) D. H. R. Barton, *Quart. Rev.*, **10**, 44 (1956).
2) B. Capon, *ibid.*, **18**, 45 (1964).
3) S. Wintein, E. Grunwald, R. E. Bruckles and C. Hanson, *J. Am. Chem. Soc.*, **70**, 816 (1948); S. Winstein, H. V. Hess and R. E. Bruckles, *ibid.*, **64**, 2796 (1942).
4) S. Winstein, E. Grunwald and L. L. Ingraham, *ibid.*, **70**, 821 (1948); E. Grunwald, *ibid.*, **73**, 5458 (1951).
5) S. Winstein and R. B. Henderson, *ibid.*, **65**, 2196 (1943); D. S. Noyce, B. R. Thomas and B. N. Bastian, *ibid.*, **82**, 885, 1246 (1960).
6) W. Hückel, M. Meiel, E. Jordan and W. Seeger, *Ann.*, **616**, 46 (1958).
7) C. C. Price and J. V. Karabinos, *J. Am. Chem. Soc.*, **62**, 1159 (1940).

I: X=OTs
Ia: X=OH

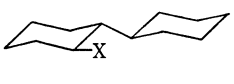

II: X=OTs
IIa: X=OH

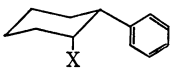

III: X=OTs
IIIa: X=OH

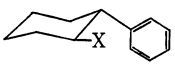

IV: X=OTs
IVa: X=OH

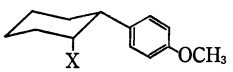

V: X=OTs
Va: X=OH

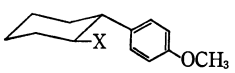

VI: X=OTs
VIa: X=OH

The infrared spectra of these isomeric alcohols obtained above are consistent with the conformational assignment. It has been pointed out that alkyl substituted cyclohexanol with an equatorial hydroxyl can be distinguished from the epimers with an axial hydroxyl by the position of C–O stretching frequency.[8] The *cis* isomer (axial) of 2-cyclohexyl, 2-phenyl and 2-*p*-anisylcyclohexanol showed absorption at 968, 964 and 965 cm^{-1} (KBr) respectively, the *trans* isomers (equatorial) at 1044, 1057 and 1056 cm^{-1}.

p-Methoxybenzalcyclopentane (XIV) which might be formed as the ring contraction product was obtained through the path A as shown in Scheme I. On the other hand, from the path B the alcohol XIII was not obtained, since the alcohol XV was easily dehydrated to give *p*-methoxybenzalcyclopent-1-ene (XVI).

Kinetic Experiments. The results of the kinetic measurements are listed in Table 1. Acetolyses of the isomeric *p*-toluenesulfonates in the presence of pottasium acetate are first order and the rates are increased only slightly over that observed in the absence of added acetate ion except *trans*-2-*p*-anisylcyclohexyl *p*-toluenesulfonate.[9]

The *cis* isomers are solvolyzed faster than the *trans* isomers respectively. However, the

TABLE 1. FIRST ORDER RATE CONSTANT OF 2-CYCLOHEXYL, 2-PHENYL AND 2-*p*-ANISYL *p*-TOLUENESULFONATES

Ester	Temp. °C	ROTs 10^2 M	KOAc 10^2 M	$10^5 \times k_1$ sec^{-1}	ΔH^* kcal/mol	ΔS^* e.u.
I	44.90	0.819	1.93	8.88±0.26		
	44.91	0.819	1.93	8.92±0.12		
	49.69	1.60	2.80	18.3±0.2		
	59.74	1.55	2.01	51.9±0.5		
	75.0			278	24.3	−0.77
II	59.84	2.21	3.04	2.46±0.05		
	74.67	1.85	2.31	15.8±0.3		
	75.0	2.26	2.03	16.5	28.2	+4.9
III	59.79	1.83	3.12	1.40±0.04		
	74.51	1.83	3.19	7.70±0.15		
	89.98	1.41	2.22	42.7±0.4		
	75.0			8.38	26.5	−1.3
IV	74.73	0.684	2.28	0.455±0.004		
	90.46	0.785	1.16	3.39±0.07		
	99.94	0.775	2.17	10.7±0.2		
	75.0			0.520	30.4	+4.3
V	74.62	1.50	2.53	12.4±0.7		
	89.93	1.50	3.12	72.9±0.1		
	100.09	1.60	2.53	230±5		
	75.0			13.2	29.1	+6.9
VI	74.67	1.26	1.57	4.06±0.19		
	89.83	1.85	3.50	21.8±0.3		
	99.88	1.20	2.50	54.5±0.4		
	75.0			4.31	25.7	−5.1
VI	74.62	2.49	—	2.33±0.04		
	89.84	2.49	—	15.3±0.2		
	99.77	2.49	—	46.7±0.5		
	75.0			2.41	30.7	+6.5

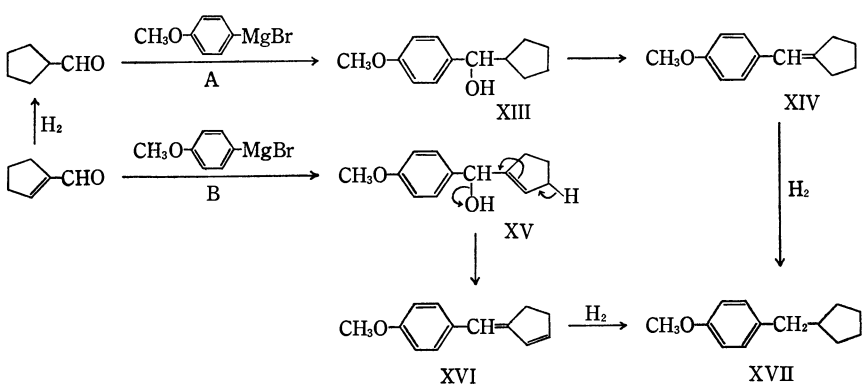

Scheme I.

8) W. Hückel and Y. Riad, *Ann.*, **637**, 33 (1960); W. Hückel and J. Kunze, *ibid.*, **645**, 194 (1961).

9) Special salts effect has been observed about *trans*-2-*p*-anisylcyclohexyl *p*-bromobenzenesulfonate (A. N. Fainberg, G. C. Robinson and S. Winstein, *J. Am. Chem. Soc.*, **78**, 2278 (1956)).

acetolysis rate of *trans*-2-*p*-anisylcyclohexyl *p*-toluenesulfonate is smaller than that of *cis* isomer, and the value of $\Delta H^{\neq}$ of *trans* isomer is larger than that of *cis* isomer. In the system without lyate ion, the rate is approximately half of that containing lyate ion, and showes $\Delta H^{\neq}=30.7$ kcal/mol and $\Delta S^{\neq}=6.7$ e.u.

Products. The lyate ion salt was present in slightly excess and the products were isolated after the reaction proceeded to ten half lives. The results are shown in Table 2. The solvolysis products were extracted followed by injecting to preparative v. p. c. The control experiments showed that the products were stable under the condition of the reactions, and fractionation during the isolation process was found to be slight and probably not significant. The analytical data by means of v. p. c. were suported by another method shown in Table 2. The acetolysis products of *trans*-2-*p*-anisylcyclohexyl *p*-toluenesulfonate were separated by column chromatography followed by reduction with lithium aluminum hydride, and it was ascertained the main product was *trans*-2-*p*-anisylcyclohexanol. It is noted that the main product is *trans*-2-*p*-anisylcyclohexyl acetate, which has the retention of configuration. Furthermore, the formation of *p*-methoxybenzalcyclopentane (2%) was detected by means of v. p. c.

TABLE 2. THE PRODUCTS FROM ACETOLYSIS OF 2-CYCLOHEXYL, 2-PHENYL AND 2-*p*-ANISYLCYCLOHEXYL *p*-TOLUENESULFONATES (%)

p-Toluenesulfonate	1-Olefin	3-Olefin	Acetate	Undetected Product
I (*cis*)	99[a]			
II (*trans*)	67[a]	12	*cis*-19	2
	84[b]		16	
III (*cis*)	91[d]	6	3	
	93[c]			
IV (*trans*)	36[d]	28	*cis*-20	16
V (*cis*)	86[d]	4	2	8
VI (*trans*)[f]	11[d]	16	*trnas*-69	2
	9[e]	15	*trans*-70	4

a) Yield by v.p.c. (Carbowax 6000, 150°C).
b) Yield by column-chromatographic isolation (alumina).
c) Yield of total olefin determined by Lucas-Pressmann method.
d) Yield by v.p.c. using biphenyl as internal standard substance (Carbowax 6000, 200°C).
e) Similar to d) (Apiezon L, 250°C).
f) *p*-Methoxybenzalcyclopentane was detected as low as 2% yield.

TABLE 3. COMPARISON OF RATES FOR ACETOLYSIS OF 2-CYCLOHEXYL, 2-PHENYL AND 2-*p*-ANISYLCYCLOHEXYL *p*-TOLUENESULFONATE (75°C)

p-Toluenesulfonate	$k_1\times10^5$(sec^{-1})	*a/e*	Rel. Rate
I (*cis*)	278		66
II (*trans*)	16.5	17	3.9
III (*cis*)	8.38		2.0
IV (*trans*)	0.520	16	0.125
V (*cis*)	13.2		3.1
VI (*trans*)	4.31	3.1	1.0
Cyclohexyl-	4.28		1.0

Discussion of Results. The data on all of the compounds are summarized in Table 3, giving extrapolated or interpolated rate constants at 75°C. In addition, relative rates for cyclohexyl *p*-toluenesulfonate[10] are given for reference. As shown in Table 3 *cis* isomer (axial) solvolyzes faster than the *trans* isomer (equatorial) respectively.

In these substances the sizes of cyclohexyl, phenyl and *p*-anisyl groups are sterically large enough to suppose these groups occupy the equatorial position ; in other words tosyl group occupies the axial position in the *cis* isomer, on the other hand the equatorial position in the *trans* isomer.

It appears that the greater reactivity of 2-cyclohexylcyclohexyl *p*-toluenesulfonate is due to steric acceleration. Scale model indicates that the 2-cyclohexylcyclohexyl system, unlike the 2-phenyl and 2-*p*-anisylcyclohexyl system, is quite congested and rotation of cyclohexyl and tosyl groups is restricted.

The axial-equatorial ratio of cyclohexyl *p*-toluenesulfonate is three owing to the 1,3-diaxial interaction.[11] In the case of 2-cyclohexyl and 2-phenylcyclohexyl *p*-toluenesulfonate the *cis*/*trans* ratio is respectively 16 and 17, so the *cis* isomers are more accelerated than the trans isomers. Inspection of these relative reactivities shows that in both isomers, there may be some factors to be account for the acceleration except that of 1,3-diaxial interaction. In order to aspect this factor, the products of acetolysis were investigated. As shown in Table 2 *cis* isomers gave mainly 1-olefin accompanied with a small amount of 3-olefin and acetate, although *trans* isomers gave 1-olefin and considerable large amounts of 3-olefin and *cis* acetate. Thus the formation of different products from the two

10) H. C. Brown and G. Ham, *ibid.*, **78**, 2735 (1956).
11) I. Moritani, S. Nishida and M. Murakami, *ibid.*, **81**, 3420 (1959).

isomers shows that the products are not derived entirely from a dissociated 2-substituted cyclohexyl cation, since this intermediate would be common to both isomers. These results suggest that in the case of *trans* isomer, the transition state involves the classical carbonium ion. On the other hand in the *cis* isomer two explanations may offer themselves to rationalize these results; (a) E_1 type elimination involving the bridged ion XVIII or (b) E_2 type elimination by the solvent as illustrated by XIX.

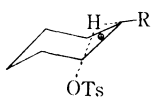

XVIII

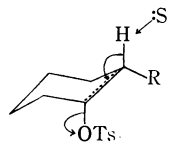

XIX

The high solvolysis rate of vicinally *cis* alkylcyclohexyl *p*-toluenesulfonates is due to participation of the adjacent hydrogen atom, though no details of the reaction products are given.[12] Recently this was supported by the study of β-deuterium isotope effect in solvolytic reaction.[13] However, by the systematic study of 2-alkylsubstituted cyclohexyl *p*-toluenesulfonate, it was revealed that the reaction was E_2 type elimination involving nucleophilic participation by the solvent.[14]

The acetolysis rates of *trans*-2-alkylcyclohexyl *p*-toluenesulfonates increase as the bulk of the substituent becomes larger, $CH_3 < i\text{-}C_3H_7 < C_6H_{11} < t\text{-}C_4H_9$. This may be also interpreted in terms of increasing steric effect by substituent. Nevertheless, the order of the rate ratio of *cis*/*trans* for each *p*-toluenesulfonate is found to $t\text{-}C_4H_9 < C_6H_{11} < i\text{-}C_3H_7 < CH_3$. This tendency may not be due to inductive effect but hyperconjugation. Therefore in the transition state of acetolysis of *cis* isomers the reaction may proceed through the *trans* elimination. Furthermore, it has been reported that the hydrogen participation is not effective in the solvolysis of neomenthyl,[15] 3-cyclohexyl-2-butyl[16] and 2-*t*-butylcyclohexyl *p*-toluenesulfonate.[17] Thus the accelerated rate of *cis*-2-cyclohexylcyclohexyl *p*-toluenesulfonate is considered to be arised from a predominating bimolecular solvolysis (*trans*-elimination).

TABLE 4. RATES AND RELATIVE RATES FOR ACETOLYSIS OF 2-ALKYLCYCLOHEXYL *p*-TOLUENESULFONATES (75°C)

2-Alkyl substituted cyclohexyl *p*-toluenesulfonate	CH_3	$i\text{-}C_3H_7$-	C_6H_{11}-	$t\text{-}C_4H_9$-
k_1^{trans} (10^5)	1.56	9.22	16.5	352
k_1^{trans}/k_0^{trans}	1.00	5.91	10.6	226
k_1^{cis} (10^5)	79.5	221	278	634
k_1^{cis}/k_0^{cis}	1.00	2.78	3.50	7.98
cis(a)/*trans*(e)	51	24	17	1.8

Turing to the π-electron neighbouring system, the similar result was obtained concerning to 2-phenylcyclohexyl *p*-toluenesulfonate as shown in Tables 2 and 3. The data suggest that the reaction mechanism of acetolysis of this *p*-toluenesulfonate is same as that of 2-alkylcyclohexyl *p*-toluenesulfonate. The rate retardation observed is presumably due to the inductive effect of phenyl group.

The *trans* isomer solvolyzes not faster but slower, at one-eighth of the rate of cyclohexyl *p*-toluenesulfonate, and one-sixteenth times smaller than that of the *cis* isomer. The slow rate of the *trans* isomer cannot be interpreted in terms of significant phenyl participation. In the present case we can rationalize the failure to observe participation to the high cost in energy required to place the phenyl group in the axial position where it would be a favourable position to participate.

For the sake of comparison, rate and products of acetolysis were studied on 2-*p*-anisylcyclohexyl *p*-toluenesulfonate. In the case of *cis* isomer, the results shown in Tables 3 and 4 are similar to that of *cis*-2-phenylcyclohexyl *p*-toluenesulfonate. This indicates that *cis* isomer proceeds through *trans* elimination. On the contrary, *trans*-2-*p*-anisylcyclohexyl *p*-toluenesulfonate gave different products from those obtained from 2-alkylcyclohexyl *p*-toluenesulfonate, *viz.* the main product was not 1-olefin but acetate (70 %), which was produced by retention of configuration, *trans* acetate.

The products of retention of configuration might be obtained from double inversion, that is, phenyl participation. It leads to the

12) S. Winstein, B. K. Moore, E. Grunwald, H. W. Jones, J. Corse, D. Trifan and H. Marshall, *ibid.*, **74**, 1127 (1952); S. Winstein and N. J. Holness, *ibid.*, **77**, 5562 (1955); S. Winstein and J. Takahashi, *Tetrahedron*, **2**, 316 (1958); D. J. Cram and J. Tadanier, *J. Am. Chem. Soc.*, **81**, 2737 (1959).

13) V. J. Shiner, Jr., and J. G. Jewett, *ibid.*, **87**, 1382, 1383 (1965).

14) I. Moritani, N. Obata and S. Nishida, to be published.

15) W. Hückel and C. M. Jennewein, *Ann.* **683**, 100 (1965).

16) H. C. Brown, K. J. Morgan and F. J. Chloupec, *J. Am. Chem. Soc.*, **87**, 2137 (1965).

17) K. Okamoto and K. Saito, The Abstract of the 18th Conference on the Reaction Mechanism of Organic Reaction at Kyoto 1967, page 81.

rate enhancement and retention of configuration through bridging of phenyl group. The powerful participation effect of *p*-anisyl group[18] and the formation of bridged *p*-anisonium ion in strong acid[19] have been observed. However, since the *trans* isomer VI solvolyzes slower than cyclohexyl *p*-toluenesulfonate, it seems likely that *p*-anisyl participation is not important in the reaction of this compound. This may be due to high cost in energy required to place the *p*-anisyl group in the axial position where it would be in a favourable position to participate.

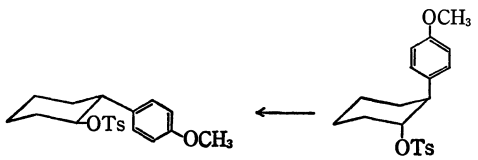

XX XXI

We therefore propose the following mechanism. The rate determining step is the formation of classical carbonium ion. *p*-Anisyl group can migrate just before carbonium ion is formed at C_1, then the intermediate XXII may be formed. The newly formed bridged ion XXII may be a considerable stable intermediate of so called dienon type.[20]

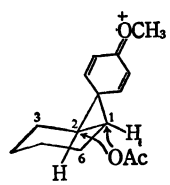

XXII

When the bridged ion is opened by acetate ion, the products, which possess the same configuration as the starting materials, are obtained. Olefins might be obtained through abstraction of proton by solvent. The fact that 3-*p*-anisylcyclohexene is mainly obtained may be rationalized by suspecting the easy abstraction of proton at C_3 or C_6.

It is noteworthy that *p*-methoxybenzal cyclopentane, the rearranged ring contracted product, was detected only as low as 2% yield. The migration of methylene group may be far less than that of *p*-anisyl group in this compound.

Experimental

All melting points ware uncorrected. The IR spectrum was recorded by the use of an EPI-S2 apparatus. The UV spectrum was recorded by the use of an EPS-2U apparatus.

Materials. *2-Cyclohexylcyclohexanone.* 1-Chlorocyclohexylcyclohexanone was prepared by condensation of cyclohexanone by the method of Kunze,[21] in 70% yield, bp 115°C/6 mmHg (lit.[22] bp 140°C/18 mmHg), semicarbazone, mp 182—183°C (lit.[22] mp 182—183°C). This ketone was converted to 2-cyclohexylidenecyclohexanon by treatment with sodium methoxide in 82% yield, mp 57°C (methanol) (lit.[23] mp 57°C), semicarbazone mp 186.5—188°C. Moreover hydrogenation of 2-cyclohexylidenecyclohexanone over PdO_2-$CaCO_3$ catalysts gave 2-cyclohexylcyclohexanone in 98% yield, bp 126°C/8 mmHg (lit.[23] bp 135°C/11mmHg), n_D^{20} 1.4913 (lit.[23] n_D^{20} 1.4915).

cis-2-Cyclohexylcyclohexanol (*Ia*). This material was prepared by hydrogenation of 2-cyclohexylcyclohexanone over platinum black in acetic acid in 74% yield, mp 59—60°C (petroleum ether, bp 40—50°C) (lit.[6] mp 60.8°C).

trans-2-Cyclohexylcyclohexanol (*IIa*). This material was prepared by reduction with lithium aluminum hydride of 2-cyclohexanone at 0°C, bp 106—107°C/6 mmHg, n_D^{20} 1.5010. This alcohol was esterificated with phthalic acid and recrystallized several times with chloroform followed by hydrolysis, and pure alcohol was obtained, mp 53—54°C (lit.[6] 52.8°C).

1-Cyclohexylcylohexene (*VII*). 1-Cyclohexylcylohexanol, mp 53-54°C (lit.[24] mp 51°C), bp 114—115 °C/7 mmHg was dehydrated by iodine at 150°C in 50% yield, bp 64—66°C/7 mmHg, n_D^{20} 1.4965 (lit.[25] n_D^{20} 1.4949).

3-Cyclohexylcyclohexene (*VIII*). This material was prepared from cyclohexylmagnesium bromide and 3-cyclohexenyl bromide, bp 73—74°C/7 mmHg, n_D^{20} 1.4964 (lit.[25] n_D^{20} 1.4941).

cis-2-Phenylcyclohexanol (*IIIa*). *o*-Phenylphenol was hydrogenated using Raney nickel as catalyst in ethanol.[7] The oily mixture of alcohol (6.5 g) obtained was chromatographed over 100 g of activated alumina. Elution with petroleum ether (bp 40—50 °C) gave 4.1 g of *cis* alcohol, mp 40—42°C (petroleum ether, bp 40—50°C) (lit.[7] mp 40—42°C).

Found: C, 81.54; H, 9.16%. Calcd for $C_{12}H_{16}O$:

18) S. Winstein *et al.*, *J. Am. Chem. Soc.*, **74**, 1140 (1952); **75**, 147 (1953); **78**, 328 (1956); S. Winstein and R. Baker, *ibid.*, **86**, 2071 (1964); H. C. Brown and H. M. Bell, *ibid.*, **86**, 5003, 5006 (1964); P. von R. Schleyer, D. C. Kleinfelter and H. G. Richey, Jr., *ibid.*, **85**, 479 (1963); H. C. Brown, R. Bernheimer, C. J. Kim and S. E. Schepple, *ibid.*, **89**, 370 (1967).

19) G. A. Olah, E. Namanworth, M. B. Comisarow and B. Ramsey, *ibid.*, **89**, 711 (1967).

20) R. Baird and S. Winstein, *ibid.*, **84**, 788 (1962); A. A. Guiswold and O. L. Chapman, *J. Org. Chem.*, **29**, 2047 (1964); L. Eberson and S. Winstein, *J. Am. Chem. Soc.*, **87**, 3506 (1965).

21) K. Kunze, *Ber.*, **59**, 2085 (1926).

22) W. Hückel, O. Neuenfoeffer, A. Gerke and E. Frank, *Ann.*, **477**, 119 (1930).

23) J. Reese, *Ber.*, **75**, 384 (1942).

24) F. Signaigo and P. Cramer, *J. Am. Chem. Soc.*, **55**, 3326 (1933).

25) W. Hückel *et al.*, *Ann.*, **637**, 33 (1960).

C, 81.77; H, 9.14%. *cis*-2-phenylcyclohexyl phthalate, mp 174—175°C. Further elution with the petroleum ether (bp 40—60°C) gave small amount of *trans* isomer (IVa).

trans-2-Phenylcyclohexanol (*IVa*). This material was prepared from 2-phenylcyclohexanone[7] by lithium aluminum hydride reduction, mp 52—54°C (petroleum ether, bp 40—50°C) (lit.[7] mp 52—53°C).

Found: C, 81.60; H, 9.04%. Calcd for $C_{12}H_{16}O$: C, 81.77; H, 9.14%.

1-Phenylcyclohexene (*IX*). 1-Phenylcyclohexanol was dehydrated by heating with potassium acid sulfate,[26] bp 125—127°C/15 mmHg, n_D^{20} 1.5692.

3-Phenylcyclohexene. This material prepared from 3-bromocyclohexene and phenylmagnesium bromide, bp 114—115°C/15 mmHg, n_D^{20} 1.5448 (lit.[26] n_D^{20} 1.5448).

2-p-Anisylcyclohexanone. This ketone was prepared by the reaction of *p*-anisylmagnesium bromide with 2-chlorocyclohexanone in 46% yield, mp 88.0—88.5°C (lit.[27] mp 89°C).

Found: C, 76.61; H, 7.90%. Calcd for $C_{13}H_{16}O$: C, 76.44; H, 7.90%.

1-p-Anisylcyclohexene(*XI*). 1-*p*-Anisylcyclhexanol prepared from cyclohexanone and *p*-anisylmagnesium bromide was easily dehydrated during distillation, bp 138—139°C/6 mmHg. Completely dehydration by heating with potassium acid sulfate gave the pure 1-*p*-anisylcyclohexene in 52% yield, mp 32—33°C.

Found : C, 82.94 ; H, 8.60%. Calcd for $C_{13}H_{16}O_2$: C, 82.93 ; H, 8.57%. This olefin was hydrogenated with paladium black in alcohol at atmospheric pressure. After absorbing theoretical amount of hydrogen, crystalline material was obtained, which was ascertained to be *p*-anisylcyclohexene by comparison with IR spetrum and mixed melting point of the authentic sample, mp 57—58°C (lit.[27] 57—58°C).

Found: C, 81.60; H, 9.30%. Calcd for $C_{13}H_{18}O$: C, 82.08: H, 9.53%.

trans-2-p-Anisylcyclohexanol (*VIa*). This material was prepared by two methods. First, 2-*p*-anisylcyclohexanone (14 g) in dry ether (100 m*l*) was added with stirring to the ethereal solution (100 m*l*) of lithium aluminum hydride (1.5 g) below 10°C. After treatment with the usual manner, alcohol VIa (12.6 g) was obtained, mp 70—71°C (petroleum ether, bp 40—50°C).

Found: C, 75.47; H, 8.85%. Calcd for $C_{13}H_{18}O_2$: C, 75.69; H, 8.80%. On the other hand, 1-*p*-anisylcyclohexene (30 g) in tetrahydrofuran (100 m*l*) was treated with diborane generated from 30 mmol of boron trifluoride ethelate.[28] After destroying excess diborane the organoborane was treated with 18.5 m*l* of 3N sodium hydroxide followed by addition of 18.5 m*l* of 30% hydrogen peroxide at 30—50°C. The reaction mixture was stirred for an additional hour, then extrated with ether. After treatment with the usual manner recrystallization by petroleum ether (bp 50—70°C) gave *trans-2-p*-ansylcyclohexanol (29 g), mp 70.8—71.2°C.

Found: C, 75.77; H, 8.88%. Calcd for $C_{13}H_{18}O_2$: C, 75.69; H, 8.80%. These two alcohols obtained above showed the same IR spectra and mixed melting points.

cis-2-p-Anisylcyclohexanol (*Va*). A mixture of 2-*p*-anisylcyclohexanone (6.7 g), acetic acid (70 m*l*) and conc. hydrochloric acid (1 m*l*) was hydrogenated over platin-mohr catalysis at atmospheric pressure until the theoretical amount of hydrogen had been absorved. After treatment with the usual manner *cis*-2-*p*-anisylcyclohexyl acetate (Vb) was obtained, mp 81—82°C.

Found: C, 72.49; H, 8.05%. Calcd for $C_{15}H_{20}O_3$: C, 72.55; H, 8.12%. *cis-p*-Anisylcyclohexanol was prepared by hydrolysis of the acetate in 66% yield (from ketone), mp 53—54°C (petroleum ether, bp 40—50°C).

Found: C, 75.82; H, 8.73%, Calcd for $C_{13}H_{18}O_2$: C, 75.69; H, 8.80%. This alcohol was identical with the one obtained from the reduction of 2-*p*-anisylcyclohexanone by aluminum isopropoxide.[27]

trans-2-p-Anisylcyclohexyl Acetate (*VIb*). This material was prepared from *trans*-2-*p*-anisylcyclohexanol and acetic acid anhydride in dry pyridine in 98% yield, mp 58—59°C (petroleum ether, bp 40—50°C).

Found: C, 71, 94; H, 8.00%. Calcd for $C_{15}H_{20}O_3$: C, 72.55; H, 8.12%.

3-p-Anisylcylohexene (*XII*). This material was obtained from 3-bromocyclohexene and *p*-anisylmagnesium bromide in 40% yield, n_D^{25} 1.5498 (lit.[29] 1.5500).

Cyclopentyl Aldehyde. 1-Cyclopent-1-ene aldehyde[30] was prepared from oxidation of *trans*-cyclohexane-1,2-diol by sodium paraperiodate followed by condensation by potassium hydroxide solution at pH 4, bp 57°C/25 mmHg, ν 1640 (C=C), 1679 cm^{-1} (C=O), λ_{max}^{EtOH} 234.5 mμ. A solution of this aldehyde (40 g) in ether (50 m*l*) was hydrogenated over 8% paradium-charcoal catalyst (8 g). After absorption of the theoretical amount of hydrogen (10 *l*), the catalysts were filtered off, and the distillation of the filtrate gave cyclopentyl aldehyde[31] (20 g), bp 34°C/24 mmHg, ν 1720 cm^{-1}.

p-Anisylcylopentylcarbinol (*XIII*). To a solution of *p*-anisylmagnesium bromide (0.23 mol) in ether (400 m l) was added a solution of cyclopentyl aldehyde (20 g) in ether (200 m*l*) with reflux. After treatment with the usual manner *p*-anisylcyclopentylcarbinol (20 g) was obtained. Phenyl urethane, mp 237—238°C.

p-Methoxybenzalcyclopentane (*XIV*). *p*-Anisylcyclopentylcarbinol was dehydrated by heating with aqueous oxalic acid, bp 82—84°C/0.001 mmHg, n_D^{20} 1.5710.

Found: C, 82.94; H, 8.54%. Calcd for $C_{13}H_{16}O$:

26) E. L. Eliel, J. W. McCoy and C. C. Price, *J. Org. Chem.*, **22**, 1533 (1957).

27) W. E. Bachmann, G. I. Fujimoto and L. B. Wick, *J. Am. Chem. Soc.*, **72**, 1995 (1950).

28) H. C. Brown and G. Zweifel, *ibid.*, **83**, 2544 (1961).

29) W. R. Biggerstaff, A. P. Menditto and I. Yokoyama, *J. Org. Chem.*, **19**, 934 (1954).

30) J. B. Brown, H. B. Herbest and E. H. Jones, *J. Chem. Soc.*, 3634 (1950).

31) P. M. Union, *Ann. chim.*, [11] **43**, 1 (1934).

C, 82.93; H, 8.57%.

p-Methoxybenzalcyclopentene (*XVI*). To a solution of *p*-anisylmagnesium bromide (0.42 mole) in ether (350 m*l*) a solution of 1-cyclopent-1-ene aldehyde (38 g) in ether (100 m*l*) was added slowly with stirring at 0°C. After reflux for additional half of hour, the mixture was poured into a cold saturated aqueous solution of ammonium chloride. The organic layer was washed with water and dried over magnesium sulfate, and the ether was removed. The residual oil was distilled, bp 118—119°C/0.15 mmHg, mp 70—71°C (ethanol) (56%).

Found: C, 83.35; H, 7.40%. Calcd for $C_{13}H_{14}O$: C, 83.83; H, 7.58%. ν_{Nujol} 1255, 1247 ($-OCH_3$), 1606, 1537, 1510, 1179, 814 (phenyl), 1306 cm^{-1}, λ_{max}^{EtOH} 297.5 mμ. The olefin (mp 70—71°C) above obtained was hydrogenated by absorbing two moles of hydrogen, and *p*-anisylcyclopentylmethane was obtained, n_D^{20} 1.5238.

Found: C, 81.86; H, 9.49%. Calcd for $C_{13}H_{18}O$: C, 82.06; H, 9.54%. This material was also obtained by hydrogenation of *p*-methoxybenzal cyclopentane by the absorption of one mole of hydrogen.

Kinetic Measurements. Solvolysis kinetics were measured by our previous methods.[11] In the solvolysis of the *p*-toluenesulfonates, no unusual feature was noted in the kinetic behavior except *trans*-2-*p*-anisylcyclohexyl *p*-toluenesulfonate. In this case special salt effect was found.[32]

Acetolysis products. *Acetolysis of cis and trans-2-Cyclohexylcyclohexyl p-Toluenesulfonate. a) Vapor Phase Chromatography.* The mixture of *trans*-2-cyclohexylcyclohexyl *p*-toluenesulfonate (4.95 g) and potassium acetate (2.25 g) was acetolyzed at 99.8°C until the reaction proceeded to ten-half lives. The reaction mixture was poured into cold water followed by continuous extraction by petroleum ether (bp 40—50°C). After washing with sodium bicarbonate solution and water, the petroleum ether solution was dried, concentrated and injected to v. p. c. (Carbowax 6000, 3m, 150°C). The data obtained is shown in Table 2. For the acetolysis of *cis*-2-cyclohexylcyclohexyl *p*-toluenesulfonate the data was obtained by the same treatment.

b) Product Isolation. A solution of *trans*-2-cyclohexylcyclohexyl *p*-toluenesulfonate (3.36 g) and potassium acetate (1.10 g) in acetic acid (100 m*l*) was acetolyzed and treated similarly as described above. The concentrated petroleum ether solution was chromatographed over alumina. Elution with petroleum ether gave olefins (1.99 g) selectively and further elution with benzene gave acetate (0.32 g). Treatment of the acetate with lithium aluminum hydride gave an alcohol, which was identified to be *cis*-2-cyclohexylcyclohexanol by comparison of IR spectrum with that of an authentic sample.

Acetolysis of cis and trans-2-Phenylcyclohexyl p-Toluenesulfonates. The acetolysis products were determined by v. p. c. (Carbowax 6000, 3m, 200°C).

Acetolysis of cis and trans-2-p-Anisylcyclohexyl p-Toluenesulfonates. a) Vapor Phase Chromatography. A solution of *trans*-2-*p*-anisylcyclohexyl *p*-toluenesulfonate (5.02 g) in acetic acid (140 m*l*) and potassium acetate (2.20 g) was heated at 99.8 °C until the reaction proceeded to ten-half lives. Further work up essentially as above for the *cis*-2-cyclohexyl *p*-toluenesulfonate yielded oily liquid (3.81 g), this was submitted to v. p. c. (Apiezon L, 2m, 250°C, and Carbowax 6000, 2m, 200°C, biphenyl was used as an internal standard substance). *p*-Methoxybenzalcyclopentane which was formed through ring contraction was identified, but *p*-anisylcyclopentylcarbinyl acetate and *p*-anisylmethylcyclopentene-1 were not detected.

A solution of *cis*-2-*p*-anisylcyclohexyl *p*-toluenesulfonate (0.788 g) in acetic acid (140 m*l*) and potassiun acetate (0.457 g) was solvolyzed. The reaction products (0.408 g) was analyzed by v. p. c.

b) Product Isolation. A solution of *trans*-2-*p*-anisylcyclohexyl *p*-toluenesulfonate (250g) in acetic acid (100 m*l*) potassium acetate (1.02 g) were heated at 99.8°C until ten half lives. After treatment as described above the oily reation products (1.42 g) obtained were dissolved in petroleum ether and submited to v. p. c. Elution with benzene gave olefins and further elution with benzene-methanol gave acetate. Treatment of the acetate with lithium aluminum hydride gave alcohol (mp 70—71°C), which was identified to be *trans*-2-*p*-anisylcyclohexanol by comparison with IR spectrum and mixed mp. The ratio of olefin and *trans* acetate is 12/88.

TABLE 5. DECOMPOSITION TEMPERATURE, ANALYTICAL DATA AND YIELDS OF 2-SUBSTITUTED CYCLOHEXYL *p*-TOLUENESULFONATES[a]

Ester	Decompt. point(°C)	Found C%	Found H%	Calcd C%	Calcd H%	Yield %
I	84.5 (84.2)[8]	67.88	8.34	67.80	8.39	68
II	122 (125.8)[8]	67.49	8.21	67.80	8.39	84
III	114 (102—103)[33]	68.96	6.77	69.06	6.71	60
IV	129 (126—128)[33]	69.36	6.78	69.06	6.71	69
V	117	66.61	6.65	66.64	6.65	81
VI	119	66.69	6.62	66.64	6.65	94

a) *p*-Toluenesulfonates were prepared from the method of Tipson.[34]

32) S. Winstein and R. M. Roberts, *J. Am. Chem. Soc.*, **75**, 2297 (1953).

33) S. J. Cristol and F. R, Stermitz, *ibid.*, **82**, 4692 (1960).

34) R. S. Tipson, *J. Org. Chem.*, **9**, 235 (1944).

BULLETIN OF THE CHEMICAL SOCIETY OF JAPAN VOL. 41 1891—1896 (1968)

Condensation Reaction of Ferrocene with Carbonyl Compounds

Mikio SHIGA, Izumi MOTOYAMA and Kazuo HATA

Department of Chemistry, Faculty of Science, Tokyo Metropolitan University, Setagaya, Tokyo

(Received December 27, 1967)

The condensation reactions of ferrocene with various ketones and with trichloroacetaldehyde in the presence of aluminum chloride were investigated. The formation of carbinol (**7**) as an intermediate was postulated in these reactions. In the reaction of acetone with ferrocene, the intermediate carbinol underwent further condensation with other ferrocene molecules to give oligomers (**9**). On the other hand, in the cases of methyl ethyl ketone, acetophenone, propiophenone, cyclohexanone, and trichloroacetaldehyde, the condensation reactions produced olefinic compounds *via* the intermediate carbinols. The intermediate carbinol was isolated together with the olefin in the reaction with trichloroacetaldehyde.

The codensation reactions of ferrocene with aldehydes catalyzed by Lewis acid have already been reported by several workers.[1—5] In the reaction of formaldehyde with ferrocene, Rinehart *et al.* isolated 1,2-diferrocenylethane (**6**, R=H) as the main product,[3,4] whereas Pauson *et al.* obtained diferrocenylmethane (**4**, R=H) by the same reaction under different conditions.[1] These facts have been reasonably interpreted by postulating a ferrocenylmethyl radical (**3**,R=H) derived from the ferrocenylmethyl cation (**2**,R=H) by internal electron-migration from the iron to the α-carbon atom.[1]

It is expected that the substituent on the α-carbon of the intermediate carbinol (or carbonium ion) will electronically affect such an electron-migration process. To date, however, few papers have been published on the reaction of ferrocene with ketone and polyhaloaldehyde. This paper will report on the condensation reactions of ferrocene with various ketones and with trichloroacetaldehyde in the presence of aluminum chloride.

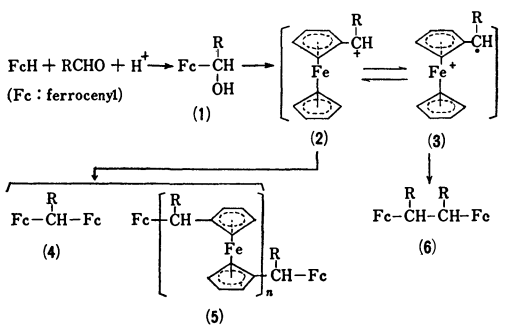

Results and Discussion

The reaction of ferrocene with acetone in the presence of aluminum chloride in anhydrous chloroform under an atmosphere of nitrogen at room temperature gave a mixture of oligomers (**9**). The formation of such polycondensation products suggests that the reaction proceeded through a carbonium ion (**8**), derived from carbinol (**7**), as is shown in the scheme.

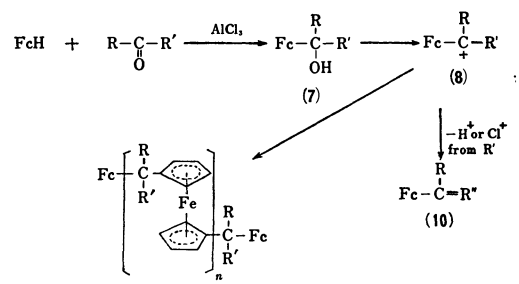

(**9**) R=R′=CH_3, n=1—7
(**9′**) R=R′=CH_3, n=1—6
(**9″**) R=R′=CH_3, n=7

	R	R″
a	CH_3	$CHCH_3$
b	C_6H_5	CH_2
c	C_6H_5	$CHCH_3$
d	1-cyclohexenyl	
e	H	CCl_2

1) P. L. Pauson and W. E. Watts, *J. Chem. Soc.*, **1962**, 3880.
2) E. W. Neuse and D. S. Trifan, *J. Am. Chem. Soc.*, **85**, 1952 (1963).
3) K. L. Rinehart and C. J. Michejda, *ibid.*, **81**, 3162 (1959).
4) K. L. Rinehart and C. J. Michejda, *Angew. Chem.*, **72**, 38 (1960).
5) A. N. Nesmeyanov and I. I. Kritskaya, *Izvestia Akad. Nauk S. S. S. R., Otdel. Khim. Nauk*, **1962**, 352.

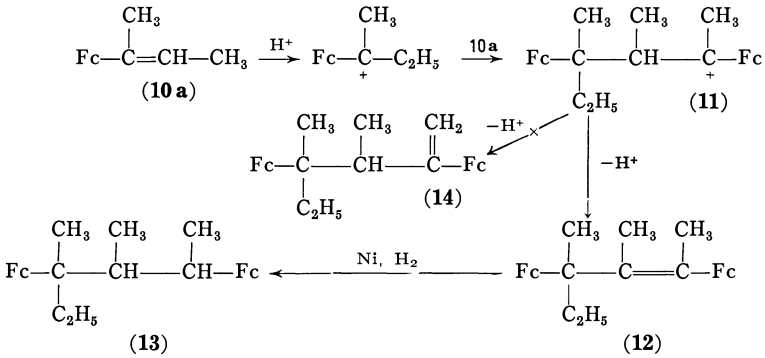

In the case of the reaction with methyl ethyl ketone, only 2,4-diferrocenyl-3,4-dimethyl-2-hexene (**12**) (mp 47—52°C) was isolated. The structure of **12** was supported by the IR spectrum. An absorption band at the 1625 cm^{-1} of **12** due to the ethylenic bond disappeared upon its catalytic hydrogenation to the alkane **13**, mp 41—49°C. It is most likely that the product **12** was produced as a result of the dimerization of an olefin **10a**, which was expected to arise upon the dehydration of the carbinol **7**, although it could not be isolated in this experiment. An alternative structure **14** for **12** was excluded by its IR spectrum.

Acetophenone also gave a dimerized product, 1,3-diferrocenyl-1,3-diphenyl-1-butene (**15**), mp 137.5—138.5°C. The NMR spectrum of **15** shows the integrated intensity ratio of the protons in ferrocenyl : phenyl and olefinic (overlapped) : methyl to be 18.3 : 11.2 : 3.0, which is nearly equal to that calculated on the basis of the formula **15**. An alkane **16**, mp 118—126°C, was obtained quantitatively by the hydrogenation of the dimer **15**. The formation of the dimer **15** may be interpreted through a mechanism analogous to that for the dimer **12**.

Neither of these reactions gave any oligomeric product, unlike the reaction of acetone with ferrocene. The absence of oligomeric products in these reactions strongly suggests that no electrophilic attack of the carbonium ion **8**, which might be created from the carbinol **7**, occurred on the other ferrocene nuclei during these reactions. Therefore, the carbinol or the carbonium ion might, upon the elimination of the water molecule or the α-proton, be converted into the two olefins, **10a** and **10b**, which would be immediately dimerized to **12** and **15** respectively by the action of aluminum chloride and a trace of water.

The condensation reaction of propiophenone with ferrocene gave only an olefinic product, 1-ferrocenyl-1-phenylpropene **10c**, a part of which was oxidized, when chromatographed on alumina, to give benzoylferrocene (**18**), mp 111—112°C. When it was refluxed with a Raney nickel catalyst in methanol,[6] the olefin **10c** was converted almost quantitatively into the hydrogenated product **17** (mp 59—60°C), which was identified by comparing it with the authentic sample prepared from the reaction of benzoylferrocene with ethylmagnesium bromide, followed by treatment with zinc dust and hydrochloric acid.[7] The NMR

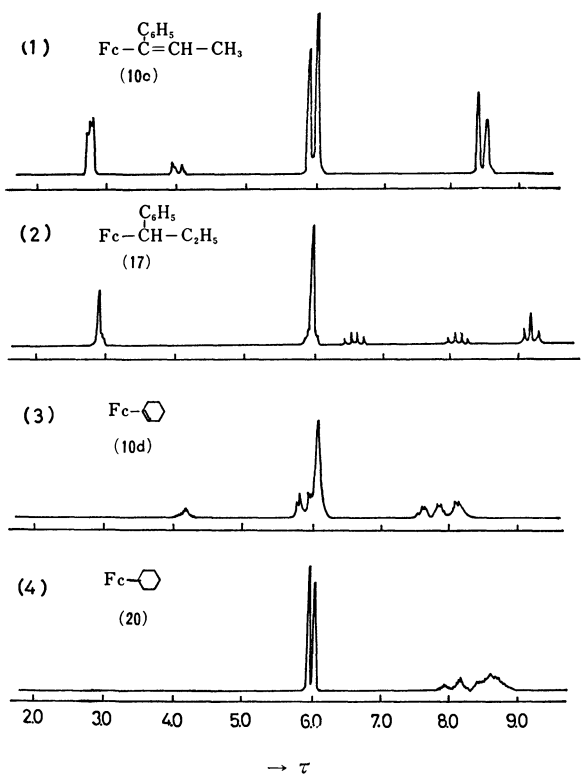

Fig. 1 The NMR spectra of the products.

6) K. Sakai, T. Ito and K. Watanabe, This Bulletin, **39**, 2230 (1966).

7) G. L. K. Hoh, W. E. McEwen and J. Kleinberg, *J. Am. Chem. Soc.*, **83**, 3949 (1961).

TABLE 1. THE NMR SPECTRA OF CONDENSATION PRODUCTS AND THEIR DERIVATIVES (τ-Value, in $CDCl_3$)

Compound	Cyclopentadienyl ring protons			CH_3	CH_2	CH	-C=CH-	C_6H_5	OH
	2,5-	3,4-	Unsubstd.						
15	5.74(s) (·····18.3·····)*	5.84(s)	5.92(d)	8.5(s) (3)*			3.4 (·····11.2·····)*	2.86(m)	
10c	·····5.93(s)····· (·····4.1·····)		6.02(s) (5.1)*	8.49(d) (3)*			6.02(m) (0.9)*	2.76(m) (5.2)*	
17	·····6.06····· (·····8.6·····)*			9.2(t) (3)*	8.13 (1.7)*	6.59(q) (1.1)*		2.85(m) (4.9)*	
10d	5.80(t) (2)*	5.95(t) (2.1)*	6.03(t) (5.2)*		7.75(b) 8.02(b) 8.35(b) (8.2)[a]*		4.2(m)		
20	·····6.06(s)····· (·····4.0·····)		6.01(s) (5.2)*		8.17(b) 8.70(b) (·····10.7·····)*	8.17(b)			
10e	5.44(t) (2.1)*	5.72(t) (2)*	5.82(s) (5.1)*				3.43(s) (1.1)*		
25	·····5.53(t)····· (2)*		5.80(s) (·····6.8·····)*			5.20(s) (1.1)*			7.13(s) (1.1)*

a) The observed methylene proton signals at $C_{4,5}$, C_3 and C_6 in compound **10d** were 3.9 : 2.2 : 2.1.
* The figures in parentheses shown below each τ-value indicate the corresponding integrated intensity ratios.
The figures shown between ····· indicate those for overlapped peaks.

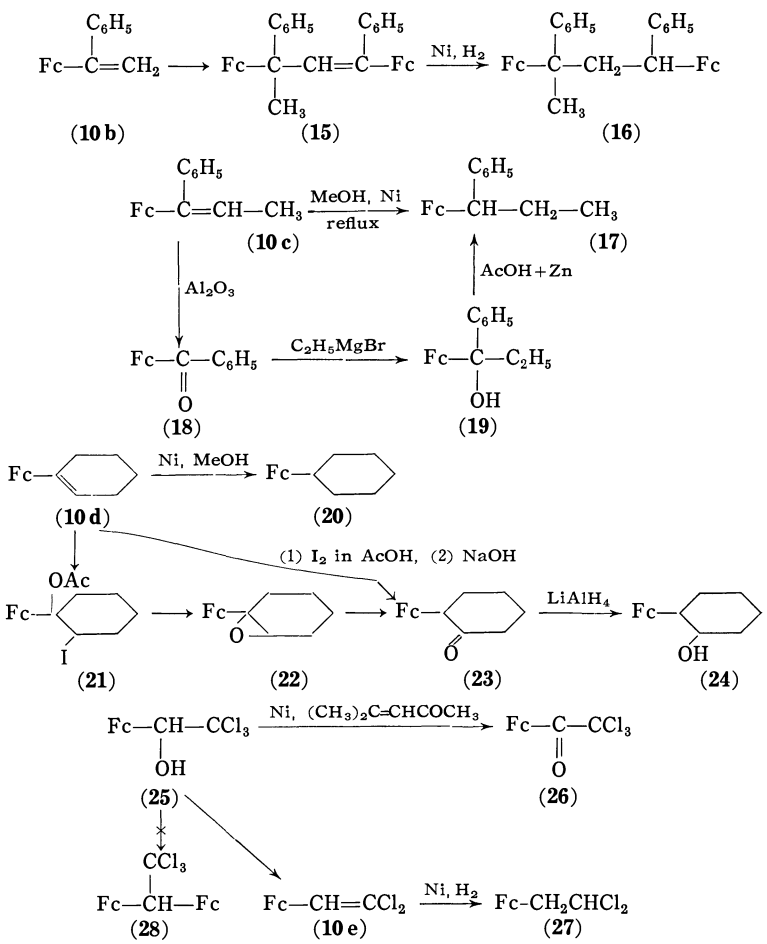

spectrum of **10c** had a doublet peak at τ 8.49 for methyl protons and two singlets, at τ 5.93 and τ 6.02, for the substituted cyclopentadienyl ring protons and the unsubstituted ones respectively, as is shown in Table 1 and Fig. 1-(1). The NMR signal due to the methyl protons of **17** showed a higher τ-value (τ 9.2, triplet) than that of **10c**. An analogous tendency was observed also in the resonance peaks of ring protons between these two compounds.

The reaction of cyclohexanone with ferrocene afforded cyclohexenylferrocene (**10d**), mp 67—68°C, in a good yield (96%). The olefin **10d** was quantitatively converted to cyclohexylferrocene (**20**), mp 40—41°C, when it was refluxed with a Raney nickel catalyst in methanol. The NMR spectrum of **10d** showed three triplets assignable to the 2,5- and 3,4-protons of the substituted cyclopentadienyl ring and the five protons of the unsubstituted ring respectively, whereas in the hydrogenated product **20** these three triplets changed into two singlets, at τ 6.06 and τ 6.01, corresponding to those of the substituted and the unsubstituted rings respectively, as is shown in Figs. 1-(3) and 1-(4). Cyclohexenylferrocene (**10d**) was transformed into 2-ferrocenylcyclohexanone (**23**), mp 99—101°C, probably through the intermediates **21** and **22**, when treated with iodine in glacial acetic acid and then with aqueous alkali. The reduction of the product **23** with lithium aluminum hydride gave 2-ferrocenylcyclohexanol (**24**), mp 88—90°C.

Trichloroacetaldehyde condensed with ferrocene to give 1,1-dichloro-2-ferrocenylethylene (**10e**), mp 55.5—56.5°C, and trichloromethylferrocenylcarbinol (**25**). The IR spectrum of the latter showed that the OH stretching band shifted toward a lower-frequency region (3430 cm^{-1}), suggesting the presence of intramolecular hydrogen-bonding between the hydroxyl group and the iron atom. The integrated intensity ratios in the NMR spectra of the olefin **10e** and the carbinol **25** were found to be as shown in Table 1. They are nearly equal to the values calculated on the basis of the formulas **10e** and **25**. When the carbinol **25** was heated with mesityl oxide in the presence of a Raney nickel catalyst, a mild redox reaction[6] afforded the corresponding ketone **26**, which sublimes easily. The olefin **10e** was catalytically hydrogenated in methanol to 1,1-dichloro-2-ferrocenylethane (**27**). The fact that the expected product **28** could not be isolated in the reaction of trichloroacetaldehyde with ferrocene can not simply be explained in terms of the steric effect of substituents on the

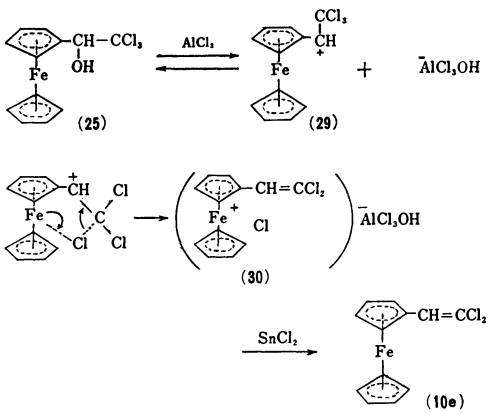

also-expected carbonium ion **29**. On the other hand, it has been suggested that the participation of the iron atom may facilitate the formation of the olefin from the carbonium ion **29** through the ferricinium ion **30**, as is shown in the scheme.[8]

The fact that the intermediate carbinol was isolated only in the case of trichloroacetaldehyde indicates that the formation of the carbonium ion was retarded by the strong electron-withdrawing nature of the trichloromethyl group in the carbinol **25**. The extraordinary stability of the ferrocenylmethyl carbonium ion (**2**, R=CH_3) over the phenyl analog has previously been demonstrated in many cases,[9,10] and it is considered that the carbonium ion can be an important intermediate in the condensation reaction of ferrocene with a carbonyl compound, although there is no positive evidence that the carbonium ion was produced during any reaction except in that with acetone.

The results described above indicate that the presence of a substituent on the α-carbon of the intermediate carbonium ion facilitates the formation of olefin and seems to prevent the formation of a radical from the carbonium ion by electron-migration.

Experimental

General Procedure. The reaction conditions and the products of the condensation reactions of ferrocene and carbonyl compounds are summarized in Table 2. A typical reaction procedure was as follows: To 0.16 mol (24 g) of anhydrous aluminum chloride in 20 *ml* of chloroform at 0°C, under an atmosphere of nitrogen, there was slowly added

8) M. Rosenblum, J. O. Santer and W. G. Howells, *J. Am. Chem. Soc.*, **85**, 1450 (1963).

9) J. H. Richards and E. A. Hill, *ibid.*, **81**, 3484 (1959).

10) D. S. Trifan and R. Bacskai, *Tetrahedron Letters*, **1960**, 1.

TABLE 2. CONDENSATION REACTION OF FERROCENE WITH CARBONYL COMPOUNDS

Carbonyl compound	Time (hr)	Product	Mp (Bp) (°C)	Yield (g)	Yield (%)
Acetone	20	Oligomers (9′)	oil	6.5	—
		(9″)	162—168	2.2	—
Methyl ethyl ketone	3	2,4-Diferrocenyl-3,4-dimethyl-2-hexene (**12**)	47—52	7.9	62
Acetophenone	5	1,3-Diferrocenyl-1,3-diphenyl-1-butene (**15**)	137.5—138	4.3	32
Acetophenone	20	1,3-Diferrocenyl-1,3-diphenyl-1-butene (**15**)	137.5—138	8.5	55
Propiophenone	5	1-Ferrocenyl-1-phenylpropene (**10c**)	(105—110/0.4 mmHg)	7.1	44
Cyclohexanone	5	Cyclohexenylferrocene (**10d**)	67—68	13.7	96
Trichloroacetaldehyde	20	1,1-Dichloro-2-ferrocenylethylene (**10e**)	55.5—56.5	3.1	21
		Trichloromethylferrocenylcarbinol (**25**)	140—141	0.85	5

In each reaction, 10 g (0.054 mol) of ferrocene was treated with 0.16 mol of carbonyl compounds in the presence of 24 g (0.16 mol) of $AlCl_3$ at 0°C.

0.16 mol of the respective carbonyl compound. Subsequently, 0.054 mol (10 g) of ferrocene, dissolved in 30 m*l* of chloroform, was added dropwise to the mixture with good stirring. After it had been stirred for several hours at room temperature, the reaction mixture was poured into 200 m*l* of water containing 5 g of stannous chloride, and then stirred for another 30 min. Finally, the chloroform layer which separated from the aqueous layer was washed three times with 50-m*l* portions of water and dried over anhydrous magnesium sulfate. Then, the chloroform and the unreacted carbonyl compound were removed by distillation to give a crude reaction product. The subsequent treatment and purification were conducted in different ways for the different products, as will be described below.

Isolation of Oligomers 9′ and 9″. The red brown oil (11.5 g), obtained from the reaction of acetone (9.3 g) with ferrocene (10 g) was dissolved in 2 m*l* of chloroform, and then the solution was poured into 200 m*l* of methanol. After the mixture had been kept standing overnight, 2.5 g of a yellow solid separated as a precipitate. The recrystallization of the precipitate from $CHCl_3$-CH_3OH gave 2.2 g of a yellow solid, mp 162—168°C.

Found: C, 68.95; H, 5.98%; mol wt(Rast), 2010. Calcd for the formula **9″**: C, 68.60; H, 6.11%; mol wt, 1944.

By the evaporation of the solvent from the filtrate, 6.5 g of an amber liquid was obtained.

Neither of these compounds showed any olefinic absorption band in its IR spectrum. The amber liquid was assumed to be a mixture of oligomers (**9′**) with lower molecular weights.

2,4-Diferrocenyl-3,4-dimethyl-2-hexene (12). The condensation product of the reaction of methyl ethyl ketone (11.6 g) with ferrocene (10 g) was extracted with methanol in a Soxhlet extractor for three hours. Then, the residual, insoluble part in methanol was dissolved in 2 m*l* of chloroform and the solution was poured into 200 m*l* of methanol. A yellow solid (8.1 g) was thus obtained as a precipitate. It was recrystallized from $CHCl_3$-CH_3OH. Yield 7.9 g (62%), mp 47—52°C.

Found: C, 70.21; H, 5.48%; mol wt, 496. Calcd for $C_{28}H_{32}Fe$: C, 70.05; H, 6.67%; mol wt, 481.

2,4-Diferrocenyl-3,4-dimethylhexane (13). A solution of 2 g of 2,4-diferrocenyl-3,4-dimethyl-2-hexene (**12**) in 30 m*l* of methanol was refluxed for 3 hr in the presence of Raney Ni (1 g).[6] The reaction mixture was then allowed to cool to room temperature and filtered in order to remove the catalyst. The methanol solution was poured into 200 m*l* of water and extracted with chloroform. The extract was concentrated to a small volume and poured into 100 m*l* of methanol. Another treatment of the mixture in the way described above gave a solid. It was recrystallized from $CHCl_3$-CH_3OH to yield 1.98 g (98% yield) of a yellow product, mp 41—48°C. Its IR spectrum had no absorption band at 1625 cm^{-1}, a band which had been assigned in **12** to the ethylenic bond.

Found : C, 69.85; H, 7.10%; mol wt, 499. Calcd for $C_{28}H_{34}Fe$: C, 69.56; H, 7.03%; mol wt, 483.

1,3-Diferrocenyl-1,3-diphenyl-1-butene (15). The condensation of acetophenone with ferrocene gave **15**. The procedure was similar to that employed for the isolation of **12**. The crude product was recrystallized from ether after the removal of the unreacted ferrocene by sublimation to give 8.5 g (55% yield) of orange yellow crystals, mp 137.5—138°C.

Found: C, 74.87; H, 5.50%; mol wt, 570. Calcd for $C_{26}H_{32}Fe$: C, 74.79; H, 5.55%; mol wt, 577.

The reduction[6] of **15** was carried out in the way which has been described for **12**. Yellow crystals of 1,3-diferrocenyl-1,3-diphenylbutane (**16**), mp 118—126°C; (1.9 g, 98% yield) were obtained from 2 g of **15**.

Found: C, 74.12; H, 5.84%; mol wt, 582. Calcd for $C_{26}H_{34}Fe$: C, 74.53; H, 5.86%; mol wt, 579.

1-Ferroceny-1-phenylpropene (10c). The crude product (11.6 g), obtained from the condensation reaction of ferrocene (10 g) with propiophenone (21.6 g) was distilled under reduced pressure to give 7.1 g (44% yield) of **10c** as a reddish-brown liquid (bp 105—110°C/0.4 mmHg) ; this liquid partially decomposed when chromatographed on alumina to give benzoylferrocene (**18**), mp 111.5—112°C. This anomalous behavior of **10c** toward alumina was confirmed by repeated experiments, and the benzoylferrocene obtained in this reaction was identified by comparing it with an authentic sample.

Found: C, 75.41; H, 6.02%; mol wt, 305. Calcd

for $C_{19}H_{18}Fe$ (**10c**): C, 75.49; H, 5.96%; mol wt, 302.

1-Ferrocenyl-1-phenylpropane (**17**). The olefinic compound **10c** was hydrogenated by the procedure described above, and the crude product was chromatographed on alumina to give 1.92 g (98%) of yellow needles, mp 59—60°C.

Found: C, 74.92; H, 6.67%; mol wt, 309. Calcd for $C_{19}H_{20}Fe$: C, 75.04; H, 6.58%; mol wt, 304.

1-Ferrocenyl-1-phenylpropane (**17**) was also prepared[7] from benzoylferrocene (**18**) by the Grignard reaction with ethylmagnesium bromide and by the successive reduction of the product with zinc dust and hydrochloric acid.

Cyclohexenylferrocene (**10d**). The crude condensation product obtained from cyclohexanone (15.6 g) and ferrocene (10 g) was chromatographed on alumina to give 13.7 g (96%) of golden yellow crystals, mp 67—68°C. The IR spectrum of **10d** showed an olefinic absorption band at 1630 cm^{-1}.

Found: C, 72.06; H, 6.89%; mol wt, 264. Calcd for $C_{16}H_{18}Fe$: C, 72.23; H, 6.77%; mol wt, 266.

Cyclohexenylferrocene (**10d**) was treated with Raney Ni in the way described above, and the crude product was purified by chromatography on alumina to yield 1.19 g (79%) of cyclohexylferrocene (**20**) as yellow crystals (mp 40—41°C).

Found: C, 71.69; H, 7.34%; mol wt, 265. Calcd for $C_{16}H_{20}Fe$: C, 71.69; H, 7.46%; mol wt, 268.

2-Ferrocenylcyclohexanone (**23**). A solution of 2 g of cyclohexenylferrocene and 0.4 g of iodine in 40 m*l* of glacial acetic acid was heated to 95°C for 1.5 hr. After it had been cooled, the reaction mixture was added, drop by drop, to 200 m*l* of a 30% aqueous potassium hydroxide solution. The solution was stirred for 1 hr and then extracted with benzene. The extract was washed once with water and dried over anhydrous magnesium sulfate. After the drying agent had been removed, the solvent was distilled off. The residue was chromatographed on alumina, using benzene as a solvent, to yield 0.44 g (21%) of orange yellow crystals, mp 99—101°C. The IR spectrum of this compound showed a sharp carbonyl band at 1685 cm^{-1}.

Found: C, 67.89; H, 6.19%; mol wt, 299. Calcd for $C_{16}H_{18}FeO$: C, 68.13; H, 6.38%; mol wt, 282.

2-Ferrocenylcyclohexanol (**24**). 2-Ferrocenylcyclohexanone (**23**) (0.5 g), dissolved in 20 m*l* of anhydrous ether, was treated with lithium aluminum hydride in the usual way to afford a yellow solid (0.42 g). Recrystallization from *n*-hexane gave 0.24 g (48%) of yellow crystals, mp 88—90°C. Its IR spectrum showed a hydroxyl band at 3380 cm^{-1}.

Found: C, 68.33; H, 6.70%; mol wt, 262. Calcd for $C_{16}H_{20}FeO$: C, 67.60; H, 6.33%; mol wt, 284.

1,1-Dichloro-2-ferrocenylethylene (**10e**) **and Trichloromethylferrocenylcarbinol** (**25**). The dark orange solid product, obtained by the condensation of trichloroacetaldehyde (23.5 g) with ferrocene (10 g), was chromatographed on alumina with chloroform. The first fraction afforded a mixture of 1,1-dichloro-2-ferrocenylethylene (**10e**) and unreacted ferrocene. After the removal of the ferrocene by sublimation, 4.2 g of dark orange crystals were obtained. These crystals were purified by chromatography on alumina using benzene - *n*-hexane to give 3.1 g (21%) of dark orange crystals, mp 55.5—56.5°C.

Found: C, 51.77; H, 3.72%; mol wt, 284. Calcd for $C_{12}H_{10}FeCl_2$: C, 51.46; H, 3.57%; mol wt, 280.

The second fraction of the chromatography yielded 0.91 g of yellow crystals. Recrystallization from *n*-hexane gave 0.85 g (5%) of yellow crystals, decomp. at 140—141°C, whose IR spectrum had a hydroxyl band at 3420 cm^{-1}.

Found: C, 43.48; H, 3.21%; mol wt, 329. Calcd for $C_{12}H_{11}FeOCl_3$: C, 43.24; H, 3.33%; mol wt, 332.

Trichloromethyl Ferrocenyl Ketone (**26**). A solution of 1 g of trichloromethylferrocenylcarbinol (**25**) and 0.5 g of a Raney nickel catalyst in 15 m*l* of mesityl oxide was heated at 95°C for 5 hr.[6] After cooling, the catalyst was filtered off and the filtrate was distilled under reduced pressure to remove the mesityl oxide. Subsequently, the residue was chromatographed on alumina with benzene to obtain 0.41 g of red crystals from the first fraction. Purification by sublimation then gave 0.38 g (38%) of red crystals, mp 84—86°C.

Found: C, 44.21; H, 2.93%; mol wt, 335. Calcd for $C_{12}H_9FeOCl_3$: C, 43.66; H, 2.72%: mol wt, 330.

1,1-Dichloro-2-ferrocenylethane (**27**). 1,1-Dichloro-2-ferrocenylethylene (**10e**) was treated by the same procedure as has been described for the reduction of **12**. The crude product was purified by chromatography on alumina with *n*-hexane to give 1.84 g (92%) of an amber liquid product **27**.

Found: C, 52.11; H, 4.87%; mol wt, 278. Calcd for $C_{12}H_{12}FeCl_2$: C, 51.06; H, 4.25%; mol wt, 282.

The authors wish to express their hearty thanks to the Ministry of Education for a grant-in-aid for fundamental scientific research.

BULLETIN OF THE CHEMICAL SOCIETY OF JAPAN VOL. 41 1897—1901 (1968)

Nitroalkenylferrocene. I. Preparation of 2-Nitro-1-ferrocenylalkenes

Mikio SHIGA, Hiromichi KONO, Izumi MOTOYAMA and Kazuo HATA

Department of Chemistry, Faculty of Science, Tokyo Metropolitan University, Setagaya, Tokyo

(Received December 27, 1967)

A wide variety of nitroalkenylferrocenes and their derivatives were synthesized by the condensation of formylferrocene and nitroalkanes. As a condensing agent, either sodium methoxide or a cyclic amine, such as piperidine, pyrrolidine and morpholine, was employed. Condensation using a cyclic amine, which is analogous to the Mannich reaction in nature, gave better results than that using sodium methoxide. The mechanism of the Mannich-type reaction has been discussed, and the formation of a molecular complex between formylferrocene and piperidine has been proposed as an intermediacy.

Many condensation reactions involving formylferrocene have been appeared in the literature. However, the reaction of the aldehyde with nitroalkane has not yet been studied except with nitromethane.

The present paper will report the preparation of several kinds of nitroalkenylferrocenes by two different methods; one is a method using sodium alkoxide[1,2] as a condensing agent, while the other uses a cyclic amine.[3-5] The reaction mechanism of the latter method, which is analogous to that of the Mannich reaction in nature, will also be discussed.

The Condensation Using Sodium Methoxide. The condensation of formylferrocene with nitroalkane by sodium methoxide was carried out as follows: A methanolic solution of sodium methoxide was gradually added to a cooled mixture of formylferrocene (**1**) and nitromethane in methanol. At the end of the reaction, an insoluble sodium salt of nitroalcohol (**2**) separated out as a yellow solid; this solid was apt to decompose to the starting materials in the presence of water. Dark violet crystals of 2-nitro-1-ferrocenylethylene (**3a**) (mp 139—140 ℃), which has been reported on as an oil by Flores *et al.*,[6] were isolated in an excellent yield by acidifying the salt with dilute hydrochloric acid. The NMR spectrum of **3a** exhibits two singlet peaks, at τ 5.46 and τ 5.81, corresponding to protons in the substituted and in the unsubstituted cyclopentadienyl ring respectively, and two doublets, centered at τ 2.03 and τ 2.80 ($J_{\alpha\beta}$= 12.5 cps), assignable to the vinyl α-proton and the vinyl β-proton*1 respectively. The IR spectrum of the nitroolefin showed absorption peaks at 1290 and 950 cm^{-1}; these peaks are indicative of *trans*-olefin.

In the reaction of formylferrocene with nitroethane, 2-nitro-1-ferrocenylpropene (**3b**), (mp 57—58℃), obtained in a low yield (12%), was the only isolated product; no salt intermediate **2** was isolated. The NMR spectrum of **3b** exhibits two singlet peaks, at τ 5.49 and τ 5.83, corresponding to the ring protons, and two singlets, at τ 2.08 and τ 7.70, assignable to the vinyl α-proton and the methyl proton respectively (Table 3).

The Condensation Using Cyclic Amines. This condensation was conducted by using a cyclic amine, such as piperidine, pyrrolidine, or morpholine, as the condensing agent in a way similar to that using sodium methoxide. The nature of this condensation seems to be analogous to the Mannich reaction; in fact, the reaction afforded a Mannich-type product,[7] aminonitroalkane (**4**), which could eventually converted into a nitroolefin (**3**) if the right conditions were employed. The condensation

1) L. Bouveault and A. Wahl, *Compt. rend.*, **135**, 41 (1902).
2) B. Preib, *Ber.*, **18**, 1362 (1885).
3) N. Campbell, W. Anderson and J. Gillore, *J. Chem. Soc.*, **1940**, 446.
4) E. Pratt and E. Werble, *J. Am. Chem. Soc.*, **72**, 4638 (1950).
5) M. Kamlet, *ibid.*, **77**, 4896 (1955).
6) B. Loev and M. Flores, *J. Org. Chem.*, **26**, 3595 (1961).

*1 The α- and β- symbols refer to the ferrocene ring throughout this paper.

7) "Organic Reactions," Vol. 1, p. 304 (1942).

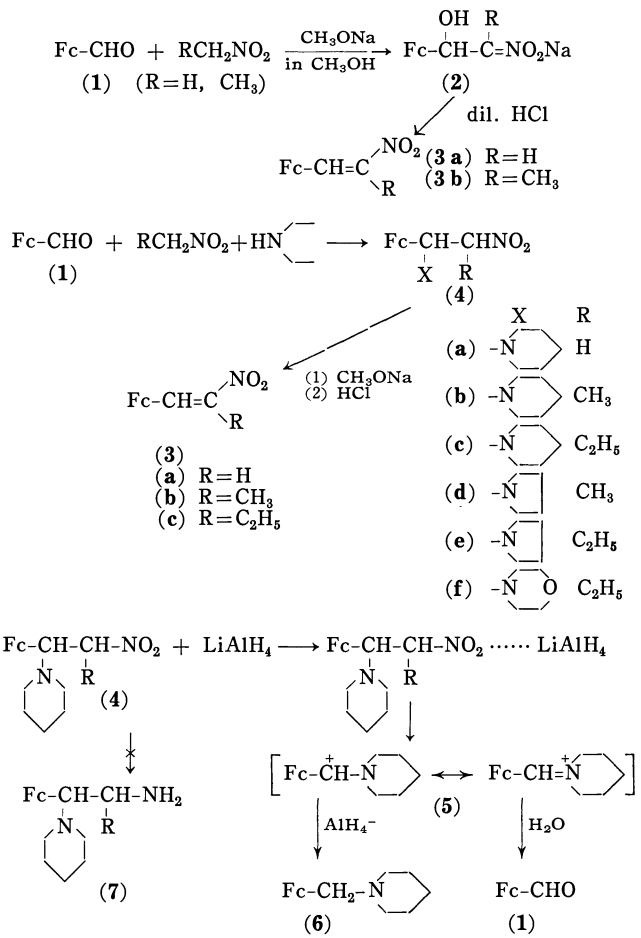

of nitromethane, nitroethane, and 1-nitropropane with formylferrocene in the presence of piperidine gave only aminonitroalkanes (**4**) as yellow crystals. The reduction of these products with $LiAlH_4$ afforded reddish-orange crystals (mp 84—86℃), along with the original aldehyde **1**; the expected amino compounds **7** were not obtained. The reddish-orange substance was identified as piperidinomethylferrocene (**6**)[8] by means of elementary analysis and a study of the IR spectrum and the NMR spectrum. Accordingly, it appears that the reaction proceeds through a cationic intermediate **5**, as is shown in the scheme.

On the other hand, nitromethane condensed with formylferrocene in the presence of pyrrolidine to form nitroolefin **3a** exclusively, while nitroethane and 1-nitropropane gave only aminonitroalkanes, **4d** and **4e** respectively. Furthermore, in the presence of morpholine, which is a weaker base than the others, the condensation of nitromethane and nitroethane with formylferrocene gave exclusively nitroolefin **3a** and **3b** respectively, whereas 1-nitropropane gave only aminoalkane **4f** as is shown in Table 1. When the Mannich bases, **4c** and **4e**, were converted to sodium salt by sodium methoxide and then treated with hydrochloric acid, the basic group on α-carbon was readily eliminated to afford quantitatively 2-nitro-1-ferrocenyl-1-butene **3c**, mp 77—78℃, whose NMR spectrum is shown in Table 3. A characteristic color change from yellow to violet was observed when a Mannich base **4** was converted into a nitroolefin **3**.

Discussion of the Mechanism of the Condensation Reaction. As the mechanism of the Mannich-type reaction[9] affording an aminonitroalkane **4**, the three courses shown in Fig. 1 can be considered. Course A involves the nucleophilic substitution of cyclic amine on the nitroalcohol **8** formed by the nucleo-

8) J.M. Osgerby and P.L. Pauson, *J. Chem. Soc.*, **1958**, 656.

9) J. Hine, "Physical Organic Chemistry," McGraw-Hill Book Company, New York (1956), p. 263.

TABLE 1. THE CONDENSATION OF FORMYLFERROCENE WITH NITROALKANE AND CYCLIC AMINE

Nitroalkane	Cyclic amine	Product	Yield (%)
Nitromethane	Piperidine	$FcCHCH_2NO_2$[a] (**4a**)	86
		X_1	
Nitroethane	Piperidine	$FcCHCH(CH_3)NO_2$[a] (**4b**)	88
		X_1	
1-Nitropropane	Piperidine	$FcCHCH(C_2H_5)NO_2$[a] (**4c**)	95
		X_1	
Nitromethane	Pyrrolidine	$FcCH=CHNO_2$ (**3a**)	81
Nitroethane	Pyrrolidine	$FcCHCH(CH_3)NO_2$[b] (**4d**)	89
		X_2	
1-Nitropropane	Pyrrolidine	$FcCHCH(C_2H_5)NO_2$[b] (**4e**)	94
		X_2	
Nitromethane	Morpholine	$FcCH=CHNO_2$ (**3a**)	74
Nitroethane	Morpholine	$FcCH=C(CH_3)NO_2$ (**3b**)	—
1-Nitropropane	Morpholine	$FcCHCH(C_2H_5)NO_2$[c] (**4f**)	72
		X_3	

a) X_1 = -N⟨ ⟩ b) X_2 = -N⟨ ⟩ c) X_3 = -N⟨ ⟩O

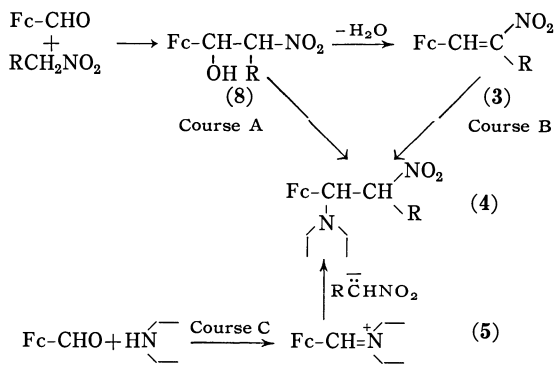

Fig. 1. Eventual mechanism of the Mannich-type condensation.

philic attack of nitroalkane on formylferrocene. Course B involves the addition of amine to the nitroolefin **3** produced by the dehydration of the nitroalcohol 8. Course C involves the intermediacy of the enamine **5**,[10] which is subjected to attack by a carbanion derived from nitroalkane. Of these three possibilities, Course A may be eliminated because of the fact that no alcoholic product was isolated from the reaction. In addition, Courses A and B can both be ruled out by the fact that the formation of aminonitroalkane **4** is not retarded, but even accelerated, when the nitroalkane with a bulkier alkyl substituent is used.

In order to obtain further information, condensation reactions of formylferrocene with compounds less acidic than nitroalkane, such as acetonitrile, α- and γ-picoline, and ethyl acetate, were attempted in the presence of piperidine in methanol. Neither the expected alcohol **9** nor the olefin **10** was thus formed; the only product isolated was a yellow, crystalline substance. When an ethereal solution of the yellow substance was shaken with dilute hydrochloric acid, the substance easily transferred to the aqueous layer to give a red solution. The neutralization of the aqueous layer with alkali gave the original aldehyde and amine. Moreover, the yellow substance was not isolated in the absence of a nucleophile, such as acetonitrile and the like, under the same conditions as above. This substance, therefore, seems to be something like a molecular complex; its elementary analysis suggests a structure corresponding to the formula **11**. The proposed structure is consistent with the following observations. The IR spectrum showed the characteristic absorption band of the carbonyl group of

10) S.P. Makarov, *J. Prakt. Chem.*, **141**, (2), 77 (1934).

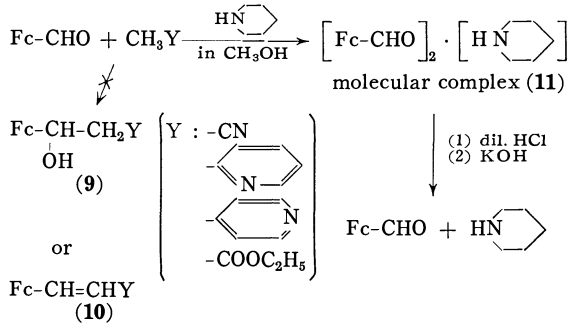

formylferrocene and that of the methylene group of piperidine, but no peak in the region of ν_{NH}. The UV spectrum of this compound is almost identical with that of formylferrocene. The complex **11** gradually decomposed into formylferrocene and piperidine when left standing in the air. Furthermore, the aminonitroalkane **4** was produced when the complex was dissolved in nitroalkane.

On the basis of these experimental results, it seems reasonable to conclude that Course C is the most likely, although there is no direct evidence for the formation of the enamine **5**.

For the preparation of 2-nitro-1-ferrocenylalkanes, piperidine is the most effective condensing agent among the cyclic amines employed in those reactions. The reactions of the nitroalkenes and the aminonitroalkanes will be reported in the following papers.

Experimental

Materials. Commercial cyclic amines and nitroalkanes were used without any further purification. Formylferrocene was prepared by the modified Vilsmeier reaction previously reported.[11]

TABLE 2. THE IR SPECTRA OF 1-FERROCENYL-2-NITROALKENES (KBr disk)

Compound	Mp(°C)	Frequency (cm^{-1})	
		$\nu_{C=C}$	ν_{NO_2}
FcCH=CHNO$_2$ (**3a**)	139—140	1630	1503 1328
FcCH=C(CH$_3$)NO$_2$ (**3b**)	57—58	1655	1499 1303
FcCH=C(C$_2$H$_5$)NO$_2$ (**3c**)	77—78	1639	1509 1298

Identification of the Reaction Products. The reaction products were identified by means of the NMR spectra, the IR spectra, and the results of elementary analyses. These results are tabulated in Tables 2, 3, and 4 respectively.

2-Nitro-1-ferrocenylethylene (3a). To an ice-cooled solution of formylferrocene (21.4 g, 0.1 mol) and nitromethane (12.2 g, 0.2 mol) in 60 m*l* of absolute methanol, there was gradually added a methanolic solution of sodium methoxide (10.8 g, 0.2 mol). Within a few minutes, about 30 g of a yellow-brown solid separated out. The solid salt was collected and washed with dry ether. Treating the solid with dilute hydrochloric acid gave 19.5 g (76% yield) of 2-nitro-1-ferrocenylethylene (**3a**) as violet crystals, mp 139—140 °C. The analytical sample was prepared by recrystallization from ethanol.

The nitroolefin **3a** was also well prepared as

TABLE 4. RESULTS OF THE ELEMENTARY ANALYSES

Compound	Found			Calcd		
	C%	H%	N%	C%	H%	N%
3a	55.64	4.79	5.36	56.07	4.28	5.42
3b	57.00	4.90	5.63	57.61	4.80	5.17
3c	57.08	5.24	4.62	58.99	5.27	4.92
4a	59.67	6.53	8.04	59.66	6.48	8.19
4b	60.69	6.79	7.86	60.05	6.78	7.81
4c	61.63	7.08	7.57	61.45	6.97	7.61
4d	59.09	6.39	7.69	59.68	6.44	8.19
4e	59.92	6.82	8.19	60.71	6.75	7.87
4f	57.69	6.46	7.34	58.10	6.46	7.53
6	67.45	7.38	4.66	68.10	7.42	4.92
11	65.58	7.41	2.59	65.40	6.10	2.88

TABLE 3. THE NMR SPECTRA OF 1-FERROCENYL-2-NITROALKENES (τ-value, in $CDCl_3$)

Compound	Unsubstituted ring protons	Substituted ring protons	Vinyl protons α	Vinyl protons β	Alkyl protons	
FcCH=CHNO$_2$ (**3a**)	5.81 (s) 5[a]	5.46 (s) 4	2.03 (d) 1	2.80 (d)[b] 1		
FcCH=C(CH$_3$)NO$_2$ (**3b**)	5.83 (s) 5	5.49 (s) 4	2.08 (s) 1		7.70 (s) 3	
FcCH=C(C$_2$H$_5$)NO$_2$ (**3c**)	5.80 (s) 5	5.49 (s) 4	2.09 (s) 1		7.21 (q) 2	8.75 (t)[c] 3

a) Figures under the τ-values indicate the ratio of intensities.
b) $J_{\alpha\beta}$=12.5 cps. c) J=6.7 cps.

11) M. Sato, H. Kono, M. Shiga, I. Motoyama and K. Hata, This Bulletin, **41**, 252 (1968).

follows: (a) Pyrrolidine (1.42 g, 0.02 mol) or morpholine (1.74 g, 0.02 mol) was gradually added to an ice-cooled solution of formylferrocene (2.14 g, 0.01 mol) and nitromethane (1.22 g, 0.02 mol) in 10 m*l* of absolute methanol. After standing for a few hours, the reaction mixtue was poured into dilute hydrochloric acid in order to be acidified, and then extracted with chloroform. The extract was washed with water, and then dried over anhydrous magnesium sulfate. After the removal of the solvent, the residue was chromatographed on alumina, using benzene as a solvent, to give the olefin **3a** in an excellent yield (Table 1).

(b) Aminonitroalkane (**4a**) (1.7 g, 0.005 mol), to be described below, was added to 10 m*l* of absolute methanol containing 1.08 g (0.02 mol) of sodium methoxide. The reaction mixture was stirred for an hour on an ice bath and then acidified with dilute hydrochloric acid to give the olefin **3a** quantitatively.

2-Nitro-1-ferrocenylpropene (**3b**). Sodium methoxide (3.6 g, 0.07 mol) in methanol was gradually added with cooling to a solution of formylferrocene (4.00 g, 0.02 mol) and nitroethane (3.0 g, 0.04 mol) in 20 m*l* of absolute methanol. After it had then been let stand for four days at room temperature, the reaction mixture was poured into 70 m*l* of 15% hydrochloric acid and extracted with chloroform. The organic layer was separated, washed with water, and dried over anhydrous magnesium sulfate. After the evaporation of the solvent, the crude product was chromatographed on alumina, using dry benzene as a solvent. From the first fraction, 2-nitro-1-ferrocenylpropene was obtained as violet crystals, mp 57—58 °C. From the following fractions 2.26 g (57%) formylferrocene were recovered.

For the preparation of nitroolefin **3b**, pyrrolidine and piperidine gave much better results than sodium methoxide, but morpholine gave only a low yield.

Aminonitroalkane, **4b** (1.78 g, 0.005 mol) and **4d** (1.71 g, 0.005 mol), prepared in excellent yields by the procedure to be described below, were quantitatively converted to the nitroolefin **3b** by treating them for an hour with 10 m*l* of a methanolic solution containing 1.08 g (0.02 mol) of sodium methoxide, followed by acidification with dilute hydrochloric acid.

2-Nitro-1-ferrocenyl-1-butene (**3c**). By the same procedure as has been described above, 2-nitro-1-ferrocenyl-1-butene was quantitatively prepared from the aminoalkanes **4c**, **4e**, and **4f** as violet crystals, mp 77—78 °C.

1-Ferrocenyl-1-piperidino-2-nitroethane (**4a**). Formylferrocene (2.14 g, 0.01 mol), nitromethane (1.22 g, 0.02 mol), and piperidine (1.70 g, 0.02 mol) were dissolved in 20 m*l* of absolute methanol. The solution was let stand at room temperature for a few hours to give 1-ferrocenyl-1-piperidino-2-nitroethane as yellow-brown crystals (2.9 g, 86%). It was filtered and washed with water and then with a small portion of ether. The pale yellow crystals obtained by recrystallization from dichloromethane - *n*-hexane melted at 116°C (dec.).

1-Ferrocenyl-1-piperidino-2-nitropropane (**4b**). Following the procedure described above, 1-ferrocenyl-1-piperidino-2-nitropropane was prepared from formylferrocene, nitroethane, and piperidine in a 94% yield. The pale yellow crystals obtained by recrystallization from dichloromethane - *n*-hexane melted at 121—122°C (dec.).

1-Ferrocenyl-1-piperidino-2-nitrobutane (**4c**). Yellow crystals of 1-ferrocenyl-1-piperidino-2-nitrobutane, mp 132°C (dec.), were similarly obtained.

Piperidinomethylferrocene (**6**). A mixture of 1-ferrocenyl-1-piperidino-2-nitropropane (**4b**) (1 g, 0.003 mol) and lithium aluminum hydride (0.8 g, 0.02 mol) in 50 m*l* of dry ether was stirred for 3 hr on an ice bath, and then 30 m*l* of methanol was gradually poured into the reaction mixture, followed by 100 m*l* of water. The mixture was then extracted with ether, and the extract was washed with water and dried over anhydrous magnesium sulfate. After the removal of the solvent, the residue was chromatographed on alumina, using benzene - *n*-hexane as a solvent. Reddish-orange crystals of piperidinomethylferrocene (**6**), mp 84—86°C, were obtained from the second fraction; yield 0.13 g (17%). The same compound **6** was obtained in a 15—17% yield from 1-ferrocenyl-1-piperidino-2-nitroethane (**4a**) by a similar procedure. The NMR spectrum of **6** exhibits two broad peaks, at τ 8.58 and τ 7.67, due to the methylene protons of the piperidine ring, and two singlets, at τ 6.66 and τ 5.93, due to α-methylene protons and ferrocene ring protons respectively.

1-Ferrocenyl-1-pyrrolidino-2-nitropropane (**4d**). By a procedure, using pyrrolidine as a condensing agent, similar to that used for the preparation of **4a**, **4d** was prepared in an 89% yield. The analytical sample, recrystallized from dichloromethane-*n*-hexane, melted at 75°C (dec.).

1-Ferrocenyl-1-pyrrolidino-2-nitrobutane (**4e**). From formylferrocene, 1-nitropropane, and pyrolidine, **4e** was obtained in a 88% yield as pale yellow crystals, mp 101—102°C, after recrystallization from dichloromethane - *n*-hexane.

1-Ferrocenyl-1-morpholino-2-nitrobutane (**4f**). A similar reaction of formylferrocene with 1-nitropropane and morpholine afforded **4f** as yellow-brown crystals, mp 139—140°C, in a 72% yield.

Molecular Complex (11) of Formylferrocene and Piperidine. Formylferrocene (1 g) was added to an ice-cooled solution of piperidine (1 g) and acetonitrile (0.5 g) in 5 m*l* of absolute methanol. After half an hour, the complex **11** separated from the solution as yellow crystals, which were then filtered and washed with methanol (yield, 0.7 g). Some discrepancies in the analytical data shown in Table 4 may be due to its instability in the air.

When 0.2 g of the complex **11** was dissolved in 2 g of nitromethane with stirring under ice cooling, the reaction mixture immediately turned to a brownish-violet. From the solution, 0.1 g of 1-ferrocenyl-1-piperidino-2-nitroethane (**4a**) was obtained as yellow crystals.

BULLETIN OF THE CHEMICAL SOCIETY OF JAPAN VOL. 41 1902—1908 (1968)

Novel Reduction of Various Organic Compounds with Water in the Presence of Precipitated Metals[1)]

Koji SAKAI, Masayoshi ISHIGE, Hiromichi KONO, Izumi MOTOYAMA, Ken-ichi WATANABE and Kazuo HATA

Department of Chemistry, Faculty of Science, Tokyo Metropolitan University, Setagaya, Tokyo

(Received December 27, 1967)

It was found that various organic compounds were reduced in good yields by refluxing them with precipitated metals in water. Water was proved to be indispensable as a hydrogen donor. The reduction of compounds which are insoluble in water was facilitated by using a mixture of dioxane and water. It is of interest that the reduction of nitriles with this catalyst afforded the hydrochlorides of the corresponding primary amines. The results imply the participation of the chloride ion on the ppt-metal catalyst. A selective reduction of C=C was observed in some α,β-unsaturated ketones, such as mesityl oxide and 1,3-diferrocenyl-2-buten-1-one. The relative activity of the various precipitated metals depends not only upon the kinds of the metals but also upon their combination. It is assumed that the surface of the ppt-Ni is acidic as a result of the coexisting chloride ion, which might participate in the catalytic reaction.

In 1952, Urushibara and Chuman discovered a new nickel catalyst[2)] and named it Urushibara nickel (abbreviated as U-Ni). It is prepared by the acid- or base-treatment of precipitated nickel (ppt-Ni in abbreviation), which is itself obtained by an ion-exchange reaction between a nickel chloride solution and zinc dust. This new nickel catalyst was proved to be useful for the catalytic hydrogenation of various organic compounds[3)] and also for other organic catalytic reactions[4)]; it has also been found that the catalytic activity of U-Ni is comparable to that of Raney-Ni. However, the nature of ppt-Ni as a precursor of the U-Ni had not yet been well studied. In a previous communication,[1)] it was reported that some organic compounds, such as olefins, ketones and nitro compounds, were catalytically reduced by refluxing them with water in the presence of ppt-Ni. It is noticeable that this reduction is performed by a simple procedure without any hydrogen gas, and that the ppt-Ni is generally useful for the reduction of various organic compounds. The present paper will deal with an extended investigation of reduction with water in the presence of ppt-Ni, and will discuss the function of ppt-Ni as a catalyst.

Results

The Reduction of Organic Compounds in the Presence of Ppt-Ni. The ppt-Ni is easily prepared by adding a hot aqueous solution of nickel chloride to zinc dust. After it has been dried under reduced pressure, it is so stable that it can be preserved in the air for a long time. Various organic compounds involving C=C, NO_2, C≡N, and C=O groups were reduced in satisfactory yields when refluxed with water in the presence of ppt-Ni; the results are summarized in Table 1.

In these reactions, it is noteworthy that water plays a dual role, serving both as a solvent and as a hydrogen donor. Indeed, while water was proved to be effective enough as a hydrogen donor,*1 methanol and ethanol are

1) Preliminary report: K. Sakai and K. Watanabe, This Bulletin, **40**, 1548 (1967).

2) Y. Urushibara, *ibid.*, **25**, 280 (1952); Y. Urushibara and S. Nishimura, *ibid.*, **28**, 446 (1955).

3) K. Hata and S. Taira, *Yuki Gosei Kagaku Kyokai Shi (J. Soc. Org. Syn. Chem. Japan)*, **16**, 596 (1958).

4) K. Watanabe, This Bulletin, **32**, 1281 (1959); K. Watanabe and K. Sakai, *ibid.*, **39**, 8 (1966); K. Sakai, T. Ito and K. Watanabe, *ibid.*, **40**, 1660 (1967).

*1 According to a private communication from Y. Urushibara and H. Tomoda, an effective reaction occurs without refluxing when an aqueous solution of acids or bases, such as HCl or NaOH, is added, drop by drop and in admixture with the sample to be reduced, into a stirred mixture of ppt-Ni and water.

TABLE 1. THE REACTION BETWEEN VARIOUS ORGANIC COMPOUNDS AND WATER IN THE PRESENCE OF PRECIPITATED NICKEL

Each run was carried out by refluxing for 12 hr.

Exp. No.	Compound		Nickel content of catalyst	Solvent		Reduction Product[a]		Recovered material
		g	g		ml		%	%
1	Styrene[b]	10	4	Water	100	Ethylbenzene	81.4	19.6
2	Nitrobenzene[b]	10	4	Water	100	Aniline	98	—
3	*p*-Nitrobiphenyl	1	2	Water Dioxane	30 10	*p*-Aminobiphenyl	80	20
4	*o*-Nitrobiphenyl	1	2	Water Dioxane	30 10	*o*-Aminobiphenyl	70	30
5	Benzonitrile[c]	10	4	Water	100	Benzylamine-HCl[d] Benzamide	90 Trace	+
6	2-Cyanopyridine	0.5	1	Water	20	Nickel chelate[e] of 2-pyridylmethylamine	>80	—
7	3-Cyanopyridine	0.5	1	Water Dioxane	40 20	3-Pyridylmethylamine[d]	>80	—
8	4-Cyanopyridine	0.5	1	Water Dioxane	40 20	4-Pyridylmethylamine[d]	>80	—
9	Benzaldehyde[b]	10	4	Water	100	Benzyl alcohol	>90	—
10	*m*-Nitrobenzaldehyde	1	2	Water Dioxane	30 10	*m*-Aminotoluene	>90	+
11	Ethyl methyl ketone[b]	10	4	Water	100	2-Butanol	87	13
12	Cyclohexanone[b]	10	4	Water	100	Cyclohexanol	90	+
13	2-Methylcyclohexanone	1	0.4	Water	10	2-Methylcyclohexanol	42	58
14	Menthone	5	2	Water Dioxane	40 20	*exo*-Menthol *endo*-Methol	3 1	>95
15	Camphor	5	2	Water Dioxane	40 10	*exo*-Borneol *endo*-Borneol	2 0.4	>97
16	Ethyl cyclopentanone-2-carboxylate	1	0.4	Water	10	Ethyl cyclopentanol-2-carboxylate	71	29
17	Acetophenone[g]	8	2	Water	70	1-Phenylethanol Ethylbenzene	25 26	49
18	Benzophenone[g]	8	2	Water Dioxane	40 30	Benzhydrol Diphenylmethane	31 40	29
19	Formylferrocene	0.5	1	Water Dioxane	20 10	Methylferrocene 1-Methyl-2-(ferrocenyl-methyl)ferrocene	80 10	—
20	Acetylferrocene	0.5	1	Water Dioxane	20 10	Ethylferrocene	30	60
21	Benzoylferrocene	1	2	Water Dioxane	20 10	Benzylferrocene	<80	—
22	Diacetylferrocene	0.5	1	Water Dioxane	20 10	Diethylferrocene 1-Ethyl-1′-acetyl-ferrocene 1-Acetyl-1′-(1-hydroxy-ethyl)ferrocene	10 40 Trace	>40
23	Mesityl oxide[b]	10	4	Water	100	Isobutyl methyl ketone	95[f]	—
24	1,3-Diferrocenyl-2-buten-1-one	0.5	1	Water Dioxane	20 10	1,3-Diferrocenyl-1-butanone	>90	—
25	Dypnone	1	2	Water Dioxane	30 10	1,3-Diphenylbutane	>90	—
26	Benzylideneacetone[g]	1	2	Water Dioxane	30 10	*n*-Butylbenzene 4-Phenyl-2-butanone 4-Phenyl-2-butanol	6 26 68	—

a) The yields were calculated from the results of gas chromatographic analysis, except for Exp. No. 5. b) The reaction time was 16 hr. c) The reaction time was 20 hr. d) The amine was obtained as hydrochloride from the reaction mixture by evaporation. e) The composition of the nickel chelate was found to be $[Ni_2(2\text{-pyridylmethylamine})_5(2\text{-pyridinecarboxylic acid})(H_2O)_3Cl]$. f) More than 90% even when refluxed for 5 hr. g) Each product was identified by infrared spectra after the isolation by gas chromatography.

unsatisfactory. Whereas compounds insoluble in water were reduced only in poor yields, the use of a mixture of dioxane and water facilitated the reaction.

As may be seen in Table 1, ethylenic double bonds were easily hydrogenated in high yields; for example, ethylbenzene was obtained in an 81.4% yield from styrene, and isobutyl methyl ketone, in a 95% yield from mesityl oxide. In the reduction of unsaturated ketones, such as mesityl oxide and 1,3-diferrocenyl-2-buten-1-one,[5] the ethylenic double bonds were preferentially hydrogenated, while the carbonyl groups were unaffected.

Ketones were generally reduced to the corresponding secondary alcohols. In some cases a reduction of the carbonyl group to the methylene group was observed, as in the Clemmensen reduction.[6] Thus, dypnone, acetylferrocene, and benzoylferrocene[7] were mainly converted to 1,3-diphenylbutane, ethylferrocene, and benzylferrocene respectively. The reduction of acetophenone yielded a mixture containing 1-phenylethanol and ethylbenzene, while benzophenone similarly gave benzhydrol and diphenylmethane. Benzylideneacetone gave a more complicated product consisting of 4-phenyl-2-butanol, 4-phenyl-2-butanone, and *n*-butylbenzene. Menthone and camphor were respectively 96% and 97% recovered unchanged, while only a small amount of the corresponding alcohols were obtained.

Nitriles were predominantly converted to primary amines without the formation of secondary amines, which are often produced as by-products in ordinary catalytic hydrogenations. It is noteworthy that the amines were obtained as their hydrochlorides, the chloride anion presumably being supplied from ppt-Ni. 2-Cyanopyridine characteristically afforded a metal complex of the amine when treated with water in the presence of ppt-Ni or ppt-Cu, while 3- and 4-cyanopyridine gave only the corresponding amine hydrochlorides. *m*-Nitrobenzaldehyde was converted to *m*-methylaniline by a Clemmensen-type reduction, whereas benzaldehyde afforded only benzyl alcohol, no appreciable amount of the expected formation of toluene being observed.

The Reduction of Organic Compounds in the Presence of Ppt-Ni, Al. Another type of ppt-Ni (denoted as ppt-Ni,Al) was prepared using aluminum grains of 40—80 meshes instead of zinc dust. The U-Ni-BA,[8] prepared from the ppt-Ni,Al, has already been reported to be a good catalyst for the hydrogenation of aromatic nuclei. The X-ray diffraction pattern of ppt-Ni,Al showed sharp, proper peaks of nickel at 38.7°, 44.7°, 51.7°, and 76.5° in 2θ, whereas in ppt-Ni the peaks of nickel were little observed.

The results of the reduction in the presence of ppt-Ni,Al are given in Table 2. The activity of the ppt-Ni,Al was found to be high enough to reduce phenol to cyclohexanone and cyclohexanol. However, in the reduction of *o*- and *m*-cresol, most of the

TABLE 2. THE REDUCTION OF ORGANIC COMPOUNDS BY WATER IN THE PRESENCE OF PRECIPITATED NICKEL, PPT-Ni, Al

Exp. No.	Compound		Nickel content of catalyst	Solvent		Reaction time	Product[a]		Recovered
		g	g		ml	hr		%	%
1	Phenol	8	1	Water	70	15	Cyclohexanol Cyclohexanone[b]	60 1.4	38.6
2	*o*-Cresol	10	2	Water	100	12	2-Methylcyclohexanol	5	95
3	*m*-Cresol	8	1	Water	70	7	3-Methylcyclohexanol	2	98
4	Styrene	8	1	Water	100	12	Ethylbenzene	29	77
5	Benzaldehyde	8	1	Water	100	12	Toluene Benzyl alcohol	Trace 94	6
6	Acetophenone[c]	8	1	Water	70	7	Ethylbenzene 1-Phenylethanol	4 36	60
7	Benzophenone	5	1	Water Methanol	40 20	7	Diphenylmethane	33	67

a) The yields were calculated from the results of gas chromatographic analysis.
b) Cyclohexanone was derived to oxime, mp 86—89°C (lit. 89—90°C).
c) Products were identified by infrared spectra after the isolation by gas chromatography.

5) P. L. Pauson and W. E. Watts, *J. Chem. Soc.*, **1962**, 3880.
6) E. L. Martin, "Organic Reactions," Vol. 1, p. 155 (1942).
7) M. Rosenblum, "Chemistry of Iron Group Metallocenes," John Wiley & Sons, New Yok (1965), p. 120.
8) K. Hata, S. Taira and I. Motoyama, This Bulletin, **31**, 776 (1958); I. Motoyama, *ibid.*, **33**, 232 (1960).

phenols were recovered unchanged. The results of the reduction of acetophenone, benzophenone, styrene, and benzaldehyde were very similar to those obtained with the ordinary ppt-Ni.

Features of the Precipitated Metals. It has been reported[9,10] that ppt-Ni contains Ni, Zn, ZnO, Zn(OH)Cl, and $Zn(OH)_2$, and that the zinc in ppt-Ni is gradually oxidized to zinc oxide with the progress of the catalytic reaction in the presence of ppt-Ni; thus, the zinc not only acts as a carrier, but also protects the nickel from oxidation.

Since the behavior of zinc might be assumed to contribute greatly to the function of ppt-Ni, we tried to determine to what extent a variation in the Zn/Ni ratio in ppt-Ni affects the reaction. In Fig. 1 the correlation is expressed in terms of the yield of cyclohexanol obtained by the reduction of cyclohexanone. As Fig. 1 shows, the maximum yield of cyclohexanol was attained by a catalyst whose Zn/Ni ratio was 10. This ratio coincides with that of the ppt-Ni, from which the U-Ni catalyst with the highest activity was prepared. It might be concluded from this finding that zinc participates in the reaction by interacting with nickel as well as with water.

From these considerations, some other precipitated metals produced by treating a certain metal chloride with zinc may be

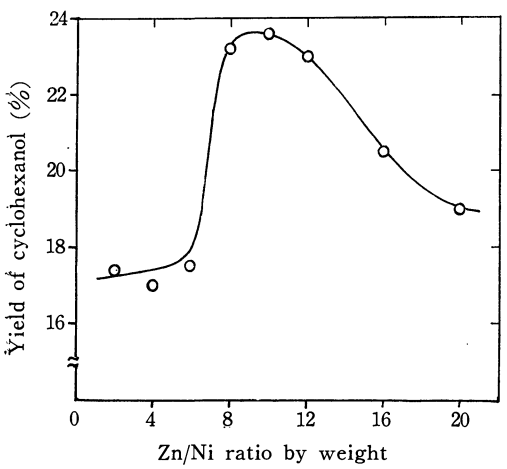

Fig. 1. The correlation between the ratio of zinc to nickel and the yield of cyclohexanol in the catalytic reduction with precipitated nickel.
Cyclohexanone 1g, catalyst 0.3g, water 1m*l*, heated to 111—115°C for 24 hr in a sealed tube.

9) Y. Urushibara, S. Yamaguchi and M. Kobayashi, *ibid.*, **29**, 815 (1956).

10) Y. Urushibara, M. Kobayashi, S. Nishimura and H. Uebara, *Shokubai* (*Catalyst*) (Tokyo), **12**, 111 (1956).

TABLE 3. THE RELATIVE ACTIVITIES OF THE PRECIPITATED METALS

Cyclohexanone 1 g, catalyst 0.3 g, water 1 m*l*, heated to 111—114°C for 12 hr in a sealed tube.

Exp. No.	Catalyst	Composition of the reaction product[a] (%)	
		Cyclohexanol	Cyclohexanone
1	Ppt-Ni	15.3	84.7
		15.0	85.0
2	Ppt-Co	10.0	90.0
3	Ppt-Cu	3.5	96.5
4	Ppt-Fe	3.4	96.6
5	Ppt-Ni-Co	17.7	82.3
6	Ppt-Ni-Cu	5.5	94.5
7	Ppt-Ni-Fe	15.2	84.8

a) Products were determined by gas chromatography; column 1.5 m, silicone grease DC 550 on Celite 30—40 meshes; temp., *ca.* 150°C; flow rate, 60 cc/min; carrier gas, H_2.

expected to be more reactive than the ppt-Ni. Thus, the following precipitated metals were prepared: ppt-Co, ppt-Cu, ppt-Fe, and mixed precipitated metals, such as ppt-Ni-Co, ppt-Ni-Cu, and ppt-Ni-Fe. The relative activities of these precipitated metals were then examined in the reduction of cyclohexanone. The results of representative experiments, shown in Table 3, exhibit the relative activities in the following order: ppt-Ni-Co > ppt-Ni > ppt-Ni-Fe > ppt-Co > ppt-Ni-Cu > ppt-Cu > ppt-Fe. This indicates that the activity of precipitated metal may be increased by a proper combination of metals.

The behavior of ppt-Ni contrasts with that of ordinary hydrogenation catalysts. Thus, a rapid decomposition of hydrogen peroxide was observed in the presence of U-Ni, "Stabilized nickel," copper chromite, or zinc chromite, but it could not be observed with ppt-Ni. On the other hand, the effective reduction of the cited compounds by water was observed only in the presence of the "precipitated metals," whereas U-Ni, Raney-Ni, and other hydrogenation catalysts were very feeble. The difference between them is reflected in the X-ray diffraction diagrams. The results of X-ray diffraction analysis, suggest[11] that the surface of ppt-Ni never consists of nickel itself, but rather is convered with alloy-like layers composed of nickel and zinc, contaminated with OH^- and Cl^-.

Some of the experimental results are compatible with this view. Thus, it was found that the reduction of nitriles in the presence

11) S. Taira, "Shokubai Kogaku Koza (Catalytic Engineering)," Vol. 10, Chijinshokan & Co., Tokyo (1967), p. 498.

of ppt-Ni produced amine hydrochlorides, while scarcely any free amines were detectable. When the ppt-Ni was soaked in water, a silver nitrate test for chloride anion was negative after 24 hr and only slightly positive after 72 hr. However, when the ppt-Ni was digested in hot water for 72 hr, a distinct deposit of silver chloride was observed in a silver nitrate test of the solution. Consequently, the surface of the ppt-Ni may be assumed to be relatively acidic as a result of coexisting chloride ions, which might participate in the catalytic reaction.

The Acidity and Acid Strength[12] of the Surface of Ppt-Ni. To measure the acidity and acid strength of the surface of ppt-Ni, *n*-butylamine titration was applied to the ppt-Ni in benzene, using Methyl Red as an indicator (pK_a 4.8). Though Methyl Red generally turns into a red acidic form when it reacts with an acidic solid, the dark gray color of the ppt-Ni makes it impossible to detect any color change in the adsorbed indicator on the solid surface. Therefore, the point of neutralization was determined by noting the change in color on anhydrous magnesium sulfate, which had previously been mixed with the ppt-Ni. The relation between the weight of the ppt-Ni used and the amounts of the *n*-butylamine adsorbed is shown in Fig. 2. From the slope of the line in Fig 2, the acidity of ppt-Ni was calculated to be 1.05×10^{-5} (eq/g) at pK_a 4.8. On the other hand, the acidity of ppt-Ni was nearly zero when Methyl Yellow was used as an indicator (pK_a 3.3). These results imply that the acid strength of the surface is at least more acidic than pK_a 4.8, while the number of acid sites is comparatively small.

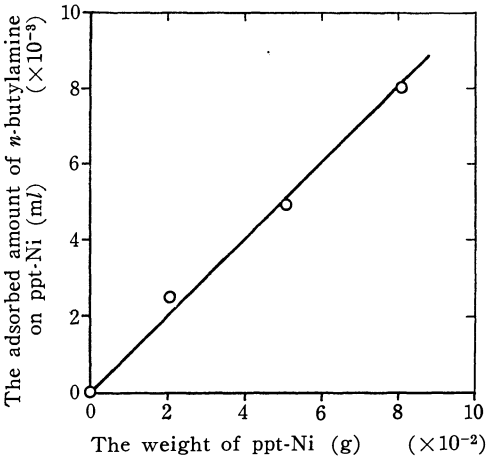

Fig. 2. *n*-Butylamine titration of the precipitated nickel.

12) O. Johnson, *J. Phys. Chem.*, **59** 827 (1955); H. A. Benesi, *J. Am. Chem. Soc.*, **78**, 5496 (1956).

Discussion

It is well known that both zinc amalgam[6] and zinc itself[13] can be used for reduction in acidic, basic, or neutral solutions. However, the reduction generally requires the cooperation of acid to increase the yield of the reaction product, and subsequent undesirable side-reactions due to the acid are inevitable. A unique characteristic of the reduction with ppt-Ni is the use of water as a hydrogen donor, thus making the use of any acid generally unnecessary. Consequently, the reduction can be performed under practically neutral conditions.

The results shown in Table 1 suggest that the reduction may proceed in a manner somewhat similar to that in the Clemmensen reduction. However, there are some differences between these two reduction reactions. The Clemmensen reduction of a ketone often results in the formation of alcohol, saturated hydrocarbon, olefin, and a dimerization or rearrangement product; for example, benzophenone yields benzhydrol, diphenylmethane, tetraphenylethylene, and benzopinacol. In regard to the formation of the pinacol, a radical intermediate has been proposed for the mechanism of the Clemmensen reduction.[14] On the other hand, the reduction of benzophenone in the presence of the ppt-Ni affords only benzhydrol and diphenylmethane. A radical mechanism may be excluded on the base of the fact that no formation of the pinacol was observed. The presence of a large quantity of water as a solvent also supports this presumption.

Among three analogous α,β-unsaturated ketones $RC(CH_3)=CHCOR$ ($R=CH_3$, C_6H_5, ferrocenyl), the reduction of carbonyl to methylene was observed only in dypnone ($R=C_6H_5$). It has been reported[15] that the carbonyl group in mesityl oxide also remains unaffected by the Clemmensen reduction, the reason being discussed by postulating the intermediacy of a cyclopropanol form. On the other hand, Rinehart *et al.*[16] have pointed out the differ-

13) Y. Ogata, "Oxidation and Reduction of Organic Compounds" (in Japanese), Nankodo, Tokyo (1963), p. 656.

14) W. Steinkopf and A. Wolfram, *Ann.*, **430**, 113 (1923).

15) B. R. Davis and P. D. Woodgate, *J. Chem. Soc.* (C), **1966**, 2006.

16) L. Rinehart, Jr., J. Curby, Jr., H. Gustafson, K.G.Harrison, R.E. Bozak and D.E.Bublity, *J. Am. Chem. Soc.*, **84**, 3263 (1962).

ence in behavior between 1,3-diferrocenyl-2-buten-1-one and dypnone toward reaction with methylmagnesium bromide, the former not bringing about either the 1,4- or 1,2-addition of the Grignard reagent, whereas the latter does so. The present results on the reduction in the presence of ppt-Ni are compatible with these observations.

Bradlow *et al.*[17] have examined the substituent effect in the Clemmensen reduction of benzophenone derivatives; they found that substituents in the ortho position or electron-withdrawing substituents facilitate the formation of diphenylmethanes, whereas electron-donating substituents promote the formation of pinacols. In the present reduction of carbonyl groups, the trend of the reaction must be affected not only by the electronic factor but also by the steric factor. A molecule of dypnone can take a planar conformation in which the C=C, C=O, and two phenyl groups lie on a common plane, as is indicated by a molecular model. The planar conformation may facilitate the approach of the molecule toward the catalyst metal, resulting in the reduction of both ethylenic and carbonyl groups. On the other hand, a voluminous ferrocenyl group is assumed to hinder the approach of the carbonyl group toward the catalyst metal, thus preventing the catalytic reduction.

At any rate, the ppt-metal catalyzed reaction has been found to be relatively complex, and it is difficult to explain the function of ppt-metal in terms of the electrode potential of the metals. It was found that the ppt-Ni prepared with a 0.25 M sodium chloride solution instead of water increased the yield of the product, and the X-ray diffraction analysis has indicated an increase in the amount of Zn(OH)Cl in this particular ppt-Ni.

Though the mechanism of the ppt-metal-catalyzed reaction has not yet been sufficiently elucidated, the reaction may be assumed to involve at least two processes—the decomposition of water and the reduction of substrates, and the reduction may follow a course similar to that in an ordinary hydrogenation reaction. A more detailed discussion of the mechanism of this reaction will, however, be reported in a subsequent paper.

Experimental

Catalysts. *Precipitated Metals.* Zinc dust (10 g) and distilled water (3 m*l*) were placed in an Erlenmeyer flask and heated on a water bath. An aqueous solution (10 m*l*) containing either 4.04 g of nickel(II) chloride ($NiCl_2 \cdot 6H_2O$),[2] 4.04 g of cobalt(II) chloride ($CoCl_2 \cdot 6H_2O$), 2.69 g of copper(II) chloride ($CuCl_2 \cdot 2H_2O$), or 4.84 g of iron(III) chloride (anhydrous), previously heated to 60°C, was added to the heated zinc dust mud with vigorous shaking. A violent exchange reaction took place, depositing nickel on the surface of the zink dust. The whole solid was collected on a glass filter by suction, washed with water three times and then with methanol and ether, and dried under reduced pressure. The precipitated metal thus obtained contains about 1 g of each metal, supported on the zinc dust.

Mixed Precipitated Metals. Ppt-Ni-Co, ppt-Ni-Cu, and ppt-Ni-Fe were prepared by the same procedure using a mixture of 2 g of nickel(II) chloride and either 2 g of $CoCl_2 \cdot 6H_2O$, 1.5 g of $CuCl_2 \cdot 2H_2O$, or 1.4 g of $FeCl_3$, instead of 4.04 g of nickel chloride alone.

Ppt-Ni,Al. Aluminum grains of 40—80 meshes (50 g) were washed with 250 m*l* of a 3% sodium hydroxide solution and then with water. The aluminum grains were placed in a 300-m*l* Erlenmeyer flask along with a small quantity of water, and were heated on a water bath. An aqueous solution of nickel chloride (100 m*l*) containing 40 g of $NiCl_2 \cdot 6H_2O$, previously heated to 80°C, was poured on the aluminum grains. Occasional stirring with a glass rod was continued until the slushy reaction mixture became nearly solid. The solid was then washed three times with water and then with methanol and ether, and dried under reduced pressure.

The Reduction of Styrene. A suspension of styrene (10 g) in 100 m*l* of water was refluxed vigorously in the presence of the ppt-Ni containing 4 g of nickel. After the solution had been refluxed for 12 hr, the ppt-Ni was separated by filtration while hot, and washed with water and with ether. The filtrate and the washings were combined and extracted with ether. The extract was dried over anhydrous magnesium sulfate, and the ether was carefully evaporated away on a water bath. The residue was analyzed by gas chromatography (column, 30% Carbowax 1500 on Celite 30—40 meshes; length, 2 m; column temp., *ca.* 180°C; flow rate, 14—20 cm/sec; carrier gas, H_2). The yield of ethylbenzene was 81.4%. The ethylbenzene (bp 129—131°C) was identified by infrared spectrum analysis.

The Reduction of Benzonitrile. The reaction procedure was almost the same as that described above. After the reaction, the ppt-Ni was filtered off. The filtrate was carefully evaporated to dryness under reduced pressure, and the residue was extracted with ether. The evaporation of the ether extract gave a small quantity of a white solid which was identified as benzamide. A major part of the product, which consisted of a white solid insoluble in ether, was recrystallized from hot water (mp >240°C). It was identified as benzylamine hydrochloride by IR analysis (ν_{max}^{KBr} 3012, 1520, 1500, 750, and 695 cm^{-1}) and by NMR analysis (benzene ring protons τ 2.55, methylene protons τ 5.8 in D_2O). The hydrochloride (yield, *ca.* 90%) liberated benzyl-

17) H. L. Bradlow and C. A. van der Werf, *J. Am. Chem. Soc.*, **69**, 1254 (1948).

amine when treated with sodium hydroxide.

The Reduction of Formylferrocene.[18] After the reaction had been conducted in a similar manner, the ppt-Ni was separated and the product was obtained by extraction with ether. The gas chromatographic analysis (column, 20% APL on Celite 30—40 meshes; length, 2 m; column temp., *ca.* 180°C; flow rate, 20—15 cm/sec; carrier gas, H_2) indicated a sole compound as the reduction product. The crude product was dissolved in benzene and separated by column chromatography on active alumina (*ca.* 100—200 meshes), using *n*-hexane for elution. A careful evaporation of the yellow elute afforded yellow crystals of methylferrocene (yield, *ca.* 80%), mp 34.9—35.2°C (lit. 35.5—36.5 °C). This substance was identified by comparing its infrared spectrum with that of an authentic specimen. A successive elution of the column chromatography exhibited a small quantity of a yellow crystalline product, which could not be detected on gas chromatography and which was assumed to be 1-methyl-2-(ferrocenylmethyl)ferrocene on the basis of its NMR spectrum.

The Reduction of 2-Cyanopyridine. 2-Cyanopyridine (0.3 g) and water (10 m*l*) were refluxed vigorously in the presence of ppt-Ni or ppt-Cu (containing 0.4 g of the catalyst metal) for 10 hr. After the ppt-Ni or ppt-Cu had then been filtered off, the filtrate was carefully evaporated to dryness on a water bath; a green solid was thus obtained. The solid was washed with ether, dissolved in ethanol, and separated by column chromatography on active alumina. The evaporation of the solvent from the elute gave a greenish-blue solid. Recrystallization from hot water afforded a nickel or copper chelate in the form of greenish-blue (nickel) or pale blue (copper) needles. Elementary analyses were carried out with samples dried at 56°C under reduced pressure for 1 hr.

Nickel complex, Found: C, 49.67; H, 5.52; N, 17.68%. Calcd for $C_{36}H_{50}O_5N_{11}ClNi_2$: C, 49.7; H, 5.75; N, 17.7%.

Copper complex, Found: C, 31.09; H, 3.91; N, 12.42%. Calcd for $C_6H_8N_2Cl_2Cu$: C, 29.7; H, 3.30, N, 11.5%.

These metal complexes were confirmed to be metal chelates of 2-pyridylmethylamine by means of their infrared and ultraviolet spectra.[19] The composition of the nickel chelate corresponds to the formula. $Ni_2(C_5H_5NCH_2NH_2)_5(C_5H_5NCO_2H)(H_2O)_3Cl$ Nickel complex: IR, ν_{max}^{KBr} 3220,2924,1670(s), 1608 cm^{-1} UV, $\lambda_{max}^{H_2O}$ 267,261,254 mμ. Copper complex: IR, ν_{max}^{KBr} 3220, 2924, 1604 cm^{-1}. UV, $\lambda_{max}^{H_2O}$ 253, 247, 240 mμ.

Acid Strength Measurement[12] **of Ppt-Ni.** The ppt-N powder was completely dried for an hour at 80°C under reduced pressure. A sample of the ppt-Ni (0.0215 g) was then placed in a 50-m*l* Erlenmeyer flask, together with 0.500 g of anhydrous magnesium sulfate. Dry benzene (5 m*l*) and a drop of a 0.1% benzene solution of Methyl Red (pK_a 4.8) were added to the mixture. The indicator immediately gave a red color on the magnesium sulfate. Then, a 0.0999 N benzene solution of *n*-butylamine was added, drop by drop, through a micropipet until a color change from red to yellow was observed on the surface of the magnesium sulfate. Referring to a blank test in order to evaluate the acid strength of the magnesium sulfate itself, the amount of *n*-butylamine adsorbed on the acid sites of the ppt-Ni was then calculated. Similar titrations were made with 0.0516 g and 0.0817 g of ppt-Ni; the results are plotted on Fig. 2.

Using Methyl Yellow as an indicator, the same titration method was applied to measure the acid strength of ppt-Ni in pK_a 3.3. In order to ensure that no excess of amine was present on the solid at the end point, a drop of 0.05 N trichloroacetic acid in benzene was added; the red color then reappeared.

The authors wish to express their hearty thanks to Professor Dr. Michio Kobayashi for his helpful advice, and also to Mr. Yasuharu Nakaido and Mr. Satoshi Kobayashi of Gunma University and Dr. Masami Ichikuni of this University for their X-ray analyses.

18) Formylferrocene was prepared by a modified method of the Vilsmeyer reaction: M. Sato, H. Kono, M. Shiga, I. Motoyama and K. Hata, This Bulletin, **41**, 252 (1968).

19) S. Utsuno and K. Sone, *ibid.*, **37**, 1038 (1964).

BULLETIN OF THE CHEMICAL SOCIETY OF JAPAN VOL. 41 1909—1916 (1968)

Studies of Peptide Antibiotics. XIII. Synthesis of Retrogramicidin S[1]

Michinori WAKI and Nobuo IZUMIYA

Laboratory of Biochemistry, Faculty of Science, Kyushu University, Hakozaki, Fukuoka

(Received January 22, 1968)

In order to investigate a contribution for an antibacterial activity of a direction of the peptide bonds in gramicidin S molecule, retrogramicidin S with the reverse peptide sequence was prepared through a cyclization reaction of linear decapeptide active ester in pyridine. The cyclization of linear pentapeptide active ester yielded a mixture of retrocyclosemigramicidin S and retrogramicidin S. Retrogramicidin S thus obtained exhibited a weak activity against *Bacillus subtilis* and *Staphylococcus aureus*, whereas retrocyclosemigramicidin S showed no activity against any of microorganisms tested.

In studies of the relationship between chemical structure and biological activity of gramicidin S, various analogs wherein several amino acid residues are replaced by other amino acids have been synthesized in this laboratory.[2] For example, it was found that [5,5′-glycine]-gramicidin S[3,4] possessed a stronger activity in several-fold than natural gramicidin S. As a different type of synthetic analogs of gramicidin S, we have designed the synthesis of retrogramicidin S in order to determine what degree the direction of the peptide bonds contributes to a biological activity. The retrogramicidin S can be regarded as a cyclodiastereomer, which has been called by Prelog,[5] of gramicidin S.

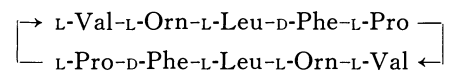

gramicidin S

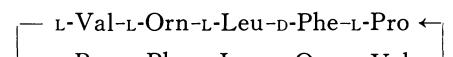

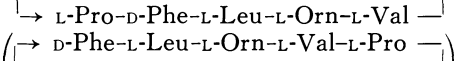

retrogramicidis S (XXII)

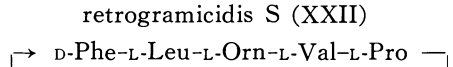

retrocyclosemigramicidin S (XXIII)

In the studies of synthetic analogs of linear biologically active peptides, a retro-analog of bradykinin has been synthesized by two groups,[6] they observed that the retrobradykinin was completely inactive in the rat uterus assay. As an analog of cyclic active peptides, Shemyakin *et al.* demonstrated that the retroenantio-[5,5′-glycine]-gramicidin S was highly active as the parent compound, [5,5′-glycine]-gramicidin S.[7]

For the conformation of gramicidin S in the solid- and solution-state, several models have been proposed.[8] A possible model (Fig. 1) is the intramolecular antiparallel β form with four hydrogen bond which has been suggested by Hodgkin and Oughton with the results of X-ray crystallographic investigation.[9] Schwyzer also suggested the same model with the occurrence of dimerization reaction on the

1) A part of this work was presented at the 5 th Symposium of Peptide Chemistry, Kyoto, November, 1967, and communicated briefly in *Tetrahedron Letters*, **1968**, 3083.

2) See for recent example, M. Waki, O. Abe, R. Okawa, T.Kato, S. Makisumi and N. Izumiya, This Bulletin, **40**, 2904 (1967).

3) We followed the rules naming synthetic modifications of natural peptides in *Biochemistry*, **6**, 362 (1967).

4) H. Aoyagi, T. Kato, M. Ohno, M. Kondo and N. Izumiya, *J. Am. Chem. Soc.*, **86**, 5700 (1964); This Bulletin, **38**, 2139 (1965).

5) V. Prelog and H. Gerlach, *Helv. Chim. Acta*, **47**, 2288 (1964).

6) S. Lande, *J. Org. Chem.*, **27**, 4558 (1962) ; K. Vogler, P. Lanz and W. Lergier, *Helv. Chim. Acta*, **45**, 561 (1962).

7) M.M. Shemyakin, Yu. A. Ovchinnikov, V.T. Ivanov and I.D.Ryabova, *Experientia*, **23**, 326 (1967). These authors have mentioned that retro-[5,5′-glycine]-gramicidin S is highly active as [5,5′-glycine]-gramicidin S in foot note.

8) See for recent example, D. Balasubramanian, *J. Am. Chem. Soc.*, **89**, 5445 (1967).

9) D. C. Hodgkin and B. M. Oughton, *Biochem. J.*, **65**, 752 (1957).

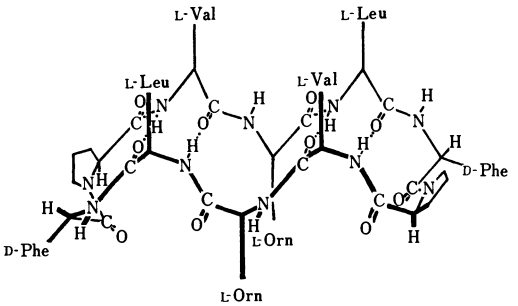

Fig. 1. A possible structure of gramicidin S.

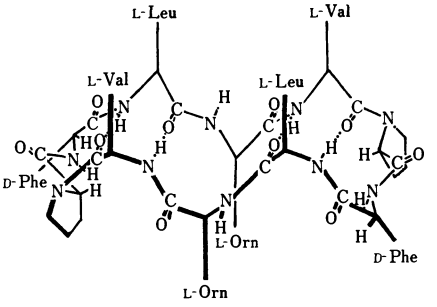

Fig. 2. A possible structure of retrogramicidin S.

occasion of gramicidin S synthesis.[10] In this model, the hydrophilic ornithyl side chains are on one side of the pleated sheet, thus the model appears to be a cationic detergent. Rothen's surface studies on gramicidin S, quoted in Craig's article,[11] also seem to support this model. We attempted to construct the retrogramicidin S model (Fig. 2) with the antiparallel β form, which has been suggested by Hodgkin and Oughton, as a principal frame by molecular model study. It is observed that the hydrophobic proline residues are directed to the side where the ornithyl side chains are located on. Since the character as a specific cationic detergent for gramicidin S is an important factor for the antibacterial activ-

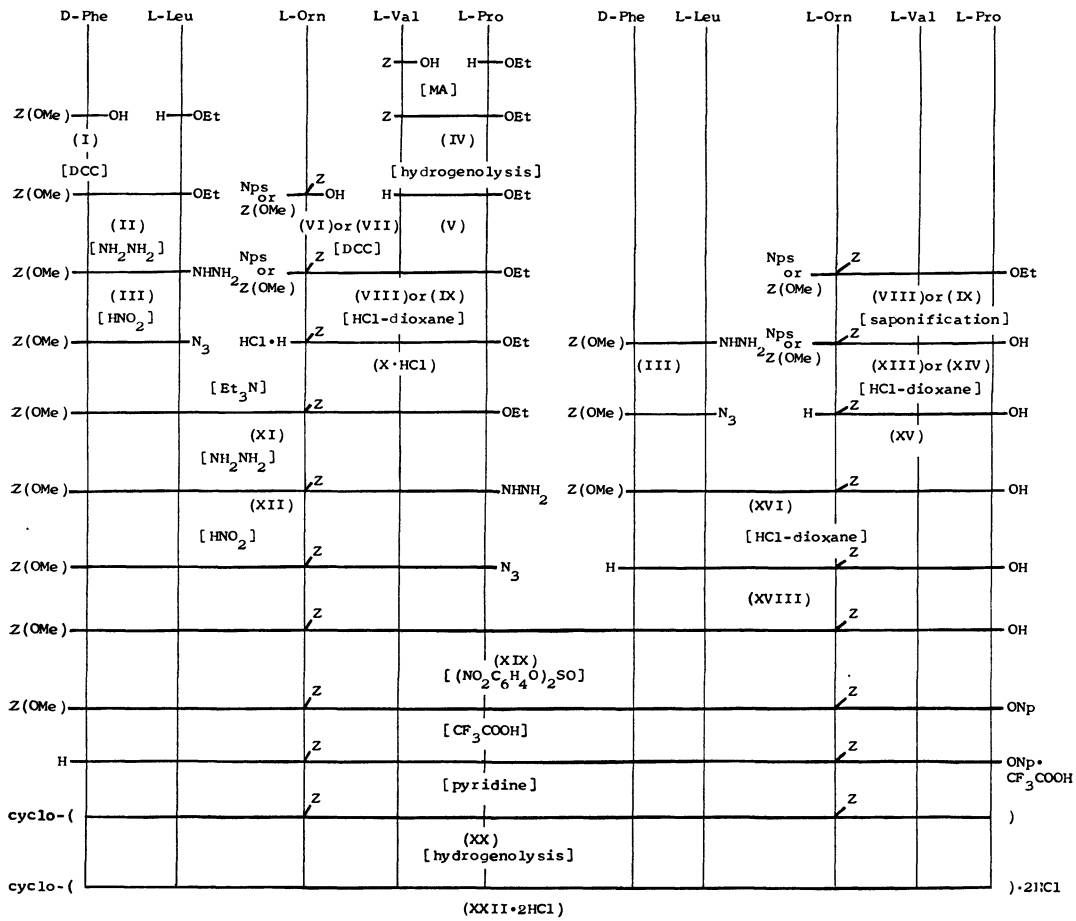

Fig. 3. Synthesis of retrogramicidin S.

10) R. Schwyzer, *Chimia*, **12**, 53 (1958).

11) L.C. Craig, *Science*, **144**, 1093 (1964).

ity,[12] two proline residues in retrogramicidin S may disturb an interaction of the compound and a microorganism. Thus, we tended to surmise that retrogramicidin S would possess weaker or no activity compared with gramicidin S.

The sequence of reaction employed for the synthesis of retrogramicidin S (XXII) from a linear decapeptide nitrophenyl ester is shown in Fig. 3. The sequence of steps was chosen specifically to preclude racemization. The tripeptide ester (X) was obtained by treatment of hydrogen chloride on either VIII or IX. In this step, the use of *o*-nitrophenylsulfenyl group seemed more advantageous than that of *p*-methoxybenzyloxycarbonyl; *o*-nitrophenylsulfenyl chloride,[13] which was used for VI synthesis, was prepared more easily than *p*-methoxybenzyloxycarbonyl azide,[14] and the selective removal of nitrophenylsulfenyl group from VIII or XIII was easier than that of methoxybenzyloxycarbonyl group from IX or XIV. The condensation of the azide derived from acyldipeptide hydrazide (III) with X gave acylpentapeptide ester (XI).

To obtain an acylpentapeptide acid (XVI), the acylpentapeptide ester (XI) was subjected to saponification. When XI was treated with dilute alkali (Fig. 4), there was formed a crude product which was composed of two compounds. The mixture was separated into two pure components by use of a Sephadex LH-20 column; the desired acylpeptide acid (XVI) was obtained from the faster eluting fraction, and a compound with mp 121—123 ℃ was obtained from the slower fraction. The elemental analysis of the latter compound and the neutral equivalent by quantitative titration procedure favored the dibasic acid of structure

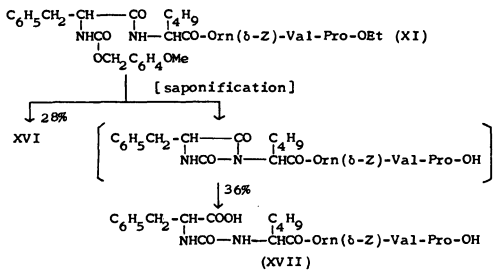

Fig. 4. Saponification of acylpentapeptide ethyl ester (XI).

XVII. It appeared that the cyclization with loss of *p*-methoxybenzyl alcohol, followed by hydrolytic opening of the hydantoin intermediate, had occurred in addition to the desired hydrolysis reaction. Such rearrangements have been observed already by Maclaren[15] and Bodanszky *et al.*,[16] the latter group demonstrated that alkaline treatment of *α*-benzyloxycarbonyl-*ω*-nitroarginyl-tetraglycine ethyl ester yielded a dibasic acid, 5-[1-carboxy-4(3-nitroguanidino)butyl]-hydantoyl-triglycine.

The acylpentapeptide acid (XVI) was prepared more efficiently as follows. Saponification of acyltripeptide ester (VIII or IX) gave the acyltripeptide acid (XIII or XIV) without appreciable side reactions, then either XIII or XIV was transformed to the free tripeptide (XV). The condensation of the azide from III with XV afforded the acylpentapeptide acid (XVI) in a good yield. Then, the condensation of the azide from XII with free pentapeptide (XVIII), which had been obtained from XVI, gave the acyldecapeptide acid(XIX). The successive treatments of XIX with di-*p*-nitrophenyl sulfite, trifluoroacetic acid and excess pyridine afforded the benzyloxycarbonyl-substituted cyclic decapeptide (XX) in a good yield (49% from XIX). The hydrogenation of XX in the presence of two equivalents of hydrogen chloride yielded the desired retrogramicidin S dihydrochloride as colorless crystals containing water of crystallization.

The synthesis of the protected cyclic decapeptide (XX) was also attempted by possibe dimerization reaction of the pentapeptide active ester (XXIV) (Fig. 5). The compound XXIV was treated with excess pyridine, and after evaporation the reaction mixture was passed through Dowex 1 and 50 columns; the subsequent evaporation of the effluent yielded a semisolid residue. This

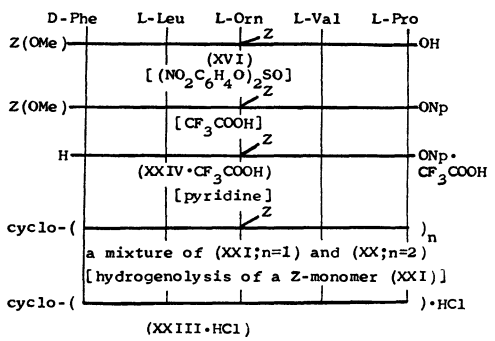

Fig. 5. Synthesis of retrocyclosemigramicidin S.

12) E.P.Abraham, "Comprehensive Biochemistry," Vol. 11, Elsevier, Amsterdam (1963), p. 181.

13) M. H. Hubacher, "Organic Syntheses," Coll. Vol. II, p. 455 (1943); L. Zervas, D. Borvas and E. Gazis, *J. Am. Chem. Soc.*, **85**, 3660 (1963).

14) F.Weygand and K.Hunger, *Chem. Ber.*, **95**, 1 (1962).

15) J.A.Maclaren, *Austral. J.Chem.*, **11**, 360(1958); M. Bodanszky, J. T. Sheehan, M. A. Ondetti and S Lande, *J. Am. Chem. Soc.*, **85**, 991 (1963).

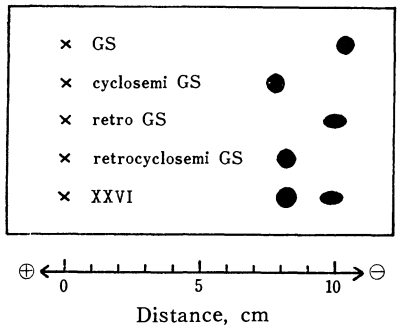

Fig. 6. Paper electrophoresis of the compounds. GS, gramicidin S; XXVI, hydrogenated material after cyclization of pentapeptide ester (XXIV).

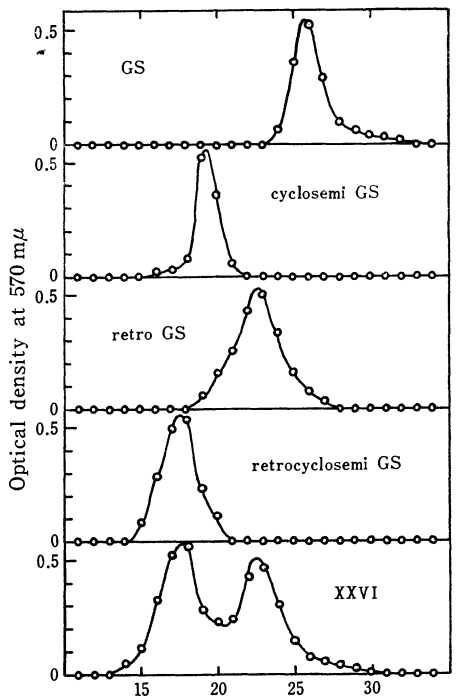

Fig. 7. Carboxymethylcellulose column chromatography of the compounds.

residue was found to be a mixture of two components by analyses with a hydrogenated material of a small part of the residue (see, Figs. 6 and 7). The residue was applied with a Sephadex LH-20 column to be separated into the components; dimer (XX) was obtained in a yield of 22.6% and the monomer (XXI) obtained in 25.3%. Thus, the weight ratio of XXI and XX is calculated as 53 : 47; the result indicates that an appreciable portion of the active ester (XXIV) is present in a transition state favored for the formation of the cyclic dimer even though some active esters are directed to the intramolecular cyclization reaction. We reported already that the cyclization reaction of H-Val-Orn(δ-Z)-Leu-D-Phe-Pro-ONp (XXVII) had afforded a mixture of the protected cyclosemigramicidin S and the protected gramicidin S with a weight ratio of 32 : 68.[16] In spite of the profound difference of the amino acid sequences between XXIV and XXVII, the formation of the protected cyclic decapeptides in considerable amount by the dimerization reaction in both cases favors for the stable comformation of a XX and protected gramicidin S molecule.

The antibacterial activity of gramicidin S, retrogramicidin S (XXII) and retrocyclosemigramicidin S (XXIII) toward several microorganisms was examined. The monomer XXIII showed no activity for any of the microorganisms even at 100 μg/ml of the assay medium.[17] Gramicidin S and XXII showed also no activity for the Gram negative microorganisms (*E. coli* and other), whereas minimum concentrations of growth-inhibition for the Gram positive microorganisms (*B. Subtilis* and other) were found to be 5 μg/ml with gramicidin S and 50 μg/ml with XXII. Since this results agree in some extent with the surmise described already, the proposed structure (Fig. 2) for a retrogramicidin S molecular as a possible conformation will be useful for understanding the mode of antibacterial activities of gramicidin S and its analogs.

Experimental

All the melting points are uncorrected. Prior to analysis, the compounds were dried over phosphorus pentoxide to a constant weight at 80°C and 2 mmHg, except for the cyclic peptide hydrochlorides.

Z(OMe)-D-Phe-OH·DCHA(I·DCHA).[18] A solution of dicyclohexylamine (6 ml) in ether (10 ml) was added to *p*-methoxybenzyloxycarbonyl-D-phenylalanine which was prepared from D-phenylalanine (0.03 mol).[19] Ether was evaporated *in vacuo*, and the residual oil was crystallized by the addition of petroleum ether. It was recrystallized from ethyl acetate-petroleum ether; yield, 9.85 g (64% from

16) M. Waki and N. Izumiya, This Bulletin, **40**, 1687 (1967); *J. Am. Chem. Soc.*, **89**, 1278 (1967).

17) We have observed that the cyclic pentapeptides synthesized in this laboratory, cyclosemigramicidin S[15] and its analogs, exhibit no activity.

18) The following abbreviations are from *Biochemistry*, **5**, 2485 (1966); Z-, benzyloxycarbonyl; Z(OMe)-, *p*-methoxybenzyloxycarbonyl; Nps-, *o*-nitrophenylsulfenyl; -ONp, *p*-nitrophenoxy; ·DCHA; dicyclohexalammonium salt; DCC, dicyclohexylcarbodiimide; DMF, dimethylformamide. Amino acid symbols except D-Phe denote the L-configuration.

19) T. Kato and N. Izumiya, This Bulletin, **39**, 2242 (1966).

D-phenylalanine); mp 154—155°C; $[\alpha]_D^{20}$ −23.6° (*c* 1, methanol); R_f 0.77.[20]

Found: C, 70.36; H, 8.27; N, 5.22%. Calcd for $C_{30}H_{42}O_5N_2$: C, 70.56; H, 8.29; N, 5.49%.

Z(OMe)-D-Phe-Leu-OEt (II). To a solution of I·DCHA (10.21 g, 20 mmol), L-leucine ethyl ester *p*-toluenesulfonate[21] (6.63 g, 20 mmol) in chloroform (120 ml) was added dicyclohexylcarbodiimide[22] (4.13 g, 20 mmol) at 0 °C. The reaction mixture was stirred for 1 hr at 0 °C, and then kept overnight in a refrigerator. The mixture was evaporated *in vacuo*, and ethyl acetate (150 ml) was added to the residue. After the dicyclohexylurea was filtered off, the filtrate was washed successively with 0.5 M citric acid, 4% sodium bicarbonate and water, and dried over sodium sulfate. The filtrate was evaporated *in vacuo*, and the residue was crystallized by the addition of ether and petroleum ether. It was recrystallized from methanol-ether-petroleum ether; yield, 7.25 g (77%); mp 108—109°C; $[\alpha]_D^{25}$ −0.6° (*c* 1, DMF); R_f 0.97.[20]

Found: C, 66.31; H, 7.35; N, 6.01%. Calcd for $C_{26}H_{34}O_6N_2$: C, 66.36; H, 7.28; N, 5.95%.

Z(OMe)-D-Phe-Leu-NHNH$_2$ (III). A solution of II (7.06 g, 15 mmol) and hydrazine hydrate (14.6 ml, 300 mmol) in dimethylformamide (20 ml) was allowed to stand at room temperature for 2 days. The hydrazine was evaporated *in vacuo*, and then water (250 ml) was added to the residue. The resulting crystals were collected by filtration; yield, 6.51 g (95%); mp 176—177°C; $[\alpha]_D^{20}$ −7.5° (*c* 1, DMF); R_f 0.87.[20]

Found: C, 63.23; H, 7.05; N, 12.18%. Calcd for $C_{24}H_{32}O_5N_4$: C, 63.14; H, 7.07; N, 12.27%.

Z-Val-Pro-OEt (IV). To a chilled solution of benzyloxycarbonyl-L-valine (10.05 g, 50 mmol) and triethylamime (5.6 ml, 40 mmol) in tetrahydrofuran (60 ml), isobutylchloroformate (5.24 ml, 40 mmol) was added. After 15 min, a mixture of L-proline ethyl ester *p*-toluenesulfonate[21] (12.61 g, 40 mmol), triethylamine (5.6 ml, 40 mmol) and chloroform (60 ml) was added to the solution. The reaction mixture was allowed to stand overnight and then evaporated to dryness *in vacuo*. After the residual oil was dissolved in ethyl acetate, the solution was washed successively with 3% hydrochloric acid, 4% sodium bicarbonate and water, dried over sodium sulfate, and then the filtrate was evaporated. The product was obtained as an oil; yield, 10.36 g (69%); R_f 0.94.[20]

HCl·H-Val-Pro-OEt (V·HCl). A solution of IV (7.53 g, 20 mmol) dissolved in a mixture of 3.97 N ethanolic hydrogen chloride (5.04 ml) and ethanol (100 ml) was hydrogenated in the presence of palladium black. After 3 hr, the filtrate from the catalyst was evaporated to dryness *in vacuo*. The oil weighed 5.35 g (96%); R_f 0.79.[20]

Nps-Orn(δ-Z)-OH·DCHA(VI·DCHA). δ-Benzyloxycarbonyl-L-ornithine (10.65 g, 40 mmol) was dissolved in a mixture of 2 N sodium hydroxide (40 ml, 80 mmol) and dioxane (160 ml). To the solution, *o*-nitrophenysulfenyl chloride[13] (7.59 g, 40 mmol) and 2 N sodium hydroxide (15 ml, 30 mmol) was added 5 portions over a period of 30 min under vigorous stirring. The reaction mixture was diluted with water (600 ml), a small amount of the insoluble material was filtered off and the filtrate was acidified with 0.5 M citric acid at 0 °C. The solution was extracted with ethyl acetate, and the extract was washed with water and dried over sodium sulfate. The filtrate from the salt was evaporated *in vacuo*. To the residue the solution of dicyclohexylamine (8 ml) in ether (10 ml) was added. This solution was treated following the same procedure described for the preparation of I·DCHA. The crude product was recrystallized from methanol-ether-petroleum ether; yield, 17.06 g (71%); mp 167—169 °C; $[\alpha]_D^{25}$ −25.0° (*c* 1, DMF); R_f 0.85.[20]

Found: C, 61.81; H, 7.38; N, 9.06%. Calcd for $C_{31}H_{44}O_6N_4S$: C, 61.97; H, 7.38; N, 9.33%.

Z(OMe)-Orn(δ-Z)-OH·DCHA (VII·DCHA). *p*-Methoxybenzyloxycarbonyl-δ-benzyloxycarbonyl-L-ornithine[23] was prepared from δ-benzyloxycarbonyl-ornithine (0.05 mol) and then changed to VII·DCHA as described for the preparation of I·DCHA; yield, 20.56 g (67%), mp 121—122 °C; $[\alpha]_D^{20}$ −4.0° (*c* 1, methanol); R_f 0.81.[20]

Found: C, 66.80; H, 8.15; N, 6.77%. Calcd for $C_{34}H_{49}O_7N_3$: C, 66.75; H, 8.09; N, 6.87%.

Nps-Orn(δ-Z)-Val-Pro-OEt (VIII). To a suspension of VI·DCHA (6.01 g, 10 mmol) in ethyl acetate (100 ml) at 0 °C, 0.5 M citric acid (40 ml) was added under stirring. After 1 hr, the organic layer was separated and washed with water. It was then dried over sodium sulfate and evaporated to dryness to give an oily product (4.20 g) of VI. To a solution of the oily VI in chloroform (60 ml) was added V·HCl (3.07 g, 11 mmol) and triethylamine (1.54 ml, 11 mmol). Dicyclohexylcarbodiimide (2.06 g, 10 mmol) was added to the solution at 0 °C, and then the reaction mixture was treated in the same manner as that used for the preparation of II. The residual oil weighed 6.37 g (99%); R_f 0.98.[20]

Z(OMe)-Orn(δ-Z)-Val-Pro-OEt (IX). A crystalline product VII (4.35 g) from VII·DCHA (6.12 g, 10 mmol) was coupled with V·HCl (3.07 g, 11 mmol) by dicyclohexylcarbodiimide (2.06 g, 10 mmol) following essentially the same procedure described above. The oily residue obtained weighed 6.29 g (96%); R_f 0.94.[20]

HCl·H-Orn(δ-Z)-Val-Pro-OEt (X·HCl). From VIII. To a solution of VIII (5.15 g, 8 mmol) in

20) The R_f value of the thin-layer chromatography with Merck silica gel refers to a solvent system of *n*-butanol-acetic acid-pyridine-water (4 : 1 : 1 : 2, v/v). Spots of materials possessing a free amino group on a thin-layer plate were detected by spraying ninhydrin, and those of the amino group-blocked materials, by spraying 47% hydrobromic acid and then ninhydrin.

21) T.Kato, S.Makisumi, M.Ohno and N.Izumiya, *Nippon Kagaku Zasshi* (*J. Chem. Soc. Japan, Pure Chem. Sect.*), **83**, 1151 (1962).

22) J.C. Sheehan and G.P. Hess, *J. Am. Chem. Soc.*, **77**, 1067 (1955).

23) M. Kondo, H.Aoyagi, T.Kato and N.Izumiya, This Bulletin, **39**, 2234 (1966).

dioxane (16 ml), 2 N hydrogen chloride in dioxane (16 ml) was added. After the solution was allowed to stand at room temperature for 30 min, the solution was evaporated *in vacuo*. The residual oil was washed several times with ether by the way of decantation ; yield of the oily X·HCl, 5.11 g (97 %); R_f 0.82.[20]

From IX. A solution of IX (5.24 g, 8 mmol) and anisole (2 ml) in dioxane (20 ml) was treated with 3 N hydrogen chloride in dioxane (53 ml) for 3 hr; yield of the oily X·HCl, 5.27 g (100%); R_f 0.82.[20]

Z(OMe)-D-Phe-Leu-Orn(δ-Z)-Val-Pro-OEt (XI). To a chilled solution of III (4.57 g, 10 mmol) in glacial acetic acid (140 ml) and dimethylformamide (70 ml), there were stirred 1 N hydrochloric acid (22 ml), sodium nitrite (0.76 g) in water (2 ml). After 10 min, cold water (500 ml) was added. The azide which thereupon precipitated was collected by filtration, washed with water, a saturated sodium bicarbonate solution and water, and then dried in a desiccator. The azide was added to a solution of X·HCl (5.27 g, 10 mmol) and triethylamine (14 ml) in dimethylformamide (50 ml). The mixture was then stirred for 3 days at 0 °C and evaporated *in vacuo*. The precipitate which was formed upon the addition of water (400 ml) was collected, and then washed with 4 % sodium bicarbonate, 0.5 M citric acid and water. It was recrystallized from dioxane-ether-petroleum ether. Yield, 6.26 g (68%); mp 158—159 °C; $[\alpha]_D^{20}$ −31.0° (*c* 1, DMF); R_f 0.98[20]

Found: C, 64.38; H, 7.31; N, 9.00 %. Calcd for $C_{49}H_{66}O_{11}N_6$: C, 64.31; H, 7.27; N, 9.19 %.

Z(OMe)-D-Phe-Leu-Orn(δ-Z)-Val-Pro-NHNH$_2$ (XII). To a solution of XI (0.92 g, 1 mmol) in dimethylformamide (8 ml), hydrazine hydrate (1.21 ml, 25 mmol) was added and the solution was allowed to stand for 7 days at room temperature. The reaction mixture was then evaporated *in vacuo*. The hydrazide which precipitated upon the addition of water was collected by filtration and dried. The product was recrystallized from methanol-ether; yield, 0.75 g (83 %); mp 160—161 °C; $[\alpha]_D^{20}$ −29.4° (*c* 0.5, DMF); R_f 0.88[20].

Found: C, 62.14; H, 7.27; N, 12.12 %. Calcd for $C_{47}H_{64}O_{10}N_8 \cdot 1/2H_2O$: C, 62.03; H, 7.20; N, 12.31 %.

Nps-Orn(δ-Z)-Val-Pro-OH (XIII). To a solution of VIII (5.31 g 8 mmol) in methanol (40 ml) and dioxane (40 ml), N sodium hydroxide (32 ml) was added; the solution then was allowed to stand for 24 hr at room temperature. After the addition of water (40 ml), the solution was evaporated *in vacuo* to remove organic solvents. After the solution was extracted with ether, it was acidified with 0.5 M citric acid at 0 °C. The solution was extracted with ethyl acetate and the organic layer was dried over sodium sulfate. The filtrate was evaporated to dryness *in vacuo* to afford an oily product; yield, 3.05 g (62%); R_f 0.86.[20]

Z(OMe)-Orn(δ-Z)-Val-Pro-OH (XIV). To a solution of IX (3.27 g, 5 mmol) in methanol (50 ml), 1 N sodium hydroxide (10 ml) was added. The solution was treated following the same procedure described above. The residual oil weighed 1.89 g (60 %); R_f 0.84.[20]

HCl·H-Orn(δ-Z)-Val-Pro-OH (XV·HCl). From XIII. To a solution of XIII (3.08 g, 5 mmol) in dioxane (20 ml), 2 N hydrogen chloride in dioxane (15 ml) was added at room temperature. After 30 min the solution was evaporated to dryness, and the residue was washed repeatedly with ether by decantation. The remaining hygroscopic crystals were collected by filtration with the aid of ether; yield, 1.90 g (76 %); mp 135—140 °C (decomp.); $[\alpha]_D^{20}$ −18.0° (*c* 0.5, DMF); R_f 0.71.[20]

Found: C, 53.60; H, 7.19; N, 10.57 %. Calcd for $C_{23}H_{34}O_6N_4 \cdot HCl \cdot H_2O$: C, 53.43; H, 7.21; N, 10.84%.

From XIV. XV·HCl was also prepared from XIV (1.88 g, 3 mmol), anisole (0.9 ml) and 2.53 N hydrogen chloride in dioxane (23.7 ml) for 2 hr following the same procedure described above; yield, 1.03 g (69 %); $[\alpha]_D^{25}$ −17.9° (*c* 0.4, DMF); R_f 0.71.[20]

H-Orn(δ-Z)-Val-Pro-OH (XV). XV·HCl (998 mg, 2 mmol) was dissolved in small volume of a mixture of water and methanol. After triethylamine (0.28 ml) had been added, the solution was evaporated to dryness *in vacuo*. The crystalline product was collected by filtration with the aid of water ; yield, 898 mg (97 %); mp 174—176 °C (decomp.); $[\alpha]_D^{25}$ −34.0° (*c* 0.4, acetic acid); R_f 0.71.[20]

Found: C, 53.34; H, 7.68; N, 10.91 %. Calcd for $C_{23}H_{34}O_6N_4 \cdot 2H_2O$: C, 55.41; H, 7.68; N, 11.24 %.

Z(OMe)-D-Phe-Leu-Orn(δ-Z)-Val-Pro-OH (XVI). From III and XV. The azide derived from III (2.15 g, 4.7 mmol) was added to a solution of XV·HCl (2.50 g, 5 mmol) and triethylamine (1.4 ml, 10 mmol) in dimethylformamide (25 ml), and the mixture was stirred for 3 days at 0 °C. The mixture was evaporated *in vacuo*, and the residue was added to ethyl acetate (300 ml). The mixture was washed successively with water, 0.5 M citric acid, and water, and then dried over sodium sulfate. After the filtrate was evaporated, the residual crystals were collected with the aid of a mixture of ether and petroleum ether. It was recrystallized from methanol-ether-petroleum ether; yield, 2.92 g (70 %); mp 137—138°C; $[\alpha]_D^{25}$ −29.5° (*c* 0.5, DMF); R_f 0.82,[20] 0.68.[24]

Found: C, 63.53; H, 6.75; N, 9.66 %. Calcd for $C_{47}H_{62}O_{11}N_6$: C, 63.64; H, 7.65; N, 9.48 %.

From XI. To a solution of XI (275 mg, 0.3 mmol) in ethanol (4 ml) and dioxane (2 ml), 1 N sodium hydroxide (0.6 ml) was added at room temperature. The hydrolysis was almost complete after 4 hr. The solution was concentrated *in vacuo* to small volume, and acidified with 0.5 M citric acid under cooling. The separated crystalline solid was taken up with ethyl acetate, and the ethyl acetate solution was washed with water, dried over sodium sulfate. The filtrate was evaporated, and the residual crystals were collected by filtration with the aid of a mixture of ether and petroleum ether; yield of the crude product, 208 mg. The crude product was separated into the two pure components as follows. A solution of the crude product (200 mg) in dioxane (0.6 ml)

24) The R_f value of the thin-layer chromatography refers to a solvent system of chloroform-methanol (5 : 1, v/v).

was applied to a column (0.9×48 cm) with Sephadex LH-20, and the development continued with dioxane. Elution was carried out at room temperature, the flow rate 7 ml per hr, and 1.5 ml fraction collected. When the peptide content in the fractions was determined on a thin-layer plate, two compounds appeared separately in tube numbers 10 to 13 and 14 to 20. The fractions of 10—13 were combined, evaporated and the crystals of XVI were obtained. Yield, 73 mg (28 % from XI); mp 136—137 °C; $[\alpha]_D^{25}$ −30.6° (*c* 0.2, DMF); R_f 0.82[20], 0.68.[24]

2-Isobutyl-5-[1-carboxy-2-(phenyl)-ethyl]-hydantoyl-Orn(∂-Z)-Val-Pro-OH (XVII). The fractions of 14—20 obtained in above was evaporated *in vacuo*, and the residual product was recrystallized from methanol-water; yield, 80 mg (36 % from XI); mp 121—123 °C; $[\alpha]_D^{25}$ −23.3° (*c* 0.3, DMF); R_f 0.65.[24]

Found: C, 61.21; H, 7.49; N, 10.55 %; neut equiv, 784. Calcd for $C_{39}H_{54}O_{10}N_6$: C, 61.08; H, 7.10; N, 10.96 %; neut equiv, 767.

HCl·H-D-Phe-Leu-Orn(∂-Z)-Val-Pro-OH (XVIII·HCl). To a solution of XVI (1.06 g, 1.2 mmol) and anisole (0.3 ml) in dioxane (6 ml), 2.57 N hydrogen chloride in dioxane (9.3 ml) was added at room temperature. After 4 hr, the solution was treated following the same procedure for the preparation of XV·HCl. Yield, 0.82 g (90 %); mp 201—203 °C (decomp.); $[\alpha]_D^{25}$ −53.6° (*c* 0.3, DMF); R_f 0.77.[20]

Found: C, 58.72; H, 7.25; N, 10.75 %. Calcd for $C_{38}H_{54}O_8N_6 \cdot HCl \cdot H_2O$: C, 58.71; H, 7.39; N, 10.81 %.

H-D-Phe-Leu-Orn(∂-Z)-Val-Pro-OH (XVIII). XVIII·HCl (152 mg, 0.2 mmol) was dissolved in a mixture of water and methanol. After triethylamine (0.06 ml) had been addded, the solution was evaporated to dryness *in vacuo*. The crystalline product was collected by filtration with the aid of methanol. It was recrystallized from hot methanol-ether, and washed with a small amount of water; yield, 105 mg (72 %); mp 199—201°C (decomp.); $[\alpha]_D^{20}$ −84.3° (*c* 0.3, acetic acid); R_f 0.77.[20]

Found: C, 60.35; H, 7.50; N, 11.04 %. Calcd for $C_{38}H_{54}O_8N_6 \cdot 2H_2O$: C, 60.14; H, 7.70; N, 11.08 %.

Z(OMe)-D-Phe-Leu-Orn(∂-Z)-Val-Pro-D-Phe-Leu-Orn(∂-Z)-Val-Pro-OH (XIX). The azide was prepared from XII (451 mg, 0.5 mmol), 1N hydrochloric acid (1.1 ml), and sodium nitrite (38 mg) in a mixture of acetic acid (6 ml) and dimethylformamide (3 ml) as in the case of the preparation of XI. Then the azide dried was added to a solution of XVIII·HCl (380 mg, 0.5 mmol) and triethylamine (0.14 ml, 1 mmol) in dimethylformamide (10 ml). After the reaction mixture was stirred for 3 days at 0°C, it was treated following the same procedure that employed for the preparation of XVI. The crude product was recrystallized from hot dioxane-methanol-ether; yield, 600 mg (75 %); mp 174—175 °C; $[\alpha]_D^{25}$ −31.4° (*c* 0.5, DMF); R_f 0.94,[20] 0.45.[24]

Found: C, 62.78; H, 7.24; N, 10.58 %. Calcd for $C_{85}H_{114}O_{18}N_{12} \cdot 2H_2O$: C, 62.71; H, 7.31; N, 10.33 %.

***cyclo*-(D-Phe-Leu-Orn(∂-Z)-Val-Pro-)$_2$ (XX).** **From XIX.** To a solution of XIX (557 mg, 0.35 mmol) in pyridine (10 ml), di-*p*-nitrophenyl sulfite[25] (2.27 g, 7 mmol) was added. After the mixture had been allowed to stand for 24 hr at room temperature, it was evaporated *in vacuo*. The residual solid was collected by filtration with the aid of a mixture of ether-petroleumether (1 : 1, v/v); 589 mg. The *p*-nitrophenyl ester content for this product was estimated to be 85 % by measuring the optical density of the compound at 412 mμ.[26] To the acyldecapeptide *p*-nitrophenyl ester (585 mg) thus obtained, anisole (0.5 ml) and trifluoroacetic acid (3.5 ml) were added at 0 °C. After the solution was evaporated *in vacuo*, the residual powder was collected by filtration with the aid of ether. The decapeptide *p*-nitrophenyl ester trifluoroacetate thus obtained was dissolved in dimethylformamide (10 ml) and acetic acid (0.1 ml). The solution was then stirred, drop by drop and over a period of 4 hr, into pyridine (170 ml) which had been kept at 60 °C; the stirring was then continued for an additional 2 hr at the same temperature. After the solvent had been removed, the residue was dissolved in a mixture of methanol (40 ml) and water (10 ml). After the insoluble substance was removed, the filtrate was passed successively through columns (1.8×10 cm, each) of Dowex 1 (OH^- form) and Dowex 50 (H^+ form). The columns were washed with the same solvent (200 ml), and the combined effluent was evaporated *in vacuo* to yield a crystalline product. The product was collected by filtration with the aid of water, and recrystallized from methanol-ether-petroleum ether; yield, 242 mg (49 % from XIX); mp 250—251°C (decomp.); $[\alpha]_D^{20}$ −41.3° (*c* 0.3, acetic acid).

Found: C, 64.44; H, 7.46; N, 11.73 %; mol wt, 1413.[27] Calcd for $C_{76}H_{104}O_{14}N_{12} \cdot 1/2H_2O$: C, 64.34; H, 7.46; N, 11.85 %; mol wt, 1419.

From XVI. The acylpentapeptide XVI (2.22 g, 2.5 mmol) was converted to the pentapeptide *p*-nitrophenyl ester trifluoroacetate (XXIV·CF_3COOH) following the same procedure as described above. XXIV·CF_3COOH (2.39 g) thus obtained was added to pyridine (800 ml). After the filtrate was passed through columns of Dowex 1 and Dowex 50 as described above, the effluent was evaporated to dryness, the residual product was collected by filtration with the aid of water; yield of the crude product (XXV), 830 mg. The solution of XXV (50 mg) in methanol (1 ml) was applied to a column (2.7×50 cm) with Sephadex LH-20, and the development continued with methanol. Elution was carried out at room temperature, the flow rate 30 ml per hr, and 3 ml fraction collected.

When the peptide content in the fractions was determined on a thin-layer plate, the peak of XX appeared from the test tube numbers 45 to 52 and the peak of XXI from 54 to 65. The same chromatography was repeated further nine times; thus, 500 mg of XXV was separated into two component. The ten fractions of 45—52 were combined, evapo-

25) B. Iselin and R. Schwyzer, *Helv. Chim. Acta*, **43**, 1760 (1960).

26) R. Schwyzer and P. Sieber, *ibid.*, **40**, 624 (1957).

27) Molecular weight was determined by a Hitachi Osmometer, type 115 (solvent, methanol).

TABLE 1. INHIBITORY ACTIVITY OF FOUR COMPOUNDS ON MICROORGANISMS
Minimum inhibitory concentration, $\mu g/ml$

A. Bouillon agar medium[a)]

	Escherichia coli	*Proteus vulgaris*	*Staphylococcus aureus*	*Bacillus subtilis*	*Mycobacterium avium*
GS	>100	>100	5	5	>100
retro GS	>100	>100	50	50	>100
retrocyclosemi GS	>100	>100	>100	>100	>100

B. Synthetic medium[b)]

	Escherichia coli	*Proteus vulgaris*	*Staphylococcus aureus*	*Bacillus subtilis*	*Mycobacterium avium*
GS	>100	>100	5	5	>100
retro GS	>100	>100	50	50	>100
retrocyclosemi GS	>100	>100	>100	>100	>100

a) Usual bouillon agar medium, pH 7.0.
b) Stephenson-Whetham's medium (modified).

rated *in vacuo* and the crystals (240 mg, 22.6 % from XVI) of XX were obtained; yield after recrystallization, 234 mg (22 %); mp 251—252 °C (decomp.); $[\alpha]_D^{20}$ −40.8° (*c* 0.3, acetic acid).

***cyclo*-D-Phe-Leu-Orn(δ-Z)-Val-Pro (XXI).** The ten fractions of the test tube numbers 54—65 obtained in above were evaporated *in vacuo* to afford an oily residue. It was crystallized after standing of several days in a refrigerator ; 271 mg (25.5 % from XVI). It was recrystallized from methanol-ether-petroleum ether (235 mg, 22 %); mp 230—232 °C (decomp.); $[\alpha]_D^{20}$ −50.9° (*c* 0.2, acetic acid).

Found: C, 63.19; H, 7.20; N, 11.33 %; mol wt, 697.[27)] Calcd for $C_{38}H_{52}O_7N_6 \cdot H_2O$: C, 63.13; H, 7.53; N, 11.62 %; mol wt, 723.

Retrogramicidin S, *cyclo*-(D-Phe-Leu-Orn-Val-Pro-)$_2$ (XXII). A solution of XX (85 mg, 0.06 mmol) in methanol (3 ml) and 0.4 N methanolic hydrogen chloride (0.32 ml), was subjected to hydrogenolysis in the presence of palladium black for 3 hr. The solution, after being filtered from the catalyst, was evaporated *in vacuo*. The residual product was recrystallized from methanol-ether-petroleum ether; yield of the air-dried product, 69 mg (94%); mp 272—276°C (decomp.); $[\alpha]_D^{20}$ −36.3° (*c* 0.1, etnanol); R_f 0.96,[28)] 0.75[20)]; amino acid ratios in acid hydrolysate, $Phe_{0.8}Leu_{1.0}Orn_{1.1}Val_{1.0}Pro_{1.0}$.

Found; C, 54.64; H, 7.89; N, 12.51%. Calcd for $C_{60}H_{92}O_{10}N_{12} \cdot 2HCl \cdot 6H_2O$: C, 54,49; H, 8.08; N, 12.71%. The air-dried product lost 8.6% of its weight after being dried for 3 hr at 80°C and 2 mmHg. Calcd for $6H_2O$; 8.2%.

Retrocyclosemigramicidin S, *cyclo*-D-Phe-Leu-Orn-Val-Pro (XXIII). XXI (42 mg, 0.06 mmol) was treated as described for the preparation of XXII·2HCl; yield, 31 mg (84 %); mp 252—253 °C (decomp.); $[\alpha]_D^{20}$ −60.0° (*c* 0.5, ethanol); R_f 0.92,[28)] 0.61; [20)] amino acid ratios in acid hydrolysate, $Phe_{0.9}Leu_{1.0}Orn_{1.0}Val_{0.9}Pro_{1.1}$.

Found: C, 54.27; H, 7.77; N, 12.85 %. Calcd for $C_{30}H_{46}O_5N_6 \cdot HCl \cdot 3H_2O$: C, 54.49; H, 8.08; N, 12.71%. The air-dried product lost 8.7 % of its weight after drided for 3 hr at 80 °C and 2 mmHg. Calcd for $3H_2O$: 8.2 %.

Electrophoresis and Carboxymethylcellulose (CMC) Chromatography. These experiments were carried out as has been described before.[16)] A part of the crude product (XXV), which was obtained after the cyclization reaction of the pentapeptide *p*-nitrophenyl ester (XXIV), was hydrogenated, and the hydrogenated product thus obtained was designated as XXVI. As shown in Figs. 6 and 7, retro GS and retrocyclosemi GS was clearly separated in the electrophoresis, whereas these compounds could be only partially separated with a column (0.9×50 cm) of CMC.

Microbiological Assays.[29)] The microorganisms employed are listed in Table 1. The minimum amount of the compound necessary for the complete inhibition of growth was determined by a dilution method using a bouillon agar medium and a synthetic medium. As is shown in Table 1, retrogramicidin S (XXII) was found to exhibit weak antibacterial activity against *Bacillus subtilis* and *Staphylococcus aureus*. Whereas retrocyclosemigramicidin S (XXIII) exhibited no antibacterial activity against the microorganisms tested.

28) The R_f value of the paper chromatography refers to the same solvent system described.[20)]

29) We are indebted to Dr. M. Shibata of Takeda Chemical Industries, Ltd. for the assay.

BULLETIN OF THE CHEMICAL SOCIETY OF JAPAN VOL. 41 1917—1921 (1968)

The Chemiluminescence of Indole Derivatives. IV. Correlation between Chemiluminescence and Structure of 2,3-Dimethylindoles

Noboru SUGIYAMA, Hiroshi YAMAMOTO and Yoshimori OMOTE

Department of Chemistry, Tokyo Kyoiku University, Otsuka, Tokyo

and Masamoto AKUTAGAWA

Department of Chemistry, Faculty of Education, Kumamoto University, Kurokamicho, Kumamoto

(Received January 30, 1968)

Four 5-substituted and three 6-substituted 2,3-dimethylindoles and unsubstituted 2,3-dimethylindole were synthesized and their light emission was measured in the presence of atmospheric oxygen and potassium *t*-butoxide in dimethyl sulfoxide. It was found that the Hammett equation was applicable to their chemiluminescent reaction with ρ value of -1.24. For the 6-position of indole nucleus σ_p was used, and for the 5-position σ_m was used. Also, four hydroperoxides of 2,3-dimethylindole bearing substituents at the 5- or 6-position, which emitted light in the presence of potassium *t*-butoxide in dimethyl sulfoxide, gave linear Hammett plots with ρ value of -2.04. The relationship between the Hammett equation and the chemiluminescence of these inole derivatives has been discussed further.

Previously we found that forty-one of substituted indoles were chemiluminescent in the presence of atmospheric oxygen and potassium hydroxide in dimethyl sulfoxide.[1] Also, we proposed the mechanism of the chemiluminescence of 2,3-dimethylindole (I) involving the hydroperoxide anion (II) as an intermediate.[2] McCapra *et al.*[3,4] independently suggested the same intermediate and discussed the mechanism of the chemiluminescence from the standpoint of the decomposition of the hydroperoxide.

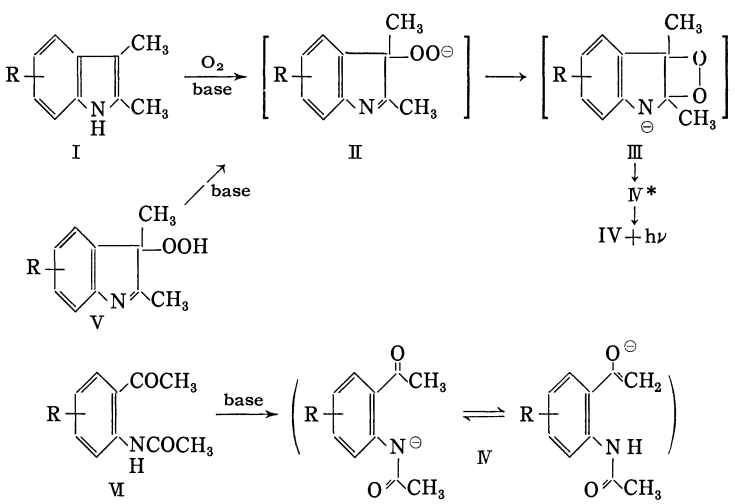

Scheme 1

1) N. Sugiyama, M. Akutagawa, T. Gasha, Y. Saiga and H. Yamamoto, This Bulletin, **40**, 347 (1967).

2) N. Sugiyama and M. Akutagawa, *ibid.*, **40**, 240 (1967).

3) F. McCapra, D.G. Richardson and Y.C. Chang, *Photochem. Photobiol.*, **4**, 1111 (1965).

4) F. McCapra and Y. C. Chang, *Chemical Commun.*, **1966**, 522.

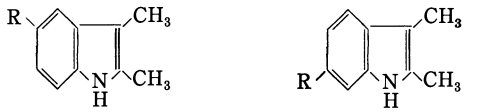

Ia R=H, Ib R=CH_3
Ic R=CH_3CONH
Id R=CH_3O, Ie R=Cl
If R=CH_3
Ig R=CH_3CONH
Ih R=Cl

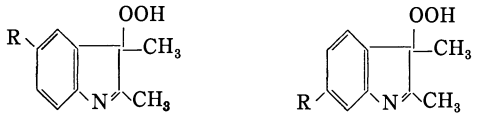

Va R=H, Vb R=CH_3
Vd R=CH_3O
Vf R=CH_3

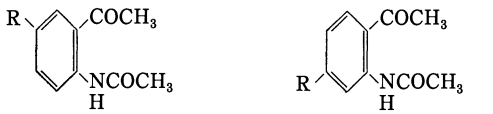

VIa R=H, VIb R=CH_3
VIc R=CH_3CONH
VId R=CH_3O, VIe R=Cl
VIf R=CH_3
VIg R=CH_3CONH
VIh R=Cl

Scheme 2

Furthermore, we speculated the mechanism of the chemiluminescent reaction of I as shown in Scheme 1.[5] The compound I changes to hydroperoxide anion (II), with oxygen and base, while the hydroperoxide (V) requires only base for conversion to II. Then II is converted to four-membered cyclic peroxide (III) which decomposes to an excited *o*-acetamidoacetophenone anion (IV*). And IV* falls to the ground state with an emission of light.

Recently we have prepared some substituted 2,3-dimethylindoles, measured their chemiluminescence, and found that the Hammett equation was applicable to their chemiluminescent reaction. The Hammett relationship was first found to apply to the chemiluminescent reaction of lophine by Philbrook *et al.*[6] There is, however, no example of the application of the Hammett equation to the chemiluminescence of indoles. It is interesting to examine the relationship between the Hammett equation and the chemiluminescence of indole derivatives.

Results and Discussion

We prepared eight 2,3-dimethylindoles, four of which had substituents at the 5-position of indole ring (Ib, Ic, Id and Ie), and three of which had substituents at the 6-position (If, Ig and Ih). Also we synthesized four hydroperoxides of 2,3-dimethylindoles (Va, Vb, Vd and Vf). The chemiluminescence maxima are shown in Table 1 and the fluorescence maxima after the chemiluminescent reaction are shown in Table 2. It can be concluded that the emitting species of the chemiluminescent reaction of I and V are the same and might be *o*-acetamidoacetophenone anion (VI*) in an excited singlet state, because the maxima of the fluorescence spectra of VI under the same condition as the chemiluminescence agreed closely with the maxima of the chemiluminescence spectra of I and V and also with the maxima of their fluorescence spectra after the chemiluminescent reaction.

TABLE 1. CHEMILUMINESCENCE MAXIMA OF 2,3-DIMETHYLINDOLES (I) AND THEIR HYDROPEROXIDES (V)

R of I or V		Chemiluminescence maxima of I	V
a.	H	520 mμ	520 mμ
b.	5-CH_3	532	532
c.	5-CH_3CONH	537	
d.	5-CH_3O	548	546
e.	5-Cl	532	
f.	6-CH_3	519	520
g.	6-CH_3CONH	530	
h.	6-Cl	518	

TABLE 2. FLUORESCENCE MAXIMA OF 2,3-DIMETHYLINDOLES (I), HYDROPEROXIDES (V) AND CHEMILUMINESCENCE PRODUCTS (VI)

R of I, V or VI		Fluorescence maxima of I	V	VI+
a.	H	520 mμ	520 mμ	520 mμ
b.	5-CH_3	531	531	532
c.	5-CH_3CONH	539		539
d.	5-CH_3O	549	546	546
e.	5-Cl	532		533
f.	6-CH_3	521	520	520
g.	6-CH_3CONH	532		530
h.	6-Cl	518		519

+ synthesized product under the same condition as the chemiluminescent reaction.

We found that σ values of para and meta substitution in benzene ring were favorably used for the 6- and 5-positions of indole nucleus respectively. In the cases of eight indoles, Ia, Ib, Ic, Id, Ie, If, Ig and Ih, the plot of $\log A/A_0$ against σ given by McDaniel and Brown,[7] was a straight line, where A and A_0 are the amount of light emitted during the chemiluminescent reaction of substituted 2,3-dimethylindoles and that of 2,3-dimethyl-

5) N.Sugiyama, M.Akutagawa and H.Yamamoto, This Bulletin, **41**, 936 (1968).

6) a) G. E. Philbrook and M. A. Maxwell, *Tetrahedron Letters*, **1964**, 1111.

b) G.E. Philbrook, M.A. Maxwell, R. E. Taylor and J.R.Totter, *Photochem. Photobiol.*, **4**, 1175 (1965).

7) D.H.McDaniel and H.C.Brown, *J. Org. Chem.*, **23**, 420 (1958).

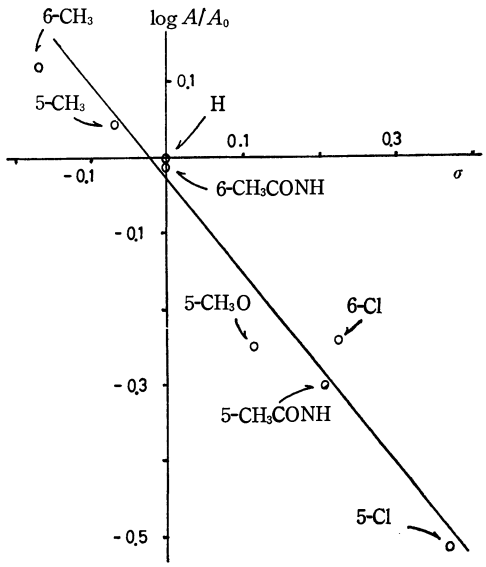

Fig. 1. Hammett plot based on the relative total light emission for substituted 2,3-dimethylindoles.

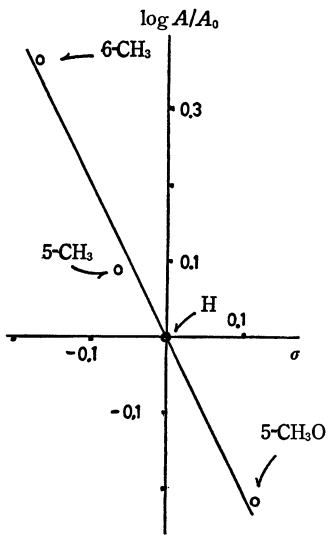

Fig. 2. Hammett plot based on the relative total light emission for substituted 2,3-dimethylindolenyl-3-hydroperoxides.

indole, respectively. (Fig. 1) The value of the reaction constant ρ determined by least squares method is -1.24. Also we proved the Hammett relationship in the chemiluminescent reaction of four indole hydroperoxides, Va, Vb, Vd and Vf. The value of ρ is -2.04. (Fig. 2).

The negative values of ρ indicate that these chemiluminescent reactions are facilitated by a high electron density at the reaction site. Both Fig. 1 and Fig. 2 show that an electron-releasing substituent favors the chemiluminescent reaction and the negative slope is consistent with the interpretation described above.

TABLE 3. RELATIVE TOTAL LIGHT EMISSION (A/A_0) OF 2,3-DIMETHYLINDOLES (I) AND THEIR HYDROPEROXIDES (V)

R of I or V		I^+	V^{++}
a.	H	1.00	1.00
b.	5-CH_3	1.11	1.22
c.	5-CH_3CONH	0.50	
d.	5-CH_3O	0.56	0.60
e.	5-Cl	0.30	
f.	6-CH_3	1.32	2.34
g.	6-CH_3CONH	0.97	
h.	6-Cl	0.57	

$^+$ A_0=Total emission of Ia
$^{++}$ A_0=Total emssion of Va

TABLE 4. HALF-LIVES OF CHEMILUMINESCENCE OF 2,3-DIMETHYLINDOLES (I) AND THEIR HYDROPEROXIDES (V)

R of I or V		I	V
a.	H	22 sec	1.6 sec
b.	5-CH_3	21	1.7
c.	5-CH_3CONH	25	
d.	5-CH_3O	31	1.9
e.	5-Cl	82	
f.	6-CH_3	12	1.5
g.	6-CH_3CONH	9.8	
h.	6-Cl	62	

From intensity of chemiluminescence-time curves, decay constants were calculated by the equation $I=I_0\exp(-t/\alpha)$, where I and I_0 are the intensity at time t and zero respectively, and $1/\alpha$ is a decay constant. A plot of $\log I$ *vs.* time t gave α. The half-lives of chemiluminescence calculated by the equation $t_{1/2}=2.303\times\alpha\times\log 2$ for indoles and hydroperoxides are shown in Table 4. The hydroperoxides (V) emitted light instantaneously, the duration being a few seconds, $t_{1/2}=1.5-1.9$ sec, while the parent indoles (I) emitted light more slowly, the duration being from 40 to 170 seconds, $t_{1/2}=9.8-82$ sec. Considering the facts that the reaction rate of the chemiluminescence of V is very fast, and that the amount of the light is different with different substituents, it is tentatively assumed that the quantum yield of the chemiluminescence of V is correlated with the Hammett σ function.

Finally, we attempt to show a reasonable explanation for the slope of the curve in Fig. 1 or in Fig. 2, which is consistent with the reaction mechanism shown in Scheme 1. In the intermediate III an electron-releasing substituent R at the 6-position contributes to an increase of an electron density on the para

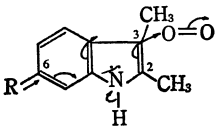

position to R. This negative charge will facilitate the homolytic fission of the bond between C-2 and C-3. This is the reason why the reaction from V to IV or from I to II is favored by high electron availability.

Also, we can explain the fact that the absolute value of ρ, 1.24, for the reaction from I to IV is less than that of ρ, 2.04, for the reaction from V to IV. If we assume that the rate from I to II in the reaction from I to IV is slow, the substituent R at the 6-position increases an electron density on the para position to R and it is probably unfavorable for the increase of the electron density at the 3-position of indole nucleus. Then the electron-releasing substituent in the 6-position retards the reaction from I to III, and this makes the absolute value of ρ decrease from 2.04 to 1.24.

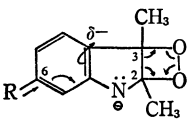

Now, we can conclude that the Hammett relationship may be applied to interpret the influence of a substituent on an indole ring upon the quantum yield of the chemiluminescent reaction of 5- or 6-substituted 2,3-dimethylindole hydroperoxides as well as upon the light emission of the parent 2,3-dimethylindoles.

Experimental

5-Acetamido-2,3-dimethylindole (Ic). Powdered 5-amino-2,3-dimethylindole,[8] 0.5 g, was dissolved in 4.7 m*l* of acetic anhydride and kept for 3 hr at room temperature. Then the solution was poured onto crushed ice. White precipitates, 0.52 g, were collected and recrystallized from ethanol-water to give colorless long plates, mp 171.0—171.5 °C.

Found: C, 71.26; H, 6.71; N, 13.95 %. Calcd for $C_{12}H_{14}ON_2$: C, 71.26; H, 6.98; N, 13.85 %.

UV: λ_{max}^{EtOH} mμ (log ε), 245(4.45), 298(3.68, sh.), 310(3.44). IR: ν^{KBr} cm^{-1} 3370, 3250, 1650, 1550, 860, 810.

6-Acetamido-2, 3-dimethylindole (Ig). By the same method as Ic, 6-amino-2,3-dimethylindole was acetylated. Colorless leaflets from ethanol, mp 204—206°C.

Found: C, 71.08; H, 7.08; N, 13.97 %. Calcd for $C_{12}H_{14}ON_2$: C, 71.26; H, 6.98; N, 13.58 %.

UV: λ_{max}^{EtOH} mμ (log ε), 218(4.24), 248(4.37), 294 (4.01). IR: ν^{KBr} cm^{-1} 3290, 3210, 1625, 1525, 860, 810.

2, 3, 6-Trimethylindole (If).[9] White leaflets from ethanol-water, mp 119.5—121.0 °C.

UV: λ_{max}^{EtOH} mμ (log ε), 230(4.55), 280(3.79), 295 (3.69, sh.). IR: ν^{KBr} cm^{-1} 3360, 2950, 2890, 2840, 853, 802.

6-Chloro-2,3-dimethylindole (Ih).[9] White leaflets, from ether-petroleum ether, mp 164.5—165.5 °C.

UV: λ_{max}^{EtOH} mμ (log ε), 235(4.57), 286(3.83), 296 (3.78, sh.). IR: ν^{BKr} cm^{-1} 3360, 848, 804, 740.

2,3,6-Trimethylindolenyl-3-hydroperoxide (Vf). 1f, 200 mg, was dissolved in warm light petroleum (bp 60—80 °C, 30 m*l*) and a trace of benzoyl peroxide was added to the solution in the presence of atmospheric oxygen. After an hour the solution began to deposit the hydroperoxide, 110 mg, as white crystals, mp 112.5—113.0 °C (decomp.).

Found: C, 69.09; H, 6.79; N, 7.24 %. Calcd for $C_{11}H_{13}O_2N$: C, 69.05; H, 6.85; N, 7.33 %.

UV: λ_{max}^{EtOH} mμ (log ε), 218(4.31, sh.), 223(4.37), 230(4.26, sh.), 274(3.43). IR: ν^{KBr} cm^{-1} 3410, 3050, 2920, 2770, 878, 820.

Preparation of 2-Acetamidoacetophenone Derivatives (VI). Corresponding substituted indoles were dissolved in acetic acid and treated with ozonized oxygen at room temperature until the indole spot had disappeared on thin-layer chromatography. The products were isolated by neutralization followed by extraction with ether.

2,4-Diacetamidoacetophenone (VIg). Colorless leaflets from ethanol-water, mp 217—218 °C.

UV: λ_{max}^{EtOH} mμ (log ε), 254(4.42), 296(4.27). IR: ν^{KBr} cm^{-1} 3260, 3180, 1692, 1665, 1640, 1545, 883, 825.

2-Acetamido-4-methylacetophenone (VIf).[10] Colorless crystals, mp 75—76 °C.

UV: λ_{max}^{EtOH} mμ (log ε), 235(4.43), 239(4.44), 266 (4.04), 274(4.02), 325(3.58). IR: ν^{KBr} cm^{-1} 3200, 1680, 1640, 1525, 880, 810.

2-Acetamido-4-chloroacetophenone (VIh).[9] White plates from methanol, mp 146.5—148.0 °C.

UV: λ_{max}^{EtOH} mμ (log ε), 236(4.53, sh.), 240(4.57), 266(4.15), 274(4.11), 323(3.67). IR: ν^{KBr} cm^{-1} 3160, 1680, 1640, 875, 810, 750.

2,5-Diacetamidoacetophenone (VIc).[11] White needles from ethanol, mp 190—191 °C.

UV: λ_{max}^{EtOH} mμ (log ε), 243(4.43), 276(4.18), 351 (3.40). IR: ν^{KBr} cm^{-1} 3190, 1680, 1650, 882, 820.

Chemiluminescence. In the case of the chemiluminescence of I, 1 m*l* of potassium *t*-butoxide DMSO solution (10^{-2} mol/*l*) was at once added to 1 m*l* of the sample DMSO solution (10^{-3} mol/*l*), continuous tiny bubbles of oxygen being passed through the solution. The change in the intensity of light with time was recorded and total light emission

8) E. Shaw and D.W.Woolley, *J. Am. Chem. Soc.*, **75**, 1877 (1958).

9) D.W.Ockenden and K. Schofield, *J. Chem. Soc.*, **1957**, 3175.

10) D. W. Ockenden and K. Schofield, *ibid.*, **1953**, 612.

11) N.J. Leonard and S.N.Boyd, Jr., *J. Org. Chem.*, **11**, 405 (1946).

(A) was determined by the area of emission curve. Then relative total light emission (A/A_0) was calculated. A_0 is the area of Ia which was taken as the reference substance. In the case of V, continuous bubbles of argon was passed through the DMSO solution and the area of emission curve of Va was taken as the reference area. (Table 3).

Chemiluminescence Spectra and Fluorescence Spectra. Chemiluminescence spectra of I and V were measured by the same method as described in the preceeding paper.[5] Fluorescence spectra of substituted 2-acetamidoacetophenone (VI) were measured under the same condition as chemiluminescent reaction of I. Chemiluminescence and fluorescence maxima are shown in Table 1 and Table 2.

BULLETIN OF THE CHEMICAL SOCIETY OF JAPAN VOL. 41 1921—1924 (1968)

Electrochemical Fluorination of Glycols and Esters of Dicarboxylic Acids*1

Shunji NAGASE, Takashi ABE and Hajime BABA

Government Industrial Research Institute, Nagoya, Kita-ku, Nagoya

(Received February 1, 1968)

The electrochemical fluorination of glycols (1,3-propanediol and 1,4-butanediol), and dimethyl or diethyl esters of dicarboxylic acids (malonic, succinic, and maleic acids) was carried out. Difluoromalonic acid from esters of malonic acid, and perfluorosuccinic acid from esters of succinic acid or maleic acid, were obtained in reasonable yields, while 1,3-propanediol and 1,4-butanediol were cleaved or underwent ring formation and yielded only small amounts of perfluoro-dicarboxylic acids. Perfluoromonocarboxylic acids and fluorocarbons were among the by-products of these esters and glycols.

Alcohols and esters have been known to give perfluoro-carboxylic acid fluorides upon electrochemical fluorination.[1,2] The perfluorocarboxylic acid fluorides can be converted into the parent acids by hydrolysis. The present paper will deal with the syntheses of difluoromalonic acid and perfluorosuccinic acid by the use of this method.

Perfluoro-dicarboxylic acids have commonly been prepared by the oxidation of fluorinated cycloölefins[3-5] or diolefins.[6,7]

The oxidation of unsaturated fluoro-carboxylic acid[8] and the hydrolysis of chlorofluoro-carboxylic acid[9] have also been reported to yield perfluoro-dicarboxylic acids. The preparation of perfluorosuccinic acid from succinic acid and anhydride,[10,11] maleic acid and anhydride,[11] or from succinoyl fluoride[12] by the electrochemical process has been described.

Accordingly, glycols (1,3-propanediol and 1,4-butanediol), and dimethyl or diethyl esters of dicarboxylic acids (malonic, succinic, and

*1 Presented in part at the Symposium on Organic Halogen Compounds, Tokyo, November, 1967.

1) S. Nagase and R. Kojima, *Kogyo Kagaku Zasshi* (*J. Chem. Soc. Japan, Ind. Chem. Sect.*), **64**, 1397 (1961); Japanese Pat. 417721 (1963); S. Nagase and R. Kojima, This Bulletin, **34**, 1468 (1961); Japanese Pat. 417722 (1963).

2) S. Nagase, "Fluorine Chemistry Reviews," Vol. I, ed. by P. Tarrant, Marcel Dekker, New York (1967), p. 77.

3) A. L. Henne and W. J. Zimmerschied, *J. Am. Chem. Soc.*, **69**, 281 (1947).

4) M. W. Buxton, D. W. Ingram, F. Smith, M. Stacey and J. C. Tatlow, *J. Chem. Soc.*, **1952**, 3830.

5) D. E. M. Evans and J. C. Tatlow, *ibid.*, **1954**, 3779.

6) A. L. Henne and E. G. DeWitt, *J. Am. Chem. Soc.*, **70**, 1548 (1948).

7) R. N. Haszeldine, *J. Chem. Soc.*, **1955**, 4302.

8) R. N. Haszeldine, *ibid.*, **1954**, 4026.

9) D. C. England, R. V. Lindsey, Jr., and L. R. Melby, *J. Am. Chem. Soc.*, **80**, 6442 (1958).

10) M. A. Okatov, *Khim. Nauka i Prom.*, **4**, 675 (1959).

11) S. Nagase, H. Baba, K. Tanaka and T. Abe, *Kogyo Kagaku Zasshi* (*J. Chem. Soc. Japan, Ind. Chem. Sect.*), **67**, 2062 (1965).

12) H. M. Scholberg and H. G. Bryce, U. S. Pat. 2717871 (1955); Japanese Pat. 221494 (1956).

maleic acids) were subjected to electrochemical fluorination. No work had previously been reported on the electrochemical fluorination of these compounds.

It was found that the esters of dicarboxylic acids afforded the expected perfluoro-dicarboxylic acids in a reasonable yield, along with degraded products, while glycols were cleaved extensively or underwent cyclization, yielding smaller amounts of perfluoro-dicarboxylic acids. Perfluoro-monocarboxylic acids and fluorocarbons, including perfluoro-ethers and bis(trifluoromethyl) peroxide, were among the by-products in these fluorination reactions.

Experimental

Materials and Apparatus. The samples subjected to fluorination were commercial-grade chemicals. Their purities were confirmed by gas chromatography.

All the features of the apparatus used for this fluorination reaction were essentially the same as those of the apparatus diagrammed in a previous paper,[11] except that a part of the electrolytic cell used was that described in another paper.[13]

Procedures. As a typical example, the procedures for the fluorination of diethyl succinate (Run 6 in Table 1) will be described. Diethyl succinate (31.4 g, 0.18 mol) was introduced into anhydrous hydrogen fluoride (1 *l*) which had been purified by electrolysis, and then the electrolysis of the solution was carried out with an anodic current density of 2.9 A/dm^2, at a cell voltage of 5—6 V and at a cell temperature of 5—6°C. The electrolysis was continued until the voltage rose to 6.8 V. The amount of electricity required for this fluorination was 191 A hr. To aid agitation, helium was introduced into the hydrogen fluoride solution at the flow rate of 15 m*l*/min from the bottom of the cell through a bubbler.

The outgoing gases, such as hydrogen, hydrogen fluoride, monobasic and dibasic perfluoro-acid fluorides, oxygen difluoride, and fluorocarbons, from the electrolytic cell were passed through the reflux condenser (kept at −15°C) into the hydrogen fluoride absorber (A), an iron tube containing sodium fluoride pellets, and the perfluoro-acid fluoride absorber (B), a pair of polyethylene bottles containing water. The gases were then led into gas-washing bottles (C), an Ichinose bottle containing an aqueous solution of sodium sulfite and sodium hydroxide with a small amount of potassium iodide, and then finally conducted into traps (D) kept in ice and liquid nitrogen.

The hydrogen fluoride in the gas stream was removed in A, perfluoro-acid fluorides were converted into the parent acids in B, oxygen difluoride and carbon dioxide were removed in C, and fluorocarbons were collected in D. The hydrogen was allowed to escape into the air.

The products in B were worked up as usual[11] to give an ether extract of perfluoro-carboxylic acids. This ether extract was dried and, after the removal of the ether, distilled under reduced pressure (20 mmHg) at a bath temperature of below 100°C. The distillate was a mixture of trifluoroacetic acid and perfluoropropionic acid, which were converted into their sodium salts (23.8 g). These were analyzed quantitatively by the base-line technique of the IR spectrum, as has previously been described in detail.[1] The composition (wt%) of the product was $CF_3COONa : C_2F_5COONa = 64 : 36$. A trace of sodium perfluorobutyrate was also present. The residue was crude perfluorosuccinic acid, which was dissolved into hot benzene; a small amount of inorganic impurity was filtered off, and the filtrate was allowed to stand overnight. The crystalline precipitate which was thus separated was recrystallized from benzene, giving white needles of perfluorosuccinic acid (5.8 g, 17.0% yield), mp 116—116.5°C (lit.[4] mp 116—116.5°C). The IR spectrum of this product was identical with that of an authentic specimen prepared by another method.[4]

Fluorocarbons (18.0 g) trapped in D were analyzed quantitatively by low-temperature distillation, gas chromatography, and IR spectroscopy, much the same methods as had been used in a series of electrochemical fluorinations of gaseous organic compounds.[14] The composition (mol%) of the fluorocarbons was as follows: carbon tetrafluoride (45.3%), fluoroform (24.2%), perfluoroethane (19.2%), perfluoropropane (3.7%), perfluorodiethyl ether (2.6%) perfluorodimethyl ether (2.2%), pentafluoroethane (1.9%), and 1,1,1,2-tetrafluoroethane (0.9%). A small quantity of unidentified compounds (0.9 g) was also found.

The experimental procedures for all the other runs, including those giving difluoromalonic acid, were similar to the one illustrated above. Difluoromalonic acid was obtained as very hygroscopic white needles, mp 117—118°C (lit.[5] mp 117—118°C) (Found: C, 25.25; H, 1.64; F, 27.0%).

Results and Discussion

The reaction conditions and the results obtained are summarized in Table 1. The product distribution of the fluorocarbon by-products obtained from five representative samples are shown in Table 2.

1,3-Propanediol was cleaved extensively into fluorocarbons and perfluoro-monocarboxylic acids, and difluoromalonic acid was produced in only a low yield. The main components of fluorocarbons were carbon tetrafluoride, perfluoroethane, and fluoroform, but perfluoropropane, perfluorodiethyl ether, perfluorodimethyl ether, perfluoro-*n*-butane, and pentafluoroethane were also formed.

13) S. Nagase, H. Baba and T. Abe, This Bulletin, **39**, 2304 (1966).

14) Preceding paper: S. Nagase, H. Baba and T. Abe, *ibid.*, **40**, 2358 (1967).

TABLE 1. FLUORINATION OF GLYCOLS AND ESTERS OF DICARBOXYLIC ACIDS[a)]

Run No.	Sample mol		Perfluoro-dicarboxylic acid Yield %	Perfluoro-monocarboxylic acid (sodium salt) Yield %[b)]			Fluorocarbon g	Electricity passed A·hr
				CF_3-COONa	C_2F_5-COONa	C_3F_7-COONa		
1	$HOCH_2CH_2CH_2OH$	(0.3)	$CF_2(COOH)_2$ (2.6)	10.8	10.9	—	13.6	190
2	$CH_2OH(CH_2)_2CH_2OH$	(0.18)	$(CF_2COOH)_2$ (1.8)	14.2	6.3	1.1	22.2	185
3	$CH_2(COOCH_3)_2$	(0.18)	$(CF_2COOH)_2$ (12.0)	30.5	3.1	—	5.7	136
4	$CH_2(COOC_2H_5)_2$	(0.18)	$CF_2(COOH)_2$ (11.8)	107.0	4.2	—	15.5	145
5	$(CH_2COOCH_3)_2$	(0.18)	$(CF_2COOH)_2$ (15.1)	2.2	25.3	—	10.6	152
6	$(CH_2COOC_2H_5)_2$	(0.18)	$(CF_2COOH)_2$ (17.0)	62.2	25.6	—	18.0	191
7	$(:CHCOOCH_3)_2$	(0.18)	$(CF_2COOH)_2$ (8.4)	1.5	26.1	—	14.1	147
8	$(:CHCOOC_2H_5)_2$	(0.18)	$(CF_2COOH)_2$ (9.5)	71.3	28.1	—	16.8	176

a) Anodic current density: 2.9 A/dm², Cell temperature: 5—6°C.
b) (Mole of each sodium salt obtained/mole of sample used) × 100.

TABLE 2. COMPOSITION OF FLUOROCARBON PRODUCTS

Sample	Fluorocarbon mol %[a)]							Others, %
	CF_4	CHF_3	CF_3CF_3	CHF_2CF_3	C_3F_8	n-C_4F_{10}	CF_3OCF_3	
$HOCH_2CH_2CH_2OH$	55.0	8.7	22.4	1.4	5.8	0.8	1.9	$C_2F_5OC_2F_5$ (4.0)
$CH_2OH(CH_2)_2CH_2OH$	25.3	4.9	12.7	—	16.6	2.7	0.7	$CF_2(CF_2)_2CF_2$ (37.1) O
$CH_2(COOCH_3)_2$	42.4	36.6	3.0	0.4	—	—	12.5	CH_2F_2 (1.0), CF_3OOCF_3 (4.1)
$(CH_2COOCH_3)_2$	35.7	24.9	22.4	1.0	4.6	—	10.2	CH_2F_2 (1.2)
$(:CHCOOCH_3)_2$	42.7	17.1	19.6	—	16.4	0.5	3.0	$CF_2(CF_2)_2CF_2$ (0.7) O

a) A small amount of unidentified products was not considered.

These compounds appeared to be derived by the fluorination reaction *via* a free-radical mechanism on the anode surface; the progressive replacement of hydrogen and some oxygen of the glycol by fluorine atoms occurred, with accompanying extensive fragmentation of the carbon skeleton due to the high reaction heat. The combination of the fragment radicals yielded perfluorodimethyl ether, perfluorodiethyl ether, and perfluoro-*n*-butane. Difluoromalonyl fluoride, which yields difluoromalonic acid by hydrolysis, may be formed through the malonyl fluoride produced by the mechanism involving fluorination, followed by dehydrofluorination at the α-carbon atoms of the glycol, much as with that of monohydric alcohols.[1)]

The electrochemical fluorination of 1,4-butanediol produced perfluorotetrahydrofuran as the principal product (23.7% yield).*2 Perfluorosuccinic acid, perfluoro-monocarboxylic acids, and fluorocarbons were also obtained. Such cyclization reactions are often observed in the electrochemical fluorination of some oxygen-containing compounds.[15,16)] In this case, cyclization could have occurred at an early stage of the process, since the ring formation of this glycol takes place easily in acid media, and even the cyclic skeleton thus formed may be further ruptured into straight-chain fluorinated products in the fluorination. The results of the electrochemical fluorination of tetrahydrofuran (0.18 mol), which was found to afford perfluorotetrahydrofuran in a 34.7% yield, may be consistent with this interpretation.

The electrochemical fluorination of 1,2-ethanediol (0.3 mol) was examined under similar conditions. Trifluoroacetic acid was formed in a 6.1% yield, together with fluorocarbons. The fluorocarbons*3 contained mainly carbon tetrafluoride and fluoroform. Bis(trifluoromethyl) peroxide, perfluoroethane, and perfluorodimethyl ether were also among the products.

The esters of malonic acid afforded difluoro-

*2 9.2 g.

15) E. A. Kauck and J. H. Simons, U. S. Pat 2644823 (1953); Brit. Pat. 718318 (1954).

16) Saline Ludwigshalle A.-G., German Pat. 1069638 (1959); Brit. Pat. 862538 (1961).

*3 The amount of the fluorocarbon mixture was 16.5 g, but a considerable portion (4.0 g) of it went unidentified.

malonic acid in a fair yield. Perfluoropropionic acid was produced in addition to trifluoroacetic acid from these esters; both the carbonyl carbons were incorporated into the perfluoropropionic acid. The formation of a large amount of trifluoroacetic acid from the ethyl esters indicates its additional formation from the two ethoxyl groups of the ester.

For the sake of comparison, the electrochemical fluorination of free acid, malonic acid, was also performed; only traces of difluoromalonic acid and trifluoroacetic acid were yielded. The free acid was cleaved almost completely into fluorocarbons (carbon tetrafluoride, fluoroform, and methylene fluoride) and carbon dioxide in the course of the fluorination.

The esters of succinic acid and even those of maleic acid gave perfluorosuccinic acid in reasonable yields, yields which were greater than the yields from the free acids and their anhydrides.[11] Perfluoro-monocarboxylic acids and fluorocarbons, exemplified by those obtained from the methyl esters of the acids shown in Table 2, were common by-products in these fluorination reactions.

The sequence of the formation of dibasic perfluoro-acid fluorides from the esters may involve the hydrofluorolysis of the esters in hydrogen fluoride to form dibasic acid fluorides and alcohols. The alcohols formed in this way would be converted into acid fluorides through the mechanism involving fluorination, followed by dehydrofluorination, at the oxygen-bonded carbon atom.[1] Both the acid fluorides thus produced would then be fluorinated further to the corresponding perfluoro-acid fluorides. For example, in the case of diethyl succinate, this reaction would be represented by the following formulae:

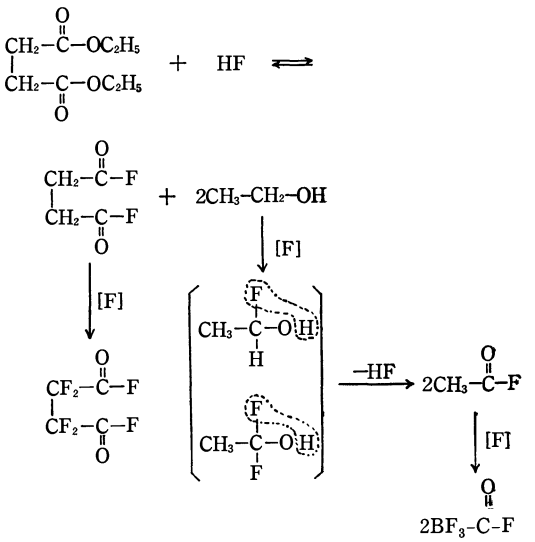

Although fragmentation or cyclization prevailed in the fluorination of glycols, dibasic perfluoro-acid fluorides were produced. The mechanism of the formation of dibasic perfluoro-acid fluorides from glycols could be considered to be similar to that of monohydric alcohols.[1] The production of a considerable amount of perfluorotetrahydrofuran from 1,4-butanediol shows the ease of five-membered-ring formation and the stability of an ether linkage in the fluorination reaction.

BULLETIN OF THE CHEMICAL SOCIETY OF JAPAN VOL. 41 1925—1928 (1968)

The Reactions of Esters of Amidosulfurous Acid

Hisashi TAKEI, Hideo SHIMIZU, Moriaki HIGO and Teruaki MUKAIYAMA

Laboratory of Organic Chemistry, Tokyo Institute of Technology, Ookayama, Meguro-ku, Tokyo

(Received February 6, 1968)

It was found that benzhydryl dimethylamidosulfite, obtained from *N,N,N',N'*-tetramethylsulfurous diamide-phenyl isocyanate adduct and benzhydrol, decomposed to give benzhydryldimethylamine and sulfur dioxide. Similarly, triphenylmethyl and 1,3-diphenylallyl dimethylamidosulfite gave corresponding tertiary amines when these esters were refluxed in benzene. On the other hand, benzoin dimethylamidosulfite gave benzil, the oxidized product of benzoin. When β-anilinoethyl and β-*N*-methylaminoethyl dimethylamidosulfite were heated at 120—130℃ for 10 min, cyclic esters of amidosulfurous acid, 3-phenyl- and 3-methyl-1,2,3-oxathiazolidine-2-oxide, were obtained along with evolution of dimethylamine. Further, the thermal decomposition of the cyclic compounds was studied.

In the preceding paper, it has been shown that tetraalkylsulfurous diamides(I) and phenyl isocyanate gave 1 : 1 adducts (II), which react readily with active hydrogen compounds such as alcohols, carboxylic acids and mercaptans to give *N,N*-dialkyl-*N'*-phenylureas (III), and alkyl dialkylamidosulfites, *N,N*-dialkylcarboxylic amides and *S*-alkyl dialkylamidothiosulfites, respectively.[1] This reaction is considered to be a convenient route for the synthesis of amidosulfurous acid derivatives, since I and phenyl isocyanate are readily available and the products are obtained in excellent yields under mild conditions by simple procedure.

As part of the investigation of the reactions of amidosulfurous acid derivatives,[1,2] the reactions of II with various alcohols such as α-substituted benzyl alcohols, α-ketoalcohols and aminoalcohols were studied in order to prepare the corresponding esters and to know the nature of the esters. When benzhydrol was added to a solution of II in dry ether, *N,N*-dimethyl-*N'*-phenylurea (III) was separated quantitatively and, after removal of the solvent, a viscous oily substance remained. The structure of this oily substance was assigned to be benzhydryl dimethylamidosulfite (IVa) by its infrared spectrum which has characteristic bands attributable to ester of amidosulfrous acid (1150 and 900 cm^{-1}). However, an attempt to purify this oily substance by vaccum distillation resulted in decomposition with evolution of sulfur dioxide. From the residue, benzhydryldimethylamine (Va) was isolated in a 50 % yield. Similar decomposition was observed when triphenylmethyl and 1,3-diphenylallyl dimethylamidosulfites (IVb and IVc), obtained as viscous oily substance by the above mentioned procedure, were refluxed in dry benzene, and corresponding tertiary amines (Vb and Vc) were obtained in 50% and 59% yields, respectively.

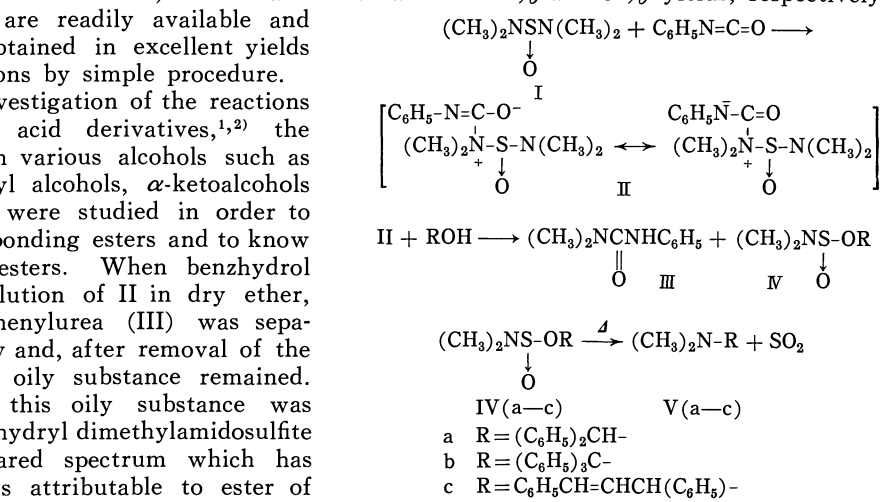

While, ethyl, allyl, cyclohexyl and benzyl dimethylamidosulfites are fairly stable and are able to be distilled under reduced pressure without decomposition.[1] Concerning the above results, Zinner[3] has reported that attempts to

1) T. Mukaiyama, H. Shimizu and H. Takei, *J. Org. Chem.*, **32**, 3475 (1967).

2) T. Mukaiyama, H. Shimizu and H.Takei, This Bulletin, 40, 939 (1967).

3) G. Zinner, *Angew. Chem.*, **69**, 93 (1959).

distill ethyl dialkylamidosulfites at atmospheric pressure resulted in decomposition with evolution of sulfur dioxide, but the corresponding tertiary amines could not be isolated. It can be noted that electron-withdrawing substituents, *e. g.* two phenyl groups, on α-carbon atom of the esters favor the reaction to afford tertiary amines probably proceeding through an internal nucleophilic attack by the amino group on α-carbon atom (S_Ni Mechanism).

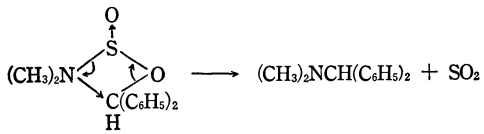

Next, it was established that the reaction of II with benzoin afforded benzoin dimethylamidosulfite (VI) as a viscous oily substance along with III. The structure of VI was confirmed by its infrared spectrum and the fact that treatment of VI with ethanol gave benzoin and ethyl dimethylamidosulfite (VII), transesterification products, in good yields. When VI was refluxed in dry benzene for an hour, the expected products, dimethylaminodeoxybenzoin and sulfur dioxide, could not be detected, instead, benzil, the oxidized product of benzoin, was obtained in a 74 % yield.

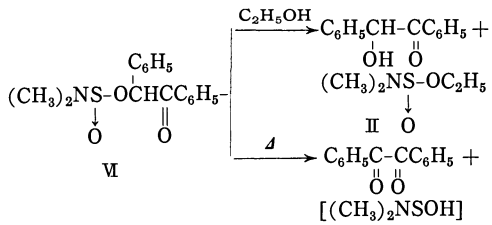

It seemed reasonable to assume that benzil may be produced through radical intermediates based on the following results: When VI was heated in benzene in the presence of diphenylpicrylhydrazyl, violet color of the radical disappeared soon. In addition, it was found that addition of diethylaniline, which is known to be a radical scavenger, inhibit the decomposition of VI. Based on these results, the oxidation reaction can be explained by assuming the following radical chain mechanism.

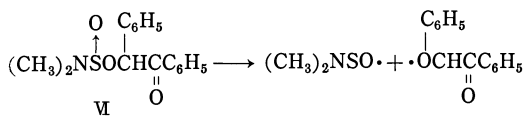

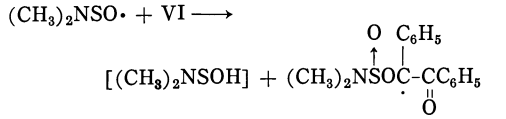

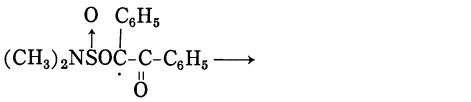

In a similar fashion, when hydrazobenzene was treated with II in benzene at room temperature, azobenzene was obtained in a 78 % yield along with III.

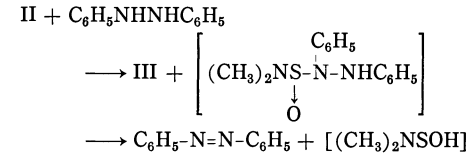

In the case of the reaction of II with α-hydroxycarboxylic esters such as ethyl lactate and ethyl mandelate, however, the thermal decomposition of the corresponsing esters of dimethylamidosulfurous acid obtained as undistillable oily substance did not afford the expected products, α-ketocarboxylic esters, but a large amount of dark colored tarry product and a small amount of unpleasant smelling, low-boiling substances resulted.

Finally, the reaction of II with aminoalcohol was examined. When *N*-phenylethanolamine was added to II in dry ether, III was obtained in a quantitative yield and, after removal of the solvent under reduced pressure, a viscous oily substance remained. The structure of the oily substance was assigned to be β-anilinoethyl dimethylamidosulfite (VIIIa) by its infrared spectrum which has characteristic bands of nitrogen-hydrogen linkage (3200 cm^{-1}) and of ester of amidosulfurous acid (1180 and 900 cm^{-1}). When IXa was heated at 120—130 ℃ for 10 min, evolution of dimethylamine was observed and vacuum distillation of the residue gave cyclic ester of amidosulfurous acid, 3-phenyl-1,2,3-oxathizolidine-2-oxide(IXa), in an 81 % yield. In a similar way, 3-methyl-1,2,3-oxathiazolidine-2-oxide(IXb) was prepared by the reaction of II with *N*-methylethanolamine.

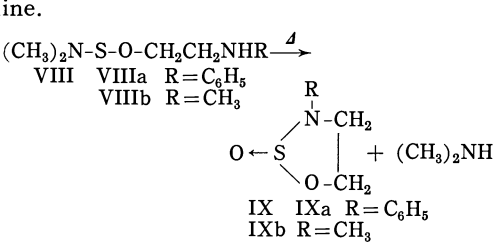

These cyclic compounds were unstable to prolonged heating. For example, when IXa was refluxed in dry xylene for 5 hr, evolution of sulfur dioxide was observed and a large

amount of dark colored tarry material was deposited in the flask. From the hot xylene layer, a small amount (6 %) of *N,N'*-diphenylpiperazine was obtained. Further, it was found that when IXa was refluxed in xylene in the presence of benzoic acid or aniline, β-anilinoethyl benzoate or *N,N'*-diphenylethylenediamine was obtained in a 54% or 33% yield, respectively.

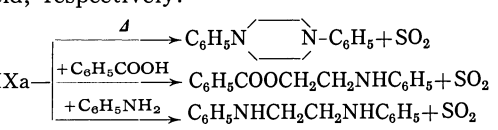

Experimental

All melting points and boiling points are uncorrected.

Reaction of *N,N,N',N'*-Tetramethylsulfurous Diamid-Phenyl Isocyanate Adduct (II) with Benzhydrol. To an ice-cooled solution of *N,N,N',N'*-tetramethylsulfurous diamide (I) (1.36 g, 10 mmol) in 5 m*l* of dry ether, a solution of phenyl isocyanate (1.19 g, 10 mmol) in 10 m*l* of dry ether was added dropwise with stirring. The mixture was kept standing at room temperature for an hour, and then a solution of benzhydrol (1.84 g, 10 mmol) in ether was added. An exothermic reaction took place and *N,N*-dimethyl-*N'*-phenylurea (III) was precipitated soon. The III was collected and recrystallized from water: yield 1.6 g, mp 134 °C. The filtrate was evaporated at room temperature under reduced pressure, and a viscous oily substance remained. The infrared spectrum of this colorless oily substance shows characteristic bands attributable to ester of amidosulfurous acid (1150 and 900 cm^{-1}). An attempt to purify the oily substance by vacuum distillation led to the decomposition giving 1.05 g (50 %) of benzhydryldimethylamine (Va), bp 130°C/8 mmHg, which solidified soon. It was recrystallized from aqueous ethanol, mp 70.5—71 °C (lit. mp 68.5—70°C).[4]

Found: C, 85.27; H, 8.05; N, 6.67 %. Calcd for $C_{15}H_{17}N$: C, 85.26; H, 8.11; N, 6.63 %.

Similarly, the reaction of II (10 mmol) with 1,3-diphenylallyl alcohol (2.10 g, 10 mmol) gave the corresponding ester of dimethylamidosulfurous acid (IVc) as an oily substance. Its infrared spectrum shows characteristic bands attributable to ester of amidosulfurous acid (1170 and 960 cm^{-1}). When this oily substance was refluxed in benzene for an hour, evolution of sulfur dioxide was observed. After removal of the solvent, the residual liquid was distilled to give 1.40 g (59 %) of 1-dimethylamino-1,3-diphenyl-2-propene (Vc), bp 120—122 °C/0.1 mmHg.

Found: C, 85.87; H, 8.27; N, 6.12 %. Calcd for $C_{17}H_{19}N$: C, 86.03; H, 8.07; N, 5.90 %.

Picrate, mp 175—177 °C (decomp).

Found: C, 59.46; H, 4.96; N, 11.99 %. Calcd for $C_{23}H_{22}N_4O_7$: C, 59.22; H, 4.75; N, 12.01 %.

4) M.M.Sommelet, *Compt. rend.*, **175**, 1150 (1922).

The reaction of II (10 mmol) with triphenylcarbinol (2.60 g, 10 mmol) gave 1.44 g (50 %) of dimethyl(triphenylmethyl) amine (Vb), mp 93—95 °C (lit. mp 97°C).[5]

Reaction of II with Benzoin. To a solution of 10 mmol of II in dry benzene, a solution of benzoin (2.12 g, 10 mmol) in dry tetrahydrofuran was added dropwise with stirring. After stirring for half an hour at room temperature, the solvent was removed under reduced pressure. Precipitated urea (III) (quantitative yield) was filtered off and the residual liquid (VI) was dissolved in dry benzene. Then the solution was refluxed for an hour, cooled and concentrated under reduced pressure. After standing the residue overnight, precipitated benzil was collected, washed with a small amount of ethanol and recrystallized from ethanol: yield 1.56 g (74%), mp and mixed mp 95—96°C.

Reaction of VI with Ethanol. Ethanol (5 m*l*) was added to the VI prepared by the procedure described above, and the mixture was refluxed for half an hour, cooled and concentrated under reduced pressure. Precipitated benzoin was collected, washed with a small amount of ethanol and recrystallized from ethanol: yield 1.40 g (70 %), mp and mixed mp 134 °C. The filtrate was distilled to give ethyl dimethylamidosulfite (VII): yield 0.8 g (60 %), bp 65—67°C/18 mmHg[1].

Thermal Decomposition of VI in the Presence of *N,N*-Diethylaniline. A solution of VI (10 mmol) and *N,N*-diethylaniline (1.5 g, 10 mmol) in dry benzene was refluxed for an hour. Then 2 m*l* of ethanol was added and the mixture was refluxed for 15 min, cooled and concentrated under reduced pressure. Precipitated benzoin (1.60 g, 76 %), mp and mixed mp 134 °C, was filtered off and the filtrate was distilled to give VII (0.9 g, 66 %), bp 66—68°C/18 mmHg.[1]

Reaction of II with Hydrazobenzene. To a solution of 10 mmol of II in dry ether, 1.84 g (10 mmol) of hydrazobenzene in dry benzene was added dropwise with stirring at room temperature. Precipitated urea (quantitative yield) was filtered off and the orange-red filtrate was concentrated under reduced pressure. The residual liquid was distilled to give azobenzene (1.42 g, 78 %), bp 145—150°C/12 mmHg, which solidified soon. It was recrystallized from aqueous ethanol, mp and mixid mp 67—68°C.

Reaction of II with *N*-Phenylethamine. To an ice-cooled solution of 10 mmol of II in dry ether, a solution of *N*-phenylethanolamine (1.37 g, 10 mmol) in dry ether was added dropwise with stirring. Precipitated urea (III) (quantitative yield) was filtered off and the filtrate was concentrated under reduced pressure. The infrared spectrum of the oily residue shows characteristic bands attributable to nitrogen-hydrogen linkage (3200 cm^{-1}) and ester of amidosulfurous acid (1180 and 900 cm^{-1}). When this oily substance was heated at 120—130°C for 10 min, evolution of dimethylamine was observed. The residual liquid was distilled to give 3-phenyl-1,2,3-oxathiazolidine-2-oxide (IXa), which solidified

5) E. Hemilian and H. Silberstein, *Ber.*, **17**, 746 (1884).

immediately: yield 1.48 g (81 %), bp 144 °C/0.07 mmHg.

Found: C, 53.18; H, 5.36; N, 8.37 %. Calcd for $C_8H_9NO_2S$: C, 52.45; H, 4.95; N, 7.65 %.

In a similar manner, 3-methyl-1,2,3-oxathiazolidine-2-oxide (IXb) was obtained in a 21 % yield by treating II with *N*-methylethanolamine, bp 100—102°C/23 mmHg.

Found: C, 30.15; H, 6.56; N, 11.31 %. Calcd for $C_3H_7NO_2S$: C, 29.74; H, 5.82; N, 11.57 %.

Attempts to prepare 3-unsubstituted. oxathiazolidine or benzoxathiazoline by treating II with ethanolamine or *o*-aminophenol were unsuccessful though the urea was obtained in a quantitative yield.

Thermal Decomposition of IXa. When a solution of IXa (1.83 g, 10 mmol) in dry xylene was refluxed for 5 hr, evolution of sulfur dioxide was observed and a large amount of dark colored tarry product was deposited. The hot xylene layer was decanted and the residue was heated with benzene. The hot benzene layer was decanted and combined with the xylene solution. After removal of the benzene and xylene under reduced pressure, the residue solidified. It was recrystallized from ethanol to give *N,N'*-diphenylpiperazine: yield 0.07 g (6 %), mp 164 °C. (lit. mp 164—165 °C).[6]

When the thermal decomposition of IXa was carried out in the presence of *N*-phenylethanolamine, *N,N'*-diphenylpiperazine was obtained in a 25 % yield.

Reaction of IXa with Benzoic Acid. When a solution of IXa (1.83 g, 10 mmol) and benzoic acid (1.22 g, 10 mmol) in xylene was refluxed for 7 hr, vigorous evolution of sulfur dioxide was observed. After removal of the solvent under reduced pressure, colorless crystalline product was obtained. It was recrystallized from ethanol to give β-anilinoethyl benzoate: yield 1.30 g (54 %), mp 73.5—76 °C (lit. mp 77 °C).[7]

In a similar manner, the reaction of IXa with aniline gave *N,N'*-diphenylethylenediamine. It was recrystallized from aqueous ethanol: yield 0.73 g (33%), mp 65.5—67 °C (lit. mp 65 °C).[8]

6) G. R. Clemo and W. H. Perkin, Jr., *J. Chem. Soc.*, **121**, 647 (1922).

7) E. Bergs, *Ann.*, **332**, 209 (1904).

8) C.A. Bishoff and O. Nastvogel, *Ber.*, **22**, 1783 (1889).

BULLETIN OF THE CHEMICAL SOCIETY OF JAPAN VOL. 41 1928—1937 (1968)

Hydrogen Abstraction Reaction of α-Heteroatom Substituted Compounds by *t*-Butoxy Radical*1

Kenji UNEYAMA, Hiroshi NAMBA and Shigeru OAE

Department of Applied Chemistry, Faculty of Engineering, Osaka City University, Sugimoto-cho, Sumiyoshi-ku, Osaka

(Received February 19, 1968)

Hydrogen abstraction reactions of various α-substituted compounds were examined in chlorobenzene using di-*t*-butyl peroxide. The reactivities are not satisfactorily correlated with σ^* values of the substituents. The relative rates of substituted anisoles, *N,N*-dimethylanilines and phenyl methyl sulfones give good correlations with Hammett σ values with ρ values of -0.39, -0.42 and -0.2 respectively, but those of thioanisoles requires an additional term due to conjugative effect as described in $\log k/k_0 = -0.11(\sigma + 0.75\Delta\sigma_{R^+})$ in order to get a good Hammett correlation. These results were discussed in terms of a combination of an inductive effect, an electron-releasing and an electron-sharing conjugation.

In connection with our recent work on the 3d orbital resonance in divalent sulfides, we have extended our investigation to the hydrogen abstraction reaction of various sulfur compounds and related α-heteroatom substituted compounds by *t*-butoxyl radical. In the carbanion forming reaction such as the base catalyzed hydrogen-deuterium exchange reaction of various mercaptoles,[1] the base catalyzed decarboxylation reactions of various α-alkyl- and arylmercaptoacetic acids,[2] the E_2 reaction of β-chloroethyl phenyl sulfides[3] and also the acid dissociation equilibria of phenols

*1 Paper XI on 3d-orbital Resonance in Divalent Sulfides.

1) S. Oae, W. Tagaki and A. Ohno, *Tetrahedron*, **20**, 417, 427 (1964).

2) a) S. Oae, W. Tagaki, K. Uneyama and I. Minamida, *ibid.*, in press. b) W. Tagaki, K. Uneyama, I. Minamida, Kim Yon Hey, Y. Ikeda and S. Oae, This Bulletin, **39**, 917 (1966).

3) Y. Yano and S. Oae, *Tetrahedron*, in press.

which bear either mercapto or other related sulfur substituents in the benzene rings,[4] all the mercapto groups showed rate enhancing effect, while the corresponding oxygen counterparts showed rate retardation and these results are explained on the basis of the stabilization of carbanion incipiently formed in the transition state by the 3d orbital resonance effect of divalent sulfur atom as shown in Eq. (1).[5] Meanwhile in the carbonium ion forming reaction such as the solvolyses of α-substituted methyl chlorides, alkoxyl group is known to give greater rate enhancement than mercapto group[6] due to the more effective electron-releasing conjugative effect of alkoxy group than that of the sulfur counterpart. The effects of divalent sulfur and alkoxy group in the radical forming reaction have not been investigated quantitatively and hence are quite interesting subjects for investigation in connection with these conjugative effects, namely electron-releasing conjugation[7] like (2) and electron-sharing conjugation like (3), since the electric environment of the radical reaction is vastly different from these of the ionic reactions and other factor may become important.

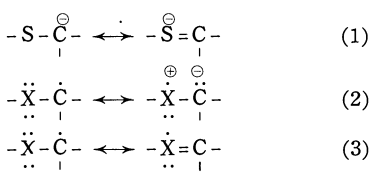

(1)

(2)

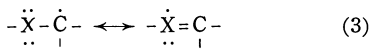

(3)

Russell *et al.* investigated the hydrogen abstraction from α-methyl or methylene group attached to heteroatoms by phenyl radical and found that alkoxyl, mercapto and amino groups have substantial rate enhancing effects as compared with phenyl group and explained these rate-enhancements in terms of the stabilization of the incipient radicals by electron-releasing conjugative effect of α-substituents as shown in Eq. (2). Meanwhile, the electron-sharing conjugation[8,9] like (3) has been proposed on the basis of the remarkably large Q values of alkyl vinyl sulfides and vinylidene mercaptals as compared with those of the oxygen analogs, methyl vinyl sulfone and trimethylvinylsilane in the copolymerization with styrene. The stabilization of the radicals, namely the large Q values, has been proposed to be due to the delocalization of an odd electron into the hybridized orbital between 2p-orbital on α-carbon atom and 3d-orbital on sulfur atoms, and this type of conjugative effect can display only with those groups of the 2nd row elements bearing at least one lone electron pair and not with these without any lone-pair or with those of the lst row elements. The electron-sharing conjugation also can satisfactorily explain the orientation of the thiyl radical to mercapto- and alkoxyacetylenes.[10] However, the hypothesis of the electron-sharing conjugation effect has to be tested with more critical and quantitative experiments. With these background thoughts, we have studied the hydrogen abstraction reaction of various α-substituted compounds by *t*-butoxy radical and this paper will discribe the detailed account of the results and discussion especially as to what extent, electron-releasing or/and electron-sharing conjugative effects would control the reactivities and also change the mechanism of the reaction.

Results and Discussion

Kinetics. The decomposition of di-*t*-butyl peroxide was carried out in chlorobenzene at 130℃ ±0.5℃, for 42 hr during which the peroxide was completely decomposed.[11] The *t*-butoxy radical formed by the thermal decomposition of the peroxide is mainly consumed through the following two processes. The one is the β-scission of *t*-butoxy radical into acetone and methyl radical as shown by Eq. (4) and the other is the hydrogen abstraction from a hydrogen donor compound (RH) giving *t*-butanol Eq. (5). In these experiments, the total yields of acetone and *t*-butanol combined were always more than 95 % with all the substrates examined; therefore, the hydrogen abstraction and the β-scission consist of the main portion of the reaction. Thus, the relative reactivity of reactions (4) to (5) is given by Eq. (6),[12]

4) S. Oae, M. Yoshihara and W. Tagaki, This Bulletin, **40**, 951 (1967)

5) C.C.Price and S.Oae, "Sulfur Bonding," Ronald Press Co., N.Y. (1962).

6) H. Böhme, H.Fischer and R.Frank, *Ann.*, **563**, 54 (1949)

7) R.F. Bridger and G.A. Russell, *J. Am. Chem. Soc.*, **85**, 3754 (1963)

8) C.C.Price and J.Zomlefer, *ibid*, **72**, 14 (1950); C.C. Price and T.C. Schman, *J. Polymer Sci.*, **16**, 577 (1955); C.E.Scott and C.C. Price, *J. Am. Chem. Soc.*, **81**, 2670, 2672 (1959). See also Ref. 5, p. 26.

9) W.Tagaki, S.Kiso, T.Tada, R.Nomura and S. Oae, This Bulletin, submitted.

10) H.C.Volger and J.F.Arens, *Rec. Trav. Chim.*, **77**, 1170 (1958); J. Bonnema and J. F. Arens, *ibid*, **79**, 1137 (1960); H.J. Alkema and J.F. Arens, *ibid*, **79**, 1257 (1960).

11) J.H. Raley, F.F. Rust and W.E. Vaughan, *J. Am. Chem. Soc.*, **70**, 1336 (1948)

12) J.H. Raley, F.F. Rust and W. E. Vaughan, *J. Am. Chem. Soc.*, **70**, 1336 (1948).

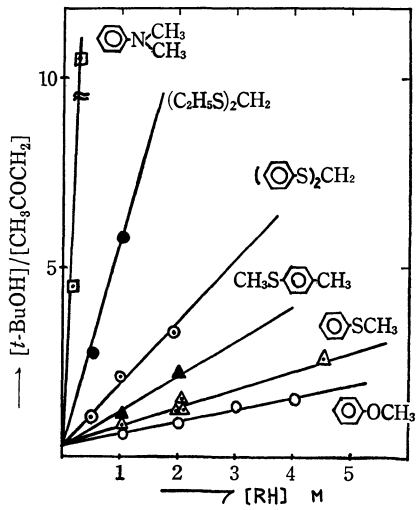

Fig. 1. Plot of [t-BuOH]/[CH_3COCH_3] against [RH].

$$t\text{-BuO}\cdot \xrightarrow{k_d} CH_3COCH_3 + CH_3\cdot \quad (4)$$

$$t\text{-BuO}\cdot + RH \xrightarrow{k_a} t\text{-BuOH} + R\cdot \quad (5)$$

$$t\text{-BuOH}/CH_3COCH_3 = k_a/k_d \times [RH] \quad (6)$$

where k_d and k_a are the rate constants of the decomposition and the hydrogen abstraction respectively, while [RH] is the concentration of a substrate. Applicability of this Eq. (6) to all the substrates can be tested by plotting their t-BuOH/CH_3COCH_3 values againt [RH] and we got a straight line, from whose slope k_a/k_d was able to be calculated. Applications for a few substrates are illustrated in Fig. 1.

Influence of α-Substituent. The relative reactivities k_a/k_d of all the substrates and those of hydrogen abstraction relative to toluene are summarized along with the σ^* values of all the substituents in Table 1. Inspection of the data reveals a few interesting points worthy to be noted in the following paragraphs. 1) Anisole, thioanisole and *N,N*-dimethylaniline react much faster than

TABLE 1. RELATIVE REACTIVITIES OF α-HYDROGEN ATOM[a)]

Compound	$k_a/k_d \times 10$[d)]	Rel. reactivity[c)]	σ^*[d)]
	0.944	1.00	0.215
	1.36	1.44	0.95[e)]
	2.00	2.12	0.77
	77.3	81.9	
	0.05	0.05	1.32[f)]
$(CH_3C_2)_2S$[h)]	6.70	7.10	0.46
$(C_2H_5S)_2CH_2$[i)]	15.4	16.3	1.12
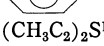	46.4	49.2	1.02
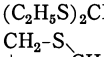	9.44	10.0	1.54
	13.1	13.9	2.31
	3.91	4.14	1.90

a) In chlorobenzene at 130°C. Most of substrates were examined in 0.5—2.0 M concentration and di-t-butyl peroxide was 0.107 M.

b) Reactivity per one hydrogen.

c) Relative reactivity to toluene.

d) See Ref. 2c), and R. W. Taft. Jr., "Steric Effects in Org. Chem.," ed. by M.S. Newman, John Wiley & Sons, Inc., New York (1956).

e) Reported value is 0.85 by R.W.Taft, Jr., See Ref. d.

f) σ^* value of $CH_3SO_2CH_2$- group.

g) 0.1—0.3M of substrate and 0.043 M of (t-BuO)$_2$.

h) Methylene was assumed to be a reactive hydrogen source.

i) Reactivity of hydrogen (H_α) surrounded by two geminal sulfur atom was calculated as follows.

$(k_a/k_d)H_\alpha = 1/2\{$Total reactivity of $(C_2H_5S)_2CH_2$ —Total reactivity of $(C_2H_5)_2S\}$

TABLE 2. RELATION OF REACTIVITY WITH THE NUMBER OF α-SUBSTITUENT[a)]

X_nCH_{4-n} \ X						CH_3[d)]	CH_3[e)]
Primary	$n=1$	1	1	1	1	1	1
Secondary	2	4.7	2.9	4.7	4.2	3.2	8
Tertiary	3	6.6	—	9.6		5.1—6.4	44

a) Reactivity of α-hydrogen atom toward t-BuO· as the number of substituents was changed.

b) By t-BuOCl at 40°C, C. Walling and B.B. Jacknow, *J. Am. Chem. Soc.*, **82**, 6108 (1960).

c) By (t-BuO)$_2$ at 135°C. A.L. Willams, E.A. Oberright and J.B. Brooks, *ibid.*, **78**, 1190 (1956).

d) By (t-BuO)$_2$ at 135°C, toluene, ethylbenzene, and cumene are substrates.

e) Hexamethylethane, neopentane, and n-butane are substrates by t-BuOCl at 40 °C. C. Walling and W. Thaler, *ibid.*, **83**, 3877 (1961).

toluene, while *N,N*-dimethylaniline is the fastest reacting substrate among all of the substrates examined and thioanisole has a slightly larger rate than anisole, whereas very little hydrogen abstraction takes place with phenyl methyl sulfone. This markedly slow rate of phenyl methyl sulfone is quite contrary to the case of the carbanion forming reaction as seen in the decarboxylation reaction,[2] in which phenylsulfonyl group accelerates the reaction more than phenylmercapto group. 2) The ring compound (ethanedithioformal) reacts faster than the corresponding acyclic compound (diethylmercaptoformal). 3) Successive substitution of either phenylmercapto or phenoxyl group at α-carbon atom of either thioanisole or anisole respectively leads to a gradual rate increment (see Table 2). 4) No reasonable correlation between reactivities of substrates (XCH_3) and σ^* values of substituents (X) is found and only scattered points are obtained when one plots $\log k_a/k_d$ against σ^* values as shown in Fig. 2. These observations reveal that the reactivities of α-hydrogen are not determined simply by inductive effect of α-substituents and that those substituents that have heteroatoms bearing at least one lone electron pair at α-position enhance the rate of hydrogen absotraction. The successive substitution of phenylmercapto and phenoxyl groups at α-position appears to increase the relative rate considerably. Thus diphenylmercaptoformal is 5 times as reactive as thioanisole, while tris (phenylmercapto) methane has rate 7 times larger than that of thioanisole. This gradual rate enhancement with additional substitution of same substituent on α-carbon atom can be seen with all the substituents, however, the amount of the rate enhancement by one additional substituent seems to be nearly identical independently of the nature of substituent in spite of the different induc-

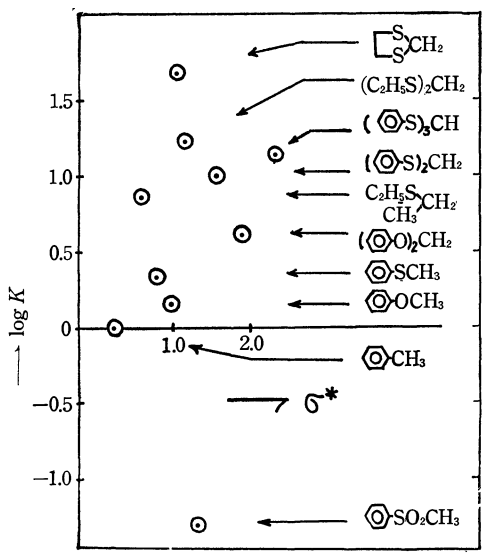

Fig. 2. Correlation of Reactivity of Hydrogen of X_nCH_{4-n} toward *t*-BuO· radical with σ^* of Substituent.

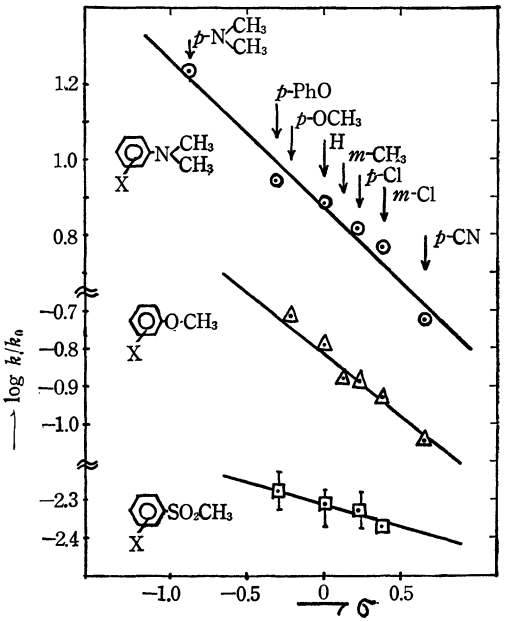

Fig. 3. Hammett correlation of anisole, *N,N*-dimethylaniline and methyl phenyl sulfone.

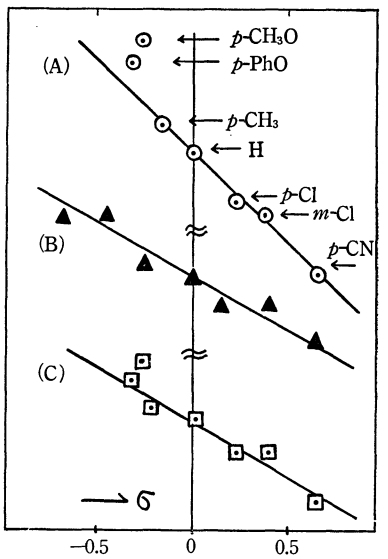

Fig. 4. Hammett correlation of substituted thioanisoles.
(A) $\log k/k_0 = -0.12\ \sigma$
(B) $\log k/k_0 = -0.11\ (\sigma + 0.75\ \Delta\sigma_{R+})$
(C) $\log k/k_0 = -0.11\ \sigma + 0.1 \cdot E_R$

TABLE 3. RING SUBSTITUENT EFFECTS OF ANISOLE, THIOANISOLE *N,N*-DIMETHYLANILINE AND METHYL PHENYL SULFONE[a)]

Substituent \ $k_a/k_d \times 10$	-OCH_3[b)]	-SCH_3[b)]	-SO_2CH_3[c)]	-$N(CH_3)_2$[d)]
p-$N(CH_3)_2$	—	—	—	172
p-PhO	—	2.33	0.053	88.4
p-CH_3	1.74	2.40[e)]	—	—
p-CH_3	—	2.10[f)]	—	—
H	1.36	2.00	0.048	77.4
p-Cl	1.12	1.87	0.047	65.2
m-Cl	1.00	1.83	0.040	58.1
p-CN	0.78	1.67	—	36.6
m-CH_3O	1.13	—	—	—

a) All the values of k_a/k_d are the averages of more than two runs.
b) 2.00 M in chlorobenzene with 0.107 M of di-*t*-butyl peroxide.
c) 1.00 M.
d) 0.1 M solution with 0.043 M of $(t\text{-BuO})_2$.
e) The reactivity of hydrogen of methoxyl group was subtracted from the total reactivity (3.76) as follows. Substituted anisole gave a satisfactory Hammett σ correlation and σ value of para-methylmercapto group is 0.00, therefore, the reactivity of hydrogen of methylmercapto group in para methoxythioanisole is 3.76—1.36 (reactivity of anisole) = 2.40.
f) Substituted toluene is known to give σ^+ correlation (see Ref. 22) and ρ is −0.38 (σ^+) at 125 °C with di-*t*-butyl peroxide.
The reactivity of para-methyl group is

$$\log k = -0.38(-0.604) + \log 0.944 = 0.205,\ k = 1.60.$$

Therefore, the reactivity of hydrogen of methylmercapto group is

$$3.70(\text{total reactivity}) - 1.60 = 2.10.$$

TABLE 4. HAMMETT ρ VALUE OF HYDROGEN ABSTRACTION REACTION BY *t*-BUTOXYL RADICAL

Substrate	Solvent	Temp. (°C)	ρ	r[d)]
-CH_3	Chlorobenzene	125	−0.55	
		135	−0.38(σ^+)[a)]	
		45	−0.32(σ^+)[b)]	0.973
	Freon-113	45	−0.35(σ^+)[b)]	0.989
-OCH_3	Chlorobenzene	130	−0.39	0.986
		45	−0.41[c)]	
-SCH_3	Chlorobenzene	130	−0.15	0.956
			−0.11(σ^+)	0.970
			−0.11(σ+0.75 $\Delta\sigma_R^+$)	0.986
-$N(CH_3)_2$	Chlorobenzene	130	−0.42	0.981
-SO_2CH_3	Chlorobenzene	130	−0.2	—

a) T. Yamamoto, M. Hasegawa and T. Nakamura, see Ref. 22.
b) H. Sakurai and A. Hosomi, *J. Am. Chem. Soc.*, **89**, 458 (1967).
c) H. Sakurai and A. Hosomi, *Conference on Org. Reaction Mechanism, Kyoto* (1067). Di-*t*-butyl peroxalate was used.
d) Correlation coefficient.

tive effects of these substituents, if one carefully examines the data in Table 2, which includes other reported data on methyl[13] and phenyl[14] groups. This fact suggests that all the substituents including methyl, phenyl, phenoxyl and phenylmercapto groups when they are substituted additionally at α-position give some additional stabilization to the incipiently developing radicals by the conjugative effect of the respective groups.

Hamett Relationship. The relative reactivities found for these substituted anisole, thioanisole, *N,N*-dimethylaniline, and phenyl methyl sulfone derivatives are treated with the Hammett equation. The results are shown in Figs. 3 and 4, and Tables 3 and 4, while the Hammett ρ values of these reactions are listed in Table 4. Table 4 shows that the logarithms of the relative rates of the substituted anisoles and *N,N*-dimethylanilines can be satisfactorily correlated with normal Hammett σ values with ρ values of -0.39 and -0.42 respectively and the sulfones also give σ correlation with $\rho=-0.2$ although reproducibility of k_a/k_d values is by no means excellent for the sulfonyl compounds. The substituted thioanisoles show somewhat different pattern of substituent effect. While *p*-CN, *p*-Cl, *m*-Cl, H and *p*-CH_3 groups are well correlated with σ values, *p*-CH_3O and *p*-PhO groups give slight deviations from the linearity of correlation line with the value of $\rho=-0.15$ and the correlation coefficient of 0.956. Yukawa-Tsuno's treatment[15] gave the best line with $r=0.75$, to give an equation $\log k/k_0=-0.11(\sigma+0.75\,\Delta\sigma_R^+)$ with correlation coefficient of 0.986, while Brown-Okamoto's σ^+[16] correlation gave $\rho=-0.11$, correlation coefficient of 0.970. Yamamoto's treatment[17] of E_R value also gave a relatively good correlation with $\rho=-0.12$, and the correlation coefficient of 0.980, but methoxyl group falls off substantiallyl.

We used Yukawa-Tsuno'st reatment because of the following reasons. 1) calculated r value, which is a rough measure of resonance contribution[17] is very small, namely, 0.1, in this free radical reaction of hydrogen abstraction of thioanisole when one compares the value with those observed in many other examples.[18] 2) The carbon atom of the reacting center is considered to bear a partial positive charge in the transition state because the hydrogen abstracting agent in this reacton is *t*-butoxyl radical. 3) The trend of the α-substituent effects in this hydrogen abstraction reaction is similar to that found in the solvolyses of α-substituted methyl chlorides, but not to that in the carbanion-forming reactions as seen in Table 5. 4) The kinetic isotope effect of the reaction measured with both α-deuterated and undeuterated thioanisoles, *i.e.* 3.2 at 130℃, which is considered to be a relatively large as compared to the others[19] listed in Table 6, indicates that C–H bond of thioanisole

TABLE 5. COMPARISON OF THE EFFECT OF SULFUR SUBSTITUENTS TO CARBANION, RADICAL AND CARBONIUM IONS ON α-CARBON ATOM

Substituent	$-X-\overset{\ominus}{C}-$ [a]	$-X-\dot{C}-$ [b]	$-X-\overset{\oplus}{C}-$ [c]
C_2H_5S-	1.0	1.0	1.0
-S-	10^3	0.6	0.005
-SO_2-	$>10^5$	0.02	no reaction

a) Base catalyzed decarboxylations of α-substituted carboxylic acids. S. Oae, W. Tagaki, K. Uneyama and I. Minamida, *Tetrahedron*, in press.

b) Hydrogen abstraction by *t*-butoxyl radical in this work.

c) Solvolysis reaction of α-substituted methyl chlorides (X-CH_2Cl). H. Böhme, H.Fischer and R. Frank, *Ann.*, **563**, 54 (1949).

TABLE 6. KINETIC ISOTOPE EFFECT.

Substrate	k_H/k_D	Solvent	Radical	Temp. ℃
-SCH_3 [a]	3.2	PhCl	*t*-BuO·	130
-CH_2CH_3 [b]	3.7	PhCl	*t*-BuO·	120
-CH_3 [c]	2.4	Freon-113	*t*-BuO·	45

a) Hydrogen of methyl group was 33% of deuterium content.
$k_H=0.200$, $k_{obs}=0.153$, hence, k_D calcd$=0.062$, see experimental.

b) G. A. Russell, *J. Am. Chem. Soc.*, **79**, 3871 (1957).

c) H. Sakurai, *Symposium on Hammett Relationship, Kyoto*, (1967).

13) C.Walling and W.Thaler, *J. Am. Chem. Soc.*, **85**, 3754 (1963).

15) C. Walling and B.B. Jacknow, *ibid*, **82**, 6108 (1960) ; J. H. Brooks, *Trans. Faraday Soc.*, **53**, 327 (1957).

15) Y. Yukawa and Y.Tsuno, This Bulletin, **32**, 960, 965, 971 (1959).

16) H.C. Brown and Y. Okamoto, *J. Am. Chem. Soc.*, **79**, 1913 (1957); Y. Okamoto and H. C. Brown, *J. Org. Chem.*, **22**, 485 (1957).

17) T.Azumi and T.Yamamoto, *Reports of Himeji Institute of Techn.*, **11**, 152 (1960); T. Otsu and T. Yamamoto, *Yuki Gosei Kagaku Kyokaishi* (*J. Soc. Org. Synth. Chem. Japan*), **23**, 643 (1965).

18) See T. Yamamoto, his Ph. D. works in Osaka City Univ. (1966), in which various Hammett relation of radical reactions are summarized.

19) G. A. Russell, **79**, 3871 *J. Am. Chem. Soc.*, (1957).

is broken at the transition state sufficiently enough to receive a noticeable assistance of the conjugative effect of the ring substituents *via* the divalent sulfur atom.

Therefore, electron-releasing conjugative effect of substituent must be responsible. Alkoxyl, mercapto and amino groups are known to be markedly electron-releasing in the electron-donating reactions, and the order of the effect is the following, $R_2N- \gg R-O- > R-S- > Ph- \gg PhSO_2-$.*2 This order of electron-releasing effect can explain the sequence of the relative reactivities of the heteroatom-substituted compounds. This is quite understandable in view of the fact that *t*-butoxyl radical is highly electronegative and the transition state of this hydrogen abstraction reaction would be of somewhat polar nature as was postulated previously by Russell in the similar hydrogen abstraction reaction with phenyl radical. The slightly larger reactivity of thioanisole as compared with anisole may be due to the stronger inductive effect of phenoxyl group than that of phenylmercapto group and/or a possible electron-releasing effect from aryl group additionally transmitted to the reaction center through the divalent sulfur atom. Russell *et al.* also reported that thioanisole is three times as reactive as anisole in hydrogen abstraction by phenyl radical. Taking into account the less electronegativity of phenyl radical and the larger kinetic isotope effect (k_H/k_D), (which means the greater bond breaking in the transition state) than that with *t*-butoxy radical, this rather large rate difference is considered to be due to the greater stabilization of thiophenylmethyl radical ($PhSCH_2\cdot$) by the electron-sharing conjugation. Such an effect which we call electron-sharing conjugation is not conceivable in the case of anisole because of the lack of available 3d-orbitals. Though the effect is small, this conjugative effect by divalent sulfur atom is playing a definite role in the reaction of thioanisole derivatives as will be discussed.

In the previous paragraph it was shown that both anisole*3 and *N,N*-dimethylaniline give good correlations with Hammett σ constants. This successful σ-correlation for both substituted anisoles and *N,N*-dimethylanilines indicates that electron-releasing π-inductive effects of these *p*-substituents like *p*-methoxyl and *p*-phenoxyl groups are transmitted inductively to the terminal carbon atom through the chain as illustrated by (B).

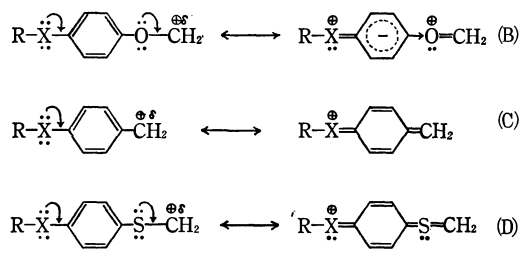

Meanwhile, thioanisole derivatives apparently display an additional conjugative effect of substituents and its Hammett relationship is described in Eq. (7),

$$\log k/k_0 = -0.11\ (\sigma + 0.75\Delta\sigma_R^+) \qquad (7)$$

although the degree of the additional conjugative effect is somewhat smaller ($r=0.75$) than benzyl radical ($r=1.0$), in which σ^+ plot is known to give a satisfactory correlation.[22] The successful σ^+ correlation suggests that a direct conjugative interaction between the reacting carbon center and the substituents is operative and such a conjugation is possible only through the 3d-orbital resonance of divalent sulfur atom shown by (D). Sulfonyl group, having no electron pair available for such a conjugation retards the rate of hydrogen abstraction by *t*-butoxyl radical and σ correlation gives a better fit than σ^+ correlation for the rates of substituted sulfonyl compounds.

As a final remark, we may conclude that the rate enhancement by α-heteroatoms in this reaction is mainly due to the electron-releasing conjugative effect and both substituted anisoles and *N,N*-dimethylanilines give good Hammett σ correlations, while in the

*2 ($\sigma_p^+ - \sigma_m^+$) values of $(CH_3)_2N$, CH_3O, CH_3S, C_6H_5, and CH_3SO_2- are -1.49, -0.83, (-0.75 for Ph-O), -0.76, -0.29 and 0.12 respectively from H. C. Brown and Y. Okamoto, *J. Am. Chem. Soc.*, **80**, 4979 (1958) ; H.H. Jaffe, *Chem. Revs.*, **53**, 222 (1953). σ_m^+s of phenyl, *N,N*-dimethyl and phenoxy are not available, hence σ_m values were used for σ_m^+. σ^+ of sulfonyl group is not available, therefore ($\sigma_p - \sigma_m$) was used instead of $\sigma_p^+ - \sigma_m^+$. This treatment is reasonable when one recalls the similarity of σ_p^+ values with σ_p values of electron-withdrawing group.

*3 Sakurai and Hosomi reported also $\rho = -0.41$ in the hydrogen abstraction of substituted anisoles by *t*-butoxyl radical at 45°C[20] ,and the thermal decomposition of ring substituted *t*-butyl perphenoxyacetate in ethylbenzene is known to give σ correlation with ρ value of -1.18.[21]

20) H.Sakurai an A.Hosomi, *Conference on Org. Reaction Mechanism, Kyoto, Japan* (1967).

21) C. Ruchardt, H. Bock and I. Ruthardt, *Ang. Chem.*, **78**, 268 (1966).

22) H.Sakurai and A.Hosomi, *J. Am. Chem. Soc.*, **89**, 458 (1967); T. Yamamoto, M. Hasegawa and T. Nakamura, *Anual Meeting of the Chem. Soc., Japan, Chugoku-Shikoku Area Meeting* (1965).

case of substituted thioanisoles, an additional conjugative effect of substituents such as *p*-methoxyl and *p*-phenoxyl group, appears to be transmitted *via* sulfur atom perhaps using 3d-orbitals of divalent sulfur atom and the rates are correlated better with σ^+ values. More clear evidence of electron-sharing conjugation of divalent sulfur atom may be obtained in the hydrogen abstraction reaction with more neutral phenyl radical and the work on this line is in progress in these laboratories.

Experimental

Preparations of Materials. *Substituted Anisoles.* *p*-Chloro-, *m*-chloro-, *p*-methoxy- and *m*-methoxyanisoles were synthesized by methylation of the corresponding phenols with dimethyl sulfate in alkaline methanol solution. *p*-Cyanoanisole was prepared by Sandmeyer reaction of diazonium salt of *p*-anisidine.

Substituted Thioanisoles. The methylation of thiophenol, *p*-chloro- and *p*-methylthiopheno land *p*-methylmercaptophenol by dimethyl sulfate gave the corresponding thioanisole derivatives in good yields. *p*-Methylmercaptobenzonitrile was prepared from Sandmeyer reaction of *p*-methylmercaptoaniline in 23% yield and recrystallized from methanol as colorless crystals melting at 63—64°C. *p*-Methylmercaptoaniline was obtained by the usual methylation of *p*-aminothiophenol, which was prepared by the treatment of *p*-chloronitrobenzene with sodium sulfide nonanhydrate as described by Gilman.[23] *m*-Chlorothioanisole was prepared by allowing to react sodium methylmercaptide with diazonium salt of *m*-chloroaniline in an aqueous alkaline solution.[24] *p*-Methylmercaptophenyl phenyl ether was prepared by heating the mixture of *p*-methylmercaptophenol[25] and bromobenzene in a concentrated aqueous potassium hydroxide solution in the presence of a small amount of copper powder at 150°C as described by Brewster.[26]

Preparation of Substituted N,N-Dimethylaniline Derivatives. *p*-Dimethylaminobenzonitrile was prepared by Sandmeyer reaction of *p*-amino-*N,N*-dimethylaniline and purified by recrystallization from methanol as colorless crystals melting at 73—74°C. 4-*N,N*-dimethylaminodiphenyl ether was prepared by methylation of 4-aminodiphenyl ether with dimethyl sulfate in aqueous $NaHCO_3$ solution as described by Evans[27]. 4-Aminodiphenyl ether was prepared by the reduction of 4-nitrodiphenyl ether with zinc dust as described by Suter.[28] 4-Chloro-*N,N*-dimethylaniline and 3-chloro-*N,N*-dimethylaniline were prepared by the usual methylation of *p*-chloro- and *m*-chloroanilines with dimethyl sulfate in dioxane. Distillation gave crude products, which were then purified through an alumina column chromatography with *n*-hexane in order to remove trace amount of secondary and primary amines and finally distilled. *N,N,N',N'*-tetramethyl-*p*-phenylenediamine was prepared as follows.[29] A mixture of 8 g of hydrochloric acid and 8 g of methanol was placed in a sealed tube and heated at 180—200°C for 3 hr. After breaking the tube, the reaction mixture was poured into a sufficient amount of 10% aqueous sodium hydroxide solution to afford a precipitate, which was then filtered and washed several times with water, dried and finally recrystallized from *n*-hexane. Mp 49—50. Yield 50%.

Substituted Phenyl Methyl Sulfones. *p*-Chloro-, *m*-chloro-, *p*-phenoxyphenyl methyl sulfones and unsubstituted phenyl methyl sulfone were prepared by the oxidation of the corresponding sulfides with an execess amount of hydrogen peroxide in acetic acid and recrystallized twice from benzene-*n*-hexane.

Other α-Substituted Compounds. Ethanedithioformal, diethylthioformal, diphenylthioformal and diphenylformal were prepared by the substitution reaction of methylene chloride with corresponding sodium mercaptides and phenoxide in ethanol. After the usual work-up, ethanedithioformal, diethylthioformal, and diphenylformal were distilled under reduced pressure through an efficient column. Diphenylthioformal was recrystallized from petroleum ether. Tris(phenylmercapto) methane was prepared by the substitution reaction of ethyl orthoformate with thiophenol in benzene using boron trifluoride as a catalyst and recrystallized from methanol to give colorless crystals melting at 39—40 °C.

Di-t-butyl peroxide. Di-*t*-butyl peroxide was prepared by Milas and Surgenor's method.[30] This peroxide was distilled to give distillate boiling at 109—110 °C. No detectable amount of *t*-butyl hydroperoxide was found to be contained from the IR and NMR spectra.

Elemental analysis. Found: C, 65.35; H, 12.30%. Calcd: C, 65.70, H, 12.40%.

Deuterated Thioanisole. Thioanisole 2.0 g (*ca.* 0.016 mol) was poured into 12.5 g (*ca.* 0.12 mol) of *t*-BuOD (70% deuterated) containing 0.6 g (*ca.* 0.012 mol) of metal potassium and the mixture was sealed into an ampoule *in vacuo*, which was kept at 90°C for 48 hr. The usual work-up gave 1.8 g of 33% deuterated thioanisole by NMR measurement.

Chlorobenzene. Chlorobezene used for solvent was purified by washing commercial grade of chlorobenzene with concentrated sulfuric acid, and then distillation over phosphorus pentoxide. The distillate was distilled again through an efficient column. Bp 130.5—131.0°C. Purities of all the substrates used in this experiment were carefully checked by IR, NMR, Gas chromatography and elemental analyses. Properties of all these compounds used

23) H. Gilmann and G. C. Gainer, *J. Am. Chem. Soc.*, **71**, 1749 (1949).

24) E. Miller, F.S.Crossley and M.L.Moore, *ibid.*, **64**, 2322 (1942).

25) E. Goethals and P. de Radgitzky, *Bull. Soc. Chem. Belges.*, **73**, 546 (1964).

26) R.Q.Brewster and T.Groening, "Org. Syntheses," Coll. Vol. II, p. 445 (1943).

27) D.P. Evans and R. Williano, *J. Chem. Soc.*, **1939**, 1199.

28) C.M.Suter, *J. Am. Chem. Soc.*, **51**, 2581 (1929).

29) C. Wurster, *Ber.*, **12**, 526 (1879).

30) N.A. Milas and D.M. Surgenor, *J. Am. Chem. Soc.*, **68**, 205, 643 (1946).

TABLE 7. THE MELTING AND BOILING POINTS, ELEMENTAL ANALYSES AND CHEM. SHIFT OF α-PROTON OF SUBSTRATES USED IN THIS EXPERIMENT

Compound	Bp °C/mmHg (mp °C)	Elemental analysis Found (C, H)	Calcd (C, H)	Chem. shift[a] (ppm)
X-C$_6$H$_4$-OCH$_3$				
X = H	155—155.5			
p-Cl	98.5—98.7/30			3.73
m-Cl	114.5—115/65			
p-CH_3O	(78—79)			
m-CH_3O	91.5—92.5/12			
p-CN	(59—60)	72.00, 5.13	72.16, 5.30	
X-C$_6$H$_4$-SCH$_3$				
H	93.2—93.5/31.5			2.42
p-Cl	94.4/2			
m-Cl	90.5—91/1.5			
p-CH_3O	132/24			
p-CH_3	110/29			
p-PhO	172—173/2			
p-CN	(63—64)	64.53, 4.65	64.39, 4.73	
X-C$_6$H$_4$-N(CH$_3$)$_2$				
H	100—1.005/40			2.88
p-Cl	85/5(32)			2.88
m-Cl	76/1.5			2.89
p-PhO	152—153/5	79.16, 7.22	78.84, 7.09	2.89
p-N(CH$_3$)$_2$	(49—50	73.35, 9.84	73.12, 9.82	2.79
p-CN	(73—74)	74.13, 6.99	73.94, 6.90	3.01
X-C$_6$H$_4$-SO_2CH_3				
H	(88.5—89.2)			2.94
p-Cl	(96—97)			2.95
m-Cl	(108—109.5)			2.96
p-PhO	(85—86)			2.92
C$_6$H$_5$-CH_3	110.3—110.7			2.33
(C$_6$H$_5$-S)$_2CH_2$	(36—37)			4.24
(C$_6$H$_5$-S)$_3$CH	(39.4—39.8)	67.09, 4.70	67.01, 4.74	5.30
(C$_6$H$_5$-O)$_2CH_2$	121—122/1.6			5.67
$C_2H_5SC_2H_5$	91.3—91.5			
$(C_2H_5S)_2CH_2$	96.0—96.5/45	43.62, 8.54	44.12, 8.82	3.70
$CH_2(S)CH_2$ $CH_2(S)$	8.5—86/53	33.65, 5.63	33.96, 5.66	3.89

a) In 10% CCl_4, TMS was used as an internal standard.

for kinetics are listed in Table 7.

Kinetic Procedure. Each sample substrate was weighed in a 5 m*l* volumetric flask and diluted with chlorobenzene to make the total volume of the solution exactly 5 m*l*. The solution, 2 m*l* was pipetted out into a glass tube (*ca.* 10 m*l* volume), into which 2 m*l* of 0.214 M of di-*t*-butyl peroxide-chlorobenzene solution was pipetted to make the total volume of 4 m*l*. The tube was cooled with dry ice-acetone, evacuated three times and sealed. The tubes were set in a paraffin bath kept at 130 ±0.5°C for 42 hr.

The cooled tube was opened, into which 1 m*l* of toluene solution containing 0.74 mmol of benzene

per 1 m*l* was added for the internal standard of gas chromatography. The mixture in the tube was placed in a distilling flask and distilled. The distillate below 130°C was collected and the amounts of acetone and *t*-butanol were analyzed by gas chromatography using PEG 6000 4 m column at 81°C using hydrogen as a carrier gas. From the relative areas of two peaks, the moles of acetone and *t*-butanol produced in the reaction were calculated using the calibration line.

Values of k_a/k_d were calculated by Eq. (6).

BULLETIN OF THE CHEMICAL SOCIETY OF JAPAN VOL. 41 1937—1939 (1968)

Macrocyclic Dilactone. II. The General Synthesis of Macrocyclic Dilactone

Noboru SUGIYAMA, Hiroaki MARUYAMA,
Taketoshi GASHA and Choji KASHIMA

Department of Chemistry, Tokyo Kyoiku University, Otsuka, Tokyo

(Received February 19, 1968)

One previous papar reported the synthesis of 7-hydroxyoctanoic acid dilactone through the dimeric ester. This paper will describe how the dilactone of 12-hydroxystearic acid is synthesized by this method. The dilactone from two kinds of hydroxy alkanoic acid, 7-hydroxyoctanoic acid and 12-hydroxystearic acid, is also otained. From these results, it seems that this new method can be of general use in the synthesis of various kinds of dilactones.

Previously, the present authors reported on the preparation of the dilactone of 7-hydroxyoctanoic acid by two methods, the pyrolytic depolymerization of the polyester and the cyclization of the dimeric ester.[1] The latter method was found to be superior for the synthesis of 7-hydroxyoctanoic acid dilactone (I).

This paper will describe the synthesis of dilactone from 12-hydroxystearic acid (III), which can cyclize to a thirteen-membered monolactones from 12-hydroxystearic acid (III).

As a result of the action of thionyl bromide, III gave 12-bromostearoyl bromide (IV), which was then treated with the original acid III to produce the dimeric ester, 1′-carboxy-11′-heptadecyl 12-bromostearate (V). The infrared absorption spectrum of V showed absorption bands at 1730 and 1180 cm^{-1} of the ester carbonyl group. The NMR spectrum of V is shown in Table 1. These spectral data and the molecular weight measurment support the structure of V. By means of the high-dilution method in methyl ethyl ketone,[2] V

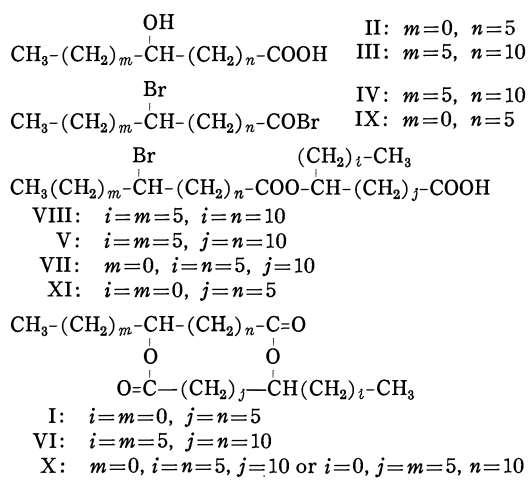

was cyclized to 12-hydroxystearic acid dilactone, 1,14-dioxa-2,15-dioxo-13,26-dihexylcyclohexacosane (VI). The structre of VI was comfirmed as follows. The infrared absorption spectrum showed the ester carbonyl bands at 1730 and 1180 cm^{-1}, and no absorption in the region of carboxyl bands. The NMR spectrum, listed in Table 2, showed the multiplet at τ 5.16 of the methine protons at C-13 and C-26, the triplet at τ 7.79 of the methylene protones

1) N. Sugiyama, T. Gasha and C. Kashima, This Bulletin, **40**, 2713 (1967).

2) J. Plesek, *Collection Czech. Chem. Commun.*, **22**, 49 (1957).

TABLE 1. THE NMR SPECTRAL DATA OF V, VII, VIII AND XI (τ)

	V	VII	VIII	XI
Carboxyl	−0.05	1.50	−0.43	0.05
Methine (CH-O)	5.21	5.40	5.21	5.18
Methine (CH-Br)	5.91	6.02	6.00	6.57
Methylene (CH_2-C=O)	7.78	7.75	7.80	7.78
Methylene (CH_2-CBr)	8.10	8.34	8.10	—*
Methyl (CH_3CBr)	—	8.30	—	8.29
Methyl (CH_3-C-O)	—	—	8.85	8.83
Methyl (CH_3-CH_2)	9.11	9.12	9.09	—
Other methylenes	8.72	8.71	8.68	8.56

* The methylene (CH_2-CBr) signal was indistinguishable from the multiplet of other methylenes.

TABLE 2. THE IR AND THE NMR SPECTRAL DATA OF I, VII, AND X

	I	VI	X
$\nu_{C=H}$	1730	1730	1730
τ_{CH} (CH-O)	5.24	5.16	5.21
τ_{CH_2} (CH_2-C=O)	7.83	7.79	7.79
τ_{CH_3} (CH_3-C-O)	8.85	—	8.86
τ_{CH_3} (CH_3-CH_2)	—	9.12	9.14
τ_{CH_2} (other methylenes)	8.62	8.73	8.73

at C-3 and C-16, the triplet at τ 9.21 of the methyl protons, and multiplet centered at τ 8.73 of the methylene protons. The molecular weights and the results of the elemental analysis supported the structure of VI.

Using this new method, it is effected that a dilactone can be obtained from two kinds of hydroxy alkanoic acids. The dilactone which is formed from two kinds of hydroxy carboxylic acids can be called a mixed dilactone. The preparation of a mixed dilactone has not been found described in the literature except for the heating a miture of two kinds of acids; by this method the corresponding dilactone can not be selectively obtained. The present authors succeded in synthesizing the dilactone selectively from two kinds of acids, II and III. Since two kinds of ester are expected as the intermediates in the synthesis of the mixed dilactone, two synthetic routes were examined for obtaining the mixed dilactone from II and III. One route was the cyclization of 1′-carboxy-11′-heptadecyl 7-bromooctanoate (VII), and the other, that of 1′-carboxy-6′-heptyl 12-bromostearate (VIII).

The dimeric ester VII was obtained from 7-bromooctanoyl bromide (IX) by treatment with III. The structure of VII was confirmed as follows. The infrared absorption spectrum was similar to that of V; the NMR srectrum was as shown in Table 1. The molecular weight measurements and the elemental analysis supported the structure of VII. Similarly, the dimeric ester VIII was obtained from 12-bromostearoyl bromide (IV) by treatment of 7-hydroxyoctanoic acid (II). The infrared absorption spectrum was similar to that of VII, while the NMR spectrum was as listed in Table 1. The spectral data, the molecula weight measurements, and the elemental analysis showed the structure of the dimeric ester VIII.

By the high-dilution method,[2] VII was cyclized in the presence of potassium carbonate. The infrared absorption spectrum of this cyclized product showed ester carbonyl bands at 1730 and 1180 cm^{-1}, and no band characteristic of the carboxyl group. The NMR spectrum, listed in Table 2, showed the multiplet at τ 5.21 assigned to methine protons, the triplet at τ 7.79 of methylene protons, and the signals at τ 8.86 and 9.14 of methyl protons, while other protons appeared at τ 8.73 as a multiplet. The spectral data, the molecular weight measurements, and the elemental analysis confirmed this cyclized product to be the mixed dilactone, 1,14-dioxa-2,15-dioxo-13-hexyl-21-methylcycloheneicosane (X). Under the same conditions, catalyzed by potassium carbonate, VIII was cyclized, and the cyclized product was identified with X by the spectral data and by the R_f value on silicagel thin-layer chromatograpy.

In conclusion, these results suggest that the new synthetic method is generally applicable to the preparation of the dilactone from hydroxy alkanoic acids. Moreover, the mixed dilactones can be obtained from two different kinds of hydroxy alkanoic acids by this methods.

Experimental

1′-Carboxy-11′-heptadecyl 12-bromostearate (V). A mixture of 10 g of III and 10 m*l* of thionyl bromide in 100 m*l* of dry chloroform was refluxed for 3 hr with stirring. After the removal of the solvent and the excess thionyl bromide, the residue was dissolved in 100 m*l* of dry benzene, and then 9 g of III was added. The mixture was refluxed for 4 hr with stirring, and then washed with water and dried over anhydrous sodium sulfate. After the evaporation of the solvent, the residue, which showed three spots on silica-gel thin-layer chromatography, was passed through a silica-gel (Merck 7734) column with a benzene - chloroform (7 : 3 v/v) mixture. When the second fraction was then collected, 8.5 g of V were obtained, mp 55°C.

Found: C, 66.95; H, 10.68%; mol wt (titration), 625. Calcd for $C_{36}H_6O_4Br$: C, 66.93; H, 10.79%; mol wt, 645.97. IR (liquid film): 3500—2400, 1730,

1710, 1180 and 970 cm^{-1}.

1,14-Dioxa-2,15-dioxo-13,26-dihexylcyclohexacosane (VI). Over a 28 hr-period, a solution of 2.5 g of V in 50 m*l* of methyl ethyl ketone was added, through a reflux condenser, to 600 m*l* of methyl ethyl ketone containing 15 g of anhydrous potassium carbonate under vigorous stirring and refluxing. After the additon of V, the stirring and refluxing were continued for 8 more hours. The reaction mixture was concentrated after the removal of potassium carbonate, and the residue was dissolved in ether. The ethereal solution was washed with water and dried over anhydrous sodium sulfate. The solvent was removed, and the residue was passed through a silica-gel (Merck 7729) column with a benzene-ethyl acetate (4 : 1 v/v) mixture. The first fraction was then collected, and the solvent was removed. The first fraction was then collected, and the solvent was removed. The residue was chromatographed on an alumina (Wako alumina) column with a benzene-ethyl acetate (20 : 1 v/v) mixture. A fraction which showed a R_f value of 0.60 on silica-gel (Wakogel B-5) thin-layer chromatograph with a benzene-ethyl acetate (10 : 1 v/v) mixture was then collected; yield 1 g.

Found: C, 76.92; H, 12.27%; mol wt (Rast), 619. Calcd for $C_{36}H_{68}O_4$: C, 76.54; H, 12.13%; mol wt, 564.90. IR (liquid film): 2940, 2860, 1730, 1460, 1180 and 1110 cm^{-1}.

1'-Carboxy-11'-heptadecyl 7-Bromooctanoate (VII). A mixture of 4 g of II and 6 m*l* of thionyl bromide in 100 m*l* of dry benzene was refluxed for 3.5 hr with stirring. After the removal of the solvent and the excess thionyl bromide, the residue was distilled under reduced pressure, bp 146—150°C/10 mmHg, 2.1 g of IX were thus obtained. IR (liquid film): 2940, 2860, 1800, 1460 and 970 cm^{-1}. The mixture of 2.1 g IX and 3 g of III in 50 m*l* of dry chloroform was refluxed for 3 hr with stirring. The reaction mixture was then treated by the same procedure as V. Four grams of VII were then obtained by recrystallization from chloroform; mp 65°C.

Found: C, 61.84; H, 9.88%; mol wt (titration), 494. Calcd for $C_{26}H_{49}O_4Br$: C, 61.81; H, 9.72%; mol wt, 505.67. IR (liquid film): 3500—2400, 1730, 1710, 1470, 1190 and 970 cm^{-1}.

1'-Carboxy-6'-heptyl 12-Bromostearate (VIII). 12-Bromostearoyl bromide, which had been obtained from 10 g of III and 10 m*l* of thionyl bromide, was added to a solution of 3.5 g of II in 100 m*l* of dry benzene, after which the mixture was refluxed for 4.5 hr with stirring. The reaction mixture was then treated by the same procedure as were V and VII; 1.5 g of VIII were thus obtained.

Found: C, 61.59; H, 10.14%; mol wt (titration), 594. Calcd for $C_{26}H_{49}O_4Br$: C, 61.81; H, 9.72%; mol wt, 505.67. IR (liquid film): 3500—2400, 1730, 1710, 1460, 1180 and 970 cm^{-1}.

1,14-Dioxa-2,15-dioxo-13-hexyl-21-methylcycloheneicosane (X). For 20 hr, a solution of 1 g of VII in 50 m*l* of methyl ethyl ketone was slowly added, under vigorous stirring and refluxing, through a reflux condenser to 600 m*l* of methyl ethyl ketone containing 15 g of anhydrous potassium carbonate. After continuous stirring and refluxing for 4 hr, the reaction mixture was treated by the same procedure as VI. The yield of X was 0.5 g; the R_f value on silica-gel (Wokogel B-5) thin-layer chromatography with a benzene-ethyl acetate (10 : 1 v/v) mixture was 0.53.

Found: C, 72.68; H, 11.19%; mol wt (Rast), 422. Calcd for $C_{26}H_{48}O_4$: C, 73.53; H, 11.39%; mol wt, 424.64. IR (liquid film); 2940, 1730, 1460, 1180 and 1110 cm^{-1}.

X was also obtained by the cyclization of VIII by the same procedure; it was identified by means of the infrared absorption, the NMR spectra, and the R_f value of thin-layer chromatography.

NMR Spectra. The NMR spectra were measured on a Hitachi H-60 High resolution Nuclear Magnetic Resonance Spectrometer. The solvent was carbon tetrachloride, while tetramethylsilane was used as the internal standard.

BULLETIN OF THE CHEMICAL SOCIETY OF JAPAN VOL. 41 1940—1944 (1968)

Anionic Copolymerization of Styrene and *trans*-Stilbene with *n*-Butyllithium

Heimei YUKI, Masahiko KATO and Yoshio OKAMOTO

Department of Chemistry, Faculy of Engineering Science, Osaka University, Toyonaka, Osaka

(Received February 19, 1968)

The anionic copolymerization of styrene (M_1) and *trans*-stilbene (M_2) by *n*-butyllithium was investigated. *trans*-stilbene, which can not homopolymerized by itself, could be copolymerized with styrene in tetrahydrofuran and in benzene by an anionic catalyst. The copolymerization in tetrahydrofuran proceeded with a chain transfer to *trans*-stilbene, while that in benzene seemed to proceed without the chain transfer. The monomer reactivity ratio, r_1, was obtained from the copolymer composition at the complete consumption of M_1, assuming that the rate constant, k_{22}, is zero. The r_1 values were 2.3 in tetrahydrofuran at 0°C and 18 in benzene at 30°C. The color of the solution changed from red to purple in tetrahydrofuran, while in benzene no change occurred.

The present authors have found that, if a suitable combination of monomers is chosen, an alternating copolymer can be obtained by an anionic mechanism.[1] In the previous paper, an investigation of the anionic copolymerization of styrene (M_1) and 1,1-diphenylethylene (M_2) was reported in detail.[2] The copolymerization proceeded in a living system, and monomer reactivity ratios, r_1, were obtained as 0.2 in tetrahydrofuran(THF) at 30°C and as 0.4 in benzene at 30°C, assuming that a 1,1-diphenylethylene anion does not add to 1,1-diphenylethylene.

In this paper, a detailed study of the copolymerization of styrene (M_1) and *trans*-stilbene (M_2) will be described, and the results will be correlated with the results of the copolymerization of styrene and 1,1-diphenylethylene.

Experimental

Materials. *Styrene.* This was purified by the usual method and was distilled on a vacuum line from calcium hydride.

trans-Stilbene. The monomer synthesized from benzoin[3] was recrystallized from methanol and then twice from *n*-hexane.

Tetrahydrofuran (THF). The solvent, refluxed over metallic sodium and then over lithium aluminum hydride, was distilled onto sodium-potassium alloy and naphthalene. From the characteristic green solution, it was then distilled on a vacuum line to a reaction vessel.

Benzene. Benzene was purified by the standard method[4] and was stored over sodium. Before use, it was transferred to a flask containing *n*-butyllithium, and then it was distilled on a vacuum system to a reaction vessel.

n-Butyllithium (n-BuLi). According to the method of Ziegler,[5] *n*-BuLi was prepared in *n*-heptane and the concentration was determined by double titration.[6]

Polymerization. *trans*-Stilbene was first placed in a glass ampoule and dried *in vacuo*. Then, the solvent and styrene were transferred into the ampoule by vacuum distillation. The solution was immersed in a bath at a constant temperature, and *n*-BuLi was added under dry argon with a syringe. The reaction was terminated by adding methanol, after which the contents of the ampoule were poured into a large amount of methanol. The precipitated polymer was collected by filtration, washed with methanol, dried, and weighed. The mother liquor and the washings of the polymer precipitation were then combined and evaporated at reduced pressure, and the residual unchanged monomer and lithium compound were weighed.

Measurement. *Viscosity.* The viscosity of the polymer was measured in a benzene solution (C= 1.0 g/d*l*) at 30.0°C.

1) H. Yuki, K. Kosai, S. Murahashi and J. Hotta, *J. Polymer Sci.*, **B2**, 1121 (1964).

2) H. Yuki, J. Hotta, Y. Okamoto and S. Murahashi, This Bulletin, **40**, 2659 (1967).

3) R. L. Shriner and A. Berger, "Organic Syntheses," Coll. Vol. III, p. 786 (1955).

4) A. Weissberger, E. S. Proskauer, J. A. Riddick and E. E. Toops, Jr., "Organic Solvents," 2nd. Ed., Interscience Publishers, New York (1955).

5) K. Ziegler and H. Colonius, *Ann.*, **479**, 135 (1930).

6) H. Gilman and A. H. Haubein, *J. Am. Chem. Soc.*, **66**, 1515 (1944).

Electronic Spectrum. The spectrum of a living anion was measured in THF with a Cary 15 Spectrophotometer.

Results

Polymerization in THF. The copolymerization of styrene (M_1) and *trans*-stilbene (M_2) with *n*-BuLi was carried out in THF at 0°C, the initial molar ratio of styrene to *trans*-stilbene, $[M_1]_0/[M_2]_0$, being 1.0/1.5. The results are shown in Fig. 1. The reaction came instantaneously to an end, always giving a copolymer in a 68% yield against the total amount of monomers, regardless of the reaction time measured.

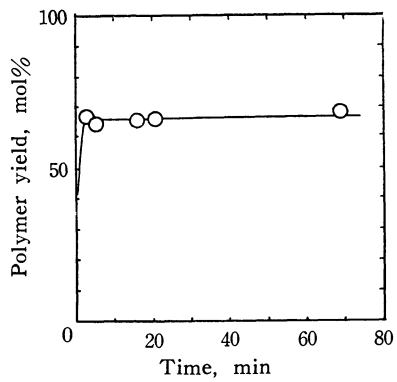

Fig. 1. Anionic copolymerization of styrene (M_1) and *trans*-stilbene (M_2) in THF.—Time *vs.* polymer yield.
$[M_1]_0+[M_2]_0$ 7.0 mmol, $[M_1]_0/[M_2]_0$ 1/1.5, THF 15 m*l*, Temp. 0°C, *n*-BuLi 5.8×10^{-2} mmol.

The copolymerization was carried out by varying the ratio, $[M_1]_0/[M_2]_0$, the total amounts of monomers, $[M_1]_0+[M_2]_0$, being kept constant. The results are summarized in Table 1. Attempts to determine the copolymer composition were made with elementary analysis, UV and NMR spectroscopies, but no satisfactory results were obtained because these monomers all have similar structures. On the other hand, the residues recovered from the mother liquor of polymer precipitates were solid and were found to be a mixture of lithium compounds, mainly carbonate, and unchanged *trans*-stilbene, which was identified by IR and UV spectroscopies. The sum of the amounts of the polymer and the unchanged monomer, $P+M_r$, just balanced the total amounts (weight) of the monomers, M_1+M_2, indicating the complete incorporation of the charged styrene into the copolymer. The amount of unchanged *trans*-stilbene was also determined by studying the UV spectrum of a part of the reaction mixture; it was found to be nearly equal to the value obtained by gravimetry. Thus, the copolymer composition can be determined from the polymer yield as $M_1/P-M_1$; this value is converted into the molar ratio of the monomers in the copolymer, $[m_1]/[m_2]$, in Table 1. Below, the composition of the copolymer is always calculated from the polymer yield on the assumption that the charged styrene is completely consumed by the copolymerization. We have found that the polymer yield and the $[m_1]/[m_2]$ ratio decrease with a decrease in the $[M_1]_0/[M_2]_0$ ratio.

The copolymerization at 0°C in THF was investigated by varying the ratio, $[M_1]_0/[M_2]_0$, while the amount of the M_1 monomer was kept constant. The results are listed in Table

TABLE 1. ANIONIC COPOLYMERIZATION OF STYRENE (M_1) AND *trans*-STILBENE (M_2) IN THF
$[M_1]_0+[M_2]_0$ 3.4 mmol, [*n*-BuLi] 5.7×10^{-2} mmol, THF 10 m*l*, temp. 0°C, time 40—60 min

Monomer, g		$[M_1]_0$	Polymer	Unchanged M_2		$[m_1]$
M_1	M_2	$[M_2]_0$ [a]	P, g	M_r, g [b]	M_r, g [c]	$[m_2]$ [d]
0.244	0.187	2.26	0.353	0.080	0.059	3.9
0.206	0.250	1.42	0.338	0.127	0.100	2.7
0.170	0.314	0.94	0.320	0.165	0.118	2.0
0.140	0.374	0.65	0.285	0.235	0.191	1.7

a) Initial molar ratio in monomer mixture.
b) Obtained by gravimetry. Weight (8 mg) of Li_2CO_3 was subtracted from the weight of residue obtained from mother liquor of polymer.
c) Estimated from UV spectrum.
d) Molar ratio of monomers in copolymer.

TABLE 2. ANIONIC COPOLYMERIZATION OF STYRENE (M_1) AND *trans*-STILBENE (M_2) IN THF
$[M_1]_0$ 3.47 mmol, THF 15 m*l*, [*n*-BuLi] 5.7×10^{-2} mmol, temp. 0°C, time 2.5 hr

$[M_2]_0$ mmol	$[M_1]_0/[M_2]_0$ [a]	Yield %	$[m_1]/[m_2]$ [b]	η_{sp}/c [c] dl/g	s.p. [d] °C
0.41	8.09	85.5	43	0.652	135
0.92	3.76	85.6	6.8	0.391	157
1.26	2.71	87.0	4.2	0.296	160
2.34	1.50	79.6	2.4	0.188	165
3.44	1.00	72.8	1.8	0.126	176
5.28	0.67	62.5	1.4	0.104	190
8.12	0.43	51.1	1.1	0.010	200

a) Initial molar ratio in monomer mixture.
b) Molar ratio of monomers in copolymer.
c) Benzene solution at 30.0°C.
d) Softening point of copolymer.

2. The polymer yield against the total amount of the monomers, the copolymer composition expressed in the $[m_1]/[m_2]$ ratio, and the viscosity of the polymer all decreased with an increase in the amount of M_2 in the monomers charged, while the softening point rose. The data in Table 2 suggest that a lower monomer composition, $[M_1]_0/[M_2]_0$, than 0.4 may give an essentially alternating copolymer of M_1 and M_2 monomers with a very low molecular weight.

If, in the copolymerization, the M_2 monomer can not add to the $\sim M_2^-$ anion, and if the M_1 comonomer is completely incorporated into the copolymer, the monomer reactivity ratio, r_1, can easily be obtained from the polymer yield by assuming that $k_{22}=0$ and $[M_1]=0$ in the Mayo-Lewis copolymer composition equation.[2] The copolymerization in THF at 0°C gave the value, $r_1=2.3$, as is show in Fig. 2, the plots in which were obtained from the data in Tables 1 and 2.

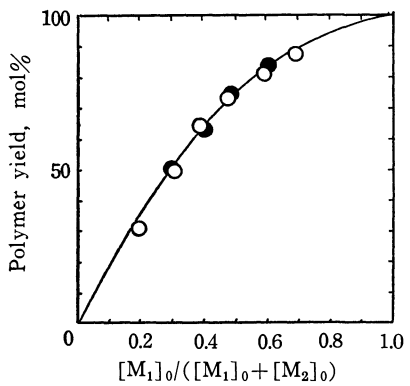

Fig. 2. Anionic copolymerization of styrene (M_1) and *trans*-stilbene (M_2) in THF.— Monomer reactivity ratio, r_1.
○: $[M_1]_0+[M_2]_0$ 3.4 mmol, THF 10 m*l*, Time 40—60 min
●: $[M_1]_0$ 3.47 mmol, THF 15 m*l*, Time 2.5 hr, *n*-BuLi 5.7×10^{-2} mmol, Temp. 0°C

Polymerization in Benzene. The reaction rate was investigated in the copolymerization in benzene with *n*-BuLi at 30°C; the molar ratio of the initial monomer concentrations, $[M_1]_0/[M_2]_0$, was 1.0/3.0. The results are shown in Fig. 3. The reaction proceeded slowly in comparison with that in THF, a constant yield (24%) being obtained after about 24 hr. It was confirmed that, in this case, styrene was also completely incorporated into the copolymer after a sufficient reaction time.

The effects of the initial molar ratio, $[M_1]_0/[M_2]_0$, on the copolymerizaton in

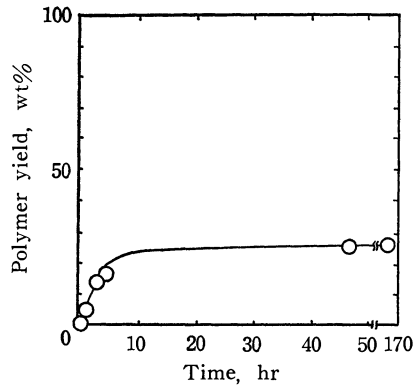

Fig. 3. Anionic copolymerization of styrene (M_1) and *trans*-stilbene (M_2) in benzene.— Time *vs.* polymer yield.
$[M_1]_0+[M_2]_0$ 14.8 mmol, $[M_1]_0/[M_2]_0$ 1.0/3.0, Benzene 20 m*l*, Temp. 30°C, *n*-BuLi 1.14×10^{-1} mmol.

TABLE 3. ANIONIC COPOLYMERIZATION OF STYRENE (M_1) AND *trans*-STILBENE (M_2) IN BENZENE

$[M_1]_0$ 3.4 mmol, benzene 15 m*l*, [*n*-BuLi] 1.14×10^{-1} mmol, temp. 30°C, time 90 hr

$[M_2]$ mmol	$[M_1]_0$[a] / $[M_2]_0$	Yield %	$[m_1]$[b] / $[m_2]$	η_{sp}/c[c] dl/g
0.38	9.00	85.1	99	0.095
0.87	4.00	75.1	19	0.099
1.49	1.90	63.7	13	0.105
2.33	1.44	54.5	9.0	0.093
3.51	0.96	45.2	6.7	0.145
5.26	0.64	36.9	4.9	0.132
7.13	0.47	31.4	3.8	0.101

a) Initial molar ratio in monomer mixture.
b) Molar ratio of monomers in copolymer.
c) Benzene solution at 30.0°C.

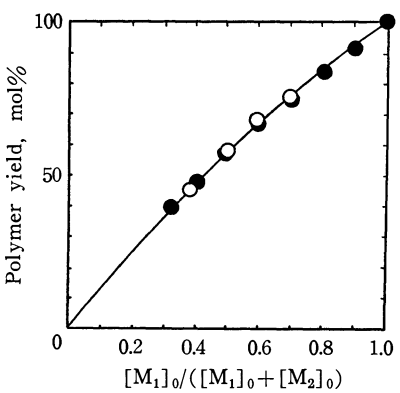

Fig. 4. Anionic copolymerization of styrene (M_1) and *trans*-stilbene (M_2) in benzene.— Monomer reactivity ratio, r_1.
○: $[M_1]_0+[M_2]_0$ 8.0 mmol, ●: $[M_1]_0$ 3.4 mmol, Benzene 15 m*l*, Cat. *n*-BuLi, Temp. 30°C, Time: ○ 40 hr, ● 90 hr.

benzene were investigated with a constant concentration of the M_1 monomer. The results are listed in Table 3. The relative reactivity of styrene against *trans*-stilbene was much greater in benzene than in THF. The solution viscosity of the polymer was constant regardless of $[M_1]_0/[M_2]_0$.

The monomer reactivity ratio, r_1, was calculated from the polymer yield as has been described above. As Fig. 4 shows, r_1 is 18 in the copolymerization in benzene at 30°C.

Electronic Spectrum of the Reaction Mixture. In the copolymerization of styrene and *trans*-stilbene by *n*-BuLi in THF, the red color gradually turned purple, even at 0°C. The change in the electronic spectra of the solution was followed; it is shown in Fig. 5. The red color of the solution diminished gradually and an absorption appeared at 555 mμ after about 30 min, by which time the copolymerization reaction had already finished. In the homopolymerization of styrene carried out under the same conditions, the red color of the reaction mixture did not change when it stood for a prolonged period. Therefore, this change in spectra may be attributed to the anion of *trans*-stilbene. The same spectral change was also observed in the reaction of *trans*-stilbene with *n*-BuLi in THF.[7] The purple solution initiated the polymerization of styrene to give a polymer quantitatively. On the other hand, in the copolymerization in benzene the orange color of the solution did not change in several hours, even at 30°C.

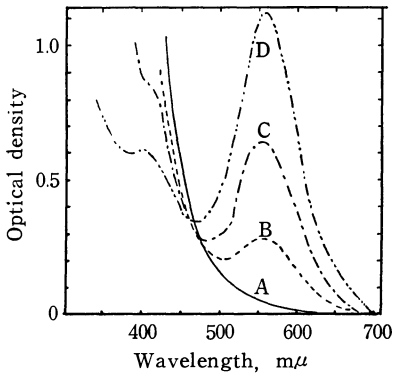

Fig. 5. Anionic copolymerization of styrene (M_1) and *trans*-stilbene (M_2) in THF.— Electronic spectra of reaction mixture.
$[M_1]_0+[M_2]_0$ 8.8 mmol, Cat. *n*-BuLi, Temp. 0°C, Time : A 20 min, B 33 min, C 1.6 hr, D 4.8 hr

7) H. Yuki, Y. Okamoto and M. Kato, This Bulletin, to be published.

Discussion

Reactivity of Monomers. The monomer reactivity ratios, r, in the copolymerization of styrene (M_1) and *trans*-stilbene (M_2) or 1,1-diphenylethylene (M_2)[2] with *n*-BuLi are summarized in Table 4. The r_1 values obtained in the copolymerization with 1,1-diphenylethylene were less than unity in THF and also in benzene, while the ratios in the copolymerization with *trans*-stilbene were more than unity in both the solvents. These results show that, in the following reactions, the order of the rate constants is $k_{12D}>k_{11}>k_{12S}$.

$$\sim CH_2-\underset{\underset{Ph}{|}}{CH^-}+CH_2=\underset{\underset{Ph}{|}}{CH} \xrightarrow{k_{11}} \sim CH_2-\underset{\underset{Ph}{|}}{CH^-} \qquad (1)$$

$$\sim CH_2-\underset{\underset{Ph}{|}}{CH^-}+CH_2=\underset{\underset{Ph}{|}}{\overset{\overset{Ph}{|}}{C}} \xrightarrow{k_{12D}} \sim CH_2-\underset{\underset{Ph}{|}}{\overset{\overset{Ph}{|}}{C^-}} \qquad (2)$$

$$\sim CH_2-\underset{\underset{Ph}{|}}{CH^-}+\underset{\underset{Ph}{|}}{\overset{\overset{Ph}{|}}{CH}}=CH \xrightarrow{k_{12S}} \sim \underset{\underset{Ph}{|}}{\overset{\overset{Ph}{|}}{CH}}-CH^- \qquad (3)$$

1,1-Diphenylethylene is the most reactive monomer to a styryl anion, for the monomer reacts with the anion to give a more stable anion conjugating with two benzene rings. On the other hand, *trans*-stilbene is the least reactive monomer because of its steric hindrance. The copolymerization of styrene and *trans*-stilbene in THF proceeded rapidly, while the copolymerization of styrene and 1,1-diphenylethylene proceeded so slowly that the reaction finished in 24 hr, even in THF at 0°C.[2] This may have been because the *trans*-stilbene anion produced in the reaction (3) has the same structure as the styryl anion, which is reactive enough to end instantaneously the homopolymerization of styrene, while the 1,1-diphenylethylene anion is very stable and has a big steric hindrance, therefore giving a very small k_{21}.

As Figs. 1 and 3 show, the overall rate of the copolymerization is greater in THF than in benzene. This may be becanse in THF a free ion plays a great part in the chain growth,[8] while in benzene living chain ends form ion pairs to associate themselves.[9] The

8) D.N. Bhattachayryya, C.L. Lee, J.Smid and M. Szwarc, *J. Phys. Chem.*, **69**, 612 (1965); H. Hostalka, R. V. Figini and G. V. Schulz, *Makromol. Chem.*, **71**, 198 (1964).

9) D. J. Worsfold and S. Bywater, *Can. J. Chem.*, **38**, 1891 (1960); M. Morton, L. J. Fetters and E. E. Bostick, *J. Polymer Sci.*, **C1**, 311 (1963).

TABLE 4. MONOMER REACTIVITY RATIO, r_1, IN ANIONIC COPOLYMERIZATION OF STYRENE (M_1) AND 1,1-DIPHENYLETHYLENE (M_2)[2] OR *trans*-STILBENE (M_2) WITH *n*-BULI

Monomer		r_1 value	
M_1	M_2	in THF	in Benzeen
Styrene	1,1-Diphenyl-ethylene	0.13[a]	0.71[a]
Styrene	*trans*-Stilbene	2.3[b]	18[a]

a) At 30°C. b) At 0°C.

$1/r_1$ value (k_{12}/k_{11}) is smaller in benzene than in THF, as is shown in Table 4; this suggests that the relative reactivity of a M_2 monomer toward a $\sim St^-Li^+$ ion pair is smaller than that toward a styryl free anion, when the reactivities of styrene toward its chain ends are taken as standards.

Chain Transfer and Electronic Spectrum of the Living Anion. The viscosity of the copolymer decreased with an increase in the *trans*-stilbene, as is shown in Table 2. This indicates that a chain transfer to the *trans*-stilbene occurred in THF. This transfer may proceed as follows:

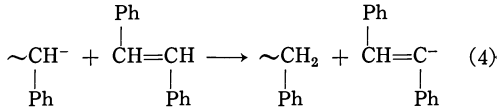

(4)

The production of the anion with a λ_{max} at 555 mμ may be connected with the chain transfer reaction shown by the process (4). On the other hand, the copolymerization in benzene (Table 3) seemed to proceed without the chain transfer, for no change in the red color of the reaction mixture was observed and the solution viscosity of the copolymer did not decrease with an increase in the *trans*-stilbene charged, although the exact molecular weight of the copolymer could not be determined.

BULLETIN OF THE CHEMICAL SOCIETY OF JAPAN VOL. 41 1945—1950 (1968)

Constituents of Fruit Oil from Japanese Pepper

Tsutomu SAKAI, Kazuo YOSHIHARA and Yoshio HIROSE

The Institute of Food Chemistry, Dojimanaka, Kita-ku, Osaka

(Received February 19, 1968)

The steam-volatile constituents from ripe fruits of Japanese pepper have been studied using column and gas chromatographic separations, followed by characterization on the basis of infrared, nuclear magnetic resonance, and mass spectrometry. The capillary gas chromatography of the volatile oil from ripe fruits of Japanese pepper revealed the presence of approximately 130 components. Among the components identified were the following: 19 hydrocarbons (α-pinene, camphene, β-pinene, sabinene, myrcene, α-phellandrene, limonene, β-phellandrene, *p*-cymene, terpinolene, α-copaene, β-caryophyllene, humulene, γ_2-cadinene, α-muurolene, δ-cadinene, γ-cadinene calamenene, and α-calacorene), 15 alcohols (linalool, isopulegol, *trans*- and *cis*-2,8-*p*-menthadien-1-ol, terpinen-4-ol, limonen-4-ol, α-terpineol, 1(7), 8-*p*-menthadien-*trans*-2-ol, citronellol, *trans*- and *cis*-carveol, geraniol, cuminalcohol, β-caryophyllene alcohol, and nerolidol), 9 aldehydes and ketones (citronellal, dihydrocarvone, cryptone, carvone, piperitone, phellandral, cuminaldehyde, perillaldehyde, and piperitenone), 7 esters (isobutyl isovarelate, isobutyl caproate, linalyl acetate, citronellyl acetate, terpinyl acetate, geranyl acetate, and methyl cinnamate), and 6 oxides (1,8-cineol, β-terpinen-3,4-oxide, *trans*- and *cis*-limonen-1,2-oxide, terpinolen-4,8-oxide, and methyl chavicol).

Japanese pepper (*Zanthoxylum piperitum* DC., in Japanese, "Sansho," and its variety *Z. piperitum var. inerme* Makino, "Asakura-sansho") is a popular spicy plant in our country. The young leaves and fruits of Japanese pepper, possessing a pleasant odor and a strong pungent taste, are widely used as spice.

The essential oil from fruits of Japanese pepper have been studied by several authors. Earlier work on the volatile oil has been reviewed by Guenther.[1] Later, Katayama[2] reported the identification of several terpenes on the basis of the R_f value on a chromatostrip. The compounds reported on hitherto were 1,8-cineol, limonene, β-phellandrene, terpinolene, citronellal, linalool, α-terpineol, citronellyl acetate, geraniol, geranyl acetate, and cuminalcohol.

This paper will present the results of our investigation of the volatile oil isolated from ripe fruits of "Asakura-sansho."

Experimental

Apparatus. *Gas Chromatography.* The components were separated on a Varian Aerograph Model 90-P. The columns were : (1) a 25 ft-by-1/4 inch stainless steel column packed with 20% Triton X 305; (2) a 10 ft-by-3/8 inch aluminum column, 20% Carbowax 20 M ; and (3) the same column as (2), 20% SF-96; solid support, 60—80 mesh chromosorb W. These runs were isothermal or programmed. The flow rate of the helium carrier gas was 30—60 ml/min. The separated components were trapped in thin-walled glass capillaries following the method developed by Jennings and his co-workers.[3]

For analytical chromatography we used a Hitachi Perkin-Elmer Model F-6D gas chromatograph equipped with a flame-ionization detector. 45 m-by-0.25 mm stainless steel capillary columns coated with HB-2000, with FS-45, and with Q-45 were used. The column temperature was programmed from 70 to 150 °C (HB-2000), and was held isothermally at 80, 130, 150, and 200°C. The nitrogen carrier-gas inlet pressure was 1.0 kg/cm^2.

Infrared Spectroscopy. The infrared spectra were taken as thin films between sodium chloride plates on a Hitachi EPI-G2 spectrometer, equipped with a custom-made beam condenser.

Nuclear Magnetic Resonance Spectrometry. The NMR spectra were measured on a JEOL Model C-60 spectrometer at 60 MHz in carbon tetrachloride, using tetramethylsilane as an internal reference. The microcell technique was adopted.[4]

Mass Spectrometry. Mass spectra were obtained

1) E. Guenther, "The Essential Oils," Vol. III, Van Nostrand, New York (1949), p. 376.

2) T. Katayama, *Bull. Japanese Soc. Sci. Fisheries*, **24**, 511 (1958).

3) W.G. Jennings, R.K. Creveling and D.E. Heinz, *J. Food Sci.*, **29**, 730 (1964).

4) S. Ito and I. Miura, This Bulletin, **38**, 2197 (1965).

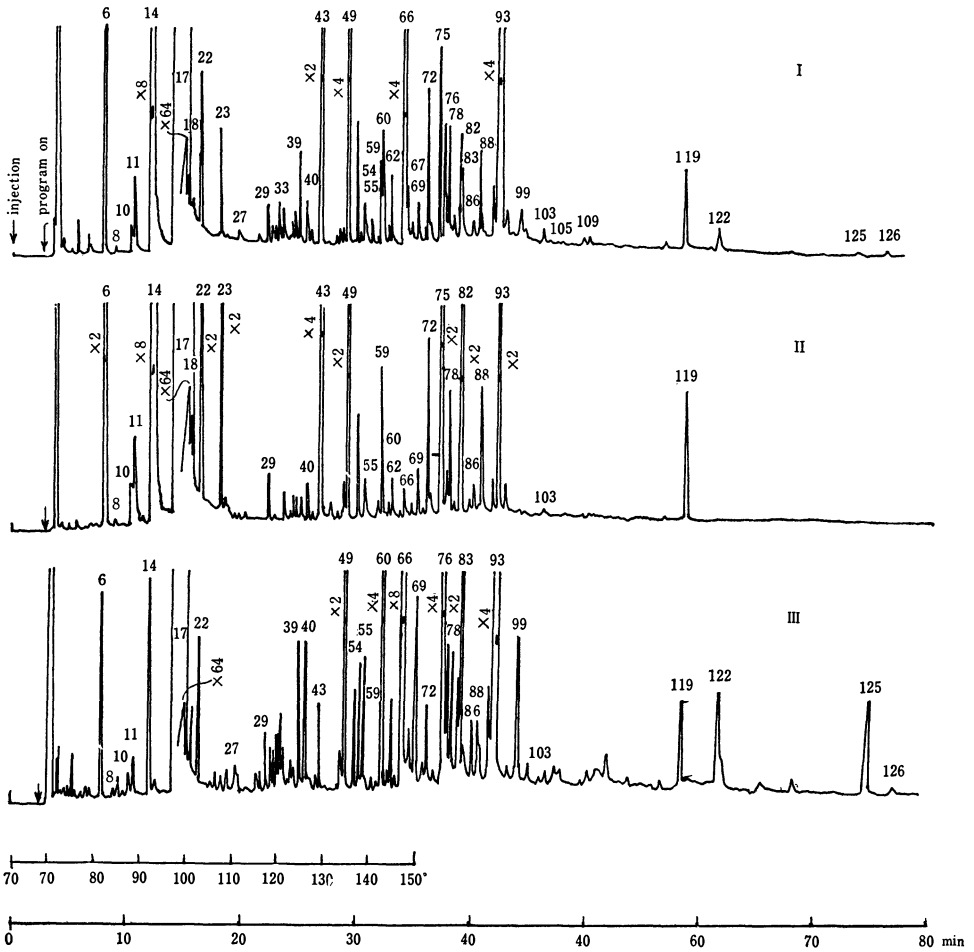

Fig. 1. Gas chromatograms of Japanese pepper fruit oil I. Ripe fruit oil, II. Unripe fruit oil, III. Stored ripe fruit oil 45 m×0.25 mm HB-2000 column; temperature isothermal at 70°C for 3 min then programmed at 2.5°C per minute to 150°C and run isothermal thereafter; sample 1.0—2.0 μl ; range 1×1 except as indicated.

on a Hitachi RMU-6 mass spectrometer. The operating conditions were as follows: ionization voltage, 80 eV; ion-accelerating voltage, 2000 V; temperatures of ionization chamber and sample injection block, 250 and 150°C respectively.

Preparation and Separation of the Volatile Oil. Ripe fruits of "Asakura-sansho," cultivated in the Yoshino district, Nara Prefecture, were crushed and steam-distilled. The yield of the volatile oil was 0.96 per cent of the raw material.

The neutral volatile oil (104 m*l*), freed from acids and bases, was fractionated into sixteen fractions by distillation under reduced pressure, utilizing a Podbielniak 13 mm-by-24 inch Heli-Grid column. Each fraction was further fractionated by means of silica gel column chromatography and preparative gas chromatography. The individual components were then purified by reinjection into various columns.

Results and Discussion

Figure 1 shows the comparative capillary chromatograms of ripe fruit oil (top of Fig. 1), unripe fruit oil*[1] (middle), and ripe fruit oil stored for a long time at room temperature (bottom). Each chromatogram was obtained by using a flame-ionization detector and by injecting 1.0 μl of the raw volatile oil into a HB-2000 capillary column. The column temperature was held initially at 70°C for 3

*[1] The oleoresin was obtained by extraction with hexane from unripe fruits of "Asakura-sansho" which were cultivated in Minô, Osaka Prefecture. By steam-distillation of oleoresin, the volatile oil was isolated.

TABLE 1. IDENTIFICATION OF CONSTITUENTS OF VOLATILE OIL FROM RIPE FRUITS OF JAPANESE PEPPER USING CAPILLARY GLC, IR, NMR AND MS SPECTRAL ANALYSES

Peak No. in Fig. 1	Identified component	IR, NMR, MS Lit. Ref.	Authentic sample
6	α-Pinene	IR[a,b] MS[c]	commercial
8	Camphene	IR[a,b] MS[c]	commercial
10	β-Pinene	IR[a,b] MS[c]	commercial
11	Sabinene	IR[a,b] MS[c]	Juniper berry oil[d]
14	Myrcene	IR[a,b] MS[c]	Juniper berry oil[d]
15	α-Phellandrene	IR[a] MS[c]	commercial
17	Limonene	IR[a,b] MS[c]	commercial
	1,8-Cineol	IR[b]	commercial
18	β-Phellandrene	IR[a] MS[c]	not available
22	*p*-Cymene	IR[a,b] MS[c]	commercial
23	Terpinolene	IR[a,b]	dehydration of α-terpineol
27	Isobutyl isovarelate		esterification
29	Isobutyl caproate		esterification
33	β-Terpinen-3,4-oxide		not available
39	*trans*- and *cis*-		oxidation of
40	Limonen-1,2-oxide	IR[e]	limonene[e]
43	Citronellal	MS[f]	commercial
49	Linalool	IR[b] MS[g]	commercial
54	Terpinolen-4,8-oxide		not available
55	Isopulegol	IR[h] NMR[h] MS[h]	commercial
	trans-2,8-*p*-Mentha-dien-1-ol	IR[i] NMR[i]	autoxidation of limonene[i]
59	Terpinen-4-ol	IR[b,j] MS[g]	Juniper berry oil[d]
	Linalyl acetate	IR[b]	commercial
60	*cis*-2,8-*p*-Mentha-dien-1-ol	IR[i] NMR[i]	autoxidation of limonene[i]
	Dihydrocarvone		reduction of carvone
62	α-Copaene	IR[k]	Cubeb oil[l]
66	Cryptone		autoxidation of β-phellandrene[m]
67	Methyl chavicol		oil of *Fagara mantchurica*[n]
69	Limonen-4-ol		not available
72	α-Terpineol	IR[j] MS[g]	commercial
75	β-Caryophyllene	IR[b]	Juniper berry oil[d]
76	Carvone	IR[b] MS[f]	commercial
	Piperitone	MS[f]	Mentha species[o]
	Citronellyl acetate		commercial
78	Phellandral		reduction of perillaldehyde
82	Terpinyl acetate		commercial
83	Cuminaldehyde	MS[f]	commercial
86	Perillaldehyde		commercial
88	Humulene	IR[b]	Juniper berry oil[d]
	1(7),8-*p*-Menthadien-*trans*-2-ol	IR[i] NMR[i]	not available
	Citrodellol	MS[g]	commeircal
90	γ_2-Cadinene	IR[p]	not available
93	Geranyl acetate	MS[q]	commercial
	trans-Carveol	NMR[r]	autoxidation of limonene[i]
99	α-Muurolene	IR[s]	oil of *Mentha piperita*[s]
	cis-Carveol	NMR[r]	autoxidation of limonene[i]
	Geraniol	MS[g]	commercial
103	δ-Cadinene	IR[b]	Juniper berry oil[d]
	γ-Cadinene	IR[b]	Juniper berry oil[d]
105	Piperitenone	IR[b,t] MS[f,t]	Mentha species[o]
109	Calamenene	IR[b] MS[u]	Cubeb oil[l] Yomena oil[u]
118	α-Calacorene	IR[b] MS[u]	Yomena oil[u]
119	Methyl cinnamate		commercial
122	Cuminalcohol	MS[g]	reduction of cuminaldehyde
125	β-Caryophyllene alcohol	mp 96 °C[v]	hydration of β-caryophyllene[v]
126	Nerolidol		commercial

a) B.M. Mitzner, E.T. Theimer, J.K. Freeman, *Appl. Spectroscopy*, **19**, 169 (1965). b) J.Pliva, M. Horak, V. Herout, F.Sorm, Terpenspektren, Sammlung der Spektren und PhysikalishenKonstanten, Bd. I and II. Akademie Verlag, Berlin1960 and1963. c) R.Ryhage, E. von Sydow, *Acta Chem. Scand.*,**17**, 2025 (1963). d) K. Nishimura, Y. Hirose, *Nippon Kagaku Zasshi* (*J. Chem. Soc. Japan, Pure Chem. Sect.*), **83**, 350 (1962). e) W.F. Newhall, *J. Org. Chem.*, **29**, 185 (1964). f) E. von Sydow, *Acta Chem. Scand.*, **18**, 1099 (1964). g) E.von Sydow, *ibid.*, **17**, 2504 (1963). h) R.Teranishi, "Flavor Chemistry," Am. Chem. Soc., Washington, D.C. (1966). i) C.S.Foote, S.Wexler, W.Ando, *Tetrahedron Letters*, **1965**, 4111. j) B.M.Mitzner, S.Lemberg, *Am. Perf. & Cosm.*, **81**, March 25; May 27 (1965). k) P. de Mayo, R.E. Williams, G. Büchi, S.H.Feairheller, *Tetrahedron*, **21**, 619 (1965). l) Y.Ohta, T. Sakai, Y. Hirose, unpublished m) O. Wallach, *Ann.*, **343**, 28 (1905). n) Y. Ohta, Y. Hirose, unpublished o) S.Shimizu, *Perf. Essen. Oil Rec.*, **56**, 212 (1965). p) C.C.Karta, P.S.Kalsi, A.M. Shaligram, K. K. Chakravarti, S. C. Bhattacharyya, *Tetrahedron*, **19**, 241 (1963). q) E. von Sydow, *Acta Chem. Scand.*, **19**, 2083 (1965). r) S.H.Schroeter, E.L.Eliel, *J.Org. Chem.*, **30**, 1 (1963). s) R. Vlahov, M. Holub, I. Ognjanov, V. Herout, *Coll. Czech. Chem. Commun.*, **31**, 808 (1966). t) M.G. Moshonas, *J. Food Sci.*, **32**, 206 (1967). u) N. Tsubaki, K. Nishimura, Y. Hirose, This Bulletin, **39**, 312 (1966). v) Y. Asahina, T. Tsukamoto, *J. Pharm. Soc. Japan*, **484**, 463 (1922).

min, then programmed at 2.5℃ per minute to 150℃, and run isothermally at 150℃ until all the components had emerged. For the determination of the location of a particular peak, an authentic sample or a purified component was mixed with the original oil and chromatographed using the same analytical conditions as above. The location was confirmed by an appreciable increase in the particular peak.

Among the more than 130 component peaks observed in the chromatogram of fruits oils, fifty-six compounds were isolated and determined. Table 1 lists the components which were confirmed by a comparison of their infrared, nuclear magnetic resonance, and mass spectra with those of authentic samples and the literature data. Authentic samples were obtained from reliable commercial sources or synthesized by well-established methods, and were purified by gas chromatographic separation before use. In a few cases authentic samples were not available.

The mono- and sesqui-terpenic hydrocarbons were identified by direct comparison with authentic samples, except for β-phellandrene and γ_2-cadinene. The main components were limonene and β-phellandrene. Most of the hydrocarbons in the fruit oil of Japanese pepper are commonly found also in other oils of the same family (*Rutaceae*)-citrus oils, orange oil,[5,6] lemon oil[7,8] and natsudaidai oil.[9]

Among the oxygenated components, geranyl acetate, linalool, cryptone, and citronellal were present in quite large amounts. The two isobutyl esters were supposed to be related by a poignant principle, sanshool.[10]

It is most interesting that almost all of the auto- and photo-oxidation products from limonene[11-13] were isolated from fruits of Japanese pepper. These were *trans*- and *cis*-limonen-1,2-oxide, *trans*- and *cis*-2,8-*p*-menthadien-1-ol, *trans*- and *cis*-carveol, 1(7),8-*p*-menthadien-*trans*-2-ol, carvone, and perillaldehyde. Some of them were also found in citrus oils, orange oil,[5,14,15] and grapefruit oil.[16] Cryptone was also derived from the autoxidation of β-phellandrene.[17] These facts are indicated in Fig. 1.

The three monoterpenic oxygenated compounds, β-terpinen-3,4-oxide, terpinolen-4,8-oxide, and limonen-4-ol, had not previously been found in natural products. Besides, it seems that this is the first report on the isolation of β-caryophyllene alcohol from natural sources.

β-Terpinen-3,4-oxide. The IR (Fig. 2) and NMR spectra of this substance showed the presence of an isopropyl group (ν_{max}^{film} 1380, 1360 cm^{-1}; δ 0.92, 0.94 ppm, each 3H d. *J* 7 Hz), an exocyclic methylene group (ν_{max}^{film} 3060, 1640, 880 cm^{-1}; δ 4.62 ppm, 2H s.), and a proton linked to an epoxide ring (ν_{max}^{film} 850 cm^{-1}, 1,2-epoxide; δ 2.87 ppm, 1H unresolved). Its mass spectrum showed a molecular ion peak at *m/e*

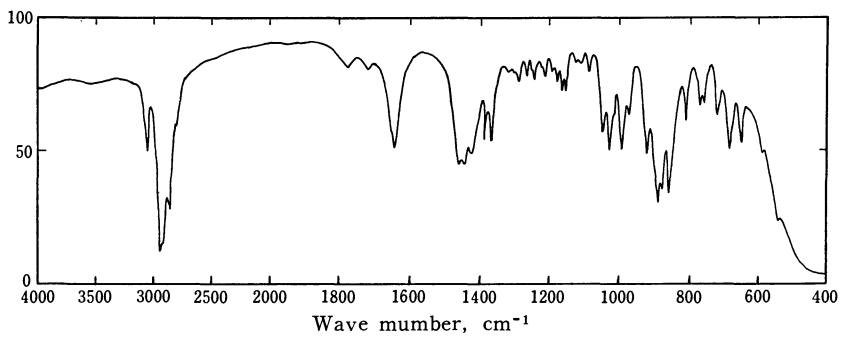

Fig. 2. IR spectrum of β-terpinen-3,4-oxide.

5) R.W. Wolford and J. A.Attaway, *J. Agr. Food Chem.*, **15**, 369 (1967).
6) K. Maekawa, M. Kodama, M. Kushii and M. Mitamura, *Agr. Biol. Chem.*, **31**, 373 (1967).
7) W.H.D. McLeod,Jr., W.H.McFadden and N.M. Buigues, *J. Food Sci.*, **31**, 591 (1966).
8) J.R. Clark and R.A. Bernhard, *Food Research*, **25**, 389 (1960).
9) Y. Ohta and Y. Hirose, *Agr. Biol. Chem.*, **30**, 1196 (1966).
10) M.Asano and T.Aihara, *J.Pharm. Soc. Japan*, **69**, 79 (1949).
11) G. O. Schenck, K. Gollnick, G. Buchwald, S. Schroeter and G. Ohloff, *Ann.*, **674**, 93 (1964).
12) G.O. Schenck, O.-A. Neumüller, G. Ohloff and S.Schroeter, *ibid.*, **687**, 26 (1965).
13) C. S. Foote, S. Wexler and W. Ando, *Tetrahedron Letters*, **1965**, 4111.
14) G. L. K. Hunter and M. G. Moshonas, *Anal. Chem.*, **37**, 378 (1965).
15) T. H. Schultz, R. Teranishi, W. H. Mc Fadden, P.W.Kilpatrick and J. Corse, *J. Food Sci.*, **29**, 790 (1964).
16) G.L. K. Hunter and M. G. Moshonas, *ibid.*, **31**, 167 (1966).
17) O. Wallach, *Ann.*, **28**, 340 (1904).

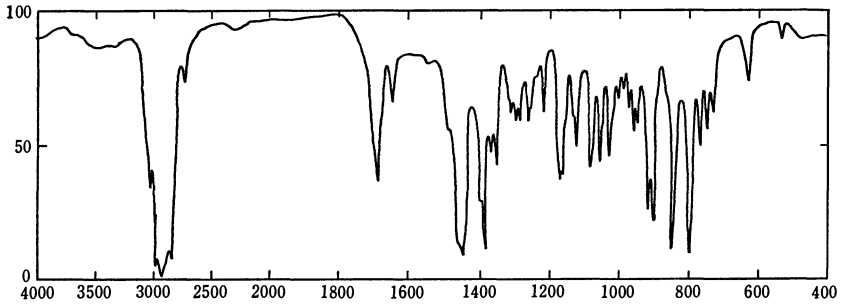

Fig. 3. IR spctrum of terpinolen-4,8-oxide.

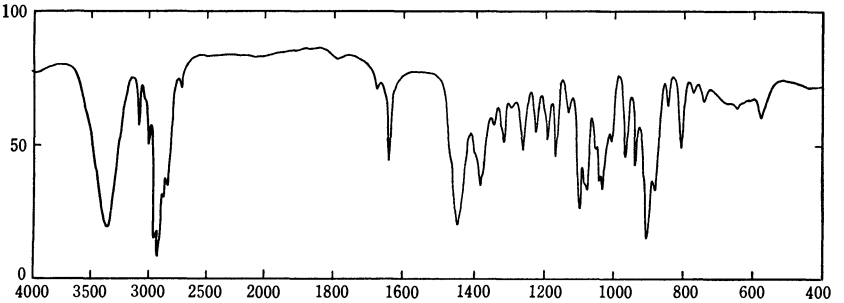

Fig. 4. IR spectrum of limonen-4-ol.

152 ($C_{10}H_{16}O$, 6%), a base peak at *m/e* 43, and conspicuous peaks at *m/e* 109 (48%), and 81 (83%).

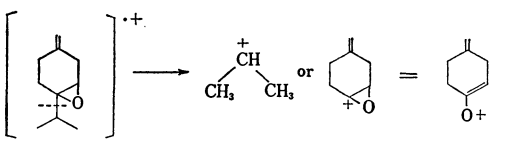

m/e 152 *m/e* 43 *m/e* 109

Terpinolen-4,8-oxide. The mass spectrum of this substance showed a molecular ion peak at *m/e* 152 ($C_{10}H_{16}O$, 3%) and a base peak at *m/e* 94 ($M^+-CH_3COCH_3$). The mass spectrum of the dihydro-oxide showed a molecular ion peak at *m/e* 154 and a base peak at *m/e* 58 (CH_3COCH_3). According to the NMR spectrum, two methyl groups were assigned to the *gem*-dimethyl group attached to a carbon-bearing oxygen (δ 1.20 ppm, 6 H s.) and one methyl group to $-CH=C-CH_3$ (ν_{max}^{film} 1685, 790 cm^{-1}; δ 1.62 ppm, 3H s., 5.34, 1H unresolved). Its IR spectrum (Fig. 3) showed an absorption peak at 840 cm^{-1} due to an 1,2-epoxide ring.

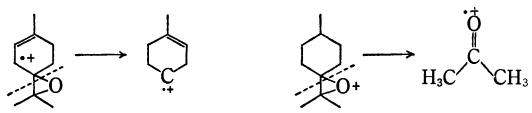

Limonen-4-ol. From the IR (Fig. 4) and NMR spectra of this substance the presence of a hydroxyl group (ν_{max}^{film} 3370 cm^{-1}), an isopropenyl group (ν_{max}^{film} 3100, 1640, 900 cm^{-1}; δ 1.75 ppm, 3H s., 4.74, 4.92, each 1H broad s.), and a methyl group attached to a trisubstituted double bond (δ 1.65 ppm, 3H s., 5.20, 1H unresolved) were inferred. This alcohol was hydrogenated with platinium oxide in methanol to give a tetrahydro-derivative, which was identified with the known tetrahydroterpinen-4-ol.[18] Its mass spectrum showed a molecular ion peak at *m/e* 152 ($C_{10}H_{16}O$, 11%), a base peak at *m/e* 69, and strong peaks at *m/e* 84 (85%) and 41 (60%), which were explained by the following fission mode:

From these facts the structure of this alcohol was deduced to be 1,8-*p*-menthadien-4-ol.

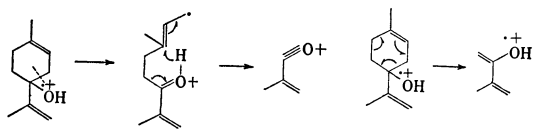

m/e 152 *m/e* 69 *m/e* 152 *m/e* 84

As is shown in Fig. 1, the amounts of citronellal and β-phellandrene decreased when the fruit oil stood at room temperature. On the contrary, the amounts of isopulegol and cryptone increased. Citronellal was also isomerized to isopulegol by distillation and by column

18) B.M. Mitzner and S. Lemberg, *Amer. Perf. & Cosm.*, **81**, June 80 (1966).

chromatographic separation. Schulte-Elte and Ohloff[19] reported that the thermal isomerization of citronellal yielded a mixture of isopulegol and neoisopulegol.

During the study of the chemical characteristics of the fruit oil, we attempted to identify the principal flavor components other than citronellal in Japanese pepper, but we were not able to reach any conclusions. Its seems that the characteristic aroma of Japanese pepper is chiefly attributable to citronellal after all.

A comparison of the constituents of volatile oils of unripe fruit oil and ripe fruit oil stored for a long time is in progress. Our results will be reported later.

The authors thank Dr. C. S. Foote, University of California, Los Angels, for supplying authentic samples and IR and NMR spectra of 1(7),8-*p*-menthadien-*trans*-2-ol, *trans*- and *cis*-2,8-*p*-menthadien-1-ol, *etc.*, which led to its identification. The authors are also grateful to Dr.S. Shimizu, The Shinshu Uniersity, Ina, for samples of piperitone and piperitenone, and to Dr. M. Romanuk, Czechoslovak Academy of Science, Prague, for authentic α-muurolene. Thanks are also due to Mr. M. Shiga, Shiono Koryo Kaisha Ltd., Osaka, who kindly provided oleoresin from unripe fruits of "Asakura-sansho."

19) K. H. Schulte-Elte and G. Ohloff, *Helv. Chim. Acta*, **50**, 153 (1967).

BULLETIN OF THE CHEMICAL SOCIETY OY JAPAN VOL. 41 1950—1953 (1968)

Constituents of Leaf Oil from Japanese Pepper

Shoichi KUSUMOTO, Akio OHSUKA and Munio KOTAKE

Institute of Organic Chemistry, Faculty of Science, Osaka City University, Kita-ku, Osaka

and Tsutomu SAKAI

Institute of Food Chemistry, Kita-ku, Osaka

(Received February 20, 1968)

The steam-volatile constituents from leaves of Japanese pepper were separated by column chromatography and GLC, and their chemical structures were studied by IR, NMR, and mass spectrometry. The volatile oil was found to be composed of about 100 components; those identified were as follows: 15 hydrocarbons (α- and β-pinene, camphene, sabinene, myrcene, α- and β-phellandrene, limonene, *p*-cymene, terpinolene, α-copaene, caryophyllene, humulene, α-muurolene, and γ-cadinene), 16 alcohols (2-penten-1-ol, *n*-hexanol, 3-hexen-1-ol, *trans*- and *cis*-sabinene hydrate, *cis*-linalool oxide, linalool, isopulegol, neoisopulegol, terpinen-4-ol, α- and δ-terpineol, limonen-4-ol, benzyl alcohol, β-phenylethyl alcohol, and nerolidol), 2 aldehydes (2-hexenal and citronellal), 1 ketone (cryptone), 7 esters (isobutyl caproate, linalyl acetate, citronellyl acetate, terpinyl acetate, geranyl acetate, methyl salicylate, and methyl cinnamate) and 2 ethers (1,8-cineol and methyl chavicol).

The fruits and the young leaves of Japanese pepper (*Xanthoxylum piperitum* DC. (Japanese name, "Sanshoo"), and a variety of it, *X. piperitum var. inerme* Makino ("Asakura-sanshoo")) are widely used as spice in our country because of their characteristic odor and burning taste.

The essential oil of the fruits has been studied by several investigators, and recently almost all the components of the oil were identified by one of the present authors, Tsutomu Sakai.[1] The components responsible for its pungent taste have been shown to be α- and β-sanshool by Crombie and Tayler.[2] However, the constitution of the leaves has not yet been studied. Therefore, the study of the composition of the volatile oil isolated from the young leaves of "Asakura-sanshoo"

1) T. Sakai, K. Yoshihara and Y. Hirose, This Bulletin, **41**, 1945, (1968).

2) L. Crombie and J. L. Tayler, *J. Chem. Soc.* **1957**, 2760.

was undertaken.

Experimental

Extraction and Steam Distillation. 1) Twenty-six kilograms of fresh young leaves of *X. piperitum* DC. *var. inerme* Makino (collected at the beginning of June in Kyoto Prefecture) were extracted three times with redistilled petroleum ether (bp below 50 °C) at room temperature. The residue obtained by the evaporation of the solvent was steam-distilled under reduced pressure (30—40 mmHg). The distillate was saturated with sodium chloride and extracted with petroleum ether. The solvent was evaporated after the removal of acids to give a colorless oil (about 37 g).

2) Twelve kilograms of the leaves (see above) were extracted with ether instead of petroleum ether. About 11 g of a pale yellow oil was obtained.

Silica-gel Chromatography of the Essential Oil. The essential oils obtained in 1) and 2) were combined and placed in a column packed with 300 g of silica-gel (Merck 0.05—0.2 mm). This mixture was eluted first with petroleum ether, and then with petroleum ether containing various concentrations of ether (from 2 to 50%). The fractions obtained are summarized in Table 1.

TABLE 1. FRACTIONS OF THE SILICA GEL CHROMATOGRAPHY

Fraction	Wt, g	Constituent
A	26.0	Hydrocarbons
B	7.0	Ethers and esters
C	1.9	Ethers, aldehydes, esters and alcohols
D	0.4	Ethers, aldehydes, esters and alcohols
E	1.4	Alcohols
F	1.0	Alcohols
G	0.2	Alcohols
H	0.3	Alcohols

The Isolation of the Components by Preparative Gas-liquid Chromatography (GLC). Each fraction obtained by silica-gel chromatography was distilled under reduced pressure, and the components of the distillate were isolated by preparative GLC under suitable conditions. A Shimadzu GC-2B-type gas chromatograph with a copper spiral column (4 mm in diameter, 5 m in length) was used in the preparation. Glass capillaries were employed as receivers, and hydrogen, as the carrier gas. The conditions employed are shown in Table 2.

The Identification of the Isolated Components. The isolated components were identified by means of IR, NMR,*1 and mass spectrometry, and by a direct comparison of the retention times in an analytical GLC with those of authentic samples. The analytical GLC was carried out using a Hitachi Perkin-Elmer Model F-6D gas chromatograph provided with a flame-ionization detecter. Stainless-steel capillary columns (0.25 mm in diameter and 45 m in length) were coated with HB-2000 and FS-45. The column temperature was programmed from 70 to 150°C, or was held isothermally at 80, 110, and 130°C. The nitrogen-carrier gas-inlet pressure was 1.0 kg/cm^2.

TABLE 2. CONDITIONS OF PREPARATIVE GAS CHROMATOGRAPHY

	Stationary phase	Column temp. °C	H_2 Flow rate m*l*/min
a)	PEG 6000	120	20
b)	PEG 20M	160	25
c)	PEG 20M	170	35
d)	PEG 20M	175	25
e)	DEGSPE*	120	20
f)	DEGSPE	140	20
g)	DEGSPE	160	25
h)	DEGSPE	170	30

* Diethyleneglycol succinate polyester

Synthesis of *trans*- and *cis*-Sabinene Hydrate. A mixture of sabinene (1.05 g), potassium permanganate (0.21 g), potassium periodate (7.35 g), and potassium carbonate (0.52 g) in 200 m*l* of water was stirred continuously for 39 hr at room temperature. After the manganese dioxide precipitated had been removed by filtration, the aqueous layer was extracted with ether; this ether extract was then washed with water, dried, and concentraed under reduced pressure to give 0.6 g of a colorless oil; ν_{max}^{film} 1720 cm^{-1}. The oil was found by its gas chromatogram to be composed of almost pure sabinaketone.

A solution of this product in 3 m*l* of absolute ether was added, drop by drop, to a solution of methylmagnesium bromide (which had been prepared from 0.21 g of magnesium) in 10 m*l* of absolute ether; the mixture was refluxed for 40 min with occasional shaking, and then, after cooling, the excess reagent was decomposed with crushed ice. The product was isolated by steam distillation and by the extraction of the distillate with ether. *trans*- and *cis*-Sabinene hydrate were isolated from this crude product (0.53 g) by preparative GLC (PEG 20M, 170°C); the *trans*-isomer, mp 59—60°C (Lit.[4] 60—61°C), and the *cis*-isomer, mp 36—37.5 °C (Lit.[4] 38—39°C).

Results and Discussion

Since the essential oils prepared from fresh leaves of "Asakura-sanshoo" by extraction with either ether or petroleum ether were found through their gas chromatograms to be composed of almost identical substances, the

*1 NMR spectra were measured in carbon tetrachloride using TMS as internal reference at 60 Mc on a JEOL model C-60 spectrometer.

3) B. M. Mitzner and S. Lemberg, *Am. Perf. & Cosm.*, **81**, 25 March, 37 May (1966).

4) J. W. Daly, E. C. Green and R. H. Eastman, *J. Am. Chem. Soc.*, **80**, 6330 (1958).

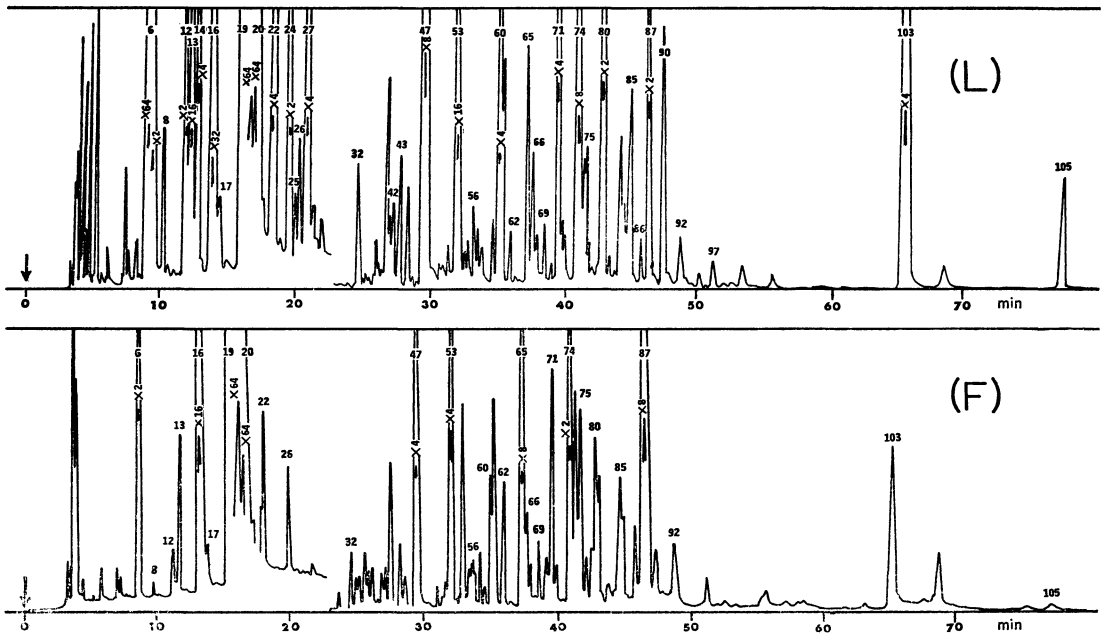

Fig. 1. Analytical gas liquid chromatograms of the essential oils.
(L) The essential oil of the leaves
(F) The essential oil of the fruits

two oils were combined for further study. Figure 1 shows the gas chromatograms of the whole essential oil obtained from young leaves by ether extraction and the whole volatile oil of the fruits.[1] These chromatograms were obtained by injecting 1.0 μl of each oil into an HB-2000 capillary column. The column temperature was initially held at 70°C for 3 min, then programmed at 2.5°C/min to 150°C and ran isothermally at 150°C until all the components had emerged. Table 3 lists the components, which were identified by means of spectral studies.

The compounds responsible for the characteristic odor of Japanese pepper, however, were not obtained in this instance, just as in the earlier work.[1] Therefore, the natural odor may be attributed to a mixed effect of many components.

Limonene and β-phellandrene were the main constituents of the monoterpene hydrocarbons, accounting for about 60% of the total volatile oil.

The major components of the oxygenated compounds were 1,8-cineol, citronellal, linalool, and methyl cinnamate, followed by terpinen-4-ol, α-terpineol, terpinyl acetate, and geranyl acetate.

Although citronellal could be isolated directly from the essential oil by preparative GLC, it disappeared completely after the oil had been subjected to silica-gel column chromatography, and the amounts of isopulegol and neoisopulegol were more than those found to be present in the original oil. Therefore, these alcohols may partly be formed as a result of the isomerization of citronellal on the silica-gel column.

One compound, which was masked by the peak (53) due to linalool in Fig. 1, was isolated from fractions E and F by preparative GLC. Its IR spectrum showed the presence of the tertiary hydroxyl group (ν_{max}^{film} 3370, 1135 cm^{-1}), the isopropyl group (1380, 1364 cm^{-1}), and the methylene group in a cyclopropane ring (3050 cm^{-1}). Its NMR spectrum also suggested the presence of an isopropyl group (δ=0.88, 0.93 ppm, each 3H d, J=6 cps), two protons of a cyclopropane ring (δ=0.23 ppm, 1 H dd, J=9, 5.3 cps and δ=0.70 ppm, 1H dd, J=4.5, 5.3 cps), and a methyl group on a carbon atom bearing an oxygene function(δ= 1.28 ppm, 3H s). No sign of a double bond was found in either of the spectra. The mass spectrum showed a molecular-ion peak at m/e 154 ($C_{10}H_{18}O$, 4%) and a base peak at m/e 93. Furthermore, its mass spectrum lower than m/e 136 ($M-H_2O$) was similar in every respect to that of sabinene. These results suggest that this alcohol is sabinene hydrate (4-thujanol). In order to confirm this, *cis*- and

TABLE 3. COMPOUNDS IDENTIFIED FROM LEAF OIL OF JAPANESE PEPPER

Peak No. in Fig. 1.	Compound	Fr. in Table 1.	Conditions in Table 2
6	α-Pinene	A	a
8	Camphene*	A	
12	β-Pinene*	A	
13	Sabinene	A	a
14	2-Hexenal**	C	g, e
16	Myrcene	A	a
17	α-Phellandrene*	A	f, g
19	1,8-Cineol	B, C	f
19	Limonene	A	a
20	β-Phellandrene	A	a
22	p-Cymene	A	a
24	2-Penten-1-ol**	F, G	b
25	n-Hexanol**	F, G	b
26	Terpinolene*	A	
27	3-Hexen-1-ol**	F, G	b, d
32	Isobutyl caproate*		
42	*cis*-Linalool oxide**	F	d
43	*trans*-Sabinene hydrate**	E	d
47	Citronellal		
53	Linalool	E	d
53	*cis*-Sabinene hydrate**	E, F	d
56	Isopulegol	C, D, E, F	d
56	Neoisopulegol	C, D	g
60	Linalyl acetate	B	d
60	Terpinen-4-ol	C, D, E	d
62	α-Copaene	A	c
65	Cryptone*		
66	Methyl chavicol*		
69	Limonen-4-ol	E	d
70(?)	δ-Terpineol[3]	F	d
71	α-Terpineol	F	d
74	Caryophyllene	A	c
75	Citronellyl acetate	B	d
80	Terpinyl acetate	B	d
85	Humulene	A	c
86	Benzyl alcohol**	G, H	g
	Methyl salicylate**	B	d
87	Geranyl acetate	B	d
90(?)	β-Phenyl ethyl alcohol**	G, H	g
92	α-Muurolene	A	c
97	γ-Cadinene	A	c
103	Methyl cinnamate	C, D	h
105	Nerolidol		h

* These were not isolated but identified by analytical GLC in comparison with the retention times of the components of fruits.
** These were not isolated from the fruit oil.

trans-sabinene hydrate were synthesized according to the method of Daly.[4] The alcohol thus isolated was found to be identical with the synthetic *cis*-isomer with respect to the IR, NMR, and GLC spectra. On the other hand, the *trans*-isomer was isolated in an impure state, as was indicated by an analytical gas chromatogram.

The IR spectrum of peak (24) in Fig. 1 indicates the presence of the primary hydroxyl group (ν_{max}^{film} 3350, 1040, 1000 cm^{-1}) and the double bond (1650 cm^{-1}). Its mass spectrum showed a molecular-ion peak at *m/e* 86 ($C_5H_{10}O$, 9%), a base peak at *m/e* 57, and strong peaks at *m/e* 68 ($M-H_2O$, 16%), 44 (33%), 41 (41%), and 29 (38%). These results suggest that this alcohol is a primary pentenol possessing no terminal methylene group. There are four possible structures consistent with the data given above, 2-methyl-2-buten-1-ol, 3-methyl-2-buten-1-ol, 3-penten-1-ol, and 2-penten-1-ol. The isolated alcohol was found not to be identical with the former two when examined by IR and mass spectra. It was considered to be the last one because of the fact that its mass spectrum showed a strong base peak at *m/e* 57, suggesting the presence of the $-CH=CH-CH_2OH$ group. The configuration of the double bond is probably the cis form, judging from its IR spectrum.

In addition to the compounds listed in Table 3, several esters, monoterpenic alcohols, and sesquiterpenic hydrocarbons were isolated, but their structures could not be deduced because of the small quantities present.

It is apparent from Fig. 1 that the main components of the leaves mentioned above are also present in high concentrations in the oil obtained from the fruit. However, their relative quantities varied considerably from case to case. For instance, cryptone, a relatively large amount of which was found in the fruit oil, was shown to exist in a much smaller amount in the leaf oil. Other carbonyl compounds, such as carvone, piperitenone, phellandral, and cuminaldehyde, isolated from fruit oil were not isolated from the leaf oil. In the leaf oil, on the other hand, caryophyllene was found in greater quantities than in the fruit oil.

Moreover, the aliphatic compounds, such as 2-hexenal (leaf aldehyde), 2-penten-1-ol, *n*-hexanol, and *cis*-3-hexen-1-ol (leaf alcohol), had the characteristic odor of the leaves.

It is still impossible at the present time to show the differences between the leaf and fruit oil, since they were not collected in the same localities and seasons and since different methods were used to obtain the oils.

The authors are grateful to Dr. Yoshio Hirose of the Institute of Food Chemistry for his suggestions and helpful discussions during the course of this work.

BULLETIN OF THE CHEMICAL SOCIETY OF JAPAN VOL. 41 1954—1958 (1968)

Organic Syntheses by Means of Noble Metal Compounds. XXXVII.[1] Carbonylation of Allene-Palladium Chloride Complexes

Tosaku SUSUKI and Jiro TSUJI

Basic Research Laboratories, Toyo Rayon Co., Kamakura

(Received February 22, 1968)

The reaction of allene with palladium chloride and a carboxylate anion gave di-μ-chloro-bis(2-acyloxy-π-allyl) dipalladium which was converted into an acetoacetate by carbonylation. Carbonylation of allene in ethanol in the presence of palladium chloride produced ethyl itaconate. The carbonylation of di-μ-chloro-bis(2-chloro-π-allyl) dipalladium in ethanol formed 3-chloro-3-butenoate. 4-Hydroxy-3,4-dimethyl-2-pentenoic acid γ-lactone, 3-isopropylideneglutarate and 3-(ethoxycarbonylmethyl)-4-methyl-3-hexenedioate were isolated by the carbonylation of di-μ-chloro-bis[2-(1-(chloromethyl)vinyl)-π-allyl] dipalladium. The mechanisms of these reactions are discussed.

Olefinic double bonds react with palladium chloride easily to form π-complexes or π-allyl complexes.[2] Of particular interest is the complex formation with dienes. Thus 1 3-butadiene reacts with palladium chloride to form 1-(chloromethyl)-π-allylpalladium chloride.[3] Allene is a 1,2-diene and its reaction with palladium chloride gives either complex I or II, depending on the reaction conditions.[4,5] The formation of the complexes I and II can be explained in the following way.

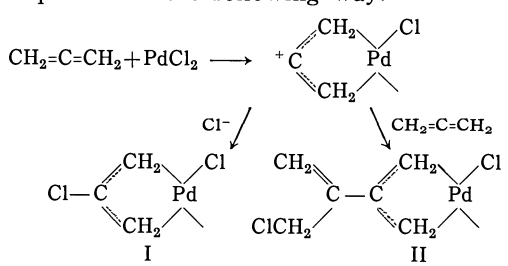

By the displacement of a chlorine atom of palladium chloride by one of the double bonds of allene, the center carbon atom of allene becomes cationic and a nucleophilic attack at this carbon is expected. When the displaced chloride anion attacks the carbon, the complex I is formed and this reaction proceeds in a benzene solution. In other words, this reaction is the insertion of the double bond of allene between the Pd–Cl bond. When the reaction is carried out in methanol, the cationic center is somewhat stabilized and another molecule of allene attacks the carbon to give the complex II. The consideration of this mechanism led us to expect that the attack of other nucleophiles at the center carbon of allene in the presence of palladium chloride should give π-allylic complexes substituted at the center carbon. From these considerations, the π-allylic complex formation from allene in the presence of a carboxylate anion and carbon monoxide was studied.

The carbonylation of π-allylic palladium complexes to form β,γ-unsaturated carboxylic acid derivatives is a well established reaction.[6,7] Therefore, it is expected that the carbonylation of the allene complexes should give 3-substituted 3-butenoic acid derivatives. A part of these studies has already been reported.[8]

Results

At first the reaction of allene with palladium chloride in the presence of carboxylate anions

1) Part XXXVI. H. Takahashi and J. Tsuji, *J.Am. Chem. Soc.*, **90**, 2387 (1968).

2) E.O. Fischer and H. Werner, "Metal π-Complexes", Vol. 1, Elsevier Pub. Co., Amsterdam (1966).

3) S.D. Robinson and B.L. Shaw, *J. Chem. Soc.*, **1963**, 4806; 1964, 5002.

4) R.G. Schultz, *Tetrahedron Lettesrs*, **1964**, 301; *Tetrahedron*, **20**, 2809 (1964).

5) M. S. Lupin and B. L. Shaw, *Tetrahedron Letters*, **1964**, 883; M.S. Lupin, J. Powell, and B. L. Shaw, *J. Chem. Soc.*, *A*, **1966**, 1687.

6) J. Tsuji, J. Kiji and M. Morikawa, *Tetrahedron Letters*, **1963**, 1811; J. Tsuji, J. Kiji, S. Imamura, and M. Morikawa, *J. Am. Chem. Soc.*, **86**, 4359 (1964).

7) W. T. Dent, R. Long and G. G. Whitfield, *J. Chem. Soc.*, **1964**, 1588.

8) J. Tsuji and T. Susuki, *Tetrahedron Letters*, **1965**, 3027.

was studied. When allene was bubbled into acetic acid solution of sodium chloropalladate and sodium acetate, di-μ-chloro-bis(2-acetoxy-π-allyl) dipalladium (complex III) was isolated. Similarly, the reaction in propionic acid gave a propionyl substituted π-allyl complex. Although the reaction was carried out in protic solvents, a complex corresponding to II was not isolated.

$$CH_2{=}C{=}CH_2 + PdCl_2 + CH_3CO_2^- \longrightarrow$$

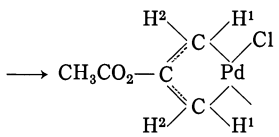

III

The structure of the complex III was proved by its NMR spectrum (Fig. 1), which showed

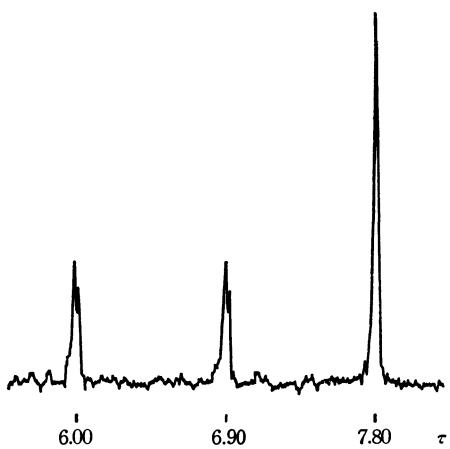

Fig. 1. NMR spectrum of di-μ-chloro-bi (2-acetoxy-π-allyl) dipalladium.

a pattern typical of π-allylpalladium chloride. In this spectrum, the peaks at τ 6.90 and 6.00 assignable to H^1 and H^2 appeared as doublets and their coupling constant ($J_{1,2}$) was found to be 2.4 cps. The coupling of H^1 and H^2 is not observed with most of π-allylic complexes and the only exception so far reported is the complex I, which has $J_{1,2}=2.0$.[5] Thus it seems likely that only the π-allyl complexes substituted with electronegative groups at the center carbon show the coupling of H^1 and H^2.

The attack of carbon monoxide on olefins coordinated to palladium to form acid derivatives is well known.[9] It is expected that the attack of carbon monoxide on the center carbon of allene should form a carbonyl substituted π-allyl complex which is further attacked by carbon monoxide to give itaconate as shown below. Based on this assumption, the reaction of allene, carbon monoxide and palladium chloride in ethanol was carried out, and actually itaconate was isolated, although the yield was poor.

$$CH_2{=}C{=}CH_2 + CO + PdCl_2 \longrightarrow$$

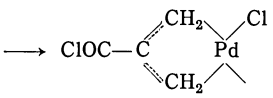

$$\xrightarrow{CO}$$

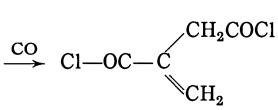

$$\xrightarrow{ROH}$$

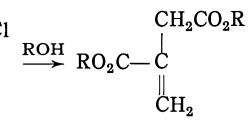

Then the carbonylation of the complexes I, II and III was studied. The product of the carbonylation of the complex I was 3-chloro-3-butenoate as expected.

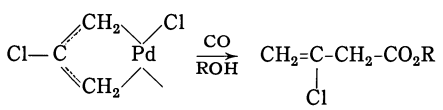

I

The carbonylation of the complex III was carried out in benzene and the product was treated with ethanol. An ester was isolated by distillation and identified as ethyl acetoacetate (V), which was presumably formed by ethanolysis of ethyl 3-acetoxy-3-butenoate (IV) formed initially.

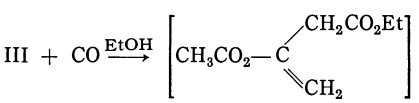

IV

$$\longrightarrow CH_3COCH_2CO_2Et$$

V

Different from the complexes I and III, which gave 3-substituted 3-butenoates, the carbonylation of the complex II seems to be complicated. In addition to the π-allylic structure, this complex contains allylic chloride and conjugated diene structures, both of which are expected to be carbonylated. Actually the carbonylation of the complex II in ethanol produced three products, which were formed by the stepwise attack of one, two and three molecules of carbon monoxide. The first product was an unsaturated lactone (IR 1750 cm^{-1}) and identified as 4-hydroxy-3,4-dimethyl-2-pentenoic acid γ-lactone (VI) by

9) J. Tsuji, M. Morikawa and J. Kiji, *J. Am. Chem. Soc.*, **86**, 4851 (1964).

NMR and IR spectra and mixed melting point measurement with an authentic sample.

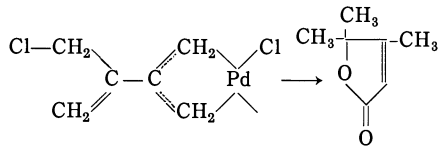

II VI

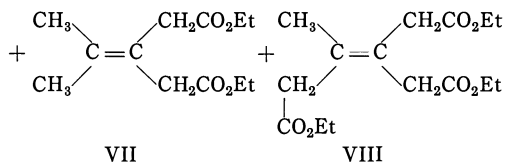

VII VIII

The second one was an unsaturated diester. The NMR spectrum showed two singlets due to two methyl groups (6H at τ 8.26) and two methylene groups (4 H at τ 6.94). The ozonization, followed by the treatment with dinitrophenylhydrazine produced two hydrazones. They were the hydrazones of acetone and ethyl 3-oxoglutarate. From these evidences, the ester is determined as ethyl 3-isopropylideneglutarate (VII). The third, higher boiling fraction was a triester. The ozonization gave ethyl acetoacetate and ethyl 3-oxoglutarate, which suggests that the triester is ethyl 3-(ethoxycarbonylmethyl)-4-methyl-3-hexenedioate (VIII). The NMR spectrum supports the structure (Fig. 2).

The formation of these three esters can be explained by the following mechanism. At first carbon monoxide attacks the π-allylic system to form IX, which is converted into the lactone VI by double bond isomerization and hydrogenolysis of the chlorine as shown below. The intermediate lactone X is an allylic lactone and can react with palladium by oxidative addition to form another π-allylic complex XI. The carbonylation of this complex leads to the formation of a diester (XII), which gives VII by hydrogenolysis.

The intermediate diester XII has an allylic chloride structure and can be converted into another π-allylic complex XIII by the reaction with palladium. The carbonylation of this complex gives the triester VIII.

Experimental

Materials. Allene was purchased from the Matheson Co. It was distilled from a cylinder into a glass vessel and its volume was measured. Then it was redistilled into a stainless steel autoclave. The NMR specptra were determined with high resolution spectrometer, models DP 60 and HR 100, the peak positions are expressed in terms of τ values. The molecular weights were determined in benzene using a Mechrolab vapor pressure osmometer, or by mass spectrometer.

Formation of the Complex III. Sodium chloropalladate (9.0 g) and sodium acetate (2 g) were dissolved in acetic acid (220 m*l*) and allene was bubbled into the solution at room temperature with stirring. The deep brown solution turned gradually to pale brown, and the complex began to precipitate slowly. After one hour, the complex was collected by filtration (6.7 g) and recrystallized from a mixture of chloroform and methanol, mp 178.5—179.5°C (decomp).

Found; C, 24.96 ; H, 3.09 ; Cl, 15.15%, mol wt, 478.7. Calcd for $(C_5H_7O_2PdCl)_2$; C, 24.84 ; H, 2.90; Cl, 14.70%, mol wt, 481.8. NMR. Fig. 1.

By the similar procedure, the propionyl complex

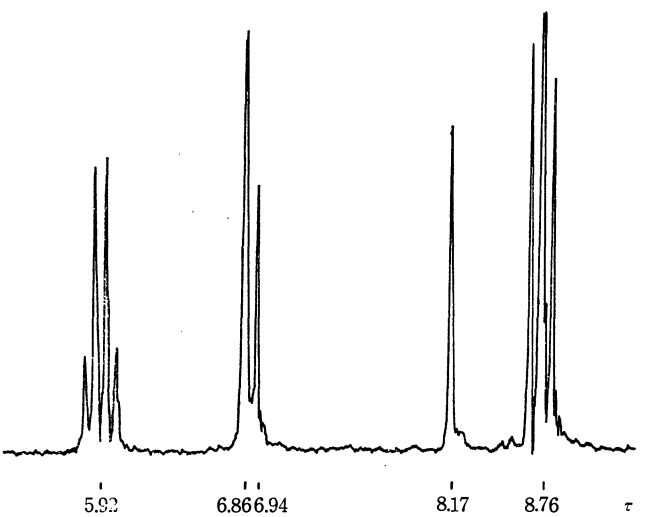

Fig. 2. NMR spectrum of ethyl 3-(ethoxycarbonylmethyl) 4-methyl-3-hexenedioate.

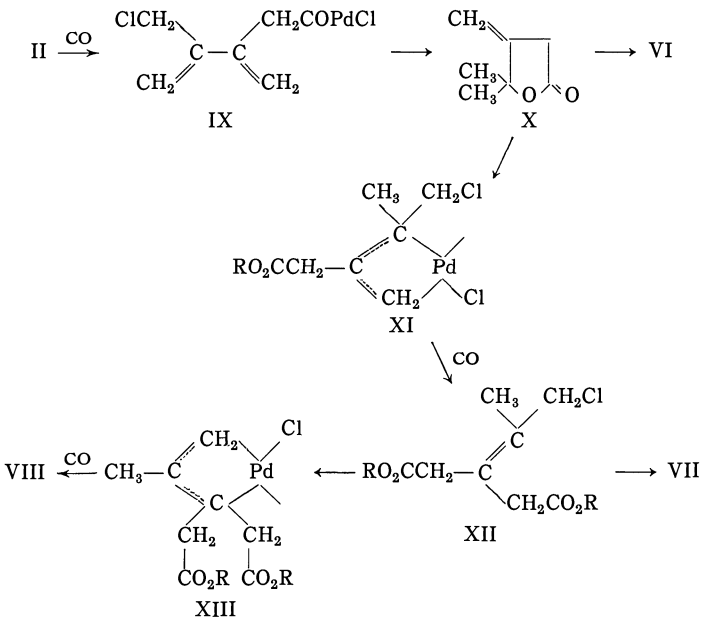

(3.9 g) was obtained from sodium chloropalladate (6.0 g) and sodium propionate in propionic acid (200 m*l*) and methanol (100 m*l*). The complex was recrystallized from chloroform-methanol mixture, mp 169—170°C (decomp).

Found: C, 28.30; H, 3.53; Cl, 14.38%, mol wt, 516. Calcd for $(C_6H_9O_2PdCl)_2$: C, 28.26; H, 3.56; Cl, 13.90%, mol wt, 510. NMR. 8.80 (triplet, CH_3-), 7.51 (quartet, -CH_2-CO-), 6.88, and 5.96 (doublets), $J_{1,2}=2.4$ cps.

Carbonylation of the Complex I. The complex I (9.5 g) in methanol (60 m*l*) was carbonylated at 100°C under carbon monoxide pressure (100 atm) for 15 hr. After the usual work-up, 4.0 g of the product was isolated by distillation at 145—146°C. It was identified as methyl 3-chloro-3-butenoate by the following evidences. IR, 1750 and 1640 cm^{-1}, NMR spectrum, 6.55 (-CH_2-), 6.11 (CH_3), 4.44 (=CH_2).

Found: C, 44.81; H, 5.31; Cl, 26.24%, mol wt, 134. Calcd for $C_5H_7O_2Cl$: C, 44.63; H, 5.24; Cl, 26.35%, mol wt, 134.5.

Carbonylation of the Complex III. The complex (2.5 g) and benzene (40 m*l*) were placed in a glass vessel with a gas inlet capillary, and then the vessel was placed in an autoclave. The carbonylation was carried out at 100°C under carbon monoxide pressure (100 atm) for 16 hr with shaking. The product was heated with 10 m*l* of ethanol and the solvents were removed by distillation. The residue was distilled under reduced pressure (50°C/14 mmHg) to give 0.3 g of the product, which was identified as ethyl acetoacetate by gas chromatography, IR spectrum and the mixed melting point determination of its dinitrophenylhydrazone (mp 95—96°C).

Carbonylation of Allene. Ethanol (50 m*l*) and palladium chloride (3 g) were placed in the glass vessel which was placed in the autoclave. Allene (10 m*l*) was distilled into the autoclave and then carbon monoxide was charged (100 atm). The autoclave was shaken at 150°C for 20 hr. The precipitated palladium was removed by filtration and ethanol was removed by distillaton. The residue was subjected to the distillation under reduced pressure (103°C/9 mmHg) to give 0.5 g of ethyl itaconate. The structure was determined by IR and NMR spectra. IR 1730, 1640 cm^{-1}, NMR 3.76, 4.35 (=CH_2), 5.85 (-CH_2-), 6.76(CH_2) 8.73 (CH_3).

Found: C, 58.32; H, 7.68%, mol wt, 189. Calcd for $C_9H_{14}O_4$: C, 58.05; H, 7.58%, mol wt, 186.2.

Carbonylation of the Complex II. The complex (10 g) was carbonylated in ethanol (60 m*l*) at 110°C under carbon monoxide pressure (110 atm) for 15 hr with shaking, and pressure drop of 13 atm was observed. After the usual work-up, the residue was distilled under reduced pressure to give the following two fractions. The first fraction (80—110°C/3 mmHg, 4.6 g) was found to be a mixture of two compounds and they were separated by preparative gas chromatography. One of them solidified on standing and was recrystallized from ether-hexane mixture, mp 43.5—45°C (reported mp 44.5—46.5°C[10]), yield 24.4%. This compound was identified as 4-hydroxy-3,4-dimethyl-2-pentenoic acid γ-lactone by the following evidence. IR, 1750, 1630 cm^{-1}, NMR 8.53(CH_3), 7.94(CH_3), 4.40 (=CH-).

Found: C, 66.54; H, 7.97%, mol wt, 130. Calcd for $C_7H_{10}O_2$: C, 66.64; H, 7.99%, mol wot, 126.

The compound was identified by the comparison with the authentic sample which was prepared by

10) J. M. Stewart and D. W. Wooley, *J. Am. Chem. Soc.*, **81**, 4951 (1959).

11) S. G. Matsoyan, G. A. Chukhadzhyan and S. A. Vartanyan, *Zhur. Obshchei. Khim.*, **30**, 1202 (1960); *Chem. Abstr.*, **55**, 374 (1961).

the known method.[10,11] The other one was redistilled (132℃/10 mmHg, 20.2%) and found to be ethyl 3-isopropylideneglutarate by the following evidence. IR, 1740 cm^{-1} NMR, 8.75 (6H, $-CH_3$), 8.26 (6H, $-CH_3$), 6.94 (4H $-CH_2-$), 5.98 (4H, $O-CH_2-$).

Found : C, 63.01 ; H, 8.79%, mol wt, 220. Calcd for $C_{12}H_{20}O_4$: C, 63.13 ; H, 8.83%, mol wt, 228.

The ester was ozonized in ethyl acetate containing tetracyanoethylene and the ozonide was treated with dinitrophenylhydrazine. The hydrazone was separated by passing through a silica column using benzene as an eluate to give two hydrazones. One of them was recrystallized from ethanol and identified as the hydrazone of acetone, mp 125—126℃. The other was recrystallized from aqueous ethanol, mp 85—86 ℃. The hydrazone was identified as that of ethyl 3-oxoglutarate by mixed melting point determination with an authentic sample.

Found: C, 47.20; H, 4.77; N, 14.64%. Calcd for $C_{15}H_{18}N_4O_8$: C, 47.12; H, 4.75; N, 14.66%.

The second fraction was redistilled (125—127℃/3 mmHg) to give 1.1 g of a triester which was identified as ethyl 3-(ethoxycarbonylmethy)-4-methyl-3-hexenedioate by the following evidences. IR, 1735 cm^{-1}, NMR (Fig. 2) 8.76 and 5.92 (3 ethyl groups), 8.17 (methyl), 6.94 and 6.86 (3 methylene groups).

Found : C, 59.84 ; H, 8.04%, mol wt, 306. Calcd for $C_{15}H_{24}O_6$: C, 59.98 ; H, 8.05%, mol wt, 300.

The ester was ozonized as before and the product was converted into dinitrophenylhydrazones, which were separated into two fractions by column chromatography through silica gel using benzene as an eluate. One of them was identified as the hydrazone of ethyl acetoacetate by IR and mixed melting determination (95—96℃) with an authentic sample.

Found : C, 46.51 ; H, 4.45 ; N, 18.07%. Calcd for $C_{12}H_{14}N_4O_6$: C, 46.45 ; H, 4.55 ; N, 18.06%.

The other hydrazone was identified as that of ethyl 3-oxoglutarate (mp 85—86℃).

NOTES

Studies on the Thin Layer Chromatography of Condensed Phosphates

Takeo YAMABE, Takaya IIDA and Nobuharu TAKAI

The Institute of Industrial Science, The University of Tokyo, Roppongi, Minato-ku, Tokyo

(Received January 12, 1968)

It is said that the chemistry of phosphates has been developed through the improvement of the techniques of the separation and the analysis of phosphates. The separation and the analysis of phosphates with various degrees of condensation have been tried by many methods.[1-3] Among them, the thin layer chromatography is one of the most effective, because a relatively short time of running and a small amount of samples are required and the separation is fairly good.

Thin layers are usually made by fixing silica gels or alumina powders with gypsum, but gypsum cannot be used for substances such as phosphates which react with it. Accordingly, the present authors have improved the method and the result will be presented.

Experimental

Silica gel (Wakogel B-O, 10 g) or cellulose powder (Toyo-Roshi >300 mesh, 10 g) was suspended in a 0.05% aqueous sodium polyacrylate (30 m*l*) or a 1% cellulose acetate solution in *N, N*-dimethylformamide (35 m*l*). The thin layers with the following combinations were prepared as usual; silica gel-sodium polyacrylate, silica gel-cellulose acetate, cellulose powder-sodium polyacrylate, and cellulose powder-cellulose acetate. As samples of phosphates with various degrees of condensation, sodium salts of orthophosphate, pyrophosphate, tripolyphosphate, trimetaphosphate, and tetrametaphosphate were used.

On the thin layer plates, 1 μl of 0.2% aqueous solution of each phosphate was spotted with a microsyringe, and developed in a closed chamber at room temperature. When the solvent was developed up to 10 cm from the spotting point, the plates were taken out and dried in air. Then the phosphates were hydrolyzed with an aqueous nitric acid solution (1 : 1) and colored with ammonium molybdate and stannous chloride.[4,5] The developing solvents are shown in Table 1.

TABLE 1. DEVELOPING SOLVENTS

Acidic solvent		Basic solvent	
No.	Main solvent	No.	Main solvent
A1	M	B1	M-*n*B
A2	E	B2	E-*n*P
A3	*i*P	B3	E-*i*B
A4	*i*P	B4	*n*P
A5	*i*P-*t*B	B5	*n*P-*i*B
A6	*i*P-D	B6	Py
A7	*i*P-EG		
A9	*t*B		
A11	D		
A12	A		
A0	A: 175 m*l*, AA: 55 m*l*, W: 45 m*l*		
B0[6]	M: 150 m*l*, Am: 45 m*l*, TC: 10 m*l*, W: 90 m*l*		

1) M: methanol, E: ethanol, *n*P: *n*-propanol, *i*P: isopropanol, *n*B: *n*-butanol, *i*B: isobutanol, *t*B: *t*-butanol, D: dioxane, Py: pyridine, EG: ethylene glycol monomethyl ether, A: acetone, AA: acetic acid, Am: ammonia water(28%), TC: aqueous trichloroacetic acid (10%), W: water

2) A1—A12 and B1—B6: for detail see S. Ohashi, Mukikagaku-Zensho IV-6 "Phosphorus," p. 42.

Results and Discussion

The R_f values and the time of running are shown in Tables 2, 3, 4, and 5.

When acidic solvents are used, the order of R_f values is

orthophosphate > polyphosphate > metaphosphate

1) S. Ohashi, Mukikagaku-Zensho IV-6 "Phosphorus," Maruzen, Tokyo (1965), p. 37.

2) J. R. Van Wazer, "Phosphorus and Its Compounds," Vol. I, Interscience Publishers, Inc., New York (1964), p. 441.

3) T. Kubo and E. Niki, *Bunseki Kagaku*, **11**, 1085 (1962).

4) E. Karl-Kroupa, *Anal. Chem.*, **28**, 1091 (1956).

5) D. N. Bernhart and W. B. Chess, *ibid.*, **31**, 1026 (1959).

6) H. Seiler, *Helv. Chim. Acta*, **44**, 1753 (1961).

TABLE 2. R_f VALUES
(Cellulose powder-Cellulose acetate)

No.	O	P	Tr	TrM	TeM	Time (min)
A0	.72	.10	.04	.10	.00	18
A1	.97	.90	.74	—	.30	17
A2	.99	.90	.80	—	.74	28
A3	.88	.60	.37	.31	.13	45
A4	.67	.21	.15	.08	.02	22
A5	.80	.55	.43	.37	.24	56
A6	.88	.52	.36	.22	.17	36
A7	1.00	.94	.91	—	.79	63
A9	.83	.46	.17	.10	.10	90
A12	.15	.03	.02	—	.37	29
B0	.00	.00	.00	.93	.90	15
B1	.50	.00	.00	.78	.68	19
B2	.49	.20	.26	.73	.63	40
B3	.45	.26	.33	.60	.56	45
B4	.29	.00	.00	.42	.30	35
B5	.44	.27	.33	.59	.52	55
B6	.15	.00	.02	.71	.53	30

O: orthophosphate, P: pyrophosphate,
Tr: tripolyphosphate, TrM: trimetaphosphate,
TeM: tetrametaphosphate

TABLE 3. R_f VALUES
(Cellulose powder-Sodium polyacrylate)

No.	O	P	Tr	TrM	TeM	Time (min)
A0	.63	.07	.02	.09	.00	14
A1	.87	.77	.62	—	.32	15
A2	.93	.83	.84	—	.32	26
A3	1.00	.48	.15	—	.00	27
A4	.62	.24	.12	.12	.05	24
A5	.83	.58	.50	.43	.25	57
A6	.73	.45	.31	.24	.14	34
A7	.94	.86	.82	—	.71	77
A9	.80	.45	.20	.15	.03	71
A11	.91	.88	.79	.17	.46	30
A12	.19	.07	.09	—	.34	17
B0	.57	.13	.60	.91	.90	17
B1	.42	.06	.08	.80	.74	21
B2	.49	.20	.26	.73	.63	40
B3	.45	.26	.33	.60	.56	45
B4	.32	.15	.13	—	.48	35
B5	.44	.27	.33	.59	.52	55
B6	.15	.00	.02	.71	.53	30

TABLE 4. R_f VALUES
(Silica gel-Cellulose acetate)

No.	O	P	Tr	TrM	TeM	Time (min)
A1	.28	.05	.20	—	.03	75
A4	.36	.06	.02	.00	.00	390
A9	.44	.05	.03	.06	.02	390
B0	.62	.13	.24	.77	.68	75
B2	.25	.05	.09	.56	.43	180
B3	.14	.02	.05	.26	.20	110

TABLE 5. R_f VALUES
(Silica gel-Sodium polyacrylate)

No.	O	P	Tr	TrM	TeM	Time (min)
A5	.51	.00	.10	.55	.54	360
A7	.39	.29	.30	—	.54	360
B0	.62	.00	.05	.83	.69	62
B2	.20	.05	.05	.61	.48	150
B3	.29	.00	.00	.46	.44	175
B6	.13	.02	.01	.58	.18	120

and when basic solvents are used, the order of R_f values is

metaphosphate > orthophosphate > polyphosphate.

These orders agree with those in the paper chromatography.[3] It was proved that the thin layer chromatography by the method proposed in this report was very useful for the separation and the analysis of condensed phosphates. The cellulose acetate, used as the binder, gave almost the same results for all the solvents, but when the system of silica gel, sodium polyacrylate, and acidic solvent was used, it is apt to take much time of running and caused tailing of spots.

The authors wish to express thanks to Dr. S. Hayano and Dr. M. Seno in our Institute for their kind advices.

Quenching of Fluorescence of Pyrene and Anthracene by Electron-accepting Substances

Akira NAKAJIMA*[1] and Hideo AKAMATU

Department of Chemistry, Faculty of Science, The University of Tokyo, Hongo, Tokyo

(Received January 22, 1968)

In despite of many investigations,[1] the inner mechanism of fluorescence quenching is not clearly understood. It has been pointed out that fluorescence quenching by foreign substances might be closely related to the electron transfer reaction or the charge-transfer interaction between an excited fluorescent molecule and a quencher molecule.[2-8] If such a reaction or an interaction plays an important role in the mechanism of fluorescence quenching, the quenching ability of a quencher molecule may be connected with its electron-affinity or ionization potential.[9] As far as we know, however, only a few works[9-11] have been done along this line.

In this investigation, the electron-accepting substances were employed for quenching the fluorescence of pyrene and anthracene, and a study was attempted on the relation between the quenching constants and the electron-affinities of the quencher molecules, on the basis of the quenching mechanism involving the charge-transfer interaction between the fluorescent hydrocarbons and the quenchers.

Experimental

Pyrene and anthracene were purified by recrystallization, zone-refining and sublimation in vacuum. The substances employed as quenchers were repeatedly recrystallized and then sublimed in vacuum. The solvents used were dried and distilled benzene for the pyrene solution and G. R. grade acetone for the anthracene solution.

The measurements of the fluorescence spectra and the fluorescence intensities were made with a Hitachi EPS-2U recording spectrophotometer mounted with an attachment for fluorescence measurement. The light source for fluorescence excitation was a super-high pressure mercury lamp with a suitable UV filter (mainly 365 mμ). The measurements were made at room temperature for the benzene solution of pyrene and the acetone solution of anthracene, the concentrations of which were 2.52×10^{-3} and 1.00×10^{-3} (mol/l), respectively. These solutions were not degassed, but it is usually assumed that the quenching action of a quencher is independent of dissolved oxygen.[8b]

Since the shape of the fluorescence spectra of these aromatic hydrocarbons did not practically change in the presence of a quencher, the relative fluorescence intensities were obtained from the heights at a given wavelength for the various quencher concentrations. At higher quencher concentrations, however, the absorption of exciting light by the quencher as well as the reabsorption of fluorescence gave rise to serious errors in the observed fluorescence intensities. They were appropriately corrected by taking account of the optical geometry of excitation and observation and of the quencher concetrations.[12]

From a plot of the relative fluorescence intensities against the logarithms of quencher concentrations, the quenching constant was obtained as the reciprocal of the half-value-concentration, where the value of the relative fluorescence intensity was reduced to half the value in the absence of the quencher.

*1 Present address: Research Institute of Applied Electricity, Hokkaido University, Sapporo.

1) Th. Förster, "Fluoreszenz Organischer Verbindungen," Vandenhoeck & Ruprecht, Göttingen (1951).

2) E. Bauer, *Z. phys. Chem.*, **B16**, 465 (1932).

3) J. Weiss and H. Fischgold, *ibid.*, **B32**, 135 (1936); J. Weiss, *Trans. Faraday Soc.*, **35**, 48(1939).

4) L. Orgel and D. Phil, *Quart. Rev.*, **8**, 422 (1954).

5) H. Leonhardt and A. Weller, "Luminescence of Organic and Inorganic Materials," ed. by H. Kallmann and G. Spruch, John Wiley & Sons Inc., New York (1962), p.74; *Ber. Bunsenges. physik. Chem.*, **67**, 791 (1963).

6) N. Mataga, *Mol. Phys.*, **10**, 201, 203 (1966).

7) H. Beens, H. Knibbe and A. Weller, *J. Chem. Phys.*, **47**, 1183, 1184 (1967).

8) a) T. Miwa and M. Koizumi, This Bulletin, **39**, 2588 (1966). b) T. Miwa and M. Koizumi, *ibid.*, **40**, 2254 (1967).

9) D. Majumdar and S. Basu, *J. Chem. Phys.*, **33**, 1199 (1960).

10) P. McCartin, *J. Am. Chem. Soc.*, **85**, 2021 (1963).

11) G. Schenk and N. Radke, *Anal. Chem.*, **37**, 910 (1965).

12) The observed fluorescence intensities, I_f^{obs}, were corrected by the following formula:

$$I_f^{cor} = \frac{D_Q+D_A}{1-10^{-(D_Q+D_A)}} \frac{1-10^{-D_A}}{D_A} \frac{1-10^{-D_F}}{2.303 D_F} I_f^{obs}$$

where D_A and D_Q are the absorbances at the exciting wavelength of a fluorescer and a quencher, respectively, and D_F is the absorbance of the solution at the wavelength where the fluorescence intensities were measured.

For the pyrene solution, the quenching constants were estimated for both monomer and excimer fluorescence bands with the peaks at 396 mμ and 480 mμ, respectively.[13]

Results and Discussion

The quenching constants obtained for a series of electron-accepting substances are shown in Table 1 together with the values of their electron affinities. For the pyrene solution the equilibrium constants, K, for charge transfer complex formation with these electron-accepting substances, are also given.

In studies on fluorescence quenching, it is important to know the type of the molecular process and the nature of the inner mechanism of fluorescence quenching. Two types of quenching processes, static and dynamical ones, can be assumed.[1,14] In a static quenching process, the non-fluorescent molecular complex, (AQ), is formed between a fluorescer, A, and a quencher, Q, in the ground state and only the uncomplexed fraction of the fluorescer contributes to the observed emission. This is given by the following scheme:

$$\begin{array}{ccc} A + Q & \rightleftharpoons & (AQ) \\ {\scriptstyle h\nu_a}\downarrow\uparrow{\scriptstyle h\nu_f} & {\scriptstyle K} & {\scriptstyle h\nu_a}\downarrow\uparrow{\scriptstyle \text{heat}} \\ A^* & & (AQ)^* \end{array}$$

The equilibrium constant, K, is expressed as

$$K = \frac{[(AQ)]}{[A][Q]}.$$

If a static quenching process can be assumed, the quenching constant, k, may be approximately given by the following form:

$$k = \frac{K}{KC+1}$$

where C is the initial concentration of fluorescer. This equation can easily be derived for 1 : 1 complex formation, if the complexed fraction is sufficiently small, as is usually the case. For the pyrene solutions, as is seen from Table 1, $C = 2.52 \times 10^{-3}$ (mol/l) and K= 0.1—20 (l/mol); therefore, k should be 0.1—20, which is, however, inconsistent with the observed k-values, *i.e.*, 10^2—10^3.

The fact that the observed k-values are much larger than those estimated on the assumption of a static quenching process, leads to the predominance of the dynamical quenching process.[10,11,13,14] in which a quencher molecule encounters an excited fluorescer molecule by diffusion through the solution, forming an excited complex in which deactiva-

13) K. Kasper, *Z. physik. Chem., N. F.*, **12**, 52 (1957).
14) A. Weller, *Discussions Faraday Soc.*, **27**, 28 (1959).

TABLE 1. QUENCHING CONSTANTS OF ELECTRON-ACCEPTING QUENCHERS FOR FLUORESCENCE OF PYRENE AND ANTHRACENE

Quencher	Electron-affinity[a] (eV)	K[b] (l/mol)	Quenching constant, k(l/mol) Pyrene		Anthracene
			Monomer	Excimer	
Phthalic anhydride	0.15	c)	238	385	122
Maleic anhydride	0.57	c)	345	770	35[e]
Tetrachlorophthalic anhydride	0.58	2.7	303	500	227
p-Benzoquinone	0.6	c)	417	833	185
sym-Trinitrobenzene	0.7	3.7	476	909	278
Pyromellitic dianhydride	0.85	—	—	—	132
2,5-Dichlorobenzoquinone	1.15	c)	870	1110	370
p-Chloranil	1.37	c)	—	—	1100[d]
p-Bromanil	1.4	c)	2040[d]	2940[d]	—
2,3-Dicyanobenzoquinone	1.7	0.2	1790	2270	556
Tetracyanoethylene	1.8	19	2380	2380	376[e]
Iodine	(1.8)	c)	690	1000	—
2,4-Dinitrochlorobenzene		—	—	—	278
2,3-Dichloronaphthoquinone		—	—	—	1000[d]

a) G. Briegleb, *Angew. Chem.*, **76**, 326 (1964).
b) Estimated by the Benesi-Hildebrand's method.
c) The charge transfer spectra were not separably observed.
d) This large value may have resulted from the insufficient correction for the reabsorption of fluorescence by the quencher.
e) The observed small value is probably due to the Diels-Alder reaction.

tion of energy is effective. That the absorption spectra of the aromatic hydrocarbon were not affected by the addition of a quencher, is also favorable to a dynamical quenching process.

As for the inner mechanism, the possibility of the electronic energy transfer can be eliminated because of the small overlap of the fluorescence spectra of the fluorescers with the absorption spectra of the quenchers. Further, it can be seen from Table 1 that the quenching abilities of these quenchers can not consistently be explained by the heavy atom effect, which enhances the intersystem-crossing from the excited singlet state to the triplet state in the fluorescer molecule.

Comparing the k-values with the electron-affinities enables one to find a fairly good correlation between them. This parallelism between the quenching constants[15] and the electron-affinities suggests that the charge transfer interaction should play an important role in the fluorescence quenching mechanism for these systems.

The charge transfer mechanism of fluorescence quenching may be interpreted in terms of the formation of excited-state charge transfer complex due to the increased mixing of the locally excited (A*Q) and the charge transfer (A^+Q^-) configurations on the mutual approach of A* and Q.[6,7]

For the systems of pyrene-phthalic anhydride and pyrene-tetrachlorophthalic anhydride, the complex emissions were observed at 510 mμ and 550 mμ,[16] respectively, in benzene solution at room temperature. The intensity of these complex emissions increased with the rise of temperature. Since the viscosity of the solvent decreases at higher temperatures, the molecules diffuse in solution more easily to form the excited complexes, resulting in the complex emission. This phenomenon will also support a diffusional process in excited complex formation.

Since the observed 'apparent' quenching constants for excimer fluorescence, k_e, are larger than the quenching constants for monomer fluorescence, k_m, it can safely be said that the quenching of pyrene excimer by these quenchers does occur.[17] Furthermore, the fact that $k_e < 2.4\,k_m$ shows that the excimer is less sensitive to the quenching action of these quenchers,[13] indicating that the electron-donating ability of excimer is smaller than that of the excited monomer.

The authors are indebted to Professor Hiroaki Baba of Hokkaido University for his valuable advices.

15) Strictly speaking, the k-value for a quencher depends on its diffusion constant in solution. However, the differences among the diffusion constants of these quenchers are too small to change the order of k-values.

16) The complex emission of pyrene-tetrachlorophthalic anhydride was the mirror image of the corresponding charge transfer complex absorption.

17) A kinetic analysis gives the following relation:

$$k_e \geqq k_m + k_{te}$$

where k_{te} is the 'true' quenching constant for excimer fluorescence, defined as an analogous expression to k_m.

In the case where no 'true' quenching of excimer occurs, $k_e = k_m$; otherwise holds the inequality. It can also be shown that when the quenching of excimer occurs to the same extent as the quenching of excited monomer,

$$k_e = (1+\sqrt{2})k_m = 2.4\,k_m.$$

Zinc 2,2,2-Trichloroethoxide. A Soluble Zinc Alcoholate

Takeo SAEGUSA and Takashi UESHIMA

Department of Synthetic Chemistry, Kyoto University, Sakyo-ku, Kyoto

(Received January 24, 1968)

In our previous studies,[1-3] aluminum 2,2,2-trichloroethoxide (I) was prepared and its properties were compared with those of such usual aluminum alcoholates as aluminum isopropoxide and *t*-butoxide. I is distinguished from usual aluminum alcoholates by the following properties: i) I dissociates to a monomer in donor solvents, whereas usual aluminum alcoholates are in associated form even in donor solvents. ii) I is a strong

1) T. Saegusa and T. Ueshima, *Inorg. Chem.*, **6**, 1679 (1967).

2) T. Saegusa and T. Ueshima, to be published in This Bulletin.

3) T. Saegusa, S. Tomita and T. Ueshima, *J. Organometal. Chem.*, **10**, 360 (1967).

Lewis acid and causes the cationic polymerization of vinyl monomers and cyclic ethers. iii) The insertion reaction of methylene into the Al-OR linkage in the reaction with diazomethane is observed in I, but not in usual aluminum alcoholates. The present study deals with the preparation and the properties of zinc 2,2,2-trichloroethoxide (II).

Experimental

Synthesis of II. Under a nitrogen atmosphere, 0.1 mol of diethylzinc in 20 m*l* of ethyl ether was added slowly with vigorous stirring into a mixture of CCl_3CH_2OH (0.2 mol) and ethyl ether (50 m*l*) at −50—−20°C. Then the reaction system was allowed to warm to room temperature and finally heated to reflux for 2 hr. A white precipitate separated from the solution; this was washed repeatedly with tetrahydrofuran to remove C_2H_5Zn-OCH_2CCl_3[4] and the starting materials. Reprecipitation was performed by the solvent-precipitant combination of pyridine and *n*-heptane. The yield was about 75%. Found: Zn, 18.08%. Calcd for $C_4H_4Cl_6O_2Zn$: Zn, 18.02%. The trichloroethoxy group was quantitatively determined by the v.p.c. analysis of trichloroethanol in the acid hydrolysis mixture. The CCl_3CH_2OH/Zn ratio was 1.94 (Calcd 2.00). II was decomposed without subliming under reduced pressure (0.08 mmHg) at *ca.* 120°C.

Results and Discussion

Zinc dialcoholates of unsubstituted alcohols, such as methanol and ethanol are known to be insoluble in organic solvents as a result of the strong tendency of the association through the oxygen atom of an alkoxy group.[5] The II prepared in the present study, however, was found to be soluble in the systems containing strong donor solvents, such as pyridine, quinoline, dimethylaniline, morpholine, piperidine, *N*-ethylpiperidine, and dimethyl sulfoxide. Ethers, ketones, esters, and trialkylamines were not effective in solubilizing II. In the present study, reference experiments showed that $Zn(OEt)_2$ was not soluble in any solvents which solubilized II. The specific solubility character of II may be due to the three chlorine atoms of the Cl_3CCH_2O-group, which have an electron-withdrawing effect to decrease the nucleophilicity of the oxygen of the Cl_3CCH_2O-group. The coordination of a donor molecule of a solvent onto zinc prevails over that of the oxygen of the Cl_3CCH_2O-group of another molecule of II. Thus, the coordination of a donor to zinc breaks the association through the oxygen-zinc bond and, hence, solubilizes II. On the contrary, the oxygen atom in usual zinc dialcoholates has a stronger nucleophilicity and a donor molecule does not break the association.

This explanation has been supported by the IR spectrum study. Three bands, at 1605, 1580, and 1572 cm^{-1} of the IR spectrum of the II-pyridine system (in Nujol), were due to the stretching vibration ($\nu_{C=N}$ or $\nu_{C=C}$) of pyridine. The first band, at 1605 cm^{-1}, can reasonably be ascribed to the pyridine which is coordinating onto the zinc atom,[1,6] whereas the latter two bands are due to free pyridine. On the other hand, the IR spectrum of the $Zn(OCH_2CH_3)_2$-pyridine system (in Nujol) showed only the two bands of free pyridine. Thus, the IR study has indicated that pyridine coordinates onto the zinc of II, but not onto the zinc of $Zn(OCH_2CH_3)_2$.

The coordination of pyridine to II, however, was not so strong that the pyridine-II complex could not be isolated. The recrystallization and evaporation of the excess pyridine-II mixture was attempted to isolate the pyridine-II complex. Pyridine was easily removed from the complex, and II was always left in these trials. A rather weak coordination of pyridine to II was further indicated by the finding that more than 10 mol of pyridine were required in order to dissolve 1 mol of II in a large amount of benzene. The IR spectrum indicated that a large portion of pyridine existed in a free, non-coordinating form.

The NMR spectrum of the solution of II in the benzene-pyridine mixture showed a sharp singlet at 4.70 ppm (δ) at temperatures from −30 to 23°C. This observation is taken to indicate that II is in a monomeric form in the solvent system containing pyridine. The effect of the CCl_3 group in II corresponds to that in $Al(OCH_2CCl_3)_3$.[1] These two halo-alcoholates differ from each other in acid strength. The shift of the $\nu_{C=N(or\ C=C)}$ of pyridine by coordination was 30 cm^{-1} in the pyridine-$Al(OCH_2CCl_3)_3$ complex; this shift was larger than that of 25 cm^{-1} in the pyridine-II complex (not isolated). In addition, the 1 : 1 complex of $Al(OCH_2CCl_3)_3$ with pyridine was isolated,[1] whereas no complex of II was isolated.

4) T. Saegusa and T. Ueshima, *ibid.*, **13**, 249 (1968).

5) G. E. Coates and D. Ridley, *J. Chem. Soc.*, **1965**, 1870.

6) M. R. Basila, T. R. Kanter and K. H. Rhee, *J. Phys. Chem.*, **68**, 3197 (1967).

Studies of Thin-layer Chromatography of Inorganic Salts. I. The Separation of Inert Metallic Complexes by Means of Thin-layer Chromatography on Silica Gel[1]

Tetsuo BABA,[2] Hayami YONEDA[3] and Masayuki MUTO

Department of Chemistry, Wakayama University, Masagocho, Wakayama

(Received February 5, 1968)

Two kinds of equilibrium, partition and adsorption, can be considered as the main types of retention of solutes onto adsorbing material during development. In paper chromatography, partition mechanism has been widely accepted because adsorption sites of paper are covered with water or hydrophilic solvent, so that the direct adsorption of solute molecules is considered to be negligible. However, one of the present authors[4] studied the paper chromatography of inert cobalt(III) complexes having different ionic charges using an aqueous ethylamine solution as a developer and found that the R_f values of the complexes increase with the decrease of their positive ionic charge to reach nearly unity in the case of complex anions. Thus an adsorption mechanism was established at least in the case where inorganic salts are developed with an aqueous solution.

A similar kind of adsorption mechanism is expected in thin-layer chromatography. In this case, one can select adsorbents as well as developers so that one can carry out the development under much wider range of conditions than in paper chromatography. Therefore much more informations can be expected from the study of thin-layer chromatography. The present paper will discribe the results obtained in thin-layer chromatography, in which inert metallic complexes were developed on silica gel with aqueous solutions of simple inorganic salts.

Experimental

As an adsorbent, Merck's silica gel H, prepared for thin-layer chromatography according to Stahl's method was used without further purification.

The compounds developed in this investigation were inert metallic complexes having various ionic charges: $[Co(NH_3)_6](ClO_4)_3$, $[CoCH_3CO_2(NH_3)_5](ClO_4)_2$, *cis*-$[Co(CHCO_3)_2en_2]NO_3$, α-$[Cogly_3]$, Na-$[Co(S_2O_3)_2en_2]$, $Na_3[Co(NO_2)_6]$ and $K_3[Crox_3]$, where *en*, *gly* and *ox* denote ethylenediamine, glycinate anion and bivalent oxalate anion, respectively. The development was carried out at room temperatures of 22—25°C. The spots of the cobalt complexes were detected by spraying a potassium sulfide solution, while the spot of the chromium complex could be easily identified by its characteristic blue color.

Results and Discussion

Figure 1 shows the chromatogram developed with distilled water. A marked contrast can be seen between the behavior of the anionic and the neutral complexes and that of the complex cations; $[Crox_3]^{3-}$, $[Co(NO_2)_6]^{3-}$, $[Co(S_2O_3)_2en_2]^-$ and $[Co\,gly_3]^0$ show large R_f values, while $[Co(NH_3)_6]^{3+}$, $[CoCH_3CO_2(NH_3)_5]^{2+}$ and $[Co(CH_3CO_2)_2en_2]^+$ remained near the origin. This fact indicates that the adsorptive power of silica gel is acting selectively upon the complex cations but not upon the complex anions and the neutral complex.

Next, in order to palliate the strong adsorption of the complex cations and to see the effect of the different ionic charges, the

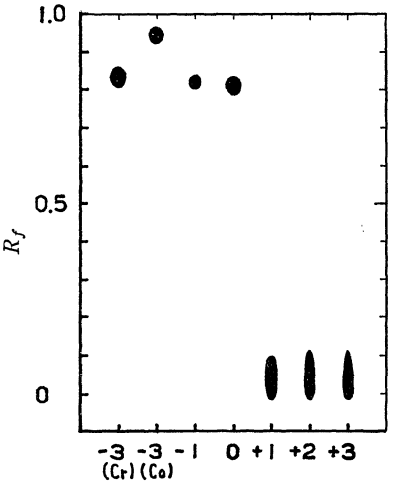

Fig. 1. Chromatogram for distilled water system.

1) Presented at the 17th Symposium of Coordination Chemistry at Hiroshima University, December, 1967.

2) On leave from the Minoshima High School, Arita-shi, Wakayama.

3) Correspondence to be addressed to this author.

4) H. Yoneda, This Bulletin, **40**, 2442 (1967).

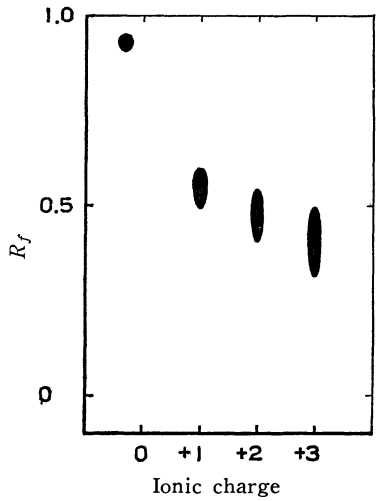

Fig. 2a Chromatogram for 0.1M KCl system.

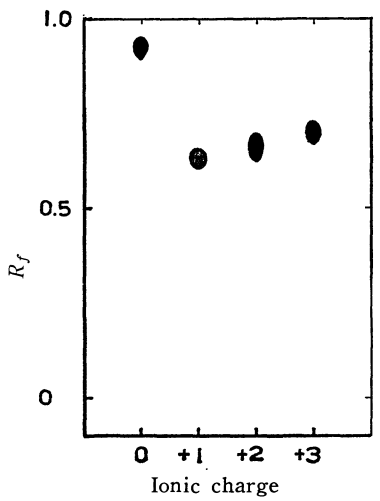

Fig. 2b Chromatogram for 0.2M KCl system.

development was carried out with several potassium chloride solutions of stepwisely varied concentration. Thus the complex cations moved from the origin, and their R_f values increased with the increase of the salt concentration. At low concentrations up to 0.1M, the R_f values of the complex cations showed a regular increase with the decrease of the ionic charge as can be seen in Fig. 2a (+1> +2>+3). However, this regular trend in variation of R_f values became irregular above 0.1M, and at 0.2M the order of the R_f values was completely reversed as is seen in Fig. 2b (+3>+2>+1). This order of the R_f values (+3>+2>+1) was maintained above 0.2M and at 0.5M all the R_f values became near 0.9. A similar variation of R_f value was also observed in the case of ammonium chloride

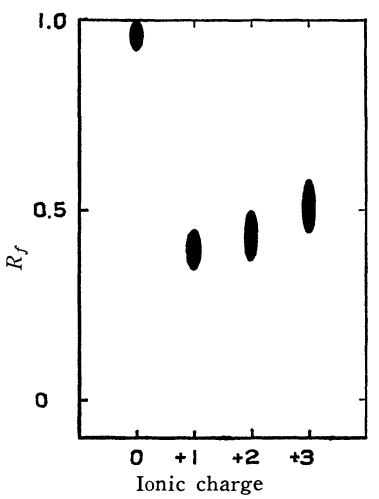

Fig. 3. Chromatogram for 0.05M Na_2SO_4 system.

solution.

When sodium sulfate solutions were used as developer, the above-mentioned phenomena were observed at much lower concentrations; at 0.01M the complex cations moved from the origin, and the order of the R_f values was +1>+2>+3, and at 0.05M this order was completely reversed as is seen in Fig. 3.

The R_f value of the neutral $[Cogly_3]^0$ complex was always about 0.9 and did not show the salt effect.

These results can be explained as follows. Since silica gel is charged negatively in contact with water, it adsorbs strongly the complex cations. This kind of electrostatic attraction can be reduced by the addition of an electrolyte such as potassium chloride or sodium sulfate. The R_f value of the complex cation increases with the decrease of positive ionic charge, which reflects decrease of the electrostatic attraction. As the electrolyte concentration increases, association of anions around the complex cation takes place to a considerable extent to result in appreciable decrease of the apparent charge of the complex cation. Since such association proceeds to a greater extent at higher concentrations of the salt anions and for higher positive ionic charges of the complex cation, the order of the apparent charges of the complex cations $[Co(NH_3)_6]^{3+}$, $[CoCH_3CO_2(NH_3)_5]^{2+}$ and $[Co(CH_3CO_2)_2en_2]^+$ becomes reverse to their ionic charges. Thus the electrostatic adsorption onto silica gel is in the order of $[Co(CH_3CO_2)_2en_2]^+$-anions > $[CoCH_3CO_2(NH_3)_5]^{2+}$-anions > $[Co(NH_3)_6]^{3+}$-anions, and the reverse of the R_f value order can be understood.

Studies on Heteroaromaticity. XVII.[1] Photorearrangement of *N*-(2-Oxo-3-indolylidene)-aniline *N*-Oxides

Tadashi SASAKI and Masahiko TAKAHASHI

Institute of Applied Organic Chemistry, Faculty of Engineering, Nagoya University, Chikusa-ku, Nagoya

(Received February 7, 1968)

It is well known that the photochemical rearrangement of heterocyclic *N*-oxides is followed by ring-enlargement or -contraction,[2] but little has been reported on the similar reactions of exocyclic nitrones, though there are several papers published concerning their photochemical reactions.[3,4]

The present note deals with the experimental results of photochemical ring-enlargement of *N*-(2-oxo-3-indolylidene)-aniline *N*-oxide[5] (I), its 5,7-dibromo- (IV) and 5-nitro analog (VI), exocyclic ketonitrones of isatin and its analogs. The photochemical reactions of isatin itself[6] and isatin ylid[7] have been reported.

I was irradiated in tetrahydrofuran at room temperature with a 100 watt high pressure mercury lamp to afford III as colorless needles, which was identical with an authentic sample of 3-phenyl-2,4-(1*H*,3*H*)-quinazolinedione[8] in every respect.

Irradiation of some nitrones leads to the formation of the isomeric oxaziridines which are convertible to the corresponding amides[3] by further thermal or photochemical rearrangement and thermal rearrangement of some spiro-oxaziridines often gives the ring-enlarged lactams.[9] Considering above facts, it may be reasonably assumed that a spiro-type oxaziridine intermediate (II) might be involved in the present reaction, but several attempts to isolate II were unsuccessful.

Similar treatment of *N*-(5,7-dibromo-2-oxo-3-indolylidene)-aniline *N*-oxide (IV) afforded expected 6,8-dibromo-3-phenyl-2,4-(1*H*,3*H*)-quinazolinedione (V) in 13% yield, accompanied with III in 23% yield; other products were intractable tars.

It should be noteworthy that the formation of III from IV in this reaction has revealed occurrence of the photochemical elimination of two aromatic bromine atoms under the above reaction conditions; similar photochemical behaviors have been observed quite seldom,[10] except in some iodine-substituted aromatic compounds.[11]

Photolysis of *N*-(5-nitro-2-oxo-3-indolylidene)-aniline *N*-oxide (VI) only resulted in the formation of intractable tars under the same reaction conditions as described above.

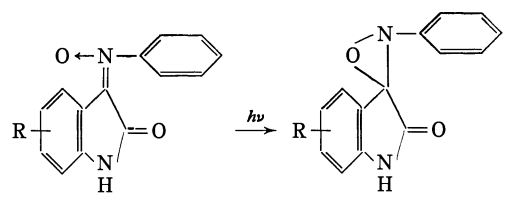

(I) R=H
(IV) R=5,7-dibromo
(VI) R=5-nitro

(II)

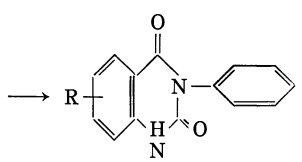

(III) R=H
(V) R=6,8-dibromo

1) Part XVI of this series: T. Sasaki and T. Yoshioka, submitted to this Bulletin.

2) O. Buchardt, C. Lohse, A. M. Duffield and C. Djerassi, *Tetrahedron Letters*, **1967**, 2741; M. J. Haddadin and C. H. Issidorides, *ibid*, **1967**, 753 and references cited therein.

3) J. Hammer and A. Macaluso, *Chem. Revs.*, **64**, 473 (1964); G. R. Deloierre and M. Lamchen, *Quart. Rev.*, **19**, 329 (1965).

4) J. S. Splitter and M. Calvin, *J. Org. Chem.*, **30**, 3427 (1965).

5) H. Ruppe and E. Sückline, *Helv. Chim. Acta*, **7**, 577 (1924).

6) S. Capuano and L. Giammanco, *Gazz. Chim. Ital.*, **86**, 126 (1956).

7) P. de Mayo and J. J. Ryan, *Tetrahedron Letters*, **1967**, 827.

8) S. Toyoshima, K. Shimada, H. Hamano and T. Daigo, *Yakugaku Zasshi*, **85**, 502 (1965).

9) W. D. Emmons, *J. Am. Chem. Soc.*, **79**, 5739 (1957); H. Kirmm, *Chem. Ber.*, **91**, 1057 (1958); E. Schmidt and D. Murauski, *Chem. Ber.*, **98**, 2525 (1965).

10) E. Latowska and T. Latowski, *Rocz. Chem.*, **40**, 1977 (1966); *Chem. Abstr.*, **67**, 32155d (1967); N. Kharasch, R. K. Sharma and H. B. Lewis, *Chem. Commun.*, **1966**, 418.

11) W. Wolf and N. Kharasch, *J. Org. Chem.*, **26**, 283 (1961); N. Kharasch, W. Wolf, T. J. Erpelding, P. C. Naylor and L. Tokes, *Chem. Ind.* (London); **1962**, 1720; J. A. Kampmeier and E. Hoffmeister, *J. Am. Chem. Soc.*, **84**, 3787 (1962).

Experimental[12]

Starting Materials. *N-(2-Oxo-3-indolylidene)-aniline N-Oxide (I).* This was prepared by the known method,[8] mp 218—220°C (decomp).

N-(5,7-Dibromo-2-oxy-3-indolylidene)-aniline N-Oxide (IV). To a solution of 2g of 5,7-dibromoisatin[13] in 50m*l* of ethanol was added 0.88g of phenylhydroxylamine and the reaction mixture was refluxed on a water bath for 1 hr. After cooling, the precipitated crystals were collected and recrystallized from dioxane to afford 2.5g (96%) of IV, mp 283—284°C.

Found: C, 42.62; H, 1.82; N, 7.27%. Calcd for $C_{14}H_8O_2N_2Br_2$: C, 42.44; H, 2.04; N, 7.07%.

N-(5-Nitro-2-oxo-3-indolylidene)-aniline N-Oxide (VI). This was prepared from 5-nitroisatin[14] and phenylhydroxylamine in the similar way as IV in 40% yield, mp 229—231°C.

Found: C, 59.60; H, 2.87; N, 14.92%. Calcd for $C_{14}H_9O_4N_3$: C, 59.38; H, 3.20; N, 14.84%.

Irradiation of I. A solution of 0.5g of I in 80 m*l* of tetrahydrofuran was irradiated for 17 hr. After removing the solvent, the residue was treated with a small amount of ethanol and the insoluble products were recrystallized from ethanol to afford 0.255g of white crystals, mp 287—289°C, which was identified to be III by infrared-spectroscopic comparison with a specimen prepared by the known method.[8]

Irradiation of IV. A solution of 0.5g of IV in 100m*l* of tetrahydrofuran was irradiated for 15hr. After removing the solvent, the residual oil was dissolved in chloroform and chromatographed on a silica-gel column (17g), using chloroform as an eluent. From the first fraction, 0.067g (13%) of white needles, mp 238—241°C from methanol, was obtained; this was identified to be V from the elemental analysis and by comparison with a specimen prepared by the reported method[15] infrared-spectroscopically. From the second fraction, 0.13g (23%) of III was isolated.

12) All melting points reported in this note were determined on a microhot stage and are not corrected. Microanalyses were carried out with a Yanagimoto C, H, N-Corder, MT-1 type.

13) H.G. Lindwall, J. Bandes and I. Weinberg, *J. Am. Chem. Soc.*, **53**, 317 (1931).

14) H.O. Calvery, C.R. Noller and R. Adams, *ibid.*, **47**, 3059 (1925); W. C. Sumpter and W.F. Jones, *ibid.*, **65**, 1802 (1943).

15) F.E. Sheibley, *J. Org. Chem.*, **17**, 221 (1952).

Room-Temperature Polycondensation of β-Amino Acid Derivatives. IV.*1 Solvent Effect on the Michael Reaction of Acrylates

Kohei SANUI and Naoya OGATA

Chemistry Department, Sophia University, Chiyoda-Ku, Tokyo

(Received February 17, 1968)

It was previously shown[1,2] that acrylates add with amino alcohols, followed by polycondensation at room temperature to form polyamide in alcohol solution in the presence of basic catalysts. When ethanolamine and acrylate are mixed in a solvent, an addition reaction of ethanolamine with acrylate takes place at the amino group and *N*-(hydroxyethyl) β-alanine ester is formed.

In this addition reaction, it was found that amino alcohol has a much higher reaction rate than amine itself and the addition of amine to acrylate is accelerated to a large extent in the presence of alcohol.[3] Also, it was found[4] that solvent has a great influence on the course of the polycondensation in the presence of basic catalysts, and polyamide is formed in methanol solution *via* route I, while polyamide ether is mainly formed in tetrahydrofuran *via* route II through rearrangement.

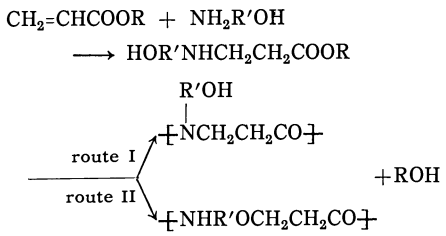

*1 Part III: K. Sanui and N.Ogata, This Bulletin, **40**, 1727 (1967).

1) N. Ogata and T. Asahara, *J. Polymer Sci.*, Part B, **4**, 273 (1966).

2) N. Ogata and T. Asahara, This Bulletin, **39**, 1359 (1966).

3) K. Sanui and N. Ogata, *ibid.*, **40**, 1727 (1967).

4) N. Ogata, T. Asahara and K. Sanui, *J. Polymer Sci.*, Part A-1, **6**, 1195 (1968).

TABLE 1. SOLVENT EFFECT OF THE COMPETITIVE ADDITION REACTION OF ACRYLATES
(Concn., 1 mol/*l*., Catalyst, ROK=5 mol%, * at 30°C., ** at 25°C)

Acrylate R	Solvent	ε (20°C)	Amount of acrylate A (%)	*n*-BuNHCH$_2$CH$_2$COOR [I] B (%)	[I] C (%)	ROCH$_2$CH$_2$COOR [II] D (%)	[II] E (%)	[II]/[I] F
Ethyl*	Cyclohexanone	18.3	39	61	99	1	1	0.01
	Ethanol	24.3	2	81	81	17	19	0.23
	Acetone	21.4	69	17	36	14	14	0.39
	Dioxane	2.21	27	46	71	27	29	0.41
	Ethanol/THF =50/50		5	55	55	40	45	0.82
	n-Heptane	1.92	3	42	42	55	58	1.4
	DMF	36.6	6	40	40	54	60	1.5
	THF		6	32	38	62	62	1.6
	Acetonitrile	37.5	0	20	20	80	80	4.0
Methyl**	Dioxane	2.21	25	70	95	5	5	0.05
	Methanol	32.6	0	91	91	9	9	0.10
	THF		0	30	30	70	70	2.3

A, B, D: after 3 hr, C, E: final yield, ε: Dielectric constant

These results suggest that the nucleophilicity of amino and hydroxyl groups may depend on solvent, hence the variation of the solvent results in the change in the course of the polycondensation.

Therefore, the solvent effect on the course of the competitive addition reaction of acrylate with aliphatic amine and alcohol was investigated in the presence of alkali metal alkoxide.

$$CH_2{=}CHCOOR + R\text{-}OH + R\text{-}NH_2 \xrightarrow{\text{base}} R\text{-}NHCH_2CH_2COOR + R\text{-}OCH_2CH_2COOR$$

The reaction was carried out as follows: methyl or ethyl acrylate, *n*-butylamine and methanol or ethanol were dissolved in various solvents each in the concentration of 1 mol/*l* in the presence of 5 mol% of potassium methoxide or ethoxide, and the amount of each reactants and also products in the solution were determined by gas chromatographic analysis using a dioctyl phthalate column.

Figure 1 shows the rate of the addition reaction of acrylate in methanol and tetrahydrofuran solutions, where it is seen that the addition of alcohol to acrylate takes place mainly in tetrahydrofuran and the ratio of the addition products of alcohol and amine is 7/3, while acrylate adds almost exclusively with amine in methanol without the addition of methanol.

Table 1 shows results of the competitive addition reaction in various solvents. Solvents in which the addition takes place almost exclusively with amine were cyclohexanone, methanol and dioxane. Methyl acrylate is more reactive than ethyl acrylate. Ethyl acrylate adds with both amine and ethanol in the ethanol solution, although the addition with amine still predominated. In a mixed solvent of ethanol and tetrahydrofuran, the addition reaction with both amine and alcohol took place as can be seen in Table 1. In all other solvents except acetone the addition reaction of acrylate proceeded almost quantitatively, leaving very small amount of unchanged acrylate in the solution. In the acetone solution, almost half amount of ethyl acrylate remained unchanged and the addition reaction did not further proceed even after several days. Several unidentified peaks were detected in the gas chromatographic analysis of the acetone solution after the reaction occurred. When only *n*-butylamine was dissolved in acetone, the amount of *n*-butylamine in the

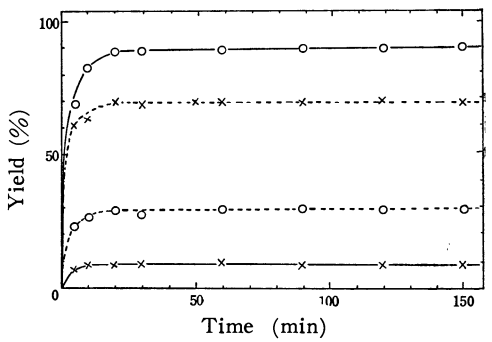

Fig. 1. The competition reaction of methyl acrylate with *n*-butylamine and methanol in methanol (——) and tetrahydrofuran (----).
(Concn., 1 mol/*l*, at 25°C., Catalyst, CH_3OK=5 mol%)
○ : *n*-BuNHCH$_2$CH$_2$COOCH$_3$
× : CH$_3$OCH$_2$CH$_2$COOCH$_3$

solution decreased very rapidly to a trace after 30 min, and a new peak appeared in the gas chromatograph which coincided with one of the unidentified peaks.

The dielectric constant of solvent does not necessarily affect the course of the competitive addition reaction as can be seen in Table 1, whereas the rate of the addition reaction increased generally in a solvent with a higher dielectric constant.

The observed solvent effect on the Michael-type reaction of acrylate might be due to the change of the nucleophilicity of amine and alcohol in different solvents.

In the tetrahydrofuran solution, the rate of the simple addition of acrylate with alcohol alone in the presence of potassium alkoxide is much faster than that with amine alone.[2] However, when an acrylate and an amine are dissolved in an alcohol, the addition reaction of the acrylate takes place almost exclusively with the amine, and the alcohol does not react at all. Dioxane and cyclohexanone had the same solvent effect on the addition reaction of acrylates. Therefore, amines are more nucleophilic than alkoxide ions in such solvents as alcohol, dioxane and cyclohexanone.

Thus, the formation of polyamide through the polycondensation between amino and ester groups in an alcohol solution is explained from the increase in the nucleophilicity of the amino group in alcohol, while the formation of polyamide ether in tetrahydrofuran is attributed to the increase in the nucleophilicity of the hydroxyl group in this solvent.

It is known that the interfacial polycondensation of aromatic amine and dicarboxylic acid chloride in ordinary organic solvents resulted in a low molecular weight polyamide, because of low basicity of aromatic diamine. However, a very high molecular weight polyamide is formed[5] when cyclohexanone is used as the solvent for the aromatic amine. This might be correlated with the present results that the nucleophilicity of amine is greater in cyclohexanone solutin.

The above-mentioned results on the course of the addition reaction of acrylates offer a cue to obtain a high molecular weight polymer by the room-temperature polycondensation of the β-alanine derivatives.

5) H. F. Mark, S. M. Atlas and N. Ogata, *ibid.*, **61**, s 49 (1962).

SHORT COMMUNICATIONS

New Cyano-Ammine Cobalt(III) Complexes

Nobufumi MAKI, Masaharu MOCHIZUKI and Shukichi SAKURABA
Depertment of Chemistry, Faculty of Engineering, Shizuoka University, Johoku, Hamamatsu

(Received March 15, 1968)

Shibata *et al.*[1] reported the synthesis of $[Co(CN)(NH_3)_5]Cl_2$ and $[Co(CN)_3(NH_3)_3]$, while Siebert[2] independently published the preparation of the former-type of complex, $[Co(CN)(NH_3)_5]X_2$ (X=Cl, Br, NO_3, ClO_4, or 1/2 SO_4). Several years ago, Cambi *et al.*[3] reported the preparation of $K_2[Co(CN)_5(NH_3)]$.

In the cyano-ammine series, however, the complexes of cis- and trans-isomers described below are now still missing members: $[Co(CN)_2(NH_3)_4]X$ and $M[Co(CN)_4(NH_3)_2]$.

In the present communication, the preparation of complexes *cis*-$[Co(CN)_2(NH_3)_4]NO_3 \cdot H_2O$, *cis*-$[Co(CN)_2en(NH_3)_2]NO_3$ and $[Co(CN)_3en(NH_3)] \cdot H_2O$ are reported.

Preparation of *cis*-$[Co(CN)_2(NH_3)_4]NO_3 \cdot H_2O$.[4] Forty grams of *trans*-$[Co(CN)Cl(NH_3)_4]NO_3$[5] were mixed with 29 g of AgCN in 400 m*l* of water at room temperature and heated on a water bath (40—50°C) for three hours. Special care was taken to warm gently, because the complex solution tends to decompose above 50°C. No smell of ammonia should be present. The mixture was filtered and the residue repeatedly extracted with hot water (50°C).

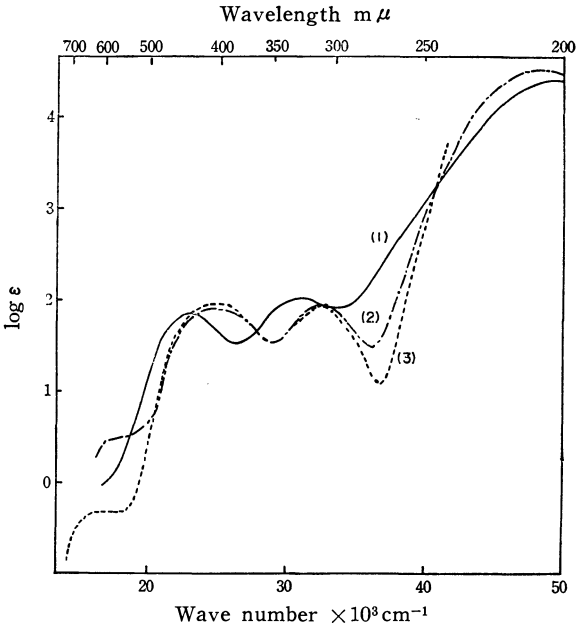

Fig. 1. The absorption spectra of dicyano cobalt (III) complexes: (1) —— *cis*-$[Co(CN)_2(NH_3)_4]NO_3 \cdot H_2O$; (2) —·— *cis*-$[Co(CN)_2en(NH_3)_2]NO_3$; (3) ------ *cis*-$[Co(CN)_2en_2]NO_3$.

TABLE 1. THE ABSORPTION MAXIMA OF DICYANO-COBALT (III) COMPLEXES

Compound			
cis-$[Co(CN)_2(NH_3)_4]NO_3 \cdot H_2O$	23.04 (1.86)	31.28 (2.03)	47.26 (4.31)
trans-$[Co(CN)_2(NH_3)_4]NO_3 \cdot 2H_2O$	*ca.* 22 (1.81) 24.02 (1.95)	31.60 (2.05)	47.80 (4.14)
cis-$[Co(CN)_2en(NH_3)_2]NO_3$	24.63 (1.91)	32.46 (1.96)	47.31 (4.41)
cis-$[Co(CN)_2en_2]NO_3$	24.73 (1.91)	32.37 (1.93)	47.37 (4.32)
trans-$[Co(CN)_2en_2]NO_3$	*ca.* 22 (1.38) 24.33 (1.90)	32.38 (1.93)	47.62 (4.44)
$[Co(CN)_3en(NH_3)] \cdot H_2O$	25.51 (1.90)	32.36 (1.92)	48.31 (4.45)
$[Co(CN)_3dien]$	26.45 (2.45)	33.33 (2.39)	48.54 (4.11)

Unit: wave number 10^3/cm (log ε) dien=diethylenetriamine

1) M. Shibata, M. Mori and E. Kyuno, *Inorg. Chem.*, **3**, 1573 (1964).
2) H. Siebert, *Z. anorg. u. allgem. Chem.*, **327**, 63 (1964).
3) L. Cambi and E. Daglia, *Gazz. chim. ital.*, 88, 691 (1964).
4) Independent of this work, the complex, *cis*-$[Co(CN)_2(NH_3)_4]Cl$, has been reported by Nishikawa *et al.*; Proc. 21st Annual Meeting Chem. Soc. Japan, p. 1108 (1968).
5) K. Ohkawa, J. Hidaka and Y. Shimura, This Bulletin, **39**, 1715 (1966).

A New Series of Chromium(III) Complexes of Schiff Bases obtained from Substituted Salicylaldehydes and Amines

Shoichiro YAMADA and Katsumoto IWASAKI
Institute of Chemistry, College of General Education, Osaka University, Toyonaka, Osaka

(Received June 4, 1968)

Schiff base complexes of various transition elements have been reported in the literature.[1,2] However, synthesis of chromium(III) complexes of *C*, *N*-disubstituted salicylideneimines has been considered to be very difficult, and the complexes of the $Cr(X\text{-sal. }R)_3$ type, for example, have never been isolated (Fig. 1). The present paper deals with successful preparation of a series of these chromium (III) complexes.

The new chromium(III) complexes, which are given in Table 1, were prepared by the following general method. To a suspension of chromium(III) acetate hydrate (0.01 mol) in ethylene glycol were added salicylaldehyde or 5,6-benzosalicylaldehyde (0.03 mol), an alkyl or an aryl amine (0.03 mol) and an aqueous solution of sodium carbonate (0.01 mol, 67% of the theoretical amount), and the resulting solution was heated on an oil-bath at about 120°C for two or three hours. After the red solution was cooled to room temperature, the precipitate was filtered off, washed with ethanol and recrystallized from ethanol. Brown-purple to orange-red crystals of the compound, the colour depending appreciably upon the size of the particles, were obtained in good yield. The crystals are soluble in common organic solvents.

TABLE 1. ANALYTICAL DATA OF CHROMIUM(III) COMPLEXES OF THE $Cr(X\text{-sal. }R)_3$ TYPE

X	R	Calcd, % C	H	N	Found, % C	H	N
H	CH_3	63.42	5.32	9.25	63.09	5.18	9.05
	C_2H_5	65.31	6.09	8.46	65.56	6.27	8.14
	n-C_3H_7	66.89	6.74	7.80	66.24	6.84	7.61
	iso-C_3H_7	66.89	6.74	7.80	66.48	6.73	7.86
	Ph*	73.11	4.72	6.56	72.76	4.59	6.41
5,6-Benzo	CH_3	71.51	5.00	6.95	71.14	5.19	6.70
	C_2H_5	72.43	5.61	6.50	72.13	5.46	6.50
	n-C_3H_7	73.23	6.15	6.10	72.67	6.10	6.03
	iso-C_3H_7	73.23	6.15	6.10	72.98	6.06	6.10
	Ph	77.45	4.59	5.31	77.69	4.20	5.04

* The notation Ph denotes a phenyl group.

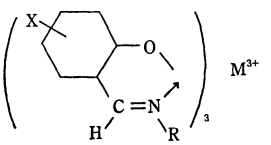

Fig. 1. $M(X\text{-sal. }R)_3$.

Elemental analyses, as shown in Table 1, indicate that these complexes have the formulae of $Cr(X\text{-sal. }R)_3$, in agreement with the formulae expected on the basis of the magnetic moments, which were determined to be about 3.79 to 3.86 B.M. at room temperature corresponding to three unpaired electrons. Infrared spectra of these complexes show an absorption band at about 1530 to 1540 cm^{-1} due to the C=N stretching vibration, indicating the formation of the Schiff bases.

Although the two types of configuration, a *mer*- and a *fac*-form, are possible for these complexes, only one form of the two was isolated as crystals in the present work. In any case, it is likely that all the chromium-(III) complexes so far prepared take the same type of configuration, since they show nearly identical electronic absorption spectra having a d-d band maximum at about 18000 cm^{-1}.

It is interesting to note that the complexes of the $Cr(X\text{-sal. }iso\text{-}C_3H_7)_3$ type, X being H and 5,6-benzo, have been prepared in the present work, since it was believed to be very difficult due to the steric hindrance to synthesize the corresponding complexes of cobalt(III), which have only recently been isolated.[3]

The details of this work will be reported elsewhere later.

1) R. H. Holm, G. W. Everett, Jr., and A. Chakravorty, "Progress in Inorganic Chemistry," Vol. VII, ed. by F. A. Cotton, Interscience Publishers, New York, N.Y. (1966), p. 83.
2) S. Yamada, *Coordin. Chem. Reviews*, **1**, 415 (1966).
3) S. Yamada, E. Ohno and K. Yamanouchi, This Bulletin, **41**, 535 (1968).

Thermal Racemization of the Optically Active Chlorosilane

Hideki SAKURAI, Masashi MURAKAMI and Makoto KUMADA
Department of Synthetic Chemistry, Kyoto University, Sakyo-ku, Kyoto

(Receivd June 10, 1968)

Incidentally to studies on chlorination of an optically active hydrosilane, (+)-α-naphthylphenylmethylsilane (I),[1] to the corresponding chlorosilane, (−)-α-naphthylphenylmethylchlorosilane (II), we have found that II was configurationally unstable at moderately high temperature (200—300°C) and recemized rather rapidly in the vapor phase as well as in the liquid state. Interestingly, I was configurationally more stable than II.

The optically active chlorosilane, II, mp 63.8°C, $[\alpha]_D$ −6.00(*c* 10.68, cyclohexane)[lit.,[1] mp 63.5—64°C, $[\alpha]_D$ −6.28 (*c* 10.5, cyclohexane)] was passed through a preparative g.l.c. (3m column of Apiezon L grease on Celite 545) at 300°C with retention time of 35—50 min and recovered. Contrary to our expectation, the recovered II exhibited no optical rotation. However, I, mp 63.7—64.3°C, $[\alpha]_D$ +33.7 (*c* 10.9, cyclohexne) [lit.,[1] mp 63.5—64.5°C, $[\alpha]_D$ +34.3 (*c* 10.9, cyclohexane)], did not racemize under the same condition. Thus, I passed through the preparative g.l.c. at 300°C (retention time of 30—35 min) showed an optical activity, $[\alpha]_D$ +30.5 (*c* 1.40, cyclohexane). Accordingly, this figure indicates at least 95% retention of configuration of I.

To test that racemization of II proceeds non-catalytically, reactions were carried out in clean small sealed tubes. The results are listed in Table 1.

Obviously, II racemizes thermally even in the liquid state. Several possibilities responsible to racemization may be considered and elucidation of the mechanism is now in progress.

TABLE 1. THERMAL RACEMIZATION OF OPTICALLY ACTIVE CHLOROSILANE

No.	Wt. of II (g)	Temp. (°C)	Reaction time (min)	$[\alpha]_D$	Optical purity (%)
1	1.085	200	65	−5.54	92.3
2	1.054	250	65	−4.74	79.0
3	1.136	300[a]	67	−1.06	17.7

a) After the reaction, the sample colorized slightly, but an examination by g.l.c. showed that no detectable chemical change had occurred.

1) L. H. Sommer, "Stereochemistry, Mechanism, and Silicon," McGraw-Hill, New York (1965); L. H. Sommer, C. L. Frye, G. A. Parker and K. W. Michael, *J. Am. Chem. Soc.*, **86**, 3271 (1964); L. H. Sommer, C. L. Frye and G. A. Parker, *ibid.*, **86**, 3276, 3280 (1964); L. H. Sommer, *Angew. Chem.*, **76**, 176 (1962).

Molecular Complex between Two Free Radicals. A Complex between the *p*-Phenylenediamine Cation Radical and the *N,N,N′,N′*-Tetramethyl-*p*-phenylenediamine Cation Radical

Katsuo TAKEMOTO, Shigeki NAKAYAMA, Keisuke SUZUKI and Yuzuru OOSHIKA

Faculty of Science, Kwansei Gakuin University, Nishinomiya

(Received June 11, 1968)

Dimerizations of the cation radicals of *p*-phenylenediamine and its analogues[1-6] have already been studied by spectroscopic[1-4,6] and ESR[5] techniques. In the present communication, a spectroscopic study of a molecular complex formed between the cation radical of *p*-phenylenediamine (PD^+) and that of *N, N, N′, N′*-tetramethyl-*p*-phenylenediamine ($TMPD^+$) will be reported.

The temperature and the concentration dependence of the UV and visible spectra of solutions containing PD^+ and $TMPD^+$*1 were determined by using a Cary Model 14 recording spectrophotometer. From the analyses of these results, it was concluded that a (1 : 1) molecular complex $(PD^+)_1(TMPD^+)_1$ is formed below −80°C. A typical run is shown in Fig. 1. The spectrum at room temperature is only a weighted sum of the spectra of PD^+ and $TMPD^+$. The spectrum at −195°C consists of three new bands (C, R′, and Y′) which are characteristic of the complex. The spectra in the intermediate-temperature range may be explained as sums of the absorption bands of PD^+, $TMPD^+$, $(PD^+)_2$, and the complex.*2

The spectrum of the present complex closely resembles those of the dimers of PD^+ and its methyl-derivatives.[1] The ν_{max} and the heat of complex formation (which was obtained from the temperature dependence of the equilibrium constant determined from the above spectra) of the present complex are compared with those for the above dimers in Table 1.

From these results, it may be considered that the present complex is formed by the pairing action of odd electrons in the PD^+ and the $TMPD^+$, and that the C band is due to a charge-transfer transition[7] between the covalent (PD^+-$TMPD^+$) and charge-transferred states (resonance between PD^{2+}-TMPD and PD-$TMPD^{2+}$).

More detailed research is now progress at this laboratory.

TABLE 1

Substance	ν_{max} (kK) of absorption C	R′	Y′	Heat of complex formation (or dimerization)
$(PD^+)_1(TMPD^+)_1$	14.7	24.0	34.8	*ca.* 6.0 kcal/mol
$(PD^+)_2$	16.5	27.4	36.0	8.0
$(DMPD^+)_2$	15.0	24.3	35.3	10
$(TMPD^+)_2$	13.1	19.7	32.1	5.0

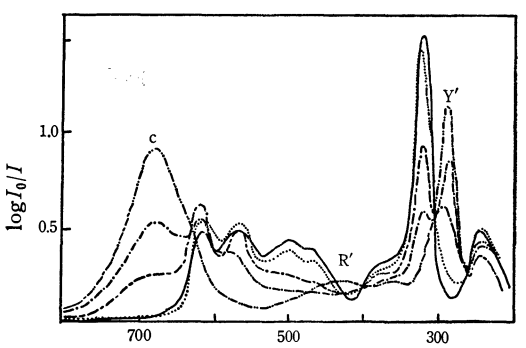

Fig. 1. Temperature dependent spectra of a solution containing PD^+ (0.347 mol/*l*) and $TMPD^+$ (0.430 mol/*l*). Solvent used was a ethanol-ethyl ether (2 : 1) mixture. Molar ratio [PD^+] : [$TMPD^+$] = 0.807 : 1.
—— 25°C, ····· −87.9°C, —·— −114.2°C, —·— −128.5°C, —··— −159.2°C

1) K. Uemura, S. Nakayama, Y. Seo, K. Suzuki and Y. Ooshika, This Bulletin, **39**, 1348 (1966).
2) T. Sakata and S. Nagakura, *Technical Report of ISSP. Ser. A*, No. 244 (1967).
3) G. T. Pott and J. Kommandeur, *J. Chem. Phys.*, **47**, 395 (1967).
4) Y. Nakato, N. Yamamoto and H. Tsubomura, This Bulletin, **40**, 2480 (1967).
5) A. Kawamori, A. Honda, N. Joo, K. Suzuki and Y. Ooshika, *J. Chem. Phys.*, **44**, 4363 (1963).
6) K. Takemoto, H. Matsusaka, S. Nakayama, K. Suzuki and Y. Ooshika, This Bulletin, **41**, 764 (1968).
7) K. H. Hausser and J. N. Murrell, *J. Chem. Phys.*, **27**, 500 (1957).

*1 PD bromide and TMPD perchlorate were used.
*2 Amount of $(TMPD^+)_2$ was very small in these conditions.

Determination of Optical Constants of Single Crystal by ATR*1

Koji Tsuji and Haruka Yamada
Department of Chemistry, Kwansei Gakuin University, Nishinomiya

(Received June 13, 1968)

Very few measurements of absolute absorption intensities have been made on the infrared spectra of single crystals, because the thin layers of single crystals required are quite difficult to prepare, and it is also difficult to measure the thickness. It is, however, desirable to measure the intensities for single crystals, as they provide important knowledge related to the intermolecular forces when compared with those for the polycrystalline films.[1] Recently the infrared spectra of a single crystal, an anisotropic medium, have been successfully obtained by applying the ATR technique.[2] The determination of the infrared intensities of single crystals will also be possible if the optical constants can be obtained by the same method.[3] No attempt to do so has, however, yet been made, because there is an inevitable difficulty in making a good contact between the crystal sample and the high-index material.

We are developing a method of measuring optical constants of single molecular crystals by the ATR technique. The method is based on the determination of the true reflectivity for the perpendicular polarization, R_s. The reflecting surface of the sample is polished, and it is fixed firmly to the KRS-5 hemicylinder. After the R_s curve is recorded, we correct the R_s for the incompleteness of the contact as follows: A) The reflectivity for parallel polarization, R_p, goes down to zero at the principal angle, θ_p, in non-absorbing regions. If the optical contact is not complete, then the appreciable energy at θ_p, which is due to the lack of optical contact, is detected as R_p. Measuring the minimum R_p at θ_p, we obtain $R_s(\text{true}) = R_s\ (\text{observed}) - R_p$ (at $\theta = \theta_p, k = 0$). B) In non-absorbing regions the R_s is observed at a small angle of incidence, one where the total reflection does not occur. Then it is compared with the R_s calculated theoretically at the same incident angle. The difference between observed and calculated R_s values may be attributed to the energy resulting from the incompleteness of the contact. After the true R_s curves are thus obtained with two different incident angles, the n and k values are calculated on the basis of Frenel's formulae.

To illustrate the results obtainable with this method, we have measured the ATR spectra of an iodoform single crystal for the ν_4(E) CH bending band. Using a hexagonal bipyramidal iodoform, and taking the reflecting surface as the (0001) plane, the R_s (true) curves have been obtained. Then the n, k and α have been calculated by following Fahrenfort's method,[4] with some modifications suggested by Hansen,[5] using a FACOM 270—20 computer.

The calculated n and α values are shown in Fig. 1. The intensity $A_{\text{crystal}(0001)}$ is

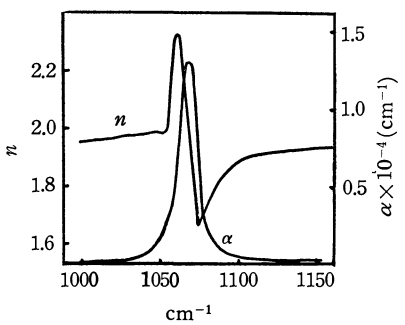

Fig. 1. Refractive index, n, and absorption coefficient, α, of CHI_3 single crystal in (0001) plane.

19.4 ± 4 cm/μmol, which is compared with the value 9.9 ± 0.5 cm/μmol for $A_{CS_2\,\text{soln.}}$. Iodoform belongs to the C_6^6 space group and the molecular axes of CHI_3 lie perpendicular to the (0001) plane, so that the ν_4 has all the intensity in this plane if the oriented gas model is assumed. $A_{\text{crystal}(0001)} = (3/2) A_{\text{soln.}} \times$ (field parameter). The details and a discussion will be published in the near future.

*1 Presented at the 21st Annual Meeting of the Chemical Society of Japan, Osaka, April, 1968.

1) D. A. Dows, "Physics and Chemistry of the Organic Solid States," Vol. I, Ed. Fox, Labes and Weissberger, Interscience Publishers, Inc., New York (1963), p. 657; Vol. II, p. 88 (1965).
2) H. Yamada and K. Suzuki, *Spectrochim. Acta*, **23A**, 1735 (1967).
3) N. J. Harrick, "Internal Reflection Spectroscopy," Interscience Publishers, Inc., New York (1967), p. 243.
4) J. Fahrenfort, *Spectrochim. Acta*, **18**, 1103 (1962).
5) W. N. Hansen, *ibid.*, **21**, 209, 815 (1965).

Energy Difference between Rotational Isomers of Methyl Ethyl Ether

Teizo KITAGAWA and Tatsuo MIYAZAWA
Institute for Protein Research, Osaka University, Kita-ku, Osaka

(Received June 18, 1968)

Raman lines due to skeletal bending modes of methyl ethyl ether were observed at 381 (weak) and 471 cm^{-1} (strong) for the liquid phase.[1-3] Corresponding infrared bands were observed at 370 and 464 cm^{-1} for the vapor phase at room temperature.[2,3] However, the band at 370 cm^{-1} was not observed in the solid state and was assigned to the gauche isomer, whereas the band of the solid phase at 472 cm^{-1} was assigned to the trans isomer.[4] The molecular structure of the trans isomer was determined by microwave analysis.[5] Measurement of the energy difference between the rotational isomers of methyl ethyl ether is also important for studying conformations of polymers, *e.g.*, polyethyleneglycol[6] in solution.

In the present study, the infrared spectra of methyl ethyl ether in the gaseous, liquid and solid states were measured in the region 550—200 cm^{-1}. The length of the gas cell used was 105 mm and the sample pressure was 660 mmHg at 303°K. The liquid cell (about 0.2 mm thick) was connected to a vacuum line and was kept at 204°K. The ether sample was distilled into the cell. For preparing a solid film, vapor was condensed on a cesium iodide window at 98°K and the solid was then annealed at 145°K. Typical spectra of the vapor, liquid, and solid phases are shown in Fig. 1. Temperature dependence of the intensities of liquid bands was observed and the bands at 258 and 300 cm^{-1} were found to become stronger as temperature was lowered. Accordingly, the area intensities of

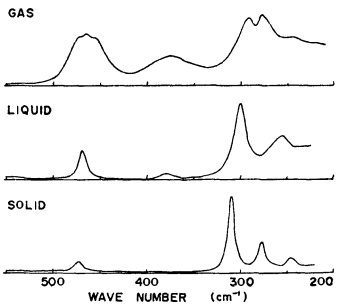

Fig. 1. Infrared absorption (optical density) curves of methyl ethyl ether.

the bands at 380 cm^{-1} (gauche) and 300 cm^{-1} (trans) were measured at 259, 248, 237, 228, 223, 216, 210, 204, and 198°K, and the energy difference between the rotational isomers was found as $\Delta H = H(\text{gauche}) - H(\text{trans}) = 1.5 \pm 0.1$ kcal/mol for the liquid phase. Temperature dependence of the vapor bands at 465, 375, and 280 cm^{-1} was also observed. After making corrections for emission from the cell at elevated temperatures, area-intensity ratios were measured at 303, 333, 375, and 423°K and the energy difference was found as $\Delta H = 1.5 \pm 0.2$ kcal/mol for the vapor phase. (From this value, the population of the gauche isomer is calculated to be as small as ~5% at ~200°K where microwave absorption lines of the gauche isomer were not identified.[5]) Thus, the ΔH values for the vapor and liquid phases of methyl ethyl ether are like, as expected from small dipole-moment difference between the two isomers.

The band of the liquid and vapor phase at ~465 cm^{-1} was previously assigned to the trans isomer, because the corresponding band was also observed in the solid phase. However, apparent relative intensities of the bands at 375 cm^{-1} (gauche) and 465 cm^{-1} were found to be independent of temperature, indicating that the bands of the trans and gauche isomers overlap at 465 cm^{-1} and the intensity of the composite band is largely due to the gauche isomer.

1) K. W. F. Kohlrausch, *Monatsh. Chem.*, 88, 349 (1936).
2) Y. Mashiko, *Nippon Kagaku Zasshi* (*J. Chem. Soc. Japan, Pure Chem. Sect.*), **80**, 593 (1959).
3) A. D. H. Clague and A. Danti, *Spectrochim. Acta*, **24A**, 439 (1968).
4) R. G. Snyder and G. Zerbi, *ibid.*, **23A**, 391 (1967).
5) K. Ono, M. Hayashi and H. Murata, Symposium on Molecular Structure, Sapporo, Japan, October, (1967).
6) J. E. Mark and P. J. Flory, *J. Am. Chem. Soc.*, 88, 3702 (1966).

BULLETIN OF THE CHEMICAL SOCIETY OF JAPAN VOL. 41 1977—1982 (1968)

Studies of Photosensitive Resins. IV. Photosensitization Mechanism of Polyvinyl Cinnamate

Kenichiro NAKAMURA and Shinichi KIKUCHI

The Institute of Industrial Science, The University of Tokyo, Roppongi, Minato-ku, Tokyo

(Received October 3, 1967)

The photosensitization mechanism of polyvinyl cinnamate was investigated by measuring the phosphorescence spectra of cinnamic acid and sensitizers. The peak of phosphorescence for *trans*-cinnamic acid was found to be 20100 cm^{-1}, and the triplet energies of the effective sensitizers were found to be situated near or higher than that of cinnamic acid. It was established that the phosphorescences of sensitizers were exceedingly quenched when cinnamic acid was introduced into their solutions. This finding can be understood if it is assumed that the excitation energy is transferred from the triplet state of the sensitizer to that of cinnamic acid. The critical separation of donor and acceptor and the configuration of the triplet state for cinnamic acid are also discussed.

Polyvinyl cinnamate is one of the most common photosensitive resins which become insoluble upon irradiation with light. The sensitized polyvinyl cinnamate is sensitive to visible light, while the non-sensitized resin is sensitive only to ultraviolet light. Many sensitizers, such as aromatic nitro and keto compounds, are reported to have this effect.

The photo-crosslinking mechanism of polyvinyl cinnamate has been made fairly clear. However, the sensitization mechanism of the resin is still the subject of frequent discussion. Tsuda[1,2] measured the photosensitivities of resins sensitized by mixtures of aromatic compounds, and showed that the mixing effect of a sensitizer can be fairly well understood by assuming a triplet energy transfer. He also measured the phosphorescence spectra of cinnamic acid, and reported that the limit of the spectral sensitization of polyvinyl cinnamate coincided with the wavelength of phosphorescence emitted from cinnamic acid. However, the triplet energy transfer mechanism has not been reported more definitely. Studies of the quenching of sensitizers' phosphorescence would seem to make the mechanism clearer. Therefore, the authors have measured the phosphorescence spectra of various sensitizers and have studied the quenching effect on a sensitizer's phosphorescence of the addition of cinnamic acid.

The photo-crosslinking of polyvinyl cinnamate is a reaction similar to the photo-dimerization of cinnamic acid in a solid phase. Therefore, the authors also studied the photochemistry of cinnamic acid. When cinnamic acid is irradiated with ultraviolet light in a solution, a photoisomerization reaction occurs. The quantum yields of the cis→trans and trans→cis isomerization of cinnamic acid were found by Vaidya[3] to be 0.21 and 0.61 respectively. The sum of the two quantum yields was about unity. This fact suggests that the excited states of *cis*- and *trans*-cinnamic acid concerned are the same.

Hammond *et al.*[4] discussed the cis-trans isomerization of stilbene in detail, and emphasized that a phantom triplet exists in the lowest triplet state of stilbene. There has, however, been no report which gives information about phantom triplet of cinnamic acid. Therefore, the authors intended to investigate the configuration of the triplet state by measuring the phosphorescence spectra of *cis*- and *trans*-cinnamic acid. The phosphorescence spectrum of trans-cinnamic acid was measured by Tsuda,[5] but that of cis isomer has not yet been measured.

Energy transfer from the triplet state has been observed between a number of donor-acceptor pairs.[6,7] Hammond *et al.*[8] have shown that the photosensitized cis-trans isomerization of stilbene is caused by the transfer of the triplet excitation. Porter *et al.*[9] have studied the quenching of the triplet state by measuring the triplet-triplet absorption spectra; they reported that there is no evidence for long-range resonance transfer of the kind found

1) M. Tsuda, *J. Soc. Sci. Photography Japan*, **28**, 7 (1965).
2) M. Tsuda, *J. Polymer Sci.*, **B2**, 1143 (1964).
3) B. K. Vaidya, *Proc. Roy. Soc.* (*London*), **A129**, 299 (1930).
4) G. S. Hammond *et al.*, *J. Am. Chem. Soc.*, **83**, 2396 (1961); *ibid.*, **84**, 4983 (1962); *ibid.*, **86**, 3197 (1964); *ibid.*, **88**, 4769 (1966).
5) M. Tsuda, International Conference of Photographic Science, Tokyo, 1967.
6) V. Ermolaev, *Soviet Physics, Uspekhi*, **80**, 333 (1955).
7) A. Terenin, V. Ermolaev. *Trans. Faraday Soc.*, **52** 1042 (1956).
8) G. S. Hammond, J. Soltiel, A. A. Lamola, N. J. Turro, J. S. Bradshow, D. O. Cowan, R. C. Counsell, V. Vogt and C. Dalton, *J. Am. Chem. Soc.*, **86**, 3197 (1964).
9) G. Porter, F. R. S. and F. Wilkinson, *Proc. Roy. Soc.* (*London*), **A264**, 1 (1961).

in the anlogous singlet energy transfer process. In this paper, the distance of the energy transfer between the acceptor and donor molecules will also be discussed.

Experimental

The phosphorescence spectra of sensitizers were measured in an EPA solution at 77°K. The concentration of the sensitizer was 10^{-3} M, and 0.01—0.2 M *trans*-cinnamic acid was added to the sensitizer's solution. In the quenching measurements, the concentration of the sensitizer was kept at a constant value.

cis-Cinnamic acid was prepared from phenyl propiolic acid by the hydrogen reduction method described by Paal.[10] Colloidal palladium[11] was used as a catalyst in the reduction. The synthesized product was slightly colored, but the product recrystallized three times from ligroin was white, mp 68°C. *trans*-Cinnamic acid, guaranteed reagent, was purified two times by recrystallization from ethanol. The phosphorescence spectra were measured by an Aminco-Bowman spectrophotofluorometer.

Results and Discussion

Phosphorescence Spectra of Cinnamic Acid. The phosphorescence spectrum of *trans*-cinnamic acid in an EPA solution is shown in Fig. 1. The 0–0 band (20100 cm^{-1}) and the 0–2 band (18600 cm^{-1}) are strong in this phosphorescence spectrum, while 0–1 band is rather weak. The excitation wavelength was 280 mμ; it corresponds to the K-absorption band of cinnamic acid.

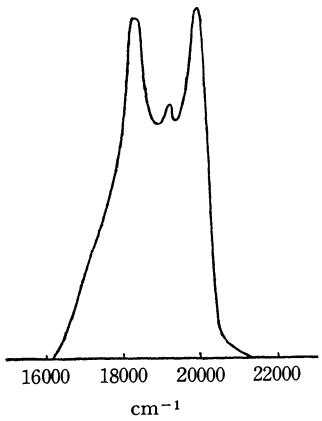

Fig. 1. Phosphorescence spectrum of *trans*-cinnamic acid.

In order to study the solvent effect on the phosphorescence, the authors also measured it in petroleum ether. However, no change in spectra could be found between EPA and petroleum ether. It may, therefore, be concluded that the phosphorescence of cinnamic acid is not affected by the solvent.

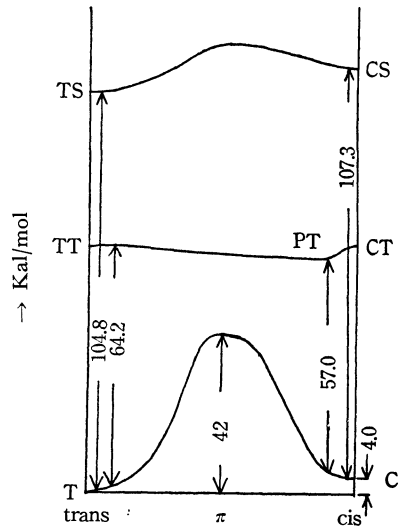

Fig. 2. Possible potential function for rotation in cinnamic acid.

The phosphorescence spectra of *cis*-cinnamic acid in EPA and in petroleum ether were also measured; They were the same as those of *trans*-cinnamic acid. This fact suggests that the triplet state of *trans*-cinnamic acid is the same as that of *cis*-cinnamic acid, and that the phantom triplet state proposed by Hammond *et al.*[4] exists in the triplet state of cinnamic acid. Therefore, the configuration of the potential function for rotation in cinnamic acid may be as is shown in Fig. 2.

The energies necessary for exciting *trans*- and *cis*-cinnamic acid are 104.8 kcal/mol (273 mμ) and 107.3 kcal/mol (266 mμ) respectively. The energy difference between the ground state of *trans*-cinnamic acid and that of *cis*-cinnamic acid was estimated to be 4.0 kcal/mol from the difference in hydrogenation energy between the two compounds.[12]

The activation energy for the thermal isomerization of cinnamic acid has not been measured, because the decomposition reaction takes precedence over the isomerization reaction at higher temperatures. However, its esters are stable for heat and they thermally isomerize. The activation energy for the thermal isomerization of methyl cinnamate has been reported to be 41.6 kcal/mol. A similar activation energy, about 41.6 kcal/mol, is necessary to cause the isomerization of styryl compounds.[13] Consequently, the activation energy of cinnamic acid may not be very different from that of cinnamic acid.

At a photostationary state, the ratio of the cis product to the trans product is about 3.0.[3] The

10) C. Paal and C. Hartman, *Ber.*, **42**, 3930 (1909).
11) C. Paal and C. Amberger, *ibid.*, **38**, 1398 (1905).
12) R. B. Williams, *J. Am. Chem. Soc.*, **64**, 1395 (1942).
13) G. B. Kistiakowsky and W. R. Smith, *ibid.*, **57**, 269 (1935).

irradiated solution contains more of the cis isomer than that of the trans isomer. Therefore, the phantom triplet state may be located near the cis position, as is shown in Fig. 2. It may be seen in this figure that, when cinnamic acid at the phantom triplet is degraded to the ground state, the cis isomer may be mainly produced.

In a previous paper,[14] the present authors calculated the electronic structure and energy levels of *trans*-cinnamic acid by the LCAO-SCF-MO method. The calculated energy of the first triplet, 2.79 eV, corresponds to the T-TT energy in Fig. 2. In Fig. 3, all the energy levels are the calculated values.

The flourescence of cinnamic acid was measured, but no fluorescence could be detected. This may be due to the intersystem-crossing from the singlet state to the triplet state. The intersystem-crossing from the first excited singlet state to the second triplet state is probable, because the second triplet state is located near the first excited singlet state, as is shown in Fig. 3.

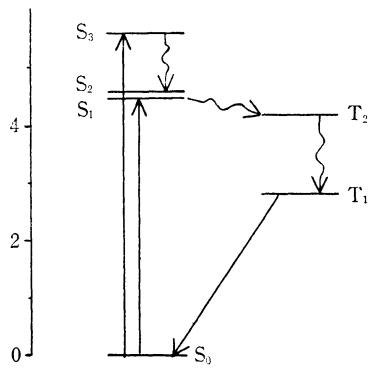

Fig. 3. State diagram for cinnamic acid.

Phosphorescence Spectra of Sensitizers. All the effective sensitizers for polyvinyl cinnamate emit phosphorescence near the 20000 cm^{-1} region, as is shown in Table 1. In this table, the wavelengths for the phosphorescence and absorption peaks and the values of the photosensitivities of the sensitized resins are shown. The triplet state energy of phenol is larger than that of cinnamic acid, but it is not an effective sensitizer for the resin. In photosensitization, phosphorescence is not the only important factor; the absorption of a sensitizer is also essential. For the irradiation of the resin, a mercury lamp is generally used. The photosensitivities shown in Table 1 are those obtained by irradiation with a mercury lamp. The wavelength of the emission peak of a mercury lamp is about 350 mμ. Therefore, the effective sensitizers must have absorption peaks near this region. In this table the intersystem-crossing efficiency from the singlet state to the triplet state is also shown. The efficiencies of 5-nitroacenaphthene and *p*-nitroaniline have not yet been reported. However, their efficiency may be about 1 because their absorptions are caused by n–π^* and the efficiency for the n–π^* compound is generally large. The efficiency of Michler's ketone is about 1, and its photosensitivity is very large. These results can be understood if the excitation energy is transferred from the triplet state of the sensitizer's molecule to that of the resin.

In order to make the triplet energy transfer more clear, the quenching of a sensitizer's phosphorescence was studied. The phosphorescence spectra of 2-nitrofluorene are shown in Fig. 4. The spectrum was measured at 77°K in a 10^{-3} M EPA solution. The uppermost curve in this figure is the spectrum of 2-nitrofluorene alone. The other curves are the spectra of 2-nitrofluorene, which includes 0.01—0.2 M cinnamic acid. It may be seen in this figure

Table 1. Photosensitivities of sensitized resins

Sensitizer	Abs. cm^{-1}	Phos. cm^{-1}	Intersystem[16] crossing efficiency	Photosensitive[1,17] value
Naphthalene	36400	22000	0.39	2.6
Phenanthrene	26700	19000		7.7
Chrysene	27800	19800	0.67	18
Phenol	37000	28600		1.8
2-Nitrofluorene	30300	20600		113*
5-Nitroacenaphthene	27000	19800		84*
p-Nitroaniline	27000	19700		110
Michler's ketone	25600	21300	1.01	650

* The method employed for these two values is different from that for other values. 5-Nitroacenaphthene is about 10 times more sensitive than *p*-nitroaniline.

14) K. Nakamura and S. Kikuchi, This Bulletin, **40**, 1028 (1967).
15) T. Forster, *Discussions Faraday Soc.*, **27**, 1 (1959).
16) M. J. Turro, "Molecular Photochemistry," W. A. Benjamine, Inc., New York (1965), p. 131.
17) L. M. Minsk, J. S. Smith, W. P. VanDeusen and J. F. Wright, *J. Appl. Pol. Sci.*, **2**, 302 (1959).

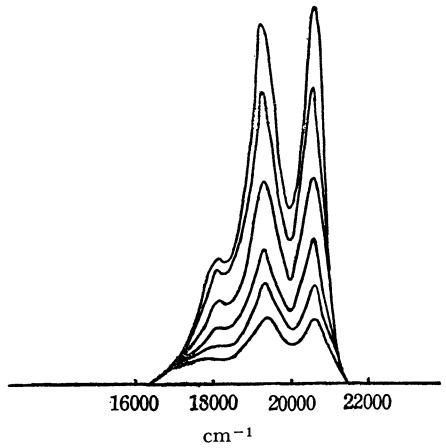

Fig. 4. Phosphorescence spectra of 2-nitrofluorene.
the uppermost curve: added 0 M cinnamic acid
the second curve: added 0.01 M cinnamic acid
the third curve: added 0.05 M cinnamic acid
the fourth curve: added 0.1 M cinnamic acid
the fifth curve: added 0.15 M cinnamic acid
the lowest curve: added 0.2 M cinnamic acid

that the phosphorescence of 2-nitrofluorene is remarkably quenched by the addition of cinnamic acid. The solutions were irradiated by a 350-mμ light. There is no absorption of cinnamic acid in this region, while 2-nitrofluorene has an intensive absorption band there. Therefore, the addition of cinnamic acid does not affect the phosphorescence spectrum. The quenching of the phosphorescence is considered to be due to the energy transfer from the triplet state of 2-nitrofluorene to cinnamic acid.

In Fig. 5, the intensities of the 0–0 bands of the sensitizers' phosphorescence are plotted against the concentrations of cinnamic acid. The quenching curves of other bands of 2-nitrofluorene are uniformly quenched. The concentration of the acceptor molecule, $[A]_{1/2}$, is estimated when the decay of the donor's phosphorescence, in the presence of the acceptor, is equal to one-half of its value in the absence of the acceptor. Thus, it is found from this

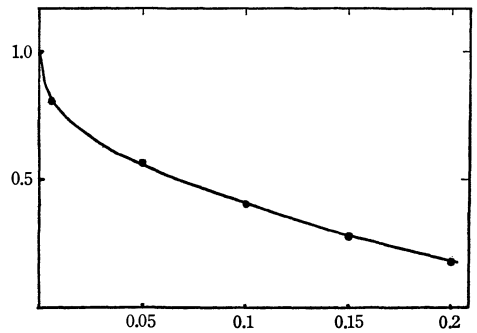

Fig. 5. The decay curve of phosphorescence of 2-nitrofluorene with addition of cinnamic acid.

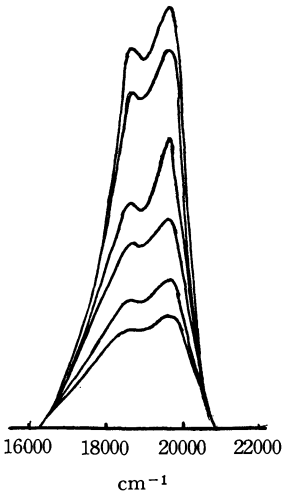

Fig. 6. Phosphorescence spectra of *p*-nitroaniline.
the uppermost curve: added 0 M cinnamic acid
the second curve: added 0.01 M cinnamic acid
the third curve: added 0.05 M cinnamic acid
the fourth curve: added 0.1 M cinnamic acid
the fifth curve: added 0.15 M cinnamic acid
the lowest curve: added 0.2 M cinnamic acid

figure that the concentration of $[A]_{1/2}$ is 0.063 M.

The phosphorescence spectra of *p*-nitroaniline are shown in Fig. 6. The samples were irradiated with a 350 mμ light. The remarkable quenching of the phosphorescence occurs just as in the case of 2-nitrofluorene. The 0–0 band of *p*-nitroaniline was found to be 19700 cm^{-1}. Therefore, the triplet state of *p*-nitroaniline is also an effective sensitizer of polyvinyl cinnamate. However, *o*-nitroaniline is not effective for sensitizing the resin. The intensity of the phosphorescence of *o*-nitroaniline was found

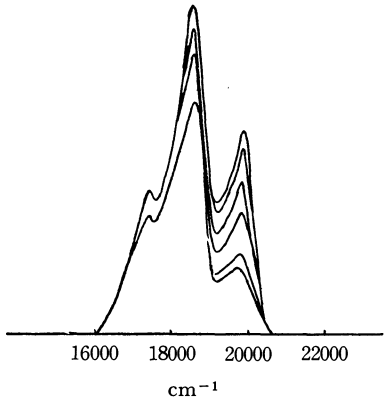

Fig. 7. Phosphorescence spectra of 5-nitroacenaphthene.
the uppermost curve: added 0 M cinnamic acid
the second curve: added 0.01 M cinnamic acid
the third curve: added 0.05 M cinnamic acid
the fourth curve: added 0.1 M cinnamic acid
the fifth curve: added 0.15 M cinnamic acid
the lowest curve: added 0.2 M cinnamic acid

to be very weak, in comparison with that of the *p*-isomer, although the phosphorescences of the two compounds are quite similar in shape and are equally quenched by the addition of cinnamic acid. In the case of *o*-nitroaniline, the same energy transfer could be found as in the *p* isomer. This suggests that the structural effect on the triplet transfer is small, and that the smaller sensitization effect of *o*-nitroaniline can be correlated with the weak intensity of the phosphorescence in comparison with that of *p*-nitroaniline.

The phosphorescence spectra of 5-nitroacenaphthene are shown in Fig. 7. The exciting light was 350 mμ. The remarkable quenching by cinnamic acid could also be observed. The triplet state of 5-nitroacenaphthene is situated near that of cinnamic acid, and the effect of the sensitization on the resin is very large.

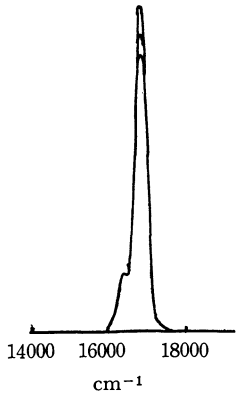

Fig. 8. Phosphorescence spectra of 1,2-benzanthracene.
the uppermost curve: added 0 M and 0.01 M cinnamic acid
the second curve: added 0.05 M and 0.1 M cinnamic acid
the lowest curve: added 0.15 M and 0.2 M cinnamic acid

The phosphorescence spectra of acenaphthene were also measured. It was found that its phosphorescence is greatly quenched by the addition of cinnamic acid. However, this compound is not an effective sensitizer. This lack of effectiveness is attributable to the absorption wavelength. The wavelength of the absorption peak for 5-nitroacenaphthene is about 320 mμ.

As is shown in Fig. 8, the phosphorescence of 1,2-benzanthracene is not quenched by the addition of cinnamic acid. The triplet energy of this compound is 16700 cm^{-1}, much smaller than that of cinnamic acid. Therefore, it is impossible for the triplet energy of 1,2-benzanthracene to be transferred to cinnamic acid.

The above quenching measurements make it clear that sensitization is due to the triplet-energy-transfer mechanism. The authors also tried to detect the sensitized phosphorescence of cinnamic acid. However, it could not be detected. The strength of the phosphorescence of cinnamic acid is smaller than that of the sensitizer, and the wavelengths of the two phosphorescence peaks are similar. Therefore, it seems reasonable to say that it is covered by that of the sensitizer.

In the measurement of the quenching of the sensitizer's phosphorescence, the authors could estimate $[A]_{1/2}$. Once $[A]_{1/2}$ is known, the experimental value of R_0 may be calculated by the equation:[15]

$$R_0 = \frac{7.35}{\sqrt[3]{[A]_{1/2}}} \quad (Å)$$

The critical separation estimated from the above equation is shown in Table 2. There is no evidence for a long-range resonance transfer of the kind found in the analogous singlet-energy-transfer process. Therefore, the exchange transfer mechanism may be applied to the triplet energy transfer from the sensitizer molecule to cinnamic acid.

The rate of the production of the triplet state can be written by:

$$\frac{d[T]}{dt} = \phi I_{abs} - (k_1[T] + k_q[Q][T]) \qquad (1)$$

where I_{abs} is the number of the absorbed photons, ϕ is the quantum yield which represents the efficiency of the absorbed photon in creating the triplet state, k_1 is the first-odrer rate constant of the decay of the triplet donor T, k_q is the bimolecular-quenching rate constant, and [Q] is the concentration of the quencher, cinnamic acid.

Table 2. Critical separation of sensitizer

Sensitizer	Phos. energy cm^{-1}	$[A]_{1/2}$ M	R_0 Å	α mol^{-1}
5-Nitroacenaphthene	19800	0.12	14.9	9
Acenaphthene	20900	0.019	17.5	52
1,2-Benzanthracene	16700	—	—	1
p-Nitroaniline	19700	0.094	16.2	8
o-Nitroaniline	19700	0.105	15.5	7
2-Nitrofluorene	20600	0.063	18.4	21
Pyrene	19700	0.113	15.2	15

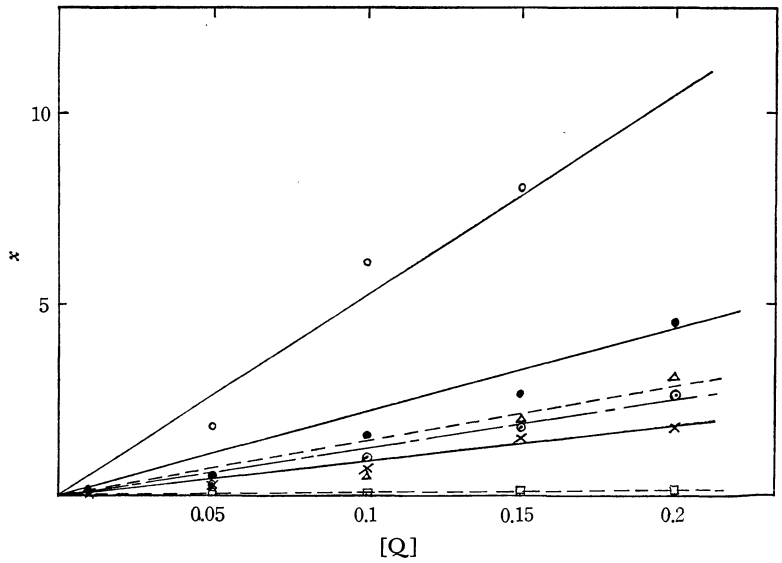

Fig. 9. The quenching effect of sensitizers.
—○— acenaphthene —●— 2-nitrofluorene
--△-- *o*-nitroaniline --⊙— *p*-nitroaniline
—×— 5-nitroacenaphthene --□— 1,2-benzanthracene

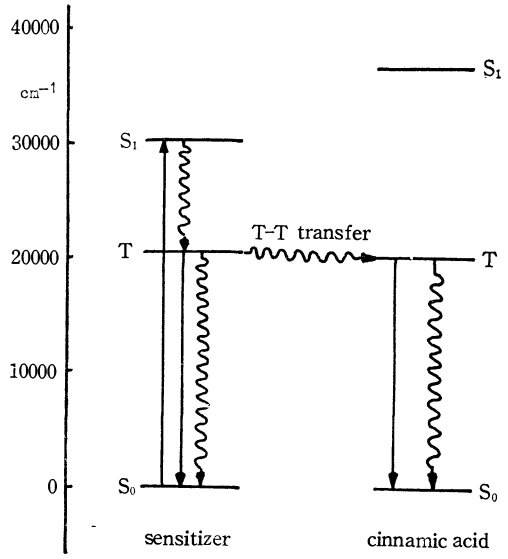

Fig. 10. The electronic levels of the sensitizer, 2-nitrofluorene, and cinnamic acid in the phenomenon of sensitization.

At the stationary state, the following equation can be derived:

$$[T]_Q = \frac{\phi I_{abs}}{k_1 + k_Q[Q]} \tag{2}$$

The emission strength of the donor phosphorescence is proportional to the triplet concentration [T]. Therefore, the ratio of phosphorescences, P_Q/P_0, can be estimated by:

$$\frac{P_Q}{P_0} = \frac{1}{1 + \alpha[Q]} \tag{3}$$

where P_0 and P_Q are the emission strengths of the phosphorescences of the donor and the quenched donor, and α is k_Q/k_1. From the above equation, the following relation can be derived:

$$x = \alpha[Q] \tag{4}$$

where $x=(P_0/P_Q-1)$.

In Fig. 9, the relations obtained experimentally are shown. The linear relation between them is fairly satisfactory. The inclination of the line shows the value of α. In Table 2 the obtained values of α are presented in the last column.

Finally, the electronic levels of the energy donor and acceptor in the phenomenon of sensitization can be expressed as is shown in Fig. 10. The energy difference in the donor between the lowest singlet and the triplet is much smaller than that in the acceptor, and the phosphorescence of the donor is quenched by the addition of an acceptor.

On the basis of the above results, it can be concluded that the photosensitization of polyvinyl cinnamate is caused by the triplet-state mechanism.

BULLETIN OF THE CHEMICAL SOCIETY OF JAPAN VOL. 41 1983—1989 (1968)

Hydrolysis of Uranium Monocarbide and Oxidation Potentials

Yoshio HORI and Takashi MUKAIBO

Department of Industrial Chemistry, Faculty of Engineering, The University of Tokyo, Hongo, Tokyo

(Received February 6, 1968)

The hydrolysis of UC with 1 N H_2SO_4 was carried out in the presence of various oxidants at 80°C. The amount of gaseous products was measured by means of a gas chromatograph; the dissolved, carbon-containing compounds, and the insoluble residues produced in the reaction were analyzed for carbon. Analyses of the uranium and oxidants consumed were also made by volumetric and gravimetric methods. The results may be summarized: (1) The hydrolysis of UC with 1 N H_2SO_4 proceeds by an electro-chemical mechanism. (2) The hydrolysis products fundamentally depend upon the oxidation potential of the oxidants in the solution. (3) The oxidation potential at which the hydrolysis of UC with 1 N H_2SO_4 proceeds can be explained in terms of the partial ionic character of UC. (4) The application of this experimental method to other carbides would serve to clarify the chemical reaction and the bond character of the carbides.

Reactions between carbides and aqueous solutions containing oxidants have been studied by several authors. According to these studies, the hydrolyses of some carbides, such as uranium and actinides with nitric acid, yield products with different compositions from those obtained from aqueous solutions without any oxidants.[1-5] Others, such as CaC_2, give rise to products of the same composition whether containing nitric acid or not.[6] The present study seeks to clarify the mechanism of the hydrolysis of uranium monocarbide, which has not been discussed by previous authors.

Experimental

Experimental Procedure. About 250—500 mg of a UC sample was placed in a reactor. The reactor (volume: *ca.* 200 m*l*) consists of a glass tube 40 mm in diameter, connected with two vacuum stop cocks. After evacuation through one of the stop cocks, 35 m*l* of an aqueous reagent solution was introduced into the reactor as fast as possible in order to prevent air dissolution. Then it was immersed in a thermostated water bath at 80±0.1°C or placed in an air bath at the same temperature; in the latter case the reaction had to continue for more than ten hours. After the reaction, the reactor was cooled to room temperature, and the products were analyzed as will be described below.

Materials (1) Uranium Monocarbide. The same powdered sample as had been used in a previous work[7] was employed in this study.

Materials (2) Aqueous Reagent Solution. The solutions were prepared by dissolving oxidizing reagents into 1.1 N H_2SO_4, which had been flushed with purified nitrogen before the reaction. In order to control the oxidation potentials of the reactant solutions, the following reagents were employed (the standard oxidation potentials at 25°C are shown in parentheses): $FeSO_4 \cdot 7H_2O$(Fe^{2+}/Fe −0.44 V), JIS GR grade reagent. $CoSO_4 \cdot 7H_2O$(Co^{2+}/Co −0.277 V), JIS GR grade reagent. $NiSO_4 \cdot 7H_2O$(Ni^{2+}/Ni −0.250 V), JIS GR grade reagent. $SnSO_4$ (Sn^{2+}/Sn −0.140 V), the reagent solution of Sn^{2+}, was prepared by dissolving a ten-fold excess of Sn metal, 99.9% purity, into GR grade $CuSO_4$ and an H_2SO_4 aqueous solution in a purified nitrogen atmosphere. The resultant solution was analyzed to ascertain the absence of Cu^{2+} and Sn^{4+} concentrations. By the use of a KI and starch solution, Cu^{2+} was not detectable. The concentration of Sn^{2+} was equal to the total concentration of Sn ions within 1%; this indicates the absence of Sn^{4+} in the solution. $CuSO_4 \cdot 5H_2O$ (Cu^{2+}/Cu +0.377 V), JIS GR grade reagent. Ag_2SO_4 (Ag^+/Ag +0.799 V), the Ag_2SO_4 was obtained as a precipitate by the addition of H_2SO_4 to a GR grade $AgNO_3$ solution. The precipitate was filtered and then washed with alcohol and ethyl ether. NO_3^- was not detectable in the compound. $Fe_2(SO_4)_3 \cdot xH_2O$ (Fe^{3+}/Fe^{2+} +0.771 V), JIS GR grade reagent.

Chemical Analysis (1). The aqueous systems which involved Fe^{2+} and Co^{2+} were not analyzed for the corresponding metal after the reaction, because no metal deposit was found in these systems after the reaction had been completed. Ni^{2+} was weighed as nickel dimethyl glyoxime.[8] Sn^{2+} was determined as follows. A known amount of $FeCl_3$ solution was added to the test solution, and the Fe^{2+} reduced by Sn^{2+} was titrated

1) J. L. Drummond, B. J. McDonald and H. M. Ockenden, *J. Chem. Soc.*, **1957**, 4785.
2) P. L. Pausen, J. McLean and W. J. Clelland, *Nature*, **197**, 1200 (1963).
3) D. M. Donaldson, K. Hartley, P. Lees and N. Parkinson, *Trans. AIME*, **227**, 191 (1963).
4) F. H. Pollard, G. Nickless and S. Evered, *J. Chromatog.*, **15**, 223 (1964).
5) L. M. Ferris and M. J. Bradley, *J. Am. Chem. Soc.*, **87**, 1710 (1965).
6) M. B. Sears and L. M. Ferris, *J. Inorg. Nucl. Chem.*, **29**, 1255 (1967).
7) Y. Hori and T. Mukaibo, This Bulletin, **40**, 1878 (1967).
8) I. M. Kolthoff and E. B. Sandell, "Textbook of Quantitative Inorganic Analysis," Macmillan, New York (1952).

by 0.05 N $K_2Cr_2O_7$ using sodium diphenyl amine sulfonate as an indicator. An Sn metal, precipitated during the hydrolysis of UC, was dissolved into a mixed solution of HCl and H_2SO_4; after conversion to Sn^{4+} by chlorine gas, Sn^{2+} was precipitated as SnS_2 by H_2S. It was weighed as SnO_2 after vigorous heating. The concentration of Cu^{2+} was determined by iodometry.[8] The Fe^{2+} concentration in the solutions was determined by titration with 0.05 N $K_2Cr_2O_7$, and the total Fe was treated similarly after having been passed through a Jones reductor. Ag^+ was weighed as AgCl as usual.[8] The uranium test solution was reduced by a Jones reductor after appropriate separations, and was titrated by 0.05 N $K_2Cr_2O_7$ after air-bubbling for 10 min.[9]

Chemical Analysis (2). The carbon which was initially included in the UC powder was found in the gaseous products, in the reactant solution, and in the solid products after the reaction. The total pressure of the gaseous products was measured by a conventional mercury manometer, and the volume at STP was obtained by the correction of the water vapor pressures at room temperatures. The analysis of the gaseous products was made for N_2, H_2, CO, CO_2, CH_4, C_2H_6, C_3H_8, C_3H_6, i-C_4H_{10}, 1-C_4H_8, and unidentified C_4 and C_5 products by means of a gas chromatography equipped with a thermal conductivity detector. They were separated by means of a 4 m-long column containing 38% dimethyl formamide - activated alumina with H_2 carrier gas, a 2.5 m-long column containing 2.5% squarene-silica gel, with H_2 carrier gas, and a 1 m-long column containing a 13X molecular sieve, with H_2 and N_2 carrier gas. All these four operations were carried out at room temperature, and all gave accurate and reproducible results concerning the composition of the gaseous products. The carbon - containing compounds in the solutions were analyzed for carbon by persulfate oxidation.[10] The solid products were treated in warm hydrochloric acid in order to dissolve the deposited metals, and the insoluble residues were burned to CO_2, which was then weighed in a usual way.

Results

Table 1 presents the products of reactions between UC and various aqueous systems.

Aqueous Systems Which Contain Fe^{2+}, Co^{2+}, Ni^{2+}. Apparently from Table 1, the products and the compositions obtained for the systems containing Fe^{2+}, Co^{2+}, and Ni^{2+} (columns 4 to 6) are virtually equal to those without any oxidant (column 2). No metal deposition was observed for any of these systems. For comparison a reaction between UC powder mixed with *ca.* 20 mg of Ni powder and Ni^{2+} solution was also carried out. The result (column 7) differs a little from that obtained for the system without Ni powder (column 6). The difference between the solutions with and without nickel metal (columns 6 and 7) may be attributed mainly to the nucleation overpotential of nickel. It indicates that the hydrolysis of UC is influenced by the oxidant at the oxidation potential of -0.26 V for $Ni^{2+}+2\,e \rightarrow Ni$ (concentration 0.10 M and at 80°C). The uranium ion was found to exist as U^{4+} in all the solutions.

Sn^{2+} Systems. The reaction proceeded as readily as in the non-oxidant solution. The gaseous products decreased with the Sn^{2+} concentration. The amount of hydrogen and methane considerably decreased. Ethane and the other higher hydrocarbons, the dissolved carbon-containing compounds, and the greenish-black insoluble residues increased. It is also significant that the quantity of the unsaturated hydrocarbons (C_3H_6 and 1-C_4H_8) became

Table 1. Product of the reaction between UC and aqueous systems (80°C, 1.1 N H_2SO_4)

Oxidant	Non-oxidant	Au powder	Fe^{2+}	Co^{2+}	Ni^{2+}	Ni^{2+} and Ni	Sn^{2+}	Sn^{2+}	Cu^{2+}	Ag^+	Fe^{3+} and Fe^{2+}
Concn. (M)	—	—	0.30	0.30	0.30	0.10	0.025	0.100	0.191	0.118	1.94/1
Time (hr)	3.0	9.0	2.5	2.5	5.0	1.5	6.0	6.0	69	9.0	69
	ml/g	ml/g	ml/g	ml/g	ml/g	ml/g	ml/g	ml/g	ml/g	ml/g	ml/g
H_2	8.20	13.78	8.48	8.53	9.72	8.55	2.67	1.34	1.16	0.00	0.95
CH_4	85.2	76.7	84.1	83.0	82.4	76.0	64.9	42.3	9.00	0.17	2.17
C_2H_6	0.23	0.39	0.54	0.57	0.91	0.61	1.64	1.50	0.61	0.21	0.00
C_3H_8	0.07	0.21	0.09	0.14	0.20	0.12	0.42	0.42	0.00	0.00	0.00
C_3H_6	0.03	0.10	0.05	0.08	0.14	0.06	0.56	0.77	0.00	0.00	0.00
i-C_4H_{10}	0.00	0.00	0.00	0.00	0.00	0.00	0.18	0.25	0.00	0.00	0.00
n-C_4H_{10}	0.02	0.11	0.02	0.03	0.08	0.00	0.37	0.56	0.00	0.00	0.00
1-C_4H_8	0.02	0.07	0.05	0.03	0.07	0.00	0.07	0.17	0.00	0.00	0.00
C_5H_{12}	0.00	0.00	0.07	0.09	0.00	0.00	0.00	0.25	0.00	0.00	0.00
CO_2	0.00	0.30	0.00	0.00	0.00	0.00	0.00	0.22	17.4	5.15	14.9
	mg/g	mg/g	mg/g	mg/g	mg/g	mg/g	mg/g	mg/g	mg/g	mg/g	mg/g
Solubles	0.00	0.29	0.00	0.00	0.00	1.54	1.52	3.78	68.7	2.74	7.05
Residues	0.20	3.72	0.21	0.57	0.25	0.72	1.05	8.75	35.9	48.8	30.2

9) I. M. Kolthoff *et al.*; "Volumetric Analysis," Vol. III (1957).

10) J. Katz, S. Abraham and N. Baker, *Anal. Chem.*, **26**, 1503 (1954).

more than that of the saturated hydrocarbons (C_3H_8 and C_4H_{10}, respectively). A gray sponge identified as metallic tin was produced.

Cu^{2+} Solution. The reaction was so slow that after 69 hr only 20% of the UC has reacted. Thus, the precision of the analysis of the products was lower than in the other systems. Though traces of hydrogen and methane were produced, the main products were dissolved, carbon-containing compounds and insoluble black residues. A small amount of CO_2 was also detected. A grain-like copper metal was produced, and some of the copper deposit was found to adhere to he carbide surface. The valence of uranium in the product solution was +6.

Ag^+ Solution. The reaction proceeded rather readily. Virtually no hydrogen and no methane were produced. The insoluble residues and carbon dioxide were obtained dominantly. Dendritic silver was deposited, and the uranium in the solution was in the +6 state.

Fe^{3+} and Fe^{2+} Solution. Although the reaction rate was not high, the reaction was completed after 69 hr. Virtually no hydrocarbons evolved. A large amount of an insoluble powder and/or sponge-like residue was found. The quantity of the dissolved carbon-containing compounds decreased. The evolution of CO_2 increased. A trace of CO was detected, but no quantitative analysis was made. After the reaction, Fe^{3+} was found to be reduced to Fe^{2+} quantitatively.*1

Au Powder System. The reaction between UC and 1.1 N H_2SO_4 in the presence of Au powder was studied in order to determine whether or not the reaction products differ when UC came into contact with non-reactive metal. About 250 mg of UC and 3 g of 325 mesh under Au powder were mixed in a mortar, and then charged into a reactor. There were more hydrogen and more insoluble residues, and less methane, compared with the non-oxidant solution (Table 1, columns 2 and 3). These results will be discussed in the following section.

Discussion

The Relation between the Oxidation Potentials and the Hydrolysis Reaction of UC. The hydrolysis of UC with 1 N H_2SO_4 is considered, on the basis of the experiment with Au powder to be discussed below, to proceed by the electrochemical mechanism:

TABLE 2. CARBON AND HYDROGEN BALANCE OF THE REACTION (80°C, 1.1 N H_2SO_4)

Oxidant	Non-oxidant		Au powder		Fe^{2+}		Co^{2+}		Ni^{2+}		Ni^{2+} and Ni	
Concn. (M)	—		—		0.30		0.30		0.30		0.10	
	mg atom/mmol		mg atom/mmol		mg atom/mmol		mg atom/mmol		mg atom/mmol		mg atom/mmol	
	C	H	C	H	C	H	C	H	C	H	C	H
H_2		0.183		0.307		0.189		0.190		0.217		0.191
CH_4	0.950	3.800	0.855	3.420	0.938	3.75	0.927	3.71	0.917	3.678	0.848	3.39
C_2-C_5	0.011	0.033	0.027	0.070	0.024	0.062	0.028	0.084	0.039	0.103	0.020	0.05
CO_2	0.000		0.004		0.000		0.000		0.000		0.000	
Solubles	0.000		0.006		0.000		0.000		0.000		0.032	
Residues	0.004		0.078		0.005		0.012		0.005		0.015	
Total	0.965*	4.016	0.970	3.797	0.967	4.00	0.967	3.98	0.961	4.00	0.915	3.63

Oxidant	Sn^{2+}		Sn^{2+}		Cu^{2+}		Ag^+		Fe^{3+}/Fe^{2+}	
Concn. (M)	0.025		0.100		0.191		0.118		1.94/1	
	mg atom/mmol		mg atom/mmol		mg atom/mmol		mg atom/mmol		mg atom/mmol	
	C	H	C	H	C	H	C	H	C	H
H_2		0.060		0.030		0.026		0.000		0.022
CH_4	0.724	2.89	0.471	1.883	0.100	0.400	0.002	0.008	0.024	0.096
C_2-C_5	0.096	0.251	0.133	0.317	0.014	0.042	0.005	0.014	0.000	0.000
CO_2	0.000		0.002		0.194		0.057		0.166	
Solubles	0.033		0.079		0.923		0.057		0.146	
Residues	0.023		0.182		0.745		1.018		0.625	
Total	0.876	3.201	0.867	2.230	1.976	0.468	1.075	0.022	0.961	0.118

* UC contained 0.968 mg atom/mmol of carbon, initially.

*1 The valence of uranium was not determined. Titration with a $K_2Cr_2O_7$ solution is employed as a conventional volumetric analysis of uranium. As the direct oxidation of U^{4+} to UO_2^{2+} by $Cr_2O_7^{2-}$ proceeds slowly, it is recommended to add a Fe^{3+} solution first, then oxidize U^{4+} to UO_2^{2+}, and finally determine the resultant Fe^{2+} by titration. Therefore, uranium ions coexisting with Fe^{3+} can be regarded as UO_2^{2+}.

Table 3. The material balance for oxidation and reduction

Oxidant	Non-oxidant		Au powder		Fe^{2+}		Co^{2+}	
Concn. (M)	—		—		0.30		0.30	
Oxidation* potential					−0.455		−0.292	
	mg eqv/mmol		mg eqv/mmol		mg eqv/mmol		mg eqv/mmol	
	Oxid.	Red.	Oxid.	Red.	Oxid.	Red.	Oxid.	Red.
$UC \rightarrow U^{n+}$	4.00		4.00		4.00		4.00	
$C \rightarrow CO_2$			0.01					
$H^+ \rightarrow H^0$								
H_2		0.183		0.307		0.189		0.190
Hydrocarbon		3.833		3.49		3.81		3.790
Oxidant consumption						0.00		0.00
Total	4.00	4.02	4.01	3.80	4.00	4.00	4.00	3.98

Oxidant	Ni^{2+}		Ni^{2+} and Ni		Sn^{2+}		Sn^{2+}	
Concn. (M)	0.30		0.10		0.025		0.100	
Oxidation potential	−0.266		−0.260		−0.208		−0.187	
	mg eqv/mmol		mg eqv/mmol		mg eqv/mmol		mg eqv/mmol	
	Oxid.	Red.	Oxid.	Red.	Oxid.	Red.	Oxid.	Red.
$UC \rightarrow U^{n+}$	4.00		4.00		4.00		4.00	
$C \rightarrow CO_2$							0.01	
$H^+ \rightarrow H^0$								
H_2		0.217		0.191		0.060		0.030
Hydrocarbon		3.781		3.44		3.14		2.200
Oxidant consumption		0.00		0.00		0.566		1.384
Total	4.00	4.00	4.00	3.63	4.00	3.77	4.01	3.61

Oxidant	Cu^{2+}		Ag^+		Fe^{3+}/Fe^{2+}	
Concn. (M)	0.191		0.118		1.94/1	
Oxidation	+0.312		+0.711		+0.846	
	mg eqv/mmol		mg eqv/mmol		mg eqv/mmol	
	Oxid.	Red.	Oxid.	Red.	Oxid.	Red.
$UC \rightarrow U^{n+}$	6.00		6.00		6.00	
$C \rightarrow CO_2$	0.78		0.23		0.67	
$H^+ \rightarrow H^0$						
H_2		0.026		0.00		0.022
Hydrocarbon		0.442		0.022		0.096
Oxidant consumption		2.91		6.28		6.51
Total	6.78	3.38	6.23	6.30	6.67	6.63

* Oxidation potentials were calculated from thermochemical data (at 80°C).[11,12]

$$UC \rightarrow U^{4+} + (C + 4e)_{carbide}$$

$$(C + 4e)_{carbide} + 4H^+ \rightarrow CH_4$$

As UC is a good electric conductor, a part of the electrons liberated by the dissolution of U are able to migrate to Au powder, which is in contact with UC. Then the electrons will reduce protons to hydrogen radicals on Au particles.

Partially, $H^+ + e \rightarrow H\cdot$ (on Au particles)

Since there is no carbon atom available for the formation of methane on Au particles, these radicals will react with each other and will result in hydrogen molecules:

$$H\cdot + H\cdot \rightarrow H_2 \text{ (on Au particles)}$$

11) W. Latimer, "Oxidation Potentials," Prentice Hall, Englewood Cliffs, N. J. (1952).
12) A. J. deBethune, T. S. Licht and N. Swendeman, *J. Electrochem. Soc.*, **106**, 616 (1959).

As a result, carbon atoms which failed to react with hydrogen atoms would polymerize and precipitate, because the overall ratio of H to C remains 4.0.

$$C \rightarrow \text{insoluble residues}$$

Evidently the composition of the reaction products changes with the oxidation potential, as may be seen from Tables 1, 2, and 3. In solutions without any oxidant, the overall reaction will proceed as below:

$$(UC)_{carbide} \rightarrow U^{4+} + (C + 4e)_{carbide}$$

$$(C + 4e)_{carbide} + 4H^+ \rightarrow CH_4 + \text{a small quantity of higher hydrocarbons, and hydrogen.}$$

The same discussion holds also in the solution containing Fe^{2+} and Co^{2+}. At a potential higher than about -0.26 V of the oxidation potential (*i.e.*, Ni^{2+}/Ni solution), the composition of the reaction products is found to change with the potential. The overall reaction in the Sn^{2+}/Sn solution can be written:

$$UC + xH^+ + (4-x)/2\ Sn^{2+} \rightarrow U^{4+} + (4-x)/2\ Sn + CH_x$$

where x is the average ratio of H to C in the products. From Table 2, x is found to be $2.23/0.867=2.57$ in the 0.1 M solution of Sn^{2+}. The value of x decreases with the concentration of Sn^{2+}.

As is shown in Table 2 concerning the material balance, the total carbon exceeds 0.968 in the Cu^{2+}/Cu system, and the material balance for oxidation and reduction (Table 3) is not matched. The reason for this will be explained below. After the reaction, the insoluble residue was treated with warm hydrochloric acid in order to dissolve the unchanged UC. In this procedure, hydrogen probably evolved on copper metal adherent to the unchanged UC, and carbon atoms in UC were polymerized and precipitated by the mechanism described in connection with the Au powder system. The insoluble residues containing carbon which resulted from this procedure entered the product of the reaction in the Cu^{2+}/Cu system.

In the system of Ag^+/Ag and Fe^{3+}/Fe^{2+}, the overall reaction can be expressed:

$$UC + 2H_2O + 6Ag^+ \rightarrow UO_2^{2+} + 4H^+ + 6Ag + C^{*2}$$

Carbon atoms result in the insoluble residue, the dissolved compounds, and carbon dioxide in the above reaction.

The Production of CO_2. When the reactant solution did not include any oxidant, a substantial number of the carbon atoms in UC were converted to CH_4. As the oxidation potential becomes higher, C_2H_6, C_3H_8, C_3H_6, the soluble compounds, the insoluble residues, and CO_2 increase. Figure 1 presents the average oxidation number of the carbon atom. In its calculation a hydrogen atom bonded to a carbon atom is estimated at -1, and an oxygen, at $+2$. Obviously CH_4 is produced when no oxidation occurs, and the increase of C_2H_6, C_3H_8, C_3H_6, the soluble compounds, and the insoluble residues corresponds to partial oxidation, while CO_2 evolves as a result of full oxidation.

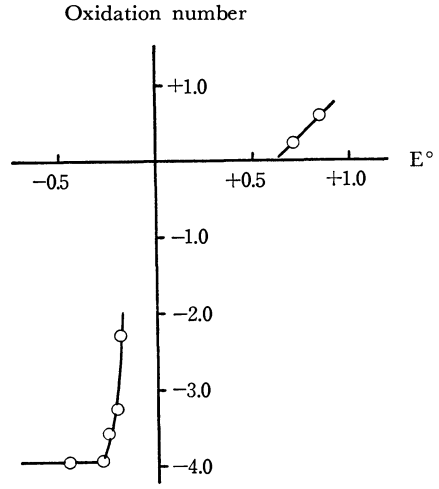

Fig. 1. Oxidation number of carbon *versus* oxidation potential.

The formation of CO_2 is interesting, since the oxidation potential for the reaction:

$$2H_2O = O_2 + 4H^+ + 4e$$

is about $+1.2$ V at 80°C.[11,12] It is impossible that CO_2 evolves through the oxygen molecules or atoms that come from the oxidation of water by such oxidants as ferric ions. CO_2 would be formed from the direct reduction of H_2O with the carbon atom which is recovered from the carbide lattice. Without presence of oxidants, the carbon atom will not react with H_2O to produce CO_2, because Coulombic repulsion will be caused between $^{\delta+}H\diagdown\diagup O^{\delta-}\diagup H^{\delta+}$: and the partially-ionic carbon atom, as will be discussed below. Accordingly, the carbon atom can reduce H_2O after losing some fraction of its electrons.

Comparison with Other Studies. Damiens[13] studied the hydrolysis of cerium carbide with HCl solution which contained $FeCl_3$; the found that the products differed considerably from those obtained in a solution not containing an oxidant. The reaction between UC and HNO_3 has been studied by many authors in connection with the reprocessing of nuclear fuel.[1-5] Except for the report by Pollard

*2 The oxidation-reduction potential for the reaction

$$U^{4+} + 2H_2O \rightarrow UO_2^{2+} + 4H^+ + 2e$$

is $+0.264$ V at 80°C.[11]

13) A. Damiens, *Ann. chim.*, **10**, 137 (1918).

et al.,[4] most of their studies are in general agreement, showing that carbide carbon is converted to CO_2, oxalic acid, mellitic acid, other aromatic compounds, and free carbon in some papers. Pollard *et al.*, however, reported that most of the carbide carbon was found in hydrocarbons, the composition of which was virtually equal to that obtained in dilute acid not containing nitric acid. This discrepancy has not been explained. The formation of CO_2 and other organic compounds is consistent with the present experimental results, since the oxidation-reduction potential for the reaction:

$$NO_3^- + 4H^+ + 3e \rightarrow NO + 2H_2O \qquad E^\circ_{25^\circ} = 0.96\ V$$

$$2NO_3^- + 4H^+ + 2e \rightarrow N_2O_4 + 2H_2O \qquad E^\circ_{25^\circ} = 0.80\ V$$

Baudin[14] *et al.* reported the hydrolysis of UC with 3 N HCl - 0.25 N $K_2Cr_2O_7$. According to them, hydrogen decreased markedly (11.2%→1.1% of total gases), compared with a non-oxidant solution, and C_3, C_4 ethylenics evolved (C_3H_6 1.65%, C_4H_8 1%). Their report, however, indicates that the composition of products of a 0.25 N $K_2Cr_2O_7$ solution is rather equal to that for the nonoxidant solution, since more than 90% of the carbide carbon is converted to methane. In our preliminary 1 N HCl-0.25 N $K_2Cr_2O_7$ experiment, the reaction rate was rather low; about half of the reacted carbide carbon was found in CO_2, and the other half in insoluble residues. A more critical comparison of these marked differences between the two cannot be made since their experimental procedures were not reported in detail by Baudin *et al.* Greenwood and Osborn[15] described the hydrolysis of LaC_2 and La_2C_3 with 4 N H_2SO_4 and 2 N HNO_3. According to them, hydrogen was markedly lessened in 2 N HNO_3, but most of the carbide carbon was converted into C_2H_2, C_2H_4, and free carbon in both 2 N HNO_3 and 4 N H_2SO_4. Pollard *et al.*[16] reported the hydrolysis of LaC_2, CeC_2, NdC_2, GdC_2, and $YC_{1.6}$ with 4 N HNO_3. The hydrolysis of carbides with 4 N HNO_3 gave results virtually equal to those for water and 4 N H_3SO_4, in spite of the considerable evolution of nitric oxides. This problem cannot be further discussed critically, however, since the experimental details were not described.

Sears and Ferris[6] studied the reactions of CaC_2 and BaC_2 with different concentrations of nitric acid. The reactions of CaC_2 with 0—16 M HNO_3 and BaC_2 with 0—8 N HNO_3 yielded C_2H_2 as the only carbon-containing product, but when reacted with 10—16 M HNO_3, BaC_2 gave rise to free carbon and carbon oxides by the partial oxidation of carbide carbon simultaneously with the production of acetylene.

The Potential at Which UC Reacts with Aqueous Acid. On the basis of the present experiment, E_H, the oxidation potential at which the hydrolysis of UC proceeds really may be said to be near −0.26 V since the Ni^{2+} ion has the basest oxidation potential among any oxidants that show the oxidant effect. As an extreme case, the reaction:

$$UC = U^{4+} + 4e + C(\beta\text{-graphite}) \qquad E^\circ = -1.2\ V \qquad (1)$$

can be interestingly compared with the present one. In this case the reaction:

$$4H^+ + 4e + C(\beta\text{-graphite}) = CH_4 \qquad E^\circ = 0.13\ V \qquad (2)$$

would correspond to the cathodic one. The oxidation potentials for these two reactions, (1) and (2), can readily be calculated to be −1.2 V and +0.13 V, respectively from the thermochemical data.[11,17] E_H will depend upon the overpotentials for the evolution of methane and the dissolution of uranium. In general, the anodic dissolution of metals occurs at a rather low polarization; the cathodic evolution of gases, such as H_2 and O_2, is accompanied by rather high overpotentials. Accordingly, if it is assumed that the Reactions (1) and (2) actually proceeds in the hydrolysis of UC, E_H may be observed to be roughly equal to E_R,*3 the oxidation potential for (1), that is −1.2 V. Thus, the difference between the experimental E_H values near −0.26 V and E_R, −1.2 V would indicate the variation in the reactivity of the carbon in the carbide lattice from that in the graphite lattice.

From the behavior of CaC_2 and BaC_2 reported by Sears and Ferris,[6] the E_H value is estimated to be about 1.0 V for BaC_2 and higher than 1.0 V for CaC_2. The oxidation potential, E_R, for the (1)-type reaction.

$$BaC_2 = Ba^{2+} + 2e + 2C(\beta\text{-graphite})$$

may be said to be −2.62 V and that for CaC_2 −2.56 V on the basis of the thermochemical data.[11,18,19] $E_H - E_R$ is then, rather a large value of 3.6 V. CaC_2 is reported to be an ionic crystal, $Ca^{2+}C_2^{2-}$, on the basis of the neutron diffraction.[20] If it is tentatively assumed that the $E_H - E_R$ value becomes larger as the ionic character of carbides increases, the $E_H - E_R$ value of 0.9 V for UC may be

14) G. Baudin, J. Besson, P. Blum and J. Spitz, *Compt. Rend.*, **254**, 4179 (1962).
15) N. N. Greenwood and A. J. Osborn, *J. Chem. Soc.*, **1961**, 1775.
16) F. H. Pollard, G. Nickless and S. Evered, *J. Chromatog.*, **15**, 211 (1964).
17) M. H. Rand and O. Kubaschewski, "The Thermochemical Properties of Uranium Compounds," Oliver & Void, London (1963).
*3 Oxidation potential for reference reaction.
18) R. H. Flowers and E. G. Rauh, *J. Inorg. Nucl. Chem.*, **28**, 1355 (1966).
19) R. L. Faircloth, R. H. Flowers and F. C. W. Pummery, *J. Inorg. Nucl. Chem.*, **29**, 311 (1967).
20) M. Atoji, *J. Chem. Phys.*, **35**, 1950 (1961).

said to be due to the partially ionic character of UC, *i.e.*, $U^{n+}C^{n-}$. The partial ionic character is also confirmed by the fact that the work function for U is about 3.5 eV,[21,22] while that for graphite is about 4.4 eV.[23] This suggests that electrons will be transferred from U atoms to C atoms in the UC crystal lattice. The reaction between UC and an acid aqueous solution would proceed as below:

$$U^{n+}C^{n-} \rightarrow U^{4+} + C^{n-} + (4-n)e_{\text{in crystal}}$$

$$C^{n-} + (4-n)e_{\text{in crystal}} + 4H^{+} \rightarrow CH_4$$

As has been discussed above, the $E_H - E_R$ value would reflect the bond nature of carbide and could be employed as a parameter for the reactivity of various carbides.

21) J. C. Riviere, *Proc. Phys. Soc.*, **80**, 116, (1962).
22) R. K. Fry and A. B. Cardwell, *Phys. Rev.*, **125**, 471 (1962).
23) G. Montet, M. Hoch and G. Hennig, USAEC ANL-6804 (1964).

Conclusion

1) The reaction between UC and 1 N H_2SO_4 proceeds by an electrochemical mechanism.

2) The hydrolysis products of UC with aqueous acid solution depend fundamentally upon the oxidation potential of the oxidant in the solution.

3) The potential, E_H, where the hydrolysis proceeds is about -0.26 V for UC, and UC would be partial ionic crystal.

4) E_H can be employed as a parameter which expresses the reactivity of carbides.

The authors are grateful to Dr. K. Fueki for his valuable discussions during the course of this work.

BULLETIN OF THE CHEMICAL SOCIETY OF JAPAN VOL. 41 1989—1997 (1968)

An MO-theoretical Interpretation of the Nature of Chemical Reactions. I. Partitioning Analysis of the Interaction Energy*[1]

Kenichi FUKUI and Hiroshi FUJIMOTO

Faculty of Engineering, Kyoto University, Sakyo-ku, Kyoto

(Received February 20, 1968)

The molecular interaction energy, without considering the nuclear configuration change, is discussed by partitioning it into the Coulomb, exchange, delocalization, and polarization terms. A succinct approximate expression for each term is derived, and its magnitude is discussed. The expressions obtained as the second-order perturbation terms for the delocalization and the polarization energies are in accord with those of the well-established reactivity indices, the delocalizability, and the self-atom polarizability respectively. The chemical reactivity can thus be measured by the combined sum of these four terms. In usual ionic reactions the Coulomb and the delocalization terms are more important than the exchange and the polarization terms respectively.

The molecular orbital (MO) approach can be used to interpret the chemical reactivity of organic molecules, both saturated[1)] and unsaturated.[2)] Most of these MO criteria for the chemical reactivity are based on the use of various reactivity indices defined as the theoretical quantities of isolated reactant molecules, each based on an appropriately-assumed model for the chemical reaction. The classification of these indices has tentatively been made by dividing them into three groups, the static, the localization, and the delocalization approaches.[3)] The comparison of these approaches appeared promising for acquiring knowledge of the reaction mechanism.[2)] However, the semiempirical character of calculation made an absolute comparison of the various methods difficult. In addition, as a result of the existence of several theoretical correlations among the reactivity indices,[4)] no unequivocal conclusion has yet been obtained. Although the formal introduction of

*1 The basic idea of this paper was presented by one of the present authors (K.F.) at the International Summer School of Quantum Chemistry, Istanbul, August, 1964, while a skeletal presentation was made in K. Fukui, *Kogyo Kagaku Zasshi* (*J. Chem. Soc. Japan, Ind. Chem. Sect.*), **69**, 794 (1966).

1) K. Fukui, "Modern Quantum Chemistry," Vol I, ed. by O. Sinanoğlu, Academic Press, New York (1965), p. 49, and the references cited therein.

2) A. Streitwieser, Jr., "Molecular Orbital Theory for Organic Chemists," John Wiley & Sons, New York (1961), Chapter 11, and the references cited therein.

3) K. Fukui, "Molecular Orbitals in Chemistry, Physics and Biology," ed. by P.-O. Löwdin and B. Pullman, Academic Press, New York (1964), p. 513.

4) K. Fukui, T. Yonezawa and C. Nagata, *J. Chem. Phys.*, **26**, 831 (1957), and the references cited therein.

the "transition-state" concept in the absolute-rate theory has doubtless been illuminating, the basic principle of the activated complex formation is not yet clear. The nature of chemical reactions, therefore, still remains obscure in many details from the quantum-mechanical point of view.

It is the aim of the present approach to make a contribution to this problem through a formulation of the energy of chemical interaction, to derive at the same time a prototype of several reactivity indices in a unified manner, and also to discuss the characteristic features of the reaction path on the potential energy surface. The method is based chiefly on the Roothaan-type linear combination of atomic orbitals (LCAO) MO approach, with some use of the configuration interaction (CI) procedure.[5]

Electron Delocalization in the Chemical Interaction. Since 1933[6] several theories were proposed one after another to explain the chemical reactivity of conjugated molecules along the static[6-8] and the localization approaches.[9] In 1952 the "frontier electron" concept[10] was put forth; it pointed out that the electrophilic aromatic substitution should take place at the carbon atom of the largest density of the highest energy electrons. Similarly, the nucleophilic replacement was later shown to occur at the position of the largest density of the lowest unoccupied MO. In comparison with the theoretically well-established character of the other reactivity theories then existing, the lack of a solid physical foundation for the infant frontier electron theory suggested instead the possibility of the involvement of a new principle for the mode of chemical interaction.

It was coincidentally in the same year that the elegant theory of the charge-transfer interaction was developed by Mulliken with regard to the molecular complex formation between a donor and an acceptor.[11] In this connection, the "overlap and orientation" principle was proposed;[12] it considered only the overlap interaction between the highest energy occupied MO of the donor and the lowest energy unoccupied MO of the acceptor.

Since the behavior of the frontier electrons was attributed to some type of electron delocalization between the reactant and the reagent,[13] it was natural for the charge-transfer mechanism and the overlap and orientation principle to be connected to the problem of ionic reactions. Brown combined the charge-transfer theory with the frontier electron concept to derive a consistent theory of chemical reactivity.[14] All of these treatments[10-15] together may be termed the "delocalization approach" to chemical reactivity theory.

Applying the donor and acceptor concept to the substitution reactions in conjugated molecules, the electrophilic and the nucleophilic reactions were discussed from a unified point of view. Thus, the highest occupied (HO) MO of the donor molecule and the lowest unoccupied (LU) MO of the acceptor molecule were considered to behave as frontier orbitals in ionic reactions,[10] not only in substitutions but also in additions, and even in multicentric reactions.[8] When the overlap and orientation principle was applied to odd-electron molecules or radicals, the half-occupied nonbonding (NB) MO was responsible for the reactive interaction. A similar behavior of these particular MO's has also been pointed out in nonplanar saturated molecules.[1] In addition, the conspicuous property of HO and LU in determining the steric course of organic reactions has been discovered and has attracted much attention.[3,16]

In this view, it may be of interest to discuss the energy of reacting systems by dividing it into various kinds of interactions. Such a treatment will be useful in helping us to understand what factor is really important in the chemical reaction.

Interaction with No Nuclear Configuration Change

The energy of the interaction between two independent systems, in which, tentatively, no nuclear configuration change is considered, is defined by the following equation:

5) C. C. J. Roothaan, *Revs. Mod. Phys.*, **23**, 69 (1951). Longuet-Higgins and Murrell applied the concept of configuration interaction in discussing the electronic spectra of composite alternant hydrocarbons. They introduced the idea of polarization and charge-transfer interaction between the two fragments of a composite molecule. H. C. Longuet-Higgins and J. N. Murrell, *Proc. Phy. Soc.*, **A68**, 601 (1955); J. N. Murrell, *ibid.*, **A68**, 969 (1955).

6) L. Pauling and G. W. Wheland, *J. Chem. Phys.*, **1**, 362 (1933).

7) T. Ri and H. Eyring, *ibid.*, **8**, 433 (1940); T. Ri, *Rev. Phys. Chem. Japan*, **17**, 1, 16 (1943); A. Pullman and B. Pullman, *Experientia*, **2**, 364 (1946); M. J. S. Dewar, *Trans. Faraday Soc.*, **42**, 764 (1946).

8) a) C. A. Coulson, *Discussions Faraday Soc.*, **2**, 9 (1947); *J. chim. phys.*, **45**, 243 (1948); b) C. A. Coulson and H. C. Longuet-Higgins, *Proc. Roy. Soc. (London)* **A191**, 39; **A192**, 16 (1947); other papers cited in Ref. 3.

9) G. W. Wheland, *J. Am. Chem. Soc.*, **64**, 900 (1942); M. J. S. Dewar, *ibid.*, **74**, 3357 (1952).

10) K. Fukui, T. Yonezawa and H. Shingu, *J. Chem. Phys.*, **20**, 722 (1952); see also the subsequent papers: K. Fukui, T. Yonezawa, C. Nagata and H. Shingu, *ibid.*, **22**, 1433 (1954), and the papers cited in Ref. 3.

11) R. S. Mulliken *J. Am. Chem. Soc.*, **74**, 811 (1952).

12) R. S. Mulliken, *Rec. Trav. Chim.*, **75**, 845 (1956).

13) K. Fukui, T. Yonezawa and C. Nagata, This Bulletin, **27**, 423 (1954); K. Fukui, T. Yonezawa and C. Nagata, *J. Chem. Phys.*, **27**, 1247 (1957).

14) R. D. Brown, *J. Chem. Soc.*, **1959**, 2232; *cf.* K. Fukui, K. Morokuma, T. Yonezawa and C. Nagata, *J. Chem. Phys.*, **32**, 1743 (1960).

15) S. Nagakura and J. Tanaka, *Nippon Kagaku Zasshi* (*J. Chem. Soc. Japan, Pure Chem. Sect.*), **75**, 933 (1954); T. Yonezawa, K. Hayashi, C. Nagata, S. Okamura and K. Fukui, *J. Polymer Sci.*, **14**, 312 (1954), and other, related papers cited in Refs. 2 and 3.

16) R. B. Woodward and R. Hoffmann, *J. Am. Chem. Soc.*, **87**, 395, 2511 (1965).

$$\Delta W = W - (W_{A0} + W_{B0}) \quad (1)$$

where ΔW is the interaction energy, W_{A0} and W_{B0} being the energies of the initial stationary states of two isolated systems, A and B, and W, the lowest total energy of the two mutually-interacting systems. The energies of all the systems were calculated in the frame of the Born-Oppenheimer approximation[17] and obtained in the form of the adiabatic potential.

The Hamiltonian operator of the combined system in atomic units is:

$$H = \sum_{\lambda} H(\lambda) + \sum_{\lambda<\lambda'} \frac{1}{r_{\lambda\lambda'}} + \sum_{\gamma<\gamma'} \frac{Z_\gamma Z_{\gamma'}}{R_{\gamma\gamma'}}$$

$$H(\lambda) = -\frac{1}{2}\Delta(\lambda) + V(\lambda)$$

$$V(\lambda) = V_A(\lambda) + V_B(\lambda)$$

$$V_A(\lambda) = -\sum_{\alpha} \frac{Z_\alpha}{r_{\lambda\alpha}}, \quad V_B(\lambda) = -\sum_{\beta} \frac{Z_\beta}{r_{\lambda\beta}} \quad (2)$$

in which:

$H(\lambda)$:	One-electron Hamiltonian operator of the electron λ.
$Z_\alpha, Z_\beta, Z_\gamma$:	The positive charges of the nuclei α, β, and γ, which specify their belonging to the system A, the system B, and the combined system, AB, respectively.
$r_{\lambda\lambda'}$:	The distance between the two electrons λ and λ'.
$r_{\lambda\alpha}$, *etc.*:	The distance of the electron λ from the nucleus α, *etc.*
$R_{\alpha\alpha'}$, *etc.*:	The distance between the nuclei α and α', *etc.*

The unperturbed normalized wave-functions of the A and B systems are assumed to be represented in terms of Slater determinants composed of orthonormal spin-orbitals with LCAO MO spatial functions, which are Roothaan-type SCF (self-consistent-field) MO's with respect to the *ground state* of each isolated system.[18] The wave-functions of an excited or charge-transferred configuration may be made up of the MO's associated with the realistic and non-realistic roots of the Fock equation for the ground state. Therefore, all of the MO's are definite and fixed, with a given nuclear configuration in each isolated system.

The spatial parts of LCAO MO are represented by:

$$a(1) = \sum_{t} C_t t(1) \quad \text{for the system } A \quad (3a)$$

and

$$b(1) = \sum_{u} C_u u(1) \quad \text{for the system } B \quad (3b)$$

where t and u are the AO's belonging to the nuclei of A and B respectively. No particular restriction is placed on the type of these AO's. Usually they may be taken to be Slater-type or Gaussian AO's. However, it is often convenient for the later discussion of reactivity criteria to employ the valence atomic orbitals (VAO's).[19] Our present purpose allows us to take all functions as real.

The occupied and unoccupied MO's in the ground state are distinguished in the following way:[20]

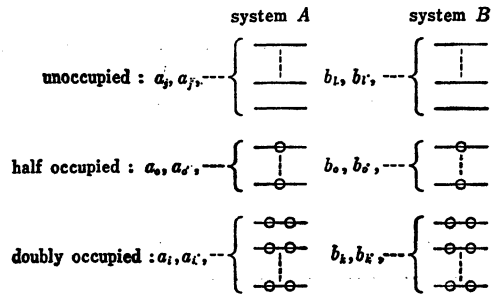

The configurations to be taken into account are as follows:

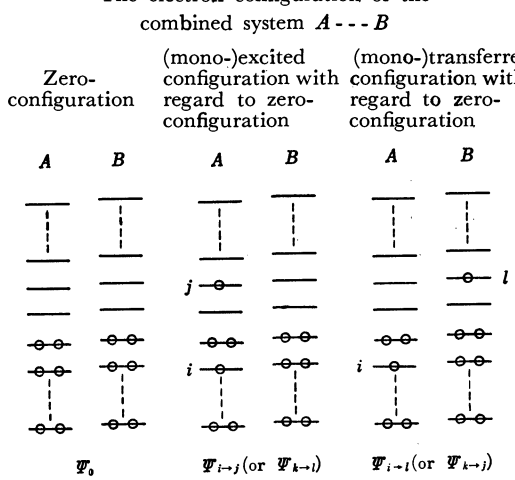

The perturbed normalized wave-functions of the combined-system Ψ_J's are constructed by means of

17) M. Born and J. R. Oppenheimer, *Ann. Physik*, **84**, 457 (1927).

18) Either A and B, or both, may be an odd-electron system. For such a system the "restricted" open-shell SCF MO theory (*e.g.*, see G. Berthier, "Molecular Orbitals in Chemistry, Physics, and Biology," ed. by P.-O. Löwdin and B. Pullman, Academic Press, New York (1964), p. 57) should be applied to compose the wave-function. A calculation similar to the present one was early made by Mori (Y. Mori, This Bulletin, **35**, 1584 (1962)) with respect to the interaction between a molecule and a radical.

19) K. Ruedenberg, *Rev. Mod. Phys.*, **34**, 326 (1962); compare R. McWeeny, *ibid.*, **32**, 335 (1960).

20) For the presentation of an "unoccupied" MO to interact with another molecule, the Roothaan LCAO MO approach, with a basis set of a limited number of AO's chosen so as to be suitable for describing the occupied MO's is not necessarily appropriate.

the Slater determinants, composed of a_i's, a_j's, b_k's, and b_l's according to each electron configuration. The subscript J stands for all configurations, 0, $i\to j$, $k\to l$, $i\to l$, $k\to j$, and other highly-excited or transferred ones, such as $(i\to j, i'\to j')$, $(i\to j, i'\to l)$, $(i\to l, i'\to l')$, and so on.[21] The wave-function Ψ_J may further be specified by the superscript $(2S+1)$ and the subscript M_S as represented by ${}^{2S+1}_{M_S}\Psi_J$, where S and M_S designate the usual total spin quantum numbers. For instance, ${}^{3}_{0}\Psi_{i\to l}$ is represented by:

$$\frac{1}{\sqrt{2}}[NA\,|a_1\bar{a}_1a_2\bar{a}_2\cdots a_{i-1}\bar{a}_{i-1}a_ia_{i+1}\bar{a}_{i+1}\cdots a_n\bar{a}_nb_1\bar{b}_1\cdots b_m\bar{b}_m\bar{b}_l| + NA\,|a_1\bar{a}_1a_2\bar{a}_2\cdots a_{i-1}\bar{a}_{i-1}\bar{a}_ia_{i+1}\bar{a}_{i+1}\cdots a_n\bar{a}_nb_1\bar{b}_1\cdots b_m\bar{b}_mb_l|]$$

where NA signifies the normalization-antisymmetrization operator; the nonbarred and barred MO's represent the spin-orbitals with spin-functions of α and β respectively, and n and m indicate the number of doubly-occupied MO's of A and B respectively in the zero-configuration.

The secular determinant is represented by:

$$\begin{vmatrix} H_{I,I}-E & H_{I,J}-S_{I,J}E\cdots \\ H_{J,I}-S_{J,I}E & H_{J,J}-E\cdots \\ \cdots\cdots & \end{vmatrix} = 0 \quad (4)$$

where the subscript I signifies the initial J, and where:

$$H_{J,J'} = \int \Psi_J^* H \Psi_{J'} d\tau$$

$$S_{J,J'} = \int \Psi_J^* \Psi_{J'} d\tau$$

The orders of magnitude of the overlap integrals are estimated as:

$$S_{0,i\to l} = S_{0,k\to j} = O(s_{ab})$$

$$S_{0,i\to j} = S_{0,k\to l} = S_{i\to l,\,k\to j} = S_{i\to j,\,k\to l} = O(s_{ab}^2)$$

$$S_{i\to j,i'\to l} = S_{i\to j,k\to j'} = S_{i\to l,k\to l'} = S_{k\to j,k'\to l} = O\ (s_{ab}^3)$$

$$S_{i\to j,i'\to j'} = S_{k\to l,k'\to l'} = O\ (s_{ab}^4)$$

$$S_{i\to j,(i\to j,i'\to l)} = S_{i\to j,(i\to j,k\to j')} = S_{i\to j,i\to l} = S_{i\to j,k\to j} = O(s_{ab})$$

$$S_{i\to j,(i\to j,i'\to j')} = S_{i\to j,(i\to j,k\to l)} = S_{i\to j,i'\to j} = O(s_{ab}^2)$$

and so forth, where s_{ab} represents an overlap integral of an MO of the system A and an MO of the system B. The general relation is given by:

$$S_{J,J'} = O\ (s_{ab}^{\nu}) \quad (5)$$

in which ν is the minimum number of electron transfers between A and B required to shift the electron configuration from J to J'.

In order to calculate W in Eq. (1), which is given by the lowest root of the secular equation (4), it is assumed that the lowest $H_{J,J}$ is $H_{I,I}$ and that no others are equal to $H_{I,I}$.[22] On the basis of the second assumption, that $S_{J,J'}$ and $H_{J,J'}$ $(J\neq J')$ are small, W can be expanded in approximately the following form:

$$W = H_{I,I} - \left(\sum_p^{\text{monotr.}} + \sum_p^{\text{monoex.}} + \sum_p^{\text{ditr.}} + \sum_p^{\text{monotr.-monoex.}} + \sum_p^{\text{diex.}} + \cdots\right)\frac{|H_{I,p}-S_{I,p}H_{I,I}|^2}{H_{p,p}-H_{I,I}} + \cdots \quad (6)$$

where monotr., diex., *etc.* imply monotransferred, diexcited, *etc.* configurations with respect to the initial configuration, I.[23] The third term $(+\cdots)$ designates the remaining terms, which cover the difference from the exact root of Eq. (4).

If it is assumed[12] that the interaction between A and B is not yet very strong and that $H_{I,p}$ is almost linear with $S_{I,p}$, it follows that, in light of Eq. (5), the terms from monotransferred configurations will possess magnitudes of the order of s_{ab}^2, and that the monoex. and the ditr. terms are of s_{ab}^4, the monotr.-monoex. term is of s_{ab}^6, and so on. In addition to this, if SCF MO's are employed, the well-known Brillouin theorem[24] makes the $H_{I,p}$ values of monoex. terms small. Moreover, the denominator of the second term, $H_{p,p}-H_{I,I}$, can usually not be small in excited configuration terms, while in transferred configuration terms it can be, and sometimes, as in Eq. (7'), even a first-order term appears in place of the second-order transferred configuration terms of Eq. (6). In these circumstances the monotransferred term will become uniquely important.

21) The wave-functions for these electron configurations should be regarded as those adopted to describe the perturbed wave-function in terms of that of the isolated reactant molecules, and not necessarily as corresponding to any realistic " excited " or " transferred " states.

22) This assumption reflects the adiabaticity requirement for the interaction. There are two other possibilities. In one the lowest $H_{J,J}$ is $H_{I,I}$ and the other $pH_{J,J}$'s ($H_{1,1}$, $H_{2,2}\cdots$, $H_{q,q}\cdots$, $H_{p,p}$) are equal to $H_{I,I}$, where the suffix q stands for one of the monotransferred configurations with reference to I. In this case the equation corresponding to Eq. (7) becomes:

$$W = H_{I,I} - \left\{\sum_{q=1}^{p}|H_{I,q}-S_{I,q}H_{I,I}|^2\right\}^{1/2} + \cdots \quad (7')$$

The other is the case in which the lowest $H_{J,J}$ is not $H_{I,I}$ but $pH_{C,C}$'s ($H_{C1,C1}$, $H_{C2,C2}\cdots$, $H_{Cq,Cq}\cdots$, $H_{Cp,Cp}\cdots$) of an equal energy, where C_q stands for one of the monotransferred configurations of I. In this case

$$W = H_{C,C} - \frac{\sum_{q=1}^{p}|H_{I,C_q}-S_{I,C_q}H_{C,C}|^2}{H_{I,I}-H_{C,C}} + \cdots \quad (7'')$$

23) When the initial configuration is an excited one, the term " excited " configuration should include "di"-excited configurations, too.

24) L. Brillouin, *Actualités sci. et ind.*, **71** (1933); **159** (1934).

Thus, if we take only the terms not smaller than s_{ab}^2, namely, the monotransferred terms in the second term of Eq. (6), we get:

$$W = H_{I,I} - \sum_{p=1}^{N} \frac{|H_{I,p} - S_{I,p}H_{I,I}|^2}{H_{p,p} - H_{I,I}} \tag{7}$$

where p stands for the pth monotransferred configuration with reference to I, and where N is the number of monotransferred configurations.

Combined Reactivity Index

The interaction energy, ΔW, in Eq. (1), appropriately calculated with respect to a given nuclear configuration, will serve as a reasonable measure of the stability of that configuration. A comparisen of ΔW with the various nuclear configurations which are possible in a given chemical interaction will make it possible to discuss the preferred orientation theoretically. Thus, ΔW can be a general scale of reactivity. The singlet interaction energy,[25] ΔW, of Eq. (1), which has reference to the initial state, with a zero-configuration composed of two even-electron ground-state systems, is written by Eq. (6) as:

$$\Delta W = \varepsilon_0 - D - \Pi \tag{8}$$

where:

$$\varepsilon_0 = H_{0,0} - (W_{A0} + W_{B0}) \tag{8a}$$

$$D = \sum_{i}^{\text{occ}} \sum_{l}^{\text{uno}} \frac{|H_{0,i\to l} - S_{0,i\to l}H_{0,0}|^2}{H_{i\to l,i\to l} - H_{0,0}} + \sum_{k}^{\text{occ}} \sum_{j}^{\text{uno}} \frac{|H_{0,k\to j} - S_{0,k\to j}H_{0,0}|^2}{H_{k\to j,k\to j} - H_{0,0}} \tag{8b}$$

$$\Pi = \sum_{i}^{\text{occ}} \sum_{j}^{\text{uno}} \frac{|H_{0,i\to j} - S_{0,i\to j}H_{0,0}|^2}{H_{i\to j,i\to j} - H_{0,0}} + \sum_{k}^{\text{occ}} \sum_{l}^{\text{uno}} \frac{|H_{0,k\to l} - S_{0,k\to l}H_{0,0}|^2}{H_{k\to l,k\to l} - H_{0,0}} \tag{8c}$$

Coulomb and Exchange Interaction Terms. Among the three terms on the right side of Eq. (8), ε_0 is a first order term which arises from the Coulomb and the exchange interaction terms between A and B: it can be calculated easily as:

$$\varepsilon_0 = \varepsilon_Q + \varepsilon_K \tag{9}$$

where the Coulomb interaction energy, ε_Q, is:

$$\varepsilon_Q = 2\sum_i V_{Bii} + 2\sum_k V_{Akk} + 4\sum_i \sum_k (ii|kk) + \sum_\alpha \sum_\beta \frac{Z_\alpha Z_\beta}{R_{\alpha\beta}} \tag{10}$$

and where the exchange interaction energy, ε_K, is:

$$\varepsilon_K = -2\sum_i \sum_k [(ik|ki) + s_{ik}[V_{ik} + \sum_{i'} \{2(ik|i'i') - (ii'|i'k)\} + \sum_{k'} \{2(ik|k'k') - (ik'|k'k)\}]] \tag{11}$$

in which:

$$V_{Bii} = \int a_i(1)V_B(1)a_i(1)\mathrm{d}v(1), \text{ etc.}$$

$$V_{ik} = \int a_i(1)V(1)b_k(1)\mathrm{d}v(1), \text{ etc.}$$

$$(ij|kl) = \int a_i(1)b_k(2)\frac{1}{r_{12}}a_j(1)b_l(2)\mathrm{d}v(1)\mathrm{d}v(2), \text{ etc.}$$

$$s_{ik} = \int a_i(1)b_k(1)\mathrm{d}v(1), \text{ etc.}$$

If we here employ the Mulliken approximation:[26]

$$\int \cdots \int t(1)t'(1)f\cdots \mathrm{d}v(1)\cdots \cong \frac{1}{2}s_{tt'}\left\{\int \cdots \int t(1)t(1)f\cdots \mathrm{d}v(1)\cdots + \int \cdots \int t'(1)t'(1)f\cdots \mathrm{d}v(1)\cdots\right\}$$

we can easily obtain:[27]

$$\varepsilon_Q \cong \sum_t N_{At}v_{Btt} + \sum_u N_{Bu}v_{Auu} + \sum_t \sum_u N_{At}N_{Bu}(tt|uu) + \sum_\alpha \sum_\beta \frac{Z_\alpha Z_\beta}{R_{\alpha\beta}} \tag{12}$$

25) The term "singlet interaction" signifies an interaction of two systems, A and B, with a conservation of the total spin zero. Similarly, "doublet interaction" and "triplet interaction" will later be used in the cases of the interaction of a radical with a molecule or with a radical.

26) R. S. Mulliken, *J. chim. phys.*, **46**, 497 (1949).

27) In the doublet interaction between an even-electron system (A) and an odd-electron system (B), a similar equation is obtained:

$$\varepsilon_Q = 2\sum_i V_{Bii} + 2\sum_k V_{Akk} + V_{Ao'o'} + 4\sum_i \sum_k (ii|kk) + 2\sum_i (ii|o'o') + \sum_\alpha \sum_\beta \frac{Z_\alpha Z_\beta}{R_{\alpha\beta}} \cong \sum_\alpha \sum_\beta \frac{(Z_\alpha - N_\alpha)(Z_\beta - N_\beta)}{R_{\alpha\beta}} \tag{12'}$$

The singlet and the triplet interactions between two odd-electron systems give an analogous relation.

where N_{At} is the population of the tth AO of the isolated system, A, and is given by:

$$N_{At} = 2\sum_{i}^{occ}\sum_{t'} C_t^{(i)}C_{t'}^{(i)}s_{tt'}$$

and:

$$v_{Btt} = \int t(1)V_B(1)t(1)\mathrm{d}v(1) = \sum_{\beta} v_{\beta tt},\ etc.,$$

in which $C_t^{(i)}$ means the coefficient of Eq. (3a) for MO a_i, and in which

$$s_{tt'} = \int t(1)t'(1)\mathrm{d}v(1)$$

$$v_{\beta tt} = -\int t(1)\frac{Z_\beta}{r_{1\beta}}t(1)\mathrm{d}v(1),\ etc.$$

Further approximation which puts

$$v_{\beta tt} \cong -\frac{Z_\beta}{R_{\alpha\beta}}$$

etc., where α denotes the nucleus to which the tth AO belongs, may be possible if the distance between A and B is not very short. This approximation at once gives rise to the succinct expression:

$$\varepsilon_Q \cong \sum_{\alpha}\sum_{\beta}\frac{(Z_\alpha - N_\alpha)(Z_\beta - N_\beta)}{R_{\alpha\beta}} \qquad (13)$$

where N_α is the population of the atom α, that is, it is equal to $\sum_{t}^{(\alpha)} N_{At}$.[28] This equation is very convenient for grasping the meaning of the Coulomb interaction term, since $(Z_\alpha - N_\alpha)$ and $(Z_\beta - N_\beta)$ represent the net plus charge of the atom α of A and of the atom β of B respectively. In neutral nonpolar molecules, therefore, ε_Q is not very important.

The exchange interaction term, ε_K, is almost solely responsible for the multiplet separation. In the ground-state interactions it is usually repulsive except for the singlet interaction of two ground-state odd-electron systems.[29]

The case of single-site overlapping, namely, when overlapping between only one AO (say r) of A and one AO (say r') of B is appreciable, may often be important. This is nearly the case in the aromatic substitution by a reagent with essentially one AO. If VAO's are employed as the basis AO's, the MO overlapping with reagent orbitals becomes single-sited in many cases.

In the case of single-site overlapping, Eq. (11) becomes, by the use of the Mulliken approximation:

$$\varepsilon_K \cong -\frac{1}{8}s_{rr'}{}^2P_{rr}P_{r'r'}[2v_{rr} + 2v_{r'r'} + (rr|rr) + (r'r'|r'r') + 2(rr|r'r') + P_{rr}\{(rr|rr) + (rr|r'r')\} + P_{r'r'}\{(r'r'|r'r') + (rr|r'r')\}] \qquad (14)$$

in which:

$$v_{rr} = v_{Arr} + v_{Brr},\ etc.,$$

$$P_{rr} = 2\sum_{i}^{occ} C_r^{(i)}C_r^{(i)},\ etc.$$

indicating that the exchange interaction varies with the square of the overlap integrals and is, accordingly, less important than the Coulomb interaction at the initial stage of interaction in polar reactions.

Charge-transfer Interaction Term. The second term appearing on the right side of Eq. (8) comes from the electron-delocalization interaction due to the mixing of monotransferred configurations. The calculation of the matrix elements and overlap integrals gives:

$$H_{i\to l,i\to l} - H_{0,0} = -(E_{Bl} + \Delta E_{Bl}) + (I_{Ai} + \Delta I_{Ai}) + a_{il} \qquad (15)$$

in which:[30]

$$E_{Bl} = -[H_{Bll} + \sum_{k}\{2(ll|kk) - (lk|kl)\}]$$

$$I_{Ai} = -[H_{Aii} + \sum_{i'}\{2(ii|i'i') - (ii'|i'i)\}]$$

---

28) If we put $s_{tt'}$'s and $s_{uu'}$'s equal to zero, Eq. (13) becomes identical to the equation obtained by Rein and Pollak (R. Rein and M. Pollak, *J. Chem. Phys.*, **47**, 2039 (1967)). They also assumed $s_{ab}=0$ in obtaining the exchange interaction energy. See also G. Klopman and R. F. Hudson, *Theoret. chim. Acta (Berl.)*, **8**, 165 (1967).

29) In this case

$$\varepsilon_K = -2\sum_i\sum_k[(ik|ki) + s_{ik}[V_{ik} + \sum_{i'}\{2(ik|i'i') - (ii'|i'k)\} + \sum_{k'}\{2(ik|k'k') - (ik'|k'k)\}]] - \sum_i\sum_k s_{ik}[\{2(ik|oo) - (io|ok)\} + \{2(ik|o'o') - (io'|o'k)\}] - \sum_i[(io'|o'i) + s_{io'}[V_{io'} + \sum_{i'}\{2(io'|i'i') - (ii'|i'o')\} + \sum_k\{2(io'|kk) - (ik|ko')\} + (io'|oo) + (io|oo')]] - \sum_k[(ok|ko) + s_{ok}[V_{ok} + \sum_i\{2(ok|ii) - (oi|ik)\} + \sum_{k'}\{2(ok|k'k') - (ok'|k'k)\} + (ok|o'o') + (oo'|o'k)]] + \delta_{oo'}$$

where:

$$\delta_{oo'} = (oo'|o'o) + s_{oo'}[V_{oo'} + \sum_i\{2(oo'|ii) - (oi|io')\} + \sum_k\{2(oo'|kk) - (ok|ko')\}]$$

Since the magnitude of ε_K is essentially determined by the orbital overlapping between the two systems, the attractive term, $\delta_{oo'}$, is in this case dominant, as is the case of hydrogen molecule formation from two hydrogen atoms.

30) The terms of the s_{ab} $(cd|ef)$ type are omitted in order to avoid intricacy of expression in the subsequent equations, where a, b,··· denote MO's. These are obtainable in a manner similar to that of 29). The terms of $s_{ab}{}^2$ are all neglected.

$$\Delta E_{Bl} = -\{V_{All} + 2\sum_{i'}(ll|i'i')\} + \sum_{i'}\{V_{li'}s_{li'} + (li'|i'l)\}$$

$$\Delta I_{Ai} = -\{V_{Bii} + 2\sum_{k}(ii|kk)\} + \sum_{k}\{V_{ik}s_{ik} + (ik|ki)\}$$

$$a_{il} = -(ii|ll) + 2\{V_{il}s_{il} + (il|li)\}$$

$$H_{Aii} = \int a_i(1)H_A(1)a_i(1)\mathrm{d}v(1), \text{ etc.}$$

$$H_A(\lambda) = -\frac{1}{2}\Delta(\lambda) + V_A(\lambda), \text{ etc.}$$

and:

$$H_{0,i\to l} - S_{0,i\to l}H_{0,0} = \sqrt{2}\,[Q_{il} + K_{il}] \quad (16)^{31}$$

where

$$Q_{il} = \{V_{Bil} + 2\sum_{k}(il|kk)\} - s_{il}\{V_{Bii} + 2\sum_{k}(ii|kk)\}$$

is the Coulomb interaction part, and where

$$K_{il} = -\sum_{k}\{(ik|kl) - s_{il}(ik|ki)\}$$

is the exchange interaction part.

The Koopmans theorem[32] makes a possible physical interpretation of the quantities in Eq. (15). The quantity I_{Ai} is the vertical ionization potential, with no rearrangement of the nuclear configuration, of the isolated system A with respect to the electron in the ith MO; similarly, E_{Bl} is the vertical "electron affinity"[33] of the isolated system B with respect to the lth MO, while ΔI_{Ai} is the change in I_{Ai} due to the approach of the system B, and ΔE_{Bl} is the change in E_{Bl} due to the approach of the system A. With regard to a_{il}, the following relations hold:

$$a_{il} = I_{Ai}^{(B+l)} - I_{Ai}^{(B)} = E_{Bl}^{(A)} - E_{Bl}^{(A-i)}$$

where:

$$I_{Ai}^{(B)} = I_{Ai} + \Delta I_{Ai}$$
$$E_{Bl}^{(A)} = E_{Bl} + \Delta E_{Bl}$$

where $I_{Ai}^{(B+l)}$ is the value of I_{Ai} in the case of the approach of the system B with an additional electron occupying the lth unoccupied MO, and where $E_{Bl}^{(A-i)}$ is the value of E_{Bl} in the case of the approach of the system A in which one electron occupying the ith MO is subtracted.

Then, we derive the useful equation:

$$H_{i\to l,i\to l} - H_{0,0} = I_{Ai}^{(B)} - E_{Bl}^{(A-i)} = I_{Ai}^{(B+l)} - E_{Bl}^{(A)} \quad (17)$$

which shows that this quantity is not simply written as $(I_{Ai}-E_{Bl})$. As a matter of fact, Eq. (17) is self-evident, as is directly elucidated by the following diagram:

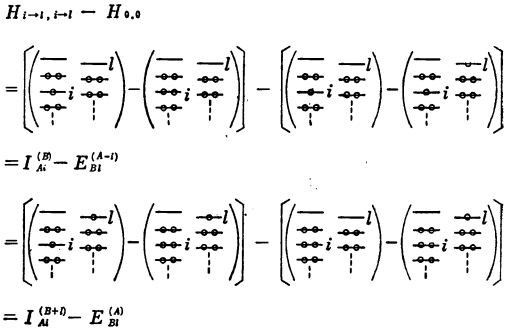

Relations of such a kind are completely general in character (*cf.* Eq. (21)).

Equation (16) indicates that the numerator of each term on the right side of Eq. (8b) consists of two parts, the Coulomb interaction part and the exchange interaction part. Since the latter is small compared with the former except in a perfectly nonpolar case, we will consider only the case in which the exchange part can be neglected.

The approximation of *multiple-site overlapping*, in which the paired AO's are denoted by the r of A and the r' of B, leads to the expression:

$$H_{0,i\to l} - S_{0,i\to l}H_{0,0} \cong \sqrt{2}\sum_{r} C_r^{(i)}C_{r'}^{(l)}\gamma_{rr'}^{(i)} \quad (18)$$

where:

$$\gamma_{rr'}^{(i)} \cong s_{rr'}\left[\frac{1}{2}(v_{Brr} + v_{Br'r'}) + \frac{1}{2}\sum_{u}N_{Bu}\{(rr|uu) + (r'r'|uu)\} + \sum_{\alpha}\sum_{\beta}\frac{n_\alpha^{(ii)}(Z_\beta - N_\beta)}{R_{\alpha\beta}}\right] \quad (19)$$

in which:

$$n_\alpha^{(ii)} = \sum_{t}^{(\alpha)}\sum_{t'}C_t^{(i)}C_{t'}^{(i)}s_{tt'}$$

Eq. (19) indicates a linear relationship of the right side of Eq. (16) with orbital overlapping. Equation (19) can also be written:

$$\gamma_{rr'}^{(i)} \cong -\int r(1)\left(\sum_{\beta}\frac{Z_\beta - N_\beta}{r_{1\beta}}\right)r'(1)\mathrm{d}v(1) + s_{rr'}\sum_{\alpha}\sum_{\beta}\frac{n_\alpha^{(ii)}(Z_\beta - N_\beta)}{R_{\alpha\beta}} \quad (19')$$

which shows the remarkable characteristic that the charge-transfer interaction is large with the local net

31) To derive this equation, it must be remembered that the MO's are assumed to satisfy the Fock equation for the isolated system.

32) T. Koopmans, *Physica*, **1**, 104 (1933).

33) With respect to the physical significance of the energy level of a Fock-Roothaan unoccupied MO, one should in any event be cautious. To connect E_{Bl} with any experimental value, it is recommended that one adopts an extended-basis set of AO's in the Roothaan LCAO. This point will be discussed in a subsequent paper.

charge near the reaction center of the acceptor molecule.

Thus, we can obtain this approximate expression of D:

$$D \cong 2\left\{\sum_{i}^{\text{occ}}\sum_{l}^{\text{uno}} \frac{(\sum_r C_r^{(i)} C_{r'}^{(l)} \gamma_{rr'}^{(i)})^2}{I_{Ai}^{(B)} - E_{Bl}^{(A-i)}} + \sum_{k}^{\text{occ}}\sum_{j}^{\text{uno}} \frac{(\sum_r C_r^{(j)} C_{r'}^{(k)} \gamma_{rr'}^{(k)})^2}{I_{Bk}^{(A)} - E_{Aj}^{(B-k)}}\right\} \quad (20)$$

in which:

$$\gamma_{rr'}^{(k)} \cong -\int r(1)\left(\sum_\alpha \frac{Z_\alpha - N_\alpha}{r_{1\alpha}}\right) r'(1)\mathrm{d}v(1) + s_{rr'}\sum_\alpha\sum_\beta \frac{n_{\alpha\beta}^{(kk)}(Z_\alpha - N_\alpha)}{R_{\alpha\beta}}$$

If we consider the special case of a single-site interaction between the rth AO of the reactant, A, and a reagent, B, assuming that the reagent possesses only one AO (designated as r') and, accordingly, only one MO to be taken into account, and that $C_{r'}^{(l)}\gamma_{rr'}^{(i)}(=\gamma_r)$ and $C_{r'}^{(k)}\gamma_{rr'}^{(k)}(=\gamma_{r'})$ are constant with respect to a given reagent, then it follows that:

$$D \cong \begin{cases} 2\sum_{i}^{\text{occ}} \dfrac{C_r^{(i)2}}{\varepsilon_B - \varepsilon_{Ai}}\gamma_r^2 & \text{when the reagent orbital is unoccupied} \\ 2\sum_{j}^{\text{uno}} \dfrac{C_r^{(j)2}}{\varepsilon_{Aj} - \varepsilon_B}\gamma'^2_r & \text{when the reagent orbital is occupied,} \end{cases} \quad (20')$$

in which:

$$\varepsilon_{Ai} = -I_{Ai}^{(B)}, \quad \varepsilon_{Aj} = -E_{Aj}^{(B-k)}$$

and

$$\varepsilon_B = \begin{cases} -E_B^{(A-i)} & \text{when the reagent orbital is unoccupied} \\ -I_B^{(A)} & \text{when the reagent orbital is occupied} \end{cases}$$

The quantity on the right side of Eq. (20′) is nothing but *superdelocalizability*[13] and *delocalizability*[34] previously defined by one of the present authors in discussing the reactivity of unsaturated and saturated compounds. These relations are useful for estimating the value of the quantities employed in semi-empirical reactivity theories.

The same equations as in Eqs. (17)—(19′) hold in the interaction of an even-electron system and an odd-electron system. In this case, however, Eq. (20) becomes:

$$D \cong 2\left\{\sum_{i}^{\text{occ}}\sum_{l}^{\text{uno}} \frac{(\sum_r C_r^{(i)} C_{r'}^{(l)} \gamma_{rr'}^{(i)})^2}{I_{Ai}^{(B)} - E_{Bl}^{(A-i)}} + \sum_{k}^{\text{occ}}\sum_{j}^{\text{uno}} \frac{(\sum_r C_r^{(j)} C_{r'}^{(k)} \gamma_{rr'}^{(k)})^2}{I_{Bk}^{(A)} - E_{Aj}^{(B-k)}}\right\} + \left\{\sum_{i}^{\text{occ}} \frac{(\sum_r C_r^{(i)} C_{r'}^{(o')} \gamma_{rr'}^{(i)})^2}{I_{Ai}^{(B)} - E_{Bo'}^{(A-i)}} + \sum_{j}^{\text{uno}} \frac{(\sum_r C_r^{(j)} C_{r'}^{(o')} \gamma_{rr'}^{(o')})^2}{I_{Bo'}^{(A)} - E_{Aj}^{(B-o')}}\right\} \quad (21)$$

and, corresponding to Eq. (20′), we obtain:

$$D \cong \sum_{i}^{\text{occ}} \frac{C_r^{(i)2}}{\varepsilon_B - \varepsilon_{Ai}}\gamma_r^2 + \sum_{j}^{\text{uno}} \frac{C_r^{(j)2}}{\varepsilon_{Aj} - \varepsilon_{B'}}\gamma_{r'}^2 \quad (21')$$

in which ε_B is equal to $(-E_{Bo'}^{(A-i)}$ and $\varepsilon_{B'}$ is equal to $(-I_{Bo'}^{(A)})$. This equation is similar to the form of superdelocalizability and that of delocalizability for this case of interaction. It is noteworthy that, even in the interaction of a neutral molecule with a neutral radical, the local charge of atoms determines the magnitude of D.[35]

Polarization Term. The third interaction term corresponds to the polarization due to the mutual approach of A and B. The necessary matrix elements to calculate are as follows:

$$H_{i\to j, i\to j} - H_{0,0} = I_{A+j,i}^{(B)} - E_{Aj}^{(B)} = I_{Ai}^{(B)} - E_{A-i,j}^{(B)} \quad (22)$$

where $I_{A+j,i}^{(B)}$ is the ionization potential of an electron of the ith MO of the system A, with one additional electron occupying the jth MO, in the approach of the system B, and $E_{A-i,j}^{(B)}$ is the electron affinity with respect to the jth unoccupied MO of the system A, with one electron of the ith MO subtracted, in the approach of the system B. Moreover,

$$H_{0,i\to j} - S_{0,i\to j}H_{0,0} = \sqrt{2}[V_{Bij} + 2\sum_k (ij|kk)] + O(s_{ab}^2) \quad (23)$$

This reduces, by the aid of the Mulliken approximation, to:

$$H_{0,i\to j} - S_{0,i\to j}H_{0,0} \cong -\sqrt{2}\zeta_{AB}^{(ij)} \quad (23')$$

in which:

$$\zeta_{AB}^{(ij)} = \sum_\alpha\sum_\beta \frac{n_\alpha^{(ij)} + n_\alpha^{(ji)}}{2} \cdot \frac{Z_\beta - N_\beta}{R_{\alpha\beta}} \quad (24)$$

where:

$$n_\alpha^{(ij)} = \sum_t^{(\alpha)}\sum_{t'} C_t^{(i)} C_{t'}^{(j)} s_{tt'}$$

The case of a single-site interaction between the atom α of A and the atom β of B is taken for the

34) K. Fukui, H. Kato and T. Yonezawa, This Bulletin, **34**, 1111 (1961).

35) This fact does not imply that the term D is not important in the radical interaction of a molecule. One must note that a majority of radicals involve a polar character, so the Coulomb interaction part of Eq. (16) still remains important.

sake of simplicity, in which the overlap integrals are neglected. This is a case of aromatic substitution in which only the 2 pπ AO's are taken into account. Then, we have:

$$\zeta_{AB}^{(ij)} \cong C_r^{(i)} C_r^{(j)} \frac{Z_\beta - N_\beta}{R_{r\beta}} \tag{24'}$$

which is proportional to the net charge of the atom β of the system B. This equation is useful for understanding the physical meaning of Eq. (23). The approximate formula of Π can be obtained by using Eq. (23'):

$$\Pi \cong 2\left\{ \sum_i^{\text{occ}} \sum_j^{\text{uno}} \frac{(\zeta_{AB}^{(ij)})^2}{I_{Ai}^{(B)} - E_{A-i,j}^{(B)}} + \sum_k^{\text{occ}} \sum_l^{\text{uno}} \frac{(\zeta_{BA}^{(kl)})^2}{I_{Bk}^{(A)} - E_{B-k,l}^{(A)}} \right\} \tag{25}$$

If we consider that the quantity $(Z_\beta - N_\beta)/R_{r\beta}$ in Eq. (24') for a definite distance of approach is consant with regard to a given reagent, B, and denote it by δ_r, we obtain as the first half of Π:

$$\Pi \sim \frac{1}{2} \pi_{Arr} (\delta_r)^2$$

in which:

$$\pi_{Arr} = 4 \sum_i^{\text{occ}} \sum_j^{\text{uno}} \frac{C_r^{(i)2} C_r^{(j)2}}{\varepsilon_{Aj} - \varepsilon_{Ai}} \overline{\beta} \tag{26}$$

($\varepsilon_{Aj} = -E_{A-i,j}^{(B)}$, $\varepsilon_{Ai} = -I_{Ai}^{(B)}$; $\overline{\beta}$ is an appropriately-chosen energy unit)

is of the same form as the well-known *self-atom polarizability* defined by Coulson and Longuet-Higgins in discussing the property of conjugated molecules.[8a]

In this way, it has been demonstrated that the generalized scale of reactivity for an interaction between two chemical systems breaks up into the Coulomb interaction term of the atomic charge, the exchange interaction term, the delocalizability term, and the polarizability term. In some chemical reactions, some of these terms may be less important than the others. As has been discussed earlier, the polarizability term is usually less important than the delocalizability term in ionic reactions, and the exchange interaction term is not important except in special cases. In a case in which one of the charge-transfer configurations possesses nearly the same energy as the initial one, the corresponding term becomes particularly important, whereas none of excited configurations can be important since none of them can possess the same energy as the initial one. The Coulomb interaction of the atomic charge is appreciable in a long-range interaction, but it will become less and less important as the reaction proceeds and as an appreciable amount of charge is transferred from the donor to the acceptor, which thus " neutralize " each other.

The nuclear configuration change which is caused by the interaction described above and which is left out of account in the present paper will be discussed in a forth coming paper with reference to the general features of the chemical reaction.

BULLETIN OF THE CHEMICAL SOCIETY OF JAPAN VOL. 41 1998—2004 (1968)

Electronic Properties of Some Complexes of Tetracyanoquinodimethan with Aromatic Diamines

Masatake OHMASA, Minoru KINOSHITA, Mizuka SANO and Hideo AKAMATU

Department of Chemistry, Faculty of Science, University of Tokyo, Hongo, Tokyo

(Received February 23, 1968)

Complexes of tetracyanoquinodimethan have been prepared with a number of aromatic diamines which are varied in their molecular shape and ionization potential. Infrared absorption spectra have revealed most of the complexes to be ionic in character. They showed a strong ESR absorption; in regard to its temperature dependence, however, three modes of variation were observed for these solid complexes. The complexes with *N,N'*-diphenyl-*p*-phenylenediamine and *N,N'*-di-β-naphthyl-*p*-phenylenediamine were considered to be of non-bonding type and showed no ESR absorption. However, no appreciable difference in semiconductive properties has been found between the ionic type and the non-bonding type complexes, except the complex of diaminodurene-TCNQ (1 : 2). The latter showed a high electrical conductivity and a paramagnetic behavior which was nearly independent of temperature.

In recent years, Weiss' idea[1] that some organic molecular complexes are ionic in their ground state has been proved by studies of their visible[2] and infrared[3,4] absorption spectra. Usually, as expected, such ionic complexes are formed by an electron transfer from a good electron-donor to a good electron-acceptor, provided that the resulting ion radicals are sufficiently stable.

Although these ion radicals are themselves paramagnetic, it is of interest to see how their paramagnetism is modified upon aggregation. This was studied by Kainer *et al.*[5-8] in 1950's for the complexes formed between aromatic diamines and halogenated benzoquinones. They discussed three possible modes of variation of the paramagnetism with temperature. One is a normal magnetic behavior of Curie type, and others are paramagnetism controlled by thermal equilibration between magnetic and non-magnetic states.

Most complexes studied by Kainer *et al.*[5-8] showed the paramagnetism of Curie type in their temperature range. In these years, however, the complexes of *p*-chloranil with diaminodurene[9] and *p*-phenylenediamine,[10,11] and the complexes of iodine with perylene,[12] pyrene[12] and benzidine[11] have been shown to be of the other type having a magnetic state at thermally accessible position. We have also found a similar magnetic property with the complex obtained from *N,N,N',N'*-tetrametyl-*p*-phenylenediamine and 7,7,8,8-tetracyano-*p*-quinodimethan (TCNQ).[13]

Our study has been extended to a number of complexes based on TCNQ as an acceptor, using various aromatic diamines as a donor. Tetracyanoquinodimethan is known to possess a marked acceptor ability, and furthermore, it shows remarkable stability in its anion radical form, which is an important property suited to our systematic study. The complexes studied are tabulated in Table 1, in which the corresponding abbreviations are also given.

Experimental

Chemicals. 7,7,8,8-Tetracyano-*p*-quinodimethan was synthesized from 1,4-cyclohexanedione by the method described by Acker and Hertler,[14] and purified by recrystallization from acetonitrile. Diaminodurene was synthesized from durene by nitration followed by reduction, and purified by sublimation in a vacuum. Other aromatic amines were obtained from commercial sources,

1) J. Weiss, *Nature*, **147**, 512 (1941).
2) R. Foster and T. J. Thomson, *Trans. Faraday Soc.*, **59**, 296 (1963).
3) Y. Matsunaga, *Nature*, **205**, 72 (1965).
4) Y. Matsunaga, *J. Chem. Phys.*, **41**, 1609 (1964).
5) H. Kainer, D. Bijl and A. C. Rose-Innes, *Naturwissenschaften*, **41**, 303 (1954).
6) H. Kainer, D. Bijl and A. C. Rose-Innes, *Nature*, **178**, 1462 (1956).
7) H. Kainer and A. Überle, *Chem. Ber.*, **88**, 1147 (1955).
8) D. Bijl, H. Kainer and A. C. Rose-Innes, *J. Chem. Phys.*, **30**, 765 (1959).
9) D. B. Chesnut and W. D. Phillips, *ibid.*, **35**, 1002 (1961).
10) A. Ottenberg, C. J. Hoffman and J. Osiecki, *ibid.*, **38**, 1898 (1963).
11) V. A. Benderskii, I. B. Shevchenko and L. A. Blyumenfeld, *Opt. and Spectry.*, **16**, 254 (1964).
12) L. S. Singer and J. Kommandeur, *J. Chem. Phys.*, **34**, 133 (1961).
13) M. Kinoshita and H. Akamatu, *Nature*, **207**, 291 (1965).
14) D. S. Acker and W. R. Hertler, *J. Am. Chem. Soc.*, **84**, 3370 (1962).

Table 1. The complexes studied and solvents used in preparation

Donor	Complex	Solvent used in preparation
p-Phenylenediamine	*p*-PD·TCNQ	Chloroform
N,N-Dimethyl-*p*-phenylenediamine	DMPD·TCNQ	Dichloromethane
N,N-Diethyl-*p*-phenylenediamine	DEPD·TCNQ (2 : 3)	Chloroform
N,N,N',N'-Tetramethyl-*p*-phenylenediamine	TMPD·TCNQ	Methanol
Diaminodurene	DAD·TCNQ (1 : 1)	Tetrahydrofuran
	DAD·TCNQ (1 : 2)	Ethanol and chloroform
o-Phenylenediamine	*o*-PD·TCNQ (2 : 1)	Dichloromethane
Benzidine	BD·TCNQ	Dichloromethane
N,N'-Diphenyl-*p*-phenylenediamine	DϕPD·TCNQ	Chloroform
N,N'-Di-β-naphthyl-*p*-phenylenediamine	DNPD·TCNQ	Dichloromethane

Table 2. Determination of the chemical composition of the complexes

Complex	Wavelength used mμ	Extinction coefficient *l*/mol·cm		Composition (Donor : Acceptor)	
		Amine	TCNQ[a]	Spectral analysis	Stoichiometry
p-PD·TCNQ	249	7800	2460	1 : 0.95	1 : 1
DMPD·TCNQ	260	11400	1570	1 : 0.96	1 : 1
DEPD·TCNQ (2 : 3)	265	9730	1000	1 : 1.35	2 : 3
DAD·TCNQ (1 : 1)	243	7850	2870	1 : 0.85	1 : 1
	(400)	(100)[b]			
o-PD·TCNQ (2 : 1)	245	6020	2940	1 : 0.47	2 : 1
BD·TCNQ	287	25800	450	1 : 1.03	1 : 1
DϕPD·TCNQ	304	28000	1400	1 : 1.09	1 : 1
	(400)	(200)[b]			
DNPD·TCNQ	319	26000	3300	1 : 0.82	1 : 1

a) The concentration of TCNQ was first determined from the absorbance at 400 mμ; its extinction coefficient at 400 mμ was taken to be 67600 *l*/mol·cm.
b) The contribution at 400 mμ was neglected in determining the TCNQ concentration.

and used after purification by recrystallization, sublimation or distillation under a reduced pressure. All solvents used for complex formation were commercial ones, and were used without further purification.

Complex Preparation *p*-PD·TCNQ. Deep purple polycrystals were obtained by mixing a solution of 25 mg of TCNQ in 60 m*l* of chloroform with a solution of 14 mg of *p*-phenylenediamine in 20 m*l* of chloroform at room temperature.

TMPD·TCNQ. To a saturated solution of Würster's blue perchlorate in methanol was added a saturated solution of lithium salt of TCNQ in methanol at room temperature, and dark green crystals thus formed were collected.

DAD·TCNQ (1:2). To a solution of 95 mg of diaminodurene in 70 m*l* of ethanol was introduced hydrogen iodide and then added 150 m*l* of diethyl ether. White precipitate was obtained. To a solution of 101 mg of the precipitate in 25 m*l* of ethanol was added a solution of 102 mg of TCNQ in 150 m*l* of chloroform, and the mixture was allowed to stand overnight at room temperature. Black rod crystals were obtained.

Other complexes were prepared from neutral components in a similar manner to that adopted in the preparation of *p*-PD·TCNQ. Solvents used are given in Table 1. In some cases, a complex was prepared under a nitrogen atmosphere and sealed into a sample tube without being exposed to air. Its ESR absorption was found to be identical, in every way, with that of the corresponding complex prepared in air.

Visible Absorption Measurement. To determine composition of a complex, visible absorption spectrum was examined for a dilute solution of the complex in dichloromethane, in which the complex dissociated into components of their neutral form. Their extinction coefficients at the relevant wavelengths were determined separately, as shown in Table 2. Using these values, the composition of a complex was estimated from the observed absorption spectra. In some cases, an elementary analysis was also adopted for comparison.

Infrared Absorption Measurement. Absorption spectra in the infrared region were measured using the method of Nujol mulls to determine whether the complexes were ionic or not. Lithium salt of TCNQ and bromide of the amines, as well as neutral TCNQ and amines, were used as references.

ESR Absorption Measurement. Electron spin resonance (ESR) measurements were made with a Hitachi X-band spectrometer. To control temperature, nitrogen gas at various temperatures was introduced into a cavity through a quartz dewar and blown toward a sample tube. The temperature was measured by means of a thermocouple attached to a sample. The relative spin concentrations at various temperatures were obtained by integration of derivative curves recorded. The absolute number of spins was determined at room temperature by comparing the integrated absorption intensity of a sample with that of a standard specimen

of 1,1-diphenyl-2-picrylhydrazyl, which was calibrated by a static susceptibility measurement.

Electrical Resistivity. Electrical resistivity of a complex was measured in a form of compressed pellet by a DC-method.

Results and Discussion

Composition of the Complexes. Chemical composition (donor to acceptor ratio) obtained from an analysis of visible absorption spectra is given in Table 2. To a molecular complex, however, it is quite reasonable to assume the stoichiometric ratio as is given in the last column of Table 2. The composition of the complex of DEPD·TCNQ was found to be 2 : 3. The ratio was different from the one determined by Melby *et al.*[15] They have given the ratio of 1 : 2 to the complex obtained in the same manner on the basis of an elementary analysis. An elementary analysis, however, was not sensitive enough to distinguish the ratios in question. We thus tentatively adopted the ratio of 2 : 3.

Characterization of the Complexes. Recently, Matsunaga[4] has shown that infrared absorption spectra can be used successfully in characterization of charge transfer complexes of halogenated *p*-benzoquinones. This method is also applicable to TCNQ complexes. The key band in the latter case is that of the C≡N stretching vibration located around 2200 cm^{-1}. For neutral TCNQ, the band is located at 2223 cm^{-1}, and it shifts to 2203 cm^{-1} and becomes somewhat broadened for a typical ion radical salt of TCNQ with lithium.*1

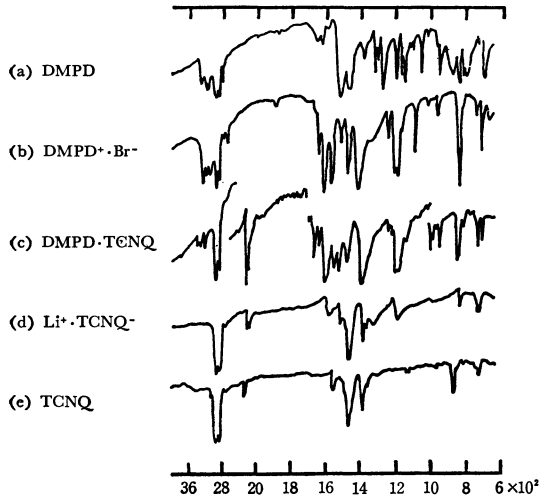

Fig. 1. Infrared absorption spectrum of the complex of DMPD·TCNQ is compared with that of related compounds; (a) DMPD, (b) its bromide, (c) the complex, (d) Li^+TCNQ^- and (e) TCNQ.

15) L. R. Melby, R. J. Harder, W. R. Hertler, W. Mahler, R. E. Benson and W. E. Mochel, *J. Am. Chem. Soc.*, **84**, 3374 (1962).

In Fig. 1 are shown,*2 as an example, the infrared absorption spectra of DMPD, its bromide, DMPD·TCNQ, lithium salt of TCNQ, and TCNQ. The C≡N stretching band is broadened and shifted to 2200 cm^{-1} for the complex. These features are identical to those of lithium salt of TCNQ, and suggest the complex is primarily ionic in its ground state. Further supports are obtained from a comparison of the spectra in Fig. 1. For instance, the C-N stretching vibration band at 1275 cm^{-1} in DMPD disappears and, instead, a new band appears at 1385 cm^{-1} by the formation of the complex. The latter band is considered to correspond to that of the bromide at 1410 cm^{-1}. It is thus concluded that the complex of DMPD·TCNQ is of ionic type.

In a similar way, the complexes of *p*-PD·TCNQ, and DAD·TCNQ (1 : 1) were characterized as essentially of ionic type. The complex of TMPD·TCNQ was also shown to be ionic.[18] In these complexes, therefore, both donor and acceptor are considered to exist as paramagnetic ion radicals. The complex of *o*-PD·TCNQ (2 : 1) belongs almost certainly to this group because of an observed shift and broadening in the C≡N stretching vibration band, but we are not certain about the structure of the amine part.

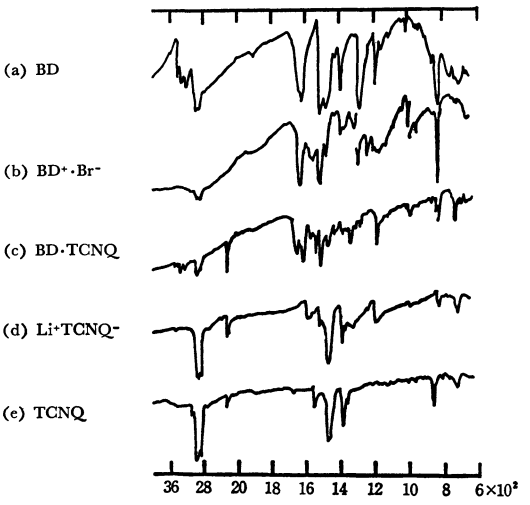

Fig. 2. Infrared absorption spectra of (a) BD, (b) its bromide, (c) the complex of BD·TCNQ, (d) Li^+TCNQ^- and (e) TCNQ.

On the other hand, the infrared absorption spectra of DNPD·TCNQ and DϕPD·TCNQ were found to be quite in accord with a superposition of spectra of neutral components. These complexes are thus

*1 Actually, the band consists of three lines at 2171, 2189 and 2203 cm^{-1} for the anion radical salt. The absorption at 2203 cm^{-1} is the most intense one.

*2 Note that the absorption bands due to Nujol are not deleted from the spectra in Figs. 1, 2 and 3.

considered to be of non-bonding type. The complex of BD·TCNQ may also fall into this group, for which the C≡N stretching vibration band was found to be sharp and located closely to that of neutral TCNQ. As is compared in Fig. 2, however, the entire spectrum of this complex is not explained either by a superposition of ionic components or by a superposition of neutral components. At this moment, therefore, we are not conclusive, but we are of opinion that the complex may also be of non-bonding type.

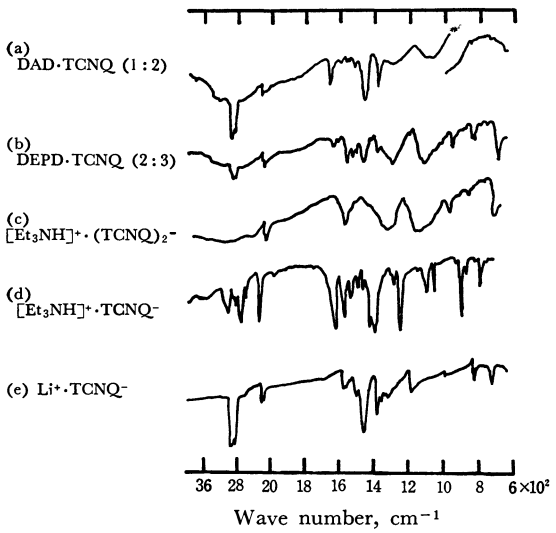

Fig. 3. Infrared absorption spectra of (a) DAD·TCNQ (1 : 2), (b) DEPD·TCNQ (2 : 3), (c) $[Et_3NH]^+(TCNQ)_2^-$, (d) $[Et_3NH]^+(TCNQ)^-$ and (e) Li^+TCNQ^-.

The infrared absorption spectra of DAD·TCNQ (1 : 2) and DEPD·TCNQ (2 : 3) are shown in Fig. 3, together with those of $[Et_3NH]^+(TCNQ)_2^-$, $[Et_3NH]^+(TCNQ)^-$ and lithium salt of TCNQ. In these complexes, it was found that the key band around 2200 cm^{-1} was broadened, and that two new broad absorptions appeared at 1100 and 1300 cm^{-1}. These features are quite in accordance with the spectrum of $[Et_3NH]^+(TCNQ)_2^-$.[15] Therefore, the TCNQ part of the complexes was considered to possess a similar character to that of the latter salt. The amine part of DAD·TCNQ (1 : 2) and the 1 : 2 complex of DEPD·TCNQ, on the other hand, has been assigned to an onium type cation by Melby *et al.*[15] This is very likely for the complex of DAD·TCNQ (1 : 2) because of its preparation procedure. From an infrared absorption, we could not determine whether the amine part in our 2 : 3 complex of DEPD·TCNQ takes an onium form or a positive ion radical form. When it was dissolved in acetonitrile, the complex showed a visible absorption spectrum characteristic of a positive ion radical of Würster's blue type. We thus concluded that DEPD exists as an ion radical form in the complex.

Magnetic and Electrical Properties. The magnetic and electrical properties observed for the complexes are summarized in Table 3, in which the complexes are divided into four groups, A, B, C and D for convenience, according to differences observed in the temperature dependence of ESR absorption intensities. The complexes in group A show a rapid intensity drop with the decrease in temperature, while the complex in group B shows a very slow descent. Group C includes the complexes for which the paramagnetism is of Curie type, and group D stands for the complexes of no ESR absorption.

The complexes of *p*-PD·TCNQ, DMPD·TCNQ, DAD·TCNQ (1 : 1) and *o*-PD·TCNQ (2 : 1), as well as TMPD·TCNQ,[13] fall into group A. The intensity-temperature curves are shown in Figs. 4 and 5. A common feature of this group is that the ESR absorption loses its intensity rather sharply in the higher temperature region when the temperature is lowered. In the lower temperature region, however, these complexes behave differently. For *p*-PD·TCNQ and TMPD·TCNQ, the intensity reaches to its minimum and then increases as the

Table 3. Magnetic and electrical properties of the complexes

Complex	Spin concentration[a]	J (eV)	$\rho_{15°C}$, Ω·cm	E (eV)	Type
p-PD·TCNQ	3×10^{22}	0.15	4.2×10^{3}	0.17	A
DMPD·TCNQ	3×10^{22}	0.21	4.0×10^{7}	0.48	A
TMPD·TCNQ	2×10^{23}	0.08	6.8×10^{5}	0.36	A
o-PD·TCNQ (2 : 1)	7×10^{21}	0.07	1.4×10^{7}	0.45	A
DAD·TCNQ (1 : 1)	1×10^{22}	0.13	1.5×10^{6}	0.27	A
DAD·TCNQ (1 : 2)	3×10^{23}	—[b]	1.5×10^{1}	0.04	B
DEPD·TCNQ (2 : 3)	8×10^{23}	0	3.3×10^{3}	0.08	C
BD·TCNQ	5×10^{21}	0	5.1×10^{3}	0.08	C
DϕPD·TCNQ	No signal	—	4.9×10^{5}	0.33	D
DNPD·TCNQ	No signal	—	6.7×10^{7}	0.67	D

a) Number of spins per one mole of a complex at room temperature, 296°K.
b) Slight change in intensity; about 20% decrease from 300 to 120°K.

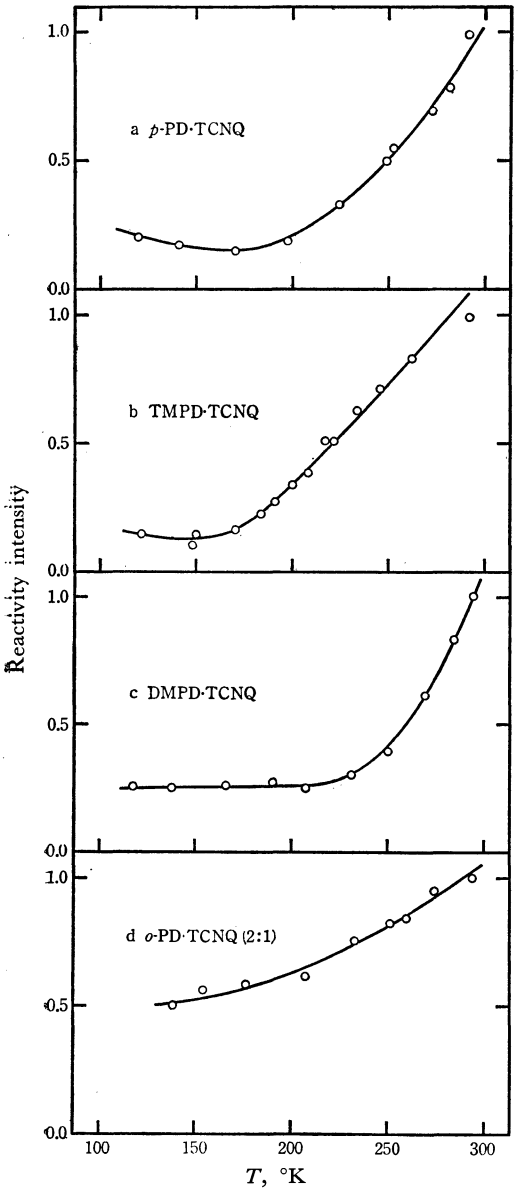

Fig. 4. Relative ESR absorption intensities of the complexes of (a) *p*-PD·TCNQ, (b) TMPD·TCNQ, (c) DMPD·TCNQ and (d) *o*-PD·TCNQ (2 : 1) are plotted against temperature. The intensities are arbitrarily normalized to unity at room temperature.

temperature decreases, while the other complexes show no minimum and their intensity traces a plateau. For these complexes, the ESR absorption intensity I in the higher temperature region was analysed by an equation

$$I = C\exp(-J/kT)/T$$

where C is a constant and J is an activation energy for generation of a magnetic state. A plot of $\ln(IT)$ *vs.* $1/T$ yielded a straight line, whence the J-values

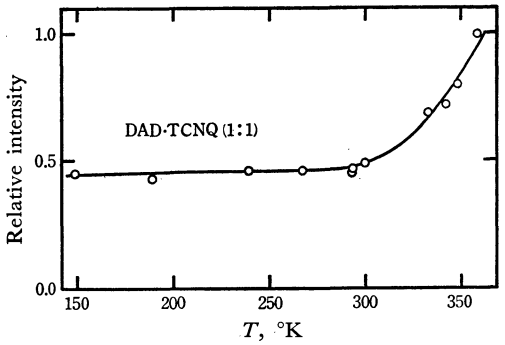

Fig. 5. Plot of relative ESR absorption intensities as a function of temperature for complex of DAD·TCNQ (1 : 1).

in Table 3 were obtained.*3

For the complex of DAD·TCNQ (1 : 1), there was only a slight decrease in its ESR absorption intensity below room temperature. As shown in Fig. 5, however, we observed a sharp increase in intensity when the temperature was raised above room temperature. This change was found to be completely reversible, and the J-value listed was determined from this part of temperature dependence.

Other ESR behaviors of the complexes in group A are more or less identical with each other. The line width was found to change with temperature with a single exception of *p*-PD·TCNQ. The line width was, in general, very sharp at room temperature, but it was broadened by factors of 2—5 by lowering the temperature. The complex of *p*-PD·TCNQ showed virtually no broadening effect over the whole temperature range. The absorption for the complexes of DAD·TCNQ (1 : 1), *o*-PD·TCNQ (2 : 1) and DMPD·TCNQ consisted of a single line, while the other complexes showed a structure characteristic of *g*-factor anisotropy. The line shape was not affected by an introduction of air for all complexes in group A.

It should be noted that the spin concentrations at room temperature are not consistent with the order of the J-values. Higher concentration may be expected for a complex with smaller J-value. The complex of *o*-PD·TCNQ (2 : 1) is of the smallest J-value, but it has the lowest concentration.

Electrical resistivity of these complexes was found to be rather high at room temperature compared to that of groups B and C. The activation energy E for electrical conduction in the equation of $\sigma = \sigma_0 \exp(-E/kT)$ was also relatively large, and always larger than that for spin excitation (J). For the complex of *p*-PD·TCNQ, however, both activation energies were found to be virtually coincident within

*3 A correction was made for the intensities in the higher temperature region of the complexes, *p*-PD·TCNQ and TMPD·TCNQ, by subtracting the intensities obtained by an extrapolation from the lower temperature side to the high temperature side.

a range of experimental accuracy, which would have some significance in a sense that a similar observation[12] was reported for the complexes of iodine with perylene and pyrene. In the latter complexes, the parallelism in both activation energies has strongly supported a prediction that conduction electrons (or holes) are responsible for the observed paramagnetism. However, it seems rather hasty to draw the same conclusion for the complex of *p*-PD·TCNQ by reason of the general tendency of $E > J$ in this group of complexes.

Group B consists of only one member, DAD·TCNQ (1 : 2). It should be, however, noted that this salt is different structurally from other complexes studied here. It has, as shown in Fig. 6, a

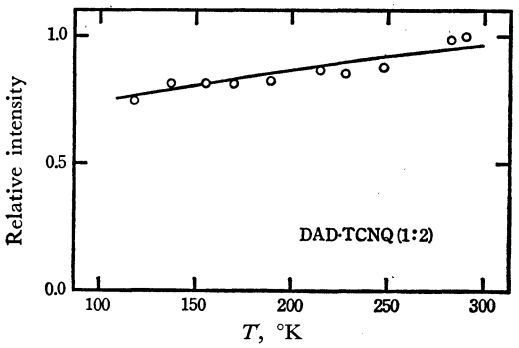

Fig. 6. Temperature dependence of relative ESR absorption intensities for DAD·TCNQ (1 : 2).

unique paramagnetism similar to that found with the salts of (quinolinium)$^+$(TCNQ)$_2^-$ type.[16,17] The intensity-temperature curve was very similar to that of the lower temperature portion of DAD·TCNQ (1 : 1). To check the behavior at higher temperatures, we raised the temperature above room temperature, but we could not observe any steep rise of its ESR absorption intensity. Furthermore, in contrast to the complexes in group A, the absorption width was found to be very sensitive to air. In a vacuum, it gave a sharp absorption with a structure due to *g*-factor anisotropy. An introduction of air caused a remarkable broadening in the width and the structure was smeared out. The effect of air on line width is given in Table 4.

Table 4. Effect of air on the ESR absorption line width

Complex	Line width* (in gauss)	
	in a vacuum	in air
DAD·TCNQ (1 : 2)	1.4_4	2.2_7
BD·TCNQ	1.1_4	3.1_2

* The line width was measured at the half height of an integrated absorption curve.

16) R. G. Kepler, P. E. Bierstedt and R. E. Merrifield, *Phys. Rev. Letters*, **5**, 503 (1960).
17) R. G. Kepler, *J. Chem. Phys.*, **39**, 3528 (1963).

The electrical resistivity of DAD·TCNQ (1 : 2) was found to be very low and the activation energy was also small. These are again a similar feature of the salt of quinolinium-TCNQ type.[16,18] The ESR line shape of DAD·TCNQ (1 : 2) was sometimes distorted by skin-effect because of its low resistivity. Therefore, a possibility that the observed ESR absorption is due to conduction electrons may be considered. In the case of the salt of (quinolinium)$^+$(TCNQ)$_2^-$, the magnetic susceptibility-temperature curve has been interpreted in terms of conduction electrons.[19]

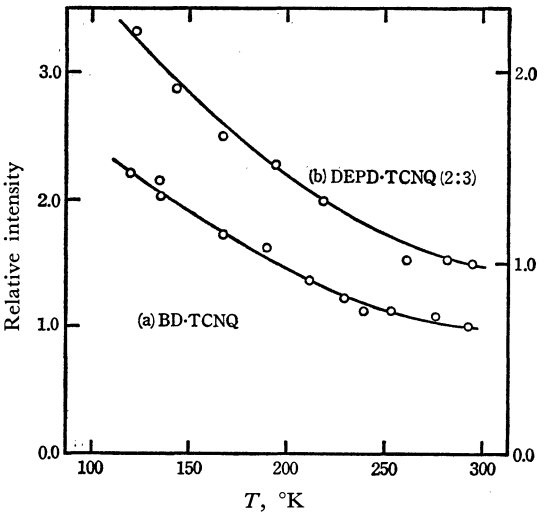

Fig. 7. The variations of ESR absorption intensities with temperature are illustrated in relative units for the complexes of (a) BD·TCNQ and (b) DEPD·TCNQ (2 : 3). The scale for (a) is shown on left, while for (b) on right. The actural intensity for (a) is smaller by a factor of about 10^2 than that for (b) at room temperature (see Table 3).

There are two complexes, DEPD·TCNQ (2 : 3) and BD·TCNQ, in group C. These complexes exhibited Curie type paramagnetism, as shown in Fig. 7, and they showed relatively low electrical resistivity and small activation energy. However, other properties of these complexes were found to differ remarkably from one another. The spin concentration of DEPD·TCNQ (2 : 3) was very high. The absorption line shape was not varied either by temperature or by air. On the other hand, the spin concentration of BD·TCNQ was found to be very low; indeed, there was only one unpaired electron over about 100 donor-acceptor pairs. The ESR absorption line shape and width of BD·TCNQ were found to be sensitive to air, whereas there was no temperature effect on them.

18) W. J. Siemons, P. E. Bierstedt and R. G. Kepler, *J. Chem. Phys.*, **39**, 3523 (1963).
19) T. Kondow, K. Siratori and H. Inokuchi, *J. Phys. Soc. Japan*, **23**, 98 (1967).

A change of line width by air is indicated in Table 4.

A low spin concentration in the complex of BD·TCNQ suggests its non-bonding character, because, in complexes of non-bonding type, the spin concentration is usually very low and the ESR absorption intensity varies, in most cases, following Curie law. However, a relatively high conductivity and a small activation energy of BD·TCNQ suggest some difference in property from those of usual weak complexes. These features seem to be correlated to a difficulty found in characterizing the complex by the infrared absorption spectrum.

The complexes DφPD·TCNQ and DNPD·TCNQ were found to be diamagnetic and classified under group D. The diamagnetism is consistent with the results in their infrared absorption spectra.

Conclusion

The complexes studied are found to show a variety of properties, magnetically, electrically and optically, even though they are formed between chemically resembling donors and the same acceptor. An ionization potential of a donor, for example, is not a determining factor of a complex character by itself. To gauge the ionization potential of these donors, we used wavelengths of absorption maxima of charge-transfer bands for the complexes of *p*-bromanil with the amines in carbon tetrachloride.*4 The results are given in Table 5. The donors fall into two groups; most donors have the maxima in the range of 900—970 mμ, and only three donors have the maxima in 620—670 mμ. However, in the former group, for which the ionization potential is lower than that for the latter, the donors which give rise to a complex of non-bonding type are included, as well as those giving rise to an ionic complex. The donors in the latter group give also an ionic complex, although their ionization potentials are higher than those of DφPD and DNPD. Within our experimental range, therefore, it is concluded that a character, dative or non-bonding, of a complex with a particular acceptor is determined by a conflict between ionization potential of a donor and its steric factors. This can be easily seen in a comparison between a character of TMPD·TCNQ or *p*-PD·TCNQ and that of DφPD·TCNQ or DNPD·TCNQ.

Table 5. Charge transfer absorption maxima of the complexes of *p*-bromanil with the amines in carbon tetrachloride, as an indication of the ionization potentials

Donor	Absorption maximum
p-PD	672 mμ
DMPD	908
DEPD	950
TMPD	918
DAD	973
o-PD	646
BD	624
DφPD	942 (453)[a]
DNPD	931 (485)[a]

a) There are two charge transfer absorption bands for the complex.

*4 Since the complexes of TCNQ with some of the amines are scarcely soluble in a less polar solvent and since they dissociate into ions in a polar solvent, it is very difficult to observe a charge-transfer band of the TCNQ complexes itself.

Once an ionic character is obtained for a complex, its magnetic behavior is dominated by an electronic interaction between the unpaired electrons on donor and acceptor ion radicals. If there is no interaction, the complex will show the paramagnetism of the Curie type. However, an appreciable amount of interaction may result, as discussed by Kainer *et al.*,[8] in the paramagnetism of the other type. For such an interaction, charge-transfer stabilization of the non-magnetic ground state has been suggested to explain a somewhat large activation energy for spin excitation.[20,21]

All the ionic charge-transfer complexes studied except DEPD·TCNQ (2 : 3) exhibit the latter type of paramagnetism.*5 Therefore, the paramagnetic behavior of type in group A seems very common to the ionic complexes. In the case of DEPD·TCNQ (2 : 3), the interaction is, in our opinion, hindered by the large substituents and possibly by its anomalous composition.

Finally, it could be mentioned that the ESR behaviors of the complexes in group A are consistent, at least qualitatively, with a prediction for the ESR absorption of Wannier spin excitons.[22] The crystal structure of the 1 : 1 complexes in group A is very well considered to be similar to that of the complex of TMPD·TCNQ. In the latter complex, the donor and acceptor ions are stacked alternately and equidistantly in a face-to-face manner forming a linear chain.[23] For such a structure, it has been predicted that spin excitation produces Wannier type spin excitons, which are observable in ESR. The line width of the ESR absorption for Wannier type excitons is suggested to be approximately independent of temperature.[22]

The line width for *p*-PD·TCNQ did not change with temperature, and our attempts to observe any fine-structure and $\Delta m = \pm 2$ transition have failed for the complexes in group A. These observations may suggest the possibility of Wannier spin excitons in these solid complexes.

20) P. L. Nordio, Z. G. Soos and H. M. McConnell, *Ann. Rev. Phys. Chem.*, **17**, 237 (1966).
21) H. M. McConnell, B. M. Hoffman and R. M. Metzger, *Proc. Natl. Acad. Sci. U. S.*, **53**, 46 (1965).
*5 DAD·TCNQ (1 : 2) is eliminated in this discussion, because of its exceptional structure.
22) Z. G. Soos, *J. Chem. Phys.*, **46**, 4284 (1967).
23) A. W. Hanson, *Acta Cryst.*, **19**, 610 (1965).

BULLETIN OF THE CHEMICAL SOCIETY OF JAPAN VOL. 41 2005—2007 (1968)

Hydrogen Produced by the Hot-Atom-Process in the Radiolysis of Ethane

Masao INOUE, Taiko UNO, Shin SATO and Shoji SHIDA

Department of Applied Physics, Tokyo Institute of Technology, Ookayama, Meguro-ku, Tokyo

(Received February 29, 1968)

The mechanism of the formation of " molecular " hydrogen in the ethane radiolysis at 300 Torr has been studied with ethane-ethane-d_6-ethylene mixtures. The *G*-value of the hydrogen has been found to be 3.3. The addition of electron and positive ion scavengers scarcely affected the formation of the hydrogen at all. From the isotopic composition of the hydrogen, it was demonstrated that most of the hydrogen is formed by molecular detachment from the ethane molecule, while the rest is formed by the abstraction of a hydrogen atom from the ethane molecule by a hot hydrogen atom, the *G*-value being estimated to be 0.6.

Hydrogen is one of the important products in the radiolysis of hydrocarbons; the mechanisms of its formation may be divided into two types, radical and " molecular " processes. The former is the abstraction of a hydrogen atom from a molecule by a thermal hydrogen atom which is scavengeable by the additives, the so-called radical scavengers. The latter may include different modes of hydrogen formation which cannot be inhibited by the radical scavengers.

The abstraction of a hydrogen atom from a molecule by a hot hydrogen atom, which has a kinetically or electronically excess energy due to the dissociation of a molecule in superexcited states, is a mode of " molecular " hydrogen formation suggested by several authors.[1-3] Recently, some experimental evidence for this mode of formation has been given by the radiolysis of several olefins in the liquid phase.[4,5] In this experiment, we attempted to study the mechanism of the formation of " molecular " hydrogen, especially the hydrogen formation by the hot-atom-process in the radiolysis of ethane in the gas phase.

It seems well established by previous studies of ethane radiolysis near atmospheric pressure[2,6,7] that the *G*-value of the total hydrogen is 8.3—8.8, and that about 60% of it is formed by radical process. These authors have also shown that the additives, such as ethylene, propylene, and nitric oxide, can completely suppress the hydrogen formation due to thermal hydrogen atoms.

In order not only to confine ourselves to " molecular " hydrogen but to discriminate the hydrogen formed by the hot-atom-process from that formed by the molecular detachment process, we irradiated mixtures of ethane and ethane-d_6 containing ethylene as a radical scavenger and examined the isotopic composition of the hydrogen formed. The effects of other types of additives, such as electron scavengers and positive-ion scavengers, were also investigated to see if electrons and/or ionic species were involved in the formation of " molecular " hydrogen. Furthermore, the variation in the isotopic composition of hydrogen as a function of the ratio of ethane to ethane-d_6 was studied; this permitted us to estimate tentatively the relative importance of the hydrogen formation due to the hot-atom-process in comparison with other processes.

Experimental

Research-grade ethane and ethylene purchased from the Takachiho Trading Co. were used after degassing and bulb-to-bulb distillations. The ethane-d_6 was synthesized from acetylend-d_2 which had been obtained by passing deuterium oxide vapor over purified carbide at room temperature. The addition of deuterium to acetylene-d_2 was carried out at 190°C over a palladium catalyst. The ethane-d_6 produced was used after gas-chromatographic purifications and bulb-to-bulb distillations. The isotopic purity was found by mass spectrometry to be 99.6 at% D.

Samples were irradiated in Pyrex-glass tubes (about 80 m*l* in volume) with a breakable seal attached. The sample pressure was 300 Torr, and each sample contained 8 mol% of ethylene as a radical scavenger. Irradiations were carried out by gamma-rays of 6000Ci ^{60}Co at a dose rate of 1.1×10^6 R/hr. After irradiation, the hydrogen and methane were separated off at −196°C. The yield of hydrogen was measured, and its isotopic composition was determined by mass spectrometry.

1) H. H. Carmichael, R. Gorden, Jr., and P. Ausloos, *J. Chem. Phys.*, **42**, 343 (1965).
2) C. M. Wodetzki, R. A. Casker and D. B. Peterson, *J. Phys. Chem.*, **69**, 1045 (1965).
3) for the radiolysis of other systems see Ref. 5.
4) Y. Hatano and S. Shida, *J. Chem. Phys.*, **46**, 4784 (1967).
5) Y. Hatano, S. Shida and S. Sato, This Bulletin, **41**, 1120 (1968).
6) R. A. Back, *J. Phys. Chem.*, **64**, 124 (1960).
7) Kang Yang and P. L. Gant, *ibid.*, **65**, 1861 (1961).

Results and Discussion

Table 1 shows a variation in the hydrogen yield as a function of the absorbed dose. The *G*-value of non-radical hydrogen was calculated to be 3.3, a value which is in good agreement with those obtained by previous investigations.[2,6,7] The linearity of the hydrogen yield with the absorbed dose, as well as the absence of any effect of the temperature on the hydrogen yield or on the isotopic composition between −78.5°C and 125°C, shown in Table 2, confirmed that hydrogen is not formed by a radical process.

TABLE 1. VARIATION OF HYDROGEN YIELD AS A FUNCTION OF ABSORBED DOSE. RADIOLYSIS OF 90 : 10 : 8 ETHANE - ETHANE-d_6 - ETHYLENE

Irradiation time hr	Absorbed dose eV/g	Yield μmol
5	2.5×10^{19}	1.6
10	5.0×10^{19}	2.8
15	7.5×10^{19}	4.5

TABLE 2. EFFECT OF TEMPERATURE ON THE HYDROGEN YIELD AND ISOTOPIC COMPOSITION. RADIOLYSIS OF 90 : 10 : 8 ETHANE - ETHANE-d_6 - ETHYLENE

Temperature °C	Yield μmol	Isotopic composition*		
		H_2	HD	D_2
−78.5	2.83	89.7	2.3	8.0
0	2.46	89.7	2.2	8.0
25	2.83	90.8	2.5	6.7
125	2.77	90.8	2.3	6.9

* Contribution from ethylene to H_2 and HD% in the isotopic composition of hydrogen was found to be negligible from the study of ethane-ethylene-d_4 radiolysis.

Because of its large proton affinity and its weak reactivity towards electron and radicals, ammonia is considered to be an efficient proton acceptor and is often used in the study of hydrocarbon radiolysis to ascertain whether the cationic reactions are effective.[8,9] On the other hand, sulfur hexafluoride has been found to be an efficient scavenger of thermalized electrons, such as nitrous oxide and carbon tetrachloride.[10,11] In Table 3 it may be seen that the addition of ammonia and sulfur hexafluoride scarcely affects either the hydrogen yield or its isotopic composition at all. The results exclude the possible participation of a recombination of the positive ion with the electron and/or of an ion-molecule reaction in the formation of hydrogen in this system.

TABLE 3. EFFECTS OF POSITIVE ION SCAVENGER AND OF ELECTRON SCAVENGER ON THE HYDROGEN YIELD AND ISOTOPIC COMPOSITION. RADIOLYSIS OF 90 : 10 : 8 ETHANE - ETHANE-d_6 - ETHYLENE

Additive mol%	Yield μmol	Isotopic composition		
		H_2	HD	D_2
NH_3				
0	2.8	90.8	2.5	6.7
5	2.9	90.3	2.1	7.6
10	2.5	90.4	2.1	7.5
15	2.7	90.6	2.0	7.4
SF_6				
0	2.8	90.8	2.5	6.7
5	2.9	89.9	2.0	8.1
10	2.9	91.1	2.5	6.4
15	3.0	90.8	2.5	6.7

TABLE 4. VARIATION OF THE ISOTOPIC COMPOSITION OF HYDROGEN AS A FUNCTION OF ETHANE-d_6 CONCENTRATION

Concentration ratio			Isotopic composition		
C_2H_6	C_2D_6	C_2H_4	H_2	HD	D_2
99	1	8	98.9	0.3	0.7
98	2	8	98.2	0.5	1.3
96	4	8	96.2	1.1	2.7
93	7	8	93.1	1.9	4.9
90	10	8	90.8	1.5	6.7

The existence of HD in the isotopic composition of hydrogen, even though it is present in only a small amount, confirms that part of the "molecular" hydrogen is formed by a bimolecular process; on the basis of the above results, we can reasonably attribute its formation to the abstraction

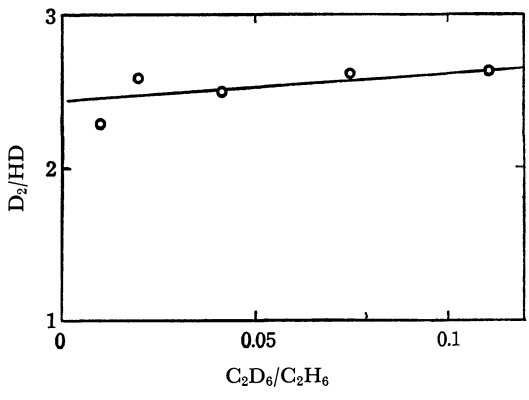

Fig. 1. D_2/HD as a function of ethane-d_6 concentration.

8) W. R. Busler, D. H. Martin and F. Williams, *Discussions Faraday Soc.*, **36**, 102 (1963).
9) H. Okamoto, K. Fueki and Z. Kuri, *J. Phys. Chem.*, **71**, 3222 (1967).
10) G. R. A. Johnson and J. M. Warman, *Nature*, **203**, 73 (1964).
11) W. T. Hoslander and G. R. Freeman, *J. Phys. Chem.*, **71**, 2562 (1967).

of a hydrogen atom from an ethane molecule by a hot hydrogen atom. Table 4 shows the variation in the isotopic composition of hydrogen as a function of the concentration of ethane-d_6. From a kinetic analysis of the reaction mechanisms in the radiolysis of butenes - butenes-d_8, Hatano and Shida[4] pointed out that the value of D_2/HD extrapolated to a zero concentration of butenes-d_8 is equal to one-half of the ratio of the unimolecular to the bimolecular process. Figure 1 shows the plots of D_2/HD as a function of the ethane-d_6 concentration. The application of the above method enables us to estimate the *G*-value of the formation of the hydrogen by the hot-atom-process to be 0.6.

In conclusion, the neutralization of ions and the ion-molecule reactions do not play significant roles in the hydrogen formation by the " molecular " process; the modes of the formation of all the hydrogen in the radiolysis of ethane may be classified as the radical process, the molecular detachment process and the hot-atom-process, whose *G*-values are, respectively, 5.0—5.5, 2.7, and 0.6.

BULLETIN OF THE CHEMICAL SOCIETY OF JAPAN VOL. 41 2007—2017 (1967)

The Crystal Structure of the Copper(II) Chelate of *N,N'*-Ethylenebis(*l*-ephedrine)

Michio MOTOHASHI, Yoshiharu AMANO and Toyozo UNO

Faculty of Pharmaceutical Sciences, Kyoto University, Sakyo-ku, Kyoto

(Received March 4, 1968)

The crystal structure of the copper(II) chelate of *N,N'*-ethylenebis(*l*-ephedrine), where two molecules of *l*-ephedrine are connected through an ethylene group, has been determined by three dimensional X-ray analysis. The dimensions of the orthorhombic unit cell with the space group $P2_12_12_1$-D_2^4 are $a=8.431$, $b=15.92$, $c=16.70$ Å, $Z=4$ and $\rho_0=1.34$ g/cm^3. The intensity data were collected by multiple film technique, and the structure was determined by the heavy atom method. The positions of the copper atom simulated the symmetry of a higher space group than that of $P2_12_12_1$ and the phases calculated from them gave two pseudo mirrors in the Fourier map based on the copper atom only. The structural determination was made with the use of the methods of successive approximations and diagonal and block diagonal least-squares. The problems concerning the pseudo mirrors were solved mainly from the behaviors of the thermal parameters. The final results were obtained by correcting some unsuitable positional and thermal parameters found by the block diagonal least-squares refinement. The final *R*-factor is 13.0%. The structure shows that two crystalline water molecules do not coordinate to the copper atom and that the N–C–C–N bridge causes distortion of the square planar coordination around the copper atom.

In a previous paper,[1] we reported that the *trans*-bis(*l*-ephedrine)copper(II)[2] chelate reacted with carbon tetrachloride and chloroform. Considering that this peculiar reaction might be concerned with the structure of the chelate, we attempted synthesis of some *N,N'*-polymethylenebis(ephedrine) by combining two molecules of ephedrine with a polymethylene group and preparation of their copper(II) chelates in order to investigate their properties from the structural point of view.

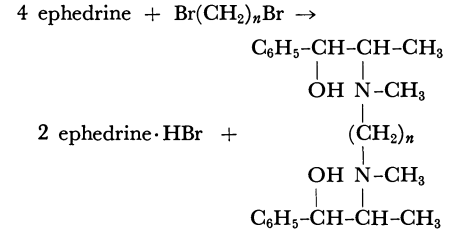

When *n* is equal to one, the corresponding substance could not be obtained, and oxazolidine was obtained instead.[3] When *n* is equal to three, neither *N,N'*-trimethylenebis(*l*-ephedrine) nor its hydrochloride was obtained in the pure state. *N,N'*-Hexamethylenebis(*l*-ephedrine) hydrochloride*1 with $n=6$ was isolated, but its copper(II) chelate could not be prepared because of its instability. When *n* is equal to two, the copper(II) chelate of

1) Y. Amano and T. Uno, *Nippon Kagaku Zasshi* (*J. Chem. Soc. Japan, Pure Chem. Sect.*), **86**, 1105 (1965).
2) Y. Amano, K. Osaki and T. Watanabe, This Bulletin, **37**, 1363 (1964).
3) H. Williams, *J. Pharm. Pharmacol.*, **16**, *Suppl.*, 166 T (1964).
*1 Anal., Found: C, 64.22; H, 8.88; N, 5.99; Cl, 14.64%. Calcd for $C_{26}H_{42}O_2Cl_2$: C, 64,31; H, 8.72; N, 5.77; Cl, 14.60% mp: 249°C.

meso-*N*,*N*′-ethylenebis(ephedrine),[4] where one molecule of *l*-ephedrine is connected with one molecule of *d*-ephedrine through an ethylene group, was obtained as a green crystalline powder, but the purification was not feasible. On the other hand, *N*,*N*′-ethylenebis(*l*-ephedrine)[4] reacted with copper sulfate in the presence of sodium hydroxide to give *N*,*N*′-ethylenebis(*l*-ephedrinato) copper(II) chelate (abbreviated as EBECu hereafter). From the results of the elemental analysis and the continuous variations, it became clear that this chelate has a ligand in the ratio of 1 : 1 to copper(II) and that one molecule of this chelate has two water molecules.

The IR spectrum of this chelate shows two absorption bands at 1670 and 1710 cm^{-1}. On recrystallization from deuterium oxide, two new absorption bands appear at 1170 and 1210 cm^{-1} with the decrease of the intensities of the original bands, so we assigned the original two absorption bands to the bending vibrations of water, but there seemed to be some ambiguities about the assignment, because the frequency (1710 cm^{-1}) was higher than the frequencies found for ordinary H_2O bending vibrations. The existence of two different absorption bands was supposed to show either that there were two water molecules in the different states in the crystal or that two molecules of water approached so near that they had influence on each other with consequent splitting of the bands.

It was reported that the copper(II) chelate coordinated by oxygen and nitrogen were blue or blue violet (trans coordination)[5,6] or green (cis coordination).[7,8] From the chemical structure of the ligand, EBECu was presumed to have cis coordination structure for oxygen and nitrogen, but it was blue. When it was dissolved in acetone and some of acetone was distilled, the color turned green but changed to original blue on addition of water. From this fact it was presumed that the blue chelate had two molecules of water which coordinated to the copper atom and that the chelate had an octahedral structure around the copper atom. In order to make clear the state of the water molecules in the chelate and to compare the structure with that of *trans*-bis(*l*-ephedrine) copper(II) chelate, we carried out three dimensional X-ray crystal structure analysis.

Experimental

N,N′-Ethylenebis(*l*-ephedrianto) Copper(II) Chelate. Sixty milliliters of 20% aqueous solution of sodium hydroxide was slowly added under cooling in ice to a mixture of 3.6 g of *N*,*N*′-ethylene bis(*l*-ephedrine) in dilute hydrochloric acid and 2.4 g of $Cu(SO_4)_2 \cdot 5H_2O$ in water. At this time light blue precipitates were once formed and they turned deep blue gradually. The blue precipitates were filtered and washed with small volumes of water and diethyl ether and dried well in a desiccator under reduced pressure. The blue precipitates were dissolved in dry pyridine, and the blue solution was filtered, concentrated *in vacuo*, and water was added, when blue needles separated. This reprecipitation procedure was repeated two more times (mp 156—157°C, decomp.). Found: C, 58.45; H, 7.66; N, 6.19; Cu, 14.27%. Calcd for $C_{22}H_{30}O_2N_2Cu \cdot 2H_2O$: C, 58.19; H, 7.55; N, 6.17; Cu, 13.99%;

Continuous Variations. An aqueous solution of copper sulfate (10^{-2} M) was mixed at various ratios with a solution of *N*,*N*′-ethylenebis(*l*-ephedrine) in dilute hydrochloric acid (10^{-2} M) to make the total volume 10 m*l*. After 10 min the blue substance was extracted with 15 m*l* of isoamyl alcohol, dried with anhydrous sodium sulfate, and the absorbance was measured at 620 mμ. The results are shown in Fig. 1.

Intensity Data. From the precession and Weissenberg photographs of the crystals prepared by the method described above, the unit cell dimensions were determined and are shown in Table 1. The reflection data were collected by multiple film technique. They

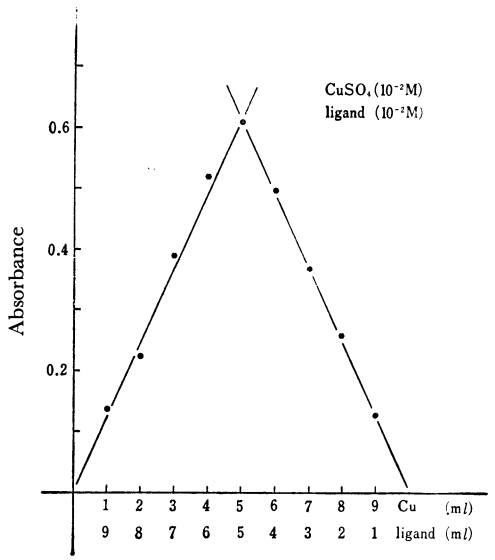

Fig. 1. Continuous variations.

Table 1. Crystallographic data

Space group:	$P2_12_12_1$-D_2^4
a =	8.431 ± 0.005 Å
b =	15.92 ± 0.03
c =	16.70 ± 0.03
V =	2241.5 Å^3
Z =	4
$\rho_{calcd.}$ =	1.345 g/cm^3
$\rho_{obs.}$ =	1.34 g/cm^3
$M_{calcd.}$ =	454.1
$M_{obs.}$ =	452.3
μ(for Cu$K\alpha$) =	16.78 cm^{-1}

4) H. Nishimura, O. Yamauchi and H. Takamatsu, *Chem. Pharm. Bull.*, **12**, 1004 (1964).
5) K. Tomita, This Bulletin, **34**, 297 (1961).
6) R. F. Bryan, R. J. Poljak and K. Tomita, *Acta Cryst.*, **14**, 1125 (1961).
7) F. J. Lewellyn and T. N. Waters, *J. Chem. Soc.*, **1960**, 2639.
8) D. Hall and T. N. Waters, *ibid.*, **1960**, 2644.

were recorded on equi-inclination Weissenberg photographs around *a* axis ((0*kl*)—(5*kl*)) and 30° precession photographs ((*hk*0), (*hk*1), (*h*0*l*)). The copper $K\alpha$ radiation with a nickel filter was used for the Weissenberg and the precession photographs, and 1968 independent reflections were observed. For 1752 reflections the intensities were measured by visual comparison with the standard intensity scale prepared from the same crystal. The intensities ranged from 0.5 to 10^4 for 1752 reflections. The 216 reflections, which had too weak intensities, to be measured were given the intensities 0.2. The Lorentz and polarization corrections and calculations of Wilson's scaling were made in the usual way by the program which was written by the author. No corrections were made for the absorptions because the crystal size was small ($\mu R=0.166$). The overall thermal parameter of the crystal was 5.0 Å^2. The computations in the present study were carried on the electronic computer KDC-II (Hitachi, HITAC 5020) of the Kyoto University Computation Center and on the HITAC 5020E of the Tokyo University Computation Center.

Structure Determination

The ordinary heavy atom method was applied to phase determination. From Haker sections, the positional parameters of copper atom were determined: $x/a=0.250, y/b=0.075$ and $z/c=0.000$. The structure amplitudes were calculated on the basis

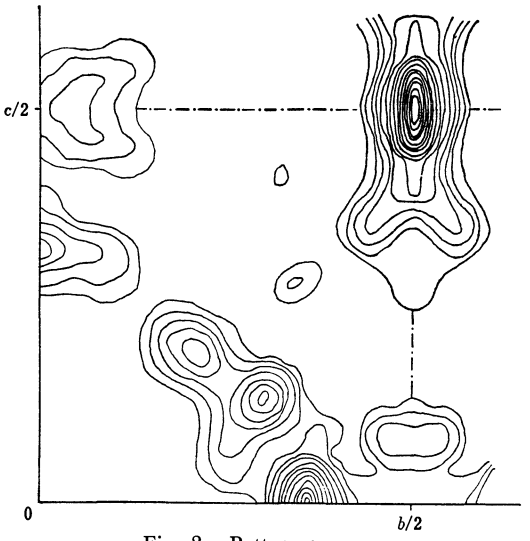

Fig. 2. Patterson map.

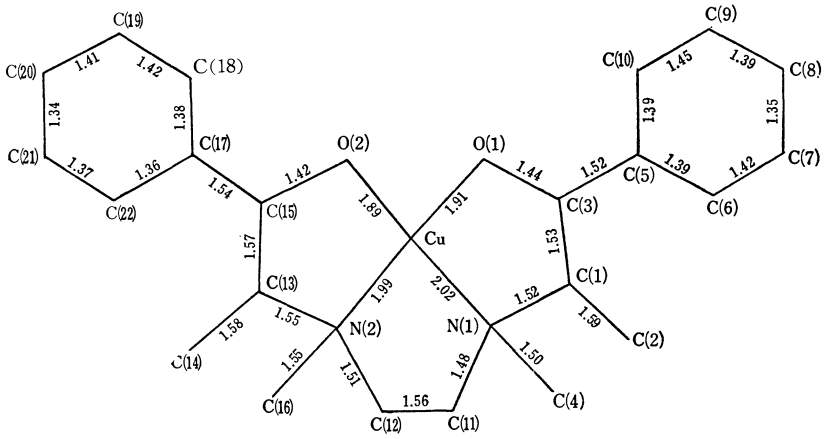

Fig. 3(a). Bond lengths of EBECu (in Å).

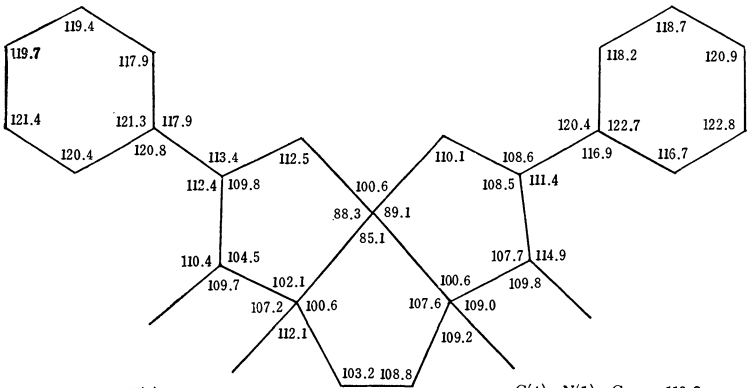

Fig. 3(b). Bond angles of EBECu (in °).

of this atom only, and the R-factor

$$R = \sum ||F_o| - |F_c|| / \sum |F_o|$$

was found to be 74%. The atomic scattering factors were taken from the International Tables for X-ray Crystallography, and no dispersion corrections for atomic scattering factors were applied. As the copper atom, the only heavy atom in an asymmetric unit, had the positional parameters $x/a=1/4$ and $z/c=0$, two pseudo mirrors were found in the Fourier synthesis using the phases calculated on the basis of the copper atom only, and there were four peaks having the same height for one atom. Accordingly it was very difficult to discriminate the correct peaks out of them. From the copper-copper peaks in the Haker sections somewhat extended along b axis as shown in Fig. 2 for example, it was supposed that two or more copper-copper peaks overlapped one another. Therefore, the positional parameters of copper atom x and z were shifted by 1/60 of the unit cell dimensions and the structure amplitudes were calculated. The R-factor was 45%. After the Fourier synthesis the four peaks, which had shown the same peak height when copper had the positional parameters $x/a=1/4$ and $z/c=0$, gained different positions and different peak heights. So the method of successive approximations was applied.

First, as the results of the Fourier synthesis with phases calculated on the basis of the copper atom only, 15 peaks of light atoms were found, and then the Fourier synthesis based on 16 atoms, namely, copper and 15 light atoms, gave additional six peaks. This process was repeated once more, giving

TABLE 2. FINAL ATOMIC COORDINATES AND TEMPERATURE FACTORS

The anisotropic temperature factors are expressed in the form of

$$\exp[-(B_{11}h^2+B_{22}k^2+B_{33}l^2+B_{12}hk+B_{13}hl+B_{23}kl)]$$

Atom	x $\sigma(x)$	y $\sigma(y)$	z $\sigma(z)$	B_{11} $\sigma(B_{11})$	B_{22} $\sigma(B_{22})$	B_{33} $\sigma(B_{33})$	B_{12} $\sigma(B_{12})$	B_{13} $\sigma(B_{13})$	B_{23} $\sigma(B_{23})$
Cu	0.2219	0.0719	0.0119	1387	376	391	13	147	−41
	2	2	2	47	7	7	32	31	13

(B_{11} *etc.*: $\times 10^{-5}$, $\sigma(B_{11})$ *etc.*: $\times 10^{-5}$, $\sigma(x)$ *etc.*: $\times 10^{-3}$ Å)

Atom	x	$\sigma(x)$	y	$\sigma(y)$	z	$\sigma(z)$	B	$\sigma(B)$
O(1)	0.0145	12	0.0255	10	−0.0054	10	5.26	0.22
O(2)	0.1952	12	0.1182	10	0.1150	10	5.10	0.22
W(1)	0.1389	18	0.6088	16	0.3841	16	9.82	0.44
W(2)	0.1157	18	0.9589	16	0.1616	16	9.82*	0.45
N(1)	0.2286	15	0.9488	11	0.3951	11	4.38	0.24
N(2)	0.4542	13	0.0856	10	0.0249	10	4.00	0.22
C(1)	0.3452	19	0.0192	15	0.3761	15	4.97	0.33
C(2)	0.2767	21	0.1063	16	0.4071	16	6.12	0.39
C(3)	0.5068	19	0.9945	15	0.4113	15	4.74	0.32
C(4)	0.2703	20	0.8729	15	0.3459	15	5.33	0.33
C(5)	0.3762	18	0.5659	15	0.0954	14	4.76	0.31
C(6)	0.2936	20	0.5736	17	0.1679	16	6.05	0.37
C(7)	0.1872	25	0.6421	20	0.1749	20	7.68	0.51
C(8)	0.1591	24	0.6965	19	0.1145	20	7.25	0.49
C(9)	0.2362	24	0.6880	19	0.0414	18	7.52	0.48
C(10)	0.3480	21	0.6195	17	0.0311	17	6.22	0.41
C(11)	0.0565	19	0.9646	15	0.3889	15	4.73	0.31
C(12)	0.0329	20	0.4015	17	0.0554	16	5.70	0.38
C(13)	0.4648	18	0.1629	14	0.0814	14	4.21	0.29
C(14)	0.4168	19	0.2448	14	0.0343	14	4.55	0.31
C(15)	0.3414	19	0.1441	15	0.1494	15	4.81	0.32
C(16)	0.5247	21	0.0099	17	0.0707	17	5.88	0.39
C(17)	0.3233*	17	0.2183*	13	0.2081*	13	4.02	0.27
C(18)	0.1722	20	0.2570	15	0.2131	15	5.00	0.33
C(19)	0.1609	22	0.3260	17	0.2667	18	6.34	0.42
C(20)	0.2925	21	0.3519	16	0.3122	16	5.59	0.36
C(21)	0.4318*	22	0.3109*	19	0.3051*	18	6.45	0.43
C(22)	0.4481	20	0.2448	16	0.2529	16	5.33	0.36

($\sigma(x)$ *etc.*: $\times 10^{-3}$ Å, $\sigma(B)$: Å^2)

TABLE 3. OBSERVED AND CALCULATED STRUCTURE FACTORS

($\times 10$)

H	FO	FC	H	FO	FC	H	FO	FC	H	FO	FC	H	FO	FC	H	FO	FC	H	FO	FC	H	FO	FC
K,L= 1	0		1e 20	40	2e 33	49	1e317	310	K,L=10	3		5e211	197		5e316	307	K,L= 1	6		4e 47	61	0e 27	29
1e(A)1154			2e 66	77	3e108	122	2e114	138	0e164	194	K,L= 7	4		K,L=	4	5	0e576	551		5e 25	40	1e 70	62
2e560	591		3e 8	9	4e 45	49	3e186	213	1e450	412	0e 56	57		0e287	306		1e554	520	K,L=18	6		2e 50	49
3e654	663	K,L=20	0		5e 49	62	4e127	139	2e 11	42	1e553	565		2e144	183		0e114	107	3e 68	74			
4e389	439	0e 77	63	K,L=17	1		5e 94	101	3e374	398	2e303	316		2e196	170		3e 28	25		1e 20	19	4e 9	29
5e644	520	2e 49	69	0e135	111	K,L=14	2		4e 78	74	3e289	327		3e436	441		4e214	246		2e 8	14	5e 31	45
K,L= 2	0	K,L= 0	1	1e 51	44	0e905	884		5e237	218	4e121	129		4e156	83		5e109	150		3e 37	44	K,L=16	7
1e562	526	1e373	347	2e 97	108	1e124	100	K,L=11	3		5e155	149		5e208	220	K,L= 2	6		4e 26	42	0e 69	53
2e129	64	2e 44	64	3e 12	41	4e163	156	0e506	456	K,L= 8	4		K,L= 5	5		0e503	474	K,L=19	6		1e 95	96
3e486	465	3e359	386	4e 73	87	3e 60	54	1e102	100	0e409	478		0e(E)1067			1e381	349	0e 27	20	2e 11	22	
4e624	583	4e693	697	5e 8	24	4e 85	109	2e418	445	1e458	438		1e491	492		2e273	291	1e 66	65	3e 37	52	
5e298	369	5e 46	45	K,L=18	1	5e 11	18	3e 39	31	2e470	519		2e345	404		3e 99	137	2e 6	24	4e 50	56	
K,L= 3	0	K,L= 1	1	0e 12	22	K,L=15	2		4e170	179	3e132	99		3e162	150		4e186	188	K,L= 0	7		5e 43	49
1e853	939	1e493	557	1e159	123	0e 15	23		5e104	88	4e317	321		4e181	195		5e336	331	1e251	227	K,L=17	7	
2e473	398	2e329	188	2e 10	11	1e169	147	K,L=12	3		5e 55	50		5e179	154	K,L= 3	6		2e242	233	0e145	121	
3e 64	3	3e707	824	3e 76	84	2e 73	59	0e103	54	K,L= 9	4		K,L= 6	5		0e378	366	3e236	181	1e 53	29	
4e358	321	4e303	315	4e 13	36	3e134	149	1e210	196	0e 12	48		0e272	316		1e223	237	4e313	324	2e 53	68	
5e 16	27	5e424	386	5e 23	39	4e 83	112	2e 68	99	1e291	259		1e126	74		2e109	151	5e 51	34	3e 33	27	
K,L= 4	0	K,L= 2	1	K,L=19	1	5e 58	76	3e110	101	2e 10	17		2e108	148		3e 23	71	K,L= 1	7		4e 47	62	
0e424	423	0e487	536	0e 65	50	K,L=16	2		4e163	171	3e267	284		3e158	172		4e440	413	0e351	336	K,L=18	7	
1e365	364	2e393	384	1e 10	12	0e 87	81		5e109	138	4e200	197		4e386	366		5e164	155	1e453	427	0e 85	82	
2e(8)1110		3e686	620	2e 65	72	1e 51	46	K,L=13	3		5e 67	68		5e215	182	K,L= 4	6		2e287	322	1e 93	88	
3e 67	136	4e260	157	3e 18	20	2e126	151	0e 68	54	K,L=10	4		K,L= 7	5		0e384	397	3e218	209	2e 42	43	
4e 44	73	5e345	348	K,L=20	1	3e 44	41	1e 40	43	0e 81	85		0e347	212		1e255	200	4e295	289	3e 52	75	
5e432	372	K,L= 3	1	0e 40	37	4e 9	28	2e149	142	1e 54	43		1e159	97		2e203	214	5e393	331	K,L=19	7	
K,L= 5	0	1e814	882	2e 16	25	5e 46	64	3e191	208	2e 96	71		2e183	175		3e222	180	K,L= 2	7		0e 32	22
1e660	656	2e699	713	K,L= 0	2	K,L=17	2		4e 71	50	3e295	300		3e329	344		4e228	205	0e 31	76	2e 30	52	
2e 85	49	3e230	245	1e454	520	0e 13	16		5e127	143	4e 82	53		4e 97	119		5e302	260	1e583	571	K,L= 0	8	
3e643	648	4e864	811	2e174	64	1e 32	22	K,L=14	3		5e223	189		5e383	338	K,L= 5	6		2e315	300	0e750	736	
4e473	441	5e227	163	3e169	157	2e 33	35	0e 64	22	K,L= 11	4		K,L= 8	5		0e465	367	3e512	504	1e704	698	
5e359	365	K,L= 4	1	4e767	842	3e 19	43	1e 77	102	0e 13	41		0e 97	67		1e281	300	4e283	246	2e440	457	
K,L= 6	0	0e115	55	5e177	197	4e 8	38	2e144	136	1e196	196		1e347	326		2e208	229	5e171	204	3e187	127	
0e685	712	1e548	667	K,L= 1	2	5e 7	18	3e 79	101	2e 27	26		2e206	251		3e146	138	K,L= 3	7		4e153	148	
1e106	141	2e184	197	0e423	440	K,L=18	2		4e139	148	3e 69	68		3e117	95		4e423	416	0e852	869	5e235	242	
2e755	723	3e530	567	1e875	965	0e 53	53	2e 37	49	4e254	257		4e161	140		5e219	204	1e174	183	K,L= 1	8	
3e404	374	4e198	148	2e320	286	1e 12	36	K,L=15	3		5e 38	71		5e265	195	K,L= 6	6		2e571	641	0e489	467	
4e279	215	5e443	367	3e666	658	2e 10	12	0e198	193	K,L=12	4		K,L= 9	5		0e524	438	3e141	115	1e794	775	
5e 56	67	K,L= 5	1	4e271	259	3e 35	43	1e 83	73	0e391	402		0e467	438		1e491	498	4e292	301	2e184	168	
K,L= 7	0	0e940	984	5e434	438	4e 7	20	2e 96	118	1e118	84		1e269	243		2e270	264	5e266	257	3e880	329	
1e547	553	1e229	212	K,L= 2	2	5e 41	72	3e 66	94	2e189	224		2e341	341		3e 11	22	K,L= 4	7		4e254	238	
2e204	233	2e360	398	1e566	502	K,L=19	2		4e107	109	3e167	187		3e222	227		4e318	302	0e336	361	5e296	293	
3e514	464	3e748	735	2e416	414	0e 10	3	5e 46	57	4e142	151		4e147	178		5e128	158	1e573	597	K,L= 2	8	
4e337	188	4e678	619	3e485	461	1e 80	70	K,L=16	3		5e101	113		5e261	240	K,L= 7	6		2e171	189	0e955	958	
5e337	312	5e252	204	4e569	539	2e 21	36	0e 20	36	K,L=13	4		K,L=10	5		0e411	435	3e341	370	1e447	446	
K,L= 8	0	K,L= 6	1	5e332	270	3e 46	55	1e106	87	0e179	187		0e 97	106		1e499	447	4e288	319	2e355	346	
0e132	174	0e245	313	K,L= 3	2	K,L=20	2		2e 12	19	1e381	362		1e317	314		2e259	246	5e338	318	3e287	249	
1e 23	2	1e358	372	0e570	654	0e 74	69	3e 73	81	2e 12	20		2e188	213		3e211	230	K,L= 5	7		4e189	179	
2e468	497	2e156	135	1e472	471	1e 41	50	4e 30	43	3e182	175		3e263	289		4e101	88	0e117	99	5e261	233	
3e217	265	3e185	173	2e542	492	K,L= 0	3	5e 67	76	4e 48	65		4e147	164		5e105	131	1e502	462	K,L= 3	8	
4e207	214	4e344	330	3e584	553	1e330	247	K,L=17	3		5e130	154	5e169	197	K,L= 8	6		2e110	85	0e442	584	
5e 28	32	5e278	272	4e527	475	2e279	234	0e183	178	K,L=14	4		K,L=11	5		0e410	386	3e255	252	1e168	150	
K,L= 9	0	K,L= 7	1	5e208	185	3e265	244	1e 13	32	0e171	153		0e336	306		1e209	174	4e274	296	2e168	148	
1e111	134	0e201	225	K,L= 4	2	4e312	348	2e 96	109	1e 55	36		1e258	209		2e181	164	5e198	189	3e 84	69	
2e237	281	1e249	195	0e223	272	2e 97	73	3e 32	39	2e220	222		2e234	223		3e348	334	K,L= 6	7		4e261	279	
3e118	50	2e186	208	1e 88	102	K,L= 1	3	4e 70	69	3e 77	78		3e144	155		4e245	269	0e305	320	5e 70	78	
4e189	180	3e300	326	2e268	265	0e535	573	5e 7	12	4e142	138		4e 89	73		5e178	181	1e 76	94	K,L= 4	8	
5e155	178	4e200	201	3e150	184	1e538	542	K,L=18	3		5e 41	45	5e 72	97	K,L= 9	6		2e316	305	0e 15	12	
K,L=10	0	5e261	212	4e 96	51	2e231	202	0e116	79	K,L=15	4		K,L=12	5		0e257	272	3e112	119	1e 11	274	
0e167	140	K,L= 8	1	5e338	302	3e145	149	1e155	117	0e 33	36		0e116	113		1e248	236	4e301	343	2e223	232	
1e 12	6	0e858	737	K,L= 5	2	4e272	238	2e 9	38	1e187	181		1e185	155		2e201	179	5e118	123	3e181	186	
2e157	184	1e216	221	0e145	147	5e435	435	3e 73	76	2e 89	86		2e102	77		3e159	138	K,L= 7	7		4e145	167	
3e268	266	2e213	218	1e554	589	K,L= 2	3	4e 9	18	3e 90	103		3e208	250		4e290	309	0e 12	26	5e263	254	
4e 72	24	3e129	151	2e148	150	0e(C)1331		K,L=19	3		4e 45	60		4e156	179	5e 11	45	1e136	111	K,L= 5	8	
5e 93	90	4e196	165	3e570	541	1e421	363	0e 53	40	5e 44	51		5e 80	68	K,L=10	6		2e 71	77	0e191	186	
K,L=11	0	5e 42	32	4e138	150	2e630	517	1e 9	22	K,L=16	4		K,L=13	5		0e157	157	3e112	314	1e410	399	
1e141	129	K,L= 9	1	5e278	263	3e225	202	2e 54	58	0e 88	63		0e 43	46		1e 83	53	4e182	150	3e159	144	
2e102	161	0e 96	102	K,L= 6	2	4e178	145	3e 7	23	1e 92	86		1e 48	44		2e199	206	5e238	198	3e329	316	
3e 67	92	1e126	104	0e736	720	5e237	216	K,L=20	3		2e 65	63		2e 13	24		3e254	223	K,L= 8	7		4e148	164
4e250	295	2e338	396	1e486	412	K,L= 3	3	0e 29	26	3e 84	101		3e130	148		4e177	184	0e 91	88	5e178	184	
5e 42	3	3e 18	40	2e597	628	0e(D)1158		K,L= 0	4		4e 20	16		4e 49	42		5e116	89	1e224	218	K,L= 9	8	
K,L=12	0	4e169	141	3e251	242	1e497	438	0e101	1		5e 58	59		5e 77	83	K,L=11	6		2e199	201	0e477	447	
0e342	251	5e115	101	4e159	150	2e645	618	1e169	187	K,L=17	4		K,L=14	5		0e 48	35	3e224	205	1e211	203	
1e 42	73	K,L=10	1	5e360	290	3e537	441	2e 89	40	0e 26	21		0e 15	20		1e103	99	4e195	182	2e256	266	
2e 45	44	0e104	48	K,L= 7	2	4e646	592	3e167	101	1e 23	41		1e107	105		2e 56	49	5e118	109	3e118	108	
3e 14	64	1e487	459	0e174	170	5e188	177	4e590	529	2e 37	30		2e 96	89		3e151	143	K,L= 9	7		4e301	305	
4e158	156	2e 84	92	1e552	600	K,L= 4	3	5e370	317	3e 11	22		3e 50	67		4e 64	85	0e250	264	5e298	283	
5e 93	109	3e258	260	2e 59	85	0e298	270	K,L= 1	4		4e 78	94		4e103	123		5e112	154	1e202	188	K,L= 7	8	
K,L=13	0	4e114	114	3e 75	408	1e(E)1037		0e320	298		5e 7	4		5e 10	18	K,L=12	6		2e204	214	0e466	408	
1e231	184	5e169	182	4e 98	94	2e185	198	1e187	194	K,L=18	4		K,L=15	5		0e 82	60	3e 21	38	1e262	227	
2e 62	62	K,L=11	1	5e330	295	3e196	211	2e417	382	0e 97	79		0e160	156		1e 70	63	4e 98	91	2e255	201	
3e 79	78	0e426	354	K,L= 8	2	4e 77	92	3e422	404	1e 11	18		1e 14	47		2e233	244	5e 28	70	3e197	215	
4e 35	56	1e104	65	0e449	462	3e188	189	4e429	437	2e 9	6		2e112	119		3e 89	129	K,L=10	7		4e143	181	
5e 80	72	2e365	392	1e247	214	K,L= 5	3	5e313	267	3e 9	38		3e110	131		4e 54	62	0e268	267	5e171	206	
K,L=14	0	3e143	138	2e586	600	0e(F)1077		K,L= 2	4		4e 40	56		4e 10	41		5e 69	78	1e231	225	K,L= 8	8	
0e160	165	4e151	136	3e267	291	1e368	370	0e577	492	K,L=19	4		5e 62	72	K,L=13	6		2e237	250	0e266	212	
1e182	120	5e 79	69	4e322	322	2e347	308	1e176	128	0e 68	50	K,L=16	5		0e175	159	3e246	216	1e305	256		
2e239	267	K,L=12	1	5e114	140	0e306	267	2e201	210	1e 72	56		0e 14	7	1e235	202	4e162	175	2e242	256		
3e 14	18	0e 15	54	K,L= 9	2	4e279	270	3e216	217	2e 23	36		1e158	160	2e 96	87	5e 57	54	3e389	409		
4e106	128	1e390	378	0e 11	2	5e 96	91	4e506	501	3e 42	55		2e 39	46	3e117	114	K,L=11	7		4e189	195		
5e 22	25	2e 78	82	1e483	448	K,L= 6	3	5e101	236	K,L=20	4		3e 77	90	4e 90	79	0e226	216	5e167	187		
K,L=15	0	3e177	195	2e 72	120	0e343	273	K,L= 3	4		0e 80	71		4e 51	71	5e 55	68	1e263	247	K,L= 9	8	
1e156	121	4e148	145	3e190	196	1e659	606	0e281	195	K,L= 0	5		5e 72	78	K,L=14	6		2e210	226	0e186	211	
2e 12	42	5e 69	77	4e193	183	2e211	228	1e610	537	1e580	605	K,L=17	5		0e289	252	3e153	153	1e214	192		
3e155	206	K,L=13	1	5e 98	112	0e354	332	2e550	557	2e405	364	0e171	151		1e 86	61	4e 79	89	2e241	227		
4e 51	66	0e 14	16	K,L=10	2	4e440	426	3e422	387	3e421	351	1e 47	47		2e216	245	5e 11	32	3e242	250		
5e 10	24	1e108	100	0e168	167	5e243	230	4e191	193	4e 41	81	2e 73	85		3e 77	97	K,L=12	7		4e 47	58	
K,L=16	0	2e312	316	1e105	98	K,L= 7	3	5e117	116	5e221	210	3e 35	46		4e 94	109	0e207	186	5e 90	106		
0e142	148	3e 85	86	2e113	96	0e367	410	K,L= 4	4	K,L= 1	5		4e 52	57	5e 29	30	1e187	179	K,L=10	8		
1e 50	66	4e 47	54	3e315	336	1e355	290	0e483	412	0e 64	76		5e 6	29	K,L=15	6		2e138	139	0e122	65	
2e121	146	5e 75	87	4e 68	74	2e171	144	1e546	544	1e492	446	K,L=18	5		0e 58	74	3e 97	129	1e 98	71		
3e 36	41	K,L=14	1	5e204	174	3e225	245	2e127	84	2e274	274	0e 82	45		1e168	148	4e 55	64	2e114	118		
4e 9	40	0e 66	46	K,L=11	2	4e202	184	3e529	549	3e232	184	1e100	80		2e 55	53	5e 78	61	3e100	117		
5e 61	85	1e102	118	0e 13	1	5e301	255	4e144	126	4e234	260	2e 9	26		3e 75	78	K,L=13	7		4e 50	85	
K,L=17	0	2e 47	58	1e142	153	K,L= 8	3	5e457	359	5e398	339	3e 47	58		4e 61	55	0e130	110	5e 71	77		
1e 13	18	3e 92	118	2e 64	13	0e 37	110	K,L= 5	4	K,L= 2	5		4e 36	46	5e 48	67	1e111	97	K,L=11	8		
2e 66	61	4e 70	75	3e 13	14	1e337	334	0e439	431	0e248	223	K,L=19	5		K,L=16	6		2e 58	61	0e 15	2	
3e 51	82	5e 46	66	4e191	187	2e333	316	1e360	379	1e948	880	0e 61	55		0e 48	30	3e115	115	1e 48	27		
4e 80	105	K,L=15	1	5e 29	32	3e163	193	2e216	268	2e382	319	1e 8	20		1e 13	30	4e 66	73	2e 67	92		
5e 31	33	0e155	134	K,L=12	2	4e402	424	3e140	95	3e383	409	2e 59	63		2e 72	86	5e 83	93	3e 14	7		
K,L=18	0	1e140	99	0e272	254	3e174	175	4e311	319	4e304	311	3e 30	48		3e 54	76	K,L=14	7		4e 98	109	
0e 62	57	2e 40	49	1e108	76	K,L= 9	3	5e130	127	5e183	196	K,L= 0	6		4e 38	46	0e 14	10	5e 83	104		
1e 12	29	3e 49	51	2e166	159	0e505	469	K,L= 6	4	K,L= 3	5		0e599	561	5e 22	35	1e 57	59	K,L=12	8		
2e 10	5	4e 67	80	3e105	119	1e122	97	0e794	799	0e 76	135		1e793	797	K,L=17	6		2e 58	71	0e 56	37	
3e 20	11	5e 60	77	4e179	160	2e349	329	1e433	436	1e456	437		2e788	799	0e 12	17	3e 13	46	1e116	96		
4e 7	5	K,L=16	1	5e194	166	3e 88	94	2e293	332	2e159	168		3e177	185	1e 12	14	4e 16	86	2e155	138		
5e 45	72	0e 75	68	K,L=13	2	4e186	192	3e205	222	3e352	312		4e305	249	2e 10	19	5e 16	26	3e 97	105		
K,L=19	0	1e141	144	0e134	90	5e973	228	4e276	276	4e363	413		5e229	228	3e 33	48	K,L=15	7		4e 44	58	

TABLE 3. (Continued)

H	FO	FC	H	FO	FC	H	FO	FC	H	FO	FC	H	FO	FC	H	FO	FC	H	FO	FC	H	FO	FC
5* 51	56	0*176	142	3*107	016	5* 47	54	2*181	169	4*107	119	2* 87	80	1*133	110	2* 12	5	0*120	84				
K,L=18	8	1*209	233	4* 77	92	K,L= 9	11	3* 86	101	5* 69	97	3* 79	102	2* 43	59	3* 51	56	1* 11	17				
0*188	160	2*228	229	5* 68	94	0*124	103	4* 55	80	K,L= 9	13	4* 75	88	3* 80	76	4* 35	69	2* 80	85				
1*174	149	3* 86	67	K,L=10	10	1*145	103	5* 24	25	0* 15	37	5* 63	75	4* 7	42	5* 46	70	3* 9	17				
2* 81	95	4*105	123	0* 15	0	2*237	239	K,L= 9	12	1*168	143	K,L=10	14	5* 25	37	K,L= 2	17	4* 11	28				
3*105	122	5* 66	82	1* 14	20	3*114	99	0* 15	9	2* 60	61	0* 30	21	K,L=12	15	0* 94	99	K,L= 8	18				
4* 59	54	K,L=12	9	2*114	97	4* 43	56	1*106	77	3*111	139	1* 74	65	0*119	102	1* 14	28	0* 40	38				
5* 10	31	0*103	90	3*108	127	5* 97	119	2*105	103	4* 30	34	2* 41	49	1* 11	18	2* 57	56	1* 81	73				
K,L=14	8	1*139	103	4*101	112	K,L=10	11	3* 39	50	5* 10	51	3* 78	92	2* 92	91	3* 65	91	2* 8	17				
0* 79	44	2*111	127	5* 66	99	0*110	98	4*111	123	K,L=10	13	4* 47	72	3* 92	74	4* 60	82	3* 40	42				
1* 78	57	3*108	111	K,L=11	10	1*181	171	5* 21	34	0*226	222	5* 45	53	4* 25	33	5* 9	33	K,L= 9	18				
2*105	111	4* 81	105	0*103	79	2* 13	24	K,L=10	12	1*125	107	K,L=11	14	K,L=13	15	K,L= 3	17	0* 59	57				
3*102	117	5* 53	70	1*111	78	5* 68	88	0* 83	81	2* 76	85	0* 73	61	0* 9	12	0*128	133	1* 9	11				
4* 68	76	K,L=13	9	2*146	142	4*103	104	1* 73	76	3* 52	48	1* 30	42	1* 45	32	1*194	189	2* 40	51				
5* 9	29	0*109	96	3* 27	40	5* 35	70	2* 12	32	4* 75	79	2* 24	56	2* 7	10	2* 56	56	K,L= 0	19				
K,L=15	8	1* 57	58	4* 80	67	K,L=11	11	3* 14	19	5* 21	41	3* 26	49	3* 18	24	3*109	101	1* 98	81				
0* 89	70	2* 65	75	5* 48	68	0* 63	45	4* 33	55	K,L=11	13	4* 45	58	K,L=14	15	4* 9	13	2* 10	16				
1*129	116	3* 70	76	K,L=12	10	1*122	106	5* 25	26	0* 47	41	5* 34	52	0* 49	21	5* 8	48	3* 97	70				
2* 11	25	4* 10	54	0* 13	32	2*108	111	K,L=11	12	1*130	97	K,L=12	14	2* 5	1	K,L= 4	17	4* 6	20				
3* 71	98	5* 31	34	1* 68	68	3* 83	79	0*109	70	2* 75	89	0*105	92	K,L= 0	16	0*167	164	K,L= 1	19				
4* 28	41	K,L=14	9	2* 68	87	4* 74	92	1* 51	51	3* 50	49	1*111	87	0* 15	19	1* 58	53	0* 83	54				
5* 32	48	0* 20	4	3* 60	64	5* 50	77	2* 12	13	4* 28	38	2* 39	58	1*205	176	2*108	123	1* 11	30				
K,L=16	8	1* 80	71	4* 39	48	K,L=12	11	3* 54	62	5* 40	66	3* 41	51	2* 12	7	3* 24	44	2* 92	59				
0*101	63	2* 12	28	5* 47	76	0* 56	22	4* 58	63	K,L=12	13	4* 48	58	3* 94	88	4* 64	84	3* 47	56				
1* 46	37	3* 13	29	K,L=13	10	1*156	135	5* 47	60	0*157	96	5* 20	46	4* 23	43	5* 33	35	4* 28	45				
2* 56	81	4* 29	35	0*181	144	2* 12	23	K,L=12	12	1* 66	82	K,L=13	14	5* 28	68	K,L= 5	17	K,L= 2	19				
3* 27	36	5* 47	54	1* 74	54	3* 90	108	0*124	125	2* 50	48	0*116	82	K,L= 1	16	0* 27	35	0* 99	69				
4* 29	42	K,L=15	9	2* 47	63	4* 44	69	1* 62	78	3* 18	36	1* 96	86	0*224	236	1*103	104	1* 22	31				
5* 19	40	0* 37	38	3* 58	72	5* 37	51	2* 52	47	4* 21	36	2* 70	72	1* 88	46	2* 11	11	2* 76	79				
K,L=17	8	1* 51	48	4* 37	46	K,L=13	11	3* 47	71	5* 7	22	3* 42	48	2*126	117	3* 67	63	3* 10	41				
0* 11	4	2* 11	18	5* 21	31	0* 27	21	4* 55	67	K,L=13	13	4* 47	51	3* 14	47	4* 16	40	4* 38	51				
1* 11	22	3* 37	49	K,L=14	10	1* 63	54	5* 57	72	0* 34	17	K,L=14	14	4* 80	105	5* 8	42	K,L= 3	19				
2* 9	17	4* 8	31	0*124	108	2* 11	40	K,L=13	12	1* 12	8	0*110	75	5* 10	37	K,L= 6	17	0* 11	22				
3* 9	25	5* 7	29	1* 78	81	3* 53	75	0*150	103	2* 37	42	1*137	94	K,L= 2	16	0*105	68	1*117	97				
4* 15	30	K,L=16	9	2* 68	70	4* 31	44	1* 60	59	3* 46	61	2* 14	30	0* 65	60	1* 46	43	2* 9	22				
K,L=18	8	0*104	77	3* 47	53	5* 35	47	2* 59	76	4* 56	72	3* 48	59	1*120	126	2* 56	67	3* 38	38				
0* 53	44	1* 56	33	4* 34	40	K,L=14	11	3* 34	53	5* 22	35	K,L=15	14	2* 47	53	3* 48	48	4* 8	18				
1* 23	21	2* 44	58	5* 41	59	0* 53	18	4* 55	66	K,L=14	13	1* 63	58	3* 93	117	4* 16	33	K,L= 4	19				
2* 7	26	3* 22	30	K,L=15	10	1* 29	19	5* 20	42	0* 11	14	2* 45	64	4* 10	37	5* 35	51	0*116	83				
3* 22	43	4* 32	47	0*135	9A	2* 10	26	K,L=14	12	1* 73	41	K,L= 0	15	5* 65	88	K,L= 7	17	1* 37	31				
K,L= 0	9	5* 13	30	1* 12	40	0* 11	22	0*154	106	2* 9	6	1* 94	124	K,L= 3	16	0* 29	4	2* 88	91				
1* 76	81	K,L=17	9	2* 37	52	4* 50	58	1*117	85	3* 39	44	2*138	154	0* 15	2	1* 42	49	3* 25	44				
2*100	46	0* 81	47	3* 42	68	5* 18	28	2* 46	61	4* 31	41	3* 76	89	1* 88	92	2* 42	42	4* 34	55				
3*151	99	1* 90	75	4* 41	58	K,L=15	11	3* 49	52	K,L=15	13	4* 10	1	2* 66	66	3* 11	7	K,L= 5	19				
4*254	314	2* 47	53	5* 6	17	0* 41	39	4* 9	30	0* 97	75	5* 11	6	3* 36	55	4* 15	40	0* 11	17				
5*168	205	3* 8	14	K,L=16	10	1* 73	58	5* 35	52	1* 25	21	K,L= 1	15	4* 10	18	5* 25	39	1* 77	64				
K,L= 1	9	K,L=18	9	0* 24	68	2* 30	29	K,L=15	12	2* 28	36	0* 97	92	5* 10	42	K,L= 8	17	2* 8	28				
0*384	360	0* 77	56	1* 89	64	3* 17	37	0* 73	53	3* 15	28	1*110	121	K,L= 4	16	0* 35	17	3* 47	64				
1*359	292	1* 80	65	2* 22	37	4* 37	59	1* 50	38	K,L=16	13	2* 87	92	0* 15	16	1* 33	23	4* 22	49				
2*362	337	2* 38	40	3* 29	35	K,L=16	11	2* 71	76	0* 53	33	3* 57	57	10 14	22	2* 42	31	K,L= 6	19				
3*166	144	K,L= 0	10	4* 37	47	0* 54	55	3* 31	42	1* 53	52	4* 60	72	2* 95	98	3* 45	53	0* 10	17				
4*228	210	0*718	645	K,L=17	10	1* 99	68	4* 47	65	K,L= 0	14	5* 11	44	3* 21	26	4* 7	28	1* 28	37				
5*277	264	1*377	375	0* 50	24	2* 29	34	K,L=16	12	0* 15	27	K,L= 2	15	4* 71	95	5* 16	47	2* 11	34				
K,L= 2	9	2*332	319	1* 9	18	3* 37	52	0* 30	28	1*242	228	0*175	200	5* 9	30	K,L= 9	17	3* 15	34				
0*367	390	3*302	291	2* 48	56	K,L=17	11	1* 78	67	2* 34	25	1* 74	69	K,L= 5	16	0* 67	40	K,L= 7	19				
1*306	313	4*212	247	3* 25	48	0* 66	39	2* 16	21	3* 71	31	2* 84	75	0* 81	57	1* 78	69	0* 9	0				
2*244	228	5*166	159	K,L= 0	11	1* 64	68	3* 15	24	4* 89	81	3*104	136	1* 14	24	2* 38	42	1* 9	2				
3*140	103	K,L= 1	10	1* 57	44	2* 33	44	K,L= 0	13	5* 51	77	4* 86	105	2* 47	45	3* 39	49	K,L= 8	19				
4*237	241	0*346	300	2*145	146	K,L= 0	12	1*101	115	K,L= 1	14	5* 28	37	3* 23	46	4* 21	28	0* 67	30				
5*160	134	1*418	360	3*159	161	0*227	220	2* 35	40	0*135	144	K,L= 3	15	4* 46	60	K,L=10	17	1* 8	7				
K,L= 3	9	2*276	330	4*133	166	1*269	259	3*167	194	1*172	150	0*112	112	5* 9	40	0* 78	63	K,L= 9	19				
0*631	628	3*274	300	5*183	229	2* 11	25	4* 11	35	2*141	116	1*156	131	K,L= 6	16	1* 54	38	1* 40	52				
1*408	335	4*191	188	K,L= 1	11	3*159	153	5* 68	77	3* 79	96	2* 71	82	0* 14	32	2* 51	54	K,L= 0	20				
2*375	356	5*254	241	0* 12	14	4*209	252	K,L= 1	13	4* 44	57	3* 83	92	1*128	117	3* 8	33	0* 54	22				
3*254	256	K,L= 2	10	1*328	274	5* 57	63	0*106	109	5* 11	42	4* 48	57	2* 12	16	K,L=11	17	1*110	96				
4*197	219	0*449	407	2*111	86	K,L= 1	12	1*117	104	K,L= 2	14	5* 76	126	3* 93	97	0*		2* 8	22				
5* 96	86	1*231	199	3*189	163	0*170	112	2*153	167	0* 55	58	K,L= 4	15	4* 39	55	1* 77	74	3* 59	86				
K,L= 4	9	2* 10	132	4*130	186	1*187	164	3* 42	42	1*225	208	0*167	179	5* 27	54	3* 34	51	K,L= 1	20				
0*249	278	3*209	223	5*148	155	2*222	213	4*141	165	2* 54	47	1* 71	56	K,L= 7	16	K,L=12	17	0* 68	57				
1*439	425	4*233	266	K,L= 2	11	3*228	206	5*116	166	3* 79	74	2*127	147	0*197	177	0* 41	44	1* 10	27				
2*242	199	5*215	194	0*442	419	4*123	157	K,L= 2	13	4* 63	97	3* 87	98	1* 71	62	K,L= 0	18	2* 52	62				
3*238	205	K,L= 3	10	1*215	210	5*113	127	0*315	302	5* 11	18	4* 97	111	2*106	133	0* 13	23	K,L= 2	20				
4*200	206	0* 93	92	2*271	255	K,L= 2	12	1* 96	64	K,L= 3	14	5* 10	5	3* 64	61	1* 62	61	0* 10	3				
5*237	250	1*184	160	3*111	109	0*332	338	2*161	150	0* 64	47	K,L= 5	15	4* 78	86	2* 59	84	1* 9	22				
K,L= 5	9	2* 73	84	4* 90	96	1*128	109	3* 87	101	1*110	113	0* 73	44	5* 8	5	3*118	133	2* 8	32				
0*514	515	3*246	251	5*126	147	2*108	125	4*101	121	2*137	131	1*173	160	K,L= 8	16	4* 8	14	K,L= 3	20				
1*392	353	4*185	208	K,L= 3	11	3* 81	102	5* 32	37	3* 79	105	2* 84	44	0* 13	30	5* 67	94	0* 10	25				
2*271	262	5*129	112	0*230	202	4*172	181	K,L= 3	13	4* 39	52	3*134	156	1*115	110	K,L= 1	18	1* 9	24				
3*209	251	K,L= 4	10	1*340	313	5* 76	86	0*139	110	5* 48	51	4* 10	29	2* 41	47	0*183	154	2* 7	28				
4*243	233	0*132	49	2*195	179	K,L= 3	12	1*219	197	K,L= 4	14	5* 37	71	3* 94	88	1* 49	44	K,L= 4	20				
5*236	247	1*135	126	3*232	249	0*141	98	2*139	104	0* 60	43	K,L= 6	15	4* 8	13	2* 94	112	0* 9	4				
K,L= 6	9	2*118	119	4*109	117	1* 71	93	3*199	214	1*126	134	0*103	76	5* 36	61	3* 11	41	1* 9	28				
0* 65	83	3*108	105	5*173	188	2*112	124	4* 49	58	2* 33	39	1* 68	63	K,L= 9	16	4* 67	90	2* 28	35				
1*431	409	4*180	185	K,L= 4	11	3*280	279	5* 68	77	3* 95	95	2* 86	101	0*142	106	5* 7	26	K,L= 5	20				
2*168	158	5*213	193	0*293	294	4* 79	101	K,L= 4	13	4* 51	74	3* 13	19	1* 33	37	K,L= 2	18	0* 67	52				
3*256	269	K,L= 5	10	1*378	346	5*104	125	0*255	273	5* 75	108	4* 47	51	2* 61	66	0* 97	75	1* 8	15				
4*219	253	0*512	504	2*180	138	K,L= 4	12	1*170	142	K,L= 5	14	5* 51	79	3* 11	25	1*107	109	2* 34	45				
5* 76	78	1*169	179	3*242	251	0* 14	58	2*221	214	0* 88	76	K,L= 7	15	4* 54	69	2* 58	67	K,L= 6	20				
K,L= 7	9	2*251	214	4*187	188	1*146	149	3* 88	124	1* 95	67	0* 14	4	K,L=10	16	3* 69	77	1* 53	63				
0* 38	46	3*195	162	5* 56	48	2*219	216	4* 85	107	2*113	126	1* 14	26	0* 12	21	4* 53	69	K,L= 0	21				
1* 93	107	4*109	148	K,L= 5	11	3* 86	79	5* 11	23	3*110	122	2* 65	74	1* 51	54	5* 7	39	1* 17	36				
2*161	155	5* 81	119	0*208	211	4*125	121	K,L= 5	13	4* 87	115	3* 13	10	2* 23	42	K,L= 3	18	K,L= 1	21				
3*128	147	K,L= 6	10	1*249	227	5* 87	104	0* 25	59	5* 53	93	4* 50	71	3* 19	18	0* 13	13	0* 10	39				
4*264	258	0*188	203	2*211	230	K,L= 5	12	1* 90	81	K,L= 6	14	5* 43	63	4* 59	75	1* 13	20	1* 37	40				
5* 98	128	1*333	292	3*146	131	0*266	306	2* 51	74	0* 15	17	K,L= 8	15	K,L=11	16	2* 10	1	K,L= 2	21				
K,L= 8	9	2*463	470	4*254	262	1*162	133	3* 71	71	1*160	153	0* 42	44	0* 11	9	3* 49	59	0* 14	20				
0*139	138	3*155	117	5* 40	48	2*148	145	4* 11	44	2*165	178	1* 63	58	1* 50	38	4* 8	30	1* 18	20				
1*223	186	4* 78	63	K,L= 6	11	3* 84	82	5* 77	98	3*106	112	2* 31	47	2* 8	13	5* 37	59	K,L= 3	21				
2*103	100	5*105	95	0* 45	30	4*141	163	K,L= 6	13	4* 60	54	3* 87	67	3* 50	56	K,L= 4	18	1* 35	45				
3*264	220	K,L= 7	10	1*210	157	5* 40	34	0* 30	35	5* 34	59	4* 42	59	4* 20	18	0* 13	0						
4*132	109	0*355	347	2*126	96	K,L= 6	12	1* 94	78	K,L= 7	14	5* 63	73	K,L=12	16	1* 68	69			FO			
5* 12	22	1*371	342	3*211	199	0* 43	45	2*159	171	0*183	172	K,L= 9	15	0* 9	6	2* 10	20						
K,L= 9	9	2*174	144	4* 61	63	1*128	216	3* 67	66	1* 77	73	0*101	70	1* 55	48	3* 11	17	(A)	967				
0* 79	74	3*318	326	5* 89	112	2*232	247	4* 65	68	2* 99	109	1* 94	114	2* 14	48	4* 18	30	(B)	1119				
1*111	131	4*128	139	K,L= 7	11	3*107	80	5* 55	85	3* 59	62	2* 81	94	3* 36	44	K,L= 5	18	(C)	1128				
2*228	229	5* 91	101	0*242	230	4* 11	48	K,L= 7	13	4*120	157	3* 80	82	K,L=13	16	0*127	103	(D)	984				
3*193	172	K,L= 8	10	1*140	130	5*100	130	0*173	114	5* 10	0	4* 54	77	0* 91	75	1* 19	19	(E)	954				
4*125	111	0*268	277	3* 87	49	K,L= 7	12	1*106	103	K,L= 8	14	5* 64	75	2* 42	53	2* 80	52	(F)	942				
5* 76	71	1* 80	70	3*154	201	0*217	237	2*100	115	0* 40	32	K,L=10	15	K,L= 0	17	3* 35	39	(G)	1118				
K,L=10	9	2*148	159	4* 81	75	1*156	160	3*117	107	1*179	153	0*207	164	1* 73	76	4* 17	22						
0*162	146	3*106	116	5* 89	112	2* 97	79	4*105	131	2* 49	56	1* 37	46	2* 82	119	K,L= 6	18						
1*234	223	4* 90	85	K,L= 8	11	3*103	121	5* 62	78	3* 75	89	2* 69	77	3* 55	89	0* 65	32						
2*145	143	5* 61	74	0*335	301	4*100	121	K,L= 8	13	4* 10	19	3* 11	29	4* 21	19	1*109	94						
3*112	141	K,L= 9	10	1*117	49	5* 11	50	0*222	203	5* 69	94	4* 62	81	5* 9	25	2* 35	46						
4*158	169	0* 14	25	2* 36	22	K,L= 8	12	1* 29	59	K,L= 9	14	5* 7	39	K,L= 1	17	3* 86	81						
5* 11	21	1*155	147	3* 67	88	0*189	146	2* 12	27	0*171	150	K,L=11	15	0* 48	68	4* 6	33						
K,L=11	9	2*126	119	4*114	117	1*155	136	3* 71	75	1* 56	54	0* 63	28	1*109	91	K,L= 7	18						

all 29 peaks except the peaks for hydrogen atoms. At this stage the *R*-factor was found to be 33%. The validity of the determined positional parameters of all the atoms except hydrogen atoms was examined by refining them by the method of diagonal least squares using 655 reflection data ($0.1 \leqq \sin\theta \leqq 0.6$). Only the real part of dispersion corrections were taken into account at this stage. After five cycles, there was one atom whose thermal parameter diverged, so that the new positional parameters were determined from the Fourier map obtained by the structure amplitude from 28 atoms except that atom with the use of all reflection data. After four cycles there was no atom with diverging thermal parameter. At this stage the thermal parameters of the atoms were generally small owing to the use of only a part of the observed reflection data in the least-squares treatment, but some of them were exceptionally small. By considering the bond lengths and angles, the positions of some atoms were found to be opposite to the correct ones with respect to the pseudo mirrors. We revised these erroneous positions and carried out five cycles of diagonal least-squares treatment using all reflection data. After this calculation, all the thermal parameters, bond lengths and angles were found to be nearly satisfactory, the *R*-factor being 16.4%. The data were then refined by the block diagonal least-squares method by using all the reflection data and the isotropic temperature factors for all the atoms. For this stage we used the computer program which was written by Dr. T. Ashida and is reserved at the Tokyo University Computation Center. As described in the diagonal least-squares method, only the real part of the dispersion corrections was considered. All reflection data were weighted equally. After four cycles, the *R*-factor was found to be 14.4%. However, two unreasonable results were obtained; the thermal factor of one crystal water W(2) was 12.3 Å^2 and the C(21)–C(22) bond length was 1.26 Å. Using the anisotropic temperature factor for the copper atom and excluding seven reflection data supposed to have the extinction effects, we attempted the refinement by the block diagonal least-squares method but failed to obtain better results. The *R*-factor was 12.8%. Considering the fact that the thermal parameter of W(2) remained large, we supposed that the correct position of this atom might be on the opposite side of the pseudo mirrors, and without changing the parameters of the other 28 atoms, we calculated the atomic distances by assuming the three positions on the opposite side of the pseudo mirrors. However, the results were not satisfactory because the three positions calculated were unreasonably close to the chelating molecules.

Taking account of these facts, we set thermal parameter of W(2) equal to that of W(1) and corrected the positional parameters of C(17) and of C(21) so as to have a reasonable atomic distance between C(21) and C(22). The final parameters thus obtained are shown in Table 2, where the values with asterisk refer to the corrected parameters. The bond lengths and angles calculated from these parameters are shown in Fig. 3. The *R*-factor calculated from these corrected parameters was found to be 13.0%. The observed and calculated structure factors computed from corrected parameters are listed in Table 3.

Results and Discussion

Figure 4 shows one molecule of the copper chelate and the two nearest crystallization water. As described in the previous section, the copper atom has the position near $x/a=1/4$ and $z/c=0$, and the distances from copper atom to this position along *a*

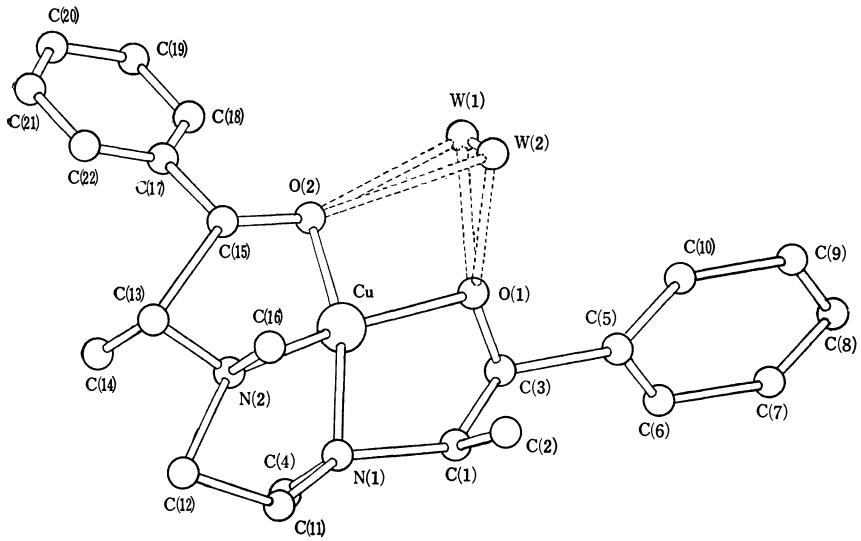

Fig. 4. The molecular structure of EBECu.

Table 4. Best plane

[a] Each plane is represented by $Z=AX+BY+D$, where X, Y and Z are coordinates in Å. For this calculation the positional parameters are translated from Table 2 by symmetric codes.

Plane	A	B	D	Atoms
Benzene ring (I)	2.1874	1.7764	−23.089	C(3), C(5)-C(10)
Benzene ring (II)	0.3690	−0.8694	12.716	C(15), C(17)-C(22)
Chelate ring (III)	−1.5472	−4.3636	57.953	Cu, O(1), C(3), N(1)
Chelate ring (IV)	−0.1654	−2.1405	28.679	Cu, O(2), C(15), N(2)

[b] Displacement of atoms from the planes (in Å).

Plane(I)		Plane(II)		Plane(III)		Plane(IV)	
C(3)	−0.019	C(15)	−0.005	Cu	−0.018	Cu	−0.020
C(5)	0.002	C(17)**	0.003	O(1)	0.032	O(2)	0.026
C(6)	0.023	C(18)	0.005	C(3)	−0.026	C(15)	−0.019
C(7)	−0.009	C(19)	−0.001	N(1)	0.013	N(2)	0.013
C(8)	−0.013	C(20)	−0.007	C(1)*	0.657	C(13)*	−0.695
C(9)	0.000	C(21)**	0.006				
C(10)	0.016	C(22)	−0.002				

* shows that the atom was not included in the evalution of the equation of the plane.
** shows corrected positional parameters (see Text).

and c axis are 0.028 (0.239 Å) and 0.021 (0.191 Å), respectively, whereas the distance along b axis is 0.072 (1.144 Å).

The copper atom is situated at the center of a distorted square plane where the two oxygen atoms O(1), O(2) and two nitrogen atoms N(1), N(2) assume the cis configuration. The bond lengths of Cu–O(1), Cu–O(2), Cu–N(1) and Cu–N(2) are 1.91, 1.89, 2.02 and 1.99 A, respectively, which are in good agreement with those of *trans*-bis(*l*-ephedrine)-copper(II) chelate (Cu–O: 1.88, Cu–N: 2.05 Å). These five-atom system is non-planar. The oxygen atom, O(1), is −0.516 Å from the plane through N(1), Cu and N(2), and O(2) is +0.423 Å from this plane. The fact that the O(1)–Cu–N(2) and O(2)–Cu–N(1) angles are 163.3 and 165.5°, respectively, indicates the probable distortion of the square-planar structure owing to the N(1)–C(11)–C(12)-N(2) bridge formation. This bridge is in the *gauche* form with the internal rotation angle of 53.8°, and C(11) is −0.354 Å from the plane through N(1), Cu and N(2), and C(12) is +0.392 Å from this plane (Table 4).

As to the five membered chelate ring formed by Cu, O(2), C(15), C(13) and N(2), the atom C(13) deviates from the least-square plane through the other four atoms; C(13) is 0.695 Å apart from this plane, while the distances between each of the four atoms and the plane is in the range 0.013—0.026 Å. Similary, in the system formed by Cu, O(1), C(3), C(1) and N(1), the atom C(1) is 0.657 Å apart from the least-square plane through the other four atoms, while the distances from this plane are between 0.013 and 0.032 Å with respect to the other four atoms. In these chelate rings the carbon atoms adjacent to the nitrogen atoms are far from the plane., These results also coincide well with the *trans*-bis(*l*-ephedrine)copper(II) chelate.

The thermal parameters of N(1) and N(2) are small as compared with those of the other atoms. This fact may be interpreted in terms of the distortion of the tetrahedral structure around the nitrogen atoms and the restriction of the movements caused by the N–C–C–N bridge. Some of C–N bond lengths, 1.55 Å for C(16)–N(2) or C(13)–N(2). appear to be somewhat longer than he mean value for C–N single bond (1.47 Å). We can find, however, the cases such as quaternary ammonium salts where C–N bonds are between 1.50 and 1.55 Å.[9] Therefore our results are not unreasonable.

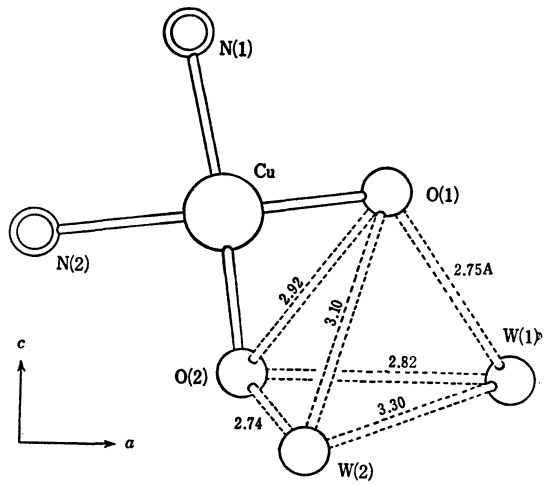

Fig. 5. Interatomic distances of oxygen atoms.

9) R. Eisenberg and J. A. Ibers, *Inorg. Chem.*, **4**, 605 (1965).

Four oxygen atoms projected on *ac* are shown in Fig. 5. As shown in the figure, the interatomic distances of these four atoms are between 2.74 and 3.30 Å, and the interatomic angles are 50—73° (Table 5). Accordingly the four atoms are nearly at the corners of a tetrahedron, and it is impossible to consider that one atom has the hydrogen bond with other special oxygen atom. However, because the thermal parameters of W(1) and W(2) are larger than the corresponding values of the other atoms, we consider that, as Bryan *et al.* reported about bis(β-aminobuthyrato)-copper(II) dihydrate,[6] a water molecule forms a hydrogen bond with each of the two oxygen atoms alternately. It is improbable that the two hydrogen atoms of a water molecule are hydrogen-bonded with the oxygen atoms at the same time. As there is no obvious difference between W(1) and W(2) and the two water molecules approach each other, the splitting of the absorption bands near 1700 cm^{-1} may be ascribed to the interaction between the two water molecules.

Table 5. Interatomic angles of oxygen atoms

O(2)-O(1)-W(1)	59.6°
O(2)-O(1)-W(2)	53.9
W(1)-O(1)-W(2)	68.4
O(1)-O(2)-W(1)	57.1
O(1)-O(2)-W(2)	66.4
W(1)-O(2)-W(2)	72.8
O(1)-W(1)-W(2)	61.0
O(1)-W(1)-O(2)	63.3
O(2)-W(1)-W(2)	52.4
O(1)-W(2)-W(1)	50.7
O(1)-W(2)-O(2)	60.0
W(1)-W(2)-O(2)	54.8

About the reversible color change of EBECu, it was presumed first that the octahedral chelate of EBECu containing two molecules of water would be blue and that the anhydrous square planar chelate would be green, but on the contrary the present X-ray studies show that the blue chelate has the square planar structure. This phenomenon may be

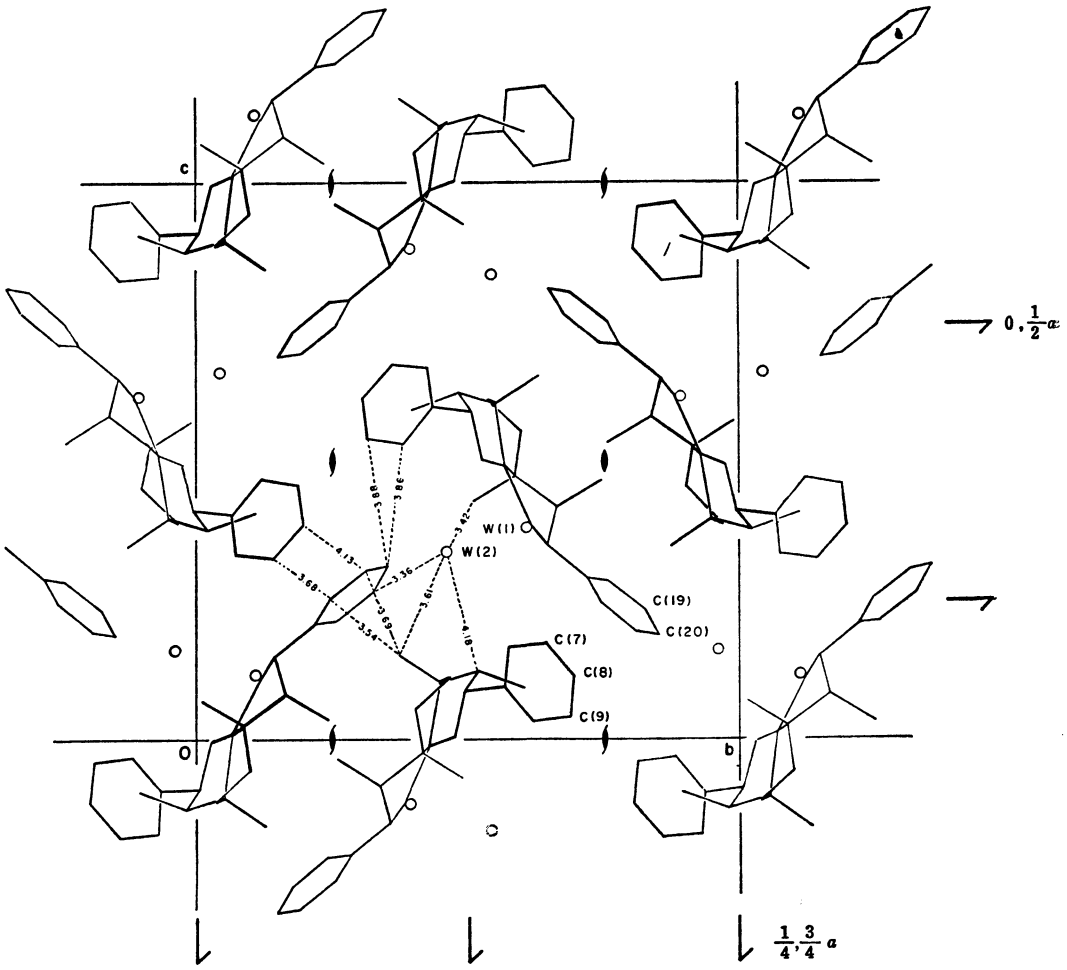

Fig. 6(a). Projection of the structure along the *a* axis.

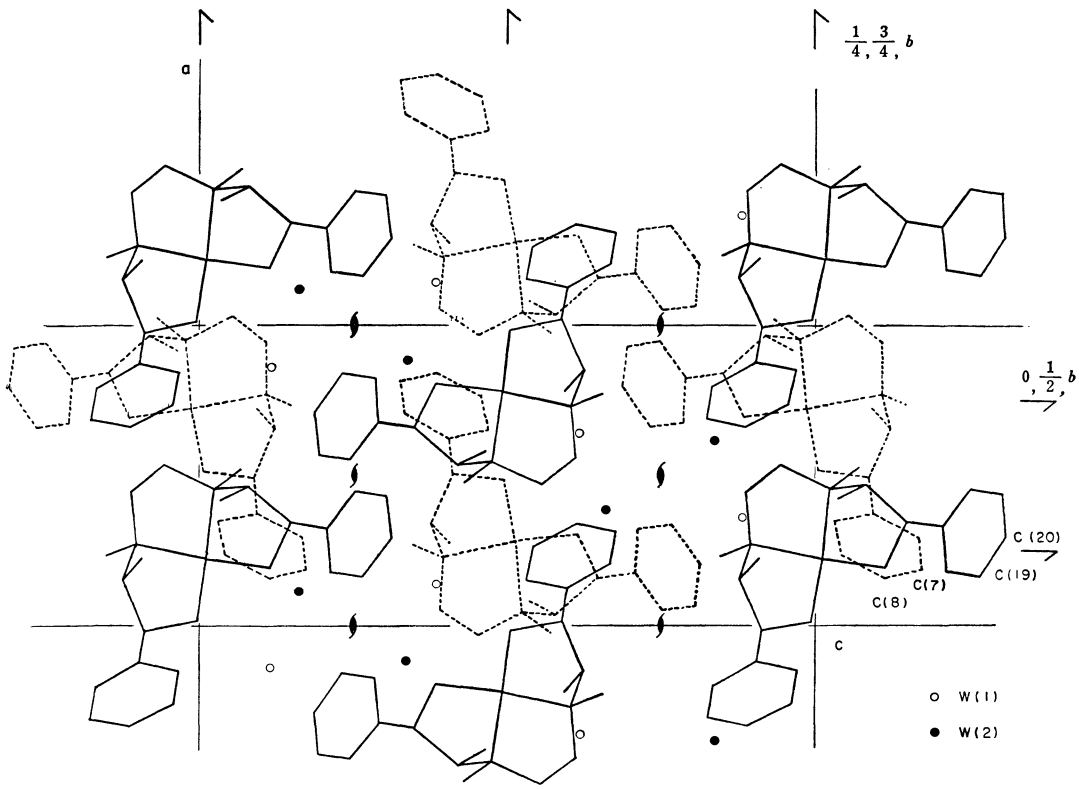

Fig. 6(b). Projection of the structure along the *b* axis.

Table 6. Intermolecular atomic distances

[a] from benzene carbon atoms (less than 3.9Å)						[b] from other atoms (less than 4.0Å)					
C(22)	C(4)	[−1+x,	1+y,	1+z]*	3** 3.54Å	W(1)	C(16)	[1+x,	y,	x]	1 3.33
C(20)	C(16)	[1+x,	y,	z]	4 3.54	W(1)	C(14)	[x,	1+y,	1+z]	3 3.46
C(7)	C(11)	[1+x,	y,	z]	1 3.65	W(1)	C(13)	[1+x,	y,	z]	1 3.50
C(22)	C(7)	[1+x,	1+y,	−1+z]	2 3.69	C(6)	C(11)	[1+x,	y,	z]	1 3.55
C(22)	C(2)	[1+x,	1+y,	−1+z]	2 3.69	W(2)	C(4)	[1+x,	1+y,	−1+z]	2 3.61
C(21)	C(4)	[−1+x,	1+y,	1+z]	3 3.70	W(1)	N(2)	[1+x,	y,	z]	1 3.77
C(18)	C(12)	[x,	1+y,	1+z]	3 3.70	O(1)	C(14)	[x,	1+y,	1+z]	3 3.78
C(22)	C(6)	[1+x,	1+y,	−1+z]	2 3.73	W(2)	C(11)	[1+x,	1+y,	−1+z]	2 3.83
C(17)	C(2)	[1+x,	1+y,	−1+z]	2 3.79	C(14)	C(4)	[−1+x,	1+y,	1+z]	3 3.89
C(21)	C(16)	[1+x,	y,	z]	4 3.80	Cu	C(14)	[x,	1+y,	1+z]	3 3.96
C(19)	C(11)	[x,	1+y,	1+z]	3 3.87	C(6)	C(12)	[1+x,	y,	z]	1 3.98
C(19)	C(12)	[x,	1+y,	1+z]	3 3.88	W(1)	C(12)	[1+x,	y,	z]	1 3.98
C(21)	C(2)	[1+x,	1+y,	−1+z]	2 3.90						

* lattice translation

** symmetry translation in the unit cell

1 $+x, +y, +z$, 2 $\frac{1}{2}-x, -y, \frac{1}{2}+z$, 3 $\frac{1}{2}+x, \frac{1}{2}-y, -z$, 4 $-x, \frac{1}{2}+y, \frac{1}{2}-z$

explained as follows; on dissolving the chelate in acetone the hydrogen bonds connecting the crystal water with the oxygen atoms in the chelate are cleaved, affecting the coordinating abilities of the oxygen atoms of the chelate and consequently the color of the chelate. The orientation of molecules in the crystal projected on *bc* and *ac* are shown in Fig. 6. Table 6 shows the intermolecular atomic distances which are less than 3.9 Å from one of the carbon atoms of benzene ring and less than 4.0 Å from one of the other atoms. The distances are considered to be reasonable. The benzene rings in four different molecules fairly approach one another, and if this state is projected on *bc* the twofold screw

axis along *b* axis is found at the center of the four benzene rings. There are hydrogen bonds between the two water molecules and the nearest chelate molecule, but the atomic distances from these water molecules to the oxygen atoms of the other chelate molecules are more than 5.0 Å, so that there are no intermolecular hydrogen bonds.

For *trans*-bis(*l*-ephedrine)copper(II) chelate, we presumed in earlier publiciation[1] that the hydrogen bonds were cleaved in polar solvents and that halogenated hydrocarbons could easily approach the copper atom and react with it. There are active hydrogen atoms on the nitrogen coordinating to the copper atom, but it is not clear whether they are concerned with this reaction or not. EBECu chelate dissolved in ethyl alcohol also reacts with carbon tetrachloride. It is probable that the cleavage of the hydrogen bonds due to solvation results in the formation of a vacant space near the copper atom, allowing carbon tetrachloride molecules to approach the copper atom. Although EBECu has no active hydrogen, it reacts with carbon tetrachloride. It seems therefore that in the case of *trans*-bis(*l*-ephedrine)copper(II) chelate, the existence of active hydrogen is not an important factor for these reactions.

The authors are grateful to Professor K. Osaki and Mr. T. Taga, Faculty of Pharmaceutical Sciences, Kyoto University, for their kind advices and supplying some of the computer programs used in the present studies. We also thank Mr. T. Nishio for the synthesis of some *N*,*N*′-polymethylenebis(ephedrines).

BULLETIN OF THE CHEMICAL SOCIETY OF JAPAN VOL. 41 2017—2026 (1968)

ASMO-SCF-CI Calculation on the Electronic Structures of the Bases of Nucleic Acids with Special Emphasis on the Configuration Interaction

Hiroko FUJITA, Akira IMAMURA and Chikayoshi NAGATA

Biophysics Division, National Cancer Center Research Institute, Tsukiji, Chuo-ku, Tokyo

(Received March 14, 1968)

The calculation was carried out on the electronic structures of the bases of nucleic acids by means of semi-empirical self-consistent field configuration interaction (SCF-CI) method taking into account of the CI calculation. The effects of mixed configurations, *e.g.*, doubly excited ones, on the transition energies and oscillator strengths, were remarkable. On the other hand, the effects on the direction of the transition moments and the π-electron densities were small. The more configurations were involved, the better the calculated data agreed with the experimental result, but the change of the calculated values with increasing number of configurations from twenty to thirty was small. The agreement between the calculated singlet transition energies and the observed ones obtained by the vapor spectra of the bases was satisfactory, when twenty or thirty configurations including doubly excited ones were considered. The direction of the transition moment calculated by the present authors for thymine agreed well with the experimental result by Stewart and Davidson. For adenine, the calculated direction of transition moment of the main band was polarized parallel to long-axis and it coincided not with the result obtained by Stewart and Davidson, but with that proposed by Mason. Variation of the core resonance integral exerted the influence on the elcetronic structures, and K in Eq. (1), *viz.*, -0.49 was better than -0.431 when doubly excited configurations were taken into calculation.

The approximate calculations were already carried out on the electronic structures of the bases of nucleic acids by Hückel MO, semi-empirical SCF MO, or SCF-MO-CI (configuration interaction) methods. Pullman and Pullman,[1] and Ladik and Hoffman[2] used Hückel MO, while Berthod *et al.*,[3] Nagata *et al.*[4] and Veillard and Pullman[5] used SCF-MO. While, Nesbet,[6] Tanaka and Nagakura,[7] Ladik and Appel,[8] and Denis and Pullmen[9]

1) A. Pullman and B. Pullman, *Bull. Soc. Chim. France*, **1958**, 766; **1959**, 594.
2) J. Ladik and T. A. Hoffman, *Biopolymers Symp. No.* **1**, 117 (1964).
3) H. Berthod, C. Giessner-Prettre and A. Pullman, *Theoret. chim. Acta*, **5**, 53 (1966).
4) C. Nagata, A. Imamura, Y. Tagashira and M. Kodama, This Bulletin, **38**, 1638 (1965).
5) A. Veillard and B. Pullman, *J. Theoret. Biol.*, **4**, 37 (1963).
6) R. K. Nesbet, *Biopolymers Symp. No.* **1**, 129 (1964).
7) M. Tanaka and S. Nagakura, *Theoret. chim. Acta*, **6**, 320 (1966).
8) J. Ladik and K. Appel, *ibid.*, **4**, 132 (1966).
9) A. Denis and A. Pullman, *ibid.*, **7**, 110 (1967).

adopted the SCF-MO-CI method considering singly excited configurations. Imamura *et al.*[10] have included the doubly excited configurations as well as singly excited ones in the SCF-MO-CI calculation. However, in this paper transition energy and oscillator strength were not given.

Murrell and McEwen[11] carried out the calculation on the electronic structure of aromatic hydrocarbons and emphasized the importance of doubly excited configurations in CI calculation.

Similarly, Koutecký *et al.*,[12] on the basis of their calculation of the electronic structures of benzene, showed that tri-, tetra-, and hexa-excited configurations had practically no effect on the singlet energy levels. On the contrary, doubly excited configuration had remarkable effect on them irrespective of its dependence on the parametrization of the integrals.

It may be worthy to study afresh the effect of mixed configurations, excited singly and/or doubly, on the electronic structures of the bases of nucleic acids. The present paper deals with the systematic study of the effect of mixed configurations on the transition energy, oscillator strength, direction of the transition moment, and π-electron density of bases of nucleic acids. The importance of doubly excited configurations was stressed. Furthermore, the parametrization of core integral, in the CI calculation which included doubly excited configurations, was studied to verify the proposition of Anno and Sado,[13] *viz.*, -2.7217 eV for β_{cc} of benzene was better than -2.39 eV. The calculated transition energies were depend greatly on the values of β_{cc}, and, if β_{cc} was assumed to be -2.7217 eV, they agreed well with the experimental values derived from the vapor spectra of bases.

Method

We have used the semi-empirical ASMO-SCF-CI method. One center Coulomb repulsion integrals were evaluated in terms of $I-A$ according to the Pariser-Parr approximation,[14] where I and A were ionization potential and electron affinity, respectively. The values of I and A were the same as our previous papers.[4,10] For two center repulsion integrals, Mataga-Nishimoto's approximation[15] was used. The core resonance integral, different from our previous papers,[4,10] was represented by Wolfsberg-Helmhotz's approximate equation,[16]

$$\beta_{rs} = K\, S_{rs}(I_r+I_s), \qquad (1)$$

were K is a constant, *i.e.*, -0.431 or -0.490 when β_{cc} in benzene is -2.39 eV or -2.7217 eV, respectively, and S_{rs} is the overlap integral between the rth and sth atomic orbitals. As usual, the differential overlap integral and penetration integral were neglected.

The electron density was calculated by the equation used in our previous paper,[10],*1 and the expersions of the transition moment and oscillator strength were the same as our previous ones.[4,17]

The configurations taken into CI calculation contained the ground, singly excited and doubly excited ones. Doubly excited configurations were due to the excitations of electrons in the same occupied level from this to the another same unoccupied one. The four CI calculations were denoted by 2, 3, 4 and 5, respectively, and the SCF calculation was denoted by calculation 1. The classification of CI calculation and the configuration used are shown in Table 1.

Results and Discussion

Singlet Transition Energy and Oscillator Strength. The calculated singlet excited energies and oscillator strengths for adenine, guanine, thymine, cytosine, and uracil are shown in Tables 2 and 3. As is seen in Table 2, the lowest singlet excited energy or those near to it were reduced when the singly excited configurations were alone considered. This tendency can easily be explained in terms of that the ground configuration has zero matrix element when the singly excited configurations are considered in the SCF-CI calculation, but the excited levels with lower energies are depressed by interaction of singly excited configurations. On the other hand, CI calculation of singly and doubly excited configurations gave rather complicated results; *viz.*, some calculated results showed the states shifted to longer and others to shorter wavelength. The doubly excited configurations depress the ground state energy, which contributes to the blue shift. The tendency of this shift of the spectra is originated from the change of the energies of the ground and the excited states. The difference between the energy level of the ground state in CI calculation involving thirty configurations and that in SCF calculation was about 0.4 eV in all bases. This value was rather small as compared with that of benzene, *i.e.*, 1.5 eV.[11]

As shown in Tabl 2, the calculation including 5 singly excited configurations (calculation 2) showed little change on the SCF excitation energies, but those including several doubly excited configurations

10) A. Imamura, H. Fujita and C. Nagata, This Bulletin, **40**, 21 (1967).
11) J. N. Murrell and K. L. McEwen, *J. Chem. Phys.*, **25**, 1143 (1956).
12) J. Koutecký, K. Hlavatý and P. Hochmann, *Theoret. chim. Acta*, **3**, 341 (1965).
13) T. Anno and A. Sado, *J. Chem. Phys.*, **39**, 2293 (1963).
14) R. Pariser and R. G. Parr, *ibid.*, **21**, 767 (1953).
15) N. Mataga and K. Nishimoto, *Z. Physik. Chem. Neue Folge*, **13**, 140 (1957).
16) M. Wolfsberg and L. Helmholtz, *J. Chem. Phys.*, **20**, 837 (1952).
17) A. Imamura, H. Fujita and C. Nagata, This Bulletin, **40**, 522 (1967).
*1 In this definition, cross terms between the configurations are neglected.

TABLE 1. CLASSIFICATION OF CALCULATIONS WITH NUMBER OF CONFIGURATIONS IN THE CI CALCULATIONS*

		Adenine (A)	Guanine (G)	Thymine (T)	Cytosine (C)	Uracil (U)
Calculation 2		0— 0, 6— 7, 6— 8,	0— 0, 7— 8, 7— 9,	0— 0, 6— 7, 6— 8,	0— 0, 5— 6, 5— 7,	0— 0, 5— 6, 5— 7,
CI 5 (G+4S)		6— 9, 5— 7	7—10, 7—11	5— 7, 6— 9	5— 8, 4— 6	4— 6, 4— 7
Calculation 2		0— 0, 6— 7, 6— 8,	0— 0, 7— 8, 7— 9,	0— 0, 6— 7, 6— 8,	0— 0, 5— 6, 5— 7,	0— 0, 5— 6, 5— 7,
	A($G+8S+4D$**)	6— 9, 5— 7, 5— 9,	7—10, 7—11, 6— 8,	5— 7, 6— 9, 5— 8,	4— 6, 5— 8, 3— 6,	4— 6, 4— 7, 5— 8,
	G($G+7S+3D$)	5— 8, 4— 7, 6—10,	6— 9, 5— 8, 7— 8	4— 7, 6— 7 6— 8	4— 7, 5— 6 5— 7	3— 6, 5— 6 5— 7
	T($G+6S+2D$)	6— 7 6— 8 6— 9	7— 8,	6— 7, 6— 8	5— 6, 5— 7	5— 6, 5— 7
	C($G+6S+2D$)	6— 7 6— 8, 6— 9,	7— 9 7—10			4— 6
	U($G+6S+3D$)	5— 7	7— 9, 7—10			4— 6
		5— 7				
Calculation 4		0— 0, 6— 7, 6— 8,	0— 0, 7— 8, 7— 9,	0— 0, 6— 7, 6— 8,	0— 0, 5— 6, 5— 7,	0— 0, 5— 6, 5— 7,
		6— 9, 6—10, 5— 7,	7—10, 7—11, 6— 8,	6— 9, 6—10, 5— 7,	5— 8, 4— 6, 4— 7,	5— 8, 4— 6, 4— 7,
		5— 8, 5— 9, 4— 7,	6— 9, 6—10, 5— 8,	5— 8, 5— 9, 4— 7,	4— 8, 3— 6, 3— 7,	4— 8, 3— 6, 3— 7,
		4— 8, 4— 9, 3— 7,	5— 9, 5—10, 4— 8,	4— 8, 3— 7, 3— 8,	3— 8, 2— 6, 2— 7,	3— 8, 2— 6, 2— 7,
	CI 20	3— 8, 6— 7 6— 8	4— 9, 7— 8 7— 9	2— 7, 6— 7 6— 8	1— 6, 5— 6 5— 7	1— 6, 5— 6 5— 7
	($G+12S+7D$)	6— 7, 6— 8,	7— 8, 7— 9,	6— 7, 6— 8,	5— 6, 5— 7,	5— 6, 5— 7,
		6— 9 5— 7 5— 8	7—10 7—11 6— 8	6— 9 5— 7 5— 8	4— 6 5— 8 3— 6	5— 8 4— 6 4— 7
		6— 9, 5— 7, 5— 8,	7—10, 7—11, 6— 8,	6— 9, 5— 7, 5— 8,	4— 6, 5— 8, 3— 6,	5— 8, 4— 6, 4— 7,
		5— 9 4— 7	6— 9 5— 8	4— 7 4— 8	4— 7 3— 7	4— 8 3— 6
		5— 9, 4— 7	6— 9, 5— 8	4— 7, 4— 8	4— 7, 3— 7	4— 8, 3— 6
Calculation 5		0— 0, 6— 7, 6— 8,	0— 0, 7— 8, 7— 9,	0— 0, 6— 7, 6— 8,	0— 0, 5— 6, 5— 7,	0— 0, 5— 6, 5— 7,
		6— 9, 6—10, 5— 7,	7—10, 7—11, 6— 8,	6— 9, 6—10, 5— 7,	4— 6, 5— 8, 3— 6,	5— 8, 4— 6, 4— 7,
		5— 8, 5— 9, 5—10,	6— 9, 5— 8, 5— 9,	5— 8, 5— 9, 5—10,	4— 7, 3— 7, 4— 8,	4— 8, 3— 6, 3— 7,
		4— 7, 4— 8, 4— 9,	6—10, 4— 8, 4— 9,	4— 7, 4— 8, 4— 9,	3— 8, 2— 6, 2— 7,	3— 8, 2— 6, 2— 7,
		4—10, 3— 7, 3— 8,	5—10, 4—10, 6—11,	4—10, 3— 7, 3— 8,	1— 6, 2— 8, 1— 7,	2— 8, 1— 6, 1— 7,
	CI 30	3— 9, 6— 7 6— 8	3— 8, 7— 8 7— 9	2— 7, 6— 7 6— 8	1— 8, 5— 6 5— 7	1— 8, 5— 6 5— 7
	($G+15S+14D$)	6— 7, 6— 8,	7— 8, 7— 9,	6— 7, 6— 8,	5— 6, 5— 7,	5— 6, 5— 7,
		6— 9 6—10 5— 7	7—10 7—11 6— 8	6— 9 6—10 5— 7	4— 6 5— 8 3— 6	5— 8 4— 6 4— 7
		6— 9, 6—10, 5— 7,	7—10, 7—11, 6— 8,	6— 9, 6—10, 5— 7,	4— 6, 5— 8, 3— 6,	5— 8, 4— 6, 4— 7,
		5— 8 5— 9 5—10	6— 9 5— 8 5— 9	5— 8 5— 9 5—10	4— 7 3— 7 4— 8	4— 8 3— 6 3— 7
		5— 8, 5— 9, 5—10,	6— 9, 5— 8, 5— 9,	5— 8, 5— 9, 5—10,	4— 7, 3— 7, 4— 8,	4— 8, 3— 6, 3— 7,
		4— 7 4— 8 4— 9	6—10 4— 8 4— 9	4— 7 4— 8 4— 9	3— 8 2— 6 2— 7	3— 8 2— 6 2— 7
		4— 7, 4— 8, 4— 9,	6—10, 4— 8, 4— 9,	4— 7, 4— 8, 4— 9,	3— 8, 2— 6, 2— 7,	3— 8, 2— 6, 2— 7,
		3— 7 3— 8 3— 9	5—10 4—10 6—11	3— 7 3— 8 2— 7	1— 6 2— 8 1— 7	2— 8 1— 6 1— 7
		3— 7, 3— 8, 3— 9	5—10, 4—10, 6—11	3— 7, 3— 8, 2— 7	1— 6, 2— 8, 1— 7	2— 8, 1— 6, 1— 7

* SCF without CI was denoted by Calculation 1. ** G: ground, S: singly excited, D: doubly excited configuration.

(calculation 3) exhibited remarkable changes. As was anticipated, the more the number of configurations increased, the better the calculated data agreed with the experimental results (calculation 4). But the inclusion of more than twenty configurations showd no better result (calculation 5). The results of calculation 5 are depicted in Fig. 1 together with the observed absorption curves obtained from the vapor,[18] liquid,[19] and solid film states,[20] respectively. The absorption maxima recorded in the liquid and solid states, occured at longer wavelengths than in the vapor state, and these shifts would be due to the hydrogen-bonding in the liquid and solid states. Therefore, the values obtained in the vapor state were the most preferable for comparing them with the calculated ones. Since we had a few data on the vapor state the comparison was mainly made with the data obtained from the liquid state, in this paper. As is seen in Fig. 1 and Table 2, the agreement between the calculated and the observed data in the liquid state was especially good for adenine. It is of interest that the two lowest absorption bands of adenine were interchangeable when doubly excited configurations were included in the CI calculation. In the SCF or in the CI calculation with 5 singly excited configurations and in the CI calculations involving doubly excited configurations, the (6—7) transition and the (6—8) transition were contained in the lowest energy transition, respectively. In order to know the contribution of the singly excited configurations and doubly excited ones to the change of transition energy of adenine, the calculation with singly excited configurations alone was carred out in claculation 3. No interchange of the transition energies resulted in this case showing an important contribution of

TABLE 2. SINGLET TRANSITION ENERGIES (E) AND OSCILLATOR STRENGTHS (f) IN BASES OF NUCLEIC ACIDS CALCULATED WITH NUMBER OF MIXED CONFIGURATIONS IN COMPARISON WITH THE EXPERIMENTAL VALUES (K IN EQ. (1) IS -0.431, AND UNIT OF eV IS E)

(a) Calculated transition energy and oscillator strength

	Calc. 1		Calc. 2		Calc. 3		Calc. 4		Calc. 5	
	E	f	E	f	E	f	E	f	E	f
A	4.461(6— 7)	0.608	4.419(6— 7)	0.565	4.399(6— 8)	0.080	4.484(6— 8)	0.096	4.533(6—8*)	0.089
	4.747(6— 8)	0.378	4.645(6— 8)	0.176	4.518(6— 7)	0.354	4.556(6— 7)	0.298	4.616(6—7**)	0.288
	5.221(6— 9)	0.030	5.222(6— 9)	0.145	5.112(6— 9)	0.177	5.153(6— 9)	0.129	5.099(6— 9)	0.116
	5.590(5— 7)	0.400	5.734(5— 7)	0.571	5.695(5— 7)	0.560	5.742(5— 7)	0.491	5.821(5— 7)	0.492
	6.353(5— 8)	0.379			6.191(6—10)	0.265	6.217(6—10)	0.211	6.261(5— 8)	0.233
G	3.941(7— 8)	0.425	3.900(7— 8)	0.369	3.779(7— 8)	0.299	3.832(7— 8)	0.277	3.895(7— 8)	0.277
	4.363(7— 9)	0.532	4.374(7— 9)	0.508	4.349(7— 9)	0.385	4.239(7— 9)	0.301	4.252(7— 9)	0.263
	4.758(7—10)	0.108	4.780(7—10)	0.187	4.712(7—10)	0.142	4.741(7—10)	0.137	4.779(7—10)	0.134
	6.271(7—11)	0.026	6.281(7—11)	0.041	5.761(7—11)	0.009	5.737(7—11)	0.018	5.766(7—11)	0.023
	6.496(6— 8)	0.059			6.578(6— 8)	0.157	6.624(6— 8)	0.287	6.546(6— 9)	0.352
T	4.841(6— 7)	0.756	4.759(6— 7)	0.624	4.853(6— 7)	0.378	4.895(6— 7)	0.370	4.895(6— 7)	0.374
	5.425(6— 8)	0.273	5.275(6— 8)	0.213	5.356(6— 8)	0.118	5.146(6— 8)	0.143	5.184(6— 8)	0.147
	5.875(5— 7)	0.061	6.040(5— 7)	0.258	5.987(5— 7)	0.173	5.938(5— 7)	0.125	5.945(5— 7)	0.109
	6.550(6— 9)	0.040	6.618(6— 9)	0.059	6.559(6— 9)	0.142	6.563(6— 9)	0.154	6.593(6— 9)	0.136
	6.699(5— 8)	0.574			6.947(5— 8)	0.522	6.859(5— 8)	0.457	6.864(5— 8)	0.412
C	3.952(5— 6)	0.142	3.933(5— 6)	0.157	3.818(5— 6)	0.120	3.931(5— 6)	0.102	3.976(5— 6)	0.102
	5.579(5— 7)	0.625	5.180(5— 7)	0.076	4.728(5— 7)	0.061	4.549(5— 7)	0.054	4.561(5— 7)	0.053
	5.840(4— 6)	0.578	5.963(4— 6)	1.047	5.872(5— 8)	0.886	5.847(4— 6)	0.830	5.934(4— 6)	0.636
	6.677(5— 8)	0.048	6.971(5— 8)	0.168	6.363(4— 6)	0.492	6.062(5— 8)	0.133	6.136(5— 8)	0.346
	6.795(3— 6)	0.212			7.221(3— 6)	0.024	6.966(3— 6)	0.285	6.980(3— 6)	0.242
U	5.108(5— 6)	0.754	5.000(5— 6)	0.481	5.032(5— 6)	0.349	4.940(5— 6)	0.271	4.948(5— 6)	0.267
	5.679(5— 7)	0.221	5.462(5— 7)	0.111	5.511(4— 6)	0.029	5.377(5— 7)	0.145	5.380(5— 6)	0.145
	5.882(4— 6)	0.047	6.150(4— 6)	0.286	6.001(5— 7)	0.255	6.071(5— 7)	0.141	6.046(5— 7)	0.151
	6.711(4— 7)	0.566	6.768(4— 7)	0.785	6.725(5— 8)	0.341	6.737(5— 8)	0.071	6.953(4— 7)	0.263
	7.001(5— 8)	0.003			7.155(4— 7)	0.354	6.959(4— 7)	0.497	7.053(4— 7)	0.326

* Mixing of (6—8) transition is 65.6% and that of (5—7) transition is 9.4%.
** Mixing of (6—7) transition is 87.9% and that of (6—9) transition is 3.6%.

18) L. B. Clark, G. G. Peschel and I. Tinoco, *J. Phys. Chem.*, **69**, 3615 (1965).

19) D. Voet, W. B. Greatzer, R. A. Cox and P. Doty, *Biopolymers*, **1**, 193 (1963).

20) T. Yamada and H. Fukutome, *ibid.*, **6**, 43 (1968).

TABLE 2 (b). Experiments

	E Voet *et al.*	*E* Tanaka and Nagakura	*E* Clark *et al.*	*f* Voet *et al.*[*5]	*f* Tanaka and Nagakura	*f* Clark *et al.*
A	4.6(sh[*3])	4.61		0.049	$\sim 10^{-3}$	
	4.758	4.73	4.975	0.249	0.27	0.24
	5.988	5.98	5.988	0.529	0.40	
		6.77			0.26	
G	4.507		4.230	0.123		
	5.039		4.364	0.236		
	6.324			0.564		
T	4.686	4.68		0.183	0.21	
	6.046	6.05		0.314	0.31	
		6.9(*4)				
C	4.642		4.274	0.116		
	6.308			0.698		
U	4.776		5.080	0.175		
	6.121		6.046(*sh*)	0.248		
			6.628			

*3 *sh* designates a shoulder.
*4 The value measured with evaporated film on quartz plate. (Ref. 7)
*5 The values were obtained by using the effective wave number limited method.

TABLE 3. SINGLET TRANSITION ENERGIES AND OSCILLATOR STRENGTHS IN BASES OF NUCLEIC ACIDS (K IN EQ. (1) IS -0.49)

		SCF *E*(eV)	*f*		Calc. 5′ *E*(eV)	*f*
A	6— 7	4.881	0.674	1—2*(6— 7)	4.994	0.164
	6— 8	5.211	0.420	1—3*(6— 7)	5.052	0.323
	6— 9	5.703	0.035	1—4 (6— 9)	5.572	0.064
	5— 7	6.103	0.468	1—5 (5— 7)	6.346	0.582
	5— 8	6.928	0.453	1—6 (5— 8)	6.867	0.266
G	7— 8	4.403	0.527	1—2 (7— 8)	4.307	0.327
	7— 9	4.697	0.530	1—3 (7— 9)	4.710	0.285
	7—10	5.241	0.122	1—4 (7—10)	5.249	0.151
	7—11	6.864	0.027	1—5 (7—11)	6.454	0.010
	6— 8	7.097	0.061	1—6 (6— 8)	7.048	0.282
T	6— 7	5.168	0.820	1—2 (6— 7)	5.194	0.419
	6— 8	5.900	0.333	1—3 (6— 8)	5.585	0.150
	5— 7	6.244	0.060	1—4 (5— 7)	6.408	0.171
	6— 9	7.177	0.037	1—5 (6— 9)	7.115	0.258
	5— 8	7.179	0.653	1—6 (5— 8)	7.428	0.429
C	5— 6	4.288	0.144	1—2 (5— 6)	4.364	0.116
	5— 7	6.042	0.704	1—3 (5— 7)	5.120	0.048
	4— 6	6.284	0.619	1—4 (4— 6)	6.417	0.978
	5— 8	7.301	0.047	1—5 (5— 8)	6.778	0.136
	4— 7	7.506	0.192	1—6 (3— 6)	7.621	0.322
U	5— 6	5.443	0.801	1—2 (5— 6)	5.329	0.333
	5— 7	6.177	0.271	1—3 (4— 6)	5.771	0.120
	4— 6	6.260	0.049	1—4 (5— 7)	6.525	0.205
	4— 7	7.196	0.641	1—5 (4— 7)	7.425	0.433
	5— 8	7.664	0.003	1—6 (5— 8)	7.694	0.288

* (1—2) transition is mixed with (6—7) transition (45.6%) and (6—8) transition (35.8%) and (1—3) transition is mixed with (6—7) transition (46.8%) and (6—8) transition (36.1%)

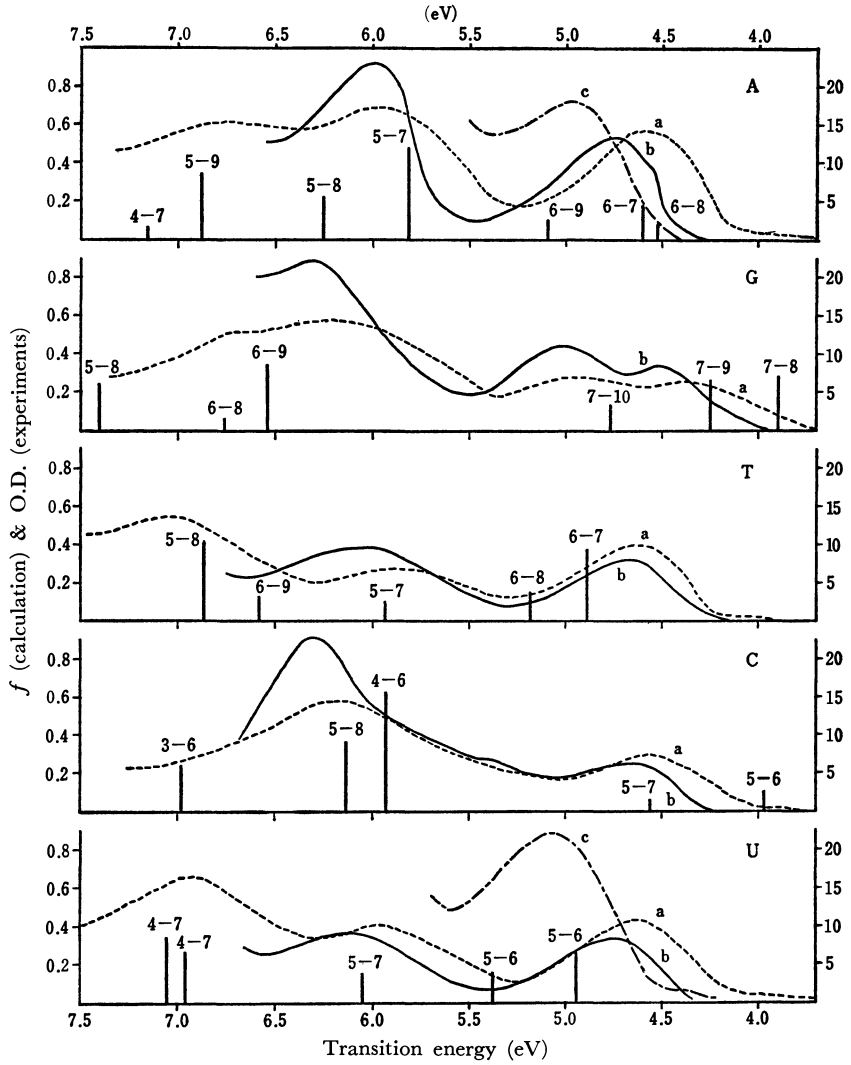

Fig. 1. The calculated singlet transition energies and oscillator strengths (f) in bases of nucleic acids in comparison with the observed absorption curves, measured (a) with evaporated film on puartz plate (Ref. 20) in O. D., (b) in aqueous solution (Ref. 19) in $\varepsilon \times 10^{-3}$ and (c) in vapor state (Ref. 18) in O. D., respectively. (Value of K in Eq. (1) is -0.431.)

doubly excited configurations to the transition energy, although some authors[6-8] calculated the structures of the bases including singly excited configurations alone, predicted the lowest energy transition with small oscillator strength.

In our previous report,[4] the (6—8) transition of adenine showed larger value of transition energy than the (6—7) transition, and its oscillator strength showed almost the same order with the (6—7) transition. On the basis of this, it was difficult to assign the shoulder band of adenine around 268 mμ to π–π^* transition. Recently, Tanaka and Nagakura,[7] on the basis of their experiments and theoretical considerations, have clearly shown that the shoulder band was π–π^* transition. Appearance of the lowest (6—8) transition with very small value of oscillator strength in our CI calculation of adenine would also be explained in terms of the appearance of shoulder band.

The calculated excitation energies of the lowest transition for thymine and uracil were larger than the observed ones. However, if we compared the calculated values with that obtained from vapor spectra of uracil,[18] the agreement became better. Although the vapor spectra of thymine have not yet been reported, the same may be true of this compound.

The calculated values of the lowest transitions for guanine and cytosine were too small to compare them with the observed ones. Especially agreement was not good for cytosine. But in these cases, if we took the vapor spectra of cytosine and guanine into

TABLE 4. TRIPLET TRANSITION ENERGIES (IN UNIT OF eV) IN BASES OF NUCLEIC ACIDS CALCULATED WITH NUMBER OF MIXED CONFIGURATIONS AND TWO K VALUES

		$K=-0.431$				$K=-0.490$	
	Cal. 1	Cal. 2	Cal. 3	Cal. 4	Cal. 5	Cal. 1′	Cal. 5′
A	2.572(6— 7)	2.567(6— 7)	2.640(6— 7)	2.570(6— 7)	2.646(6— 7)	2.971(6— 7)	3.083(6— 7)
	3.403(6— 8)	3.319(6— 8)	3.382(6— 8)	3.486(6— 8)	3.560(6— 8)	3.889(6— 8)	4.027(6— 8)
	3.586(6— 9)	3.593(6— 9)	3.614(6— 9)	3.657(6— 9)	3.698(6— 9)	4.093(6— 9)	4.200(6— 9)
G	2.563(7— 9)	2.453(7— 9)	2.560(7— 9)	2.552(7— 9)	2.598(7— 9)	2.966(7— 8)	2.953(7— 9)
	2.586(7— 8)	2.555(7— 8)	2.675(7— 8)	2.671(7— 8)	2.748(7— 8)	2.975(7— 9)	3.227(7— 8)
	3.181(7—10)	3.214(7—10)	3.272(7—10)	3.115(7—10)	3.163(7—10)	3.683(7—10)	3.651(7—10)
T	2.155(6— 7)	2.052(6— 7)	2.277(6— 7)	2.109(6— 7)	2.160(6— 7)	2.546(6— 7)	2.554(6— 7)
	4.419(6— 8)	4.185(6— 8)	4.173(5— 8)	3.553(6— 8)	3.585(6— 8)	4.760(6— 8)	4.079(6— 8)
	4.471(5— 8)	5.039(5— 7)	4.381(6— 8)	4.310(5— 8)	4.262(5— 8)	4.985(5— 8)	4.809(5— 8)
C	2.556(5— 6)	2.409(5— 6)	2.252(5— 6)	2.352(5— 6)	2.418(5— 6)	2.940(5— 6)	2.833(5— 6)
	3.688(4— 6)	3.251(5— 7)	3.356(5— 7)	3.391(5— 7)	3.500(5— 7)	4.166(4— 6)	3.958(5— 7)
	3.769(5— 7)	3.600(4— 6)	3.705(4— 6)	3.704(4— 6)	3.774(4— 6)	4.180(5— 7)	4.263(4— 6)
U	2.224(5— 6)	2.121(5— 6)	2.224(5— 6)	2.251(5— 6)	2.324(5— 6)	2.650(5— 6)	2.734(5— 6)
	4.273(4— 7)	3.706(5— 7)	3.906(4— 7)	3.441(5— 7)	3.546(4— 7)	4.830(4— 7)	4.070(5— 7)
	4.501(5— 7)	4.853(4— 6)	3.974(5— 7)	4.160(4— 7)	4.331(4— 7)	4.859(5— 7)	4.893(4— 7)

account, the circumstances were improved.

Expectedly, the magnitude of the calculated oscillator strengths for all bases were decreased with increasing number of the mixed configurations. However, this tendency was not seen when the number of configuration was increased from twenty to thirty (Table 2). The effect of CI calculation with doubly excited configurations was especially remarkable (calculation 3).

In the discussions stated above, K in Eq. (1) was equal to -0.431. If K was equal to -0.490, the coincidence of the calculated values with the observed ones was satisfactory: thus, the agreement of the calculated transition energies with the experimental ones was better than the above case (*cf.* Tables 2 and 3). This result was fairly consistent with the conclusion of Anno and Sado[13] who assigned -2.7217 eV for β_{cc} in benzene in the CI calculation including doubly excited configurations.

Triplet Excitation Energy. As shown in Table 4, the change in triplet transition energies against the numbers of mixed configurations was similar to that in singlet transition energies. The phosphorescence spectra of DNA or bases of nucleic acids have already been measured,[21-26] but phosphorescence spectra of DNA were not yet interpreted. Lamola

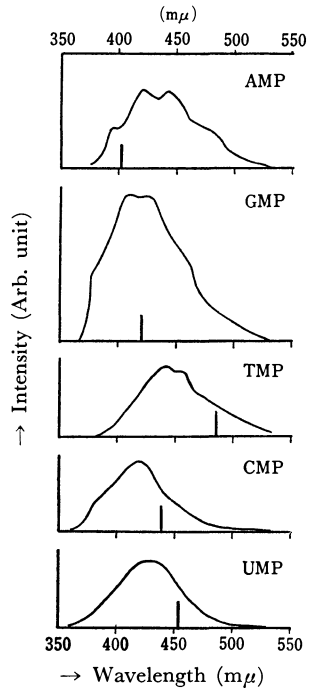

Fig. 2. The calculated triplet transition energies in bases of nucleic acids in comparison with the observed phosphorescence spectra. (Ref. 25) (K in Eq. (1) is -0.490)

et al.[26] have concluded that the triplet state in DNA was formed in the thymine residue, while Imakubo *et al.*[25] assumed that DNA phosphorescence spectra were not due to one base alone, but more than two bases. Both reports agreed with each other in that thymine had the lowest triplet energy among the five others. In agreement with this, our calculation

21) R. Bersohn and I. Isenberg, *J. Chem. Phys.*, **40**, 3175 (1964).
22) R. O. Rahn, J. W. Longworth, J. Eisinger and R. G. Shulman, *Proc. Nat. Acad. Sci.*, **51**, 1299 (1964).
23) R. O. Rahn, R. G. Shulman and J. W. Longworth, *ibid.*, **53**, 893 (1965).
24) C. Hélène, P. Douzou and A. M. Michelson, *ibid.*, **55**, 376 (1966).
25) K. Imakubo, T. Higashimura and T. Sidei, *J. Phys. Soc. Japan*, **22**, 339 (1967).
26) A. A. Lamola, M. Guéron, T. Yamane, J. Eisinger and R. G. Shulman, *J. Chem. Phys.*, **47**, 2210 (1967).

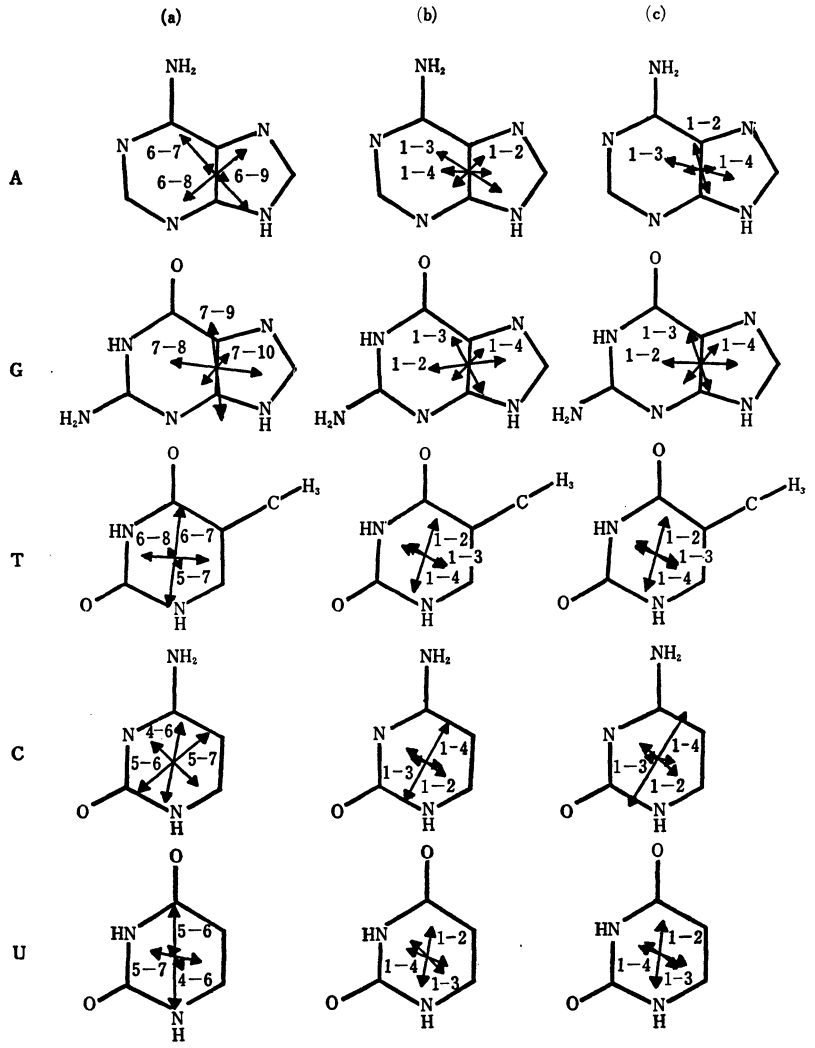

Fig. 3. Predicted direction of polarization of the transitions in bases of nucleic acids.
(a): SCF MO method, (b): SCF CI method including thirty configurations ($K=-0.431$),
(c): SCF CI method including thirty configurations ($K=-0.490$).

predicted the lowest triplet energy of thymine among five bases as seen in Table 4. (Fig. 2 and Table 4). Berthod *et al.*[3] predicted that the triplet energy of uracil whose structure is akin to thymine was the smallest among adenine, guanine, cytosine and uracil.

Direction of Transition Moment. The direction of transition moment of bases was not known. Thus, on the basis of their measurement of polarized absorption spectra of single crystal of 9-methyladenine, Stewart and Davidson,[27] have concluded that the intense band at 275 mμ which corresponded to the main band at 260 mμ of adenine in solution was polarized parallel to short-axis. This conclusion was not harmony with Mason's proposition that it was polarized parallel to long-axis,[28] although Mason has derived his conclusion from indirect measurement.

Therefore, it may be worthy to study the polarization of transition moment by means of MO calculation. As shown in Fig. 3, (a), in the SCF calculation without CI calculation, (6—7) and (6—8) transitions in adenine were neither polarized parallel to long-axis nor short-axis but parallel to the middle of both directions. But the effect of CI calculation on the direction of polarization and the oscillator strength was not small, especially on those of (6—7) and (6—8) transitions in adenine. Therefore, the SCF calculation without CI calculation was not fitted for discussing the direction of transition moment. A slight change in the direction of (6—7)

27) R. F. Stewart and N. Davidson, *ibid.*, **39**, 255 (1963).

28) S. F. Mason, *J. Chem. Soc.*, **1954**, 2071.

TABLE 5. TOTAL π-ELECTRON DENSITY IN BASES OF NUCLEIC ACIDS IN THE GROUND STATE

		1	2	3	4	5	6	7	8	9	10	11
Adenine	Cal. 1	1.352	0.790	1.352	0.916	1.070	0.797	1.326	0.900	1.672	1.825	
	Cal. 2	1.352	0.790	1.352	0.916	1.070	0.797	1.326	0.900	1.672	1.825	
	Cal. 3	1.353	0.791	1.350	0.915	1.063	0.800	1.327	0.903	1.674	1.823	
	Cal. 4	1.349	0.795	1.348	0.917	1.063	0.801	1.326	0.905	1.673	1.822	
	Cal. 5	1.349	0.795	1.348	0.918	1.065	0.802	1.324	0.904	1.673	1.822	
		1	2	3	4	5	6	7	8	9	10	11
Guanine	Cal. 1	1.722	0.800	1.440	0.963	1.070	0.771	1.290	0.934	1.669	1.512	1.830
	Cal. 2	1.722	0.800	1.440	0.963	1.070	0.771	1.290	0.934	1.669	1.512	1.830
	Cal. 3	1.723	0.802	1.437	0.962	1.063	0.777	1.293	0.933	1.670	1.509	1.830
	Cal. 4	1.723	0.804	1.436	0.963	1.066	0.779	1.290	0.933	1.669	1.507	1.830
	Cal. 5	1.723	0.804	1.436	0.964	1.066	0.778	1.290	0.935	1.669	1.506	1.829
		1	2	3	4	5	6	7	8	9	10	
Thymine	Cal. 1	1.739	0.757	1.737	0.945	1.069	0.753	1.520	1.478	0.995	1.006	
	Cal. 2	1.739	0.757	1.737	0.945	1.069	0.753	1.520	1.478	0.995	1.006	
	Cal. 3	1.741	0.759	1.732	0.958	1.061	0.762	1.516	1.475	0.994	1.002	
	Cal. 4	1.739	0.764	1.733	0.957	1.063	0.763	1.514	1.472	0.993	1.003	
	Cal. 5	1.738	0.764	1.733	0.957	1.064	0.762	1.514	1.472	0.994	1.003	
		1	2	3	4	5	6	7	8			
Cytosine	Cal. 1	1.394	0.748	1.706	0.891	1.130	0.773	1.540	1.817			
	Cal. 2	1.394	0.748	1.706	0.891	1.130	0.773	1.540	1.817			
	Cal. 3	1.390	0.751	1.705	0.894	1.132	0.777	1.533	1.818			
	Cal. 4	1.390	0.754	1.705	0.898	1.128	0.780	1.533	1.813			
	Cal. 5	1.390	0.754	1.704	0.897	1.129	0.780	1.533	1.813			
		1	2	3	4	5	6	7	8			
Uracil	Cal. 1	1.738	0.756	1.738	0.932	1.083	0.753	1.521	1.478			
	Cal. 2	1.738	0.756	1.738	0.932	1.083	0.753	1.521	1.478			
	Cal. 3	1.741	0.758	1.732	0.947	1.073	0.763	1.516	1.470			
	Cal. 4	1.738	0.764	1.734	0.945	1.076	0.764	1.512	1.468			
	Cal. 5	1.737	0.764	1.733	0.944	1.076	0.763	1.513	1.469			

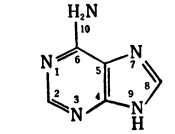
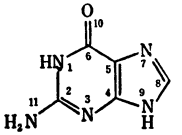
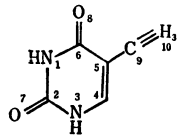
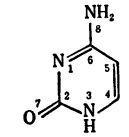
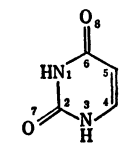

transition in adenine parallel to long-axis was brought about by the CI calculation (Fig. 3, (b)). This tendency was more remarkable if $-0.490(=K)$ was used (Fig. 3, (c)). As was discussed before, (1—3) transition in adenine was assigned to the main band at 260 mμ. This transition is rather long-axis polarized in contrast with the experimental result of Stewart and Davidson. This direction of the calculated lowest transition in adenine ((1—2) transition in Fig. 3, (b) or (1—2) transition in Fig. 3, (c)) which was assigned for the shoulder band around 268 mμ, could be determined to be polarized parallel to neither long-axis nor short-axis. However, we dare to think that it was polarized parallel to short-axis, as seen in Fig. 3, (c). But this lowest transition was difficult to be assigned to the observed short-axis polarized transition because of its small oscillator strength. As seen in Fig. 3 (b) and (c), the direction of this lowest transition was greatly influenced by the change of β_{cc}.

Stewart and Davidson[27] found that for 1-methylthymine, the first absorption band ($\lambda_{max}=275$ mμ) was polarized parallel to the N_1–C_4 axis, and the second band ($\lambda_{max}=230$ mμ) was polarized nearly perpendicular to the first. Upon comparison of the calculated electronic structures of uracil and thymine, it was clear that the effect of the substitution of methyl group for hydrogen was slight. Hence, the comparison of the calculated result for thymine with experimental one for 1-methylthymine was of interest. As shown in Fig. 3, the lowest transition was polarized parallel to the N_1–C_4 axis, and the second and third transitions were polarized nearly perpendicular to the first in agreement with the experiment. Since no available experimental data has been given for the bases except adenine and thymine, so far as the calculated results are shown in Fig. 3. The calculated directions of polarizations for these compounds were slightly changed by CI calculation.

Total π-Electron Density. As shown in Table 5, the effect of CI calculation on the total π-electron density was negligibly small. However, the CI calculation affected the SCF π-electron density in such a way that the carbon atom became less polar, and the electron density approached to the value of 1.0. It is well known that SCF method always overestimates the polar resonance structure of the molecule, and consequently, the effect of CI calculation seems to decrease the polarity of the molecule.

This investigation was partly supported by a grant of the Japanese Ministry of Education, and the calculations were performed on an IBM 7090 computer at the Japan IBM Co., with the permission of the UNICON Committee.

BULLETIN OF THE CHEMICAL SOCIETY OF JAPAN VOL. 41 2026—2029 (1968)

Infrared Spectra of the Addition Compounds of Trimethylamine Oxide with Zinc, Cadmium and Mercuric Halides in the Range 1500—250 cm^{-1}

Masao KIMURA,*1 Yoko KURODA and Ikutoshi SHIBUYA*1

Department of Chemistry, Faculty of Science, Nagoya University, Nagoya

(Received March 18, 1968)

Infrared spectra were taken in the region 4000—250 cm^{-1} for trimethylamine oxide complexes of the type ZnX_2L_2 and Cd(or Hg)X_2L(L=$(CH_3)_3NO$ and X=Cl, Br or I). Two new bands at about 550 and 400 cm^{-1} were observed for all complexes. The zinc complexes gave rise to more bands at about 955 and 270 cm^{-1}. Except for these bands, no appreciable change was observed in the vibrational frequencies of trimethylamine oxide upon coordination. These results suggest that the complexes form a tetrahedral arrangement about a metal atom with weak coordinate bonds, and that the crystals of the zinc complexes consist of monomers and those of the cadmium and the mercury complexes of halogen bridged dimeric molecules $[MX_2L]_2$.

In previous infrared and Raman studies[1] of trimethylamine oxide dihydrate, assignments of vibrational frequencies were based upon the polarization properties of the Raman lines and normal coordinate treatment. According to the results, the N–O bond of trimethylamine oxide in the solid state absorbs at 936 cm^{-1}. This value is in the same frequency region as for the N–O bonds of unconjugated oximes. The N–O stretching force constant obtained for trimethylamine oxide, 3.580 mdyn/Å,

*1 Present address: Department of Chemistry, Faculty of Science, Hokkaido University, Sapporo.

*2 Present address: Hitachi Chemical Co., Ltd., Hitachi.

1) Y. Kuroda and M. Kimura, *Spectrochim. Acta*, **22**, 47 (1966).

was also very close to values ranging from 3.8 to 4.0 mdyn/Å for unconjugated oximes.[2,3] From these results, the N–O bond of trimethylamine oxide was concluded to have a pure single bond character in accordance with conclusions drawn from the results of X-Ray structure analysis[4] and electric dipole moment measurement.[5]

Recently, metal complexes with tertiary phosphine oxides[6] and tertiary arsine oxides[7] were prepared and studied by means of electronic spectra, infrared spectra, magnetic measurements and so on. It is known that the oxygen atom of tertiary amine oxide behaves as an electron donor and forms a coordinates to metal atoms.[8-11] Since the possibility of π-bond character is not present in trimethyl amine oxide, these studies were undertaken to compare the coordination of oxygen atoms in trimethyl amine oxide complexes and other types of complexes. However, the bond characters and molecular configurations in these kinds of complexes are not systematically interpreted yet.

In the present infrared study, addition compounds between trimethylamine oxide and the halides of the 2nd *b*-subgroup elements were dealt with, and attention was focused on the effect of coordination on ligand vibrations.

Experimental

Preparation. $ZnBr_2$ *and* ZnI_2 *Addition Compounds.* A solution of 0.01—0.02 mol of $(CH_3)_3NO\cdot 2H_2O$ in about 50 m*l* of ethanol was slowly added to a solution of 0.01 mol zinc halide in about 50 m*l* of ethanol. Needle crystals were formed in from a few hours to a few days. These crystals were collected, washed several times with ethanol and dried over phophorus pentoxide for several days. These complexes are slightly soluble in water, methanol and ethanol at room temperature, but decompose in warm solutions. Found: Zn, 17.4; C, 19.2; H, 4.85; N, 7.07%. Calcd for $ZnBr_2[(CH_3)_3NO]_2$: Zn, 17.41; C, 19.20; H, 4.83; N, 7.46%. Found: Zn, 14.0; C, 15.24; H, 3.91; N, 5.88%. Calcd for $ZnI_2[(CH_3)_3NO]_2$: Zn, 13.93; C, 15.34; H, 3.87; N, 5.97%.

$CdCl_2$, $CdBr_2$ *and* CdI_2 *Addition Compounds.* These compounds were prepared by the same procedure as that used for the zinc complexes. Precipitates were formed immediately from solutions. All complexes are soluble in water, methanol and ethanol. Found: Cd, 42.6; C, 14.22; H, 3.60; N, 5.21%. Calcd for $CdCl_2[(CH_3)_3NO]$: Cd, 43.5; C, 13.94; H, 3.51; N, 5.24%. Found: Cd 33.0%. Calcd for $CdBr_2[(CH_3)_3NO]$: Cd, 32.4%. Found: Cd, 25.1%. Calcd for $CdI_2[(CH_3)_3NO]$: Cd, 25.5%.

$HgCl_2$ *and* $HgBr_2$ *Addition Compounds.* The procedure of preparation was the same as for the zinc and cadmium complexes. White needle crystals were formed in a few minutes after the solutions were mixed. They decompose in water solutions. Found: Hg, 57.1%. Calcd for $HgCl_2[(CH_3)_3NO]$: Hg, 57.9%. Found: Hg, 46.7%. Calcd. for $HgBr_2[(CH_3)_3NO]$: Hg, 46.1%.

Measurement. Infrared spectra were taken using a grating infrared spectrophotometer model DS-402G of the Japan Spectroscopic Co., Ltd. The samples were run as Nujol mulls in the region 4000—250 cm^{-1}, and the regions of Nujol absorptions were examined with hexachlorobutadiene mulls. The 3 μ region was employed for checking the absence of hydrated water molecules in the complexes.

The observed frequencies for the complexes are listed in Table 1 together with those for trimethylamine oxide.[1]

Results and Discussion

All bands due to trimethylamine oxide remain practically unaltered in the spectrum of every complex under investigation. In addition, two new bands appear at about 550 and about 400 cm^{-1}. These additional bands are also observed at approximately the same position irrespective of the type of compounds. The zinc complexes give rise to more absorption bands at about 955 and about 270 cm^{-1}. Rodley *et al.* also dealt with this type of zinc halide complex, but mentioned nothing about these bands.[11] Bands at 946 and 492 cm^{-1} for the complex of cadmium iodide are relatively wide and are probably composite bands corresponding to the doublet bands of the other cadmium complexes.

Vibrations Associated with the Ligand. The cadmium and mercury complexes have two bands near 950 cm^{-1} corresponding to the degenerate C–N stretching vibration, $\nu(C_3N)$, and the N–O stretching vibration, ν(N–O), of the ligand, while the zinc complexes have three bands near 950 cm^{-1}. Kida *et al.*[12a] also observed two N–O stretching bands, ν(N–O), at about 1210 and about 1205 cm^{-1}, only for zinc and copper complexes of pyridine *N*-oxide, the former of which, $Zn(PyO)_2Cl_2$, is analogous to $ZnCl_2[(CH_3)_3NO]_2$ in its formula.

2) H. J. Bernstein, *J. Chem. Phys.*, **6**, 718 (1938).
3) K. Torii and T. Shimanouchi, Preprints for the 17th Annual Meeting of the Chemical Society of Japan (Tokyo, 1964).
4) A. Caron, G. J. Palenik, E. Goldish and J. Donohue, *Acta Cryst.*, **17**, 102 (1964).
5) E. P. Linton, *J. Am. Chem. Soc.*, **62**, 1945 (1940).
6) a) D. M. L. Goodgame, M. Goodgame and F. A. Cotton, *Inorg. Chem.*, **1**, 239 (1962). b) F. A. Cotton, R. Barnes and E. Bannister, *J. Chem. Soc.*, **1960**, 2199.
7) See G. A. Rodley, D. M. L. Goodgame and F. A. Cotton, *J. Chem. Soc.*, **1965**, 1499.
8) K. Issleib and A. Kreibich, *Z. anorg. u. allgem. Chem.*, **313**, 338 (1961).
9) S. Kida, This Bulletin, **36**, 712 (1963).
10) R. S. Drago, J. T. Donoghue and D. W. Herlocker, *Inorg. Chem.*, **4**, 836 (1965).
11) Private communication from G. A. Rodley; S. H. Hunter, V. M. Langford, G. A. Rodley and C. J. Wilkins, *J. Chem. Soc.*, to be published. Also S. H. Hunter, G. A. Rodley and C. J. Wilkins, Proceedings for the 10th International conference on Coordination Chemistry, Tokyo (1967), p. 334.
12) a) S. Kida, J. V. Quagliano, J. A. Walmsley and S. Y. Tyree, *Spectrochim. Acta*, **19**, 189 (1963). b) Y. Kakiuti, S. Kida and J. V. Quagliano., *ibid.*, **19**, 201 (1963).

TABLE 1. OBSERVED FREQUENCIES FOR THE COMPLEXES OF TRIMETHYLAMINE OXIDE WITH THE METAL HALIDES (in cm^{-1})

L*	$ZnBr_2 \cdot L_2$	$ZnI_2 \cdot L_2$	$CdCl_2 \cdot L$	$CdBr_2 \cdot L$	$CdI_2 \cdot L$	$HgCl_2 \cdot L$	$HgBr_2 \cdot L$
1482	1482 s	1480 s	1481 s	1480 s	1476 s	1476 s	1473 s
1472	1473 s	1474 s	1470 s	1465 s	~1460 sh	1456 s	1451 s
1457	1459 s	1456 s	1462 s	1459 s	1454 s	1427 w	1434 w
1442	1435 m	1435 m	1455 s	1455 s	1393 m	1403 m	1400 s
1432	1428 m	1428 m	1425 w	1425 m			
1398	1390 s	1392 s	1413 m	1412 m			
			1397 w	1386 w			
1240	1233 s	1229 s	1244 s	1241 s	1232 s	1230 m	1226 m
1124	1116 m	1115 m	1132 w	1128 w	1121 w	1124 m	1115 m
946	955 s	953 sh	956 s	953 s	946 vs	942 s	942 s
	946 s	945 s					
936	940 s	942 sh	947 s	942 s		935 s	926 s
756	766 s	764 s	762 s	757 s	760 s	757 m	752 m
	555 s	550 s	542 s	537 s	528 m	542 s	540 s
497	489 m	487 m	500 m	495 sh	492 m	485 m	486 m
469	476 s	475 s	483 s	481 s		470 s	473 s
380	402 m	395 m	403 m	402 m	400 m	395 m	395 m
	378 m	374 m	388 m	388 m	380 m	382 m	382 m
	276 m, b	274 m					

* L≡$(CH_3)_3NO$

Generally, Zn(II) has a very strong tendency to appear in tetrahedral environments as indicated by the following examples: $ZnCl_2(NH_3)_2$ and $ZnBr_2(NH_3)_2$ crystals,[13] and $ZnCl_2$[thiourea]$_2$.[14] The zinc atoms of the addition compounds studied here probably follow this general tendency of coordination. If the two N-O bonds are arranged in close proximity to each other so as to have no center of symmetry, the ν(N-O) bands are possibly observed as two bands, even though the frequency separation between them might be small. Unlike Zn complexes, Cd and Hg complexes in the crystalline state form either a tetrahedral or octahedral arrangement about a metal atom according to the constitution of the complexes. The crystal of the type LCd(or Hg)X_2, such as [trimethyl-phosphine]$CdBr_2$ consists of halogen bridged dimeric molecules expressed by $L_2(CdX_2)_2$.[15] The single dimeric molecules, then, have a center of symmetry and approximately tetrahedral arrangement about the metal atoms. The type of Cd and Hg complexes treated in the present study is the same as the type compounds mentioned above. Therefore, it is quite probable that the crystals of the complexes in question are also built from dimeric molecules with a center of symmetry. Then, only one ν(N-O) should be observed. The metal-halogen stretching frequencies ν(M-X) of some complex halides of Zn, Cd and Hg were discussed by Coates and Ridley, and were successfully interpreted from this view point of structures as described above.[15]

It is reasonable to consider that the band near 400 cm^{-1} was caused by splittin of the de enerate vibration of the ligand upon coordination. Similarly, it is probable that the degenerate C-N stretching vibration of the ligand near 950 cm^{-1} splits appreciably and gives rise to the additional bands for zinc complexes. Furthermore, a band near 550 cm^{-1} is due probably to the splitting of the degenerate N-O rocking vibration of the ligand at 497 cm^{-1}.

No appreciable change in observed frequencies for trimethylamine *N*-oxide could be seen upon coordination to Zn, Cd and Hg atoms, except for some splittings of the degenerate vibrations. Similar phenomena were observed for $M[(CH_3)_3NO]_4^{2-}$ by Kida[9] and Drago *et al.*,[10] and for $Zn[(CH_3)_3NO]_2X_2$ by Rodley *et al.*[11] This is quite interesting upon comparison with changes in the vibrational frequencies of pyridine *N*-oxide or tertiary phosphine oxides upon coordination. The ν(N-O) of pyridine *N*-oxide[12] are lowered by about 45 cm^{-1} and the ν(P-O) of tertiary phosphine oxides[6b] by about 50 cm^{-1} upon coordination. These frequency shifts can be explained by a decrease in the double bond character of the N-O or P-O bonds upon coordination. Such an origin of frequency lowering can hardly be found for trimethylamine oxide. Therefore, the coordination of trimethylamine oxide to a metal atom will result in no appreciable change in the N-O bond nature.

Vibrations Associated with Metal-oxygen. The bands at about 270 cm^{-1} proper to the zinc

13) C. H. MacGillavry and J. H. Bijvoet, *Z. Krist.* **A94**, 231 (1936).

14) N. R. Kunchur and M. R. Truter, *J. Chem. Soc.*, **1958**, 3478.

15) G. E. Coates and D. Ridley, *ibid.*, **1964**, 166.

complexes appear to be associated with Zn–O, not with halogen atoms, because both the $ZnBr_2$ and the ZnI_2 complexes have bands at the same frequency and generally the zinc-bromine stretching frequencies of $ZnBr_4^{2-}$ or $ZnBr_2$ complexes are present in a lower frequency region.[15,16]

The band near 550 cm^{-1} appeared in a clear region of the ligand bands. On closer examination, these bands show slight but regular variations in positions according to the species of complexes. Rodley *et al.* proposed the assignment[11] to a metal-oxygen stretching vibration, ν(M–O). Although this possibility of assignment cannot be ruled out for the present case, a value of 550 cm^{-1} for ν(M–O) seems too high. Therefore, we adopt the assignment to the ligand vibration as mentioned in the foregoing section.

For a definite discussion of the origin and nature of the bands near 550 cm^{-1} and near 270 cm^{-1}, it is desirable to obtain other lower frequency bands below 250 cm^{-1}. Toward this end, far infrared studies are now in progress.

16) R. J. H. Clark and T. M. Dunn, *ibid.*, **1963**, 1198.

BULLETIN OF THE CHEMICAL SOCIETY OF JAPAN VOL. 41 2029—2032 (1968)

A Theoretical Consideration on Chemical Reactions in the Kjeldahl Digestion

Yazaemon MORITA

Government Chemical Industrial Research Institute, Tokyo, Shibuya-ku, Tokyo

(Received September 12, 1967)

The decomposition of organic nitrogen compounds by Kjeldahl digestion was discussed and some experiments were carried out. The relationship between the amount of sulfuric acid consumed and the amount of ammonia produced at various stages including final ones of the decomposition was examined. As a result, chemical reaction of decomposition was evaluated, and the temperature at the initial stage reveals one of the important factors which determine the ratio of oxidative action of hot concentrated sulfuric acid to reductive action of sulfur dioxide produced in the reaction system. It is concluded that, if the temperature of initial stage is adjusted properly, it is possible to decompose mostly nitro and azo compounds into ammonia by sulfuric acid containing potassium sulfate without reductive pretreatment which has previously been believed to be indispensable.

Since publication of the Kjeldahl method for nitrogen analysis,[1] a number of studies have been carried out on its applications and improvements, and this method, together with the Dumas', is extensively used in various fields for the determination of nitrogen. As reported previously,[2] however, many problems must be solved before this method is applicable to all types of nitrogen compounds. This statement is supported, for example, by a series of many years' studies by Bradstreet.[3]

As is known, the most important and fundamental of the Kjeldhal method is the digestion of nitrogen compounds with hot concentrated sulfuric acid, and a detailed study of this step is necessary for its application and its improvement. The decomposition reaction is extremely complicated and only very few studies concerning kinetics by Bredig *et al.*[4] and Schwab *et al.*[5] have been made. These studies gave some light on the rate of decomposition, but not on the applicability of this method.

This paper deals, experimentally as well as theoretically, with the thermal decomposition in concentrated sulfuric acid and the applicability of the Kjeldahl method.

Theoretical and Experimental

Thermal decomposition of organic compounds without nitrogen in concentrated sulfuric acid can be expressed by Eq. (1) as known previously;

1) J. Kjeldahl, Z. *anal. Chem.*, **22**, 336 (1883).
2) Y. Morita and Y. Kogure, *Nippon Kagaku Zasshi* (*J. Chem. Soc. Japan, Pure Chem. Sect.*), **88**, 1179 (1967).
3) R. B. Bradstreet, *Ind. Eng. Chem., Anal. Ed.*, **10**, 696 (1938); *ibid.*, **12**, 657 (1940); *Chem. Revs.*, **27**, 331 (1940); *Anal. Chem.*, **21**, 1012 (1949); *ibid.*, **26**, 185 (1954); *ibid.*, **26**, 235 (1954); *ibid.*, **29**, 944 (1959); *ibid.*, **32**, 114 (1960).
4) C. Bredig and J. W. Brown, Z. *physik. Chem.*, **46**, 502 (1903).
5) G. M. Schwab and E. Schwab-Agallidis, *J. Am. Chem. Soc.*, **73**, 803 (1951); *Angew. Chem.*, **65**, 418 (1953); *Mh. Chem.*, **86**, 341 (1955); *ibid.*, **88**, 288 (1957).

$$C_nH_mO_l + (2n+m/2-l)\cdot H_2SO_4 \rightarrow n\cdot CO_2 + (2n+m/2-l)\cdot SO_2 + (2n+m-l)\cdot H_2O \quad (1)$$

where n, m, and l denote the numbers of atoms C, H, and O, respectively.

On the other hand, oxidative decomposition of various organic nitrogen compounds in a chromic acid-sulfuric acid mixture can be expressed by Eq. (2). This is derived from Eq. (1) by taking into account the nitrogen contained and the type of linkage of nitrogen shown in the studies of Jurecek *et al.*[6] as well as the present author[7]:

$$C_nH_mO_lN_{d=a+b+c} + (2n+m/2-l-1.5a+2.5b)\cdot O \rightarrow n\cdot CO_2 + (m/2-3a-b)\cdot H_2O + a\cdot NH_3 + b\cdot HNO_3 + c/2\cdot N_2 \quad (2)$$

where n, m, l, and $d(=a+b+c)$ denote the numbers of atoms C, H, O, and N, respectively, and a, b, and c denote respectively the numbers of nitrogen atoms present in the functional groups are shown in Table 1.

In such oxidative decomposition, the decomposition products are ammonia, nitric acid, and nitrogen molecule or a mixture whose proportion depends upon the nitrogen functional groups, and the consumption of oxigen varies with these groups.[6-7]

It is desirable in the Kjeldhal digestion to convert all the nitrogen atoms into ammonia and not to react as shown in Eq. (2).

But the actual decomposition reaction is mainly oxidation accompanied by reduction, dehydration, hydrolysis, substitution, and other complicated reaction, and can not be simply expressed by Eq. (2).

For example, the nitro group of 3-nitrosalicylic acid is quantitatively converted into nitric acid when oxidized with a chromic acid-sulfuric acid mixture,[7] but yields a calculated amount of ammonia when decomposed with hot concentrated sulfuric acid.[2] Thus, the Kjeldahl digestion does not proceed in accordance with Eq. (2).

Now, if the Kjeldahl digestion is the following oxidation-reduction reaction,

$$C_n + 2n\cdot H_2SO_4 \rightarrow n\cdot CO_2 + 2n\cdot SO_2 + 2n\cdot H_2O$$

$$H_m + m/2\cdot H_2SO_4 \rightarrow m/2\cdot SO_2 + m\cdot H_2O$$

$$O_l + l\cdot SO_2 + l\cdot H_2O \rightarrow l\cdot H_2SO_4$$

$$N_{d=a+b+c} + 1.5d\cdot SO_2 + 3d\cdot H_2O \rightarrow d\cdot H_2SO_4 + d/2\cdot (NH_4)_2SO_4$$

the sum of these reactions can be written as follows.

$$C_nH_mO_lN_d + (2n+m/2-l-d)H_2SO_4 \rightarrow n\cdot CO_2 + (2n+m/2-l-1.5d)\cdot SO_2 + (2n+m-l-3d)\cdot H_2O + d/2\cdot (NH_4)_2SO_4 \quad (3)$$

If the decomposition of nitrogen compounds proceeds ideally according to Eq. (3), Eq. (4) can be obtained.

$$\frac{x}{w} = \frac{(2n+m/2-l-d)\cdot H_2SO_4}{C_nH_mO_lN_d} (=K_1) \quad (4)$$

x=amount of sulfuric acid consumed.

w=weight of sample.

K_1=a proportional constant characteristic of a given sample.

As the Kjeldahl method does not fit the determination of nitrogen in all nitrogen compounds, it is obvious that Eqs. (3) and (4) have not universal validity.

In order to study this subject more closely, Eq. (4) must be replaced by Eq. (5) which is applicable to most cases.

$$\frac{x}{w} = K_1\alpha = K_1' \quad (5)$$

α=a factor which depends upon the mode of decomposition.

The value of K_1' is experimentally given and α can be calculated from Eq. (4).

When $\alpha=1$, Eq. (5) becomes identical with Eq. (4), but when $\alpha>1$, it does not so and in this case

TABLE 1. VARIOUS FUNCTIONAL GROUPS CONTAINING NITROGEN INVOLVED IN OXIDATIVE DECOMPOSITION PRODUCTS BY THE CHROMIC ACID-SULFURIC ACID MIXTURE

Functional group		Decomposition product	
$-CONH_2$	(Carbamoyl group)	a	NH_3
-OCN	(Cyanato group)		
-NCO	(Isocyanato group)		
-SCN	(Thiocyanato group)		
-NCS	(Isothiocyanato group)		
-CN	(Cyano group)		
-NC	(Isocyano group)		
$-NH_2$	(Amino group)		
=NH	(Imino group)		
=N-	(Nitrogen heteroatom without N-N linkage)		
$-NO_2$	(Nitro group)	b	NHO_3
-NOOH	(Isonitro group)		
-NHOH	(Hydroxyamino group)		
=NOH	(Hydroxyimino group)		
$-NHNH_2$	(Hydrazino group)	c	N_2
-N=N-	(Azo group)		
=N-N=	(Azino group)		
$-\overset{+}{N}\equiv N$	(Diazonium group)		

6) M. Jureček, *Mikrochim. Acta*, **1962**, 926; *ibid.*, **1962**, 1101; *ibid.*, **1963**, 643; V. Novák, P. Kozák, P. Matousek and M. Jureček, *Collect. Czechoslov. Chem. Commun.*, **28**, 487 (1963); *ibid.*, **28**, 3443 (1963).

7) Y. Morita and Y. Kogure, *Nippon Kagaku Zasshi* (*J. Chem. Soc. Japan, Pure Chem. Sect.*), **86**, 87 (1965); *ibid.*, **86**, 508 (1965); *ibid.*, **86**, 601 (1965).

nitric acid or nitrogen molecule is produced by the decomposition. Some examples are now given below.

Two gramms of concentrated sulfuric acid is put into a micro Kjeldahl flask containing sample, and heated by 100 W electric heater with a variable resistor. When the solution in the flask becomes light brown, 0.5 g of potassium sulfate is added and the mixture is heated until it turns clear and colorless. In this way the decomposition is completed.

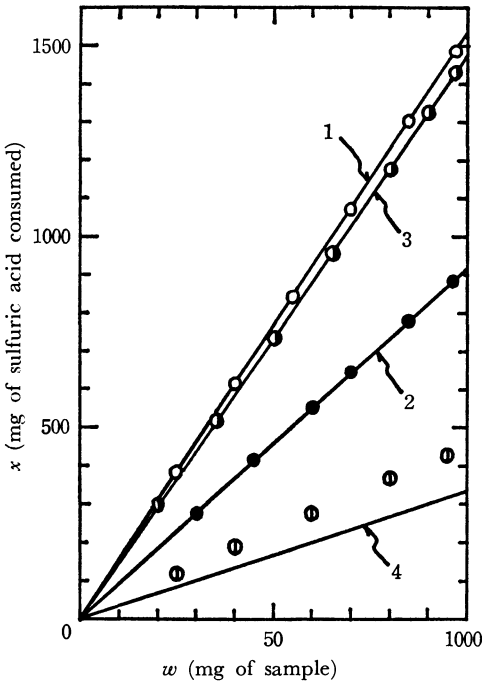

Fig. 1. Amount of sulfuric acid consumed *vs.* weight of sample in Kjeldahl digestion.
○, ●, ◑, ⓘ: Observed ——: Calculated
○, 1: Aniline ●, 2: Nitrobenzene
◑, 3: Azobenzene ⓘ, 4: 2,4-DNPH

The mixture is then diluted with water, boiled to drive off SO_2 and the remaining sulfuric acid is titrated. The blank test is made and the actual amount of sulfuric acid consumed is obtained by subtracting the blank value from the titrated one. In Fig. 1, mg of sulfuric acid consumed (x) is plotted against mg of sample (w).

As shown in Fig. 1, Eq. (4) is not applicable to 2,4-dinitro-phenylhydrazine (2,4-DNPH) alone. Consequently, the decomposition of this compound can not be expressed by Eq. (3), but corresponds to

Table 2. Calculated values of α in decomposition of 2,4-DNPH and observed ones

Mode of reaction	I	II	III	IV	Observed
α	1.00	1.29	2.00	2.29	1.29

the case where $\alpha > 1$ in Eq. (5). Four possible decomposition reactions of 2,4-DNPH are shown below, and the values of α calculated for each reaction are shown in Table 2.

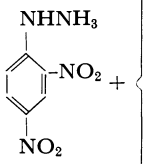

$$+ \begin{cases} 7\cdot H_2SO_4 \rightarrow 6\cdot CO_2 + 5\cdot SO_2 + 2\cdot H_2O + 2(NH_4)_2SO_4 & \text{(I)} \\ 9\cdot H_2SO_4 \rightarrow 6\cdot CO_2 + 8\cdot SO_2 + 8\cdot H_2O + (NH_4)_2SO_4 + N_2 & \text{(II)} \\ 14\cdot H_2SO_4 \rightarrow 6\cdot CO_2 + 13\cdot SO_2 + 12\cdot H_2O + (NH_4)_2SO_4 + 2\cdot HNO_3 & \text{(III)} \\ 16\cdot H_2SO_4 \rightarrow 6\cdot CO_2 + 16\cdot SO_2 + 18\cdot H_2O + 2\cdot HNO + N_2 & \text{(IV)} \end{cases}$$

It appears from Table 2 that in the decomposition of 2,4-DNPH, (II) may occur and this assumption is supported by the measurements of ammonia described below.

In this way, it is possible to interpret the reaction at the completion of the decomposition in terms of the amount of sulfuric acid consumed.

Because of the complex nature of the decomposition reaction, it is necessary to elucidate the steps involved to clarifiy the overall decomposition. For this purpose, the relationship between the amount of sulfuric acid consumed (x_t) and that of ammonia produced (y_t) after $t$hr must be considered.

If the amount of sulfuric acid consumed in Eq. (3) and the amount of ammonia produced are assumed to be proportional at all time, the degree of decomposition is x_t/x which is equal to y_t/y. Therefore, the equation

$$y_t = \frac{y}{x} x_t = K_2 \cdot x_t \qquad (6)$$

must be valid.

Equation (6) shows that the ratio of the amount of sulfuric acid consumed (x) to the amount of ammonia produced (y) at the completion of the decomposition is constant for a given sample, and K_2 can be determined by measuring x_t and y_t at various stages of decomposition. A comparison of these observed values with those calculated ones on the basis of Eq. (3) will give some insight into the mechanism of the reaction. It is clear from this experiments that the decomposition which is obeyed Eq. (6) always includes the chemical reaction shown by Eq. (3). However, Eq. (6) can not be applicable to acid amides and nitriles which yield ammonia on acid hydrolysis.

Next, some example are shown below ; the relationship between observed x_t and y_t at various stages of decomposition of typical organic nitrogen compounds is shown in Fig. 2. Conveniently, if y_t is plotted against x_t/x, $x_t/x=1$ means that the decomposition is completed and the solution becomes colorless and clear, whereas, $x_t/x<1$ means that the mixture is incompletely decomposed and the solution develops varying colors. The degree of decomposition can be controlled by adjusting the time of heating.

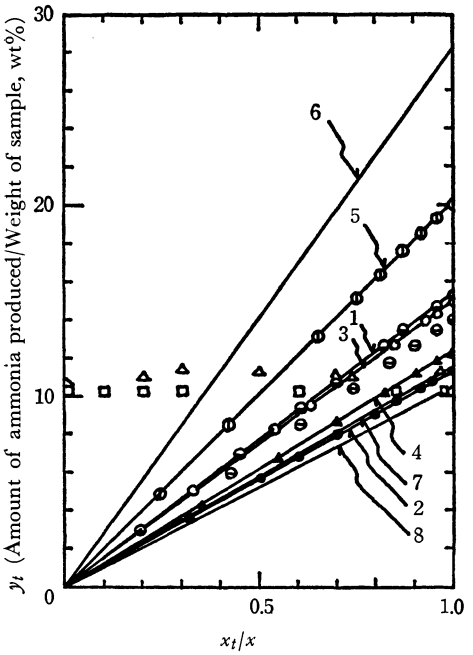

Fig. 2. Amount of ammonia produced *vs.* digestion degree in Kjeldahl digestion.
○, ●, ◒, ▲, ⓘ, ⊖, △, □: Observed
——: Calculated
○, 1: Aniline ●, 2: Nitrobenzene
◒, 3: Azobenzene
▲, 4: Cyclohexanone oxime
ⓘ, 5: 2,4-Dinitrophenylhydrazone of cyclohexanone ⊖, 6: 2,4-DNPH
△, 7: Benzamide □, 8: Anisonitrile

As shown in Fig. 2, aniline, nitrobenzene, cyclohexanone oxime, azobenzene, and 2,4-dinitrophenylhydrazone of cyclohexanone are decomposed in accordance with Eq. (6), and a complete agreement is obtained between observed and calculated values. It may be concluded that Eq. (3) is applicable to the main decomposition reaction of these compounds. It is found that 2,4-DNPH are decomposed according to Eq. (6). However, the reaction (II) mentioned earlier is the main reaction of this compound because that y at $x_t/x=1$ is 50% of the calculated value and the observed value of α in Eq. (5) supports the validity of Eq. (II). Contrarily, anisonitrile and benzamide are not decomposed in accordance with Eq. (6).

All amino compounds unexceptionally converted into ammonia by the oxidative decomposition as shown in Table 1. By the reductive preteatment, nitro and azo compounds are believed to be analyzed quantitatively, but nitrobenzene, azobenzene, and other nitro compounds are found by the author to be analyzed without the above-mentioned treatment as shown in Fig. 2.

This finding indicates that oxidation and reduction may occur side by side in the course of reaction depending upon the condition, and that the compounds containing nitro and azo groups are reduced preferentially.

On the other hand, a concentrated sulfuric acid mainly reacts oxidatively with a reducing functional group such as the hydrazino group. Consequently, when the hydrazino group becomes less reductive by substitution to form hydrazono group like 2,4-dinitrophenylhydrazone of cyclohexanone, the reductive effect of hydrazono group is the same as that of azo group.

The reduction reaction for nitro and azo groups is accompanied by the carbonization of organic samples at the initial stage of the decomposition and takes place slowly as the decomposition proceeds. Therefore, it is desirable to heat the sample initially at a temperatures as low as possible and to suppress excessive oxidation reaction and after appropriate decomposition, to raise the temperature to increase the oxidative action of sulfuric acid.

It may be concluded that nitro and azo compounds can be decomposed quantitatively into ammonia by sulfuric acid containing potassium sulfate similarly as amino compounds, and the reductive pretreatment hitherto made is found to be needless. Furthermore, failures in the past endeavor to decompose these compounds seem mostly to be due to a lack of the study on the heating condition.

BULLETIN OF THE CHEMICAL SOCIETY OF JAPAN VOL. 41 2033—2040 (1968)

Kinetics of Multidentate Ligand Substitution Reaction. III. Substitution Reactions of BT with Cobalt(II) and Nickel(II) Chelates of *N*-(2-Hydroxyethyl)-ethylenediamine-*N*,*N*′,*N*′-triacetic Acid and 2,2′-Ethylenedioxybis[ethyliminodi(acetic acid)]

Mutsuo KODAMA, Chifumi SASAKI and Tomohiko NODA

Department of Chemistry, Ibaraki University, Mito, Ibaraki

(Received October 25, 1967)

BT can displace EDTA-OH and GEDTA from their cobalt(II) and nickel(II) chelate as in the case of the substitution reaction of BT with cobalt(II)-EDTA chelate or nickel(II)-EDTA chelate. In this paper, kinetics of the substitution reactions of BT with cobalt(II)- and nickel(II)-chelates of EDTA-OH and of GEDTA was studied spectrophotometrically. All substitution reactions were found to be first-order in BT and first-order in metal(II)-chelate of EDTA-OH or GEDTA, and to proceed through two simultaneous reaction paths analogous to those proposed for the substitution reaction of BT with cobalt(II)-EDTA chelate. Although EDTA-OH differs from EDTA by the presence of a hydroxyethyl group in place of one acetate group, its metal(II) chelate behaves in a nearly identical manner with EDTA chelate in the substitution reaction and the cleavage of the metal-nitrogen bond of the glycinate group is considered to be the probable rate-determining step. The substitution reactions of BT with GEDTA chelates are considered to be more favored thermodynamically over the reactions of EDTA-OH chelates, but were found to be less favored kinetically. This fact may suggest that the geometrical structure of metal(II)-GEDTA plays an important role in determining the rate of the substitution reaction of GEDTA.

In the previous papers,[1,2] kinetics of the substitution reactions of Eriochrom Black T (BT) with cobalt(II) and nickel(II) chelates of ethylenediaminetetraacetic acid (EDTA) and of nitrilotriacetic acid (NTA) were studied. Reactions were first-order in BT and first-order in metal(II) chelate of 1 to 1 composition.

BT can also displace *N*-(2-hydroxyethyl)-ethylenediamine-*N*,*N*′,*N*′-triacetate (EDTA-OH) and 2,2′-ethylenedioxybis[ethyliminodi(acetate)] (GEDTA) from their chelates of cobalt(II) and nickel(II). In this paper, the kinetics of the substitution reactions of BT with EDTA-OH and GEDTA chelates of these metal ions were dealt with spectrophotometrically. From comparison of the rate constants of the substitution reactions of EDTA-OH chelates of cobalt(II) and nickel(II) with those of EDTA chelates, the reaction mechanism was assigned in detail.

Experimental

Reagents. The preparation and the standardization of solutions of cobalt(II) and nickel(II) perchlorates were described in the previous papers.[1,2] Reagent grade EDTA-OH and GEDTA were recrystallized from water. The concentration of EDTA-OH solution was standardized against the standard copper(II) solution by a volumetric titration with Murexide as indicator.[3] The standard solution of GEDTA was prepared by dissolving a known amount of GEDTA dried for two hours at 115°C into a diluted alkaline solution. The purification of BT was also described in the previous paper.[4] Other reagents were of guranteed reagent grade and used without further purification.

Apparatus and Procedure. The apparatus and the experimental procedures were the same as described previously.[1] In this study, all measurements were conducted in solutions of ionic strength 0.30 ($NaClO_4$), and no buffer reagent was used, because free EDTA-OH and GEDTA can have enough buffer capacity to maintain the pH values of solutions constant at the pH range from 8.00 to 10.50.

Results and Discussion

All exchange reactions were studied in solutions of pH from 8.00 to 10.50 containing large excesses of complexed and uncomplexed EDTA-OH or GEDTA. Therefore, the exchange reactions can be treated as pseudo first-order reactions. All exchange reactions of BT were found to give invariably the linear relations between log $(A_D/(A-A_{MD}))$ and time, t, with the intercept identical to log $(\varepsilon_{BT}/(\varepsilon_{BT}-\varepsilon_{MD}))$, holding the following relation (Fig. 1).

1) M. Kodama, This Bulletin, **40**, 2575 (1967).
2) M. Kodama, C. Sasaki and M. Murata, *ibid.*, **41**, 1333 (1968).
3) The same procedure as was proposed for the EDTA titration of copper was employed.
4) M. Kodama and H. Ebine, This Bulletin, **40**, 1857 (1967).

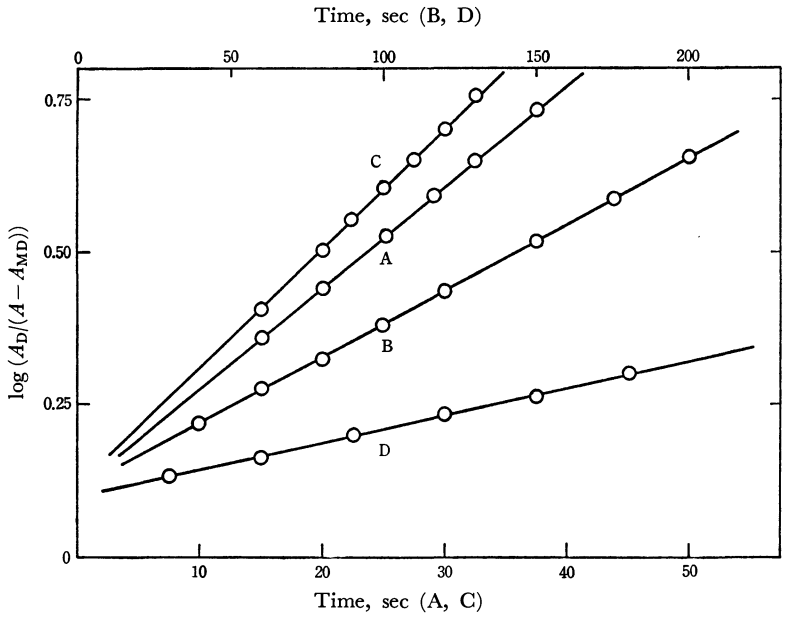

Fig. 1. The plot of log $[A_D/(A-A_{MD})]$ against t.
$\mu=0.30$, $\lambda=630$ mμ

A: Co(II)EDTA-OH system
$[BT]_0=1.50\times10^{-5}$ M, pH=8.23, $[CoZ^-]=1.0$ mM
Concentration of uncomplexed EDTA-OH=10.0 mM

B: Ni(II)-EDTA-OH system
$[BT]_0=3.05\times10^{-5}$ M, pH=10.17, $[NiZ^-]=8.25_5$ mM
Concentration of uncomplexed EDTA-OH=8.0 mM

C: Co(II)-GEDTA system
$[BT]_0=1.00\times10^{-5}$ M, pH=8.80, $[CoZ^{2-}]=0.30$ mM
Concentration of uncomplexed GEDTA=10.0 mM

D: Ni(II)-GEDTA system
$[BT]_0=2.90\times10^{-5}$ M, pH=10.10, $[NiZ^{2-}]=6.60$ mM
Concentration of uncomplexed GEDTA=10.0 mM

$$\log\frac{A_D}{A-A_{MD}}-\log\frac{\varepsilon_{BT}}{\varepsilon_{BT}-\varepsilon_{MD}}=\frac{k^+}{2.303}\cdot t \qquad (1)$$

where simbols, A_D and A, have the same meanings as used in the previous paper[4] and the other notation definitions are as follows. A_{MD}: Absorbance of the solution where all BT ions in the solution is considered to form the complex with nickel(II) or cobalt(II); ε_{BT}: The apparent extinction coefficient of uncomplexed BT at the given pH[2]; ε_{MD}: The true extinction coefficient of metal (II)-BT chelate.

As was stated previously,[1,2] when the stability constants of metal(II)-BT chelate are much greater than those of metal(II)-EDTA-OH or GEDTA chelates, and hence, the concentration of uncomplexed BT at equilibrium, $[BT]_e$, can be neglected as compared with the intial concentration of BT, $[BT]_0$, and with the BT concentration, [BT], at time t, in an early stage of the reaction, the left hand side of Eq. (1) must be equal to $\log([BT]_0-[BT]_e)/([BT]-[BT]_e)$. Therefore, if the above conditions are fulfilled by the systems, the slope of the linear relation between $\log(A_D/(A-A_{MD}))$ and t should correspond to the apparent rate constant of the forward reaction of the pseudo first-order reaction (2).

$$\left.\begin{matrix}HD^{2-}\\D^{3-}\end{matrix}\right\} \overset{k^+}{\underset{k^-}{\rightleftharpoons}} MD^- \qquad (2)$$

where HD^{2-}, D^{3-} and MD^- mean doubly and completely deprotonated BT anion and metal(II)-BT chelate, respectively.

Reported stability constants of metal(II)-BT chelate, K_{MD},s[1,2] indicate that the requirements are satisfied by the present systems. The following experimental facts were also found in the preliminary experiments where free EDTA-OH or GEDTA ranged from 5.0 mM to 25 mM, and its cobalt(II) or nickel(II) chelate from 0.30 mM to 25.0 mM.

i) In solutions of a given pH, given concentrations of cabalt(II) or nickel(II) chelate of EDTA-OH or GEDTA and the given initial concentration of BT, the slope of $\log(A_D/(A-A_{MD}))$ *vs.* t plot is independent of the concentration of uncomplexed EDTA-OH or GEDTA (Table 1).

Table 1. Dependence of the slope on the concentration of uncomplexed chelating agent

$\mu=0.30$

i) Cobalt(II)-EDTA-OH system

Concentration of EDTA-OH, mM	Slope, sec^{-1}	
10	1.62×10^{-2}	pH=8.23
15	1.68×10^{-2}	$[BT]_0=1.83\times10^{-5}$ M
20	1.65×10^{-2}	$[CoZ^-]=1.0$ mM

ii) Nickel(II)-EDTA-OH system

Concentration of EDTA-OH, mM	Slope, sec^{-1}	
8.0	1.90×10^{-3}	pH=10.0
15.0	1.87×10^{-3}	$[BT]_0=3.05\times10^{-5}$ M
25.0	1.91×10^{-3}	$[NiZ^-]=8.25_5$ mM

iii) Cobalt(II)-GEDTA system

Concentration of GEDTA, mM	Slope, sec^{-1}	
5	$1.18_2\times10^{-2}$	pH=8.10
10	$1.18_2\times10^{-2}$	$[BT]_0=1.00\times10^{-5}$ M
15	$1.16_5\times10^{-2}$	$[CoZ^{2-}]=0.30$ mM

iv) Nickel(II)-GEDTA system

Concentration of GEDTA, mM	Slope, sec^{-1}	
10	1.04×10^{-3}	pH=10.10
15	1.05×10^{-3}	$[BT]_0=2.90\times10^{-5}$ M
25	1.02×10^{-3}	$[NiZ^{2-}]=6.60$ mM

Table 2. Dependence of the slope on the initial concentration of BT

$\mu=0.30$

i) Cobalt(II)-EDTA-OH system

Concentration of BT, M	Slope, sec^{-1}	
7.31×10^{-6}	1.63×10^{-2}	pH=8.23
1.83×10^{-5}	1.62×10^{-2}	Concentration of free
2.56×10^{-5}	1.61×10^{-2}	EDTA-OH=10 mM
		$[CoZ^-]=1.0$ mM

ii) Nickel(II)-EDTA-OH system

Concentration of BT, M	Slope, sec^{-1}	
1.22×10^{-5}	1.45×10^{-3}	pH=9.86
2.14×10^{-5}	1.40×10^{-3}	Concentration of free
3.05×10^{-5}	$1.43\times10_{-3}$	EDTA-OH=8.0 mM
		$[NiZ^-]=8.25_5$ mM

iii) Cobalt(II)-GEDTA system

Concentration of BT, M	Slope, sec^{-1}	
8.45×10^{-6}	2.44×10^{-2}	pH=8.16
2.11×10^{-5}	2.40×10^{-2}	Concentration of free
2.54×10^{-5}	2.44×10^{-2}	GEDTA=10 mM
		$[CoZ^{2-}]=0.60$ mM

iv) Nickel(II)-GEDTA system

Concentration of BT, M	Slope, sec^{-1}	
5.80×10^{-6}	1.06×10^{-3}	pH=10.10
1.45×10^{-5}	1.02×10^{-3}	Concentration of free
2.90×10^{-5}	1.04×10^{-3}	GEDTA=10.0 mM
		$[NiZ^{2-}]=6.60$ mM

ii) In solutions of a given pH, given concentrations of uncomplexed EDTA-OH or GEDTA and of cobalt(II)- or nickel(II) chelate of EDTA or GEDTA, the slope of the linear relation is independent of the initial concentration of BT, $[BT]_0$ (Table 2).

iii) In solutions of a given pH, given concentrations of uncomplexed EDTA-OH or GEDTA, and of the given initial concentration of BT, the slope of the linear relation is proportional to the concentration of metal(II) chelate of EDTA-OH or GEDTA (Table 3).

iv) In solutions of a given initial concentration of BT, given concentrations of uncomplexed EDTA-OH or GEDTA, and of cobalt(II) or nickel(II) chelate of EDTA-OH or GEDTA, the slope of the linear relation is a linear function of the reciprocal of the concentration of hydrogen ion (Fig. 2), and given by

$$\text{slope} = k_\alpha + k_\beta/[H^+] \qquad (3)$$

These facts clearly indicate that the present substitution reactions of BT have the same reaction mechanism as was proposed for the substitution reaction of BT with cobalt(II)-EDTA chelate.[1] Consequently, k^+ in Eq. (1) or (2) should be given by

$$k^+ = (k_1^+ + k_2^+ \cdot k_2/[H^+]) \cdot [MZ] \qquad (4)$$

where k_2 refers to the dissociation of the second phenolic group of BT,[5] and [MZ] to the concentration of cobalt(II) or nickel(II) chelate of EDTA-OH or of GEDTA. Here, k_1^+ and k_2^+ in Eq. (4) are the second-order rate constants of the following reactions

$$\text{i)}\quad HD^{2-} + MZ^{2-n} \underset{k_1^-}{\overset{k_1^+}{\rightleftharpoons}} MD^- + HZ^{1-n}$$

$$\text{ii)}\quad HD^{2-} \overset{\text{rapid}}{\rightleftharpoons} H^+ + D^{3-}$$

$$D^{3-} + MZ^{2-n} \underset{k_2^-}{\overset{k_2^+}{\rightleftharpoons}} MD^- + Z^{n-} \qquad \text{rate determining step}$$

where MZ^{2-n} means metal(II)-EDTA-OH or -GEDTA chelate and Z^{n-}, completely deprotonated EDTA-OH or GEDTA anion.

From slopes of the linear relation between $k^+/[MZ]$ and $1/[H^+]$ and the intercepts, k_1^+'s and k_2^+'s

5) G. Schwarzenbach and W. Biedermann, *Helv. Chim. Acta*, **31**, 678 (1948).

TABLE 3. DEPENDENCE OF THE SLOPE ON THE CONCENTRATION OF METAL(II) CHELATE

$\mu=0.30$

i) Cobalt(II)-EDTA-OH system

Concentration of Co(II)-EDTA-OH, mM	Slope, sec^{-1}	Slope ratio calcd	Slope ratio obsd	
0.40	$6.6_6\times10^{-3}$	1.00	1.00	pH=8.23
1.00	1.68×10^{-2}	2.50	2.54	Concentration of free
1.40	2.34×10^{-2}	3.50	3.52	EDTA-OH=10 mM
2.00	3.33×10^{-2}	5.00	5.00	$[BT]_0=1.83\times10^{-5}$ M

ii) Nickel(II)-EDTA-OH system

Concentration of Ni(II)-EDTA-OH, mM	Slope, sec^{-1}	Slope ratio calcd	Slope ratio obsd	
8.25_5	1.90×10^{-3}	1.00	1.00	pH=10.0
16.51	3.74×10^{-3}	2.00	1.97	Concentration of free
24.77	5.70×10^{-3}	3.00	3.00	EDTA-OH=8.0 mM
				$[BT]_0=3.05\times10^{-5}$ M

iii) Cobalt(II)-GEDTA system

Concentration of Co(II)-GEDTA, mM	Slope, sec^{-1}	Slope ratio calcd	Slope ratio obsd	
0.15	5.66×10^{-3}	1.00	1.00	pH=8.00
0.30	$1.13_5\times10^{-2}$	2.00	1.95	Concentration of free
0.45	$1.72_0\times10^{-2}$	3.00	2.94	GEDTA=10 mM
0.60	$2.26_5\times10^{-2}$	4.00	3.88	$[BT]_0=1.40\times10^{-5}$ M

iv) Nickel(II)-GEDTA system

Concentration of Ni(II)-GEDTA, mM	Slope, sec^{-1}	Slope ratio calcd	Slope ratio obsd	
3.30	5.18×10^{-4}	1.00	1.00	pH=10.10
6.60	1.04×10^{-3}	2.00	1.97	Concentration of free
13.20	2.07×10^{-3}	4.00	3.99	GEDTA=10.0 mM
				$[BT]_0=2.90\times10^{-5}$ M

were determined (Fig. 2). These values are listed in Table 4 together with those for the substitution reactions of BT with EDTA chelates reported previously.[1,2]

We have mentioned previously[2] the importance of mixed ligand complexes as reaction intermediates in the proposed mechanism of the substitution reactions of BT with cobalt(II) and nickel(II)-EDTA chelates; prior to the complete dissociation of EDTA anion (Y^{4-}) from metal ion, BT may form coordinate bonds with metal ions, block the reformation of metal-EDTA bonds, and, thus, greatly increase the rate of dissociation of EDTA anion from the metal ion.

Electrostatically, the incompletely deprotonated BT anion (HD^{2-}) would have less repulsion against the negatively charged metal(II)-EDTA chelate. Therefore, kinetically, the reaction which proceeds through incompletely deprotonated BT anion can be expected to have an advantage over that proceeds through compltely deprotonated BT anion (D^{3-}). However, rate constants for the reactions through compltely deprotonated BT anion were much greater than those for the reactions through doubly deprotonated BT anion (HD^{2-}). This may suggest the need for the second phenolic oxygen to form the second metal(II)-oxygen bond prior to the rate determining step. Thus, the structure of a mixed ligand chelate as a reaction intermediate in the substitution reaction of BT with EDTA chelate should have metal-D^{3-} segment where two metal-oxygen bonds and one metal-nitrogen bond are included. Therefore, in this structure, at least, one half of Y^{4-} must be unwrapped.

Although EDTA-OH differs from EDTA by the presence of a hydroxyethyl group in place of one acetate group, its metal(II) chelate behaves kinetically in a nearly identical manner with EDTA chelate. Therefore, the structure of the reaction intermediate in the substitution reaction involving EDTA-OH chelate may be identical with that in the reaction of EDTA chelate.

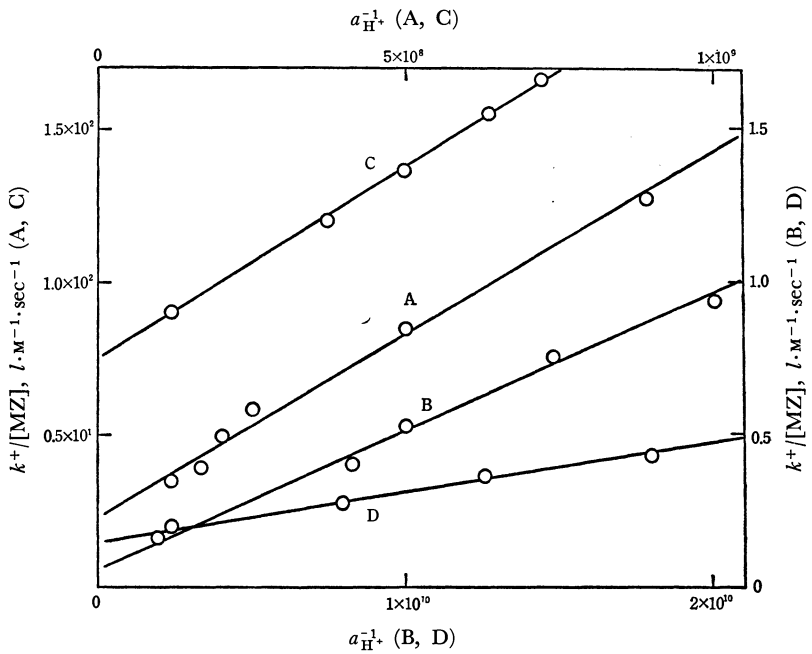

Fig. 2. Relation between $k^+/[MZ]$ and the concentration of hydrogen ion.
$\mu=0.30$, $\lambda=630$ mμ

A: Co(II)-EDTA-OH system
$[BT]_0=1.50\times10^{-5}$ M, $[CoZ^-]=1.00$ mM
Concentration of uncomplexed EDTA-OH=10.0 mM

B: Ni(II)-EDTA-OH system
$[BT]_0=3.05\times10^{-5}$ M, $[NiZ^-]=8.25_5$ mM
Concentration of uncomplexed EDTA-OH=8.0 mM

C: Co(II)-GEDTA system
$[BT]_0=2.00\times10^{-5}$ M, $[CoZ^{2-}]=0.60$ mM
Concentration of uncomplexed GEDTA=10.0 mM

D: Ni(II)-GEDTA system
$[BT]_0=2.90\times10^{-5}$ M, $[NiZ^{2-}]=6.60$ mM
Concentration of uncomplexed GEDTA=10.0 mM

Table 4. Rate constants for the substitution reactions of BT with cobalt(II) and nickel(II) chelates of EDTA, EDTA-OH and GEDTA

	EDTA chelates[1,2]		EDTA-OH chelates		GEDTA chelates	
	k_1^+	k_2^+	k_1^+	k_2^+	k_1^+	k_2^+
Co(II)	0.40	3.28×10^{3}[a]	2.20×10^{1}	3.24×10^{4}[b]	7.37×10^{1}	2.28×10^{4}[c]
Ni(II)	0	1.25[d]	0.08	6.93[d]	0.16	3.30[d]

Rate constants, $M^{-1} \cdot sec^{-1}$, $\mu=0.30$: a) 24.5°C b) 26°C c) 25°C d) 15°C.

In the kinetic studies of the electrophilic and the nucleophilic substitution reactions involving multidentate ligands, Margerum *et al.*[6,7] determined the detailed reaction mechanism by relating the experimental rate constant of the substitution reaction to the stability of the proposed reaction intermediate (a dinuclear complex or a mixed ligand complex). As was discussed above, the reaction intermediate in the present substitution reaction of BT may have one of these four structures listed in Fig. 3. To assign the detailed reaction mechanism, the treatment proposed by Rorabacher and Margerum[7] for the nucleophilic substitution reaction between EDTA and nickel(II)-polyamine complexes was applied directly to the present substitution reactions of BT with cobalt(II) and nickel(II) chelates of EDTA and of EDTA-OH. The direct application of their treatment leads to the conclusion that

6) T. J. Bydalek and D. W. Margerum, *Inorg. Chem.*, **2**, 678 (1963).
7) D. B. Rorabacher and D. W. Margerum, *ibid.*, **3**, 382 (1964).

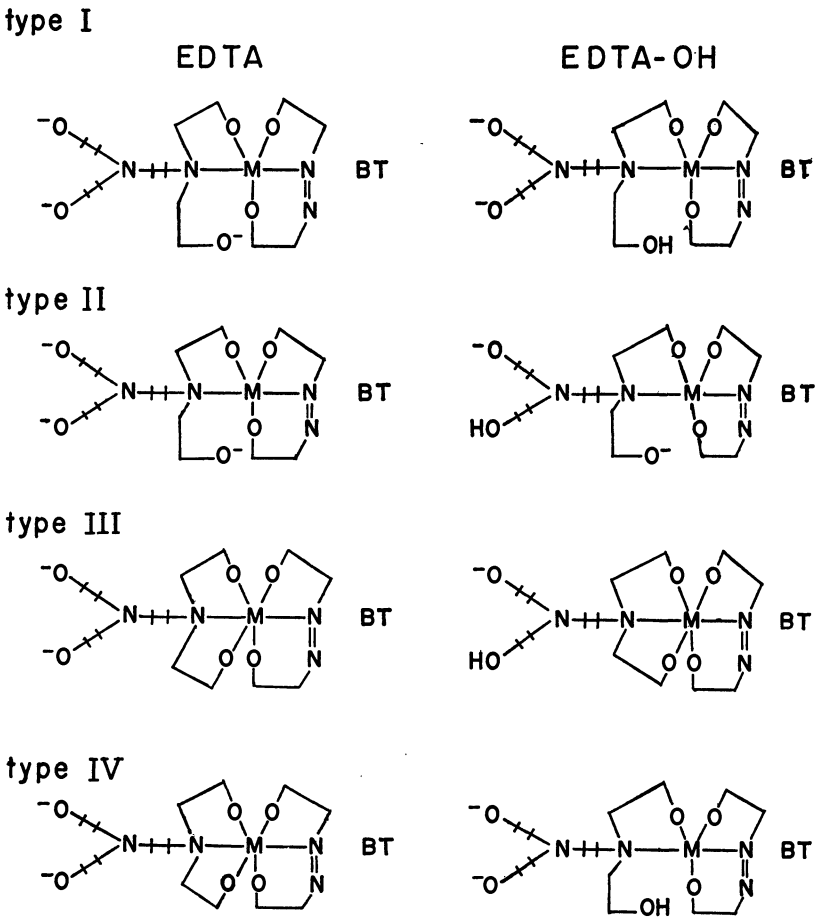

Fig. 3. Reaction intermediates.

TABLE 5. STABILITY CONSTANTS ($\mu=0.30$)*

1)	Co(II)-EDTA chelate[8]	$K_{CoY}=10^{15.71}$
2)	Ni(II)-EDTA chelate[8]	$K_{NiY}=10^{18.02}$
3)	Co(II)-EDTA-OH chelate[9]	$K_{CoZ}=10^{13.95}$
4)	Ni(II)-EDTA-OH chelate[9]	$K_{NiZ}=10^{16.55}$
5)	Ni(II)-EDTP chelate[10]	$K_{NiZ}=10^{9.10}$
6)	Ni(II)-NTA chelate[11]	$K_{NiX}=10^{11.09}$
7)	α-Amino, α-methylpropionate[12]	
	Co(II) chelate	$K_{CoX}=10^{3.51}$
	Ni(II) chelate	$K_{NiX}=10^{4.56}$
8)	*N*-Methyliminodiacetate[13]	
	Co(II) chelate	$K_{CoX}=10^{7.32}$
	Ni(II) chelate	$K_{NiX}=10^{8.43}$
9)	BT chelates[1,2]	
		$K_{CoD}=10^{20.0}$
		$K_{NiD}=10^{20.8}$
10)	Co(II)-GEDTA chelate[14]	
		$K_{CoZ}=10^{11.70}$
11)	Ni(II)-GEDTA chelate[14]	
		$K_{NiZ}=10^{13.00}$

* These values are calculated from the related stability constants in solutions of ionic strength 0.10 and the activity constants of the ions calculated by means of Davies equation.[1]

experimental rate constant ratio between EDTA and EDTA-OH systems should be equal to the ratio of the reaction intermediate stability, provided that the rate of the dissociation of tervalent EDTA-OH anion Z^{3-} from the reaction intermediate can be equated with that of Y^{4-}. As suggested by Margerum *et al.*,[7] the relative stability for the reaction intermediate given by the following relation was used in place of the actual one.

$$K_r^{7)} = \frac{K_{\text{chelon-segment}} \cdot K_{\text{BT-segment}}}{K_{MZ}} \qquad (5)$$

Where $K_{\text{chelon-segment}}$ corresponds to the stability

8) G. Schwarzenbach, R. Gut and G. Anderegg, *Helv. Chim. Acta*, **37**, 937 (1954).
9) S. Chaberek, Jr., and A. E. Martell, *J. Am. Chem. Soc.*, **77**, 1477 (1955).
10) R. C. Courtney, S. Chaberek, Jr., and A. E. Martell, *ibid.*, **75**, 4814 (1953).
11) G. Schwarzenbach and R. Gut, *Helv. Chim. Acta*, **39**, 1583 (1956).
12) H. Irving and L. D. Pettit, *J. Chem. Soc.*, **1963**, 1946.
13) G. Schwarzenbach, G, Anderagg, W. Schneider and H. Senn, *Helv. Chim. Acta*, **38**, 1147 (1955).
14) J. H. Holloway and C. N. Reilley, *Anal. Chem.*, **32**, 249 (1960).

TABLE 6. REACTION INTERMEDIATES AND RATE CONSTANT RATIOS

			EDTA	EDTA-OH	Rate constant ratio Calcd	Rate constant ratio Obsd
Type I	Ni(II)	$\log K_r$	7.34	8.81		
		$\log K_{elcc}$	0.50	—	2.35	5.54
		statistical factor	4.0	1.0		
	Co(II)	$\log K_r$	7.80	9.56		
		$\log K_{elec}$	0.50	—	4.57	9.85
		statistical factor	4.0	1.0		
Type II	Ni(II)	$\log K_r$	7.34	8.81		
		$\log K_{elec}$	0.50	0.50	14.8	5.54
		statistical factor	4.0	2.0		
	Co(II)	$\log K_r$	7.80	9.56		
		$\log K_{elec}$	0.50	0.50	28.9	9.85
		statistical factor	4.0	2.0		
Type III	Ni(II)	$\log K_r$	11.24	12.71		
		$\log K_{elec}$	—	—	14.8	5.54
		statistical factor	2.0	1.0		
	Co(II)	$\log K_r$	11.61	13.37		
		$\log K_{elec}$	—	—	28.9	9.85
		statistical factor	2.0	1.0		
Type IV	Ni(II)	$\log K_r$	11.11	9.56		
		$\log K_{elec}$	—	—	1/317	5.54
		statistical factor	2.0	1.0		
	Co(II)	$\log K_r$	11.41	8.81		
		$\log K_{elec}$	—	—	1/224	9.85
		statistical factor	2.0	1.0		

constant of metal(II)-glycinate or -iminodiacetate chelate, $K_{BT-segment}$, to the stability constant of metal(II)-BT chelate, and K_{MZ}, the stability constant of metal(II)-EDTA or -EDTA-OH chelate.

The relative stability of the proposed reaction intermediate calculated from the numerical values given in Table 5 are listed in Table 6 together with the rate constants. In the evaluation of the stability, the additional stability due to the electrostatic attraction of acetate group, K_{elec} (3.17),[6] and the statistical factor[6] were also taken into consideration. Here, *N*-methyl iminodiacetate and α-amino, α-methylpropionate were chosen as intermediate models.[6] Clearly, the structures type I fit the observed data best and are considered to be the preferred intermediates.

If the rupture of the second (EDTA or EDTA-OH anion) nitrogen-nickel bond accompanied by the rotation around a C–N or C–C bond and the formation of nickel-water bond is the rate determining step, the products of the rate constant for the rupture of nickel-nitrogen bond corrected for the rotational barrier involved[7] and K_r values must be equal to the experimental rate constants. However, K_r values in Table 6 clearly show that the experimental rate constants are much smaller than these products. Generally, it is very hard to consider that the rupture of the last nickel-oxygen bond is involved in the rate determining step, because the nickel-acetate cleavage is much faster than the nickel-amine cleavage.[6] Consequently, the above fact may indicate that the BT anion coordinated to the nickel(II) ion gives a serious effect on the rupture of nickel-nitrogen bond, the accompanied rotation around the C–N or the C–C bond of the leaving EDTA or EDTA-OH anion, other structural transformation or the formation of nickel(II)-water bond. To get additional information about this effect, further systematic investigations should be conducted.

As was tried in the substitution reaction of BT with EDTA-OH chelate, if the same reaction mechanism (glycinate intermediate) also fits the substitution reaction with GEDTA chelate, the rate of the reaction of BT with GEDTA chelate can be compared with that of EDTA chelate theoretically on the basis of the reaction intermediates.

Stability constant ratios of reaction intermediates between reactions with GEDTA chelates and those with EDTA chelates were also calculated by choosing α-amino, α-methylpropionate as an intermediate model and using stability constants listed in Table 5. Calculated values for cobalt(II) and nickel(II) systems were 1.02×10^4 and 1.07×10^5, respectively. This may suggest that the substitution reactions of BT with GEDTA chelates must be much favored thermodynamically over the reactions of BT with

EDTA chelates. However, rate constant ratios experimentally found for cobalt(II) and nickel(II) systems were 6.80 and 2.64, in a remarkable disagreement with the theoretically predicted ones. This probably means that the substitution reaction of BT with GEDTA chelate involves the reaction intermediate quite different from that for the reaction of EDTA chelate, or that the substitution reaction of BT with GEDTA chelate may have the same reaction intermediate as the reaction with EDTA, but, the steric effect due to the $-O-CH_2-CH_2-O-CH_2-CH_2-N-(CH_2COO^-)_2$ segment in GEDTA makes the reaction intermediate less stable to make the reaction less favorable kinetically. The latter explanation may be probable, because the rate constant ratio for the reaction of cobalt(II) chelate is not diffrent considerably from that for the reaction of nickel(II)-chelate.

If the glycinate mechanism also fits the reaction of BT with nickel(II)-NTA chelates, the stability constant ratio of reaction intermediates between the reaction with nickel(II)-NTA chelate and that with nickel(II)-EDTA chelate can be calculated to be 6.30×10^6. This result clearly suggests that if the reaction of BT with nickel(II)-NTA chelate had the same reaction mechanism as that with EDTA chelate had, the reaction of nickel(II)-NTA chelate would proceed very rapidly as compared with that of nickel(II)-EDTA chelate. As was reported previously,[2] the reaction was found to proceed rapidly in accordance with the above prediction.

Finally, we can mention that the kinetic study of substitution reactions of metal chelates with dyes other than BT would provide the additional information about the mechanism of multidentate ligand substitution reactions.

BULLETIN OF THE CHEMICAL SOCIETY OF JAPAN VOL. 41 2040—2044 (1968)

Studies of the Grinding of Condensed Phosphates. IV. Grinding of Sodium Trimetaphosphate at Low Pressure

Itaru MOTOOKA, Genzo HASHIZUME and Masamitsu KOBAYASHI

Department of Chemistry, Faculty of General Education, Kobe University, Nada-ku, Kobe

(Received December 22, 1967)

The change in sodium trimetaphosphate by grinding at low pressure was examined by the X-ray diffraction method and paper chromatography. The crystalline sodium trimetaphosphate became amorphous more rapidly when ground at low pressure than in dry air or nitrogen gas, and in these cases the chain phosphates higher than triphosphate were produced in addition to ortho-, pyro- and tri-phosphates.

In the previous papers,[1,2] it has been reported that the P–O–P linkages of cyclic sodium trimetaphosphate were severed to the chain phosphates due to grinding and the chain-length of some long-chain phosphates such as lithium, sodium and potassium polyphosphates decreased as a result of the cleavage of the P–O–P linkages upon grinding.

It was reported by Baramboim[3] that organic high polymers such as polystyrene depolymerize to the shorter-chain molecules upon grinding in the manner similar to the previous papers.[1,2] On the contrary, Kargin *et al.*[4] reported that styrene and other monomers polymerize by mechanical treatment.

In the case of phosphates, the possibility of producing the longer-chain phosphates by condensation can be anticipated. As the polymerization of phosphates is a condensation reaction in which water molecules are expelled, this reaction will be affected by the water molecules and so sodium trimetaphosphate was ground at low humidity and at low pressure, namely, one to several mmHg.

Experimental

Materials. Trisodium dihydrogen triphosphate, $Na_3H_2P_3O_{10}\cdot 1.5H_2O$, was prepared by the addition of alcohol to the aqueous solution of sodium salt which was adjusted to pH 4.6 with perchloric acid. The X-ray diffraction pattern of the precipitate*1 obtained was

1) Part I: I. Motooka, G. Hashizume and M. Kobayashi, *Nippon Kagaku Zasshi* (*J. Chem. Soc. Japan, Pure Chem. Sect.*), **87**, 255 (1966).
2) Part II: I. Motooka, G. Hashizume and M. Kobayashi, *ibid.*, **87**, 953 (1966).
3) N. K. Baramboim, *Zh. Fiz. Khim.*, **32**, 432 (1958).
4) N. A. Plate and V. A. Kargin, *J. Polymer Sci.*, **62**, 1027 (1962).

*1 This precipitate contained ortho- and pyrophosphates of 10 to 20% in the analysis of paper chromatography.

identical with Corbridge's data.[5]

The preparation of sodium trimetaphosphate, $Na_3P_3O_9$, disodium dihydrogen pyrophosphate, $Na_2H_2P_2O_7$, and monosodium dihydrogen orthophosphate, NaH_2PO_4, has been described in a previous paper.[1]

Apparatus. The apparatus used in grinding was an Ishikawa's vacuum grinder (AGZ-type) and, in case of need, the same as in the previous paper[2] was used.

Procedure. One gram of phosphate was ground for a difinite time. The atmosphere during grinding was controlled in the following way. (1) In dry air: after the air in the grinding apparatus had been removed with a vacuum pump, the air dried by passing it successively through concentrated sulfuric acid, silica gel and phosphorus pentoxide was introduced into the apparatus. New phosphorus pentoxide was always provided in the apparatus. The relative humidity in it was 5 to 10% by a hair hygrometer. (2) In nitrogen gas: after the air had been removed, the apparatus was filled with dry nitrogen gas. New phosphorus pentoxide was also provided in it. The relative humidity was the same as in (1). (3) At low pressure: sample was ground while evacuating with a vacuum pump to below 5 mmHg pressure. The relative humidity was below 5% by a hair hygrometer.

Results and Discussion

Grinding of Sodium Trimetaphosphate at Low Pressure. As stated in the previous paper,[6] water molecules participate in the mechanism of the change which takes place when sodium trimetaphosphate is ground. Therefore, in order to investigate further the effect of water molecules, the grinding was carried out in an atmosphere evacuated to below 5 mmHg pressure as one method for reducing the water molecules.

Figure 1 shows the changes in X-ray diffraction patterns of sodium trimetaphosphate due to grinding in various atmospheres. It can be seen that the effect of grinding at low pressure is larger than that of grinding in dry air or nitrogen gas. For example, although the diffraction lines of sodium trimetaphosphate remain even after grinding for 6 hr in the dry air and nitrogen gas, the product ground for 6 hr at low pressure is amorphous. As regards the relative humidity, this result agrees with that of the previous paper[6]—that is, the grinding effect decreases with increase in relative humidity.

Rehbinder *et al.*[7] have investigated the effect of water on grinding of quartz, and reported that more amorphous layer was produced as the water content decreased. There is a good agreement between their results and ours. The results described above, however, can not be interpreted simply as due to low humidity since factors*2 other than water molecules must be taken into account in the case of low pressure.

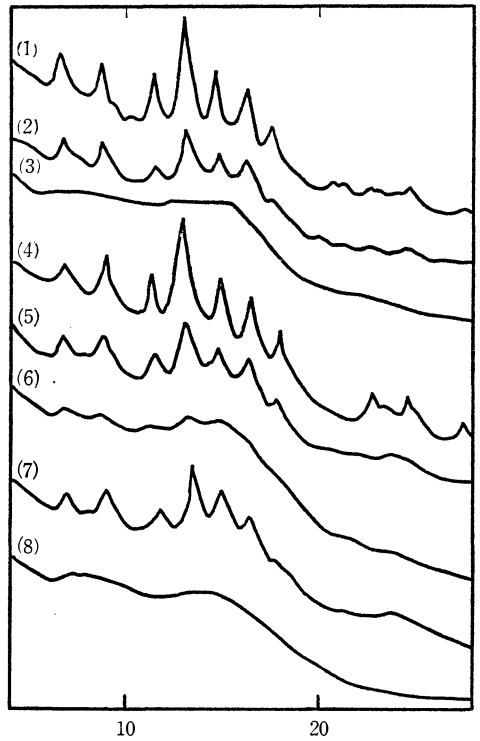

Fig. 1. X-ray diffraction patterns of $Na_3P_3O_9$ in various atmospheres.

(1) 3 hr grinding in dry air
(2) 6 hr grinding in dry air
(3) 24 hr grinding in dry air
(4) 3 hr grinding in nitrogen gas
(5) 6 hr grinding in nitrogen gas
(6) 9 hr grinding in nitrogen gas
(7) 3 hr grinding at low pressure
(8) 6 hr grinding at low pressure

The results of analyses of these ground samples by paper chromatography are given in Table 1.*3 The rate of decrease of trimetaphosphate molecules by grinding at low pressure is the fastest and this supports the results of the change in X-ray diffraction patterns in Fig. 1. They differ from those in the preceding paper[1] in that considerable tetra- and

5) E. C. Corbridge and F. R. Tromans, *Anal. Chem.*, **30**, 1101 (1958).
6) Part III: I. Motooka, G. Hashizume and M. Kobayashi, This Bulletin, **40**, 2095 (1967).
7) P. A. Rehbinder and G. S. Chodakow, *Silikattechn.*, **13** [6], 200 (1962).
*2 For example, the flow of air in the apparatus.[8]
8) G. Jimbo, *Hyomen (Surface)*, **1**, 47 (1963).

*3 Although the grinders used in this experiment were of the Ishikawa type, the grinding effect—for example, the rate of production of amorphous substance or the distribution of the various kinds of phosphates—was affected by its kind (AG-type or AGA-type) and by the use of other grinder even if of the same kind. An example is given in Table 2. In the case of grinder of AGA-type No. 2, the grinding effect is largest, and especially the amounts of tetra- and higher-polyphosphates is largest at humidity of 20% and temperature of 20°C. Even in the case of the same grinder, the grinding effect becomes poor because of the defacement of the rotating shaft and the weakening of the force by which the pestle is pressed when used for a long time.

TABLE 1. DISTRIBUTION OF PHOSPHORUS AMONG THE SAMPLES GROUND AT VARIOUS ATMOSPHERES

Atmosphere	Grinding time (hr)	Analytical value by paper chromatography (%)				
		Ortho	Pyro	Tri	Tetra~	Trimeta
Dry air	3	0	0	0	0	100
	6	0.2	0.8	1.0	0.4	97.6
	9	1.0	1.4	3.4	18.8	75.4
	24	7.1	6.9	7.1	45.4	33.5
Nitrogen gas	3	0	0	0	0	100
	6	3.0	5.4	3.5	17.5	70.6
	9	3.7	3.7	6.9	23.3	62.5
Low pressure	3	0	0.5	0.9	30.1	68.5
	6	0.3	0.5	2.8	41.2	55.2
	9	2.4	3.0	3.5	64.2	26.8

TABLE 2. EFFECT OF GRINDER

Grinder	Grinding time (hr)	Atmosphere		Analytical value (%)				
		Temp. (°C)	Humidity (%)	Ortho	Pyro	Tri	Tetra~	Trimeta
AGA-type No. 1	72	30	40	5.0	5.9	9.7	0.4	79.1
AGA-type No. 2	72	30	40	12.7	12.8	30.3	4.0	40.2
AG-type	72	30	40	3.7	7.6	9.3	0.1	79.3
AGA-type No. 1	72	20	20	6.7	10.2	14.0	0.7	68.4
AGA-type No. 2	72	20	20	12.8	13.3	16.8	21.8	35.3

TABLE 3. DISTRIBUTION OF PHOSPHORUS AMONG THE SAMPLES GROUND AT LOW PRESSURE

Sample	Atmosphere	Grinding time (hr)	Analytical value (%)			
			Ortho	Pyro	Tri	Tetra~
NaH_2PO_4	Low pressure	56	100	0	0	0
$Na_2H_2P_2O_7$	Low pressure	2	7.3	80.3	12.4	0
		6	17.1	49.8	20.8	12.4
	Dry air	6	5.8	94.2	0	0
$Na_3H_2P_3O_{10}$	Low pressure	3	10.3	37.7	40.7	11.3
		6	11.7	38.2	32.9	17.2
		9	13.3	37.8	26.3	22.7
	Relative humidity of 40%	6	14.5	28.0	57.5	0
		24	16.1	33.8	50.1	0
		48	20.1	44.0	35.9	0

higher- polyphosphates are produced in all cases of dry air, nitrogen gas and the evacuated state. This is due to the presence of smaller amounts of water molecules in the atmosphere of grinding and the following mechanisms can be assumed:

(1) Cyclic trimetaphosphates are severed to chain phosphates due to grinding and these chain phosphates are condensed to higher polyphosphates.

(2) The active molecules produced when the P–O–P linkages are severed are combined into longer-chain phosphates.

$$Na_3P_3O_9 \rightarrow Na_3P_3O_9: \quad (I)$$

$$Na_3P_3O_9: + H_2O \rightarrow Na_3H_2P_3O_{10} \quad (II)$$

$$Na_3H_2P_3O_{10} + H_2O \rightarrow Na_2H_2P_2O_7 + NaH_2PO_4 \quad (III)$$

$$Na_2H_2P_2O_7 + H_2O \rightarrow 2NaH_2PO_4 \quad (IV)$$

$$Na_kH_2P_kO_{3k+1} + Na_lH_2P_lO_{3l+1} \rightarrow Na_{k+l}H_2P_{k+l}O_{3(k+l)+1} + H_2O \quad (k, l = 1, 2, 3,\cdots) \quad (V)$$

$$m\mathrm{Na_3P_3O_9}: + n\mathrm{Na_3P_3O_9}: \rightarrow \mathrm{Na_{3(m+n)}P_{3(m+n)}O_{9(m+n)}}: \quad \text{(VI)}$$

$$\mathrm{Na_{3(m+n)}P_{3(m+n)}O_{9(m+n)}}: + \mathrm{H_2O} \rightarrow \mathrm{Na_{3(m+n)}H_2P_{3(m+n)}O_{9(m+n)+1}} \quad (m, n = 1, 2, 3, \cdots) \quad \text{(VII)}$$

Equations (I) to (V) show the mechanism of (1) and Eqs. (I), (VI) and (VII) the mechanism of (2). It has been reported in the previous papers[1,6] that the reactions shown in Eqs. (I) to (IV) take place. It is considered that, in the present investigation, the reactions in Eqs. (V) and (VI) take place much more easily than the ones in Eqs. (II), (III) and (IV) since the amount of water molecules in atmosphere is small.

Grinding of Monosodium Dihydrogen Orthophosphate, Disodium Dihydrogen Pyrophosphate and Trisodium Dihydrogen Triphosphate at Low Pressure. In order to examine the possibility of Eq. (V), the grinding of NaH_2PO_4, $Na_2H_2P_2O_7$ and $Na_3H_2P_3O_{10}\cdot 1.5H_2O$ was studied in an atmosphere containing a small amount of water molecules. The X-ray diffraction patterns of NaH_2PO_4, $Na_2H_2P_2O_7$ and $Na_3H_2P_3O_{10}\cdot 1.5H_2O$ by grinding are shown in Figs. 2, 3 and 4, respectively. The X-ray diffraction pattern of NaH_2PO_4 ground for 56 hr is essentially identical with the original sample. $Na_2H_2P_2O_7$ becomes almost amorphous when ground for 6 hr at low pressure, but in dry air some diffraction lines of $Na_2H_2P_2O_7$ remain after grinding for 6 hr. $Na_3H_2P_3O_{10}$ changes similarly.

The distribution of various phosphates determined by paper chromatography is given in Table 3. Sample of NaH_2PO_4 ground for 56 hr is entirely orthophosphate. This is probably due to the fact

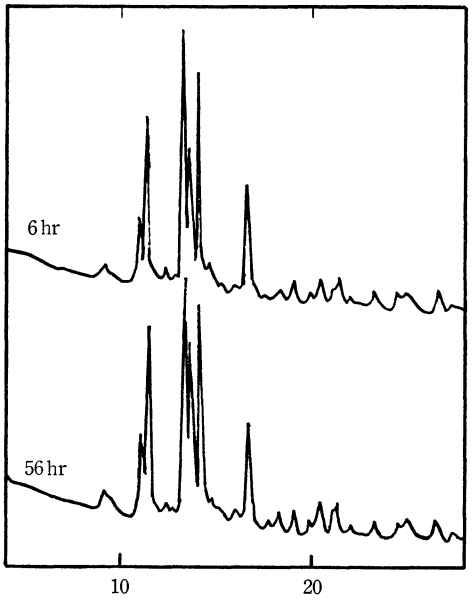

Fig. 2. X-ray diffraction patterns of NaH_2PO_4 ground at low pressure.
The numbers represent the grinding time.

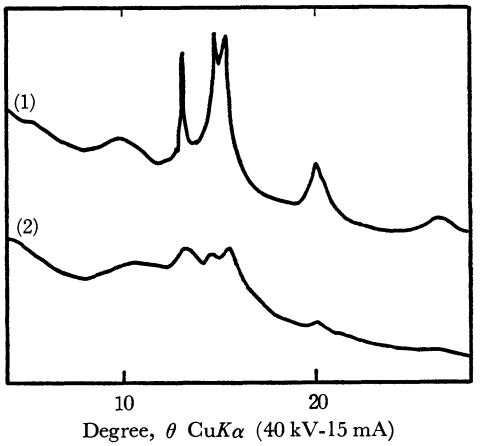

Fig. 3. X-ray diffraction patterns of $Na_2H_2P_2O_7$ ground in dry air and at low pressure.
(1) 6 hr grinding in dry air
(2) 6 hr grinding at low pressure

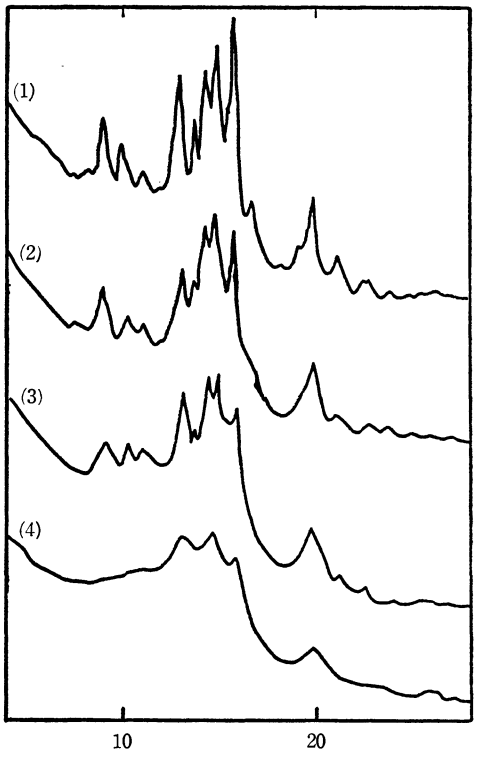

Fig. 4. X-ray diffraction patterns of the ground $Na_3H_2P_3O_{10}\cdot 1.5H_2O$.
(1) 3 hr grinding at the relative humidity of 40%
(2) 6 hr grinding at the relative humidity of 40%
(3) 3 hr grinding at low pressure
(4) 6 hr grinding at low pressure

that the crystal of NaH_2PO_4 is very stable for grinding or recrystallizes easily even if the lattice is disturbed.*4 Although $Na_2H_2P_2O_7$ becomes orthophosphates by grinding in air, it also condenses to tri- and higher-polyphosphates simultaneously at low pressure. $Na_3H_2P_3O_{10}$ shows a tendency similar to $Na_2H_2P_2O_7$, namely, some tetra- and higher- polyphosphates are produced at low pressure.

From the above results, it is possible for the mechanism of (1) to take place. However, it is difficult to confirm the mechanism of (2) and this must be studied further in the future but the fact that the amounts of tetra- and higher-polyphosphates produced when $Na_3P_3O_9$ is ground at low pressure are much more than those produced by grinding $Na_2H_2P_2O_7$ and $Na_3H_2P_3O_{10}$ indicates the possibility of the mechanism of (2).

*4 Monosodium dihydrogen orthophosphate is ready to adhere to the mortar during grinding, and it may decrease the efficiency of grinding.

BULLETIN OF THE CHEMICAL SOCIETY OF JAPAN VOL. 41 2044—2049 (1968)

Syntheses and Properties of Some Dithio-β-diketonato Complexes*1

Akira OUCHI, Mitsuhisa NAKATANI and Yoshiaki TAKAHASHI

Department of Chemistry, College of General Education, The University of Tokyo, Komaba, Meguro-ku, Tokyo

(Received February 9, 1968)

Some compounds of type $M(L_{ss})_2$, where M is Ni(II) or Co(II) and HL_{ss} is some dithio derivative of β-diketones (benzoylacetone, trifluoroacetylacetone, trifluorobenzoylacetone or dibenzoylmethane), were obtained by passing hydrogen chloride and hydrogen sulfide into ethanol solutions containing β-diketone and metal chloride. Such compounds seem to be isostructural to the bis(dithioacetylacetonato) complexes and are stable. They are all deeply colored and their solutions show a characteristic absorption in the visible region, 16700 cm^{-1} for bis(dithiobenzoylacetonato)nickel(II) and 15200 cm^{-1} for bis(dithiodibenzoylmethanato)nickel(II). On the other hand, infrared spectra of these complexes show ν(C=S) bands at 1220—1240, 1170—1180 and 840 cm^{-1}. $M(L_{ss})_2Cl_4$ type complexes (where M=Fe(II) or Co(II) and HL_{ss}=dithiobenzoylacetone) were also obtained and they seem to be isostructural to $Fe(C_5H_7S_2)_2Cl_4$. Their magnetic susceptibilities and electronic and infrared spectra are shown and discussed.

The dithio-derivatives of acetylacetonato complexes were previously synthesized[1-5] and they seem to have very interesting properties. Recently, the present authors reported the syntheses of the dithioacetylacetonato complexes of various metals and found that (1) there are two kinds of dithioacetylacetonato complexes the $M(L_{ss})_2$ type and the $M(L_{ss})_2Cl_4$ type,[4] (2) in the case of nickel complexes of thio-derivatives of acetylacetonates, there is a regular change in the wave numbers of infrared and visible spectra from $Ni(C_5H_7SO)_2$ *via* $Ni(C_5H_7S_2)$-(C_5H_7SO) to $Ni(C_5H_7S_2)_2$.[3] As these compounds have characteristic absorption bands in infrared spectra as well as in electronic spectra owing to the metal-sulfur bond and the pseudo-aromaticity of their chelate ring, an investigation of the same type of complexes of other dithio-β-diketones, comparing them with the dithioacetylacetonates, should be interesting.

The dithio-β-diketonato complexes of nickel(II) were obtained using benzoylacetone, trifluoroacetylacetone, trifluorobenzoylaceton and dibenzoylmethane in the same manner as the synthesis of dithioacetylacetonates from acetylacetonates. However, the dithio-derivatives of hexafluoroacetylacetone, ethylacetoacetate and methylacetoacetate could not be obtained by the same method, being too unstable. In the case of monothio-β-diketonato complexes of nickel(II), the wavelength of the visible absorption spectral band of thioethylacetoacetate is longer than that of the monothio-derivative of acetylacetonate, although both can be synthesized.[6] In the case of the nickel complexes of dithio-β-diketones, the longer the wavelength of the above band, the less stable the complex. Perhaps this fact is related to the instability of these complexes.

*1 This peper was presented at the 17th Symposium on Coordination Chemistry, Hiroshima, December, 1967.

1) L. Martin, I. M. Stewart, *Nature*, **210**, 522 (1966).
2) K. Knauer, P. Hemmerich and J. D. W. Van Voorst, *Angew. Chem. Intern. Ed. Engl.*, **6**, 262 (1967).
3) A. Ouchi, M. Hyodo and Y. Takahashi, This Bulletin, **40**, 2819 (1967).
4) A. Furuhashi, K. Watanuki and A. Ouchi, *ibid.*, **46**, 110 (1968).
5) R. Beckett and B. F. Hoskins, *Chem. Commun.*, **1967**, 909.
6) S. H. H. Chaston, S. E. Livingstone and T. N. Lockyer, *Aust. J. Chem.*, **19**, 1401 (1966).

Experimental

Materials and Instruments. Starting materials of GR grade were used without further purification. Infrared spectra were obtained with a potassium disc using Japan Spectroscopic Co., Ltd.'s, DS 403 G infrared spectrophotometer. Electronic spectra were obtained with a Hitachi EPS-2 automatic recording spectrophotometer. Magnetic moments were measured with a Gouy balance at room temperature (15°C).

Synthesis of Bis(dithiotrifluoroacetylacetonato)nickel(II). One and three tenth grams (0.01 mol) of anhydrous nickel(II) chloride and 3.1 g (0.02 mol) of trifluoroacetylacetone were dissolved in 20 m*l* of absolute ethanol. Into the clean, green solution, hydrogen chloride gas was bubbled for 30 min, then hydrogen sulfide for one hour. The solution was allowed to stand for one day at about 0°C. The black precipitate obtained was recrystallized from benzene and dried in vacuum. The yield was about 2.1 g (25% calculated for nickel(II) chloride).

Synthesis of Bis(dithiotrifluoroacetylacetonato)cobalt(II). This complex was obtained by almost the same method as the corresponding nickel(II) complex. As it is fairly soluble in ethanol, 5 m*l* of ethanol was enough par 0.01 mol of cobalt chloride. The yield was only about 15%.

Synthesis of Bis(dithiotrifluorobenzoylacetonato)nickel(II). The crude compound, obtained by the same method as was used for dithiotrifluoroacetylacetonates, contains by-products. The main impurity seems to be the dimer of dithio-β-diketone, but dithiolate salts may also be present. Repeated recrystallization was carried out with a mixture of chloroform and petroleum ether. The chromatographic method may also be applied to purification. The yield was about 30% or less due to loss in the recrystallization process.

Synthesis of Bis(dithiobenzoylacetonato)nickel(II). The crude complex, prepared in a manner similar to the above, was purified by the column chromatography. Alumina column chromatography, using benzene as the eluent, was effective. The yield was about 30%. Bis-(dithiodibenzoylmethanato)nickel(II) was also synthesized by the same method as was used in the synthesis of dithiobenzoylacetonate. The yield was less, about 20%.

Synthesis of Bis(dithiobenzoylacetonato)cobalt(II) Tetrachloride and Bis(dithiobenzoylacetonato)iron(II) Tetrachloride. The method of synthesizing the dithio-β-diketonato complex was applicable, using anhydrous cobalt(II) chloride or ferric chloride as the source of metal salts, respectively. Analytically pure products precipitated from the mother liquor, and chromatographic separation was not necessary. The yield was 30% and 42%, respectively (calculated for the metal salts).

Results and Discussion

Analytical data and the magnetic moments of these compounds are summarized in Tables 1 and

Table 1. Analysis of complexes (Figures are given in %.)

		Metal	C	H	S	Cl
$Ni(sbzsac)_2$	Calcd	13.18	53.94	4.07	28.80	
	Found	12.75	53.97	4.19	29.10	
$Co(sbzsac)_2Cl_4$	Calcd	10.03	40.90	3.09	21.84	24.14
	Found	10.36	40.96	3.37	22.50	24.50
$Fe(sbzsac)_2Cl_4$	Calcd	9.56	41.11	3.11	21.95	24.27
	Found	9.95	40.73	3.15	22.40	24.70
$Ni(sbzsbz)_2$	Calcd	10.31	63.27	3.89	22.52	
	Found	10.10	62.39	4.54	22.60	
$Ni(sfasac)_2$	Calcd	13.68	27.99	1.88	29.89	
	Found	12.90	27.98	1.37	30.07	
$Co(sfasac)_2$	Calcd	13.73	27.98	1.88	29.87	
	Found	13.50	27.72	1.72	30.10	
$Ni(sfasbz)_2$	Calcd	10.61	43.42	2.18	23.18	
	Found	10.56	43.15	2.20	23.50	

sbzsac=dithiobenzoylacetone ($C_{10}H_9S_2$)
sbzsbz=dithiodibenzoylmethane ($C_{15}H_{11}S_2$)
sfasac=dithiotrifluoroacetylaetone ($C_5F_3H_4S_2$)
sfasbz=dithiotrifluorobenzoylacetone ($C_{10}F_3H_6S_2$)

Table 2. Magnetic moment of complexes (Figures are given in B. M. per 1 mol of metal.)

$Ni(sbzsac)_2$	diamagnetic	$Co(sfasac)_2$	1.34
$Ni(sbzsbz)_2$	diamagnetic	$Co(sbzsac)_2Cl$	4.12
$Ni(sfasac)_2$	diamagnetic	$Fe(sbzsac)_2Cl_4$	5.10
$Ni(sfasbz)_2$	diamagnetic		

* Refer to Table 1 about the abbreviations in this table.

Table 3. Infrared frequencies of the dithio-β-diketonato complexes (cm^{-1})

s=strong, m=medium, w=weak, sh=shoulder, $L_{so}=(C_5H_7SO)$, $L_{ss}=(C_5H_7S_2)$. Refer to Table 1 for the abbreviations of the names of the complexes.

$Ni(L_{so})_2$	$Ni(L_{so})(L_{ss})$	$Ni(L_{ss})_2$	$Ni(sbzsac)_2$	Ni(sbzsbz)	$Ni(sfasac)_2$	$Co(sfasac)_2$	$Ni(sfasbz)_2$	$Fe(L_{ss})_2Cl_4$	$Fe(sbzsac)_2Cl_4$	$Co(sbzsac)_2Cl_4$	Tentative assignments
1567(s)*	1558 s*						1595 w		1593 w	1593 w	aryl, *=ν(C=O)
1480, 1476 s	1490 s	1495 s	1470 s 1465 s	1471 s 1448 s	1505 s 1490 s	1490 s	1490 s	1470 s	1500 w 1475 s	1500 w 1475 s	ν(C=C), δ(C-H)
1445, 1440, 1430 m	1425, 1415 m	1433 w	1445 s			1440 w	1450 s	1430, 1420 s	1455 w		$\delta(CH_3)$
1375 m 1340 m	1360 m 1340 m	1353 m	1360 m 1350 s	1347 m	1363 m 1340 w	1363 m 1340 w	1390 m	1375 s 1353 s	1372 w 1340 m	1350 w 1340 m	$\delta(CH_3)$ and others
	1312 w 1294 w	1314 m 1290 m	1298 s 1273 m	1295 s 1282 m	1302 s	1303 s	1295 s		1312 w	1303 m	ν(C=C), ν(C-R)
1235 s	1232 s 1162 s	1154 s	1219 m 1209 w 1180 m	1223 s 1175 m	1237 s 1170 s	1234 s 1170 s	1240 s 1212 w 1170 s	1230 m 1200 s	1258 s 1218 w	1257 s 1220 m	ν(C=S), δ(C-H) ν(C-C) or the mix. of them
1120 m	1125 w 1115 w		1155 w 1108 w 1073 w	1155 w 1100 w 1074 m	1142 s 1135 s 1118 s	1138 s 1120 s	1145 s 1110 s	1073 w	1145 m 1098 m	1145 m 1110 w 1100 m	ν(C-F) and others
1170 m 987 w 937 w*	1015 m 937 w*	1013 m	1025 m 1018 m 998 m** 908 m	999 m** 965 w 945 m 922 w 905 m	1010 w 928 s	1015 w 928 s	1030 m 1000 m** 965 s 920 w	1007 m 997 m 982 w	1018 m 998 s** 923 s	1013 m 988 s** 922 s	$\rho(CH_3)$ and others; *, $\nu(C-CH_3)$; **, aryl
815 s 810 s	831 s 810 s	841 s	840 m	840 m	848 s	845 s	850 s 825 w	860 s	877 s 865 s	878 s 860 m	ν(C=S)
723 s 667 m 647 m 501, 494 m 420 w	748 m 727 m 712 w 656 m 553 m 522 m 498 m 422 w	749 m 705 w 558 s 422 w	763 s 736 s 690 s 677 m 633 m 525 m 458 w	753 s 730 w 692 s 655 m 618 w 560 w 493 w 420 w	765 s 712 w 695 s 650 m 565 w 538 w 481 m	763 s 695 s 648 m 565 w 539 w 490 m	750 s 695 s 646 m 618 w 602 w 592 m 563 w 548 s 478 w 447 w	710 w 696 s 573 w 557 s 523 w 459 w 431 s 422 w	760 s 708 m 675 s 638 w 600 w 559 w 508 m	760 s 708 m 676 s 637 m 600 w 560 m 508 m 444 m	π, aryl ring and others

TABLE 4. ELECTRONIC SPECTRA OF THE DITHIO-β-DIKETONATO COMPLEXES (cm^{-1} (log ε))
br=broad, sh=shoulder. Refer also to Table 1 for the abbreviations of the names of the complexes.

$Ni(L_{so})_2$	$Ni(L_{so})(L_{ss})$	$Ni(L_{ss})_2$	$Ni(sbzsac)_2$	$Ni(sbzsbz)_2$	$Ni(sfasbz)_2$	$Ni(sfasac)_2$	$Co(sfasac)_2$	$Fe(L_{ss})_2Cl_4$ (Reflectance)	$Fe(L_{ss})_2Cl_4$	$Fe(sbzsac)_2Cl_4$	$Co(sbzsac)_2Cl_4$		
Methanol	Methanol	Methanol	Methanol	Benzene	Benzene	Methanol	Methanol		Methanol	Methanol	Benzene	Methanl	Solvent
	49000 (4.38)												Tentative assign-ment
	41600 (4.14)	41300 (4.18)	39060 (4.28)						37700 (4.13)	39700 (4.60)		39700 (4.27)	
39700 (4.29)	38500 (4.40)					37040 (4.71)	37040 (4.65)						π-π
37100(sh) (4.03)	37300 (4.40)	36900 (4.53)	33550 (4.34)	31530 (4.40)	32800 (4.42)				34500 (4.19)	34500 (3.93)	33200 (3.62)	34900 (3.92)	
32300 (4.03)	30400 (4.23)	29700 (4.30)	28740 (4.34)	27400 (4.62)	27200 (5.57)	29600 (4.03)	29600 (4.31)	30300					
								27700	27400 (2.19)	28260 (3.72)	28590 (3.35)	28360 (4.30)	π-π or d-π
26800 (3.53)								25300					
22500 (3.37)	22600 (3.34)	23800(sh) (3.55)	23000 (3.62)			23250(sh) (3.37)	23250(sh) (3.37)	21000(br)	21720(br) (2.07)	20000(br) (2.64)	22720(sh) (2.59)	20210(br) (2.69)	
18900 (2.94)	21300 (3.35)	20900 (2.92)		21360(sh) (3.91)	21730(sh) (3.52)								
		17850 (3.54)						17850(vw)					d-d
	16380 (2.82)		16660 (3.02)			16800 (3.17)	16800 (3.19)		16650(sh) (1.71)		16660 (2.08)		or d-π
15400 (2.29)				15200 (3.30)	15110 (3.28)								or mix. of them

2, respectively. The relevant infrared frequencies of these complexes are shown in Table 3, and the wave numbers of their electronic spectra in Table 4 together with those of some related compounds.

From the magnetic moment data, the $M(L_{ss})_2$ type compounds are all low spin types; the nickel(II) complexes are all diamagnetic and the cobalt(II) complex has about one unpaired electron. This result is the same as that for the bis(dithioacetylacetonato) complexes, and these compounds would also have a planar structure as was the case of bis(dithioacetylacetonato)cobalt (II), which was found through X-ray crystallographic analysis.[5] The $M(L_{ss})_2Cl_4$ complexes are high spin octahedral types, as bis(dithioacetylacetonato)iron(II) tetrachloride, although the exact structure has not yet been determined.[2,4]

The general features of the spectra of these complexes resemble those of the acetylacetonates and dithioacetylacetonates, except for many additional bands due to the introduction of a phenyl or trifluoromethyl group. The tentative assignments given in Table 3 were made by referring to the acetylacetonates.

Sometimes, the compounds containing phenyl groups show a sharp weak band near 1590 cm^{-1}, but the band is different in shape from the ν(C=O) band; perhaps it is a skeletal inplane vibration band of the benzene ring.

The ν(C=S) bands of these compounds appear near 1220—1240; 1170 and 840—850 cm^{-1} in the case of $M(L_{ss})_2$ type compounds.

Thioacetylacetonato complex, $Ni(L_{ss})(L_{so})$, also exhibited three ν(C=S) at 1232, 1162 and 830 cm^{-1}. On the other hand, those of bis(dithioacetylacetonato)nickel(II) and cobalt(II) appear near 1160 and 840 cm^{-1} only. This fact seems to indicate that the C=S bond character of the $M(L_{ss})_2$ complexes resemble those of $M(L_{ss})(L_{so})$ type compounds, and there are two kinds of C=S bonds in these complexes; one sulfur atom may at least be more weakly bonded to the central metal atom than the other. Thus the chelate ring of the complexes now investigated may be more or less deformed, although it has been reported from X-ray crystallographic analysis that bis(dithioacetylacetonato)cobalt(II) has four identical Co–S bonds.[5]

The infrared spectra of bis(dithiobenzoylacetonato)cobalt(II) (or iron(II)) tetrachloride have ν(C=S) bands near 1257 and 870 cm^{-1}, as bis(dithioacetylacetonato-iron(II) tetrachloride. Generally, the infrared spectra of these three complexes resemble one another, and they seem to be isostructural.

The intensities of the visible region bands of these compounds are very strong compared with those of the corresponding β-diketonato complexes, as in the case of the thio-derivatives of acetylacetonates. From a comparison of the spectra of these complexes with those of the acetylacetonates,[7,8] tentative assignments are given in Table 4. The band near 16000 cm^{-1} of $M(L_{ss})_2$ type complexes may be taken as the d–d band from the wave number, but as its intensity is too high, it seems to be d–π band or at least a mixture of d–d and d–π bands.

The wave number of this band of nickel complexes of dithiotrifluoroacetylacetone and dithiobenzoylacetone is about 16800 cm^{-1}, and that of the dithiodibenzoylmethanato and dithiotrifluorobenzoylacetonato complexes about 15200 cm^{-1}.

On the other hand, the wavelengths of the bands of the series of thioacetylacetonatonickel(II) complexes are as follows; 17850 for bis(dithioacetylacetonate), 16380 for monothioacetylacetonatodithioacetonate and 15400 for bis(monothioacetylacetonato) (cm^{-1}).

From a comparison of the spectra of these two series of complexes, it is deduced at least that the substitution of trifluoromethyl or phenyl groups into the dithioacetylacetone chelate in place of methyl groups has the same effect as the substitution of sulfur by oxygen. Although the intensity of the band is almost the same in these substituted dithio-β-diketonato complexes, that of the oxygen substituted complexes is lowered when the number of oxygen atoms is increased.

These facts may be explained as follows. The introduction of oxygen into the chelate decreases the electron density of the six membered ring to some extent since the oxygen atom bonds to the central metal atom in a pure coordination bond. Thus, the sulfur-metal bond of the chelate ring is weakned. In the same way, the substitution of the methyl group of the acetylacetonato chelate with a phenyl or trifluoromethyl group also decreases the electron density of the ring by withdrawing electrons to the group. As a result, the electronic energy levels of these two series of compounds, as well as the wave numbers of the d–π band, should resemble each other.

From the absorption coefficients of the complexes of both series, back donation seems to be possible only from the central metal to sulfur, and not to oxygen in these chelate rings.

A benzene solution of bis(dithiobenzoylacetonato)-cobalt(II) tetrachloride shows a similar spectrum as the $M(L_{ss})_2$ type complexes; a band at 16660 cm^{-1} appears, although the intensity of this band is only one tenth that of $M(L_{ss})_2$ type complexes. This band does not occur in an alcoholic solution of the same complex. This fact suggests that the compound does not have simple ionic bonding between the tetrachloroiron(II) anion and the dithiolium cation, but has a kind of coordination bond between them. In alcoholic solution, as well as in aqueous solution, this complex seems to decompose into a

7) J. P. Fackler, Jr., F. A. Cotton and D. W. Barnum, *Inorg. Chem.*, **2**, 97 (1963).
8) D. W. Barnum, *J. Inorg. Nucl. Chem.*, **21**, 221; **22**, 183 (1961).

solvated metal ion and dithiolium ion, as is found from the absorption spectra.

To confirm the structure definitely, further investigation, especially X-ray analysis, is necessary, and is now going on in our laboratory.

The authors wish to thank Professor Mikio Katayama and the Analytical Division of the Department of Pharmacy for the infrared measurements and the elementary analyses. Helpful discussions with Professor Yukichi Yoshino, Dr. Kunihiko Watanuki and colleagues of our laboratory are also gratefully acknowledged.

BULLETIN OF THE CHEMICAL SOCIETY OF JAPAN VOL. 41 2049—2054 (1968)

Syntheses and Properties of Some Tetrabromobis(dithioacetylacetonato) Complexes

Akiko FURUHASHI, Toshio TAKEUCHI*1 and Akira OUCHI*1

Department of Chemistry, College of Engineering and Science, Aoyama Gakuin Uuiversity, Megurisawa, Setagaya-ku, Tokyo

(Received March 14, 1968)

Some compounds of type $M(L_{ss})_2Br_4$, where M is Mn(II), Fe(II), Co(II), Cu(II), Zn(II) and Cd(II) and HL_{ss} are dithioacetylacetone, were obtained by passing hydrogen bromide, adding bromine and passing hydrogen sulfide through an ethanolic solution containing an anhydrous metal bromide and acetylacetone. Such compounds, which seem to be isostructural with tetrachlorobis-(dithioacetylacetonato)iron(II), are stable. They are all of high spin, and their infrared spectra show characteristic bands at about 1200, 1000 and 860 cm^{-1}. $Cu^I(L_{ss})_2Br_3$ was also obtained from cupric bromide by the same method without using bromine, but from cupric chloride, an isostructural complex was not obtained but $[Cu(C_5H_8S_2)Cl]_n$. Electronic spectra are also shown and discussed.

The tetrachlorobis(acetylacetonato) complexes of iron(II),[1] manganese(II)[2] and mercury(II)[2] have already been synthesized and discussed. The present authors investigated the syntheses of the homologue of the complex, but chloro-complexes of other metals were hardly obtained. This seems due to the fact that, 1) the chloro complexes are relatively unstable and especially sensitive to water and alcohol, and the products may be decomposed by the solvent during synthesis; 2) in these complexes, dithioacetylacetone is probably in the form of dithiolium ion of unipositive charge; then some oxidant must be added during synthesis.

In the case of $Fe^{II}(L_{ss})_2Cl_4$, ferric chloride was used as the starting material and a tervalent ferric salt works as the oxidant. Manganese and mercury have another relatively stable oxidation state other than the bivalent state, and they may act as a kind of autooxidation catalyst in the process. On the other hand, zinc and cadmium, for example, have a very stable bivalent state and no oxidation ability nor oxidation catalytic effects are expected.

Consequently, an improved synthetic method for the $M^{II}(L_{ss})_2X_4$ (where HL_{ss} is dithioacetylacetone, X is Cl or Br) has been investigated in our laboratory and the complexes of many metals are newly obtained.

The $M^{II}(L_{ss})_2Br_4$ type complexes thus obtained are all of high spin, and show almost the same infrared spectra as that of $Fe^{II}(L_{ss})_2Cl_4$, and not that of $Co(L_{ss})_2$.[3]

When cupric bromid was used as the starting material and bromine not added, the cuprous complex $Cu^I(L_{ss})_2Br_3$ was obtained; but if bromine was added, the cupric complex precipitates. From cupric chloride, however, an isostructural complex was not obtained but $[Cu(C_5H_8S_2)Cl]_n$.

Experimental

Materials and Instruments. The starting materials were of GR grade and were used without further purification. Infrared spectra were obtained by the KBr

*1 College of General Education, The University of Tokyo, Komaba, Meguro-ku, Tokyo.

1) K. Knauer, P. Hemmerich and J. D. W. Van Voorst, *Angew. Chem. Intern. Ed. Engl.*, **6**, 262 (1967).

2) A. Furuhashi K. Watanuki and A. Ouchi, This Bulletin, **41**, 110 (1968).

3) A. Ouchi, M. Hyodo and Y. Takahashi, *ibid.*, **40**, 2819 (1967).

disc procedure using a Type DS 403 G infrared spectrophotometer of the Japan Spectroscopic Co., Ltd. Electronic spectra were obtained with a Hitachi EPS-2 type automatic recording spectrophotometer. Reflectance spectra were obtained with an Ito Model QV-3 spectrophotometer, using a reflectance attachment and a magnesium oxide standard. Magnetic moments were measured with a Gouy balance at room temperature (15°C).

Syntheses of Tetrabromobis(dithioacetylacetonato)manganese(II). Three and three tenth grams (0.015 m*l*) of anhydrous manganese(II) bromide and 3.00 g (0.030 mol) of acetylacetone were mixed with 20.0 m*l* of absolute ethanol, and all solid materials*2 dissolved. To the solution cooled on ice, were added first dry hydrogen bromide for 30 min, then 1.1 m*l* (0.042 mol) of bromine dropwise while shaking and finally hydrogen sulfide for 5 min until a some precipitate appeared. The precipitate was filtered off and the filtrate kept in an ice bath for about one hour. The yellow precipitate thus obtained was filtered off and washed with carbon disulfide, ethyl alcohol, chloroform and petroleum ether in succession. The product was dried in a vacuum desiccator. The yield was about 4.0 g (42.0%). Though the product is soluble in water or polar organic solvents, it reacts with them and it is insoluble in non-polar organic solvents. For this reason recrystallization has not yet succeeded.

The syntheses of cobalt(II), zinc(II), cadmium(II) and copper(II) complexes were carried out by almost the same method; the yields were about 30—50%.

The iron(II) complex was obtained from ferric bromide without using bromine, as ferric ion itself worked as the oxidizing agent. The copper(I) complex was obtained from cupric bromide without bromine.

Synthesis of Chlorodithioacetylacetonatocopper(I). One and seven tenth grams of cupric chloride (0.010 mol) and 2.0 g (0.020 mol) of acetylacetone were dissolved in 30 m*l* of absolute ethanol, and the solution refluxed for 2 hr. The clean solution thus obtained was cooled on an ice bath and hydrogen chloride was bubbled in, then hydrogen sulfide. Yellow precipitate appeared immediately. The precipitated product was very unstable, but when washed with absolute ethanol repeatedly, a pale brownish white product was obtained which was very stable even in air. The yield was about 2.1 g (91.5%).

The attempt to synthesize $Zn(L_{ss})_2Cl_4$ or $Cu(L_{ss})_2Cl_4$ from the bivalent metal chloride using chlorine as an oxidant was not successful; perhaps the product is not stable to the solvent during synthesis. On the other hand, the bromo-complexes of these metals are sufficiently stable, and moreover, bromine is easier to handle quantitatively than chlorine; as the addition of a large exess of halogen should be avoided to minimize the side reaction. The syntheses of the iodo-complexes were also attempted, but iodine did not react easily, and the bonding was not very stable; consequently, stable iodo-complexes were not obtained. When ferric bromide was used as the starting material and bromine added, the iron(III) complex did not precipitate. Perhaps tervalent iron complex is not stable, as the formula of the iron(III) complex should be $Fe(L_{ss})_2Cl_5$ from the valence equilibrium, and the central metal ion should be heptacoordinated; it is probably not a stable state.

The attempt to synthesize the isostructural nickel complex was not successful by the same method, perhaps this is due to the fact that the dithioacetylacetonato complex is very stable.

*2 After the dissolution some crystal may appear, which is redissolved into the solvent when hydrogen bromide is passed.

Results and Discussion

Analytical data for these compounds are summarized in Table 1. Their magnetic moments are given in Table 2.

From the magnetic data, the $M(L_{ss})_2Br_4$ type complexes are all high spin types. Though their exact structures have not been determined yet, it may be octahedral.[1,2] $Co(L_{ss})_2Br_5$, for example, seems to have three unpaired electrons, though the observed value is higher than the calculated value, 3.8, as is commonly recognized for many cobalt(II) octahedral complexes.[4] On the other hand, bis(dithioacetylacetonato)cobalt(II), which has a planer structure,[5] is a low spin type and has only one unpaired electron.

Consequently, there are two types of dithioacetylacetonato complexes of the same metal; one is $M(L_{ss})_2$ and the other $M(L_{ss})_2X_4$ (general formulae).

The infrared spectral data for the complexes are summarized in Tables 3 and 4 together with those of some related compounds.[2,3] The general features of the infrared spectra of these complexes rather resemble that of $Fe(L_{ss})_2Cl_4$ and not that of $Co(L_{ss})_2$.

The wave numbers of the main peaks of $Fe(L_{ss})_2Cl_4$ and $Fe(L_{ss})_2Br_4$ are very similar in the 2000—400 cm^{-1} region, indicating that these two complexes are almost isostructural and chlorine or bromine does not affect the vibrational frequencies in that region seriously. This fact seems to suggest that the halogen atoms do not bond directly to the carbon atom in these complexes.[6]

Then one of the formulae proposed by Knauer,[1] (I), is not probable.

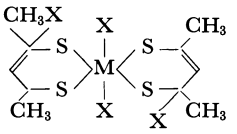

(I)

The characteristic bands which seem to be ν(C=S) bands or mixed bands containing ν(C=S)[7] appear

4) F. A. Cotton and G. Wilkison, "Advanced Inorganic Chemistry," 2nd ed., Interscience Publ. (Div. of Wiley and Son Co.) New York, N.Y. (1966), p. 870.

5) R. Becket and B. F. Itokins, *Chem. Commun.*, **1967**, 909.

6) D. Gibson, C. Oldham, J. Lewis, D. Lawton, R. Mason and G. B. Robertson, *Nature*, **208** (**5010**), 580 (1965).

7) S. H. H. Chaston, S. E. Livingstone, T. N. Lockyer, V. A. Pickles and J. S. Shannon, *Aust. J. Chem.*, **18**, 673 (1965).

TABLE 1. ANALYSIS OF COMPLEXES (Figures are given in %.)

		Metal	C	H	S	X
$Mn(L_{ss})_2Br_4$	Calcd	8.62	18.85	2.22	20.13	50.17
	Found	9.45	19.71	2.40	19.90	50.02
$Fe(L_{ss})Br_4$	Calcd	8.74	18.83	2.21	20.11	50.10
	Found	9.02	19.01	2.55	20.58	50.05
$Co(L_{ss})_2Br_4$	Calcd	9.19	18.74	2.20	20.01	49.86
	Found	10.00	19.67	2.61	20.78	50.03
$Cu^{I}(L_{ss})_2Br_3$	Calcd	11.23	21.23	2.49	22.67	42.37
	Found	11.25	21.65	2.52	21.18	42.30
$Cu^{II}(L_{ss})_2Br_4$	Calcd	9.84	18.60	2.19	19.86	49.51
	Found	9.80	19.73	2.29	20.56	49.70
$Zn(L_{ss})_2Br_4$	Calcd	10.10	18.55	2.18	19.81	49.37
	Found	10.78	18.21	2.48	20.50	50.40
$Cd(L_{ss})_2Br_4$	Calcd	16.18	17.29	2.03	18.47	46.02
	Found	17.05	17.42	1.95	19.21	47.00
$Cu(C_5H_3S_2)Cl$	Calcd	27.48	25.95	3.49	27.73	15.33
	Found	27.54	25.76	3.30	27.58	15.43

L_{ss}=dithioacetylacetone; $(C_5H_7S_2)^+$
X=Cl or Br

TABLE 2. MAGNETIC MOMENTS OF COMPLEXES (at 15°C)

Compound	Magnetic moment* (B.M.)	Number of unpaired electrons	Oxidation number of the central metal
$Mn(L_{ss})_2Br_4$	6.02	5	+2
$Fe(L_{ss})_2Br_4$	5.51	4	+2
$Co(L_{ss})_2Br_4$	4.82	3	+2
$Cu^{II}(L_{ss})_2Br_4$	1.84	1	+2
$Cu^{I}(L_{ss})_2Br_3$	diamagnetic	0	+1
$Zn(L_{ss})_2Br_4$	diamagnetic	0	+2
$Cd(L_{ss})_2Br_4$	diamagnetic	0	+2
$Cu(C_5H_3S_2)Cl$	diamagnetic	0	+1

* per one mol of metal

near 1230 and 860 cm^{-1}. The exact assignment of these bands has not yet been made; those written in Table 3 are only tentative. But the general features of the infrared spectra of these complexes resemble those of potassium dichloroacetylacetonato-platinate(II) and related complexes.[8,9] In the latter compounds, there is a ring structure of acetylacetone, which is bonded to the central metal atom by γ-carbon atom or by the π-electrons of the C=C double bond. Strong 1200, 1000 and 860 cm^{-1} bands are also recognized in the spectra of the platinum complexes, but the band at 800 cm^{-1} is absent. However, this fact should not be taken as evidence of the existence of a γ-carbon bonding structure, since the thio- and dithioacetylacetonato chelate rings seem to have an electronic structure different from that of acetylacetonato chelate. The final decision should be arrived from an X-ray crystallographic analysis. But we can expect at least that the halogenobis(dithioacetylacetonato) complexes do not have usual MS_4 type coordination which is found in the $Co(L_{ss})_2$ complex. The dithioacetylacetonato ligands of these compounds seem to form rings themselves, unipositive dithiolium ion for example, and this is the reason that the infrared spectra of these compounds and that of γ-carbon bonding acetylacetonate coincide with each other. The ring form ligand may be a unidentate in these complexes, although it is not yet clear by which atom it bonds to the central metal.

This reflection spectra between 28000 and 13500 cm^{-1} are shown in Table 5. Cabalt(II) complex has an intense band at about 15900 cm^{-1}, and this peak seems to be not only the d–d band but a mixture of d–d and d–π bands. Iron(II) and copper(II) complexes also have an intense color, but their peaks are not clear; shoulders at about 20000—19000 cm^{-1} seem to correspond to them. The intense color of these compounds disappears when they are dissolved in water or methanol. Although weak bands are recognized in this absorption spectra, log ε is only about 2 in both cases; in other words, only about one tenth that of bis-(dithioacetylacetonato)cobalt(II).[3] This intense color of these solid complexes seems to indicate that there is a kind of bonding between the central metal and the ligands. They are not the MX_4^{2-}-$(L_{ss}^{+})_2$ type simple ionic bonding compounds, though, because the metal ion, as well as the dithiolium ion,

8) G. T. Behnke and K. Nakamoto, *Inorg. Chem.*, **6**, 433, 440 (1967), **7**, 330 (1968).
9) D. Gibson, J. Lewis and C. Oldham. *J. Chem. Soc.* (*A*), **1967**, 72

Table 3. Infrared spectra of complexes (Figures are given in cm^{-1}.)
s=strong, m=medium, w=weak, $L_{ss}=(C_5H_7S_2)$

$Ni(L_{ss})_2$*	$Fe(L_{ss})_2Cl_4$**	$Mn(L_{ss})_2Br_4$	$Fe(L_{ss})_2Br_4$	$Co(L_{ss})_2Br_4$	$Cu^{I}(L_{ss})_2Br_3$	$Cu^{II}(L_{ss})_2Br_4$	$Zn(L_{ss})_2Br_4$	$Cd(L_{ss})_2Br_4$	$Cu(C_5H_8S_2)Cl$	Tentative assignments
1490 s	1470 s	1480 s	1478 s	1475 s	1475 s	1475 s	1478 s	1480 s		ν(C=C)
1433 w	1430 s	1425 m	1428 m	1425 m	1415 m	1425 m	1425 m	1438, 1425 m	1452 sh, 1445 s, 1415 w	δ(C-H)
	1420 s	1400 w	1400 w	1400 w	1400 w		1398 w		1405 m	
	1375 s	1380 m	1380 m	1375 m	1370 m	1360 m	1375 m	1370 s	1385 s	
1353 m	1353 s	1356 m	1355 m	1353 m			1355 m		1375 w	
1314 m										
1290 m										$\delta_s(CH_3)$
	1230 m	1230 m	1231 m	1230 m	1233 m	1232 m	1230 m	1236 m	1151 s	ν(C=C)
	1200 s	1205 s	1205 s	1204 s	1205 s	1204 s	1205 s	1200 s		ν(C=S)
1154 s										or the mixture of them
	1073 w	1095 w	1095 w	1095 w	1100 w	1098 w	1095 m	1100 w	1100 vs	δ(C-H) or ν(C-C)
1013 m	1007 m	1020 w	1020 w	1020 w	1018 s	1010 s	1020 w	1020 s	1035 s	$\rho(CH_3)$
	997 m	1010 s	1010 s	1008 s	998 w	998 w	1010 s	1000 w	990 w	$\nu(C-CH_3)$
	982 w	1000 w	998 w	998 w			997 w		955 w	
		982 w	983 w	980 w			980 w		945 m	
									940 m	
841 s	860 s	862 s	865 s	861 s	883 w	881 m	860 s	876 m		$\nu(C-CH_3)$
					845 s	840 s		886 s		ν(C=S)
										or the mixture of them
749 m	710 w	702 m	715 w	700 s	700 m	700 m	700 m	705 m	670 s	π(C-H)
705 w	696 s		702 m							

* See Ref. 2, ** See Ref. 3, δ_s: symmetric bending, π( ): out-of-plane bending

TABLE 4. FAR INFRARED SPECTRA OF COMPLEXES (Figures are given in cm^{-1}.)

$Fe(L_{ss})_2Cl_4$	$Fe(L_{ss})_2Br_4$	$Co(L_{ss})_2Br_4$	$Cu^{I}(L_{ss})_2Br_3$	$Cu^{II}(L_{ss})_2Br_4$
573 w	571 w	571 w	573 w	571 w
557 s	558 s	558 s	548 s	556 s 545 s
523 w	519 w	520 w	517 w	516 w
436 s	457 w	455 w	454 w	453 w
436 s	434 s	435 s	433 s	431 s

TABLE 5. ELECTRONIC SPECTRA OF COMPLEXES

(Figures are given in cm^{-1} for wave numbers and log ε for intensities (in parentheses).) (vs: very strong, s: strong, m: medium, w: weak, sh: shoulder) (absorption means the absorption spectra of the methanol solution.*)

$Mn(L_{ss})_2Br_4$	absorption		37300	34700		22750		
			(4.09)	(4.18)		(2.17)		
	reflectance					22700(m)		14280(vw)
$Fe(L_{ss})_2Br_4$	absorption		37500	34500	27200	23270	20300	16660
			(3.49)	(3.79)	(2.75)	(2.68)	(2.67)	(2.43)
	reflectance				27800(s)	24400(w)	20000(sh)	16950(sh)15150(w)
$Co(L_{ss})_2Br_4$	absorption		37600	34800	27500	22730		
			(4.12)	(4.14)	(2.48)	(2.39)		
	reflectance				27800(w)	22200(m)	18500(w)	15900(vs)
$Cu^{I}(L_{ss})_2Br_3$	absorption		37600	34500	26600	23280	19240	16670
			(3.76)	(3.89)	(2.61)	(2.51)	(2.40)	(2.33)
	reflectance				27000(w)	23300(s)	20900(w)	1638(sh)
$Cu^{II}(L_{ss})_2Br_4$	absorption	42900	37900	34900	26600	23580		17070
		(3.81)	(4.03)	(4.10)	(2.85)	(2.66)		(2.45)
	reflectance				27800(s)	23800(w)	19050(sh)	16250(sh)
$Zn(L_{ss})_2Br_4$	absorption	43700	37500	34800	27600	22720		
		(3.61)	(3.65)	(3.82)	(2.21)	(2.16)		
	reflectance					23800(s)	19650(w)	
$Cd(L_{ss})_2Br_4$	absorption		37600	34500		23300		
			(4.02)	(4.09)		(2.38)		
	reflectance					23000(s)	19420(w,sh)	

* These absorption spectra of the solutions should be those of some decomposition product of complexes with solvents and may not be the spectra of the complex itself.

do not have such intense color. Copper(I), manganese(II), zinc(II) and cadmium(II) complexes also have a less intense peak in this region in the solid state, but not in solution.

The absorptions near 23000 cm^{-1} and 28000 cm^{-1} are found both in their reflection and absorption spectra. These bands and the ones near 34500 and 37500 cm^{-1} of the methanolic solution can probably be assigned to π–π transitions of the dithiolium salts.[10,11] The latter two are also found for 3,5-dimethyl-1,2-dithiolium perchlorate too.[12] From this result, the dithiolium cation seems to exist without decomposition even if the metal-ligand bond is broken by dissolution of the compelexes in methanol, or other similar polar solvents. All of these $M_{ss}^{II}(L_{ss})_2X_4$ type complexes seem to dissociate almost completely into M^{++}, $(L_{ss})^+$ and X^-, as in the case of $Fe_{ss}^{II}(L_{ss})_2Cl_4$.[1] Although this fact was recognized previously, it is also recognized from the qualitative electric conductivity measurement of the aqueous and acetonitrilic solution of these compounds.

From these results, structure (III) is preferable to that proposed by Knauer,[1] which is shown in (II).

10) E. Klingsberg, *J. Am. Chem. Soc.*, **83**, 2934 (1961).
11) E. Klingsberg, *ibid.*, **84**, 2941 (1962).
12) M. Schmidt and H. Schulz, *Chem. Ber.*, **101**, 277 (1968).

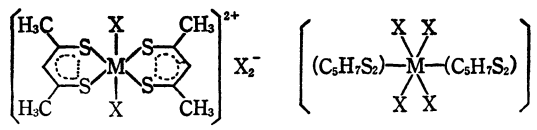

(II) (III)

An X-ray crystallographic study of these compounds, which is now in progress by the present authors, may clarify the detailed structure of these comples.

The infrared spectra of $[Cu(C_5H_8S_2)Cl]_n$ is very unique and resembles that of dithioacetylacetone dimer. But it is insoluble in nonpolar solvents and is stable. Though the exact structure is not yet clear, it may be a kind of adduct; a $(-Cu(C_5H_8S_2)-Cl-)_n$ type chain, in which dithioacetylacetone, $C_5H_8S_2$, molecules are bonded to each other copper atom as an unidentate is tentatively proposed.

The authors wish to thank the Analytical Division of the Department of Pharmacy, Professor Mikio Katayama, and the Biochemistry Laboratory of the College of General Education, The University of Tokyo for the elementary analyses of these complexes as well as for the measurement of the infrared spectra. The authors wish to express their appreciation to Professor Yasumasa Hayakawa and the staff of the Department of Chemistry of Aoyama Gakuin University; helpful discussions by Professors Yukichi Yoshino, and Kunihiko Watanuki and colleagues of our laboratory are also gratefully acknowledged.

BULLETIN OF THE CHEMICAL SOCIETY OF JAPAN VOL. 41 2054—2058 (1968)

Studies on Coprecipited Phases in the Calcium-Gadolinium Oxalate System

Hsiu CHI

Department of Chemistry, New Asia College, The Chinese University of Hong Kong, Kowloon, Hong Kong

and Kozo NAGASHIMA

Department of Chemistry, Faculty of Science, Tokyo Kyoiku University, Otsuka, Bunkyo-ku, Tokyo

(Received March 4, 1968)

Calcium oxalate is often used as a carrier for precipitating rare earth elements. Gadolinium was chosen as a rare earth element and X-ray powder diffractometry used for the identification of coprecipitated solids. The X-ray lattice spacings are tabulated for each of the coprecipitates of varying composition in the calcium-gadolinium oxalate system. From the spacings, the following facts were obtained: (1) The uptake mechanisms of gadolinium in calcium oxalate, and calcium in gadolinium oxalate are completely due to the formation of solid solutions. (2) Several new solid solution phases were formed. (3) When the gadolinium to calcium ratio is proper, precipitates having a weddellite structure, which is not obtained in usual analytical procedures, are formed.

The purpose of the present work is to show that the various forms of the hydrated calcium-gadolinium oxalate system can be built up from a trace amount to a large percentage of gadolinium ions in aqueous solutions, with emphasis laid on the fact that some of the unstable forms of hydrated calcium oxalate may be stabilized by the addition and intervention of the tripositive gadolinium ions.

It is well-known that calcium oxalate is often used as a good carrier to precipitate the rare earth elements and other elements. Among these may be mentioned the separation of rare earth elements from uranium, beryllium, aluminum and zirconium by simply agitating an acetic acid solution of the mixture with solid calcium oxalate monohydrate. A similar technique has been used to separate the rare earth elements and strontium from zirconium, niobium and ruthenium.[1-3]

Following an intensive study of the coprecipitation of rare earth elements with various calcium oxalate hydrates, it has been found that calcium oxalate dihydrate carries small amounts of rare earth elements through mixed crystal formation and that the uptake of rare earth elements by calcium monohydrate follows the Freundlich adsorption isotherm.[1] In the case of thorium, calcium oxalate trihydrate

1) B. C. Purkayastha and S. N. Bhattacharyya, *J. Inorg. Nucl. Chem.*, **10**, 103 (1959).
2) B. C. Purkayastha and S. N. Bhattacharyya, *J. Indian Chem. Soc.*, **41**, 71 (1964).
3) T. Shigematsu, M. Tabushi and M. Matsui, *Bull. Inst. Chem. Res., Kyoto Univ.*, **40**, 381 (1962).

does not take up thorium by way of mixed crystal formation, while dihydrate does.[2]

It was reported that the coprecipitation of a number of elements with calcium oxalate followed the logarithmic distribution law, and that some discrepancies existed in such systems as yttrium-calcium oxalates and scandium-calcium oxalates.[4] The former followed the logarithmic distribution law through a wide range of pH, while the latter obeyed the same law only below pH 3.5, and deviated gradually with increase in pH until pH 4 was reached, after which the system followed the homogeneous distribution law entirely.[8]

From the investigations cited above, it is obvious that the processes of coprecipitation are essentially affected by the forms of calcium oxalate crystals. A number of studies on the crystal forms of hydrated calcium oxalate are found in the literature.[5-7] Those on the phase diagrams and thermodynamic properties[8] have also been reported. For the most part of them, the description and identification of these crystalline species were given in terms of thermogravimetry, X-ray powder diffractometry and infrared spectrophotometry.

The conclusion may be drawn from the results of the above studies, that among various hydrates of calcium oxalate, the most stable one at room temperature is the monohydrate,[5] and the more unstable forms are the dihydrate, the trihydrates and the intermediate hydrates with nonintegral numbers of water molecules between two and three.[6] Some authors designated the monohydrate as form A, and the trihydrates as forms B, C, and D.[5,9] However, more proper names from mineralogy of whewellite[10] for form A and weddellite[11] for form B may be adopted in the investigation of the crystal structures.

Although the formation of solid solutions of trace amounts of rare earth elements with calcium oxalate has been studied by several groups of workers in recent years, little attention was paid to the study of precipitated phases of the calcium-rare earth element oxalate system when the percentage of rare earth element became high. On the other hand, many studies have been made on the phase relations by thermolysis between one hydrate and another, as well as between two forms of the anhydrous salt of calcium oxalate.[7,8,12] Nevertheless, investigations along these lines were scarcely extended beyond detailed information as to whether or not the phases of the calcium oxalate hydrates may have tendency to be changed or stabilized by other cations of similar size.

Experimental

Reagents. Gadolinium nitrate solution was prepared from 99.9% Gd_2O_3, supplied by Miyazaki Chemical Co., Tokyo, Japan. Calcium nitrate solution was prepared from the special grade (JIS) calcium carbonate. Concentrations of these solutions were determined by titration with standard EDTA solution.

Apparatus. All X-ray measurements were carried out with a Rigaku-Denki "Geigerflex" X-ray difractometer, and operated throughout this investigation at 30 kV and 15 mA, using a copper target.

Procedure. For the most of the data in this paper, a total of 200 m*l* of the solution containing about 3 mM of total ions was prepared as nitrate. Methyl red was used as an indicator, and a few drops of dilute ammonium hydroxide and then dilute nitric acid were added until the color just changed from yellow to pink. Most of the experiments were performed at the room temperature around 30°C.

To the above solution was added, with vigorous stirring, 50 m*l* of reagent solution containing 2 g of ammonium oxalate, sufficient to precipitate both the gadolinium and the calcium ions. The turbid mixture was allowed to settle over-night. Precipitated oxalates were collected on filter paper, and washed with a small amount of 0.5% ammonium oxalate, and then with deionized water.

The precipitation from hot solutions was made in the same manner as described above, except that the solutions containing calcium and gadolinium ions were heated to boil, and then hot solutions containing the ammonium oxalate were poured with vigorous stirring. Rapid precipitation set in almost immediately, and was usually completed within a few minutes.

Results

Since the main purpose of this experiment is to determine the forms of phases of the precipitates by means of X-ray powder diffraction, the d-spacings of the precipitates have been carefully compared with those of whewellite[10] and of weddellite.[11] The results are summarized and compiled in two tables.

(1) Precipitates prepared at room temperature

The precipitates containing 0—1 atomic % of gadolinium formed at room temperature consist of fine crystals with the characteristic spacings of whewellite. When the gadolinium content exceeds 2%, the precipitates no longer show whewellite-like structure, but exhibit the characteristic spacings of weddellite until the atomic percentage of gadolinium increases up to 30. The sharp contrast is readily seen in Table 1. For convenience, the two phases consisting of whewellite-like and weddellite-like

4) T. Shigematsu, M. Tabushi and M. Matsui, This Bulletin, **37**, 1610 (1964).
5) J. Lecomte, T. Pobeguin and J. Wyart, *J. Phys. Radium*, **6**, 22 (1945).
6) L. Walter-Levy and J. Laniepce, *Compt. Rend.*, **254**, 1073 (1962).
7) P. L. Waters, *Nature*, **178**, 324 (1956).
8) N. Gerard and G. Watelle-Marion, *Compt. Rend.*, **261**, 2363 (1965).
9) Fink, Inorganic Index to the Powder Diffraction File, **14**, 768—771, ASTM Publication (1965).
10) A. J. Gude, 3rd, E. J. Young, V. C. Kennedy and L. B. Riley, *Am. Mineralogist*, **45**, 1257 (1960).
11) C. O. Hutton and W. H. Taft, *Mineral. Mag.*, **34** (268), 256 (1965).
12) H. J. Arnott, F. G. E. Pautard and H. Steinfink, *Nature*, **208**, 1197 (1965).

Table 1. X-Ray powder diffraction data for Ca and Gd oxalate precipitated at room temperature (Cu$K\alpha$, λ=1.5418 Å)

Whewellite		Weddellite		Spacing	Atomic % of gadolinium										Phase
d(Å)	I	d(Å)	I	d(Å)	0	0.3	1	2	5	15	30	70	85	100	
				7.90										24	G
				7.63									100		γ
				7.56								86		53	γ, G
				7.53							17				γ
				7.50						24					γ
				6.24					16	11	9	4	4		β, γ
		6.17	90	6.22				16							β
5.95	75			5.97	11	12	13								α
5.79	27			5.83	6	4	4								α
				5.75								5	6		γ
				5.74						3	5				γ
				4.93										3	G
				4.80								4	4		γ
				4.79						3	5				γ
		4.40	60	4.44				7	8	4	2				β
				4.35									3	3	γ, G
				4.34						2	2	2			γ
				3.92										7	G
				3.91									4		G
				3.90							3	3			γ
				3.75								6	7		γ
				3.74						3	2				γ
3.63	100			3.66	30	13	12								α
				3.45									2	2	γ, G
				3.21						2	2	2	2	1	γ, G
		3.09	40	3.10				3	4	3	3	2			β
		2.82	10	2.83				5	5	3	2	2	2		β, γ
		2.77	100	2.79				12	16	11	5				β
				2.47								2	3		γ
				2.46							2				γ
		2.42	40	2.43				3	3	3	1				β
		2.40	40	2.41				5	5	3	2				β
				2.38							2	2	3	1	γ, G
2.36	68			2.37	11	7	6								α
		2.24	70	2.25				7	8	4	2				β
2.21	10	2.21	20	2.21	1	1	1	2	3	2	2				α, β
		2.12	50	2.12				2	3	2	1				β
				2.11										2	G
				2.10							2	2	3		γ

structures are respectively designated as α and β forms of the Ca-Gd oxalate system.

As the gadolinium content attained a range of between 30 and 85% in the solution, the coprecipitated phases give diffraction patterns with entirely different spacings, comprising 4.80, 3.90, 3.21, 2.46, 2.38, 2.10 A, *etc.* These are designated as the γ form so as to be distinguishable from the other forms. It is noteworthy that the values of the d-spacings for any form stated above do not vary over a wide range of composition.

Pure hydrated calcium oxalate and pure hydrated gadolinium oxalate were also prepared by the same method as described in the paragraph under the heading of " Procedure." The former is a typical artificial whewellite, and is distinctly recognizable from its characteristic spacings. The latter is not known in nature, and the name " G form " is given to this solid phase that has spacings of 7.56, 4.93, 4.35, 3.92, 3.45 A, *etc.* Among these, the 7.56 A spacing gives the strongest diffraction.

(2) Precipitates prepared at elevated temperature

The results are quite different when the coprecipitation was carried out at an elevated temperature. The precipitates thus obtained with amounts of

TABLE 2. X-RAY POWDER DIFFRACTION DATA FOR Ca AND Gd OXALATE PRECIPITATED AT ELEVATED TEMPERATURE (Cu$K\alpha$, $\lambda = 1.5418$ Å)

Whewellite		Spacing	Atomic% of gadolinium							Phase
d(Å)	I	d(Å)	0	10	30	50	70	85	100	
		6.17							100	G′
		6.09						33		δ
		6.07					29			δ
		6.01			51	32				α, δ
		5.99		63						α
5.95	75	5.95	59							α
		4.84							15	G′
		4.80			4	3	6	10		δ
		4.32							33	G′
		4.30					4	7		δ
3.63	100	3.65	55	45	40	27	28	11		α, δ
		3.13							11	G′
		3.12						4		δ
		3.11					4			δ
		3.04							8	G′
		3.03					10	9		δ
		3.02							10	G′
		2.98		31	29	19	17	9		α
2.97	100	2.97	31							α
		2.92		11	9	7	7	6	12	α, δ, G′
2.90	18	2.91	10							α
		2.52				4	5	6	7	δ, G′
		2.51						5		δ
2.49	35	2.50	12	9	8	7	7			α, δ
		2.45						7	15	δ, G′
		2.44						7		δ
2.36	68	2.36	31	21	19	15	13	11		α, δ
		2.34							15	G′
2.25	25	2.26	9	7	5	5				α
		2.15						5	10	δ, G′
		2.12							7	G′
		2.09						5		δ
2.07	21	2.08	9	4	5	7	5			α, δ
		1.99							7	G′
1.98	20	1.98	8	7	7	6	7	7		α, δ
		1.96						5		δ
1.95	16	1.95	7	7	10	7	5			α, δ
1.93	22	1.93	7	7	5	3				
		1.83							12	G′
1.81	13	1.82	7	5	5	4	6	7		α, δ

gadolinium varying from traces to a very large percentage are identified as fine crystals with characteristic spacings of whewellite, the α form according to our designation. No weddellite-like structure (β form) is found.

Pure hydrated gadolinium oxalate was also prepared. At temperatures around 100°C, a lower hydrate rather than a higher hydrate is formed. Its spacings are remarkably different from those of the G form, hence the name of G′ form is given to this phase. From solutions of high concentrations of gadolinium, still another phase appeared, which gave weak diffraction patterns. This phase is designated as the δ form. The various forms obtained from the solutions at the elevated temperature are summarized in Table 2.

Discussion

From the experimental results, proper formulas can be used to depict the various forms of the hydrated calcium and gadolinium oxalates which were precipitated in the respective solutions either at room temperature or at elevated temperatures.

TABLE 3. FORMULAS SUGGESTED FOR THE HYDRATED Ca-Gd OXALATES PRECIPITATED AT ROOM TEMPERATURE*

Form of phase	Formula
α	$(Ca_{1-x}, Gd_{2x/3})(COO)_2 \cdot H_2O$
β	$(Ca_{1-x}, Gd_{2x/3})(COO)_2 \cdot 2H_2O$*
γ	$(Gd_{1-x}, Ca_{3x/2})_3(COO)_3 \cdot mH_2O$
G	$(Gd_{1-x}, Ca_{3x/2})_2(COO)_3 \cdot nH_2O$

* The formula for the β form may be also expressed as

$$(Ca_{1-x}, Gd_{2x/3})(COO)_2 \cdot (2+y)H_2O$$

in which y has a value varying between 0 and 0.5. The fractional portion of the H_2O content is zeolitic.

TABLE 4. FORMULAS SUGGESTED FOR THE HYDRATED Ca-Gd OXALATES PRECIPITATED AT ELEVATED TEMPERATURES

Form of phase	Formula
α	$(Ca_{1-x}, Gd_{2x/3})(COO)_2 \cdot H_2O$
δ	$(Gd_{1-x}, Ca_{3x/2})_2(COO)_3 \cdot m'H_2O$
G'	$(Gd_{1-x}, Ca_{3x/2})_2(COO)_3 \cdot n'H_2O$

The formulas are listed in Tables 3 and 4.

Because no β form appears in the mixed crystals prepared at elevated temperatures, this form is evidently less stable toward heat than the α form. When the concentration of calcium ion is very high compared with that of gadolinium ion, the precipitated host lattice must be in the most stable form of whewellite. Owing to the very small amount of the guest gadolinium ions absorbed on the surface or entrapped by successive layers of the host lattice, the total amount of hydrated water of the guest lattice will also be small, and as a result, the α form rapidly aggregates.

When the concentration of gadolinium ions exceeds 2%, the number of water molecules brought into the lattice would be much greater than in the former case, and they may be capable of changing the monohydrate into the dihydrate of calcium oxalate. In other words, the host lattice of the whewellite-like phase is smoothly transformed into the other host lattice of weddellite-like phase following the reinforcement of gadolinium ions together with an abundant supply of hydrated water, resulting in the formation of the β form.

At elevated temperatures gadolinium ions are capable of migrating gradually into the lattice of calcium oxalate monohydrate up to a large amount without altering any spacing of the latter; as a result, words, the substitution of calcium ions by gadolinium ions in the α form phase under the experimental conditions can preceed to a great extent, sometimes expanding into the range of the δ form.

On the other hand, the G' form phase does not admit calcium ions into its lattice to an extent greater than a few percent. It follows that the phase of the δ form may be considered as a distorted phase of the G' form. With reference to Table 2, it is seen that any one set of spacings, possibly regarded as characteristic of the δ form, is almost identical with that of the G' form, or with only a very slight shift.

From the present study, it is tentatively suggested that a metastable solid phase like the β form may coexist temporarily with a more unstable phase like the γ form under ordinary experimental conditions. This is clearly seen from the data on the phases when the gadolinium content reaches 30%, as shown in Table 1. The same fact is observed with the α form and δ form which coexist with each other, as shown in Table 2.

BULLETIN OF THE CHEMICAL SOCIETY OF JAPAN VOL. 41 2059—2064 (1968)

Polarographic Behavior of Tris(2,2′-bipyridine)cobalt(II) and Tris(2,2′-bipyridine)cobalt(III) in Acetonitrile Solutions

Nobuyuki TANAKA and Yuichi SATO

Department of Chemistry, Faculty of Science, Tohoku University, Katahira-cho, Sendai

(Received March 18, 1968)

The electrode processes of tris(2,2′-bipyridine)cobalt(II) and tris(2,2′-bipyridine)cobalt(III) complexes at the dropping mercury electrode in acetonitrile solutions have been investigated by the measurement of direct current, alternating current and Kalousek polarograms. The cobalt(II) complex gave a one-step oxidation and a four-step reduction wave and the cobalt(III) complex, a five-step reduction wave, when tetraethylammonium perchlorate was used as supporting electrolyte. The solution containing the cobalt(II) and the cobalt(III) complexes gave a reversible composite wave. The limiting currents of the first two steps named from positive to negative potentials of the reduction wave of the cobalt(II) complex were diffusion-controlled, the first step being of a one-electron reduction process and the second step, of a two-electron reduction process. From the effect of free 2,2′-bipyridine and water on the reduction wave of the cobalt(II) complex and from the Kalousek polarograms, the electrode processes of the first two steps taking place in the presence of a large concentration of free 2,2′-bipyridine were estimated as,

$$[Co(bipy)_3]^{2+} \underset{-e}{\overset{e}{\rightleftharpoons}} [Co(bipy)_3]^{+} \underset{-2e}{\overset{2e}{\rightleftharpoons}} [Co(bipy)_3]^{-}$$

The effect of a small concentration of acrylonitrile on the reduction wave of the cobalt(II) complex was studied.

As acetonitrile is an aprotic solvent and has less oxidizing power than water, the electrode process in acetonitrile is sometimes quite different in water. Tris(2,2′-bipyridine)iron(II) complex cation in acetonitrile solutions is reduced to univalent tris-(2,2′-bipyridine)ferrate anion which cannot exist in aqueous solutions.[1,2] Such a low valent state is expected in bipyridine complexes of other metals.

In the present paper, the electrode processes of tris(2,2′-bipyridine)cobalt(II) and tris(2,2′-bipyridine)cobalt(III) complexes at the dropping mercury electrode (DME) are presented and the effect of acrylonitrile on the reduction wave of the cobalt(II) complex is discussed.

Experimental

Tris(2,2′-bipyridine)cobalt(II) perchlorate and tris-(2,2′-bipyridine)cobalt(III) perchlorate were prepared according to Burstall and Nyholm[3] and identified by elementary analysis. Acetonitrile, tetraethylammonium perchlorate and sodium perchlorate were the same as described in a previous paper.[2] Acrylonitrile used was of a reagent grade. The dropping mercury electrode used had an m value of 0.63_1 mg/sec and a drop time t_d of 4.84 sec, when measured in an air-free acetonitrile solution containing 0.05 M of $(C_2H_5)_4NClO_4$ at 25°C and at −0.5 V *vs.* SCE at 50 cm of the height of mercury reservoir. An aqueous saturated calomel electrode (SCE) served as a reference electrode. The electrolysis cell and other apparatus are the same as previously described.[2]

Results

Tris(2,2′-bipyridine)cobalt(II) complex gave a one-step oxidation wave from cobalt(II) to cobalt-(III) around +0.2 V *vs.* SCE, while tris(2,2′-bipyridine)cobalt(III) complex gave a reduction wave from cobalt(III) to cobalt(II) at almost the same potential. The plots of $\log \bar{i}/(\bar{i}_d - \bar{i})$ *vs.* E for the anodic and the cathodic wave gave straight lines. Half-wave potentials and the values of the slopes determined from the log-plot analysis were given in Table 1. The solution containing the same concentrations of the cobalt(II) and the cobalt(III) complexes showed a continuous oxidation-reduction wave and an equilibrium potential which was equal to the half-wave potentials of the oxidation wave of the cobalt(II) complex and the reduction wave of the cobalt(III) complex.

When tetraethylammonium perchlorate was used as supporting electrolyte, tris(2,2′-bipyridine)cobalt-(II) complex gave a four-step reduction wave as reproduced in Fig. 1 (curve a). In the solutions

1) N. Tanaka and Y. Sato, *Inorg. Nucl. Chem. Letters*, **2**, 359 (1966).
2) N. Tanaka and Y. Sato, *Electrochim. Acta*, **13**, 335 (1968).
3) F. H. Burstall and R. S. Nyholm, *J. Chem. Soc.*, **1952**, 3570.

TABLE 1. LOG-PLOT ANALYSIS FOR THE OXIDATION OF THE COBALT(II) AND THE REDUCTION OF THE COBALT(III) COMPLEXES (25°)*

Reaction	$E_{1/2}$, V *vs.* SCE	Slope, mV
Oxidation process	0.241	62
Reduction process	0.235	65

* Electrolytic solutions contain 0.5 mM complex and 0.05 M $(C_2H_5)_4NClO_4$.

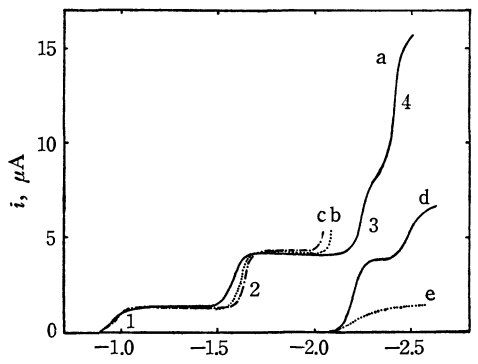

Fig. 1. D.c. polarograms of (a) 0.5 mM $[Co(bipy)_3](ClO_4)_2$, (b) (a) with 10.0 mM 2,2'-bipyridine, (c) (a) with 50.0 mM 2,2'-bipyridine, (d) 1.0 mM 2,2'-bipyridine and (e) 0.38 mM CH_2CHCN. Supporting electrolyte is 0.05 M $(C_2H_5)_4NClO_4$.

containing sodium perchlorate as supporting electrolyte, the first two steps were observed, which were followed by the reduction of sodium ions. The cobalt(III) complex gave a five-step reduction wave, of which the second to the fifth steps were exactly the same as the first to the fourth steps of the cobalt(II) complex. In this paper, the polarographic behavior of the cobalt(II) complex is presented.

The limiting currents of the first (at −1.2 V) and the second step (at −1.8 V) named from positive to negative potentials were found to be proportional to the square root of the mercury pressure on the DME between 45 and 60 cm. The limiting currents were also proportional to the concentration of the complex. Upon the addition of free 2,2'-bipyridine to the solution containing 0.5 mM of the complex, the limiting currents of the first two steps were not affected, but those of the third and the fourth step were increased. The half-wave potential and the slope of the log-plot analysis (57 mV) of the first step were not affected, whereas the half-wave potential of the second step shifted to more negative potentials and the slope of the log-plot approached to the value of that of a reversible two-electron electrode process with increasing concentrations of free bipyridine (see Table 2). The half-wave potential of the third and the fourth step shifted to less negative potentials. Free 2,2'-bipyridine gave a two-step

TABLE 2. LOG-PLOT ANALYSIS FOR THE SECOND STEP OF THE REDUCTION OF THE COBALT(II) COMPLEX AT VARIOUS CONCENTRATIONS OF 2,2'-BIPYRIDINE*

Conc. of 2,2'-bipyridine, mM	$E_{1/2}$, V *vs.* SCE	Slope, mV
0	−1.580	57
10	−1.617	40
50	−1.632	35

* Electrolytic solutions contain 0.5 mM $[Co(bipy)_3](ClO_4)_2$, 0.05 M $(C_2H_5)_4NClO_4$ and various concentrations of 2,2'-bipyridine.

reduction wave at potentials corresponding nearly to the third and the fourth step of the polarogram of the complex as shown in Fig. 1.

By the addition of a small concentration of water into the acetonitrile solution containing 0.5 mM of the complex and 0.05 M of $(C_2H_5)_4NClO_4$, the limiting currents of the first two steps of the reduction wave were scarcely affected, but the third and the fourth step shifted to less negative potentials and the limiting current of the third step increased (Fig. 2). By further addition of water, the third step shifted to less negative potentials and the second step became ill-defined. The polarogram of free 2,2'-bipyridine was also affected by the addition of water; its reduction potential shifted to less negative potentials and its limiting current increased.

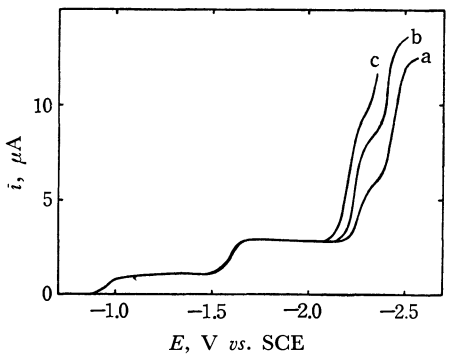

Fig. 2. D.c. polarograms of 0.5 mM $[Co(bipy)_3](ClO_4)_2$ (a) in the absence and in the presence of (b) 0.028 M and (c) 0.139 M of water. Supporting electrolyte is 0.05 M $(C_2H_5)_4NClO_4$.

The reversibilities of the first two steps were confirmed by the measurement of Kalousek polarograms, which are shown in Fig. 3. A two-step oxidation wave was obtained, when the electrode potential was set up at −1.9 V (curves b and b' in Fig. 3).

Acetonitrile often contains acrylonitrile as impurity, which gives a drawn-out cathodic wave at about −2.3 V as reproduced in Fig. 1 (curve e). Kalousek polarogram of acrylonitrile gave a one-step oxidation wave at about −0.6 V, when the electrode potential was set up at the potential of the

limiting current of the reduction wave of acrylonitrile. When acrylonitrile was present in the solution, the reduction wave of cobalt(II)-bipyridine complex was affected and two new steps appeared, which were named 2 A and 2 B (curves b and c in Fig. 4). The 2 A step started from about −1.3 V followed by the second step, and its limiting current

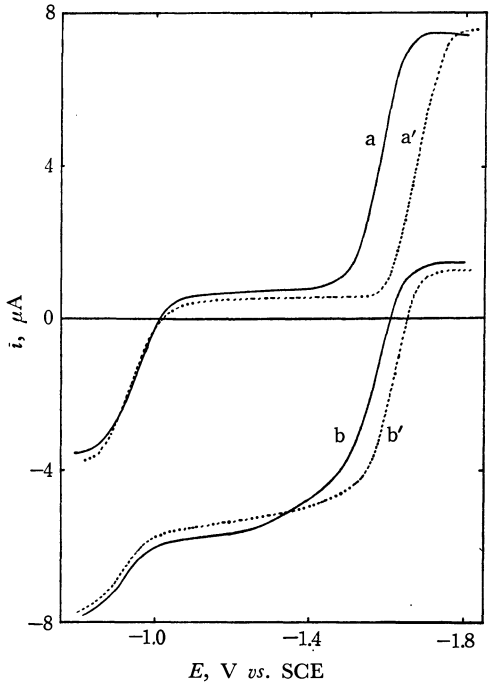

Fig. 3. Kalousek polarograms of 0.5 mM $[Co(bipy)_3](ClO_4)_2$ (a and b) in the absence and (a′ and b′) in the presence of 50 mM of 2,2′-bipyridine. Supporting electrolyte is 0.05 M $(C_2H_5)_4NClO_4$. E_2 potentials are set up at −1.20 V for a and a′ and −1.90 V for b and b′.

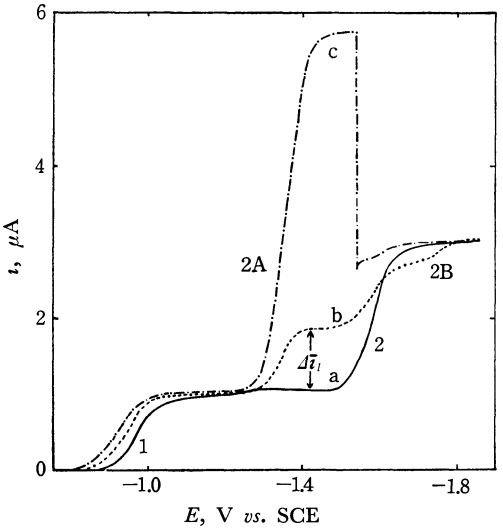

Fig. 4. D.c. polarograms of 0.5 mM $[Co(bipy)_3](ClO_4)_2$ (a) in the absence and in the presence of (b) 0.38 mM and (c) 1.9 mM of CH_2CHCN. Supporting electrolyte is 0.05 M $(C_2H_5)_4NClO_4$.

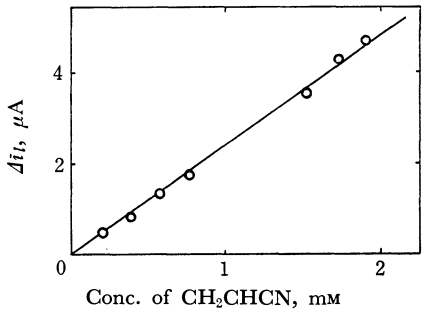

Fig. 5. Limiting current of the 2A step as a function of the concentration of acrylonitrile, obtained with the solutions containing 0.5 mM $[Co(bipy)_3](ClO_4)_2$, CH_2CHCN and 0.05 M $(C_2H_5)_4NClO_4$. For Δi_l, see curve b in Fig. 4.

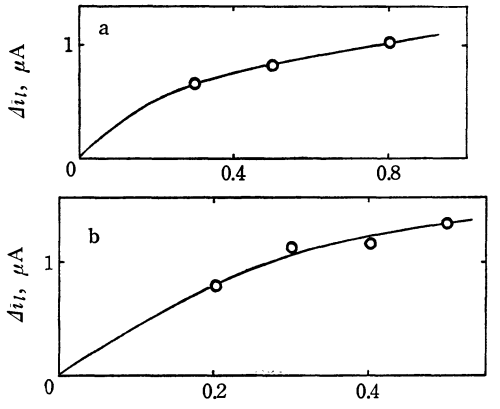

Fig. 6. Limiting current of the 2A step as a function of concentration of the complex, obtained with the solutions containing $[Co(bipy)_3](ClO_4)_2$, 0.05 M $(C_2H_5)_4NClO_4$ and (a) 0.38 mM CH_2CHCN and (b) 0.57 mM CH_2CHCN. For Δi_l, see curve b in Fig. 4.

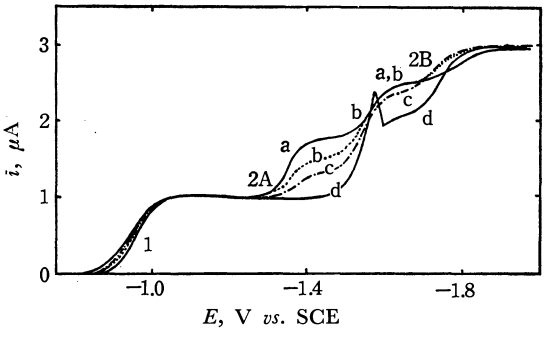

Fig. 7. D.c. polarograms of 0.5 mM $[Co(bipy)_3](ClO_4)_2$ in the presence of 0.38 mM CH_2CHCN and (a) 0, (b) 1.0 mM, (c) 2.0 mM and (d) 10.0 mM 2,2′-bipyridine. Supporting electrolyte is 0.05 M $(C_2H_5)_4NClO_4$.

(the difference of the limiting currents at -1.45 V in the presence and the absence of acrylonitrile, Δi_l) was proportional to the concentration of acrylonitrile at the constant concentration of the complex (see Fig. 5), and to the square root of the height of the mercury reservoir. Although the limiting current of the 2 A step was increased with increasing concentrations of the complex at the constant concentration of acrylonitrile, Δi_l was not proportional to the concentration of the complex, but approached to a definite value (Fig. 6). When the concentration of acrylonitrile was about five times larger than that of the complex, the 2 A step gave a peak current and its reproducibility was poor. By adding free 2,2′-bipyridine to the solution the 2 A step was depressed and the 2 B step became more noticeable, as seen in Fig. 7. In the solution containing 0.5 mM of the complex and 0.38 mM of acrylonitrile, the 2 A step almost disappeared by the addition of about 6 mM of free bipyridine.

A.c. polarograms of the cobalt(II) complex were recorded in the presence and in the absence of acrylonitrile and free bipyridine (Fig. 8). The solution containing only the complex showed four peakss which corresponded to the above-mentioned four steps of the d.c. polarogram. In Fig. 8, the first two peaks are reproduced. The other two peaks which appeared at more negative potentials are considered to be the reduction of the ligand coordinated to cobalt. By adding acrylonitrile two new peaks named 2 A and 2 B appeared. The addition of 10 mM of free bipyridine depressed the 2 A peak as shown in Fig. 8 (curve c). The solution

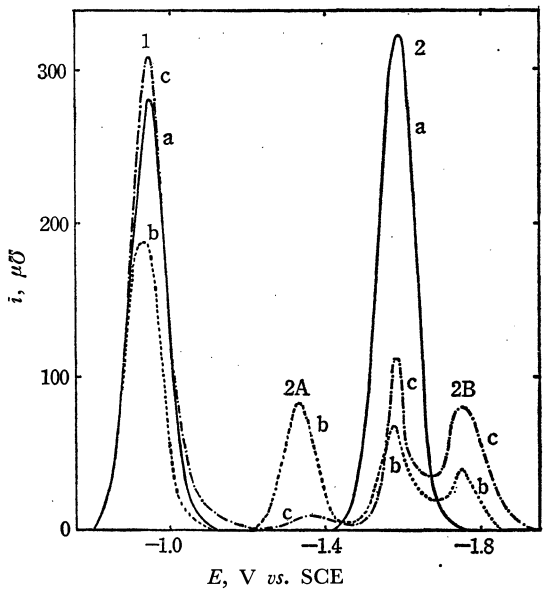

Fig. 8. A.c. polarograms of 0.5 mM $[Co(bipy)_3](ClO_4)_2$ (a) in the absence and in the presence of (b) 0.38 mM CH_2CHCN and (c) 0.38 mM CH_2CHCN and 10.0 mM 2,2′-bipyridine. Supporting electrolyte is 0.05 M $(C_2H_5)_4NClO_4$.

containing only acrylonitrile showed a small peak of irreversible-type at about -2.2 V.

Discussion

The slopes of the log-plot and the half-wave potentials for the reduction of the cobalt(III) and the oxidation of the cobalt(II) complexes show that the electrode process of the coabalt(III) and the cobalt(II) system,

$$[Co(bipy)_3]^{3+} + e \rightleftharpoons [Co(bipy)_3]^{2+}$$

is reversible at the DME. The continuous oxidation-reduction wave which was obtained with a solution containing the same concentrations of the cobalt(III) and the cobalt(II) complex confirmed the above conclusion.

The limiting currents of the first two steps of the reduction wave of the cobalt(II) complex are concluded to be diffusion-controlled from the linearities of the limiting currents on the square root of the mercury pressure and on the concentration of the complex. The diffusion current constant for the first step obtained by the Ilkovič equation is 2.17, which is nearly equal to the value of a one-electron reduction of tris(2,2′-bipyridine)iron(II) complex.[2] The ratio of the wave heights of the first two steps is 1 : 2 after corrected for the drop time. The fact that the wave heights of the first two steps of the complex are not influenced by the addition of free 2,2′-bipyridine and a small concentration of water but those of the last two steps are influenced shows that the electrode processes of the first two steps and the latter two steps are different in nature.

From the same considerations as in the case of the reduction of the iron(II) complex[2] in addition to the fact that the reduction potential of free 2,2′-bipyridine is equal to the potential of the third and the fourth step of the reduction wave of the complex (see Fig. 1), the first two steps are concluded to be due to the reduction of the cobalt(II) complex itself and the latter two steps, the reduction of free bipyridine liberated from the complex. The second step seems to be a two-electron reduction from the cobalt(I) complex to the cobalt(-I) complex and the electrode process is considered to consist of various paths, such as a reduction from $[Co(bipy)_3]^+$, and that from $[Co(bipy)_{3-n}]^+$, the reduction potentials of the latter being less negative than the former. As the concentration of free bipyridine is increased, the reaction path from $[Co(bipy)_3]^+$ will be predominant because the half-wave potential shifted to more negative potentials and the reciprocal slope of the log-plot became smaller and approached to the theoretical value of a two-electron reversible process (see Table 2).

Kalousek polarograms also suggested the formation of the cobalt(I) and the cobalt(-I) complex at the electrode surface at the potentials of the first and the second step, respectively. Thus, the reaction

scheme may be written as,

$$
\begin{array}{ccc}
[Co(bipy)_3]^{2+} & & \\
+ & & \\
e & & \text{(the first step)} \\
\downarrow\uparrow & & \\
[Co(bipy)_3]^{+} & \rightleftharpoons & [Co(bipy)_{3-n}]^{+} + n\ \text{bipy} \\
+ & & + \\
2e & & 2e \qquad \text{(the second step)} \\
\downarrow\uparrow & & \downarrow\uparrow \\
[Co(bipy)_3]^{-} & \rightleftharpoons & [Co(bipy)_{3-n}]^{-} + n\ \text{bipy}
\end{array}
$$

Vlček[4] and Waind and Martin[5] found the cobalt(I) state polarographically and were successful in preparing the compound. Herzog, Klausch and Lantos[6] prepared the cobalt(0) complex, $[Co(bipy)_3]$, from $CoCl_2$ and Li_2bipy in tetrahydrofuran. The bipyridine complex of cobalt(-I) has not been prepared yet according to the author's knowledge. The reason why the reduction process to the cobalt(0) complex is not observed at the DME is probably in the fact that the cabalt(0)-bipyridine complex is not sufficiently stable in acetonitrile and the cobalt(I) complex is reduced directly to the cobalt(-I) state.

The reduction mechanism of acrylonitrile at the DME in acetonitrile has not been discussed,[7] although the reduction wave is often used for the analysis of residual acrylonitrile monomer in styrene-acrylonitrile copolymer.[8] The electrode process of acrylonitrile is considered to be irreversible from the shape of the drawn-out wave (curve e in Fig. 1) and the small peak current of the a.c. polarogram. Kalousek polarogram also confirmed the irreversibility of the electrode process. Proton will not take part in the reduction process because the electrode reaction proceeds in acetonitrile of aprotic solvent. If proton took part in, the reduction product of acrylonitrile at the electrode surface would be propionitrile, CH_3CH_2CN, as was found in aqueous solutions.[9] This is not the case because propionitrile gives no oxidation wave at about -0.6 V[10] where an oxidation wave is observed in a Kalousek polarogram. Since acrylonitrile polymer radical has been observed by e.s.r.[11] the reduction product of acrylonitrile is likely to be an acrylonitrile radical, but not a propionitrile molecule. Stylene, $C_6H_5CH=CH_2$, and crotonic acid, $CH_3CH=CHCOOH$ also give a reduction wave at about -2.45V and -2.3V, respectively, and at the Kalousek circuit, an anodic wave at about -1.15 V and $+0.1$ V, respectively. Although acrylonitrile itself is reduced at such a negative potential as -2.3 V, the reduction wave of the cobalt(II) complex is affected at about -1.4 V (2 A wave) and -1.7 V (2 B wave) in the presence of a small concentration of acrylonitrile (curve b and c in Fig. 4). From the proportionalities of the limiting current of the 2 A step on the concentration of acrylonitrile at the constant concentration of the complex (Fig. 5) and on the square root of the height of the mercury reservoir, the 2 A step seems to be controlled by the diffusion of acrylonitrile. The temperature coefficient of the limiting current of the 2 A step was found to be 1.3%/deg at 25°. Even when the concentration of acrylonitrile is larger than that of the complex, the limiting current of the 2 A step is proportional to the concentration of acrylonitrile. However, the limiting current suddenly decreased at the potential of the first half of the second step and the limiting current at -1.9 V is constant irrespective of the concentration of acrylonitrile as far as the concentration of the complex is the same (curve c in Fig. 4). The dependency of $\Delta\bar{i}_l$ on the concentration of the complex at the constant concentration of acrylonitile is almost in agreement with the Langmuir isotherm. All these results suggest that the 2 A step is not due to a reduction of the complex but due to that of acrylonitrile in the presence of cobalt(I) species at the electrode. Since the 2 A step was suppressed by the addition of free 2,2′-bipyridine as shown in Fig. 7, the reduction of acrylonitrile seems to require the species of $[Co(bipy)_{3-n}]^{+}$ at the electrode surface. The cobalt(I) complex formed at the electrode is considered to be substitution-labile, because the half-wave potential of the second step was shifted to more negative potentials with increasing concentrations of free bipyridine. Therefore, in the absence of free bipyridine, cobalt(I) species formed at the electrode surface at -1.1 to -1.5 V may be mainly $[Co(bipy)_{3-n}]^{+}$. An acrylonitrile molecule to be reduced approaches to the electrode and may be coordinated to the central cobalt ion in $[Co(bipy)_{3-n}]^{+}$ which is adsorbed on the surface of the electrode. The reduction of acrylonitrile will occur at this state. If free bipyridine is present in the solution, the coordination of acrylonitrile to the central cobalt(I) ion is hindered and consequently the limiting current of the 2 A step is decreased. In this electrode process, the cobalt(I) species acts as a role of bridge for the electron transfer from the electrode to acrylonitrile molecule. The complex formation between acrylonitrile and $[Co(bipy)_{3-n}]^{+}$ does not occur in the bulk of the solution but at the electrode surface, because the limiting current of the 2 A step is proportional to the concentration of acrylonitrile but not to that of the complex. An acrylonitrile molecule seems to be coordinated at its double bond

4) A. A. Vlček, *Nature*, **180**, 753 (1957).
5) G. M. Waind and B. Martin, *J. Inorg. Nucl. Chem.*, **8**, 551 (1958).
6) S. Herzog, R. Klausch and J. Lantos, *Z. Chem.*, **4**, 150 (1964).
7) J. F. Coetzee, G. P. Cunningham, D. K. McGuire and G. R. Padmanabhan, *Anal. Chem.*, **34**, 1139 (1962).
8) G. C. Claver and M. E. Murphy, *ibid.*, **31**, 1682 (1959).
9) T. Asahara, S. Hayano, M. Senō and H. Kaneko, *Denki Kagaku*, **35**, 882 (1967).
10) R. C. Larson and R. T. Iwamoto, *J. Am. Chem. Soc.*, **82**, 3526 (1960).
11) C. H. Bamford, A. D. Jenkins, D. J. E. Ingram and M. C. R. Symons, *Nature*, **175**, 894 (1955).

rather than at its CN group, because a solvent molecule (acetonitrile) has also a CN group and its concentration is about 5×10^4 times greater than that of acrylonitrile. In the case of iron(I) tetracarbonyl acrylonitrile ($Fe(CO)_4CH_2$=CHCN), both a double-bonded type and a σ-bonded type of bonding of acrylonitrile to the central iron are known.[12,13] The potential of the 2 A step is nearly the middle between the reduction potential of acrylonitrile and the oxidation potential of its reduction product obtained by the Kalousek circuit. The overpotential of acrylonitrile appears to be lessened by the coordination to cobalt(I) at the electrode surface. At the potentials of the 2nd step where cobalt(I) is reduced to cobalt(−I) state, the 2 A step vanishes, and acrylonitrile cannot coordinate to the cobalt(−I) and consequently the limiting current of the second step is constant at about −1.9 V irrespective of the concentration of acrylonitrile. A similar phenomenon as the 2 A step is observed in the case of crotonic acid but the situation seems to be more complicated. The 2B step appears to occur by the retardation of the electrode process of the acrylonitrile as the current-potential curve at the second step is seen to be cut off and the limiting current at about −1.9 V is always constant.

The authors wish to thank the Ministry of Education for the financial support granted for this research.

12) S. F. A. Kettle and L. E. Orgel, *Chem. Ind. (London)*, **1960**, 49.
13) E. H. Schubert and R. K. Sheline, *Inorg. Chem.*, **5**, 1071 (1966).

BULLETIN OF THE CHEMICAL SOCIETY OF JAPAN VOL. 41 2064—2066 (1968)

Polarographic Behavior of Tris(2,2′-bipyridine)manganese(II) in Acetonitrile Solutions

Yuichi SATO and Nobuyuki TANAKA

Department of Chemistry, Faculty of Science, Tohoku University, Katahira-cho, Sendai

(Received March 27, 1968)

Polarographic behavior of tris(2,2′-bipyridine)manganese(II) perchlorate at the dropping mercury electrode in acetonitrile solutions has been investigated by the measurement of d.c., a.c. and Kalousek polarograms. The manganese(II) complex gave a five-step reduction wave and a one-step oxidation wave at the dropping mercury electrode when tetraethylammonium perchlorate was used as supporting electrolyte. In the presence of a large concentration of free 2,2′-bipyridine, the limiting currents of the first three steps of the reduction of the manganese(II) complex are all diffusion-controlled and of a one-electron reduction process. The electrode processes for these steps have been concluded to be the reductions to $[Mn(bipy)_3]^+$, $[Mn(bipy)_3]$ and $[Mn(bipy)_3]^-$, respectively.

The electro-reduction of tris(2,2′-bipyridine)manganese(II) complex at the dropping mercury electrode (DME) in ethanol solutions and the formation of tris(2,2′-bipyridine)manganese(I) cation, $[Mn(bipy)_3]^+$, at the electrode surface were briefly reported.[1]

In acetonitrile solutions the electro-reduction of tris(2,2′-bipyridine)manganese(II) complex is expected to proceed to the lower oxidation state as was observed with tris(2,2′-bipyridine)iron(II)[2] and tris(2,2′-bipyridine)cobalt(II)[3] complexes.

The present paper is concerned with the polarographic behavior of tris(2,2′-bipyridine)manganese(II) complex and the support on the formation of $[Mn(bipy)_3]$ and $[Mn(bipy)_3]^-$ at the DME in acetonitrile solutions.

Experimental

Tris(2,2′-bipyridine)manganese(II) perchlorate, $[Mn(bipy)_3](ClO_4)_2$ was prepared according to Burstall and Nyholm[4] and identified by chemical analysis. Acetonitrile, tetraethylammonium perchlorate and sodium perchlorate were the same as described in a previous paper.[2] The dropping mercury electrode used had an m value of 0.63_1 mg/sec and a drop time t_d of 4.83 sec when measured in an air-free acetonitrile solution

1) A. A. Vlček, *Pure and Applied Chem.*, **10**, 61 (1965).
2) N. Tanaka and Y. Sato, *Inorg. Nucl. Chem. Letters*, **2**, 359 (1966); *Electrochim. Acta*, **13**, 335 (1968).
3) N. Tanaka and Y. Sato, This Bulletin, **41**, 2059 (1968).
4) F. H. Burstall and R. S. Nyholm, *J. Chem. Soc.*, **1952**, 3570.

containing 0.05 M of $(C_2H_5)_4NClO_4$ at 25°C and at −0.5 V *vs.* SCE at 50 cm of the height of mercury reservior. An aqueous saturated calomel electrode (SCE) served as reference electrode. The electrolysis cell and other apparatus are previously reported.[2)]

Results

Tris(2,2'-bipyridine)manganese(II) complex gave a five-step reduction wave with a maximum at the second step when tetraethylammonium perchlorate was used as supporting electrolyte (Fig. 1). In the solutions containing sodium perchlorate as supporting electrolyte only the first two steps were observed which were followed by the reduction of sodium ions.

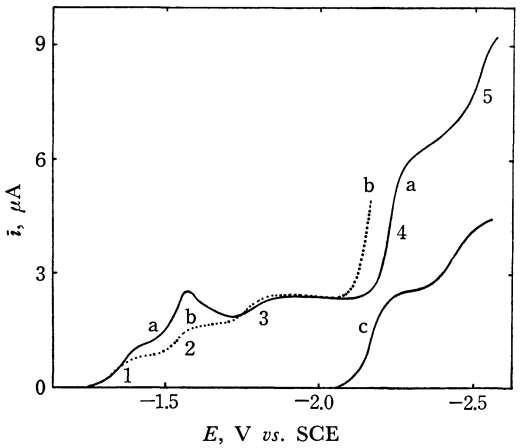

Fig. 1. D.c. polarograms of 0.5 mM $[Mn(bipy)_3](ClO_4)_2$ (a) in the absence and (b) the presence of 5.0 mM 2,2'-bipyridine and (c) that of 0.5 mM free 2,2'-bipyridine. Supporting electrolyte is 0.05 M $(C_2H_5)_4NClO_4$.

Upon the addition of free 2,2'-bipyridine, the maximum at the second step was depressed (Fig. 2) and the limiting currents of the fourth and the fifth step increased. In the presence of 5.0 mM or more, the reduction potentials and the limiting currents of the first three steps which are shown by curve d in Fig. 2 were almost the same irrespective of the concentration of bipyridine. Therefore, the nature of the limiting currents of the first three steps was investigated with the solutions containing excess 2,2'-bipyridine. The limiting currents of the first three steps were found to be proportional to the square root of the mercury pressure between 45 cm and 60 cm on the DME and also to the concentration of the complex. The results of log-plot analysis of the first step of the reduction at various concentrations of 2,2'-bipyridine are given in Table 1. At a large concentration of 2,2'-bipyridine compared with the complex, the half-wave potentials and the slopes of log-plot seem to be constant irrespective of the concentration of bipyridine. Free 2,2'-bipyridine gave a two-step reduction wave at the potentials

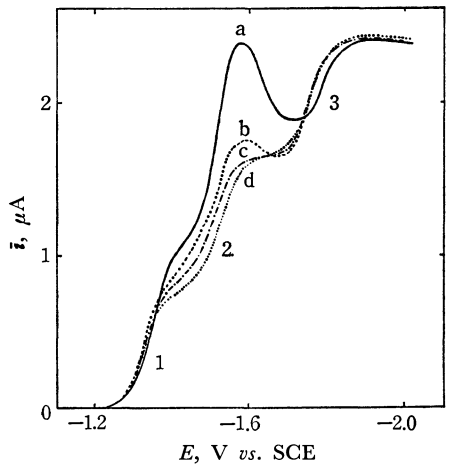

Fig. 2. The effect of free 2,2'-bipyridine upon the first three steps of the reduction wave of 0.5 mM $[Mn(bipy)_3](ClO_4)_2$. The concentrations of 2,2'-bipyridine are (a) 0, (b) 0.5 mM, (c) 1.0 mM and (d) 5.0 mM.

Table 1. Half-wave potentials and slopes of log-plots for the first step of the reduction wave of 0.5 mM $[Mn(bipy)_3](ClO_4)_2$ in acetonitrile solutions containing various concentrations of 2,2'-bipyridine and 0.05 M $(C_2H_5)_4NClO_4$ at 25°C.

Concn. of 2,2'-bipyridine mM	$E_{1/2}$ V *vs.* SCE	Slope mV
0	−1.347	69
0.5	−1.340	75
1.0	−1.335	71
2.0	−1.329	65
5.0	−1.333	65
10.0	−1.327	64

where tris(2,2'-bipyridine)manganese(II) complex gave the fourth and the fifth wave, respectively, as shown in Fig. 1.

Upon the addition of a small concentration of water into the acetonitrile solution, the first three steps of the reduction wave were scarcely affected, but the fourth and the fifth step shifted to less negative potentials and the limiting currents increased as seen in the five-step reduction wave of tris(2,2'-bipyridine)iron(II) cmplex.[2)]

The reversibilities of the first three steps were confirmed by the measurement of Kalousek polarograms, which are shown in Fig. 3. A one-step, a two-step and a three-step oxidation wave were obtained, when the electrode potentials were set up at −1.40 V, −1.65 V and −1.95 V respectively.

A.c. polarograms of the complex gave five peaks; their peak potentials were found to coincide with the half-wave potentials of the corresponding steps of the

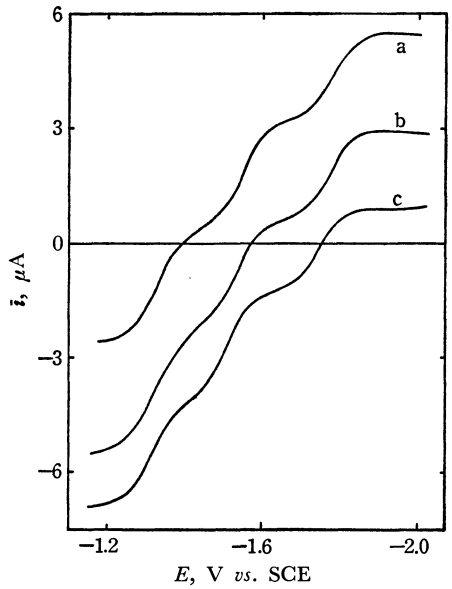

Fig. 3. Kalousek polarograms of the solution containing 0.5 mM $[Mn(bipy)_3](ClO_4)_2$, 50.0 mM 2,2′-bipyridine and 0.05 M $(C_2H_5)_4NClO_4$. Electrode potentials are set up at (a) −1.40 V, (b) −1.65 V and (c) −1.95 V. Exchange frequency is about 14 Hz.

d.c. polarogram. The addition of free 2,2′-bipyridine to the solution of the complex increased the fourth and the fifth peak current, but gave almost no influence on the first, the second and the third one.

The complex gave a one-step anodic wave at about +0.3 V which was almost the same as the potential of anodic wave of free 2,2′-bipyridine. However, neither the manganese(II) complex nor free 2,2′-bipyridine gave an anodic wave at less positive potentials than +1.9 V,[2] when the rotated platinum electrode was used as a working electrode.

Discussion

The limiting currents of the first three steps of the reduction wave of tris(2,2′-bipyridine)manganese(II) complex in the presence of excess 2,2′-bipyridine are concluded to be diffusion-controlled from the linearities of the limiting currents on the square root of the mercury pressure and the complex concentrations. The diffusion current constant for the first step calculated by the Ilkovič equation is 1.95, which is nearly equal to the values of one-electron reduction of various metal ions[5] and tris(2,2′-bipyridine)iron(II)[2] and tris(2,2′-bipyridine)cobalt(II)[3] in acetonitrile solutions. The ratio of the wave height for the first three steps obtained at a large concentration of 2,2′-bipyridine is 1 : 1 : 1 after corrected for the drop time. The slope of log-plot analysis for the first step approaches to the value of a reversible one-electron reduction with increasing concentrations of 2,2′-bipyridine (Table 1). 2,2′-Bipyridine seems to act as a maximum suppressor. The effect of 2,2′-bipyridine and water on the d.c. ploarogram suggests that the first three steps and other two steps observed at more negative potentials are different in nature from the same consideration as in the case with the reduction of the iron(II)[2] and the cobalt(II)[3] complexes. From all these results mentioned above, each of the first three steps of the manganese(II) complex is concluded to be a one-electron reduction of the complex itself as given by

$$[Mn(bipy)_3]^{2+} \underset{-e}{\overset{e}{\rightleftharpoons}} [Mn(bipy)_3]^{+} \underset{-e}{\overset{e}{\rightleftharpoons}}$$

$$[Mn(bipy)_3] \underset{-e}{\overset{e}{\rightleftharpoons}} [Mn(bipy)_3]^{-}$$

and the other two steps, the reduction of the ligand liberated from the complex. Kalousek polarograms show that the electrode process of each of the first three steps is reversible and also confirm the existence of low oxidation states such as $[Mn(bipy)_3]^+$, $[Mn(bipy)_3]$ and $[Mn(bipy)_3]^-$ at the electrode surface in acetonitrile.

The formation of tris(2,2′-bipyridine)manganese(I) state at the DME in ethanol was already reported by Vlcek,[1] though the compound seems not to be isolated. Herzog and Schmidt prepared tris(2,2′-bipyridine)manganese(0), $[Mn(bipy)_3]$,[6] and lithium tris(2,2′-bipyridine)manganate(−I), $Li[Mn(bipy)_3]\cdot 4THF$,[7] in tetrahydrofuran(THF). These facts confirm the above explanation for the first three steps of the reduction wave of the manganese(II) complex in acetonitrile. It may be concluded from the results obtained with the rotated platinum electrode that the anodic wave observed at +0.3 V is not the oxidation of manganese(II) to higher oxidation state but the oxidation of mercury to form mercury-bipyridine complexes, bipyridine being liberated from the manganese(II) complex at the electrode surface.

The authors wish to express their thanks to the Ministry of Education for the financial support granted for this research.

5) I. M. Kolthoff and J. F. Coetzee, *J. Am. Chem. Soc.*, **79**, 1852 (1957).

6) S. Herzog and M. Schmidt, *Z. Chem.*, **2**, 24 (1962).

7) S. Herzog and M. Schmidt, *ibid.*, **3**, 392 (1963).

BULLETIN OF THE CHEMICAL SOCIETY OF JAPAN VOL. 41 2067—2072 (1968)

Polarographic and Spectroscopic Studies on the Ion-pair Formation of Trioxalatocobaltate(III) Ions with Cations in Aqueous Solutions

Nobuyuki TANAKA and Kazuo KOSEKI

Department of Chemistry, Faculty of Science, Tohoku University, Katahira-cho, Sendai

(Received March 18, 1968)

The ion association between trioxalatocobaltate(III) anion and uni-, bi- and tervalent cations in aqueous solutions has been studied by polarographic and ultraviolet, visible and infrared spectroscopic methods. The association constants have been obtained by the measurement of the polarographic diffusion current of trioxalatocobaltate(III) ions in the presence of varied concentrations of cations at ionic strength 0.1 (NH_4NO_3) and 25°C. The influence of ammonium ion was taken into consideration in the treatment of polarographic data. The values obtained are 7.9 for $(CH_3)_4N^+[Co(ox)_3]^{3-}$, 3.7 ± 0.4 for $(C_2H_5)_4N^+[Co(ox)_3]^{3-}$, 22 ± 1 for $Na^+[Co(ox)_3]^{3-}$, 56 ± 6 for $Mg^{2+}[Co(ox)_3]^{3-}$, 55 ± 4 for $Ca^{2+}[Co(ox)_3]^{3-}$, 53 ± 3 for $Sr^{2+}[Co(ox)_3]^{3-}$, 55 ± 7 for $Ba^{2+}[Co(ox)_3]^{3-}$ and 118 ± 17 for $Al^{3+}[Co(ox)_3]^{3-}$. The association constant of $NH_4^+[Co(ox)_3]^{3-}$ was determined by the conductivity measurement to be 33.6 ($\log K=1.5_3$) at zero ionic strength. No change was observed in the visible, the ultraviolet and the infrared absorption spectra of trioxalatocobaltate(III) ions upon the addition of various cations even at the concentration at which the ion-pair formation is assumed to occur from the polarographic studies. These facts indicate that, in a sense of equilibrium study, there is no direct interaction between the complex anion and the cation, but one or more water molecules interpose between the two ions.

In recent years a number of investigations have been made of the ion-pair formation in solutions by many kinds of method. However, their results are not necessarily consistent with each other. The so-called "ion-pair" involves many different types, *e.g.*, a contact ion-pair, a solvent shared ion-pair and a solvent separated ion-pair.[1] Different types of ion-pairs are detected according to the characteristics of the methods used in the investigation. This may be a cause of the disagreement.

One of the purposes of this study is to determine the association constants between trioxalatocobaltate (III) anion and univalent, bivalent and tervalent cations using the polarographic method presented in a previous paper.[2] The other is to obtain some informations of the outer-sphere ion association from the comparison of the polarographic data with the visible, the ultraviolet and the infrared absorption spectra.

Experimental

Materials. Potassium trioxalatocobaltate(III) and ammonium trioxalatocobaltate(III) were prepared by the usual method.[3] The preparation of calcium, strontium and barium salts of trioxalatocobaltate(III) was made as follows. Calcium perchlorate which was prepared by the procedure of Smith and Koch[4] was added in excess to the solution of potassium trioxalatocobaltate(III) to precipitate potassium perchlorate. After filtration, calcium trioxalatocobaltate(III) was precipitated by the addition of ethanol. It was purified from aqueous solution by precipitating with ethanol. Strontium and barium trioxalatocobaltates(III) were prepared in the same way. Tetramethylammonium nitrate was prepared from $(CH_3)_4NBr$ and $AgNO_3$, and was recrystallized from water. Tetraethylammonium perchlorate was obtained according to Cokal and Wise.[5] All other chemicals used were of a guaranteed reagent grade.

Measurements. For the measurement of the limiting diffusion current, polarograms were recorded with a Shimadzu RP-2 polarograph in the solution of ionic strength 0.1 (adjusted with NH_4NO_3) containing 0.005% gelatin. The cell temperature was maintained at 25.0°C by means of a water thermostat. To avoid the effect of light, all the measurements were made with a brown-colored cell in a dark room. Since the trioxalatocobaltate(III) ions were reduced gradually to cobalt(II) in the presence of metallic mercury, the polarographic measurements were made as soon as possible after the dissolution of the complex and the removal of the dissolved oxygen in the solution.

The conductivity measurements were made in a glass cell equipped with platinized platinum electrodes using a Yokokawa BV-Z-103 B Wheatstone bridge. The cell constant was obtained to be 0.421 cm^{-1} by measuring

1) T. R. Griffiths and C. R. Symons, *Mol. Phys.*, **3**, 90 (1960).
2) N. Tanaka, K. Ogino and G. Satô, This Bulletin, **39**, 366 (1966).
3) S. P. L. Sörensen, *Z. Anorg. Chem.*, **11**, 2 (1896).
4) G. F. Smith and E. G. Koch, *Z. Anorg. Allg. Chem.*, **223**, 18 (1935).
5) E. J. Cokal and E. N. Wise, *J. Electroanal. Chem.*, **11**, 406 (1966).

the conductivity of 0.1 M KCl solution. The conductivity water of a specific conductivity of 4.2×10^{-7} ohm^{-1} cm^{-1} was prepared by passing the redistilled water through the ion-exchange column. Its specific conductivity, however, raised to 1.36×10^{-6} ohm^{-1}cm^{-1} when it was shaked and kept in a flask for about one hour, and this value was used for the water conductivity correction. All the solutions used were kept at 25.0°C in a water thermostat.

The visible and ultraviolet spectra were obtained with a Hitachi EPS-3 spectrophotometer at room temperature. The ionic strength of the solution was adjusted to be 0.09. The infrared absorption spectra were measured with a Hitachi EPI-2G recording infrared spectrophotometer. Cells with windows of calcium fluoride were used when the measurements were made with solutions. Platinum foil of 0.05 mm thick was used for a spacer. The infrared absorption spectra of solid samples were obtained by the KBr disk method. The wave-length calibration was precisely made with water vapor and carbon dioxide.

Results

The Determination of the Association Constants Using the Polarographic Diffusion Current. In the investigation of the ion association, the addition of a certain salt is often required in order to adjust the ionic strength. In that case, the salt of the ions which seem not to associate with other ions must be chosen. However, in the case that the multivalent ions are involved in the system investigated, the association between the multivalent ions and the ion that is added in order to adjust the ionic strength cannot be sometimes ignored.

A modified equation of the equation which was presented in the previous paper[2] was derived for the determination of the association constant using the polarographic diffusion current. The influence of the ion which is added in order to adjust the ionic strength was taken into consideration in the treatment of polarographic data.

In the solution containing two different cations M^{m+} and $M'^{m'+}$ and complex anion X^{x-}, there exist the following equilibria

$$M^{m+} + X^{x-} \rightleftarrows M^{m+}X^{x-} \quad (1)$$

$$M'^{m'+} + X^{x-} \rightleftarrows M'^{m'+}X^{x-} \quad (2)$$

where $M^{m+}X^{x-}$ and $M'^{m'+}X^{x-}$ represent an ion-pair of M^{m+} with X^{x-} and that of $M'^{m'+}$ with X^{x-} respectively. Since the dissociation and the association of ion-pairs are very rapid, the apparent diffusion coefficient D is given by

$$D = \frac{D_X + D_{MX}K_{MX}C_M + D_{M'X}K_{M'X}C_{M'}}{1 + C_MK_{MX} + C_{M'}K_{M'X}} \quad (3)$$

where D_X, D_{MX} and $D_{M'X}$ are the diffusion coefficients of X^{x-}, $M^{m+}X^{x-}$ and $M'^{m'+}X^{x-}$, respectively, C_M and $C_{M'}$ are the concentrations of M^{m+} and $M'^{m'+}$ respectively, and K_{MX} and $K_{M'X}$ are the association constants of the corresponding ion-pairs expressed in concentration. When the ionic strength is kept constant, a relation given by the equation,

$$iC_M + jC_{M'} = a \quad (4)$$

holds for C_M and $C_{M'}$ where a is the ionic strength, i and j are the values calculated as follows. Assuming that M salt is of a u-v electrolyte, the value of i is given by $i=(vu^2+uv^2)/2v$. In a similar fashion, M' salt being u'-v' electrolyte, the value of j is given by $j=(v'u'^2+u'v'^2)/2v'$. Introducing $C_{M'}$ derived from Eq. (4) into Eq. (3), Eq. (5) is obtained, which is rearranged to Eq. (6).

$$D = \frac{D_X + \frac{a}{j}D_{M'X}K_{M'X} + \left(K_{MX}D_{MX} - \frac{i}{j}K_{M'X}D_{M'X}\right)C_M}{1 + \frac{a}{j}K_{M'X} + \left(K_{MX} - \frac{i}{j}K_{M'X}\right)C_M} \quad (5)$$

$$\frac{C_M}{\dfrac{D_X + \frac{a}{j}D_{M'X}K_{M'X}}{1 + \frac{a}{j}K_{M'X}} - D} = \frac{1 + \frac{a}{j}K_{M'X} + \left(K_{MX} - \frac{i}{j}K_{M'X}\right)C_M}{\dfrac{\left(D_X + \frac{a}{j}D_{M'X}K_{M'X}\right)\left(K_{MX} - \frac{i}{j}K_{M'X}\right)}{1 + \frac{a}{j}K_{M'X}} - \left(K_{MX}D_{MX} - \frac{i}{j}K_{M'X}D_{M'X}\right)} \quad (6)$$

The first term of the denominator of the left-hand side of Eq. (6) indicates the diffusion coefficient which is obtained in the absence of M^{m+}, that is, the expression which is obtained when C_M equals zero in Eq. (5).

The left-hand side of Eq. (6) can be obtained experimentally. If the left-hand side of Eq. (6) is plotted against C_M, a straight line must be obtained, and the ratio of the slope to the intercept gives

$$\frac{\text{Slope}}{\text{Intercept}} = \frac{K_{MX} - \frac{i}{j}K_{M'X}}{1 + \frac{a}{j}K_{M'X}} \quad (7)$$

When the value of either of K_{MX} and $K_{M'X}$ is known, that of the other can be calculated from Eq. (7). If the association between M' and X can be neglected, *i.e.*, $K_{M'X} \fallingdotseq 0$, Eq. (6) yields

$$\frac{C_M}{D_M - D} = \frac{1 + K_{MX}C_M}{(D_X - D_{MX})K_{MX}} \quad (8)$$

The association constant K_{MX} can be obtained directly from the ratio of the slope to the intercept. In the present investigation, M′ represents ammonium ion which is added in order to adjust the ionic strength, M represents other cations, and X, trioxalatocobaltate(III) anion.

Since it has been found that the ammonium ion forms ion-pair with trioxalatocobaltate(III) anion from the measurement of the conductivity of ammonium trioxalatocobaltate(III) solution, the results of the measurements of all systems investigated in the present study was treated with Eq. (6). The value of association constant of trioxalatocobaltate(III) ion with ammonium ion which is necessary to solve Eq. (7) was calculated from the conductivity of ammonium trioxalatocobaltate(III) solution. Figure 1 shows the experimental conductivity curve in which observed values of Λ are plotted against $C^{1/2}$. The equivalent conductivity at zero concentration Λ° was obtained from the extrapolation of the curve. The Λ_i° of trioxalatocobaltate(III) ion was obtained to be 91.4 Ω^{-1}cm^2 by subtracting Λ_i° of ammonium ion from Λ°. The association constant corresponding to the reaction,

$$NH_4^+ + [Co(ox)_3]^{3-} \rightleftharpoons NH_4^+[Co(ox)_3]^{3-}$$

was calculated according to the method of Jenkins and Monk.[6] The thermodynamic association constant was calculated to be 33.6 (log K=1.5$_3$) from the concentration association constants K_c obtained, using activity coefficients which were calculated by the Debye-Hückel equation. The concentration association constant $K_{M'X}$ at ionic strength 0.1 was calculated to be 7.9 from the thermodynamic association constant by using the activity coefficient. This value was employed to solve Eq. (7).

The change in current at -0.7 V *vs.* SCE was

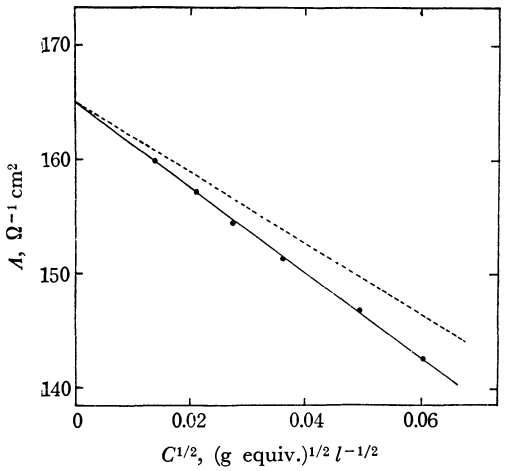

Fig. 1. Equivalent conductivity of $(NH_4)_3[Co(ox)_3]$ solutions as a function of the concentration. A broken line indicates the theoretical values calculated by Onsager's limiting equation.

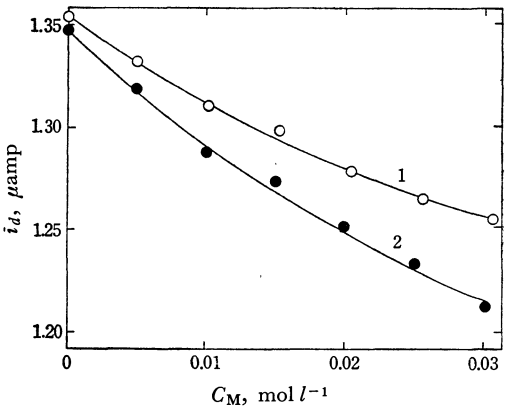

Fig. 2. Variation of the mean diffusion current ($\bar{i}_d$) of the reduction wave of $[Co(ox)_3]^{3-}$ with the change of concentrations of (1) magnesium and (2) barium ions.

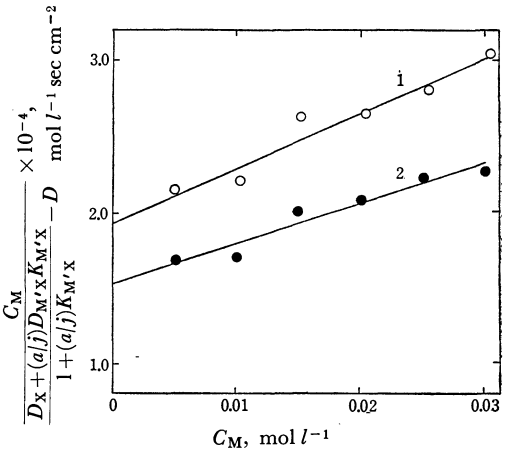

Fig. 3. Left-hand side of Eq. (6) as a function of concentrations of (1) magnesium and (2) barium ions.

TABLE 1. ASSOCIATION CONSTANTS OF TRIOXALATOCOBALTATE(III) ION WITH VARIOUS CATIONS AT 25°C

Cation	Slope / Intercept	K_{MX} (μ=0.1)	log K_{MX} (μ=0)
Na^+	8±1	22± 1	1.9$_4$
Mg^{2+}	18±2	56± 6	2.8$_9$
Ca^{2+}	17±1	55± 4	2.9$_2$
Sr^{2+}	16±1	53± 3	2.9$_4$
Ba^{2+}	17±2	55± 7	2.9$_5$
Al^{3+}	39±3	118±17	3.7$_0$
$(CH_3)_4N^+$	0	7.9	1.5$_2$
$(C_2H_5)_4N^+$	−2.4±0.3	3.7±0.4	1.1$_8$

6) I. L. Jenkins and C. B. Monk, *J. Chem. Soc.*, **1951**, 68.

measured with the increase of the cation concentration in neutral solution. Typical examples of these plots are given in Fig. 2. The diffusion coefficient was calculated by the Ilkovič equation from the mean diffusion current. The experimental values in Fig. 2 were treated with Eq. (6). The plots thus obtained are given in Fig. 3. The values of the ratio of slope to intercept were determined by a least square method with the plots in Fig. 3. The association constant K_{MX} was obtained by introducing the value of $K_{M'X}$ and that of the ratio of slope to intercept into Eq. (7), which is given in Table 1.*1 The thermodynamic association constants were calculated from those concentration association constants, using the activity coefficients which were calculated by the Debye-Hückel equation with the following ion-size parameters:[8] 4 Å for Na^+, 8Å for Mg^{2+}, 6Å for Ca^{2+}, 5 Å for Sr^{2+} and Ba^{2+}, 9Å for Al^{3+}, 6 Å for $[Co(ox)_3]^{3-}$ and 6.5 Å for all the ion-pairs $M^{m+}[Co(ox)_3]^{3-}$. The thermodynamic association constants are also given in Table 1.

The treatment with Eq. (6) was successfully extended to the systems containing tetraalkylammonium cations and trioxalatocobaltate(III) anions. The changes in diffusion coefficient with the increase in the concentrations of tetramethylammonium and tetraethylammonium ions are shown in Fig. 4, which are much different from those observed with the other systems. A similar experiment was carried out with the system containing hexamminecobalt(III) and tetraethylammonium cations in which no ion association is likely to take place. Although the addition of tetraethylammonium ion caused a slight decrease in the limiting current of hexamminecobalt(III), the decrease was confirmed to arise from the decrease in the drop time of the mercury electrode due to the surface-active properties of tetraethylammonium ions. These plots are also shown in Fig. 4 (3 in Fig. 4). The great change in current in the system containing $[Co(ox)_3]^{3-}$ anions and tetraalkylammonium cations cannot be accounted for by the decrease in drop time of mercury electrode. This may be attributed to ion-pair formation between $[Co(ox)_3]^{3-}$ anions and tetraalkylammonium cations. Equation (5) indicates that, when $K_{MX}/K_{M'X} \geqq 1 > D_{MX}/D_{M'X}$, plots of the diffusion coefficient D against C_M give curves similar to curves 1 and 2 in Fig. 4. The sign of equality gives a straight line similar to curve 1, while the sign of inequality gives a convex curve similar to curve 2. The experimental values in Fig. 4 corrected for the drop time of mercury electrode were treated with Eq. (6). The plots thus obtained are shown in Fig. 5. The association constants K_{MX} which were obtained with a procedure similar to other cases are given in the last two lines of Table 1.

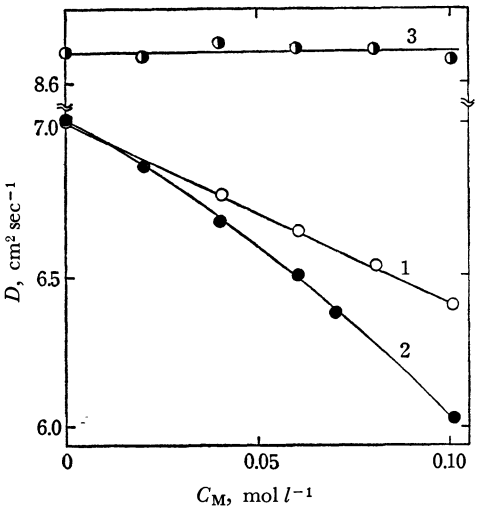

Fig. 4. Apparent diffusion coefficient (D) calculated from the reduction wave of cobalt complexes as a function of the concentration of tetraalkylammonium ions. The systems are: (1) $(CH_3)_4N^+$-$[Co(ox)_3]^{3-}$, (2) $(C_2H_5)_4N^+$-$[Co(ox)_3]^{3-}$ and (3) $(C_2H_5)_4N^+$-$[Co(NH_3)_6]^{3+}$. All the values are corrected for the drop time of DME.

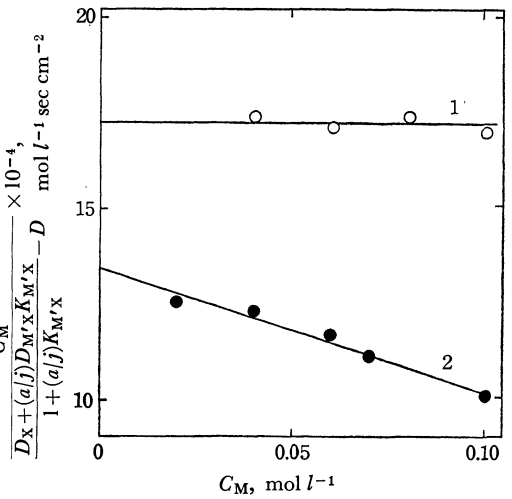

Fig. 5. Left-hand side of Eq. (6) as a function of concentrations of (1) tetramethylammonium and (2) tetraethylammonium ions.

*1 In the case of aluminum(III) ion, the association between aluminum(III) and nitrate ions seems not to be ignored. In this study, however, the correction for the effect of nitrate ions was not made, because no accurate value has been reported for the association constant of the ion-pair of these two ions. If it is assumed that the association constant of the ion-pair of aluminum with nitrate ions is the same with that of hexamminecobalt(III) with nitrate ions, which is, reported to be 1.6_3 in logarithmic unit at infinite dilution,[7] the association constant of $Al^{3+}[Co(ox)_3]^{3-}$ at ionic strength 0.1 is calculated to be 140 instead of 118 given in Table 1.

7) S. Katayama and R. Tamamushi, presented at the 20th Annual Meeting of the Chemical Society of Japan, Tokyo (April, 1967).

8) J. Kielland, *J. Am. Chem. Soc.*, **59**, 1675 (1937).

Visible and Ultraviolet Spectra. The visible and ultraviolet absorption spectra of trioxalatocobaltate(III) in aqueous solutions were measured in order to know what changes occur on the absorption spectra when an ion-pair $M^{m+}[Co(ox)_3]^{3-}$ is formed, where M^{m+} represents metal ions, such as Na^+, Mg^{2+}, Ca^{2+}, Sr^{2+}, Ba^{2+} and Al^{3+}. The solutions containing potassium trioxalatocobaltate and metal chloride were prepared as about 60—70% of trioxalatocobaltate ions exist in the form of ion-pair. The ion-pair formation gave no effect on the absorption spectra over the range of 210 mμ to 700 mμ.

Infrared Spectra. In order to investigate how the ion association affects the vibration of ligand, the infrared absorption due to $\nu_s(C\text{-}O)+\nu(C\text{-}C)$ was measured with the solution of potassium, magnesium, calcium and strontium trioxalatocobaltate(III). The solution of 0.02 M potassium trioxalatocobaltate(III) in which a great part of trioxalatocobaltate(III) ions seemed to exist in the form of free ions gave an absorption maximum due to $\nu_s(C\text{-}O)+\nu(C\text{-}C)$ at 1389 cm^{-1}. The solutions which contained 0.02 M potassium trioxalatocobaltate(III) and 0.15 M magnesium, calcium and strontium chloride gave also an absorption due to $\nu_s(C\text{-}O)+\nu(C\text{-}C)$ at 1389 cm^{-1}. From the value of the association constants obtained by the polarographic method it was estimated that 80—90% of trioxalatocobaltate-(III) ions were present in the form of ion-pair $M^{2+}[Co(ox)_3]^{3-}$ in these solutions. The absorption spectra of potassium, calcium, strontium and barium trioxalatocobaltate(III) in solid state were measured and compared with the spectra of the solutions mentioned above. They are given in Fig. 6.

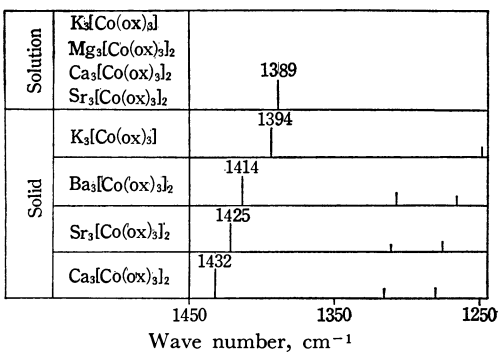

Fig. 6. Wave numbers of the absorption bands of trioxalatocobaltate(III) in aqueous solutions and in solid state.

Discussion

The association constants of trioxalatocobaltate-(III) anion with cations were compared with those of ferricyanide anion with cations and also those of hexamminecobalt(III) cation with anions (see Table 2). The values given for comparison in Table 2 are those of being determined from conductivity measurements, because the conductivity method seems to detect the same type of ion-pair as the polarographic method does. The association constants for the ion-pair $M^{m+}[Fe(CN)_6]^{3-}$ agree well with our results. The radii of $[Co(ox)_3]^{3-}$ and $[Fe(CN)_6]^{3-}$ ions are calculated to be 3.0Å and 2.8Å, respectively, by applying Stokes' law. That both complex anions have similar radii may be a cause of the good agreement. On the other hand, the association constants of hexamminecobalt(III) cation with anions are about five times larger than those of tervalent complex anion with cations except for the case of ion-pairs of 3-1 electrolytes, though the application of Stokes's law gives the radius of $[Co(NH_3)_6]^{3+}$ ion to be 2.8 Å, which is nearly equal to those of the complex anion described above. This great difference on association constant was, therefore, considered to arise from the difference in size between the ions paired with complex ions. The bi- and tervalent metal cations are strongly hydrated than the anions owing to their small sizes, so that the metal cations seem to associate with complex anions in a state of hydrated cations. Hence the apparent size of hydrated cation in a associated state appears to be larger than the size of hydrated anion. This may be a cuase of the great difference. The discussion for the results of spectroscopic study on ion association will lead some support to this consideration.

It would be expected that, if a trioxalatocobaltate(III) anion is associated with a cation, the complex anion is polarized and in consequence the change of absorption band in visible or ultraviolet

Table 2. Logarithmic association constants of complex ions with hydrated ions at zero ionic strength at 25°C

$[Co(ox)_3]^{3-}$		$[Fe(CN)_6]^{3-}$		$[Co(NH_3)_6]^{3+}$	
Ion	log K	Ion	log K	Ion	log K
Na^+	1.9_4	K^+	1.40[9]	Cl^-	1.49[6] 1.5[12,13]
NH_4^+	1.5_3			NO_3^-	1.6_3[7]
$(CH_3)_4N^+$	1.5_2			ClO_4^-	1.4_0[7]
$(C_2H_5)_4N^+$	1.1_8				
Mg^{2+}	2.8_9	Mg^{2+}	2.79[10]	SO_4^{2-}	3.56[6]
Ca^{2+}	2.9_2	Ca^{2+}	2.83[10]		
Sr^{2+}	2.9_4	Sr^{2+}	2.85[10]		
Ba^{2+}	2.9_5	Ba^{2+}	2.88[10]		
Al^{3+}	3.7_0	La^{3+}	3.74[11]	$P_3O_9^{3-}$	4.44[14]

9) C. B. Monk, *J. Chem. Soc.*, **1949**, 423.
10) C. W. Gibby and C. B. Monk, *Trans Faraday Soc.*, **48**, 632 (1952).
11) H. S. Dunsmore and J. G. James, *J. Chem. Soc.*, **1951**, 2925.
12) S. Katayama, *Rikagaku Kenkyusho Hokoku*, **42**, 243 (1966).
13) R. Tamamushi, T. Isono and S. Katayama, This Bulletin, **40**, 334 (1967).
14) C. B. Monk, *J. Chem. Soc.*, **1952**, 1317.

TABLE 3. DIFFUSION COEFFICIENTS OF ION-PAIRS AND COMPLEX IONS

Ion-pair	$D\times10^6$ cm^2 sec^{-1}	Ion-pair	$D\times10^6$ cm^2 sec^{-1}	Complex ion	$D\times10^6$ cm^2 sec^{-1}
$Na^+[Co(ox)_3]^{3-}$	5.8			$[Co(ox)_3]^{3-}$	8.1
$NH_4^+[Co(ox)_3]^{3-}$	5.6			$[Co(NH_3)_6]^{3+}$	8.4[16]
$(CH_3)_4N^+[Co(ox)_3]^{3-}$	4.3			$[Cr(NH_3)_6]^{3+}$	8.5[17]
$(C_2H_5)_4N^+[Co(ox)_3]^{3-}$	2.4			$[Co(en)_3]^{3+}$	6.4[18]
				$[Cr(en)_3]^{3+}$	5.9[19]
$Mg^{2+}[Co(ox)]^{3-}$	4.8	$[Co(NH_3)_6]^{3+}SO_4^{2-}$	5.7[15]		
$Ca^{2+}[Co(ox)_3]^{3-}$	4.4	$[Cr(NH_3)_6]^{3+}SO_4^{2-}$	5.7[15]		
$Sr^{2+}[Co(ox)_3]^{3-}$	4.2	$[Co(en)_3]^{3+}SO_4^{2-}$	5.3[15]		
$Ba^{2+}[Co(ox)_3]^{3-}$	4.2	$[Cr(en)_3]^{3+}SO_4^{2-}$	5.1[15]		
$Al^{3+}[Co(ox)_3]^{3-}$	3.8				

region occurs. However, any change was not observed on the absorption over the range of 210 mμ to 700 mμ. Moreover, if the ion-pair formation occurs, the decrease of the degree of degeneracy and the shift of the absorption band would be expected on the infrared absorption spectra. No changes, however, were observed in all the systems, although in solid state trioxalatocobaltates(III) of potassium and alkali earth metals gave the frequency shift. That is to say, the existence of ion-pairs could not be detected by the measurement of visible, ultraviolet and infrared absorption spectra. On the other hand, the existence of ion-pair was distinctly detected by the polarographic method. The explanation of this apparent discrepancy is that the complex anion has no direct interaction with metal ion, but one or more water molecules interpose between the two ions. The separation of the ions by several water molecules can greatly decrease the polarization effect of the complex anion, so that the absorption spectra show no indication of the ion-pair formation.

The consideration that the metal ion forms the ion-pair in a hydrated state was supported further by the discussion on the diffusion coefficient of ion-pair. The diffusion coefficients of the ion-pairs D_{MX} were obtained by substituting D_X, $D_{M'X}$, K_{MX} and $K_{M'X}$ into the slope of the plots of Eq. (6). D_X was calculated by the application of the Nernst equation to the limiting mobility of complex anion. $D_{M'X}$ was obtained with Eq. (3), when C_M equaled zero. The value of D_{MX} thus obtained are given in the first column of Table 3. The diffusion coefficients of ion-pairs decrease with increasing positive charges on the metal ion. This fact clearly demonstrates the influence of hydration of the cation. The increase in cation charge is accompanied by the increase in size of hydrated cation, and consequently give raise to the decrease in the diffusion coefficient of metal ion. The diffusion coefficients of the ion-pairs of trioxalatocobaltate(III) anion and alkali earth metal cations are further compared with those of the ion-pairs of tervalent complex cations and sulphate anion (see also Table 3). The diffusion coefficients of complex ions are also given in Table 3. It is seen from Table 3 that the diffusion coefficients of ion-pairs of complex anion and cation are smaller than those of complex cation and anion. Since the diffusion coefficient of complex anion is nearly equal to or somewhat larger than those of complex cation, the ions paired with complex ions seem to be responsible for the difference between these two sets of figures in Table 3.

The possibility of the existence of several water molecules between the complex anion and the metal cation was examined also by the estimation of the closest approach of the paired ions. The value of the closest approach was calculated in the same way as presented in the previous paper,[20] and was found to be in good agreement with the sum of Stokes' law radius of trioxalatocobaltate(III) ion and the radius of the hydrated metal ion. From these discussions it may be concluded that in a sense of equilibrium study a trioxalatocobaltate(III) anion and a metal cation has no direct interaction, but one or more water molecules interpose between the two ions.

The closest approach for ion-pair $R_4N^+[Co(ox)_3]^{3-}$ was also calculated. The values are 6.0 Å and 8.0 Å for $(CH_3)_4N^+[Co(ox)_3]^{3-}$ and $(C_2H_5)_4N^+$-$[Co(ox)_3]^{3-}$, respectively. They are in good agreement with the distance which were obtained by adding the crystallographic radius of R_4N^+ ion to the radius of $[Co(ox)_3]^{3-}$ ion.

The authors wish to thank the Ministry of Education for the financial support granted for this research.

15) N. Tanaka and A. Yamada, *Z. Anal. Chem.*, **224**, 117 (1967).
16) H. A. Laitinen, J. C. Bailar, Jr., H. F. Holtzclaw, Jr., and J. V. Quagliano, *J. Am. Chem. Soc.*, **70**, 2999 (1948).
17) N. Tanaka, K. Ebata and G. Satô, This Bulletin, **36**, 912 (1963).
18) H. A. Laitinen and M. W. Grieb, *J. Am. Chem. Soc.*, **77**, 5201 (1955).
19) N. Tanaka and A. Yamada, This Bulletin, **39**, 920 (1966).
20) N. Tanaka, Y. Kobayashi and M. Kamada, This Bulletin, **39**, 2187 (1966).

BULLETIN OF THE CHEMICAL SOCIETY OF JAPAN VOL. 41 2073—2077 (1968)

Syntheses of *trans*-Isoflavan-4-ols

Shozo YAMAGUCHI, Shoei ITO, Ikuko SUZUKI and Naoto INOUE

College of General Education, Tohoku University, Kawauchi, Sendai

(Received November 14, 1967)

The reaction of nitrous acid and three 4-aminoisoflavan hydrochlorides (III, IV, and V) obtained by the catalytic hydrogenation of isoflavanone oximes, and the hydroboration of three isoflavenes (XII, XIII, and VIII), were investigated in the hope of finding a general method of synthesizing *trans*-isoflavan-4-ols. The reaction of III and IV with nitrous acid afforded the corresponding *trans*-4-ols, though in a poor yield, but that of V produced no expected compound, the corresponding isoflavene (VIII) being obtained instead. The hydroboration of XII, XIII, and VIII afforded the corresponding *trans* alcohols (VI, VII, and XIV) in good yields. In addition, it became clear that 4-aminoisoflavans obtained by the catalytic reduction of the oximino compounds possess the 3,4-*cis* configuration.

Inoue obtained *cis*-7-methoxyisoflavan-4-ol (X) as a main product and *trans*-7-methoxyisoflavan-4-ol (VII) as a by-product by the reduction of 7-methoxyisoflavanone with sodium borohydride. However, the hydride reduction of isoflavanone and 4′,7-dimethoxyisoflavanone did not afford the *trans*-4-ols.[1,2] Later, the present authors[3] obtained VII by the reaction of 4-amino-7-methoxyisoflavan hydrochloride (IV) with nitrous acid, but we could not apply this reaction to other aminoisoflavans, since these amines had not yet been prepared in our laboratory.

In order to find out a general method of synthesizing *trans*-isoflavan-4-ols, we undertook the

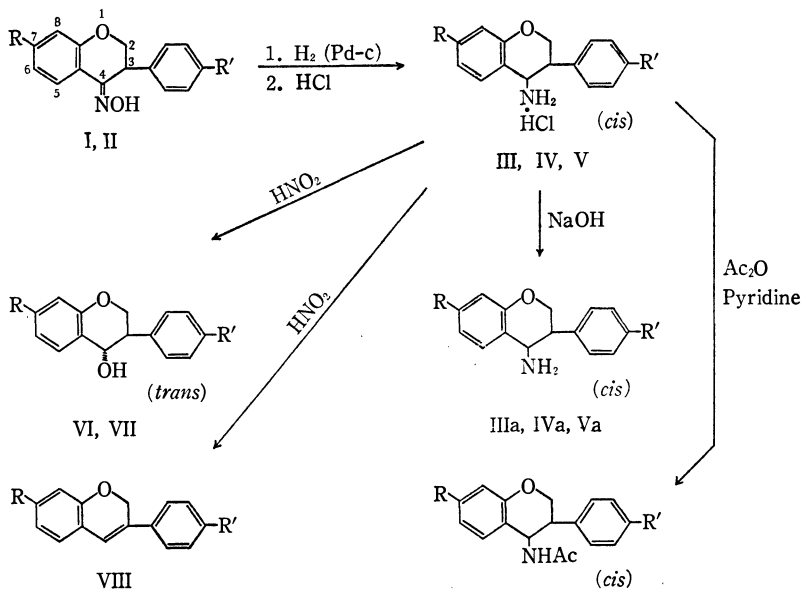

I, II — III, IV, V — VI, VII — IIIa, IVa, Va — VIII — IIIb, IVb, Vb

I, III, IIIa, IIIb, VI	R=R′=H
IV, IVa, IVb, VII	R=OMe, R′=H
II, V, Va, Vb, VIII	R=R′=OMe

Chart 1

1) N. Inoue, This Bulletin, **37**, 601 (1964).
2) S. Yamaguchi, S. Ito, A. Nakamura and N. Inoue, *ibid.*, **38**, 2187 (1965).
3) N. Inoue, S. Yamaguchi and S. Fujiwara, *ibid.*, **37**, 604 (1964).

TABLE 1. CHEMICAL SHIFTS OF METHYL PROTONS OF ACETYL GROUPS OF 4-AcO-F*, 4-AcO-IF* and 4-AcNH-IF

Entry	Compound	cis (ppm)	trans (ppm)	$\Delta\delta$ (ppm)
1	4-AcO-F	2.05	2.05	0.0
2	4-AcO-7-MeO-F**	2.07	2.05	0.02
3	4-AcO-IF	1.83	2.02	0.19
4	4-AcO-7-MeO-IF	1.83	2.05	0.22
5	4-AcO-4',7-$(MeO)_2$-IF		2.04	
6	4-AcNH-IF	1.83		
7	4-AcNH-7-MeO-IF	1.83		
8	4-AcNH-4',7-$(MeO)_2$-IF	1.83		

* F: Flavan; IF: Isoflavan.

** Unpublished results. The syntheses and the stereochemistry of these compounds will be reported elswhere.

synthesis of 4-aminoisoflavan (IIIa) and 4-amino-4',7-dimethoxyisoflavan (Va), and also the examination of their reaction with nitrous acid and of the hydroboration of isoflavenes. The results obtained will be presented in this paper.

4-Aminoisoflavans were synthesized according to the following reaction scheme. The catalytic hydrogenation of isoflavanone oxime (I) and 4',7-dimethoxyisoflavanone oxime (II) in acetic acid containing a small amount of perchloric acid in the presence of palladium on carbon produced the corresponding amines (IIIa and Va), which were then isolated as hydrochlorides (III and V), and the treatment of III and V with acetic anhydride and pyridine gave 4-acetamido derivatives (IIIb and Vb).

The stereochemistry of three 4-aminoisoflavans (IIIa, IVa, and Va) was determined on the basis of the NMR spectra. In the NMR spectra of these amines, the signals assigned to three protons of the 2- and 4- positions are observed around 4.0—4.9 ppm and overlap with each other. In the case of 4-acetamidoisoflavans (IIIb, IVb, and Vb), the proton signals of the 4-position shift to a lower field and appear quite broad. Therefore, it is difficult to determine the value of $J_{3H,4H}$ directly from the signals of the chroman-ring protons. As is shown in Table 1, the methyl proton signals of the acetyl group of 4-acetoxyflavan (*cis*, *trans*), 4-acetoxy-7-methoxyflavan (*cis*, *trans*), and *trans*-4-acetoxyisoflavans are observed at 2.02—2.07 ppm (Entries 1, 2, 3, 4, and 5). On the other hand, these signals of *cis*-4-acetoxyisoflavans shift to a field higher by approximately 0.19—0.22 ppm and appear at 1.83 ppm (Entries 3 and 4). In *cis*-4-acetoxyisoflavans, the acetyl group is above the plane of the adjacent phenyl group at the 3-position (Fig. 1): consequently, the acetyl group suffers the shielding effect of the C_8 phenyl group and shifts to a higher field. This upfield shift seems to be characteristic of 3,4-*cis*-isoflavans. A quite similar phenomenon is observed in the NMR spectra of the 4-acetamidoisoflavans (IIIb, IVb, and Vb). The methyl proton signals of the acetyl group of these acetamido compounds appear at 1.83 ppm (Entries 6, 7, and 8 in Table 1). A comparison of these values with those of *cis*-acetoxyisoflavans suggests the *cis* configuration of IIIb, IVb, and Vb.

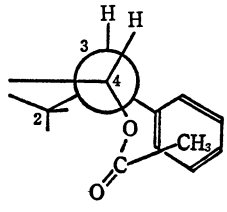

Fig. 1

The above inference is also supported by the stereochemistry of the catalytic hydrogenation of cyclohexanone oximes[4] and isoflavanones.[1-3] Furthermore, as will be shown in the Experimental part of this paper and as has been shown in a previous report,[3] in the reactions of 4-aminoisoflavan hydrochloride (III) and the 4-amino-7-methoxy derivative (IV) with nitrous acid, the yields of *trans*-isoflavan-4-ols (VI and VII) were as low as 26% and 15% respectively, and the 4-amino-4',7-dimethoxy derivative (V) gave only 4',7-dimethoxyisoflavene (VIII).[5] In view of the reported stereochemistry of the reaction of aminocyclohexanes with nitrous acid,[6] the results described above also support the *cis* configuration assigned to 4-aminoisoflavans.

The reaction of two 4-aminoisoflavan hydrochlorides (III and V) with nitrous acid was also carried out. From III, a compound with a mp of 97°C was obtained in a 26% yield; this compound had the molecular formula $C_{15}H_{14}O_2$, but it was not identical with *cis*-isoflavan-4-ol (IX).[1] Therefore, the compound may be supposed to be *trans* alcohol (VI). This was confirmed by comparing the NMR

4) J. H. Brewster, *J. Am. Chem. Soc.*, **76**, 6361 (1954).
5) R. B. Bradburry and D. E. White, *J. Chem. Soc.*, **1953**, 871.
6) a) E. L. Eliel, N. L. Allinger, S. J. Angyal and G. A. Morrison, "Conformation Analysis," Interscience Publishers, New York, N. Y. (1965), p. 89. b) M. Hannack, "Conformation Analysis," Academic Press, New York, N. Y. (1965).

TABLE 2. NMR SPECTRA OF ISOFLAVAN-4-OLS AND THEIR DERIVATIVES

Compound	Position of peaks in ppm	No of protons (assignment)	Remarks	Configuration
Isoflavan-4-ol (IX)[1,2,3]	4.60	1 (4-H)	Doublet $J_{3,4}=2.9$ Hz	3(ax), 4(eq) cis
Acetate[2]	6.16	1 (4-H)	Doublet $J_{3,4}=3.0$	3(ax), 4(eq) cis
Isoflavan-4-ol (VI)	4.92	1 (4-H)	Doublet $J_{3,4}=8.0$	3(ax), 4(ax) trans
Acetate	6.19	1 (4-H)	Doublet $J_{3,4}=6.0$	3(ax), 4(ax) trans
4',7-Dimethoxy-isoflavan-4-ol (XI)[2]	4.66	1 (4-H)	Doublet $J_{3,4}=2.9$	3(ax), 4(eq) cis
4',7-Dimethoxy-isoflavan-4-ol (XIV)	4.82	1 (4-H)	Quartet $J_{3,4}=7.9$	3(ax), 4(ax) trans
Acetate	6.06	1 (4-H)	Doublet $J_{3,4}=5.0$	3(ax), 4(ax) trans

spectra of VI and its acetate with those of *cis*-isoflavan-4-ol (Table 2). The reaction between V and nitrous acid at room temperature gave an olefinic compound with a mp of 161°C which was identified as VIII.[5] Even the reaction at a lower temperature (ice-cooling) gave no expected *trans*-4',7-dimethoxyisoflavan-4-ol (XIV); rather, the starting amine was recovered, together with VIII.

The synthesis of *trans*-isoflavan-4-ols by the hydroboration of isoflavenes was attempted next. The hydroboration of substituted double bonds and subsequent oxidation by hydrogen peroxide has been reported to lead to *cis*-type hydration, following the anti-Markownikoff rule.[7] Therefore, it was anticipated that the application of this reaction to isoflavenes would result in the formation of *trans*-isoflavan-4-ols. 7-Methoxyisoflavene (XIII) and

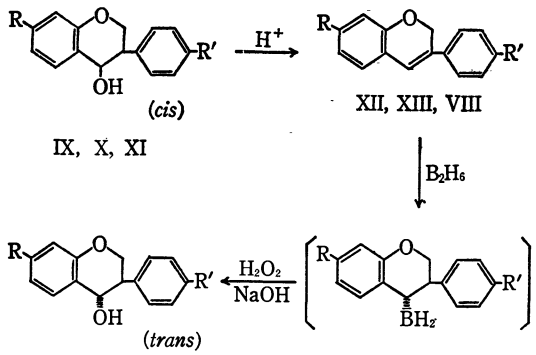

VI, IX, XII R=R'=H
VII, X, XIII R=OMe, R'=H
VIII, XI, XIV R=R'=OMe

Chart 2

VIII were prepared from the corresponding *cis* alcohols (X and XI) by heating in acetic acid. Isoflavene (XII) was prepared by refluxing a solution of the *cis* alcohol (IX) in acetic acid containing a small amount of concentrated hydrochloric acid.

A 1-mol equivalent of diborane (2.0 M equivalent in BH_3) and a 2.5 1-mol equivalent of XIII were allowed to react in tetrahydrofuran. At appropriate intervals of time, samples were withdrawn and analysed for remaining XIII by measuring the extinction at 333 mμ. The amounts of remaining unreacted XIII observed 30 min, 2 hr, and 17 hr after the beginning of the reaction were 65%, 35%, and 10% respectively. In order to transform the remaining XIII into the organoborane completely, a diborane-THF solution was then added until the molar ratio of XIII and diborane became 1.62 : 1. The XIII disappeared 70 min after the addition of the final diborane solution.

It has been reported[7] that, in the hydroboration of trisubstituted olefins such as α-pinene, the reaction proceeds rapidly to the dialkylborane stage. In our experiment, however, when the molar ratio of XIII (trisubstituted olefin) to diborane was 2.5 : 1, unreacted XIII was detected, but when the ratio was 1.62 : 1, no XIII was detected. The above experimental results indicate that the reaction proceeds predominantly to the monoalkylborane. After the usual treatment, a compound with a mp of 131°C was obtained in a 44% yield; this compound was identical with *trans*-7-methoxyisoflavan-4-ol (VII).[1-3] A similar reaction of XII gave *trans*-isoflavan-4-ol (VI) in a 73% yield. A compound (XIV) with a mp of 124°C was obtained in a 66% yield from VIII. It was different from *cis*-4',7-dimethoxyisoflavan-4-ol (XI)[1,2] and may, therefore, be supposed to be a *trans* modification. The NMR spectra of XIV and its acetate (Table 2) support the *trans* configuration.

In conclusion, the hydroboration of isoflavenes seems valuable as a general method of synthesizing *trans*-isoflavan-4-ols.

7) a) H. C. Brown, "Hydroboration," Benjamin Inc., New York, N. Y. (1962). b) H. C. Brown and J. Zweifel, "Organic Reaction," Vol. 13, ed. by R. Adams, John Wiley & Sons, Inc., New York, N. Y. (1963), p. 1.

Experimental

The NMR spectra were determined with a Varian A-60 spectrometer at 60 MHz, using deuterochloroform as the solvent and tetramethylsilane as the internal reference.

4',7-Dimethoxyisoflavanone Oxime (II). A solution of 2.2 g of 4',7-dimethoxyisoflavanone[8] and 2.2 g of hydroxylamine hydrochloride in a mixture of 22 m*l* of pyridine and 22 m*l* of ethanol was refluxed for 10 hr. The reaction mixture was then poured into water to precipitate crystals. The recrystallization of the crystals from ethanol gave 1.7 g (74% yield) of crystals, mp 142—143°C.

Found: C, 68.47; H, 5.43; N, 4.65%. Calcd for $C_{17}H_{17}O_4N$: C, 68.21; H, 5.73; N, 4.68%.

4-Aminoisoflavan (IIIa). A solution of 3 g of isoflavanone oxime (I)[9] in 200 m*l* of acetic acid containing 0.5 m*l* of 70% perchloric acid was hydrogenated under atmospheric pressure in the presence of 3 g of 5% palladium on carbon.*1 After 2.43 mol of hydrogen had been absorbed at room temperature (18°C), the catalyst was filtered off. The acetic acid was removed under reduced pressure, and 6 N hydrochloric acid was added to the residue, thus affording crystals. Recrystallization from ethanol gave 2 g (64% yield) of 4-aminoisoflavan hydrochloride (III), mp 243—245°C (decomp.) ν_{N^+-H} 3200—2700 cm^{-1} (KBr). pK_a[10] 7.67(in H_2O); 7.25 (in 34% aqueous ethanol).

Found: C, 68.71; H, 5.98; N, 5.54%. Calcd for $C_{15}H_{16}ONCl$: C, 68.83; H, 6.16; N, 5.35%.

The crystals obtained by the neutralization of an aqueous solution of 300 mg of III with 5% sodium hydroxide were recrystallized from dilute methanol to give 150 mg of 4-aminoisoflavan (IIIa), mp 74—76°C.

Found: C, 79.69; H, 6.73; N, 6.01%. Calcd for $C_{15}H_{15}ON$: C, 79.97; H, 6.71; N, 6.22%.

4-Acetamidoisoflavan (IIIb). A solution of 100 mg of III in pyridine was acetylated with acetic anhydride by the usual method. Recrystallization from diluted ethanol then gave 70 mg of the acetate (IIIb), mp 182—183°C. ν_{NH} 3260 cm^{-1} (KBr), $\nu_{C=O}$ 1660 cm^{-1} (KBr).

Found: C, 76.74; H, 6.45; N, 5.13%. Calcd for $C_{17}H_{17}O_2N$: C, 76.38; H, 6.41; N, 5.24%.

Reaction of 4-Aminoisoflavan Hydrochloride (III) with Nitrous Acid. To a swirling solution of 1 g of III in 80 m*l* of 50% acetic acid, there were added, drop by drop and under cooling with ice, 25 m*l* of an aqueous solution containing 700 mg of sodium nitrite. After the stirring had continued for 1 hr under cooling, and then a further 30 min at room temperature, the reaction mixture was poured into water, and subsequently extracted with ether. The extract was washed with a sodium hydrogen carbonate aqueous solution and with water, dried on sodium sulfate, and distilled. The recrystallization of the residue from petroleum ether gave *trans*-isoflavan-4-ol (VI), mp 96—97°C, in a 26% yield. The NMR spectrum of VI shows a signal of the C_4 proton at 4.92 ppm as a doublet, $J_{3H,4H}$ 8.0 Hz, ν_{OH} 3350 cm^{-1} (KBr).

Found: C, 76.32; H, 6.43%. Calcd for $C_{15}H_{14}O_2$: C, 76.62; H, 6.24%.

***trans*-4-Acetoxyisoflavan.** A solution of 100 mg of *trans*-isoflavan-4-ol (VI) in pyridine was acetylated with acetic anhydride by the usual method. The recrystallization of the crude product from diluted ethanol gave 70 mg of acetate, mp 72—73°C. $\nu_{C=O}$ 1739 cm^{-1}.

Found: C, 75.95; H, 6.24%. Calcd for $C_{17}H_{16}O_3$: C, 76.10; H, 6.01%.

4-Acetamido-7-methoxyisoflavan (IVb). A solution of 100 mg of 4-amino-7-methoxyisoflavan hydrochloride[3] (pK_a 7.45 in 34% aqueous ethanol) in pyridine was acetylated with acetic anhydride by the usual method. The recrystallization of the product from ethanol gave 80 mg of acetate, mp 238—239°C. ν_{NH} 3250 cm^{-1} (KBr), $\nu_{C=O}$ 1640, 1665 cm^{-1} (KBr).

Found: C, 73.08; H, 6.66; N, 4.65%. Calcd for $C_{18}H_{19}O_3N$: C, 72.70; H, 6.44; N, 4.71%.

4-Amino-4',7-dimethoxyisoflavan (Va). A solution of 1.5 g of 4',7-dimethoxyisoflavanone oxime (II) in 250 m*l* of acetic acid containing 2 m*l* of 70% perchloric acid was hydrogenated in the presence of 1.5 g of 5% palladium on carbon under atmospheric pressure. After the solution had absorbed 2.20 mol of hydrogen at room temperature (17°C), the catalyst was filtered off and the solvent was removed under reduced pressure. To the residue, 6 N hydrochloric acid was added to give crystals. Recrystallization from ethanol gave 700 mg (45% yield) of 4-amino-4',7-dimethoxyisoflavan hydrochloride (V), mp 213—215°C (decomp.). ν_{N^+-H} 3200—2700 cm^{-1} (KBr). pK_a 7.50 in 34% aqueous ethanol.

Found: C, 63.62; H, 6.12; N, 4.13%. Calcd for $C_{17}H_{20}O_3NCl$: C, 63.41; H, 6.23; N, 4.35%.

The neutralization of an aqueous solution of 200 mg of the hydrochloride (V) with 5% sodium hydroxide afforded a crystalline material, which was then recrystallized from diluted ethanol to give 100 mg of 4-amino-4',7-dimethoxyisoflavan (Va), mp 89—90°C.

Found: C, 71.34; H, 6.79; N, 4.77%. Calcd for $C_{17}H_{19}O_3N$: C, 71.56; H, 6.71; N, 4.91%.

4-Acetamido-4',7-dimethoxyisoflavan (Vb). A solution of 100 mg of V in pyridine was acetylated with acetic anhydride in the usual manner. Recrystallization from ethanol gave 70 mg of acetate (Vb), mp 240—242°C. ν_{NH} 3250 cm^{-1} (KBr), $\nu_{C=O}$ 1643, 1665 cm^{-1} (KBr).

Found: C, 69.92; H, 6.35; N, 4.17%. Calcd for $C_{19}H_{21}O_4N$: C, 69.70; H, 6.47; N, 4.28%.

Reaction of 4-Amino-4',7-dimethoxyisoflavan Hydrochloride (V) with Nitrous Acid. To a swirling solution of 500 mg of the hydrochloride (V) in 60 m*l* of 50% acetic acid, there was added, drop by drop and under cooling with ice, a solution of 300 mg of sodium nitrite in 20 m*l* of water. After it had then been allowed to stand for 2 hr under the cooling and a further hour at room temperature, the reaction mixture was poured into water and subsequently extracted with ether. The extract was washed with a sodium hydrogen carbonate solution and with water, and dried on anhydrous sodium sulfate. The residue remaining after the removal of the ether was recrystallized from ethanol to yield 150 mg

8) N. Inoue, *Nippon Kagaku Zassi* (*J. Chem. Soc. Japan, Pure Chem. Sect.*), **79**, 215 (1958).

9) N. Inoue, *Sci. Repts. Tohoku Univ., First Ser.* **XLV**; 63 (1961).

*1 Five percent palladium on carbon, obtained from the Kawakami Research Institute, was used in all the following experiments.

10) K. Nakanishi, "Yuki Kagaku no Shinpo," Vol. 12, ed. by M. Murakami, Kyoritsu Shuppan, Tokyo, Japan (1957), p. 19.

(36% yield) of crystals, mp 160—161°C, which were identified as 4′,7-dimethoxyisoflavene (VIII). When V was treated with nitrous acid for 2 hr under milder reaction conditions (ice cooling), the expected *trans*-4′,7-dimethoxyisoflavan-4-ol (XIV) was not obtained, but 50 mg of VIII and 200 mg of unreacted V were recovered.

Isoflavene (XII). A solution of 1 g *cis*-isoflavan-4-ol (IX) in 30 m*l* of acetic acid containing 2 drops of concentrated hydrochloric acid was refluxed for 1 hr. After the removal of the acetic acid under reduced pressure, 50 m*l* of water were added. The crystals thus obtained were recrystallized from methanol to give 0.8 g of the crystals (XII), mp 90—91°C.

Found: C, 86.32; H, 5.92%. Calcd for $C_{15}H_{12}O$: C, 86.51; H, 5.81%.

Preparation of the Diborane-Tetrahydrofuran Solution[7]. All the reactions were carried out under a nitrogen atmosphere. To a swirling solution of 3 g of sodium borohydride in 18 m*l* of diglyme (dried on calcium hydride and then on lithium aluminum hydride, and subsequently distilled), there were added, drop by drop over a period of 30 min under cooling with ice, 15 m*l* of boronfluoride etherate (distilled under reduced pressure after adding anhydrous ethyl ether and calcium hydride). The stirring was then continued for 30 more min, after which the mixture was heated at 110°C for 1 hr for the complete generation of diborane. The generated diborane was cooled by dry ice - acetone to remove the ether, and then passed through 15 m*l* of THF (dried on lithium aluminum hydride and distilled) containing 0.2 g of sodium borohydride in order to remove the borontrifluoride. Then the diborane was introduced to 25 m*l* of THF in an absorption bottle cooled by ice water. The concentration of diborane in the diborane-THF solution was determined from the volume of the hydrogen generated by pouring a constant volume of the solution into a mixture of water-diglyme-THF.

***trans*-7-Methoxyisoflavan-4-ol (VII).** To a solution of 635 mg (2.67 mmol) of 7-methoxyisoflavene[3] (XIII) in 10 m*l* of THF, there were added 1.60 m*l* (1.06 mmol) of a diborane-THF solution (concentration 0.66 mol/*l*) with stirring and under cooling with ice. Every hour, a small portion of the solution was taken up in order to determine the unreacted XIII by means of the change in the absorption intensity at 333 mμ by reference to a previously-prepared calibration curve. The flask was permitted to remain for 2 hr at 0°C, and then kept for 15 hr at room temperature. After 17 hr, 0.9 m*l* (0.59 mmol) of the diborane-THF solution was added. After it had been confirmed that the unreacted XIII had disappeared after 70 min, 5 m*l* of THF and 0.5 m*l* of water were carefully added with stirring and under cooling with ice in order to decompose the excess diborane. To the above solution, there were then added, drop by drop, 1.25 m*l* of 3 N sodium hydroxide over a period of approximately 3 min and then 0.32 m*l* of 30% hydrogen peroxide over a period of about 2 min. The stirring was continued for 1 hr under cooling with ice, and then for 1 more hr at room temperature, after which the solution was poured into water and extracted with ether. In order to remove any phenolic substances, the extract was washed with 1 N sodium hydroxide and with water, dried on sodium sulfate, and distilled under reduced pressure. The residual oil was crystallized by the addition of ethanol, which afforded 300 mg (44% yield) of crystals, mp 130—131°C. The melting point of this compound was not depressed on admixture with authentic *trans*-7-methoxyisoflavan-4-ol.

***trans*-Isoflavan-4-ol (VI).** To a swirling solution of 1.0 g of isoflavene (XII) in 7 m*l* of THF, there were added 4.0 m*l* of the diborane-THF solution under cooling with ice. The reaction mixture was then worked up in a manner similar to that of Experiment XIII described above. After the ether had been removed, 5 m*l* of *n*-hexane were added to the residual oil, giving 0.8 g (73% yield) of crystals. Recrystallization from *n*-hexane - benzene afforded crystals, mp 97—97.5°C, which did not show any depression of melting point on admixture with authentic *trans*-isoflavan-4-ol.

***trans*-4′,7-Dimethoxyisoflavan-4-ol (XIV).** To a solution of 700 mg of 4′,7-dimethoxyisoflavene (VIII)[5] in 15 m*l* of THF, 2.2 m*l* of the diborane-THF solution were added under cooling with ice. The crystals obtained by the usual treatment were recrystallized from benzene to give 490 mg (66% yield) of crystals, mp 123.5—124°C. This compound (XIV) was not identical with the reduction product of 4′,7-dimethoxyisoflavanone. $J_{3H,4H}$ 7.9 Hz.

Found: C, 71.87; H, 6.44%. Calcd for $C_{17}H_{18}O_4$: C, 71.31; 6.34%.

By the usual manner, the acetate of XIV was prepared by reaction with pyridine - acetic anhydride, mp 131—132.5°C. $J_{3H,4H}$ 5.0 Hz.

Found: C, 69.77; H, 6.09%. Calcd for $C_{19}H_{20}O_5$: C, 69.50; H, 6.14%.

The authors wish to express their sincere thanks to Professor Yoshio Kitahara for his making convenient the NMR spectra measurements.

BULLETIN OF THE CHEMICAL SOCIETY OF JAPAN VOL. 41 2078—2082 (1968)

The Rearrangement of Isoflavanone Oximes with Lithium Aluminum Hydride

Naoto INOUE, Shozo YAMAGUCHI, Shoei ITO and Ikuko SUZUKI

College of General Education, Tohoku University, Kawauchi, Sendai

(Received December 19, 1967)

The reaction of isoflavanone oxime (III), 7-methoxyisoflavanone oxime (IV), and 4',7-dimethoxyisoflavanone oxime (V) with lithium aluminum hydride in ether for 20 hr under refluxing gave 3-phenyl-2,3,4,5-tetrahydro-1,5-benzoxazepine derivatives (XVII, XVIII and XIX) but not the expected 4-aminoisoflavans. When a similar reaction was carried out using flavanone oxime and 7-methoxyflavanone oxime, only 4-aminoflavans were obtained, and the rearrangement reaction observed in isoflavanone oximes did not occur. Therefore, it may be considered that, in the reaction of chromanone oximes and lithium aluminum hydride, the position (C_2 or C_3) and the size of the substituent exerts a remarkable influence on the rearrangement reaction, while the methoxyl group at the 7-position (*para* position to the oximino group) has little effect.

By the catalytic hydrogenation of flavanone oxime (I), Bognár and his co-workers[1] obtained 4-aminoflavan (II), which is an intermediate in the course of the synthesis of one of the stereoisomers of flavan-4-ol. They also reported that, in the reduction of I using diborane or lithium aluminum hydride or aluminum amalgam, II was always obtained. In the preceding paper[2] it was reported that the catalytic hydrogenation of isoflavanone oximes in the presence of palladium on carbon gave 4-aminoisoflavans, which are intermediates for the synthesis of *trans*-isoflavan-4-ols. In order to obtain 4-aminoisoflavans, an ether solution of isoflavanone oximes was reduced with lithium aluminum hydride. However, the expected 4-aminoisoflavans were not obtained; a different kind of compouds was isolated. This paper will describe the results of these reactions.

When an ether solution of isoflavanone oxime (III), 7-methoxyisoflavanone oxime (IV), and 4',7-dimethoxyisoflavanone oxime (V) was refluxed with lithium aluminum hydride for 20 hr and then treated with 6 N hydrochloric acid, hydrochlorides of unknown basic compounds, were obtained, IX mp 220°C, X mp 247°C, and XI mp 186°C respectively. These compounds (IX, X, and XI) are different from the hydrochlorides[2] of 4-aminoisoflavans (XII, XIII, and XIV), which are the catalytic hydrogenation products of III, IV, and V respectively. The IX, X, and XI compounds, show a broad ν_{N^+-H} band between 2800—2300 cm^{-1} in their infrared spectra, and may be assumed to be hydrochlorides of secondary amines in view of the infrared spectra[2] of XII, XIII, and XIV. In the infrared spectra of *N*-acetyl derivatives of the amines, no band corresponding to the N–H stretching vibration is observed, but one assigned to the carbonyl group of $N-COCH_3$ appears at 1640 cm^{-1}. The above data also support the idea that IX, X, and XI are secondary amine hydrochlorides. From the reactions of IX and X with nitrous acid, the nitroso compounds XV and XVI, possessing the characteristic absorption ($\nu_{N=O}$) of N–N=O at 1450 cm^{-1}, are obtained. These compounds are converted to the original amine hydrochlorides (IX and X), after catalytic hydrogenation with Raney Ni and subsequent treatment with hydrochloric acid. Therefore, it is clear that the reaction with nitrous acid and the successive catalytic hydrogenation does not change the skeletons of these compounds.

The molecular weights of the amines (XVIII and XIX) were determined to be 255 and 285 respectively by mass spectrometry; these values accord with those of 4-amino-7-methoxyisoflavan (VII) and 4-amino-4',7-dimethoxyisoflavan (VIII). The elemental analyses of XVIII and XIX agree with $C_{16}H_{17}ON$ and $C_{17}H_{19}O_3N$ respectively, which correspond to the molecular formulae of VII and VIII. In the mass spectra of 4-aminoisoflavans, the peaks of $M-NH_3$ and $M-NH_3-H$ are observed, while, in those of XVIII and XIX, no corresponding peaks are observed*1 (Fig. 2).

On the basis of these data, it may reasonably be concluded that the unknown compounds, IX, X, and XI, obtained by the lithium aluminum hydride reduction of isoflavanone oximes are secondary amine hydrochlorides isomeric with 4-aminoisoflavan hydrochlorides.

1) R. Bognár, M. Rakosi, H. Fletcher, D. Kohoe, E. M. Philibin and T. S. Wheeler, *Tetrahedron*, **18**, 135 (1962).

2) S. Yamaguchi, S. Ito, I. Suzuki and N. Inoue, This Bulletin, **41**, 2073 (1968).

*1 The details will be reported elsewhere.

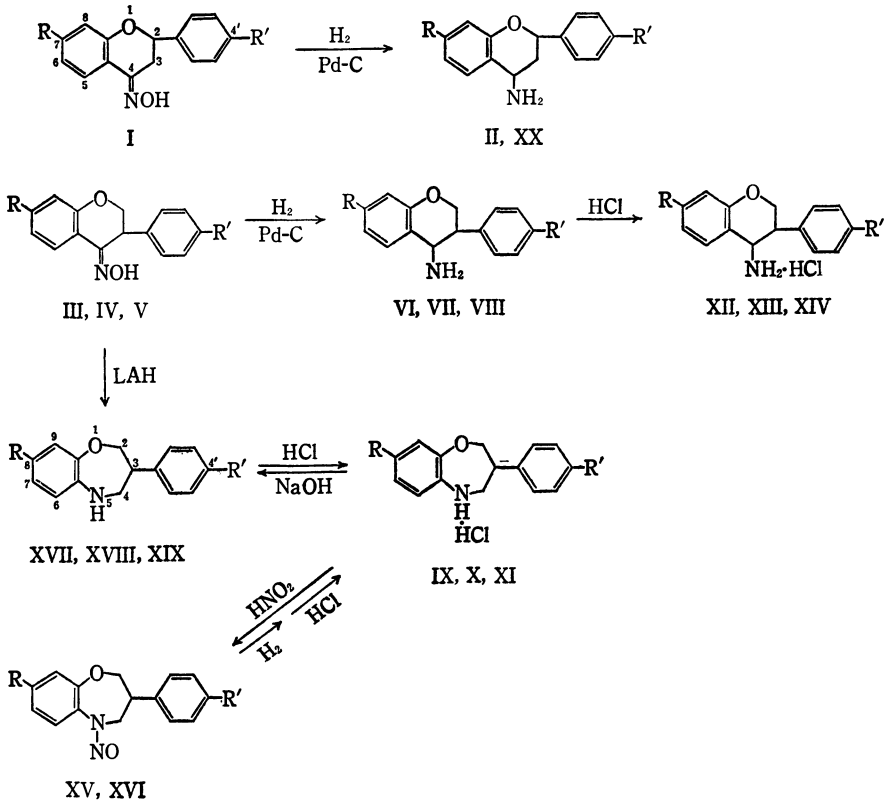

I, II, III, VI, IX, XII, XV, XVII: R=R'=H
IV, VII, X, XIII, XVI, XVIII, XX: R=OCH_3, R'=H
V, VIII, XI, XIV, XIX: R=R'=OCH_3

Fig. 1

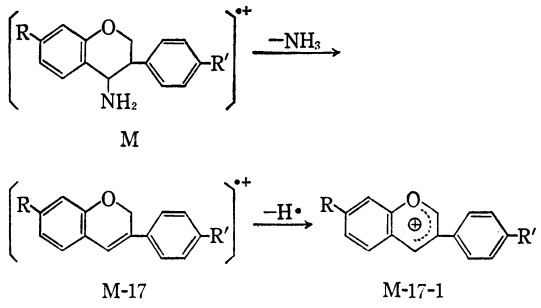

M M-17 M-17-1

Fig 2.

Recently, a few examples of secondary amines being produced by rearrangement in the reduction of oximes with lithium aluminum hydride have been found. Smith and his co-workers[3] have reported that, in the reduction of oximes of aldehydes or ketones, the rearrangement products were obtained together with the corresponding normal reduction products. For example, the reduction of oximes of acetophenone and propiophenone afforded phenylethylamine (16%) and phenylpropylamine (14%), together with α-aminoethylbenzene and α-aminopropylbenzene, respectively.

Harfenist and Magniens[4] have reported that, in the lithium aluminum hydride reduction of oximes of six-membered ring ketones fused to phenothiazine, seven-membered cyclic amines (Table 1) were formed by ring enlargement. Graham and Williams[5] mentioned that, in the lithium aluminum

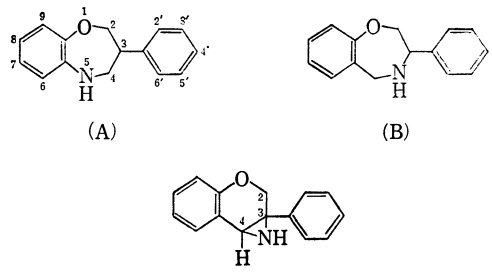

(A) (B) (C)

Fig. 3

3) D. R. Smith, M. Maienthal and J. Tiptor, *J. Org. Chem.*, **17**, 294 (1952).

4) M. Harfenist and E. Magniens, *J. Am. Chem. Soc.*, **80**, 6080 (1965).

5) S. H. Graham and A. J. S. Williams, *Tetrahedron*, **21**, 3263 (1965).

TABLE 1. pK_a VALUES OF AMINE HYDROCHLORIDES

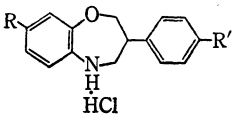

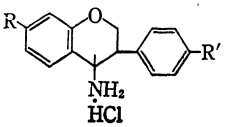

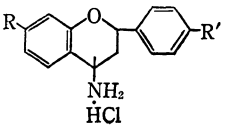

	pK_a*		pK_a[2]		pK_a	
R=R'=H	IX	4.05	XII	7.25	II	7.40
R=OCH_3, R'=H	X	4.60	XIII	7.45	XX	7.95
R=R'=OCH_3	XI	4.65	XIV	7.50		

* measured in 15% aq. EtOH.

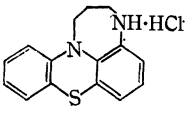

3.75 (in 50% Me_2SO)[4]

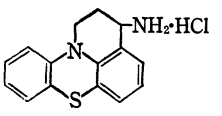

8.11 (in 50% Me_2SO)[4]

Aziridine 7.98[7]

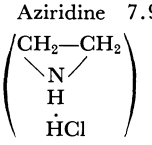

hydride reduction of phenyl alkyl ketone oximes, bulky alkyl group increase the yields of secondary amines produced by rearrangement. On the other hand, Kitahonoki *et al.*[6] found that the reduction of ketoximes and aldoximes with lithium aluminum hydride in tetrahydrofuran causes a rearrangement affording azirizines.

The number of *aliphatic hydrocarbon protons* (4.67—3.08 ppm)*2 indicated by the NMR spectra of IX, X and XI is five,*3 this fact also supports the idea that these compounds are not azirizine derivatives (Fig. 3 (C).).

The pK_a values of azirizines are reported to be around 7.97[7]. However, as will be described later, those of IX, X, and XI are 4.05, 4.60, and 4.65 respectively (Table 1). In addition, azirizine compounds cause ring opening during catalytic reduction, affording primary amines. Since the *N*-nitroso derivatives of the compounds obtained in this experiment, as has been mentioned, gave the original secondary amines upon high-pressure hydrogenation, the formation of azirizine derivatives is also obviated.

Accordingly, it may be considered that the IX, X, and XI compounds possess the A- or B-type structure, as shown in Fig. 3, structures which are derived by the enlargement of the chromane ring, involving the rearrangment of the benzenoid carbon adjacent to the C_4 of isoflavanone oximes to the nitrogen atom of the oximino group.

Since A is a monoalkyl aniline derivative and B is a benzylamine derivative, there must be remarkable difference between their pK_a values. The pK_a values of IX, X, and XI were measured by the ultraviolet absorption method[8] using a Britton-Robinson buffer solution. These values were then compared with those of 4-aminoisoflavans reported in the preceding paper,[2] and with those[4] of the rearrangement products of oximes of phenothiazine derivatives (Table 1). From the data shown in Table 1, it may reasonably be concluded that the amines (XVII, XVIII, and XIX) obtained by the lithium aluminum hydride reduction of isoflavanone oximes possess the A-type structure.

Lyle and Troscianec[9] indicated that, in the lithium aluminum hydride reduction of oximes of acetophenone derivatives, the electron-releasing group at the *para* position gave more rearrangement products, and the electron-attracting group gave less. Different from Lyle's results, in this experiment the rearrangement product was obtained in a good yield (70—90%), irrespective of the presence or absence of the methoxyl group at the 7-position of isoflavanone oximes. It has been reported[1] that the reduction of flavanone oxime afforded only the normal reduction product even though lithium aluminum hydride was used. The present authors reinvestigated the reduction of flavanone oximes following the method of Bognár and found that the product was only 4-aminoflavan (*II*), identical with the product obtained by the catalytic hydrogenation of flavanone oxime. When a similar experiment was carried out using 7-methoxyflavanone oxime, only 4-amino-7-methoxyflavan (XX) was obtained, and the rearrangment product was not isolated. The pK_a values of hydrochlorides of II and XX are

6) K. Kitahonoki, K. Kodera, Y. Matsukawa, S. Miyazaki, T. Okuda, H. Takahashi and Y. Takano, *Tetrahedron Letters*, **1965**, 1059.

*2 The NMR spectra were determined with a Varian A-60 spectrometer, at 60 Mc, using deuterochloroform as the solvent and tetramethylsilane as the internal reference.

*3 If the secondary amines obtained in this experiment are aziridine derivatives, they must have three aliphatic hydrocarbon protons.

7) G. J. Buistand and H. Lucas, *J. Am. Chem. Soc.*, **79**, 6157 (1957).

8) K. Nakanishi, "Yukikagaku no Shinpo," Vol. XII, ed. by M. Murakami, Kyoritsu Shuppan, Tokyo (1947), p. 19.

9) R. E. Lyle and H. J. Troscianec, *J. Org. Chem.*, **20**, 1757 (1955).

7.40 and 7.95 respectively; these values are close to those of 4-aminoisoflavans. Therefore, it may be considered that, in the reaction of chromanone oximes with lithium aluminum hydride, the position (C_2 or C_3) and the size of the substituent exerts a remarkable influence on the rearrangement reaction, but that the methoxyl group at the 7-position (the *para* position to the oximino group) has little effect. From a similar reaction using chromanone oximes substituted with various groups at the C_2 or C_3 position, the following conclusions were drawn: first, chromanone oximes without a C_2 substituent gave only the rearrangement products; second, chromanone oximes with a C_2 substituent gave a mixture of the normal reduction products (primary amines) and the rearrangement products (secondary amines); third, the more bulky substituents at C_2 gave the more normal reduction products and the fewer rearrangement products. This problem will be reported on later in more detail.

The mechanism concerning the rearrangement reaction of chromanone oxime with lithium aluminum hydride will be reported on by Kitahara and the present authors in the near future.

Experimental*4

Reduction of Isoflavanone Oxime (III) with $LiAlH_4$. To a swirling suspension of 1 g of $LiAlH_4$ in 80 m*l* of ether, there was added, drop by drop, a solution of 1 g of III in 70 m*l* of ether at room temperature. After having been allowed to reflux for 20 hr, the reaction mixture was decomposed with water under cooling with ice. The ether layer was washed with 1 N sodium hydroxide and water, and then dried over anhydrous sodium sulfate. After the removal of the ether, 6 N hydrochloric acid was added, giving 0.8 g (80% yield) of crude crystals. Recrystallization from ethanol gave 0.6 g of 3-phenyl-2,3,4,5-tetrahydro-1,5-benzoxazepin hydrochloride (IX), mp 218—220°C. ν_{N^+-H} 2800—2300 cm^{-1}.

Found: C, 68.53; H, 6.02; N, 5.21%. Calcd for $C_{15}H_{16}ONCl$: C, 68.83; H, 6.16; N, 5.35%.

By the usual method, 200 mg of the hydrochloride (IX) was acetylated with pryidine-acetic anhydride, giving 150 mg of acetate, mp 190—191°C (from ethanol). ν_{COCH_3} 1653 cm^{-1}.

Found: C, 76.17; H, 6.49; N, 5.02%. Calcd for $C_{17}H_{17}O_2N$: C, 76.38; H, 6.41; N, 5.24%.

A solution of 100 mg of the acetate in 5 m*l* of ethanol and 0.5 m*l* of concentrated hydrochloric acid was refluxed for 10 hr. The crystals obtained after the removal of the ethanol were recrystallized from ethanol to give the hydrochloride (IX). The neutralization of 100 mg of IX with 1 N sodium hydroxide gave an oily substance, which was extracted with ether and dried over anhydrous sodium sulfate; the solvent was then removed, but did not give crystals.

Reduction of 7-Methoxyisoflavanone Oxime (IV) with $LiAlH_4$. A solution of 2 g of IV in 120 m*l* of ether was added, drop by drop, to a swirling suspension of 2 g of $LiAlH_4$ in 80 m*l* of ether at room temperature. After it had been refluxed for 20 hr, the reaction mixture was decomposed with water under cooling with ice. The ether layer was washed with 1 N sodium hydroxide and water, and then dried over anhydrous sodium sulfate. After the removal of the ether, 6 N hydrochloric acid was added to effect crystallization (1.8 g, 90% yield). Recrystallization from acetic acid gave 1.5 g of 3-phenyl-8-methoxy-2,3,4,5-tetrahydro-1,5-benzoxazepine hydrochloride (X), mp 240—243°C. ν_{N^+-H} 2800—2300 cm^{-1}.

Found: C, 66.06; H, 6.18; N, 4.61%. Calcd for $C_{16}H_{18}O_2NCl$: C, 65.86; H, 6.22; N, 4.83%.

By the usual method, 200 mg of X was acetylated with pyridine - acetic anhydride, thus affording 170 mg of acetate, mp 142—143°C. ν_{CO} 1651 cm^{-1}.

Found: C, 73.09; H, 6.65; N, 4.64%. Calcd for $C_{18}H_{19}O_3N$: C, 72.70; H, 6.44; N, 4.71%.

The crystals obtained by the neutralization of 200 mg of X with 1 N sodium hydroxide were recrystallized from methanol, giving 100 mg of free amine (XVIII), mp 81—82°C. ν_{NH} 3350 cm^{-1}.

Found: C, 75.39; H, 6.64; N, 5.24%. Calcd for $C_{16}H_{17}O_2N$: C, 75.27; H, 6.71; N, 5.49%.

Reduction of 4',7-Dimethoxyisoflavanone Oxime (V) with $LiAlH_4$. A solution of 1.3 g of V in 60 m*l* of tetrahydrofuran was added, drop by drop, to a swirling suspension of 1.3 g of $LiAlH_4$ in 50 m*l* of ether at room temperature. After it had been refluxed for 24 hr, the reaction mixture was decomposed with water under cooling with ice. The ether layer was washed with 1 N sodium hydroxide and water, and then dried over anhydrous sodium sulfate. After the removal of the solvent, 6 N hydrochloric acid was added to give a solid, (0.97 g). Recrystallization from ethanol gave 0.5 g of 3-(4'-methoxyphenyl)-8-methoxy-2,3,4,5-tetrahydro-1,5-benzoxazepine hydrochloride (XI), mp 185—186°C. ν_{N^+-H} 2800—2300 cm^{-1}.

Found: C, 63.65; H, 6.14; N, 4.56%. Calcd for $C_{17}H_{20}O_3NCl$: C, 63.41; H, 6.23; N, 4.35%.

The acetylation of 100 mg of XI with pyridine-acetic anhydride by the general method gave 90 mg of acetate, mp 158—159°C. ν_{COCH_3} 1651 cm^{-1}.

Found: C, 69.52; H, 6.34; N, 4.07%. Calcd for $C_{19}H_{21}O_4N$: C, 69.70; H, 6.47; N, 4.28%.

The crystals obtained by the neutralization of 200 mg of XI with 1 N sodium hydroxide were recrystallized from ethanol, giving free amine (XIX), mp 83—84°C. ν_{NH} 3355 cm^{-1}.

Found: C, 71.31; H, 6.78; N, 4.97%. Calcd for $C_{17}H_{19}O_3N$: C, 71.56; H, 6.71; N, 4.91%.

Reaction of 3-Phenyl-2,3,4,5-tetrahydro-1,5-benzoxazepine Hydrochloride (IX) and Nitrous Acid. To a swirling solution of 700 mg of IX in 30 m*l* of 50% acetic acid, there was added, drop by drop, a solution of 600 mg of sodium nitrite in 30 m*l* of water under cooling with ice. After the solution had been stirred for 1 hr, the crystals produced were filtered and washed with water; 500 mg of crude crystals (mp 78—80°C) were thus obtained. Recrystallization from diluted methanol gave a *N*-nitroso compound (XV), mp 56—58°C. $\nu_{N=O}$ 1450 cm^{-1}.

Found: C, 71.02; H, 5.42; N, 10.92%. Calcd for $C_{15}H_{14}O_2N_2$: C, 70.85; H, 5.55; N, 11.02%.

Reaction of 3-Phenyl-8-methoxy-2,3,4,5-tetrahydro-1,5-benzoxazepine Hydrochloride (X) and Nitrous Acid. A solution of 0.8 g of sodium nitrite in

*4 All melting points are uncorrected. The ether used in these experiments was dried over $LiAlH_4$.

70 m*l* of water was added, drop by drop, to a swirling solution of 1.2 g of X in 250 m*l* of 50% acetic acid under cooling with ice. After the solution had been stirred for 1 hr, the crystals produced were filtered and washed with water; 1.1 g of crude crystals, mp 86—88°C, were thus obtained. Recrystallization from ethanol gave a *N*-nitroso compound (XVI), mp 64—66°C. $\nu_{N=O}$ 1450 cm^{-1}.

Found: C, 67.42; H, 5.34; N, 9.55%. Calcd for $C_{16}H_{16}O_3N_2$: C, 67.59; H, 5.67; N, 9.85%.

Catalytic Reduction of the 3-Phenyl-2,3,4,5-tetrahydro-1,5-benzoxazepine-*N*-nitroso Compound (XV) by Raney-Ni. A mixture of 100 mg of XV and 100 mg of Raney-Ni (W-4) in 30 m*l* of ethanol was submitted to hydrogenation in an autoclave (hydrogen pressure: 62 atm) at 65°C for one and a half hr. After the removal of the solvent, 6 N hydrochloric acid was added to crystallize the residue. Recrystallization from ethanol gave crystals, mp 218—219°C, whose mixed melting point with IX was undepressed.

Catalytic Reduction of the 3-Phenyl-8-methoxy-2,3,4,5-tetrahydro-1,5-benzoxazepine-*N*-nitroso Compound (XVI) by Raney-Ni. A mixture of 100 mg of XVI and 100 mg of Raney-Ni (W-4) in 50 m*l* of ethanol was submitted to hydrogenation in an autoclave (hydrogen pressure: 62 atm) at 60°C for 1.5 hr. After the removal of the solvent, 6 N hydrochloric acid was added to afford crystals. Recrystallization from acetic acid gave crystals of a mp of 240—242°C, which was undepressed on admixture with X.

Reduction of Flavanone Oxime (I) by $LiAlH_4$. A solution of 1 g of I in 70 m*l* of ether was added, drop by drop, to a swirling suspension of 1 g of $LiAlH_4$ in 80 m*l* of ether at room temperature. The mixture was refluxed for 20 hr, and then decomposed with water under cooling with ice and worked up as has been described above for III. The crystals obtained, 0.78 g, were recrystallized from ethanol, affording 4-aminoflavan hydrochloride, mp 267—270°C, which did not show any depression of melting point on admixture with the compound obtained by the catalytic reduction of I using palladium on carbon as a catalyst.

Reduction of 7-Methoxyflavanone Oxime by $LiAlH_4$. To a swirling suspension of 1 g of $LiAlH_4$ in 80 m*l* of ether, there was added, drop by drop, a solution of 1 g of 7-methoxyflavanone oxime in 100 m*l* of ether at room temperature. The mixture was then refluxed for 20 hr. By working up in the usual manner, 910 mg of crystals were obtained. Recrystallization from ethyl acetate gave 4-amino-7-methoxyflavan, mp 220°C (undepressed on admixture with the compound[10] obtained by the catalytic reduction of 7-methoxyflavanone oxime using palladium on carbon as a catalyst).

The authors wish to express their thanks to Mr. Hideji Abe for his measurement of the mass spectra.

10) N. Inoue, S. Yamaguchi and S. Fujiwara, This Bulletin, **37**, 588 (1964).

BULLETIN OF THE CHEMICAL SOCIETY OF JAPAN VOL. 41 2082—2086 (1968)

Polar Conjugative Effect of Aryldithia Group on the Dissociation and Ultraviolet Spectra of Substituted Phenols[1]

Shigeru OAE and Masakuni YOSHIHARA

Department of Applied Chemistry, Faculty of Engineering, Osaka City University, Sugimoto-cho, Sumiyoshi-ku, Osaka

(Received October 2, 1967)

A few substituted aryldithiaphenols have been synthesized and their acid dissociations, NMR chemical shifts and UV spectra have been determined. The relatively stronger acidic nature of *p*-aryldithiaphenols over that of the meta-isomers is interpreted as being caused by the 3d-orbital resonance effect of the aryldithia group.

Some years ago, small blue shifts of UV spectra of dialkyl disulfides in the following order, *i.e.*, methyl, ethyl, isopropyl and *t*-butyl, were suggested to be due to the decrease of acidity of α-hydrogen in these dialkyl disulfides.[2] Meanwhile, the acidic nature of α-hydrogen in dialkyl disulfides has been demonstrated in several cases, where the disulfides have another electron-withdrawing group such as carboxyl or carboalkoxy group at α-carbon.[3-7] A typical example would be the alkaline cleavage of dithioglycolic acid, in which the initial step is presumed to be the removal of α-proton:

1) Paper on "3d Orbital Resonance in Divalent Sulfides" (XII).

2) N. A. Rosenthal and G. Oster, *J. Am. Chem. Soc.*, **83**, 4445 (1961).

3) A. Schoberl and H. Eck, *Ann.*, **552**, 105 (1936).

4) J. P. Danehy and J. A. Kreuz, *J. Am. Chem. Soc.*, **83**, 1109 (1961).

5) E. G. Howard, *J. Org. Chem.*, **27**, 2212 (1962).

6) J. P. Danehy and E. Hunter, *ibid.*, **32**, 2047 (1967).

7) J. P. Danehy, "The Alkaline Decomposition of Aliphatic Disulfides," in "Organic Sulfur Compounds," Vol. II, ed. by N. Kharasch and Cal Y. Meyers, Pergamon Press, New York (1963).

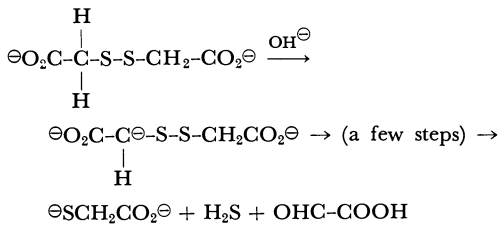

Although this apparent acidity is presumed to be due to the following 3d-orbital resonance of dithia group, there is no unambiguous evidence to support it.

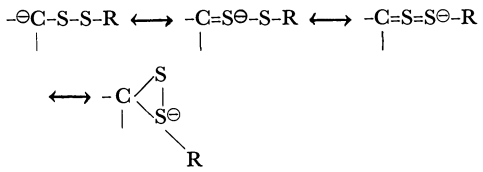

Therefore it is desirable to have a set of quantitative data to illustrate the existence of 3d-orbital resonance of dithia group.

We have synthesized a few dithia-substituted phenols and measured their dissociation constants, chemical shifts and UV spectra. This paper will describe the results and their implications.

Experimental

Bis(4-hydroxyphenyl) Disulfide. Into 2 g of 4-hydroxythiophenol suspended in 30 m*l* of water was added a solution containing a little over an equivalent amount of ferric chloride. The mixture was warmed for 30 min, the resulting precipitate was collected and recrystallized from benzene-*n*-hexane mixture: 80% yield, mp 149—150°C, colorless needles. (Found: C, 57.87; H, 4.14%)

Bis(3-hydroxyphenyl) Disulfide. The reaction of 3-hydroxythiophenol with ferric chloride solution similarly gave bis(3-hydroxy-phenyl) disulfide in 80% yield: colorless needles, mp 94—95°C. (Found: C, 57.93; H, 4.15%. Calcd for $C_{12}H_{10}OS_2$: C, 57.58; H, 4.03%.)

4-Nitro-4'-hydroxydiphenyl Disulfide. 4-Nitrobenzenesulfenyl chloride prepared from bis(4-nitrophenyl) disulfide (4.9 g) and dry Cl_2 gas was dissolved in 30 m*l* of absolute ether. This solution was added dropwise into an absolute ether solution of 4-hydroxy-thiophenol (4 g) with cooling and stirring. After refluxing 10 min, the solvent was evaporated and the remaining product was recrystallized from aqueous ethanol; yellow needles, 8 g (90% yield), mp 118—120°C. (Found: C, 51.69; H, 3.47%. Calcd for $C_{12}H_9NO_3S_2$: C, 51.60; H, 3.25%.)

It is advisable that the refluxing should not be kept too long, since prolonged heating leads to a disproportionation to bis(4-nitro-phenyl) disulfide.

2-Nitro-4'-hydroxydiphenyl Disulfide. This compound was prepared in the same manner as in the case of 4-nitro-4'-hydroxy-diphenyl disulfide, from 4.9 g of bis(2-nitrophenyl) disulfide and 4 g of 4-hydroxythiophenol. Recrystallization from aqueous methanol gave yellow needles of mp 118—119°C, 70% yield. (Found: C, 51.60; H, 3.41%. Calcd for $C_{12}H_9NO_3Se$: C, 51.60; H, 3.25%.)

4-Nitro-3'-hydroxydiphenyl Disulfide. Into 50 m*l* of absolute ether solution containing 2 g of 3-hydroxythiophenol was added dropwise 4-nitrobenzenesulfenyl chloride dissolved in 50 m*l* of absolute ether under cooling and stirring. After stirring and cooling for 30 min, the solvent was removed *in vacuo*. The resulting oil was recrystallized from benzene-*n*-hexane mixture (without warming); 70% yield, mp 98—100°C. Found: C, 51.59; H, 3.41%. Calcd for $C_{12}H_9NO_3S_2$: C. 51.60; H, 3.25%.

Results and Discussion

Syntheses and Stabilities of Aryldithiaphenols. Symmetrical disulfides are relatively easy to prepare and quite stable. The unsymmetrical diaryl disulfides not bearing hydroxyl group are also quite stable even under refluxing in chloroform or carbon tetrachloride. However, unsymmetrical phenolic diaryl disulfides are rather unstable and disproportionate readily. Hence, the preparation and the recrystallization of unsymmetrical disulfides bearing a hydroxyl group have to be carried out rather quickly under the condition in which temperature is always kept below 40—50°C. Prolonged heating in ethanol, benzene, and chloroform always leads to the disproportionation. Many attempts to prepare 3- or 4-hydroxydiphenyl disulfide were all unsuccessful, though various conditions were applied changing the temperature, the reaction time, *etc.*

Acid Dissociations. The acid dissociation constants of all the aryldithiaphenols and the related compounds measured in 50 vol% aqueous ethanol solution are summarized in Table 1.

Table 1. Dissociation constants of several dithia-substituted phenols and the related compounds
(25°C, 0.001 M solns. in 50 vol% aqueous ethanol)[a]

Compound		pK_{a_1}	pK_{a_2}	ΔpK_a
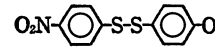	(I)	9.91		
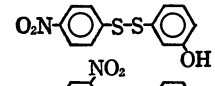	(II)	10.30		
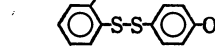	(III)	9.98		
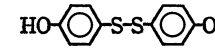	(IV)	10.08	10.68	0.60
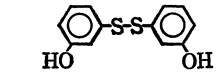	(V)	10.38	10.78	0.40
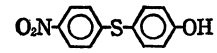	(VI)	9.86		
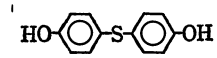	(VII)	10.35	11.0	0.65

a) pK_a values were estimated using 0.01 N KOH by a standard calculation (A. Albert and E. P. Serjeant, "Ionization Constants of Acids and Bases," Methuen and Co. (1962), p. 45).

It is interesting to note that the acidity of *p*-nitrophenyldithiaphenol (I) is stronger than that of the meta-isomer (II) by about 0.4 pK_a unit. These observations suggest strongly that the *p*-nitrophenyldithia group does operate an electron-accepting conjugation through benzene ring, involving the expansion of valence shell of the sulfur atoms of the dithia group in the dissociation of the *p*-substituted phenol, as shown below:

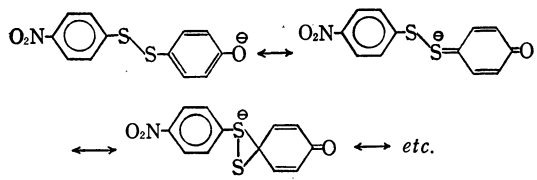

TABLE 2. COMPARATIVE σ-CONSTANTS

Group			$\Delta(\sigma_p-\sigma_m)$	Ref.
	m- *p*-	0.18 0.29	+0.11	8
	m- *p*-	0.16 0.03	−0.13	8
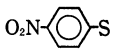	*m*- *p*-	0.34 0.44	+0.10	8
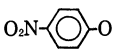	*m*- *p*-	0.31 0.19	−0.12	8
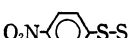	*m*- *p*-	0.26 0.42	+0.16	This
	m- *p*-	0.52 0.71	+0.19	8

These values are calculated from the corresponding pK_a and the ρ-value of 2.50.

Hammett's σ-values of the dithia and the related groups in the dissociations of various substituted phenols are listed in Table 2. While only the inductive or π-inductive effect is transmitted through the benzene ring, the $\Delta(\sigma_p-\sigma_m)$ value becomes negative, as seen in the values of both phenoxy and *p*-nitrophenoxy substituted phenols, the positive values of $\Delta(\sigma_p-\sigma_m)$ for phenylthia and *p*-nitrophenylthia groups[8] and various other sulfur groups[9] have been taken to indicate the operation of the 3d-orbital resonance effect of these sulfur groups in the dissociations of the *p*-substituted phenols as shown below:

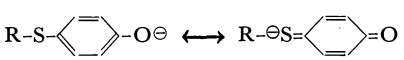

The $\Delta(\sigma_p-\sigma_m)$ value for *p*-nitrophenyldithia group (0.16) is even somewhat larger than that for the corresponding monothia group (0.10) and comes close to that for phenylsulfinyl group (0.19) which has been known to display 3d-orbital resonance effect both in the dissociation of the substituted phenols and the carbanion forming reactions.[10]

Though the *m*-hydroxyphenyl is not identical to *p*-hydroxyphenyl group, it is interesting to compare the acidities of the two isomers, IV and V, because the inductive effects of both groups are presumed not to be much different in view of our previous work on the dissociations of bis(hydroxyphenyl) sulfides, sulfoxides, sulfones and tris(hydroxyphenyl)sulfonium compounds.[11] The fact that the compound IV is a stronger acid than the compound V, apparently suggests that the 3d-orbital resonance effect is operating in the former compound.

The less acidic nature of *o*-nitrophenyldithiaphenol (III) as compared to the *p*-nitrophenyl isomer (I) is probably due to the non-bonding interaction of the following type which results in the decrease of

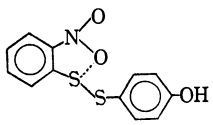

electronegativity of the sulfur atom attached nitrophenyl group, thus decreasing both the 3d-orbital resonance effect and electron-withdrawing inductive effect of the dithia group. A similar non-bonding interaction is already known from the X-ray structural determination of *o*-nitrobenzenesulfenic acid.[12]

TABLE 3. NMR SPECTRA (IN 1,4-DIOXANE, ppm)

Compound	OH proton	Ring proton
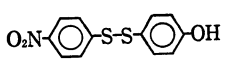	7.87	8.10, 7.95, 7.61, 7.46, 7.30, 7.16, 6.61, 6.48
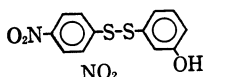	7.77	8.14, 7.99, 7.62, 7.47, 6.26 (multiplet)
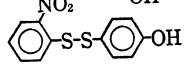	7.77	8.27—8.05, 7.35, 7.19, 6.61, 6.48
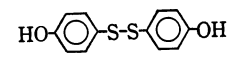	7.69	7.24, 7.10, 6.61, 6.47
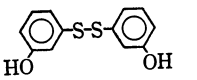	7.69	6.74 (multiplet)
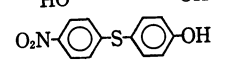	8.02	7.95, 7.80, 7.33, 7.18, 7.02, 6.87, 6.76, 7.61
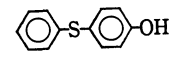	7.71	7.27, 7.12, 6.99, 6.69, 6.53
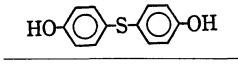	7.54	7.11, 6.96, 6.60, 6.47

8) S. Oae, "3d Orbital Resonance Involving the Sulfur Atom in Organic Sulfide," in "Organic Sulfur Compounds," Vol. III (in Press); Cal. Y. Meyers, *Gazz. Chim. Ital.*, **93**, 1206 (1963).

9) C. C. Price and S. Oae, "Sulfur Bonding," Ronald Press, New York (1962).

10) D. J. Cram, "Fundamentals of Carbanion Chemistry," Academic Press, New York (1965).

11) S. Oae and C. Zault, *J. Am. Chem. Soc.*, **82**, 5359 (1960); S. Oae, M. Yoshihara and W. Tagaki, This Bulletin, **40**, 951 (1967).

12) W. C. Hamilton and S. J. LaPlaca, *J. Am. Chem. Soc.*, **86**, 2289 (1964).

NMR Spectra. The proton chemical shifts of OH groups of some aryldithiaphenols and the related compounds in 1,4-dioxane are summarized in Table 3.

Although only a few compounds are available for the study, apparently there are good correlations between the acid strength and the chemical shifts for both para- and meta- substituted dithiaphenols and monothiaphenols, whose slopes of chemical shifts (ppm) against pK_a values are found to be -1 (Fig. 1). These observations suggest that the chemical shifts are dependent on the molecular structures while the electron densities of hydroxyl

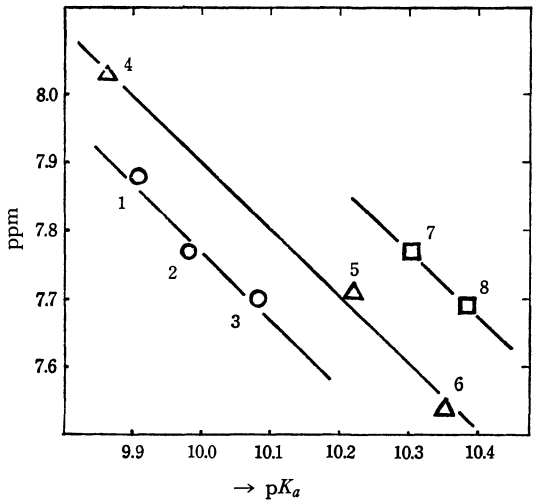

Fig. 1. The relationship between pK_a and the chemical shift of phenolic proton.

(1) 4-Nitro-4'-hydroxydiphenyl disulfide
(2) 2-Nitro-4'-hydroxydiphenyl disulfide
(3) Bis(4-hydroxyphenyl) disulfide
(4) 4-Nitro-4'-hydroxydiphenyl sulfide
(5) 4-hydroxydiphenyl sulfide
(6) Bis(4-hydroxyphenyl) sulfide
(7) 4-Nitro-3'-hydroxydiphenyl disulfide
(8) Bis(3-hydroxyphenyl) disulfide

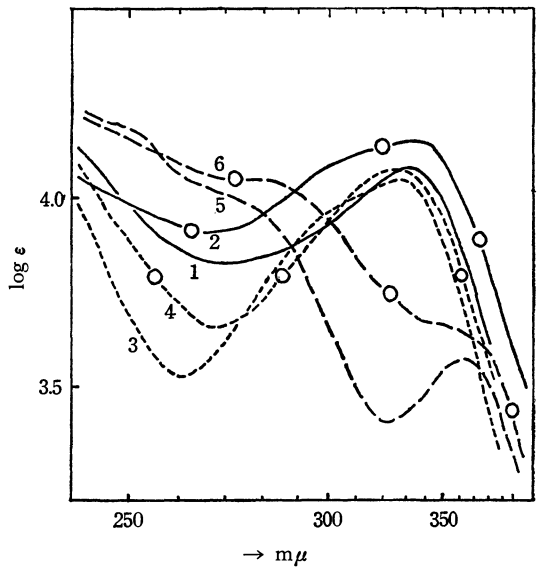

Fig. 2. UV spectra of some nitro-substituted dithiaphenols in 50 vol % ethanol and alkaline solutions.

4-Nitro-4'-hydroxydiphenyl disulfide (1, neutral; 2, alkaline)
4-Nitro-3'-hydroxydiphenyl disulfide (3, neutral; 4, alkaline)
2-Nitro-4'-hydroxydiphenyl disulfide (5, neutral; 6, alkaline)

Table 4. UV spectra in 50% ethanol and alkaline solution

Compound	In neutral mμ (log ε)	In alkaline mμ (log ε)
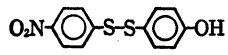	335 (4.07)	sh. 305 (4.10) 336 (4.15)
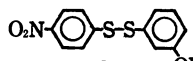	sh. 295 (3.92) 327 (4.05)	328 (4.07)
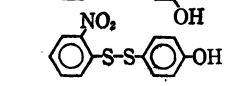	sh. 250 (4.19) sh. 280 (3.92) 367 (3.57)	sh. 290 (4.04) sh. 362 (3.62)
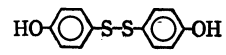	240 (4.15) sh. 280—290 (3.87—3.91)	253 (4.11) 302 (4.13) sh. 330 (4.07)
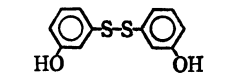	285.5 (4.32) 292 (4.34)	sh. 286 (4.28) 295.5 (4.32)
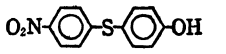	sh. 260 (4.34) 352 (4.69)	264.5 (4.73) 356 (4.68)
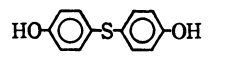	231.2 (4.16)[a] 248.6 (4.16)	265 (4.39)[a]

a) These values are those in 6% ethanol and alkaline solutions in preceding paper (This Bulletin, **40**, 951 (1967)).

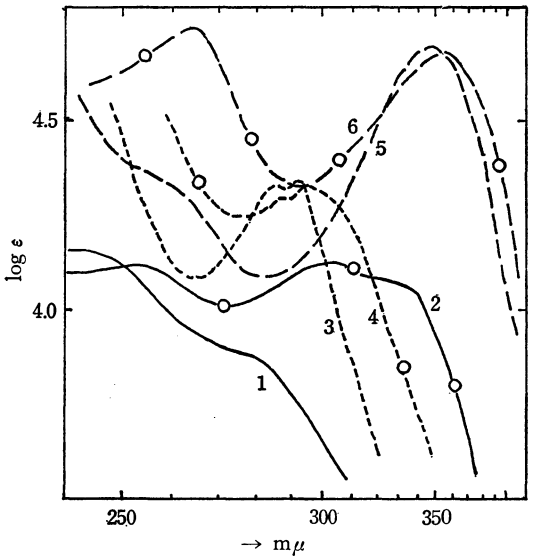

Fig. 3. UV spectra of some hydroxy-substituted dithiaphenols and monothiaphenol in 50 vol % ethanol and alkaline solutions.
Bis(4-hydroxyphenyl) disulfide (1, neutral; 2, alkaline)
Bis(3-hydroxyphenyl) disulfide (3, neutral; 4, alkaline)
4-Nitro-4'-hydroxydiphenyl sulfide (5, neutral; 6, alkaline)

groups are in a direct correlation with the free energies of dissociation.

Ultraviolet Absorption Spectra. The ultraviolet absorption spectra of dithia- and monothiaphenols are taken in 50% ethanol and alkaline solution and summarized in Table 4 and Figs. 2 and 3.

One notices that the λ_{max} for 4-nitro-4'-hydroxydiphenyl disulfide (I), 335 mμ, is at a longer wavelength than that for the meta-isomer (II). Perhaps the chromophore, *p*-nitrophenyldithia group in this case, is perturbed by the *p*-hydroxyphenyl group due to the electron-donation than by the meta group which cannot come in conjugation with the chromophore. It is interesting to note that the λ_{max} (352 mμ) of 4-nitro-4'-hydroxydiphenyl sulfide is at a longer wavelength (17 mμ) than that of the corresponding dithia group (335 mμ), perhaps because of the easy transmission of the electron-withdrawing inductive effect of 4-nitrophenylmercapto group. A question arises as to the possibility through conjugation using 3d-orbitals with the expansion of outer shell of the sulfur atom. However, this possibility does not seem to appear in the ultraviolet absorption spectra. Thus, the λ_{max} of 4-nitro-4'-hydroxydiphenyl sulfide in 50% ethanol solution shifts only slightly to a longer wavelength in alkaline solution (4 mμ), while there are also no red shifts of λ_{max} from neutral to alkaline solutions in the case of the dithia-substituted phenols.

BULLETIN OF THE CHEMICAL SOCIETY OF JAPAN VOL. 41 2086—2095 (1968)

Preparation and Oxidation of Dihydrothiophenes*1

Takao TAKAYA, Shigeo KOSAKA, Yoshio OTSUJI and Eiji IMOTO

Department of Applied Chemistry, College of Engineering, University of Osaka Prefecture, Sakai, Osaka

(Received November, 15, 1967)

The preparation and oxidation of 3,4-disubstituted 2,5- and 4,5-dihydrothiophenes are described. The oxidation of these dihydrothiophenes with 30% hydrogen peroxide in acetic acid gave the corresponding thiophene derivatives. However, the oxidation of the same compounds with perbenzoic acid in chloroform gave the corresponding sulfone derivatives. The mechanisms for these oxidation are discussed.

During the course of our studies of the chemistry of dihydrothiophenes, we happened to find that 2,5-dihydrothiophene-3,4-dicarboxylic acid (Ia_1, R=H)[1] is oxidized to thiophene-3,4-dicarboxylic acid (IIa_1, R=H)[1] by 30% hydrogen peroxide in acetic acid. This fact is not consistent with the previously-reported findings that the oxidation of 2,5-dihydrothiophene[2] and 2-methyl-4,5-dihydrothiophene-3-carboxylic acid[3] with the same reagent gives the corresponding sulfones. These observations prompted us to study the oxidation of

*1 Part VIII of the series entitled "Studies of the Syntheses of Heterocyclic Compounds." This paper was presented at the 19th Annual Meeting of the Chemical Society of Japan, Yokohama, April, 1966. Part VII: T. Takaya, H. Yoshimoto and E. Imoto, This Bulletin, **41**, 2176 (1968).

1) Suffix 1 represents R=H and suffix 2 represents $R=CH_3$.

2) S. F. Birch and D. T. McAllan, *J. Chem. Soc.*, **1951**, 2556.

3) F. Korte and K. Löhmer, *Chem. Ber.*, **90**, 1290 (1957).

several 3,4-disubstituted 2,5- or 4,5-dihydrothiophenes in detail.

Results and Discussion

Oxidation of 3,4-Disubstituted 2,5-Dihydrothiophenes. When 3,4-disubstituted 2,5-dihydrothiophenes (I) were treated with 30% hydrogen peroxide in acetic acid, the corresponding thiophene (II) and/or sulfone derivatives (III) were obtained, depending on the nature of the substituents. The results are summarized in Chart 1 and in Table 1.

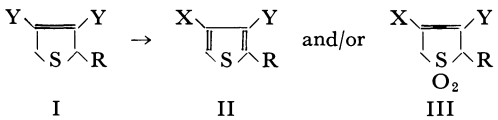

I II and/or III

These results suggest that: 1) when both of the two substituents are electron-withdrawing groups, the oxidation tends to produce the corresponding thiophene derivatives, II; 2) when one substituent is an electron-releasing group and the other is an electron-withdrawing group, the oxidation tends to produce the sulfone derivatives, III; and 3) 3,4-dimethoxycarbonyl-2,5-dihydrothiophene (Ic_1, R=H) and its 2-methyl derivative (Ic_2, R=CH_3) are exceptional. Upon oxidation the former produced a mixture of $IIIc_1$ and IIc_1 in an approximate molar ratio of 7 : 3, and the latter, a mixture of $IIIc_2$ and IIc_2 in an approximate molar ratio of 8 : 2.

The oxidation of 3,4-disubstituted 2,5-dihydrothiophenes, I, was also carried out with perbenzoic acid in chloroform. The products obtained in this oxidation are summarized in Table 1. The results show that the oxidation of 3,4-disubstituted 2,5-dihydrothiophenes with perbenzoic acid in chloroform produces the corresponding sulfone derivatives irrespective of the nature of the substituents, except that 2,5-dihydrothiophene-3,4-dicarboxylic acid, Ia_1, forms the corresponding sulfoxide (V). The exceptional formation of this compound may be due to its insolubility in chloroform. In fact, this compound precipitated out during the reaction.

The structure of the products obtained by the above oxidations was confirmed as follows. The thiophene derivatives were identified by comparison with the respective authentic samples which had been obtained by the oxidation of the corresponding dihydrothiophenes with chloranil. The sulfone derivatives were identified from the results of elemental analyses and from the presence of the absorption bands corresponding to the sulfone group in

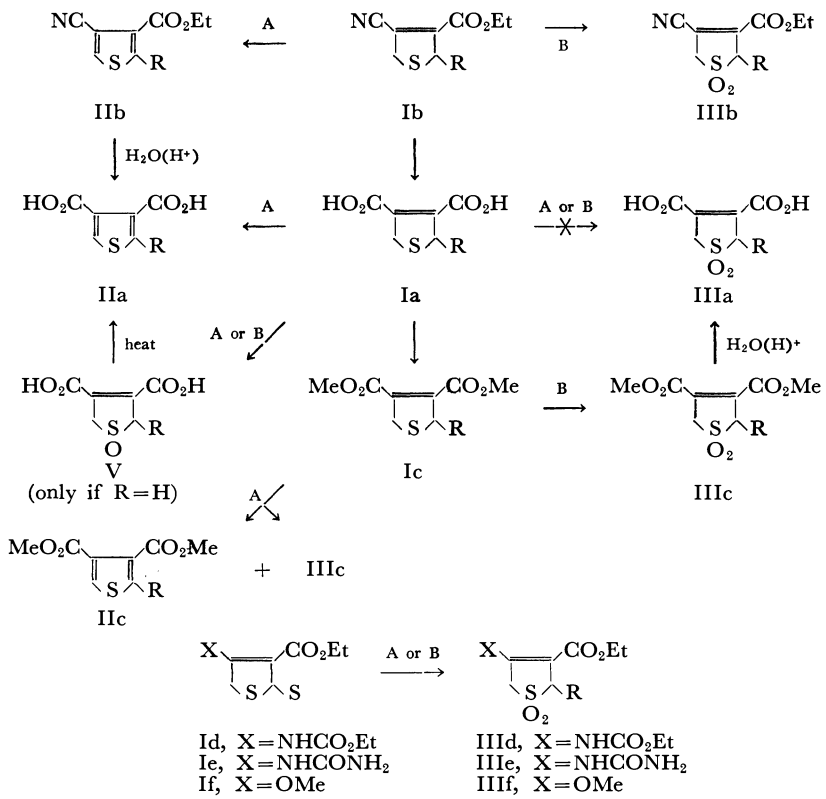

Chart 1

TABLE 1. OXIDATION OF 2,5-DIHYDROTHIOPHENES

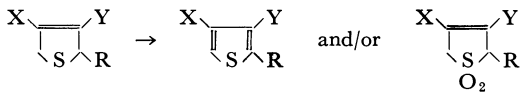

I II III

Starting material	Substituents X	Y	R	Procedure*	Product	Yield %
Ia_1	COOH	COOH	H	A	IIa_1	68
Ia_1	COOH	COOH	H	A	V	83
Ia_2	COOH	COOH	Me	A	IIa_2	90
Ib_1	CN	CO_2Et	H	A	IIb_1	92
Ib_1	CN	CO_2Et	H	A	IIb_1**	88
Ib_2	CN	CO_2Et	Me	A	IIb_2 $IIIb_2$	92 trace
Ic_1	CO_2Me	CO_2Me	H	A	IIc_1 $IIIc_1$	23 53
Ic_2	CO_2Me	CO_2Me	Me	A	IIc_2 $IIIc_2$	13 53
Id_1	$NHCO_2Et$	CO_2Et	H	A	$IIId_1$	69
Ie_1	$NHCONH_2$	CO_2Et	H	A	$IIIe_1$	67
Ie_2	$NHCONH_2$	CO_2Et	Me	A	$IIIe_2$	78
If_1	OMe	CO_2Et	H	A	$IIIf_1$	52
Ia_1	COOH	COOH	H	B	V	84
Ib_1	CN	CO_2Et	H	B	$IIIb_1$	84
Ib_2	CN	CO_2Et	Me	B	$IIIb_2$ IIb_2	77 trace
Ic_1	CO_2Me	CO_2Me	H	B	$IIIc_1$	95
Ic_2	CO_2Me	CO_2Me	Me	B	$IIIc_2$	75
Id_1	$NHCO_2Et$	CO_2Et	H	B	$IIId_1$	86
If_1	OMe	CO_2Et	H	B	$IIIf_1$	82

* A, the oxidation with 30% hydrogen peroxide - acetic acid; B, the oxidation with perbenzoic acid - chloroform. See Experimental for the detailed procedure.

** The reaction was conducted by standing the reaction mixture for 90 min at 100°C.

their infrared spectra. The structure of 3,4-dicarboxy-2,5-dihydrothiophene-1-oxide, V, was confirmed on the bases of the following observations: a) the elemental analysis, $C_6H_6O_5S$ (MW 189), shows that this compound contains one more oxygen atom than Ia_1, b) the infrared spectrum has no characteristic absorption bands in the sulfone and thiophene regions, and c) this compound produces the pyrazoline derivative (VI) when V is treated with diazomethane. The first two pieces of evidence, a) and b), suggest that either the sulfoxide V or the epoxide (IV) is a possible structure. However, the third piece of evidence, c), indicates that the most probable structure is the sulfoxide V. It is of interest to note here that when the sulfoxide V was heated for several minutes in a protic solvent such as aqueous ethanol or glacial acetic acid, it was converted into thiophene-3,4-dicarboxylic acid, IIa_1.[4]

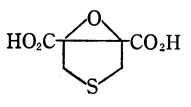

IV

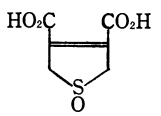

V

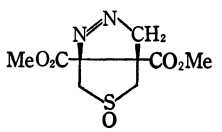

VI

A similar dehydration reaction has recently been found by Cava and Pollack[5] in 1,3-dihydrobenzo[*c*]-thiophene (VII); the pyrolysis of VII on neutral alumina afforded isothianaphthene (VIII) in a 94% yield.

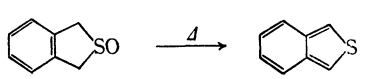

VII VIII

4) This compound was kindly provided by Professor S. Oae.

5) M. P. Cava and N. M. Pollack, *J. Am. Chem. Soc.*, **88**, 4112 (1966).

These facts suggest that the transformation of dihydrothiophenes to the corresponding thiophene derivatives proceeds through the corresponding sulfoxide derivatives, even though attempts to isolate sulfoxides of 3,4-disubstituted dihydrothiophenes other than Ia_1 have been unsuccessful.

A probable mechanism for the transformation of the 2,5-dihydrothiophene Ia_1 to the thiophene IIa_1 *via* the sulfoxide V is illustrated in Chart 2. The

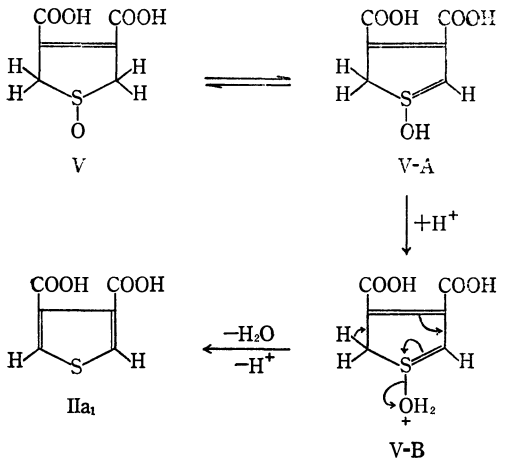

Chart 2

first step of this transformation is the oxidation of the sulfide to the sulfoxide. Since the hydrogen atom of the methylene group adjacent to the sulfoxide group is acidic, and since its acidity is also enhanced by two carboxyl groups, the electron-withdrawing groups at the 3- and 4-positions, the sulfoxide V may take a tautomeric form (V-A). The V-A tautomer would be dehydrated under acidic conditions to produce the thiophene derivative IIa_1 *via* V-B. A similar mechanism would hold for the other 2,5-dihydrothiophene which has electron-withdrawing groups at the 3- and 4- positions. In fact, in these cases the thiophene derivatives were produced. However, when one substituent is an electron-releasing group and the other is an electron-withdrawing group in 3,4-disubstituted 2,5-dihydrothiophenes, the hydrogen atom of the methylene group placed between the sulfoxide and the carbon atom bearing the electron-withdrawing group will not be acidic enough to be removed as a proton. In these cases a tautomeric equilibrium of the V⇌V-A type can not exist and the mechanism shown in Chart 2 can not be applied. As a result, the subsequent oxidation of the sulfoxide to the sulfone will take place. The proposed mechanism was further supported by the observation that tetrahydrothiophene-3,4-dicarboxylic acid (IX) afforded the corresponding sulfone (X) exclusively when IX was treated with 30% hydrogen peroxide in acetic acid.

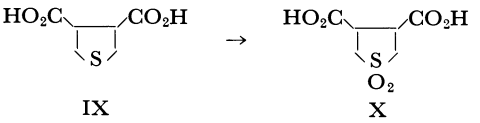

In this case, the hydrogen atoms of the methylene group adjacent to the sulfur atom are not acidic enough to be removed as a proton. Consequently, the compound IX can not undergo the subsequent reaction indicated in Chart 2, and the sulfone derivative X is produced.

Oxidation of 3,4-disubstituted 4,5-Dihydrothiophenes. The oxidation of 3,4-disubstituted 4,5-dihydrothiophenes (XI) with 30% hydrogen peroxide or perbenzoic acid was carried out in a manner similar to that of 3,4-disubstituted 2,5-dihydrothiophenes I. The results are summarized in Table 2.

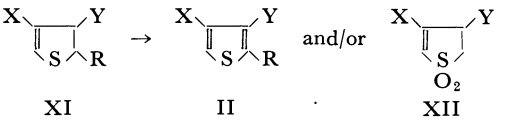

As may be seen in Table 2, 4,5-dihydrothiophene-3,4-dicarboxylic acid (XIa_1, R=H) and its 5-methyl derivative (XIa_2, R=CH_3) were, with 30% hydrogen peroxide in acetic acid, oxidized to the corresponding thiophene derivatives, IIa_1 and IIa_2. However,

Table 2. Oxidation of 4,5-dihydrothiophenes

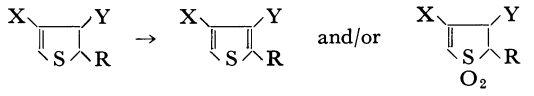

Starting material	Substituents X	Y	R	Procedure*	Product	Yield %
XIa_1	COOH	COOH	H	A	IIa_1	97
XIa_2	COOH	COOH	Me	A	IIa_2	83
XIb_1	CO_2Me	CO_2Me	H	A	IIc_1	10
					$XIIb_1$	60
XIb_1	CO_2Me	CO_2Me	H	B	$XIIb_1$	97

* A, the oxidation with 30% hydrogen peroxide-acetic acid; B, the oxidation with perbenzoic acid-chloroform. See Experimental for the detailed procedure.

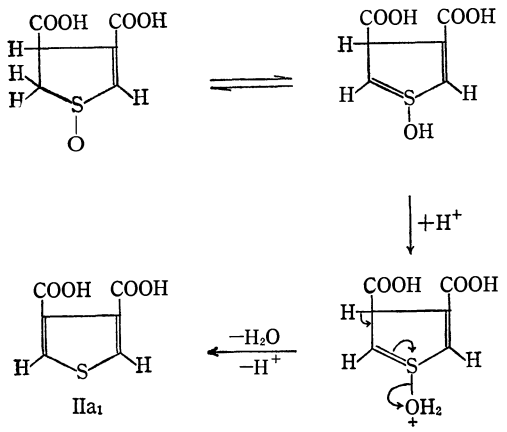

Chart 3

with the same reagent 2-methyl-4,5-dihydrothiophene-3-carboxylic acid[3] was not oxidized to the thiophene derivative, but to the corresponding sulfone derivative, in a 90% yield. These facts can probably be explained in terms of the mechanism outlined in Chart 3. Since the methylene group in XIa_1 is placed between an electron-withdrawing substituent and the sulfoxide group, one of the hydrogen atoms of the methylene group will be acidic enough to be removed as a proton*2 and the thiophene derivatives can be formed; otherwise, the dihydrothiophenes would be further oxidized to the corresponding sulfone derivatives.

The dissociation of the hydrogen atom of the methylene or methine group to a proton in the 3,4-disubstituted 2,5- or 4,5-dihydrothiophene would be much more favored in a protic solvent than in an aprotic solvent. This assumption would explain why the thiophene derivatives were produced in a protic solvent such as acetic acid, while sulfone derivatives were produced in an aprotic solvent such as chloroform. However, no explanation can be given of the fact that the oxidation of 3,4-dimethoxycarbonyl-2,5-dihydrothiophene, Ic_1, and its 2-methyl derivative, Ic_2, and 3,4-dimethoxycarbonyl-4,5-dihydrothiophene (XIb_1, R=H) with 30% hydrogen peroxide in a protic solvent such as acetic acid gave the corresponding sulfone derivative as the main product.

Preparation of Dihydrothiophenes. All of the dihydrothiophenes used in this paper, except for Ia_1, Ib_1, and XIa_1, were new compounds; they were synthesized by the following routes (see Chart 4). The starting compound ($XIIIa_2$, R=CH_3) was obtained by refluxing a solution of ethyl β-mercaptopropinate and ethyl crotonate in benzene in the presence of sodium ethoxide, ethyl β-ethoxycarbonylmethylmercaptobutyrate (XIV) was supposed to be an intermediate in this cyclization reaction. However, Larsson and Dahlström[6] have reported that, in contrast to our product, $XIIIa_2$, 2-ethoxycarbonyl-5-methyl-3-ketotetrahydrothiophene (XV) is produced by warming XIV in toluene in the presence of sodium ethoxide on a water bath. Although the reason for this inconsistency is not clear at the present time, it might be due to the differences in the reaction conditions employed.

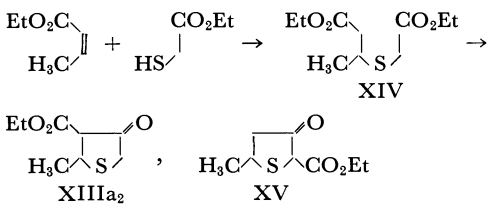

The structures of the compounds $XIIIa_2$, Ib_2, Ia_2, Ic_2 and XIa_2 obtained in our experiments were confirmed by a comparison of their spectroscopic

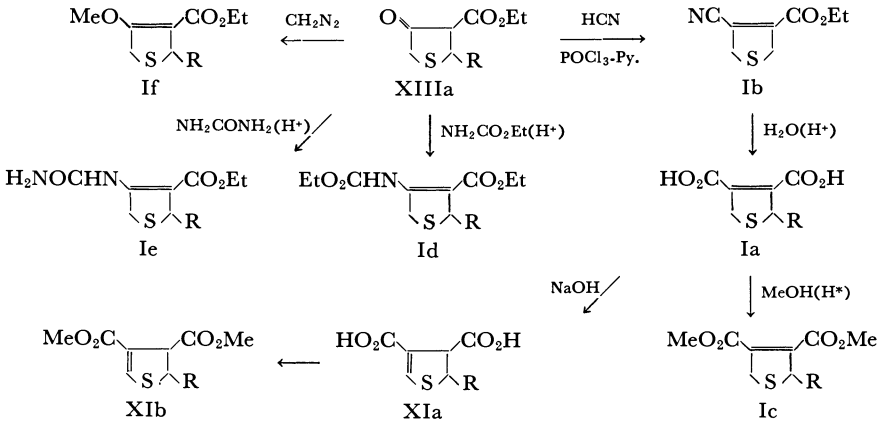

Chart 4

*2 In the case of the compound XIa_2, the hydrogen atom of the methine group to which the methyl group is attached will still be acidic enough to be removed as a proton. Thus, compound XIa_2 gave the IIa_2 thiophene upon oxidation.

6) E. Larsson and H. Dahlström, *Svensk. Kem. Tid.*, **37**, 248 (1945); *Chem. Abstr.*, **40**, 2444 (1946).

TABLE 3. SPECTROSCOPIC DATA FOR 2-METHYL-3-ETHOXYCARBONYL-4-KETOTETRAHYDROTHIOPHENE AND ITS RELATED COMPOUNDS

		$XIIIa_1$***	Ib_1	Ia_1	Ic_1	XIa_1
UV* (mμ)	λ_{max}	249	228	223	212	293
	ε	2700	7600	10000	—	9900
IR** (cm^{-1})	$\nu_{C=C}$	1625	1635	1640	1655	1570
		$XIIIa_2$***	Ib_2	Ia_2	Ic_2	XIa_2
UV* (mμ)	λ_{max}	251	225	224	212	291
	ε	1900	7100	9000	8000	9200
IR** (cm^{-1})	$\nu_{C=C}$	1620	1630	1655	1660	1570

* Measured in 99% EtOH.

** Measured in CCl_4 for $XIIIa_1$, $XIIIa_2$, Ib_1, Ib_2, Ic_1, and Ic_2: measured in a KBr disk for Ia_1, Ia_2, XIa_1, and XIa_2.

*** The infrared spectra of $XIIIa_1$, and $XIIIa_2$ showed the following absorptions: $XIIIa_1$; 1760 (ester carbonyl), 1735 (ketone), 1670 (ester carbonyl after chelation to the enolic hydroxyl group), and 1625 cm^{-1} (C=C linkage); $XIIIa_2$; 1750 (ester carbonyl), 1730 (ketone), 1660 (ester carbonyl after chelation to the enolic hydroxyl group), and 1620 cm^{-1} (C=C linkage).

TABLE 4. THE COMPOUNDS OBTAINED BY THE OXIDATION OF 2,5- AND 4,5-DIHYDROTHIOPHENE DERIVATIVES

Compound	Mp (Bp, °C/mmHg)	Recryst. solvent	Formula	Analytical data					
				Calcd %			Found %		
				C	H	N	C	H	N
IIa_1	225—227[a]	Water							
IIa_2	204—205	10% Ethanol	$C_7H_6O_4S$	45.17	3.25		45.38	3.54	
IIb_1	96— 97	Cyclohexane	$C_8H_7O_2NS$	53.04	3.90	7.73	53.18	4.03	7.67
IIb_2	82— 83	Petroleum ether-chloroform	$C_9H_9O_2NS$	55.38	4.65	7.18	55.16	4.57	7.22
IIc_1	59— 60[b]	Petroleum ether							
IIc_2	(123—124)		$C_9H_{10}O_4S$	50.47	4.71		50.70	4.78	
$IIIb_1$	111—113	Petroleum ether-chloroform	$C_8H_9O_4NS$	44.66	4.22	6.51	44.67	4.52	6.67
$IIIc_1$	104—105	Petroleum ether-chloroform	$C_8H_{10}O_6S$	41.03	4.30		40.91	4.18	
$IIIc_2$	70— 71.5	Petroleum ether-ether	$C_9H_{12}O_6S$	43.55	4.87		43.32	4.98	
$IIId_1$	90— 91	Chloroform-ligroin	$C_{10}H_{15}O_6NS$	43.32	5.45	5.05	43.56	5.20	4.81
$IIIe_1$	186—187	95% Ethanol	$C_8H_{12}O_5N_2S$	38.71	4.87	11.29	38.58	4.77	11.21
$IIIe_2$	189—190	95% Ethanol	$C_9H_{14}O_5N_2S$	41.22	5.38	10.68	41.50	5.17	10.38
$IIIf_1$	72— 74	Petroleum ether-ether	$C_8H_{12}O_5S$	43.64	5.49		43.85	5.42	
V	216—220		$C_6H_6O_5S$	37.90	3.18		37.79	3.29	
$XIIa_1$	125—126	Ether	$C_8H_{10}O_6S$	41.03	4.30		40.91	4.18	

a) Lit. mp 230—231°C, J. Sice, *J. Org. Chem.*, **19**, 70 (1954).

b) Lit. mp 60—61°C, E. C. Kornfeld and R. G. Jones, *ibid.*, **19**, 1671 (1954).

properties with those of the related compounds. The spectroscopic data are summarized in Table 3.

First, note that the compounds Ib_1, Ia_1, Ic_1, and XIa_1 have been derived from $XIIIa_1$, and that the structures of all of these compounds have been confirmed. (Although Ic_1 was first obtained in our experiment, the structure of this compound should be correct since Ic_1 was prepared simply by the esterification of Ia_1.) In addition, note also that the compounds Ib_2, Ia_2, Ic_2, and XIa_2 were experimentally derived from $XIIIa_2$ by the same methods as those employed for the derivation of Ib_1, Ia_1 Ic_1, and XIa_1 from $XIIIa_1$. This means that Ib_2, Ia_2, Ic_2, and XIa_2 have structures corresponding to those of Ib_1, Ia_1, Ic_1, and XIa_1 respectively. An inspection of the spectroscopic data in Table 3 indicates that the compound XIa_1, in which the double bond in the ring is in conjugation with the sulfur atom, shows the absorption band at the longer-wavelength side both in the ultraviolet and the infrared ($\nu_{C=C}$) spectra as compared with those for the compounds Ib_1, Ia_1 and Ic_1, in which no such

a conjugation is involved. The similarity of the spectroscopic data of compounds $XIIIa_2$, Ib_2, Ia_2 Ic_2, and XIa_2 to those of the corresponding compounds, $XIIIa_1$, Ib_1, Ia_1, Ic_1 and XIa_1, strongly suggests that the structures for the compounds $XIIIa_2$, Ib_2, Ia_2, Ic_2, and XIa_2 shown in Chart 4 are all correct. For the compound XIa_2, the above arguments lead to the structure of either XIa_2 or XIa'_2. The NMR spectrum of the compound showed, however, that the XIa_2 structure is also correct (see Experimental Section).

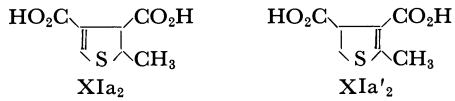

XIa_2 XIa'_2

The preparation of the compounds which have an electron-releasing and an electron-withdrawing group in 3,4-disubstituted 2,5-dihydrothiophenes was carried out as follows. 3-Ethoxycarbonyl-4-ethoxycarbonylamino-2,5-dihydrothiophene (Id_1, R=H) and its 2-methyl derivative (Id_2, R=CH_3) were prepared by the condensation of $XIIIa_1$ or $XIIIa_2$ with urethan in the presence of *p*-toluenesulfonic acid. The position of the double bond in Id_1 was confirmed from the fact that the NMR spectrum of Id_1 showed two protons at C-2 and two protons at C-5. 3-Ethoxycarbonyl-4-ureido-2,5-dihydrothiophene (Ie_1, R=H) and its 2-methyl derivative (Ie_2, R=CH_3) were also synthesized by the condensation of $XIIIa_1$ or $XIIIa_2$ with urea. 3-Methoxy-4-ethoxycarbonyl-2,5-dihydrothiophene (If_1, R=H) was obtained by treating $XIIIa_1$ with an excess ethereal diazomethane by a method similar to that of Blake and his co-workers.[7]

Experimental

All the melting points are uncorrected. The infrared spectra were recorded with a Hitachi EPI-S_2 infrared spectrophotometer. The ultraviolet spectra were obtained with a Hitachi EPS-20 recording spectrophotometer. The NMR spectra were obtained with a Nihondenshi JNM-3H-60 high-resolution nmr spectrometer in a 10% carbon tetrachloride solution of the samples, using a TMS reference at 22°C.

Materials. 3-Cyano-4-ethoxycarbonyl-2,5-dihydrothiophene Ib_1, 3,4-dicarboxy-2,5-dihydrothiophene Ia_1, and tetrahydrothiophene-3,4-dicarboxylic acid IX were prepared by the method of Baker and his co-workers from 3-ethoxycarbonyl-4-ketotetrahydrothiophene $XIIIa_1$.[8]

2-Methyl-3-ethoxycarbonyl-4-ketotetrahydrothiophene ($XIIIa_2$, R=CH_3). Eighty-seven grams of ethyl thioglycolate in 250 m*l* of dry benzene was added to dry sodium ethoxide prepared from 23 g of sodium and absolute ethanol. To the reaction mixture there was then added, drop by drop and with shaking, 82 g of ethyl crotonate over a period of 10 min. After being refluxed for 3 hr, the benzene solution was extracted with ice water. The aqueous layer was acidified with acetic acid and then extracted with benzene. The benzene extract was washed successively with water, dilute aqueous sodium bicarbonate, and water. The distillation of the benzene extract gave 5.1 g (41%) of $XIIIa_2$ boiling at 107—108°C/6 mmHg, n_D^{25} 1.497. This compound was used for the preparation of Ib_2 without further purification. The semicarbazone of $XIIIa_2$ was prepared by the usual method. Three recystallizations from aqueous ethanol gave an analytical sample, mp 149—150°C.

Found: C, 43.90; H, 6.01; N, 17.15%. Calcd for $C_9H_{15}N_3O_3S$: C, 44.08; H, 6.17; N, 17.14%.

2-Methyl-3-ethoxycarbonyl-4-cyano-2,5-dihydrothiophene (Ib_2, R=CH_3). This compound was prepared in a 70% yield from $XIIIa_2$ by applying the method of Baker and his co-workers,[8] who prepared Ib_1 from $XIIIa_1$, bp 106—108°C/1 mmHg.

Found: C, 54.74; H, 5.90%. Calcd for $C_9H_{11}NO_2S$: C, 54.82; H, 5.62%.

2-Methyl-2,5-dihydrothiophene-3,4-dicarboxylic Acid (Ia_2, R=CH_3). This compound was obtained in a 67% yield by the acid hydrolysis of Ib_2 according to the method of Baker and his co-workers,[8] mp 145—147°C (from acetone-benzene).

Found: C, 44.95; H, 4.43%. Calcd for $C_7H_8O_4S$: C, 44.70; H, 4.29%.

5-Methyl-4,5-dihydrothiophene-3,4-dicarboxylic Acid (XIa_2, R=CH_3). A solution of 1 g of Ia_2 in 5 m*l* of ethanol was refluxed for 5 hr with 1 g of potassium hydroxide in 5 m*l* of water. The solution was then acidified with dilute hydrochloric acid and extracted three times with ethyl acetate. The extracts were dried over anhydrous sodium sulfate and evaporated to dryness *in vacuo*. The residue (0.4 g, mp 124—132°C) was recrystallized from acetone-benzene-petroleum ether to give 0.2 g (20%) of colorless crystals, mp 161—162°C. The infrared spectrum showed bands at 1570 cm^{-1} (double bond conjugated with a sulfur atom), 1705 cm^{-1} (carboxylic acid), 1660 cm^{-1} (α,β-unsaturated carboxylic acid) and 3050 cm^{-1} (olefinic proton), and the nmr spectrum of the dimethyl ester of XIa_2 showed a characteristic vinyl proton at 2, 6 τ (doublet, J=1.5 cps; a long-range coupling with a proton at C-3).

Found: C, 44.50; H, 4.32%. Calcd for $C_7H_8O_4S$: C, 44.69; H, 4.29%.

2-Methyl-3,4-dimethoxycarbonyl-2,5-dihydrothiophene (Ic_2, R=CH_3). A solution of 3.76 g of Ia_2 in dry ether containing a small amount of absolute methanol was treated with an excess of ethereal diazomethane. After the evaporation of the solvent, the distillation of the residue gave 3.1 g (70%) of a yellow liquid, bp 118—124°C/4 mmHg, n_D^{23} 1.502.

Found: C, 50.20; H, 5.34%. Calcd for $C_9H_{12}O_4S$: C, 50.00; H, 5.60%.

3,4-Dimethoxycarbonyl-2,5-dihydrothiophene (Ic_1, R=H). A mixture of 10.5 g of Ia_1, 1.0 g of *p*-toluenesulfonic acid, 80 m*l* of chloroform, and 60 m*l* of methanol was refluxed for 50 hr in a Soxhlet apparatus containing anhydrous sodium sulfate in a thimble. After the mixture had then been distilled through a Vigreux column at an atmospheric pressure in order to remove the solvent, the distillation of the residue gave 7.7 g (70%) of a colorless liquid, bp 130—131°C/3 mmHg, n_D^{23} 1.516.

Found: C, 47.68; H, 5.01%. Calcd for $C_8H_{10}O_4S$: C, 47.53; H, 4.99%.

7) J. Blacke, C. D. Willson and H. Rapoport, *J. Am. Chem. Soc.*, **86**, 5294 (1964).

8) B. R. Baker, M. V. Querry and A. F. Kadish, *J. Org. Chem.*, **13**, 123 (1948).

3,4-Dimethoxycarbonyl-4,5-dihydrothiophene (XIb$_1$, R=H). 4,5-Dihydrothiophene-3,4-dicarboxylic acid (XIa$_1$, R=H) was prepared by the method of Baker and his co-workers.[9] Recrystallization from acetone-benzene gave XIa$_1$, mp 180—181°C. A solution of 4.5 g of XIa$_1$ in dry ether containing a small amount of absolute methanol was terated with an excess of ethereal diazomethane. After the evaporation of the solvent, the residue was distilled to give 4.1 g (90%) of XIb$_1$, bp 122—124°C/3 mmHg, n_D^{30} 1.525. The infrared spectrum showed bands at 1730 cm^{-1} (ester C=O), 1700 cm^{-1} (α,β-unsaturated ester C=O), and 1575 cm^{-1} (double bond conjugated with a sulfur atom), and the nmr spectrum showed a characteristic vinyl proton at 2.55 τ (doublet, J=1.5 cps; a long-range coupling with a proton at C-3).

Found: C, 47.53; H, 4.99%. Calcd for $C_8H_{10}O_4S$: C, 47.65; H, 5.21%.

2-Methyl-3-ethoxycarbonyl-4-ethoxycarbonylamino-2,5-dihydrothiophene (Id$_2$, R=CH$_3$). A mixture of 11 g of the β-ketoester XIIIa$_2$, 6 g of urethane, 1 g of *p*-toluenesulfonic acid, and 200 m*l* of dry benzene was refluxed for 15 hr in a Soxhlet apparatus containing anhydrous sodium sulfate in a thimble. The mixture, was then washed thoroughly with water to remove the *p*-toluenesulfonic acid and the excess urethane. The evaporation of the solvent gave 14 g (93%) of the product, Id$_2$. This crude product was purified by chromatography using an alumina column and chloroform as an eluent, or by recrystallization from methanol-water, to give an analytical sample, mp 68—69.5°C.

Found: C, 50.72; H, 6.44; N, 5.17%. Calcd for $C_{11}H_{17}O_4NS$: C, 50.96; H, 6.61; N, 5.40%.

3-Ethoxycarbonylamino-4-ethoxycarbonyl-2,5-dihydrothiophene (Id$_1$, R=H). A mixture of 3.5 g of XIIIa$_1$, 1.8 g of urethane, 300 mg of *p*-toluenesulfonic acid, and 70 m*l* of dry benzene was refluxed for 15 hr in a Soxhlet apparatus. The mixture was then worked up in the manner described above to give 4.10 g (83%) of Id$_1$ (mp 70—71.5°C (from methanol-water)). The NMR spectrum of Id$_1$ ($CHCl_3$) showed a triplet at 8.7 τ (6H) (J=7.5 cps), a triplet at 6.3 τ (2H) (J=3 cps), a quartet at 4.85 τ(2H) (J=7.5 cps), a quartet at 5.75 τ(2H) (J=7.5 cps), a triplet at 5.6 τ(2H) (J=3 cps), and a singlet at 4.45 τ(1H).

Found: C, 49.13; H, 5.95; N, 5.53%. Calcd for $C_{10}H_{15}O_6NS$: C, 48.97; H, 6.17; N, 5.71%.

3-Ethoxycarbonyl-4-ureido-2,5-dihydrothiophene (Ie$_1$, R=H). A) A mixture of 5.0 g of finely-ground urea, 13 g of XIIIa$_1$, 1.5 m*l* of absolute ethanol, and three drops of concentrated hydrochloric acid was placed in an evaporating dish covered loosely with a watch glass, and then evacuated continuously by an aspirator in a desiccator containing concentrated sulfuric acid as a drying agent. After about a week, the dried mixure was recrystallized from 95% ethanol to give 12.9 g (80%) of Ie$_1$, mp 198—203°C. Repeated recrystallizations from 99% ethanol gave crystals melting at 201—203°C.

B) A mixture of 3.48 g of XIIIa$_1$, 1.20 g of urea, 40 m*l* of absolute ethanol, 90 m*l* of dry benzene, and 0.3g of *p*-toluenesulfonic acid was refluxed for 48 hr in a Soxhlet apparatus containing anhydrous sodium sulfate in a thimble. The mixture was then evaporated to dryness, and the residue was recrystallized from 95% ethanol to give 3.56 g (82%) of Ie$_1$, mp 201—203°C.

Found: C, 44.52; H, 5.27; N, 12.91%. Calcd for $C_8H_{12}O_3N_2S$: C, 44.44; H, 5.60; N, 12.96%.

2-Methyl-3-ethoxycarbonyl-4-ureido-2,5-dihydrothiophene (Ie$_2$, R=CH$_3$). By treating 4.70 g of XIIIa$_2$ and 1.65 g of urea such as has been described above in the case of Id$_1$ (method A), 3.0 g (78%) of crude Ie$_2$, mp 180—184°C, were obtained. Three recrystallizations from 95% ethanol gave pure Ie$_2$, mp 187—188.5°C.

Found: C, 47.20; H, 6.26; N, 12.18%. Calcd for $C_9H_{14}O_3N_2S$: C, 46.95; H, 6.13; N, 12.17%.

3-Ethoxycarbonyl-4-methoxy-2,5-dihydrothiophene (If$_1$, R=H). To a solution of 7 g of XIIIa$_1$ in dry ether there was added an excess of dry ethereal diazomethane. The resultant solution was kept in a refrigerator for 16 hr, and then evaporated; the residue was fractionally distilled to give 6 g of If$_1$, bp 118—120°C/5 mmHg.

Found: C, 50.95; H, 6.28%. Calcd for $C_8H_{12}O_3S$: C, 51.06; H, 6.43%.

Direct Conversion of Ia$_1$ to IIa$_1$. To a solution of 0.87 g of Ia$_1$ in 5 m*l* of acetone and 10 m*l* of acetic acid 1.5 m*l* of 30% hydrogen peroixde were added while the mixture was being cooled to prevent the temperature from rising above 50°C. The reaction mixture was then allowed to stand for 24 hr at 50°C. After the evaporation of the solvent under reduced pressure, the residue was recrystallized from water to give 585 mg (68%) of IIa$_1$.

Oxidation of the Cyanoester Ib$_1$ with 30% Hydrogen Peroxide in Acetic Acid (Procedure A). A mixture of 3.0 m*l* of 30% hydrogen peroxide and 20 m*l* of acetic acid was allowed to stand at 40°C for 3 hr. To the above cooled solution there was then added, in portions, a solution of 1.83 g of the Ib$_1$ cyanoester in 10 m*l* of acetone at a temperature below 25°C. The reaction mixture was allowed to stand for 38 hr at 25°C. The solvent was then removed under reduced pressure below 50°C. The residue was triturated with a mixture of petroleum ether and acetone to give 3-cyano-4-ethoxycarbonylthiophene (IIb$_1$, R=H).

Oxidation of Id$_1$, If$_1$, XIa$_1$ and XIa$_2$ with 30% Hydrogen Peroxide in Acetic Acid. This was carried out in a manner similar to that described for Ib$_1$.

Oxidation of the Cyanoester Ib$_2$ with 30% Hydrogen Peroxide in Acetic Acid. The oxidation of the Ib$_2$ cyanoester (1.970 g) in acetone (1.5 m*l*) with 30% hydrogen peroxide (3.0 m*l*) in acetic acid (20 m*l*) was carried out according to the procedure A. The reaction mixture was then worked up in a manner similar to that described for Ib$_1$, and the residue was chromatographed on alumina. The corresponding thiophene, IIb$_2$ (1.9 g), was eluted with a mixture of petroleum ether and chloroform (9 : 1), and a small amount of the corresponding sulfone, IIIb$_2$ (*ca.* 10 mg), was eluted with a mixture of petroleum ether and chloroform (4 : 6).

Oxidation of the Diester, Ic$_1$, Ic$_2$ and XIb$_1$ with 30% Hydrogen Peroxide in Acetic Acid. This oxidation was carried out in a manner similar to that described for Ib$_1$ (Procedure A). When the reaction mixture was worked up according to the procedure A, the residue gave a mixture of the corresponding thiophene and sulfone derivatives. The approximate molar ratio of the two derivatives in the mixture was estimated by a

9) G. B. Brown, B. R. Baker, S. Bernstein and S. R. Safir, *J. Org. Chem.*, **12**, 155 (1947).

comparison of the infrared spectra of the reaction mixture and those of a mixture of the authentic samples, IIc and IIIc, the relative concentrations of IIc and IIIc being varied correspondingly. The approximate molar ratio of the sulfone and the thiophene derivative in the oxidation products was : (70% $IIIc_1$: 30% IIc_1), (80% $IIIc_2$: 20% IIc_2), and (85% $XIIb_1$: 15% IIc_1), respectively. Attempts to separate the mixture completely by chromatography using an alumina or a silica gel column were unsuccessful.

Oxidation of Ie_1 and Ie_2 with 30% Hydrogen Peroxide in a Mixture of Acetic Acid and Acetic Anhydride. A mixture of 1.5 m*l* of 30% hydrogen peroxide, 4.5 m*l* of acetic anhydride, and 9.0 m*l* of acetic acid was allowed to stand at 45°C for 3 hr (or at 25°C for 12 hr). To the cooled solution there was then added, in portions, 1.08 g of Ie_1, with occasional cooling to prevent the temperature from rising above 45°C. Then the reaction mixture was kept at 45°C for 17 hr. After the evaporation of the solvent under reduced pressure below 45°C, the residue was recrystallized from 95% ethanol to give the product, mp 174—179°C. The infrared spectrum of the product showed a weak absorption band at 1020 cm^{-1} in the sulfoxide region. This product was presumed to be a mixture of the corresponding sulfoxide and sulfone derivative, but it was not separated by fractional recrystallizations. The product was refluxed with Raney nickel in ethanol for 1 hr, and the residue, after the evaporation of the solvent, was recrystallized to give 0.63 g (53%), of the $IIIe_1$ sulfone.

The 2-methyl derivative, Ie_2 was treated in a manner similar to that described for Ie_1 to give the corresponding sulfone, $IIIe_2$.

Oxidation of the Cyanoester Ib_1 with Perbenzoic Acid in Chloroform (Procedure B). To 46.8 m*l* (0.01 mol) of a solution of perbenzoic acid in dry chloroform there was added, portion by portion, a solution of 0.916 g (0.005 mol) of Ib_1 in 2 m*l* of acetone, while the temperature was maintained at 25°C. The mixture was then allowed to stand at 25°C for 24 hr. The reaction mixture was washed successively with two 15-m*l* portions of 5% sodium thiosulfate, with 10% aqueous sodium carbonate, and with three 20-m*l* portions of water, and then dried overnight over anhydrous sodium sulfate. After the removal of the solvent, 1.05 g of the corresponding sulfone, $IIIb_1$ was obtained. The characteristic infrared absorptions in the sulfone region were at 1343 and 1160 cm^{-1}.

Oxidation of the Cyanoester Ib_2 with Perbenzoic Acid in Chloroform. After a mixture of the Ib_2 cyanoester (591 mg, 3 mmol) and perbenzoic acid (6 mmol) in chloroform (23 m*l*) had been worked up as has been described for Ib_1 (Procedure B), the residue was chromatographed on alumina; a small amount of the corresponding thiophene, IIb_2 (*ca.* 20 mg), was eluted with a mixture of petroleum ether and chloroform (9 : 1), and 0.43 g of the corresponding sulfone, $IIIb_2$[10], with a (4 : 1) mixture of petroleum ether and chloroform.

Oxidation of Ic_1, Ic_2, Id_1, If_1, and XIb_1 with Perbenzoic Acid in Chloroform. This oxidation was carried out according to the procedure B to give the corresponding sulfones. The infrared spectra of these sulfone derivatives showed characteristic absorption bands in the sulfone region.

Oxidation of 2,5-Dihydrothiophene-3,4-dicarboxylic Acid Ia_2 to 2,5-Dihydrothiophene-3,4-dicarboxylic Acid-1-oxide (V). With 30% Hydrogen Peroxide-Acetic Acid. A mixture of 70 m*l* of acetic acid and 9.0 m*l* of 30% hydrogen peroxide was allowed to stand at 40°C for 3 hr. To this solution there was then added, portion by portion, 5.22 g of the Ia_1 diacid dissolved in 20 m*l* of acetone, while the temperature was maintained below 20°C; the reaction mixture was then kept at 20°C for 24 more hours. The colorless precipitate which was gradually formed was collected by filtration, washed with cold acetone, and then dried to give 4.70 g (83%) of the sulfoxide V, λ_{max}^{EtOH} 226 mμ ($\varepsilon = 11900$), ν_{max}^{KBr} 1870 w, 1710 s, 1674 s, 1645 s, 1295 s, 1225 s, 1010 s, 955 m and 730 cm^{-1} (m), neut. equiv. 190 (calcd 190). A second crop of the product (0.62 g) was obtained by the concentration of the mother liquor under reduced pressure. This minor product was identical in infrared and ultraviolet spectra with the authentic sample of thiophene-3,4-dicarboxylic acid.[4] The melting point of an admixture with the authentic sample was also undepressed.

With Perbenzoic Acid-Chloroform. To a solution of 4.4 g of perbenzoic acid in 10 m*l* of dry chloroform, there was added, portion by portion, a solution of 1.74 g of the Ia_1 diacid in 3 ml of acetone, while the temperature was kept below 25°C. A colorless precipitate soon appeared from the mixture. The reaction mixture was kept at 20°C for 24 hr. The precipitate was collected by filtration, washed with cold acetone, and dried to give 1.60 g (84%) of the sulfoxide V, which was identical in infrared and ultraviolet spectra with the product obtained by the treatment of Ia_1 with hydrogen peroxide-acetic acid.

Conversion of the Sulfoxide V to Thiophene-3,4-dicarboxylic Acid IIa_1. Two grams of the V sulfoxide were dissolved in 20 m*l* of water by warming the solution on a hot-plate. After the mixture had been cooled, long colorless, needles crystallized out. The crystals were collected by filtration and dried to give 1.6 g (89%) of IIa_1. Its mixed melting point with the authentic sample showed no depression. When acetic acid or aqueous ethanol was used as the solvent, the solvent was evaporated to dryness *in vacuo*, and then the residue was recrystallized from water.

Reaction of the Sulfoxide V with Diazomethane in Ether. A solution of 570 mg of the V sulfoxide in 1 m*l* of dry methanol was treated with an excess of diazomethane in ether. The reaction mixture, after standing for 24 hr at room temperature, was dried over anhydrous sodium sulfate. After the removal of the solvent, the residue was recrystallized from benzene-chloroform to yield 390 mg (56%) of VI, mp 155—156°C. A characteristic infrared spectrum in the sulfoxide region was at 1045 cm^{-1}.

Found: C, 41.61; H, 4.65; N, 10.86%. Calcd for $C_9H_{12}O_5N_2S$: C, 41.54; H, 4.65; N, 10.77%.

Oxidation of Tetrahydrothiophene-3,4-dicarboxylic Acid (IX). Compound IX (0.82 g) was oxidized to X in a 80% yield, by a mixture consisting of 30% hydrogen peroxide (1.35 m*l*) and acetic acid (12 m*l*), in a manner similar to that described for Ib_1 except that the reaction was carried out at 50°C. The compound X had a mp of 201—203°C after recrystallization from acetic acid.

10) The structure of the sulfone $IIIb_2$ was confirmed by hydrolysis of $IIIb_2$ to $IIIa_2$ because of an unsuccessful purification of $IIIb_2$.

Found: C, 34.68; H, 3.74%. Calcd for $C_6H_8O_6S$: C, 34.62; H, 3.87%.

Dehydrogenation of the Ib_1 Cyanoester with Chloranil to the IIb_1 Thiophene. A mixture of 550 mg of the Ib_1 cyanoester and 787 mg of chloranil in 20 m*l* of dry toluene was refluxed for 6 hr. The mixture was then concentrated to a small volume under a stream of nitrogen. When the residue was diluted with 20 m*l* of dry chloroform, yellow crystals (chloranil) precipitated immediately. After filtration, the chloroform solution was concentrated to a small volume (*ca.* 5 m*l*), which was then chromatographed on alumina (20 g) using a mixture of chloroform and petroleum ether (5 : 1) as an eluent. After the evaporation of the solvent, the residue was triturated with petroleum ether to give 158 mg of the IIb_1 thiophene, which was identical in all respects (infrared, ultraviolet spectrum, and mixed melting point) with the prodct prepared from Ib_1 by the procedure A.

2-Methyl-3,4-dimethoxycarbonylthiophene (IIc_2, R=CH_3). Prepared by treating the IIa_2 diacid with diazomethane in ether, showed a bp of 123—124°C/3 mmHg, n_D^{15} 1.526.

Found: C, 50.70; H, 4.78%. Calcd for $C_9H_{10}O_4S$: C, 50.47; H, 4.71%.

Acid Hydrolysis of IIb_1 to IIa_1. A mixture of 180 mg of IIb_1, 1.5 m*l* of acetic acid, and 1 m*l* of concentrated hydrochloric acid was refluxed for 22 hr. The solvent was then evaporated to dryness *in vacuo*. Recrystallization from water gave 105 mg of IIa_1, mp 214—216°C, identical in all respects with thiophene-3,4-dicarboxylic acid, IIa_1.

Hydrolysis of $IIIc_1$ to 2,5-Dihydrothiophene-3,4-dicarboxylic Acid-1,1-dioxide ($IIIa_1$, R=H). A mixture of 2.0 g of $IIIc_1$ and 100 m*l* of saturated hydrobromic acid was stirred at 60°C for 20 hr. The reaction mixture was then concentrated to dryness under reduced pressure below 60°C. The residue was recrystallized from ether - petroleum ether to give 1.50 g (85%) of colorless crystals, mp 172—176°C. Found: C, 32.05; H, 3.58%. Calcd for $C_6H_6O_6S$: C, 32.15; H, 3.60%. The dehydration of the crystals over phosphorus pentoxide at 100°C *in vacuo* gave $IIIa_1$, mp 180—181°C.

Found: C, 34.94; H, 2.91%. Calcd for $C_6H_6O_6S$: C, 34.96; H, 2.93%.

Hydrolysis of $IIIc_2$ to 2-Methyl-2,5-dihydrothiophene-3,4-dicarboxylic Acid-1,1-dioxide ($IIIa_2$, R=CH_3). By refluxing a mixture of 592 mg of $IIIc_2$ and 10 m*l* of saturated hydrobromic acid in the manner described above for $IIIc_1$, 387 mg (72%) of $IIIa_2$ was obtained; mp 172—174°C (from ether-petroleum ether).

Found: C, 38.06; H, 3.68%. Calcd for $C_7H_8O_6S$: C, 38.19; H, 3.66%.

The authors are indebted to Dr. Syunichi Kawamura of the Radiation Center of Osaka Prefecture for the nmr measurements.

BULLETIN OF THE CHEMICAL SOCIETY OF JAPAN VOL. 41 2095—2101 (1968)

Synthesis and Properties of Nitrosoazulenes[1)]

Tetsuo NOZOE, Paw Wang YANG,[2a)] Hiroshi OGAWA[2b)] and Takashi TODA

Department of Chemistry, Faculty of Science, Tohoku University, Katahira-cho, Sendai

(Received January 27, 1968)

Ethyl 2-amino-3-nitrosoazulene-1-carboxylate (II) was synthesized from ethyl 2-aminoazulene-1-carboxylate by treatment with isoamyl nitrite. The structure of the amino-nitrosoazulene was proved by the reductive acetylation of the azulene to give ethyl 2,3-diacetylaminoazulene-1-carboxylate. This nitrosation method was then applied to several azulenes possessing different substituents; it yielded some stable nitrosoazulene derivatives. The spectral properties of the nitrosoazulenes will be discussed. The condensation reactions of II with aromatic amines failed to give azo-dyes, but with diethyl malonate and malononitril they gave the corresponding pyrazinoazulene derivatives.

Although Hafner and his co-workers reported the formation of 1-nitrosoazulene in 1961,[3)] they could not succeed in isolating the pure substance. Kitahara and Kato obtained 2-amino-1-cyano-3-nitroso-7-isopropylazulene in a poor yield;[4)] however, its chemical and physical properties have not been investigated. The present authors have observed the formation of ethyl 2-amino-3-nitrosoazulene-1-carboxylate (II) in a fairly good yield[5)] accompanied

1) Presented at the Local General Meeting of the Tohoku District of the Chemical Society of Japan, Morioka, October, 1964.

2) Present address: a) Department of Chemistry, Faculty of Science, National Taiwan University, Taipei, Taiwan. b) Research Laboratory, Dai Nippon Ink Chemical Co., Urawa-shi, Saitama-ken.

3) K. Hafner, A. Stephan and C. Bernhard, *Ann.*, **650**, 42 (1961).

4) Y. Kitahara and T. Kato, *Bulletin of the Chemical Research Institute of Non-Aqueous Solutions, Tohoku University*, **14**, 53 (1964).

5) T. Nozoe, T. Toda, T. Asao and A. Yamanouchi, This Bulletin, **41**, No. 12 (1968), in press.

by the exchange of the tropyl group and the nitroso group when ethyl 2-amino-3-tropylazulene-1-carboxylate (I) was treated with isoamyl nitrite (IAN) in alcohol or benzene. It is very interesting that the deamination reaction of I did not take place and that II was obtained in a good yield even though the reaction was carried out in the presence of a reducing reagent such as alcohol. We applied this method to several azulenes and investigated the properties of the nitrosoazulenes thus obtained.

Although 1-nitrosoazulene has been reported to be very unstable and could not be isolated,[3] II is a

Table 1

Starting substances	No.		Products No.	mp °C	Yield %	Recovery %	N analysis as mononitrosoazulene Calcd	Found
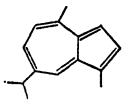	(V)	reddish brown powder	(XVIII)	>300	72	9	6.16	7.20
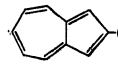	(VI)	reddish brown powder	(XIX)	>200	30		7.31	7.81
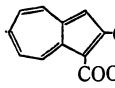	(VII)	black powder		>200	7	80		
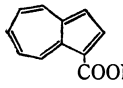	(VIII)	black powder	(XX)	152—160	20	75	6.11	6.53
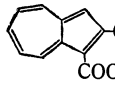	(IX)	black powder	(XXI)	>300	39	36	5.76	7.05
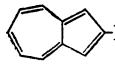	(X)	dark brown powder			10			
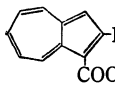	(XI)	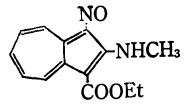	(XXII)	156	100		10.85	10.45
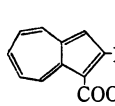	(XII)	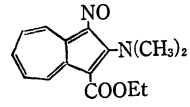	(XXIII)	oil 244 as picrate	58	25	13.97 as picrate	13.65
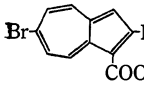	(XIII)	dark brown powder		138—145	77			
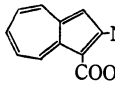	(XIV)	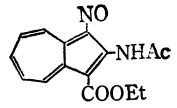	(XXIV)	>300	4	95	9.79	9.38
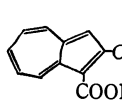	(XV)	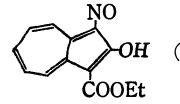	(XXV)	156	77		5.51	5.27
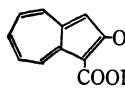	(XVI)	black powder	(XXVI)		65		5.40	4.74
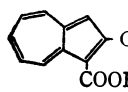	(XVII)	black powder	(XXVII)	>200	20	36	4.88	4.92

very stable entity. Therefore, ethyl 2-aminoazulene-1-carboxylate (III), which does not possess a tropyl group at the C-3 position, was treated with IAN in alcohol or benzene; II was thus obtained in a 95% yield. The addition of a trace amount of hydrogen chloride or concentrated sulfuric acid to the reaction mixture did not affected the yield of II. However, when III was treated with sodium nitrite together with a mineral acid in alcohol, II could not be isolated and intractable resinous substances were formed. Since I and III afforded the same product, II, the position of the introduced nitroso group should be C-3 position of the azulene ring. This was confirmed by the reductive acetylation of II, which yielded ethyl 2,3-diacetylaminoazulene-1-carboxylate (IV).[6]

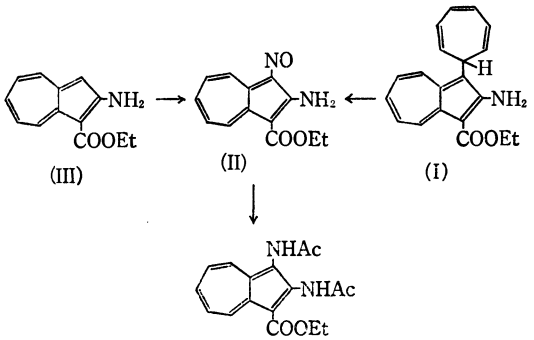

In order to investigate the effect of substituents on the nitrosation reaction, the reactions of several azulenes (V—XVII),[7] possessing different substituents, such as alkyl, alkylamino, ethoxycarbonyl, or hydroxyl groups, have been carried out under the same reaction conditions; the results obtained are shown in Table 1.

II and ethyl 2-methylamino-3-nitrosoazulene-1-carboxylate (XXII) are very stable, but 2-dimethylamino-, 2-acetylamino-, and 2-hydroxy-3-nitrosoazulene derivatives (XXIII, XIV, and XXV respectively) are not very stable and change to black, resinous substances when heated for a long time during the purification process or when stored for a long period. The products in other cases should be nitrosation products, according to their analytical data; however, they are very unstable and are obtained only as amorphous powders, accompanied by large amounts of tarry substances, and they could not be purified. The reductive acetylation of those substances (XVIII, XX, XXI, XXVI and XXVII) was then attempted. Although almost two equivalent moles of hydrogen were taken up in each case, only resinous products were obtained. On the other hand, XXV afforded ethyl 3-acetylamino-2-hydroxyazulene-1-carboxylate (XXVIII) in a good yield under the same conditions. XXVIII was also obtained by the same reductive acetylation of ethyl 3-(*p*-tolyl)azo-2-hydroxyazulene (XXIX), which had been obtained from XV.

The results presented above suggested that the nitrosation reaction of the azulenes takes place first, but the nitrosoazulenes formed are unstable, except for II, XXII XXV, *etc.*, and the polymerization and/or other reactions occur to give resinous materials. The molecular weights of XVIII, XIX, *etc.*, could not be measured because of their insolubility. It can reasonably be understood that 1-nitrosoazulenes can possess A- and B-type canonical formulae and that the self-condensation reactions occur to form C- and other-type polymers.

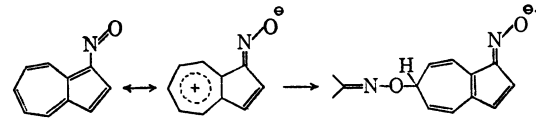

The nitrosoazulenes which have an amino or hydroxyl group at the C-2 position are stable entities. Therefore, one of the canonical formulae of those nitrosoazulenes is a D-type formula (and also A' and B'); this plays an important role in the stability of those nitrosoazulenes. D-type entities are able to tautomerize with E-type entities with an exchange of hydrogen atoms; this tautomerization may contribute to the stabilization of those nitrosoazulenes.

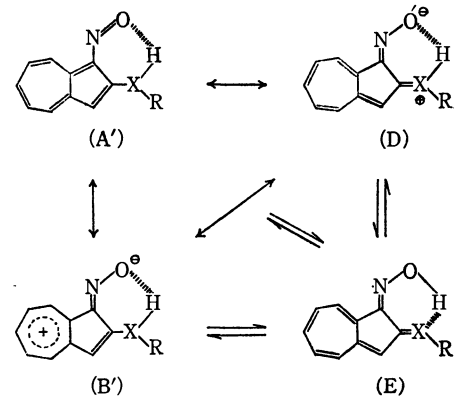

The nitrosation of azulenes with IAN may proceed by a radical mechanism. However, it is well-known that the cationoid substitution reactions of azulenes readily occur at C-1 and C-3 positions.[7a] The results shown in Table 1 indicate that azulenes which possess electron-releasing groups readily afford

6) M. Kobayashi, Master's thesis submitted to Tohoku University, March, 1961.

7) The methods of synthesizing known azulenes are described in the following articles and in the litratures cited therein: a) T. Nozoe and T. Asao, "Dai Yuki Kagaku, (Comprehensive Organic Chemistry)," Vol. 13, ed. by M. Kotake, Asakura Shoten, Tokyo (1960), pp. 439—534. b) T. Nozoe, S. Seto, K. Takase, S. Matsumura and T. Nakazawa, *Nippon Kagaku Zasshi* (*J. Chem. Soc. Japan, Pure Chem. Sect.*), **86**, 346 (1965).

nitroso derivatives, whereas azulenes which have electron-withdrowing groups do not give the corresponding nitrosoazulenes easily, but rather resulted in the recovery of the original azulenes under the same reaction conditions. Furthermore, I readily yielded II with the exchange of the tropyl group. In view of the above facts, it seems rather reasonable to say that the reaction proceeds through an ionic process.

Generally, the UV and visible spectra of azulenes show fine structures; however, the spectrum of II shows a fairly broad structure compared with that of III, as is shown in Fig. 1. The spectrum of azulene in concentrated sulfuric acid[8] and the spectrum of 1-ethoxycarbonylazulene-3-tropylium perchlorate[9] do not show such fine structures either. These facts suggest that the contribution of B- and D-type canonical formulae to II is fairly important.

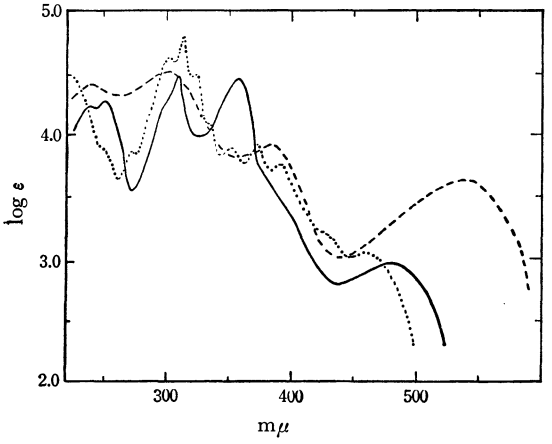

Fig. 1

—— II
---- III
— — 1-Ethoxycarbonylazulene-3-tropylium perchlorate

The IR spectrum of 5-nitrosotropolone, which is said to exist as a tropo-quinone oxime form,[10] shows strong bands at 1603 and 1325 cm^{-1}, a weak band at 1522 cm^{-1}, and a very weak band at 1439 cm^{-1}. On the other hand, the IR spectra of the nitrosoazulenes show several bands between 1530—1480 cm^{-1} as follows II, 1600 (s), 1570 (m), 1540 (m), 1515 (s), 1450 (m) and 1430 (s) cm^{-1}; XXII, 1605 (S), 1570 (m), 1525 (s), 1480 (w) and 1440 (s) cm^{-1}; XXIII, 1600 (s), 1570 (w), 1520 (s), 1480 (w) and 1430 (s) cm^{-1}; XXV, 1620 (m), 1580 (w), 1495 (v.s.), 1450 (v.s) and 1405 (w) cm^{-1}; XXVI, 1600 (m), 1545 (s), 1520 (s), 1475 (w), 1440 (s) and 1404 (s) cm^{-1}; and an ester carbonyl band near 1670 cm^{-1} in all the nitrosoazulenes above.[11] Although XXIII and XXVI do not have oxime-type tautomeric forms, they possess a strong band between 1525—1520 cm^{-1}. Therefore, the absorptions of the nitrosoazulenes are assigned to N=O stretching vibrations of the nitroso group this is in agreement with those of the nitroso group of aromatic compounds.[12] However, XXV does not show such a band in this region, but shows a very strong band at 1490 cm^{-1}. Presumably this is due to the contribution of the E-type canonical form; the band at 1700 cm^{-1} of XXV may be assigned to a C=O or C=N stretching vibration of the five-membered ring of D- or E-type entities of XXV, because no band is observed near 1700 cm^{-1} in other nitrosoazulenes.

Azulenes which possess a condensed imidazole ring fused to the C-1 and C-2 of the azulene nucleus have been synthesized.[6] The synthesis of the same type azulenes which possess an oxazole ring fused to C-1 and C-2 was attempted. XXV and XXIX were reduced over palladized charcoal in formic acid, providing ethyl 3-formamide-2-hydroxyazulene 1-carboxylate (XXX). However, the treatment of XXVIII and XXX in anhydrous formic acid and in acetic anhydride resulted in only the recovery of the starting substances and 3-diacetylamino-2-acetoxyazulene-1-carboxylate (XXXI) respectively. When the reactions were carried out with a small amount of concentrated sulfuric acid or under more drastic conditions, only tarry materials were formed. The treatment of XXXI with sodium hydroxide in alcohol regenerated XXVIII readily.

It is well known that the aromatic nitroso compounds afford azo-dyes and Shiff bases upon treatment with the corresponding amines and active methylene compounds respectively. The reaction of II with *p*-toluidine, *p*-nitroaniline, 2,4-dichloroaniline in benzene, pyridine or xylene resulted in the recovery of II under mild conditions; under more drastic conditions, only black, intractable, resinous substances were obtained. When the reaction was carried out in boiling aniline, red-violet needles were obtained. However, they were not identical with ethyl 2-amino-3-(phenylazo)azulene-1-carboxylate. The amount of this substances was insufficient for further investigation.

The treatment of II with diethyl malonate and malononitril gave diethyl 3(4*H*)-oxoazuleno[1,2-*b*]pyrazine-2,5-dicarboxylate (XXXII) and ethyl 2-cyano-3(4*H*)-oxoazuleno[1,2-*b*]pyrazine-5-carboxylate (XXXIII) respectively. They are hardly soluble in most organic solvents, and XXXIII could not be

8) Pl. A. Plattner, E. Heilbronner and S. Weber, *Helv. Chim. Acta*, **35**, 1036 (1952).
9) A. Yamanouchi, M.Sc. thesis submitted to Tohoku University, March, 1964; T. Nozoe, A. Yamanouchi and T. Toda, to be published.
10) T. Nozoe, K. Takase and H. Matsumura, "Dai Yuki Kagaku, (Comprehensive Organic Chemistry)," Vol. 13, ed. by M. Kotake, Asakura Shoten, Tokyo (1960), p. 274.
11) The IR spectra of the nitrosoazulenes were measured in the solid state by the KBr pellet method.
12) J. L. Bellamy, "the Infra-red Spectra of Complex Molecules," Methuen, London (1958), p. 305.

obtained in an analytically-pure state. However, the spectral and analytical data indicate that a pyrazine ring is formed during the condensation

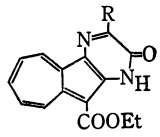

XXXII: R=COOEt
XXXIII: R=CN

reactions. Their UV spectra are very similar to that of 2,3-dimethylazuleno-[1,2-*b*]pyrazine,[6] as is shown in Fig. 2.

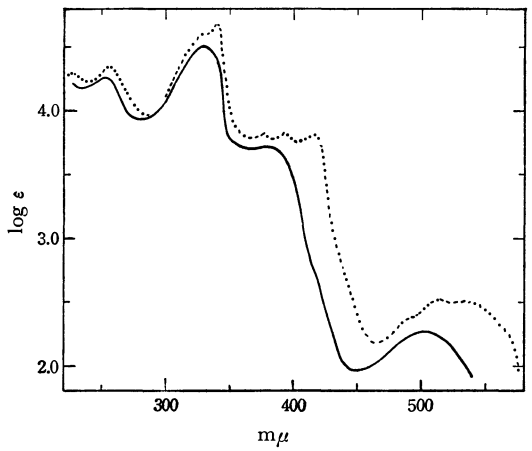

Fig. 2.
—— XXXII
---- 2,3-dimethylazuleno[1,2-*b*]pyrazine

Experimental[13]

Ethyl 2-Methylaminoazulene-1-carboxylate (XI). To a solution of 0.36 g of VII in 2 m*l* of dioxane, 0.50 g of 30% aqueous methylamine was added, and then the mixture was heated under reflux for 12 hr. The solvent was removed under reduced pressure, and the residue was dissolved in benzene. The benzene layer was washed with water, dried over sodium sulfate, filtered, and concentrated to give 0.365 g of a reddish-brown oil. The oil was chromatographed on alumina, and the cyclohexane eluate gave 50 mg of the recovered starting material, while the ether eluate gave 0.285 g of yellow needles of XI, mp 66—67°C. The recrystallisation of this from light petroleum raised its mp to 67.5—68°C; orange plates.

Found: C, 73.32; H, 6.52; N, 6.04%. Calcd for $C_{14}H_{15}O_2N$: C, 73.34; H, 6.59; N, 6.11%.

Ethyl 2-Diethylaminoazulene-1-carboxylate (XII). A solution of 0.80 g of VII and 0.83 g of 40% aqueous dimethylamine in 5 m*l* of alcohol was heated under reflux for 3 hr, and then the reaction mixture was treated as above. A brown oil, 0.835 g, was obtained and gave trinitrobenzoate (mp 159.5°C from alcohol) as reddish-brown needles.

13) All melting points are uncorrected.

Found: C, 55.79; H, 4.46; N, 11.89%. Calcd for $C_{21}H_{20}O_8N_4$: C, 55.26; H, 4.42; N, 12.28%.

Ethyl 2-Amino-6-bromoazulene-1-carboxylate (XIV). A solution of 0.427 g of diethyl 2-amino-6-bromoazulene-1,3-dicarboxylate[14] and 0.28 g of potassium hydroxide in 10 m*l* of alcohol was heated under reflux for 3 hr. The alcohol was then removed, and 8 m*l* of water was added to the reaction mixture to give 8.5 mg of the recovered starting material, which was separated by filtration. The water layer was acidified with N hydrochloric acid to form yellow precipitate. The separated precipitate was dried in a desiccator to give 0.38 g of a yellow-green powder. The powder was heated under reflux for 2.5 hr in 3 m*l* of pyridine and then concentrated. The residue was submitted to chromatography after having been dissolved in benzene, and then washed with water and dried over sodium sulfate. The benzene-ether (1: 1) eluate afforded 32 mg of 2-amino-6-bromoazulene, and the same mixed solvent (1: 4) gave 66 mg of brown micro needles of XIV, which did not show any clear melting point.

Found: C, 54.47; H, 3.80; N, 5.79%. Calcd for $C_{13}H_{12}O_2NBr$: C, 54.20; H, 3.48; N, 6.32%.

Ethyl 2-Acetoxyazulene-1-carboxylate (XVII). A solution of 0.454 g of XV in 3 m*l* of acetic anhydride was heated on a water bath for 5 min, and then the excess acetic anhydride was removed under reduced pressure to give 0.462 g of deep red needles of XVII, mp 62—63°C from alcohol.

Found: C, 69.50; H, 5.59%. Calcd for $C_{15}H_{14}O_4$: C, 69.75; H, 5.46%.

Ethyl 2-Amino-3-nitrosoazulene-1-carboxylate (II). a) Into an ice-cold solution of 0.30 g of III in 9 m*l* of benzene, 0.216 g of IAN was stirred drop by drop; the solution was then allowed to stand overnight at room temperature. The solution was washed with water, dried over sodium sulfate, and concentrated to give 0.324 g of dark brown needles of II. The recrystallisation of crude II from benzene raised its mp to 177—178°C; brown needles.

Found: C, 63.61; H, 4.73; N, 11.25%. Calcd for $C_{13}H_{12}O_3N_2$: C, 63.92; H, 4.95; N, 11.47%.

When alcohol was used instead of benzene, the same results were obtained.

b) When benzene which had been saturated with dry hydrogen chloride or which contained a drop of conc. sulfuric acid was used and treated as above, 0.304 g of II was obtained from 0.30 g of III.

c) Into an ice-cold solution of 0.30 g of III in 10 m*l* of alcohol containning 0.4 m*l* of N hydrochloric acid, a solution of 0.22 g of sodium nitrite in 2 m*l* of water was stirred. After having been allowed to stand overnight at room temperature, the solution was neutralized with aqueous sodium bicarbonate, and then concentrated under reduced pressure to give a black residue, which failed to give a pure substance by means of column- or thinlayer-chromatography or other methods. When III was treated for a shorter period under the same conditions, the recovered III and some intractable gummy substances were obtained.

Ethyl 2-Methylamino-3-nitrosoazulene-1-carboxylate (XXII). By the same treatment as in the case of III, 50 mg of XI and 34 mg of IAN gave 59 mg of XXII as brown plates, mp 157°C from benzene.

14) T. Nozoe, S. Seto and S. Matsumura, This Bulletin, **35**, 1990 (1962).

Found: C, 65.47; H, 5.14; N, 10.45%. Calcd for $C_{14}H_{14}O_3N_2$: C, 65.10; H, 5.46; N, 10.85%.

Ethyl 2-Dimethylamino-3-nitrosoazulene-1-carboxylate (XXIII). From 0.30 g of XII and 0.30 g of IAN, 0.37 g of crude products was obtained; this was then submitted to chromatography. The benzene-ethyl acetate (1:1) eluate afforded 71 mg of the recovered substance, and the ethyl acetate eluate gave 0.193 g of a brown oil which did not give trinitrobenzolate, but a picrate as yellow-brown prism, mp 240—244°C from alcohol.

Found: N, 10.38%. Calcd for $C_{15}H_{16}O_3N_2$: N, 10.29%.

Found: C, 50.62; H, 4.07; N, 13.51%. Calcd for $C_{21}H_{19}O_{10}N_5$: C, 50.30; H, 3.82; N, 13.97%.

Ethyl 2-Hydroxy-3-nitrosoazulene-1-carboxylate (XXV). A solution of 0.60 g of XV in 18 m*l* of benzene and 0.36 g of IAN was treated as before. After the solution had been allowed overnight at room temperature, the formed precipitate was separated by filtration, and from the benzene layer a black powder was obtained. When the powder was recrystallized from benzene, acetone, or alcohol, this changed to an intractable gummy substance. The powder was washed with alcohol to give 0.522 g of XXV, mp 156°C (dec.).

Found: C, 61.85; H, 4.73; N, 5.27%. Calcd for $C_{13}H_{11}O_4N \cdot \frac{1}{2}H_2O$: C, 61.41; H, 4.76; N, 5.51%.

The ir spectrum of this shows a broad band at 3510 cm^{-1}.

Nitrosation of Other Azulenes. The other azulenes listed in Table 1 (V—XVII) were treated with IAN as above or with modified methods. However, the nitrosoazulenes formed were very unstable, and during the recrystallisation process they turned to intractable tarry or resinous substances. Some of them became resinified even when allowed to stand at room temperature or stored in an ice box. Therefore, the nitrosoazulenes obtained were washed with suitable organic solvents and submitted to analysis.

Reduction of II; Ethyl 2,3-Diacetylaminoazulene-1-carboxylate (IV). II (0.10 g) in 5 m*l* of acetic anhydride was reduced over 0.10 g of 10% palladised charcoal, and two equivalent moles of hydrogen was taken up. After the catalyst had been removed by filtration, the solution was concentrated and the residue was chromatographed on alumina. From the ethyl acetate eluate, pale violet crystals were obtained; the recrystallization of this from benzene afforded 43 mg of IV, mp 218—219°C, which failed to show any depression when mixed with an authentic sample of ethyl 2,3-diacetylaminoazulene-1-carboxylate.[6]

Ethyl 3-Acetylamino-2-hydroxyazulene-1-carboxylate (XXVIII). A solution of 0.12 g of XXV in 10 m*l* of acetic anhydride was treated as above over 0.12 g of 10% palladised charcoal. The residue obtained was recrystallized from alcohol to give 70 mg of XXVIII as reddish-brown micro needles, mp 220—220.5°C.

Found: C, 65.58; H, 5.62; N, 5.11%. Calcd for $C_{15}H_{15}O_4N$: C, 65.92; H, 5.53; N, 5.13%.

By the same method, 0.10 g of ethyl 3-(*p*-tolyl)azo-2-hydroxyazulene-1-carboxylate afforded 50 mg of XXVIII, and the mixed-melting-point measurement of XXVIII obtained from different starting substances did not show any depression.

Ethyl 3-(*p*-Tolyl)azo-2-hydroxyazulene-1-carboxylate (XXIX). A solution of 4.0 g of XV in 40 m*l* of pyridine was cooled in an ice bath, and into this *p*-tolyldiazonium chloride, prepared from 2.16 g *p*-toluidine in the usual way, was stirred drop by drop. After the mixture had been allowed to stand for a couple hours at room temperature, the precipitate formed was separated by filtration and recrystallized from alcohol to give 5.88 g of reddish-brown needles of XXIX, mp 146—147°C.

Found: C, 71.79; H, 5.64; N, 8.18%. Calcd for $C_{20}H_{18}O_3N_2$: C, 71.84; H, 5.43; N, 8.38%.

Ethyl 3-Formamide-2-hydroxyazulene-1-carboxylate (XXX). The catalytic reduction of 1.2 g of XXV over 0.20 g of 10% palladised charcoal in 15 m*l* of anhydrous formic acid caused the absorption of two moles of hydrogen. After the catalyst had been separated by filtration and the formic acid was removed, the residue was washed with water and dried in a desiccator; recrystallization from benzene then gave 1.05 g of reddish-brown micro needles of XXX, mp 187°C.

Found: C, 65.18; H, 5.34; N, 4.88%. Calcd for $C_{14}H_{13}O_4N$: C, 64.86; H, 5.05; N, 5.40%.

XXX was also obtained in a good yield by the catalytic reduction of XXIX in formic acid.

Cataltyic Reduction of Other Nitrosoazulenes. The catalytic reduction of XX,XXI, XXVI, and others over palladised charcoal was attempted. Although about two equivalent moles of hydrogen were taken up in every case, no pure substances could be obtained. Example: after reduction, 97 mg of brown powder were obtained from 0.15 g of crude XXVI and was submitted to chromatography. The benzene eluate was recrystallized from light petroleum-benzene to give 32 mg of a brown powder, mp 186°C, which did not give a correct analysis.

λ_{max}^{MeOH}, mμ; 238, 294, 305 and 275. IR in $CHCl_3$; 3450, 3000, 2950, 1680, 1430, 1370 and 1200 cm^{-1}.

Attempted Isooxazole-ring Formation. *a*) A solution of 0.10 g of XXX in 5 m*l* of anhydrous formic acid was heated under reflux for one hour; the formic acid was then removed under reduced pressure. The residue was washed with water and recrystallized from alcohol to give 85 mg of the recovered starting material. The addition of concentrated sulfuric acid or prolonged heating at an elevated temperature gave a black, intractable resinous substance.

b) Ethyl 3-Diacetylamine-2-acetoxyazulene-1-carboxylate (XXXI). A solution of 0.15 g of XXVIII in 10 m*l* of acetic anhydride was dissolved in benzene, washed with water, and dried over sodium sulfate, and the benzene was removed. The recrystallisation of the residue from alcohol-light petroleum afforded 0.14 g of pure XXXI as dark red prisms, mp 137.5—138.5°C.

Found: C, 63.41; H, 5.42; N, 3.88%. Calcd for $C_{19}H_{19}O_6N$: C, 63.86; H, 5.36; N, 3.92%.

Hydrolysis of XXXI. To a solution of 66 mg of XXXI in 2 m*l* of alcohol, 0.17 m*l* of N sodium hydroxide was added, and then the resulting solution was heated on a water bath for 2 hr. After the ethanol had been removed, water was added to the solution and the pH of the solution was adjusted to about 4 with N hydrochloric acid. The recrystallisation of the precipitate obtained above from alcohol gave 47 mg of micro needles, mp 219—220°C, which did not show any depression on admixture with the authentic sample of XXVIII.

Reaction of II with Aromatic Amines. A solution of 0.50 g of II in 10 m*l* of aniline was heated under

reflux for 2 hr, and then the excess aniline was removed under reduced pressure. The residue was dissolved in benzene, washed with water, dried over sodium sulfate, and chromatographed on alumina. The light petroleum eluate gave 88 mg of violet-brown needles, mp 232—234°C.

Found: C, 72.67; H, 5.49; N, 12.55%. λ_{max}^{MeOH}, mμ; 255, 320, 370 and 535; this is analogous to that of ethyl 2-amino-3-(phenylazo)azulene-1-carboxylate.

The condensation reactions of II with *p*-toluidine, *p*-nitroaniline, and 2,4-dichloroaniline in benzene, alcohol, xylene, or pyridine resulted in the recovery of II under milder conditions or in the formation of intractable tar under drastic conditions.

Ethyl 2-Amino-3-(phenylazo)azulene-1-carboxylate. Into a cold solution of 0.215 g of II in 5 m*l* of alcohol, 1 m*l* of phenyl diazonium chloride prepared from 0.15 g of aniline in an ordinary way was stirred drop by drop. The solution was then allowed to stand for 1 hr at room temperature. The precipitate formed was then separated by filtration and recrystallized from alcohol to give 0.275 g of violet needles, mp 136—137°C.

Found: N, 13.27%. Calcd for $C_{19}H_{17}O_2N_3$: N, 13.16%.

Diethyl 3(4*H*)-Oxoazuleno[1,2-*b*]pyrazine-2,5-dicarboxylate (XXXII). A solution of 0.25 g of II and 0.24 g of diethyl malonate in 3 m*l* of acetic anhydride was allowed to stand at room temperature for 4 hr with stirring, and then the excess acetic anhydride was removed under reduced pressure. The residue was dissolved in chloroform, washed with water, and dried over sodium sulfate; the concentration of the solution left a brown resinous substance which was submitted to chromatography. The ether - ethyl acetate (1 : 3) eluate afforded 28 mg of a violet-brown powder; the recrystallisation of this from light petroleum - benzene gave pale violet micro prisms of XXXII, mp 204—207°C.

Found: C, 62.43; H, 5.41; N, 8.09%. Calcd for $C_{18}H_{16}O_5N_2{\cdot}\frac{1}{2}H_2O$: C, 61.90; H, 4.90; N, 8.02%.

Ethyl 2-Cyano-3(4*H*)-oxoazuleno[1, 2-*b*]pyrazine-5-carboxylate (XXXIII). Into a solution of 0.25 g of II in 6 m*l* of anhydrous alcohol cooled in an ice bath, a solution prepared from 30 mg of sodium and 0.10 g of malononitril in 1 m*l* of anhydrous alcohol was stirred drop by drop; the reaction mixture was then stored in ice box overnight. The solvent was then removed under reduced pressure, and the residue was washed with water and dried in a desccator to give 0.16 g of a brown solid. The recrystallisation of this from methanol gave a dark violet powder of XXXIII, mp <250°C. Although the UV spectrum of XXXIII is very similar to that of XXXII, and although the IR spectrum of XXXIII agrees with the proposed structure (3300, 2180, 1670, 1600, 1540, 1470, 1440, 1430, 1255, 1110 and 860 cm^{-1}, KBr pellet), we failed to obtain analytically-pure substances.

BULLETIN OF THE CHEMICAL SOCIETY OF JAPAN VOL. 41 2102—2111 (1968)

The Synthesis and Electrophilic and Nucleophilic Substitution Reactions of 6-Chloro-1-azaazulan-2-ones and 2,6-Dichloro-1-azaazulenes[1]

Takashi TODA, Shuichi SETO[2] and Tetsuo NOZOE

Department of Chemistry, Faculty of Science, Tohoku University, Katahiracho, Sendai

(Received February 19, 1968)

6-Chloro-1-azaazulan-2-ones and 2,6-dichloro-1-azaazulenes have been synthesized from 2-amino-5-chlorotropone. By the investigation of their electrophilic and nucleophilic substitution reactions, it is proved that the electrophilic substitutions take place at the C-3 positions of those compounds, and that the nucleophilic substitutions occur at the C-6 positions and then at the C-2 positions. The tautomerism of 6-amino-2-chloro-1-azaazulene derivatives is discussed.

1-Azaazulenes and their 2-hydroxy derivatives (1-azaazulan-2-ones) are important and interesting substances not only as non-benzenoid analogues of indoles and isomers of quinolines, but also as heterocyclic azulene-type compounds. Several derivatives of 1-azaazulene (I) and 1-azaazulan-2-one (II) have been synthesized.[3-10] The electrophilic substitution reactions of those compounds[3a,8,10a] and the nucleophilic substitution reactions of 2-chloro-1-azaazulene (III)[3b,5b,7] have been investigated. However, 1-azaazulenes and those related compounds which possess functional groups other than alkyl groups in their seven-membered ring have not been known.[11] The purpose of the present paper is to synthesize 1-azaazulenes which possess halogen atoms in their five- and seven-membered rings, and to investigate the chemical properties of these synthesized 1-azaazulenes.

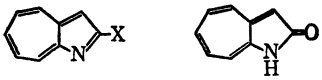

(I): X=H (II) (IV)
(III): X=Cl

It has long been known that abnormal substitutions take place during the nucleophilic reactions of halo-tropolones,[12] 2-halo-tropones,[13] and tropolone arylsulfonates,[14,15] and that abnormal ring formations occurd in the cases of azulenes,[4,15] 1-azaazulan-2-ones,[6] and 1-oxaazulan-2-one (IV) derivatives[14,15] obtained from 2-halo-tropones and tropolone arylsulfonates. Therefore, a method which is known to give a normal condensation product was employed: that is, the condensation reaction of 2-aminotropone derivatives with diethyl malonate.[6]

1) Part of the D. Sc. thesis of Takashi Toda, Tohoku University, March, 1958. Presented in part at the Local Meeting of the Tohoku District of the Chemical Society of Japan, June, 1956, at Yonezawa and at the 11th General Meeting of the Chemical Society of Japan, April, 1958, at Tokyo.

2) Present address: the Chemical Research Institute of Non-Aqueous Solutions, Tohoku University.

3) T. Nozoe, S. Seto, S. Matsumura and T. Terasawa, a) *Chem. Ind.*, **1954**, 1356. b) *ibid.*, **1954**, 1357.

4) a) T. Nozoe, S. Seto, S. Matsumura and T. Asano, *Proc. Japan Acad.*, **32**, 339 (1956). b) S. Matsumura, This Bulletin, **34**, 1362 (1961); **35**, 677 (1962).

5) a) T. Nozoe, Y. Kitahara and T. Arai, *Proc. Japan Acad.*, **30**, 478 (1954). b) J. Shin, D.Sc. thesis submitted to Tohoku University, March, 1958.

6) a) T. Nozoe, S. Seto and S. Nozoe, *Proc. Japan Acad.*, **32**, 472 (1956). b) S. Seto and S. Nozoe, *ibid.*, **32**, 765 (1956).

7) S. Seto and K. Suzuki, report presented at the General Local Meeting of the Tohoku District of the Chemical Society of Japan, at Hirosaki, Oct., 1956.

8) a) Y. Murase, M.Sc. thesis submitted to Tohoku University, March, 1955. b) S. Nozoe, *ibid.*, March, 1957. c) A. Sato, *ibid.*, March, 1959.

9) a) G. Sunagawa, N. Soma, H. Nakao and Y. Matsumoto, *Yakugaku Zasshi* (*J. Pharm. Soc. Japan*), **81**, 1799 (1961). b) G. Sunagawa and N. Soma, *ibid.*, **82**, 418 (1962). c) G. Sunagawa and H. Nakao, *Chem. & Pharm. Bull. Japan*, **13**, 450 (1965). d) H. Nakao, N. Soma, Y. Sato and G. Sunagawa, *ibid.*, **13**, 473 (1965). e) H. Nakao, N. Soma and G. Sunagawa, *ibid.*, **13**, 828 (1965).

10) a) T. Toda, This Bulletin, **40**, 590 (1967). b) T. Nozoe, S. Seto and T. Toda, *ibid.*, **41**, 208 (1968).

11) After this work had been completed, a few examples of the nucleophilic substitution reactions of 1-azaazulenes which possess halogen atoms in their seven-membered ring were reported by Shin (Ref. 5b) and by Sunagawa and Soma (Ref. 8a, b).

12) a) T. Nozoe and Y. Kitahara, *Proc. Japan Acad.*, **30**, 204 (1954). b) Y. Kitahara, *Sci. Repts. Tohoku Univ., Ser. I*, **39**, 258, 265, 275 (1955); **40**, 74 (1956). c) K. Doi, This Bulletin, **34**, 497 (1961). d) T. Toda, *ibid.*, **40**, 588 (1967).

13) a) S. Seto, *Sci. Repts. Tohoku Univ., Ser. I*, **38**, 377 (1953). b) T. Nozoe, S. Seto and T. Sato, *Proc. Japan Acad.*, **30**, 473 (1954). c) T. Sato, *Nippon Kagaku Zasshi* (*J. Chem. Soc. Japan, Pure Chem. Sect.*), **80**, 1056, 1167, 1171, 1340 (1959).

14) a) T. Sato, *ibid.*, **80**, 1342, 1345, 1347, 1349 (1959). b) H. Takeshita, M.Sc. essay submitted to Tohoku Univ., March, 1957.

15) a) T. Nozoe, S. Seto, K. Takase, S. Matsumura and T. Nakazawa, *Nippon Kagaku Zasshi* (*J. Chem. Soc. Japan, Pure Chem. Sect.*), **86**, 346 (1965). b) M. Kato. D.Sc. thesis submitted to Tohoku Univ., March, 1965. c) M. Kaneko, M.Sc. thesis submitted to Tohoku Univ., March, 1965.

The Synthesis and Electrophilic Substitution Reactions of 6-Chloro-1-azaazulan-2-ones and 2,6-Dichloro-1-azaazulenes. 2-Amino-5-chlorotropone (V) was prepared by the action of liquid ammonia[16,17] on 5-chlorotropolone methyl ether (VI).[18] The reaction of V with diethyl malonate in the presence of sodium ethoxide afforded ethyl 6-chloro-1-azaazulan-2-on-3-carboxylate (VII) in *ca.* a 70% yield. The UV spectrum of VII is very similar to that of ethyl 1-azaazulan-2-on-3-carboxylate (VIII). The treatment of VII with aqueous alkali did not touch the chlorine atom, but gave a free carboxylic acid (VIIa).

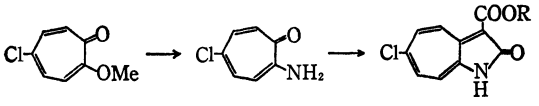

(VI) (V) (VII): R=Et (VIIa): R=H

The hydrolysis of VII with concentrated hydrochloric acid also gave VIIa; the following decarboxylation reaction of VIIa in quinoline or collidine resulted in only tarry substances.

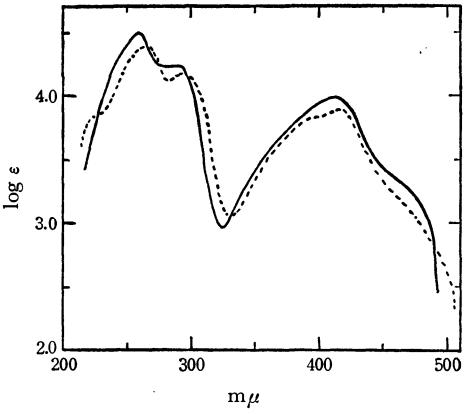

Fig. 1

—— II ---- IX

When VII was treated with concentrated hydrochloric acid in a sealed tube at about 130°C, 6-chloro-1-azaazulan-2-one (IX) was obtained by hydrolysis and by the decarboxylation of VII. On the other hand, the prolonged treatment of VII in concentrated hydrobromic acid under reflux afforded the 6-bromo derivative (X) with an exchange of halogen atoms, and the same treatment of X with concentrated hydrochloric acid gave back IX *vice versa.*

16) a) T. Nozoe, S. Seto, H. Takeda, S. Morosawa and K. Matsumoto, *Proc. Japan Acad.*, **27**, 556 (1951). b) *Sci. Repts. Tohoku Univ., Ser. I*, **36**, 126 (1952).

17) W. von E. Doering and L. H. Knox, *J. Am. Chem. Soc.*, **73**, 828 (1952).

18) T. Sato, *Bulletin of the Chemical Research Institute of Non-Aqueous Solutions, Tohoku Univ.*, **8**, 47 (1959).

The catalytic reduction of IX and VIIa over palladized charcoal with alkali resulted in the formation of, respectively, the known 1-azaazulan-2-one (II)[3a] and its 3-carboxylic acid (VIIIa)[3a] in good yields. It is interesting and noteworthy to point out that 1-azaazulene and its derivatives, are readily reduced to give perhydro compounds by the catalytic reduction,[19] but not 1-azaazulan-2-one derivatives.

The electrophilic substitution reactions of 6-halo-1-azaazulan-2-ones were investigated.

The bromination of IX in acetic acid afforded a monobromo compound (XI) in a good yield; this XI was also obtained from VIIa, with the evolution of carbon dioxide, by the same treatment. Since the bromination of 1-azaazulan-2-on-3-carboxylic acid (VIIIa) gave the 3-bromo-1-azaazulan-2-one,[3a] XI must be 3-bromo-6-chloro-1-azaazulan-2-one.

The nitration of IX and X in acetic acid with fuming nitric acid gave the corresponding nitro compounds (XII and XIII respectively). The reaction of X with *p*-tolyl diazonium chloride formed the 3-(*p*-tolyl)azo compound (XIV).

The catalytic reduction of XII and XIV over palladized charcoal gave the same 3-amino-6-chloro-1-azaazulan-2-one, which was very unstable and which could not be isolated in a free state, but which afforded a stable acetylamino derivative (XV) by the subsequent acetylation:

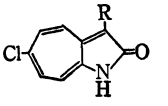

(IX): R=H
(XI): R=Br
(XII): R=NO_2
(XIV): R=*p*-tolylazo
(XV): R=NHAc

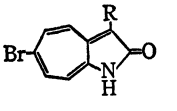

(X): R=H
(XIII): R=NO_2

The treatment of VII, VIIa, IX, X, and XI with acetic anhydride gave the respective corresponding acetates. The UV spectra of these acetates are similar to that of II,[3a] but not to that of I,[3b] and their IR spectra show two strong carbonyl bands, near 1720 and 1700 cm^{-1}. Therefore, they are *N*-acetyl derivatives of the original compounds. A careful examination, by means of chromatography and IR and UV spectroscopy, of the acetylation reaction mixtures and their mother layers after recrystallization did not show any evidence of the presence of *O*-acetyl derivatives.

Ethyl 2,6-dichloro-1-azaazulen-3-carboxylate (XVI) and 2,6-dichloro-1-azaazulene (XVII) were obtained by the treatment of VII and IX with phosphorus oxychloride, respectively. By the action of phosphorus tribromide, IX afforded 2,6-dibromo-1-azaazulene (XVIII), with an exchange of halogen atoms. The halogen atoms of XVII were

19) Unpublished observations made in the authors' laboratory.

exchanged by the treatment of hydrogen bromide in acetic acid to give XVIII, while, *vice versa*, those of XVIII were changed to XVII with the use of hydrogen chloride.

The bromination of XVII and XVIII in acetic acid proceeded readily and gave the corresponding trihalo derivatives (XIX and XX, respectively). XIX was also obtained by the bromination of 2,6-dichloro-1-azaazulen-3-carboxylic acid, which had been prepared from VIIa with phosphorus oxychloride. However, the rate of the bromination of 2,6-dichloro-1-azaazulen-3-carboxylic acid was not as fast as in the case of VIIa. The UV spectra of the obtained 2,6-dihalo-1-azaazulenes are similar to that of 2-chloro-1-azaazulene,[3b] as is shown in Fig. 2.

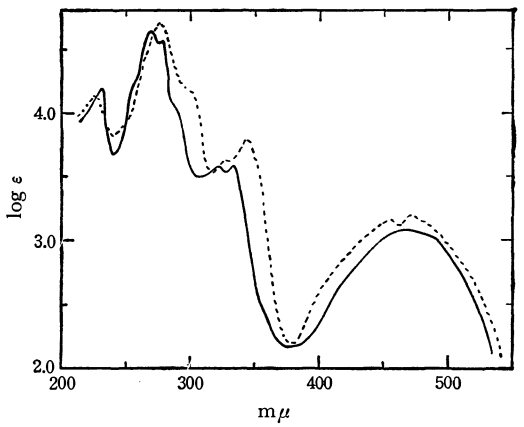

Fig. 2

—— III ---- XVII

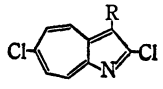

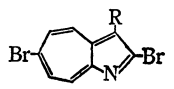

(XVI): R=COOEt (XVIII): R=H
(XVII): R=H (XX): R=Br
(XIX): R=Br
(XXI): R=COOH

The nitration and azo-coupling reactions of XVII resulted in the recovery of the starting substance.

The electron density of the 1-azaazulene nucleus is high at 1,3-positions because of the contributions of such resonance hybrids as A_1, A_2, and A_3.[3b,20] Therefore, the electrophilic substitution reactions take place easily at the C-3 position, especially if C-2 is replaced by an electron-donating group.[3] However, if an electronegative group is introduced into them, electrophilic substitution reactions might not be easy under milder conditions, such as azo-coupling, and/or under acidic conditions, such as nitration, because protonation occurs on the nitrogen atom (or the C-3 position), and this makes for a lower electron density of the 1-azaazulene nucleus. On the other hand, 1-azaazulan-2-one derivatives possess a hydrogen which can dissociate as a proton. Therefore, II forms an anion the canonical forms of which are such as B_1, B_2, B_3, *etc.*; electrophiles can readily attack the C-3 position of this type of anion, especially under basic conditions.

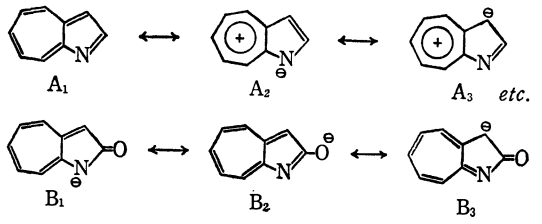

The Nucleophilic Substitution Reactions of 6-Chloro-1-azaazulan-2-one and 2,6-Dichloro-1-azaazulenes. The treatment of IX with excess aqueous potassium hydroxide, sodium methoxide, liquid ammonia, sodium cyanide, *p*-toluidine, *etc.* resulted in the recovery of the starting substance. With dimethylamine in methanol, IX afforded a very small amount of orange needles, but almost all of the IX was recovered. However, 6-(*p*-tolyl)thio-1-azaazulan-2-one (XXII) was obtained in a good yield when IX was treated with the sodium salt of *p*-thiocresol in methanol. The reaction of XXII with phosphorus oxychloride gave 2-chloro-6-(*p*-tolyl)thio-1-azaazulene (XXIII), which was also obtained from XVII with one equivalent mole of *p*-thiocresol. The further treatment of XXIII with *p*-thiocresol formed 2,6-di(*p*-tolyl)thio-1-azaazulene (XXIV), which was also obtained from XVII with an excess of *p*-thiocresol.

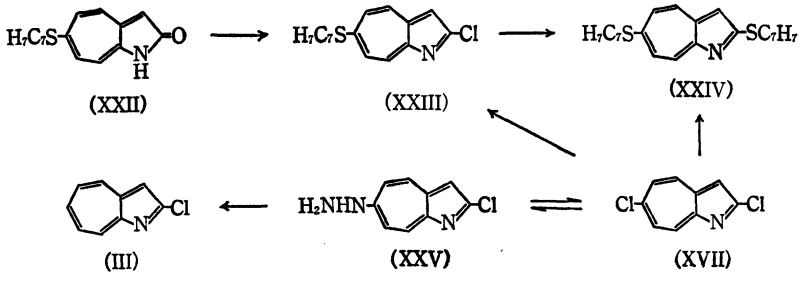

20) H. Kon, *Sci. Repts. Tohoku Univ., Ser. I*, **38**, 67 (1954).

The treatment of XVII with hydrazine hydrate in alcohol afforded a dark reddish-violet hydrazino compound (XXV) which was very unstable and which could not be isolated in a pure state. The decomposition reaction of this crude hydrazino compound with concentrated hydrochloric acid and cuprous sulfate, and with acetic acid and cuprous sulfate,[21,22] gave 2,6-dichloro-1-azaazulene, XVII, and 2-chloro-1-azaazulene, III, respectively. Therefore, the structure of XXV should be 2-chloro-6-hydrazino-1-azaazulene.

It has been predicted, on the basis of measurement of the dipole moment[23,24] and on the basis of theoretical considerations,[20,25] that the electron densities of azulenes and azaazulenes are lower in their seven-membered-ring part than in the five-membered-ring moiety. Thus, it was predicted that the nucleophilic substitution reactions of XVII would take place at the C-6 position first. The facts presented above prove this prediction from the point of view of the chemical reactivity of XVII.

On the other hand, 1-azaazulan-2-ones under the basic conditions are favoured to exist in their anion forms, such as B_1, B_2, *etc.*, as has been mentioned above. As a result of this, the nucleophilic substitution reactions of IX become difficult under the basic conditions. However, 1-azaazulenes and 1-azaazulan-2-ones can form tropyrium-type cations (C_1 and C_2) by protonation under acidic conditions. The nucleophiles readily attack such protonated species, such as in the halogen exchange reactions of IX and XVII described above. This is a phenomenon analogous to the halogen-exchange reaction of halo-tropones under acidic conditions.[26]

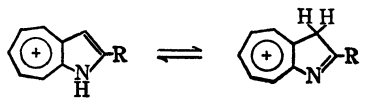

C_1 C_2

R=H or OH

The products obtained by the action of several nucleophilic reagents on XVII are shown in Table 1. The reaction of XVII with other nucleophiles than those listed in Table 1, such as sodium hydroxide, potassium cyanide, cuprous cyanide, and nitromethane, resulted in the recovery of the starting substance or did not give any clear-cut results.

TABLE 1. NUCLEOPHILIC SUBSTITUTION REACTION PRODUCTS OF XVII AND THEIR CHARACTERISTIC IR SPECTRA IN THEIR FINGER PRINT REGION

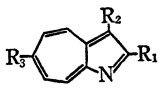

No.	R_1	R_2	R_3	Color	IR△, cm^{-1}
XVI	Cl	COOEt	Cl	Yellow	845
XVII	Cl	H	Cl	Orange-red	834
XVIII	Br	H	Br	Orange-red	831
XIX	Cl	Br	Cl	Carmine	838
XXIII	Cl	H	$SC_7H_7(p)$	Orange-red	837 (806)*
XXIV	$SC_7H_7(p)$	H	$SC_7H_7(p)$	Orange-red	838 (805)*
XXVI	Cl	H	OMe	Yellow	847
XXVII	Cl	H	OEt	Yellow	845
XXVIII	Cl	H	NH_2	Yellow-brown	840
XXIX	Cl	H	NHMe	Yellow-brown	825
XXX	Cl	H	NMe_2	Yellow-brown	825
XXXI	Cl	H	SEt	Orange	823
XXXII	Cl	H	NO_2	Violet-red	828
XXXIII	Cl	H	$CH(COOEt)_2$	Yellow-brown	840
XXXIV	Cl	H	$CH\langle^{CN}_{COOEt}$	Yellow-brown	842
XXXV	Cl	H	$NHC_7H_7(p)$	Brown-red	830 (821)*
XXXVI	Cl	H	$NHC_6H_4NO_2(p)$	Brown	828

△ KBr pellet

* Two adjacent hydrogens in phenyl group.

21) L. Gatterman and R. Holze, *Ber.*, **25**, 1074 (1892).
22) S. Seto, *Sci. Repts. Tohoku Univ., Ser. I*, **38**, 286, 295 (1953).
23) G. W. Wheland and D. E. Man, *J. Chem. Phys.*, **17**, 264 (1949).
24) Y. Kurita and M. Kubo, *J. Am. Chem. Soc.*, **79**, 5460 (1957).
25) a) A. Julg, *J. chim. phys.*, **52**, 377 (1956). b) A. Julg and P. Francois, *ibid.*, **59**, 339 (1962).
26) W. von E. Doering and L. H. Knox, *J. Am. Chem. Soc.*, **74**, 5683 (1952).

Table 2. Characteristic IR spectra of 1-azaazulan-2-ones in their finger print region

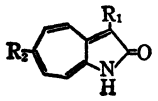

No.	R_1	R_2	Color	IR$^{\Delta}$, cm^{-1}
VII	COOEt	Cl	Yellow	850
	N-Acetate of VII		Yellow	847
VIIa	COOH	Cl	Yellow	842
	N-acetate of VIIa		Yellow	843
IX	H	Cl	Pale orange	823
	N-Acetate of IX		Yellow	822
X	H	Br	Pale orange	822
	N-Acetate of X		Yellow	820
XI	Br	Cl	Orange	841
	N-Acetate of XI		Pale orange	840
XII	NO_2	Cl	Orange	839
XV	NHAc	Cl	Orange	825
XXII	H	$SC_7H_7(p)$	Orange	825 (808)*

$^{\Delta}$ KBr pellet
* Two adjacent hydrogens in phenyl group.

After the substitution took place at C-6, no other substitution reaction occurred at C-2, even though excess reagents were used. Only a strong nucleophile such as the *p*-thiocresol anion[27] could afford the disubstituted product.

It has been shown that abnormal substitution reactions sometimes occur during the nucleophilic substitution reactions of troponoid compounds.[4,6,12-15] Therefore, the reactions described above might take place in such abnormal ways. To clarify this situation, the IR spectra of the nucleophilic substitution products were investigated. The fingerprint regions of the IR spectra of troponoid and azulenoid compounds show strong characteristic bands between 815—860 cm^{-1} and 770—820 cm^{-1} if they possess, respectively, two adjacent hydrogens and one hydrogen in their seven-membered ring.[28] The IR spectra of the 1-azaazulenes in Table 1 and of the 1-azaazulan-2-one derivatives in Table 2 show strong absorption bands between 815—850 cm^{-1}, but not between 770—820 cm^{-1} nor between 850—900 cm^{-1}. Thus, it is proved that the nucleophilic substitution reactions of XVII take place at the C-6 position in the normal way.

The IR spectrum of 6-amino-2-chloro-1-azaazulene (XXVIII) shows strong absorption bands at 1660 and 1602 cm^{-1} and bands at 3350, 3175, and 1585 cm^{-1} of a medium intensity. On the other hand, the 6-methylamino derivative (XXIX) possesses a strong band at 1598 cm^{-1} and medium bands at 3025, 1547 and 1502 cm^{-1}, while 6-dimethylamino compound (XXX) shows strong band at 1599 cm^{-1} and medium bands at 1588 and 1500 cm^{-1}. The assignment of these bands is rather difficult, because usually NH stretching appears between 3100—3500 cm^{-1}, NH deformation shows bands between 1550—1640 cm^{-1}, and the skeletal vibrations of aromatic compounds are between 1650—1480 cm^{-1}.[29] If the band of XXVIII at 1660 cm^{-1} is due to the imino C=N stretching, XXVIII has two tautomeric forms, such as D_1 and D_2. However, the UV spectra of XXVIII, XXIX

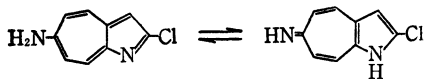

D_1 D_2

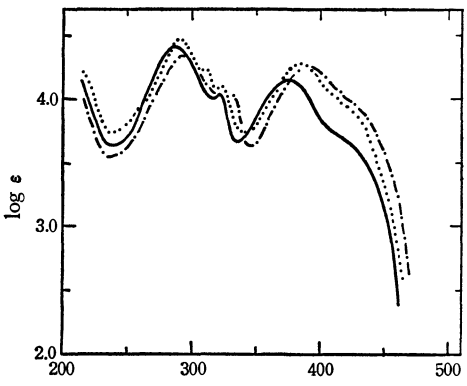

Fig. 3

—— XXVIII ---- XXIX —·—· XXX

27) L. F. Bunnett and R. E. Zahler, *Chem. Revs.*, **49**, 273 (1952).
28) Y. Ikegami, "Kagaku no Ryoiki Special Issue, Infrared Spectra," No. 8, Nanko-Do, Tokyo (1958), p. 33.
29) L. J. Bellamy, "Infra-red Spectra of Complex Molecules," 2nd ed., Methuen, London (1958).

and XXX are very similar to each other, and XXX can not take the type-D_2 tautomeric form. Therefore, it is difficult to decide toward which form the equilibria of these compounds tend. Also, the UV and IR spectra were measured in very different states; the UV spectra were measured in highly-diluted solutions, and the IR spectra, in solid states. Therefore, the tautomeric forms may be different in the different states. As a rational explanation of those phenomena, the contribution of zwitter-ion structures, such as E_1 and E_2, to these three compounds is suggested. This would explain why the UV spectra of those three compounds, and also their IR spectra, show analogous figures.

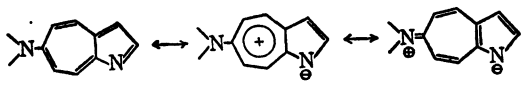

E_1 E_2 *etc.*

Wheland has proposed the contributions of such zwitter-ion structures to 2-hydroxy- and 4-hydroxy-pyrimidines;[30] Tsubomura also pointed out the contributions of the same type of zwitter-ion structures to hydroxy- and amino-pyrimidines on the basis of a consideration of their IR and UV spectra.[31]

Experimental[32]

2-Amino-5-chlorotropone (V). In an ice-cold, sealed tube, 9.0 g of VI[18] were placed, and to this *ca.* 50 m*l* of liquid ammonia were introduced; then this mixture was allowed to stand at room temperature for 4 days. After the ammonia had then been removed, the residue was recrystallized from benzene-methanol to give 7.7 g of V, mp 157—159°C; further recrystallization from the same mixed solvents raised its mp to 159—159.5°C.

Found: C, 53.89; H, 3.45; N, 9.12%. Calcd for C_7H_6ONCl: C, 54.04; H, 3.89; N, 9.00%.

Ethyl 6-Chloro-1-azaazulan-2-on-3-carboxylate (VII). A mixture of 0.95 g of V in 5.0 m*l* of absolute alcohol and a solution of 3 m*l* of alcohol containing 0.3 g of sodium and 1.95 g of diethyl malonate in a sealed tube was heated at 100°C for 5 hr. After cooling, the alcohol was removed under reduced pressure, and water was added to the residue. The pH of the water layer was adjusted to *ca.* 4.5 with 1 N sulfuric acid, and then the precipitate formed was separated by filtration and dried in a desiccator. The recrystallization of the precipitate from ethyl acetate-alcohol gave 1.15 g of orange needles of VII; mp 227.5—228°C.

Found: C, 53.35; H, 4.52; N, 5.54%. Calcd for $C_{12}H_{10}O_3NCl \cdot H_2O$: C, 53.15; H, 4.79; N, 5.54%. λ_{max}^{MeOH} mμ (log ε); 225 (4.19), 283 (4.39) and 430 (4.18).

The mother layer of the recrystallization was chromatographed on alumina to give a further 0.12 g of VII, and 80 mg of V was recovered by the elution of the ethyl acetate.

30) G. W. Wheland, "Advanced Organic Chemistry," 2nd ed., John Wiley, New York (1949), p. 636.
31) H. Tsubomura, *Nippon Kagaku Zasshi* (*J. Chem. Soc. Japan Pure Chem. Sect.*), **78**, 1528 (1957).
32) All melting points are uncorrected.

***N*-Acetate of VII.** A solution of 40 mg of VII in 0.5 m*l* of acetic anhydride was heated for reflux for 3 hr; then, after cooling, the precipitate formed was recrystallized from benzene-cyclohexane to give 40 mg of orange-yellow micro needles of the *N*-acetate of VII, mp 181°C.

Found: N, 5.13%. Calcd for $C_{14}H_{12}O_4NCl$; N, 4.77%. IR ($CHCl_3$); 1720 and 1705 cm^{-1}.

6-Chloro-1-azaazulan-2-on-3-carboxylic Acid (VIIa). A mixture of 0.25 g of VII, 1.0 g of pottassium hydroxide, 7 m*l* of water, and 20 m*l* of methanol was heated on a water bath for 2 hr. When the VII had dissolved completely, the pH of the solution was adjusted with 1 N sulfuric acid to *ca.* 3 to give the precipitate. The precipitate was separated by filtration, washed with water, and dried in a desiccator to give 0.21 g of yellow micro needles of VIIa. Recrystallization from alcohol afforded pure VIIa, mp 231—232°C (decomposed). The mother layer of the hydrolysis did not give any precipitate upon the addition of silver nitrate after the solution had been made acidic with nitric acid.

Found: C, 53.60; H, 2.72; N, 6.67%. Calcd for $C_{10}H_6O_3NCl$: C, 53.68; H, 2.70; N, 6.26%.

The *N*-acetate of VIIa was prepared by the same method as was used for the *N*-acetate of VII; yellow needles, mp 205—206°C (blacken).

Found: N, 5.31%. Calcd for $C_{12}H_8O_4NCl$: N, 5.27%. IR (KBr pellet); 1702 and 1685 cm^{-1}.

The Decarboxylated Bromination. a) *Bromination of 1-Azaazulan-2-on-3-carboxylic Acid.* The carboxylic acid (50 mg) was suspended in 1 m*l* of acetic acid and to this 50 mg of bromine was added. The acid was dissolved while carbon dioxide evolved, and the precipitate was formed after a while. The precipitate was then recrystallized twice from methanol to give 50 mg of orange needles mp 210—211°C which were found to be identical with 3-bromo-1-azaazulan-2-one by mixed-melting-point measurements.

b) *Bromination of VIIa.* VIIa (0.10 g) was treated with 80 mg of bromine in 2 m*l* of acetic acid as above to give 0.10 g of XI; orange silky needles from alcohol, mp 243—243.5°C.

Found: N, 5.62%. Calcd for $C_9H_5ONBrCl$: N, 5.41%.

N-Acetate of XI: orange-red needles, mp 190—191°C, from alcohol.

Found: N, 4.57%. Calcd for $C_{11}H_7O_2NBrCl$: N, 4.66%. IR ($CHCl_3$); 1723 and 1708 cm^{-1}.

6-Chloro-1-azaazulan-2-one (IX). A mixture of VII (0.80 g) and 8 m*l* of concentrated hydrochloric acid in a sealed tube was heated for 5 hr at 130°C. The hydrochloric acid was removed under reduced pressure, and then the residue was treated with aqueous bicarbonate to adjust its pH to *ca.* 8, washed with water, and dried in a desiccator. The precipitate was recrystallized from methanol to give yellow prisms of IX, mp 232—233°C; yield, 0.48 g.

Found: C, 59.79; H, 3.52; N, 7.49%. Calcd for C_9H_6ONCl: C, 60.19; H, 3.37; N, 7.79%. λ_{max}^{MeOH} mμ (log ε); 262 (4.38), 293 (4.15) and 410 (3.86).

N-Acetate of IX; yellow silky needles from ethyl acetate, mp 228—229°C.

Found: N, 6.42%. Calcd for $C_{11}H_8O_2NCl$: N, 6.32%. IR ($CHCl_3$); 1722 and 1705 cm^{-1}.

The Catalytic Reduction of VIIa and IX. a) In a solution of 50 mg of VIIa in 2 m*l* of 2 N sodium

hydroxide, 10 mg of 5% palladium on charcoal were suspended, and then the reduction was carried out in the usual way. The catalyst was removed by filtration, and the solution was acidified with 1 N sulfuric acid to give a yellow precipitate, the recrystallization of which from alcohol afforded yellow needles of VIIIa, mp 204°C (decompose); yield, 30 mg.

Found: N, 7.05%. Calcd for $C_{10}H_7O_3N$: N, 7.41%.

b) A solution of 0.10 g of IX and 50 mg of sodium acetate in 50 m*l* of methanol was reduced by means of palladised charcoal as above to give 60 mg of orange needles, mp 164—165°C after recrystallization from ethyl acetate; this melting point was identical with that of an authentic sample of II.[3a]

3-Bromo-6-chloro-1-azaazulan-2-one (XI). A solution of 0.10 g of IX in 2 m*l* of acetic acid was treated with 90 mg of bromine and then allowed to stand overnight at room temperature. After the acetic acid had been removed, the residue was washed with aqueous sodium bicarbonate and water, and recrystallized from alcohol to give orange silky needles of XI, mp 245°C; yield, 0.12 g. This was identical with the product of the decarboxylated bromination of VIIa.

Found: C, 41.47; H, 2.19; N, 5.75%. Calcd for $C_9H_5ONBrCl$: C, 41.81; H, 1.95; N, 5.41%.

6-Chloro-3-nitro-1-azaazulan-2-one (XII). To a solution of 0.20 g of IX in 5 m*l* of acetic acid, 0.3 m*l* of fumed nitric acid was added, and then the mixture was allowed to stand overnight at room temperature. The precipitate which formed was separated by filtration, washed with water and alcohol, and then recrystallized from a large amount of alcohol-dioxane to give greenish-brown scales of XII, mp >300°C; yield, 0.18 g.

Found: C, 47.53; H, 1.99; N, 12.20%. Calcd for $C_9H_5O_3N_2Cl$: C, 47.68; H, 2.24; N, 12.47%.

6-Chloro-3-(*p*-tolyl)azo-1-azaazulan-2-one (XIV). Into a solution of 0.10 g of IX in 5 m*l* of 50% of dioxane which had been cooled in an ice bath, *p*-toluene diazonium chloride prepared from 60 mg of *p*-toluidine in the ordinary way was added, drop by drop; the pH of the solution was then adjusted to *ca.* 8.5 with 5% aqueous sodium carbonate, after which the solution was allowed to stand overnight at room temperature. The precipitate formed was separated by filtration, washed with water, and dried in a desiccator to give 0.15 g of a red-purple powder. However, the purification of this powder by means of recrystallization or chromatography failed to produce an analytically-pure substance. The UV spectrum of this shows a figure analogous to that of 3-(*p*-tolyl)azo-1-azaazulan-2-one,[3a] but it shift to a longer wavelength. λ_{max}^{MeOH} mμ (log ε); 247 (4.21), 277 (4.22), 322 (4.13) and 480 (4.16).

3-Acetylamino-6-chloro-1-azaazulan-2-one (XV). a) *The Reduction of XII.* A suspension of XII in 100 m*l* of alcohol was reduced over 10 mg of 5% palladized charcoal in the usual way. The XII dissolved gradually. After 3 mol of hydrogen had been taken up, the catalyst was removed by filtration and the alcohol was concentrated. The residue turned to a black, resinous substances upon concentration. Acetic anhydride (2 m*l*) was added to the residue and the mixture was heated on a water bath. After the acetic anhydride had been removed under reduced pressure, the residue was recrystallized from acetone-methanol to give orange micro needles of XV; mp 276—277°C; yield, 40 mg.

Found: C, 55.57; H, 3.95; H, 11.51%. Calcd for $C_{11}H_9O_2N_2Cl$: C, 55.82; H, 3.83; N, 11.84%.

b) The Reduction of XIV. From 0.10 g of XIV, 40 mg of XV were obtained by the same procedure.

6-Bromo-1-azaazulan-2-one (X). In a sealed tube, 0.10 g of IX and 2 m*l* of acetic acid which had been saturated with dry hydrogen bromide were heated for 6 hr at 100°C. The acetic acid and hydrogen bromide were removed, and then the obtained residue was washed with aqueous sodium bicarbonate and water, and dried in a desiccator. The recrystallization of this solid from methanol gave 0.11 g of orange needles of X, mp 211—212°C. The mixed melting point of X with IX was 224—226°C.

Found: C, 48.59; H, 2.51; N, 6.59%. Calcd for C_9H_6ONBr: C, 48.24; H, 2.69; N, 6.25%.

By the same treatment of X in acetic acid saturated with hydrogen chloride, IX was obtained, mp 232°C. Found: N, 7.91%.

N-Acetate of X; mp 204—205°C. IR ($CHCl_3$); 1720 and 1700 cm^{-1}.

Found: N, 4.82%. Calcd for $C_{11}H_8O_2NBr$: N, 5.21%.

6-Bromo-3-nitro-1-azaazulan-2-one (XIII). By the same treatment as in the nitration of IX, 0.10 g of X afforded 80 mg of pale-greenish-brown leaflets of XIII, mp >300°C, from a large amount of dioxane.

Found: C, 40.58; H, 2.01; N, 10.96%. Calcd for $C_9H_5O_3N_2Br$: C, 40.17; H. 1.87; N, 10.41%.

Ethyl 2,6-Dichloro-1-azaazulen-3-carboxylate (XVI). In a sealed tube, 0.10 g of VII and 1.0 m*l* of phosphorus oxychloride were heated at 100°C for 3 hr, and then the phosphorus oxychloride was removed under reduced pressure. The residue was poured into crushed ice, and the pH of the water layer was adjusted to *ca.* 8.5 with sodium bicarbonate. The precipitate formed was separated by filtration, dried in a desiccator, and recrystallized from benzene to give 90 mg of yellow needles of XVI, mp 185—186°C.

Found: C, 53.05; H, 3.69; N, 5.51%. Calcd for $C_{12}H_9O_2NCl_2$: C, 53.36; H, 3.36; N, 5.19%.

2,6-Dichloro-1-azaazulene (XVII). a) From 8.0 g of IX and 50 m*l* of phosphorus oxychloride treated as above, 7.0 g of orange red needles of XVII were obtained; mp 183°C from cyclohexane. The second crop was 0.8 g, mp 177°C.

Found: C, 53.50; H, 2,87; N, 6.91%. Calcd for $C_9H_5NCl_2$: C, 53.56; H, 2.54; N, 7.07%. λ_{max}^{MeOH} mμ (log ε); 228 (4.16), 275 (4.71), 342 (3.84), 456 (3.19) and 464 (3.20).

b) By the same treatment of 0.10 g of X with 1 m*l* of phosphorus oxychloride, 0.10 g of IX was obtained. Found: N, 7.25%.

c) XVIII (0.10 g) was treated with 5 m*l* of acetic acid, which had been saturated with hydrogen chloride, for 5 hr at 140°C in a sealed tube. After cooling, the product was treated as above to give 80 mg of XVII, mp 181—182°C. Found: N, 7.11%.

2,6-Dichloro-1-azaazulen-3-carboxylic Acid (XXI). VIIa (0.20 g) in 1 m*l* of phosphorus oxychloride was treated as above, and then the pH of the water layer was adjusted to *ca.* 5 with sodium bicarbonate. The precipitate formed and the water-layer extracts obtained by means of benzene were combined, washed with water, and recrystallized from benzene to give 0.10 g of yellow needles of XXI, which did not have

a clear melting point.

Found: C, 49.20; H, 1.88; N, 5.63%. Calcd for $C_{10}H_5O_2NCl_2$: C, 49.64; H, 2.09; N, 5.79%.

2,6-Dibromo-1-azaazulene (XVIII). a) In a sealed tube, 0.10 g of IX and 1 m*l* of phosphorus tribromide were heated at 150°C for 3 hr; after cooling, the reaction mixture was treated as in the case of XVII. The crude XVIII was chromatographed on alumina, and the benzene eluate was recrystallized from benzene-cyclohexane to give orange-red needles of XVIII, mp 202—204°C; yield, 0.10 g.

Found: C, 37.61; H, 2.12; N, 5.24%. Calcd for $C_9H_5NBr_2$: C, 37.66; H, 1.76; N, 4.88%. λ_{max}^{MeOH} mμ (log ε); 230 (4.07), 280 (4.67), 331 (3.83), 347 (3.93) and 466 (3.23).

b) XVII (0.10 g) was heated in 5 ml of acetic acid which had been saturated with hydrogen bromide, for 5 hr at 140°C, and then treated as above to give 0.12 g of XVIII, mp 202.5—203.5°C. Found: N, 5.02%.

3-Bromo-2,6-dichloro-1-azaazulene (XIX). a) A solution of 50 mg of XXI in 1 m*l* of acetic acid was treated with 40 mg of bromine at room temperature. This oily substance formed gradually solidified. The reaction mixture was then allowed to stand for 3 hr, the acetic acid was removed under reduced pressure, and the pH of the residue was adjusted to *ca.* 8.5 with aqueous sodium bicarbonate. The precipitate which formed was then washed with water and dried in a desiccator, and the benzene solution of this was chromatographed on alumina. The benzene eluate was recrystallized from benzene to give 40 mg of reddish-carmine needles of XIX, mp 208—209°C.

Found: C, 39.14; H, 1.55; N, 5.58%. Calcd for $C_9H_4NBrCl_2$: C, 39.03; H, 1.45; N, 5.06%.

b) When 60 mg of XVII in 1 m*l* of chloroform were treated with 50 mg of bromine, the reaction proceeded exothermically and the precipitate formed immediately. The precipitate was then treated as above to give 80 mg of XIX, mp 208—209°C.

2,3,6-Tribromo-1-azaazulene (XX). To a mixture of 20 mg of XVIII and 5 mg of sodium carbonate in 2 m*l* of chloroform, 10 mg of bromine were added; the mixture was then allowed to stand at room temperature for 5 hr. The chloroform was removed, and the residue was washed with water, dried in a desiccator, and recrystallized from benzene - light petroleum to give 25 mg of reddish-carmine needles of XX, mp 215—216°C.

Found: C, 29.98; H, 0.86; N, 4.16%. Calcd for $C_9H_4NBr_3$: C, 29.54; H, 1.10; N, 3.83%.

An Attempted Nitration of XVII. To a solution of 50 mg of XVII in 1 m*l* of acetic acid, 0.2 m*l* of fumed nitric acid was added, after which the mixture was allowed to stand at room temperature overnight. After the acetic acid had then been removed under reduced pressure, the pH of the residue was adjusted to *ca.* 8 with aqueous sodium bicarbonate and the precipitate thus formed was washed with water and dried. The recrystallization of the residue from cyclohexane gave 40 mg of red needles, mp 180—182°C, which did not show any depression when the needles were mixed with the starting substance. The second crop was 5 mg. When the reaction mixture was heated on a water bath, no crystalline substances were obtained, and in concentrated sulfuric acid instead of acetic acid, the starting substance was recovered.

An Attempted Azocoupling Reaction of XVII. XVII (50 mg) was treated with 50 mg of diazotized toluidine in the ordinary way and then allowed to stand in a refrigerator overnight. The precipitate thus formed was then extracted with benzene, and the benzene layer was washed with water, dried over sodium sulfate, and chromatographed on alumina. The benzene eluate was recrystallized from cyclohexane to give 40 mg of orange-red needles, mp 182—183°C, which did not show any depression when the needles were mixed with the starting substance.

The Reaction of XVII with Hydrazine and the Decomposition of 2-Chloro-6-hydrazino-1-aza-azulene. a) A solution of 0.20 g of XVII and 80 mg of hydrazine hydrate in 2 m*l* of alcohol was warmed on a water bath for 30 min. The color of the solution changed from orange to dark orange, and then gradually to dark red. The alcohol was removed under reduced pressure and extracted with ethyl acetate. The ethyl acetate extracts were washed with water and dried over sodium sulfate, and the ethyl acetate was removed under reduced pressure to give 0.16 g of a red-violet powder, which decomposed *ca.* 210°C. The powder was unstable and could not be obtained in a pure state because when it was heated in a solvent the color of the powder changed and gave tarry substances.

A solution of 0.14 g of the crude XXV in 2 m*l* of acetic acid was poured all at once into a boiling solution of 0.70 g of cuprous sulfate in 2 m*l* of water. After cooling, the pH of the solution was adjusted to *ca.* 8 with sodium bicarbonate, and the solution was extracted with benzene; the combined benzene extracts were then dried over sodium sulfate and chromatographed on alumina. The benzene eluate was recrystallized from cyclohexane to give 50 mg of orange needles, mp 72°C, which did not show any depression when the needles were mixed with 2-chloro-1-azaazulene (III); the UV spectrum of the product was identical with that of III.

b) Freshly-prepared XXV (80 mg) was dissolved in 2 m*l* of concentrated hydrochloric acid, after which the solution was poured into a boiling solution of 0.60 g of cuprous sulfate in 2 m*l* of water. After cooling, the solution was treadted as above; 20 mg of orange needles were obtained; the mp of 182°C, did not show any depression when the needles were mixed with XVII.

6-(*p*-Tolyl)thio-1-azaazulan-2-one (XXII). IX (0.18 g) was added to a solution prepared from 0.20 g of *p*-thiocresol and 0.10 g of sodium methoxide in 10 m*l* of absolute methanol, and the mixture was heated in a sealed tube for 2 hr at 100°C. The methanol was then removed under reduced pressure, and the precipitate formed was washed with water, dried in a desiccator, and recrystallized from ether-alcohol to give brownish-red prisms of XXII, mp 220—220.5°C; yield, 0.23 g.

Found: C, 71.58; H, 5.36; N, 5.49%. Calcd for $C_{16}H_{13}ONS$: C, 71.90; H, 4.90; N, 5.24%. λ_{max}^{MeOH} mμ (log ε); 221 (4.31), 261 (4.50), 329 (4.21) and 416 (4.19).

2-Chloro-6-(*p*-tolyl)thio-1-azaazulene (XXIII). a) In a sealed tube, 80 mg of XXII in 1 m*l* of phosphorus oxychloride were heated for one hour. After the reaction, the product was treated as the ordinary way. The crude substances thus obtained were recrystallised from cyclohexane-benzene to give 70 mg of orange needles of XXIII, mp 128—129°C.

Found: C, 67.55; H, 4.01; N, 5.33%. Calcd for

$C_{16}H_{12}NSCl$: C, 67.25; H, 4.23; N, 4.90%.

b) To a solution of 60 mg of *p*-thiocresol and 30 mg of sodium methoxide in 5 m*l* of absolute methanol, 0.10 g of XVII was added, and then the mixture was heated under reflux for 15 min. The solution was concentrated under reduced pressure and extracted with benzene, and the benzene extracts were washed with water, dried with water, dried over sodium sulfate, and chromatographed on alumina. The benzene eluate was then recrystallized from cyclohexane-benzene to give orange prisms of XXIII, mp 127.5—129°C; yield, 0.12 g.

2,6-Di(*p*-tolylthio)-1-azaazulene (XXIV). a) A solution of 0.10 g of XVII in 3 m*l* of absolute methanol containing 0.14 g of *p*-thiocresol and 60 mg of sodium methoxide was heated under reflux for 15 min; after reaction, this mixture was treated as above. Orange prisms of XXIV were obtained, mp 189—190°C, yield, 0.16 g.

Found: C, 73.91; H, 5.21; N, 3.91%. Calcd for $C_{23}H_{19}NS_2$: C, 73.88; H, 5.13; N, 3.75%.

b) To a solution of 50 mg of *p*-thiocresol and 20 mg of sodium methoxide in 2 m*l* of absolute methanol, 0.10 g of XXIII was added; the mixture was heated under reflux for 20 min and then treated as above to give 0.12 g of orange prisms mp 189—190°C, which did not show any depression when the prisms were mixed with the XXIV obtained above.

2-Chloro-6-methoxy-1-azaazulene (XXVI). In 2 m*l* of absolute methanol containing 30 mg of sodium, 0.10 g of XVII was heated under reflux for 30 min; after cooling, the methanol was removed under reduced pressure. The precipitate thus formed was washed with water, dried in a desiccator, and recrystallized from benzene-cyclohexane to give 80 mg of yellow needles of XXVI, mp 103—104°C.

Found: C, 61.55; H, 4.29; N, 7.37%. Calcd for $C_{10}H_8ONCl$: C, 61.56; H, 4.16; N, 7.23%. Picrate, mp 206°C. Found: N, 13.18%. Calcd for $C_{16}H_{11}O_8N_4Cl$: N, 13.25%.

2-Chloro-6-ethoxy-1-azaazulene (XXVII). XVII (0.10 g) was treated as above in 2 m*l* of absolute alcohol, containing 30 mg of sodium, to give 0.10 g of yellow needles of XXVII, mp 117—118°C, from benzene-light petroleum.

Found: N, 6.97%. Calcd for $C_{11}H_{10}ONCl$: N, 6.75%.

The Reaction of XVII with Aqueous Alkali. To a solution of 60 mg of potassium hydroxide in 1 m*l* of water, 0.20 g of XVII was added, and the mixture was heated under reflux for 2 hr. The solvent was then removed, and the residue was washed with water and dried in a desiccator to give 0.18 g of yellow needles, mp 179—181°C, which did not show any depression when the needles were mixed with the original XVII. The silver nitrate test of the aqueous layer of the reaction mixture was negative.

The Reaction of XVII with Ammonia. *a) In Methanol.* A solution of 0.10 g of XVII in 15 m*l* of methanol was saturated with ammonia gas at 0°C and then allowed to stand at room temperature for 2 days. After the solvent and ammonia had been removed, the residue was extracted with benzene and chromatographed on alumina. The benzene eluate afforded 50 mg of yellow needles, mp 181—183°C, which did not show any depression when the needles were mixed with XVII.

The ethyl acetate eluate afforded 20 mg of yellow needles, mp 102°C, which did not show any depression when the needles were mixed with XXVI.

b) XVII (0.70 g) was dissolved in 50 m*l* of liquid ammonia which had been cooled in a sodium chloride-ice bath, and then the mixture was allowed to stand at room temperature for 4 days. After the ammonia had been removed the residue was washed with water, dried in a desiccator, and fractionally-recrystallized from benzene and acetone. From the benzene-soluble part, 0.15 g of XVII was recovered, and from the acetone-soluble part, 0.35 g of orange brown prisms of XXVIII, mp 218—220°C, was obtained.

Found: C, 54.60; H, 4.69; N, 13.83%. Calcd for $C_9H_7N_2Cl \cdot H_2O$: C, 54.97; H, 4.61; N, 14.25%.

2-Chloro-6-methylamino-1-azaazulene (XXIX). A solution of 0.10 g of XVII, 70 mg of methylamine hydrochloride, and 50 mg of sodium carbonate in 2 m*l* of methanol was heated in a sealed tube at 100°C for one hr, and then the methanol was removed. The residue was washed with water and recrystallized from acetone-methanol to give 70 mg of yellow-brown micro prisms of XXIX, mp 224—225°C.

Found: C, 62.05; H, 4.38; N, 14.11%. Calcd for $C_9H_7N_2Cl$: C, 62.34; H, 4.71; N, 14.54%.

2-Chloro-6-dimethylamino-1-azaazulene (XXX). A solution of 0.20 g of XVII and 0.5 m*l* of 40% of aqueous dimethylamine in 4 m*l* of methanol was heated under reflux for one hour, and then treated as above to give 0.19 g of pale brown XXX, mp 158—162°C. Recrystallization from benzene raised its mp to 194—195°C; yellow brown scales; yield, 0.16 g.

Found: C, 64.15; H, 5.32; N, 13.43%. Calcd for $C_{11}H_{11}N_2Cl$: C, 63.89; H, 5.36, N, 13.56%.

2-Chloro-6-ethylthio-1-azaazulene (XXXI). A solution of 0.10 g of XVII, 60 mg of sodium methoxide, and 70 mg of ethyl mercaptan in 2 m*l* of absolute methanol was heated under reflux for 15 min, and then the methanol was removed. The residue was dissolved in benzene, washed with water, dried over sodium sulfate, and chromatographed on alumina. The benzene eluate gave 90 mg of orange prisms of XXXI, mp 94°C, from benzene.

Found: C, 58.73; H, 4.46; N, 6.46%. Calcd for $C_{11}H_{10}NSCl$: C, 59.05; H, 4.51; N, 6.26%.

2-Chloro-6-nitro-1-azaazulene (XXXII). A solution of 0.10 g of XVII and 70 mg of sodium nitrite in 3 m*l* of methanol was heated under reflux for 2 hr, concentrated, and extracted with ethyl acetate. The combined ethyl acetate extracts were washed with water, dried over sodium sulfate, and chromatographed on alumina. The ethyl acetate eluate was then recrystallized from the same solvent to give silky, reddish-violet needles of XXXII, mp 220°C (decomp.); yield, 60 mg.

Found: C, 51.37; H, 2.57; N, 12.86%. Calcd for $C_9H_5O_2N_2Cl$: C, 51.82; H, 2.42; N, 13.43%.

Diethyl (2-Chloro-1-azaazulen-6-yl)malonate (XXXIII). To a solution of 50 mg of sodium in 3 m*l* of diethyl malonate, 0.20 g of XVII was added; the mixture was heated at 50°C for one hour, and then the diethyl malonate was removed under reduced pressure. The residue was poured into crushed ice, and the pH of the solution was adjusted to *ca.* 8 by the addition of acetic acid; this giving a precipitate. The precipitate was separated by filtration, washed with water, dried in a desiccator, and extracted with benzene. The benzene

extracts gave 20 mg of the starting substances. The benzene-insoluble solid was dissolved to ethyl acetate and chromatographed on alumina. The ethyl acetate eluate gave a resinous substance. The repeated recrystallization of this from ethyl acetate gave brown micro needles, mp 255°C (decomp. and gradually blacken about 220°C); yield, 40 mg.

Found: N, 3.97%. Calcd for $C_{16}H_{16}O_4NCl$: N, 4.35%.

When the reaction was carried out at room temperature, 90% of XVII was recovered, and the treatment of XVII in absolute methanol with diethyl malonate and sodium methoxide under reflux resulted in a 15% recovery of the XVII, a 20% recovery of the XXVI, and some intractable tar.

Ethyl 1-Cyano-1-(2-chloro-1-azaazulen-6-yl)acetate (XXXIV). To a solution which had been prepared from 0.24 g of ethyl cyanoacetate and 50 mg of sodium in 5 m*l* of benzene, 0.20 g of XVII was added, after which the mixture was heated at 70°C for 5 hr. After cooling, the reaction mixture was poured into crushed ice, and the pH of the water layer was adjusted to *ca.* 6.5 with acetic acid. The reaction mixture was then separated into a benzene-soluble part and an insoluble precipitate. The benzene layer afforded 0.10 g of the recovered XVII after concentration. The precipitate (0.10 g) was dissolved in ethyl acetate - alcohol (10: 1) and chromatographed on alumina three times. The recrystallization of the ethyl acetate - alcohol eluate gave 40 mg of yellow-brown micro prisms of XXXIV, mp 260°C (decomp., blacken *ca.* 200°C).

Found: C, 61.64; H, 4.15; N, 9.99%. Calcd for $C_{14}H_{11}O_2N_2Cl$: C, 61.21; H, 4.40; N, 10.19%.

2-Chloro-6-(*p*-tolyl)amino-1-azaazulene (XXXV). A solution of 50 mg of XVIII and 50 mg of *p*-toluidine in 3 m*l* of methanol was heated under reflux for one hour and then concentrated under reduced pressure; the precipitate thus formed was washed with aqueous sodium bicarbonate and then water. After having been dried in a desiccator, this was dissolved in benzene, and the benzene solution was chromatographed on alumina. The benzene eluate was recrystallized from cyclohexane -benzene to give 70 mg of reddish-brown micro prisms of XXXV, mp 200—201°C.

Found: N, 10.24%. Calcd for $C_{16}H_{13}N_2Cl$: N, 10.42%.

2-Chloro-6-(*p*-nitrophenyl)amino-1-azaazulene (XXXVI). A solution of 50 mg of XVII and 70 mg of *p*-nitroaniline in 4 m*l* of methanol was heated under reflux for one hour after which the methanol was removed under reduced pressure. The residue was washed with aqueous sodium bicarbonate and water, and recrystallized from acetone - methanol to give 60 mg of brown micro needles of XXXVI, mp 241—242°C.

Found: N, 14.07%. Calcd for $C_{15}H_{10}O_2N_3Cl$: N, 14.02%.

The support of this project by the Takasago Perfumery Co. is gratefully acknowledged.

BULLETIN OF THE CHEMICAL SOCIETY OF JAPAN VOL. 41 2111—2114 (1968)

The Formation and Reactions of α-Keto Sulfoxide

Takanobu KUMAMOTO and Teruaki MUKAIYAMA

Laboratory of Organic Chemistry, Tokyo Institute of Technology, Ookayama, Meguro-ku, Tokyo

(Received February 3, 1968)

The reactions of α-keto sulfoxide, produced by the oxidation of thiolester, were studied. It was established that the oxidation of *S*-ethyl thiobenzoate with *N*-bromosuccinimide and isopropyl alcohol afforded benzoyl ethyl sulfoxide. Similarly, butyryl ethyl sulfoxide was produced by the oxidation of *S*-ethyl thiobutyrate with iodosobenzene. α-Keto sulfoxide, produced by the above-mentioned oxidations, reacts with alcohols, phenols, amines or sodium carboxylates to afford acylated products such as esters, amides or carboxylic anhydrides in good yields.

It has been found that hexahydrophthalic anhydride is obtained in good yield by the reaction of sodium hexahydrophthalate with benzenesulfenyl chloride at room temperature. This result can be explained by assuming an initial formation of a condensation product, sodium benzenesulfenyl hexahydrophthalate, which in turn cyclizes to yield acid anhydride by the elimination of sodium benzenesulfenate.

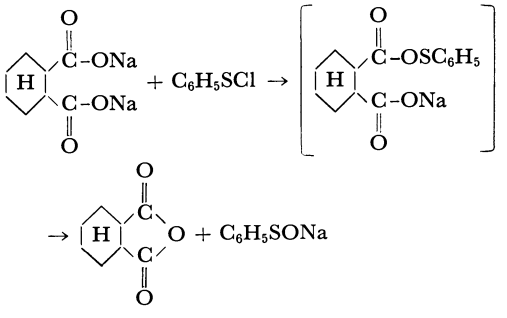

Based on this finding, the oxidation of thiolesters was investigated with the assumption that α-keto

TABLE 1. THE REACTION OF 1 mol OF THIOLESTER WITH 1 mol OF *N*-BROMOSUCCINIMIDE AND 2 mol OF ALCOHOL

Thiol ester	Alcohol	Ester		Yield of succinimide
		Yield	Bp	
C_6H_5-C(=O)-SC_2H_5	C_2H_5OH	72%	88—91°C/12 mmHg	92%
C_6H_5-C(=O)-SC_2H_5	$C_6H_5CH_2OH$	61%	120—122°C/3 mmHg	99%
C_6H_5-C(=O)-SC_6H_5	C_2H_5OH	60%	96—100°C/20 mmHg	60%
C_6H_5-C(=O)-SC_6H_5	*n*-C_4H_9OH	65%	122—124°C/14 mmHg	84%

sulfoxide, an isomer of sulfenyl carboxylate, would be an active acylating reagent when it was treated with active hydrogen compounds.

The oxidation of thiolester with either aqueous peracetic acid[1] or potassium permanganate[2] as an oxidant resulted in the formation of carboxylic acid, instead of the expected α-keto sulfoxide. In order to perform the above mentioned acylation reaction by the use of thiolester through α-keto sulfoxide, it is necessary to explore a convenient method for the oxidation of thiolester under anhydrous condition.

Recently, it has been reported that the treatment of *N*-bromosuccinimide with sulfide in hydrous dioxane at room temperature afforded sulfoxide.[3] In the present investigation, a modified oxidation of thiolester was tried by the use of alcohol instead of water in the above reaction as shown in the following equation. It was expected that oxidation by this procedure would be successfully carried out under anhydrous condition. Indeed, when 2 mol of benzyl alcohol was added to a mixture of 1 mol of *S*-ethyl thiobenzoate and 1 mol of *N*-bromosuccinimide, benzyl benzoate (61%), succinimide (99%) and benzyl bromide (64%) were obtained.

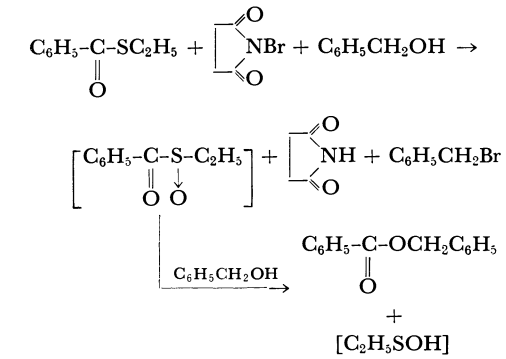

In a similar manner, various esters were obtained from the reaction of 1 mol each of thiolester and *N*-bromosuccinimide, and 2 mol of alcohols (see Table 1).

In order to extend this type of acylation to various active hydrogen compounds, such as amines or phenols, the oxidation of thiolester with equimolar amounts of *N*-bromosuccinimide and alcohol was investigated. The reaction of equimolar amounts of *S*-ethyl thiobenzoate, *N*-bromosuccinimide and isopropyl alcohol under ice-cooling, followed by the addition of butyl alcohol, resulted in the formation of butyl benzoate (93%), succinimide (88%), diethyl disulfide (68%) and *S*-ethyl thioethyl sulfonate (65%). Diethyl disulfide and *S*-ethyl thioethyl sulfonate would be the products resulted by the decomposition of ethanesulfenic acid formed. Of importance in this reaction is the fact that isopropyl benzoate, an undesirable by-product, was not obtained at all.

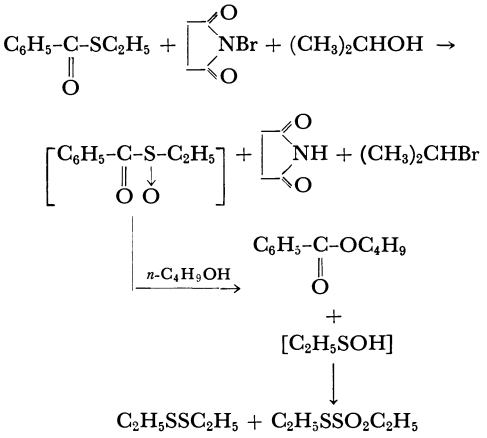

In a similar manner, various esters were obtained in good yields by the reactions of α-keto sulfoxide, produced from thiolester, *N*-bromosuccinimide and isopropyl alcohol, with various alcohols (see Table 2).

The existence of the α-keto sulfoxide, an intermediate, was confirmed by the infrared spectra of

1) C. J. Carallito and D. M. Freuhauf, *J. Am. Chem. Soc.*, **71**, 2248 (1949).
2) R. Otto and R. Luders, *Ber.*, **13**, 1285 (1880).
3) W. Tagaki, K. Kikukawa, K. Ando and S. Oae, *Chem. Ind.*, **38**, 1624 (1964).

Table 2. The reaction of benzoyl ethyl sulfoxide with alcohols

ROH	$C_6H_5CO_2R$ Yield	$C_6H_5CO_2R$ Bp °C/mmHg	Yield of succinimide	Yield of $(C_2H_5S)_2$	Yield of $C_2H_5SSO_2C_2H_5$
n-C_4H_9OH	93%	126—128/20	88%	68%	65%
n-$C_8H_{17}OH$	74%	128—132/1	93%	69%	—
$C_6H_5CH_2OH$	55%	127—128/2	91%	—	—
cyclo-$C_6H_{11}OH$	65%	109—113/1	91%	55%	—

Table 3. The reaction of α-keto sulfoxide, produced by the oxidation of thiolester with iodosobenzene, with alcohols

Thiol ester	Alcohol	Ester Yield	Ester Bp °C/mmHg	Yield of iodobenzene
C_3H_7-C(=O)-SC_2H_5	C_2H_5OH	72%	101—110/760	94
C_3H_7-C(=O)-SC_2H_5	i-C_3H_7OH	48%	110—115/760	80%
C_3H_7-C(=O)-SC_2H_5	n-$C_8H_{17}OH$	65%	120—126/24	—
C_6H_5-C(=O)-SC_2H_5	n-$C_8H_{17}OH$	37%	130—132/2	75%

the reaction mixture which was obtained from the reaction of the *S*-ethyl thiobenzoate, *N*-bromosuccinimide and isopropyl alcohol: 1720 cm^{-1}, 1780 cm^{-1} (>C=O), 1180 cm^{-1} (>S→O). This spectrum was identical with that of the reaction mixture which was obtained from the reaction of *S*-ethyl thiobenzoate and iodosobenzene mentioned below.

Next, α-keto sulfoxide, produced by the above mentioned procedure, was treated with phenol, phenyl benzoate (56%) and succinimide (87%) were obtained. The reactions of benzoyl ethyl sulfoxide with substituted phenol, such as *p*-chlorophenol and *p*-nitrophenol gave *p*-chlorophenyl benzoate and *p*-nitrophenyl benzoate in 34% and 10% yields, respectively along with a tarry product.

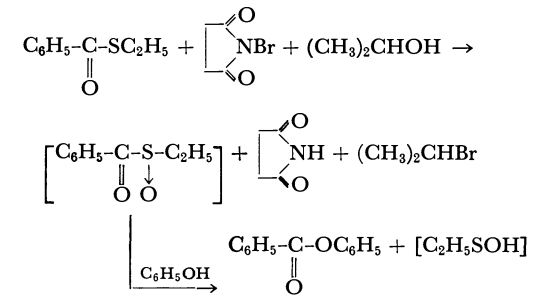

When benzoyl ethyl sulfoxide was allowed to react with benzoic acid, benzoic anhydride could not be obtained, while benzoic acid was recovered quantitatively along with unidentifiable tarry materials. However, when sodium benzoate was used instead of benzoic acid in the above reaction, benzoic anhydride was obtained in 65% yield.

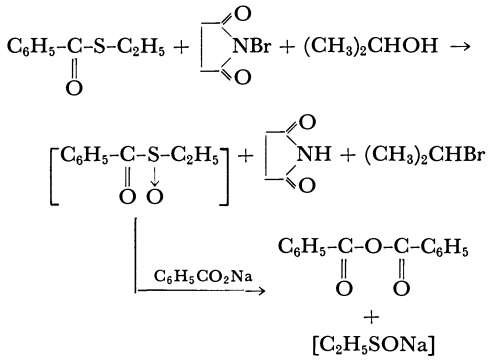

In addition, benzoyl ethyl sulfoxide was found to react vigorously with aniline to afford benzanilide (70%) and succinimide (72%).

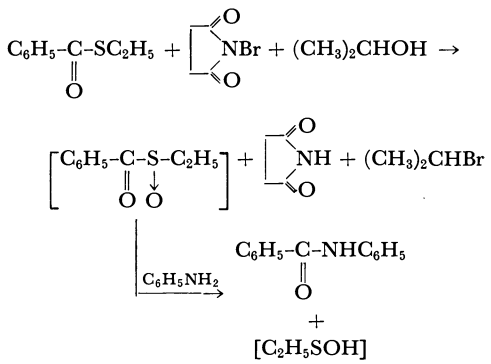

Then, the oxidation of thiolesters was tried by the use of iodosobenzene. When a mixture of *S*-ethyl thiobutyrate and iodosobenzene was refluxed in chloroform for 45 min, a precipitates of iodosobenzene disappeared. Successive addition of *n*-octyl alcohol to the reaction mixture at room temperature resulted in the formation of *n*-octyl butyrate in 65% yield.

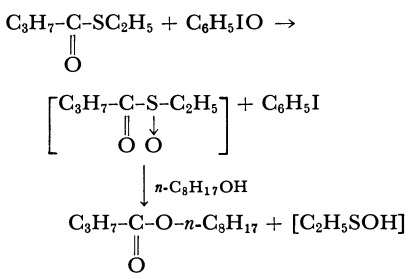

Various esters were obtained in a similar manner by the reaction of thiolesters, iodosobenzene and alcohols (see Table 3).

Experimental

The Reaction of Sodium Hexahydrophthalate with Benzenesulfenyl Chloride. A mixture of sodium hexahydrophthalate (2.16 g, 0.01 mol) and benzenesulfenyl chloride (2.89 g, 0.02 mol) was stirred in tetrahydrofuran for 6 hr at room temperature. After the precipitates formed was removed by filtration, the residue was evapolated under reduced pressure. Distillation *in vacuo* gave hexahydrophthalic anhydride (1.00 g, 65%, bp 100—106°C/0.15 mmHg) with much amount of tarry product.

The Reaction of 1 mol of *S*-Ethyl Thiobenzoate with 1 mol of *N*-Bromosuccinimide and 2 mol of Benzyl Alcohol. Into a mixture of *S*-ethyl thiobenzoate (1.66 g, 0.01 mol) and *N*-bromosuccinimide (1.78 g, 0.01 mol) in carbon tetrachloride (20 m*l*), a solution of benzyl alcohol (2.16 g, 0.02 mol) in carbon tetrachloride (10 m*l*) was added drop by drop under stirring. After stirring had been continued for 3 hr, white precipitates were collected, washed with carbon tetrachloride; succinimide was obtained, 0.92 g (93%), mp 122—123°C. The filtrate was concentrated, and the distillation under reduced pressure gave a mixture of benzyl bromide and benzyl alcohol (bp 80—89°C/12 mmHg) and benzyl benzoate (bp 120—122°C/12 mmHg), 1.21 g (61%). The mixture of benzyl bromide and benzyl alcohol was refluxed with thiourea (1 g) in ether for 2 hr, and benzyl thioureyl bromide 1.53 g was obtained. From the weight of benzyl thioureyl bromide, the yield of benzyl bromide was estimated to be 1.06 g (62%).

Similarlly, various esters were obtained by the reaction of thiolesters and *N*-bromosuccinimide and alcohols. The results are listed in Table 1. All the esters were identified by the direct comparison of their IR spectra with those of corresponding authentic samples.

The Oxidation of *S*-Ethyl Thiobenzoate with *N*-Bromosuccinimide and Isopropyl Alcohol, and Reaction of Benzoyl Ethyl Sulfoxide, produced by the Oxidation, with Butyl Alcohol. Into a mixture of *S*-ethyl thiobenzoate (1.66 g, 0.01 mol) and *N*-bromosuccinimide (1.78 g, 0.01 mol) in carbon tetrachloride (10 m*l*), a solution of isopropyl alcohol (0.60 g, 0.01 mol) in carbon tetrachloride (10 m*l*) was added drop by drop under ice-cooling. After stirring for 2 hr, butyl alcohol (0.74 g, 0.01 mol) was added to the reaction mixture. The reaction mixture was stirred for 30 min. The succinimide, which precipitated, was filtered and was washed with carbon tetrachloride, 0.87 g (88%), mp 124—125°C. After removal of solvent, distillation under reduced pressure gave diethyl disulfide, (40—55°C/20 mmHg), 0.21 g (68%), *S*-ethyl thioethyl sulfonate, (90—100°C/20 mmHg), 0.25 g (65%) and butyl benzoate, (126—128°C/20 mmHg), 1.65 g (93%). Diethyl disulfide and butyl benzoate were identified by direct comparison of their IR spectra with those of corresponding authentic sample.

By a similar procedure, various esters were obtained by the reaction of benzoyl ethyl sulfoxide, produced by the reaction of *S*-ethyl thiobenzoate and *N*-bromosuccinimide and isopropyl alcohol, with various alcohols. The results are listed in Table 2. Butyl benzoate and benzyl benzoate were identified by direct comparison of their IR spectra with those of the authentic samples. The elemental analyses of octyl benzoate and cyclohexyl benzoate are as follows;

Found: C, 76.59; H, 9.43%. Calcd for $C_{15}H_{22}O_2$: ($C_6H_5CO_2$*n*-C_8H_{17}): C, 76.88; H, 9.46%.

Found: C, 76.34; H, 8.14%. Calcd for $C_{15}H_{16}O_2$ ($C_6H_5CO_2C_6H_{11}$): C, 76.44; H, 7.90%.

Reaction of Benzoyl Ethyl Sulfoxide with Sodium Benzoate. Sodium benzoate (1.44 g, 0.01 mol) was added to the carbon tetrachloride solution of benzoyl ethyl sulfoxide produced by the above mentioned procedure. After stirring for 30 min, white precipitates were collected. The solution was concentrated and distillation under reduced pressure gave benzoic anhydride (bp 140—142°C/1 mmHg) 1.46 g (65%).

Reaction of Benzoyl Ethyl Sulfoxide with Aniline. Similarly, *S*-ethyl thiobenzoate (1.66 g, 0.01 mol), *N*-bromosuccinimide (1.78 g, 0.01 mol) and isopropyl alcohol (0.60 g, 0.01 mol) were allowed to react under ice cooling. After removal of precipitated succinimide (0.70 g, 71% yield), excess amount of aniline (1.86 g, 0.02 mol) was added to the filtrate and a vigorous reaction took place in a short time. The reaction mixture was concentrated and the residue was washed with water and recrystallization from alcohol gave benzanilide, 1.38 g (70%), mp 162°C.

The Oxidation of *S*-Ethyl Thiobutyrate with Iodosobenzene and Reaction of Butyryl Ethyl Sulfoxide with Ethyl Alcohol. A mixture of *S*-ethyl thiobutyrate (1.32 g, 0.01 mol) and iodosobenzene (2.20 g, 0.01 mol) was refluxed in chloroform for 45 min. Ethyl alcohol (0.46 g, 0.01 mol) was added to the reaction mixture at room temperature. Distillation gave ethyl butyrate (bp 112—116°C/760 mmHg), 0.81 g (72%) and iodobenzene (bp 89—92°C/28 mmHg), 1.92 g (94%).

By a similar procedure, various esters were obtained by the reaction of butyryl ethyl sulfoxide, produced from thiolesters and iodosobenzene, with alcohols. Results are listed in Table 3.

BULLETIN OF THE CHEMICAL SOCIETY OF JAPAN VOL. 41 2115—2117 (1968)

Stereochemical Studies of the 4-Hydroxyl Group of Polymethoxyflavan-3,4-diols

Shinzaburo HISHIDA, Misao UMEHARA, Fujiyuki KAYANUMA and Ryoichi MIYAZAKI

Department of Chemistry, Nihon University, Setagaya-ku, Tokyo

(Received February 17, 1968)

In the previous papers, it was suggested that the 4-hydroxyl group of flavan-3,4-*trans*-diols altered in configuration upon the formation of the isopropylidene derivatives. In order to confirm this suggestion, the isopropylidene derivatives were prepared by the reaction of 4-^{16}OH with acetone-^{18}O, and of 4-^{18}OH with acetone-^{16}O, and the contents of oxygen-18 were analyzed. The oxygen atom from acetone was found in the isopropylidene derivatives of *trans*-3′,4′,5,7-tetramethoxy-*cis*- and *trans*-3′,4′,5′,5,7-pentamethoxy-flavan-3,4-diols.

The formation of isopropylidene derivatives has frequently been used for the assignment of vicinal dihydroxyl groups in a cyclohexane ring to a cis configuration. However, it has been shown that this procedure is not diagnostic for a cis configuration in the case of 3,4-dihydroxyl groups of flavan-3,4-diols.[1] We have shown that identical isopropylidene derivatives were obtained from pairs of flavan-3,4-*cis*- and *trans*-diols which had methoxyl groups at the 5,7-position. Non-substituted flavan-3,4-*cis*-diol, its 4′-methoxy, and 7-methoxy derivatives gave the respective isopropylidene derivatives, but their trans isomers gave no isopropylidene derivatives by the reaction of flavan-3,4-diols with acetone in the presence of cupric sulfate.[2] In contrast to them, the trans isomers of 3′,4′,5,7-tetramethoxy- and 3′,4′,5′,5,7-pentamethoxyflavan-3,4-diol afforded the same isopropylidene derivatives as those from the respective cis isomers.[3] This anomaly may be explained by the benzylic character at the 4-position, which was enhanced by the presence of methoxyl groups at the 5,7-position and which then facilitated the formation of carbonium ions and the attack of the oxygen atom of acetone from the less strained site.[4]

We will report here the determination of the origin of the oxygen atom at the 4-position of the isopropylidene derivatives, whether it is from the 4-hydroxyl group or from acetone. The isopropylidene derivatives were prepared from 3′,4′,5,7-tetramethoxyflavan-3,4-*cis*- and *trans*-diol, which contained natural oxygen atoms, as a result of a reaction with acetone enriched with oxygen-18 in the presence of cupric sulfate, and from 3′,4′,5′,5,7-pentamethoxyflavan-3,4-*cis*- and *trans*-diol, which contained natural oxygen atoms, as a result of a reaction with enriched acetone. 3′,4′,5′,5,7-Pentamethoxyflavan-3,4-*cis*- and *trans*-diol, which were enriched at the 4-hydroxyl group with oxygen-18, were prepared by the reduction of the corresponding 3-hydroxyflavanone (ampelopsin pentamethyl ether), enriched with oxygen-18 at the 4-carbonyl oxygen atom, and submitted to a reaction with natural acetone.

Results and Discussion

The results of the measurements of the oxygen-18 contents are summarized in Table 1. The values of the oxygen-18 contents were calculated from the M+2/M ratio of the isopropylidene derivatives[5] and carbon dioxides,[6] which were obtained by the combustion of the samples, in the mass-spectra. It seems that the values from carbon dioxides are more appropriate, because in them the undesirable disturbance of contaminated deuterium atoms is excluded.

The cis and trans isomers of 3′,4′,5,7-tetramethoxyflavan-3,4-diols were readily separated through the formation of the boron complex of the cis isomer.

1) E. J. Corey, E. M. Philbin and T. S. Wheeler, *Tetrahedron Letters*, No. 13, 429 (1961); M. M. Bokadia, B. R. Brown, P. L. Kolker, C. W. Love, J. Newbould, G. A. Somerfield and P. W. Wood, *J. Chem. Soc.*, **1961**, 4663; S. Fujise, S. Hishida, T. Onuma, K. Adachi, Y. Fujise and T. Munekata, This Bulletin, **35**, 1245 (1962).

2) S. Fujise, T. Munekata, E. Ishikawa, T. Kobayashi, I. Sakai, M. Ueno, T. Yuki and S. Hishida, *Nippon Kagaku Zasshi* (*J. Chem. Soc. Japan, Pure Chem. Sect.*), **84**, 81 (1963).

3) S. Fujise, K. Adachi and S. Hishida, *ibid.*, **83**, 1294 (1962); S. Fujise, T. Onuma and S. Hishida, *ibid.*, **83**, 1298 (1962).

4) S. Fujise, Y. Fujise and S. Hishida, *ibid.*, **84**, 78 (1963).

5) G. A. Hamilton and F. H. Westheimer, *J. Am. Chem. Soc.*, **81**, 6332 (1959); G. Swain, G. Tsuchihashi and L. J. Taylor, *Anal. Chem.*, **35**, 1415 (1963).

6) S. Oae, T. Kitao and Y. Kitaoka, *J. Am. Chem. Soc.*, **84**, 3359 (1962) (*cf.* D. Rittenberg and L. Ponticorvo, *J. Appl. Rad. Isotopes*, **1**, 208 (1956)).

TABLE 1. THE CONTENTS OF OXYGEN-18 AT THE 4-POSITION

	Methoxyflavan-3,4-diols	Acetone	Isopropylidene derivatives
3′,4′,5,7-$(OMe)_4$-			
cis-diol	0.2(nat.)	1.45	0.2(0.2)
trans-diol	0.2(nat.)	1.45	1.4(1.7)
3′,4′,5′,5,7-$(OMe)_5$-			
cis-diol	0.2(nat.)	2.7	2.7(3.2)
	4.6(6.1)	0.2(nat.)	0.2(0.2)
trans-diol	0.2(nat.)	2.7	2.7(2.6)
	4.8(5.1)	0.2(nat.)	0.2(0.2)

The values were calculated from the M+2/M ratio of CO_2. The values in parenthesis were calculated from the M+2/M ratio of flavan-3,4-diols and isopropylidene derivatives.

After the reduction of 3′,4′,5,7-tetramethoxy-3-hydroxyflavanone with sodium borohydride in boiling methanol, the reaction mixture was concentrated to a small volume and diluted with water; then the crystallization of the pure trans isomer took place. The aqueous solution which contained the boron complex of cis isomer gave the pure cis isomer on acidification with acetic acid. Their purities were checked by thin-layer chromatography. The distinct separation of the spots of the cis and trans isomers on a chromatogram was achieved by using silica gel treated with sodium borate. An incomplete separation of the cis and trans isomers was observed when 3′,4′,5′,5,7-pentamethoxy-3-hydroxyflavanone was reduced with sodium borohydride. According to the same procedure, the cis isomer obtained on the aqueous solution was found to be pure by thin layer chromatography, but the trans isomer proved to be contaminated with the cis isomer. The purification of the trans isomer was difficult, and the impure sample was submitted to the oxygen-18 experiment.

From Table 1, it is evident that the isopropylidene derivative from the cis isomer of tetramethoxyflavan-3,4-diol contained no oxygen-18 atom of acetone; it is supposed to be formed with a retention of the 4-hydroxyl group through the normal process (A).

The S_N1-type mechanism was postulated, because all the experimental results were covered by using the formation of carbonium ions. However, the S_N2-type and S_Ni-type mechanisms were valid in only a few cases.

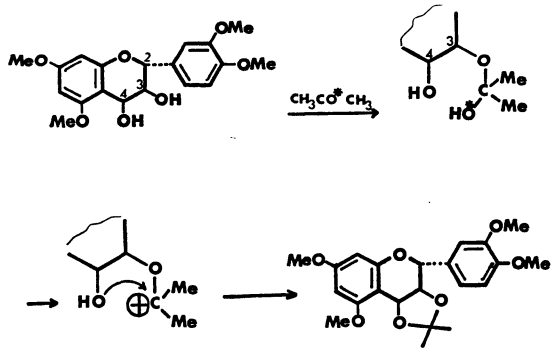

However, it was found that the trans isomer readily formed the identical isopropylidene derivative incorporated with the oxygen-18 of acetone. This anomalous reaction may be explained as follows (process (B));

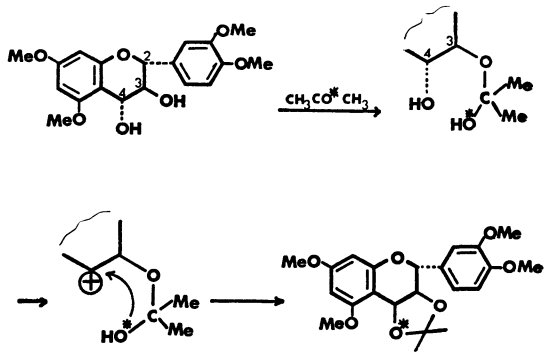

The formation of the dioxolane ring from the flavan-3,4-*trans*-diol through the process (A) requires more distortion of the pyran ring than that from the flavan-3,4-*cis*-diol. The dioxolane ring should be formed through the process that requires the less distortion. The enhanced benzylic character at the 4-carbon atom by the methoxyl groups facilitates the formation of carbonium ions, and the hydroxyl group of acetone hemiketal more readily attacks the carbonium ion from the less distorted site, the cis-direction, than from the trans-direction.

Both cis and trans isomers of pentamethoxyflavan-3,4-diol gave the same isopropylidene derivative, which was incorporated with acetone oxygen. Although the trans isomer was impure because of contamination with the cis isomer, the incorporation of acetone oxygen is not unexpected (*via* process (B)). However, the fact that the cis isomer incorporated acetone oxygen is very interesting and shows that the formation of carbonium ions at the 4-carbon atom and the reaction of the 4-carbonium ion with the hydroxyl group of acetone hemiketal (process (B)) exceeds the normal process (A).

The readiness of the formation of the 4-carbonium ion and of the attack of the hydroxyl group of

acetone hemiketal in the case of pentamethoxyflavan-3,4-diol, relative to the case of the tetramethoxy derivative, is not clearly explained by the resonance stabilization and the steric factors of the reaction process.

Experimental

3′,4′,5,7-Tetramethoxyflavan-3,4-diols. As has been described in the previous papers,[3] 3′,4′,5,7-tetramethoxy-3-hydroxyflavanone was reduced with sodium borohydride (in a large excess) in boiling methanol. The reaction mixture was concentrated to a small volume *in vacuo* and diluted with water. The pure trans isomer soon began to crystallize, and it separated from methanol as prisms, mp 205—206°C. On the acidification of the aqueous solution with acetic acid, the cis isomer was separated in a gelatinous form; it was changed to needles when shaken with ether, and was separated from methanol as needles, mp 165—166°C.

Thin-layer chromatography on silica-gel, using ethyl acetate saturated with water, showed that the cis and trans isomers were both pure. Silica-gel films were prepared as follows. Silica-gel (5 g) was suspended in a 2% aqueous solution of sodium borate (10 ml) and sprayed on glass plates (20 pieces 25 mm × 70 mm). Pink spots were developed by spraying of sulfuric acid and by gentle heating. The trans isomer is more mobile than the cis isomer.

3′,4′,5′,5,7-Pentamethoxyflavan-3,4-diols. The cis and trans isomers were prepared by the procedure described above. The cis isomer separated from methanol as needles, mp 195—196°C, and showed the one spot on a thin-layer chromatogram. However, the trans isomer, recrystallized repeatedly from methanol and benzene (as needles, mp 183—184°C), showed two spots. The lower spot corresponded to the spot of the cis isomer.

3′,4′,5′,5,7-Pentamethoxy-3-hydroxyflavanone-4-^{18}O. To a solution of 3-hydroxyflavanone (2.5 g) in 140 m*l* of dioxane there were added 10 m*l* of heavy water (^{18}O; 5.2%) and a trace of hydrochloric acid, and the solution was kept at 30°C for 2 days. After the removal of the solvent under reduced pressure, the remaining white crystals were separated from methanol as needles, mp 194.5—195.5°C, 2.0 g. The analysis of oxygen-18 showed an ^{18}O content of 5.1%, which was calculated from the M+2/M ratio of CO_2 (^{18}O; 5.4%, calculated from M+2/M ratio of the flavanone-4-^{18}O).

Analysis of Oxygen-18. The mass spectra of flavan-3,4-diols and isopropylidene derivatives were measured with a Hitachi RMU-6D mass spectrometer and a direct-inlet system, operating with an ionization energy of 70 eV. The M+2/M ratio was determined from the intensities of peaks by slow scanning and was corrected by considering the incorporated deuterium atoms.

To analyze oxygen-18 in the form of carbon dioxide, samples were decomposed with mercuric cyanide and mercuric chloride in a vacuum, according to the method of Rittenberg and Ponticorvo.[6]

The authors wish to thank Professor S. Oae and Dr. S. Kozuka of Osaka City University for their guidance in the analysis of oxygen-18.

BULLETIN OF THE CHEMICAL SOCIETY OF JAPAN VOL. 41 2118—2123 (1968)

Ring-butylamination of Toluquinone: Isolation of Products by TLC and an Observation of Their Reaction Course on the Basis of Molecular Reactivity Index

Ju KUMANOTANI, Fumio KAGAWA, Aizo HIKOSAKA and Kazuyuki SUGITA

The Engineering Research Institute, Faculty of Engineering, The University of Tokyo, Yayoi, Bunkyo-ku, Tokyo

(Received February 20, 1968)

The ring-butylamination of toluquinone with *n*-butyl-amine was carried out in a chloroform or ethanolic solution at room temperature or at 25.0°C with various molar ratios of the quinone to the amine (designated as Q/A). For the successful separation of each product, TLC was applied, while polarography was used for following the change in the composition of the reacting mixture as well as for measuring the amount of the amino-quinone separated from the reacting mixture by TLC. In the butylamination of toluquinone with excess butylamine (Q/A: 1/5) for 10 hr, the major products were 3,6-bis-(*n*-butylamino)-toluquinone (32%) and 2,5-bis(*n*-butylamino)-*p*-benzoquinone (8%), accompanied by a relatively large amount of unknown by-products: with a Q/A of 2/1 for 2 hr, the major products were 3- and 4-*n*-butylamino-toluquinone (17% and 21%) and 3,6-bis(*n*-butylamino)-toluquinone (3.3%) together with toluhydroquinone (47%). The quantitative formation of 3,6-bis(*n*-butylamino)-toluquinone from 3-*n*-butylamino-toluquinone or the formation of 2,5-bis(*n*-butylamino)-*p*-benzoquinone (34%) and 3,6-bis-(*n*-butylamino)-toluquinone (1%) from 4-*n*-butylamino-toluquinone was also found (Q/A: 1/4, 3 hr or 13 hr), where a faster reaction was found for the 3-isomer than for the 4-isomer under the present conditions. The pathway of the formation of each product was discussed on the basis of the calculated reactivity index of toluquinone or its butylaminated toluquinone isomers toward the amine-attacking.

It is well known that the reactions of *p*-benzoquinone and its derivatives with amines can be classified into three types: (a) the nucleophilic 1,4-addition of an amine to a quinone to give an amino-quinol which, on oxidation, yields the corresponding amino-quinone,[1] (b) the amination of a substituted quinone by replacing the labile substituent (*e.g.*, halogen and alkoxyl) already present[2] and (c) the methylamination of the methylated quinones.[3] Among these reactions, the 1,4-addition reaction of an amine to a quinone was studied by Hofmann *et al.* with aromatic amines.[4] Regarding the reaction mechanism of the 1,4-addition of amines to quinones, however, few papers have been published, though this reaction seems to involve an interesting and attractive redox reaction system, judging from the standpoint of organic chemistry as well as from that of biochemistry. Moreover, the exact mechanism of the reaction of a quinone with an amine still remaines unsolved, since, for example, the amination of *p*-benzoquinone with an amine is so fast that its kinetic treatment is impossible by the usual analytical means.

The aim of this study, which has the ultimate purpose of revealing the quinone-amine reaction mechanism, is to find a quinone-amine reaction which proceeds at a rate measurable by conventional analytical means. Therefore, the system of toluquinone and *n*-butylamine was chosen and examined for the products made in a chloroform or ethanolic solution at room temperature or at 25.0°C, while the molar ratio of toluquinone to the amine was varied. Moreover, the concept of the reactivity index calculated by means of quantum chemistry was applied to the discussion of the product distribution of the amino-quinone formed in the quinone-amine reacting system.

Experimental

Materials. Toluquinone, mp 67.3—67.8°C, was prepared by the oxidation of toluidine by the method described in the literature.[5] The *n*-butylamine, obtained commercially, was of a chemically pure grade and was used without further purification.

TLC Analysis. TLC was carried out to separate each of the reaction products obtained in the reaction of

1) See, *e.g.*, L. Fieser and M. Fieser, "Advanced Organic Chemistry," Reinhold, New York (1961), p. 853.

2) See, *e.g.*, D. Buckley, H. B. Henbst and P. Slade, *J. Chem. Soc.*, **1957**, 4891.

3) D. W. Cameron, P. M. Scott and L. Todd, *ibid.*, **1964**, 42; D. W. Cameron and P. M. Scott, *ibid.*, **1964**, 5569.

4) See, *e.g.*, A. W. Hofmann, *Jahresber. für Chemie*, **1863**, 415; T. Zincke, *Ber.*, **12**, 1641 (1879).

5) "Handbuch der präparativen Chemie," 2. Band, Ferdinand Enke, Stuttgart (1937), p. 690.

toluquinone with *n*-butylamine, prior to the identification or polarographic analysis of the products, by the ascending chromatographic technique. In this technique Silica Rider, a commercially-available silica-gel purchased from the Daiichi Pure Chemicals Co., Ltd., was used after its activation by heating at 110°C for 2 hr. The chromatography was conducted, in most cases, in a chloroform tank. In the TLC, chromatography was repeated twice in order to obtain sufficiently-separated zones.

Polarographic Study of the Butylamination of Quinone. *Polarographic Potential $E_{(1/2)}$ (vs. SCE).* This was measured at 25.0°C on a pure quinoid compound in a mixed solvent of isopropyl alcohol - aqueous phosphate buffer (pH 6.8) (1 : 1 by volume), using a Yanagimoto Polarograph PA-102. The $E_{(1/2)}$ thus measured can be used for deciding whether an alkylamino-quinoid compound is mono- or di-substituted, since, under the present quinoid system, $E_{(1/2)}$ is *ca.* −0.3 V for the mono-substituted quinone and *ca.* −0.5 V for the di-substituted quinone.

Polarographic Study of the Progress of the Alkylamination of Quinone. In the nucleophilic 1,4-addition of an amine to *p*-benzoquinone, the aminoquinol first formed yields the corresponding amino-quinone upon its oxidation with the parent quinone present in the reacting system; the latter may undergo a second amination in the same way to yield 2,5-bis(*n*-butylamino)-*p*-benzoquinone.[1] When the reaction is carried out in air, however, according to the different redox potentials of the quinone and the related amino-quinones that are participating in the reaction, there is a possibility of hydrogen abstraction with oxygen in air from the amino-hydroquinones formed in the course of the reaction. Therefore, in the polarographic studies of the reaction course of toluquinone and *n*-butylamine, the change in the composition of the reacting mixture *vs.* the reaction time was examined under various conditions for such products detectable by polarography as toluhydroquinone, toluquinone (−0.06 V), and mono- and di-butylaminated toluquinones, as well as hydrogen peroxide (−1.2 V). (None of the three possibly existing isomeric mono-butylaminated toluquinones could be detected in their mixture, nor could the di-butylaminated quinones be distinguished from each other under the present polarographic conditions.)

An example of polarographic analysis of the reacting mixture is as follows: To an ethanolic solution of toluquinone, which had been kept at 25.0°C in a water bath, was instantly added an ethanolic solution of *n*-butylamine, after which the reaction was continued under stirring for a certain time interval. During this reaction 0.1 m*l* portions of the reacting solution were pipetted out at certain time intervals and dissolved into 10.0 m*l* of an isopropyl alcohol solution; then 2.0 m*l* of the resultant solution, mixed with the same volume of the aqueous phosphate buffer (pH 6.0), was submitted to polarographic analysis.

Butylamination of Toluquinone with n-Butylamine. Derivation of 3,6-Bis(n-butylamino)-toluquinone and 2,5-Bis(n-butylamino)-p-benzoquinone by the Reaction of Toluquinone with Excess n-Butylamine. To a mixture of toluquinone (4.88 g, 40 mmol) in ethanol (100 m*l*) in an Erlenmeyer flask, *n*-butylamine (14.6 g, 200 mmol) was added drop by drop, over 30-min period at room temperature; after that the stiaring was continued for 5 hr, and the resultant solution was refrigerated for 2 days and filtered to remove violet crystals (3.4 g). This substance (1.0 g) was submitted to TLC, where the amount of the sample treated per plate (0.14×20×20 cm) was *ca.* 200 mg; a solution of this substance (200 mg) in chloroform (2 m*l*) was applied in line on the silica-gel layer and developed in a chloroform tank. After the solvent had reached the upper edge of the plate, the plate was dried in air for 30 min and then again developed with chloroform. The two separated zones (C′ and D′) were then scrapped from the plate and extracted with 10 m*l* of chloroform and then 10 m*l* of methanol; the extracts thus obtained were collected for C′ or D′, and evaporated to dryness under a reduced pressure of nitrogen to give violet crystals (C, 140 mg) and reddish crystals (D, 45 mg). These substances were recrystallizable from chloroform or ethanol.

Compound C; mp 119.7—120.7°C.

Found: C, 67.8; H, 9.3; N, 10.2%. Calcd for $C_{15}H_{24}O_2N_2$: C, 68.1; H, 9.1; N, 10.6%.

$E_{(1/2)}$, −0.53 V. R_f, 0.17.

IR in CCl_4[6]; 3355 and 3297 (m, ν_{N-H}), 1644 (m, $\nu_{C=C}$), 1613 and 1580 (s, $\nu_{C=O}$), 1502 cm^{-1} (s, amido II type).

NMR in $CDCl_3$ (see (1)): 9.05 and 8.95 τ (6 H_h), 8.50 τ (8 H_g), 7.93 τ (3 H_f), 6.87 τ (2 H_e, quartet coupled with H_g and H_a), 6.46 τ (2 H_d, quartet coupled with H_g and H_b), 4.80 τ (1 H_c) and 3.32 τ (1 H_a and 1 H_b, broadened).

Compound D; mp 163.5—164.5°C.

Found: N, 11.2%. Calcd for $C_{14}H_{22}O_2N_2$: N, 11.2%.

$E_{(1/2)}$, −0.57 V. R_f, 0.08.

IR in CCl_4[6]: 3355 (m, ν_{N-H}), 1650 (m, $\nu_{C=C}$), 1589 (s, $\nu_{C=O}$), 1503 cm^{-1} (s, amido II type).

NMR in $CDCl_3$ (see (2)): 9.07 and 8.96 τ (6 H_e), 8.44 τ (8 H_d), 6.84 τ (4 H_c, quartet coupled with H_d and H_b), 4.73 τ (2 H_a) and 3.36 τ (2 H_b, broadened).

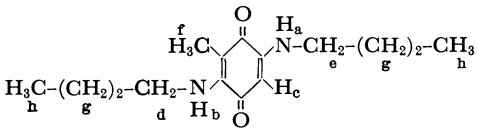

(1)

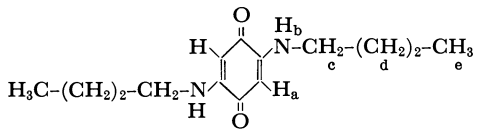

(2)

From the above results, it was concluded that Compound C is 3,6-bis(*n*-butylamino)-toluquinone and that Compound D is 2,5-bis(*n*-butylamino)-*p*-benzoquinone.

The change in the composition of the reacting mixture *vs.* the reaction time was followed polarographically for a reaction carried out at a moderate reagent concentration in an ethanolic solution; it is shown in Fig. 1.

To determine the amount of each of the di-butylaminated quinones, 1.0 m*l* of the reacting solution obtained 10 hr after the beginning of the reaction was

6) Unpublished data; a paper on the spectral data of the amino-quinoid compound will be shortly submitted for publication.

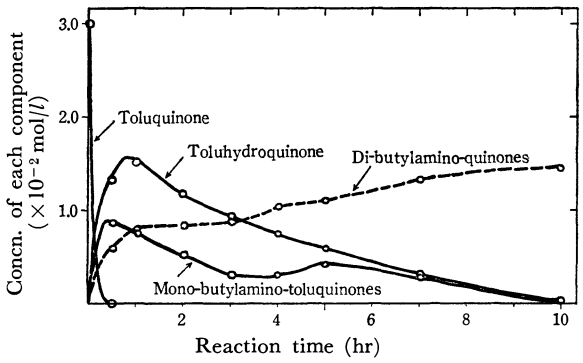

Fig. 1. Change of composition *vs.* reaction time in the reaction of toluquinone with excess *n*-butylamine (Q/A: 1/5); ethanolic solutions of toluquinone (36.6 mg, 0.3 mmol in 10 m*l*) and *n*-butylamine (1.0 m*l* of 15 vol%).

pipetted out, submitted to the TLC (thickness of the silica-gel layer: 0.6 mm), and chromatographed in a chloroform tank such as has already been described. The product (C or D) thus separated was dissolved in 5.0 m*l* or 10.0 m*l* of isopropyl alcohol to prepare a solution with a suitable concentration for the polarographic analysis; 2.0 m*l* of the resultant solution was mixed with the same volume of the aqueous phosphate buffer (pH 6.0) and submitted to the polarographic analysis. The product ratio of C to D was found to be 4/1.

Derivation of 3- and 4-n-Butylamino-toluquinone with a Q/A of 2:1. A solution of toluquinone (2.44 g, 20 mmol) in chloroform (10 m*l*) was instantly mixed with achloroform solution of *n*-butylamine (5 m*l* of 19.3 vol %) at room temperature in an Erlenmeyer flask and stirred magnetically for 1 hr, refrigerated for a day, and filtered to remove the precipitated crystals of toluhydroquinone. The resultant chloroform solution was submitted to the TLC in the same manner as has already been described, thus affording the crystals in yields of 450 mg (A′) and 290 mg (B′); 30 m*l* of dried ether were used for the extraction (200 mg of the sample were treated per plate).

The A′ (20—30 mg), shown by its polarogram to consist of two components, A and C, was dissolved in a small amount of chloroform, applied on the silica-gel layer (thickness, 0.6 mm) and chromatographed with a mixed solvent of ethyl acetate - carbon tetrachloride (1 : 15 by volume). The chromatogram thus obtained was again developed in the same solvent tank to give pure A and C. The purity of the substance, A or C, was confirmed by a.c. polarography. A was isolated as a sublimate from its mixture with Compound C by heating the mixture under reduced pressure. B gave only one peak in its polarogram. The chemical and physical constants of the compounds, A and B, are shown below.

Compound A recrystallizable from *n*-hexane: mp 63.6—65.6°C.

Found: N, 7.2%; mol wt (v.p.o.), 207. Calcd for $C_{11}H_{15}O_2N$: N, 7.3%; mol wt 193.

$E_{(1/2)}$, −0.30 V. R_f, 0.15.

UV: λ_{max}^{EtOH} 214 (ε 28200), 275 (ε 12200), 485 mμ (ε 2740).

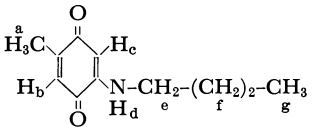

(3)

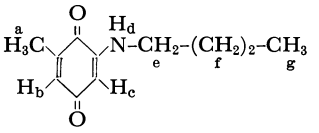

(4)

NMR in $CDCl_3$ (see (3)); 9.05 and 8.95 τ(3 H_g), 8.42 τ(4 H_f), 7.95 τ(3 H_a, doublet coupled with H_b[7]), 6.90 τ(2 H_e, quartet coupled with H_d and H_f), 4.60 τ(H_c), 4.46 τ(H_d), broadened), 3.60 τ(H_b, quartet coupled with H_a).

Compound B recrystallizable from *n*-hexane: mp 72.2—73.3°C.

Found: C, 67.6; H, 7.8; N, 7.2%; mol wt (v.p.o.), 189. Calcd for $C_{11}H_{15}O_2N$: C, 68.4; H, 7.8; N, 7.3%; mol wt, 193.

$E_{(1/2)}$, −0.28 V. R_f, 0.07.

UV: λ_{max}^{EtOH} 218 (ε 22800), 278 (ε 9150), 485 mμ (ε 2940).

NMR in $CDCl_3$ (see (4)); 9.05 and 8.93 τ(3 H_g), 8.48 τ(4 H_f), 7.98 τ(3 H_a, doublet coupled with H_b), 6.88 τ(2 H_e, quartet coupled with H_d and H_f), 4.59 τ (H_c, doublet (J=2.5 cps) coupled with H_b[8]), 4.38 τ (H_d, broadened), 3.58 τ(H_b, quartet or quintet coupled with H_a and H_c).

Compound C: $E_{(1/2)}$, −0.53 V. Its infrared spectrum was in agreement with that of the authentic sample given in the preceding section.

According to the study made by Yates *et al.*[9] of the out-of-plane bending of the C-H of *p*-benzoquinone and its derivatives by infrared spectroscopy, it became evident that neither A nor B, each having a characteristic absorption band at 880 cm^{-1} or 894 cm^{-1} in CS_2 respectively, was identical with the 2,3-disubstituted *p*-benzoquinone isomer. Upon determining which compound, A or B was identical with one of the two possible isomers, 3- and 4-*n*-butylamino-toluquinone, we attempted to acertain the difference between the wave numbers of the two carbonyl groups within a molecule of each 3- and 4-*n*-butylaminotoluquinone. The results thus obtained were correlated with the expected $\Delta\nu_{C=O}$, originating from the different " aufrichtung " effect of the carbonyl group, which was given by the different hyperconjugation and the electron-donating effects of the existing methyl group or the different inductomeric effect of the *n*-butylamino group already present; (5) and (6) show 3-*n*-butylamino-toluquinone, and (7) and (8), 4-*n*-butylamino-toluquinone.

7) E. R. Wagner, R. D. Moss and R. M. Brooker, *Tetrahedron Letters*, **47**, 4236 (1965).
8) J. H. Day and A. Jaochim, *J. Org. Chem.*, **30**, 4108 (1965).
9) P. Yates, M. I. Ardao and L. F. Fieser, *J. Am. Chem. Soc.*, **78**, 652 (1956).

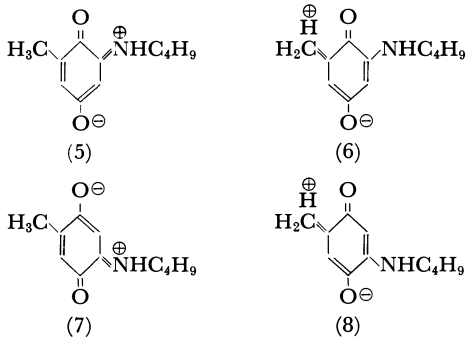

Thus, on the basis of a comparison between the observed facts that $\Delta\nu_{C=O}$ is 36 cm^{-1} for A and 47 cm^{-1} for B, it is concluded that Compound A is 4-*n*-butylamino-toluquinone and Compound B is 3-*n*-butylamino-toluquinone.

This is in agreement with the NMR spectra.

The change in the composition of the reacting mixture *vs.* the reaction time was followed polarographically (see Fig. 2).

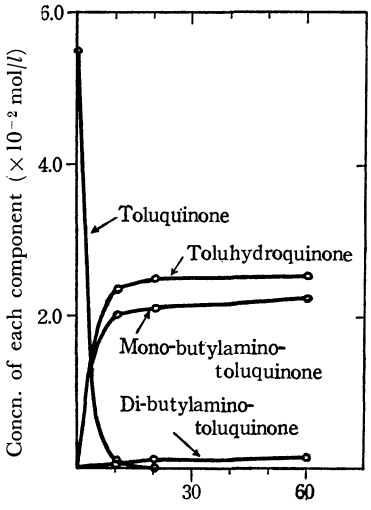

Fig. 2. Change of composition *vs.* reaction time in the reaction of toluquinone with *n*-butylamine-(Q/A: 2/1); a solution of toluquinone (36.6 mg, 0.3 mmol in ethanol (5.0 m*l*) was reacted with an ethanolic *n*-butylamine solution (0.5 m*l* of 3.0 vol%)

To determine the amount of each of the butylamino-toluquinones, 1.0 m*l* of the reacting solution obtained was, 2 hr after the beginning of the reaction, pipetted out and submitted to the TLC (thickness, 0.6 mm). Each of the substances, A′ and B′ extracted with 30 m*l* of ether, was submitted to polarographic analysis in the same way as has been described before; the A: B: C ratio was found to be 51 : 41 : 8.

Derivation of 3,6-Bis(n-butylamine)-toluquinone by the Reaction of 3-n-Butylamino-toluquinone and n-Butylamine with a Q/A of 1/4. A solution of 3-*n*-butylamino-toluquinone (63.7 mg, 0.33 mmol) in ethanol (10 m*l*) was instantly mixed with an ethanolic *n*-butylamine solution (1.0 m*l* of 12 vol%) at 25.0°C, stirred for 3 hr, and then submitted to the TLC on a silica-gel layer such as has been described for the mono-butylamination of toluquinone. The major separated zone was extracted with 5.0 m*l* of chloroform and then 5.0 m*l* of methanol; the extracts thus obtained were combined, and the solution was submitted to evaporation to dryness under reduced nitrogen pressure to give crystals as the residue; recrystallization from chloroform or ethanol gave violet crystals; mp 119.7—120.7°C; $E_{(1/2)}$, −0.53 V; R_f, 0.17; (Found: C, 68.2; H, 9.2; N, 10.3%). The identity of this compound with 3,6-bis(*n*-butylamino)-toluquinone was also established by its infrared spectral agreement with an authentic sample already prepared in the reaction of toluquinone with excess amine.

The relation obtained polarographically regarding the change in the reacting mixture *vs.* the reaction time is shown in Fig. 3.

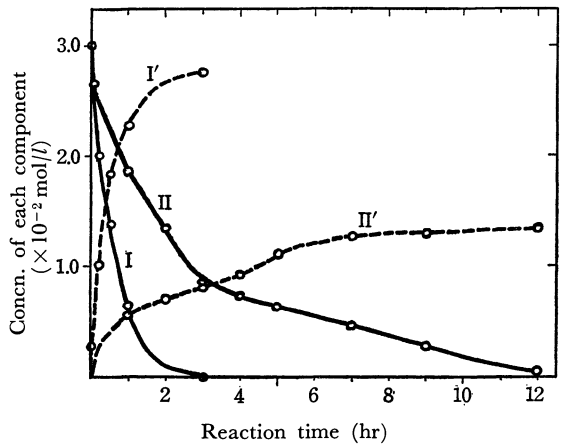

Fig. 3. Reaction of 3-*n*-butylamino-toluquinone (I) and 4-*n*-butylamino-toluquinone (II) with *n*-butylamine; (I) ethanolic solutions of 3-aminoquinone (63.7 mg, 0.33 mmol in 10 m*l*) and *n*-butylamine (1 m*l* of 12 vol%), (II) ethanolic solutions of 4-aminoquinone (28.9 mg, 0.15 mmol in 5 m*l*) and *n*-butylamine (0.5 m*l* of 12 vol%).

Upon the measurement of the yield, a 1.0 m*l* portion of the reacting solution pipetted out was submitted to TLC similar as that used in the preceding section; the yield of this substance was 95%.

Derivation of 2,5-Bis(n-butylamino)-p-benzoquinone and 3,6-Bis(n-butylamino)-toluquinone by the Reaction of 4-n-Butylamino-toluquinone with Excess n-Butylamine. A solution of 4-*n*-butylamino-toluquinone (28.9 mg, 0.15 mmol) in ethanol (5.0 m*l*) was reacted with an ethanolic *n*-butylamine solution (0.5 m*l* of 12 vol%) for 13 hr such as has already been described in connection with other reactions, and a half volume of the reacting solution was applied in line on the silica-gel layer (thickness: 0.6 mm) and chromatographed in the chloroform tank in the manner already described. Then, each of the violet- and pink-colored zones obtained was extracted with 5 m*l* of chloroform and then 5 m*l* of methanol. The extracts thus obtained gave violet- and pink-colored crystals after the removal of the solvent; the infrared spectra were identical with those of 3,6-bis-(*n*-butylamino)-toluquinone and 2,5-bis(*n*-butylamino)-*p*-benzoquinone respectively. The yield of each of these

products was measured by submitting a 1.0 ml portion of the remaining half volume of the reacting solution to an analysis combining TLC and polarography, as had already been used for the other cases; the yields of 3,6-bis-(*n*-butylamino)-toluquinone and 2,5-bis (*n*-butylamino)-*p*-benzoquinone were 1.0% and 34% respectively.

The change in the composition of the ethanolic reacting mixture *vs.* the reaction time was followed polarographically; it is plotted in Fig. 3.

Results and Discussion

Correlation of Each of the Butylaminated Quinones. In the reaction of toluquinone with an ethanolic solution of excess *n*-butylamine, the major butylaminated quinone derivatives were 3,6-bis(*n*-butylamino)-toluquinone (32% for the toluquinone used) and 2,5-bis(*n*-butylamino)-*p*-benzoquinone (8%), together with a relatively large amount of by-products. Upon the determination of the reaction course producing each of the butylaminated toluquinones, the reaction of toluquinone with the amine was carried out with a Q/A molar ratio of 2/1 ; as expected, this led to the formation of mono-butylaminated toluquinones, the products being toluhydroquinone (47%), 3- and 4-*n*-butylamino-toluquinone (17% and 21%), and 3,6-bis-(*n*-butylamino)-toluquinone (3.3%).

Among these products, 3,6-bis(*n*-butylamino)-toluquinone can be considered to be made through either 3- or 6-*n*-butylamino-toluquinone. It will be clearly explained below.

Further in the reaction of 3-*n*-butylamino-toluquinone with an ethanolic solution of *n*-butylamine (Q/A: 1/4), 3,6-bis(*n*-butylamino)-toluquinone was prepared approximately quantitatively, while, with 4-*n*-butylamino-toluquinone (Q/A: 1/4), 2,5-bis(*n*-butylamino)-*p*-benzoquinone (34%) and a trace of 3,6-bis(*n*-butylamino)-toluquinone were obtained, with a complete consumption of the amino-toluquinone. The former was, presumably, a result of the methylamination mechanism already proposed by Cameron *et al.*[3] for the methylamination of toluquinone with methylamine; the latter found by the TLC technique, was readily assumed to be produced by such a complex reaction as is illustrated by the formation of larger amounts of by-products, *e.g.*, through the redistribution of the butylamino-residue of the amino-quinones between the products existing in the reaction course.

Concerning the alkylamination of toluquinone or its derivation with alkylamine, the formation of 3,6-bis(methylamino)-toluquinone[3,10,11] from toluquinone and that of 2,5-bis(methylamino)-*p*-benzoquinone from 4-methoxyl-toluquinone[3,10] by reaction with methylamine have been reported. However, in the former case the pathway leading to the amino-quinone has not yet been established, and in the latter case 4-methylamino-toluquinone has been proposed as an intermediate on the basis of no evidence. The results obtained by the present authors for the reactions of *n*-butylamine and toluquinone or its amino-derivatives give exact evidence for the pathway of the alkylamination of toluquinone with an amine.

Polarographic Study of the Progress of the Reaction of Toluquinone with *n*-Butylamine. In the reaction of *n*-butylamine with toluquinone (Q/A: 2/1) it was revealed that the reaction was saturated within 20 min (see Fig. 2). The major products were mono-butylaminated toluquinones plus a minor quantity of dibutylaminated quinones; no detectable amount of hydrogen peroxide was found, indicating that the hydrogen-abstraction from the alkylamino-hydroquinone was made first with the parent quinone, not with oxygen in air.

With a Q/A of 3/2, due to the decrease in the amount of the mono-butylaminated toluquinone once formed through its further reaction, the reaction product obtained 2 hr after the beginning of the reaction was found to be contaminated with relatively large amounts of mono- and dibutylaminated quinones; this procedure is, then, unsuitable for the selective preparation of either mono- or di-butylaminated toluquinone in an excellent yield. Under the present conditions, the formation of hydrogen peroxide was detected by observing a polarographic wave corresponding to that of hydrogen peroxide at -1.2 V.

With a Q/A of 1/5, as may be seen from Fig. 1, the step-by-step butylamination of toluquinone to 3,6-bis(*n*-butylamino)-toluquinone through the well-known reaction course, the participation of toluquinone in the further reaction made through the air-oxidation of toluhydroquinone accumulated at the early stage of the reaction, and the saturation of the product distribution 10 hr after the beginning of the reaction can clearly be seen; the fact that the conversion curve observed on the rate of mono-butylaminated toluquinone shows two upward peaks indicates the complexity of the reaction. Of course, in this system the formation of hydrogen peroxide was also found polarographically.

An Observation of the Reactivity of Toluquinone toward *n*-Butylamine in Terms of the Reactivity Index Calculated. In the methylamination of *p*-benzoquinone leading to the formation of 2,5-bis(methylamino)-*p*-benzoquinone, it was proposed by Cameron *et al.*[3] that the first step is the nucleophilic 1,4-addition of the amine to the quinone, thus giving monomethylamino-hydroquinone. Then, as a parameter of the reactivity of toluquinone toward the attack by *n*-butylamine, the reactivity index was calculated for toluquinone and its mono-butylamino derivatives by utilizing the ω-technique in a simple linear combination of

10) F. Fichter, *Ann.*, **361**, 400 (1908).
11) W. K. Anslow and H. Raistrick, *J. Chem. Soc.*, **1939**, 1447.

TABLE 1. REACTIVITY INDEX FOR THE NUCLEOPHILIC SUBSTITUTION

Compound	Superdelocalizability $S_r^{(N)}$ (Formal charge Q_r) Position			
	1	3	4	6
Toluquinone	0.9724 (+0.087)	0.9614 (+0.064)	1.0202 (+0.070)	0.8825 (+0.043)
3-Alkylaminotoluquinone	0.9796 (+0.078)	0.9924 (+0.084)	0.8627 (+0.018)	1.0107 (+0.044)
6-Alkylaminotoluquinone	0.8848 (+0.041)	1.1817 (+0.067)	1.0910 (+0.059)	0.9790 (+0.064)
4-Alkylaminotoluquinone	1.1125 (+0.090)	0.8017 (+0.013)	1.0551 (+0.090)	0.8772 (+0.033)

the atomic orbital theory, using the Streitwieser heteroatom parameter.[12] (The calculations were performed on the HITAC 5020 Computer, in the Computer Center, The University of Tokyo; see Table 1.)

Ring Butylamination. The preferential attack at the 3 or 4 position of toluquinone with *n*-butylamine, and the subsequent amine-attack at the para-position of the first substituted amino group on the quinoid ring, can be readily predicted from their reactivity index, presented in Table 1. (The ring carbon to which the methyl or alkylamino group is linked is not considered, because of its steric effect toward the amine-attack.)

Moreover, it is obviously shown that a greater contribution by 3-*n*-butylamino-toluquinone than by the 6-isomer to the formation of 3,6-bis(*n*-butylamino)-toluquinone can be considered. The participation of 6-*n*-butylamino-toluquinone, of course, can not always be obviated, since, if this amino-quinoid compound were an intermediate in the present reaction course, the reactivity index of this compound toward butylamination would be relatively large.

Side-chain Butylamination. In order to elucidate the reactivity of the substituted methyl group on the quinoid ring toward the methyl-butylamination, the reactivity indices of the three possible monobutylaminated toluquinone isomers were compared; the formal charge or superdelocalizability calculated for the three isomers (at 1 position) shows that the carbon atom of the quinoid ring to which the methyl group is linked is most positive, causing the hydrogens of the methyl group to be more positive and then to undergo the formation of quinone methide readily, followed by methyl-butylamination.

In comparison with those reactivty indices (see Table 1) calculated for the three mono-alkylaminated toluquinone isomers, a larger reactivity for the methyl-butylamination can be predicted for the 4-alkylamino-toluquinone; this is in agreement with the experimental result of the preferential methyl-butylamination of 4-*n*-butylamino-toluquinone, whereas 3-*n*-butylamino-toluquinone could not be methyl-butylaminated and was converted quantitatively into 3,6-bis(*n*-butylamino)-toluquinone.

12) A. Streitwieser, Jr., *J. Am. Chem. Soc.*, **82**, 4123 (1960), A. Streitwieser, Jr. and P. M. Nair, *Tetrahedron*, **1959** 149.

BULLETIN OF THE CHEMICAL SOCIETY OF JAPAN VOL. 41 2124—2128 (1968)

Reactions of *N,N'*-Dichlorobarbital and Related Compounds with Organic Compounds*1,*2,*3

Yoshio Otsuji, Tokuyuki Kuroda and Eiji Imoto

Department of Applied Chemistry, Faculty of Engineering, University of Osaka Prefecture, Sakai-shi, Osaka

(Received February 28, 1968)

N,N'-Dichlorobarbital (NDCB) reacted as a highly-reactive oxidizing or chlorinating reagent with ether, aldehyde, ketone, olefin and toluene. NDCB also showed a stereospecific chlorination of *d*-camphor, giving exclusively *exo*-3-chloro-*d*-camphor, and one of chloestanone, giving 2β-chlorocholestanone in part. The reactivities of a variety of *N*-halo compounds were compared and discussed in terms of the polarographic reduction potentials of the N-halogen bond in the compounds.

N-Halogenoimides have been known as effective halogenating or oxidizing reagents for olefins, alcohols and carbonyl compounds.[1] In the past, attention has been paid mostly to *N*-bromosuccinimide (NBS) because of its accessibility.[1] However, the usefulness of other *N*-halo compounds as reagents for organic syntheses seems to be open for further investigation.

During the course of our studies of the chemistry of barbital derivatives, we have found that *N,N'*-dichlorobarbital (NDCB) is a reactive reagent for organic compounds. NDCB has been synthesized by Ziegler *et al.* and found to be effective for the halogenation of olefins.[2] However, the other chemical properties of NDCB have not been much elucidated.

This paper will deal with the reactions of NDCB with a variety of organic compounds. A comparison of the reactivity of NDCB with those of other *N*-halo compounds will also be made in the light of the polarographic reduction potentials.

Results and Discussion

Reactions of NDCB with Organic Compounds. When NDCB was added to tetrahydrofuran at room temperature, a vigorous reaction took place. The product isolated after an acid-catalyzed hydrolysis was 3-hydroxybutyraldehyde.

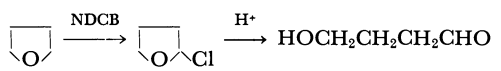

A similar vigorous reaction was also observed in carbon tetrachloride at room temperature, but no reaction took place with NBS in carbon tetrachloride even at the reflux temperature.

NDCB reacted smoothly with toluene under reflux to give benzyl chloride in a high yield both in the absence of a solvent and in carbon tetrachloride. NBS did not react with toluene at all under these conditions. These results clearly demonstrate that NDCB is a reagent more reactive than NBS. The results are summarized in Table 1.

Benzaldehyde readily reacted with both NDCB and NBS to form benzoyl chloride and bromide reaspectively. The reaction of NDCB with excess butanol without a solvent afforded a mixture of *n*-butyraldehyde (47%) and *n*-butyric acid (16%), plus a trace of butyl butyrate, while the reaction in carbon tetrachloride yielded butyl butyrate as the main product, along with traces of butyraldehyde and butyric acid. With NBS, butyl butyrate was obtained as the main product irrespective of the presence or absence of carbon tetrachloride. Butyl butyrate would be obtained by the oxidation of the hemiacetal (**1**), which had been produced by the reaction of butyraldehyde and butanol, with *N*-halo compounds.

$$C_3H_7CHO + C_4H_9OH \rightarrow \underset{\mathbf{1}}{C_3H_7CH(OH)OC_4H_9}$$

$$\mathbf{1} + \text{NDCB or NBS} \rightarrow C_3H_7CO_2C_4H_9$$

Butyraldehyde, when oxidized with NDCB and NBS, usually gave butyric acid in a relatively high yield. However, when NDCB was allowed to react with butyraldehyde in the absence of a solvent at room temperature, a vigorous reaction took place to give a mixture of butyric acid and a condensation product, 2-ethyl-2-hexenylaldehyde, in a molar

*1 Part XII of a series on "Reactivities of the Heterocyclic Compounds."

*2 Part XI: Y. Ueno, S. Asakawa and E. Imoto, *Nippon Kagaku Zasshi* (*J. Chem. Soc. Japan, Pure Chem. Sect.*), **89**, 101 (1968).

*3 Presented at the 20th Annual Meeting of the Chemical Society of Japan, Tokyo, April, 1967.

1) For example, L. Horner and E. H. Winkelmann, "Newer Methods of Preparative Organic Chemistry," Vol. 3, ed. by W. Foerst, Academic Press, New York (1964), p. 151.

2) K. Ziegler, A. Späth, Eschaaf, W. Schumann and E. Winkelmann, *Ann.*, **551**, 80 (1942).

TABLE 1. PRODUCTS OBTAINED BY THE REACTIONS OF NDCB AND NBS WITH ORGANIC COMPOUNDS

Compound	NDCB[a]			
	No Solvent	Yield (%)	In CCl_4	Yield (%)
Tetrahydrofuran	3-Hydroxybutyraldehyde	51	3-Hydroxybutyraldehyde	21
Toluene	Benzyl chloride	72	Benzyl chloride	—
Benzaldehyde	Benzoyl chloride	96	Benzoyl chloride	76
Butanol	Butyraldehyde	47	Butyraldehyde	trace
	Butyric acid	16	Butyric acid	trace
	Butyl butyrate	trace	Butyl butyrate	29
Butyraldehyde	Butyric acid	58	Butyric acid	74
	2-Ethyl-2-hexenylaldehyde	37		

Compound	NBS[b]			
	No Solvent	Yield (%)	In CCl_4	Yield (%)
Tetrahydrofuran	———		None[c]	
Toluene	None[c]		None[c]	
Benzaldehyde	Benzoyl bromide	—	Benzoyl bromide	—
Butanol	Butyraldehyde	7	Butyraldehyde	trace
	Butyric acid	trace		
	Butyl butyrate	44	Butyl butyrate	12
Butyraldehyde	Butyric acid	65	———	

a) The yield was calculated on the basis that two chlorine atoms in NDCB were paticipated in the reaction as active halogen atoms.
b) The yield was calculated on the basis that one bromine atom in NBS was participated in the reaction.
c) The starting material was recovered.

ratio of 3 : 2. A similar condensation was also observed in cyclohexanone; it will be described later.

These results suggest that NDCB reacts in two distinct ways, depending on the reaction medium. In heterogeneous media (in non-polar solvents such as carbon tetrachloride) the reaction chiefly proceeds in homolytic fashion, causing free radical halogenation. On the other hand, in homogeneous media (in polar solvents) the reaction proceeds in heterolytic fashion, the N–Cl bond reacting in the polarized form and behaving like a Lewis acid. A tendency of this kind, though to a lesser extent, has also been observed for NBS.[1]

Stereochemistry. The stereochemistry of halogenation with NDCB was studied, taking *d*-camphor and cholestanone as substrates. *d*-Camphor has been found to be halogenated with molecular chlorine to give *endo*-3-chloro-camphor (**2**)[3] exclusively. However, when an equimolar mixture of *d*-camphor and NDCB was heated at 140°C for 40 min, *exo*-3-chlorocamphor (**3**) was obtained in a 95% yield. The similar treatment of *d*-camphor with NBS gave *endo*-3-bromocamphor in an 80% yield.

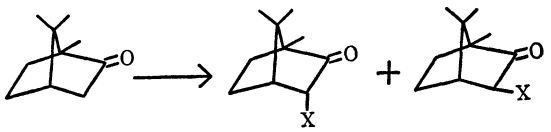

	2	**3**
NDCB	0	95%
NBS	80%	0

An abnormal stereochemistry in the halogenation with NDCB was also found for cholestanone. The literature has shown that the chlorination of cholestanone can be carried out by passing chlorine gas into the solution of the compound in carbon tetrachloride or acetic acid, affording the 2α-chloro-derivative exclusively.[4] However, when a mixture of NDCB and cholestanone was heated at 140°C for 30 min, a mixture consisting of 3 parts of 2α-chloro- and 4 parts of 2β-chloro-derivatives was obtained in a total yield of 73%.

These products were nicely separated by column chromatography on alumina, using chloroform as an eluent, and were identified by the measurement of their melting points, infrared spectra, and optical rotations, which were all in satisfactory agreement

3) S. H. Harper, "Chemistry of Carbon Compounds," Vol. II, ed. by E. H. Rodd, Elsvier Publishing Company, New York, N. Y. (1953), p. 602.

4) a) J. J. Beereboom, C. Djerassi, D. Ginsburg and L. F. Fieser, *J. Am. Chem. Soc.*, **75**, 3500 (1953); b) B. Ellis and V. Petrow, *J. Chem. Soc.*, **1953**, 3869.

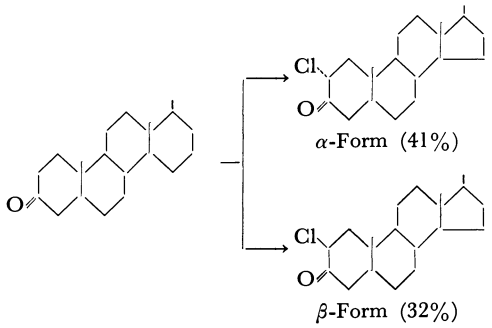

with the literature values. Unfortunately, we can not reasonably explain the abnormal stereochemistry observed in the reaction of NDCB.

Polarographic Reduction Potentials of *N*-Halo Compounds. There have been found many *N*-halo compounds which can potentially serve as halogenating or oxidizing reagents for organic compounds. The reactivities of these *N*-halo compounds can primarily be characterized by the polarity of the *N*-halogen bonds, which in turn determines the reductivity of those bonds. The polarographic half-wave potential seems to be a good index for the reductivity.

Very few polarographic data of *N*-halo compounds have been published. Recently, however, *N*-bromosuccinimide has been polarographically investigated in detail in water by Nagai and Matsuda.[5] The polarograms obtained have shown the appearance of complicated waves due to the hydrolysis of *N*-halo compounds. For this reason, we measured the half-wave potentials for *N*-halo compounds in dimethylformamide (DMF). Figure 1 shows the

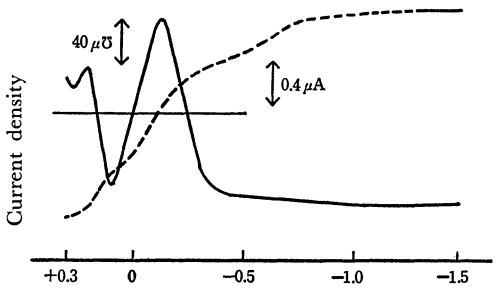

Fig. 1. Polarogram of *N,N'*-dichlorobarbital in DMF at 20°C.
—— AC Polarogram
---- DC Polarogram

polarogram for NDCB. The peaks in the AC polarogram were in accordance with the $E_{1/2}$ values obtained by DC polarography, and the shape of the polarogram was reproducible in three experiments. These results indicate that the waves are attributable to the true electrochemical reduction. Barbital itself did not show the reduction waves above −1.5 V. The wave at −0.12 V would seem, therefore, to be the result of the reduction of the N–Cl bond. Other *N*-halo compounds behaved similarly. The $E_{1/2}$ values (V) measured at 20°C were as follows: *N,N',N''*-trichloroisocynanuric acid (−0.07), NDCB (−0.12), *N*-chlorophthalimide (−0.15), *N*-chlorosuccinimide (−0.21), and NBS (−0.26). These values indicate that the polarity of *N*-halo compounds decreases in the above order.

Correlation between the Reactivities of *N*-Halo Compounds and Their $E_{1/2}$ Values. *Rractions of Cyclohexanone with N-Halo Compounds.* It is reasonable to assume that, if the more polar N–halogen bond is contained in the *N*-halo compound, a much higher yield would be expected in the condensation product, since the condensation should be a polar reaction which could sometimes be catalyzed by Lewis acid.[6] On the basis of this assumption, the reactions of cyclohexanone with several *N*-halo compounds were studied. The treatment of cyclohexanone with the *N*-halo compounds in the absence of a solvent afforded 2-halogeno-cyclohexanone and 2-(1-halogenocyclohexyl)cyclohexanone (**4**) in yields depending on the *N*-halo compounds used, as is represented in Table 2.

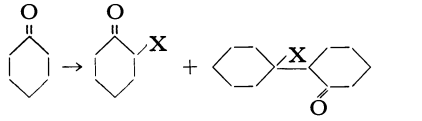

4

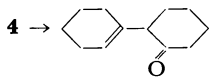

5

The structure of **4** was established as follows: **4** was converted to 2-(1-cyclohexenyl)cyclohexanone (**5**) by treatment with pyridine. The properties of **5** thus obtained were identical with those of

Table 2. Products obtained by the reactions of *N*-halo compounds with cyclohexanone

N-Halo compound	Yield of the product (%) 2-Halogeno-cyclohexanone	2-(1-Halogeno-cyclohexyl)-cyclohexanone
N,N',N''-Trichloro-isocyanuric acid	39	61
N,N'-Dichlorobarbital	50	45
N-Bromosuccinimide	75	0

* The yield was calculated on the basis that three chlorine atoms in *N,N',N''*-trichloroisocyanuric acid, two chlorine atoms in NDCB, and one bromine atom in NBS were participated in the reactions.

5) T. Nagai and T. Matsuda, *Nippon Kagaku Zasshi* (*J. Chem. Soc. Japan, Pure Chem. Sect.*), **88**, 66 (1967).

6) J. Reese, *Ber.*, **75**, 384 (1942).

5 prepared by the method described in the literature.[7]

Table 2 shows that *N,N',N''*-trichloroisocyanuric acid, which contains the most polar N–Cl bond, produced the condensation product in the highest yield. The second highest yield of the condensation product was obtained with NDCB, which has less polarity in the N–Cl bond. The weakest polar compound, NBS, did not afford the condensation product in a detectable yield.

Halogenation of Cyclohexene. The halogenation of cyclohexene with *N*-halo compounds can be a good measure of the polarity of the N–halogen bond in the compounds. The compounds which contain more polar N–halogen bond would facilitate the addition of halogen to the double bond over an allylic halogenation which proceeds through a free radical mechanism. If the *N*-halo compound contains a less polar N–halogen bond, the allylic halogenation would be favored over the addition reaction. This expectation was verified by those of our experiments shown in Table 3. The reaction of NDCB with cyclohexene afforded a mixture of 3-chlorocyclohexene, the product due to the radical substitution and 1,2-dichlorocyclohexane, the product due to the polar addition, in the molar ratio of 53 : 14. However, with the less polar *N*-halo compound, NBS, the sole product isolated was 3-bromocyclohexene, which was the product due to the free radical substitution. Thus, we may suppose that the polarity of the N–halogen bond which could be estimated by the polarographic measurement, would provide a good method for the systematization of the reactivities of *N*-halo compounds.

Table 3. Products obtained by the reactions of *N*-halo compounds with cyclohexene

Product	Yield of product (%)*		
	NDCB	NCS	NBS
3-Chlorocyclohexene	53	42	—
3,6-Dichlorocyclohexene	trace	21	—
1,2-Dichlorocyclohexane	14	4	—
3-Bromocyclohexene	—	—	68
3,6-Dibromocyclohexene	—	—	17
1,2-Dibromocyclohexane	—	—	—

* The yield was calculated on the basis that two chlorine atoms in NDCB, one chlorine atom in NCS and one bromine atom in NBS were participated in the reactions.

Experimental

All melting points are uncorrected. The infrared spectra were recorded with a Hitachi EPI-S_2 infrared spectrometer. The glc data were obtained using a Yanagimoto GCG-5 DH gas chromatograph. Microanalyses were performed with a Yanagimoto MT-1 CHN Corder. The optical rotations were measured with a Perkin-Elmer 141 Polarimeter.

Materials. *N*-Bromosuccinimide (NBS), mp 174—175°C,[1] *N*-chlorosuccinimide (NCS),[8] mp 148—149°C, *N*-chlorophthalimide, mp 183°C,[1] and *N,N',N''*-trichloroisocyanuric acid, mp 245°C (dec.),[9] were prepared by the methods described in the literature and were used after purification by recrystallization from benzene.

N,N'-Dichlorobarbital (NDCB) was prepared by passing chlorine gas into an aqueous solution of barbital at room temperature. After the chlorine had been saturated, the reaction mixture was cooled and filtered. The solid thus obtained was washed with water and recrystallized from benzene, mp 125—127°C. The yield was almost quantitative.

Found: C, 38.19; H, 3.64; N, 11.29%. Calcd for $C_8H_{10}O_3N_2Cl_2$: C, 37.97; H, 3.98; N, 11.07%

The other reagents were of a commercial grade and were used after purification by recrystallization or distillation.

Proof of Structure and Determination of Yields of Products. The reaction products were usually identified by a comparision of their infrared spectra with those of the respective authentic samples. For liquid products, the retention times in glc were compared with those of the authentic samples. For solid products, mixture-melting point examinations and microanalyses were also performed.

The yields of products were determined by glc analyses or by measurement of the weights of the products.

The glc analysis was used for toluene, tetrahydrofuran, butanol, cyclohexene, butyraldehyde and cyclohexanone.

In the cases of carbonyl compounds, they were also converted to their 2,4-dinitrophenylhydrazones and weighed.

Preparation of the Authentic Samples. Authentic samples of butyl butyrate,[10] 2-chlorocyclohexanone,[11] 2-bromocyclohexanone,[12] 3-chlorocyclohexene,[2] 3-bromocyclohexene,[2] 1,2-dichlorocyclohexane,[13] and 2-(1-cyclohexenyl)cyclohexanone[5] were prepared according to the procedures described in the literature. 2-Ethyl-2-hexenylaldehyde was kindly provided by the Kyowa Hakko Kogyo Co., Ltd.

General Procedure for Reactions with NDCB. *In the Absence of a Solvent.* To an excess organic compound (20—30 g) NDCB (5—10 g) was added at room temperature with shaking. The reaction usually proceeded smoothly and exothermally. The mixture was then warmed for 30 min, if necessary. After standing for 30 min, the mixture was cooled and then filtered to remove the precipitated barbital. The filtrate was distilled, and the distillate was subjected to analysis.

In Carbon Tetrachloride. A saturated solution of 10 g of NDCB in carbon tetrachloride was added to a solution of 10 g of an organic compound in 50 m*l* of the same

7) W. S. Rapson, *J. Chem. Soc.*, **1941**, 16.

8) E. L. Hirst and A. K. MacBeth, *ibid.*, **121**, 2174 (1922).

9) H. J. Schmidt and K. Geiersberger, German Pat. 1141641 (1962).

10) G. R. Robertson, "Organic Syntheses," Coll. Vol. 1, p. 138 (1941).

11) M. S. Newman, M. D. Farbman and H. Hipsher, "Organic Syntheses," Coll. Vol. 3, p. 188 (1955).

12) P. Z. Bedoukian, *J. Am. Chem. Soc.*, **67**, 1430 (1945).

13) S. Kharasch and H. C. Brown, *ibid.*, **61**, 3432 (1939).

solvent at room temperature. The mixture was then usually heated at reflux for 1 hr and cooled. The precipitated barbital was separated by filtration, the filtrate was concentrated to remove the solvent, and then the residue was distilled. The distillate was subjected to analysis.

General Procedure for Reactions with NBS. *In the Absence of a Solvent.* To an excess organic compound (10—15 g) NBS (2 g) was added at room temperature with shaking, and then the mixture was refluxed for several hours under nitrogen. (In the reactions with NBS, much more severe reaction conditions were required for the completion of reactions than those used for the reactions with NDCB.) After the mixture had then been cooled, succinimide was separated as a solid and removed by filtration. The filtrate was distilled, and the distillate was subjected to analysis.

In Carbon Tetrachloride. A solution of 2 g of an organic compound in 10 m*l* of carbon tetrachloride was added to a solution of 2 g of NBS in 20 m*l* of carbon tetrachloride at room temperature. After the mixture had then been refluxed for several hours and cooled, the solvent was evaporated. The residue was distilled, and the distillate was subjected to analysis. Succinimide was usually recovered from the residue as a solid.

Reactions of Camphor. *With NDCB.* A mixture of 5 g of NDCB and 5 g of *d*-camphor was heated at 140°C for 40 min and then sublimed at 80°C/5 mmHg. Sublimation gave 5.8 g (95%) of *exo*-3-chlorocamphor, mp 117—118°C; $[\alpha]_D^{20}$ +47.7° (*c* 0.52, C_2H_5OH) (lit., mp 117°C,[3] $[\alpha]_D^{20}$ +35°[3] (*c* 10, C_2H_5OH)).

Found: C, 60.39; H, 8.05%. Calcd for $C_{10}H_{15}OCl$: C, 60.77; H, 7.81%.

With NBS. A mixture of 4 g of NBS and 4 g of *d*-camphor was treated in the manner described above. The sublimation of the mixture at 60—70°C/4 mmHg afforded 4.1 g (80%) of *endo*-3-chlorocamphor, mp 75—77°C, $[\alpha]_D^{18}$ +117.0° (*c* 0.52, benzene) (lit., mp 77°C,[3] $[\alpha]_D^{18}$ +117.1°[3] (*c* 10, benzene)).

Found: C, 51.98; H, 6.54%. Calcd for $C_{10}H_{15}OBr$: C, 52.01; H, 6.46%.

Reaction of Cholestanone with NDCB. A mixture of 1 g of NDCB and 2 g of cholestanone was heated at 150°C for 30 min. The reaction mixture was then chromatographed on a column of alumina, using chloroform as an eluent. One fraction contained 700 mg (32%) of 2β-chlorocholestanone, which, after recrystallization from ethanol - water, showed a mp of 119—121°C, $[\alpha]_D^{22}$ +120.6° (*c* 0.34, $CHCl_3$) (lit., mp 120°C,[14] $[\alpha]_D^{22}$ +124°[14] (EtOH)), $\nu_{C=O}$; 1715 cm^{-1}.

Found: C, 77.32; H, 11.19%. Calcd for $C_{27}H_{45}OCl$: C, 77.00; H, 10.79%.

The other fraction contained 900 mg (41%) of 2α-chlorocholestanone, which, after recrystallization from ethanol-water, showed a mp of 174—179°C, $[\alpha]_D^{20}$ +42° (*c* 0.67, EtOH) (lit., mp 182°C, $[\alpha]_D^{20}$ +41° (EtOH)), $\nu_{C=O}$; 1730 cm^{-1}.

Found: C, 77.27; H, 10.66%. Calcd for $C_{27}H_{45}OCl$: C, 77.00; H, 10.79%.

Polarographic Measurements. The polarographic data were obtained with a Yanagimoto Model PA-102 recording polarograph, using a H-cell equipped with a Hg reference electrode. The capillary characteristics were: $m=0.544$ mg/sec, $t=3.5$ sec/drop at 60 cm. Sample solutions were prepared by dissolving *N*-halo compounds in dry DMF at a concentration of 0.1 mol/*l*. Potassium perchlorate, 0.1 mol/*l* and a few drops of a solution of polyvinyl chloride in DMF were added to the sample solutions as a supporting electrolyte and as a maximum suppressor, respectively. Measurements were made at room temperature after bubbling nitrogen into the solutions for 30 min.

Reaction of Cyclohexanone with *N,N',N''*-Trichloroisocyanuric Acid. A mixture of 3 g of *N,N',N''*-trichloroisocyanuric acid and 10 g of cyclohexanone was refluxed for 1 hr and then cooled. Cyanuric acid, which was separated as a solid, was removed by filtration. The distillation of the filtrate under reduced pressure afforded 1.42 g (39%) of 2-chlorocyclohexanone, 94—96°C/14 mmHg and 2.23 g (61%) of 2-(1-chlorocyclohexyl)cyclohexanone, 108—110°C/4 mmHg.

Conversion of 2-(1-Chlorocyclohexyl)cyclohexanone to 2-(1-Cyclohexenyl)cyclohexanone. A solution of 1 g of 2-(1-chlorocyclohexyl)cyclohexanone in 10 m*l* of pyridine was refluxed for 1 hr. After cooling, the mixture was acidified with dilute hydrochloric acid and extracted with ether. The ether was then evaporated, and the residue was distilled under reduced pressure; bp 105—108°C/3 mmHg. The product was identical with the authentic sample of 2-(1-cyclohexenyl)-cyclohexanone in every respect.

Reaction of Cyclohexene with NCS. A mixture of 1.5 g of NCS and 10 m*l* of cyclohexene was refluxed for 1 hr, and then cooled. The precipitated succinimide was removed by filtration, and the filtrate was distilled under reduced pressure. The glc analysis of the distillate showed that the distillate consisted of 3-chlorocyclohexene (42%), 3,6-dichlorocyclohexene (21%) and 1,2-dichlorocyclohexane in the yields indicated in parentheses.

The authors wish to thank Dr. J. Nakaya for his suggestions concerning the polarographic measurements.

14) G. H. Alt and D. H. R. Barton, *J. Chem. Soc.*, **1954**, 4284.

BULLETIN OF THE CHEMICAL SOCIETY OF JAPAN VOL. 41 2129—2134 (1968)

The Preparation and Cycloaddition Reactions of Pentafluoro-1,3-pentadienes

Hiroshige MURAMATSU, Kan INUKAI and Teruo UEDA

Government Industrial Research Institute, Nagoya, Kita-ku, Nagoya

(Received March 1, 1968)

3,4,5,5,5-Pentafluoro-1,3-pentadienes were prepared from 1 : 1 adducts of perfluoropropylene and alcohols by dehydration followed by dehydrofluorination. When 2-methyl-3,4,5,5,5-pentafluoro-1,3-pentadiene was heated at 130—220°C, an intramolecular cyclization occurred to give 1-methyl-2,3-difluoro-3-trifluoromethylcyclobutene in 73—87% yields. α-Trifluoromethyl-β-acetylacrylic acid and 1-trifluoromethyl-2-fluoro-3-methylenecyclobutene were synthesized from the cyclobutene by oxidation and dehydrofluorination, respectively. Several polyfluorocyclobutanes with a perfluoropropenyl group were prepared by the cross-cycloaddition of the pentafluoro-1,3-pentadienes with the fluoroolefins such as 1,1-difluoro-2,2-dichloroethylene, trifluorochloroethylene, and perfluoropropylene.

Though fluorine-containing 1,3-butadienes have been prepared by various methods,[1] only a few papers[2] dealt with the syntheses of the polyfluoro-1,3-pentadienes. As the (2-hydroperfluoropropyl)-alkylcarbinols were found to be prepared in an excellent yield by the addition of alcohols to perfluoropropylene under γ-irradiation,[3] these carbinols were considered to be suitable intermediates for the syntheses of pentafluoro-1,3-pentadienes. Accordingly, (2-hydroperfluoropropyl)dimethylcarbinol was treated with phosphorus pentoxide to yield 2-methyl-3,3,4,5,5,5-hexafluoro-1-pentene,[3] which was subsequently dehydrofluorinated with potassium hydroxide to give 2-methyl-3,4,5,5,5-pentafluoro-1,3-pentadiene.

$$CF_3CF{=}CF_2 + CH_3CHROH \xrightarrow{\gamma\text{-ray}}$$

$$CF_3CHFCF_2CR(CH_3)OH \xrightarrow{P_2O_5}$$

$$CF_3CHFCF_2CR{=}CH_2 \xrightarrow{KOH} CF_3CF{=}CFCR{=}CH_2$$

(Ia R=H; Ib R=CH_3)

The pentafluoro-1,3-pentadienes (Ia,b) consisted of *cis* and *trans* isomers, the former being predominant.[4] The ratio of *cis* to *trans* varied with the condition of dehydrofluorination. Whereas the *cis* isomer was formed almost exclusively in dehydrofluorination with solid potassium hydroxide in the absence of a solvent, the ratio of *cis* to *trans* was about 2 : 1 in the presence of methanol or ethanol.

The assignment of the isomers to *cis* and *trans* were made unambiguously on the basis of the coupling constants[5] between vicinal F and CF_3, and those between vicinal F and F in their ^{19}F NMR spectra, whose parameters are shown in Table 1. Both isomers of pentafluoro-1,3-pentadienes polymerized upon standing in air and the rates of polymerization of the *trans* isomers were much greater than those of the *cis* isomers. From the NMR spectra, the structures of the polymers were found to be $[-CF(CF_3)CF{=}CRCH_2-]_n$, formed through the 1,4-polymerization.

Several papers have reported on the intramolecular cyclization of polyfluoro-1,3-dienes. Perfluoro-,[6] 2,3-dichloro-1,1,4,4-tetrafluoro-,[7] and 1,4-dichloro-1,2,3,4-tetrafluoro-1,3-butadiene[8] have produced the corresponding perhalocyclobutenes upon heating. When 2-methyl-3,4,5,5,5-pentafluoro-1,3-pentadiene was heated at 130—220°C, an intramolecular cyclization took place to give 1-methyl-2,3-difluoro-3-trifluoromethylcyclobutene (II) in approximately 80% yield. The effect of reaction temperature on the yield was shown in

1) A. M. Lovelace, D. A. Rausch and W. Postelnek, "Aliphatic Fluorine Compounds," Reinhold Publishing Corp., New York (1958), p. 100.

2) A. L. Henne and P. E. Hinkamp, *J. Am. Chem. Soc.*, **76**, 5147 (1954); P. Tarrant and E. G. Gillman, *ibid.*, **76**, 5423 (1954); P. Tarrant and M. R. Lilyquist, *ibid.*, **77**, 3640 (1955).

3) H. Muramatsu, K. Inukai and T. Ueda, This Bulletin, **40**, 903 (1967).

4) The predominance of the *cis* form over the *trans* form has been observed in the preparation of perfluoropropenes and chlorofluoroethylenes containing an ethereal group; H, Muramatsu *et al.*, *ibid.*, **40**, 1284 (1967).

5) The coupling constants of $J_{F,F}$ and J_{F,CF_3} were in agreement with those of polyfluoropropenes reported in the literature; J. W. Emsley, J. Feeney and L. H. Sutcliffe, "High Resolution Nuclear Magnetic Resonance Spectroscopy," Vol. 2, Pergamon Press, Oxford, (1966), p. 909.

6) M. Prober and W. T. Miller, *J. Am. Chem. Soc.*, **71**, 598 (1949); Ref. 7.

7) W. T. Miller, U. S. Pat. 2729613 (1956).

8) R. N. Haszeldine and J. E. Osborne, *J. Chem. Soc.*, **1955**, 3880.

TABLE 1. ^{19}F NMR SPECTRAL PARAMETERS OF PENTAFLUORO-1,3-PENTADIENES, $CF_3CF_a=CF_bCR=CH_2$

R	Isomer	Chemical shift,* ppm			Coupling constant, cps			
		δ_{CF_3}	δ_{Fb}	δ_{Fa}	$J_{CF_3,Fa}$	$J_{CF_3,Fb}$	$J_{Fa,Fb}$	$J_{Fb,H}$**
H	*cis*	−9.7	61	78	12	8	2	24
	trans	−8.1	78	94	11	22	128	22
CH_3	*cis*	−10.7	42	79	13	8	8	—
	trans	−9.0	68	90	10	23	129	—

* The chemical shifts of fluorines are with respect to external trifluoroacetic acid increasing to upfield.
** Coupling between the fluorine and hydrogen on vicinal carbon atoms.

TABLE 2. RESULTS OF CYCLIZATION REACTIONS*

Reaction temp. °C	Pentadiene added g	Pentadiene recovered g	Cyclobutene g	Polymer g	Yield** of cyclobutene %
130	73	13	47	11	78
140	107	8	87	11	87
150	93	4	75	11	84
160	112	4	87	17	80
180	109	5	87	16	84
200	95	5	75	13	84
220	140	6	98	30	73

* In each run, about 10 g of Terpene B was added as an inhibitor and the reaction mixture was heated for a period of 21 hr.
** Based on the amount of pentadiene charged.

TABLE 3. NMR SPECTRAL PARAMETERS OF ESTERS OF α-TRIFLUOROMETHYL-β-ACETYLACRYLIC ACIDS, $CH_3COCH=C(CF_3)COOR$

R	Isomer	Chemical shifts,* ppm					Coupling constant, cps
		δ_{CF_3}	τ_{COCH_3}	τ_{CH_3}	τ_{CH_2}	$\tau_{=CH}$	$J_{CF_3,H}$
CH_3	*cis*	−12.5	7.68	6.24		2.95	1.5
	trans	−13.1	8.31	6.76		2.28	1.8
C_2H_5	*cis*	−12.1	7.69	8 74	5.82	2.99	1.3
	trans	−12.7	8.34	8.85	6.57	2.28	2.0
H		−12.7	8.30			2.52	1.6

* The chemical shifts of fluorines are with respect to external trifluoroacetic acid increasing to upfield.

TABLE 4. YIELDS AND PHYSICAL PROPERTIES OF POLYFLUOROCYCLOBUTANES WITH A PERFLUOROPROPENYL GROUP,

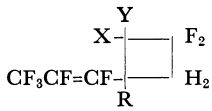

R	X	Y	Yield %	Bp °C(mmHg)	n_D^{20}	d_4^{20}	C, %		H, %		$\nu_{C=C}$ cm^{-1}
							Found	Calcd	Found	Calcd	
H	F	Cl*	49	119—120	1.3602	1.568	31.47	30.62	1.68	1.10	1729
H	Cl	Cl	55	84— 85(77)	1.3882	1.593	29.75	28.89	1.37	1.04	1723
H	F	CF_3	6	117—118	1.3234	1.617	31.49	31.19	1.05	0.98	1723
CH_3	F	Cl*	49	91— 92(44)	1.3690	1.600	34.87	33.30	2.10	1.75	1723
CH_3	Cl	Cl	36	90— 92(64)	1.3950	1.552	32.46	31.50	1.86	1.65	1720
CH_3	F	CF_3	3	126—132	1.3350	1.545	33.13	33.56	1.59	1.56	1726

* Contained a small amount of the dimer of pentafluoropentadiene.

Table 2. The cyclization of 3,4,5,5,5-pentafluoro-1,3-pentadiene was unsuccessful due to polymerization to give viscous polymeric substance.

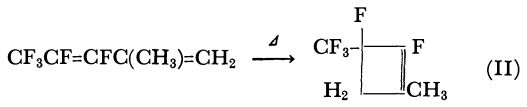

(II)

The structure of II was confirmed by elemental analysis, IR, and NMR spectra. In the ^{19}F NMR spectrum, a peak for the CF_3 group appeared as a doublet at 3.4 ppm caused by the splitting of a geminal fluorine ($J_{CF_3,F}$ 8.1 cps) and those for the =CF– and –CF– as a triplet and a multiplet at 37 and 100 ppm, respectively. The triplet may be due to a long range coupling with hydrogens of methylene group ($J_{F,H}$ 13.2 cps).[9]

The structure of II was further substantiated by the following reactions. Oxidation of II with potassium permanganate gave α-trifluoromethyl-β-acetylacrylic acid (III), which was obviously formed by dehydrofluorination of an intermediate, α-fluoro-α-trifluoromethyl-β-acetylpropionic acid (IV). Though two isomers of the disubstituted acrylic acid were possible, only the *trans* isomer was identified.

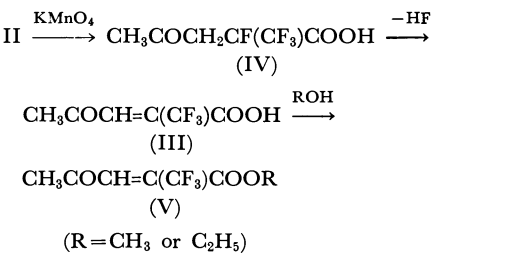

(R=CH_3 or C_2H_5)

In esterification of III using *p*-toluenesulfonic acid as a catalyst, an isomerization took place to give a mixture of the *trans* and *cis* isomers, the *trans* ester being predominant (about 8 to 1 for R=CH_3; 6 to 1 for R=C_2H_5).

It has already been known[10] that carbonyl-containing groups in substituted olefins have long range deshielding effects on *cis*-β-hydrogen atoms and *cis*-β-methyl groups. The peak for the vinylic hydrogen of one isomer obtained in esterification appeared in a lower field by 0.7 ppm than that of the other isomer, but the peak for the methyl hydrogens in acetyl group of the former isomer appeared in a higher field by 0.6 ppm than that of the latter isomer. These chemical shifts of protons indicate the former to have the *trans* structure and the latter the *cis*. For the trifluoromethyl group, a deshielding effect of 0.6 ppm by the carbonyl group in the *cis* position was also observed in the ^{19}F NMR spectra. Table 3 gives the NMR parameters for methyl and ethyl α-trifluoromethyl-β-acetyl acrylates. It is seen that J^{cis}_{H,CF_3} is smaller than J^{trans}_{H,CF_3} in each of the esters.[11]

Treatment of II with potassium hydroxide produced 1-trifluoromethyl-2-fluoro-3-methylenecyclobutene (VI) through a 1,4-elimination. To a mixture of II and VI was added bromine under ultraviolet irradiation to yield the dibromocyclobutenes, (VII) and (VIII) in a ratio of 1 : 1.2. Debromination of VII and VIII gave the pure VI, which polymerized upon standing overnight, yielding a white solid polymer.

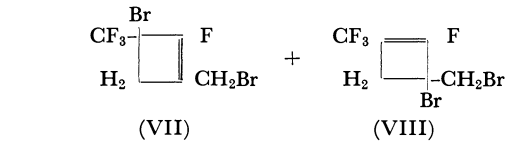

(VI)

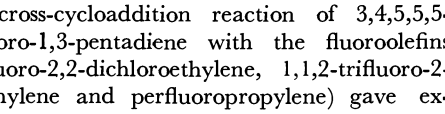

(VII) (VIII)

The cross-cycloaddition reaction of 3,4,5,5,5-pentafluoro-1,3-pentadiene with the fluoroolefins (1,1-difluoro-2,2-dichloroethylene, 1,1,2-trifluoro-2-chloroethylene and perfluoropropylene) gave exclusively (perfluoropropenyl)cyclobutanes (IXa), no cyclohexenes being found.[12] In all the cases, the telomers of the pentadiene were formed as by-products. Similarly, 2-methyl-3,4,5,5,5-pentafluoro-1,3-pentadiene reacted with the fluoroolefins to give the (perfluoropropenyl)polyfluorocyclobutanes (IXb) together with II.

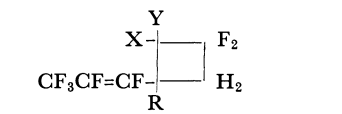

(IXa R=H; IXb R=CH_3)
(X, Y=Cl, F or CF_3)

Table 4 summarizes the yields based on the pentadienes added and the physical properties of polyfluorocyclobutanes containing a perfluoropropenyl group.

The cycloadducts IXa,b were identified by their NMR spectra and IR spectra ($\nu_{C=C}$ 1723—1729cm^{-1} for R=H, 1720—1726 cm^{-1} for R=CH_3). Further the 1-perfluoropropenyl-2-halo-3,3-difluorocyclobutenes (Xa,b) were synthesized by dehydrochlorination of the cycloadducts IXa. Xa was identical

9) In some polyfluorocyclobutenes such as 1-phenyl-3,3,4-trifluoro-4-chlorocyclobutene and 1-phenyl-2,3,3-trifluorocyclobutene, the cross-ring couplings between H and F with $J_{H,F}$ of 8—12 cps were reported; C. M. Sharts and J. D. Roberts, *J. Am. Chem. Soc.*, **79**, 1008 (1957).

10) Ref. 5, p. 735.

11) For coupling constants between the vicinal F–F, F–CF_3, F–CH_3, or CF_3–CF_3 on the double bond in fluoroalkenes, it was found that $J^{cis}_{F,F}<J^{trans}_{F,F}$; $J^{cis}_{F,CF_3}>J^{trans}_{F,CF_3}$; $J^{cis}_{F,CH_3}<J^{trans}_{F,CH_3}$; $J^{cis}_{CF_3,CF_3}>J^{trans}_{CF_3,CF_3}$.

12) For a recent review on Diels-Alder reactions of organic fluorine compounds, see D. R. A. Perry, "Fluorine Chemistry Reviews," Vol. 1, P. Tarrant, ed., Marcel Dekker, Inc., New York (1967), p. 253.

with the product obtained in the dehydrohalogenation of the (2-hydroperfluoropropyl)polyhalocyclobutanes (XI), which was prepared by the cycloaddition of 3,3,4,5,5,5-hexafluoro-1-pentene and trifluorochloroethylene.

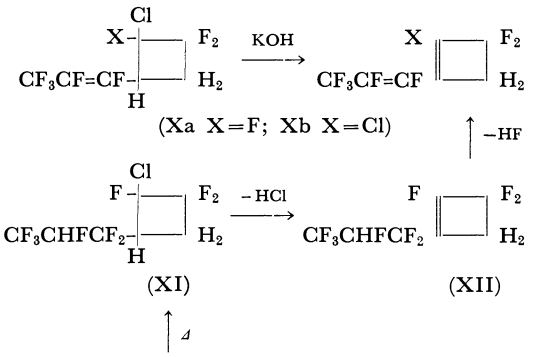

$CF_3CHFCF_2CH=CH_2 + CF_2=CFCl$

The cycloadducts formed in the cycloadditions of trifluorochloroethylene or perfluoropropylene with I were found from their ^{19}F NMR spectra to consist of the two isomers A and B in approximately equal amounts.

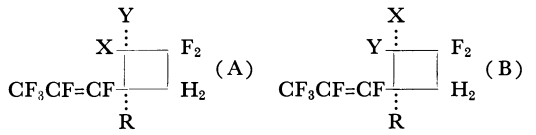

Experimental[13]

The NMR spectra were obtained using a JNM-C-60 high resolution spectrometer (60 Mc for ^1H and 56.4 Mc for ^{19}F). Tetramethylsilane was used for ^1H as an internal standard and trifluoroacetic acid for ^{19}F as an external standard.

3,4,5,5,5-Pentafluoro-1,3-pentadiene (Ia). 3,3,4,5,5,5-Hexafluoro-1-pentene was prepared as reported in a previous paper.[3] In a 200 m*l* flask equipped with a stirrer and a reflux condenser was placed 105 g (0.59 mol) of the hexafluoro-1-pentene. After powdered potassium hydroxide (30 g) was added, the mixture was heated at 65—75°C for 1 hr with stirring. A gas chromatogram of the reaction mixture indicated that about 20% of the reactant was dehydrofluorinated. Addition of potassium hydroxide (30 g) and heating of the reaction mixture (65—75°C, 1 hr) were repeated four times. Distillation of the mixture gave 81 g (0.51 mol, 86% yield) of 3,4,5,5,5-pentafluoro-1,3-pentadiene, bp 40—41°C, n_D^{20} 1.3372, d_4^{20} 1.266, $\nu_{C=C}$ 1696 and 1612 cm^{-1}. The gas chromatogram and ^{19}F NMR spectrum of the pentadiene indicated that it consisted of almost exclusively the *cis* form.

Found: C, 38.65; H, 2.90%. Calcd for $C_5H_3F_5$: C, 37.99; H, 3.19%

When the pentadiene was stored in air, it polymerized gradually to yield viscous polymer, whose structure was confirmed to be $[-CF(CF_3)CF=CHCH_2-]_n$ from its ^{19}F NMR spectrum. δ_{CF_3} 2.3 ppm, $\delta_{-CF=}$ 41 ppm (broad doublet, $J_{H,F}$ 30 cps), $\delta_{-\underset{|}{CF}-}$ 95 ppm.

2-Methyl-3,4,5,5,5-pentafluoro-1,3-pentadiene (Ib). *a) Dehydrofluorination with Solid Potassium Hydroxide.* 2-Methyl-3,3,4,5,5,5-hexafluoro-1-pentene (86 g, 0.43 mol) prepared as reported[3] was treated with powdered potassium hydroxide (144 g) as mentioned above to give 63 g (0.37 mol, 86% yield) of 2-methyl-3,4,5,5,5-pentafluoro-1,3-pentadiene, bp 61—62°C, n_D^{20} 1.3357, d_4^{20} 1.211, $\nu_{C=C}$ 1719 and 1644 cm^{-1}. The gas chromatogram (DOP column, 2 m, 84°C, carrier gas He, 37 m*l*/min) of the pentadiene obtained showed two peaks, that of the *cis* isomer (retention time, 5.0 min) and of the *trans* isomer (6.7 min), in a ratio of 97: 3.

Found: C, 41.81; H, 2.95%. Calcd for $C_6H_5F_5$: C, 41.87; H, 2.93%.

b) Dehydrofluorination with Alcoholic Potassium Hydroxide Solution. In a 300 m*l* flask with a stirrer was placed 50.2 g (0.26 mol) of the 2-methylhexafluoro-1-pentene. A solution of 25 g (0.45 mol) of potassium hydroxide in 150 m*l* of ethanol was added drop by drop and the mixture was poured into water. The organic layer (39.5 g) was separated, dried and distilled to give 34.5 g (0.20 mol, 77% yield) of the 2-methylpentafluoro-1,3-pentadiene, whose gas chromatogram showed presence of the *cis* and *trans* isomers in a ratio of 7: 3.

A similar treatment of the 2-methylhexafluoro-1-pentene with potassium hydroxide in methanol gave the 2-methylpentafluoro-1,3-pentadiene in a yield of 45%. The ratio of *cis* and *trans* was 6: 4.

1-Methyl-2,3-difluoro-3-trifluoromethylcyclobutene (II). A 300 m*l* stainless-steel autoclave was charged with 93 g (0.54 mol) of 2-methyl-3,4,5,5,5-pentafluoro-1,3-pentadiene (*cis* : *trans* 97: 3) and 10 g of Terpene B. The mixture was kept at 150°C for 21 hr. The resultant mixture was distilled to give a fraction boiling at 78—82°C and a viscous residue (20 g), which was presumed to be a mixture of Terpene B and the telomer of the pentadiene. The distillate consisted of 3.6 g of the unchanged pentadiene and 74 g (0.43 mol, 80% yield) of 1-methyl-2,3-difluoro-3-trifluoromethylcyclobutene, which was redistilled to give the pure II, bp 79—80°C, n_D^{20} 1.3291, d_4^{20} 1.263, $\nu_{C=C}$ 1738 cm^{-1}.

Found: C, 42.09; H, 2.99%. Calcd for $C_6H_5F_5$: C, 41.87; H, 2.93%.

The effect of the reaction temperature on the yield was shown in Table 2, which indicates an optimum temperature to be in 140—200°C. Above 200°C, the yield decreased presumably because of the polymerization of the pentadiene.

α-Trifluoromethyl-β-acetylacrylic Acid (III). An aqueous solution of potassium permanganate (58 g, 0.37 mol) was added to 42 g (0.24 mol) of 1-methyl-2,3-difluoro-3-trifluoromethylcyclobutene in acetone. After removal of manganese dioxide by filtration, the filtrate was acidified with sulfuric acid and extracted with ether. Vacuum distillation of the extract gave 24 g (0.13 mol, 54% yield) of crude α-trifluoromethyl-β-acetyl acrylic acid, bp 106—107°C/7 mmHg, and a tarry residue (11 g). The crude acid containing a small amount of α-fluoro-α-trifluoromethyl-β-acetylpropionic acid, δ_{CF_3} 2.1 ppm (doublet), $J_{CF_3,F}$ 7.5 cps, $\delta_{-\underset{|}{CF}-}$ 87 ppm (multiplet), was recrystallized from benzene to give white needles, mp 70—71°C.

Found: C, 38.72; H, 2.65%; Neut. equiv. 180.

13) All temperature readings are uncorrected.

Calcd for $C_6H_5O_3F_3$: C, 39.57; H, 2.77%; Neut. equiv. 182.

Methyl and Ethyl α-Trifluoromethyl-β-acetylacrylate (V). A mixture of α-trifluoromethyl-β-acetylacrylic acid (9 g), methanol (50 ml), benzene (30 ml), and *p*-toluenesulfonic acid was refluxed for 6 hr and extracted with ether. Distillation of the extract gave 3.5 g of methyl α-trifluoromethyl-β-acetylacrylate (a mixture of *trans* and *cis* isomers), bp 90—92°C/18 mmHg, n_D^{20} 1.3992, d_4^{20} 1.305.

Found: C, 42.53; H, 2.65%. Calcd for $C_7H_7O_3F_3$: C, 42. 87; H, 3.60%.

The gas chromatogram (Silicone DC-550 column, 2 m, 167°C, carrier gas He, 58 ml/min) of the methyl ester showed two peaks of the *trans* isomer (retention time, 6.6 min) and the *cis* isomer (10.7 min) in an area ratio of 8: 1.

Ethyl α-trifluoromethyl-β-acetylacrylate (10 g) was prepared from the acrylic acid (9 g) in a similar way as described above. The gas chromatogram of the ethyl ester showed two peaks, that of the *trans* (8.8 min) and of thd *cis* (19.8 min) in a ratio of 6: 1. bp 95—99°C/18 mmHg, n_D^{20} 1.3998, d_4^{20} 1.248.

Found: C, 45.40; H, 4.25%. Calcd for $C_8H_9O_3F_3$: C, 45.72; H, 4.32%.

1-Fluoro-2-bromomethyl- 4 - bromo - 4 - trifluoromethylcyclobutene (VII) and 1-Fluoro-2-trifluoromethyl-4-bromo-4-bromomethyl-cyclobutene(VIII). A mixture of 130 g (0.76 mol) of 1-methyl-2,3-difluoro-3-trifluoromethylcyclobutene and 30 g of powdered potassium hydroxide was heated at about 110°C for 1 hr with stirring. Addition of potassium hydroxide (30 g) was repeated seven times and the gas chromatogram of the reaction mixture indicated the formation of 27 g (0.18 mol, 24% yield) of 1-trifluoromethyl-2-fluoro-3-methylenecyclobutene. To the reaction mixture, bromine (29 g, 0.18 mol) was added drop by drop under UV irradiation, and the distillation of the mixture gave a fraction boiling at 63—68°C/18.5 mmHg (43 g, 0.14 mol, 78% yield), which was a mixture of the dibromocyclobutenes, 1,4-adduct VII and 1,2-adduct VIII in a ratio of 1: 1.2. The dibromocyclobutenes were separated by a preparative gas chromatograph.

VII: n_D^{20} 1.4630, d_4^{20} 1.953, $\nu_{C=C}$ 1724 cm^{-1}, δ_{CF_3} −4.0 ppm (singlet), $\delta_{-CF=}$ 21 ppm (triplet), $J_{CH_2,F}$ 13 cps.

Found: C, 23.11; H, 1.37%. Calcd for $C_6H_4F_4Br_2$: C, 23.11; H, 1.29%.

VIII: n_D^{20} 1.4441, d_4^{20} 1.927, $\nu_{C=C}$ 1736 cm^{-1}, δ_{CF_3} −14.0 ppm (doublet), $\delta_{-CF=}$ 11 ppm (triplet of quartet), $J_{CF_3,F}$ 10 cps, $J_{CH_2,F}$ 13 cps.

Found: C, 22.71; H, 1.42%. Calcd for $C_6H_4F_4Br_2$: C, 23.11; H, 1.29%.

1-Trifluoromethyl - 2 - fluoro - 3 - methylenecyclobutene (VI). The dibromocyclobutenes described above was treated with zinc dust in hexanol to give quantitatively 1-trifluoromethyl-2-fluoro-3-methylenecyclobutene, bp 42—43°C, n_D^{20} 1.3640, d_4^{20} 1.191, $\nu_{C=C}$ 1720 and 1671 cm^{-1}, δ_{CF_3} −13.6 ppm (doublet), $\delta_{-CF=}$ 17 ppm (multiplet), $J_{CF_3,F}$ 12 cps.

Found: C, 42.37; H, 2.85%. Calcd for $C_6H_4F_4$: C, 42.61; H, 2.89%.

Preparations of the (Perfluoropropenyl)polyfluorocyclobutanes (IXa). A mixture of 136 g (0.86 mol) of 3,4,5,5,5-pentafluoro-1,3-pentadiene, 99 g (0.85 mol) of trifluorochloroethylene, and 10 g of Terpene B in a 300 ml autoclave was heated at 200°C for 21 hr. The content was poured into methanol to yield white polymers (48 g), which were separated by filtration. The filtrate was treated with water to remove methanol, and an organic layer was distilled to give the unchanged pentadiene, hexafluorodichlorocyclobutane (14.2 g), and 116 g (0.42 mol, 49% yield) of 1-(perfluoropropenyl)-2-chloro-2,3,3-trifluorocyclobutane, bp 119—120°C.

The cross-cycloaddition of 3,4,5,5,5-pentafluoro-1,3-pentadiene and other polyfluoroolefins was carried out under similar conditions.

Preparations of the (Perfluoropropenyl)methylpolyfluorocyclobutanes (IXb). A mixture of 85 g (0.49 mol) of 2-methyl-3,4,5,5,5-pentafluoro-1,3-pentadiene, 70 g (0.53 mol) of 1,1-difluoro-2,2-dichloroethylene, and 10 g of Terpene B was charged into an autoclave and heated at 202°C for 24 hr. The contents were poured into methanol to give dark colored polymers (27 g), which were then filtered. After the filtrate had been treated with water, the organic layer was separated, dried, and distilled to give a small amount of tetrafluorotetrachlorocyclobutane, 8 g (0.04 mol, 9% yield) of II, and 54 g (0.18 mol, 36% yield) of 1-methyl-1-perfluoropropenyl -2,2- dichloro - 3,3 - difluorocyclobutene, bp 90—92°C/64 mmHg.

The cross-cycloaddition of 2-methyl-3,4,5,5,5-pentafluoro-1,3-pentadiene and other polyfluoroolefins was carried out under similar conditions.

1-Perfluoropropenyl - 2, 3, 3 - trifluorocyclobutene (Xa). To 49 g (0.18 mol) of 1-perfluoropropenyl-2,3,3-trifluoro-2-chlorocyclobutane, 15 g (0.27 mol) of potassium hydroxide in 100 ml of ethanol were added drop by drop over a 1 hr period at room temperature. The mixture was stirred for 30 min and then poured into water. The organic layer (42 g) was separated, dried, and distilled to give 20 g (0.085 mol, 48% yield) of Xa, bp 80—81°C, n_D^{20} 1.3551, d_4^{20} 1.219, $\nu_{C=C}$ 1715 and 1663 cm^{-1}.

Found: C, 35.69; H, 1.19%. Calcd for $C_7H_2F_8$: C, 35.31; H, 0.85%.

1-Perfluoropropenyl-2-chloro - 3, 3 - difluorocyclobutene (Xb). 1-Perfluoropropenyl-2,2-dichloro-3,3-difluorocyclobutane (33 g, 0.11 mol) was treated with potassium hydroxide as mentioned above to give 19.4 g (0.076 mole, 67% yield) of Xb, bp 120—121°C, n_D^{20} 1.3958, d_4^{20} 1.561, $\nu_{C=C}$ 1687 and 1601 cm^{-1}.

Found: C, 32.03; H, 0.79; Cl, 13.2%. Calcd for $C_7H_2F_7Cl$; C, 31.18; H, 0.87; Cl, 13.9%.

1-Hexafluoropropyl-2-chloro - 2,3,3-trifluorocyclobutane (XI). A mixture of 117 g (0.65 mol) of 3,3,4,5,5,5-hexafluoro-1-pentene, 98 g (0.84 mol) of trifluorochloroethylene, and 5 g of Terpene B was charged into a 300 ml autoclave and heated at 200°C for 48.5 hr. Distillation yielded 32 g (0.11 mol, 17% yield) of 1-hexafluoropropyl-2-chloro-2,3,3-trifluorocyclobutane, bp 80—82°C/138 mmHg, n_D^{20} 1.3504, d_4^{20} 1.592.

Found: C, 28.54; H, 1.37%. Calcd for $C_7H_4F_9Cl$: C, 28.72; H, 1.24%.

1 - Hexafluoropropyl - 2,3,3 - trifluorocyclobutene (XII). To 28 g (0.094 mol) of XI, 6.3 g (0.11 mol) of potassium hydroxide in 50 ml of ethanol were added dropwise at room temperature. The mixture was poured into water and the organic layer (25 g) was separated and distilled to give 8.2 g (0.032 mole, 34% yield) of 1-hexafluoropropyl-2,3,3-trifluorocyclobutene, bp 93—96°C, n_D^{20} 1.3202, d_4^{20} 1.529, $\nu_{C=C}$ 1733 cm^{-1}.

Found: C, 32.57; H, 1.17%. Calcd for $C_7H_3F_9$: C, 32.01; H, 1.33%.

Treatment of XII with powdered potassium hydroxide produced (perfluoropropenyl)trifluorocyclobutene Xa in a yield of 50%.

The authors wish to thank Mr. H. Sugita of Government Industrial Research Institute, Tokyo, for the carbon and hydrogen analyses.

BULLETIN OF THE CHEMICAL SOCIETY OF JAPAN VOL. 41 2134—2140 (1968)

Studies on Separation of Amino Acids and Related Compounds. IV. Separation of Diastereomeric Tripeptides Containing Basic and Acidic Amino Acid Residue[1]

Masako MURAOKA, Norio YOSHIDA, Kosaku NODA and Nobuo IZUMIYA

Laboratory of Biochemistry, Faculty of Science, Kyushu University, Hakozaki, Fukuoka

(Received March 4, 1968)

Twelve pure tripeptides have been synthesized and the separation of each mixture composed of two diastereomeric tripeptides with an amino acid analyzer has been studied. Among six model systems of diastereomeric mixture studied, a mixture of the LL and LD isomers of glycyl-ornithyl-glutamic acid was separated most efficiently.

The several methods of measuring the extent of racemization of the step of the peptide bond formation have been reported in the literature.[2] Anderson *et al.*[3] found that benzyloxycarbonyl-glycyl-L-phenylalanyl-glycine ethyl ester can be separated from the racemate by fractional crystallization in which the less soluble racemate separates in the first crops; many investigators have used this Anderson's test for the study of racemization as a model system in different coupling procedures.[2] Williams *et al.* suggested the fractional crystallization of benzoyl-leucyl-glycine ethyl ester which is synthesized from benzoyl-L-leucine and glycine ethyl ester with a coupling procedure.[4] Clayton *et al.* indicated that a diastereomeric mixture of benzyloxycarbonyl-glycyl-alanyl-L-phenylalanyl-glycine can be separated by countercurrent distribution.[5] Weygand *et al.* have taken advantage of separating diastereomeric trifluoroacetyl-dipeptide methyl esters by gas chromatography for the study of racemization.[6] Taschner *et al.* were able to detect a small amount of the LD diastereomer in an LL dipeptide by paper chromatography; they have applied this technique in order to examine the degree of racemization caused by the activation of an acyl-dipeptide acid.[7] Halpern *et al.* have described the use of NMR procedure for detection of racemization.[8]

We have been attempting to find a convenient procedure of racemization-test with the application an of amino acid analyzer. A procedure which we have designed is as follows. When an acyl-dipeptide acid is condensed with an amino acid benzyl ester by an usual coupling method, an acyl-tripeptide benzyl ester will be obtained. The crude product is subjected directly to hydrogenolysis, and the hydrogenated material is submitted to an amino acid

$$\text{Z-Gly-L-A-OH} + \text{H-L-B-OBzl} \xrightarrow[\text{racemization of A residue)}]{\text{(with partial or complete}} \text{Z-Gly-A-B-OBzl (LL isomer + DL isomer)} \xrightarrow[H_2]{} \text{H-Gly-A-B-OH (LL isomer + DL isomer)}$$

Fig. 1. Supposed sequence of synthesis of tripeptide diastereomers.
Z-, benzyloxycarbonyl; -OBzl, benzyl ester; A or B, certatin amino acid residue bearing an asymmetrical carbon.

1) Part III of this series: K. Noda, H. Okai, T. Kato and N. Izumiya, This Bulletin, **41**, 401 (1968).
2) E. Schröder and K. Lübke, "The Peptides," Vol. I, Academic Press, New York (1966), p. 319; M. Bodanszky and M. A. Ondetti, "Peptide Synthesis," Interscience Publishers, New York (1966), p. 137.
3) G. W. Anderson, J. Blodinger and A. D. Welcher, *J. Am. Chem. Soc.*, **74**, 5309 (1952).
4) M. W. Williams and G. T. Young, *J. Chem. Soc.*, **1964**, 881.
5) D. W. Clayton, J. A. Farrington, G. W. Kenner and J. M. Turner, *ibid.*, **1957**, 1398.
6) F. Weygand, A. Prox and W. König, *Chem. Ber.*, **99**, 1451 (1966).
7) E. Taschner, A. Chimiak, J. F. Biernat, T. Sokolowska, C. Wasielewski and B. Rzeszotarska, "Peptide Symposium," Pergamon, Oxford (1963), p. 109.
8) B. Halpern, L. F. Chew and B. Weinstein, *Tetrahedron Letters*, **1967**, 3075; *J. Am. Chem. Soc.*, **89**, 5051 (1967).

analyzer (Fig. 1). In the present paper we describe the syntheses of several model peptides and the separation experiments of each mixture of diastereomeric peptides by the analyzer.

The literature survey on the separation of dipeptide diastereomers by an amino acid analyzer, has revealed that two groups reported the separation of a mixture of alanyl-alanines.[9] We also described in the previous paper the separation of leucyl-valine diastereomers.[1] Though the model dipeptides are not true diastereomers it would be of interest to note that Kornguth *et al.* have reported the complete separation of a mixture of ε-(α-L-glutamyl)-L-lysine and ε-(γ-L-glutamyl)-L-lysine.[10] A separation study of tripeptide diastereomers by an amino acid analyzer has not been performed to date as far as we recognize.

For model peptide, we chose tripeptide, which is composed of glycine, a basic and an acidic amino acid, with the surmise that a diastereomeric mixture of this polyfunctional neutral tripeptide might be efficiently separated under an appropriate condition. Each pure diastereomer of glycyl-lysyl-glutamic acid, glycyl-lysyl-aspartic acid, glycyl-ornithyl-glutamic acid and glycyl-ornithyl-aspartic acid were prepared in the conventional manner as the first step of the study. For example, glycyl-L-lysyl-L-glutamic acid was synthesized as shown in Fig. 2. Thus eight tripeptides (XXIII—XXX) of Gly-Lys-Glu type were obtained as hygroscopic crystals and their homogeneity was ascertained by paper and thin-layer chromatographies and electrophoresis.

As the control material for the experiment with the analyzer, several dipeptides (VII—X) of Lys-Glu type were also synthesized by the usual way.

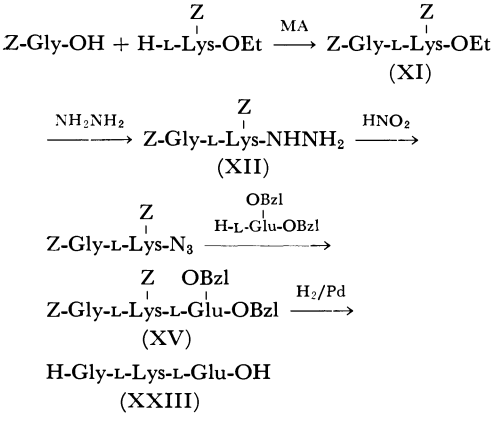

Fig. 2. Sequence of synthesis of tripeptide (XXIII).
MA, the mixed anhydride method.

9) F. C. Neuhas, *J. Biol. Chem.*, **237**, 778 (1962); K. Harada and S. W. Fox, *Arch. Biochem. Biophys.*, **109**, 49 (1965).
10) M. L. Kornguth, A. Neidle and H. Waelsch, *Biochemistry*, **2**, 740 (1963).

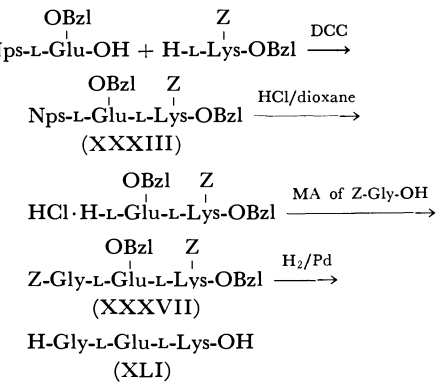

Fig. 3. Sequence of synthesis of tripeptide (XLI).
Nps-, *o*-nitrophenylsulfenyl; DCC, dicyclohexylcarbodiimide.

Since any mixture of diastereomeric tripeptides of Gly-Lys-Glu type was not separated completely by the analyzer as described later, syntheses of model tripeptides of Gly-Glu-Lys type were further attempted. Each pure diastereomer of glycyl-glutamyl-lysine and glycyl-aspartyl-lysine was prepared in the manner of the stepwise elongation to preclude racemization. For example, synthetic sequence of glycyl-L-glutamyl-L-lysine was noted in Fig. 3.

As a preliminary experiment, separation studies of mixture of diastereomeric peptides with paper chromatography and electrophoresis were performed. As noted in Table 1, it was observed that the mixture of dipeptide diastereomers was separated each other more efficiently in general than a mixture of tripeptides.

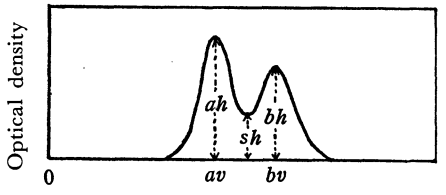

Fig. 4. Model elution pattern of a diastereomeric mixture.

A model elution pattern of a mixture composed of two diastereomers in the same amounts by an amino acid analyzer was indicated in Fig. 4. For the approximate expression of the efficiency of separation, we introduced the term rs, apparent ratio of separation; rs is calculated by the equation of $[sh/(ah+bh)\times 2]\times 100$.

Each mixture of the diastereomeric dipeptides or tripeptides was subjected to the analyzer. For the elution of columns three procedures were employed and the results obtained were summarized in Table 2. In procedure (i) the elution was carried out with a medium column (0.9×50 cm) and pH 5.28 buffer; any peptide mixture was found not to be

TABLE 1. R_f AND R_{Gly} VALUES OF PEPTIDES ON PAPER CHROMATOGRAPHY AND ELECTROPHORESIS

Compound		Paper chromatography R_f[b]	Paper electrophoresis R_{Gly}[a]		
			pH 1.8[c]	pH 3.25[d]	pH 4.25[d]
Lys-Glu,	L-L	0.23	1.13	1.14	1.10
Lys-Glu,	L-D	0.18	1.13	1.09	1.10
Lys-Asp,	L-L	0.18	1.09	1.14	1.12
Lys-Asp,	L-D	0.17	1.09	1.10	1.12
Gly-Lys-Glu,	L-L	0.15	1.03	1.21	1.08
Gly-Lys-Glu,	L-D	0.15	1.03	1.21	1.08
Gly-Lys-Asp,	L-L	0.12	1.11	1.18	1.14
Gly-Lys-Asp,	L-D	0.12	1.11	1.18	1.14
Gly-Orn-Glu,	L-L	0.15	1.10	1.23	1.12
Gly-Orn-Glu,	L-D	0.15	1.10	1.23	1.12
Gly-Orn-Asp,	L-L	0.13	1.44	1.22	1.11
Gly-Orn-Asp,	L-D	0.13	1.44	1.22	1.11
Gly-Glu-Lys,	L-L	0.16	1.12	1.14	1.03
Gly-Glu-Lys,	D-L	0.14	1.12	1.14	1.03
Gly-Asp-Lys,	L-L	0.13	1.12	1.13	1.01
Gly-Asp-Lys,	D-L	0.12	1.12	1.13	1.01

a) Calculated relatively from a distance travelled of glycine as a control compound.
b) Solvent system: *n*-butanol - acetic acid - pyridine - water (4 : 1 : 1 : 2, v/v).
c) Solvent system: formic acid - acetic acid - methanol - water (1 : 3 : 6 : 10, v/v).
d) Solvent system: 0.2 M sodium citrate buffer.

TABLE 2. VALUES RELATING TO CHROMATOGRAPHY OF PEPTIDES WITH AMINO ACID ANALYZER

		Effluent volume (av or bv, m*l*) and apparent ratio of separation (rs, %)					
		(i)[a]		(ii)[b]		(iii)[c]	
		av or bv	rs	av or bv	rs	av or bv	rs
Lys-Glu,	L-L	46	0	62	77	411	91
Lys-Glu,	L-D	46		51		399	
Lys-Asp,	L-L	43	0	44	77	288	100
Lys-Asp,	L-D	43		36		236	
Gly-Lys-Glu,	L-L	47	0	88	0	409	50
Gly-Lys-Glu,	L-D	47		88		418	
Gly-Lys-Asp,	L-L	59	0	61	0	332	0
Gly-Lys-Asp,	L-D	59		61		332	
Gly-Orn-Glu,	L-L	41	0	74	0	397	64
Gly-Orn-Glu,	L-D	41		74		403	
Gly-Orn-Asp,	L-L	45	0	49	0	274	0
Gly-Orn-Asp,	L-D	45		49		274	
Gly-Glu-Lys,	L-L	42	0	51	0	400	0
Gly-Glu-Lys,	D-L	42		51		400	
Gly-Asp-Lys,	L-L	33	0	31	0	396	10
Gly-Asp-Lys,	D-L	33		31		393	

a) With medium column (0.9×50 cm) and 0.2 M sodium citrate buffer (pH 5.28).
b) With small column (0.6×10 cm) and 0.2 M sodium citrate buffer (pH 4.25).
c) With the small column, 0.2 M sodium citrate at pH 3.25 was applied until 360 m*l*, and then the system was changed to the pH 4.25 buffer.

separated. In scheme (ii) a smaller column (0.6 ×10 cm) was used and eluted with pH 4.25 buffer; any tripeptide system of Gly-Glu-Lys or Gly-Lys-Glu type was no separated though both dipeptide systems separated considerably. In scheme (iii) the elution was initiated with pH 3.25, and at fraction 360 m*l* the eluting solution was changed to pH 4.25 buffer. At first four systems of Gly-Lys-Glu type were studied; although separation of glycyl-ornithyl-glutamic acid diastereomers occurred most efficiently, the separation was not still completed (Fig. 7). Therefore, the analysis was further extended to two model systems of glycyl-glutamyl-lysine and glycyl-aspartyl-lysine; the results were

worse than that of the system of glycyl-ornithyl-glutamic acid. Several chromatographic patterns obtained were indicated in Figs. 5—7 for examples.

Though it appears that a reaction sequence to afford glycyl-ornithyl-glutamic acid from benzyloxycarbonyl-glycyl-δ-benzyloxycarbonyl-L-ornithine and L-glutamic acid dibenzyl ester can be used for the detection of racemization, the separation study of several dipeptide diastereomers, such as α-acetyl-lysyl-alanine, and tripeptide diastereomers is being continued in this laboratory in order to find a model system in better separation.

Experimental

The melting points were uncorrected. Optical rotations were determined with a Yanagimoto Photometric Polarimeter, OR-20 type.

D-Glutamic Acid Dibenzyl Ester *p*-Toluenesulfonate (I). This compound was obtained according to the procedure for the L-isomer.[11] Yield, 72%; mp 140—141°C; $[\alpha]_D^{20}$ −6.9° (*c* 2, methanol). Reported value for the L-isomer; mp 142°C; $[\alpha]_D$ +7.6° (methanol).[11]

D-Aspartic Acid Dibenzyl Ester *p*-Toluenesulfonate (II). This compound was obtained according to the procedure for the L-isomer.[11] Yield, 81%; mp 155—156°C; $[\alpha]_D^{20}$ +1.0° (*c* 2, methanol). Reported value for the L-isomer; mp 151—152°C; $[\alpha]_D^{20}$ +1.0° (methanol).[11,12]

Dibenzyloxycarbonyl-lysyl-glutamic Acid Dibenzyl Ester. *The LL Isomer (III).* A suspension of dibenzyloxycarbonyl-L-lysine dicyclohexylammonium salt[13] (1.78 g, 3 mmol) in ethyl acetate was stirred with 0.5 M citric acid (12 m*l*) during 1 hr. The ethyl acetate layer was separated and washed with water, and dried over sodium sulfate. The filtrate was evaporated *in vacuo* and the residual oil (dibenzyloxycarbonyl-L-lysine) was dissolved in tetrahydrofuran (6 m*l*). The solution was treated with triethylamine (0.42 m*l*, 3 mmol) and isobutyl chloroformate (0.39 m*l*, 3 mmol) at −5°C.[14] After 15 min, a mixture of L-glutamic acid dibenzyl ester *p*-toluenesulfonate (1.50 g, 3 mmol) in chloroform (6 m*l*) and triethylamine (0.42 m*l*, 3 mmol) was added. The mixture was left to stand overnight at room temperature, and then evaporated *in vacuo*. The residue was dissolved in ethyl acetate (20 m*l*), then the solution was washed successively with 4% sodium bicarbonate, 2% hydrochloric acid and water, and dried over sodium sulfate. The filtrate was evaporated *in vacuo*, and the oily residue was solidified by the addition of ether and petroleum ether. The product was recrystallized from ethyl acetate - ether - petroleum ether. Yield, 1.51 g (70%); mp 113°C; $[\alpha]_D^{25}$ −14.2° (*c* 1, dimethylformamide).

Found: C, 67.85; H, 6.42; N, 5.98%. Calcd for $C_{41}H_{45}N_3O_9$: C, 68.03; H, 6.27; N, 5.81%.

The LD Isomer (IV). This compound was obtained from dibenzyloxycarbonyl-L-lysine and I by the mixed anhydride method described above. Yield, 55%; mp 95°C; $[\alpha]_D^{20}$ +6.4° (*c* 1, dimethylformamide).

Found: C, 68.03; H, 6.32; N, 5.98%.

Dibenzyloxycarbonyl-lysyl-aspartic Acid Dibenzyl Ester. *The LL Isomer (V).* This compound was obtained from dibenzyloxycarbonyl-L-lysine and L-aspartic acid dibenzyl ester by the mixed anhydride method. Yield, 74%; mp 139—140°C; $[\alpha]_D^{25}$ −9.4° (*c* 1, dimethylformamide).

Found: C, 67.68; H, 6.11; N, 5.92%. Calcd for $C_{40}H_{43}N_3O_9$: C, 67.44; H, 6.52; N, 5.92%.

The LD Isomer (VI). This compound was obtained from dibenzyloxycarbonyl-L-lysine and II. Yield, 66%; mp 97—98°C; $[\alpha]_D^{20}$ +6.2° (*c* 1, dimethylformamide).

Found: C, 67.65; H, 6.19; N, 5.98%.

Lysyl-glutamic Acid (Lys-Glu). *The LL Isomer (VII).* A solution of III (0.72 g, 1 mmol) in a mixture of acetic acid (3 m*l*), methanol (1.2 m*l*) and water (0.6 m*l*) was treated with hydrogen in the presence of palladium black. The filtrate from the catalyst was evaporated *in vacuo* to dryness. The residual crystals were recrystallized from water - ethanol. Yield, 0.23 g (85%); mp 194—196°C (decomp.); $[\alpha]_D^{20}$ +20.1° (*c* 3.1, water) (Found as a hemihydrate: C, 46.34; H, 7.91; N, 14.49%). Bergmann *et al.*[15] reported the synthesis of this compound by hydrogenolysis of Z-L-Lys(ε-Z)-L-Glu-OH which was obtained through the saponification of Z-L-Lys(ε-Z)-L-Glu(γ-OEt)-OEt; mp 197°C; $[\alpha]_D^{19}$ +22.9° (water).

The LD Isomer (VIII). This compound was obtained by hydrogenolysis of IV as described above; yield, 96%; $[\alpha]_D^{20}$ +33.4° (*c* 1, water). The elemental analysis could not be performed because of its hygroscopic character compared with the LL isomer (VII), however the homogeneity of this compound VIII was confirmed by paper chromatography and electrophoresis.

Lysyl-aspartic Acid (Lys-Asp). *The LL Isomer (IX).* This compound was obtained by hydrogenolysis of V. Yield, 86%; $[\alpha]_D^{25}$ +25.3° (*c* 1.3, water) (Found as a monohydrate: C, 42.81; H, 7.73; N, 14.68%). Bergmann *et al.*[16] reported the synthesis of this compound by hydrogenolysis of Z-L-Lys(ε-Z)-L-Asp-OH; $[\alpha]_D^{25}$ +23° (water).

The LD Isomer (X). The compound VI was hydrogenated and the filtrate from the catalyst was evaporated to dryness. The residual crystals were collected with the aid of ethanol. Yield, 86%; mp 180—182°C (decomp.); $[\alpha]_D^{25}$ +30.6° (*c* 1, water).

Found: C, 42.66; H, 7.86; N, 14.68%. Calcd for $C_{10}H_{19}O_5N_3 \cdot H_2O$: C, 43.00; H, 7.58; N, 15.03%.

Benzyloxycarbonyl-glycyl-ε-benzyloxycarbonyl-L-lysine Ethyl Ester (XI). This compound was obtained from benzyloxycarbonyl-glycine and ε-benzyloxycarbonyl-L-lysine ethyl ester *p*-toluenesulfonate[17] by the mixed anhydride method as described for the preparation of III. Yield, 76%; mp 77—78°C; $[\alpha]_D^{21}$ +3.2° (*c* 1, ethyl acetate).

11) N. Izumiya and S. Makisumi, *Nippon Kagaku Zassi* (*J. Chem. Soc. Japan, Pure. Chem. Sect.*), **78**, 662, 1768 (1957).

12) We wish to correct the value of the L-isomer as $[\alpha]_D^{20}$ −1.0° (*c* 2, methanol).

13) S. Guttmann and R. A. Boissonas, *Helv. Chim. Acta*, **41**, 1852 (1958); E. Klieger, E. Schröder and H. Gibian, *Ann.*, **640**, 157 (1961).

14) J. R. Vaughan, Jr., and R. T. Osato, *J. Am. Chem. Soc.*, **73**, 5553 (1951).

15) M. Bergmann, L. Zervas and J. P. Greenstein, *Ber.*, **65**, 1692 (1932).

16) M. Bergmann, L. Zervas, H. Rinke and H. Schleich, *Z. Physiol. Chem.*, **224**, 26 (1934).

17) T. Kato, S. Makisumi, M. Ohno and N. Izumiya, *Nippon Kagaku Zasshi* (*J. Chem. Soc. Japan, Pure Chem. Sect.*), **83**, 1151 (1962).

Found: C, 62.50; H, 6.66; N, 8.42%. Calcd for $C_{26}H_{33}O_7N_3$: C, 62.49; H, 6.87; N, 8.43%.

Benzyloxycarbonyl-glycyl-ε-benzyloxycarbonyl-L-lysine Hydrazide (XII). A solution of XI (4.99 g, 10 mmol) and hydrazine hydrate (1.21 ml, 25 mmol) in methanol was allowed to stand at 30°C for 48 hr. The excess hydrazine was evaporated *in vacuo*, and then water (50 ml) was added to the residue. The resulting crystals were collected by filtration and washed with water. Yield, 4.3 g (91%); mp 163—165°C; $[\alpha]_D^{25}$ −1.2° (*c* 1, dimethylformamide) (Found: C, 59.25; H, 6.31; N, 14.41%). Erlanger and Brand[18] reported the synthesis of this compound from Z-Gly-L-Lys(ε-Z)-OMe with hydrazine; mp 167°C.

Benzyloxycarbonyl-glycyl-δ-benzyloxycarbonyl-L-ornithine Ethyl Ester (XIII). This compound was obtained from benzyloxycarbonyl-glycine and δ-benzyloxycarbonyl-L-ornithine ethyl ester *p*-toluenesulfonate[19] by the mixed anhydride method as described for the preparation of III. Yield, 71%; mp 79—80°C; $[\alpha]_D^{20}$ −7.6° (*c* 1, dimethylformamide).

Found: C, 61.84; H, 6.44; N, 8.66%. Calcd for $C_{25}H_{31}O_7N_3$: C, 61.58; H, 6.32; N, 8.56%.

Benzyloxycarbonyl-glycyl-δ-benzyloxycarbonyl-L-ornithine Hydrazide (XIV). The compound XIII was converted to the hydrazide as described for the preparation of XII. Yield, 87%; mp 141—143°C; $[\alpha]_D^{20}$ +0.8° (*c* 1, dimethylformamide).

Found: C, 58.10; H, 6.25; N, 14.75%. Calcd for $C_{23}H_{29}O_6N_5$: C, 58.18; H, 6.24; N, 14.62%.

Benzyloxycarbonyl-glycyl-ε-benzyloxycarbonyl-lysyl-glutamic Acid Dibenzyl Ester. *The LL Isomer (XV).* To a chilled solution of XII (1.94 g, 4 mmol) in glacial acetic acid (40 ml) and 2 N hydrochloric acid (2.4 ml) was added sodium nitrite (0.32 g) with stirring. After the solution had been allowed to stand for 5 min at −5°C, it was diluted with cold water (100 ml), and the protected dipeptide azide was extracted three times with 50 ml portions of ethyl acetate. The combined ethyl acetate solution was washed with 4% sodium bicarbonate and water, dried over sodium sulfate, and then added to a cold solution of L-glutamic acid dibenzyl ester *p*-toluenesulfonate (2.00 g, 4 mmol) in triethylamine (0.56 ml, 4 mmol) and dimethylformamide (10 ml). After the mixture had been stirred for 3 days at 0°C and evaporated *in vacuo*, the residue was dissolved in ethyl acetate and washed successively with 4% sodium bicarbonate, 2% hydrochloric acid and water, and dried over sodium sulfate. The filtrate was evaporated *in vacuo* and the oily residue was solidified by the addition of ether and petroleum ether. The product was recrystallized from ethyl acetate - ether - petroleum ether. Yield, 2.17 g (69%); mp 117—118°C; $[\alpha]_D^{20}$ −10.8° (*c* 1, dimethylformamide). For the elemental analysis, a part of the crystals was purified further by column chromatography of Sephadex LH-20 (column size; 0.9×50 cm) using dioxane as a solvent.

Found: C, 65.82; H, 6.20; N, 7.28%. Calcd for $C_{43}H_{48}O_{10}N_4$: C, 66.14; H, 6.20; N, 7.18%.

The LD Isomer (XVI). This compound was obtained from XII and I by the azide method. Yield, 63%; mp 122°C; $[\alpha]_D^{20}$ +3.6° (*c* 1, dimethylformamide).

Found: C, 65.87; H, 6.26; N 7.38%.,

Benzyloxycarbonyl-glycyl-ε-benzyloxycarbonyl-lysyl-aspartic Acid Dibenzyl Ester. *The LL Isomer (XVII).* The protected tripeptide ester (XVII—XXII) were obtained in the same manner from the corresponding protected dipeptide hydrazide (XII or XIV) and the corresponding amino acid dibenzyl ester as described for the preparation of XV. Yield, 64%; mp 122—123°C; $[\alpha]_D^{20}$ −8.6° (*c* 1, dimethylformamide).

Found: C, 65.72; H, 6.10; N, 7.44%. Calcd for $C_{42}H_{46}O_{10}N_4$: C, 65.76; H, 6.05; N, 7.31%.

The LD Isomer (XVIII). Yield, 60%; mp 105—106°C; $[\alpha]_D^{20}$ +6.2° (*c* 1, dimethylformamide).

Found: C, 65.31; H, 6.15; N, 7.76%.

Benzyloxycarbonyl-glycyl-δ-benzyloxycarbonyl-ornithyl-glutamic Acid Dibenzyl Ester. *The LL Isomer (XIX).* Yield, 61%; mp 84°C; $[\alpha]_D^{20}$ −10.0° (*c* 1, dimethylformamide).

Found: C, 65.46; H, 6.05; N, 7.18%. Calcd for $C_{42}H_{46}O_{10}N_4$: C, 65.76; H, 6.05; N, 7.31%.

The LD Isomer (XX). Yield, 76%; mp 96°C; $[\alpha]_D^{20}$ +5.2° (*c* 1, dimethylformamaide).

Found: C, 65.37; H, 6.00; N, 7.33%.

Benzyloxycarbonyl-glycyl-δ-benzyloxycarbonyl-ornithyl-aspartic Acid Dibenzyl Ester. *The LL Isomer (XXI).* Yield, 64%; mp 127—129°C; $[\alpha]_D^{20}$ −8.0° (*c* 1, dimethylformamide).

Found: C, 65.03; H, 5.83; N, 7.84%. Calcd for $C_{41}H_{44}O_{10}N_4$: C, 65.41; H, 5.89; N, 7.44%.

The LD Isomer (XXII). Yield, 61%; mp 103—104°C; $[\alpha]_D^{20}$ +6.4° (*c* 1, dimethylformamide).

Found: C, 64.98; H, 5.83; N, 7.77%.

Glycyl-lysyl-glutamic Acid (Gly-Lys-Glu), LL Isomer (XXIII) and LD Isomer (XXIV); Gly-Lys-Asp, LL Isomer (XXV) and LD Isomer (XXVI); Gly-Orn-Glu, LL Isomer (XXVII) and LD Isomer (XXVIII); Gly-Orn-Asp, LL Isomer (XXIX) and DL Isomer (XXX). Each of benzyloxycarbonyl-tripeptide benzyl ester (XV—XXII) (2 mmol) obtained above was suspended in a solution (20 ml) of acetic acid, methanol and water (6:1:3), and the mixture was treated with hydrogen in the presence of palladium black. As the hydrogenolysis had proceeded the suspended material went into the solution. The catalyst was removed by filtration, and the filtrate was evaporated *in vacuo* to dryness. The residual oil become hygroscopic crystals upon treatment with ethanol. The yields were almost quantitative. The homogeneity of these peptides was established by paper chromatography and electrophoresis. Elemental analysis was not performed because of its highly hygroscopic character. Amiard and Goffinet[20] reported the synthesis of XXIII by saponification and detritylation of Tri-Gly-L-Lys(ε-Tri)-L-Glu(γ-OEt)-OEt.

***o*-Nitrophenylsulfenyl-γ-benzyl-D-glutamic Acid Dicyclohexylammonium Salt (XXXI).** This compound was obtained according to the procedure for the L isomer.[21] Yield, 66%; mp 167—168°C; $[\alpha]_D^{20}$ +33.7° (*c* 3.5, chloroform). Reported value for the L isomer,[21] mp 168°C; $[\alpha]_D^{20}$ −34.0° (chloroform).

18) B. F. Erlanger and E. Brand, *J. Am. Chem. Soc.*, **73**, 4025 (1951).
19) N. Izumiya, T. Kato, Y. Fujita, M. Ohno and M. Kondo, This Bulletin, **37**, 1809 (1964).
20) G. Amiard and B. Goffinet, *Bull. Soc. Chim. France*, **1957**, 1133.
21) L. Zervas, D. Borovas and E. Gazis, *J. Am. Chem. Soc.*, **85**, 3660 (1963).

o-Nitrophenylsulfenyl-β-benzyl-D-aspartic Acid Dicyclohexylammonium Salt (XXXII). This compound was obtained according to the procedure for the L isomer.[22] Yield, 59%; mp 165°C; $[\alpha]_D^{20}$ +41.0° (*c* 4, chloroform). Reported value for the L isomer;[22] mp 165—166°C; $[\alpha]_D^{20}$ −38.0° (chloroform).

o-Nitrophenylsulfenyl-γ-benzyl-glutamyl-ε-benzyloxycarbonyl-lysine Benzyl Ester. *The LL Isomer (XXXIII).* To a solution of o-nitrophenylsulfenyl-γ-benzyl-L-glutamic acid dicyclohexylammonium salt[21] (1.72 g, 3 mmol) and ε-benzyloxycarbonyl-L-lysine benzyl ester *p*-toluenesulfonate[23] (1.63 g, 3 mmol) in chloroform (12 m*l*) was added dicyclohexylcarbodiimide (0.62 g, 3 mmol) with stirring at −5°C. After 2 hr at −5°C, the stirring was continued at room temperature overnight. After the reaction mixture was evaporated *in vacuo*, the residue was treated with ethyl acetate (20 m*l*), and insoluble precipitate of dicyclohexylurea was removed by filtration. The filtrate was washed successively with 4% sodium bicarbonate, 0.5 M citric acid and water, dried over sodium sulfate and evaporated *in vacuo* yielding an oily residue. Yield of the oil, 2.01 g (90%). This oil did not crystallize on prolonged standing in a refrigerator.

The DL Isomer (XXXIV). This compound was obtained from XXXI and ε-benzyloxycarbonyl-L-lysine benzyl ester as described above. The product was recrystallized from ethyl acetate - ether - petroleum ether. Yield, 73%; mp 87—88°C; $[\alpha]_D^{20}$ +19.2° (*c* 1, chloroform).

Found: C, 63.07; H, 5.79; N, 7.59%. Calcd for $C_{39}H_{12}O_9N_4S$: C, 63.06; H, 5.70; N, 7.54%.

o-Nitrophenylsulfenyl-β-benzyl-aspartyl-ε-benzyloxycarbonyl-lysine Benzyl Ester. *The LL Isomer (XXXV).* This compound was obtained from o-nitrophenylsulfenyl-β-benzyl-L-aspartic acid dicyclohexylammonium salt[22] and ε-benzyloxycarbonyl-L-lysine benzyl ester as described above and recrystallized from ethyl acetate - ether - petroleum ether. Yield, 88%; mp 128—129°C; $[\alpha]_D^{20}$ −17.2° (*c* 1, dimethylformamide).

Found: C, 62.58; H, 5.51; N, 7.83%. Calcd for $C_{35}H_{40}O_9N_4S$: C, 62.62; H, 5.53; N, 7.69%.

The DL Isomer (XXXVI). This compound was obtained from XXXII and ε-benzyloxycarbonyl-L-lysine benzyl ester as described above. Yield, 82%; mp 118—119°C; $[\alpha]_D^{20}$ +11.8° (*c* 1, chloroform).

Found: C, 61.76; H, 5.40; N, 7.84%. Calcd for $C_{38}H_{40}O_9N_4S \cdot 1/2H_2O$: C, 61.86; H, 5.60; N, 7.60%.

Benzyloxycarbonyl-glycyl-γ-benzyl-glutamyl-ε-benzyloxycarbonyl-lysine Benzyl Ester. *The LL Isomer (XXXVII).* To a solution of the nitrophenylsulfenyl-dipeptide ester XXXIII (1.54 g 2 mmol) in dioxane (6 m*l*), 2 N hydrogen chloride in dioxane (4 m*l*) was added. After the solution was allowed to stand at room temperature for 30 min, it was evaporated *in vacuo*. The residual oil was washed several times with ether by the way of decantation; yield of the oily dipeptide ester monohydrochloride, 1.26 g (102%). Then the compound XXXVII was prepared from benzyloxycarbonyl-glycine (2 mmol) and the dipeptide ester monohydrochloride (1.26 g) obtained above by the mixed anhydride method as described for the preparation of III. The product was recrystallized from ethyl acetate - ether - petroleum ether. Yield, 1.11 g (71%); mp 97°C; $[\alpha]_D^{20}$ −9.0° (*c* 1, dimethylformamide).

Found: C, 66.23; H, 6.11; N, 7.21%. Calcd for $C_{43}H_{48}O_{10}N_4$: C, 66.14; H, 6.20; N, 7.18%.

The DL Isomer (XXXVIII). The crystalline dipeptide ester monohydrochloride (1.23 g) was obtained from the nitrophenylsulfenyl-dipeptide ester XXXIV (2 mmol) with the treatment of hydrogen chloride in dioxane as has been described above. Then, XXXVIII was prepared from benzyloxycarbonyl-glycine and the dipeptide ester monohydrochloride (1.23 g) by the mixed anhydride method. The product was recrystallized from ethyl acetate - ether - petroleum ether. Yield, 1.09 g (70%); mp 126°C; $[\alpha]_D^{20}$ −4.4° (*c* 1, dimethylformamide).

Found: C, 66.21; H, 6.13; N, 7.22%.

Benzyloxycarbonyl-glycyl-β-benzyl-aspartyl-ε-benzyloxycarbonyl-lysine Benzyl Ester. *The LL Isomer (XXXIX).* This compound was prepared from benzyloxycarbonyl-glycine and the crystalline dipeptide ester monohydrochloride which was obtained from XXXV with hydrogen chloride in dioxane. The product was recrystallized from ethyl acetate - ether - petroleum ether. Yield, 61%; mp 117°C; $[\alpha]_D^{20}$ −18.6° (*c* 1, dimethylformamide).

Found: C, 65.76; H, 6.07; N, 7.27%. Calcd for $C_{42}H_{46}O_{10}N_4$: C, 65.76; H, 6.05; N, 7.31%.

The LD Isomer (XL). This compound was synthesized as described above from benzyloxycarbonyl-glycine and the crystalline dipeptide ester monohydrochloride which was obtained from XXXVI. Yield, 73%; mp 91°C; $[\alpha]_D^{20}$ +6.2° (*c* 1, dimethylformamide).

Found: C, 65.60; H, 6.08; N, 7.21%.

Glycyl-glutamyl-lysine (Gly-Glu-Lys). *The LL Isomer (XLI).* The compound XXXVII (0.78 g) was hydrogenated as has been described for the preparation of Lys-Glu (VII) and the filtrate from the catalyst was evaporated to dryness. The residual crystals were recrystallized from water-ethanol. Yield, 0.247 g (70%); $[\alpha]_D^{20}$ −22.4° (*c* 1, water).

Found: C, 44.28; H, 7.25; N, 15.66%. Calcd for $C_{13}H_{24}O_6N_4 \cdot H_2O$: C, 44.56; H, 7.48; N, 15.99%.

The DL Isomer (XLII). This was obtained by the

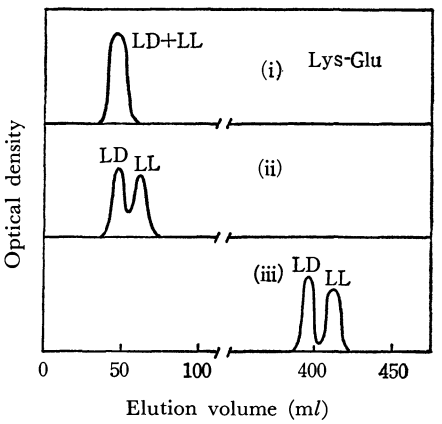

Fig. 5. Elution pattern of a diastereomeric mixture of Lys-Glu.
(i) 0.9×50 cm column and pH 5.28 buffer,
(ii) 0.6×10 cm column and pH 4.25 buffer,
(iii) 0.6×10 cm column, pH 3.25 buffer (360 m*l*) and then pH 4.25 buffer.

22) L. Zervas and C. Hamilidis, *ibid.*, **87**, 99 (1965).
23) O. Abe, H. Takiguchi, M. Ohno, S. Makisumi and N. Izumiya, This Bulletin, **40**, 1945 (1967).

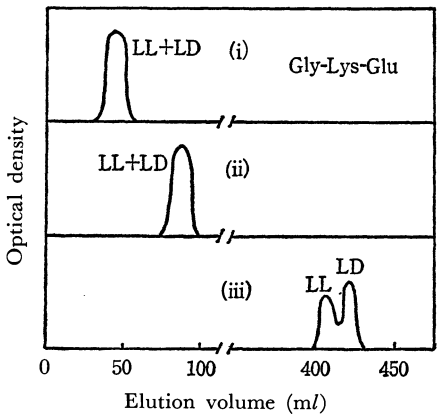

Fig. 6. Elution pattern of a diastereomeric mixture of Gly-Lys-Glu.
(i), (ii) and (iii); see Fig. 5.

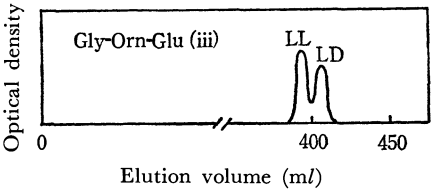

Fig. 7. Elution pattern of a diastereomeric mixture of Gly-Orn-Glu.
(iii); see Fig. 5.

hydrogenolysis of XXXVIII as described above. Yield, 82%; $[\alpha]_D^{20}$ +13.0° (*c* 1, water).

Found: C, 46.20; H, 7.28; N, 16.03%. Calcd for $C_{13}H_{24}O_6N_4 \cdot \frac{1}{2}H_2O$: C, 45.92; H, 7.35; N, 16.33%.

Glycyl-aspartyl-lysine (Gly-Asp-Lys). *The* LL *Isomer* (*XLIII*). This was obtained by hydrogenolysis of XXXIX. Yield, 71%; $[\alpha]_D^{20}$ −4.6° (*c* 1, water).

Found: C, 42.65; H, 7.10; N, 16.31%. Calcd for $C_{12}H_{22}O_6N_4 \cdot H_2O$: C, 42.85; H, 7.19; N, 16.66%.

The DL *Isomer* (*XLIV*). This was obtained by hydrogenolysis of XL. Yield, 85%; $[\alpha]_D^{20}$ +14.8° (*c* 1, water).

Found: C, 43.16; H, 7.42; N, 16.29%. Calcd for $C_{12}H_{22}O_6N_4 \cdot H_2O$: C, 42.85; H, 7.19; N, 16.66%.

Paper Chromatography and Paper Electrophoresis. A paper chromatography was carried out with ascending technique using Toyo Roshi No. 52, and a peptide on the paper was revealed with ninhydrin. As shown in Table 2, it was observed that the diastereomers of several peptides were separated on the chromatogram. The electrophoresis was carried out under the following condition: 500 V/30 cm with formic acid - acetic acid - methanol - water solution and 300 V/30 cm with 0.2 M sodium citrate buffer. As indicated in Table 2, it appeared that the ability to separate a diasteremeric mixture was less than that in the paper chromatography.

Separation Studies with Amino Acid Analyzer. A mixture of 0.6 μmol each of the LL form and the LD (or DL) form of di- or tripeptides was analyzed by Hitachi amino acid analyzer with spherical resin (No 3105), model KLA-3B, under the following conditions: flow rate, 60 ml/hr and jacket temperature, 55°C. Three different analyses were performed for each diastereomeric mixture as follows: (i) with 0.9×50 cm column, 0.2 M sodium citrate buffer at pH 5.28 was used; (ii) with 0.6×10 cm column, 0.2 M sodium citrate at pH 4.25 was used; (iii) with 0.6×10 cm column, 0.2 M sodium citrate at pH 3.25 was applied for 6 hr (toltal effluent volume, 360 ml), and then the buffer system was changed to pH 4.25. The results obtained were summarized in Table 2. The several chromatographic patterns with the amino acid analyzer were indicated in Figs. 5—7.

The authors wish to express their thanks to Dr. Haruhiko Aoyagi, in this laboratory for his valuable discussions.

BULLETIN OF THE CHEMICAL SOCIETY OF JAPAN VOL. 41 2141—2148 (1968)

Studies on Pyrimidine Derivatives and Related Compounds. LVII.[1] Cyclization Mechanisms of Ethyl 2-(5-Pyrazolyl)aminoalkylidenecyanoacetates

Akira TAKAMIZAWA, Yoshio HAMASHIMA and Shoji SAKAI

Shionogi Research Laboratory, Shionogi & Co., Ltd., Fukushima-ku, Osaka

and Saburo NAGAKURA

The Institute for Solid State Physics, The University of Tokyo, Azabu, Tokyo

(Received March 4, 1968)

It was found that the orientation of cyclization reaction of ethyl 2-(5-pyrazolyl)aminomethylenecyanoacetates (Va—c) and ethyl 1-cyano-2-(5-pyrazolyl)aminocrotonates (Xa—c) largely depends on the catalyst used: for example, the cyclization of Va by the acid catalyst results in only 7-amino derivative; on the other hand, the mixture of 7-amino derivative and 7-hydroxy derivative is obtained in the presence of the base catalyst. In order to clarify the mechanism of this reaction, we studied spectrophotometrically the behaviors of these compounds in basic solution, taking ethyl 2-(1,4-dimethylpyrazol-5-yl)aminomethylenecyanoacetate (XV), and ethyl 1-cyano-2-(1,4-dimethylpyrazol-5-yl)aminocrotonate (XVI) as model compounds. Consequently, it was found that the proton dissociation of the C_2-amino group is greatly disturbed by the methyl substitution on that carbon atom. This finding is used for explaining the fact that the base catalyzed cyclization of X is insensitive to the amount of catalyst used while that of V shows some dependency on the concentration of alkali.

Detailed investigation on the cyclization mechanism of 2-aminoalkylidenecyanoacetates has not yet been carried out. Recently, Midorikawa, *et al.*[2] reported that the condensation of methyl *cis*-1-cyano-2-methoxyacrylate and methyl *trans*-1-cyano-2-methoxycinnamate with hydrazine to pyrazole derivatives was mainly controlled by their geometric factors.

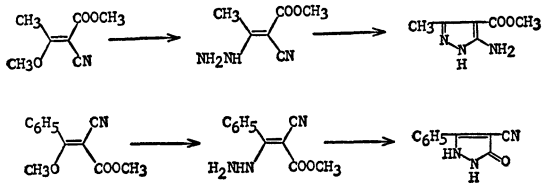

Chart 1

Previously,[3,4] it was suggested that the synthesis of 7-amino- or 7-hydroxypyrazolo[1,5-*a*]pyrimidine derivatives by the cyclization of ethyl 2-(5-pyrazolyl)-aminoalkylidenecyanoacetates was characteristically effected by acid or base catalysts, and, particularly in the latter case, was also effected by the amount of the catalyst used. This paper deals with the details of these reaction mechanisms.

Jones prepared ethyl ethoxymethylenecyanoacetate[5] (III) by the reaction of ethyl cyanoacetate (I), acetic anhydride, and ethyl orthoformate (II) and measured its NMR spectrum. He found a sharp singlet signal at τ 1.95 corresponding to the C_2 proton. We have prepared ethyl 2-(5-pyrazolyl)-aminomethylenecyanoacetates (Va—c) by the condensation of III with 5-aminopyrazoles (IVa—c) and have measured their NMR spectra with the results shown in Fig. 1. According to this figure, the NMR spectra of Va and Vc show the doublet signals of =CH-N< at τ 1.92 (J=13.8 cps) and at τ 1.86 (J=13.0 cps), respectively, each doublet being due to the coupling with adjacent NH proton. This indicates that Va and Vc consist of single ester, respectively. On the contrary, Vb shows the two doublet proton signals of =CH-N< at τ 1.72 (J=13.8 cps) and τ 2.00 (J=14.4 cps). From the intensities of these two doublet signals, the ratio of isomers is known to be approximately 1 : 1. Each doublet is converted into singlet by an addition of deuterium oxide. Jackman[6-8] and other several

1) Part LVI. A. Takamizawa, K. Hirai and S. Matsumoto, *Tetrahedron Letters*, **1968**, 4027.
2) H. Midorikawa, H. Baba and I. Hori, Presented at the 17th Annual Meeting of Chem. Soc. Japan, Tokyo, April, 1964.
3) A. Takamizawa, S. Hayashi, Y. Hamashima and R. Kido, *Yakugaku Zasshi* (*J. Pharmac. Soc. Japan*), **83**, 745 (1963).
4) S. Hayashi, *ibid.*, **85**, 442 (1965).
5) R. G. Jones, *J. Am. Chem. Soc.*, **74**, 4889 (1952).
6) L. M. Jackman and R. H. Wiley, *Proc. Chem. Soc.*, **1958**, 196.
7) L. M. Jackman and R. H. Wiley, *J. Chem. Soc.*, **1960**, 2881.
8) L. M. Jackman and R. H. Wiley, *ibid.*, **1960**, 2886.

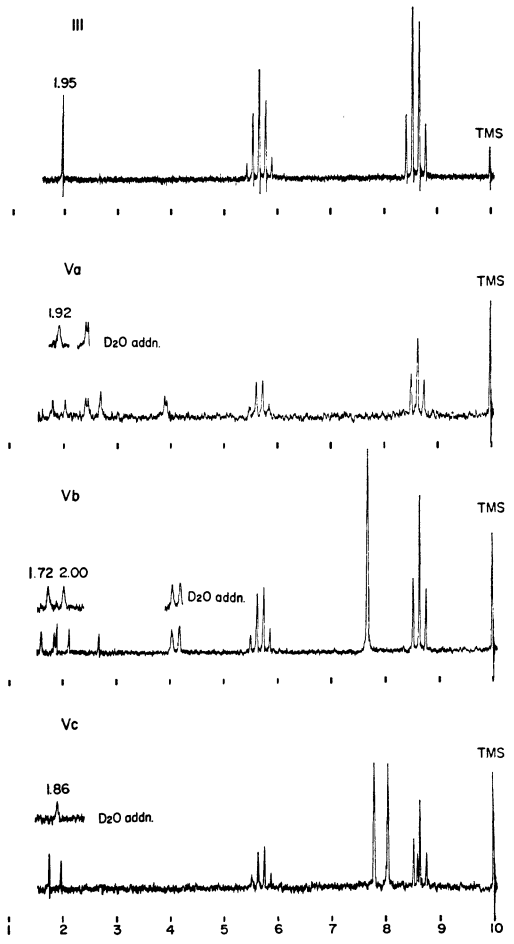

Fig. 1. The NMR spectra of III and Va—c at 60 Mc.

authors[9-12] demonstrated that, provided both isomers of a pair are available, NMR spectroscopy can be used to establish the geometric configurations of some α,β-unsaturated esters. This method is based on the fact that the protons of a *cis*-β-methyl group are more deshielded than those of a *trans*-β-methyl group. More recently, Hayashi, Hori, Baba and Midorikawa[13] and also McGreer *et al.*[14,15] reported that a *cis*-β-methyl group against the ester group of methyl 1-methoxyethylidenecyanoacetate is more

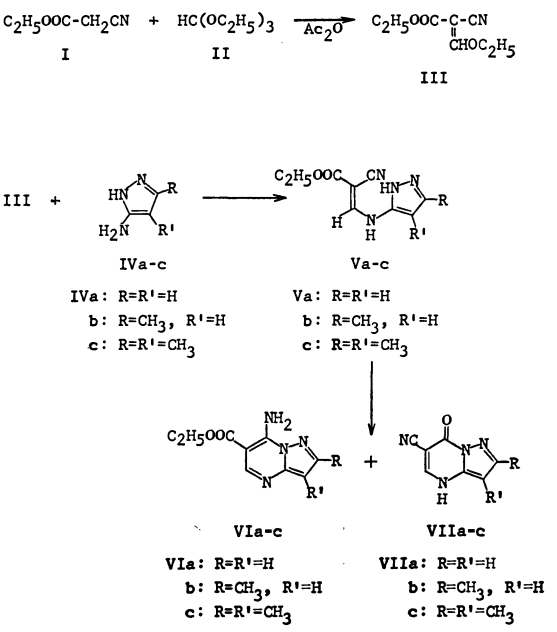

Chart 2

deshielded than that of *trans*-isomer, but the authors have no definite confidence for deciding the geometric configurations of Va—c from the data or NMR.

Now let us turn to the cyclization reaction of Va—c. The results obtained under various conditions are fairly systematic as is shown in Table 1a-d. The cyclization reaction of Va—c in the presence of acid catalysts gives only 7-amino derivatives (VIa—c). On the other hand, the reaction is rather complicated under base catalysts, and the mixture of VIa—c and 7-hydroxy derivatives (VIIa—c) can be obtained with

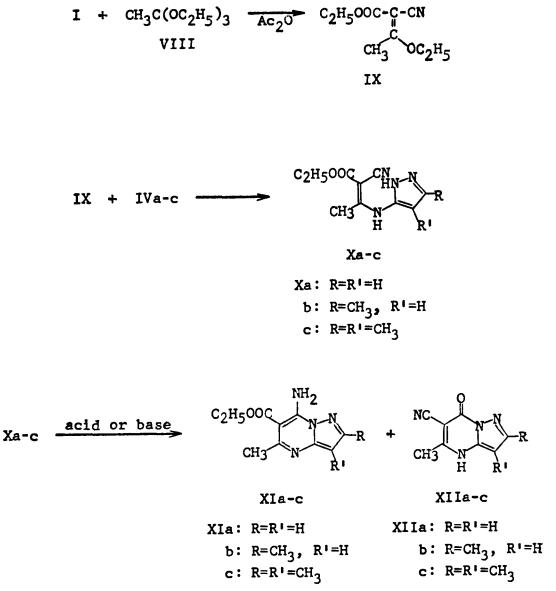

Chart 3

9) J. W. Burrcel, L. M. Jackman and B. C. L. Weedon, *Proc. Chem. Soc.*, **1959**, 233.
10) R. O. Morris, C. A. Vernon and R. F. M. White, *ibid.*, **1958**, 304.
11) D. E. Jones, R. O. Morries, C. A. Vernon and R. F. M. White, *J. Chem. Soc.*, **1960**, 2349.
12) S. Fujiwara, H. Shimizu, Y. Arata and S. Akabori, This Bulletin, **33**, 428 (1960).
13) T. Hayashi, I. Hori, H. Baba and H. Midorikawa, *J. Org. Chem.*, **30**, 695 (1965).
14) D. E. McGreer, R. S. McDanniel and M. G. Vinje, *Can. J. Chem.*, **43**, 1389 (1965).
15) D. E. McGreer, N. W. K. Chiu and M. G. Vinje, *ibid.*, **43**, 1398 (1965).

Table 1a. Ratios of VIa and VIIa prepared under various reaction conditions

Run	Va, mol	$NaOC_2H_5$,[a] mol	Time, hr	Temp., °C	Total yield, %	VIa/VIIa
1	0.002	0.001	91	Room	96.2	41.5/58.5
2	0.002	0.002	91	Room	86.1	29.9/70.1
3	0.002	0.004	43	Room	91.7	67.2/32.8
4	0.002	0.006	43	Room	86.7	77.7/22.3
5	0.002	0.001	2	Reflux	92.2	47.4/52.6
6	0.002	0.002	2	Reflux	91.7	30.8/69.2
7	0.002	0.004	2	Reflux	88.9	76.5/23.5
8	0.002	0.006	2	Reflux	83.6	88.8/11.2

Table 1b. Ratios of VIb and VIIb prepared under various reaction conditions

Run	Vb, mol	$NaOC_2H_5$,[a] mol	Time, hr	Temp., °C	Total yield, %	VIb/VIIb
1	0.002	0.001	148	Room	98.5	53.2/46.8
2	0.002	0.002	148	Room	94.2	54.6/45.4
3	0.002	0.004	148	Room	97.7	71.1/28.9
4	0.002	0.006	148	Room	96.3	81.0/19.0
5	0.002	0.001	2	Reflux	87.5	52.0/48.0
6	0.002	0.002	2	Reflux	94.3	43.6/56.4
7	0.002	0.004	2	Reflux	90.5	77.3/22.7
8	0.002	0.006	2	Reflux	92.6	81.9/18.1

Table 1c. Ratios of VIc and VIIc prepared under various reaction conditions

Run	Vc, mol	$NaOC_2H_5$,[a] mol	Time, hr	Temp., °C	Total yield, %	VIc/VIIc
1	0.002	0.001	144	Room	96.6	51.7/48.3
2	0.002	0.002	68	Room	90.3	62.4/37.6
3	0.002	0.004	43	Room	97.3	74.2/25.8
4	0.002	0.001	2	Reflux	95.5	60.4/39.6
5	0.002	0.002	2	Reflux	88.3	62.8/37.2
6	0.002	0.004	2	Reflux	95.3	79.4/20.6
7	0.002	0.006	2	Reflux	95.1	85.6/14.4
8	0.002	0.006	2	Reflux	92.3	89.8/10.2

Table 1d. Ratios of VI and VII prepared under various reaction conditions

Run	Starting material mol	Catalyst[a] mol	Time hr	Temp. °C	Total yield %	VI/VII
1	Va, 0.002	conc. HCl 0.004	2	Reflux	95.0	100/ —
2	Vb, 0.002	conc. HCl 0.004	2	Reflux	98.8	100/ —
3	Vc, 0.002	conc. HCl 0.004	2	Reflux	94.5	100/ —
4	Va, 0.002	CH_3COOH[b]	3	100	97.2	100/ —
5	Vb, 0.002	CH_3COOH[b]	3	100	97.7	100/ —
6	Vc, 0.002	CH_3COOH[b]	3	100	95.5	100/ —
7	Va, 0.002	Na_2CO_3[c]	0.02	100	84.5	—/100
8	Vb, 0.002	Na_2CO_3[c]	1	100	62.5	7.8/92.2
9	Vc, 0.002	Na_2CO_3[c]	1	100	80.0	34.3/65.7
10	Va, 0.002	NaOH[d]	0.03	100	81.6	—/100
11	Vb, 0.002	NaOH[d]	1	100	76.1	—/100
12	Vc, 0.002	NaOH[d]	1	100	78.5	—/100

a) 40 m*l* of C_2H_5OH was used as a solvent.
b) 3 m*l* of CH_3COOH was used as a solvent.
c) 10 m*l* of 10% aqueous Na_2CO_3 solution was used.
d) 10 m*l* of 5% aqueous NaOH solution was used.

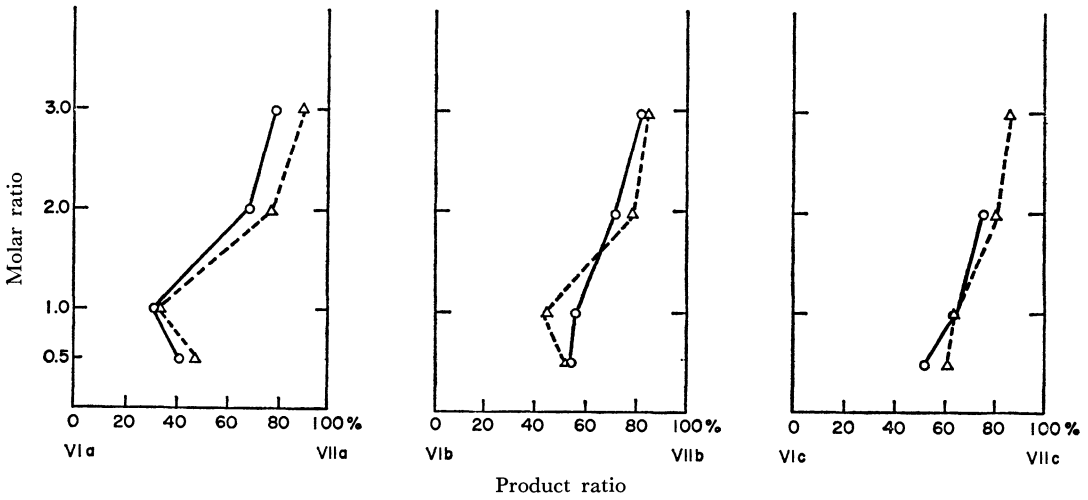

Fig. 2. Plot of the ratios of the products (VI and VII) at room temperature (——) and at refluxing temperature (----).

TABLE 2. RATIOS OF XI AND XII PREPARED UNDER VARIOUS REACTION CONDITIONS

Run	Starting material mol	Catalyst, mol	Solvent[a]	Time hr	Temp. °C	Total yield %	XI/XII
1	Xa, 0.002	conc. HCl, 0.004	C_2H_5OH	2	Reflux	86.5	54.6/45.4
2	Xb, 0.002	conc. HCl, 0.004	C_2H_5OH	2	Reflux	90.2	55.6/44.4
3	Xc, 0.002	conc. HCl, 0.004	C_2H_5OH	2	Reflux	95.0	38.3/61.7
4	Xa, 0.002	$NaOC_2H_5$,[b] 0.006	DMF	2	100	90.1	0/100
5	Xb, 0.002	$NaOC_2H_5$,[b] 0.006	DMF	2	100	98.3	0/100
6	Xc, 0.002	$NaOC_2H_5$,[b] 0.006	DMF	2	100	96.5	0/100
7	Xa, 0.002	$NaOC_2H_5$, 0.002	C_2H_5OH	2	Reflux	90.6	0/100
8	Xa, 0.002	$NaOC_2H_5$, 0.004	C_2H_5OH	2	Reflux	94.0	0/100
9	Xa, 0.002	$NaOC_2H_5$, 0.006	C_2H_5OH	24	Room	94.2	0/100
10	Xb, 0.002	$NaOC_2H_5$, 0.004	C_2H_5OH	2	Reflux	87.8	0/100
11	Xc, 0.002	$NaOC_2H_5$, 0.004	C_2H_5OH	2	Reflux	93.2	0/100
12	Xa, 0.002	CH_3COOH,	CH_3COOH[c]	3	100	94.4	58.9/41.1
13	Xa, 0.002	NaOH	H_2O[d]	24	Room	75.8	0/100

a) 40 m*l* of each solvent was used.
b) 1% $NaOC_2H_5$ in C_2H_5OH was used.
c) 3 m*l* of CH_3COOH was used as a solvent.
d) 10 m*l* of 5% NaOH solution was used as a solvent.

the general tendency that the proportion of VIa—c increases with the increasing amount of catalysts. Correlations of the ratios of the products with the amounts of catalysts are summarized in Fig. 2. The correlation curves for Va and Vb show the minimum ratios of VI to VII when an equimolar amount of catalyst is used.

Ethyl 1-cyano-2-ethoxycrotonate (IX) obtained by the reaction of I with ethyl orthoacetate (VIII) in acetic anhydride consists of the geometric isomers in the ratio of approximately 96 : 4. IX was used without further purification to prepare ethyl 1-cyano-2-(5-pyrazolyl)aminocrotonates (Xa—c), which were all decided by the NMR measurement to consist of a single component, respectively. The treatment of Xa—c with acid or alkali gives cyclization products in good yield. The results are given in Table 2. As is clearly seen in this table, only 7-hydroxy derivatives (XIIa—c) can be obtained under basic conditions regardless of the amount of the catalysts. On the other hand, the cyclization reaction of Xa—c under acidic conditions gives 7-amino- (XIa—c) and 7-hydroxy derivatives (XIIa—c) in the ratio of approximately 1 : 1.

From the above-mentioned results, it is clear that the orientation of cyclization reaction of Va—c is effected by the kind of catalyst used, namely, by acid or base catalyst used. Moreover, in the case of the base catalyzed cyclization, the reaction is sensitive to the amount of the catalyst. The similar situation concerning the dependence on the kind of catalyst was found for the reaction of Xa—c. In this

case, however, we could not observe the dependence upon an amount of base. In order to clarify the reason for the difference in the reaction between Va—c and Xa—c, their behaviors in alkaline medium have been studied by measuring ultraviolet absorption spectra of ethyl 2-(1,4-dimethylpyrazol-5-yl)-aminomethylenecyanoacetate (XV), and ethyl 1-cyano-2-(1,4-dimethylpyrazol-5-yl)aminocrotonate (XVI) which are similar in their structures to V and X, respectively, but cannot be expected to take pyrazolopyrimidine condensation because of the methylation on the N atom. In XV, as is shown in Fig. 3, the ultraviolet absorption maximum at 286 mμ shifts to 318 mμ by an addition of the base even in alcoholic medium, indicating the occurrence of deprotonation at the C_2-amino group.[16] The

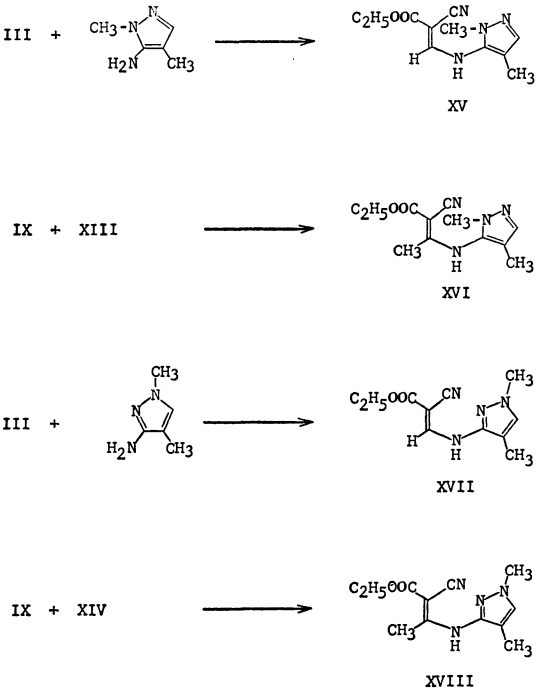

Chart 4

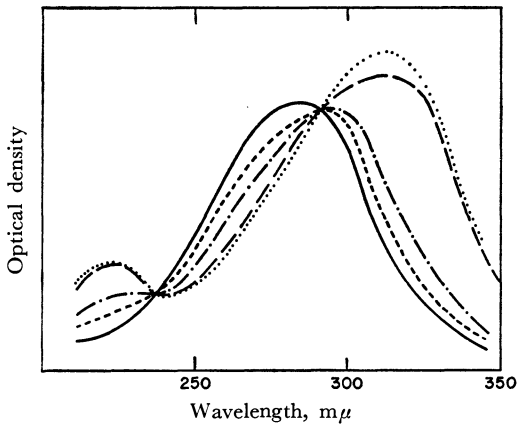

Fig. 3. Ultraviolet absorption curves of XV under various conditions.
——: Neutral in C_2H_5OH (λ_{max} 286 mμ)
----: In the presence of 0.5 eq. mole of $NaOC_2H_5$
·—·: In the presence of 1.0 eq. mole of $NaOC_2H_5$
——: In the presence of 3.0 eq. mole of $NaOC_2H_5$
·····: In the presence of excess of $NaOC_2H_5$

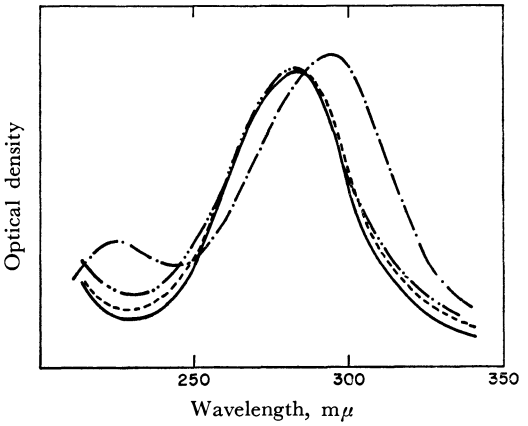

Fig. 4. Ultraviolet absorption curves of XVI under various conditions.
——: Neutral in C_2H_5OH (λ_{max} 285 mμ)
----: In the presence of $NaOC_2H_5$ (λ_{max} 285 mμ)
·—·: In the presence of NaOH dil. C_2H_5OH (λ_{max} 227.5, 296 mμ)
·——·: In the presence of conc. HCl in C_2H_5OH (λ_{max} 285 mμ)

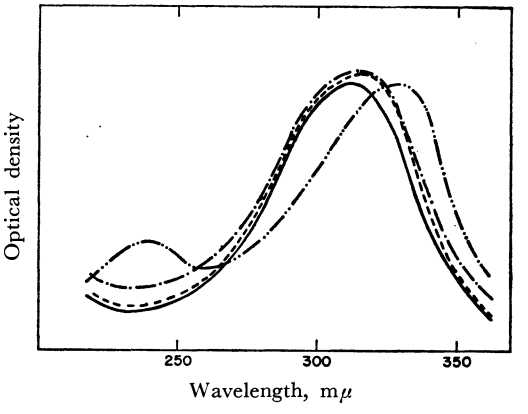

Fig. 5. Ultraviolet absorption curves of Vb under various conditions.
——: Neutral in C_2H_5OH (λ_{max} 314 mμ)
----: In the presence of excess of $NaOC_2H_5$ (λ_{max} 318 mμ)
·—·: In the presence of NaOH in dil. C_2H_5OH (λ_{max} 318 mμ)
·——·: In the presence of excess of NaOH in H_2O (λ_{max} 239, 327 mμ)

16) Deprotonation may conceivably occur in the other groups. For example, the C_2-H of XV may dissociate proton in basic media. This possibility, however, is very likely excluded, because the C_2-H dissociation product is less stabilized by the resonance than the C_2-N-H dissociation product.

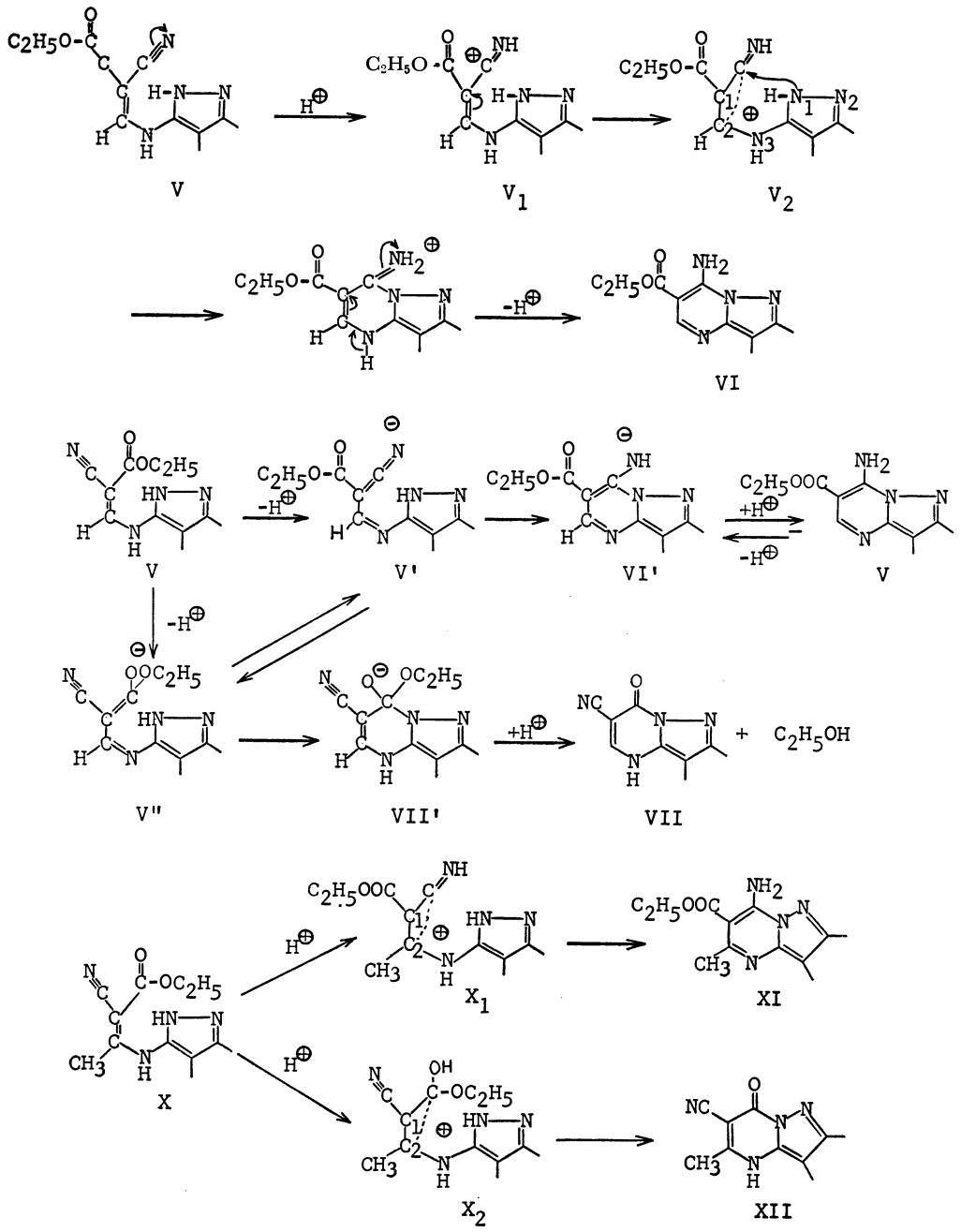

Chart 5

pK_a value of XV can be evaluated to be 8.45 by the aid of the usual equation.[17] In the presence of more than 5 equivalents of the base, the absorption curve becomes constant because of the complete dissociation. In XVI the dissociation hardly occurs in alcoholic medium, but by the addition to water, the dissociation may be thought to occur in view of the appearance of a new absorption maximum at 227.5 mμ (Fig. 4). This means that the methyl substitution at the C_2 position makes the dissociation more difficult.[18]

17) $pK_a = pH - \log((A-b)/(b-B))$ (A, B and b are the molecular extinction coefficients of the acidic form, the basic form and the equilibrium mixture of them, respectively, under the conditions that the total concentration of XV is constant).

18) The ultraviolet absorption spectra of ethyl 2-(1,4-dimethylpyrazol-3-yl)aminomethylenecyanoacetate (XVII) and ethyl 1-cyano-2-(1,4-dimethylpyrazol-3-yl)aminocrotonate (XVIII) were measured in solutions with various pH values. The results show that XVIII is dissociated with more difficulty than XVII is.

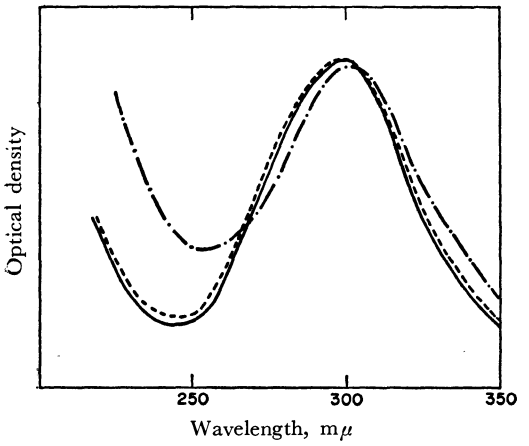

Fig. 6. Ultraviolet absorption curves of Xa under various conditions.
——: Neutral in C_2H_5OH (λ_{max} 298 mμ)
----: In the presence of $NaOC_2H_5$ (λ_{max} 298 mμ)
·—·: In the presence of excess of NaOH in H_2O (λ_{max} 303 mμ)

The same tendency was also observed in Va—c and Xa—c. For example, at room temperature dissociation of Vb in basic alcohol, which could hardly be expected to cause the cyclization reaction, was not detected, but the dissociation proceeded by the addition of water and the maximum at 318 mμ shifted to 327 mμ accompanied with an appearance of a new maximum at 239 mμ. On the contrary, as is shown in Fig. 6, dissociation was scarcely detected in Xa by the addition of excess of base in alcohol or even in water. From the above-mentioned experimental results of ultraviolet absorption spectra, it may be obvious that the dissociation of 2-(5-pyrazolyl)aminoalkylidenecyanoacetates in alkaline medium becomes difficult by the substitution of methyl group at the C_2 position. This seems to correspond to the fact that the cyclization of Va—c is more sensitive to the amount of alkali as catalyst than Xa—c.

As a whole, possible cyclization mechanisms of this series may be considered as follows: As is shown in Chart 5, protonation will occur in acidic medium at the cyano group[19] in V to give a carbonium ion intermediate such as V_2. In this intermediate cation, rotation may be possible around the C_1-C_2 bond, and the nucleophilic attack of pyrazole N_1 to the cyano group may preferentially give VI. With base catalyst, deprotonation from the N_3 amino group may easily give V′ or V″. The orientation of the reaction will be influenced by the stability of V′ and V″,[20] and the equilibrium (V′ ⇌V″) will be inclined towards V′ with the increasing amount of the base.

In X protonation occurs at the cyano or carbonyl group and the carbonium ions such as X_1 and X_2 are produced. In these ions rotation around the C_1-C_2 bond may be somewhat hindered sterically by the methyl group resulting in a mixture of 7-amino- (XI) and 7-oxo (XII) compounds. In the consideration of the base catalyzed cyclization of X, we must give attention to the spectrophotometric observation that deprotonation at the N_3 amino group is prohibited by the steric effect of the adjacent methyl group in addition to its hyperconjugation effect. From this it may be inferred that only 7-oxo compound (XII) is produced mainly because of its original geometric factor. In this series of reactions, the details of orientation mechanism may be thought to be controlled by various factors such as solvent effect, reaction temperature and so on. Further work on the reaction mechanisms for this series is in progress.

Experimental[21]

Cyclization Reactions of Va—c under Various Conditions. A. Vc (0.4685 g) was dissolved in 40 ml of ethanol by warming. After being cooled, the solution was mixed with 2 ml of ethanol containing 0.046 g of sodium, and stirred at room temperature for 68 hr. Evaporation of the mixture gave solids. To the residue was added water and the precipitated solids were filtered, washed and dried to give 0.268 g (56.3%) of VIc. The filtrate was made acidic by acid and the precipitated solids were filtered and dried. Recrystallization from methanol gave colorless needles, which were proved to be identical with an authentic sample. Yield, 34%.

B. Vb (0.44 g) was dissolved in 40 ml of ethanol by warming. After cooled, the solution was mixed with 1 ml of ethanol containing 0.023 g of sodium, and heated to reflux for 2 hr, and concentrated. To the residue was added water and the precipitated solids were collected and dried to give 0.2 g (45.5%) of VIb. From the mother liquid was obtained 0.146 g (42.0%) of VIIb neutralized by acetic acid.

C. To 10 ml of 5% sodium hydroxide in water was suspended 0.4124 g of Va, and the mixture was heated at 100°C for 20 min to become clear solution. After cooled, the solution was neutralized by acetic acid to give 0.261 g (81.6%) of VIIa as colorless prisms.

D. To 10 ml of 10% sodium carbonate in water was added 0.4685 g of Vc, and the mixture was heated on a steam bath for 1 hr resulting to obtain clear solution. After being cooled, the precipitated solids were collected and washed to give 0.103 g (27.4%) of VIc. The filtrate

19) The intermediate produced by protonation on the carbonyl oxygen atom can be considered. This intermediate, however, is disregarded for the cyclization of V, because the actual reaction does not occur through it.

20) In Chart 5, V′ and V″ are, respectively, represented by one of various resonance structures. In these intermediates, the negative charge may be considered to be delocalized all-around the molecule.

21) All NMR spectra were obtained on the Varian A-60 spectrometer in deuterio chloroform using tetramethylsilane (TMS) as an internal reference. The ultraviolet absorption spectra were recorded by Hitachi ELS-3 recording spectrophotometer.

was neutralized with acetic acid to precipitate a colorless solid, which was proved to be VIIc by the comparisons of infrared spectra. Yield, 0.246 g (52.6%).

E. To the suspension of 0.4124 g of Va in 40 m*l* of ethanol was added 0.42 g of conc. hydrochloric acid, and the mixture was heated to reflux on a steam bath for 2 hr. Evaporation of the solution resulted colorless residue, which was dissolved in water and neutralized with sodium carbonate to precipitate VIa as colorless needles, yield, 0.391 g (95%).

Cyclization Reactions of Xa—c under Various Conditions. A. To a solution of 0.4405 g of Xa in 40 m*l* of ethanol was added 0.42 g of conc. hydrochloric acid, and the mixture was heated to reflux for 2 hr and evaporated. The residues were dissolved in water and neutralized with sodium carbonate to obtain colorless solids, which were extracted with cold sodium hydroxide solution and filtered. The solid was proved to be identical with XIa by the comparisons of their infrared spectra. Yield, 0.137 g (39.4%). Sodium hydroxide solution was neutralized with acetic acid to obtain XIIa as colorless needles, yield, 0.208 g (47.2%).

B. To a solution of 0.4405 g of XIa in 40 m*l* of ethanol was added 0.092 g of sodium in ethanol (9 m*l*), and the mixture was heated to reflux on a steam bath for 2 hr. Evaporation of the solution gave colorless solid, which was dissolved in water and neutralized with acetic acid to give XIIa as colorless sticks, yield. 0.327 g (94%).

Ethyl 2-(1,4-Dimethylpyrazol-5-yl)aminomethylenecyanoacetate (XV). A solution of 1.7 g of III and 1.12 g of XIII in 30 m*l* of ethanol was heated to reflux for 3 hr, and concentrated. The residue was recrystallized from ethanol - ether to give XV as colorless sticks, mp 112—113°C, yield, 2.12 g (90.6%).

Found: C, 56.50; H, 6.35; N, 23.98%. Calcd for $C_{11}H_{14}O_2N_4$: C, 56.40; H, 6.02; N, 23.92%.

Ethyl 1-Cyano-2-(1,4-dimethylpyrazol-5-yl)aminocrotonate (XVI). A solution of 0.366 g of IX and 0.222 g of XIII in 3 m*l* of ethanol was heated to reflux for 10 hr, and concentrated to afford colorless residue, which was recrystallized from acetone - ether to give XVI as colorless rhombi, mp 142—144°C. Yield, 0.42 g (84.6%).

Found: C, 58.28; H, 6.32; N, 22.63%. Calcd for $C_{12}H_{16}O_2N_4$: C, 58.05; H, 6.50; N, 22.57%.

Ethyl 2-(1,4-Dimethylpyrazol-3-yl)aminomethylenecyanoacetate (XVII). A mixture of 0.85 g of III and 0.56 g of XIV in 20 m*l* of ethanol was heated on a steam bath for 5 hr, and concentrated to give colorless solid, which was recrystallized from ethanol to give XVII as colorless needles, mp 122—123°C. Yield, 1.02 g (87.2%).

Found: C, 56.50; H, 6.35; N, 23.98%. Calcd for $C_{11}H_{14}O_2N_4$: C, 56.40; H, 6.02; 23.92%.

Ethyl 1-Cyano-2-(1,4-dimethylpyrazol-3-yl)aminocrotonate (XVIII). A solution of 1.5 g of XIV and 2.6 g of IX in 10 m*l* of ethanol was stirred at room temperature for 30 min to give colorless solid, which was filtered and recrystallized from ether to obtain XVIII as colorless silky needles, mp 143°C. Yield, 2.3 g (71.7%).

Found: C, 58.36; H, 6.72; N, 22.83%. Calcd for $C_{12}H_{16}O_2N_4$: C, 58.05; H, 6.50; N, 22.57%.

BULLETIN OF THE CHEMICAL SOCIETY OF JAPAN VOL. 41 2148—2150 (1968)

Oxazolidone Derivatives of Hydroxyamino Acids. V.[1] New Synthesis of *threo*- and *erythro*-β-Hydroxy-DL-aspartic Acids*[1]

Toshishige INUI,*[2] Yoshimoto OHTA,*[3] Toshiaki UJIKE,*[4]
Hakuji KATSURA and Takeo KANEKO

Department of Chemistry, Faculty of Science, Osaka University, Toyonaka, Osaka

(Received March 8, 1968)

threo- and *erythro*-β-Hydroxy-DL-aspartic acids (VI and X) were synthesized by oxidation and subsequent hydrolysis of DL-*trans*- and DL-*cis*-5-furyl-2-oxo-oxazolidine-4-carboxylic acids (IV and VIII) derived from *threo*- and *erythro*-β-furyl-DL-serines (III and VII) respectively.

β-Hydroxyaspartic acids were first synthesized by Dakin.[2] Later, Kornguth[3] synthesized these amino acids by condensation of glyoxalic acid with copper glycinate. Recently, *threo*- and *erythro*-β-hydroxy-DL-aspartic acids were synthesized stereochemically by the reaction of *cis*- and DL-*trans*-epoxysuccinic acids with ammonia[4] or benzylamine[5] respectively.

1) Part IV: T. Inui, *Nippon Kagaku Zasshi* (*J. Chem. Soc. Japan, Pure Chem. Sect.*), **83**, 493 (1962).

*1 Presented at the 14th Annual Meeting of the Chemical Society of Japan, Tokyo, April, 1961.

*2 Present address: Institute of Chemistry, College of General Education, Osaka University, Toyonaka, Osaka.

*3 Present address: The Institute of Food Chemistry, Dojima, Kita-ku, Osaka.

*4 Present address: Sun Star Dentifrice Co., Takatsuki, Osaka.

2) H. D. Dakin, *J. Biol. Chem.*, **48**, 273 (1921); **50**, 410 (1922).

3) M. L. Kornguth and H. J. Sallach, *Arch. Biochem. Biophys.*, **91**, 39 (1960).

4) T. Kaneko and H. Katsura, This Bulletin, **36**, 899 (1963); H. Okai, N. Imamura and N. Izumiya, *ibid.*, **40**, 2154 (1967).

5) Y. Liwschitz, Y. Rabinsohn and A. Haber, *J. Chem. Soc.*, **1962**, 3589.

The present paper is concerned with another stereospecific synthesis of *threo-* and *erythro-*β-hydroxy-DL-aspartic acids from the corresponding β-furyl-DL-serines respectively.

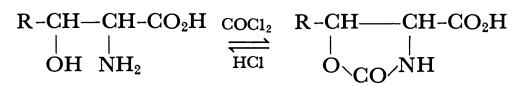

(I) (II)

In the previous report,[6] hydroxyamino acids (I) such as threonine were easily cyclized with phosgene to the corresponding oxazolidone derivatives (II) without any configurational change at the either asymmetric center. If *trans-* and *cis-*furyloxazolidone-carboxylic acids (II, R = C_4H_3O) derived from *threo-* and *erythro-*β-furylserines (I, R = C_4H_3O) were oxidized to the corresponding oxazolidone-dicarboxylic acids (II, R = CO_2H), the dicarboxylic acids thus obtained would be hydrolyzed to *threo-* and *erythro-*β-hydroxyaspartic acids (I, R = CO_2H) maintaining the same configurations with those of the starting β-furylserines.

*threo-*β-Furyl-DL-serine (III) was prepared from furfural and glycine by the directions of Hayes.[7] On the other hand, *erythro-*β-furyl-DL-serine (VII)

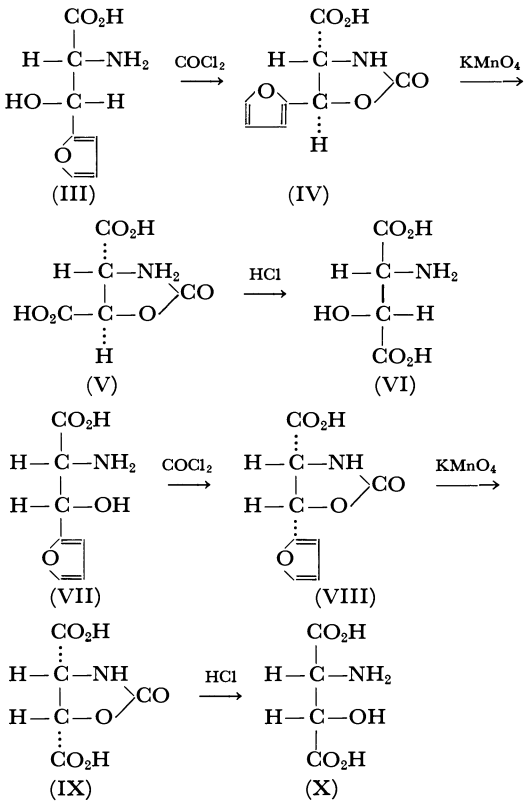

(III) (IV) (V) (VI) (VII) (VIII) (IX) (X)

Table 1. R_f Values on paper chromatogram

threo-Isomer	R_f	*erythro*-Isomer	R_f
III	0.28	VII	0.18
threo-β-Phenyl-DL-serine	0.42	*erythro*-β-Phenyl-DL-serine	0.27
Threonine	0.18	Allothreonine	0.13

Solvent: *n*-Butanol-acetone-concentrated aqueous ammonia-water (8:1:1:6).[8]

was separated as its dioxane adduct from the mixture of III and VII, which was obtained by condensation of furfural with copper glycinate, by applying the method for separation of *erythro-*β-phenyl-DL-serine from its *threo-*isomer.[8] The R_f values of III and VII on paper chromatogram were compared with those of threonine, allothreonine and *threo-* and *erythro-*β-phenylserines (Table 1), and their structures were confirmed as the assigned ones. Then, III and VII were cyclized with phosgene to DL-*trans-* and DL-*cis-*5-furyl-2-oxo-oxazolidine-4-carboxylic acids (IV and VIII) respectively. Oxidation of IV with aqueous potassium permanganate solution provided DL-*trans-*2-oxo-oxazolidine-4,5-dicarboxylic acid (V) as a crystalline state in a yield of 30%, which was hydrolyzed with hydrochloric acid to *threo-*β-hydroxy-DL-aspartic acid (VI). However, oxidation and subsequent hydrolysis of IV without isolation of V gave VI in an overall yield of 40%. Similarly, *erythro-*β-hydroxy-DL-aspartic acid (X) was obtained by oxidation and subsequent hydrolysis of VIII in a yield of 39%. The properties tested of VI and X were identical with those of the corresponding authentic samples.

Experimental*5

***threo*-β-Furyl-DL-serine (III).** According to the directions of Hayes,[7] III was prepared by condensation of 293 g (3.05 mol) of furfural with 115 g (1.53 mol) of glycine in the presence of 170 g (3.03 mol) of potassium hydroxide in 1200 m*l* of ethanol. Yield, 126 g (48%), mp 197°C (decomp.) after recrystallization from water and ethanol.

Found: C, 49.47; H, 5.41; N, 8.28%. Calcd for $C_7H_9NO_4$: C, 49.12; H, 5.30; N, 8.18%.

***erythro*-β-Furyl-DL-serine (VII).** Using the method for preparation of threonine by Akabori,[9] a mixture of 10.2 g (0.106 mol) of furfural and 11.3 g (0.0534 mol) of copper glycinate in 200 m*l* of 1 N potassium hydroxide was stirred for 2 hr at 10—20°C. After it had been kept overnight at room temperature, undissolved material was filtered off and the filtrate was acidified with 20 m*l* of acetic acid. The acidic solution was washed with ether and bubbled with a stream of hydrogen sulfide to decompose the resulting copper complex. The filtrate from copper sulfide was evaporated *in vacuo* to a small

6) T. Kaneko and T. Inui, *Nippon Kagaku Zasshi (J. Chem. Soc. Japan, Pure Chem. Sect.)*, **82**, 1075 (1961); T. Inui and T. Kaneko, *ibid.*, **82**, 1078 (1961).

7) K. Hayes and G. Geber, *J. Org. Chem.*, **16**, 269 (1951).

8) K. N. F. Shaw and S. W. Fox, *J. Am. Chem. Soc.*, **75**, 3421 (1953).

*5 All melting points are uncorrected.

9) M. Sato, K. Okawa and S. Akabori, This Bulletin, **30**, 937 (1957).

volume and diluted with ethanol to separate *threo*-isomer III (9.1 g; 50%), which was collected by filtration. The residue obtained by evaporation of solvent from the filtrate was dissolved into 30 m*l* of water and 30 m*l* of dioxane was added to the aqueous solution to precipitate VII as its dioxane adduct. Yield, 5.0 g (22%). Recrystallization from water-dioxane (1: 1) gave 3.3 g of chromatographically pure VII melting at 169°C (decomp.).

Found: C, 50.44; H, 6.06; N, 6.55%. Calcd for $C_7H_9NO_4 \cdot \frac{1}{2}C_4H_8O_2$: C, 50.23; H, 6.09; N, 6.51%.

DL-*trans*-5-Furyl-2-oxo-oxazolidine-4-carboxylic Acid (IV). To a solution of 29.0 g (0.168 mol) of III in 645 m*l* (0.645 mol) of 1 N potassium hydroxide, a solution of 20.2 g (0.204 mol) of phosgene in 80 m*l* of toluene was added dropwise over 30 min with stirring at 0—3°C and the reaction mixture was stirred for an additional 3 hr below 5°C. The aqueous layer separated from organic layer was acidified with 14 m*l* of concentrated hydrochloric acid to separate a crude product (28.0 g, mp 199—200°C (decomp.)), which was shown to be a mixture of IV and its potassium salt by detecting with flame test.

A stream of dry hydrogen chloride was passed through a suspension of the crude product in about 30 volumes of ethyl acetate and the resulting mixture was washed thoroughly with water. Evaporation of the dried solution provided IV as a pure state. Yield, 21.0 g (63%); mp 126—128°C (decomp.) after recrystallization from ethyl acetate - petroleum ether.

Found: C, 48.70; H, 3.64; N, 7.12%. Calcd for $C_8H_7NO_5$: C, 48.74; H, 3.58; N, 7.11%.

DL-*cis*-5-Furyl-2-oxo-oxazolidine-4-carboxylic Acid (VIII). In a similar way, a solution of 5.0 g (0.0232 mol) of dioxane adduct of VII in 50 m*l* (0.0891 mol) of 10% aqueous potassium hydroxide solution was treated with a solution of 2.8 g (0.0283 mol) of phosgene in 15 m*l* of toluene. The aqueous layer separated from organic layer was acidified with concentrated hydrochloric acid and the acidic solution was extracted with ethyl acetate. The dried extract was evaporated *in vacuo* leaving VIII as a crystalline solid. Yield, 2.8 g (61%); mp 143—144°C (decomp.) after recrystallization from ethyl acetate.

Found: C, 48.77; H, 3.71; N, 6.78%. Calcd for $C_8H_7NO_5$: C, 48.74; H, 3.58; N, 7.11%.

DL-*trans*-2-Oxo-oxazolidine-4, 5-dicarboxylic Acid (V). Three grams (0.0152 mol) of IV was dissolved into 200 m*l* of water and neutralized with 15 m*l* (0.0150 mol) of 1 N potassium hydroxide. The resulting solution was oxidized with 270 m*l* (0.0683 mol; 96% of required ammount) of 4% aqueous potassium permanganate solution for 2 hr at 15—20°C. After manganese dioxide precipitated had been removed, the aqueous solution was acidified with 10 m*l* of concentrated hydrochloric acid and evaporated to dryness *in vacuo*. The residue was extracted three times with 50-m*l* portions of hot dioxane and the combined extracts were evaporated *in vacuo* to give crystals. Yield, 0.8 g (30%); mp 159—160°C (decomp.) after recrystallization from ethyl acetate - petroleum ether.

Found: C, 34.90; H, 3.07; N, 7.95%; mol wt (titration with alkali), 177, 180. Calcd for $C_5H_5NO_6$: C, 34.29; H, 2.88; N, 8.00%, mol wt, 175.1.

The treatment of V with an ethereal diazomethane solution gave dimethyl DL-*trans*-2-oxo-oxazolidine-4,5-dicarboxylate melting at 97—99°C after recrystallization from benzene.

Found: C, 41.96; H, 4.54; N, 6.96%. Calcd for $C_7H_9NO_6$: C, 41.38; H, 4.47; N, 6.90%.

***threo*-β-Hydroxy-DL-aspartic Acid (VI).** *By Hydrolysis of V.* A solution of 1.0 g (0.0057 mol) of V in 20 m*l* of 6 N hydrochloric acid was refluxed for 6 hr and VI was isolated from the hydrolyzate in an usual way. Yield, 0.6 g (70%).

It was identified by comparing its physical properties such as infrared spectra with those of an authentic sample. Analytical sample was recrystallized from water and dried over phosphorus pentoxide in a vacuum desiccator.

Found: C, 32.53; H, 4.81; N, 9.55%. Calcd for $C_4H_7NO_5$: C, 32.22; H, 4.73; N, 9.41%.

By Oxidation and Subsequent Hydrolysis of IV. In the same way as the above, a neutralized solution of 5.0 g (0.0254 mol) of IV in 240 m*l* of water was oxidized with 475 m*l* (0.120 mol; 101% of required ammount) of 4% aqueous potassium permanganate solution. After manganese dioxide precipitated had been removed, the residue obtained from the filtrate was hydrolyzed with 30 m*l* of 6 N hydrochloric acid under refluxing for 6 hr. Yield, 1.5 g (40% based on IV).

***erythro*-β-Hydroxy-DL-aspartic Acid (X).** A neutralized solution of 3.0 g (0.0152 mol) of VIII in 200 m*l* of water was oxidized with 290 m*l* (0.0734 mol; 103% of required ammount) of 4% aqueous potassium permanganate solution. After removing manganese dioxide, the residue obtained from the filtrate by evaporation of the solvent was dissolved into 30 m*l* of 6 N hydrochloric acid and the resulting solution was refluxed for 6 hr. From the hydrolyzate, X was isolated as its hydrochloride in an usual way. Yield, 1.1 g (39%), mp 215°C (decomp.).

The properties tested of this compound such as infrared spectra were identical with those of an authentic sample.

Found: C, 25.86; H, 4.40; N, 7,66; Cl, 19.49%. Calcd for $C_4H_7NO_5 \cdot HCl$: C, 25.89; H, 4.35; N, 7.55; Cl, 19.11%.

BULLETIN OF THE CHEMICAL SOCIETY OF JAPAN VOL. 41 2151—2155 (1968)

Photochemical Rearrangement of Azoxybenzene to 2-Hydroxyazobenzene and *cis-trans* Isomerization

Rikuhei TANIKAGA

Department of Chemistry, Faculty of Science, Kyoto University, Sakyo-ku, Kyoto

(Received March 11, 1968)

The photochemical oxygen migration and *cis-trans* isomerization of azoxybenzene have been investigated. The direct irradiation of *trans*-azoxybenzene leads to both rearrangement to 2-hydroxyazobenzene and *cis-trans* isomerization, whose rate is faster in a polar protic solvent and is never affected by a quencher. Direct irradiation does not afford any azobenzene formed from an excited triplet state of azoxybenzene. On the basis of these observations, the author proposes a mechanism in which 2-hydroxyazobenzene and *cis*-azoxybenzene are formed directly from an excited singlet state of *trans*-azoxybenzene. This mechanism is analogous to that for the photochemical rearrangement of nitrone to oxaziridine. Nitro- or dimethylamino-substituted azoxybenzene undergoes neither photochemical rearrangement nor *cis-trans* isomerization. Oxygen migration is not sterically hindered by a substituent in the 3-position of azoxybenzene.

The photochemical rearrangement of *trans*-azoxybenzene (I) to 2-hydroxyazobenzene (II) was first reported by Knipscheer,[1] and an intramolecular pathway was postulated by Badger *et al.*[2] because an oxygen atom was found to migrate from the azo-nitrogen atom, to which it was originally attached, to an ortho position of the aromatic nucleus adjoining the other azo-nitrogen atom.

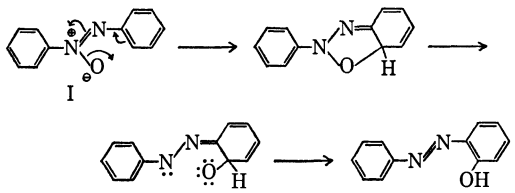

I

II

This intramolecular mechanism was confirmed by means of tracer methods.[3,4] Although it has not definitely been established whether or not an excited triplet state intermediate is involved, it may be suggested that II is formed directly from an excited singlet state of I, because an excited triplet state of I has been found to take a completely different course, *i.e.*, to undergo photochemical reduction to azobenzene.[5] Thus it is necessary to clarify this situation.

The photolysis of I affords *cis*-azoxybenzene (III) besides II,[6] but no effort has been made to discuss the rearrangement and the isomerization at the same time.

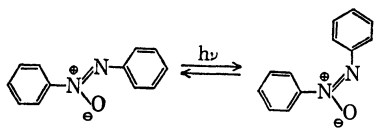

I III

A principal objective of this work is to propose a mechanism for these two photochemical reactions and to discuss the effect of solvents and substituents.

It is interesting to note that neither the photochemical rearrangement of *N*,α-diphenylnitrone (IV) to 2,3-diphenyl-oxaziridine (V)[7] nor the *cis-trans* isomerization of azobenzene[8] proceeds *via* its excited triplet state.

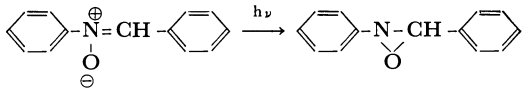

IV V

Results and Discussion

Reactive Intermediate. The photochemical rearrangement of *trans*-azoxybenzene (I) to 2-hydroxyazobenzene (II) was initiated with wavelengths longer than 300 mμ. The sole absorption

1) H. M. Knipscheer, *Rec. Trav. Chim.*, **22**, 14 (1903).
2) G. M. Badger and R. G. Buttery, *J. Chem. Soc.*, **1954**, 2243.
3) M. M. Shemyakin, V. J. Maimind and B. K. Vaichunaite, *Chem. & Ind.*, **1958**, 755; M. M. Shemyakin, T. E. Agadzhanyan, V. J. Maimind, R. V. Kudryavtsev and D. N. Kursanov, *Doklady Akad. Nauk S. S. S. R.*, **135**, 346 (1960).
4) S. Oae, T. Fukumoto and M. Yamagami, This Bulletin, **34**, 1873 (1961); **36**, 601 (1963).
5) R. Tanikaga, K. Maruyama, R. Goto and A. Kaji, *Tetrahedron Letters*, **1966**, 5925; R. Tanikaga, This Bulletin, **41**, 1664 (1968).
6) D. Webb and H. H. Jaffé, *Tetrahedron Letters*, **1964**, 1875; *J. Am. Chem. Soc.*, **86**, 2419 (1964), and other references cited therein.
7) K. Shinzawa and I. Tanaka, *J. Phys. Chem.*, **68**, 1205 (1964); **69**, 2545 (1965).
8) L. B. Jones and G. S. Hammond, *J. Am. Chem. Soc.*, **87**, 4219 (1965).

(λ_{max}^{EtOH}=323 mμ, ε_{max}=14700) above 300 mμ in the electronic spectrum of I is assigned to a $\pi\rightarrow\pi^*$ transition,[9,10] and $n\rightarrow\pi^*$ transition is assumed to be submerged under the high-intensity band of the $\pi\rightarrow\pi^*$ transition.[9] Therefore, the photochemical rearrangment of I probably starts from its $\pi\rightarrow\pi^*$ transition.

The irradiation of I in a solution or in a solid phase yielded II and *cis*-azoxybenzene (III). An example of the time dependencies of their yields is given in Fig. 1.

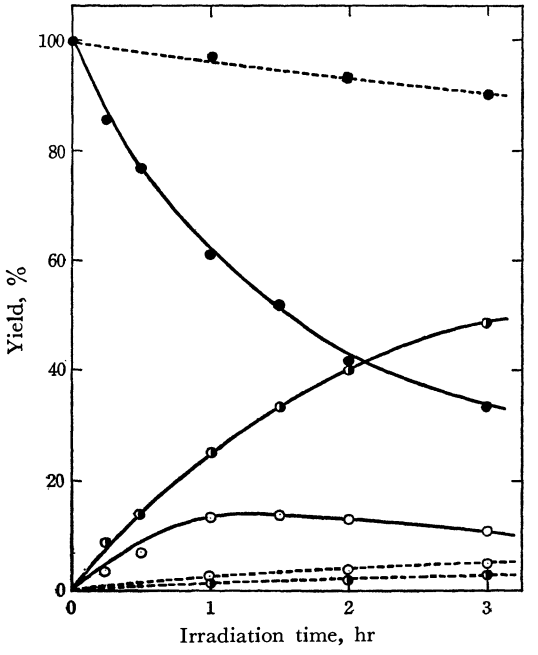

Fig. 1. Irradiation of azoxybenzene (10^{-2} M) at 25.0±0.1°C.
● *trans*-Azoxybenzene (I)
◑ 2-Hydroxyazobenzene (II)
○ *cis*-Azoxybenzene (III)
—— In ethanol ----- In *n*-hexane

Figure 1 shows the photostationary state of a *trans*-isomer I; a *cis*-isomer III was not established so easily. The thermal isomerization of III to I was slow under these experimental conditions.

Even if an oxygen-saturated or degassed solution of I containing naphthalene or iodine was irradiated, no difference from the results shown in Fig. 1 was found; that is to say, neither the rearrangement to II nor the isomerization to III was affected by a quencher. On the other hand, when a degassed solution of I with a sensitizer was irradiated, azobenzene was obtained as a major product. This photochemical reduction was thought to proceed *via* the excited triplet state of I.[5] However, the direct irradiation of I without a sensitizer never afforded azobenzene. These results show that the rearrangement to II probably occur directly from the excited singlet state, S_1, of I, not from its excited triplet state.

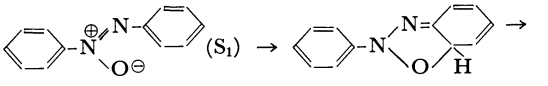

I

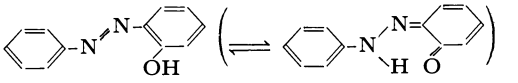

II

The driving force of cyclization may be attributed to the attack of an oxyanion, as has been implied by Badger *et al.*[2] Interestingly the excited singlet state S_1 of I is more basic than its ground state.[11]

II and III were obtained upon the irradiation of I in carbon tetrachloride or in a solid phase, while acetone was not formed upon the irradiation of I in isopropanol. These results are consistent with the above-mentioned mechanism, in which hydrogen abstraction is not expected to take place. On the other hand, the photochemical reduction of the excited triplet state of I is followed by hydrogen abstraction.[5]

The mechanism for the rearrangement of I to II is assumed to be similar to that for the photochemical rearrangement of *N*,α-diphenylnitrone (IV) to 2,3-diphenyl-oxaziridine (V).[7]

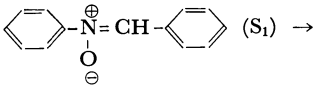

IV

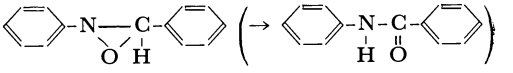

V

The rearrangement of I to II is always accompanied by *cis-trans* isomerization. A *cis-trans* isomerization is often considered to involve an excited triplet state; indeed, the isomerization of IV is thought to proceed *via* the excited triplet state.[7] However, the *cis-trans* isomerization of I probably occur directly from the excited singlet state, not the triplet state for the reaction was not affected by a quencher, and azobenzene, which could be expected to be formed from the excited triplet state of I, was not obtained.

Solvent Effect. The results of the photolysis of I in various solvents using a Pyrex filter are given in Table 1.

The finding that the yield of II was higher in a polar protic solvent can be explained by an ionic

9) H. H. Jaffé and M. Orchin, "Theory and Applications of Ultraviolet Spectroscopy," John Wiley & Sons, Inc., New York (1962), p. 282.
10) C. Tosi, *Spectrochim. Acta*, **22**, 1701 (1966), and other references cited therein.
11) H. H. Jaffé, D. L. Beveridge and H. L. Jones, *J. Am. Chem. Soc.*, **86**, 2932 (1964); H. H. Jaffé and H. L. Jones, *J. Org. Chem.*, **30**, 964 (1965).

TABLE 1. IRRADIATION OF AZOXYBENZENE (10^{-2} M) FOR 2 HR AT 25.0±0.1°C

Solvent	Dielectric constant	Yield of Product (%)		
		I	II	III
EtOH	24.3	42.3	40.3	12.8
iso-PrOH	18.3	47.2	38.8	12.0
MeCN	37.5	58.3	11.7	12.8
Benzene	2.28	80.0	4.1	14.9
n-Hexane	1.89	93.0	2.0	4.3

mechanism containing the attack of an oxyanion. The solvent effect on the rearrangement and the isomerization of I is in contrast to the effect on the reduction, whose reactivity is controlled by the hydrogen-donating ability of the solvent used (for example, isopropanol>ethanol).[5] Photolysis for different times showed that the faster II was formed, the faster was the photostationary state of I and III established.

Substituent Effect. Although the irradiation of an ethanolic solution of 4,4′-dimethyl-, 4,4′-dichloro-, 4,4′-dibromo-, and 4,4′-dimethoxy-azoxybenzene gave the corresponding 2-hydroxyazobenzene and *cis*-azoxybenzene, 4,4′-dinitro- and 4,4′-bis-(dimethylamino)-azoxybenezene were photochemically unreactive. This is presumably the result of an excitation of a nitro- or dimethylamino-group, not an azoxy-group. It is interesting to note that both the rearrangement and the isomerization always take place at the same time.

Steric Effect. Cumming's report that the irradiation of an ethanolic solution of 3,3′-dimethyl-*azoxybenzene (VI) yielded only 2-hydroxy-3,3′*-dimethylazobenzene[12] is difficult to understand in view of the steric effect of a methyl group. In order to discuss whether or not a substituent at a 3-position of the aromatic nucleus hinders an oxygen atom from migrating to a 2-position, an ethanolic solution of VI, 3,3′-dichloroazoxybenzene (VII) or 3,3′-dibromoazoxybenzene (VIII), was irradiated. The ratios of the migration of an oxygen atom to the 2- and 6-positions were as follows:

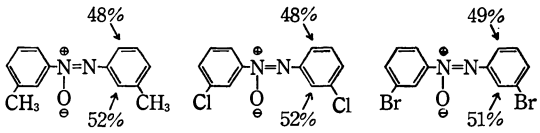

VI VII VIII

A bulky substituent like a bromo-group had no steric effect on the rearrangement. This can be explained by the fact that a migrating group is a small oxyanion. The 2-hydroxy-3,3′-dimethylazobenzene obtained by Cumming *et al.* may have been a mixture of 2-hydroxy-3,3′-dimethyl-azobenzene and 6-hydroxy-3,3′-dimethylazobenzene.

Experimental

Materials. The azoxybenzenes were prepared by the reduction of the corresponding nitro compound (Method A) or nitroso compound (Method B), or by the oxidation of the corresponding azobenzene (Method C). They were purified by recrystallization or column chromatography until their thin-layer chromatography (TLC) showed only one spot (see Table 2).

Photolysis of Azoxybenzene (I). An irradiation source was a 100 W high-pressure mercury arc lamp fitted with a water-cooled immersion well (Eikosha Halos PIH 100). A degassed solution (10 m*l*) of I (10^{-2}M) was irradiated in a Pyrex tube (inner diameter, 15 mm) directly attached to the lamp, and was thermostated at 25.0±0.1°C. TLC (Merck silica gel G, *n*-hexane-benzene (2: 1)) showed two products, namely, 2-hydroxyazobenzene (II) and *cis*-azoxybenzene (III). The yield of the product was determined as follows. After irradiation, 2-hydroxy-4,4′-dichloroazobenzene (IX) was added to the solution as an internal standard. Each

TABLE 2

Substituent	Preparation method	Mp (°C)	λ_{max}^{EtOH} (mμ)	ε_{max}^{EtOH}	Ref.
—	A	35.5	323	14700	13
4,4′-Me	A	70.5	331	18100	14
4,4′-Cl	A	155.5	332	18700	15
4′4′-Br	A	172.0	333	22100	15
4,4′-MeO	A	113.0	356	13900	16
4,4′-NO_2	C	192.5	342	25700	17
4,4′-Me_2N	B	247.0	427	41000	18
3,3-Me	A	34.0	325	14700	14
3,3′-Cl	A	98.0	324	12500	15
3,3′-Br	A	110.0	323	15700	15

12) W. M. Cumming and G. S. Ferrier, *J. Chem. Soc.*, **127**, 2377 (1925).
13) A. Lachman, *J. Am. Chem. Soc.*, **24**, 1180 (1902).
14) L. Zechmeister and P. Rom, *Ber.*, **59**, 870 (1926).
15) C. M. Suter and F. B. Dains, *J. Am. Chem. Soc.*, **50**, 2734 (1928).
16) D. Vorländer, *Ber.*, **40**, 1422 (1907).
17) A. Werner and E. Stiasny, *ibid.*, **32**, 3272 (1899).
18) J. Pinnow and G. Pistor, *ibid.*, **26**, 1313 (1893).

TABLE 3. IRRADIATION OF 4,4'-DISUBSTITUTED AZOXYBENZENE

Substituent	2-Hydroxyazobenzene				*cis*-Azoxybenzene
	Mp (°C)	$\lambda_{max}^{CHCl_3}$ (mμ)	ε_{max}	Yield (%)	Yield (%)
H	84.5	325	18000	60	9
Me	153.5	339	19100	51	8
Cl	176.5	339	19500	35	8
Br	181.5	342	21100	29	9
MeO	133.0	384	23700	17	2
NO_2	—	—	—	0	0
Me_2N	—	—	—	0	0

component was separated by TLC on silica gel and extracted with chloroform. The yield was determined from the intensity of the maximum absorption of the extract in an electronic spectrum, whose extinction coefficient had previously been determined by means of an authentic sample. Before the absorption of the extract containing a *cis*-isomer III was measured, the extract had been left at *ca.* 35°C in the dark for 10 hr to transform it to a more thermally-stable *trans*-isomer. The extinction coefficients used in this work were: I $\varepsilon_{326\ m\mu}$= 14800, II $\varepsilon_{325\ m\mu}$=18000, and IX $\varepsilon_{339\ m\mu}$=19500 (in chloroform).

The time dependencies of the product composition are given in Fig. 1.

The results of the irradiation of I in various solvents for 2 hours are given in Table 1.

No change in the product ratio was detected from the irradiation of I with a quencher like oxygen (saturated), naphthalene (10^{-1}—1 M), or iodine (10^{-1} M).

A degassed isopropanolic solution of I (5×10^{-2}M) was irradiated for 20 hr as described above, and then analyzed by gas chromatography (Yanagimoto GCG-5DH, polyethylene glycol 20M 4.5 m, He), but no acetone was detected.

Photolysis of 4,4'-Disubstituted Azoxybenzene. A degassed ethanolic solution (10 m*l*) of 4,4'-disubstituted azoxybenzene (10^{-2}M) was irradiated in a Pyrex tube at 48.0±0.1°C for 3 hr. TLC on silica gel showed two products, namely, the corresponding 2-hydroxyazobenzene and *cis*-azoxybenzene. Their yields were determined as above. The results obtained are shown in Table 3.

Photolysis of 3,3'-Dimethylazoxybenzene (VI). *Qualitative Analysis of Products.* An ethanolic solution (200 m*l*) of VI (10^{-2}M) in a flask was irradiated with an unfiltered internal lamp for 100 hr. TLC on silica gel showed two products, which were supposed to be azobenzene derivatives from their color reactions with concentrated sulfuric acid on silica gel thin-layer chromatography. After the removal of the ethanol, the chromatography of the residue on a column of silica gel and elution with petroleum ether (bp 40—60°C) - benzene (2: 1) gave two compounds, A and B.

The first compound, A, was red crystals, mp 69°C (from ethanol).

Found: C, 74.49; H, 6.44; N, 12.11%. Calcd for $C_{14}H_{14}N_2O$: C, 74.31; H, 6.24; N, 12.38%.

The second compound, B, was red needles, mp 101°C (from ethanol).

Found: C, 74.45; H, 6.40; N, 12.32%. Calcd for $C_{14}H_{14}N_2O$: C, 74.31; H, 6.24; N, 12.38%.

From the results of elemental analysis and the usual example of the photochemical rearrangement of azoxybenzene, the two compounds, A and B, may be supposed to be 2-hydroxy-3,3'-dimethylazobenzene (X) and 6-hydroxy-3,3'-dimethylazobenzene (XI). On the other hand, the reaction products from diazotized *m*-toluidine and *o*-cresol were separated by TLC on silica gel to give a compound identical with Compound A in its melting point, R_f value, ultraviolet spectrum, and infrared spectrum; it did not give any Compound B. Hence Compound A was assigned to X. Similarly, the reaction of diazotized *m*-toluidine and *p*-cresol[19] gave Compound B, which was assigned to XI.

Quantitative Analysis of Products. A degassed ethanolic solution (10 m*l*) of VI (10^{-2}M) was irradiated in a Pyrex tube for 30 hr as has been described in discussing the photolysis of I. The products were separated by TLC, and their yields were determined from the absorption intensities in their electronic spectra in a manner described earlier. The extinction coefficients used were: X $\varepsilon_{332\ m\mu}$=19300 and XI $\varepsilon_{326\ m\mu}$=19000 (in chloroform). The product ratio of X to XI was 52 to 48.

Photolysis of 3,3'-Dichloroazoxybenzene (VII) and 3,3'-Dibromoazoxybenzene (VIII). *Qualitative Analysis of Products.* An ethanolic solution (200 m*l*) of VII or VIII (10^{-2}M) was irradiated for 100 hr. The products were separated by TLC (silica gel, *n*-hexane). Two products, C and D, were obtained from the photolysis of VII, and two others, E and F, from the photolysis of VIII. On the other hand, the reaction of diazotized *m*-chloroaniline and *p*-chlorophenol gave Compound C, and the reaction of diazotized *m*-bromoaniline and *p*-bromophenol gave Compound E. Thus Compound C was assigned to 6-hydroxy-3,3'-dichloroazobenzene(XII); D, to 2-hydroxy-3,3'-dichloroazobenzene (XIII); E, to 6-hydroxy-3,3'-dibromoazobenzene (XIV), and F, to 2-hydroxy-3,3'-dibromoazobenzene (XV).

XII was orange crystals, mp 158°C (from ethanol).

Found: C, 54.12; H, 3.26; N, 10.41; Cl, 26.57%. Calcd for $C_{12}H_8N_2OCl_2$: C, 53.97; H, 3.02; N, 10.49; Cl, 26.55%.

XIII was orange needles, mp 144°C (from ethanol).

Found: C, 54.21; H, 3.26; N, 10.72; Cl, 26.74%. Calcd for $C_{12}H_8N_2OCl_2$: C, 53.97; H, 3.02; N, 10.49; Cl, 26.55%.

XIV was reddish orange crystals, mp 171°C (from ethanol).

Found: C, 40.59; H, 2.49; N, 7.86; Br, 44.99%. Calcd for $C_{12}H_8N_2OBr_2$: C, 40.48; H, 2.27; N, 7.87; Br, 44.89%.

19) P. Jacobson and P. Piepenbrink, *ibid.*, **27**, 2703 (1894).

XV was reddish-brown crystals, mp 144°C (from ethanol).

Found: C, 40.76; H, 2.39; N, 7.79; Br, 45.11%. Calcd for $C_{12}H_8N_2OBr_2$: C, 40.48; H, 2.27; N. 7.87; Br, 44.89%.

Quantitative Analysis of Products. A degassed ethanolic solution (10 m*l*) of VII or VIII (10^{-2}M) was irradiated in a Pyrex tube for 30 hr as has been described in connection with the photolysis of I. The yields of the products were determined as has been described above. The extinction coefficients used were: XII $\varepsilon_{316\ m\mu}$=16700, XIII $\varepsilon_{330\ m\mu}$=18800, XIV $\varepsilon_{318m\mu}$=16400, and XV $\varepsilon_{332\ m\mu}$=19100 (in chloroform). The product ratio of XI to XII was 48 to 52, and that of XIV to XV was 49 to 51.

The author wishes to thank Professor Ryozo Goto for his helpful discussions and encouragement throughout the course of this work. He is also indebted to Professors Aritsune Kaji and Kazuhiro Maruyama for their valuable discussions.

BULLETIN OF THE CHEMICAL SOCIETY OF JAPAN VOL. 41 2155—2161 (1968)

Selective Chemical Cleavage of Threonine Peptides[1)]

Takeo KANEKO, Shoichi KUSUMOTO,*1 Toshishige INUI*2 and Tetsuo SHIBA

Department of Chemistry, Faculty of Science, Osaka University, Toyonaka, Osaka

(Received March 13, 1968)

Threonine peptide was converted to an oxazolidone derivative *via* an *O*-chlorocarbonyl derivative by treatment with phosgene and dimethylaniline followed by refluxing in xylene, wherever the threonine residue was located in peptide chain, that is, either at amino or carboxyl terminal, or in the middle of the chain. When the oxazolidone peptide was treated with alkali at room temperature, the peptide bond of the original threonine residue of which the amino group participated was selectively cleaved giving a mixture of the carboxylic acid derived from the *N*-terminal amino acid or peptide, and 5-methyl-2-oxo-oxazolidine-4-carbonyl derivative, whereas other peptide bonds remained unchanged in this reaction. Several threonine peptides were synthesized and were subjected to the cleavage reaction. In all cases the expected cleavage occurred in a satisfactory yield.

Selective cleavage reaction of a peptide bond at the residue of β-hydroxy-α-amino acid by a strong acid such as sulfuric acid[2-5)] or hydrogen fluoride[6)] has been known. This cleavage is based on the N→O acyl migration. However, an entirely different principle can be applied to the same purpose. As already mentioned in the preliminary report,[1)] methyl *N*-benzoylthreoninate was found to be cyclized to *N*-benzoyloxazolidone derivative which was then hydrolyzed to 5-methyl-2-oxo-oxazolidine-4-carboxylic acid by sodium hydroxide under a mild condition accompanied with removal of the benzoyl group. This finding leads to an idea that the peptide bond in which the amino group of the hydroxyamino acid participated would be cleaved by cyclization to the oxazolidone derivative followed by hydrolysis with alkali as shown in Fig. 1, inasmuch as *N*-acyl

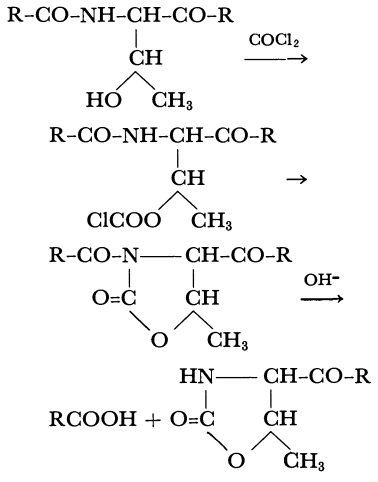

Fig. 1

1) This work was partly reported in a preliminary form: T. Kaneko and T. Inui, This Bulletin, **36**, 1541 (1963), and also presented at the 16th and 17th Annual Meetings of the Chemical Society of Japan, Tokyo, April, 1963 and Tokyo, April, 1964.

*1 Present address: Institute of Organic Chemistry, Faculty of Science, Osaka City University, Nishiogimachi, Kitaku, Osaka.

*2 Present address: Institute of Chemistry, College of General Education, Osaka University, Toyonaka, Osaka.

2) D. F. Elliott, "The Chemical Structure of Protein," ed. by G. E. W. Wolstenholme and M. P. Cameron, Little, Brown, Massachusetts (1953), p. 129.

3) D. F. Elliott, *Biochem. J.*, **50**, 542 (1952).

4) G. D. Fasman, *Science*, **131**, 420 (1960).

5) K. Iwai, *Nippon Kagaku Zasshi* (*J. Chem. Soc. Japan, Pure Chem. Sect.*), **81**, 1302 (1960).

6) K. H. Shin, S. Sakakibara, W. Schneider and G. P. Hess, *Biochem. Biophys. Res. Commun.*, **8**, 288 (1962).

group attached to nitrogen atom in oxazolidone ring might be so labile to basic reagent as to cause the hydrolytic cleavage at the linkage between the acyl group and the ring nitrogen atom.

Actually *N*-protected serine peptide was cleaved selectively by this method to give the *N*-protected amino acid or peptide and the oxazolidone derivative as reported in the previous paper.[7] In this paper, the results obtained when threonine peptides were subjected to the similar reaction were presented.

All threonine peptides used in this study were synthesized mainly through the dicyclohexylcarbodiimide method by the usual precedure. Authentic 5-methyl-2-oxo-oxazolidine-4-carbonyl derivatives were prepared either from threonine itself or from threonyl peptide by treatment with phosgene and the base as shown below in the case of the cleavage reaction.

Di- or tripeptide in which the threonine residue was located at a *C*-terminal position, *e.g.*, *N*-benzyloxycarbonylalanylthreonine methyl ester (I, V), *N*-benzyloxycarbonylglycylthreonine methyl ester (VIII) or *N*-benzyloxycarbonylalanylalanylthreonine methyl ester (XI), was investigated as a first type of a model threonine peptide for the cleavage reaction. *N*-Benzyloxycarbonyl-DL-alanyl-DL-threonine methyl ester (I) or *N*-benzyloxycarbonyl-L-alanyl-L-threonine methyl ester (V) was converted to the *O*-chlorocarbonyl compound in almost quantitative yield according to the procedure by Skinner *et al.*[8] or by Bergel *et al.*[9] The *O*-chlorocarbonyl compound was then cyclized to an oxazolidone derivative by heating in xylene under reflux with evolution of hydrogen chloride. In this reaction, L-L compound V gave an oily oxazolidone derivative (VII) as the sole product, whereas DL-DL compound I afforded a mixture of crystalline and oily substances (IIIa and IIIb respectively). In the latter case, formation of the two substances may be due to a diastereoisomerism. When the compound V was treated with phosgene and pyridine under the condition which was used to prepare cyclic carbonic esters of vicinal glycol of sugars,[10] the oxazolidone derivative VII was obtained directly without isolation of the intermediate, the *O*-chlorocarbonyl compound. An infrared spectrum of this product was identical to that of the product of the stepwise synthesis as mentioned above.

The L-oxazolidone compound VII was treated with potassium hydroxide in methanol at room temperature to afford a mixture of *N*-benzyloxycarbonyl-L-alanine and L-*trans*-5-methyl-2-oxo-oxazolidine-4-carboxylic acid (L-IV) in yields of 71 and 60% respectively, while, in a similar reaction of the crystalline racemic oxazolidone compound IIIa, yields of the corresponding products were 87 and 90% respectively. Under the same condition of alkaline treatment, the original dipeptide, *i.e.*, *N*-benzyloxycarbonylalanylthreonine methyl ester (I or V) was only saponified and no cleavage of the peptide bond took place.

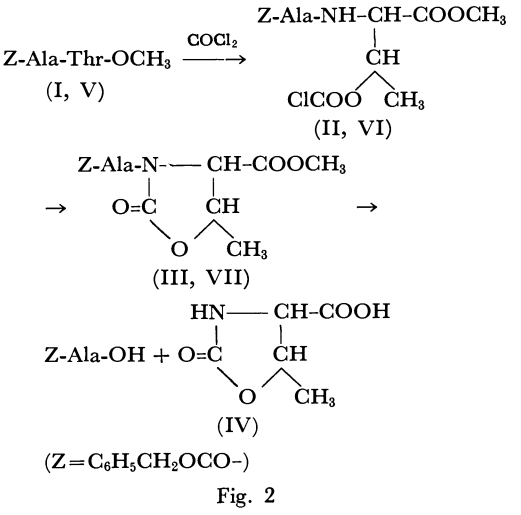

Fig. 2

Similar cleavage reactions also occurred on *N*-benzyloxycarbonylglycyl-DL-threonine methyl ester (VIII) and *N*-benzyloxycarbonyl-L-alanyl-L-alanyl-L-threonine methyl ester (XI), both giving fairly good yields of the corresponding degradation products as shown in Table 1. The reaction of the latter peptide ester XI with phosgene in benzene did not proceed well and only the starting material was recovered, while the reaction in dioxane gave the *O*-chlorocarbonyl compound (XII) in a good yield. From the results obtained above, it is now concluded that the cleavage reaction takes place selectively at the peptide linkage involving the amino group of the threonine residue without any effect on other peptide bonds, and all amino acid residues in the peptide are not subjected to racemization during the reaction.

In order to confirm the conclusion that the cleavage reaction occurs only at the linkage of the amino side of the threonine residue wherever threonine is located in the peptide chain, a reaction of *N*-benzyloxycarbonylglycyl-L-threonyl-L-phenylalanine methyl ester (XIX) was next investigated. In a similar way, the tripeptide XIX was converted to *N*-benzyloxycarbonylglycyl-L-5-methyl-2-oxo-oxazolidine-4-carbonyl-L-phenylalanine methyl ester (XXI) through a corresponding chlorocarbonyl compound (XX) as shown in Fig. 3. This oxazolidone peptide XXI was also cleaved by alkaline hydrolysis to give *N*-benzyloxycarbonylglycine and

7) T. Kaneko, I. Takeuchi and T. Inui, This Bulletin, **41**, 974 (1968).
8) C. G. Skinner, T. J. McCord, J. M. Ravel and W. Shive, *J. Am. Chem. Soc.*, **78**, 2412 (1956).
9) F. Bergel and R. Wade, *J. Chem. Soc.*, **1959**, 941.
10) B. P. Vaterlaus and H. Spiegelberg, *Helv. Chim. Acta*, **47**, 508 (1964).

TABLE 1. RESULTS OF SELECTIVE CLEAVAGE OF THREONINE PEPTIDES

Peptide	Oxazolidone derivative	Product isolated by cleavage reaction (yield)*	
I	IIIa	Z-Ala-OH (DL) (87%)	IV (DL) (90%)
I	IIIb	Z-Ala-OH (DL) (79%)	IV (DL) (67%)
V	VII	Z-Ala-OH (71%)	IV (60%)
VIII	X	Z-Gly-OH (71%)	IV (76%)
XI	XIII	Z-Ala-Ala-OH (86%)	IV (62%)
XIX	XXI	Z-Gly-OH (54%)	XVII (50%)

* Unless otherwise stated, the amino acid residue has an L-configuration.

L-5-methyl-2-oxo-oxazolidine-4-carbonyl-L-phenylalanine (XVII) in 54% and 50% yields respectively. The latter oxazolidone derivative XVII was crystallized as cyclohexylammonium salt and identified by comparison with the authentic compound which was obtained by treatment of L-threonyl-L-phenylalanine with phosgene and potassium carbonate.

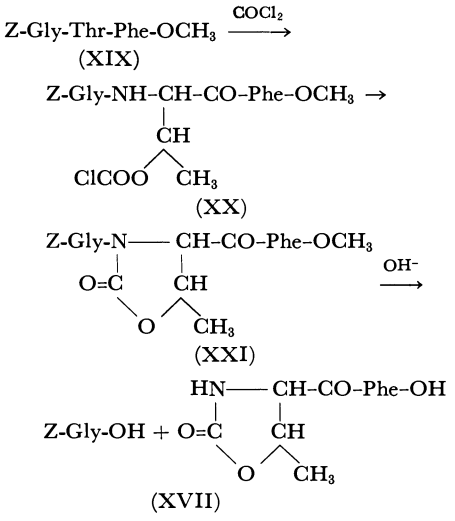

Fig. 3

In conclusion, it is ascertained that the peptide of β-hydroxy-α-amino acid, not only serine but threonine, can be cleaved selectively at the peptide linkage which involves an amino group of the hydroxyamino acid through formation of oxazolidone derivative without any racemization of amino acid residues and any cleavage of other peptide bonds.

Experimental*3

N-Benzyloxycarbonyl-DL-alanyl-O-chlorocarbonyl-DL-threonine Methyl Ester (II). Phosgene was passed through a suspension of 6.8 g (0.020 mol) of N-benzyloxycarbonyl-DL-alanyl-DL-threonine methyl ester[11] (I) in 80 m*l* of benzene at 8—11°C for 20 min after addition of 2.4 g (0.020 mol) of dimethylaniline until the solid was dissolved. The reaction mixture was stirred below 20°C for 2 hr and then allowed to stand overnight. Through the solution, carbon dioxide was passed to remove excess phosgene. The benzene solution was washed with water and dilute hydrochloric acid, and then dried. Evaporation *in vacuo* gave an oily substance which was readily crystallized; wt 7.8 g (97%). Recrystallization from benzene-petroleum ether gave pure crystals of II; mp 103.5—104.0°C.

Found: C, 51.12; H, 5.26; N, 6.91%. Calcd for $C_{17}H_{21}O_7N_2Cl$: C, 50.94; H, 5.28; N, 6.99%.

In order to confirm a structure of the *O*-chlorocarbonyl compound II, this was converted to *N*-benzyloxycarbonyl-DL-alanyl-*O*-(*N*-phenylcarbamoyl)-DL-threonine methyl ester by a reaction with aniline; mp 155—156°C.

Found: C, 60.38; H, 5.94; N, 9.22%. Calcd for $C_{23}H_{27}O_7N_3$: C, 60.38; H, 5.95; N, 9.19%.

Methyl DL-3-(*N*-Benzyloxycarbonyl-DL-alanyl)-5-methyl-2-oxo-oxazolidine-4-carboxylate (IIIa, b). A solution of 8.6 g of crude II in 80 m*l* of xylene was heated under reflux. An evolution of hydrogen chloride gas ceased after 1 hr. Upon concentration of the reaction mixture to about half a volume, a crystalline solid was formed. It was filtered off; wt 3.8 g (49%), and then recrystallized from ethyl acetate to give crystalline IIIa of mp 129.5—130.0°C; wt 2.8 g.

Found: C, 56.16; H, 5.52; N, 7.60%. Calcd for $C_{17}H_{20}O_7N_2$: C, 56.04; H, 5.53; N, 7.69%.

A mother liquor from the crystals was evaporated *in vacuo* to yield 4.5 g of an oily product IIIb.

Cleavage of IIIa and IIIb by Alkaline Hydrolysis. *a) Hydrolysis of Crystalline IIIa.* To a solution of 2.46 g (6.76 mmol) of IIIa in 38 m*l* of methanol, 1.51 m*l* of 0.90 N aqueous potassium hydroxide solution was added with stirring for 20 min. Stirring at room temperature was continued for an additional 1.5 hr. After evaporation *in vacuo*, water was added to the residue. Undissolved part was extracted with ethyl acetate. The aqueous layer was acidified with concentrated hydrochloric acid to pH 3 to deposit an oily substance which was then extracted with ethyl acetate. Evaporation of the solvent from the latter extract *in vacuo* after drying gave crystals; wt 1.32 g (87%), mp 113—114°C. It was recrystallized from ethyl acetate-petroleum ether; mp 113.5—114.0°C. The melting point and infrared spectrum of this compound were identical to those of authentic *N*-benzyloxycarbonyl-DL-alanine.

The aqueous layer of pH 3 which was separated from the ethyl acetate layer was further acidified to pH 1 by addition of concentrated hydrochloric acid, and evaporated *in vacuo*. The residue obtained was extracted with hot ethyl acetate three times. The ethyl acetate solution

*3 All melting points given are uncorrected.

11) Mp 103.5—105.0°C. This compound had been prepared by Th. Wieland, K. Freter and E. Gross, *Ann.*, **626**, 154 (1959) through the mixed anhydride method. In this study, the same compound was synthesized by the carbodiimide method in a similar way to that of the preparation of L-L-isomer (V) as shown below.

was concentrated after decolorization to give crystals; wt 0.89 g (90%), mp 117—119°C. Recrystallization from ethyl acetate - petroleum ether raised the melting point to 126.5—127.0°C. The melting point and the infrared spectrum of this crystals were identical to those of authentic DL-*trans*-5-methyl-2-oxo-oxazolidine-4-carboxylic acid (DL-IV)[12].

b) *Hydrolysis of Oily IIIb.* In a way similar to the hydrolysis of IIIa, 4.5 g of IIIb was dissolved in 60 m*l* of methanol and treated with 27 m*l* of 1 N potassium hydroxide solution. As reaction products, 2.2 g (79%) of *N*-benzyloxycarbonyl-DL-alanine and 1.2 g (67%) of DL-5-methyl-2-oxo-oxazolidine-4-carboxylic acid (DL-IV) were obtained. Both compounds were identified by comparison with the authentic samples in their melting points and infrared spectra respectively.

N-Benzyloxycarbonyl-L-alanyl-L-threonine Methyl Ester (V). To a mixed solution of 22.3 g (0.10 mol) of *N*-benzyloxycarbonyl-L-alanine and methyl L-threoninate, prepared from 17.0 g (0.10 mol) of the hydrochloride and 10.2 g of triethylamine, in 180 m*l* of chloroform, a solution of 20.6 g (0.10 mol) of *N,N'*-dicyclohexylcarbodiimide in 50 m*l* of chloroform was added with stirring for 30 min. After standing overnight, *N,N'*-dicyclohexylurea formed was removed by filtration. The chloroform solution was washed with water, dilute hydrochloric acid, water, aqueous sodium hydrogen carbonate solution and water successively. Concentration of the solution after drying gave 29.5 g (87%) of a crude product which was then recrystallized from ethyl acetate to yield 22.9 g (68%) of V; mp 132.0—132.8°C, $[\alpha]_D^{16.5}$ −23.6° (*c* 2.88, methanol).

Found: C, 57.15; H, 6,63; N, 8.15%. Calcd for $C_{16}H_{22}O_6N_2$: C, 56.79; H, 6.55; N, 8.28%.

N-Benzyloxycarbonyl-L-alanyl-O-chlorocarbonyl-L-threonine Methyl Ester (VI). Phosgene was passed through a suspension of 6.8 g (0.020 mol) of V in 80 m*l* of benzene in the presence of 2.4 g (0.020 mol) of dimethylaniline at about 8°C for 30 min. The reaction mixture was treated in a manner similar to that in the preparation of DL-compound II to yield 8.0 g (100%) of crude crystals of VI. This was recrystallized from benzene-petroleum ether (1 : 1); mp 79.5—81.0°C, $[\alpha]_D^{13.5}$ +30.8° (*c* 3.05, benzene).

Found: C, 51.08; H, 5.15; N, 6.96; Cl. 8.48%. Calcd for $C_{17}H_{21}O_7N_2Cl$: C, 50.94; H, 5.28; N, 6.99; Cl, 8.85%.

Methyl L-3-(N-Benzyloxycarbonyl-L-alanyl)-5-methyl-2-oxo-oxazolidine-4-carboxylate (VII). *a*) *Stepwise Synthesis from VI.* A solution of 7.2 g of the crude VI in 60 m*l* of xylene was heated under reflux. A similar treatment of the reaction mixture to that in the preparation of DL-compound III gave 6.8 g of an oily product VII, $[\alpha]_D^{12}$ −58.8° (*c* 3.0, methanol).

b) *Direct Synthesis from V.* A mixture of 5.0 m*l* (0.062 mol) of pyridine and 12 m*l* of anhydrous benzene was added to 19.8 g of 10% phosgene solution in benzene at 2—4°C for 20 min with stirring. To this sticky half-frozen mixture, a solution of 3.2 g (9.4 mmol) of V in 50 m*l* of anhydrous dioxane was added dropwise at about 0°C for 40 min with stirring. Though the stirring became increasingly difficult, it was continued at this temperature for 1 hr, and then at room temperature for an additional 1 hr. After addition of 80 m*l* of ice-water, the reaction mixture was extracted with ethyl acetate several times. Combined organic layer was washed with 1 N hydrochloric acid, 5% aqueous sodium hydrogen carbonate solution and water successively, and dried with magnesium sulfate. After the solution had been evaporated *in vacuo*, 3.5 g of a pale brownish oil remained which was identified with authentic VII in infrared spectrum. This product seemed to be not so pure, because, on the cleavage reaction, it gave cyclohexylammonium salts of *N*-benzyloxycarbonylalanine and 5-methyl-2-oxo-oxazolidine-4-carboxylic acid in relatively poor yields of 42 and 26% respectively.

Cleavage of VII by Alkaline Hydrolysis. In a way similar to that in the cleavage of DL-compound III, hydrolysis of 3.11 g (8.54 mmol) of the crude VII in 80 m*l* of ethanol and 18 m*l* of 0.95 N potassium hydroxide solution was carried out. Extraction with ethyl acetate from an aqueous solution of pH 3 gave crude crystals of *N*-benzyloxycarbonyl-L-alanine of mp 72—76°C; wt 1.36 g (71%). It was recrystallized from chloroform-petroleum ether (1 : 1); wt 0.68 g, mp 86—87°C, $[\alpha]_D^{13.2}$ 13.8° (*c* 3.32, acetic acid). Further acidification of the remaining aqueous solution by hydrochloric acid gave 0.75 g (60%) of crude crystals of IV; mp 129—133°C. Recrystallization from ethyl acetate gave pure crystals of mp 139.0—139.8°C, $[\alpha]_D^{19.8}$ +40.7° (*c* 2.75, water). These physical constants as well as the infrared spectrum of this compound were all identical to those of authentic L-IV.[13]

N-Benzyloxycarbonylglycyl-DL-threonine Methyl Ester (VIII). A solution of 25.1 g (0.12 mol) of *N*-benzyloxycarbonylglycine in 260 m*l* of a mixture of chloroform and dioxane (1 : 1) was added to a solution of methyl DL-threoninate which was prepared from 20.4 g (0.12 mol) of the hydrochloride and 12.3 g (0.12 mol) of triethylamine, in 100 m*l* of chloroform. To the reaction mixture, a solution of 24.7 g (0.12 mol) of *N,N'*-dicyclohexylcarbodiimide in 50 m*l* of chloroform was added for 40 min with stirring. After stirring for 2 hr at room temperature, it was allowed to stand overnight. By the usual procedure, 37 g (95 %) of a crude product of VIII was obtained. It was recrystallized from ethyl acetate; wt 26.2 g (67%), mp 110.5—111.8°C.

Found: C, 55.57; H, 6.31; N, 8.87%. Calcd for $C_{15}H_{20}O_6N_2$: C, 55.55; H, 6.22; N, 8.64%.

Cleavage Reaction of VIII. *N*-Benzyloxycarbonylglycyl-*O*-chlorocarbonyl-DL-threonine methyl ester (IX) was obtained from 6.5 g (0.020 mol) of VIII by action of phosgene in the presence of 2.4 g of dimethylaniline in 80 m*l* of benzene at 5—8°C; wt 7.2 g (94%). Whole amount of the crude product IX thus obtained was cyclized by heating in 60 m*l* of xylene under reflux for 1 hr to yield 6.2 g of an oily substance (X) which was then dissolved in 80 m*l* of methanol and hydrolyzed by treatment with 35 m*l* of 1 N potassium hydroxide at room temperature for 1.5 hr. The reaction mixture was acidified to pH 3 by hydrochloric acid, and extracted with ethyl acetate to give crude *N*-benzyloxycarbonylglycine; wt 3.0 g (71% based on VIII). It was recrystallized from ethyl acetate - petroleum ether (4 : 1); mp 121.0—121.8°C. The remaining aqueous solution was acidified to pH 1 and treated by the usual procedure to

12) Lit.: T. Kaneko and T. Inui, *Nippon Kagaku Zasshi* (*J. Chem. Soc. Japan, Pure Chem. Sect.*), **82**, 1075 (1961); mp 127—128°C.

13) Lit.: T. Kaneko and T. Inui, *Nippon Kagaku Zasshi* (*J. Chem. Soc. Japan, Pure Chem. Sect.*), **82**, 1078 (1961); mp 139.5—140.5°C, $[\alpha]_D^{25}$ +41.2° (*c* 3.04, water).

give 2.2 g (76% based on VIII) of DL-IV. It was recrystallized from ethyl acetate - petroleum ether (4 : 1); mp 126.5—127.0°C. Both products were identified by comparison with the authentic samples.

N-Benzyloxycarbonyl-L-alanyl-L-alanyl-L-threonine Methyl Ester (XI). *a) Azide Method.* To a cold solution of 6.5 g (0.021 mol) of *N*-benzyloxycarbonyl-L-alanyl-L-alanine hydrazide[14] in a mixture of 43 m*l* of acetic acid, 21.5 m*l* of 5 N hydrochloric acid and 170 m*l* of water, there was added a cold solution of 18.0 m*l* of 10% aqueous sodium nitrite solution at −5°C. An oily product formed solidified immediately. The solid was extracted with a mixture of ethyl acetate and ether (1 : 1). The extract was washed with water, 3% aqueous sodium hydrogen carbonate solution and water successively in the cold, and then dried with sodium sulfate. On the other hand, 3.5 g (0.035 mol) of triethylamine was added to a suspension of 5.8 g (0.034 mol) of methyl L-threoninate hydrochloride in 40 m*l* of chloroform. After addition of 120 m*l* of anhydrous ether, triethylamine hydrochloride formed was filtered off. Free ester solution thus obtained was poured into the azide solution prepared above on ice-cooling. The reaction mixture was stirred for 3 hr and then kept in a refrigerator overnight. A crystalline product of XI was filtered; wt 5.9 g (69%), mp 179—180°C. It was recrystallized from methanol - ethyl acetate (3 : 1); wt 5.0 g, mp 181.0—181.5°C, $[\alpha]_D^{11}$ −56.5° (*c* 1.82, methanol).

Found: C, 55.87; H, 6.68; N, 10.26%. Calcd for $C_{19}H_{27}O_7N_3$: C, 55.73; H, 6.65; N, 10.26%.

b) Carbodiimide Method. A solution of 3.1 g (0.030 mol) of triethylamine and methyl L-threoninate prepared from 5.1 g (0.030 mol) of the hydrochloride, in 30 m*l* of chloroform was added to a solution of 8.8 g (0.030 mol) of *N*-benzyloxycarbonyl-L-alanyl-L-alanine in 40 m*l* of a mixture of dioxane and chloroform (1 : 1). To the mixture, a solution of 6.2 g (0.030 mol) of *N,N'*-dicyclohexylcarbodiimide in 15 m*l* of chloroform was added dropwise. The reaction mixture was stirred at room temperature for 4 hr and then allowed to stand overnight. A mixture of dicyclohexylurea and a condensed product was filtered off. This was heated in 80 m*l* of dioxane under reflux to dissolve the latter only, keeping the former insoluble. To the filtrate, 100 m*l* of petroleum ether was added to crystallize the product; wt 5.3 g (43%), mp 177—179°C. This was recrystallized from methanol-ethyl acetate (3 : 1); wt 3.6 g, mp 181.5—182.8°C, $[\alpha]_D^{12.5}$ −56.3° (*c* 1.83, methanol). All properties of these crystals were quite identical to those of the compound XI obtained by the azide method.

Found: C, 55.79; H, 6.64; N, 10.35%.

The organic layer separated from the solid product was washed with water, dilute hydrochloric acid, aqueous sodium hydrogen carbonate solution and water successively, and then concentrated *in vacuo* to give crystals; wt 3.5 g. It was recrystallized from ethyl acetate - petroleum ether (25 : 10); wt 2.5 g mp 141.5—142.5°C, $[\alpha]_D^{12.5}$ −5.4° (*c* 1.84, methanol).

Found: C, 56.27; H, 6.89; N, 9.91; H_2O, 2.53%. Calcd for $C_{33}H_{43}O_{11}N_5 \cdot H_2O$: C, 56.32; H, 6.45; N, 9.95; H_2O, 2.56%.

From the results of the elementary analysis and an infrared spectrum, a structure of this compound is presumed to be *O,N*-di-(*N*-benzyloxycarbonyl-L-alanyl-L-alanyl)-L-threonine methyl ester hydrate.

N-Benzyloxycarbonyl-L-alanyl-L-alanyl-O-chlorocarbonyl-L-threonine Methyl Ester (XII). Through a suspension of 4.1 g (0.01 mol) of XI in 40 m*l* of dioxane, phosgene was passed at 8—10°C for 45 min in the presence of 1.2 g (0.01 mol) of dimethylaniline. After stirring for 3.5 hr, the reaction mixture was allowed to stand overnight. After removal of excess phosgene by passage of carbon dioxide, the solution was concentrated *in vacuo* to give crystals. It was filtered, washed with water and then dried; wt 4.2 g (89%), mp 149—150°C (decomp.). Recrystallization from benzene gave 3.5 g of pure crystals; mp 150.5—151.°C (decomp.), $[\alpha]_D^{15}$ +8.6° (*c* 3.02, benzene).

Found: C, 50.87; H, 5.59; N, 8.81%. Calcd for $C_{20}H_{26}O_8N_3Cl$: C, 50.90; H, 5.55; N, 8.91%.

Methyl L-3-(N-Benzyloxycarbonyl-L-alanyl-L-alanyl)-5-methyl-2-oxo-oxazolidine-4-carboxylate (XIII). Heating of 3.1 g (0.066 mol) of XII in 30 m*l* of xylene under reflux for 75 min followed by evaporation *in vacuo* gave a product of a closed ring as a syrup; wt 2.8 g (98%), $[\alpha]_D^{15}$ −84.6° (*c* 3.6, methanol). This was used for the following cleavage reaction without further purification.

Cleavage of XIII by Alkaline Hydrolysis. Hydrolysis of 2.19 g (5.03 mmol) of XIII was carried out in 30 m*l* of methanol by addition of 11.1 m*l* of 0.9 N aqueous potassium hydroxide and keeping the solution at room temperature for 1.5 hr. After methanol had been evaporated *in vacuo*, water was added to the reaction mixture, pH of which was then adjusted to 3 by addition of hydrochloric acid. Extraction with ethyl acetate followed by evaporation of the solvent gave 1.27 g (86%) of crude crystals of mp 135.0—139.5°C. It was recrystallized from chloroform to yield a pure material; mp 149.0—150.0°C, $[\alpha]_D^{13.5}$ −32.5° (*c* 3.26, methanol), which was identified to be *N*-benzyloxycarbonyl-L-alanyl-L-alanine by comparison with the authentic sample.

On the other hand, the aqueous layer separated from the ethyl acetate extract was further acidified and evaporated *in vacuo* to give a residue. This was extracted with hot ethyl acetate and the solvent was removed by evaporation to give L-IV; wt 0.45 g (62%), mp 128—132°C. It was recrystallized from ethyl acetate; mp 138—140°C, $[\alpha]_D^{13.8}$ +41.8° (*c* 2.70, water). These were identical to those of the authentic sample.

N-Benzyloxycarbonyl-L-threonyl-L-phenylalanine Methyl Ester (XIV). To a mixed solution of 51 g (0.20 mol) of *N*-benzyloxycarbonyl-L-threonine in 400 m*l* of acetonitrile and methyl L-phenylalaninate, prepared from 48 g (0.22 mol) of the hydrochloride, in 60 m*l* of acetonitrile, a solution of 42 g (0.20 mol) of *N,N'*-dicyclohexylcarbodiimide in 100 m*l* of acetonitrile was added at room temperature with stirring. Stirring at room temperature was continued for 4 hr. After standing overnight, the urea derivative precipitated was filtered off, and the solvent was removed by evaporation *in vacuo*. Syrupy residue thus obtained was dissolved in ethyl acetate, washed with 5% aqueous potassium hydrogen carbonate solution, 0.5 N hydrochloric acid and water successively, and then dried with sodium sulfate. To a concentrated solution, petroleum ether was added to give

14) This compound was prepared from *N*-benzyloxycarbonyl-L-alanyl-L-alanine methyl ester by the usual procedure; mp 212—213°C, $[\alpha]_D^{7.3}$ −51.0° (*c* 1.92, methanol), $[\alpha]_D^{18}$ −67.4° (*c* 1.84, 0.5 N hydrochloric acid). Lit.: B. F. Erlanger and E. Brand, *J. Am. Chem. Soc.*, **73**, 3508 (1951).

crystals; wt 74 g (89%), mp 104—106°C. Repeated recrystallization from ethyl acetate - petroleum ether raised the melting point up to 108.5—109.0°C, $[\alpha]_D^{19}$ +3.9° (*c* 1.15, ethanol).

Found: C, 63.72; H, 6.36; N, 6.66%. Calcd for $C_{22}H_{26}O_6N_2$: C, 63.75; H, 6.32; N. 6.76%.

***N*-Benzyloxycarbonyl-L-threonyl-L-phenylalanine (XV).** To a solution of 1.03 g (2.5 mmol) of XIV in a mixture of 35 m*l* of dioxane and 5 m*l* of water, there was added 5.5 m*l* of 0.5 N aqueous sodium hydroxide solution dropwise for 8 hr with stirring. After standing overnight, 5.5 m*l* of 0.5 N hydrochloric acid was added, and the reaction mixture was evaporated *in vacuo* to dryness. The residue obtained was triturated with ethyl acetate to remove insoluble sodium chloride. Ethyl acetate solution was extracted with 5% sodium hydrogen carbonate solution. The aqueous extract was acidified with 2 N hydrochloric acid to yield crystals of XV; wt 0.51 g (51%), mp 152—154°C. It was recrystallized from ethyl acetate - petroleum ether; mp 156—157°C, $[\alpha]_D^{20}$ +23.2° (*c* 1.94, ethanol).

Found: C, 62.74; H, 6.04; N, 6.76%. Calcd for $C_{21}H_{24}O_6N_2$: C, 62.99; H, 6.04; N, 7.00%.

From the mother liquor of the first crystallization of the product, a considerable amount of XVII was obtained.

L-Threonyl-L-phenylalanine (XVI). Hydrogen gas was passed through a solution of 8.0 g (0.020 mol) of XV in a mixture of 150 m*l* of methanol and 20 m*l* of water at room temperature for 6 hr in the presence of palladium black. When a crystalline product was formed during the hydrogenation, water was added to dissolve it. The catalyst was removed by filtration and the filtrate was concentrated to a small volume. On addition of ethanol, crystals of dipeptide XVI were formed; wt 5.9 g (95%). It was recrystallized from water-ethanol; mp 251—253°C (decomp.), $[\alpha]_D^{21}$ +24.8° (*c* 2.02, water).

Found: C, 57.31; H, 7.77; N, 9.16%. Calcd for $C_{13}H_{18}O_4N_2 \cdot C_2H_6O$: C, 57.67; H, 7.74; N, 8.97%.

L-5-Methyl-2-oxo-oxazolidine-4-carbonyl-L-phenylalanine (XVII). To a solution of 3.1 g (0.01 mol) of XVI containing one mole of ethyl alcohol as crystallization solvent in 20 m*l* of water there were added 10 m*l* of 1 N aqueous potassium hydroxide solution and 2.8 g (0.02 mol) of solid potassium carbonate. To the mixture, 9.1 g of toluene solution containing 1.5 g (0.015 mol) of phosgene was added dropwise at 1—5°C for 20 min with vigorous stirring. The reaction mixture was stirred at the same temperature for 1.5 hr and then at room temperature for 40 min. An aqueous layer was separated, washed with ether and then acidified with 2 N hydrochloric acid to give crystals; wt 0.6 g. The filtrate was evaporated *in vacuo* to a residue, which was then triturated with ethyl acetate. To the concentrated ethyl acetate solution, petroleum ether was added to yield a second crop of the crystalline product; wt 2.3 g. Total yield, 2.9 g (99%). This was purified as cyclohexylammonium salt; mp 210.0—210.5°C, $[\alpha]_D^{20}$ +25.2° (*c* 1.27, water).

Found: C, 61.15; H, 7.53; N, 10.56%. Calcd for $C_{14}H_{16}O_5N_2 \cdot C_6H_{13}N$: C, 61.36; H, 7.47; N, 10.74%.

L-Threonyl-L-phenylalanine Methyl Ester Hydrochloride (XVIII). Hydrogen gas was passed through a solution of 8.3 g (0.020 mol) of XIV in 100 m*l* of methanol and 3.5 m*l* of concentrated hydrochloric acid in the presence of palladium black at room temperature for 20 hr. After removal of the catalyst by filtration, the solution was evaporated *in vacuo*. An oily residue thus obtained was dissolved in a small amount of methanol, and on addition of ether needles were obtained; wt 5.2 g (83%). It was recrystallized from methanol - ether; wt 4.4 g, mp 136—138°C.

Found: C, 53.10; H, 6.78; N, 8.67; Cl, 11.06%. Calcd for $C_{14}H_{21}O_4N_2Cl$: C, 53.08; H, 6.68; N, 8.84; Cl, 11.19%.

***N*-Benzyloxycarbonylglycyl-L-threonyl-L-phenylalanine Methyl Ester (XIX).** To a mixed solution of 4.2 g (0.020 mol) of *N*-benzyloxycarbonylglycine in 20 m*l* of tetrahydrofuran and 4.1 g (0.020 mol) of *N,N'*-dicyclohexylcarbodiimide in 20 m*l* of tetrahydrofuran, there was added a solution of a free dipeptide ester, prepared from 6.3 g (0.020 mol) of XVIII and an equivalent amount of triethylamine, in 80 m*l* of tetrahydrofuran. After the reaction mixture had been stirred at room temperature for 4 hr, it was allowed to stand overnight. A precipitate formed upon addition of acetic acid was filtered off and the filtrate was evaporated *in vacuo*. An oily residue obtained was crystallized from ethyl acetate; wt 6.9 g (73%), mp 146.0—148.5°C. It was recrystallized from ethyl acetate; mp 146.5—149.0°C, $[\alpha]_D^{22}$ −14.0° (*c* 2.0, chloroform).

Found: C, 61.25; H, 6.38; N, 8.78%. Calcd for $C_{24}H_{29}O_7N_3$: C, 61.13; H, 6.20; N, 8.91%.

***N*-Benzyloxycarbonylglycyl-*O*-chlorocarbonyl-L-threonyl-L-phenylalanine Methyl Ester (XX).** Phosgene was passed through a solution of 4.7 g (0.010 mol) of XIX and 1.2 g (0.010 mol) of dimethylaniline in 120 m*l* of anhydrous dioxane at 9—11°C 30 min. Stirring at this temperature was continued for 1.5 hr and then at room temperature for 1 hr. After standing overnight, the solvent was removed by evaporation *in vacuo*. A solution of the residue thus obtained in ethyl acetate was washed with 0.3 N hydrochloric acid and then dried with magnesium sulfate. Again, the solution was evaporated *in vacuo* to an oily residue, which was then crystallized from chloroform; wt 4.1 g (62%), mp 90—92°C (decomp.), $[\alpha]_D^{20}$ +36.3° (*c* 0.96, chloroform).

Found: C, 47.70; H, 4.50; N, 6.73; Cl, 21.56%. Calcd for $C_{25}H_{28}O_8N_3Cl \cdot CHCl_3$: C, 47.79; H, 4.48; N, 6.43; Cl, 21.71%.

3-(*N*-Benzyloxycarbonylglycyl)-L-5-methyl-2-oxo-oxazolidine-4-carbonyl-L-phenylalanine Methyl Ester (XXI). A solution of 9.1 g (0.014 mol) of XX in 90 m*l* of xylene was heated under reflux for 30 min. After evaporation *in vacuo*, a crystalline residue obtained was recrystallized from ethyl acetate - petroleum ether; wt 4.2 g (60%), mp 155.0—159.5°C. Repeated recrystallization gave a pure sample; mp 165.0—166.5°C, $[\alpha]_D^{20}$ +4.8° (*c* 1.05, ethanol).

Found: C, 60.05; H, 5.61; N, 8.32%. Calcd for $C_{25}H_{27}O_8N_3$: C, 60.35; H, 5.47; N, 8.45%.

Cleavage of XXI by Alkaline Hydrolysis. To a solution of 3.0 g (6.0 mmol) of XXI in 50 m*l* of methanol, there was added 14.4 m*l* of 1 N sodium hydroxide. After the reaction mixture had been stirred at room temperature for 2.5 hr, 2 N hydrochloric acid was added to pH 3. Methanol was removed by evaporation *in vacuo*. To a residue obtained, 1 N sodium hydroxide solution was added and extracted with ethyl acetate. The aqueous layer was separated and acidified to pH 3.2

with 1 N hydrochloric acid. An oily material formed was separated by decantation and the solution was further acidified to pH 2.5 to yield colorless crystals; wt 0.17 g, mp 122—123°C. Its infrared spectrum was identical to that of *N*-benzyloxycarbonylglycine. More amount of the same compound was obtained when the oily material was dissolved in ethyl acetate, extracted with 0.5 N sodium hydroxide solution and then the aqueous solution was acidified; wt 0.51 g. Total yield; 54%.

The aqueous solution of pH 2.5 was evaporated *in vacuo*. A residue thus obtained was treated with ethyl acetate. An oily residue obtained by evaporation of the solvent was then dissolved in ethanol. An addition of cyclohexylamine and ether to the solution gave colorless crystals of cyclohexylammonium salt; wt 1.17 g (50%), mp 199—201°C (decomp.). Its infrared spectrum was quite identical to that of cyclohexylammonium salt of XVII prepared from XVI by treatment with phosgene. Recrystallization from ethanol - ether gave a pure salt; mp 209—210°C (decomp.), $[\alpha]_D^{13}$ +24.9° (*c* 2.21, water).

The authors wish to express their thanks to Central Research Laboratories of Ajinomoto Co., Inc. for donation of amino acids.

BULLETIN OF THE CHEMICAL SOCIETY OF JAPAN VOL. 41 2161—2164 (1968)

The Reaction between Hydrocarbon and Hydrogen Cyanide in Silent Electrical Discharge. II.[1] The Formation of Acrylonitrile from Ethylene and Hydrogen Cyanide*[1]

Kazuaki KAWAMOTO

Institute of Commodities, Faculty of Economics, Kagawa University, Takamatsu

(Received March 14, 1968)

The present investigation was undertaken to examine the possibility of the direct introduction of a cyano radical into ethylene by means of a silent discharge. When a mixture of ethylene and hydrogen cyanide was discharged in an ozonizer under atmospheric pressure, the main liquid product was acrylonitrile, though the formation of telomers, such as ethyl cyanide, *n*-butyl cyanide and *n*-hexyl cyanide, was also observed. Besides these compounds, the reaction products were confirmed to consist of *s*-butyl, *n*-propyl, isopropyl, *n*-amyl, and isoamyl cyanides, and a gaseous product. The yield of acrylonitrile was affected by the temperature and voltage of the discharge. It has been found that the yields of the liquid products and the gaseous product increase with the rise in the temperature and voltage of the discharge, while the relative ratio of acrylonitrile to the other liquid product decreases. Judging from the relative concentration of each compound in the reaction products, it may be said that the vinyl radical and the cyano radical are the main intermediates in this reaction system.

Studies concerning the reaction of ethylene alone in electrical discharge have been reported by many investigators.[2] Moreover, in recent years, the reactions of ethylene and ammonia or oxygen under silent electrical discharge have been investigated by Sugino *et al.*[3] and by Tsutsumi *et al.*[4]

In a previous study,[1] it was found that, when a mixture of cyclohexane and hydrogen cyanide was discharged in an ozonizer, cyclohexyl cyanide could be prepared in one step, and that the relative amounts of this compound depended not only upon the discharge voltage, but also upon the discharge temperature.

The direct synthesis of acrylonitrile from ethylene and cyano-compounds has been established in several patents. (1) Acrylonitrile was obtained by the addition of cyanogen chloride or cyanogen bromide to ethylene in the presence of $AlCl_3$ and CH_3NO_2.[5] (2) It was found by Oberbacher[6] that

1) K. Kawamoto, N. Sonoda and S. Tsutsumi, This Bulletin, **41**, 1376 (1968).

*1 The results of this investigation were presented at the 18th Annual Meeting of the Chemical Society of Japan, Osaka, April, 1965; some of them were also presented at the 19th Annual Meeting of the Chemical Society of Japan, Yokohama, April, 1966.

2) These reports are summarized by C. L. Thomas, G. Egloff and J. C. Morell, *Chem. Revs.*, **28**, 1 (1941).

3) T. Matsuda, K. Oto and K. Sugino, *Nippon Kagaku Zasshi (J. Chem. Soc. Japan, Pure Chem. Sect.)*, **79**, 325 (1958); K. Sugino, E. Inoue, K. Shirai, T. Koseki and T. Gomi, *ibid.*, **86**, 114 (1965).

4) S. Yamamoto, N. Sonoda and S. Tsutsumi, Preprints for of the 17th Annual Meeting of the Chemical Society of Japan, (April, 1964), p. 24.

5) Brit. Pat. 686692; *Chem. Abstr.*, **48**, 8251 (1954).

6) B. Oberbacher, German Pat. 1034625; *Chem. Abstr.*, **54**, 11996 (1960).

acrylonitrile could be prepared by the reaction of ethylene with cyanogen at 300—700°C at low pressures. (3) Porter and Nesty[7] and Sandner and Fierce[8] found that, in the absence of a catalyst, when ethylene was reacted with cyanogen or hydrogen cyanide at about 750—900°C it was transformed into acrylonitrile.

Francesconi and Ciurlo[9] reported that when a mixture of ethylene and hydrogen cyanide was subjected to the electrical discharge, ethyl cyanide and ethyl isocyanide were obtained.

In the present paper, the author wishes to report the direct formation of acrylonitrile in a reaction between ethylene and hydrogen cyanide in a silent discharge, and to establish, if possible, the most suitable conditions for the formation of acrylonitrile.

Experimental

Materials. The ethylene used in this experiment showed no impurity in gas-chromatographic analysis. (Columns of activated charcoal and dimethyl sulfolane were used.) The hydrogen cyanide was prepared according to Brauer's method.[10]

Apparatus and Procedure. The apparatus employed was similar to that used by the passing method in the previous paper.[1] The discharge tube used was a Pyrex tube 40 cm in effective length, 4 cm in outside diameter, and with a space gap of 0.25 cm. Ethylene and hydrogen cyanide vapor were passed through the discharge tube at a constant velocity for the period of the reaction. The amount of hydrogen cyanide used in each experiment was about a 2-mol. A 60-cycle alternating current was sent through a voltage regulator, and the voltage was stepped up by a transformer (Capacity: 15 kV) to give the required value. The products coming out of the discharge tube were removed by being passed through a condenser cooled with ice water, supplemented by two traps which were cooled with ice. The liquid products were analyzed by the method described below, while the noncondensable gas was analyzed by gas chromatography at intervals of 30 min.

Identification and Analysis of the Reaction Products. The reaction products were identified by comparing them with the authentic samples*2 by gas chromatography. (Columns of tricresyl phosphate, PEG-6000, and silicone DC 550 were used.) In addition, the reaction products were fractionally distilled in the presence of a small amount of hydroquinone, and the constituents of the cut were identified by the formation of the derivatives described below and by the infrared absorption.

The fraction boiling at 75—79°C was confirmed to consist mainly of acrylonitrile by transforming it into the *N-t*-butyl acrylamide,*3 mp 126—128°C, and the picrate of β-piperidinopropionitirle, *4 mp 160—161°C. They showed no depression in their melting points when mixed with authentic specimens. The infrared spectrum of this fraction agreed with that of authentic acrylonitrile. Besides acrylonitrile, the reaction products were identified by the methods described below.*5

The gaseous products, when analyzed by gas chromatography, were found to consist of ethane, acetylene, hydrogen, *n*-butane, 1-butene, 1,3-butadiene, methane, propane, and propylene. (Columns of activated charcoal, tricresyl phosphate, acetonylacetone, and dimethyl sulfolane were used.) The gaseous products could not be determined quantitatively. The liquid products were analyzed quantitatively by gas chromatography using a 5-m column of PEG-6000, a 3-m column of silicone DC 550, and a 3-m column of tricresyl phosphate at 140°C. Further, the content of acrylonitrile was also determined by the method of Beesing *et al.*[11] However, the difference between this method and gas-chromatographic analysis was less than 2 per cent.

Results and Discussion

By running ethylene with hydrogen cyanide only one time in an ozonizer under the conditions described in Table 1, a large number of compounds were obtained, along with acrylonitrile as the object substance. Among these, the identified compounds are summarized in Table 2. The compositions of the reaction products given in this table are reproducible within 1 per cent. In the presence of a small quantity of air, a solid brown deposit was formed on the glass wall. Accordingly, the air was completely removed from the reaction system. The liquid product absorbed oxygen from the air quite readily, and it was polymerized upon standing at room temperature.

Influences of the Discharge Temperatures and Voltages on the Reaction between Ethylene and Hydrogen Cyanide. As may be seen from

7) F. Porter and G. A. Nesty, U. S. Pat. 2445693; *Chem. Abstr.*, **42**, 8209 (1948).

8) W. J. Sandner and W. L. Fierce, U. S. Pat. 2803641; *Chem. Abstr.*, **52**, 5449 (1958).

9) L. Francesconi and A. Ciurlo, *Gazz. Chim. Ital.*, **53**, 327 (1923).

10) G. Brauer, "Handbuch der Präparativen Anorganischen Chemie," Ferdinand Enke Verlag, Stuttgart (1954), p. 500.

*2 *s*-Butyl, isoamyl, *n*-amyl, and *n*-hexyl cyanides were prepared according to the procedure of Jeffery and Vogel; G. H. Jeffery and A. I. Vogel, *J. Chem. Soc.*, **1948**, 679. Further, the following commercial chemicals were used for identification: acrylonitrile, ethyl cyanide, *n*-propyl cyanide, isopropyl cyanide and *n*-butyl cyanide.

*3 *N-t*-Butyl acrylamide was prepared according to the procedure of Plaut and Ritter; H. Plaut and J. J. Ritter, *J. Am. Chem. Soc.*, **73**, 4076 (1951).

*4 The picrate of β-piperidinopropionitrile was prepared by Brockway's method; C. E. Brockway, *Anal. Chem.*, **21**, 1207 (1949).

*5 (1) Ethyl cyanide was present in a fraction boiling at 92—97°C, and the ethyl 2,4,6-trihydroxyphenyl ketone, mp 175—176°C, was obtained. (2) *n*-Butyl cyanide was present in the fraction distilling at 136—141°C; this compound gave the *n*-butyl 2,4,6-trihydroxyphenyl ketone, mp 87—88°C. These alkyl (2,4,6-trihydroxyphenyl) ketones were prepared by the procedure of Howells and Little; H. P. Howells and J. G. Little, *J. Am. Chem. Soc.*, **54**, 2451 (1932). The infrared spectrum showed a strong absorption band at 2250 cm^{-1} (C≡N). (3) The other products were identified by comparing their retention times on the gas chromatography with those of authentic compounds.

11) D. W. Beesing, W. P. Tyler, D. M. Kurty and S. A. Harrison, *Anal. Chem.*, **21**, 1073 (1949).

Table 1. The reaction between ethylene and hydrogen cyanide in silent electrical discharge (Experimental conditions)

Experiment No.	1	2	3	4	5
Ethylene used, *l*	22.17	22.67	27.59	27.54	27.69
Velocity, *l*/hr	3.70	3.78	3.07	3.06	3.08
Discharge time, hr	6	6	9	9	9
Second. voltage, kV	13	13	12	13.5	15
Second. current, mA	1.8	1.8	1.7	1.9	2.1
Temp. of discharge tube					
Inside, °C	30—67	10—26	10—26	10—26	10—26
Outside, °C	30—60	10	10	10	10

Table 2. The reaction between ethylene and hydrogen cyanide in silent electrical discharge (Experimental results)

Experiment No.	1	2	3	4	5
Liquid product collected, g	31.28	33.12	35.41	35.62	34.09
Reaction product, g	4.59	3.25	4.44	5.21	6.47
Conversion efficiency,*1 %	16.5	11.4	12.8	15.1	18.6
Composition of liquid reaction products*2					
Acrylonitrile, %	45.8	57.9	59.9	52.1	45.9
Ethyl cyanide, %	12.6	7.1	7.0	9.2	12.9
n-Butyl cyanide, %	17.2	12.6	11.4	15.2	17.1
s-Butyl cyanide, %	10.6	6.7	5.9	8.0	10.2
n-Propyl cyanide, %	2.6	2.8	2.5	2.9	2.9
Isopropyl cyanide, %	2.0	1.9	1.8	1.7	2.0
n-Hexyl cyanide, %	T	T	T	T	T
n-Amyl cyanide, %	T	T	T	T	T
Isoamyl cyanide, %	T	T	T	T	T
Unidentified product, %	9.2	11.0	11.5	10.9	9.0

*1 The conversion efficiency was given by (grams of reaction product/grams of ethylene used)×100.
*2 The yields of each compound produced were given by (grams of each compound/grams of total reaction product)×100.
T: Trace

Experiments Nos. 1 and 2 in Table 2, the conversion efficiency (grams of reaction product/grams of ethylene used×100) depends upon the temperature at which the discharge is carried out; it has been found that the yields of the liquid product and the gaseous product increase with a rise in the discharge temperature, and that, further, in the case of a high-temperature discharge, the proportion of acrylonitrile in the liquid product decreases and the yeilds of ethyl cyanide, *n*-butyl cyanide, and *s*-butyl cyanide increase. Thus, it may be said that a low temperature favors the formation of acrylonitrile. Ethyl, *n*-butyl, and *n*-hexyl cyanides seem to be formed by the telomerization between ethylene and hydrogen cyanide. However, the formation of *n*-octyl cyanide (1 : 4 telomer) and one-to-five or more products could not be observed by gas-chromatographic analysis. Further, the author could not find any dicyano-compounds and isocyano-compounds in the present research.

As may be seen from Experiments Nos. 3, 4 and 5 in Table 2, the yield of the reaction product was also affected by the discharge voltage; it has been found that increasing the voltage increases the yields of the liquid product and the gaseous product. Thus, the amount of ethylene reacted was at a maximum at the maximum voltage used in this experiment.

The Mechanism of the Formation of Acrylonitrile. It was reported by Egloff *et al.*[2] that the radical from ethylene in the electrical discharge was a vinyl radical, and that it was produced by breaking a carbon-hydrogen bond. Tsutsumi[12] reported that the vinyl radical was obtained by two molecular processes,*6 as is shown below.

12) S. Tsutsumi, *Chem. Ind.* (*Kagaku Kogyo*), **16**, 623 (1965).

*6 $CH_2=CH_2 + e^* \rightarrow CH_2=CH_2^* + e$

$CH_2=CH_2^* + CH_2=CH_2 \rightarrow$

$CH_2=\dot{C}H + CH_3-\dot{C}H_2$

The formation of acrylonitrile by the reaction of ethylene with hydrogen cyanide in a silent discharge may be represented as follows: The first step is the activation of the ethylene molecule and the hydrogen cyanide molecule by electron impact, while the second step consists of both (1) the reaction of the activated ethylene molecule with a normal ethylene molecule to give the vinyl radical and the ethyl radical, and (2) the decomposition of the activated molecules to give the vinyl radical, the cyano radical, and the hydrogen atom. Acrylonitrile may be formed by a combination of the vinyl radical and the cyano radical thus obtained. Further, the formation of acetylene, 1,3-butadiene, and 1-butene may show the existence of the vinyl radical.

The Reaction Occurring in the Silent Discharge. Although the reaction of ethylene with hydrogen cyanide in a silent discharge is somewhat complicated by a secondary reaction, the principal reaction can be interpreted as including the formation of the vinyl radical, the ethyl radical, the cyano radical, and the hydrogen atom and the combination of these radicals, telomerization, hydrogenation, and dehydrogenation.

Besides acrylonitrile, considerable quantities of one-to-one products and one-to-two products, such as ethyl cyanide and *n*-butyl cyanide, were produced. Since the investigated reaction is presumed to be a radical reaction, the mechanisms of these telomers may be described as below:

$$HCN + e^* \rightarrow HCN^* + e \rightarrow \cdot H + \cdot CN \quad (1)$$

$$CH_2{=}CH_2 + \cdot CN \rightarrow \cdot CH_2CH_2CN \quad (2)$$

$$\cdot CH_2CH_2CN + HCN \rightarrow CH_3CH_2CN + \cdot CN \quad (3)$$

$$\cdot CH_2CH_2CN + CH_2{=}CH_2 \rightarrow \cdot CH_2(CH_2)_3CN \quad (4)$$

$$\cdot CH_2(CH_2)_3CN + HCN \rightarrow CH_3(CH_2)_3CN + \cdot CN \quad (5)$$

$$\cdot CH_2(CH_2)_3CN + CH_2{=}CH_2 \rightarrow \cdot CH_2(CH_2)_5CN \quad (6)$$

$$\cdot CH_2(CH_2)_5CN + HCN \rightarrow CH_3(CH_2)_5CN + \cdot CN \quad (7)$$

The addition reaction of the $C_6H_{12}CN$ radical to ethylene in these reaction mechanisms need not be considered, since no products beyond *n*-hexyl cyanide were obtained. In addition, a part of the ethyl cyanide may be formed by the reaction between the ethyl radical obtained by two molecular processes*6 and the cyano radical. Further, it seems that ethane, *n*-butane, and 1-butene are obtained by the ethyl radical.

Beer and Besprozvannyi[13] found, from their data on the telomerization of ethylene in carbon tetrachloride and chloroform, that compounds ($ClCH_2(CH_2)_3CCl_3$ and $CH_3(CH_2)_3CCl_3$) with $n=2$ were formed over a wide range of ethylene concentration. They suggested that the predominance of telomers with $n=2$ resulted from the stabilization of the trichloroamyl radical by a "pseudo cyclic" configuration between the unpaired electron of the end CH_2 and the electrophilic CCl_3 groups. As may be seen from Table 2, the yield of the telomer (*n*-butyl cyanide) with $n=2$ was higher than that of the telomer (*n*-hexyl cyanide) with $n=3$. Accordingly, the existence of a pseudo cyclic arrangement may be supported in the reaction of ethylene with hydrogen cyanide under a silent discharge. The formation of *s*-butyl cyanide was also observed. This is presumably due to the isomerization of *n*-butyl cyanide to *s*-butyl cyanide.

The author wishes to express his hearty thanks to Professor S. Tsutsumi of Osaka University for his kind guidance and valuable suggestions throughout this work.

13) A. A. Beer and M. A. Besprozvannyi, *Khim. Nauka i Prom.*, **4**, 547 (1959).

BULLETIN OF THE CHEMICAL SOCIETY OF JAPAN VOL. 41 2165—2168 (1968)

The Effect of the ω-Cyano Group on the Reactivity of Secondary Bromides in the Formolysis Reaction and on the Reactivity of Primary Bromides in the Reaction with Silver Nitrate[1—4]

Peter S. STRILKO,[5a] Hiroyuki MORITA and Shigeru OAE[5b]

Department of Applied Chemistry, Faculty of Engineering, Osaka City University, Sugimoto-cho, Sumiyoshi-ku, Osaka

(Received March 18, 1968)

Several ω-cyano-2-bromoalkanes have been synthesized and their formolysis rates were determined. The reactivity of these compounds was found to decrease with a decrease in chain length and have a parallerism with a chemical shift (>CH–, $-CH_3$) of NMR spectra. A similar sequence was observed in the reactivity of ω-cyano-1-bromoalkanes in the reaction with silver nitrate.

In the previous paper[6] of this series, rates of formolysis of several 5-substituted 2-bromopentanes were studied. While the 5-acetoxy and 5-bromo groups exhibited essentially no effect upon the reactivity, it was found that the methoxy group at the 5 position accelerated the formolysis by a factor of about thirty and that the cyano group at the same position caused nearly a five-fold retardation. The large accelerating effect of the methoxy group was ascribed to the five-membered ring neighboring group participation of the δ-methoxy group. This interpretation was confirmed later by Winstein and his co-workers.[7] As for the retarding effect of the ω-cyano group, the electrostatic attraction between the unshared electron pairs of covalently bonded bromine and the cyano group was suggested as a possible explanation, since the electron-withdrawing inductive effect is known to virtually disappear after being transmitted through more than three saturated methylene linkages in both S_N1 and S_N2 reactions[8,9] of primary organic halides. One way to test this assumption is to compare the reactivity of ω-cyanobromoalkanes of different methylene chain length, because direct electrostatic interactions of this nature should be quite insensitive to ring size. Therefore, the present investigation was undertaken to deal with the rates of formolysis of several 2-bromo-ω-cyanoalkanes, namely 2-bromo-3-cyanopropane, 2-bromo-4-cyanobutane, 2-bromo-5-cyanopentane and 2-bromo-6-cyanohexane. Contrary to our earlier expectation, the reactivity of 2-bromo-5-cyanopentane was much greater than that of 2-bromo-4-cyanobutane, which in turn, had remarkably greater reactivity than 3-cyano homolog, while the reactivity of 2-bromo-6-cyanohexane was found not to reach that of 2-bromobutane after being transmitted through four saturated methylene linkages, though it was greater than that of 2-bromo-5-cyanopentane.

The investigation has been extended to the kinetic study of the reaction of silver nitrate in absolute ethanol with 1-bromo-ω-cyanoalkanes, namely, 1-bromo-2-cyanoethane, 1-bromo-3-cyanopropane, 1-bromo-4-cyanobutane, 1-bromo-5-cyanopentane and 1-bromo-6-cyanohexane. Here again the reactivity was found to decrease as the cyano group more closely approached the reacting center and to be insensitive to the size of the chain length contrary to that expected from the assumption in the previous paper.[6]

Experimental

Materials. Commercially available extra pure 98% formic acid was diluted with distilled water to give a solution of specific gravity of 1.2086 at 20°C. This corresponds to 92.4% formic acid by weight. The purification of absolute ethanol and the preparation of a silver nitrate solution were discussed elsewhere.[10]

1) Contribution from the Department of Chemistry, Drexel Institute of Technology, Philadelphia, Pennsylvania, and the Department of Applied Chemistry, Faculty of Engineering, Osaka City University, Osaka, Japan.

2) Paper VII on "Relative Reactivities of Organic Halides in Displacement Reactions"; Paper VI, *J. Am. Chem. Soc.*, **79**, 3118 (1957).

3) We are indebted to Sigma Xi Society for the Grant-in-Aid.

4) Presented in part before the Fourth Delaware Valley Regional Meeting, Philadelphia, Pennsylvania, January 26, 1962.

5) a) Present Address: E. I. Dupont de Nemours Co. Wilmington, Delaware, U.S.A. b) Present Address: Department of Applied Chemistry, Faculty of Engineering, Osaka City University, Osaka, Japan.

6) S. Oae, *J. Am. Chem. Soc.*, **78**, 4032 (1956).

7) S. Winstein, E. Allred, R. Heck and R. Glick, *Tetrahedron*, **3**, 1 (1958); E. L. Allred and S. Winstein, *J. Am. Chem. Soc.*, **89**, 3991 (1967).

8) S. Oae and C. A. VanderWerf, *ibid.*, **78**, 4034 (1956).

9) K. Akagi, S. Oae and M. Murakami, *ibid.*, **78**, 4032 (1956).

10) S. Oae and C. A. VanderWerf, *ibid.*, **75**, 2724 (1953).

2-Bromo-6-cyanohexane was synthesized by a following method. Commercially available α-picoline was reduced to 2-methyl-piperidine by catalytic hydrogenation with Raney nickel at 200°C and 150 atm of hydrogen, and 2-methyl-piperidine thus prepared was converted to 1,5-dibromohexane by the von Braun reaction.[11] Equivalent amounts of 1,5-dibromohexane and sodium cyanide were refluxed in ethanol for 4 hr and 2-bromo-6-cyanohexane was obtained in a 25% yield. The fraction boiling at 103—103.5°C/2 mmHg was collected and used.

Found: C, 44.23; H, 6.37%. Calcd for $C_7H_{12}NBr$: C, 44.23; H, 6.03%. n_D^{30} 1.4784.

2-Bromo-5-cyanopentane was prepared by a procedure described.[6]

2-Bromo-4-cyanobutane was made similarly, starting from 1,3-dibromobutane and sodium cyanide. The fraction boiling at 86—86.5°C/8 mmHg was collected and used.

Found: C, 37.74; H, 5.08%. Calcd for C_5H_8NBr: C, 37.74; H, 4.98%. n_D^{30} 1.4692.

2-Bromo-3-cyanopropane was made similarly, starting from 1,2-dibromopropane and sodium cyanide. The fraction boiling at 65°C/75 mmHg was collected and used.

Found: C, 32.30; H, 4.16%. Calcd for C_4H_6NBr: C, 32.46; H, 4.16%. n_D^{30} 1.5147.

1-Bromo-2-cyanoethane was an Eastman white labeled product. 1-Bromo-3-cyanopropane, 1-bromo-4-cyanobutane, 1-bromo-5-cyanopentane and 1-bromo-6-cyanohexane were obtained from Aldrich Chemical Company. All were washed with diluted alkaline solutions, dried over anhydrous calcium chloride and carefully fractionated. Boiling points and refractive indices of the respective compounds are shown below. (Table. 1)

TABLE 1. PHYSICAL CONSTANTS OF ω-CYANO-1-BROMOALKANES

Compound	Boiling point	Refractive index
1-Bromo-2-cyanoethane	76.2—76.3°C/9 mmHg	1.4768
1-Bromo-3-cyanopropane	99.6—99.9°C/14 mmHg	1.4753
1-Bromo-4-cyanobutane	108.4—108.6°C/9.4 mmHg	1.4754
1-Bromo-5-cyanopentane	118.0—118.2°C/7 mmHg	1.4744
1-Bromo-6-cyanohexane	133.5—134.5°C/7.6 mmHg	1.4728

2-Bromobutane and 1-bromopentane were both Eastman white labeled products and were purified as in the previous work.[6,8]

Determination of Rate Constant. Kinetic measurements and rate calculations for the formolysis of secondary bromides were made by the same procedure previously used.[6] In this case, 5 m*l* portions were sealed in ampoules and the reaction was carried out at 85.00±0.01°C, 95.00±0.01°C and 105.00±0.01°C, respectively, while the titration was accomplished by Volhard's method, using ammonium alum as the indicator. First order rate constants were calculated according to the equation,

$$k = \frac{2.303}{t} \cdot \log \frac{a}{a-x}$$

The activation parameters were obtained graphically.

Isolation of Product in the Reaction of 2-Bromobutane with Formic Acid. A solution of 2-bromobutane in 90% formic acid was refluxed on a steam bath for 48 hr. This was poured into cold water and extracted with ether. The ethereal extracts were washed three times with water, three times with diluted sodium carbonate and three times again with water. They were dried over potassium carbonate and the solvent was distilled to give a pale yellow residue. This was found to have very similar index of refraction, infrared spectrum and identical retention time in the vapor phase chromatograph with an authentic sample of secondary butyl formate prepared by the method of Pickard, Kenyon and Hunter.[12]

Primary bromides are known to react with ethanolic silver nitrate to give the corresponding nitrate ester.[10] 1-Bromo-5-cyanopentane was treated in the same concentration solutions as those used for the kinetics, but allowed to reflux on a steam bath for several days. The silver bromide was filtered, followed by evaporation of the solvent, removal of any additional solid and distillation of the filtrate through a packed column. The yellow distillate, bp 113—114°C/15 mmHg, showed infrared bands at 1276 cm^{-1} and 1632 cm^{-1}, indicating the presence of nitrate ester and a strong aliphatic ether band at 1108 cm^{-1} in addition to those bands present in the starting material.[13]

Result and Discussion

The first-order rate constants, $\Delta H^{\neq}$ and $\Delta S^{\neq}$ of secondary bromides at 85.0°C, 95.0°C and 105.0°C are given in Table 2.

The results clearly indicate that low reactivity of 2-bromo-5-cyanopentane is not the unique phenomenon. In fact, the rate decreases with the decrease in chain length. However, when one plots the logarithms of the rates against *n*, one finds that 2-bromo-3-cyanopropane falls off the line while the others are in a fairly good correlationship (Fig. 1). Apparently the formolysis of this particular bromide proceeds through a different path. Indeed, both the enthalpy and entropy of activation of the reaction are vastly different from those of the other compounds. The strong electron-withdrawing inductive effect of ω-cyano group probably makes the S_N1 type heterolysis of C–Br bond so difficult that S_N2 type process, in which formolysis is assisted by the nucleophilic attack of formate, becomes predominant. As one expected, the NMR chemical shifts of methyne proton at 2 position of substitued

11) Adapted from a method of J. Von Braun, "Organic Syntheses," Coll. Vol. I, p. 428 (1941).

12) R. H. Pickard, J. Kenyon and H. Hunter, *J. Chem. Soc.*, **1923**, 123.

13) L. J. Bellamy, "The Infra-red Spectra of Complex Molecules," John Wiley and Sons, Inc., New York, N.Y. (1958).

TABLE 2. FIRST-ORDER RATE CONSTANTS, AND ACTIVATION PARAMETERS OF FORMOLYSIS OF SECONDARY ORGANIC BROMIDES IN 92.4% FORMIC ACID

Compound	Temp (°C)	k_1(sec^{-1})	$\Delta H^{\neq}$(kcal/mol)	$\Delta S^{\neq 95°C}$(e.u.)
$NCCH_2CHBrCH_3$	85.0	$1.31\pm0.11\times10^{-6}$		
	95.0	$2.19\pm0.07\times10^{-6}$		
	105.0	$4.12\pm0.03\times10^{-6}$	15.3	−43.1
$NC(CH_2)_2CHBrCH_3$	85.0	$5.68\pm0.05\times10^{-6}$		
	95.0	$1.44\pm0.04\times10^{-5}$		
	105.0	$3.44\pm0.13\times10^{-5}$	25.9	−16.1
$NC(CH_2)_3CHBrCH_3$	85.0	$1.99\pm0.06\times10^{-5}$		
	95.0	$6.19\pm0.03\times10^{-5}$		
	105.0	$1.37\pm0.08\times10^{-4}$	25.6	−9.87
$NC(CH_2)_4CHBrCH_3$	85.0	$2.49\pm0.08\times10^{-5}$		
	95.0	$7.53\pm0.05\times10^{-5}$		
	105.0	$1.89\pm0.01\times10^{-4}$	25.1	−9.96
$CH_3CH_2CHBrCH_3$	85.0	$1.62\pm0.02\times10^{-4}$		
	95.0	$3.97\pm0.04\times10^{-4}$		
	105.0	$9.77\pm0.30\times10^{-4}$	24.0	−9.29

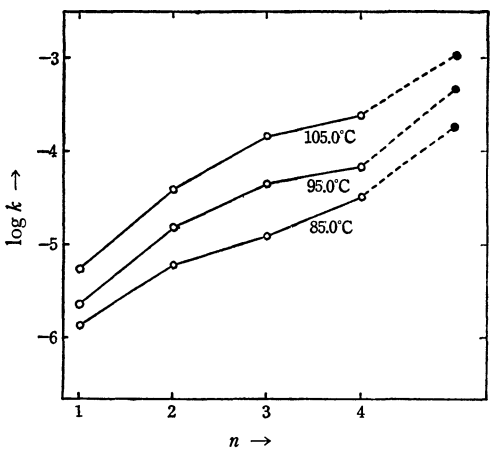

Fig. 1. Correlationship between the formolysis rates of $NC(CH_2)_nCHBrCH_3$ and n.
—○— $NC(CH_2)_nCHBrCH_3$
—●— $CH_3CH_2CHBrCH_3$

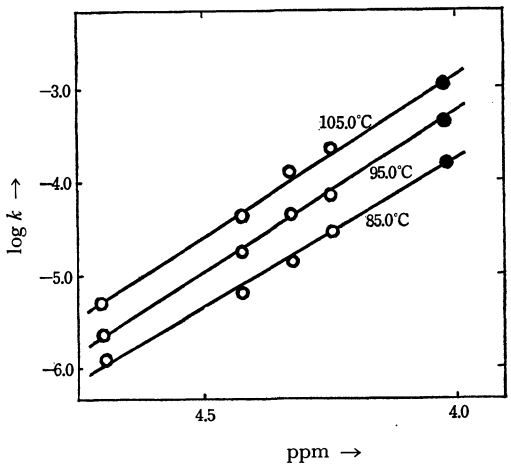

Fig. 2. Correlationship between the formolysis rates and NMR methyne chemical shifts of $NC(CH_2)_nCHBrCH_3$ and $CH_3CH_2CHBrCH_3$.
—○— $NC(CH_2)_nCHBrCH_3$
—●— $CH_3CH_2CHBrCH_3$

2-bromoalkanes can be correlated with the methylene chain lengths, while a rough linear correlationship is observed between the rates and the NMR chemical shifts of these organic bromides. (Fig. 2) A similar relationship between the chemical shifts and the electron-withdrawing properties has been reported in the case of ω-nitroalkanes,[14] however, in this case the inductive and/or field effects disappear rapidly after being transmitted through more than four methylene linkages. Perhaps in the case of nitro group, negative oxygen atoms display negative field effect and decrease the electron-withdrawing effect so markedly beyond more than two methylene groups away. While cyano group being uncharged yet electronegative and polarizable, may perturb the electrons further away, both directly and indirectly. From the NMR data, the transmission coefficient, ε, of cyano group is calculated to be 0.45–0.50. Transmission coefficient has been accepted to be nearly constant, *i.e.*, 0.35, in many reactions.[15] Therefore the value we obtained is somewhat larger than the ordinary one. In this case not only an inductive effect through methylene but also some field effect of highly electro-negative groups are in operation. To clarify this problem, $\rho\sigma^*$

14) W. Hofman, L. Stefariak, T. Urbanski and M. Witanowski, *J. Am. Chem. Soc.*, **86**, 554 (1964).

15) M. J. S. Dewar and P. J. Grisdale, *ibid.*, **84**, 3539, 3548 (1961).

treatment[16] was carried out in which σ^* values were calculated by using the transmission coefficient obtained in this experiment. A very good linear correlationship was found as in Fig. 3. This may mean that the formolysis of ω-cyano-2-bromoalkanes is controlled by the inductive effect alone.

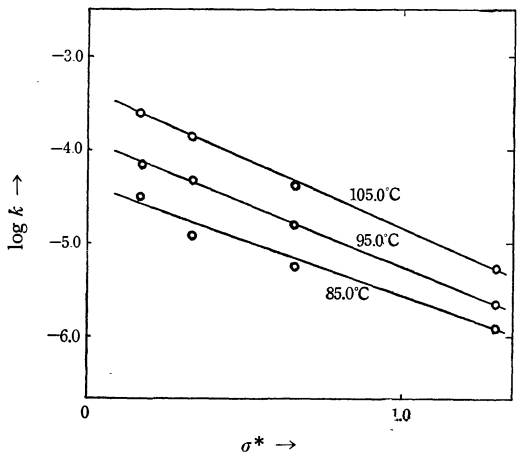

Fig. 3. Correlationship between the formolysis rates of $NC(CH_2)_nCHBrCH_3$ and σ^* of $-(CH_2)_n-CN$.

The second order rate constants for the reaction of the primary bromides with silver nitrates in absolute ethanol at 50.04±0.02°C are tabulated in Table 3.

There are numerous sources of evidence to support the fact that carbon-halogen bond fission is the rate determining step for the reaction between silver nitrate and alkyl halides. Therefore, one would expect that the slow reacting primary 1-bromo-ω-cyanoalkanes would show a similar sequence of reactivities in the reaction with silver nitrate. In fact, the cyano group was found to retard the reactivity considerably as it approaches closer to the reacting site. However, in this case the retarding effect of the cyano group virtually disappeared beyond three saturated methylene groups.

TABLE 3. SECOND-ORDER RATE CONSTANTS FOR THE REACTION OF PRIMARY BROMIDES WITH SILVER NITRATE IN ABSOLUTE ETHANOL AT 50.04±0.02°C

Compound	$k_2 \times 10^4$ $l\ mol^{-1}sec^{-1}$
1-Bromo-2-cyanoethane	2.98
1-Bromo-3-cyanopropane	5.01
1-Bromo-4-cyanobutane	14.0
1-Bromo-5-cyanopentane	23.4
1-Bromo-6-cyanohexane	21.6
1-Bromopentane	16.9

It is interesting to note that 1-bromo-5-cyanopentane and 1-bromo-6-cyanohexane were found to react faster than 1-bromo-pentane. This may be due to an altering of the electron-withdrawing ability of the cyano group by coordination with silver ion, as is known to occur in ũ bonded systems, or by some interaction with solvent such as hydrogen bonding.[17]

The presence of an ether in the product may be accounted for by a transition state model in which silver ion is exerting an attracting force on the halogen which results in partial carbonium ion character at the seat of reaction. Displacement could be effected by nitrate ion to give the expected product or by solvent with the subsequent loss of a proton to give rise to the ethoxy derivative.

We are indebted to Mr. Clyde Zault who checked some of the kinetic runs.

16) R. W. Taft, Jr., "Separation of Polar, Steric, and Resonance Effects in Reactivity," in "Steric Effects in Organic Chemistry," ed. by M. S. Newman, John Wiley and Sons, Inc., New York (1956), p. 595.

17) P. von R. Schleyer and A. Allerhand, *J. Am. Chem. Soc.*, **84**, 1322 (1962).

BULLETIN OF THE CHEMICAL SOCIETY OF JAPAN VOL. 41 2169—2172 (1968)

Effect of Pressure on Graphitization of Carbon. IV. Abrupt Graphitization of Hard Carbon under 5 kbar

Kan-ichi KAMIYA, Michio INAGAKI, Masato MIZUTANI and Tokiti NODA*1

Faculty of Engineering, Nagoya University, Chikusa-ku, Nagoya

(Received February 15, 1968)

A hard carbon, phenolformaldehyde resin char carbonized to 700°C, was heat-treated under a quasi-hydrostatic pressure of 5 kbar at various temperatures between 1100—1800°C for the residence times of 3, 20 and 60 min. The graphitization process of the hard carbon under pressure consisted of three stages. In the first stage of the graphitization, the profile of (002) diffraction line was symmetrical. It means that there is only one component A_H in the sample. In the second and third stages of graphitization, the (002) profile became composite. In the second stage, three components A_H, G'_H and G''_H coexisted in the sample. The sum of the contents of the components G'_H and G''_H was less than 20% and increased gradually with heat treatment temperature. In the third stage, two components A_H and G''_H coexisted. The content of the component G''_H increased abruptly up to more than 70% at about 1400, 1500 and 1700°C for the residence time of 60, 20 and 3 min, respectively. The components A_H and G''_H have the turbostratic and graphitic structures, respectively. The component G'_H seemed to have the intermediate structure between turbostratic and graphitic structures.

Hard carbons or non-graphitizing carbons are hardly graphitized even at very high temperatures such as 3000°C. So-called two- or three-phase graphitization was often observed for hard carbons at high temperatures of heat treatment.[1-4] Recently, Oberlin and Rousseaux gave a beautiful representation of two-phase graphitization of a sugar charcoal by means of dark field electron micrographs and electron microdiffraction.[5] On the other hand, soft carbons are easily graphitized under the same condition and multi-phase graphitization has never been observed. Under high pressure above 3 kbar, the graphitization of soft carbons was found to proceed very rapidly at relatively low temperatures as 1500°C and the phenomenon similar to the two-phase graphitization was observed.[6,7] It was found that even glassy carbon, a typical hard carbon, was graphitized around 1500°C under 10 kbar.[6] In the present work, phenolformaldehyde resin char, one of hard carbons, was heat-treated under the pressure of 5 kbar at various temperatures for three different residence times. The graphitization process of the sample was precisely followed by analyzing the profile of (002) diffraction line and was compared with that of soft carbon under the same pressure.

Experimental and Results

The sample used was a carbon prepared at 700°C from phenolformaldehyde resin, which was made by a conventional method using ammonium hydroxide as catalyst. The sample was a hard carbon and was

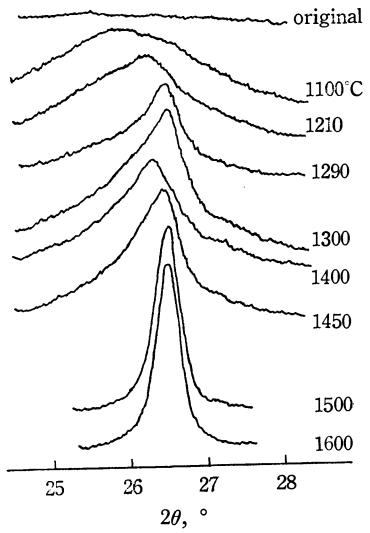

Fig. 1. Change of profile of (002) diffraction line of the hard carbon, heat-treated under 5 kbar for 60 min, with HTT.

*1 Present address; Mie University, Tsu, Mie-ken

1) R. E. Franklin, *Proc. Roy. Soc.*, **A 209**, 196 (1951).
2) H. Akamatu, H. Inokuchi, H. Takahashi and Y. Matsunaga, This Bulletin, **29**, 574 (1956).
3) M. Inagaki and T. Noda, *ibid.*, **35**, 1652 (1962).
4) H. Honda and K. Kobayashi, private communication.
5) A. Oberlin and F. Rousseaux, *Compt. Rend.*, **265**, C 436 (1967).
6) T. Noda and H. Kato, *Carbon*, **3**, 289 (1965).
7) T. Noda, K. Kamiya and M. Inagaki, This Bulletin, **41**, 485 (1968).

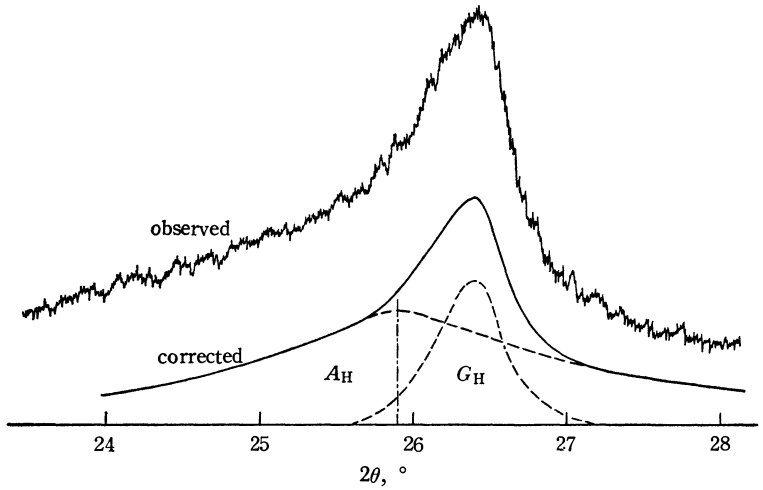

Fig. 2. Schema of separation of composite profile observed on the hard carbon.

named as PH-7 in order to make easy to distinguish from the sample of a soft carbon PV-7, which was used in the previous works.[6-9] The particle size of the sample was limited in the range of 0.1—0.4 mm. The used high pressure apparatus and the arrangement of specimen cell were the same as reported previously.[7] The heat treatments of the sample were performed under a quasi-hydrostatic pressure of 5 kbar at various temperatures between 1100—1800°C for residence times of 3, 20 and 60 min. The heat treatment temperature (HTT) was evaluated from the electric input power by using the relation between temperature and input power, which was determined beforehand for the same arrangement and sample. For the heat-treated sample, the profile of (002) diffraction line was measured by using Ni-filtered Cu$K\alpha$ radiation and a recording goniometer.

Change of (002) diffraction profile with HTT for the residence time of 60 min. is shown in Fig. 1. Above 1200°C, the profile appeared to be composite, consisting of at least two component profiles. Such a composite profile was separated into the component profiles by almost the same procedure as previously described.[7,8] In the present work, however, the profile on the low angle side is folded at the angular position where the tail of the folded profile coincides well with the tail of the composite profile on the high angle side (Fig. 2). When this profile on the low angle side is subtracted from the composite profile, the balance gives another component profile, which is on the high angle side. In the present work, these two components corresponding to the profiles on the low angle side and high angle side are designated as A_H and G_H, respectively.*2

For each separated profile, the c_0-spacing was measured by referring to the inner standard of silicon and the area under the profile was measured by using a planimeter. In order to obtain the content of the component G_H, the ratio of the area under the profile for the component G_H to the total area of the composite profile was obtained and then corrected for the preferred orientation of crystallite in the specimen by using the same calibration curve as reported previously.[8] Changes of c_0-spacing of two components with HTT are shown in Fig. 3 and the

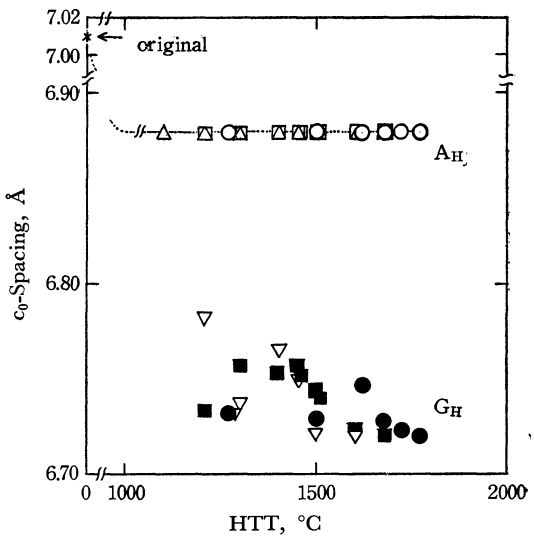

Fig. 3. Changes of c_0-spacing of two components A_H and G_H with HTT.

A_H	G_H	
○	●	3 min
□	■	20 min
△	▽	60 min

8) M. Inagaki, K. Kamiya and T. Noda, *Kogyo Kagaku Zasshi* (*J. Chem. Soc. Japan, Ind. Chem. Sect.*), **71**, 652 (1968).
9) M. Inagaki, K. Kamiya and T. Noda, *ibid.*, **71**, 812 (1968).

*2 The suffix " H " stands for the component observed on hard carbon.

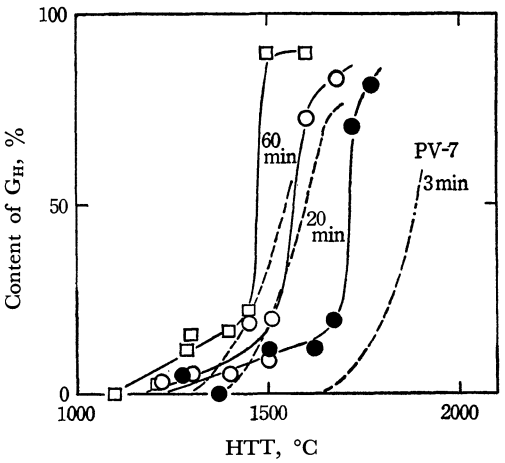

Fig. 4. Changes of content of the component G_H with HTT
● 3 min ○ 20 min □ 60 min
Changes of content of the component G_S of the soft carbon PV-7[7] were shown by the broken lines.

change of content of the component G_H with HTT is shown in Fig. 4.

Discussion and Summary

On the graphitization process of the hard carbon PH-7 under 5 kbar, the profile of (002) diffraction line showed the composite one. Similar composite profiles of (00 *l*) diffraction line had been observed on the soft carbon PV-7 heat-treated under the same pressure.[6-9] The graphitization process of PH-7 under pressure seemed to be composed of two stages; in the early stage the (002) profile of the heat-treated sample being symmetrical and in the later stage it consisting of two component profiles A_H and G_H. However, the later stage could be divided into two more stages from the view points of c_0-spacing, symmetry of the profile and content of the component G_H, which will be described below. Therefore, the graphitization process of PH-7 under pressure was considered to consist of three stages. On the soft carbon PV-7, the graphitization process under the same pressure was divided into two stages.

In the first stage of the graphitization, the (002) profile is symmetrical though being very broad. It means that there is only one component A_H in the sample. The presence of the high angle component G_H was not indicated. The c_0-spacing of the component A_H decreases from the original value to 6.88 A with the increase in HTT.

In the second stage of graphitization (above 1200°C), the (002) profile becomes composite, consisting of the components A_H and G_H. The content of the component G_H increases gradually up to about 20% and its apparent c_0-spacing decreases from about 6.79 to 6.72 Å with the increase in HTT. The profile of the component G_H in this stage is not exactly symmetrical and therefore may consist of two components G'_H and G''_H. Assuming that the component G'_H has a relatively large c_0-spacing as 6.78 Å and the component G''_H has 6.72 Å and that the component G'_H transforms to G''_H, the gradual decrease of the apparent c_0-spacing and the lack of symmetry of profile of the component G_H may be explained. On the other hand, the component A_H becomes to have a constant c_0-spacing of 6.88 Å through this stage, though the angular position of this component profile has not been assumed as constant before the separation of the composite profile. On the soft carbon PV-7,[7] the component A_S on the low angle side had a little smaller c_0-spacing and its profile was much sharper than that of the compoent A_H observed on the hard carbon PH-7 in the present work.

In the third stage of graphitization, the content of the component G_H increases abruptly to more than 70% at about 1400, 1500 and 1700°C for the residence time of 60, 20 and 3 min, respectively. The profile of the component G_H is almost symmetrical

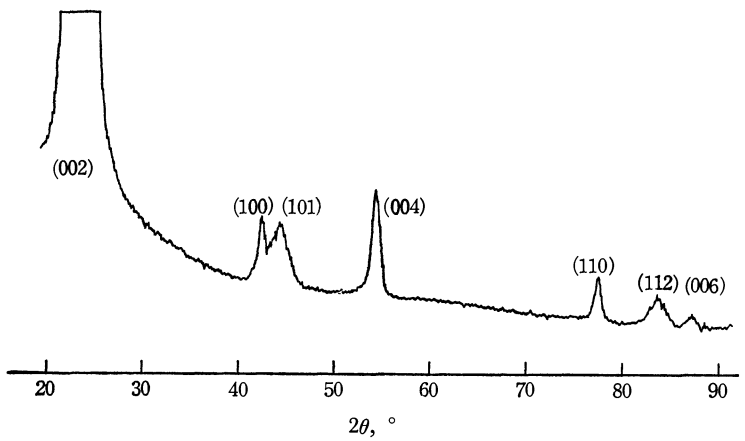

Fig. 5. Diffraction pattern of the hard carbon heat-treated at 1500°C for 60 min under 5 kbar.

and has the c_0-spacing of around 6.72 Å. Therefore, component G_H may consist of only one component the G''_H in this stage. The c_0-spacing of the component A_H is also constant at 6.88 Å through stage. The sample obtained in this stage (the content of G_H is more than 70%) was found to have the three-dimensional diffraction lines such as (101) and (112) lines (Fig. 5).

These experimental facts suggest the followings; The component A_H has turbostratic structure and its c_0-spacing in the second and third stages is the same as that has been assigned for this structure by others.[1,10] The component G_H is considered to consist of two components G'_H and G''_H. The component G''_H, which has the c_0-spacing of 6.72 Å and shows the three-dimensional diffraction lines, corresponds to graphitic structure and it may be the same as the component G_S observed on the soft cabon PV-7. The component G'_H, whose c_0-spacing is between 6.72 and 6.88 Å, corresponds to the intermediate structure between turbostratic and graphitic structures. The component G'_H is observed only in the second stage of graphitization and its content is much less than 20%. No component having such an intermediate structure as G'_H was observed on the soft carbon PV-7.

As shown in Fig. 4 (for the convenience of comparison the change of content of the component G_S in the soft carbon PV-7 are also shown), it is surprising that the hard carbon PH-7 is graphitized as abruptly as the soft carbon PV-7 at low temperature as 1500°C under 5 kbar. For the residence time of 3 min, the hard carbon PH-7 seems to be graphitized somewhat faster than the soft carbon PV-7.

From the results of the present work, it is deduced that the hard carbon heat-treated under pressure consists of two or three components, each of which has enough extent to produce the coherent X-ray scattering. Such a constitution of the structural components is very similar to that oberved on the soft carbon.[7]

The authors wish to thank Tokai Electrode Mfg. Co. for supplying the graphite materials used.

10) B. E. Warren, "Proceedings of the Conferences on Carbon," Univ. of Buffalo (1956), p. 49.

NOTES

Reaction of Triethylaluminum with Ketone

Yoshio BABA

Resources Research Institute, Kawaguchi, Saitama

(Received April 17, 1967)

It has been found that the reaction of alkylaluminum compounds with ketones involves normal addition, reduction and enolization reactions.[1-4]

Pasynkiewicz and Sliwa[5] have carried out studies of the reaction of triethylaluminum with diethyl ketone and diisopropyl ketone. As a result of these experiments, they concluded that the normal addition and reduction are affected by the mole ratio of ketone/$AlEt_3$ and by the reaction temperature, while the enolization reaction is not subject to such influences.

In the course of an investigation of the reactions of methyl ketones with triethylaluminum, the present author has been interested in the fact that, although the reactions of triethylaluminum and its diethyl ether adduct with ketones yield three kinds of products resulting from addition, reduction and enolization-condensation reactions, a considerable quantity of ethane has been obtained as a further product. The amount of this gaseous product was much greater than was to be expected from the amount of the enolization-condensation product.

The present investigation was undertaken to reveal the source of these gaseous products and the mechanism of the formation of the enolization-condensation product in the reaction of ketones with triethylaluminum and its diethyl ether adduct.

Experimental

All the melting points uncorrected.

Materials. Commercial acetone (bp 55°C), methylethyl ketone (bp 78°C), methyl *n*-propylketone (bp 101°C), methyl isopropyl ketone (bp 94°C), methyl *s*-butyl ketone (bp 116°C), methyl *t*-butyl ketone (bp 105°C) methyl *n*-amyl ketone (bp 148°C), methyl isoamyl ketone (bp 142°C), and acetophenone (bp 201°C) were purified by distillation. Triethylaluminum purchased from the Ethyl Corp. was used without further purification.

Solvent. Petroleum ether was distilled, and a fraction with a bp of 35—45°C was dried over metallic sodium.

Analytical Procedure. The amounts of recovered ketone and secondary alcohol were determined by the Iddles[6] and Verbeck[7] methods respectively. The tertiary alcohol content was calculated from the total amount of alcohol itself determined by the active hydrogen analysis, and from the secondary alcohol content. The amounts of the gaseous products were measured, and then their components were analyzed by gas chromatography using a Okura Gas Chromatograph, Model-4000 (dimethyl sulfolane 5 m; 20°C; hydrogen gas as carrier gas). The active hydrogen content of the condensation products was determined by the Niederl[8] method, based on the reaction with methylmagnesium iodide.

General Procedure. All the reactions were carried out in an atmosphere of dry nitrogen. A thirty-weight-percent solution of triethylaluminum or its diethyl ether adduct in dry petroleum ether, containing 0.1 mol of the aluminum compound, was added to a gently-refluxing 30 wt % solution of ketone (0.1 mol) in dry petroleum ether. A gaseous product which evolved during the addition of the aluminum compound solution was led through a gas meter to a gas receiver. The reaction solution was then refluxed for an additional 0.5 hr, by which time the gas evolution practically terminated. The reaction solution was cooled in an ice bath, and the aluminum compound was decomposed by adding diethyl ether containing a theoretical amount of water. After the addition of cracked ice, precipitated aluminum hydroxide was removed by filtration and the filter cake was washed thoroughly with ether. The organic layer was separated and dried over anhydrous magnesium sulfate. The solvent was removed by distillation using a Widmer column (30 cm), and the residue was then distilled. The components of the distillate were determined by the methods described in the "Analytical Procedure" section, while the residue of the distillation was weighed and its active hydrogen content determined.

Reaction of Acetone with Triethylaluminum. A rectification of the product obtained from the reaction

1) H. Gilman and K. E. Marple, *Rec. trav. chim.*, **55**, 133 (1936).
2) H. Meerwein, G. Hinz and H. Majert, *J. prakt. Chem.*, (2), **147**, 226 (1937).
3) K. Ziegler, K. Schneider and J. Schneider, *Ann.*, **623**, 9 (1959).
4) G. Wittig and O. Bub, *ibid.*, **566**, 113 (1950).
5) S. Pasynkiewicz and E. Sliwa, *J. Organometal. Chem.*, **3**, 121 (1965).
6) H. Iddles and C. Jackson, *Ind. Eng. Chem., Anal. Ed.*, **6**, 454, (1934).
7) S. Siggia, "Quantitative Organic Analysis *via* Functional Group," 2nd Ed., John Wiley & Sons, Inc., New York (1954), p. 11.
8) " Micromethods of Quantitative Organic Analysis," 2nd Ed. (1942), p. 263.

of acetone (5.8 g) with triethylaluminum yielded the following three fractions:

Fraction 1 bp 75—78°C, 0.6 g
Fraction 2 bp 95—98°C, 2.0 g
Fraction 3 bp 70—75°C/25 mmHg, 2.2 g

3,5-Dinitrobenzoates of Fraction 1 (mp 121—122°C, from ethanol) and Fraction 2 (mp 116—117°C, from ethanol) were identified as those of isopropyl alcohol and dimethylethylcarbinol, respectively, by mixed-melting-point determinations with the authentic substances. The Fraction 3 was converted into its 2,4-dinitrophenylhydrazone (mp 202—203°C, from ethanol, undepressed by admixture with the authentic hydrazone of diacetone-alcohol).

Reaction of Acetophenone with Triethylaluminum - diethyl ether Adduct. A crude product obtained from the reaction of acetophenone (8.2 g) with the triethylaluminum - diethyl ether adduct was separated by vacuum distillation into a low-boiling fraction (bp 85—95°C/5 mmHg, 6.5 g) and a high-boiling condensation product (bp 195—197°C/5 mmHg, 2.0 g). The low-boiling fraction, after its secondary alcohol content had been determined, was esterified by refluxing it with a solution of phthalic anhydride in dry pyridine containing a slightly excessive amount of anhydride. The tertiary alcohol fraction (3.8 g) was collected by the distillation of the reaction mixture, while the secondary alcohol (0.6 g) was recovered by the hydrolysis of the monoester of phthalic acid obtained as the residue of the distillation. No depression in the melting points of the 3,5-dinitrobenzoate of the secondary alcohol fraction (mp 94—95°C, from ethanol) or in the *p*-nitrobenzoate of the tertiary alcohol fraction (mp 99.0—99.5°C, from ethanol) was observed upon admixture with authentic derivatives of phenylmethylcarbinol and phenylmethylethylcarbinol respectively. The melting point of the semicarbazone (mp 150—151°C, from methanol) of the high-boiling condensation product (bp 195—197°C/5 mmHg) corresponded with that reported for the semicarbazone of dypnone.[9]

Results and Discussion

The results obtained in the reactions of ketones with triethylaluminum and its diethyl ether adduct are cited in Tables 1 and 2.

The reaction of methyl ketone with triethylaluminum with a ketone/$AlEt_3$ mole ratio of 1 and at the temperature of 50—60°C gave considerable quantities of condensation products. The yields of these condensation products in eight experiments, but not with pinacoline, were about 50 wt% based on the ketones used. These high-boiling products appear to be produced by the enolization condensation

Table 1. Reactions of triethylaluminum with methyl ketones

Methyl ketone	mol	Reaction product: Condensation prod. g	Condensation prod. active H (mol)	Ethane (mol)	*s*-Alcohol %	*s*-Alcohol (mol)	Ethylene (mol)	*t*-Alcohol %	Recovered ketone
CH_3CO-CH_3	0.100	2.2	0.019	0.019	17.4	0.017	0.017	44.7	0
$-C_2H_5$	0.082	2.8	0.021	0.026	25.2	0.021	0.022	27.3	0
$-C_3H_7$-*n*	0.073	3.2	0.019	0.024	14.9	0.011	0.011	34.3	0
$-C_3H_7$-*i*	0.052	2.2	0.013	0.042	40.8	0.021	0.019	10.4	0
$-C_4H_9$-*s*	0.078	5.5	0.009	0.028	25.1	0.020	0.019	4.4	0
$-C_4H_9$-*t*	0.062	0.1	0.001	0.049	39.1	0.024	0.025	59.3	0
$-C_5H_{11}$-*n*	0.078	4.3	0.019	0.020	31.6	0.025	0.024	20.1	0
$-C_5H_{11}$-*i*	0.086	2.8	0.012	0.018	20.2	0.017	0.015	51.2	0
$-C_6H_5$	0.073	4.7	0.017	0.016	46.6	0.034	0.036	0	trace

Table 2. Reactions of triethyl aluminum diethyl ether adduct with methyl ketones

Methyl ketone	mol	Reaction product: Condensation prod. g	Condensation prod. active H (mol)	Ethane (mol)	*s*-Alcohol %	*s*-Alcohol (mol)	Ethylene (mol)	*t*-Alcohol %	Recovered ketone
$CH_3-CO-C_2H_5$	0.073	1.0	0.007	0.054	10.8	0.008	0.008	70.4	0
$-C_3H_7$-*i*	0.078	0.3	0.002	0.048	15.6	0.012	0.013	80.6	0
$-C_4H_9$-*s*	0.062	0.8	0.008	0.044	16.1	0.001	0.001	71.0	0
$-C_4H_9$-*t*	0.065	0.2	0.002	0.058	28.5	0.019	0.020	68.4	0
$-C_5H_{11}$-*n*	0.065	1.5	0.007	0.046	4.5	0.003	0.003	75.2	0
$-C_6H_5$	0.068	2.0	0.008	0.040	6.1	0.004	0.005	36.9	32.6

9) N. O. Calloway, *J. Am. Chem. Soc.*, **59**, 809 (1937).

reaction, as is shown in Eq. (1). In fact, in the experiments with acetone and acetophenone, diacetonealcohol and dypnone were obtained respectively. The amounts of ethane in the gaseous products nearly corresponded to that calculated from the active hydrogen content of the condensation products.

$$RCOCH_3 + \text{al-}C_2H_5 \rightarrow \underset{(I)}{RCOCH_2\text{al}} + C_2H_6$$

$$(I) + RCOCH_3 \rightarrow R\text{-}\underset{\displaystyle CH_2COR}{\overset{\displaystyle Oal}{\overset{|}{C}}}\text{-}CH_3 \xrightarrow{H_2O}$$

$$R\text{-}\underset{\displaystyle CH_2COR}{\overset{\displaystyle OH}{\overset{|}{C}}}\text{-}CH_3 \xrightarrow{\text{or } (-H_2O)} R\text{-}\overset{\displaystyle CH_3}{\overset{|}{C}}\text{=}CHCOR \qquad (1)$$

However, in the reaction of pinacoline with triethylaluminum, although considerable quantities of ethane were collected, neither the high-boiling product nor the recovered ketone were obtained; secondary and tertiary alcohols were obtained in yields of 39.1% and 59.3%, respectively. Such an inconsistency between the amount of ethane produced in the course of the reaction and the amount of active hydrogen in the high-boiling condensation product was markedly observed in the case of the reaction with the triethylaluminum diethyl ether adduct.

The reactions of ketone with an equimolar amount of triethylaluminum diethyl ether adduct differ from those with free triethylaluminum; the former afforded a smaller amount of condensation product than the latter. In the experiments with five methyl ketones, but not acetophenone, no ketones were recovered, while the amount of ethane evolved during the reaction was much greater than that obtained from the experiments with free triethylaluminum.

It may be concluded from the results of these experiments that the reaction of methyl ketone with triethylaluminum or its diethyl ether adduct proceeds through the courses indicated by Eqs. (2) and (3).

The enolate (II) produced by the reaction of ketone with free triethylaluminum appears to be so reactive as to react readily with the second molecule of the ketone and thus yield the condensation product. The enolate (III) formed by the reaction of ketone with the diethyl ether adduct of triethylaluminum, however, probably inhibits the condensation reaction because of the blocking effect of the coordinated diethyl ether.[10]

In the case of pinacoline, the reaction with free

$$RCOCH_3 + \text{al-Et} \begin{cases} \xrightarrow{\text{Addition}}\ \xrightarrow{(H_2O)}\ R\text{-}\overset{\displaystyle OH}{\overset{|}{C}}\text{-}CH_3 \\ \qquad\qquad\qquad\quad \underset{\displaystyle Et}{|} \\ \xrightarrow{\text{Reduction}}\ \xrightarrow{(H_2O)}\ R\text{-}\overset{\displaystyle H}{\overset{|}{C}}\text{-}CH_3 + C_2H_4 \\ \qquad\qquad\qquad\quad \underset{\displaystyle OH}{|} \\ \xrightarrow{\text{Enolization}}\ \underset{(II)}{RCOCH_2\text{al}} + C_2H_6 \end{cases} \qquad (2)$$

$$(II) \xrightarrow{RCOCH_3}\ \xrightarrow{(H_2O)}\ R\text{-}\overset{\displaystyle OH}{\overset{|}{C}}\text{-}CH_3 \quad \text{or} \quad R\text{-}\overset{}{\overset{\|}{C}}\text{-}CH_3$$
$$\qquad\qquad\qquad\qquad\qquad\qquad\qquad\qquad\qquad\qquad\quad \underset{\displaystyle CH_2COR}{|} \qquad\qquad\quad \underset{\displaystyle CHCOR}{|}$$

$$RCOCH_3 + \text{al-Et}\cdot Et_2O/3 \xrightarrow{\text{Enolization}} \underset{(III)}{RCOCH_2\text{al}\cdot Et_2O/3} + C_2H_6$$

$$(III) + \text{al-Et}\cdot Et_2O/3 \begin{cases} \xrightarrow{\text{Addition}}\ \xrightarrow{(H_2O)}\ R\text{-}\overset{\displaystyle OH}{\overset{|}{C}}\text{-}CH_3 \\ \qquad\qquad\qquad\quad \underset{\displaystyle Et}{|} \\ \xrightarrow{\text{Reduction}}\ \xrightarrow{(H_2O)}\ R\text{-}\overset{\displaystyle OH}{\overset{|}{C}}\text{-}CH_3 + C_2H_4 \\ \qquad\qquad\qquad\quad \underset{\displaystyle H}{|} \end{cases} \qquad (3)$$

10) K. Ziegler, *Ann.*, **629**, 251 (1960).

triethylaluminum affords a sterically-hindered enolate comparable to those produced in the reaction of simple ketone with the triethylaluminum diethyl ether adduct; this is because of the accumulated methyl groups on the α-carbon atom of the carbonyl group. As a result of this steric effect, the addition of the second molecule of pinacoline to the enolate is completely suppressed; thus the reaction does not afford the condensation product.

The author wishes to thank Dr. J. Yoshimura, Professor of the Tokyo Institute of Technology, for many helpful discussions and suggestions made during this work.

Selective Deethoxycarbonylation of β-Ethoxycarbonylamino-α,β-Unsaturated Carboxylic Esters*[1]

Takao TAKAYA, Hataaki YOSHIMOTO and Eiji IMOTO

Department of Applied Chemistry, College of Engineering, University of Osaka Prefecture, Sakai, Osaka

(Received May 22, 1967)

An ethoxycarbonyl group attached to a carbon atom is usually more easily hydrolysed in either an alkaline or an acidic medium than is an ethoxycarbonyl group attached to an amino group. We have, however, found that the hydrolysis of the compounds represented as having the general structure I with sodium ethoxide in ethanol occurs at different positions, depending on the nature of the group, G, intervening between ethoxycarbonyl and ethoxycarbonylamino groups.

$$EtO_2CNH\text{-}G\text{-}CO_2Et$$
(I)

When G was a group containing a double bond between the two functional groups, as in the compound III, the ethoxycarbonyl group attached to the amino group was selectively hydrolysed to give IV, in which the ethoxycarbonyl group attached to the carbon atom remained unchanged.

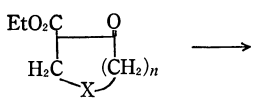

(II)

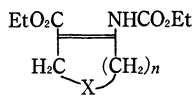

(III)

IIa_1: X=CH_2, n=1 $IIIa_1$: X=CH_2, n=1
IIa_2: X=CH_2, n=2 $IIIa_2$: X=CH_2, n=2
IIb_1: X=S, n=1 $IIIb_1$: X=S, n=1
IIb_2: X=S, n=2 $IIIb_2$: X=S, n=2

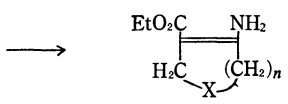

(IV)

IVa_1: X=CH_2, n=1
IVa_2: X=CH_2, n=2
IVb_1: X=S, n=1
IVb_2: X=S, n=2

Although β-amino-α, β-unsaturated carboxylic esters, such as IVa_1 and IVa_2, were also obtained from the corresponding β-ketoester II and ammonia according to the method of Prelog and Szpilfogel,[1] a similar reaction of 3-ethoxycarbonyl-4-ketotetrahydrothiophene IIb_1 resulted in the complete recovery of the starting material. However, IVb_1 was obtained in only a moderate yield by the alkaline hydrolysis of 3-ethoxycarbonyl-4-ethoxycarbonylamino-2,5-dihydrothiophene $IIIb_1$.

On the contrary, when G was a group containing a single bond between the two functional groups, as in the compound V[2] or VI,[2] the ethoxycarbonyl group attached to the carbon atom was selectively hydrolysed with sodium ethoxide in ethanol to give VII or VIII, in which the ethoxycarbonyl group attached to the amino group remained unattacked. The acid hydrolysis of V and VI, as usual, gave VII and VIII, respectively.

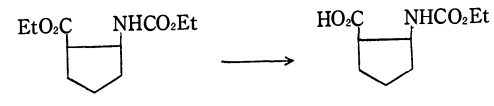

(V) (VII)

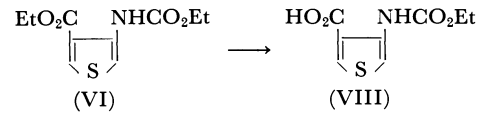

(VI) (VIII)

The starting materials, β-ethoxycarbonylamino-α, β-unsaturated carboxylic esters, III, were prepared in good yields by refluxing the corresponding β-ketoester, II, and urethane in the presence of *p*-toluenesulfonic acid.

*1 Studies on the Syntheses of Heterocyclic Compounds. Part VII. Part VI: M. Fujimori, E. Haruki and E. Imoto, This Bulletin, in press.

1) V. Prelog and S. Szpilfogel, *Helv. Chim. Acta*, **28**, 1684 (1946).

Table 1. The preparation of III

Compound	Mp, °C	Yield, %	Formula		Analysis C	H	N
$IIIa_1$	50—52	75	$C_{11}H_{17}O_4N$	Calcd	58.13	7.54	6.16
				Found	58.28	7.30	6.26
$IIIa_2$	46.5—48.5	81	$C_{12}H_{19}O_4N$	Calcd	59.73	7.94	5.81
				Found	59.71	8.18	6.02
$IIIb_1$	70—71.5	90	$C_{10}H_{15}O_4NS$	Calcd	48.97	6.17	5.71
				Found	48.87	6.17	5.80
$IIIb_2$	32—33	76	$C_{11}H_{17}O_4NS$	Calcd	50.96	6.61	5.40
				Found	51.03	6.59	5.24

Table 2. Selective hydrolysis of III, V and VI

Compound	Mp (Bp, °C/mmHg)	Recryst. solvent	Yield, %	Formula		Analysis C	H	N
IVa_1	58—60	Petroleum ether*1	77	$C_8H_{13}O_2N$	Calcd	61.91	8.44	9.03
					Found	62.03	8.21	8.81
IVa_2	71—73	Petroleum ether	62	$C_9H_{15}O_2N$	Calcd	63.88	8.94	8.28
					Found	64.01	9.01	8.01
IVb_1	80—82	EtOH-H_2O	58	$C_7H_{11}O_2NS$	Calcd	48.55	6.40	8.09
					Found	48.23	6.40	7.74
IVb_2	(108—109/0.2)		65	$C_8H_{13}O_2NS$	Calcd	51.33	7.00	7.48
					Found	51.58	7.30	6.89*2
VII	124—125	Benzene	70	$C_9H_5O_4N$	Calcd	53.72	7.51	6.97
					Found	53.78	7.65	6.70
VIII	152—154	Benzene	73	$C_8H_9O_4NS$	Calcd	44.66	4.22	6.51
					Found	44.80	4.10	6.47

*1 Bp 40—60°C.
*2 Partly decomposed into 3-ethoxycarbonyltetrahydro-1,4-thiapyrone and ammonia.

Experimental[3]

β-Ketoester, II. Several β-ketoesters, 2-ethoxycarbonylcyclopentanone IIa_2,[4] 2-ethoxycabonylcyclohexanone (IIa_3),[5] 3-ethoxycabonyl-4-ketotetrahydrotiophene (IIb_1),[6] and 3-ethoxycarbonyltetrahydro-1,4-thiapyrone (IIb_2),[7] were sythesized by the methods given in the literature.

General Procedure for the Preparation of III. A mixture of 0.6 mol of II, 0.7 mol of urethane, and 1 g of *p*-toluenesulfonic acid dissolved in 100 m*l* of benzene was refluxed for 15 hr in a Soxhlet apparatus containing sodium sulfate in a thimble. The reaction mixture was then washed thoroughly with water to remove the *p*-toluenesulfonic acid and the excess urethane. After the evaporation of the solvent, a crude product was purified by chromatography using a column packed with alumina, plus chloroform - petroleum ether as an eluent, or by recrystallization from methanol-water (9: 1). The yield and properties for each compound are given in Table 1.

General Procedure for the Deethoxycarbonylation of III. A solution of 0.25 mol of sodium metal in 100 m*l* of ethanol containing 0.05 mol of III was refluxed for 17 hr. The cooled reaction mixture was diluted with water and then extracted with ether, after which the ethereal solution was treated with active charcoal and dried over sodium sulfate overnight. The solvent was removed, and the residue was recrystallized from an appropriate solvent or distilled under reduced pressure to give IV. The yield, properties, and recrystallizing solvent for IV are given in Table 2.

Hydrolysis of V or VI. After the treatment of 6 mmol of V or VI with 0.5 g of sodium metal in 50 m*l* of ethanol in the manner described above, the cooled reaction mixture was diluted with water, acidified with hydrochloric acid, and extracted with ether. The ethereal solution was then worked up in the usual manner and recrystallized from benzene. The products, VII and VIII, were obtained by refluxing V and VI respectively with 6 N hydrochloric acid for 8 hr. The analytical data and physical constants of VII and VIII are summarized in Table 2.

2) The preparation of V and VI will be described in another paper.
3) All melting points are uncorrected.
4) P. S. Pinkney, "Organic Syntheses," Coll. Vol. II, p. 116 (1943).
5) H. R. Snyder, L. A. Brooks and S. H. Shapiro, *ibid.*, Coll. Vol. II, p. 531 (1943).
6) G. B. Brown, B. R. Baker, S. Bernstein and S. R. Safir, *J. Org. Chem.*, **12**, 155 (1947).
7) E. A. Fehnel and M. Carmack, *J. Am. Chem. Soc.*, **70**, 1813 (1948).

Syntheses of 3,3-Dimethyl-2-hydroxybutyric Acid and Tertiary Leucine and Their Optical Resolutions

Tadashi TANABE, Shinichi YAJIMA and Masami IMAIDA

Division of Organic Chemistry, Institute for Protein Research, Osaka University, Kita-ku, Osaka

(Received July 8, 1967)

DL-3,3-Dimethyl-2-hydroxybutyric acid (I) was prepared by the reduction of trimethylpyruvic acid (II) with sodium amalgam[1] and by catalytic hydrogenation with palladium black.[2] The optical resolution of I has not yet been attempted, however.

DL-*t*-Leucine (III) was prepared by the reduction of trimethylpyruvic acid oxime[3] and resolved into its optical isomers by the treatment of the *N*-formyl derivative of III with brucine.[4] The absolute configuration of the (−) isomer (IIIa) was finally determined to be L by Izumiya *et al.*[5]

In the present work, I was prepared by the catalytic hydrogenation of II with a Raney nickel catalyst and was resolved into optically-active isomers with brucine and cinchonidine. The absolute configuration of the (+) isomer (Ia) was determined to be L_s by the deamination of L-(−)-*t*-leucine (IIIa) with nitrous acid to Ia.

III was prepared by the reductive amination of II with a Raney nickel catalyst and was converted into the *N*-acetyl derivative and the amide. The (−) isomer was obtained with cinchonidine from the former and with D-tartaric acid from the latter.

Experimental

Preparation of DL-3,3-Dimethyl-2-hydroxybutyric Acid (I). The ether extracts of the oxidized product of 120 g of pinacolone with pottasium permanganate[6] were concentrated, and then the residue was neutralized with 5 N sodium hydroxide. The resulting solution was hydrogenated at 50°C in the presence of a Raney nickel catalyst prepared from 5 g of alloy.[7] After the catalyst had been removed by filtration, the filtrate was passed through a column of sulfonic resin (H^+ form) and then concentrated to dryness *in vacuo* at below 50°C. Crude crystals were dissolved in a minimal volume of benzene, and then petroleum benzin was added. The crystals were collected to give 80 g of I. Mp 87—88°C.

Found: C, 54.36; H, 9.11%. Calcd for $C_6H_{12}O_3$: C, 54.53; H, 9.15%.

Optical Resolution of I into L-(+)-3,3-Dimethyl-2-hydroxybutyric Acid (Ia). Seventy-five grams of I and 224 g of brucine were dissolved in 1 *l* of water, and then the solution was concentrated to 500 m*l*. After the solution had been allowed to stand overnight in a refrigerator, the brucine salts were collected. Six recrystallizations of the salt from water yielded the pure brucine salt of Ia. Yield 22 g; mp 223—224°C (decomp.), $[\alpha]_D^{20}$ −31° (*c* 1, alcohol).

Found: N, 5.32 Calcd for $C_{29}H_{38}N_2O_7$: N, 5.33%.

Twenty grams of the salts were treated with 5 N sodium hydroxide, and the liberated brucine was removed by filtration. The filtrate was treated with sulfonic resin to remove a trace of brucine and sodium ions, and then concentrated to dryness under reduced pressure. The crystallization of the crude material from benzene-petroleum benzin gave optically-pure Ia. Yield 3.9 g; mp 51—52°C, $[\alpha]_D^{20}$ +4.5° (*c* 4, water). $[\alpha]_D^{20}$ −63° (*c* 1, water, 48.5 mg ammonium molybdate in 10 m*l*).

Found: C, 54.75; H, 9.30%.

Optical Resolution of I into D-(−)-3,3-Dimethyl-2-hydroxybutyric Acid (Ib). Thirty-five grams of cinchonidine and 15.8 g of I were dissolved in 100 m*l* of alcohol, and then the solution was allowed to stand overnight in a refrigerator to give 33 g of the cinchonidine salt. Five recrystallizations of the salt from alcohol gave pure cinchonidine salt of Ib. Yield 9 g; Mp 220—221°C, $[\alpha]_D^{20}$ −10.2° (*c* 1, alcohol).

Found: C, 69.46; H, 8.11; N, 6.24%. Calcd for $C_{25}H_{34}N_2O_4$: C, 70.09; H, 8.03; N, 6.57%.

Nine grams of the salt obtained were suspended in 100 m*l* of hot water, and then decomposed with 5 m*l* of 5 N sodium hydroxide under vigorous stirring for a day. After the removal of the cinchonidine by filtration, the filtrate yielded pure Ib when treated by the procedure described above. Yield 2.3 g; mp 50—51°C, $-[\alpha]_D^{20}$ −4.3° (*c* 4, water), $[\alpha]_D^{20}$ +65° (*c* 1, water, 51 mg of ammonium molybdate in 10 m*l*).

Found: C, 54.36; H, 9.38%.

Preparation of (+)-3,3-Dimethyl-2-hydroxybutyric Acid (Ia) from L-(−)-*t*-Leucine (IIIa). A solution of 0.77 g of sodium nitrite in 10 m*l* of water was added, drop by drop, to a solution of 1.4 g of L-(−)-*t*-leucine (IIIa) ($[\alpha]_D^{20}$ −8.5) in 10 m*l* of 2 N sulfuric acid. After the evolution of nitrogen had ceased, 5 m*l* of 2 N sulfuric acid was added and the product was extracted with ether. The ether extract was concentrated, and the residue was dissolved in 10 m*l* of water and decolorized with charcoal. After concentration *in vacuo*, the residual crude crystals were dissolved in a minimal volume of benzene, and then petroleum benzin was added. The resulting solution was cooled to give an acid (Ib). Yield, 70 mg; mp 43°C, $[\alpha]_D^{20}$ −58° (*c* 1, water, 50 mg of ammonium molybdate in 10 m*l*).

1) C. Glücksmann, *Monatsh.*, **10**, 770 (1889); **12**, 356 (1891).
2) F. Knoop and H. Oesterlin, *Z. Physiol. Chem.*, **148**, 307 (1925).
3) F. Knoop and G. Landmann, *ibid.*, **89**, 157 (1914).
4) E. Abderhalden, W. Faust and E. Haase, *ibid.*, **228**, 187 (1934).
5) N. Izumiya, S.-C. J. Fu, S. M. Birnbaum and J. P. Greenstein, *J. Biol. Chem.*, **205**, 221 (1953).
6) R .Adams and E. W. Adams, "Organic Syntheses," Coll. Vol. II, p. 459 (1948).
7) Y. Izumi, M. Imaida, H. Fukawa and S. Akabori, This Bulletin, **36**, 24 (1963).

Preparation of DL-*t*-Leucine Hydrochloride (IV). Sodium trimethylpyruvate prepared from 62 g of II was subjected to reductive amination in 300 m*l* of concentrated aqueous ammonia (at 100 atm and 60°C) with a Raney nickel catalyst prepared from 3 g of alloy. The reaction mixture was then concentrated under reduced pressure. After the addition of sufficient 6 N hydrochloric acid to form the hydrochloride, the solution was evaporated to dryness and the IV was taken up with methanol. After the removal of the methanol, there remained 50 g of IV.

Preparation of *N*-Acetyl-DL-*t*-Leucine (V). III prepared from 50 g of IV by neutralization with 10 N sodium hydroxide was acetylated with a mixture of 90 m*l* of acetic anhydride and 20 m*l* of acetic acid at room temperature for 6 hr. The reaction mixture was then evaporated to dryness, and the product was taken up with alcohol. After the removal of the alcohol, the residual substance was recrystallized from alcohol. Yield 31.5 g; mp 229—231°C.

Found: C, 55.39; H, 8.59; N, 8.02%. Calcd for $C_6H_{14}NO_2Cl$: C, 55.47; H, 8.73; N, 8.39%.

Optical Resolution of V and Isolation of L-*t*-Leucine (IIIa). Sixty-five grams of V and 110 g of cinchonidine were dissolved in 200 m*l* of hot alcohol, after which the solution was allowed to stand overnight in a refrigerator. The crystalline precipitates were then collected. Six recrystallizations of the salt from alcohol gave 12 g of pure cinchonidine salt of IIIa. Twelve grams of the salt were decomposed with 1 N sodium hydroxide, and the liberated cinchonidine was filtered off. The filtrate was shaken with chloroform, acidified with 2 N hydrochloric acid, concentrated to 100 m*l* and extracted with ethyl acetate. The extract was evaporated to dryness, and the residue was recrystallized from a mixture of water and alcohol. 1.2 g of (−)-*N*-acetyl-*t*-leucine (VI) were obtained; mp 228—229°C, $[\alpha]_D^{20}$ −40° (*c* 1, water).

1.2 g of VI were hydrolyzed with hydrochloric acid, and then the hydrolysate was concentrated and the excess hydrochloric acid was removed by azeotropic distillation with water. The resulting crystals were dissolved in 20 m*l* of water and neutralized with diethylamine, and then 2 m*l* of alcohol were added. After the solution had stood overnight, IIIa was obtained. Yield 820 mg; mp 280°C (sublimed), $[\alpha]_D^{20}$ −9.5° (*c* 2, water).

Preparation of DL-*t*-Leucine Methylester Hydrochloride (VII). The product obtained from the reductive amination of 50 g of II was concentrated *in vacuo*, and the residue was extracted with 300 m*l* of methanol. Then to the extract there were added 100 m*l* of toluene, and the solution was evaporated to dryness under reduced pressure. The residue was dissolved in 300 m*l* of methanol, and the solution was saturated with hydrogen chloride, refluxed for 6 hr, and concentrated to dryness *in vacuo* at below 60 °C. A trace of water remaining in the residue was removed by azeotropic distillation with toluene; the subsequent addition of 5 m*l* of ether to the residue gave 27 g of VII. Mp 180—181°C.

Preparation and Optical Resolution of DL-*t*-Leucine Amide and Isolation of (−)-*t*-Leucine (III). Twenty-seven grams of VII were dissolved in 1 *l* of chloroform, and then dry ammonia was bubbled into the solution at 0°C. The ammonium chloride formed was filtered off, and the chloroform was removed under reduced pressure. The residual syrup was shaken with 200 m*l* of liquid ammonia in a 1-*l* autoclave for 12 hr at 55—60°C. After the ammonia had been evaporated off, the residue and 33.5 g of D-tartaric acid were dissolved in 45 m*l* of water. Storage overnight in a refrigerator gave 24.4 g of the salt. The salt was twice recrystallized from water to give 13.6 g of the pure D-tartrate of IIIa. $[\alpha]_D$ +0.88 (*c* 5, water).

13.6 g of the salt was hydrolyzed with 230 m*l* of 4 N hydrochloric acid for 6 hr, and the hydrolysate was concentrated to dryness. The residue was dissolved in 200 m*l* of water, and the solution was passed through a column of a weakly basic resin (Amberlite GC-45, OH^- form) to remove the tartaric acid and hydrochloric acid. *t*-Leucine was eluted with 400 m*l* of 0.5% aqueous acetic acid, after which to the eluate there was added 10 m*l* of concentrated hydrochloric acid. The resulting solution was concentrated to dryness. The residue was dissolved in a mixture of 9 m*l* of methanol and 4 m*l* of water, and the pH of the resulting solution was adjusted to 6.5 with diethylamine to yield 3 g of crude IVa, which was then recrystallized from a mixture of water and alcohol. Yield 1.7 g, $[\alpha]_D^{20}$ −9.0° (*c* 4, water). Found: C, 54.78; H, 10.09; N, 10.74%.

The authors wish to express their thanks to Professor Yoshiharu Izumi for his continuous guidance and help. They also wish to thank Miss Kiku Koike and Miss Nobuko Ohya for carrying out the elemental microanalyses.

The Cyanation of Ethylene with Cyanogen by a Silent Discharge

Tomiya ISSHIKI,*1 Noboru SONODA and Shigeru TSUTSUMI

Department of Chemical Technology, Faculty of Engineering, Osaka University, Yamadakami, Suita, Osaka

(Received November 21, 1967)

There have been several patents[1-3] on the reaction of cyanogen with olefins. It has been shown that the reaction of cyanogen with ethylene over a nichrome wire coil above 815°C gives rise to succinonitrile,[1] whereas in the absence of a catalyst acrylonitrile was produced at 750—900°C,[2] or at 300—700°C under low pressure.[3] These facts show that the reaction of cyanogen with olefin may require high temperatures because of the high activation energy. In connection with our study on the reaction under an electrical discharge, a similar reaction was undertaken in a silent discharge, which seemed to resemble a high LET radiation process.[4] It was observed that the reaction proceeded smoothly at room temperature under atmospheric pressure.

The reaction of equimolar amounts of cyanogen and ethylene gave acrylonitrile as the main product in a yield of 40.0%, based on unrecovered ethylene, and propionitrile and valeronitrile were also formed in yields of 5.3 and 9.5%, respectively. A trace amount of adiponitrile was detected, and some undetectable solid, deposited on the surface of the discharge tube, was obtained. The gaseous products indentified were acetylene (7.6%), ethane (1.9%) and small amounts of butane, 1-butene, methane, hydrogen cyanide and hydrogen.

It was reported that acetylene was the main product of a silent discharge reaction with ethylene,[5] and that the reaction of cyanogen[6] in a silent discharge would give cyanoradical as an intermediate. Although little information was obtained about the reaction mechanism in the present experiment, acetylene may not be the precursor of acrylonitrile, because the addition of a small amount of acetylene to the reaction mixture did not cause any increase in the yield of the cyanated products.

Experimental

The silent discharge tube used was a Siemens type tube made of hard glass; discharge length, 24 cm; space gap, 3.5 mm; discharge space volume, 50 m*l*. The secondary voltage applied was 15 kV, and secondary current 1.0 mA at 60 cycles.

A gaseous mixture of 25.3 *l* of ethylene (0.503 mol) and cyanogen (0.503 mol) was circulated at the rate of 1.4 *l* min through the Siemens tube, and the effluent gas, before returning to the gas container, was passed through a cold trap at −20°C to collect condensable products.

After the discharge was continued for 7 hr, the components of the gaseous products were analyzed by v. p. c. using columns of activated charcoal and tricresyl phosphate: ethylene (0.293 mol), cyanogen (0.394 mol), acetylene (0.016 mol), ethane (0.004 mol), methane (0.001 mol), and trace amounts of 1-butene, butane, hydrogen, hydrogen cyanide and acrylonitrile were detected. To the condensed liquid products (8.2 g) was added a small amount of hydroquinone to prevent the polymerization of unsaturated products, and the resulting mixture was distilled under reduced pressure in a nitrogen atmosphere to give 5.7 g of a fraction boiling at 110°C/7 mmHg and 2.4 g of residue. Vapor phase chromatographic analysis of the fraction and the residue using a tricresyl phosphate column showed the presence of acrylonitrile (4.5 g), propionitrile (0.6 g), valeronitrile (0.8 g), adiponitrile (trace) and a small amount of unidentified products.

The acrylonitrile formed was also confirmed as its dibromo derivative; bromination of the liquid sample boiling at 76—78°C, obtained by redistillation of the above fraction, gave 2,3-dibromopropionitrile, which was identified by elementary analysis and the complete coincidence of the infrared spectrum with that of an authentic sample.

Found: C, 16.82; H, 1.56; N, 6.49; Br, 75.00%. Calcd for $C_3H_3NBr_2$: C, 16.93; H, 1.42; N, 6.58; Br, 75.04%.

*1 Inquiries should be addressed to: Research Institute, Mitsubishi Edogawa Chemical Co., Ltd., 6-3 Chome, Kanda, Surugadai, Chiyoda-ku, Tokyo.

1) G. W. Ayers, U. S. Pat. 2780638; *Chem. Abstr.*, **51**, 13906 (1957).
2) B. Oberbacher, Ger. Pat. 1034625; *Chem. Abstr.*, **54**, 11896 (1960).
3) W. L. Fierce and W. J. Sandner, U. S. Pat. 2803642; *Chem. Abstr.*, **52**, 5449 (1958).
4) A. Yokohata and S. Tsuda, This Bulletin, **39**, 46 (1966).
5) G. Egloff, C. L. Thomas and I. C. Morrell, *Chem. Revs.*, **28**, 1 (1941).
6) M. Kondo, *Nippon Kagaku Zasshi*, (*J. Chem. Soc. Japan, Pure Chem. Sect.*), **77**, 486 (1955).

Nitration of Phenylacetaldehyde

Yoshimori OMOTE, Naoaki FUKADA, Masakata HAYAKAWA and Noboru SUGIYAMA

Department of Chemistry, Tokyo Kyoiku University, Otsuka, Tokyo

(Received December 9, 1967)

There has been only one report about the direct nitration of phenylacetaldehyde (I); in that experiment Forrer[1] used concentrated nitric acid as a nitrating agent, but failed to obtain *o*-nitrophenylacetaldehyde (II). II is one of most important materials for preparing indole[2] and *N*-hydroxyindole,[3] but it is not convenient to synthesize II from *o*-nitrocinnamamide[2] or 1-chloro-4-(*o*-nitrophenyl)-2-butene.[4] We attempted to obtain II by the direct nitration of I with fuming nitric acid in acetic anhydride. The conditions were similar to those in the *o*-nitration with acetylnitrate.[5] Contrary to our expectations, however, II could not thus be obtained. Four compounds were isolated instead; they were identified as phenylacetaldehyde-diacetate (III), *p*-nitrophenylacetaldehyde-diacetate (IV), bis-(α-acetoxy-β-phenylethyl)-ether (V), and bis-(α-acetoxy-β-*o*-nitrophenylethyl)-ether (VI).

To an acetic anhydride solution of I, an equivalent amount of fuming nitric acid was added slowly at 0°C. An ether solution of the reaction mixture afforded an insoluble solid. The fractional distillation of the ether solution under reduced pressure gave two main fractions. The thin-layer chromatography of the yellow distillate, with a lower boiling point, showed that it contained the known compound III[6,7] as a main component. The orange distillate, with a higher boiling point, partly solidified upon cooling or standing for several days. After recrystallization, two crystalline compounds were isolated. One of them was identified with an authentic compound, V.[6,7] The structure of the other crystal (mp 102°C) was established to be IV by elemental analyses, and by a study of the IR, UV and NMR spectra. The NMR spectrum contained two symmetrical doublets with the same relative area centered at τ 1.82 and τ 2.59. The methine triplet was centered at τ 3.08.

The solid which was insoluble in the ether solution from the reaction mixture was recrystallized four times from acetone to afford colorless crystals (mp 196°C). The NMR spectrum showed an extensively split doublet (2 H) centered at τ 1.88 (the proton *ortho* to the nitro group) and a complex multiplet (6 H) with the strongest peak at τ 2.80 (the remaining three aromatic protons). The methine triplet was centered at τ 3.88. These data, as well as the results of elemental analyses and the IR and UV spectra of the crystal, were consistent with the structure of VI.

From a consideration of the reaction products, III, IV, V and VI, it seems reasonable to assume that direct nitration with fuming nitric acid in acetic anhydride cannot give II, but it can give III, from which IV and V are formed, and V can change into VI.

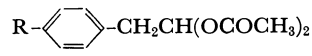

III, R=H

IV, R=NO_2

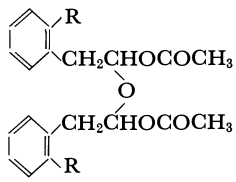

V, R=H

VI, R=NO_2

Experimental

All boiling points and melting points are uncorrected.

Nitration of Phenylacetaldehyde. To 100 g of phenylacetaldehyde (I) in 200 m*l* of acetic anhydride in a 500 m*l*, three-necked flask equipped with a mechanical stirrer, 53 g of fuming nitric acid (d 1.50) were added, drop by drop, over a period of 6 hr at 0°C. The liquid mixture was then stirred for 6 hr, during which the ice in the bath melted and the solution warmed to room temperature. The mixture was poured onto ice and left to stand overnight. The oily product was separated by decantation from the aqueous acidic solution, and washed with a sodium carbonate solution and water. By extraction with ether, the oily product was separated into two parts; part A was an oily solid, only slightly soluble in ether, while part B was readily soluble in ether.

Bis-(α-acetoxy-β-*o*-nitrophenylethyl)-ether (VI). Part A, a crude oily solid (about 10 g), was recrystallized four times from acetone to give colorless leaflets of VI, mp 196°C. NMR spectrum in deuterochloroform: τ 1.88 (doublet, 2 H), τ 2.80 (multiplet, 6 H), τ 3.88 (triplet, 2 H), τ 6.95 (doublet, 4 H) and τ 8.13 (singlet, 6 H). ν^{KBr} 2920, 2850, 1440, 1435 and 1375 (–CH_3 and –CH_2–); 1740 (CO); 3070, 1605 and 1495 (aromatic); 1510 and 1350 (NO_2); 1245 and 1230 (C–O–C) cm^{-1}.

1) C. Forrer, *Ber.*, **17**, 982 (1884).
2) R. A. Weerman, *Ann.*, **401**, 1 (1913).
3) M. Mousseron-Canet and J. P. Boca, *Bull. Soc. Chim. France*, **1967**, 1296.
4) W. E. Noland and J. H. Sellstedt, *J. Org. Chem.*, **31**, 345 (1966).
5) A. Pictet and E. Khotinsky, *Ber.*, **40**, 1163 (1907).
6) A. Wohl and R. Maag, *ibid.*, **43**, 3293 (1910).
7) E. Spath, *Monatsh. Chem.*, **36**, 29 (1915).

λ_{max}^{EtOH} (log ε) 270 (3.97) mμ. $\lambda_{max}^{0.1N\ NaOH\text{-}EtOH}$ (log ε) 263 (4.09) and 470 (4.64) mμ.

Found: C, 55.91; H, 4.66; N, 6.17%; mol wt (Rast), 448. Calcd for $C_{20}H_{20}O_9N_2$: C, 55.55; H, 4.66; N, 6.48%; mol wt, 432.38.

Phenylacetaldehyde-diacetate (III). Part B was concentrated on a rotary evaporator, and then the residue was, under reduced pressure, distilled into three fractions, together with 30—50 g of a tarry residue. Fraction 1, 5 g of a yellow liquid, bp 50—125°C/2.5 mmHg; fraction 2, 26 g of a yellow liquid, bp 125°C/2.5 mmHg, and fraction 3, 27 g of an orange liquid, bp 125—175°C/2.5 mmHg. Most of the fraction 1 consisted of the starting material, I. Fraction 3 was redistilled to give two main fractions; fraction a, 17 g of a yellow liquid, bp 126°C/2.5 mmHg, and fraction b, 6 g of an orange liquid, bp 165—178°C/2.5 mmHg. Fraction 2 and fraction a were combined and redistilled to give a faint yellow liquid of III (35 g), bp 126°C/2.5 mmHg (lit. 146—148°C/10 mmHg[6,7]). NMR spectrum in carbon tetrachloride: τ 2.82 (multiplet, 5 H), τ 3.18 (triplet, 1 H), τ 6.98 (doublet, 2 H) and τ 8.04 (singlet, 6 H). ν 2950, 2850, 1455, 1435 and 1375 ($-CH_3$ and $-CH_2-$); 1760 (CO); 3050, 1605 and 1495 (aromatic); 1240 and 1200 (C-O-C) cm^{-1}. λ_{max}^{EtOH} 253 and 259 mμ. $\lambda_{max}^{0.1N\ NaOH\text{-}EtOH}$ 250 and 297 mμ.

***p*-Nitrophenylacetaldehyde-diacetate (IV).** Fraction b was partly solidified in the flask by cooling or standing for several days. Recrystallization several times from methanol afforded prisms of IV (3 g), mp 102°C. NMR spectrum in deuterochloroform: τ 1.82 and τ 2.59 (two symmetrical doublets with the same relative area, 4 H), τ 3.08 (triplet, 1 H), τ 6.78 (doublet, 2 H) and τ 7.92 (singlet, 6 H). ν^{KBr} 2950, 2850, 1440, 1430 and 1378 ($-CH_3$ and $-CH_2-$); 1750 (CO); 3080, 1608 and 1490 (aromatic); 1512 and 1350 (NO_2); 1240 and 1200 (C-O-C) cm^{-1}. λ_{max}^{EtOH} (log ε) 268 (4.02) mμ. $\lambda_{max}^{0.1N\ NaOH\text{-}EtOH}$ (log ε) 270 (4.03) and 471 (4.39) mμ.

Found: C, 54.18; H, 4.98; N, 5.10%. Calcd for $C_{12}H_{13}O_6N$: C, 53.93; H, 4.90; N, 5.24%.

Bis-(α-acetoxy-β-phenylethyl)-ether (V). The mother liquid of the recrystallization of IV was concentrated to give crude crystals, from which 0.05 g of V was obtained by recrystallization from ethanol, mp 126—127°C. The melting point was identical with that of an authentic sample.[7] ν^{KBr} 2930, 2850, 1455, 1435 and 1380 ($-CH_3$ and $-CH_2-$); 1740 (CO); 3050, 1605 and 1495 (aromatic); 1255 and 1240 (C-O-C) cm^{-1}. λ_{max}^{EtOH} 260 mμ. $\lambda_{max}^{0.1N\ NaOH\text{-}EtOH}$ 297 mμ.

Identification of Azulene Compounds in the Dehydrogenation Products of the Sesquiterpene Hydrocarbon Fraction of Camphor Oil

Shûichi HAYASHI, Shinji KUROKAWA and Tamon MATSUURA

Department of Chemistry, Faculty of Science, Hiroshima University, Hiroshima

(Received December 28, 1967)

In a previous investigation[1] of the colored matter in blue camphor oil,*1 in which S- and Se-guaiazulene (85 : 5 ratio) were identified, the authors pointed out that a mixture of azulene compounds obtained on the sulfur dehydrogenation of the sesquiterpene hydrocarbon fraction of the blue camphor oil behaved differently on thin-layer chromatography from a mixture extracted directly from the blue oil.

The present experiment was undertaken to clarify the structure of azulenes obtained from the sulfur dehydrogenation of the sesquiterpene hydrocarbon fraction of the blue camphor oil; the sesquiterpene hydrocarbon fraction was dehydrogenated with sulfur, and then a mixture of azulene compounds extracted from the reaction mixture was separated, by the use of silica gel - *n*-hexane chromatography, to yield S-guaiazulene (85%), vetivazulene (8%), and 3,5,8-trimethylazuleno[6,5-*b*]thiophene (7%).

This composition is remarkably different from the azulene composition in the blue camphor oil. The detection of vetivazulene was the first such case in the dehydrogenation products of camphor oil, and presented interesting information for the study of the constituents of camphor oil, because no constituent which may be considered to be a precursor has not been detected. 3,5,8-Trimethylazuleno[6,5-*b*]-thiophene may be a secondary reaction product of the S-guaiazulene produced in the dehydrogenation of camphor oil, for the azulenothiophene had also been produced in a similar yield in the high-temperature reaction of S-guaiazulene and sulfur.[2]

Experimental

Dehydrogenation of the Sesquiterpene Hydrocarbon Fraction. A high-boiling fraction of camphor oil,

*1 The high-boiling fraction of camphor oil containing sesquiterpene hydrocarbons and alcohols and other high-boiling constituents is called blue camphor oil, because of its color.

1) S. Hayashi, T. Matsuura, O. Yamamoto and M. Okano, *Nippon Kagaku Zasshi* (*J. Chem. Soc. Japan, Pure Chem. Sect.*), **81**, 1186 (1960).

2) S. Hayashi, S. Kurokawa, M. Okano and T. Matsuura, *Tetrahedron Letters*, **1967**, 3443; *J. Sci. Hiroshima Univ., Ser. A-II*, **31**, 79 (1967).

obtained by distilling out a monoterpene fraction, bp above 215°C, d_4^{25} 0.9625, n_D^{25} 0.5057, $[\alpha]_D^{25}$ +40.0°, was fractionated through a Dixon-packed distillation column, and then the whole sesquiterpene hydrocarbon fraction, bp 104—120°C/9 mmHg, d_4^{25} 0.9289, n_D^{25} 1.5060, $[\alpha]_D^{25}$ +11.54°, was collected.

The fraction was dehydrogenated by heating it together with powdered sulfur at 180—240°C for 4 hr. The dehydrogenation products separated by distillation were then treated in the usual manner, phosphoric acid extraction and silica gel - benzene chromatography; a mixture of azulene compounds free from non-azulene products was thus obtained. This azulene mixture was then separated by chromatography on a silica-gel column using *n*-hexane. The results are shown in Table. 1

Table 1. Separation of azulene compounds produced in the dehydrogenation of the sesquiterpene hydrocarbon fraction

Eluting order	Appearance	Yield, g (%)
1	Blue, solidifiable	6.470 (84.9)
2	Violet, liquid	0.647 (8.3)
3	Dark violet, solid	0.517 (6.8)

Identification of the Azulene Compound. *S-Guaiazulene.* The blue azulene which was first eluted out from the column, solidified when stored. Its gas chromatogram (Chromosorb-W impregnated with 10% Silicone SE-30, Diasolid-L with 10% neopentyl glycol succinate, each column 1 m in length), IR,[3] UV,[4] visible[4] and NMR[5] spectra are in good agreement with those of S-guaiazulene. It gave the trinitrobenzoate,[6] mp 149—150°C, and the picrate,[6] mp 121—122°C, of S-guaiazulene (admixing).

Vetivazulene. The violet oil obtained from the second eluate was then purified by repeated phosphoric acid extraction and silica gel - *n*-hexane chromatography. The azulene oil thus obtained showed only one peak in gas chromatography, and its IR,[7] UV[8] and visible[4,8] absorption spectra agreed well with those of vetivazulene. The NMR and mass spectra of the oil can reasonably be explained by the structure of vetivazulene.

3,5,8-*Trimethylazuleno*[6,5-*b*]*thiophene.* From the third eluate, a dark violet crystalline mass, mp 95—107°C, was obtained after the solvent had been evaporated. It was further purified by repeated silica gel - *n*-hexane chromatography, and by subsequent recrystallization from methanol, to give dark violet needles melting at 116.0—116.5°C. A mixed-melting-point determination with 3,5,8-trimethylazuleno[6,5-*b*]thiophene[2] showed no depression. The NMR spectra of the compounds measured in chloroform and in trifluoroacetic acid both coincided with those of the azulenothiophene.[2] These findings were also supported by the IR and mass spectra.

3) Hs. H. Günthard and Pl. A. Plattner, *Helv. Chim. Acta*, **32**, 284 (1948).
4) Pl. A. Plattner, *ibid.*, **24**, 283E (1941).
5) D. Meuche, B. B. Molloy, D. H. Reid and E. Heilbronner, *ibid.*, **46**, 2483 (1963).
6) Pl. A. Plattner, A. Fürst and L. Marti, *ibid.*, **32**, 2452 (1949).
7) J. Pliva, H. Horak, V. Herout and F. Šorm, "Terpenspektren," Akademie-Verlag, Berlin (1960), p. 161.
8) B. Susz, A. St. Pfau and Pl. A. Plattner, *Helv. Chim. Acta*, **20**, 469 (1937).

Studies of the Chemistry of Azole Derivatives. VII. *N*-Substituted-2-amino-5-ketothiazolidino[4,5-*d*]thiazoles

J. M. SINGH

School of Chemistry, Meerut College, Meerut, India

(Received January 6, 1968)

In extension to our previous work on thiazoles[2,3] the present communication deals with the study of reaction of compounds having $-\overset{O}{\overset{\|}{C}}-CH_2-$ function in cyclic structure with lodine and monosubstituted thioureas. Dodson[4] reported the preparation of 2-amino-4-methyl-5-carbethoxythiazole by the reaction of acetoacetic ester, iodine and thiourea. In order to extend the application of this reaction, 2,4-diketothiazolidine was condensed with thiourea and iodine (1 : 2 : 1). The reaction can be represented as given below.

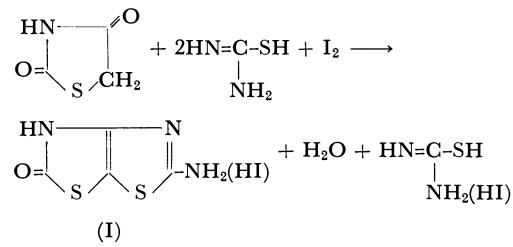

(I)

On treatment with ammonium hydroxide (I) afforded the free base which could be diazotised using phosphoric acid and on acetylation it gave

1) Present address: Scientific Officer, Defence Science Laboratory, Delhi-6, India.
2) J. M. Singh, *Can. J. Chem.*, in press.
3) J. M. Singh and G. R. Chaudhry, *J. Indian Chem. Soc.*, **43**, 273 (1966).
4) R. M. Dodson and W. King, *J. Am. Chem. Soc.*, **67**, 2242 (1945).

TABLE 1. *N*-SUBSTITUTED-2-AMINO-5-KETOTHIAZOLIDINO[4,5-*d*]THIAZOLES

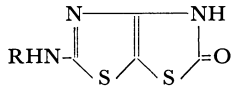

Sample	R	Yield %	Mp °C	Molecular formula	N% Found	N% Calcd	S% Found	S% Calcd
1	Phenyl-	41	200	$C_{10}H_7N_3OS_2$	16.72	16.87	25.54	25.73
2	*o*-Tolyl-	35	190	$C_{11}H_9N_3OS_2$	15.99	15.97	24.65	24.71
3	*p*-Tolyl-	39	195	$C_{11}H_9N_3OS_2$	15.85	15.92	24.59	24.71
4	*p*-Chlorophenyl-	40	176	$C_{10}H_6ClN_3OS_2$	14.72	14.81	22.35	22.57
5	*p*-Bromophenyl-	45	250	$C_{10}H_6BrN_3OS_2$	12.65	12.80	19.39	19.51
6	2,4-Dichlorophenyl-	40	300	$C_{10}H_5Cl_2N_3OS_2$	13.06	13.26	20.31	20.13
7	*α*-Naphthyl-	35	220	$C_{14}H_9N_3OS_2$	14.25	14.05	21.32	21.45
8	*β*-Naphthyl-	35	190	$C_{14}H_9N_3OS_2$	14.13	14.05	21.35	21.45
9	*p*-Nitrophenyl-	30	160	$C_{10}H_6N_4O_3S_2$	19.25	19.05	21.58	21.77
10	*o*-Nitrophenyl-	34	185	$C_{10}H_6N_4O_3S_2$	19.19	19.05	21.68	21.77

monoacetylated derivative. These reactions, supported by analysis, confirmed the presence of an amino group.

Monosubstituted thioureas were prepared and condensed with 2,4-diketothiazolidine in presence of iodine (2 : 1 : 1) to give, *N*-substituted-2-amino-5-ketothiazolidino[4,5-*d*]thiazoles.

Experimental

Substituted thioureas were prepared following the method of De Clermont.[6]

2-Amino-5-ketothiazolidino[4,5-*d*]thiazole.

A mixture of 2,4-diketothiazolidine (0.1 mol), iodine (0.1 mol) and thiourea (0.2 mol) was heated on a water bath for 20 hr. The condenser was removed and heating was continued for another 12 hr. It was then kept in contact of ether for 12 hr. The excess of iodine was removed by sodium thiosulfate solution. 2-Amino-5-ketothiazolidino[4,5-*d*]thiazole hydroiodide thus formed was dissolved in water and neutralized with ammonium hydroxide solution to liberate the free base, recrystallized from alcohol, mp 175—177°C.

Found: N, 24.34; S, 36.35%. Calcd for $C_4H_3N_3S_2O$: N, 24.27; S, 36.99%.

The mono acetyl derivative melted at 220°C after recrystallization from benzene.

Found: N, 20.31; S, 30.31%. Calcd for $C_6H_5N_3S_2O_2$: N, 19.54; S, 29.76%.

Following this procedure other compounds were prepared.[7] Data of these products are listed in the table.

The author expresses sincere gratitude to the Head, Chemistry Department, Meerut College, Meerut, for providing necessary facilities.

5) K. Ganapthai and Venkataraman, *Proc. Indian Acad. Sci.*, **224**, 359 (1945).

6) Ph. De Clermont and E. Wehrlin, *J. Chem. Soc.*, **31**, 70 (1877).

7) All melting points are uncorrected and ethanol was used for recrystallization.

Halogenation of Palladium(II) Complexes of β-Ketoamines

Akira KASAHARA and Takeo IZUMI

Department of Chemistry, Faculty of Liberal Arts and Science, Yamagata University, Yamagata

(Received January 16, 1968)

Recenty, Collman has described electrophilic substitution reactions of chromium (III), cobalt (III), and rhodium (III) acetylacetonates[1]; furthermore, we have reported that divalent palladium acetylacetonate has a pseudo-aromatic nature and undergoes an electrophilic substitution at the central carbon of the chelate ring.[2] An investigation of the chemistry of the inert metal chelates of β-ketoamine, the mononitrogen analogs of acetylacetonates, seems a logical sequel to these earlier studies; along these lines, Collman and Kittleman[3] have reported on the bromination of the chromium (III) complexes of β-ketoamines. In the present work, the palladium(II) complexes (1) of β-ketoamines derived from aromatic amines (aniline, *p*-toluidine, and α-naphthylamine) and acetylacetone were found to undergo facile halogenation with *N*-halosuccinimides at the central carbon atom of the chelate ring in the manner of a quasi-aromatic system (*cf.* Fig. 1).

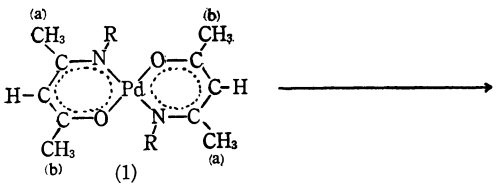

(1)

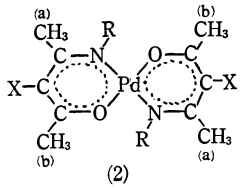

(2)

Fig. 1

Experimental[4]

Materials. Bis(4-anilino-3-penten-2-one)palladium-(II) (1, R=phenyl) and bis(4-*p*-toluidino-3-penten-2-one)palladium(II) (1, R=*p*-tolyl) were prepared by the procedure of Yamada.[5] Bis(4-α-naphthylamino-3-penten-2-one)palladium(II) (1, R=α-naphthyl) was prepared from potassium tetrachloropalladate and α-naphthylamino-3-penten-2-one according to Yamada's method[5] (dec. p. 220—223°C).

General Procedure for Preparing the Halogenated Palladium(II) Complex. Bis(3-chloro-4-anilino-3-penten-2-one)palladium(II). A solution of 0.454 g (0.001 mol) of bis(4-anilino-3-penten-2-one)palladium-(II) and 0.267 g (0.002 mol) of *N*-chloro succinimide in 25 m*l* of chloroform was boiled for 5 min, and then evaporated to dryness. The crude complex was separated from succinimide by ether extraction. After the removal of the ether, the resulting residue was chromatographed

TABLE 1. CHARACTERIZATION OF BIS(3-HALO-β-KETOAMINO)PALLADIUM(II) COMPLEXES (2)

R	X	Mp, °C	C%		H%		N%	
			Calcd	Found	Calcd	Found	Calcd	Found
Phenyl	Cl	214—215	50.45	50.64	4.23	4.18	5.34	5.45
Phenyl	Br	191—194*	43.13	43.31	3.61	3.78	4.57	4.49
p-Tolyl	Cl	216—217**	52.22	52.37	4.74	4.71	5.07	5.11
p-Tolyl	Br	185—187**	44.96	44.86	4.09	4.15	4.37	4.44
α-Naphthyl	Cl	205—207*	57.75	57.80	4.20	4.09	4.99	4.87
α-Naphthyl	Br	180—182**	50.55	50.66	3.67	3.55	3.93	3.91

* Decomposed point. ** Melted with decomposition.

1) a) J. P. Collman, "Reactions of Coordinated Ligands and Homogeneous Catalysis," ed. by R. F. Gould, Advances in Chemistry Series, No. 37, American Chemical Society, Washigton, D. C. (1963), p. 78. b) J. P. Collman, *Angew. Chem.*, **77**, 154 (1965). c) J. P. Collman, "Transition Metal Chemistry," Vol. II, ed. by R. L. Carlin, Marcel Dekker, New York (1966), p. 1.

2) A. Kasahara, K. Ujiie and K. Tanaka, This Bulletin, **39**, 2227 (1966).

3) J. P. Collman and E. T. Kittleman, *Inorg. Chem.*, **1**, 499 (1962).

4) All melting points are uncorrected. The infrared spectra were measured on KBr disks with a Hitachi EPI-S infrared spectrometer, while the ultraviolet absorption spectra were measured with a Hitachi recording spectrophotometer, model EPS-3T. The NMR spectra were recorded by a Hitachi H-60 instrument.

5) E. Yoshida and S. Yamada, This Bulletin, **38**, 2179 (1965).

TABLE 2. ULTRAVIOLET SPECTRA* AND NUCLEAR MAGNETIC SPECTRA** (AT 60 Mc/sec) OF PALLADIUM COMPLEXES OF β-KETOAMINES (2)

Compound R	Compound X	λ_{max}, mμ (log ε)	Chemical shifts of protons CH_3(a)	CH_3(b)	X	H of aromatic rings	CH_3 on aromatic rings
Phenyl	H	344(3.93)	8.66(3)	8.37(3)	5.18(1)	3.14—2.55(5)	
Phenyl	Cl	362(4.01)	8.38(3)	8.13(3)	—	3.22—2.65(5)	
Phenyl	Br	361(4.07)	8.31(3)	8.05(3)	—	3.20—2.60(5)	
p-Tolyl	H	345(3.90)	8.61(3)	8.34(3)	5.19(1)	3.28—2.85(4)	7.70(3)
p-Tolyl	Cl	360(3.96)	8.36(3)	8.12(3)	—	3.25—2.84(4)	7.69(3)
p-Tolyl	Br	361(3.98)	8.28(3)	8.00(3)	—	3.23—2.80(4)	7.68(3)
α-Naphthyl	H	345(3.95)	8.64(3)	8.35(3)	5.20(1)	3.25—2.60(7)	
α-Naphthyl	Cl	360(4.02)	8.35(3)	8.11(3)	—	3.24—2.54(7)	
α-Naphthyl	Br	361(4.03)	8.30(3)	8.07(3)	—	3.25—2.55(7)	

* Chloroform was used as solvent.

** NMR data are expressed as τ value and deuterochloroform was used as solvent, using tetramethylsilane as an internal reference. Relative peak intensities in parentheses.

on alumina using dichlorometane. Recrystallization from benzene afforded 0.254 g (45% yield) of yellow crystals, mp 214—215°C (dec.). IR Spectrum (KBr): 1560, 1434, and 1380 cm^{-1}.

Table 1 summarizes the halogenated complexes that have been synthesized by this method. The yields of the purified complexes ranged from 30 to 50%.

Discussion

The infrared spectrum of bis(4-anilino-3-penten-2-one)palladium(II) (1, R=phenyl) exhibits strong and characteristic peaks at 1585 and 1512 cm^{-1}. This characteristic pattern of the infrared maxima is shown by all of the β-ketoamine complexes examined. The replacement of the hydrogen by the halogen at the central carbon atom resulted in the disappearance of the bands at 1585 and 1512 cm^{-1} and their replacement by a strong peak at 1560 cm^{-1}. This behavior is analogous to that of the spectra of the metal acetylacetonates. Dryden[6] observed that the replacement of the hydrogen by other groups at the central carbon of metal acetylacetonate rings caused the infrared doublet in the 1500—1600 cm^{-1} region to become a singlet at about 1550 cm^{-1}. An example of this empirical rule has also been observed in the series of the chromium(III) complexes of β-ketoamines.[3] Furthermore, bis(4-anilino-3-penten-2-one)palladium (II) (1, R=phenyl) shows a medium band at 1204 cm^{-1}, but there is no absorption peak at 1200 cm^{-1} in the spectra of the halogenated complexes. The medium band at 1199 cm^{-1} in the spectra of palladium acetylacetonate has previously been assigned to the bending mode of the hydrogen at the central carbon atom;[7] the absence of this peak is unequivocal evidence of the replacement at the central carbon of acetylacetonates.[8]

The nuclear magnetic resonance spectra summarized in Table 2 provide conclusive proof of the structure assigned to the halogenated complexes (2). The unhalogenated complex (1, R=phenyl) exhibits proton signals at 8.66, 8.37, 5.18, and 3.14—2.55 τ, with relative intensities of 3 : 3 : 1 : 5. These signals may be assigned to the methyl protons (a), methyl protons (b), the hydrogens on the center carbon, and the aromatic protons (*cf.* Fig. 1). On the other hand, the halogenated complex, bis(3-chloro-4-anilino-3-penten-2-one)palladium(II (2, R=phenyl, X=Cl), gives signals at 8.38, 8.13, and 3.22—2.65 τ, with relative intensities of 3 : 3 : 5. These signals may be assigned to the methyl protons (a), methyl protons (b), and the aromatic protons, respectively. The ultraviolet spectra of the palladium(II) complexes of β-ketoamines are summarized in Table 2. The introduction of the halogen into the chelate rings gives rise to a bathochromic shift in each of the ultraviolet maxima, suggesting an increased conjugated system.

Preliminary attempts to carry out the nitration and acetylation of this complex system were unsuccessful. Under the same conditions that had previously effected the nitration of palladium(II) acetylacetonate,[2] the β-ketoamine complexes were destroyed. The latter showed much less stability under acidic conditions.

6) R. P. Dryden and A. Winston, *J. Phys. Chem.*, **62**, 635 (1958).

7) K. Nakamoto, P. J. McCarthy and A. E. Martell, *J. Am. Chem. Soc.*, **83**, 1272 (1961).

8) J. P. Collman, R. L. Marshall, W. L. Young, II, and S. D. Goldby, *Inorg. Chem.*, **1**, 704 (1962).

Hydrogen Bonds between *p*-Chlorophenol and Alkylbenzenes

Masato IGARASHI and Tadatoshi WATABE

Department of Chemistry, Faculty of Science, Tokyo Kyoiku University, Bunkyo-ku, Tokyo

(Received January 31, 1968)

Hydrogen bonds between organic hydroxy compounds and aromatic compounds, *i.e.*, the so-called π–H bonds, have been studied by many authors, for example, methyl alcohol - methylated benzene complexes were examined by Krueger and Mettee.[1)]

When *p*-chlorophenol was used instead of methyl alcohol, the shift of the OH-stretching frequency was greater than in the case of methyl alcohol. In this case *p*-chlorophenol was used as the proton donor, and methylated, ethylated and isopropylated benzenes were used as proton acceptors.

The OH-stretching frequency shifts, $\Delta\nu$, the enthalpy changes, $-\Delta H$, the entropy changes, $-\Delta S$, and the equilibrium constants, K, for π–H complexes formed in a carbon tetrachloride solution were obtained and compared with other findings on hydrogen-bonded complexes.

Experimental

The infrared absorption spectra were recorded with a Jasco Diffraction Grating Infrared Spectrophotometer, Model DG 201.

The concentrations of *p*-chlorophenol were regulated so as to have an order of magnitude of 0.001 mol/*l* and so as not to form hydrogen bonds among themselves, while those of alkylbenzenes were 0.5 mol/*l*, except for penta- and hexamethylbenzenes, which had a 0.2 mol/*l* concentration because of their low solubilities.

The temperatures of the solutions were altered by 10° stages from 15°C to 74°C in order to obtain $-\Delta H$ and $-\Delta S$ from the change in the absorption intensities of the free and hydrogen-bonded OH-stretching frequencies.

Results and Discussion

The observed values of $\Delta\nu$, $-\Delta H$, $-\Delta S$, and K are listed in Table 1. The frequency shift, $\Delta\nu$, seems to correlate extremely well with the number, n, of alkyl groups and little with their mutual configurations. The correlations are represented by a linear relation, *i.e.*, $\Delta\nu = an + 47$, shown in Fig. 1.

The gradients, a, were 9.0 in methylated benzenes, 7.9 in ethylated benzenes, and 9.7 in isopropylated benzenes, while the standard deviations were 0.3, 0.2, and 0.1 respectively.

The same linear correlation may be found from the table of methyl alcohol - methylated benzene complexes,[1)] where a is 8.7 ± 1.7 and where the 47 constant is replaced by 23. It is interesting to see that the gradients are nearly equal to each other irrespective of the species of alkyl groups in the proton acceptors and of the proton donors.

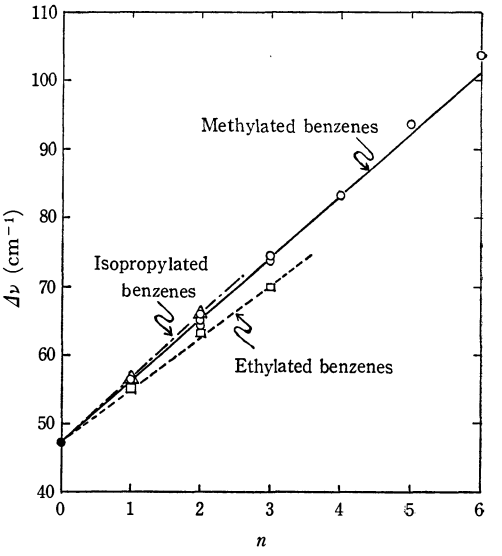

Fig. 1. The correlations between the OH frequency shifts $\Delta\nu$ of *p*-chlorophenol and the number n of alkyl groups in alkylbenzenes.

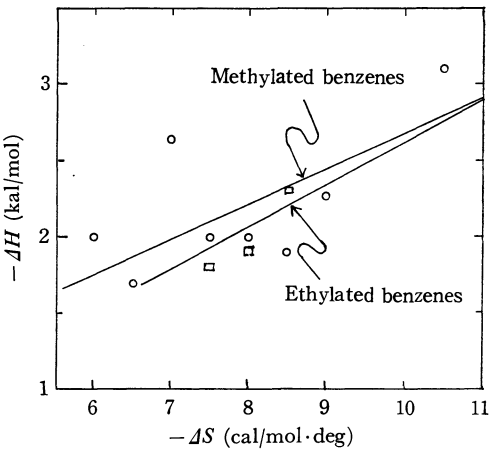

Fig. 2. The correlations between $-\Delta H$ and $-\Delta S$ of *p*-chlorophenol - alkylbenzene complxes.

The linear relationship between $\Delta\nu$ and ΔH (Badger-Bauer's rule) does not hold in this study

1) P. J. Kruegar and H. D. Mettee, *Can. J. Chem.*, **42**, 288 (1964).

TABLE 1. VALUES OF $\Delta\nu$, $-\Delta H$, $-\Delta S$ AND K OF π-H COMPLEXES OF *p*-CHLOROPHENOL AND PROTON ACCEPTORS

Proton acceptor	$\Delta\nu$ (cm^{-1})	$-\Delta H$ (kcal/mol)	$-\Delta S$ (cal/mol·deg)	K (at 23°C)
Benzene	47	4.4	18	0.21
Toluene	56	1.9	8.5	0.35
o-Xylene	63.5	2.3	9	0.53
m-Xylene	66	2.0	8	0.50
p-Xylene	65	1.7	6.5	0.60
Mesitylene	74	1.7	6.5	0.60
Pseudocumene	73.5	2.0	7.5	0.62
Durene	82.5	3.1	10.5	0.80
Pentamethylbenzene	93.5	2.0	6	1.45
Hexamethylbenzene	103	2.4	7	1.82
Ethylbenzene	55	1.9	8	0.43
Diethylbenzene	62.5	2.3	8.5	0.60
Triethylbenzene	70	1.8	7.5	0.55
Cumene	56.5	2.6	10	0.60
Diisopropylbenzene	66.5	2.8	10.5	0.51
t-Butylbenzene	57.5	1.9	8	0.48

either, as Pimentel and McClellan have pointed out that it does not hold for many other examples of hydrogen-bonded complexes.[2)]

The ΔH *vs.* ΔS relation seems to be nearly linear, as in many other complexes,[1,2)] although the deviation from linearity is rather large (Fig. 2). The equilibrium constant, K, tends to increase monotonously as n increases. This trend is quite different from that of the methyl alcohol - methylated benzene series,[1)] which has shown the minimum value when $n=2$.

The authors wish to express their gratitude to Professor Keizo Suzuki for his kind encouragement throughout this study.

2) G. C. Pimentel and A. L. McClellan, "The Hydrogen Bond," W. H. Freeman and Company, San Francisco and London (1960), p. 85.

Reaction of Butadiene in the Presence of a Three-component Catalyst Consisting of Iron(III)acetylacetonate, a Phosphorus Compound, and Bis(diethylaluminum)sulfate

Masao IWAMOTO

Central Research Laboratories, Toyo Rayon Company, Ltd., Sonoyama, Otsu

(Received February 2, 1968)

It has been reported that a catalyst composed of iron(III)acetylacetonate and triethylaluminum is active in the reaction of butadiene with ethylene, yielding 1,4-hexadiene,[1] and also in the trimerization of butadiene, yielding *n*-dodeca 1,3,6,10-tetraene.[2] Hidai and his co-workers[3] studied the effect of adding triphenylphosphine as an electron donor to the catalyst system in the reaction of butadiene ; they found that the selectivity of the reaction was altered with an increase in the molar ratio of triphenylphosphine to iron(III)acetylacetonate. They obtained liquid polybutadiene as a by-product when the molar ratio was larger than five. On the other hand, we obtained a solid polymer composed of 1,2-addition sequences when three or four moles of triphenylphosphine per mole of iron(III)acetylacetonate were added to the catalyst system.[4]

In this note, the author will describe the characteristics of a three-component catalyst containing bis(diethylaluminum)sulfate as an organoaluminum compound. In a previous paper,[5] we reported on

1) G. Hata, *J. Am. Chem. Soc.*, **86**, 3903 (1964).
2) M. Hidai, Y. Uchida and A. Misono, This Bulletin, **38**, 1243 (1965).
3) M. Hidai, K. Tamai, Y. Uchida and A. Misono, *ibid.*, **39**, 1357 (1966).
4) M. Iwamoto, Unpublished work.

TABLE 1. REACTIONS OF BUTADIENE IN THE PRESENCE OF $Fe(acac)_3$-$P(C_4H_9)_3$-$[(C_2H_5)_2Al]_2SO_4$ CATALYST

Benzene ml	$Fe(acac)_3$ mmol	$P(C_4H_9)_3$ mmol	$[(C_2H_5)_2Al]_2SO_4$ mmol	Butadiene g	React. temp.[a] °C	React time hr	Products (g)		
							MHT	OT	Residue
20	1	0	4.1	40	55—60	18.5	0.8	—	4.9
20	1	1	4.1	40	55—60	2	16.9	5.3	9.5
20	1	2	4.1	40	55—60	2	19.2	3.8	10.9
20	1	4	4.1	40	55—60	2	12.7	1.6	14.3
20	1	4	6.0	40	30—32	2	24.6	6.0	10.5
40	0.25	1	3.0	33.5	40	2	21.0	4.5	3.2
40	0.25	1	3.0	20	r.t.[b]	1	8.0	3.5	7.6
40	0.25	1	3.0	20	r.t.	2	8.7	4.0	7.8
40	0.25	1	3.0	20	r.t.	4	10.3	4.7	6.1

a) bath temperature b) r.t.=room temperature

the vinyl-polymerization of butadiene and isoprene in the presence of a catalyst composed of the cobalt thiocyanate - triphenylphosphine complex and bis-(diethylaluminum) sulfate. Bis(diethylaluminum)-sulfate has been found to act somewhat differently from triethylaluminum.

A mixture of butadiene linear dimers composed of 9.5 g of 3-methyl-1,4,6-heptatriene (MHT) and 12.7 g of 1,3,6-octatriene (OT) was obtained, along with 4 g of a by-product, in a reaction of butadine carried out at 50—60°C for 5 hr in the presence of a catalyst consisting of 0.5 mmol of iron(III)acetyl-acetonate, 2 mmol of triphenylphosphine, and 3.6 mmol of bis(diethylaluminum)sulfate. In this case, there was a selective formation of the linear dimers, and more 1,4-addition product, OT, than 1,2-addition product, MHT, was formed. The results obtained in the reaction of butadiene with a catalyst, using tributylphosphine as an electron donor, are summarized in Table 1. It was found that the amount of MHT in the dimer mixture was affected by the P/Fe molar ratio, and that the residue in the atmospheric distillation of the reaction mixture increased with an increase in the P/Fe molar ratio. As compared with the catalyst containing triphenylphosphine, the catalyst containing tributyl-phosphine tends to form more of the 1,2-addition product than of the 1,4-addition product, just as cobalt catalysts do.[6]

When diphenylphosphine was added to the catalyst system as an electron donor, a rubber-like polymer was obtained as the main product, together with a small amount of linear dimers. The infrared spectrum of the polymer shows strong absorption peaks at 910 and 955 cm^{-1}, suggesting a high content of the 1,2-addition sequence in the polymer chain. Triethylphosphite also promoted the polymerization of butadiene, yielding a colorless polymer mainly composed of the 1,2-addition sequence. When tributylphosphite or phosphorus oxychloride was added, the reaction proceeded less selectively to yield both the dimers and a polymeric substance.

It is considered that the catalytic formation of the oligomers is closely related to the vinyl-polymerization of butadiene, and these facts in turn suggest a similarity in the catalytically-active complex for both the reactions. The variation in the properties of the catalytic system is considered to depend on the physical and chemical characteristics of the electron donor added and may be explained in a way similar to that presented in a previous report.[3] Moreover, it has been found that the organoaluminum compound also affects the properties and the activity of the catalyst system.

5) M. Iwamoto and S. Yaguchi, *Polymer Letters*, **5**, 1007 (1967).

6) T. Saito, T. Ohno, Y. Uchida and A. Misono, *Kogyo Kagaku Zasshi (J. Chem. Soc. Japan, Ind. Chem. Sect.)*, **66**, 1099 (1963); This Bulletin, **37**, 105 (1964).

The Acid-catalyzed S_N1-like Acylation of *l*-Menthol

Fuminori AKIYAMA and Niichiro TOKURA

Department of Applied Chemistry, Faculty of Engineering, Osaka University, Suita, Osaka

(Received February 8, 1968)

In a preceding paper[1] we reported that the propionylation of *l*-menthol in acetonitrile or liquid sulfur dioxide was a first-order-like reaction at a high initial concentration of *l*-menthol, even though the reaction was studied with equivalent amounts of *l*-menthol and propionyl chloride. This evidence will be studied in more detail in the present paper.

The second-order plot and the first-order plot in acetonitrile are visualized in Fig. 1 and Fig. 2. The slopes, k_1, of the apparent first-order plot were obtained at various concentrations of *l*-menthol, propionyl chloride, and *l*-menthyl propionate; they are shown in Table 1. The effect of the hydrogen chloride on the slope of the apparent first-order plot was also studied (*cf.* Fig. 3).

Table 1 and Fig. 3 indicate that the apparent first-order reaction is dependent on the concentrations of *l*-menthol and hydogen chloride, but not on the concentrations of propionyl chloride and *l*-menthyl propionate:

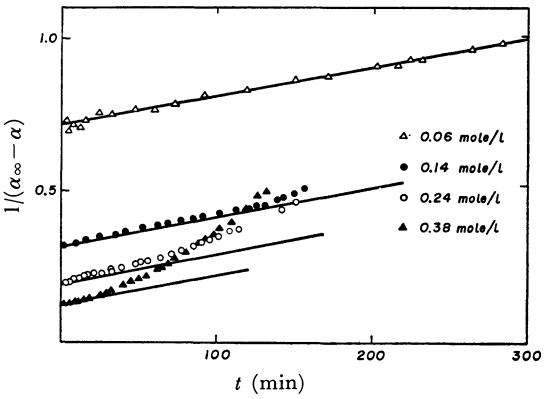

Fig. 1. Second-order plots in acetonitrile at 25°C.

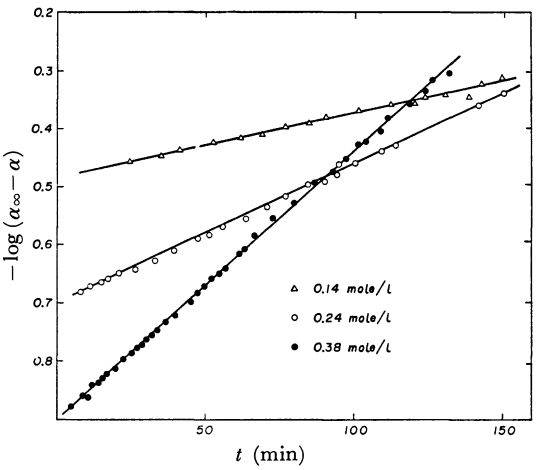

Fig. 2. First-order plots in acetonitrile at 25°C.

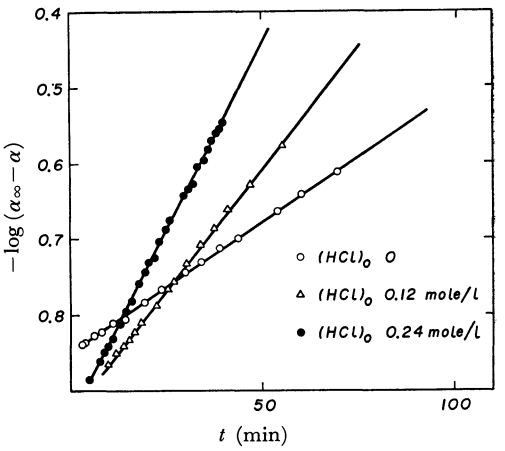

Fig. 3. Effect of hydrochloric acid on k_1 at 25°C. $(C_{10}H_{19}OH)_0$ 0.36 mol/*l*

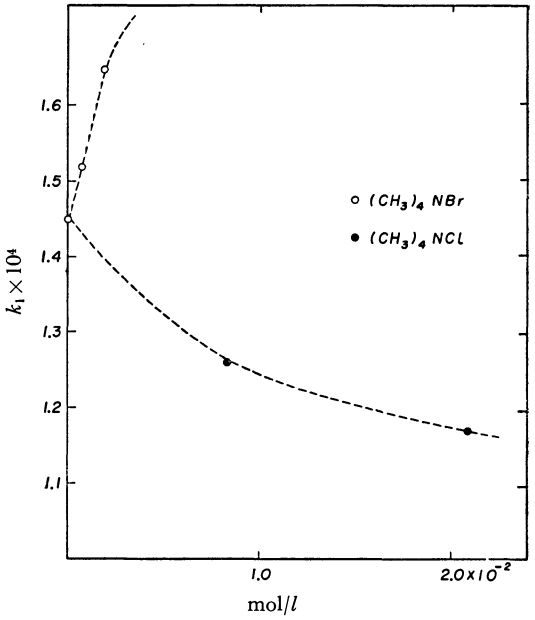

Fig. 4. Effect of $(CH_3)_4NBr$ and $(CH_3)_4NCl$ $(C_{10}H_{19}OH)_0$ 0.36 mol/*l*.

1) F. Akiyama and N. Tokura, This Bullettin, **39**, 131 (1966).

Table 1. The effect of the initial concentrations of *l*-menthol, propionyl chloride and *l*-menthyl propionate on the first-order reaction rate in acetonitrile at 25°C

$(C_{10}H_{19}OH)$ mol/*l*	(CH_3CH_2COCl) mol/*l*	$(CH_3CH_2COOC_{10}H_{19})$ mol/*l*	k_1, sec^{-1}
0.14	0.14	0	3.85×10^{-5}
0.24	0.24	0	9.19×10^{-5}
0.24	0.24	0.25	8.75×10^{-5}
0.24	0.24	0.35	8.87×10^{-5}
0.36	0.24	0	1.43×10^{-4}
0.38	0.38	0	1.63×10^{-4}
0.38	0.19	0	1.53×10^{-4}
0.48	0.24	0	2.28×10^{-4}
0.67	0.38	0	3.11×10^{-4}

$$k_1 = k_1^\circ(C_{10}H_{19}OH) + k_1^\circ(HCl) \quad (1)$$

Therefore, the apparent first-order propionylation may not be an intrinsic first-order reaction. The effect of tetramethylammonium bromide and tetramethylammonium chloride on the apparent first-order propionylation was also studied; it is shown in Fig. 4.

This figure shows the acceleration of the reaction by tetramethylammonium bromide and the retardation of the reaction by tetramethylammonium chloride. Therefore, the apparent first-order propionylation may be assumed to contain a S_N1-like reaction. Perhaps the second term of Eq. (1), the propionylation catalyzed by hydrogen chloride, is the S_N1-like acylation:

$$CH_3CH_2COCl \xrightarrow{HCl} CH_3CH_2CO^+ + Cl^-\cdots HCl \quad (2)$$

The catalytic effect of hydrogen chloride is assumed to be that of a general acid catalysis. Other general acids, propionic acid and acetic acid, accelerate the apparent first-order reaction, as is shown in Fig. 5.

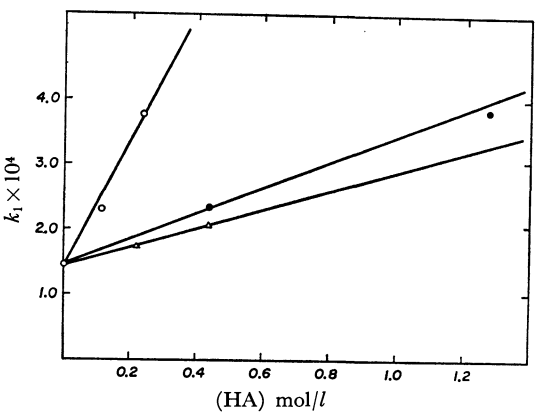

Fig. 5. The catalytic effect of hydrochloric acid, acetic acid and propionic acid. $(C_{10}H_{19}OH)_0$ 0.36 mol/*l*
○ hydrochloric acid+propionic acid
● acetic acid
△ propionic acid

Hydrogen chloride may have a retardation effect by means of the free chloride ion which is generated by the dissociation of hydrogen chloride, as well as an acceleration effect. Furthermore, hydrogen chloride may escape from the reaction solution partially. Therefore, an exact quantitative explanation of the effect of hydrogen chloride is difficult in the case of such a high concentration of hydrogen chloride.

However, the present authors can explain the propionylation of *l*-menthol at a high initial concentration of *l*-menthol as follows. In the initial stage of the reaction, a S_N2-type propionylation of *l*-menthol takes place. With the progress of the reaction, hydrogen chloride is generated and a S_N1 like propionylation, catalyzed by hydrogen chloride, takes place. As the decrease in the reaction rate with the consumption of *l*-menthol is compensated for by the acceleration of the reaction with the generation of hydrogen chloride, the propionylation is apparently a first-order reaction. At a low initial concentration of *l*-menthol, the propionylation of *l*-menthol is a second-order reaction, as is shown in Fig. 1. Perhaps the S_N1-like acylation does not take place without a general acid catalyst.

In a less polar solvent, benzene or chloroform no S_N1-like propionylation catalyzed by hydrogen chloride takes place, as has been shown in the preceding paper.[1] Because of the lack of the stabilization of the acylium ion in acyl halide in compared with that of the carbonium ion from the tertiary alkyl halide, the S_N1-like mechanism of acylation may require the aid of the acid catalyst in the polar solvent.

Experimental

Materials. Commercial extra-pure-grade *l*-menthol was used without further purification. Acetonitrile was dried with phosphorus pentoxide and distilled. The acetonitrile was distilled over potassium carbonate. Commercial propionyl chloride was distilled.

The Kinetic Procedure. The polarimetric procedure used for kinetic followings was described previously. A graphic representation of the apparatus was also found therein[1,2] The details of the kinetic procedure was also explained in a preceding paper.[1] Hydrogen chloride was generated by the following reaction:

$$CH_3COCl + H_2O \rightarrow CH_3COOH + HCl$$

After the addition of a definite amount of water, the effect of hydrogen chloride was studied.

2) N. Tokura and F. Akiyama, This Bulletin, **37**, 1723 (1964).

Hydrogen Cyanide Formation in the Gas-phase Radiolysis of Mixtures of Nitrogen and Ethylene

Takefumi OKA, Ryo KATO, Shin SATO and Shoji SHIDA

Department of Applied Physics, Tokyo Institute of Technology, Ookayama, Meguro-ku, Tokyo

(Received February 9, 1968)

Recently, several studies have been reported on the radiolytic isotopic exchange of nitrogen, in which the *G*-values of nitrogen atoms have been estimated to range from 9 to 19.[1-3] These values prompted us to investigate the radiolysis of gaseous mixtures of nitrogen and ethylene in an attempt to study the reactions of nitrogen atoms with ethylene molecules.

Experimental

Gaseous mixtures of nitrogen and ethylene in various pressures and ratios were irradiated with ^{60}Co γ-rays in sealed, 80-m*l* vessels made of Pyrex glass.

The nitrogen was purchased from the Takachiho Shoji Co. and was used without further purification. Gas chromatographic analysis showed that it contained 0.01% oxygen.

The dose rate was 1.25×10^6 R/hr; it was measured with a Fricke dosimeter, assuming that $G(Fe^{3+})=15.5$.

Products were analyzed by gas chromatography; for hydrocarbons, use was made of a column packed with silica gel, and for hydrogen cyanide, a column of dioctyl phthalate.

Results

The major products observed are shown in Fig. 1 as a function of the nitrogen pressure.

Since hydrogen cyanide was the only observed product containing nitrogen atoms, the *G*-values were measured under a variety of conditions.

1. Table 1 shows the irradiation-time dependence of *G*(HCN).*1

2. The pressure change of nitrogen from 250 to 750 Torr did not vary the value (0.5) of *G*(HCN), where the pressure of ethylene was 6 Torr and the irradiation time was 5 hr.

3. When the ethylene pressure was varied from 6 to 34 Torr, while the pressure of nitrogen (550 Torr) and the irradiation time (10 hr) were kept constant, *G*(HCN) was again found to be constant (0.4).

4. In the presence of sulfur hexafluoride (1 to

TABLE 1. IRRADIATION TIME DEPENDENCE OF HYDROGEN CYANIDE FORMATION
$P(N_2)=564$ Torr, $P(C_2H_4)=6$ Torr

Irrad. time, hr	HCN, μmol	G(HCN)
5	0.18	0.51
10	0.29	0.42
20	0.28	0.20
30	0.25	0.12

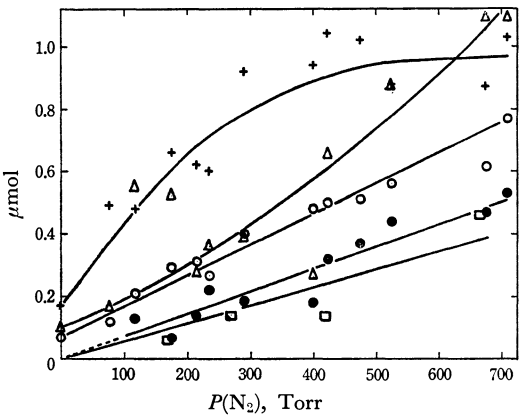

Fig. 1. Nitrogen pressure dependence of main product formation.
$P(C_2H_4)=33$ Torr, Irrad. time; 9 hr
+ Acetylene △ *n*-Butane
○ Ethane ● Propane
□ Hydrogen cyanide

*1 Calculation of G(HCN) is based on the energy absorbed by the nitrogen.

1) M. Anbar and P. Perlstein, *J. Phys. Chem.*, **68**, 1234 (1964).
2) D. H. Dawes and R. A. Back, *ibid.*, **69**, 2385 (1965).
3) R. Shimozawa and K. Ooshima, Proceedings for the 10th Discussion Meeting of Radiation Chemistry, Hiroshima (October, 1967).

3 Torr), G(HCN) increased up to 0.8 from 0.4 (the latter value being obtained in the absence of sulfur hexafluoride), where the nitrogen was at 560 Torr, the ethylene was at 7 Torr, and the irradiation time was 10 hr.

5. When *trans*-2-butene (7 Torr) was used in place of ethylene, where the nitrogen was at 550 Torr and the irradiation time was 10 hr, practically no hydrogen cyanide formation was observed. When both ethylene (6 Torr) and *trans*-butene (7 Torr) were present, G(HCN) found was 0.1_7.

Discussion

Since G(HCN) does not vary with the change in the pressure of ethylene (result 3), it is obvious that hydrogen cyanide is formed by the reaction of active species from nitrogen with ethylene. By extrapolating the values in Table 1 to zero time, the initial G(HCN) value is estimated to be 0.8. The decrease in G(HCN) with the irradiation time may be due to the electron scavenging of the product, hydrogen cyanide,[4] followed by decomposition. The value of 0.8 is in agreement with that obtained in the presence of sulfur hexafluoride (result 4). Consequently, the G-value of active species responsible for the formation of hydrogen cyanide may be estimated to be 0.8.

The independency of G(HCN) of the pressure of nitrogen suggests that the active species are not excited nitrogen molecules. If excited nitrogen molecules are responsible for the formation of hydrogen cyanide, a decrease in G(HCN) should be observed with an increase in the pressure of nitrogen because of the deactivation. Moreover, it is generally accepted, in the study of active nitrogen produced by electric discharge, that the species responsible for the formation of hydrogen cyanide are nitrogen atoms, but not excited molecules.[5] Therefore, we can safely say that the active species leading to the formation of hydrogen cyanide in the present system are nitrogen atoms and/or nitrogen atom ions. The reaction may be as follows:

$$N \text{ (or } N^+) + C_2H_4 \rightarrow HCN + CH_3 \text{ (or } CH_3^+)$$

The methyl radical or ion formed here probably reacts with ethylene and yields propane as the final product.

When *trans*-2-butene was used in place of ethylene, we could not detect the formation of hydrogen cyanide, but in the presence of both olefins we found a small amount of hydrogen cyanide (result 5). This suggests that *trans*-butene reacts with active species produced from nitrogen, but does not yield hydrogen cyanide. Therefore, we carried out a careful search for products containing nitrogen atoms, but could not find any. One possibility is the interference of some impurity in *trans*-butene, although none could be detected.

Nitrogen atoms may be considered to be formed as follows:

$$N_2 \text{—} \sim\!\!\!\rightarrow N_2^+ + e \quad (1)$$

$$N_2 \text{—} \sim\!\!\!\rightarrow N + N^+ + e \text{ (or } N + N) \quad (2)$$

$$N_2^+ + e \rightarrow 2N \quad (3)$$

In the presence of ethylene, however, the reaction (3) competes with ion-molecule reactions, including the following reaction:

$$N_2^+ + C_2H_4 \rightarrow N_2 + C_2H_4^+ \quad (4)$$

The ions produced may decompose immediately or may react with other ethylene molecules. The rate of the reaction (4) will be more than 10^{-10} cc molecule^{-1} sec^{-1}, judging from a similar reaction in rare gases,[6] while the rate of the reaction (3) may be less than 10^{-6} cc molecule^{-1} sec^{-1}.[7] Under the conditions of the present experiment (a few Torr of ethylene and a dose rate of about 10^6 R/hr), the contribution of the reaction (3) to the formation of nitrogen atoms may be negligibly small.

According to a recent report on the electron impact of nitrogen,[8] a part of the ionization is dissociative. If we take 14% for the fraction of the dissociative ionization (this value corresponds to that obtained by the impact of 50 eV-electrons), the G-values of the nitrogen atoms and nitrogen atom ions estimated above can be interpreted well.

4) M. Inoue, *J. Chim. Phys.*, **63**, 1061 (1966).
5) B. Brocklehurst and K. R. Jennings, "Progress in Reaction Kinetics," Vol. 4, ed. by G. Porter, Pergamon Press, Oxford (1967).
6) J. L. Franklin and F. H. Field, *J. Am. Chem. Soc.*, **83**, 3555 (1962).
7) H. S. W. Massey and E. H. S. Burhop, "Electronic and Ionic Impact Phenomena," Clarendon Press, Oxford (1952), p. 631.
8) D. Rapp, P. Englander-Golden and D. D. Briglia, *J. Chem. Phys.*, **42**, 4081 (1965).

Hydrogenation and Hydrogenolysis. X. The Hydrogenation of Methoxy- and Ethoxyanilines with Rhodium Catalysts[1]

Shigeo NISHIMURA, Hiroshi UCHINO and Hisashi YOSHINO

Department of Industrial Chemistry, Tokyo University of Agriculture and Technology, Koganei, Tokyo

(Received February 26, 1968)

The catalytic hydrogenation of alkoxyanilines is usually accompanied by the hydrogenolysis of the alkoxyl group, which lowers the yields of corresponding alkoxycyclohexylamines.[2,3] Hydrogenolysis occurs most extensively in hydrogenation of methoxy- and ethoxyanilines. Freifelder and Stone hydrogenated various alkoxyanilines in methanol or ethanol at elevated temperature and pressure, using ruthenium dioxide, a catalyst that has proved useful in reduction of aromatic amines.[4] However, the yields of methoxy- and ethoxycyclohexylamines were rather low except in the case of *o*-ethoxyaniline where 2-ethoxycyclohexylamine was obtained in 78.7% yield. A low-pressure hydrogenation of alkoxyanilines over 5% rhodium-on-alumina in ethanol in the presence or absence of an equivalent of acetic acid was also reported.[3] Although hydrogenolysis occurred to a somewhat less extent under these conditions, it appears that, in most instances, rates of hydrogenation were small and considerable amounts of starting materials remained unchanged, even after a long reaction period with a 40% weight ratio of catalyst to alkoxyaniline. Thus, no satisfactory method for hydrogenation of alkoxyanilines, especially for methoxy- and ethoxyanilines, seems to have ever been described in the literature.

As reported in a previous paper,[5] decrease in the rate during the rhodium-catalyzed hydrogenation of aniline was considerably improved by the presence of a small amount of alkali which was added to or contained in the catalyst. Presence of alkali also depressed formation of secondary amine almost completely. Subsequently, we have studied the hydrogenation of alkoxyanilines with the alkali-promoted rhodium catalysts and found that the rhodium oxide prepared by fusion of rhodium chloride with lithium nitrate affords excellent yields of methoxy- and ethoxycyclohexylamines in hydrogenation of the corresponding methoxy- and ethoxyanilines. Over this catalyst, hydrogenolysis occurred only to a small extent (3.1—5.9%) and hydrogenation was completed within a few hours at 80—90°C under a high pressure of hydrogen with use of less than 2% weight ratio of catalyst to the substrate. Formation of secondary amines was also completely suppressed or only at a very low level over this catalyst. The results of the hydrogenation of isomeric methoxy- and ethoxyanilines are summarized in Table 1. The hydrogenation of ortho isomers was rather difficult to be completed at 80°C, but this difficulty was overcome at a higher reaction temperature. Approximate relative rates of hydrogenolysis, obtained on the basis of the amounts of cyclohexylamine formed during half-hydrogenation time, are also shown in the last column of Table 1, taking the rate for *o*-ethoxyaniline as unity. It will be seen that generally methoxyanilines hydrogenolyze more rapidly than do the corresponding ethoxyanilines, and that the rate of hydrogenolysis is in the order of ortho<meta<para isomers in both methoxy- and ethoxyanilines, although the proportion of hydrogenolysis is not always in the same order.[6]

Hydrogenation with the usual rhodium oxide, prepared by sodium nitrate fusion, was often inhibited at a later stage of reaction, although this oxide was as effective in hydrogenation of *p*-methoxyaniline as that by lithium nitrate fusion.[7] With rhodium hydroxide and lithium hydroxide, which was shown to be an effective catalyst system for hydrogenation of aniline,[5] *p*-methoxyaniline hydrogenated with a much smaller rate and gave a larger amount of hydrogenolysis product than with the rhodium oxide catalysts. The hydrogenation was strongly inhibited by the addition of sodium hydroxide. From these results, it will be probable that the hydrogenation of an alkoxyaniline is more easily inhibited by presence of a stronger alkali than in the case of aniline, and that the alkali contained in the oxide catalysts works as a weaker base than the corresponding alkali hydroxides. A similar difference in the action of alkali has also been observed in the rhodium-catalyzed hydrogenation of nitriles, where the reaction was retarded by addition of alkali in the order: LiOH<NaOH<KOH.[8]

1) Part IX: S. Nishimura and M. Hama, This Bulletin, **39**, 2467 (1966).
2) M. Freifelder and G. R. Stone, *J. Org. Chem.*, **27**, 3568 (1962).
3) M. Freifelder, Y. H. Ng and P. F. Helgren, *ibid.*, **30**, 2485 (1965).
4) P. N. Rylander, "Catalytic Hydrogenation over Platinum Metals," Academic Press Inc., New York (1967), p. 352.
5) S. Nishimura, T. Shu, T. Hara and Y. Takagi, This Bulletin, **39**, 329 (1966).
6) *Cf.* Refs. 2 and 3.
7) The rhodium oxide by potassium nitrate fusion was much less active for this hydrogenation (unpublished results).
8) Y. Takagi, S. Nishimura, K. Taya and K. Hirota *Sci. Papers Inst. Phys. Chem. Research (Tokyo)*, **61**, 114 (1967).

TABLE 1. HYDROGENATION OF METHOXY- AND ETHOXYANILINES WITH RHODIUM CATALYSTS[a]

RO in $RO\text{-}C_6H_4NH_2$	Catalyst[b]	Amount of the catalyst (g)	Reac. temp. (°C)	Reac. time (hr)	Mol% composition of products[c] I	II	III[d]	IV	Yield of I by distillation (%)	Relative rate of hydrogenolysis
o-CH_3O	Rh oxide(Li)	0.2	80	8.5	59.1	3.7	7.2	30.0		1.47
o-CH_3O	Rh oxide(Li)	0.2	90	2.5	91.4	4.6	3.7	0.3	77[e]	
o-CH_3O	Rh oxide(Na)	0.2	90	2.5	73.6	5.8	7.3	13.3		
m-CH_3O	Rh oxide(Li)	0.2	80	2.5	94.9	5.1	0.0	0.0	84[f]	3.10
p-CH_3O	Rh oxide(Li)	0.1	80	1.8	94.3	5.3	0.4	0.0	85[g]	3.39
p-CH_3O	Rh oxide(Na)	0.1	80	2.3	95.1	4.9	0.0	0.0		
p-CH_3O	Rh hydroxide[h]	0.1	80	5.0	24.5	5.2	0.9	69.4		
o-C_2H_5O	Rh oxide(Li)	0.2	80	2.7	89.9	4.1	1.6	4.4	81[i]	1.00
o-C_2H_5O[j]	Rh oxide(Li)	0.15	90	2.3	94.1	5.9	0.0	0.0	88	
o-C_2H_5O[j]	Rh oxide(Na)	0.15	90	4.0	92.7	3.1	trace	4.2		
m-C_2H_5O	Rh oxide(Li)	0.2	80	1.7	96.9	3.1	0.0	0.0	86[k]	2.20
p-C_2H_5O	Rh oxide(Li)	0.2	80	1.5	96.8	3.2	0.0	0.0	86[l]	2.28

a) Unless otherwise noted, 0.1 mol of alkoxyaniline was hydrogenated in 30 m*l* of anhydrous *t*-butyl alcohol at 80 or 90°C under 80—100 kg/cm² of hydrogen pressure. b) Li or Na in parentheses indicates the oxide prepared by lithium nitrate fusion or by sodium nitrate fusion, respectively. c) I: Alkoxycyclohexylamine. II: Cyclohexylamine. III: Secondary products. Gas-chromatographic analysis shows that these are not saturated secondary amines, but cyclohexylidenecyclohexylamine derivatives which probably resulted from the products of insufficient hydrogenation. IV: Alkoxyaniline. d) Based on the moles of starting alkoxyaniline. e) Bp 70—71.5°C/20 mmHg; n_D^{25} 1.4592. f) Bp 80.5—83°C/23 mmHg; n_D^{25} 1.4620. g) Bp 93.5—95.5°C/42 mmHg; n_D^{25} 1.4638. h) $LiOH \cdot H_2O$ (10 mg) was added. i) Bp 73.5—74.5°C/16.5 mmHg; n_D^{25} 1.4532. j) Anhydrous isopropyl alcohol was used as solvent. k) Bp 89.5—90.5°C/25 mmHg; n_D^{25} 1.4581. l) Bp 81—82.5°C/17.5 mmHg; n_D^{25} 1.4595.

Experimental

Catalysts. *The Rhodium Oxide Prepared by Lithium Nitrate Fusion.* A mixture of 3 g of rhodium chloride trihydrate and 45 g of lithium nitrate was fused in the same way as in the preparation of Adams platinum oxide.[9] After violent evolution of the oxides of nitrogen, the temperature was raised and kept at 420—460°C for about 15 min. After cooling, the solidified mass was rinsed in distilled water. The solid was collected, washed with 1—2% aqueous solution of lithium nitrate, and then dried over soda lime.

The Rhodium Oxide Prepared by Sodium Nitrate Fusion. This oxide was prepared according to the procedure described previously.[10]

Rhodium hydroxide. This was prepared from aqueous solutions of rhodium chloride and lithium hydroxide as described previously.[1]

Hydrogenation. The hydrogenation was carried out in a 200-m*l* autoclave of an electromagnetically-stirring type under the conditions described in Table 1. Isopropyl and *t*-butyl alcohols used as solvent were carefully dehydrated over calcium oxide, otherwise the hydrolysis products, alkoxycyclohexanols, were often produced during hydrogenation.

Analysis of Products. Products were analyzed by gas chromatography using a column of 10% PEG 6000-10% KOH on Chromosorb W (60—80 mesh). The gas chromatograms of alkoxycyclohexylamines were separated into two peaks except in the case of 2-methoxycyclohexylamine, where only one peak was obtained probably because of incomplete separation. The areas of the larger peaks, which probably correspond to the cis isomers, were 80.7, 69.2, 91.8, 85.3 and 74.1% for 3-methoxy, 4-methoxy-, 2-ethoxy-, 3-ethoxy- and 4-ethoxycyclohexylamine, respectively, in the experiments carried out at 80°C. Methoxy- and ethoxycyclohexylamines were further isolated by distillation at reduced pressure, after most of solvent had been distilled off at atmospheric pressure, with equipment of soda lime tubes.

This work was supported in part by the Mitsubishi Chemical Industries Co., Ltd., to which our thanks are due.

9) R. Adams, V. Voorhees and R. L. Shriner, "Organic Syntheses," Coll. Vol. I, 2nd Ed., p. 463 (1961).
10) S. Nishimura, This Bulletin, **34**, 1544 (1961).

Electronic Structures of Methylenecyclopropene and Cyclopropenone

Akiyoshi WATANABE, Hiroyuki YAMAGUCHI, Yoshito AMAKO and Hiroshi AZUMI

Department of Chemistry, Faculty of Science, Tohoku University, Katahira-cho, Sendai

(Received March 11, 1968)

Recently, Saga[1] reported on the dipole moments and pK values of cyclopropenone derivatives. It seemed that it would be very interesting to compare his experimental data with the results of theoretical calculations. This report will describe an application of the semiempirical LCAO SCF MO method, including CI, to the electronic structures of these molecules.

In each iteration process of the SCF procedure, the values of the molecular integrals were recalculated by using the new bond distances, l_{rs}, obtained from the $l_{rs}=1.520-0.186\,p_{rs}$ relation,[2] where p_{rs} is the bond order between the two carbon atoms r and s obtained by the previous iteration process. However, the bond distance of C=O was kept constant throughout the calculation. One- and two-center Coulomb integrals were calculated by the usual approximation proposed by Parr and Pariser[3] and using the values of I_p and A given by Pritchard and Skinner[4] and the value of β obtained by Kon's formula.[5] In the CI calculation only the one-electron excitation configurations were taken into account. The final results may be tabulated as follows:

The calculated dipole moment of cyclopropenone, 4.428 D, seems to be reasonable when it is compared with the observed dipole moment of 3,4-diphenylcyclopropenone, 5.00 D.[1] The bond distances shown in the figures, which were obtained from the SCF p_{rs}'s, may serve to suggest the structures of these molecules. The formal negative charge at the oxygen atom of cyclopropenone seems to be too high to correspond to the pK value, −2.8 (25°C), of 3,4-diphenylcyclopropenone,[1] since the pK value of

(1) Methylenecyclopropene:

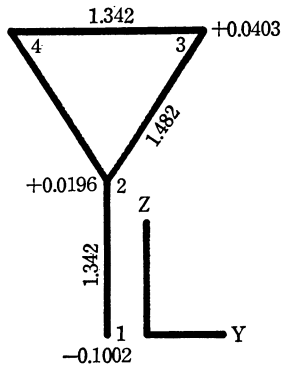

a. Dipole moment 1.157 D

b. Molecular orbitals and energies

Symm.	ε_i	C_1	C_2	C_3	C_4
$1b_1$	−14.9557	0.3509	0.5440	0.5390	0.5390
$2b_1$	−11.0664	−0.6535	−0.4408	0.4351	0.4351
$1a_2$	0.4870	0.0000	0.0000	−0.7071	0.7071
$3b_1$	1.2590	0.6707	−0.7140	0.1420	0.1420

c. Transition energies and oscillator strengths (without CI)

Symm.	Transition	Polarization	Energy (eV)	f
$^1B_2$	3←2	y	5.746	0.17
$^1A_1$	4←2	z	6.792	0.67
$^1A_1$	4←1	z	9.191	0.021
$^1B_2$	3←1	y	9.225	0.42

d. Transition energies and oscillator strengths (after CI)

Symm.	Wave function	Energy (eV)	f
$^1A_1$	$0.9332\Phi_{4\leftarrow2}+0.3594\Phi_{4\leftarrow1}$	5.374	0.41
$^1B_2$	$0.9665\Phi_{3\leftarrow2}+0.2567\Phi_{3\leftarrow1}$	5.483	0.27
$^1B_2$	$0.2567\Phi_{3\leftarrow2}-0.9665\Phi_{3\leftarrow1}$	9.489	0.25
$^1A_1$	$0.3594\Phi_{4\leftarrow2}-0.9332\Phi_{4\leftarrow1}$	9.609	0.23

1) M. Saga, M. S. Thesis submitted to Tohoku Univ., 1964.
2) T. Nakajima and S. Katagiri, *Mol. Phys.*, **6**, 149 (1963).
3) R. Pariser and R. G. Parr, *J. Chem. Phys.*, **21**, 767 (1953).
4) H. A. Skinner and H. O. Pritchard, *Trans. Faraday Soc.*, **49**, 1254 (1953).
5) H. Kon, This Bulletin, **28**, 275 (1955).

(2) Cyclopropenone:

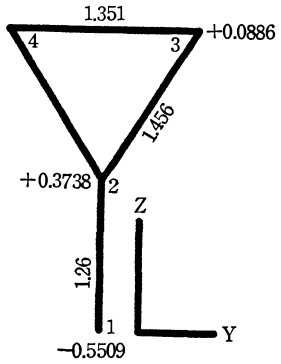

a. Dipole moment 4.428 D

b. Molecular orbitals and energies

Symm.	ε_i	C_1	C_3	C_3	C_4
$1b_1$	−15.8377	0.3855	0.4991	0.5488	0.5488
$2b_1$	−12.3455	−0.7917	−0.2531	0.3932	0.3932
$1a_2$	−0.6787	0.0000	0.0000	−0.7071	0.7071
$3b_1$	0.0798	0.4739	−0.8288	0.2104	0.2104

c. Transition energies and oscillator strengths (without CI).

Symm.	Transition	Polarization	Energy (eV)	f
$^1B_2$	3←2	y	6.066	0.15
$^1A_1$	4←2	z	6.177	0.51
$^1A_1$	4←1	z	8.942	0.007
$^1B_2$	3←1	y	8.997	0.43

d. Transition energies and oscillator strengths (after CI).

Symm.	Wave function	Energy (eV)	f
$^1B_2$	$0.9940\Phi_{3\leftarrow 2}+0.1094\Phi_{3\leftarrow 1}$	6.030	0.20
$^1A_1$	$0.9925\Phi_{4\leftarrow 2}+0.1123\Phi_{4\leftarrow 1}$	6.134	0.51
$^1A_1$	$0.1123\Phi_{4\leftarrow 2}-0.9925\Phi_{4\leftarrow 1}$	8.985	0.0002
$^1B_2$	$0.1094\Phi_{3\leftarrow 2}-0.9940\Phi_{3\leftarrow 1}$	9.033	0.36
$^3B_2$	$0.5148\Phi_{3\leftarrow 2}+0.8573\Phi_{3\leftarrow 1}$	2.872	
$^3A_1$	$0.9989\Phi_{4\leftarrow 2}-0.0470\Phi_{4\leftarrow 1}$	4.204	
$^3A_1$	$0.0470\Phi_{4\leftarrow 2}+0.9989\Phi_{4\leftarrow 1}$	8.630	
$^3B_2$	$0.8573\Phi_{3\leftarrow 2}-0.5148\Phi_{3\leftarrow 1}$	8.789	

the tropone molecule has been reported to be −1.02 (20°C) by Hosoya and Nagakura.[6] However, since the correspondence relation between the pK values and π electron densities should be limited within similar molecules, the reason for such a high negative formal charge at the oxygen atom as in cyclopropenone can be attributed to its special structure.

6) H. Hosoya and S. Nagakura, *ibid.*, **39**, 1414 (1966).

An Easy Conversion of 2,3,4,5,6-Pentamethylbenzyl Derivatives to Hexamethylbenzene by Catalysis of Sulfuric Acid[1)]

Hitomi SUZUKI and Kiyomi NAKAMURA

Department of Chemistry, Faculty of Science, Kyoto University, Sakyo-ku, Kyoto

(Received March 13, 1968)

In the acidic decomposition of 2,3,4,5,6-pentamethylbenzyl nitrate, an appreciable amount of hexamethylbenzene (HMB) was obtained as one of the main products.[2)] Since the intermolecular migration of the methyl group can hardly be possible under those mild conditions, HMB must have been formed by some other ways. Perhaps the most satisfactory interpretation is that the nitrate underwent the complex ionization to yield pentamethylbenzyl cation (PMB^+),[3)] which was then converted into HMB by the hydrogen atom abstraction.[4)]

1) The Reaction of Polysubstituted Aromatics. Part X; Part IX: This Bulletin, **39**, 1201 (1966).

2) K. Maruyama, K. Nakamura and H. Suzuki, *Nippon Kagaku Zasshi* (*J. Chem. Soc. Japan, Pure Chem. Sect.*), **89**, 78 (1968).

3) L. P Kuhn, *J. Am. Chem. Soc.*, **69**, 1974 (1947).

4) H. M. Buck, L. J. Oosterhoff, M. J. v. d. Sluys-v. d. Vlugt and K. G. Verhoeven, *Rec. Trav. Chim.*, **86**, 923 (1967).

Table 1. Yield of HMB

X in $C_6(CH_3)_5CH_2X$	(g)	H_2SO_4 (ml)	Conditions	Yield (g)	Yield (%)*
OH	2.0	10	30 min at 13°C	0.66	72
ONO_2	2.0	20	2 hr at 0—10°C	0.04	6[2]
$OCOCH_3$	2.0	10	30 min at 13°C	0.51	70
$OCOCH_3$	2.0	10	30 min at 13°C in methylcyclohexane (30 ml)	0.86	118
Cl	2.0	10	30 min at 13°C	0.53	64

* Calculated on the assumption that one mole of HMB was formed from two moles of the starting material.

With an intent to confirm this, some 2,3,4,5,6-pentamethylbenzyl derivatives were prepared and subjected to the action of sulfuric acid. All these compounds were found to be reduced with great ease to HMB, the yield of which could be increased considerably when the reaction was carried out in alkane medium. The characteristic color changes from purple-red into dark purple were observed during these transformations. Although the similar color change was observed by dissolving 2,3,4,5,6-pentamethylbenzyl alcohol in trifluoroacetic acid, the reduction was slow and incomplete at room temperature. However, PMR spectroscopy has revealed that the addition of small amounts of sulfuric acid to the solution can complete the reduction within a few minutes. Rather surprisingly, an attempted synthesis of bis(2,3,4,5,6-pentamethylbenzyl) ether by heating the alcohol with tosyl chloride in presence of pyridine also led to the formation of some HMB. The alcohol and its esters were especially subject to the easy reduction; even from the chloride HMB was slowly formed with continuous evolution of hydrogen chloride. The remarkable stability of PMB^+ has recently been established in strong acid system (SbF_5-SO_2),[5] but the present work has shown that PMB^+ is readily reduced to HMB under ordinary conditions. No pentamethylbenzene could be detected during these reactions.

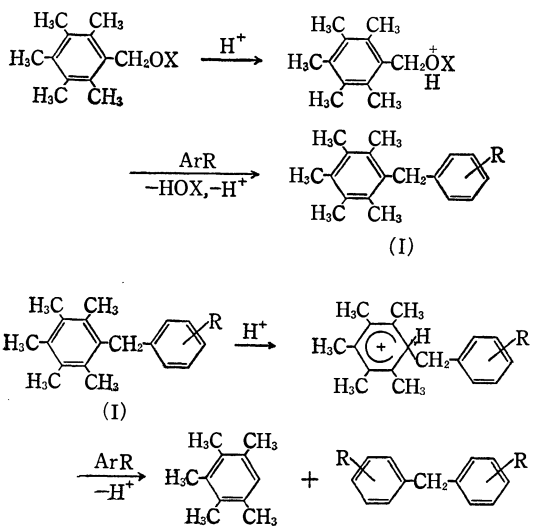

In the medium of an aromatic hydrocarbon, the methylene group was transferred from PMB^+ to the solvent with the consequent formation of pentamethylbenzene and diphenylmethane derivatives. The process must be similar to those of the transcarbonylation,[6] the transbenzylation,[7] and the transsulfonation,[8] and may be explained in terms of steric crowdedness and strong electrophilic character of PMB^+.

Experimental

2,3,4,5,6-Pentamethylbenzyl derivatives were prepared as described in the literature: the alcohol (mp 160—161°C),[9] the nitrate (mp 95—97°C),[2] the acetate (mp 84.5—86.5°C),[9] and the chloride (mp 81—82°C).[10]

All these compounds dissolved readily in sulfuric acid to give a purple solution which was, after having stood for some time, diluted with excess of water. A solid precipitate was chromatographed on alumina using light petroleum to give HMB as an early eluate; it was spectroscopically identical with the authentic specimen, and showed no depression of the mixed melting point (mp 164—165°C).[11] A dark brown powder of no definite melting point (on heating, it turned to yellow with gradual decomposition) remained on the top of the column, and dissolevd readily in carbon tetrachloride to give a brown-red solution, the PMR spectrum of which showed a broad methyl absorption at around 7.8—8.0 τ. Thus it is a polymeric substance probably formed as a result of the hydrogen atom abstraction by PMB^+. Yields of HMB from various sources were recorded in Table 1.

2,3,4,5,6-Pentamethylbenzyl acetate (2.0 g) in methylcyclohexane (30 ml) was treated with sulfuric acid

5) J. M. Bollinger, M. B. Comisarow, C. A. Cupas and G. A. Olah, *J. Am. Chem. Soc.*, **89**, 5687 (1967).
6) R. C. Fuson, G. R. Bakker and B. Vittimberga, *ibid.*, **81**, 4858 (1959).
7) C. Serres and E. K. Fields, *ibid.*, **82**, 4685 (1960).
8) H. Drews, S. Meyerson and E. K. Fields, *ibid.*, **83**, 3871 (1961).
9) O. Jacobsen, *Ber.*, **22**, 1217 (1889).
10) F. Bennington, R. D. Morin and L. C. Clark, *J. Org. Chem.*, **23**, 2034 (1958).
11) L. I. Smith and F. H. MacDougall, *J. Am. Chem. Soc.*, **51**, 3001 (1929).

(10 m*l*) under vigorous agitation at 13°C for 30 min. The mixture immediately turned into dark purple and some heat was evolved. Quenching with water, extraction by ether, and removal of the solvent under reduced pressure left a light brown solid, the chromatography of which on alumina using light petroleum gave HMB (mp 164—165°C, 0.86 g) as an early eluate.

A deep purple solution of 2,3,4,5,6-pentamethylbenzyl alcohol (0.5 g) in a large excess of trifluoroacetic acid was stirred at room temperature for 40 hr. Ordinary working-up and the subsequent chromatography on alumina gave HMB (0.03 g, 14%*) from the light petroleum eluates. Most products (mainly trifluoroacetate) remained on the top of the column.

The transfer of the methylene group of PMB^+ to another aromatic nucleus was realized by stirring a mixture of a pentamethylbenzyl derivative (2.0 g) with an aromatic hydrocarbon (40 m*l*) and sulfuric acid (15 m*l*) at 10°C for 1.5—2 hr. Products were analyzed by gas chromatography and identified by comparison with the authentic specimens; pentamethylbenzene and diphenylmenthane were formed nearly in equal quantity. Small amounts of another diphenylmethane compound (probably *unsym*-polymethyldiphenylmethane of the type I) were not further investigated.

A Facile Synthesis of 1,2 ; 5,6-Di-*O*-cyclohexylidene-α-D-allose*[1]

Masajiro KAWANA, Hiroshi OHRUI and Sakae EMOTO

Rikagaku Kenkyusho (The Institute of Physical and Chemical Research), Yamato-machi, Kita-Adachi-gun, Saitama

(Received March 14, 1968)

1,2;5,6-Di-*O*-cyclohexylidene-α-D-allose (III) is required for a study of asymmetric synthesis with sugar derivatives. It has been shown that 1,2 ; 5,6-di-*O*-cyclohexylidene-α-D-glucose (I) is more effective for some asymmetric reactions than the corresponding isopropylidene derivative.[1]

Sowa and Thomas[2] reported that 1,2; 5,6-di-*O*-isopropylidene-α-D-allose was prepared in a 62% yield from the corresponding glucose by oxidation with dimethyl sulfoxide - acetic anhydride (DMSO-Ac_2O), followed by reduction with sodium borohydride. This synthetic procedure, however, involves complicated manipulations, such as the removal of the excess DMSO-Ac_2O *in vacuo* at 35—40°C and the purification of the product by column chromatography.

The authors have found that the use of I,[3] which is more readily available than the corresponding isopropylidene derivative,[4] afforded a convenient method for preparing III and related compounds without the cumbersome treatment described above. The method, because of its simplicity, seems to be suitable for studies of allose chemistry.

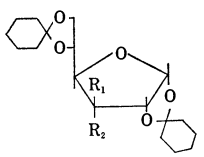

I: R_1=OH, R_2=H
II: R_1, R_2=OH
III: R_1=H, R_2=OH

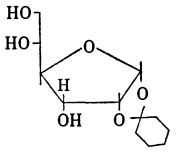

IV

The oxidation of I with DMSO-Ac_2O was carried out in the usual manner, and the reaction mixture was treated with aqueous potassium carbonate and ammonium hydroxide to give gummy materials, which were then reduced with sodium borohydride in a mixture of ether and methanol. The removal of the solvents provided crystalline products, which then gave pure III in a 50% yield after recrystallization. The relatively low yield of III was attributed to the formation of by-products, which presumably consist mainly of methylthiomethylene and acetyl derivatives of I formed in the oxidation step,[5] judging from the results of thin-layer chromatography. The *allo* configuration of III was confirmed by the conversion of the product into D-allose.

The selective cleavage of the 5,6-cyclohexylidene group of III was performed with aqueous acetic acid, affording 1,2-*O*-cyclohexylidene-α-D-allose (IV) in a 88% yield.

1,2;5,6-Di-*O*-cyclohexylidene-α-D-*ribo*-hexofuranos-3-ulose could also be easily obtained from the gummy

*1 In a journal which came to hand after this manuscript had been contributed to this Bulletin, K. James, A. R. Tatchell and P. K. Ray (*J. Chem. Soc.*, (*C*), **1967**, 2681) describe the synthesis of the title compound, but their techniques differ in some details.

1) M. Kawana and S. Emoto, This Bulletin, **41**, 259 (1968).

2) W. Sowa and G. H. S. Thomas, *Can. J. Chem.*, **44**, 836 (1966).

3) R. C. Hockett, R. E. Miller and A. Scattergood, *J. Am. Chem. Soc.*, **71**, 3072 (1949).

4) W. L. Glen, G. S. Myers and G. A. Grant, *J. Chem. Soc.*, **1951**, 2568.

5) J. D. Albright and L. Goldman, *J. Am. Chem. Soc.*, **89**, 2416 (1967); W. W. Epstein and F. W. Sweat, *Chem. Revs.*, **67**, 247 (1967).

materials as a crystalline mono hydrate (II), although in a low yield. The infrared spectrum of II in potassium bromide showed the presence of the hydroxyl group but no carbonyl group; however, the absorption band of the latter appeared in carbon tetrachloride, as in the case of the corresponding isopropylidene derivative.[6] The reduction of II with sodium borohydride yielded III stereospecifically under conditions similar to those of the reduction of the gummy materials.

Experimental

All melting points are uncorrected. The infrared spectra were measured with a Perkin-Elmer Model 521 grating infrared spectrophotometer. The optical rotations were determined with a Perkin-Elmer Model 141 photoelectric polarimeter in a 1-dm tube. The elemental analyses were performed by the Organic Analysis Laboratory of this Institute.

The thin-layer chromatography was performed by the ascending technique on a 250μ-layer of silica gel G (E. Merck, Darmstadt, Germany), activated for 2 hr at 120°C. The spray reagent was a mixture of methanol, sulfuric acid, and *p*-methoxybenzaldehyde (85: 10: 5, v/v).

1,2;5,6-Di-*O*-cyclohexylidene-α-D-allose (III). A mixture of 1,2;5,6-di-*O*-cyclohexylidene-α-D-glucose[3] (I; 3.4 g, 0.01 mol), dimethyl sulfoxide (15 m*l*), and acetic anhydride (10 m*l*) was allowed to stand at room temperature for 24 hr. A thin-layer chromatogram of the solution showed three main spots (one at R_f 0.43 due to the hydrate (II) of D-*ribo*-hexos-3-ulose, and those at 0.56 and 0.73 due to by-products) with benzene-ether (85 : 15, v/v). The reaction mixture was then stirred into an ice-water mixture (100 m*l*) containing potassium carbonate (15 g). After 30 min, 38% ammonium hydroxide (10 m*l*) was added, and the stirring was continued for 20 more min. The resulting gummy materials were washed with aqueous potassium carbonate and dissolved in ether (40 m*l*). The ethereal solution was washed with 10% aqueous potassium carbonate (10 m*l*) and then water (4×10 m*l*), and diluted with ether (5 m*l*) and methanol (10 m*l*).

To this solution there was added solid sodium borohydride (420 mg, 0.011 mol) under cooling in an ice-water bath; the mixture was stirred for 30 min, and then water (5 m*l*) was added. After the stirring had been continued for 5 min, the reaction mixture, now diluted with ether (20 m*l*), was washed with water (4×10 m*l*), and then the solution was dried over sodium sulfate. A thin-layer chromatogram of the solution showed four spots with benzene-ether (85 : 15, v/v) (R_f 0.25 due to III, 0.44 (faint) due to an unknown substance which was distinguishable from II by color, and 0.56 and 0.71 presumably due to by-products produced in the oxidative reaction). The evaporation of the solvents gave a crystalline product, which in turn provided III (1.7 g, 50%) after recrystallization from ligroin - ethyl acetate (9 : 1, v/v): mp 125—126°C; $[\alpha]_D^{25}$ +41.4° (*c* 0.65, ethanol); IR (KBr), 3495 cm^{-1}.

Found: C, 63.64; H, 8.02%. Calcd for $C_{18}H_{28}O_6$: C, 63.51; H, 8.29%.

A thin-layer chromatogram of III showed one spot (R_f 0.71) which could be distinguished from a spot (R_f 0.59) of I with chloroform-methanol (97 : 3, v/v).

A mixture of III (681 mg, 2.0 mmol) and Dowx 50W-X8 (H^+; 3 g (wet)) in dioxane (4 m*l*) and water (4 m*l*) was stirred as 80 °C for 45 min. The spots of the starting material and of 1,2-*O*-cyclohexylidene-α-D-allose (IV) on the thin-layer chromatograms almost completely disappeared; as solvent systems, chloroform-methanol (97: 3, v/v) and (85: 15, v/v) were employed respectively. The resin was filtered and washed with water, and the filtrate was extracted with chloroform (3×10 m*l*). The water layer was concentrated to dryness at 60°C in a rotary evaporator with the aid of a water aspirator, and the residue was crystallized from ethanol-water, affording analytically-pure D-allose (175 mg, 48.6%) (Found: C, 39.78; H, 6.61%): mp 127—131°C; $[\alpha]_D^{20}$ +2.1° (4 min) → +13.5° (20 hr) (*c* 1.46, water) (lit.[7] mp 128—128.5°C, $[\alpha]_D^{20\cdot1}$ +2.10° (4 min) → +14.41° (20 hr)). The X-ray powder diffraction patterns of the product were identical with those of an authentic sample.

The Hydrate of 1,2;5,6-Di-*O*-cyclohexylidene-α-D-*ribo*-hexofuranos-3-ulose (II). The oxidation of 1,2;5,6-di-*O*-cyclohexylidene-α-D-glucose (I; 3.4 g, 0.01 mol) was carried out in the same manner as has been described for the synthesis of the allose derivative (III). The ethereal solution of gummy materials was washed successively with aqueous potassium carbonate (10 m*l*) and water (40 m*l*), and then most of the ether was distilled out at 60°C under ordinary pressure and then at room temperature with the aid of a water aspirator. The oily residue gave, after the addition of *n*-hexane (15 m*l*), a crystalline product (1.3 g). Recrystallization from *n*-hexane - ethyl acetate (2 : 1, v/v) afforded II, which was then dried over phosphorus pentoxide at room temperature under reduced pressure (3 mmHg) for 2 hr. The yield of II was 0.9 g (25%): mp 119—121°C under rapid heating); $[\alpha]_D^{20}$ +40.0° (3 min) → +40.7° (5 min) → 41.8° (10 min) → +44.3° (30 min) → +44.3° (3 hr; constant) (*c* 0.28, 80% aqueous dioxane); IR, 3400 cm^{-1} (KBr), 1773 cm^{-1} (CCl_4, 40 min after solution).

Found: C, 60.87; H, 7.96%. Calcd for $C_{18}H_{28}O_7$: C, 60.66; H, 7.92%.

Solid sodium borohydride (57 mg, 1.5 mmol) was added to a solution of II (535 mg, 1.5 mmol) in a mixture of ether (16 m*l*) and methanol (4 m*l*) under cooling in an ice-water bath, and then the mixture was stirred for 30 min. Water (1 m*l*) was then added, after which the stirring was continued for 5 min. The resulting mixture, now diluted with ether (20 m*l*), was washed with water (4×5 m*l*), and the solution was dried over sodium sulfate. A thin-layer chromatogram of the solution showed only one spot due to III with chloroform-methanol (97: 3, v/v). The removal of the solvents gave analytically-pure III (483 mg, 94.5%) (Found: C, 63.60; H, 8.17%). Its melting point, specific rotation and infrared spectrum were identical with those of a sample prepared from the gummy materials.

1,2-*O*-Cyclohexylidene-α-D-allose (IV). The method reported by Gramera *et al.*,[8] but slightly modified,

6) O. Theander, *Acta Chem. Scand.*, **18**, 2209 (1964).

7) F. P. Phelps and F. Bates, *J. Am. Chem. Soc.*, **56**, 1250 (1934).

8) R. E. Gramera, A. Park and R. L. Whistler, *J. Org. Chem.*, **28**, 3230 (1963).

was used for this preparation. A solution of 1,2;5,6-di-*O*-cyclohexylidene-α-D-allose (III; 20 g, 0.059 mol) in acetic acid (210 m*l*) was diluted with water (90 m*l*). This solution was kept at 75°C for 35 min, and then poured into a shallow evaporating dish and allowed to evaporate to dryness in a hood at room temperature. The resulting crystalline mass was thoroughly dried by the repeated evaporation of its benzene solution (3× 100 m*l*) under reduced pressure at 60°C. The crude crystals (*ca.* 20 g) were recrystallized from ligroin - ethyl acetate (2: 1, v/v), yielding IV (13.5 g, 88%): mp 111—112°C; $[\alpha]_D^{25}$ +46.1° (*c* 0.56, ethanol); Fehling test, negative; IR (KBr), 3430 (shoulder), 3300, 3160 (shoulder) cm^{-1}.

Found: C, 55.60; H, 7.49%. Calcd for $C_{12}H_{20}O_6$: C, 55.37; H, 7.75%.

The authors wish to thank Dr. Kiyoshi Isono of the Institute of Physical and Chemical Research for the X-ray powder diffraction data, and Dr. Hiroyoshi Kuzuhara of this Institute for his helpful suggestions.

The Heat of Dilution of Poly(vinyl acetate) in Benzene and Methyl Ethyl Ketone

Akihiro KAGEMOTO and Ryoichi FUJISHIRO

Department of Chemistry, Osaka Institute of Technology, Omiyakitano-cho, Asahi-ku, Osaka
Department of Chemistry, Faculty of Science, Osaka City University, Sumiyoshi-ku, Osaka

(Received March 15, 1968)

In our previous papers[1-4] we have measured the heats of dilution of atactic polystyrene,[1] *cis*-polybutadiene,[2] poly(ethylene oxide),[3] and polymethyl methacrylate[4] solutions; derived the interaction parameter between the polymer and solvent, and found that the interaction heat parameter, χ_H, is considerably dependent not only on the concentration of the polymer, but also on its molecular weight. In order to confirm this fact for other polymer solutions, the heats of dilution of poly(vinyl acetate) (PVAc) with the degrees of polymerization of 480, 1480, and 2450, and also the heat of mixing of the monomer of PVAc, were measured at 25.0±0.01°C using a twin micro-calorimeter, with methyl ethyl ketone (MEK) and benzene as solvents.

The heats of dilution of the polymer solutions were measured over the concentration range from 0.2 to 0.08 in the volume fraction of the polymer, by adding a successive of 10-m*l* and 30-m*l* portions of the solvent to a solution of a known concentration. The data obtained are shown in Table 1.

The benzene solution is endothermic, while the MEK solution is exothermic.

As has been shown in previously published paper,[1] the heats of dilution, $\Delta\overline{H}_d$, are related to the initial volume fraction of the polymer, ϕ_2, and the final one, ϕ_2', as follows:

$$\Delta\overline{H}_d = RT\chi_H\phi_2\phi_2'\Delta n_1 \quad (1)$$

when the interaction heat of parameter, χ_H, is not dependent on the concentration, or

$$\Delta\overline{H}_d/RT\phi_2\phi_2'\Delta n_1 = \chi_1 + \chi_2(\phi_2+\phi_2')/2 \quad (2)$$

when the χ_H parameter depends linearly on the concentration, according to the equation that $\chi_H=\chi_1+\chi_2\phi_2$.

In these equations Δn_1 is the number of moles of the solvent added.

By using the experimental data listed in Table 1 and Eq.(1), the interaction heat parameter, χ_H, has been obtained for each dilution process of each system; these parameters are given in the last column of Table 1.

According to Eq.(1), $\Delta\overline{H}_d$ must vary linearly with $\phi_2\phi_2'\Delta n_1$. However, these plots are not linear, as may be seen in Figs. 1 (a) and (b), indicating that χ_H depends on the concentration.

This tendency has been confirmed by plotting the $\Delta\overline{H}_d/\phi_2\phi_2'\Delta n_1$ against the average volume fraction $(\phi_2+\phi_2')/2$ for each system according to Eq. (2). In order to obtain the accurate values of χ_1 and χ_2, the least-squares treatment of the data was carried out according to Eq. (2); the results are shown in Table 2.

In a good solvent the χ_H parameter is considerably dependent on the concentration, while in the poor solvent, benzene, it is not.

Such a tendency can be explained according to the dilution theory of polymer solutions by Flory,[5] and

1) A. Kagemoto, S. Murakami and R. Fujishiro, This Bulletin, **39**, 15 (1966).
2) A. Kagemoto, S. Murakami and R. Fujishiro, *ibid.*, **39**, 1814 (1966).
3) A. Kagemoto, S. Murakami and R. Fujishiro, *Makromol. Chem.*, **105**, 154 (1967).
4) A. Kagemoto, S. Murakami and R. Fujishiro, This Bulletin, **40**, 11 (1967).
5) P. J. Flory, and W. R. Krigbaum, *J. Chem. Phys.*, **18**, 1086 (1950).

TABLE 1. THE HEAT OF DILUTION OF POLYVINYL ACETATE SOLUTION AT 25°C

I. Polyvinyl acetate - Benzene systems

V cc	ϕ_2	V' cc	ϕ_2'	$\Delta\overline{H}_d$ cal	χ_H
Monomer					
5	1.000	10	0.500	3.491	0.22
10	0.500	15	0.333	1.301	0.24
15	0.333	20	0.250	0.623	0.23
20	0.250	25	0.200	0.358	0.22
5	1.000	10	0.500	3.420	0.21
10	0.500	15	0.333	1.193	0.22
15	0.333	20	0.250	0.623	0.23
$\overline{P}=480$					
10	0.265	20	0.128	0.163	0.074
20	0.128	30	0.088	0.065	0.089
30	0.088	40	0.066	0.034	0.090
20	0.212	30	0.141	0.141	0.072
30	0.141	50	0.085	0.122	0.078
20	0.197	30	0.131	0.138	0.082
30	0.131	40	0.098	0.072	0.086
40	0.098	50	0.078	0.045	0.090
50	0.078	60	0.065	0.025	0.076
$\overline{P}=1850$					
10	0.220	20	0.110	0.087	0.055
20	0.110	30	0.077	0.040	0.072
30	0.095	40	0.074	0.032	0.070
30	0.080	50	0.050	0.034	0.065
10	0.196	30	0.065	0.125	0.075
10	0.156	20	0.078	0.055	0.070
20	0.078	30	0.052	0.017	0.058
10	0.220	30	0.077	0.127	0.058
10	0.156	30	0.052	0.072	0.068
30	0.105	50	0.063	0.056	0.065
$\overline{P}=2450$					
10	0.196	20	0.098	0.053	0.042
20	0.098	30	0.065	0.020	0.048
10	0.092	20	0.046	0.011	0.040
30	0.098	40	0.073	0.023	0.049
10	0.151	20	0.076	0.036	0.048
40	0.062	50	0.050	0.008	0.039
20	0.085	30	0.056	0.014	0.045
30	0.123	50	0.074	0.059	0.050
20	0.176	30	0.117	0.052	0.039
30	0.117	40	0.088	0.030	0.045

II. Polyvinyl acetate - Methyl ethyl ketone systems

V cc	ϕ_2	V' cc	ϕ_2'	$-\Delta\overline{H}_d$ cal	χ_H
Monomer					
5	1.000	10	0.500	2.443	−0.15
10	0.500	15	0.333	0.813	−0.15
15	0.333	20	0.250	0.380	−0.14
20	0.250	25	0.200	0.212	−0.13
5	1.000	10	0.500	2.280	−0.14
10	0.500	15	0.333	0.813	−0.15
15	0.333	20	0.250	0.380	−0.14
$\overline{P}=480$					
10	0.256	20	0.128	0.209	−0.098
20	0.128	30	0.085	0.060	−0.085
30	0.085	40	0.064	0.032	−0.090
10	0.205	20	0.104	0.122	−0.088
20	0.104	30	0.068	0.044	−0.095
30	0.086	50	0.051	0.045	−0.079
10	0.167	30	0.055	0.108	−0.090
20	0.237	30	0.158	0.244	−0.100
30	0.158	40	0.059	0.053	−0.087
40	0.156	70	0.089	0.239	−0.088
10	0.256	30	0.085	0.269	−0.094
10	0.256	40	0.064	0.301	−0.094
10	0.205	30	0.068	0.166	−0.091
10	0.205	50	0.051	0.211	−0.077
$\overline{P}=1850$					
10	0.210	20	0.105	0.115	−0.080
20	0.105	30	0.070	0.036	−0.075
10	0.198	20	0.099	0.088	−0.069
20	0.099	30	0.066	0.028	−0.065
20	0.125	40	0.063	0.077	−0.075
10	0.157	20	0.079	0.053	−0.065
20	0.087	30	0.058	0.021	−0.065
10	0.231	20	0.116	0.148	−0.085
20	0.116	30	0.077	0.044	−0.075
30	0.085	40	0.064	0.025	−0.070
10	0.210	30	0.070	0.151	−0.079
10	0.198	30	0.066	0.116	−0.069
10	0.231	30	0.077	0.192	−0.083
$\overline{P}=2450$					
10	0.156	20	0.078	0.046	−0.058
10	0.115	20	0.058	0.024	−0.055
10	0.186	20	0.093	0.066	−0.069
20	0.093	30	0.062	0.023	−0.060
20	0.075	30	0.050	0.014	−0.059
10	0.135	20	0.068	0.030	−0.050
30	0.084	40	0.063	0.020	−0.059
40	0.069	50	0.055	0.012	−0.049
10	0.109	20	0.055	0.023	−0.060
50	0.082	60	0.068	0.020	−0.055

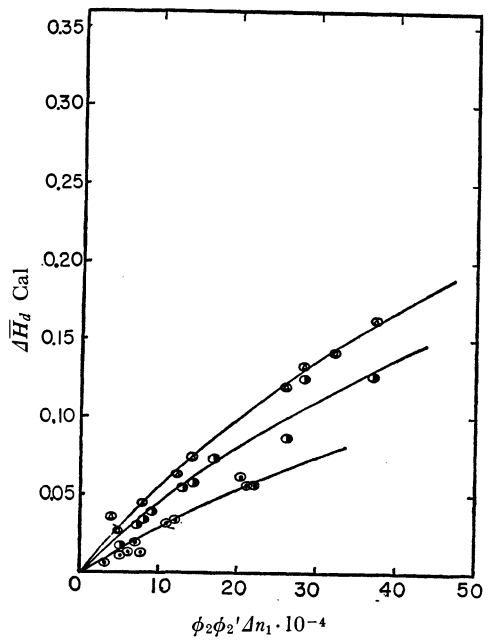

Fig. 1(a). The plot of the heat of dilution, $\Delta\overline{H}_d$, against $\phi_2\phi_2'\Delta n_1$.
Mn { $4\cdot10^4$ △ / $15\cdot10^4$ ◑ / $20\cdot10^4$ ⊙ }
P.V.Ac.—Benzene

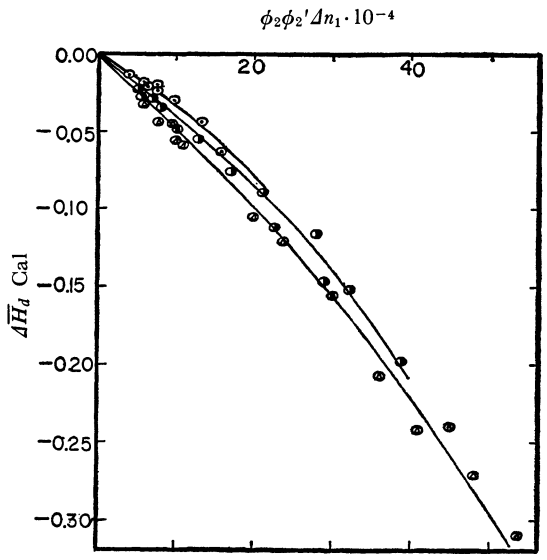

Fig. 1(b). The plot of the heat of dilution, $\Delta\overline{H}_d$, against $\phi_2\phi_2'\Delta n_1$.
Mn { $4\cdot10^{-4}$ △ / $15\cdot10^{-4}$ ◑ / $20\cdot10^{-4}$ ⊙ }
P.V.Ac.—M.E.K.

also according to the Huggins[6] theory. The Huggins theory, however, includes various factors characteristic of polymer solutions, so our results can not be quantitatively compared with those of this theory because of the lack of information concerning the chain configuration of the polymer molecules in the solution.

Table 2. Dependence of the interaction heat parameter on the concentration: $\chi_H = \chi_1 + \chi_2\phi_2$

	χ_1	χ_2
PVAc-Benzene		
$\overline{P}=1$	0.230	
$\overline{P}=480$	0.095	−0.096
$\overline{P}=1850$	0.071	−0.047
$\overline{P}=2450$	0.046	−0.011
PVAc-MEK		
$\overline{P}=1$	−0.140	
$\overline{P}=480$	−0.088	−0.10
$\overline{P}=1850$	−0.059	−0.12
$\overline{P}=2450$	−0.048	−0.11
$\overline{P}=3500$[7]	−0.038	−0.17

* $\overline{P}$: degree of polymerization.

Further, the value of χ_1, which is the interaction heat parameter in the dilute solution, decreases in absolute value as the molecular weight increases, as is shown in the first column in Table 2.

Such a dependence of the χ_1 parameter on the molecular weight has been found for other polymer solutions in previous papers.[3-4]

The dependence of the χ_1 parameter on the molecular weight has been theoretically derived by Huggins, who also explained it by using the dilute solution theory of polymers. For example, according to the theory the second virial coefficient can generally be given by the following equation:

$$A_2 = (\bar{u}_2^2/V_1)\phi_1(1-\theta/T)F(X)$$

where $F(X)$ is the complicated function of the molecular weight and the excluded volume (β); it decreases as the molecular weight increases.

The approximate treatment of the second virial coefficient gives the apparent interaction parameter, χ_1, as:

$$\chi_1 = (\psi_1\theta/T)F(X)$$

which is written as:

$$\chi_1 = \chi_1(X=0)F(X)$$

Since $F(X)$ decreases with an increase in the molecular weight, the apparent interaction parameter, χ_1, decreases with an increase in the molecular weight of the polymer.

Our results seem to be qualitatively in good agreement with the dilute solution theory of Flory.

6) M. L. Huggins, *J. Am. Chem. Soc.*, **86**, 3535 (1964).

7) J. D. Ferry, *J. Chem. Phys.*, **17** 1107 (1949).

Spin Correlation in Metal-Chelate-TCNQ Radical Salts

Mizuka SANO, Toshiaki OHTA and Hideo AKAMATU

Department of Chemistry, Faculty of Science, The University of Tokyo, Hongo, Tokyo

(Received March 16, 1968)

We have been interested in the paramagnetism of anion radical salts of 7,7,8,8-tetracyano-*p*-quinodimethan (TCNQ), and our study has been extended to the salts with metal-chelates. We synthesized a new kind of organo-metallic radical salts by the reaction between octahedral tris-dipyridyl (dip) metal-chelate compounds and TCNQ, and examined paramagnetic behavior of the salts as a function of temperature in the temperature region from 77 to 300°K, by a Faraday-type magnetic balance. The experimental procedure was the same as described in a previous paper.[1]

Preparation. $Fe(dip)_3(TCNQ)_2 \cdot 3H_2O$ (reddish black crystals), $Ni(dip)_3(TCNQ)_2 \cdot 3H_2O$ (greenish black crystals) and $Cu(dip)_3(TCNQ)_3Cl \cdot 4H_2O$ (black powder) were obtained by the reactions of $Fe(dip)_3Cl_2 \cdot 7H_2O$, $Ni(dip)_3Cl_2 \cdot 6H_2O$, and of $Cu(dip)_3Cl_2 \cdot 7H_2O$ with Li·TCNQ in methanol, respectively.

Results and Discussion

$Fe(dip)_3^{2+}(TCNQ^-)_2 \cdot 3H_2O$. The magnetic susceptibility decreased with decreasing temperature, although a small rise was observed in the lower temperature region. The curve (a) in Fig. 1 shows the temperature dependence of the paramagnetic susceptibility observed, after the correction was made for molecular diamagnetism of dipyridyl, TCNQ and H_2O, using the values determined experimentally and Pascal's constants. The curve (b) shows the susceptibility for $Fe(dip)_3Cl_2 \cdot 7H_2O$, after diamagnetism due to dipyridyl, Cl^- and H_2O was subtracted from the observed susceptibility. The corrected value showed a small paramagnetism of unknown character. The difference between (a) and (b), the curve (c), means the paramagnetic susceptibility resulted from the salt formation with TCNQ. If it is assumed that the rise in the lower temperature region originated from impurities, and that the susceptibility of impurities obeys Curie law as expressed by the curve (d), the difference between (c) and (d) could be attributed to the paramagnetism for TCNQ radicals in the salt, which is indicated by black circles in Fig. 1. The impurities would be TCNQ radicals which are improperly located in a lattice, as suggested by Kepler for other TCNQ salts.[2]

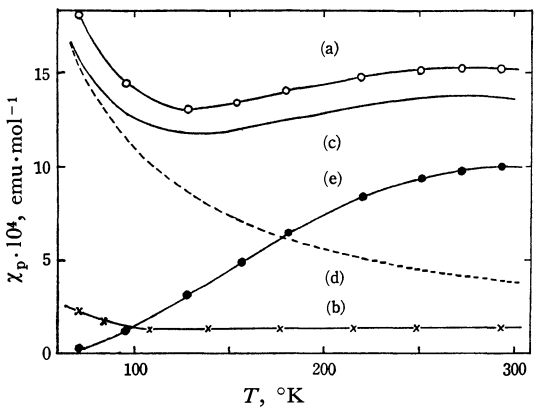

Fig. 1. Susceptibilities of (a) $Fe(dip)_3(TCNQ)_2 \cdot 3H_2O$, and (b) $Fe(dip)_3Cl_2 \cdot 7H_2O$, after correction for diamagnetism. (c) The difference between (a) and (b). (d) The assumed susceptibility for impurities. (e) The calculated, and ● the observed paramagnetic susceptibilities for TCNQ radicals in pairs.

According to the recent development in theoretical treatments of paramagnetism for organic free radicals, the paramagnetism can be reasonablv interpreted in terms of an exchange-coupled linear chain model.[3-5] For the case, in which spin correlation exists only in a pair of free radicals and gives rise to a ground singlet state and a thermally accessible triplet state (a singlet-triplet model), the paramagnetic susceptibility is expressed by

$$\chi_p = (2N'g^2\beta^2/kT) \cdot [3+\exp(\delta/kT)]^{-1},$$

where δ is the singlet-triplet energy separation, and N' is the number of spin pairs.

As can be seen in Fig. 1, the estimated susceptibility for TCNQ radicals finds a good fit to the value calculated from the singlet-triplet model, the curve (e), for which δ was taken to be 0.047 eV, and N', 5.17×10^{23}. The result reveals that the majority of anion radicals of TCNQ are pairing in the salt.

$Ni(dip)_3^{2+}(TCNQ^-)_2 \cdot 3H_2O$. The susceptibilities for this TCNQ salt and $Ni(dip)_3^{2+}Cl_2^- \cdot 6H_2O$ were both paramagnetic at room temperature, and increased with decreasing temperature. Figure 2 shows an appreciable amount of difference between

1) Y. Sato, M. Kinoshita, M. Sano and H. Akamatu, This Bulletin, **40**, 2539 (1967).

2) R. G. Kepler, *J. Chem. Phys.*, **39**, 3528 (1963).

3) R. M. Lynden-Bell and H. M. McConnell, *ibid.*, **37**, 794 (1962).

4) A. S. Edelstein, *ibid.*, **40**, 488 (1964).

5) Z. G. Soos, *ibid.*, **43**, 1121 (1965).

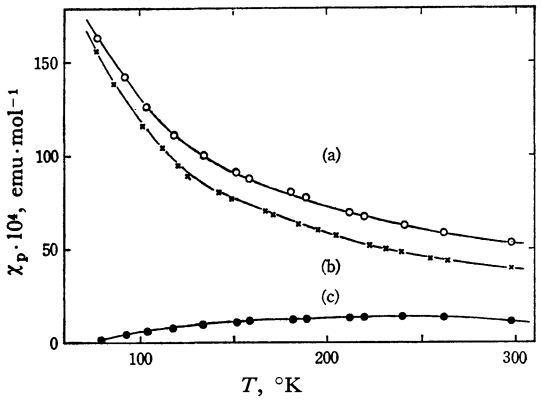

Fig. 2. Paramagnetic susceptibilities of (a) Ni(dip)$_3$(TCNQ)$_2 \cdot 3H_2O$, and (b) Ni(dip)$_3Cl_2 \cdot 6H_2O$. (c) The calculated, and ● the observed paramagnetic susceptibilities for TCNQ radicals in pairs.

the susceptibility values for these compounds. TCNQ radicals in the salt are thus found to contribute considerably to the observed paramagnetism. The temperature dependence of the susceptibility for the radicals in pairs could be explained on the basis of the singlet-triplet model for $\delta = 0.04$ eV, and $N' = 5.45 \times 10^{23}$.

This result indicates that the paramagnetism for the TCNQ salt could be explained without considering superexchange interaction between *d*-electrons in Ni(dip)$_3^{2+}$ and π-electrons in TCNQ radicals, and that spin correlation exists only in a pair of TCNQ anion radicals.

Cu(dip)$_3^{2+}$(TCNQ$^-$)(TCNQ)$_2$Cl$^- \cdot 4H_2O$. The paramagnetic susceptibility changed anomalously with the change in temperature. The susceptibility for TCNQ radicals, which was estimated tentatively from the difference between the value for the salt and that for Cu(dip)$_3^{2+}$Cl$_2^- \cdot 7H_2O$ is shown by the curve (c) in Fig. 3. It was nearly independent of temperature above 130°K, but it increased steeply

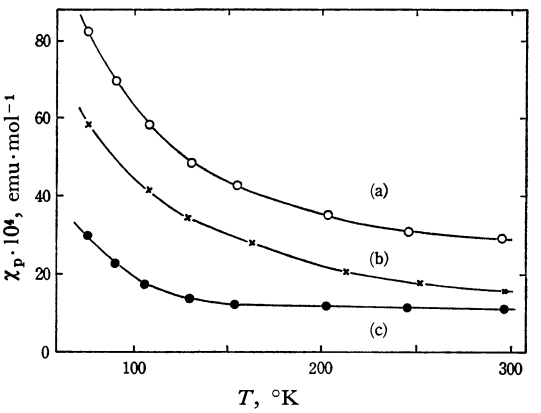

Fig. 3. Paramagnetic susceptibilities of (a) Cu(dip)$_3$(TCNQ)$_3$Cl$\cdot 4H_2O$, and (b) Cu(dip)$_3Cl_2 \cdot 7H_2O$. (c) The difference between (a) and (b).

in the temperature region below 130°K. The steep rise could not be fitted either to the values estimated by Curie law or by the Curie-Weiss law with a negative Weiss temperature. The electrical resistivity for this TCNQ salt was found to be as low as 270 Ω·cm at room temperature.

Ba^{2+}(TCNQ$^-$)$_2 \cdot 2H_2O$, Ni^{2+}(TCNQ$^-$)$_2 \cdot 3H_2O$, Fe^{2+}(TCNQ$^-$)$_2 \cdot 3H_2O$, and Cu$^+$(TCNQ$^-$)(TCNQ). The reciprocal values of paramagnetic susceptibility for the former three salts were plotted against temperature, as shown in Fig. 4, after

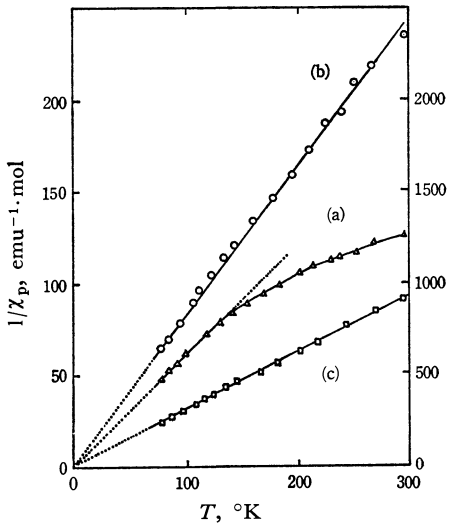

Fig. 4. Inverse paramagnetic susceptibilities of (a) Ba(TCNQ)$_2 \cdot 2H_2O$, (b) Ni(TCNQ)$_2 \cdot 3H_2O$, and (c) Fe(TCNQ)$_2 \cdot 3H_2O$. The scale for (a) is shown on right, while for (b) and (c) on left.

correction was made for their molecular diamagnetism. The paramagnetism of the nickel and ferrous salts was found to obey Curie law, and the value of the susceptibility agreed with the value expected on the basis of the cation alone. The same result has been reported by Kepler.[2)]

The plots for the barium salt, on the other hand, deviate from a straight line. Ba^{2+} itself is diamagnetic, so that the paramagnetism observed could be associated entirely with TCNQ radicals, and the deviation exhibits a strong spin exchange interaction between radicals. The temperature dependence of the susceptibility for the spin-paired radicals was explained by the singlet triplet model for which δ was taken to be 0.080 eV, and N', 4.77×10^{23}.

The product from metathesis of cupric sulfate with Li·TCNQ in methanol was found to have the composition of Cu(TCNQ)$_2$ by an elementary analysis. The inclusion of neutral TCNQ and its 1 : 1 ratio to TCNQ anion in the salt were determined by the measurement of an infrared absorption spectrum, which revealed that an electron transfer occurred from a TCNQ anion to Cu^{2+}, forming a diamagnetic Cu$^+$. The paramagnetic susceptibility of the salt

was low, 1.90×10^{-4} emu/mol at room temperature, and was independent of temperature.

Conclusion

The paramagnetic susceptibility for the TCNQ salts studied here, except for the copper salts, could be explained by a simple summation of the susceptibility value for the cation and that for anion radicals of TCNQ. The majority of the radicals in a salt are pairing in the sense of their spin exchange interaction, and the paramagnetism for the radicals in pairs is explained quantitatively on the basis of the singlet-triplet model. The singlet-triplet energy separation for the paired radicals in the metal-chelate-TCNQ salts is smaller than that in the simple metal-TCNQ salts.

Studies on Heteroaromaticity. XVI.[1] Further Studies on the Thermal 1,3-Dipolar Cycloaddition Reactions of Some Aromatic Hydroxamoyl Chlorides

Tadashi SASAKI and Toshiyuki YOSHIOKA

Institute of Applied Organic Chemistry, Faculty of Engineering, Nagoya University, Chikusa-ku, Nagoya

(Received February 8, 1968)

With a view of extending the synthetic utility of the thermal 1,3-dipolar cycloaddition reactions,[2] 5-nitro-2-furyl- (Ia), phenyl- (Ib), *p*-nitrophenyl- (Ic) and *m*-nitrophenylhydroxamoyl chloride (Id) were treated with i) triphenylphosphine, ii) benzonitrile or acetonitrile, iii) aromatic aldehydes, iv) quinones, v) anthranilate and vi) cyclic non-conjugated polyenes; each reaction proceeded smoothly with evolution of hydrogen chloride gas except when basic dipolarophiles were used. By this reaction, the yields of products were better than those *via* the routine nitrile oxide methods.

In the previous report,[2] the thermal 1,3-dipolar cycloaddition reactions of furyl- and 5-nitro-2-furylhydroxamoyl chloride with olefinic and acetylenic compounds was described and this paper deals with further experimental results carried out on several dipolarophiles with a view of extending the synthetic potentials of the thermal procedure. Reactions were carried out by using 5-nitro-2-furyl- (Ia), phenyl- (Ib), *p*-nitrophenyl- (Ic) and *m*-nitrophenylhydroxamoyl chloride (Id) and each reactivity was compared with those of the corresponding nitrile oxides, if possible.

Results and Discussion

Reaction with Triphenylphosphine. Stable aromatic nitrile oxides such as tri- and tetramethyl-substituted benzonitrile oxides are known to react with triphenylphosphine to afford the corresponding aromatic nitriles accompanied with the formation of triphenylphosphine oxide[3] but no description about the reaction of triphenylphosphine with benzonitrile oxide can be found. The corresponding nitrile oxides derived from Ia–d were treated with triphenylphosphine under the given reaction conditions[3] to afford the furoxane-type products instead of nitriles presumably because of strongly basic character of triphenylphosphine, but when Ia–d were directly heated in toluene with an equimolecular amount of triphenylphosphine for several hours, the corresponding nitriles, IIa–d, were obtained in good yields as shown in Table 1, also accompanied with the formation of triphenylphosphine oxide in almost quantitative yields. Such different yields might come from the different stability of each

Table 1. Nitriles (IIa—d)

Dipolar	Reflux hr	Yield %	Melting point, °C	IR (KBr) ν_{CN}, cm^{-1}
Ia	9	52	65—67[19]	2290
Ib	5	60	bp 190—192	2290
Ic	7	65	140—143[15]	2290
Id	9	71	119—118[16]	2290

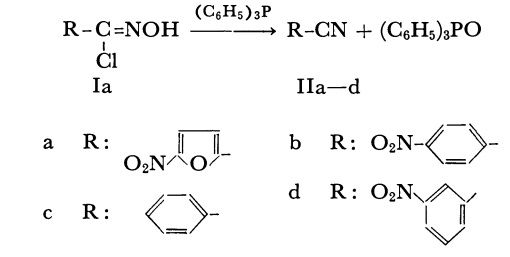

1) Part XV of this series: T. Sasaki, S. Eguchi and K. Kojima, *J. Heterocyclic Chem.*, **5**, (1968) in press.

2) T. Sasaki and T. Yoshioka, This Bulletin, **40**, 2604 (1967).

3) C. Grundmann and H.-Q. Frommeld, *J. Org. Chem.*, **30**, 2077 (1965).

hydroxamoyl chloride, Ia—d, under the given creation conditions. It should be added that by this thermal procedure, no furoxane formation was observed as reported in the previous paper.[2]

Reaction with Benzonitrile or Acetonitrile. Benzonitrile oxide has been converted to oxadiazoles by the 1,3-dipolar cycloaddition reactions with both aromatic nitriles[4] and the nitriles activated by an electron-attracting substituent,[5] but the reaction with aliphatic nitriles was unsuccessful, though the catalytic action of boron trifluoride in the cycloaddition of benzonitrile oxide with nitriles and carbonyl compounds has been reported by Morrocchi, *et al.*[6]

Ia was heated in toluene with benzonitrile for 11 hr giving the corresponding oxadiazole IIIa in only 8% yield; the similar procedure in the presence of boron trifluoride etherate as a catalyst gave the same product in a 36% yield, while the reaction of 5-nitro-2-furocarbonitrile oxide with benzonitrile only afforded intractable tars. Ib also afforded IIb in a 65% yield even without the catalyst and almost quantitatively with the catalyst. IIIb has been prepared by the 1,3-dipolar cycloaddition of benzonitrile oxide with benzonitrile without a catalyst in a 55% yield.[7] These results obviously indicate that the presence of boron trifluoride can improve the yields of the thermal 1,3-dipolar cycloaddition products. The reaction of Ia with acetonitrile did not occur even in the presence of the catalyst and Ia was recovered, though Ib afforded IVb in a 35% yield under the similar reaction conditions. IVb has been prepared by the reaction of benzonitrile oxide with acetonitrile in the presence of the catalyst in a 35% yield.[6]

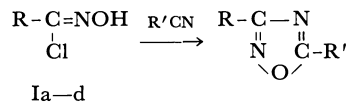

Ia—d

IIIa—d (R′: C_6H_5), IVb (R′: CH_3)

These results are summarized in Table 2 except IVb.

Reaction with Aromatic Aldehydes. Similar 1,3-dipolar cycloaddition reactions of benzonitrile oxide with such carbonyl compounds as aromatic

Table 2. 1,2,4-Oxadiazoles (IIIa—d)

Dipolar	Reflux hr	Yield %	Melting point °C	Microanalysis Found (Calcd) C	H	N	UV λ_{max}^{EtOH} mμ (ε)
Ia	11	8	IIIa 206	56.10	2.73	16.13	313 (18600)
	11*	36		(56.03	2.74	16.34)	255 (22900)
Ib	16	65	IIIb 110[7]				244 (50500)
	10*	Quantitative					
Ic	10	<5	IIIc 210	62.74	3.05	15.48	275† (22200)
	10*	25		(62.92	3.39	15.73)	262 (28400)
Id	24	50	IIId 165	63.54	2.73	15.91	250† (31100)
	24*	80		(62.92	3.39	15.48)	232 (36000)

* In the presence of boron trifluoride etherate as a catalyst.
† Shoulder.

Table 3. Dioxazoles (Vb, VIb and VId)

Dipolar	Dipolarophile	Yield %	Product (Mp, °C)	Microanalysis Found (Calcd) C	H	N	UV λ_{max}^{EtOH} mμ (ε)	NMR ($CDCl_3$) C-5-H (τ)
Ib	*p*-NO_2-C_6H_4-CHO	55	Vb (133)	61.93 (62.22	3.37 3.73	10.52 10.37)	258 (23000)	3.00 (singlet)
Ib	5-NO_2-C_4H_2O-CHO	45	VIb (127)	54.99 (55.39	2.63 3.10	10.73 10.77)	288 (12200) 265 (11000)	3.02 (singlet)
Id	5-NO_2-C_4H_2O-CHO	10	VId (110)	47.51 (47.22	2.29 2.31	13.91 13.77)	290 (13900) 252 (18000)	

4) G. Leamdri and M. Palotti, *Ann. Chim. (Rome)*, **47**, 376 (1957).
5) R. Huisgen, W. Mack and E. Anneser, *Tetrahedron Letters*, **1961**, 583.
6) S. Morrocchi, A. Ricca and L. Velo, *ibid.*, **1967**, 331.
7) F. Floy and R. Lenaers, *Helv. Chim. Acta*, **46**, 1067 (1961).

aldehydes, α-ketoesters and α-diketones have been reported to afford dioxazoles, but no reactions have been reported to occur with aliphatic aldehydes, acetophenone and aliphatic ketones in general.[5] Treatment of Ia with benzaldehyde, *p*-nitrobenzaldehyde and 5-nitro-2-furfural in the presence of the catalyst resulted in the formation of intractable tars, while Ib afforded with *p*-nitrobenzaldehyde and 5-nitro-2-furfural the corresponding dioxazoles, Vb, and VIb, respectively and similarly VId from Id and 5-nitro-2-furfural even in the absence of the catalyst. These results are summarized in Table 3.

A role of such electrophilic catalyst as a Lewis acid in the thermal 1,3-dipolar cycloaddition reactions is uncertain at the present stage, but it could be said that the presence of boron trifluoride etherate might accelerate the removal of hydrogen chloride from hydroxamoyl chlorides and increase the polarization of a carbonyl group of dipolarophiles as predicted by Morrocchi, *et al.*[6]

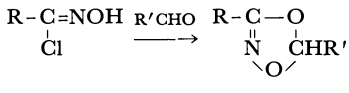

Vb (R′: O_2N-C$_6$H$_4$-) VIb (R′: O_2N-furyl-) VId (R′: O_2N-furyl-)

Reaction with Quinones. Benzonitrile oxide is also known to react with 1,4-benzoquinone and 1,4-naphthoquinone giving the corresponding 1 : 1 adducts, with subsequent oxidation to quinones having condensed benzene-isoxazole and naphthalene-isoxazole nuclei respectively.[8]

Ia was heated with 1,4-benzoquinone for 9 hr to afford VIa in a 31% yield: the structure was confirmed by the NMR spectrum in DMSO-d_6, showing a chemical shift at 2.90 τ (singlet, 2 H) attributable to two equivalent aromatic protons of benzoqinone. Similar treatment of Ia with 1,4-naphthoquinone afforded VIIa in a 25% yield and similarly, VIIb from Ib and 1,4-benzoquinone in a 36% yield. The structure of VIIa was confirmed from the elemental analysis and the NMR spectrum and furthermore, from the mass spectrum as described in Experimental, and the structure of VIIb was characterized as a 1 : 2 adduct from the elemental analysis and the NMR spectrum in DMSO-d_6, showing no aromatic proton originated from benzoquinone. It is noteworthy that the thermal procedure always afforded the products possessing an isoxazole structure instead of the simple adducts with an isoxazoline structure without any side-formation of furoxanes.[2]

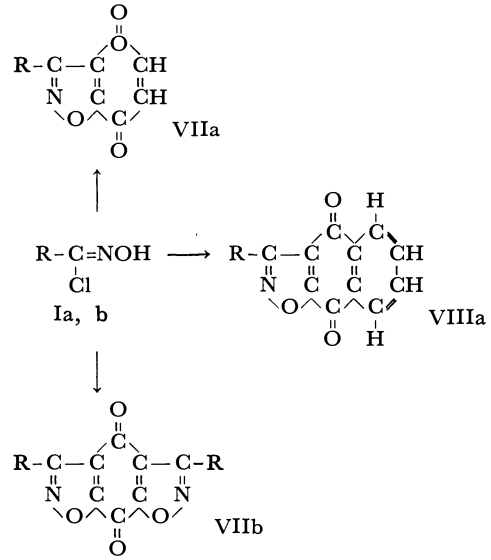

VIIa, VIIIa, VIIb

Reaction with Anthranilate. Dornow and Fischer[9] have reported the formation of a quinazoline-type product from Ib and two equivalent amounts of methyl anthranilate on keeping the reaction mixture at room temperature. Similar treatment of Ia with methyl anthranilate also afforded IXa in a 60% yield; the structure was consistent with 3-hydroxy-4-oxo-2-(5′-nitro-2′-furyl)-3,4-dihydroquinazoline on the basis of the elemental analysis and the spectral data. The infrared spectrum (KBr disc) exhibited a strong absorption of ν_{CO} at 1695 and that of intramolecular hydrogen bonding at 2500 cm^{-1}, supporting its *N*-hydroxyl structure rather than its *N*-oxide.[10] In the ultraviolet spectrum in ethanol, the absorption maxima at 374 mμ (ε = 16700) and at 268 (18200) resembled to those of the known product IXb.[9]

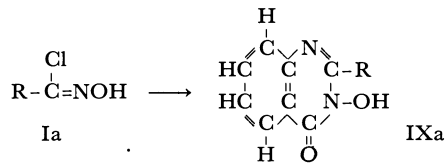

Ia → IXa

Reaction with Olefins. In addition to the previous report,[2] Ia was treated with non-conjugated cyclic polyenes like 1,5-cyclooctadiene and 1,5,9-cyclodecatriene to afford 1 : 1 adducts, Xa and XIa, in 55 and 70% yields, respectively. Ic also afforded a 1 : 1 adduct Xc in a 55% yield. However, the reactions of Ia with conjugated polyenes like 1,3-cyclooctadiene, myrcene and butadiene did not occur at all and the starting materials were

8) A. Quilico, C. Stagno and D'Alcontres, *Gazz. Chim. Ital.*, **80**, 140 (1950); *Chem. Abstr.*, **45**, 606c (1951). The yields of the products are very low and diphenylfuroxane and benzonitrile are always accompanied as the by-products.

9) A. Dornow and K. Fischer, *Chem. Ber.*, **99**, 72 (1966).

10) Similar phenomena have been observed in 2-hydroxypyridine *N*-oxide (E. Shaw, *J. Am. Chem. Soc.*, **71**, 67 (1949)) and 2-hydroxyquinoline *N*-oxide (K. G. Cunningham, G. T. Newbold, F. S. Spring and J. Sharp, *J. Chem. Soc.*, **1949**, 2091).

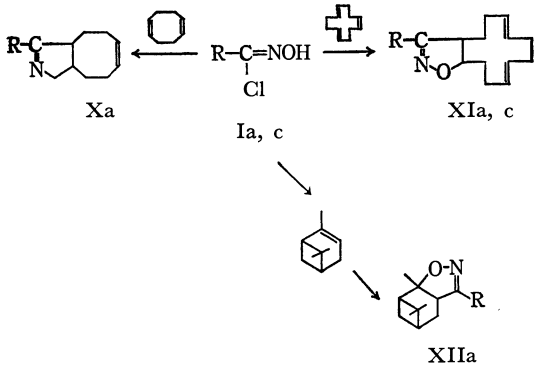

Xa Ia, c XIa, c XIIa

recovered, though benzonitrile oxide is known to react with conjugated dienes[11] or myrcene.[12]

As is pointed out in the previous paper,[2] cyclic monoolefins like cyclohexene, cyclooctene give good yields in the thermal 1,3-dipolar cycloaddition reactions; similarly, α-pinene underwent the same reaction with Ia giving a 1 : 1 adduct XIIa in a 90% yield.

As a conclusion, the thermal 1,3-dipolar cycloaddition reactions using hydroxamoyl chloride can be said to have more versatile applicability than those using the corresponding nitrile oxides; the reaction proceeds with evolution of hydrogen chloride gas which is a very convenient clue for determining the end-point of the reaction except when basic dipolarophiles are used. In the latter case, two equivalent amounts of bases are used and care should be paid to control the reaction temperature as low as possible enough to proceed the reaction. This is the case when basic dipolarophiles are readily decomposed by hydrogen chloride evolved, as is observed in the formation of IXa.

Experimental

The melting points were measured on a microhot stage and are not corrected. The microanalyses were carried out with a Yanagimoto C. H. N. Corder, Model MT-1 type. The infrared spectra were measured on a Nippon-Bunko IR-S type spectrophotometer and the ultraviolet spectra, on a Nippon-Bunko optical rotary dispersion recorder, Model ORD/UV-5. The NMR spectra were determined on a Varian A-60 spectrometer, with tetramethylsilane as an internal standard and the peak positions are expressed by τ-values. The mass spectrum was obtained with a Hitachi RMU-6D mass spectrometer with an energy of 70 eV.

Hydroxamoyl Chlorides. Ia,[12] Ib,[13] Ic[14] and Id[15] were prepared by the known procedures.

Reaction of Ia—d with Triphenylphosphine. A solution of 1.0 g (5 mmol) of Id and 1.3 g (5 mmol) of triphenylphosphine in 30 m*l* of dry toluene was refluxed at 140—150°C for 9 hr until evolution of hydrogen chloride gas had completely ceased. The solvent and surplus triphenylphosphine were removed under reduced pressue and the residue was dissolved in chloroform and chromatographed on a silica-gel (Mallinckrodt, 100 mesh) column, using chloroform as an eluent. From the first fraction, 0.57 g of *m*-nitrobenzonitrile was obtained. This was identified by the comparison with an authentic sample[16] spectroscopically (IR). From the second fraction, 1.4 g (96%) of triphenylphosphine oxide, mp 166°C (lit.,[17] mp 166°C) was obtained. Similar treatment of Ia—c with triphenylphosphine afforded the corresponding nitriles as shown in Table 1.

Reaction of Ia—d with Benzonitrile. A solution 0.75 g (5 mmol) of Ib and 0.55 g (5 mmol) of benzonitrile in 20 m*l* of dry toluene was refluxed at 140—150°C for 16 hr until evolution of hydrogen chloride gas had completely ceased. After removing toluene and surplus benzonitrile under reduced pressure, ethanol was added to the residue and the precipitated colorless needles were collected and recrystallized from ethanol-benzene to give 0.6 g of 3,5-diphenyl-1,2,4-oxadiazole, mp 110°C (lit.,[7] mp 109°C, no depression by the mixed melting point). Similar treatment of Ia—d with benzonitrile afforded the corresponding oxadiazoles as indicated in Table 2.

Reaction of Ib with Acetonitrile. A solution of 0.74 g (5 mmol) of Ib and 0.25 g (5 mmol) of acetonitrile in 25 m*l* of dry toluene was refluxed for 32 hr in the presence of a catalytic amount of boron trifluoride etherate. After the removal of distillable parts from the reaction mixture under reduced pressure, the residue was purified according to the procedure given by Tieman and Krueger[18] to afford 3-phenyl-5-methy-1,2,4-oxadiazole, mp 41°C (lit.,[18] mp 41°C) in a 35% yield.

Reaction with Aromatic Aldehydes. A solution of 0.72 g (5 mmol) of Ib and 0.73 g (5 mmol) of *p*-nitrobenzaldehyde in 20 m*l* of dry toluene was refluxed for 21 hr. After toluene was removed under reduced pressure, the residue was dissolved in chloroform and chromatographed on a silica-gel column, using chloroform as an eluent. The first fraction afforded 0.7 g of 3-phenyl-5-(*p*-nitrophenyl)-1,2,4-dioxazole (Vb). Similarly, 3-phenyl-5-(5′-nitro-2′-furyl)- (VIb) and 3-(*m*-nitrophenyl)-(5′-nitro-2′-furyl)-1,2,4-dioxazole (VId) were prepared from the corresponding components after 11 and 24 hrs' refluxing, respectively. These results are summarized in Table 3.

Reaction of Ia—b with Quinones. A solution of 0.9 g (5 mmol) of Ia and 1.0 g (10 mmol) of 1,4-benzoquinone in 30 m*l* of dry toluene was refluxed for 9 hr. The reaction mixture was filtered while hot and the filtrate was allowed to stand. The resulting precipitates were collected and recrystallized from ethanol-benzene to give 0.4 g of VIIa, mp 200—202°C. IR (KBr) cm^{-1}: 1690, 1670 (CO). UV λ_{max}^{EtOH} mμ (ε): 314 (13800), 246 (11600).

Found: C, 50.65; H, 1.40; N, 10.48%. Calcd for $C_{11}H_4O_6N_2$: C, 50.78; H, 1.54; N, 10.77%.

Similar treatment of Ib with 1,4-benzoquinone afforded VIIb, mp 264°C, after 22 hrs' refluxing.

11) A. Quilico, P. Grünanger and R. Mazzini, *Gazz. Chim. Ital.*, **82**, 349 (1952).
12) T. Sasaki, S. Eguchi and T. Ishii, in preparation.
13) M. H. Benn, *Can. J. Chem.*, **42**, 2393 (1964).
14) H. R. Rheinboldt, *Liebigs Ann.*, **451**, 166 (1927).
15) M. T. Bogert and L. Kohnstamm, *J. Am. Chem. Soc.*, **25**, 478 (1903).
16) M. T. Bogert and H. T. Beans, *ibid.*, **26**, 464 (1904).
17) V. F. Kucherov, *Zhur. Obshch. Khim.*, **19**, 126 (1949); *Chem. Abstr.*, **43**, 6178 (1949).
18) Tieman and Krueger, *Ber.*, **17**, 1685 (1884).

Table 4. Reactions with cyclic polyenes

Dipolar	Olefin	Product (Mp, °C)	Microanalysis Found (Calcd) C	H	N	UV λ_{max}^{EtOH}, mμ (ε)
Ia	A*	Xa (117)	59.47 (59.53	5.17 5.38	10.85 10.68)	348 (15800), 258 (8200), 235 (8000)
Ic	A*	Xc (110)	65.86 (66.16	5.68 5.92	9.97 10.29)	311 (16200), 225 (11000)
Ia	B*	XIa (164)	64.26 (64.54	6.53 6.37	9.08 8.86)	350 (14900), 260 (7600), 236 (7400)

A*: 1,5-Cyclooctadiene B*: 1,5,9-Cyclododecatriene

Found: C, 70.54; H, 2.53; N, 7.82%. Calcd for $C_{20}H_{10}O_4N_2$ for 1:2 adduct: C, 70.17; H, 2.94; N, 8.18%. Calcd for $C_{13}H_7O_3N$ for 1:1 adduct: C, 69.33; H, 3.13; N, 6.22%.

Similarly, VIIIa was obtained from Ia and 1,4-naphthoquinone after 30 hrs' refluxing. IR (KBr) cm^{-1}: 1685 (CO). UV λ_{max}^{EtOH} mμ (ε): 325 (16900). NMR (DMSO-d_6) τ: 1.90 (multiplet, 4 H, phenyl protons). Mass: M^+ 314 (Calcd 314).

Found: C, 58.18; H, 1.94; N, 9.25%. Calcd for $C_{15}H_6O_6N_2$: 58.07; H, 1.95; N. 9.03%.

Reaction of Ia with Methyl Anthranilate. A solution of 0.95 g (5 mmol) of Ia and 1.5 g (10 mmol) of methyl anthranilate in 30 m*l* of dry ether was kept standing at room temperature for 6 months. Solidified crystals were collected, washed with water and recrystallized from ethanol to give 1.1 g of IXa, mp 223°C (decomp).

Found: C, 52.95; H, 2.59; N, 15.09%. Calcd for $C_{12}H_7O_5N_3$: C, 52.75; H, 2.58; N, 15.38%.

Reaction with Olefins. A solution of 0.95 g (5 mmol) of Ia and 1 m*l* of 1,5-cyclooctadiene in 20 m*l* of dry toluene was refluxed for 9 hr. After toluene and surplus 1,5-cyclooctadiene were removed under reduced pressure, the residual oil was dissolved in chloroform and chromatographed on a silica-gel column, using chloroform as an eluent. 0.73 g of Xa, mp 116°C, was obtained from the first fraction. Analytical values are shown in Table 4 with those of other products.

Similar treatment of Ia with α-pinene afforded XIIa, mp 197°C, after 24 hrs' refluxing and purifying the crude product by means of column chromatography. UV λ_{max}^{EtOH} mμ (ε): 350 (14600), 255 (8500). NMR ($CDCl_3$) τ: 6.55 (1 H, quartet, J=4.0 and 10.0 cps, H_A*).

Found: C, 61.60; H, 6.25; N, 9.65%. Calcd for $C_{15}H_{20}O_4N_2$*: C, 62.05; H, 6.25; N, 9.65%.

The authors wish to express their gratitude to Mr. Akiho Ishihara of their laboratories for microanalyses and to the Dainippon Pharmaceutical Co. for measuring NMR spectra.

19) T. Sasaki and T. Yoshioka, *Yukigosei Kagaku Kyokaishi* (*J. Synth. Org. Chem. Japan*), **25**, 665 (1967).

* Two possible structures, XII and XIIa′, are

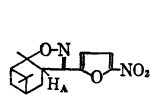

XIIa

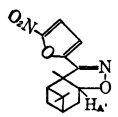

XII′a

presumable for this formula. If XIIa′ is assumed to be a correct structure, H_A' should be appeared in more lower magnetic field than the observed value, 6.55 τ, by the presence of a neighboring oxygen atom.

Studies on Heteroaromaticity. XVIII.[1] Reaction of Aromatic Hydroxamoyl Chlorides with Methyl Dithiocarbazinate

Tadashi SASAKI and Toshiyuki YOSHIOKA

Institute of Applied Organic Chemistry, Faculty of Engineering, Nagoya University, Chikusa-ku, Nagoya

(Received February 19, 1968)

Dornow and Fischer[2] have reported interesting reactions of aromatic hydroxamoyl chlorides with methyl dithiocarbazinate to give 2-substituted amino-5-methylmercapto-1,3,4-thiadiazoles; for example, 2-anilino-5-methylmercapto-1,3,4-thiadiazole, mp 126°C,[3] was obtained in 48% yield, from phenylhydroxamoyl chloride.

Since this kind of reactions is obviously involved in the thermal 1,3-dipolar cycloaddition reactions,[1,4] we attempted the similar reactions with 5-nitro-2-furyl- (I), *p*-nitrophenyl- (II), and *m*-nitrophenylhydroxamoyl chloride (III) and we wish to report on some interesting results.

I was refluxed in ethanol with two equivalent amounts of methyl dithiocarbazinate to afford a product in 50% yield, the structure of which was, however, characterized from the elemental analysis and the NMR measurement as 2-(5′-nitro-2′-furyl)-5-methylmercapto-1,3,4-thiadiazole, IV, instead of the expected 2-substituted amino-1,3,4-thiadiazole, IV′. The NMR spectrum of IV in DMSO-d_6 manifested a chemical shift at 7.14 τ (singlet, 3 H, $-SCH_3$) besides those due to nitrofuran ring protons.[5] Similar treatment of II afforded, however, a mixture of VI and VII in 45 and 27% yields respectively. The structural elucidation of both compounds was done from their elemental analyses and NMR sepctra and VI was confirmed to be 2-(*p*-nitroanilino)-5-methylmercapto-1,3,4-thiadiazole and VII, to be 2-(*p*-nitrophenyl)-5-methylmercapto-1,3,4-thiadiazole. Similarly, a mixture of the corresponding *m*-nitro compounds, VIII and IX, was obtained from III in 45 and 20% yields respectively. Treatment of I with two equivalent amounts of thiosemicarbazide under the similar reaction conditions resulted in the formation of intractable tars only, but when semicarbazide was used in place of thiosemicarbazide, normal substitution reaction had occurred between a chlorine atom of I and an amino group of semicarbazide affording X in 50% yield; the similar substitution has been observed in the reaction of I with some amino- and hydrazino compounds.[6]

About the mechanism of the formation of IV from I, VI and VII from II, and VIII and IX from III, we would propose here two competitive reactions, a) and b): in a), simple substitution reaction, followed by elimination of hydroxylamine afforded IV, VII and IX respectively; on the contrary, in b), thermal 1,3-dipolar cycloaddition might take place at first between hydroxamoyl chloride and carbon-sulfur double bond as shown in the usual nitrile oxide reactions[7] and this assumption seems to be reasonable from our previous findings on the parallel

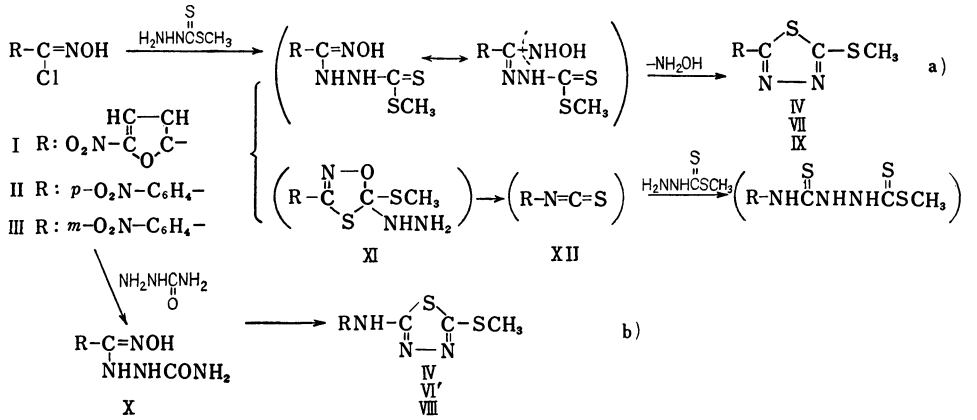

1) Part XVII of this series: T. Sasaki and M. Takahashi, This Bulletin, **41**, 1967 (1968).
2) A. Dornow and K. Fischer, *Chem. Ber.*, **99**, 72 (1966).
3) M. Busch, *J. prakt. Chem.*, **93**, 352 (1916).
4) T. Sasaki and T. Yoshioka, This Bulletin, **40**, 2604 (1967).
5) 2.10 τ (1 H, doublet, J=4.0 cps, 4′-C-H) and 2.41 τ (1 H, doublet, J=4.0 cps, 3′-C-H).
6) T. Sasaki and T. Yoshioka, *Yûkigosei Kagaku Kyôkaishi* (*J. Synth. Org. Chem. Japan*), **25**, 665 (1967).
7) R. Huisgen, M. Mark and E. Anneser, *Angew. Chem.*, **73**, 656 (1961); *ibid.*, **75**, 604 (1963).

reactivity between thermal 1,3-dipolar cycloaddition of hydroxamoyl chloride and the corresponding nitrile oxide cycloaddition.[1,4] As is suggested by Huisgen,[7] the intermediate thioisocyanate XII, produced by decomposition of the adduct XI *via* route b), seems to react with an equivalent amount of methyl dithiocarbazinate to give VI and VIII, which is the known procedure for preparing 2-anilino-5-methylmercapto-1,3,4-thiadiazole.[3] Other examples of the thermal 1,3-dipolar cycloaddition of hydroxamoyl chlorides with compounds possessing carbon-sulfur double bond are under investigation. The reason why phenylhydroxamoyl chloride affords exclusively 2-substituted amino compound through b)[2] and 1, giving 2-substituted IV through a), while the corresponding *p*- (II), and *m*-nitrophenylhydroxamoyl chloride (III) gave a mixture of the products through a) and b) at the same time, is uncertain at the present stage.

Experimental

Reaction of 5-Nitro-2-furylhydroxamoyl Chloride (I). A solution of 0.95 g (5 mmol) of I[1] and 1.15 g (11 mmol) of methyl dithiocarbazinate[8] in 40 m*l* of ethanol was refluxed for 12 hr. After removal of ethanol, the residue was digested with 20 m*l* of a ethanol-water mixture (1: 1). The resulting crystals were collected and recrystallized from ethanol to give 0.6 g of IV as yellow crystals, mp 180—181°C. UV λ_{max}^{EtOH} mμ (ε); 356 (14500), 282 (6300).

Found: C, 34.02; H, 1.76; N, 16.92%. Calcd for $C_7H_6O_3N_4S_2$: C, 34.58; H, 2.07; N, 17.28%.

Reaction of *p*-Nitrophenylhydroxamoyl Chloride (II). A solution of 0.6 g (3 mmol) of II[1] and 0.75 g (6 mmol) of methyl dithiocarbazinate[8] in 20 m*l* of ethanol was refluxed for 10 hr. The resulting crystals were collected after cooling and extracted with hot chloroform. The insoluble part was recrystallized several times from pyridine-ethanol to afford 0.36 g of yellow needles, VI, mp 270—271°C. IR (KBr) cm^{-1}; 3310, 3250 νNH). UV λ_{max}^{EtOH} mμ (ε); 354 (22800). NMR (DMSO-d_6) τ; 6.5 (broad, 1 H, -NH-), 7.25 (singlet, 3 H, -SCH$_3$).

Found: C, 41.13; H, 2.74; N, 20.57%. Calcd for $C_9H_8O_2N_4S_2$: C, 40.62; H, 3.01; N, 20.89%.

From the chloroform solution, 0.2 g of VII as colorless plates, mp 222—223°C, were obtained after removing chloroform, followed by recrystallization from benzene-ethanol. IR (KBr) cm^{-1}; no νNH. UV λ_{max}^{EtOH} mμ (ε); 335 (16300), 254 (8500). NMR (DMSO-d_6) τ; 7.14 (singlet, 3 H, -SCH$_3$).

Found: C, 42.13; H, 2.46; N, 16.72%. Calcd for $C_9H_7O_2N_3S_2$: C, 42.68; H, 2.74; N, 16.59%.

Reaction of *m*-Nitrophenylhydroxamoyl Chloride (III). Similar treatment of III[1] and work-up as above afforded VIII as yellow crystals, mp 234—236°C, in 45% and IX as colorless crystals, mp 172—173°C, in 20% yield.

VIII: IR (KBr) cm^{-1}; 3310, 3260 (νNH). UV λ_{max}^{EtOH} mμ (ε); 350 (2600, shoulder), 300 (24200), 245 (13400). NMR (DMSO-d_6)τ; 6.5 (broad, 1 H, -NH-) 7.25 (singlet, 3 H, -SCH$_3$).

Found: C, 40.43; H, 2.64; N, 20.59%. Calcd for $C_9H_8O_2N_4S_2$: C, 40.62; H, 3.01; N, 20.89%.

IX: IR (KBr) cm^{-1}; no νNH. UV $\lambda_{max}^{CHCl_3}$ mμ (ε); 306 (16600), 273 (12000). NMR (DMSO-d_6) τ; 7.15 (singlet, 3 H, -SCH$_3$).

Found: C, 42.68; H, 2.51; N, 16.21%. Calcd for $C_9H_7O_2N_3S_2$: C, 42.68; H, 2.78; N, 16. 59%.

Reaction of I with Semicarbazide. A solution of 0.93 g (5 mmol) of I[1] and 0.75 g (10 mmol) of semicarbazide in 10 m*l* of ethanol was refluxed for 1 hr. The resulting crystals were collected after cooling, washed with a small amount of water and recrystallized from water-ethanol-DMF to afford 0.5 g (44%) of X as pale yellow crystals, mp 195—197°C (decomp). IR (KBr) cm^{-1}; 3500, 3250 (νNH), 1660 (νCO).

Found: C, 31.00; H, 2.84; N, 29.94%. Calcd for $C_6H_7O_5N_5$: C, 31.45; H, 3.08; N, 30.56%.

8) F. Audrieth, F. S. Scott and P. S. Kippur, *J. Org. Chem.*, **19**, 733 (1954).

Studies on Heteroaromaticity. XIX.[1] Direct 1,3-Dipolar Cycloaddition of Hydroxamoyl Chlorides with Enamines

Tadashi SASAKI and Toshiyuki YOSHIOKA

Institute of Applied Organic Chemistry, Faculty of Engineering, Nagoya University, Chikusa-ku, Nagoya

(Received February 26, 1968)

Minami and Matsumoto[2] have reported the 1,3-dipolar cycloaddition of 5-nitro-2-furonitrile oxide with a series of enamines, affording 1 : 1 adducts with a 5-amino-substituted isoxazoline structure and making for facile conversion to the corresponding isoxazoles by subsequent acid treatment. This paper will deal with our finding that the same products can be obtained directly from hydroxyamoyl chloride as from the corresponding nitrile oxide in better yields and by simpler procedures. Furthermore, we will report a novel one-step procedure for preparing isoxazole derivatives using enamines with

1) Part XVIII of this series: T. Sasaki and T. Yoshioka, This Bulletin, **41**, 2211 (1968).
2) S. Minami and J. Matsumoto, *Chem. Pharm. Bull. (Tokyo)*, **15**, 366 (1967).

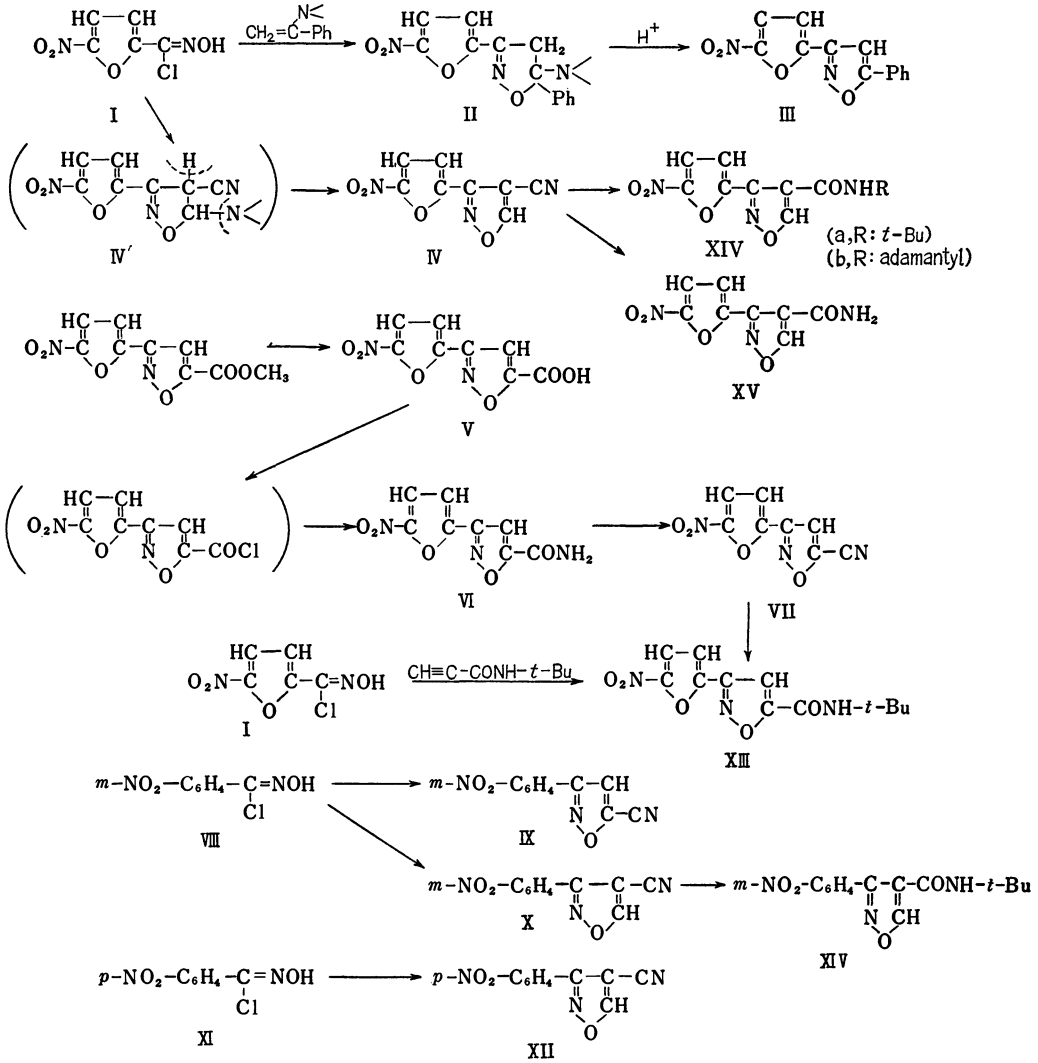

a specific structure.

5-Nitro-2-furylhydroxamoyl chloride (I)[1] was treated with morpholino-1-phenylethylene in ether at room temperature to afford an adduct (1 : 1), II, in a 80% yield, though the same product was obtained from 5-nitro-2-furonitrile oxide[3] and the same enamine in but a 50% yield. This somewhat lower yield might be caused by the difficult solubility of the nitrile oxide in ether. From the fact that the acid hydrolysis of II supplied a known compound, 3-(5′-nitro-2′-furyl)-5-phenylisoxazole, III, with a mp of 209—210°C,[2] II was concluded to be 3-(5′-nitro-2′-furyl)-5-phenyl-5-morpholinoisoxazoline. When 1-morpholino-2-cyanoethylene[4] was used as a dipolarophilic enamine, one which has a strong electronegative cyano group instead of the electropositive alkyl or alicyclic group in general enamines such as the above-described 1-morpholino-1-phenylethylene, the product, IV, was proved to be 3-(5′-nitro-2′-furyl)-4-cyanoisoxazole as a result of the structural elucidation on the basis of the spectral data; the NMR spectrum in $CDCl_3$ manifested a chemical shift at 0.86 τ (singlet, 1 H, 5-C–H),[3] and the ultraviolet spectrum showed an absorption maximum at 309 mμ (ε=14100)[3] in ethanol.

It is noteworthy that IV has an isoxazole structure instead of the expected isoxazoline (IV′) structure after the spontaneous *cis*-elimination of a morpholine molecule from the latter,[5] presumably

3) T. Sasaki and T. Yoshioka, This Bulletin, **40**, 260 (1967).

4) T. Sasaki, unpublished data.

5) The NMR spectrum of 1-morpholino-2-cyanoethylene showed an AB-quartet about its olefinic protons. This compound was concluded to take a *trans*-configuration, considering that the coupling constant is 14 cps, causing a facile *cis*-elimination of a morpholine molecule. The same thing could be said about 1-pyrrolidino- and 1-piperidino-2-cyanoethylene.

by facile aromatization after removal of hydrogen cyanide on account of the strong tendency toward protonation of a hydrogen atom attached to a carbon bearing a cyano group. All attempts at the direct preparation of an isomer, VII, 3-(5'-nitro-2'-furyl)-5-cyanoisoxazole, were unsuccessful, whether the routine nitrile-oxide method or the direct treatment of I with cyanoacetylene was employed. This compound was finally prepared by the dehydration of 3-(5'-nitro-2'-furyl)-5-carbamidoisoxazole (VI); VI was prepared by the following sequence of reactions starting from a known 5-carbomethoxyisoxazole[3] →V→VI. VII was found to be hardly purified at all even by column chromatography; therefore, it was converted to the corresponding amide (XIII) by a Ritter reaction with *t*-butyl alcohol, which was compared with a product, XIV, derived from IV by the Ritter reaction. XIII and XIV showed similar ultraviolet spectral patterns, but they were quite different in their NMR spectra, as will be shown in the Experimental Section. IV was also prepared from 1-pyrrolidino-,[4,5] and 1-piperidino-2-cyanoethylene[4,5] under similar reaction conditions, indicating that this direct isoxazole-formation is a general characteristic of the above cyano-enamines. Similarly, *m*-nitrophenylhydroxazovl chloride (VIII) afforded the corresponding 5-cyano- (IX) and 4-cyanoisoxazole (X) by the reactions of the nitrile oxide with cyanoacetylene[6] and of VIII with 1-morpholino-2-cyanoethylene; IX and X were afforded in 30 and 70% yields respectively. On the other hand, from *p*-nitrophenylhydroxamoyl chloride (XI), only the 4-cyanoisoxazole (XII) could be isolated in a 80% yield by a reaction with 1-morpholino-2-cyanoethylene; X underwent a Ritter reaction to afford the corresponding amide (XIV). Acidic hydrolysis of the nitrile in IV was carried out and an almost quantitative yileld of the corresponding amide (XV) was obtained and its infrared spectrum was different from its 5-amide.[3]

Experimental[6]

Reaction of I with 1-Morpholino-1-phenylethylene. A solution of 0.95 g (5 mmol) of I[1] and 1.9 g (10 mmol) of 1-morpholino-1-phenylethylene[7] in 30 m*l* of dry ether was kept standing at room temperature for 1 month. The resulting crystals were collected and recrystallized three times from benzene to afford 1.5 g of II as pale yellow crystals, mp 215—216°C. UV λ_{max}^{EtOH} mμ (ε): 348 (13500), 253 (8600).

Found: C, 59.47; H, 4.88; N, 12.24%. Calcd for $C_{17}H_{17}O_5N_3$: C, 59.47; H, 4.99; N, 12.29%.

The nitrile oxide procedure[3] afforded II, but in only a 50% yield. With hydrochloric acid, II was readily converted to III[2] almost quantitatively.

Reaction of I with 1-Morpholino-2-cyanoethylene. A solution of 0.82 g (4.3 mmol) of I[1] and 1.3 g (10 mmol) of 1-morpholino-2-cyanoethylene[4] in 60 m*l* of dry ether was kept standing at room temperature for 1 month. After the ether had then been removed, the residual oil was digested with 30 m*l* of water; the resulting crystals were collected and recrystallized several times from ethanol to give 0.7 g (80%) of IV as pale yellow crystals, mp 130—132°C. IR (KBr) cm^{-1}: 2300 ($\nu_{C\equiv N}$).

Found: C, 46.90; H, 1.09; N, 20.32%. Cacld for $C_8H_3O_4N_3$: C, 46.87; H, 1.47; N, 20.49%.

The Ritter Reactions of IV. Into a solution of 0.15 g (0.8 mmol) of IV in 7 m*l* of *t*-butanol, there was stirred 0.7 m*l* of concentrated sulfuric acid at room temperature. An exothermic reaction occurred. After the reaction mixture had then been allowed to stand at room temperature for 1 day, it was poured into ice water and the resulting crystals were recrystallized from benzene - petroleum ether to give 0.15 g (70%) of XIVa, mp 169—171°C. IR (KBr) cm^{-1}: 3320 (ν_{NH}), 1665 (ν_{CO}). UV λ_{max}^{EtOH} mμ (ε): 319 (14000). NMR ($CDCl_3$) τ: 1.10 (singlet, 1 H, 5-C-H), 2.55 (singlet, 2 H, nitrofuran ring protons*[1]), 3.70 (broad, 1 H, NH), 8.51 (singlet, 9 H, t-Bu).

Found: C, 52.15; H, 4.79; N, 14.92%. Calcd for $C_{12}H_{13}O_5N_3$: C, 51.61; H, 4.69; N, 15.05%.

Similarly, from 0.22 g (1.1 mmol) of IV, 0.29 g (1.4 mmol) of adamantly bromide,[9] 10 m*l* of acetic acid and 1 m*l* of 98% sulfuric acid, 0.28 g (70%) of XIVb, mp 174—175°C, was obtined after purification by column chromatography*[2] and recrystallization from ethanol-petroleum ether. IR (KBr) cm^{-1}: 3410, 3380 (ν_{NH}), 1665 (ν_{CO}). UV λ_{max}^{MeOH} mμ (ε): 318 (8700).

Found: C, 60.28; H, 5.60; N, 11.05%. Calcd for $C_{18}H_{21}O_5N_3$: C, 60.16; H, 5.89; N, 11.69%.

Acidic Hydrolysis of IV. IV, 0.32 g (1.5 mmol), was dissolved in 4 m*l* of 98% sulfuric acid and this solution was kept standing at room temperature for 1 day and poured into ice water. The resulting crystals were collected and recrystallized from ethanol to give 0.31 g (95%) of XV, mp 271—272°C. IR (KBr) cm^{-1}: 3450, 3360, 3300 (ν_{NH}), 1690 (ν_{CO}). UV λ_{max}^{MeOH} mμ (ε): 315 (12700).

Found: C, 43.03; H, 2.30; N, 18.65%. Calcd for $C_7H_5O_5N_3$: C, 43.06; H, 2.26; N, 18.83%.

---

6) Melting points are uncorrected. The ultraviolet absorption spectra were recorded on a Nippon-Bunko optical rotary dispersion recorder, Model ORD/UV-5. The infrared spectra were obtained with a Nippon-Bunko IR-S spectrophotometer. Microanalyses were carried out with a Yanagimoto C. H. N. Corder MT-1 type. The NMR spectra were determined with a Varian A-60 spectrometer, using tetramethylsilane as the internal standard. The chemical shifts are recorded in τ-values.

7) S. Hünig, K. Hübner and E. Benzig, *Chem. Ber.*, **95**, 926 (1962).

8) S. Murahashi, S. Kurioka and S. Maikawa, *Nippon Kagaku Zasshi* (*J. Chem. Soc. Japan, Pure Chem. Sect.*), **77**, 1689 (1956).

*1 This is the first example of the appearance of a singlet of two nitrofuran-ring protons in 2,5-disubstituted furan derivatives. The reason is uncertain at present.

9) T. Sasaki, S. Eguchi and T. Toru, This Bulletin, **41**, 236 (1968).

*2 XIVb was obtained from the second fraction by silica-gel (Mallinckrodt, 100 mesh) chromatography, using chloroform as an eluent. From the third fraction, there was obtained 30 mg (10%) of 3-(5'-nitro-2'-furyl)-isoxazole-4-carbamide, mp 265—257°C, which was identical with XV.

Preparation of an Isomer, XIII. 3-(5′-Nitro-2′-furyl)-5-carbomethoxyisoxazole[3] was quantitatively hydrolyzed with hydrochloric acid to the corresponding acid, V (mp 222°C). IR (KBr) cm^{-1}: 1685 (ν_{CO}).

Found: C, 42.81; H, 1.63; N, 12.52%. Calcd for $C_8H_4O_6N_2$: C, 42.87; H, 1.80; N, 12.50%.

V was treated with thionyl chloride by the routine procedure to afford the corresponding acid chloride, which, without further purification, was then dissolved in benzene. Ammonia gas was introduced into this solution to give VI (mp 246—247°C) in a 92% yield.

Found: C, 43.16; H, 1.88; N, 19.25%. Calcd for $C_8H_5O_5N_3$: C, 43.06; H, 2.26; N, 18.83%.

VI was treated with thionyl chloride or phosphorus pentachloride, and the crude nitrile (its existence was demonstrated by the presence of the 2300 cm^{-1} absorption due to $\nu_{C\equiv N}$ in the IR spectrum) was treated with *t*-butanol in concentrated sulfuric acid, as has been described above, to afford XIII, which was also prepared in a 34% yield from the thermal 1,3-dipolar cycloaddition reaction of I with *N*-*t*-butylpropiolamide.[10] Mp 214—215°C. UV λ_{max}^{EtOH} mμ (ε): 318 (14000). NMR ($CDCl_3$) τ: 2.79 (singlet, 1 H, 4-C–H), 2.60 and 2.87 (each doublet, 1 H, J=3.8 cps, nitrofuran-ring protons), 3.50 (broad, 1 H, NH), 8.50 (singlet, 9 H, *t*-Bu).

Found: C, 51.87; H, 4.70; N, 15.00%. Calcd for $C_{12}H_{13}O_5N_3$: C, 51.61; H, 4.79; N, 15.05%.

3-(*m*-Nitrophenyl)-5-cyanoisoxazole (IX). VIII (0.61 g; 3.0 mmol) was dissolved in 100 m*l* of ether, and into this solution there was stirred an equivalent amount of 1% aqueous sodium hydroxide at room temperature. After 2 min, an ether layer was separated and dried; a solution of 0.3 g (3.0 mmol) of cyanoacetylene[8] was then added. The reaction mixture was kept standing at room temperature for 1 day, and then the residue, obtained after the removal of the ether, was chromatographed on a silica-gel column. From the second fraction there was obtained 0.20 g (30%) of IX, mp 122—123°C from ethanol. IR (KBr) cm^{-1}: 2300 (ν_{CN}). UV λ_{max}^{EtOH} mμ (ε): 248 (13200). NMR ($CDCl_3$) τ: 2.62 (singlet, 1 H, 4-C–H).

Found: C, 55.58; H, 2.01; N, 19.47%. Calcd for $C_{10}H_5O_3N_3$: C, 55.82; H, 2.34; N, 19.53%.

3-(*m*-Nitrophenyl)-4-cyanoisoxazole (X). VIII (0.61 g; 3.0 mmol) and 0.91 g (6.6 mmol) of 1-morpholino-2-cyanoethylene[4] were dissolved in 40 m*l* of ether, and then the reaction mixture was kept standing at room temperature for 1 month. The resulting crystals were recrystallized from ethanol to give 0.52 g (80%) of X, mp 101—103°C. IR (KBr) cm^{-1}: 2300 (ν_{CN}). UV λ_{max}^{EtOH} mμ (ε): 247 (13000). NMR ($CDCl_3$) τ: 0.82 (singlet, 1 H, 5-C–H).

Found: C, 55.99; H, 1.91; N, 19.53%. Calcd for $C_{10}H_5O_3N_3$: C, 55.82; H, 2.34; N, 19.53%.

The Ritter Reaction of X. X (0.2 g; 1 mmol) was dissolved in a mixture of 5 m*l* of *t*-butanol and 1 m*l* of concentrated sulfuric acid. The mixture was kept standing at room temperature for 6 days. It was poured into ice water and the resulting crystals were recrystallized from ethanol - petroleum ether to give 0.21 g (75%) of XIV, mp 141—143°C. IR (KBr) cm^{-1}: 3290 (ν_{NH}), 1650 (ν_{CO}). UV λ_{max}^{MeOH} mμ (ε): 252 (12600).

Found: C, 58.37; H, 5.21; N, 14.39%. Calcd for $C_{14}H_{15}O_4N_3$: C, 58.12; H, 5.23; N, 14.53%.

3-(*p*-Nitrophenyl)-4-cyanoisoxazole (XII). Much as above, XII was prepared from XI and 1-morpholino-2-cyanoethylene[4] in a 80% yield. Mp 165—167°C, from ethanol. IR (KBr) cm^{-1}: 2300 (ν_{CN}). UV λ_{max}^{EtOH} mμ (ε): 265 (14700). NMR ($CDCl_3$) τ: 0.87 (singlet, 1 H, 5-C–H).

Found: C, 55.63; H, 1.84; N, 20.00%. Calcd for $C_{10}H_5O_3N_3$: C, 55.82; H, 2.34; N, 19.53%.

10) T. Sasaki, S. Eguchi and K. Shoji, submitted to *J. Chem. Soc.*

Studies on Heteroaromaticity. XXII.[1] Bromination of 6-Substituted Uracils with NBS

Tadashi SASAKI and Moriyasu ANDO

Institute of Applied Organic Chemistry, Faculty of Engineering, Nagoya University, Chikusa-ku, Nagoya

(Received March 9, 1968)

N-bromosuccimide (NBS) is known to effect the side-chain bromination of aromatic hydrocarbons[2] and of 3-methylthiophene[3] and the allylic bromination.[4] Nishiwaki and Goto[5] have reported that 6-methyl- (Ia), 2-mercapto-6-methyl- and 2-amino-6-methyluracil are brominated with NBS in the presence of benzoyl peroxide (BPO) to afford the corresponding brominated products at the 5-position of a pyrimidine ring and from this fact, they have disclosed that the reactions proceed *via* an ionic mechanism by the electrophilic attacks of NBS at the 5-position, since the yields did not change even in the absence of BPO. However, the yield of the produced 5-bromo-6-methyluracil (IIa), for instance, is as low as 45%. We presumed that this

1) Part XXI of this series: T. Sasaki and M. Ando, This Bulletin, in press.
2) N. B. Chapman and J. F. A. Williams, *J. Chem. Soc.*, **1952**, 5044.
3) F. L. Greenwood, M. D. Kellert and J. Sedlak, "Org. Synth.," Coll. Vol. IV, p. 108 (1963).
4) E. Campaigne and B. F. Tuller, *ibid.*, IV, 921 (1963).
5) T. Nishiwaki and T. Goto, This Bulletin, **33**, 26 (1960).

Table 1. Bromination of 6-substituted uracils

Uracil	Reaction temp., °C	Reaction time, hr	Product (Mp, °C)	Yield %	Microanalysis Found (Calcd) C	H	N
Ia	55	12	IIa	85	29.20	2.42	13.66
	r*	2	(270—275♯)	88	(29.29	2.46	13.67)
Ib	70	10	IIb	88			
	r*	2	(295♯♯)	88			
	r*	2		88			
Ic	r*	2	IIc	88	34.92	3.21	10.30
			(228—230**)		(34.69	3.27	10.11)
Id	r*	2	IId	65	36.78	4.41	9.29
	r*	8	(193—195)	85	(36.88	4.47	9.56)
Ie	r*	2	IIe	57	32.12	2.53	10.43
	r*	8	(264—265)	70	(31.96	2.68	10.65)

r*: reflux
**: decomposition
♯: mp 230°C, R. Behrend, *Ann.*, **229**, 17 (1885).
mp 247°C (decomp), T. Matsukawa *et al.*, *Yakugaku Zasshi*, **70**, 134 (1950).
mp 241°C (decomp), B. Kurtev *et al.*, *Chem. Abstr.*, **47**, 1607 (1953).
mp 251°C (decomp).[9]
♯♯: mp 293°C, G. H. Hitchings, G. B. Elion and E. A. Falco, *J. Biol. Chem.*, **185**, 643 (1950).

result is due to the poor solubility of Ia in carbon tetrachloride used as the solvent, though this solvent is commonly used in this type of reactions.[6] We changed the solvent from this non-polar carbon tetrachloride to polar ethanol, in which the solubility of uracil derivatives is larger than that in carbon tetrachloride. This increased solubility might favor the ionic reactions and as a result, the yield of IIa could be improved up to 85%. This note deals with the results of the similar procedure applied to other 6-substituted uracils. The structural elucidation of the products was done by the NMR spectra, since Nishiwaki and Goto[5] have demonstrated the site of the bromine atom to be at the 5-position by its characteristic reactivity[7] and by the chemical conversion to the known compounds. The NMR spectrum of IIa in DMSO-d_6, as an example, showed the presence of methyl protons and the absence of a C-5 proton, indicating IIa to be 5-bromo-6-methyluracil. The bromination is expected to proceed more readily as the electron-density at the 5-position of a pyrimidine ring increases by the stronger electron-donating nature of a 6-substituent R. Uracil[8] (Ib, R=H), 6-uracil acetate[9] (Ic, R=CH_2COOEt), orotaldehyde[10] (Id, R=CHO), and orotate[11] (Ie, R=COOEt) were treated with NBS and the considerable yields of the corresponding 5-

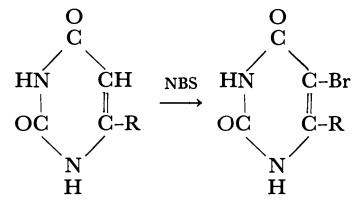

I a (R=CH_3) II a (R=CH_3)
b (R=H) b (R=H)
c (R=CH_2COOEt) c (R=CH_2COOEt)
d (R=CHO) d (R=$CH(OEt)_2$)
e (R=COOEt) e (R=COOEt)

bromo compounds were obtained, except the case when the bromination of Id afforded IId. The structure of IId was found to be the diethylacetal instead of the expected 5-bromoorotaldehyde from the elemental analysis and the spectral data; the NMR spectrum in DMSO-d_6 exhibited the chemical shifts at $-1.53\ \tau$ (s, -NH, disappeared on deuteration), -0.78 (s, -NH, disappeared on deuteration), 4.50 (s), 6.36 (q, J=6.8 cps) and 8.22 (t, J=6.8 cps) in the proton ratio of 1 : 1 : 1 : 4 : 6, among which a signal at $4.50\ \tau$ is assignable either to an acetal proton[12] or to a C-5 proton[13] and therefore, the ultraviolet spectrum was inspected. As shown in Table 2, an absorption maximum is

6) C. Djerassi, *Chem. Revs.*, **43**, 271 (1948).
7) J. Chesterfield, *J. Chem. Soc.*, **1955**, 3478.
8) D. Davidson and O. Bandisch, *J. Am. Chem. Soc.*, **48**, 2379 (1926).
9) G. E. Hilbert, *ibid.*, **54**, 2076 (1932).
10) K. Y. Zee-Cheng and C. C. Cheng, *J. Heterocyclic Chem.*, **4**, 163 (1967).
11) M. Ridi and G. Aldo, *Gazz. Chim. Ital.*, **82**, 13 (1952).

12) $5.28\ \tau$ for $MeCH(OEt)_2$: N. S. Bhacca, L. F. Johnson and J. N. Shoolery, "NMR Spectra Catalog," Varian Associates, Palo Alto, Calif. U.S.A. (1962). Spectrum No. 143.
13) NMR of Ia (DMSO-d_6) τ: -0.85 (broad s, -NH, disappeared on deuteration), 4.65 (s, C-5-H), 7.95 (s, $-CH_3$).
It should be noted here that a broad signal due to NH protons was split into two sharp signals after bromination.

TABLE 2. UV ABSORPTION OF 6-SUBSTITUTED URACILS AND THEIR 5-BROMO DERIVATIVES

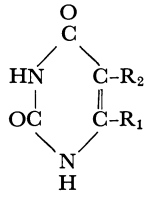

R_1	R_2=H		R_2=Br	
	λ_{max}^{MeOH} mμ	log ε	λ_{max}^{MeOH} mμ	log ε
H	258	3.80	270	3.90
CH_3	259	4.02	273	3.96
COOEt	286	3.87	290	3.82
CH_2COOEt	260	4.02	278	3.94
$CH(OEt)_2$*	260	3.90	278	3.93

* T. Sasaki, unpublished data.

located at 278 mμ, which is shifted 18 mμ bathochromically from that of 5-unsubstituted orotaldehyde diethylacetal and this is in good accordance with the general trend of other products as manifested in this table. From these facts, IId was concluded to be 5-bromoorotaldehyde diethylacetal. It should be mentioned as a conclusion that the yields decreased in the following sequence as the electron-donating nature decreased:

$$R = CH_3 \geq H \geq CH_2COOEt > CH(OEt)_2 > COOEt$$

Experimental[14]

5-Bromo-6-methyluracil (IIa). 0.6 g of 6-methyluracil (Ia)[13] and 1 g of NBS were suspended in 50 m*l* of ethanol and the reaction mixture was stirred at 55°C for 12 hr after addition of a catalytic amount of BPO. After the suspension dissolved, precipitation occurred again. Precipitated crystals were collected and recrystallized from ethanol. NMR (DMSO-d_6) τ: -1.40 (s, NH[13]), -1.28 (s, NH[13]), 7.80 (s, CH_3).

The above reaction without BPO afforded the same product in almost the same yield.

The yields, melting points and elemental analyses are summarized in Table 1 and the data on the ultraviolet analyses are summarized in Table 2, with those of other products.

14) The melting points were measured on a micro hot stage and were not corrected. The microanalyses were carried out with a Yanagimoto C. H. N. Corder, Model MT-1. The ultraviolet spectra were measured on a Nippon-Bunko optical rotary dispersion recorder, Model ORD/UV-5. The NMR spectra were taken on a Varian A-60 spectrometer, using tetramethylsilane as an internal standard and the chemical shifts are presented in terms of τ-values; where singlet is designated as s, doublet as d, triplet as t, quartet as q and multiplet as m.

SHORT COMMUNICATIONS

The Preparation of Mesoionic 5-Imino-3,5-dihydro-1,3-oxazole Derivatives

Shigeru SATO, Toshiyasu MASE*1 and Masaki OHTA

Laboratory of Organic Chemistry, Tokyo Institute of Technology, Ookayama, Meguro-ku, Tokyo

(Received May 30, 1968)

Of the mesoionic oxazoles with an exo-imino group, only fused ring compounds called Reissert-imine salts (II), have isolated and characterized as intermediates in the acid hydrolysis of Reissert compounds (I).[1,2]

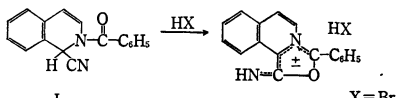

I II X=Br X=ClO4

However, in the case of the acid hydrolysis of *N*-benzoylanilinoacetonitrile (III), the intermediacy of the mesoionic compound (IV) seemed to be unlikely, since III, in contrast with I, underwent normal hydrolysis to benzoic acid instead of to benzaldehyde.[3]

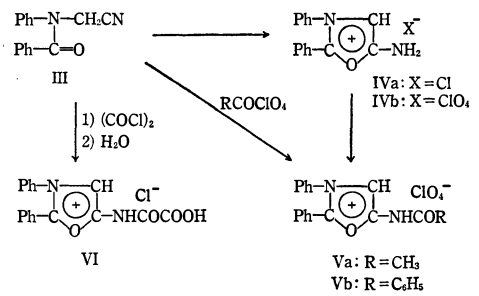

IVa: X=Cl IVb: X=ClO4

VI Va: R=CH3 Vb: R=C6H5

We wish to report here the successful preparation of IV (a and b) and exo-*N*-acyl derivatives (Va and Vb) from III.

Hydrogen chloride was introduced into a solution of III in methylene chloride until the saturation point had been reached. By adding ether to the resulting solution, 5-imino-2,3-diphenyl-3,5-dihydro-1,3-oxazole hydrochloride (IVa), mp 130—135°C (decomp.)[4] was separated out in an almost quantitative yield. The treatment of IVa with silver perchlorate in chloroform gave the hydroperchlorate (IVb), mp 200—202°C (decomp.). IVb was acetylated with acetic anhydride to give the exo-*N*-acetyl derivative (Va) in a 90% yield. Va was also obtained in an almost quantitative yield by the treatment of III with acetyl perchlorate in benzene. The *N*-benzoyl derivative of IV (Vb), mp 215—220°C (decomp.), was formed similarly in a 65% yield by the treatment of III with benzoyl perchlorate. The treatment of III with oxalyl chloride, followed by hydrolysis with water, gave VI, mp 180—185°C (decomp.).

The details of the present investigation will be present in a subsequent paper.

*1 Present address: Yamanouchi Pharmaceutical Co., Ltd., Hasunecho, Itabashi-ku, Tokyo.

1) L. W. Davis, *J. Org. Chem.*, **25**, 376 (1960).
2) I. W. Elliott and J. O. Leflore, *ibid.*, **28**, 3181 (1963).
3) I. W. Elliott, *J. Am. Chem. Soc.*, **77**, 4408 (1955).
4) All the melting points were determined on a hot plate and were not corrected.

The Photoreaction of β-Acyl- and β-Aroyl-acrylic Acids

Noboru SUGIYAMA, Hiroshi KATAOKA and Choji KASHIMA

Department of Chemistry, Tokyo Kyoiku University, Otsuka, Tokyo

and Kazutoshi YAMADA

Departmet of Synthetic Chemistry, Chiba University, Yayoi-cho, Chiba

(Received June 4, 1968)

During the course of an investigation of the reaction of β-acyl- and β-aroyl-acrylic acids,[1,2] we have found that the methanol adduct, β-benzoyl-α-methoxypropionic acid (1d),[3] and *cis*-β-benzoylacrylic acid (1b) were obtained from *trans*-β-benzoylacrylic acid (1a) by irradiation in methanol.*1 We have studied the photoreaction of 1a in various solvents as well as the analogous photoreactions of β-acyl- and β-aroyl-acrylic acids and their esters (2a—8a).

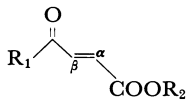

a

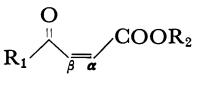

b

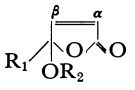

c

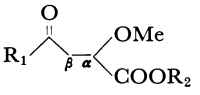

d

1) R_1=Ph R_2=H; 2) R_1=Ph, R_2=Me;
3) R_1=*p*-MeC_6H_4, R_2=H;
4) R_1=*p*-$MeOC_6H_4$, R_2=H;
5) R_1=*p*-BrC_6H_4, R_2=H;
6) R_1=Me, R_2=H; 7) R_1=R_2=Me;
8) R_1=*t*-Bu, R_2=H

Following three types of reaction were observed in the photoreaction listed in Table 1. a→b: *trans* to *cis* isomerization. a→c: isomerization to angelica lactones. a→d: alcohol addition to the olefinic double bond.

These reactions occurred complicatedly. For example, compound 1a in ether exclusively afforded the *cis*-isomer 1b, whereas that in methanol gave two products, the *cis*-isomer 1b and methanol adduct 1d. On the other hand, the irradiation of the methanol solution of 3a gave rise to both 3c and 3d. A methanol solution of 6a and 8a produced only the angelica lactone type compounds 6c and 8c. The details of these photoreactions will be reported elsewhere.

Table 1. Photoreaction products of β-acyl- and β-aroyl-acrylic acids

Compd.	Solv.	Time (hr)	Product (%) b	c	d
1a	no	45	12	0	0
1a	MeOH	12	17	0	14
1a	MeOH	120	0	0	100[a]
1a	EtOH	72	0	0	25
1a	ether	45	20	0	0
2a	MeOH	17	90	0	0
3a	MeOH	120	0	23[b]	77[c]
4a	MeOH	1 week	18	0	82[a]
5a	MeOH	72	0	4[b]	88[c]
6a	no	44	0	80	0
6a	MeOH	45	0	85	0
7a	no	1 week	90	0	0
7a	acetone	17	78	0	0
8a	MeOH	31	0	100	0

a) Type d products (1d and 4d) were obtained as free acids (R_2=H), which were esterified with diazomethane and subjected to NMR analysis. The methyl ester of 1d was also identified by comparison with authentic sample.[2]
b), c) Irradiation gave directly methyl esters and methyl ethers.

Table 2. The NMR data (τ) of α and β protons of starting materials and products

	a	b	c	d
1	2.04,3.17	2.89,3.68	—	5.55,6.50
2	2.02,3.12	3.13,3.76	—	—
3	2.04,3.17	3.76	2.68,3.86	5.52,6.59
4	2.01,3.17	2.84,3.60	—	5.55,6.63
5	2.14,3.26	—	3.77*	5.55,6.63
6	3.20	—	2.84,3.95	—
7	3.29	3,84	—	—
8	2.37,3.24	—	2.62,3.84	—

* R_2=Me

1) N. Sugiyama, T. Gasha, H. Kataoka and C. Kashima, This Bulletin, **41**, 971 (1968).
2) N. Sugiyama, T. Gasha, H. Kataoka and C. Kashima, *J. Chem. Soc.*, in press.
3) This photoaddition of methanol was reported independently by D. B. Rao *et al.* in *Tetrahedron Letters*, p. 1613 in **1968**.
*1 Taika 500 W high pressure mercury lamp was used as a light source and pyrex tube as a filter.

The d-d Bands of Hexachloroferrate(III) Ion

Hideo YAMATERA and Akemi KATO

Department of Chemistry, Nagoya University, Chikusa-ku, Nagoya

(Received June 13. 1968)

Spectra of finely powdered solid samples of hexacoordinated iron(III) chloride complexes were obtained in the visible and near infrared region with a Carl Zeiss PMQII spectrophotometer equipped with the reflectance attachment RA3.

The spectrum of $(NH_4)_4[FeCl_6][SbCl_6]$, which is representative of hexachloroferrate(III) spectra, is shown in Fig. 1. The bands associated with $[FeCl_6]^{3-}$ can easily be distinguished from those due to NH_4^+ vibrations by comparing the spectrum with that of $(NH_4)_2SnCl_6$, which is essentially isomorphous with $(NH_4)_4[FeCl_6][SbCl_6]$. The band at 12800 cm^{-1} corresponds to the first (lowest in wave number) band so far observed,[1-3] and the band at 8900 cm^{-1} has not been reported.

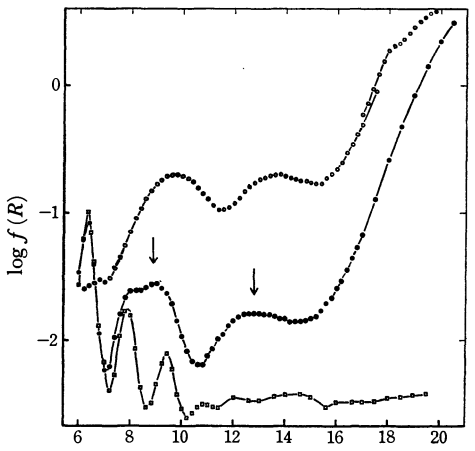

Fig. 1. Spectra* of $(NH_4)_4[FeCl_6][SbCl_6]$ (-●-), $Cs_3Fe_2Cl_9$ (-○-) and $(NH_4)_2[SnCl_6]$ (-□-).

The bands at 8900 cm^{-1} and 12800 cm^{-1} are assigned to the $^6A_{1g}\rightarrow{}^4T_{1g}(G)$ and $^6A_{1g}\rightarrow{}^4T_{2g}(G)$ transitions, respectively. With this assignment, a narrow band due to the $^6A_{1g}\rightarrow{}^4A_{1g}$, $^4E_g(G)$ transitions is expected to appear near 18000 cm^{-1}. Closer examination of the spectrum in this region disclosed a slight but discernible rise at about 18000 cm^{-1} on the slope of the intense charge transfer band. Moreover, the spectrum of $Cs_3Fe_2Cl_9$, which also contains $FeCl_6$ chromophores, clearly showed a shoulder at 17900 cm^{-1}, in addition to the two bands at 9800 cm^{-1} and 13600 cm^{-1}.

This assignment unfortunately disagrees with the assignment given by Hatfield *et al.*,[2] but it gives more reasonable values for the ligand field and interelectronic repulsion parameters: $\Delta=$ 11100 cm^{-1} and $B=605$ cm^{-1} (with the assumption $C=4B$). Jørgensen's estimation[4] of his spectrochemical and nephelauxetic functions, $f=$ 0.80 and $h=2.0$ for Cl^- and $g=1.4$kK and $k_{35}=$ 0.24 for Fe(III), leads to a prediction of $\Delta=$ 11200 cm^{-1} and $B=572$ cm^{-1}, if B for the free Fe^{3+} is assumed to be 1100 cm^{-1} by interpolation. Our result compares well with this prediction.

Full results and detailed discussions will be given elsewhere.

* $f(R)$ $[=(1-R)^2/2R$, where R represents the reflecting power] is nearly proportional to the absorption coefficient for finely powdered weakly absorbing substances. [See, for example, G. Kortüm and H. Schöttler, *Z. Electrochem.*, **57**, 253 (1953).]

1) H. L. Schläfer, *Z. Physik. Chem. Neue Folge*, **3**, 222 (1955).

2) W. E. Hatfield, R. C. Fay, C. E. Pfluger and T. S. Piper, *J. Am. Chem. Soc.*, **85**, 265 (1963).

3) A. P. Ginsberg and M. B. Robin, *Inorg. Chem.*, **2**, 817 (1963).

4) C. K. Jørgensen, *Discussions Faraday Soc.*, **26**, 110 (1958); "Structure and Bonding," Vol. 1, ed. by C. K. Jørgensen, J. B. Neilands, R. S. Nyholm, D. Reinen and R. J. P. Williams, Springer-Verlag, Berlin (1966), p. 3.

Ionic Processes in the Radiolysis of Nitrous Oxide

Satoshi TAKAO, Shoji SHIDA, Yoshihiko HATANO and Hideo YAMAZAKI

Laboratory of Physical Chemistry, Tokyo Institute of Technology, Meguro-ku, Tokyo

(Received June 14, 1968)

Although many studies have been made of the gas-phase radiolysis of nitrous oxide,[1] almost nothing definite has yet been established about its mechanism. In the present study SF_6 and CO_2 were used as electron scavengers, and various rare gases, as electron suppliers.

The irradiations were done with ^{60}Co-γ rays at 25°C to a total dose of 7.2×10^{20} eV·g^{-1}. The products, N_2 and O_2, were analyzed by gas chromatography, and the amounts of NO were calculated stoichiometrically.

The observed G-values of the products of the radiolysis of pure N_2O at 50—400 mmHg were $G(N_2)=10.1$, $G(O_2)=3.8$, and $G(NO)=5.1$, independent of the pressure. On the addition of only 0.01% SF_6 to the N_2O at 200 mmHg, these G-values all decreased rapidly, they then remained constant on the further addition of up to at least 0.3%. The decreases were $-\Delta G(N_2)=2.1$, $-\Delta G(O_2)=0.6$ and $-\Delta G(NO)=1.8$; accordingly, $-\Delta G(N_2O)=3.0$. The experiments with CO_2 gave similar results, except for a much slower leveling off of the G-values.

When increasing amounts (up to 600 mmHg) of rare gases were added to N_2O of a constant pressure of 60 mmHg, the amounts of N_2, O_2, and NO, all increased linearly in the case of He and Ne, while in the case of Ar, Kr, and Xe, although N_2 and O_2 increased linearly, NO did not appreciably increase at all. The increases in the G-values of the product by sensitization, G_{sens}, based on the energy absorbed by the rare gases, are shown in Table 1.

TABLE 1. G_{sens} FOR VARIOUS RARE GASES

	G_{sens}				
	He	Ne	Ar	Kr	Xe
N_2	7.3	6.3	3.0	2.9	3.8
O_2	2.8	2.4	1.5	1.6	1.8
NO	3.0	3.2	~0.0	~0.5	~0.5

If it is assumed that all electrons are scavenged by SF_6, and that SF_6^- does not contribute in any way to the decomposition of N_2O, one may infer from the above $-\Delta G$-values and with $W(N_2O)=33.0$ eV that one electron produced by the ionization of N_2O decomposes just one molecule of N_2O and yields 0.7 molecule of N_2. In the rare-gas experiments, the charge transfer from Xe^+ to N_2O is energetically impossible, and that from Kr^+ and Ar^+ appears not to occur either in spite of their higher ionization potentials than that of N_2O (12.9 eV), for their G_{sens} values are rather similar to those of Xe. As may be seen from the G_{sens} values, one excess (excess with respect to the positive ion produced by the ionization of N_2O) electron from these three rare gases, either as itself or through neutralization, decomposes one or less molecule of N_2O and yields one or less molecule of N_2. In the cases of He and Ne, the G_{sens} are remarkably higher than those for the other rare gases, and the ionization of N_2O by charge transfer and excitation transfer surely occurs. The fact that the formation of NO is not appreciably sensitized by Xe, Kr, and Ar indicates that N_2O^+ is necessary for the formation of NO. The results obtained here can not be accounted for by the often-assumed mechanism[2];

$$e^- + N_2O \rightarrow N_2 + O^-$$

$$O^- + N_2O \rightarrow N_2 + O_2^- \text{ and } NO + NO^-$$

because, according to this mechanism, more than one molecule of N_2 should be produced per electron. In order to explain the observed fact that one electron produces one or less molecule of N_2, one must assume the long-lived N_2O^- suggested by Freeman.[3] Recently Warman[4] has also obtained evidence for the initial formation of N_2O^- upon electron capture by N_2O. Thus, the major reaction may be tentatively described as follows:

$$e^- + N_2O \xrightarrow{M} N_2O^-$$

$$N_2O^- + N_2O^+ \rightarrow N_2 + O + N_2O$$

$$\text{and } N + NO + N_2O$$

followed by the combination of O and N to form O_2 and NO through NO_2. For the final conclusion to be attained, however, more supporting evidences are required.

1) For example, F. T. Jones and T. J. Sworski, *J. Phys. Chem.*, **70**, 1546 (1966).

2) For example, J. M. Warman, *Nature*, **213**, 381 (1967).

3) W. J. Holtslander and G. R. Freeman, *J. Phys. Chem.*, **71**, 2562 (1967).

4) J. M. Warman, private communication.

Glass Transition in Dehydrated Amorphous Solid

Natsuo ONODERA, Hiroshi SUGA and Syûzô SEKI

Department of Chemistry, Faculty of Science, Osaka University, Toyonaka, Osaka

(Received June 17, 1968)

Glass is considered as a kind of rigid, non-crystalline material. Usually glass is obtained by supercooling of liquid and therefore this condition is invariably adopted in its numerous definitions.

Non-crystalline solids can be, however, prepared by other unusual methods.[1] Dehydration process of some hydrated crystals also yields amorphous anhydrides.[2] Then a question arises as to whether these non-crystalline solids can be called glasses or not. One approach to this problem is to find out glass transition phenomena in these amorphous materials. This phenomenon is always accompanied with usual glass and characterizes boundary between glassy and supercooled liquid states.

Magnesium acetate tetrahydrate was dehydrated in solid state under vacuum (10^{-3} mmHg). The anhydride is known to give only one broad band in the low angle range of its X-ray diffraction pattern indicating an amorphous material, which transforms spontaneously into crystalline anhydride at about 250°C on heating.[3] About 20 mg of the anhydride was packed into an aluminum pan and mounted on sample holder of Perkin-Elmer DSC-1B scanning calorimeter. In order to keep a constant condition, sample was first heated up to 500°K, kept for a short time, and finally quenched to 400°K. Measurements were then carried out with heating rates between 1.25 and 80 deg·min^{-1}. The results are shown in Fig. 1.

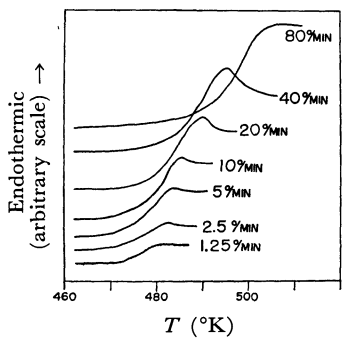

Fig. 1. DSC curve for the glass transition of magnesium acetate.

An endothermic anomaly always appears just before an exothermic effect due to crystallization. The shape and the temperature of the anomaly strongly depend on the heating rate employed. These results clearly show that the anomaly is due to glass transition phenomenon of the amorphous anhydride. Activation plot of the type developed by McMillan[4] is given in Fig. 2. From the slope of the bestfit straight line, apparent enthalpy of activation governing relaxation process becomes 131 ± 5 kcal·mol^{-1}.

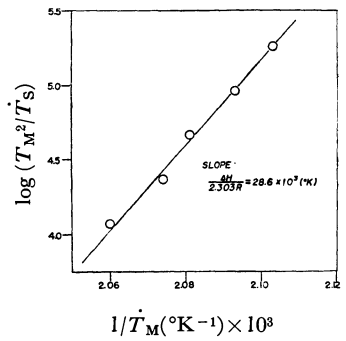

Fig. 2. Activation plot for the glass transition of magnesium acetate (T_M, inflection point; $\dot{T}_S$, heating rate).

We have discovered the first example of the non-crystalline solid prepared by dehydration exhibiting a glass transition phenomenon. This fact coincides with our previous observations[5] that the non-crystalline solid deposited on the chilled substrate from vapor state shows the same phenomenon. These observations lead to the conclusion that amorphous solids prepared by unusual methods other than supercooling of liquid can be firmly regarded as glasses. The details of the results will be given in due course.

1) D. R. Secrist and J. D. Mackenzie, "Modern Aspect of the Vitreous State," Vol. 3, 6, ed. by J. D. Mackenzie, Butterworths Sci. Publ., Ltd., London (1964), p. 149.
2) M. Volmer and G. Seydel, *Z. physik. Chem.*, **A179**, 153 (1937).
3) K. Manabe and T. Kubo, *Kogyo Kagaku Zasshi (J. Chem. Soc. Japan, Ind. Chem. Sect.)*, **70**, 13 (1967).
4) J. A. McMillan, *J. Chem. Phys.*, **42**, 3497 (1965).
5) M. Sugisaki, H. Suga and S. Seki, This Bulletin, **40**, 2984 (1967); **41**, No. 11 (1968).

Auto-correlation Function of the Maximum Wave Current in Polarography

Shizuo FUJIWARA, Yoshio UMEZAWA and Teruhiko KUGO*1

Department of Chemistry, Faculty of Science, The University of Tokyo, Hongo, Bunkyo-ku, Tokyo

(Received June 25, 1968)

Antweiler first reported noise-like fluctuations in the 1st kind maximum wave current of a polarographic *i-t* curve.[1] In connection with our series of investigations of the maximum wave current in polarography, we have recently obtained an auto-correlation function for these noise-like fluctuations with the use of a digitalized polarograph, where the mercury drop, voltage sweep and data sampling are synchronized.

The polarographic current of a drop of mercury at a constant voltage, *i. e.*, the *i-t* curve, is recorded automatically with the use of a digital computer (JEOL RA-5).

It is observed that the *i-t* curves are very smooth for the ordinary diffusion current, whereas, very noisy in the region of the maximum wave current. Fig. 1 a shows a typical example for a system of 2.5 mM copper(II) sulfate as depolarizer and 0.1 M potassium chloride as supporting electrolyte.

The result of analysis of the auto-correlation function for the noise-like current in Fig. 1a-(i) is as shown in Fig. 1b. The Fourier components of the auto-correlation function are shown in Fig. 1c. The 1st largest peak of the power spectrum of Fig. 1c refers to the direct current component, and the 4th peak refers to that of about 17 Hz. Accordingly, there exists a dominant hidden periodicity in the noise-like fluctuations in Fig. 1a-(i).

The details of the instrumentation and of the discussion of the results will be published in this journal. Further investigation is in progress.

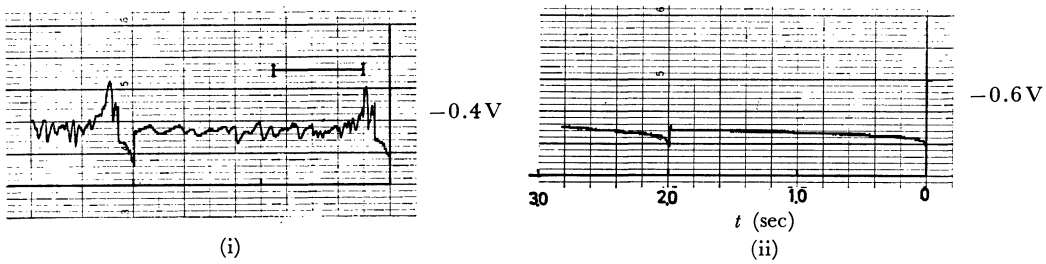

Fig. 1 a.

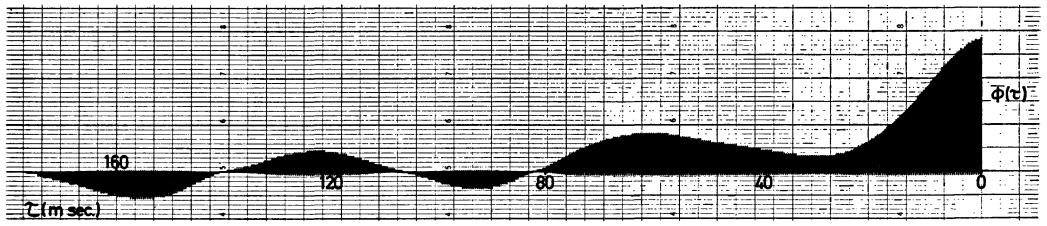

Fig. 1 b.

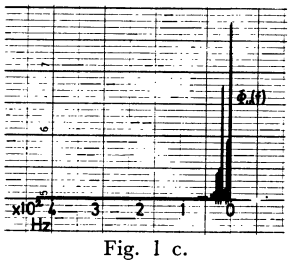

Fig. 1 c.

Fig. 1 a. Noise-like fluctuations in *i-t* curves at different voltages.
Chemical system
2.5 mM Copper sulfate as depolarizer
0.1 M Potassium chloride as supporting electrolyte
b. Auto-correlation function of the noise-like fluctuations in the portion indicated by I—I in Fig. 1a-(i).
c. Power spectrum of the noise-like fluctuations in the indicated portion in Fig. 1a-(i).

*1 Research fellow of the University of Tokyo on leave from Yanagimoto Co., Ltd.

1) H. J. Antweiler, *Z. Electrochem.*, **44**, 888 (1938).

Novel Isomers of the *trans*-(O–CN)-Cyanoaminoacidatodiethylenetriamine Cobalt(III) Complex Ion

Kuwako OHKAWA,*1 Shigenobu YANO and Junnosuke FUJITA

Department of Chemistry, Faculty of Science, Tohoku University, Sendai

(Received June 26, 1968)

Recently we prepared many complexes containing the *trans*-(O–X)-[Co·X·am·dien]$^+$ type ions, (X=CN^-, Cl^-, NO_2^-, am=α-aminoacidato ion and dien=$NH_2CH_2CH_2NHCH_2CH_2NH_2$), and confirmed the geometrical structure of these ions from an analysis of their ultraviolet absorption spectra.[1] In these new complex ions, dien occupies the cis-trans (mer) position, and their NMR spectra (60 Mc) give the methylene signal of meridional dien ring in the same region as reported before.[2]

As Fig. 1-a shows, however, the NMR spectrum

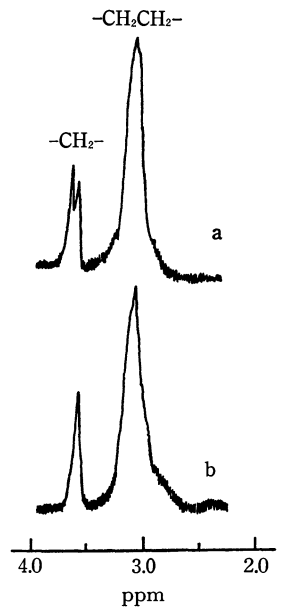

Fig. 1. The NMR spectra (60 Mc) of *trans*-(O–CN)-[Co(CN)gly·dien]$^+$ in D_2O.
a) Sample prepared from [Co(CN)$(SO_3)(NH_3)_4$]
b) Sample prepared from *trans*-(O–Cl)-[Co·Cl·gly·dien]$^+$
NaTMS was used as an internal reference.

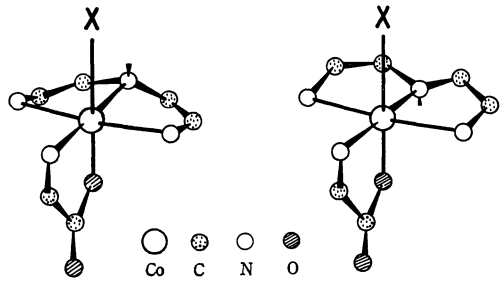

Fig. 2. Two isomers of *trans*-(O–X)-[Co·X·gly·dien]$^+$.

of the *trans*-(O–CN)-[Co(CN)gly·dien]$^+$ ion (gly=glycine), which was prepared from [Co(CN)$(SO_3)(NH_3)_4$] *via* Co(CN)dien$(OH_2)Br_2$, shows two kinds of methylene signal due to glycine ring at 210.5 and 213.5 cps. On the other hand, the corresponding chloro or nitro complex exhibits only one methylene signal at 216.3 and 213.4 cps, respectively. Such a difference was also observed in L-alaninate and α-aminoisobutyrate complexes.

The appearance of the two kinds of methylene signal in the cyanoglycinato complex would be due to existence of the two isomers shown in Fig. 2, or to any other reason coming from the coordination of CN^-. The latter reason, however, will be ruled out by the evidence that another sample of *trans*-(O–CN)-[Co(CN)gly·dien]$^+$, derived from the corresponding chloro complex by reaction of CN^- in DMSO, exhibits the same absorption spectrum with that prepared from [Co(CN)$(SO_3)(NH_3)_4$], but its NMR gives only one methylene signal (Fig. 1-b). This singlet signal coincides with one of the two signals mentioned above to support the existence of such an isomerism.

This isomerism would be attributed to the coordination of CN^- on either of the non-equivalent sides of the N_4 plane involving the puckered rings of dien. Hence such an isomerism cannot be substantiated in such complexes as [Co$(NO_2)_3$-dien],[3] in which both sides of the N_4 plane are occupied by two NO_2^- ions.

*1 Present address: Department of Chemistry, Osaka University, Toyonaka, Osaka.

1) Presented at the 21th Annual Meeting of the Chemical Society of Japan, Osaka, April, 1968.

2) J. I. Legg and D. W. Cooke, *Inorg. Chem.*, **5**, 594 (1966).

3) Y. Kushi, K. Watanabe and H. Kuroya, This Bulletin, **40**, 2985 (1967).

ESR Spectrum of Tropone Anion Radical

Yusaku IKEGAMI and Shuichi SETO

Chemical Research Institute of Non-Aqueous Solutions, Tohoku University, Katahira-cho, Sendai

(Received July 4, 1968)

Tropone is a particularly interesting compound in which to compare experimentally and theoretically estimated pi-electron densities because it is a peculiar conjugate ring system. The Hückel MO treatment for tropone molecule results in that the unpaired electron in its anion radical does not distribute to the carbonyl group.[1] This fact is likely related to the instability of the anion radical. Treatment of tropone, for example, with alkali metal in degassed tetrahydrofuran or dimethoxyethane displays the immediate color change into reddish-violet solution, but it does not show any ESR signal. This paper reports the ESR spectrum of tropone anion radical prepared with the electrolytic technique, which have proven a valuable tool for the preparation of radical ions for ESR study.[2]

Tropone was thoroughly purified by distillation in a high-vaccum apparatus. The electrochemical reduction of the solution in degassed *N,N*-dimethylformamide (DMF) presented the spectrum shown in Fig. 1. Tetra-*n*-propylammonium perchlorate was used as the supporting electrolyte. The radical is not so stable that the signal strength decreased to one half during 15 min at room temperature after the current was shut off.

Hyperfine structure of the spectrum is analyzed with three splitting constants, which are reasonably assigned in consideration of the calculated spin densities, as given in Table 1. The calculations of unpaired spin densities (ρ_i^π) for tropone anion radical were carried out by Hückel and McLachlan's methods[3] on some cases changed Coulomb integral parameter (α_O) at oxygen atom and resonance integral parameter ($\beta_{C=O}$) of C=O bond. We neglected all other bond length variations. The parameters given for the carbonyl group do not affect so much on the spin densities of carbon atoms at 2-, 4-, 5- and 7-positions. A good results is shown in Table 1 in which the parameters, $\alpha_O=\alpha+1.8\,\beta$ and $\beta_{C=O}=1.4\,\beta$, were applied for the calculation.

TABLE 1. OBSERVED SPLITTING CONSTANTS AND CALCULATED SPIN DENSITIES FOR TROPONE ANION RADICAL

Ring position (Number of H)	Observed a_i^H gauss	Spin density, ρ_i^π Experimental[a]	Calculated Hückel	Calculated McLachlan
1			0	−0.05342
2, 7 (2H)	8.578	0.3619	0.27157	0.37221
3, 6 (2H)	0.10	0.004	0.05379	−0.02019
4, 5 (2H)	5.050	0.2131	0.17464	0.18427
8			0	−0.01916

a) Spin densities using the relation, $a_i^H=Q_{CH}^H\rho_i^\pi$, where $|Q_{CH}^H|=23.7$ gauss.

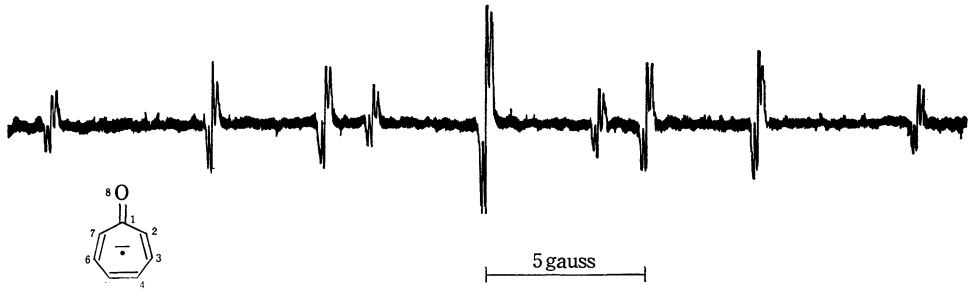

Fig. 1. ESR spectrum of tropone anion radical generated by the electrolytic reduction in DMF.

1) H. Yamaguchi, Y. Amako and H. Azumi, *Tetrahedron*, **24**, 267 (1968).
2) For example, M. Hirayama, This Bulletin, **40**, 1822 (1967).
3) A. D. McLachlan, *Mol. Phys.*, **3**, 233 (1960). The λ-parameter in McLachlan's procedure was fixed at the value $\lambda=1.2\,\beta$.

Isomerization Reactions of Dideuteroethylene and *cis*-2-Butene Photosensitized by $Zn(^3P_1)$

Shun-ichi HIROKAMI and Shin SATO

Department of Applied Physics, Tokyo Institute of Technology, Ookayama, Meguro-ku, Tokyo

(Received June 28, 1968)

Unimolecular isomerizations of monoolefins have extensively been used for the study of the photosensitizations in which the energies transferred from photosensitizers to reactants are less than the dissociation energies of any hydrocarbon bond.[1-4] More than twenty years ago, for instance, Steacie and his collaborators showed that excited zinc atoms were capable of sensitizing the reaction of ethylene.[5] Since then, however, no paper has appeared on zinc-photosensitization except a short note.[6]

A zinc lamp emits two resonance lines, one at 3076 Å, the other at 2139 Å. The latter is easily filtered out with a glass filter such as UV29 supplied by the Toshiba Denki Co. The lifetime of $Zn(^3P_1)$ has been reported to be 2×10^{-5} sec.[7] The energy transferred from $Zn(^3P_1)$ is 93.0 kcal, which is in between the values with $Cd(^3P_1)$ and $Hg(^3P_1)$.

Using the detecting method previously reported,[2] we examined the reaction of *trans*-dideuteroethylene photosensitized by $Zn(^3P_1)$ over the temperature range from 320 to 350°C in the expectation that the reactions could be explained by a mechanism similar to that of the photosensitization by $Cd(^3P_1)$.[3] However, unexpected results were obtained. The main reaction observed was *cis-trans* isomerization, the quantum yield of which increased with an increase in the pressure of the reactant, reaching more than twenty at the pressure of 40 mmHg. On the other hand, the isomerization to 1,1-dideuteroethylene, which is one of the main reactions in the Cd-photosensitization at low pressures,[3] was observed to occur very slowly.

With *cis*-2-butene as a reactant, slow *cis-trans* isomerizations were observed to occur both with and without the irradiation of the zinc resonance line at 3076 Å. The reaction with the irradiation was much slower than that of ethylene. When a small amount of acetylene was added to this system, however, the dark reaction was inhibited and the reaction photosensitized by $Zn(^3P_1)$ was much enhanced. The results are shown in Fig. 1.

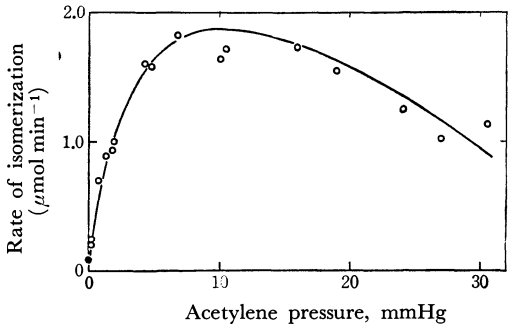

Fig. 1. Rate of the isomerization from *cis* to *trans*-2-butene photosensitized by $Zn(^3P_1)$ as a function of the pressure of acetylene added. (Initial pressure of *cis*-2-butene is 10 mmHg. Irradiation time is 2 min)

These results obviously show that excited zinc atoms react with ethylene or acetylene to produce catalyzers for the *cis-trans* isomerization of olefins. These catalyzers must be short-lived, because the isomerizations do not proceed after the termination of the irradiation. The mechanism of these reactions and the nature of the catalyzer are now being investigated.

1) T. Terao, S. Hirokami, S. Sato and R. J. Cvetanović, *Can. J. Chem.*, **44**, 2173 (1966).
2) S. Hirokami and S. Sato, *ibid.*, **45**, 3181 (1967).
3) S. Tsunashima, S. Hirokami and S. Sato, *ibid.*, **46**, 995 (1968).
4) S. Tsunashima and S. Sato, This Bulletin, **41**, 284 (1968).
5) H. Habeeb, D. J. LeRoy and E. W. Steacie, *J. Chem. Phys.*, **10**, 261 (1942).
6) R. F. Sullivan, *Dissertation Abstr.*, **18**, 1650 (1958).
7) F. W. Byron, M. N. McDermott, R. Novick, B. W. Perry and E. Saloman, *Phys. Rev.*, **134A**, 47 (1964).

BULLETIN OF THE CHEMICAL SOCIETY OF JAPAN VOL. 41 2227—2233 (1968)

Kinetic Studies of the Catalytic Ortho-Parahydrogen Conversion and Hydrogen-Deuterium Equilibration on γ-Alumina

Seigo OHNO and Iwao YASUMORI

Department of Chemistry, Tokyo Institute of Technology, Ookayama, Meguro-ku, Tokyo

(Received July 10, 1967)

Kinetic studies of the catalytic ortho-parahydrogen conversion and hydrogen-deuterium equilibration on highly purified γ-alumina were conducted in the range of temperature from 77 to 221°K and in the range of pressure from 10 to 120 mmHg. The rate equation obtained can be well explained by a mechanism which involves the reaction between an adsorbed atom and a molecule. The true activation energy, E, and the heat of adsorption of the reactive molecule, Q, were estimated as $E=0.51$—0.80 and $Q=0.51$—0.72 kcal/mol for the conversion (77—195°K), and $E=4.6$ and $Q=1.9$ kcal/mol for the equilibration (145—221°K). The conversion at temperatures below 90°K was found to proceed mostly *via* the magnetic mechanism. A thermal desorption study of adsorbed ethylene showed that there are three types of adsorption on γ-alumina with different activation energies of desorption, and that these species occupy a total of only a few hundredths of the surface. It was concluded that the most strongly-adsorbed ethylene blocks the reactions *via* the chemical mechanism, while the most weakly-adsorbed one retards the conversion *via* the magnetic mechanism. The nature of active sites for the reactions was discussed by taking the results of the ESR measurement into consideration.

During the past three decades, a number of investigations have been made in an attempt to ascertain the mechanisms of the ortho-parahydrogen conversion and of the hydrogen-deuterium equilibration on various solid surfaces, and several mechanisms have been proposed. Bonhoeffer and Farkas[1] proposed a dissociation-recombination mechanism of hydrogen on the surface. Later, Rideal[2] proposed an alternative mechanism, *i. e.*, the exchange of hydrogen atoms between an adsorbed hydrogen molecule and an atom, in order to account for the fact that the reaction rate is appreciable on some catalysts at which the rate of atomic recombination is extremely slow. Couper and Eley[3] have modified this mechanism by assuming the reaction of an adsorbed atom with a gaseous molecule. Further, Boreskov and Vassilevitch[4] proposed a mechanism in which the molecule, after the exchange, migrates to the site of weakest adsorption and then desorbs. A mechanism of bimolecular reaction between adsorbed molecules was proposed by Schwab and Killmann.[5,6]

Besides the chemical mechanisms expressed above, the interconversion between nuclear spin isomers, para- and orthohydrogen or ortho- and paradeuterium, proceeds physically by means of perturbations due to the inhomogeneous magnetic field of paramagnetic substances.

More detailed and accurate kinetic studies are needed in order to clarify which mechanism is operative and to determine whether adsorbed molecular hydrogen participates in the reactions. Only a few studies, however, have concerned themselves with these problems.

Among a number of active substances for these reactions, it has recently been reported[7,8] that evacuated or irradiated alumina is catalytically active to both the ortho-parahydrogen conversion*1 and the hydrogen-deuterium equilibration.*1 The fact that alumina, originally diamagnetic and a poor adsorbent of hydrogen, accelerates the conversion at such a low temperature as 77°K and the equilibration at higher temperatures suggests the existence of paramagnetic sites and of dissociatively-adsorbed hydrogen on the surface.

1) K. F. Bonhoeffer and A. Farkas, *Z. physik. Chem.*, **12B**, 231 (1931).
2) E. K. Rideal, *Proc. Cambridge Phil. Soc.*, **35**, 130 (1939).
3) A. Couper and D. D. Eley, *Discussions Faraday Soc.*, **8**, 172 (1950).
4) G. K. Boreskov and A. A. Vassilevitch, Actes Congr. Intern. Catalyse, 2e, Paris, 1960, **1**, 1095 (Editions Technip, Paris, 1961).
5) G. M. Schwab and E. Killmann, *ibid.*, 2e, Paris, 1960, **1**, 1047 (Editions Technip, Paris, 1961).
6) G. M. Schwab and E. Killmann, *Z. physik. Chem. (N. F.)*, **24**, 119 (1960).
7) G. J. K. Acres, D. D. Eley and J. M. Trillo, *J. Catalysis*, **4**, 12 (1965).
8) I. Yasumori and S. Ohno, This Bulletin, **39**, 1302 (1966).

*1 Hereafter these will be called simply as conversion and equilibration.

The kinetics of the conversion and of the equilibration on the surface of highly-purified γ-alumina were examined in detail in the present experiment. In addition, studies of the effect of adsorbed ethylene on the reaction rates, on the thermal desorption of ethylene, and on ESR of γ-alumina were carried out in order to obtain some information on the nature of the active sites.

Experimental

Apparatus and Procedure. Kinetic studies of the conversion and of the equilibration on γ-alumina were carried out using an apparatus which consisted of a conventional high-vacuum system with a grease-free reaction vessel of about 950 m*l* combined with a circulation pump and arrangements for the preparation and storage of normal hydrogen, para-rich hydrogen, and deuterium. The reaction system was connected with a low-pressure-type gas chromatograph[8] *via* a greaseless valve and a trap cooled at 77°K.

The temperature of the catalyst vessel was maintained using the following cooling agents: liquid nitrogen (77°K), liquid oxygen (90°K), a mixture of *n*-propanol and methanol (100 : 30) cooled with liquid nitrogen (145°K), *n*-propanol cooled with liquid nitrogen (159°K), methanol cooled with solid carbon dioxide (195°K), and *n*-hexanol cooled with liquid nitrogen (221°K). The effective volume of the reaction vessel at each temperature was measured using hydrogen.

A measured amount of the reactant gas was introduced into the reaction vessel and left in contact with the catalyst for a given time; then about 1% of the gas was sampled for the gas-chromatographic analysis.

In case of the thermal desorption study, alumina was preliminally exposed to 5×10^{-2} mmHg of ethylene, at various temperatures, and then evacuated at the same temperature. The temperature of the alumina was then raised linearly with the time up to 350°C; the pressure change due to the desorption under pumping was simultaneously registered. The details of this apparatus will be reported later.

The amounts of irreversibly-adsorbed ethylene on γ-alumina were estimated as follows. Gamma-alumina in a small vessel was evacuated at 500°C. A known amount of ethylene was then introduced into the vessel at 195 or 298°K and left in contact with the alumina for 0.5 hr. The amount of ethylene remaining in the gas phase was then measured by collecting it into a side tube at the temperature of liquid nitrogen. The difference between the amounts of introduced ethylene and of collected one was equated with that of irreversibly-adsorbed ethylene.

The surface area of γ-alumina was determined by the BET method in a constant-volume system using nitrogen at 77°K.

The ESR spectra were measured at 9194 Mc/s on an X-band spectrometer (Japan Electron Optics Laboratory Co., JES-3B 365) using powdered γ-alumina placed in a quartz tube 4 mm in inside diameter. After calcination at 500°C, the samples were evacuated at various temperatures for 5 hr *via* a cold trap at 77°K and then sealed off prior to ESR measurements.

Materials. Cylinder hydrogen was purified by diffusing it through a heated thimble made of palladium-silver alloy. High-purity deuterium and ethylene from the Takachiho Chemical Co. were used without further purification. Cylinder helium was passed through a liquid-nitrogen trap, filled with Linde molecular sieve 13X, in order to remove the oxygen and other condensables.

Normal hydrogen was used as the reactant of the conversion at temperatures of 77 and 90°K, while para-rich hydrogen prepared by equilibrating it at 77°K was used in the temperature range from 145 to 195°K. In the case of equilibration, an equimolar mixture of hydrogen and deuterium was used as the reactant.

Aluminum oxide was prepared by the hydrolysis of aluminum isopropoxide which had been distilled three times under reduced pressure. The spectroscopic analysis of the oxide showed that the contents, as impurities, of iron, copper, magnesium, and manganese are all less than 1 ppm except for silicon (20 ppm). An X-ray diffraction study showed that the oxide, after having been calcined at 100 and 250°C, has the structure of pseude-böhmite, and that it changes to γ-alumina upon calcination at 500°C.

The γ-alumina catalyst finally adopted was calcined at 500°C for 10 hr in air, and then evacuated at the same temperature for 20 hr *in vacuo* at better than 1×10^{-6} mmHg. Prior to each run of reaction, the catalyst was evacuated at 500°C for 2 hr and cooled down to the reaction temperature by introducing about 10 mmHg of helium into the reaction vessel.

In some runs, the catalyst evacuated at 500°C was preliminarily brought into contact with 10 mmHg of ethylene for 1 hr at 195 or 298°K and then evacuated for 1 hr.

Results and Discussion

Experimental-rate Expression. It was verified that the diffusion through the catalyst pore has no influence on the rate; a calculation of the Thile modulus, by assuming a pore radius of 10 Å showed that the effectiveness factor of the surface was almost unity under the present reaction conditions.

As may be seen from the time course of the reaction under constant pressures (Fig. 1), the experimental-rate constants, k_e, of both conversion and equilibration were expressed as:

$$k_e = \frac{1}{t}\ln\frac{X_0-X_e}{X_t-X_e}\ \mathrm{min}^{-1} \qquad (1)$$

where X_0 is the initial mole fraction of the species which disappears with the progress of the reaction, and where X_t and X_e are those of the same species at the time t and the equilibrium at the experimental temperature, T, respectively. A specific rate, k_m, was calculated by the following equation:

$$k_m = n\frac{k_e}{60S} = \frac{k_ePV}{60SkT}\ \mathrm{molecules\cdot sec^{-1}cm^{-2}} \qquad (2)$$

whene n is the number of molecules in the reaction system; P, the total pressure of the reactant; V, the effective volume of the reaction

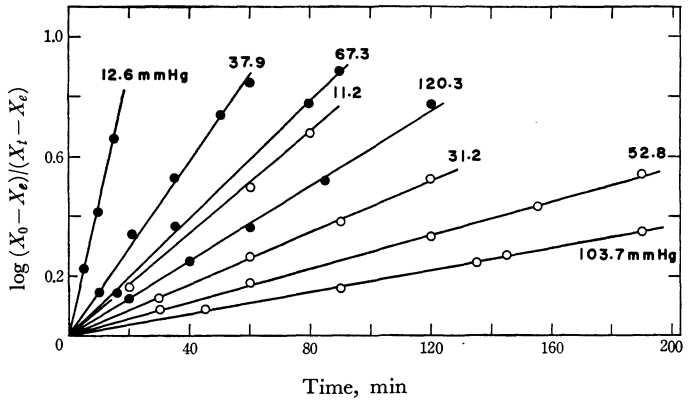

Fig. 1. Time course of the conversion and the equilibration on γ-alumina at various pressures.
●, conversion at 77°K; ○, equilibration at 159°K: catalyst, 33.4 mg

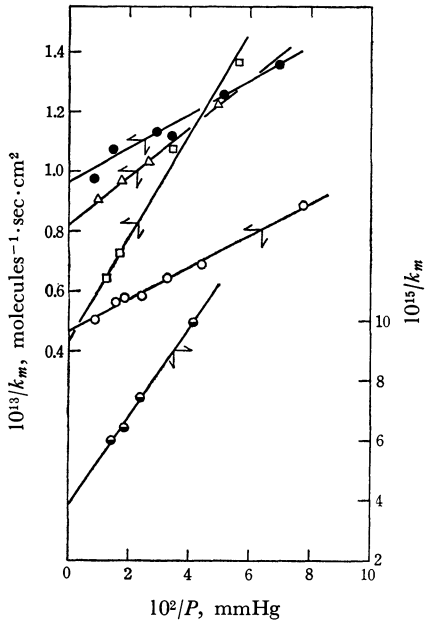

Fig. 2. Dependence of the conversion reaction rate on the total pressure.
●, 77°K; ○, 90°K; ◒, 145°K on unpoisoned γ-alumina: △, 90°K on γ-alumina poisoned by ethylene at 298°K: □, 195°K on γ-alumina poisoned by ethylene at 195°K

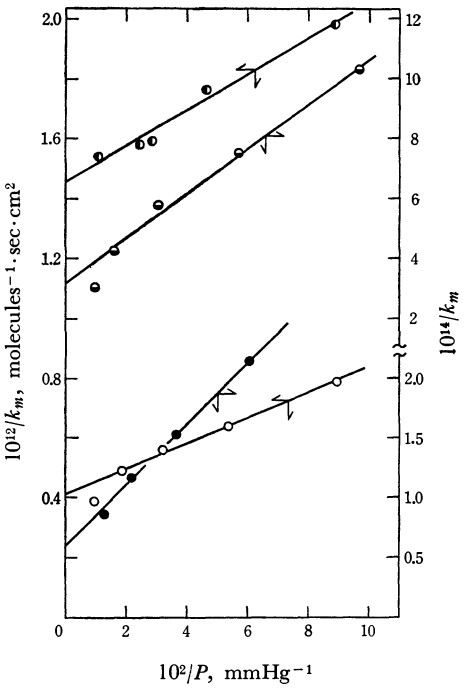

Fig. 3. Dependence of the equilibration reaction rate on the total pressure.
◐, 145°K; ○, 159°K; ◒, 195°K and ●, 221°K

system; S, the surface area of the catalyst, and k, the Boltzmann constant.

Figure 2 shows that the linear relationship holds between $1/k_m$ and $1/P$ for the conversion in the range of temperature from 77 to 195°K and in the range of pressure from 12.8 to 120.3 mmHg. Similar behavior can also be seen in Fig. 3 for the equilibration in the range of temperature from 145 to 221°K and in the range of pressure from 10.3 to 106.5 mmHg.

From these results, a rate expression which fits both the reactions may be given as:

$$-\frac{n}{S}\cdot\frac{dX_t}{dt}=k\frac{aP}{1+aP}(X_t-X_e)$$

molecules·sec^{-1}cm^{-2} (3)

where k corresponds to the value of k_m extrapolated to an infinite pressure. The Arrhenius plots of k shown in Fig. 4, may be expressed as:

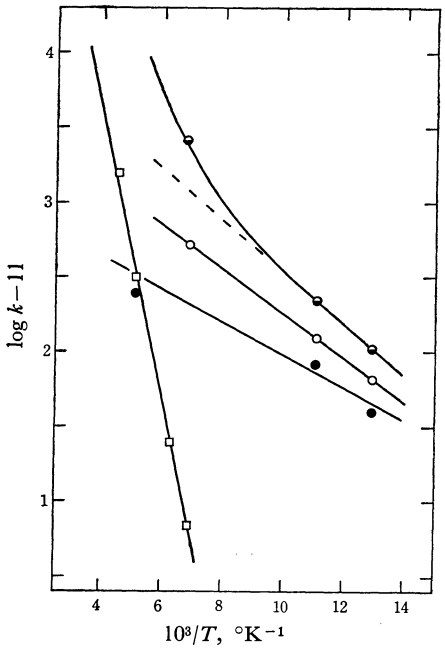

Fig. 4. Arrhenius plots of the extrapolated rate, k, in the conversion and the equilibration.
◒, conversion on unpoisoned γ-alumina; ○, conversion on γ-alumina poisoned by ethylene at 298°K and ●, at 195°K: □, equilibration on unpoisoned γ-alumina

$$k = A\exp(-E/\boldsymbol{R}T) \tag{4}$$

where A and E are constants.

The a parameter in Eq. (3) was determined from the slopes of the plots in Figs. 2 and 3. This parameter, as a function of the temperature, is shown in Fig. 5; it may be expressed as:

$$a = a_0\exp(\boldsymbol{Q}/\boldsymbol{R}T), \tag{5}$$

by taking two constants, a_0 and $\boldsymbol{Q}$. The estimated values of these constants are shown in Table 1.

It is found that the Arrhenius plot of k for the conversion deviates upward from a straight line with increasing temperatures and that it approaches that for the equilibration. This deviation does not, however, appear when the catalyst is preliminarily

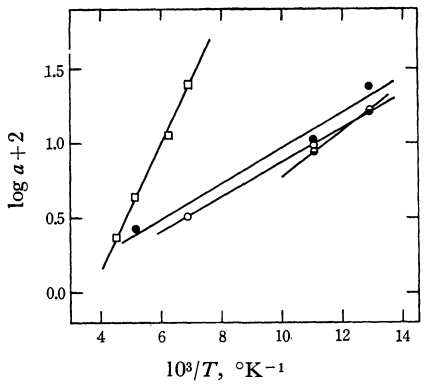

Fig. 5. Relationship between parameter, a, and temperature. Symbols are the same as those in Fig. 4.

treated by ethylene at 195 or 298°K. These results suggest that the reactions *via* a chemical mechanism are mostly retarded by adsorbed ethylene which remains on the surface of the catalyst evacuated at 298°K, while the low-temperature conversion is stopped by ethylene adsorbed at 195°K. It may, therefore, be concluded that the conversion at high temperatures proceeds *via* a mechanism similar to that of the equilibration, but that the reaction *via* another, probably physical, mechanism becomes predominant at low temperatures.

Mechanism of the Conversion. *Derivation of Rate Expression.* By assuming that the conversion takes place magnetically at low temperatures, the reaction may be described by the following scheme:

$$\begin{array}{ccc} o\text{-}H_2(g) & & p\text{-}H_2(g) \\ {\scriptstyle k_1}\big\downarrow\big\uparrow{\scriptstyle k_{-1}} & & {\scriptstyle k_2}\big\downarrow\big\uparrow{\scriptstyle k_{-2}} \\ o\text{-}H_2(a) & \underset{k_{-3}}{\overset{k_3}{\rightleftharpoons}} & p\text{-}H_2(a) \\ \vdots & & \vdots \\ S_m & & S_m \end{array} \tag{I}$$

where S_m is a paramagnetic site on the surface. The rate equations for these steps may be written as:

$$\frac{dN_{go}}{dt} = \frac{V}{\boldsymbol{k}T}\cdot\frac{dP_o}{dt} = -k_1P_o(1-\theta)\sigma_1S + k_{-1}\theta_o\sigma_1S \tag{6}$$

Table 1. Kinetic constants in the conversion and the equilibration

Reaction	Catalyst treatment	E (kcal/mol)	Q (kcal/mol)	a_0 mmHg^{-1}	A molecules·sec^{-1}cm^{-2}
o-H_2=p-H_2	(A); evacuated at 500°C	0.80*	0.72*	1.7×10^{-3}	19×10^{14}
	C_2H_4 adsorbed at 298°K after (A)	0.70	0.50	5.3×10^{-3}	5.8×10^{14}
	C_2H_4 adsorbed at 195°K after (A)	0.51	0.51	6.3×10^{-3}	1.2×10^{14}
H_2+D_2=2HD	evacuated at 500°C	4.6	1.9	2.8×10^{-4}	5.0×10^{18}

* Calculated from rates at 77 and 90°K.

$$\frac{dN_{gp}}{dt} = \frac{V}{kT}\cdot\frac{dP_p}{dt} = -k_2P_p(1-\theta)\sigma_1 S + k_{-2}\theta_p\sigma_1 S \quad (7)$$

$$\frac{d\theta_o}{dt} = k_1P_o(1-\theta) - k_{-1}\theta_o - k_3\theta_o + k_{-3}\theta_p \quad (8)$$

$$\frac{d\theta_p}{dt} = k_2P_p(1-\theta) - k_{-2}\theta_p + k_3\theta_o - k_{-3}\theta_p \quad (9)$$

where:

$$\theta = \theta_o + \theta_p$$

P_o and P_p are the partial pressures of ortho- and parahydrogen; N_{go} and N_{gp}, the numbers of the respective molecules in the gas phase; θ_o and θ_p, the surface coverages of these species, and σ_1, the number of active sites per unit area of the catalyst surface. At a steady state where $d\theta_o/dt = d\theta_p/dt = 0$, the expressions for the surface coverage are obtained as:

$$\theta_o = \frac{1}{D}\{k_1(k_{-2}+k_{-3})P_o + k_2k_{-3}P_p\} \quad (10)$$

$$\theta_p = \frac{1}{D}\{k_1k_3P_o + k_2(k_{-1}+k_3)P_p\} \quad (11)$$

where:

$$D = k_1(k_{-2}+k_3+k_{-3})P_o + k_2(k_{-1}+k_3+k_{-3})P_p + (k_{-1}k_{-2}+k_{-1}k_{-3}+k_{-2}k_{-3}).$$

By substituting these relations into Eqs. (6) and (7), we obtain the equations:

$$\frac{dP_o}{dt} = \frac{\rho}{D}(k_{-1}k_2k_{-3}P_p - k_1k_{-2}k_3P_o) \quad (12)$$

and

$$\frac{dP_p}{dt} = \frac{\rho}{D}(k_1k_{-2}k_3P_o - k_{-1}k_2k_{-3}P_p) \quad (13)$$

where:

$$\rho \equiv \sigma_1 S k T/V.$$

Assuming that there is no difference between the adsorption behavior of these isomers, *i. e.*, that $k_1=k_2$ and that $k_{-1}=k_{-2}$, Eq. (12) can be rewritten in the form:

$$-\frac{d(PX_o)}{dt} = \rho\frac{k_{-1}(k_3+k_{-3})}{k_{-1}+k_3+k_{-3}}\cdot\frac{(k_1/k_{-1})P}{1+(k_1/k_{-1})P}\times\left[X_o - \frac{1}{1+k_3/k_{-3}}\right] \quad (14)$$

where X_o is the mole fraction of orthohydrogen. This equation can easily be reduced to Eq. (3). The E and Q constants in Table 1 can, therefore, be expressed as:

$$E = -R\frac{d\ln\{k_{-1}(k_3+k_{-3})/(k_{-1}+k_3+k_{-3})\}}{d(1/T)} \quad (15)$$

$$Q = R\frac{d\ln(k_1/k_{-1})}{d(1/T)} = R\frac{d\ln a}{d(1/T)} \quad (16)$$

which have physical significance as the activation energy and the heat of adsorption, respectively.

Rate-determining Step of the Conversion. There are two extreme cases which depend on the relative order of the magnitude of rate constants, $k_{-1} \gg k_3$, k_{-3} and *vice versa*, corresponding to the cases where the rate is controlled by the surface conversion or by the desorption, respectively. In the former case, Eq. (14) can be simplified to:

$$-\frac{d(PX_o)}{dt} = \rho(k_3+k_{-3})\frac{(k_1/k_{-1})P}{1+(k_1/k_{-1})P}(X_o - X_e) \quad (17)$$

while in the latter case it can be simplified to the same equation except that k_{-1} replaces (k_3+k_{-3}) in Eq. (17).

The former case is preferable to the latter, as will be dicussed below. If the latter case were operative, the observed rate would correspond to the rate of desorption. On the basis of the activated complex theory, the rate of desorption is given as:

$$v = k_d n_{H_2(a)} = \frac{kT}{h}\exp(-E/RT)\sigma_1\theta_{H_2(a)} \text{ molecules}\cdot\text{sec}^{-1}\text{cm}^{-2} \quad (18)$$

The frequency factor, A, is equivalent to the $kT/h\cdot\sigma_1$ in Eq. (18). Hence, the observed value of A, 19×10^{14} molecules·sec^{-1}·cm^{-2}, in Table 1 results in the value of σ_1 of 1—3×10^3 sites·cm^{-2} at 77—90°K, a value which is too small to keep the rate of surface conversion faster than that of desorption.

Isotope Effect. As may be seen in Table 1, the activation energy of the conversion at temperatures below 90°K is smaller than that of the equilibration by about 4 kcal/mol. This difference is larger than that in the zero-point energies between gaseous hydrogen and deuterium, 1.8 kcal/mol. The latter should be the maximum difference in activation energy due to the isotope effect, as has been pointed out by Eley *et al.*[7] There ia a difference of 1.2 kcal/mol between the heats of adsorption determined from the kinetics of equilibration and of conversion. Moore and Ward[9] have estimated the heats of the molecular adsorption of para-, orthohydrogen, hydrogen deuteride, ortho-, and paradeuterium on alumina by gas chromatography. The obtained values, ranging from 1.40 (p-H_2) to 1.65 kcal/mol (p-D_2), lead to a maximum difference of 0.25 kcal/mol due to the isotope effect.

The above kinetic results can not be explained by the isotope effect only. The conversion at temperatures below 90°K, therefore, proceeds *via* a mechanism different from that of the equilibration.

9) W. R. Moore and H. R. Ward, *J. Phys. Chem.*, **64**, 832 (1960).

Mechanism of the Equilibration. The equilibration can only occur *via* a chemical mechanism. On the assumption that the Rideal mechanism is operative, the reaction scheme may be expressed as:

$$\begin{array}{ccccc} H_2(g) & & 2HD(g) & & D_2(g) \\ k_1' \downarrow\uparrow k'_{-1} & & k_2' \downarrow\uparrow k_{-2}' & & k_1'' \downarrow\uparrow k_{-1}'' \\ H_2(a) & & 2HD(a) & & D_2(a) \\ + & \underset{k_{-3}'}{\overset{k_3'}{\rightleftharpoons}} & + & \underset{k_{-3}''}{\overset{k_3''}{\rightleftharpoons}} & + \\ D(a) & & H(a)\ D(a) & & H(a) \end{array} \qquad \text{(II)}$$

By a treatment similar to the above, when the exchange of atoms is the rate-controlling step a rate equation may be derived as follows:

$$-\frac{d(PX)}{dt} = \rho'\theta_a(k_3'+2k_{-3}')\frac{(k_1'/k'_{-1})P}{1+(k_1'/k'_{-1})P} \times\left[X-\frac{1}{1+k_3'/2k'_{-3}}\right] \qquad (19)$$

with:

$$\rho' \equiv \sigma_2 S\boldsymbol{k}T/V,$$

where X is the sum of the mole fractions of hydrogen and deuterium in the gas phase and σ_2 is the number of active sites per unit area of the catalyst surface. The precise form of σ_2 is given in Eq. (20).

A thermal desorption study of hydrogen adsorbed on the alumina showed that no appreciable desorption occurred up to 250°K. Hence, by assuming that the surface coverage of the adsorbed hydrogen atom, θ_a, remains unaltered throughout the present experiment, it may be seen that Eq. (19) coincides with the experimental results, Eq. (3).

The heat of adsorption, 1.9 kcal/mol, estimated from the kinetic study is quite similar to those obtained by gas chromatography. To judge from these coincidences, it is probable that the equilibration proceeds mainly through a reaction of molecularly-adsorbed hydrogen with the adsorbed hydrogen atom.

The application of the activated complex theory to this mechanism gives the following expression for the rate of the surface process:

$$v = \sigma_2 k_3'\theta_a\theta_m = \frac{z\sigma_a\sigma_m}{n_0} k_3'\theta_a\theta_m\ . \qquad (20)$$

The rate constant, k_3', has the form $k_3' = \boldsymbol{k}T/\boldsymbol{h}\cdot\exp(-E/\boldsymbol{R}T)$ if the ratio of partition functions, $f(X_\ddagger)/f(H(a))\cdot f(H_2(a))$, is unity. σ_a and σ_m are the number of sites which hold hydrogen atoms and molecules respectively. z is the number of nearest neighbors around the respective site; θ_m, the fraction of the surface covered by adsorbed hydrogen molecules, and n_0, the total number of active sites, $\sigma_a+\sigma_m$. This equation can be used to evaluate the number of adsorption sites on the present catalyst surface. Assuming that σ_a and σ_m are of the same order of magnitude, that $z=4$, and that $n_0=1\times10^{15}$ cm^{-2}, σ's can be evaluated as 0.5×10^{10} cm^{-2} from the observed value, 5.0×10^{18}, of A shown in Table 1.

A separate study of the poisoning effect of ethylene adsorbed at 298°K showed that the amount of adsorbed ethylene which completely blocks the reaction can be estimated to be 2×10^{12} molecules·cm^{-2} from the initial decrease in the equilibration rate. Dolidze *et al.*[10] have reported that γ-alumina, calcined at 500°C in air and evacuated at 320°C, can adsorb 3×10^{11} hydrogen atoms per unit area at 523°K under pressures below 10^{-2} mmHg. These values seem to be in satisfactory agreement with one another in view of the approximations made.

A rate equation similar to Eq. (19) can be derived on the basis of the Boreskov-Vassilevitch reaction scheme as:

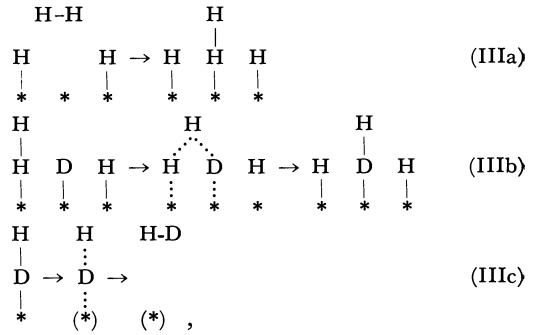

(IIIa)

(IIIb)

(IIIc)

provided that (IIIb) is the rate-controlling step, where * represents an active site and (*), the site for the weakest adsorption.

The Schwab-Killmann mechanism (IV).

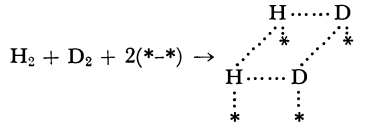

(IV)

does not fit the observed kinetic equation. This mechanism results in the rate equation:

$$-\frac{d(PX)}{dt} = \rho''\left(\frac{aP}{1+aP}\right)^2\left[k_4\frac{X^2}{4} - k_{-4}(1-X)^2\right] \qquad (21)$$

where $\rho''\equiv\sigma_3^2 S\boldsymbol{k}T/2V$, where k_4 and k_{-4} are the rate constants of HD formation and its reverse on the surface respectively, and σ_3, the number of dual sites per unit area. This equation does not agree with Eq. (3) in two aspects, *i. e.*, the time-course characteristics and the pressure dependence.

Properties of Active Sites. It may be seen from Fig. 4 that the adsorbed ethylene affects the

10) G. M. Dolidze, Yu. A. Kobanovskii and L. S. Polak, *Kinetika i Kataliz*, **6**, 897 (1965).

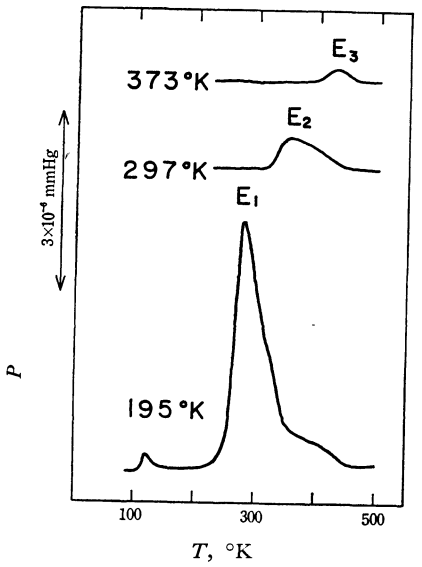

Fig. 6. Desorption spectra of adsorbed ethylene on γ-alumina.
Rate of temperature rise, 2.70°K/min

rate of conversion in different ways depending upon the reaction temperatures. Figure 6 shows the thermal desorption spectra of the adsorbed ethylene on the alumina preliminarily evacuated at 500°C. Irreversibly-adsorbed ethylene at 195°K gave a spectrum consisting of a small peak at 110°K, a large peak, E_1, with a maximum at 280°K, and a shoulder on the high-temperature side of E_1. With an adsorption sample at 297°K, an unsymmetrical peak, E_2, with a maximum at 355°K was obtained, but not the E_1 peak. Finally, a sample of adsorption at 373°K gave only a small, symmetrical peak, E_3. The relative areas of the peaks were estimated to be $16.3(E_1) : 3.3(E_2) : 1.0(E_3)$, and the activation energies of the desorption of the respective peaks were determined[11] to be $19(E_1)$, $25(E_2)$ and $31(E_3)$ kcal/mol on the assumption that the desorption obeys the first-order law. The peak at 110°K was attributed to the desorption of ethylene physically adsorbed on the alumina and/or the wall of the apparatus.

It was found, by a static measurement of the adsorption, that the fraction of the surface occupied by ethylene is quite small; the sum of the fractions of the surface covered by adsorbed ethylene which give the E_1, E_2, and E_3 peaks was 0.024, while that corresponding to E_2 and E_3 was 0.0021. The E_2 and E_3 peaks were found to coincide with those observed by Amenomiya and Cvetanović by a method of inert-gas flow.[11]

The γ-alumina in the present experiment gave a sharp, symmetrical ESR signal 12 oe wide, corresponding to $g=2.004$. The intensity of this signal changed with the evacuation temperatures, as is shown in Table 2. A similar signal with $g=2.003$ has been reported by Berger and Roth.[12]

Table 2. Changes in the intensity of ESR signal ($g=2.004$) of γ-alumina with evacuation

Evacuation	Intensity of ESR signal
30°C—5 hr	1.8×10^{14} spins/g
500°C—5 hr	0.75
550°C—5 hr	0.71
C_2H_4 adsorbed at 30°C after 550°C—5 hr	0.94

Provided that the conversion at low temperatures takes place only on these ESR active sites, its rate at 77°K is estimated to be 1×10^5 molecules·sec^{-1}·$spin^{-1}$ under a total pressure of 12.6 mmHg.

Eley *et al.*[7] have reported that there is a linear relationship between the rate of conversion and the number of unpaired electrons produced on α-alumina by γ-ray irradiation. On the basis of their findings, the rate of conversion at 77°K may be estimated as 2 molecules·sec^{-1}·$spin^{-1}$ under a total pressure of 4 mmHg provided that all these electrons are effective for the reaction. In the present study, the decrease in the conversion rate per ethylene molecule adsorbed at 195°K, which mostly retards the low-temperature conversion, is estimated as 0.5 under similar conditions. This value agrees in order of magnitude with the result reported by Eley *et al.* The ESR active sites do not, therefore, correspond to that for the low-temperature conversion.

This consideration leads to the following conclusions. There are two kinds of paramagnetic centers on or in evacuated γ-alumina; one gives an ESR signal, but has little effect on the low-temperature conversion, while the other gives no ESR signal, but accelerates the conversion. These active sites, including those for the equilibration, exist over only a small percentage of the whole surface. The most strongly-adsorbed ethylene retards the reaction *via* the chemical mechanism, while the most weakly-adsorbed one retards the conversion *via* the physical mechanism.

The authors wish to express their thanks to Professor Emeritus Yasuo Inamura of their Institute for his encouragement and to Mr. Tetsuo Maruyama of the Japan Electron Optics Laboratory Co. for his help in the ESR measurements.

11) Y. Amenomiya and R. J. Cvetanović, *J. Phys. Chem.*, **67**, 144 (1963).

12) P. A. Berger and J. F. Roth, *J. Catalysis*, **4**, 717 (1965).

BULLETIN OF THE CHEMICAL SOCIETY OF JAPAN VOL. 41 2234—2239 (1968)

Oxygen Oxidation of Ferrous Ions Induced by Chelation

Yoshimi KURIMURA,*1 Ryoji OCHIAI*2 and Niro MATSUURA

Department of Chemistry, College of General Education, The University of Tokyo, Meguro-ku, Tokyo

(Received November 20, 1967)

The oxidation of ferrous ions by dissolved oxygen in aqueous solutions in the presence of such chelating agents as EDTA, DTPA, EDTAOH, EDTP, CyDTA and NTA was studied spectrophotometrically. The rate equation for the oxidation reaction is:

$$d[Fe^{III}]/dt = 4k_p[Fe^{II}HZ][O_2] + 4k_n[Fe^{II}Z][O_2]$$

where k_p is the rate constant for the (1) reaction; k_n, the rate constant for the (2) reaction; $Fe^{II}HZ$, protonated chelate, and $Fe^{II}Z$, the normal chelate.

$$Fe^{II}HZ + O_2 \xrightarrow{k_p} Fe^{III}Z + HO_2 \quad (1)$$

$$Fe^{II}Z + O_2 \xrightarrow{k_n} Fe^{III}Z + O_2^- \quad (2)$$

The linear relationship between $\log k$ and $\log R_f$ shown by Eq. (3), was obtained from all the experimental results except for those on the EDTPA and CyDTA systems:

$$\log k = 0.92 + 0.13 \log R_f \quad (3)$$

In Eq. (3), k is $4k_p$ and R_f is $K_{Fe^{III}L}/K_{Fe^{II}HL}$ for the protonated chelate, while k is $4k_n$ and R_f is $K_{Fe^{III}L}/K_{Fe^{II}L}$ for the normal chelate. In the cases of the DTPA and CyDTA systems, a deviation from the straight line was observed. This can be explained by steric hindrance of the oxygen attack by these chelates.

The oxidation of ferrous ions by dissolved oxygen in aqueous solutions in the presence of simple anions, such as chloride,[1] sulfate,[2] perchlorate[3] and phosphate,[4] has been extensively investigated. The oxidation reaction has been found to be accelerated in the presence of pyrophosphate anions.[5-8] King and Davidson suggested that the oxidation rate of ferrous ions increases as the complexing affinity of the anion for ferric ions increases.[7] Thus, at a given pH, the rate can be found to decrease in the order of pyrophosphate, phosphate, chloride, sulfate, and perchlorate.

The oxidation reaction is also accelerated in the presence of such chelating agents as ethylenediaminetetraacetic acid (EDTA), nitritotriacetic acid (NTA), diethylenetriaminepentaacetic acid (DTPA), 1,2-cyclohexanediaminetetraacetic acid (CyDTA), *N*-Hydroxyethylenediamine-*N*,*N*',*N*'-triacetic acid (EDTAOH), and ethylenediaminetetrapropionic acid (EDTP). This acceleration may be ascribed to the stabilization of the oxidized form by the chelation. In this connection, a relationship between the oxidation rate of ferrous ions and the chelation of ferrous and ferric ions is expected. The rate and mechanism of the oxidation reaction of ferrous ions by dissolved oxygen were studied spectrophotometrically; the effect on the reaction rate of the chelation of ferrous and ferric ions will also be discussed.

Experimental

Materials. The ferrous ammonium sulfate, perchloric acid, and sodium hydroxide used were all commercially-available G. R.-grade reagents. Redistilled water was used in the preparation of the solutions.

Preparation of Samples. The hydrogen ion concentration in the chelating-agent solution containing sodium perchlorate was adjusted by the addition of dilute perchloric acid or a dilute sodium hydroxide

*1 Present address: Chemical Laboratory, College of Liberal Arts, Ibaraki University, Watari-machi, Mito, Ibaraki.

*2 Present address: Depertment of Chemistry, Faculty of Sience, Tokyo Metropolitan University, Setagaya-ku, Tokyo.

1) A. M. Posner, *Trans. Faraday Soc.*, **49**, 382 (1953).
2) A. B. Lamb and L. W. Elder, *J. Am. Chem. Soc.*, **53**, 137 (1931).
3) P. George, *J. Chem. Soc.*, **1954**, 4349.
4) M. Cher and N. Davidson, *J. Am. Chem. Soc.*, **77**, 793 (1955).
5) H. A. Spoehr, *ibid.*, **46**, 1497 (1924).
6) J. H. C. Smith and H. A. Spoehr, *ibid.*, **48**, 107 (1926).
7) J. King and N. Davidson, *ibid.*, **80**, 1542 (1958).
8) S. Utsumi and K. Muroshima, *Nippon Kagaku Zasshi (J. Chem. Soc. Japan, Pure Chem. Sect.)*, **86**, 593 (1965).

solution. A ferrous ion solution was prepared by mixing appropriate amounts of a ferrous ammonium sulfate solution, a sodium perchlorate solution, and water. The ionic strengths of these solutions were maintained at 0.1 by sodium perchlorate.

Measurement of Reaction Rate. The chelating agent and the ferrous ion solutions were kept in a thermostated bath at 25°C for about one hour. By the mixing of the air-saturated chelating-agent and the air-saturated ferrous ion solutions, the reaction was initiated. A portion of the reaction mixture was poured into a 1-cm quartz cell, and the variation in the optical density in the ultraviolet region due to the ferric chelate was recorded automatically on a Hitachi recording spectrophotometer. Thus, twelve seconds after the initiation of the reaction, reproducible results could be obtained. When the reaction proceeded at a moderate rate, the variation in the optical density was measured by using a Hitachi EPU-type spectrophotometer. The molar extinction coefficients used to determine the concentrations of the ferric chelates of EDTA, NTA, DTPA, CyDTA, EDTAOH, and EDTP were 9300 at 258 mμ, 7100 at 258 mμ, 9600 at 258 mμ 8200 at 260 mμ 7900 at 259 mμ, and 5600 at 258 mμ respectively. The variation in the molar extinction coefficients of these chelates under the present experimental conditions was within $\pm 3\%$ in each case.

The oxidation rates in the oxygen-saturated solutions were determined by the following procedure. A 20 m*l* test tube with two small pipes at the end of its was used. These pipes were used to bubble oxygen gas through the solution. One of the test tubes was used for the oxygenation of the ferrous-ion solution, and the other, for the oxygenation of the chelating agent solution. Oxygen bubbling was continued about two hours at 25°C. Then, one or two m*l* of the ferrous ion solution were pipetted into 10 m*l* of the chelating agent solution, in which oxygen bubbling was continued until the end of the measurements. A portion of the oxygen-saturated reaction mixture was poured into a 1 cm quartz cell equipped with a cap. The variation in the optical density was measured in the manner described above.

Results

Dependence of the Rate on the Concentrations of Ferrous Ions, Chelating Agent, and Oxygen. The variation in the ferric-ions concentration with the time at various concentrations of ferrous ions at a given pH and a given concentration of the chelating agent for the DTPA system is shown in Fig. 1. The initial oxidation rate was determined from the initial slope of the curve. The dependence of the rate on the concentration of Fe(II) for the DTPA system is shown in Fig. 2. A linear relationship between the rate and the concentration of Fe(II) was observed in this case. A linear relationship was also obtained between the rate and the concentration of the chelating agents, as Fig. 3 shows.

Under the present experimental conditions, the reaction was first-order with respect to the total concentrations of both ferrous ions and the chelating agent. However, this linear relationship was not observed in the relatively high pH region.

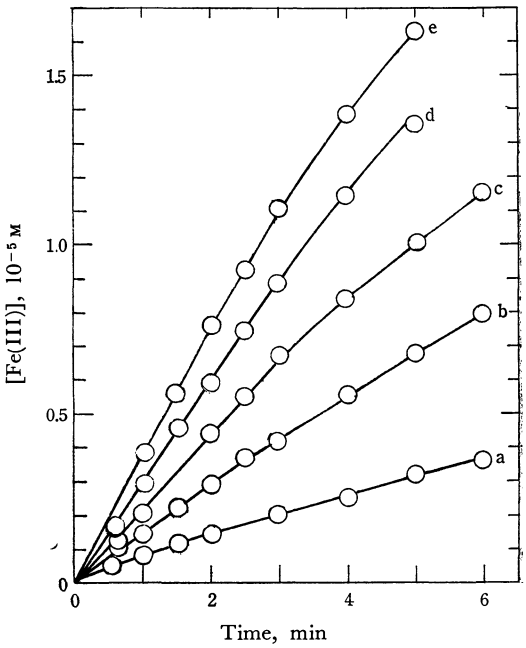

Fig. 1. Variation of the Fe(III) concentrations with time in the air saturated Fe(II)-DTPA system.
Fe(II) concentration:
a 8.0×10^{-6} M b 1.2×10^{-5} M c 1.6×10^{-5} M
d 2.4×10^{-5} M e 4.0×10^{-5} M
1.06×10^{-4} M DTPA pH 2.30 ± 0.01
0.1 M $NaClO_4$ 25°C

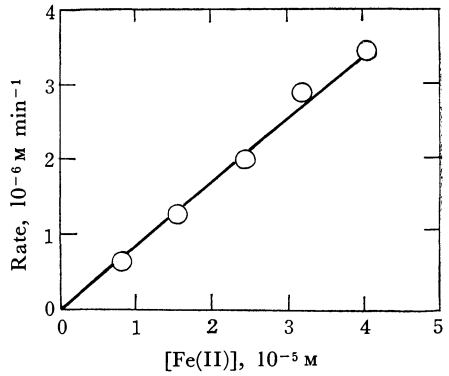

Fig. 2. Dependence of the oxidation rate on Fe(II) concentration in the air saturated Fe(II)-DTPA system at low pH region.
1.06×10^{-4} M DTPA pH 2.30 ± 0.01
0.1 M $NaClO_4$ 25°C

The oxidation reaction in these systems was also first-order with respect to the concentration of dissolved oxygen in the solution. This first order dependence was examined by comparing the specific rate in the air-saturated solution with that in the oxygen-saturated solution. The ratio of the concentrations of oxygen in the aerated and

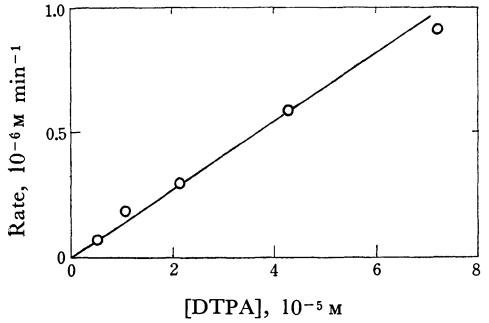

Fig. 3. Dependence of the oxidation rate on DTPA concentration in the air saturated Fe(III)-DTPA system at low pH region.
4.0×10^{-5} M Fe(II) pH 2.22 ± 0.01
0.1 M $NaClO_4$ 25°C

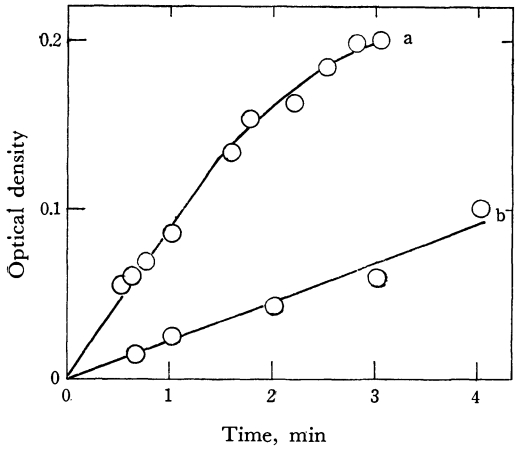

Fig. 4. Comparison of the oxidation rate in the air saturated solution and in the oxygen saturated solution.
a oxygen saturated solution
b air saturated solution
pH 2.00 ± 0.01 0.1 M $NaClO_4$ 25°C

oxygenated solutions was estimated to be about 1 to 4.7. This ratio was nearly equal to the ratio of the reaction rate in an aerated solution to that in the corresponding oxygenated solution, as is shown in Fig. 4 for the DTPA system.

The results suggested that the rate equation for Fe(II)-chelating agent-O_2 reaction system at a low pH is:

$$d[Fe(III)]/dt = k_a[Fe(II)]_t[Z]_t[O_2] \quad (1)$$

where k_a is the apparent rate constant; $[Fe(II)]_t$, the total concentration of the ferrous iron, and $[z]_t$, the total concentration of the chelating agent.

Dependence of the Rate on the pH. The variation in the rate with the pH in the DTPA, EDTA, CyDTA, and EDTAOH systems is shown in Figs. 5 and 6. The reaction rate in the EDTA system in the pH region from 3 to 5 under these experimental conditions could not be deterimned

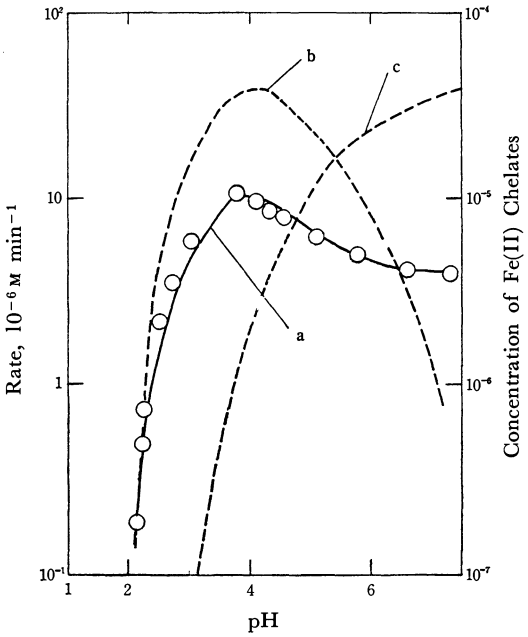

Fig. 5. Dependence of the oxidation rate on pH in the air saturated Fe(II)-DTPA system.
○ observed value
a calculated curve
b concentration of protonated chelate ($Fe^{II}HDTPA$)
c concentration of normal chelate ($Fe^{II}DTPA$)
9.4×10^{-4} M DTPA 4.0×10^{-5} M Fe(II)
0.1 M $NaClO_4$ 25°C

because the rate was too rapid to determine its value. The oxidation rate in the DTPA system, as shown in Fig. 5, increases simply with an increase pH values of the solution under the conditions employed and reaches its maximum at pH 4. Then, with the increase in the pH, the rate begins to decrease, becoming nearly constant at pH values higher than 6.5. In the EDTA and the CyDTA systems, such a maximum in the reaction rate was also observed. On the other hand, under these experimental conditions the reaction rates in the NTA and the EDTAOH systems increase simply with an increase in the pH values and become nearly constant at higher pH values, without any distinctive maximum.

Discussion

The concentrations of Fe(II) chelate for the EDTA and the DTPA systems under the present experimental conditions can be calculated by using the formation constants of Fe(II) chelates and the acid dissociation constants of the chelating agents. The results of the calculation are shown in Fig. 5 for DTPA chelates. By comparing these two curves with the observed rate, it is made clear that the oxidation reaction of Fe(II) chelates proceeds

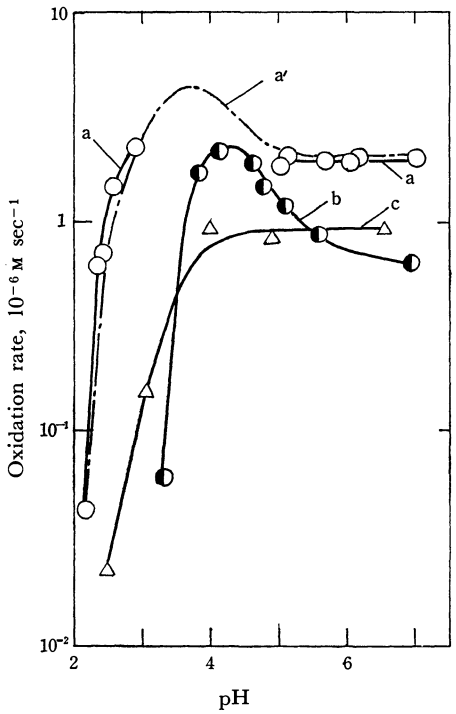

Fig. 6. Dependence of the oxidation rate on pH in the air saturated Fe(II)-chelating agent systems.
a EDTA system, 3.1×10^{-5} M EDTA
a' calculated curve for the EDTA system
b CyDTA system, 4.6×10^{-5} M CyDTA
c EDTAOH system, 1.5×10^{-4} M EDTAOH
2.9×10^{-5} M Fe(II) 0.1 M $NaClO_4$ 25°C

through two simultaneous reaction paths, one of which involves the oxidation of the protonated chelate while the other involves the oxidation of the normal chelate. In a similar way, it may be suggested that the oxidation of Fe(II) in the EDTA system also preceeds through two simultaneous reaction paths. The maximum in the oxidation rate for the CyDTA system, shown in Fig. 6, indicates the presence of the protonated chelate in a low pH region, though the formation constant of the protonated chelate has not yet been reported. As is clear from the foregoing discussion, the rate equation (2) can be assumed for the oxidation of Fe(II) chelates discussed here:

$$d[Fe(III)]/dt = 4k_p[Fe^{II}HZ][O_2] + 4k_n[Fe^{II}Z][O_2] \quad (2)$$

In Eq. (2), k_p and k_n represent the rate constants of the two oxidation reactions, (3) and (4), respectively:

$$Fe^{II}HZ + O_2 \xrightarrow{k_p} Fe^{III}Z + HO_2 \quad (3)$$

$$Fe^{II}Z + O_2 \xrightarrow{k_n} Fe^{III}Z + O_2^- \quad (4)$$

The first term in the right-hand side of Eq. (2) corresponds to the oxidation of the protonated chelate, and the second, to that of the normal chelate. The k_n value for the oxidation of Fe(II) in the DTPA system can be determined from the reaction rate obtained in the high pH region and the concentration of the corresponding nornal chelate at the pH where the reaction rate is obtained.*3 Thus, using this k_n value, the rate obtained at a low pH, and the concentrations of the protonated and normal chelates, the value can be obtained. For the NTA and the EDTAOH systems, the first term of Eq. (2) can be neglected, so the k_n value can be obtained simply from a comparison of the oxidation rate with the concentration of the normal chelate at a given pH.

The rate-pH curves shown in Fig. 5 (curve a) for the DTPA and in Fig. 6 (curve a') for the EDTA system were calculated by using the k_p and k_n values for the corresponding systems. The agreement between the observed rates and the calculated curves confirms that the proposed rate equation is satisfactory. Such an agreement was also observed in the other systems.

Table 1. Rate constants for the oxidation of Fe(II) chelates and the formation constants of Fe(II) and Fe(III) chelates

Fe(II) chelate	(M^{-1} sec^{-1})	Logarithmic stability constant[9]		
		$K_{Fe^{II}HL}$	$K_{Fe^{II}L}$	$K_{Fe^{III}L}$
FeHEDTA	6.8×10^3	2.8		
FeEDTA	2.7×10^2		14.3	25.1
FeNTA	80		8.8	15.9
FeHDTPA	18	5.4		
FeDTPA	7.0		16.0	27.5
FeEDTAOH	1.0×10^2		12.2	19.8
FeEDTP	90		6.2	14.4
FeCyDTA	89		18.2	29.3

The values of the rate constants for several systems are listed in Table 1, along with the corresponding chelate formation constants for Fe(II) and Fe(III). It is interesting to note here that the rate constant for the oxidation of the normal chelate does not always increase with an increase in the corresponding formation constant of ferric chelate. This is contrary to the findings of King and Davidson for the oxidation of Fe(II)-simple anion systems.[7] The oxidation reaction

*3 The concentration of oxygen in the air-saturated solution in the pH region from 2 to 8 is estimated to be 2.4×10^{-4} M under the present experimental conditions.

9) J. Bjerrum, G. Schwarzenbach and L. G. Sillen, "Stability Constants," Chem. Soc., London (1956); A. Ringbom, "Complexation in Analytical Chemistry," John Wiely and Sons Inc., New York, N. Y. (1963).

of the protonated chelates always proceeds more rapidly than that of the corresponding normal chelates. For example, the rate constant for the oxidation reaction of the protonated Fe(II)-EDTA chelate is about thirty times greater than that of the normal chelate. This suggests that the addition of a proton to the normal chelate makes it liable to oxygen attack.

It may be suggested that the reaction mechanism for the oxidation of Fe(II) by oxygen in the presence of a chelating agent is as follows:

$$Fe^{2+} + HZ \rightleftharpoons Fe^{II}HZ \quad (a)$$

$$+H^+ \uparrow\downarrow -H^+$$

$$Fe^{2+} + Z \rightleftharpoons Fe^{II}Z \quad (b)$$

$$Fe^{II}HZ + O_2 \xrightarrow{k_p} Fe^{III}Z + HO_2 \quad (3)$$

$$Fe^{II}Z + O_2 \xrightarrow{k_n} Fe^{III}Z + O_2^- \quad (4)$$

$$O_2^- + H^+ \rightarrow HO_2 \quad (5)$$

$$Fe(II) + HO_2 + H^+ \rightarrow Fe(III) + H_2O_2 \quad (6)$$

$$Fe(II) + H_2O_2 \rightarrow Fe(III) + OH^- + OH \quad (7)$$

$$Fe(II) + OH \rightarrow Fe(III) + OH^- \quad (8)$$

In these equation, Fe(III) and Fe(II) represent the ferric and ferrous iron species respectively. In the reaction of Fe(II)-EDTA chelates, the mechanism of reactions (3) and (4) may be represented as follows:

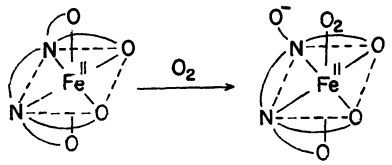

$$+ O_2^- \quad (9)$$

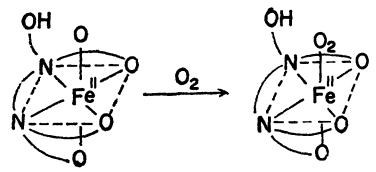

$$+ HO_2 \quad (10)$$

The reaction (9) corresponds to Eq. (4), and the reaction (10), to Eq. (3).

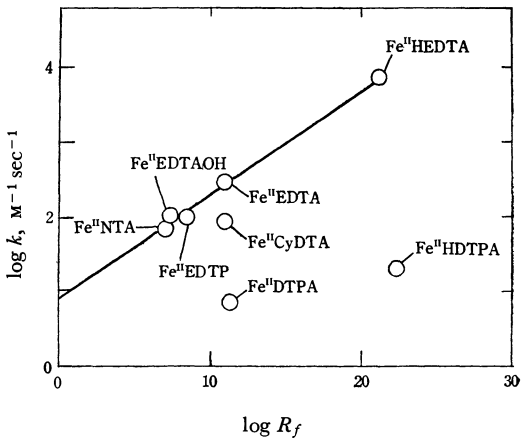

Fig. 7. Relation between log k and log R_f.
k: rate constant for the oxidation of Fe(II) chelate
R_f: $K_{Fe^{III}L}/K_{Fe^{II}L}$*4 for normal chelate
$K_{Fe^{III}L}/K_{Fe^{II}HL}$*4 for protonated chelate

If the relationship between the rate constant for the oxidation of Fe(II) and the formation constants of the chelates of Fe(II) and Fe(III) are examined, in all except a few cases a straight line is obtained, as shown in Fig. 7. Thus, the experimental equation (11) can be obtained from the straight line:

$$\log k = 0.92 + 0.13 \log R_f \quad (11)$$

Then:

$$\log k_x = 0.32 + 0.13 \log R_f \quad (12)$$

where k_x is k_p or k_n and where k is equal to $4k_n$ and R_f, to $K_{Fe^{III}L}/K_{Fe^{II}L}$ in the case of the normal chelate, and where k is equal to $4k_p$ and R_f, to $K_{Fe^{III}L}/K_{Fe^{II}HL}$ in the case of the protonated chelate. Daviation from the straight line is observed in the CyDTA and the DTPA systems. In view of the geometrical structure of these metal chelates, the oxygen attack on them might be restricted by steric hindrance.

If the activation entropies of these reactions are assumed to be identical with each other, a relationship between log k and log R_f can be obtained, as is described below. Equation (13) is obtained on the basis of the above assumption. It represents a linear relationship between standard free energy change, ΔG_0, and the corresponding standard free energy of activation, $\Delta G_0^{\neq}$, in the reactions.

$$\Delta G_0^{\neq} = \alpha + \beta \Delta G_0 \quad (13)$$

where α and β are the constants. The rate constant is given kinetically by the equation:

$$k_x = \frac{kT}{h} \exp(\Delta G_0^{\neq}/RT) \quad (14)$$

*4 $K_{Fe^{III}L}$, $K_{Fe^{II}L}$ and $K_{Fe^{II}HL}$ are the formation constants of normal Fe(III), normal Fe(II) and protonated Fe(II) chelates, respectively.

and the standard free energy change in the reaction is:

$$\Delta G_0 = -FE^0 + RT \ln R_f \quad (15)$$

where F is the Faraday constant and E^0, the standard oxidation potential of Reaction (16):

$$Fe^{2+} = Fe^{3+} + e^- \quad (E^0 = -0.77\ V)^{10)} \quad (16)$$

Combining Eqs. (13), (14), and (15) and by rewriting the resulting equation in logarithmic form, Eq. (17) is obtained:

$$\log k_x = \log \frac{kT}{h} + \frac{1}{2.303RT}\{\beta FE^0 - \alpha\} - \beta \log R_f \quad (17)$$

This equation represents the linear relationship between $\log k_x$ and $\log R_f$. By combining Eqs. (12) and (17), $\alpha = 16$ kcal mol^{-1} and $\beta = -0.13$ are obtained.

For the oxidation of the chelates described here, the straight line shown in Fig. 7 can be obtained, because the activation entropies are approximately identical with each other and because there is a compensation effect[11] between the activation enthalpy, $\Delta H^{\neq}$, and the activation entropy, $\Delta S^{\neq}$. Therefore, the principle of a linear-free energy relation (LFER) appears in the reactions. In the cases of DTPA and CyDTA, an exception is observed, as is shown in Fig. 7. This can be explained by lowering of the oxidation rate due to steric hidrance of the oxygen attack on these chelates.

The authors wish to express their thanks to Professor Yukichi Yoshino and Professor Mutsuo Kodama for their helpful discussions of this work.

10) W. M. Latimar, "The Oxidation Sates of the Elements and their Potentials in Aqueous Solutions," 2nd Ed., Prentice-Hall, New York N. Y. (1952).

11) R. A. Fairclough and C. N. Hinshelwood, *J. Chem. Soc.*, **1937**, 1573.

BULLETIN OF THE CHEMICAL SOCIETY OF JAPAN VOL. 41 2239—2247 (1968)

An Energetic Consideration of the Monomer Reactivity in Catalytic Polymerization

Tsutomu KAGIYA, Yūzō SUMIDA and Tetsuya NAKATA

Faculty of Engineering, Kyoto University, Sakyo-ku, Kyoto

(Received December 29, 1967)

The elementary processes constituting the polymerization reaction are energetically considered, and the relation between the activation energy of each process and the structures of reagents or the kind of solvents is theoretically discussed. The solvation energy of ion has been evaluated with the ionization potential of anion or the electron affinity of cation, and the ionization potential or the electron affinity of the growing radical with that of the corresponding monomer. The energy of the highest occupied ($\varepsilon_{ho}=\alpha+\lambda_{ho}\beta$) or the lowest vacant ($\varepsilon_{lv}=\alpha-\eta_{lv}\beta$) π level of the monomer has been calculated, and the π bond dissociation energy has been evaluated with the summation ($\lambda_{ho}+\eta_{lv}$). On the basis of these considerations, the monomer reactivity in catalytic polymerization can be compared with the relative magnitude of the electronic natures of monomer and components of catalyst, *i. e.*, ionization potential or electron affinity.

In recent years, a number of experimental informations has been accumulated on the polymerization of vinyl compounds. On the basis of the data, Alfrey and Price[1,2] have systematically made a study of the correlations between the monomer reactivities in radical polymerization and the structural factors of vinyl monomers in terms of the empirical values of Q and e. Yonezawa, Fukui and their coworkers,[3-5] from the standpoint of the simple molecular orbital theory, have calculated the stabilization energy arising from π conjugation in the transition state in radical or ionic polymerization of vinyl monomer and the

1) T. Alfrey, Jr. and C. C. Price, *J. Polymer Sci.*, **2**, 101 (1947).
2) G. E. Ham, *ibid.*, **14**, 483 (1954).
3) T. Yonezawa, K. Hayashi, C. Nagata, S. Okamura and K. Fukui, *ibid.*, **14**, 312 (1954).
4) K. Hayashi, T. Yonezawa, C. Nagata, S. Okamura and K. Fukui, *ibid.*, **20**, 537 (1956).
5) T. Yonezawa, T. Higashimura, K. Katagiri, K. Hayashi, S. Okamura and K. Fukui, *ibid.*, **26**, 311 (1957).

localization energy indicating the facility of the initiation reaction in ionic polymerization, and have considered the relation between these characteristic values and the reactivities of monomers.

The latest experimental results, however, have indicated that the monomer reactivity is remarkably affected by the structure of catalyst[6,7] and the nature of solvent.[8,9] Hence it appears that these theories based on the free ion model are insufficient to explain the accumulated experimental data.

The purpose of the work is to study quantitatively the monomer reactivity in catalytic polymerization. The elementary processes constituting the polymerization reaction are energetically considered in connection with the electronic structures of the monomer and the catalyst. On the basis of the conclusion, the monomer reactivity in catalytic polymerization should be correlated with the electronic structures of a monomer and components of catalyst.

Theoretical

(I) The Overall Rate of Polymerization. It is generally assumed that the catalytic polymerization consists of the elementary processes of (i) the formation of the active ion-pair (the initiation), (ii) the monomer addition to the active ion-pair (the propagation), (iii) the formation of the polymer and the active ion-pair (the chain transfer) and (iv) the deactivation of the active ion-pair (the termination). In order to discuss theoretically the monomer reactivity in catalytic polymerization, an energetic consideration was forcused on the first two steps, that is, the initiation and the propagation. Then, the followings are postulated.

(i) The initiation process is that forms the solvated active ion-pair by the reaction of monomer and catalyst.

(ii) The propagation process consists of the formation reaction of the intermediate and its rearrangement reaction to make the chain growth. The former is that to form the complex in which the monomer co-ordinates to the solvated ion-pair nucleophilically and electrophilically. The latter is the unimolecular rearrangement reaction of the complex.

According to the above postulations, the elementary processes controlling the overall polymerization are illustrated by the following models for the anionic polymerization of the vinyl monomer as an example.

Initiation:

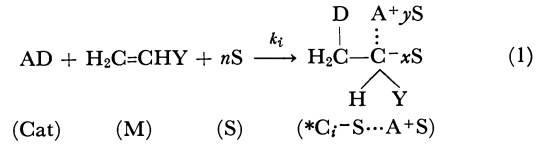

(1)

(Cat) (M) (S) ($*C_i$-S···A^+S)

Propagation:

The formation of the intermediate complex:

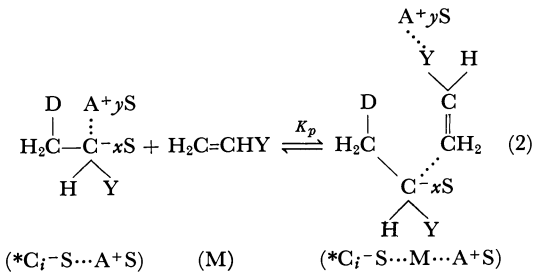

(2)

($*C_i$-S···A^+S) (M) ($*C_i$-S···M···A^+S)

The rearrangement of the intermediate complex:

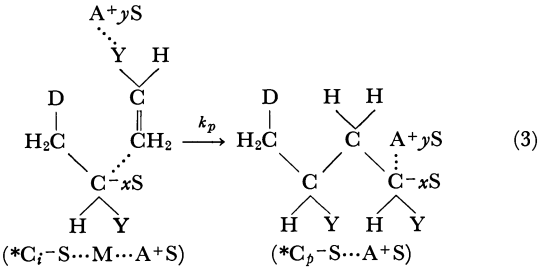

(3)

($*C_i$-S···M···A^+S) ($*C_p$-S···A^+S)

In the above models, AD represents a catalyst, and the conjugated component A is an electron acceptable group and D an electron donative group. The expression in ( ) indicates the abbreviation of the model compound. Where Cat: catalyst, M: monomer, S: solvent, $*C_i$-S···A^+S: initiating active ion-pair solvated, $*C_p$-S···A^+S: propagating active ion-pair solvated, $*C_t$-S···M···A^+S: intermediate complex, Y: electron donative group such as a carbonyl group in the monomer molecule, x and y: the number of solvent molecules solvating to the anion and the cation, and $x+y=n$. k_i and k_p are the rate constants of the initiation and the rearrangement reaction, and K_p the equilibrium constant of the intermediate formation.

Based on the assumption of the first order rate with respect to all components, the rate of consumption of the catalyst is

$$-\frac{d[Cat]}{dt} = k_i[S][M][Cat] \quad (4)$$

Since the concentration of the solvent and the monomer can be regarded as constant in the first stage of the polymerization, the remaining concentration of the catalyst is expressed by Eq. (5),

$$[Cat] = [Cat]_0 e^{-k_i[S][M]t} \quad (5)$$

where $[Cat]_0$ is the initial concentration of the catalyst. While, from the equilibrium reaction (2),

6) Y. Imanishi, T. Higashimura and S. Okamura, *Kobunshi Kagaku (Chemistry of High Polymers)*, **18**, 333 (1961).
7) T. Kagiya, T. Kondo and K. Fukui, This Bulletin, **41**, 2473 (1968).
8) T. Kagiya, T. Shimidzu and K. Fukui, *Shokubai (Catalyst)*, **5**, 304 (1963).
9) H. L. Hsieh, *J. Polymer Sci.*, **A3**, 153 (1965).

$$[*C_i\text{-}S\cdots M\cdots A^+S] = K_p[M] \times ([Cat]_0 - [Cat] - [*C_i\text{-}S\cdots M\cdots A^+S] - [*C_p\text{-}S\cdots A^+S]) \quad (6)$$

In the beginning of the polymerization, the polymer concentration $[*C_p\text{-}S\cdots A^+S] \approx 0$, hence

$$[*C_i\text{-}S\cdots M\cdots A^+S] = \frac{K_p[M][Cat]_0}{1+K_p[M]}(1-e^{-k_i[S][M]t}) \quad (7)$$

In the case of the first order propagation reaction with respect to the intermediate, the overall rate of polymerization is generally given as follows,

$$R = \frac{d[*C_p\text{-}S\cdots A^+S]}{dt} = k_p[*C_i\text{-}S\cdots M\cdots A^+S][M] = \frac{k_pK_p[M][Cat]_0}{1+K_p[M]}(1-e^{-k_i[S][M]t}) \quad (8)$$

It is apparent from Eq. (8) that the overall rate is simplified as follows by the relative magnitude of the K_p value, in both polymerization with the slow initiation ($k_i \ll 1$) and the rapid initiation ($k_i \gg 1$) defined by us previously,[10]

The polymerization with the slow initiation ($k_i \ll 1$):

$$K_p[M] \ll 1 \quad R = k_ik_pK_p[M]^2[S][Cat]_0t \quad (9)$$

$$K_p[M] \gg 1 \quad R = k_ik_p[M][S][Cat]_0t \quad (10)$$

The polymerization with the rapid initiation ($k_i \gg 1$):

$$K_p[M] \ll 1 \quad R = k_pK_p[M][Cat]_0 \quad (11)$$

$$K_p[M] \gg 1 \quad R = k_p[Cat]_0 \quad (12)$$

Equations (9) and (10) in the slow initiation system show that the polymerization rate in the early stage increases with the polymerization time.

Since the equilibrium constant K_p is considered to be small, the overall rate of polymerization can be generally discussed by Eq. (9). The observed specific rate k in the slow initiation system (9) involves that the equilibrium constant of the formation of the intermediate and both rate constants of the formation of the active ion-pair and the rearrangement reaction of the complex.

$$k = k_ik_pK_p \quad (13)$$

(II) An Energetic Study of the Catalytic Polymerization. Based on Eq. (13), the overall activation energy ΔE is given as follows by using each activation energy (ΔE_i, ΔE_p) and the Gibbs' free energy change (ΔG_p) of the reactions,

$$\Delta E = \Delta E_i + \Delta E_p + \Delta G_p \quad (14)$$

In order to evaluate quantitatively the activation energy and the Gibbs' free energy change of each reaction, an energetic study was made as follows.

(a) The Overall Activation Energy of the Initiation Reaction. As shown in Eq. (1), it has been considered in ionic polymerization whether the polymerization takes place by an anionic mechanism (the formation of the D-C covalent bond) or a cationic mechanism (the formation of the A-C covalent bond) is dependent on the relative electronic properties of the catalyst and the monomer.

In order to study energetically the rate of initiation, we assume the following elementary reactions of the initiation for an anionic polymerization as an example,

$$AD \rightarrow A\cdot + D\cdot \quad (i)$$

$$H_2C{=}CHY \rightarrow H_2\dot{C}{-}\dot{C}HY \quad (ii)$$

$$D\cdot + H_2\dot{C}{-}\dot{C}HY \rightarrow H_2C(D){-}\dot{C}HY \quad (iii)$$

$$H_2C(D){-}\dot{C}HY + e \rightarrow H_2C(D){-}C^-(H)(Y) \quad (iv)$$

$$A\cdot \rightarrow A^+ + e \quad (v)$$

$$H_2C(D){-}C^-(H)(Y) + xS \rightarrow H_2C(D){-}C^-(H)(Y)\,xS \quad (vi)$$

$$A^+ + yS \rightarrow A^+yS \quad (vii)$$

$$H_2C(D){-}C^-(H)(Y)\,xS + A^+yS \rightarrow H_2C(D){-}C^-(H)(Y)\,xS \quad (viii)$$

The reactions (i) and (ii) are the bond dissociation of the catalyst AD and the π bond dissociation of the vinyl monomer, and the component radical D· of catalyst combines with the monomer radical to give the polymer end (iii). The growing radical produced by the reaction (iii) and the other component radical A· of catalyst ionize ((iv), (v)) and form the corresponding solvated ions ((vi), (vii)). The two solvated ions having an opposite charge form a solvated ion-pair by an electrostatic force (viii).

According to Polanyi - Horiuchi - Semenov's empirical rule, the overall rate of the growing radical ($H_2DC\text{-}\dot{C}HY$) formation is considered to be large as both of the bond dissociation energy B(A-D) of the A-D bond and the π bond dissociation energy B(C=C) of the monomer are small or as B(D-C) of the $D\text{-}CH_2\dot{C}HY$ large. It is supposed that the reactions (iv) and (v) take place easily when the electron affinity $E_a(*C_i\cdot)$ of the radical $CH_2D\dot{C}HY$ indicated by $*C_i\cdot$ is large and the ionization potential $I_p(A\cdot)$ of a component A· is small, and that the reactions (vi) and (vii) occur facilely

10) T. Kagiya, M. Izu and K. Fukui, This Bulletin, **40**, 1045 (1967).

as the solvation energies, *i.e.*, $-\Delta G_s(*C_i^- \cdots S)$ and $-\Delta G_s(A^+ \cdots S)$, of the growing anion H_2-DCHYC$^-$ indicated by $*C_i^-$ and the counter cation A^+ are large. The two solvated ions having an opposite charge exist usually in the solution as a solvated ion-pair. It is, however, considered that the facility of the polymerization increases with a decrease in the electrostatic energy $-\Delta G_e(*C_i^- S \cdots A^+ S)$ arised between two solvated ions, because the rate of polymerization by a free ion mechanism is larger than that by an ion-pair mechanism.[11]

On the basis of the above considerations, it has been assumed that the activation energy (ΔE_i) of the initiation is expressed as follows, by the use of the free energy changes of these elementary reactions and the electronic natures of the catalyst components,

Anionic Polymerization;

$$\begin{aligned}\Delta E_{i(A)} = {} & c_1 B(\text{A-D}) + c_2 B(\text{C=C}) - c_3 B(\text{D-C}) \\ & + c_4[I_p(\text{A}\cdot) - E_a(*C_i\cdot)] \\ & + c_5[\Delta G_s(*C_i^- \cdots S) + \Delta G_s(A^+ \cdots S)] \\ & - c_6 \Delta G_e(*C_i^- S \cdots A^+ S) \end{aligned} \quad (15)$$

Cationic Polymerization;

$$\begin{aligned}\Delta E_{i(C)} = {} & c_1' B(\text{A-D}) + c_2' B(\text{C=C}) - c_3' B(\text{A-C}) \\ & + c_4'[I_p(*C_i\cdot) - E_a(\text{D}\cdot)] \\ & + c_5'[\Delta G_s(*C_i^+ \cdots S) + \Delta G_s(D^- \cdots S)] \\ & - c_6' \Delta G_e(*C_i^+ S \cdots D^- S) \end{aligned} \quad (16)$$

where $c_1, \cdots, c_6, c_1', \cdots, c_6'$ are the positive constants disregarding the kinds of monomer, catalyst and solvent.

(b) The Overall Activation Energy of the Propagation Reaction. As Eq. (2) shows, the formation reaction of the intermediate complex is that the monomer co-ordinates to the solvated ion-pair nucleophilically and electrophilically. Then, it is considered that the Gibbs' free energy of the co-ordination of the monomer to the growing chain and the counter ions can be estimated with the nucleophilic and electrophilic co-ordination energies and the electrostatic energy of the solvated ion-pair. Therefore, the Gibbs' free energy of the reaction is written as follows,

Anionic Polymerization;

$$\begin{aligned}-\Delta G_{p(A)} = {} & -\Delta G_e(A^+ S \cdots M) \\ & - \Delta G_c(*C_i^- S \cdots M) + \Delta G_e(*C_i^- S \cdots A^+ S) \end{aligned} \quad (17)$$

Cationic Polymerization;

$$\begin{aligned}-\Delta G_{p(C)} = {} & -\Delta G_e(D^- S \cdots M) \\ & - \Delta G_c(*C_i^+ S \cdots M) + \Delta G_e(*C_i^+ S \cdots D^- S) \end{aligned} \quad (18)$$

where $-\Delta G_p$ represents the Gibbs' free energy of the formation reaction of the intermediate and $-\Delta G_c$ the co-ordination energy, and the abbreviation $*C_i^- S \cdots M$ or $*C_i^+ S \cdots M$ indicates the monomer co-ordinating to the solvated growing anion or cation and $A^+ S \cdots M$ or $D^- S \cdots M$ indicates the monomer co-ordinating to the counter cation or anion.

On the other hand, in a similar manner as the initiation reaction, the following elementary reactions of the chain growth reaction of the intermediate for an anionic polymerization as an example were assumed,

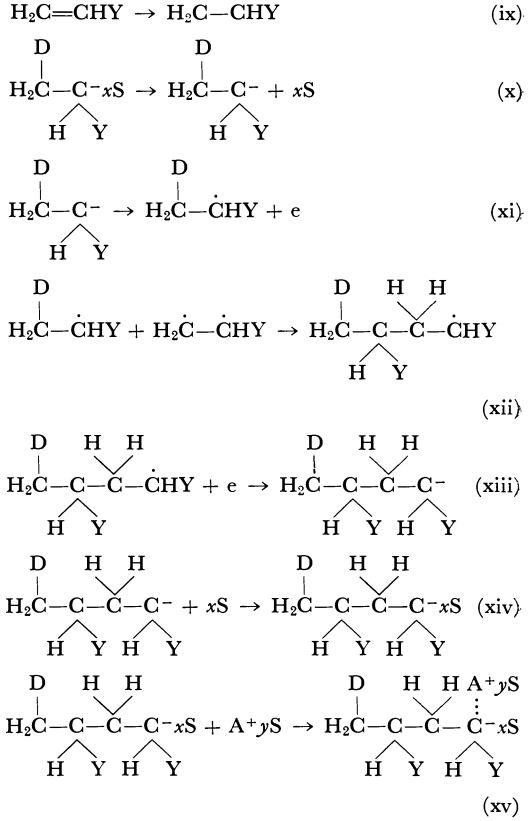

(ix) (x) (xi) (xii) (xiii) (xiv) (xv)

In the above elementary reactions, the reaction (ix) is the π bond dissociation to form the monomer radical, (x) and (xi) are the desolvation of the solvated growing ion and the formation of the growing radical, (xii) is the recombination of the growing radical with the monomer radical to make growth of the chain. The growing radical produced by the reaction (xii) ionizes (xiii) and forms the corresponding solvated ion (xiv), and the two solvated ions having an opposite charge form a solvated ion-pair by an electrostatic force (xv).

In the same way of the initiation reaction, the activation energy (ΔE_p) of the chain growth reaction may be considered to be small as the π bond dissociation energy B(C=C) of monomer is small and the bond dissociation energy B(*C-C) of the

11) D. N. Bhattacharyya, J. Smid and M. Szwarc, *J. Phys. Chem.*, **69**, 612, 624 (1965).

growing radical with the monomer radical large. It is supposed that the reactions (x) and (xi) are easily arised as the desolvation energy $-\Delta G_{ds}$ ($*C_i^- \cdots S$) of the solvated ion $H_2DCHYC^- \cdots xS$ indicated by $*C_i^- \cdots S$ and the ionization potential $I_p(*C_i^-)$ of the ion H_2DCHYC^- are small, and that the reactions (xiii) and (xiv) take place easily when the electron affinity $E_a(*C_p\cdot)$ of the radical $H_2DCHYCH_2CHYC\cdot$ indicated by $*C_p\cdot$ and the solvation energy $-\Delta G_s(*C_p^- \cdots S)$ of the propagating growing ion $H_2DCHYCH_2CHYC^-$ indicated by $*C_p^-$ are large. On the basis of the reason described in the initiation reaction, it is also considered that the rate of polymerization increases with a decrease in the electrostatic energy $-\Delta G_e$-($*C_p^- S \cdots A^+ S$) of (xv) arised between two solvated ions.

On the basis of the above considerations, it has been assumed that the activation energy of the chain growth reaction is expressed as follows,

Anionic Polymerization;

$$\begin{aligned}\Delta E_{p(A)} &= c_7 B(C{=}C) - c_8 B(*C\text{-}C) \\ &\quad - c_9[\Delta G_{ds}(*C_i^- \cdots S) - \Delta G_s(*C_p^- \cdots S)] \\ &\quad + c_{10}[I_p(*C_i^-) - E_a(*C_p\cdot)] \\ &\quad - c_{11}\Delta G_e(*C_p^- S \cdots A^+ S) \end{aligned} \tag{19}$$

Cationic Polymerization;

$$\begin{aligned}\Delta E_{p(C)} &= c_7' B(C{=}C) - c_8' B(*C\text{-}C) \\ &\quad - c_9'[\Delta G_{ds}(*C_i^+ \cdots S) - \Delta G_s(*C_p^+ \cdots S)] \\ &\quad + c_{10}'[I_p(*C_p\cdot) - E_a(*C_i^+)] \\ &\quad - c_{11}'\Delta G_e(*C_p^+ S \cdots D^- S) \end{aligned} \tag{20}$$

where $c_7, \cdots, c_{11}, c_7', \cdots, c_{11}'$ are the positive constants disregarding the kinds of monomer, catalyst and solvent. In Eqs. (19) and (20), the ionization potential $I_p(*C_i^-)$ or the electron affinity $E_a(*C_i^+)$ of the initiating anion or cation is approximately equal to the electron affinity $E_a(*C_p\cdot)$ or the ionization potential $I_p(*C_p\cdot)$ of the propagating radical, respectively. The desolvation energy $-\Delta G_{ds}$-($*C_i^- \cdots S$) or $-\Delta G_{ds}(*C_i^+ \cdots S)$ is also equal to the solvation energy $-\Delta G_s(*C_p^- \cdots S)$ or $-\Delta G_s$-($*C_p^+ \cdots S$). Equations (19) and (20) may, therefore, be written,

Anionic Polymerization;

$$\begin{aligned}\Delta E_{p(A)} &= c_7 B(C{=}C) - c_8 B(*C\text{-}C) \\ &\quad - c_{11}\Delta G_e(*C_p^- S \cdots A^+ S) \end{aligned} \tag{21}$$

Cationic Polymerization;

$$\begin{aligned}\Delta E_{p(C)} &= c_7' B(C{=}C) - c_8' B(*C\text{-}C) \\ &\quad - c_{11}'\Delta G_e(*C_p^+ S \cdots D^- S) \end{aligned} \tag{22}$$

(c) The Overall Activation Energy of the Polymerization. From a series of these energetic considerations, it seems reasonable to conclude that the overall activation energy, in any cases of the slow initiation and the rapid initiation,[10] is expressed as follows by using Eqs. (15)—(22),

The Slow Initiation System (9)

Anionic Polymerization;

$$\begin{aligned}\Delta E_{(A)} &= c_1 B(A\text{-}D) + (c_2 + c_7) B(C{=}C) \\ &\quad - c_3 B(D\text{-}C) - c_8 B(*C\text{-}C) \\ &\quad + c_4[I_p(A\cdot) - E_a(*C_i\cdot)] \\ &\quad + c_5[\Delta G_s(*C_i^- \cdots S) + \Delta G_s(A^+ \cdots S)] \\ &\quad + [\Delta G_c(A^+ S \cdots M) + \Delta G_c(*C_i^- S \cdots M)] \\ &\quad - (c_6 + 1 + c_{11})\Delta G_e(*C_i^- S \cdots A^+ S) \end{aligned} \tag{23}$$

Cationic Polymerization;

$$\begin{aligned}\Delta E_{(C)} &= c_1' B(A\text{-}D) + (c_2' + c_7') B(C{=}C) \\ &\quad - c_3' B(A\text{-}C) - c_8' B(*C\text{-}C) \\ &\quad + c_4'[I_p(*C_i\cdot) - E_a(D\cdot)] \\ &\quad + c_5'[\Delta G_s(*C_i^+ \cdots S) + \Delta G_s(D^- \cdots S)] \\ &\quad + [\Delta G_c(D^- S \cdots M) + \Delta G_c(*C_i^+ S \cdots M)] \\ &\quad - (c_6' + 1 + c_{11}')\Delta G_e(*C_i^+ S \cdots D^- S) \end{aligned} \tag{24}$$

The Rapid Initiation System (11)

Anionic Polymerization;

$$\begin{aligned}\Delta E_{(A)} &= c_7 B(C{=}C) - c_8 B(*C\text{-}C) \\ &\quad + [\Delta G_c(A^+ S \cdots M) + \Delta G_c(*C_i^- S \cdots M)] \\ &\quad - (1 + c_{11})\Delta G_e(*C_i^- S \cdots A^+ S) \end{aligned} \tag{25}$$

Cationic Polymerization;

$$\begin{aligned}\Delta E_{(C)} &= c_7' B(C{=}C) - c_8' B(*C\text{-}C) \\ &\quad + [\Delta G_c(D^- S \cdots M) + \Delta G_c(*C_i^+ S \cdots M)] \\ &\quad - (1 + c_{11}')\Delta G_e(*C_i^+ S \cdots D^- S) \end{aligned} \tag{26}$$

In the above Eqs. (23)—(26), we may regard the value of $B(*C\text{-}C)$ as a constant, because the dissociation energy of the *C-C bond is about 81 ± 3 kcal/mol. And $B(D\text{-}C)$ is constant (83 ± 4 kcal/mol) in the case of CH_3, OCH_3, NH_2 and OH as a component D, and $B(A\text{-}C)$ is constant because the hydrogen atom acts as a component A in the cationic polymerization. $B(A\text{-}D)$ is remarkably affected by the kind of catalyst (Table 1).[12,13] It is obvious in Table 1 that $B(A\text{-}D)$ varies more remarkably with the change in the electron affinity of component D than the ionization potential of component A. Then, it may be allowed that $B(A\text{-}D)$ is tentatively expressed as follows,

$$B(A\text{-}D) = c_{12} + c_{13}E_a(D) + c_{14}I_p(A) \qquad (c_{13} \gg c_{14} > 0) \tag{27}$$

where c_{12}, c_{13} and c_{14} are assumed to be the constants disregarding the kind of catalyst.

Subsequently, we tried to evaluate the solvation energy of ion with its electronic properties. Little information has, however, been reported on the

12) C. J. Schexnayder, Jr., "National Aeronautics and Space Administration, Technical Note," D-1791, Washington (1963).

13) C. T. Mortimer, "Reaction Heats and Bond Strengths," Pergamon, Oxford (1962).

TABLE 1. BOND DISSOCIATION ENERGY OF A–D COMPOUND*1

A	I_p(A), eV	D				
		H	OH	Br	Cl	F
		E_a(D), eV				
		0.7	2.6	3.5	3.8	4.3
H	13.6	103.1	116	86.5	102.0	133.8
Li	5.4	57.6	101.9	100.4	110.3	136.0
Na	5.1	47.2	80.9	88.5	97.7	107.2
K	4.3	42.9	86.0	90.8	101.0	116.9
Rb	4.2	39.2	—	90.5	101.9	119.9
Cs	3.8	41.5	91.0	90.9	101.0	122.8

*1 In units of kcal/mol. Data in Ref. 12 and 13.

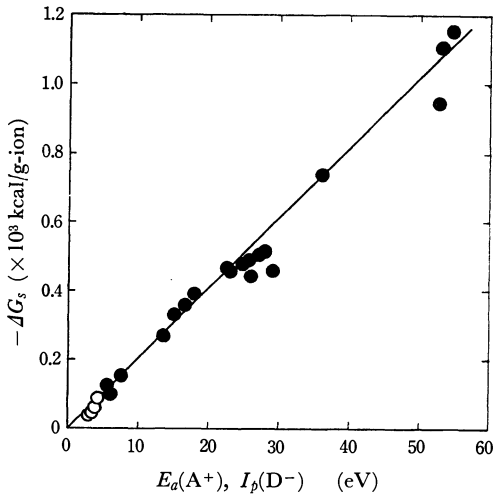

Fig. 1. Relation between the hydration energy ($-\Delta G_s$) of ion and the electron affinity ($E_a(A^+)$) of cation or the ionization potential ($I_p(D^-)$) of anion.
● metal cation, ○ halogen anion

solvation energies of ions determined in the various organic solvents all but water. Then, the plots of the hydration energies of ions[14] against the electron affinities of cations and the ionization potentials of anions were drawn in Fig. 1. In Fig. 1, as an electron affinity of divalent cation, the sum of the first and the second electron affinities was used, which is required to make the radical from the divalent cation. The hydration energy of the metal cation or the halogen anion has a linear relation through an origin with the electron affinity of cation or the ionization potential of anion. If there is a linear free energy relationship between the solvation energy in organic solvent and the hydration energy, the solvation energy of ion is generally expressed as follows,

$$-\Delta G_s(A^+\cdots S) = c_{15}E_a(A^+) + c_{16} \quad (c_{15} > 0) \qquad (28)$$

$$-\Delta G_s(D^-\cdots S) = c_{15}'I_p(D^-) + c_{16}' \quad (c_{15}' > 0) \qquad (29)$$

where c_{15}, c_{16}, c_{15}' and c_{16}' are the constants depending on the kind of solvents.

Moreover, it may be considered that the solvation energy of the polymer chain anion or cation is a constant in the same solvent system in consideration of the sufficient length of the polymer chain.

$$-\Delta G_s(*C_i^-\cdots S) = c_{17} \qquad (30)$$

$$-\Delta G_s(*C_i^+\cdots S) = c_{17}' \qquad (31)$$

On the other hand, it seems reasonable, from a point of quantum chemical view, that the nucleophilicity or the electrophilicity of monomer is approximately estimated by its ionization potential or electron affinity, respectively. That is, the nucleophilicity of monomer increases with a decrease in its ionization potential and the electrophilicity of monomer increases with an increase in its electron affinity. Hence, it is assumed that the co-ordination energy of monomer to ion and the electrostatic energy arised between two solvated ions are tentatively expressed as follows,

$$-\Delta G_c(A^+S\cdots M) = c_{18}E_a(A^+) - c_{19}I_p(M) + c_{20} \quad (c_{18}, c_{19} > 0) \qquad (32)$$

$$-\Delta G_c(D^-S\cdots M) = c_{18}'I_p(D^-) + c_{19}'E_a(M) + c_{20}' \quad (c_{18}', c_{19}' > 0) \qquad (33)$$

$$-\Delta G_c(*C_i^-S\cdots M) = c_{21}E_a(M) + c_{22} \quad (c_{21} > 0) \qquad (34)$$

$$-\Delta G_c(*C_i^+S\cdots M) = -c'_{21}I_p(M) + c_{22}' \quad (c_{21}' > 0) \qquad (35)$$

$$-\Delta G_e(*C_i^-S\cdots A^+S) = c_{23}E_a(A^+) - c_{24}I_p(*C_i^-) + c_{25} \quad (c_{23}, c_{24} > 0) \qquad (36)$$

$$-\Delta G_e(*C_i^+S\cdots D^-S) = -c_{23}'I_p(D^-) + c_{24}'E_a(*C_i^+) + c_{25}' \quad (c_{23}', c_{24}' > 0) \qquad (37)$$

where c_{18},$\cdots$, c_{25}, c_{18}',$\cdots$, c_{25}' are constants. And Eqs. (34) and (35) are simplified by using the relations (30) and (31).

The ionization potential and the electron affinity

14) J. D. Bernal and R. H. Fowler, *J. Chem. Phys.*, **1**, 515 (1933).

of the initiating growing radical can be considered in connection with the electronic porperties of the corresponding monomer. Although these values of all monomers are scarcely available up to the present, it is possible to evaluate those with the method of the molecular orbital theory or using some values relating to those. For instance, the ionization potential and the electron affinity are approximately expressed by the energies of the highest occupied ε_{ho} and the lowest vacant ε_{lv} π orbitals, respectively.

$$\varepsilon_{ho} = \alpha + \lambda_{ho}\beta = -I_p \tag{38}$$

$$\varepsilon_{lv} = \alpha - \eta_{lv}\beta = -E_a \tag{39}$$

(α, β: negative constants)

It is apparent from the above equations that the ionization potential is large as the λ_{ho} value is large, and that the electron affinity is large as the η_{lv} value is small.

The observed ionization potential[15] or the observed electron affinity[16] of the radical is plotted against the λ_{ho} or η_{lv} value of the corresponding monomer (in Figs. 2 and 3). Figure 4 shows the linear relation between the ionization potential of the radical and that of the monomer. From these figures, it is found that the ionization potential or the electron affinity of the initiating radical and

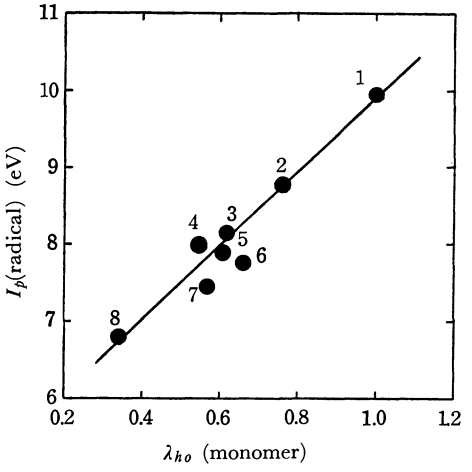

Fig. 2. Relation between the ionization potential of radical and the λ_{ho} value of monomer.
Monomer (radical); (1) CH_2=CH_2 ($\cdot CH_2CH_3$), (2) CH_2=$CHCH_3$ ($\cdot CH_2CH_2CH_3$), (3) CH_2=$CHCH$=CH_2, ($\cdot CH_2CH$=CH_2), (4) CH_2=$C(CH_3)CH$=CH_2 ($\cdot CH_2C(CH_3)$=CH_2), (5) CH_2=$C(CH_3)_2$ ($\cdot CH(CH_3)_2$), (6) CH_2=CH-ϕ ($\cdot CH_2$-ϕ), (7) CH_2=CH-ϕ-p-CH_3 ($\cdot CH_2$-ϕ-p-CH_3), (8) CH_2=CH-ϕ-p-OCH_3 ($\cdot CH_2$-ϕ-p-OCH_3)

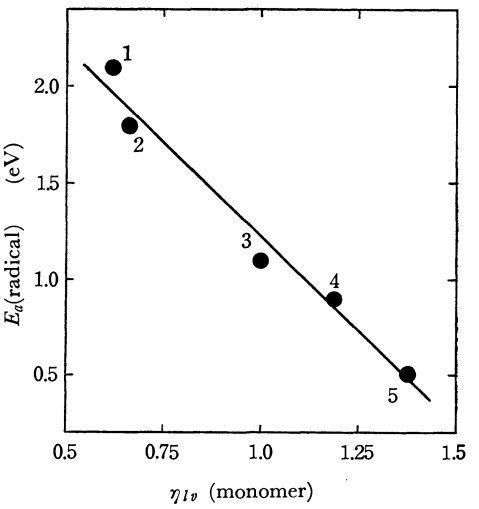

Fig. 3. Relation between the electron affinity of radical and the η_{lv} value of monomer.
Monomer (radical); (1) CH_2=$CHCH$=CH_2 ($\cdot CH_2$-CH=CH_2), (2) CH_2=CH-ϕ ($\cdot CH_2$-ϕ), (3) CH_2=CH_2 ($\cdot CH_3$), (4) CH_2=$CHCH_3$ ($\cdot CH_2CH_3$), (5) CH_2=$C(CH_3)_2$ ($\cdot CH(CH_3)_2$)

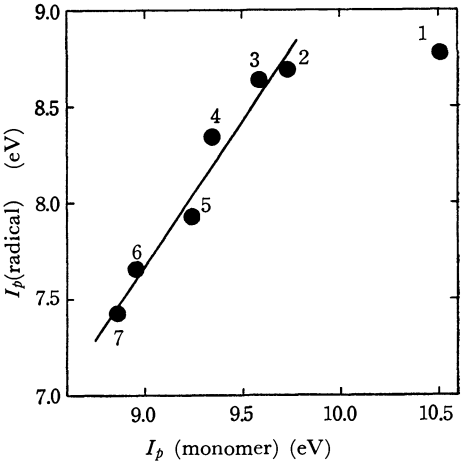

Fig. 4. Comparison of the ionization potential of radical with that of monomer.
Monomer (radical); (1) CH_2=CH_2 ($\cdot CH_2CH_3$), (2) CH_2=$CHCH_3$ ($\cdot CH_2CH_2CH_3$), (3) CH_2=$CHCH_2CH_3$ ($\cdot CH_2CH_2CH_2CH_3$), (4) CH_2=C-$(CH_3)_2$ ($\cdot CH_2CH(CH_3)_2$), (5) CH_3CH=$CHCH_3$ ($\cdot CH(CH_3)CH_2CH_3$), (6) 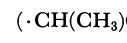 ( ), (7) CH_3CH=$C(CH_3)_2$ ($\cdot CH(CH_3)CH(CH_3)_2$)

ion is expressed by that of the corresponding monomer, as follows,

$$E_a(*C_i\cdot) = I_p(*C_i^-) = c_{26}E_a(M) + c_{27} \quad (c_{26} > 0) \tag{40}$$

$$I_p(*C_i\cdot) = E_a(*C_i^+) = c_{26}'I_p(M) + c_{27}' \quad (c_{26}' > 0) \tag{41}$$

15) A. Streitwieser, Jr., "Progress in Physical Organic Chemistry," Vol. 1, ed. by S. G. Cohen, A. Streitwieser, Jr., and R. W. Taft, Interscience Publishers, New York. N. Y. (1963).
16) H. O. Pritchard, *Chem. Revs.*, **52**, 529 (1953).

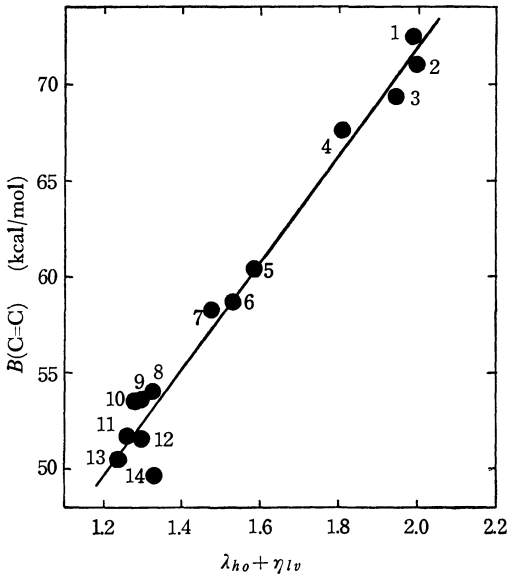

Fig. 5. Relation between the π bond dissociation energy B(C=C) and the $(\lambda_{ho}+\eta_{lv})$ value of monomer.
(1) Isobutylene, (2) Ethylene, (3) Propylene, (4) Vinyl acetate, (5) Methyl vinyl ketone, (6) Methyl acrylate, (7) Acrolein, (8) Styrene, (9) *p*-Methylstyrene, (10) *p*-Chlorostyrene, (11) Acrylonitrile, (12) α-Methylstyrene, (13) Butadiene, (14) Methyl methacrylate

Lastly, we tried to evaluate the π bond dissociation energy B(C=C) of monomer H_2C=CHY with its characteristic values of the electronic structures. The observed values of B(C=C) have, however, been reported. Then, we estimated B(C=C) in term of the localization energy.[17]

$$H_2C{=}CHY \rightarrow H_2\dot{C}\text{-}\dot{C}HY \qquad \text{(ii)}$$

On the assumption that the two odd electrons of the product in the above reaction are the p-electrons, it is considered that B(C=C) may be expressed by the difference between the total energies of the radical and the monomer, as follows,

$$B(\text{C=C}) = \sum_i^{occ} \nu_i \varepsilon_{i(CH_2Y)} + \varepsilon_{(CH_3)} - \sum_j^{occ} \nu_j \varepsilon_{j(CH_2=CHY)} \qquad (42)$$

$$= \sum_i^{occ} \nu_i \lambda_i \beta_{(CH_2Y)} - \sum_j^{occ} \nu_j \lambda_j \beta_{(CH_2=CHY)} \qquad (43)$$

In Eq. (42), the first, the second and the third terms indicate the total energies of π electrons of the radicals CH_2Y and CH_3 and the monomer CH_2=CHY, respectively. Where $\sum^{occ}$ means a summation with respect to the occupied orbitals, ε_i is the π energy of the ith orbital, λ_i the coefficient of β_i in Eq. (38) and ν_i the number of π electron in the ith orbital.

It is found from the results that B(C=C) of monomer CH_2=CHY varies remarkably with the kind of substituent Y. In order to evaluate B(C=C) with its characteristic values, the plots of B(C=C) against the summation $(\lambda_{ho}+\eta_{lv})$ of the coefficinets of β in the highest occupied and the lowest vacant π orbitals of monomer were drawn in Fig. 5. From the linear relationship between B(C=C) and $(\lambda_{ho}+\eta_{lv})$, the π bond dissociation energy may be expressed as follows,

$$B(\text{C=C}) = c_{28}(\lambda_{ho}+\eta_{lv}) + c_{29} \quad (c_{28} > 0) \qquad (44)$$

$$= c_{30}(I_p(\text{M}) - E_a(\text{M})) + c_{31} \quad (c_{30} > 0) \qquad (45)$$

From a series of the above considerations (27)—(45), it is concluded that the overall activation energy of ionic polymerization may be expressed as follows,

The Slow Initiation System (9)
Anionic Polymerization;

$$\Delta E_{(A)} = k_1 + k_2 E_a(\text{D}) \pm k_3 I_p(\text{A}) - k_4 E_a(\text{M}) + k_5 I_p(\text{M}) \qquad (46)$$

Cationic Polymerization;

$$\Delta E_{(C)} = k_1' + k_2' I_p(\text{A}) - k_3' E_a(\text{D}) + k_4' I_p(\text{M}) - k_5' E_a(\text{M}) \qquad (47)$$

where $k_1,\cdots, k_5, k_1',\cdots, k_5'$ are the positive constants. The coefficient of I_p(A) in Eq. (46) represents the term, $(c_4+c_{23}+c_1c_{14}+c_6c_{23}+c_{11}c_{23})-(c_{18}+c_5c_{15})$, and might change in sign since the constants c_{15}, c_{18} and c_{23} are those to depend on the kind of solvent.

The Rapid Initiation System (11)
Anionic Polymerization;

$$\Delta E_{(A)} = k_6 \pm k_7 I_p(\text{A}) - k_8 E_a(\text{M}) + k_9 I_p(\text{M}) \qquad (48)$$

Cationic Polymerization;

$$\Delta E_{(C)} = k_6' - k_7' E_a(\text{D}) + k_8' I_p(\text{M}) - k_9' E_a(\text{M}) \qquad (49)$$

where $k_6,\cdots, k_9, k_6',\cdots, k_9'$ are the positive constants and the coefficient of I_p(A) in Eq. (48) might change in sign by the kind of solvent.

In the polymerization that the contribution to the activation energy of the monomer co-ordination to the growing ion is larger than that to the counter ion, these equations lead to the reasonable conclusion that the monomer reactivity in anionic polymerization increases as the electron affinity of the monomer increases, and that in cationic polymerization increases as the ionization potential of

17) G. W. Wheland, *J. Am. Chem. Soc.*, **64**, 900 (1942).

the monomer decreases.*1 On the attention to the catalyst in the polymerization of the same monomer, the catalytic activity in anionic polymerization increases as the electron affinity of component D decreases, whereas that in cationic polymerization increases as the electron affinity of D increases and as the ionization potential of A decreases.

On the basis of these energetic considerations, the monomer reactivity and the catalytic activity will be quantitatively discussed in the subsequent paper.

The authors are grateful to Professor Kenichi Fukui and Professor Teijiro Yonezawa for their valuable suggestions while carrying out this study.

*1 As Eq. (41) shows, $I_p(M)$ is positively proportional to $I_p(*C_i\cdot)$. It is found in a homologous series that there exists the positive linear relation between $I_p(*C_i\cdot)$ and $I_p(*C_i^-)$, *cf.*, $I_p(*C_i\cdot)$ and $I_p(*C_i^-)$ for the alkyl radicals are in units of eV 9.95 and 1.1 for methyl, 8.78 and 0.9 for ethyl, 8.69 and 0.8 for *n*-propyl, 8.64 and 0.65 for *n*-butyl, and 7.90 and 0.5 for isopropyl radical. According to this relation, the activation energy of the anionic polymerization is given as follows, $\Delta E_{(A)}=k_{10}-k_{11}E_a(M)+k_{12}I_p(*C_i^-)$. This equation indicates that the activation energy of the anionic polymerization decreases as the electron affinity of monomer is large and the ionization potential of the corresponding growing anion is small, in other words, that it is dominated with the energetic difference between the lowest vacant level of monomer and the highest occupied level of the growing anion. Similarly, the activation energy of the cationic polymerization is given as follows, $\Delta E_{(C)}=k_{10}'+k_{11}'I_p(M)-k_{12}'E_a(*C_i^+)$, and it is dominated with the energetic difference between the highest occupied level of monomer and the lowest vacant level of the growing cation. In words of the quantum chemical view, the concept that one may discuss the reactivity of monomer in ionic polymerization with the relative difference of the electronic states between the monomer and the growing ion, can be considered to correspond to the treatment of the zero-order perturbation.

BULLETIN OF THE CHEMICAL SOCIETY OF JAPAN VOL. 41 2247—2253 (1968)

A Structural Study on the Catalytic Activity in Ionic Polymerization

Tsutomu KAGIYA, Yūzō SUMIDA and Tetsuya NAKATA

Faculty of Engineering, Kyoto University, Sakyo-ku, Kyoto

(Received December 29, 1967)

According to the theoretical conclusion reported previously on the activation energy of the catalytic polymerization, the experimental results relating to the monomer reactivity and the catalytic activity in anionic or cationic polymerization were interpreted. The catalytic activity in ionic polymerization can be quantitatively compared with the relative magnitude of the ionization potential or the electron affinity of monomer and components (A, D) of catalyst (AD). As a measure of the ionization potential or the electron affinity of monomer, the energy of the highest occupied ($\varepsilon_{ho}=\alpha+\lambda_{ho}\beta$) or the lowest vacant ($\varepsilon_{lv}=\alpha-\eta_{lv}\beta$) π level of the monomer has been used, and as a measure of the electron affinity of component D, the pK_a of the acid HD or the σ_I value. In anionic polymerization, it was found that the polymerization by the catalyst with the same component A took place only in the combination of the monomer and the catalyst in which the η_{lv}/pK_a value was less than about 2.5×10^{-2}, and that the catalytic activity, with the same component D, depends on the kind of solvent. The results in cationic polymerization were also discussed in connection with the electron affinity of component D or co-catalyst. And the monomer reactivity in ionic polymerization with the same catalyst was quantitatively discussed with the η_{lv} or λ_{ho} value of monomer. From the accordance between the theoretical consideration and the experimental data, the present treatment was found to be useful for the purpose of the quantitative study of the catalytic activity and the monomer reactivity in ionic polymerization.

In the past ten years, many works on ionic polymerization have been accumulated. Little attention has, however, been paid to the relation between the catalytic activity and the structure of the catalyst.

In the previous paper,[1] the authors made a study on the energetic consideration of ionic polymerization and reported that the monomer reactivity could be compared with the relative magnitude of the electronic natures of monomer and catalyst components.

1) T. Kagiya, Y. Sumida and T. Nakata, This Bulletin, **41**, 2239 (1968).

The purpose of this paper is to determine the relation between the catalytic activity and the structure of the catalyst on the basis of the energetic study reported previously. It was found that the relative magnitude of the catalytic activity is closely related to the electronic structures of catalyst and monomer. The theoretical treatment was found to be useful for the purpose of a systematical interpretation of many kinds of experimental results.

Theoretical

As have been described in the previous paper,[1] the overall activation energy of ionic polymerization with the slow or the rapid initiation[2] is expressed as follows,

The Slow Inititation System
Anionic Polymerization;

$$\Delta E_{(A)} = k_1 + k_2 E_a(\mathrm{D}) \pm k_3 I_p(\mathrm{A}) - k_4 E_a(\mathrm{M}) + k_5 I_p(\mathrm{M}) \quad (1)$$

Cationic Polymerization;

$$\Delta E_{(C)} = k_1' - k_2' E_a(\mathrm{D}) + k_3' I_p(\mathrm{A}) + k_4' I_p(\mathrm{M}) - k_5' E_a(\mathrm{M}) \quad (2)$$

The Rapid Initiation System
Anionic Polymerization;

$$\Delta E_{(A)} = k_6 \pm k_7 I_p(\mathrm{A}) - k_8 E_a(\mathrm{M}) + k_5 I_p(\mathrm{M}) \quad (3)$$

Cationic Polymerization;

$$\Delta E_{(C)} = k_6' - k_7' E_a(\mathrm{D}) + k_8' I_p(\mathrm{M}) - k_5' E_a(\mathrm{M}) \quad (4)$$

where $k_1, \cdots, k_8, k_1', \cdots, k_8'$ are the positive constants. k_3 and k_7 depend on the kind of solvents. M: monomer, AD: catalyst, D: conjugated component acting as the electron donor, A: conjugated component acting as the electron acceptor. E_a and I_p are an electron affinity and an ionization potential, respectively. In the polymeriaztion that the contribution to the activation energy of the monomer co-ordination to the growing ion is larger than that to the counter ion, the last terms in these equations (1)—(4) contribute less to the change in the overall activation energy of the polymerization.

According to the energetic consideration of the catalytic polymerization, the catalyst give mainly an effect on the initiation and propagation reactions.[1,3] And, since the activation energy of the initiation reaction is larger than that of the propagation in the polymerization with the slow initiation, the overall catalytic activity can be discussed quantitatively with Eqs. (1) and (2). It is evident from Eqs. (1) and (2) that the overall activation energy of the anionic polymerization decreases as the electron affinity of D decreases, whereas that of the cationic polymerization decreases as that of D increases. The electron accepting component A of the catalyst is usually a metal or hydrogen atom, and the data of the ionization potentials of their compounds have been reported, while those of the electron affinities of D have not.

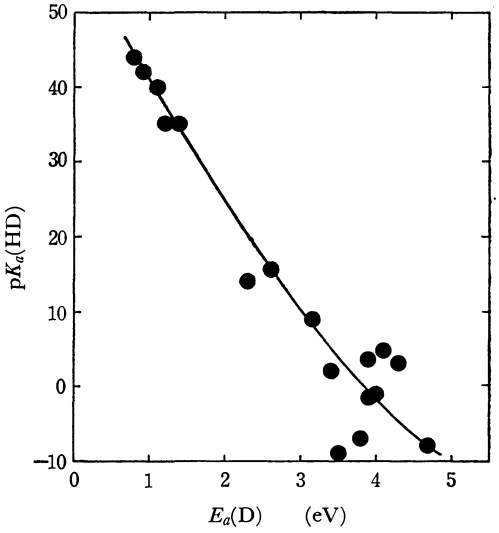

Fig. 1. Relation between the electron affinity of component D and the pK_a value of the conjugated acid HD.

In order to evaluate the electron affinity of D with the parameter corresponding to it, the relation between the E_a(D) value and the pK_a value of the conjugated acid HD[4,5] was investigated as shown in Fig. 1. E_a(D) can be approximately evaluated with pK_a(HD) as follows,

$$E_a(\mathrm{D}) = -k_9 \mathrm{p}K_a(\mathrm{HD}) + k_{10} \quad (k_9 > 0) \quad (5)$$

Therefore, the overall activation energy of the polymerization with the slow initiation by the catalyst with the same component A is given as follows, neglecting the last terms,

$$\Delta E_{(A)} = k_{11} - k_{12} \mathrm{p}K_a(\mathrm{HD}) - k_4 E_a(\mathrm{M}) \quad (6)$$

$$\Delta E_{(C)} = k_{11}' + k_{12}' \mathrm{p}K_a(\mathrm{HD}) + k_4' I_p(\mathrm{M}) \quad (7)$$

where k_{11}, k_{12}, k_{11}' and k_{12}' are constants.

Since the electron affinity of D is one of the measures of the electron withdrawing character of D, it is considered to be related to the inductive substituent constant σ_I. Figure 2 shows the relation between them. In a similar manner as described above, the overall activation energy can

2) T. Kagiya, M. Izu and K. Fukui, *ibid.*, **40**, 1045 (1967).
3) T. Kagiya, T. Kondo and K. Fukui, This Bulletin in press.
4) D. J. Cram, "Fundamentals of Carbanion Chemstry," Academic Press, New York and London (1965), pp. 4—19.
5) A. Albert and E. P. Serjeant, "Ionization Constants of Acids and Bases," First Edition, Methuen & Co., Ltd. (1962).

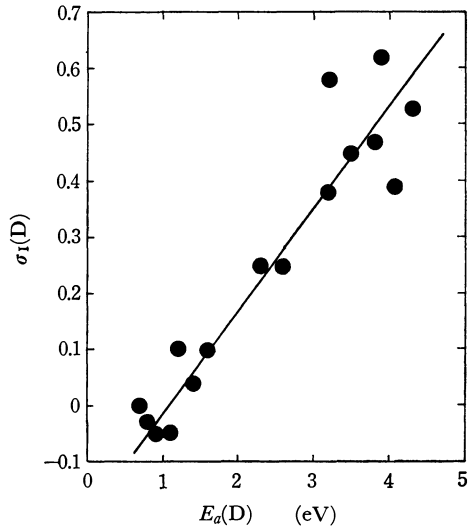

Fig. 2. Relation between the electron affinity of component D and the inductive substituent constant σ_I.

be expressed by the following equations, neglecting the last terms, instead of Eqs. (1) and (2),

$$\Delta E_{(A)} = k_{13} + k_{14}\sigma_I(D) - k_4 E_a(M) \quad (k_{14}>0) \tag{8}$$

$$\Delta E_{(C)} = k_{13}' - k_{14}'\sigma_I(D) + k_4' I_p(M) \quad (k_{14}'>0) \tag{9}$$

where k_{13}, k_{14}, k_{13}' and k_{14}' are constants.

The Eqs. (1)—(9) were used to discuss whether a certain compound in connection with the structures of catalyst and monomer has a catalytic activity or not.

Interpretation of Experimental Data

Monomer Reactivity and Catalytic Activity in Anionic Polymerization. As have been described in the preceding chapter, the monomer reactivity and the catalytic activity in anionic polymerization can be compared with the electron affinity of monomer and catalyst component D. Little information has, however, been reported on the electron affinities of various monomers except those of some components D. Then, as described in the previous paper,[1] the η_{lv} values of vinyl monomers were calculated as the parameter relating to the electron affinity and the results were summarized in Table 1 in the order of the smaller value. The observed half wave reduction potential[6] relating to the electron affinity is also tabulated in Table 1.

There is a general tendency that the monomer polymerizes more easily as its η_{lv} value is small, and that the order of the monomer reactivity is nearly in accordance with the empirical informations. In order to discuss quantitatively this fact, Fig. 3 was drawn. The half wave reduction potential was adopted as a measure of the electron affinity, and the reactivity[7] of monomer with the CH_3O^- or n-$C_{12}H_{25}S^-$ anion as its reactivity in anionic polymerization.

Table 1. Monomer reactivity in anionic polymerization and energy of the lowest vacant π level of monomer

Monomer	*1	η_{lv}*2	$-E_{1/2}$*3
CH_2=CH-C$_6$H$_4$-NO_2	+	0.2658	
CH_2=$CHNO_2$	+	0.2714	
CH_2=$C(CN)_2$	+	0.3106	
CH_2=CHCHO	+	0.3147	(2.50)*4
CH_2=$C(COOCH_3)_2$	+	0.3346	
CH_2=CH-C$_6$H$_4$-CN	+	0.3845	
CH_2=CHCN	+	0.4065	2.90
CH_2=$C(CH_3)$CN	+	0.4311	3.13
CH_2=$CHCOCH_3$	+	0.4476	(2.65)*4
CH_2=$CHCOOCH_3$	+	0.4527	2.95
CH_2=$C(CH_3)COOCH_3$	+	0.4872	3.07
CH_3CH=CHCHO	+	0.4917	
CH_2=CH-C$_5$H$_4$N	+	0.5709	
CH_2=$CHCH=CH_2$	+	0.6180	3.27
CH_2=CH-C$_6$H$_5$	+	0.6622	3.19
CH_2=CH-C$_6$H$_4$-Cl	−	0.6742	
CH_2=CH-C$_6$H$_4$-Br	−	0.6769	
CH_2=CH-C$_6$H$_4$-OCH_3	−	0.7065	
CH_2=$C(CH_3)$-C$_6$H$_5$	+	0.7163	
CH_2=CHCl	−	0.8556	no wave
CH_2=$CHOCOCH_3$	−	0.9581	no wave
CH_2=CHS-C$_6$H$_5$	−	0.9600	
CH_2=CH_2	+	1.0000	
CH_2=$CHOCH_3$	−	1.1175	
CH_2=$CHCH_3$	?	1.1838	
CH_2=$C(CH_3)_2$	−	1.3808	

*1 + and − indicate the occurrence and the nonoccurrence of the anionic polymerization.
*2 η_{lv} is the coefficient of the energy of the lowest vacant π level, $\varepsilon_{lv}=\alpha-\eta_{lv}\beta$.
*3 $-E_{1/2}$ is the half wave reduction potential in units of eV. Data in Ref. 6.
*4 An approximate value.

6) N. Yamazaki, I. Tanaka and S. Nakahama, paper presented at the 16th Symposium on Polymer Chemistry, Kyushu, October 1967, preprint, p. 91.

7) Y. Yasuda and T. Tsuruta, paper presented at the 16th Symposium on Polymer Chemistry, Kyushu, October 1967, preprint, p. 105.

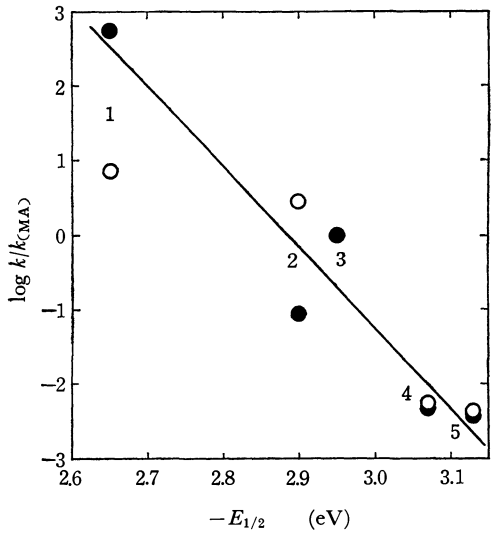

Fig. 3. Relation between the reactivity of monomer with CH_3^- or n-$C_{12}H_{25}S^-$ anion and the half wave reduction potential of monomer.
○ CH_3O^-, ● n-$C_{12}H_{25}S^-$
(1) Methyl vinyl ketone, (2) Acrylonitrile, (3) Methyl acrylate, (4) Methyl methacrylate, (5) Methacrylonitrile

On the other hand, Higginson *et al.*[8] studied the reactivity of some vinyl monomers catalysed by the sodium salts of various weak acids and pointed out that the occurrence of the polymerization had some relations to the pK_a of the original acids and the color resulting from the addition of the catalyst into the monomer.

In Eq. (6), the overall activation energy of anionic polymerization with the same component A is given by the following equation,

$$\Delta E_{(A)} = k_{15} - k_{12}pK_a(HD) + k_{16}\eta_{lv}(M) \quad (k_{12},\ k_{16}>0) \quad (10)$$

In order to discuss the catalytic activity in connection with the property of monomer, it is necessary to claculate the value of $(-k_{12}pK_a(HD)+k_{16}\eta_{lv}(M))$. This value, however, cannot be calculated in practice. Then the η_{lv}/pK_a value was examined here and summarized in Table 2. Table 2 shows that the polymerization occurs in the combination of the monomer and the catalyst in which the η_{lv}/pK_a value is less than about 2.5×10^{-2}.

Tsuruta *et al.*[9] discussed the possibility of the anionic polymerization in connection with the structures of monomer and catalyst as shown in Table 3. In Table 3, (a) group of catalyst gives the polymer of the monomer in group (A), (B) and (C), (b) group (B) and (C) groups but not (A), and (c) group (C) group but not (A) and (B) groups. In order to study the result by using the above conclusion, the η_{lv}/pK_a values have been calculated. The results obtained also indicate that the polymerization takes place only in the combination of the catalyst and the monomer in which the η_{lv}/pK_a value is less than about 2.5×10^{-2}. It is concluded from the above facts that η_{lv}/pK_a value is an important parameter for evaluation of the catalytic activity in anionic polymerizations.

It is also considered that the analogous condition described above is preserved in the propagation reaction in anionic polymerization. In order to examine this inference, the η_{lv}/pK_a value was calculated as to the several vinyl monomers, where CH_3Y may be considered to be employed as the conjugated acid CH_2DCHY - CH_2CH_2Y of the propagating anion CH_2DCHY - CH_2C^-HY of the monomer CH_2=CHY. It is apparent in Table 4 that the η_{lv}/pK_a parameter is a good index to predict the occurrence of the anionic polymerizations.

Szwarc *et al.*[10] studied the anionic polymerization of styrene in tetrahydrofuran and in dioxane, and observed that the rate of propagation is dependent on the kind of counter ions and the nature of solvents. This result may be also discussed by Eq. (3). In the case of the same monomer and the

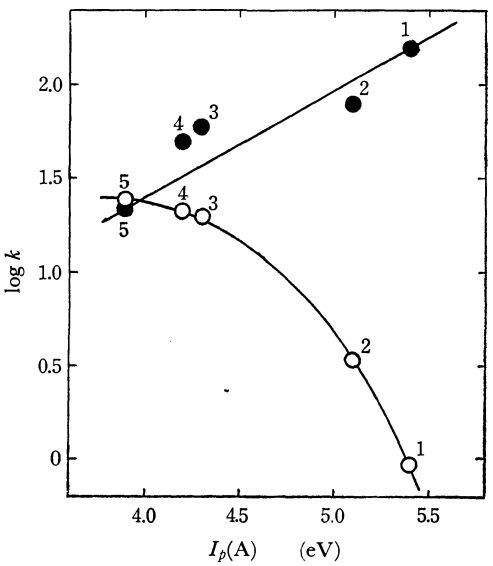

Fig. 4. Effect of the ionization potential of counter metal on the rate constant of propagation in anionic polymerization of styrene.
●, tetrahydrofuran; ○, dioxane.
(1) Li, (2) Na, (3) K, (4) Rb, (5) Cs

8) N. S. Wooding and W. C. Higginson, *J. Chem. Soc.*, **1952**, 774.
9) T. Tsuruta, "Atarashii Kobunshi Gosei Kagaku (Kagaku Zokan 13)," ed. by E. Imoto, M. Imoto, R. Oda, S. Kambara, J. Furukawa and S. Murahashi, Kagaku Dojin (1964), p. 109.
10) D. N. Bhattacharyya, J. Smid and M. Szwarc, *J. Phys. Chem.*, **69**, 612, 624 (1965).

TABLE 2. THE RATIO OF THE η_{lv} VALUE OF THE ENERGY OF THE LOWEST VACANT π LEVEL OF MONOMER TO THE pK_a VALUE OF THE ORIGINAL ACID OF THE CATALYST

Original acid	pK_a	Cloro of anion	$\eta_{lv}/pK_a \times 10^2$ *		
			Acrylonitrile $\eta_{lv}=0.4065$	Methyl methacrylate $\eta_{lv}=0.4872$	Styrene $\eta_{lv}=0.6622$
Methanol	16	Colorless	+ 2.54	− 3.05	− 4.14
Ethanol	18	Colorless	+ 2.26	− 2.71	− 3.68
Acetophenone	19	Yellow	+ 2.14	− 2.57	− 3.48
Triphenylcarbinol	19	Green	+ 2.14	− 2.57	− 3.48
Indene	21	Yellow	+ 1.94	+ 2.32	− 3.16
Phenylacetylene	21	Colorless	+ 1.94	+ 2.32	− 3.16
Diphenylamine	23	Colorless	+ 1.77	+ 2.12	− 2.88
Fluorene	25	Red	+ 1.63	+ 1.95	− 2.65
Acetylene	26	Colorless	+ 1.56	+ 1.87	− 2.55
Aniline	27	Colorless	+ 1.50	+ 1.81	+ 2.45
p-Methoxyaniline	27	Colorless	+ 1.50	+ 1.81	+ 2.45
Xanthen	29	Red	+ 1.40	+ 1.68	+ 2.28
Triphenylmethane	33	Red	+ 1.23	+ 1.48	+ 2.01
Ammonia	35	Colorless	+ 1.16	+ 1.39	+ 1.89

* + indicates the formation of polymer, − indicates the absence of polymer.

TABLE 3. THE RATIO OF THE η_{lv} VALUE OF THE ENERGY OF THE LOWEST VACANT π LEVEL OF MONOMER TO THE pK_a VALUE OF THE CONJUGATED ACID OF THE CATALYST

Catalyst	Conjugated acid	pK_a*1	$\eta_{lv}/pK_a \times 10^2$	Monomer	η_{lv}*2
(a) NaR	RH	35	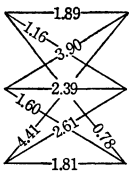	(A) $CH_2=CH-C_6H_5$	0.6622
(b) NaOR	ROH	17		(B) $CH_2=CHCN$	0.4065
(c) (H_2O)	H_2O	15		(C) $CH_2=CHNO_2$	0.2714

*1 Data of Refs. 4 and 5.
*2 η_{lv} is the coefficient of the energy of the lowest vacant π level, $\varepsilon_{lv}=\alpha-\eta_{lv}\beta$.

TABLE 4. THE η_{lv} VALUE OF THE ENERGY OF THE LOWEST VACANT π LEVEL OF MONOMER AND THE pK_a VALUE OF THE CONJUGATED ACID

Monomer	η_{lv}*1	Conjugated acid	pK_a*2	*3	$\eta_{lv}/pK_a \times 10^2$
$CH_2=CHNO_2$	0.2714	CH_3NO_2	11	+	2.47
$CH_2=C(CN)_2$	0.3106	$CH_2(CN)_2$	12	+	2.59
$CH_2=CHCHO$	0.3147	CH_3CHO	14.5	+	2.17
$CH_2=C(COOCH_3)_2$	0.3346	$CH_2(COOCH_3)_2$	13.3	+	2.52
$CH_2=CHCN$	0.4065	CH_3CN	25	+	1.63
$CH_2=CHCOCH_3$	0.4476	CH_3COCH_3	20	+	2.24
$CH_2=CHCOOCH_3$	0.4527	CH_3COOCH_3	24.5	+	1.85
$CH_2=CH-C_6H_5$	0.6622	$CH_3-C_6H_5$	35	+	1.89
$CH_2=CHCl$	0.8556	CH_3Cl	22	−	3.89
$CH_2=CHOCOCH_3$	0.9581	CH_3OCOCH_3	24.5	−	3.91
$CH_2=CH_2$	1.0000	CH_4	40	+	2.50
$CH_2=CHCH_3$	1.1838	CH_3CH_3	42	?	2.81
$CH_2=C(CH_3)_2$	1.3808	$CH_3CH_2CH_3$	44	−	3.14

*1 η_{lv} is the coefficient of the energy of the lowest vacant π level, $\varepsilon_{lv}=\alpha-\eta_{lv}\beta$.
*2 Data of Refs. 4 and 5.
*3 + and − indicate the occurrence and the nonoccurrence of the anionic polymerization.

same conjugated component D of catalyst, Eq. (3) may be written as follows,

$$\log k = k_{17} \pm k_{18} I_p(\mathrm{A}) \quad (k_{18} > 0) \qquad (11)$$

where k is a rate constant of the propagation reaction, k_{17} and k_{18} are constants, and k_{18} depends on the kind of solvent. Figure 4 indicates that Eq. (11) can approximately express the change of the propagation rate with the counter metals.

Monomer Reactivity and Catalytic Activity in Cationic Polymerization. As the same manner, the λ_{ho} values of various vinyl monomers were calculated in the order of the smaller value as shown in Table 5. There is a general tendency that the monomer polymerizes more easily as its λ_{ho} value is smaller, and that the monomer whose ionization potential[11-14] is larger than about 10.2 eV occurs no longer a cationic polymerization. The order of the monomer reactivity is nearly in accordance with the empirical informations. Figure 5 shows the relation between the rate constant of propagation in the cationic polymerization of the styrene derivatives[15] and their ionization potentials.[11] These results also lead to the conclusion that the quantitative treatment in the previous paper[1] represents satisfactorily many experimental data on the monomer reactivity in the cationic polymerization.

TABLE 5. MONOMER REACTIVITY IN CATIONIC POLYMERIZATION AND ENERGY OF THE HIGHEST OCCUPIED π LEVEL OF MONOMER

Monomer	*1	λ_{ho}*2	$-I_p$*3
CH_2=CH-C$_6$H$_4$-OCH_3	+	0.3424	7.92
CH_2=$CHOCH_3$	+	0.3542	9.97
CH_2=$C(CH_3)CH$=CH_2	+	0.5460	8.86
CH_2=CHS-C$_6$H$_5$	+	0.5654	
CH_2=$C(CH_3)$-C$_6$H$_5$	+	0.5793	(8.2)*4
CH_2=CH-C$_6$H$_4$-CH_3	+	0.5793	8.20
CH_2=CH-C$_6$H$_4$-Br	+	0.5875	
CH_2=CH-C$_6$H$_4$-Cl	+	0.6051	8.47
CH_2=$C(CH_3)_2$	+	0.6082	9.35
CH_2=$CHCH$=CH_2	+	0.6180	9.07
CH_2=CH-C$_6$H$_5$	+	0.6622	8.47
CH_2=CH-C$_5$H$_4$N	−	0.7176	
CH_2=$C(CH_3)CN$	−	0.7202	(10.5)*4
CH_2=$CHCH_3$	+	0.7632	9.70
CH_2=$CHOCOCH_3$	−	0.8500	(10.5)*4
CH_2=CHCN	−	0.8547	10.75
CH_2=CHCl	−	0.9420	10.39
CH_3CH=CHCHO	+	0.9905	9.73
CH_2=$CHCOOCH_3$	−	1.0774	(10.7)*4
CH_2=$CHCOCH_3$	+	1.1368	(10.2)*4
CH_2=CHCHO	+	1.1607	10.10

*1 + and − indicate the occurrence and the non-occurrence of the cationic polymerization.
*2 λ_{ho} is the coefficient of the energy of the highest occupied π level, $\varepsilon_{ho} = \alpha + \lambda_{ho}\beta$.
*3 I_p is the ionization potential in units of eV. Data in Refs. 11, 12, 13 and 14.
*4 An approximate value.

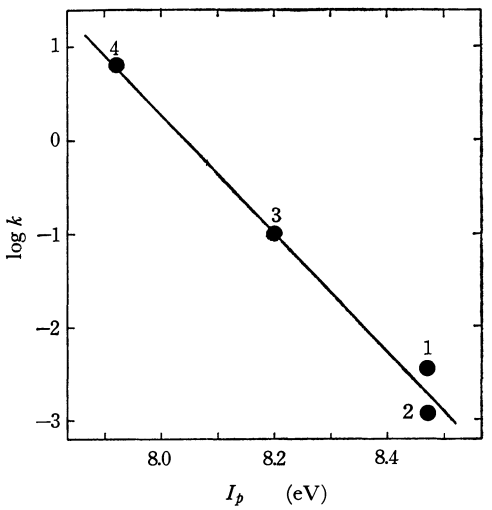

Fig. 5. Relation between the rate constant of propagation in cationic polymerization of styrene derivative and its ionization potential.
(1) Styrene, (2) *p*-Chlorostyrene,
(3) *p*-Methylstyrene, (4) *p*-Methoxystyrene

On the other hand, Yokota *et al.*[16] studied the kinetics of the polymerization of formaldehyde by the various proton acids in liquid carbon dioxide, and reported that this polymerization belonged to a type of the stationary successive with the rapid initiation[2] and the catalytic activity was remarkably changed by the kind of counter anions. Substituting Eq. (5) into Eq. (4), it is expected that the following relation exists between the rate of polymerization and the pK_a value of the acid of the catalyst,

$$\log R = k_{19} - k_{20} \mathrm{p}K_a(\mathrm{HD}) \quad (k_{20} > 0) \qquad (12)$$

where R is a rate of polymerization, k_{19} and k_{20}

11) N. Tamura, M. Hatano and S. Kambara, paper presented at the 20th Annual Meeting of the Chemical Society of Japan, Tokyo, March 1967, preprint IV, p. 277.
12) K. Watanabe, *J. Chem. Phys.*, **26**, 542 (1957).
13) K. Watanabe, T. Nakayama and J. Mottl, "Final Report on Ionization Potentials of Molecules by a Photoionization Method," December, 1959, Dept. Army No. 5B-99-01-004, ORD TB2-0001-OOR-1624.
14) A. Streitwieser, *J. Am. Chem. Soc.*, **82**, 4123 (1960).
15) N. Kanoh, T. Higashimura and S. Okamura, *Makromol. Chem.*, **56**, 65 (1962).
16) H. Yokota and M. Kondo, *J. Polymer Sci., Part A*, in press.

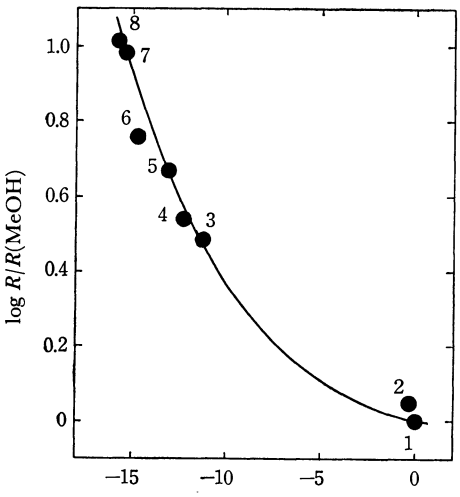

Fig. 6. Effect of the pK_a value of catalyst on the rate of cationic polymerization of formaldehyde. (1) Methanol, (2) Water, (3) Acetic acid, (4) Formic acid, (5) Monochloroacetic acid, (6) Dichloroacetic acid, (7) Trichloroacetic acid, (8) Trifluoroacetic acid.

are constants. As shown in Fig. 6, the relation (12), that is, Eq. (4) holds good in the cationic polymerization.

In both of the cationic polymerization of styrene catalysed by Lewis acids[17] and the racemization of 1-phenylethyl chloride,[18] the cationic activity of Lewis acids is in the order as follows,

$$\underset{(252)}{SbCl_5} \gg \underset{(175)}{TiCl_4} > \underset{(163)}{AlBr_3} > \underset{(133)}{SnCl_4} \gtrsim \underset{(141)}{FeCl_3} > \underset{(57)}{ZnCl_2} > \underset{(52)}{HgCl_2}$$

These Lewis acids react with the co-catalyst to form the counter anions of the growing chain end. Therefore, it is expected that an increase in the cationic activity of Lewis acid is arised from an increase in its acidity. Okamura *et al.*[17] employed the heat of solution of Lewis acid and ethyl acetate as a measure of the acidity of Lewis acid. Present authors used the shift of the characteristic band of the carbonyl group in the infrared spectrum of the Lewis acid-xanthone complex,[19] and reported[20] that an increase in the shift showed an increase in the acidity of Lewis acid. The values in parentheses in the above relation represent the magnitude of the carbonyl shift. There is a good correlation between the catalytic acitivity and the carbonyl shift in the Lewis acid-xanthone complex.

Similarly, the activity of co-catalysts in the polymerization system of the same monomer and the same Lewis acid catalyst, for example, in the cationic polymerization of isobutene catalysed by tin chloride,[21] decreases in the order,

$$\underset{(pK_a=0.64)}{CCl_3COOH} > \underset{(2.87)}{CH_2ClCOOH} > \underset{(4.76)}{CH_3COOH} > \underset{(9)}{CH_3CH_2NO_2} > \underset{(11)}{CH_3NO_2} > \underset{(10)}{C_6H_5OH} > \underset{(15)}{H_2O}$$

As the pK_a value of co-catalyst decreases, its activity increases, and Eq. (7) is satisfied.

As described above, in any cases of anionic and cationic polymerization the energetic treatment in the previous paper was found to be useful to explain quantitatively many kinds of experimental data.

The authors are grateful to Professor Kenichi Fukui and Professor Teijiro Yonezawa for their valuable suggestions while carrying out this study.

17) S. Okamura, T. Higashimura and H. Sakurada, *Kogyo Kagaku Zasshi (J. Chem. Soc. Japan, Ind. Chem. Sect.)*, **61**, 1640 (1958).
18) K. Bodendorf and H. Boehme, *Ann.*, **516**, 1 (1935).
19) D. Cook, *Can. J. Chem.*, **41**, 522 (1963).
20) T. Kagiya, Y. Sumida and T. Inoue, This Bulletin, **41**, 767 (1968).
21) K. E. Russell, *Trans. Faraday Soc.*, **48**, 114 (1952).

BULLETIN OF THE CHEMICAL SOCIETY OF JAPAN VOL. 41 2254—2257 (1968)

SCFMO Parameters for Heteroatoms donating Lone Pairs

Kichisuke NISHIMOTO*1 and Leslie S. FORSTER

Department of Chemistry, University of Arizona, Tucson, Arizona, U.S.A.

(Received January 26, 1968)

The interrelationships between the semi-empirical parameters involved in SCFMO calculations have been considered. The calculated transition energies for molecules containing an atom that donates two electrons to the π-system are mainly dependent upon the first valence state ionization energy of the heteroatom, and the nearest-neighbor two center repulsion integrals.

The proliferation of semi-empirical SCFMO calculations has been accompanied by an ever widening array of parameter sets. This diversity is particularly evident in the parameters assigned to nitrogen and oxygen atoms donating two electrons to the π-system. Thus, good results have been obtained for the aniline spectrum when the nitrogen valence state ionization energy has been varied from 22.49 to 28.63 eV[1,2] and as an extreme cases, a successful calculation has been made with the nitrogen and carbon valence state ionization energies (V.S.I.E.) set equal.[3]

In addition to the V.S.I.E., I_μ, the parameters involved in SCFMO calculations in the Pariser-Parr-Pople approximation are the one and two center repuslion integrals, $\gamma_{\mu\mu}$ and $\gamma_{\mu\nu}$, and the core resonance integrals, $\beta_{\mu\nu}$. A number of systematic studies have been made on the effects of these parameters upon the electronic structure of aniline.[1,2,4,5] In some of this work, the interrelationships between the parameters have been implicit but insufficiently stressed. It is the purpose of the present note to focus attention on the more important aspects of the parameterization problem.

Method of Calculation

In the SCF variant of the Pariser-Parr-Pople method,[6] the $\boldsymbol{F}$ matrix is diagonalized, $\boldsymbol{F}\psi_i=\varepsilon_i\psi_i$. The eigenvalues, ε_i, and eigenvectors, $\psi_i=\sum C_{i\mu}\phi_\mu$, may then be used to compute the energies of an excited singlet configuration, χ_{i-j}, from the expression $E_{i-j}=\varepsilon_j-\varepsilon_i-(ii/jj)+2(ij/ij)$. Configuration interaction is then invoked. The off-diagonal elements of the CI matrix involve the repulsion integrals, $(kl/mn)=\int\psi_k(1)\psi_l(1)(1/r_{12})\cdot\psi_m(2)\psi_n(2)\mathrm{d}v$, that depend on the coefficients of the molecular orbitals. The elements of $\boldsymbol{F}$ are

$$F_{\mu\mu}=-I_\mu+\frac{1}{2}q_\mu\gamma_{\mu\mu}+\sum_{\nu\neq\mu}(q_\nu-n_\nu)\gamma_{\mu\nu} \quad (1)$$

$$F_{\mu\nu}=\beta_{\mu\nu}-\frac{1}{2}p_{\mu\nu}\gamma_{\mu\nu} \quad . \quad (2)$$

Where q_μ and $p_{\mu\nu}$ are the diagonal and off-diagonal elements, respectively, of the bond order-charge density matrix and n_ν is the number of electrons. 1 or 2, donated to the π-system by the νth atom.

The $\boldsymbol{F}$ matrix is then solved iteratively to self-consistency. The solutions are mainly dependent on the diagonal and nearest neighbor off-diagonal elements of $\boldsymbol{F}$.

Diagonal F Elements

For most of neutral molecules, $q_\nu-n_\nu$ is rather small and Eq. (1) can be written

$$F_{\mu\mu}\simeq-I_\nu+\frac{1}{2}q_\mu\gamma_{\mu\mu}$$

In the Pariser-Parr approximation, $\gamma_{\mu\mu}=I_\mu-A_\mu$. For $n_\mu=1$ and $q_\mu\simeq1$

$$F_{\mu\mu}\simeq-\frac{1}{2}I_\mu-\frac{1}{2}A_\mu$$

where A_μ, the electron affinity, is generally small. When $n_\mu=2$, $\gamma_{\mu\mu}=I_2-I_1$, the difference in the first and second V.S.I.E. For $q_\mu\simeq2$

$$F_{\mu\mu}\simeq-I_1=-I_\mu$$

Consequently, the diagonal elements of $\boldsymbol{F}$ are dependent principally upon the first V.S.I.E.

The validity of this approximation can be appreciated by reference to Table 1 and Fig. 1, wherein the computations of the aniline spectrum by a number of workers are summarized. With the exception of calculations 6, 9, and 10 which

*1 Permanent address, Department of Chemistry, Faculty of Science, Osaka City University, Sumiyoshi-ku, Osaka.

1) M. Klessinger, *Theor. Chim. Acta*, **5**, 236 (1966).
2) S. Kwiatkowski, *Bull. Acad. Polon.*, **13**, 817 (1965).
3) P. Knowton and W. R. Carper, *Mol. Phys.*, **11**, 213 (1966).
4) I. Fischer-Hjalmers, *Arkiv Fysik*, **21**, 123 (1962).
5) J. E. Bloor, P. N. Daykin and P. Boltwood, *Can. J. Chem.*, **42**, 121 (1964).
6) J. A. Pople, *Proc. Phys. Soc.*, **A68**, 81 (1955).

TABLE 1. KEY TO FIG. 1 CALCULATION. NM AND PP REFER TO NISHIMOTO-MATAGA[12] AND PARISER-PARR[9] TECHNIQUES, RESPECTIVELY

Calcd. No.	$I_N = I_N^+ - \gamma_{N-N}^{++}$	I_N^+	γ_{N-N}^{++}	I_C	γ_{CC}	$\gamma_{\mu\nu}$	β_{CC}	β_{CN}	Ref.
1	8.46	24.38	15.92	11.28		NM	−2.39	−2.50	5
2	9.26	26.7	17.44	11.16	11.13	NM	−2.35	−2.46	7
3	9.80	22.63+	12.83	11.16+	11.08	NM	−2.32	−2.30	1
4	10.02	24.38	14.36	11.28		NM	−2.35	−2.74	5
5	10.13	23.46	13.31	11.22	10.80	NM	−2.39	−2.40	2
6	11.42	28.63+	17.21	11.16+	11.08	PP	−2.32	−2.30	1
7	11.64	24.38	12.74	11.28		NM	−2.35	−2.74	5
8	11.96	24.30	12.34	11.16	11.13	NM	−2.39	−2.40	2
9	14.18	28.63+	14.45	11.16+	11.08	PP	−2.32	−2.30	1
10	15.80	28.63+	12.83	11.16+	11.08	PP	−2.32	−2.30	1
11	15.80	28.63+	12.83	11.16+	11.08	PP++	−2.32	−2.30	1

\+ $I_N - I_C$ given
++ nearest neighbor $\gamma_{\mu\nu}$ reduced

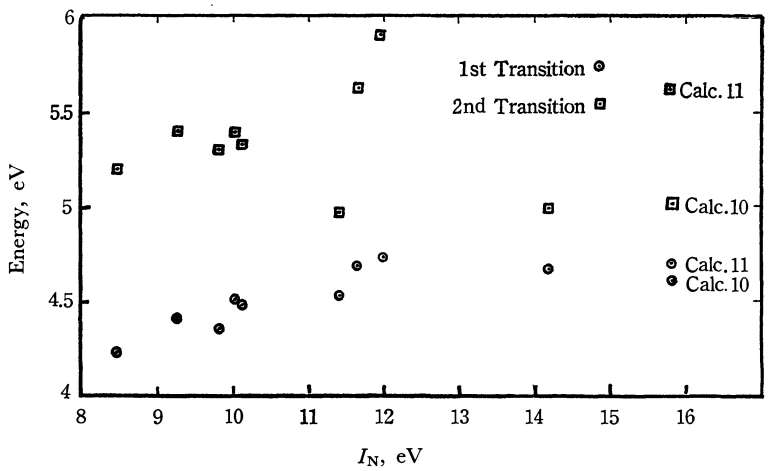

Fig. 1. Dependence of the two lowest aniline transition energies on $I_1 = I_2 - \gamma_{N-N}^{++}$. Parameters employed with each I_1 are listed in Table 1.

will be discussed below, the energies of the two lowest transitions lie close to a smooth curve, indicating a functional relationship depending only on the first V.S.I.E. of nitrogen.

This dependence upon I_1 is shown more graphically in Fig. 2 where only I_1 is varied for each curve. For the $-NH_2$ group, a constant β approximation ($\beta_{CC} = \beta_{CN} = -2.38$ eV) and the variable β approximation ($\beta_{CC} = -0.51p - 2.04$ eV and $\beta_{CN} = 0.53p - 2.24$ eV) yield the same curves. The repulsion integrals were claculated by the NM prescription[7];

$$\gamma_{\mu\nu} = 14.397/(a_{\mu\nu} + r_{\mu\nu}) \text{ eV}.$$

It is interesting to note that the phenol spectrum is well represented by the Fig. 2 curves. In the phenol calculation

$$I_O^+ - \gamma_{O-O}^{++} = 11.4 \text{ eV}$$

This leads to (Fig. 2) 4.67 and 5.75 eV which may be compared to 4.62 and 5.76 eV obtained from the usual variable β computation.[7] The aniline experimental transition energies are 4.34 and 5.29 eV and good results are obtained when $I_N^+ - \gamma_{N-N}^{++} \simeq 9$ eV.

Off-diagonal *F* Elements

Bloor, Daykin and Boltwood[5] have determined the effect of β_{CN} on the aniline transition energies and found that a variation from −2.00 to −2.75 eV leaves the lowest transition energy essentially unchanged, and produces only a 0.30 eV change in the second transition energy.

The nearest neighbor $\gamma_{\mu\nu}$ and $\beta_{\mu\nu}$ are interrelated by Eq. (2) and $F_{\mu\nu}$ would be but little affected by changes in $\gamma_{\mu\nu}$. Thus, the ***F*** matrix, and therefore

7) K. Nishimoto and L. S. Forster, *Theor. Chim. Acta*, **4**, 155 (1966).

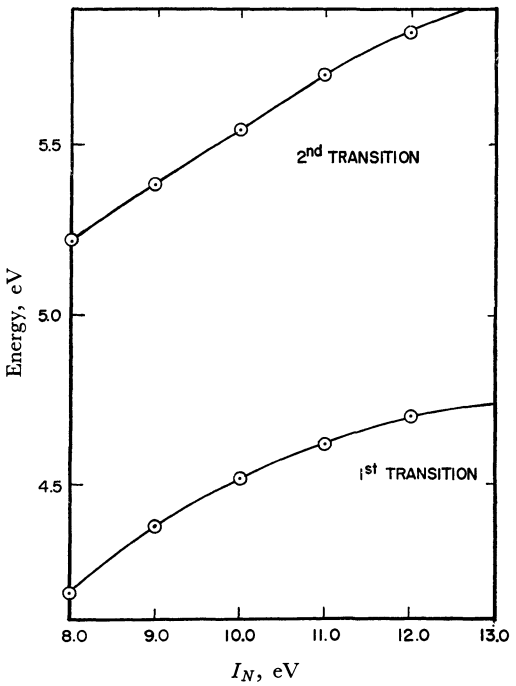

Fig. 2. Dependence of the two lowest aniline transition energies on I_1. Variable parameterization (NM integrals)[7] employed in all calculations.

the ground state charge distribution, are not very dependent on the repulsion integrals.

The statements in this section are applicable only to the systems with weakly interacting substituents, wherein, the spectrum of the parent molecule is not perturbed too greatly by the substituent(s). When many heteroatoms are incorporated into the π-system, *e. g.* uracil and isoalloxazine,[8] the off-diagonal $F_{\mu\nu}$ may be quite dependent upon the parameter choice.

Configurational Energies and Configuration Interaction

As noted above, neither the $\gamma_{\mu\mu}$ nor $\gamma_{\mu\nu}$ choice markedly affects the eigenvalues or the eigenvectors of the $\boldsymbol{F}$ matrix. Both the diagonal elements (configurational energies) and off-diagonal elements of the CI matrix depend upon the repulsion integrals over molecular orbitals, (kl/mn). These in turn are functions of the eigenvectors of the $\boldsymbol{F}$ matrix and the $\gamma_{\mu\mu}$ and $\gamma_{\mu\nu}$ integrals. The effect of nearest-neighbor $\gamma_{\mu\nu}$ is marked. In the Pariser-Parr calculation, $\gamma_{\mu\nu}$ were computed by a quadratic interpolation and the calculated energy of the 2nd benzene transition was 0.7 eV too small.[9] Reducing the nearest-neighbor $\gamma_{\mu\nu}$ rectifies this problem.[10,11] The drastic lowering or the second aniline transition in calculations 6, 9, and 10 can be ascribed to the larger $\gamma_{\mu\nu}$ employed.[1]

The use of the Nishimoto-Mataga technique for evaluating $\gamma_{\mu\nu}$[12] circumvents this difficulty.[1,3,7]

Core Charge Effect

In all of the calculations described in Table 1 and Figs. 1 and 2, N^{++} ($n_N=2$) was assumed. It should be possible by a suitable adjustment of the parameters to obtain appropriate $F_{CC}-F_{NN}$ differences (3—4 eV) when $n_N=1$, and we find that this is indeed the case. In contrast to the situation for transition energies where only the differences in diagonal F elements are imporatant, computation of ionization potentials from the orbital energies requires appropriate absolute values of the diagonal F elements. In this regard the N^+ core is quite unsuitable since very small (or even negative) ionization potentials are obtained with this assumption.

One Center Repulsion Integrals

Paolini[13] has suggested that $\gamma_{\mu\mu}$ is proportional to the Z_{eff} (computed from the Slater rules) of the neutral species. In the Pariser-Parr method:

$$\gamma^{+}_{N-N^{+}} = I_N - A_N$$

$$N[(sp^2)^4p_z, V_3] \rightarrow \overset{+}{N}[(sp^2)^4, V_2]: I_N$$

$$\bar{N}[(sp^2)^4p_z^2, V_2] \rightarrow N[(sp^2)^4p_z, V_3]: A_N$$

and

$$\gamma^{++}_{N-N^{++}} = I_2 - I_1$$

$$N[(sp^2)^3p_z^2, V_3] \rightarrow \overset{+}{N}[(sp^2)^3p_z, V_3]: I_1$$

$$\overset{+}{N}[(sp^2)^3p_z, V_4] \rightarrow \overset{++}{N}[(sp^2)^3, V_3]: I_2$$

Thus, $\gamma^{++}_{N-N^{++}}$ and $\gamma^{+}_{N-N^{+}}$ represent the repulsion between two p_z electrons in systems with different Z_{eff}. If we relate these quantities by

$$\gamma^{++}_{N-N^{++}}/\gamma^{+}_{N-N^{+}} = Z_{\text{neutral}}/Z_{\text{anion}} \qquad (3)$$

then $\gamma^{++}_{N-N^{++}}=1.1\gamma^{+}_{N-N^{+}}$. However, $\gamma_{\mu\mu}$ as used in Eq. (1) will depend upon the net charge on the μth atom. A large net positive charge will occur when $n_N=2$ and $\gamma^{++}_{N-N^{++}}$ should be larger than estimated by Eq. (3). The ratio of the two $\gamma_{\mu\mu}$ quantities used in our previous work is 1.4,[7] a reasonable value. In any event, whenever the

8) J. L. Fox, S. P. LaBerge, K. Nishimoto and L. S. Forster, *Biochim. Biophys. Acta*, **136**, 544 (1967).

9) R. Pariser and R. G. Parr, *J. Chem. Phys.*, **21**, 767 (1953).

10) R. Pariser, *ibid.*, **24**, 250 (1956).

11) K. Nishimoto and L. S. Forster, *Theor. Chim. Acta*, **3**, 407 (1965).

12) K. Nishimoto and N. Mataga, *Z. Physik. Chem. (Frankfurt)*, **12**, 335 (1957).

13) L. Paolini, *Nuov. Cim.*, **4**, 410 (1956).

results are sensitive to $\gamma_{\mu\mu}$ choice, the $\gamma_{\mu\mu}$ magnitudes assigned to the $n=2$ and $n=1$ atoms should differ as indicated above.

Conclusion

If semi-empirical SCFMO calculations are used for spectral interpretations of systems with weakly interacting substituents, good results can be obtained by the appropriate choice of I_μ and nearest-neighbor $\gamma_{\mu\nu}$; the other parameters may be varied over a wide range with minor effect.

The experimental ionization potential for CH_3NH_2 is 9.26 eV,[14] a value suitable for I_1, in the calculation of the aniline transition energies. This suggests that the experimental ionization potentials for CH_3X can be used for I_1 whenever X is a substituent donating two electrons to the π-system. Consequently, the following I_1 quantities are recommended.

X	I_1 (eV)[14]
-OH	11.37
$-OCH_3$	10.52
$-NH_2$	9.26
$-NHCH_3$	8.53
$-N(CH_3)_2$	8.11

The nearest-neighbor off-diagonal F elements are approximately -4 eV. This corresponds to β in a Hückel calculation. Since $F_{NN}-F_{CC}\simeq-4$ eV, it is reasonable to express the Hückel coulomb parameter as $\alpha_N=\alpha+\beta$ for NH_2 group.

This work was supported by the U. S. Public Health Service (Grant GM-13218).

14) K. Watanabe, T. Nakayama and J. Mottl, *J. Quant. Spectry. Radiative Transfer*, **2**, 369 (1959).

BULLETIN OF THE CHEMICAL SOCIETY OF JAPAN VOL. 41 2257—2263 (1968)

Changes in Catalytic Activity and Surface Properties of Nickel Oxide with Gamma-Irradiation

Toshiro YAMASHINA, Takaaki NAGAMATSUYA*1 and Masakatsu SANO

Faculty of Engineering, Hokkaido University, Sapporo

(Received January 27, 1968)

The nature of the active sites of nickel oxide has been studied by changing surface properties by means of γ-irradiation technique. Using powdered nickel oxide catalyst, catalytic activities, surface excess oxygen contents, electrical conductivity changes during thermal desorption of gases, and reactivities of the sample with CO_2, CO and H_2 were compared as a function of γ-ray dose of preirradiation. It has been found that the catalytic activity, the excess oxygen content and the conductivity change with the increase in the irradiation dose, and the change is remarkable when a total dose is greater than 1×10^8R. The catalytic activity for the decomposition of H_2O_2 was observed to increase, while that for the decomposition of i-C_3H_7OH vapor was observed to decrease with the irradiation dose. Measurements on the desorption of excess oxygen and the adsorption of CO_2 simultaneously with electrical conductivity have indicated that the adsorbed state of surface oxygen may be changed into a strong form by the irradiation, as $O^-_{(ad)} \rightsquigarrow O^{2-}_{(ad)}$. Discussions have been made on the correlation between the catalytic sites and surface properties of the irradiated nickel oxide.

Many studies have been made on the surface chemistry of nickel oxide as well as that of other transition-metal oxides, and particular interest is shown in the surface heterogeneity of the oxides. The surface heterogeneity of powdered nickel oxide has been investigated by various methods, including the determination of the distribution of surface excess oxygen,[1] isotopic exchange reaction technique,[2,3] electrical conductivity measurement during adsorption or desorption,[4] deactivation with CO_2 adsorption[5,6] and so on. However, there has been discrepancy among the results of

* Present address: Japan Atomic Energy Institute, Ooarai, Ibaragi.

1) H. Gossel, *Z. Elektrochem.*, **65**, 98 (1961).

2) G. K. Boreskov, "Advances in Catalysis," Vol. 15, ed. by D. D. Eley, H. Pines and P. B. Weisz, Academic Press, New York (1965), p. 285.

3) K. Klier and M. Jiratova, Proc. Intern. Congr. Catalysis, 3rd, Amsterdam, 1965 (1966), p. 763.

4) H. Saltsburg, D. P. Snowden and M. C. Garrison, *J. Phys. Chem.*, **68**, 3765 (1964).

5) G. Parravano and C. A. Demonicali, *J. Chem. Phys.*, **26**, 359 (1957).

6) J. Kondo, T. Uchijima and Y. Yoneda, This Bulletin, **40**, 1040 (1967).

different workers. This may be due to the difference in the method of sample preparation or experimental procedures. Accordingly, many unresolved problems on active sites and the chemical reactivity of nickel oxide surface have been remained.

The present investigation was undertaken to obtain some informations as to the state of surface excess oxygen in connection with active sites and the surface reactivity of nickel oxide. By means of irradiation the surface state of the oxide could be changed selectively. Thus the surface state has been examined from many viewpoints such as catalytic activity, the nature of excess oxygen, electrical conductivity and adsorption of gases as a function of irradiation dose of γ-rays.

Some results on the nature of the irradiated nickel oxide, *i. e.*, on the catalytic activity for the decomposition of H_2O_2 solution[7] and the reduction kinetics by H_2,[8] have been reported previously by the present authors. The purpose of this report is to describe some additional results of the previous study and some preliminary results obtained by using an apparatus connected with a quadrupole mass spectrometer for the adsorption and the desorption of CO_2 and i-C_3H_7OH.

Experimental

Materials. NiO sample was obtained by decomposing and firing CP grade nitrate in air at 500°C for 5 hr after a gentle evaporation of the dilute solution of the nitrate. The oxide product was reduced to a granular form (100—200 mesh). The BET surface area of this sample measured by nitrogen adsorption was 9—10 m^2/g. Carbon monoxide (99.5%), carbon dioxide (99.95%) and isopropanol (spectro-grade) were obtained commercially. Hydrogen was purified by diffusing the crude gas through a palladium film.

Irradiation of sample was carried out in air at room temperature with Co-60 γ-rays, the intensity of which was 5.85×10^5 R/hr; total dose reached about 1×10^9 R.

Catalytic Activity. The catalytic activity of NiO was determined by using the decomposition of a 7.5% hydrogen peroxide solution as a model reaction. The rate of reaction was followed by measuring the volume of oxygen evolved per minute with the apparatus shown previously.[9] A 0.2 g catalyst sample was used for each run and the reaction temperature was 25—45°C. Before each run, the decomposition rate without catalyst was measured. Negligibly small amount of decomposition less than about 5% of that with catalyst was found to occur. The reproducibility in the determination of the catalytic activity was found to be better than 5%. The activity for the decomposition of i-C_3H_7OH was also measured by means of the apparatus described previously.[10]

Excess Oxygen Content and Electrical Conductivity Measurements. The quantity of excess oxygen in NiO was determined by an iodometric titration[9] and a gravimetric method with a vacuum microbalance. Chemical analysis by the iodometry was performed as follows: 0.5 g of KI, 50 m*l* of 35% HCl and 100 m*l* of H_2O were added to 0.5 g of catalyst sample and the sample was dissolved by heating gently. Under a nitrogen flow, the solution was cooled and allowed to stand in darkness, then the titration was made with a 0.01 N $Na_2S_2O_3$ solution as quickly as possible. Replicate titration experiments were made at least five times, the reproducibility in the determination being found to be better than 10%.

Electrical conductivity measurements were made by means of AC and DC potentiometric methods with a cell for powdered NiO shown in Fig. 1. An 1.0 g catalyst

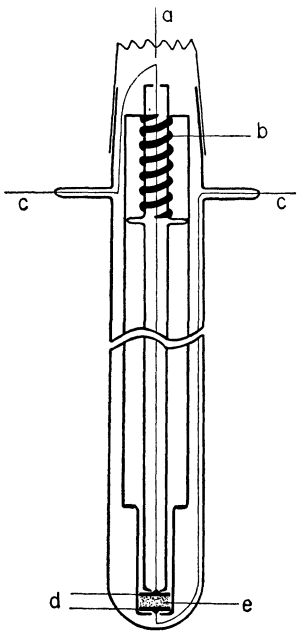

Fig. 1. Electrical conductivity cell.
a: to vacuum system, b: spring,
c: Pt leads for electrical measurements,
d: Pt disc, e: powdered sample

sample was inserted between two platinum plates (disc of 1 cm in diameter) and pressure of about 2 kg/cm^2 was applied with a steel spring. The closed end of a quartz tube containing the cell connected to a vacuum line was inserted into an electric furnace, then changes in the conductivity during the adsorption or the desorption of gases were measured. The resistivities of NiO were observed to be in the range from 10^5 to 10^8 Ω. Determinations both by the AC and DC methods gave nearly identical values of the resistance, and no polarization effect was observed in the measurement by the DC method. Accordingly, the following results in the present paper were obtained mainly by the DC method.

Adsorption and Desorption Measurements. Changes in the weight of catalyst samples during adsorption or desorption of gases were measured in an all

7) T. Yamashina and M. Sano, This Bulletin, **38**, 1801 (1965).
8) T. Yamashina and T. Nagamatsuya, *ibid.*, **38**, 507 (1965).
9) T. Yamashina and M. Sano, *Nippon Kagaku Zashi (J. Chem. Soc. Japan, Pure Chem. Sect.)*, **87**, 553 (1966).
10) T. Yamashina, *Shokubai (Catalyst)*, **9**, 9 (1967).

glass closed system of a Gulbransen type microbalance having the sensitivity of 7.21×10^{-7} g/div. (1 div.= 0.01 mm). The total volume of the system was about 1800 m*l*, and the system could be evacuated below 1×10^{-5} mmHg.

The rate of decomposition of i-C_3H_7OH adsorbed on nickel oxide was measured by using a vacuum apparatus having a mass spectrometer described previously.[10] The essential feature of the apparatus was the connection of the reaction vessel to a Mitsubishi MF1-T4 quadrupole mass filter by a variable leak (Granville-Phillips). Using the apparatus, the reaction mixture can be analyzed continuously throughout the course of the reaction.

Results

Effect of γ-Preirradiation on the Properties of NiO. Changes in the catalytic activity, the content of excess oxygen and the electrical conductivity of NiO were examined as a function of the preirradiation of γ-rays. The results are summarized in Fig. 2, in which the catalytic activity

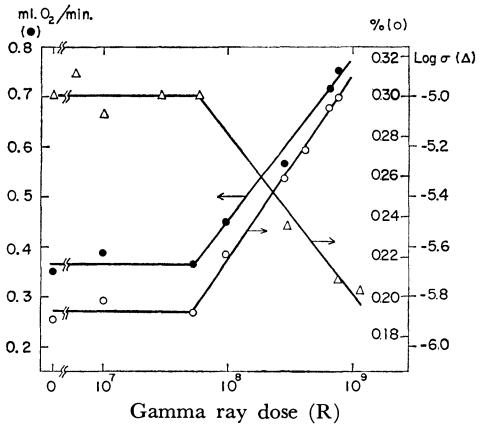

Fig. 2. Catalytic activity, excess oxygen and electrical conductivity of NiO as a function of γ-ray dose of preirradiation.
●: catalytic activity (40°C)
○: excess oxygen (iodometry)
△: electrical conductivity

is the decomposition rate of the H_2O_2 at 40°C. Each value was found to change with the increase of irradiation dose. The change is remarkable when a total dose is greater than about 1×10^8 R. No distinct changes due to the irradiation were observed in the BET surface area and the X-ray diffraction pattern. In Fig. 3, the catalytic activity and the conductivity are shown as a function of the amount of excess oxygen with the irradiation. Linear relationships are seen in both cases. It must be noted that the electrical conductivity of NiO, a p-type semiconductor, was observed to decrease in spite of an increase in the excess oxygen content with the irradiation.

Several properties of the non-irradiated and

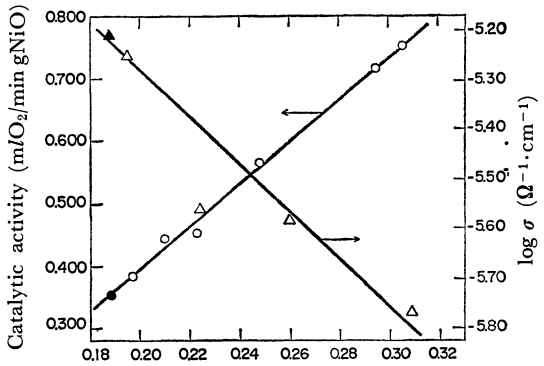

Fig. 3. Catalytic activity and conductivity *vs.* amount of excess oxygen with irradiation.
○: catalytic activity
△: electrical conductivity
●▲: non-irradiated

irradiated (8.8×10^8 R) NiO are summarized in Table 1.

The anomaly observed in the relation between the conductivity and the excess oxygen content induced by the irradiation could be ascribed to the changes in the adsorption state of surface oxygen and the defect structure. The some properties of the excess oxygen have been compared on the non-irradiated NiO with the irradiated NiO; in the experiments described below, the authors have examined on two samples, NiO(I)-non-irradiated, NiO(II)-irradiated (8.8×10^8R).

Flash Desorption of Surface Oxygen. By means of a microbalance technique and by raising the temperature at a 1°C/min rate *in vacuo*, desorption curves of the oxygen from NiO(I) and from NiO(II) were obtained. The experimental results are shown in Fig. 4.

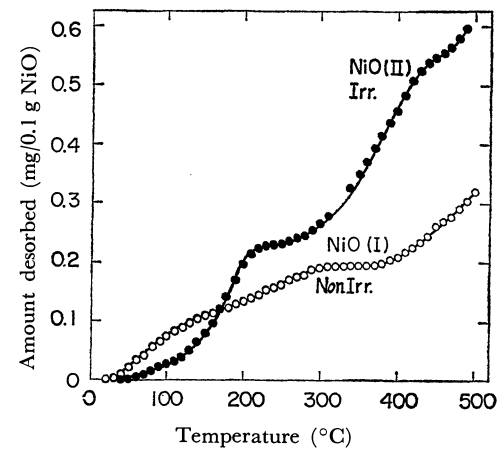

Fig. 4. Amount of excess oxygen desorbed during raising temperature (1°C/min) *in vacuo*.
○: non-irradiated NiO
●: irradiated (8.8×10^8r) NiO

TABLE 1. EFFECT OF IRRADIATION ON VARIOUS PROPERTIES OF NiO

	NiO(I) non-irradiated	NiO(II) irradiated (8.8×10^5R)
Catalytic activity (decomposition of 7.5% H_2O_2, 40°C)	0.36 (ml·O_2/min)	0.76
Activation energy (25—45°C)	11.1 (kcal/mol)	20.4
Excess oxygen { iodometric	0.188 (%)	0.305
Excess oxygen { gravimetric	8.50 (%)	9.29
Electrical conductivity (25°C)	3.65×10^{-6} ($\Omega^{-1}\cdot cm^{-1}$)	0.965×10^{-6}
Reduction rate { by H_2 (60 mmHG, 190°C)	72 min (10% reduction)	108
Reduction rate { by CO (70 mmHg, 250°C)	150 min (4% reduction)	not reacted
Surface area (B. E. T.)	10.6 (m^2/g)	9.9
X-Ray diffraction (powder method)	no difference	

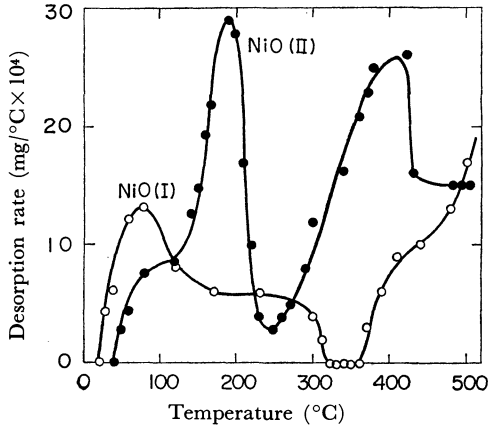

Fig. 5. Desorption rate of excess oxygen during raising temperature (1°C/min) *in vacuo*.

Further, the rates of oxygen desorption are plotted as a function of the desorption temperature in Fig. 5. As can be seen in these figures, the amount of oxygen desorbed from NiO(II) was less than that from NiO(I) in the temperature range below about 200°C, and the peaks of the desorption rate appeared at about 100°C for NiO(I) and about 200°C for NiO(II).

Changes in the electrical conductivity of the both samples during the desorption of excess oxygen are shown in Fig. 6, where $\log\sigma$ *versus* $1/T$ is plotted. As can be seen from the figure, NiO samples after irradiation have a lower conductivity than before, and when NiO(II) was heated up to higher temperatures *in vacuo*, a much different curve from that of NiO(I) was observed. Namely, an irregular "S" shaped change was observed for the NiO(II) in the temperature range 150—250°C. After heating up to 500°C NiO(II) became to behave like NiO(I). This fact seems to show a disappearence of the irradiation effect by the heating. The temperature of 200°C which gave the lowest conductivity in the irregular region corresponds with the temperature giving a high peak on the desorption rate curve in Fig. 5. The

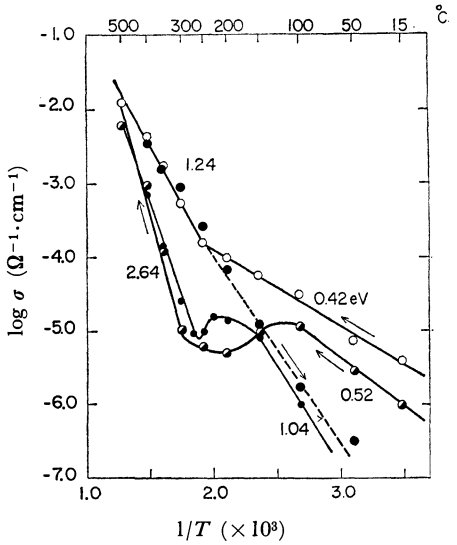

Fig. 6. Temperature dependence of electrical conductivity of NiO before and after irradiation, *in vacuo*.
○: non-irradiated sample (NiO(I))
◑: irradiated (8.8×10^8R) sample (NiO(II))
●: NiO(I) and NiO(II), cooled *in vacuo*
●: conductivity change of NiO in H_2 (2 mmHg), obtained by Dereń *et al.*[16]

irregular "S" shaped curve in the conductivity-temperature relationship is a characteristic feature for the irradiated samples, and the extent of the curvature becomes larger with increasing irradiation dose.

Adsorption of CO_2. Using the vacuum microbalance, adsorption measurements of CO_2 at room temperature were carried out on NiO(I) and NiO(II). Because the adsorption was a very rapid process, comparisons between NiO(I) and NiO(II) were not possible from the kinetics of adsorption. The amount of CO_2 adsorbed during 30 min at room temperature and under the pressure of 20 mmHg was shown in Table 2. It is to be noted that the amount of CO_2 adsorbed by

Table 2. Amount of CO_2 adsorbed by NiO CO_2: 20 mmHg, at 25°C

	NiO (I) non-irradiated	NiO (II) irradiated (8.8×10^8R)
Total amount of CO_2 adsorbed	0.0590(mg/0.1 g NiO)	0.0136
Amount of CO_2 desorbed by evacuation	0.0405	0.0063
Amount of CO_2 remained on NiO	0.0185	0.0073

NiO(II) is much less than the amount adsorbed by NiO(I). The process of electrical conductivity change during the adsorption of CO_2 at room temperature is given in Fig. 7, where the temperature at which the thermal treatments *in vacuo* were made is indicated along each curve. Conductivity changes resulted from adsorption were larger in NiO(I) than in NiO(II) in the cases of the pretreatment below 200°C.

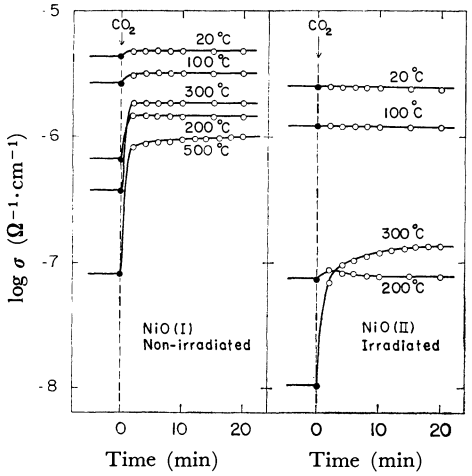

Fig. 7. Variation of electrical conductivity of NiO(I) and NiO(II) with adsorption of CO_2 (20 mmHg) at room temperature.
Sample was heated for one hour *in vacuo*, at the each temperature shown in figure, before CO_2 admission.

Decomposition of *i*-C_3H_7OH in Adsorbed Layer. To obtain another evidence on the reactivity of the irradiated oxide surface, the catalytic decomposition of *i*-C_3H_7OH by NiO(I) and NiO(II) has been examined. After *i*-C_3H_7OH was allowed to adsorb on the oxide at room temperature and under 30 mmHg pressure for 20 hr, the vapor of *i*-C_3H_7OH remained in the gas phase was removed by the evacuation at room temperature, then the strongly chemisorbed *i*-C_3H_7OH was desorbed by raising the temperature. The change in pressure of the system was read and the products were analyzed at every 50°C.

Results are presented in Fig. 8 and Fig. 9 where the relative intensities of main products, *i*-C_3H_7OH, $(CH_3)_2CO$, C_3H_6 and CO_2 are compared. With rise of desorption temperature, the

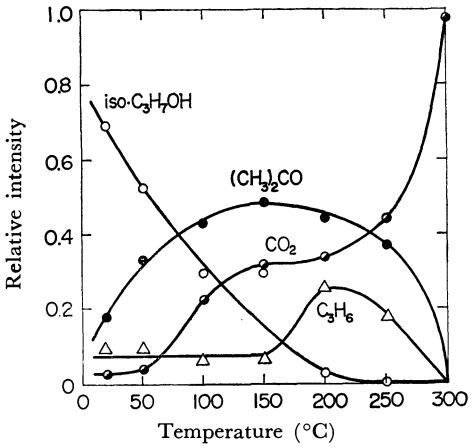

Fig. 8. Relative intensities of main products desorbed from adsorbed layer of *i*-C_3H_7OH, analysed by a quadrupole spectrometer; non-irradiated NiO (NiO(I)).

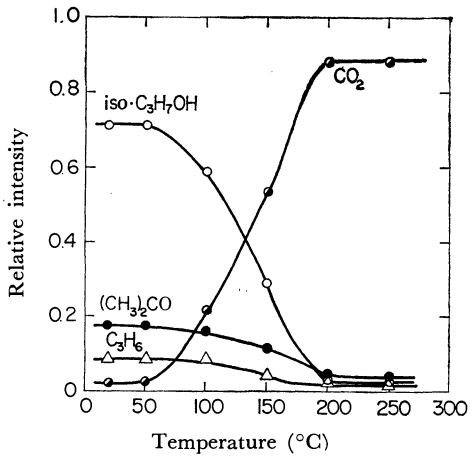

Fig. 9. Relative intensity of main products desorbed from adsorbed layer of *i*-C_3H_7OH, analysed by a quadrupole spectrometer; irradiated (8.8×10^8R) NiO (NiO(II)).

Table 3. Dehydrogenation of *i*-C_3H_7OH on irradiated NiO
(rising rate of temperature 1°C/min, analyzed by quadrupole spectrometer)

	Non-irradiated	Irradiated (6.7×10^8R)	Irradiated (8.8×10^8R)
Starting temperature of dehydrogenation of *i*-C_3H_7OH	115°C	140°C	210°C
Completion temperature of dehydrogenation of *i*-C_3H_7OH	250	280	330

composition of i-C_3H_7OH in the products decreased and that of CO_2 increased, on the other hand, $(CH_3)_2CO$ and C_3H_6 were observed to form only in the case of NiO(I) sample. The experimental results concerning the dehydrogenation of i-C_3H_7OH on NiO(I) and NiO(II) are summarized in Table 3. It can be seen that the reaction was retarded by the irradiation.

Reductive Properties of Irradiated NiO. Reduction rates of NiO(I) and NiO(II) by H_2 and CO were measured with the vacuum microbalance. Velocity curves for the reduction by H_2 (60 mmHg, at 190°C) and CO(70 mmHg, at 250°C) are presented in Fig. 10, where the reduction rate of NiO(II) is much lower than that of NiO(I).

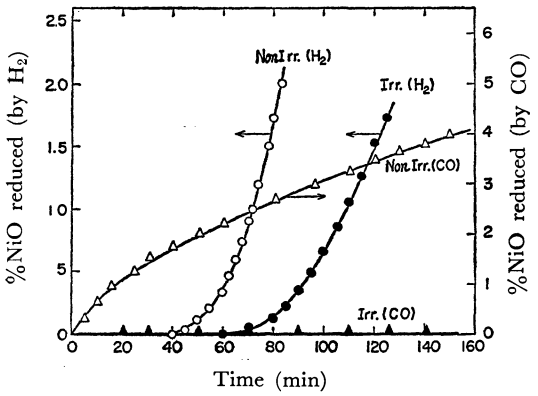

Fig. 10. Reduction curves of NiO samples by H_2 (60 mmHg, 190°C) and CO (70 mmHg, 250°C), ○△: non-irradiated, (NiO(I)) ●▲: irradiated (8.8×10^8R)(NiO(II).

Discussion

Measurements for the catalytic activity, the content of excess oxygen and the electrical conductivity of NiO as a function of γ-ray irradiation dose have shown abrupt changes when a total dose is greater than about 1×10^8 R. In the previous study on the hydrogen reduction of NiO with the irradiation,[8] the authors have found nearly the same phenomena as the present resulst. However, it is difficult at the present time to give full interpretation on the phenomena of the abrupt changes in terms of the irradiation.

In the present paper, discussion has been made on the surface state and the active sites of the irradiated NiO.

Surface State of the Irradiated NiO. Many works have been described on the surface properties of nickel oxide affected by nuclear irradiation.[11-13] Experiments by Charman and Dell[11] and Maxim and Braun[12] have shown that the amount of surface excess oxygen in NiO was increased by the reactor irradiation. The correlation between electrical properties and the content of excess oxygen of the reactor irradiated NiO has been investigated by Nachman *et al.*[13] They concluded that the complicated change in conductivity could be attributed to the radiation-induced defects in the lattice.

In the present study, the electrical conductivity was found to decrease and the amount of excess oxygen was found to increase as the irradiation dose was increased (Fig. 2). Such results can not be expected in ordinary p-type semiconductors. Therefore, the change in the conductivity seems to have no connection with the change in the excess oxygen content due to the irradiation. The descrease in the conductivity would be due to the decrease in the concentration of positive holes, *i. e.*, the charge-carriers, because the irradiation introduces deep trapping level on the vacant cation site as pointed out by several authors[13,14] in the study of nuclear radiation. According to the study by Young,[14] the conductivity of NiO was found to decrease after the nuclear irradiation *in vacuo* while to increase after the irradiation in oxygen. His results are much different from those of the present study which have shown the decrease in the conductivity after the γ-ray irradiation both *in vacuo* and in oxygen. The difference could be due to the conditions of irradiation and also the preparation of NiO samples, *i. e.*, Young prepared it by the complete oxidation of nickel foil at 1000°C.

Iodometric titration measurements with the partial dissolution method[9] have shown that the most of excess oxygen induced by the irradiation appeared to be near the surface of NiO particles. In view of the above facts, the most reasonable conclusion is that irradiation might cause two different effects against the surface properties of NiO: one is the induced chemisorption of oxygen and the other is the hole-trapping which makes to decrease in the concentration of charge-carrier. By the irradiation of γ-rays, surface excess oxygen may be converted to an adsorbed state bonding more strongly with the NiO lattice than the one before the irradiation, as

$$O^-_{(ads)} \rightsquigarrow O^{2-}_{(ads)}.$$

Changes in the electrical conductivity of NiO(II) during the CO_2 adsorption were much less than those of NiO(I) as shown in Fig. 7. The adsorption processes of CO_2 on the both samples could be considered as follows[3]:

11) H. B. Charman and R. M. Dell, *J. Phys. Chem. Solids*, **23**, 1967 (1962); *Trans. Faraday Soc.*, **59**, 470 (1963).

12) I. Maxim and T. Braun, *J. Phys. Chem. Solids*, **24**, 537 (1963).

13) M. Nachman, L. Cojocaru and L. Ribco, *Nukleonik*, **10**, 1 (1967).

14) D. A. Young, *Discussions Faraday Soc.*, **31**, 267 (1961).

for NiO(I).

$$CO_2 + O^-_{(ads)} + Ni^{2+} = CO_3^{2-} + Ni^{3+} \quad (1)$$

and for NiO(II).

$$CO_2 + O^{2-}_{(ads)} + Ni^{2+} = CO_3^{2-} + Ni^{2+} \quad (2)$$

According to this mechanism, the concentration of Ni^{3+} ions in NiO(I) may be increased by the adsorption of CO_2, and the conductivity would be increased. Changes in the conductivity during the CO_2 adsorption was found to increase gradually as the pretreatment temperature was raised, and remarkable change was found above 200—250°C. This may be attributed to the change in the adsorbed state. Considering from the model proposed by Eischens *et al.*[15] and that proposed by Alexeyev *et al.*,[16] the change would be as follows:

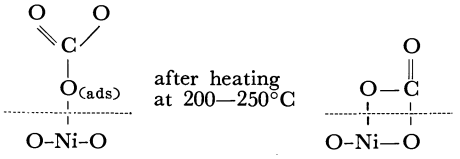

This model requires that, after a heat treatment at higher temperature, CO_2 should become to adsorb on nickel ions which formed as a result of desorption of surface excess oxygen.

The irregular variation observed in the electrical conductivity of irradiated NiO when the temperature of sample was raised *in vacuo*, seems to be associated with the abrupt desorption of excess oxygen (Figs. 4 and 5) in nearly the same temperature range. It can be concluded that the strongly chemisorbed oxygen produced by the irradiation ($O^-_{(ads)} \rightsquigarrow O^{2-}_{(ads)}$) may start to desorb suddenly at 150°C. Consequently the concentration of charge-carriers (positive holes) diminished and it caused the decrease of conductivity. The phenomena of "S" shaped variation in $\log \sigma$ *vs.* $1/T$ curve have been found in the case of n-type semiconductors,[15] *e. g.*, ZnO, CdS, *etc.* Experiments carried out by Dereń *et al.*[16] on the conductivity of NiO have shown that the $\log \sigma$-$1/T$ curve in hydrogen (2 mmHg) was nearly the same as that found in the present study for the irradiated NiO (Fig. 5). The same experiments in this laboratory have given the same result as above.

The suggestion drawn from these experiments was that semiconducting property of the surface layer of NiO would be changeable from p-type to n-type. However, the clear explanation of these phenomena remains as a problem for the future.

15) B. M. Arghiropoulos and S. J. Teichner, *J. Catalysis*, **3**, 477, (1964).

16) J. Dereń, J. Haber and J. Sloczynski, *Bull. de L'academie Polonaise des Sciences(Série des Sciences chimiques VIII)*, 391 (1960).

Interpretaion of Catalytic Sites on Irradiated NiO. Many groups of workers have studied in recent years on the radiation effects on the catalytic activity of powdered catalysts. However their results have been rather conflicting and varied considerably with experimental systems and procedures. Consequently, it is very difficult to interpret the mutual relation between active sites and the surface structure changed in terms of irradiation. In the present study, the catalytic activity of NiO for decomposition of H_2O_2 was increased, while that for decomposition of i-C_3H_7OH was decreased by the irradiation. It can be concluded that active sites on NiO produced by irradiation should be different in each reaction. Considering the proportional relation between the amount of excess oxygen determined by the iodometric titration and the catalytic activity changed by the irradiation, it can be concluded that the active sites for decomposition of H_2O_2 correspond to the positive holes.

In his considerations regarding the mechanism of catalytic decomposition of H_2O_2 on NiO, Roginsky[17] has assumed that the positive holes produced by oxygen adsorption could be the acceptors of electrons from reactants. According to this assumption, the catalysts with higher concentration of positive holes would have the higher catalytic activity. The model proposed by Roginsky might be applied to the interpretation in the case of irradiated NiO.

On the other hand, the active sites for decomposition of i-C_3H_7OH, adsorption of CO_2 would not relate to the positive holes, but to the adsorption state of oxygen on irradiated NiO. Experiments on reductive properties of NiO, showed that reactivity of surface oxygen on irradiated NiO was much less than that on non-irradiated NiO.

The amount of CO_2 adsorbed by irradiated sample (NiO(II)) was only one-fourth of that by NiO(I). The nature of adsorption sites for CO_2 on NiO seems to be affected by the state of surface excess oxygen, *i. e.*, whether the surface excess oxygen is chemisorbed strongly or weakly. The adsorption measurements have shown that the ratio of the amount of i-C_3H_7OH adsorbed by the both samples at room temperature, was nearly the same as that of CO_2 at room temperature. From the above consideration, it seems to be most reasonable to conclude that the weakly chemisorbed oxygen ($O^-_{(ad)}$) might be more reactive than the strongly chemisorbed one ($O^{2-}_{(ad)}$) for decomposition reaction of i-C_3H_7OH. However, further clarification on the active sites produced on NiO by the irradiation must await more detailed studies.

17) S. Z. Roginsky, *J. Chem. Sci. Ind.*, **2**, (2) (1957).

BULLETIN OF THE CHEMICAL SOCIETY OF JAPAN VOL. 41 2264—2269 (1968)

UV and Visible Absorption Spectra of Monohalogenated Anthracenes. I. The First Absorption Bands

Isao OHNO

Department of Electronic Engineering, Faculty of Engineering, Tamagawa University, Machida, Tokyo

and Kaoru IGUCHI

Department of Chemistry, School of Science and Engineering, Waseda University, Nishiokubo, Tokyo

(Received February 3, 1968)

UV and visible absorption spectra of monohalogenated anthracenes are measured, and the first absorption band are reported. When anthracene is monohalogenated, the first absorption band slightly shifts toward red or does not shift in accordance with the change in the position and the species of the substituting halogen atom, but the vibrational structure remains unchanged. The sequence of magnitude of red shift due to the position is 9-halo>1-halo>2-halo-anthracene, while that due to the species is different depending on the substituted position: in the 9-position, it is monobromo>monochloro>monofluoro>monoiodo anthracene, and, in the 1 or 2-position, it is monochloro>monofluoro>monobromo≃monoiodo anthracene. For the sequence of red shift due to the species of the substituting halogen atom, there are similarities between the first absorption band of monohalogenated anthracenes and the K or B-band of monohalogenated benzenes. These results are discussed in terms of the simple LCAO MO perturbation treatment.

The effect of monohalogenation and other substitution of aromatic hydrocarbons on UV and visible absorption spectra has been studied by many authors,[1-5] where the shift and the intensity-variation of the absorption peaks have been examined. In polyacene, this effect of monohalogenation is so weak that the theoretical consideration may be treated with a perturbation theory containing some parameter determinations. The perturbation consists of two factors; the variation of 1) the steric configuration and 2) the electronic structure.

In UV and visible absorption spectra of anthracene, the first absorption band appears at near 380 mμ, and the second band at near 250 mμ. The first band has a prominent vibrational structure which is characteristic of polyacene, and the calculated energy[6] and the assignment of the transition, A_{1g}–B_{2u}, are well supported by many experimental data.[7] Since early, UV and visible absorption spectra of some of monochloro and monobromo anthracenes have been reported together with other simple substituted anthracenes.[8] Recently, the charge transfer band,[9] the excimer fluorescence and dimer absorption spectra[10] of these have been studied, but the complete systematic examination has never been reported.

For the extensive study of monohalogenated anthracenes, we have synthesized and purified all isomers of monofluoro, monochloro, monobromo and monoiodo anthracene. In this paper, we will report UV and visible absorption spectra corresponding to the first absorption band; wavelengths for O–O transition, the vibrational assignment and molar extinction coefficients of the first band. Also, these results are discussed systematically in terms of the simple LCAO MO perturbation treatment.

Experimental and Results

Samples were synthesized in the process as shown in Table 1, and purified by recrystallization from a suitable solvent, sublimation and column chromatography. The detail of sample preparation will be reported in another paper, (together with some of their properties and results of their elementary analysies). In this paper, the existence of halogen atoms except fluorine was confirmed qualitatively by Beilstein Method.

1) A. L. Sklar, *J. Chem. Phys.*, **7**, 984 (1939).
2) F. A. Matsen, *J. Am. Chem. Soc.*, **72**, 5243 (1950); W. W. Robertson and F. A. Matsen, *ibid.*, **72**, 5252 (1950).
3) Y. I'haya, *J. Am. Chem. Soc.*, **81**, 6120 (1959).
4) S. Nagakura and K. Kimura, *Nippon Kagaku Zasshi (J. Chem, Soc. Japan, Pure Chem. Sect.)*, **86**, 1 (1965).
5) K. Iguchi, T. Nozaki, A. Imamura and S. Takahashi, This Bulletin, **36**, 697 (1963).
6) R. Pariser, *J. Chem. Phys.*, **24**, 250 (1956).
7) J. W. Sidman, *ibid.*, **25**, 115 (1956).
8) J. A. Christiansen, *Z. Physik. Chem., (B)*, **33**, 133 (1936).
9) A. Kuboyama, *Rep. Gov. Chem. Ind. Res., Tokyo*, **59**, 1 (1964).
10) E. A. Chandrass and J. Ferguson, *J. Chem. Phys.*, **45**, 3554 (1966).

TABLE 1. PREPARATIONS OF MONOHALOGENATED ANTHRACENES

Halide	Starting material	Reaction	
9-Fluoro anthracene	Anthracene	*p*-Tolyliododifluoride →	
9-Chloro anthracene		Cl_2 →	
9-Bromo anthracene		Br_2 →	
9-Iodo anthracene	9-Bromo anthracene	Mg+I →	
1-Fluoro anthracene	1-Amino anthraquinone	The Schieman reaction	Reduction
1-Chloro anthracene		The Sandmeyer reaction	
1-Bromo anthracene			
1-Iodo anthracene			
2-Fluoro anthracene	2-Amino anthraquinone	Same as the above reaction	
2-Chloro anthracene			
2-Bromo anthracene			
2-Iodo anthracene			

The sample (*ca.* 1 mg) was dissolved in purified *n*-hexane (10 m*l*); then a definite volume (*ca.* 1 m*l*) of the solution was withdrawn and added to the same solvent (10 m*l*) in absorption cell. The absorption spectra were measured at room temperature with a Hitachi EPS-3 spectrophotometer in the range 290—410 mμ. They correspond to the first excitation band and are illustrated in Figs. 1—4. Wavelengths of absorption peaks, molar extinction coefficients*1 and the vibrational assignment are given in Table 2.

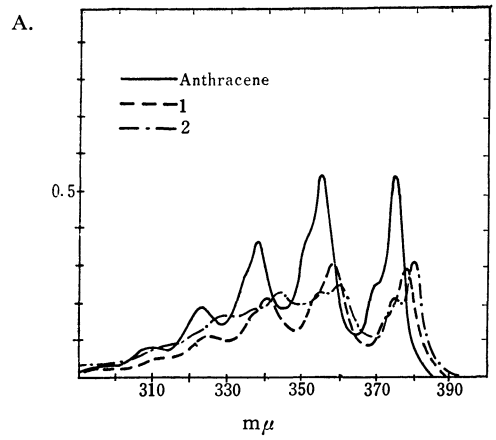

Fig. 1. The first absorption bands of anthracene and monofluoro anthracenes.
Concentration (10^{-5} mol/*l*)
$C_a=5.72$
$C_1=4.60$
$C_2=5.68$

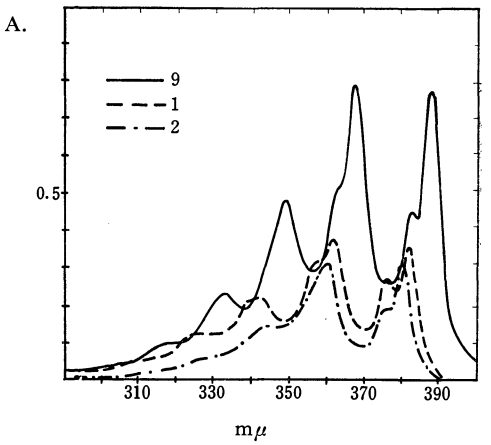

Fig. 2. The first absorption bands of monochloro anthracenes.
Concentration (10^{-5} mol/*l*)
$C_9=8.68$
$C_1=4.90$
$C_2=5.40$

The vibrational structure of the first absorption band of monohalogenated anthracene, two prominent vibrational progressions, appear clearly as those of anthracene. The wavelength of the absorption peak slightly shifts toward red or does not in accordance with the position and the species of the substituting halogen atom. The magnitude of shift is so small that the effect of monohalogenation on the electronic state of anthracene may be regarded as a perturbation, and so we will make a perturbation treatment in later section.

*1 We calculated the molar extinction coefficients by k=[absorbance]/[mole concentration]·[light path (cm)].

Though the monofluorination and the monochlorination have an influence on the first absorption band, the monobromination has an influence only when it is made at the 9-position, while the monoiodination has no influence. The sequence of red shift due to the atomic species is varied in accordance with the substituted position. In 9-position, it is monobromo > monochloro > (monofluoro)*2 > monoiodo anthracene, and in the 1 or 2-position, it is monochloro > monofluoro > monobromo > monoiodo anthracene. It is notable that the sequence of red shift due to the species of the substituting halogen atom in the 1 or 2-halo-anthracene is similar to that in the first absorption band, *i.e.*, B-band (A_{1g}–B_{2u}), of monohalogenated benzene, and the sequence in 9-halo-anthracene is almost similar to that in the second absorption band, *i.e.*, K-band (A_{1g}–B_{1u}).

Prominent vibrational frequencies are the same as those of anthracene; they are about 1400 cm^{-1} and about 400 cm^{-1}, which slightly depend on states of aggregation (gas, liquid, crystal phase or solvent used). The vibration of 1400 cm^{-1} is assigned to the stretching of carbon skeleton (Gamma Carbon Stretching) and another vibration is assigned to the skeletal bending.[7]

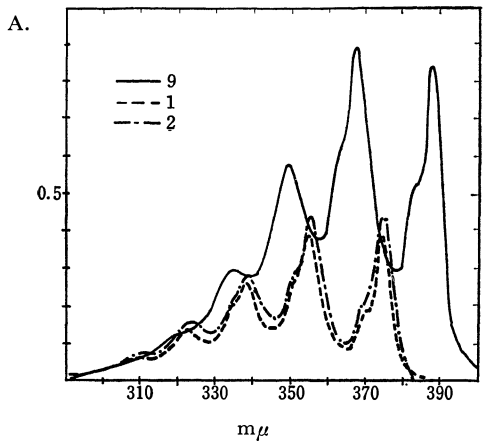

Fig. 3. The first absorption bands of monobromo anthracenes.
Concentration (10^{-5} mol/l)
C_9=9.03
C_1=4.93
C_2=4.49

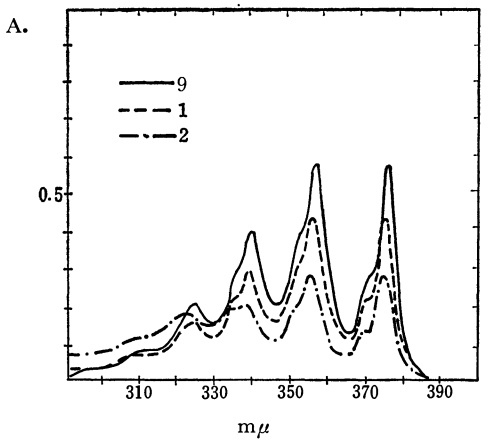

Fig. 4. The first absorption bands of monoiodo anthracenes.
Concentration (10^{-5} mol/l)
C_9=6.26
C_1=3.83
C_2=4.20

*2 Separation of 9-fluoro anthracene from unchanged anthracene was very difficult. We obtained the absorption peak at 386 mμ which is sure to be O-O transition of the first absorption band of 9-fluoro anthracene, but the other vibrational components could not be separated from those of the unchanged anthracene.

Discussion

Since early, experimental and theoretical studies of monosubstituted benzenes have accumulated a lot of information on electronic spectra of aromatic molecules.[1-4] These benzene derivatives are divided into two groups[4]: one has the substituents such as NO_2, NH_2 which interact strongly with the π-electron system of benzene, another has the substituents which interact weakly with it. Fluorine, chlorine and bromine atoms have a weak interaction with benzene, or more generally, with aromatic molecules. Iodine atom shows special effects, in which the Rydberg transition of iodine atom is mixed in the absorption spectra of benzene derivatives[4] and the steric effect appears in *p*-terphenyl derivatives,[5] but such special effects were not observed by us in the first absorption band of anthracene derivatives.

In spite of the simplicity, LCAO MO perturbation treatment gives many useful and intuitional informations. So this treatment has been used by many authors[2,3,5] since early to elucidate the effect of substitution on electronic spectra of aromatic molecules. Iguchi and his co-workers[5] applied the perturbation theory[11] to *p*-terphenyl derivatives, and obtained a good qualitative agreement between theory and experiment. Now, we intend to explain our experimental data with the same treatment.

It is known that a forbidden transition exists in the neighobrhood of this allowed transition (the first absorption band). In the Hückel approximation, however, both the highest occupied (No. 7) and lowest unoccupied (No. 7′) MO's, are well separated from other MO's. The first absorption corresponds principally to the transition No. 7—No. 7′ of MO's, and the forbidden transition to No. 7—No. 6′ (see Pariser[6]). Thus the effect

11) K. Fukui, C. Nagata, T. Yonezawa, H. Kato and K. Morimura, *J. Chem. Phys.*, **31**, 287 (1959).

TABLE 2. WAVELENGTHS, WAVE NUMBERS AND MOLAR EXTINCTION COEFFICIENTS OF THE ABSORPTION PEAKS OF ANTHRACENE AND MONOHALOGENATED ANTHRACENES

[λ in mμ, ν in 10^4 cm^{-1} and k in 10^3 mol^{-1} l cm^{-1}]

λ	ν	k	λ	ν	k	λ	ν	k	λ	ν	k
i) Anthracene			iv) 9-Cl			vii) 9-Br			x) 9-I		
375*	2.66	9.51	387*	2.58	8.99	388*	2.57	10.46	375*	2.66	9.08
370	2.70	4.47	383	2.62	5.30	383	2.61	5.75	370	2.70	4.35
356	2.80	9.56	367	2.72	9.08	368	2.71	9.99	356	2.80	9.19
351	2.84	6.26	362	2.76	5.87	363	2.75	6.67	351	2.84	6.32
339	2.94	6.35	349	2.86	5.53	350	2.85	6.44	339	2.94	4.42
335	2.98	4.73	344	2.90	4.03	345	2.89	4.99	335	2.98	3.32
324	3.08	3.28	333	3.00	2.74	334	2.99	3.33	324	3.08	2.53
319	3.13	2.29	329	3.04	2.19	330	3.03	2.44	319	3.13	1.26
310	3.22	1.35	318	3.14	0.92	319	3.13	1.39	310	3.22	0.95
297	3.36	0.52	304	3.28	0.46	305	3.27	0.55	297	3.36	0.47
ii) 1-F			v) 1-Cl			viii) 1-Br			xi) 1-I		
377*	2.65	6.37	382*	2.62	7.38	375*	2.66	7.87	375*	2.66	11.22
372	2.69	3.68	376	2.66	5.75	370	2.70	3.86	370	2.70	5.48
358	2.79	6.72	362	2.76	7.85	356	2.81	7.91	356	2.81	11.27
353	2.83	4.77	357	2.80	6.67	351	2.85	5.27	351	2.85	7.30
341	2.93	4.73	344	2.90	5.50	339	2.95	5.35	339	2.95	7.62
336	2.97	3.58	340	2.94	4.89	335	2.99	3.95	335	2.99	5.61
325	3.07	2.60	329	3.04	2.95	324	3.09	2.84	324	3.09	4.04
321	3.11	2.08	324	3.08	2.55	320	3.13	2.03	320	3.13	3.13
311	3.21	1.30	314	3.32	1.34	310	3.23	1.23	310	3.23	1.85
			301	3.32	0.77	296	3.37	0.63	297	3.37	0.86
iii) 2-F			vi) 2-Cl			ix) 2-Br			xii) 2-I		
379*	2.63	5.49	380*	2.63	5.92	375*	2.66	9.76	375*	2.67	6.66
374	2.67	3.80	375	2.67	3.38	370	2.70	4.68	370	2.71	3.49
360	2.77	4.45	360	2.77	6.03	356	2.81	9.81	355	2.81	6.73
354	2.82	4.04	356	2.81	5.18	351	2.85	6.13	351	2.85	4.40
343	2.91	4.04	342	2.92	4.31	339	2.95	6.24	339	2.95	4.48
338	2.95	3.34	339	2.95	4.10	335	2.99	4.91	335	2.99	4.45
329	3.04	2.97	327	3.05	2.51	323	3.09	3.59	323	3.09	4.28
322	3.10	2.16	323	3.09	2.47	320	3.13	2.67	319	3.13	3.76
313	3.19	1.58	313	3.19	1.29	310	3.23	1.69	310	3.23	2.66
301	3.32	0.79	300	3.33	0.74	309	3.31	0.67	297	3.37	1.76

* denotes O–O transition

of forbidden transition is neglected in our treatment.

The effect of monohalogenation on electronic spectra of aromatic molecules may be divided into three types: 1) steric effect, 2) inductive effect and 3) resonance effect. Other types may not be considered for the first approximation. Type 1) may be neglected in polyacene because of the rigidity of the framework. while it is essential in polyphenyl such as *p*-terphenyl.[5] It is assumed that the inductive and resonance effects by the halogen atom are restricted to the AO of carbon atom to which the halogen is attached. So, when the anthracene molecule is monohalogenated, the change of energy of the ith MO is given by[12]:

$$\Delta \boldsymbol{e}_i = \boldsymbol{e}_i - \boldsymbol{e}_i^0 = (\boldsymbol{C}_t^i)^2\alpha^{(1)} + (\boldsymbol{C}_t^i)^2/[\boldsymbol{e}_i^0 + (\boldsymbol{C}_t^i)^2\alpha^{(1)} - \alpha_x]\cdot\gamma^2 \quad (1)$$

Where $\boldsymbol{e}_i^0$ and $\boldsymbol{C}_t^i$ are the energy and coefficient of the tth AO in the ith MO, respectively; t denotes the position of monohalogenation. Also, α_x designates the energy of the highest occupied orbital (p-orbital) of halogen atom, while γ is the resonance integral of the bond between halogen atom and anthracene, $\alpha^{(1)}$ is the change of core integral of carbon atom by the inductive effect of halogen atom. Here we may neglect the change of α_x (H_{77} in Matsen's notation) by the inductive effect of anthracene molecule.[2] In the estimation

12) K. Iguchi, *ibid.*, **30**, 319 (1959).

of the order of magnitude $(-\boldsymbol{e}_i^0)$ and $(-\underline{\alpha_x})$ may be regarded almost equal to ionization potentials of anthracene and methyl halides, respectively.[13] So, we have $(-\boldsymbol{e}_i^0) \simeq 7$ eV, $(-\alpha_x) \simeq 10$ eV, $(\boldsymbol{C}_t^i)^2 \lesssim 0.2$ and $\alpha^{(1)} \lesssim 3.3$ eV (see Table 3 and Fig. 5), then $(-\boldsymbol{e}_i^0)$ and $(-\alpha_x) \gg (\boldsymbol{C}_t^i)^2\alpha$.[1] Thus we may neglect the term $(\boldsymbol{C}_t^i)^2\alpha^{(1)}$ in denominator in Eq. (1). In alternant hydrocarbons the square of each AO coefficient is the same for both the highest occupied MO and the lowest unoccupied MO. Thus, the shift, δ, of the first absorption peak is expressed simply as

$$\Delta\boldsymbol{e}_{i'} - \Delta\boldsymbol{e}_i = \delta$$
$$= (\boldsymbol{C}_t^i)^2[1/(\alpha - k_t) - 1/(\alpha + k_t)]\cdot\gamma^2$$
$$\text{and} \qquad \alpha = \alpha_c^0 - \alpha_x,\ \boldsymbol{e}_i^0 = \alpha_c^0 + k_t \qquad (2)$$

Here α_c^0 is the core integral of carbon atom and k_t is the root of Hückel seqular equation.

Since $(\alpha - k_t)$ is larger than $(\alpha + k_t)$, δ is always negative. Thus, so far as the resonance effect is dominant, the red shift of absorption peak occures in anthracene derivatives, or more generally in alternant hydrocarbon derivatives. The magnitude of the red shift is determined by three factors: 1) $(\boldsymbol{C}_t^i)^2$, *i.e.*, the square of the coefficient of the tth AO in the ith MO, 2) the energy of the highest occupied orbital (p-orbital) of halogen atom and 3) the resonance integral between anthracene and halogen atom.

Now, let us consider the sequence of red shift. First, we consider the sequence due to the monohalogenated position. In this case, factor 2) and 3) are common for all position, so that the shift is determined by factor 1). From Fig. 5, giving the value of $(\boldsymbol{C}_t^i)^2$ calculated by Hückel approximation, the theoretical prediction of the sequence of red shift due to the position may be 9-halo > 1-halo > 2-halo-anthracene. This prediction is almost in harmony with our experimental data. Next, we consider the sequence of red shift due to the atomic species. In this case, factor 1) is common for all species, so that the sequence is determined by factor 2) and factor 3). Ionization potentials of halogenated methyls and the pure anthracene are listed in Table 3, and the sequence of its value is F > Cl > Br > I-methyls > anthracene. The evaluation of the resonance integral between halogen atom

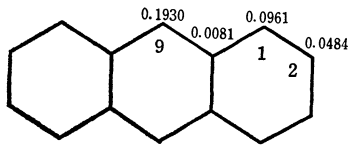

Fig. 5. The square of MO coefficients in the highest occupied orbital (same as the lowest unoccupied orbital).

13) R. S. Mulliken, *Phys. Rev.*, **74**, 736 (1948).

Table 3. Ionization potentials of methyl halides[a] and the pure anthracene[b], resonance integral of C-X bond[c], and changes of core integral of carbon atom by the inductive effect of halogen atom ($\alpha^{(1)}$ in our notation)[d]

i)	Ionization potentials (eV)	
	CH_3F	12.61
	CH_3Cl	11.34
	CH_3Br	10.50
	CH_3I	9.55
	Anthracene	7.4
ii)	Resonance integral, γ (eV)	
	C-F	1.28
	C-Cl	1.58
	C-Br	1.93
	C-I	1.20
iii)	Changes of core integral, $\alpha^{(1)}$ (eV)	
	F	3.3
	Cl	2.4
	Br	1.8
	I	

a, c) See Ref. 4.
b) F. Gutmann and L. E. Lyons, "Organic Semiconductors," John Wiley and Sons, Inc., New York, N. Y. (1967).
d) See Ref. 2. These values were roughly estimated from the oscillator strengths of phenyl halides.

and anthracene is one of the most important problem in discussion of the effect of substitution and will be discussed elsewhere. Here we will use semiempirical values determined by Nagakura[4] in electronic spectra of monohalogenated benzene. The sequence of magnitude is Br > Cl > I > F, as shown in Table 3. So, the theoretical prediction for the sequence of red shift of the absorption peak is monobromo > monochloro > monoiodo > monofluoro anthracene. The agreement between this prediction and our experimental data is not satisfactory; this prediction is only in harmony with the sequence of 9-bromo and 9-chloro anthracene, but does not the other monohalogenated anthracenes. And further the difference of the sequence due to the species in accordance with the substituted position cannot be explained by this treatment.

Some reasons for this disagreement will be thought as following. Essentially, the magnitude of the shift is too small to predict exactly with the simple LCAO MO perturbation treatment. Scince the density of π-electron in the highest occupied orbital and that in the lowest unoccupied orbital are largest at the 9-position, it may be allowed to neglect the resonance between halogen atom and carbon atoms to which the halogen atom is not attached, in the case of 9-halo-anthracenes. But in the cases of the other halogenated anthracenes,

it may not be allowed. We neglected the steric effect. If the substitution of the heavy atom such as bromine and iodine causes the distortion of the skeletal framework, it may affect the electronic structure. Our experimental fact is well explained if we assume that this distortion effect causes the blue shift and cancels out the red shift by the resonance effect in monohalogenated anthracene. However, there is no decisive evidence to support this assumption. On the contrary, it is reported that the distortion of skeletal framework causes red shift in substituted benzene.[14]

14) J. Dale, *Chem. Ber.*, **94**, 2821 (1961).

In this experiment it is found that the wavelengths of absorption peaks of monoiodo anthracenes and 1 or 2-bromo anthracene are not different from those of anthracene. This point will require a more detail examination. We are planning the elementary analysis and the measurement of infrared spectra to make sure the structure of monohalogenated anthracenes, and the results will be published in another paper.

One of the authors (I. O.) wishes to express his gratitude to Professor S. Aono of Kanazawa University for his continual encouragements, and also to Professor H. Miyazawa of Tamagawa University for his invaluable suggestion.

BULLETIN OF THE CHEMICAL SOCIETY OF JAPAN VOL. 41 2269—2273 (1968)

Nuclear Magnetic Double-resonance Study of the Hindered Internal Rotation in Formamide

Hirotake KAMEI

Electrotechnical Laboratory, Tanashi, Tokyo

(Received February 13, 1968)

The nitrogen-14 quadrupole relaxation broadening effect on the proton spectrum of formamide was eliminated by a $^{1}H-\{^{14}N\}$ double resonance technique. The completely-decoupled proton spectra of formamide in the neat liquid and in acetone, dioxane, and water solutions were observed at several temperatures. The spectra observed at room temperature were analyzed on the basis of an ABC system, while the spectra at higher temperatures ($\sim$100°C) were analyzed on the basis of an AB_2 system. From the changes in the resonance lines of the formyl proton with the temperature, the values of the activation energy for the hindered internal rotation about the C-N bond, E_a^{rot}, and for the intermolecular proton exchange involving the amine protons, E_a^{ex}, were obtained. It has been found that the hydrogen-bond formation on the carbonyl oxygen of formamide increases the E_a^{rot} value and the magnitude of the vicinal coupling constants, while it decreases the magnitude of the geminal coupling constant.

The hindered internal rotation in amides has been attributed to the partial double-bond character in the C-N bond resulting from a contribution from a resonance form such as II.

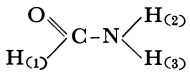

I

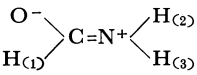

II

The stability of the II resonance form must be affected by the nature of the intermolecular interactions between amide and the solvent molecule. One would predict a solvent effect on the activation energy for rotation about the C-N bond. Such solvent effect has been demonstrated for *N,N*-disubstituted amides[1,2] and thioamides[3] using a nuclear magnetic resoance technique. Effects due to protonation[4] and complex formation[5] have also been observed. Such solvent effects are also found for unsubstituted amides. However, the resonance lines of the protons bonded directly to nitrogen are broadened, and a complete analysis of the spectrum is usually not possible. The broad nature of the lines is derived from the quadrupole coupling of the ^{14}N nucleus. The quadrupole broadening can be eliminated by a technique of

1) J. C. Woodbrey and M. T. Rogers, *J. Am. Chem. Soc.*, **84**, 13 (1962).

2) A. G. Whittaker and S. Siegel, *J. Chem. Phys.*, **42**, 3320 (1965); **43**, 1745 (1965).

3) A. Loewenstein, A. Melera, P. Rigny, and W. Walter, *J. Phys. Chem.*, **68**, 1597 (1964).

4) G. Fraenkel and C. Franconi, *J. Am. Chem. Soc.*, **82**, 4478 (1960).

5) E. S. Gore, D. J. Blears, and S. S. Danyluk, *Can. J. Chem.*, **43**, 2135 (1965).

nuclear magnetic double resonance[6] and also by the substitution of the isotope, ^{15}N. Sunners *et al.*[7] studied ^{15}N-substituted formamide and found the activation energy for rotation, E_a^{rot}, to be 18±3 kcal/mol for formamide in a 10 mol% acetone solution.

In the present work the quadrupole broadening was eliminated by the nuclear magnetic double-resonance technique. The completely-decoupled proton spectra of formamide were then obtained under different conditions. The values of E_a^{rot} have been determined in several solutions. The solvent effects on E_a^{rot} and NMR parameters will be discussed.

Experimental

Measurements. Double resonance experiments were carried out on a ^1H-{^{14}N} double resonance spectrometer which made possible the complete decoupling of the ^1H-^{14}N coupling by the irradiation of the large second radio-frequency field at about 2.9MHz and the observation of the proton resonance at 40MHz. Details of the spectrometer and associated equipments have been described elsewhere.[8]

Double-resonance proton spectra were obtained for each sample at several temperatures. The accuracy of the sample temperature determinations was about ±1°C. The frequency and width of each resonance line were determined by a method of sideband audio modulation, with an accuracy of ±(0.5%+0.05)Hz. In order to monitor the homogeneity of the field, the line width of cyclohexane, which was used as a reference, was measured in each measurement.

The measurements were made at a constant second radio-frequency field. The frequency was 2.88950 MHz, while the amplitude, H_2, was 4.3 gauss. The value of H_2 was determined from the Bloch-Siegert shift,[9] $\delta_B \sim \gamma^2 H_2^2/2\Delta\omega$, where $\Delta\omega$ is the frequency difference between the proton resonacne and the second radio-frequency field. Figure 1 shows typical spectrum

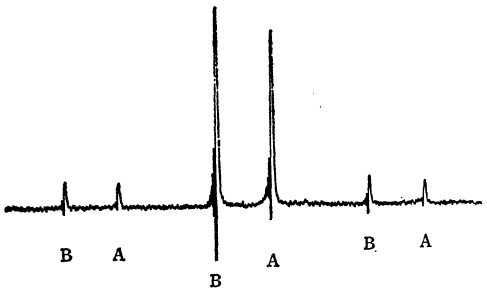

Fig. 1. Bloch-Siegert shift in cyclohexane resonance. A, normal resonance; B, H_2 supplied

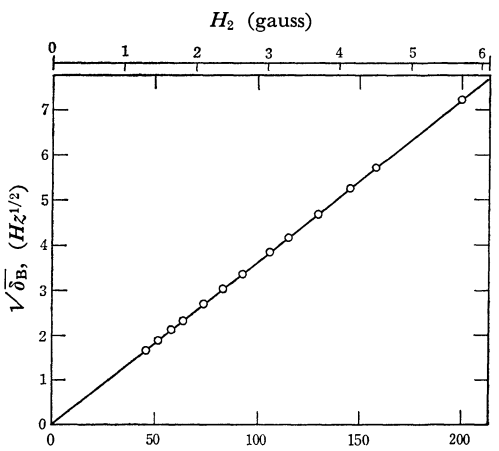

Fig. 2. Plot of $\sqrt{\delta_B}$ *vs.* the voltage of the second *r-f* field.

of cyclohexane with the bracketing side-band signals. When the second radio-frequency field is supplied, the resonance shifts to a lower field (from A to B). A plot of $\sqrt{\delta_B}$ *vs.* the voltage of second radio-frequency, to which H_2 is proportional, resulted in a straight line, as is shown in Fig. 2. Thus, H_2 can be determined precisely from the Bloch-Siegert shift in the hetero-nuclear double resonance.

Preparation of Samples. Formamide was purified as follows: With bromothymol blue as an indicator, reagent-grade formamide was neutralized with solid sodium hydroxide. Sodium formate was added to the neutral liquid, and formamide was fractionally distilled under reduced pressure by passing dry argon through. All the solvents were reagent-grade quality and were dried and doubly-distilled prior to use. The samples were degassed and sealed *in vacuo*. The compositions of the samples were determined by means of their weight.

Results and Discussion

Chemical Shifts and Coupling Constants at Room Temperature. The double-resonance proton spectra of formamide in the neat liquid and in water, acetone, and dioxane solutions at 27°C are shown in Fig. 3. The spectra can be assigned on the basis of three nonequivalent protons. This indicates that the rotation about the C–N bond is very slow at room temperature. The assignment of the spectra has been described previously.[10] The spectra have been analyzed on the basis of an ABC system, employing the Castellano-Waugh method.[11] Details of the method of spectrum analysis have been described elsewhere.[12]

6) J. D. Baldeschwieler and E. W. Randall, *Chem. Revs.*, **63**, 81 (1963).
7) B. Sunners, L. H. Piette, and W. G. Schneider, *Can. J. Chem.*, **38**, 681 (1960).
8) H. Kamei, *Japan. J. Appl. Phys.*, **4**, 212 (1965).
9) F. Bloch and A. Siegert, *Phys. Rev.*, **57**, 522 (1940); W. A. Anderson and R. Freeman, *J. Chem. Phys.*, **37**, 85 (1962).
10) H. Kamei, This Bulletin, **38**, 1212 (1965).
11) S. Castellano and J. S. Waugh, *J. Chem. Phys.*, **34**, 295 (1961).
12) M. Shibuya, H. Kamei, and T. Yonemoto, *Shizuoka-daigaku Denshikogaku-kenkyujo Kenkyuhokoku (Bull. Research Institute of Electronics, Shizuoka Univ.)*, **1**, 131 (1966).

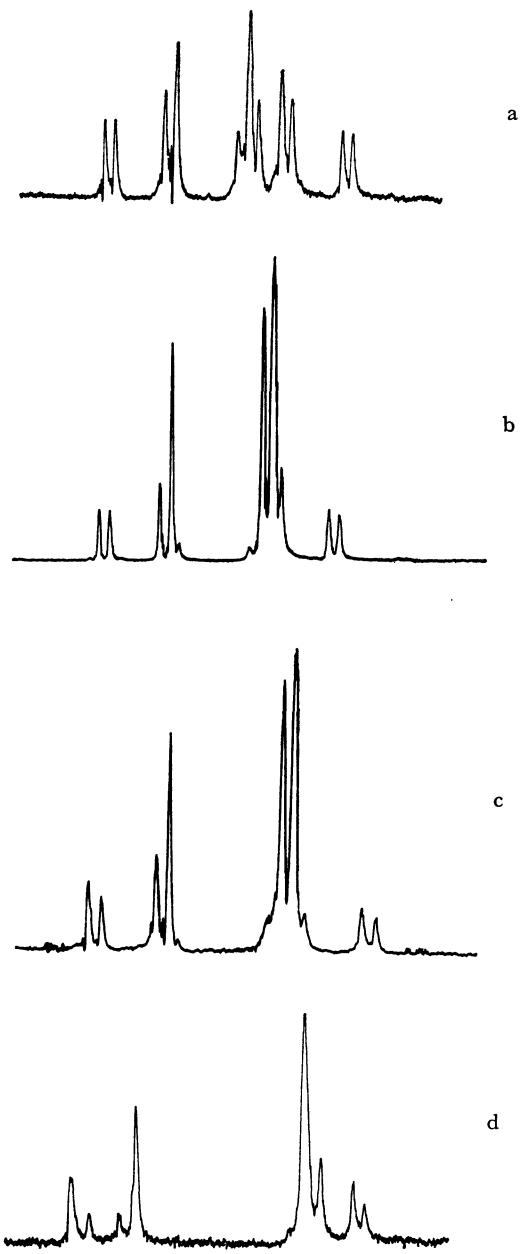

Fig. 3. ^{14}N decoupled proton spectra of formamide a) in the neat liquid, and in the solutions with b) water, c) acetone, and d) dioxane at 27°C.

The chemical shifts and coupling constants are given in Table 1. All the coupling constants have the same sign. The same results have been obtained for formamide-^{15}N by Bourn and Randall using a proton-proton double-resonance technqiue.[13]

A solvent effect on the chemical shift and the coupling constant is observed. This may arise from the different natures of the hydrogen-bond interactions in the different systems. Amine protons engage in the intermolecular hydrogen bond and the chemical shift is strongly dependent on the nature of the interactions with the solvent. No remarkable solvent dependence is found in the chemical shift of the formayl proton.

The coupling constant also shows a solvent dependence. This indicates that the molecular geometry or the electronic structure is affected by the intermolecular interactions.

Temperature Effects on the Spectrum. The spectra of formamide in the neat liquid at several temperatures are shown in Fig. 4. On raising the temperature, the rate of the hindered internal rotation about the C–N bond is increased,

Table 1. NMR Parameters (in Hz) of ABC type spectrum of formamide at 27°C

Solvent	Neat	Water	Acetone	Dioxane
Concentration mol%	100	22.8	22.2	24.6
δ_1	−266.8*1	−264.7*1	−266.4*2	−262.7*2
δ_2	−232.1*1	−228.9*1	−221.5*2	−215.8*2
δ_3	−239.9*1	−242.2*1	−229.4*2	−219.3*2
J_{12}	±13.6	±13.8	±13.5	±13.5
J_{13}	±2.0	±2.2	±1.7	±1.4
J_{23}	±2.4	±2.2	±2.7	±2.7

*1 Relative to cyclohexane as external reference and corrected for bulk diamagnetic susceptibility, χ_v. The values of $\chi_v(\times 10^6)$ for formamide, water, and cyclohexane at 27°C are taken to be −0.549, −0.717, and −0.626, respectively.
*2 Relative to cyclohexane as internal reference.

Table 2. NMR parameters (in Hz) of AB_2 type spectrum of formamide at higher temperatures

Solvent	Neat	Water	Dioxane
Concentration mol%	100	22.8	24.6
Temperature °C	102	93	101
δ_1	−268.2*1	−265.3*1	−263.8*2
$\delta_{2,3}$	−221.0*1	−221.1*1	−198.6*2
J	7.5	7.5	7.3
$\bar{\delta}$*3	−236.0	−235.5	−217.3
$\bar{J}$*3	7.8	8.0	7.5

*1 Relative to cyclohexane as external reference and corrected for bulk diamagnetic susceptibility, χ_v. The values of $\chi_v(\times 10^6)$ for formamide (93°C), formamide (102°C), water (93°C), cyclohexane (93°C), and cyclohexane (102°C) are taken to be −0.522, −0.519, −0.694, −0.572, and −0.564, respectively.
*2 Relative to cyclohexane as internal reference.
*3 $\bar{\delta}=(\delta_2^{27}+\delta_3^{27})/2$ and $\bar{J}=(J_{12}^{27}+J_{13}^{27})/2$.

13) A. J. R. Bourn and E. W. Randall, *Mol. Phys.*, **8**, 567 (1964).

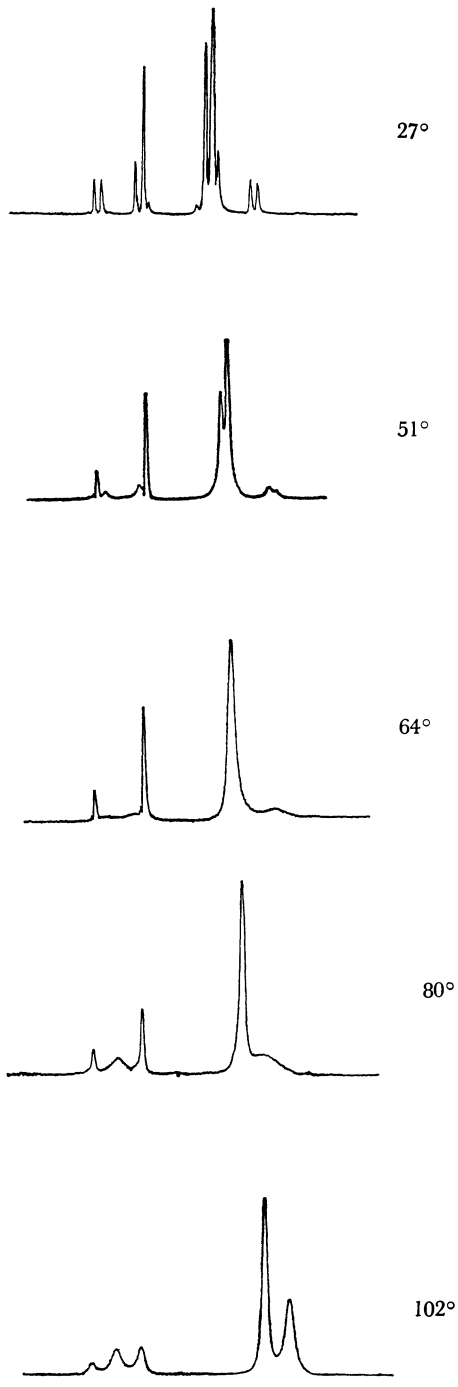

Fig. 4. ^{14}N decoupled proton spectra of formamide in the neat liquid at various temperatures.

and the spectrum is changed. At higher temperatures the rate of rotation becomes very rapid, so the amine protons are indistinguishable one from the other and the spectrum changes to an AB_2-type pattern. The coupling constants and the chemical shifts of the AB_2-type spectrum are given in Table 2, along with the average chemical shifts and the coupling constants at 27°C, $\bar{\delta}=(\delta_2^{27}+\delta_3^{27})/2$ and $\bar{J}=(J_{12}^{27}+J_{13}^{27})/2$. The signal of the amine protons is progressively shifted toward higher field with the increase in the temperature. This higher-field shift can be attributed to the increasing dissociation of the hydrogen bond involving these protons.

Hindered Internal Rotation and Intermolecular Proton Exchange. The signal shapes are influenced not only by the hindered internal rotation, but also by the intermolecular proton exchange involving the amine protons. As the temperature is raised, the rate of these rate processes increases and the lines broaden and coalesce. It is not possible to obtain the information concerning the hindered internal rotation separately from the information concerning changes in the signal of the amine protons. Although the formyl proton does not participate in the rate processes, its signal is affected by the rate processes through the spin-spin interaction. To the first-order approximation, the two outer lines of the $H_{(1)}$ quartet are unaffected by the internal rotation, and the line width and the separation between the two lines are not altered. Since the intermolecular proton exchange influences all the lines in the spectrum, the broadening of the two outer lines is attributable to the intermolecular proton exchange. The two inner lines broaden and ultimately coalesce. Changes in the separation between the two outer lines have not been observed up to 80°C.

The mean lifetime, 2τ, of the intermolecular proton exchange was evaluated from the broadening of the two outer lines in the $H_{(1)}$ quartet by employing the following relation:[14]

$$1/2\tau = \pi(\Delta' - \Delta) \qquad (1)$$

where Δ' (in Hz) is taken as the half-line width of the broadened line and where Δ is the line width in the absence of exchange. From 15°C to 30°C, changes in the line width have been lost in the experimental error. At lower temperatures a line broadening has been observed; this may arise from the increase in the viscosity of the sample. The line width at 27°C has been used as Δ. The values of the activation energy, E_a^{ex}, for the intermolecular proton exchange have been obtained from the plots of $\log 1/2\tau$ *vs.* $1/T$; the results are shown in Table 3. The value for the neat liquid is in good agreement with the value of 10 ± 3 kcal/mol reported by Sunners *et al.*[7] for formamide-^{15}N at higher temperatures, where internal rotation is already rapid.

In view of the above facts, it is possible to deal with the $H_{(1)}$ quartet by means of the approximation presented above.

14) J. A. Pople, W. G. Schneider, and H. J. Bernstein, "High-resolution Nuclear Magnetic Resonance," McGraw-Hill Book Co., New York, N. Y. (1959), p. 218.

TABLE 3. ACTIVATION ENERGY AND FREQUENCY FACTOR*

Solvent	Neat	Water	Acetone	Dioxane
Concentration mol%	100	22.8	22.2	24.6
E_a^{rot} (kcal/mol)	18.9±1.0	21.3±1.3	16.9±1.9	16.8±1.0
log A^{rot}	12.9±0.6	14.9±1.3	12.1±1.3	11.9±0.7
E_a^{ex} (kcal/mol)	12.1±2.5	14.5±5.5		11.7±1.3
log A^{ex}	7.6±1.5	9.3±3.5		7.1±0.8

* The errors quoted are 95% confidence limits.

At a given temperature the mean lifetime, 2τ, of the protons at the $H_{(2)}$ and $H_{(3)}$ positions was evaluated from the relation (1) (at lower temperatures) and the following relation[14] (at higher temperatures):

$$1/2\tau = \pi(\delta\nu)^2/2(\Delta' - \Delta) \qquad (2)$$

where $\delta\nu$ (in Hz) is the separation between two inner lines in the absence of rotation. The values of E_a^{rot} were obtained from the plots of log $1/2\,\tau$ *vs.* $1/T$. The results are given in Table 3, with the frequency factors.

The observed changes in E_a^{rot} with the solvent may be associated with the effects of the solvent on the partial double-bond character in the C–N bond. The predominant effect is a hydrogen-bonding effect. The hydrogen-bond formation on the carbonyl oxygen in the formamide molecule tends to favor the contribution of the II resonance form, and it increases the double bond character in the C–N bond. In acetone and dioxane solutions, the amine protons may be strongly bonded to the oxygen atoms in the acetone or dioxane molecule, while the carbonyl oxygen in the formamide molecule is left relatively free. Thus, the double-bond character in the C–N bond decreases and the activation energy is lowered compared to that in the neat liquid. In a water solution, the hydrogen bond between formamide and water is stronger than that of amide with itself, and a higher activation energy is found.

BULLETIN OF THE CHEMICAL SOCIETY OF JAPAN VOL. 41 2274—2280 (1968)

Studies on the Radical Species in Solid Methylene Blue as Revealed from the ESR Spectra

Michio OKUDA, Takeo KOWATA, Yoshiharu USUI and Masao KOIZUMI

Department of Chemistry, Faculty of Science, Tohoku University, Katahira-cho, Sendai

(Received February 19, 1968)

The ESR signals of polycrystalline methylene blue (MB) salts have been investigated in respect to a) temperature effect, b) anion effect, c) influence of the addition of donor and acceptor and d) response to visible light irradiation. a) The signal intensity in general increases with the rising temperature, but a sharp difference in the ESR behavior has been found above and below room temperature. Response to the temperature change at low temperature is reversible and the apparent activation energy is *ca.* 0.03 eV (L-type behavior) whereas the high temperature behavior has a marked tendency of irreversibility and the activation energy is at least one order larger (H-type behavior). b) No essential anion effect has been observed on *g*-value, line shape and spin concentration for chloride, iodide and phosphate. c) The addition of trinitrobenzene and paraphenylenediamine in 10 : 1 to MB chloride also had no essential effect. d) Corresponding to the L-type and H-type behavior observed in a), visible light irradiation has been found to cause a decrease or an increase in signal intensity respectively at low and high temperature. From these findings it has been concluded that there are at least two kinds of defect (L-type and H-type) and that the formation of radical species occurs only on such defect sites. Some suggestions have been made on the nature of these two types of defects and on the molecular processes occurring at or near these defect sites. The radical formation reaction is most likely to be connected with dye-dye interaction, $D^+ + D^+ \rightleftarrows D^{++} + D$.

The past work has shown that some kinds of dye give ESR signals in the solid state; various mechanisms have been proposed for their appearance, but they are not always amply established. Terenin *et al.*[1] have proposed a conduction electron theory for xanthene and triphenylmethan dyes, on the basis of the similar dependence of conductivity and of the ESR signal intensity upon the addition of water or oxygen. Nelson *et al.*[2] has claimed for the case of crystal violet, the occurrence of electron transfer between dye cation and its paired anion, because of great dependence of the features of the signal on the paired anion. Other mechanisms conceivable from relevant work are the biradical theory which has been mentioned by Simpson *et al.*,[3] and the defect theory suggested by Lagercrantz *et al.*[4] for methylene blue.

In the present paper attention is focused on the possibility of electron transfer between two dye cations. Since the occurrence of the analogous process has been well established by our group[5] and by Lindqvist[6] in the case of the photoreaction of some dyes in solution, it is quite natural to expect its occurrence also in the solid state where dye ions exist close with each other.

Choosing methylene blue, we have investigated the effect of temperature, of paired anions, of the addition of typical electron donor or acceptor and of the visible light illumination on the ESR signal of the polycrystalline sample. ESR in methylene blue was studied previously by Lagercrantz *et al.*[4] and by Simpson *et al.*[3] in the solid state but there is disagreement in many respects. On the other hand, ESR signals of methylene blue radical have been reported by Heineken *et al.*[7] and by Tuck *et al.*[8] in the acidic or alkaline solution.

Experimental

Materials. Methylene blue chloride, Merck G. R. grade was purified by two methods, by recrystallization from *n*-buthanol and by the method reported by Bergmann *et al.*[9] The latter is particularly effective

1) V. Holmogorov and S. Terenin, *Naturwiss.*, **50**, 299 (1963).
2) R. C. Nelson and L. C. Brown, *J. Chem. Phys.*, **39**, 499 (1963).
3) L. P. Simpson, J. S. Kirby-Smith and M. L. Randolph, *Nature*, **199**, 243 (1963).
4) C. Lagercrantz and M. Yjheland, *Acta Chem. Scand.*, **15**, 1204 (1961).
5) S. Kato, M. Morita and M. Koizumi, This Bulletin, **37**, 117 (1964); Y. Usui, K. Itoh and M. Koizumi, *ibid.*, **38**, 1015 (1965).
6) L. Lindqvist, *Arkiv. Kemi*, **16**, 79 (1960); J. Kaoshe and L. Lindqvist, *J. Phys. Chem.*, **68**, 817 (1964).
7) F. W. Heineken, M. Bruin and F. Bruin, *J. Chem. Phys.*, **37**, 1479 (1962).
8) L. D. Tuck and D. W. Schiesor, *J. Phys. Chem.*, **66**, 937 (1962).
9) K. Bergmann and C. T. O'Konski, *ibid.*, **67**, 2169 (1963).

for removing a trace of trimethylthionine, which can be preferentially extracted from the aqueous 0.01 N ammonia-alkaline solution of methylene blue (0.1 g 100c) with benzene layer. Ten to twenty times extraction was necessary for the disappearance of the purple color of trimethylthionine in benzene layer. The solution of methylene blue purified, was concentrated under reduced pressure at room temperature and the obtained sample was dried below 40°C for 7 hr in an ampule at 10^{-5} mmHg.

s-Trinitrobenzene of Wakō G. R. grade was recrystallized from benzene at least three times. Paraphenylenediamine was purified by sublimation *in vacuo*.

The mixture of methylene blue with trinitrobenzene or paraphenylenediamine was prepared in the following way. The mixture at a desired composition was milled in a mortar and pressed at 4000 kg/cm^2 after degassing. The pressed sample was crashed to the size less than 1.5 mm and then desiccated in an ampule similarly as in the case of polycrystalline sample.

Procedure. All the samples dried in ampules were transferred to ESR sample tubes (5 mm in diameter) *in vacuo* and then sealed off. All the above procedures were performed in the dark. The ESR spectra were measured by a JEOL JESP-10 type ESR spectrometer (X-band, 100KC field modulation). The temperature was controlled over the range from 137°K to 373°K by passing a cold gas from liquid nitrogen or hot air through the inside of the cavity. The constancy was ±0.5°C. A light source was usually a projector incandescent lamp (Kondo 100V-500W, operated at 90V). Y2 cut off filter ($\lambda>470$ nm) and a $CuSO_4$ aq. solution filter were employed. For the investigation of the wavelength effect, Xe-arc lamp (Ushio UXL 500W) was used with a set of suitable interference filters. The light was focused on the sample tube with a condenser lens ($f\simeq1.8$). Intensity was not controlled in particular but was ascertained to be nearly the same.

Results and Discussion

To examine the possible effect of impurity, the samples purified by different methods have been compared at first. The samples recrystallized five times and eight times from *n*-buthanol showed the ESR signal of nearly equal intensity; it was always a single line of Lorentzian type with $\Delta H_{msl}=9.6$ and $g=2.0049$. Figure 1 shows one example. The spin concentration was respectively 1.3×10^{18} and 1.4×10^{18} per unit gram. The sample purified by Bergmann's method also gave the spin concentration of $\sim1\times10^{18}$ spins/g. These values are of the same order as the one reported by Simpson, 1.2×10^{18} spin/g and also are not very different from 10^{15}—10^{18} spin/g of Lagercrantz. On the basis of the above agreement irrespective of the different procedures in making samples, one may safely conclude that the signal is intrinsic for methylene blue.

Temperature Effect. As the first attempt to elucidate the origin of ESR signal, measurements were made at different temperatures from 143 to 343°K. Such studies are expected to be helpful to distinguish the defect theory, the conduction electron theory and the biradical theory.

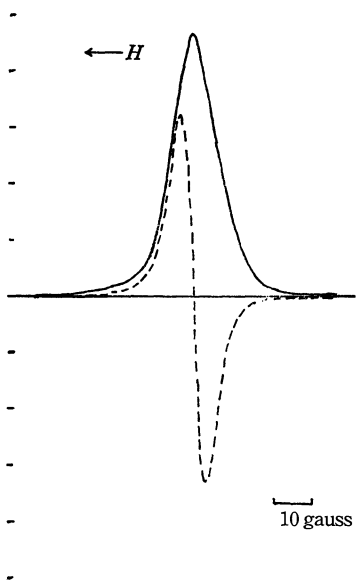

Fig. 1. ESR line shape of methylene blue chloride in the solid state.
Solid line: Integrated curve
Dotted line: Differential curve

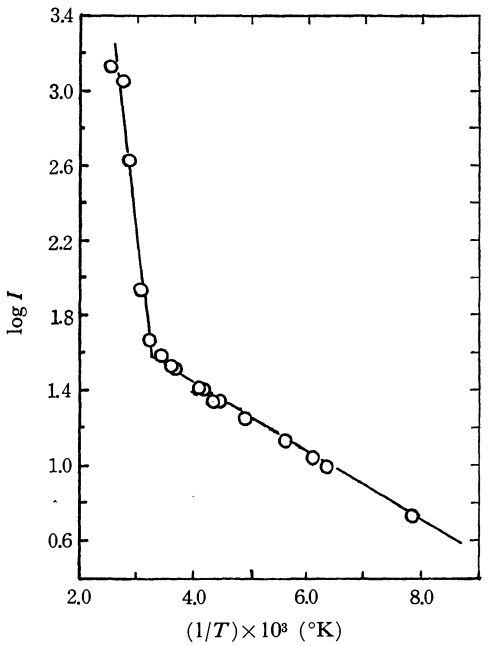

Fig. 2. Temperature dependence of the signal intensity of polycrystalline MB.

The essential features of the signal remain the same throughout the entire temperature region. The intensity increases monotonously with the rise of temperature. This agrees with Lagercrantz

at least qualtitatively, but not with Simpson. A notable finding is that in the response to temperature change, a clear difference exists above and below room temperature. Thus in the lower temperature region, the response is rather rapid and the change is reversible. At higher temperature, on the other hand, the response is very slow, requiring as long as several hours to get the final state at ~340°K. Around this temperature the equilibrium intensity is difficult to determine; the behavior appeared often to be even irreversible. The temperature dependence of the signal intensity (I) in the high and low temperature regions was found to be different in the order of magnitude. Figure 2 gives the plot of log I (corrected for Curie Law) against $1/T$. In the higher temperature region, the I-value at one to two hours after fixing temperature in heating experiments, was conventionally adopted. It is evident that the plot consists of two linear parts; from the slopes of the two linear lines, the energy difference between the two states with and without unpaired electron, was evaluated as 0.036 eV (ΔE^{L}) and 0.28 eV (ΔE^{H}) respectively for low and high temperature regions.

Although there is some ambiguity in the latter value, yet it is quite definite that ΔE^{L} is of the order of van der Waals energy and ΔE^{H} is more than one order larger.

If the electrons raised to the conduction band were the origin of the signal, as in the case of triphenylmethane and xanthene dyes,[1] the values of ΔE should be of the same order as the one evaluated from the temperature dependence of the electric conductivity. The latter value of Meier[10] is 1.36 eV and the value of Matsumoto is 1.6 eV[11] in the room temperature region; these values differ from the above ΔE values in the order of magnitude. Hence the conductive electron theory in a simple form may be rejected for the present sample. The biradical theory may also be ruled out from the similar reasoning, since the triplet level is expected to be located much higher than ΔE^{H} and ΔE^{L}.

On the other hand, the defect theory proposed by Lagercrantz[4] seems to be satisfactory if it is complemented by the following two assumptions. The first is that at low temperature, the radical formation reaction is in equilibrium only at certain defect sites, and the second is that at higher temperature, other type(s) of defect gradually come to play a dominant role. The first assumption is necessary, because the number of unpaired spins is less than 1% of the entire dye ions and yet the ΔE^{L} value is so small that quite an appreciable quantity of unpaired spin should exists in the equilibrium. Provided several % of the entire lattice sites exist as defects, the present result may be satisfactorily interpreted. The second assumption is less compulsive, but it is reasonable because an alternative assumption that two kinds of reaction occur at a single type of defect depending upon temperature, seems unlikely from the general theory of defect in solid state.

In the further investigations, emphasis was placed on the clarification of the process occurring at lower temperature, because the phenomena at lower temperature were thought to be more simple than at higher temperature.

Anion Effect and Donor, Acceptor Effect. Provided the electron transfer were occurring between dye cation and its paired anion, as has been established by Nelson *et al.*[2] for crystal violet, other salts than chloride would display quite different features in their ESR signals. Hence iodide and phosphate of methylene blue were investigated. Further, the effect of the addition of some inorganic salts and of a typical electron donor and acceptor was examined in a pressed form. The effect of pressing was also examined using polycrystalline methylene blue chloride.

ESR spectra of iodide and phosphate of methylene blue were measured at various temperatures from 143 to 293°K, quite similarly as in the case of chloride. The shapes of ESR spectra were essentially the same as the one of chloride. The data for the line width (ΔH_{msl}), the g-value, spin concentration at ordinary temperature and the values of ΔE^{L} are given in Table 1. It is seen that there is no significant difference in the three salts. Slight differences in the spin concentration and in

Table 1. ESR parameters of the various samples

	ΔH_{msl} (G)	g-Value	Spin concn.**	ΔE^{L} (eV)
$MB^{+}Cl^{-}$	9.6	2.0049	1×10^{18}	0.036
$MB^{+}I^{-}$	13.6	2.004	$\sim10^{17}$	0.041
$(MB^{+})_2HPO_4^{2-}$	6.3	2.0056	3×10^{18}	0.051
$MB^{+}Cl^{-}$ pressed	9.2	2.0041	$\sim10^{19}$	0.026
MB : TNB (1 : 10)	9.0_6	2.0040	2×10^{18}	0.017*
MB : PPD (1 : 10)	—	2.004	2.5×10^{18}	0.011

* for the sample MB : TNB=1 : 50
** per g of MB

10) H. Meier, *Z. physik. Chem.*, **208**, 325 (1958).

11) Private communication from S. Matsumoto.

ΔE^{L} are not compatible with the hypothesis of electron transfer between cation and anion. The pressed sample of methylene blue mixed with trinitrobenzene or paraphenylenediamine (TNB, PPD) (at the mole ratio, MB : TNB=1 : 10) as well as the similarly pressed sample of methylene blue alone gave essentially the similar signals. The ESR parameters such as line width, *g*-value and the ΔE^{L} value of these samples are given in Table 1. All of them are not different significantly from the values of the polycrystalline methylene blue unpressed. Furthermore it was found that the addition of sodium chloride, potassium bromide and pottassium iodide to chloride of methylene blue in the mole ratio of 2 : 1, do not essentially affect the characteristics of the signal.

All these findings support the afore-mentioned view that the formation of unpaired electron occurs at some defect points; because it is reasonable to consider that the added substances do not affect the nature of the defect so much as they may affect the average properties of the sample. Although the nature of the reaction related to the formation of unpaired electron is still unknown at this stage, it seems natural to consider the occurrence of reaction $D^{+}+D^{+}\rightleftharpoons D^{++}+D\cdot$ at defect sites, because the electron transfer between paired anion and cation has been ruled out and further because it is well-known that an analogous reaction, $D^{+}*+D^{+}\rightarrow D^{++}+D\cdot$ occurs photochemically in solutions.

Irradiation Effect. The investigation of the effect of light will give information on the nature of the molecular processes which may occur at normal and defect sites.

The effect of illuminating the polycrystalline methylene blue chloride by the visible light, has proved to be very unique in that it occurrs in the opposite direction at high and low temperature regions. At very low temperatures (<223°K) the signal intensity decreases upon irradiation, quite rapidly and reaches the steady value within a few minutes. When the illumination is stopped, the intensity recovers its initial value also in a few minutes. At higher temperatures ($\gtrsim 293$°K) the intensity increases, upon irradiation, but more slowly. When the light is off, the increase still continues for a few minutes and then begins to decrease. At an extremely high temperature of 373°K, this increase after the light being off, is not observable. At high temperatures, the recovery of the original intensity is very slow and in some cases seems to be even irreversible. Some examples of the intensity *vs.* time plot are shown in Fig. 3. It is evident that at 291°K and at 273°K, *i. e.*, in the medium temperature region, the plot can be interpreted as a superposition of the high and low temperature behaviors. Thus the slight increase observed when the light is off, is due to the existence of the low temperature type process. Although the intensity change upon irradiation is

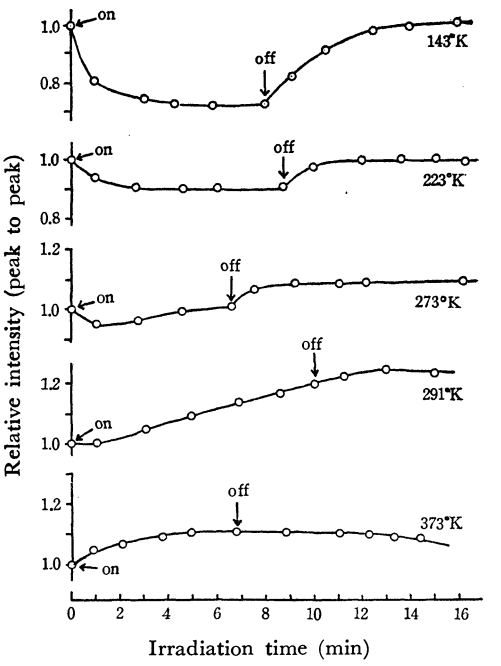

Fig. 3. Effect of photo-irradiation on the signal intensity of polycrystalline MB (measured by peak to peak distance of differential curve of ESR spectra).

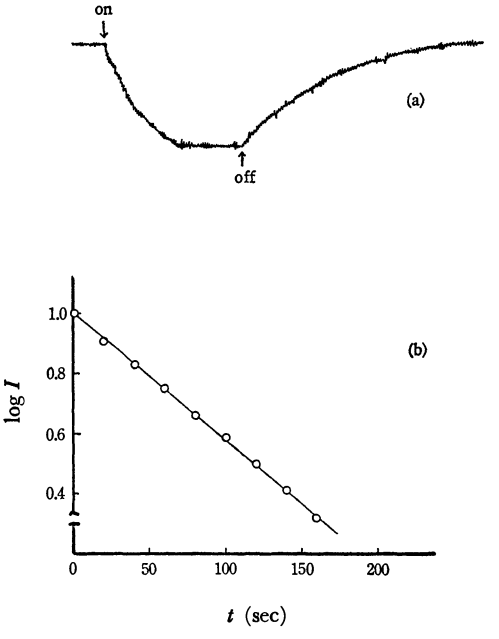

Fig. 4. Recovery processes of the signal intensity after the light is cut off. (at 183°K)
a: Recovery curve
d: Logarithmic plot of the amount of decrease of signal intensity *vs.* time.

quite remarkable, as stated above, there is no essential change in the signal shape as well as in

the line width and the g-value. The kinetics of the recovery at low temperatures could be investigated accurately by measuring the peak to peak distance in the differential curve of ESR signal. The recovery is satisfactorily exponential as is shown in Fig. 4. From the measurements at different temperatures, the apparent activation energy of 0.5 kcal/mol (0.02 eV) was obtained (ΔE_R).

All the above findings are consistent with the view which has been proposed; there are apparently two kinds of defect playing a dominant role respectively at high and low temperatures. The value of the activation energy for the recovery process (0.02 eV) at low temperature, which approximates the ΔE^L value, strongly suggests that the similar process as in the thermal one is occurring for the recovery.

Figure 5 gives the comparison of chloride, iodide and phosphate when they are irradiated at low temperatures. It is seen that the anion effect is

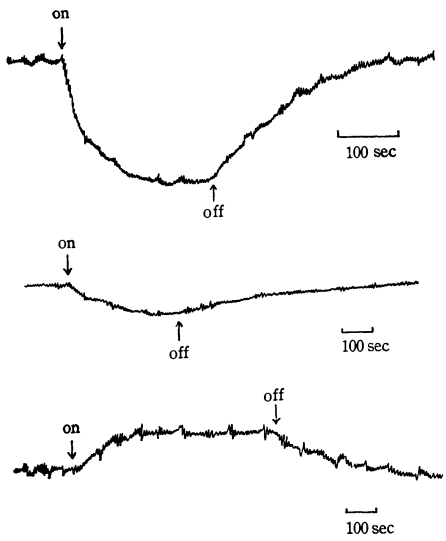

Fig. 5. Comparison of the effects of photo-irradiation on the signal intensity of different salts of MB. (from up to down)
a: MB^+Cl^- (at 215°K)
b: MB^+I^- (at 222°K)
c: $(MB^+)_2HPO_4^{2-}$ (at 243°K)

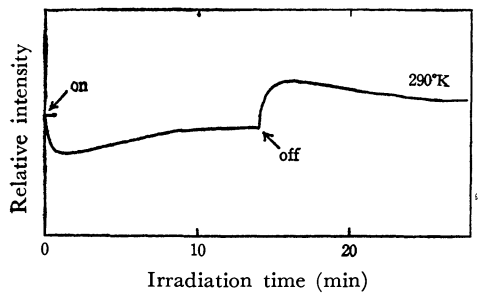

(a)

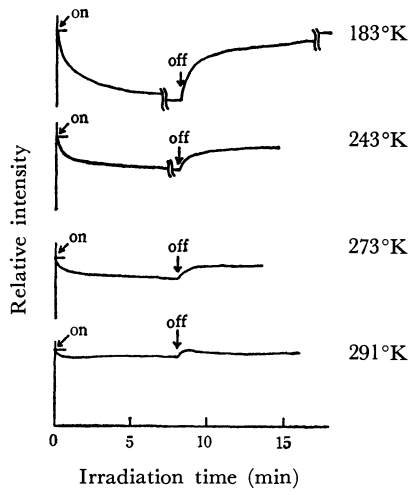

(b)

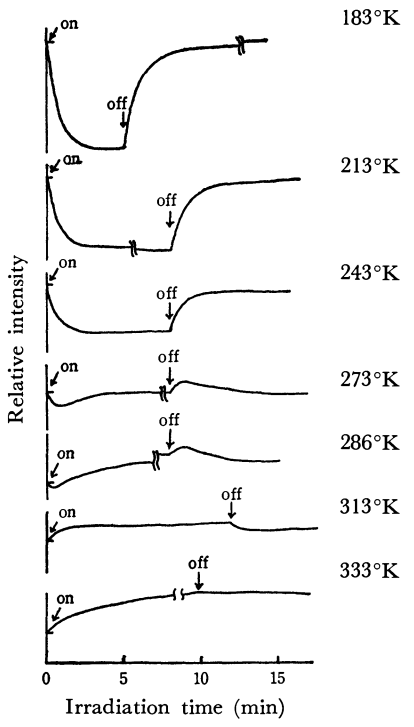

(c)

Fig. 6. Effect of photo-irradiation on the signal intensity of pressed MB alone and those dispersed into electron donor or acceptor media at several lower temperatures.
a: Pressed MB (at room temperature)
b: MB+PPD (1 : 10)
c: MB+TNB (1 : 10)

remarkable. Thus the L-type behavior is very prominent in chloride, less in iodide whereas in phosphate the H-type one is notable even at 243°K.

It is to be noted that the H-type behavior in this case appears quite reversible. Careful inspection

Table 2. Kinetics of the photoresponse

Sample	1st order decay constant when the light is "ON" $\times 10^{-2}$sec^{-1} Temperature			Recovery process when the light is "OFF" (Half period several ten sec) Temperature		
	183°K	213°K	243°K	183°K	213°K	243°K
MB pressed						2nd order (room temp.)
MB+TNB (1 : 10)	2.7	3.0	3.6	1st order	1st order +2nd order	2nd order
MB+TNB (1 : 50)	2.4	2.8	3.5	1st order		2nd order
MB+PPD (1 : 10)	2.5		3.5	1st order		~2nd order

of the irradiation effect upon various samples leads to the suggestion that H-type defects in general consists of the reversible type and the other one(s) at which the ESR behavior is almost irreversible.

At any rate it seems plausible to attribute these differences in the three salts to the different contributions of the H-type defects in these salts, because the thermal behavior at L-type defects are so similar that it is difficult to attribute them to the L-type defect.

In the pressed methylene blue sample, the L-type behavior is quite prominent even at 290°K, as is shown in Fig. 6. The effect of the addition of donor or acceptor is not so pronounced but a general tendency is seen that the addition of TNB or PPD respectively enhances and suppresses the H-type behavior (when compared with the pressed methylene blue sample). This is clearly seen from Fig. 6(a)—(c). These results can be interpreted to be due to the opposite influence of a donor and an acceptor on the photochemical formation of radical species at H-type defects. Furthermore, the energy transfer by exciton mechanism is improbable, because if it really occurs, it would be greatly suppressed and consequently the photoeffect should be much reduced by the addition of donor and acceptor. Thus it may be concluded that most of the acts induced by illumination take place only in the close neighborhood of the defect sites.

Since the slow response when the light is on or off, suggests an appreciable structural change near defects, or mass transfer, some further kinetic studies were made in terms of the intensity change, when the light is on or off at low temperatures. The results are given in Table 2. It is seen that at low temperatures where the L-type defect plays a dominant role, the kinetic feature is essentially the same in all the samples. The second order process at 243°K suggests that the transient species produced by illumination, are two particles existing independently with each other. The activation energy for the disappearance reaction of radical species, as estimated from the data in Table 2 is 0.001—0.002 eV (ΔE_D).

Figure 7 shows the time dependence of the signal intensity when the pressed sample of methylene blue was irradiated by the light of narrow region at 18°C. The clear tendency is seen that the light of shorter wavelength enhances the H-type behavior. Since 660—670 nm and 625—630 nm correspond respectively to the main peak of methylene blue and the dimer absorption, it is tempting to consider that the dye ions at the H-type defects or in its close neighborhood take a dimer-like configuration.

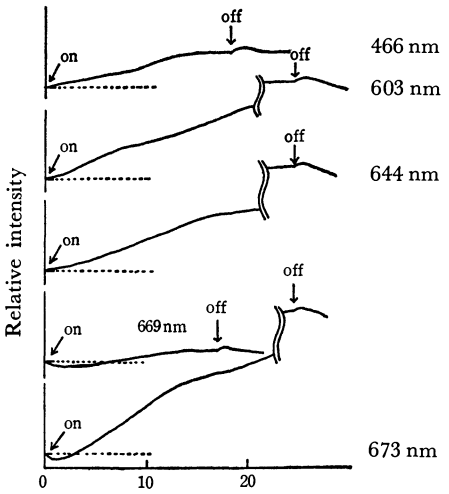

Fig. 7. Wavelength dependency of photo-irradiation effect on the signal intensity of pressed MB.

Summarized Discussion and a Possible Molecular Model

The existence of more than two types of defect, where unpaired electrons are located in the polycrystalline methylene blue chloride, have been verified from the temperature dependence of the signal intensity and the response to the irradiation. This has been further supported by the finding that the change from L-type to H-type behavior occurs

at about the same temperature in both phenomena. The formation of radical species is considered to occur mainly on these defect sites in both the illuminated and unilluminated conditions, on the basis that electron donor and acceptor of the high concentration does not essentially affect the signal intensity. The process occurring at L-type defects is mild and reversible and the one occurring at H-type defects is drastic. From the values of ΔE^{L}, ΔE_{D} and ΔE_{R}, the energy levels for the two states wth and without unpaired spin at L-type defects are given as Fig. 8.

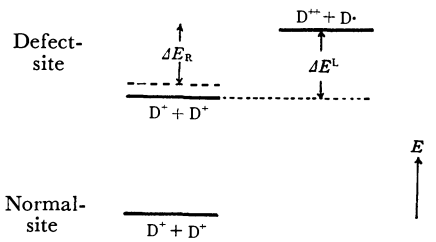

Fig. 8. Energy levels for the two states with and without unpaired spin at L-type defects.

It is particulary interesting that L-type defects show the decrease in signal intensity upon irradiation, while H-type defects show the increase. The magnitude of the contribution of L-type and H-type defects depends upon the kind of anion but at very low temperatures the L-type defect plays a dominant role irrespective of the salt type. Thus the characteristics of the signals in dark are not essentially affected by the anion. Sharp contrasts observed in the response to illumination in three salts, are concerned with the magnitude of the contribution of H-type defect, which is at most about 20% of the entire intensity at room temperature.

As to the molecular process occurring at L-type defects, the most plausible process is the electron transfer between two dye ions,

$$D^+ + D^+ \rightleftharpoons D^{++} + D\cdot \quad (\text{or } D^{++}\cdots D\cdot)$$

Although there is no strong evidence for this mechanism, all the other hypothesis cannot interpret the present results. Especially, the absence of a large anion effect on the features of the signal in dark, rules out the electron transfer between anion and cation.

The decrease in radical species upon irradiation may be due to the reaction of $(D^{++}\cdots D\cdot)$ with a near-by D^{+*} ion which may produce three ground state dye ions in a slightly different configuration, which is of course unstable. When the light is off, it returns to the original cofiguration and ultimately yield $D^{++}\cdots D\cdot$ to restore the equilibrium state. First order kinetics at very low temperatures justifies this view, in addition to the approximate agreement of ΔE^{L} and ΔE_{R}. However, with the rise of temperature, the process becomes more complicated as judged from the second order kinetics at 243°K. Further details of the process are quite unknown at the present stage.

Although detailed studies have not been attempted to elucidate the nature of the H-type defect, it is quite notable that the H-type response to illumination is brought about conspicuously by the wavelength corresponding to dimer absorption. This suggests the hypothesis that the dye ions exist as a dimer-like configuration at or around the H-type defects, and that the process occurring upon illumination is the reaction

$$(D^+\cdots D^+) \rightarrow D^{++} + D\cdot$$

In connection with this hypothesis, it is interesting that the phosphate of methylene blue displays the H-type behavior to a great extent, as has been shown in the H-type-response to illumination even at a low temperature of 243°K. This may be due to the circumstance that two dye ions attached to the bivalent anion are rather easy to take the dimer-like configuration. The results given in Table 1, seem to be interpreted along the similar reasoning. Thus a slightly higher spin concentration, narrowing of the linewidth and a slightly larger value of ΔE^{L} for the phosphate can be attributed to a larger contribution of the H-type defect in this salt.

The above discussion on the molecular process is of course still speculative. It will be interesting to extend the investigation to the salts involving other polyvalent anions and also to mixed dyes along the above picture.

The authors are grateful to Professor H. Kokubun for discussion.

BULLETIN OF THE CHEMICAL SOCIETY OF JAPAN VOL. 41 2281—2284 (1968)

The Reactions of Acetylene Photosensitized by Cd($^3P_1$)

Shigeru TSUNASHIMA and Shin SATO

Department of Applied Physics, Tokyo Institute of Technology, Ookayama, Meguro-ku, Tokyo

(Received February 29, 1968)

The reactions of acetylene photosensitized by Cd($^3P_1$) have been investigated at 270±1°C. The main products were benzene and vinylacetylene. The formations of polymer and hydrogen were not observed. From the studies of the effects of pressures and foreign gases on the quantum yields, the product formations were successfully explained by the reactions of excited molecules. The investigation of the reaction of a mixture of hydrogen and acetylene photosensitized by Cd($^3P_1$) suggests that benzene is also formed from the reactions of hydrogen atoms and acetylene molecules.

Since Bates and Taylor investigated the reactions of acetylene photosensitized by mercury,[1] many investigations have been made of the reactions of this compound.[2-8] However, the mechanism of benzene formation has not yet been completely resolved. LeRoy has proposed a radical mechanism for the benzene formation,[7] while Shida and Tsukada have proposed a mechanism involving both free radicals and excited molecules.[8]

If benzene is formed only from the reaction of free radicals, its formation is not expected in the cadmium-photosensitization, because the dissociation energy of the C–H bond of the acetylene molecule (114 kcal)[9] is larger than the energy of triplet cadmium (87.7 kcal) even when the heat of the formation of cadmium hydride (15.5 kcal) is considered.

In the present paper, a detailed investigation of the reactions of acetylene photosensitized by cadmium will be reported.

Experimental

Acetylene, ethylene, isobutene, and *cis*-2-butene supplied by the Takachiho Shoji Co. were used after bulb-to-bulb distillations. The gas-chromatographic analysis showed that the impurities were less than 0.5%. Hydrogen supplied by the Suzuki Shokan Co. was used after it had been passed through a trap at the temperature of liquid nitrogen. Acetylene-d_2 was synthesized from calcium carbide and deuterium oxide. Mass-spectrometric analysis showed that the isotopic purity was larger than 98%.

The apparatus and the light source used were practically the same as have been described previously.[10]

The reaction products were analyzed by gas chromatography. The column used was packed with silicon DC-550 on celite (supplied by the Shimazu Co., 7 m long) and was operated at 60°C.

The intensity of the cadmium resonance line at 3261 Å was measured using the cadmium-photosensitized *cis-trans* isomerization of *cis*-2-butene under the assumption of the quantum yield being 0.5.[10]

Results and Discussion

Mechanism of Product Formations. In the reaction of acetylene photosensitized by cadmium at 270±1°C, the main products were identified as benzene and vinylacetylene by gas chromatography and by mass spectrometry. No hydrogen formation was observed; if present at all, the quantum yield is less than 10^{-5}.

Figure 1 shows the irradiation-time dependence of the products. A slight disappearance of acetylene was observed; the amount was almost equal to the sum of three times the amount of benzene and twice the amount of vinylacetylene. This fact suggests that the formation of polymers, such as cuprene, is negligibly small.

The isotopic hydrogen-atom distribution of benzene formed in the reaction of a mixture of acetylene-d_0 and -d_2 could not be determined, because intermolecular hydrogen-deuterium exchange reaction occurred rapidly, even in a dark reaction at 270±1°C.

1) R. Bates and H. S. Taylor, *J. Am. Chem. Soc.*, **49**, 2438 (1927).
2) H. W. Melville, *Trans. Faraday Soc.*, **32**, 258 (1936).
3) D. J. LeRoy and E. W. R. Steacie, *J. Chem. Phys.*, **12**, 117 (1944).
4) J. K. Cashion and D. J. LeRoy, *Can. J. Chem.*, **32**, 906 (1954).
5) A. G. Scherwood and H. E. Gunning, *J. Phys. Chem.*, **69**, 1732 (1965).
6) S. Shida, Z. Kuri and T. Furuoya, *J. Chem. Phys.*, **28**, 131 (1958).
7) D. J. LeRoy, *ibid.*, **45**, 3482 (1966).
8) S. Shida and M. Tsukada, *ibid.*, **44**, 3133 (1966); S. Shida, M. Tsukada and T. Oka, *ibid.*, **45**, 3483 (1966).
9) B. E. Knox and H. B. Palmer, *Chem. Revs.*, **61**, 247 (1961).
10) S. Tsunashima and S. Sato, This Bulletin, **41**, 284 (1968).

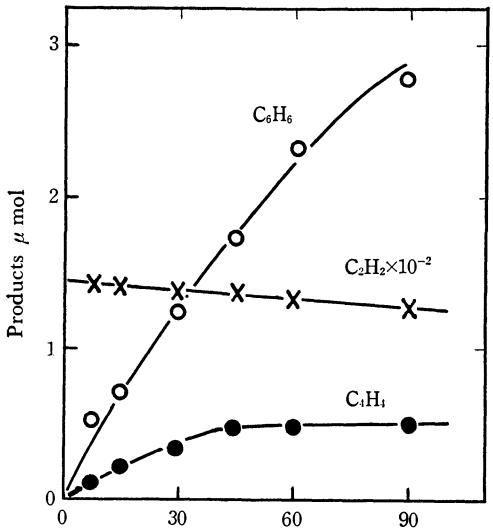

Fig. 1. Time dependence of the amounts of the products. (initial pressure, 36.6 mmHg)

Table 1 shows the quantum yields of the products formed in the reaction of acetylene at 80 mmHg, together with those in the presence of foreign gases.

The products of the cadmium-photosensitization are different from those of the mercury-photosensitization,[1-8] the direct photolysis,[11] and the radiolysis.[12] If benzene and vinylacetylene are formed from the reaction of free radicals, the formations of ethylene, 1,3-butadiene, and diacetylene can be expected, besides the formation of vinylacetylene. However, they were not observed in the cadmium-photosensitization. Furthermore, the energy available for the C-H-bond splitting in the cadmium-photosensitization is smaller than the dissociation energy of the C–H bond of the acetylene molecule. Benzene and vinylacetylene may be formed from the reaction of excited molecules. The energy levels of the excited singlet molecule are above the excitation energy of triplet cadmium.[13] The triplet state of the acetylene molecule is not known, although Bowman and Miller observed a peak at 2.0 eV in the electron-energy-loss spectrum of acetylene and tentatively surmised that the peak was caused by the triplet state of the acetylene molecule.[14]

Pressure-dependence of the Products. The quantum yields of benzene and vinylacetylene formations were measured over the pressure range from 10 to 330 mmHg (Fig. 2). Their maximum values were found at about 80 mmHg and at about 40 mmHg respectively. Even at the maximum values, the sum of their quantum yields is less than unity. That is, most of the energy absorbed by cadmium atoms is not used for the product formations. This fact can not be explained by the incomplete quenching of triplet cadmium atoms by acetylene, because the quenching efficiency of acetylene is almost equal to that of 2-butene[15] and the pressure range used here is the complete quenching region for 2-butene.[10]

To explain the pressure dependence of the quantum yields, the following reaction mechanism may be considered in terms of the excited molecules:

$$Cd(^3P_1) + A \rightarrow CdA^* \quad (1)$$
$$CdA^* \rightarrow Cd + A_1^* \quad (2)$$
$$CdA^* + A \rightarrow Cd + 2A \quad (3)$$
$$A_1^* + A \rightarrow A_2^* \quad (4)$$
$$\rightarrow 2A \quad (5)$$
$$A_2^* \rightarrow 2A \quad (6)$$
$$A_2^* + A \rightarrow A_3^* \quad (7)$$
$$A_3^* \rightarrow 3A \quad (8)$$
$$\rightarrow C_4H_4 + A \quad (9)$$
$$\rightarrow C_6H_6 \quad (10)$$
$$A_3^* + A \rightarrow C_6H_6 + A \quad (11)$$

TABLE 1. EFFECTS OF FOREIGN GASES ON THE PRODUCT FORMATIONS*

Foreign gas	mmHg	Products (quantum yield × 10^2)					
		H_2	C_2H_6	C_2H_4	C_4H_4**	C_4H_6***	C_6H_6
	0	nil	nil	nil	2.0	nil	9.4
C_2H_4	10.1	nil	nil	—	0.4	nil	2.0
iso-C_4H_8	2.2	nil	nil	nil	—	—	2.2
H_2	110.	—	0.7	44.0	1.8	2.3	32.

* pressure of acetylene: 80 mmHg
** C_4H_4: vinylacetylene
*** C_4H_6: 1,3-butadiene

11) For example, H. Zelikoff and L. M. Aschenbrand, *J. Chem. Phys.*, **24**, 1034 (1956).
12) For example, J. T. Futrell and L. W. Sieck, *J. Phys. Chem.*, **69**, 892 (1965).
13) G. Herzberg, "Electronic Spectra and Electronic Structure of Polyatomic Molecules," D. Van Norstand Co. Inc., New York (1966), p. 611.
14) C. R. Bowman and W. D. Miller, *J. Chem. Phys.*, **42**, 681 (1965).
15) S. Tsunashima and S. Sato, This Bulletin, **40**, 2987 (1967).

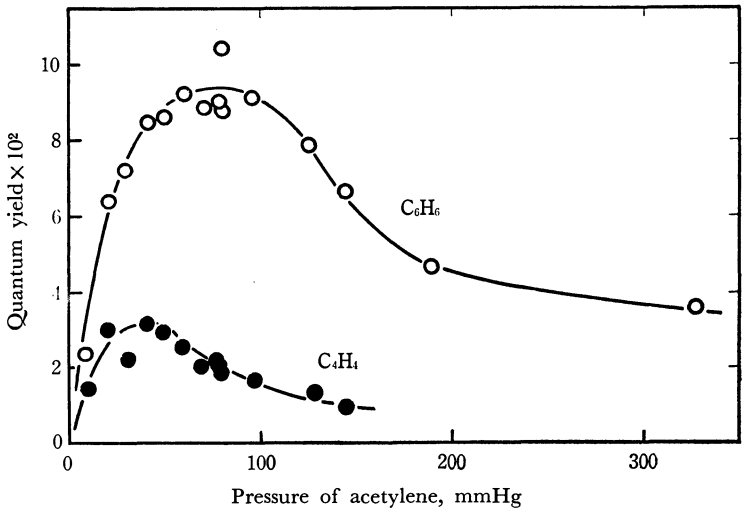

Fig. 2. Pressure dependence of the quantum yields of benzene and vinylacetylene formation.

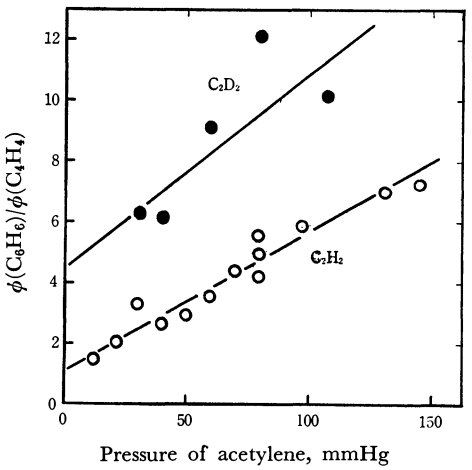

Fig. 3. Plots of the ratio, $\phi(C_6H_6)/\phi(C_4H_4)$ against the pressure of acetylene.

where acetylene is denoted as A and where CdA* is the transient complex of a triplet cadmium atom and an acetylene molecule. The symbols A_1*, A_2*, and A_3* represent, respectively, an excited acetylene molecule (presumably, a triplet acetylene molecule), a transient dimer, and a transient trimer. The steady-state treatment derives the following relation:

$$\phi(C_6H_6)/\phi(C_4H_4) = k_{10}/k_9 + (k_{11}/k_9)[A] \qquad (I)$$

where $\phi(C_6H_6)$ and $\phi(C_4H_4)$ are the quantum yields of the benzene and vinylacetylene formations respectively. The plots of the $\phi(C_6H_6)/\phi(C_4H_4)$ ratio *vs.* the acetylene pressure are shown in Fig. 3. From the slopes and the intercepts, the k_{10}/k_9 and k_{11}/k_9 values are calculated by the method of least squares (Table 2).

TABLE 2. VALUES OF k_{10}/k_9 AND k_{11}/k_9

	k_{10}/k_9	k_{11}/k_9 (mmHg^{-1})
C_2H_2	1.2±0.3	4.6±0.4
C_2D_2	4.6±2.1	6.5±3.0

Effects of Ethylene and Isobutene. As is shown in Table 1, ethylene and isobutene inhibit the formations of benzene and vinylacetylene. Figure 4 shows the plots of ϕ_0/ϕ *vs.* the foreign gas

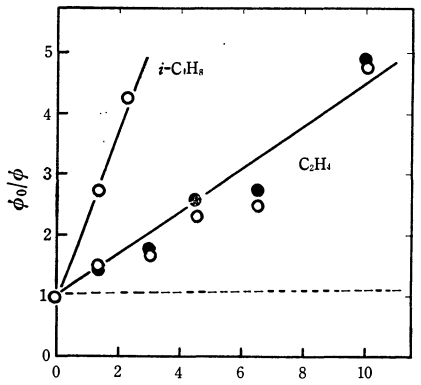

Fig. 4. Plots of ϕ_0/ϕ against the pressure of foreign gas.
(dotted line: expected curve from competitive quenching for Cd($^3P_1$) atoms, pressure of acetylene: 80 mmHg, ○: benzene, ●: vinylacetylene)

pressure in the reaction of acetylene at 80 mmHg. Here, ϕ_0 and ϕ are the quantum yields of benzene or vinylacetylene formations in the absence and in the presence of foreign gas respectively. The efficiency of isobutene for the inhibition is about five times that of ethylene. A similar trend has been reported in the efficiency of quenching

triplet benzene (about five times)[16,17] and triplet acetone (about four times),[18] and also in the efficiency of scavenging hydrogen atoms (about five times).[19]

The inhibition by ethylene or isobutene can not be explained by the competitive quenching for triplet cadmium atoms, since the observed $(\phi_0/\phi-1)$ values, as is shown in Fig. 4, are more than forty times as large as that calculated by assuming competitive quenching. The products expected by the addition of ethylene and isobutene were not detected in spite of careful research. The inhibition, therefore, may be explained by the quenching of excited molecules by foreign gases. Including the quenching reactions by foreign gases, the following relations are obtained:

$$(\phi_0/\phi)_{C_4H_4} = (1+k_{10}'[M]/(k_{10}+k_{11}[A]))(\phi_0/\phi)_{C_6H_6}$$
$$= (1+k_{11}'[M]/(k_8+k_9+k_{10}+k_{11}[A]))(1+k_7'[M]/(k_6+k_7[A]))(1+k_5'[M]/(k_4+k_5)[A])$$
$$\times (1+k_3'[M]/(k_2+k_3[A])) \quad \text{(II)}$$

Here, k_3', k_5', k_7', and k_{11}' represent, respectively, the rate constants of a foreign gas (M) for quenching CdA*, A_1*, A_2*, and A_3*.

As is shown in Fig. 4, the (ϕ_0/ϕ) value for vinylacetylene formation is almost equal to that for benzene formation; therefore, the $k_{11}'[M]/(k_{10}+k_{11}[A]) \ll 1$ relation holds under the conditions of this experiment. That is, the process of quenching A_3* by foreign gas is not effective for the inhibition of the formation of benzene and vinylacetylene. However, the linear relationship in Fig. 4 suggests that one of the quenching processes (reaction (3'), (5'), or (7')) is effective. However, no definite conclusion can be drawn as to which quenching process is the most effective on the basis of these experiments alone.

Isotope Effect. As is shown in Table 3, there are large isotope effects on the formations of benzene and vinylacetylene. In the mercury-photosensitization, no such large isotope effect has been observed on the formation of benzene.[8] The isotope effect can not be explained by the difference in the quenching efficiencies of acetylene-d_0 and -d_2.[15] The effect may result from the isotope effect on the rates of the reactions (9), (10), and (11), as is shown in Table 2.

Table 3. Isotope effects on the formations of benzene and vinylacetylene

Pressure mmHg	C_4H_4/C_4D_4	C_6H_6/C_6D_6
30	2.6	1.4
40	3.5	1.5
60	3.8	1.5
80	4.3	1.9
100	3.5	1.9

Effect of Hydrogen. As is shown in Table 1, the addition of an excess amount of hydrogen caused an increase in the quantum yield of benzene formation, together with those of ethylene and 1,3-butadiene formations. Cashion and LeRoy observed a similar effect of the addition of hydrogen in the mercury-photosensitization and proposed the importance of free radicals in the mechanism.[4] Benzene formed from the reaction of a mixture of acetylene-d_2 and hydrogen photosensitized by cadmium consisted of a mixture of C_6D_6(69.2%), C_6HD_5(26.6%), and $C_6H_2D_4$(3.5%). This suggests that a part of the benzene is formed by the reaction of hydrogen atoms. The reaction mechanism may be described as follows;

$$Cd(^3P_1) + H_2 \rightarrow CdH + H \quad (12)$$
$$H + C_2H_2 \rightarrow C_2H_3 \quad (13)$$
$$2\,C_2H_3 \rightarrow C_2H_2 + C_2H_4 \quad (14)$$
$$\rightarrow C_4H_6 \quad (15)$$
$$C_2H_2 + C_2H_2 \rightarrow C_4H_5 \quad (16)$$
$$2\,C_4H_5 \rightarrow C_4H_4 + C_4H_6 \quad (17)$$
$$\rightarrow \text{dimer} \quad (18)$$
$$C_4H_5 + C_2H_2 \rightarrow C_6H_7 \quad (19)$$
$$C_6H_7 \rightarrow C_6H_6 + H \quad (20)$$
$$\rightarrow \text{polymer} \quad (21)$$

This reaction mechanism interprets the formations of butadiene and ethylene as well as the formation of benzene. That is, benzene can also be formed from the reaction of free radicals.

The authors are indebted to Mr. H. Sakurai for the mass spectrometric analyses and to Mr. S. Hirokami for synthesizing acetylene-d_2.

16) C. A. Haninger and E. K. C. Lee, *J. Phys. Chem.*, **71**, 3104 (1967).
17) A. Morikawa and R. J. Cvetanović, private communication.
18) R. E. Rebbert and P. Ausloos, *J. Am. Chem. Soc.*, **87**, 5569 (1965).
19) K. R. Jennings and R. J. Cvetanović, *J. Chem. Phys.*, **37**, 543 (1962).

BULLETIN OF THE CHEMICAL SOCIETY OF JAPAN VOL. 41 2285—2288 (1968)

Gel Filtration of Surfactants on Sephadex

Fumikatsu TOKIWA, Kenji OHKI and Isao KOKUBO

Research Laboratories, Kao Soap Company, Minato-Yakushubata, Wakayama-shi

(Received March 7, 1968)

An attempt has been made to apply gel filtration on Sephadex to micellar solutions of surfactants. The data on the gel filtration of surfactants were interpreted by taking into account the fact that there exist both micellized and unmicellized species in the solutions. A simple method for obtaining the retention volume of the micelle (V_M) of a surfactant directly from the elution curve was developed. Further, the relation between the values of V_M and the micellar molecular weights (MMW) was examined for various types of surfactants. A linear relation was found between V_M and log MMW, with the exception of a surfactant with a heterocyclic structure. It appears that gel filtration offers a convenient way for roughly estimating the MMW's of surfactants.

Gel filtration is a type of partition chromatography in which substances are separated largely on the basis of the molecular size. If a mixture of low-molecular-weight substances and high-molecular-weight substances moves through a gel column, the former are slowed down as a result of their penetration into the gel, enabling the latter to flow faster down through the column. The sizes of surfactant micelles are, in general, within the range to which this gel filtration is applicable. However, few studies have been made of the application of gel filtration to micellar solutions of surfactants.[1]

In the present work, an attempt has been made to apply gel filtration on Sephadex, a cross-linked dextran gel, to micellar solutions of surfactants, especially those of sodium dodecyl sulfate (SDS) and sodium tetradecyl sulfate (STS). The results were interpreted by taking into account the fact that micelles always exist in equilibrium with monomolecularly-dispersed species above the critical micelle concentration (CMC). Further, the relation between the retention volumes of micelles and their molecular weights was examined for various types of surfactants.

Experimental

Materials. Sephadex G-50 and G-75, with particle sizes of 20—80 and 40—120 micron respectively, and Blue Dextran 2000, with a molecular weight of 2×10^6, were obtained from Pharmacia, Sweden. The sodium decyl-, dodecyl-, and tetradecyl-sulfates were prepared from the respective alcohols by the method of Dreger *et al.*[2] and were purified by repeated recrystallizations from a mixture of isopropanol-water and by extraction with petroleum ether. The sodium decylbenzene sulfonate and sodium dodecyltrioxyethylene sulfate were the same samples as those used in previous works.[3,4] The sodium dodecane sulfonate was a product of Farbenfabrik Bayer, Germany. The dodecyl decaoxyethylene ether and octylphenyl decaoxyethylene ether were samples prepared and purified by a method described elsewhere.[4] The dodecylamine hydrochloride and hexadecyl pyridinium chloride were obtained from Tokyo Kasei and were purified by repeated recrystallizations from acetone. The oil-soluble dyes Yellow OB and Aniline Blue, which were used as solubilizates, were specially-prepared commercial samples.

Procedure. Sephadex G-50 or G-75 was allowed to swell in distilled water for at least 24 hr, and then decanted before being poured into a jacketed column, 1.3 cm in diameter $\times$38 cm in height, with a sintered glass plate at the bottom. After the column had then been filled with the Sephadex gel, a filter paper disk was placed on the top of the gel to prevent its disturbance when the sample solution was added. The column was maintained at 25 ± 0.1°C or 32 ± 0.1°C. The gel column was then washed with distilled water overnight. The void volume of the column, V_0, was checked on the first run of each freshly-packed column, and then on alternate runs, using Blue Dextran 2000.

The sample solution of a surfactant was applied continuously to the top of the column through a siphon connected to the sample reservoir. After about 30 m*l* of the sample solution had sunk into the gel, the eluant, which was the same solution as that which had previously filled the column, was allowed to flow down. An automatic fraction-collector was employed, and fractions of approximately 1 m*l* were collected. The electrical conductivity of each fraction was measured in

1) T. Sasaki and T. Siki, Paper presented at Symposium on Oil Chemistry in Japan, Nagoya, Oct., 1966; T. Sasaki, *Yukagaku (J. Japan Oil Chemists' Soc.)*, **16**, 49 (1967).

2) E. E. Dreger, G. I. Keim, G. D. Miles, L. Shedlovsky and J. Ross, *Ind. Eng. Chem.*, **36**, 610 (1944).

3) F. Tokiwa and K. Ohki, *Kolloid-Z. Z. Polymere*, **223**, 38 (1968).

4) F. Tokiwa and K. Ohki, *J. Phys. Chem.*, **71**, 1343 (1967).

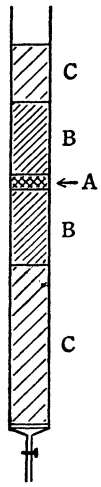

Fig. 1. The gel filtration in measurement of the retention volume of the micelle tagged with Yellow OB.
A: 1 m*l* of the sample solution in 2.0 g/d*l* tagged with Yellow OB.
B: 10 m*l* of the sample solution in 2.0 g/d*l* untagged.
C: the solution in 0.5 g/d*l* of the same surfactant as that in the sample solution.

order to determine the retention volume of the surfactant.

An alternative procedure was employed to examine the relation between the retention volumes of the micelles and their molecular weights. A 1 m*l* portion of the sample solution in a concentration of 2.0 g/d*l*, which had been tagged by solubilized Yellow OB, was allowed to flow down, in the form of a sandwich (shown in Fig. 1) with two untagged 10 m*l* portions of the sample solution, through a column filled with the solution in a concentration of 0.5 g/d*l* of the same surfactant as that in the sample solution. This minimizes the widening of the sample band by diffusing the tagged micelles. The volume of the solution flowing down before and after the tagged sample solution was set at 10 m*l* after several examinations. The retention volume of the sample was determined with the naked eye.

Results and Discussion

Figure 2 shows the elution curves of SDS in water at various concentrations, using a Sephadex G-50 column. Below the CMC the retention volume obtained from the curve is independent of the concentration of the surfactant. Above the CMC, on the other hand, the retention volume decreases, at first rapidly and then more and more gradually, with an increase in the concentration. The surfactant solution, the concentration of which is higher than the CMC, contains both micellized and unmicellized (monomeric) species. The retention volume observed, V_{obs}, may, therefore, be separated into the retention volume of the monomer, V_m, and that of the micelle, V_M. The values of

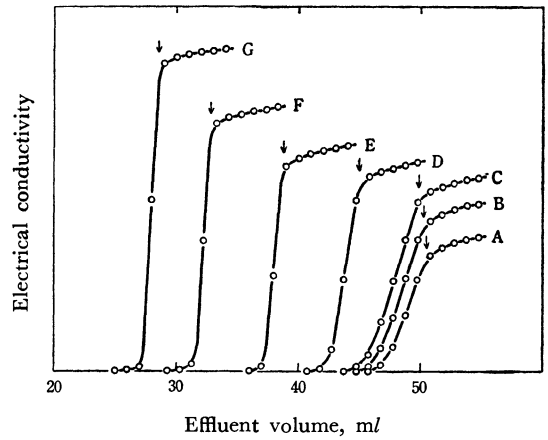

Fig. 2. Elution curves of sodium dodecyl sulfate in water at various concentrations with a Sephadex G-50 column at 32°C:
A 0.0030 M; B 0.0060 M; C 0.0080 M;
D 0.010 M; E 0.013 M; F 0.020 M;
G 0.040 M. The arrow indicates the retention volume of the surfactant at each concentration.

V_{obs}, V_m, and V_M are related by the expression:

$$V_{obs} = xV_m + (1-x)V_M$$
$$= V_M + x(V_m - V_M),\ x = C_m/C \qquad (1)$$

where C is the total concentration of the surfactant and C_m is the concentration of the monomer species. Below the CMC, $C_m=C$; therefore $V_{obs}=V_m$, since x is equal to unity. Above the CMC, C_m is nearly a constant ($C_m \simeq$CMC).[5] Thus, plots of V_{obs} *vs.* $1/C$ consist of two straight lines; one intersects the ordinate at V_M, and one is parallel to the abscissa at $V_{obs}=V_m$. These two lines intersect at $1/C=1/\text{CMC}$. Figure 3 shows the V_{obs}-*vs.*-$1/C$ plots for SDS and STS in water. The

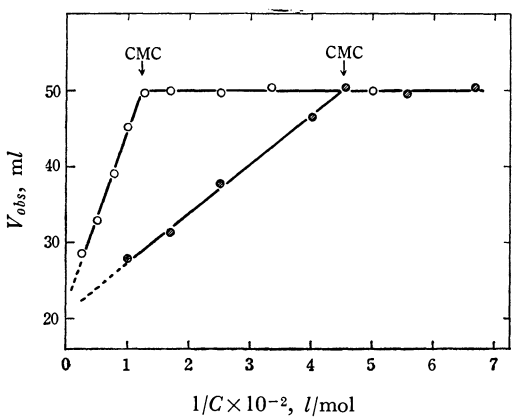

Fig. 3. Plots of V_{obs} *vs.* $1/C$ for sodium dodecyl sulfate (○) and sodium tetradecyl sulfate (◍) in water with a Sephadex G-50 column at 32°C.

5) E. Hutchinson, *Z. Physik. Chem. (Frankfurt)*, **21**, 38 (1959); E. Hutchinson, V. E. Sheaffer and F. Tokiwa, *J. Phys. Chem.*, **68**, 2818 (1964).

values of V_m for SDS and STS are almost the same, while the value of V_M for SDS is slightly larger than that for STS. The CMC values of SDS and STS obstained from the breakpoint of the V_{obs}-*vs.*-$1/C$ plots are in good agreement with their published values.[6,7]

If the gel column has previously been filled with the solution of the surfactant, which is the same as that in the sample solution, of a concentration of C_s, the x in Eq. (1) may be written in the following forms. When C_s is smaller than CMC:

$$x = (C_m - C_s)/(C - C_s)$$

When C_s is larger than CMC:

$$x = 0$$

Therefore, we have:

$$V_{obs} = V_M + \frac{C_m - C_s}{C - C_s}(V_m - V_M) \quad \text{for } C_s < \text{CMC} \qquad (2)$$

and:

$$V_{obs} = V_M \quad \text{for } C_s \geq \text{CMC} \qquad (3)$$

Figure 4 shows the V_{obs}-*vs.*-$1/(C-C_s)$ plots for SDS at different values of C_s. When $\text{CMC} > C > C_s$, $C_m = C$; therefore, the value of V_{obs} is again equal to V_m, and the plots of V_{obs} *vs.* $1/(C-C_s)$ in this region become straight lines parallel to the abscissa at $V_{obs} = V_m$. When $C \geq \text{CMC} > C_s$, C_m is nearly equal to the CMC and is independent of C, so the slope of the plots of V_{obs} *vs.* $1/(C-C_s)$ (*i. e.*, the value of $(C_m - C_s)\cdot(V_m - V_M)$) decreases with an increase in C_s and becomes zero at $C_s = C_m (\simeq \text{CMC})$, as may be expected from Eq. (2). When $C > C_s \geq$ CMC, the plots of V_{obs} *vs.* $1/(C-C_s)$ are straight lines parallel to the abscissa at $V_{obs} = V_M$, as described in Eq. (3). Thus, the value of V_M can easily be obtained from the retention volume observed, V_{obs}, at $C_s \geq$ CMC.

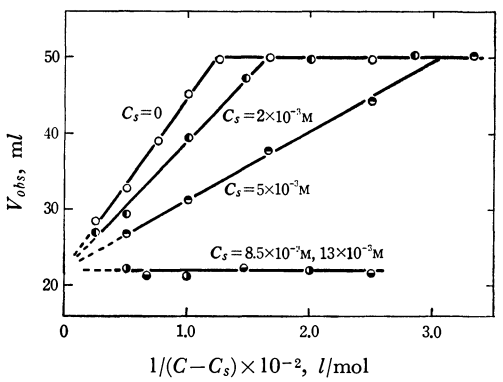

Fig. 4. Plots of V_{obs} *vs.* $1/(C-C_s)$ for sodium dodecyl sulfate at different values of C_s with a Sephadex G-50 column at 32°C.

6) K. J. Mysels and L. H. Princen, *J. Phys. Chem.*, **63**, 1696 (1959).
7) H. Lange, *Kolloid-Z.*, **131**, 96 (1953).

The retention volumes of substances have some relation with their molecular weights. In the field of biochemistry numerous attempts have been made to determine the molecular weights of proteins from their retention volumes.[8-10] It is

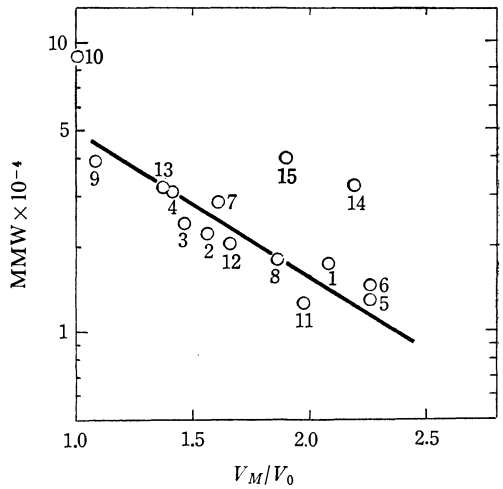

Fig. 5. Relation between retention volumes and micellar molecular weights for various types of surfactants at 25°C, using a Sephadex G-75 column.

(1) $C_{12}H_{25}OSO_3Na$ in water[a]
(2) $C_{12}H_{25}OSO_3Na$ in 0.05 M NaCl[a]
(3) $C_{12}H_{25}OSO_3Na$ in 0.10 M NaCl[a]
(4) $C_{12}H_{25}OSO_3Na$ in 0.25 M NaCl[a]
(5) $C_{10}H_{21}OSO_3Na$ in water[b]
(6) $C_{12}H_{25}SO_3Na$ in water[b]
(7) $C_{12}H_{25}O(CH_2CH_2O)_3SO_3Na$ in 0.10 M NaCl[c]
(8) $C_{10}H_{21}$-C$_6$H$_4$-SO_3Na in 0.10 M NaCl[d]
(9) $C_{12}H_{25}O(CH_2CH_2O)_{10}H$ in water[e]
(10) C_8H_{17}-C$_6$H$_4$-$O(CH_2CH_2O)_{10}H$ in water[f]
(11) $C_{12}H_{25}NH_2HCl$ in water[b]
(12) $C_{12}H_{25}NH_2HCl$ in 0.016 M NaCl[b]
(13) $C_{12}H_{25}NH_2HCl$ in 0.046 M NaCl[b]
(14) $C_{16}H_{33}$-N-Cl in 0.018 M NaCl[g]
(15) $C_{16}H_{33}$-N-Cl in 0.058 M NaCl[g]

MMW was taken a) from Ref. 6; b) from Ref. 11; c) from Ref. 4; d) from Ref. 3; e) from Ref. 12; f) from Ref. 13; g) from Ref. 14.

8) J. R. Whitaker, *Anal. Chem.*, **35**, 1950 (1963).
9) T. I. Pristoupil, *J. Chromatog.*, **19**, 64 (1965).
10) A. A. Leach and P. C. O'shea, *ibid.*, **17**, 245 (1965).
11) H. V. Tarter and A. L. M. Lelong, *J. Phys. Chem.*, **59**, 1185 (1955).
12) F. Tokiwa and T. Isemura, This Bulletin, **35**, 1737 (1962).
13) L. M. Kushner, W. D. Hubbard and A. S. Doan, *J. Phys. Chem.*, **61**, 371 (1957).
14) E. W. Anacker, *ibid.*, **62**, 41 (1958).
15) B. Gelott, *J. Chromatog.*, **3**, 330 (1960).

of interest and also of importance to learn whether there is any possibility of estimating the micellar molecular weights (MMW) of surfactants directly from their gel filtration data. For this purpose, the V_M values for various types of surfactants of known MMW were determined. In the present experiment the micellar solution of the surfactant examined, which was tagged with solubilized Yellow OB, was allowed to flow down in the form of a sandwhich, as has been described in the Experimental section, through a Sephadex G-75 column. The Sephadex G-75 was chosen after taking into account its fractionation range of molecular weight (3×10^3—6×10^4). The effect of oil-soluble dyes on the values of V_M was checked by using two different types of dyes, Yellow OB and Aniline Blue. It was confirmed that the retention volumes are not influenced by the addition of the dyes.

In Fig. 5, the MMW's of various types of surfactants are plotted against the V_M/V_0 ratios, where V_0 is the void volume of the column. There is a linear relation between log MMW and V_M/V_0 except in the cases of hexadecyl pyridinium chloride and octylphenyl decaoxyethylene ether, as may be seen in Fig. 5. The values of V_M for these surfactants deviate from the linear relation. Probably the derivation in the case of hexadecyl pyridinium chloride may be attributed to the interaction of the dextran gel with the pyridine ring in the surfactant molecule. Such interactions have been found in experiments with heterocyclic substances.[15] The reason for the deviation found in octylphenyl decaoxyethylene ether is not clear, because its MMW is outside the fractionation range of the gel used.

From the data presented above, it appears that gel filtration on Sephadex offers a convenient way of roughly estimating the MMW of a surfactant unless the surfactant has a heterocyclic structure.

The authors wish to express their thaks to Dr. H. Kita, Director of the Research Laboratories, for his encouragement and the permission to publish this paper.

BULLETIN OF THE CHEMICAL SOCIETY OF JAPAN VOL. 41 2288—2292 (1968)

Retardation of Polarographic Oxidation of Ethylenediaminetetraacetatocobaltate(II) by Mercury(I) Iodide Film Formation

Nobuyuki TANAKA, Setsuko YAMAMOTO and Yuichi SATO

Department of Chemistry, Faculty of Science, Tohoku University, Katahira-cho, Sendai

(Received March 13, 1968)

The electrode process of ethylenediaminetetraacetatocobaltate(II) ($Co^{II}Y^{2-}$) at the dropping mercury electrode has been studied in the presence of iodide ions. It was found that polarographic anodic waves of $Co^{II}Y^{2-}$ were affected by the film of mercury(I) iodide which was formed electrolytically at the electrode surface. The measurement of current-time curves during the life of a mercury drop and the coulometric studies revealed that the electro-oxidation of $Co^{II}Y^{2-}$ was completely inhibited by the formation of monomolecular layer of mercury(I) iodide on the mercury surface.

The electrode processes of ethylenediaminetetraacetatocobaltates(II, III) at various kinds of electrodes have been studied by several investigators;[1-6] the polarographic behaviors of these complexes have been investigated in detail.[1-4] Anson[5] reported the effect of adsorbed halide ions on the electro-oxidation of ethylenediaminetetraacetatocobaltate(II) ($Co^{II}Y^{2-}$) at a platinum electrode. According to his paper, adsorbed halide ions act catalytically on the electro-oxidation of $Co^{II}Y^{2-}$ and inhibit the oxidation of the platinum electrode especially in acid solutions. Voltammetric and chronopotentiometric behaviors of the anodic oxidation of $Co^{II}Y^{2-}$ at a carbon paste electrode were reported by T. Kitagawa and S. Tsushima.[6] They found, however, that the adsorbable halide ions did not show any pronounced effect on the kinetics of the electrode reaction at the carbon paste electrode.

1) C. N. Reilley, W. G. Scribner and C. Temple, *Anal. Chem.*, **28**, 450 (1956).
2) N. Maki, This Bulletin, **37**, 765 (1964).
3) N. Tanaka and H. Ogino, *ibid.*, **38**, 1054 (1965).
4) H. Ogino, *ibid.*, **38**, 771 (1965).
5) F. C. Anson, *J. Electrochem. Soc.*, **110**, 436 (1963).
6) T. Kitagawa and S. Tsushima, *Review of Polarography (Kyoto)*, **14**, 17 (1966).

The present paper is concerned with the effect of iodide ions on the electro-oxidation of $Co^{II}Y^{2-}$ to $Co^{III}Y^{-}$ at the dropping mercury electrode (DME). Iodide ions depolarize the dropping mercury anode with the formation of slightly soluble merucry(I) iodide. In the presence of iodide ions, a direct current (d. c.) polarogram showed the decrease in anodic limiting current of $Co^{II}Y^{2-}$ and a current-time curve during the life of a mercury drop showed a peculiar shape. The influence of iodide ions on the polarogram and current-time curve of $Co^{II}Y^{2-}$ was explained as a result of the film formation of mercury(I) iodide on the electrode surface.

Experimental

A standard solution of cobalt(II) nitrate was obtained by the same procedure as reported previously.[7] Its concentration was determined with a standardized disodium dihydrogen ethylenediaminetetraacetate solution by amperometric titration. The concentration of iodide ions was determined by the Volhard method. All other chemicals used were of analytical reagent grade.

D.c. polarograms were recorded with a Yanagimoto Galvarecorder Model AP-1 with an automatic potential scanner. A Rikendenshi SP-J1 recorder with a Rikadenki DC-201 preamplifier was used to measure current-time curves. The dropping mercury electrode used had an m value of 1.397 mg/sec and a drop time t_d of 5.38 sec, being measured in an air-free 1 M potassium chloride solution containing 0.01% gelatin at 25°C and -0.5 V *vs.* SCE at a 70 cm height of the mercury reservoir. A saturated calomel electrode (SCE) was used as a reference electrode. All measurements were carried out in a thermostat of 25°C, and the dissolved oxygen in the solution was removed by passing pure nitrogen gas through the solution.

Current-potential and current-time curves presented in this paper are all corrected for residual currents. In the case of current-potential curves, the average current was measured and denoted by $\bar{i}$. The plus sign is given for the anodic current and the minus sign for the cathodic one according to the electrochemical nomenclature and definitions by CITCE. The quantity of electricity was calculated by weighing the area of current-time recording chart with a maximum relative error due to weighing of $\pm 1\%$.

Results and Discussion

Inhibition of the Electrode Reaction by Mercury(I) Iodide Film Formation. Cobalt(II)-EDTA anions gave a polarographic anodic wave as a result of the electrode reaction,

$$Co^{III}Y^{-} + e \rightleftarrows Co^{II}Y^{2-} \qquad (1)$$

Its half-wave potential $E_{1/2}$ was obtained at $+0.13_8$ V *vs.* SCE, independent of the ionic strength from 0.1 to 1.0 and of the concentration of gelatin from zero to 0.05%. This value of $E_{1/2}$ is in good agreement with that reported by Reilley *et al.*[1] independent of pH from 4.5 to 10.5. The limiting current of the oxidation wave was diffusion-controlled.

It is also well known that iodide ions give a polarographic anodic wave based on the electrode reaction,[8]

$$Hg_2I_2 + 2e \rightleftarrows 2Hg + 2I^{-} \qquad (2)$$

The wave showed a well-defined shape at a small concentration of iodide, but when the concentration of iodide was greater than about 5×10^{-4} M the limiting current showed irregular fluctuations. Accordingly, 0.05% gelatin was used in this experiment to improve the iodide limiting current.

The current-time curve of iodide ions showed a normal shape, provided that an appropriate concentration of gelatin was present in the solution. However, in the presence of iodide ions, polarograms of $Co^{II}Y^{2-}$ were found not to be diffusion-controlled and current-time curves of $Co^{II}Y^{2-}$ showed peculiar shapes. In Fig. 1 are shown

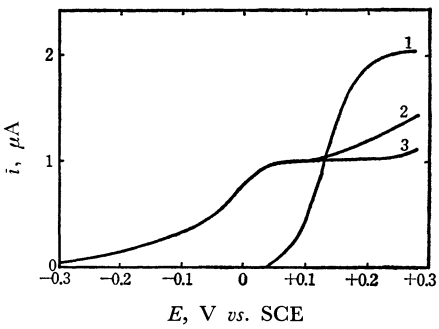

Fig. 1. Polarograms of 1.0 mM $Co^{II}Y^{2-}$ obtained in the solutions containing 0.1 M acetate buffer and 0.05% gelatin (1) in the absence and (2) in the presence of 3×10^{-4} M KI. Curve 3 is a polarogram of 3×10^{-4} M KI in 0.1 M acetate buffer containing 0.05% gelatin.

polarograms of 1.0 mM $Co^{II}Y^{2-}$ which were obtained in the solution containing 3×10^{-4} M potassium iodide, 0.1 M acetate buffer (pH 4.59) and 0.05% gelatin. Comparing curve 2 with curve 1, it is clear that the limiting current of $Co^{II}Y^{2-}$ is much smaller in the presence of iodide ions, whereas iodide ions yield a wave proportional to their concentration even in the presence of the complex. This phenomenon was also observed in the measurement of current-time curves.

Figure 2 presents the current-time curves during the life of a mercury drop measured at $+0.25$ V *vs.* SCE where the electrode reactions according to Eqs. (1) and (2) can take place. The abnormal

7) N. Tanaka and H. Ogino, This Bulletin, **38**, 439 (1965).

8) I. M. Kolthoff and J. J. Lingane, "Polarography," Vol. 2, Interscience Publishers, New York (1952), p. 577.

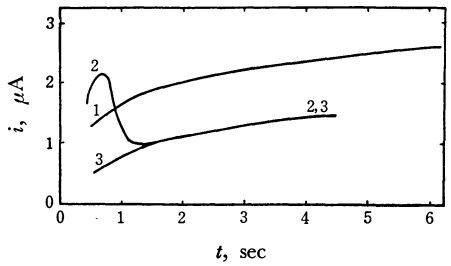

Fig. 2. Current-time curves obtained at +0.25 V *vs.* SCE with the same solutions as given in Fig. 1.

shape of current-time curve of $Co^{II}Y^{2-}$ was obtained in the presence of iodide ions (curve 2 in Fig. 2). During the earlier period of the growth of the mercury drop, the current-time curve (curve 2) follows the pattern of the normal diffusion-controlled current-time relationship, that is, the current observed is equal to the sum of the anodic current of $Co^{II}Y^{2-}$ (curve 1) and that of iodide (curve 3). Then, the current begins to decrease and at the end of the drop life it coincides exactly with the curve obtained in the solution containing only iodide ions. This suggests that mercury(I) iodide, which is the product of the electrode reaction according to Eq. (2), is adsorbed on the mercury surface and inhibits the electro-oxidation of $Co^{II}Y^{2-}$. In the earlier period of the drop life, the amount of adsorbed mercury(I) iodide is not enough to retard the electrode reaction of $Co^{II}Y^{2-}$, so that no deviation from the diffusion-controlled current occurs.

As the rate of mercury(I) iodide film formation is greater than the rate of the growth of the mercury drop, the ratio of the area occupied by the adsorbed mercury(I) iodide to the area of the mercury surface, *i. e.* the surface coverage θ, becomes larger with the time. This results in the retardation of the electro-oxidation of $Co^{II}Y^{2-}$ and the decrease in the current.

In Fig. 3 are shown the current-time curves obtained at various concentrations of iodide in the presence and the absence of $Co^{II}Y^{2-}$. These current-time curves demonstrate systematically the effect of adsorbed mercury(I) iodide on the oxidation of $Co^{II}Y^{2-}$ with increasing concentrations of iodide; the increase in the iodide concentration gradually changes the shape of the current-time curve. At a very low concentration of iodide such as 4×10^{-5} M, the current-time curve showed a normal shape during the whole life of the mercury drop (curve 1); this concentration of iodide is not sufficiently large enough to cause the retardation of the electro-oxidation of $Co^{II}Y^{2-}$. As the concentration of iodide increases, a remarkable change appears in the current-time curves (curves 2 and 3). When the concentration of iodide ions is equal to 1×10^{-3} M, the oxidation reaction of $Co^{II}Y^{2-}$ does

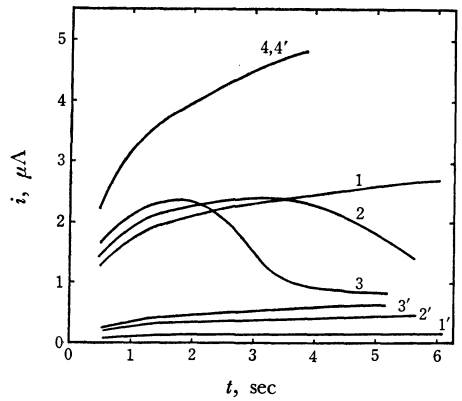

Fig. 3. Current-time curves of 1.0 mM $Co^{II}Y^{2-}$ obtained at +0.25 V *vs.* SCE in the solutions containing 0.1 M acetate buffer and 0.05% gelatin in the presence of (1) 4×10^{-5} M, (2) 1×10^{-4} M (3) 1.4×10^{-4} M and (4) 1×10^{-3} M KI. Curves 1' to 4' are current-time curves obtained in the same solutions as curves 1 to 4 but in the absence of $Co^{II}Y^{2-}$.

not occur even at the very beginning of the drop life; curves 4 and 4' are almost the same. In Fig. 4 are shown the d. c. polarograms which were obtained with the same solutions as shown in Fig. 3. Polarographic behaviors were found to be analogous to those of the current-time curves. With increasing concentrations of iodide, the anodic current of $Co^{II}Y^{2-}$ gradually decreases, until no difference could be seen between two polarograms of iodide ions with (curve 4) and without $Co^{II}Y^{2-}$ ions (curve 4').

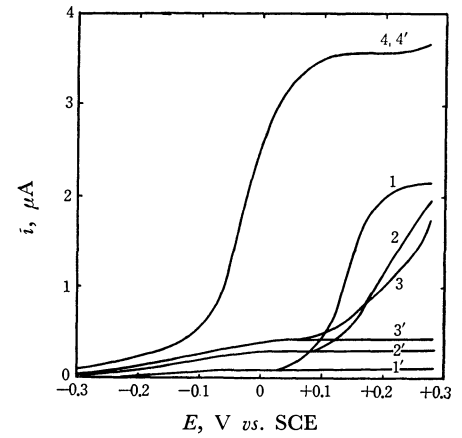

Fig. 4. Polarograms obtained with the same solutions as given in Fig. 3.

From the results mentioned above, it may be said that adsorbed mercury(I) iodide inhibits the electro-oxidation of $Co^{II}Y^{2-}$, but not that of mercury taking place in the presence of iodide ions. The electro-oxidation of mercury which took place in the presence of ethylenediaminetetraacetate

anion to form ethylenediaminetetraacetatomercurate(II) (HgY^{2-}) was also observed. It occurred at almost the same potentials as the electro-oxidation of $Co^{II}Y^{2-}$, but it was not so inhibited as $Co^{II}Y^{2-}$ in the presence of iodide ions.

Quantitative Evaluation of Adsorbed Mercury(I) Iodide. The inhibition of the electrode reaction of $Co^{II}Y^{2-}$ by mercury(I) iodide film formation at the surface of the dropping mercury electrode was investigated quantitatively in the following way. The quantity of electricity q which was consumed to form mercury(I) iodide (Hg_2I_2) at the electrode surface was measured from the area of the current-time curve of iodide ions. Let us denote the time when the current-time curve of $Co^{II}Y^{2-}$ began to decrease in the presence of iodide to be t_1, and the quantity of electricity consumed until t_1 to be q_1. The former was determined from the current-time curve which was prepared by subtracting the current-time curve obtained with the solution containing iodide only from that obtained with the solution containing $Co^{II}Y^{2-}$ and iodide. (See Fig. 5). The values of q were determined at various concentrations of iodide ions. Plots of q_1 *vs.* A_1 gave a straight line passing through the origin, where A_1 is the area of the electrode surface at time t_1 expressed in cm^2 ((1) in Fig. 6). Therefore it can be concluded that when the inhibition of the electro-oxidation of $Co^{II}Y^{2-}$ begins during the life of a mercury drop the extent of coverage of the electrode surface by mercury(I) iodide is constant irrespective of the iodide ion concentrations. A linear relationship between q_2 and A_2 was also obtained, as is shown by (2) in Fig. 6, where q_2 and A_2 mean the electricity consumed and the surface area, respectively, at time t_2 when the electro-oxidation of $Co^{II}Y^{2-}$ at the DME is completely inhibited.

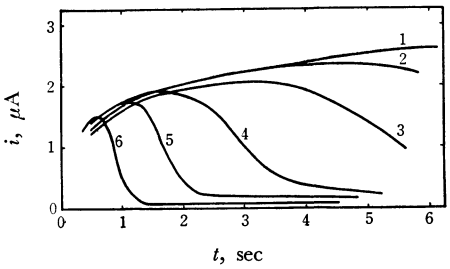

Fig. 5. Current-time curves of 1.0 mM $Co^{II}Y^{2-}$ at +0.25 V *vs.* SCE after correction for those of the corresponding concentration of iodide. The supporting electrolyte solutions contain 0.1 M acetate buffer and 0.05% gelatin. Concentrations of iodide ions are (1) none, (2) 8×10^{-5} M, (3) 1×10^{-4} M, (4) 1.4×10^{-4} M, (5) 2×10^{-4} M and (6) 3×10^{-4} M.

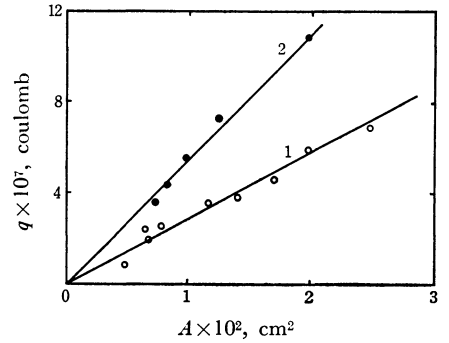

Fig. 6. The quantity of electricity versus the area of the DME (1) when inhibition of the electrode reaction begins and (2) when the electrode reaction is completely inhibited.

The surface coverage θ can be calculated with the equation,

$$\theta = \frac{n \times S}{A} \tag{3}$$

where n is the number of mercury(I) iodide molecules formed on the mercury surface, S is the area covered by one adsorbed molecule of mercury(I) iodide in cm^2, and A is the area of the electrode surface in cm^2. The value of n was calculated from the quantity of electricity consumed.

The crystal structure of mercury(I) iodide has been investigated by Havighurst.[9] If it is assumed that mercury(I) iodide forms a molecular film of the same structural arrangement as in the crystal, the effective area which one molecule of mercury(I) iodide occupies on the surface of mercury can be calculated with the aid of the structural parameters. When the amount of mercury(I) iodide produced by the electro-oxidation is less, the molecule is considered to be adsorbed in such a way that the c axis (the direction of I-Hg-Hg-I) is parallel with the surface of mercury. In this case, if the (110) plane is parallel with the surface, the effective area S is equal to 4.04×10^{-15} cm^2, while if the (100) plane is parallel with the surface, the value of S is equal to 5.71×10^{-15} cm^2.

On the other hand, if mercury(I) iodide is assumed to form a monomolecular film at time t_2 when the electro-oxidation of $Co^{II}Y^{2-}$ is completely inhibited, the effective area of one adsorbed molecule of mercury(I) iodide (Hg_2I_2) is calculated,

Table 1. Effective surface area S_2 of mercury(I) iodide at time t_2

$[I^-]\times10^4$ mol/l	t_2 sec	$q_2\times10^7$ coulomb	$A_2\times10^2$ cm^2	$S_2\times10^{15}$ cm^2
2.0	2.52	10.8	2.0	5.9
3.0	1.26	7.3	1.2	5.4
4.0	0.88	5.5	1.0	5.7
5.0	0.69	4.4	0.8	6.1
6.0	0.57	3.6	0.7	6.5
			Average	5.9×10^{-15} cm^2

9) R. T. Havighurst, *J. Am. Chem. Soc.*, **48**, 2113 (1926).

with the values of q_2 and A_2 obtained experimentally, to be approximately 5.9×10^{-15} cm^2 irrespective of the iodide concentration (see Table 1). This value is very close to the value of 5.71×10^{-15} cm^2 which was obtained with the assumption that the (100) plane of mercury(I) iodide covers the mercury surface.

As was mentioned above, the retardation of the electro-oxidation of $Co^{II}Y^{2-}$ begins at time t_1, when the mercury surface is covered by a smaller amount of mercury(I) iodide. The surface coverage θ_1 at time t_1 was calculated with the effective area of 5.71×10^{-15} cm^2 for mercury(I) iodide as given in Table 2, which seems to indicate

Table 2. Surface coverage θ_1 at time t_1

$[I^-] \times 10^4$ mol/l	t_1 sec	$q_1 \times 10^7$ coulomb	$A_1 \times 10^2$ cm^2	θ_1
0.8	3.53	6.9	2.5	0.5
1.0	2.52	5.9	2.0	0.5
1.2	2.02	4.6	1.7	0.5
1.4	1.51	3.8	1.4	0.5
2.0	1.13	3.6	1.2	0.6
3.0	0.63	2.6	0.8	0.6
4.0	0.50	1.9	0.7	0.5
5.0	0.47	2.4	0.7	0.7
6.0	0.32	0.8	0.5	0.3

that the retardation of the electro-oxidation of $Co^{II}Y^{2-}$ begins to occur when the fraction of the covered surface reaches nearly a half of the whole area of the electrode, again irrespective of the iodide concentration.

Conclusion. The electro-oxidation of ethylenediaminetetraacetatocobaltate(II) at the DME was found to be retarded and inhibited by the film formation of mercury(I) iodide. The effective area of one adsorbed molecule of mercury(I) iodide (Hg_2I_2) agreed with the area which one molecule of mercury(I) iodide covers if the (100) plane is considered to be parallel with the surface of mercury, being calculated with the aid of the structural parameters of the compound. It seems difficult, however, to decide at the present moment whether this agreement is fortuitous or not.

The film formation of mercury(I) iodide did not interfere with the electro-oxidation of mercury to form mercury(I) iodide, and less interfere with that of mercury to form ethylenediaminetetraacetatomercurate(II) under the conditions that the electro-oxidation of ethylenediaminetetraacetatocobaltate(II) is completely inhibited.

The authors wish to thank the Ministry of Education for the financial support granted for this research.

BULLETIN OF THE CHEMICAL SOCIETY OF JAPAN VOL. 41 2292—2297 (1968)

Silent Discharge Reactions in Aqueous Solutions. VIII. Effects of Discharge Gap Distance and Discharge Current on the Yield of Decomposition Products Formed from Water in Argon Atmosphere

Akira YOKOHATA, Katsuyuki HARAKON and Satoru TSUDA

Department of Chemistry, Faculty of Engineering, Hiroshima University, Senda-machi, Hiroshima

(Received March 14, 1968)

In order to elucidate the effects of discharge gap distance and discharge current on ${}^{s}G(H_2O_2)$, ${}^{s}G(OH)$ and ${}^{s}G(H)$, the study of this series was further made by using a new discharge apparatus. Both of acidic aqueous solutions of ferrous sulfate and ferrous sulfate-cupric sulfate have been selected as the reaction systems suitable for this purpose. Experiments were made in the range from 3 mm to 9 mm of discharge gap distance and from 0.2 mA to 0.5 mA of discharge current. Each ${}^{s}G$ value of H_2O_2, OH and H varied with gap distance (5→9 mm) and current (0.2 →0.5 mA) as follows; in the former, 1.0→1.2, 1.8→0.9 and 1.1→0.9: in the latter, 1.4→1.2, 0.6→ 0.9, 0.8→0.9. Based on the value of $Y(H_2O_2)/Y(H+OH)$, it was concluded that (1) the silent discharge reactions under a longer gap distance correspond to the radiolysis having a value of higher LET, that (2) although those under a lower current do also to a higher one, the effect of discharge current on the value of apparent LET is relatively small.

In the previous reports,[1] the authors have elucidated that in the silent discharge reactions of the aqueous solutions under the atmosphere of inert gas, the actions of the slow electrons generated in the gas phase to water molecules play a main

1) A. Yokohata and S. Tsuda, This Bulletin, **39**, 46, 53, 1636 (1966); **40**, 294, 1339, 2502, 2507 (1967).

role. In other words, the silent discharge reactions can be well interpreted in terms of an indirect effect: the primary one being the radiolysis of the water to give the intermediates like hydrogen atoms or hydroxyl radicals through the interaction of slow electrons with water molecules, in which the molecular products; hydrogen and hydrogen peroxide can also be obtained.

Each apparent G value (denoted by ${}^{s}G$) determined through the series of this study was as follows:

In argon; ${}^{s}G(\mathrm{H})=0.6$, ${}^{s}G(\mathrm{OH})=0.7$ and ${}^{s}G(\mathrm{H_2O_2})=1.5$

Of course, these values are meaningful only in the discharge tube used by us and not so universal as in the radiation chemistry. They appear to vary with the shape of discharge tube, the discharge gap distance and the discharge current, because the numbers and the mode of the streamers produced by discharge depend on them.

In order to get more informations on these points, a new discharge apparatus to make possible the variation of discharge gap distance was devised. The effect of electric discharge current has been also checked.

It is of interest and important to clear up these problems in the field of silent discharge. The aqueous solutions of ferrous ions and ferrous-cupric ions acidified with 0.4 N sulfuric acid were selected as the reaction systems suitable for this purpose.

Experimental

Apparatus. Figure 1 shows an experimental apparatus. It is composed of a discharge vessel having an electrode (A) of glass disk on which a tin foil (a) is wrapped and a gas washing bottle (B). A glass disk connected with glass holder (b) by adhesive is movable up and down through the wax-sealed part (c), which makes the variation of discharge gap distance possible. This disk was used as one electrode of the high tension side, and the tin foil part wrapped on the outer side (d) of vessel as another electrode (earth side).

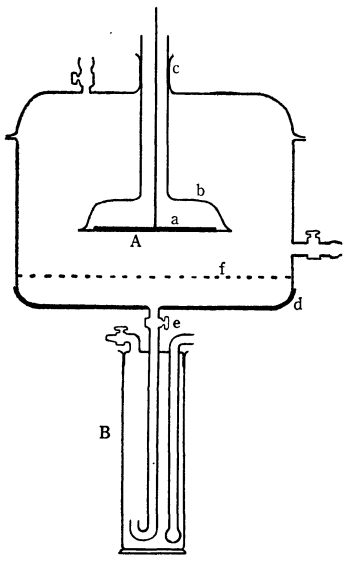

Fig. 1. Experimental apparatus.

After the sample solution deaerated previously by argon had been introduced into the vessel through the stopcock (e) of gas-washing bottle, the discharge was made by applying a high tension among those two electrodes, flowing argon gas through the vessel.

The discharge gap distance between the glass disk and the water surface was measured by the scale previously marked on the glass holder, while the level of the solution in the vessel was always kept constant (f).

The value of applied voltage was always calibrated by a static voltmeter. The electric discharge current was measured by the electric circuit shown in Fig. 2.

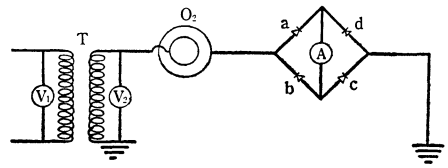

Fig. 2. Electric circuit.

V_1: Voltmeter V_2: Static electric voltmeter
a, b, c, d: Cu_2O rectifier A: Direct ammeter
Oz: Discharge tube T: Transformer

All experiments were made at room temperature, and at the constant solution volume of 100 m*l*. Flow velocity of argon gas was about 120 m*l*/min.

Materials. For the reliable performance, triple distilled water was always used throughout the work. All other materials were of reagent grade. Argon (purity$\gtrsim$99.998%) was used without further procedure.

Analysis. Ferric ion was determined from its optical density using a spectrophotometer at 304 mμ where $\varepsilon=2160\ \mathrm{M^{-1}cm^{-1}}$. Hydrogen peroxide was determined by the Ghormley method.[2]

Results

Figure 3 shows the relation between the applied voltage and electric current under each discharge gap distance of 5, 7 and 9 mm. As previously described, the discharge tube may be considered to be a sort of condenser having the capacitance C,[3] which consists of two parts, C_{die} and C_a; the former depends on the thickness and surface area of the glass disk and of the part covered by tin foil on the vessel, and the latter, on the gap distance among the glass disk and the water surface.

In Fig. 3, B, B', and B'' show respectively the firing voltage (V_1) for gap distance of 5, 7 and 9 mm. The AB, AB' and AB'' parts before discharge are

2) A. O. Allen, C. J. Hochanadel, J. A. Ghormley and T. W. Davis, *J. Phys. Chem.*, **56**, 575 (1952).
3) T. Biyodo, *J. Japan Chem. (Kagaku-no-Ryoiki)*, **3**, 172 (1950).

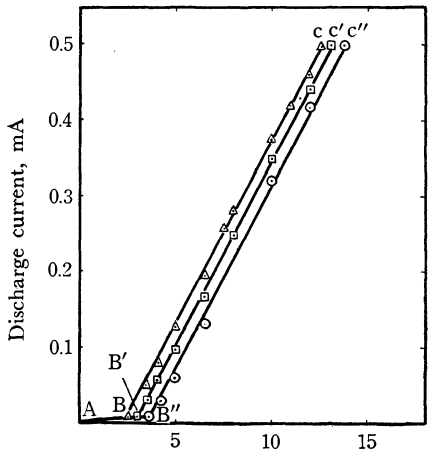

Fig. 3. Relation between applied voltage and discharge current.
Discharge gap distance: ⊙ 9 mm, ⊡ 7 mm, △ 5 mm

expressed by the formula $I=\omega CV$. For BC, B′C′ and B″C″ during discharge, $I=\omega CV_1+\omega C_{die}(V-V_1)$: $\omega=2\pi f$; V_1: firing voltage; V: applied voltage; f: frequency.

Table 1 summarizes the values of C, C_{die} and C_a against each discharge gap distance. These values are the ones needed for when calculating the energy dissipated by the silent discharge, as discussed later.

TABLE 1. RELATION BETWEEN DISCHARGE GAP DISTANCE AND CAPACITANCE

Gap distance mm	C, pF	C_{die}, pF	C_a, pF
5	6.3_7	131	6.7_0
7	5.3_1	131	5.5_3
9	4.4_2	131	4.5_7

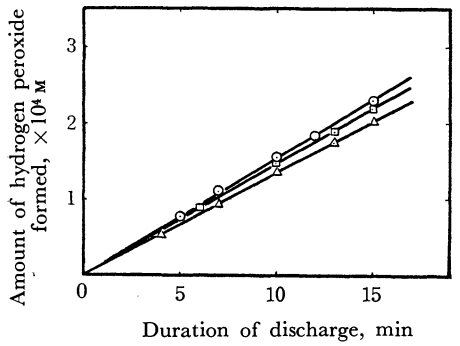

Fig. 4. Relation between amount of hydrogen peroxide formed and duration of discharge in 0.4 N sulfuric acid solution.
Discharge current: 0.5 mA
Discharge gap distance: ⊙ 9 mm, ⊡ 7 mm, △ 5 mm

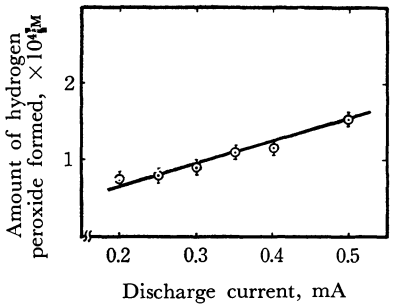

Fig. 5. Relation between amount of hydrogen peroxide formed and discharge current in 0.4 N sulfuric acid solution.
Discharge gap distance: 9 mm
Duration of discharge: 10 min

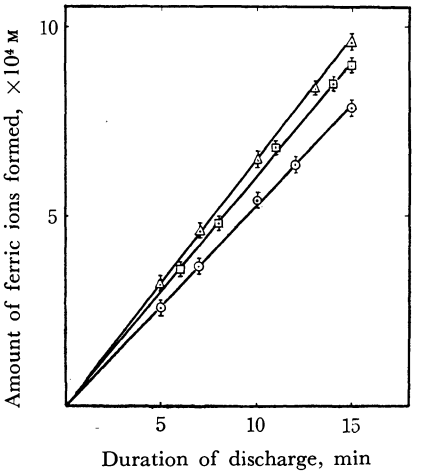

Fig. 6a

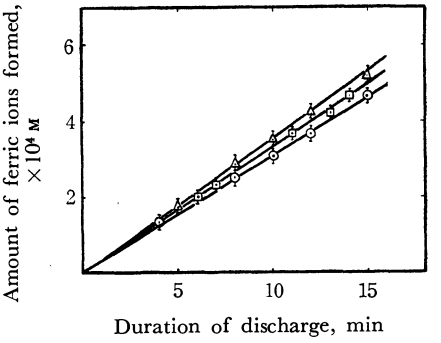

Fig. 6b

Fig. 6. Relation between amount of ferric ions formed and duration of discharge.
Discharge current: 0.5 mA
Dischrge gap distance:
⊙ 9 mm, ⊡ 7 mm, △ 5 mm
a Ferrous ion system: 2×10^{-3} M $FeSO_4$, 0.4 N H_2SO_4
b Ferrous-cupric ion system: 2×10^{-3} M $FeSO_4$—2×10^{-2} M $CuSO_4$, 0.4 N H_2SO_4

In the aqueous solution of 0.4 N sulfuric acid deaerated by argon, silent discharge leads to the formation of hydrogen peroxide.

Figure 4 shows the relation between the amount of hydrogen peroxide formed and the duration of discharge under the constant electric discharge current, 0.5 mA, where the discharge gap distance was changed in the range from 5 mm to 9 mm. In every case a good linearity has been found.

Figure 5 shows the relation between the amount of hydrogen peroxide formed and discharge current under a condition of discharge gap distance=9 mm and duration of discharge=10 min. In the experimental condition from 0.2 mA to 0.5 mA a good linearity was also found respectively.

As shown in the previous reports,[1] the silent discharge leads to the oxidation of ferrous ions to ferric ions. Then, the yield of ferric ions was independent of the concentration of ferrous ions in the range from 2×10^{-3} M to 4×10^{-1} M, and of the concentration of sulfuric acid in the range from 2×10^{-2} N to 1.5 N.

On the other hand, the addition of cupric ions reduces the yield of ferric ions because of the competition reaction of cupric ions and ferrous ions for the hydrogen atom. Then, it is also known that the existence of cupric ions of about 10 times as much as the ferrous ions is sufficient to scavenge the hydrogen atoms through the competition with ferrous ions.[1] In the ferrous ion system 2×10^{-3} M ferrous sulfate, and in the ferrous-cupric ion system 2×10^{-3} M ferrous sulfate and 2×10^{-2} M cupric sulfate were used respectively.

Figure 6 shows the relation between the amount of ferric ions formed and the duration of discharge (Fig. 6a for ferrous ion system and Fig. 6b for ferrous-cupric ion system), where the discharge current was 0.5 mA and the discharge gap distance was changed in the range from 5 mm to 9 mm. In all cases a good linearity has been found.

Figure 7 shows the relation between the amount of ferric ions formed and electric discharge current (Fig. 7a for ferrous ion system and Fig. 7b for ferrous-cupric ion system), where the discharge gap distance was 9 mm and the discharge current was changed in the range from 0.2 mA to 0.5 mA. In both cases a good linearity has been also found.

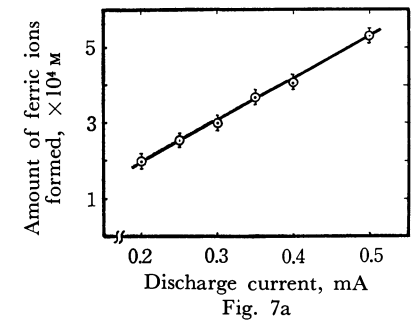

Fig. 7a

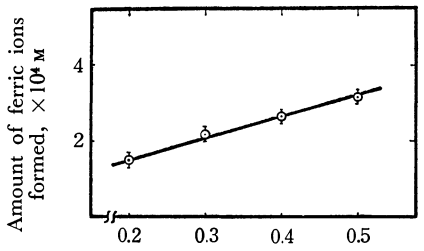

Fig. 7b

Fig. 7. Relation between amount of ferric ions formed and discharge current.
Discharge gap distance: 9 mm
Duration of discharge: 10 min
a Ferrous ion system: 2×10^{-3} M $FeSO_4$, 0.4 N H_2SO_4
b Ferrous-cupric ion system: 2×10^{-3} M $FeSO_4$–2×10^{-2} M $CuSO_4$, 0.4 N H_2SO_4

Discussion

On the basis of the well-known reaction mechanisms of the radiolysis of these systems, Eqs. (1) and (2) can be obtained. For the ferrous ion system,

$$G(Fe^{3+}) = 2G(H_2O_2) + G(OH) + G(H) \quad (1)$$

For the ferrous-cupric ions system,

$$G(Fe^{3+}) = 2G(H_2O_2) + G(OH) - G(H) \quad (2)$$

Since the silent discharge reactions correspond to ones induced by ionizing radiations of high LET (linear energy transfer), Eqs. (3) and (4) should be obtained respectively.[1]

$$Y(Fe^{3+}) = 2Y(H_2O_2) + Y(OH) + Y(H) \quad (3)$$

$$Y(Fe^{3+}) = 2Y(H_2O_2) + Y(OH) - Y(H) \quad (4)$$

where, Y shows respectively the yield of each product under a given discharge conditions. Thus, $Y(OH)$ and $Y(H)$ can be separately estimated from $Y(Fe^{3+})$ in the ferrous ion system, $Y(Fe^{3+})$ in the ferrous-cupric ion system, and $Y(H_2O_2)$ in the aqueous 0.4 N sulfuric acid.

Table 2. Relation between discharge gap distance and Y value

Gap distance mm	$Y(H_2O_2)$ $\times10^4$ M	$Y(H+OH)$ $\times10^4$ M	$Y(OH-H)$ $\times10^4$ M	$Y(H_2O_2)/Y(H+OH)$
5	1.3_6	3.7_8	0.8_1	0.36
7	1.4_7	3.1_1	0.4_0	0.47
9	1.5_5	2.2_4	0.0_6	0.69

By the same treatment as described in the previous report,[1] we can estimate $G(Fe^{3+})$ value from the value of apparent LET estimated on the basis of the relation between $G(H_2O_2)/G(H+OH)$ and LET. By combining $G(Fe^{3+})$ value estimated in this way with $Y(Fe^{3+})$, the absorbed dose can be determined. Of course, this means the dose determined by a chemical dosimeter; in other word, ones normalized to the scale of radiation chemistry. Let us call it "the apparent dose." The significance and the usefullness of this dose have been discussed in detail through the series of this study.

Effect of Discharge Gap Distance. Table 2 shows the respective value of $Y(H_2O_2)$, $Y(H+OH)$, $Y(OH-H)$ and $Y(H_2O_2)/Y(H+OH)$ under each discharge gap distance of 5, 7 and 9 mm, where discharge current=0.5 mA and duration of discharge=10 min. Thus, it can be understood that the silent discharge reactions of the aqueous solutions in argon atmosphere under each discharge gap distance of 5 mm, 7 mm and 9 mm correspond to the ones induced by the ionizing radiations having the value of LET of about 2, 4 and 6 (eV/Å).

By the use of each $G(Fe^{3+})$ value estimated from the value of LET,[4] the apparent dose rate can be respectively estimated to be 7.9×10^5 R/hr in 5 mm, 8.0×10^5 R/hr in 7 mm and 7.5×10^5 R/hr in 9 mm.

In general, the energy dissipated per second by the silent discharge is known to be expressed as follows:[5]

$$A=\frac{\left[f(C_{die}+C_a)(V_i+V_d)\{2E_m-(V_i+V_d)\{1+C_a/C_{die})\}\right]}{1+C_a/C_{die}} \qquad (5)$$

where V_i is correlated by the $V_i=V_1(C_{die}/(C_a+C_{die}))$ formula to the firing voltage, V_1. Table 3 shows the results of the calculation of A for each case of $V_d/V_i=0.2$ and 0.4.[1]

Since it is very difficult to determine exactly a value of firing voltage, the values calculated from Eq. (5) should be considered to be approximate ones.

Table 3. Calculated results of dissipated energy under each discharge gap distance of 5, 7 and 9 mm (normalized to the case of 5 mm)

Discharge gap distance mm	V_d/V_i	Dissipated energy
5		1
7	0.2	1.2
9		1.4
5		1
7	0.4	1.2
9		1.4

In spite of the fact that the dissipated energy increases with increasing discharge gap distance, the absorbed dose determined was almost the same. This finding suggests that the chemical utilization efficiency is rather better in a short discharge gap distance.

Table 4 shows each ${}^sG$ value of hydrogen peroxide, hydroxyl radical and hydrogen atom in relation to discharge gap distance. The increments of ${}^sG(H_2O_2)$ and the decrement of ${}^sG(OH)$ or ${}^sG(H)$ with the increasing discharge gap distance tend to confirm that the silent discharge reactions under a longer gap distance correspond to them induced by the ionizing radiations having a higher LET.

Table 4. Relation between discharge gap distance and ${}^sG$ value; discharge current=0.5 mA

Gap distance mm	${}^sG(H_2O_2)$	${}^sG(OH)$	${}^sG(H)$
5	1.0	1.8	1.1
7	1.1	1.3	1.0
9	1.2	0.9	0.9

In general, a higher applied voltage is needed for with an increasing discharge gap distance under

Table 5. Relations of the values of Y and apparent LET to each discharge current; discharge gap distance=9 mm

Discharge current, mA	$Y(H_2O_2)$ $\times10^4$ M	$Y(H+OH)$ $\times10^4$ M	$Y(OH-H)$ $\times10^4$ M	$\frac{Y(H_2O_2)}{Y(H+OH)}$	LET eV/Å
0.2	0.6_7	0.6_7	0.1_6	1.0	8
0.3	0.9_7	1.2	0.1_1	0.8	7
0.4	1.2_5	1.7	0.1_0	0.7	6
0.5	1.5_5	2.2	0.0_2	0.7	6

4) A. O. Allen, "Radiation Chemistry of Water and Aqueous Solutions," D. Van Nostrand Company, New York (1961), p. 54.

5) S. Fuji and N. Takimura, *Bulletin of the Electrotechnical Laboratory (Denki Shikensho Hokoku)*, **16**, 837 (1952).

A: the energy dissipated per second by the silent discharge

f: the frequency of the electric source used

C_{die}: the total capacitance of the insulator

C_a: the capacitance due to the gap distance in the discharge tube

V_i: the voltage across the gap space at the firing voltage

V_d: the stopping voltage

E_m: the maximum value of the applied voltage

a constant discharge current. A higher applied voltage would result in a localty of discharge which will induce the chemical reactions corresponding to them by a more densely ionizing radiations. The findings obtained support this interpretation.

Effect of Discharge Current. By the same procedure as above mentioned, the effect of discharge current was checked. Table 5 shows the respective value of $Y(H_2O_2)$, $Y(H+OH)$, $Y(OH-H)$, $Y(H_2O_2)/Y(H+OH)$ and apparent LET under each discharge current of 0.2, 0.3, 0.4 and 0.5 mA, where discharge gap distance= 9 mm and duration of discharge=10 min. From the value of apparent LET, the apparent dose rates under each discharge current of 0.2, 0.3, 0.4 and 0.5 mA were respectively estimated to be 2.9×10^5 R/hr, 4.4×10^5 R/hr, 6.0×10^5 R/hr and 7.5×10^5 R/hr. Table 6 shows the relation between each ${}^sG$ value of products and discharge current.

Table 6. Relation between discharge current and ${}^sG$ value; discharge gap distance=9 mm

Discharge current mA	${}^sG(H_2O_2)$	${}^sG(OH)$	${}^sG(H)$
0.2	1.4	0.6	0.8
0.3	1.3	0.8	0.9
0.4	1.3	0.8	0.8
0.5	1.2	0.9	0.9

These findings show that the silent discharge reactions under a lower current tend to correspond to the radiolysis having a value of higher LET. However, it can be concluded that the effect of discharge current on the value of apparent LET is relatively small.

BULLETIN OF THE CHEMICAL SOCIETY OF JAPAN VOL. 41 2297—2305 (1968)

Solvent Effect in NMR Spectroscopy. II. A Repulsive Interaction between the Benzene Solvent Molecule and the Nitrogen Lone-Pair, and the Effects Induced by the Addition of Protic Substances

Teijiro YONEZAWA, Isao MORISHIMA and Kazuhiko FUKUTA

Department of Hydrocarbon Chemistry, Faculty of Engineering, Kyoto University, Sakyo-ku, Kyoto

(Received March 28, 1968)

The variations in the chemical shifts of proton resonances in imines, aziridines, and oximes, all of which have oriented nitrogen lone-pair electrons, on going from a carbon tetrachloride solution to a benzene solution ("benzene solvent shift") are determined. Also determined are the changes in the corresponding proton chemical shifts in a benzene solution when protic substances, such as methanol or trifluoroacetic acid, are added ("addition shift"). It is generally found that the upfield benzene-solvent shift is more sensitive to the protons *trans* to the oriented nitrogen lone-pair than to the *cis*. This observation indicates that the formation of a benzene-solute collisional complex is most likely to occur at a site as far as possible from the nitrogen lone-pair. The repelling of a benzene solvent molecule by the nitrogen lone-pair may occur due to the repulsive interaction between lone-pair electrons and benzene π-electrons. It is also found that the addition shift is upfield and is larger for the proton *trans* to the nitrogen lone-pair than for that *cis*. These general observations are of predictive value in the determination of the orientation of the nitrogen lone-pair electrons and in the assignment of the signals of proton groups in the vicinity of the nitrogen lone-pair.

A great number of studies of the specific solvent effects on the proton chemical shifts of polar solutes in aromatic solvents have been reported,[1,2] and the study of these effects has been proved to be a very powerful technique for use in structure elucidation and conformational analysis. For a complex molecule, the size and sign of the benzene-solvent shft (the difference in the chemical shift of a signal in a benzene solvent and in an inactive solvent) have been linked with the position of the protons relative to the polar functional groups.[2]

This benzene-induced chemical shift depends on the equilibrium formation of a stereospecific collisional complex between the solute and the benzene solvent.[2c] The orientation of the solvent molecule

1) T. Yonezawa, I. Morishima and K. Takeuchi, This Bulletin, **40**, 1807 (1967).

2) a) N. S. Bhacca and D. H. Williams, "Application of NMR Spectroscopy in Organic Chemistry," Holden-Day, San Francisco, Calif. (1964), Chap. 7. b) See T. Ledaal, *Tetrahedron Letters*, **1966**, 1653 and the references cited therein. c) J. Ronayne and D. H. Williams, *J. Chem. Soc., (B)*, **1967**, 540.

with respect to the dipolar functional groups is non-random. The ketones in a benzene solution form a solute-solvent collisional complex in which the π-electrons of the benzene ring interact with the partial positive charge on the carbonyl carbon atom in such a manner that the benzene ring locates as far as possible from the partial negative charge on oxygen.[2]

In addition to these benzene solvent shifts, we have found a solvent effect induced by the addition of protic substances, such as methanol or trifluoroacetic acid, to a benzene solution of several polar solute molecules.[1] In the previous paper,[1] we have pointed out that the addition of a protic substance to the benzene solution of the carbonyl compounds causes an upfield shift of the protons of the solute molecules. This effect is more pronounced on the protons lying in close proximity to the proton-accepting site of a solute molecule than on those remote from it. The use of this addition shift in structural analysis has been described.

Despite these abundant potential uses of the benzene-induced shift in solving structural and other physical problems, there have been few investigations aimed at elucidating the intrinsic nature of this stereospecific intereaction in aromatic solvents. In the present study we have tried to investigate the benzene-solvent effect of the nitrogen-containing molecules with oriented lone-pair electrons from two viewpoints. First, in order to make clear the nature of the repulsive interaction of the benzene solvent molecule with the negatively-charged site of the polar functional groups of a solute; a limiting case of this interaction between a benzene-solvent molecule and the nitrogen lone-pair electrons is studied. Second, the effect induced by the addition of a protic substance to the benzene solution is further examined for solute molecules with an oriented nitrogen lone-pair which is available as a proton-accepting site. In this work we have determined the benzene-solvent shift and the effect induced by the addition of protic substances on the protons of imines (I), aziridines (II), and oximes (III).

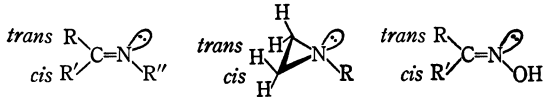

I II III

We now wish to propose the generalization that a benzene-solvent molecule is repelled by the nitrogen lone-pair and has a more remarkable shielding effect on the protons remote from the lone pair; this phenomenon to be of considerable predictive value in structural determination. The addition shift is also shown to have a definite tendency for various solute molecules.

Experimental

Materials. All the chemicals used in this study were obtained from commerical sources unless otherwise noted, and all were carefully purified by distillation before use. The aldimines and ketimines were prepared according to the procedure of Campbell *et al.*[3] To 29.5 g (0.5 mol) of *n*-propylamine, 29.0 g (0.5 mol) of acetone were added gradually over a period of two hours in a nitrogen atmosphere. Potassium hydroxide flakes were then added, and the mixture was allowed to stand in a refrigerator overnight. The dried material was distilled over a few pellets of potassium hydroxide. The *N*-phenylacetonimine was prepared by the condensation of the corresponding ketal[4] with aniline by the method of Hoch.[5] The 1-methyl- and 1-ethylaziridines were prepared from commercially-avaiable 2-methylaminoethanol and 2-ethylaminoethanol respectively by the method of Cairn.[6] The *O*-methylacetoxime ether was prepared by adding dimethylsulfate to a sodium hydroxide solution of acetoxime.[7]

NMR Measurements. Solutions for NMR measurements were prepared in such a way that the concentrations were 7.5 mol% in both the benzene and the carbon tetrachloride solutions. The details of the preparation of the samples for measuring the addition shift have been reported in a previous paper.[1] All the samples were run on a JEOL JNM-3H-60 spectrometer operation at 60 MHz, using an internally-locked field-frequency stabilization control system.[1] The chemical shifts were monitored by an electronic-frequency counter in Hz from an internal TMS.

Results and Discussion

Benzene-solvent Shift. Tables 1, 2, and 3 summarize the chemical shift, in benzene and carbon tetrachloride solutions, of protons of imines (Table 1), aziridines (Table 2), and oximes and oxime ether (Table 3). Before discussing the benzene-solvent shift, however, we wish to discuss briefly the signal assignment of the *cis* and *trans* proton groups for imines (I), aziridines (II), and oximes (III). The basis of the assignment of I is the proton-proton coupling constant between N-$CH_2(\alpha)$ and C-CH_3 protons. The lower-field methyl signal of *N-n*-propylacetonimine shows a splitting ($J=1.4$ Hz) by N-$CH_2(\alpha)$ protons, while the higher-field one gives $J=0.7$ Hz. For *N-n*-propylaldimine the corresponding coupling constant is 1.4 Hz. In light of the general trend, *trans* coupling constant > *cis* coupling constant, the lower-field methyl signal, resonating at about $\tau=8.1$, can be assigned to *trans* methyl protons. Accordingly, the NMR spectrum giving a single

3) K. N. Campbell, A. H. Sommers and B. K. Campbell, *J. Am. Chem. Soc.*, **66**, 82 (1944).
4) W. J. Croxall, F. J. Clavis and H. T. Neher, *ibid.*, **70**, 2805 (1948).
5) M. J. Hoch, *C. R. Acad. Sci. Paris*, **199**, 1428 (1934).
6) T. L. Cairn, *J. Am. Chem. Soc.*, **63**, 871 (1941).
7) Ponzio and Charrier, *Gazzetta Chimica Italiana*, **37**, I, 506 (1907).

TABLE 1. CHEMICAL SHIFTS INDUCED BY THE ADDITION OF METHANOL TO THE BENZENE SOLUTIONS OF IMINES

Solute	Proton	ν_{CCl_4}[a,b]	$\nu_{C_6H_6}$[a,b]	$\Delta\nu_{CCl_4}^{C_6H_6}$[c]	$\Delta\nu_{C_6H_6}^{MeOH}$[d]
N-*n*-Propylacetonimine	*trans*-CH_3	114.5	110.6	+ 3.9	+ 8.8
	cis-CH_3	104.4	83.7	+20.7	+10.6
trans[e] CH_3, *cis*[e] CH_3, $CH_2CH_2CH_3$	α-CH_2	184.2	184.5	− 0.3	+10.7
	β-CH_2	89.9	99.0	− 0.1	+ 8.3
α β γ	γ-CH_3	54.4	59.2	− 4.8	+ 7.5
N-*n*-Propylacetaldimine	*trans*-CH_3	112.6	100.9	+11.7	+ 5.2
	cis-H	450.3	437.7	+12.6	+ 9.4
trans CH_3, *cis* H, $CH_2CH_2CH_3$	α-CH_2	193.4	191.4	+ 2.0	*
	β-CH_2	89.0	77.5	+11.5	+ 4.2
α β γ	γ-CH_3	52.3	51.5	+ 0.8	+ 5.6
N-Phenylacetonimine	*trans*-CH_3	122.5	112.0	+10.5	+ 1.9
trans CH_3, *cis* CH_3, C_6H_5	*cis*-CH_3	103.0	83.7	+19.3	+ 3.4

a) Chemical shift in Hz from an internal TMS.
b) 7.5 mol in carbon tetrachloride and benzene solution.
c) Benzene solvent shifts in Hz.
d) Addition shifts in Hz (added methanol; 1.4 mmol).
e) The notation "*trans*" or "*cis*" is referred to the *N*-substituent.

methyl proton signal for *N*-*n*-propylaldimine shows the presence of a single *trans* isomer. These assignments correspond to results of recent work by Olah *et al.*[8] The assignment of the ring methylene proton signals for 1-methyl- and 1-ethylaziridine has been well established,[9] as have the facts that the higher-field one of the two separate ring proton signals belongs to the *cis* group, and the remaining one, the *trans*. For oximes, C-methyl protons when *cis* to the hydroxy group resonate at higher fields than when *trans*; both C-methylene and C-methine protons when *cis* to the hydroxyl group resonate at lower fields than when *trans*. These assignments are based upon the studies by Karabatsos[10] and Huitric.[11] The benzene-solvent shift, $\Delta\nu_{CCl_4}^{C_6H_6}$, is defined as the difference in the chemical shift of a signal between that in a benzene solution and in a carbon tetrachloride solution.

It can be seen from Table 1 that benzene causes a shielding of C-alkyl proton resonances relative to the carbon tetrachloride solution and a shielding or deshielding of N-alkyl protons for several imines. The benzene-solvent shift values, $\Delta\nu_{CCl_4}^{C_6C_6}$, for

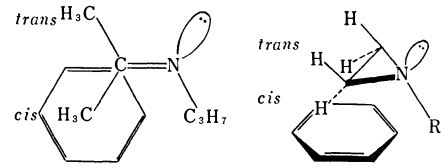

Fig. 1. Model representation of benzene-imine complex. Benzene solvent molecules are repelled by the nitrogen lone pair.

C-alkyl groups of *N*-*n*-propylacetonimine are very different for the *cis* and *trans* groups. A larger shift is observed for the *cis* methyl protons than for the *trans* ones; indeed, the difference is unexpectedly large. This observation makes one picture a benzene-imine stereospecific collisional complex in which the benzene-solvent molecule is repelled by the nitrogen lone-pair, as is shown in Fig. 1. This type of complex has a more effective shielding effect on the *cis* protons than on the *trans* ones. Table 1 also shows the results for *N*-*n*-propylacetaldimine. Contrary to the results for *N*-*n*-propylacetonimine, both C-alkyl and N-alkyl protons are shielded by the benzene solvent here. No shielding or deshielding effect by the benzene solvent for *n*-propyl protons of *N*-*n*-propylacetonimine and *N*-*n*-propylacetaldimine is yet clear in its origin. The larger value of the benzene-solvent shift for methine protons than for methyl protons on the C-alkyl group also indicates that aldimine exists in a single conformation with the C-alkyl group *trans* to the N-alkyl group. In the case of

8) G. A. Olah and P. Kreienbühl, *J. Am. Chem. Soc.*, **89**, 4756 (1967).
9) T. Yonezawa, I. Morishima and K. Takeuchi, *ibid.*, Submitted for the publication; H. Saitô, K. Nuckada, T. Kobayashi and K. Morita, *ibid.*, **89**, 6605 (1967).
10) G. J. Karabatsos, R. A. Taller and F. M. Vane, *ibid.*, **85**, 2326, 2327 (1963).
11) A. C. Huitric, D. B. Roll and J. R. DeBoer, *J. Org. Chem.*, **32**, 1661 (1967).

TABLE 2. CHMICAL SHIFTS INDUCED BY THE ADDITION OF METHANOL TO THE BENZENE SOLUTIONS OF AZIRIDINES

Solute	Proton	ν_{CCl_4} [a,b]	$\nu_{C_6H_6}$ [a,b]	$\Delta\nu_{CCl_4}^{C_6H_6}$ [c]	$\Delta\nu_{C_6H_6}^{MeOH}$ [d]
1-Methylaziridine	*trans*-H	94.2	90.3	+ 3.9	+11.5
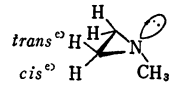	*cis*-H	52.3	38.6	+13.7	+12.2
	N-CH_3	131.0	122.6	+ 8.4	+13.1
1-Ethylaziridine	*trans*-H	93.2	90.8	+ 2.4	+11.8
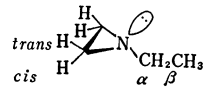	*cis*-H	54.0	41.8	+12.2	+12.6
	α-CH_2	126.6	118.7	+ 7.9	+12.9
	β-CH_3	64.7	63.5	+ 1.2	+ 8.4

a) Chemical shifts in Hz from an internal TMS.
b) 7.5 mol in carbon tetrachloride and benzene solution.
c) Benzene solvent shifts in Hz.
d) Addition shifts in Hz (added methanol; 1.4 mmol).
e) The notation "*trans*" or "*cis*" is referred to the *N*-substituent.

TABLE 3. CHEMICAL SHIFTS INDUCED BY THE ADDITION OF TFA TO THE BENZENE SOLUTION OF OXIMES AND OXIME ETHER

Solute	Proton	ν_{CCl_4} [a,b]	$\nu_{C_6H_6}$ [a,b]	$\Delta\nu_{CCl_4}^{C_6H_6}$ [c]	$\Delta\nu_{C_6H_6}^{TFA}$ [d]
Acetoxime	*trans*-CH_3	112.0	96.3	+15.7	+16.9
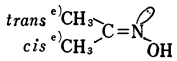	*cis*-CH_3	111.1	101.5	+ 9.6	+18.7
Cyclohexanone oxime	α-*trans*	132.3	128.2	+ 4.1	+14.2
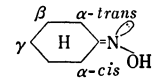	α-*cis*	154.6	148.0	− 1.7	+16.6
	β,γ-CH_2	97.6	77.5	+20.1	+ 9.6
Acetaldoxime					
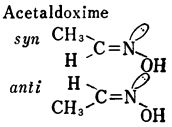	*syn* CH_3	112.8	84.8	+28.0	+ 9.3
	syn H	440.8	431.0	+ 9.8	+10.9
	anti CH_3	112.8	93.1	+19.7	+12.4
	anti H	404.9	386.1	+18.8	+19.6
Propionaldoxime					
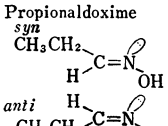	*syn* β-CH_3	66.0	46.0	+20.0	+ 8.5
	syn α-CH_2	133.9	112.8	+21.1	+ 8.3
	syn α-H	439.7	435.7	+ 4.0	+14.8
	anti β-CH_3	65.3	43.7	+21.6	+ 7.4
	anti α-CH_2	140.8	134.5	+ 6.3	+17.7
	anti α-H	396.4	383.6	+12.8	+23.7
Ethyl methyl ketoxime					
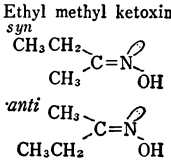	*syn* α-CH_3	109.8	103.0	+ 6.8	+15.0
	syn β-CH_3	65.6	52.6	+13.0	+10.2
	syn α-CH_2	131.9	118.4	+13.5	+14.2
	anti α-CH_3	110.3	96.3	+14.0	+16.8
	anti β-CH_3	64.5	51.7	+12.8	+12.8
	anti α-CH_2	133.3	137.5	− 4.2	+18.5
O-Methylacetoxime ether	O-CH_3	227.7	223.0	+ 4.7	+22.1
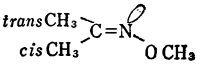	*trans*-CH_3	107.8	96.3	+11.5	+24.0
	cis-CH_3	105.3	97.4	+ 7.9	+26.5

a) Chemical shift in Hz from an internal TMS.
b) 7.5 mol in carbon tetrachloride and benzene solution.
c) Benzene solvent shifts in Hz.
d) Addition shifts in Hz (added trifluoroacetic acid; 0.167 mmol).
e) The notation "*trans*" or "*cis*" is referred to the *N*-substituent.

the *N*-phenylacetonimine in Table 1, *cis* methyl protons are shifted more upfield by the benzene solvent than are *trans* methyl protons; this implies also that the benzene molecule is repelled by the nitrogen lone-pair and that it approaches the *cis* methyl group. The replacement of the *n*-propyl group by the phenyl group does not significantly affect this specific solvent shift.

This repulsive interaction between a benzene molecule and lone-pair electrons is further evident from the data for aziridine compounds compiled in Table 2. All the compounds in Table 2 perform a slow internal inversion at the nitrogen atom and show the *cis* and *trans* proton signals separately at room temperature. The $\Delta\nu_{CCl_4}^{C_6H_6}$ values are larger for *cis* methylene protons than for *trans* ones. This observation again indicates that the benzene-solvent molecule locates preferentially as far away as possible at the opposite side of the effective lone-pair (the nitrogen lone-pair) (Fig. 1). This repulsive interaction does not depend on the *N*-substituent alkyl group, as can be seen in Table 2, on passing from 1-methyl- to 1-ethylaziridine. Namely, for 1-ethylaziridine, which has the bulkier ethyl group, the $\Delta\nu_{CCl_4}^{C_6H_6}$ values are not significantly changed; this indicates that the benzene-solvent molecules lying at the *cis* ring methylene protons are not sterically repelled by the 1-substituent alkyl group. The difference in the solvent shift, $\Delta\nu_{CCl_4}^{C_6H_6}$, between the protons of the lone-pair side (the *trans* group) and the opposite side (*cis* group and 1-alkyl protons) is quite large, indicating that the benzene-solvent molecule locates preferentially on one side (the 1-alkyl side) of the three-membered-ring plane.

From these data and from our discussion of the benzene-solvent shift, it can now be concluded that the benzene π-electrons and the nitrogen lone-pair electrons interact repulsively and that this interaction causes a specific benzene-solvent effect on the nitrogen-containing solute molecules.

Oxime has two interaction sites with the benzene-solvent molecule; the nitrogen lone-pair and the hydroxyl group. The partial negative charge on the hydroxyl oxygen repels the benzene molecule and causes a more effective specific shielding of the *trans* C-alkyl protons than of the *cis*. This is analogous to the effect frequently encountered with the polar carbonyl group.[1,2] However, another repulsive site, the nitrogen lone-pair, is also active in benzene-oxime solvent interaction.

The observed benzene-solvent shift may result from the two competitive repulsive interactions between the benzene-hydroxyl group and the benzene-nitrogen lone-pair electrons. Although the benzene-solvent shifts for a few examples of oximes have been determined by Karabatsos,[10] we carried out further, extended studies in order to examine the above-mentioned type of competitive interaction. As is evident in Table 3, the difference in the $\Delta\nu_{CCl_4}^{C_6H_6}$ values for the *cis* and *trans* protons of acetoxime and cyclohexanone oxime is small compared with that between such protons of imines and aziridines (Tables 1 and 2), the value for the *trans* protons being only slightly larger. This observation may reflect the two competitive repulsive interactions mentioned above. Compared with the $\Delta\nu_{CCl_4}^{C_6H_6}$ values of imines with only one repulsive interaction site of the nitrogen lone-pair (Table 1), the reduced value of the difference in $\Delta\nu_{CCl_4}^{C_6H_6}$ for *cis* and *trans* protons of oximes supports the competitive repulsive interaction. This observation has also been encountered in a previous paper[1] regarding nitrosamine, which has two possible repulsive sites, the nitrogen lone-pair and the negatively-charged oxygen atom of the nitroso group.

For acetaldoxime and propionaldoxime, which are mixtures of the *syn* and *anti* isomers consisting of 67% and 45% *syn* isomers for the two aldoximes respectively, the repulsive interaction mentioned above can be expected. For acetaldoxime, the $\Delta\nu_{CCl_4}^{C_6H_6}$ value of the methyl protons is larger for the *syn* isomer than for the *anti*, while for the methine protons the situation is just the reverse. This observation also reflects the fact that the benzene-hydroxyl group repulsive interaction is stronger than the benzene-nitrogen lone-pair interaction. It should be noted that the difference in the $\Delta\nu_{CCl_4}^{C_6H_6}$ values for methyl and methine protons is quite a bit smaller for the case of the *anti* isomer of acetaldoxime compared with that of the *syn* isomer. A similar trend of the solvent shifts is also obtained for ethyl methyl ketoxime.

The last example is *O*-methyl acetoxime ether. In a carbon tetrachloride solution *cis* methyl protons (*cis* to the *O*-methyl group) resonate at a slightly lower field. The addition of benzene to this solution causes the signals to cross, and in the benzene solution the *cis* methyl protons resonate at a very slightly higher field, as may be seen in Table 3. Therefore, the value of $\Delta\nu_{CCl_4}^{C_6H_6}$ is larger for *trans* methyl protons than for *cis* methyl protons. This oxime ether also has two interaction centers with the benzene molecule, the nitrogen lone-pair and the oxygen lone-pair. From the above observation, it can also be said that the benzene-solvent molecule is repelled more effectively by the oxygen lone-pair electrons. This finding is compatible with the finding of Karabatsos and Hsi.[12]

Chemical Shifts Induced by the Addition of Protic Substances to Benzene Solutions. Tables 1—3 also present the chemical shifts for protons induced by the addition of portion of methanol (MeOH) or trifluoroacetic acid (TFA) to

12) G. J. Karabatsos and N. Hsi, *Tetrahedron*, **23**, 1079 (1967).

benzene solutions of imines, aziridines, oximes, and oxime ether. The addition shift, $\Delta\nu^{TFA}_{C_6H_6}$ or $\Delta\nu^{MeOH}_{C_6H_6}$ corresponds to the difference between the chemical shift induced by the addition of the protic substances to a benzene solution of the solute and the chemical shift induced by the addition of a protic substance to a carbon tetrachloride solution of the same solute.[1] This correction for the protonation shift is important for the solute molecules of the present case, which are sensitive to the protic additivities resulting from the hydrogen bonding interaction with the nitrogen lone-pair, causing downfield shifts of the protons in the vicinity of the nitrogen atom.

Figures 2—12 give the plots of the addition shift, $\Delta\nu^{TFA}_{C_6H_6}$ or $\Delta\nu^{MeOH}_{C_6H_6}$ *vs.* the concentration of the added protic substances. A considerable induced upfield shift for the protons in the vicinity of the nitrogen lone-pair is observed, as is to be expected from the various carbonyl compounds discussed in the previous work.[1] For *N*-*n*-propylacetonimine, the protons of the *n*-propyl group suffer larger upfield addition shifts in the groups closer to the nitrogen atom (Table 1 and Fig. 2). It may be seen in Fig. 2 that the aparent addition shift is enhanced by the increase in the concentration of added methanol, until the downfield shift induced by the OH···N hydrogen bond formation appears. For the methyl protons of the $N{=}C(CH_3)_2$ fragment, the relative value of the addition shift is in the order of the solvent shift for *cis* and *trans* methyl groups, and the general tendency of the addition shift does not hold, as was established for carbonyl compounds in the previous work.[1] In the case of carbonyl compounds, the order of the upfield addition shift is just the opposite of that of the solvent shift, and this addition shift is more sensitive to the protons lying in close proximity to the proton-accepting site of the solute molecule than to those remote from it.[1]

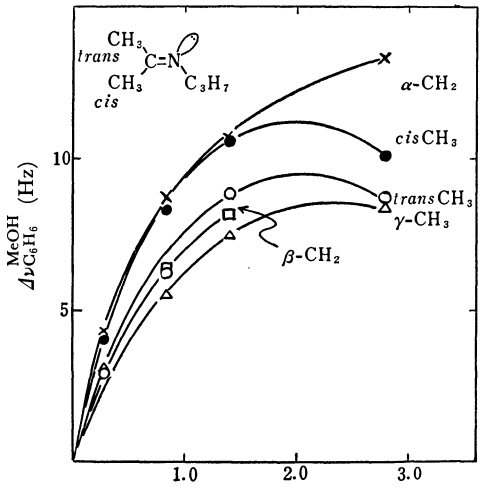

Fig. 2. Plots of $\Delta\nu^{MeOH}_{C_6H_6}$ *vs.* mol of added methanol for *N*-*n*-propylacetonimine.

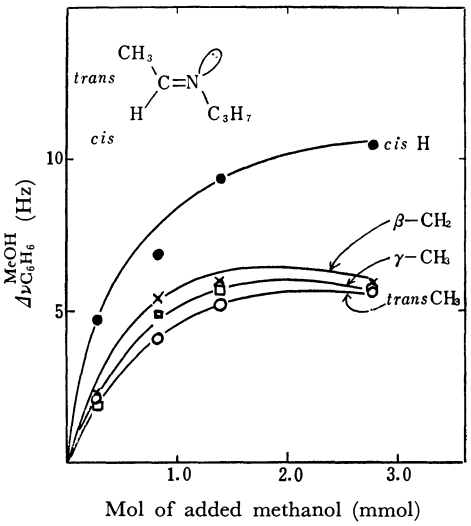

Fig. 3. Plots of $\Delta\nu^{MeOH}_{C_6H_6}$ *vs.* mol of added methanol for *N*-*n*-propylacetaldimine.

For *N*-*n*-propylacetaldimine, upfield addition shifts are observed for all the protons. It may be observed in Fig. 3 that this addition shift is more remarkable with the methine proton than with the methyl protons, which are *cis* to the nitrogen lone-pair. This addition shift has the same order as the solvent shift. The upfield addition shift increases with the concentration of added methanol, as is shown in Fig. 3. The upfield addition shift for the *N*-*n*-propyl proton is in the order of β-methylene $>\gamma$-methyl (the α-methylene signal is hidden in the methanol methyl proton signal). This

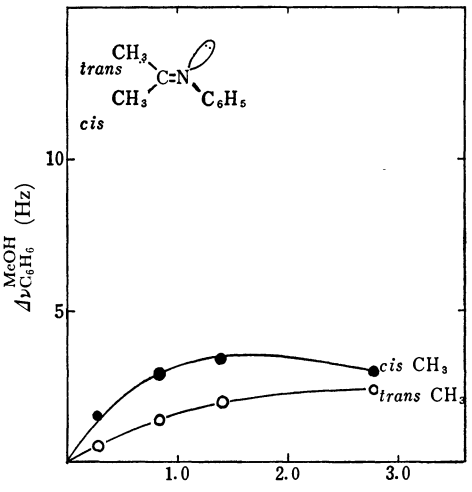

Fig. 4. Plots of $\Delta\nu^{MeOH}_{C_6H_6}$ *vs.* mol of added methanol for *N*-phenylacetonimine.

may also be seen for *N*-phenylacetonimine in Table 1 and Fig. 4 and for *N*-*n*-propylacetonimine in Fig. 2.

For 1-methyl- and 1-ethylaziridines, *cis* ring methylene protons undergo greater upfield addition shifts than do the *trans* protons, but the difference is very small (Figs. 5 and 6).

Oxime has two possible proton-accepting sites, the nitrogen lone-pair and the oxygen lone-pair of the hydroxyl group. Saito and Nukada[13] investigated the structure of oxime hydrochloride and showed that the protonation of the oximes occurs exclusively at the nitrogen lone-pair rather than at the hydroxyl oxygen atom. We will, therefore, in interpreting the addition shift for oximes, henceforth assume that, in solution with protic substances, the hydrogen-bonding interaction of oxime occurs exclusively at the nitrogen lone-pair. Judging from the addition shift for imines, the slightly larger value (Table 3 and Figs.

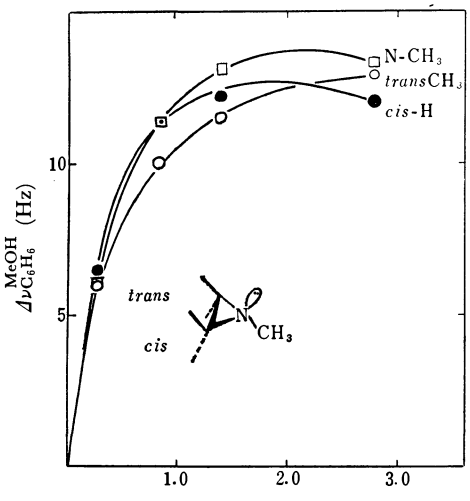

Fig. 5. Plots of $\Delta\nu_{C_6H_6}^{MeOH}$ *vs.* mol of added methanol for 1-phenylacetonimine.

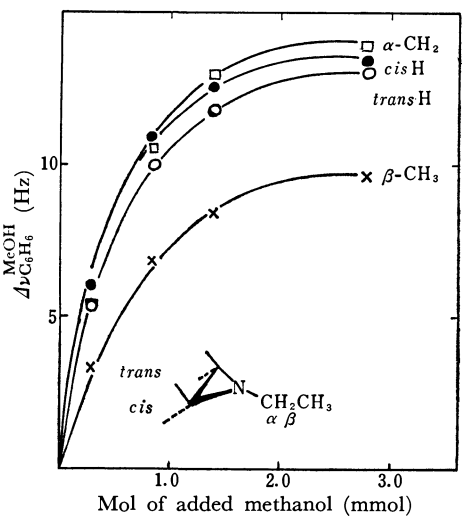

Fig. 6. Plots of $\Delta\nu_{C_6H_6}^{MeOH}$ *vs.* mol of added methanol for 1-methylaziridine.

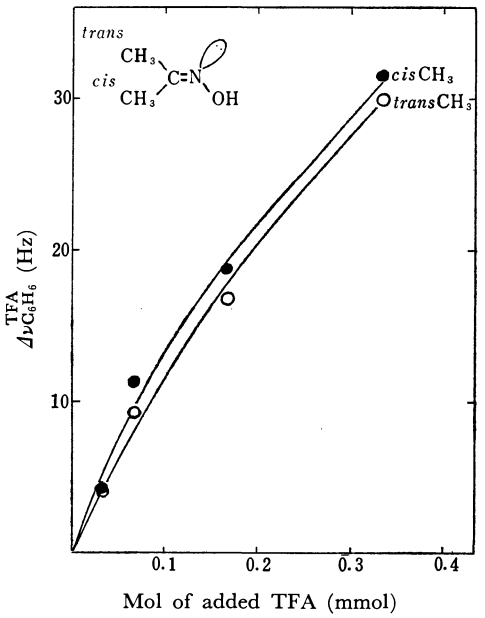

Fig. 7. Plots of $\Delta\nu_{C_6H_6}^{TFA}$ *vs.* mol of added TFA for acetoxime.

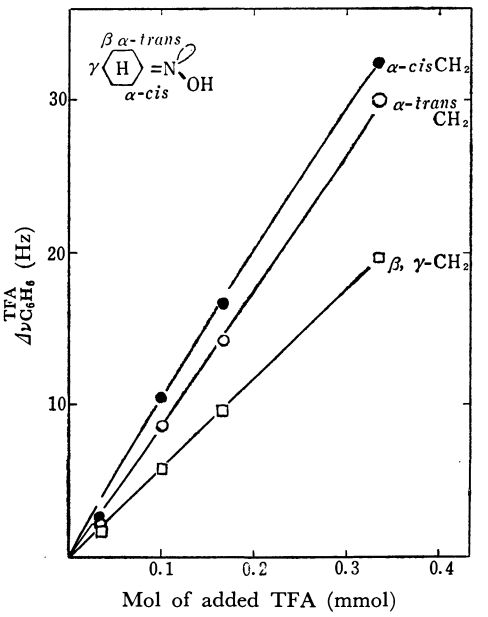

Fig. 8. Plots of $\Delta\nu_{C_6H_6}^{TFA}$ *vs.* mol of added TFA for cyclohexane oxime.

13) H. Saito, K. Nukada and M. Ohno, *Tetrahedron Letters*, **1964**, 2124; H. Saitô, *Nippon Kagaku Zasshi (J. Chem. Soc. Japan, Pure Chem. Sect.)*, **85**, 724 (1964).

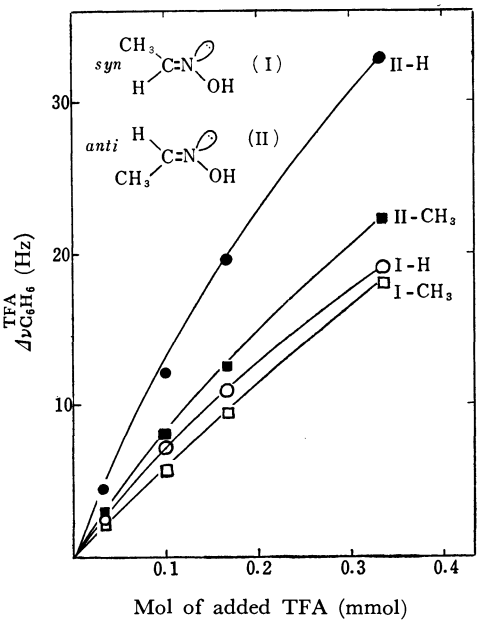

Fig. 9. Plots of $\Delta\nu^{TFA}_{C_6H_6}$ *vs.* mol of added TFA for acetaldoxime.

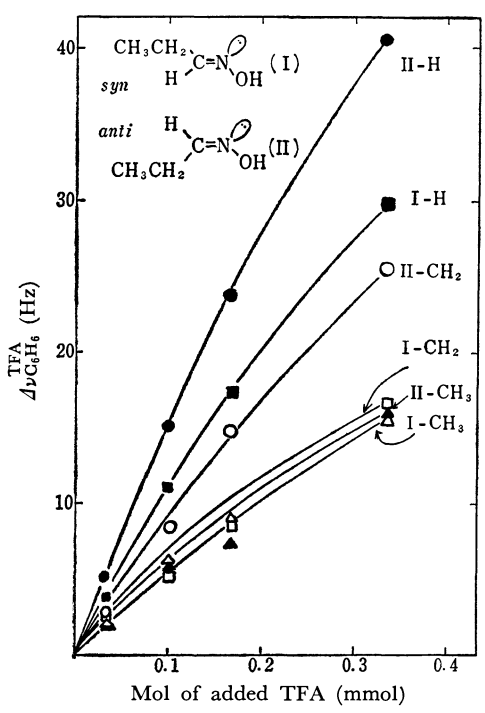

Fig. 10. Plots of $\Delta\nu^{TFA}_{C_6H_6}$ *vs.* mol of added TFA for propionaldoxime.

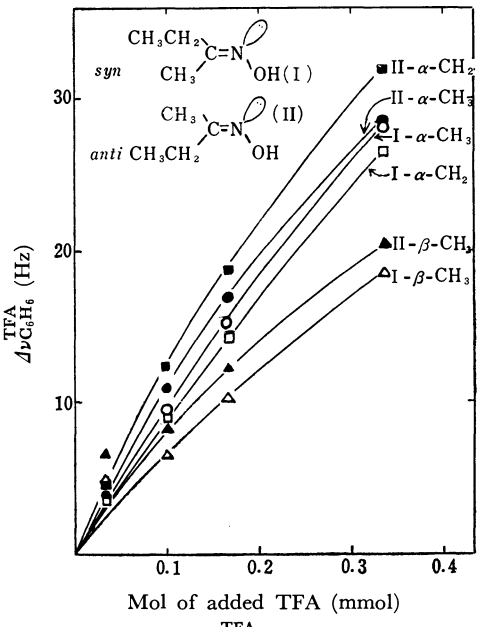

Fig. 11. Plots of $\Delta\nu^{TFA}_{C_6H_6}$ *vs.* mol of added TFA for ethyl methyl ketoxime.

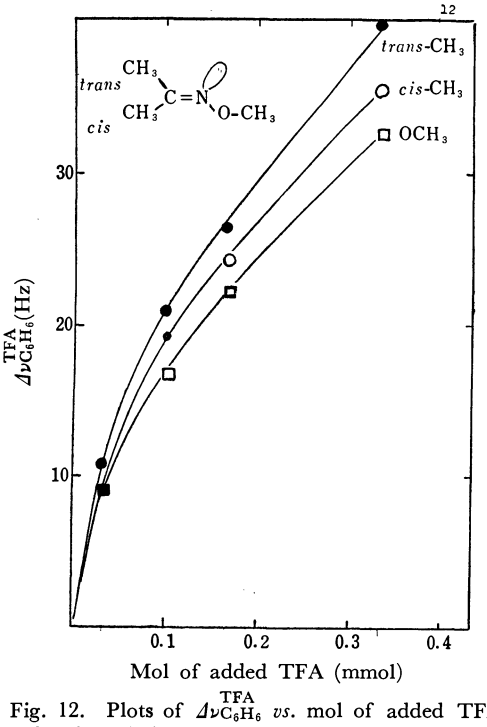

Fig. 12. Plots of $\Delta\nu^{TFA}_{C_6H_6}$ *vs.* mol of added TFA for *O*-methylacetoxime ether.

7—11) of $\Delta\nu^{TFA}_{C_6H_6}$ for the *cis* protons than for the *trans* protons of acetoxime and cyclohexanone oxime may reflect the fact that the hydrogen-bonding interaction preferentially occurs at the nitrogen lone-pair rather than at the hydroxyl oxygen. This will be verified in the discussion below of the results for *O*-methylacetoxime ether. It indicates that the generalization valid for the carbonyl compounds regarding the specific addition shift does not hold for oximes or for imines and aziridines.

As is shown in Table 3 and Fig. 9, the $\Delta\nu^{TFA}_{C_6H_6}$ values for methyl protons of acetaldoxime are larger for the *anti* isomer than for the *syn*. The $\Delta\nu^{TFA}_{C_6H_6}$ values of the methine proton are also larger for the *anti* isomer than for the *syn* isomer, as is also the case for $\Delta\nu^{TFA}_{C_6H_6}$ values. The same relation is observed for the methylene and methine protons of propionaldoxime. We interpreted this observation by assuming that the *anti* isomer is more subject to the hydrogen-bond interaction than the *syn* isomer, thus causing the greater upfield addition shift for the *anti* isomer than for the *syn*. The $\Delta\nu^{TFA}_{C_6H_6}$ value for the methyl protons of propionaldoxime is quite small and is slightly larger for the *syn* isomer than for the *anti* isomer, as is shown in Table 3 and Fig. 10. Ethyl methyl ketoxime gives results (Table 3 and Fig. 11) analogous to the case of propionaldoxime, as well as to that of the solvent shift.

Figure 12 shows the results for O-methylacetoxime ether. These results are anologous to those for acetoxime (see Fig. 8). The *cis* methyl group undergoes a larger upfield addition shift, $\Delta\nu^{TFA}_{C_6H_6}$, than does the *trans* methyl group when more methanol is added. The value of the addition shift, $\Delta\nu^{TFA}_{C_6H_6}$, for O-methyl protons is the smallest of those for the three methyl groups. These two observations imply that the hydrogen-bonding interaction preferentially occurs at the nitrogen lone-pair rather than at the oxygen lone-pair, as is the case with oximes. If the hydrogen-bonding interaction preferentially occurs at the oxygen lone-pair, the O-methyl group should undergo the largest upfield addition shift.

In conclusion, it is clear that, for compounds with a fixedly-oriented nitrogen lone-pair, the upfield addition shift is larger for the protons *trans* to the nitrogen lone-pair than for those *cis* to it. This tendency is different from the trend earlier established for the carbonyl compounds.[1] The origin of these conflicting observations is not clear at present; the problem will be investigated in the future.

However, it should be remarked that the present measurements of the benzene-solvent shift and the addition shift may themselves be useful in strucutal and stereochemical problems concerning the nitrogen lone-pair orientation.

BULLETIN OF THE CHEMICAL SOCIETY OF JAPAN VOL. 41 2305—2311 (1968)

The Crystal Structure of *l*-Cysteic Acid

Hideaki KONISHI,*1 Tamaichi ASHIDA and Masao KAKUDO

Institute for Protein Research, Osaka University, Joancho, Kita-ku, Osaka

(Received April 1, 1968)

The crystal structure of cysteic acid, $C_3H_7NO_5S$, has been determined. The crystal is orthorhombic with a space group of $P2_12_12_1$, and four molecules are in a unit cell with these dimensions: $a=8.35$, $b=10.16$, and $c=7.44$ Å. The molecule is a zwitter ion, $^-O_3SCH_2CH(NH_3^+)COOH$; its dimensions are generally similar to those found in other amino acids and sulfonic acids. The acidic groups occupy the trans positions with respect to the C_α–C_β bond, while the amino group is in a gauche position to the sulfonic group and forms an intramolecular hydrogen bond between them.

The X-ray crystal structure analysis of some α-amino acids and peptides has long been in progress in this Laboratory; the present work on cysteic acid was undertaken as part of this program. This amino acid is, in nature, found normally in sheep's fleece.

Recently, Hirota and Izumi[1] employed cysteic acid as a resolution reagent in the optical resolution of 2-amino-2'-nitro-6,6'-bitolyl; they obtained an optically highly pure compound. Izumi and others have also studied the asymmetric hydrogenation of methyl acetoacetate into methyl 2-hydroxybutyrate with catalysts modified with 2-amino acids or 2-hydroxy acids.[2] A characteristic result has been found in the asymmetric hydrogenation with the catalysts modified by cysteic acid.[3] In connection with the mechanisms of these resolutions and asymmetric reductions, it is worthwhile clarifying the ionic state of cysteic acid in the

*1 Present address: Shinto Paint Co., Ltd., Komatsu-Kitadoori, Higashi-yodogawa-ku, Osaka.

1) K. Hirota and Y. Izumi, private communication.

2) Y. Izumi, *Yuuki Goosei Kagaku Kyookai-shi (J. Soc. Org. Synth. Chem., Japan)*, **25**, 1013 (1967).

3) Y. Izumi, private communication.

crystal, since two types of zwitter ions are possible for this amino acid.

Experimental

Cysteic acid, $C_3H_7NO_5S$, prepared from cystine by treatment with aqueous bromine was supplied to the authors by Professor Yoshiharu Izumi. Colorless, transparent, and prism-like crystals were obtained by recrystallization from a methanol-water solution. They showed a pronounced cleavage perpendicular to the b axis. The lattice constants were obtained by oscillation and Weissenberg photographs taken around the b and c axes. More accurate values of the unit cell dimensions obtained on a single crystal diffractometer, using Mo$K\alpha$ radiation ($\lambda=0.7107$ Å), are: $a=8.35\pm0.01$, $b=10.16\pm0.01$, $c=7.44\pm0.01$ Å. The crystal belongs to the orthorhombic system; the absence of all ($h00$), ($0k0$), and ($00l$) reflections having odd values of h, k, and l respectively showed the space group to be $P2_12_12_1$. The observed density of the crystal obtained by the flotation method in a mixture of CH_3I and CCl_4 is 1.77 g cm^{-3}, while the calculated value is 1.77 g cm^{-3} (assuming four molecules in a unit cell).

The diffraction was measured on an AFC-model-1 (Automatic Four Circle) diffractometer made by Rigaku Denki Co., Ltd. The intensities in the $0<2\theta$(Mo$K\alpha$) $<55°$ range, which corresponds to the limiting sphere of Cu$K\alpha$ radiation, were collected. Zr-filtered Mo$K\alpha$ radiation was used with the pulse-height analyzer. The diffractometer was operated in an "open-loop" manner by a NEAC-2101 electronic computer. The $\omega/2\theta$-scan method was adopted for measuring the integrated intensities. The background was estimated from the measurements at the starting and end points of the scan. The programs designed by Tatzuo Ueki were used for the goniostat setting and the data processing.

The intensities were corrected only for Lorentz and polarization factors. In this way the integrated intensities of 1044 independent reflections were recorded, of which 121 (11.6%) were observed to be zero.

Structure Determination

The coordinates of the sulfur atom were deduced from the Patterson function. The first electron density map was synthesized by the use of the phases estimated from the coordinates of the S atom. Since the z parameters of S is nearly 1/4, the resulting map revealed the pseudo mirror plane on $z=1/4$. However, all the non-hydrogen atoms except for two carboxyl oxygen atoms could be located on the basis of the knowledge of the bond lengths and angles. In the succeeding Fourier map, all the non-hydrogen atoms of a

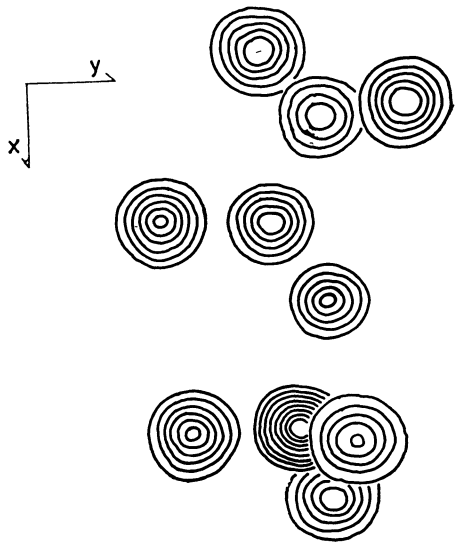

Fig. 1. A composite drawing of the final electron density map. Contour intervals: sulfur, 5 e.Å^{-3} starting at 2 e.Å^{-3}; other atoms 2 e.Å^{-3} starting at 2 e.Å^{-3}.

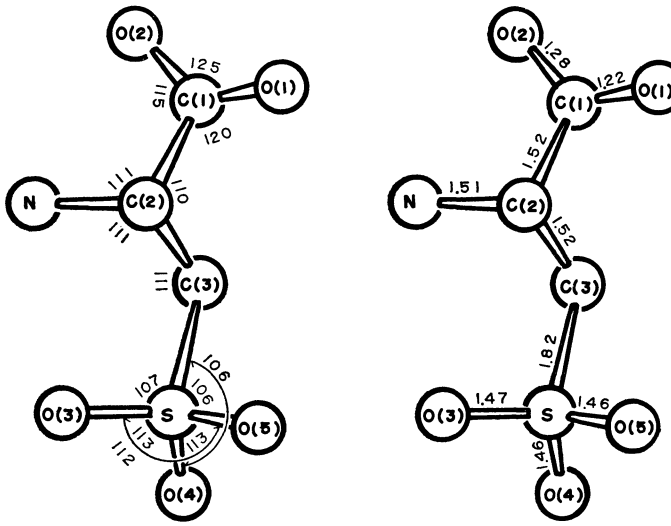

Fig. 2. Bond distances and angles.

Table 1(a). The atomic coordinantes and their standard deviations

	x/a	y/b	z/c	$\sigma(x)$	$\sigma(y)$	$\sigma(z)$
S	0.5579	0.3430	0.2640	0.003 Å	0.003 Å	0.003 Å
C(1)	0.0701	0.3756	0.2642	0.014	0.012	0.012
C(2)	0.2324	0.3121	0.2951	0.011	0.012	0.012
C(3)	0.3585	0.3797	0.1801	0.012	0.012	0.012
N	0.2261	0.1660	0.2564	0.010	0.010	0.011
O(1)	0.0474	0.4901	0.3068	0.011	0.009	0.011
O(2)	−0.0360	0.3012	0.1905	0.009	0.010	0.012
O(3)	0.5612	0.2007	0.3019	0.010	0.009	0.012
O(4)	0.6682	0.3819	0.1221	0.009	0.012	0.010
O(5)	0.5765	0.4212	0.4272	0.012	0.012	0.010

Table 1(b). The anisotropic thermal parameters and their standard deviations ($\times 10^4$)

The thermal parameters are of the from

$$T=\exp(-(B_{11}h^2+B_{22}k^2+B_{33}l^2+B_{12}hk+B_{13}hl+B_{23}kl))$$

	B_{11}	σ	B_{22}	σ	B_{33}	σ	B_{12}	σ	B_{13}	σ	B_{23}	σ
S	84	3	77	3	117	4	5	6	36	8	−45	7
C(1)	137	18	67	10	87	17	4	25	− 7	38	30	25
C(2)	78	14	68	11	104	19	− 1	21	31	29	13	25
C(3)	92	16	69	11	118	20	−27	23	85	32	71	26
N	121	14	61	9	128	18	−29	21	−25	31	−13	27
O(1)	148	16	70	9	219	23	5	22	39	37	96	25
O(2)	88	12	91	10	316	30	12	20	164	34	83	31
O(3)	108	13	75	9	276	27	5	20	46	38	−88	27
O(4)	84	12	140	14	156	18	48	23	− 5	28	−85	29
O(5)	189	20	134	13	110	16	−49	31	97	36	5	26

Table 1(c). The coordinates of the hydrogen atoms and their isotropic thermal parameters

	Bonded to	x/a	y/b	z/c	B
H(1)	C(3)	0.345	0.462	0.187	3.5 Å^2
H(2)	C(3)	0.379	0.352	0.040	0.7
H(3)	C(2)	0.260	0.322	0.423	2.6
H(4)	O(2)	−0.154	0.335	0.173	1.2
H(5)	O(5)	0.196	0.127	0.355	7.1
H(6)	O(4)	0.212	0.147	0.129	4.5
N(7)	O(3)	0.317	0.161	0.243	5.2

$\sigma<(x)>=0.17$ Å $\quad \sigma<(y)>=0.17$ Å $\quad \sigma<(z)>=0.18$ Å $\quad \sigma<(B)>=4.4$ Å

molecule were clearly defined. The final Fourier map is given in Fig. 1.

The positional and thermal parameters were refined by block-diagonal least-squares calculations, which minimize $\sum w(|F_o|-|F_c|)^2$. The weighting scheme was: $w=0$ when $F_o=0$ and $w=1$ when $F_o \neq 0$. The scattering factors for all the atoms were taken from "International Tables for X-Ray Crystallography (1959)". After several cycles of the least-squares calculation, the R index reached 15.6%. In the next calculation, all the hydrogen atoms were included. Their coordinates were assigned so that they are consistent with the tetrahedral bond angles and the optimum hydrogen bonding. Then, the maximum shift of the parameters (0.007 Å) became less than a half of the estimated standard deviation. It was, therefore, felt that further refinement would not improve the accuracy of the final parameters. The R index was 14.2% ($R=17.2\%$ with $F_o=0$). The mean value of the e.s.d.'s of the atomic coordinates of C, N, and O was 0.011 Å (0.009—0.014 Å). Difference-Fourier synthesis was carried out to confirm the hydrogen positions, but there still remained a little ambiguity about their positions, for there were many false peaks at other than the hydrogen atom positions. The atomic parameters are listed in Table 1, while the observed and calculated structure factors are listed in Table 2.

The computations were made on a NEAC 2200-model 500 in the computing center of this university. The program for the Patterson function was written by Noritake Yasuoka, and the others, by one of the authors (T. A).

TABLE 2. OBSERVED AND CALCULATED STRUCTURE FACTORS ($\times 5$)

L	FO	FC	L	FO	FC	L	FO	FC	L	FO	FC	L	FO	FC	L	FO	FC	L	FO	FC	L	FO	FC	L	FO	FC
H=K= 0	0		0	83	99	0	221	214	3	116	108	6	69	64	7	33	30	0	84	94	3	57	60	1	36	29	2	22	29
2	742	779	1	64	72	1	156	153	4	137	124	7	28	21	8	58	53	1	74	78	4	45	47	2	84	76	3	17	25
4	202	198	2	108	119	2	25	26	5	79	66	8	59	51	9	27	29	2	66	66	5	15	23	3	60	47	H=K=	8	10
6	114	129	3	153	149	3	163	150	6	54	57	9	19	6	H=K=	3	5	3	48	47	6	22	31	4	57	45	0	0	11
8	5	27	4	78	77	4	29	34	7	42	39	H=K=	2	4	0	9	14	4	33	28	7	18	8	5	37	30	H=K=	0	11
10	21	19	5	50	47	5	45	28	8	45	50	0	71	67	1	130	143	5	55	54	H=K=	7	7	6	26	19	1	20	10
H=K= 1	0		6	84	88	6	78	82	9	11	20	1	93	89	2	74	66	6	24	16	0	0	6	7	21	19	2	10	9
1	153	179	7	44	40	7	24	24	10	11	22	2	29	36	3	128	138	7	22	25	1	26	39	H=K=	2	9	3	18	8
2	71	72	8	39	44	8	29	24	H=K=	2	3	3	116	111	4	37	45	8	31	23	2	16	19	0	0	14	4	10	2
3	45	34	9	12	12	9	37	17	0	126	137	4	72	77	5	64	62	H=K=	5	6	3	44	48	1	29	31	5	0	1
4	45	42	10	13	15	10	19	14	1	117	104	5	63	60	6	23	18	0	19	21	4	15	11	2	31	27	6	0	1
5	95	100	H=K=	2	1	H=K=	2	2	2	93	93	6	56	51	7	40	45	1	47	65	5	43	35	3	58	50	H=K=	1	11
6	15	19	0	295	312	0	33	13	3	64	67	7	65	64	8	23	27	2	23	24	6	11	10	4	26	15	0	0	2
7	57	54	1	174	173	1	235	227	4	65	66	8	0	22	9	34	27	3	82	76	H=K=	8	7	5	46	39	1	17	13
8	0	9	2	179	190	2	71	73	5	70	70	9	24	40	H=K=	4	5	4	0	11	0	0	11	6	18	14	2	25	15
9	10	14	3	33	11	3	155	160	6	60	59	H=K=	3	4	0	53	62	5	35	30	1	0	33	7	33	21	3	25	12
10	34	18	4	73	72	4	37	43	7	84	78	0	0	11	1	38	44	6	0	1	2	26	22	H=K=	3	9	4	16	8
H=K=	2	0	5	59	67	5	133	137	8	29	30	1	51	58	2	117	123	7	14	19	3	0	5	0	70	84	5	29	14
0	360	411	6	88	97	6	81	82	9	33	35	2	67	66	3	32	30	8	11	8	4	41	41	1	31	42	6	22	10
1	156	163	7	58	56	7	55	60	10	30	27	3	90	83	4	106	110	H=K=	6	6	5	0	6	2	62	63	H=K=	2	11
2	169	198	8	46	52	8	33	35	H=K=	3	3	4	32	36	5	0	19	0	48	66	H=K=	9	7	3	0	5	0	34	25
3	148	159	9	0	20	9	58	38	0	125	125	5	63	54	6	57	55	1	0	22	0	18	10	4	35	35	1	0	3
4	107	106	10	25	20	10	9	9	1	151	123	6	0	39	7	21	33	2	72	81	1	0	1	5	0	14	2	21	25
5	118	139	H=K=	3	1	H=K=	3	2	2	127	120	7	0	7	8	32	40	3	73	62	2	29	22	6	6	18	3	0	8
6	49	42	0	6	6	0	170	174	3	140	140	8	10	21	9	34	24	4	47	52	3	0	14	7	37	25	4	27	26
7	89	92	1	403	382	1	159	134	4	56	62	9	24	19	H=K=	5	5	5	45	45	H=K=	0	8	H=K=	4	9	5	0	7
8	0	5	2	194	196	2	68	49	5	46	54	H=K=	4	0	23	23	6	30	19	0	12	13	0	34	45	6	28	19	
9	14	9	3	171	176	3	65	60	6	36	31	0	73	76	1	65	67	7	39	24	1	80	66	1	54	52	H=K=	3	11
10	27	21	4	72	89	4	118	134	7	15	26	1	66	56	2	0	10	H=K=	7	6	2	0	10	2	47	59	0	10	5
H=K=	3	0	5	99	106	5	0	10	8	16	11	2	46	44	3	80	80	0	19	10	3	95	72	3	34	31	1	39	51
1	93	80	6	44	62	6	59	56	9	17	16	3	17	9	4	12	12	1	23	26	4	30	20	4	37	34	2	0	15
2	133	123	7	36	41	7	38	38	H=K=	4	3	4	37	42	5	38	32	2	0	23	5	37	31	5	27	31	3	44	39
3	88	101	8	8	18	8	17	17	0	76	84	5	18	25	6	38	37	3	30	39	6	0	13	6	9	8	4	6	9
4	0	1	9	25	10	9	0	7	1	36	34	6	24	23	7	12	9	4	10	23	7	21	16	7	29	31	5	32	37
5	94	106	10	18	9	H=K=	4	2	2	42	42	7	21	23	8	41	45	5	32	29	8	0	3	H=K=	5	9	H=K=	4	11
6	58	59	H=K=	4	1	0	101	94	3	124	125	8	17	18	H=K=	6	5	6	18	12	H=K=	1	8	0	47	78	0	10	24
7	37	31	0	124	143	1	64	59	4	55	59	9	22	33	0	69	98	7	23	21	0	99	92	1	9	3	1	0	10
8	42	39	1	191	167	2	141	119	5	106	117	H=K=	5	4	1	22	28	H=K=	8	6	1	36	36	2	57	61	2	14	16
9	20	15	2	137	134	3	35	32	6	10	35	0	0	5	2	107	104	0	28	43	2	121	107	3	22	21	3	20	15
10	9	5	3	105	109	4	18	14	7	72	76	1	36	41	3	30	27	1	43	41	3	42	35	4	69	45	4	9	19
H=K=	4	0	4	134	125	5	27	25	8	0	19	2	57	52	4	76	75	2	48	54	4	105	88	5	17	14	5	9	1
0	81	78	5	101	105	6	24	24	9	42	45	3	26	30	5	29	24	3	31	29	5	56	44	6	45	41	H=K=	5	11
1	206	184	6	58	66	7	0	13	H=K=	5	3	4	22	14	6	47	42	4	48	41	6	54	51	H=K=	6	9	0	23	15
2	126	117	7	31	30	8	33	41	0	117	136	5	28	23	7	24	19	5	27	19	7	31	19	0	19	30	1	0	22
3	147	151	8	28	20	9	18	12	1	41	34	6	22	20	8	18	22	6	21	25	8	37	29	1	0	15	2	12	17
4	74	74	9	13	12	H=K=	5	2	2	166	149	7	0	8	H=K=	7	5	H=K=	9	6	H=K=	2	8	2	10	27	3	17	18
5	46	52	H=K=	5	1	0	0	12	3	14	18	8	20	22	0	0	6	0	30	34	0	0	6	3	17	17	4	0	9
6	12	7	0	23	25	1	71	68	4	104	106	H=K=	6	4	1	76	77	1	37	51	1	100	106	4	17	12	H=K=	6	11
7	52	65	1	160	137	2	0	18	5	19	25	0	12	16	2	24	20	2	26	22	2	34	36	5	11	21	0	23	19
8	15	1	2	0	29	3	69	58	6	42	42	1	21	25	3	57	54	3	64	54	3	89	78	H=K=	7	9	1	27	9
9	38	35	3	108	94	4	43	36	7	17	16	2	52	43	4	33	31	4	0	11	4	46	48	0	10	20	2	13	21
H=K=	5	0	4	60	58	5	43	42	8	27	22	3	54	51	5	38	28	H=K=	10	6	5	45	45	1	0	10	3	13	15
1	126	116	5	57	52	6	7	6	9	18	14	4	77	73	6	18	14	0	36	44	6	0	18	2	27	22	H=K=	7	11
2	11	11	6	39	35	7	13	12	H=K=	6	3	5	18	13	7	19	17	1	13	16	7	37	26	3	13	4	0	9	2
3	47	41	7	16	7	8	14	16	0	51	58	6	43	46	H=K=	8	5	2	36	39	8	27	11	4	0	23	1	0	11
4	64	69	8	0	14	9	24	24	1	51	45	7	0	21	0	0	2	H=K=	0	7	H=K=	3	8	H=K=	8	9	H=K=	0	12
5	27	32	9	0	5	H=K=	6	2	2	55	47	8	32	25	1	0	3	1	49	36	0	41	50	0	11	24	0	15	15
6	28	20	H=K=	6	1	0	51	50	3	48	45	H=K=	7	4	2	0	16	2	35	29	1	43	60	1	19	15	1	8	2
7	0	0	0	150	147	1	31	27	4	29	29	0	52	54	1	0	17	2	86	92	2	34	38	2	0	10	2	29	17
8	16	16	1	121	111	2	70	65	5	56	47	1	12	14	2	23	19	3	23	25	3	26	23	3	26	18	3	26	18
9	0	4	2	167	138	3	76	69	6	13	10	2	61	43	5	36	28	4	111	104	4	49	38	4	15	20	H=K=	0	14
H=K=	6	0	3	99	88	4	45	45	7	35	28	3	30	24	6	11	21	6	65	51	5	19	30	0	16	12	4	47	31
0	131	130	4	88	78	5	87	81	8	0	16	4	56	47	H=K=	9	5	7	37	11	6	0	25	1	18	22	H=K=	1	12
1	49	48	5	41	40	6	42	40	H=K=	7	3	5	38	33	0	12	19	8	15	25	7	15	16	2	0	11	0	53	48
2	131	117	6	42	42	7	29	30	0	81	111	6	48	44	1	15	10	9	0	9	8	37	20	3	12	12	1	27	20
3	95	88	7	24	31	8	16	32	1	16	13	7	39	19	2	10	5	H=K=	1	7	H=K=	4	8	4	58	44	2	54	36
4	139	128	8	35	25	H=K=	7	2	2	90	76	H=K=	8	4	3	18	16	0	38	40	0	48	62	5	0	13	3	31	26
5	85	84	H=K=	7	1	0	21	23	3	25	18	0	32	37	4	22	27	1	49	47	1	9	6	6	65	46	4	34	24
6	73	79	0	28	37	1	19	48	4	26	20	1	25	25	5	0	7	2	69	57	2	35	40	7	0	5	5	45	35
7	59	60	1	123	129	2	25	29	5	5	8	2	41	32	H=K=	0	7	3	21	16	3	23	20	H=K=	1	10	H=K=	2	12
8	11	17	2	42	37	3	48	35	6	19	9	3	56	45	0	14	20	4	63	46	4	40	42	0	52	49	0	0	3
H=K=	7	0	3	77	56	4	65	55	7	0	12	4	37	33	1	20	15	5	23	16	5	0	14	1	69	64	1	27	26
1	0	15	4	13	13	5	31	32	8	0	2	5	43	37	2	24	16	6	33	23	6	0	27	2	51	36	2	0	1
2	43	42	5	27	20	6	49	56	H=K=	8	3	6	35	38	3	30	6	7	0	5	7	0	7	3	60	56	3	29	25
3	24	13	6	17	15	7	28	29	0	26	15	H=K=	9	4	H=K=	0	6	8	32	22	H=K=	5	8	4	47	37	4	0	3
4	7	13	7	6	13	8	29	29	1	13	11	0	10	17	0	265	255	9	17	16	0	19	7	5	64	39	5	30	22
5	47	44	8	27	13	H=K=	8	2	2	14	11	1	46	58	1	108	97	H=K=	2	7	1	42	39	6	45	32	H=K=	3	12
6	37	43	H=K=	8	1	0	25	20	3	17	4	2	31	29	2	298	267	0	40	41	2	16	13	7	20	17	0	16	28
7	11	25	0	28	39	1	73	74	4	17	6	3	39	34	3	47	40	1	103	106	3	40	31	H=K=	2	10	1	0	28
8	28	24	1	0	16	2	30	33	5	31	25	4	31	31	4	171	157	2	96	91	4	10	9	0	0	1	2	21	17
H=K=	8	0	2	40	38	3	65	54	6	0	10	5	23	23	5	24	24	3	106	87	5	41	32	1	0	16	3	17	19
0	125	133	3	37	21	4	54	39	7	42	34	H=K=	10	4	6	67	57	4	105	102	6	6	10	2	13	7	4	0	8
1	0	3	4	16	23	5	75	63	H=K=	9	3	0	17	32	7	14	28	5	41	30	7	28	23	3	17	12	H=K=	0	18
2	103	93	5	34	23	6	27	27	0	0	6	1	29	34	8	35	37	6	61	51	H=K=	6	8	4	32	29	0	6	22
3	29	26	6	25	24	7	50	47	1	15	15	2	29	30	9	35	15	7	25	29	0	18	33	5	16	17	1	11	10
4	79	67	7	16	17	H=K=	9	2	2	17	21	3	42	31	H=K=	1	6	8	37	32	1	21	39	6	34	21	2	0	19
5	41	41	H=K=	9	1	0	47	58	3	16	20	4	23	21	0	189	182	H=K=	3	7	2	14	23	7	19	17	3	6	7
6	50	57	0	0	20	1	55	52	4	23	16	H=K=	11	4	1	34	28	0	0	20	3	27	33	H=K=	3	10	H=K=	5	12
7	0	7	1	11	15	2	36	34	5	47	34	0	13	6	2	120	107	1	128	141	4	8	22	0	32	43	0	13	3
H=K=	9	0	2	25	14	3	51	38	6	0	5	1	15	21	3	129	118	2	39	32	5	0	12	1	43	46	1	9	17
1	115	99	3	26	12	4	17	22	H=K=	10	3	H=K=	0	5	4	0	10	3	108	109	6	0	10	2	22	21	2	25	4
2	9	14	4	48	37	5	14	19	0	26	23	1	82	75	5	90	92	4	17	23	H=K=	7	8	3	27	23	H=K=	0	13
3	73	50	5	22	16	6	30	21	1	29	38	2	20	14	6	35	34	5	54	58	0	36	57	4	18	11	1	6	3
4	0	1	6	44	39	H=K=	10	2	2	6	10	3	7	3	7	57	58	6	26	24	1	23	29	5	8	7	2	40	24
5	45	38	H=K=	10	1	0	23	29	3	0	19	4	44	35	8	20	17	7	22	35	2	13	61	6	0	16	3	13	3
6	37	43	H=K=	11	1	1	73	62	4	0	3	5	80	70	9	32	32	8	24	28	3	0	14	H=K=	4	10	H=K=	1	13
H=K=	10	0	1	48	33	2	44	36	H=K=	11	3	6	5	19	H=K=	2	6	H=K=	4	7	4	51	40	0	21	5	0	29	33
0	80	103	2	34	18	3	51	42	0	0	14	7	60	48	0	62	70	0	21	39	5	9	8	1	15	16	1	0	11
1	10	16	3	0	8	4	36	24	1	15	4	8	18	10	1	33	40	1	132	155	H=K=	8	8	2	11	6	2	42	30
2	95	80	4	22	5	5	30	24	2	15	11	9	54	46	2	85	85	2	48	44	0	0	2	3	12	8	3	31	10
3	46	28	5	23	18	H=K=	11	2	H=K=	0	4	H=K=	1	5	3	71	85	3	141	134	1	42	49	4	0	11	H=K=	2	13
4	60	43	H=K=	11	1	0	37	15	0	315	307	0	84	70	4	58	53	4	21	17	2	12	7	5	19	8	0	13	9
5	6	5	0	17	13	1	19	3	1	49	46	1	61	48	5	73	68	5	46	46	3	39	42	6	20	7	1	4	29
H=K=	11	0	1	17	24	2	19	22	2	139	117	2	32	29	6	37	42	6	13	16	4	0	3	H=K=	5	10	2	13	18
1	0	1	2	9	6	H=K=	0	3	3	136	126	3	32	21	7	27	20	7	15	29	H=K=	9	8	0	14	11	3	23	18
2	13	5	3	23	14	1	16	13	4	63	65	4	76	74	8	0	20	8	6	21	0	10	28	1	0	7	H=K=	3	13
3	18	10	H=K=	0	2	2	182	182	5	43	34	5	24	16	9	6	21	H=K=	5	7	1	7	20	2	21	19	0	0	21
H=K=	0	1	0	242	252	3	74	77	6	91	93	6	39	26	H=K=	3	6	0	34	39	2	43	33	3	16	14	1	16	13
1	9	8	1	535	525	4	55	58	7	28	24	7	31	28	0	7	1	1	37	40	H=K=	0	9	4	28	27	2	24	18
2	25	17	2	266	255	5	16	9	8	49	51	8	21	22	1	69	61	2	59	63	1	8	15	5	24	18	H=K=	4	13
3	10	12	3	40	42	6	33	30	9	19	12	9	0	11	2	42	41	3	20	31	2	0	35	H=K=	6	10	0	16	0
4	18	16	4	127	117	7	38	49	10	33	27	H=K=	2	5	3	70	71	4	18	51	3	25	14	0	15	17	1	29	40
5	84	85	5	72	75	8	36	43	H=K=	1	4	0	87	94	4	52	47	5	29	32	4	34	16	1	10	12			
6	73	85	6	33	31	9	8	6	0	105	102	1	63	61	5	36	45	6	19	20	5	8	19	2	23	17			
7	96	95	7	52	44	10	36	34	1	230	219	2	164	150	6	24	26	7	46	37	6	0	3	3	25	11			
8	53	50	8	11	28	H=K=	1	3	2	58	51	3	40	36	7	32	28	H=K=	6	7	7	0	0	4	22	9			
9	45	42	9	21	9	0	139	143	3	70	61	4	91	89	8	15	23	0	25	45	8	0	2	H=K=	7	10			
10	0	11	10	0	5	1	18	9	4	98	89	5	19	26	9	15	16	1	72	89	H=K=	1	9	0	17	43			
H=K=	1	1	H=K=	1	2	2	121	116	5	34	31	6	72	70	H=K=	4	6	2	35	47	0	53	59	1	24	27			

Discussion

The bond distances and angles given in Fig. 2 are generally in good agreement with those previously reported for α-amino acids and sulfonic acids. The estimated standard deviations of the bond distances and angles are: 0.01 Å for S–O and S–C, 0.02 Å for other bonds, and 1.0° for the angles. In the molecule O(4)–S–C(3)–C(2)–C(1) possesses a trans-zigzag conformation, and N and S have a gauche form around the C(2)–C(3) methylene linkage (see Fig. 3).

The asymmetry about the C(1)–C(2) bond in the carboxyl group (C(2)–C(1)–O(1), 120°; C(2)–C(1)–O(2), 115°) is in good agreement with the foregoing findings. The two C–O distances, 1.22 and 1.28 Å, are significantly different from each other. The longer one is that of the oxygen atom with a hydrogen atom. The carboxyl group and C(2) are coplanar, and the equation for the best plane is;

$$0.2922X - 0.2990Y - 0.9061Z + 0.7324 = 0,$$

where X, Y, and Z are in the Å unit. The deviations of the individual atoms from the plane are:

O(1), 0.002; O(2), 0.001

C(1), −0.004; C(2), 0.001 Å.

The N atom also lies nearly on the plane, its deviation from the plane being −0.20 Å. The projection along the C(1)–C(2) bond is shown in Fig. 3.

The bond distances and angles of the sulfonic group are compared with those of other related compounds[4,5] in Table 3. The shape and size of the sulfonic group are substantially the same as in other compounds. The three S–O bonds seem to be nearly equivalent to each other, showing that there is no hydrogen atom bonded to this group.

Around the amino group there are four close N–O contacts (I, II, III, and V in Fig. 4) available for hydrogen-bond formations. Considering the configuration around N, the I, II, and III contacts are favorable for hydrogen bonds (see Table 4); of these, the I contact is an intramolecular hydrogen bond. Such a bond has also been found in taurine.[4] If V is assumed to be a hydrogen bond, an unfavorable conformation occurs around N. The three hydrogen atoms, H(7), H(6), and H(5), as refined by least-squares calculation, lie nearly on I, II, and III. These three are, therefore, favorable for hydrogen bonds. The cleavage perpendicular to the b axis can be well interpreted by taking V not to be a hydrogen bond. The fourth hydrogen bond (IV in Fig. 4) was found between O(2) of the carboxyl group and O(4) of the sulfonic group.

In the sulfonic group, each oxygen atom forms an NH–O hydrogen bond. In addition, O(4) accepts the OH–O hydrogen bond from the carboxyl group.

In view of the configurations of the carboxyl

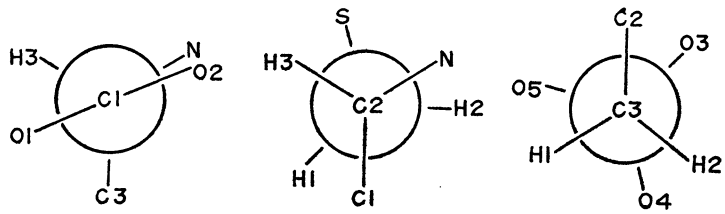

(a) (b) (c)

Fig. 3

(a) A view down the C(1)-C(2) bond.
(b) A view down the C(2)-C(3) bond.
(c) A view down the C(3)-S bond.

TABLE 3. COMPARISON OF THE DIMENSIONS OF THE SULFONIC GROUPS

	Taurine[4] $NH_3^+CH_2CH_2SO_3^-$	Potassium α-hydroxy-benzylsulfonate[5] $C_6H_5CH(OH)SO_3^-K^+$	Cysteic acid $^-O_3SCH_2CH(NH_3^+)COOH$
∠OSO	110.9°—113.7°	111°—114°	112°—113°
∠CSO	105.8°—106.9°	106°—108°	106°—107°
S-C	1.78_0 Å	1.83 Å	1.82 Å
S-O	1.44_8—1.46_5 Å	1.42—1.45 Å	1.46—1.47

4) Y. Okaya, *Acta Cryst.*, **21**, 726 (1966).

5) T. Kuroda T. Ashida, Y. Sasada and M. Kakudo, This Bulletin, **40**, 1377 (1967).

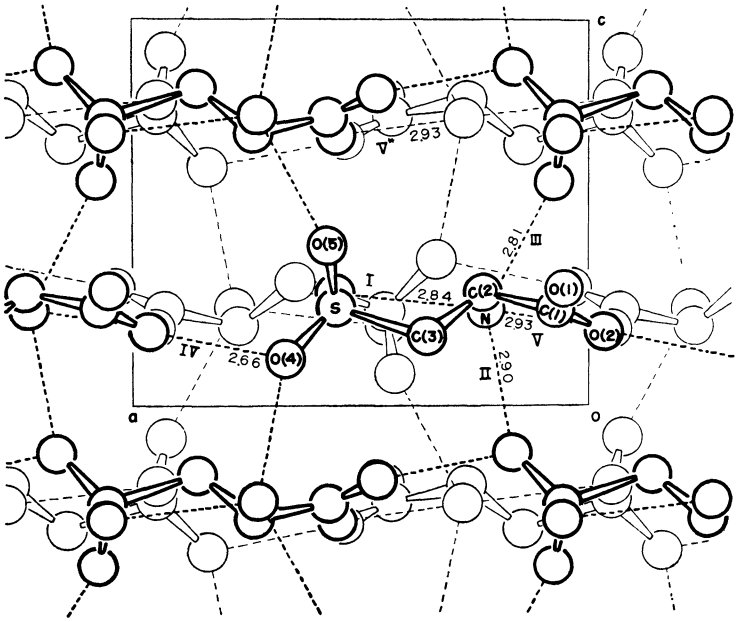

Fig. 4(a). The crystal structure viewed down the *b* axis. Chain lines show the close contacts available for hydrogen bonding.

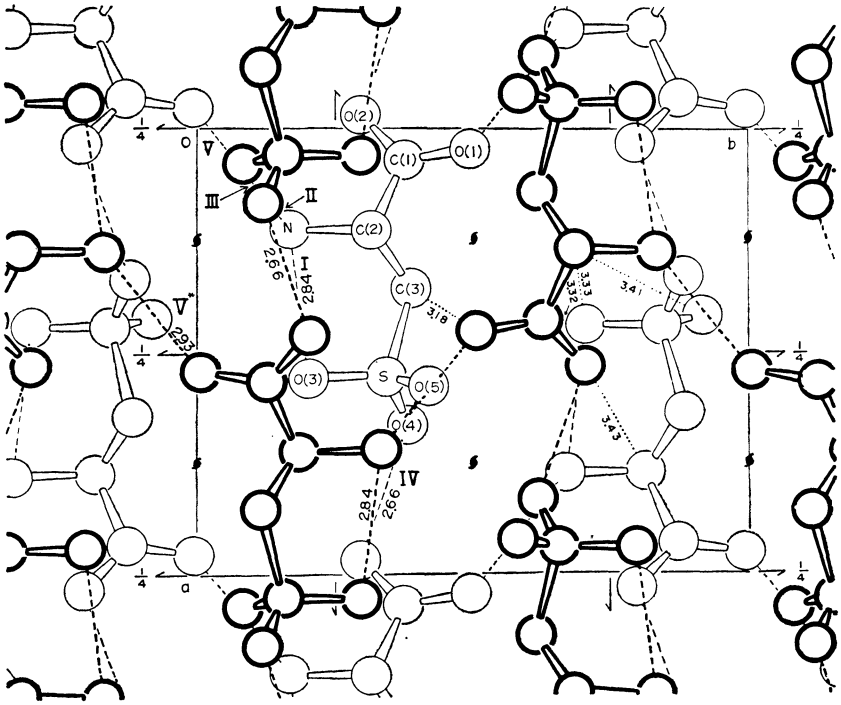

Fig. 4(b). The crystal structure viewed down the *c* axis. Some van der Waals contacts are shown by dotted line.

TABLE 4. THE HYDROGEN BONDS

(a) Short N···O, and O···O contacts.

No.	From	To	Distance	Hydrogen atom involved
I	N	O(3)	2.84 Å	H(7)
II	N	O(4)	2.90	H(6)
III	N	O(5)	2.81	H(5)
IV	O(4)	O(2)	2.66	H(4)
V	N	O(1)	2.93	

(b) Configuration around N.

Angle between		and		
	C-N		I	80°
	C-N		II	111
	C-N		III	110
	C-N		V	131
	I		II	107
	I		III	112
	II		III	133
	I		V	150
	II		V	67
	III		V	66

and sulfonic groups, together with the hydrogen-bond system in the crystal, the cysteic acid molecule can be said to have the zwitter ion form:

$$^{-}O_3SCH_2CH(NH_3^{+})COOH\,.$$

This could be expected from the difference between the dissociation constants of the carboxyl and the sulfonic groups. On the other hand, it has been expected, in the study of the optical resolution,[1] that cysteic acid is weaker than usual sulfonic acid. This seems reasonable if the molecule takes such a zwitter ion structure. It is also expected that, in an asymmetric hydrogenation,[3] this acid will be absorbed on the Raney nickel catalyst in a fairly different manner from common amino acids. This would explain the characteristic result obtained in the hydrogenation with the catalyst modified by this acid.

Fairly close van der Waals contacts are shown in Fig. 4(b). The molecules are at nearly $z=1/4$, and form a sheet parallel to the (010) plane by the three hydrogen bonds, II, III, and IV. No hydrogen bond seems to contribute to the contacts among these sheets.

The authors wish to express their deep thanks to Professor Yoshiharu Izumi for supplying material and for his continued interest, and to Drs. Tsunehiro Takano and Tatsuo Ueki for their kind cooperation. The authors' thanks are also due to the Matsunaga Science Foundation for its financial support.

BULLETIN OF THE CHEMICAL SOCIETY OF JAPAN VOL. 41 2312—2319 (1968)

Fluorescence Quenching and the Charge Transfer in the Excited State. III. Flash Photolytic Studies*[1]

Hiroshi YAMASHITA, Hiroshi KOKUBUN and Masao KOIZUMI

Department of Chemistry, Faculty of Science, Tohoku University, Katahira-cho, Sendai

(Received April 1, 1968)

It has been established by the flash photolysis that the *N,N*-dimethyl β-naphthylamine (DMN) cation is produced by the interaction of excited DMN with dimethyl isophthalate (DMP). The assignment has been made by comparing the transient spectrum with that obtained by the γ-radiolysis of DMN in *s*-butyl chloride. The decay of the DMN cation is first order in acetone (DK, 20.7), ethanol (24.3) DMF (36.7), second order in formamide (109.5) and it is the superposition of first and second order in acetonitrile. This strongly suggests that the radical cation exists as the solvent-shared ion pair in medium polar solvents while as free species in highly polar solvents. The decay of the former has been found to be not essentially affected by oxygen. The finding that the transient spectrum is observed even in the aerated solution supports the view that it is produced at the singlet excited state. From the effect of [DMP] on the yield of triplet DMN, it has been inferred that the radiationless process occurring in the ex-CT complex is mainly internal conversion. The reactivity of the triplet DMN against DMP has been found very small as compared with that of the signlet excited state; the rate constant for $(DMN)^T + DMP \rightarrow DMN + DMP$ was $k_{10} \simeq 10^5\ M^{-1}\ sec^{-1}$. The erroneous discussion given in the previous paper has been corrected; the decrease both in the quenching constant (for normal fluorescence) and in the emissivity of the ex-CT emission with the solvent polarity (in slightly polar solvents) is most likely to be attributed to the solvent-solute interaction, the increase of which (with the increase in solvent polarity) is unfavorable both to the formation of the ex-CT complex and to the emissivity of the ex-CT emission.

In 1961 Weller *et al.*[1] discovered anomalous fluorescence in the system of perylene and aromatic amines dissolved in non polar solvents, the emission due to the charge transfer complex which is formed only in the excited state. At the same time, they also established by means of a flash technique, the formation of radical anions for the similar systems dissolved in polar solvents. These discoveries are the first confirmative evidence for charge transfer (CT) and electron transfer (ET) mechanisms for the quenching of fluorescence. Since then, extensive studies on the similar systems have been made by Mataga *et al.*[2-6] as well as Weller's group[7-9] and much information has been obtained in particular, on the behavior of excited CT (ex-CT) complexes.

In our previous papers,[10,11] one of the present authors (M. K.) with collaborators, has shown that the quenching action of methylbenzoate and dimethyl isophthalate (DMP) on the fluorescence of *N,N*-dimethyl β-naphthylamine (DMNA) can be interpreted satisfactorily by CT and ET mechanisms. Thus in support of CT mechanism, a new emission with a longer wavelength peak and with a large solvent effect, was observed in non polar or slightly polar solvents. ($DK < 10$), the emission which is most likely to be ascribed to ex-CT complex. In highly and medium polar solvents ($DK \gtrsim 20$) on the other hand, such an emission was absent and yet the quenching constant was very large and increased with the polarity of the solvent, in consistence with

*1 A short communication was published in *Z. physik. Chem. N. F.*, **57**, 103 (1968).

1) H. Leonhard and A. Weller, *ibid.*, **29**, 277 (1961); *B. Bunsenges. physik. Chem.*, **67**, 791 (1963); "Luminescence of Organic and Inorganic Materials," ed. by H. P. Kellmann and G. M. Spruch, John Wiley & Sons, New York (1962), p. 74.

2) N. Mataga, T. Okada and N. Yamamoto, This Bulletin, **39**, 2562, 2563 (1966).

3) N. Mataga, T. Okada and K. Ezumi, *Mol. Phys.*, **10**, 201 (1966).

4) N. Mataga, K. Ezumi and T. Okada, *ibid.*, **10**, 203 (1966).

5) N. Mataga, T. Okada and N. Yamamoto, *Chem. Phys. Letters*, **1**, 119 (1967).

6) N. Mataga and K. Ezumi, This Bulletin, **40**, 1355 (1967).

7) H. Beens, H. Knibbe and A. Weller, *J. Chem. Phys.*, **47**, 1183 (1967).

8) H. Knibbe, K. Röllig, F. P. Schäffer and A. Weller, *ibid.*, **47**, 1184 (1967).

9) H. Knibbe, D. Rehm and A. Weller, *Z. physik. Chem. N. F.*, **56**, 95, 99 (1967).

10) T. Miwa and M. Koizumi, This Bulletin, **39**, 2603 (1966).

11) K. Kaneta and M. Koizumi, *ibid.*, **40**, 2254 (1967).

ET mechanism. A difference between our system and Weller-Mataga's systems (W-M systems) are that the donor-acceptor relation is inversed, namely the fluorescer is a donor in our system while it is an acceptor in W-M systems.

The present paper is concerned with the flash photolytic studies on the system consisting of DMP and DMNA or β-napthyl ethyl ether (NEE) in various solvents. The principal purpose is of course, to detect the radical cation of fluorescer in highly or medium polar solvents in order to confirm definitely ET mechanism in our system. This has been verified in the case of DMNA; the transient spectrum observed, agreed satisfactorily with that of the radical cation obtained by the γ-radiolysis of DMNA in *s*-butyl chloride. In the case of NEE, the similar transient spectrum was observed but it did not agree with the one obtained by the γ-ray radiolysis. The conclusive assignment, therefore, must await further studies.

The second purpose of the present work, *i. e.*, the investigation of the behavior of the radical cation in various solvents, has been carried out, in view of the above results, mainly on the DMNA radical. It has been established that the free radical cation or the solvent-shared ion pair is formed depending on the polarity of the solvent.

The third purpose is to elucidate, in relation to the solvent effect, the radiationless processes occurring in the ex-CT complex. This has been done by examining the influence of quencher concentration on the yield of triplet DMNA. It has been found that the non radiative process in question is mainly the internal conversion to the ground state molecule. In connection with this investigation, the reactivity of triplet DMNA toward the quencher in various solvents has also been investigated. This has been found to be far less than that of the singlet excited state.

Finally comprehensive discussion has been given in which an erroneous discussion made in the previous paper[11] has been corrected.

Experimental

Materials. *N,N*-Dimethyl β-naphthylamine, *m*-dimethyl isophthalate, cyclohexane, benzene, isopropyl ether, ethyl ether, ethyl acetate, methyl acetate, ethyl benzoate and dimethyl formamide were purified in the same way as in a previous paper.[10]

β-Naphthyl ethyl ether was prepared according to reference.[12] The crude product was recrystallized four times from ethanol and finally sublimed *in vacuo*.

Phthalic anhydride of Kanto-Kagaku G. R. grade was recrystallized twice from benzene and was dried *in vacuo*.

Phthalonitrile of Wakojunyaku was recrystallized from the water-ethanol mixture (1 : 1 in volume) three times.

Liquid paraffin of Kanto-Kagaku G. R. grade was used without purification.

Bromobenzene of Wakojunyaku E. P. grade was fractionally distilled. Bp 155.0—155.5°C.

Ethanol of Wakojunyaku G. R. grade was distilled with a column of precision type. Bp 78.3°C.

Methanol of Wakojunyaku G. R. grade was treated with metallic magnesium and iodine, and then distilled. Bp 64.5°C.

Formamide of Wakojunyaku G. R. grade was purified by fractional solidification three times.

Apparatus and Procedure. The flash apparatus and the procedures were the usual ones.

Results and Discussion

Transient Spectra in the Presence and in the Absence of a Quencher. Figure 1 gives a transient spectrum obtained upon flashing the solution of DMNA in cyclohexane. This spectrum can safely be ascribed to T–T absorption on the ground of its short life time of about 60 μsec (first order decay, see below) and of the non-appearance in the aerated solution. A similar spectrum was obtained in liquid paraffin and in isopropyl ether*2 but was not in bromobenzene, ethyl acetate and ethyl benzoate, all of which belong to slightly polar solvent. This seems very curious and should be reinvestigated.

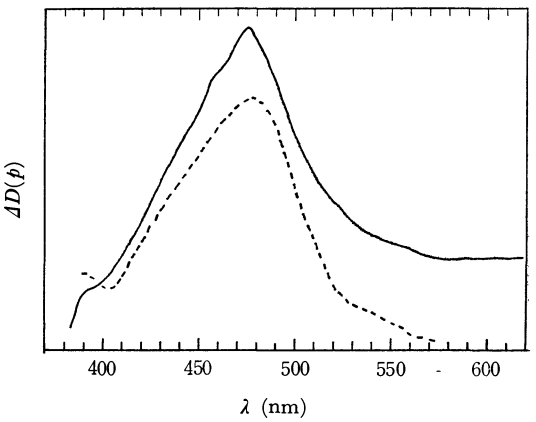

Fig. 1. T–T absorption spectra of DMNA in cyclohexane in the absence and in the presence of quencher.
30 μsec after flash
——: [DMNA] = 5×10^{-4} M, [DMP] = 0 M
– – –: [DMNA] = 5×10^{-4} M, [DMP] = 5×10^{-2} M

Upon addition of DMP as much as 5×10^{-2} M to the DMNA solution in cyclohexane, a similar T–T absorption was still observed although the intensity was somewhat weakened, and no new transient absorption was detected. This is just the result expected, since the ex-CT complex formed in nonpolar solvents, being very short-lived, cannot be observed by the usual flash technique.

12) W. A. Davis, *J. Chem. Soc.*, **77**, 33 (1900).

*2 The statement that no T–T absorption appeared in isopropylether, in the previous paper, should be corrected.

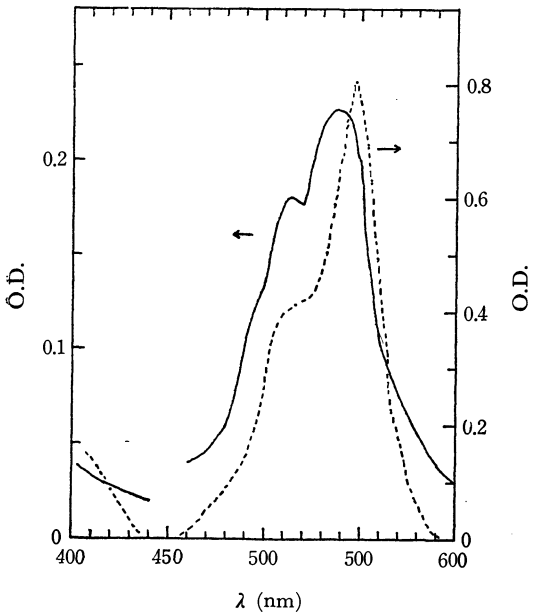

Fig. 2. Transient absorption of DMNA radical cation.
[DMNA] = 10^{-3} M, [DMP] 5×10^{-2} M
——: in DMF at room temp. by flash photolysis
- - -: in *s*-butylchloride at 77°K by γ-radiolysis

In highly or medium polar solvents (DK$\gtrsim$20) such as acetone, ethanol, acrylonitrile, dimethylformamide (DMF) and formamide, DMNA gave somewhat broadened T–T absorption.

Upon addition of $\gtrsim10^{-2}$ M DMP, a new absorption with a peak around 540 nm appeared in all the above solvents. Figure 2 shows as an example, a transient spectrum in the DMF solution. This is compared with the absorption spectrum of the DMNA cation obtained by the γ-ray radiolysis of the solution in *s*-butyl chloride at 77°K.*3 Fairly good agreement of the two spectra supports the assignment of our transient species as a radical cation.*4

Figure 3 gives the transient spectra in the acetone solutions. One can see the similar spectrum in the aerated solution. This indicates that the formation of radical cation occurs at the singlet excited state and that it is insensitive to oxygen, in agreement with the general behavior of radical cation.[13]

Furthermore, the usage of phthalic anhydride and phthalonitrile as quencher, gave the similar transient spectra.

*3 The authors are gratefull to Dr. T. Shida (*Inst. Phys. Chem. Research, Tokyo*) for having performed this experiment.

*4 Possibility that the absorption of radical cation and anion overlaps in the same region cannot altogether be denied (although not likely), since the latter could not be detected in the present work.

13) T. Ohno, S. Kato and M. Koizumi, This Bulletin, **39**, 232 (1966).

According to the unpublished results of our group, the fluorescent behavior of NEE-DMP system is similar to that of DMNA-DMP system in the points that it gives ex-CT emission in a slightly polar solvent but not in highly or medium polar solvents where high quenching is significant.

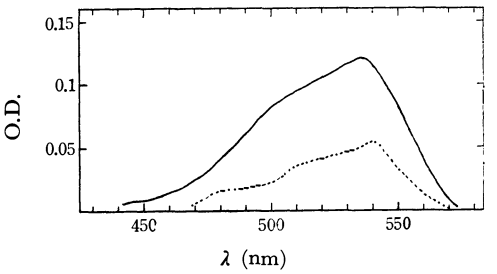

Fig. 3. Transient absorption spectra of DMNA radical cation in acetone in the absence and in the presence of oxygen, 30 μsec after flash.
[DMNA] = 5×10^{-4} M, [DMP] = 5×10^{-2} M
——: in degassed acetone
- - -: in aerated acetone

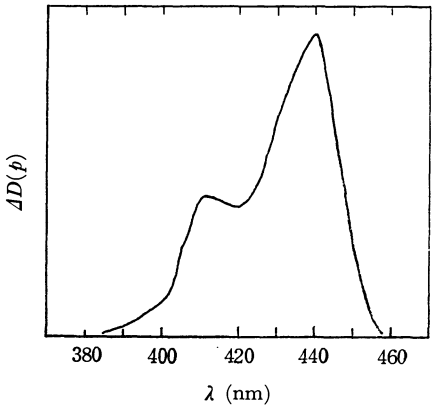

Fig. 4. T–T absorption spectra of NEE in cyclohexane, 30 μsec after flash.
[NEE] = 1.2×10^{-3} M

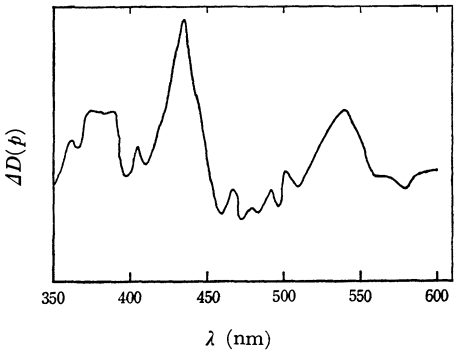

Fig. 5. Transient absorption spectra of NEE in DMF in the presence of quencher, 30 μsec after flash.
[NEE] = 10^{-3} M, [Q] = 10^{-1} M

TABLE 1. THE DECAY CONSTANTS AND THE YIELDS OF THE DMNA RADICAL CATION IN VARIOUS CONDITIONS

Concentrations of		k (sec^{-1})		D_{540}	
DMNA, M	m-DMP, M	degassed	aerated	degassed	aerated
5×10^{-4}	10^{-2}	1.7×10^{4}	2.7×10^{4}	0.106	0.05
5×10^{-4}	5×10^{-2}	2.6×10^{4}	1.9×10^{4}	0.15	0.08
5×10^{-4}	10^{-1}	2.0×10^{4}	2.7×10^{4}	0.30	0.08
10^{-3}	5×10^{-2}	2.0×10^{4}	2.0×10^{4}	0.10	0.06
10^{-3}	10^{-1}	1.8×10^{4}	2.6×10^{4}	0.18	0.06

TABLE 2. THE HALF-LIFE PERIODS AND THE YIELDS OF THE DMNA RADICAL CATION IN ACETONITRILE

Concentration of		τ sec		D_{540}	
DMNA, M	m-DMP, M	degassed	aerated	degassed	aerated
5×10^{-4}	10^{-2}	3.4×10^{-4}	4.8×10^{-4}	0.097	0.064
5×10^{-4}	5×10^{-2}	4.1×10^{-4}	4.1×10^{-4}	0.098	0.086
5×10^{-4}	10^{-1}	4.4×10^{-4}	5.0×10^{-4}	0.11	0.084
10^{-3}	5×10^{-2}	3.3×10^{-4}	3.2×10^{-4}	0.084	0.074
10^{-3}	10^{-1}	4.7×10^{-4}	6.0×10^{-4}	0.093	0.075

Hence the similar flash experiments were performed on this compound.

Figure 4 gives a T-T absorption spectrum of NEE in cyclohexane, which agrees with the one reported by Porter and Windsor.[14] In the case of slightly polar solvents, the addition of $\sim10^{-2}$ M DMP gives essentially the similar transient spectrum.

In highly polar solvents such as DMF and acetonitrile, quite a different spectrum is observed as shown in Fig. 5. The spectra in these solvents are very similar to each other with two peaks around $\sim$540 and 500 nm and furthermore they resemble that of DMNA to some extent. It seems most likely to ascribe this spectrum to a radical cation of NEE, but the spectrum of the radical cation obtained by the γ-radiolysis in s-butyl chloride was quite different and the conclusive assignment should await further sutdies.

The Behavior of DMNA Radical Cation in Various Polar Solvents. In DMF, the decay rate and the yield of the radical cation immediately after flashing (measured by the optical density at 540 nm) were investigated in various conditions. The results are listed in Table 1. The decay was first order.

One can say that the first order rate constant is essentially the same for both aerated and deaerated solutions. The yield in the degassed solution increases evidently with the increase in the concentration of DMP. The yield in the aerated solution is less than half that in the degassed solution. This may be due to the competitive deactivation reaction of the singlet excited DMNA by oxygen. All the above results support the view that the radical cation is produced at the singlet excited state.

In the case of acetone and ethanol used as solvents, the decay obeys first order in the degassed solution. The rate constants is $4.1\times10^{3}\,sec^{-1}$ for ethanol, and $7.5\times10^{3}\,sec^{-1}$ for acetone. In the aerated solution, the yield is negligible in the case of ethanol and very small for acetone.

In acetonitrile, the decay is always the superposition of the first and the second order processes. Table 2 gives the yield as measured at the maximum of the optical density at 540 nm and the half life period (τ) (not very accurate) as evaluated from the decay curves.

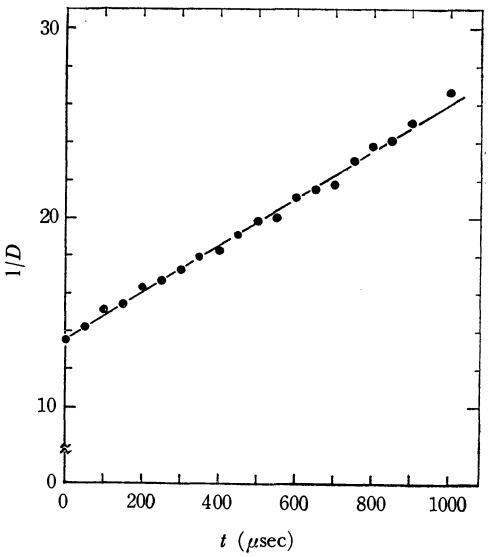

Fig. 6. Second order decay of DMNA radical cation in formamide.
[DMNA] = 1×10^{-3} M, [DMP] = 5×10^{-2} M

14) G. Porter and M. W. Windsor, *Proc. Roy. Soc.*, **A245**, 238 (1958).

TABLE 3. THE RATE CONSTANTS AND THE YIELD OF THE DMNA RADICAL CATION IN FORMAMIDE (PA, phthalic anhydride)

Concentration of			k (M^{-1} sec^{-1})		D_{540}
DMNA, M	DMP, M	PA, M	(degassed)	(aerated)	(degassed)
1.5×10^{-3}	5×10^{-2}	—	1.35×10^{5}	1.0×10^{5}	0.264
1.5×10^{-3}	—	5×10^{-2}	4.3×10^{4}	7×10^{4}	0.305

TABLE 4. HALF-LIFE VALUES AND THE YIELDS OF THE DMNA RADICAL ION

Solvent		[DMNA], M	Acceptor, M	τ sec	D_{540}
Acetone		5×10^{-4}	5×10^{-2} (DMP)	1.3×10^{-4}	0.116
	Aerated	5×10^{-4}	5×10^{-2}	3.3×10^{-4}	0.056
Ethanol		5×10^{-4}	5×10^{-2}	2.5×10^{-4}	0.115
DMF		5×10^{-4}	5×10^{-2}	3.8×10^{-5}	0.047
	Aerated	5×10^{-4}	5×10^{-2}	5.3×10^{-5}	0.036
		5×10^{-4}	5×10^{-2} (PA)	2.6×10^{-5}	0.056
Acetonitrile		5×10^{-4}	5×10^{-2} (DMP)	4.1×10^{-4}	0.098
	Aerated	5×10^{-5}	5×10^{-2}	4.1×10^{-4}	0.086
Formamide		1.5×10^{-3}	5×10^{-2}	5.4×10^{-4}	0.264
		1.5×10^{-3}	5×10^{-2} (PA)	7.7×10^{-4}	0.305
		1.0×10^{-3}	5×10^{-2} (DMP)	1×10^{-3}	0.074

In this case the yield in the aerated solution is not so different from that for the degassed solution.

In the case of formamide, the decay of the DMNA radical cation is second order as is shown in Fig. 6. The similar result was obtained when phthalic anhydride was used instead of DMP. The results are listed in Table 3.

Summarizing the behavior of the radical cation of DMNA in various solvents, the notable finding is that the radical cation decays according to first order in the solvents of medium polarity (acetone (DK=20.7), ethanol (24.3) and DMF (36.7)) while in a solvent of high polarity (formamide (DK=109.5)), it is second order and in acetonitrile (intermediate in the above two groups), the decay is a superposition of the first and second order. In view of the quite similar absorption spectra observed in all the cases, there seems to be no other interpretation than the following. In the medium polar solvents, the radical cations and anions exist as solvent-shared ion pairs which reconvert to the stable species by a unimolecular process, while in the highly polar solvents the free radical ions exist as two separate species and recombined bimolecularly. In acetonitrile, the separated radical species and the ion pairs may coexist.

In Table 4, half-life values and the yields of the DMNA radical ion in various solvents are summarized.

The result that the half-life in DMF is one order smaller than in formamide despite the several ten times smaller yield in the former, reconfirms that the radical cation exists as ion pair in the former and further it indicates that the ion pair in DMF is rather unstable. The order in the τ-values (DMF<ethanol, acetone<acetonitrile) suggests that the ion pair becomes more stable in this order.

Interaction between Triplet DMNA and DMP in Nonpolar Solvents. It is interesting to examine the influence of the addition of DMP on the yield of triplet DMNA and on its decay. The former is expected to afford the information as to the radiationless processes for the ex-CT complex while the latter will enable us to compare the reactivity of singlet and triplet excited states against the acceptor-type quencher. Cyclohexane is the most suitable solvent because the yield of ex-CT complex is very high and accordingly the quenching constant is also very high (K=65) in this solvent.

Before describing the results, it is convenient to list up the usuful relations which can be derived on the basis of the following plausible scheme.

$F + h\nu \rightarrow {}^1F^*$	I_{ab}	
${}^1F^* \rightarrow F + h\nu$	k_1	free fluorescer molecule
${}^1F^* \rightarrow F$	k_2	
${}^1F^* \rightarrow {}^3F$	k_3	
${}^1F^* + Q \rightarrow {}^1F^*\cdots Q$	k_4	encounter complex
${}^1F^* \cdots Q \rightarrow {}^1F^* + Q$	k_{-4}	
${}^1F^* \cdots Q \rightarrow (F^+\cdots Q^-)^*$	k_5	
$(F^+\cdots Q^-)^* \rightarrow F + Q + h\nu_{CT}$	k_6	ex-CT complex
$(F^+\cdots Q^-)^* \rightarrow F + Q$	k_7	
$(F^+\cdots Q^-)^* \rightarrow {}^3F + Q$	k_8	

The above scheme is essentially the same as the one proposed in the previous paper;[11] small

differences are 1) discrimination of the internal conversion and intersystem crossing processes (k_2, k_3 and k_7, k_8) and 2) neglect of any kinds of deactivation process, such as $(^1F^*\cdots Q)\rightarrow F+Q$ or $(^1F^*\cdots Q)\rightarrow {}^3F+Q$, for the encounter-complex. The former is necessary to treat the triplet yield. The latter neglect may be permitted since in the present system, the formation of ex-CT complex is considered to be a principal process for quenching. It is to be added that the ex-CT complex is assumed to behave irreversibly.

On the basis of the above scheme, the application of the steady method leads to the following formulas straighforwardly.

$$D_T/D_{T_0} = \frac{1+\frac{k_4k_8}{k_3}\gamma\tau_2[Q]}{1+\gamma k_4\tau_1[Q]} \quad (1)$$

$$I_F/I_{F_0} = \frac{1}{1+k_4\tau_1\gamma[Q]} \quad (2)$$

$$I_{F,CT} = \frac{k_4k_6\gamma\tau_1\tau_2[Q]I_{ab}}{1+k_4\tau_1\gamma[Q]} \quad (3)$$

where

$$\gamma = k_5/(k_{-4}+k_5),\ \tau_1 = 1/(k_1+k_2+k_3)$$
$$\tau_2 = 1/(k_6+k_7+k_8)$$

From the above equations and by using the relations

$$K = k_4\gamma\tau_1 \quad (4)$$
$$\Phi_{CT} = k_6\tau_2 \quad (5)$$
$$\Phi_0 = k_1\tau_1 \quad (6)$$

where K is a quenching constant and Φ_{CT} is a probability of CT emission, the follwoing relations can easily be obtained.

$$I_{F,CT} = \frac{K\phi_{CT}[Q]}{1+K[Q]} \quad (7)$$

$$I_{F,CT}/I_F = \frac{I_F}{I_{F_0}}k_4k_6\gamma\tau_1\tau_2[Q]I_{ab} = \frac{k_4k_6\gamma\tau_2[Q]}{k_1} = \frac{K\Phi_{CT}[Q]}{\Phi_0} \quad (8)$$

$$\frac{D_T}{D_{T_0}} = \frac{I_F}{I_{F_0}}\left(1+\frac{k_4k_8}{k_3}\gamma\tau_2[Q]\right) = \frac{I_F}{I_{F_0}}\left(1+\frac{k_8\tau_2}{k_3\tau_1}K[Q]\right) \quad (9)$$

Turning to the experimental results, examples of the decay for triplet DMNA are shown in Fig. 7. From such decay curves the triplet yields and the apparent first order rate constants were evaluated for several concentrations of DMP. From the latter values, the following values were obtained as the genuine rate constants for the processes,

$$F^T \xrightarrow{k_9} F$$

$$F^T + Q \xrightarrow{k_{10}} F + Q$$

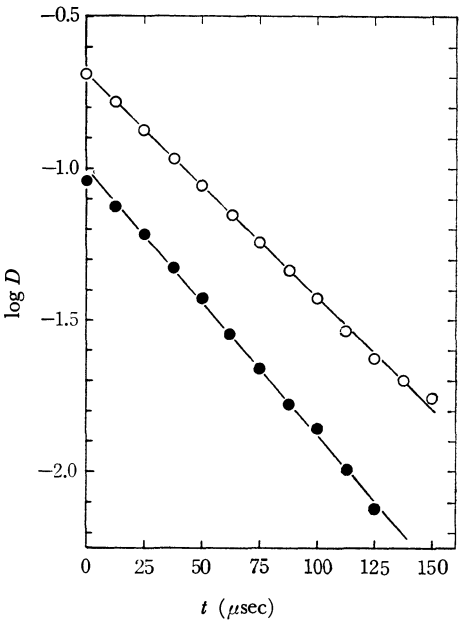

Fig. 7. First order decay of DMNA triplet in cyclohexane in the absence and in the presence of quencher.
○ [DMP]=0 M
● [DMP]=5×10⁻² M
[DMNA]=5×10⁻⁴ M

$$k_9 = 1.68\times10^4\ \text{sec}^{-1} \quad k_{10} \simeq 10^5\ \text{M}^{-1}\,\text{sec}^{-1}$$

It can be concluded from the above k_{10}-value that the reactivity of the triplet DMNA toward DMP is very small as compared with that of the singlet excited state.

Table 5 gives the relative yields of the triplet state $[F^T]/[F^T]_0$ (suffix 0 denotes the absence of Q) as evaluated from the optical densities at 480 nm, and the relative fluorescence intensities obtained from the data given in previous paper.[11]

Although the data are rather scanty, the ratio $[F^T]/[F^T]_0$ is larger than I_F/I_{F_0} only by less than 10% or so. From Eq. (9) it may be concluded that $k_8\tau_2$ is several times smaller than $k_3\tau_1$.

Table 5. Relative yields of triplet and relative fluorescence intensities

[Q], M	$[F^T]/[F^T]_0$	I_F/I_{F_0}	$K[Q]$
0	1	1	0
5×10^{-3}	0.80	0.75	0.33
10^{-2}	0.65	0.6	0.65
5×10^{-2}	(0.59)	0.23	3.3

Summary and Comprehensive Discussion

The present investigation has demonstrated clearly that the electron transfer occurs from the excited DMNA molecule to DMP in polar solvents.

The evidence for the view that the radical ions do not always exist as free ions but exist as solvent-shared ion pair, is afforded by the finding that the transient species in medium polar and in highly polar solvents, give essentially the similar spectrum and yet the decay feature in the former is first order whereas the latter is second order.

In nonpolar or slightly polar solvents, the ex-CT complexing has already been amply demonstrated in the previous paper, and some additional information has been obtained by the present flash studies. Since some papers dealing with the ex-CT complex appeared last year at about the same time as Part II of the present series, and since a part of the discussion given in the previous paper,[11] has been found to be improper, the authors would like to take up some of the previous results as well as the present ones and generally discuss them, referring also the results of other workers.

In the previous paper it was shown that the relative quenching efficiencies $(a\gamma)_i/(a\gamma)_2$ (2; cyclohexane) and the relative emissivity of ex-CT complex $(\phi_{0,CT})_i/(\phi_{0,CT})_2$ in slightly polar solvents, ($\phi_{0,CT}$; a ratio of the acts of an emitting process to those of the effective quenching process for normal fluorescence) decrease with the polarity of the solvent in somewhat similar manner. The result itself is correct, but the interpretation was erroneous. Thus the statement*5 "... one common process for CT emission and the quenching process, *i. e.*, the process of formation of the ex-CT complex essentially affects both CT emission and the quenching process ... and that this perhaps the main reason why ϕ_{CT} and $a\gamma$ decreases with the solvent polarity." is not correct. As is clear from the definition, ϕ_{CT} should reflect the emissivity of ex-CT complex itself. As long as the CT mechanism prevails, the decrease in $a\gamma$ naturally causes the decrease in the quantum yield of ex-CT emission, but the parallel decrease in ϕ_{CT} and $a\gamma$ should be interpreted to indicate that the more difficult the formation of ex-CT complex becomes, the less emitting the ex-CT complex becomes. This is very plausible on the basis of solvent-solute interaction, because as the solvent becomes more polar, the reorientation of solvent molecules becomes more and more difficult and at the same time, the interaction between the pdrouced ex-CT complex and solvent molecules becomes also larger, and this will cause the decrease in emissivity of ex-CT complex.

The previous results reinterpreted in this way is quite consistent with other workers' results. Thus Mataga *et al.*[5] showed that in the ex-CT complex of pyrene and dimethylaniline, the rate constant for emission, k_f', decreases while that for radiationless process, k_i' increases and that the quantum yield, Q_F', largely decreases with the polarity of the solvent. Weller *et al.*[8] also found that in the anthracen-diethylaniline system, the relative intensity of the ex-CT complex decreases with the solvent polarity and decreases far more than the lifetime of ex-CT emission. This is because, they interpreted, the former depends on the tendency with which the ex-CT complex is formed and also on the emissivity of the ex-CT complex, while the latter is concerned with the ex-CT complex itself.

As to the molecular processes which cause the decrease in the emissivity of the ex-CT complex with the solvent polarity, Mataga stressed the interaction between fluoresent species and solvent molecules which affect not only the molecular configurations (the configuration of the ex-CT complex and that of the surrounding solvent molecules) but also the electronic state of the ex-CT complex. Weller on the other hand considered that the increase in the solvent polarity enhances the process

$$(A^-\cdots D^+) \xrightarrow{k_{IP}} A_S^-\cdots D_S^+ \qquad (a)$$

where $A_S^-\cdots D_S^+$ is nonfluorescent. Furthermore he attributed the decrease in the probability of ex-CT complexing with the increase of solvent polarity, to the competition of the following two processes,

$$A^* + D \rightarrow (A^-\cdots D^+) \qquad (b)$$

$$A^* + D \rightarrow (A_S^-\cdots D_S^+) \rightarrow A + D \qquad (c)$$

of which the latter prevails over the former as the solvent becomes more polar.

Although there is no doubt that such processes must generally be taken into consideration, the authors are inclined that Mataga's picture fits better to our system at least in slightly polar solvents. Because in slightly polar solvents ($DK \lesssim 10$) the formation of the ion pair was not observed. More strong evidence is, as reported in the previous paper, that the addition of a small quantity of the highly polar solvent to the DMNA solution in nonpolar solvents causes a decrease of $a\gamma$ itself. This result can never be interpreted if only the competition between Process (b) and (c) is essential for quenching phenomena. That reorientation of solvent molecules is necessary for the ex-CT complexing was also clearly demonstrated by Mataga *et al.*[6] by comparing the fluorescent spectra of aromatic hydrocarbons dissolved in aromatic dimethyl amines at low and high temperatures.

As to the radiationless processes occurring in the ex-CT complex, the authors, in the present paper, have demonstrated fairly clearly that in our system it is the internal conversion to the ground state molecule and not the intersystem crossing. This is somewhat similar to Mataga's result,[5] that pyrene in acetonitrile involving dimethylamine gives no T-T absorption, but is contrary to Weller's result for the perylene-aromatic amine system.[1]

*5 p. 2262 in Part II, Ref. 11.

The finding that the reactivity of triplet DMNA toward DMP is much smaller than that of singlet state agrees with the current view that the triplet state generally resembles the ground state rather than the singlet excited state and it is of radical nature rather than ionic. Similar results have been reported also by Mataga *et al.*;[6] they found that the phosphorescent spectra of some hydrocarbons in dimethylaniline are practically the same as those in *n*-hexane and that the phosphorescent decay times are also the same in the both solvents.

BULLETIN OF THE CHEMICAL SOCIETY OF JAPAN VOL. 41 2319—2324 (1968)

Studies on the Electronic Spectra of the Semiquinones of Anthracene and Its Related Heterocycles. I

Hiroshi MASUHARA, Michio OKUDA and Masao KOIZUMI

Department of Chemistry, Faculty of Science, Tohoku University, Katahira-cho, Sendai

(Received April 1, 1968)

Electronic absorption spectra of two types of half reduced acridine, *i. e.*, C-radical (unpaired electron on 9-C-atom) and N-radical (unpaired electron on N-atom), of half-reduced anthracene and of xanthene deprived of one hydrogen atom, are measured in several rigid solvents at 77°K. It has been established that these radicals can be produced conveniently by irradiating the rigid solutions of the reduced forms, by a medium high pressure mercury lamp. It has been found that the absorption spectra of these radical species are generally classified into three groups, a) ~250 nm (4.9 eV), b) ~350 nm (3.5 eV) and c) visible (2.3—2.8 eV). Peculiar features for each radical species are; i) anthracene radical has no visible absorption, ii) acridine N-radical has no absorption at ~250 nm, and iii) acridine C-radical has a prominent sharp peak at 281 nm. Flash photolytic and ESR studies have also been performed on the radical species produced upon irradiation of dihydroanthracene and xanthene; the results obtained have substantiated the assignment of the intermediates observed in rigid solvents.

Our group has long been engaged in the studies of the primary processes of the photoreduction of some typical dyes and also of acridine.[1-5] Further studies on the photoreduction in relation to acridine are now being extended to phenazine and anthracene. Under such circumstances, it is highly desirable to measure the accurate electronic absorption spectra of the semiquinones of anthracene and its related heterocycles and also to investigate theoretically their electronic structures. Such studies are considered also to be important as the basic information of dye photochemistry, since the foregoing types of compound are the skeletones of various dyes.

From such a view point, accurate measurement of the absorption spectra of semiquinones of anthracene, acridine and xanthene were made in rigid solvents, and the open shell SCF calculation including CI was attempted to discuss the electronic structures of these semiquinones. The present paper is mainly concerned with the experimental results, deferring the theoretical ones to the next paper.

It has been found that these types of semiquinone can be produced most conveniently by the photochemical dehydrogenation of the reduced forms (acridan, dihydroanthracene, xanthene). Since they have no absorption below 300 nm and since they were almost completely converted to semiquinones by irradiation, reliable measurement could be performed throughout the region from 230 to 1000 nm.

It has been established that the absorption spectra of these semiquinones are well correlated with each other as is expected from the resemblance of the absorption spectra of the oxidized form (except xanthene) apart from minor differences. ESR and flash experiments have also been performed to confirm the assignment of the intermediate species in question.

1) A. Kira, S. Kato and M. Koizumi, This Bulletin, **39**, 1221 (1966).
2) A. Kira, Y. Ikeda and M. Koizumi, *ibid.*, **39**, 1673 (1966).
3) S. Niizuma, Y. Ikeda and M. Kiozumi, *ibid.*, **40**, 2249 (1967).
4) A. Kira and M. Koizumi, *ibid.*, **40**, 2486 (1976).
5) M. Koizumi, H. Yamashita and Y. Ikeda, *ibid.*, **41**, 1056 (1968); *J. Chem. Phys.*, **48**, 1869 (1968).

Experimental

Materials. 9,10-Dihydroanthracene and xanthene of G. R. grade were purified by repeated recrystallization from ethanol. Acridan was synthesized by reducing acridine with sodium amalgum.

Solvents used for Low Temperature Spectroscopy. Ethanol (99.5 vol%) of G. R. grade was used without any treatment, while the one of E. P. grade was purified by distillation. Isopentane and ethyl ether were dried over sodium and then distilled. Methylcyclohexane was treated with fuming sulfuric acid several times, washed with alkaline aqueous solution and then with water, shaken with alkaline $KMnO_4$ solution, rewashed with water, desciccated over $CaCl_2$ and silica gel and finally distilled with a fractionating column. All the solvents purified were checked by UV spectra. No absorption was observed above 210 nm for isopentane and above 220 nm for methylcyclohexane.

Solvents used for ESR Measurements. Poly-trifluorochloroethylene (Daiflon) was used without any purification. Tetrahydrofuran of First Grade from Wako-junyaku was refluxed with sodium for several hours, and then distilled.

Degassing of the samples was performed by at least five cycles of freeze-pump-thaw or by distillation method, both on a vacuum line.

Apparatus and Procedure. *Low Temperature Spectroscopy.* After having tried various types of apparatus, the final and most satisfactory one which is shown in Fig. 1, was manufactured.

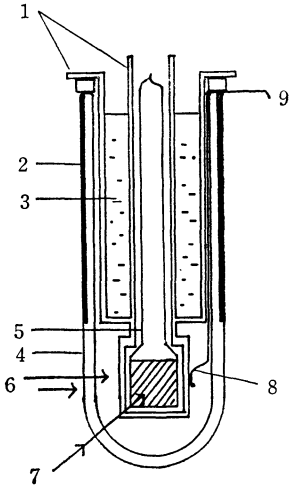

Fig. 1. (1) cell-holder of copper, (2) plated with silver, (3) liquid nitrogen, (4) quartz Dewar vessel, (5) quartz cell, (6) analysing beam, (7) exciting beam, (8) copper-constantan thermopile, (9) to microampere-meter

A quartz cell (5) settled in a copper cell-holder (1) was cooled slowly by pouring liquid nitrogen into the cell-holder. The apparatus was mechanically stable. A constant and sufficient low temperature of 77°K was attained in about ten minutes. There was no fear of the depression of the meniscus below the center of the cell, which would have interfered with an accurate measurement. After being kept at 77°K for more than twenty minutes, the sample was irradiated by a medium pressure mercury lamp (Toshiba Chokoatsu SHLUV, with a cover glass removed) with no filter.

All the absorption spectra were measured by a Hitachi EPS-3 spectrophotometer. Temperature was measured by a copper-constantan thermopile (8), the tip of which was fixed on the cell-holder (1) near the quartz cell.

The solvents used were

1) isopentane and methylcyclohexane mixture (1 : 1 — 1 : 4)

2) EPA (5 : 5 : 2 — 5 : 2 : 3)

3) ethanol. When not evacuated, a little water (6 vol%) was sometimes added; this procedure was very efficient for preventing cracking of rigid matrix. This was unnecessary for the evacuated ethanol solution.

Flash Apparatus. Same one as has been described in previous papers.[1,4]

ESR Spectra. A Nippon Denshi (Japan Electron Optics) P-10-type ESR spectrometer (X-band) with 100 kc field modulation, was used. As solvents, benzene, tertiary butanol, tetrahydrofuran and Daiflon were used; good ESR signals were obtained in the last two solvents. The reason for not having used the usual rigid solvents is that they often give rise to some free radicals of their own origin and complicate the ESR signals;[6] all the foregoing solvents have no easily detachable hydrogen atoms. Although the solutions when cooled to a low temperature of 77°K, assume the polycrystalline state, it was expected from the previous work,[6] that they would give the ESR spectra originating from only the solute species. 500 W medium pressure mercury lamp was used as a light source. The light was passed through a water layer 1 cm thick and focused on the quartz cell by means of a lens.

Results and Discussion

Anthracene Semiquinone. When the solutions of dihydroanthracene 1.0×10^{-4} M in rigid solvents were illuminated by a mercury lamp at 77°K, they always colored slightly yellow. At

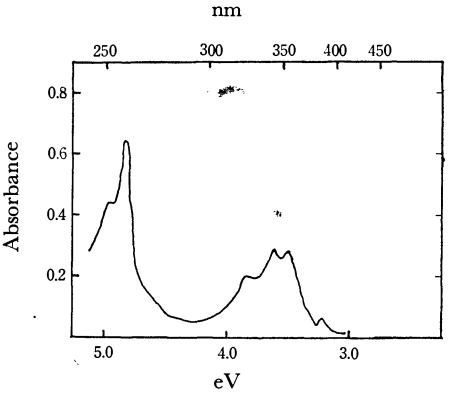

Fig. 2. The electronic spectrum of anthracene semiquinone obtained by irradiating MP (9 : 3) solution of 9,10-dihydroanthracene, 1.0×10^{-4} M at 77°K.

6) S. Niizuma and M. Koizumi, This Bulletin, **41**, 1090 (1968).

this temperature, the color remained unaltered for more than an hour when the light was off. Figure 2 gives the absorption spectrum in MP (9 : 3). Prominent peaks are seen around 250 and 340 nm regions. When the sample was warmed to room temperature, the major part of these bands disappeared and the absorption spectra of the resulting solution clearly showed that a small quantity of anthracene was produced. Hence it is most likely to attribute the above absorption bands to anthracene semiquinone, which is produced during the dehydrogenation reaction of 9,10-dihydroanthracene. It is, however, worthy noticing that the spectral shape of 340 nm region resembles closely that of anthracene, apart from a slight blue shift and the non-existence of 380 nm peak of anthracene. As to the assignment, therefore, the authors at first conceived of the possibility of the detachment of two hydrogen atoms in one act, yielding a certain anthracene-like intermediate such as distorted anthracene stabilized in rigid solvents. But such a view has proved to be ruled out; the assertion that the spectrum in question is really to be ascribed to semiquinone, has been substantiated from the following flash photolytic and ESR investigations.

Figure 3 gives the transient absorption spectrum obtained when the solution of dihydroanthracene 5×10^{-4} M, in ethanol was illuminated by the flash. The absorption in the region around 425 nm is most likely to be ascribed to the triplet state, while the one in the region 305—360 nm, to semiquinone, because the former decays as the superposition of the first and second order processes with a half life of 60 μsec and the latter, on the other hand, decays in second order with a much longer life of 370 μsec. Evidently the asorption around 305—360 nm corresponds to the one in rigid solvents. No transient absorption spectrum was detected in the aerated solution. The finding that the absorption in question decays as of second order and with a large half-value period can never be reconciled with the view of the distorted anthracene.

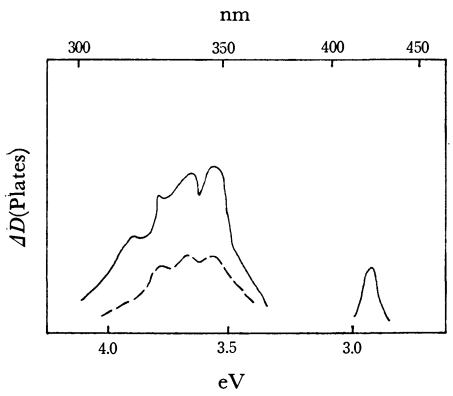

Fig. 3. The transient absorption spectra from the ethanol solution of 9,10-dihydroanthracene, degassed and 5.0×10^{-4} M at room temperature.
—— 93 μsec, ---- 360 μsec

Table 1 gives the solvent effect on the absorption spectrum.

Table 1. Solvent effects on the wave numbers of the absorption maxima of anthracene semiquinone

Solvent			
MP	30860	29760	28410
Ethanol[a)]	31150	29330	28410
Ethanol[b)]	31550	29500	28740

a) contains a little water (6 vol%)
b) obtained from the flash photolysis

ESR studies were performed by using the solution of dihydroanthracene 5×10^{-2} M in Daiflon and tetrahydrofuran. When irradiated by a mercury lamp at 77°K, the sample colored yellow and gave good ESR signals. Some parameters of the signals are listed in Table 2.

Table 2. Parameters of ESR signals of anthracene semiquinone

Solvent	g-Value	ΔH_{msl}(geuss)
Daiflon	2.0029	20.4
Tetrahydrofuran	2.0028	32.5

Somewhat larger value of ΔH_{msl} for tetrahydrofuran will be discussed later. From the g-value and the value of ΔH_{msl} there is scarcely any doubt that the signal is due to a π-radical, which in the present case is most likely to have the following structure.

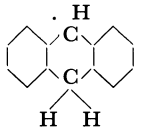

Although the media for the spectral and ESR studies are different, it is reasonable to consider, from the similar coloration, that the same reaction is occurring in the two cases.

One more point to be worthy noticing in respect to the feature of UV spectrum is that anthracene semiquinone has no absorption in the visible region, in sharp contradistinction to other semiquinones investigated in the present investigation.

Acridine Semiquinone. When solutions of acridan in rigid solvents were irradiated by mercury lamp at 77°K, the solution always colored brown. The color remained for more than an hour after the light was off, but it disappeared upon warming the sample to room temperature. Two examples of the absorption spectrum are shown in Fig. 4, a and b. The bands in three wavelength regions

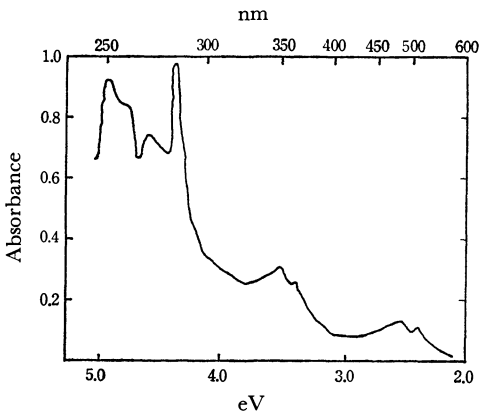

Fig. 4a. The electronic spectrum of acridine semiquinone obtained by irradiating aerated EPA (4:4:2) solution of acridan, 3.6×10^{-5} M at 77°K.

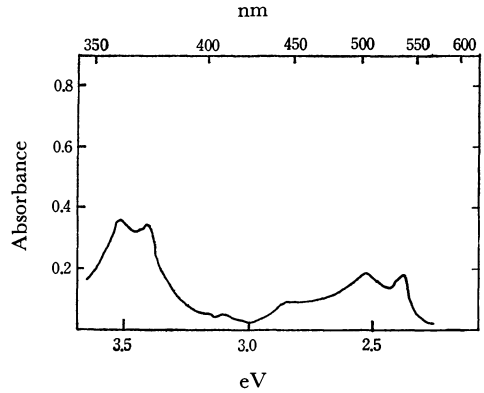

Fig. 4b. The electronic spectrum of acridine-C semiquinone obtained by irradiation of the degassed MP (4:1) solution of acridan, 3×10^{-4} M at 77°K.

are distinguished, the prominent peaks being (253, 281 nm*1) (365 nm) (480, 520 nm). In the flash experiment[1] using ethanol solution of acridine, the region around 365 nm had escaped the observation because of the superposition of the acridine absorption. The peaks at 281, 480 and 522 nm mentioned above, agree fairly well with the ones published before as well as with the ones obtained by the photolysis of diacridan.[6] Hence the above spectrum is safely assigned to a C-radical (see Fig. 6). The values of molar absorbance evaluated under the assumption that the entire acridan is converted to semiquinone, are given in Table 3.

Besides the aforementioned peaks, a broad absorption extending from 500 to 700 nm was observed in EPA and in ethanol. This may be due to solvated electrons but there is no definite evidence at present.

*1 According to theory, the appearance of this only in this case, is peculiar.

TABLE 3. ESTIMATED MOLAR ABSORBANCE OF ACRIDINE C-RADICAL

Solvent	365 nm	488 nm	523 nm
MP	0.9×10^{4}	4.0×10^{3}	3.5×10^{3}
EPA (4:4:2)	0.8×10^{4}	2.2×10^{3}	1.8×10^{3}
EPA (5:2:3)	1.0×10^{4}	1.7×10^{3}	1.8×10^{3}
Ethanol[a]	1.1×10^{4}	2.6×10^{3}	3.0×10^{3}
Ethanol[b]	$3\pm1\times10^{4}$		1.0×10^{4}

a) contains a little water (6 vol%)
b) by Kira[1]

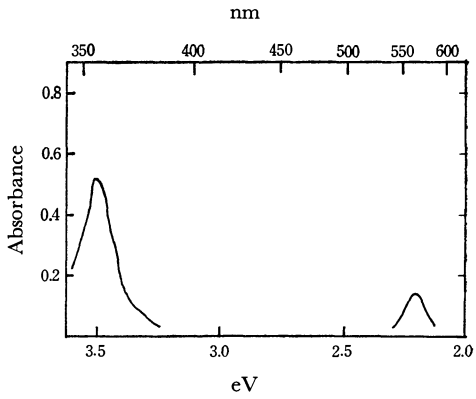

Fig. 5. The electronic spectrum of acridine-N semiquinone obtained by irradiating the aerated ethanol solution of acridan, 1.0×10^{-4} M at 77°K. This ethanol solution included a little water (6%).

Figure 5 gives the absorption spectrum of the intermediate produced by the irradiation of the aerated ethanol solution of acridan at 77°K. This spectrum is quite different from the ones shown in Fig. 4. At the time when the above results were obtained, it was a puzzling matter how to interpret these differences, because Kira and Koizumi's work[7] was not yet commenced at that time. Now that strong evidence has been given for the formation of C-radical and N-radical according to the experimental conditions, the absorption spectrum given in Fig. 5 can safely be

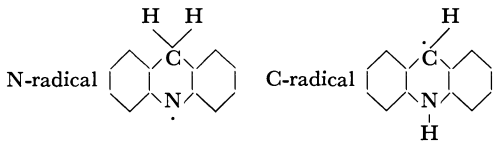

Fig. 6.

ascribed to N-radical from the agreement of the peak positions. Although there seems to be no doubt as to the assignment, a problem still remains why the N-radical is formed in the aerated ethanol solution whereas only the C-radical is formed in the

7) A. Kira, and M. Koizumi, to be published.

Table 4. Solvent effects on the wave numbers of the absorption maxima of acridine C-radical

Solvent									
MP	39525	38610	36630	35580	28409	27400		20490	19120
EPA (4:4:2)	39525	38760	36630	35580	28410	25700	25700	20490	19160
Ethanol[a)]	39525	38760	36760	35580	28320	27470	25700	20400	19190
Ethanol[b)]								20615	19230

a) Contains a little water (6 vol%)
b) Flash photolysis data by Kira[1)]

Table 5. Solvent effects on the wave numbers of absorption maxima of xanthene semiquinone

Solvent									
MP	31150	30030	28990	26600	25380	23810	22220	20830	17240
Ethanol	30960	30030	29150	27030	25560	24153	22420	20830	17240
Ethanol[a)]			29410						

a) From the flash data

aerated EPA solution as well as in the degassed MP solution. The problem awaits further studies, together with the ESR studies which are now in progress. Table 4 gives the solvent effect on the absorption spectrum of C-radical.

From the absence of the solvent effect, all the absorption may safely be attributed to the π-π^* transition.

Xanthene Semiquinone. When the xanthene solutions in ethanol or MP were irradiated, the solutions became yellow in color. As shown in Fig. 7, the absorption spectrum displays peaks at 255 nm (with a shoulder near 270 nm), 340 nm, 580 nm and a broad absorption band extending from 370 to 400 nm. When the sample was warmed up to room temperature, the shoulder at 270 nm and the last broad band still remained to exist while the other bands disappeared completely. This implies that along with a radical

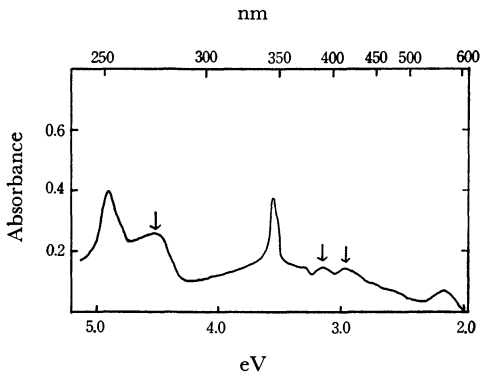

Fig. 7. The electronic spectrum of xanthene semiquinone obtained by the irradiation of the degassed ethanol solution, 1.2×10^{-4} M at 77°K. This spectrum includes the absorption of the photoproduct (↓), which is not separated from semiquinone.

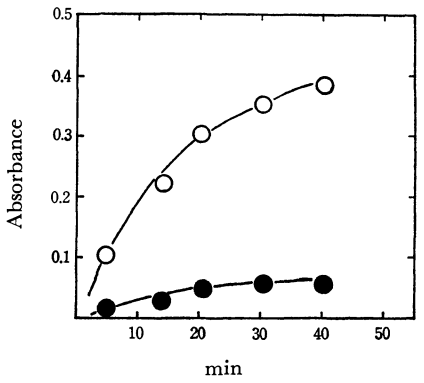

Fig. 8. A build-up of xanthene semiquinone (○ 343 nm) and that of photoproducts (● 390 nm). 8×10^{-5} M ethanol solution of xanthene.

species, some stable compound was produced simultaneously. Judging from the build-up curves shown in Fig. 8, the formation of the radical species and the stable compound in question, appears to proceed as two independent reactions. It is to be noted that the absorption bands at 252 and 270 nm were interfered with the bands of the original compound. Further, it is likely that most of xanthene semiquinone reconverts to xanthene by regaining a hydrogen atom when the solvent is melted, because the amount of xanthene was found to be almost the same as that before irradiation. The solvent effects are given in Table 5.

Good ESR signals were obtained when 5×10^{-2} M of xanthene in tetrahydrofuran or Daiflon was irradiated. The sample became yellow upon irradiation. The ESR spectrum in the case of tetrahydrofuran medium, as shown in Fig. 9, is somewhat asymmetric and broad, similarly as in the case of anthracene semiquinone in the same medium.

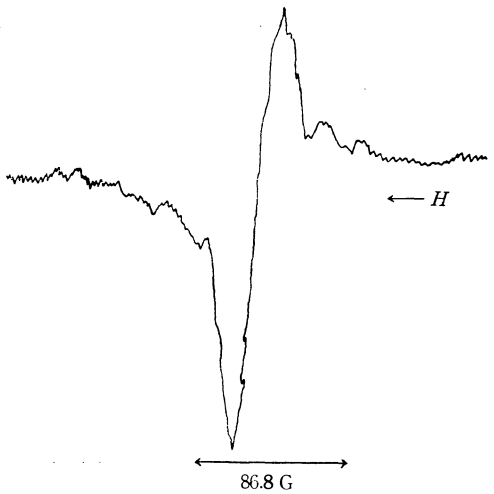

Fig. 9. ESR spectra obtained by the irradiation of tetrahydrofuran solution of xanthene, 5×10^{-2} M.

This is perhaps due to the coexistence of the tetrahydrofuran radical, which was produced through a secondary reaction between xanthene semiquinone and tetrahydrofuran molecules.[8] ESR parameters are given in Table 6.

TABLE 6. ESR PARAMETERS OF XANTHENE SEMIQUINONE

Solvent	g-Value	ΔH_{msl}(gauss)
Diflon	2.0043	16.2
Tetrahydrofuran	2.0046	26.0

From the g-value and the value of ΔH_{msl}, there is no doubt that the radical is a π-radical with the following structure:

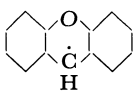

8) S. Niizuma and M. Koizumi, to be published. T. Maruyama *et al.*, the 19th Annual Meeting of the Chemical Society of Japan, Tokyo, 1966.

In the flash experiments, two transient absorptions were observed around 340 nm and 420 nm of which the latter was attributed to the triplet state, because of its short decay rate. That no absorption was detected in the vicinity of 580 nm, may be due to a very small absorbance of 580 nm as is evident from Fig. 7. The absorption around 340 nm evidently corresponds to the one in rigid solvents and is acribed to xanthene semiquinone.

Comprehensive Discussion

The present investigation has established that the absorption spectra of semiquinones in question, are classified into three groups, ~250 nm (4.9 eV), ~350 nm (3.5 eV) and visible (2.3—2.8 eV).

According to an open shell SCF-CI calculation (Longuet-Higgins-and-Pople-type) the details of which will be reported in the next paper, one obtains the similar classification except for some shifts (toward shorter wavelength), *i. e.*, ~1 eV, ~0.6 eV and ~0.5 eV respectively for 4.9 eV group, 3.5 eV group and for a visible group. This correspondence between theory and experiment is considered to be an additional evidence for the assignment of the intermediates as semiquinones. As to the peculiarities of the spectrum of each semiquinone, the most significant findings are;

a) Acridine C-radical has a prominent sharp peak at 281 nm.

b) For acridine N-radical, the band around 250 nm is very weak.

c) Anthracene semiquinone has no visible absorption.

As to these three characteristics, reasonable interpretations will be given in the theoretical part. Finally, it will be added that the difference in reactivity toward oxygen, between acridine C- and N-radicals, may be attributed to the energy difference of the half occupied molecular orbitals of the two species. This will also be discussed in the next paper.

BULLETIN OF THE CHEMICAL SOCIETY OF JAPAN VOL. 41 2325—2330 (1968)

The Rectification Effects Using the Ices Doped with Electrolytes

Kuniyoshi SHIMIZU, Yoshiaki YOSHIDA, Manabu SENŌ and Hiroshi NOZAKI

The Institute of Industrial Science, The University of Tokyo, Roppongi, Minato-ku, Tokyo

(Received April 2, 1968)

The rectifying properties of the combined systems of two crystals, one being doped with a proton donor (poly(styrene sulfonic acid) or hydrogen fluoride) and the other being doped with a proton acceptor (poly(2-vinyl-*N*-*n*-butylpyridinium bromide), poly(2-vinyl-*N*-*n*-butylpyridinium hydroxide) or lithium hydroxide) are examined and discussed. In the case of the combination of the ices doped with poly(styrene sulfonic acid) and poly(2-vinyl-*N*-*n*-butylpyridinium hydroxide) or poly(2-vinyl-*N*-*n*-butylpyridinium bromide), the current *versus* voltage curves have the hysteresis loops and the rectification ratio defined as the ratio of the forward current to the backward current is low. The dynamic rectification effect is slightly observed. In the case of the combination of the ices doped with lithium hydroxide and hydrogen fluoride, the rectification ratios exceed 100 and the rectification mechanism is presumed to be the same as in the system of the aqueous solutions. The dynamic characteristics depend on the frequencies; the rectification phenomena are not observed when the alternating voltages with frequencies higher than 30 kc are applied.

Reiss and Fuller[1] pointed out that the proton excess and the proton defficiency in an aqueous solution exert a similar function to the electron excess and the electron defficiency in a usual semiconductor, respectively. In the previous paper,[2] the rectification effect on the liquid junction of the aqueous solution of poly(2-vinyl-*N*-*n*-butylpyridinium hydroxide) and the aqueous solution of poly(styrene sulfonic acid) was investigated. The rectification effect was also found by some authors[3] on the composite membrane consisting of cation- and anion-exchange membrane. On the basis of the mobility of the charge carriers, the electron in a semiconductor is more analogous to the proton in ice than the proton in an aqueous solution. As a matter of fact, Eigen and de Maeyer[4] suggested the possibility of rectification effect on the ices doped with LiOH and HF.

In the present investigation, the rectifying properties are examined and discussed on the combined systems of two ices, one being doped with a proton donor (poly(styrene sulfonic acid) or HF) and the other being doped with a proton acceptor (poly(2-vinyl-*N*-*n*-butylpyridinium hydroxide), poly(2-vinyl-*N*-*n*-butylpyridinium bromide) or LiOH).

1) H. Reiss, *J. Chem. Phys.*, **21**, 1209 (1953); C. S. Füller, *Rec. Chem. Progr.*, **17**, 75 (1956).
2) K. Shimizu, M. Senō and H. Nozaki, This Bulletin, **41**, 802 (1968).
3) B. Lovrecek, A. Despic and J. O'M. Bockris, *J. Phys. Chem.*, **63**, 750 (1959); V. P. Läuger, *Ber. Buns. Phys. Chem.*, **68** (No. 6), 534 (1964); M. Senō and T. Yamabe, This Bulletin, **37**, 668 (1964); T. Teorell, *Z. Physik. Chem. Neue. Folge.*, **15**, 385 (1958).
4) M. Eigen and L. de Maeyer, *Proc. Roy. Soc.*, **A247**, 505 (1958).

Experimental

Materials. Poly(styrene sulfonic acid) (PVSA), molecular weight, 100000, was prepared by the same method as in the literature.[5] One molecule of PVSA has 450 sulfonic groups. Poly (2-vinyl-*N*-*n*-butylpyridinium bromide) (NBPB), molecular weight, 15000, was prepared by the method in the literature.[6]

Found: N, 8.0; Br. 21.2%. Calcd for complete quarternarization: N, 5.8; Br, 33.0%.

Poly(2-vinyl-*N*-*n*-butylpyridinium hydroxide) (NBOH) was prepared by the same method as in the previous paper.[2] Lithium hydroxide and hydrogen fluoride of reagent grade were used without further purification. Water used was treated as follows. The deionized water was distilled in a pyrex cell still containing a small amount of $KMnO_4$ and was collected in a polyethylene vessel. Then the distilled water was degassed by using the apparatus reported in the literature.[7] The specific conductivity was of the order, 10^{-7} ohm^{-1} cm^{-1}.

Apparatus and Procedure for Measurements. For measurements of the static conductivity of the ices doped with electrolytes, the electrolyte solutions in the silica tube (Fig. 1) were frozen in a dry-ice - methanol bath while nitrogen gas was flowed through the silica tube. The measurements were started at five hours after the electrolytes solution was poured into the silica tube (diameter: 4.0 cm). For the investigation of the rectification effect using the ices doped with electrolytes, the procedure of solidification of electrolyte solutions was conducted as follows. At first, the solution of NBOH (or NBPB, LiOH) was transferred into the silica tube maintained at −10°C in an alcohol bath and was

5) H. H. Roth, *Ind. Eng. Chem.*, **49**, 1820 (1957).
6) R. M. Fuoss and U. P. Strauss, *J. Polymer Sci.*, **3**, 246 (1948).
7) R. Goto, "Butsurikagaku Zittsukenho," Kyoritsu Shuppan, Tokyo (1965), p. 103.

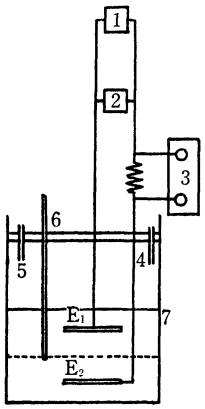

Fig. 1. Apparatus.

1: Voltage source, 2: voltmeter, 3: oscilloscope or X-Y recorder, 4 and 5: inlet and outlet of N_2 gas, 6: thermometer, 7: silica tube, E_1 and E_2: platinum electrodes.

frozen therein. After three hours, the solution of PVSA (or HF) which was supercooled at a few degrees below 0°C was poured above the NBOH (or NBPB, LiOH)-doped ice in the silica tube and was solidified in the alcohol bath for three hours. Then, the electric current was read at 30 sec after the voltage was applied. A constant voltage was supplied by a battery, and an alternating voltage was supplied by an ultra-low frequency oscillator (10^{-3}—10^{6} sec).

Results

I. The D. C. Electric Conductivity of Ice Doped with Polyelectrolyte. The d. c. electric conductivities of ices doped with PVSA, NBPB or NBOH were measured by using the apparatus as shown in Fig. 1. In Figs. 2, 3 and 4, the dependence of the electric conductivity (σ) of the ices doped with polyelectrolytes on temperature is shown, where the concentrations of polyelectrolytes are 1.36×10^{-2} and 0.68×10^{-2} equiv/l. Although an irregular change was observed near the freezing point, the Arrhenius-type relationship holds in a range of sufficiently low temperatures. From the straight line portions in Figs. 2, 3 and 4, we obtained the following relations.

$$\sigma_p = \sigma_{p,o}\exp(-8.23\times10^3/\boldsymbol{R}T) \quad (1)$$

$$\sigma_h = \sigma_{h,o}\exp(-13.94\times10^3/\boldsymbol{R}T) \quad (2)$$

$$\sigma_{h'} = \sigma_{h',o}\exp(-13.94\times10^3/\boldsymbol{R}T) \quad (3)$$

where the indeces p, h and h' refer to the ices doped with PVSA, NBOH and NBPB, respectively.

The dependence of the electric conductivity of the ices doped with polyelectrolytes on the concentrations of the polyelectrolytes at -10°C is shown in Fig. 5.

II. The Rectification Phenomena Using the Ices Doped with Electrolytes. Making the solid junction of two ices, one doped with a

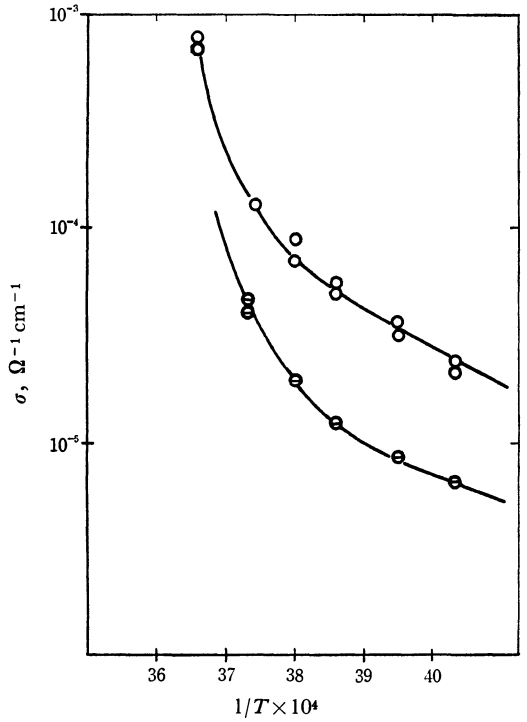

Fig. 2. Dependence of d. c. conductivity of the ice doped with PVSA on temperature.
○: $C_p=1.36\times10^{-2}$ equiv/l
⊖: $C_p=0.68\times10^{-2}$ equiv/l

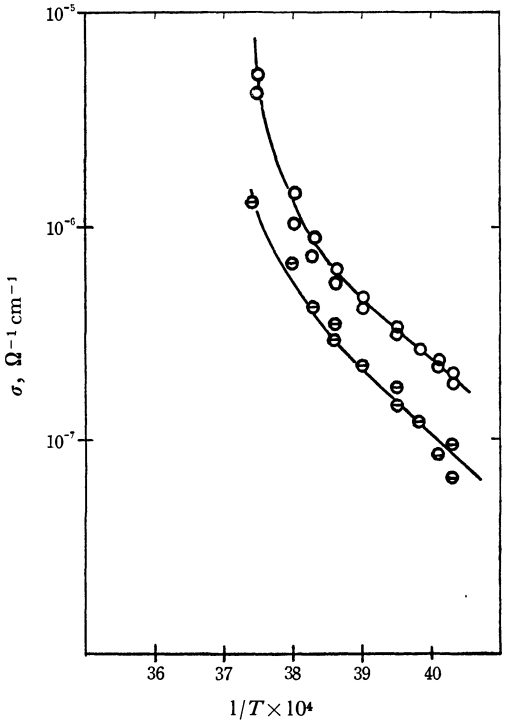

Fig. 3. Dependence of d. c. conductivity of the ice doped with NBPB on temperature.
○: $C_{h'}=1.36\times10^{-2}$ equiv/l
⊖: $C_{h'}=0.68\times10^{-2}$ equiv/l

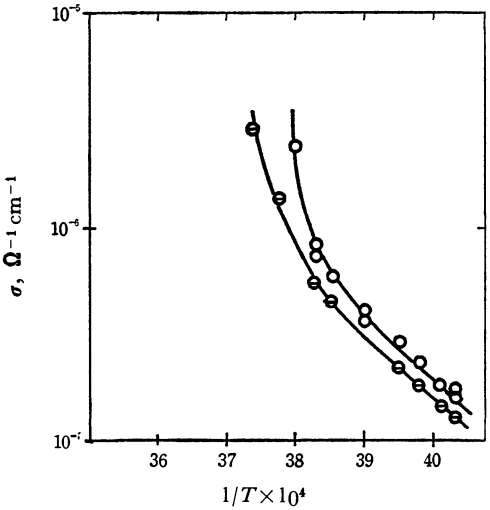

Fig. 4. Dependence of d. c. conductivity of the ice doped with NBOH on temperature.
○: $C_h=1.36\times10^{-2}$ equiv/l
⊖: $C_h=0.68\times10^{-2}$ equiv/l

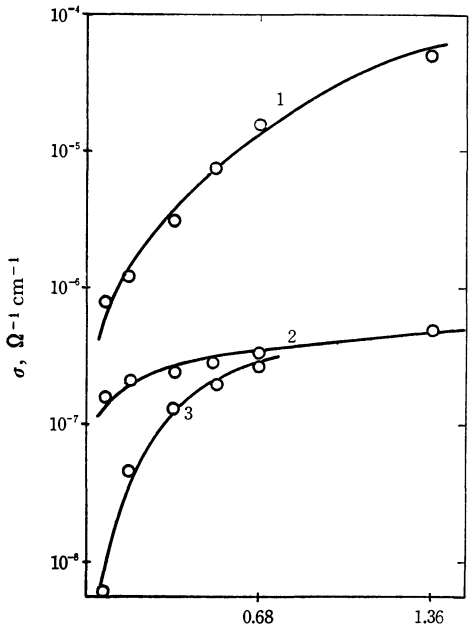

Fig. 5. Dependence of d. c. conductivity of the ice doped with polyelectrolyte on the concentration of charge carrier.
1: PVSA, 2: NBPB, 3: NBOH $T=-10$°C

proton donor (PVSA or HF) and the other doped with a proton acceptor (NBOH, NBPB or LiOH), we investigated the rectification effects, in analogy to the *p-n* junction in an electronic semiconductor.

NBOH-PVSA and NBPB-PVSA Systems. When the positive electrode is placed in the region of ice doped with a proton acceptor and the negative

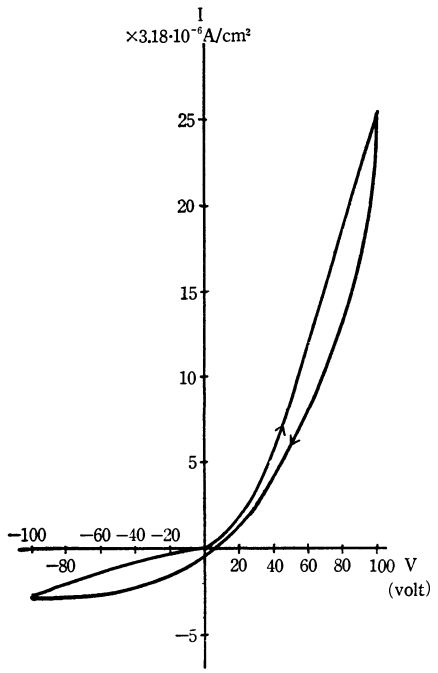

Fig. 6. Current plots *versus* constant voltages of NBPB-PVSA systems.
$C_p=0.34\times10^{-2}$ equiv/l
$C_{h'}=1.36\times10^{-2}$ equiv/l

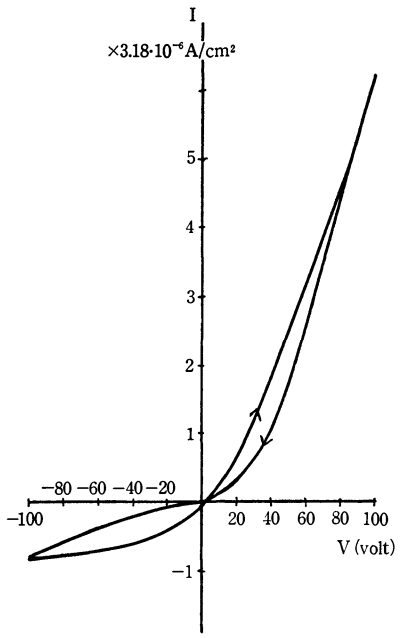

Fig. 7. Current plots *versus* constant voltages of NBOH-PVSA systems.
$C_p=0.34\times10^{-2}$ equiv/l
$C_h=1.36\times10^{-2}$ equiv/l

electrode is placed in the region of ice doped with a proton donor, the system exhibits a greater electric resistance than the case when the voltages with the reverse polarity were applied. The typical curves of the static current *versus* voltage are shown in Figs. 6 and 7. The data given in Figs. 6 and 7 were read at 30 sec after the voltages were applied. From these figures we can see that the curves have the hysteresis loops in both the NBOH-PVSA and the NBPB-PVSA systems.

The dynamic characteristics of rectification phenomena were remarkable when the alternating voltages of ultra-low frequencies were applied to the systems. The rectification effect was slightly observed even when the alternating voltage of 10 kc was applied. An example is shown in Fig. 8.

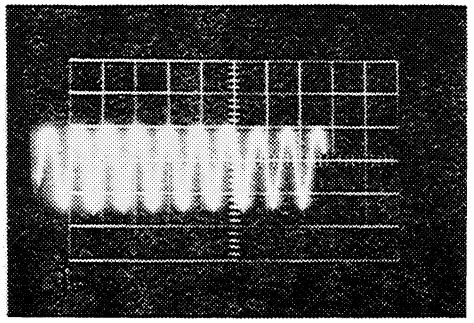

Fig. 8. Rectification of alternating sine-wave current in NBPB-PVSA system.
$C_p=0.34\times10^{-2}$ equiv/l
$C_{h'}=1.36\times10^{-2}$ equiv/l
Frequency: 5 kc

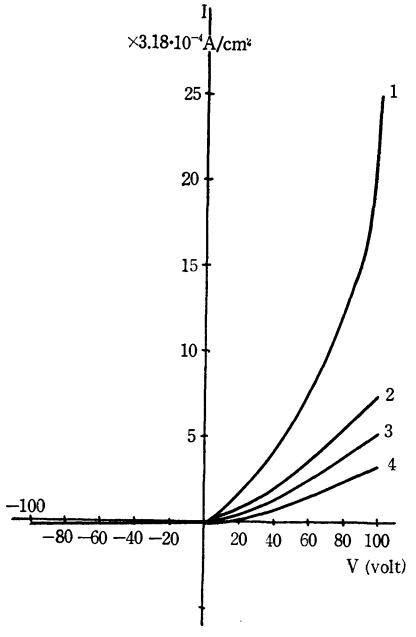

Fig. 9. Current plots *versus* constant voltages of LiOH-HF systems.
1: $C_p=0.0776$, $C_h=0.1$
2: $C_p=0.0388$, $C_h=0.1$
3: $C_p=0.0194$, $C_h=0.1$
4: $C_p=0.0097$, $C_h=0.1$
All values are in equiv/l.

LiOH-HF System. The static and dynamic rectification phenomena of this system are more remarkable than those of NBOH-PVSA and NBPB-PVSA systems. The static characteristics are shown in Figs. 9 and 10. The curves in Fig. 9 were measured under the condition where the concentration of LiOH was maintained at 0.1 equiv/l and the concentration of HF was varied from 0.0097 to 0.0776 equiv/l. The curves in

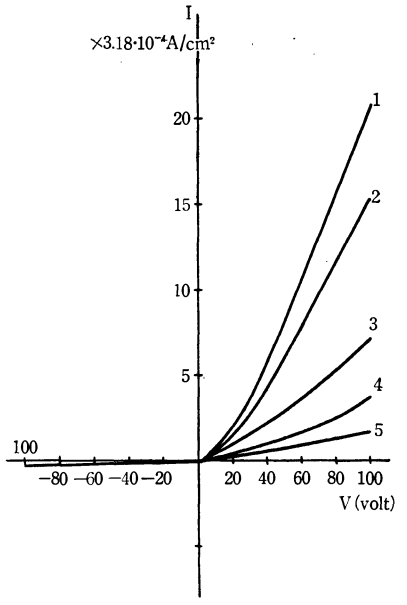

Fig. 10. Current plots *versus* constant voltages of LiOH-HF systems.
1: $C_p=0.0388$, $C_h=0.3$
2: $C_p=0.0388$, $C_h=0.2$
3: $C_p=0.0388$, $C_h=0.1$
4: $C_p=0.0388$, $C_h=0.05$
5: $C_p=0.0388$, $C_h=0.025$
All values are in equiv/l.

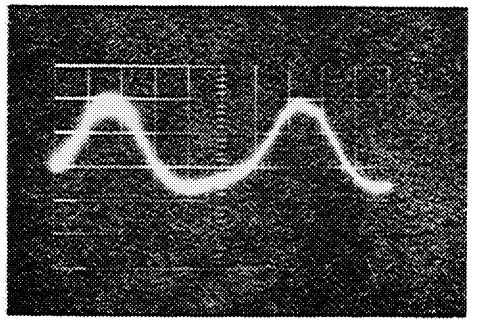

Fig. 11. Dependence of rectification ratio on frequency in LiOH-HF system.
$C_p=0.0388$ equiv/l $C_h=0.1$ equiv/l

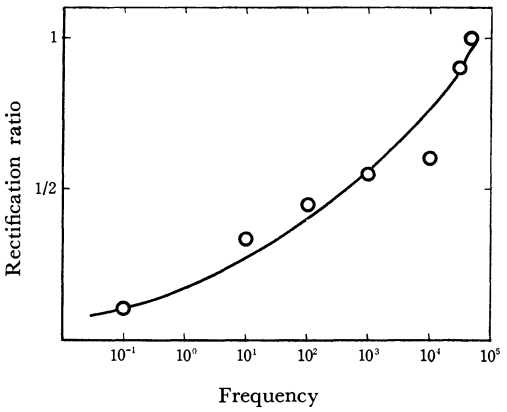

Fig. 12. Rectification of alternating sine-wave current in LiOH-HF system.
C_p=0.0388 equiv/l C_h=0.1 equiv/l
Frequency: 1 kc

Fig. 10 were obtained under the condition where the concentration of HF was maintained at 0.0388 equiv/l and the concentration of LiOH was varied from 0.025 to 0.3 equiv/l. A dynamic characteristic is shown in Fig. 11. The rectification ratio (the ratio of the forward current to the backward one) strongly depends on the frequency of the applied voltage and an example is shown in Fig. 12. The rectification phenomena were slightly observed even when the alternating voltage of 30 kc was applied.

Discussion

The d. c. electrical conductivity of the pure ice measured by Johnstone,[8] Bradley[9] and Granicher[10] was about 10^{-9} ohm^{-1}cm^{-1} at -10°C and the activation energy was 13.8 kcal/mol (by Granicher[10]). In the ice crystal, each oxygen atom is surrounded tetrahedrally by four hydroxyl ions at a distance of 2.76 Å. The pure ice is a good example of a protonic conductor. The mobility of a proton is ten times higher than a hydroxyl ion in ices (the mobilities of hydroxyl ion and proton are $\leq 5\times10^{-2}$ cm^{2}V^{-1}sec^{-1} and 0.1 to 0.5 cm^{2}V^{-1}sec^{-1}, respectively). The results in Figs. 2, 3 and 4 may be understood on this basis. Furthermore, the activation energy observed in the pure ice would reflect one for a protonic conduction, and the activation energy for a hydroxyl ion conduction should be greater. The activation energies of the electrical conduction of the ices doped with PVSA, NBPB and NBOH were measured to be 8.23, 13.94 and 13.94 kcal/mol, respectively. From these observations, it can be said that the inclusion of the linear polymers would contribute to the increase in the electrical conduction, owing to an increase in carrier concentrations and a lowering in activation energies caused by the generation of the structural defect in ices. The similarity in the conductivities of ices doped with NBPB and NBOH suggests that the charge carrier in both ices is the same one (OH^-).

Form the above consideration, it should be clear that the charge carriers of the ices doped with electrolytes are protons in the case of addition of PVSA and HF, and hydroxyl ions in the case of addition of NBOH, NBPB and LiOH. Then, by making the solid junction of two ices, one doped with a proton donor and the other with a proton acceptor, the rectification effect could be observed, such as in a *p-n* junction of a semiconductor.

In the case of the liquid junction analogous to a *p-n* junction,[2] the following equations were proposed for the rectification effect; when the forward bias voltages are applied;

$$J = e(D_pC_p/L_p+D_hC_h/L_h)\{\exp(\alpha eV/kT)-1\} \quad (4)$$

when the backward bias voltages are applied;

$$J = eg[\exp(\beta eV/kT)-\exp\{-(1-\beta)eV/kT\}] \quad (5)$$

where J is the electric current, e is the elementary charge, D_p and D_h are the diffusion coefficients of proton and hydroxyl ion, respectively, C_p and C_h are the concentrations of electrolytes in the proton excess region and the proton defficiency region, respectively, L_p and L_h are the mean distances by which proton and hydroxyl ion proceed in the proton defficient and proton excess regions until their disappearance, α is the coefficient showing the effective portion of the applied voltage, β is the transfer number for the neutralization reaction, g is the exchange velocity at the dissociation equilibrium of H_2O, k is the Boltzmann constant and V is the applied voltage. Equation (4) was derived under the assumption that the rate of electrical conduction is controlled by the diffusion of charge carriers in the transition region. On the other hand, Eq. (5) was derived under the assumption that the dissociation reaction of H_2O is the rate-determining step in the electrical conduction mechanism and from this equation the backward currents are shown to be independent of the concentrations of the charge carriers.

In the case of NBPB-PVSA and NBOH-PVSA systems, the recitification effects were observed as expected, but the static characteristics are not explained by Eqs. (4) and (5), and, moreover, the hysteresis is observed in the current *versus* voltage curves even in the forward direction (Figs. 6 and 7). The rectification effects were also slightly

8) J. H. L. Johnstone, *Proc. Trans. Nova Scotian Inst. Sci.*, **13**, 126 (1912).
9) R. S. Bradley, *Trans. Faraday Soc.*, **53**, 687 (1957).
10) H. Gränicher, C. Jaccard, P. Scherrer and A. Steinman, *Discussions Faraday Soc.*, **23**, 50 (1957).

observed when the ultra-low frequency a.c. ($\leq$10 kc) was applied. The causes of the hysteresis, which is a principal discrepancy from the theoretical prediction, are considered to be due to the capacitance of the system, the space charge effect or the polarization effect. The capacitance of the system would play a more significant role, as the concentrations of charge carriers becomes lower. The polarization effects are caused by the electrode effects and by the difference in mobilities between the charge carriers in the bulk of ices. The polarization connected with the electrode processes can be neglected at sufficiently high voltages.

In the case of LiOH-HF systems, the rectification curves as shown in Figs. 9 and 10 are well reproduced by Eqs. (4) and (5). The backward currents are almost independent of the concentrations of charge carriers, although the values are higher than in the pure ice. The constancy of the backward currents is well explained by the dissociation controlled mechanism, as derived for the liquid junction. The dynamic characteristics are remarkable when the alternating voltage with frequencies ranged to 30 kc was applied. This could be expected from the higher mobilities of H^+ and OH^- in ice. It is not possible to give detailed discussions here, for the uniform distribution of the doped electrolytes is not confirmed in the present investigation. It may be noticed, however, that the rectification effect observed in the HF-LiOH system is the most excellent of the junction diodes with the ionic conduction mechanism reported up to the present.

BULLETIN OF THE CHEMICAL SOCIETY OF JAPAN VOL. 41 2330—2336 (1968)

Dilute Solution Properties of Monodisperse Poly(α-methyl styrene). I. Sedimentation Coefficient in Theta Solvent

Mitsuo ABE,*1 Kuniaki SAKATO, Takashi KAGEYAMA, the late Masaaki FUKATSU and Michio KURATA*2

Institute for Chemical Research, Kyoto University, Uji, Kyoto

(Received April 5, 1968)

The sedimentation behavior of anionically polymerized poly(α-methyl styrene) has been studied as a function of molecular weight, concentration and speed of centrifugation under the theta condition of solvent and temperature, *i. e.*, in cyclohexane at 39°C. Analysis of the data was made by use of Fujita's equation for the pressure- and concentration-dependent sedimentation. It was found that the sedimentation coefficient at zero concentration and one atmosphere was given as $s_0^0=2.00\times10^{-15}M^{1/2}$ sec, where M is molecular weight. The concentration dependence coefficient k and the pressure dependence coefficient μ appearing in the Fujita equation were obtained as $k=6.2\times10^{-4}M^{1/2}$ dl/g, and $\mu=1.6\times10^{-9}$ cm²/dyne, respectively. The intrinsic viscosity in the theta solvent was also determined as $[\eta]_\theta=7.60\times10^{-4}M^{1/2}$ dl/g.

The purpose of this series is to present the results of systematic measurements carried out on the dilute solution properties of anionically prepared poly(α-methyl styrene). This polymer was taken as working material since its molecular weight distribution had been reported to be extremely sharp compared with other species of anionically prepared polymers.[1] Studies along the same line as the present have been published recently by Bywater and associates,[2] and by Nagasawa and associates.[3] They studied the behavior of intrinsic viscosity, sedimentation coefficient and polymer coil dimensions as functions of molecular weight and solvent nature, and compared the results with the current theories. However, no extensive measurement on the viscoelastic properties of dilute solutions of monodisperse polymer has been

*1 Visiting scientist (1966—67) from the Research Center, Japan Synthetic Rubber Co., Ltd., Ikuta, Kawasaki, Kanagawa.

*2 Reprint requests should be addressed to M. Kurata.

1) T. Fujimoto, N. Ozaki and M. Nagasawa, *J. Polymer Sci.*, **A3**, 2259 (1965).

2) A. F. Sirianni, D. J. Worsfold and S. Bywater, *Trans. Faraday Soc.*, **55**, 2124 (1959); J. M. G. Cowie, S. Bywater and D. J. Worsfold, *Polymer*, **8**, 105 (1967).

3) I. Noda, S. Saito, T. Fujimoto and M. Nagasawa, *J. Phys. Chem.*, **71**, 4048 (1967).

published yet but some preliminary measurements.[4,5] Thus, in this series, we intend to investigate not only the viscosity and sedimentation behavior but also the viscoelastic behavior of dilute solutions under varying conditions of molecular weight, concentration and solvent nature.

In this paper, we present a series of velocity sedimentation data obtained for the monodisperse poly(α-methyl styrene) in a theta solvent. The sedimentation coefficient at zero concentration and one atmosphere is determined as a function of molecular weight using Fujita's equation for the pressure- and concentration-dependent sedimentation.[6]

The Fujita equation for the apparent sedimentation coefficient s_{app} is written in the form that

$$s_{app} = \frac{\ln(r/r_m)}{\omega^2(t-t_0)} = s_c^0\left\{1 + K\left[\left(\frac{r}{r_m}\right)^2 - 1\right]\right\} \quad (1)$$

with

$$s_c^0 = s_0^0/(1 + kc) \quad (2)$$

$$K = \frac{kc - m(1 + kc)}{2(1 + kc)} \quad (3)$$

$$m = \frac{1}{2}\mu\omega^2\rho_0^0 r_m^2 . \quad (4)$$

Here r is the radial distance of the boundary from the axis of rotation, r_m is the radial distance of the meniscus, ω is the angular velocity, t is the time measured from the moment the acceleration of the rotor commenced, t_0 is the zero-time correction for the acceleration period, and ρ_0^0 is the density of solvent at one atmosphere. s_c^0 and s_0^0 represent values of the sedimentation coefficient at initial concentration c of the solution and at infinite dilution, respectively: the both are referred to one atmosphere of the pressure. k and μ are constants characteristic of the polymer-solvent system: the former is called the concentration dependence coefficient and the latter is called the pressure dependence coefficient.

An experimental test of Eq. (1) has been made by Billick using anionically polymerized polystyrene.[7] He has shown that the pressure and concentration dependence effects of the sedimentation velocity can be treated adequately by Eq. (1) in both poor and good solvents. However, as was noted by Blair and Williams,[8] the evaluation of the pressure dependence coefficient μ and also of the concentration dependence coefficient k is very sensitive to the zero-time correction t_0 applied for the acceleration period, and accordingly it is subjected to a rather large experimental error. In fact, Billick[7] has reported rather scattering values, $\mu = 1.2—3.4\times10^{-9}$ cm²/dyne; while Blair-Williams[8] and Wales-Rehfeld[9] have reported $(1.6\pm0.2)\times10^{-9}$ and 2.2×10^{-9}, respectively, for the system polystyrene in cyclohexane.

In view of the existing uncertainty in the value of μ, we found it worthwhile to remeasure the pressure-dependent sedimentation rate using monodisperse polymer samples. After the present work was completed, Noda *et al.*[3] published velocity sedimentation data on the same polymer-solvent system as the present, though their measurements were less extensive with respect to the variation of speed of centrifugation than ours. They reported $\mu = 2.3\times10^{-9}$ for the system poly(α-methyl styrene) in cyclohexane.

Experimental

Polymer Samples and Their Molecular Weights. Nine samples of poly(α-methyl styrene) with narrow distribution of the molecular weight were prepared in our laboratory by the anionic polymerization technique.[1,10] The initiator used was *n*-butyl lithium for BH-1 and seven samples of BB series, and sodium naphthalene for sample A-1. The terminator used was *n*-butanol for the BB and A series, and water for the BH series. The polymerization was carried out at −78°C in a purified water-free tetrahydrofuran as solvent. All polymers were fractionated in a large-scale Desreux column at 25°C by using benzene-ethanol mixtures, and the middle fraction of each polymer was utilized for measurements. These polymers were then freed from solvents by freeze-drying from benzene solutions followed by evacuation for about 24 hr at 60°C, and were sealed into ampules under argon atmosphere or at 10^{-6} mmHg pressure. More details of the sample preparation will be described elsewhere.[11]

The weight-average molecular weights M_w were determined by light scattering in benzene at 30°C and in cyclohexane at 39°C using a Brice type photoelectric photometer. The refractive index increments in these two solvents were 0.134 and 0.200 ml/g, respectively, for the light of 436 mμ wavelength. The number-average molecular weights M_n were determined by osmometry for samples BB-4, 6, 8, BH-1, and A-1 in toluene at 37°C. Details of these measurements will be described in Part II of this series, but a part of the results is given in Table 1.

The ratios M_w/M_n of our samples were in the range 0.93—1.07 if they were evaluated directly from the values of M_w and M_n. This ratio M_w/M_n, however, can be evaluated with a higher accuracy from the

4) J. E. Frederick and J. D. Ferry, *ibid.*, **69**, 346 (1965).
5) A. Sakanishi and H. Tanaka, *J. Soc. Material Sci.*, **16**, 528 (1967); *Repts. Progr. Polymer Phys. Japan*, **10**, 89 (1967).
6) H. Fujita, *J. Am. Chem. Soc.*, **78**, 3598 (1956). See also, H. Fujita, "Mathematical Theory of Sedimentation Analysis," Academic Press, Inc., New York, N. Y. (1962).
7) I. H. Billick, *J. Phys. Chem.*, **66**, 1941 (1962).
8) J. E. Blair and J. W. Williams, *ibid.*, **68**, 161 (1964).
9) M. Wales and S. J. Rehfeld, *J. Polymer Sci.* **62**, 179 (1962).
10) M. Morton, A. A. Rembaum and J. L. Hall, *ibid.*, **A1**, 461 (1963).
11) Y. Tsunajima, K. Sakato, M. Fukatsu and M. Kurata, *Bull. Inst. Chem. Res. Kyoto Univ.*, **46**, 37 (1968).

TABLE 1. MOLECULAR WEIGHTS, SEDIMENTATION COEFFICIENTS AND INTRINSIC VISCOSITIES OF ANIONICALLY PREPARED POLY(α-METHYL STYRENE)

Sample No.	M_w $\times 10^{-4}$	M_n $\times 10^{-4}$	$[\eta]_\theta$ (dl/g)	k'	s_0^0 $\times 10^{13}$ (sec)	k (dl/g)
BB-7	168[a]	—	0.983	0.55	—	—
BB-5	143[a]	—	0.910	0.53	23.9±0.5	0.79±0.15
A-1	97.0[a]	93.2	0.706	0.53	19.3±0.5	0.52±0.10
BB-10	64.0[a]	—	0.600	0.53	—	—
BB-6	48.8[a]	48.7	0.528	0.58	13.0±0.3	0.44±0.07
BB-9	35.5[b]	—	0.430	0.53	—	—
BH-1	26.0[c]	24.2	0.395	0.59	10.25±0.20	0.28±0.07
BB-4	4.87[c]	5.26	0.177	0.53	4.26±0.10	0.16±0.04
BB-8	4.03[b]	4.07	0.142	0.56	—	—

a) Determined in both benzene and cyclohexane.
b) Determined in benzene. c) determined in cyclohexane.

sedimentation boundary curve obtained in theta solvent.[12] The results of such measurements indicated that M_w/M_n were less than 1.01 for the samples BB-4, 5, 6, BH-1 and A-1. It is clear from these measurements that all our samples have an extremely narrow molecular weight distribution.

Theta Solvent and Temperature. Reagent grade cyclohexane was dried over a molecular sieve of 4A after the removal of a trace of benzene by a silica gel column, and was fractionally distilled with metallic sodium. The theta temperature was 38.6°C in cyclohexane as determined by the light-scattering second virial coefficient A_2. Figure 1 shows the A_2 *versus* temperature relationship obtained for sample A-1.

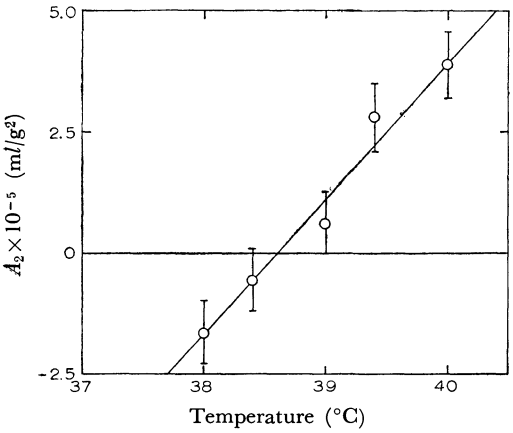

Fig. 1. Variation of the light-scattering second virial coefficient with temperature of sample A-1 in cyclohexane.

Sedimentation Velocity. Sedimentation velocity measurements were carried out in a Spinco model E ultracentrifuge equipped with an RTIC temperature control unit. In all experiments, the temperature was controlled at 39.0±0.1°C. A double sector cell of 12 mm long was used, and measurements were made at four rotor speeds, *i. e.*, 59780, 50740, 42040 and 29500 rpm, and at three or four initial concentrations of about 0.03 to 0.25 g/dl. Schlieren diagrams were read on a' 'Universal" contour projector (made by Nihon Kogaku Co., Ltd., Tokyo, Japan) to the accuracy of some 0.005 mm. The boundary position r in Eq. (1) was determined from the maximum of the refractive index gradient, since the schlieren diagrams were of good gaussian distribution curves.

Partial Specific Volume. A measuring-cylinder pycnometer of the Lipkin type was used to determine solution densities. The volume was approximately 10 ml. The density ρ_0 of cyclohexane was 0.7598 at 39°C. The partial specific volume v of poly(α-methyl styrene) was found to be 0.882 ml/g in this solvent.

Intrinsic Viscosity. Viscosity measurements were carried out in cyclohexane at 39°C using dilution viscometers of the Ubbelohde type. The corrections for the kinetic energy and shear rate effect were both negligible under the experimental conditions. The intrinsic viscosity $[\eta]_\theta$ and the Huggins coefficient k' determined are given in Table 1. The solvent viscosity η_0 was 0.730 centi-poise at 39°C.

Results

Zero-time Correction for Sedimentation. Among several methods so far proposed for the evaluation of the zero-time correction t_0 in sedimentation experiments, the so-called "best-fit" method of Blair and Williams[8] was found to be most appropriate for analysis of the present measurements. In this method, the value of t^0 is determined so as to minimize the "standard deviation" σ which is defined by

$$\sigma = [(1/n)\sum_{i=1}^{n} R_i^2]^{1/2} \tag{5}$$

with

$$R = s_c^0\omega^2(t-t_0) + s_c^0K\omega^2(t-t_0)[(r/r_m)^2-1] - \ln(r/r_m) \tag{6}$$

Here n denotes the number of observation in a given run of experiments. Figure 2 illustrates

12) T. Homma, K. Kawahara, H. Fujita and M. Ueda, *Makromol. Chem.*, **67**, 132 (1963).

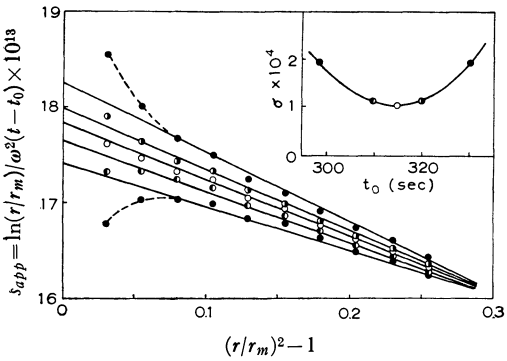

Fig. 2. Determination of the zero-time correction t_0 by the " best-fit " method of Blair and Williams. The five lines and different marks show the apparent sedimentation coefficients plotted against the quantity $(r/r_m)^2-1$ with five different choices of t_0 value. The insert shows variation of the standard deviation σ with the assumed values of t_0. Sample, A-1; rotor speed, 50740 rpm; concentration, 0.131 g/dl.

the procedure for the determination of t_0, in which the apparent sedimentation coefficients s_{app} obtained for various assumed values of t_0 are plotted against the quantity $(r/r_m)^2-1$. With aid of the best-fit line to each set of experimental points, a pair of values of s_c^0 and K can be determined, and then the standard deviation σ can be calculated using Eqs. (5) and (6). The values of σ thus obtained are shown in the insert of Fig. 2 as a function of t_0, and the "best-fit" value of t_0 is determined to be 315 sec. This value of t_0 was considerably larger than the time, 260 sec in this example, required for the so-called "2/3-acceleration".[7,13]

Pressure- and Concentration-dependence Coefficients. The values of s_c^0 and K corresponding to the best-fit value of t_0 were determined for samples BB-4, 5, 6, BH-1 and A-1 under various conditions of the concentration and the speed of centrifugation. The results are summarized in Table 2. For illustration, the values of s_c^0 of sample BB-5 thus determined are plotted in Fig. 3 against the concentration c. No systematic effect of the speed of centrifugation is observed in these s_c^0 *versus* c plots, and we can evaluate the concentration dependence coefficient k within an accuracy of about ten or twenty percent. The values of k thus obtained are listed in Table 1, and are plotted against the square-root of the molecular weight in Fig. 4. This plot suggests the relationship,

$$k = 6.2\times10^{-4}\,M^{1/2}\ \text{dl/g}.$$

The pressure dependence coefficient μ can be readily evaluated by substituting the values of K and k into Eqs. (3) and (4). The results are

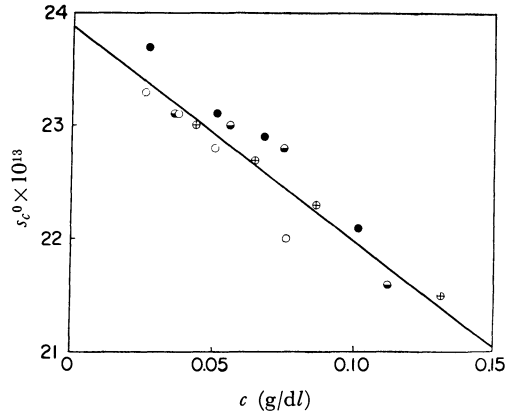

Fig. 3. Variation of sedimentation coefficient s_c^0 with the concentration c of sample BB-5 in cyclohexane at 39°C. Rotor speeds: ○, 59780; ⊕, 50740; ◒, 42040; ●, 29500 rpm.

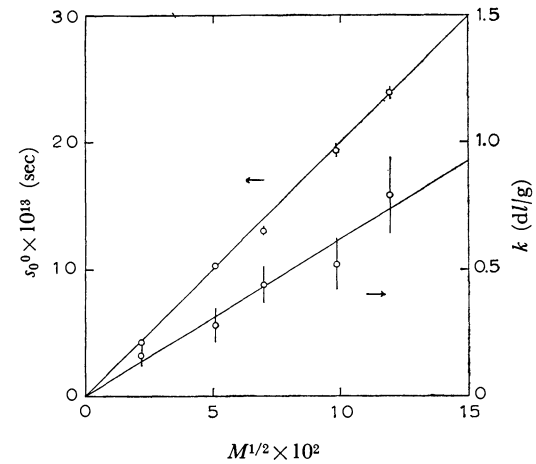

Fig. 4. The sedimentation coefficient s_0^0 and its concentration dependence coefficient k as functions of the molecular weight M.

tabulated in Table 2. No systematic variation of the μ values with the polymer molecular weight nor concentration is observed, and the averaging of these sixty four values of μ yields

$$\mu = (1.6 \pm 0.2)\times10^{-9}\ \text{cm}^2/\text{dyn}. \qquad (8)$$

Sedimentation Coefficient at Infinite Dilution. The sedimentation coefficient s_0^0 at zero concentration of the polymer and at one atmosphere are listed in Table 1. As shown in Fig. 4, this quantity s_0^0 is proportional to the square root of the molecular weight:

$$s_0^0 = (2.00 \pm 0.03)\times10^{-15}\,M^{1/2}\ \text{sec}. \qquad (9)$$

Intrinsic Viscosity. The intrinsic viscosities given in Table 1 are also proportional to the square root of the molecular weight:

$$[\eta]_\theta = (7.60 \pm 0.07)\times10^{-4}\,M^{1/2}\ \text{dl/g}. \qquad (10)$$

13) R. Trautman, *J. Phys. Chem.*, **60**, 1211 (1956).

TABLE 2. PRESSURE- AND CONCENTRATION-DEPENDENCE OF THE SEDIMENTATION COEFFICIENT OF POLY(α-METHYL STYRENE) IN CYCLOHEXANE AT 39°C

Sample	ω (rpm)	c (g/dl)	$s_c^0 \times 10^{13}$ (sec)	$-K$	$\mu \times 10^9$ (cm²/dyne)	$\sigma \times 10^4$
BB-5	59780	0.026	23.3	0.43	1.5	0.7
		0.038	23.1	0.44	1.6	1.0
		0.051	22.8	0.45	1.6	1.5
		0.076	22.0	0.46	1.7	0.9
	50740	0.044	23.0	0.31	1.6	1.4
		0.065	22.7	0.30	1.5	1.8
		0.087	22.3	0.32	1.7	1.3
		0.131	21.5	0.33	1.8	1.7
	42040	0.037	23.1	0.24	1.7	1.3
		0.056	23.0	0.24	1.8	1.1
		0.075	22.8	0.24	1.8	1.2
		0.112	21.6	0.21	1.7	1.8
	29500	0.027	23.7	0.11	1.7	0.9
		0.051	23.1	0.070	1.3	0.8
		0.068	22.9	0.12	2.1	0.8
		0.102	22.1	0.14	2.4	0.6
A-1	59780	0.040	18.9	0.44	1.6	1.6
		0.061	18.6	0.46	1.7	2.0
		0.122	17.9	0.46	1.7	0.8
		0.159	17.5	0.48	1.7	1.3
	50740	0.036	18.8	0.31	1.6	1.8
		0.066	18.7	0.33	1.7	1.3
		0.087	18.2	0.31	1.6	0.9
		0.131	17.8	0.32	1.7	1.0
	42040	0.099	18.7	0.23	1.7	1.5
		0.149	18.2	0.23	1.7	1.4
		0.199	17.7	0.23	1.8	1.0
		0.298	16.9	0.24	1.9	1.1
	29500	0.077	18.6	0.092	1.6	1.5
		0.102	18.5	0.092	1.7	1.6
		0.152	18.0	0.072	1.5	0.7
BB-6	59780	0.049	12.92	0.49	1.8	1.0
		0.074	12.55	0.41	1.5	1.4
		0.098	12.48	0.43	1.6	1.9
		0.147	12.30	0.44	1.6	0.9
		0.294	11.43	0.41	1.5	1.2
	50740	0.047	12.63	0.30	1.6	1.6
		0.067	12.44	0.31	1.6	0.8
		0.089	12.23	0.29	1.5	1.0
		0.134	12.07	0.29	1.6	1.1
	42040	0.038	12.76	0.20	1.5	2.3
		0.051	12.81	0.21	1.6	1.3
		0.077	12.70	0.22	1.7	2.0
		0.102	12.46	0.21	1.6	1.0
	29500	0.075	12.62	0.095	1.6	1.9
		0.150	12.38	0.056	1.1	1.1
		0.225	11.90	0.10	1.9	1.2
BH-1	59780	0.077	9.98	0.40	1.5	1.5
		0.115	9.90	0.38	1.4	1.5
		0.153	9.78	0.45	1.6	1.3
		0.230	9.40	0.40	1.5	0.7
	50740	0.062	10.10	0.34	1.7	2.0
		0.093	10.00	0.31	1.6	3.5
		0.124	9.87	0.31	1.6	1.6
		0.187	9.71	0.34	1.7	1.4
	42040	0.077	10.03	0·17	1.3	1.4
		0.153	9.90	0.20	1.5	2.7
		0.230	9.64	0.24	1.8	2.3
	29500	0.153	9.83	0.082	1.5	0.8
		0.229	9.64	0.093	1.8	1.2
BB-4	59780	0.176	4.15	0.44	1.6	1.0
		0.264	4.07	0.39	1.4	1.1
		0.396	4.00	0.38	1.4	1.6
		0.528	3.90	0.38	1.4	1.0

Discussion

The present measurements indicate that the concentration dependence of the sedimentation coefficient does not vanish at the theta temperature. According to Pyun and Fixman,[14] the concentration dependence coefficient k, as expressed in units of dl/g, is given as:

$$k = k^{\varphi}(4/300)(M/N_A\pi)^2[(1-v\rho_0)^2/6\eta_0 s_0^0]^3 \quad (11)$$

where N_A is the Avogadro number, and ρ_0 and η_0 are the density and viscosity of solvent. k^{φ} denotes the value of the concentration dependence coefficient when the concentration is expressed in the volume fraction. The Pyun and Fixman theory shows that k^{φ} depends on the thermodynamic interaction between polymer segmants and that it takes a value between 2 and 3 at the theta point. The substitution of the present results, Eqs. (7) and (9), into Eq. (11) yields $k^{\varphi}=3.08$. This value is favorably compared with the above theoretical estimate, especially with the value, $k^{\varphi}=2.96$, which is derived by their "spherocylinder" approximation.[14]

As for the pressure dependence coefficient μ of the sedimentation coefficient, Noda *et al.* have reported the value, $\mu=2.3\times10^{-9}$, for the same polymer-solvent system as the present.[3] They referred to the agreement of this value with the theoretical value, $\mu=2.0\times10^{-9}$, which is calculated from the pressure-dependence coefficient λ of the solvent viscosity using the relationship,[15]

$$\mu = \lambda + [v\rho_0/(1-v\rho_0)]\kappa. \quad (12)$$

Here κ is the isothermal compressibility of the solution. The value of λ, however, is known only roughly in the case of cyclohexane,[15] and therefore the above comparison of μ values will not be given a much significance. The present estimate of μ given in Eq. (8) is in good agreement with the values which were obtained for polystyrene in cyclohexane by Blair-Williams,[8] Billick,*3 and Cowie-Bywater.[16] Thus, we prefer the present estimate $\mu=1.6\times10^{-9}$, and conclude that μ is primarily independent of polymer species but characteristic of solvent.

In spite of the above discrepancy in μ values, no discrepancy is observed in the values of s_0^0 between the measurements by Noda *et al.*[3] and ours. This can be demonstrated by plotting s_0^0 against $[\eta]_\theta$. As shown in Fig. 5, the two series of data support the single correlation line:

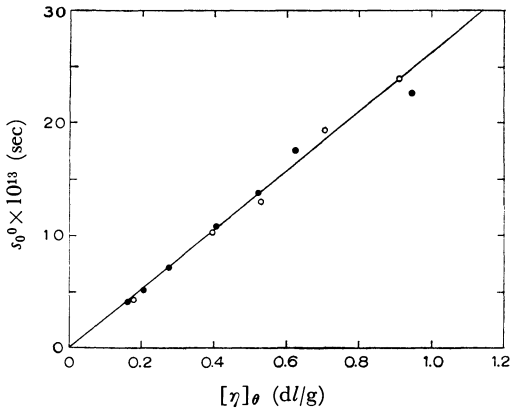

Fig. 5. Relationship between the sedimentation coefficient and the intrinsic viscosity. White circles, the present data; black circles, the data of Noda, Saito, Fujimoto and Nagasawa.[3]

$$s_0^0 = 2.63 \times 10^{-12}[\eta]_\theta. \quad (13)$$

This is probably due to the fact that in measurements of Noda *et al.*, the rotor speed was chosen as slow as possible to reduce the pressure effect. At such a low speed of centrifugation, the estimation of the pressure coefficient μ is subjected to a rather large experimental error, but the determination of s_0^0 itself can be performed with a sufficient accuracy.

The sedimentation coefficient *vs.* molecular weight relationship, Eq. (9), is slightly different from the relationship presented by Noda *et al.*:[3]

$$s_0^0 = 2.04 \times 10^{-15} M^{1/2}$$
(in cyclohexane at 39°C). (14)

The intrinsic viscosity *vs.* molecular weight relationship, Eq. (10), is also different from the relationships,

$$[\eta]_\theta = 7.13 \times 10^{-4} M^{0.51}$$
(in cyclohexane at 39°C) (15)

$$[\eta]_\theta = 7.80 \times 10^{-4} M^{0.50}$$
(in cyclohexane at 37°C) (16)

which were presented by Noda *et al.*[3] and Cowie *et al.*,[2] respectively. These discrepancies seem to arize from small but systematic errors involved in the molecular weight determination in these three laboratories. With the present data, we obtain from Eqs. (9) and (10)

$$\beta = \frac{s_0^0[\eta]_\theta^{1/3}\eta_0 N_A}{(1-v\rho_0)M^{2/3}} = \Phi^{1/3}P^{-1}$$
$$= (2.41 \pm 0.07) \times 10^6, \quad (17)$$

where P and Φ are the Flory universal constants for the sedimentation coefficient and the intrinsic viscosity, respectively. This value of the Scherage-Mandelkern constant β is slightly lower than the value $(2.5—2.6)\times10^6$ which is predicted by the

14) C. W. Pyun and M. Fixman, *J. Chem. Phys.*, **41**, 937 (1964).
15) R. L. Baldwin and K. E. van Holde, *Fortschr. Hochpolymer Forsch.*, **1**, 451 (1960).
16) J. M. G. Cowie and S. Bywater, *Polymer*, **6**, 197 (1965).
*3 The average of thirteen values of μ given in Table IIa of Ref. 7 yields 1.75×10^{-9} cm²/dyne.

current theories. It is, however, difficult to decide whether this discrepancy is attributed to underestimate of M in our light scattering measurements or to overestimate of Φ in the current theories.

We are indebted to Professor Hiroshi Fujita for valuable discussions, and to the Ministry of Education for a grant-in-aid. One of us (M. A.) thanks the Japan Synthetic Rubber Company for having allowed him to participate in this research program at the Institute for Chemical Research, Kyoto University during the period 1966—67.

BULLETIN OF THE CHEMICAL SOCIETY OF JAPAN VOL. 41 2336—2342 (1968)

Electronic Structures and Reactivities of Aliphatic Polycyclo Compounds. I. Fused Three-membered-ring Compounds*[1]

Teijiro YONEZAWA,* Kiyoshi SIMIZU** and Hiroshi KATO*

* *Faculty of Engineering, Kyoto University, Sakyo-ku, Kyoto*

** *Research Laboratory for Chemical Fibers, Nitto Boseki Co. Ltd., Fukuyama Koriyama-shi, Fukushima*

(Received April 11, 1968)

The electronic structures of bicyclo(1.1.0)butane, tricyclo(3.1.0.0)hexane, tricyclo(2.1.0.0)-pentane, tricyclo(1.1.0.0)butane, prismane, and spiro(2.2)pentane are studied by the extended Hückel method. The calculated total energies of bicyclo(1.1.0)butanes with various dihedral angles, θ, and bridgehead C–C–H angles, α, show that the most stable configuration of bicyclobutane is at $\alpha=135°$ and $\theta=115$—$120°$. It is made clear that the s-nature of the carbon atoms of the $C\text{–}H_{axial}$ and $C\text{–}H_{equatorial}$ depends greatly on the dihedral angle of the two cyclopropane rings. The double-bond character between the bridgehead carbon atoms in the bicyclobutane and its homologues is pointed out. The stabilities of the C–C bonds of prismane are shown to be largely dependent on the angle between the C–H bond and the four-membered-ring plane. The electronic structures of some configurations of spiropentane with different dihedral angles are discussed. The physico-chemical properties of these compounds are briefly investigated.

It is well known that the cyclopropane ring has a small C–C–C bond angle of 60° and exhibits aromaticity and peculiar reactivities in most reactions.[1-3] Therefore, it is interesting to examine the physico-chemical properties of the following compounds: bicyclo(1.1.0)butane (I) in which two cyclopropane rings are fused with each other, with one C–C bond in common, and its homologues: tricyclo(3.1.0.0)-hexane (II), tricyclo(2.1.0.0)pentane (III) and tricylo(1.1.0.0)butane (IV), prismane (V), and spiro(2.2)pentane (VI), in which two cyclopropane rings hold a carbon atom in common.

Spiro(2.2)pentane (VI) was synthesized by Murray and Stevenson[4] about twenty years ago. The other compounds have, however, been prepared quite recently. The preparation of bicyclo(1.1.0)-butane (I) has been reported by Lemal *et al.*[5] and Srinivasan[6] independently. Tricyclo(3.1.0.0)-hexane and tricyclo(2.1.0.0)pentane derivatives were prepared by Meinwald[7] and by Masamune.[8] The preparation of tricyclo(1.1.0.0)butane, the structure of which seems to be tetrahedron, has not been reported as yet. Prismane derivatives have been synthesized by Viehe *et al.*,[9] and the properties of these small cage compounds have recently been reported on by Wiberg *et al.*[10]

As for theoretical investigations, Weltner[11] suggested that tricyclo(1.1.0.0)butane (IV) consists of "acetylenic" sp hybridized carbon atoms and

---

*1 Presented at the Meeting of Chemical Society of Japan (1966).

1) A. D. Walsh, *Trans. Faraday Soc.*, **45**, 179 (1949).

2) C. A. Coulson and W. E. Moffitt, *Phil. Mag.*, **40**, 1 (1949).

3) See for example, a) S. Nishida and T. Tsuji, *J. Soc. Org. Syn. Chem. Japan*, **22**, 272 (1964); b) M. T. Rogers, *J. Am. Chem. Soc.*, **69**, 2544 (1947); c) M. S. Kharasch, M. Z. Fineman and F. R. Mayo, *J. Am. Chem. Soc.*, **61**, 2139 (1939).

4) M. J. Murray and E. H. Stevenson, *J. Am. Chem. Soc.*, **66**, 812 (1944).

5) D. M. Lemal, F. Menger and G. W. Clark, *ibid.*, **85**, 2529 (1963).

6) R. Srinivasan, *ibid.*, **85**, 4045 (1963).

7) J. Meinwald, C. Swithenbank and A. Lewis, *ibid.*, **86**, 735 (1964).

8) S. Masamune, *ibid.*, **86**, 736 (1964).

9) H. G. Viehe, R. Merényi, J. F. M. Oth, J. R. Senders and P. Valange, *Angew. Chem.*, **76**, 922 (1964).

10) K. B. Wiberg, G. M. Lampman, R. P. Ciula, D. S. Connor, P. Schertler and J. Lavanish, *Tetrahedron*, **21**, 2749 (1965).

11) W. Weltner, Jr., *J. Am. Chem. Soc.*, **75**, 4224 (1953).

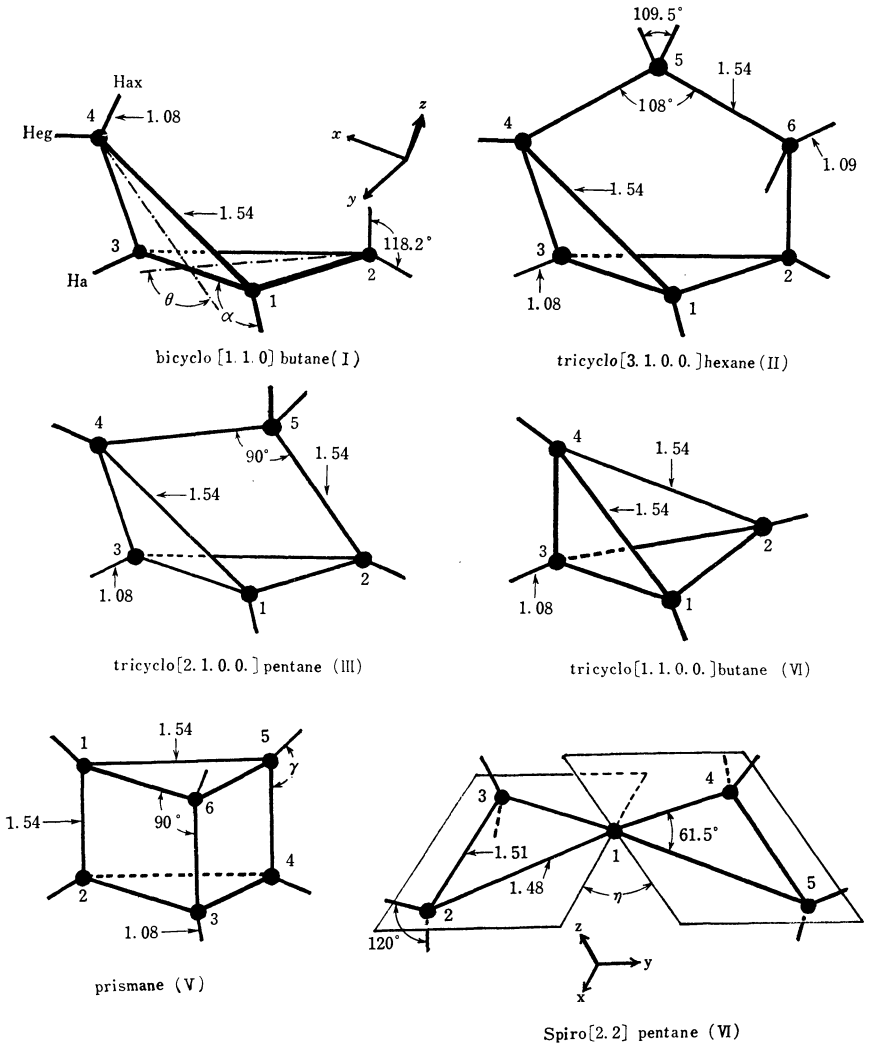

Fig. 1. Molecular structures of polycyclo compounds.

pointed out the large s-nature of the carbon atom in the C–H bond, basing his observations on the maximum overlap method.[12] Maksić *et al.*[13] calculated the electronic structure of bicyclobutane (I) by the same method and indicated the remarkable s-nature of bridgehead carbon atoms. Pomerantz *et al.*[14] suggested qualitatively that the central bond has an olefinic π-character.

Quite recently, Baird and Dewar[15] have calculated the strain energies of many cyclopropanes and cyclopropenes by means of the NDDO method[16] and be established that tricyclobutane (IV) would have very large strain energies (150.5 kcal/mol).

In the present paper, the correlation between the electronic structures and the dihedral angle of bicyclobutane will be studied first. Then, we will discuss how the electronic structures change for a series of bicyclobutane homologues: tricyclohexane (II), tricyclopentane (III), and tricyclobutane (IV). Secondly, the electronic structures of two possible configurations of prismane (V) will be investigated in relation to their stabilities. Finally, the stabilities of spiropentane (VI) with several dihedral angles will be discussed in comparison with that of 1,1-dimethylcyclopropane.

The extended Hückel method[17] is used for the

12) For example, J. D. Dunitz and V. Schomaker, *J. Chem. Phys.*, **20**, 1703 (1952).
13) Z. Maksić, L. Klasinc and M. Randić, *Theort. chim. Acta*, **4**, 273 (1966).
14) M. Pomerantz and E. W. Abrahamson, *J. Am. Chem. Soc.*, **88**, 3970 (1966).
15) a) M. J. S. Dewar and G. Klopman, *ibid.*, **89**, 3089 (1967); b) N. C. Baird and M. J. S. Dewar, *ibid.*, **89**, 3966 (1967).
16) J. A. Pople and G. A. Segal, *J. Chem. Phys.*, **43**, S 136 (1965); **44**, 3289 (1966).
17) R. Hoffmann, *ibid.*, **39**, 1397 (1958).

calculation. The parameters used in the present paper are identical with those previously reported.[17,18]

For all the compounds mentioned above except for spiro(2.2)pentane (VI)[19] the bond lengths and bond angles have never been reported. We assume them by referring to the observed values of cycloalkanes,[20] shown in Fig. 1.

Electronic Structures of Various Configurations of Bicyclo(1.1.0)butane and Its Homologues. *Stable Configuration of Bicyclo(1.1.0)-butane I.* The relation between the dihedral angle, θ, and the total electronic energies of bicyclobutane with the constant value of $\alpha=180°$ is shown in Fig. 2. The calculated results indicate that the total electronic energy reaches a minimum at the dihedral angle, θ, of 115—120°, while the bicyclobutane seems to be bent more than cyclobutane, which has the dihedral angle of 160°.

Next, the calculations were carried out, changing the value of the bridgehead C–C–H angle, α, in the range of 90—180° but keeping the constant dihedral angle of 120°, which corresponds to a local minimum of total electronic energy. In Fig. 3 the total electronic energy of bicyclobutane is plotted against the value of α. It is found that the total electronic energy has a minimum at an α value of about 135°.

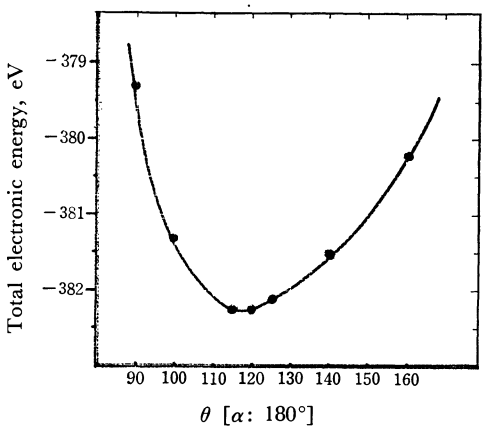

Fig. 2. Total electronic energies of various configurations of bicyclobutane.

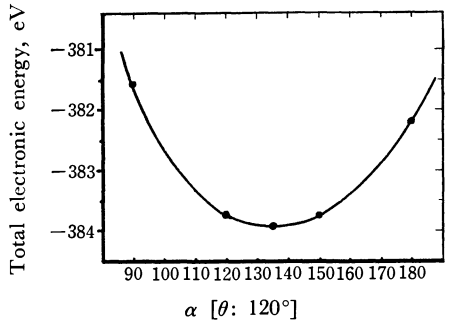

Fig. 3. Total electronic energies of various configurations of bicyclobutane.

As to the molecular structure of bicyclobutane, Haller and Srinivasan[21] suggested the following on the basis of their IR spectral data: $\theta=126°$, $\alpha=163°$, $\angle HCH=118°$, C_1–C_2; 1.53 Å, C_1–C_3; 1.54 Å and C–H; 1.08 Å.

On the other hand, Harmony and Cox[22] have recently reported the following values, based on their microwave spectroscopic data: $\theta=121°$, $\alpha=130°$, $\angle HCH=116°$, C_1–C_2; 1.51 Å, C_1–C_3; 1.49 Å and C–H; 1.08 Å. Our results seem to support the structure reported by Harmony and Cox.

Stability of Bicyclo(1.1.0)butane and Its Homologues. Tricyclo(3.1.0.0)hexane (II), tricyclo(2.1.0.0)-pentane (III), and tricyclo(1.1.0.0)butane (IV)*2 are considered to be cage molecules which are constructed by connecting perihedral secondary carbon atoms (*i. e.*, C_2 and C_4 in Fig. 1) with a ethylenic group, with a methylenic group, and directly.

Table 1 shows the dihedral angle, θ; the bridgehead C–C–H angle, α*3; the highest occupied HO orbital energy; the lowest vacant LV orbital energy, and the gap energy between these energies. The HO orbital energies of these compounds are about −11——12 eV, as is shown in Table 1; they are higher by 1—2 eV than that of cyclopropane, whose HO orbital energy is −13.052 eV. The ionization potentials for these compounds seem to be smaller than that of cyclopropane. The LV orbital energies for these compounds are much lower than those for acyclic saturated hydrocarbons (*n*-butane, 2.492 eV; isobutane, 1.374 eV; neopentane, 0.837 eV); thus, the electron affinities of these compounds may be very large. These levels of bicyclobutane and its homologues, however, are higher than those of acyclic unsaturated hydrocarbons (*e. g.*, ethylene; −8.253 eV); therefore, the LV energy levels of these compounds are located midway between those for common saturated hydrocarbons and unsaturated hydrocarbons. The energy gaps between the HO and LV orbital energies for these compounds are 4—7 eV, much

18) T. Yonezawa, K. Simizu and H. Kato, This Bulletin, **40**, 456 (1967).
19) J. Donohue, G. L. Humphrey and V. Schomaker, *J. Am. Chem. Soc.*, **67**, 332 (1945).
20) "Tables of Interatomic Distances and Configurations in Molecules and Ions," Special Publication, No. 11, The Chemical Society, London (1958).
21) I. Haller and R. Srinivasan, *J. Chem. Phys.*, **41**, 2745 (1964).
22) M. D. Harmony and K. Cox, *J. Am. Chem. Soc.*, **88**, 5049 (1966).

*2 Tricyclo(1.1.0.0)butane (IV) has not as yet been synthesized.

*3 Since the configurations of bicyclobutane homologues have not yet been reported, as is mentioned above, the values of α are calculated from the configuration assumed in Fig. 1.

Table 1. Dihedral angles: θ, α, HO and LV energies and their gaps of bicyclobutane and its homologues

Structural formula	Name	θ	α	HO energy eV	LV energy eV	Gap energy eV
	Tricyclo(3.1.0.0)hexane (II)	138°12′	121°43′	−10.914	−6.813	4.101
	Bicyclo(1.1.0)butane (I)	120°	135°	−11.950	−5.904	6.046
	Tricyclo(2.1.0.0)pentane (III)	109°28′	135°	−10.837	−5.405	5.432
	Tricyclo(1.1.0.0)butane (IV)	70°32′	144°14′	−11.969	−4.344	7.626

Table 2. HO and LV orbitals of bicyclobutane and its homologues

HO orbital

Compound	$C_{1Z}+C_{3Z}$	$C_{1X}-C_{3X}$[a]	$C_{2Z}-C_{4Z}$
Tricyclo(3.1.0.0)hexane (II)	0.4862	0.3474	−0.2560
Bicyclo(1.1.0)butane (I)	0.4828	0.3843	−0.2018
Tricyclo(2.1.0.0)pentane (III)	0.4537	0.2868	−0.4225

LV orbital

Compound	$C_{1Z}-C_{3Z}$	$C_{1X}+C_{3X}$	$C_{2X}+C_{4X}$
Tricyclo(3.1.0.0)hexane (II)	0.4851	0.4958	−0.5275
Bicyclo(1.1.0)butane (I)	0.5785	0.4750	−0.5089
Tricyclo(2.1.0.0)pentane (III)	0.5822	0.4957	−0.5138

a) C_1-C_3 line denotes the x axis. See Fig. 1.

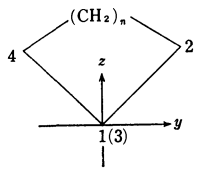

$n=2,1,0$

less than that for cyclopropane (8.709 eV). It is well known that cyclopropane has its UV absorption spectra near the wavelength of 190 mμ.[23] Therefore, the absorption spectra of present compounds exist in rather a longer wavelength region than those of cyclopropane, and their conjugative abilities may be large. The conjugative property will be discussed below.

Nature of the Central Bond of Bicyclo(1.1.0)-butane and Its Homologues. In this section the double-bond character of the central bonds (C_1–C_3 bonds in Fig. 1) of bicyclobutane and its homologues will be elucidated.

The AO coefficients of the HO and LV orbitals of the bicyclobutane with the most stable configuration and its homologues are cited in Table 2. They mainly consist of the $2p_Z$ and $2p_X$ of C_1, C_2, C_3 and C_4; other, very small AO coefficients are neglected.

These results indicated that a π-type interaction takes place between two p_Z AO's of the carbon atoms in the central bonds of these compounds. Further, the HO and LV orbitals are respectively, the bonding and the antibonding orbital with respect to the p_Z–p_Z bond. The natures of the two orbitals of these compounds resemble those of the π-orbitals of mono-olefins.

Wiberg *et al.*[10] have reported that the reaction of bicyclobutane-1-methanol with a dilute acid occurs almost instantaneously, accompanying the cleavage of the central bond, and that 1-hydroxycyclobutanemethanol is obtained. It is known that this addition reaction follows the Markownikoff rule.[10]

In addition, peculiar properties have been

23) H. Weitkamp, U. Hasserodt and F. Korte, *Chem. Ber.*, **95**, 2280 (1962).

observed in bicyclobutane, such as that the absorption spectra of methyl-3-methylbicyclobutane-1-carboxylate appears at 210 mμ (ε: 7000), just as in the corresponding α,β-unsaturated ester,[10] and that the addition of iodine to bicyclobutane proceeds *via* an intermediate such as a benzene-iodine complex.[10] Further, the derivatives of tricyclohexane (II) and tricyclopentane (III) with conjugative substituents on carbon atoms, C_1 and C_3, show their UV absorption spectra in rather a longer-wavelength region.[8,24]

Our present conclusion, indicating the existence of the π-type conjugation in the central bond, is compatible with the suggestion of Pomerantz *et al.*,[14] and it explains fairly well the above peculiar properties.

s-Nature of the C-H Bonds of Bicyclo(1.1.0)butane and Its Homologues. The s-nature of the bonds of bicyclobutane and its homologues has been studied in terms of Y_{CH}, which was difined in a previous paper[18] as representing the contribution of the 2s AO of the carbon atom to the C-H bond:

$$Y_{CH} = \frac{N_{C(S)H(S)}}{M_{CH}} \times 100\%$$

where the notation C(S) implies the 2s AO of a carbon atom.

The relation between the values of Y_{CH} and the dihedral angle, θ, of bicyclobutane is shown in Fig. 4.

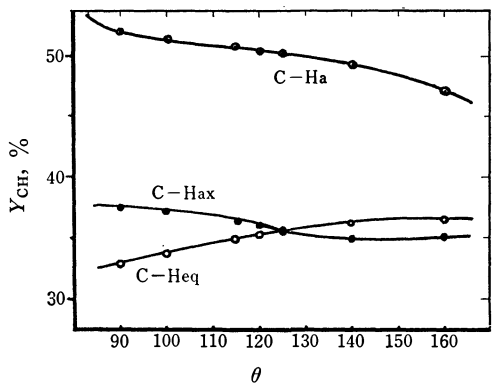

Fig. 4. Values of Y_{CH} of various configurations of bicyclobutane.

The value of Y_{CH_a} decreases with the increase in θ. However, the value of Y_{CH_a} is much larger than those of $Y_{CH_{axial}}$ and $Y_{CH_{equatorial}}$. Hence, the s-nature of the carbon-hybridized orbital of the C-H_a bond may be expected to be large. The value of $Y_{CH_{axial}}$ decreases with the increase in $Y_{CH_{equatorial}}$ the two curves cross at the value of $\theta = 125°$.

The observed ^{13}C-H coupling constants,[8,10,25,26] the fractional s-character of the carbon hybrid atomic orbital for the C-H bond estimated by experiments or from the values calculated by Weltner[11] and Maksić *et al.*,[13] the values of Y_{CH}, and the squares of the bond order, $(P_{CsHs})^2$, are given in Table 3, where P_{CsHs} in dicates the bond order between the 2s orbital of the carbon atom and the ls orbital of the hydrogen atom in a C-H bond.

It may be seen in Table 3 that these theoretical indices run approximately parallel to the magnitude of the s-nature estimated and the ^{13}C-H coupling constants. However, for C-H axial and C-H equatorial bonds in bicyclobutane, the calculated results contradict the ^{13}C-H coupling constants.

However, it may be noted that, as has been stated above, the s-natures of these two C-H bonds very sensitively with the change in the dihedral angle and the two Y_{CH} curves cross at 125°, which is very close to the dihedral angle, 120°, adopted in the present calculations. If, for the dihedral angle, the value of 126° reported by Haller and Srinivasan is adopted, our results agree with the experimental results. This point should be checked further both experimentally and theoretically with regard to the reliability of the extended Hückel approximation.

As to tricyclobutane (IV), the value of Y_{CH} for its four equivalent C-H bonds amounts to 50%. This indicates the fractional s-character of the carbon hybrid AO in this compound is very large and that the C-H bond is markedly polar.

Electronic Structures of Prismane (V). Two structures of prismane were studied; one is a rather hypothetical configuration (V'), which consists of two interacting cyclopropenyl radicals, as is shown in Fig. 5. The other is a more real configuration

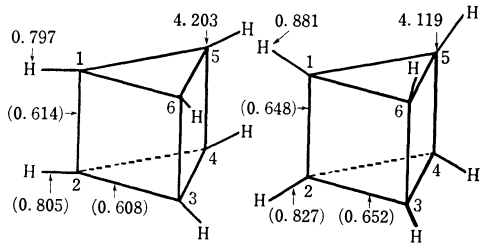

Fig. 5. Atomic populations and atomic bond populations of two configurations of prismane.
( ): atomic bond population

(V), where the C-H bonds of the cyclopropenyl radicals are bent to the outside. In Table 4 the total electronic energies and the energies of the highest occupied and lowest vacant orbitals of the two configurations of prismane (C_6H_6) are given,

24) A. Small, *J. Am. Chem. Soc.*, **86**, 2091 (1964).
25) D. Seebach, *Angew. Chem.* **77**, 119 (1965); C. Juan and H. S. Gutowsky, *J. Chem. Phys.*, **37**, 2198 (1962).
26) S. Masamune, *Tetrahedron Letters*, **1965**, 945.

TABLE 3. BOND NATURE OF C-H BONDS OF BICYCLOBUTANE AND ITS HOMOLOGUES

Compnund		J^{13}_{C-H} c/s	S-% estimated obs.	Present calcd. Y_{CH} %	Present calcd. P^2
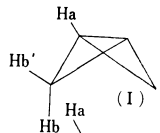 (I)	Ha	202[10]	40.4 38.61[13]	46.073	0.1104
	Hb'	170[10]	34	35.001	0.0637
	Hb	152[10]	30.4	35.996	0.0685
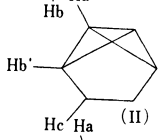 (II)	Ha	—	—	41.445	0.0907
	Hb'	171[26]*a	34.4	45.017	0.1059
	Hc	—	—	30.757	0.0504
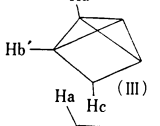 (III)	Ha	—	—	46.278	0.1096
	Hb'	190[25]*a	38	45.695	0.1074
	Hc	—	—	32.599	0.0566
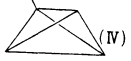 (IV)	Ha	—	32[11] 45.45[13]	50.127	0.1263

*a Observed values of their derivatives are listed.

TABLE 4. TOTAL ELECTRONIC ENERGIES, HO AND LV ORBITAL ENERGIES OF TWO CONFIGURATIONS OF PRISMANE AND BENZENE

		Benzene	Prismane V′ γ: 90°	Prismane V γ: 149°
Table electronic energy	eV	−527.825	−513.977	−521.209
HO energy	eV	−12.820	−11.514	−11.368
LV energy	eV	−8.361	−6.167	−1.167

TABLE 5. HO AND LV ORBITALS OF SOME CONFIGURATIONS OF SPIROPENTANE AND OF 1,1-DIMETHYL CYCLOPROPANE

HO orbitals

1,1-Dimethylcyclopropane		$0.5925C_{1X} + 0.4210(C_{2Y}-C_{3Y}) - 0.2035(C_{5X}+C_{4X})$
Spiropentane	$\eta=90°$	$\begin{cases} 0.6058C_{1X} + 0.4386(C_{2Y}-C_{3Y}) \\ 0.6058C_{1Z} + 0.4386(C_{5Y}-C_{4Y}) \end{cases}$
	$\eta=45°$	$-\{0.2772C_{1X}+0.3087(C_{2Y}-C_{3Y})\} + \{0.6691C_{1Z}+0.3087(C_{5Y}-C_{4Y})\}$
	$\eta=0°$	$1.0118C_{1Z}$

LV orbitals

1,1-Dimethylcyclopropane		$0.8101C_{1X} - 0.6673(C_{2Y}-C_{3Y}) - 0.3928(C_{2X}+C_{3X})$
Spiropentane	$\eta=90°$	$\begin{cases} 0.8043C_{1X} - 0.6550(C_{2Y}-C_{3Y}) - 0.4202(C_{2X}+C_{2X}) \\ 0.8043C_{1Z} - 0.6550(C_{5Y}-C_{4Y}) - 0.4202(C_{5Z}+C_{4Z}) \end{cases}$
	$\eta=45°$	$-\{0.2723C_{1X}-0.4800(C_{2}-C_{3Y})\} + \{0.6574C_{1Z}-0.4800(C_{5Y}-C_{4Y})\}$
	$\eta=0°$	$0.5761\{(C_{2Y}-C_{3Y})-(C_{5Y}-C_{4Y})\}$

together with those of benzene for comparison. The present calculations show that these two configurations of prismane are less stable than benzene and that the V configuration is more stable than the V′. Therefore, it may be concluded that the value of the C–C–H angle, γ, plays an important role in determining the stability of prismane. The highest occupied orbitals for both configurations are higher than that for benzene; the energy levels of the lowest vacant orbital for both configurations are higher by about 2 eV than that for benzene, but are markedly lower than those for ordinary saturated hydrocarbons (*e. g.*, *n*-butane, 2.492 eV) and for cyclopropane (−4.244 eV).

The atomic population and the atomic bond population of both configurations of prismane are given in Fig. 5.*4

Photodecomposition of Prismane (V). Breslow *et al.*[27] proposed a reaction mechanism for the photodecomposition of prismane, where bicyclo(2.2.0)-hexa-1,5-diene is produced at first with cleavages of the C_1–C_5 and C_2–C_4 bonds, not of the C_1–C_2 bond, followed by isomerization to benzene. We assume this reaction in the following mechanism: the irradiation of light first causes the excitation of one electron from the HO orbital to the LV orbital, while in the next stage the cleavage of the weakest bond takes place. For this singlyexcited state, the values of $M_{C_1C_2}$ and $M_{C_1C_5}$ are obtained as 0.814 and 0.419 respectively. This implies that the cleavage of C_1–C_5 bond may occur more easily. These calculated results support the reaction mechanism proposed by Breslow *et al.*

Electronic Structures of Spiro(2.2)pentane (VI). As to spiro(2.2)pentane (VI), the dihedral angle, η, is experimentally known to be 90°. In the present treatment, the electronic structures for three configurations, with η=90, 45 and 0°, were investigated in order to reveal the correlation between the dihedral angle and the stability of spiro pentane. They were compared with the electronic structure of 1,1-dimethylcyclopropane, which is considered to be derived from spiropentane by opening one cyclopropane ring.

Spiropentane is the most stable at η=90° (−488.38 eV) (this is in accordance with the experimental result) and gradually becomes more unstable as η decreases from 90 (−486.90 eV) to 0° (−484.09 eV). The HO orbital energy for spiropentane with the configuration of η=90° (−12.551 eV) is lower than that for 1,1-dimethylcyclopropane (−12.325 eV), but higher than those for methylcyclopropane (−12.612 eV) and for cyclopropane (−13.052 eV).

The AO coefficients of the HO and LV orbitals for spiropentane and dimethylcyclopropane are given in Table 5. In spiropentane with η=90° both orbitals are doubly degenerated, and each orbital consists of the carbon 2p orbitals of a cyclopropane ring. The LV and HO orbitals at η=45° are nearly equal to a linear combination of the corresponding doubly degenerated orbitals at η=90°. At the value of η=0°, the HO orbital is exclusively made of the $2p_Z$ AO of the carbon atom C_1, just as is a lone-pair orbital, further, the LV orbital is constructed only from the $2p_Y$AO's of the four carbon atoms, C_4, C_5, C_2 and C_3. Therefore, spiropentane of this configuration has extremely peculiar electron distribution.

An the basis of a comparison of the atomic bond populations, the C_2–C_3 bond for spiropentane ($M_{C_2C_3}$=0.592) may be expected to be weaker than those for 1,1-dimethylcyclopropane (M_{C_2C},= 0.611) and cyclopropane (M_{CC}=0.628). In fact, in the hydrogenation which accompanies the ring-opening reaction, the heat of formation, ΔH, for spiropentane is −42.0 kcal/mol, which seems to be required for the cleavage of the C_2–C_3 bond; on the other hand, the ΔH for cyclopropane is −37.6 kcal/mol.[28]

These experimental results indicate that the cleavage of the C_2–C_3 bond occurs more easily in spiropentane than in cyclopropane; this is in accordance with our calculated results.

The calculations were carried out on the HITAC 5020 Computer at the University of Tokyo.

*4 As prismane of the V′ configuration is transformed into the V configuration, all the atom bond populations increase and the value of M_{cc} for a three-member ring becomes larger than that of cyclopropane, 0.629. This fact may also indicate that the bending of C-H bonds is closely correlated with the stabilization of prismane.

27) R. Breslow, P. Gal, H. W. Changand and L. J. Altman, *J. Am. Chem. Soc.*, **87**, 5139 (1965).

28) J. Newham, *Chem. Revs.*, **63**, 123 (1963).

BULLETIN OF THE CHEMICAL SOCIETY OF JAPAN VOL. 41 2343—2349 (1968)

Photochemistry of Acetanilide. I. Quantum Yields of the Rearrangement and Benzene Photosensitized Reaction

Haruo SHIZUKA[1] and Ikuzo TANAKA

Laboratory of Physical Chemistry, Tokyo Institute of Technology, Ookayama, Meguro-ku, Tokyo

(Received April 12, 1968)

The photochemical rearrangement of acetanilide under 2537 Å irradiation has been studied by spectrophotometry. The quantum yield of the rearrangement in cyclohexane solution was independent of the irradiation time, concentration of acetanilide, presence of oxygen and light intensity. It was found that electronic energy transfer from the electronically excited benzene to acetanilide occurred in the mixed solution, and the transfer mechanism was explained by singlet-singlet nonradiative energy transfer. It was observed that the energy transfer rate constant was about 22 times greater than that predicted by diffusion theory (the transfer rate constant, $k_3=1.45\times10^{11}\ l\cdot mol^{-1}\cdot sec^{-1}$). From these studies, it is proposed that the rearrangement of acetanilide is an introamolecular reaction and does not occur from the triplet state but from the lowest singlet excited state.

It is known that organic carbonyl compounds give rise photochemically to many interesting reactions; abstraction, rearrangement, addition, dimerization and decomposition.

The photochemical reactions of phenyl esters in solution yield products of rearrangement similar to those of the Fries reaction. Hence, this rearrangment is termed the photo-Fries-rearrangement.

Anderson and Reese[2] reproted that phenyl esters rearrange to yield *ortho*-hydroxyl aryl ketones as well as *para* isomers by irradiation with UV light, as indicated by Eq. (1).

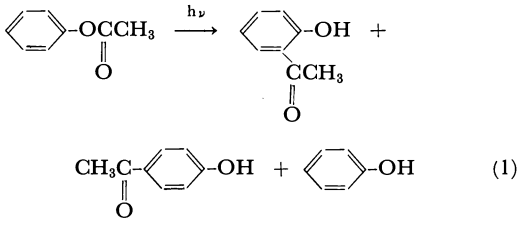

(1)

Kobsa[3] and Finnegan *et al.*[4] reported similar findings. Elad and coworkers reported the photochemical reaction of anilide, another carbonyl derivative.[5]

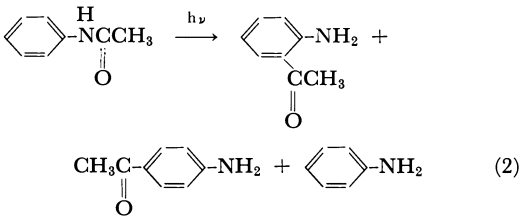

(2)

Kobsa suggested a mechanism for the photo-Fries-reaction involving homolysis of the phenyl ester into a free-radical pair, held together in a solvent cage, with subsequent rearrangement.[3] However, little mechanistic work on the photo-Fries-rearrangement has been reported.

On the other hand, a molecular-orbital calculation has been carried out to determine the π-electronic structure of acetanilide.[6] The subject of electronic energy transfer between unlike molecules in solution through a resonance interaction has received considerable interest.[7-15] The study of electronic energy transfer is very useful for investigating the role of excited states in photochemical

1) Present address, Department of Chemistry, Faculty of Engineering, Gunma University, Tenjincho, Kiryu, Gunma.

2) J. C. Anderson and C. B. Reese, a) *Proc. Chem. Soc. (London)*, **1960**, 217; b) *J. Chem. Soc.*, **1963**, 1781.

3) H. Kobsa, *J. Org. Chem.*, **27**, 2293 (1962).

4) R. A. Finnegan and A. W. Hagen, *Tetrahedron Letters*, **1963**, 365.

5) a) D. Elad, *ibid.*, **1963**, 873; b) D. Elad, D. V. Rao and V. I. Stenberg, *J. Org. Chem.*, **30**, 3252 (1965).

6) H. Baba and S. Suzuki, *J. Chem. Phys.*, **32**, 1706 (1960).

7) Th. Förster, *Ann. Physik*, **2**, 55 (1948).

8) Th. Förster, *Discussions Faraday Soc.*, **27**, 7 (1959).

9) Th. Förster, a) *Z. Elektrochem.*, **53**, 93 (1949); b) *Z. Naturforschung*, **4**, 321 (1949); c) *Trans. Faraday Soc.*, **51**, 774 (1955).

10) W. F. Watson and R. Livingston, *J. Chem. Phys.*, **18**, 802 (1950).

11) E. J. Bowen and B. Brocklehurst, *Trans. Faraday Soc.*, **49**, 1131 (1953).

12) E. J. Bowen and R. Livingston, *J. Am. Chem. Soc.*, **76**, 6300 (1954).

13) W. R. Ware, *ibid.*, **83**, 4374 (1961).

14) J. B. Birks and K. N. Kuchela, *Proc. Phys. Soc. (London)*, **77**, 1083 (1961).

15) D. W. Ellis and B. S. Solomon, *J. Chem. Phys.*, **46**, 3497 (1967).

reactions. It is very interesting to elucidate the correlation between the photochemical reaction and the electronically excited state for acetanilide through photosensitization by benzene in the liquid phase. The photosensitizations by benzene have been studied in the gas phase.[16-19]

This paper reports measurements of quantum yields under various conditions and the mechanism of electronic energy transfer from the excited benzene to acetanilide, in order to make clear the mechanism of the photo-Fries-rearrangement.

Experimental

Materials. Acetanilide was a Tokyo Kasei Co. G. R. grade product and was purified by repeated recrystallization from water. *o*-Amino acetophenone, *p*-amino acetophenone and piperylene were Tokyo Kasei Co. G. R. grade products. Benzene was a Kokusan Chemical Works Ltd. G. R. grade product and was purified by vapor-phase chromatography. Cyclohexane was a Nichiri Co. reagent grade product and was purified by passage through silicagel and by distillation.

Light Source. A low pressure mercury resonance lamp containing neon was used as the 2537 Å radiation source with a Vycor glass filter.

Light Intensity Measurement. Actinometry was carried out in a reaction cell (quartz) using a ferric oxalate actinometer solution. The light intensity at 2537 Å was determined by the difference in light intensities with and without the benzene solution filter which cut off the wavelengths below 2700 Å. In the case of benzene photosensitization, a reaction cell of 1 cm length was used and the light intensity (I_0) at 2537 Å was 9.7×10^{14} photons·sec^{-1}·cm^{-2}.

Analysis. The amounts of *o*-amino acetophenone and *p*-amino acetophenone produced by the photochemical reaction were determined spectrophotometrically. Ultraviolet absorption spectra at room temperature were taken with Hitachi 139 and Hitachi EPS 2 spectrophotometers.

Results and Discussion

Reaction Products. The spectrum of the solution of acetanilide changed markedly upon irradiation with 2537 Å light as shown in Fig. 1. Absorption Band II (240 mμ) of acetanilide decreased and new bands with maxima at 225, 287 and 355 mμ appeared as the irradiation time increased, with two isosbestic points at 233 and 255 mμ. The reaction products corresponded to *o*-amino acetophenone (absorption peaks 225 and 355 mμ) and *p*-amino acetophenone (absorption peaks 224 and 287 mμ) as shown in Table 1.

Therefore, quantum yields of *o*-amino acetophenone, *p*-amino acetophenone and the disappearance of acetanilide were measured spectrophotometrically. The samll amount of aniline which was produced from the primary process of the photochemical reaction for acetanilide[5] could not be directly determined by means of the

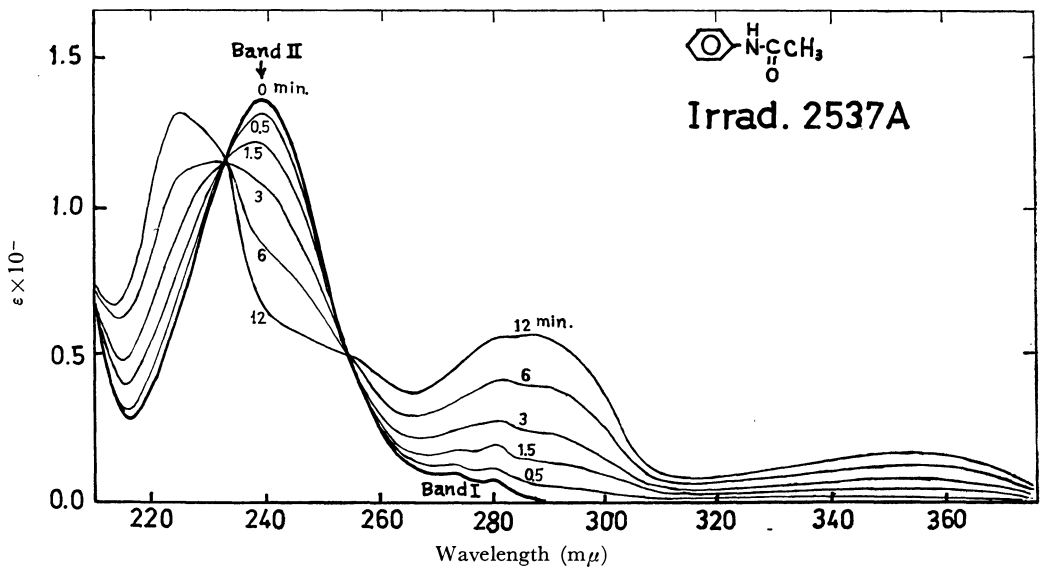

Fig. 1. Spectral change of acetanilide in cyclohexane solution with lapse of time at room temperature by irradiation with 2537 Å light. Numbers refer to time at measurement in minutes.

16) H. Ishikawa and W. A. Noyes, *ibid.*, **37**, 583 (1962).
17) R. B. Cundall, F. J. Fletcher and D. G. Milne, a) *Trans. Faraday Soc.*, **60**, 1146 (1964); b) *J. Chem. Phys.*, **39**, 3536 (1963).
18) S. Sato, K. Kikuchi and M. Tanaka, *J. Chem. Phys.*, **39**, 239 (1963).
19) a) E. K. C. Lee and N. W. Lee, *J. Phys. Chem.*, **71**, 1167 (1967); b) E. K. C. Lee, *ibid.*, **71**, 2804 (1967).

TABLE 1. MOLAR DECADIC EXTINCTION COEFFICIENTS[a]

Substance	λ mμ	$\varepsilon \times 10^{-4}$
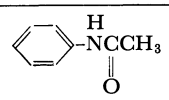	240 274	1.36 0.093
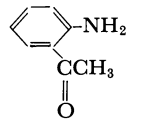	225 355	2.84 0.53
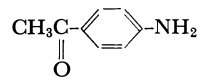	224 287	1.12 2.00

a) In cyclohexane solution

spectrophotometric method, because of the overlapping acetanilide, *o*-amino acetophenone and *p*-amino acetophenone spectra.

Effect of Irradiation Time, Concentration, Oxygen, and Light Intensity on Quantum Yields. Quantum yields were obtained under various conditions (Fig. 2). The quantum yields of the rearrangement in cyclohexane did not change with variation in irradiation time, concentration of acetanilide and light intensity (Fig. 2 a, b and d). The effect of oxygen dissolved in the solution on the quantum yield was probably absent because there was no difference in quantum yields between an aerated solution and one deaerated by flushing with nitrogen at room temperature (Fig. 2c) The quantum yields of *o*-amino acetophenone and *p*-amino acetophenone in cyclohexane solution at 20°C were 0.07 and 0.06, respectively. The quantum yield of the disappearance of acetanilide was about 0.15. The addition of piperylene as a triplet quencher (E_T ~2.48 eV)[20] did not affect the quantum yield of this isomerization in a concentration range 10^{-4} to 10^{-2} mol/*l* (Fig. 2e).

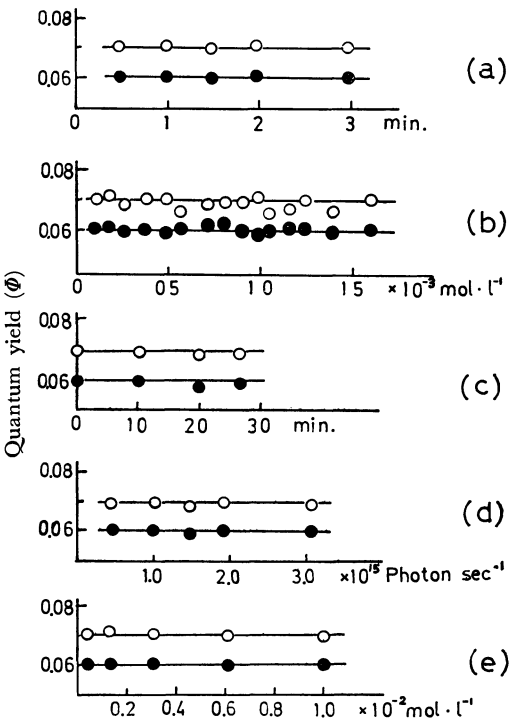

Fig. 2. Dependence of quantum yield in cyclohexane solution.
(a) On irradiation time at 20°C with initial concentration of 9.48×10^{-4} mol/*l*
(b) On concentration at 20°C
(c) On deaeration by flushing with nitrogen at room temperature
(d) On light intensity at 20°C
(e) On addition of piperylene
○···Φ of *o*-amino acetophenone
●···Φ of *p*-amino acetophenone

From these results, it is assumed that acetanilide does not react from the triplet state $T_1(\pi-\pi^*)$. The photochemical rearrangement of acetanilide may be an intramolecular reaction in dilute solutions ($<\sim 10^{-3}$ mol/*l*) as suggested for phenyl acetate by Anderson and Reese.[2] However, it has been reported that an intermolecular reaction occurred in the rearrangement of acetanilide.[5a] It is though that the intermolecular reaction occurs at high concentrations.

Energy Transfer from the Electronically Excited Benzene to Acetanilide. The photosensitization has been studied quantitatively in a cyclohexane solution at room temperature through a determination of the relative rate R/R_0 of product formation, varying the concentrations of benzene and acetanilide, where R and R_0 are the reaction rates with and without benzene in acetanilide solution, respectively. The reaction rates of the

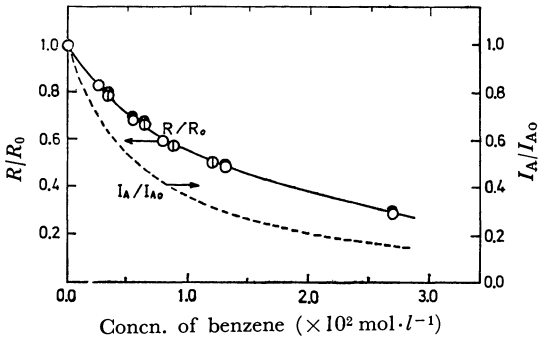

Fig. 3. Plot of R/R_0 against the concentration of benzene. Acetanilide concentration is 5.22×10^{-5} mol/*l* in cyclohexane. Dotted line denotes plot of I_A/I_{A0} against the concentration of benzene.
○···*o*-amino acetophenone } open air
●···*p*-amino acetophenone }
①···*o*-amino acetophenone } N_2 saturated
◑···*p*-amino acetophenone }

20) a) P. E. Eaton, W. S. Hurt, *J. Am. Chem. Soc.*, **88**, 5038 (1966); b) E. Y. Y. Lam, D. Valentine and G. S. Hammond, *ibid.*, **89**, 3482 (1967).

product formations (*o*-amino acetophenone and *p*-amino acetophenone) were measured spectrophotometrically. Figure 3 shows the dependences of the relative rates R/R_0 on the concentration of benzene in aerated or deaerated cyclohexane solutions. An effect of dissolved oxygen ($\sim 10^{-3}$ mol/*l*) was not observed within the experimental error as shown in Fig. 3. An increase in the rate of rearrangement could not be detected even in a carefully degassed solution. This could be explained by the fact that the maximum rate of the quenching reaction by dissolved oxygen of 10^{-3} mol/*l* was about one tenth of the overall deactivation rate of the excited singlet benzene ($^1B_{2u}$), considering it to be diffusion controlled, as is discussed later. Figure 4 shows the dependence of the relative rate R/R_0 on the concentration of acetanilide. The

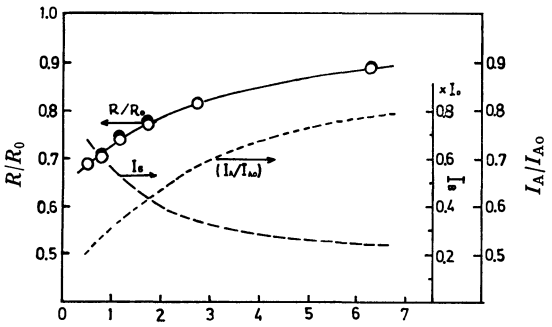

Fig. 4. Plot of R/R_0 against the concentration of acetanilide. Benzene concentration is 5.4×10^{-3} mol/*l* in cyclohexane. Dotted line denotes plot of I_A/I_{A0} and broken line denotes plot of I_B against the concentration of benzene, respectively.
○···*o*-amino acetophenone} open air
●···*p*-amino acetophenone}

energy transfer efficiency γ from the excited benzene to acetanilide was calculated from the following equation;

$$\gamma = \frac{I_\Sigma - I_A}{I_B} \tag{3}$$

where

$$I_\Sigma = \frac{R}{R_0} I_{A0} \tag{4}$$

and I_{A0} is the light intensity absorbed by acetanilide in the absence of benzene, which was determined experimentally, I_A and I_B are the light intensities absorbed by acetanilide and by benzene in the mixed solution, respectively, which have been calculated using Beer's law. Figure 5(a) or 6(a) shows the transfer efficiency γ as a function of the concentration of benzene (donor) or of acetanilide (acceptor), respectively. It seems that the excited state of benzene for this energy transfer should be the lowest singlet excited state ($^1B_{2u}$) since the effect of dissolved oxygen on the photo-

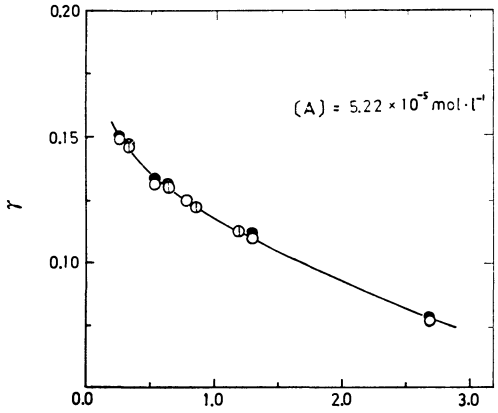

Fig. 5(a). The dependence of the transfer efficiency γ on the concentration of benzene.
○···*o*-amino acetophenone} open air
●···*p*-amino acetophenone}
◑···*o*-amino acetophenone} N_2 saturated
◐···*p*-amino acetophenone}

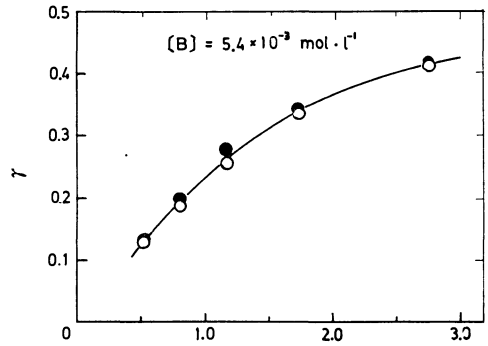

Fig. 6(a). The dependence of the transfer efficiency γ on the concentration of acetanilide.
○···*o*-amino acetophenone} open air
●···*p*-amino acetophenone}

sensitization was absent as shown in Fig. 5(a). If the energy transfer had occurred from the triplet state of benzene ($^3B_{1u}$), the reaction rate of an aerated solution would be small in comparison with that in a deaerated solution.

The characteristics of the lower excited state of benzene and acetanilide are summarized in Table 2. If energy considerations are kept in mind, the following reactions may occur when benzene molecules absorb radiation at 2537 Å in the mixed solution;

$$\begin{array}{ccccc} B^* & \xrightarrow{k_3} & A^* & \xrightarrow{\phi} & \text{Reaction product} \\ & & (+A) & & \\ & & (+B) & & \\ h\nu \uparrow & \downarrow k_1 & \downarrow k_2 & & \\ B & & & & \end{array} \qquad k_1 = k_B^c + k_B^s + k_B^f$$

$$B \xrightarrow{h\nu} B^* \tag{5}$$

TABLE 2. ENERGIES, OSCILLATOR STRENGTHS AND WAVE FUNCTIONS FOR LOWER EXCITED STATES OF BENZENE AND ACETANILIDE

	Symmetry	Observed excitation energy, eV	Observed oscillator strength	Wave function	Band assignment
Benzene[a)]	$^1B_{2u}(D_{6h})$	4.88	0.0014	$1/2(V_{24}-V_{35})$	I
Acetanilide[b)]	$^1B_2(C_{2v})$	4.53_2	0.01	$0.481V_{24}$ $-0.875V_{35}$	I
	$^1A_1(C_{2v})$	5.18_3	0.28	V_{34}	II

a) See Ref. 21.
b) See Ref. 6.

$$B^* \xrightarrow{k_{B^c}} B_T \quad (6)$$

$$B^* \xrightarrow{k_{B^a}} B \quad (7)$$

$$B^* \xrightarrow{k_{B^f}} B + h\nu' \quad (8)$$

$$B^* + B \xrightarrow{k_2} 2B \quad (9)$$

$$B^* + A \xrightarrow{k_3} B + A^* \quad (10)$$

where B and A are the ground states of benzene and acetanilide, respectively, B* is the excited singlet state of benzene ($^1B_{2u}$), B_T the lowest triplet state of benzene ($^3B_{1u}$), A* the lowest singlet excited state of acetanilide ($^1B_2$) and Φ the quantum yield of the product. Then, using a steady-state treatment, the following equations are obtained.

$$[B^*] = \frac{I_B}{k_1 + k_2[B] + k_3[A]} \quad (11)$$

$$\gamma = \frac{k_3[B^*][A]}{I_B} = \frac{k_3[A]}{k_1 + k_2[B] + k_3[A]} \quad (12)$$

The transfer efficiency γ decreased as the concentration of benzene increased (Fig. 5(a) and Eq. (12)), due to self-quenching (Eq. (9)). On the other hand, γ increased when the concentration of the acceptor (acetanilide) increased, as shown in Fig. 6(a) and Eq. (12).

Equation (13) is derived from Eq. (12),

$$\frac{1}{\gamma} = \frac{k_1 + k_2[B]}{k_3[A]} + 1 \quad (13)$$

Figure 5(b) shows that the results corresponding to Eq. (13) are well represented by a linear plot of $1/\gamma$ *vs.* [B], where $[A]=5.22\times10^{-5}$ mol/*l*. From the slope and intercept of the plot shown in Fig. 5(b), k_2 and k_3 can be obtained.

$$\frac{k_2}{k_3[A]} = 2.3\times10^2\ l/\text{mol}$$

$$\frac{k_1}{k_3[A]} + 1 = 6.1$$

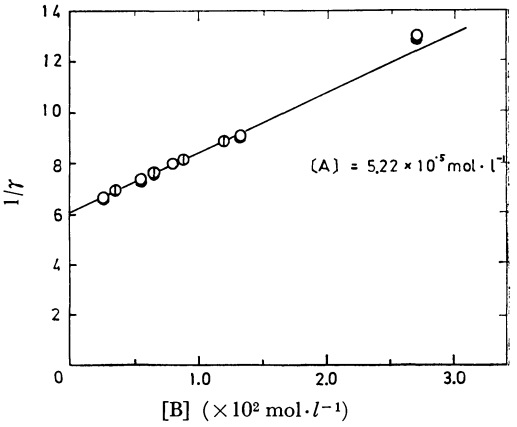

Fig. 5(b). Plot of $1/\gamma$ against the concentration of benzene.

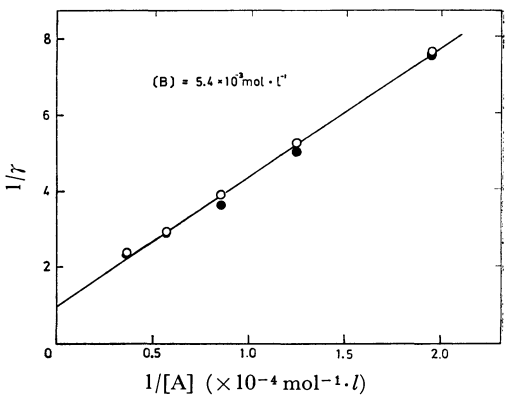

Fig. 6(b). Plot of $1/\gamma$ against the reciprocal of acetanilide concentration.

$$k_2 = 4.51 \times 10\ \ k_1\ l/\text{mol} \quad (14)$$

$$k_3 = 3.76 \times 10^3\ k_1\ l/\text{mol} \quad (15)$$

Figure 6(b) shows that the results corresponding to Eq. (13) give also good linearity of $1/\gamma$ *vs.* 1/[A], where $[B]=5.4\times10^{-3}$ mol/*l*. The slope of the plot in Fig. 6(b)

$$\frac{k_1+k_2[B]}{k_3} = 3.35 \times 10^{-4}\ \text{mol}/l \quad (16)$$

21) H. B. Klevens and J. R. Platt, Tech. Rept., Laboratory of Molecular Structure and Spectra, University of Chicago, Part 1, p. 145 (1953—1954).

From Eqs. (14) and (15), Eq. (17) is derived

$$\frac{k_1+k_2[\mathrm{B}]}{k_3} = \frac{k_1+4.51\times 10k_1\times 5.4\times 10^{-3}}{3.76\times 10^3\times k_1}$$

$$= 3.32\times 10^{-4}\ \mathrm{mol}/l \qquad (17)$$

These two values of the slope which are derived in different ways are in good agreement.

From the work of Ivanova *et al.*,[22] the lifetime of the benzene singlet excited state ($^1B_{2u}$) in the absence of acetanilide is given by

$$\tau_B = \frac{1}{k_1} = 2.6\times 10^{-8}\ \mathrm{sec}$$

$$k_1 = 3.85\times 10^7\ \mathrm{sec}^{-1} \qquad (18)$$

Therefore, the self-quenching rate constant k_2 and the energy transfer rate constant k_3 are calculated from Eqs. (14) and (15), respectively.

$$k_2 = 1.74\times 10^9\ l\cdot\mathrm{mol}^{-1}\,\mathrm{sec}^{-1} \qquad (14')$$

$$k_3 = 1.45\times 10^{11}\ l\cdot\mathrm{mol}^{-1}\,\mathrm{sec}^{-1} \qquad (15')$$

It is interesting to note that the value of k_3 in this experiment is close to the 1.4—$2.5\times 10^{11}\ l\cdot\mathrm{mol}^{-1}\cdot\mathrm{sec}^{-1}$ obtained by Bowen and Livingston[12] for the mixture of anthracene derivatives and perylene (or rubrene) at room temperature in various solvents.

The rate constant of a diffusion-controlled bimolecular reaction is represented approximately by the modified Debye equation.[23,24]

$$k_D = \frac{8RT}{3000\eta} \qquad (19)$$

where k_D is in units of $l\mathrm{mol}^{-1}\mathrm{sec}^{-1}$ when η, the viscosity of the solvent, is in units of poise.

The value of k_D corresponding to cyclohexane at 20°C is $6.6\times 10^9\ l\cdot\mathrm{mol}^{-1}\cdot\mathrm{sec}^{-1}$.[25] The empirical value of the rate constant k_2 corresponding to the self-quenching of benzene might not exceed the value of k_D. In contrast to this, the energy transfer rate constant k_3 is about 22 times greater than the value of k_D.

The possibility that complex formation between benzene and acetanilide is responsible for this energy transfer was shown to be unlikely by the fact that the spectral intensities and the positions of the mixed solution were identical with those of the separate solutions as shown in Fig. 7.

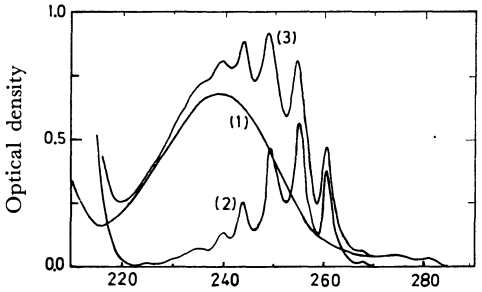

Fig. 7. Absorption curves of CH soln's of acetanilide, benzene and their mixture.
(1) Acetanilide $5.0\times 10^{-5}\ \mathrm{mol}\cdot l^{-1}$
(2) Benzene $2.6\times 10^{-3}\ \mathrm{mol}\cdot l^{-1}$
(3) Acetanilide $5.0\times 10^{-5}\ \mathrm{mol}\cdot l^{-1}$, benzene $2.6\times 10^{-3}\ \mathrm{mol}\cdot l^{-1}$

The critical transfer distance R_0 is given by[7,8]

$$R_0^6 = \frac{9000\ln 10\ \chi^2\varphi_s^0}{128\pi^6 n^4 N}\int_0^\infty f_s(\bar{\nu})\varepsilon_A(\bar{\nu})\frac{d\bar{\nu}}{\bar{\nu}^4} \qquad (20)$$

where $\bar{\nu}$ is the wave number, $\varepsilon_A(\bar{\nu})$ the molar extinction coefficient of the acceptor, $f_s(\bar{\nu})$ the spectral distribution of fluorescence of the sensitizer (measured in quanta and normalized to unity on a wave number scale), N Avogadro's number,

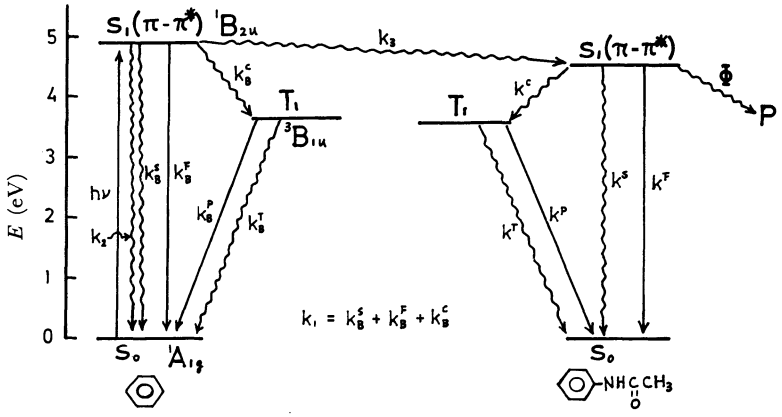

Fig. 8. Energy state diagram for energy transfer between benzene and acetanilide.

22) T. V. Ivanova, P. I. Kudryashov and B. Ya. Sveshnikov, *Doklad. Akad. Nauk. SSSR*, **138**, 572 (1961).
23) P. Debye, *Trans. Electrochem. Soc.*, **82**, 265 (1942).
24) E. J. Bowen, *Trans. Faraday Soc.*, **50**, 97 (1954).
25) J. G. Calvert and J. N. Pitts, Jr., "Photochemistry," John Wiley and Sons, New York (1966), p. 627.

χ^2 an orientation factor equal to 2/3, n the index of refraction of the solvent and φ_s^0 the fluorescence efficiency of the sensitizer for [A]=0. The integral was evaluated graphically (6.72×10^{-14}). φ_s^0 was obtained from the work of Ivanova *et al.*[22] (0.1). Then,

$$R_0 \approx 26\ \text{Å}$$

Though the $^1B_{2u}\leftarrow{}^1A_{1g}$ transition in benzene is a symmetry forbidden transition, the Förster equation (20) might be applied to this energy transfer because the overlap integral (6.72×10^{-14}) is not so small.

Considering the magnitude of the energy transfer rate constant k_3, it is thought that the transfer from the electronically excited benzene to acetanilide is singlet-singlet nonradiative energy transfer; a resonance transfer for a weak interaction.

Figure 8 shows the energy level diagram for the energy transfer between benzene and acetanilide

$$B^*(^1B_{2u}) + A(^1A_1) \xrightarrow{k_3} B(^1A_{1g}) + A^*(^1B_2) \quad (21)$$

In conclusion, it is said that acetanilide does not react from the triplet state, but *via* the lowest singlet excited state formed by the benzene-photosensitized reaction.

The authors are greatly indebted to Associate Professor Yuji Mori of the Tokyo Institute of Technology for his generous and very helpful discussions concerning this paper.

BULLETIN OF THE CHEMICAL SOCIETY OF JAPAN VOL. 41 2349—2352 (1968)

Bond Distances of Cyanogen as Determined by Gas Electron Diffraction

Yonezo MORINO, Kozo KUCHITSU, Yasurō HORI*1 and Mitsutoshi TANIMOTO

Department of Chemistry, Faculty of Science, The University of Tokyo, Hongo, Bunkyo-ku, Tokyo

(Received April 18, 1968)

The internuclear distances of cyanogen were determined by gas electron diffraction to be $r_g(C\equiv N)=1.163_4\pm0.001_9$ Å and $r_g(C-C)=1.392_5\pm0.002_2$ Å. The average moment of inertia calculated from this structure agreed with Maki's infrared results as corrected for rotation-vibration interaction. The spectroscopic moment of inertia obtained by Maki was used for calibrating the electron-diffraction scale factor, and the zero-point average distances, with their limits of error, were obtained as $r_z(C\equiv N)=1.155_2\pm0.001_3$ Å and $r_z(C-C)=1.387_1\pm0.001_4$ Å.

It has long been known that the length of a CC single bond depends on its environment. A carbon-carbon single bond adjacent to multiple bonds is found to be appreciably shorter than one in normal hydrocarbons, and the shortening is most conspicuous when the single bond is located between triple bonds.[1] Cyanogen, C_2N_2, is one of the simplest molecules of this category. Earlier electron-diffraction measurements of this molecule by Pauling, Springall and Palmer[2] and by Langseth and Mφller[3] gave $r(C\equiv N)=1.16\pm0.02$ and 1.15 ± 0.02 Å, and $r(C-C)=1.37\pm0.02$ and 1.38 ± 0.02 Å, respectively. The precise rotational constants, B_0, for two isotopic species, $^{12}C_2{}^{14}N_2$ and $^{12}C_2{}^{15}N_2$, have been obtained by Maki[4] from his rotational analysis of the infrared spectra. The resulting bond distances are $r_0(C\equiv N)=1.15_4\pm0.017$ Å and $r_0(C-C)=1.38_9\pm0.030$ Å.

On the basis of more recent developments in experiment and theory, a reliable average structure can be determined by the use of a combination of rotational constants obtained from high-resolution spectroscopy and internuclear distances obtained from electron diffraction.[5] The present study aims to apply this method to determining the average structure of cyanogen in the ground vibrational state.

Experimental

A sample of cyanogen, which contained 0.6% carbon dioxide and 0.4% air, was kindly offered by Dr. Shizuo Nakamura of the Sagami Chemical Research Center. It was purified before use by pumping off any impurities from the sample while it was held at dry ice temperature.

*1 Present address: Institute for Solid State Physics, The University of Tokyo, Minato-ku, Roppongi, Tokyo.

1) G. Herzberg, F. Patat and H. Verleger, *J. Phys. Chem.*, **41**, 123 (1937).

2) L. Pauling, H. D. Springall and K. J. Palmer, *J. Am. Chem. Soc.*, **61**, 927 (1939).

3) A. Langseth and C. K. Mφller, *Acta Chem. Scand.*, **4**, 725 (1950).

4) A. G. Maki, *J. Chem. Phys.*, **43**, 3193 (1965).

5) K. Kuchitsu and S. Konaka, *ibid.*, **45**, 4342 (1966); K. Kuchitsu, T. Fukuyama and Y. Morino, *J. Mol. Structure*, **1**, 463 (1968).

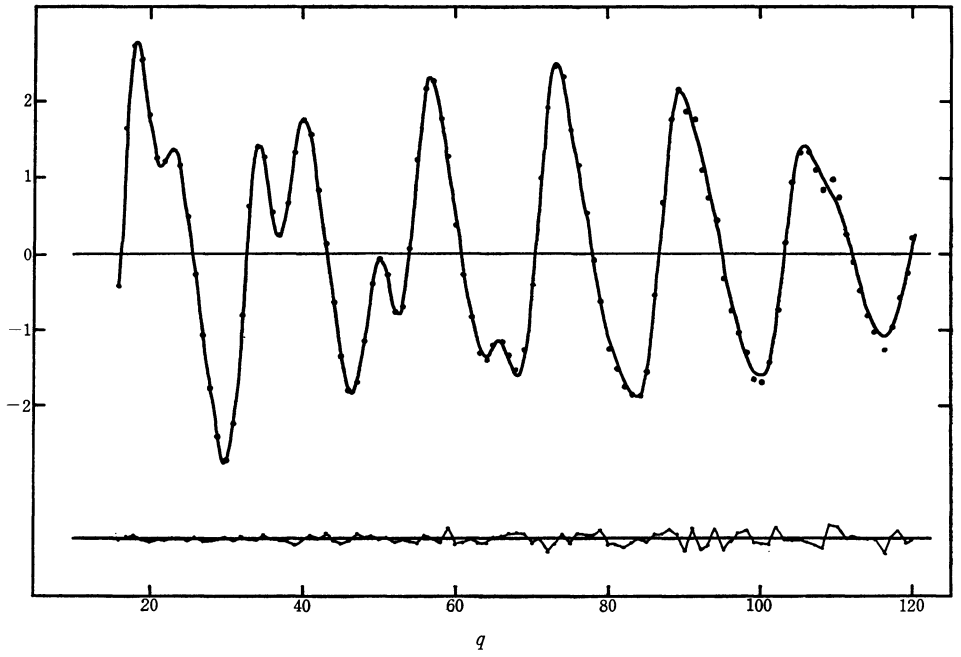

Fig. 1. Reduced molecular intensity curves (dots for observed values and the solid curve calculated from the best-fit model) and the residuals (below).

A diffraction apparatus with an r^3-sector previously reported[5] was used for the present study. The camera distances were measured as 243.22±0.02 and 107.78± 0.02 mm. The accelerating voltage (about 40 kV) was stabilized within 0.1%. The wavelength of the electron beam was calibrated to 0.15% with reference to the r_a(C=O) bond distance (1.164$_6$ Å) of carbon dioxide measured under the same experimental conditions. The gas, stored in a 2-*l* flask with a pressure of about 50 mmHg at 293°K, was led into the apparatus through a nozzle 0.2 mm in diameter. The pressure in the apparatus was less than 1×10^{-4} mmHg during photographic exposure. The beam current was about 0.16 μA. Diffraction photographs were recorded on Fuji Process Hard plates.

Four photographs from each camera distance were traced with a microphotometer, and the optical densities were measured by an integrating digital voltmeter, TR-65A15.[6] Photographs were taken so as to keep the optical densities in the region proportional to the electron intensities.

Analysis

The electron intensity was analyzed by a standard least-squares method[7] after correction for small extraneous scattering. The calculations were made by using the HITAC 5020E at the Computation Center of the University of Tokyo. The experimental reduced molecular intensity, $qM(q)$, for q values of 16 to 120 was fitted to the theoretical expression by an estimated weight function:

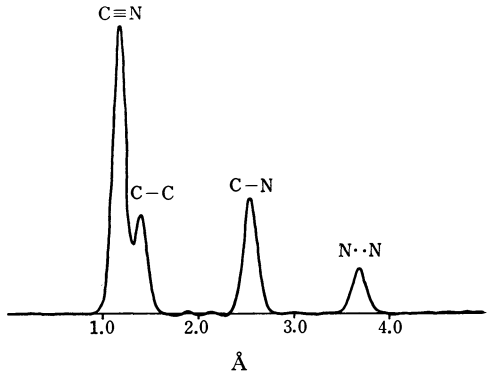

Fig. 2. Radial distribution curve for cyanogen.

$$qM(q) = k\sum c_{ij}\exp\left[-\frac{1}{2}l_{ij}^2\left(\frac{\pi}{10}\right)^2q^2\right] \times \sin\frac{\pi}{10}q\left[r_{aij}-\kappa_{ij}\left(\frac{\pi}{10}\right)^2q^2\right]\Big/r_{aij} \quad (1)$$

The asymmetry parameters, κ, were fixed at their estimated values,[8] κ(C≡N)$=5.5\times10^{-7}$ Å^3 and κ(C–C)$=12.0\times10^{-7}$ Å^3. The κ parameters for nonbonded atom pairs were assumed to be zero. Figure 1 shows some typical reduced molecular intensities (experimental and best-fit) and the difference between the observed and the calculated values from the best-fit parameters. The r_a distances and the mean amplitudes obtained from the above analysis are listed in Table 1, along with their limits of error, which were estimated from

6) Y. Morino, K. Kuchitsu and T. Fukuyama, This Bulletin, **40**, 423 (1967).
7) Y. Morino, K. Kuchitsu and Y. Murata, *Acta Cryst.*, **18**, 549 (1965).
8) K. Kuchitsu, This Bulletin, **40**, 498 (1967).

Table 1. Internuclear distances, mean amplitudes and shrinkages of cyanogen (in Å units)

	r_a	l_{obs}	l_{calc}
C≡N	$1.162_3 \pm 0.001_9$	$0.035_3 \pm 0.000_8$	0.0347
C-C	$1.391_3 \pm 0.002_2$	$0.041_6 \pm 0.002_6$	0.0428
C·N	$2.542_3 \pm 0.003_5$	$0.050_8 \pm 0.001_3$	0.0470
N··N	$3.695_9 \pm 0.005_8$	$0.056_3 \pm 0.004_0$	0.0515

	r_g	δ_{obs}	δ_{calc}
C≡N	1.163_4	—	—
C-C	1.392_5	—	—
C·N	2.543_3	$0.012_6 \pm 0.004_5$	0.011
N··N	3.696_7	$0.022_6 \pm 0.006_8$	0.024

the internal consistency and the reproducibility of the results from four sets of electron intensities. The last column of Table 1 gives the values of the mean amplitudes calculated by the use of quadratic force constants. The F_{11}, F_{12}, and F_{22} force constants were calculated from the ν_1 and ν_2 for $^{12}C_2{}^{14}N_2$ and from the ν_1 for $^{12}C_2{}^{15}N_2$, which was estimated from the $\nu_1+\nu_5$ for this isotopic species by the use of the ν_5 and x_{55} for the normal species;[4] they were found to be $F_{11}=16.78$, $F_{12}=0.42$, and $F_{22}=6.71$ md/Å. The other force constants were determined uniquely from the vibrational frequencies, since the secular equations are all one-dimensional: $F_{33}=17.73$, $F_{44}=0.18$, and $F_{55}=0.17$ md/Å. The observed shrinkage effects, δ_g, agree with the calculated values reported by Cyvin and Meisingseth,[9] and are shown in Table 1.

Average Distances

With the force constants obtained above, the zero-point average distance, $r_\alpha{}^0$, was derived from r_α in three steps:[5] (i) The thermal average of the instantaneous internuclear distance was calculated by:

$$r_g = r_a + l^2/r_a \qquad (2)$$

(ii) The r_g distance was converted to the absolute-zero temperature:

$$r_g(0°K) = \lim(T \to 0°K) r_g \qquad (3)$$

(iii) The average distance, $r_\alpha{}^0$, was obtained by the subtraction of the centrifugal correction and the perpendicular contribution:

$$r_\alpha{}^0 = r_g(0°K) - (\langle \Delta x^2 \rangle_0 + \langle \Delta y^2 \rangle_0)/2r_e - \delta r \qquad (4)$$

In the second step the parameters characterizing the anharmonicity of the bond-stretching vibrations were assumed to be equal to those of the corresponding diatomic molecules. The anharmonic term, $\langle \Delta z \rangle$, which is latent in the expression of r_g, was estimated for bonded atom pairs in a way described elsewhere.[5] Those for nonbonded atom pairs were calculated by the summation of the linear terms for the constituent bonded pairs. The mean-square perpendicular and parallel amplitudes of vibration, $\langle \Delta x^2 \rangle$, $\langle \Delta y^2 \rangle$ and $\langle \Delta z^2 \rangle$ were calculated by the general formulas given by Morino and Hirota.[10]

The $r_\alpha{}^0$ distances determined in this way, listed in Table 2, are essentially equivalent to the spectroscopic distances, r_z, between the average positions of the atoms in the ground vibrational state.

Table 2. Zero-point average distances from electron diffraction (in Å units)

	$r_\alpha{}^0$		$r_\alpha{}^0$
C≡N	$1.156_6 \pm 0.002_0$	C·N	$2.544_3 \pm 0.003_5$
C-C	$1.388_8 \pm 0.002_2$	N··N	$3.707_0 \pm 0.005_8$

Table 3. Average moments of inertia for $^{12}C_2{}^{14}N_2$ and $^{12}C_2{}^{15}N_2$ (in amu Å^2 units)

	$^{12}C_2{}^{14}N_2$	$^{12}C_2{}^{15}N_2$	
$I_\alpha{}^0$(ED)	107.53 ± 0.35	114.36 ± 0.38	
I_z(IR)	107.27 ± 0.03	114.09 ± 0.03	set A[a]
	107.31 ± 0.03	114.12 ± 0.03	set B[a]

a) See Ref. 4.

The average distances are shown to be additive:

$$r_\alpha{}^0(C\cdot\cdot N) - r_\alpha{}^0(C\text{-}C) - r_\alpha{}^0(C\equiv N) = -0.001_1 \pm 0.004_6 \text{ Å}$$

and:

$$r_\alpha{}^0(N\cdot\cdot N) - 2r_\alpha{}^0(C\equiv N) - r_\alpha{}^0(C\text{-}C) = 0.005_0 \pm 0.006_8 \text{ Å}$$

The linearity of the molecule has thus been confirmed by the present study of gas electron diffraction. The moments of inertia, $I_\alpha{}^0$, of $^{12}C_2{}^{14}N_2$ and $^{12}C_2{}^{15}N_2$ corresponding to the $r_\alpha{}^0$ distances are listed in Table 3.

Average Moment of Inertia as Detemined by Infrared Spectrocopy

The moment of inertia, I_z, for the average configuration was calculated from the effective rotational constant for the ground vibrational state, B_0, by[11]:

9) S. J. Cyvin and E. Meisingseth, *Acta Chem. Scand.*, **15**, 1289 (1961).

10) Y. Morino and E. Hirota, *J. Chem. Phys.*, **23**, 737 (1955).

11) V. W. Laurie and D. R. Herschbach, *ibid.*, **37**, 1687 (1962).

$$I_z = \frac{h}{8\pi^2 B_0} - \frac{h}{8\pi^2} \times \left[\frac{1}{\omega_1} + \frac{1}{\omega_2} + \frac{1}{\omega_3} + \frac{1}{\omega_4} + \frac{1}{\omega_5} - \frac{4}{\omega_3+\omega_5} - 4(\zeta_{14})^2\left(\frac{1}{\omega_2} + \frac{1}{\omega_1+\omega_4}\right) - 4(\zeta_{24})^2\left(\frac{1}{\omega_1} + \frac{1}{\omega_2+\omega_4}\right)\right] \quad (5)$$

The correction term was calculated to be -0.012 amu Å^2. The average moments of inertia are listed in Table 3.

Average Structure of Cyanogen

The average moments of inertia obtained from electron diffraction and from infrared spectroscopy agree well with each other, differing only about 0.24%. The difference is within the limit of error of the electron-diffraction experiment. Infrared spectroscopy gives moments of inertia more accurate than those of electron diffraction. On the other hand, uncertainties in the spectroscopic bond distances are still a few hundredths of an angstrom, as assigned by Maki.[4] The principal reasons for this are that the distances derived from the isotopic moments of inertia are sensitive to small errors in the moments (as is illustrated in Fig. 3) and that the dependence of the average bond distances on isotopic substitution is uncertain. On the other hand, the essential part of the above-mentioned discrepancy in the moments of inertia can be ascribed to the systematic error of 0.12% in the measurement of the electron wavelength. Such being the circumstances, the scale factor was calibrated by the spectroscopic moments of inertia (Maki's set A); the corrected average bond distances turned out to be:

$$r_z(\text{C}\equiv\text{N}) = 1.155_2 \pm 0.001_3 \text{ Å}$$

and:

$$r_z(\text{C-C}) = 1.387_1 \pm 0.001_4 \text{ Å}$$

The use of his alternative set, B, which was regarded by Maki as less plausible, led to an increase of 0.0002 Å in both distances. The r_z structure obtained above is, accidentally, close to the effective r_0 structure reported by Maki.

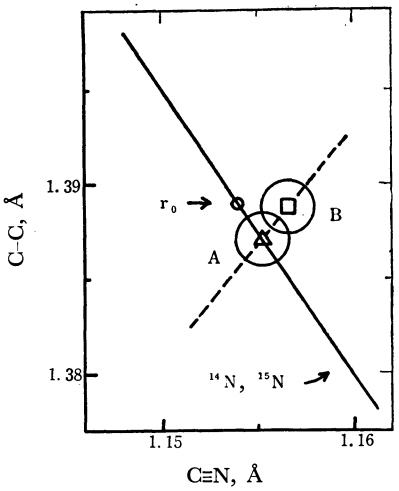

Fig. 3. Plot of the C-C distance *versus* the C-N distance in cyanogen. The solid line represents the relationship between the distances r(C-C) and r(C≡N). Two lines for $^{12}C_2{}^{14}N_2$ and $^{12}C_2{}^{15}N_2$ are virtually indistinguishable in the region shown in the figure. The broken line is a locus of the most probable distances as the electron-diffraction scale factor is varied. The square corresponds to the $r_\alpha{}^0$ distances observed by electron diffraction, while the triangle represents the average distances r_z. The circles indicate the limits of random error in electron-diffraction experiment. The limits of uncertainties of the r_z parameters are set by the crossings of the solid lines and the circle A. The limits of error of the r_0 distances reported by Maki (± 0.030 Å for C-C and ± 0.017 Å for C-N) are outside the illustrated region.

The CC bond length determined above is about 0.01 Å longer than the value expected from the empirical rule proposed by Stoicheff,[12] r(C-C≡) $= 1.299 + 0.040 \times 2 = 1.379$ Å. This slight discrepancy can be explained, at least qualitatively, in terms of the difference in bond order. The details will be published in a forthcoming paper.

12) B. P. Stoicheff, *Tetrahedron*, **17**, 135 (1962).

BULLETIN OF THE CHEMICAL SOCIETY OF JAPAN VOL. 41 2353—2356 (1968)

Infrared Spectra and Conformations of Succinonitrile in Silver and Copper Complexes

Masako SUZUKI and Takehiko SHIMANOUCHI

Department of Chemistry, Faculty of Science, The University of Tokyo, Hongo, Bunkyo-ku, Tokyo

(Received April 22, 1968)

Succinonitrile silver nitrate $[Ag(NCCH_2CH_2CN)]NO_3$ and succinonitrile disilver nitrate $[Ag(NCCH_2CH_2CN)Ag](NO_3)_2$ were prepared and the infrared spectra down to 60 cm^{-1} were measured. It was shown that the ligand molecule takes only the trans form in these complexes. The far infrared spectra were also measured for the free succinonitrile ligand at room and liquid nitrogen temperatures and for the copper complex. The assignments of bands for the nitrate ion and the trans and the gauche forms of succinonitrile were given.

Vibrational spectra of succinonitrile show that this molecule takes both the trans and gauche forms in the solid state at room temperature and only the latter form remains at low temperature.[1,2] As for the crystal of bis(succinonitrile)copper(I) nitrate, $[Cu(NCCH_2CH_2CN)_2]NO_3$, infrared spectra,[3] and X-ray analysis[4] show that the ligand succinonitrle takes the gauche form.

We have succeeded in preparing two kinds of silver complexes, succinonitrile silver nitrate $[Ag(NCCH_2CH_2CN)]NO_3$ and succinonitrile disilver nitrate $[Ag(NCCH_2CH_2CN)Ag](NO_3)_2$. We have measured the infrared spectra of these complexes down to 60 cm^{-1} and found that the ligand succinonitrile molecule takes only the trans form in these complexes. This fact has been confirmed for the disilver nitrate by the X-ray analysis as reported by Nomura and Saito.[5] In the present paper the results of the infrared spectra of silver nitrate and disilver nitrate complexes are reported. The fact that we have only the trans form in the silver complexes and only the gauche form in the copper complex enables us to obtain the spectra of the two conformations separately. Accordingly, the spectra of the copper complex and the free succinonitrile ligand have also been measured down to 60 cm^{-1} and the assignments of bands have been reinvestigated.

Experimental

Silver complexes were prepared from succinonitrile and silver nitrate. Succinonitrile (bp 158—160°C/20 mmHg) was melted at about 60°C and silver nitrate powder was added. The excess nitrile was extracted by an alcohol-ether mixture. The complexes were recrystallized from ethanol and colorless needle-like crystals were obtained. Microscopic investigation showed that two kinds of crystals exist. One was transparent and of regular shapes and the other was opaque and of irregular shape. These two kinds of crystals were separated manually. The following elementary analysis showed that the former kind is succinonitrile disilver nitrate and the latter is succinonitrile silver nitrate.

Found: C, 11.80; H, 0.84; N, 13.32%. Calcd for $[Ag(NCCH_2CH_2CN)Ag](NO_3)_2$: C, 11.44; H, 0.96; N, 13.34%.

Found: C, 19.57; H, 1.77; N, 16.91%. Calcd for $[Ag(NCCH_2CH_2CN)]NO_3$: C, 19.22; H, 1.61; N, 16.80%.

The copper complex was prepared according to the method given by Morgan.[6]

The infrared spectra were recorded by the following grating spectrometers: Hitachi EPI-2 and Perkin-Elmer 112G (4000—650 cm^{-1}), Japan Spectroscopic Co. 401G (700—300 cm^{-1}) and Hitachi FIS-1 (500—60 cm^{-1}). Nujol mull and HCB mull were used except in the far infrared region, where the samples mixed with paraffin were used. The copper complex in a KBr disk or in contact with alkali halide windows was reported to decompose gradually.[3] For the present complexes the same phenomena were observed. In order to avoid the decomposition, thin polyethylene films were inserted between the alkali halide windows and the sample. Sometimes the sample was purposely put in contact with the KBr window, since the changes in spectra were useful for discriminating the nitrate ion bands from those belonging to the ligand molecule. Succinonitrile was melted and solidified between the KBr plates in the 4000—500 cm^{-1} region or between the silicon plates in the 500—60 cm^{-1} region and was used for the measurement at room temperature and at liquid nitrogen temperature. The spectra are shown in Fig. 1.

Result and Discussion

The complexes dealt with in the present study contain nitrate ions and the absorption bands

1) W. E. Fitzgerald and G. J. Janz, *J. Mol. Spectry.*, **1**, 49 (1957).
2) T. Fujiyama, K. Tokumaru and T. Shimanouchi, *Spectrochim. Acta*, **20**, 415 (1964).
3) I. Matsubara, This Bulletin, **34**, 1710 (1961).
4) Y. Kinoshita, I. Matsubara and Y. Saito, *ibid.*, **32**, 741 (1959).
5) T. Nomura and Y. Saito, *ibid.*, **39**, 1468 (1966).
6) H. H. Morgan, *J. Chem. Soc.*, **123**, 2901 (1923).

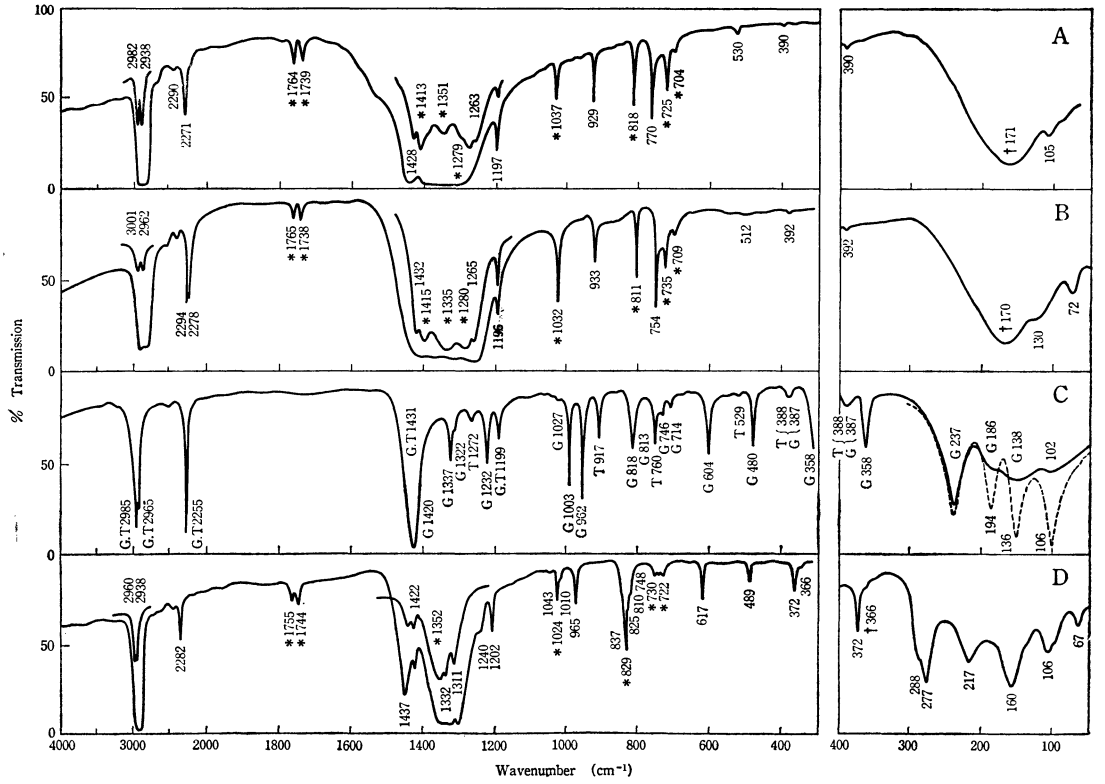

Fig. 1. Infrared spectra of succinonitrile and complexes.
(A) $[Ag(sn)]NO_3$, (B) $[Ag(sn)Ag](NO_3)_2$, (C) free succinonitrile, solid at room temperature, (D) $[Cu(sn)_2]NO_3$.
The dotted line of (C) gives the spectrum at liquid nitrogen temperature. Bands with an asterisk are assigned to the modes of the nitrate ion. Bands with a dagger are assigned to the metal-ligand stretching and deformation vibrations.

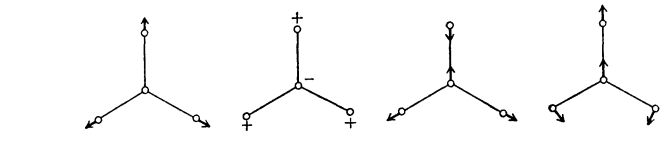

	ν_1	ν_2	ν_3	ν_4
	A_1'	A_2''	E'	E'
Infrared	ia	a	a	a
Raman	a	ia	a	a
	~1050	~800	1350~1400	700~750

Fig. 2. Vibrational modes of nitrate ion, symmetry species, infrared and Raman selection rule and approximate region (in cm^{-1}) in which these vibration bands appear.

due to this ion are discussed first. Figure 2 shows the modes of normal vibrations, their selection rule in infrared and Raman spectra and the frequencies which these vibrational modes are expected to have. The spectra given in Fig. 1 were compared with those of some inorganic nitrate salts and the bands asterisked in Fig. 1 are assigned to the nitrate ion vibrations. The totally symmetric vibration, ν_1, is infrared inactive. However, a weak band appears near 1035 cm^{-1} for the three complexes and is assigned to this mode which becomes infrared active owing to the crystalline field effect. The out-of-plane vibration, ν_2, is infrared active and appears near 820 cm^{-1} as a sharp band. The degenerate N-O stretching vibration, ν_3, appears very strongly in the region 1250—1450 cm^{-1}.

TABLE 1. FREQUENCIES OF INFRARED BANDS DUE TO NITRATE ION IN cm^{-1}

$[Ag(sn)]NO_3$	$[Ag(sn)Ag](NO_3)_2$	$[Cu(sn)_2]NO_3$	Assignment
{1764 {1739	{1765 {1738	{1755 {1744	$\nu_1+\nu_4$ (E′)
{1413 {1351 {1279	{1415 {1335 {1280	1352	ν_3 (E′)
1037	1032	1024	ν_1 (A_1')
818	811	829	ν_2 (A_2'')
{ 725 { 704	{ 735 { 709	{ 730 { 722	ν_4 (E′)

TABLE 2. OBSERVED FREQUENCIES IN cm^{-1} AND ASSIGNMENTS OF SUCCINONITRILE AND COMPLEXES

Succinonitrile	Complexes*			Assignment
	Ag(i)	Ag(ii)	Cu	
2985 (T, G)	2982	3001	2960	CH str. (a_u, b)
2965 (T, G)	2938	2962	2938	CH str. (b_u, a)
2255 (T, G)	2290 2271	2294 2278	2282	CN str. (b_u, a, b)
1431 (T, G)	1428	1432	1437	CH_2 scis. (b_u, b)
1420 (G)			1422	CH_2 scis. (a)
1337 (G)			1332	CH_2 wag. (b)
1322 (G)			1311	CH_2 wag. (a)
1272 (T)	1263	1265		CH_2 wag. (b_u)
1232 (G)			1240	CH_2 twist. (b)
1199 (T, G)	1197	1196	1202	CH_2 twist. (a_u, a)
1027 (G)			1043	CC str. (a)
1003 (G)			1010	CH_2 rock. (a)
962 (G)			965	CCN str. (b)
917 (T)	929	933		CCN str. (b_u)
818 (G)			825	CCN str. (a)
813 (G)			810	CH_2 rock. (b)
760 (T)	770	754		CH_2 rock. (a_u)
604 (G)			617	CCC deform. (b)
529 (T)	530	512		CCC deform. (b_u)
480 (G)			489	CCC deform. (a)
388 (T)	390	392		CCN deform. (a_u)
387 (G)				CCN deform. (a)
358 (G)			372	CCN deform. (b)
			366	Cu···N str.
237 (G)			{288 {277	CCN deform. (b)
186 (G)			217	CCN deform. (a)
	171	170		{Ag···ligand vibration {CCN deform. (b_u)
138 (G)			160	CC torsion (a)
	105	130		CC torsion (a_u)
102		72	{106 { 67	intermolecular vibrations

* Ag(i), and Ag(ii) and Cu denote succinonitrile silver nitrate, disilver nitrate, and copper nitrate, respectively.

For the copper complex only one peak appears at 1352 cm^{-1}. For the silver complexes three bands appear in this region as shown in Fig. 1. When the sample was fresh, the central peak at 1351 cm^{-1} for silver nitrate and at 1335 cm^{-1} for disilver nitrate appeared strongly. The intensities of the two bands near 1410 cm^{-1} and 1280 cm^{-1} relative to that of the central peak increased when the sample was in contact with alkali halide plates. We did not investigate the spectral changes in

detail, since they were not related with the problem dealt with in the present study. The degenerate ONO deformation vibration, ν_4, appears as a doublet near 725 and 704 cm^{-1}, the splitting being caused by the crystalline field effect. In addition to the fundamental bands discussed above two peaks appear at 1764 and 1739 cm^{-1} for silver nitrate. These peaks are assigned to the combination bands, 1037+725 and 1037+704 in cm^{-1}. For the disilver nitrate and copper complexes the doublets near 1750 cm^{-1} are interpreted similarly. The results are summarized in Table 1.

As for the free ligand, the spectra of succinonitrile are interpreted as the overlap of the trans and gauche bands.[1,2] In the present measurement the spectrum was extended down to 60 cm^{-1} and three very broad bands were found at 186, 138 and 102 cm^{-1} and a sharp band at 237 cm^{-1} at room temperature. In this region the CCN deformation vibration (b_u) and the CC torsion (a_u) of the trans form and the CCN deformation vibration (a) and the CC torsion (a) of the gauche form are expected to appear. In order to make the situation clear, the spectrum at liquid nitrogen temperature was measured and is shown as a dotted line in Fig. 1. The spectrum above 300 cm^{-1} shows that only the gauche form exists at liquid nitrogen temperature and, accordingly, the four bands at 237, 186, 138 and 102 cm^{-1} should be assigned to the gauche form. The frequencies of the 237 and 186 cm^{-1} bands are compared with the calculated[2] and are assigned to the two CCN deformation bands. The remaining two bands at 138 and 102 cm^{-1} are tentatively assigned to CC torsion and an intermolecular vibration, since for the nitrile group a considerably strong intermolecular interaction is expected. The results are summarized in Table 2 and Fig. 1, where the trans and gauche forms are denoted by T and G, respectively.

The spectrum of the copper complex shown in Fig. 1 supports the conclusion obtained by Matsubara[3] and Kinoshita, Matsubara and Saito[4] that only the gauche form exists. As shown in Table 2 almost all the bands are assigned to those of the gauche form. There are some very weak bands, such as those at 837 and 748 cm^{-1}, which are not given in the table. They are assigned to the combination bands. In the region lower than 400 cm^{-1} metal-ligand vibrations are also expected. They may be coupled with the low frequency vibrations of the ligand gauche molecule. In fact, six bands appear below 300 cm^{-1} instead of the four bands of the free ligand gauche form. They are tentatively assigned as shown in Table 2, although they may be strongly coupled with each other.

The spectra of silver nitrate and disilver nitrate are of interest, when they are compared with those of the free ligand and copper complex. It is surprising that all the bands assigned to the gauche form disappear and only those assigned to the trans form remain. From these spectra we can conclude undoubtfully that the ligand molecule takes the trans form in the silver nitrate and disilver nitrate complexes. This conclusion was confirmed by the X-ray analysis by Nomura and Saito.[5] The detail of the assignments are given in Table II. The gauche bands at 962, 604, 480, 358, 237, 186 and 138 cm^{-1} disappear. Silver nitrate has two bands at 929 and 530 cm^{-1} and disilver nitrate has two bands at 933 and 512 cm^{-1}. They definitely correspond to the 917 and 529 cm^{-1} bands of the trans form of free ligand. As for the region below 300 cm^{-1}, silver nitrate has two bands at 171 and 105 cm^{-1} and disilver nitrate has three bands at 170, 130 and 72 cm^{-1}. In this region, CCN deformation (b_u), CC torsion (a_u), and metal ligand vibrations are expected to appear. The band at 170 cm^{-1} is very broad and is interpreted to be the overlapped band. Tentative assignments are given in Table 2, although three vibrations are strongly coupled with each other.

BULLETIN OF THE CHEMICAL SOCIETY OF JAPAN VOL. 41 2357—2361 (1968)

Certain Interactions between Transition Metal Ions and the NCS Group in Chromium(III) Isothiocyanato Complexes. I. Reinecke's Salt Type Complexes Involving Cobalt(II) and Copper(II) Ions*1

Hisaya OKI, Eishin KYUNO and Ryokichi TSUCHIYA

Department of Chemistry, Faculty of Science, Kanazawa University, Kanazawa

(Received August 21, 1967)

Cobalt(II) tetraisothiocyanatochromate(III), $Co[Cr(NCS)_4(NH_3)_2]_2$, was prepared from cobalt(II) chloride and Reinecke's salt in an aqueous solution. The absorption spectrum gave evidence that the so-called "cobalt-salt" dissociated into cobalt(II) cation and Reineck's anion in aqueous solution. The reflection spectrum showed a remarkably strong absorption band at $14.08 \times 10^{13}\,sec^{-1}$, which might be assigned to bonding between cobalt(II) and sulfur in an NCS^- ligand. The three absorption peaks observed at 2158, 2095 and 2065 cm^{-1} in the IR spectrum due to C-N stretching vibrations also emphasized the strong interaction between cobalt and sulfur. The effective magnetic moment estimated was 4.58 B. M. at 18.3°C. The corresponding copper(II) salt, $Cu(OH)[Cr(NCS)_4(NH_3)_2]$, was obtained from an aqueous solution of copper(II) sulfate and Reinecke's salt as a yellow powder. It was a sparingly soluble in water. In the reflection spectrum, the red-shifted band covered much of the first band region of Reinecke's salt and in the IR spectrum, the C-N band had only a small splitting. The magnetic moment was found to be 3.84 B. M. at 16.0°C, which is close to the predicted value in the complex when copper is reduced, becoming univalent. X-Ray diffraction analysis also showed a relatively stronger contraction of the unit cell in the copper salt than in the cobalt salt. On the basis of the above points, it was proposed that in the copper salt there is considerable π-bonding between copper and the two adjacent isothiocyanate groups.

It has already been reported[1] that the so-called "cobalt(II) salt" prepared from cobalt(II) chloride and Reinecke's salt exhibited a gradual color change from reddish-purple to grayish-green when it was exposed to dry air, and the color changed back to the original purple upon absorption of water, while the corresponding "copper(II) salt" gave a yellow color quite different from Reinecke's salt, when it was prepared from copper-(II) sulfate and Reinecke's salt. However, no further attempts to obtain information on the structures of these salts has been made.[1]

The green color in the cobalt(II) salt in the dry, solid state and the yellow color in the copper(II) salt suggest the presence of a certain interaction between cobalt or copper ion and Reinecke's anion. Our interest lies particularly in investigating such color changes in the cobalt and copper salts in relation to a structural discussion based on the spectra, magnetic behavior and measurements of chemical properties.

Experimental

Preparation of Compounds. *Cobalt(II) Tetraisothiocyanatochromate(III)* (called "Co-salt"). To a solution of Reinecke's salt (8 g/800 m*l* of H_2O) at 60°C, a solution of cobalt(II) chloride hexahydrate (225 g/700 m*l* of H_2O) at 5°C was added. Being kept in a refrigerator over night, reddish-purple scale-like crystals precipitated out. After filtration, the crystals were washed with a small amount of ether, and when dried over sulfuric acid *in vacuo*, their color changed to grayish-green.

Found: Cr, 14.39; Co, 8.47; N, 23.64%. Calcd for $Co[Cr(NCS)_4(NH_3)_2]_2$, Cr, 14.94; Co, 8.47; N, 24.16%.

In reverse, the color changed back to the original upon washing with water.

Copper(III) Tetraisothiocyanatochromate(III). (called "Cu-salt"). To a solution of Reinecke's salt at 60°C, a solution of copper(II) sulfate pentahydrate was added in a stoichiometric ratio (1 : 1). As soon as both solutions were mixed together, a yellow powder was obtained. The color does not change in a dry or moist atmosphere. The crystal was insoluble in water, alcohol, ether, dioxane and several organic solvents.

When the solids of Reinecke's salt and copper(II) sulfate hydrate were mixed in a motar, the same salt was also obtained.

Found: Cr, 13.05; Cu, 15.84; N, 21.57; C, 12.27; H, 1.70%. Calcd for $Cu(OH)[Cr(NCS)_4(NH_3)]_2$: Cr, 13.03; Cu, 15.94; N, 21.07; C, 12.29; H, 1.75%.

Apparatus for Measurement. Molar conductivity, electronic and reflection spectra, IR and far-infrared absorption spectra, magnetic suceptibility and

*1 Presented at the 15th and 16th Symposiums on Coordination Compounds of the Chemical Society of Japan; Kanazawa, Oct., 1965 and Tokyo, Dec., 1966.

1) O. Christensen, *J. pr. Chem.*, **45**, 371 (1892).

X-ray diffraction were measured with a Yokogawa Universal Bridge BV-Z-13A, a Hitachi EPU-2A spectrophotometer with a standard reflection attachement, a Nippon Bunko IR Spectrometer DS-301 and a Hitachi ERI-101 Grating IR Spectrometer, a Gouy balance and a Rigaku-denki Geigerflex X-ray Analyser, respectively.

Results and Discussion

Conductivity and pH Measurements. The value of the molar conductivity of the "Co-salt" was 196.4 $cm^2ohm^{-1}(1\times10^{-2}$ mol/l) at 25°C and that of Reinecke's salt 103.1 cm^2ohm^{-1} (2×10^{-2} mol/l). This suggests that the Co-salt is a 1 : 2 valency type salt, being capable of dissociating into a cobalt cation and Reinecke's anion in aqueous solution according to the following equation,

$$Co[Cr(NCS)_4(NH_3)_2]_2 \rightarrow Co^{2+} + 2[Cr(NCS)_4(NH_3)_2]^-.$$

For the corresponding Cu-salt, the conductivity could not be measured because of its insolubility in water. Christensen[1] reported that copper was univalent in the salt, but in the present work, it was concluded that the Cu-salt involves a hydroxyl group, as indicated by the chemical formula $Cu(OH)[Cr(NCS)_4(NH_3)_2]$.

In order to ascertain the composition of the Cu-salt, the following experiments were carried out.

Solutions of different concentrations of Reinecke's salt were added to solutions containing a constant number of moles of copper(II) sulfate pentahydrate. The precipitation formed was filtered off and the absorbancy of the filtrates measured at peaks of both the first and second absorption bands in Reinecke's salt. The results are shown in Fig. 1. It suggests that the Cu-salt obtained above has a simple mole ratio 1 : 1 as confirmed by the elementary analysis.

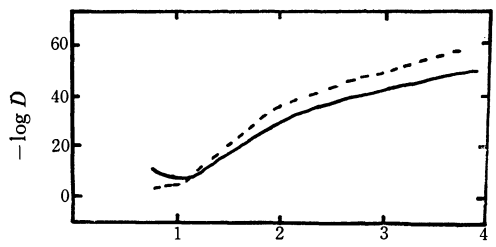

Fig. 1. The absorbancy of the filtrates after the Cu-salt formation.
----- at 520 m (the first band of Reinecke's salt)
—— at 392 m (the second band of Reinecke's salt)

The pH values of Reinecke's salt and copper(II) sulfate hydrate were found to be 4.84 and 4.50, respectively, in their aqueous solutions, whereas that of the filtrate was found to be in the range 2.70 to 2.50. In addition, it was found that the tendency to form the Cu-salt was extremely decreased in strongly acidic solutions. These results also indicate the existence of a hydroxo group in the Cu-salt.

Visible and UV Spectra. The visible and ultraviolet absorption spectra of the Co-salt measured are shown in Fig. 2, together with those of Reinecke's salt; numerical values are 57.69 ($\log\varepsilon=2.03$), 76.53 ($\log\varepsilon=2.00$) and 99.67×10^{13} sec^{-1} ($\log\varepsilon=4.12$) for the Co-salt, and 57.69 ($\log\varepsilon=2.01$), 76.53 ($\log\varepsilon=1.96$) and 99.67×10^{13} sec^{-1} ($\log\varepsilon=4.14$) for Reinecke's salt, respectively.

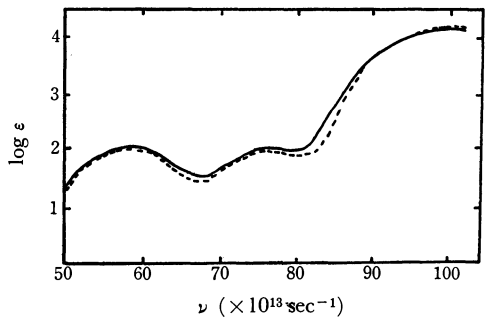

Fig. 2. The absorption spectra of the Co-salt (——) and Reinecke's salt (-----).

It is obvious in Fig. 2 that the absorption spectrum of the Co-salt is in approximate agreement with that of Reinecke's salt within the range of wavelength measured. This may support the assumption concerning the dissociation of the Co-salt as a 1 : 2 valency type, since the contribution of the spectrum of cobalt(II) cation in aqueous solution to that of the Co-salt is very small in the corresponding wavelength region.

Reflection Spectra. Reflection spectra of the Co- and Cu-salts were measured for powdered crystals, the latter being especially meaningful due to its lesser solubility in water. The results are shown in Figs. 3 and 4 for the Co- and Cu-salts, respectively, in which the logarithm of $f(R_d)$ coordinate is equal to $(1-R_d)^2/2R_d$ in the Kubelka-Munk equation, where R_d is the relative diffuse-reflection index.

The reflection spectrum of the grayish-green Co-salt showed two bands: the one appearing at 42.55×10^{13} sec^{-1} ($\log f(R_d)=0.67$) may probably be assigned to charge transfer from sulfur to cobalt, which could not be found in Reinecke's salt, and the other, at 60.00×10^{13} sec^{-1} ($\log f(R_d)=0.068$), may correspond to the first absorption band of Reinecke's salt. On the other hand, the band corresponding to the second band of Reinecke's salt could not be observed in the Co-salt.

In the Cu-salt, the first absorption band corresponding to that of Reinecke's salt is only observed as a shoulder, but the second band could not be observed due to the great shift of the charge transfer

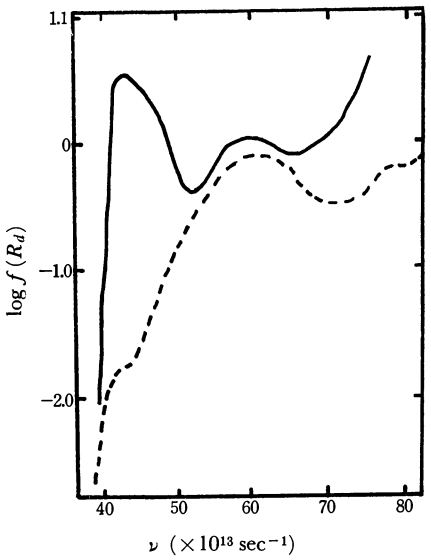

Fig. 3. The reflection spectra of the Co-salt (——) and Reineck's salt (-----).

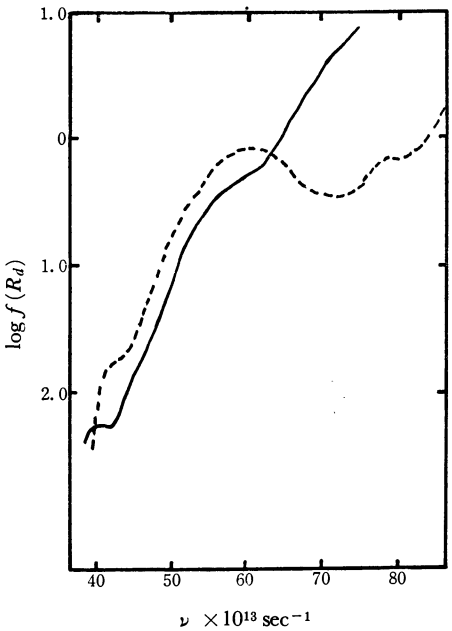

Fig. 4. The reflection spectra of the Cu-salt (——) and Reineck's salt (-----).

band to the visible region. Such a great shift suggests a strong interaction between the copper ion and Reinecke's anion.

IR Spectra. The bond between metal ions and isothiocyanate groups has been known and is classified according to the following three types:

1) a bond through the nitrogen atom in NCS, like M–NCS

2) a bond through the sulfur atom in NCS, like M–SCN

3) a bond through an NCS group bridge with an another metal, like M–NCS–M',
where M and M' are two different metals.

Jones[2] has reported on the three normal vibrational modes of thiocyanate ion in KNCS. Mitchell and Williams[3] proposed that the stretching frequencies of C–N bonding in isothiocyanato type complexes increase in the order $NCS^- < M-NCS \leqslant M-SCN < M-NCS-M'$, and that, especially, the frequencies in the bridged M–NCS–M' become higher as the electronegativity of M' becomes smaller.

Lewis, Nyholm and Smith,[4] on the other hand, noted that the C–S stretching frequency peak of 2) appears in a region lower than that of 1). It may be expected from such information that the peak due to C–S stretching in 3) will appear between the peaks in the above two cases.

The IR spectra of the Co- and Cu-salts with respect to C–N and C–S stretching vibrations are shown in Figs. 5 and 6, respectively, together with that of Reinecke's salt. Numerical data are summarized in Table 1, where data on a few Reinecke type salts by Fujita *et al.*[5] are cited for comparison with values obtained in the present work.

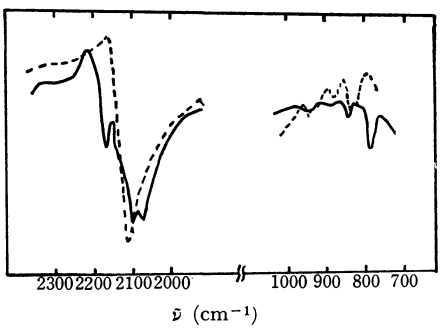

Fig. 5. IR spectra of the Co-salt (——) and Reineck's salt (-----).

The presence of peaks at 2158 cm^{-1} and 795 cm^{-1}, assigned to the C–N and C–S stretching vibrations, respectively, in the Co-salt, as shown in Table 1, suggest a relatively strong bond between cobalt(II) ion and the sulfur atom in the NCS^- group, forming a bridged structure such as Cr–NCS–Co, analogous to a Reinecke type Hg-salt, owing to the complete similarity of the IR spectra of these two salts.

On the other hand, in the Cu-salt, the peak assigned to the C–N stretching vibration did not

2) L. H. Jones, *J. Chem. Phys.*, **25**, 1069 (1956).
3) P. C. H. Mitchell and R. J. P. Williams, *J. Chem. Soc.*, **1960**, 1912.
4) J. Lewis, R. S. Nyholm and P. W. Smith, *ibid.*, **1961**, 4590.
5) J. Fujita, K. Nakamoto and M. Kobayashi, *J. Am. Chem. Soc.*, **83**, 4157 (1961)

Table 1. The infrared absorption peaks of the Reinecke's type salts

	ν_{C-N}			ν_{C-S}		δ_{NCS}			
Reinecke's salt	2120	2080							by Fujita *et al.*[5]
Cholin-salt	2180								
Ba-salt	2000	2130							
Hg-salt	2160	2098	2073						
Reinecke's salt	2119			840	860	467			by authors
Co-salt	2158	2095	2065	795	855	471	464	444	
Cu-salt	2110	2095	2075	810	825	475	460		
Hg-salt	2160	2095	2065	798	845				

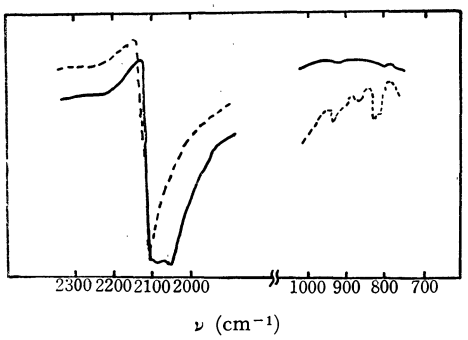

Fig. 6. IR spectra of the Cu-salt (——) and Reinecke's salt (----).

shift from the corresponding one in Reinecke's salt. Therefore, the bridged structure concluded for the Co-salt, M–NCS–M′, must be excluded for the Cu-salt.

However, since the band in the C–N stretching region is found to split into three peaks and the C–S band shifts to a lower wave number region than that of Reinecke's salt, but not so low as that of the Co-salt, another kind of the interaction should be considered between the copper(II) ion and Reinecke's anion.

Thus, a structure in which the copper is weakly coordinated to Reinecke's anion through two sulfur atoms in both adjacent NCS^- groups square planar around the copper atom can be assumed. But such a structure may also be unacceptable, since X-ray analysis data[6] give about 7 Å for the S–S distance between the two sulfur atoms in the adjacent NCS^- groups.

Taking into account also the reflection spectra of the Cu-salt, a structure may be conclusively proposed in which the copper(II) ion is not bound to sulfur atoms, but to the NCS^- groups as a whole, concluding considerable π-bonding character due to the transfer of the π-electron spread over the NCS^- group to the copper ion. Although such a structure, allowing π-bonding with respect to the NCS^- groups, is unknown to date, it may be most reasonable, and is also supported by the far-infrared absorption spectra described below.

Far-IR Absorption Spectra. The far-infrared absorption spectrum of the Co-salt is shown in Fig. 7, togehter with that of Reinecke's salt. The absorption band at 500 cm^{-1} in Reinecke's salt may be assigned to the Cr–N stretching vibrations on the ammonia, since it did not shift even when ammonium ion was replaced by cobalt ion, and it is coincident with the corresponding band in the ammine complexes.

The band at 467 cm^{-1} in Reinecke's salt may be assigned to the NCS bending vibration since it is in good agreement with the corresponding band which has been reported by Sabatini *et al.*[7] concerning metal cyanato, thiocyanato and selenocyanato complexes. In the Co-salt, the corresponding band splits into three peaks, which may be due to the NCS bending vibration free from the counter cation and due to some interactions with the counter cation through the bridged Cr–NCS–Co bond.

The band at 347 cm^{-1} is probably due to the Cr–N stretching vibration in thiocyanate as suggested in the literature.[4,7] The bands observed in the wave number region, 270—245 cm^{-1}, may be assigned to Co–S stretching, but there is no further verification for it.

The far-infrared absorption spectra of the Cu-salt and of Reinecke's salt are shown in Fig. 8. The band near 490 cm^{-1} is assigned to Cr–N stretching involving NH_3. It has a weak shoulder at 505 cm^{-1}, which was not detected in any other

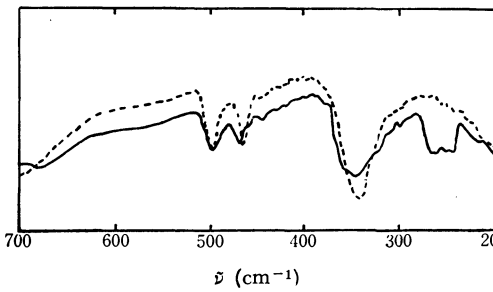

Fig. 7. The far infrared spectra of the Co-salt (——) and Reinecke's salt (----).

6) Y. Takeuchi and Y. Saito, This Bulletin, **30**, 319 (1957).
7) A. Sabatini and I. Bertini, *Inorg. Chem.*, **4**, 959 (1965).

TABLE 2. THE ANALYSES OF THE X-RAY DIFFRACTION AND DENSITY OF THE REINECKE'S TYPE SALTS

	c/a	a (Å)	c (Å)	Density, ρ		Z	Ref.
				Calcd	Found		
Reinecke's salt	1	13.25		1.50		6	6
Co-salt	1.1	10.30	11.34	1.96	1.87	8	
Cu-salt	0.89	9.03	8.07	2.01	1.96	2	

salts treated in the present work. However, it is not clear whether the shoulder is due to the distorted structure of Reinecke's anion in the crystal or not.

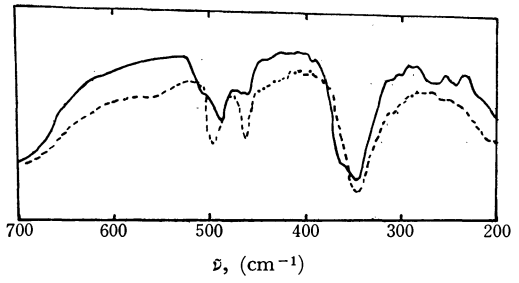

Fig. 8. The far infrared spectra of the Cu-salt (——) and Reinecke's salt (----).

The band assigned to the NCS bending vibration splits into two bands, but does not show the presence of a direct bond between the copper ion and a sulfur atom.

If the copper was bound to an NCS group through a sulfur atom, the absorption band assigned to the Cr–N stretching vibrations involving the NCS group should shift to a lower wave number range as is the case with the Co-salt. However, the corresponding bands were all shifted to a higher wave number region. From the various information described above, it may be reasonable to introduce the concept that the π-electron bond between an isothiocyanate group and copper ion plays an important role in the interaction between copper and Reinecke's anion in the Cu-salt.

Magnetic Susceptibility. From the magnetic susceptibility measurements, a value of 4.50 B. M. was obtained for the Co-salt as the effective magnetic moment. If the divalent cobalt ion is in a high spin state, the number of unpaired electrons contained may be amount to 4.5 (therein 3 for Cr and 1.5 for Co) per molecule of the salt; and then, the spin-only value should be 5.41 B. M. The value obtained in the present work seems to be remarkably small compared with that in the high spin state of cobalt. This supports in addition to the results from absorption and IR spectra, some kind of "superexchange interaction" between Co and Cr ions through an NCS^- group.

The magnetic moment of the Cu-salt is expected to be 4.9 B. M. by evaluating the total number of spins contained. But the value obtained is 3.84 B. M. at 16°C, which is smaller. It may also alow that the copper is bound to Reinecke's anion through the π-electron in the NCS^- groups as explained above on the basis of the IR spectra.

X-Ray Diffraction Measurement. The results of analysis of the X-ray diffraction patterns for the Co- and Cu-salts are summarized in Table 2, together with those for Reinecke's salt already published by Y. Saito *et al.*[6] The structures of these salts are indicated to be tetragonal, except for Reinecke's salt which has a cubic structure. The density of the Co-salt was measured in Nujol, whereas that of the Cu-salt, in water. The result that the Cu-salt has the largest density of these three salts suggest that there is the strongest contraction of the unit cell in the Cu-salt.

The authors wish to express their gratitude for a grant from the Ministry of Education for this study.

BULLETIN OF THE CHEMICAL SOCIETY OF JAPAN VOL. 41 2362—2366 (1968)

Certain Interactions between Transition Metal Ions and the NCS Group in Chromium(III) Isothiocyanato Complexes. II. Reinecke's Salt Type Complexes Involving Nickel(II), Manganese(II) and Iron(III) Ions*[1]

Hisaya Oki, Eishin Kyuno and Ryokichi Tsuchiya

Department of Chemistry, Faculty of Science, Kanazawa University, Kanazawa

(Received September 18, 1967)

Nickel(II), manganese(II) and black iron(III)-tetraisothiocyanatochromate(III) were prepared by the reaction of nickel(II) nitrate, manganese(II) sulfate and iron(III) chloride with Reinecke's salt, respectively. Each salt exhibits a gradual color change from reddish-purple to brownish-orange, red and black, respectively, when exposed to dry air after preparation, except for the orange iron(III) salt prepared in hydrochloric acid solution, which shows no color change from the original orange. Their absorption spectra give evidence that each salt will dissociate into a metal cation and Reinecke's anion in aqueous solution. Splittings due to the C–N stretching vibration were not observed in the IR spectra. The effective magnetic moments were evaluated as 3.96, 5.13, 5.0 and 4.81 B. M. for the nickel(II)-, the manganese(II)-, the black iron(III)- and the orange iron(III)-salts, respectively. They show that the salts are nearly low spin types, or a type somewhere between low and high spin. From X-ray diffraction analyses, the unit cell of all the salts were found to be tetragonal.

In a preceding paper,[1] cobalt(II) and copper(II) isothiocyanatochromate(III) were prepared and it was concluded that the gradual color change from reddish-purple to grayish-green for the cobalt(II) salt was due to the appearance of an interaction between cobalt ion and the sulfur atom of an NCS group in Reinecke's anion, and that the formation of the insoluble, yellow copper(II) salt showed the presence of the assumed π-bonding between copper ion and an NCS group.

In the present work, the preparation of the nickel(II), manganese(II) and iron(III) salts of Reinecke's salt type has been carried out, and the structures of these compounds discussed with respect to the interaction between the transition metal cations and NCS groups in Reinecke's anion on the basis of electronic and IR spectra, magnetic susceptibility measurements and other chemical techniques.

Experimental

Nickel(II) Salt of Reinecke's Salt Type (called "Ni-salt"). To a solution of Reinecke's salt (1.5 g/100 m*l* of H_2O) at 60°C, crystals of nickel(II) nitrate (4 g) were added. After being kept in a refrigerator over night, reddish-purple scale-like crystal precipitated from the solution. After recrystallizing the precipitate obtained, it was washed with water. When the crystals were dried *in vacuo* over sulfuric acid at room temperature, their color changed to brownish-orange. If they were then heated at 68°C, the color changed further to greensih-brown, but the brownish-orange color was immediately reproduced when exposed to air.

Found: Cr, 14.07; Ni, 7.55; N, 22.96; H_2O, 2.4%. Calcd for $Ni[Cr(NCS)_4(NH_3)_2]_2 \cdot H_2O$: Cr, 14.32; Ni, 8.06; N, 23.56; H_2O: 2.52%.

Manganese(II) Salt of Reinecke's Salt Type (called "Mn-salt"). To a solution of Reinecke's salt (1.5 g/100 m*l* of H_2O) at 60°C, crystals of manganese(II) sulfate tetrahydrate (6 g) were added. When the solution was kept in a refrigerator over night, reddish-purple, scale-like crystals precipitated out. Separated by filtration, the crystals were washed with water. With drying *in vacuo* over sulfuric acid, their color changed to red, and the original color was reproduced when exposed to moist air.

Found: Cr, 13.84; Mn, 8.09; N, 22.91; H_2O, 5.0%. Calcd for $Mn[Cr(NCS)_4(NH_3)_2]_2 \cdot 2H_2O$: Cr, 14.29; Mn, 7.55; N, 23.10; H_2O, 4.95%.

Iron(III) Salts of Reinecke's Salt Type. *a) Black Iron(III) Salts of Reinecke's Salt Type* (called "black Fe-salt"). To a solution of Reinecke's salt (1.5 g/100 m*l* of H_2O) at 60°C, a solution of iron(III) chloride hexahydrate (8 g/10 m*l* of H_2O) was added. When the solution was kept in a refrigerator over night, reddish-purple, scale-like crystals pricipitated out, which were then separated by filtration. After being washed with a small amount of water, and dried *in vacuo* over sulfuric acid, the color of the crystals changed from reddish-purple to black. As recrystallization was repeated in water, the color of the crystal was gradually changed from black to purple or somewhat reddish-purple. This

*1 Read in part at the 16th Symposium on Coordination Compounds of the Chemical Society of Japan, Tokyo, Dec., 1966.

1) H. Oki, E. Kyuno and R. Tsuchiya, This Bulletin, **41**, 2357 (1968).

is probably due to the sublimation of iron(II) trithiocyanate, produced as the result of the partial decomposition of the black Fe-salt, leaving a small amount of ferric oxide. Thus, recrystallization was unsuccessful even in an acidic solution.

Found: Cr, 11.87; Fe, 9.60; N, 23.53%. Calcd for $Fe[Cr(NCS)_4(NH_3)_2]_3 \cdot Fe(NCS)_3$: Cr, 12.57; Fe, 9.00; N, 23.70%.

b) Orange Iron(III) Salt of Reinecke's Salt Type (called "orange Fe-salt"). To a solution of iron(III) chloride hydrate (8 g/10 m*l* of 8 N HCl), a solution of Reinecke's salt (10 g in 6 N hydrochloric acid) at 60°C was added. When the solution was kept in a refrigerator over night, a reddish-orange or orange powder separated out, which was filtered and washed with a small amount of ether. The orange crystals did not show any color change, even when upon drying, differing from the black Fe-salt described above.

Found: Cr, 13.06; Fe, 6.69; N, 22.17; Cl, 9.24%. Calcd for $FeHCl_2[Cr(NCS)_4(NH_3)_2]_2$: Cr, 13.60; Fe, 7.30; N, 21.98; Cl, 9.28%.

Apparatus for Measurement. Conductivity, visible and UV absorption spectra, IR and far-IR absorption spectra, reflection spectra, magnetic susceptibility and X-ray diffractions were measured with the same apparatus described in the preceding paper.[1]

Results and Discussion

Conductivities and Behavior toward Ion Exchangers. Values of the molar conductivity of the salts per equivalent Reinecke's anion in aqueous solution at 25°C are listed in Table 1. They suggest, first, that the Ni- and Mn-salts are 1:2 valency types which can dissociate into a metal cation and two Reinecke anions in aqueous solution.

Table 1. The molar conductivity (at 25°C)

Sample	Concentration mol/*l*	Molar conductivity cm^2ohm^{-1}	Type
Reinecke's salt	2×10^{-2}	103.1	1 : 1
Ni-salt	5×10^{-2}	115.3	1 : 2
Mn-salt	2×10^{-2}	106.3	1 : 2
Black Fe-salt	4×10^{-2}	194.8	1 : 3
Orange Fe-salt	4×10^{-2}	374.8	

On the other hand, the condutivity of the black Fe-salt per equivalent Reinecke anion was found to be much greater than expected for 1 : 3 type salts in general. This can be explained reasonably by their behavior toward ion exchangers.

When an aqueous solution of the black Fe-salt was poured onto a column of anion exchange resin (Dowex 1×8), pink solution passed through, leaving some red material adsorbed on the exchanger. It is thought that the pink solution, in part, contains $Fe(NCS)_3$ and the appearance of the red color on the exchanger is due to the adsorption of Reinecke's anion. The presence of $Fe(NCS)_3$ in the pink solution was verified by detecting the chromium ion formed by the reaction of Reinecke's anion with ferric ion.

Moreover, the orange Fe-salt has the largest molar conductivity of all the complexes, as given in Table 1. This is due to the presence of hydrogen ion which is capable of dissociation in aqueous solution, as indicated by the formula proposed in the Experimental section.

When an aqueous solution of the orange Fe-salt was poured onto the column of the same exchanger as was used above, yellow solution passed through, leaving red material on the exchanger. It is thought that the yellow color of the solution indicates the presence of iron(III) ion, and the red material on the exchanger indicates the adsorption of Reinecke's anion.

Electronic Absorption Spectra. The electronic absorption spectra of the Ni(II)- and Mn(II)-salts of Reinecke's salt type were in approximate agreement with that of Reinecke's salt itself, which supports their complete dissociation to Ni(II) or Mn(II) cations and Reinecke's anion in aqueous solution. The numerals of the electronic spectra of these complexes are listed in Table 2, including those of both Fe-salts described below.

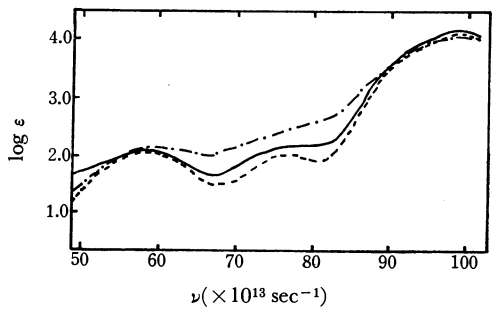

Fig. 1. The absorption spectra of the black Fe- (——), and the orange Fe-salts (— - —) and Reinecke's salt (- - -).

The electronic spectra of the black and orange Fe-salts are shown in Fig. 1, together with that of Reinecke's salt. As seen in this figure, the spectra of these compounds are also similar to that of Reinecke's salt except for the second band being changed to a shoulder. It shows that both Fe-salts dissociate into iron(III) cations and Reinecke's anions in an aqueous solution, the same as the Ni- and Mn-salts, but some amount of hydroxo-iron(III) is formed.

Reflection Spectra. Absorption spectra of the Ni-, Mn- and orange Fe-salts in the solid state were measured by the diffusion-reflection method and are shown in Fig. 2 together with that of Reinecke's salt. In the Ni- and Mn-salts, only the first band corresponding to that of Reinecke's salt is observed, the second band being undetectable probably because of the shift of the intense charge transfer band to the visible region, which can not

Table 2. The absorption spectra of the Reinecke's type salts

	The first band		The second band		The specific band	
	$\nu(10^{13}\,\mathrm{sec}^{-1})$	$(\log \varepsilon)$	$\nu(10^{13}\,\mathrm{sec}^{-1})$	$(\log \varepsilon)$	$\nu(10^{13}\,\mathrm{sec}^{-1})$	$(\log \varepsilon)$
Reinecke's salt	57.69	(2.01)	76.53	(1.96)	99.67	(4.14)
Ni-salt	57.69	(2.01)	76.53	(1.96)	99.67	(4.14)
Mn-salt	57.69	(2.03)	76.53	(1.96)	99.67	(4.14)
Black Fe-salt	57.69	(2.05)			99.01	(4.18)
Orange Fe-salt	60.00	(2.11)			99.01	(4.11)

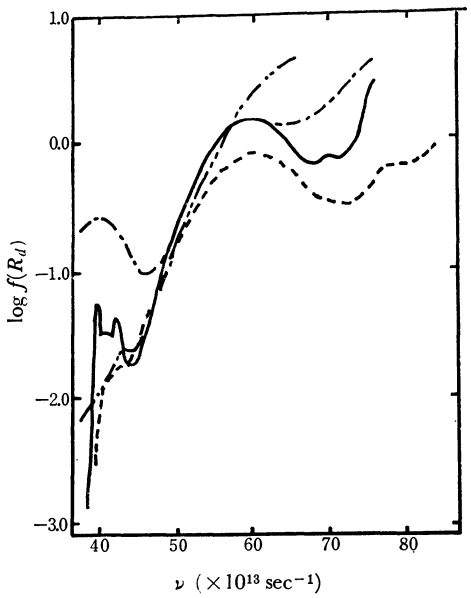

Fig. 2. The reflection spectra of the Mn-salt (——), the Ni-salt (— - —), the orange Fe-salt (— - - —) and Reinecke's salt (- - -).

be observed in the visible absorption spectra of these compounds in aqueous solution.

In the Mn-salt, an absorption peak which seems assignable to the second absorption band of manganese sulfate in aqueous solution is also faintly observed at $69.77\times10^{13}\,\mathrm{sec}^{-1}$. Besides, three absorption bands are observed in the frequency range from $38.71\times10^{13}\,\mathrm{sec}^{-1}$ to $44.44\times10^{13}\,\mathrm{sec}^{-1}$, which are thought probably due to the overlapping of the electron spin forbidden band with the first bands of manganese(II) cation and Reinecke's anion.

In the orange Fe(III)-salt, both the first and second bands corresponding to those of Reinecke's salt could not be observed, and only an electron spin forbidden band was found.

In the reflection spectrum of the black Fe(III) salt, no positive peak was detected because of the black color due to an intense absorbance over all wavelengths measured.

IR Spectra. The infrared absorption spectra of the Ni- and Mn-salts, which are very similar, are shown in Fig. 3, together with those of the Co-salt[1] and Reinecke's salt. Since the absorption peaks assigned to the C-N stretching vibration of the Ni- and the Mn-salts does not shift so greatly, and the peaks due to C-S stretching are also observed in a higher wave number region than that of the Co-salt,[1] but lower than that of Reinecke's salt, the bond between the sulfur atom in an NCS group and nickel(II) or manganese(II) ion is not so strong as the corresponding bond in the Co-salt.

The IR spectra of the black and orange iron(III)-salts are shown in Fig. 4. In the black Fe(III)-salt, two peaks, assigned to C-N stretching at 2117 and 2075 cm^{-1}, are observed; the former peak may be due to an appreciable interaction between the sulfur in coordinated NCS and iron,

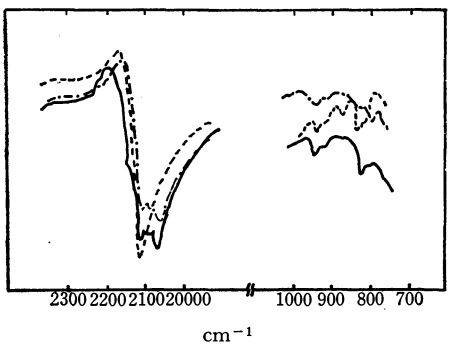

Fig. 3. The infrared spectra of the Mn-salt (——), the Ni-salt (— - —) and Reinecke's salt (- - -).

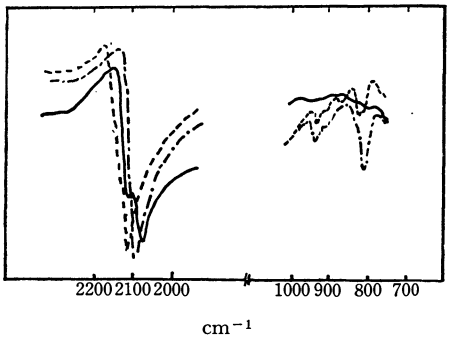

Fig. 4. The infrared spectra of the black Fe-salt (——), the orange Fe-salt (— - —) and Reinecke's salt (- - -).

TABLE 3. THE ANALYSES OF THE X-RAY DIFFRACTION AND DENSITY OF THE REINECKE'S TYPE SALTS

	c/a	a(Å)	c(Å)	ρ Calcd	ρ Found	Z
Reinecke's salt	1	13.42	13.42	1.50		6
Ni-salt	1.3	13.08	17.35	1.59	1.53	8
Mn-salt	0.96	11.41	10.95	1.69	1.12	4
Black Fe-salt	0.9	15.81	14.23	1.55	1.60	8
Orange Fe-salt	1.2	12.24	14.70	1.73	1.45	8

but assumably it will be weaker than that in the corresponding Co-salt; the latter should be independent of such an interaction.

There was found, on the other hand, only one peak at 2098 cm^{-1} due to the C–N stretching vibration in the orange iron(III)-salt as shown in Fig. 4. This may be attributed to the iron being surrounded by large coordinated chloride atoms, as pointed out by Fujita *et al.*[2] In the cholin-salt, the effective charge is small, since the positive charge on the nitrogen atom is screened by bulky aliphatic groups and so the interaction between the thiocyanate group and cholin ion may be negligibly small.

Far-IR Absorption Spectra. The far infrared absorption spectra of the Ni(II)-, Mn(II)-, black Fe(III)- and orange Fe(III)- salts are shown in Fig. 5. In the Ni(II)- and Mn(II)-salts, the band near 500 cm^{-1} assigned to the Cr–N stretching vibration involving NH_3 does not shift or split, whereas the band appearing in the region immediately to lower wave number than that of the former band assigned to NCS bending slightly splits into two peaks, but the splitting is not so large as that in the Co-salt. Thus it is thought that the nickel and manganese ions bind weakly with isothiocyanate groups through the sulfur atom.

The spectrum of the black Fe(III) salt resembles that of the Ni-salt, except for the appearance of a small band at 393 cm^{-1} which is probably due to slight contamination with $FeCl_3$. Hence, the interaction between iron and thiocyanate may have a strength similar to the Ni-salt.

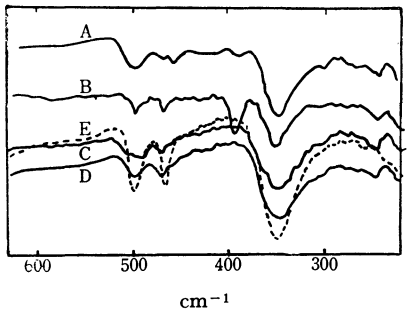

Fig. 5. The far infrared spectra of the Mn-salt (A), the orange Fe-salt (B), the black Fe-salt (C), the Ni-salt (D) and Reinecke's salt (E) (- - -).

The orange Fe(III)-salt has, on the other hand, a new band at 390 cm^{-1}, which has never been observed in the other Reinecke type salts. It consists of two absorption peaks. They are assigned to Fe-Cl stretching vibrations which are attached to hydrogen ion and which are not. Besides, the band assigned to the Cr–N stretching vibration involving an NCS group is commonly observed at 347 cm^{-1} in all Reinecke type salts, and Reinecke's salt itself treated in these papers.[1]

Magnetic Susceptibility. The calculated value of the effective magnetic moment from the magnetic susceptibility in the brownish-orange Ni-salt was 3.96 B. M. and the corresponding calculated value when the nickel is in a low spin state should be 3.87 B. M., which is in good agreement with the observed value described above. It may suggest that the nickel ion is probably surrounded by four sulfur atoms in a square planar arrangement. It is known that when the coordination of four sulfur atoms around nickel ion is square planar, the complex exhibits a brown or orange color; when it is tetrahedral, the complex becomes gray in color. Therfore, it can be predicted that when the former square planar complex is changed to the latter tetrahedral one, the value of the magnetic moment should increase. Nevertheless, the value of the magnetic moment in the Ni-salt heated at 68°C is found to be 4.01 B. M., being not so large as that calculated assuming a tetrahedral configuration around the nickel ion. This is probably due to the incompleteness of the structure change from square planar to tetrahedral.

The observed value of the magnetic moment in the Mn(II)-salt was 5.13 B. M. It is much smaller than the calculated value for a high spin state for manganese, 6.41 B. M. However, it is still larger than that for low spin type manganese, 4.39 B. M. The value of 5.41 B. M. is also expected for the square planar structure for the Mn-salt. These results, therefore, indicate that manganese ion is surrounded by four sulfur atoms in a square planar arrangement in the salt. However, such an interpretation is still inconsistent with that obtained from the reflection spectrum measurement. In addition, the bond between manganese ion and

2) J. Fujita, K. Nakamoto and M. Kobayashi, *J. Am. Chem. Soc.*, **78**, 3256 (1956).

sulfur atoms in a thiocyanate group is weak enough since no shift of the band due to the C–N stretching vibration can be detected in the infrared spectrum. At present, no successful explanation for these phenomena has been given without any discrepancies.

The effective magnetic moment of the black Fe(III)-salt was obtained as 5.0 B. M. The interpretation for the configuration of coordinated atoms around the iron(III) ion can not be appropriately given due to a mixing of iron(III) trirhodanate into the Fe(III)-salt.

The value obtained for the magnetic moment of the orange Fe(III) salt was 4.85 B. M. If iron atom is surrounded by two chloride ions and two Reinecke's anions forming a square planar structure, the calculated value obtained is 4.38 B. M. Therefore it is adequate to consider that this salt has a square planar structure and an ionic character.

X-Ray Diffraction Measurement. The results of an analysis of the X-ray diffraction patterns are summarized in Table 3.

The density of the Ni- and the black Fe-salt are nearly equal to that of Reinceke's salt. This indicates that these salts have not so strong a bond between the metal ions and Reinecke's anion as is the case in the Co- and Cu-salts. The values for the densities of the Mn- and orange Fe-salts obtained do not equal those of the salts mentioned above.

The authors wish to express their gratitude for a grant from the Ministry of Education for these studies.

BULLETIN OF THE CHEMICAL SOCIETY OF JAPAN VOL. 41 2366—2371 (1968)

Synthetic Inorganic Ion-exchange Materials. XII. Some Observation on Surface Structure and Cation-exchange Behaviour of Three Different Antimonic Acids

Mitsuo ABE and Takuji ITO

Department of Chemistry, Tokyo Institute of Technology, Ookayama, Meguro-ku, Tokyo

(Received September 20, 1967)

The cation-exchange behaviour and surface functionality of three different antimonic acids, amorphous, glassy and crystalline, were studied by thermogravimetric measurement, infrared absorption spectrometry and change in uptake of potassium ions upon heating. The ion-exchange capacities of the amorphous and glassy antimonic acids decrease with the loss of chemically bonded water. In contrast, the capacities of the crystalline acid heated within 200°C rarely change because of the loss of the interstitial (free) water and no drastic change occurs in the surface structure of the crystal. The crystalline acid with free water removed adsorbs moisture upon exposure to the atomsphere at room temperature. Upon heating above 300°C, the tenaciously bonded water was removed and the cation-exchange capacity decreased simultaneously. The infrared absorption spectra indicated that the surface functionality of the crystalline acid, similar to that of crystalline sodium antimonate $Na[Sb(OH)_6]$, is different from those of the amorphous and glassy acids. It seems that chemically bonded water in the crystalline acid is tenaciously combined as Sb-OH.

In recent years, increased interest in inorganic ion-exchangers has appeared.[1-3] Disadvantages in present types of organic ion-exchangers, such as instability at high temperature and at high levels of ionizing radiation and the limitation in selectivity, sparked the development of inorganic ion-exchangers.

In previous papers we showed that antimonic acid[4] and polyvalent antimonates[5,6] have useful cation exchange properties for akali metal ions,

1) K. A. Kraus, H. O. Philips, T. A. Carlson and J. S. Jonson, Proceedings of the Second International Conference on Peaceful Uses of Atomic Energy, Geneva, 1958, paper No. 15/p/1832 (1958).

2) C. B. Amphlett, L. A. McDonald and M. J. Redman, *J. Inorg. Nucl. Chem.*, **6**, 220 (1958).

3) For example, K. A. Kraus and H. O. Philips, *J. Am. Chem. Soc.*, **78**, 644 (1956); L. Baseste and J. Pelsmackers, *J. Inorg. Nucl. Chem.*, **21**, 124 (1961).

4) M. Abe and T. Ito, *Nippon Kagaku Zasshi (J. Chem. Soc. Japan, Pure Chem. Sect.)*, **87**, 1174 (1966).

5) M. Abe and T. Kenjo and T. Ito, *Kogyo Kagaku Zasshi (J. Chem. Soc. Japan, Ind. Chem. Sect.)*, **70**, 291 (1967).

6) M. Abe and T. Ito, *ibid.*, **70**, 440 (1967).

including a suitable rate for adsorption and desorption in column operation. The antimonic acid showed that differences in selectivity for alkali metal ions are very large and that mutual separation can be achieved with a small column ($0.8\phi \times 6.0$ cm).[7] The antimonic acid obtained through the hydrolysis of antimony pentachloride was gradually peptized by immersing it in pure water for a long period of time. Preparation of the antimonic acid under various conditions has been studied to obtain a chemically stable material[8]; at first, the hydrolyzed precipitate was in an amorphous state, but was gradually transformed into a crystalline powder when it was kept for long time in the mother liquid. Freshly prepared amorphous precipitate in a wet state was dissolved in hot water, and glassy material obtained by cooling the solution rapidly and then evaporating the moisture.

In the investigation of the Sb-O-H_2O system, the thermal decomposition of the three different antimonic acids has already been studied by thermogravimetry and differential thermal analysis, and X-ray powder diffraction analysis and chemical analysis of the oxygen content were made of the thermally decomposed products[9];

$$S_A: Sb_2O_5 \cdot nH_2O \rightarrow Sb_2O_5(\text{amorphous}) \downarrow$$

$$S_G: Sb_2O_5 \cdot nH_2O(G) \rightarrow Sb_2O_5(G) \rightarrow Sb_6O_{13}(C) \rightarrow Sb_2O_4$$

$$S_C: Sb_2O_5 \cdot 4H_2O(A) \rightarrow Sb_2O_5 \cdot 2H_2O(A) \rightarrow Sb_2O_5(B) \rightarrow Sb_6O_{13}(C)$$

(A), (B) and (C), which are cubic space groups $Fd3m(O_h^7)$, have lattice constants of 10.38_2, 10.28 and 10.305 Å, respectively. In order to clarify problems involving the mechanism of the ion exchange ability, the present paper describes the ion-exchange properties and infrared spectra of the three different antimonic acids dried at increasing temperature.

Experimental

Preparations of the Three Different Antimonic Acids. All samples were prepared as described previously[8]: concentrated antimony pentachloride solution (1 : 1), prepared by dropping liquid antimony pentachloride into the same volume of cold water, was hydrolized in a large amount of water at 25°C; $\mathbf{S_A}$, the hydrolyzed precipitate was kept in mother liquor at 25°C for 4 hr, and washed until free of Cl^- with a centrifuger (about 10000 rpm); $\mathbf{S_C}$ the crystalline antimonic acid was obtained by aging the precipitate in mother liquor at 30°C for 20 days; $\mathbf{S_G}$ the antimony pentachloride solution (30 m*l*) was hydrolyzed in 1 *l* of water at 20°C, and let stand for 4 hr. The precipitate, washed with water, was then dissolved in 300 m*l* of hot water. The glassy gel, (G) having five weak inflexions (d; 3.28, 2.63, 1.72, 1.64 and 1.38 Å), was obtained by cooling the solution rapidly and then evaporating the moisture.

When these products were dried with a fan at room temperature over a period of 6 months, they were transformed into granular material suitable for column operation. The dried samples were ground and separated into 100—200 mesh size, and in the sieves the granules of the antimonic acids were washed with water in roder to remove small quantities of adherent antimonic acid dust.

Uptake of Potassium Ions. When the antimonic acid is added to a solution of potassium chloride, hydrogen ions in the material are equivalently liberated by cation exchange in the external solution. The uptake of potassium ions was determined as follows; 50 m*l* of 0.1 N KCl solution was added to 0.4 g of the antimonic acid sample in a 100 m*l* bottle with a glass stooper, and after 48 hr, each solution, containing liberated hydrogen ions, was titrated with standard 0.1 N NaOH solution.

Measurement of Infrared Absorption Spectra. Infrared spectra was measured with a standard KBr disk and hexachloro-1,3-butadiene (H. C. B.) mulls technique, using an Hitachi EPI-S recording spectrometer. Measurements were carried out in comparison with the KBr blank disk, and the H. C. B. was previously dehydrated with anhydrous calcium sulfate.

Results and Discussion

Uptakes of Potassium Ions on Three Different Antimonic Acid at Various Drying Temperatures. The uptake of potassium ions by the antimonic acids, heated for 4 hr at 60°C to 1000°C and then kept in the atmosphere at room temperature, is shown in Fig. 1. The uptakes of

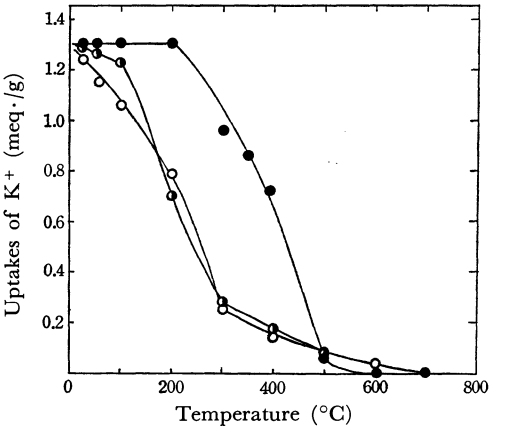

Fig. 1. K^+-uptakes on three different antimonic acids after heating to 900°C.
○: Amorphous antimonic acid
●: Crystalline antimonic acid
◑: Glassy antimonic acid

7) M. Abe and T. Ito, This Bulletin, **40**, 1013 (1967).
8) M. Abe and T. Ito, *ibid.*, **41**, 333 (1968).
9) M. Abe, *Kogyo Kagaku Zasshi (J. Chem. Soc. Japan, Ind. Chem. Sect.)*, **70**, 2226 (1967).

the heated amorphous and glassy samples decreased continuously with increasing temperature, and showed no exchange properties above 600°C. In contrast, the uptake of the crystalline samples heated at 60 to 200°C scarcely decreased with increasing temperature, but decreased rapidly above 300°C, and then the samples heated to 700°C showed no ion-exchange properties, similar to the amorphous and glassy samples.

Thermal Decomposition and Re-hydration Processes. The particular investigation of the thermal decomposition of three different antimonic acids has been reported previously.[9] The changes in weight loss of the samples heated under the same condition are illustrated in Fig. 2. The

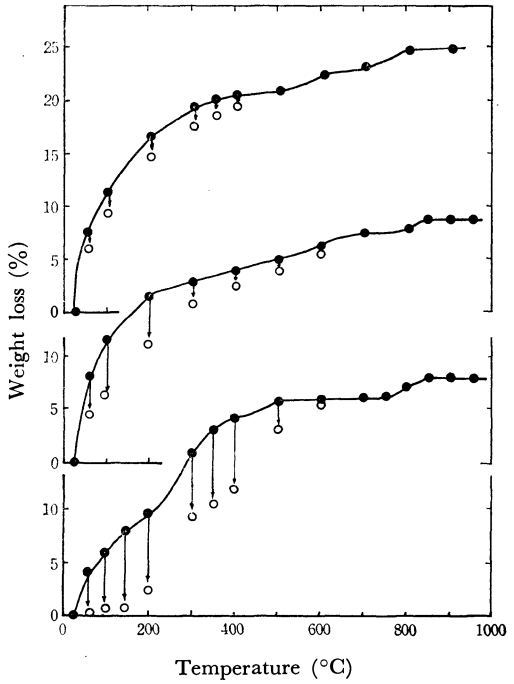

Fig. 2. Water adsorption on the heated antimonic acid samples.
(Top) amorphous antimonic acid
(Middle) glassy antimonic acid
(Bottom) crystalline antimonic acid
●: Heated for 4 hr and then weighted after 15 min
○: Weighted after admission for 1 month at room temperature

amorphous acid was continuously dehydrated without loss of oxygen by heating below 600°C, and then transformed into Sb_2O_5 (G) showing weak X-ray diffraction intensities. The loss of oxygen began from 650°C and Sb_2O_5(G) transformed into Sb_6O_{13}(C). As the decrease in potassium ion uptake is comparable to the amount of dehydration, it is evident that the ion-exchange capacity decreases with the loss of hydrated water. These results suggest that the concentration of exchangeable hydrogen ions in the material phase is decreased by this treatment.

On the crystalline antimonic acid, the decrease in the uptake is different from that obtained for the amorphous or glassy acids. The weights of all the samples, heated at below 200°C and then kept in air at room temperature for a relatively short time, return to the initial values by adsorbing moisture from the atomosphere. X-ray diffraction analysis indicated that no drastic change in the structure of the crystal occurs when the free water molecule are lost.

The loss of water, found to be reversible, is attributed to the removal of the free water which can be desorbed by heating and adsorbed by cooling without change in the crystal structure. With increasing the temperature above 300°C, the crystalline antimonic acid begins to lose bonded water which constitutes part of the crystal structure. The reversibility of the free water decreased simultaneously with increasing temperature, and samples heated above 700°C showed no adsorptive properties toward moisture. It is evident that the decrease in uptake of the crystalline acid does not occur with the removal of free water, but with a decrease in the bonded water by heating above 300°C.

Infrared Absorption Spectra of the Three Different Antimonic Acids. Any difference between the amorphous or glassy acids and the

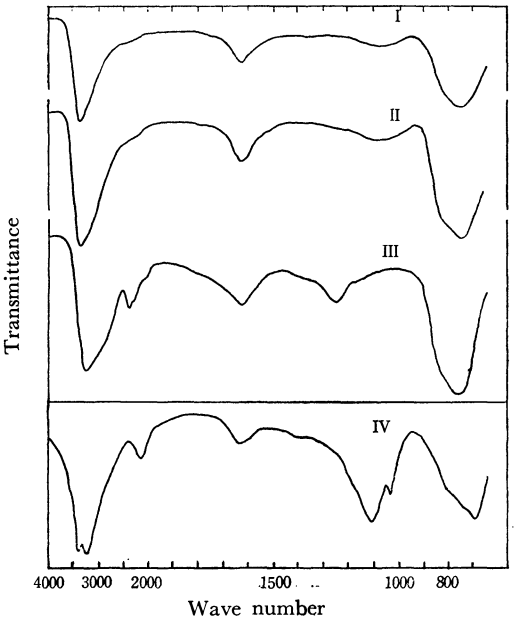

Fig. 3. Infrared absorption spectra of three different antimonic acids and sodium antimonate.
I: Amorphous acid
II: Glassy acid
III: Crystalline acid
IV: Sodium antimonate

crystalline acid in adsorptive properties toward lithium ions is expected to depend on surface functionality. Hence, surface functionality refers collectively to the chemical functional groups which terminate the bulk structure of the solid and their immediate environment, as reported by McDonald.[10]

The absorption band between 2800 and 3800 cm^{-1} with a maximum at 3350 cm^{-1} is characteristic of interstitial water and OH groups, and the band between 1500 and 1760 cm^{-1}, with a maximum at 1630 cm^{-1}, is due to the deformation vibration of the interstitial water. The absorption bands for the amorphous and glassy acids are similar to those obtained for a number of metallic hydrous oxides (such as Zr, Sn and Th[11]), with the exception of the stretching vibration of Sb-O with a maximum at 750 cm^{-1}.

The crystalline antimonic acid showed band having maxima at 2430 and 1280 cm^{-1} in addition to the bands found for the amorphous and glassy acids. Its spectrum is almost the same as that of sodium antimonate $Na(Sb(OH)_6]$ (tetragonal crystal system $P4/n$), as illustrated in Fig. 3. It has been known that the OH groups in the antimonate coordinate with one atom of antimony. Siebert[12] deduced that the intense absorption band between 1000 and 1200 cm^{-1} on the antimonate must be assigned to the Sb-OH deformation vibration of the antimonyl group in octahedra, and the maximum intensity at 2145 cm^{-1} is probably due to an overtone of the Sb-OH deformation vibration. The band between 1100 and 1350 cm^{-1} of the crystalline acid can be assigned to the Sb-OH deformation vibration, though it is shifted to higher frequency in comparison with that of the antimonate. It is concluded that the crystalline antimonic acid is different from the amorphous and glassy acids, not only in fundamental crystal structure, but also in surface functionality. The broad adsorption band between about 2700 and 3800 cm^{-1} implies that hydrogen bonding exists between OH groups and the water molecules surrounding them.

Infrared Spectra of Three Different Antimonic Acids at Various Drying temperatures. Infrared absorption spectra of the amorphous acid heated for 4 hr at 100 to 700°C are shown in Fig. 4. Absorption bands due to OH groups continuously decreased with increasing temperature, and a drastic change in the band at 750 cm^{-1} was caused by heating to 700°C, indicating the formation of Sb_6O_{13}.[9] Measurements with an H. C. B. mull showed that absorption bands involving OH groups and water disappear at 600°C. The disappearance

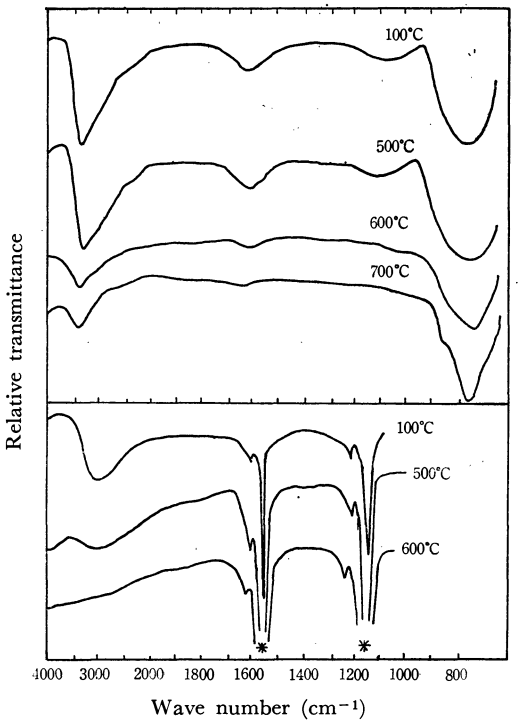

Fig. 4. Infra-red absorption spectra of amorphous antimonic acid after heating to 700°C for 4 hr.
(Top) KBr disk method
(Bottom) H.C.B. suspended method
* absorption band of H.C.B.

of both the OH and H_2O bands supports our conclusion[9] that the product heated at 700°C is not Sb_3O_6OH as reported by Dihlström *et al.*[13] and Schrevelius,[14] but Sb_6O_{13}. Similar changes were observed upon heat treatment of the glassy antimonic acid. The decrease in intensity of the OH-band below 600°C is ascribed to the condensation of acid groups in the amorphous or glassy antimonic acids to Sb-O-Sb. Sb_2O_5 was formed on heating at 600°C for 4 hr. By the condensation of acid groups, as assumed in metallic hydrous oxide,[11,15] it is possible to explain the irreversible loss of water in these acids. The condensation decreases the concentration of exchangeable hydrogen ions in the materials, and therefore causes a lower uptake of potassium ions. However, information obtained from this measurement is not enough to arrive at a proper conclusion on the surface functionality of amorphous antimonic acid. Further confirmation of the surface functionality

10) R. S. McDonald, *J. Phys. Chem.*, **62**, 1168 (1958).
11) C. H. Wirguin and A. A. Yaron, *J. Inorg. Nucl. Chem.*, **28**, 2378 (1966).
12) H. Siebert, *Z. Anorg. Allgem. Chem.*, **301**, 161 (1959).
13) K. Dihlström and A. Westgem, *ibid.*, **235**, 153 (1937).
14) N. Shrewelius, Studier över antimonat, hydroantimonate och fluoantimonat; Dissertation, University of Stockholm (1943). *Cf.* C. J. Vitaliano and B. Mason, *Am. Min.*, **37**, 982 (1952).
15) V. Vesely and V. Pekarek, *J. Inorg. Nucl. Chem.*, **25**, 697 (1963).

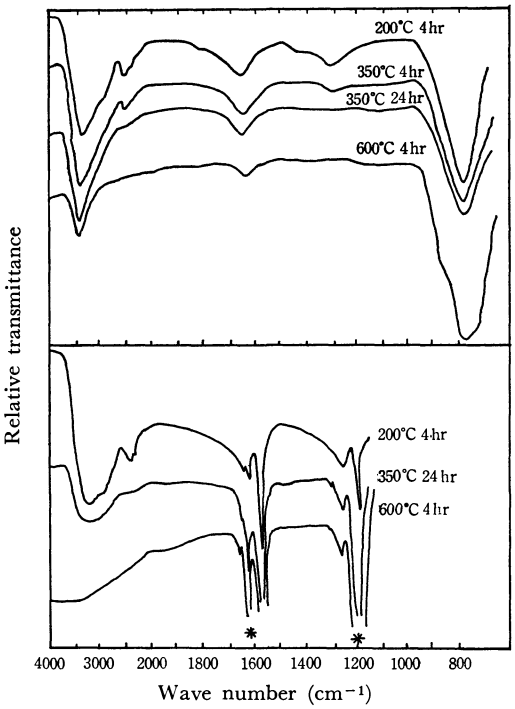

Fig. 5. Infrared absorption spectra of crystalline antimonic acid after heating to 600°C.
(Top) KBr disk method
(Bottom) H.C.B. suspended method
* absorption band of H.C.B.

must be obtained by checking other physical and chemical properties.

In the crystalline antimonic acid, little change was observed when samples were heated at 60—200°C, but at 300°C, the absorption bands of Sb-OH decreased with increasing temperature, corresponding to the removal of strongly bonded water, which comprises part of the crystal structure, as deduced from the results of X-ray examinations.[9] These results indicate the existence of strongly bonded water combined with Sb-OH. It is possible to interpret that the uptake of the alkali metal ions on the crystalline acid scarcely changes due to the removal of interstitial water, but decreases rapidly upon decomposition of the Sb-OH groups. The infrared spectra of the crystalline acid heated at 700°C showed a change in the intensity of the Sb-O stretching vibration, indicating a drastic change to Sb_6O_{13}, as in the amorphous acid.

Infrared Spectra of Three Different Antimonic Acid adsorbed Alkali Metal Ions. The ion-exchange properties of the surface sites of the hydrous oxides of metals is very important problem, but little is known concerning their immediate environment except in the case of amorphous silica.[10]

When the hydrogen forms of the amorphous samples were converted to sodium or potassium forms by treatment with a solution of 0.1 N NaCl or 0.1 N KCl, using a column technique, the infrared spectra scarcely changed from those of the hydrogen forms, as illustrated in Fig. 6.

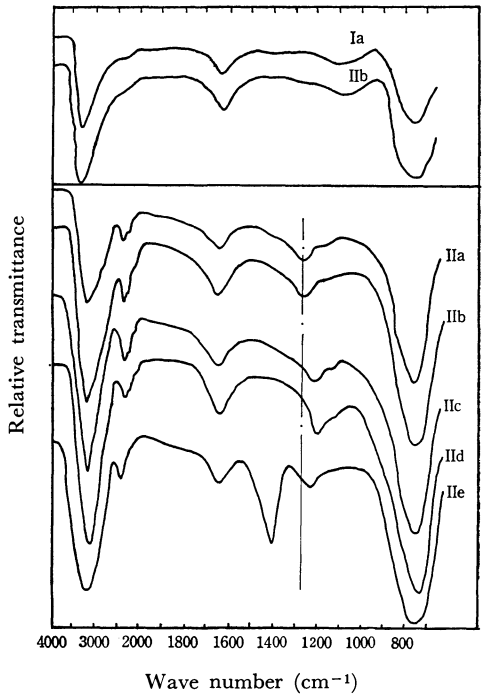

Fig. 6. The infrared absorption patterns of antimonic acids before and after exchange with alkali metals (KBr disk).
(Top) amorphous antimonic acid, Ia: H-form, Ib: K-form, (Bottom) crystalline antimonic acid, IIa: H-form, IIb: 1.1 mep.K^+/g, IIb: 2.2 meq.K^+/g, IId: 2.8 meq.Na^+/g, IIe 2.0 meq.NH_4^+/g

The spectra of the crystalline acid was similar to that of the hydrogen form, except that the deformation band of Sb-OH was shifted to a lower vibration frequency with the adsorption of alkali metal ions. It has been known that an atom or molecule adsorbed near a surface perturbs the motions of atoms of the group, causing a shift in some group vibration frequency.[10] Such a shift is evidence that the deformation frequency at 1280 cm^{-1} on the hydrogen form is affected by the chemically adsorbed ions. It is possible to explain a shift to lower frequency, assuming that an increase in reduced mass occurs near the surface groups by conversion to alkali metal forms. If hydrogen ions in Sb-OH exchange to the alkali metal ions in the external solution, the absorption intensity of Sb-OH should apparently decrease. However, little change in the intensities were observed in conversions by any alkali metal ions.

From these results, it is possible to propose the

following structure for the crystalline antimonic acid $H_2Sb_2O_5(OH)_2$:

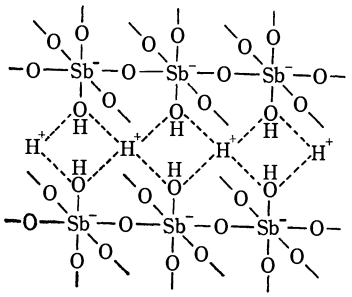

$H_2Sb_2O_5(OH)_2$

The hydrogen ions in the structure may be combined as H_3O^+. If 5 molecules of water are removed from two $H[Sb(OH)_6]$ molecules, modified from $Na[Sb(OH)_6]$, such a structure is easily deduced. It seems that, however, the hydrogen bonding surface groups are constrained by rigid three-dimensional bonding, in the same manner as the Sb_4O_6 molecule in senarmontite (cubic Sb_2O_3),[9] and that the ion-exchangeable hydrogen ions are surrounded by six oxygen atoms, as Na^+ in $Na[Sb(OH)_6]$.

In the amorphous and glassy acids, though information obtained from infrared spectra measurements is too little to allow an evaluation of the surface functionality, the results on the irreversible loss of the water by the heated samples indicates that a large part of water included in these materials are chemically bonded, and decreases continuously with increasing temperature, involving condensation of the acid groups. From a previous experiment, it was thought that the difference between the amorphous and glassy acids is only the difference in particle size.[9] The matrix of the glassy acid is Sb_2O_5 (structure G), and scarcely changes with increasing temperature (below 600°C). The ion-exchange capacity correspondingly decreased with the loss of water molecules in the material. Therefore, it seems that the water included in the amorphous or glassy acids is not simply interstitial water but bonded water. The existence of isolated OH groups was not observed through hydrogen bonding in the materials.

The following surface structure is probable for the amorphous and glassy acids, although the structure of the hydrogen bonded water molecules is uncertain.

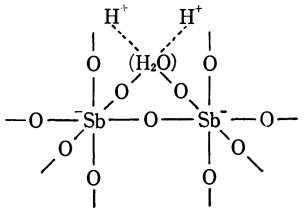

$Sb_2O_5 \cdot nH_2O$

We have already pointed out that disparity of lithium adsorptions on the antimonic acid obtained by various preparations is not due to a difference in particle size of the materials, but the existence of different typs having a difference in selectivity toward lithium ion adsorption.[8] In present experiment, it may be concluded that the difference in selectivity is closely connected to the difference in surface functionality in the antimonic acids.

BULLETIN OF THE CHEMICAL SOCIETY OF JAPAN VOL. 41 2371—2375 (1968)

Tensammetric Study of the Adsorption of Brucine

Mutsuo KODAMA, Mitsuko MURATA, Tomohiko NODA and Akiko KIMURA

Department of Chemistry, Ibaraki University, Mito, Ibaraki

(Received October 25, 1967)

This paper will present two results of experiments concerning the adsorption of brucine. We will first discuss the adsorption of brucine on D. M. E. studied tensammetrically. Brucine was found to give a tensammetric wave with two peaks, at +0.10 V and −1.15 V *vs.* SCE. The positive tensammetric peak can be ascribed to the usual adsorption process. The second peak, however, behaved differently from the first, probably due to the reformation of adsorbed brucine film involving the protonation and the reorientation of brucine. Secondly, we will present experimental facts concerning the depressive effects of brucine on the reduction waves of copper(II).

Brucine has been reported to produce a catalytic wave in the pH range from 5.0 to 12.0.[1] In previous papers,[2,3] we studied chronopotentiometrically the perturbation effect of adsorbed

1) H. F. Kirkpatrick, *Quart. J. Pharm. Pharmacol.*, **19**, 127 (1946).
2) M. Kodama and R. W. Murray, *Anal. Chem.*, **37**, 1638 (1965).
3) R. W. Murray and M. Kodama, *ibid.*, **37**, 1759 (1965).

brucine on the electroreduction of copper(II) in a tartrate medium and the discriminative effects of the brucine film toward the electroactive-metal-complex enantiomers. In the absence of brucine, the chronopotentiometry of copper(II) tartrate shows a diffusion-controlled character and the behavior of copper tartrate *d*- and *l*-enantiomers is identical. In the presence of brucine, however, the electrolysis is no longer diffusion-controlled and the product, $i \cdot \tau^{1/2}$, of the chronopotentiometric wave of copper(II) decreases linearly with an increase in the applied current. A measurable difference in $i \cdot \tau^{1/2}$ value between the copper(II) complex of *d*-tartrate and that of *l*-tartrate was also observed. These facts were ascribed to the interaction between the copper tartrate complex and the adsorbed brucine film, but no precise description of the nature of the surface interaction of brucine film with the electroactive species was given.

In view of all this, it is worthwhile to study the nature of the adsorbed brucine film. In the present paper, we will discuss our study of the adsorption of brucine on DME using the tensammetric method.

Experimental

Reagents. The tartaric acid and brucine sulfate used were of an analytical reagent grade (Tokyo Kasei). All the other chemicals were of an analytical reagent grade and were used without further purification.

Apparatus. The tensammetric waves of brucine were measured with a Yanagimoto PA-102 Pen-recording Polarograph either manualy or automatically. The d.c. potentials appllied were determined by using a Shimadzu K-2 potentiometer.

The flow rate of mercury, m, and the drop time, t_d, of the dropping mercury electrode (DME) were measured and found to be 1.24_8 mg/sec and 6.30 sec respectively in an air-free 0.10 M acetate buffer solution of pH 4.80, with an open circuit at 60 cm of a mercury column at 25°C. A saturated calomel electrode (SCE) of a large area was used as a reference electrode and connected to the cell solution through a Hume and Harris type salt bridge. In a. c. polarographic measurements, a 200-μF condenser was used to minimize the effect of cell resistance.[4] The pH of the solution was measured with a glass electrode pH meter (Hitachi-Horiba Model M-4).

All the polarographic studies were carried out at 25°C in solutions of 1.50 ionic strength, which was adjusted by adding appropriate amounts of sodium sulfate. The oxygen dissolved in the sample solution was removed by bubbling pure nitrogen gas through the solution.

Results and Discussion

Tensammetric Behaviors of Brucine. As is obvious from the curves in Fig. 1, brucine lowers the surface tension at the interface of a mercury-electrolyte solution and changes the electrocapillary

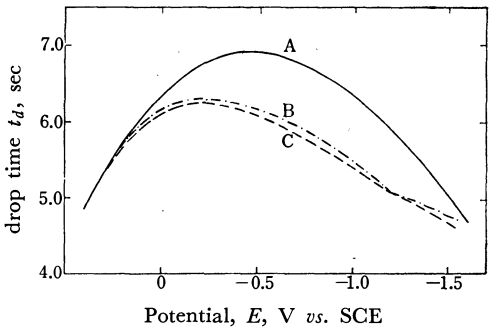

Fig. 1. Electrocapillary curves.
A pH=4.0, 0.50 M sodium sulfate
B pH=2.0, 0.50 M sodium sulfate, 1.0 mM brucine
C pH=7.0, 0.50 M sodium sulfate, 1.0 mM brucine

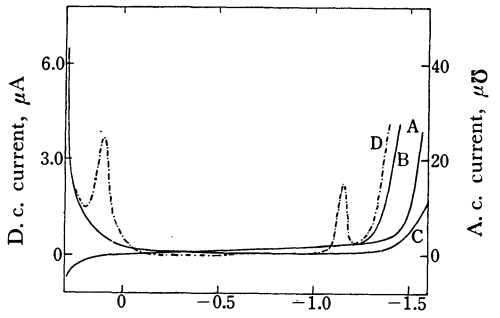

Fig. 2. D. c. and a. c. base-currents.
pH=4.0, 0.50 M sodium sulfate
A d. c. base-current, no brucine
B d. c. base-current, 1.0 mM brucine
C a. c. base-current, no brucine
D a. c. base-current, 1.0 mM brucine

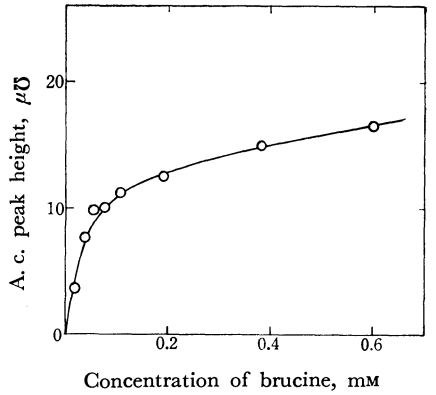

Fig. 3. The peak-height of the first a. c. polarographic wave and the concentration of brucine.
pH=4.0, 0.50 M sodium sulfate

4) B. Breyer, F. Gutmann and S. Hacobian, *Australian J. Sci. Res., Ser. A*, **4**, 595 (1951).

curve considerably. The top part of the electrocapillary curve becomes very flat. The surface-tension lowering by brucine was found to be independent of the pH value of the solution and of the nature of the supporting electrolyte (Fig. 1). The lowering of the a.c. base current and the appearance of an a.c. polarographic wave due to the presence of brucine are also shown in Fig. 2. The a.c. polarographic wave, with summit potentials at +0.10 V and −1.15 V *vs.* SCE, can be considered to be tensammetric in nature, because it is not accompanied by a corresponding d.c. step (Fig. 2). The maximum depression of the a.c. base-current was shown to occur at the potential around the e.c.m. (electrocapillary maximum). The surface-tension lowering and the a.c. base-current lowering become greater with an increase in the concentration of brucine in the bulk solution. The dependence of the peak height of the positive tensammetric wave on the brucine concentration is shown in Fig. 3. The peak height increases with the concentration up to 0.1 mM and reaches a limiting height above concentration of 0.2 mM following a typical Langmuir-type relation.

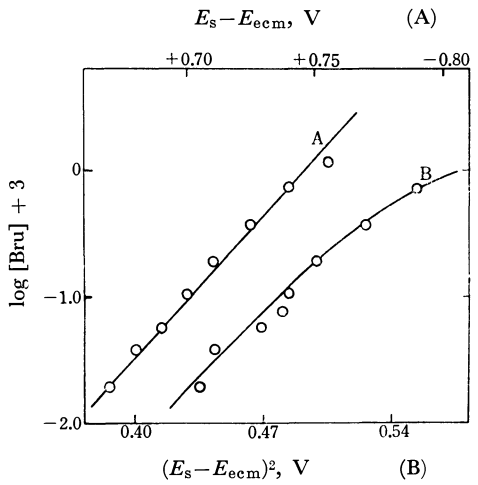

Fig. 4. Relation between log [Brucine] and $E_{ecm}-E_s$ or $(E_{ecm}-E_s)^2$ for the first peak-height.
pH=2.00, 0.50 M sodium sulfate
A: $E_{ecm}-E_s$, B: $(E_{ecm}-E_s)^2$

The positive tensammetric peak was found to shift slightly to the more positive potential with an increase in the pH value and to disappear at pH values higher than 7.0, merging with the mercury dissolution wave. As Fig. 4 shows, it was also found to shift to the more positive potential with an increase in the brucine concentration in all the supporting electrolytes tested (sulfate and tartrate) according to the following relation, given by Breyer and Bauer.[5]

$$E_s - E_{ecm} = K_1 - K_2 \log C_{Bru}$$ [5]

where E_s represents the summit potential; E_{ecm}, the electrocapillary zero potential (−0.50 V *vs.* SCE), and C_{Bru}, the bulk concentration of brucine, and where K_1 and K_2 are constants.

The above experimental results clearly indicate that the positive tensammetric peak arises from the usual adsorption process involving the neutral form of brucine. This conclusion could also be confirmed by examining the effect of adsorbed brucine on the d.c. polarograms of copper(II). As Fig. 5 illustrates, the minimum occurs in the region of the e.c.m., showing the maximum adsorbability and the maximum depression action of brucine at this potential range.[6] At potentials more negative than the e.c.m., the depression of the limiting current becomes less pronounced with an increase in the negative potential; the wave height reaches its full height again at potentials more negative than −0.90 V *vs.* SCE.

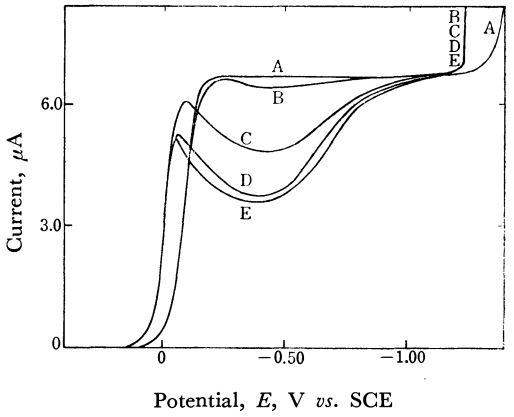

Fig. 5. Depressive effect of brucine on the reduction wave of copper(II), at ionic strength=1.50.
A 0.50 M tartrate, no brucine, pH=3.0
B 0.50 M tartrate, 1.0 mM brucine, pH=3.0
C 0.10 M tartrate, 1.0 mM brucine, pH=3.0
D 0.01 M tartrate, 1.0 mM brucine, pH=3.0
E 0.50 M Na_2SO_4, 1.0 mM brucine, pH=2.10

Conversely, the negative tensammetric peak differs considerably from the usual tensammetric wave involving the adsorption-desorption processes, in which, even at the potential where the negative peak appears, a lowering of the surface tension can still be observed (Fig. 1) and in which neither the plot of E_s-E_{ecm} nor that of $(E_s-E_{ecm})^2$ [5] against log C_{Bru} gives a linear relation, as is shown in Fig. 6.

The kink appearing in the electrocapillary curve shown in Fig. 1 corresponds exactly to the second summit potential, and a rise in the a.c. base-current can be observed on the negative side of the second wave. It is also interesting that the second tensammetric wave was always found to be accompanied by

5) B. Breyer and H. H. Bauer, "Alternating Current Polarography and Tensammetry," Interscience Publishers, New York (1963), p. 89.
6) *Ibid.*, p. 86.

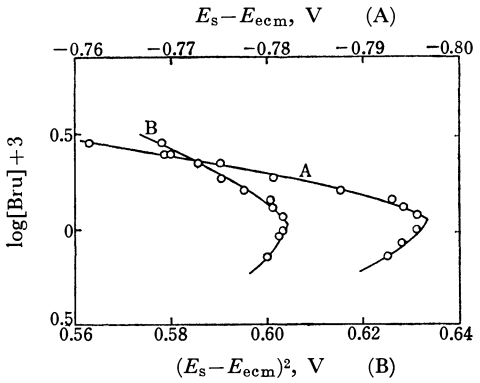

Fig. 6. Relation between log[Brucine] and $E_{ecm}-E_s$ or $(E_{ecm}-E_s)^2$ for the second peak-height.
pH=3.0, 0.50 M sodium sulfate
A: $E_{ecm}-E_s$, B: $(E_{ecm}-E_s)^2$

a catalytic wave (presumably due to the catalytic hydrogen discharge) in the pH range from 3.0 to 8.5 (contrary to the findings by Kirkpatrick[1]). At low concentrations of brucine, the catalytic wave occurs at a potential very close to the second summit potential. However, as the concentration of brucine increases, the separation between the second summit potential and the potential at which a catalytic wave occurs becomes greater.

Since the catalytic effect is generally influenced by the orientation of the catalytically-active species, and since the adsorption of positively-charged species must be advantageous compared with that neutral one at potential sufficiently negative with respective to the e.c.m., we can assume that the second tensammetric peak corresponds to a process such as the reformation of adsorbed brucine film involving the protonation and the reorientation of brucine. Here, the resulting brucine film with a relatively loose structure may be catalytically more active than that with a compact structure which is expected at high brucine concentrations.

The dependence of the peak height on the temperature was also examined in the temperature range from 15°C to 35°C. In this temperature range, both peak heights were found to decrease slightly with an increase in the temperature. On the other hand, it was also found that the peak height is little affected by the addition of 5×10^{-4} M LEO (Polyoxyethylene-Lauryl-Ether). From these results, we can deduce that brucine is firmly adsorbed on DME under the experimental conditions employed.

Strychnine was also found to be adsorbed on DME and to show exactly the same tensammetric behavior as brucine.

The Blocking Effect of Brucine on D. C. Polarographic Waves of Copper(II). Brucine was found to exert a depressive effect on the reduction waves of copper(II) in both sulfate and tartrate solutions. As has been described previously, the maximal depression of the limiting current occurs around the e. c. m.

In contrast to the sulfate system, the depressive effect of brucine on the reduction wave of copper(II) was demonstrated to become less pronounced in a tartrate solution upon an increase in the concentration of tartrate over the pH range from 2.0 to 5.0 (Fig. 5). Copper(II) has been reported to form a variety of complexes, depending on the pH value in solution and the concentration ratio between tartrate and copper(II). At a pH higher than 6 under a low ratio, mixed hydroxy-tartrate complexes have been reported.[7] A low pH value may be responsible for the formation of such a protonated

TABLE 1. FRACTION OF COPPER(II) PRESENT AS VARIOUS COMPLEX SPECIES IN 0.50 M AND 0.10 M TARTRATE SOLUTIONS

pH	Total concentration of tartrate, M	Fraction				
		Cu^{2+}	CuT	CuT_2^{2-}	CuT_3^{4-}	CuT_4^{6-}
1.20	0.10	0.998	0.002	—	—	—
	0.50	0.992	0.008	—	—	—
2.00	0.10	0.946	0.054	—	—	—
	0.50	0.786	0.211	0.003	—	—
3.00	0.10	0.207	0.687	0.106	—	—
	0.50	0.033	0.517	0.421	0.019	0.010
4.00	0.10	0.007	0.300	0.673	0.008	0.012
	0.50	—	0.057	0.623	0.040	0.280
5.00	0.10	0.001	0.113	0.744	0.027	0.115
	0.50	—	0.006	0.194	0.037	0.763
6.00	0.10	—	0.091	0.714	0.032	0.160
	0.50	—	0.003	0.145	0.033	0.819
7.00	0.10	—	0.091	0.711	0.032	0.166
	0.50	—	0.003	0.141	0.032	0.824

7) A. S. Tikhonov and V. P. Bel'skaya, *Obachxhei Khim., Akad. Nauk. S.S.S.R.*, **2**, 1211 (1953).

complex as $CuHT^+$.[8] At a low pH, in addition, a series of complexes expressed by CuT_x^{2-2x} may be expected, where $x=1$ to 4. From the step-by step formation constants for this series, reported to be 3.20, 1.91, −0.34, and 1.71 in logarithm value respectively,[9] the equilibrium compositions can be calculated. Table 1 shows the expected compositions in solution with various pH values. In a 0.50 M tartrate solution, the predominant species in the pH range from 3.0 to 7.0 are CuT_2^{2-} and CuT_4^{6-}. At pH 2.0, the major component is Cu^{2+}, while CuT is present in a small equilibrium concentration of 21%. Considering that the reported values may differ by several tenths from the logarithm values of true formation constants which can be safely used in the calculation, it can be concluded that there is no close relation between the composition of the tartrato-copper(II) complex and the minimizing action of the tartrate ion, but that the complex formation between copper(II) and the tartrate ion is essential. This conclusion is confirmed by the fact that, in a 0.10 M tartrate solution of pH 2.0, where almost all copper(II) ions were present in the form of Cu^{2+}, a pronounced depressive effect of brucine is observed. The importance of the complex formation in minimizing the depressive effect of brucine can also be seen by examining the effect of brucine on the limiting current of copper(II)-nitrilotriacetate complexes (a graph is not shown here). The depressive effect of brucine is eliminated completely by the addition of 10 mM nitrilotriacetate to 2.0 mM copper(II) at pH 4.0. Although the solution components in a 0.50 M tartrate solution of pH 6.0 are quite similar to those in the pH 5.0 solution, the effect of brucine was observed to be greater in the former solution. This clearly indicates that hydrogen ions also play an important role in the minimizing action performed the tartrate ion.

Though the detailed roles that tartrate and hydrogen ions play in the minimization of the depressive effect of brucine on the reduction of copper(II) in a tartrate solution could not completely explained in this study, and since, hence, further systematic investigations must be conducted to describe the characteristic nature of adsorbed brucine film precisely, we hope the results discussed here will provide suggestive clues for the explanation of the interaction between the adsorbed film and the electroactive substance at the electrode surface.

The authors wish to thank the Ministry of Education for the financial support given to this research.

8) H. Flashka, J. Butcher and R. Speights, *Talanta*, **8**, 400 (1961).
9) S. Froneaus, Dissertation Lund (Sweden), 1948.

BULLETIN OF THE CHEMICAL SOCIETY OF JAPAN VOL. 41 2375—2378 (1968)

The Kinetics of Substitution Reactions Involving Metal Complexes. XII. The Reactions between Copper(II) Ions and Zinc(II)-nitrilotriacetate Complexes

Nobuyuki TANAKA and Masaru KIMURA*1

Department of Chemistry, Faculty of Science, Tohoku University, Katahira-cho, Sendai

(Received November 13, 1967)

The kinetic study of the substitution reaction of copper(II) ions and zinc(II)-nitrilotriacetate complexes in acetate buffer solutions has been carried out with the same procedure as reported previously. The reaction was treated as to proceed through both hydrated metal ions and monoacetato complexes. The rate constants for eight elementary reaction paths, of which four involve the hydrated copper(II) ions and the others the monoacetatocopper(II) complexes, were determined at ionic strength 0.23 at 0°C. The values obtained indicate that all the reactions proceeding through hydrated copper(II) ions are faster than the corresponding reactions proceeding through monoacetatocopper(II) complexes.

Our previous study[1] showed that monoacetatonickel(II) ions react with nitrilotriacetate (NTA) anions faster than hydrated nickel(II) ions do. Since this was considered to be due to the characteristics of nickel(II) but not NTA ions, the confirmation was undertaken in the present study.

*1 Former name: Yu Saito.
Present address: Department of Applied Chemistry, Yamagata University, Yamagata Technical College, Zyonan, Yonezawa.

1) N. Tanaka and M. Kimura, This Bulletin, **40**, 2100 (1967).

The substitution reactions between copper(II) ions and zinc(II)-nitrilotriacetate complexes have been investigated, and the rate constants for eight reactions including the reactions between copper(II) ions and nitrilotriacetate anions have been determined.

Experimental

A solution of zinc(II) nitrate was prepared by dissolving a known amount of pure zinc metal in reagent-grade nitric acid. The preparation and standardization of all other chemicals used were the same as described in the previous paper.[1]

The rate of the reaction between copper(II) ions and zinc(II)-NTA complexes was determined by the measurement of the polarographic limiting diffusion current of copper(II) ions in acetate buffer solutions at 0°C and ionic strength 0.23. The ionic strength was adjusted with potassium nitrate. Gelatin was added as a maximum suppressor by 0.01% in concentration. The pH of the solution was measured after the polarographic measurement with a Hitachi-Horiba Model M-4 pH meter.

Result

In the acetate buffer solution containing acetate ions up to 0.2 M in concentration, the overall substitution reaction of copper(II) ions and zinc(II)-NTA complexes is written as

$$\left\{\begin{matrix}Cu^{2+}\\ \downarrow\uparrow\\ CuOAc^{+}\\ \downarrow\uparrow\\ Cu(OAc)_2\end{matrix}\right\} + ZnX^{-} \overset{k^{+}_{app}}{\rightleftharpoons} CuX^{-} + \left\{\begin{matrix}Zn^{2+}\\ \downarrow\uparrow\\ ZnOAc^{+}\end{matrix}\right\} \quad (1)$$

where X^{3-} means a tervalent NTA anion. Under the condition that both Zn(II) ions and Zn(II)-NTA complexes are present in a large excess over copper(II) ions, the substitution reaction (1) can be treated as a pseudo-first order reaction. The apparent rate constants of the forward reaction (1), k^{+}_{app}, were obtained by similar treatments as given in the previous papers.[2-4] The values of k^{+}_{app} were obtained as a function of the hydrogen ion concentration at two different concentrations of zinc(II) ions and at three different concentrations of acetate ions. Their plots against the hydrogen ion concentration are given in Fig. 1. Figure 1 clearly indicates that a linear relation exists between k^{+}_{app} and $[H^+]$, and that the values of k^{+}_{app} at $[H^+]=0$, which were obtained by extrapolation, are dependent on the concentrations of zinc(II) ions and acetate ions.

On the basis of the dependencies of the observed apparent rate constants on the concentrations of

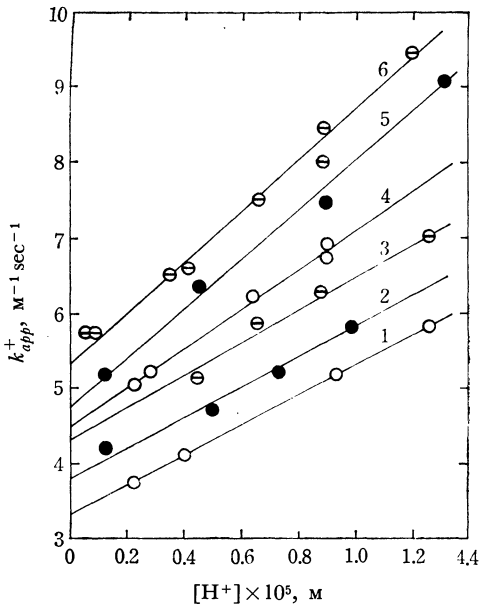

Fig. 1. k^{+}_{app} as a function of the hydrogen ion concentration in acetate buffer - potassium nitrate solutions of ionic strength 0.23 at 0°C. Initial concentrations are $[Cu^{2+}]_{0,app}=2.00\times10^{-4}$ M; $[ZnX^-]_0=4.35\times10^{-3}$ M; $[Zn^{2+}]_{0,app}=11.68\times10^{-3}$ M (plots 1, 2 and 3) and $[Zn^{2+}]_{0,app}=6.34\times10^{-3}$ M (plots 4, 5 and 6). Concentrations of free acetate are 0.048 M for ⊖, 0.097 M for ●, and 0.196 M for ○.

zinc(II) ions, Zn(II)-NTA complexes, hydrogen ions and acetate ions, which are identical to those of the substitution reaction of copper(II) ions and zinc(II)-EDTA complexes,[4] the following mechanisms were set down for reaction (1).

$$\text{(i)}\quad Cu^{2+} + ZnX^{-} \overset{k^{+}_{Ih}}{\rightleftharpoons} CuX^{-} + Zn^{2+} \quad (2)$$

$$CuOAc^{+} + ZnX^{-} \overset{k^{+}_{Ic}}{\rightleftharpoons} CuX^{-} + ZnOAc^{+} \quad (2')$$

$$\text{(ii)}\quad ZnX^{-} + H^{+} \rightleftharpoons ZnHX \quad (3)$$

$$Cu^{2+} + ZnHX \overset{k^{+}_{IIh}}{\rightleftharpoons} CuHX + Zn^{2+} \quad (4)$$

$$CuOAc^{+} + ZnHX \overset{k^{+}_{IIc}}{\rightleftharpoons} CuHX + ZnOAc^{+} \quad (4')$$

$$CuHX \rightleftharpoons CuX^{-} + H^{+} \quad (5)$$

$$\text{(iii)}\quad ZnX^{-} \rightleftharpoons \left\{\begin{matrix}Zn^{2+}\\ \downarrow\uparrow\\ ZnOAc^{+}\end{matrix}\right\} + X^{3-} \quad (6)$$

$$Cu^{2+} + X^{3-} \overset{k^{+}_{IIIh}}{\rightleftharpoons} CuX^{-} \quad (7)$$

2) N. Tanaka, K. Kato and R. Tamamushi, This Bulletin, **31**, 283 (1958).
3) N. Tanaka and K. Kato, *ibid.*, **32**, 1376 (1959).
4) K. Kato, *ibid.*, **33**, 200 (1960).

$$CuOAc^+ + X^{3-} \overset{k^+_{IIIc}}{\rightleftharpoons} CuX^- + OAc^- \quad (7')$$

(iv) $$ZnX^- + H^+ \rightleftharpoons \left\{\begin{matrix} Zn^{2+} \\ \downarrow\uparrow \\ ZnOAc^+ \end{matrix}\right\} + HX^{2-} \quad (8)$$

$$Cu^{2+} + HX^{2-} \overset{k^+_{IVh}}{\rightleftharpoons} CuHX \quad (9)$$

$$CuOAc^+ + HX^{2-} \overset{k^+_{IVc}}{\rightleftharpoons} CuHX + OAc^- \quad (9')$$

From the same treatment in principle as in the previous papers,[2-5] Eq. (10) is obtained for the rate equation for reaction (1).

$$k^+_{app} = \frac{1}{\sum_{n=0}^{2} \beta_{Cu(OAc)_n}[OAc^-]^n}\Big[k^+_{1h} + k^+_{1c}[OAc^-] + (k^+_{2h} + k^+_{2c}[OAc^-])[H^+] + \{k^+_{3h} + k^+_{3c}[OAc^-] + (k^+_{4h} + k^+_{4c}[OAc^-])[H^+]\} \times \frac{1 + \beta_{ZnOAc}[OAc^-]}{[Zn^{2+}]_{0,app}}\Big] \quad (10)$$

where,

$$\left.\begin{aligned} &k^+_{1c} = k^+_{1c}\beta_{CuOAc},\ k^+_{2h} = k^+_{IIh}K^H_{ZnHX}, \\ &k^+_{2c} = k^+_{IIc}\beta_{CuOAc}K^H_{ZnHX},\ k^+_{3h} = k^+_{IIIh}/K_{ZnX}, \\ &k^+_{3c} = k^+_{IIIc}\beta_{CuOAc}/K_{ZnX},\ k^+_{4h} = k^+_{IVh}/(K_{ZnX}K_{HX}), \\ &k^+_{4c} = k^+_{IVc}\beta_{CuOAc}/(K_{ZnX}K_{HX}) \end{aligned}\right\} \quad (10')$$

In Eq. (10), the initial concentration $[Zn^{2+}]_{0,app}$ is substituted for $[Zn^{2+}]_{app}$.

Table 1. Rate constants in Eq. (10) obtained at ionic strength 0.23 at 0°C

	Rate constant	
k^+_{1h}	5.4	$l\ mol^{-1}\ sec^{-1}$
k^+_{1c}	7.6×10	$l^2\ mol^{-2}\ sec^{-1}$
k^+_{2h}	$\sim1\times10^5$	$l^2\ mol^{-2}\ sec^{-1}$
k^+_{2c}	$\sim1\times10^6$	$l^3\ mol^{-3}\ sec^{-1}$
k^+_{3h}	1.60×10^{-2}	sec^{-1}
k^+_{3c}	3.0×10^{-1}	$l\ mol^{-1}\ sec^{-1}$
k^+_{4h}	4×10^3	$l\ mol^{-1}\ sec^{-1}$
k^+_{4c}	2×10^4	$l^2\ mol^{-2}\ sec^{-1}$

5) N. Tanaka and H. Ogino, This Bulletin, **36**, 175 (1963).

Table 2. Rate constants for reactions (2), (2'), (4), (4'), (7), (7'), (9) and (9') at ionic strength 0.23 at 0°C

	Rate constant, $l\ mol^{-1}\ sec^{-1}$
k^+_{Ih}	5.4
k^+_{Ic}	2.3
k^+_{IIh}	~30
k^+_{IIc}	~10
k^+_{IIIh}	2.0×10^8
k^+_{IIIc}	1.1×10^8
k^+_{IVh}	5×10^3
k^+_{IVc}	1×10^3

The rate constants in Eq. (10) were obtained from the analysis of those plots in Fig. 1, and are given in Table 1.

The rate constants for reactions (2), (2'), (4), (4'), (7), (7'), (9) and (9') were calculated from the relations given in Eqs. (10') and are given in Table 2. The values of K_{ZnX} and K^H_{ZnHX} which were used in the calculation are $10^{10.06}$ and $10^{3.5}$, respectively. They are the values which were determined by the polarographic method at ionic strength 0.2 at 0°C.[6] The values of K_{HX}, β_{CuOAc} and $\beta_{Cu(OAc)_2}$ are the same as those used in the previous paper.[1]

Discussion

The values in Table 2 indicate that all the reactions proceeding through hydrated copper(II) ions are faster than the corresponding reactions through monoacetatocopper(II) ions. This contrasts with the results obtained in the case of the substitution reactions involving nickel(II) ions and confirms our previous consideration.

With the rate constants obtained in this study, the ratios of the rate constants for the reactions,

$$M^{2+} + X^{3-} \underset{k^-_{IIIh}}{\overset{k^+_{IIIh}}{\rightleftharpoons}} MX^- \quad (11)$$

$$M^{2+} + HX^{2-} \underset{k^-_{IVh}}{\overset{k^+_{IVh}}{\rightleftharpoons}} MX^- + H^+ \quad (12)$$

may be discussed. For reactions (11) and (12), the following relation holds.

$$k^+_{IIIh}/k^+_{IVh} = (k^-_{IIIh}/k^-_{IVh})/K_{HX} \quad (13)$$

If it is assumed that the treatment given by Bydalek

6) Y. Saito, Ph. D. Thesis, Tohoku University (1967).

TABLE 3. THE RATIOS OF THE RATE CONSTANTS FOR REACTIONS (11) AND (12)

Metal	Temp., °C	μ	k^{+}_{IIIh}/k^{+}_{IVh}	k^{-}_{IIIh}/k^{-}_{IVh}	Investigators
Ni^{2+}	25	1.25	6.4×10^{4}	8×10^{-6}	Bydalek and Blomster[8]
Ni^{2+}	0	0.2	2×10^{4}	5×10^{-6}	Tanaka and Kimura[1]
Ni^{2+}	0	0.2	1.4×10^{4}	3×10^{-6}	Tanaka and Kimura[1]
Cd^{2+}	25	0.2		1×10^{-5}	Tanaka *et al.*[9]
Cu^{2+}	0	0.23	4×10^{4}		This stuydy

and Margerum[7] and Bydalek and Blomster[8] can be applied to these reactions, and that the same reaction intermediates given by the latter authors for the Ni(II)-NTA reactions,

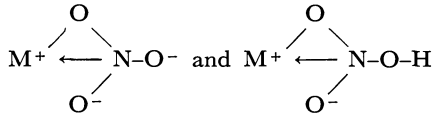

are formed in reactions (11) and (12), respectively, the ratio k^{-}_{IIIh}/k^{-}_{IVh} is considered to be equal to the value of the acid dissociation constant for acetic acid, $10^{-4.7}$. Then, the ratio k^{+}_{IIIh}/k^{+}_{IVh} was calculated to be

$$k^{+}_{IIIh}/k^{+}_{IVh} = (k^{-}_{IIIh}/k^{-}_{IVh})/K_{HX} = 10^{5.3}$$

Since this relation holds for any metal ion, the ratio must be the same irrespective of the kind of metal ions involved. The ratios obtained in the present study are given in Table 3 together with the values reported in the literatures. From Table 3, it can be seen that the observed values are in an essential agreement with the calculated ones.

In the present and the previous[1] studies, the rate constants for the complex-forming reactions of Cu-NTA and Ni-NTA complexes were determined. If the rate constants for Cu-NTA complexes are denoted with $k^{+}_{IIIh}(Cu)$ and $k^{+}_{IVh}(Cu)$ and those for Ni-NTA complexes with $k^{+}_{IIIh}(Ni)$ and $k^{+}_{IVh}(Ni)$, the values of $k^{+}_{IIIh}(Cu)/k^{+}_{IIIh}(Ni)$ and $k^{+}_{IVh}(Cu)/k^{+}_{IVh}(Ni)$ were calculated to be 2×10^{3} and 1×10^{3}, respectively. The values seem to be in an essential agreement with the ratio of the rate constants for the exchange of a water molecule from a hydrated copper(II) ion and a hydrated nickel(II) ion, which was reported by Eigen and Tamm,[10,11] and Connick and Stover.[12]

The authors wish to thank the Ministry of Education for the financial support granted for this research. Thanks are also due to the Teijin-Kumura Shogaku-kai for the scholarship granted to one of the authors (M. K.).

7) T. J. Bydalek and D. W. Margerum, *Inorg. Chem.*, **2**, 678 (1963).
8) T. J. Bydalek and M. L. Blomster, *ibid.*, **3**, 667 (1964).
9) N. Tanaka, K. Ebata, T. Takahari and T. Kumagai, This Bulletin, **35**, 1836 (1962).
10) M. Eigen, *Z. Elektrochem.*, **64**, 115 (1960).
11) M. Eigen and K. Tamm, *ibid.*, **66**, 93, 107 (1962).
12) R. E. Connick and E. S. Stover, *J. Phys. Chem.*, **65**, 2075 (1961).

BULLETIN OF THE CHEMICAL SOCIETY OF JAPAN VOL. 41 2379—2381 (1968)

Studies on Some Telluro-Tungstomolybdates

Keshawa Chandra PATHAK

Department of Chemistry, Banaras Hindu University, Varanasi-5, India

(Received December 1, 1967)

Ammonium telluro-tungstomolybdate $6(NH_4)_2O \cdot 2TeO_3 \cdot WO_3 \cdot 10MoO_3 \cdot 30H_2O$ and the corresponding salts with silver, strontium, barium, cerium, lead, iron and guanidine have been isolated, their properties studied and the composition determined by the analytical methods. IR spectra of ammonium and guanidine salts have been recorded and the characteristic peaks assigned. Thermal decomposition studies (TGA and DTA) of ammonium salt were made. Differential thermal analysis of ammonium salt was done in nitrogen atmosphere too.

Formation of heteropoly salts by tungsten and molybdenum is well known.[1] Tellurium has also been reported to form heteropoly salts with various elements such as molybdenum,[2] tungsten,[3] phosphorus, arsenic.[4]

The condensation reaction of telluric acid with tungstic acid was studied by Rosenheim and Traube.[5] Recently telluric-12 tungstic heteropoly acid[6] and its silver salt[7] was studied by Ganelina.

Formation of heteropoly salts of telluric acid with molybdic acid has been extensively studied.[8] A series of heterotrisalts containing tellurium, vanadium, molybdenum, tungsten, phosphorus has been studied in these laboratories[9-11] and the work is now extended to study the heterotrisalt formation of tellurium, tungsten and molybdenum.

The preparation, analysis and some properties of ammonium telluro-tungstomolybdate and its salts with silver, strontium, barium, cerium, lead, iron and guanidine are reported in this communication.

Experimental

All the chemicals used were of E. Merck or B. D. H. pure quality. Ammonium telluro-tungstomolybdate-telluric acid (4.6 g) and molybdic acid (21.6 g) were refluxed in ammoniacal medium for 6 hr. Five grams of tungstic acid dissolved in sufficient quantity of ammonium hydroxide was added to the above solution and refluxed for another 10 hr. The solution was then evaporated to a small bulk and kept in a refrigerator for crystallization. White crystalline ammonium telluro-tungstomolybdate was obtained which was recrystallized and analysed. The compound is stable at room temperature but decomposes on heating or treatment with acids. The analytical data are shown in Table 1.

Its silver, strontium, barium, cerium, lead, iron and guanidine salts were prepared by adding silver nitrate, strontium acetate, barium chloride, cerous nitrate, lead nitrate, ferric chloride and guanidine hydrochloride solutions to the ammonium salt solution in water.

Tellurium was estimated as metallic tellurium and ammonia as described earlier.[8] Tungstic and molybdic acids were separated by standard method. The other cations silver, strontium, barium, cerium, lead, iron were estimated by usual gravimetric methods and guanidine by microanalytical method. The results are recorded in Table 1.

IR spectra (KBr phase) of ammonium and guanidine salts were recorded on Perkin Elmer infracord in 2—15 μ region.

Thermogravimetric analysis of ammonium salt was carried out on a Stanton Thermobalance of 1 mg sensitivity. The sample of the size 150—170 mesh was heated at a uniform rate of 3°C/min. The loss in weight was obtained as the furnace temperature is increased and the temperature recorded automatically. The TGA curve of ammonium telluro-tungstomolybdate has been given in Fig. 1.

The DTA of the ammonium salt was carried out as reported in an earlier communication.[9] The heating was carried out in nitrogen atmosphere also.

Results and Discussion

Assignment of definite structure to the heteropoly acids and their salts encounters a great difficulty on account of the large size of the molecules involved. However, the composition of ammonium telluro-tungstomolybdate has been arrived at on the basis of analytical results. The stability of the

1) "Gmelins Handbuch der Anorganischen Chemie," System-Nummer 54, Verlag Chemie GMBH, Berlin, p. 324: *ibid.*, System Nummer 53, p. 312.
2) *Ibid.*, System Nummer 53, p. 321.
3) *Ibid.*, System Nummer 54, p. 325.
4) R. F. Weinland and H. Prause, *Z. anorg. Chem.*, **28**, 45 (1901).
5) A. Rosenheim and A. Traube, *ibid.*, **91**, 75 (1915).
6) E. Sh. Ganelina, *Zhur. Neorg. Khim.*, **7**, 1570 (1962).
7) E. Sh. Ganelina and T. N. Reznikova, *ibid.*, **8**, 1891 (1963).
8) S. Prasad and K. C. Pathak, *J. Indian Chem. Soc.*, **42**, 373 (1965).
9) S. Prasad and K. C. Pathak, *ibid.*, **42**, 698 (1965); **43**, 348 (1966).
10) S. Prasad and K. C. Pathak, ThisBu lletin, **39**, 2666 (1966).
11) S. Prasad and K. C. Pathak, *Indian J. Chem.*, **5**, 14 (1967).

TABLE 1. ANALYTICAL DATA FOR THE

Tellurotungsto-molybdate	Formula	Colour
Ammonium	$6(NH_4)_2O \cdot 2TeO_3 \cdot WO_3 \cdot 10MoO_3 \cdot 30H_2O$	White $(NH_4)_2O$:
Silver	$6Ag_2O \cdot 2TeO_3 \cdot WO_3 \cdot 10MoO_3 \cdot 8H_2O$	Yellowish whits Ag_2O:
Strontium	$6SrO \cdot 2TeO_3 \cdot WO_3 \cdot 10MoO_3 \cdot 12H_2O$	White SrO:
Barium	$6BaO \cdot 2TeO_3 \cdot WO_3 \cdot 10MoO_3 \cdot 15H_2O$	White BaO:
Cerium	$2Ce_2O_3 \cdot 2TeO_3 \cdot WO_3 \cdot 10MoO_3 \cdot 10H_2O$	Yellowish white Ce_2O_3:
Lead	$6PbO \cdot 2TeO_3 \cdot WO_3 \cdot 10MoO_3 \cdot 6H_2O$	White PbO:
Iron	$2Fe_2O_3 \cdot 2TeO_3 \cdot WO_3 \cdot 10MoO_3 \cdot 10H_2O$	Brownish violet Fe_2O_3:
Guanidine	$6(CN_3H_6)_2O \cdot 2TeO_3 \cdot WO_3 \cdot 10MoO_3 \cdot 20H_2O$	White $(CN_3H_6)_2O$:

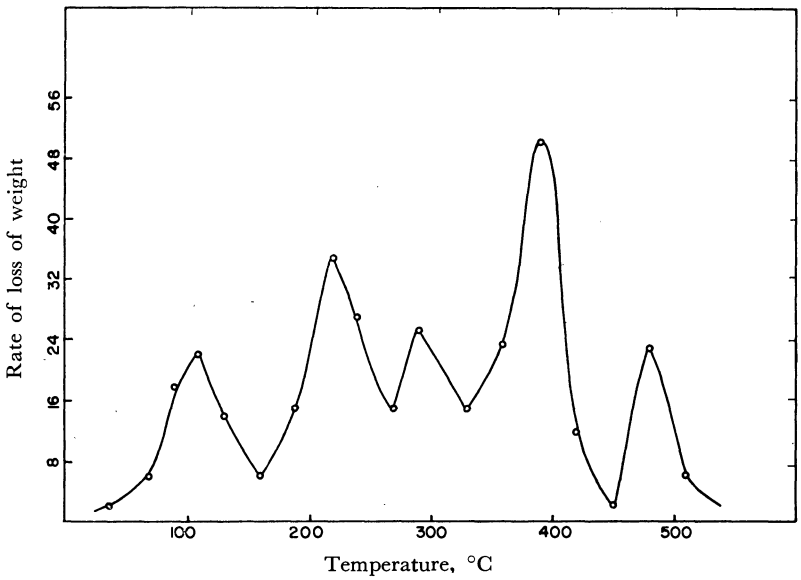

Fig. 1. TGA curve of ammonium telluro-tungstomolybdate.

anion has also been cenfirmed by passing freshly prepared solution of the ammonium salt through a cation exchange resin (Amberlite IR 120 in H^+ form). The composition of the solution after passing through the resin remained the same although free acid could not be crystallized from the solution due to its highly soluble nature. The precipitated silver, strontium, barium, cerium, lead, iron and guanidine salts conform to the same formula except that the cationic part is replaced by the respective metals.

The TGA curve of ammonium telluro-tungsto-molybdate (Fig. 1) shows the weight losses at 110, 222, 290, 390 and 480°C. The peaks upto 300°C are due to the dehydration of the compound which is in good agreement with the DTA curve (Fig. 2A) in which two endothermic peaks at 105 and 280°C are observed. After this temperature the decomposition of the compound occurs resulting in two peaks at 390 and 480°C.

The two endothermic peaks at 105 and 280°C in the DTA curve correspond to the dehydration of the compound. This clearly indicates that the water molecules are removed at two different temperatures, one at 105°C and the other at 280°C. The water molecules of crystallization are removed at 105°C and the water of constitution at a considerably higher temperature (280°C).

The characteristic exothermic peak at 380°C in DTA curve is either due to the oxidation or decomposition of ammonia at the surface of MoO_3 which acts as a ctalyst. The presence of exothermic peak due to the catalytic oxidation of ammonia has been observed by other workers while studying the thermal decomposition of ammonium molybdate[12] and ammonium vanadate[13]. The oxidation of ammonia in the last stage of decomposition has been suggested as a possible source of the exothermic heat. The nitrogen atmosphere

12) E. Ma, This Bulletin, **37**, 171 (1964).
13) M. Taniguchi and T. R. Ingraham, *Can. J. Chem.*, **42**, 2467 (1964).

VARIOUS TELLURO-TUNGSTOMOLYBDATES

Metallic oxide %		TeO_3 %		WO_3 %		MoO_3 %		H_2O %	
Found	Calcd	Found	Calcd	Found	Calcd	Found	Calcd	Found	Calcd
10.68	10.86	12.60	12.22	7.82	8.07	50.42	50.06	17.68	18.79
39.88	39.07	10.01	9.87	6.38	6.52	39.82	40.44	3.91	4.05
21.30	21.74	12.58	12.27	7.99	8.11	50.88	50.30	7.25	7.55
28.02	28.64	11.18	10.93	7.08	7.22	45.54	44.79	8.18	8.41
23.32	22.96	12.04	12.28	8.32	8.11	49.86	50.32	6.46	6.29
39.24	38.60	10.28	10.13	6.48	6.68	40.95	41.48	3.04	3.11
12.90	12.67	13.62	13.93	9.31	9.20	57.32	57.06	6.85	7.14
25.10	25.52	10.72	10.98	7.16	7.25	45.48	44.99	11.54	11.26

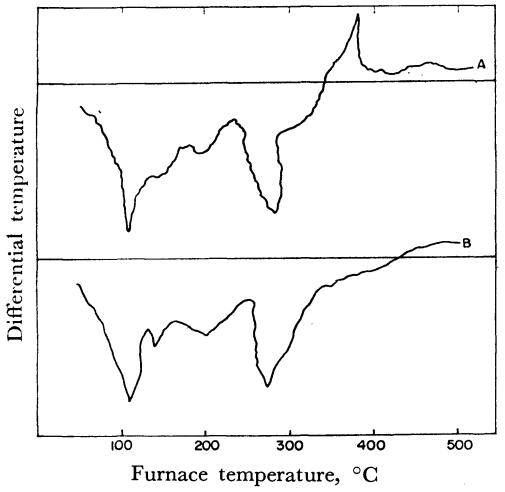

Fig. 2. Differential thermal analysis curves.
A. Ammonium telluro-tungstomolybdate
B. Ammonium telluro-tungstomolybdate in nitrogen

gives normal endothermic peaks (Fig. 2B) showing thereby that there is no oxidation of ammonia.

In IR spectra of ammonium and guanidine salts, the strong peaks at 3100 cm^{-1} and 3300 cm^{-1}, 1610 cm^{-1} and 1650 cm^{-1} respectively are due to the O–H stretch and O–H bending of water molecules present. In case of ammonium salt a strong peak at 1400 cm^{-1} is attributed to the characteristic deformation vibration of NH_4^+ ion [$\delta(NH_4)$], whereas a strong peak at 1550 cm^{-1} in case of guanidine salt is due to C=N stretch and N–H deformation of the guanidine molecule. The strong peak at 3300 cm^{-1} in case of guanidine salt may not be pure O–H stretch as it is being overlapped by N–H stretch vibrations of guanidine.

The vibrational bands appearing at 910 cm^{-1} in ammonium salt, 940 cm^{-1} and 880 cm^{-1} in guanidine salt may be due to mixed Mo–O and W–O vibrations. The regions of the absorption of the above vibrations are so close that in the compounds they overlap to a considerable extent to form broad bands. The argument may not be exactly valid since no discrete Mo–O or W–O modes of vibrations are present.

The sincere thanks of the author are due to (Late) Dr. Sarju Prasad for his keen interest and helpful suggestions, to Professor G. B. Singh and the authorities of the Banaras Hindu University for the facilities and to C. S. I. R., New Delhi for a research fellowship.

BULLETIN OF THE CHEMICAL SOCIETY OF JAPAN VOL. 41 2382—2384 (1968)

The Inert Gas Extraction-Gas Chromatographic Determination of Hydrogen in Ferrous Metals

Jiro KASHIMA and Takuo YAMAZAKI

The Castings Research Laboratory, Waseda University, Totsuka, Shinjuku-ku, Tokyo

(Received January 16, 1968)

The inert gas extraction-gas chromatographic technique has been applied for the determination of hydrogen in ferrous metals. As this method was dependent on gas chromatography, the simplification was performed on the apparatus and the analytical operation. A procedure was evolved, according to which the extracged hydrogen was measured by means of gas chromatography using the precolumn technique, *viz.*, (1) the hydrogen was rapidly transferred from the metal into an argon stream by means of H-F induction furnace, (2) this was concentrated into the cold precolumn for 4 min to collect the total amount of hydrogen from the extraction tube, (3) this was measured by gas chromatography. Analytical results obtained on 3 iron base metals suggest that the method can be widely used for the determination of hydrogen in ferrous metals.

Several methods for the determination of hydrogen in metals have recently been reviewed.[1] These include vacuum or inert gas extraction by heating or by melting and chemical methods. Among them, *viz.*, gas chromatography,[2,3] emission spectrometry[4] and isotope methods,[5,6] have recently been proposed for the determination of hydrogen in metals. Although hydrogen is generally determined by the hot-extraction method with fair accuracy, the vacuum fusion method[7] is usually employed to extract hydrogen completely in ferrous metals. Marincek and Feichtinger,[8] using a procedure based on the vacuum fusion method, found that some of hydrogen still remained in the metals over a range of temperature from 1300 to 2100°C. Bennek and Klotzbach[9] have proposed a reliable method based on tin-bath technique at 1100—1150°C using quartz crucible instead of graphite one being difficult to degass sufficiently. Bennek's method is widely used to de termine hydrogen in metals. The present paper deals with a procedure for the determination of hydrogen in ferrous metals by means of gas chromatography. The apparatus now in use consists of a compact and convenient unit. One hundred determinations of hydrogen have been carried out, and a reliable results for the extraction of hydrogen in steel and cast iron were obtained.

1) H. Kostron, *Metall*, **6**, 115 (1952).
2) H. Feichtinger, K. Brauner, H. Bächtold and F. V. Bakos, *Schweizer. Archo.*, **30**, 345 (1965).
3) S. Suzuki, *Bunseki Kagaku (Japan Analyst)*, **11**, 618 (1962).
4) O. B. Falkova, *Izvest. Akad. Nauk. SSSR, ser. Fiz.*, **19-2**, 149 (1955).
5) A. N. Zaidel and K. I. Petrov, *Zavodskaya Lab.*, **22**, 923 (1956).
6) A. N. Zaidel, A. A. Petrov and G. V. Veinberg, "The Spectrum-Isotope Method for Determining Hydrogen in Metal," Leningrad State Univ. Press (1957).
7) T. Somiya, S. Hirano, H. Kamada and I. Ogawara, *Talanta*, **11**, 581 (1964).
8) B. Marincek and H. Feichtinger, "Gases in Cast Iron," International Foundary Congress, Bruxelles, 65.
9) H. Bennek and G. Klotzbach, *Technische Mitteilungen Krupp-forschr.*, **4**, 5 (1941).

Experimental

Preparation of Samples. Steel and chill cast iron plate samples approximately 2 mm in thickness and lump ferro silicon samples were used for the test. Steel samples were prepared by cutting or breaking to an appropriate weight. Samples (1 to 1.5 g) were used after treatment of the surface. The treatment was as follows: (1) abrase with grinding paper (with exception of ferro silicon samples which break in pieces); (2) wash with carbon tetrachloride; (3) dry in hot stream of argon. It is advisable to dry the sample in the extraction tube every time just before the experiment, because the gas adsorbed on the surface of the treated sample is considerably increased during storage in a desiccator and then the removal of the gas dependent on sweeping gas is very troublesome.

Apparatus. The apparatus used for the determination of hydrogen in metals which is simplified by attaching a precolumn and is, therefore, different from usual gas collection methods, as shown in Fig. 1.

Purified argon (99.9%) was used as the carrier gas. The moisture contained in the carrier gas was removed by passing it through the desiccant tube.

Procedure. Prior to the analytical experiment, the carrier gas was passed continuously through an extraction system consisting of transparent quartz and glass tubes at 200°C for a few hours until the blank value of hydrogen could be maintained below 10^{-4} ml/min. A sample was introduced into a quartz crucible from upper part of the quartz tube under an argon flow (the flow rate is 60 ml/min) and was dried at 150°C for several minutes. After the flow rate was

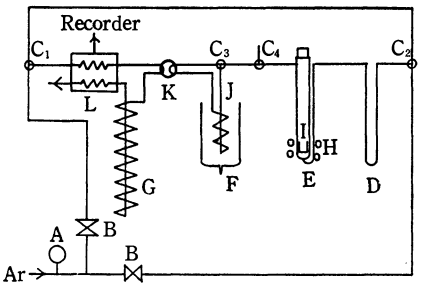

Fig. 1. Apparatus.

A: Pressure regulator
B: Needle valves
C_1—C_4: Three ways cocks
D: P_2O_5 desiccant tube
E: Transparent quartz tube (volume of about 15 m*l*)
F: Dry ice - acetone bath
G: GC column
H: H-F coil (commercially available combustion unit)
I: Quartz crucible
J: Precolumn (packed with silica-gel)
K: Gas sampling cock
L: Thermal conductivity cell of gas chromatograph

controlled to 10 m*l*/min, the system was connected with the precolumn being held below −70°C. The sample was heated to 1400°C for 4 min, and the hydrogen, collected in this precolumn, was determined by gas chromatography.

GC Measurements. Hydrogen collected in the precolumn was measured by using a copper tube (4 mm in dia. ×2.5 m long) packed with Molecular Sieve 5A. The analytical conditions were as follows; column temperature, 45°C; carrier gas (argon) speed, 60 m*l*/min. The precolumn was made of a copper tube (4 mm in dia. ×70 cm long) packed with silica-gel. The operating conditions on the precolumn were as follows: column temperature, −70°C; carrier flow rate for collecting hydrogen, 10 m*l*/min. This precolumn was capable of concentrating hydrogen for 4 min at the operating conditions, as shown in Fig. 2. The hydrogen concentrated in precolumn was introduced without any warming the precolumn.

The method of the streaming of a gas was almost the same as had been reported in a previous paper.[10] A long main column was suitable for moderating the pressure change brought about by the streaming of a gas.

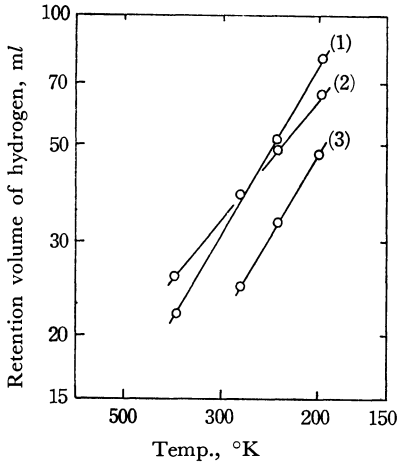

Fig. 2. Relationship between retention volume and concentration column temperature.
(1) Column: 4 mm×1 m copper, packed with silica-gel of 40—60 mesh, (2) Column: 4 mm ×1.5 m copper, packed with activated charcoal of 30—60 mesh, (3) Column: 4 mm× 70 cm copper, packed with silica-gel of 30—60 mesh

Results and Discussion

Reliability of the GC Measurements. The reliability of the GC measurements was tested by using each 0.5 m*l* of the mixed permanent gases kept in a gas container. The results are given in Table 1. This method was found to be convenient for the determination of hydrogen in metals because the gas sample could be concentrated into the precolumn in a short time. The precision was exceedingly good.

Table 1. The precision of GC measurements obtained by using the gas sample*

Concentration time, min	Peak areas, mm²		
	$H_2\times100$	$N_2\times100$	$CO\times10$
3	566	428	1469
3	531	432	1482
3	568	442	(1530)
4	529	441	1491
4	570	438	1459
Average	553	436	1486
Without precolumn	550	430	1461

* The contents of gases in the container were 42% hydrogen, 3.4% nitrogen and 6.6% carbon monoxide.

Inert Gas Extraction. Some typical examples of the extraction of hydrogen are shown in Fig. 3. These data were obtained by heating the samples at 1400°C (black circle) and by extracting hydrogen introduced into the tube without sample (white circle). The fact that, in actual practice, the extraction rate on stell sample 4 mm in thickness is almost the same as that of hydrogen evolution from the sample, reveals the possibility of the rapid extraction of hydrogen from the sample.

The degree of degassing of the sample, which

10) J. Kashima and T. Yamazaki, This Bulletin, **39**, 1448 (1966).

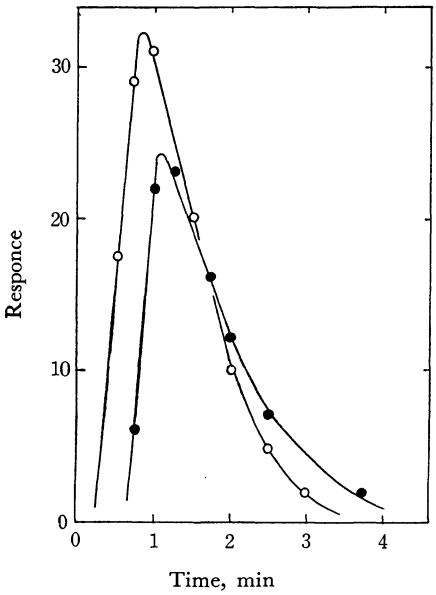

Fig. 3. Extraction curves of hydrogen.
●: Steel sample at 1400°C
○: Hydrogen introduced into the quartz tube without sample

TABLE 2. REMOVAL OF HYDROGEN FROM STEEL PLATES HEATED AT 1400°C

Plate sample	$T=D_t/R^2$	Q_t/Q_0
2 mm Cast iron	$t=20$ sec → 0.8	0.85
	$t=40$ sec → 1.65	0.96
4 mm Steel	$t=30$ sec → 0.3	0.63
	$t=2.7$ min → 1.65	0.96
5 mm Steel	$t=30$ sec → 0.19	0.53
	$t=4.5$ min → 1.7	0.97
6 mm Steel	$t=30$ sec → 0.13	0.42
	$t=6.5$ sec → 1.7	0.97

Q_t/Q_0 was graphically obtained from the following equation:

$$\frac{Q_t}{Q_0} = \sum_{i=1}^{i=\infty} - \frac{2\sin^2\lambda_i}{\lambda_i^2 + \lambda_i\sin\lambda_i\cos\lambda_i}\left(1-e^{-\lambda_i^2 D_t/R^2}\right)$$

where Q_t is the amount of hydrogen extracted from the metal in time t, Q_0 is the initial hydrogen content of the metal and T is dimentionless time dependent on diffusion coefficient D, thickness ($2R$) and time.

was dependent on sample size, time and temperature, was calaulated according to Fick equation[11] which was obtained by Fistul' for a finite thickness, using dimensionless value. The results are summarized in Table 2. It is preferable to use a steel plate 2 mm in thickness, on the basis of the fact that, when the metal was heated to about 1400°C, the total amount of hydrogen was evolved in 50—60 sec. However, it takes about 4 min to transfer hydrogen into the precolumn. It is unsuitable to use plate samples more than 5 mm in thickness because it takes still 4 min more to extract hydrogen.

Reproducibility. The analyses of steel, cast iron and ferro silicon were carried out by this proposed method. A typical chromatogram of gases concentrated in the precolumn is shown in Fig. 4. The precision of the determinations is markedly dependent on the hydrogen content, hydrogen-pick-up by the walls of the quartz tube and the amount of the surface gas, correction of which under experimental conditions varies from 4 to 9×10^{-4} ml/cm^2. This amount was determined by rewashing an extracted sample and carring out a second extraction, as had been reported in a previous paper.[12] The reproducibility of this proposed method is represented by the following examples.

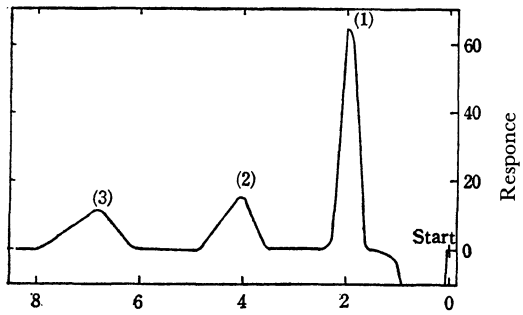

Fig. 4. Typical chromatogram of gases extracted from cast iron sample.
Hydrogen (1), nitrogen (2) and carbon monoxide (3)

(1) On a cast iron, data obtained from 8 determinations varied in the range 1.4—1.6 ppm, with a mean deviation of ±0.09 ppm.

(2) Duplicate determinations on each of 17 samples of mild steel gave results with a mean deviation of ±0.010 ppm. The hydrogen contents varied in the range 0.10—0.57 ppm.

(3) Duplicate determinations on each of 10 samples of ferro silicon gave results with a mean deviation of ±0.5 ppm. The hydrogen contents varied in the range 5.0—6.1 ppm.

Summary

A new inert gas extraction-gas chromatographic method for the determination of minute quantities of hydrogen in ferrous metals has been developed. This method was also available for trace analysis of hydrogen in the sample, because the blank value is extremely lower than that of the conventional method.

11) Yu. A. Klyachko, L. L. Kunin and S. N. Federov, Proceedings of the Commission on Analytical Chemistry, Vol. 15. Methods for Analyzing Gases in Metals (Moscow, Acad. Sci. USSR Press, 1959).

12) J. Kashima and T. Yamazaki, *Rept. Cas. Res. Lab. Waseda Univ.*, **12**, 21 (1961).

BULLETIN OF THE CHEMICAL SOCIETY OF JAPAN VOL. 41 2385—2392 (1968)

The Chromium(III) Complexes with Ammoniapropionicdiacetic Acid*[1]

Akira UEHARA, Eishin KYUNO and Ryokichi TSUCHIYA

Department of Chemistry, Faculty of Science, Kanazawa University, Kanazawa

(Received February 5, 1968)

Ammoniapropionicdiacetic acid (APDA), which belongs to a group of chelating agents similar to that of ammoniatriacetic acid, was prepared. The newly-prepared complexes containing this chelating agent were as follows: $[Cr(OH)(apdaH)(H_2O)_2]$ (red purple) (I), NH_4-$[Cr(OH)(apda)(H_2O)]\cdot 2H_2O$ (purple) (II), $(NH_4)_3[Cr(apda)_2]\cdot 2H_2O$ (pink) (III), $(Cr(apda)$-$(bipy)]\cdot 3H_2O$ (brown) (IV), $[Cr(apda)(o\text{-phen})]\cdot 3H_2O$ (brown) (V), and $[Cr(apda)(py)_2]$(pink) (VI), where apda, bipy, *o*-phen, and py are the abbreviations of the ammoniapropionatediacetate ion, *o*-phenanthroline, 2,2'-bipyridyl, and pyridine respectively. On the basis of the chemical and thermal analyses, and on the basis of the measurements of the visible, UV, reflection and IR spectra and molar conductivities, it was concluded that the ammoniapropionatediacetate acts either as a terdentate or a quadridentate ligand in these complexes. Unlike the ATA complex, no complexes in which the nitrogen dose not coordinate with chromium could be prepared in the case of APDA. The values of the effective magnetic moments for these APDA complexes were nearly equal to the spin-only values of tervalent chromium. Further comparisons of the properties of the APDA complexes with those of the ATA complexes were also made.

The preparations of the Cr(III) complexes with ammoniatriacetic acid (ATA) have already been reported;[1,2] here ATA behaves toward a chromium(III) ion not only as a terdentate, but also as a quadridentate ligand. It was also found that some complexes have different coordinating structures in a crystal state and in an aqueous solution. When an additional methylene group ($-CH_2-$) is introduced into ATA, ammoniapropionicdiacetic acid (APDA) is obtained. It was expected that this will indicate how the behavior of APDA is chemically- and sterically-different from that of ATA in complex formation. Their rational formulae are as follows;

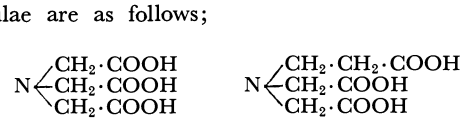

ATA APDA

The purposes of the present study were: (1) to investigate as what ligand an APDA can behave toward a chromium(III) ion; (2) to find out whether or not different structures are observed between the APDA complexes in a crystal state and in an aqueous solution, and, at the same time, (3) to compare the properties of the APDA complexes with those of ATA.

Experimental

Preparation of Ammoniapropionicdiacetic Acid, $C_7H_{11}O_6N$. The method of preparation described here is a modification of that one which has already been reported by Schwarzenbach *et al.*[3]

Ninety grams of β-alanine were neutralized with 300 m*l* of water containing 40 g of sodium hydroxide. Besides, 190 g of monochloroacetic acid were dissolved into about 300 m*l* of water and then gradually neutralized with 170 g of sodium bicarbonate. These two neutralized reagents were then mixed and heated on a water bath. When the temperature of the mixed solution reached *ca.* 70°C, 200 m*l* of water containing 80 g of sodium hydroxide were added. The temperature immediately increased because of the exothermic condensation reaction. After the reaction was over, the resultant solution was cooled to room temperature. The gradual addition of concentrated hydrochloric acid and stirring with glass rod produced white, powdered crystals. The recrystallization was achieved by dissolving the crude products into water containing an appropriate amount of sodium bicarbonate, and then by gradually adding hydrochloric acid to the solution.

Yield, about 160 g.

Found: N, 6.42; C, 40.72; H, 5.39%. Calcd for $C_7H_{11}O_6N$: N, 6.84; C, 40.98; H, 5.40%.

Preparation of the Complexes. *1) Hydroxohydrogenammoniapropionicdiacetatodiaquochromium(III),* $[Cr(OH)(apdaH)(H_2O)_2]$ (I). Thirteen grams of chromium(III) chloride hexahydrate were dissolved into 200 m*l* of water, and then 10 g of APDA were added to them. The mixed solution was heated on a water bath until no residue of the unreacted APDA could be seen. Then

*1 Presented in part at the 17th Symposium on Coordination Compounds, Hiroshima, December, 1967.

1) A. Uehara, E. Kyuno and R. Tsuchiya, This Bulletin, **40**, 2317 (1967).

2) A. Uehara, E. Kyuno and R. Tsuchiya, *ibid.*, **40**, 2322 (1967).

3) G. Schwarzenbach, H. Ackermann and P. Ruckstuhl, *Helv. Chim. Acta*, **32**, 1175 (1949).

the reddish purple crystals could easily be obtained from its cooled (room temperature) solution. The products were recrystallized from its concentrated purple solution of water. Yield, about 6 g.

Found: Cr, 16.76; N, 4.64; C, 27.61; H, 4.36%. Calcd for $[Cr(OH)(apdaH)(H_2O)_2]$: Cr, 16.84; N, 4.53; C, 27.24; H, 4.57%.

2) Ammonium Hydroxoammoniapropionicdiacetatoaquochromate(III) Dihydrate, $NH_4[Cr(OH)(apda)(H_2O)]\cdot 2H_2O$ (II). Ten grams of Complex I, obtained above, were dissolved into 200 m*l* of water containing 1.8 g of ammonium carbonate, and then the mixture was cooled to 0°C. Purple crystals were thus obtained. Recrystallization was achieved from its concentrated aqueous solution. Yield, about 2 g.

Found: Cr, 14.83; N, 7.96; C, 24.06; H, 5.87; H_2O,*2 9.8%. Calcd for $NH_4[Cr(OH)(apda)(H_2O)]\cdot 2H_2O$: Cr, 15.13; N, 8.15; C, 24.46; H, 5.57; H_2O, 10.48%.

3) Ammonium Bis-(ammoniapropionicdiacetato)chromate-(III) Dihydrate, $(NH_4)_3[Cr(apda)_2]\cdot 2H_2O$ (III). Seven grams of APDA were neutralized with 200 m*l* of water containing 4 g of ammonium carbonate, and then 10 g of Complex I were added. The mixed solution was evaporated to dryness on a water bath. Crude, pale-red crystals were thus obtained. The product was recrystallized from one percent of an aqueous ammonium carbonate solution. Yield, about 2.5 g.

Found: Cr, 9.82; N, 12.90; C, 29.94; H, 6.19; H_2O, 6.8%. Calcd for $(NH_4)_3[Cr(apda)_2]\cdot 2H_2O$: Cr, 9.52; N, 12.81; C, 30.75; H, 5.89; H_2O, 6.85%.

An attempt to obtain crystals such as $NH_4[Cr(apdaH)_2]$, in which one of the carboxyl groups of an APDA does not participate in the coordination, was unsuccessful because of the deposition of the I crystals. On the other hand, in the case of ATA, we were successful in obtaining the corresponding pink crystals of $NH_4[Cr(ataH)_2]\cdot 2H_2O$.[1]

4) Ammoniapropionicdiacetato-2,2'-bipyridylchromium(III) Trihydrate, $[Cr(apda)(bipy)]\cdot 3H_2O$ (IV). Ten grams of I were dissolved into 300 m*l* of water containing 3 g of ammonium carbonate, and then 5 g of 2,2'-bipyridyl neutralized with 6 m*l* of concentrated hydrochloric acid were added. After the mixed solution had been heated on a water bath until it changed from purple to reddish purple, it was cooled to 0°C. Then, brown crystals were separated out. The product was recrystallized from a concentrated aqueous solution or from alcohol. Yield, about 6 g.

Found: Cr, 10.76; N, 9.13; C, 44.49; H, 4.82; H_2O, 12.1%. Calcd for $[Cr(apda)(bipy)]\cdot 3H_2O$: Cr, 11.18; N, 9.04; C, 43.93; H, 4.63; H_2O, 11.72%.

5) Ammoniapropionicdiacetato-o-phenanthrolinechromium-(III) Trihydrate, $[Cr(apda)(o\text{-phen})]\cdot 3H_2O$ (V). Ten grams of I were dissolved into 300 m*l* of water containing 3 g of ammonium carbonate, and then 6 g of *o*-phenanthroline neutralized with 6 m*l* of concentrated hydrochloric acid were added. After the mixed solution had been heated on a water bath until it changed from purple to brown, it was cooled to 0°C; then, brown crystals were separated out. Recrystallization was achieved from water or from an alcohol solution. Yield, about 8 g.

Found: Cr, 10.16; N, 8.82; C, 46.70; H, 4.82; H_2O, 11.7%. Calcd for $[Cr(apda)(o\text{-phen})]\cdot 3H_2O$: Cr, 10.63; N, 8.59; C, 46.68; H, 4.53; H_2O, 11.14%.

6) Ammoniapropionicdiacetatodipyridinechromium(III), $[Cr(apda)(py)_2]$ (VI). Eleven grams of Complex II were dissolved into 30 m*l* of water containing 3 m*l* of concentrated hydrochloric acid, and then 150 m*l* (excess) of pyridine were added. This solution was heated on a water bath by using a reflux-condenser. After the solution had gradually changed in color from purple to pale red, it was immediately cooled to 0°C. Pink crystals were thus obtained. The product was recrystallized from absolute alcohol or from absolute pyridine. Yield, about 3 g.

As will be mentioned below, it was found that these crystals lost the coordinated pyridine, even at room temperature.

Found: Cr, 13.15; N, 9.38%. Calcd for $[Cr(apda)(py)_2]$: Cr, 12.61; N, 10.19%.

Apparatus. The UV and IR absorption spectra were measured with a Hitachi EPS Spectrometer and a Nippon Bunko IR-E Spectrometer respectively, while the reflection spectra were measured in a finely-powder solid state using a Hitachi EPU-2A Spectrometer equipped with the standard Hitachi reflection attachment. The thermal analyses and the conductivity and the magnetic-susceptibility measurement were carried out with a Metrimpex Derivatograph, a Yokogawa Universal Bridge BV-Z-13A, and a Gouy-Balance respectively.

Results and Discussion

Thermal Analyses. By using the derivatograph, three measurements, a thermogravimetric analysis (TGA), a differential thermogravimetric analysis (DTG), and a differential thermal analysis (DTA), can be carried out simultaneously. In this study, above all DTA and TGA were effectively used in order to ascertain the compositions of the complexes obtained. Their DTA, TGA, and temperature curves (T) are shown in Figs. 1-(A)—(F). All the measurements were carried out at a heating rate of 1°C/min in a constant nitrogen stream. The reddish-purple crystals of I gradually lose one mole of water from 130 to 160°C, and then 2 mol of water up to 230°C, as is shown in Fig. 1(A). It was found that the color changed from reddish purple to purple and then to green during the heating. These dehydration temperatures seem to be a little higher than that of crystalline water. More detailed discussions will be undertaken elsewhere.

The waters of crystallization in Complexes II, III, and V are all evolved by the decomposition up to 130°C (Figs. 1-(B), 1-(C) and 1-(E)). For Complex IV, the initial two moles of the crystalline waters and the last one were step-by-step liberated at 90°C and 150°C respectively (Fig. 1-(D)). The coordinated pyridine molecules in VI were liberated at rather a lower temperature (from room temperature to 80°C), as is shown in Fig. 1-(F).

*2 The H_2O appearing in all the analytical data in this paper shows the crystalline water estimated from the derivatogram.

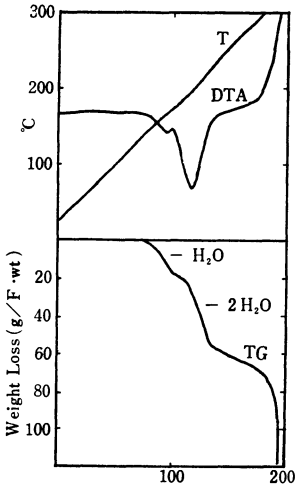

(A) $[Cr(OH)(apdaH)(H_2O)_2]$

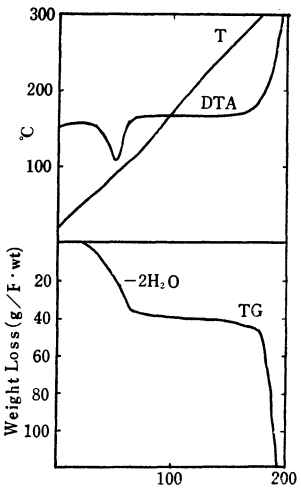

(B) $NH_4[Cr(OH)(apda)(H_2O)]\cdot 2H_2O$

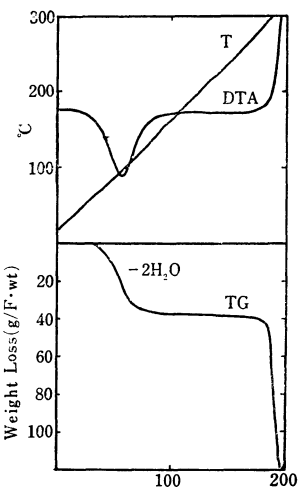

(C) $(NH_4)_3[Cr(apda)_2]\cdot 2H_2O$

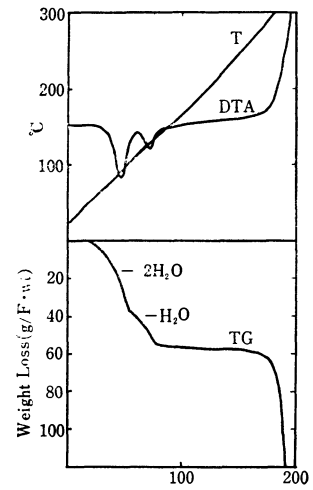

(D) $[Cr(apda)(bipy)]\cdot 3H_2O$

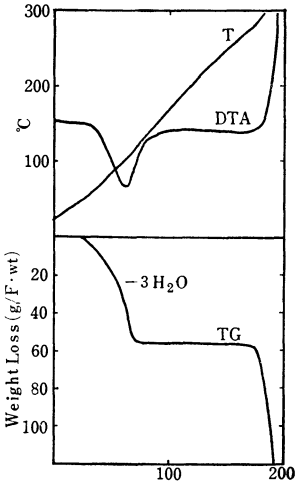

(E) $[Cr(apda)(o\text{-phen})]\cdot 3H_2O$

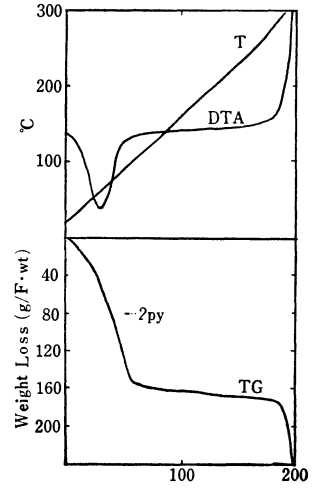

(F) $[Cr(apda)(py)_2]$

Fig. 1. Curves for thermal analyses.

Table 1. Behavior toward the ion exchanger and molar conductivities

Complex	Color of crystal	Color of solution	Adsorption to the ion exchanger		Molar conductivities (mho cm^{-1})
			Na-form	Cl-form	
I	Reddish purple	Purple	−	−	—
II	Purple	Purple	−	+	121.2
III	Pink	Pink	−	+	346.2
IV	Brown	Brown	−	−	—
V	Brown	Brown	−	−	—
VI	Pink	Pink	−	−	—

TABLE 2. ABSORPTION MAXIMA

Complex	$\nu_1(10^{13}/\text{sec})$ (log ε_1)	$\nu_2(10^{13}/\text{sec})$ (log ε_2)	$\nu_3(10^{13}/\text{sec})$ (log ε_3)
I	55.5 (2.03)	75.0 (1.93)	
II	53.5 (1.96)	73.5 (1.96)	
III	60.9 (1.87)	82.9 (1.61)	
IV	56.0 (1.98)	76.5 (2.09)	97.1 (4.30)
V	55.6 (1.94)	76.9 (2.12)	99.3 (3.66)
VI	57.0 (2.13)	77.5 (1.98)	107.1 (3.25)

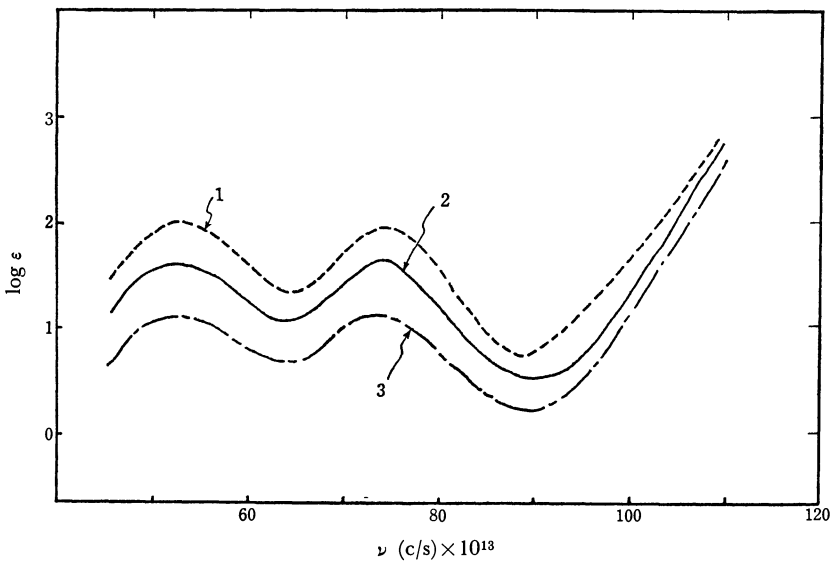

Fig. 2. Electronic absorption spectra for the solution of
1: $[Cr(OH)(apdaH)(H_2O)_2]$ 2: $[Cr(OH)(apdaH)(H_2O)_2]$ heated at 160°C
3: Purple solution of $[Cr(ata)(H_2O)_2]$.

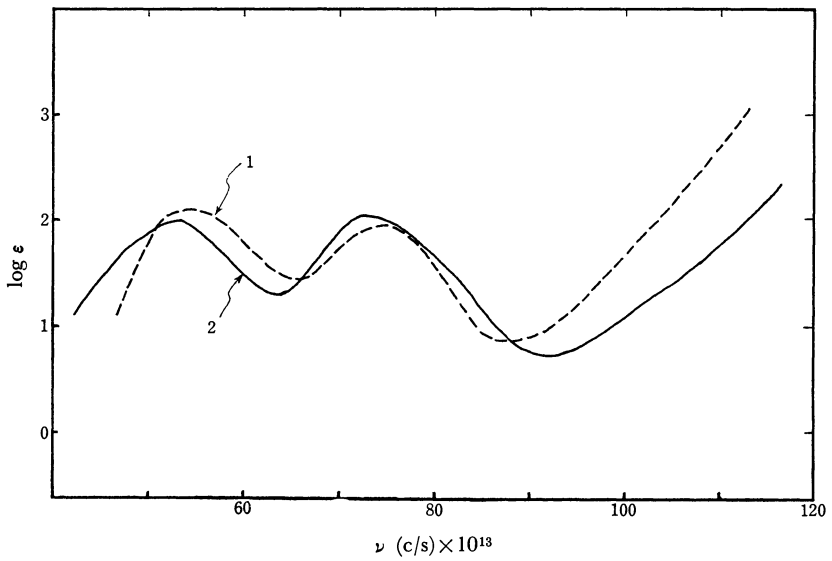

Fig. 3. Electronic absorption spectra for the solutions of
1: $NH_4[Cr(OH)(apda)(H_2O)]\cdot 2H_2O$ 2: $NH_4[Cr(OH)(ata)(H_2O)]\cdot 2H_2O$.

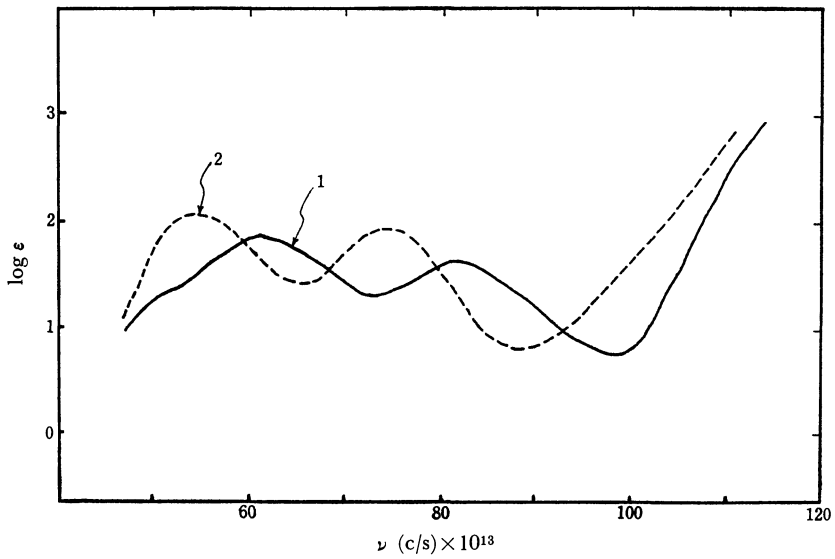

Fig. 4. Electronic absorption spectra for the solutions of
1: $(NH_4)_3[Cr(apda)_2]\cdot 2H_2O$ 2: $(NH_4)_3[Cr(apda)_2]\cdot 2H_2O$ stood overnight.

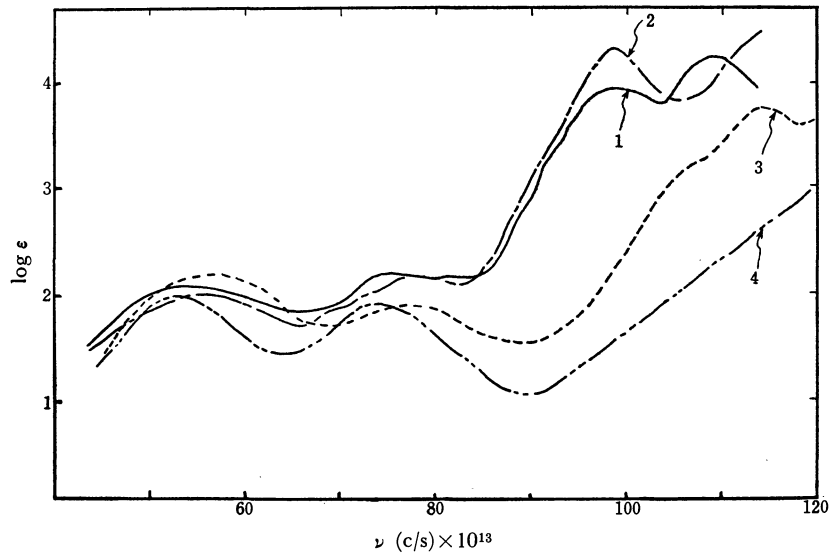

Fig. 5. Electronic absorption spectra for the solutions of
1: $[Cr(apda)(o\text{-phen})]\cdot 3H_2O$ 2: $[Cr(apda)(bipy)]\cdot 3H_2O$
3: $[Cr(apda)(py)_2]$ 4: $[Cr(apda)(py)_2]$ exposed in air.

Behavior of the Complexes in Reaction to the Ion Exchanger and Their Molar Conductivity. The behavior of the complexes in reaction to the ion exchanger and the values of their molar conductivities in a 1×10^{-3} mol/*l* solution are listed in Table 1. The + sign shows the possibility of the adsorption of the complexes by the exchanger, while — shows non-adsorption. It is shown in the table that Complexes I, IV, V, and VI were not adsorbed by either exchanger, and that their molar conductivities are extremely small (1—2 mho cm^{-1}), indicating that these complexes are non-electrolytes. On the other hand, the purple crystal, II, and the pink crystal, III, are shown to be adsorbed by the anion exchanger; additionally, their molar conductivities are 121.2 and 346.2 mho cm^{-1} respectively, showing that they are 1 : 1-type and 1 : 3-type electrolytes respectively.

Electronic Absorption Spectra. The absorption spectra for the six complexes from I through VI were all measured in aqueous solutions; those

for III and VI were measured in a buffer solution of pH 6 and in an alcohol-water solution, respectively in order to prevent gradual decomposition. Their spectra concerned are shown in Figs. 2—5, while the numerical values of their absorption maxima are summarized in Table 2.

Figure 2 shows the absorption spectra for the purple solutions of Complex I, of I heated at 160°C, and of the ATA complex (known to have the same structure as, $[Cr(ata)(H_2O)_2]$); in this figure the scale of the ordinate for the $[Cr(ata)(H_2O)_2]$ is arbitrary. Since the spectra of these three complexes show very similar forms, they are considered to have an identical structure in solutions.

The absorption spectra of I, II, and VI for the solid state, as measured by the diffuse-reflection method, are shown in Figs. 6—8. In Fig. 6, a full line shows the absorption spectrum for the solid state of I, while a dotted line gives that of a product which has lost one mole of water upon being heated at 160°C, as has been shown in thermal analyses described above. As Figs. 2 and 6 show, the spectra for the solution of I heated at 160°C and for the solution of I itself have analogous aspects, and differ from that for the solid state of I. Therefore, it may be considered that in solution Complex I has a structure identical with that of $[Cr(ata)(H_2O)_2]$, but not in a crystal state, and that certain changes in the structure occur upon heating.

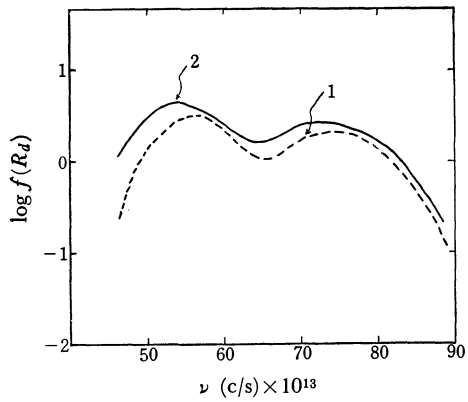

Fig. 6. Electronic absorption spectra for the solid states of
1: $[Cr(OH)(apdaH)(H_2O)_2]$,
2: $[Cr(OH)(apdaH)(H_2O)_2]$ heated at 160°C.
$f(R_d) = \frac{(1-R_d)^2}{2R_d}$
(R_d: relative reflection index)

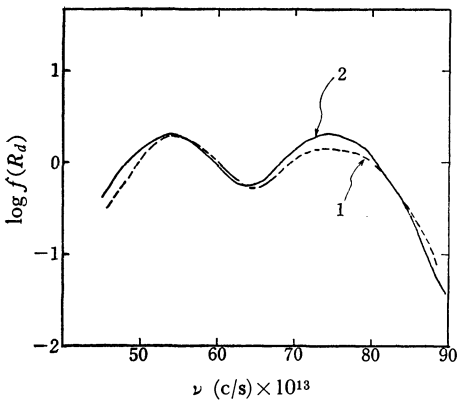

Fig. 7. Electronic absorption spectra for the solid states of
1: $NH_4[Cr(OH)(apda)(H_2O)]\cdot 2H_2O$,
2: $NH_4[Cr(OH)(ata)(H_2O)]\cdot 2H_2O$.

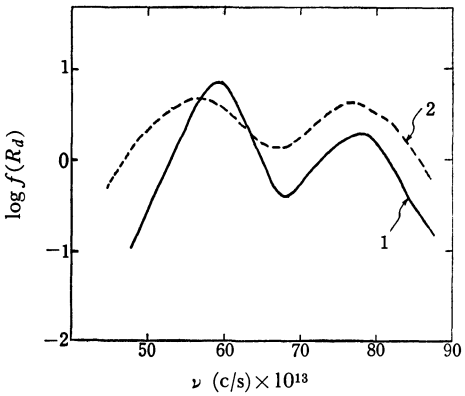

Fig. 8. Electronic absorption spectra for the solid states of
1: $[Cr(apda)(py)_2]$,
2: $[Cr(apda)(py)_2]$ exposed in air.

In Fig. 3, the absorption spectra of the purple crystals of II and the corresponding ATA complex are shown. These curves seem to be somewhat different from each other. On the other hand, Fig. 7 shows the absorption spectra of these complexes in the solid state; these spectra are quite similar to each other. One possible interpretation in these results is given below. In the preceding paper,[1] as ATA complexes corresponding to II, $NH_4[Cr(OH)(ata)(H_2O)]\cdot 2H_2O$ and $NH_4[Cr(OH)(ata)(H_2O)_2]\cdot 3H_2O$ were obtained. The former complex turned from purple to green when dissolved in water; from this it was concluded that this purple crystal is a $[Cr\cdot N\cdot O_5]$-type complex, while the product in the green solution was a $[Cr\cdot O_6]$-type one, in which the nitrogen atom is not directly coordinated to chromium. In the latter ATA complex, also, the nitrogen atom in ATA was not directly coordinated to chromium in either a solution and in a solid state. Nevertheless, in the crystal of APDA complex II, the nitrogen atom in APDA participates in coordination together with the three carboxyl groups, and we have not succeeded in preparing the $[Cr\cdot O_6]$-type complex corresponding to the green ATA complex described above.

The absorption spectra for the solutions of the pink crystal of III and of the one which was left

Table 3. IR data (cm^{-1})

Complex	-COOH	-COO-Cr	-COO-	Complement
APDA	1725(vs)			
I	1693(s)	1670(sh)—1598(vs)		
II		1670(sh)—1596(vs)		
III		1680(sh)—1595(vs)	1605(sh)	
IV		1682(sh)—1590(vs)		1588(s), 860(s), 734(s)*
V		1675(sh)—1596(vs)		1590(s), 858(s), 724(s)**
VI		1688(sh)—1590(vs)		1585(s), 753(s), 713(s)***

* The absorptions arising from 2,2'-bipyridyl.
** Those from *o*-phenanthroline.
*** Those from pyridine.

to stand overnight are shown in Fig. 4. The former spectrum indicates a splitting on the first band (a d–d electron transition). This may mean that this crystal has a *trans* structure with respect to the nitrogen atoms in APDAs. Upon standing overnight this solution gradually turned from pink to purple and its spectrum became quite similar to that of II (Figs. 3 and 4). This suggests that there is a gradual decomposition of $[Cr(apda)_2]^{3-}$ to $[Cr(OH)(apda)(H_2O)]^-$. On the other hand, $[Cr(ata)_2]^{3-}$ decomposed to $[Cr(OH)(ata)(H_2O)_2]^-$.[1]

Figure 5 shows the spectra for the solutions of the IV, V, and VI complexes, and that of III exposed to air for three days. The former two give complicated curves similar to those of the corresponding ATA complexes; this was a result of the coordination of 2,2'-bipyridyl and *o*-phenanthroline.[2] In solution, the pink crystals of VI have two absorption peaks, at 57.0 and 77.5, and a shoulder at 107.1×10^{13} c/s (in Curve 3), but the shoulder disappeared and the two peaks shifted to a longer wavelength region in VI which had been exposed to air (in Curve 4), as is shown in Fig. 5. Such a change was also found in the solid state (Fig. 8). These facts indicate that the coordinated pyridines are liberated from the crystals even at room temperature.

Infrared Spectra. The infrared spectra were measured in order to determine whether or not the carboxyl groups in the complexes were coordinated. The numerical values of the absorption bands arising from the carboxyl groups and the other ligands are listed in Table 3, while the spectra of Complex I concerning carboxyl-group stretching are shown in Fig. 9. The crystal of I gives two strong bands due to the carboxyl groups; one is a 1693 cm^{-1}, and the other is a 1670—1598 cm^{-1}. The former may be assigned to the stretching of free carboxylic acid, which disappears upon heating at 160°C, whereas the latter may be assigned to that of the coordinated carboxyl group. The shoulder at 1605 cm^{-1}, appearing only in III, suggests that it has free carboxylate ions. The other complexes show strong absorption bands in

Fig. 9. Infrared spectra for
1: $[Cr(OH)(apdaH)(H_2O)_2]$,
2: $[Cr(OH)(apdaH)(H_2O)_2]$ heated at 160°C.

the region of 1590—1680 cm^{-1}, suggesting that all the carboxyl groups are coordinated. Further, IV, V and VI show bands reflecting the vibrations of C=C, C=N, and C–H in coordinated 2,2'-bipyridyl, *o*-phenanthroline and pyridine.

Magnetic Moment. The effective magnetic moments of these complexes were evaluated from the magnetic susceptibilities as measured by the Gouy method. The numerical data, corrected by introducing each Pascal constant, are summarized

Table 4. Magnetic moments (B. M.)

Complex	B. M. (temp.)
I	3.88 (293°K)
II	3.70 (293°K)
III	3.75 (293°K)
IV	3.88 (293°K)
V	3.84 (293°K)
VI	3.82 (293°K)

in Table 4. These values, 3.7—3.9 B. M., are nearly equal to the spin-only values for tervalent chromium.

Discussion of the Structures and Some Comparisons with the ATA Complexes. The possible structues of these complexes will now be discussed and comparisons will be made with the ATA complexes on the basis of the above results. Fig. 10 shows the patterns of the possible structures, (A), (B), (C), and (D), proposed by the present authors. The classification of the success or

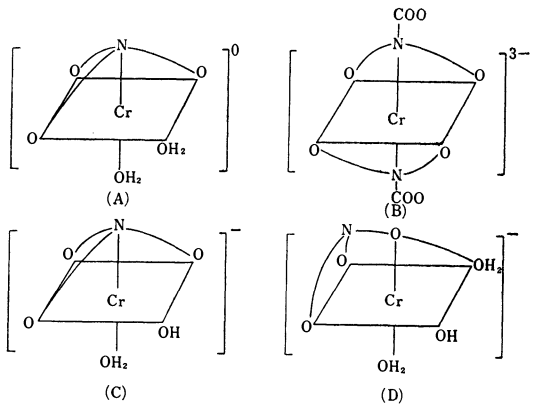

Fig. 10. Possible structures.

failure in the preparation of the ATA and APDA complexes of these four types are summarrized below:

Type	Ligand	
	ATA	APDA
A	×	○
B	○	○
C	○	○
D	○	×

where ○ indicates success in preparation and × shows failure. The crystal of the A-type complex was obtained with APDA, but not with ATA. This may be mainly due to the much lower solubility in the former complex than that in the latter. The B-type complex was prepared with both chelating agents. In the ATA complex, there was a successive decomposition from B to D, but one from B to C was found in the APDA complex. Although the C-type complex was obtained with both ligands, an instantaneous change (in an aqueous solution) into D occurred in the ATA complex, but not in the APDA complex. As has already been reported, the introduction of the methylene group ($-CH_2-$) into ATA probably results in a little more stable complex formation. The inspection by using the molecular model suggests that there is a larger strain on the nitrogen atom in coordination in the ATA complex than in that with the APDA complex. As a result of this steric factor, the nitrogen atom in APDA has the larger coordinating ability than that in ATA. This fact is consistent with the expectation as to the stability shown by Martell *et al.*[4] The failure to prepare the D-type complex, in which the nitrogen atom in APDA does not participate in the coordination, may also support such a steric reason as that described above. With all the mixed ligand complexes, the APDA always acts as a quadridentate ligand.

Finally, as is drawn below, in Complex I there are some interactions between the hydrogen atom in the free carboxylic acid and the oxygen atom in the coordinated OH group; when heated at 160°C the oxygen atom within the free carboxylic acid may participate in the coordination by losing one mole of water. A fact similar to this has previously been reported by one of the present authors.[5]

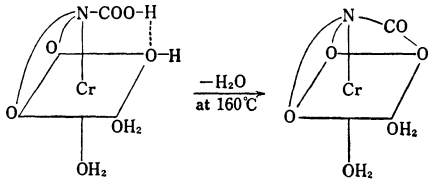

4) S. Chaberek, Jr. and A. E. Martell, *J. Am. Chem. Soc.*, **75**, 2888 (1953).
5) E. Kyuno, *Nippon Kagaku Zasshi (J. Chem. Soc. Japan, Pure. Chem. Sect.)*, **80**, 849 (1959).

BULLETIN OF THE CHEMICAL SOCIETY OF JAPAN VOL. 41 2393—2400 (1968)

The Chromium(III) Complexes with Ammoniaisopropionicdiacetic Acid*[1]

Akira UEHARA, Eishin KYUNO and Ryokichi TSUCHIYA

Department of Chemistry, Faculty of Science, Kanazawa University, Kanazawa

(Received February 19, 1968)

A new chelating agent—ammoniaisopropionicdiacetic acid (abbreviated as AIPDA), one of the derivatives of ammoniatriacetic acid, was prepared. Also, the following chromium(III) complexes containing AIPDA as a ligand were newly prepared: $NH_4[Cr(OH)(aipda)(H_2O)]\cdot 4H_2O$ (purple) (I), $NH_4[Cr(OH)(aipda)(H_2O)_2]\cdot 2H_2O$ (green) (II), $[Cr(aipda)(o\text{-phen})]\cdot 2H_2O$ (brown) (III), $[Cr(aipda)(bipy)]\cdot 3H_2O$ (brown) (IV), [Cr(aipda)(*l*-pn)] (pink) (V), $[Cr(aipda)(py)_2]$ (pink) (VI) and $NH_4[Cr(OH)(aipda)(py)]\cdot 2H_2O$ (reddish purple) (VII), where apipda, *o*-phen, bipy, *l*-pn and py are the abbreviations of the ammoniaisopropionatediacetate ion, *o*-phenanthroline, 2,2'-bipyridyl, *l*-propylenediamine and pyridine respectively. On the basis of the chemical and thermal analyses and the measurements of the electronic absorption spectra, the reflection spectra, and the IR spectra, it was found that, in these complexes, AIPDA can behave as a terdentate or a quadridentate ligand to chromium(III), but the 1 : 2 Cr(III) AIPDA complex like the corresponding ATA one could not be obtained because of the steric hindrance resulting from the introduction of a methyl group into ATA. Further information on the conductivities in an aqueous solution and the reflection spectra suggests that V and VI are gradually aquated. The properties of the AIPDA complexes obtained in the present study were compared with those of ammoniatriacetic acid and those of ammoniapropionicdiacetic acid complexes.

The preparations of the chromium(III) complexes containing ammoniatriacetic acid (ATA) and ammoniapropionicdiacetic acid (APDA) as the chelating agents have already been reported[1-3]; these two complexes behave quite differently. For example, ATA formed a more stable complex as a terdentate (O_3 type) than as a quadridentate ($N\text{-}O_3$ type) ligand in an aqueous solution, while in the solid state it formed a more stable one as a quadridentate ligand. On the other hand, AIPDA did not behave thus as a terdentate ligand (O_3 type).

When one of the hydrogen atoms in a $-CH_2-$ group in ATA is replaced with a methyl group, ammoniaisopropionicdiacetic acid (AIPDA) is obtained. This reagent is expected to indicate any chemically and sterically unique behavior in the complex formation, differing from ATA or APDA. The formula of AIPDA is drawn in Fig. 1, together with those of ATA and APDA. AIPDA has one nitrogen and three oxygen atoms capable of coordinating; therefore, it can be expected to behave either as a quadridentate ligand ($N\text{-}O_3$ type) or as a terdentate ligand ($N\text{-}O_2$ type or O_3 type). On the basis of these observations, this study aimed to find how AIPDA behaves toward a chromium(III) ion and to compare the properties of the AIPDA complexes with those of the ATA and APDA complexes.

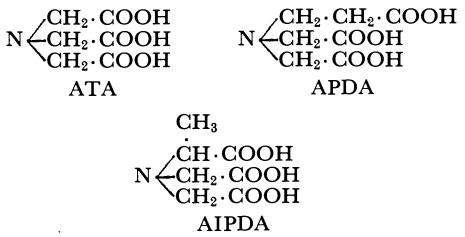

Fig. 1. Structures of the chelating agents.

Experimental

Preparation of Ammoniaisopropionicdiacetic Acid, $C_7H_{11}O_6N$. Ninety grams of *d,l*-α-alanine were neutralized with 200 m*l* of water containing 57 g of potassium hydroxide. Besides, 190 g of monochloroacetic acid was dissolved in about 300 m*l* of water and then gradually neutralized with 200 g of potassium hydrogencarbonate. The two neutralized reagents were then mixed and heated on a water bath. When the temperature of the solution was raised to *ca.* 70°C, 200 m*l* of water containing 112 g of potassium hydroxide was added. Because of the exothermic reaction, the temperature was immediately raised. After the reaction was over, an appropriate amount of concentrated hydrochloric acid was added to the solution until the

*1 Presented in part at the 17th Symposium on Coordination Compounds, Hiroshima, December, 1967.

1) A. Uehara, E. Kyuno and R. Tsuchiya, This Bulletin, **40**, 2317 (1967).
2) A. Uehara, E. Kyuno and R. Tsuchiya, *ibid.*, **40**, 2322 (1967).
3) A. Uehara, E. Kyuno and R. Tsuchiya, *ibid.*, **41**, 238 (1968).

value of pH dropped from 9 to 1—2. The potassium chloride depositing out first was filtered off. The filtrate was again concentrated to as small an amount as possible. To the resultant solution, an appropriate amount of acetone was gradually added, and then the solution was scrubbed with a glass rod until white, powdered crystals were obtained, after which the solution was kept at 0°C. Recrystallization was achieved from cold water. It is considerably soluble in water, but, is insoluble in alcohol and ether. Yield, about 100 g.

Found: N, 6.43; C, 41.21; H, 5.30%. Calcd for $C_7H_{11}O_6N$: N, 6.84; C, 40.98; H, 5.40%.

Preparations of the Complexes. The methods of preparing the complexes containing AIPDA are very simmilar to those used to prepare those with ATA.[1]

1) Ammonium Hydroxoammoniaisopropionicdiacetatoaquochromate(III) Tetrahydrate, $NH_4[Cr(OH)(aipda)(H_2O)]\cdot 4H_2O$ (purple) (I). Approximately 4.2 g of AIPDA and an appropriate amount of chromium(III) hydroxide freshly prepared from 10 g of chromium alum and aqueous ammonia were mixed in 100 m*l* of hot water; then the mixture was evaporated almost to dryness. The residue was once dissolved in 30 m*l* of not water, and the resultant purple solution was filtered from the residue undissolved. By using this purple solution as a starting material, complexes I and II were prepared as below.

To this purple solution, about 1.5 g of ammonium carbonate were added and the pH was adjusted to 5—6. After it had been cooled to 0°C, purple, scale-like crystals were obtained. The products were recrystallized from their concentrated, greenish solution. Yield, about 1 g.

Found: Cr, 13.42; N, 7.26; C, 21.96; H, 6.81; H_2O,*2 19.7%. Calcd for $NH_4[Cr(OH)(aipda)(H_2O)]\cdot 4H_2O$: Cr, 13.68; N, 7.36; C, 22.12; H, 6.12; H_2O, 19.11%.

2) Ammonium Hydroxoammoniaisopropionicdiacetatodiaquochromate(III) Dihydrate, $NH_4[Cr(OH)(aipda)(H_2O)_2]\cdot 2H_2O$ (green) (II). To the purple solution obtained above, about 2.5 g of ammonium carbonate were added and the pH was adjusted to 7—8. When it was cooled to 0°C, green, scale-like crystals were obtained. Since it was, sometimes, contaminated with purple crystals of I, the pH had to be well adjusted to the above value. The recrystallization was achieved from its concentrated, greenish solution, the pH having been adjusted to 7—8 by adding an appropriate amount of ammonium carbonate. Yield, about 1 g.

Found: Cr, 14.25; N, 7.53; C, 22.96; H, 5.71; H_2O, 9.7%. Calcd for $NH_4[Cr(OH)(aipda)(H_2O)_2]\cdot 2H_2O$: Cr, 14.73; N, 7.74; C, 23.23; H, 5.85; H_2O, 10.03%.

3) Ammoniaisopropionicdiacetato - o - phenanthrolinechromium(III) Dihydrate, $[Cr(aipda)(o\text{-phen})]\cdot 2H_2O$ (brown) (III). About 6 g of *o*-phenanthroline and 2.6 m*l* of concentrated hydrochloric acid were added to about 50 m*l* of water containing 10 g of Complex I. When the solution was then heated for several minutes on a water bath, brown crystals were separated out. The recrystallization was achieved from water. Yield, about 3 g.

Found: Cr, 11.07; N, 8.90; C, 48.09; H, 4.10; H_2O, 7.5%. Calcd for $[Cr(aipda)(o\text{-phen})]\cdot 2H_2O$: Cr, 11.04; N, 8.92; C, 48.48; H, 4.28; H_2O, 7.71%.

4) Ammoniaisopropionicdiacetato - 2,2' - bipyridylchlomium(III) Trihydrate, $[Cr(aipda)(bipy)]\cdot 3H_2O$ (brown) (IV). Five grams of 2,2'-bipyridyl and 2.6 m*l* of concentrated hydrochloric acid were added to about 50 m*l* of water containing 10 g of I. When the solution was then heated on a waterbath for several minutes, brown crystals were obtained. The products were recrystallized from water. Yield, about 4 g.

Found: Cr, 11.02; N, 9.27; C, 44.00; H, 4.11; H_2O, 12.0%. Calcd for $[Cr(aipda)(bipy)]\cdot 3H_2O$: Cr, 11.18; N, 9.04; C, 43.93; H, 4.63; H_2O, 11.72%.

5) Ammoniaisopropionicdiacetato - l - propylenediaminechromium(III), $[Cr(aipda)(l\text{-pn})]$ (pink) (V). About 2 g of *l*-propylenediamine were diluted with 20 m*l* of water and then 2.4 m*l* of concentrated hydrochloric acid were added. To this solution, a 50 m*l* portion of water containing 10 g of I was added, and resultant solution was evaporated to dryness; pink powdered crystals were thus obtained. The crude products were recrystallized from an alcohol-water (1 : 1) mixture. Yield, about 2 g. In an aqueous solution, these crystals were gradually aquated.

Found: Cr, 15.61; N, 12.21; C, 36.94; H, 5.54%. Calcd for $[Cr(aipda)(l\text{-pn})]$: Cr, 15.84; N, 12.80; C, 36.58; H, 5.52%.

The use of *d*- or racemic-propylenediamine instead of *l*-propylenediamine gave a corresponding *d*- or *d,l*-pn complex.

6) Ammoniaisopropionicdiacetato - bis (pyridine) chromium(III), $[Cr(aipda)(py)_2]$ (pink) (VI). Then grams of I were dissolved into 10 m*l* of water containing 2.4 m*l* of concentrated hydrochloric acid, and then 150 m*l* of pyridine were added to it. This mixture was heated on a water bath, using a reflux condenser in order to prevent the pyridine from vaporizing. After the solution had gradually turned from purple to pale red, it was cooled to 0°C. After it had then stood for a few days, pink crystals were obtained. The recrystallization was achieved from absolute alcohol or absolute pyridine. Yield, about 1 g.

Found: Cr, 12.91; N, 9.54%. Calcd for $[Cr(aipda)(py)_2]$: Cr, 12.61; N, 10.19%.

The elementary analyses were repeated several times, but fully satisfactory results could not be obtained since the crystals easily lose the pyridine, even at room temperature. On the basis of the derivatography, the change in the TGA curve, corresponding to two moles of pyridine, reasonably supports such a composition as $[Cr(aipda)(py)_2]$.

7) Ammonium Hydroxoammoniaisopropionicdiacetatopyridinechromate(III) Dihydrate, $NH_4[Cr(OH)(aipda)(py)]\cdot 2H_2O$ (reddish purple) (VII). Ten grams of I were dissolved into 50 m*l* of water, and then 25 m*l* of pyridine was added to the mixture. Being gradually heated on a water bath at *ca.* 40—60°C, the solution turned from green to pink. As soon as reddish purple crystals appeared, the crystals had to be quickly filtered off from the solution since the purple crystals, I, were inclined to deposit as a by-product. The recrystallization from water was always unsuccessful due to the deposition of the purple crystals, I. Moreover, since no optimum solvent for VII was found, no recrystallization could be done. Yield, about 1.5 g. For the above reasons, the results of the elementary analyses were not in

*2 The H_2O which appears in all the analytical data in this paper shows the only distinct crystalline water estimated from the derivatogram.

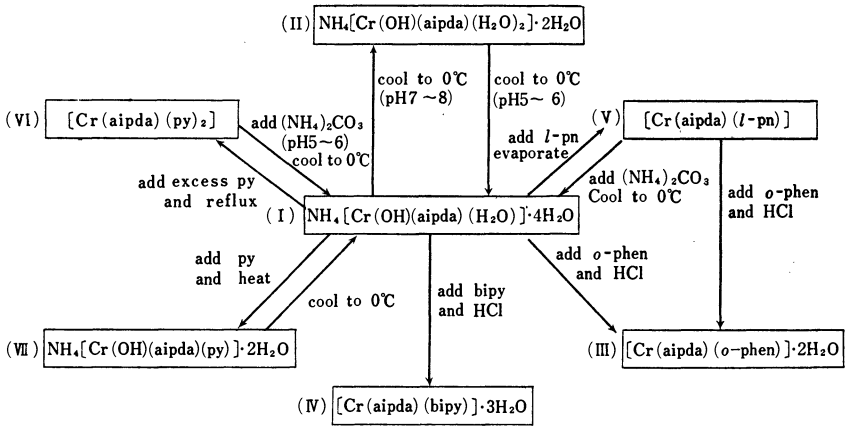

Fig. 2

excellent agreement with the calculated values shown below.

Found: Cr, 12.24; N, 9.80; C, 35.28; H, 4.97; H_2O, 8.2%. Calcd for $NH_4[Cr(OH)(aipda)(py)]\cdot 2H_2O$: Cr, 12.83; N, 10.38; C, 35.59; H, 5.45; H_2O, 8.92%.

The crystalline-water content in these complexes was estimated from the weight loss in the respective thermogravimetric curves (TGA), which were measured with a derivatograph.

Preparative Interconversion among These Complexes. Some interconversions among the complexes prepared in the present work were successful, as in the case of ATA. In Fig. 2, several interconversion procedures are shown schematically.

A) The Interconversion from I to II and Vice Versa. The pH of the greenish solution of I was adjusted to 7—8 by adding small amounts of amonium carbonate; when it had cooled to 0°C, green crystals, II, were obtained. On the other hand, when hydrochloric acid was used instead of ammonium carbonate, the pH of the greenish solution of II was descreased to 5—6 at 0°C, and purple crystals of I were obtained.

B) The Interconversion from V or VI to I. To 10 m*l* of an aqueous solution containing 1 g of V or VI, 0.2 or 0.3 g of ammonium carbonate was added respectively. These solutions turned from pink to green. When they were cooled to 0°C, purple crystals, I, were obtained.

C) The interconversion from V to III. One gram of *o*-phenanthroline was dissolved into 20 m*l* of water containing about 0.5 m*l* of concentrated hydrochloric acid. To this solution, 1.7 g of V were then dissolved by heating it on a water bath. The solution gradually changed from pink to brown. After the resultant solution had stood for several days, brown crystals, III, were obtained.

Apparatus. The apparatus used in this study was the same as has been described in a previous paper.[3)]

Results and Discussion

Thermal Measurements. The DTA, TGA, and temperature curves obtained for the complexes are shown in Figs. 3-A to 3-G, where the scale of DTA is arbitrary; the upper-side deviation of DTA indicacates the appearance of an exothermic reaction, and the under-side one, that of the endothermic reaction. All the measurements were carried out with a heating rate of 1°C/min in a nitrogen stream. As can be seen in Figs. 3-A to 3-D, the I, II, III, and IV complexes are all dehydrated between about 60 and 120°C and decomposed at about 290—300°C. Especially the step-by-step dehydration was observed for Complexes I and III. Figure 3-E shows that Complex V has no crystalline water. The complexes of VI and VII are shown in Figs. 3-F and 3-G to lose their coordinated pyridines, even at relatively low temperatures (from room temperature to 80°C). Moreover, in Complex VII, as may be seen in Fig. 3-G, the liberation of crystalline water was well detected after it had lost coordinated pyridine.

The values of the enthalpy changes in these decomposition processes, which can be evaluated from the DTA curves, will be reported elsewhere.

Behavior in Reaction to the Ion Exchanger and Molar Conductivity. The behavior in reaction to the ion exchangers and molar conductivities of a 1/1000 molar solution of the samples are shown in Table 1, in which the + symbol indicates the adsorption of the complexes by an exchanger, and −, the non-adsorption. The solutions of the purple crystals, I, and the green crystals, II, were both greenish and were adsorbed by the Cl-form anion exchanger. Their molar conductivities are 115.0 and 116.2 mho cm^{-1} respectively, suggesting that they are 1 : 1-type complexes. The value of the conductivity, 98.6 mho cm^{-1}, for VII and its ability to be adsorbed by the Cl-form exchanger indicate that it is also of this type. The complexes of III to VI were adsorbed neither by the Na-form nor the Cl-form exchanger, showing that they are all non-electrolyte molecules. A gradual decomposition in an aqueous solution was found for both V and VI, when their colors turned purple, and the decomposed solutions could not be adsorbed by the exchangers, suggesting that the aquations probably, in part at

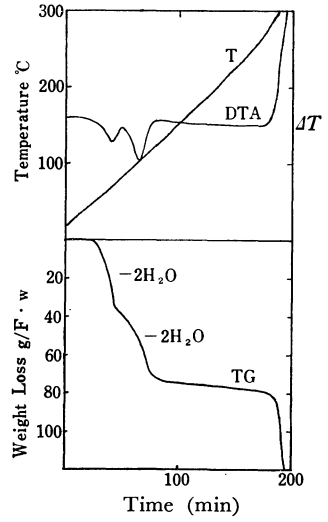

(A) $NH_4[Cr(OH)(aipda)(H_2O)]\cdot 4H_2O$

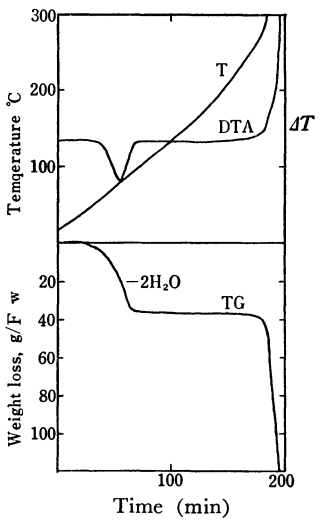

(B) $NH_4[Cr(OH)(aipda)(H_2O)_2]\cdot 2H_2O$

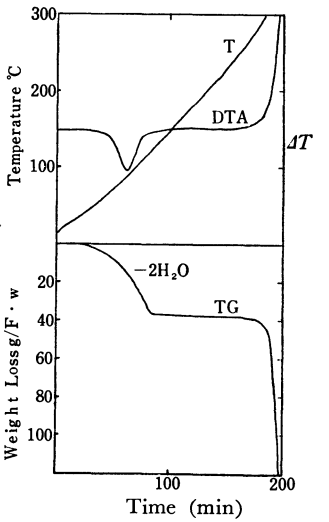

(C) $[Cr(aipda)(o\text{-phen})]\cdot 2H_2O$

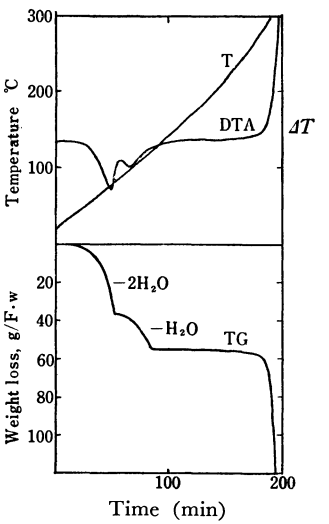

(D) $[Cr(aipda)(bipy)]\cdot 3H_2O$

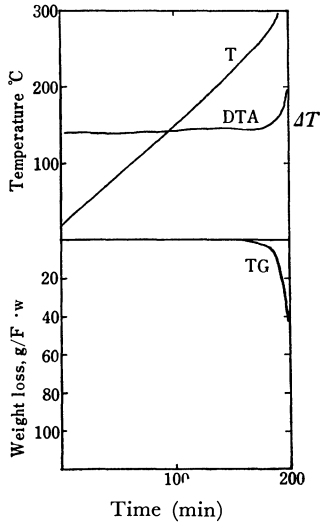

(E) [Cr(aipda)(*l*-pn)]

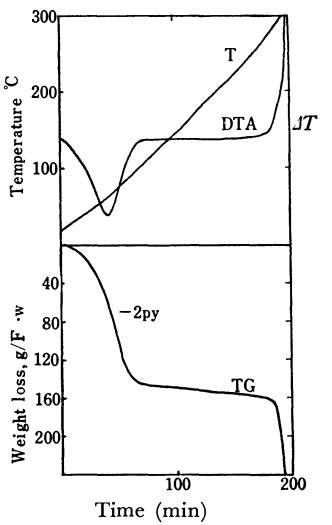

(F) $[Cr(aipda)(py)_2]$

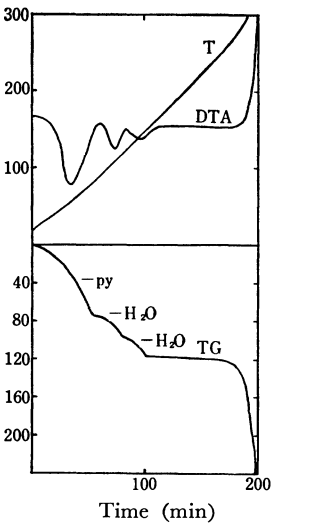

(G) $NH_4[Cr(OH)(aipda)(py)]\cdot 2H_2O$

Fig. 3. Curves for thermal analyses.

Table 1. Behavior toward the ion exchanger and molar conductivity

Complex	Color of crystal	Color of solution	Adsorption		Molar conductivity (mho cm^{-1})
			Na-form	Cl-form	
I	purple	green	−	+	115.0
II	green	green	−	+	116.2
III	brown	brown	−	−	
IV	brown	brown	−	−	
V	pink	pink	−	−	
VI	pink	pink	−	−	
VII	reddish purple	reddish purple	−	+	98.6

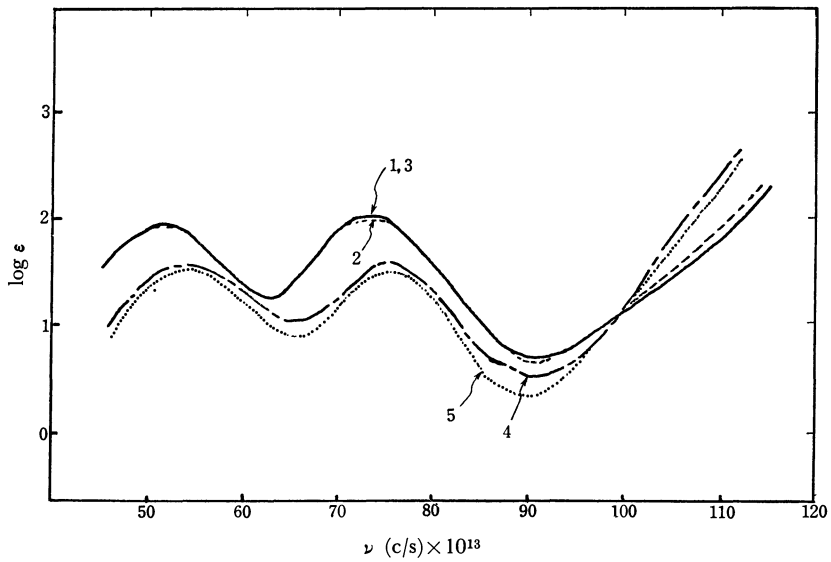

Fig. 4. Electronic absorption spectra for the solutions of
1: $NH_4[Cr(OH)(aipda)(H_2O)]\cdot 4H_2O$, 2: $NH_4[Cr(OH)(aipda)(H_2O)_2]\cdot 2H_2O$,
3: $NH_4[Cr(OH)(ata)(H_2O)]\cdot 2H_2O$, 4: $[Cr(aipda)(H_2O)_2]$, 5: $[Cr(ata)(H_2O)_2]$.

Table 2. Absorption maxima

Complex	$\nu_1(\log \varepsilon_1)$	$\nu_2(\log \varepsilon_2)$	$\nu_3(\log \varepsilon_3)$
I	51.5(1.95)	73.5(2.01)	
II	51.5(1.92)	73.5(2.00)	
III	55.9(1.91)	76.1(2.09)	99.0(3.71)
IV	56.3(1.95)	76.7(2.05)	97.1(4.18)
V	55.5(1.98)	78.5(2.04)	
VI	57.0(2.13)	77.5(1.98)	107.1(3.25)
VII	54.5(2.01)	74.3(2.08)	112.8(3.68)

least, take place.

Electronic Absorption Spectra. The Absorption spectra for Complexes I to VII were measured in an aqueous solution; of these, those for V and VI were done in a mixture of water-alcohol (1 : 1) to prevent gradual decomposition. The numerical data of the absorption maxima are summarized in Table 2. The spectra for the solutions of Complexes I and II are drawn in Fig. 4, together with

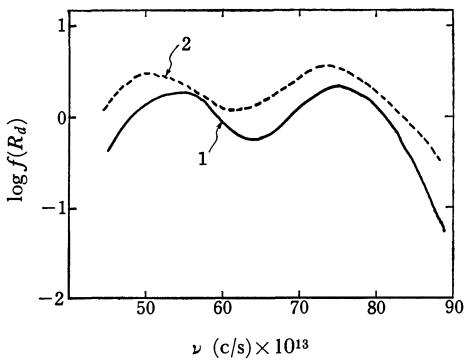

Fig. 5. Electronic absorption spectra for the solid sate of
1: $NH_4[Cr(OH)(aipda)(H_2O)]\cdot 4H_2$,
2: $NH_4[Cr(OH)(aipda)(H_2O)_2]\cdot 2H_2O$.
$f(R_d)=\dfrac{(1-R_d)^2}{2R_d}$
(R_d: relative reflection index).

TABLE 3. IR DATA (cm^{-1})

Complex	-COOH	-COO-Cr	$-COO^-$	Complement
I		1688(sh)—1598(vs)		
II		1680(sh)—1596(vs)		
III		1681(sh)—1598(vs)		1595(s), 863(s), 731(s)*
IV		1678(sh)—1595(vs)		1590(s), 861(s), 730(s)**
V		1680(sh)—1593(vs)		
VI		1675(sh)—1598(vs)		1585(s), 753(s), 712(s)**
VII		1693(sh)—1597(vs)		1583(s), 746(s), 710(s)***

* The absorption arising from *o*-phenanthroline.
** Those from 2,2'-bipyridyl.
*** Those from pyridine.

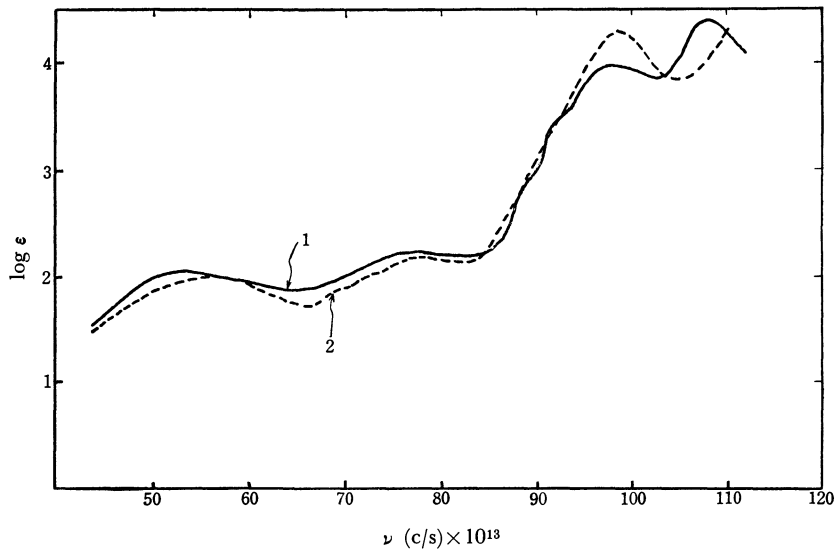

Fig. 6. Electronic absorption spectra for the solutions of
1: $[Cr(aipda)(o\text{-phen})\cdot 2H_2O$, 2: $[Cr(aipda)(bipy)]\cdot 3H_2O$.

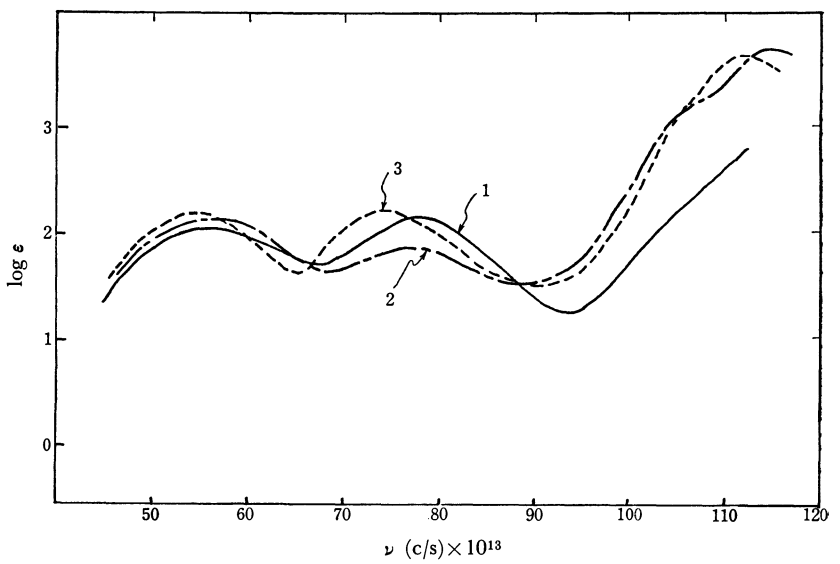

Fig. 7. Electronic absorption spectra for the solutions of
1: $[Cr(aipda)(l\text{-pn})]$, 2: $[Cr(aipda)(py)_2]$, 3: $NH_4[Cr(OH)(aipda)(py)]\cdot 2H_2O$.

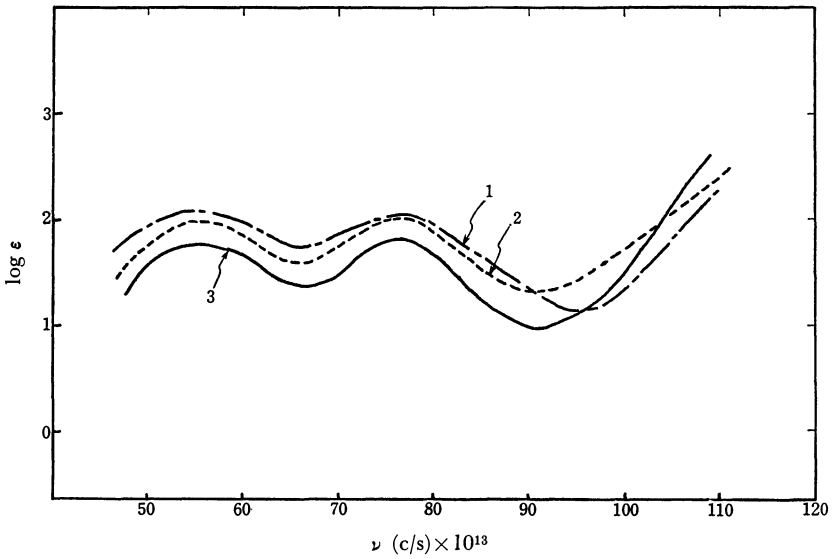

Fig. 8. Electronic absorption spectra for
1: [Cr(aipda)(*l*-pn)] stood in water, 2: [Cr(aipda)(py)$_2$] stood in water.

those for the corresponding ATA complexes and for the purple solutions of AIPDA and ATA complexes, where the scale of log ε for the purple solutions is arbitrary. A very close resemblance was seen among the spectra for the solutions of I, II, and the corresponding ATA complex.

The absorption spectra for the solid state were measured by the diffuse-reflection method. The spectra for the solid state of I and II are shown in Fig. 5. An appreciable difference between them can be seen. From these data, as with the corresponding ATA complex,[1] both the purple complex, I, and the green complex, II, may be considered to have the same structure, of the [Cr·O$_6$] type in an aqueous solution, whereas in the crystal state they have different structures (*i. e.*, the purple complex is of the [Cr·N·O$_5$] type, and the green complex, of [Cr·O$_6$] type). In addition, the purple solution used as a starting material gave a spectrum very similar to that of the corresponding purple solution of the ATA complex, showing that they have the same structure.

The spectra for the solutions of the brown crystals of III and IV gave complicated curves similar to those of the corresponding ATA and APDA complexes due to the coordination of 2,2'-bipyridyl and *o*-phenanthroline, as can be seen in Fig. 6.

The absorption spectra for the solutions of the pink crystal V, the pink crystal VI, and the reddish-purple crystal VII are drawn in Fig. 7. The complexes of VI and VII show a third absorption maximum, due to the coordinated pyridine. The complexes of V and VI in an aqueous solution have a tendency to lose *l*-propylenediamine and pyridine respectively, and their spectra are found to approach that of the purple solution used as a starting material, as is shown in Fig. 8. This indicates that these complexes may undergo aquation by losing *l*-propylenediamine and the pyridine molecule respectively. Figure 9 shows the absorption spectra for the solid states of Complex VI itself and Complex VI after it has been exposed to air for a few days. A considerable difference between them can be seen; namely, the latter has its maximum at a lower frequency region than the former. This shows that VI easily loses the coordinated pyridine molecules, even at room temperature. Such a phenomenon has also been found in the corresponding APDA complex.[3]

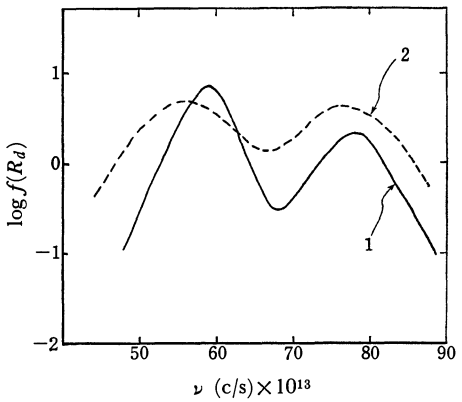

Fig. 9. Electronic absorption spectra for the solid states of
1: [Cr(aipda)(py)$_2$], 2: [Cr(aipda)(py)$_2$] exposed.

IR Spectra. The infrared spectra were measured in order to determine whether or not the carboxyl groups in the complexes are coordinating. The

numerical values of the band arising from the carboxyl groups and the other ligands concerned are listed in Table 3. Strong absorption bands in the 1589—1670 cm^{-1} region can be detected in all these complexes, indicating that all the carboxyl groups in AIPDA participate in the coordination. Furthermore, III, IV, VI, and VII gave bands connected with the vibrations of C–C, C–N, and C–H in coordinated 2,2'-bipyridyl, *o*-phenanthroline, and pyridine.

Magnetic Moments. The magnetic susceptibilities of the complexes were measured by the Gouy method. The numerical data of the effective magnetic moments, as evaluated from the above values, are listed in Table 4. The values for these complexes are 3,75—3.95 B. M., nearly equal to their spin-only values for chromium(III).

TABLE 4. MAGNETIC MOMENTS (B. M.)

Complex	μ_{eff} B. M. (temp. °K)
I	3.82 (293°K)
II	3.91 (293°K)
III	3.87 (293°K)
IV	3.85 (293°K)
V	3.87 (293°K)
VI	3.75 (293°K)
VII	3.81 (293°K)

Discussion of the Structures. *1) Possible Structures of the Complexes Obtained.* The possible structures of these complexes proposed by the present authors on the basis of the above results are given in Fig. 10. The complex species in the solution used as a starting material may have an A structure. The structure for purple crystals, I, may be identified as a C. In green crystals, II, a D structure, may hold in the same way as in the corresponding ATA complex, although the positions of the OH^- and H_2O ligands are still arbitrary. No complex with a B structure was found. In all the mixed-ligand complexes, only AIPDA acted as a quadridentate ligand.

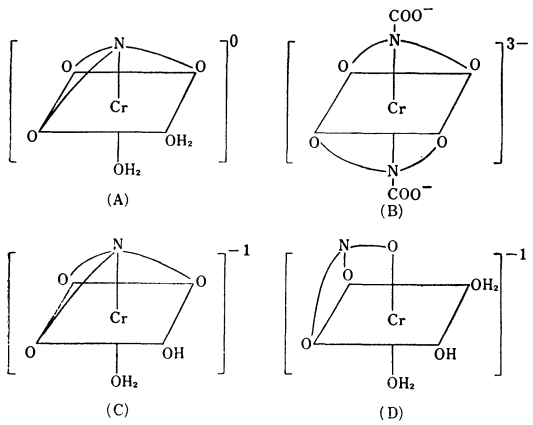

Fig. 10. Possible structures.

2) Some Comparisons among ATA, AIPDA, and APDA Complexes. Of these three ligands, ATA and AIPDA behave toward the chromium(III) ion quite similar manners, but that of APDA is somewhat different. The classification of success or failure in preparing the complexes as a crystal state are summarized in Table 5, where ○ symbolizies a successful preparation and × shows failure. It is immediately noticeable that an A-type complex can be prepared only with APDA; this may be mainly due to the lesser solubility of the complex in water. Their solubilities decrease in the order: AIPDA>ATA>APDA complexes.

TABLE 5. THE COMPLEXES OBTAINED AS A CRYSTAL STATE

	ATA	AIPDA	APDA
A type	×	×	○
B type	○	×	○
C type	○	○	○
D type	○	○	×

○, symbolizes the successful preparation.
×, the reverse.

All these ligands can form C-type complexes. Furthermore, the C-type complexes with ATA and AIPDA were changed instantly to the D-type when dissolved into water, whereas the corresponding C-type complex with APDA did not act thus. These facts may be briefly explained as follows. ATA and AIPDA form three five-membered chelate rings in the complex formation, while APDA forms two five-membered rings and one six-membered one. The inspection by using a molecular model suggests that there are larger strains on the nitrogen atom in coordinated ATA and AIPDA than that in APDA. As a result of these steric factors, the nitrogen atom in APDA has a larger coordinating ability than those in ATA and AIPDA. This fact is consistent with the expectation regarding the stability of Martell *et al.*[4] The attempt to prepare the B-type complex was not successful with AIPDA. This may be because steric hindrance due to the methyl group may arise on the formation of the 1 : 2-type complex; this possibility is supported by an inspection of the molecular model.

4) S. Chaberek, Jr., and A. E. Martell, *J. Am. Chem. Soc.*, **75**, 2888 (1953).

BULLETIN OF THE CHEMICAL SOCIETY OF JAPAN VOL. 41 2401—2405 (1968)

Use of a Hanging Mercury Drop Electrode in the Alternating Current Polarographic Analysis of Thallium(I)

Mutsuo KODAMA and Tomohiko NODA

Department of Chemistry, Ibaraki University, Mito, Ibaraki

(Received February 28, 1968)

The use of a hanging mercury drop electrode (HMDE) in the a.c. polarographic determination of thallium was studied systematically. Analysis was carried out by scanning anodically the potential of HMDE from the limiting-current potential region at a constant scanning rate and by measuring the a.c. peak-height for the anodic stripping process of thallium. Thallium could be concentrated effectively on the HMDE at the initial stage of this procedure and then stripped anodically. By employing this technique, a marked increase in sensitivity could be obtained and 1.0×10^{-6} M thallium(I) in an EDTA solution was determined accurately. The interference effects of lead, cadmium, zinc, and indium on the determination of thallium were also investigated. When the electrolysis was initiated in the limiting-current potential region of lead(II), the peak-height of thallium was found to be enhanced markedly.

Previously,[1] we have investigated the characteristics of a hanging mercury drop electrode (HMDE) in alternating current (a. c.) polarography and the possibility of using this electrode in the a.c. polarographic analysis of metal ions. Sensitivity was effectively improved by the pre-electrolysis; the metal ion was reduced to an amalgam in the limiting-current region, and then the metal was anodically stripped.

As was proposed by Underkofler and Shain[2] in the a. c. stripping analysis of cadmium(II) using a phase selective detector, the pre-electrolysis and the subsequent electro-dissolution (anodic stripping) processes can be conducted by simply scanning the potential of the working electrode in the anodic direction from the potential, where the limiting current for the metal ion to the amalgam can be observed. In the present paper, the application of this technique to the a. c. polarographic analysis of a micromolar solution of thallium(I) will be discussed.

The interference effects of other metal ions on the determination of thallium(I) in an EDTA solution will also be studied systematically.

Experimental

Reagents. The standard solution of thallium(I) was prepared by a method described previously.[3] The solutions of cadmium(II) perchlorate, zinc(II) perchlorate, lead(II) nitrate, and ethylenediaminetetraacetic acid (EDTA) were also prepared as has been described in previous papers.[4-6] The standard solution of indium(III) chloride was prepared by dissolving pure indium(III) chloride into dilute nitric acid. Its concentration was determined by titration with a standard EDTA solution.[7] The a.c. polarographic analysis showed that indium(III) was not contaminated with lead(II) and thallium(I). All the other chemicals were of an analytical reagent grade and were used without further purification.

Apparatus and Procedure. A. c. polarograms were recorded manually or automatically with a Yanagimoto PA-102 pen-recording polarograph. In a. c. polarographic measurements, a 200-μF condenser was used to minimize the effect of the cell resistance.[8] For the accurate measurement of the d. c. potential, a Shimadzu K-2-type potentiometer was used. The Kalousek circuit used in this study was also given in a previous paper.[9] A dropping mercury electrode with an m value of 1.24_0 mg/sec and a drop time, t_d, of 4.80 sec at a mercury height of 60 cm in an air-free 0.1 M acetate buffer solution of pH 4.8 at -0.60 V *vs.* SCE was used. HMDE was prepared by the method proposed by Ross, Demars and Shain.[10] In the preparation of the HMDE, one drop of mercury from the dropping mercury electrode was used.

1) M. Kodama, H. Ouchi and S. Wakui, *Nippon Kagaku Zasshi (J. Chem. Soc. Japan, Pure Chem. Sect.)*, **84**, 241 (1963).
2) W. L. Underkofler and I. Shain, *Anal. Chem.*, **37**, 218 (1965).
3) M. Kodama, T. Noda and M. Murata, This Bulletin, **41**, 354 (1968).
4) M. Kodama and C. Sasaki, *ibid.*, in press.
5) M. Kodama and H. Ebine, *ibid.*, **40**, 1857 (1967).
6) M. Kodama, *ibid.*, **40**, 2575 (1967).
7) V. Suk and M. Malat, *Chemist-Analyst*, **45**, 30 (1956).
8) B. Breyer, F. Gutmann and S. Hacobian, *Australian J. Sci. Research, Ser. A*, **4**, 595 (1951).
9) N. Tanaka, R. Tamamushi and M. Kodama, This Bulletin, **33**, 14 (1960).
10) J. W. Ross, R. D. Demars and I. Shain, *Anal. Chem.*, **28**, 1768 (1956).

Results and Discussion

A. C. Polarographic Behavior of Thallium-(I) in an EDTA Solution at a Hanging Mercury Drop Electrode. Previously,[1] we have applied the a. c. polarographic method to the stripping analysis of metals by using a HMDE as an indicator electrode. In that method, the sensitivity was improved considerably by employing the technique which consists of the pre-electrolysis step and the subsequent anodic-dissolution step. The sample was concentrated effectively on the HMDE by conducting the pre-electrolysis in the limiting current region for the reduction of the metal ion to the amalgam. However, an increase in sensitivity by pre-electrolysis could be obtained only in the analysis of metal ions which behave reversibly in a polarographic sense, such as lead(II) and cadmium(II). This may be one of the characteristic disadvantages of an analysis based on a. c. polarographic measurements. As is well known, thallium-(I) ion behaves reversibly in almost all supporing electrolyte solutions. Therefore, the a. c. polarographic analysis of thallium(I) can be effected successfully by the method involving the anodic-stripping step. For this reason, the reversibility of the electrode process of thallium(I) in an EDTA solution at HMDE was checked first by the a.c. polarographic method. As is shown in Fig. 1, the reversibility of the electrode reaction was almost perfect in an a. c. polarographic sense; the plot of $\log [(I_p/I)^{1/2}-((I_p-I)/I)^{1/2}]$ against the applied d. c. potential, E, gave a straight line with a ± 120 mV slope, which is in good agreement with the theoretically-predicted value of ± 118 mV.[3,11] Here, I_p and I indicate the a. c. peak-height and the height of the a. c. polarogram at E respectively. Under the present pH conditions, the thallium(I) ion can not form the chelate with EDTA and may exist in a hydrate-ion state.

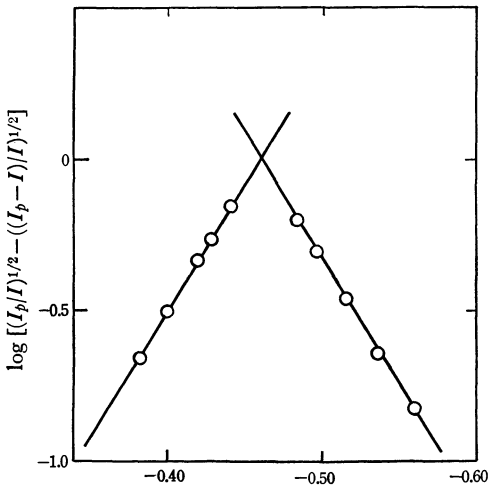

Fig. 1. The plot of $\log [(I_p/I)^{1/2}-((I_p-I)/I)^{1/2}]$ against d.c. potential, E.
pH=4.0 (acetate buffer), $\mu=0.50$
Concentration of thallium(I)$=5.0\times10^{-4}$ M
Concentration of EDTA=0.10 M
Normal scanning, non-stirred
Normal scanning means "scanned cathodically"

The Concentration of Thallium(I) on the HMDE by the Electrodeposition. Bruckenstein and Nagai[12] have shown that, in the chronopotentiometric analysis of thallium(I), a significant increase in sensitivity can be obtained by emplying the chemical stripping technique, which consists of a pre-electrolysis step and of a subsequent stripping of thallium by chemical oxidation with mercuric ions. In the a. c. polarographic determination of thallium(I), a remarkable increase in sensitivity can also be obtained by emplying the anodic stripping technique. As is illustrated by the a. c. polarograms in Fig. 2, the a. c. peak-height of thallium was greatly increased by the pre-electrolysis and by the subsequent anodic

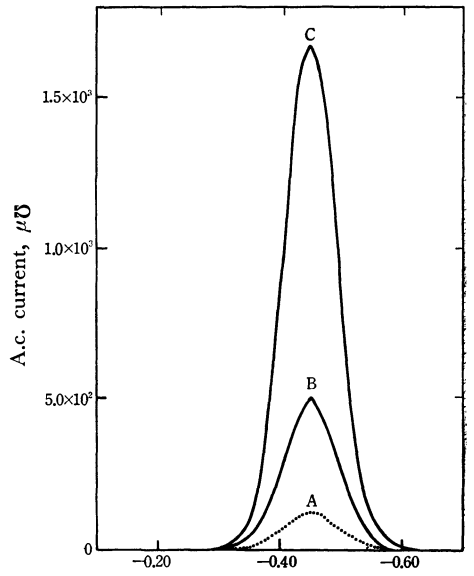

Fig. 2. A.c. polarograms of thallium(I) in 0.05 M EDTA solution.
pH=4.0 (acetate buffer), $\mu=0.50$
Concentration of thallium(I)$=1.0\times10^{-4}$ M
A. normal scanning,
B. reversal scanning, non-stirred, initial potential $=-0.80$ V *vs.* SCE,
C. revesral scanning, stirred, initial potential $=-0.80$ V *vs.* SCE
Normal and reversal scannings mean "scanned cathodically and anodically," respectively.

11) E. R. Brown, T. G. McCord, D. E. Smith and D. D. Deford, *Anal. Chem.*, **38**, 1119 (1966).
12) S. Bruckenstein and T. Nagai, *ibid.*, **33**, 1201 (1961).

stripping. In a previous paper,[1] the potential of the working electrode was scanned in the cathodic direction from the potential far anodic with respect to the reduction potential of metal ions after a timed pre-electrolysis interval. Alternatively, the pre-electrolysis and the subsequent anodic stripping can be successfully conducted by scanning anodically from the potential where the limiting current for the reduction of metal ions can be obtained. In this study, unless otherwise stated, this technique was employed. An alternating potential was superimposed on the d. c. potential throughout the experiment. However, this had not effect on the pre-electrolysis step.

At a given initial potential, from which the potential of the working electrode was scanned in the anodic direction, the a. c. peak-height of thallium(I) was linear function of the concentration of thallium(I) in the concentration range from 1×10^{-5} to 5×10^{-4} M with non-stirred solutions (Fig. 3). Although a part of the thallium deposited on the mercury electrode is lost by diffusion into the bulk of the mercury electrode, the peak-height of thallium has been found to be a linear function of the effective pre-electrolysis time (Fig. 4). Here, the pre-electrolysis time, t, can be calculated approximately by the aid of the following relation:

$$t = (E_p - E_i)/r_s + t_p \qquad (1)$$

where E_p and E_i indicate the peak potential and the initial potential respectively: r_s(2.78 mV/sec), the rate of potential scan, and t_p, the time interval during which the solution is electrolyzed at E_i. This relation can be confirmed by comparing the a.c. peak-height obtained by scanning the potential from −1.10 V *vs.* SCE without the timed interval with that obtained by scanning the potential from −0.70 V *vs.* SCE after a timed pre-electrolysis interval of 144 sec. The former agreed well with the latter within the limit of experimental error.

The a. c. stripping analysis of thallium at the HMDE was also studied in a solution stirred by a magnetic stirring bar driven by a synchronous motor. The stirring was stopped at −0.60 V *vs.* SCE to allow the solution to stand. Without stopping the agitation no improvement in sensitivity could be obtained. As is shown by the polarograms in Fig. 2 and the calibration curves in Fig. 3, the stirring of the solution made it possible to obtain a significant increase in sensitivity: the lower limit of the useful sensitivity range with this technique becomes about 1×10^{-6} M.

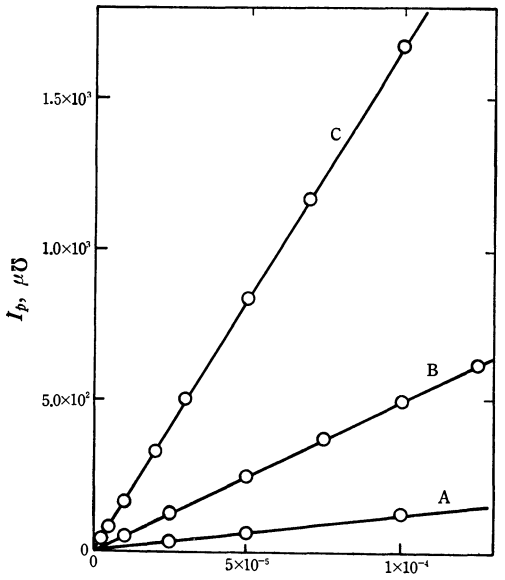

Fig. 3. The relation between the concentration of thallium(I) and a.c. peak-height.
Concentration of EDTA=0.05 M
pH=4.0 (acetate buffer), μ=0.50
A: normal scanning, non-stirred,
B: reversal scanning, non-stirred,
initial potential=−0.80 V *vs.* SCE
C: reversal scanning, stirred,
initial potential=−0.80 V *vs.* SCE
Normal and reversal scannings mean "scanned cathodically and anodically," respectively.

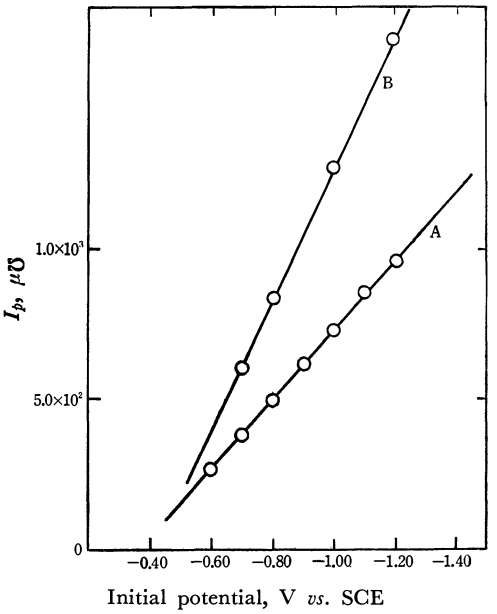

Fig. 4. The relation between a.c. peak-height of thallium(I) and the initial potential.
Concentration of EDTA=0.05 M
pH=4.0 (acetate buffer), μ=0.50
A: reversal scanning, non-stirred,
initial potential=−0.80 V *vs.* SCE
concentration of thallium(I)=1.0×10^{-4} M
B: reversal scanning, stirred,
initial potential=−0.80 V *vs.* SCE
Concentration of thallium(I)=5.0×10^{-5} M
Reversal scanning means "scanned anodically."

Interference Effects of Other Metal Ions on the Determination of Thallium(I) by the A. C. Stripping Analysis. To examine the applicability of the above technique to the practical determination of thallium in the presence of a large excess of other metal ions, the effects of the presence of lead(II), cadmium(II), zinc(II), and indium(III) ions on the peak-height of thallium(I) in EDTA solutions were studied. In solutions containing no complex-forming substance, lead(II), cadmium(II), and indium(III) ions are deposited and stripped at potentials very close to the a. c. peak potential of thallium. Therefore, those metal ions may have a considerable effect on the determination of the peak-height of thallium. In solutions containing a large excess of EDTA, however, those metal ions can be deposited on the mercury electrode only at potentials sufficiently negative with respect to the a. c. peak-height of thallium. Therefore, by choosing EDTA as the supporting electrolyte, the interference effects of those metal ions on the determination of thallium may be effectively eliminated. As predicted, when a sample is electrolyzed at the potential of −0.80 V *vs.* SCE, where only thallium(I) is reduced at the mercury electrode, those metal ions have no effect on the a. c. peak-height of thallium. In a 0.05 M EDTA solution of pH 4.0, 0.01 M indium(III) and 0.01 M zinc(II) do not affect the peak-height of 1×10^{-5} M thallium(I), even when the

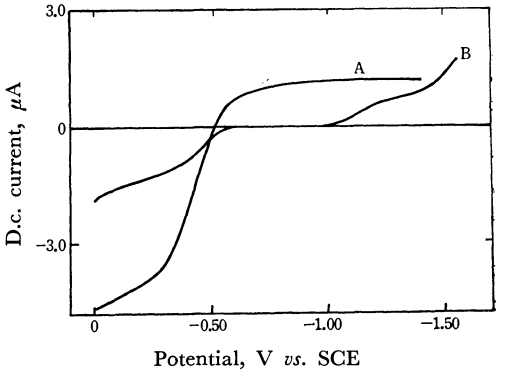

Fig. 5. Kalousek's polarograms.
Concentration of EDTA=0.05 M
pH=4.00 (acetate buffer), $\mu=0.50$
$E_{2^{1}/_{2}}=-1.20$ V *vs.* SCE
A: 3.0×10^{-4} M thallium(I)
B: 3.0×10^{-4} M lead(II)

TABLE 1. EFFECT OF THE PRESENCE OF METAL ION ON THE PEAK-HEIGHT OF THALLIUM(I)
0.05 M EDTA, acetate buffer (0.10 M) of pH 4.0, $\mu=0.50$, concentration of thallium(I)$=1.00\times10^{-5}$ M non-stirred solution

Metal ion	Concentration of metal ion, M	Initial potential V *vs.* SCE	Time interval sec	Peak-height of thallium, μ℧
—	0	−0.60	0	26.5
—	0	−0.80	0	50.0
—	0	−0.90	0	62.0
—	0	−1.10	0	85.0
—	0	−1.50	0	130.0
Pb(II)	1.0×10^{-2}	−0.80	0	48.0
		−1.10	0	170.0
		−0.60	72	49.0
		−0.60	180	84.0
Cd(II)	1.0×10^{-2}	−0.80	0	48.0
		−0.90	0	60.0
		−0.60	72	49.0
		−0.60	108	61.0
Zn(II)	1.0×10^{-2}	−0.80	0	52.0
		−1.10	0	84.0
		−0.60	72	51.2
		−0.60	180	86.0
In(III)	1.0×10^{-2}	−1.10	0	84.0
		−1.50	0	132.0
		−0.60	180	88.0
		−0.60	324	131.0
Pb(II)	1.0×10^{-2}*	−0.80	0	48.0
Cd(II)	1.0×10^{-2}	−1.10	0	180.0
Zn(II)	1.0×10^{-2}	−0.60	72	50.0
In(III)	1.0×10^{-2}	−0.60	180	86.0

* Concentration of EDTA=0.10 M

solution is electrolyzed at −1.50 V *vs.* SCE. However, in the presence of a large excess of lead(II) over thallium(I), when the solution is electrolyzed at −1.20 V *vs.* SCE, where lead(II) shows the limiting current, the a. c. peak-height of thallium(I) is markedly enhanced. This can be ascribed to the fact that thallium and lead, deposited together on mercury, are also stripped simultaneously. This explanation can be confirmed by Kalousek's polarogram, shown in Fig. 5. The electrode reaction of lead(II) ions in EDTA solution proceeds irreversibly, and the anodic oxidation of lead metal occurs at a potential far from that for the reduction of lead(II) ions, but very close to the peak potential of thallium.

The peak-height observed in the presence of lead(II), however, was considerably lower than the sum of the peak-heights of lead(II) and thallium(I) measured individually. Quite a similar phenomenon was found in the the Bi(III)-Tl(I) system also. When an excess of bismuth(III) is added to a thallium(I) solution (acidic Na_2SO_4 solution), the peak-height of the thallium obtained by employing the pre-electrolysis step become considerably lower than that obtained with a solution containing only thallium(I). Bismuth and lead are known to form stable intermetallic compounds with thallium.[13] Therefore, the above phenomenon observed in the thallium-lead system may be attributed to the formation of an intermetallic compound between thallium and lead.

In the case of cadmium, despite the fact that the electrode process also proceeds irreversibly under the present experimental conditions (EDTA solution), cadmium has no effect on the peak-height of thallium, even when the sample is pre-electrolyzed in the limiting current region in order to reduce the Cd(II)-EDTA chelate (−1.25 V *vs.* SCE). This may be ascribed to the fact that, in an EDTA solution, cadmium is stripped anodically from the amalgam at −0.60 V *vs.* SCE. Typical data obtained are given in Table 1.

Although an HMDE has the disadvantage that interference effects due to adsorption, contamination, and other surface phenomena are more frequently encountered than with a DME, where the electrode surface is renewed regularly, this electrode may be used successfully in determining traces of thallium(I) in the presence of lead, cadmium, zinc, and indium by employing the a. c. polarographic method involving pre-electrolysis and stripping.

The present authors wish to express their thanks to the Ministry of Education for the financial support granted for this research.

13) J. W. Mellor, "A Comprehensive Treatise on Inorganic and Theoretical Chemistry," Vol. V, Longmans Green and Co., London (1924).

BULLETIN OF THE CHEMICAL SOCIETY OF JAPAN VOL. 41 2405—2410 (1968)

A.C. Polarographic Determination of Lanthanum(III), Nickel(II), Calcium(II), and Magnesium(II) by Using Diethylenetriaminepentaacetic Acid as a Titrant

Mutsuo KODAMA and Mitsuko MURATA

Department of Chemistry, Ibaraki University, Mito, Ibaraki

(Received February 28, 1968)

The a.c. polarographic determination of lanthanum(III), nickel(II), calcium(II), and magnesium(II) with diethylenetriaminepentaacetic acid was studied by using a dropping mercury electrode and a hanging mercury drop electrode as indicator electrodes. Lanthanum(III) and nickel(II) in an acetate buffer solution and calcium(II) and magnesium(II) in an ammonia buffer solution could be titrated with diethylenetriaminepentaacetic acid in the concentration range from 5×10^{-5} to 1×10^{-3} M by measuring the height of the a.c. polarographic wave of diethylenetriaminepentaacetic acid after the end point. The effect of the presence of calcium-(II) ions on the a.c. polarographic determination of lanthanum(III) in an acetate buffer solution of pH 4.0 was also examined and discussed thermodynamically.

As has been reported previously,[1] diethylenetriaminepentaacetic acid (DTPA) gives a single well-defined anodic wave at a dropping mercury electrode (DME) and can be used as a titrant in the amperometric determination of electro-inactive

1) M. Kodama and A. Kimura, This Bulletin, **40**, 1639 (1967).

metal ions.*1 DTPA also shows a well-defined a. c. polarographic wave, the peak-height of which is exactly proportional to the concentration of DTPA. Therefore, electro-inactive metal ions can also be determined successfully by measuring the a. c. peak-height of uncomplexed DTPA.

In this paper, the use of DTPA as a titrant in the a. c. polarographic determination of lanthanum(III), nickel(II), calcium(II), and magnesium(II) was studied by using a DME and a hanging mercury drop electrode (HMDE) as indicator electrodes. In the a. c. polarographic analysis, especially when a stationary electrode is employed, unfavorable interference caused by the contamination by surface-active substances is frequently observed. However, as the a. c. polarographic wave of DTPA occurs at potentials sufficiently positive with respect to the electrocapillary maximum (ECM), the present method, based on the measurement of the a. c. peak-height of DTPA, is free from the effect of contamination with uncharged or positively charged surface-active substances. In this connection, the effect of camphor on the a. c. polarographic determination of lanthanum(III) was also examined.

Experimental

Reagent. The standard solution of nickel(II) perchlorate was prepared by a procedure described previously.[2] Calcium(II) and magnesium(II) perchlorate solutions were prepared by dissolving pure calcium and magnesium carbonates into a dilute perchloric acid solution. Their concentrations were then standardized against the standard EDTA solution.[3] The standard solution of lanthanum(III) nitrate was prepared by dissolving a known amount of 99.9% lanthanum oxide in a reagent-grade nitric acid. The preparation and the standardization of diethylenetriaminepentaacetic acid (DTPA) solution have also been described in the previous paper.[1] All the other chemicals were of an analytical reagent grade and were used without further purification.

Apparatus and Procedure. The a. c. polarograms were recorded manually or automatically with a Yanagimoto PA-102 pen-recording polarograph. In the a. c. polarographic measurements, a 200-μF condenser was used to minimize the effect of the cell resistance.[4] For the accurate measurement of d. c. potential, a Shimadzu K-2-type potentiometer was used.

A dropping mercury electrode (DME) with an m value of 1.24_0 mg/sec and a drop time, t_d, of 4.80 sec at a mercury height of 60 cm in an air-free 0.1 M acetate buffer solution of pH 4.80 at -0.60 V *vs.* SCE was used.

The hanging mercury drop electrode (HMDE) was prepared by the method proposed by Ross, Demars, and Shain.[5] In the preparation of the HMDE, two drops of mercury from the DME were used.

The oxygen dissolved in the solution was removed by bubbling pure nitrogen gas through the solution; measurements were conducted on solutions with a constant ionic strength of 0.50 (Na_2SO_4).

Results and Discussion

A. C. Polarographic Behavior of DTPA in the Absence of Metal Ions. As is shown by the curves in Fig. 1, DTPA in an acetate buffer solution gave a single, well-defined a. c. polarographic wave at both the DME and the HMDE corresponding to the following anodic reaction:[1]

$$\begin{array}{l} Hg + H_nZ^{n-5} \rightleftharpoons HgZ^{3-} + nH^+ + 2e^- \\ \qquad\qquad\quad \downarrow\uparrow H^+ \\ \qquad\qquad\quad HgHZ^{2-} \end{array} \qquad (1)$$

where HgZ^{3-} and $HgHZ^{2-}$ refer to normal and mono-protonated mercury(II)-DTPA chelates respectively, and where H_nZ^{n-5} indicates the incompletely-dissociated DTPA anion.

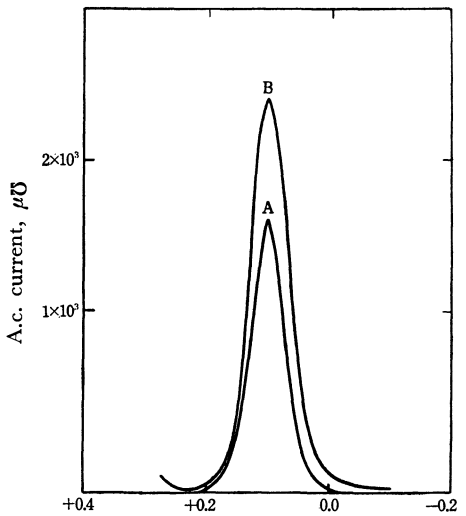

Fig. 1. A.c. polarograms of DTPA.
Concentration of DTPA = 1.0 mM, μ = 0.50
pH = 4.0 (Acetate buffer, 0.10 M)
A: DME B: HMDE

A plot of $\log [(I_p/I)^{1/2}-((I_p-I)/I)^{1/2}]$ against the d. c. potential, E,[6] gave a straight line with a slope of $\pm$85 mV. Here, I_p and I indicate the a. c. peak-height and the height of the a. c. polarogram at E respectively. Some typical examples

*1 Here, "electro-inactive metal ion" means a metal ion which does not give a polarographic wave under the usual polarographic conditions.

2) M. Kodama, C. Sasaki and M. Murata, This Bulletin, **41**, in press.

3) W. Biedermann and G. Schwarzenbach, *Chimia*, **2**, 56 (1948).

4) B. Breyer, F. Gutmann and S. Hacobian, *Australian J. Sci. Research, Ser. A*, **4**, 595 (1951).

5) J. W. Ross, R. D. Demars and I. Shain, *Anal. Chem.*, **28**, 1768 (1956).

6) M. Kodama, T. Noda and M. Murata, This Bulletin, **41**, 354 (1968).

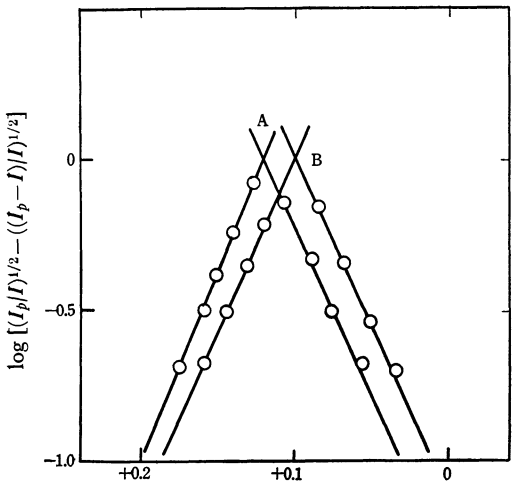

Fig. 2. The plot of log $[(I_p/I)^{1/2}-((I_p-I)/I)^{1/2}]$ against d.c. potential, E.
Concentration of DTPA = 1.0 mM, μ = 0.50
pH = 4.0 (Acetate buffer, 0.10 M)
A: DME B: HMDE

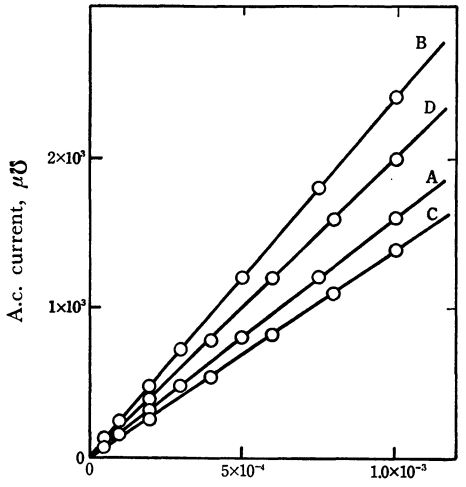

Fig. 3. The relation between the concentration of DTPA and a.c. peak-height.
μ= 0.50
A: pH= 4.0 (Acetate buffer, 0.10 M), DME
B: pH= 4.0 (Acetate buffer, 0.10 M), HMDE
C: pH=10.0 (Ammonia buffer, 0.10 M), DME
D: pH=10.0 (Ammonia buffer, 0.10 M), HMDE

are shown in Fig. 2. This clearly indicates that the electrode reaction of DTPA at the mercury electrode is not perfectly reversible in the a. c. polarographic sense, but that it can be said to be reversible to an appreciable extent. The peak-height of DTPA can be compared with that for the reduction of the copper(II)-NTA chelate.[7]

As is illustrated by the calibration curves in Fig. 3, the a. c. peak-heights were found to be exactly proportional to the bulk concentration of DTPA in the concentration range between 5×10^{-5} and 1×10^{-3} M.

In an ammonia buffer solution of pH 10.0, quite similar results were also obtained with regard to the log-plot examination and the relation between peak-hight and DTPA concentration. These results are not shown here, however.

A. C. Polarographic Titration of Metal Ions with DTPA. A good linear relation between the a. c. peak-height and the concentration of uncomplexed DTPA strongly suggests the possibility that electroinactive metal ions, such as lanthanum(III), nickel(II), calcium(II), and magnesium(II) ions, can also be titrated with DTPA by measuring the a. c. peak-height of uncomplexed DTPA after the end point.

As had been attempted previously,[1] lanthanum-(III) was titrated in an acetate buffer solution of pH 4.0. The titration curves in Fig. 4 are demonstrative examples. The end point obtained agrees well with the equivalence point, indicated by an arrow.

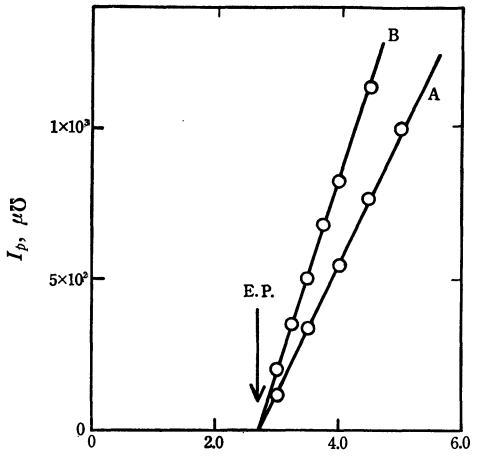

Fig. 4. Titration curves of 3.60×10^{-4} M lanthanum(III) solution with DTPA.
Volume of sample solution=75.0 ml
Concentration of DTPA=10.0 mM
pH=4.0, μ=0.50
Equivalence point was indicated by an arrow.
A: DME, B: HMDE

The conditional stability constant of the nickel-(II)-DTPA chelate, K', defined as:

$$K' = K_{NiZ}(1+K^{H}_{NZi}[H^+])/(\alpha_H)_Z \qquad (2)$$

was estimated to be $10^{10.64}$ by using the numerical values in Table 1; the table shows that the complexation reaction between 1.0 mM nickel(II) and

7) M. Kodama and N. Abe, *Nippon Kagaku Zasshi (J. Chem. Soc. Japan, Pure Chem. Sect.)*, **83**, 679 (1962).

TABLE 1. EQUILIBRIUM CONSTANTS
$\mu=0.50$

i)	pK values of DTPA[7]			
	$pK_1=1.81$,	$pK_2=2.64$,	$pK_3=4.04$	
	$pK_4=7.64$,	$pK_5=10.00$		
ii)	log K_{MZ} values			
	Mg(II):[8]	8.30	Ca(II):[7]	9.89
	Ni(II):[7]	19.32	La(III):[7]	18.96
iii)	log K^H_{MZ} values[8]			
	Mg(II):	6.60	Ca(II):	6.10
	Ni(II):	5.30	La(III):	2.30
iv)	log $K^M_{M_2Z}$ values[7]			
	Ca(II):	1.73		
	Ni(II):	5.16		

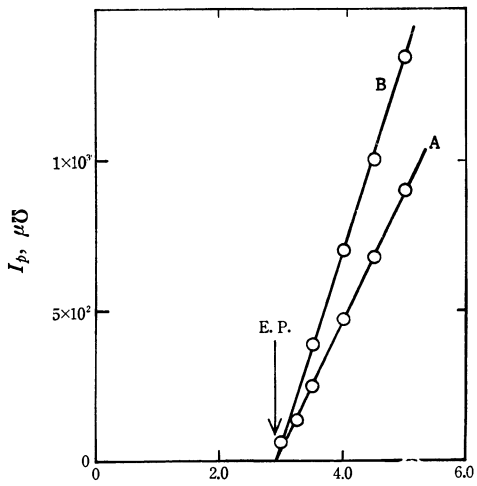

Fig. 5. Titration curve of 3.90×10^{-4} M nickel(II) lanthanum(III) solution with DTPA.
Volume of sample solution=75.0 ml
Concentration of DTPA=10.0 mM
pH=4.0, $\mu=0.50$
Equivalence point was indicated by an arrow.
A: DME B: HMDE

1.0 mM DTPA proceeds quantitatively at pH=4.0. This value is considerably larger than that of the lanthanum(III)-DTPA chelate ($10^{8.96}$). K_{NiZ}, K^H_{NiZ} and $(\alpha_H)_Z$ in Eq. (2) have their usual meanings. The values in Table 1 were calculated from the related constants in the solution with an ionic strength of 0.10 at 25°C,[8,9] while the activity coefficients of the ions were calculated by means of the well-known Davies equation.[10] Therefore, as in the case of lanthanum(III), the nickel(II) ion in an acetate buffer solution of pH 4.0 is also expected to be titrated successfully with DTPA by measuring the a. c. peak-height of DTPA after the end point. Figure 5 shows typical titration curves. The experimental end point agreed well with the stoichiometric equivalence point, indicated by an arrow.

From the thermodynamic point of view, it is expected that calcium(II) and magnesium(II) ions will form stable chelates with DTPA at pH's higher than 10.0, and that the a. c. peak-potential of DTPA in the absence of any metal ion corresponding to that in Reaction (1) must be located at a potential very negative with respect to that in the presence of calcium(II) or magnesium(II) ions, corresponding to Reaction (3):

$$\begin{array}{ccc} M_2Z^- & & \\ \Big\downarrow\Big\uparrow M^{2+} & & \\ Hg + MZ^{3-} & = HgZ^{3-} + M^{2+} + 2e^- & (3) \\ \Big\downarrow\Big\uparrow H^+ & \Big\downarrow\Big\uparrow H^+ & \\ MHZ^{2-} & HgHZ^{2-} & \end{array}$$

where M^{2+} refers calcium(II) or magnesium(II) ions.

Therefore, at pH 10.0, it is considered that calcium(II) and magnesium(II) can be determined accurately by measuring the a. c. peak-height of

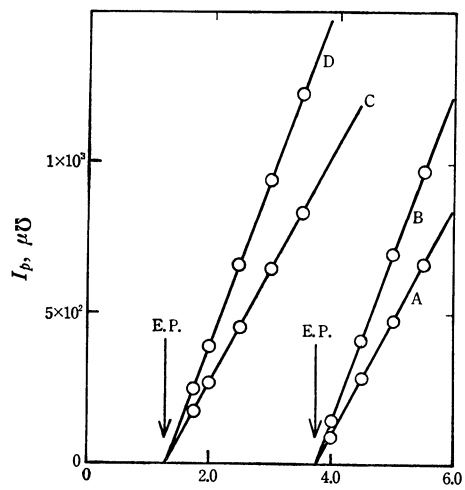

Fig. 6. Titration curves of 5.00×10^{-4} M calcium-(II) and 1.70×10^{-4} magnesium(II) solution with DTPA.
Volume of sample solution=75.0 ml
pH=10.0, $\mu=0.50$
Equivalence points were indicated by arrows.
A: Ca(II), DME B: Ca(II), HMDE
C: Mg(II), DME D: Mg(II), HMDE

8) L. G. Sillen and A. E. Martell, "Stability Constants of Metal-Ion Complexes," The Chemical Society, London (1964), p. 693.
9) A. Ringbom, "Complexation in Analytical Chemistry," Interscience, New York (1963), p. 333.
10) J. N. Butler, "Ionic Equilibrium," Addison-Wesley Publishing Co., Reading, Massachusetts (1964), p. 437.

the uncomplexed DTPA after the end point. Titrations of calcium(II) and magnesium(II) with DTPA were conducted in an ammonia buffer solution of pH 10.0. Typical titration curves are shown in Fig. 6. There is good agreement between the experimental end points and the stoichiometric equivalence points.

The results of the a. c. polarographic titration of those metal ions with DTPA are given in Tables 2, 3, and 4.

Titration of Lanthanum(III) with DTPA in the Presence of Calcium(II) Ions. In an acid medium where the lanthanum(III) ions can form a stable chelate with DTPA, but, calcium(II)

Table 2. Titration of lanthanum(III) with DTPA
volume of sample solution=75.0 m*l* concentration of DTPA=10.0 mM
acetate buffer (0.10 M) of pH 4.0 μ=0.50

Concentration of lanthanum(III) M	Electrode	Volume of DTPA, m*l* V_{calcd}	Volume of DTPA, m*l* V_{obsd}	Error, % $(V_{obsd}-V_{calcd})/V_{calcd}\times 100$
2.40×10^{-5}*	DME	1.62	1.60	−1.0
4.80×10^{-5}*	DME	3.24	3.23	−0.3
1.70×10^{-4}	DME	1.28	1.28	0
	HMDE	1.28	1.26	−1.6
3.60×10^{-4}	DME	2.70	2.68	−0.7
	HMDE	2.70	2.71	+0.4
4.80×10^{-4}	DME	3.24	3.27	+0.9
	HMDE	3.24	3.27	+0.9
7.20×10^{-4}	DME	5.40	5.40	0
	HMDE	5.40	5.40	0

* Concentration of DTPA is 1.0 mM.

Table 3. Titration of nickel(II) with DTPA
volume of sample solution=75.0 m*l* concentration of DTPA=10.0 mM
acetate buffer (0.10 M) of pH 4.0 μ = 0.50

Concentration of nickel(II) mM	Electrode	Volume, m*l* V_{calcd}	Volume, m*l* V_{obsd}	Error, % $(V_{obsd}-V_{calcd})/V_{calcd}\times 100$
0.130	DME	0.97	0.98	+1.0
	HMDE	0.97	0.98	+1.0
0.390	DME	2.91	2.90	−0.3
	HMDE	2.91	2.90	−0.3
0.780	DME	5.84	5.80	−0.7
	HMDE	5.84	5.80	−0.7

Table 4. Titration of calcium(II) and magnesium(II) with DTPA
volume of sample solution=75.0 m*l* concentration of DTPA=10.0 mM
ammonia buffer (0.10 M) of pH 10.0, μ=0.50

Metal(II)	Concentration of metal(II) mM	Electrode	Volume of DTPA, m*l* V_{calcd}	Volume of DTPA, m*l* V_{obsd}	Error, % $(V_{obsd}-V_{calcd})/V_{calcd}\times 100$
Ca(II)	0.25	DME	1.87	1.85	−1.1
		HMDE	1.87	1.89	+1.1
	0.50	DME	3.75	3.74	−0.3
		HMDE	3.75	3.70	−1.3
Mg(II)	0.17	DME	1.28	1.27	−0.8
		HMDE	1.28	1.29	+0.8
	0.42	DME	3.15	3.12	−1.0
		HMDE	3.15	3.17	+0.6

TABLE 5. TITRATION OF 75.0 ml LANTHANUM(III) SOLUTION OF 0.480 mM WITH DTPA IN THE PRESENCE OF CALCIUM(II)

concentration of DTPA=10.0 mM acetate buffer (0.10 M) of pH 4.0 μ=0.50

Concentration of calcium(II) M	Electrode	Volume of DTPA, ml V_{calcd}	Volume of DTPA, ml V_{obsd}	Error, % $(V_{obsd}-V_{calcd})/V_{calcd}\times 100$
5×10^{-4}	DME	3.24	3.25	+0.3
	HMDE	3.24	3.25	+0.3
5×10^{-3}	DME	3.24	3.23	−0.3
	HMDE	3.24	3.25	+0.3
5×10^{-2}	DME	3.24	3.23	−0.3
	HMDE	3.24	3.23	−0.3
5×10^{-1}	DME	3.24	3.19	−1.6
	HMDE	3.24	3.19	−1.6

ions can not, the end point in the titration of lanthanum(III) with DTPA may be little affected by the presence of calcium(II) ions. However, even in an acid medium, when a large excess of calcium(II) ions is present in the solution, DTPA reacts partially with calcium(II) ions. Therefore, under such conditions, some positive error may be expected in the lanthanum(III)-DTPA titration. When 1.0 mM lanthanum(III) in a solution of pH 4.0 containing 0.10 M calcium(II) is 100% over-titrated with DTPA, the concentration of the calcium(II)-DTPA chelate is calculated to be 0.85 mM with the aid of the following relation, using the numerical values in Table 1.

$$[CaZ]_t = \frac{1}{1+\dfrac{1}{\dfrac{K_{CaZ}}{(\alpha_H)_z}(1+K^H_{CaZ}[H^+]+K^{Ca}_{Ca_2Z}[Ca^{2+}])}} \quad \text{mM} \qquad (4)$$

where $[CaZ]_t = [CaZ^{3-}]+[CaHZ^{2-}]+[Ca_2Z^-]$, where K_{CaZ} is the stability constant of CaZ^{3-}, where $K^H_{CaZ}=[CaHZ^{2-}]/[CaZ^{3-}]\cdot[H^+]$, where $K^{Ca}_{CaZ}=[Ca_2Z^-]/[Ca^{2+}]\cdot[CaZ^{3-}]$, and where $(\alpha_H)_z$ corresponds to the $(\alpha_H)_Z$ value defined as $1+[H^+]/k_5+\cdots+[H^+]^5/k_1\cdot k_2\cdot k_3\cdot k_4\cdot k_5$.

In the presence of calcium(II) ions, the a. c. polarographic titration of lanthanum(III) with DTPA was also carried out at pH 4.0. The results are given in Table 5.

Even when a large excess of calcium(II) ions is present in the solution, the error in the titration is very small and the agreement between the experimental end point and the stoichiometric equivalence point can be considered to be satisfactory. This is clearly in contrast to the above theoretical prediction. An alternative explanation is possible that, under the present experimental conditions, true equilibrium constants are much smaller than the numerical values in Table 4 used in the calculation of $[CaZ]_t$, and that the actual $[CaZ]_t$ is very small. However, it is also possible to ascribe the above fact to the facts that the peak-potential corresponding to the electrode reaction (1) and that corresponding to Reaction (3) occur at the same potential, and that the a. c. peak-heights per unit of concentration for these two reactions are the same. If the d. c. half-wave potential can be equated with the a. c. peak-potential, peak-potential difference between that in the absence of and that in the presence of a large excess of calcium(II) ions can be calculated with the aid of Relation (6) in Ref. 1. The peak-potential difference calculated for 0.10 M calcium(II) was 20 mV, and the a. c. peak-height ratio obtained experimentally was 0.95 (in an ammonia buffer solution of pH 10.0). These results may support the latter explanation.

The effect of camphor on the a. c. polarographic titration of lanthanum(III) with DTPA was also examined. The presence of 1.0 mM of camphor has little effect on the titration. This can be ascribed to the fact that camphor desorps completely from the mercury electrode[11] at the potential where the a. c. polarographic wave of DTPA is observed.

Finally, it can be mentioned here that the a. c. polarographic method established in this paper may be applied successfully to the determination of rare earths in the alloy of rare earth and alkaline earth oxide.[12]

The present authors thank the Ministry of Education for the financial support granted for this research.

11) B. Breyer and H. H. Bauer, "Alternating Current Polarography and Tensammetry," Interscience Publishers, New York (1963), p. 128.

12) T. N. Nazarchuk and S. R. Boremskaya, *(Inst. Maters. Sci. Probls., Kiev) Zh. Analit. Khim.*, **21**, (6), 745 (1966).

BULLETIN OF THE CHEMICAL SOCIETY OF JAPAN VOL. 41 2411—2416 (1968)

Kinetics of Electron-Transfer Reactions Involving Ethylenediaminetetraacetatochromate(II) Ions as Reductants. II. Reactions with Some Acidopentaamminechromium(III) Complexes*1

Hiroshi OGINO and Nobuyuki TANAKA

Department of Chemistry, Faculty of Science, Tohoku University, Katahira-cho, Sendai

(Received March 1, 1968)

The rate of the electron-transfer reactions between ethylenediaminetetraacetatochromate(II) and some acidopentaamminechromium(III), $CrX(NH_3)_5^{2+}$, has been measured at ionic strength 1.0 ($NaClO_4$). The rate constants ($l\,mol^{-1}sec^{-1}$) for $X=F^-$, Cl^-, Br^- and OH^- are 2.07 at 25°C, 2×10^3 at 25°C, $>2\times10^3$ at 15°C and 2.4×10^2 at 25°C, respectively. These reactions produce ethylenediaminetetraacetatochromate(III) ions which do not contain an anion X. The mechanisms of these reactions are discussed.

It is known that the electron-transfer reactions of chromium(II) ions with halogenopentaamminechromium(III) complexes proceed through inner-sphere mechanisms,[1] in which halide ions originally coordinated to chromium(III) complexes act as bridging ligands. It is also known that the order of the efficiency of the bridging groups in the reactions between chromium(II) ions and acidopentaaquo- and hexaaquochromium(III) complexes is $Br^->Cl^->OH^->F^->NCS^->H_2O$.[2,3]

In order to know the effect of the complex formation of chromium(II) ions with ethylenediaminetetraacetate (EDTA) on the electron-transfer reactions and to elucidate the mechanism of the reactions, the kinetics of the electron-transfer reactions between chromium(II)-EDTA and acidopentaamminechromium(III) complexes are dealt with in this paper. The results are compared with those reported in the previous papers.[1-5]

Experimental

A starting material for the preparation of all acidopentaamminechromium(III) complexes used was $[CrH_2O(NH_3)_5](NO_3)_3$, which was prepared by the method of Mori,[6] and from which $[CrH_2O(NH_3)_5](ClO_4)_3$ was obtained by the procedures reported by King.[7] $[CrF(NH_3)_5](ClO_4)_2$ was prepared by the method of Linhard and Weigel[8] from $[CrH_2O(NH_3)_5](ClO_4)_3$. $[CrCl(NH_3)_5]Cl_2$ was obtained by the method reported previously.[9] Its conversion to the perchlorate was carried out by the method of Ogard and Taube[1] with the aid of Dowex 50W-X8 cation exchange resin. $[CrBr(NH_3)_5]Br_2$ was prepared by the procedures reported in literature.[1] This compound was converted to the perchlorate by the recrystallization from aqueous perchloric acid solution. The results of the analysis of the chromium(III) compounds are given in Table 1.

Chromium(II) perchlorate solutions were prepared by the reduction of hexaaquochromium(III) perchlorate with zinc amalgam. Ionic strength of the solution was adjusted to 1.0 with sodium perchlorate. The pH of the solutions was adjusted by using acetate buffer solutions. In most cases, the temperature of kinetic measurement was 25°C and, in some cases, was varied between 5°C and 35°C to determine the kinetic parameters.

Other analytical and kinetic procedures were similar to those reported previously.[4]

Results and Discussion

Kinetics of the Reactions of Chromium(II)-EDTA with $CrF(NH_3)_5^{2+}$, $CrCl(NH_3)_5^{2+}$ and $CrBr(NH_3)_5^{2+}$. Figure 1 shows a typical example of the spectral change of the $CrF(NH_3)_5^{2+}$ in the presence of excess EDTA upon the addition of chromium(II) perchlorate solution (spectra A to D).*2 The reaction seemed to be complete

*1 Presented at the 10th International Conference on Coordination Chemistry, Nikko, Japan, September, 1967.

1) A. E. Ogard and H. Taube, *J. Am. Chem. Soc.*, **80**, 1084 (1958).
2) D. L. Ball and E. L. King, *ibid.*, **80**, 1091 (1958).
3) N. Sutin, *Ann. Rev. Nucl. Sci.*, **56**, 285 (1962).
4) H. Ogino and N. Tanaka, This Bulletin, **41**, 1622 (1968).
5) A. Anderson and N. A. Bonner, *J. Am. Chem. Soc.*, **76**, 3826 (1954).
6) M. Mori, *Nippon Kagaku Zassi (J. Chem. Soc. Japan, Pure Chem. Sect.)*, **74**, 253 (1953).
7) H. J. S. King, *J. Chem. Soc.*, **127**, 2100 (1925).
8) M. Linhard and M. Weigel, *Z. Anorg. Allg. Chem.*, **278**, 24 (1955).
9) N. Tanaka, M. Kamada, J. Fujita and E. Kyuno, This Bulletin, **37**, 222 (1964).

*2 0.16 mM $[Cr^{III}(H_2O)deta]_{t=0}$ given in Fig. 1 comes from chromium(III) ions which are present as impurity in the chromium(II) perchlorate solution and may be $Cr(H_2O)_6^{3+}$ and/or $[CrOH(H_2O)_4]_2^{4+}$. It was found that, when chromium(II) solution contaminated by chromium(III) ions was injected into excess EDTA solution, the same amount of $Cr^{III}(H_2O)edta^-$ as that of chromium(III) ions in the original solution was formed within the time of mixing.[4]

Table 1. Analyses of the chromium(III) complexes

Complex	Cr, %		N, %	
	Found	Calcd	Found	Calcd
$[CrH_2O(NH_3)_5](ClO_4)_3$	11.49	11.46	15.62	15.44
$[CrF(NH_3)_5](ClO_4)_2$	14.34	14.64	20.08	19.72
$[CrCl(NH_3)_5](ClO_4)_2$	13.66	14.00	19.10	18.85
$[CrBr(NH_3)_5](ClO_4)_2$	11.93	12.50	16.75	16.84

Table 2. Rate constants of the reactions between chromium(II)-EDTA and $CrF(NH_3)_5^{2+}$ at $\mu=1.0$ ($NaClO_4$) and 25°C

pH	$[CrF(NH_3)_5^{2+}]_{t=0}$ mM	$[Cr^{II}(H_2O)edta^{2-}]$ mM	k $l\,mol^{-1}\,sec^{-1}$
4.98	3.11	5.73	2.03
4.96	3.52	2.78	2.07
4.73	3.46	5.73	2.03
4.21	2.87	2.78	2.00
4.19	2.06	20.2	1.85
3.98	2.40	20.2	1.73
3.72	1.66	20.2	1.71
3.53	2.13	20.2	2.14

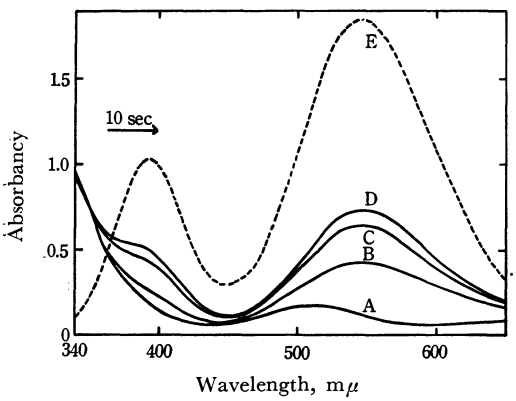

Fig. 1. Spectral change of the $CrF(NH_3)_5^{2+}$ solution in the presence of EDTA upon the addition of chromium(II) ions in sodium acetate-sodium perchlorate media: $[CrF(NH_3)_5^{2+}]_{t=0}=3.18$ mM, $[Cr(II)]_{t=0}=5.73$ mM, $[Cr^{III}(H_2O)edta^-]_{t=0}=0.16$ mM (see footnote), $[EDTA]_{t=0}=20$ mM, $\mu=1.0$, pH 4.99, 25°C, scanning speed = 3.40 mμ/sec and cell length = 1 cm. (A) Spectrum at $t=0$ over the whole range of wave length. (B) 10 sec (C) 130 sec and (D) 660 sec after the addition of chromium(II). Times given are for start of scan at 340 mμ. (E) Spectrum of the solution exposed to air after the measurement of spectrum D.

whithin 660 sec, since no change was observed in the spectrum after the measurement of spectrum D. The spectral change shown in Fig. 1 can be interpreted reasonably by the overall reaction,

$$CrX(NH_3)_5^{2+} + H_jedta^{(4-j)-} + H_2O \rightarrow Cr^{III}(H_2O)edta^- + X^- + 5NH_3 + jH^+ \quad (1)$$

where X should read F in this case. Equation (1) is generalized by writing $CrX(NH_3)_5^{2+}$ instead of $CrF(NH_3)_5^{2+}$. This equation is essentially identical with the overall reaction between chromium(II) ions and $Cr(NCS)_n(NH_3)_{6-n}^{(3-n)+}$ ions in the presence of EDTA.[4] Spectrum E was obtained when the solution was exposed to air after the completion of the reaction. The spectral change from D to E corresponds to the oxidation of $Cr^{II}(H_2O)edta^{2-}$ present in the solution to $Cr^{III}(H_2O)edta^-$ and reveals that the concentration of $Cr^{II}(H_2O)edta^{2-}$ remains constant during the reaction.

By considering the results mentioned above and those reported previously,[4] the mechanism of reaction (1) can be expressed by the following equations:

$$Cr^{2+} + H_jedta^{(4-j)-} + H_2O \rightleftharpoons Cr^{II}(H_2O)edta^{2-} + jH^+ \quad (2)$$

$$Cr^{II}(H_2O)edta^{2-} + CrX(NH_3)_5^{2+} \xrightarrow{k} Cr^{III}(H_2O)edta^- + Cr^{2+} + X^- + 5NH_3 \quad (3)$$

where reaction (3) is a rate-determining step because of the rapidity of the complex-forming reaction (2).[10,11] The rate law of the reaction (1) is given by the equation,

$$-\frac{d[CrX(NH_3)_5^{2+}]}{dt} = \frac{d[Cr^{III}(H_2O)edta^-]}{dt} = k[Cr^{II}(H_2O)edta^{2-}][CrX(NH_3)_5^{2+}] \quad (4)$$

Table 2 gives the results which were obtained on

10) K. Ogino(née Ebata) and N. Tanaka, This Bulletin, **39**, 2672 (1966).
11) N. Tanaka and A. Yamada, *Rev. Polarog. (Kyoto)*, **14**, 234 (1967).

the rate of the reaction between $Cr^{II}(H_2O)edta^{2-}$ and $CrF(NH_3)_5^{2+}$ at 25°C. These data show that the reaction is strictly of second-order. The pH dependence of the rate was analyzed by the method reported previously,[4] in which the formation of $Cr^{II}(H_2O)Hedta^-$ was considered. The rate constant of the reaction,

$$Cr^{II}(H_2O)edta^{2-} + CrF(NH_3)_5^{2+} \rightarrow Cr^{III}(H_2O)edta^- + Cr^{2+} + F^- + 5NH_3 \quad (5)$$

was obtained to be 2.07 $l\,mol^{-1}sec^{-1}$ and the rate constant of the reaction,

$$Cr^{II}(H_2O)Hedta^- + CrF(NH_3)_5^{2+} \rightarrow Cr^{III}(H_2O)Hedta + Cr^{2+} + F^- + 5NH_3 \quad (6)$$

was found to be less than 1 $l\,mole^{-1}sec^{-1}$.

Similar experiments were made on the systems containing $CrCl(NH_3)_5^{2+}$ and $CrBr(NH_3)_5^{2+}$ ions. It was found spectrophotometrically that a product of the reaction of $Cr^{II}(H_2O)edta^{2-}$ with $CrCl(NH_3)_5^{2+}$ or $CrBr(NH_3)_5^{2+}$ was not $Cr^{III}Xedta^{2-}$ but $Cr^{III}(H_2O)edta^-$. The reaction between $Cr^{II}(H_2O)edta^{2-}$ and $CrBr(NH_3)_5^{2+}$ was so rapid that the rate constant could not be determined.

Kinetics of the Reaction of Chromium(II)-EDTA with $CrH_2O(NH_3)_5^{3+}$. In the reaction between chromium(II)-EDTA and $CrH_2O(NH_3)_5^{3+}$, the observed second-order rate constants were considerably dependent on pH as shown in Fig. 2. In the pH range investigated, $CrH_2O(NH_3)_5^{3+}$ ions are appreciably hydrolyzed, because the hydrolysis constant expressed by

$$K_h = \frac{[CrOH(NH_3)_5^{2+}][H^+]}{[CrH_2O(NH_3)_5^{3+}]} \quad (7)$$

is 6.7×10^{-6} moll^{-1} at ionic strength 1.0 ($NaClO_4$) and 25°C.[12] Hence, it is reasonable to assume that the reaction in question proceeds through the following two simultaneous reaction paths:

$$Cr^{II}(H_2O)edta^{2-} + CrH_2O(NH_3)_5^{3+} \xrightarrow{k_1} Cr^{III}(H_2O)edta^- + Cr^{2+} + H_2O + 5NH_3 \quad (8)$$

$$Cr^{II}(H_2O)edta^{2-} + CrOH(NH_3)_5^{2+} \xrightarrow{k_2} Cr^{III}(H_2O)edta^- + Cr^{2+} + OH^- + 5NH_3 \quad (9)$$

By considering these reactions, the following equation can be obtained for the observed rate constant, k.

$$k = \frac{k_1 + k_2K_h/[H^+]}{1 + K_h/[H^+]} \times \frac{1}{1 + K^H[H^+]} \quad (10)$$

where

$$K^H = \frac{[Cr^{II}(H_2O)Hedta^-]}{[Cr^{II}(H_2O)edta^{2-}][H^+]} \quad (11)$$

and the value of K^H has been determined to be $10^{3.00}$.[13]

This equation is rewritten as,

$$k\alpha' = k_1 + k_2K_h/[H^+] \quad (12)$$

where

$$\alpha' = (1 + K_h/[H^+])(1 + K^H[H^+]) \quad (13)$$

If the values of left-hand side of Eq. (12) are plotted against reciprocal hydrogen ion concentrations, linear plots will be obtained. Figure 3 shows the plots of $k\alpha'$ *vs.* reciprocal hydrogen ion concentrations. The best values of intercept and slope were calculated by least square method, with the aid of the data in Fig. 3. The relation,

$$k\alpha' = (0\pm1) + (1.62\pm0.03)\times10^{-3}/[H^+] \quad (14)$$

was obtained. Uncertainties in Eq. (14) represent standard deviations. The value of intercept is practically zero. This means that the reaction proceeds through the sole path represented by Eq. (9). The rate constant of the reaction is 2.4×10^2 $l\,mol^{-1}sec^{-1}$ and the value of k_1 is less than 1 $l\,mol^{-1}sec^{-1}$.

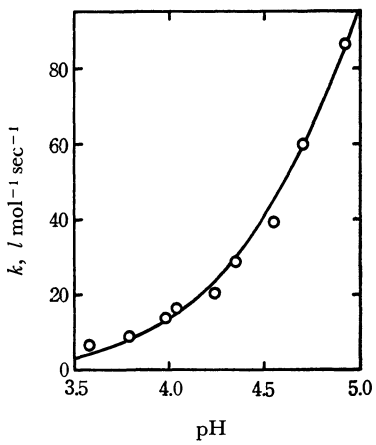

Fig. 2. The pH dependence of the observed second-order rate constant, k, for the reaction between chromium(II)-EDTA and $CrH_2O(NH_3)_5^{3+}$ at 25°C and μ=1($NaClO_4$).

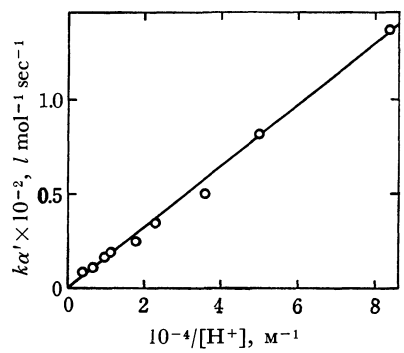

Fig. 3. The values of left-hand side of Eq. (12) as a function of reciprocal hydrogen ion concentration in the reaction between chromium(II)-EDTA and $CrH_2O(NH_3)_5^{3+}$.

12) H. Ogino, unpublished result.

13) R. L. Pecsok, L. D. Shields and W. P. Schefer, *Inorg. Chem.*, **3**, 114 (1964).

It should be noted that reactions other than Eqs. (8) and (9), such as

$$Cr^{II}(H_2O)Hedta^- + CrH_2O(NH_3)_5^{3+} \xrightarrow{k_3} Cr^{III}(H_2O)Hedta + Cr^{2+} + H_2O + 5NH_3 \quad (15)$$

and

$$Cr^{II}(H_2O)Hedta^- + CrOH(NH_3)_5^{2+} \xrightarrow{k_4} Cr^{III}(H_2O)edta^- + Cr^{2+} + H_2O + 5NH_3 \quad (16)$$

could have been considered. From the analysis of the data given in Fig. 2, it was found that there is no significant contribution of reaction (15) to the overall reaction under consideration. Reaction (16) cannot be distinguished from Eq. (8), since the interconversion of the acid and the base form of the reactants is rapid enough to maintain the equilibrium between them during the reaction. By considering both reactions (9) and (16), the following equation can be obtained instead of Eq. (12).

$$k\alpha' = k_4 K^H K_h + k_2 K_h/[H^+] \quad (17)$$

The value of intercept of the linear plots of $k\alpha'$ *vs.* reciprocal hydrogen ion concentrations corresponds to the value of $k_4 K^H K_h$. The value which was estimated with the aid of the values of K^H [13] and K_h [12] was smaller than 2×10^2 l mol^{-1}sec^{-1}.

Discussion on the Rate Constants of the Reactions between $Cr^{II}(H_2O)edta^{2-}$ and $CrX(NH_3)_5^{2+}$ Complexes. The second-order rate constants of the reaction between $Cr^{II}(H_2O)edta^{2-}$ and acido- and aquopentaamminechromium(III) complexes are given in Table 3. The kinetic parameters obtained in this study are given in Table 4 together with those of other related systems. A striking feature presented in Table 3 is a great variety of rate with the nature of the complexes.

TABLE 3. RATE CONSTANTS OF THE ELECTRON-TRANSFER REACTION BETWEEN $Cr^{II}(H_2O)edta^{2-}$ AND ACIDO- AND AQUOPENTAAMMINECHROMIUM(III) COMPLEXES AT μ=1.0 ($NaClO_4$) AND 25°C

Complex	k l mol^{-1} sec^{-1}
$Cr(NH_3)_6^{3+}$	$<10^{-2}$ a)
$CrH_2O(NH_3)_5^{3+}$	< 1
$CrOH(NH_3)_5^{2+}$	2.4×10^2
$CrF(NH_3)_5^{2+}$	2.07
$CrCl(NH_3)_5^{2+}$	2×10^3
$CrBr(NH_3)_5^{2+}$	$>2\times10^3$ b)
$CrNCS(NH_3)_5^{2+}$	0.2a)

a) μ=1.0 (NaCl), from Ref. 4.
b) At 15°C.

14) It should be noted that there is no direct evidence that the reaction between Cr^{2+} and $Cr(H_2O)_6^{3+}$ or $CrOH(H_2O)_5^{2+}$ proceeds through inner-sphere mechanism.

Table 5 shows the rate constants of the following electron-transfer reaction,

$$*Cr^{2+} + CrX(H_2O)_5^{2+} \xrightarrow{k_{Cr(II)}} *CrX(H_2O)_5^{2+} + Cr^{2+} \quad (18)$$

where *Cr denotes labeled chromium atom. It is known that the values of $k_{Cr(II)}$ given in Table 5 correspond to the rate constants of inner-sphere electron-transfer reactions, in which ligand X acts as an electron-transfer bridge and the product criteria apply.[2,3,14] The comparison of $k_{Cr(II)}$ in Table 5 reveals that the order of the efficiency of the bridging groups in reaction (18) is

$$Br^- > Cl^- > OH^- > F^- > NCS^- > H_2O$$ [2,3]

This order is in agreement with that of the rate constants of reaction (3) in Table 3. The plots of log $k_{Cr(II)Y}$ *vs.* log $k_{Cr(II)}$ give at raight line with a slope of approximately unity as shown in Fig. 4,[15] where $k_{Cr(II)Y}$ denotes the rate constant of reaction (3).

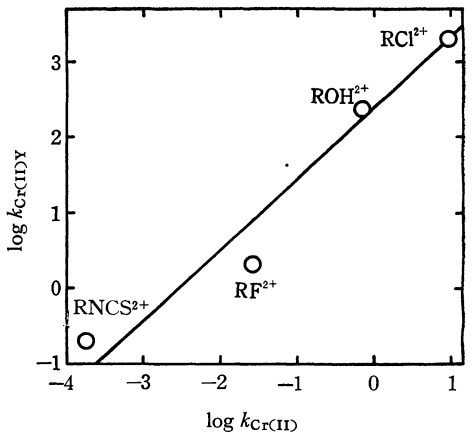

Fig. 4. Relation between the rate constant of reaction 3 ($k_{Cr(II)Y}$) and that of reaction (18) ($k_{Cr(II)}$). R denotes $Cr(NH_3)_5$ for the reaction involving $Cr^{II}(H_2O)edta^{2-}$ and $Cr(H_2O)_5$ for the reaction involving Cr^{2+}.

The facts mentioned above may suggest that the mechanism of the reactions between $Cr^{II}(H_2O)edta^{2-}$ and $CrX(NH_3)_5^{2+}$, except $Cr(NH_3)_6^{3+}$,[4] is of inner-sphere type. This leads naturally to the mechanism expressed as follows for the reaction between $Cr^{II}(H_2O)edta^{2-}$ and $CrX(NH_3)_5^{2+}$:

15) In Fig. 4, 9.1 l mol^{-1} sec^{-1} (at 0°C)[2] is used as the rate constant of the reaction between Cr^{2+} and $CrCl(H_2O)_5^{2+}$, that is, temperature dependence of the rate constant is neglected. On the other hand, the value of one sixth times of the rate constant of the Cr^{2+}-$CrOH(H_2O)_5^{2+}$ reaction should be compared with the rate constants of the other Cr^{2+}-$CrX(H_2O)_5^{2+}$ reactions, the statistical effect being considered. This correction is not made in Fig. 4. The conclusion that the slope of the plots is unity is not affected even by the consideration of these corrections, though the deviation of plots is relatively large.

Table 4. Kinetic parameters of the electron-transfer reactions of acidopentaammine-chromium(III) complexes with $Cr^{II}(H_2O)edta^{2-}$ (Cr(II)-EDTA system) and with Cr^{2+} (Cr^{2+} system)

Complex	Cr(II)-EDTA system[a]		Cr^{2+} system[b]	
	$\Delta H^{\neq}$ kcal/mol	$\Delta S^{\neq}$ e. u.	$\Delta H^{\neq}$ kcal/mol	$\Delta S^{\neq}$ e. u.
$CrF(NH_3)_5^{2+}$	13.9±0.3	−10.6±0.3	13.4	−30
$CrCl(NH_3)_5^{2+}$	9.1±1.0	−13±3	11.1	−28[c]
$CrBr(NH_3)_5^{2+}$	—	—	8.5	−33

a) This work. Uncertainties represent standard deviations.
b) From Ref. 1.
c) This value was calculated by one of the authors (H. O.) from data on the rate constants reported in the original paper.[1] The original value −23 e. u., should read −28 e. u. (H. Taube, private communication).

Table 5. Rate constants of the electron-transfer reactions between Cr^{2+} and acido- and aquopentaamminechromium(III) ions

Complex	$k_{Cr(II)}$ $l\,mol^{-1}\,sec^{-1}$	Temp. °C	Ref.
$Cr(H_2O)_6^{3+}$	$\leq 2\times10^{-5}$	24.5	5
$CrOH(H_2O)_5^{2+}$	0.7	24.5	5
$CrF(H_2O)_5^{2+}$	2.6×10^{-2}	27	2
$CrCl(H_2O)_5^{2+}$	9.1	0	2
$CrBr(H_2O)_5^{2+}$	>60	0	2
$CrNCS(H_2O)_5^{2+}$	1.8×10^{-4}	27	2

Table 6. Comparison of the rate constants of reaction (21) ($k'_{Cr(II)}$) with those of reaction (3) ($k_{Cr(II)Y}$)

Complex	$k'_{Cr(II)}$[a] $l\,mol^{-1}sec^{-1}$	$k_{Cr(II)Y}/k'_{Cr(II)}$	Temp. °C
$CrF(NH_3)_5^{2+}$	2.7×10^{-4}	7.7×10^{3}	25
$CrCl(NH_3)_5^{2+}$	5.1×10^{-2}	4×10^{4}	25
$CrBr(NH_3)_5^{2+}$	0.191	$>1\times10^{4}$	15

a) From Ref. 1.

$$Cr^{II}(H_2O)edta^{2-} + Cr^{III}X(NH_3)_5^{2+} \xrightarrow{slow} Cr^{III}Xedta^{2-} + H_2O + Cr^{2+} + 5NH_3 \quad (19)[16]$$

$$Cr^{III}Xedta^{2-} + H_2O \xrightarrow{fast} Cr^{III}(H_2O)edta^{-} + X^{-} \quad (20)$$

Product criteria did not apply to the present cases under the experimental condition. This seems to be due to the lability of $Cr^{III}Xedta^{2-}$, which dissociates rapidly to $Cr^{III}(H_2O)edta^{-}$ and anion X.

Table 6 shows the comparison of $k_{Cr(II)Y}$ with the rate constant of the following electron-transfer reaction[1]:

$$Cr^{2+} + CrX(NH_3)_5^{2+} \xrightarrow{k'_{Cr(II)}} CrX(H_2O)_5^{2+} + Cr^{2+} + 5NH_3 \quad (21)$$

Unfortunately, the comparison is restricted to only a few cases, but it is shown in Table 6 that $Cr^{II}(H_2O)edta^{2-}$ reacts with $CrX(NH_3)_5^{2+}$ faster than chromium(II) ions approximately by ten thousand times. Chromium(II) - EDTA ions are more powerful as reducing agent than chromium(II) ions. Marcus' theory predicts that the rate of electron-transfer reactions increases with free energy of the reactions,[18,19] though the thoery was derived only for outer-sphere electron-transfer reactions. It was shown recently that free energy contributes also to the rate of the inner-sphere electron-transfer reactions.[20] Considering the difference in the standard reduction potentials of $Cr(aq.)^{2+}$ - $Cr(aq.)^{3+}$ couple (−0.412 V *vs.* NHE)[21] and $Cr^{II}(H_2O)edta^{2-}$ - $Cr^{III}(H_2O)edta^{-}$ couple (−0.98$_3$ V *vs.* NHE),[13] it seems reasonable that $Cr^{II}(H_2O)edta^{2-}$ ions react more rapidly than chromium(II) ions. In addition, the electrostatic interaction between reactants is more favorable in reaction (3) than in reaction (21). If kinetic parameters of these reactions in Table 4 are compared, it will be found that the enthalpy of activation of reaction (3) is essentially identical with that of reaction (21) and that the increase in rate is mainly due to the change of the entropy of activation. For reactions between oppositely charged ions, the charge of the activated complex is reduced and hence the solvent molecules in the solvation shell will be released during the activation process. For reactions between like-charged ions, these

16) It is known that the rate for the substitution of an water molecule coordinated to chromium(II) ion is extremely rapid.[17] In Eq. (19), it is assumed that an activated complex, $[edtaCr^{II} - X - Cr^{III}(NH_3)_5]^*$, is formed after release of the coordinated water molecule in $Cr^{II}(H_2O)edta^{2-}$.
17) M. Eigen, *Ber. Bunsenges. Physik. Chem.*, **67**, 753 (1963).
18) R. Marcus, *J. Phys. Chem.*, **67**, 853 (1963).
19) R. Marcus, *J. Chem. Phys.*, **43**, 679 (1965).
20) For instance, A. Haim and N. Sutin, *J. Am. Chem. Soc.*, **88**, 434 (1966); R. D. Cannon and J. E. Earley, *ibid.*, **88**, 1872 (1966).
21) G. Grube and A. Breitinger, *Z. Elektrochem. angew. physik. Chem.*, **33**, 112 (1927).

situation is opposite. If this electrostriction effect[22,23] is considered, the smaller negative entropy of activation for reaction (3) can be understood at least qualitatively.

The authors wish to thank the Ministry of Education for the financial support granted for this research.

22) L. Laidler, "Chemical Kinetics," McGraw-Hill, Inc., New York (1965) p. 216.

23) J. Lewis and R. G. Wilkins, ed., "Modern Coordination Chemistry," Interscience Publishers Inc., New York (1960), p. 100.

BULLETIN OF THE CHEMICAL SOCIETY OF JAPAN VOL. 41 3416—3418 (1968)

Formation Constants of Chromium(III) Complexes with (N, N)-, (O, O)- and (N, O)-Type Ligands, and Their Relationship to Structure*1

Shichiro TAKATA,*2 Eishin KYUNO and Ryokichi TSUCHIYA

Department of Chemistry, Faculty of Science, Kanazawa University, Kanazawa

(Received March 15, 1968)

Formation constants of chromium(III) complexes with β-alanine, anthranilic acid, picolinic acid and 8-hydroxyquinoline, being all (N, O)-type bidentate chelate ligands, were determined by the pH method at an ionic strength $\mu=0.1$, and at 25°C. The formation constants are $\log k_1=9.69$ for β-alanine, $\log k_1=4.35$ and $\log k_2=3.67$ for anthranilic acid, $\log k_1=4.76$, $\log k_2=4.38$ and $\log k_3=4.55$ for picolinic acid and $\log k_2=9.76$ and $\log k_2=8.48$ for 8-hydroxyquinoline, respectively. The relationships between the formation constants of the complexes and the acid dissociation constants of the chelate ligands were discussed, including those for glycine and α-alanine complexes, and those, in addition, for the complexes with several (N, N)- and (O, O)-type ligands reported in a preceding paper.

Several papers have been previously published by the present authors on the formation constants of chromium(III) complexes, for example, with dicarboxylic acids such as oxalic,[1] malonic,[2] succinic,[2] phthalic[3] and maleic[4] acids as (O, O)-type ligands, with ethylenediamine[5] as an (N, N)-type ligand and glycine and α-alanine[6] as (N, O)-type ligands.

In continuation of the studies on (N, O)-type ligands, the formation constants of chromium(III) complexes with β-alanine, anthranilic acid, picolinic acid and 8-hydroxyquinoline were determined at 25°C and $\mu=0.1$, and the relationships among the formation constants of the (N, O)-type complexes presented here and those of (N, N)- and (O, O)-type complexes already published are discussed.

Experimental

Materials. Picolinic acid and β-alanine were of analytical reagent grade from Nakarai Chemicals Co., Ltd., and anthranilic acid and 8-hydroxyquinoline were of guaranteed special grade from Katayama Chemicals Co., Ltd.

Determination of Formation Constants. The formation constants of the complexes were determined by the pH method used in previous papers.[1-6] Solutions containing various concentrations of hexaaquochromium(III) perchlorate and each ligand described above were kept in a thermostat at 25°C; the ionic strength μ was adjusted to 0.1 by adding an appropriate amount of sodium perchlorate. When equilibrium was attained after one month or more, the pH of the solution was measured with a Toa Denpa pH meter, model HM-8, and the formation constants calculated.

Results

Acid Dissociation Constants of the Chelate Ligands. The acid dissociation constants of β-alanine, anthranilic acid and 8-hydroxyquinoline

*1 Presented at the 10th International Conference on Coordination Chemistry, Nikko, September, 1967.

*2 Present address, Tsubata High School, Ishikawa Prefecture.

1) K. Nagata, A. Umayahara and R. Tsuchiya, This Bulletin, **38**, 1059 (1965).
2) H. Muro and R. Tsuchiya, *ibid.*, **39**, 1589 (1966).
3) K. Higashi, K. Hori and R. Tsuchiya, *ibid.*, **40**, 2569 (1967).
4) T. Tomita, E. Kyuno and R. Tsuchiya, *ibid.*, **41**, 1130 (1968).
5) M. Ohta, H. Matsukawa and R. Tsuchiya, *ibid.*, **37**, 692 (1964).
6) H. Matsukawa, M. Ohta, S. Takata and R. Tsuchiya, *ibid.*, **38**, 1235 (1965).

TABLE 1. THE FORMATION CONSTANTS OF THE CHROMIUM(III) COMPLEXES WITH (N, O)-TYPE CHELATE LIGANDS AT $\mu=0.1$ AND AT 25°C

Ligand	$\log k_1$	$\log k_2$	$\log k_3$	pK_1	pK_2	Ref.
Glycine	8.62	7.65	5	2.43	9.62	6
α-Alanine	8.53	7.44	5.94	2.53	9.59	6
β-Alanine	9.69	—	—	3.53	10.08	*
Anthranilic acid	4.35	3.67	—	1.97	4.79	*
Picolinic acid	4.76	4.38	4.55	1.60	5.44	*
8-Hydroxyquinoline	9.76	8.48	—	4.92	9.23	*

* the present work

were determined by titrating aqueous solutions containing the ligand alone with hydrochloric acid or sodium hydroxide solution under $\mu=0.1$ and at 25°C, and they were calculated by applying the following equations,[7]

$$pK_1 = pH - \log\left(\frac{C}{A-[H^+]} - 1\right)$$

or

$$pK_2 = pH - \log\left(\frac{C}{B-[OH^-]} - 1\right)$$

where C is the total concentration of the chelate ligand, A and B are the concentrations of the hydrochloric acid and sodium hydroxide solutions calculated from their titres, respectively, and pK_1 and pK_2 are the acid dissociation constants of the ligand. The values of $[H^+]$ and $[OH^-]$ were calculated by applying the activity coefficient of hydrogen ion at $\mu=0.1$, $\gamma=0.83$,[8] to its activity obtained by pH measurement.

The acid dissociation constants of β-alanine, anthranilic acid and 8-hydroxyquinoline were determined in the manner described above, whereas those of picolinic acid were taken from the literature.[9] These values are all listed in Table 1, as well as those of glycine and α-alanine for comparison, together with the values of the formation constants of the complexes concerned.

Formation Constants of Chromium(III) Complexes with (N, O)-Type Chelate Ligands. The method used in determining the formation constants of the chromium(III) complexes with β-alanine, anthranilic acid, picolinic acid and 8-hydroxyquinoline as (N, O)-type chelate ligands was the same as used for the glycine and α-alanine complexes.[6]

By combining the values of the acid dissociation constants of the respective chelate ligands and the measured pH values with the total concentrations of the chromium ion used, of the chelate ligand concerned and of the ionizable hydrogen, the average numbers of ligands coordinated to each chromium ion, $\bar{n}$, and the reciprocal logarithmic values of the free ligand, $p[A^-]$, were calculated. The formation curves, $\bar{n}-p[A^-]$, for the (N, O)-type complexes with picolinic acid, 8-hydroxyquinoline, β-alanine and anthranilic acid, together with those of glycine and α-alanine, are shown in Fig. 1.

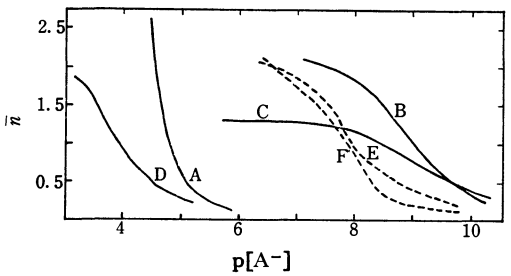

Fig. 1. Formation curves for (N, O)-type chromium(III) complexes.
A, Picolinic acid B, 8-hydroxyquinoline
C, β-Alanine D, Anthranilic acid
E, Glycine F, α-Alanine

Discussion

As given in Table 1, the first and second stepwise formation constants of the complexes, $\log k_1$ and $\log k_2$, decrease in the following order; 8-hydroxyquinoline > β-alanine > glycine > α-alanine > picolinic acid > anthranilic acid. This order runs parallel to the decreasing order of the second acid dissociation constants of these ligands, pK_2, except for 8-hydroxyquinoline.

Although a general linear relationship between the logarithms of the formation constants, $\log k_1$, and the reciprocal logarithms of the acid dissociation constants, pK_2, as expressed by

$$\log k_1 = \alpha pK_2 + C,$$

where α and C are constants, has been proposed by

7) F. Basolo and Y. T. Chen, *J. Am. Chem. Soc.*, **76**, 953 (1954).
8) J. Kielland, *ibid.*, **59**, 1675 (1937).
9) H. H. G. Jellinek and J. R. Urwin, *J. Phys. Chem.*, **58**, 548 (1954); K. Suzuki, M. Yasuda and K. Yamasaki, *ibid.*, **61**, 229 (1957).

Irving and Rossotti,[10,11] such a relationship has not always been strictly applied to many complexes, as pointed out by Jones *et al.*[12] Nevertheless, so far as both copper(II)[13] and iron(III)[14] complexes forming five-membered chelate ring with glycine and its several derivatives as (N, O)-type bidentate ligands are concerned, approximately linear relationships between $\log k_1$ and pK_2 can be obtained, respectively.

The values of the first stepwise formation constants of the complexes listed in Table 1 are plotted against pK_2 in Fig. 2, including those concerning chromium(III) asparagine and glycylglycine complexes.*3 Of these complexes, so far as glycine, α-alanine, asparagine, glycylglycine and picolinic acid, which can form five-membered chelate rings with chromium(III), are concerned, the values of $\log k_1$ against pK_2 fall approximately on a straight line, as shown in Fig. 2.

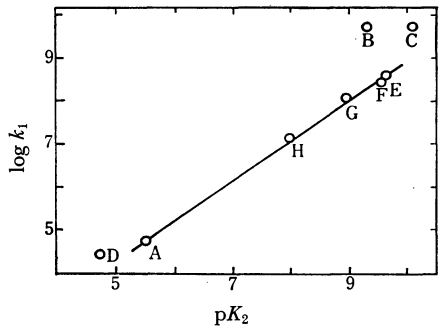

Fig. 2. Relationships between $\log k_1$ and pK_2 in (N, O)-type complexes.
A, Picolinic acid B, 8-hydroxyquinoline
C, β-Alanine D, Anthranilic acid
E, Glycine F, α-Alanine G, Asparagine
H, Glycylglycine

This fact may mean that, in these cases, the chelating tendency is not dependent upon the presence of a side-chain or end-chain in these ligands, but mainly upon the magnitude of their pK_2 values.

On the other hand, the first stepwise formation constants of the chromium(III) complexes with β-alanine and anthranilic acid, as shown in Fig. 2, deviate slightly from the straight line obtained above. This may be due to the six-membered chelate ring formation of these two ligands, which differs from glycine and its derivatives in forming five-membered chelate rings with the metal.

It has been reported by Bjerrum[11] that the values of $\log k_1/\log k_H$ are almost constant for each complex of silver(I), mercury(II), copper(II) and zinc(II) ions with various amines, where k_H is the acid formation constant.

Now, putting the values of the differences, $\Delta = \log k_1 - pK_2$, on the straight line, the relationships shown in Fig. 3 are obtained.

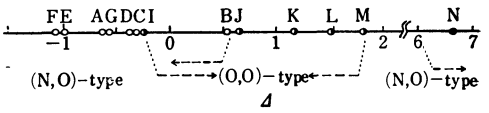

Fig. 3. The values, $\Delta = \log k_1 - pK_2$, for (N, N)-type (●), (N, O)-type (○) and (O, O)-type (◑) complexes.
A, Picolinic acid B, 8-hydroxyquinoline
C, β-Alanine D, Anthranilic acid
E, Glycine F, α-Alanine G, Asparagine
I, Maleic acid J, Phthalic acid
K, Succinic acid L, Oxalic acid
M, Malonic acid N, Ethylenediamine

The values, Δ, for the chelate ligands which can form a stronger coordinate bond with chromium than hydrogen, are placed on the right-hand side of this line, while those forming a weaker coordinate bond with chromium are placed on the left-hand side, and those which have comparable coordination tendencies toward both chromium and hydrogen are placed in the middle region of this line between the above two. Thus, their positions on the line are arranged in the order of (N, N)-, (O, O)- and (N, O)-type complexes from the right to the left. Even though values of $\log k_1$ of the (N, O)-type complexes are in the intermediate region between those of the (N, N)- and (O, O)-type complexes, the values, Δ, referred to the (N, O)-type complexes fall within a small range on the extreme left side of this line.

This may be explained by the fact that the values of pK_2 in (N, O)-type ligands, 8 to 10, except for picolinic and anthranilic acids, are not only strikingly higher than those in (O, O)-type ligands, 4 to 5, but also rather close to those in (N, N)-type ligands, about 10. Such a similarity in values of pK_2 in both (N, N)- and (N, O)-type ligands is reasonably expected, since the second acid dissociation will be, in common, concerned with the liberation of a proton from an amido group in (N, N)- and (N, O)-type ligands, whereas it will be concerned with the liberation of a hydrogen ion from a carboxyl group in (O, O)-type ligands.

That the values of Δ are found as slightly negative in (N, O)-type ligands suggests that the α-amino monobasic acids do not coordinate so strongly to chromium as to hydrogen.

10) H. Irving and H. Rossotti, *Acta Chem. Scand.*, **10**, 72 (1956).
11) J. Bjerrum, *Chem. Revs.*, **46**, 381 (1950).
12) J. G. Jones, J. B. Poole, J. C. Tomkinson and R. J. P. Williams, *J. Chem. Soc.*, **1958**, 2001.
13) B. R. Rabin, *Trans. Faraday Soc.*, **52**, 1130 (1956).
14) D. D. Perrin, *J. Chem. Soc.*, **1958**, 3125.
*3 The first stepwise formation constants and the second acid dissociation constants of these chromium(III) complexes are $\log k_1 = 8.2$ and $pK_2 = 8.85$, respectively, for asparagine and $\log k_1 = 7.2$ and $pK_2 = 8.00$ for glycylglycine, which will be published elsewhere.

BULLETIN OF THE CHEMICAL SOCIETY OF JAPAN VOL. 41 2419—2421 (1968)

Stability of Some Bivalent Metal Complexes of Benzoyl-thiobenzoylmethane in Aqueous Dioxane

Atsushi MANOME and Kazuo SAITO

Chemistry Department, Faculty of Science, Tohoku University, Katahira-cho, Sendai

(Received March 19, 1968)

Concentration equilibrium constants of benzoyl-thiobenzoylmethane (SdbmH) complexes of bivalent magnesium, cobalt, nickel, copper and zinc have been measured in 75% (v/v) aqueous dioxane containing 0.05 M sodium perchlorate. The values for the transition metal ions are greater than those of dibenzoylmethane (dbmH) complexes measured under the same conditions, although the pK value of SdbmH is smaller than that of dbmH. Contribution of d_π–d_π interaction seems to be responsible for such an unusual relationship.

Although the first example of thio homologues of β-diketones was presented by Mitra in 1933,[1] nothing had been known of their metal complexes until Chaston *et al.* prepared several monothio-β-diketones and their metal chelates.[2] Since then further varieties of mono- and di-thio-β-diketones and their transition metal chelates have been prepared and their properties described.[3-5] However, no information is available concerning the stability of their metal complexes in solution. Such studies seem very useful in discussing the characteristics of sulfur as donor atom and the a and b character of metal ions.[6]

We have attempted to measure the stabilities of metal chelates of some monothio-β-diketones in aqueous solution and found that they are soluble only in solutions containing a large amount of organic solvent such as dioxane. Monothio-β-diketones are liable to undergo hydrolysis in such media. Especially thiothenoyl-trifluoroacetone, sulfur derivative of thenoyltrifluoroacetone, is converted into thenoyltrifluoroacetone and hydrogen sulfide in 75% (v/v) aqueous dioxane (molar fraction, 0.380) within a few hours. Its absorption spectrum approaches to that of thenoyltrifluoroacetone, and an isosbestic point is observed at 307 mμ. Such a rapid change seems to be associated with its low pK value. Other monothio-β-diketones decompose more or less similarly, and the weakest acid benzoyl-monothiobenzoylmethane is expected to stand against such a hydrolysis best.

We have found that this compound is stable in the given conditions, and measured its dissociation constant and the stability constants of some of its metal chelates by an alkalimetric titration. The results have been compared with those of dibenzoylmethane (dbmH) under the identical condition.

Experimental

Materials. Thioacetylacetone, thiothenoyltrifluoroacetone, benzoylthioacetone, and benzoylthiobenzoylmethane (SdbmH) were prepared by Chaston *et al.*'s method from their oxo homologues, and identified by melting point, UV and IR spectra and the chemical analysis of carbon and hydrogen of their appropriate metal chelates.

Perchlorates of sodium, copper(II), cobalt(II), zinc, nickel and magnesium were recrystallized from aqueous solutions and dissolved in redistilled and decarbonized water. Their concentrations were determined by EDTA titration with appropriate indicators. Guaranteed grade dioxane was refluxed with concentrated hydrochloric acid and water in a current of nitrogen, shaked with solid potassium hydroxide, the aqueous layer discarded, refluxed with sodium, distilled and preserved in nitrogen atmosphere. Concentrated sodium hydroxide solution free from carbonate was diluted with water and dioxane and mixed with sodium perchlorate to produce 0.02 M sodium hydroxide solution in 0.03 M sodium perchlorate in 75% aqueous dioxane.

Measurement. Hitachi-Horiba Model P pH meter was used for the pH measurement. Horiba's Glass Electrode Type 1026-05T with a double junction mantle was used with 3.33 M potassium chloride in water and 0.05 M sodium perchlorate in 75% aqueous dioxane as bridging solution.

Metal perchlorate (1.5 to 2.0×10^{-3} M), SdbmH (5.0×10^{-3} M), perchloric acid (0.003 M) and sodium perchlorate (0.05 M) were dissolved in 75% aqueous

1) S. K. Mitra, *Indian Chem. Soc.*, **10**, 71 (1933).
2) S. H. H. Chaston, S. E. Livingstone, T. N. Lockyer and V. A. Pickles, *Aust. J. Chem.*, **18**, 673 (1965).
3) L. Martin and I. M. Stewart, *Nature*, **210**, 522 (1966).
4) A. Ouchi, M. Hyodo and Y. Takahashi, This Bulletin, **40**, 2819 (1967).
5) A. Furuhashi, K. Watanuki and A. Ouchi, *ibid.*, **41**, 110 (1968).
6) S. Ahrland, J. Chatt and N. R. Davies, *Quart. Rev.*, **12**, 265 (1958).

dioxane in a current of nitrogen. A 20 ml portion was placed in a beaker shielded with copper plates in a thermostat (25.0±0.1°C) and titrated with the alkali solution. The solution was agitated by a current of pure nitrogen saturated with the vapor of 75% aqueous dioxane. The titration was initiated *ca.* 2 hr after the electrodes were inserted into the solution. The time taken to obtain a constant reading of the meter during the course of titration was ordinarily less than 20 min, but sometimes 30 to 60 min, when the pH change between two reading points was large.

Results

In order to know the concentration of hydrogen ions in 75% aqueous dioxane, a potentiometric titration method modified by Ohtaki[7] was used. The pH_C values are interrelated with the reading of the pH meter by Eq. (1).

$$pH_C = pH_R + \Delta pH \quad (1)$$

where pH_R is the reading of the pH meter, and ΔpH is dependent on the concentration of dioxane, the ionic strength, *etc.* The ΔpH value obtained from Gran's plot[8] was +0.355±0.003 on addition of up to 2.5 ml of the sodium hydroxide solution. Hence the apparatus is useful for obtaining concentration equilibrium constants. The results were calculated by the curve fitting method.[9]

The $\log(h-H-K_wh^{-1})$ *vs.* $\log h$ diagrams for dbmH and SdbmH are shown in Fig. 1, where h and H denote the hydrogen ion concentration in equilibrium obtained from Eq. (1), and analysed excessive hydrogen ion concentration, respectively. The H values are known from the following formula,

$$H = [ClO_4^-] - [Na^+] - 2B \quad (2)$$

where B is the total concentration of the metal ion. K_w is the ion product of water under the given experimental conditions. (3.45×10^{-19}) A normalization function $y=-\log(1+x)$ is drawn and the coordinates are chosen to get the best fit with Fig. 1. The pK values are known from $\log x - \log h$. The results are given in Table 1.

Figure 2 illustrates Z *vs.* $\log a$ diagrams of bivalent metal chelates of SdbmH, where Z is the average number of the ligand bound per metal ion and a the concentration of deprotonated free ligand. The molar ratio of the formed complex is 1 to 2 and the Z is related to the overall formation constants β_1 and β_2 as follows:

$$Z = \frac{\beta_1 a + 2\beta_2 a^2}{1 + \beta_1 a + \beta_2 a^2} \quad (3)$$

This formula is simplified to

$$y = \frac{p_2 v + 2v^2}{1 + p_2 v + v^2} \quad (4)$$

where the notations are as follow: $y=Z$, $x=\log a$, $p_1=\frac{1}{2}\log\beta_2$, $x+p_1=\log v$ ($v=a\beta_2^{1/2}$) and $p_2=\beta_1\cdot\beta_2^{-1/2}$. A variety of y *vs.* $\log v$ diagrams are drawn for differing p_2 values, and one of them is chosen to get the best fit with those in Fig. 2. The $\log\beta_2$ values are then known from the reading of $\log a$ at $\log v=0$.

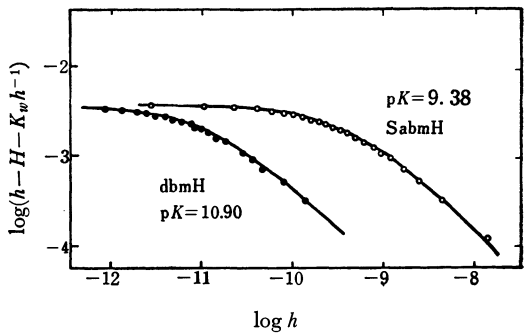

Fig. 1. Determination of pK values of dibenzoylmethane and benzoyl-thiobenzoylmethane by the curve fitting method. (25°C, in 75% aqueous dioxane containing 0.05 M $NaClO_4$)
● dbmH ○ SdbmH

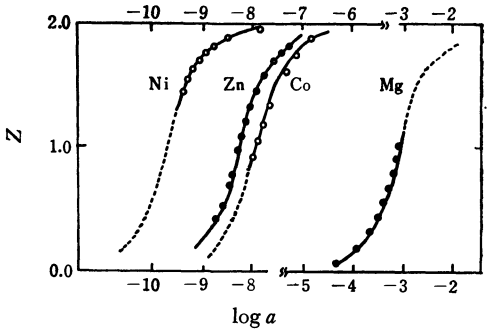

Fig. 2. Determination of concentration equilibrium constants of bivalent metal complexes of benzoyl-thiobenzoylmethane by the curve fitting method. (25°C, in 75% aqueous dioxane containing 0.05 M $NaClO_4$)

Table 1. Overall formation constants of bivalent metal chelates of benzoyl-thio benzoylmethane and dibenzoylmethane in 75% (v/v) aqueous dioxane solution at 25°C, μ, 0.05 (Concentration equilibrium constants, $\log\beta_2$)

Complex	Mg^{2+}	Co^{2+}	Ni^{2+}	Cu^{2+}	Zn^{2+}	H^+ (pK)
$M(dbm)_2$	9.9	14.4	14.7	20	13.6	10.90
$M(Sdbm)_2$	6.1	16.0	19.5	>23*	16.6	9.38
(Error)			±0.2			±0.02

* The complex formation is almost complete at the start of titration under the given condition.

7) H. Ohtaki, *Inorg. Chem.*, **6**, 808 (1967).
8) G. Gran, *Analyst*, **77**, 661 (1952).
9) L. G. Sillén, *Acta Chem. Scand.*, **10**, 186 (1956).

From similar diagrams for dibenzoylmethane complexes their β_2 values are also known. All these results are summerized in Table 1. These are all concentration equilibrium constants.

Discussion

van Uitert and his colaborators measured the pK values and the stability constants of several β-diketones and their bivalent metal chelates in 75% aqueous dioxane and discussed the conversion of concentration stability constants into thermodynamic data.[10] On evaluating the activity coefficients of the chemical species concerned, they gave several assumptions. In case of thio derivatives, however, fundamental information is missing. Dibenzoylmethane is claimed to have the biggest interaction with sodium ions among common β-diketones, and its monothio homologue is expected to have a similar trend. Neither is known its keto-enol tautometric equilibrium under the given conditions. Hence we had to give up to convert our data into thermodynamic parameters. The data in Table 1, however, were obtained under an identical condition, and we can compare them with one another. Although our experimental condition was not equal to van Uitert *et al.*'s, our data of pK and log β_2 values of dbmH and its chelates are parallel with and smaller than their thermodynamic equilibrium constants by more than 4. Such a difference is quite reasonable as they stated.[10]

The results in Table 1 are in accord with Irving-Williams series.[11] On the other hand, the log β_2 values of the thio homologue for the transition elements are greater than those of dbmH, regardless of the fact that the pK value of dbmH is greater than that of SdbmH. Hence the parallel relationship between pK and log β[12] is not seen for the transition metal ions. Only magnesium obeys this empirical law qualitatively. Such a discrepancy could be accounted for by considering the contribution of π-bonding between the transition metal ions and sulfur. Sulfur has vacant 3d orbitals, and can accept d_π electrons of transition metal ions to reinforce ordinary σ-bonding. Magnesium has no delectrons which can be donated to sulfur and gives a lower log β_2 value with SdbmH. A similar trend could have been observed with other thio homologues of β-diketones, if the experimental difficulty had been overcome. Details of the structure of monothio-β-diketone complexes are still unknown. The nickel complexes are diamagnetic and expected to have square planar structures,[2] but their geometrical isomerism is not known. Similar ambiguity remains for the copper complexes. Hence the skeletal structues of dbmH and SdbmH complexes of the semetals ions are different. Nevertheless, the difference between log β_2 values of dbmH and SdbmH complexes of various metal ions could provide an approximate measure indicating the difference in affinity of the metals towards sulfur and oxygen.

We wish to express sincere thanks to Professor M. Tanaka and Dr. H. Ohtaki of Nagoya University for their useful suggestion for the potentiometric titration technique.

10) LeGrand G. van Uitert, C. G. Hass, W. C. Fernelius and B. E. Douglas, *J. Am. Chem. Soc.*, **75**, 451, 455, 458 (1954).

11) H. M. N. H. Irving and R. J. P. Williams, *J. Chem. Soc.*, **1953**, 3192.

12) M. Calvin and K. Eilson, *J. Am. Chem. Soc.*, **67**, 2003 (1945).

BULLETIN OF THE CHEMICAL SOCIETY OF JAPAN VOL. 41 2422—2427 (1968)

Absorption Spectra and Circular Dichroisms of Metal Complexes. II. Preparation and Structure of Isomers of L-Aminoalcohol Cobalt(III) Complexes

Kousaburo OHASHI, Junnosuke FUJITA, Bun-e SHIMOYAMA*1 and Kazuo SAITO

Department of Chemistry, Faculty of Science, Tohoku University, Katahira-cho, Sendai

(Received April 13, 1968)

Seven new optically active complexes of *fac*-*Δ*- and *fac*-*Λ*-$[Co_2(L\text{-amoH})_3(L\text{-amo})_3]^{3+}$ type have been prepared, where L-amoH and L-amo denote L-aminoalcohol and L-aminoalcoholate ion, respectively. The geometrical and the absolute configuration around the metal ion of these complexes have been determined on the basis of their absorption and circular dichroism (CD) spectra. The complexes are monomeric tervalent complex ions in acid solution. In organic solvents and in crystalline states, they seem to have a dimeric structure with face-to-face O···H···O hydrogen bonds between three OH groups of the triprotonated $[Co(L\text{-amoH})_3]^{3+}$ and three oxygen atoms of the deprotonated $[Co(L\text{-amo})_3]^0$.

Although many examples of the stereospecific coordination of optically active diamines or amino acids to metal ions have been reported,[1] no work has been done concerning the complex containing optically active aminoalcohols. Yoneda and Kida[2] prepared the ethanolamine cobalt(III) complex, in which the ethanolamine coordinates to the cobalt ion as a bidentate ligand to form a five membered ring. Since the conformation of chelated ethanolamine will be a gauche form, the coordination of optically active aminoalcohols, such as L-alaninol, to the metal ion is expected to be stereospecific, as in the case of complex formation from *l*-propylenediamine and cobalt(III) ion.[3] In this paper we report the stereospecific preparation of some optically active cobalt(III) complexes of L-alaninol, -leucinol, -isoleucinol and -prolinol, and assign the geometrical and the absolute configuration of these complexes on the bases of an analysis of their absorption spectra and circular dichroism curves.

Experimental

Ligands. The optically active aminoalcohols, L-alaninol, -leucinol, -isoleucinol and -prolinol were prepared by reducing the corresponding L-amino-acid ethyl esters[4] with lithium aluminum hydride according to the method described by Karrer *et al.*[5] The aminoalcohols were distilled freshly before the use for preparation.

Preparation of the Complexes.[*2] 1) *fac*-*Δ*-$[Co_2(L\text{-alanoH})_3(L\text{-alano})_3](ClO_4)_3\cdot 2H_2O$. A mixture containing 4.0 g of $[Co(OH_2)(NH_3)_5](ClO_4)_3$ and 2.0 g of L-alaninol in 100 m*l* of water was heated on a water bath at 90°C with frequent stirring for an hour. After cooling down to the room temperature, the dark reddish violet solution was filtered to remove $[Co(NH_3)_6](ClO_4)_3$ produced during the reaction. The filtrate was evaporated gradually on a water bath at 60°C to about 20 m*l* and kept at room temperature for two or three days. The reddish violet crystals deposited gradually were filtered off and washed with ethanol and ether. The crude complex was recrystallized from 0.1 N perchloric acid solution by adding a mixture of ethanol and ether (1 : 1) and then cooling it in a refrigerator. This complex is soluble in water, methanol and perchloric acid but insoluble in ethanol and ether. The aqueous solution decomposed gradually and gave a dark brown solution.

Found: C, 24.00; H, 6.21; N, 9.46%. Calcd for $C_{18}H_{55}N_6O_{20}Cl_3Co_2 = [Co_2(L\text{-alanoH})_3(L\text{-alano})_3](ClO_4)_3 2H_2O$: C, 24.02; H, 6.16; N, 9.33%.

An attempt to prepare the corresponding bromide or sulfate was unsuccessful because of their large solubilities in accessible solvents.

2) *fac*-*Δ*-$[Co_2(L\text{-leunoH})_3(L\text{-leuno})_3]_2(SO_4)_3\cdot 3H_2O$. The crude complex was obtained by warming a mixture containing 3.4 g of L-leucinol and 2.9 g of $[Co(OH_2)_2(NH_3)_4](SO_4)_3\cdot 3H_2O$ in 25 m*l* of water at 70°C for three hours. Recrystallization was made as follows; to the 2 N sulfuric acid solution of crude complex was

*1 Present Address. Wako Pure Chemical Ind., Kawagoe, Saitama.

1) See for example, J. H. Dunlop and R. D. Gillard, "Stereoselectivity in Coordination Compounds" in "Advances in Inorganic Chemistry and Radiochemistry," H. J. Emeléus and A. G. Sharpe, Ed., Academic Press, New York (1966), Vol. 9, pp. 184—215.

2) H. Yoneda and S. Kida, *J. Am. Chem. Soc.*, **82**, 2139 (1960).

3) F. P. Dwyer, F. L. Garvan and A. Schulman, *ibid.*, **81**, 290 (1959).

4) E. Fischer, *Ber.*, **34**, 433 (1901); G. Hillmann, *Z. Naturforschg.*, **1**, 682 (1946).

*2 The following abbreviations are used; L-alaninol = L-alanoH, L-leucinol = L-leunoH, L-isoleucinol = L-isoleunoH, L-prolinol = L-prolinoH.

5) P. Karrer, P. Portmann and M. Suter, *Helv. Chim. Acta*, **31**, 1617 (1948).

added dropwise with stirring 1 N sodium hydroxide solution until the pH value of the solution reached 6. After a while, the precipitates, which might be a *Λ*-type leucinol complex contained in the crude complex, were removed by filtration. The desired *Δ*-type complex was obtained by adding more 1 N sodium hydroxide solution to the filtrate to pH 8. This procedure was repeated to give a constant CD curve. The pure complex is insoluble in water, ethanol and ether, but fairly soluble in dilute sulfuric acid, and more in a mixture of concentrated sulfuric acid and methanol (1 : 1).

Found: C, 43.84; H, 10.38; N, 8.52%. Calcd for $C_{36}H_{89}N_6O_{13}S_{3/2}Co_2$=[$Co_2$(L-leunoH)$_3$(L-leuno)$_3$]-$(SO_4)_{3/2}H_2O$: C, 44.12; H, 9.15; N, 8.57%.

3) *fac-Λ*-[Co_2(L-leunoH)$_3$(L-leuno)$_3$]Br_3. The crude complex was obtained by a procedure similar to that used for the *Δ*-leucinol complex, with 2.0 g of L-leucinol and 2.2 g of [$Co(OH_2)(NH_3)_5$]Br_3. The product was dissolved in a mixture of 47% hydrobromic acid and methanol (1 : 1), and 1 N sodium hydroxide solution was added dropwise to the solution to pH 1. The precipitate was recrystallized repeatedly by the above method to obtain a constant CD curve. The pure complex is insoluble in water and methanol, but slightly soluble in concentrated hydrobromic acid and fairly so in a mixture of concentrated hydrobromic acid and methanol (1 : 1).

Found: C, 40.63; H, 8.31; N, 7.78%. Calcd for $C_{36}H_{87}N_6O_6Br_3Co_2$=[$Co_2$(L-leunoH)$_3$(L-leuno)$_3$]$Br_3$: C, 40.88; H, 8.29; N, 7.94%.

4) *fac-Δ*-[Co_2(L-isoleunoH)$_3$(L-isoleuno)$_3$]$_2(SO_4)_3\cdot 7H_2O$ and *fac-Λ*-[Co_2(L-isoleunoH)$_3$(L-isoleuno)$_3$]$Br_3\cdot 3H_2O$. These complexes were prepared by recrystallizing the crude products which were obtained by the procedures similar to those for the corresponding L-leucinol complexes.

Found: C, 39.65; H, 9.17; N, 7.45%. Calcd for $C_{36}H_{101}N_6O_{19}S_{3/2}Co_2$ = [Co_2(L-isoleunoH)$_3$(L-isoleuno)$_3$]-$(SO_4)_{3/2}\cdot 7H_2O$: C, 39.73; H, 9.36; N, 7.72%.

Found: C, 38.88; H, 8.00; N, 7.47%. Calcd for $C_{36}H_{93}N_6O_9Br_3Co_2$ = [Co_2(L-isoleunoH)$_3$(L-isoleuno)$_3$]-$Br_3\cdot 3H_2O$: C, 38.89; H, 8.43; N, 7.56%.

5) A mixture of *fac-Δ*- and *fac-Λ*-[Co_2(L-prolinoH)$_3$-(L-prolino)$_3$]$(ClO_4)_3$. A mixture containing 2.0 g of L-prolinol and 2.3 g of [$Co(OH_2)_2(NH_3)_4$]$(ClO_4)_3$ in 40 m*l* of water was evaporated gradually with frequent stirring on a water bath at 60°C to about 20 m*l*, and kept at room temperature for a day. The reddish purple crystals were a mixture of *fac-Δ*- and *fac-Λ*-L-prolinol complex.

Separation of *Δ*- and *Λ*-Isomer. The product was dissolved in a mixture of 60% perchloric acid and methanol (1 : 1), and filtered once. The crude *Λ*-complex was precipitated by adjusting the pH of the filtrate to 1 with 2 N sodium hydroxide solution. Pure *Λ*-complex was obtained by recrystallizing these precipitates repeatedly by the same method until the CD exhibited identical curves.

To the filtrate which was made free from the *Λ*-complex was added more 2 N sodium hydroxide solution slowly and the pH of the solution was adjusted to about 4. The precipitate was filtered off and recrystallized by the same method repeatedly to have a constant CD curve. Both the *fac-Δ*- and the *fac-Λ*-complex were insoluble in water and methanol, but fairly soluble in acetone and dilute perchloric acid and more in a mixture of 60% perchloric acid and methanol (1 : 1).

Found: *fac-Δ* isomer, C, 31.26; H, 6.38; N, 7.23%. Calcd for $C_{30}H_{77}N_6O_{25}Cl_3Co_2$ = [Co_2(L-prolinoH)$_3$(L-prolino)$_3$]$(ClO_4)_3\cdot 7H_2O$, C, 31.40; H, 6.76; N, 7.32%.

Found: *fac-Λ* isomer, C, 34.17; H, 6.21; N, 7.79%. Calcd for $C_{30}H_{67}N_6O_{20}Cl_3Co_2$ = [Co_2(L-prolinoH)$_3$(L-prolino)$_3$]$(ClO_4)_3\cdot 2H_2O$, C, 34.07; H, 6.39; N, 7.95%.

Measurements. Visible and ultraviolet absorption spectra were obtained by Hitachi recording spectrophotometer Model 124. The CD curves were recorded with a Model ORD/UV-5 spectrophotometer of Japan Spectroscopic Co. All the measurements were made at room temperature, 15—20°C.

Results and Discussion

Numerical data for the absorption and the CD bands of the complexes are given in Table 1. Figures 1—5 show the absorption and the CD spectra of the complexes prepared here.

Yoneda and Kida[2] reported that the ratio of cobalt to anion in the crystalline ethanolamine cobalt(III) complex salts was always 2 : 3, and assumed that the complex should be regarded as a double salt involving two different cations, [Co eta$_2$ eta′]$^{2+}$ and [Co eta eta′$_2$]$^+$ (eta=$NH_2CH_2CH_2OH$, eta′=$NH_2CH_2CH_2O^-$) bonded with each other through O–H–O hydrogen bonds. All the aminoalcohol complexes prepared here have the same molar ratio as that of the ethanolamine complex.

Configuration of the Isomers. Since the donor atoms of an aminoalcohol are nitrogen and

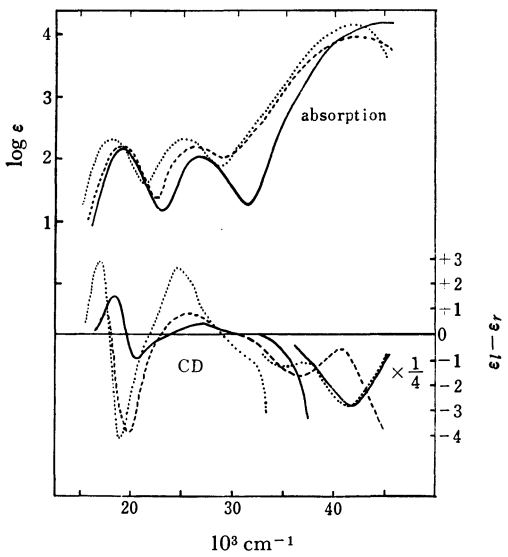

Fig. 1. Absorption and circular dichroism curves of L-alaninol complex.
—— in 30% $HClO_4$
---- in absolute methanol
..... in a mixture (1 : 1, v/v) of methanol and 0.1 N aq. NaOH soln.
log ε and $\varepsilon_l-\varepsilon_r$ are converted into per one mole of cobalt

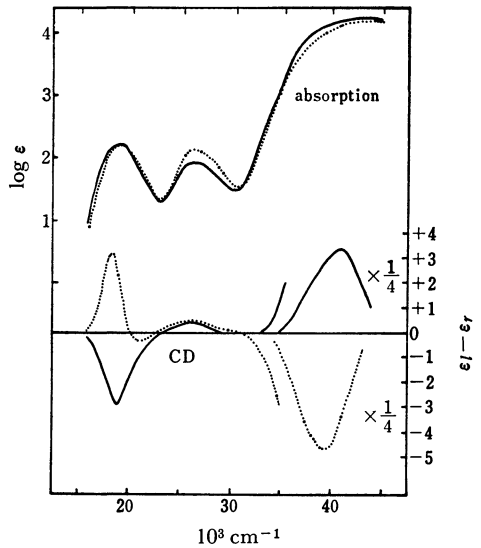

Fig. 2. Absorption and circular dichroism curves of L-leucinol complexes in 60% $HClO_4$-methanol (1 : 1).
····· *fac*-Δ isomer —— *fac*-Λ isomer
log ε and $\varepsilon_l-\varepsilon_r$ are converted into per one mole of cobalt.

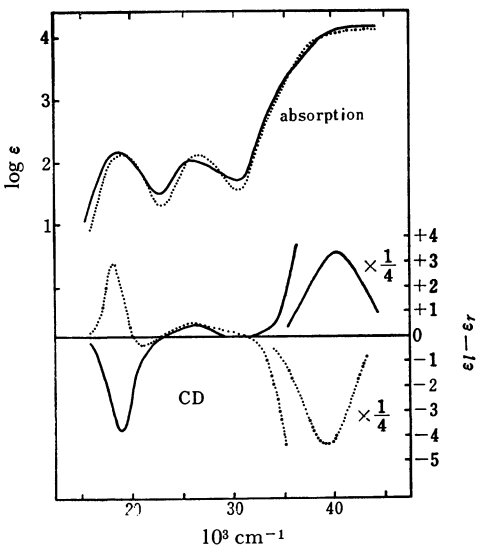

Fig. 3. Absorption and circular dichroism curves of L-isoleucinol complexes in 60% $HClO_4$-methanol (1 : 1).
····· *fac*-Δ isomer —— *fac*-Λ isomer
log ε and $\varepsilon_l-\varepsilon_r$ are converted into per one mole of cobalt.

oxygen, two geometrical isomers, facial (*fac*) and meridional (*mer*), are possible, and each of these isomers has its optical enantiomer, $\Delta(C_2)$ or D and $\Lambda(C_2)$ or L. The geometrical isomers can be distinguished from their absorption spectra; the first band of the *mer* form, having a lower symmetry

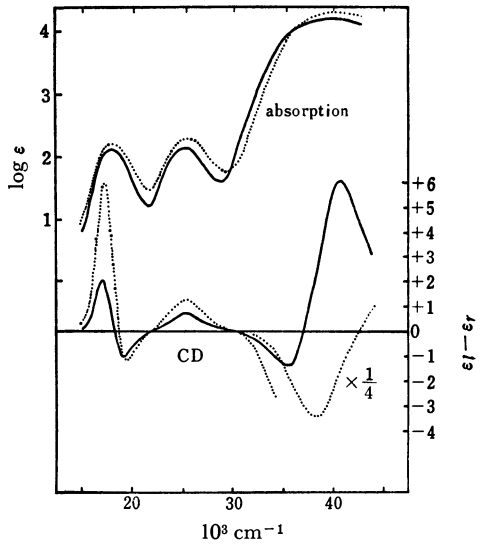

Fig. 4. Absorption and circular dichroism curves of L-prolinol complexes in 60% $HClO_4$-methanol (1 : 1).
····· *fac*-Δ isomer —— *fac*-Λ isomer
log ε and $\varepsilon_l-\varepsilon_r$ are converted into per one mole of cobalt.

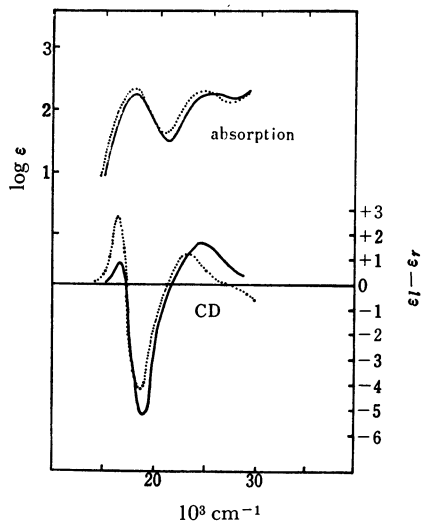

Fig. 5. Absorption and circular dichroism curves of L-prolinol complexes in acetone.
····· *fac*-Δ isomer —— *fac*-Λ isomer
log ε and $\varepsilon_l-\varepsilon_r$ are converted into per one mole of cobalt.

(C_1), should split to a much greater extent than that of the *fac* form, having a higher symmetry (C_3).[6]

As Figs. 1—4 show, the first bands of all the complexes exhibit always nearly symmetrical curves

6) Y. Shimura and R. Tsuchida, This Bulletin, **29**, 311 (1956); F. Basolo, C. J. Ballhausen and J. Bjerrum, *Acta Chem. Scand.*, **9**, 810 (1955).

TABLE 1. NUMERICAL DATA FOR ABSORPTION (AB) AND CIRCULAR DICHROISM (CD)

fac-complex ion	I Band				II Band				C. T. Band	
	AB		CD		AB		CD		CD	
	ν_{max}	log ε	ν_{max}	$\varepsilon_l-\varepsilon_r$	ν_{max}	log ε	ν_{max}	$\varepsilon_l-\varepsilon_r$	ν_{max}	$\varepsilon_l-\varepsilon_r$
Δ-[Co_2(L-alanoH)$_3$ (L-alano)$_3$]$^{3+}$	19.2[a]	2.14	18.1 20.6	+1.54 −0.84	27.0	2.04	26.2	+0.45	41.8	−11.10
	18.9[b]	2.22	17.7 19.8	+0.77 −3.92	25.9	2.19	25.3	+0.86	36.5 40.9	− 6.38 − 2.30
	17.9[c]	2.32	16.9 19.1	+2.87 −4.16	25.0	2.33	24.6	+2.65	35.7[sh] 41.5	− 5.20 −11.40
Δ-[Co_2(L-leunoH)$_3$ (L-leuno)$_3$]$^{3+}$	19.2[a]	2.18	18.3 20.8	+3.15 −0.34	26.9	2.14	25.6	+0.52	39.4	−18.58
Λ-[Co_2(L-leunoH)$_3$ (L-leuno)$_3$]$^{3+}$	18.9[a]	2.20	18.9	−2.89	26.7	1.93	26.3	+0.38	41.7	+13.55
Δ-[Co_2(L-isoleunoH)$_3$ (L-isoleuno)$_3$]$^{3+}$	19.2[a]	2.15	18.3 20.8	+2.93 −0.36	26.9	2.10	25.6	+0.51	39.2	−17.29
Λ-[Co_2(L-isoleunoH)$_3$ (L-isoleuno)$_3$]$^{3+}$	18.9[a]	2.22	18.9	−3.73	26.6	2.03	26.2	+0.45	40.3	+13.40
Δ-[Co_2(L-prolinoH)$_3$ (L-prolino)$_3$]$^{3+}$	18.1[a]	2.25	17.3 19.4	+5.99 −1.25	25.4	2.35	25.2	+1.27	38.0	−13.9
	17.8[d]	2.35	16.7 18.9	+2.84 −4.59	24.6	2.31	24.7	+0.91		
Λ-[Co_2(L-prolinoH)$_3$ (L-prolino)$_3$]$^{3+}$	18.1[a]	2.11	17.2 19.2	+2.05 −1.04	25.3	2.16	25.3	+0.79	35.6 40.7	− 1.45 + 6.10
	18.0[d]	2.20	16.5 18.5	+0.88 −5.32	25.9	2.31	23.5	+1.06		

ν in 10^3 cm^{-1}; sh shoulder; C. T. charge transfer
a) in 5 N $HClO_4$; b) in absolute methanol; c) in a mixture (1 : 1, v/v) of methanol and 0.1 N aq. NaOH soln.; d) in acetone
log ε and $\varepsilon_l-\varepsilon_r$ are converted into per one mole of cobalt.

and no indication of splitting in the solvents used here. These facts indicate that all the complexes have the *fac* configuration around the cobalt(III) ion. The shift of the first and the second absorption bands of the alaninol and the prolinol complex in the different solvents may be related to the deprotonation of the hydroxo group in coordinated aminoalcohols (Figs. 1 and 5). This can be compared to the relation between aquo and hydroxo cobalt(III) complexes in acid and alkaline solutions.

The absolute configuration of the complexes can be assigned safely from their CD spectra. The CD curve of the L-alaninol complex in acid exhibits one strong positive and one weak negative peak in the first band region (Fig. 1). Such a pattern is characteristic of the Δ-type complex with trigonal symmetry and is very similar to those of such complexes of known absolute configuration as *fac*-Δ-[Co(L-alanine)$_3$][7] or Δ-[Co(L-pn)$_3$]$^{3+}$ (pn=propylenediamine)[8]. Since the complex ion in acid will exist as a monomeric protonated tris-alaninol complex, we conclude that the complex ion is of *fac*-Δ type around the cobalt(III) ion. The sulfates of L-leucinol and L-isoleucinol complex show CD curves similar to that of *fac*-Δ L-alaninol complex and can be assigned to the *fac*-Δ type, too (Figs. 2 and 3). The CD curves of the bromides of L-leucinol and L-isoleucinol complex, on the other hand, exhibit only a strong negative peak at *ca.* 19000 cm^{-1}, and are very similar to that of Λ-[Co(D-pn)$_3$]$^{3+}$.[8] Therefore, we have assigned these bromides to the *fac*-Λ-configuration.

Figure 4 shows that both isomers of the L-prolinol complex give very different CD spectra from those of the above complexes in the first band region. Both appear to be typical of the Δ-type complex, although the CD intensity of one isomer is exceptionally large. Since both the isomers have been assigned to the *fac* form from their absorption spectra, they should be diastereomeric with each other. In order to determine the absolute configuration of these isomers, the CD in

7) B. E. Douglas and S. Yamada, *Inorg. Chem.*, **4**, 1561 (1965); E. Larsen and S. F. Mason, *J. Chem. Soc., (A)*, **1966**, 313; J. H. Dunlop and R. D. Gillard, *J. Chem. Soc.*, **1965**, 6531; R. G. Denning and T. S. Piper, *Inorg. Chem.*, **5**, 1056 (1966); M. G. B. Drew, J. H. Dunlop, R. D. Gillard and D. Rogers, *Chem. Commun.*, **1966**, 42.

8) A. J. McCaffery, S. F. Mason and B. J. Norman, *Chem. Commun.*, **1965**, 49; H. Iwasaki and Y. Saito, This Bulletin, **39**, 92 (1966).

the ultraviolet region seems to give a useful information. From the CD spectra of the alaninol, leucinol and isoleucinol complexes in the ultraviolet region, it will be recognized that the Δ-type complex in acid exhibits a strong negative CD band at *ca.* 39000 cm^{-1}, while the Λ-type complex a positive CD band at *ca.* 40000 cm^{-1} with a smaller intensity than that for the Δ-type complex. Such a relation was also observed in the CD spectra of Δ- and Λ-$[Co(L\text{-}pn)_3]^{3+}$.[9] On this empirical observation, the isomer which was separated below pH 1 could be assigned to the Λ-type, and the other isomer which precipitated at a higher pH to the Δ-type, as may be seen in Fig. 4. These CD bands may correspond to the charge transfer transition between the coordinated aminoalcohol and the cobalt(III) ion.

The higher CD intensity of Δ-prolinol complex or anomalous CD appearance of Λ-prolinol complex in the first band region as compared with those of the other aminoalcohol complexes could be explained by considering the vicinal effect of asymmetric nitrogen atoms of L-prolinols. The donor nitrogen atom of L-prolinol coordinated as a bidentate ligand becomes an asymmetric atom, and is forced to take a configuration antipodal to that of the similarly coordinated D-prolinol. The same CD behavior was observed in some L-proline complexes.[10] In the Λ-complex of L-prolinol, a negative CD band due to the Λ-configurational effect would be partly compensated by the strong vicinal effect of such an asymmetric nitrogen atom with positive CD sign. The high CD intensity of the Δ-complex of L-prolinol can be explained by the same consideration.

The Δ- and the Λ-isomer of each L-aminoalcohol complex are not enantiomeric with each other, but diastereomeric. If we assume that the stable conformation of the L-aminoalcohol, which has a similar skeletal structure to that of L-$(+)_D$-pn, is δ-gauche form, the Δ- and the Λ-tris-L-aminoalcohol complex should have the "lel" and the "ob" structure, respectively.[11] The *lel* complex is said to be more stable than the *ob* complex.[11] However, except for the case of L-alaninol complex, the reaction of L-aminoalcohols and cobalt(III) ammine complexes gave always both the *lel* and the *ob* complex of *fac*-type. The formation ratio of these isomers seemed to depend on the kind of outer-anion of starting cobalt(III) complexes, and might be related to the solubility of aminoalcohol complexes produced. More detailed study would be needed to elucidate the stereoselective coordination of such complicated ligands as L-leucinol or L-prolinol. In the case of L-alaninol complex, only a stable *lel* isomer was separated from the reaction mixture.

Attempts to prepare the other geometrical isomers, the meridional complexes, were unsuccessful. This might be related to the difficulty in forming a dimeric structure bonded with the O–H–O or N–H–O hydrogen bonding discussed later.

The higher CD intensity of charge transfer bands of the Δ-complexes than those of the Λ-complexes would be caused by a superposition of two CD bands with the same negative sign resulting from the Δ-configurational effect and the vicinal effect of L-aminoalcohols in δ-conformation. A weak negative CD band at 35600 cm^{-1} of the Λ-prolinol complex might be an imaginary minimum which appeared depending on the relation between the positive CD curve of the Λ-configuration and the negative CD curve of the δ-vicinal effect. The vicinal effect of coordinated L-pn in δ-conformation gave also a negative CD band for the charge transfer band in cobalt(III) complexes.[9]

Corresponding to the second absorption bands, both diastereomers give weak positive CD peaks. However, detailed discussion can not be made at the present stage because their origin is uncertain.

CD Spectra in Organic Solvents and in Alkaline Solutions. As is seen in Fig. 1, the CD curves of L-alaninol complex in methanol and in alkaline solution are very different from that in acid solution. The absorption spectra indicate that no substantial change of the complex itself such as decomposition or isomerization occur, but the complexes containing deprotonated L-alaninols will be present in these solvents as stated before. Therefore, such a big change in CD curves might be caused by a special interaction between the two kinds of complex in methanol or alkaline solution. Mason and Norman[12] reported that the CD curve of Δ-$[Co\,en_3]^{3+}$ (en=ethylenediamine) changes remarkably by forming an ion-pair between the complex ion and the phosphate ion, and that the complex ion and the phosphate ion might have a preferred mutual orientation in the ion-pair. The change of CD in the L-alaninol complex is much more remarkable than that in the ethylenediamine complex. A most probable structure of such an aggregate between the L-alaninol complex ions and molecules in methanol will be a dimeric form with face-to-face O···H···O hydrogen bonding between three OH groups of the triprotonated $[Co(L\text{-}alanoH)_3]^{3+}$ and three oxygen atoms of the deprotonated $[Co(L\text{-}alano)_3]^0$. The dimeric structure would also hold in the solid state as indicated by the chemical analysis. The same discussion could be made for the change on CD curves of L-prolinol complexes in acetone (Fig. 5).

In alkaline solutions, all alcoholic protons would be removed and the dimeric form would have O···H···N hydrogen bonding between three

9) K. Ogino, K. Murano and J. Fujita, *Inorg. Nucl. Chem. Letters*, **4**, 351 (1968).
10) T. Yasui, J. Hidaka and Y. Shimura, *J. Am. Chem. Soc.*, **78**, 2762 (1965); This Bulletin, **38**, 2025 (1965); T. Yasui, *ibid.*, **38**, 1746 (1965).
11) E. J. Corey and J. C. Bailar, Jr., *J. Am. Chem. Soc.*, **81**, 2620 (1959).

oxygen atoms of a complex molecule and the three amino groups of another molecule.

As in the case of the Δ-$[Co\,en_3]^{3+}$-phosphate system,[12] the change in CD of the first band in methanol and in alkaline solution might be related to the appearance of a new CD band at *ca.* 36000 cm^{-1}, which originates probably in a charge transfer transition relating to the bridging hydrogen bonding in the aggregate. The absorption spectra in these solvents indicate also the appearance of new absorption bands due to such a transition in the range between 20000 to 40000 cm^{-1}. At present, however, it is almost impossible to interpret the behavior of CD curves of the aggregates in these solvents.

12) R. Larsson, S. F. Mason and B. J. Norman, *J. Chem. Soc., (A)*, **1966**, 301.

Molecular models of the aggregates show that the O···H···O hydrogen bonding seems to be formed more easily between the Λ(*ob*)-complexes than that between Δ-(*lel*)-complexes, when we assume a tetrahedral angle for $\angle$Co–O–H and a linear O···H···O hydrogen bonding. Together with the different stabilities between the *lel* and the *ob* form,[11] two different dimeric forms, Δ-Δ and Λ-Λ, might have different stabilities, and consequently different solubilities. Therefore, the two isomers, *fac*-Δ- and *fac*-Λ- complex of each L-leucinol, L-isoleucinol and L-prolinol could be isolated by the solubility differences in solutions with different pH values.

We wish to thank the Ministry of Education for the financial support granted to this research.

BULLETIN OF THE CHEMICAL SOCIETY OF JAPAN VOL. 41 2427—2430 (1968)

Activation Analysis of Antimony in Tin Based on an Internal-Monitor Method using Thermal Neutrons

Yoshinaga OKA, Toyoaki KATO and Hui-Tuh TSAI

Department of Chemistry, Faculty of Science, Tohoku University, Katahira-cho, Sendai

(Received March 25, 1968)

An internal-monitor method proposed previously has been applied to the determination of trace amounts of antimony in tin by activation with thermal neutrons. After the antimony activity is chemically separated from the irradiated sample, the γ-ray spectrum corresponding to a mixture of ^{124}Sb and ^{125}Sb formed by the β^- decay of ^{125m,125}Sn is measured. Synthetic mixtures of antimony and tin with known weight ratios have been prepared to check the accuracy of the method. Good proportionality has been obtained between the ratios of the ^{124}Sb to ^{125}Sb activities and the ratios of the concentrations. By using this relationship, antimony analysis can easily be carried out. The content of antimony in a sample of tin down to 0.2 ppm can be determined with a relative error of $\pm 2\%$.

In cases of thermal neutron activation, where the atomic number of the element to be analyzed is higher by one unit than that of the matrix element and where the nuclear characteristics of the (n, γ) reaction product of the former and secondary β^- decay product from the latter are favorable for subsequent γ-ray spectrometric measurements, it is possible to determine the content of the element in question on the basis of the activity ratios of both radioactive species.

In a previous report,[1] the principles and applicability of this internal-monitor method to the determination of a trace amount of silver in palladium was described. By this method, errors which arise from neutron flux irregularities and self shielding effects can be avoided, and no corrections for chemical yield are neccessary. In the present work, this method was further applied to the determination of trace amounts of antimony in tin by means of thermal neutron activation.

Method of Determination

Antimony can be determined by γ-ray spectrometry through the induced ^{122}Sb or ^{124}Sb activity in an irradiated sample. Tin, on the other hand, gives nine radionuclides as (n, γ) reaction products: ^{113m}Sn, ^{113}Sn, ^{117m}Sn, ^{121m}Sn, ^{121}Sn, ^{123m}Sn, ^{125m}Sn and ^{125}Sn. However, radionuclides of present

1) Y. Oka, T. Kato, H.-T. Tsai and K. Nomura, This Bulletin, **41**, 329 (1968).

importance are formed through the following reaction scheme:

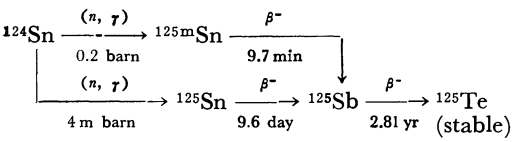

When the antimony activity is separated from the irradiated sample, therefore, a composite γ-ray spectrum which corresponds to a mixture of the 2.8 day-^{122}Sb, the 60.9 day-^{124}Sb and the 2.81 yr-^{125}Sb as β^--decay products of ^{125m,125}Sn is measured. The marked difference in energy of γ-rays emitted from ^{124}Sb (1.69 MeV) and ^{125}Sb (0.427 MeV) permits a γ-ray spectrometric determination of antimony in tin. By applying the principles illustrated in the previous report,[1] the following linear relationship is obtained between the ratio of the photopeak activities determined at identical times after each irradiation (R_{A_t}) and the ratio of the concentrations (R_W):

$$R_W = K R_{A_t}$$

The constant, K, can be determined by irradiating synthetic mixtures of antimony and tin with known compositions.

Experimental

Materials and Irradiation. A series of synthetic antimony - tin mixtures was prepared in the following manner. Tin powder 100 mg was weighed into a quartz tube with an internal diameter of 6 mm, and then known amounts of an aqua regia solution of antimony added. After evaporation to dryness, the tube was sealed.

The tin powder used was processed from tin(II) chloride of a guaranteed grade. After repeated recrystallization, the reagent was dissolved in hydrochloric acid. Tin was precipitated from this solution in the form of metallic powder by the addition of a concentrated sodium hydroxide solution with heating, repeatedly washed with water and dried in a vacuum.

The aqua regia solution of antimony was prepared through the dissolution of 99.9999% antimony metal. Proper dilution with water was made just before use. The hydrochloric acid, nitric acid and water were all redistilled. All other chemicals were of a guaranteed grade.

Commercial tin metal of a granular form and an electrolytic tin rod were tested for their antimony contents. From these samples, small pieces of approximately 60 mg were cut out and analyzed. The samples, a series of synthetic mixtures and 100 mg of the original tin powder were put together in an aluminum capsule for pile irradiation. Irradiation was performed for 180 hr in the JRR-2 reactor of the Japan Atomic Energy Research Institute. The reactor was operated at 10 MW, providing a thermal neutron flux of 2.0×10^{13} n/cm^2/sec at the irradiation site. After irradiation, the samples were cooled for 13 days and then subjected to the radiochemical procedure for the isolation of their antimony activities.

Radiochemical Procedure. Radioantimony was extracted from a hydrochloric acid solution of an irradiated tin target with isoamyl acetate. The irradiated sample was dissolved in a small amount of aqua regia, and made 8 N in hydrochloric acid to a volume of 25 m*l*. To this, 5 m*l* of isoamyl acetate was added and radioantimony extracted with 10 minutes' agitation. The organic extract was washed twice with 10 m*l* portions of 8 N hydrochloric acid, and drained into a polyethylene tube for γ-ray spectrometric measurements.

γ-Ray Measurement. For the γ-ray spectrometric measurement, a $1\frac{1}{2}'' \phi \times 1\frac{1}{2}''$NaI(Tl) crystal connected to an 800-channel pulse-height analyzer made by the Tokyo Shibaura Electric Co., Ltd., Japan was used. The graphical subtraction method[2] was employed to determine accurate photopeak areas from the γ-ray spectra obtained. Decay curve analyses have been performed for photopeak activities to confirm the radiochemical purity.

Results and Discussion

Isolation of Radioantimony. Penta-valent antimony is extractable from a hydrochloric acid solution with ethyl acetate, isoamyl acetate and other extractants,[3-5] and these properties have been utilized for the separation of a trace amount of antimony from tin.[6] To obtain the best procedure for the isolation of radioantimony from a large amount of tin, the extraction properties of both elements with isoamyl acetate have been examined further using ^{124}Sb and ^{113}Sn as tracers. Hydrochloric acid solution of varying concentrations containing definite amounts of either pentavalent antimony[7] or quadrivalent tin[8] was agitated with an equal volume of isoamyl acetate for 10 min. After agitation, both the organic and aqueous layers were γ-counted, and the percentage extraction was computed from the activity data. The extraction curves thus obtained are shown in Fig. 1. The extraction of antimony was best effected from a 7 to 8 N hydrochloric acid solution. Although up to about 20% of tin was accompanied by antimony, this could be completely removed by repeated backwashings with 8 N hydrochloric acid.

2) W. S. Lyon, Jr., Ed., "Guide to Activation Analysis," D. Van Nostrand Co., Princeton, N. J. (1964), p. 104.

3) C. E. White and H. J. Rose, *Anal. Chem.*, **25**, 351 (1953).

4) G. K. Schweitzer and L. E. Storms, *Anal. Chim. Acta*, **19**, 154 (1958).

5) N. Suzuki, *Nippon Kagaku Zasshi (J. Chem. Soc. Japan, Pure Chem. Sect.)*, **81**, 437 (1960).

6) K. Saito, N. Suzuki, K. Seto and H. Ikegami, This Bulletin, **36**, 692 (1963).

7) The neutron irradiated antimony sample was dissolved in aqua regia, and used for the extraction experiment.

8) To prepare this solution, a known amount of irradiated tin was dissolved in aqua regia with heating. From this, tin(IV) hydroxide was precipitated by the addition of a dilute aqueous sodium hydroxide solution. The precipitate was dissolved in 8 N hydrochloric acid, and the antimony activity removed by isoamyl acetate extraction. An aliquot of the aqueous layer was used for the extraction experiment.

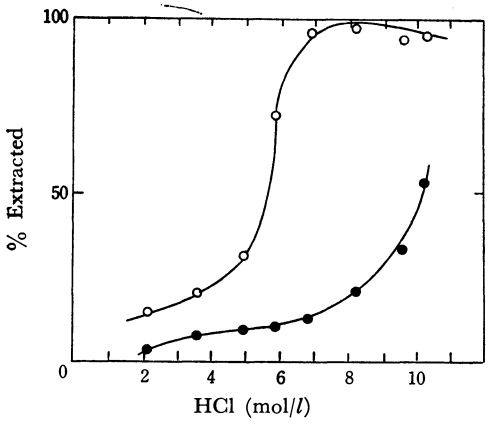

Fig. 1. Extraction curves of antimony(V) and tin(IV) from hydrochloric acid solution with isoamyl acetate.
○: Sb(V) 1.8 μg
●: Sn(IV) 2.6 mg
Org.: Aq. = 1:1 (5 ml)

When the irradiated antimony - tin mixture was subjected to the radiochemical procedure, a composite γ-ray spectrum was obtained in the final radioantimony fraction, which corresponds to a mixture of ^{122}Sb, ^{124}Sb and ^{125}Sb, as shown in Fig. 2-(1). Decontamination from other nuclides was successful.

R_W vs. R_{A_t} From the composite spectra obtained from the antimony - tin mixtures, photopeak areas were measured for 0.427 MeV γ-rays from ^{125}Sb, and for 1.69 MeV γ-ray from ^{124}Sb.

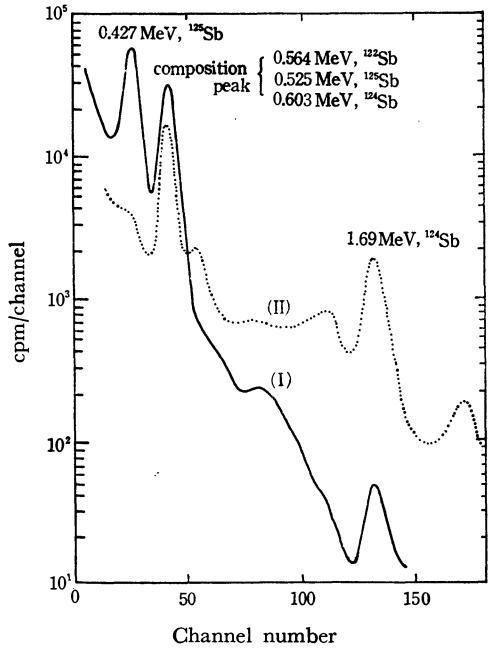

Fig. 2. γ-Ray spectra of radioantimony; (I) separated from irradiated tin - antimony mixture (Sn 101 mg+Sb 0.19 μg), 13 days after irradiation, (II) standard antimony sample.

The R_{A_t}'s were computed from the data thus obtained. At that time, the correction coefficient for ^{124}Sb arising from the original tin, α, was introduced in Eq. (1), obtaining

$$R_W = K\left(\frac{A_{^{124}\mathrm{Sb}}}{A_{^{125}\mathrm{Sb}}} - \alpha\right)_{t=13\ \mathrm{day}} \quad (2)$$

where

$$\alpha = \left(\frac{A_{^{124}\mathrm{Sb}}}{A_{^{125}\mathrm{Sb}}}\right)_{\mathrm{original}} \quad (3)$$

A's represent the photopeak activities. The α value obtained under the present conditions was 1.64×10^{-4}.[9] The reasons for this correction may arise from the antimony content in the original tin as an impurity and from the systematic second-order nuclear reactions as described later. Table 1

Table 1. R_W *vs.* R_{A_t} for tin-antimony mixtures

R_W	R_{At}[a]	R_W/R_{At}
8.67×10^{-6}	5.68×10^{-3}	1.52×10^{-3}
3.88×10^{-6}	2.59×10^{-3}	1.50×10^{-3}
1.85×10^{-6}	1.23×10^{-3}	1.50×10^{-3}
1.00×10^{-6}	6.80×10^{-4}	1.47×10^{-3}
3.13×10^{-7}	2.06×10^{-4}	1.52×10^{-3}
	Mean:	1.50×10^{-3}
	Std. dev.:	$0.01_8\times10^{-3}$ ($\pm1.2\%$)

a) 13 days after the end of irradiation

shows the relation between the weight ratios and the corrected photopeak activity ratios. Good proportionality was obtained between R_W and R_{A_t}. A relative standard deviation of ±1.2% was obtained under the present conditions. The present results show that an accurate determination can be expected using this relationship.

When a minimum photopeak area of 50 cpm is selected as the limit of detection, an antimony content in tin down to about 0.2 ppm (0.02 μg in a 100 mg sample) can be determined with a relative error of ±2%.

Interference. Interference which arises from the tin matrix has been examined. In the present case, the effects of the (n, p) and the (n, α) reactions by fast neutrons give no trouble, but interference through second-order nuclear reactions must be considered which would produce additional amounts of radioactive antimony and thus cause a positive error. ^{124}Sb is formed from tin according to the reaction scheme:

9) This corresponds to an antimony content of 0.25 ppm in the original tin. This can be attributed to the sum of antimony as an impurity and the apparent content produced by second-order reaction. The latter was computed to be 0.05 ppm as described later.

$$^{122}\mathrm{Sn}\begin{cases}(\mathrm{I}) \xrightarrow[0.16\ \text{barn}]{(n,\gamma)} {}^{123m}\mathrm{Sn} \xrightarrow[41\ \text{min}]{\beta^-} \\ (\mathrm{II}) \xrightarrow[1\ \text{m barn}]{(n,\gamma)} {}^{123}\mathrm{Sn} \xrightarrow[129\ \text{day}]{\beta^-} {}^{123}\mathrm{Sb} \xrightarrow[2.5\ \text{barn}]{(n,\gamma)} {}^{124}\mathrm{Sb}\end{cases}$$

The production rate of ^{124}Sb was computed using the Bateman equation.[10] Because of the small activation cross section for the ^{122}Sn(n, γ)^{123}Sn reaction and of the long half-life of the product, the production rate of ^{124}Sb through reaction path (II) can be excluded from the present calculation. Thus the scheme is simplified to successive reactions of the type:

$$N_1 \xrightarrow[\sigma_1]{\phi} N_2 \xrightarrow[A_1]{\lambda_2} N_3 \xrightarrow[\sigma_3]{\phi} N_4 \xrightarrow[A_4]{\lambda_4} N_5 \qquad (4)$$

where A's=activity; N's=number of atoms; λ's=disintegration constant; σ's=effective activation cross-section; and ϕ=effective neutron flux.

In order to compute the growth of the ^{124}Sb activity (A_4), a practical formula derived by De Neve *et al.*[11] was used in the present work. An apparent antimony concentration in ppb is defined by:

$$C_{\mathrm{ppb}} = \frac{A_4(\text{for 1 g Sn})}{A_4'(\text{for } 10^{-9}\text{ g Sb})} \qquad (5)$$

For an irradiation time of t, this becomes:

$$C_{\mathrm{ppb}} = \frac{N_1\sigma_1\phi}{N_4'(1-e^{-\lambda_4 t})}\left[t - \frac{\lambda_2+\lambda_4}{\lambda_2\lambda_4} + \frac{\lambda_2}{\lambda_4(\lambda_2-\lambda_4)}e^{-\lambda_4 t} - \frac{\lambda_4}{\lambda_2(\lambda_2-\lambda_4)}e^{-\lambda_2 t}\right] \qquad (6)$$

This apparent antimony content induced in the tin sample during 180 hr irradiation at a flux of 2.0×10^{13} n/cm^2/sec was computed to be 52 ppb.[12] This value must be subtracted from the gross antimony concentration to obtain the true antimony content in a sample of tin.

Antimony Analysis. This method of antimony analysis was tested on both granular tin and an electrolytic tin rod. The results obtained are shown in Table 2. These data were corrected for the effect of second-order reactions. Good agreement for antimony content in granular tin was obtained. The results for electrolytic tin, however, show an irregularity over the range of 2—3 ppm. The reason for this behavior may be inhomogeneities involving antimony as an impurity in this sample.

TABLE 2. RESULTS OF ANTIMONY ANALYSES

Sample	R_{A_t}	Antimony content (ppm)	Average
Granular tin	1.38×10^{-2}	20.7	20.4±0.3
	1.38×10^{-2}	20.7	
	1.34×10^{-2}	20.1	
	1.34×10^{-2}	20.1	
	1.37×10^{-2}	20.5	
Electrolytic tin rod	2.00×10^{-3}	2.9_5	2.7_8±0.7_9
	1.36×10^{-3}	1.9_9	
	1.98×10^{-3}	2.9_2	
	1.95×10^{-3}	2.8_8	
	2.16×10^{-3}	3.1_9	

10) G. Friedlander, J. W. Kennedy and J. M. Miller, "Nuclear and Radiochemistry," 2nd Ed., John Wiley & Sons Inc., New York (1964), p. 76.
11) R. De Neve, D. De Soete and J. Hoste, *Anal. Chim. Acta*, **36**, 508 (1966).
12) Nuclear data used for this calculation were those listed in the Nuclear Data Sheets.[13]
13) Nuclear Data Sheets, Natl. Academy of Science-Natl. Research Council, Washington, D. C. (1961).

BULLETIN OF THE CHEMICAL SOCEITY OF JAPAN VOL. 41 2431—2434 (1968)

1-Acylindoles. VI. On the Deacylation of the N¹-Position in the Formation of a 1,2,3,4-Tetrahydrocarbazole

Hisao YAMAMOTO and Toshio ATSUMI

Pharmaceuticals Division, Sumitomo Chemical Co., Kasugade-cho, Konohana-ku, Osaka

(Received November 18, 1967)

The cyclization reaction of cyclohexanone acetylphenylhydrazone to produce a tetrahydrocarbazole derivative has been reinvestigated. Although other workers obtained only a deacylated derivative in the reaction products, we found also an acylated product. It can be concluded from the experimental results that an acyl group of the N¹-position of a phenylhydrazine derivative participates only a little in the indole cyclization and that the deacetylation occurs mainly after formation of a new C–C bond.

It has been found that 1,2,3,4-tetrahydrocarbazole (II) and 9-acetyl-1,2,3,4-tetrahydrocarbazole (IIIa) could be prepared by boiling cyclohexanone acetylphenylhydrazone in dilute sulfuric acid[1,2] (Scheme I).

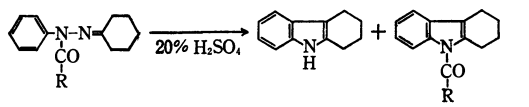

I (a: R=CH₃, b: R=C₆H₅) II III (a: R=CH₃, b: R=C₆H₅)

Scheme I

However, Suvorov *et al.* have reported that the heating of cyclohexanone acetylphenylhydrazone in 20% aqueous sulfuric acid under reflux produced 1,2,3,4-tetrahydrocarbazole, but did not give 9-acetyl-1,2,3,4-tetrahydrocarbazole, suggesting that an acyl group of the N¹ atom of the hydrazone derivative stabilizes the p-electron pair of that nitrogen atom, thus inhibiting the formation of a new C–C bond.[3] We attempted to ascertain whether the hydrolysis of the acetyl group should preceded Fischer's indole cyclization or not.

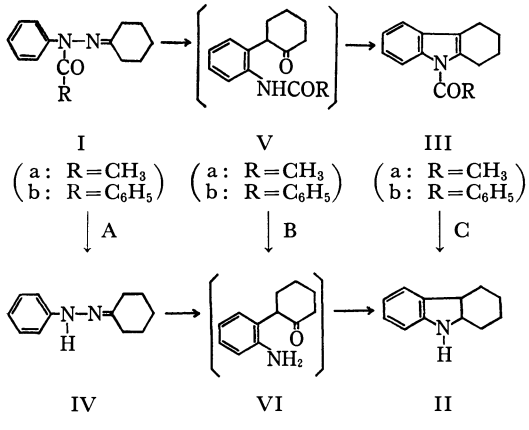

I (a: R=CH₃, b: R=C₆H₅) V (a: R=CH₃, b: R=C₆H₅) III (a: R=CH₃, b: R=C₆H₅)

A B C

IV VI II

Scheme II

The processes for preparing IIIa and II from Ia are thought to be as follows (Scheme II).

II is considered to be obtained from I through Route A, B or C. Moreover, if the indole formation of an N¹-acylated compound is retarded remarkably by the substitution of the acyl group, the deacylation should precede the formation of a new C–C bond. The assumption suggests that the reaction proceeds through Route A. Therefore, II is thought to be formed from Ia *via* Route A.

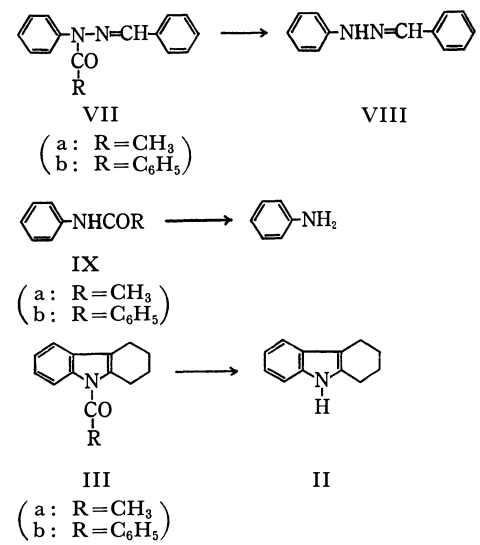

VII (a: R=CH₃, b: R=C₆H₅) VIII

IX (a: R=CH₃, b: R=C₆H₅)

III (a: R=CH₃, b: R=C₆H₅) II

Scheme III

1) H. Yamamoto, *J. Org. Chem.*, **32**, 3639 (1967).
2) W. H. Perkin and S. G. P. Plant, *J. Chem. Soc.*, **119**, 1825 (1921).
3) N. N. Suvorov and N. P. Sorokina, *Doklady Acad. Nauk S.S.S.R.*, **136**, 840 (1961).

In order to make this point clear, we studied the deacylation rates of the intermediates of each step during the reaction. The following model experiments were carried out (Scheme III). From the model experiments of VII to VIII and IX to aniline, the possibilities of Route A and B may be estimated. The rates of deacylation in all the steps of the carbazole formation can be estimated to some degree from the results of these model experiments and the process of transforming III to II. In these experiments designed to transform VII to VIII, IX to aniline, and III to II, a starting material was heated under reflux in 20% aqueous sulfuric acid for a few minutes, and the reaction products were analyzed quantitatively.

Experimental

Ultraviolet Spectrometry. The ultraviolet spectra were measured with a Shimadzu RS-27 spectrophotometer, using a 1 cm quartz cell. Quantitative analyses were carried out by means of spectra taken in ethanol. The results are shown in Table 1.

TABLE 1.

Starting material (I)	Refluxing time (min)	Reaction products (mol%) III (IIIa or IIIb	II	III+II
Ia	3	9.5	14.1	23.6
	5	10.9	21.1	32.0
	8	15.6	30.2	45.8
	12	16.0	35.6	51.6
	16	17.0	40.9	57.9
Ib	5	54.5	—	54.5
	8	65.3	3.6	68.9
	12	73.3	5.4	78.7

Thin-layer Chromatography and Photometric Analyses. The quantitative analyses of several products were carried out by thin-layer chromatography and by means of the ultraviolet absorption spectra. The products were isolated by thin-layer chromatography. The conditions for this procedure were as follows: silica gel G (Merck & Co.); thickness, 0.25 mm; solvent, carbon tetrachloride - methanol (100 : 2). The portion of the product in the thin layer was extracted with ethanol, and then the ethanol solution was analyzed by a Shimadzu RS-27 spectrophotometer. The results are shown in Table 1.

Gas Chromatography. The gas chromatographs were taken on a Yanagimoto GCG-550 F gas chromatograph. The conditions for the chromatographs of the reaction products in the process of transforming Ia to IIIa and II were as follows: column, 5% PEG-20 M 3m×1.5 mm; column temperature, 220°C; carrier gas, hydrogen; gas speed, 15 ml/min; internal standard substance, tribenzylamine.

For the gas chromatography of products in processes of transforming VIIa to VIII and VIIb to VIII, the conditions are changed in the following points: column temperature, 230°C and 210°C; internal standard substance, dicyclohexyl phthalate and diphenyl phthalate respectively.

TABLE 2.

Starting material (VII)	Refluxing time (min)	Reaction products (mol%) VIII	Recovery of starting material VII
VIIa	3	7.2	55.7
	5	9.9	61.7
	8	11.5	47.2
	12	18.2	39.2
	16	24.5	31.8
VIIb	3	3.4	87.1
	5	5.0	85.0
	12	4.7	78.8
	16	4.6	80.6

For the gas chromatography of products in the hydrolysis of transforming III to II, the conditions were as follows: column, 5% PEG-20M 0.75 m×3 mm; column temperature, 200°C; carrier gas, hydrogen; gas speed, 20 ml/min; internal standard substance, tribenzylamine.

From the areas of the individual peaks, the mol% figures were calculated for each product after a relative response date had been determined by the internal standard method using an appropriate internal standard substance. The individual peaks were identified by means of the retention times of authentic samples. The results are shown in Table 2.

Potentiometric Titration. Aniline was estimated by the potentiometric titration of a 0.1 N perchloric acid solution in glacial acetic acid, using a Hitachi-Horiba Mode M-5 glass electrode pH-meter. The results are shown in Table 3.

TABLE 3.

Starting material	Refluxing time	Reaction products (mol%) Aniline	Recovery of starting material
IXa	3	20.2	
	5	24.3	
	8	41.8	
	12	49.3	
	16	60.2	
IXb	16	0	98—99

Materials. The starting substances and authentic samples for analyses were prepared as follows:

Cyclohexanone Acetylphenylhydrazone (Ia). To a mixture of 28.8 g of cyclohexanone phenylhydrazone[4] (IV), 14 g of pyridine, and 130 ml of dry ether, 13.5 g of acetyl chloride were added drop by drop on cooling. Stirring was continued for additional 3 hr at room temperature. After the completion of the reaction, the filtrate was concentrated to an oily, yellow substance, which was then distilled in a bath of 165°C to give oily,

4) A. Baeyer, *Ann.*, **278**, 105 (1894).

yellow Ia, bp 136—141°C/0.2 mmHg (lit[2] bp 210—220°C/14 mmHg).

Cyclohexanone Benzoylphenylhydrazone (Ib). According to the above procedure, 39.2 g of cyclohexanone phenylhydrazone afforded 23.2 g of colorless prisms of Ib, mp 121—123°C (recryst. from ether). Found: C, 78.69; H, 6.76; N, 9.53%. Calcd for $C_{19}H_{20}N_2O$: C, 78.05; H, 6.90; N, 9.58%.

1,2,3,4-Tetrahydrocarbazole (II). According to the method of Perkin and Plant,[2] the heating of IV under reflux in glacial acetic acid gave white needles of II, mp 113—116°C (recryst. from aqueous alcohol).

9-Acetyl-1,2,3,4-tetrahydrocarbazole (IIIa). To a solution of 1.9 g of N¹-acetylphenylhydrazine hydrochloride in 10 m*l* of glacial acetic acid, 1.0 g of cyclohexanone was added at room temperature. The mixture was then heated at 70—75°C for 2.5 hr with stirring. After the reaction, the reaction mixture was evaporated under reduced pressure to an oily residue, to which water was added to yield an oily, brown substance. This was extracted with chloroform and dried over anhydrous sodium sulfate. The chloroform solution was concentrated to a residue, which was then recrystallized from alcohol to give white needles of IIIa, mp 77—78.3°C (lit[2] mp 77°C).

9-Benzoyl-1,2,3,4-tetrahydrocarbazole (IIIb). According to the above method, 6.4 g of white needles of IIIb, mp 83.5—84.5°C (lit.[5] mp 85°C), were prepared from 7.5 g of N¹-benzoylphenylhydrazine hydrochloride.

Benzaldehyde Acetylphenylhydrazone (VIIa). According to the method of v. Auweres and Wolter,[6] the treatment of benzaldehyde phenylhydrazone with acetyl chloride gave white needles of VIIa, mp 120—122°C (lit.[6] mp 122°C).

Benzaldehyde Benzoylphenylhydrazone (VIIb). According to the above procedure, 10 g of white needles of VIIb, mp 114—115°C (recryst. from ethanol) (lit.[6] mp 115—116°C) were prepared from 11.3 g of benzaldehyde phenylhydrazone.

Benzaldehyde Phenylhydrazone (VIII). After 5.4 g of phenylhydrazine had been added to 5.3 g of benzaldehyde, the reaction mixture was allowed to cool in an ice-water bath. The resultant precipitate was filtered and recrystallized from alcohol to give 8.3 g of white needles of VIII, mp 154—156°C (lit.[7] mp 152°C).

Acetanilide (IXa). IXa, mp 114.5—116°C, was prepared from aniline and acetic acid.[8]

Benzanilide (IXb). IXb, mp 164—165°C, was prepared from aniline and benzoic acid.[9]

General Procedure of Hydrolysis or Ring Formation. After a compound has been heated under reflux in 20% aqueous sulfuric acid for 3 min, 5 min, 8 min, 12 min, or 16 min, the reaction mixture was poured into cold water, extracted with an appropriate solvent, and analyzed quantitatively.

Results and Discussion

I was refluxed in equimolar 20% aqueous sulfuric acid to yield the deacylated compound (II) as well as the corresponding III, the yield of which was calculated with thin-layer chromatography and photometric analysis. The results are shown in Table 1.

As a model experiment, IX was heated under reflux in 20% aqueous sulfuric acid. Aniline as a hydrolyzed product of IX was quantitatively measured by the potentiometric titration. These results are shown in Table 3.

VII was hydrolyzed under reflux in 20% aqueous sulfuric acid to yield VIII, which was then quantitatively analyzed by gas chromatography (Table 2).

IIIa or IIIb was refluxed in 20% aqueous sulfuric acid. The results of analysis by gas chromatography are shown in Table 4.

Table 4.

Starting material	Refluxing time	Reaction products (mol%)	
		Deacylated compound (II)	Recovery of starting material III
IIIa	5	4.3	79.3
	8	4.3	78.4
	12	3.9	80.8
IIIb	8	0.0	89.2
	12	0.0	84.0

From the results shown in Table 4, the deacylation of IIIa or IIIb is so difficult under reflux in 20% aqueous sulfuric acid that it can be said that IIIa is hardly deacylated, and that IIIb is, in fact, practically not deacylated at all. Moreover, the formation of II from Ia proceeds much more rapidly than the formation of VIII from VIIa. As the deacylation rate of I to IV (Route A) is considered to be similar to that of VII to VIII, the formation of II from Ia has to proceed more rapidly than the deacylation of I to IV (Route A).

However, the results shown in Table 3 show that IXa is easily deacylated to aniline, therefore, it seems that a considerable part of the reaction intermediate, Va, is easily deacylated to VI, which is then cyclized to II.

These results suggest that Route B participates considerably in the formation of the deacylated compound, II. Therefore, the greater part of II is proved to be a product deacylated after the formation of a new C–C bond.

Under refluxing in dilute sulfuric acid, the acid-amide bonding of IXb is not easily cleaved. IIIb was prepared from Ib quantitatively, and the rate of the carbazole formation of Ib is little different from that of Ia.

5) W. H. Perkin, *J. Chem. Soc.*, **1923**, 676.
6) K. v. Auwers and E. Wolter, *Ann.*, **487**, 79 (1931).
7) E. Fischer, *Ber.*, **9**, 887 (1876).
8) L. F. Fieser, "Experiments in Organic Chemistry," D. C. Heath & Co., Boston (1957), p. 151.
9) C. N. Webb, "Org. Synth.," Coll. Vol. I, p. 82 (1956).

These results show that a considerable yield of 9-acetyl-1,2,3,4-tetrahydrocarbazole (IIIa) is given by treating cyclohexanone acetylphenylhydrazone (Ia) in 20% aqueous sulfuric acid under reflux, and that a 9-benzoyl derivative (IIIb) can be prepared in a much better yield from a corresponding hydrazone derivative (Ib) under the same conditions. In view of these facts, it can be concluded that a greater part of the deacylated compound is formed through the process of Route B.

Conclusion

In the case of $R=CH_3$, the refluxing of Ia in 20% aqueous sulfuric acid causes II as well as IIIa to be formed. II is considered to be formed mainly by the deacylation of Va to VI (Route B) on the basis of the following facts:

1. It can be concluded from the results of the model experiment (VIIa to VIII) that the deacylation of Ia is quite difficult under the same conditions.

2. The results of the deacylation of another model experiment (IXa to aniline) demonstrate that Va must be deacylated easily to VI.

3. It is very difficult for IIIa to be cleaved to II.

On the other hand, the same treatment of a compound, Ib, having $R = C_6H_5$ gave IIIb as the only product; it was nearly impossible to find II in the reaction products. This fact coincides with the results of the model experiments transforming VIIb to VIII, IXb to aniline, and IIIb to II.

It may be concluded that Fischer's indole cyclization is not notably affected by an acyl group of the N^1-position of a phenylhydrazine derivative and that deacylation mainly occurs in the step of V to VI (Route B) after the formation of a new C–C bond.

BULLETIN OF THE CHEMICAL SOCIETY OF JAPAN VOL. 41 2434—2439 (1968)

The Dechloro-addition of β-Chloropropionitrile to Acrylonitrile with a Sodium Amalgam

Akira MISONO, Tetsuo OSA, Takamasa ASANO and Takeo SUZUKI

Department of Industrial Chemistry, Faculty of Engineering, The University of Tokyo, Hongo, Tokyo

(Received November 22, 1967)

The reaction of a mixture of β-chloropropionitrile, acrylonitrile, and water with a sodium amalgam was investigated. The main product was adiponitrile, which was formed mainly *via* a route consisting of three steps: I. The replacement of the chloride of β-chloropropionitrile with sodium. II. The addition of the organometallic intermediate formed to acrylonitrile. III. The replacement of the sodium in the final intermediate with hydrogen. The amount formed through the Wurtz reaction was small. The by-products were propionitrile, acrylonitrile, polymers of acrylonitrile, and organometallic compounds. The details of this reaction are given in this paper.

Adiponitrile has attracted much attention from industry in connection with the production of hexamethylenediamine, the raw material of Nylon-6,6, which has been usually synthesized from adipic acid or butadiene. Recently the dimerization of acrylonitrile has aroused interest because of its simplicity.

The methods of dimerization may mainly be classified into two from the industrial point of view: The method using the various kinds of alkali metal amalgams, and the electrolytic method using an aqueous or nonaqueous solvent containing McKee's salt as a supporting salt. By the former method, adiponitrile was, in 1949, obtained by the use of a sodium amalgam, but in a yield of only 5%.[1] The yield was increased to 62% (based on the acrylonitrile) by the use of a potassium amalgam and 20 wt% hydrochloric acid, but the efficiency of the amalgam consumed was only 12%.[2] In a similar reaction, adiponitrile was formed in a 75% yield with an alkali metal amalgam in an acidic medium in the presence of a catalyzer, such as phenol, hydroquinone, or aromatic amines, and a promotor, such as ferrous, ferric, nickel, or cobalt ions, and with the addition of acetone.[3] However,

1) O. Bayer, *Angew. Chem.*, **61**, 238 (1949).
2) I. L. Knunyants and N. S. Vyazankin, *Izvest. Akad. Nauk SSSR, Otdel Khim. Nauk*, **1957**, 238.
3) A. Katchalsky, D. Vofsi and J. I. Padova, Israeli Pat. 13842, 13844 (1961).

many polymers of acrylonitrile were produced in this case.

The latter method has been reported on by Baizer since 1964;[4] much acrylonitrile was dissolved into an aqueous solution containing a high concentration of McKee's salt (for instance, tetraethylammonium *p*-toluenesulfonate), and then the solution was electrolytically dimerized. The yield reached almost 100%, and no by-products were formed. This method appears industrially promising.

The hydrodimerization of acrylonitrile has been investigated in our laboratory for the last several years, using an alkali metal amalgam in an acidic medium, in order to clarify the mechanism and the various factors of the reaction.[5]

We have found that the efficiency of the amalgam consumed was only 32% at most; the rest of the amalgam consumed was wasted in the formation of hydrogen gas. These reactions were, however, carried out in an aqueous medium. Therefore, the reaction in a non-aqueous medium was examined, but here a greater quantity of polymers of acrylonitrile was produced. The lack of a proton donor, such as water or alcohol, in the reaction system gave many organomercuric compounds.

In 1963, Knapsack proposed a method of producing adiponitrile[6] in which a mixture of β-chloropropionitrile, acrylonitrile and a small quantity of water was treated with alkali metal amalgam. The mechanism suggested was as follows:

1. $XCH_2CH_2CN + M\text{-}Hg \rightarrow \dot{C}H_2CH_2CN + MX + Hg$
2. $\dot{C}H_2CH_2CN + CH_2{=}CHCN \rightarrow NCCH_2CH_2CH_2\dot{C}HCN$
3. $\dot{C}H_2CH_2CN \rightarrow CH_2{=}CHCN + \dot{H}$
4. $NCCH_2CH_2CH_2\dot{C}HCN + \dot{H} \rightarrow NC(CH_2)_4CN$
5. $\dot{C}H_2CH_2CN + \dot{H} \rightarrow CH_3CH_2CN$
6. $2\ \dot{C}H_2CH_2CN \rightarrow NC(CH_2)_4CN$
7. $2\ \dot{C}H_2CH_2CN \rightarrow CH_3CH_2CN + CH_2{=}CHCN$

We have now developed a method similar to that of the Knapsack method in the course of our investigation of how to raise the efficiency of the alkali metal in the amalgam method. The factors affecting the reaction were not known, and the mechanism proposed by Knapsack was very doubtful; we undertook our investigation in order to clarify these problems.

Experimental

Acrylonitrile, Ethyl Acrylate and Methyl Acrylate. Commercial reagents were used after drying over "Drierite" and after distillation. The acrylates were distilled under a nitrogen atmosphere, and the distillates were kept under refrigeration in a brown bottle. Bp 78—79°C, 80—84°C, and 100—101°C respectively.

β-Chloropropionitrile, Ethyl β-Chloropropionate, and Methyl β-Chloropropionate. β-Chloropropionitrile was prepared as in the literature.[7] Bp 73—74°C/30 mmHg.

Ethyl β-chloropropionate and methyl β-chloropropionate were prepared by methods similar to the one described in the literature.[7] Ethyl β-chloropropionate: yield 80%, bp 161°C/760 mmHg; methyl β-chloropropionate: yield 72.5%, bp 147—148°C/760 mmHg.

Hydroquinone. Commercial hydroquinone was used without further purification.

Sodium Amalgam. The sodium amalgam was prepared by the electrolysis of a sodium hydroxide solution, using nickel as a cathode. The concentration of the amalgam was measured by titration.

Apparatus and an Example of the Reaction Procedure. β-Chloropropionitrile (0.3 mol), acrylonitrile (0.2 mol), and water (0.5 wt% of reaction mixture) were poured in a 100 m*l*, four-necked, round-bottomed flask equipped with a condenser, a thermometer, a dropping funnel, and a stirrer. The sodium amalgam (sodium 0.5 wt%, 0.1 g atom) was dropped from the funnel into the mixture with vigorous stirring. The temperature was kept between 40 and 42°C with water cooling. After 80 min, the reaction mixture was poured into a separatory funnel, and the amalgam separated was introduced into 4 N hydrochloric acid. The amount of residual sodium was determined quantitatively by the back titration of the acid. The pure water was charged into the separatory funnel to dissolve the neutral salt formed. Then the organic layer was separated from the aqueous layer and the aqueous layer was extracted with chloroform several times. All the organic parts were collected together and then analyzed by vapor-phase chromatography. The acrylonitrile and propionitrile were measured on a four-meter column packed with 10% dioctyl sebacate on diasolid M at 120°C. The β-chloropropionitrile was analyzed on a two-meter column packed with 10% silicone oil D. C. 550 on diasolid M at 120°C. The adiponitrile was analyzed on a three-meter column containing 10% diethyleneglycol sebacate on diasolid M at 200°C. The polymers of the yellow solid formed were not examined.

The deuterated compounds were analyzed with a mass spectrometer (Hitachi RMU-6E), using the ionization temperature of 110°C. The deuteration was determined by measuring the heights of the parent peak (P) and the (P−1) peak; the adiponitrile and the deuter ated adiponitrile were decomposed independently, and

4) M. M. Baizer, a) *Tetrahedron Letters*, **15**, 973 (1961); b) *J. Electrochem. Soc.*, **111**, 215 (1964); c) *J. Org. Chem.*, **29**, 1670 (1964).

5) T. Osa, A. Misono, these results are under contribution to "*Kyogyo Kagaku Zasshi (J. Chem. Soc. Japan, Ind. Chem. Sect.)*."

6) K. Senneward, A. Ohorodnik, H. Gudernatsch and H. Vierling, German Pat. 1151791 (1963).

7) R. Stewart and R. H. Clark, *J. Am. Chem. Soc.*, **69**, 714 (1947).

the ratio of P and P+1 does not change very much whether a compound contains a deuterium or not.[8]

The calculation may be exemplified as follows (Table 1).

Table. 1.

Mass number	107	108	109	110	111
AN*		100 (P)	7.38 (P+1)*	0.24 (P+2)*	
DAN*			100 (P)*	7.39 (P+1)*	0.24 (P+2)*
AN		100 (P)	6.71 (P+1)		0.23
Reaction product (AN+DAN)		38.1	100	6.53	0.23

* These values are quoted from Ref. 8.

The mass number, 109, of the reaction product contains not only the parent peak of the deuterated adiponitrile, but also the P+1 peak of the pure adiponitrile.

Therefore, the strength based on only the deuterated adiponitrile can be calculated by a conventional proportion using the values cited above:

$$100 - 38.1 \times \frac{6.71}{100} = 97.4$$

The deuteration is determined from the next equation:

$$\frac{97.4}{38.1 + 97.4} \times 100 = 71.9\ (\%)$$

This method of calculation gives the percentage of a monodeuterated adiponitrile. Furthermore, it is sure that the method is suitable for this investigation, because the formation of the adiponitrile containing two deuterium atoms may be neglected; the simple calculation shows that the existence of this compound results in the measurement of a larger value than the 0.23 of the 111 peak.

The symbols used in this report have the following meanings:

$$\eta_{ADN} = \frac{\text{formed adiponitrile (mol)} \times 2}{\text{consumed sodium (g atom)}} \times 100\ (\%)$$

$$\eta_{PN} = \frac{\text{formed propionitrile (mol)} \times 2}{\text{consumed sodium (g atom)}} \times 100$$

Results and Discussion

When a mixture of β-chloropropionitrile and acrylonitrile was treated with a sodium amalgam in the presence of water, the same products as those reported by Knapsack, namely, adiponitrile as the main product, and propionitrile, acrylonitrile, polymers of acrylonitrile, and organomercuric compounds as by-products, were obtained. These products were explained by him as being produced through the radical mechanism described above. However, the possibility of the mechanism could be eliminated because of the fact that hydroquinone added to the reaction solution did not disturb the reaction (Fig. 1). Therefore, the addition of β-chloropropionitrile to acrylonitrile with a sodium amalgam was dealt with in detail in order to clarify the reaction mechanism.

In the above-mentioned reaction, the water, added over a range of 0 to 1.0% by weight based

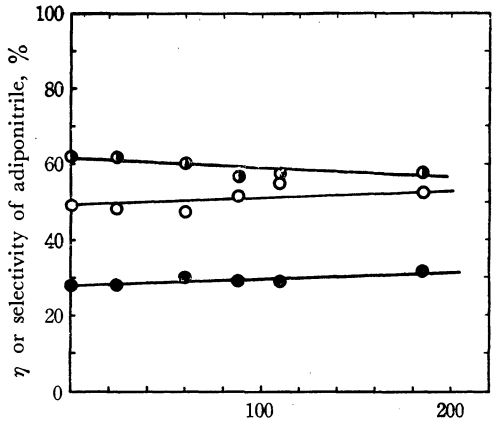

Fig. 1. The effect of hydroquinone.
○ η_{ADN}, ● η_{PN}, ◑ Selectivity of adiponitrile = $(\eta_{ADN}/\eta_{ADN}+\eta_{PN})$
Reaction conditions: β-chloropropionitrile, 0.3 mol; acrylonitrile, 0.2 mol; water, 0.5 wt%; temp., 40°C; time, 80 min

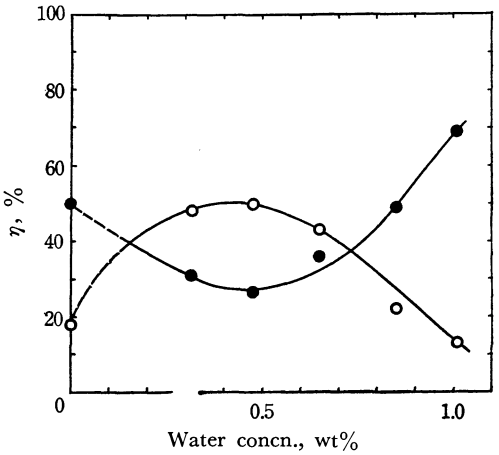

Fig. 2. The effect of water on efficiency of amalgam.
○ η_{ADN}, ● η_{PN}
Reaction conditions: β-chloropropionitrile, 0.3 mol; acrylonitrile, 0.2 mol; temp., 40°C; time, 80 min

A little amount of water (0—0.1 wt%) produces so much organomercuric compounds that the exact efficiencies are difficult to be obtained.

8) R. M. Silverstein and G. C. Bassler "Spectrometric Identification of Organic Compounds," 2nd, Johon Wiley & Sons. Inc., New York, (1963), p.p. 37, 38.

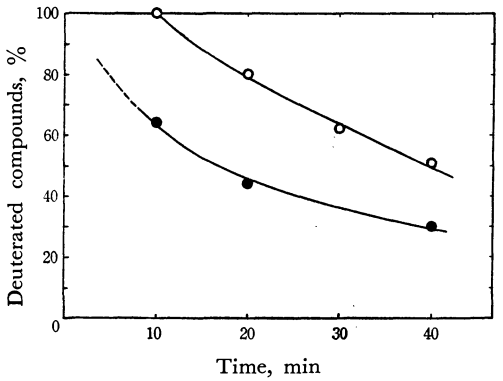

Fig. 3. Deuterations of adiponitrile and propionitrile.
○ deuterated adiponitrile
● deuterated propionitrile
Reaction conditions: β-chloropropionitrile, 0.3 mol; acrylonitrile, 0.2 mol; D_2O, 0.5 wt%; temp., 40°C

on the reaction solution, changed the η_{ADN} and η_{PN} values considerably (Fig. 2). To clarify the effect of water further, the deuterated water was added to the reaction solution in place of the water. The resulting adiponitrile and propionitrile were deuterated, whereas the reagents, such as β-chloropropionitrile and acrylonitrile, were not deuterated.

Figure 3 shows the correlation of the deuteration with the time. The deuteration of adiponitrile was 100% for the first ten minutes, after which it gradually decreased, while that of propionitrile decreased from the beginning of the reaction. The fact that deuterated compounds are obtained may mean that the water plays an important role as a proton donor and that some water is gradually formed during the reaction and then takes part in it, resulting in the decrease in the amount of deuterated products with the time. On the basis of the above findings, the reaction process producing adiponitrile may be expressed by the following equations. β-Chloropropionitrile reacts with a sodium amalgam to produce a cyanoethyl radical(I):

$$ClCH_2CH_2CN + NaHg \rightarrow \underset{\text{I}}{\dot{C}H_2CH_2CN} + NaCl + Hg \quad (1)$$

As a free radical is detected by a ESR spectrometer in a similar reaction, using methyl acrylate and methyl β-chloropropionate in place of acrylonitrile and β-chloropropionitrile[9] respectively, Eq. (1) is also adequate for this reaction. As estimated in the report that an acrylonitrile radical in a solution easily initiated the polymerization of acrylonitrile,[10] only a little of the cyanoethyl radical (I) may exist in the solution. Polyacrylonitrile was produced in this dimerization. However, relatively little of the polymer was formed, and the formation was suppressed by the addition of hydroquinone. However, hydroquinone did not disturb the desirable reaction, namely, the formation of adiponitrile. Therefore, as is generally understood, almost all the hydroquinone added may be surmised to dissolve in the reaction solution, little remaining on the surface of the amalgam. Thus the desirable reaction is disturbed little. In other words, the cyanoethyl radical (I) seems to attach to the surface of an amalgam and diffuses little into the solution, thus making it suitable for the dimerization. The compound I, then, reacts with another sodium atom to produce a cyanoethyl sodium compound (II).

$$I + NaHg \rightarrow \underset{\text{(II)}}{NaCH_2CH_2CN} + Hg \quad (2)$$

$$II + CH_2{=}CHCN \rightarrow \underset{\text{(III)}}{NCCH_2CH_2CH_2\underset{\displaystyle Na}{\underset{|}{C}}HCN} \quad (3)$$

Equation (3) is an example of the Schorigin reaction, which involves the addition of the organometallic compound to the unsaturated bonds, such as C=C, C=O, and C≡N.

The compound III may produce adiponitrile by a protonation reaction, as is generally accepted in the reaction of an organometal σ-complex with a proton, the added water acting as a proton donor.

$$III + H_2O(\text{or } D_2O) \rightarrow NC(CH_2)_4CN(\text{or } NC(CH_2)_3CHDCN) + NaOH(\text{or } NaOD) \quad (4)$$

$$NaOH + ClCH_2CH_2CN \rightarrow CH_2{=}CHCN + H_2O + NaCl \quad (5)$$

This theory is supported by the formation of deuterated adiponitrile ($NCCH_2CH_2CH_2CHDCN$). The deuterated position was determined by a mass spectrometer. The peak of the mass number 41 was considerably higher in the case of the deuterated adiponitrile than in that of adiponitrile, showing the existence of a CHDCN fragment. In addition, a little α-cyanoethyladiponitrile was formed during the dimerization reaction. These facts indicate that the α-carbon carried deuterium, that is, that contained sodium.

When a little water (usually 0.5 wt%) is present in the organic layer, the above steps proceed smoothly, because Eq. (5) holds and reproduces water as a proton donor, which then takes part in Eq. (4).

This is confirmed by independent experimental results and by the decrease in the deuteration with time (Fig. 2). Furthermore, two other mechanisms producing adiponitrile can be considered: (a) the

9) T. Osa, Doctorate thesis, Univ. of Tokyo, 112 (1967).
10) K. Ziegler, *Angew. Chem.*, **61**, 168 (1949).

Table 2. Codimerizations with some vinyl compounds and their hydrochlorinated compounds*

Raw material		Reaction products		
Hydrochlorinated compound	Polar vinyl compound	Wurtz dimer (%)	Schorign dimer (%)	Hydrodimer (%)
β-Chloropropionitrile	Ethylacrylate	Adiponitrile 0	Ethyl δ-cyanovalerate 39.8	Diethyll adipate 23.9
β-Chloropropionitrile	Methylacrylate	Adiponitrile 0	Methyl δ-cyanovalerate 29.1	Dimethyl adipate 30.4
Ethyl β-chloropropionate	Acrylonitrile	Diethyl adipate 1	Ethyl δ-cyanovalerate 11	Adipo-nitrile nitrile 5
Methyl β-chloropropionate	Acrylonitrile	Dimethyl adipate 3	Methyl δ-cyanovalerate 33.1	Adiponitrile 16.1

Reaction conditions:
hydrocholrinated compound, 0.3 mol; vinyl compound, 0.2 mol; temperature 40°C; water 0.5 wt%/reaction mixture

* The yield was calculated from the assumption that 100% of amalgam was consumed within 80 min of the reaction time, even if all the amalgam was not used at 80 min.

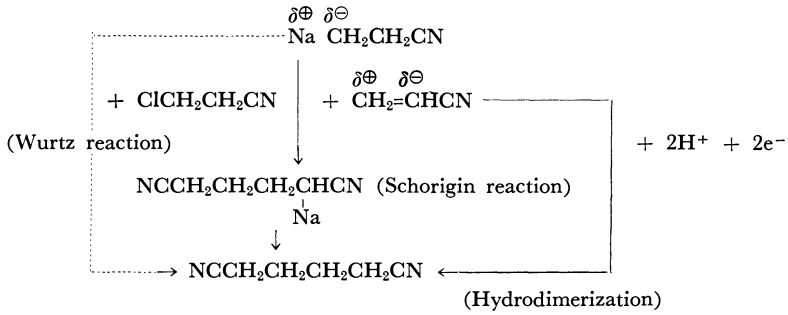

Fig. 4.

Wurtz reaction and (b) hydrodimerization. In the former reaction, the compound II reacts only with β-halogenopropionitrile, as is shown in Eq. (6):

$$II + ClCH_2CH_2CN \rightarrow NC(CH_2)_4CN + NaCl \quad (6)$$

In the latter one, on the other hand, acrylonitrile reacts with two protons and two electrons:

$$2CH_2{=}CHCN + 2H^+ + 2e^- \rightarrow NC(CH_2)_4CN \quad (7)$$

The ratio of these three types of dimerizations was determined using several hydrohalogenated compounds and polar vinyl compounds. The results of these experiments are shown in Table 2. The above-mentioned dimerization was found to occur obviously in three types of reactions: 1) the Schorigin reaction (Eq. (3)), 2) the Wurtz reaction (Eq. (6)), and 3) hydrodimerization (Eq. (7)). The yield of products by the Wurtz reaction was lowest. In general, the Schorigin reaction may be considered to occur more preferably than the hydrodimerization.

In these reaction conditions, the compound II seems to attack acrylonitrile nucleophilically, because the β-carbon of acrylonitrile has a larger $\delta\oplus$ charge than that of β-chloropropionitrile (Fig. 4).

Figure 2 showed that the formations of adiponitrile and propionitrile were competitive. Therefore, in order to obtain adiponitrile in a high yield, the water added must be suitably controlled. When water is added in an excessive amount, the propionitrile formation becomes the main process.

The increase in η_{ADN} with the addition of water in the range from 0 to 0.5 wt% suggests that the excess water participates in the reaction through Eq. (8):

$$II + H_2O \rightarrow CH_3CH_2CN + NaOH \quad (8)$$

The decrease in η_{PN} in the range between 0 to 0.5 wt% suggests that another reaction, such as Eq. (9), is predominant:

$$II + ClCH_2CH_2CN \rightarrow CH_3CH_2CN + CH_2{=}CHCN + NaCl \quad (9)$$

Accordingly, the total reaction is as follows:

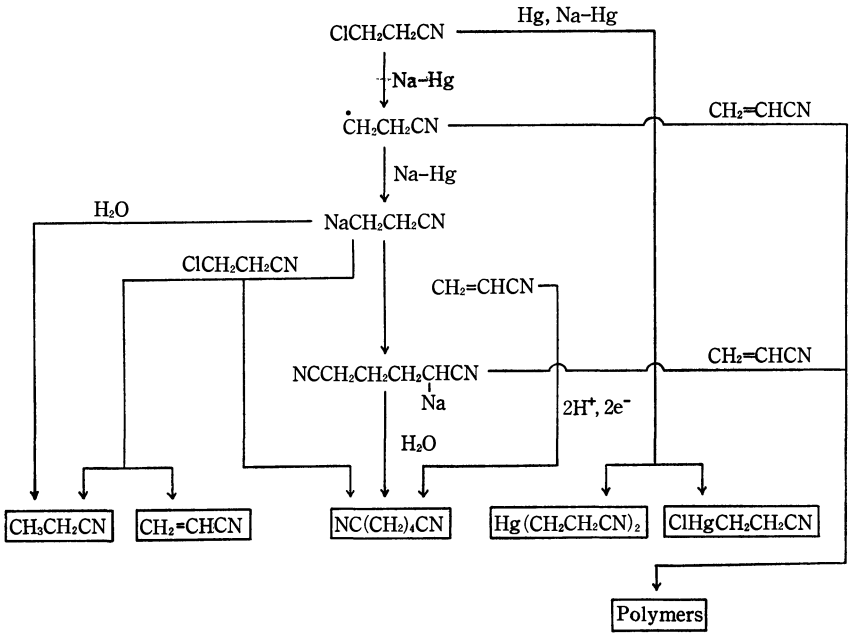

$$NaOH + ClCH_2CH_2CN \rightarrow H_2O + NaCl + CH_2{=}CHCN$$

Fig. 5. Reaction scheme.

$$2ClCH_2CH_2CN + 2NaHg \rightarrow NC(CH_2)_4CN + 2NaCl + 2Hg \quad (10)$$

and

$$2CH_2{=}CHCN + 2H^+ + 2e^- \rightarrow NC(CH_2)_4CN \quad (7)$$

Eq. (10) appears to be simply an example of the Wurtz reaction and does not show the role of acrylonitrile, because the acrylonitrile consumed by Eq. (3) is regenerated by Eqs. (5) and (9).

The polymers of acrylonitrile may be produced by the insertion reaction of III and the cyanoethyl radical diffused into the solution containing acrylonitrile:

$$III + nCH_2{=}CHCN \rightarrow \text{Polymers of acrylonitrile} \quad (11)$$

$$\dot{C}H_2CH_2CN + nCH_2{=}CHCN \rightarrow \text{Polymers of acrylonitrile} \quad (12)$$

The formation of organomercuric compounds may be explained by Eqs. (13) and (14):

$$ClCH_2CH_2CN + Hg \rightarrow ClHgCH_2CH_2CN \quad (13)$$

$$2ClCH_2CH_2CN + 2NaHg \rightarrow Hg(CH_2CH_2CN)_2 + 2NaCl + Hg \quad (14)$$

These reactions (11—14) waste the β-chloropropionitrile, sodium, and acrylonitrile.

From all these considerations, the following scheme (Fig. 5) may be proposed for this reaction. It is important that the formation of by-products shown in this scheme can be controlled by the preferable selection of additives. For example, when an adequate quantity of water is added, the formation of the organomercuric compounds can be completely suppressed, while the addition of hydroquinone can suppress the polymerization of acrylonitrile.

Consequently, adiponitrile was obtained in a yield of 50.1% (η_{ADN}) under these conditions; β-chloropropionitrile, 0.3 mol; acrylonitrile, 0.2 mol; water, 0.5 wt%; sodium amalgam, 0.5 wt% (0.1 g atom) of sodium; temperature, 40°C.

The authors wish to express their appreciation to Mr. Teruyuki Kodama for his discussions.

BULLETIN OF THE CHEMICAL SOCIETY OF JAPAN VOL. 41 2440—2442 (1968)

Catalytic Activity of Polymeric Vitamin B_{12} Model Compounds

Tadashi SASAKI and Fujinao MATSUNAGA

Institute of Applied Organic Chemistry, Faculty of Engineering, Nagoya University, Chikusa-ku, Nagoya

(Received December 11, 1967)

[$CoX(DH)_2$·P-4VP] (X: CN, Cl)-type polymeric complexes were prepared from dimethylglyoxime (DH_2) and poly-4-vinylpyridine (P-4VP) by a procedure similar to that reported for the preparation of [$CoX(DH)_2$·Pyr] (Pyr: pyridine) (T. Sasaki and F. Matsunaga, submitted to *Bull. Chem. Soc. Japan*). Moreover, their catalytic activities in the decomposition reaction of hydrogen peroxide were compared with those of the corresponding monomeric complexes [$CoX(DH)_2$·Pyr]; it was found that their activities decreases in the following order:

[$CoCl(DH)_2$·P-4VP] > [$CoCl(DH)_2$·Pyr] ≫ [$CoCN(DH)_2$·P-4VP] > [$CoCN(DH)_2$·Pyr]

About the relationship between structure and activity, it was concluded that the activity is much influenced by the nature of the X ligand of cobaloximes. It increases with a decrease in the interaction between the cobalt and nitrogen of a pyridine ring and with a weakening in the basicity of the coordinated bases. The structures of the polymeric complexes are discussed on the basis of their spectral data.

Much attention has been paid to the syntheses and catalytic behavior of polymeric chelates and studies have been made on the basis of their reactivity being similar to that of some enzymes with the object of obtaining enzymatic models from polymeric chelates. They were expected to show a "polymer effect" in their chemical character on the one hand, and to show some specific properties as polyelectrolytes on the other.[1] Akabori *et al.*[2] have found the catalytic activity of synthesized resins involving pyridoxal and salicylaldehyde in the racemization of amino acid, and Keyer[3] has reported on the catalytic activity of polymeric chelates in the decomposition reactions of hydrazine hydrate and hydrogen peroxide, though the corresponding monomeric chelates show no activity. Hatano *et al.*[4] have also described similar catalytic activity in polymeric chelates derived from some β-diketones and copper, while Roginski[5] has discussed the relationship between the electroconductivity and the catalytic activity of Cu-phthalocyanines in the oxidation of cumene, cyclohexene, and stilbene, including the decomposition reaction of hydrazine hydrate.

In a continuation of our previous examination,[6] we carried out the syntheses of polymeric vitamin B_{12} model compounds from dimethylglyoxime and poly-4-vinylpyridine according to the previous methods[6] and measured their catalytic activities in the decomposition reaction of hydrogen peroxide in comparison with the corresponding monomeric complexes, both in heterogeneous systems. The structures of the polymeric chelates will be discussed on the basis of their infrared and far-infrared spectra in the correlation with their catalytic activities.

Experimental

Materials. All the materials used in this experiment are commercially available except for poly-4-vinylpyridine, which was prepared by the procedure described by Katchalsky.[7] This polymer was soluble in hydrochloric acid and alcohol, but not in chloroform, dimethylformamide, *n*-pentane, or boiling benzene. η_{sp}=0.23 (EtOH, 0.33 g/100 m*l* at 20°C).

Preparation of Polymeric Chelates. The polymeric chelate, [$CoCN(DH)_2$·P-4VP], was prepared by the following scheme:

DH_2 (0.687 g, 0.0058 mol) and 0.35 g (0.0033 mol) of p-4VP were dissolved in 40 m*l* of hot 95% ethanol, and into this solution there was stirred a solution of 0.65 g (0.0028 mol) of $CoAc_2·4H_2O$ and 0.65 g (0.0025 mol) of KCN in 10 m*l* of water. The reaction mixture was then aerated vigorously for 4 hr while it was being heated at 70—80°C. Cobalt acetate was added last to avoid any cross-linkage of P-4VP with a cobalt atom. The precipitated brown powder was then collected and washed several times with large amounts of water,

1) M. Hatano, *J. Synth. Org. Chem. Japan*, **24**, 453 (1966), and the references citred therein.
2) K. Toi, Y. Izumi and S. Akabori, This Bulletin, **35**, 1422 (1962); *ibid.*, **36**, 734 (1963); K. Toi, *ibid.*, **36**, 739 (1963).
3) N. P. Keyer, *Kinetika i Kataliz*, **2**, 509 (1961); *ibid.*, **3**, 346, 680, 691 (1962).
4) M. Hatano, Y. Nose, T. Nozawa and S. Kambara, *Makromol. Chem.*, **98**, 136 (1966).
5) S. Z. Roginski, *Doklady Akad. Nauk*, **67**, 97 (1959); *Kinetika i Kataliz*, **4**, 431 (1963).
6) T. Sasaki and F. Matsunaga, submitted to this Bulletin.
7) A. Katchalski, K. Rosenheck and B. Altmann, *J. Poly. Sci.*, **23**, 9055 (1957).

Table 1. Microanalyses and degree of chelation

Composition	Found (Calcd) C%	H%	N%		Degree of coordination
$[CoCN(DH)_2 \cdot Pyr] \cdot \frac{1}{2}H_2O$	41.69 (41.56)	5.02 (5.00)	20.38 (20.84)		
$[CoCN(DH)_2 \cdot P\text{-}4VP]$	48.53 (47.74)	5.25 (5.63)	17.65 (17.65)		65%
$[CoCl(DH)_2 \cdot P\text{-}4VP]$	48.26 (48.01—49.25)	5.44 (5.21—5.18)	16.45 (15.82—15.89)	Cl: 7.82 (6.93—7.10)	84—86%
$[CoCl(DH)_2 \cdot Pyr]$	N: 17.19 (17.34)	Cl: 9.14 (8.78)			

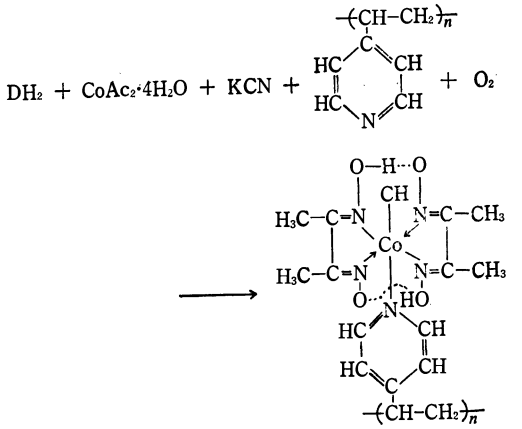

ethanol, and ether successively and dried under a vacuum. The yield was 0.9 g, mp >300°C. The microanalysis and the degree of coordination*1 are given in Table 1.

Similarly, a polymeric chelate, $[CoCl(DH)_2 \cdot P\text{-}4VP]$, was prepared by:

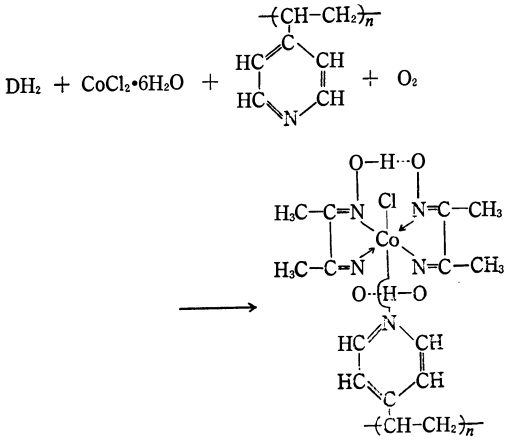

The yield was 1.4 g from 1.357 g (0.00116 mol) of DH_2. The microanalysis and the degree of coordination are given in Table 1.

Catalytic Activity of $[CoX(DH)_2 \cdot P\text{-}4VP]$ (X: CN, Cl). The decomposition rate of hydrogen peroxide in the presence of $[CoX(DH)_2 \cdot Pyr]$ and $[CoX(DH)_2 \cdot P\text{-}4VP]$ was measured at 40°C as follows: 10 m*l* of 30% aqueous hydrogen peroxide (8.8×10^{-3} mol), 10 m*l* of a phosphate buffer at pH 7.0 and a small amount of a non-ionic surface-active reagent, polyoxyethylene nonylphenol ether $\bar{P}=10$, were added to 60 m*l* of distilled water so as to bring the total volume to exactly 80 m*l*. After adding to this solution enough cobalt chelate to correspond to the 2.48×10^{-4} atom/*l* cobalt content, 5 m*l* aliquots were taken at regular time intervals, the decomposition was stopped by adding 10 m*l* of 9 N sulfuric acid, and the residual hydrogen peroxide was titrated with a 1/100 N $KMnO_4$ solution.

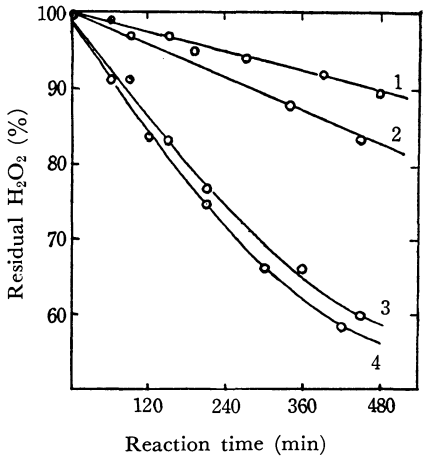

Fig. 1. Decomposition reaction of hydrogen peroxide.

Reaction temp: 40°C
Cobalt content in catalyst: 2.48×10^{-4} g atom/*l*
$[H_2O_2]_0 = 8.8 \times 10^{-3}$ mol/*l*
1 $[CoCN(DH)_2 \cdot Pyr]$
2 $[CoCN(DH)_2 \cdot P\text{-}4VP]$
3 $[CoCl(DH)_2 \cdot Pyr]$
4 $[CoCl(DH)_2 \cdot P\text{-}4VP]$

*1 The degree of coordination means the mole percentage of the chelate per monomer unit of P-4VP; it is readily calculated from the elemental analysis—that is, 100% means C, 45.71; H, 5.00; N, 20.00% calcd. for $(C_{16}H_{21}O_4N_6Co)_n$, and 0% means C, 79.96; H, 6.71; N, 13.32% calcd. for $(C_7H_7N)_n$. The observed values are located between these two values, for example, between 45.71 and 79.96 for C, and the deviations are expressed in the degree of coordination.

Table 2. Characteristic bands of monomeric and polymeric chelates (cm^{-1})

Compound	$\nu_{C=N}$	$\nu_{O-H\cdots O}$	$\nu_{C=N}$	ν_{NO}	δ_{NO}	ν_{Co-N}
[CoCN(DH)$_2$·Pyr]	2155	1745	1561	1239	1091	529, 518
[CoCN(DH)$_2$·P-4VP]	2155	1740	1563	1240	1095	529, 518
[CoCl(DH)$_2$·Pyr]		1740	1561	1239	1090	518
[CoCl(DH)$_2$·P-4VP]		1740	1562	1240	1095	518

The results are summarized in Fig. 1. When, in the above experiment, a mixture of P-4VP and DH_2 was used instead of [CoX(DH)$_2$·P-4VP], no activity was observed.

p*K* Values of the Coordinated Pyridine. The p*K*' values of pyridine and P-4VP were obtained from their titration curves. Because P-4VP was insoluble in water, P-4VP was previously dissolved in dilute hydrochloric acid of a known concentration, and this solution was titrated with 0.01 N NaOH. As NaOH was added to the solution, P-4VP was precipitated.

Infrared and Far-infrared Spectra. The infrared spectra of the chelates were measured in KBr pellets with a JASCO recording infrared spectrophotometer, Model IR-S, while the far-infrared spectra were measured with a Perkin-Elmer grating infrared spectrophotometer, Model 337.

Results and Discussion

Structural Elucidation of Polymeric Chelates. For this purpose, the infrared and far-infrared spectra of polymeric chelates were investigated and compared with the corresponding monomeric chelates. As is shown in Tables 2 and 3, the general patterns of the polymeric chelates were similar to those of the monomeric chelates except for the absorption due to the $\nu_{C=C,\ C=N}$ of a pyridine ring, which was observed to be shifted to a somewhat higher wave number by the coordination with a cobalt atom, presumably because of a lowering of the pyridine-ring conjugation.

The p*K*' values of pyridine and P-4 VP were given as 5.03 and 3.44 respectively at 20°C from their titration curves. Brown[8] has reported an increase in the basicity of pyridine derivatives upon the introduction of an alkyl group at the 4-position of the pyridine ring, but the fact that the basicity of P-4VP was less than that of pyridine can be explained by the prohibition of a proton attack on a pyridine ring caused by electrostatic repulsion by the positive-charged pyridinium ion structure in the polymer chain, an idea of which is supported by the above infrared spectral results.

Table 3. Change of frequency due to pyridine ring double bond (cm^{-1})

Compound	$\nu_{C=C,C=N}$	$\Delta\nu_{C=C,C=N}$*
[CoCN(DH)$_2$·Pyr]	1609	29
[CoCN(DH)$_2$·P-4VP]	1617	17
[CoCl(DH)$_2$·Pyr]	1609	29
[CoCl(DH)$_2$·P-4VP]	1616	16
Pyr	1580	
P-4VP	1600	

* Shifts by the coordination with a cobalt atom, for example: 1609−1580=29 and 1617−1600 =17

Relationship between Catalytic Activity and Structure. As may be clearly seen from Fig. 1, the fact that chlorocarboximatocobalt(III) showed a stronger activity than cyanocarboximatocobalt(III) in both monomeric and polymeric chelates indicates that the catalytic activity is much influenced by the X ligand and that there may be some relationship between the activity and the electronic state of the chelates. Since the characteristic absorption due to ν_{Co-N} in the far-infrared region is the same in monomeric and polymeric chelates, as Table 2 shows, their bond distances are thought to remain constant. The 29 cm^{-1} higher-frequency shift between [CoX(DH)$_2$·Pyr] and pyridine is bigger than the 16—17 cm^{-1} shift between [CoX(DH)$_2$·P-4VP] and P-4VP, indicating that the catalytic activity increased with a decrease in the interaction between a cobalt and a nitrogen atom of the pyridine ring. This result can be explained also on the basis of electronic theory: the electron-withdrawing cyano group enriches the positive charge on the cobalt atom, resulting in a stronger Co–N interaction and making the catalytic activity weaker than that of the corresponding chlorocomplexes; the reverse reasoning can be applied to an electron-donating chlorine group. About the relation between the p*K* values and the catalytic activities, it can be tentatively concluded that the weaker the coordinate base, the stronger the catalytic activity becomes, as is shown by a comparison of activity between polymeric and monomeric chelates, though further studies using several monomeric catalysts with known p*K* values are necessary to confirm this relation.

The authors wish to thank the Takeda Research Foundation for its financial support.

8) H. C. Borwn and X. R. Mihm, *J. Am. Chem. Soc.*, **78**, 1723 (1956).

BULLETIN OF THE CHEMICAL SOCIETY OF JAPAN VOL. 41 2443—2446 (1968)

Stereospecific Synthesis of 1,4-Dienes. III. The Cobalt Chloride - Phosphorus Compound - Triethylaluminum Catalyst System

Go HATA and Akihisa MIYAKE

Basic Research Laboratories, Toyo Rayon Co., Ltd., Kamakura

(Received December 31, 1967)

The admixture of cobalt chloride, $(RO)_nPCl_{3-n}$(n=0—3), and triethylaluminum catalyzes the codimerization of 1,3-dienes with ethylene to give exclusively *cis* isomers of 1,4-dienes, which result from the 1,4-addition of a C-H bond of ethylene to the 1,3-dienes. The addition of ethylene to methyl-substituted 1,3-dienes occurs predominantly on the substituted sides of the 1,3-dienes. The activity of the catalyst is strongly affected by the nature of the trivalent phosphorus components.

The admixture of first-row transition metal compounds of Group VIII of the periodic table and organoaluminum compounds catalyzes reactions between butadiene and ethylene. Wilke has reported the formation of *trans, cis*-1,5-cyclodecadiene by the reaction of butadiene with ethylene using the nickel acetylacetonate - ethoxydiethylaluminum catalyst system (zerovalent nickel).[1] On the other hand, the cobalt acetylacetonate - triethylaluminum system[2] and the iron acetylacetonate - triethylaluminum system[3] have afforded linear codimers, 1,3-hexadiene and 1,*cis*-4-hexadiene respectively. It has recently been found that admixtures of ditertiary phosphine complexes of cobalt or tertiary phosphine complexes of nickel and organoaluminum compounds also catalyze the formation of 1, 4-hexadiene.[4,5] We have investigated an effective catalyst system for this reaction. This paper will report the results of the 1,4-diene synthesis by means of a ternary catalyst system, cobalt chloride - $(RO)_nPCl_{3-n}$ triethylaluminum (n=0—3), and the effect of the nature of the phosphorus compounds upon the catalytic activity.

Results

The catalyst was prepared by mixing cobalt chloride, $(RO)_nPCl_{3-n}$ (n=0—3, R=ethyl, *n*-butyl, phenyl, chlorophenyl and tolyl) and triethylaluminum in the presence of butadiene. The addition of ethylene (40 kg/cm^2) to the resultant mixture at 60—80°C led to the formation of 1,*cis*-4-hexadiene. The preparation of the catalyst in the absence of butadiene showed a poor activity. When the molar ratio of a phosphorus component to cobalt chloride was higher than one, the catalyst showed an excellent activity and a high selectivity (95%). After the complete consumption of the butadiene, the isomerization of 1,*cis*-4-hexadiene to 2,4-hexadiene took place, as may be seen in Fig. 1. The stereospecific formation of 1,*cis*-4-hexadiene has also been observed in $Fe(acac)_3$ - Et_3Al catalyst system[3] and the $CoCl_2(Ph_2PCH_2CH_2PPh_2)_2$-$Et_3Al$ catalyst system.[4] However, the $NiCl_2(PR_3)_2$-R_2AlCl catalyst system[5] and the

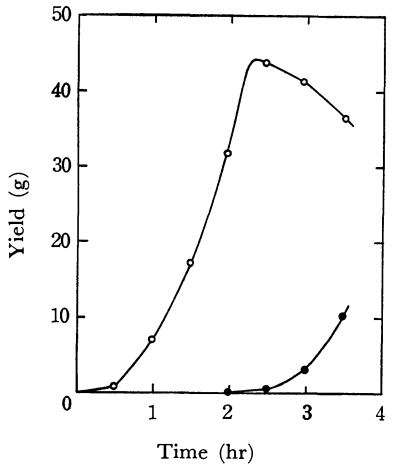

Fig. 1. Yield of 1,4- and 2,4-hexadiene *vs.* reaction time.
Reaction conditions: $CoCl_2$ 0.5 mmol, $(C_6H_5O)_3P$ 2.0 mmol, Et_3Al 12 mmol, butadiene 0.6 mol, ethylene 40 kg/cm^2, 80°C
○ 1,*cis*-4-hexadiene, ● 2,4-hexadiene

1) G. Wilke, *Angew. Chem.*, **75**, 10 (1963).
2) D. Wittenberg, *ibid.*, **75**, 1124 (1963).
3) a) G. Hata, *J. Am. Chem. Soc.*, **86**, 3903 (1964). b) G. Hata and D. Aoki, *J. Org. Chem.*, **32**, 3754 (1967).
4) M. Iwamoto and S. Yuguchi, *Kogyo Kagaku Zasshi (J. Chem. Soc. Japan, Ind. Chem. Sect.)*, **70**, 1505 (1967).
5) R. G. Miller, T. J. Kealy and A. L. Barney, *J. Am. Chem. Soc.*, **89**, 3756 (1967).

TABLE 1. REACTION OF BUTADIENE WITH ETHYLENE (80°C, ethylene 40 kg/cm²)

Run No.	Catalyst component				BD[a] ml	Time min	Product (g)		
	$CoCl_2$ mmol	Phosphorus compound	mmol	Et_3Al mmol			1,4-HD[b]	2,4-HD	Residue
1	0.5	$(C_6H_5O)_3P$	2	10	26	120	21.7	0.8	0.5
2	0.5	$(C_6H_5O)_3P$	0.5	10	26	120	15.6	1.7	3.2
3	0.5	$(o\text{-}CH_3C_6H_4O)_3P$	2	10	26	130	15.7	0.3	0.8
4	0.5	$(m\text{-}CH_3C_6H_4O)_3P$	2	10	26	130	22.6	0.2	0.6
5	0.5	$(p\text{-}ClC_6H_4O)_3P$	2	10	26	85	20.1	2.9	1.0
6	0.25	$(C_6H_5O)PCl_2$	0.5	3	52	25	41.9	3.5	0.4
7[c]	0.25	$(C_6H_5O)PCl_2$	0.5	3	52	100	42.3	0.7	0.2
8	0.5	$(C_2H_5O)_3P$	2	10	26	120	0.5	0	0.2
9	0.25	$(n\text{-}C_4H_9O)_3P$	0.5	6	52	300	0.6	0	0.2
10	0.25	$(n\text{-}C_4H_9O)PCl_2$	0.5	3	52	75	42.5	1.2	0.4

a) Liquefied butadiene (0°C) b) HD=hexadiene c) Reaction at 60°C

TABLE 2. REACTION OF ISOPRENE WITH ETHYLENE (80°C, ethylene 40 kg/cm²)

Run No.	Catalyst component				Isoprene mol	Time min	Product (g)		
	$CoCl_2$ mmol	$(RO)_nPCl_{3-n}$	mmol	Et_3Al mmol			Me-1,4-HD	Conjugated C_7-diene	Residue
11	1	$(C_6H_5O)_3P$	2	10	0.3	140	21.9	2.6	1.3
12	1	$(C_6H_5O)_3P$	1	10	0.3	140	15.5	0.3	2.8
13	0.5	$(C_6H_5O)PCl_2$	1	4	0.6	120	51.5	0.9	1.7
14	0.5	PCl_3	1	4	0.6	90	48.2	0.4	1.7

TABLE 3. EFFECT OF PHOSPHORUS COMPONENT UPON THE CATALYTIC ACTIVITY

$(C_6H_5O)_nPCl_{3-n}$	$Et_3Al/CoCl_2$ molar ratio	Time min	Product (g)		
			1,4-HD	2,4-HD	Residue
$(C_6H_5O)_3P$	20	50	4.6	trace	0.5
	10	50	1.3	0	0.2
$(C_6H_5O)_2PCl$	20	50	7.9	trace	0.5
	10	50	17.5	0	0.6
	6	50	0.1	0	0.1
$(C_6H_5O)PCl_2$	20	50	4.1	0.2	0.3
	10	50	41.7	1.2	0.5
	6	50	27.1	0.5	1.3
PCl_3	20	50	7.9	trace	0.3
	10	50	38.2	1.0	0.9
	6	30	39.8	0.6	0.7

Reaction conditions: $CoCl_2$ 0.5 mmol, $(C_6H_5O)_nPCl_{3-n}$ 1 mmol, toluene 5 ml, butadiene 0.6 mol, ethylene 40 kg/cm², 60°C

$RhCl_3$ catalyst[6] have been reported to afford a mixture of the geometrical isomers of 1,4-hexadiene.

The product corresponds to the 1,4-addition of a C-H bond of ethylene to butadiene. In unsymmetrical 1,3-dienes, there are two possible modes of the addition of ethylene. Isoprene reacted with ethylene to afford 4-methyl-1, *cis*-4-hexadiene and 5-methyl-1,4-hexadiene (in a ratio of 84 : 16) in about a 90% yield (Table 2). This reaction proceeded more slowly than that of butadiene with ethylene (Fig. 2). 1,3-Pentadiene reacted with ethylene to give 3-methyl-1,*cis*-4-hexadiene and 1,*cis*-4-heptadiene in a ratio of 91 : 9. The *trans* isomer of 1,3-pentadiene was found to be consumed faster than the *cis* isomer. These ratios of the products show that a vinyl moiety of ethylene attaches to the terminal carbon atom of the substituted double bond of a 1,3-diene system rather than to that of the non-substituted one.

6) a) T. Alderson, E. L. Jenner and R. V. Lindsey, Jr., *ibid.*, **87**, 5638 (1965). b) R. Cramer, *ibid.*, **89**, 1633 (1967).

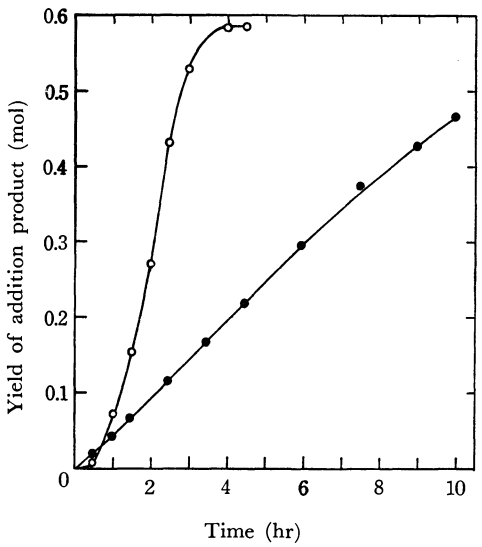

Fig. 2. Reaction of butadiene and isoprene with ethylene.
The same reaction conditions as shown in Fig. 1
○ butadiene, ● isoprene

The activity of the catalyst has been found to be strongly influenced by the nature of the trivalent phosphorus components. The results obtained by using different kinds of phosphorus components are listed in Tables 1, 3, and 4. Although the activity of the catalyst containing trialkyl phosphite was low, the catalyst containing triphenyl phosphite showed quite a high activity. The replacement of the butoxyl groups of tri-*n*-butyl phosphite or the phenoxyl groups of triphenyl phosphite by chlorine atoms increased the catalytic activity remarkably. The effect of the number of chlorine atoms in $(C_6H_5O)_nPCl_{3-n}$ upon the catalytic activity is summarized in Table 3. The results show that the phosphorus compound with more chlorine atoms directly bonded to the phosphorus atom is the more effective component of the catalyst. The effectiveness of the phosphorus components increases in the following order: $(C_6H_5O)_3P < (C_6H_5O)_2PCl < (C_6H_5O)PCl_2 < PCl_3$. In the catalyst system containing triphenyl phosphite, the higher molar ratio of triethylaluminum to cobalt chloride shows a higher activity. However, the catalyst systems of which phosphorus components have at least one P-Cl bond show a maximum activity at an appropriate molar ratio, as is shown in Table 3.

The results of the reaction using methyl or chlorine-substituted triphenyl phosphite as a catalyst component are summarized in Table 4. Tris(chlorophenyl)phosphites were more effective components than tritolyl phosphites. The effect of the *ortho*-substituents on the catalytic activity was quite large compared with that of the *para*-substituents. The *ortho*-substituted phenyl phosphites are arranged in the order of increasing effectiveness: $(o\text{-}CH_3C_6H_4O)_3P < (C_6H_5O)_3P < (o\text{-}ClC_6H_4O)_3P$.

TABLE 4. EFFECT OF A SUBSTITUENT OF TRIARYL PHOSPHITE UPON THE CATALYTIC ACTIVITY

Triaryl phosphite	Yield of 1,4-HD (g)
$(o\text{-}ClC_6H_4O)_3P$	25.9
$(p\text{-}ClC_6H_4O)_3P$	18.5
$(C_6H_5O)_3P$	17.5
$(p\text{-}CH_3C_6H_4O)_3P$	15.0
$(m\text{-}CH_3C_6H_4O)_3P$	12.3
$(o\text{-}CH_3C_6H_4O)_3P$	4.8

Reaction conditions: $CoCl_2$ 0.5 mmol, triaryl phosphite 2 mmol, Et_3Al 12 mmol, toluene 20 cc, butadiene 0.6 mol, ethylene 40 kg/cm², 80°C, 1.5 hr

Discussion

An organoaluminum compound has been found to reduce a cobalt compound to yield a cobalt hydride complex.[7] It is known that a cobalt hydride complex adds to 1,3-dienes to give substituted π-allylcobalt complexes.[8] Recently, a substituted π-allylcobalt complex has been recognized as an important intermediate in the linear dimerization of butadiene by the $CoCl_2$-$Al(C_2H_5)_3$ catalyst system.[9] These facts suggest that the most probable intermediates in this reaction are substituted π-allylcobalt complexes coordinated with the phosphorus compounds. The reaction is believed to proceed through the following steps: the addition of ethylene to the 1-methyl-π-allylcobalt complex, **1**, and the subsequent reaction of the 4-hexenylcobalt intermediate, **2**, with butadiene. A 1-methyl-π-allylcobalt complex may exist in two isomeric forms, *syn* and *anti*. Since the 1,4-hexadiene obtained consists only of the *cis* isomer, the 1-methyl-π-allyl group must be bonded to the cobalt atom in the *anti* form, **1**.

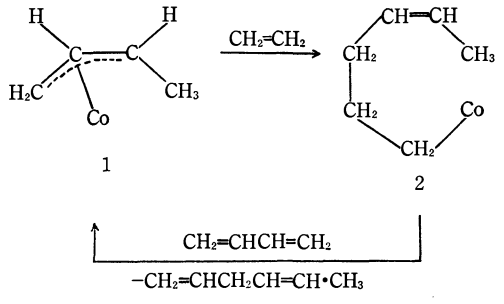

7) G. Hata, H. Kondo and A. Miyake, *ibid.*, in press.
8) a) D. W. Moore, H. B. Jonassen, T. B. Joyner and A. J. Bertrand, *Chem. Ind. (London)*, **1960**, 1304. b) J. A. Bertrand, H. B. Jonassen and D. W. Moore, *Inorg. Chem.*, **2**, 601 (1963).
9) G. Natta, V. Giannini, P. Pino and A. Cassata, *Chim. Ind. (Milan)*, **47**, 524 (1965).

The investigation of the effect of the phosphorus component upon the catalytic activity indicates that a less basic phosphorus component accelerates the reaction. Triphenyl phosphite has been reported to be less basic than triethyl phosphite,[10] as is to be expected from the electron-attracting property of a phenyl group. The former compound is a more effective catalyst component than the latter. The electron-attracting ability of a chlorine atom is expected to be greater than those of alkoxyl and phenoxyl groups. Therefore, the basicities of the phosphorus compounds would decrease in the following order: $(n\text{-}C_4H_9O)_3P > n\text{-}C_4H_9OPCl_2$; $(C_6H_5O)_3P > (C_6H_5O)_2PCl > (C_6H_5O)\text{-}PCl_2 > PCl_3$. This order accords with the increasing order of the activities of the phosphorus components.

The introduction of a substituent on each phenyl group of triphenyl phosphite affected the catalytic activity. An electron-attracting substituent accelerated the reaction, while an electron-donating substituent retarded the reaction, as expected. The increasing order of the inductive effect of the substituents is: *para* < *meta* < *ortho*. A remarkable effect of the *ortho* substituents was observed.

The catalyst systems the phosphorus components of which has P-Cl bonds were deactivated by excess triethylaluminum (Table 3). It has been reported that a P-Cl bond has been alkylated by trialkylaluminum.[11,12] This deactivation of the catalyst would be due to the alkylation of the P-Cl bond of the phosphorus components by triethylaluminum. The alkylation is accompanied by an increase in the basicity of the phosphorus components, which results in a decrease in the catalytic activity.

Trivalent phosphorus compounds can participate in both σ- and π-bonding in transition metal complexes. A decrease in the electron density on the phosphorus atom is believed to increase the π-bonding ability of the phosphorus ligand. The above results indicate that the π-bonding character of the Co–P bond of the catalyst species greatly affects the activity of the catalyst.

Experimental

Butadiene was purified by vaporization from a mixture of the liquefied diene and triethylaluminum. Isoprene and 1,3-pentadiene were distilled over calcium hydride. The solvents were refluxed over a K-Na alloy prior to distillation.

Triethyl phosphite, tri-*n*-butyl phosphite, triphenyl phosphite, and phosphorus trichloride were purified by distillation. Tris(*o*-chlorophenyl) phosphite, tris(*p*-chlorophenyl) phosphite, tri-*o*-tolyl phosphite, tri-*m*-tolyl phosphite, and tri-*p*-tolyl phosphite were each prepared by the addition of phosphorus trichloride to a *n*-hexane solution of the corresponding phenol and pyridine. *n*-Butyl phosphorodichloridite[13] and diphenyl phosphorochloridite[14] were prepared by the previously-reported methods. Phenyl phosphorodichloridite was synthesized by the following method. In a 1 *l* flask, 411 g (3 mol) of phosphorus trichloride were gently refluxed, and then 188 g (2 mol) of phenol were added. A vigorous evolution of hydrogen chloride occurred. After the addition, the unreacted phosphorus trichloride was removed under reduced pressure. Phenyl phosphorodichloridite distilled at 71°C/3 mmHg; 195 g (50% yield based on phenol). All of the above phosphorus compounds were distilled under a vacuum. Anhydrous cobalt chloride was prepared by the reaction of cobalt acetate with acetyl chloride.[15]

Addition of Ethylene to Butadiene. A 100 m*l* autoclave was charged with 20 m*l* of toluene, 5.0 m*l* of *n*-heptane (as an internal standard for gas chromatographic analysis), 0.065 g (0.5 mmol) of cobalt chloride, and 0.620 g (2 mmol) of triphenyl phosphite. After the gas within the autoclave has been replaced by ethylene, 52 m*l* (0.6 mol) of liquefied butadiene and a toluene solution of triethylaluminum (12 mmol) were added. The resultant mixture was stirred under ethylene pressure (40 kg/cm^2) at 80°C. The results are shown in Fig. 1.

Addition of Ethylene to Isoprene. A 100 m*l* autoclave was charged with 20 m*l* of xylene, 0.130 g (1 mmol) of cobalt chloride, 1.240 g (4 mmol) of triphenyl phosphite, 21.0 g (0.3 mol) of isoprene, and a xylene solution of triethylaluminum (20 mmol). The resultant mixture was stirred under ethylene pressure (40 kg/cm^2) at 80°C for 2 hr. The reaction product was decomposed with methanol and dilute hydrochloric acid. The oily layer was analyzed by gas chromatography using a squalane column. It contained 25.3 g (88% yield) of a mixture of 4-methyl-1,*cis*-4-hexadiene and 5-methyl-1,4-hexadiene and 2.6 g of C_7-conjugated dienes. The ratio of 4-methyl-1,4-hexadiene to 5-methyl-1,4-hexadiene was determined to be 84 : 16 by gas chromatography using a silver nitrate-benzyl cyanide column.

Addition of Ethylene to 1,3-Pentadiene. A 100-m*l* autoclave was charged with 10 m*l* of toluene, 0.065 g (0.5 mmol) of cobalt chloride, 0.620 g (2 mmol) of triphenyl phosphite, 20.4 g of 1,3-pentadiene (*trans*-*cis* ratio 66 : 34, purity 89%), and a toluene solution of triethylaluminum (12 mmol). The resultant mixture was stirred under ethylene pressure (40 kg/cm^2) at 80°C for 2 hr, yielding 13.8 g of 3-methyl-1,*cis*-4-hexadiene and 1.4 g of 1,*cis*-4-heptadiene in a 91% yield based on the 1,3-pentadiene consumed. The recovered 1,3-pentadiene consisted of 38% *trans* isomer and 62% *cis* isomer.

The addition products were identified by a comparison of their infrared spectra and gas chromatographic retention times with those of authentic samples.[3]

10) L. S. Meriwether and M. L. Fiene, *J. Am. Chem. Soc.*, **81**, 4200 (1959).
11) L. I. Sacharkin and O. J. Ochlobrystin, *Doklady Akad. Nauk SSSR.*, **116**, 236 (1957).
12) L. Maier, *Helv. Chim. Acta*, **47**, 27 (1964).
13) W. Gerrard, *J. Chem. Soc.*, **1940**, 1464.
14) J. P. Forsman and D. Lipkin, *J. Am. Chem. Soc.*, **75**, 3145 (1953).
15) G. W. Watt, P. S. Gentile and E. P. Helvenston, *ibid.*, **77**, 2752 (1955).

BULLETIN OF THE CHEMICAL SOCIETY OF JAPAN VOL. 41 2447—2453 (1968)

The Hydrogenation of Pyran Derivatives. IV. The Skeletal Rearrangement in the Gas-phase Dehydration of Tetrahydropyran-2-methanol

Akira MISONO, Tetsuo OSA and Yoshitomo SANAMI

Department of Industrial Chemistry, Faculty of Engineering, The University of Tokyo, Hongo, Tokyo

(Received January 24, 1968)

The gas-phase dehydration of tetrahydropyran-2-methanol (TPM), prepared by the hydrogenation of the acrolein thermal dimer (3,4-dihyro-2H-pyran-2-carboxaldehyde (AD)), was investigated over various catalysts under atmospheric pressure. In this reaction, some of the pyran ring was found to be rearranged rapidly to a seven- or five-membered ring. For example, the highly-purified and crystalline η-alumina without any carrier produced cyclopentanecarboxaldehyde (CPA) as the main product in the yield of 71% at 330°C. Over the commercial alumina catalyst, considerable amounts of 2,3,4,5-tetrahydrooxepine (THO) and oxepane (OXP) were produced as by-products, though CPA was the main product; in some cases, as much THO and OXP were produced as CPA. On the other hand, the use of a dehydrogenation catalyst resulted in THO as the main product and CPA as a by-product; in the case of the use of copper-chromium oxide supported on Kieselguhr, with hydrogen as a carrier gas at 430°C, the yields of THO and CPA were 44.8% and 4.7% respectively. In these skeletal rearrangements, the seven-membered carbonium ion compound produced by the Wagner-Meerwein-type rearrangement must be a reaction intermediate. From this intermediate, mainly CPA was produced over alumina, influencing the lone-electron pair of the ethereal oxygen. THO, on the contrary, was produced mainly over a dehydrogenation catalyst. Moreover, twice as high a yield of 1,6-hexanediol was obtained from the hydrogenation of the hydrated THO than from the hydrogenolysis of TPM or AD, as has been noted in a previous paper.

It is well known that dihydropyran is produced by the skeletal rearrangement during the dehydration of tetrahydrofurfuryl alcohol over an alumina catalyst. The reaction mechanism has been accurately established by many reports,[1,2] during the skeletal rearrangement, the carbonium ion, which is produced by the dehydroxylation of the side-chain alcohol at an acidic point on the surface of the alumina catalyst, may be rearranged to enlarge its ring *via* a step analogous to the Wagner-Meerwein rearrangement, followed by deprotonation. Accordingly, if such a reaction can be applied to the side-chain alcohol of a six-membered ring compound, the dehydration of tetrahydropyran-2-methanol (TPM) is likely to produce oxepine derivatives.

In only one patent[3] dealing with the dehydration of TPM, however, CPA has been reported as the main product; in this one case it was derived as an intermediate from the skeletal rearrangement of 2,3,4,5-tetrahydrooxepine (THO). If CPA was produced by the isomerization of THO, THO would be very unstable under the reaction conditions. However, it has been reported that the THO produced by the ring-closing dehydration of 1,6-hexanediol (1,6-D) is not changed at 250°C.[4] Therefore, the mechanism proposed by the patent is very doubtful.

In this paper, the skeletal rearrangement during the dehydration of TPM over various catalysts is accurately discussed on the basis of results concerning obtaining the unsaturated ring ether compound, THO, which is converted into 1,6-D in a good yield by hydration and by consecutive hydrogenation.

Experimental

Materials. *Acrolein Thermal Dimer (AD), 3,4-Dihydro-2H-pyran-2-methanol (DPM), and Tetrahydropyran-2-methanol (TPM).* These substances were shynthesized according to the methods described in previous papers,[5,6] except that the Diels-Alder reaction of acrolein was carried out under a 1—20 kg/cm² pressure of hydrogen instead of nitrogen, because then the yield of AD was increased a little compared with that under nitrogen.

1) C. L. Wilson, *J. Am. Chem. Soc.*, **69** 3004 (1947).
2) R. L. Sawyer and D. W. Andrews, "Organic Syntheses," Coll. Vol. III, p. 276 (1954).
3) R. R. Whetstone, (to Shell Development Co.) US 2480990 (1949).
4) D. R. Larkin, *J. Org. Chem.*, **30** 335 (1965).
5) A. Misono, T. Osa and Y. Sanami, *Kogyo Kagaku Zasshi (J. Chem. Soc. Japan, Ind. Chem. Sect.)*, **70**, 1131 (1967).
6) A. Misono, T. Osa and Y. Sanami, *ibid.*, **71** 137 (1968).

Cyclohexylcarbinol (CHC). This was also prepared according to the method described in a previous paper.[7] All the other chemicals used in the present experiment were commercial compounds of the first grade.

Catalysts. The γ-alumina catalyst without any carrier was prepared as follows. Fifty milliliters of an aqueous ammoniac solution was added to a saturated solution of 50 g of aluminum nitrate in water; the gel of aluminum hydroxide thus precipitated was rinsed with water five times and filtrated. The filtrated gel was dried in air for 10 hr at about 80°C and then sintered in air for 12 hr at about 600°C. The fine, white, sintered powder was tableted under a pressure of 150 kg/cm^2 and then crushed into particles 8—12 in mesh size. Commercial alumina catalysts, Neobead C (NC) (Al_2O_3: 100), Neobead D (ND) (Al_2O_3: 90, SiO_2: 10) and Neobead P (NP) (Al_2O_3: 88, SiO_2: 9, Na_2O: 3), were kindly supplied by the Mizusawa Chemical Co. Moreover, N631 (Al_2O_3: 15, SiO_2: 85), copper - chromium oxide (N208), copper - zinc oxide (N211), and nickel (N111), all except N631 supported on Kieselguhr were supplied by the Nikki Chemical Co.

Catalyst Activation. A catalyst was placed into the atmosphere of the feed and carrier gas for 3 hr at about 300°C, and then only a carrier gas, mostly hydrogen, was let flow through continuously until no water was formed. This pretreatment was carried out in all runs. The reaction over N111 was carried out as follows. The catalyst was renewed before each reaction, activated for 3 hr at about 450°C under the hydrogen carrier gas and at a constant flow rate of 10 ml/sec, and then placed in the atmosphere of the feed and nitrogen for 30 min.

The catalyst with tetrahydrofurfuryl alcohol (TFA) pretreated was prepared as follows; over an alumina catalyst TFA was passed by means of a nitrogen carrier for 20 min at about 300°C, and then nitrogen gas was allowed to flow through for 3 hr. The alumina catalyst obtained in this way was brown and was submitted to the reaction like other untreated aluminas.

Equipment and Methods. The dehydration reaction was carried out in the apparatus shown in Fig. 1.

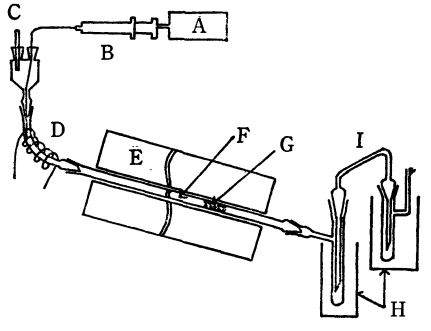

Fig. 1. Apparatus.

A	Extruder	F	Reaction tube
B	Injector	G	Catalyst
C	Gas inlet	H	Vessel with cooling material
D	Vaporizer		
E	Electric furnace	I	Trap

7) A. Misono, T. Osa and Y. Sanami, *ibid.*, **71** 680 (1968).

The reactor was equipped with a thermostat and was wrapped around with Nichrome heating wire. The reactor tube was packed with 15 ml of catalyst pellets, while the temperature was maintained at from 150°C to 500°C within ±3°C. The contact time was controlled by changing the rate of the material fed in. The majority of the product was condensed in a first trap cooled with methanol and dry ice at about −50°C, while the more volatile products were caught in a second trap cooled with methanol and dry ice below −60°C or, in some runs, with liquid nitrogen. The carrier gas was passed through the vaporizer to the reactor at a rate of from 5 to 35 ml/sec. As a carrier gas, hydrogen was generally used, because the selectivity of THO, as shown in Table 1, was slightly higher under the hydrogen carrier gas than under the nitrogen one. All the products except 1,6-hexanediol (1,6-D) were gas chromatographically analyzed using a 2 m×6 mm o.d. column containing silicon oil DC 550 on Diasolid M at 160°C. For the determination of 1,6-D and other compounds having higher boiling points, a column of 2 m×6 mm o.d. containing 10% polyphenyl ether and 2% Carbowax 20 M on Fruolopack 80 (60—80 mesh) was used at 170°C. 1,6-D recrystallyzed from a commercial product with carbon tetrachloride was used.

Identification of the Reaction Products. Pure samples of the reaction products were gas chromatographically isolated, or fractionally distilled, and identified by means of an IR spectrometer (Hitachi EPS-2) and an NMR spectrometer (Japan Electric Co. C-60). Both the preparative and analytical gas chromatographic work were carried out with a Kotaki-Superfractioner.

2,3,4,5-Tetrahydrooxepine (THO) ($C_6H_{10}O$): bp 112—114°C/760 mmHg, n_D^{25} 1.4509. IR (cm^{-1}); 2920, 2860, 1656(sh), 1650, 1302(sh), 1295, 1280(sh), 1125, 1080, and 740 (Fig. 2). NMR (ppm); multiplets at 8.3 (4 protons) and 7.95 (2 protons), a triplet at 6.15 (2 protons), a quadruplet at 5.35 (1 proton), and a doublet at 3.8 (1 proton).

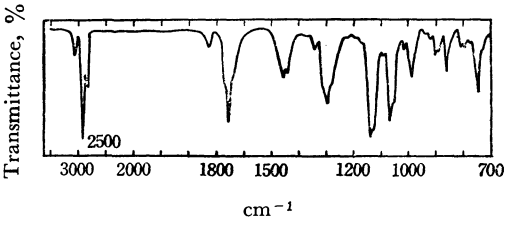

Fig. 2. IR spectrum of THO at NaCl plate.

Oxepane (OXP) ($C_6H_{12}O$): bp 124—126°C/760 mmHg, n_D^{25} 1.4349, IR (cm^{-1}); 2920, 2860, 1135, 1105, 995, and 970. NMR (ppm); a sharp peak at 8.35 (8 protons), and a peak like a triplet at 6.4 (4 protons).

2-Methyltetrahydropyran (MTHP) ($C_6H_{12}O$): bp 102—103°C/760 mmHg and n_D^{20} 1.4432 for MTHP of 96% purity. IR (cm^{-1}); 2960, 2920, 2860, 1380, 1215, 1095, 1085(sh), 1055, and 865.

6-Methyl-3,4-dihydro-2H-pyran (MDHP) ($C_6H_{10}O$): IR (cm^{-1}); 2960, 2850, 1730(sh), 1683, 1650(sh), 1450, 1390, 1300, 1240, 1170, 1095, 1070, 895, 820, and 765.

Cyclopentanecarboxaldehyde (CPA) ($C_6H_{10}O$): bp 87°C/78 mmHg and n_D^{25} 1.4379 for CPA of 98% purity. IR

TABLE 1. EFFECT OF KINDS OF CARRIER GASES UPON SELECTIVITY*1

Gas	Temp. °C	Conversion, %	Selectivity, %						
			MCPE	CHE	MDHP	THO	OXP	CPA	CPEA
H_2*2	310	54.7	6.3	5.7	1.2	18.7	13.1	37.3	5.7
	330	62.1	7.1	5.5	2.1	17.3	11.3	41.2	7.4
	350	76.1	7.2	5.9	1.2	12.7	12.9	51.0	7.7
N_2*2	310	55.3	7.0	5.7	1.3	16.7	11.7	42.3	7.3
	330	63.2	7.2	5.3	1.4	16.9	10.1	43.7	7.9
	350	79.5	7.9	6.0	1.6	10.1	10.0	52.0	5.3
H_2*3	310	52.9	6.9	4.3	1.3	41.7	1.2	29.0	6.8
	330	68.7	7.6	7.1	1.6	39.4	1.3	28.9	6.7
	350	74.3	7.2	6.9	1.5	43.5	1.4	26.9	5.4
N_2*3	310	50.1	6.2	5.0	1.3	39.9	1.4	31.5	7.3
	330	67.3	7.1	5.1	1.2	40.1	1.3	30.8	6.9
	350	78.1	7.0	5.9	1.5	38.5	1.4	32.1	6.3

*1 Feed rate of TPM and flow rate of carrier gas were constant at 10 ml/hr and 10 ml/sec, respectively. Length of catalyst bed was 7 cm.
*2 Reactions over ND catalyst.
*3 Reactions over NDF catalyst.

(cm^{-1}); 2930, 2850, 2820, 2720, 1725, and 1455. The 2,4-dinitrophenylhydrazone derivative was obtained as a yellow product, mp 158—162°C.

1-Cyclopentenecarboxaldehyde (CPEA) (C_6H_8O): IR (cm^{-1}); 2930, 2850, 2820(sh), 2720, 1720(sh), 1680, 1620, 1160, and 960 The 2,4-dinitrophenylhydrazone derivative was found to have a mp of 211—215°C

Cyclohexylidenemethane (CHYM) (C_7H_{12}): IR (cm^{-1}); 2920, 2850, 1655, 1450, and 890. NMR (ppm); a quintet peak at 8.45 (6 protons), a broad peak at 7.9 (4 protons), and a very sharp peak at 5.5 (2 protons).

1-Methylcyclohexene (MCHE) (C_7H_{12}): IR (cm^{-1}); 2920, 2860, 1455(sh), 1450, 1380, 1140, 915, 890, and 800.

Results and Discussion

In the gas-phase dehydration of tetrahydropyran-2-methanol (TPM), seven-membered compounds were detected using a catalyst other than the η-alumina catalyst, though a five-membered cyclopentanecarboxaldehyde (CPA) was mainly produced in the patent described above. Furthermore, there were many cases where an unsaturated ring ether compound, THO, was obtained in good yields. As the catalyst in this patent, there were employed one or more of the materials customarily referred to as dehydration catalysts, such oxides of the divalent or the polyvalent metals as alpha alumina, thorium oxide and titanium oxide. Catalysts with two functions, dehydration and hydrogenation, were also employed.

The results of the present investigation are illustrated in Table 2. Over the three commercial alumina catalysts, NC, ND and NP, the total amounts of the selectivities of THO and OXP were increased with a decrease in the acidity of a catalyst by analogy with its composition,[8] but that of CPA was decreased. The commercial alumina catalyst used is considered to participate with the reaction as in the dehydration of tetrahydrofurfuryl alcohol (TFA), and to produce seven-membered compounds. However, in the skeletal rearrangement during the dehydration of TPM, it might be a dominant characteristic that the selectivity of THO was higher over a catalyst used after the dehydration of TFA than over the same catalyst used directly.

The effect of pretreatment with an alumina catalyst with TFA upon the dehydration of alcohols has been little reported on; for example, the alumina catalyst pretreated with TFA decreased the rate of the dehydration of ethanol.[9] However, this effect, decreasing the selectivity of CPA and increasing that of THO, may result not only in a decrease in the dehydrating activity due to the occupation of the active points by TFA, but also in an essential change in a crystallinity of the catalyst. To elucidate these results, there is a need for further investigation of the effect of TFA on a catalyst. Therefore, the authors will report on this problem in a subsequent paper.

Over N631 as a silica-alumina catalyst, the selectivities of CPA, THO, and OXP decreased in all runs, but those of MCPE and CHE increased. MCPE and CHE are estimated to be derived from the decomposition of THO under the reaction conditions, because THO produced them selectively over N631 (Table 3).

8) H. Pines and J. Manassen, *Advance in Catalysis*, **16**, 53 (1966).
9) C. H. Kline and J. Turkevich, *J. Am. Chem. Soc.*, **67**, 498 (1945).

Table 2. Effect of reaction conditions upon selectivity*1

Catalyst*2	Temp. °C	Conversion, %	Selectivity, %						
			MCPE	CHE	MDHP	THO	OXP	CPA	CPEA
η	280	69.3	1.1	1.1	*t**3	*t*	*t*	72.5	12.0
	300	73.9	2.3	2.0	1.0	*t*	*t*	72.5	5.3
	330	89.3	3.7	2.1	*t*	*t*	*t*	79.5	3.5
NC	310	42.1	3.2	1.8	2.1	12.5	13.2	49.5	7.6
	330	57.5	3.5	2.8	1.5	11.2	13.2	42.9	8.2
	350	78.2	3.5	3.0	1.3	7.5	12.1	50.2	8.2
ND	310	50.1	5.6	5.2	2.2	15.3	14.2	36.3	6.9
	330	53.6	5.6	5.1	1.7	10.3	11.1	40.2	7.9
	350	68.5	6.3	5.7	1.5	7.5	9.2	48.1	9.5
NDF	310	38.3	5.7	3.6	2.1	42.2	1.0	28.1	7.9
	330	63.2	7.8	6.2	2.0	37.3	1.3	26.3	6.7
	350	70.2	7.8	7.0	1.5	39.3	1.1	27.3	5.8
NP	310	41.2	3.2	2.1	9.7	16.5	12.7	30.1	17.5
	330	53.6	4.9	3.7	6.7	25.1	6.5	34.5	7.9
	350	71.2	5.8	4.3	3.2	23.7	7.2	37.2	8.2
NPF	310	32.1	2.5	1.2	2.4	48.1	4.8	27.1	14.2
	330	52.1	5.1	2.5	2.3	46.5	1.2	22.1	10.7
	350	79.5	5.2	3.1	1.0	42.5	*t*	36.0	6.2
N631	310	42.3	19.2	21.3	5.3	20.4	1.0	10.8	5.6
	330	54.3	11.3	14.3	9.7	24.1	*t*	17.1	6.1
	350	63.2	18.1	20.2	6.7	22.1	*t*	15.1	3.2
N208	390	53.9	6.3	4.2	10.5	39.1	*t*	5.2	14.3
	410	61.4	5.2	3.6	10.8	49.2	*t*	6.7	10.2
	430	82.1	2.3	6.3	8.3	52.4	*t*	5.4	7.7
N211	410	50.3	5.4	2.6	13.1	34.5	*t*	10.7	10.2
	430	61.3	7.3	5.3	12.1	39.3	*t*	11.6	8.9
	450	75.2	12.3	7.6	8.3	40.7	*t*	9.6	5.2
N111	410	47.2	4.3	23.2	7.4	32.5	*t*	1.0	3.9
	430	69.5	7.0	10.3	13.2	49.3	*t*	1.2	5.4
	450	97.4	5.2	11.0	12.3	50.2	*t*	1.0	2.5

*1 Feed rate of TPM and flow rate of carrier gas were constant at 10 ml/hr and 10 ml/sec, respectively. Carrier gas was H_2 except in runs of N111 with N_2.

*2 NDF and NPF were the catalysts pretreated with tetrahydrofurfuryl alcohol. Length of catalyst bed was 5 cm. In N111 runs, it was difficult to maintain the activity of the catalyst at constant, and therefore these data were the averages of the three kinds of reactions.

*3 *t*=trace.

It has been reported[10] that a dehydrogenation catalyst, for example, copper-chromium oxide, is applicable to the dehydration of some alcohols. Though such a catalyst, as was effected, decreased the conversion to some extent, it was used in the dehydration of TPM in order to study the reaction mechanism in more detail, for the activity of a dehydrogenation catalyst for isomerization during the dehydration of alcohols is markedly less than that of such a dehydration catalyst as an alumina. The results obtained are shown in Table 2. In all runs, only a trace of OXP was formed the main product being THO. Moreover, the amounts of MDHP increased with an increase in the reaction temperature, and also that of CPA decreased considerably, especially in N111 runs.

The behavior of THO and OXP under the present reaction conditions was also investigated. The results are shown in Table 3. As is shown in Table 3, in the use of the η-alumina catalyst, CPA

10) J. Alagy, F. Defoor, S. Franckowiak, *Chem. Abstr.*, **62** 11701 (1964).

TABLE3. BEHAVIOR OF THO AND OXP UNDER REACTION CONDITIONS*

Feed	Catalyst	Temp. °C	Conversion, %	Selectivity, % MCPE	CHE	CPA
THO	η	250	25	3	2	92
		290	46	3	7	87
		310	57	7	8	81
		330	72	12	11	72
	ND	290	16	42	53	*t*
		310	17	40	54	*t*
		350	18	41	53	*t*
	N631	290	23	41	51	3
		310	28	40	50	7
		350	35	45	46	2
	N208	450	13	44	43	2
	N111	450	7	41	42	2
					MTHP	
OXP	η	290	29		96	
		310	38		95	
		330	49		97	
		350	64		98	
	ND	350	7		*t*	
	N631	350	7		*t*	
	N208	460	7		*t*	
	N111	460	5		*t*	

* Carrier gas was H_2 except in N111 runs with N_2. Feed rate and flow rate of carrier gas were constant at 10 ml/hr and 10 ml/sec, respectively. Length of catalyst bed was 5 cm. *t* = trace.

and MTHP were mainly obtained from the corresponding seven-membered compounds. However, over the other catalysts some skeletal rearrangement from seven to six or five occurred, though with difficulty.

In order to clarify the action of the catalyst in the dehydration of TPM, cyclohexyl carbinol (CHC), which is similar to TPM, was dehydrated over various catalysts. These results are shown in Table 4. It was seen that the dehydration occurred much faster over the η-alumina catalyst than over ND and N208 catalysts; that over the alumina catalyst the selectivity of CHYM was almost equal to that of MCHE; that the differences in between the selectivities of CHYM and MCHE lessened with an increase in the reaction temperature, and that, nevertheless, the differences were roughly constant until the reaction temperature over ND and N-208 catalysts. Higher reaction temperatures were, moreover, required in runs with ND and N208 catalysts than in runs with the η-alumina catalyst.

The results obtained can be explained satisfactorily by the following general estimation.[8,11] The relative rate of carbonium-ion rearrangement in the dehydration mechanisms of several alcohols over alumina catalysts can be estimated from the relative stabilities of the carbonium ions involved; the stabilities are in the order: tertiary > secondary > primary. Therefore, rearrangements to olefines

TABLE 4. DEHYDRATION PRODUCTS OF CHC*1

Catalyst	Temp. °C	Conversion, %	Selectivity, % CHYM	MCHE	CHA*2
η	280	37.5	50.3	33.7	10.5
	310	53.2	48.3	38.6	7.5
	330	89.3	47.7	42.5	3.5
	350	94.2	46.5	44.8	4.1
ND	350	45.7	72.8	11.2	6.2
	370	57.5	70.5	13.2	5.1
	390	70.2	73.5	11.0	5.3
	410	85.5	74.6	10.6	6.2
N208	350	40.3	71.3	15.5	10.2
	370	59.6	72.6	18.4	3.5
	390	62.4	72.6	20.6	3.5
	410	75.4	71.8	21.5	1.0

*1 Carrier gas was H_2. Feed rate and flow rate were constant at 10 ml/hr and 10 ml/sec, respectively. Length of catalyst bed was 5 cm.
*2 Cyclohexylcarboxaldehyde.

Over dehydration catalyst:

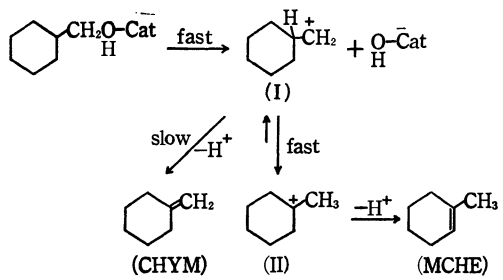

Over dehydrogenation catalyst:

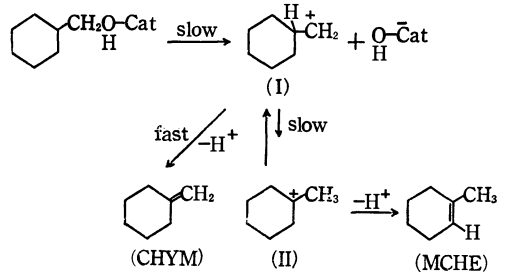

Fig. 3. Reaction pathway of dehydration of CHC.

11) J. Pines and W. O. Haag, *J. Am. Chem. Soc.*, **82**, 2471 (1960).

proceeding through primary carbonium ions are believed to occur at reasonably fast rates only on relatively strong acid sites, whereas those involving secondary and tertiary carbonium ions take place on both strong and weak acid centers.

Therefore, the reaction pathway of the dehydration of CHC may be concluded to be as shown in Fig. 3. Over a dehydration catalyst, such an alumina catalyst, the first step producing a carbonium ion (I) was very fast by virtue of its acidic sites,[8] so a large amount of I may exist in the reaction system. By the way, the deprotonation may change I into CHYM, or into MCHE *via* the methylcyclohexyl carbonium ion (II), which is produced by isomerizations and which rearranges its form to a more stable one under a high temperature. The faster the dehydration rate and the higher the reaction temperature, the smaller the difference in the selectivities between CHYM and MCHE may be. Over the dehydrogenation catalyst, on the contrary, the first dehydroxylation step producing an ionic structure (I) may be reasonably slow, and, moreover, the deprotonation may proceed extraordinarily fast as a result of the strong dehydrogenation activity of the catalyst.

Therefore, the reaction producing CHYM may be predominant, and a small quantity of MCHE may be produced by the deprotonation of the carbonium ion (II) rearranged from I.

Conclusion

The behavior of each catalyst has been clarified by elucidating the dehydration pathway of CHC. Over the dehydration catalyst, to put it simply, the rate of the dehydroxylation step is very fast, and that of the deprotonation step is very slow; therefore, the carbonium ion produced by the dehydroxylation migrates into the more stable form of the tertiary carbonium ion.[12] Over the dehydrogenation catalyst, it has been established that the deprotonation of the carbonium ion produced at the first step, contrary to the case of the dehydration catalyst, occurs faster than the migration of the primary carbonium ion to the tertiary one.

Considering the results of the dehydration of CHC and the established reaction mechanism with respect to the dehydration of TFA, the skeletal rearrangement during the dehydration of TPM over various catalysts may be estimated to be as shown in Fig. 4. Over the dehydration catalyst, the carbonium ion (I) produced II by ring enlargement through a process analogous to the Wagner-Meerwein rearrangement, after which CPA was formed by ring-shrinking isomerization. In this step, the migration of the lone-electron pair of ring ethereal oxygen to the carbonium ion resulted in simultaneous deprotonation. As a result of the

Over dehydration catalyst:

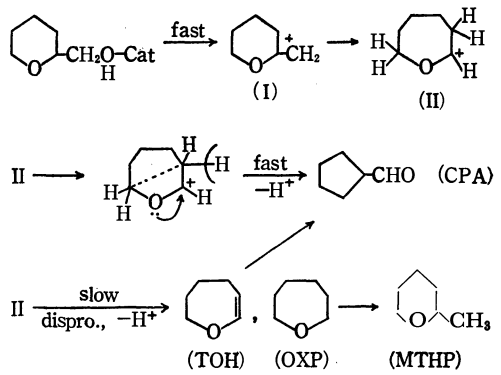

Over dehydrogenation catalyst:

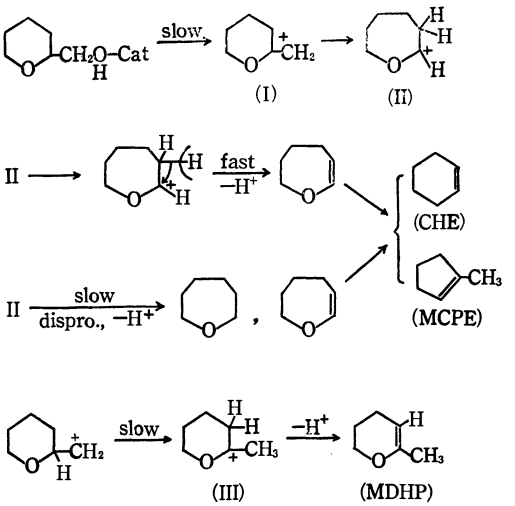

Fig. 4. Reaction pathway of dehydration of TPM.

strong influence of the acidic sites of the catalysts on the lone-electron pair of ethereal oxygen, the electron transfer from the loosened electron pair to the carbonium ion may occur with ease; on the other hand, the weaker the acidity of the catalyst, the less may the lone pair of ethereal oxygen be affected. Therefore, over each Neobead catalyst having a weaker acidity on its surface than that of η-alumina, THO and OXP may be obtained from II by deprotonation and disproportionation; then THO may go through the step from II to CPA by means of protonation. On the other hand, though OXP can be isomerized to MTHP, its very slow reaction rate scarcely produced as much MTHP as was detected. Therefore, over the dehydration catalyst, the reaction pathway of I→II→CPA may be the main route.

On the contrary, over the dehydrogenation catalyst, the reaction step producing I was very slow and THO was the main product. Since the lone-electron pair of ethereal oxygen is not affected by the catalyst at all and may be very stable in itself,

12) H. Pines and W. O. Haag, *ibid.*, **83**, 2847 (1961).

it may be difficult for the electron transfer from ethereal oxygen to the carbonium ion to occur, resulting in the predominance of the deprotonation. Moreover, a small part of the THO and OXP was produced from II by disproportionation. Taking the affinity and the basisity of the catalyst for ethereal oxygen into account, the reaction pathway from I to III can be estimated over the dehydrogenation catalyst, wherein MDHP may be produced from III by deprotonation.

The affinity of each catalyst for the lone-electron pair may depend on its acidity, so alumina may be more active in responce to it than a nickel or copper-chromium oxide catalyst.

THO was obtained in the highest yield with a copper-chromium oxide catalyst 70 mm long under a 5 ml/sec flow of a hydrogen carrier and a TPM rate of 10 ml/hr at 430°C; therefore, the selectivity of THO was about 58%, and the conversion of TPM was about 87%. However, the patent literature regarding the dehydration of TPM, as has previously been mentioned, has touched upon THO only very briefly, treating it as a mere reaction intermediate, and has not isolated it from the reaction system at all. Consequently, the dehydration of TPM with the dehydrogenation catalyst may be considered to be a new and a more useful method by which THO was obtained in better yields than by the other reactions.

Therefore, a useful application of THO may be considered to be as follows; 5 ml of THO were added to 10 ml of a 0.01 N H_2SO_4 solution and the mixture was refluxed for 30 min at 90°C. Then the mixture was hydrogenated with 0.5 g (wet) of Raney Ni (W-2) at 100°C under an initial hydrogen pressure of 20 kg/cm^2 until no more hydrogen was absorbed. After the reaction product had then been filtrated, a vacuum distillation gave about 4.7 g of 1,6-D (84% yield. Moreover, 1,6-D was synthesized directly from TPM in a 42% yield by dehydration and subsequent hydrogenation *via* THO. This skeletal rearrangement during the dehydration of TPM may become a very useful reaction for synthesizing 1,6-D.

The authors wish to thank their co-worker, Mr. Tadaomi Yamada. The authors also wish to express their gratitude to the Mizusawa Chemical Co. and the Nikki Chemical Co. for kindly suppling the various catalysts.

BULLETIN OF THE CHEMICAL SOCIETY OF JAPAN VOL. 41 2453—2457 (1968)

Further Studies on Acetoxylation of Isodihydro-*O*-acetylisophotosantonic Lactone

Tadashi SASAKI and Shoji EGUCHI

Institute of Applied Organic Chemistry, Faculty of Engineering, Nagoya University, Furo-cho, Chikusa-ku, Nagoya

(Received January 25, 1968)

Acetoxylation of *O*-acetylisophotosantonic lactone (I) and its isodihydro derivative (III) with lead tetraacetate was reinvestigated. The reaction of III in refluxing benzene afforded the known 2-acetoxy derivative (V) as the main product and α-diketone as the minor product which was isolated in its 2-keto-3-ol form (VII). The use of boron trifluoride - etherate as a catalyst in this acetoxylation, however, did not give good results. The ORD curves of dihydro-*O*-acetylisophotosantonic lactone (II), III, 2-bromo-isodihydro-*O*-acetylisophotosantonic lactone (IV), V and one of the hydrogenolysis product of I (X) were measured and some stereochemical problems of these compounds were discussed.

Acetoxylation of *O*-acetylisophotosantonic lactone (I) and its isodihydro derivative (III) by the oxidation with lead tetraacetate has been reported by White and his coworkers;[1] they isolated the corresponding 2-acetoxyl derivative XI and V, respectively in low yields but did not describe the stereochemistry of the 2-acetoxyl group, although the stereochemistry of several derivatives of *O*-acetylisophotosantonic lactone have been established, in particular, that of its 2-bromo derivative IV by X-ray analysis.[3]

In the present paper, acetoxylation of I and III has been studied and compound VII, one of the by-products, has been isolated from III in addition to the normal acetoxylation product V.

1) a) E. H. White, J. N. Marx, F. Bacheler and S. Eguchi, submitted to *Tetrahedron;* b) E. H. White and J. N. Marx, *J. Am. Chem. Soc.*, **89**, 5511 (1967).

2) J. D. Asher and G. A. Sin, a) *Proc. Chem. Soc.*, **1962**, 111; b) *J. Chem. Soc.*, **1965**, 1584.

3) a) D. H. R. Barton, P. de Mayo and M. Shafiq, *ibid.*, **1957**, 929; b) D. Arigoni, H. Boshard, H. Bruderer, G. Büchi, O. Jeger and L. J. Krebaum, *Helv. Chim. Acta*, **40**, 1732 (1957).

The optical rotatory dispersion (ORD) curves of dihydro derivatives of I (II and III), 2-bromo derivative of III (IV), V and one of the hydrogenolysis products of I (X) have been measured and their stereochemical correlations are discussed.

Results and Discussions

Acetoxylations. *O*-Acetylisophotosantonic lactone (I)[3] was hydrogenated by the known method to give the unstable dihydro derivative II which was easily converted to its C-4 epimer by treatment with alumina.[1] Hydrogenation of I afforded X, one of the hydrogenolysis products which has also been reported.[1a]

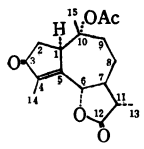

I

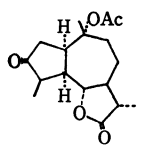

II

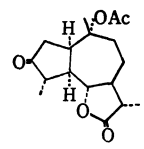

III

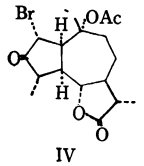

IV

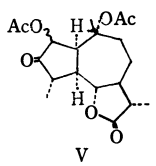

V

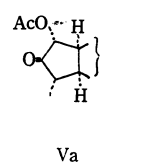

Va

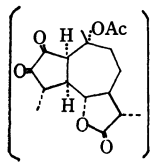

VI

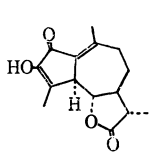

VII

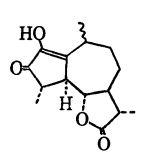

VIII

Oxidation of III with lead tetraacetate in refluxing benzene afforded the reported acetoxyl compound V[1] with a melting point of 166—168°C in a 38% yield. This yield was more or less similar to those reported.[1a] However, a new compound with a melting point of 207—210°C was isolated in a 10% yield upon alkaline hydrolysis of the residue. This compound was shown to be VII by the following evidence; the elemental analysis and the high resolution mass spectrum (M^+ at *m/e* 262.121) indicated a molecular formula $C_{15}H_{18}O_4$. The infrared spectrum which exhibited absorption bands at 3320 (OH), 1770 (γ-lactone), 1675 (cross conjugated cyclopentadienone), 1654 and 1610 (double bonds) cm^{-1}, was very similar to those of achillin[4] and desacetoxy matricarin[5] except for the presence of hydroxyl bands. The ultraviolet spectrum had maxima at 265 mμ (ε 9570) and 294 (7279) in ethanol, and at 270.5 mμ (ε 6836) and 352 (5912) in 1 N ethanolic potassium hydroxide. The NMR ($CDCl_3$) had signals at τ 3.63 (1 H, s, disappeared on deuteration, OH), 6.42 (1 H, unsym. t, J=9.5 Hz, C-6-H), 6.73 (1 H, d, J=10.0 Hz, C-5-H),[5d] 7.51 and 7.81 (each 3 H, s, two allylic methyls at C-3 and C-10) and 8.73 (3 H, d, J=6.0 Hz, methyl at C-11). The presence of an enolic hydroxyl group was indicated by a positive ferric chloride test (violet). Since White and Marx[1b] have synthesized from III desacetoxy matricarin, a C-11 epimer of achillin, VII seems to be a 3-hydroxy analogue of desacetoxy matricarin, although the isolation of this compound from natural sources has not been reported.

VII may be produced from the α-diketone VI after elimination of acetic acid, followed by enolization. This conversion to 2-keto-3-ol system is of interest, since the acetoxy compound V is known to be converted to a 3-keto-2-ol system VIII by alkaline hydrolysis.[1a] On the other hand, in steroid series, Fieser and Stevenson[6] have reported the isomerization of Δ^5-cholesten-4α-ol-3-one acetates (XII) to Δ^5-cholesten-3β-ol-4-one acetate (XIII).

Possibilities of the formation of VII from V by air oxidation upon alkaline hydrolysis were excluded

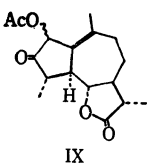

IX

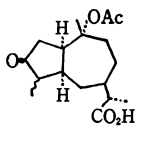

X

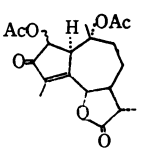

XI

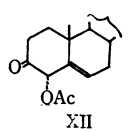

XII

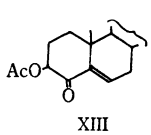

XIII

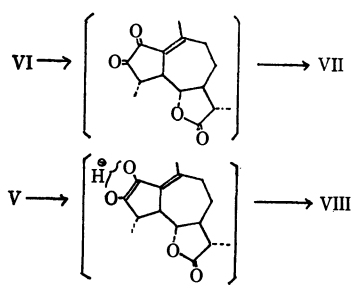

4) a) E. H. White and R. K. Winter, *Tetrahedron Letters*, **1963**, 137; b) S. J. Smolensky, C. L. Bell and L. Bauer, *Lioydis*, **30**, 144 (1967).

5) a) M. Holob and V. Herout, *Coll. Czech. Chem. Commun.*, **27**, 2980 (1962); b) K. S. Rybako, *Zh. Obshch. Khim.*, **33**, 2734 (1963); c) T. A. Geissman, T. S. Stewart and M. A. Irwin, *Phytochemistry*, **6**, 901 (1967); d) H. H. A. Linde and M. S. Ragab, *Helv. Chim. Acta*, **50**, 1961 (1967).

6) L. F. Fieser and R. Stevenson, *J. Am. Chem. Soc.*, **76**, 1728 (1954).

by the fact that V afforded exclusively compound VIII by alkaline treatment,[1] although it is known that 2-acetoxy tetrahydrosantonin gives its α-diketone derivative in a good yield upon alkaline hydrolysis.[7] The facile deacetoxylation and enolization of VI to VII was also shown by the isolation of VII from selenium dioxide oxidation of III, followed by chromatography on alumina.

Acetoxylation with lead tetraacetate is known to be catalyzed by a Lewis acid such as boron trifluoride-etherate[8] and in fact, Barton *et al.*[9] have reported the 2-acetoxylation of deoxygeigerin in an excellent yield using boron trifluoride - etherate as a catalyst. However, acetoxylation of III with lead tetraacetate by Barton's procedure using boron trifluoride-etherate as a catalyst did not proceed smoothly, and resulted in recovery of starting material, which was accompanied by a trace of a compound melting at 187—189°C. This compound had infrared absorption bands at 1770 (γ-lactone), 1750 (cyclopentanone), 1735 (acetate) and 1647 (double bond) cm^{-1}, and a weak ultraviolet absorption at 275 mμ (ε 205) and was tentatively assigned structure IX.

In the acetoxylation of I, the use of boron trifluoride-etherate was also ineffective and only the starting material was recovered, although its acetoxylation in refluxing benzene afforded 2-acetoxy derivative (XI)[1a] in a low yield.

Optical Rotatory Dispersion Studies. Successful applications of the Octant rule to the cyclopentanone series have been achieved by Klyne.[10] It is well known that ORD depends strongly on the conformation of a cyclopentanone ring itself.[11] Therefore, considerations on the conformation of the ring systems in question are required for ORD studies. The Dreiding stereomodel studies for our ring systems suggest three possible basic conformation, XIVa, b, and c.

XIVa has a very flat half-chair or an almost planar cyclopentanone ring which could enter slightly in a positive or a negative octant, and a chair cycloheptane ring.[12] In this conformation, the effect of the cyclopentanone ring on the Cotton effect will be small since C-1 and -5 more or less

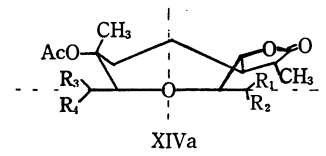

XIVa

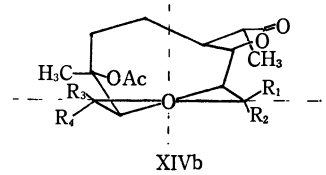

XIVb

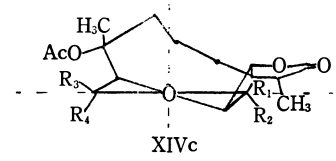

XIVc

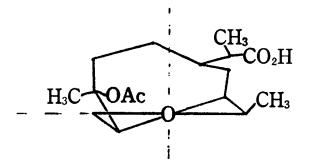

Xa

lie in the plane, and substituents at C-2 and/or C-3 are expected to contribute strongly to the Cotton effect.[13] Thus in this conformation, we can anticipate a weak positive or a weak neagtive Cotton effect, depending on substituents. XIVb has a half-chair cyclopentanone ring and a twisted-chair cycloheptane ring.[12] In this conformation, C-1 and -5 are severely skewed in negative octants and we can, therefore, expect a strong negative Cotton effect. XIVc has a half-chair cyclopentanone ring, in which C-1 and -5 are strongly skewed in the positive octants, and a boat or a twisted boat cycloheptane ring.[12] In this conformation, a strong positive Cotton effect will be anticipated.

The ORD curves of II and III are shown in Fig. 1 and those of IV, V, and X, in Fig. 2. As seen in Fig. 1, II showed a strong negative Cotton effect ($a=-112$) while III exhibited a weak positive Cotton effect ($a=+25$), but both exhibiting a fine structure of similar shape. The fact that II and III give such different values in amplitude indicates clearly that the whole molecular shape of II and III must be different, since the C-4-methyl

7) a) K. Yamakawa, *J. Org. Chem.*, **24**, 897 (1959); b) M. Yanagita and K. Yamakawa, *ibid.*, **24**, 903 (1959).

8) a) L. F. Fieser and M. Fieser, "Reagents for Organic Synthesis," John Wiley and Sons, Inc., New York, N. Y. (1967), p. 541; b) H. B. Henbest, G. H. Phillips, G. P. Slater and D. A. Thomas, *J. Chem. Soc.*, **1965**, 6.

9) D. H. R. Barton, J. T. Pinkey and R. J. Wells, *ibid.*, **1964**, 2518.

10) W. Klyne, *Tetrahedron*, **13**, 29 (1961).

11) For a recent review, see: P. Crabbe, "Optical Rotatory Dispersion and Circular Dichroism in Organic Chemistry," Holden-Day, Inc., San Francisco (1965), p. 90.

12) For recent studies on the conformation of cycloheptane ring, see: J. B. Hendrickson, a) *J. Am. Chem. Soc.*, **89**, 7036 (1967); b) *ibid.*, **89**, 7043 (1967); c) *ibid.*, **89**, 7047 (1967).

13) The effect of a cycloheptane ring on the Cotton effect will be small, since the replacement of a cyclohexane ring by a cycloheptane ring in the hexahydrindan-2-one system did not change the sign of the Cotton effect but only slightly decreased the amplitude; C. Djerrasi and J. E. Gurst, *J. Am. Chem. Soc.*, **86**, 1755 (1964).

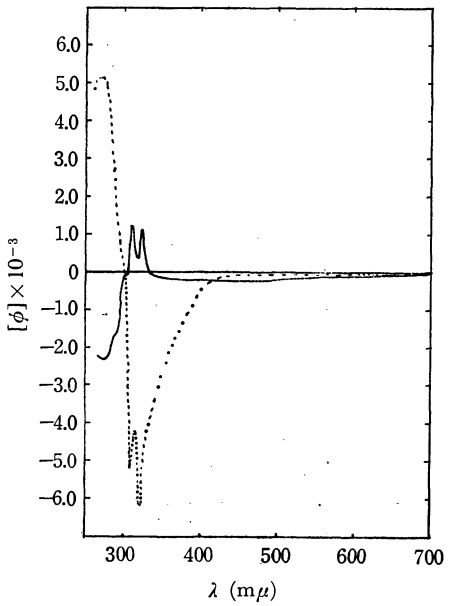

Fig. 1. ORD curves of II (·····) and III (——).

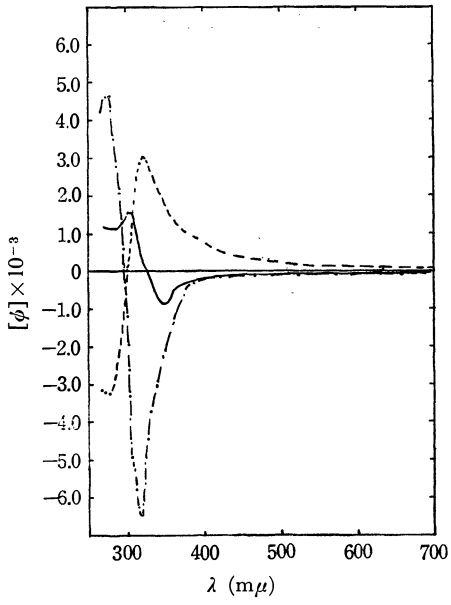

Fig. 2. ORD curves of IV (——), V (----) and X (·—·—).

alone should not cause such a large change. Only the conformation XIVb ($R_1=CH_3$; R_2, R_3, and $R_4=H$ for II) can explain the strong negative Cotton effect of II. The weak positive Cotton effect of III can not be explained by this conformation ($R_2=CH_3$; R_1, R_3, and $R_4=H$), since the negative contribution of the severely skewed cyclopentanone ring should be predominant, even if the C-4-methyl enters a positive octant. Thus, the weak positive Cotton effect of III can be explained most reasonably by conformation XIVb ($R_2=CH_3$; R_1, R_3, and $R_4=H$). The reason why II and III, respectively, adopt conformations of type XIVb and type XIVa are uncertain. The type XIVa conformation seems to be common to C-4α-methyl derivatives of this series, since IV is shown to have a very flat half-chair cyclopentanone ring and a chair cycloheptane ring by X-ray analysis.[2] Therefore, assuming that IV has the conformation of type XIVa (R_1 and $R_3=H$; $R_2=CH_3$; $R_4=Br$), a weak negative Cotton effect might be predicted, since the contribution of 2α-bromine in a negative octant may surmount that of 4α-methyl in a positive octant.[14] In fact, the observed value of IV was a weak negative Cotton effect ($a=-24$) as illustrated in Fig. 2.

The acetoxyl compound V showed a relatively weak positive Cotton effect, $a=+62$, indicating clearly that the 2-acetoxyl group is contributing more or less to the positive Cotton effect, since the amplitude is larger than that of III. Based on the conformation of type XIVa,[15] the 2-acetoxyl group seems to enter in a front positive octant (for 2α-OAc, R_1 and $R_3=H$; $R_2=CH_3$; $R_4=$OAc) or in a front negative (for 2β-OAc, R_1 and $R_4=H$; $R_2=CH_3$; $R_3=$OAc).[16] Thus, the 2α-acetoxyl structure (Va) is assigned to compound V.[17] Ketol acetates often give abnormal ORD curves,[18] even in the steroid series, and therefore, our assignment based on the ORD data might need further support, for which studies are in progress.[19]

The stereochemistry at C-4 in compound X is unknown and its ORD showed a strong negative Cotton effect ($a=-112$) which is reminiscent of the ORD of II. Such a large negative amplitude can not be expected on the basis of conformations of type XIVa and XIVc. Therefore, the conformation Xa which belongs to the conformation of type

14) For example, see C. Beard, C. Djerassi, J. Sicher, F. Sipos and M. Tichy, *Tetrahedron*, **19**, 919 (1963).

15) XIVb predicts a negative Cotton effect and XIVc, a strong positive, since the substituent effect will be small in these conformations. Such large effects of the substituents as seen in III, IV and V might also suggest the validity of the XIVa conformation.

16) The degree of the contribution of 2-OAc to the positive or the negative front octant depends on the conformation of the actoxyl group but molecular model studies indicate clearly the contribution to the front octant assuming some stable conformations of the 2-OAc.

17) It may be noted that 2α-OAc will be more stable than the 2β-isomer, since in the latter, oxygen atoms of the two acetoxyl groups at C-2 and C-10 are very close to each other and therefore, an electrostatic or a dipole-dipole repulsion might be expected.

18) For example, see; a) C. Djerassi, J. Fishman and T. Nambara, *Experientia*, **17**, 565 (1961); b) C. Djerassi, D. Halpern, V, Halpern and C. Tamm, *Helv. Chim. Acta*, **41**, 250 (1958).

19) The NMR data might be useful in some cases but in the cyclopentanone series, their application to the stereochemistry require model compounds, since for example, *cis* and *trans* lactones in our systems have almost the same coupling constants for C-6 and C-7 protons; see Refs. 1b and 5d.

XIVb, was suggested and thus, the C-4β-methyl structure was assigned to X.

Experimental[20]

***O*-Acetylisophotosantonic Lactone (I).** This was prepared by irradiation of α-santonin by the known method[3] and it melted at 182—134°C (recrystallized from methanol).

Dihydro-*O*-acetylisophotosantonic Lactone (II). Catalytic hydrogenation of I (10% Pd-C in ethyl acetate) afforded II, mp 171—173°C (from ethyl acetate).[1]

Hydrogenolysis Product of I (X). After more than 1 mol of hydrogen was uptaken in the above reduction, acidic portion was purified by crystallization from an acetone - *n*-hexane mixture to give an acid X with a melting point of 154—156°C (lit.[1a] 156—157°C).

Isodihydro-*O*-acetylisophotosantonic Lactone (III). This was obtained from II as needles with a melting point of 165.5—167°C (benzene - *n*-hexane) by epimerization on alumina.[1]

Oxidation of III with Lead Tetraacetate in Benzene. The same procedure as that of White *et al.*[1] was applied except the use of a small amount of acetic anhydride. A mixture of 1.54 g of III, 0.5 m*l* of acetic anhydride and 3.10 g of lead tetraacetate (a commerical sample was dried *in vacuo* on KOH pellets just before use) in 50 m*l* of benzene (dry benzene was distilled from $Pb(OAc)_4$) was refluxed for 12 hr until KI-strach paper became negative and the cooled reaction mixture was washed with water several times and dried over anhydrous sodium sulfate. The removal of the solvent afforded a sticky residue, from which needles with a melting point of 166—168°C was isolated in a 38% yield after crystallization from methanol. The spectral data (infrared, ultraviolet and NMR) of this compound were the same with those of the reported[1a] and thus this was identified as V.

The mother liquor was dried up to a sticky residue which was dissolved in 10 m*l* of methanol and stirred for 2 hr at room temperature in nitrogen stream after addition of 5 m*l* of 1 N aqueous potassium hydroxide. Neutralization with acetic acid and concentration afforded precipitates which were recrystallized from methanol to give needles of VII (130 mg, 9.9%), mp 207—210°C. TLC examination of the residue showed the presence of III and some unidentified materials. Mass spectrum of VII had peaks at 262.121 (M^+), 247.097 ($M-CH_3$) and 244.108 ($M-H_2O$).

Found: C, 68.21; H, 6.96%. Calcd for $C_{15}H_{18}O_4$: C, 68.16; H, 7.63%.

Oxidation of III with Selenium Dioxide. A mixture of 0.308 g of III and 0.133 g of selenium dioxide (sublimed before use) in 5 m*l* of dioxane was heated at 60°C for 5 hr. Dioxane was removed *in vacuo* and the residue was purified on alumina (neutral, activity grade III) to give crude VII from ether eluent after elution with benzene. Recrystallization from methanol gave VII with a melting point of 206—209°C in a 14% yield.

Oxidation of III with Lead Tetraacetate in the Presence of Boron Trifluoride - etherate. A mixture of 0.308 g of III, 1.0 of lead tetraacetate, 1.0 m*l* of acetic anhydride and 2.0 m*l* of BF_3 - etherate in 20 m*l* of glacial acetic acid was stirred for 24 hr at room temperature. After the TLC examination indicated that no more starting material was remained, the reaction mixture was diluted with water and extracted with chloroform (20 m*l*×5). The combined extracts were washed with water, dried over sodium sulfate and dried up to a brownish residue which was chromatographed on a silica gel column. The first fraction eluted with chloroform gave crystals of IX with a melting point of 187—189°C (from methanol) in a 3.5% yield.

Found: C, 66.53; H, 7.31%. Calcd for $C_{17}H_{22}O_5$: C, 66.65; H, 7.31%.

The second fraction gave 100 mg of the starting material (32% recovery).

Oxidation of I with Lead Tetraacetate. Oxidation was carried out in benzene by the method of White *et al.*[1a] and the acetoxyl compound XI with a melting point of 174—176°C (lit.[1a] 175—176°C) was obtained in an 11% yield. The oxidation in the presence of BF_3 - etherate was carried out as follows: A mixture of I (0.306 g), lead tetraacetate (1.0 g), acetic anhydride (0.5 m*l*) and BF_3 - etherate (1.0 m*l*) in 15 m*l* of glacial acetic acid was stirred for 20 hr at room temperature and the worked-up product was needles with a melting point of 176—181°C, infrared spectrum of which was identical with that of the starting materials (77% recovery).

2-Bromo-isodihydro - *O* - acetylisophotosantonic Lactone (IV). This was prepared by the Barton's procedure and had a melting point of 115—117°C dec. (lit.[21] 117—118°C dec.).

Optical Rotatory Dispersion Measurements. All ORD measurements were carried out in dioxane solution at room temperature (at *ca.* 20°C).

II (*c* 0.522): $[\phi]_{700}$ −29.2, $[\phi]_{350}$ −2028.7, $[\phi]_{320}$ −6086.2, $[\phi]_{313}$ −4210.4, $[\phi]_{310}$ −5186.6, $[\phi]_{290-291}$ +3725.2, $[\phi]_{278}$ +5132.5, $[\phi]_{250}$ +3725.2.

III (*c* 0.521): $[\phi]_{700}$ −94.8, $[\phi]_{390}$ −213.7, $[\phi]_{322}$ +1101.8, $[\phi]_{315}$ +391.2, $[\phi]_{311}$ +1172.8, $[\phi]_{303}$ −236.9, $[\phi]_{299}$ −79.0, $[\phi]_{290-291}$ −1409.8, $[\phi]_{274}$ −2203.6.

IV (*c* 0.336): $[\phi]_{700}$ −86.4, $[\phi]_{400}$ −331.3, $[\phi]_{346}$ −878.7, $[\phi]_{307}$ +1527.3, $[\phi]_{300-298}$ +1472.2, $[\phi]_{280}$ +1166.8.

X (*c* 0.350): $[\phi]_{700}$ −187.8, $[\phi]_{350}$ −2000.0, $[\phi]_{318}$ −6429.4, $[\phi]_{311-309}$ −5186.1, $[\phi]_{278}$ +4789.2.

The authors are much indebted to Professor E. H. White (Johns Hopkins Univ., U. S. A.) for his deep interests and kind suggestions for this studies and to the Nippon Shinyaku Co., Ltd., for his kind supply of Santonin. Thanks are also due to Mr. Akiho Ishihara for elemental analyses and ORD measurements.

20) All melting points were determined on a Yanagimoto micromelting point apparatus and are uncorrected. Microanalyses were carried out on a Yanagimoto C. H. N. Coder, Model MT-1. Infrared spectra were recorded on a JASCO Model IR-S infrared spectrophotometer and NMR spectra were obtained with a Varian A-60 spectrometer, using TMS as an internal standard. Ultraviolet spectra and ORD curves were measured on a JASCO Model ORD/UV-5 spectrophotometer. Mass spectrum of VII was obtained by a Mattauch-Herzog type high resolution mass spectrometer, JMS-O1S, using PFK as an internal standard.

21) D. H. R. Barton, J. E. B. Levisalleo and J. T. Pinkey, *J. Chem. Soc.*, **1962**, 3472.

BULLETIN OF THE CHEMICAL SOCIETY OF JAPAN VOL. 41 2458—2465 (1968)

The Stereochemistry of Perhydroacridines and Perhydrophenanthridines[1]

Tadashi MASAMUNE, Masaji OHNO,*1 Ken TAKEMURA*2 and Shigehiro OHUCHI*3

Department of Chemistry, Faculty of Science, Hokkaido University, Sapporo

(Received February 1, 1968)

The configurations of three stereoisomers, α, β and γ, of perhydroacridine and those, α, β and γ, of perhydrophenanthridine have been assigned as *trans,syn,trans, trans,anti,cis, trans,syn,cis, trans,anti,trans, trans,syn,cis* and *cis,syn,cis*, respectively, on the basis of both the process of their syntheses and the rate of formation of methiodides of the *N*-methyl derivatives. These configurations are consistent with the infrared-spectral behavior of their *N*-methyl derivatives in carbon tetrachloride solutions containing *n*-butanol as well as with the result of their exhaustive methylations. The relative steric requirement of the lone pair and the hydrogen on the N atom is also discussed.

One decade ago we reported[2] on the preparation of three stereoisomers, α, β and γ (I, II and III), of perhydroacridine, whose configurations were assigned tentatively as *trans,trans*, *trans,cis*, and *cis,cis*, respectively. In a continuing study, these compounds were converted into the corresponding *N*-methyl derivatives (Ia, IIa and IIIa), mp 38—40°C, 36—38°C and 46—48°C, and it was attempted to prepare these derivatives from *N*-methyl-*trans*- and *cis*-1,2,3,4,4a,9,9a,10-octahydroacridines[3,4] (IVa and Va). Contrary to the expectation, hydrogenation of IVa over platinum at room temperature produced Ia and IIIa in moderate yields, but no IIa, and that of Va gave IIIa as a major product along with a small amount of a new isomer (VIa), named *N*-methyl-δ-perhydroacridine. Since (1) both I and II have been obtained from *trans*-octahydroacridine (IV) by hydrogenation under the same conditions, and both II and III from the *cis* isomer (V),[2] and (2) the *trans* isomer IV has been recovered unchanged on treatment under the conditions differing from the afore-mentioned only in replacement of hydrogen by nitrogen, the configuration of III must be revised to be *trans,cis* (Chart 1).

Thus, both β- and γ-perhydroacridines II and III have one *trans* and one *cis* linkages, one of them being a *trans,anti,cis* modification, and the other a *trans,syn,cis*. On the other hand, α-perhydroacridine I involves at least one *trans* linkage[2] and, therefore, should have a *trans,trans* structure.

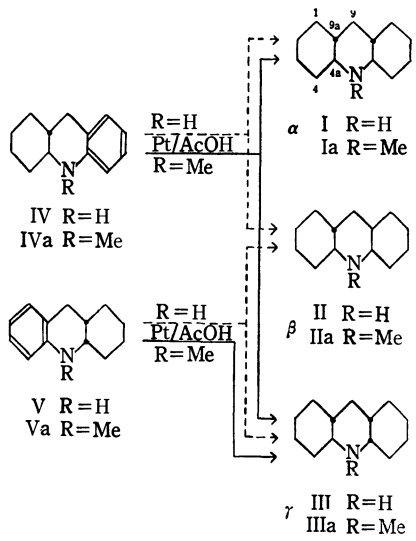

Chart 1

Only one perhydrophenanthridine (VII) has been reported: hydrogenation of 7,8,9,10-tetrahydrophenanthridine over Raney nickel at high temperature has afforded VII in a good yield, while that over platinum at room temperature a compound (VIII) assigned as a dodecahydro derivative.[5] Since VII has also been obtained from *trans*-5,6,6a,7,8,9,10,10a-octahydrophenanthridine[3] (IX) by hydrogenation over platinum at room

*1 Present address: Basic Research Laboratories, Toyo Rayon Co., Ltd., Kamakura.

*2 Present address: Research Institute of Applied Electricity, Hokkaido University, Sapporo.

*3 Present address: Mishima Plant, Toyo Rayon Co., Ltd., Mishima.

1) Part XVII of "The Condensed Polynuclear Perhydro-compounds Containing Nitrogen": Refs. 21a and 15 are considered as Parts XV and XVI of this series.

2) T. Masamune and S. Wakamatsu, *Nippon Kagaku Zasshi (J. Chem. Soc. Japan, Pure Chem. Sect.)*, **77**, 1145 (1956).

3) T. Masamune, M. Takasugi, H. Suginome and M. Yokoyama, *J. Org. Chem.*, **29**, 681 (1964).

4) D. A. Archer, H. Booth, P. C. Crisp and J. Parrick, *J. Chem. Soc.*, **1963**, 330; H. Booth, *Tetrahedron*, **19**, 91 (1963).

5) T. Masamune and Y. Kubota, *Nippon Kagaku Zasshi (J. Chem. Soc. Japan, Pure Chem. Sect.)*, **77**, 1467 (1956).

temperature,[5] reduction of the corresponding *cis* isomer[3] (X) was undertaken under the same conditions to obtain a new stereoisomer. However, the reaction led to formation of a good yield of compound VIII, which was also produced in a good yield by hydrogenation of *trans*-1,2,3,4,4a,5,6,10b-octahydrophenanthridine[6] (XI) in the presence of platinum in ethanol containing hydrochloric acid.[7] This fact, coupled with repeated analyses, led to the assignment of VIII as a perhydro compound, which was confirmed by the mass spectrum. The same treatment of a *cis* isomer[6] (XII) of XI gave a new perhydrophenanthridine (XIII), mp 37—38°C, and VIII, suggesting that the *cis* isomer XII would rearrange partially to the *trans* isomer XI under the acidic conditions used. These results (Chart 2) indicate that the stereoisomers VII, VIII and XIII, named α-, β- and γ-perhydrophenanthridines, have *trans,trans*, *trans,cis* and *cis,cis* configurations, respectively, in view of the well-known stereochemistry in hydrogenation of 1,2,3,4-tetrahydroisoquinoline.[8] The relative configurations of hydrogens at C-9a and C-8a in the perhydroacridines and those at C-10a and C-10b in the perhydrophenanthridines will be determined in the following.

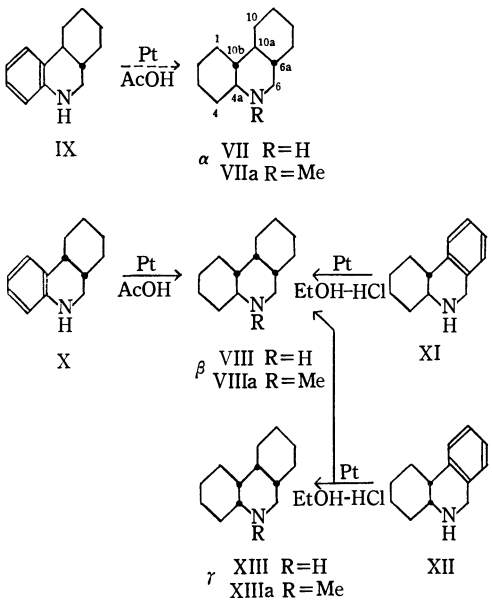

Chart 2

Formation of Methiodides of *N*-Methyl Derivatives. The rates of reaction with methyl iodide were determined for *N*-methyl derivatives of three perhydroacridines I, II and III, three perhydrophenanthridines VII, VIII and XIII, two octahydrophenanthridines XI and XII, *trans*- and *cis*-perhydroquinolines[9] (XIV and XV), piperidine (XVI), *cis*-perhydroindole[10] (XVII) and perhydrocarbazole[11] (XVIII), and the result is summarized in Table 1. In view of the fact that, in the absence of important steric hindrance, a stronger base reacts faster with a given alkyl halide,[12] the basicities of these *N*-methyl compounds were also measured. The transition state in the formation of these methiodides is supposed to have a steric arrangement similar to an ammonium cation formed by addition of a proton to each tertiary amine. Because of the small size of proton, a serious steric hindrance against the addition would hardly exist. To the contrary, it is expected that the presence of an axial methylene (β-axial methylene) group at the β-position to the N atom of a piperidine ring in these compounds would remarkably retard the rate of the quarternization, because either one of two methyl groups (N-$\underline{CH_3}$ and $\underline{CH_3}$I) on the N atom exists in an axial conformation.[13] In order to clarify these steric effects,

Table 1. The reaction rate with methyl iodide and basicity of *N*-methylperhydroacridines and related compounds

Compound (*N*-methyl derivative)	Rate constant[a] $k\times10^2$ (l/min·mol)	Basicity[b] pK_a
I	0.41	9.63
II	0.42×10^{-2}	9.67
III	0.44	9.65
VII	2.05	9.47
VIII	1.98	9.54
XIII	1.95	9.49
XI	0.52	8.54
XII	0.48	8.48
XIV	1.60	9.37
XV	1.67	9.41
XVI	1.30	9.11
XVII	3.09	9.73
XVIII	$<10^{-3}$	9.90

a) Measured at 20°C in 99.5% ethanol.
b) Measured at 20°C in 60% ethanol.

6) T. Masamune, M. Ohno, M. Koshi, S. Ohuchi and T. Iwadare, *J. Org. Chem.*, **29**, 1419 (1964).
7) *Cf.* J. M. Devereux, K. R. Payne and E. R. A. Pealing, *J. Chem. Soc.*, **1957**, 2845.
8) For example, B. Witkop, *J. Am. Chem. Soc.*, **70**, 2617 (1948); W. Hückel and F. Stepf, *Ann.*, **453**, 163 (1927).
9) M. Ehrenstein and W. Bunge, *Ber.*, **67**, 1715 (1934).
10) F. E. King, J. A. Baltrop and R. J. Walley, *J. Chem. Soc.*, **1945**, 277.
11) T. Masamune, M. Ohno and M. Koshi, *Nippon Kagaku Zasshi (J. Chem. Soc. Japan, Pure Chem. Sect.)*, **77**, 1017 (1956).
12) For example, H. C. Brown and N. R. Eldred, *J. Am. Chem. Soc.*, **71**, 445 (1949); H. C. Brown, *J. Chem. Soc.*, **1956**, 1248; R. T. Arnold, V. J. Webers and R. M. Dodson, *J. Am. Chem. Soc.*, **74**, 368 (1953); K. E. Weale, *J. Chem. Soc.*, **1954**, 2959.
13) For the stereochemistry of piperidine quaternization, see A. T. Bottini and M. K. O'Rell, *Tetrahedron Letters*, **1967**, 423, and references cited there.

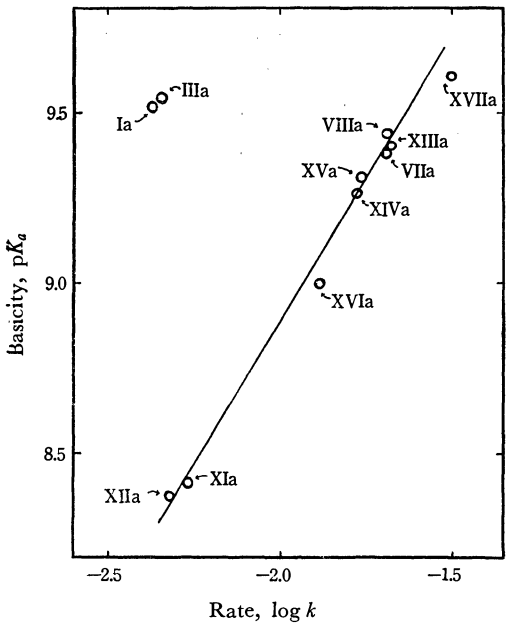

Fig. 1. The relation between the rate of *N*-methyl methiodides formation and the basicity of *N*-methylperhydroacridines and related compounds.

the logarithms of the rate constants were plotted against their pK_a values (Fig. 1).

trans-Perhydroquinoline (XIV), *trans*-octahydrophenanthridine (XI) and probably α-perhydrophenanthridine (VII) have only β-equatorial methylene substituents in the respective piperidine ring. Accordingly, the transition states in the reaction of their *N*-methyl derivatives would have approximately equal steric interactions, suggesting the presence of a linear relationship. In fact, it was true as shown in Fig. 1. Besides these bases, the corresponding *cis* isomers XVa, XIIa, VIIIa and also *N*-methyl-γ-perhydrophenanthridine (XIIIa) fell on this line, reflecting that these compounds involve the same steric requirement for the reaction as their stereoisomers. This linear relation indicates that these compounds contain no β-axial methylene substituents, as far as all the rings adopt chair conformations; namely, compounds VII, VIII and XIII have *trans,anti,trans*, *trans,syn,cis* and *cis,syn,cis* configurations, respectively.*4 *N*-Methyl derivatives, XVIa and XVIIa, of piperidine and *cis*-perhydroindole deviated slightly from the line. In the former, the deviation would be attributed to the absence of an α-substituent, and in the latter it would be due to the fact that a methylene group in a five-membered ring offers less steric hindrance than that in a six-membered ring.[14] With *N*-methyl-α- and γ-perhydroacridines Ia and IIIa, considerable deviations were observed, which apparently resulted from the substitution of two α-methylene groups in the piperidine ring. On the other hand, *N*-methyl-β-perhydroacridine IIa and *N*-methylperhydrocarbazole XVIIIa revealed conspicuous decrease in the rate (the outside of Fig. 1). Whilst the rate of the latter is not interpretable well owing to its whole ambiguous steric arrangement, it is evident that the presence of a β-axial methylene group in the piperidine ring of IIa has brought about the remarkable retardation. This result, coupled with the synthetic process, establishes that the configurations of α-, β- and γ-perhydroacridines are *trans,syn,trans*, *trans,anti,cis* and *trans,syn,cis*, respectively.

Formation of Hydrogen Bonds with *n*-Butanol.[15] The method for determination of the configurations described in the preceding section is based on measurement of the reaction rates and rather troublesome. Furthermore, no consideration is given to the conformation in tertiary amine of compounds in which ring inversion is possible. As an attempt to approach to these problems by more practical experiments under mild conditions, we examined the infrared spectra near 3400 cm^{-1} of carbon tetrachloride solutions containing the afore-mentioned tertiary amines (0.1 to 0.2 M) and *n*-butanol. To avoid the confusion due to association of the butanol itself,[16] the concentration was fixed to be 0.05 M, where only absorptions at 3640 cm^{-1} (free OH) and near 3520 cm^{-1} (dimeric OH) were observed.

The ternary solution containing *N*-methyl-α-perhydroacridine Ia exhibited a definitely different spectrum from the corresponding containing the β-isomer IIa (Fig. 2); in the former a broad band centered at *ca.* 3240 cm^{-1} appeared in addition to a sharp band at 3640 cm^{-1} due to unassociated hydroxyl groups, while in the latter a new absorption with relatively weak intensity was instead centered at *ca.* 3420 cm^{-1} along with the sharp band. These broad absorptions near 3240 and 3420 cm^{-1} are undoubtedly attributed to the hydroxyl group (OH-N) bonded with the lone pairs of N atom. Kuhn,[17] Nakamoto[18] and others[19] showed, from measurement of the infrared spectra of a number of hydrogen-bonded compounds in the crystalline state, that an approximately

*4 If compound XIII had a *cis,anti,cis* configuration, the rate of quarternization would be reduced, no matter what conformation of the piperidine ring is taken, a chair or a twist-boat form.

14) R. T. Arnold and P. N. Craig, *J. Am. Chem. Soc.*, **72**, 2728 (1950), and references cited there.
15) T. Masamune, *Chem. Commun.*, **1968**, 244.
16) W. C. Coburn, Jr., and E. Grunwald, *J. Am. Chem. Soc.*, **80**, 1318 (1958).
17) L. P. Kuhn, *ibid.*, **74**, 2492 (1952).
18) K. Nakamoto, M. Margoshes and R. E. Rundle, *ibid.*, **77**, 6480 (1955).
19) R. M. Badger, *J. Chem. Phys.*, **8**, 288 (1940); R. C. Lord and R. E. Merrified, *ibid.*, **21**, 166 (1953).

linear relation exists between the length of hydrogen bond and the shift of frequency of the associated hydroxyl group from that of the unassociated. This correlation comes into existence if the hydrogen bond is of linear type and, especially, becomes important if the relevant tertiary amines have equal basicities such as the present compounds Ia and IIa. The observed difference in the frequency shifts between Ia and IIa (400 and 240 cm^{-1}, respectively) apparently arises from that in the hydrogen bond length between both the isomers, provided that the correlation holds for the compounds in the liquid (solution) state. Thus, this result indicates that there exists a steric hindrance in IIa, which obstructs proximity of the butanol molecule to the lone pair of N atom and which must result from the presence of a β-axial methylene group. This inference is consistent with the well-established fact that the *N*-methyl group is almost exclusively oriented equatorial in *N*-methylpiperidines.[20] The ternary solutions containing *N*-methyl derivatives of γ-perhydroacridine (III), α- and β-perhydrophenanthridines (VII and VIII), *trans*-perhydroquinoline (XIV) displayed practically the same spectra in the relevant region as the corresponding containing Ia, whereas *N*-methylperhydrocarbazole (XVIIIa) showed essentially the same absorption pattern concerning the spectrum of the solution in question as IIa. These spectral behaviors are in good accord with the result obtained in the preceding section.

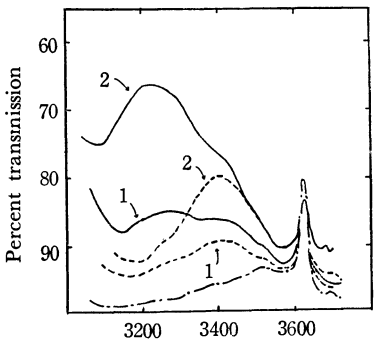

Fig. 2. Infrared spectra of *N*-methyl-α- and β-perhydroacridines (Ia and IIa) in carbon tetrachloride solutions containing *n*-butanol: —— 1, Ia (0.1 M); ——2, Ia (0.2 M); ----1, IIa (0.1 M); ----2, IIa (0.2 M); —·—, *n*-BuOH (0.05 M).

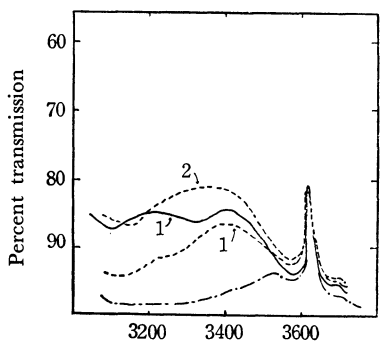

Fig. 3. Infrared spectra of *N*-methyl-γ-perhydrophenanthridine (XIIIa) and *cis*-perhydroindole (XVIIa) in carbon tetrachloride solutions containing *n*-butanol: —— 1, XIIIa (0.1 M); ---- 2, XVIIa (0.2 M); ---- 1, XVIIa (0.1 M); ——, *n*-BuOH (0.05 M).

N-Methyl derivatives of γ-perhydrophenanthridine (XIII), *cis*-perhydroquinoline (XV) and also *cis*-perhydroindole (XVII) exhibited interesting absorption bands in the spectra of their ternary solutions (Fig. 3). In the former two compounds XIIIa and XVa, both the relevant bands centered near 3240 and 3420 cm^{-1} were observed. The intensities of the latter band increased and, conversely, those of the former decreased, when compared with the corresponding bands of the respective *trans* isomers (XIIIa and VIIIa, and XVa and XIVa). With compound XVIIa such a tendency was further intensified, and the spectrum became rather similar to that of compound IIa. These facts may be explicable well on the basis of the following: compounds XIIIa and XVa involve no *trans* linkage and, therefore, would exist as an equilibrium mixture of conformers formed through ring inversion, one having β-equatorial methylene group(s) and the other β-axial. For compound XVIIa, the similar discussion would be applied, if we consider that the pyrrolidine ring adopts a half-chair conformation or we regard XVIIa as a cyclohexane derivative substituted vicinally with methylene and amino groups. This inference is not contradictory to the previous conclusion but rather supports the configuration of compound XIII.

We next measured the spectrum of the solution containing *n*-butanol (0.05 M) and the secondary amine I or II (0.15 M), in each of which both the relevant, broad and sharp bands appeared near 3240 and 3640 cm^{-1} (Fig. 4). The broad bands are ascribed to the hydroxyl groups bonded to the N atoms, because compound I or II showed only weak absorptions ($\varepsilon < 5$) near 3300 cm^{-1} at the concentration of 0.02 to 1.25 M in carbon tetrachloride and, therefore, the intensities due to the free and *N*- or *O*-bonded imino groups would be negligibly small. In the spectrum of the solution containing I, the broad band appeared with stronger intensity than the sharp. The situation became the opposite in the case of II, where the intensity of the broad band was weaker than that in the case of I. This behavior is interpretable well

20) For example, a) N. L. Allinger, J. G. D. Carpenter and F. M. Karkowski, *J. Am. Chem. Soc.*, **87**, 1232 (1965), and b) J. B. Lambert, R. G. Keske, R. E. Carhart and A. P. Jovanovich, *ibid.*, **89**, 3761 (1967).

on the basis of that the lone pair takes largely an axial conformation in both the compounds and, when the alcohol is added, only compound II is partly inverted to a less stable conformer with the lone pair equatorial and forms the hydrogen bond of almost the same length as I. This provides additional qualitative evidence supporting arguments[21] that the lone pair is smaller than the hydrogen atom.

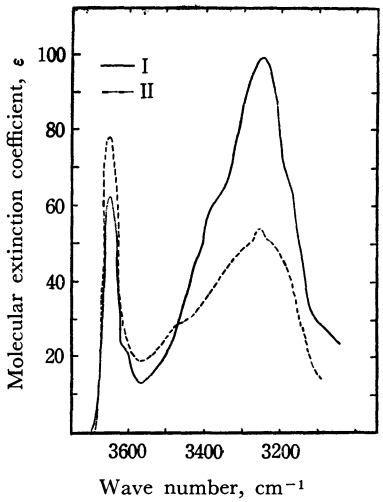

Fig. 4. Infrared spectra of α- and β- perhydroacridines (I and II) in carbon tetrachloride solutions containing *n*-butanol: I and II (0.15 M), *n*-BuOH (0.05 M), cell 0.5 mm.
The intensity ε denotes the difference of the molecular extinction coefficient between each ternary solution and the corresponding containing no *n*-butanol.

The Hofmann Degradation. The exhaustive methylation of the stereoisomers of perhydroacridine and perhydrophenanthridine was next investigated. The addition of methyl iodide into ether or acetone solutions of the *N*-methyl derivatives of the compounds readily yielded the corresponding *N*-methyl methiodides (Ib), mp 273—275°C, (IIb), mp 210—212°C, (IIIb), mp 262—264°C, (VIIb), mp 265—267°C, (VIIIb), mp 272—274°C, and (XIIIb), mp 315—316°C. Pyrolysis of the methohydroxides obtained by treatment of all the methiodides except IIb with silver oxide produced the respective original *N*-methyl compounds in 65—80% yields. On the other hand, the same treatment of IIb gave an oily product, from which a base (XVIII) $C_{15}H_{27}N$, bp 154—156°C/17 mmHg, was isolated in 65% yield in pure state through the picrate, mp 147—149°C. The compound XVIII showed absorption maxima at 1660 and 720 cm^{-1} in the infrared spectrum and gave the dihydro derivative by catalytic hydrogenation. It also afforded the glycol by oxidation with osmium tetroxide, which was readily converted into the diacetate. These facts showed the presence of a disubstituted and probably *cis* double bond. Treatment of XVIII with boiling acetic acid followed by addition of potassium iodide yielded a mixture consisting mainly of Ib, showing that no ring contraction was encountered during the pyrolysis. Hence, compound XVIII can be assigned as 3-(2'-dimethylaminocyclohexylmethyl)-cyclohexene.

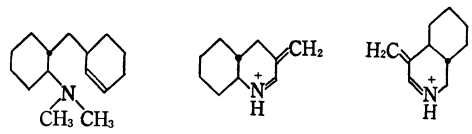

XVIII XIX XX

The methohydroxide obtained from IIb underwent the normal Hofmann degradation to give XVIII, as expected from its steric arrangement. Furthermore, with the methohydroxides which are derived from Ib, IIIb, VIIb and VIIIb and have rigid conformations, a suitable geometrical disposition[22] is not available for the normal E2 process leading to olefin, and it would not be unreasonable that only elimination of methanol took place in the degradation. On the other hand, the remaining methohydroxide derived from XIIIb may adopt at least two conformations, one having two axial β-methylene substituents in respect to the piperidine ring and the other two equatorial. The former is an unfavorable conformation owing to the severe 1,3-diaxial interaction between the axial *N*-methyl and the two methylene groups in question, although it satisfies the stereochemical arrangement required for E2 elimination. This is inferred from the observed rate in the formation of the methiodide and, in fact, the degradation has led mainly to the elimination of methanol, proving the preference of the latter conformation.

Experimental[23]

***α*-, *β*- and *γ*-Perhydroacridines (I, II and III).** These compounds were prepared according to the procedures described previously,[2] and complementary data are described here.

Compound I; mass spectrum, *m/e* 193 (M^+), 192, 151, 150, 136, and *ca.* 117 (a metastable ion). The strongest peak at *m/e* 150 would be due to an ion formulated as XIX.[24] The picrate had mp 192—194°C (lit.,[2] 173—176°C) after preparation in ether or benzene and recrystallization from ether - ethanol. The hydroiodide melted over 360°C after addition of aqueous

21) a) T. Masamune and M. Takasugi, *Chem. Commun.*, **1967**, 625 b) K. Brown, A. R. Katritzky and A. J. Waring, *J. Chem. Soc., (B)*, **1967**, 487; H. Booth and A. H. Bostock, *Chem. Commun.*, **1967**, 177; Ref. 20a.

22) *Cf.* A. C. Cope, *Org. Reactions*, **11**, 317 (1960).

23) All the melting points are uncorrected.

24) *Cf.* The mass spectra of IV and V; *m/e* 187 (M^+), 186, 144, 130, and *ca.* 110 (a metastable ion).

hydrogen iodide into I in acetone and recrystallization from ethanol.

Found: N, 13.01%. Calcd for $C_{19}H_{26}O_7N_4$: N, 13.26%.

Found: N, 4.55%. Calcd for $C_{13}H_{24}NI$: N, 4.36%.

Compound II had mp 51—53°C (lit.,[2] 48—51°C) after purification described in the following; the crude base before recrystallization was converted into the hydroiodide, mp >300°C, by addition of aqueous hydrogen iodide in acetone, which on regeneration followed by recrystallization from petroleum ether afforded II having mp 51—53°C. Compound II showed practically the same mass spectrum as I, and its benzoyl derivative had mp 87—89°C on recrystallization from petroleum ether.

Found: N, 4.88%. Calcd for $C_{20}H_{27}ON$: N, 4.71%.

Compound III showed essentially the same mass spectrum as I, and its picrate had mp 211—213°C on recrystallization from ethanol.

Found: N, 13.15%. Calcd for $C_{19}H_{26}O_7N_4$: N, 13.26%.

N-Methyl-α-, β-, γ- and δ-Perhydroacridines (Ia, IIa, IIIa and VIa) and Their Methiodides (Ib, IIb and IIIb). *a) Methylation wtih Formic Acid and Formalin.* A mixture of I (2.8 g), formic acid (1.5 m*l*) and 33% formalin (2.8 m*l*) was gently refluxed for 6 hr, and into the cooled mixture was added water (50 m*l*) and ether (30 m*l*). After separation of the aqueous layer, the ether solution was shaken with 1 N aqueous acetic acid. The aqueous and acetic acid solutions were combined and made alkaline to yield oily substance, which was extracted with ether, dried and subjected to distillation under reduced pressure. A fraction (2.3 g) boiling at 155—161°C/15 mmHg was collected and refluxed in acetic anhydride (7 g) for 30 min. The whole solution was warmed with water (50 m*l*) on a water bath for 1 hr and then treated with ether. The aqueous solution gave oil on alkalization, which was purified by distillation. The *N*-methyl derivative (Ia, 2.0 g) thus obtained had bp 158—160°C/17 mmHg and mp 38—40°C on recrystallization from petroleum ether.

Found: C, 81.20; H, 12.25; N, 6.67%. Calcd for $C_{14}H_{25}N$: C, 81.09; H, 12.15; N, 6.76%.

The picrate and the hydroiodide had mp 169—170°C (from ethanol) and mp 220—222°C (from ethanol), respectively.

Found: C, 55.28; H, 6.74; N, 13.08%. Calcd for $C_{20}H_{28}O_7N_4$: C, 55.03; H, 6.47; N, 12.84%.

Found: C, 49.93; H, 7.80; N, 3.88%. Calcd for $C_{14}H_{26}NI$: C, 50.15; H, 7.82; N, 4.18%.

N-Methyl derivatives (IIa and IIIa) of II and III were prepared in the same way as Ia. These bases and their derivatives had the following melting points. IIa, mp 36—38°C (from petroleum ether): the picrate, mp 211—213°C (from ethanol); the hydroidodie was not obtained in crystalline state.

Found: C, 81.00; H, 12.18; N, 6.65%. Calcd for $C_{14}H_{25}N$: C, 81.09; H, 12.15; N, 6.76%.

Found: C, 54.98; H, 6.53%. Calcd for $C_{20}H_{28}O_7N_4$: C, 55.03; H, 6.47%.

IIIa, mp 46—48°C (from petroleum ether); the picrate, mp 164—166°C (from ethanol); the hydroiodide was not obtained in crystalline state.

Found; C, 80.78; H, 12.20; N, 6.88%. Calcd for $C_{14}H_{25}N$: C, 81.09; H, 12.15; N, 6.76%.

Found: C, 54.89; H, 6.81%. Calcd for $C_{20}H_{28}O_7N_4$: C, 55.03; H, 6.47%.

b) Hydrogenation of N-Methyl-trans-1,2,3,4,4a,9,9a,10-Octahydroacridine (IVa) over Platinum. Compound IVa[3] (2.1 g) in acetic acid (20 m*l*) was hydrogenated over Adams' platinum (0.4 g as pltainum oxide) at room temperature for 1.5 hr, when 790 m*l* of hydrogen had been consumed (the calculated for complete hydrogenation, 770 m*l*). After removal of the catalyst and the solvent, the residue was shaken with ether and water, and the ether solution gave an oily mixture of bases on being dried and evaporated, which was dissolved in acetone. To the acetone solution was added aqueous hydrogen iodide (bp 125°C), when the hydroiodide precipitated and was collected by filtration. This compound (1.8 g) had mp 218—220°C on recrystallization from ethanol and was then reconverted to a free base (0.85 g), mp 36—38°C, which was identified as Ia. The filtrate free from this hydroiodide was concentrated under reduced pressure and then treated with 2 N sodium hydroxide solution and ether. The ether extract, after evaporation, was converted into the picrate in methanol, which had mp 153—155°C on recrystallization from ethanol and amounted to 1.5 g. This picrate was reconverted into IIIa (0.65 g), mp 46—48°C.

c) Hydrogenation of N-Methyl-cis-1,2,3,4,4a,9,9a,10-Octahydroacridine (Va) over Platinum. Compound Va (5.0 g) was hydrogenated over Adams' platinum (0.5 g) in the same manner as mentioned above, and 1850 m*l* of hydrogen was consumed (the calculated, 1770 m*l*) after 4 hr. An oily mixture of bases obtained by usual methods was dissolved in acetone and treated with aqueous hydrogen iodide, when a hydroiodide (0.4 g) separated out and was collected by filtration. It had mp 224—226°C on recrystallization from ethanol, which was depressed to 185—200°C on admixture with the hydroiodide of Ia, mp 220—222°C. Regeneration gave a free base, bp 157—160°C/20 mmHg. As the hydroiodide of IIa or IIIa was not obtained in crystalline state, this base would be a new isomer (VIa) named δ, but the compound was not further characterized because of the small amount.

Found: C, 80.80; H, 12.03%. Calcd for $C_{14}H_{25}N$: C, 81.09; H, 12.15%.

Found: C, 49.88; H, 8.03%. Calcd for $C_{14}H_{26}NI$: C, 50.15; H, 7.82%.

The aqueous acetone solution obtained on filtration of the hydroiodide of VIa was evaporated, made alkaline and extracted with ether. The ether extract, after removal of the solvent, was converted into the picrate in methanol, from which the picrate (6.0 g), mp 154—156°C, of IIIa, was isolated. Regeneration followed by distillation afforded IIIa (2.6 g), mp 45—47°C.

d) Methiodides. To an acetone or ether solution of Ia (1.7 g) was added methyl iodide (8.0 g) dropwise under cooling, when the methiodide separated out and was collected by filtration. Recrystallization from ethanol gave Ib (1.9 g), mp 273—275°C. On concentration of the mother liquor, an additional amount (0.3 g) of the crude methiodide, mp 263—266°C, was obtained.

Found: C, 51.63; H, 7.99%. Calcd for $C_{15}H_{28}NI$: C, 51.57; H, 8.08%.

Compound IIa (1.2 g) in acetone was refluxed with an excess of methyl iodide for 1 hr. Recrystallization

of the resulting methiodide from 95% ethanol afforded IIb (1.2 g), mp 210—212°C.

Found: C, 51.33; H, 8.28%. Calcd for $C_{15}H_{28}NI$: C, 51.57; H, 8.08%.

Compound IIIa (2.0 g) was converted into the corresponding methiodide (IIIb, 2.7 g) in the same manner as Ia, which had mp 262—264°C on recrystallization from ethanol.

Found: C, 51.64; H, 8.24%. Calcd for $C_{15}H_{28}NI$: C, 51.57; H, 8.08%.

α-Perhydrophenanthridine (VII). Compound VII was prepared according to the method reported previously[5] and had mp 103—104°C; mass spectrum, *m/e* 193 (M^+), 192, 151, 150, 136, and *ca.* 117 (a metastable ion). The strongest peak would be due to an ion formulated as XX.[25] The picrate had mp 231—233°C (lit.,[5] 210—212°C) on recrystallization from ethanol.

Found: N, 13.21%. Calcd for $C_{19}H_{26}O_7N_4$: N, 13.26%.

β-Perhydrophenanthridine (VIII). a) Compound VIII was obtained in 25% yield by hydrogenation of 7,8,9,10-tetrahydrophenanthridine over Adams' platinum.[5]

b) *trans*-1,2,3,4,4a,5,6,10b-Octahydrophenanthridine[6] (XI, 1.0 g) in ethanol (30 m*l*) containing 2.4 N hydrochloric acid[12] (2.5 m*l*) was hydrogenated over Adams' platinum (0.2 g) at room temperature for 5 hr, when 460 m*l* of hydrogen had been adsorbed (the calculated, 450 m*l*). The reaction mixture, after being worked up as usual, gave a solid base (0.85 g) melting at 105—118°C. Recrystallization from petroleum ether afforded a pure sample (0.7 g) of VIII, mp 122—123°C (lit.,[5] 119—121°C).

Found: C, 80.80, 80.95, 81.00; H, 12.02, 12.27, 11.74; N, 7.25%. Calcd for $C_{13}H_{23}N$: C, 80.76; H, 11.99; N, 7.25%.

Compound VIII showed essentially the same mass spectrum as VII, and the picrate had mp 223—225°C on recrystallization from ethanol.

Found: C, 54.33; H, 6.54%. Calcd for $C_{19}H_{26}O_7N_4$: C, 54.02; H, 6.20%.

c)[26] *cis*-5,6,6a,7,8,9,10,10a-Octahydrophenanthridine[5] (X, 500 mg) was hydrogenated over Adams' platinum (50 mg) at room temperature in acetic acid for 4 hr, when 200 m*l* of hydrogen had been consumed (the calculated, 180 m*l*). The reaction product, after being worked up as usual, crystallized, amounted to 522 mg, and melted at 115—120°C. Recrystallization from petroleum ether gave VIII (338 mg), mp 118—120°C.

γ-Perhydrophenanthridine (XIII). *cis*-1,2,3,4,4a,5,6,10b-Octahydrophenanthridine[6] (XII, 1.35 g) was hydrogenated over Adams' platinum (0.50 g) at room temperature in ethanol (70 m*l*) containing 2.4 N hydrochloric acid (3.5 m*l*). The reaction ceased after 24 hr, when 500 m*l* of hydrogen had been consumed (the calculated, 530 m*l*). The product (1.30 g) obtained after usual treatment was semi-solid and recrystallized from petroleum ether to yield XIII (0.32 g), mp 122—123°C. The mother liquor on the recrystallization was evaporated to dryness, and the residue (0.75 g) was converted into the picrate in ether. Upon repeated recrystallizations of the picrate from methanol, three kinds of picrates having mp 194—196°C (0.96 g), mp 178—180°C (60 mg) and mp 180—181°C (20 mg) were isolated, but the last two were not further examined. Regeneration of the picrate of mp 196°C gave a free base (348 mg), mp 35—37°C. Recrystallization from petroleum ether afforded an analytical sample (100 mg) of XIII, mp 37—38°C, which showed practically the same mass spectrum as VII.

Found: C, 80.60; H, 12.17; N, 7.48%. Calcd for $C_{13}H_{23}N$: C, 80.76; H, 11.99; N, 7.25%.

Found: N, 12.98%. Calcd for $C_{19}H_{26}O_7N_4$: N, 13.26%.

N-Methyl-α-, β- and γ-perhydrophenanthridines (VIIa, VIIIa and XIIIa) and Their Methiodides (VIIb, VIIIb and XIIIb). a) These *N*-methyl derivatives were prepared from the respective secondary amines (VII, VIII and XIII) by the same treatment (formic acid and formalin) as Ia, and had the following melting and/or boiling points. Compound VIIa had mp 26—28°C on recrystallization from petroleum ether and bp 155—157°C/20 mmHg, and the picrate mp 199—201°C after preparation in ether and recrystallization from 95% ethanol.

Found: C, 81.26; H, 11.99; N, 6.56%. Calcd for $C_{14}H_{25}N$: C, 81.09; H, 12.15; N, 6.76%.

Found: C, 54.88; H, 6.61%. Calcd for $C_{20}H_{28}O_7N_4$: C, 55.03; H, 6.47%.

Compound VIIIa and its picrate had mp 62—64°C (from petroleum ether) and mp 190—192°C (95% ethanol).

Found: C, 81.22, 80.00; H, 12.20, 11.91; N, 6.42%. Calcd for $C_{14}H_{25}N$: C, 81.09; H, 11.99; N, 6.56%.

Found: C, 55.19; H, 6.71%. Calcd for $C_{20}H_{28}O_7N_4$: C, 55.03; H, 6.47%.

Compound XIIIa, oil, boiled at 155—159°C/20 mmHg, and its picrate had mp 198—199°C after preparation in ether and recrystallization from methanol.

Found: C, 81.35; H, 11.89; N, 6.88%. Calcd for $C_{14}H_{25}N$: C, 81.09; H, 12.15; N, 6.76%.

Found: C, 55.23; H, 6.56%. Calcd for $C_{20}H_{28}O_7N_4$: C, 55.03; H, 6.47%.

b) Methiodides. Methylation of these *N*-methyl derivatives (VIIa, VIIIa and XIIIa) with methyl iodide proceeded as smoothly as Ia to give the corresponding methiodides (VIIb, VIIIb and XIIIb) in good yields, which on recrystallization from ethanol had mp 265—267°C, 272—274°C and 315—316°C, respectively.

Found (VIIb): C, 51.33; H, 8.12%. Calcd for $C_{15}H_{28}NI$: C, 51.57; H, 8.08%.

Found (VIIIb): C, 51.56; H, 8.05%. Calcd for $C_{15}H_{28}NI$: C, 51.57; H, 8.08%.

Found (XIIIb): C, 51.36; H, 7.89%. Calcd for $C_{15}H_{28}NI$: C, 51.57; H, 8.08%.

Formation of Methiodides. The rate of the methiodide formation was measured in 20 m*l* of a 99.5% ethanol solution. In practice, 10 m*l* of the ethanol solution of a tertiary amine (0.03—0.05 M) and equal volume of the ethanol solution containing 1 m*l* of methyl iodide (*ca.* 1.5 M) was separately brought to constant temperature and then mixed in a brown flask closed with a tightly fitting stopper. After suitable intervals, 2 m*l* of the solution was drawn and 5 m*l* of 0.02 N hydrochloric acid was added. The excess of the acid was back-titrated with an aqueous barium hydroxide

25) *Cf.* The mass spectra of IX and X; *m/e*, 187 (M^+), 186, 144, 130, and *ca.* 90 (a metastable ion).
26) Carried out with Mrs. Masayo Murata.

solution, using methyl-red as an indicator. It was found that 5.0 m*l* of the hydrochloric acid was equivalent to 2.96 m*l* of the barium hydroxide solution. The rate constant was then calculated using the usual expression for a second-order reaction in which methyl iodide was present substantially in a constant concentration. The result is summarized in Table 1.

Measurement of Basicity. This was carried out at 20°C in 60% aqueous ethanol according to the method of Thomson.[27] The basicity is expressed by the pK_a value of a conjugate acid of each base and the result is summarized in Table 1.

Formation of Hydrogen Bonds with *n*-Butanol. Infrared absorption spectra were determined at 20°C using a Nihon Bunko double-beam spectrophotometer, Model DS 301, equipped with sodium chloride optics. The measurement was run at 0.1—0.2 M of tertiary or secondary amines in carbon tetrachloride containing 0.05 M of *n*-butanol. The sodium chloride cell of 0.5 mm of thickness was used and the absorption of the solvent was compensated by placing a cell of the same thickness filled with the solvent in the reference beam.

Carbon tetrachloride used as the solvent was first washed with conc. sulfuric acid, dil. sodium carbonate solution and water, successively, dried with anhydrous sodium sulfate, and distilled over phosphorus pentoxide. *n*-Butanol was used after being refluxed with calcium oxide for 20 hr and distilled under reduced pressure.

The Hofmann Degradation of Methiodides of *N*-Methyl-α- and γ-perhydroacridines (Ia and IIIa) and of *N*-Methyl-α-, β- and γ-perhydrophenanthridines (VIIa, VIIIa and XIIIa). A solution of Ia (1.2 g) in 50% aqueous ethanol (20 m*l*) was shaken with silver oxide prepared from silver nitrate (0.8 g) at room temperature for 3 hr. After filtration followed by evaporation of the filtrate, the syrupy residue was heated to 180°C (bath temperature) under reduced pressure. The pyrolysis of the methohydroxide took place violently at 140—150°C. The distillate was extracted with ether, and the ether solution gave a solid base (0.45 g) on removal of the solvent, which had mp 38—40°C on recrystallization from petroleum ether and was identified as Ia. The picrate melted at 170—172°C on recrystallization from ethanol.

The pyrolysis of IIIb, VIIb, VIIIb and XIIIb was carried out in the same manner as Ia. Compound IIIb (2.8 g) produced IIIa (1.1 g), mp 46—48°C; the picrate, mp 162—164°C. Compound VIIb (1.8 g) gave VIIa (0.7 g), bp 152—153°C/18 mmHg and mp *ca.* 25°C; the picrate, mp 198—200°C. Compound VIIIb (1.1 g) afforded VIIIa (0.4 g), mp 62—64°C; the picrate, mp 190—192°C. Compound XIIIb (100 mg) gave XIIIa (52 mg), oil, which was converted into the picrate, mp 198—199°C.

The Hofmann Degradation of *N*-Methyl-β-perhydroacridine Methiodide (IIb).[28] Compound IIb (1.2 g) was converted into the syrupy methohydroxide by treatment with silver oxide prepared from silver nitrate (0.6 g), which decomposed at 120—130°C (bath temperature). The product was purified by distillation under reduced pressure followed by conversion into the picrate in ether-methanol, which had mp 147—149°C on recrystallization from ethanol. Regeneration of the picrate gave a free base, which was again distilled to yield an oily base (XVIII, 0.4 g) in pure state, bp 154—156°C/17 mmHg; IR, ν_{max}^{film} 1660 (w) and 720 (m) cm^{-1}.

Found: C, 81.25; H, 12.09; N, 6.25%. Calcd for $C_{15}H_{27}N$: C, 81.38; H, 12.29; N, 6.33%.

Found: C, 56.09; H, 6.68%. Calcd for $C_{21}H_{30}O_7N_4$: C, 55.99; H, 6.71%.

Compound XVIII (0.20 g) in acetic acid (10 m*l*) was hydrogenated over Adams' platinum (0.05 g) at room temperature for 3 hr. The reaction mixture was worked up as usual and gave the dihydro derivative (0.10 g), oil, which showed no absorption near 1660 and 720 cm^{-1} and gave the picrate, mp 147—149°C (from ethanol).

Found: C, 80.47; H, 13.23; N, 6.26%. Calcd for $C_{15}H_{29}N$: C, 80.64; H, 13.09; N, 6.27%.

Found: C, 55.51; H, 7.09; N, 12.19%. Calcd for $C_{21}H_{32}O_7N_4$: C, 55.74; H, 7.13; N, 12.38%.

Compound XVIII (100 mg) was oxidized with osmium tetroxide (173 mg) in dry benzene (5 m*l*) at room temperature. After 24 hr black osmate precipitated out, was centrifugalized and collected by filtration. The osmate (280 mg) was treated with sodium sulfite (1550 mg as $Na_2SO_3 \cdot 7H_2O$) for 5 hr in a refluxing mixture of water (10 m*l*) and ethanol (7 m*l*). After filtration of the resulting precipitate, the aqueous ethanol solution was evaporated under reduced pressure and shaken with ether repeatedly. The ether solution afforded an oily glycol (70 mg), which without further purification was acetylated with acetic anhydride (0.7 m*l*) and pyridine (0.15 m*l*) on a water bath for 2 hr. The mixture gave an oily acetate (60 mg) after being worked up as usual and distilled under reduced pressure, which showed no absorption near 3400 cm^{-1}.

Found: C, 67.28; H, 9.94; N, 3.88%. Calcd for $C_{19}H_{33}O_4N$: C, 67.22; H, 9.80; N, 4.13%.

Compound XVIII (0.30 g) was refluxed in acetic acid (10 m*l*) for 3 hr. The solution was then evaporated under reduced pressure, made alkaline with aqueous potassium hydroxide solution, and treated with ether to remove ether-soluble substance. To the aqueous solution was added potassium iodide, and the resulting solution was again evaporated to dryness and extracted with hot ethanol. Concentration of the ethanol solution gave a mixture of methiodides, from which *N*-methyl-α-perhydroacridine methiodide (Ib, 0.18 g), mp 272—275°C, was isolated on recrystallization from ethanol.

27) G. Thomson, *J. Chem. Soc.*, **1946**, 1113.

28) Carried out with Shuichi Tonooka.

BULLETIN OF THE CHEMICAL SOCIETY OF JAPAN VOL. 41 2466—2472 (1968)

Infrared-spectral Studies on the Orientation of the Lone Pairs in Piperidine Derivatives[1]

Tadashi MASAMUNE, Mitsuo TAKASUGI and Minoru MATSUKI

Department of Chemistry, Faculty of Science, Hokkaido University, Sapporo

(Received February 1, 1968)

The infrared spectra of stereoisomers of several piperidines and their *N*-methyl derivatives in carbon tetrachloride have been measured in the region of 3020 to 2500 cm^{-1}. The estimated intensities (A) of their Bohlmann bands have been analyzed, provided that Formula (1) concerning the intensity defined in the text holds for the compounds examined. The result indicates that piperidine exists mainly, but not exclusively, in the conformation with the lone pair axial.

For some years attention has been drawn to the steric requirement of a nitrogen lone pair.[2] In 1958 Aroney and LeFèvre[3] examined the Kerr constants of piperidine and *N*-methyl piperidine and concluded that the nitrogen lone pair is more bulky[4] than the hydrogen and approximately equivalent to the methyl group. Their conclusion has since been criticized by several groups,[5-11] especially by Allinger,[7] Katritzky,[5b] Lambert,[8a] and their co-workers,[12] and there remains now little doubt that the lone pair is axially oriented in *N*-substituted piperidines. However, no consistent conclusion is drawn regarding the relative orientation of the hydrogen and the lone pair in *N*-unsubstituted piperidines, although evidence has recently accumulated that the latter is smaller than the former.[13] In a preliminary communciation[11] we reported an attempt to determine a preference of the hydrogen for the equatorial position in *N*-unsubstituted piperidines on the basis of their Bohlmann bands, and the present paper describes the full details.

Bohlmann[14] reported an empirical relation between the configurations of quinolizidine derivatives and their infrared bands in the region of 2800 to 2700 cm^{-1} (general region, no exact limits) called the Bohlmann bands; namely, these bands have been correlated with the presence of at least two α-hydrogens oriented *anti*-coplanar to the lone pair. The property of this correlation has since been confirmed in the determination of configurations of related compounds[15]. Recently Hamlow and his co-workers[16] attempted to rationalize such "absorption bands" in the spectra and also "the large chemical shift difference[16,17] (0.80—0.93 ppm)" between the axial and equatorial α-protons, and proposed that these facts would be caused by the overlap of the lone pair and the anti-bonding σ^* C–H_{axial} orbital on the adjacent carbon. Apart from this rationalization, although it seems to be most valid at least concerning the infrared

1) Part XVIII of "The Condensed Polynuclear Perhydro-compounds Containing Nitrogen"; Part XVII, Ref. 20.

2) For a recent review, see F. G. Riddell, *Quart. Rev.*, **21**, 364 (1967); G. Yamamoto, *Kagaku no Ryoiki (J. Japan Chem.)*, **21**, 715, 817 (1967).

3) a) M. J. Aroney and R. J. W. LeFèvre, *J. Chem. Soc.*, **1958**, 3002. b) M. J. Aroney, C. -Y. Chen, R. J. W. LeFèvre and J. D. Saxby, *ibid.*, **1964**, 4269.

4) The "more bulky or larger" of the groups is defined in this context as that which preferentially assumes the equatorial position.

5) a) T. M. Moynehan, K. Schofield, R. A. Y. Jones and A. R. Katritzky, *J. Chem. Soc.*, **1962**, 2637; K. Brown, A. R. Katritzky and A. J. Warning, *ibid., (B)*, **1967**, 487. b) P. J. Brignell, A. R. Katritzky and P. L. Russel, *Chem. Commun.*, **1966**, 723. c) R. J. Bishop, L. E. Sutton, D. Dineen, R. A. Y. Jones, A. R. Katritzky and R. J. Wyatt, *J. Chem. Soc., (B)*, **1967**, 493.

6) N. W. J. Pumphrey and M. J. T. Robinson, *Chem. Ind.*, **1963**, 1903.

7) N. L. Allinger, J. G. D. Carpenter and F. M. Karkowski, *J. Am. Chem. Soc.*, **87**, 1232 (1965).

8) a) J. B. Lambert, R. G. Keske, R. E. Carhart and A. P. Jovanovich, *ibid.*, **89**, 3761 (1967). b) J. B. Lambert, R. G. Keske and D. K. Weary, *ibid.*, **89** 5921 (1967).

9) E. L. Eliel and Sr. M. Carmeline Knoeber, *ibid.*, **88**, 5347 (1966).

10) H. Booth and A. H. Bostock, *Chem. Commun.*, **1967**, 177.

11) T. Masamune and M. Takasugi, *ibid.*, **1967**, 625.

12) For the steric requirement of lone pairs on the atoms other than the nitrogen, see Refs. 2, 8b and 9.

13) For the contrary conclusion, see Refs. 3b and 8a.

14) F. Bohlmann, *Chem. Ber.*, **91**, 2157 (1958).

15) For examples, see R. E. Brown, D. M. Lustgarten, R. J. Stanaback and R. I. Meltzer, *J. Org. Chem.*, **31**, 1489 (1966); H. O. House, B. A. Tefertiller and C. G. Pitt, *ibid.*, **31**, 1073 (1966); W. E. Rosen, *ibid.*, **30**, 2044 (1965); M. Hesse, W. v. Philipsborn, D. Schumann, G. Spiteller, M. Spiteller-Friedmann, W. I. Taylor, H. Schmid and P. Karrer, *Helv. Chim. Acta*, **99**, 878 (1964).

16) H. P. Hamlow, S. Okuda and N. Nakagawa, *Tetrahedron Letters*, **1964**, 2553.

17) F. Bohlmann, D. Schumann and H. Schulz, *ibid.*, **1965**, 173; F. Bohlmann, D. Schumann and C. Arndt, *ibid.*, **1965**, 2703.

bands, the Bohlmann bands are expected to appear in *N*-unsubstituted piperidines as well as in quinolizidines, as far as the above-mentioned spatial requirement is satisfied for the lone pair and the α-hydrogen. However, only little attention[6,18,19] has been paid to the bands of the piperidines and no quantitative estimation appears to have been reported. In the preceding paper[20] of this series, we described the preparation and configuration of stereoisomers of perhydroacridine and perhydrophenanthridine. Having utilized these and related piperidines, it was attempted to determine the orientation of the lone pair by measurement of their Bohlmann bands and subsequent analysis of the intensities on appropriate assumptions.

Experimental

The infrared absorption bands of the following piperidine derivatives have been measured in the region of 3020 to 2500 cm^{-1}: piperidine (I), *trans*- and *cis*-perhydroquinolines[21] (II and III), *trans, syn, trans*-, *trans, anti, cis*- and *trans, syn, cis*-perhydroacridines[20,22] (IV, V and VI), *trans, anti, trans*-, *trans, syn, cis*- and *cis, syn, cis*-perhydrophenanthridines[20,23] (VII, VIII and IX), *trans*- and *cis*-2,6-dimethylpiperidines[24] (X and XI), *N*-methyl derivatives (Ia to XIa) of I to XI, and quinolizidine[25] (XII). The configurations of these compounds have all been established. The spectra of the *N*-benzoyl derivatives (Ib to XIb) of I, II, V,[26] VII, and XI have also been measured.

Materials. Most of the compounds examined were prepared by procedures described in the literatures. Solid compounds were recrystallized to constant melting point and liquids were freshly distilled before use. Only *N*-benzoyl-α-perhydrophenanthridine (VIIb) and *N*-methyl-*trans*- and *cis*-2,6-dimethylpiperidines (Xa and XIa) were new.

Treatment of VII (200 mg) in ether (10 m*l*) with benzoyl chloride (0.6 m*l*) and 3 N aqueous potassium hydroxide solution (10 m*l*) at room temperature for 20 hr gave the crude *N*-benzoyl derivative, which on recrystallization from *n*-hexane afforded a pure sample (107 mg) of VIIb, mp 98—100°C.

Found: C, 80.55; H, 9.32; N, 4.44%. Calcd for $C_{20}H_{27}ON$: C, 80.76; H, 9.15; N, 4.71%.

A mixture of XI (350 mg), formic acid (1.0 m*l*) and 33% formalin (0.9 m*l*) was heated on a steam bath for 3 hr and then cooled. The mixture was diluted with conc potassium hydroxide solution, saturated with sodium chloride and extracted with ether. The ether extract, after being dried with anhydrous sodium sulfate, was distilled over solid potassium hydroxide. The distillate was redistilled over calcium oxide and a fraction (XIa, 78 mg) of bp 139—142°C was collected. In a similar way, the corresponding *trans* isomer (Xa) was obtained and had bp 140—143°C.

Found (XIa): C, 75.35; H, 13.61%. Calcd for $C_8H_{17}N$: C, 75.52; H, 13.47%.

Found (Xa): C, 75.23; H, 13.75%. Calcd for $C_8H_{17}N$: C, 75.52; H, 13.47%.

Measurements of the Infrared Spectra. The spectra were recorded at 23°C on a Nippon Bunko 402-G spectrophotometer with 0.2 and/or 0.5 mm cells, using carbon tetrachloride solutions containing about 0.03 M of the samples. The wave numbers quoted were believed to be accurate to ± 3 cm^{-1}. The integrated intensities were expressed in this paper by $\int \varepsilon_\nu \delta\nu$, where ε_ν is the molecular extinction coefficient at the wave number ν.[27] The estimated uncertainty of the intensity was about 10%.

Results and Discussions

The spectra of several compounds are given in Figs. 1 to 4. As shown in the figures, each spectrum of *N*-unsubstituted- and *N*-methyl-piperidines and quinolizidine exhibited a sharp absorption minimum at 2820 ± 3 cm^{-1}, but, to the contrary, that of *N*-benzoyl derivatives only a plain absorption curve near the region. This strongly suggests that the Bohlmann bands must be included in the bands below 2820 cm^{-1},[28] and also indicates that, in the amides, the overlap[16] in question of the lone pair is largely forbidden due to the overlap with the benzoyl group. Thus the bands below 2820 cm^{-1} of *N*-benzoyl derivatives would be reasonably regarded as the background in the region of the corresponding piperidines. Then we have defined the difference between the integrated intensity (I_A) of the band in the 2820 to 2500 cm^{-1} range and that (I_B) of its background at that (A) of the Bohlmann band.

Before considering the intensities, it is desirable to mention the conformations of piperidine rings. *trans*-Perhydroquinoline II, three perhydroacridines IV to IV, two perhydrophenanthridines VII and VIII, and their *N*-methyl derivatives all include at least one *trans*-fused linkage and exist in rigid

18) C.-Y. Chen and R. J. W. LeFèvre, *ibid.*, **1965**, 1611.
19) R. Barchet and T. P. Forrest, *ibid.*, **1965**, 4229.
20) T. Masamune, M. Ohno, K. Takemura and S. Ohuchi, This Bulletin, **41**, 2458 (1968).
21) F. E. King, T. Henshall and R. L. St. D. Whitehead, *J. Chem. Soc.*, **1948**, 1373; M. Ehrenstein and W. Bunge, *Ber.*, **67**, 1715 (1934); C. F. Bailey and S. M. McElvain, *J. Am. Chem. Soc.*, **52**, 4015 (1930).
22) T. Masamune and S. Wakamatsu, *Nippon Kagaku Zasshi (J. Chem. Soc. Japan, Pure Chem. Sect.)*, **77**, 1145 (1956).
23) T. Masamune and Y. Kubota *ibid.*, **77**, 1467 (1956).
24) a) R. K. Hill and T. H. Chan, *Tetrahedron*, **21**, 2015 (1965); R. K. Hill, T. H. Chan and J. A. Joule, *ibid.*, **21**, 147 (1965). b) A. Marcus and R. Wolffenstein, *Ber.*, **34**, 2426 (1901); *ibid.*, **32**, 2525 (1899).
25) The authors are grateful to Dr. Ichiro Kawasaki, Osaka University, for providing them with quinolizidine.
26) "Compound IVb" in a preliminary communication (Ref. 11) should be revised to "Vb."
27) *Cf.* K. S. Seihardi and N. R. Jones, *Spectrochim. Acta*, **19**, 1013 (1963).
28) The examination of each spectrum suggests that the tailing intensity in the region above 2820 cm^{-1} of the Bohlmann band would be negligibly small as compared with that in the region below 2820 cm^{-1} of the band produced by usual C–H vibrations.

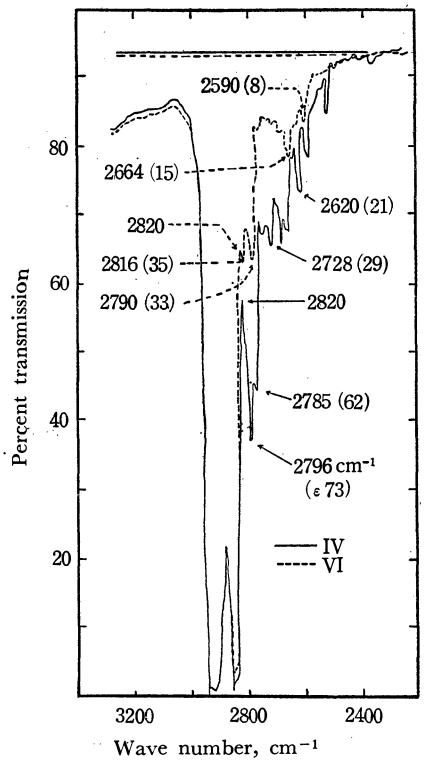

Fig. 1. Infrared spectra of α- and γ-perhydroacridines (IV and VI).
IV, 5.82 mg in 0.1 m*l* CCl_4, cell 0.2 mm
V, 4.93 mg in 0.1 m*l* CCl_4, cell 0.2 mm

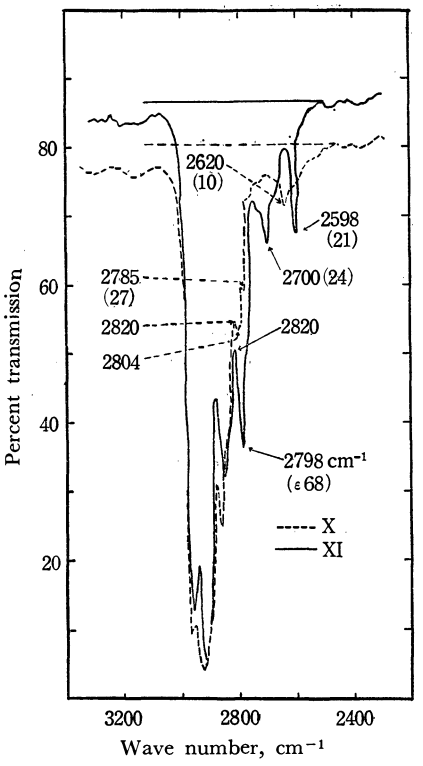

Fig. 2. Infrared spectra of *trans*- and *cis*-2.6-dimethylpiperidines (X and XI).
X, 8.0 mg in 0.2 m*l* CCl_4, cell 0.2 mm
XI, 8.0 mg in 0.2 m*l* CCl_4, cell 0.2 mm

conformations consisting of only chair-formed rings.[20] The other compounds except XII can take two conformations formed by ring inversion. In *trans*-2,6-dimethylpiperidine (X) and its *N*-methyl derivative Xa, the inversion leads to formation of the same conformer as the original, apart from the *N*-substituents, which has a conformation with one α-methyl group axial and with the other equatorial. To the contrary, the *cis* isomers XI and XIa, when flipped, are converted from a conformation with two equatorial α-methyl groups into a definitely unstable one with the two axial groups and are, therefore, essentially confined to the former. The same is the case in quinolizidine XII;[29] XII is practically fixed at one conformation with *trans*-fused rings, and only a negligible amount of the other conformer exists in the equilibrium mixture, which is formed by inversion of configuration at the nitrogen. Each of the remaining four compounds, *cis*-perhydroquinoline III, *cis, syn, cis*-perhydrophenanthridine IX, and their *N*-methyl compounds IIIa and IXa, would exist as an equilibrium mixture of conformers flipped with each other, one having two axial α-hydrogens and the other only one.*1 At the present stage it might be impossible to discuss the ratio of the conformers, as it would very largely depending on the relative steric requirement of the lone pair and the *C*-hydrogen. In summary, all the compounds other than III, IIIa, IX and IXa have rigid or essentially fixed conformations. In most of those compounds two hydrogens are oriented axial on the α-carbons in the respective piperidine rings, while in VI, VIa, X and Xa only one hydrogen and in XII three hydrogens exist at the axial conformation.

Francis[30] measured the integrated intensities of

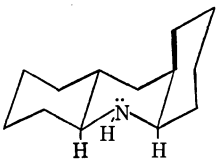

V

29) E. L. Eliel, N. L. Allinger, S. J. Angyal and G. A. Morrison, "Conformational Analysis," Interscience Publishers, New York, N. Y. (1965), p. 252.

*1 The piperidine ring of the compound IX might adopt a twisted boat form owing to the presence of 1,3-diaxial methylene groups rather than a chair form. However, whatever the conformation is, the same conclusion will be drawn, because no discussion on the intensity of IX is involved in the section "Quantitative Consideration."

30) S. A. Francis, *J. Chem. Phys.*, **18**, 861 (1950).

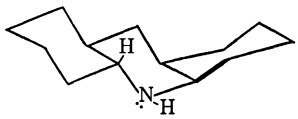

VI

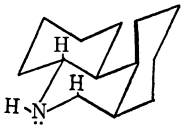

VIII

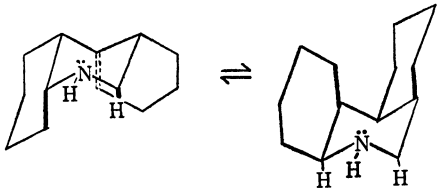

IX

the bands near 2900 cm^{-1}, produced by the in-plane and out of plane C–H vibrations, of a series of aliphatic hydrocarbons, and indicated the intensities to be interpretable well on the basis that the hydrocarbon molecule behaves like a non-interacting mixture of methyl, methylene and methine structural groups. Hence we first estimated the integrated intensities (I_t) of the bands

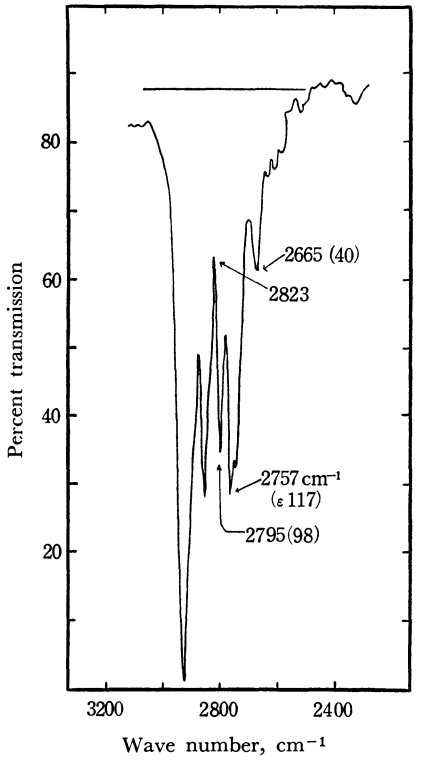

Fig. 3. Infrared spectrum of quinolizidine (XII).
XII, 5.7 mg in 0.2 m*l* CCl_4, cell 0.2 mm

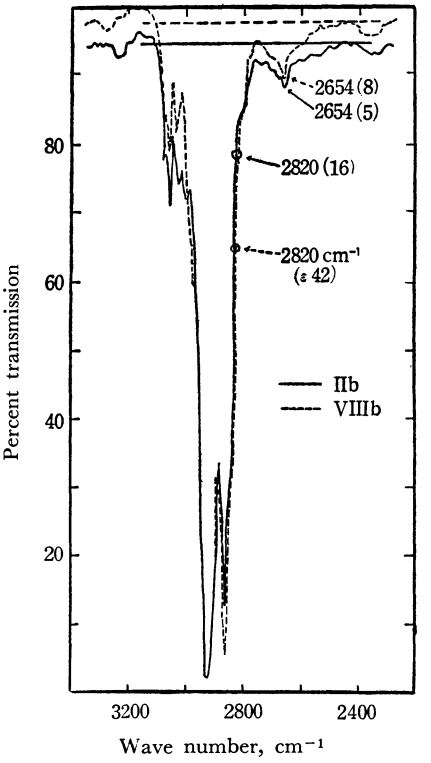

Fig. 4. Infrared spectra of *N*-benzoyl-*trans*-perhydroquinoline (IIb) and α-perhydrophenanthridine (VIIb).
IIb, 13.7 mg in 0.20 m*l* CCl_4, cell 0.2 mm
VIIb, 14.3 mg in 0.25 m*l* CCl_4, cell 0.2 mm

in the 2820 to 3000 cm^{-1} range of the present compounds. Although the intensities varied largely depending on the number of the vibrations concerned (Table 1), the average (I_m) per one C–H vibration fell within $(1.6\pm0.1)\times10^3$ $l/cm^2\cdot mol$, which was roughly equal to the corresponding, 1.3×10^3 $l/cm^2\cdot mol$,[30] for a methylene group of aliphatic hydrocarbons.

The integrated intensities (A) of the Bohlmann bands are summarized in Table 2. As shown in the table, the bands exhibited considerable intensity not only in *N*-unsubstituted piperidines having two axial α-hydrogens but also in those with only one. This observation, however, does not imply that the lone pair assumes exclusively the axial position in the piperidines.

Qualitative Consideration. The compounds examined are classified into two groups by the conformation of *N*-substituents. Compounds involved in the first class are *N*-methylpiperidines (Ia to XIa) and quinolizidine (XII). These compounds would be locked almost exclusively into a conformation with the lone pair axial. In compounds Ia, IIa, IVa Va, VIIa, VIIIa, XIa, and XII, which have two α-axial hydrogens and, accordingly, three hydrogens *anti*-coplanar to the axial lone

Table 1. Integrated intensities of the bands in the region of 3000 to 2820 cm^{-1} of piperidine derivatives

Compound	Intensities[a,b] I_t	Intensities[a,b] I_m	Compound	Intensities[a,b] I_t	Intensities[a,b] I_m	Compound	Intensities[a,b] I_t	Intensities[a,b] I_m
Ia	16.5	1.65	I	12.9	1.60	Ib	15.4	1.54
IIa	24.7	1.55	II	23.4	1.67	IIb	24.7	1.55
IIIa	25.6	1.60	III	22.4	1.60			
IVa	34.1	1.55	IV	31.8	1.59			
Va	34.1	1.55	V	30.8	1.54	Vb	34.3	1.55
VIa	36.4	1.58	VI	33.7	1.60			
VIIa	35.2	1.60	VII	32.9	1.65	VIIb	34.2	1.55
VIIIa	35.3	1.60	VIII	33.2	1.66			
IXa	37.7	1.70	IX	33.0	1.65			
Xa	23.0	1.53	X	21.2	1.63			
XIa	21.6	1.55	XI	18.5	1.54	XIb	21.8	1.55
XII	22.4	1.60						

a) The unit; $(l/cm^2 \cdot mol) \times 10^{-3}$.
b) The "I_t and I_m" refer to the total and average integrated intensities, respectively. The latter was obtained by division of I_t by the number of *C*-hydrogens which are not participating in the Bohlmann band.

Table 2. Integrated intensities of the Bohlmann bands of piperidine derivatives

Compound	Intensities[a,b] I_A	I_B	A	Compound	Intensities[a,b] I_A	I_B	A
Ia	11.4	0.8[c]	10.6	I	5.6	0.6[h]	5.0
IIa	11.2	1.2[d]	10.0	II	5.6	1.0[i]	4.6
IIIa	11.6	1.2[d]	10.4	III	6.7	1.0[i]	5.7
IVa	11.8	1.8[e]	10.0	IV	6.0	1.6[j]	4.4
Va	12.5	1.8[e]	10.7	V	7.0	1.6[j]	5.4
VIa	6.5	1.8[e]	4.7	VI	3.6	1.6[j]	2.0
VIIa	12.2	1.7[f]	10.5	VII	6.1	1.5[k]	4.6
VIIIa	10.3	1.7[f]	8.6	VIII	4.7	1.5[k]	3.2
IXa	12.6	1.7[f]	10.9	IX	7.3	1.5[k]	5.8
Xa	5.7	1.0[g]	4.7	X	2.8	0.8[l]	2.0
XIa	10.5	1.0[g]	9.5	XI	5.4	0.8[l]	4.6
XII	11.5	1.0[i]	10.5				

a) The unit; $(l/cm^2 \cdot mol) \times 10^{-3}$.
b) The "I_A, I_B and A" refer to the integrated intensities of the band in the region below 2820 cm^{-1}, its background and the Bohlmann band, respectively.
c—g) These figures denote the intensities (I_B) in the 2820 to 2500 cm^{-1} range of Ib, IIb, Vb, VIIb and XIb, respectively.
h—l) These figures were obtained by multiplication of I_B of Ib, IIb, Vb, VIIb and XIb and the following fractions, 8/10, 14/16, 20/22, 20/22 and 12/14, respectively.[31]

pair and participating in the Bohlmann band, the intensities fell within (8.6 to 10.9) $\times 10^3$ $l/cm^2 \cdot$ mol (the unit will be omitted). On the other hand, compounds VIa and Xa, having only the two relevant hydrogens, showed the weak intensity of 4.7. Compounds of the second class are *N*-unsubstituted piperidines, in which the lone pair is located in an undetermined position. Of these piperidines, compounds except VI and X have two axial α-hydrogens and showed intensities of 3.2 to 5.8, which amounted to only 46% (55—36%) of those of the respective *N*-methyl derivatives. The two compounds have only one axial α-hydrogen and exhibited the weak intensity of 2.0, which accounted for only 43% of that of VIa and Xa.

31) Both the numerator and denominator of the fraction refer to the number of hydrogens associated with the usual C-H vibrations in each compound. For example, both IIb and IIa would contain 16 relevant hydrogens, while II 14 hydrogens of such a kind. It should be mentioned that, without such a treatment which appears arbitrary, we arrive at almost the same value of N_H*.

If these decreases (46 and 43%) in intensity resulted from only a shift from axial to equatorial lone pair, it would be concluded that the lone pair assumes an equatorial conformation with a slight preference. However, the decreases are undoubtedly attributed to various factors, and one of those must be the number of the relevant hydrogens. As described above, the intensities of the compounds, when compared in the respective class, decreased to about half (55—43 and 62—35%) in passing from the three to two relevant hydrogens and from the two to one, respectively. These facts suggest that the number of α-axial hydrogens as well as the orientation of the lone pair would play a considerably great role for the decrease (46 and 43%) in question. Although it might be impossible to estimate these factors at the present stage, it would be inferred certainly that the lone pair adopts an equatorial conformation preferentially.

Quantitative Consideration. Bearing in mind the afore-mentioned qualitative consideration, we next attempted to analyze the observed intensities on the basis of the following assumptions: *the intensity (A) of the Bohlmann band in each compound is the sum of those due to individual C–H vibrations in question.* Apparently, this assumption might not strictly be correct, as bands due to overtone and/or combination would be included in the region in question. However, the perplexity due to these bands would be mostly eliminated, because the background would also include such bands. Moreover, the intensities of the bands, even if not completely eliminated, would not be great. In the previous section it has been shown that the intensity of absorption near 2900 cm^{-1} of usual C–H vibrations equals the sum of those due to individual vibrations concerned in both aliphatic hydrocarbons and the present compounds. The assumption described above was proposed on the analogy of this fact. In the present paper, we will proceed further with the analysis, leaving the detailed examination for the validity of this analogy till later on.

The intensity A of the Bohlmann band is concerned not only with the orientation of the lone pair and the number and kind of the relevant hydrogens (oriented on the α-carbon and *anti*-coplanar to the lone pair) as discussed already, but also with the extent of the overlap in question[16] and the ring distortion.[18] Hence, the above-mentioned assumption is expressed by the following formula:[32]

$$A = \sum N \times n \times I \times S \times R \qquad (1)$$

where N is N_H or N_{Me}, n is n_p, n_s or n_t, I is I_p, I_s or I_t, S is $S_{2\beta}$ or $S_{1\beta}$, and R is R_1 R_2 or R_3.

32) The intensity A might be affected by factors other than those described. If so, Formula (1) is not a mathematical expression of the first assumption but rather a new assumption. However, as far as we know, the intensity appears to depend only or mostly on these factors.

The "N_H and N_{Me}" refer to the mole fractions of conformers with an axially oriented lone pair on the nitrogen. The "n_p, n_s and n_t" are the number of relevant hydrogens in methyl, methylene and methine groups, respectively, and are given directly from the structure of the compound. The "I_p, I_s and I_t" represent the intensities for the C–H vibrations in question (whose hydrogen is present *solely* in a compound involving no distortions and located in methyl, methylene and methine groups, respectively) and are called the unit intensity. The "$S_{2\beta}$ and $S_{1\beta}$" are the ratios of the intensity produced by each vibration in question to the corresponding unit intensity, when an axial methylene or methyl substituent is present at the β-position to two α-carbons and one α-carbon bearing the relevant hydrogen(s), respectively.[18] The "$R_1(=1)$, R_2 and R_3" are the ratios of the intensity of each vibration to the corresponding unit intensity, when there are one, two and three relevant hydrogens in a compound, respectively.[16]

The second assumption follows as. *The mole fractions N_H and N_{Me} are approximately constant for all the N-unsubstituted- and N-methyl-piperidines having no methylene or methyl group syn-axial to the lone pair or the hydrogen on nitrogen, respectively;* namely, $N_H = N_H^*$ (N_H of piperidine) and $N_{Me} = 0.95$.[33] On the other hand, for compound V having the afore-mentioned axial group, the mole fraction N_H is expressed by $N_H^* \times \beta_s$, where β_s is a parameter showing the effect of the group. *In compound Va, the N-methyl group is essentially fixed at the equatorial position;* namely, $N_{Me} = 1$. On the basis of these assumptions, the following equations are obtained for all the piperidines, having rigid or essentially fixed conformations, other than III, IIIa, IX and IXa.

For compounds with R_1;

VI and X $N_H^* \times I_t \times S_{1\beta} = 2.0,\ 2.0 = 2.0$[34] (2)

For compounds with R_2;

I $N_H^* \times 2I_s \times R_2 = 5.0$ (3)

II and VII $N_H^* \times (I_s + I_s) \times R_2 = 4.6,\ 4.6 = 4.6$ (4)

IV and XI $N_H^* \times 2I_t \times R_2 = 4.4,\ 4.6 = 4.6$ (5)

V $N_H^* \times 2I_t \times R_2 \times \beta_s = 5.4$ (6)

VIII $N_H^* \times (I_s + I_t) \times R_2 \times S_{2\beta} = 3.2$ (7)

VIa and Xa $(I_p + I_t) \times R_2 \times S_{2\beta} = 4.95,\ 4.95 = 4.95$ (8)

For compounds with R_3;

Ia $(I_p + 2I_s) \times R_3 = 11.1$ (9)

33) This value is cited from the report by Allinger *et al.*[7] The mole fraction N_{Me} of Ia has recently criticized by Katritzky *et al.*[5c]

34) The unit in Eqs. of (2) to (13); $10^{-3} \times l/cm^2 \cdot mol$.

IIa and VIIa $(I_p+I_s+I_t)\times R_3$
$=10.5,\ 10.5=10.5$ (10)

IVa, Va and XIa $(I_p+2I_t)\times R_3$
$=10.5,\ 10.7,\ 10.0=10.4$ (11)

VIIIa $(I_s+I_t)\times R_3\times S_{2\beta}+I_p\times R_3=9.05$ (12)

XII $(2I_s+I_t)\times R_3=10.5$ (13)

From Eqs. (9), (10), (11) and (13), we obtain

$$I_s=0.94\times I_p \quad (14)$$

and

$$I_t=0.84\times I_p \quad (15)$$

From Eqs. (3) (4) and (5), we obtain $I_s=1.11\times I_t$, which is consistent with Eqs. (14) and (15). Inserting Eqs. (14) and (15) into Eqs. (9), (10), (11), (13) and Eqs. (3), (4) and (5) yields

$$I_p\times R_3=3.88\times 10^3\ l/\mathrm{cm}^2\cdot\mathrm{mol} \quad (16)$$

and

$$N_H{}^*\times I_p\times R_2=2.64\times 10^3\ l/\mathrm{cm}^2\cdot\mathrm{mol} \quad (17)$$

Inserting Eqs. (17) and (16) into Eqs. (7) and (12) respectively gives

$$S_{2\beta}=0.68,\ 0.74=0.71$$

From the value of $S_{2\beta}$, Eqs. (8) and (6), we obtain

$$N_H{}^*=0.70 \quad \text{and} \quad \beta_s=1.22^{35)}$$

For compounds III and IIIa of the four piperidines, in which two conformations are possible, the intensities were calculated, using the estimated values for the parameters and the above assumptions. For conformations of III and IIIa, having a methylene group *syn*-axial to the lone pair or the *N*-hydrogen and, accordingly, two axial α-hydrogens, the intensities of 5.7 and $10.8\times 10^3\ l/\mathrm{cm}^2\cdot$mol were calculated, respectively. On the other hand, for the other conformations which include only one axial α-hydrogen, the calculated intensities were 2.2 and $5.2\times 10^3\ l/\mathrm{cm}^2\cdot$mol. These values, when compared with the corresponding observed intensities (Table 2), strongly suggest that these compounds assume the former conformation mainly.

The present result $N_H{}^*=0.70$ indicates that piperidine exists preferentially in the conformer with the lone pair axial, and is consistent with that obtained by Allinger ($N_H{}^*=0.68$),[7] Katritzky,[5a,5b] Booth,[10] and their co-workers, but not with those of other authors.[3,8a] We would emphasize that, while the value for $N_H{}^*$ is derived provided that the assumptions described hold for the compounds examined, this conclusion is considerably certain qualitatively. The above disagreement might be attributed to the difference in the experimental conditions or methods, or to the assumptions involved tacitly in the analysis of the results.

The authors wish to express their thanks to Dr. Takao Iijima for helfpul discussion and Mr. Shigehiro Ohuchi for preparation of some samples.

35) The following values are obtained for the other parameters on the assumption that $S_{2\beta}$ is equal to $S_{1\beta}$, although it appears improbable:
I_p, I_s and $I_s=4.79$, 4.50 and $4.02\times 10^3\ l/\mathrm{cm}^2\cdot$mol
R_2 and $R_3=0.79$ and 0.81.

BULLETIN OF THE CHEMICAL SOCIETY OF JAPAN VOL. 41 2473—2479 (1968)

A Cationic Polymerization of *N*-Phenylethylenimine by Various Carboxylic Acid Catalysts

Tsutomu KAGIYA, Tomizo KONDO and Kenichi FUKUI

Faculty of Engineering, Kyoto University, Sakyo-ku, Kyoto

(Received February 22, 1968)

The polymerization of *N*-phenylethylenimine was carried out using various carboxylic acid catalysts (pK_a=0.23—4.87) in acetonitrile at 0°C. The number-average molecular weight was determined by measuring the allyl-group content in the infrared spectrum of the polymer initiated with allylformate. The relationship between the number-average molecular weight and the reduced viscosity was determined. Both the conversion and the number-average molecular weight increased with the reaction time when weak acid (pK_a=2.85—4.87) was used. On the other hand, when strong acid (pK_a=0.23—2.85) was used, conversion reached a limited value which increased in proportion to the amount of the catalyst. With the strong acid, the efficiency factor of the catalyst was almost unity, and was independent of the reaction time. On the other hand, with the weak acid, it was smaller than unity and increased proportionally with the amounts of the polymer formed. The rate constants of the elementary reactions were evaluated on the basis of the kinetic study. The rates of the initiation, propagation, and termination reaction increased with a decrease in the pK_a of the acid. With a weak acid, the termination reaction is slow at a low temperature (below 50°C), and increases with the reaction temperature, whereas with a strong acid the termination reaction occurs markedly even at a low temperature (above 0°C), and increases slightly with the temperature. The mechanism of the termination reaction was discussed on the basis of a structural study of the end group of the polymer.

It has already been reported by the present authors that *N*-phenylethylenimine and β-propiolactone copolymerized with various Brönsted acid catalysts, and that the monomer reactivity ratio varies with the pK_a of the acid used as the catalyst.[1]

In order to determine the role of the catalyst in the elementary reactions in the polymerization, the polymerization of *N*-phenylethylenimine was studied with various carboxylic acids, and the rate constants of the elementary reactions were determined on the basis of the kinetics. Furthermore, the mechanism of the termination reaction was discussed on the basis of the structural study of the end group of the polymer.

Experimental

Polymerization Procedure. *N*-Phenylethylenimine was prepared according to the method described in the literature[2] from β-bromoethylaniline hydrobromide. It was dried over sodium sulfate and fractionated twice before use, bp 70—70.5°C/13 mmHg. Acetonitrile was purified by the usual method.[3] Acids of guaranteed reagents were used without further purification.

Definite amounts of a catalyst and a solvent were placed into a glass ampule under a nitrogen atmosphere, and then *N*-phenylethylenimine was added to this system at −78°C. The ampule was sealed and maintained at 0—1°C for the definite period of the reaction time. The product was then washed with diethyl ether, separated by a centrifuge, and dried *in vacuo*.

Physical Analysis of the Polymer. The melting point of the polymer was measured visually in a nitrogen atmosphere in a capillary on an electric heater. The reduced viscosity of a 0.25% solution of 99—100% formic acid was measured at 35°C with an Ostwald viscometer. The infrared spectrum was obtained with the use of the potassium bromide pellet technique on a Shimadzu infrared spectrophotometer, Model IR-27. The X-ray diffraction diagram was recorded with a powder camera on a Shimadzu X-ray diffractometer, Model GX-3B. The differential thermogram was obtained with the use of a Rigaku Denki differential thermal apparatus, Model VIP-32.

Determination of Molecular Weight. It was found that *N*-phenylethylenimine polymerized with cationic reagents, such as triphenylmethyl chloride, allyl formate or allyl acetate, as well as with Brönsted acid. The absorption peak of the infrared spectrum of the polymer initiated with allyl formate at 910 cm^{-1} assigned to the vinyl group, and that at 1600 cm^{-1} assigned to the phenyl group, were used in order to determine the number-average molecular weight of the

1) T. Kagiya, T. Tomizo, S. Narisawa and K. Fukui, This Bulletin, in press.
2) H. W. Heine, B. L. Kapur and C. S. Mitch, *J. Am. Chem. Soc.*, **76**, 1173 (1954).
3) A. Weissberger, *et al.*, "Technique of Organic Chemistry, Vol. VII, Organic Solvents," Interscience Publishers, Inc., New York (1955).

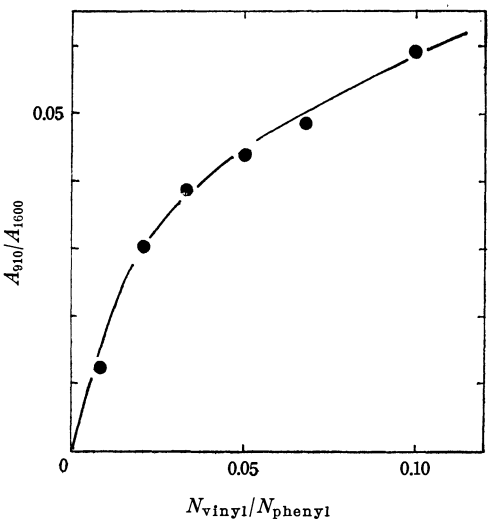

Fig. 1. Plots of A_{910}/A_{1600} *vs.* the ratio of the number of vinyl group (N_{vinyl}) in allyl urea to the number of phenyl group (N_{phenyl}) in the polymer.

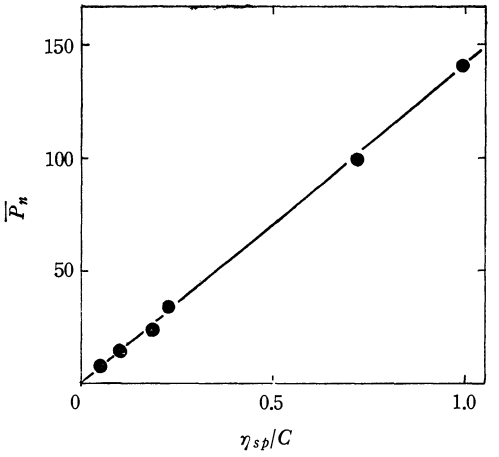

Fig. 2. The plots of the degree of the polymerization *vs.* the reduced viscosity of the polymer.

polymer. The calibration curve was obtained by plotting the optical density ratio, D_{910}/D_{1600}, in the infrared spectrum against the ratio of the number of vinyl and phenyl groups in the mixture of allyl urea and polymer obtained with formic acid (Fig. 1). The relation between the number-average molecular weight, $\overline{M}_n$, and the reduced viscosity, η_{sp}/C, is shown in Fig. 2. From Fig. 2, the following empirical equation may be obtained:

$$\eta_{sp}/C = 0.6\times10^{-4}\,\overline{M}_n$$

Results and Discussion

Physical Properties of the Polymer. The polymer is a white powdery solid soluble in formic acid, but insoluble in the other organic solvents.

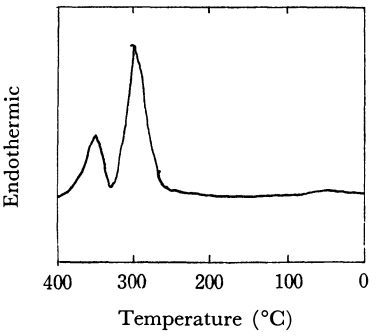

Fig. 3. Differential thermogram of the polymer.

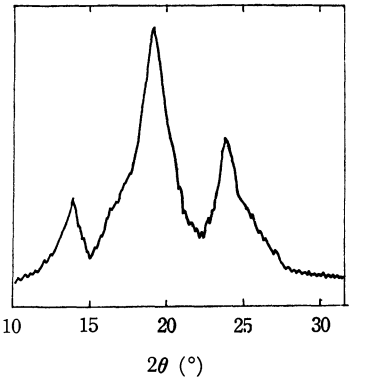

Fig. 4. X-Ray diffraction of the polymer.

The melting point of the polymer is from 287 to 292°C, and the differential thermogram of the polymer showed a sharp endothermic peak corresponding to the melting point of the polymer at 300°C (Fig. 3). In an X-ray diffraction diagram of the polymer (Fig. 4), sharp peaks were observed at 13.6, 19.4, and 23.3 θ. The figure showed that the polymer had a fairly good crystallinity.

Polymerization of *N*-Phenylethylenimine with Various Carboxylic Acids. The polymerization was carried out with various carboxylic acids (pK_a=0.23—4.87) at 0°C in acetonitrile. Figure 5 shows the variation in the polymer yield with the reaction time. With weak acid catalysts (pK_a=2.85—4.87), such as formic acid, acetic acid, and propionic acid, the polymer yield increased with the reaction time. On the other hand, with strong acids (pK_a=0.23—2.85), such as trifluoroacetic acid, dichloroacetic acid, and monochloroacetic acid, the conversion reached a saturated value ($<$ 50%) in a few minutes after the start of the polymerization. The number-average molecular weight of the polymer obtained with weak acid varied with the reaction time, whereas that obtained with strong acid remained constant (Fig. 6). With weak acid, the rate of the monomer consumption is expressed by a first-order rate equation with respect to the monomer

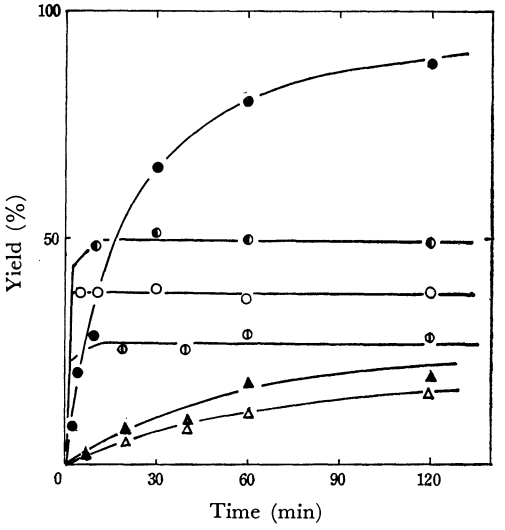

Fig. 5. Polymer yield *vs.* reaction time.
Monomer, 1 mol/*l*; Catalyst, 0.018 mol/*l*;
Solvent, Acetonitrile 5 m*l*
Reaction temperature, 0°C
○, Trifluoroacetic acid; ⓘ, Dichloroacetic acid;
◐, Monochloroacetic acid; ●, Formic acid;
▲, Acetic acid; △, Propionic acid;

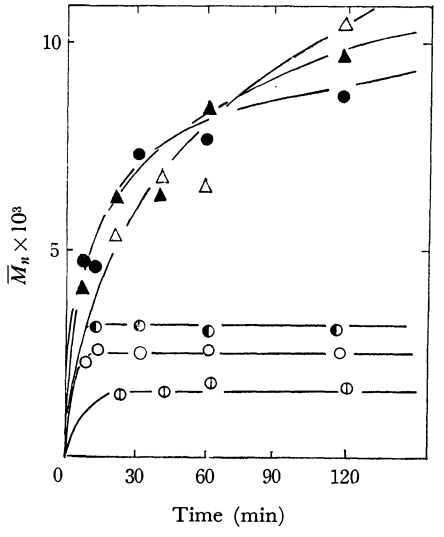

Fig. 6. The number-average molecular weight *vs.* reaction time.
(Reaction conditions and notes are the same as Fig. 5.)

concentration in the early stages of the polymerization, but not in the later stages. These facts suggest that the termination reaction occurs in this polymerization. In order to confirm that the termination reaction takes place, the following experiment was carried out. In the polymerization with monochloroacetic acid, the catalyst was added after the conversion reached the saturated value. The increase in the polymer yield in this experiment leads to the conclusion that the saturation is caused by the deactivation of the propagating species.

Kinetics of the Polymerization. The rate equations of the initiation, propagation, and transfer reactions may be assumed to be as follows:

$$R_i = k_i[\mathrm{C}][\mathrm{M}] \quad (1)$$

$$R_p = k_p[\mathrm{P}^*][\mathrm{M}] \quad (2)$$

$$R_{tr} = k_{tr}[\mathrm{P}^*][\mathrm{Y}] \quad (3)$$

where:
[C], [M], [P*], and, [Y]: the concentrations of the catalyst, monomer, the propagating species, and the substance to which the acitivity of P* is transferred.
R_i, R_p, and R_{tr}: the rates of the initiation, the propagation, and the transfer reaction.
k_i, k_p, and k_{tr}: the rate constants of the initiation, the propagation, and the transfer reaction.

The number-average degree of polymerization at a given reaction time may be written for the polymerization with no termination by recombination as follows:

$$\overline{P}_n = \int R_p dt / \left(\int R_i dt + \int R_{tr} dt \right) \quad (4)$$

By combining Eqs. (2), (3) and (4), and considering $\int R_p dt$ to be approximately equal to the polymer yield, [M_p], the reciprocal of the degree of polymerization may be expressed by the following equation:

$$1/\overline{P}_n = \int R_i dt/[\mathrm{M_p}] + (k_{tr}[\mathrm{Y}])/k_p \quad (5)$$

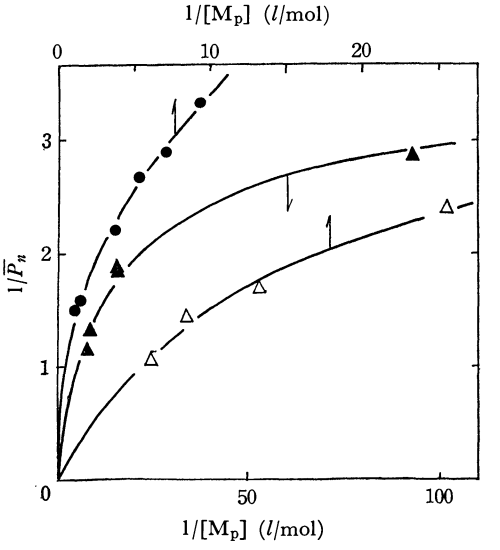

Fig. 7. Reciprocal of degree of polymerization *vs.* reciprocal of the polymer yield.
(Reaction conditions and notes are the same as Fig. 5.)

The plots of the reciprocal of $\overline{P}_n$ against the reciprocal of the polymer yield give a upward-concave curve through the point of origin, as is shown in Fig. 7. Figure 7 shows that $\int R_i dt$ increases with the reaction time. Moreover, the fact that the curve goes through the point of origin indicates that no chain transfer occurs in the polymerization with the weak acid. Equation (4) thus becomes:

$$\overline{P}_n = [M_p]/\int R_i dt \qquad (6)$$

For the polymerization without chain transfer and bimolecular termination, the value of $[M_p]/([C]_0/\overline{M}_n)$ may be called the efficiency factor of the catalyst, α. The plots of α against the reaction time are shown in Fig. 8. In the polymerization with strong acid catalysts, α is independent of the reaction time and is found to be almost unity (Fig. 8). This fact indicates that this system with strong acid involves polymerization with a rapid initiation and no chain transfer reaction. On the other hand, on the basis of the findings that, with a weak acid, α is smaller than unity and increases with the reaction time, this system may be considered to involve polymerization with a slow initiation.

The relationship between α and the amount of the polymer formed, $[M_p]$, when a weak acid is used is shown in Fig. 9. Figure 9 shows that α is proportional to the amount of the polymer formed, and is independent of the pK_a of the acid. This result may be interpreted by assuming that the stationary state is applicable, and that the termination reaction occurs with the monomer

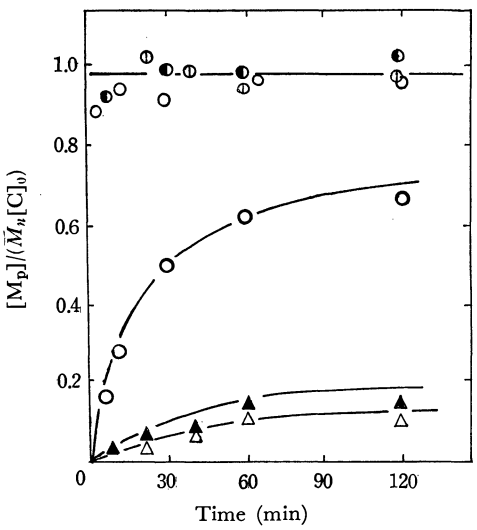

Fig. 8. The plots of efficiency factor of catalyst, *vs.* reaction time.
(Reaction condition and notes are the same as Fig. 5.)

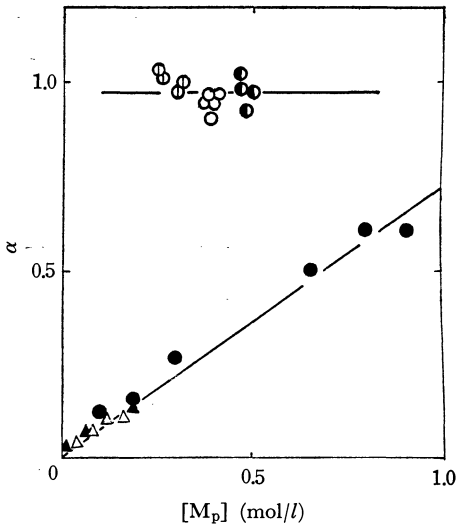

Fig. 9. The relationship between α and $[M_p]$. (Reaction conditions and notes are the same as Fig. 5.)

as is expressed by Eqs. (7) and (9):

$$R_i = R_t \qquad (7)$$

or

$$\int R_i dt = \int R_t dt = \alpha[C]_0 \qquad (8)$$

$$R_t = -d[P^*]/dt = k_t[P^*][M] \qquad (9)$$

where R_t and k_t are the rate and the rate constant of the termination respectively. By integrating Eqs. (2) and (9), and by then dividing the latter by the former,

$$\int R_t dt / \int R_p dt = k_t/k_p = \int R_t dt/[M_p] \qquad (10)$$

From Eqs. (8) and (10), Eq. (11) is derived:

$$\alpha[C]_0 = (k_t/k_p)[M_p] \qquad (11)$$

The relationship of Eq. (11) is in accord with Fig. 9; that is, α is proportional to $[M_p]$. From Eq. (11), the value of k_t/k_p was estimated to be 1.26×10^{-2}.

With a weak acid catalyst, the rate constant of the initiation reaction was obtained by using the following method. From a combination of Eqs. (1), (7), and (9), Eq. (12) is derived:

$$k_t[P^*][M] = k_t[C][M] \qquad (12)$$

By substituting the $[P^*]$ from Eq. (12) into Eq. (2), the rate of the monomer consumption becomes:

$$-d[M]/dt = (k_p k_t/k_t)[C][M] \qquad (13)$$

On the other hand, Eq. (11) may be expressed as Eq. (14):

$$[C]_0 - [C] = (k_t/k_p)([M]_0 - [M]) \qquad (14)$$

where $[M]_0$ is the initial monomer concentration. From Eqs. (13) and (14), Eq. (15) is derived:

$$-d[M]/dt = (k_p k_i/k_t)[M]\{[C]_0 - (k_t/k_p)([M]_0 - [M])\} \quad (15)$$

or:

$$\frac{-d[M]}{(k_t/k_p)[M]^2 - \{(k_t/k_p)[M]_0 - [C]_0\}[M]} = (k_p k_i/k_t)dt \quad (16)$$

On integrating, Eq. (17) is obtained:

$$\ln\left\{\frac{k_p[C]_0}{k_t[M]_0}\,\frac{[M]}{([M]-[M]_0)+(k_p/k_t)[C]_0}\right\} = k_i\{[M]_0 - (k_p/k_t)[C]_0\}t \quad (17)$$

By substituting the value, $(k_p/k_t)[C]_0 = 1.43$ mol/l, obtained from Eq. (11), $[M]_0 = 1$ mol/l and $([M]_0-[M])/[M]_0 = x$, into Eq. (17), one obtains

$$\log\{(1-0.7x)/(1-x)\} = 0.187k_i t \quad (18)$$

A plot of the left hand of Eq. (18) against t defined a straight line through the point of origin (Fig. 10). From the slope of the line, the k_i values were evaluated. The values of k_i in the polymerization with weak acid are summarized in Table 1. The fact that k_i increases with a decrease in the pK_a of the acid may be ascribed to the larger dissociation constant of the stronger acid than that of the weaker acid.

The values of k_p and k_t with a weak acid catalyst were estimated graphically as follows. The concentrations of the propagating species are expressed by Eq. (19):

$$[P^*] = \int R_i dt - \int R_t dt \quad (19)$$

By substituting Eqs. (2), (6), and (9) into Eq. (19), Eq. (20) is derived:

$$R_p/([M][M_p]) = k_p/\bar{P}_n - k_t \quad (20)$$

As is shown in Fig. 11, the plots of $R_p/([M][M_p])$ against $1/\bar{P}_n$ gave straight lines with the weak acid catalyst. Therefore, the assumption of the rate equation is considered to be suitable.

From the slope and intercept on the ordinate axis, k_p and $-k_t$ can be obtained graphically. The rate constants obtained by this method are summarized in Table 1. It is found that, with the weak acid catalyst, the rate constant of the termination reaction is about a hundredth that of the propagation, and that both k_p and k_t increase with a decrease in the pK_a of the catalyst. In the polymerization with strong acid catalysts such as trifluoroacetic acid, the rate constants can not be evaluated by the above method because the conversion is saturated immediately after the start

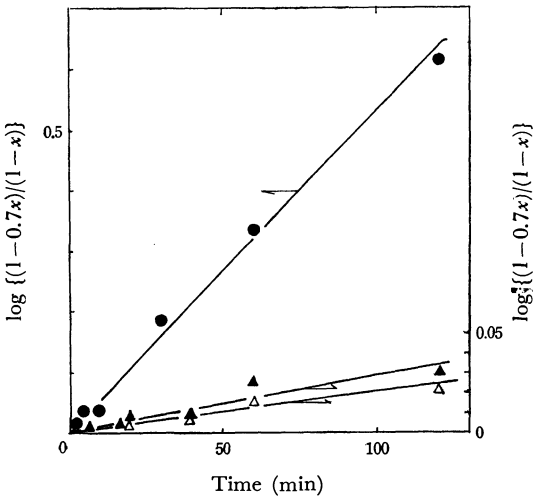

Fig. 10. The plots of $\log\{(1-0.7x)/(1-x)\}$ according to the Eq. (18).
(Reaction conditions and notes are the same as Fig. 5.)

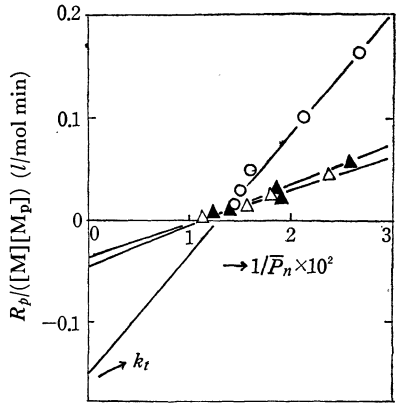

Fig. 11. The plots of $R_p/([M][M_p])$ *vs.* the reciprocal of the degree of the polymerization according to Eq. (9).
(Reaction condition and notes are the same as Fig. 5.)

Table 1. The rate constants of elementary reactions in the polymerization with weak acid catalyst

Catalyst	pK_a	$k_i \times 10^2$ l/mol min	k_p l/mol min	$k_t \times 10^2$ l/mol min	$(k_t/k_p) \times 10^2$
Formic acid	3.75	2.86	12	15	1.25
Acetic acid	4.76	0.167	3.8	4.8	1.26
Propionic acid	4.87	0.131	3.5	4.2	1.20
					mean 1.24

of the polymerization. Therefore, k_t/k_p was obtained by using the limited conversion $[M_p]_\infty$ according to the following method: From Eq. (10), Eq. (21) is derived:

$$\int R_t dt / \int R_p dt = k_t/k_p = \int R_t dt/[M_p]_\infty \quad (21)$$

On the basis of the facts that, with a strong acid catalyst, no chain-transfer reaction occurred in this polymerization, that α was almost equal to unity, and that the propagating species deactivated quantitatively, Eq. (22) can be assumed:

$$\int R_t dt = \int R_i dt = [C]_0 \quad (22)$$

By substituting Eq. (22) into Eq. (21), Eq. (23) was derived:

$$[M_p]_\infty = (k_p/k_t)[C]_0 \quad (23)$$

In the polymerization with monochloroacetic acid, the conversion reached a limited value which was dependent on the catalyst concentration. A plot of a limited conversion $[M_p]_\infty$ *versus* the initial concentration of the catalyst gave a straight line through the point of origin, as is shown in Fig. 12. This fact is in accordance with the relationship shown in Eq. (23). From the relation of $[M_p]_\infty$ and $[C]_0$ in Eq. (23), k_t/k_p can be determined.

The values of k_t/k_p are plotted against the pK_a of the catalyst in Fig. 13. This figure shows that the value of k_t/k_p decreases with an increase in the pK_a of the acid, and reaches a limited value of 1.24×10^{-2} with a weak acid. This value is almost in accord with the value, 1.26×10^{-2}, obtained from the slope of the line in Fig. 9.

Mechanism of the Termination Reaction. In order to investigate the temperature dependency of the termination reaction, the polymerization was studied with formic acid (a weak acid) or monochloroacetic acid (a strong acid) at various temperatures. A two-stage polymerization method was used. The polymerization was carried out for five minutes at a definite temperature (first stage), and then continued for 25 min at 0°C (second stage). The polymer yield obtained in the first stage, or the total of that obtained in the whole period, is plotted against the reaction temperature in Fig. 14. With the monochloroacetic

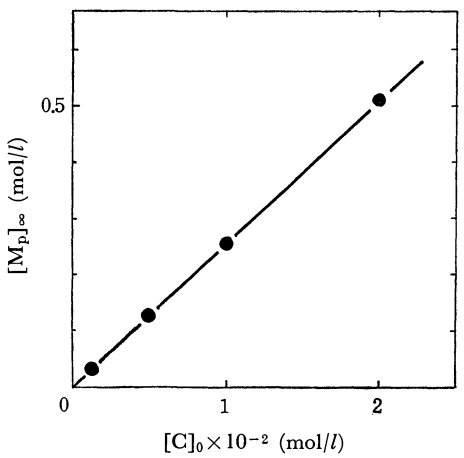

Fig. 12. Relation between the limiting conversion and initial concentration of the catalyst in the polymerization with monochloroacetic acid. (Reaction condition is the same as Fig. 5.)

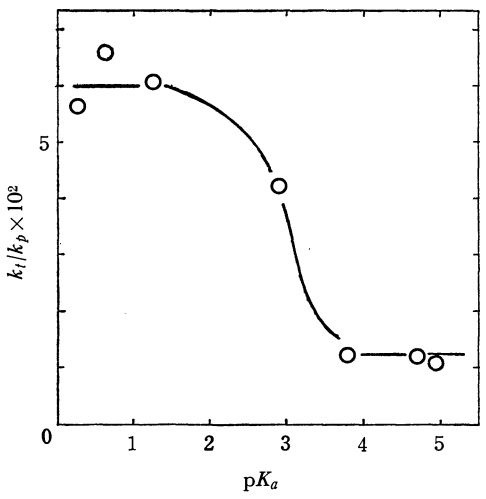

Fig. 13. The plots of k_t/k_p *vs.* pK_a of the acid catalyst.

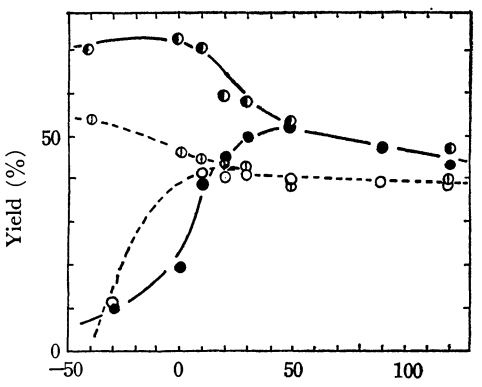

Fig. 14. The effect of temperature on the termination in the polymerization with formic acid or monochloroacetic acid.
Monomer, 1 mol/l; Catalyst, 0.018 mol/l;
Solvent, Acetonitrile 5 ml
Formic acid catalyst:
● first stage, Polymerization for 5 min at definite temperature.
◐ second stage, Continued for 25 min at 0°C.
Monochloroacetic acid catalyst:
○ first stage, Polymerization for 5 min at definite temperature.
◑ second stage, Continued for 25 min at 0°C.

acid catalyst, the conversion increased only a little in the second stage at temperatures of about 0°C. On the other hand, with formic acid the increase in conversion was observed in the second stage at temperatures below 50°C, and the termination reaction increased markedly above 50°C. This indicates that, with a weak acid, the termination reaction is slow at low temperatures and increases with the reaction temperature, while with a strong acid the termination reaction occurs remarkably at even low temperatures.

Chemical and spectral analyses of the products of the reaction of *N*-phenylethylenimine with excess amounts of monochloroacetic acid were carried out in order to elucidate the mechanism of the termination reaction. The reaction was carried out in an acetonitrile solution at room temperature for five hours. A white crystal precipitate (A) was filtered out. When this filtrate was neutralized by an 1/10 N sodium aqueous solution, a white resinous crystal (B) was precipitated. The product (A) was soluble in formic acid and insoluble in the other organic solvents. The infrared spectrum of (A) was identical to that of poly-*N*-phenylethylenimine. On the other hand, the product (B) was soluble in formic acid and ethanol, and its infrared spectrum indicated the characteristic peak at 930 cm^{-1} assigned to a piperazine ring.

It has been reported by Dick that *N*-substituted ethylenimine reacts with allyl bromide in acetone at 40°C to produce the piperazine derivatives and the polymer, and that the infrared spectrum of the polymer showed the characteristic peak of the piperazine ring at 930 cm^{-1}.[4]

In view of these facts, the *N*,*N*-diphenylpiperazine derivative and the polymer were considered to be produced in the reaction of *N*-phenylethylenimine and monochloroacetic acid by the following mechanism:

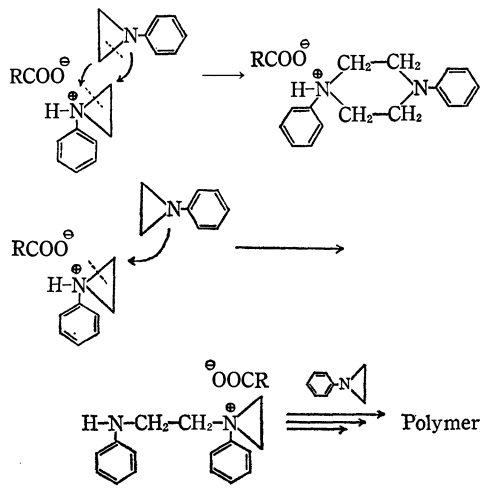

The infrared spectrum of the polymer initiated by a strong acid catalyst shows the characteristic peak of the piperazine ring at 930 cm^{-1}. Therefore, the mechanism of the termination reaction may also be considered to be piperazine ring formation at the end of the polymer.

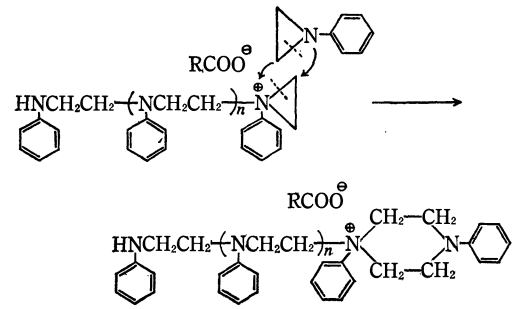

The increase in the termination reaction with a decrease in the pK_a of the acid may be ascribed to the separation of the counter anion from the growing immonium ion.

4) C. R. Dick, *J. Org. Chem.*, **32**, 72 (1967).

BULLETIN OF THE CHEMICAL SOCIETY OF JAPAN VOL. 41 2480—2483 (1968)

Ribonuclease T_1 Peptides. III. Synthesis of a Protected Heptapeptide Corresponding to Sequence 24—30

Tetsuo KATO, Nobuo MITSUYASU, Michinori WAKI, Satoru MAKISUMI and Nobuo IZUMIYA

Laboratory of Biochemistry, Faculty of Science, Kyushu University, Hakozaki, Fukuoka

(Received March 26, 1968)

A protected heptapeptide corresponding to sequence 24—30 of ribonuclease T_1, namely benzyloxycarbonyl-*O*-benzyl-L-tyrosyl-L-glutaminyl-L-leucyl-L-histidyl-γ-*t*-butyl-L-glutamyl-β-*t*-butyl-L-aspartyl-glycine ethyl ester (XI), was synthesized by coupling of benzyloxycarbonyl-*O*-benzyl-L-tyrosyl-L-glutaminyl-L-leucine azide with a tetrapeptide ester, L-histidyl-γ-*t*-butyl-L-glutamyl-β-*t*-butyl-L-aspartyl-glycine ethyl ester, which is derived from N^{α},N^{im}-dibenzyloxycarbonyl tetrapeptide ester by the catalytic hydrogenolysis. These tri- and tetrapeptide components were prepared with stepwise syntheses free from racemization.

The syntheses of the protected *N*-terminal undecapeptide (1—11) of ribonuclease T_1 containing asparagine residue in the 3rd position and the protected pentapeptide (12—16) were previously reported.[1,2] In the present paper, we will describe the synthesis of the protected heptapeptide corresponding to sequence 24—30, that is benzyloxycarbonyl-*O*-benzyl-L-tyrosyl-L-glutaminyl-L-leucyl-L-histidyl-γ-*t*-butyl-L-glutamyl-β-*t*-butyl-L-aspartyl-glycine ethyl ester (XI).

It has been known that one or more histidine residue in ribonuclease T_1 molecule play an important role to the enzymatic activity.[3] Hence the organic synthesis of peptide fragment of the enzyme containing histidine was supposed to be valuable to study the relationship of the structure and function of the enzyme molecule. Moreover this heptapeptide sequence contains acidic, basic and phenolic functional groups in a rather short peptide, so the preparation of this compound seemed to be interesting as an object of organic synthesis of a peptide.

The scheme of reactions used for the synthesis of XI was shown in Fig. 1. Benzyloxycarbonyl-β-*t*-butyl-L-aspartyl-glycine ethyl ester (I) was prepared by coupling of benzyloxycarbonyl-β-*t*-butyl-L-aspartic acid dicyclohexylammonium salt[4] with glycine ethyl ester hydrochloride using dicyclohexylcarbodiimide[5] as a coupling reagent. Furnished semisolid of I was catalytically hydrogenated to yield the dipeptide ester hydrochloride (II), which was then coupled with benzyloxycarbonyl-γ-*t*-butyl-L-glutamic acid[6] in the same manner as used for I. The protected tripeptide derivative (III) obtained was subjected to hydrogenolysis and then coupled with N^{α},N^{im}-dibenzyloxycarbonyl-L-histidine.[7] Crystals of the tetrapeptide derivative (V) thus obtained were again hydrogenated and then used to obtain the required heptapeptide derivative. The preparation of the *N*-terminal tripeptide (IX) was carried out as follows: L-leucine ethyl ester was coupled with benzyloxycarbonyl-L-glutamine *p*-nitrophenyl ester[8] to furnish the protected dipeptide ester (VII), and after the hydrogenolysis of VII, the dipeptide ester (VIII) was coupled with benzyloxycarbonyl-*O*-benzyl-L-tyrosine *p*-nitrophenyl ester.[8] The tripeptide ester derivative (IX) obtained was converted to the corresponding hydrazide (X) by the treatment with hydrazine.

The tripeptide hydrazide (X) was converted to the corresponding azide, and the azide was coupled with the tetrapeptide ester (VI). The protected heptapeptide ester derivative (XI) obtained was catalytically hydrogenated to remove the benzyloxycarbonyl and *O*-benzyl protecting groups,

1) M. Ohno, T. Kato, N. Mitsuyasu, M. Waki, S. Makisumi and N. Izumiya, This Bulletin, **40**, 204 (1967).

2) M. Waki, N. Mitsuyasu, T. Kato, S. Makisumi and N. Izumiya, *ibid.*, **41**, 669 (1968).

3) S. Yamagata, K. Takahashi and F. Egami, *J. Biochem.*, **52**, 261 (1962); F. Egami, *Nippon Kagaku Zasshi (J. Chem. Soc. Japan, Pure Chem. Sect.)*, **87**, 909 (1966).

4) R. Schwyzer and H. Dietrich, *Helv. Chim. Acta*, **44**, 2003 (1961); E. Wünsch and A. Zwick, *Z. Physiol. Chem.*, **328**, 235 (1962); E. Schröder and E. Klieger, *Ann.*, **673**, 208 (1964).

5) J. C. Sheehan and G. P. Hess, *J. Am. Chem. Soc.*, **77**, 1067 (1955).

6) R. Schwyzer and H. Kappeler, *Helv. Chim. Acta*, **44**, 1991 (1961).

7) F. Sakiyama, K. Okawa, J. Yamakawa and S. Akabori, This Bulletin, **31**, 926 (1958); A. Patchornik, A. Berger and E. Katchalsky, *J. Am. Chem. Soc.*, **79**, 6416 (1957).

8) M. Bodanszky and V. du Vigneaud, *ibid.*, **81**, 5688 (1959).

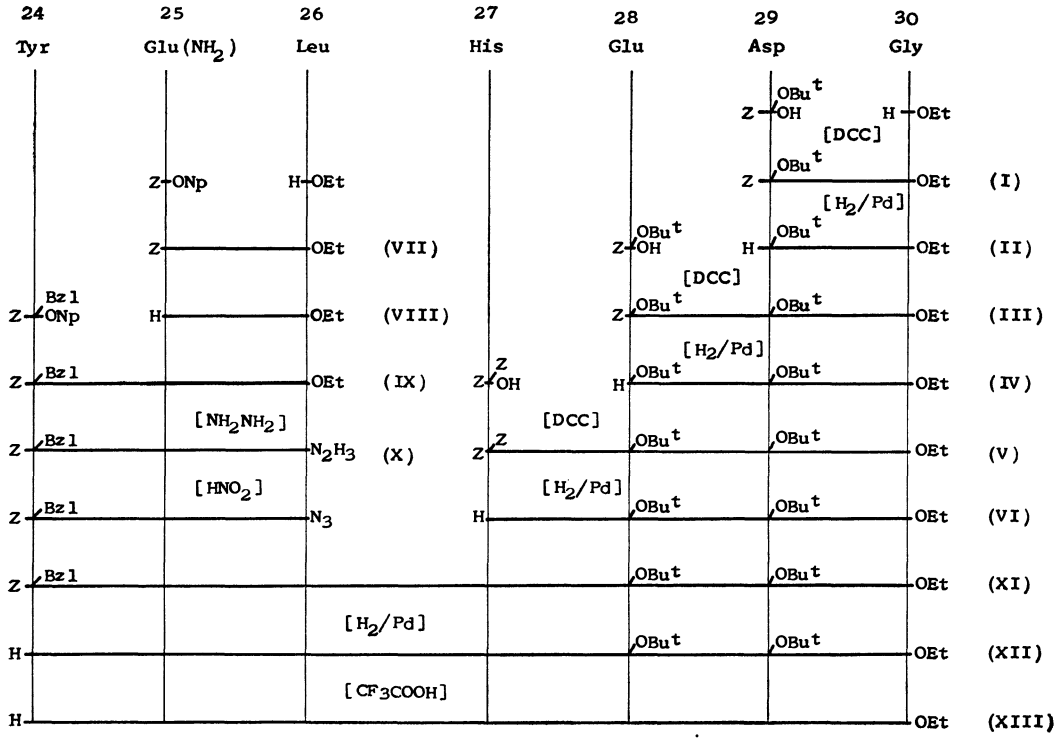

Fig. 1. Schematic diagram of synthesis of the heptapeptide ester. Z-, benzyloxycarbonyl; Bzl-, benzyl; -OBu^t, t-butyl ester; -ONp, p-nitrophenoxy ester; DCC, dicyclohexylcarbodiimide.

and the heptapeptide ester acetate (XII) obtained was then treated with trifluoroacetic acid to secure the heptapeptide ethyl ester trifluoroacetate (XIII). The peptide XIII was homogeneous as judged by the paper and thin-layer chromatography and its acid hydrolysate gave the theoretically expected amino acid ratios. Furthermore, the stereospecific purity of the peptide (XIII) was ascertained by the digestion with leucine aminopeptidase.

The syntheses of several peptides related to the ribonuclease T_1 enzyme are being continued in this laboratory.

Experimental

The melting points were not corrected. The paper chromatography and thin-layer chromatography were carried out on Toyo Roshi No. 52 paper and Merck silica gel G, respectively. Spots of materials possessing a free amino group on a thin-layer plate were detected by spraying ninhydrin, and those of the amino group-blocked materials, by spraying 47% hydrobromic acid and then ninhydrin. The developing solvent system most commonly used was n-butanol : acetic acid : pyridine : water (4 : 1 : 1 : 2). The optical rotations were measured on a Yanagimoto Photometric Polarimeter, OR-20 type. Prior to analysis, the samples were dried over anhydrous phosphorus pentoxide at 70°C and 2 mmHg to a constant weight.

Benzyloxycarbonyl-β-t-butyl-L-aspartyl-glycine Ethyl Ester (I). A suspension of benzyloxycarbonyl-β-t-butyl-L-aspartic acid dicyclohexylammonium salt[4] (5.047 g, 10 mmol) and glycine ethyl ester hydrochloride (1.396 g, 10 mmol) in chloroform (30 ml) was stirred for 30 min and the mixture was chilled to −5°C. Dicyclohexylcarbodiimide[5] (2.06 g, 10 mmol) was added to the mixture, the mixture was stirred for 2 hr at 0°C, and then it was allowed to stand overnight at 0°C. The mixture was then evaporated *in vacuo*, ethyl acetate (30 ml) was added to the residue, and the mixture was stored for several hours in a refrigerator. The dicyclohexylurea and dicyclohexylammonium hydrochloride deposited were filtered off (4.346 g, 99%), and the filtrate was washed successively with water, 10% citric acid and 4% sodium bicarbonate, and dried over sodium sulfate. The filtrate from the salt was evaporated and the residual semisolid was collected with the aid of a mixture of ether and petroleum ether (3.71 g, 91%). A portion of this was reprecipitated from ethyl acetate - ether - petroleum ether, and the semisolid obtained was analyzed; R_f 0.90 on thin-layer.

Found: C, 58.43; H, 6.99; N, 7.26%. Calcd for $C_{20}H_{28}N_2O_7$: C, 58.81; H, 6.91; N, 6.86%.

β-t-Butyl-L-aspartyl-glycine Ethyl Ester Hydrochloride (II·HCl). A solution of I (3.26 g, 8 mmol) in ethanol (30 ml) was hydrogenated in the presence of palladium black at 0°C. After 15 min, 0.52 N hydrogen chloride in ethanol (13.1 ml) was added into the solution, and hydrogenolysis was continued for 4 hr at 0°C. The filtrate from the catalyst was evaporated *in vacuo* at low temperature; yield of the hygroscopic crystals, 2.49 g (100%); R_f 0.95 on paper, 0.71 on thin-layer.

Benzyloxycarbonyl-γ-*t*-butyl-L-glutamyl-β-*t*-butyl-L-aspartyl-glycine Ethyl Ester (III). A mixture of benzyloxycarbonyl-γ-*t*-butyl-L-glutamic acid dicyclohexylammonium salt[6] (3.371 g, 6.5 mmol), II·HCl (2.03 g, 6.5 mmol), dicyclohexylcarbodiimide (1.339 g, 6.5 mmol) and chloroform (30 ml) was stirred for 2 hr at −5°C and then left to stand overnight at 0°C. The mixture was evaporated *in vacuo*, and ethyl acetate was added. After filtration, the ethyl acetate solution (*ca.* 100 ml) was washed with water, dilute acid and alkali as described for I, and dried. The filtrate from the salt was evaporated and the resulting crystals were collected by filtration with the aid of petroleum ether; yield, 3.438 g (90%); R_f 0.92 on thin-layer. A portion (134 mg) of the crystals was recrystallized from ether-petroleum ether for analysis; 119 mg; mp 58—60°C; $[\alpha]_D^{30}$ −20.0° (*c* 1, dimethylformamide).

Found: C, 58.44; H, 7.39; N, 6.92%. Calcd for $C_{29}H_{43}N_3O_{10}$: C, 58.67; H, 7.30; N, 7.08%.

γ-*t*-Butyl-L-glutamyl-β-*t*-butyl-L-aspartyl-glycine Ethy Ester Hydrochloride (IV·HCl). A solution of III (3.002 g, 5.06 mmol) in ethanol (25 ml) was hydrogenated in the presence of palladium black and 0.52 N hydrogen chloride in ethanol (10.2 ml) as described for the preparation of II. The filtrate from the catalyst was evaporated *in vacuo*; yield of the oily product (IV·HCl), 2.717 g (109%); R_f 0.97 on paper, 0.80 on thin-layer.

N^{α},N^{im}-Dibenzyloxycarbonyl-L-histidyl-γ-*t*-butyl-L-glutamyl-β-*t*-butyl-L-aspartyl-glycine Ethyl Ester (V). A mixture of N^{α},N^{im}-dibenzyloxycarbonyl-L-histidine[7] (2.27 g, 5 mmol), IV·HCl (the oily product from 5 mmol of III), triethylamine (0.73 ml), dicyclohexylcarbodiimide (1.03 g, 5 mmol) and chloroform (20 ml) was stirred for 2 hr at −5°C, allowed to stand overnight at 0°C, and evaporated *in vacuo*. Ethyl acetate (50 ml) was added to the residue, and the dicyclohexylurea deposited was filtered off (993 mg). The filtrate was washed with water, dilute citric acid and sodium bicarbonate solution as described previously. The solution dried was evaporated *in vacuo* and the residual oil was crystallized after the addition of ether and petroleum ether. Recrystallization from ethyl acetate - ether - petroleum ether gave 3.14 g (73%) of pure substance; R_f 0.93 on thin-layer; mp 85—87°C; $[\alpha]_D^{17}$ −8.0° (*c* 1, dimethylformamide).

Found: C, 59.40; H, 6.65; N, 9.41%. Calcd for $C_{43}H_{56}N_6O_{13}$: C, 59.71; H, 6.53; N, 9.72%.

L-Histidyl-γ-*t*-butyl-L-glutamyl-β-*t*-butyl-L-aspartyl-glycine Ethyl Ester Dihydrochloride (VI·2HCl). A solution of V (2.112 g, 2.5 mmol) in ethanol (30 ml) was hydrogenated at 0°C in the presence of palladium black and 0.52 N hydrogen chloride in ethanol (8 ml) as described for the preparation of II·HCl. The filtrate from the catalyst was evaporated *in vacuo*; yield of the oily product (VI·HCl), 1.696 g (101%); R_f 0.98 on paper, 0.70 on thin-layer.

Benzyloxycarbonyl-L-glutaminyl-L-leucine Ethyl Ester (VII). To a solution of L-leucine ethyl ester hydrochloride[9] (1.469 g, 7.5 mmol) dissolved in a mixture of triethylamine (1.16 ml, 8.5 mmol) and dimethylformamide (15 ml), a solution of benzyloxycarbonyl-L-glutamine *p*-nitrophenyl ester[8] (3.011 g, 7.5 mmol) in dimethylformamide (8 ml) was added. The solution was then allowed to stand overnight at room temperature and then poured into 225 ml of water. The crystalline product deposited was collected by filtration and washed successively with 3% sodium bicarbonate, M citric acid and water, and dried; 2.39 g. Recrystallization from ethanol - ether - petroleum ether gave 2.13 g (67%) of pure substance; R_f 0.97 on thin-layer; mp 128—130°C; $[\alpha]_D^{20}$ −9.4° (*c* 1.0, dimethylformamide).

Found: C, 59.74; H, 7.33; N, 9.90%. Calcd for $C_{21}H_{31}N_3O_6$: C, 59.84; H, 7.41; N, 9.97%.

L-Glutaminyl-L-leucine Ethyl Ester Hydrochloride (VIII·HCl). To a solution of VII (2.11 g, 5 mmol) dissolved in methanol (30 ml) was added 0.72 N methanolic hydrogen chloride (7.63 ml, 5.5 mmol). The solution was hydrogenated in the presence of palladium black. After 6 hr the filtrate from the catalyst was evaporated to dryness *in vacuo*; yield of the oily product (VIII·HCl), 1.667 g (103%). The homogeneity of the oil was ascertained by paper and thin-layer chromatography; R_f 0.80 on paper and 0.75 on thin-layer.

Benzyloxycarbonyl-*O*-benzyl-L-tyrosyl-L-glutaminyl-L-leucine Ethyl Ester (IX). To a solution of VIII·HCl (1.667 g, 5 mmol) dissolved in a mixture of triethylamine (0.78 ml, 5.5 mmol) and dimethylformamide (25 ml), a solution of benzyloxycarbonyl-*O*-benzyl-L-tyrosine *p*-nitrophenyl ester[8] (2.663 g, 5 mmol) in dimethylformamide (12 ml) was added. The solution was then allowed to stand overnight at room temperature and then poured into 200 ml of water. The crystalline product deposited was collected by filtration, washed and dried as described for VII. Recrystallization from methanol - ether - petroluem ether gave 2.725 g (86%) of IX; R_f 0.98 on thin-layer; mp 210—211°C; $[\alpha]_D^{15}$ −16.2° (*c* 1, dimethylformamide).

Found: C, 65.83; H, 6.90; N, 8.25%. Calcd for $C_{37}H_{46}N_4O_8$: C, 65.86; H, 6.87; N, 8.30%.

Benzyloxycarbonyl-*O*-benzyl-L-tyrosyl-L-glutaminyl-L-leucine Hydrazide (X). A solution of IX (2.022 g, 3 mmol) and hydrazine hydrate (3 ml, 60 mmol) in dimethylformamide (12 ml) was allowed to stand for 2 days at room temperature. The solution was then evaporated *in vacuo* in order to remove excess hydrazine, and then 120 ml of water was added to the residual solution. The resulting crystals (1.932 g) were collected by filtration and recrystallized from dimethylformamide-ethanol to give 1.74 g of X (90%); R_f 0.84 on thin-layer; mp 237°C; $[\alpha]_D^{15}$ −13.6° (*c* 1, dimethylformamide).

Found: C, 62.03; H, 6.76; N, 12.39%. Calcd for $C_{35}H_{44}N_6O_7 \cdot H_2O$: C, 61.93; H, 6.83; N, 12.38%.

Benzyloxycarbonyl-*O*-benzyl-L-tyrosyl-L-glutaminyl-L-leucyl-L-histidyl-γ-*t*-butyl-L-glutamyl-β-*t*-butyl-L-aspartyl-glycine Ethyl Ester (XI). Into a solution of X (1.652 g, 2.5 mmol) in a mixture of acetic acid (70 ml) and dimethylformamide (14 ml), there were added successively N hydrochloric acid (2.75 ml), sodium nitrite (190 mg) and N hydrochloric acid (2.75 ml) under stirring below −5°C. The faintly turbid solution changed to transparent in a few minutes. Then cold water (160 ml) was added to the solution, and the stirring was continued at 0°C for 30 min. The precipitate was then collected, washed successively with water, 4% sodium bicarbonate and water, and dried *in vacuo* at 0°C. The azide was then

9) F. Rohman, *Ber.*, **30**, 1978 (1897).

added to a chilled solution of VI·HCl (1.696 g, 2.5 mmol) in a mixture of dimethylformamide (40 m*l*) and triethylamine (0.73 m*l*). The solution was stirred for 3 days at 0°C, and diluted with 800 m*l* of cold water. The precipitate was collected, washed with 4% sodium bicarbonate, 10% citric acid and water, and dried; yield, 2.342 g. Recrystallization from methanol-dioxane-ether gave 2.11 g (69%) of XI; R_f 0.85 on thin-layer; mp 213—214°C; $[\alpha]_D^{30}$ −21.1° (*c* 1, dimethylformamide).

Found: C, 59.71; H, 6.78; N, 10.94%. Calcd for $C_{62}H_{84}N_{10}O_{16}\cdot H_2O$: C, 59.88; H, 6.97; H, 11.26%.

L-Tyrosyl-L-glutaminyl-L-leucyl-L-histidyl-L-glutamyl-L-aspartyl-glycine Ethyl Ester Ditrifluoroacetate (XIII·2CF$_3$COOH). A solution of XI (50 mg, 40 μmol) in 80% acetic acid (1 m*l*) was subjected to hydrogenolysis in the presence of palladium black. After 1 hr, the filtrate from the catalyst was evaporated to dryness; yield of hygroscopic crystals (XII·2AcOH), 51 mg; R_f 0.75 on thin-layer. XII·2AcOH (48 mg) was dissolved in trifluoroacetic acid (0.4 m*l*), and the solution was left to stand for 30 min and evaporated to dryness. The resulting crystals were collected by filtration with the aid of ether (46 mg); mp 180—185°C; $[\alpha]_D^{25}$ −10.0° (*c* 0.3, acetic acid); R_f 0.80 on paper, 0.71 on thin-layer; amino acid ratios in acid hydrolysate, $Tyr_{1.0}$, $Leu_{1.2}$, $His_{0.9}$, $Glu_{2.2}$, $Asp_{0.9}$, $Gly_{0.9}$.

Found: C, 44.91; H, 5.67; N, 12.30%. Calcd for $C_{39}H_{56}N_{10}O_{14}\cdot 2C_2HO_2F_3\cdot 2H_2O$: C, 44.79; H, 5.42; N, 12.15%.

The digestion of XIII·HCl by leucine aminopeptidase was carried out by the procedure of Hofmann and Yajima.[10] The paper chromatography of the digest with a solvent system of *n*-butanol : acetic acid : water (4 : 1 : 2) revealed the presence of seven ninhydrin-positive components with R_f values identical with those of authentic samples of aspartic acid (R_f, 0.25), histidine (0.28), glutamine (0.31), glycine (0.33), glutamic acid (0.36), tyrosine (0.54) and leucine (0.76).

10) K. Hofmann and H. Yajima, *J. Am. Chem. Soc.*, **83**, 2289 (1961).

BULLETIN OF THE CHEMICAL SOCIETY OF JAPAN VOL. 41 2483—2485 (1968)

Photo-induced Reactions. XIX. Photopinacolization of Unsymmetric Aromatic Ketones[1]

Teruo MATSUURA and Yoshihiko KITAURA

Department of Synthetic Chemistry, Faculty of Engineering, Kyoto University, Kyoto

(Received March 28, 1968)

Stereochemistry of the photopinacolization of unsymmetrical aromatic ketones was investigated. In the photopinacolization of aromatic ketones of type PhCOR in isopropyl alcohol, the *dl* : *meso* ratio of diastereoisomeric pinacols formed tends to increase as the size of the substituent R becomes bulkier. The *dl* : *meso* ratio of pinacols obtained from *p*-substituted acetophenone, *p*-X-C_6H_4-$COCH_3$, is about 1 in the cases that X is H, Cl, and CH_3, whereas the ratio is 1.25 in the case of X=OCH_3. The photopinacolization of acetophenone in three solvent systems cyclohexane, isopropyl alcohol, and benzene-isopropyl alcohol, was also investigated, and no solvent effect was observed on the *dl* : *meso* ratio of acetophenone pinacols.

The photoreduction of ketones, especially aromatic ketones, is one of the most extensively investigated field in organic photochemistry.[2] Unsymmetrical ketones, which can undergo photopinacolization, should give two diastereoisomeric pinacols, *dl* and *meso* forms. However, there have been only a few reports in which the ratio of such diastereoisomeric pinacols is described. It was reported that *o*-phenylbenzophenone[3] and desoxybenzoin[4] yield a higher melting pinacol predominantly over a lower melting isomer. Bencze and his coworkers found that 3-acetylpyridine yields a higher melting pinacol accompanying with a small amount of a lower melting one, while 2-acetylpyridine gives approximately an equal amount of two isomeric pinacols.[5] Brown reported that the photolysis of benzyl alcohol in acetone affords an equal amount of *dl*- and *meso*-hydrobenzoin.[6] Furthermore, acetophenone was shown to give corresponding pinacols with the *dl* : *meso* ratio of 11 : 10[7] Since there has been no systematic investigation on the

1) Part XVIII: T. Matsuura and K. Ogura, *Tetrahedron*, in press.

2) For a review see, D. C. Neckers, "Mechanistic Organic Photochemistry," Reinhold Publ. Co., New York (1967), p. 163.

3) H. H. Hatt, A. Pilgrim and E. E. M. Stephenson, *J. Chem. Soc.*, **1941**, 478.

4) F. Bergmann and Y. Hirschberg, *J. Am. Chem. Soc.*, **65**, 1429 (1943).

5) W. L. Bencze, C. A. Burkhardt and W. L. Yost, *J. Org. Chem.*, **27**, 2865 (1962).

6) W. G. Brown, *Tetrahedron Letters*, **1966**, 1845.

7) J. H. Stocker and D. H. Kern, *J. Org. Chem.*, **31**, 3755 (1966).

Tabme 1. Photopinacols III from alkyl phenyl ketone I

$C_6H_5COR \longrightarrow (C_6H_5C(OH)R)_2$
(I) (III)

R	Yield of III (%)	Chemical shifts of R-protons of III[a] (τ value) *dl*	Chemical shifts of R-protons of III[a] (τ value) *meso*	*dl*: *meso* ratio
H	70	H: 5.31 s	H: 5.18 s	0.9
CH_3	80	CH_3: 8.55 s	CH_3: 8.47 s	1.0
C_2H_5	75	CH_3: 9.40 t CH_2: 8.30 q, 7.86 q	CH_3: 9.40 t CH_2: 8.40 q, 7.60 q	1.0
i-C_3H_7	55	CH_3: 9.66 d, 8.79 d CH: 8.02 sep	CH_2: 9.36 d, 9.26 d CH: 7.81 sep	1.1_3

a) The spectra were taken in $CDCl_3$. Multiplicities of signals are shown as follows: s, singlet; d, doublet; t, triplet; q, quartet; sep, septet.

stereochemistry of the photopinacolization of unsymmetric aromatic ketones, we initiated to examine effects of substituents and solvents in this reaction. Particular attention was drawn to following three factors; namely, (i) effects of the bulkiness of the substituents R in ketones of type PhCOR, (ii) electronic effects of the para substituent in *p*-substituted acetophenone, and (iii) solvent effects with acetophenone.

A mixture of diastereoisomeric pinacols could be easily separated by a column chromatography on silica gel from the reaction mixture which was obtained by the photolysis of PhCOR (I) and *p*-X-C_6H_4-$COCH_3$ (II) in isopropyl alcohol. The *dl* : *meso* ratio of these diastereoisomeric pinacols was determined from their peak areas in the NMR spectrum of the pinacol mixture. The results are shown in Tables 1 and 2. In the case of pinacols III obtained from I, the chemical shifts of protons of the substituent R are different between *dl* and *meso* forms, and the signals of the *dl* form appear in a higher field than those of the *meso* form. The assignment of the signals was accomplished by a comparison with authentic samples.*1 The authentic sample of *dl*-hydrobenzoin (III, R=H) was prepared by a known method, and other authentic samples of the pinacols III (R=CH_3, C_2H_5, and i-C_3H_7) were obtained by fractional recrystallization of the pinacol mixture and they were characterized by a comparison of their melting points with those reported in the literature. In the case of pinacols III (R=i-C_3H_7), the *dl* and *meso* forms were characterized, from their infrared spectra, according to the method of Mosher and Heindel.[10] A mixture of the *dl* and *meso* pinacols of type IV was also separated from the reaction mixture, but each isomer was not isolated. For these pinacols, an isomer showing a methyl signal in a higher magnetic field was assigned as the *dl* form and in a lower field as the *meso* form.[8]

Table 2. Photopinacols IV from *p*-substituted acetophenone II

p-X-$C_6H_4COCH_3 \longrightarrow$ (*p*-X-$C_6H_4C(OH)CH_3)_2$
(II) (IV)

X	Yield of IV (%)	Chemical shifts of aliphatic methyl protons of IV (τ value) *dl*	Chemical shifts of aliphatic methyl protons of IV (τ value) *meso*	*dl*:*meso* ratio
H	80	8.55	8.47	1.0
CH_3	85	8.63	8.53	1.0
Cl	88	8.60	8.52	1.0
CH_3O	90	8.60	8.50	1.2_5

*1 The NMR data of acetophenone pinacols[9] and propiophenone pinacols[9] have been reported.

As shown in Table 1, the *dl* : *meso* ratio of the pinacols III obtained from I appears to have a tendency to increase slightly as the size of the substituent R becomes bulkier. Contrary to the recent results by Stocker and Kern,[7] our results indicate that the *dl* : *meso* ratio is practically 1 : 1 for R=CH_3 and C_2H_5. Although we also examined the photopinacolization of *n*-butyrophenone (I, R=*n*-C_3H_7) and *t*-butyl phenyl ketone (I, R=*t*-C_4H_9) in isopropyl alcohol, photopinacolization was found to be a minor pathway and the yield of the pinacols were so low that the *dl* : *meso* ratio could not be determined. It was found that the former undergoes the Norrish Type I process whereas the latter does the Type II process as the major pathway. The somewhat lower yield of the pinacols III (R=i-C_3H_7) is probably due to the co-occurrence of the Type I process in some extent.

Table 2 summarizes the effect of the *p*-substituent of acetophenone on the *dl* : *meso* ratio of pinacols

8) H. Agahigian, J. F. Maraveck and H. Gauther, *Can. J. Chem.*, **41**, 194 (1963).
9) H. D. Becker, *J. Org. Chem.*, **32**, 2143 (1967).
10) W. A. Mosher and N. D. Heindel, *ibid.*, **28**, 2154 (1963).

IV. The *dl* and *meso* isomers are formed practically in an equal amount in the cases of X=H, CH_3, and Cl. On the other hand, the *dl* isomer is formed predominantly over the *meso* isomer when X is a methoxyl group, a strong electron-donating group. Similarly, *p*-anisaldehyde gives a mixture of the *dl* and *meso* pinacols with 2 : 1 ratio.[11] Analogous observation has been reported by Pitts and his coworkers[12] who show that, in the Norrish Type II reaction of *n*-butyrophenone, the quantum yield is remarkably affected by introducing a *p*-methoxyl group while a *p*-methyl group has little effect.

It was reported that, in the photopinacolization of acetophenone, there is no solvent effect on the *dl* : *meso* ratio of its pinacols formed in isoproyl alcohol or cyclohexane.[12] We also carried out the photopinacolization of acetophenone in three solvent systems and similar results were obtained. A mixture of two diastereoisomeric pinacols was obtained in 80% yield in isopropyl alcohol, 87.5% in 50 : 1 benzene-isopropyl alcohol, and 68% in cyclohexane. In all cases, the *dl* : *meso* ratio was found to be 1 : 1 within experimental errors.

From the above results, it appears that there are at least two factors, which influence the *dl* : *meso* ratio of photopinacols, namely steric and electronic effects of the substituent. Further examples and mechanistic consideration will be reported in a future paper. After completion of this work, Stocker and his coworkers have reported that *p*-substitution of acetophenone with an electron-donating group results in the predominant formation of the *dl* pinacol over *meso* pinacol,[13] and that, in the photopinacolization of acetophenone, neutral organic solvents do not change appreciately the *dl* : *meso* ratio.[14] These results are essentially same as our results.

Experimental

Materials. The starting materials were commercially available. Their purities were checked by gas chromatography. The solvents, isopropyl alcohol, cyclohexane, and benzene, were dried and distilled before use. *dl*-Hydrobenzoin was prepared from *trans*-stilbene by a known method,[15] mp 123—125°C.

General Procedure for Photopinacolization. The following procedure was used for experiments of Table 1. A solution of 2.00 g of the starting aromatic ketones in 200 m*l* of isopropyl alcohol was irradiated under nitrogen at room temperature using a 100 W high-pressure mercury lamp (Ushio, UM 100) with a water-cooled Pyrex jacket. After the starting material had been consumed (6—9 hr), the mixture was evaporated under reduced pressure, and the residue was chromatographed on a silica gel column. Elution with chloroform yielded a mixture of *dl*- and *meso*-pinacols. The *dl* : *meso* ratio of the mixture was determined by NMR analysis. The results are summarized in Table 1. In the case of isobutyrophenone, 2.00 g of the ketone was dissolved in 350 m*l* of isopropyl alcohol and the solution was irradiated using a 450 W high-pressure mercury lamp (Ushio, UM 450).

For experiments of Table 2, 1.10 g of *p*-methylacetophenone, 1.00 g of *p*-methoxyacetophenone, and 0.55 g of *p*-chloroacetophenone were dissolved in 300 m*l* of isopropyl alcohol, respectively. Each solution was irradiated by a 450 W lamp for 7—8 hr as described above.

For experiments in different solvent systems, the following solution was irradiated by a 450 W lamp: 0.50 g of acetophenone in 350 m*l* of cyclohexane (12 hr) and 2.00 g of acetophenone in 500 m*l* of benzene containing 10 m*l* of isopropyl alcohol (19.5 hr).

Isolation and Characterization of Diastereoisomeric Pinacols. Some of the diastereoisomeric pinacols were separated by fractional recrystallization (*n*-hexane or petroleum ether) from the pinacol mixtures obtained as above. The melting points of pinacols isolated are listed below: *dl*-acetophonone-phinacol, 124—125°C (lit.[10] 122—123°C); *meso*-acetophenonepinacol, 119—120°C (lit.[10] 117—118°C); *dl*-hydrobenzoin, 123—125°C (lit.[16] 120°C); *meso*-hydrobenzoin, 137°C (lit.[17] 137°C); *dl*-propiophenonepinacol, 113—114°C (lit.[10] 113°C); *meso*-propiophenonepinacol, 140—141°C (lit.[10] 138—139°C); *dl*-isobutyrophenonepinacol, 159°C; *meso*-isobutyrophenone-pinacol, 130—133°C. Stereochemistry of the latter two pinacols was assigned by infrared spectroscopy[10]: $\nu_{max}^{CCl_4}$ 3568 (strong), 3612 (medium), 1150, and 1177 cm^{-1} for the *dl*-isomer and 3574 (weak) 3614 (strong), and 1121 cm^{-1} for the *meso*-isomer. Other diastereoisomeric pinacols were not separated.

11) Unpublished data from this laboratory.
12) J. N. Pitts, Jr., L. D. Hess, E. J. Baum, E. A. Schuck, J. K. S. Wan, P. A. Leermakers and G. Vesley, *Photochem. Photobiol.*, **4**, 305 (1965).
13) J. H. Stocker, D. H. Kern and R. M. Jenevein, *J. Org. Chem.*, **33**, 412 (1968).
14) J. H. Stocker and D. H. Kern, *ibid.*, **33**, 291 (1966).
15) W. A. Bonner and E. K. Raunio, *ibid.*, **31**, 293 (1966).
16) L. F. Fieser, "Experiments in Organic Chemistry," D. C. Heath and Co., Boston (1957), p. 175 and p. 188.

BULLETIN OF THE CHEMICAL SOCIETY OF JAPAN VOL. 41 2486—2489 (1968)

Azetidines. V. Preparation and Deamination of Azetidinylpropylamines[1]

Teng-Yueh CHEN[2]

Laboratory of Organic Chemistry, Tokyo Institute of Technology, Ookayama, Meguro-ku, Tokyo

(Received April 16, 1968)

The addition of 3,3-diethylazetidine to acrylonitrile and crotononitrile, followed by reduction, gave the corresponding azetidinylpropylamines. The deamination products of the amines were identical with the alcohols prepared by the addition of diethylazetidine to methyl acrylate and crotonate, followed by reduction with lithium aluminum hydride.

In Part I[3] of this series, it has been reported that azetidine gave addition products readily with active unsaturated compounds. The addition product with acrylonitrile is of particular interest since it may be converted to the corresponding amine, which then gives a cationic intermediate on deamination. It seemed to be of interest to see if the cation so generated can be attacked by the nitrogen atom in the molecule to give the spiro-azetidinium cation. The formation of such a spiro-azetidinium cations as intermediates has been suggested from time to time, and they have actually been isolated in some cases.[4]

A relatively readily accessible 3,3-diethylazetidine[5] (I) was used as the starting meterial, because the NMR spectra of its derivatives can be easily analyzed. The reaction of I with acrylonitrile proceeded readily to give β-(3,3-diethylazetidinyl-1)propionitrile (IIa), which was then reduced with lithium aluminum hydride to the corresponding amine IIIa in a good yield. The alcohol isolated after the deamination of the amine IIIa with nitrous acid was homogeneous, as judged by v.p.c., and its NMR spectrum was completely consistent with the structure IVa. It shows two triplets, at τ 6.47 and 7.43, corrresponding to the two protons on the methylene groups adjacent to the hydroxyl group and to those two adjacent to the nitrogen atom respectively (See Experimental Section). Conclusive evidence in support of the structure IVa could be obtained by the preparation of IVa by the addition of I to methyl acrylate to give Va, followed by its reduction with lithium aluminum hydride to IVa. This product was identical with the deamination product of IIIa.

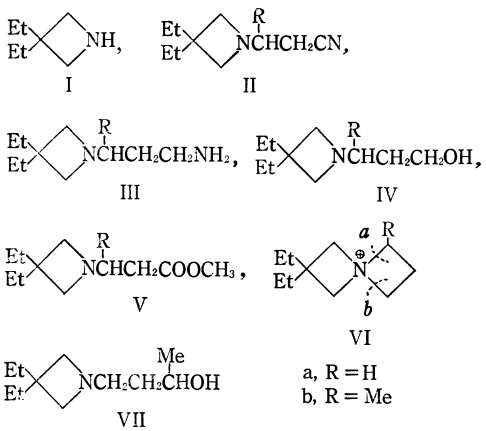

These results may be explained by considering the direct attack of an hydroxyl anion on the cation, but it does not rigorously exclude an alternative path *via* the spiro-azetidinium intermediate VIa, since it has been known that the less-heavily-substituted azetidine rings are in general more unstable than those which are more heavily substituted.[4] Hence, even if the spiro-azetidinium intermediate VIa may be formed as the intermediate, it will invariably give the alcohol IVa by the cleavage of the unsubstituted ring (at *a* or *b*).

In order to check this possibility, 3-(3,3-diethylazetidinyl-1)butylamine (IIIb) was prepared from I and crotononitrile by the method described above; it was then subjected to the deamination reaction. It was expected that if the spiro intermediate VIb was formed, it would give the product VII, resulting mainly from the cleavage of the ring at *a*.

The structure and purity of the nitrile IIb and the reduction product, amine IIIb, were determined by correct analyses, infrared spectra, and v.p.c.,

1) Part IV: T. Chen, H. Kato and M. Ohta, This Bulletin, **41**, 712 (1968).

2) Present address: National Tsing Hua University, Taiwan, The Republic of China.

3) Part I: T. Chen, H. Kato and M. Ohta, This Bulletin, **40**, 1964 (1967).

4) J. A. Moore "Heterocyclic Compounds with Three- and Four-membered Rings," Part Two, ed. by A. Weissberger, Interscience Publishers, New York, N. Y. (1964), p. 885; E. Testa, A. Wittgens, G. Maffii and G. Bianchi, *Research Progress in Organic, Biological and Med. Chem.*, **1**, 477 (1964).

5) E. Testa and L. Fontanella, *Ann.*, **625**, 95 (1959); E. Testa, L. Fontanella and G. F. Cristiani, *ibid.*, **626**, 114 (1959).

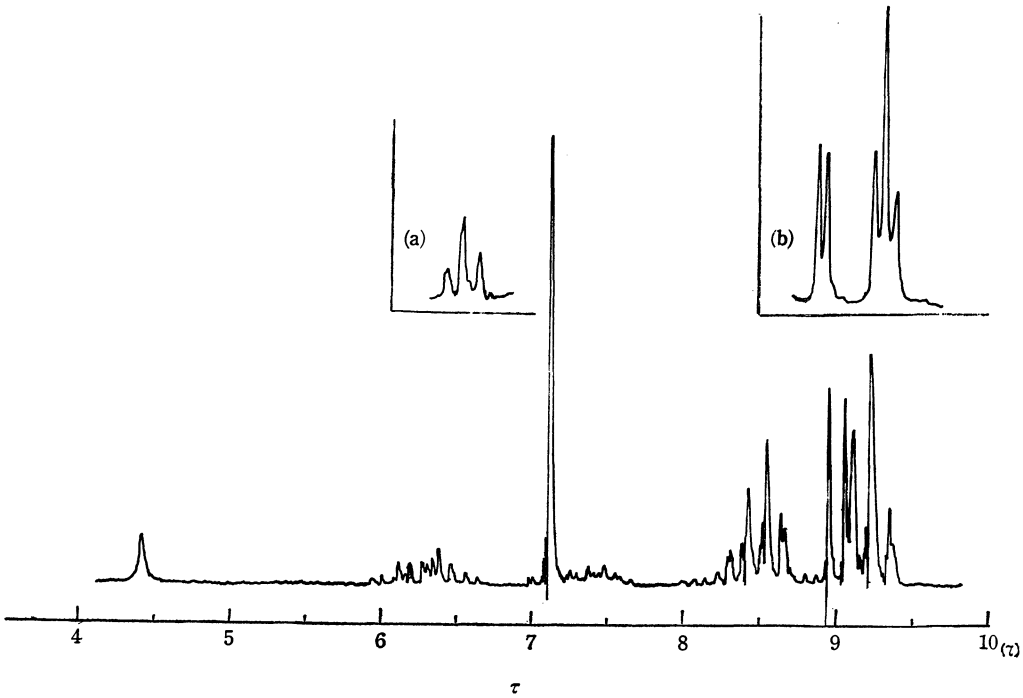

Fig. 1. The NMR spectrum of the deamination product of 3-(3,3-diethylazetidinyl)butylamine in $CDCl_3$. (a) Partial NMR spectrum of the same compound in DMSO; (b) Partial NMR spectrum of the HCl salt of the same compound in D_2O.

and were confirmed by means of a study of the NMR spectra.

The alcohol isolated after the deamination of the amine IIIb was homogeneous, as judged by v.p.c., and gave a correct analysis. The NMR spectrum shown in the figure contains ABX-pattern multiplets at τ 6.98—7.68 and 7.95—8.9 because of the asymmetric carbon adjacent to the ring nitrogen. The resonance peak of the methylene adjacent to the hydroxyl group appears at τ5.8—6.65 as complex multiplets, and the chemical shift of the hydroxyl proton appears at τ 4.41 as a singlet. The remaining part of the NMR spectrum is essentially similar to that of the amine IIIb (See Experimental Section). The integrated areas of the peaks agree well with the structure IVb. The NMR spectrum is not changed by changing the temperature of measurement. The purest sample isolated by v.p.c. also shows the same NMR spectrum as the distilled sample. However, the possibility of the formation of the alcohol VII through the nitrogen spiro intermediate VIb can not be precluded on the basis of the appearance of the NMR spectrum alone.

For purposes of confirmation, the preparation of IVb by the addition of I to methyl crotonate, followed by reduction with lithium aluminum hydride, was attempted. The product so obtained was found to be identical with the deamination product. The use of a dimethyl sulfoxide solvent for the NMR determination did not cause the expected splitting of the hydroxyl group coupled by the adjacent methylene group[6,7]; instead, a broad peak at τ 5.8 was found. It is noteworthy that the NMR spectrum of the methylene group adjacent to the hydroxyl group appears as a simple triplet at τ 6.64 in this solvent (See Fig. 1(a)).

The complex multiplicity for the methylene adjacent to the hydroxyl group in $CDCl_3$ may be explained by considering that the compound forms an intramolecular hydrogen bonding between the oxygen and the ring nitrogen; thus, the chain fixes as a six-membered ring. As a result, the free rotation of the methylene group is limited and the protons are no longer equivalent. In the dimethyl sulfoxide solvent, such hydrogen bonding is broken by forming a stronger hydrogen bonding between the alcohol and the solvent; therefore, the free rotation permits the terminal methylene to split as a normal triplet.

Moreover, the doublet at τ 9.0 and the triplet at 9.22 were found to be separated further enough to permit an accurate integration when the HCl salt of the alcohol was measured in D_2O because of the deshielding effect of the quaternary nitrogen cation; the ratio of the two peak areas was found

6) O. L. Chapman and R. W. King, *J. Am. Chem. Soc.*, **86**, 1256 (1964).
7) J. G. Traynham and G. A. Knesel, *ibid.*, **87**, 4220 (1965).

to be exactly 1 : 2 (See Fig. 1(b)).

From these results, it may reasonably be concluded that the alcohols obtained both from the deamination of the amine IIIb and from the reduction of the ester Vb are identical compounds, IVb, and that the alcohol arises from direct attack of the hydroxyl anion on the cation produced by the deamination rather than through the spiro-azetidinium intermediate.

Experimental[8]

β-(3,3-Diethylazetidinyl-1)propionitrile (IIa). This was prepared, by the general procedure described in Part I,[3] in an almost quantitative yield from 4 g of 3,3-diethylazetidine (I) and 2 g of acrylonitrile. Bp 65—67°C/1.5 mmHg, n_D^{25} 1.4502. IR: 2250 cm^{-1}.

Found: C, 72.35; H, 10.91; N, 16.77%. Calcd for $C_{10}H_{18}N_2$: C, 72.24; H, 10.91; N, 16.85%.

β-(3,3-Diethylazetidinyl-1)butyronitrile (IIb). This was prepared in a 68% yield from I and crotononitrile. Bp 68—75.5°C/1.5 mmHg, n_D^{25} 1.4511. IR: 2250 cm^{-1}. NMR(τ): 7.3—8.2 (3H, multiplet); 7.18 (4H, singlet); 8.48 (4H, quartet); 9.0 (3H, doublet); 9.22 (6H, triplet). V.p.c.: Carbowax 20 M on Diasolid A, 4 mm×150 cm, 147°C, He flow rate 50 ml/min, retention time 15 min; Apiezon Grease L on Diasolid A, 4 mm×150 cm, 147°C, He flow rate 60 ml/min, retention time 8 min.

Found: C, 73.12; H, 10.95; N, 15.43%. Calcd for $C_{11}H_{20}N_2$: C, 73.28; H, 11.18; N, 15.54%.

Picrate of IIb: mp 157—158°C.

Found: C, 49.94; H, 5.81; N, 17.27%. Calcd for $C_{17}H_{23}N_5O_7$: C, 49.87; H, 5.60; N, 17.11%.

Methyl β-(3,3-Diethylazetidinyl-1)propionate (Va). This was prepared in a 91% yield from 3 g of I and 2.3 g of methyl acrylate. Bp 64.5—67.5°C/1.5 mmHg, n_D^{25} 1.4430. IR: 1745 cm^{-1}.

Found: C, 65.99; H, 10.75; N, 7.20%. Calcd for $C_{11}H_{21}NO_2$: C, 66.29; H, 10.62; N, 7.03%.

Methyl β-(3,3-Diethylazetidinyl-1)butyrate (Vb). This was prepared in a 84% yield from I and methyl crotonate. Bp 67—68°C/1.5 mmHg, n_D^{25} 1.4445. IR; 1745 cm^{-1}. NMR in $CDCl_3$(τ): 6.38 (3H, singlet); 7.12 (4H, singlet); 7.16—8.21 (3H, multiplet); 8.42 (4H, quartet); 9.03 (3H, doublet); 9.24 (6H, triplet). V.p.c.: Silicone Grease DC550, 4 mm×225 cm, 154°C, He flow rate 60 ml/min, retention time 22 min; Apiezon Grease L on Diasolid A, 4 mm×150 cm, 150°C, He flow rate 60 ml/min, retention time 8 min; Carbowax 20 M on Diasolid 4 mm×150 cm, 150°C, He flow rate 60 ml/min, retention time 6 min.

Found: C, 67.28; H, 10.75; N, 6.76%. Calcd for $C_{12}H_{23}NO_2$: C, 67.56; H, 10.87; N, 6.57%.

Picrate of Vb: mp 88—89°C.

Found: C, 48.97; H, 5.64; N, 12.72%. Calcd for $C_{18}H_{26}N_4O_9$: C, 48.86; H, 5.92; N, 12.66%.

3-(3,3-Diethylazetidinyl-1)propylamine (IIIa). A solution of 6 g of IIa in 20 ml of ether was stirred into a suspension of 1.6 g of lithium aluminum hydride in 80 ml of ether. After two hours, the reaction mixture was hydrolyzed by the addition of dilute aqueous sodium hydroxide. The ether layer was separated, and the residue was washed several times with a total of 200 ml of ether. The combined ether extract was then dried and distilled *in vacuo* to afford 4.5 g (75% yield) of a product boiling at 55—57°C/1.5 mmHg, n_D^{25} 1.4565. IR: 3360, 3290, 1590 cm^{-1}.

Found: C, 70.35; H, 12.33; N, 15.73%. Calcd for $C_{10}H_{22}N_2$: C, 70.53; H, 13.02; N, 16.45%.[9]

Picrate of IIIa: mp 199.5—201.5°C (decomp).

Found: C, 42.39; H, 4.40; N, 17.93%. Calcd for $C_{22}H_{28}N_8O_{14}$ (dipicrate): C, 42.04; H, 4.49; N, 17.83%.

3-(3,3-Diethylazetidinyl-1)butylamine (IIIb). This was similarly prepared, in a 88% yield, from 3.2 g of IIb and 1 g of lithium aluminum hydride. Bp 62—63°C/1.5 mmHg, n_D^{25} 1.4590, IR: 3362, 3295, 1600 cm^{-1}. NMR in $CDCl_3$ (τ): 7.16 (4H, singlet); 7.34 (2H, triplet with each peak split); 7.52—8.0 (1H, multiplet); 8.1—8.85 (2H, multiplet); 8.45 (4H, quartet) (These two peaks are superimposed); 9.11 (3H, doublet); 9.23 (6H, triplet) (These two peaks separate further when the HCl salt of IIIb is measured in D_2O and the ratio of the peak area was found to be exactly 1 : 2). V.p.c.: Carbowax 20 M on Diasolid A 4 mm ×150 cm, 150°C, He flow rate 40 ml/min, retention time 9 min; Apiezon Grease L on Diasolid 4 mm× 225 cm, 150°C, He flow rate 70 ml/min, retention time 10 min.

Found: C, 71.63; H, 12.97; N, 14.99%. Calcd for $C_{11}H_{24}N_2$: C, 71.68; H, 13.13; N, 15.20%.

Picrate of IIIb: mp 238—241°C (decomp).

Found: C, 42.73; H, 4.71; N, 17.16%. Calcd for $C_{23}H_{30}N_8O_{14}$ (dipicrate): C, 42.99; H, 4.70; N, 17.44%.

γ-(3,3-Diethylazetidinyl-1)propanol (IVa). This was prepared in a 88% yield by the reduction of 4.8 g of Va with 1 g of lithium aluminum hydride. Bp 65—69°C/1.5 mmHg, n_D^{25} 1.4575. IR: a broad peak between 3500 and 3100 cm^{-1}. V.p.c.: Carbowax 20 M on Diasolid A 4 mm×225 cm, 150°C, He flow rate 60 ml/min, retention time 31.5 min.

Found: C, 70.00; H, 12.04; N, 8.09%. Calcd for $C_{10}H_{21}NO$: C, 70.12; H, 12.36; N, 8.18%.

γ-(3,3-Diethylazetidinyl-1)butanol (IVb). The reduction of 2.2 g of Vb with 0.7 g of lithium aluminum hydride afforded an alcohol fraction in a 70% yield; bp 85—90°C/1.5 mmHg, n_D^{25} 1.4615. IR: a broad peak between 3450 and 3180 cm^{-1}. NMR in $CDCl_3$ (τ): 4.41 (1H, singlet); 5.8—6.65 (2H, multiplet); 6.98—7.68 (1H, multiplet); 7.95—8.9 (2H, multiplet); 7.12 (4H, singlet); 8.48 (4H, quartet); 9.0 (3H, doublet); 9.22 (6H, triplet) (The last two peaks separate further when the HCl salt of IVb is measured in D_2O and the ratio of the peak area is exactly 1 : 2. Fig. 1 (b)). The multiplet between τ 5.8 and 6.65 appears as a simple triplet when IVb is measured in DMSO (Fig. 1(a)). V.p.c.: Apiezon Grease L on Diasolid A 4 mm× 225 cm, 160°C, He flow rate 60 ml/min, retention time 13 min; Carbowax 20 M on Diasolid A 4 mm×225 cm, 160°C, He flow rate 60 ml/min, retention time 13.4 min;

8) The general conditions for the measurements of physical constants and spectra were the same as described in Part I.[3] The v.p.c. were run on a Shimadzu Type GC-1B Gas Chromatograph.

9) Although the elemental analysis of this amine agreed only poorly with the theoretical, the picrate gave correct analysis and the v.p.c. analysis showed this compound to be homogeneous.

Silicone DC550 4 mm×225 cm, 154°C, He flow rate 60 ml/min, retention time 13 min.

Found: C, 71.42; H, 12.36; N, 7.87%. Calcd for $C_{11}H_{23}NO$: C, 71.30; H, 12.51; N, 7.56%.

Deamination of 3-(3,3-Diethylazetidinyl-1)propylamine (IIIa). A solution of 1.2 g of sodium nitrite in 7 ml of water was slowly stirred into a solution of 2 g of IIIa in 4.4 g of 50% acetic acid below 0°C. After five hours, the evolution of nitrogen was no longer observed; the mixture was made alkaline with potassium carbonate and extracted with ether. The combined extract was dried over sodium sulfate, and the solvent was removed by distillation. The crude product, which consisted of the alcohol IVa and its acetate, was treated with aqueous sodium hydroxide to hydrolize the acetate, and the mixture was extracted with ether, dried, and distilled *in vacuo* to give 1.3 g (65% yield) of IVa boiling at 70—78°C/1.5 mmHg. The IR spectrum and refractive index were identical with those of the product of the reduction of Va. NMR(τ): 5.64(1H, singlet); 6.47 (2H, triplet); 7.11 (4H, singlet, ring methylene); 7.43 (2H, triplet); 8.25—8.70 (2H, multiplet); 8.46 (4H, quartet); 9.19 (6H, triplet). V.p.c.: The results were similar to those described in the reduction of Va.

Found: C, 70.29; H, 12.24; N, 8.37%.

Deamination of 3-(3,3-Diethylazetidinyl-1)butylamine (IIIb). Two grams of IIIb were treated by the method described above except that the acetate byproduct was treated with lithium aluminum hydride instead of sodium hydroxide. The alcohol was obtained in a 62% yield. Bp 89—96°C/1.5 mmHg, n_D^{25} 1.4615, IR: a broad peak between 3450 and 3180 cm^{-1}. The NMR spectrum (See Fig. 1) was identical with that of the product obtained by the reduction of Vb; no change in the NMR spectra was observed whether it was taken at 24, 50, or 100°C. V.p.c.: this product and the mixture with the reduction product of the Vb ester showed the same retention time under the same conditions, as has been explained in the reduction of Vb.

Found: C, 71.15; H, 12.19; N, 7.95%.

The author is indebted to Professor Masaki Ohta and Dr. Hiroshi Kato for invaluable discussion and encouragement, and to Miss Mizuko Yoshida for the measurement of NMR spectra.

BULLETIN OF THE CHEMICAL SOCIETY OF JAPAN VOL. 41 2489—2494 (1968)

The Grignard Reaction of 3-Halotropolone Methyl Ethers[1]

Haruki TSURUTA and Toshio MUKAI

Department of Chemistry, Faculty of Science, Tohoku University, Katahiracho, Sendai

(Received April 17, 1968)

The Grignard reaction of the methyl ethers (I and III) of 3-bromotropolone and those (II and IV) of 3-chlorotropolone with methylmagnesium iodide or phenylmagnesium bromide were investigated. When I or II was allowed to react with methylmagnesium iodide, 2-methoxyphenyldimethylcarbinol (V) and 2-methoxy-6-isopropylphenol (VI) were obtained. The reaction of I or II with phenylmagnesium bromide afforded 2-phenyl-7-halotropones (XIII or XVII), accompanied by 2-halobenzophenones (XV or XVIII) and the triphenylcarbinol derivative (XIV). The Grignard reaction of III or IV using phenylmagnesium bromide gave 2-phenyl-3-halotropones (XVI or XIX). The mechanistic pathway for the formation of these products was discussed.

The Grignard reaction of troponoid derivatives has attracted much attention as a useful tool for the synthesis of alkyl[2,3] and aryl derivatives.[4-10] In addition, peculiar interest is also attached to the mechanism of the Grignard reactions because they are one of the most complicated nucleophilic reactions of the troponoid system. For instance, unexpected abnormal substitution reactions[6,11-13] and rearrangement reactions leading to benzenoid derivatives,[7,10-13] as well as the expected normal substitutions, usually take place, depending on the variety of substituents presented on the tropone ring, the kind of Grignard reagents,[10,11] and the

1) Reaction of the Seven-membered Aromatic Compound with Organometallic Compound. VIII. Preceding paper: T. Mukai, H. Tsuruta and Y. Momotari, This Bulletin, **40**, 1967 (1967).

2) T. Nozoe, T. Mukai and T. Tezuka, *ibid.*, **34**, 619 (1961).

3) A. P. ter Borg, R. van Helden and A. F. Bickel, *Rec. Trav. Chim.*, **81**, 591 (1962).

4) W. von E. Doering and C. F. Hisky, *J. Am. Chem. Soc.*, **74**, 5688 (1952).

5) T. Nozoe, T. Mukai and I. Murata, *Proc. Japan Acad.*, **29**, 169 (1953).

6) R. D. Haworth and P. B. Tinker, *J. Chem. Soc.*, **1955**, 911.

7) T. Nozoe, T. Mukai, J. Minegishi and T. Fujisawa, *Sci. Repts. Tohoku Univ.*, **37**, 388 (1953).

8) T. Nozoe, S. Seto, T. Ikemi, T. Sato and K. Watanabe, *ibid.*, **38**, 130 (1954).

9) K. Kikuchi, *Nippon Kagaku Zassi (J. Chem. Soc. Japan, Pure Chem. Sect.)*, **77**, 1439 (1956).

10) K. Kikuchi, *ibid.*, **81**, 505 (1960).

11) K. Kikuchi, This Bulletin, **33**, 628 (1960).

12) F. Osaki, M. S. Thesis, Tohoku Univ., 1963.

13) T. Nozoe, T. Mukai and I. Murata, *Proc. Japan Acad.*, **28**, 142 (1952).

reaction conditions used.[14]

A few papers, however, have been reported on the Grignard reactions of the troponoid with two active functional groups, such as halogen or methoxyl groups.[13,14] To elucidate in more detail the Grignard reaction of such tropone derivatives, the reactions of 3-bromotropolone methyl ethers (I and III) and 3-chlorotropolone methyl ethers (II and IV) with methylmagnesium iodide and phenylmagnesium bromide were reinvestigated. In this series of experiments, an ethereal solution of the Grignard reagent was added to an ethereal solution of I—IV at room temperature in order to avoid the further reaction of tropone derivatives with an excess of the Grignard reagents present.

I X=Br
II X=Cl

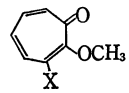

III X=Br
IV X=Cl

The reaction of I with 2.5 equivalents of methylmagnesium iodide afforded an oil in a 80% yield; this oil was found by vapor phase chromatographic analysis to be composed of four compounds in a ratio of 1 : 10 : 10 : 1. The oil was, by the use of column chromatography, separated into two main components (V and VI), both of which had the same formula, $C_{10}H_{14}O_2$. Compound (V), with a shorter retention time in the vapor phase chromatography, showed the presence of a hydroxyl group (3571 cm^{-1}) in its IR spectrum, but it was not phenolic. The NMR spectrum of V exhibited signals ascribed to two methyl groups (singlet at τ 8.51, 6H) and a methoxyl group (singlet at τ 6.14, 3H) besides a phenyl group (multiplet at τ 2.97, 4H). These data suggest that V is *o*-methoxyphenyl dimethyl carbinol. The final decision of the structure of V was made by a comparison of its infrared spectrum and vapor phase chromatographic retention time with those of an authentic sample.[15] The ultraviolet spectrum of compound VI exhibited an absorption maximum at 277 mμ, suggesting that VI is a rearranged benzenoid derivative. Compound VI indicated the presence of a hydroxyl group (3524 and 1220 cm^{-1}) and adjacent three hydrogens of substituted benzene (779 and 821 cm^{-1}) in the infrared spectrum. Its NMR spectrum showed signals due to an isopropyl group (doublet at τ 8.79 and multiplet at τ 6.77, J=7 cps, 7H), a methoxyl group (singlet at τ 6.14, 3H), a hydroxyl group (singlet at τ 4.48, 1H), and aromatic protons (ABC-type pattern centered at τ 3.33). The demethylation of VI by treating it with hydrobromic acid in acetic acid afforded an oily product (VII), $C_9H_{12}O_2$, which was soluble in a dilute sodium hydroxide solution and which showed green coloration with ferric chloride, indicating the presence of the phenolic hydroxyl group. The NMR spectrum of VII was almost the same as that of VI, except for the lack of a singlet ascribed to the methoxyl group. On the basis of the above data, two structures VIa and VIb may be proposed for the rearranged product VI, and the structure VII, for the demethylated product. However, compound VI was sparingly soluble in a dilute sodium hydroxide solution and showed no coloration with ferric chloride. These facts suggest that the phenolic hydroxyl group of VI is hindered severely, leading to VIa being preferred to VIb. The structural proof of VI was carried out by the synthesis of VI using proven manner.

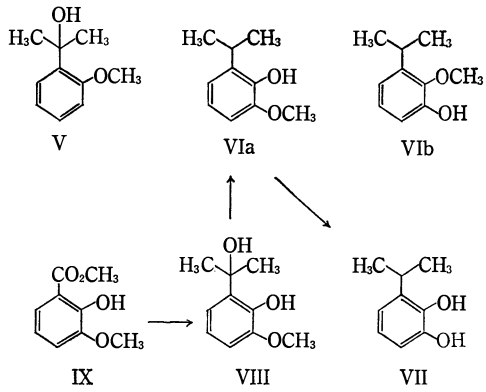

V VIa VIb

IX VIII VII

The reaction of methyl 3-methoxysalicilate (IX)[16] with methylmagnesium iodide afforded colorless crystals (VIII), $C_{10}H_{14}O_2$, which showed infrared and NMR spectra consistent with the structure of the expected 2-hydroxyisopropyl-6-methoxyphenol (see Experiment Section). Catalytic hydrogenation of VIII in the presence of a trace of acid resulted in the consumption of one equivalent of hydrogen and produced an oil, which was found to be completely identical with VI by a comparison of their infrared spectra. Thus compound VI was proved to be 6-isopropyl-2-methoxyphenol (VIa).

The Grignard reaction of 2-chloro-7-methoxytropone (II) with methylmagnesium iodide afforded an oil in a good yield; this oil was composed of seven products in a ratio of 20 : 2 : 2 : 2 : 1 : 1 : 1. The major product was found to be VI, and one of the minor products (ratio 2) was found to be V, by a comparison of their retention times in vapor phase chromatography with those of authentic

14) For example, when 3,7-dibromotropolone methyl ether was treated with *o*-tolylmagnesium bromide at room temperature, triphenyl carbinol derivatives were obtained, but 2-tolyl-3,7-dibromotropone was obtained as the main product at −30°C.

15) A. Béhal and M. Tiffeneau, *Bull. Soc. Chim. Paris*, [4], **1908**, 315; *Chem. Zentr.*, **1908**, Ib 1625.

16) I. A. Pearl, *J. Org. Chem.*, **12**, 85 (1947).

samples. The remaining products could not be elucidated because they were only minor products.

Thus, it may be concluded that the reaction of I and II with methylmagnesium iodide took place in almost the same manner, giving mainly V and VI, although the yields of the products were different. There are precedent examples similar to the formation of the rearranged product V in the Grignard reaction of other troponoids.[7-13] Thus, V apparently results from a nucleophilic attack by methylmagnesium iodide on the carbonyl carbon of the tropone ring, followed by ring contraction with the elimination of the halogen atom and by the further reaction of another molecule of methylmagnesium iodide. On the other hand, the formation of VI is an interesting example of the rearrangement of the troponoid occurring by means of the attack of the nucleophilic reagents,[17] and it can conveniently be interpreted by the following scheme. Methylmagnesium iodide may attack the C_3-position of I or II in the 1,4-addition manner, giving a cycloheptatriene-type intermediate (X) or its valence isomer (XI), which then undergos ring

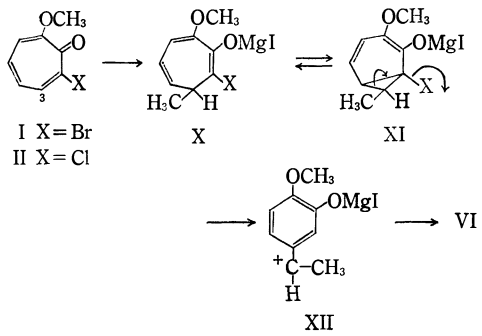

contraction with the elimination of the halogen atom, as shown by the arrow, to give a benzylium-type intermediate (XII). Another molecule of the reagent then attacks the intermediate (XII), leading to the formation of VI. Otherwise, VI may result from the concerted reaction of the intermediate (X or XI) with methylmagnesium iodide.

The Grignard reaction of another type of methyl ether (III and IV) of 3-halotropolone was investigated using methylmagnesium iodide. In the cases of both III and IV, the products were oils which were unstable and which turned into resineous tars upon standing in air. Although purification was attempted after complete hydrogenation, the reduced product showed the presence of nearly the same amounts of the nine components in the vapor-phase chromatography. This complex result made us abandon any further investigation of the reactions of III and IV.

To find what differences arise when the Grignard reagent is changed, the reactions of compounds I—IV with phenylmagnesium bromide were investigated. A preliminary report[13] has already pointed out that, upon reaction with phenylmagnesium bromide, I afforded mainly triphenylmethyl derivatives, while III gave crystals, mp 115—115.5°C, which were assumed to be bromophenyltropone. The reaction of 2-bromo-7-methoxytropone (I) with 2.2 equivalents of phenylmagnesium bromide afforded three kinds of products: 2-bromo-7-phenyltropone (XIII),[18] mp 80°C, *o*-methoxyphenyldiphenylcarbinol (XIV),[20] mp 126°C, and *o*-bromobenzophenone (XV),[19] an oil, in 20, 10 and 10% yields, respectively. The structures of these products were elucidated by mixed melting point determinations or by comparisons of the infrared spectra with those of authentic samples. The formation of XIV has already been reported,[13] but XIII and XV were isolated first in this experiment. Compound XIII is a product arising from the normal replacement of the methoxyl group at the C_7 position by the phenyl group, while XV is a rearranged product resulting from the attack of the phenyl group on the carbonyl carbon atom of I, followed by ring contraction, with the elimination of the methoxyl group. However, no other tropone derivatives, such as phenyltropolone or its methyl ether,[13] resulting from the substitution by the phenyl group could be isolated.

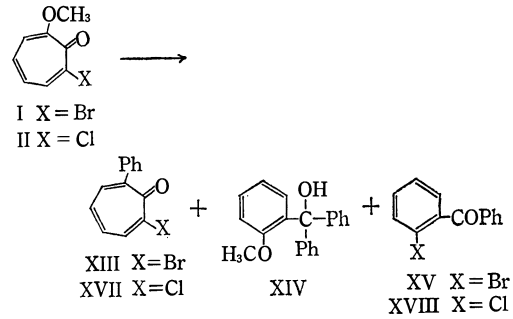

Similarly, the reaction of 2-methoxy-3-bromotropone (III) with phenylmagnesium bromide afforded 2-phenyl-3-bromotropone (XVI),[21] mp 108°C, and XV in 30 and 5% yields. However, the previously reported product, with a mp of 115—115.5°C, could not be obtained.[13] The product XVI is, of course, a normal substitution product resulting from the replacement of the methoxyl group at the C_2-position by the phenyl group.

17) E. J. Forbes, D. C. Warrell and W. J. Fry, *J. Chem. Soc., (C)*, **1967**, 1693.

18) T. Nozoe, T. Mukai and J. Minegishi, *Proc. Japan Acad.*, **28**, 287 (1952); W. von E. Doering and J. R. Mayer, *J. Am. Chem. Soc.*, **75**, 2387 (1953); T. Mukai, *Sci. Repts. Tohoku Univ., I*, **38**, 280 (1954).

19) E. Bergmann, *J. Org. Chem.*, **4**, 1 (1939).

20) A. Baeyer, *Ann.*, **354**, 168 (1900).

21) T. Toyooka, M. S. Thesis of Tohoku Univ., 1957.

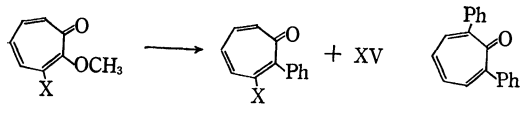

III X=Br XVI X=Br XX
IV X=Cl XIX X=Cl

The Grignard reaction of 2-chloro-7-methoxytropone (II) and phenylmagnesium bromide took place in almost the same manner as the reaction of the bromo derivative (I), giving 2-chloro-7-phenyltropone (XVII),[22] mp 74°C, 2,7-diphenyltropone (XX),[23] mp 125°C, and *o*-chlorobenzophenone (XVIII), an oil, in 8, 1.5 and 20% yields, respectively. The formation of XX can be explained by the reaction of XVII with another reagent. The Grignard reaction of 2-methoxy-3-chlorotropone (IV) with phenylmagnesium bromide also afforded 2-phenyl-3-chlorotropone (XIX),[21] mp 132°C, in 60% yield.

From the results obtained in this experiment, the following noticeable facts can be deduced. First, the reaction of methylmagnesium iodide failed to form tropone derivatives, but it did result in the formation of two benzenoid derivatives (V and VI), each with no halogen substituents. This rearrangement indicates that the reagent attacked mainly the carbonyl carbon atom and C_3-position. This may be ascribed to the fact that methylmagnesium iodide reacts as a stronger nucleophile than phenylmagnesium bromide. Second, phenylmagnesium bromide attacked the methoxyl group of the tropone ring, thus leading to the normal substitution products, phenylhalotropones. In addition, this reagent also attacked the carbonyl carbon atom to give rearranged products. It is of interest that the severely-hindered methoxyl group could be replaced by the phenyl group in a considerable yield in the cases of III and IV. Haworth and Tinker[6] have observed abnormal substitution in the reaction of 2-methoxy-6-methyltropone with phenyl magnesium bromide, in which case 2-phenyl-3-methyltropone was formed. It should be noted that no such abnormal substitution took place in the Grignard reactions of III and IV.

Unfortunately, it is impossible to explain reasonably all of the results described above. At any rate, they give some knowledge regarding the nucleophilic reactions of the troponoid systems.

Experimental

Reaction of 2-Bromo-7-Methoxytropone (I) with Methylmagnesium Iodide. Formation of V and VI. A solution of methylmagnesium iodide (7.0 mm) dissolved in ether (16 m*l*) was added, drop by drop over a 15 min period, to a solution of I (600 mg; 2.8 mm) in benzene (5 m*l*) and ether (40 m*l*). After 30 min of stirring, the reaction mixture was decomposed with 2 N sulfuric acid; the organic layer separated here was washed with 1 N potassium hydroxide solution and with water, and was dried over sodium sulfate. The evaporation of the organic layer afforded an yellow oil (455 mg). The vpc analysis (20% silicone grease at 160°C) showed it to contain four components in a relative intensity of 1 : 10 : 10 : 1 in order of retention time. When the oil was subjected to chromatographic separation using a column of neutralized alumina (Brockman II-III, 15 g), one of the main products (V) was eluted by petroleum ether - benzene (from 10 : 1 to 2 : 1). ν_{max}^{neat} 3571, 3460, 1235, 1183, 1029, 755 cm^{-1}. V was proved to be *o*-methoxyphenyldimethylcarbinol by a comparison of its infrared spectrum with that of an authentic sample.[15] Subsequent elution with petroleum ether - benzene (1 : 1) provided VI as a colorless oil; bp 122°C/25 mmHg. λ_{max}^{MeOH} mμ (log ε); 277(3.53). ν_{max}^{neat} 3571, 2967, 1284, 1272, 1220, 1063, 1048, 821, 779, 734 cm^{-1}.

Found: C, 72.22; H, 8.54%. Calcd for $C_{10}H_{14}O_2$: C, 72.26; H, 8.49%.

The aqueous alkaline extract was acidified with 6 N hydrochloric acid and extracted with ether. The evaporation of the ether layer gave a viscous yellow oil (94 mg), which in turn afforded 10 mg of VI when submitted to column chromatography using silicagel as the absorbent and benzene as the eluting solvent. The yield and the ratio of the products were practically unchanged when the amount of methylmagnesium iodide was changed from 2 to 4 equivalents.

Hydrolysis of VI. Preparation of VII. A mixture of VI (250 mg), acetic acid (2 m*l*), and 47% hydrobromic acid (2 m*l*) was refluxed for 1 hr at 140°C under a stream of nitrogen. The reaction mixture was then diluted with a large amount of water and extracted with ether. The ether layer was washed with 2 N sodium carbonate and with water, and dried over sodium sulfate. The subsequent evaporation of the ether furnished a brown oil (200 mg), which was passed through a column of silica gel (using petroleum ether-ether (10 : 2) as the eluent) and distilled to give a colorless, hygroscopic oil (VII), bp 119—121°C/26 mmHg. Compound VII was soluble in a 2 N sodium hydroxide solution, and it gave deep green complex with ferric chloride in ethanol. λ_{max}^{MeOH} mμ(log ε), 278(3.58); ν_{max}^{neat} 3497(broad), 2976, 2882, around 1250, 821, 782, 734 cm^{-1}; NMR in CCl_4 (60 Mc): τ 8.80 (doublet, J=7.0 cps, 6H), 6.88 (septet, J=7.0 cps, 1H), *ca.* 4.5 (very broad peak, 2H. Shift to a lower field in CF_3COOH), 3.38 (9 peaks, 3H).

Found: C, 68.83; H, 7.92%. Calcd for $C_9H_{12}O_2 \cdot 1/4\ H_2O$; C, 68.98; H, 8.04%.

Preparation of VIII. A solution of *o*-vanilline methyl ether (IX) (1.82 g; 10 mm) dissolved in ether (70 m*l*) was added, drop by drop, to a solution of methylmagnesium iodide (50 mm) in ether (70 m*l*) at room temperature. After the reaction mixture had then been refluxed for 30 min, it was decomposed with 20% ammonium chloride and acetic acid (4 m*l*). The organic layer separated here was washed with saturated sodium bicarbonate and with water, and dried over sodium sulfate. The evaporation of the solvent afforded crystals which were recrystallized from methanol or benzene to afford crystals (1.30 g) with a mp of 122—125°C as the first crop and then crystals containing the starting ester (410 mg), mp 54—56°C (*vide infra*).

22) T. Mukai, This Bulletin, **32**, 272 (1959).
23) T. Mukai, *ibid.*, **31**, 852 (1958).

Several recrystallizations of the crystals from methanol gave colorless prisms (VIII), mp 124—125°C. Compound VIII gave greenish-yellow complex with ferric chloride in ethanol. λ_{max}^{MeOH} mμ (log ε), 219 (3.82), 280 (3.40); ν_{max}^{KBr} 3559, 3195(b), 2985, 1290, 1266, 1222, 1056, 952, 892, 788, 746 cm^{-1}; NMR in $CDCl_3$ (60 Mc) τ 8.39 (singlet, 6H), 6.18 (singlet, 3H), 6.13 (singlet, 1H), 3.23 (singlet, 3H), 2.34 (singlet, 1H). Two peaks, those at τ 6.13 and 2.34, disappeared upon the addition of deuterium oxide.

Found: C, 65.96; H, 7.93%. Calcd for $C_{10}H_{14}O_3$: C, 65.91; H, 7.74%.

Reduction of VIII. Preparation of VI. A solution of VIII (100 mg; 0.55 mm) dissolved in ethanol (10 m*l*) containing a drop of concentrated hydrochloric acid was hydrogenated in the presence of 5% Pd-C (100 mg). It absorbed 1 equivalent of hydrogen (12.5 m*l*; Calcd 12.3 m*l*) in 2 hr. The filtration of the catalyst, followed by the evaporation of the solvent, afforded a residue. After an ethereal solution of the residue had been washed with water and dried over magnesium sulfate, the ether was removed, thus affording a pale yellow oil (87 mg) whose infrared spectrum was completely identical with that of VI.

Reaction of 2-Chloro-7-Methoxytropone (II) with Methylmagnesium Iodide. To a solution of II (500 mg; 2.9 mm) dissolved in ether (25 m*l*) and benzene (5 m*l*), there was added methylmagnesium iodide (8.7 mm) in ether (25 m*l*) for 15 min. After the reaction mixture had then been stirred for 30 min, it was decomposed with 2 N sulfuric acid and extracted with ether. The combined ether extract was washed with water, dried over sodium sulfate, and evaporated to give a yellowish-brown oil (530 mg), which showed seven peaks in a vapor-phase chromatogram (20% silicone grease at 160°C). The relative ratio of the four main peaks was 1 : 1 : 1 : 10 in order of retention time. The largest peak corresponds to VI, and one of the other three peaks to V.

Reaction of 2-Bromo-7-Methoxytropone (I) with Phenylmagnesium Bromide. *(a)* A solution of phenylmagnesium bromide (7.5 mm) in dry ether (22 m*l*) was added, drop by drop at room temperature, to a solution of I (610 mg; 2.8 mm) dissolved in a mixture of ether (50 m*l*) and benzene (15 m*l*) for 15 min. After 1 hr of stirring, the white precipitate (Grignard complex) formed was filtered off in a nitrogen stream and decomposed by adding ethanol (12 m*l*) and a large amount of ether. The organic layer was washed with 2 N sulfuric acid, 2 N potassium hydroxide, and water and dried over sodium sulfate. The evaporation of the solvent afforded a yellow oil (230 mg), which was then dissolved in benzene and passed through a column of alumina (Brockman O-I, 6 g). The evaporation of an elute with benzene gave a yellow oil (15 mg) whose infrared spectrum was identical with that of authentic *o*-bromobenzophenone.[19] The evaporation of a subsequent elute with benzene afforded yellow crystals (90 mg), which were then recrystallized from ethanol to give 2-bromo-7-phenyltropone (XIII), mp 79—80°C. Identification was made by the mixed-melting-point method and by a comparison of the infrared spectrum with that of an authentic sample.[18] Subsequent elution with ether-ethanol (1 : 25) gave crystals (30 mg), mp 84—89°C, whose infrared spectrum (ν_{max}^{KBr} 3067, 2967, 1582, 1548, 1479, 1350, 1248, 1245, 1199, 1167, 1099, 969 cm^{-1}) did not show the C=C and C=O bands characteristic of tropone derivatives. The structure of the product was not elucidated. On the other hand, the filtrate separated from the Grignard complex was treated in the usual manner to afford a yellow oil (200 mg), which was passed through a column of alumina (Brockman O-I, 5 g). A yellow oil (60 mg) obtained from an elute with benzene was proved to be *o*-bromobenzophenone (XV) contaminated by a small amount of *o*-methoxyphenyldiphenylcarbinol (XIV) by an inspection of its infrared spectrum. Subsequent elution with benzene gave XIII (30 mg), mp 73—75°C. The aqueous potassium hydroxide extract was acidified with 2 N sulfuric acid and extracted with benzene. The evaporation of the benzene extract and the recrystallization of the residue obtained from cyclohexane afforded yellow crystals (100 mg), mp 108°C, which proved to be 3-bromotropolone, a hydrolyzed product of the starting material (I).

(b) A solution of phenylmagnesium bromide (9.0 mm) in ether (30 m*l*) was added, drop by drop over a 30 min period, to a solution of I (660 mg; 3.0 mm) dissolved in a mixture of ether (50 m*l*) and benzene (12 m*l*), and then it was worked up just as in (a). The solid complex was decomposed with 2 N sulfuric acid and extracted with benzene. The benzene layer was washed with 2 N potassium hydroxide and then with water, and dried over sodium sulfate. The evaporation of the benzene afforded a brown oil (280 mg), which was then passed through a column of alumina as in (a). Elution from petroleum ether - benzene (1 : 1) to benzene afforded a mixture of XIV and XV (40 mg). Compound XIII (50 mg), mp 74°C, was obtained from the elute with benzene, and a viscous yellow oil (40 mg), from the elute with ether - methanol (1 : 25). The filtrate separated from the complex also afforded a yellowish-brown oil (470 mg), which was separated by the use of column chromatography using alumina. The evaporation of the elute with petroleum ether-benzene (1 : 1) gave XV (45 mg) and colorless crystals (75 mg), mp 105—110°C. The recrystallization of the latter crystals from ethanol afforded colorless prisms, mp 125—126°C, which were proved to be *o*-methoxyphenyldiphenylcarbinol (XIV) by the mixed melting point method and by a comparison of the infrared spectrum with that of an authentic sample.[20] Compound mp XIII (55 mg), mp 65—70°C, was obtained from the elute with benzene, and a viscous oil (*ca.* 100 mg), from an elute with ether. The aqueous alkaline extract gave no 3-bromotropolone when it was treated as has been described in (a).

Reaction of 2-Methoxy-3-Bromotropone (III) with Phenylmagnesium Bromide. *(a)* A solution of phenylmagnesium bromide (5.0 mm) dissolved in ether (10 m*l*) was added, drop by drop over a 20 min period, to a solution of III (430 mg; 2.0 mm) in ether (30 m*l*). After the mixture had then been stirred for 1.5 hr, the deposited white Grignard complex was filtered out and the solution was decomposed with ethanol (5 m*l*) and extracted with ether. The ether layer was washed with 2 N sulfuric acid, 1 N potassium hydroxide, and water, and dried over sodium sulfate. The evaporation of the ether afforded a viscous reddish-yellow oil, which, upon standing, yielded yellow crystals (85 mg), mp 96—103°C. The residual part was dissolved in petroleum ether-benzene (1 : 1) and passed through a column

of alumina (Brockman III, 13 g). Yellow crystals (75 mg), mp 93—100°C, were obtained by the evaporation of the elute with petroleum ether - benzene (1 : 1) and benzene. The crystals obtained here were combined and recrystallized from ethanol to afford 2-phenyl-3-bromotropone (XVI), mp 108°C. On the other hand, the ethereal filtrate separated from the complex was washed with 2 N sulfuric acid, 2 N potassium hydroxide, and water, and dried over sodium sulfate. The residual oil obtained by the evaporation of the ether was dissolved in petroleum ether - benzene (1 : 1) and passed through a column of alumina to give oily crystals (30 mg); these crystals did not show the bands characteristic of tropone derivatives in the infrared spectrum and could not be elucidated, because of their small amount. An aqueous potassium hydroxide solution was acidified with 2 N sulfuric acid and extracted with benzene; from the extract no clear compound could be obtained except for phenol.

(b) Reaction at −30°C. A solution of phenylmagnesium bromide (6.9 mm) dissolved in ether (20 m*l*) was added, at −30°C (dry ice-acetone) over a 15 min period, to a solution of III (500 mg; 2.3 mm) in ether (40 m*l*). The solution was then stirred at −30°C for an additional 30 min. After the complex formed had been filtered, the complex part and the filtrate were separately treated in the manner described in (a). The complex part gave a brown oil (390 mg), which was then dissolved in petroleum ether - benzene (2 : 1) and passed through a column containing alumina. The evaporation of an elute with benzene-ether (9 : 1) afforded pale yellow crystals (240 mg), mp 57—60°C, while an elute evaporated with ether gave a yellow oil (15 mg). The crystals were found by a mixed melting point determination to be recovered III. An aqueous potassium hydroxide extract was acidified with concentrated hydrochloric acid and extracted with ether. The ether was washed with water and dried over sodium sulfate. The evaporation of the solvent gave an oil with phenolic odor (165 mg); this oil was dissolved in benzene, and hydrogen bromide gas was passed into the solution. The deposited HBr-salt was neutralized with a saturated sodium bicarbonate solution and extracted with benzene. The evaporation of the benzene-extract afforded 3-bromotropolone (60 mg), mp 101—102°C. On the other hand, the filtrate separated from the complex afforded a yellow oil (102 mg); this oil was dissolved in petroleum ether - benzene (1 : 1) and passed through an alumina column. Evaporation of an elute with benzene gave XVI (32 mg), mp 104—106°C, while an elute with ether yielded a yellow oil (15 mg), which was found by an inspection of its infrared spectrum to be identical with the oily product isolated from the complex part.

Reaction of 2-Chloro-7-Methoxytropone (II) with Phenylmagnesium Bromide. A solution of phenylmagnesium bromide (8.7 mm) in ether (27 m*l*) was dropped into a solution of II (500 mg; 2.9 mm) dissolved in a mixture of benzene (5 m*l*) and ether (45 m*l*). After the mixture had been stirred for 1 hr, the precipitated complex was separated and treated in the manner described for the reaction of I with phenylmagnesium bromide. The complex part gave a brown oil (330 mg); this oil was dissolved in petroleum ether-benzene (2 : 1) and passed through a column of alumina (Brockman O-I, 12 g), The evaporation of an elute with petroleum ether - benzene (2 : 1) afforded a colorless oil (25 mg), whose infrared spectrum was very similar to that of *o*-bromobenzophenone and which afforded an oxime (mp 130°C) in a sealed tube.[24] The oil was identified as *o*-chlorobenzophenone (XVIII). Evaporation of a subsequent elute with benzene afforded a yellow oil (160 mg) which was separated using preparative thin-layer chromatography of silica gel developed by benzene; two kinds of crystals (mp 65—69°C, 50 mg; mp 121—121.5°C, 30 mg) were thus obtained. The compound with the lower melting point was recrystallized from cyclohexane to give a sample with a mp of 74—74.5°C; it was proved to be 2-chloro-7-phenyltropone (XVII) by a comparison of its infrared spectrum with that of an authentic sample[22] and by the mixed melting point method. The other crystal was found to be 2,7-diphenyltropone by a comparison of its infrared spectrum with that of an authentic sample.[23] On the other hand, the filtrate part gave a brown oil (430 mg) which was dissolved in petroleum ether - benzene (2 : 1) and separated using a column of alumina (Brockman O-I, 12 g). An elute with petroleum ether - benzene (2 : 1) was evaporated to give *o*-chlorobenzophenone (XVIII) (85 mg). Besides these products, more than ten products (each product in a quantity less than 10 mg) were obtained, but their structures could not be elucidated.

Reaction of 2-Methoxy-3-Chlorotropone (IV) with Phenylmagnesium Bromide. A solution of phenylmagnesium bromide (6.4 mm) in ether (30 m*l*) was added, drop by drop over a 10 min period, to a solution of IV (500 mg; 2.9 mm) dissolved in ether (50 m*l*). After the mixture had been stirred for 1 hr, the complex formed was filtered out and decomposed with 47% borontrifluoride etherate (4 m*l*), and the resulting solution was worked up in the usual manner. The evaporation of the ether gave crystals (400 mg) which were then recrystallized from cyclohexane to afford yellow prisms, mp 127—129°C (142 mg). The filtrate was dissolved in benzene and passed through a column of alumina (Brockman II-III, 12 g). An elute with benzene was evaporated to furnish yellow crystals (161 mg), mp 104—120°C. These crystals were combined and recrystallized from cyclohexane to afford a sample with a mp of 131—132°C; this was proved to be 2-phenyl-3-chlorotropone (XIX) by a comparison of the infrared spectra and by mixed melting point determination with an authentic sample.[21] The filtrate separated from the complex was treated like the above complex; this gave a brown oil (280 mg), which was dissolved in benzene and passed through a column of alumina (Brockman II-III, 12 g). Evaporation of an elute with benzene afforded XIX (82 mg), mp 120—122°C. The total yield of XIX was 385 mg.

The authors are indebted to Professor Tetsuo Nozoe for his encouragement throughout this work. Financial support from the Sankyo Co. is also acknowledged. The infrared spectrometer used in this study was purchased by a grant-in-aid for Fundamental and Technical Research from the Toyo Rayon Co., to which the authors are grateful.

24) J. Meisenheimer and H. Meis, *Ber.*, **57**, 295 (1924).

BULLETIN OF THE CHEMICAL SOCIETY OF JAPAN VOL. 41 2495—2503 (1968)

Acetonated Sorbofuranoses and Their Favored Conformations as Determined by Proton Magnetic Resonance Spectroscopy[1)]

Takashi MAEDA, Kazuo TORI, Shiroh SATOH and Kanji TOKUYAMA

Shionogi Research Laboratory, Shionogi & Co., Ltd., Fukushima-ku, Osaka

(Received April 23, 1968)

A series of L-sorbofuranose derivatives have been studied by PMR spectroscopy in order to determine their favored conformations from the coupling constants obtained by applying the spin-decoupling techniques and the solvent effects of benzene at 100 MHz. The coupling constants $J_{3,4}$, have disclosed that the furanose ring of methyl 1,3,4,6-tetra-*O*-acetyl-α-L-sorbofuranoside (IIa) in solutions has a conformation close to a C_3-*endo*-C_4-*exo* half-chair, while that of its β-anomer (IVa) has a C_3-*exo*-C_4-*endo* half-chair conformation. Their conformations are unchanged over the temperature range of 32—74°C, but they are affected by the introduction of a 4,6-*O*- or 2,3-*O*-isopropylidene group, either of which locks the furanose ring to a C_3-*exo*-C_4-*endo* half-chair conformation. This effect is thought to play an important role in the exclusive formation of 2,3 : 4,6-di-*O*-isopropylidene-α-L-sorbofuranose (XII) during the acetonation of L-sorbose.

The acetonation of L-sorbose yields 2,3 : 4,6-di-*O*-isopropylidene-α-L-sorbofuranose (XII) exclusively.[2)] Recent investigations of the reaction using acetone dimethyl ketal have shown the isolation of many kinds of acetonated sorbofuranoses as intermediates,[3,4)] whose relative yields are much influenced by the reaction conditions employed; *e. g.*, they were hardly detectable under usual acetonation conditions.[5-7)] The results have suggested that conformational factors play an important role in the reaction; accordingly, we were prompted to study the ring conformations of L-sorbofuranoses by mean of proton magnetic resonance (PMR) spectroscopy, as it has proved to be a powerful tool for this purpose. The present conformational study may provide important information about the differences in the stability of many intermediate L-sorbofuranoses.

Experimental

All the meting points were recorded on a Kofler microstage and have been corrected. The optical rotations were measured in acetone solutions unless otherwise stated, and the concentrations are recorded in percentages. The thin-layer chromatography (TLC) was carried out on a silica-gel plate with acetone-chloroform (1 : 9 v/v) (Solvent A) and with ether-petroleum ether (2 : 1 v/v) (Solvent B). The separated materials were developed with a Seliwanoff reagent[8)] and then heated in an oven. The preparative thin-layer chromatography (PTC) was performed on silica gel with the same solvent systems for detection, and the spots developed with iodine vapor were extracted with acetone. The evaporation of the acetone under reduced pressure yielded the materials.

Isolation of Methyl 4,6-*O*-Isopropylidene-α-L-sorbofuranoside (I). This substance was prepared essentially according to a previously-reported procedure.[4)] L-Sorbose (40 g) was refluxed in acetone dimethyl ketal (100 m*l*)[9)] containing *p*-toluenesulfonic acid (500 mg) for 2 hr. The solution was then neutralized with a slight excess of methanolic sodium methoxide. After the removal of the solvent, the residual syrup was extracted with benzene (200 m*l*); thin-layer chromatograms showed the presence of methyl 1,3 : 4,6-di-*O*-isopropylidene-β-L-sorbofuranoside (III)[4)] and 2,3 : 4,6-di-*O*-isopropylidene-α-L-sorbofuranose (XII)[2)] as the major products, and of 1,2-*O*-isopropylidene-α-L-sorbopyranose,[10)] 2,3-*O*-isopropylidene-α- (XI),[11)] 1,2 : 4,6-di-*O*-isopropylidene-α-(VIII),[3,4)] and -β- (X),[4)] 1,3 : 4,6-di-*O*-isopropylidene-β- (VI),[4)] 1-*O*-α-methoxyisopropyl-2,3 : 4,6-di-*O*- isopropylidene -α-L- sorbofuranose,[4)] and I as the minor products. The benzene solution was then extracted with water (50 m$l \times 3$). The aqueous layer was saturated with sodium chloride

1) Sorboses. XII. Part XI: M. Katsuhara, S. Wakahara and K. Tokuyama, This Bulletin, **41**, 1208 (1968).
2) T. Reichstein and G. Grüssner, *Helv. Chim. Acta*, **17**, 311 (1934).
3) K. Tokuyama and E. Honda, This Bulletin, **37**, 591 (1964).
4) T. Maeda, *ibid.*, **40**, 2212 (1967).
5) K. Tokuyama, E. Honda and N. Hōki, *J. Org. Chem.*, **29**, 133 (1964).
6) D. C. DeJongh and K. Biemann, *J. Am. Chem. Soc.*, **86**, 67 (1964).
7) J. R. Patil and J. L. Bose, *J. Indian Chem. Soc.*, **43**, 161 (1966).
8) A. Anno and N. Seno, "Jikken Kagaku Kōza," Bd. 23, ed. by Chem. Soc. Japan, Maruzen, Tokyo (1957), p. 374.
9) J. H. Brown, Jr., and N. B. Lorett, U. S. Pat. 2827494 (1958).
10) H. Ohle, *Ber.*, **71**, 762 (1938).
11) T, I. Temnikova and V. V. Sklyarava, *Zh. Prikl. Khim.*, **21**, 1131 (1954); *Chem. Abstr.*, **49**, 2952 (1955).

and extracted with chloroform (200 ml×3), and the solvent removed. From the residue (10.6 g), I (2.1 g) was separated by PTC (R_f, 0.1—0.15, Solvent A) as a crystalline syrup. Two successive recrystallizations from ether gave I as colorless needles, mp 108—109°C $[\alpha]_D^{25}$ −65.0 (*c* 1.024). Found: C, 51.47; H, 7.82; OCH_3, 13.19%. Calcd for $C_{10}H_{18}O_6$: C, 51.27; H, 7.75; OCH_3, 13.25%.

Hydrolysis of I. I (1.0 g) was treated with 60% acetic acid (10 ml) at 50°C. After 1.5 hr, the solvent was evaporated to dryness, giving L-sorbose (0.5 g).

Methyl 1,3-Di-*O*-acetyl-4,6-*O*-isopropylidene-α-L-sorbofuranoside (Ia). A mixture of I (100 mg), acetic anhydride (1 ml), and pyridine (1 ml) was kept overnight in a refrigerator, and then evaporated to dryness. The recrystallization of the residue from ether gave Ia as colorless needles (51 mg), mp 104—105°C, $[\alpha]_D^{25}$ −63.9 (*c* 0.549). Found: C, 52.53; H, 6.93%. Calcd for $C_{14}H_{22}O_8$: C, 52.82; H, 6.97%.

Methyl 1,3,4,5-Tetra-*O*-acetyl-α-L-sorbofuranoside (IIa). A solution of Ia (310 mg) in 60% acetic acid (2 ml) was allowed to stand at room temperature for 2 hr. The solvent was then removed twice by the addition of an excess of ethanol, and by concentration. Without further purification, the residual syrup was acetylated with acetic anhydride (2 ml) and pyridine (2 ml) in a refrigerator for 4 hr. The evaporation of the solvent gave a syrup (315 mg); this syrup was subsequently purified by PTC with Solvent B. IIa was obtained as a syrup, $[\alpha]_D^{22}$ −66.1 (*c* 0.672). Found: C, 50.03; H, 6.24%; mol wt, 363. Calcd for $C_{15}H_{22}O_{10}$: C, 49.72; H, 6.12%; mol wt, 362.

Hydrolysis of Methyl 1,3:4,6-di-*O*-isopropylidene-β-L-sorbofuranoside (III). A solution of III[3] (1.42 g) in 60% acetic acid (20 ml) was allowed to stand at room temperature. After 1 hr, the solution was worked-up by a procedure similar to the above. The thin-layer chromatograms of the obtained syrup (1.56 g) showed the presence of methyl 1,3,4,6-tetra-*O*-acetyl-β-L-sorbofuranoside (IVa) and methyl 1,3-*O*-isopropylidene-4,6-di-*O*-acetyl-β-L-sorbofuranoside (Va); IVa (285 mg, R_f 0.38—0.46) and Va (0.60 g, R_f 0.50—0.65) were isolated by PTC with Solvent B. IVa: colorless needles (95 mg), mp 49—50°C (recrystallized from *n*-hexane), $[\alpha]_D^{24}$ +34.7 (*c* 0.773, chloroform). Found: C, 49.53; H, 6.18%. Calcd for $C_{15}H_{22}O_{10}$: C, 49.72; H, 6.12%. Va: syrup, $[\alpha]_D^{25}$ +34.9 (*c* 0.815). Found: C, 53.02; H, 7.20%. Calcd for $C_{14}H_{22}O_8$: C, 52.82; H, 6.97%.

1,2-*O*-Isopropylidene-3,4,6-tri-*O*-acetyl-α-L-sorbofuranose (VIIa). 1,2 : 4,6-Di-*O*-isopropylidene-α-L-sorbofuranose (VIII)[3,4] (60 mg) was treated with 60% acetic acid (1.2 ml) at 40°C for 80 min. The solution was then evaporated to dryness and extracted with chloroform. The removal of the solvent gave a hygroscopic syrup (36.5 mg), which was immediately acetylated with a mixture of acetic anhydride (1 ml) and pyridine (1 ml) at room temperature. After 4 hr, the evaporation of the solution gave VIIa as a syrup, $[\alpha]_D^{23}$ −67.3 (*c* 0.989). Found: C, 52.06; H, 6.68%. Calcd for $C_{15}H_{22}O_9$: C, 52.02; H, 6.40%.

1,2-*O*-Isopropylidene-3,4,6-tri-*O*-acetyl-β-L-sorbofuranose (IXa). IXa (230 mg) was prepared from 1,2 : 4,6-di-isopropylidene-β-L-sorbofuanose (X)[4] (500 mg) in a manner similar to the above. IXa: syrup, $[\alpha]_D^{23}$ +45.6 (*c* 1.128). Found: C, 51.85; H, 6.41%. Calcd for $C_{15}H_{22}O_9$: C, 52.02; H, 6.40%.

PMR Spectra Measurements. The PMR spectra were recorded on a Varian HA-100 spectrometer by using about 5% (w/v) solutions of the samples in chloroform-d ($CDCl_3$) and/or benzene-d_6 (C_6D_6). The spectrometer was operated at 100 MHz in the frequency-swept and internal TMS-locked mode. Spin-decoupling experiments were carried out by using two Hewlett-Packard HP-200ABR audiooscillators. The spectral charts were calibrated by direct readings of the resonance frequencies by means of a Hewlett-Packard HP-5212A electronic counter. The accuracies of the chemical shifts and coupling constants described are within ±0.02 and ±0.2 Hz, respectively.

Results and Discussion

Sorbofuranosides. *a) Preparation.* Methyl 1,3,4,6-tetra-*O*-acetyl-α- (IIa) and -β-L-sorbofuranoside (IVa) could be obtained from methyl 4,6-*O*-isopropylidene-α- (I) and 1,3 : 4,6-di-*O*-isopropylidene-α-L-sorbofuranoside (III)[4] respectively. The former starting material, I, was newly isolated as a minor product from the acetonation of L-sorbose with acetone dimethyl ketal. The combined data on the elemental analysis and the mild hydrolysis yielding L-sorbose showed that I is a methyl monoacetonated sorboside. I gave a diacetate (Ia) with acetic anhydride and pyridine at an ordinary temperature. The deacetonation of Ia with 60% acetic acid, followed by acetylation, afforded a new glycoside tetraacetate, one which was not identical with the known methyl 1,3,4,5-tetra-*O*-acetyl-α-[12] or -β-L-sorbopyranoside.[12] On the basis of the negative sign of its optical rotation, the tetraacetate was identified as the desired α-furanoside IIa. Consequently, the structure of I should be either methyl 1,3- or 4,6-*O*-isopropylidene-α-L-sorbofuranoside. β-Furanoside IVa was successfully obtained by the deacetonation of III, followed by acetylation. In this case, a partially-deacetonated sorboside (Va) was also isolated as a diacetate; this should be either the diacetate of methyl 1,3- or 4,6-*O*-isopropylidene-β-L-sorbofuranoside. The determination of the I and Va structures, which are 4,6- and 1,3-*O*-isopropylidene derivatives, respectively, leaned heavily on their PMR spectral interpretations, as will be described below.

b) Conformations. The conformations of the sorbofuranosides IIa and IVa were establsihed by means of PMR spectroscopy. In their PMR spectra, singlets due to *O*-acetyl, *O*-methyl, and *O*-isopropylidene protons are easily assigned. Methylene protons at C_1 (H_1, $H_{1'}$) usually appear as an AB-type quartet, and those at C_6 (H_6, $H_{6'}$), as the AB part of an ABX system, being coupled to H_5. The remaining ring protons, H_3, H_4, and H_5, can be expected to appear as a doublet, a quartet,

12) H. H. Schulbach and G. Graefe, *Ann.*, **532**, 211 (1937).

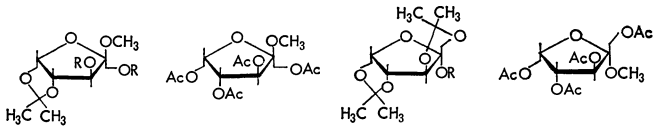

I R = H

Ia R = Ac

IIa

III R = CH_3

VI R = H

VIa R = Ac

IVa

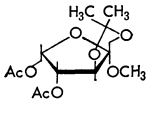

Va

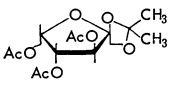

VIIa

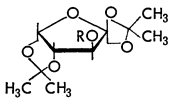

VIII R = H

VIIIa R = Ac

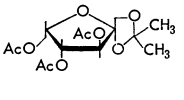

IXa

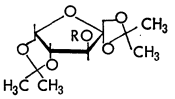

X R = H

Xa R = Ac

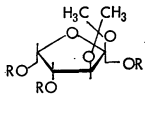

XI R = H

XIa R = Ac

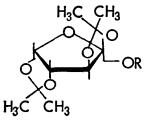

XII R = H

XIIa R = Ac

and a multiplet respectively, according to the first-order approximation. However, H_6, $H_{6'}$, H_5, H_4, and H_3 constitute an ABXYZ spin system, the signals of which can appear as a second-order pattern, depending on the $\Delta\nu_{ij}/J_{ij}$ values, where $\Delta\nu_{ij}$ is the difference in chemicals shifts (in Hz) between two interacting protons. Spin-decoupling experiments and the solvent effects of benzene[13] were mainly used to obtain the chemical shifts and coupling constants by means of the first-order approximation. However, in the present study, second-order patterns were sometimes analyzed by the usual procedure.[14]

The spectrum of IIa in $CDCl_3$ (Fig. 1a) shows a doublet at τ 4.58 due to H_3 and a doublet of doublets at τ 4.50 due to H_4 ($J_{3,4}$=5.8 and $J_{4,5}$=6.0 Hz). Double irradiation at the resonance frequency of a multiplet due to the H_5 centered at τ 5.50 changes the signal due to H_4 into a doublet, from the spacing of which the $J_{3,4}$ value (5.8 Hz) was confirmed (Fig. 1b). Reverse double-irradiation at the center of the resonance frequencies of H_3 and H_4 causes a collapse of the H_5-multiplet into a triplet, but it does not change the AB-type quartet due to H_1

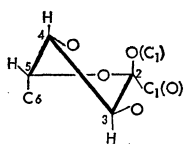

C_3-endo C_4-exo (A)

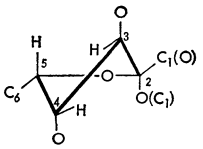

C_3-exo-C_4-endo (B)

and $H_{1'}$ at τ 5.71 and 5.78 ($J_{1,1'}$=(−)12.2 Hz); the AB-type quartet is further split into doublets by the coupling to H_5 at τ 5.75 (H_6) and 5.88 ($H_{6'}$) ($J_{5,6}$=5.0, $J_{5,6'}$=5.1, and $J_{6,6'}$=(−)11.8 Hz). Similar decoupling experiments on the spectrum in C_6D_6 also support the above assignments. The J values are unchanged by the alteration in the solvent.

The spectrum of IVa in C_6D_6 (Fig. 2a) shows a doublet at τ 4.28 due to H_3 ($J_{3,4}$=2.5 Hz) and a doublet of doublets at τ 4.58 arising from H_4 ($J_{4,5}$=5.8 Hz). Singnals appearing as the AB part of an ABX system at τ 5.68 (H_6) and 5.76 ($H_{6'}$) are due to C_6-methylene protons ($J_{5,6}$=5.3, $J_{5,6'}$=7.2, and $J_{6,6'}$=(−)11.8 Hz). On the double irradiation of H_4, a change in the shape of the H_5-multiplet centered at τ 5.45 was observed (Fig. 2b). The decoupling of H_5 changes the H_4-signal into a doublet. The observation of the spectrum in $CDCl_3$, including spin-decoupling experiments, also supports these assignments.

13) See, for example, J. Ronayne and D. H. Williams, *J. Chem. Soc., (B)*, **1967**, 540, and the reference cited therein.

14) J. W. Emsley, J. Feeney and L. H. Sutcliffe, "Highresolution Nuclear Magnetic Resonance Spectroscopy," Pergamon Press, London (1965), Chaptor 8.

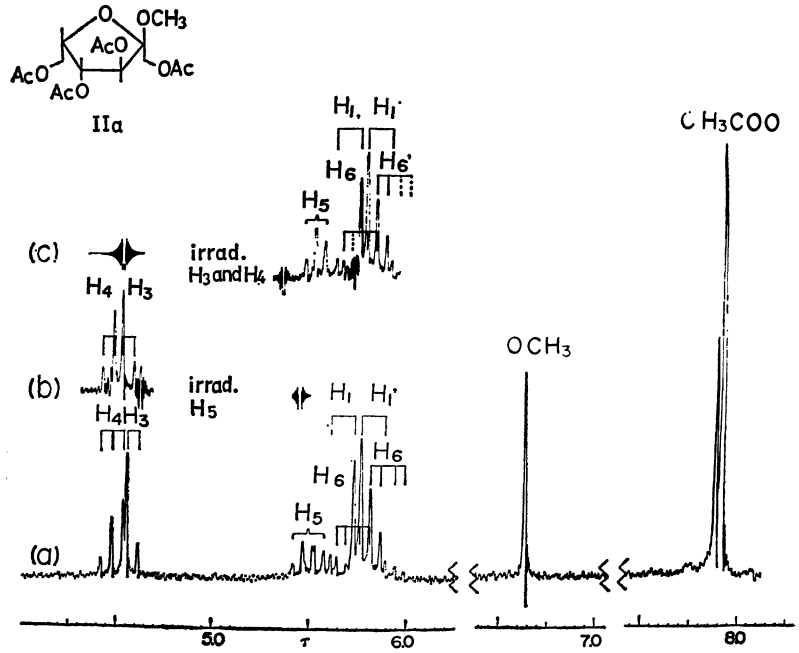

Fig. 1. PMR spectra of IIa in chloroform-d at 100 MHz.

a) Normal spectrum, b) and c) PMDR spectra

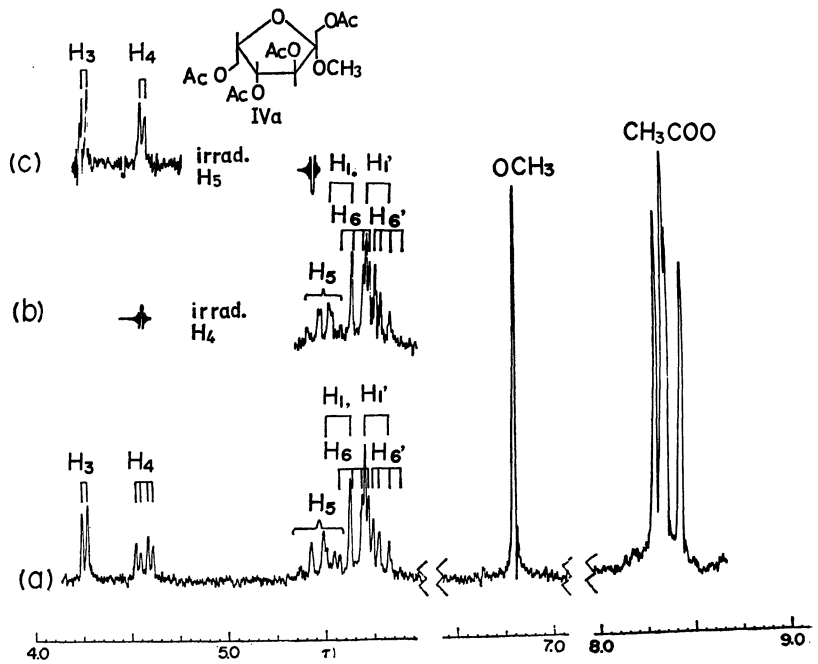

Fig. 2. PMR spectra of IVa in benzene-d_6 at 100 MHz.

a) Normal spectrum, b) and c) PMDR spectra

TABLE 1. CHEMICAL SHIFTS (τ) IN $CDCl_3$ AT 32°C[a]

Compound	H_1 and $H_{1'}$	H_3	H_4	H_5	H_6 and $H_{6'}$	CH_3-C-	CH_3COO	Other H
IIa	5.71, 5.78	4.58	4.50	5.50	5.75, 588		7.89 7.92(9H)	OCH_3 6.63
	(5.54, 5.71)	(4.28)	(4.24)	(5.61)	(5.8—6.0)		(8.23, 8.27 8.28, 8.32)	OCH_3 (6.89)
IVa	5.62, 5.90	~4.6	~4.7	~5.4	5.7—5.8		7.93(9H), 7.98	OCH_3 6.70
	(5.57, 5.75)	(4.28)	(4.58)	(5.45)	(5.68, 5.76)		(8.27, 8.32, 8.34, 8.41)	OCH_3 6.78
VIa	5.61, 5.99	5.28	5.60	5.88	5.98, 6.06	8.40, 8,63(9H)	7.93	
Ia	~5.64	4.73	5.62	~5.9	5.9—6.1	8.60(6H)	7.89	OCH_3 6.64
	(~5.41)	(4.36)	(5.82)	(~6.2)	(6.3—6.5)	(8.65, 8.88)	(8.17, 8.23)	OCH_3 (6.77)
Va	~6.12	5.88	4.75	5.30	5.6—5.7	8.57, 8.62	7.92, 7.93	OCH_3 6.70
	(6.17, 6.23)	(5.72)	(4.60)	(~5.3)	(~5.7)	(8.66, 8.78)	(8.27, 8.35)	OCH_3 (6.90)
VIIa	5.80, 5.91	4.77	4.50	5.47	5.76, 5.86	8.51, 8.63	7.89, 7.93(6H)	
VIIIa	5.70, 5.81	4.83	5.67	5.84	5.96, 6.04	(8.50, 8.58 8.63, 8.65)	7.88	
	(5.62, 5.70)	(4.65)	(5.92)	(6.12)	(6.22, 6.46)	(8.45, 8.62 8.71, 8.92)	(8.19)	
VIII	5.73, 5.89	5.96	5.88	6.04	6.20, 6.48	8.44, 8.71(6H), 8.92		OH 7.12
IXa	5.97	4.6—4.8		~5.5	6.6—6.8	8.53, 8.62	7.88(6H), 7.94	
	(5.95)	(4.38)	(4.56)	(5.3—5.8)		(8.50, 8.67)	(8.27, 8.38 8.45)	
Xa	~5.98	4.76	5.7—5.8		~6.1	8.50, 8.62(6H) 8.64	7.91	
	(5.85, 5.91)	(4.47)	(5.8—6.0)		~6.2	(8.44, 8.59, 8.65, 8.81)	(8.44)	
XIa	5.65, 5.75	5.58	4.73	5.41	5.73, 5.85	8.47, 8.64	7.91, 7.92 7.95	
XIIa	5.45, 5.85	5.58	5.68	5.7—5.9, 6.00		8.52, 8.57 8.63(6H)	7.90	
	(5.17, 5.61)	(5.48)	(5.8)	(6.1—6.2) (6.42)		(8.53, 8.68 8.69, 8.92)	(8.31)	
XII	~6.2	5.48	5.63	5.8—5.9		8.50(6H) 8.57, 8.63		OH 7.43

a) Values in parentheses are those observed in C_6D_6.

Since the only available J values for the conformational studies of ketofuranoses are $J_{3,4}$ and $J_{4,5}$, it seems rather difficult to distinguish rigorously their furanose-ring conformations from possible C_s (envelope) and C_2 (half-chair) conformations. However, it has been suggested that cyclopentane derivatives containing one hetero-atom (*e. g.*, tetrahydrofuran, tetrahydrothiophene, and pyrrolidine) exist in the half-chair conformation (C_2) with the hetero-atom located on the axis of symmetry.[15] In the case of L-sorbofuranoses, there are only two possible C_2-conformations, *i. e.*, a C_3-*endo*-C_4-*exo* (A) and a C_3-*exo*-C_4-*endo* half-chair (B).[16] By using Dreiding models, the

15) J. E. Kilpatrick, K. S. Pitzer and R. Spitzer, *J. Am. Chem. Soc.*, **69**, 2483 (1947); K. S. Pitzer and W. E. Donath, *ibid.*, **81**, 3213 (1959).

16) "*Endo*" means that the atom is located on the same side of the plane defined by the C_2–O–C_5 ring atom as the C_5–C_6 bond, while "*exo*" means that they are found on opposite side.

TABLE 2. COUPLING CONSTANTS (J, Hz)

Compound	$J_{1,1'}$	$J_{3,4}$	$J_{4,5}$	$J_{5,6}$	$J_{5,6'}$	$J_{6,6'}$
IIa	(−)12.2	5.8	6.0	5.0	5.1	(−)11.8
IVa	(−)12.2	2.5	5.8	5.3	7.2	(−)11.8
VIa	(−)12.5	0.5	4.0	4.0	4.0	(−)12.8
Ia	a)	1.5	4.0	a)	a)	a)
Va	(−)12.2	0.6	5.3	a)	a)	a)
VIIa	(−)9.0	5.3	6.2	5.2	4.8	(−)11.8
VIIIa	(−)9.0	1.5	3.0	2.8	3.0	(−)13.0
VIII	(−)9.0	1.5	3.0	2.8	3.0	(−)13.0
IXa	a)	2.5	5.8	a)	a)	a)
Xa	(−)9.0	0.3	a)	a)	a)	a)
XIa	(−)12.0	0.5	3.0	5.0	7.2	(−)11.0
XIIa	(−)12.0	0.5	2.3	a)	2.8	(−)13.8
XII	(−)12.0	0.5	2.3	a)	3.0	(−)13.8

a) Not determinable.

dihedral angles between H_3 and H_4 in the A and B conformers are found to be about 150—160° and 90—110°, respectively, whereas the angles between H_4 and H_5 are measured to be about 10—30° in both the conformers. Therefore, only the $J_{3,4}$ values in the compounds examined can be used for determining their conformations, for the dihedral angles between H_3 and H_4 in the two conformers should lead to obviously different $J_{3,4}$ values according to the Karplus equation, even though it is used in a very qualitative sense.[17] The $J_{3,4}$ values can thus be expected to be in the range of 5—6 Hz for the A conformer and in the range of 0—2.5 Hz for the B conformer.

On the basis of the $J_{3,4}$ values determined above, the conformation of IIa was concluded to be one close to C_3-*endo*-C_4-*exo* half-chair ($J_{3,4}$=5.8 Hz), and that of IVa, one close to C_3-*exo*-C_4-*endo* half-chair ($J_{3,4}$=2.5 Hz). Both conformations can satisfy the operation of the anomeric effect of the OCH_3 group and probably, the reverse anomeric effect of the CH_2OAc group[18] at the C_2 atom. The C_3-*exo*-C_4-*endo* half-chair conformation of the β-D-fructofuranose moiety of sucrose, as determined by neutron diffraction,[19] also supported the above conclusion.

The spectra of IIa and IVa in $CDCl_3$ are unchanged in chemical shifts and coupling constants over the temperature range of 32—74°C. The results show that they exist in fixed conformations in this temperature range.

Conformations of Acetonated Derivatives. The assignments of the spectra of acetonated sorbofuranoses were established in a manner similar to those described above. The data obtained are listed in Tables 1 and 2, while some of the spectra are shown in Figs. 3—6.

At the outset we investigated the conformation of the acetate (VIa) of 1,3:4,6-di-*O*-isopropylidene-β-L-sorbofuranose (VI),[4] which has two 1,3-dioxane rings. An examination of Dreiding models suggests that when the furanose-ring conformation is C_3-*exo*-C_4-*endo* half-chair, the 1,3-*O*- and 4,6-*O*-isopropylidene rings can be formed without severe non-bonded interactions, whereas when the ring has a C_3-*endo*-C_4-*exo* half-chair conformation, there are strong interactions between axial methyl groups at 1,3-dioxanes and either H_3 or H_4. As expected, the characteristic value for $J_{3,4}$ (0.5 Hz) in VIa indicates that its most favored conformation is C_3-*exo*-C_4-*endo* half-chair, where the dihedral angles are slightly contracted compared with the corresponding angles in IVa.

The determination of the spectra of the two monoisopropylidene derivatives containing one 1,3-dioxane ring, Ia and Va, provided important information. The fact that the signals due to H_3 and C_1-methylene protons are remarkably shifted downfield in the spectrum of Ia in comparison with those observed in the spectrum of VIa, confirmed the structure of I to be methyl 4,6-*O*-isopropylidene-α-L-sorbofuranoside. Similar lower-field shifts of the signals due to H_4 and C_6-methylene protons confirmed the structure of Va to be methyl 1,3-*O*-isopropylidene-4,6-di-*O*-acetyl-β-L-sorbofuranoside. The small values for $J_{3,4}$ (1.5 Hz in Ia and 0.6 Hz in Va) indicate that both monoisopropylidene furanoses also exist in a C_3-*exo*-C_4-*endo* half-chair conformation. It should be noted that the conformation of Ia is a C_3-*exo*-C_4-*endo* half-chair. This fact suggests that the restrictive influence of the 4,6-*O*-isopropylidene ring is stronger than that of the anomeric effect in the opposite direction; the 4,6-*O*-isopropylidene ring locks the

17) For instance, see N. S. Bhacca and D. H. Williams, "Applications of NMR Spectroscopy in Organic Chemistry," Holden-Day, San Francisco (1964), Chapter 6.
18) R. U. Lemieux and A. R. Morgan, *Can. J. Chem.*, **43**, 2205 (1965).
19) M. S. Sundaralingam, *J. Am. Chem. Soc.*, **87**, 599 (1965).

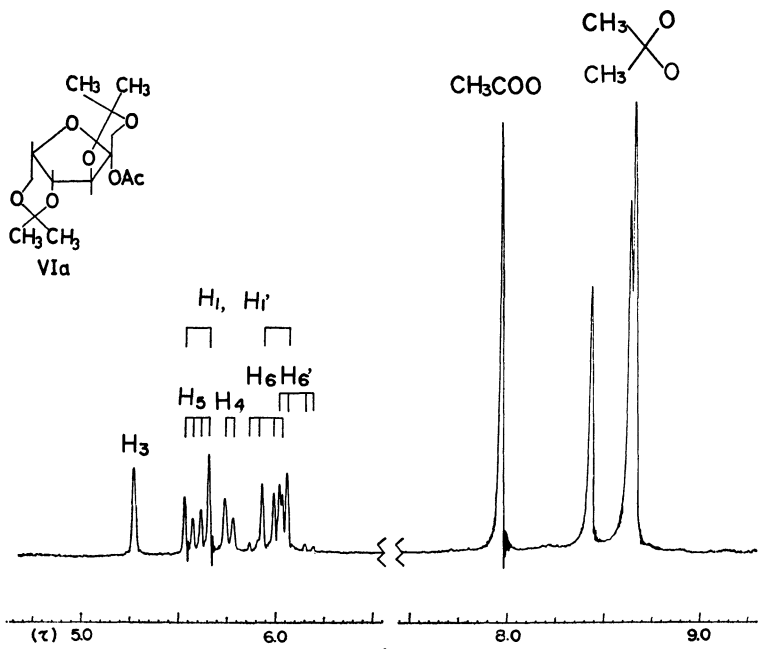

Fig. 3. PMR spectrum of VIa in chloroform-d at 100 MHz.

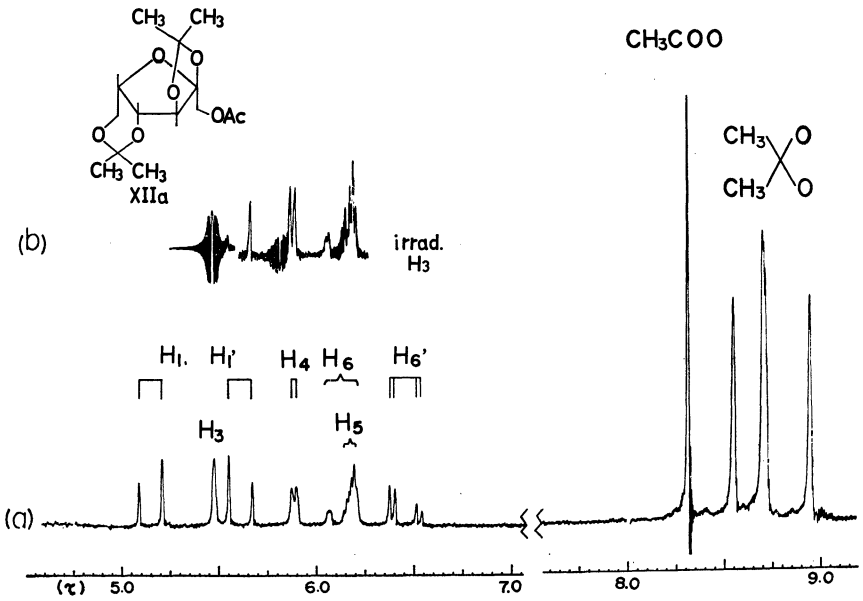

Fig. 4. PMR spectra of XIIa in benzene-d_6 at 100 MHz.
a) Normal spectrum, b) PMDR spectrum

furanose-ring to a C_3-*exo*-C_4-*endo* conformation.

This effect is also observed in other 4,6-*O*-isopropylidene-sorbofuranoses: 1,2 : 4,6-di-*O*-isopropylidene-α-L-sorbofuranose (VIII),[3,4] the acetate of VIII (VIIIa),[4] the acetate (Xa) of 1,2 : 4,6-di-*O*-isopropylidene-β-L-sorbofuranose (X),[4] XII, and the acetate of XII (XIIa).[4] The furanose-ring conformations of such furanoses were found from the small values for $J_{3,4}$ (0.3—1.5 Hz) to be C_3-*exo*-C_4-*endo* half-chairs.

The conformation of the acetate (XIa)[4] of 2,3-*O*-isopropylidene-α-L-sorbofuranose (XI),[11] the unlocked derivative of XII, seems interesting because a C_3-*endo*-C_4-*exo* half-chair conformation seems likely

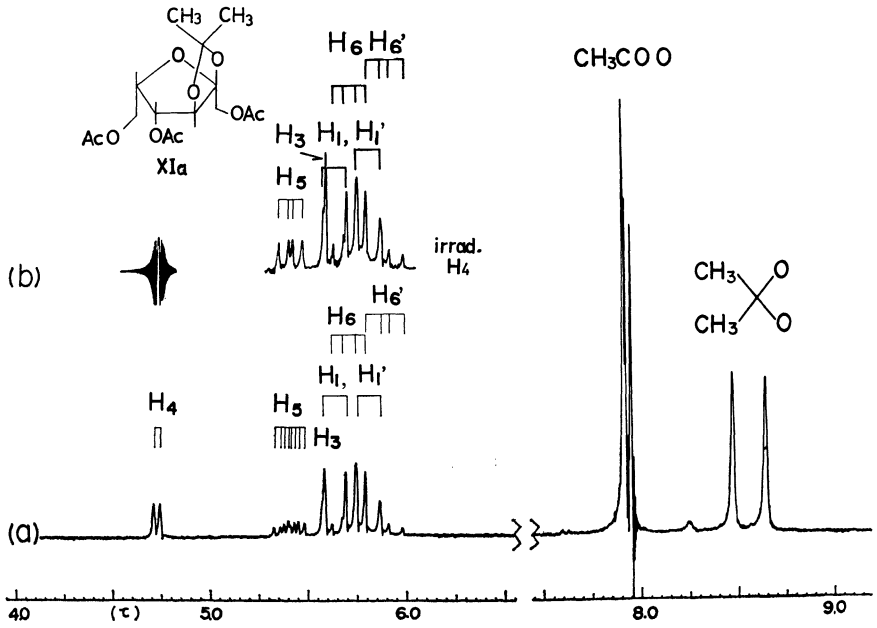

Fig. 5. PMR spectra of XIa in chloroform-d at 100 MHz.
a) Normal spectrum, b) PMDR spectrum

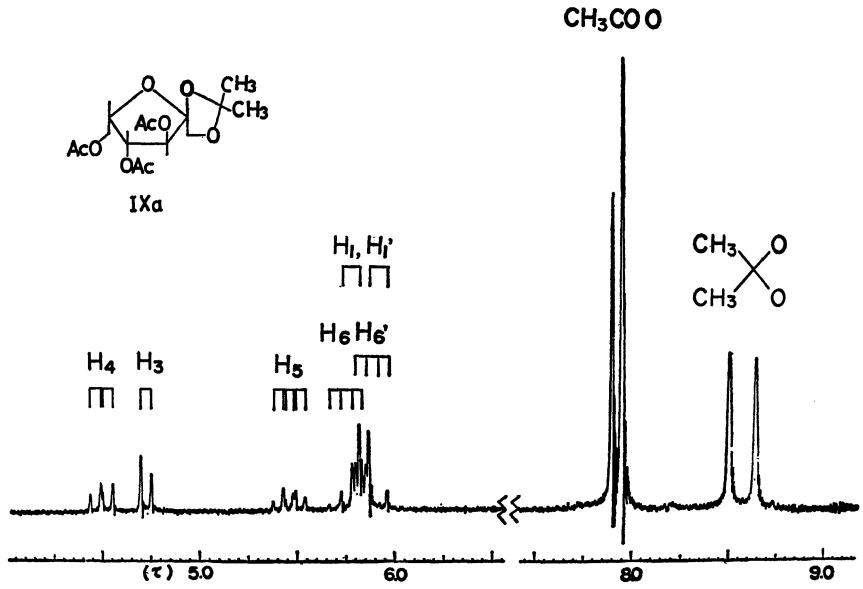

Fig. 6. PMR spectrum of IXa in chloroform-d at 100 MHz.

in view of the non-bonded interaction and the anomeric effect. However, the small $J_{3,4}$ value established that XIa adopts a similar conformation to XII. A similar situation has been found in the conformation of 1,2-*O*-isopropylidene-α-D-glucofuranose derivatives ($J_{2,3}$=0.5 Hz).[20,21] Therefore, the 2,3-*O*-isopropylidene ring was concluded to lock the furanose-ring conformation in the same direction as does the 4,6-*O*-isopropylidene ring.

20) Recently, the value of 0.5 Hz for $J_{2,3}$ in 1,2-*O*-benzylidene-α-D-xylofuranose was reported by R. J. Ferrier and L. R. Hotton, *Carbohyd. Res.*, **5**, 132 (1967).

21) R. J. Abraham, K. A. McLauchlan, L. D. Hall and L. Hough, *Chem. Ind.*, **1962**, 213; R. H. Abraham, L. D. Hall, L. Hough and K. A. McLauchlan, *J. Chem. Soc.*, **1962**, 3699.

In order to compare it with the above results, the effect of a 1,2-*O*-isopropylidene ring was studied in a similar manner by using 1,2-*O*-isopropylidene-3,4,6-tri-*O*-acetyl-α- (VIIa) and β-L-sorbofuranose (IXa), derived from VIII and X, respectively. As can be seen from Table 2, the J values in VIIa are in substantial agreement with those in IIa; the α-anomer VIIa has the same conformation as the α-furanoside IIa. Similarly, the J values provided evidence that the β-anomer IXa has the same conformation as the β-furanoside IVa. Thus, the 1,2-*O*-isopropylidene ring orients the furanose ring in the same direction as does the influence of the anomeric effect of the OCH_3 group.

Under usual reaction conditions, the acetonation of L-sorbose affords XII exclusively.[2] DeJongh and Biemann[6] suggested that the reason why VIII and X were not found might be the steric interference between the 1,3-dioxane and the 1,3-dioxolane. However, such interactions in VIII and X, if they do exist, are believed to be essentially of a degree similar to those in XII, because the VIII and X isolated by us have a similar conformation to XII. Since both the isopropylidene rings of XII lock its furanose ring in the same direction, the furanose ring of XII is thought to be stable. Both the isopropylidene rings of X similarly lock the furanose ring in the same direction. However, the difference in $J_{3,4}$ values between IXa (2.5 Hz) and Xa (0.3 Hz) suggests that there are some other factors governing the small instability in the X molecule. On the other hand, the 1,2-*O*-isopropylidene ring of VIII tends to destabilize to some extent the furanose-ring conformation restricted by the 4,6-*O*-isopropylidene ring. Therefore, a spiro-1,3-dioxolane ring at the 1,2-position of a furanose is considered to be less stable than a fused-1,3-dioxolane ring at the 2,3-position. A similar example has been reported in the acetonation of D-fructose; 2,3 : 4,6-di-*O*-isopropylidene-β-D-fructopyranose is formed as a final product *via* 1,2 : 4,5-di-*O*-isopropylidene-β-D-fructopyranose.[22]

Finally, the fact that VI has a lower stability than XII, can be reasonably explained by the lower stability of the 1,3-*O*-isopropylidene (1,3-dioxane) ring than that of the 2,3-*O*-isopropylidene ring (1,3-dioxolane), according to the Brown-Brewster-Schechter rule.[23]

On the basis of the conformational data presented above, it can be concluded that 2,3-*O*-isopropylidene derivatives are more stable than 1,2- or 1,3-*O*-isopropylidene derivatives in sorbofuranoses locked by the 4,6-*O*-isopropylidene ring. This conclusion accords well with the predominant formation of XII in the acetonation of L-sorbose under strongly acid conditions. The effect of the 4,6-*O*-isopropylidene group must play an important role in the acetonation, a mechanism for which will be proposed in future papers.

The authors wish to express their deep gratitude to Professor Toshihiko Okamoto, University of Tokyo, and Dr. Ken'ichi Takeda, Director of this Laboratory, for their encouragement.

22) E. Fisher, *Ber.*, **28**, 1164 (1895); J. C. Irvine and C. S. Garrett, *J. Chem. Soc.*, **97**, 1277 (1910); W. L. Glen, G. S. Myers and G. A. Grant, *ibid.*, **1951**, 2568; H, Ohle and I. Koller, *Ber.*, **57**, 1566 (1924).

23) H. C. Brown, J. H. Brewster and H. Shechter, *J. Am. Chem. Soc.*, **76**, 467 (1954).

BULLETIN OF THE CHEMICAL SOCIETY OF JAPAN VOL. 41 2504—2508 (1968)

Reaction of Alkylbenzene. III.*[1] The Reaction of *sec*-Butylbenzene Induced by Aluminum Chloride*[2]

Kazuyoshi ITOH, Genji YAMADA, Sawako HAMANAKA and Masaya OGAWA

Department of Applied Chemistry, Faculty of Engineering, Kansai University, Senriyama, Suita-shi, Osaka

(Received November 13, 1967)

The products successively obtained from the reaction between *sec*-butylbenzene and aluminum chloride were investigated. Transalkylation was the first observed reaction, followed by the isomerization of the side chain and then by dealkylation. The isomerization of the side chain was observed in the transalkylation products of a high basicity, such as *m*-di- and 1,3,5-tri-substituted compounds, and not in the others. The *n*-butane, resulting from dealkylation, was obtained simultaneously with 2,2di-phenylbutane. On the basis of these results, the reaction mechanism was discussed.

The reaction which alkylbenzenes undergo in the presence of aluminum chloride have been investigated by a number of workers. Transalkylation, dealkylation, and isomerization each having been considered to be a major reaction process in an early step, the reactions have been substantially clarified independently. However, the relations of these three reactions have not yet been reported on except for a few papers.[1] In fact, though, all these reaction are so complicated that the obtained products can not be attributed confidently to any reaction process.

In this investigation, the authors investigated the reaction of *s*-butylbenzene induced by aluminum chloride under comparatively mild conditions, and then detected the successive products obtained in the course of the reaction.

Experimental

Materials. *s*-Butylbenzene, which had been ascertained to be fairly pure by vpc analysis, was synthesized by the Friedel-Crafts alkylation of benzene with *s*-butylalcohol at 40°C. The purity of the products decreased at a higher reaction temperature as a result of the isomerization to isobutylbenzene.

The other hydrocarbons used as the authentic materials in vpc analysis were synthesized by the usual methods, except for *n*-butane and isobutane, which were commercially-available chemicals of the highest grade.

All the *s*-butylated benzenes (*p*-di-, *m*-di-, and 1,3,5-tri-*s*-butylbenzene) were synthesized with *s*-butylbenzene and *s*-butyl chloride in the presence of aluminum chloride at a low temperature. These products were not thoroughly pure, but were used satisfactorily for the identification of the individual alkylbenzene in vpc analysis.

2,2-Diphenylbutane was synthesized by the reaction of 2-phenyl-2-butanol with benzene in the presence of aluminum chloride, using the procedure of Serijan and Wise.[2] 2-Phenyl-2-butanol, bp 83—85°C/8 mmHg, was prepared by Grignard reaction in a 42% yield based on ethyl bromide using ethylmagnesium bromide and acetophenone. The purity was ascertained by vpc analysis to be more than 90%, and also its NMR spectrum was consistent with its formulation. The reaction of 2-phenyl-2-butanol with excess benzene was carried out at 35°C for 3 hr. The products, bp 150—152°C/3 mmHg, was found by vpc analysis to be slightly contaminated with unknown compounds, but the structure was confirmed by NMR and infrared analyses.

2,3-Diphenylbutane was synthesized by the direct reduction of 2,3-diphenylbutane-2,3-diol, which in turn had been prepared by the Grignard reaction of methylmagnesium bromide and benzil. This diol, bp 165—170°C/7 mmHg, was obtained in a 68% yield based on benzil; it was shown by vpc analysis to be more than 95% pure. The reduction of the diol was carried out in a 100 m*l* autoclave, using hydrogen and copper chromium oxide catalyst in methanol, under a pressure of 150 kg/cm² at 150—210°C for 18 hr. The reduction product, bp 112—116°C/2 mmHg, was purified by recrystallization from methanol, and the meso-isomer, mp 125°C, was isolated. (lit.[3] mp 127°C). The NMR spectrum of 2,3-diphenylbutane was consistent with its formulation.

The Reaction of *s*-Butylbenzene. *s*-Butylbenzene (0.3 mol) and aluminum chloride (0.1 mol) were placed in a 100 m*l*, three-necked flask equipped with a stirrer, a thermometer, and a condenser. After stirring, 1 m*l* of the reaction mixture was pippeted out and quenched with cold water. The hydrocarbon layer was then analyzed by vpc. As aluminum chloride was used without any particular treatment, the reaction proceeded

*1 Part II; Reference 10.

*2 Presented at the 20th Annual Meeting of the Chemical Society of Japan, Tokyo, April, 1967.

1) For example, R. L. Burwell, Jr., and A. D. Shields, *J. Am. Chem. Soc.*, **77**, 2766 (1955); R. M. Roberts, E. K. Baylis and G. J. Fonken, *ibid.*, **85**, 3454 (1963).

2) K. T. Serijan and P. H. Wise, *ibid.*, **74**, 365 (1952).

3) W. T. Somerville and P. E. Spoerri, *ibid.*, **74**, 3803 (1952).

in a heterogeneous system throughout almost all the process.

Analyses of the Products. The products were mainly analyzed by gas chromatography using a Hitachi Model KGL-2 apparatus, fitted with a 90 m, 0.25-mm i. d. capillary column coated with Apiezon grease L or polypropylene glycol (Ucon oil LB-550X) and equipped with a hydrogen-flame ionization detector. Nitrogen was used as the carrier gas, and the operating temperature was varied from 60°C to 190°C according to the boiling points of the samples. Infrared analyses were made with a Shimadzu Model IR-27 apparatus, equipped with a sodium chloride prism. The NMR spectra were taken with a JEOL Model 3H-60 spectrometer at 60 Mc and at room temperature on 10—20% (w/v) solutions of the samples in carbon tetrachloride containing tetramethylsilane as the internal standard.

Results

Identification of Products. A gas chromatogram of all the products obtained from the reaction at 70°C for 3 hr is shown in Fig. 1. In Fig. 1, A, B, and C were identified as *n*-butane, benzene, and *s*-butylbenzene, respectively. The X-group

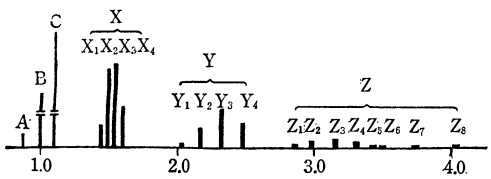

Fig. 1. Gas chromatogram of the reaction products from *s*-butylbenzene induced by $AlCl_3$ at 70°C for 3 hr.

A: *n*-Butane
B: Benzene
C: *s*-Buφ
X_1: *m*-di-*s*-Buφ
X_2: *m*-*s*-Bu-*i*-Buφ
X_3: *m*-di-*i*-Buφ
X_4: *p*-di-*s*-Buφ
Y_1: 1,3,5-tri-*s*-Buφ
Y_2: 1,3,5-di-*s*-Bu-*i*-Buφ
Y_3: 1,3,5-di-*i*-Bu-*s*-Buφ
Y_4: 1,3,5-tri-*i*-Buφ
Z_3: *meso*-2,3-di-φ-Butane
Z_4: 2,2-di-φ-Butane
Column: capillary (90 m, 0.25 mm i.d.), Apiezon grease L
Temp: 180°C
Carrier: N_2 (Press. 1.5 kg/cm²)
Detector: F.I.D. (H_2)
* Relative retention volumes

consisted of dibutylbenzenes, of which X_1 and X_4 were identified as *m*- and *p*-di-*s*-butylbenzene with each authentic compound by the internal standard method. It was also considered that X_2 and X_3 consisted of *m*-*s*-butylisobutylbenzene and *m*-diisobutylbenzene, respectively; this consideration was based on the retention volume in vpc and some other evidence, such as the conversion rate shown in Fig. 2 and the existence of an isobutyl group in the following results. The peaks of the Y-group consisted of tributylbenzenes, of which three butyl groups were either *s*- or isobutyl ones substituted at 1,3,5-positions. Y_1 was identified as 1,3,5-tri-*s*-butylbenzene by vpc with an authentic material. Y_2, Y_3, and Y_4 could not be isolated individually. However, the three components were obtained from the reaction products by fractionation; the purity was 94.5% for the three components. The fraction was ascertained to be a mixture of 1,3,5-tri-substituted benzenes on the basis of its infrared spectrum pattern in the 5—6μ region, and was also ascertained to have both the *s*-butyl- and the isobutyl-group in the side chain on the basis of its NMR spectrum,[4] which was as follows; $\tau=9.3$ (triplet, γ-methyl-H), $\tau=8.7$ (doublet, β-methyl-H), and $\tau=8.3$—8.5 (multiplet, α-methylene-H) for the *s*-butyl group, and $\tau=9.0$ (doublet, γ-methyl-H) and $\tau=7.4$ (doublet, β-methylene-H) for the isobutyl group. On the basis of this evidence, Y_2, Y_3, and Y_4 were considered to be 1,3,5-di-*s*-butyl-isobutylbenzene, 1,3,5-*s*-butyldiisobutylbenzene, and 1,3,5-triisobutylbenzene respectively. The Z-group consisted of the major products, Z_3 and Z_4, identified as 2,2-diphenylbutane and 2,3-diphenylbutane, respectively by vpc with authentic substances. Some other diphenylalkanes, such as 2-methyl-1,2-diphenylpropane and 2-methyl-1,1-diphenylpropane, were not identified in the peaks of the Z-group.

Reaction at 20°C. The yields of the products obtained at 20°C are plotted against the reaction time in Fig. 2.

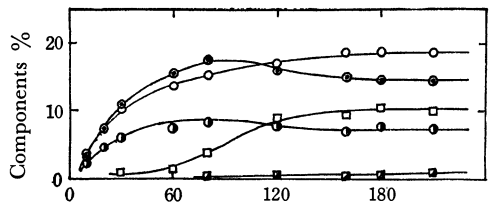

Fig. 2. Reaction product at 20°C.
○ Benzene
◉ *m*-di-*s*-Buφ (X_1)
◑ *p*-di-*s*-Buφ (X_4)
□ 1,3,5-tri-*s*-Buφ (Y_1)
◪ 1,3,5-di-*s*-Bu-*i*-Buφ (Y_2) or 1,3,5-di-*i*-Bu-*s*-Buφ (Y_3)

In the gas chromatogram of the reaction products at 20°C, neither the peak of butane nor that of any Z-component was detected during the first 3 hr. After 260 min, however, the peaks of butane and Z_3 were detected slightly. In the early steps of the reaction, X_1 and X_4 were obtained predominantly; Y_1 was detected 30 min later. The molar ratio of X_1 to X_4 was estimated to be about 2; it kept the same value throughout the reaction course. X_2 and Y_2, each with one isobutyl group,

4) K. Itoh, S. Hamanaka, F. Yamada and M. Ogawa, *Kogyo Kagaku Zasshi (J. Chem. Soc. Japan, Ind. Chem. Sect.)*, **70**, 914 (1967).

were detected 120 min later, but X_3, Y_3, and Y_4, each having two or three isobutyl groups, were not produced under the present conditions. In the reaction at 20°C, an apparent equilibrium appeared after 180 min.

Reaction at 40°C and 50°C. The X- and Y-groups of reaction products at 40°C and 50°C are shown in Fig. 3 and 4, respectively.

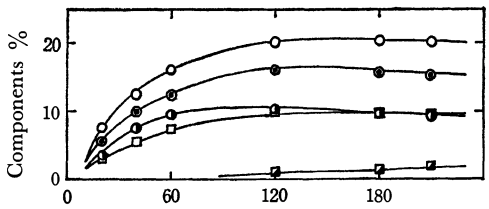

Fig. 3. Reaction products at 40°C.
- ○ Benzene
- ⊙ *m*-di-*s*-Buφ (X_1)
- ◑ *p*-di-*s*-Buφ (X_4)
- □ 1,3,5-tri-*s*-Buφ (Y_1)
- ◪ 1,3,5-di-*s*-Bu-*i*-Buφ (Y_2) or 1,3,5-di-*i*-Bu-*s*-Buφ (Y_3)

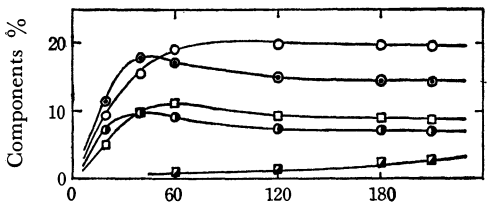

Fig. 4. Reaction products at 50°C.
- ○ Benzene
- ⊙ *m*-di-*s*-Buφ (X_1)
- ◑ *p*-di-*s*-Buφ (X_4)
- □ 1,3,5-tri-*s*-Buφ (Y_1)
- ◪ 1,3,5-di-*s*-Bu-*i*-Buφ or 1,3,5-di-*i*-Bu-*s*-Buφ (Y_2, Y_3)

These profiles are roughly the same as that of the reaction at 20°C. An apparent equilibrium could be observed after 120 min at 40°C and after 60 min at 50°C. In the latter case, the increase in X_2 and Y_2 were accelerated considerably; then X_1, X_4, and Y_1 decreased.

Reaction at 70°C. The reaction products at 70°C are shown in Fig. 5, with the X-group in the upper figure and the Y-group in the lower one; the Z-group can not be shown precisely because of the difficulty of quantitative determination. In the reaction at 70°C, X_1, X_4, Y_1, X_2, and Y_2 were obtained during the first 10 min, while the A and Z-groups were obtained 20 min later. After these initial reactions, X_3, Y_3, and Y_4, which each possessed two or more isobutyl groups, increased slowly and attained an apparent equilibrium after 180 min.

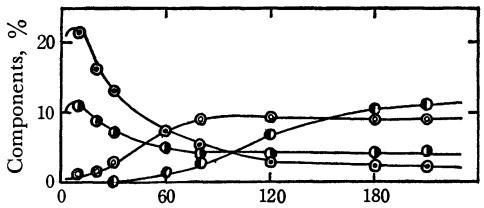

Fig. 5a. Reaction products of X-group at 70°C.
- ⊙ *m*-di-*s*-Buφ (X_1)
- ◎ *m*-*s*-Bu-*i*-Buφ (X_2)
- ◐ *m*-di-*i*-Buφ (X_3)
- ◑ *p*-di-*s*-Buφ (X_4)

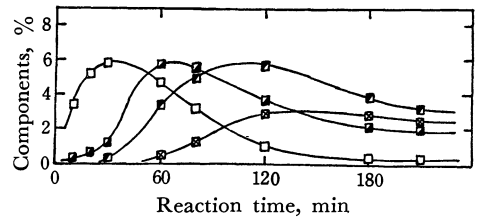

Fig. 5b. Reaction products of Y-group at 70°C.
- □ 1,3,5-tri-*s*-Buφ (Y_1)
- ◪ 1,3,5-di-*s*-Bu-*i*-Buφ (Y_2)
- ◪ 1,3,5-di-*i*-Bu-*s*-Buφ (Y_3)
- ⊠ 1,3,5-tri-*i*-Buφ (Y_4)

Discussion

In the reaction of *s*-butylbenzene induced by aluminum chloride at 20°C, transalkylation was the reaction observed first, followed by the isomerization of the side chain and dealkylation. The above reaction sequence was also ascertained at higher temperatures.

Transalkylation > Isomerization > Dealkylation

However, the rate of transalkylation under the present conditions is slower than that of the usual Friedel-Crafts alkylation, in which a reaction equilibrium is completed rapidly, sometimes within a second.[5] The present slower reaction rate may be considered to result in part from the heterogeneous reaction and in part from the structure of the attacking species.

The alkylcarbonium ion dissociated from the present reactants may be different from that liberated from alkyl halide in the Friedel-Crafts alkylation. The former ion may be unstable and not so free from the rest; hence, it has a large steric require ment. Consequently, *o*-di-, 1,2,4,-tri-, and 1,2,3-tri-substituted isomers were not obtained among the present reaction products. On the other hand, in alkylation with alkyl halide, the alkylcarbonium ion may be substantially free from paired anions

5) H. C. Brown and H. Jungh, *J. Am. Chem. Soc.*, **78**, 2182 (1956).
6) G. A. Olah *et al.*, *J. Org. Chem.*, **29**, 2310, 2313, 2315, 2689 (1964).

and can be substituted at the ortho position of alkylbenzene. For the meta-para isomer ratio of alkylbenzene, it has been generally said that the ratio is around 2 : 1, except for the case of a particular alkylbenzene such as di-*t*-butylbenzene.[6] Our present results support the above isomer ratio.

The isomerization of the side chain in which the *s*-butyl group is isomerized to the isobutyl group, which occurred after transalkylation, proceeded to a certain extent. Interestingly, the isomerized products were detected in *m*-di- and 1,3,5-trisubstituted compounds only and not in mono- and *p*-di-substituted ones. In one previous article,[7] the basicities of methylbenzenes were reported to be in the order of the following sequence:

Mesitylene > *m*-Xylene > *p*-Xylene > Toluene

Thus, the present results may be considered to be connected with the basicities of the alkylbenzene concerned. From the above consideration, the relation between transalkylation and isomerization may be represented as in Fig. 6:

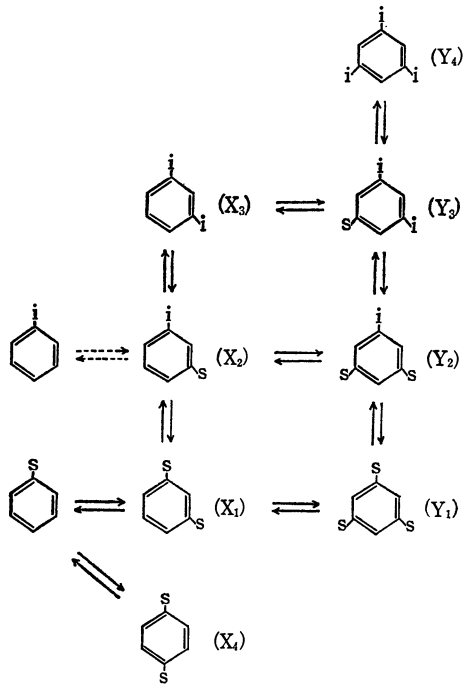

Fig. 6. Route of isomer formation.
s : *s*-butyl group
i : isobutyl group

For the isomerization of such an alkyl group, two mechanisms have been postulated; in one alkylbenzene is coordinated to the proton, isomerized through the methyl-bridged cation,[8] as is shown in Eq. (1), while in the other one the isomerization is initiated by hydride-ion abstraction from the alkyl group and then proceeds *via* a carbonium-ion mechanism, as is shown in Eq. (2).[9]

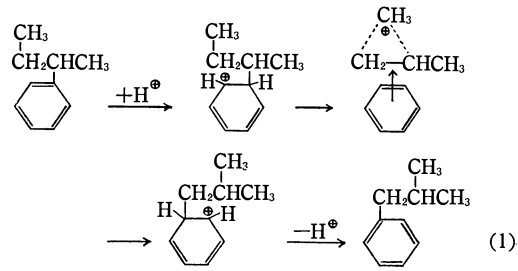

(1)

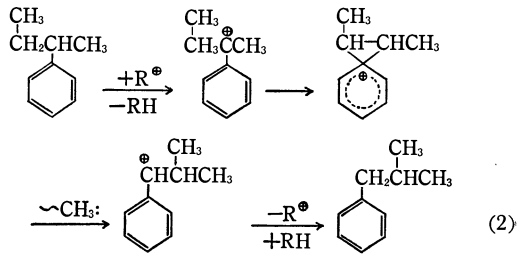

(2)

Our present results support the former mechanism. The latter mechanism can not illustrate how the isomerization in an early step proceeds without the formation of any butane or diphenylbutanes on one side or how *m*-di- and tri-*s*-butylbenzene is isomerized considerably faster than are mono- and *p*-di-*s*-butylbenzene.

Dealkylation was the last reaction in the reaction process. The dealkylation products were detected after 260 min at 20°C and after 20 min at 70°C. In the reaction at 20°C, *n*-butane was obtained simultaneously with 2,2-diphenylbutane (Z_3), while in the reaction at 70°C an unknown compound (Z_2) was first obtained, and then 2,2-diphenylbutane (Z_3), 2,3-diphenylbutane (Z_4) and other Z compounds were obtained succesively.

In a previous paper,[10] we postulated that, in secondary or tertiary alkylbenzene, the dealkylation competed with transalkylation through alkylcarbonium ions.

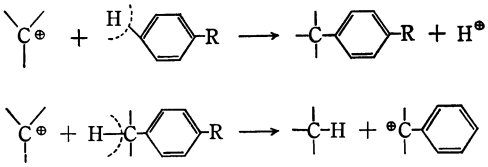

On the basis of the above results and discussion, the following reaction scheme may be suggested for the formation of 2,2-diphenylbutane:

7) S. U. Choi and H. C. Brown, *J. Am. Chem. Soc.*, **88**, 903 (1966).
8) R. M. Roberts, Y. W. Han, C. H. Schimid and D. A. Davis, *ibid.*, **81**, 640 (1959).
9) R. M. Roberts and Y. W. Han, *ibid.*, **85**, 1168 (1963).
10) K. Itoh, R. Kurashige, S. Hamanaka and M. Ogawa, *Kogyo Kagaku Zasshi (J. Chem. Soc. Japan, Ind. Chem. Sect.)*, **70**, 918 (1967).

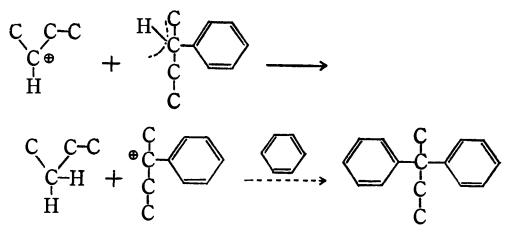

(Z_3)

Similarly, the formation of 2,3-diphenylbutane may be described as follows:

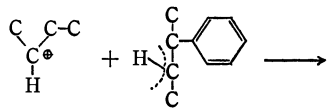

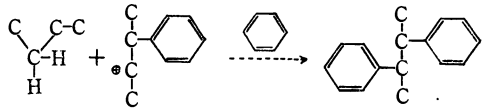

(Z_4)

In the latter case, another route could also be adopted:

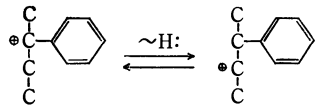

The same discussion may hold for other diphenylbutanes.

BULLETIN OF THE CHEMICAL SOCIETY OF JAPAN VOL. 41 2508—2514 (1968)

Syntheses of Citral and Citronellal by the Dehydrogenation of Geraniol Using Cu, Cu-Zn, Cu-Cr, and ZnO Catalysts

Kunio KOGAMI and Ju KUMANOTANI

The Engineering Research Institute, Faculty of Engineering, The University of Tokyo, Yayoi, Tokyo

(Received January 10, 1968)

The present paper describes the study of the syntheses of citral and citronellal by the catalytic dehydrogenation of geraniol with Cu, Cu-Zn, Cu-Cr, and ZnO catalysts under an atmospheric or a reduced pressure in vapor and liquid-phase systems. The following results were obtained: (1) the vapor-phase dehydrogenation with the Cu-Zn catalyst, conducted at a reduced pressure, was found to be most favorable, (2) when using this catalyst at 230°C, the addition of citronellal as a hydrogen acceptor prior to the dehydrogenation increased the yield of the citral from 50% to 85% (at 185°C, the highest yield of citronellal, 70%, was obtained). The composition of the product was analyzed by means of G. L. C. The reaction scheme under various conditions is also described briefly.

Citral is a raw material for the increasingly-important ionone and Vitamine A, whereas citronellal is a raw material for menthol and hydroxy-citronellal. Geraniol, a basic material for both citral and citronellal, has recently become available by means of an entirely synthetic process, instead of having to be derived from the limited natural-product source. Therefore, the present authors, in the course of their study of the synthesizing of important monoterpene compounds used for perfumery, have attempted to make citral and citronellal by the catalytic dehydrogenation of geraniol.

Concerning the present studies, only a few papers and patents have been published. Bouveault reported the quantitative conversion of geraniol into citral in the catalytic dehydrogenation of geraniol over copper at 200°C;[1] Treibs observed the formation of citronellal in the distillation of geraniol at an atmospheric pressure in the presence of copper[2]; a Russian patent described the vapor-phase dehydrogenation of geraniol at 220—230°C at a pressure of 100 mmHg, using the Cu-Cr catalyst (9% citral and 65% citronellal were thus produced)[3]; a Japanese patent[4] claimed the use of methyl ethyl ketone or butyraldehyde as a hydrogen acceptor in the liquid-phase catalyzed dehydrogenation, using a Raney-Cu, Cu-Zn or Cu-Cr catalysts, thus showing the possibility of

1) L. Bouveault, *Bull. Soc. Chim. France* (4) 3, 119 (1908).

2) W. Treibs and H. Schmidt, *Ber.*, **60**, 2335 (1927).

3) B. H. Kapabas, U.S.S.Pat. 118498 (1958).

4) T. Hashimoto and T. Shibuya, Japanese Pat. 15007 (1965).

producing citral in an improved yield of 42—43%.

The present paper will describe the syntheses of citral and citronellal by the catalyzed dehydrogenation of geraniol with a Cu, Cu-Zn, Cu-Cr, or ZnO catalyst under varying experimental conditions.

Experimental

Materials. The geraniol was purchased from the ABRAC Company, Ltd.; bp 99°C/5 mmHg, n_D^{30} 1.4740, d_{30}^{30} 0.8863. Its purity was confirmed by G.L.C. to be 98.0%. The citronellal was obtained from citronellal oil (from Formosa) by a previously described[5] method; bp 72—73°C/6 mmHg, d_{30}^{30} 0.8594, n_D^{30} 1.4492, $[\alpha]_D^{25}$ +10.8°C.

Catalysts Used. Cu-Cr-, Cu-Zn-, and ZnO-type catalysts were supplied by the Nikki Chem. Company, Ltd. Various forms of the catalyst suitable for each dehydrogenation system were used; (a), (b) and (c) were tableted catalysts 6 mm in dia. and 6 mm high, 6 mm in dia. and 3 mm high, and 3 mm in dia. and 3 mm high respectively, while (d) was a powder. The copper catalyst was used in the form of a copperwire gauze (50 mesh), as has been described by Bouvealt.[1]

Apparatus Used for Dehydrogenation. The general structure of the apparatus used for the dehydrogenation of geraniol is presented in Fig. 1. Geraniol vapor was supplied through an evaporator (2) into a reactor (3), and the reaction product was collected in a receiver (6). The catalysts were packed in the constant-temperature region of the reaction tube, as shown in Fig. 1. The evaporator (2) was heated to approximately 205°C, using Bay oil as the heating medium.

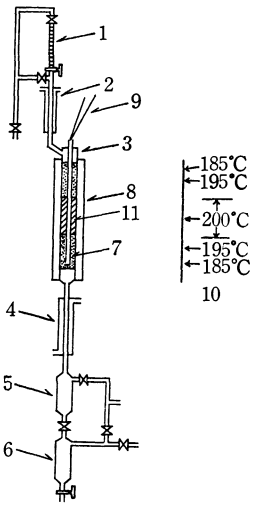

Fig. 1. Catalytic dehydrogenation apparatus.
1 Feed burette, 2 Evaporator, 3 Reactor (dia. 28 mm, length 400 mm), 4 Condenser, 5 Product receiver, 6 Product receiver, 7 Glass Rassig ring, 8 Electric-furnace, 9 Thermocouple, 10 Temperature gradient in reactor, 11 Catalyst

A portion of the glass tube leading from the evaporator to the reaction tube was also heated to 205°C by using a ribbon heater, thus keeping the temperature gradient along the reaction tube constant.

Vapor-phase Dehydrogenation Procedure at Atmospheric Pressure. After the packed catalyst had been activated with hydrogen, the reaction tube was allowed to cool to room temperature in a hydrogen stream; then the hydrogen was turned off, and nitrogen was introduced for 30 min at a rate of 500 m*l*/min. Then geraniol vapor was passed through the reacting zone of the reaction tube (kept at 200°C) under various conditions. After the reaction, the product collected in the receiver was taken with 100 m*l* of ether. The ether solution was neutralized with an aqueous solution of sodium carbonate, washed with water, dehydrated with sodium sulfate, and submitted to the evaporation of ether on a water bath to give an oily product (97—98% by weight for geraniol supplied). The composition of the product was determined by G.L.C. In the case of using a hydrogen acceptor, ethylene[6] (obtained commercially; purity 99.2%), rather than nitrogen, was passed through at a rate of 300 m*l*/min after the activation of the catalyst with hydrogen; acetone[7] or quinoline[8], mixed in geraniol, was passed through the reacting zone under a nitrogen flow.

Vapor-phase Dehydrogenation Procedure at Reduced Pressure. After the treatment of the catalyst with hydrogen and subsequent displacement with nitrogen much as has been described above, the gas inlet-cock was closed. Then the reaction system was evacuated to a certain reduced pressure, and the geraniol vapor was supplied to the reaction tube at a given L.S.V. The product was treated much as in the dehydrogenation at an atmospheric pressure. When the copper catalyst was used, the dehydrogenation was carried out under the same conditions as have been described by Bouveault.[1]

Liquid-phase Dehydrogenation Procedure at Atmospheric Pressure. A given amount of a catalyst was placed in a 300-m*l* four-necked flask equipped with an air-tight stirrer, a hydrogen inlet-tube, a Stark-Dean trap (fitted with a hydrogen outlet-tube to remove any water formed during the activation of the catalyst with hydrogen), and a thermocouple in contact with the catalyst placed at the bottom of the flask. The catalyst was heated at 200°C in an oil bath, and hydrogen was passed through the catalyst at a rate of 200 m*l*/min for 30 min; then the flask was displaced with nitrogen for 30 min at the rate of 200 m*l*/min. Thereupon, geraniol (50 g, 0.32 m) was put in the flask, and it was kept at 200°C with stirring under a nitrogen flow. The progress of the reaction was followed by G.L.C., by which the end point of the reaction was determined.

Identification and Analysis of the Product by G.L.C. In the selective dehydrogenation of geraniol to form citral or citronellal, the isolation of each product was attempted by means of a precise fractional distillation technique. The gas chromatograph Kotaki

5) P. Z. Bedoukian, "Perfumery and Flavoring Synthetics," Elsevier Publishing Company, Amsterdam (1967), p. 107.

6) W. Reeve and H. Adkins, *J. Am. Chem. Soc.*, **62**, 2874 (1940).
7) L. C. Andess, *ibid.*, **64**, 1456 (1942).
8) K. W. Rosenmund and F. Z. Zetshe., *Ber.*, **54**, 1002 (1921).

GU-21, with a thermal conductivity detector, was used, and the quantitative analysis of the composition of the product was based on the normalization method. The experimental conditions were as follows; a stainless column (dia., 3 mm; length, 2 m) packed with Dia Base A, 60—80 mesh, which was coated with 10% of Silicone DC 550, 15% of PEG 1500 and 5% of PEG 4000; helium inlet pressure, 0.78 kg/cm^2, flow rate of 30 m*l*/min; column temperature, 180°C; split temperature, 250°C; sensivity, 8 mv; chart speed, 0.5 cm/min. The standard materials used in this analysis were prepared according to the methods described in the literature or were obtained by rectifying commercially-available chemicals. Each of these materials was found to give a single peak in its respective gas chromatogram; myrcene (from the ABRAC Company, Ltd.) bp 39°C/4 mmHg, n_D^{30} 1.4690, d_{30}^{30} 0.7883; limonene (from orange oil purchased from the Polak Frutal Company, Ltd.), bp 40°C/4 mmHg, n_D^{30} 1.4717, d_{30}^{30} 0.8407; ocimene was prepared from linalool according to the Naves method,[9] bp 42°C/4 mmHg, n_D^{30} 1.4861, d_{30}^{30} 0.8655; citronellol (from the ABRAC Company, Ltd.), bp 100°C/6 mmHg, n_D^{30} 1.4539; d_{30}^{30} 0.8572; citronellal was the same as that described in the preceding section; citral was prepared by the known method[5] from lemon-grass oil; bp 102—104°C/6 mmHg, n_D^{30} 1.4881, d_{30}^{30} 0.8962; geraniol (from the ABRAC Company, Ltd.), bp 100—102°C/6 mmHg, n_D^{30} 1.4492, d_{30}^{30} 0.8594; isopulegol (from the Tokyo Kasei Ind. Compnay, Ltd.), a mixture of 20% neoisopulegol, 75% isopulegol and 5% iso-isopulegol (by G. L. C.), bp 74—78°C/6 mmHg, n_D^{30} 1.4679; d_{30}^{30} 0.9074.

Activity of the Catalyst Used. As may be seen in Table 1, the Cu-Zn catalyst gave a similar product distribution when 15 m*l* of geraniol was supplied for the 2nd and 3rd runs under the experimental conditions indicated. The results of the first run were considered to be inadequate and unreliable. On the basis of the above results and on the technical information supplied by the Nikki Chem. Company, Ltd., the data collected on the second run of 15 m*l* of geraniol was considered pertinent to this experiment (see Table 1).

Results and Discussion

Product Distribution in the Catalyzed Vapor-phase Dehydrogenation of Geraniol at Atmospheric Pressure. The results obtained are summarized in Tables 2 and 3.

a) Comparison of the Catalysts. In the dehydrogenation of geraniol over copper at 200°C or 250°C (see Table 2), contrary to Bouveault's finding indicating the quantitative transformation of geraniol into citral, a very small conversion of geraniol and, in addition, the formation of various by-products, such as terpene hydrocarbons as well as citral and citronellal, was observed; citral had a yield of only 20%. With the ZnO catalyst system, at a reaction temperature between 190°C and 230°C,

TABLE 1. CHANGES IN PRODUCT DISTRIBUTION *vs.* SUPPLYING TIME OF GERANIOL (15 m*l*) USING Cu-Zn CATALYST

Composition of products by G. L. C. (wt%)

Time of supplying	Terpene hydrocarbons	Citronellal	Isopulegol	Citronellol	Citral	Geraniol
1	17.0	30.9	12.9	6.5	32.7	
2	14.7	38.0	15.5	4.9	26.9	
3	14.4	39.2	14.4	6.1	25.8	

* The experimental condition was identical to that indicated in the first run of Table 3.

TABLE 2. VAPOR-PHASE DEHYDROGENATION OF GERANIOL USING THE REDUCED COPPER AT A REDUCED PRESSURE

Run	Reaction temperature	Reduced pressure mmHg	Geraniol flow rate	Composition of products by G.L.C. (wt%)			
				Terpene hydrocarbon	Citronellal	Citral	Geraniol
1	200°C	4— 5	65 m*l*/hr	7.3	7.2	20.6	64.9
2	200°C	41—45	65 m*l*/hr	11.7	10.1	17.1	61.1
3	230°C	3— 4	65 m*l*/hr	4.7	5.9	16.3	73.1
4	230°C	4	21 m*l*/hr	4.9	7.1	21.2	66.8
5	250°C	4	65 m*l*/hr	4.5	7.5	18.7	69.3
6	250°C	102	65 m*l*/hr	21.0	16.8	21.1	41.1
7*	200°C	4— 5	65 m*l*/hr	5.4	5.3	22.9	66.4
8*	200°C	40—45	65 m*l*/hr	8.9	8.6	20.1	62.4

* Run 7, 8: Dehydrogenation was carried out using the apparatus described in Fig. 1.

9) Y. R. Naves and F. Bondavalli, *Helv. Chim. Acta*, **48**, 563 (1965).

Table 3. Vapor-phase catalytic dehydrogenation of geraniol at atmospheric pressure

Run	Starting material, hydrogen acceptor, weight ratio for geraniol	Atmosphere, flow rate	Catalyst* ml	Reaction temperature °C	L.S.V. l/hr	Composition of products by G.L.C. (wt%)					
						Terpene hydrocarbons	Citronellal	Isopulegol	Citronellol	Citral	Geraniol
1	Geraniol	N_2, 500 ml/min	Cu-Zn, 25	200	0.25	14.7	38.0	15.5	4.9	26.9	0
2	Geraniol	N_2, 500 ml/min	Cu-Cr, 25	200	0.25	20.0	37.8	12.2	6.8	23.2	0
3	Geraniol	N_2, 500 ml/min	ZnO, 30	230	0.30	25.0	0	0	0	0	75.0
4	Geraniol-acetone*** (1 : 1)**	N_2, 500 ml/min	Cu-Zn, 25	200	0.40	17.6	25.8	15.2	6.7	24.7	10.0
5	Geraniol	Ethylene*** 300 ml/min	Cu-Zn, 25	200	0.50	9.7	45.2	16.0	3.4	25.7	0
6	Geraniol, quinoline*** (1 : 0.5)**	N_2, 500 ml/min	Cu-Zn, 25	200	0.30	9.8	13.8	3.7	5.5	26.9	24.1
7	Citral	N_2, 500 ml/min	Cu-Zn, 25	200	0.30	14.8	10.1	6.1	0	69.0	0
8	Citral	N_2:H_2=10:1, 200 ml/min	Cu-Zn, 25	200	0.30	11.4	19.8	10.1	0	58.7	0

* Form of the catalyst used was of (a). ** by weight *** Hydrogen acceptor.

Table 4. Liquid-phase catalytic dehydrogenation of geraniol

Run	Catalyst*, wt% for geraniol	Geraniol g	Hydrogen acceptor added, g (molar ratio to geraniol)	Reaction temperature °C	Reaction time hr	Composition (%) of products by G.L.C. (wt%)					
						Terpene hydrocarbons	Citronellal	Isopulegol	Citronellol	Citral	Geraniol
1	Cu-Zn, 2.0	50		200—204	3.0	0	21.5	20.6	32.5	23.2	2.2
2	Cu-Zn, 2.0	50		200—204	4.0	0	12.8	29.3	32.6	23.3	2.0
3	Cu-Cr, 2.0	50		201—205	3.5	13.2	5.3	18.3	32.0	25.5	5.7
4	Cu-Zn, 2.0	50	Citronellal 25, (1 : 0.5)	200—205	2.5	3.9	11.1	22.2	16.8	23.3 (53%)**	22.7
5	Cu-Zn, 2.0	50	Citronellal 65, (1 : 1.3)	200—205	3.5	6.1	8.8	39.5	21.0	16.8 (47%)**	7.8
6	Cu-Zn, 5.0	50	Cyclohexanone 50, (1 : 1)	180—185	3.5	0	17.2	6.0	21.2	41.0 (48.0%)**	14.6

* Form of the catalyst used was of (d). ** Yield for geraniol reacted.

no dehydrogenation reaction occurred; the terpene hydrocarbon was given in a yield of 25%, while 75% of unreacted geraniol was recovered, indicative of the inefficient catalysis of the ZnO catalyst in the dehydrogenation.

The Cu-Zn and Cu-Cr catalyst systems gave similar product distributions: citral (26%; 23% (theor.)), citronellal (37%; 38%), isopulegol (15%; 12%), terpene hydrocarbons (14%; 20%), including myrcene, limonene and ocimene, and citronellol (4%; 6%). Although the difference in the product distribution was not remarkable between them, the Cu-Zn catalyst was found to be preferable to the Cu-Cr catalyst because of its smaller formation of terpene hydrocarbons and its increased yield of citral (see Table 3).

From the above results, it was concluded that the copper or ZnO system showed less catalytic activity in the dehydrogenation of geraniol, and that, with regard to the Cu-Zn and Cu-Cr catalyst systems, various products were formed, the major product being citronellal, not citral.

b) The Effect of the Hydrogen Acceptor when Added to Reaction System. In the catalyzed dehydrogenation of geraniol, as will be described later, an equilibrium can be assumed between citral, citronellal, and geraniol in the reacting zone; it is reasonable to prevent the hydrogenating of citral into citronellal, and thereby increase the yield of citral, by using a hydrogen acceptor. Therefore, a hydrogen acceptor, such as ethylene, acetone or quinoline, was used. The results obtained are indicated in the columns for runs 4, 5 and 6 in Table 3. When acetone (1 : 1 by volume for geraniol) was used in the Cu-Zn catalyst system, the conversion of geraniol decreased and the formation of terpene hydrocarbons increased. When ethylene was used,[6] however, a decrease of a few percentage points in terpene hydrocarbons and an increase in citronellal from 37.8% (without hydrogen acceptor) to 45.2% were observed. When quinoline was used,[8] decreased yields of citral and citronellal were observed.

c) Contribution to the Hydrogenation of Hydrogen Molecules Adsorbed on the Catalyst. The product distributions already shown for various systems suggest the possibility that citronellal and citronellol may be formed by the hydrogenation of citral and citronellal, respectively. Therefore, the contribution of the adsorbed hydrogen molecules to the hydrogenation was examined in the system of citral and a catalysts pretreated with hydrogen in a stream of nitrogen or of nitrogen mixed with hydrogen (10 : 1 by volume). As may be seen in columns 7 and 8 in Table 3, citronellol was not formed, while a comparable amount of citronellal was formed. The fact that no geraniol was made in this system can be explained; in view of the polarographic redox potentials corresponding to the reduction of citral into citronellal or geraniol,[10] it is reasonable to consider that geraniol, formed first, is then dehydrogenated into citronellal.

Liquid-phase Dehydrogenation. Liquid-phase dehydrogenation as well as vapor-phase dehydrogenation is a conveniently available method for preparing citral from geraniol, not only at the laboratory but also at the plant.

When using a Cu-Zn or Cu-Cr catalyst (2% by weight of the geraniol used the dehydrogenation should be carried out in a flask under gentle boiling between 200°C and 205°C; below this temperature, for example, at 180°C, the reaction is slow and inefficient.

In a comparison of the catalytic activity of Cu-Zn and Cu-Cr catalysts, it is evident that the latter catalyst gives terpene hydrocarbons and decreased yields of both citronellal and isopulegol (see runs 2 and 3 in Table 4).

To increase the yield of citral by preventing the conversion of the once-formed citral into citronellal, either citronellal or cyclohexanone, as a hydrogen acceptor, was added at the beginning of the reaction. From the results shown in Table 4 for the system with a Cu-Zn catalyst, when citronellal or cyclohexanone was used, the reaction resulted in a relatively increased yield of citral for the converted geraniol, the yield being even larger than that obtained in the vapor-phase dehydrogenation at an atmospheric pressure. Moreover, a larger amount of isopulegol was formed in the

TABLE 5. EFFECT OF REACTION TEMPERATURE ON PRODUCT DISTRIBUTION AT REDUCED PRESSURE IN VAPOR-PHASE DEHYDROGENATION USING Cu-Zn CATALYST*

Run	Volume of catalyst ml	L.S.V. l/hr	Reduced pressure mmHg	Temperature °C	Composition of products by G.L.C. (wt%)				
					Terpene hydrocarbons	Citronellal	Isopulegol	Citral	Geraniol
1	10	0.7	8	175	6.7	48.4	4.1	28.6	12.2
2	10	0.7	8	190	6.0	36.5	4.0	23.7	29.8
3	10	0.7	8	215	6.0	34.0	3.2	30.0	26.8
4	10	0.7	8	230	6.3	32.1	2.9	37.9	20.8

* Form of the catalyst used was of (b).

10) K. Schwarbe, G. Ohloff and H. Berg, *Z. Elektrochem.*, **57**, 293 (1953).

TABLE 6. EFFECT OF CONTACT TIME ON PRODUCT DISTRIBUTION AT A REDUCED PRESSURE IN VAPOR-PHASE DEHYDROGENATION USING Cu-Zn CATALYST SYSTEM

Run	Volume of catalyst* m*l*	Reaction temperature °C	L.S.V. *l*/hr	Reduced pressure mmHg	1/S.V. sec	Terpene hydrocarbons	Citronellal	Isopulegol	Citral	Geraniol	Citronellol
1	30	230	0.7	7	6.27×10^{-3}	6.2	15.7	5.2	48.0	24.9	0
2	30	230	0.7	21	18.7×10^{-3}	10.1	18.1	6.5	43.9	21.3	0
3	30	230	0.7	30	26.8×10^{-3}	8.4	19.0	6.6	47.7	18.3	0
4	30	230	0.7	42	37.4×10^{-3}	6.5	20.1	7.0	51.4	15.0	0

Table 5 The effect of contact time on the product distribution in the vapor phase dehydrogenation with the Cu-Zn system.
* Form of the catalyst was (b).

TABLE 7. VARIATIONS OF INVERSE RELATION OF CITRAL AND CITRONELLAL FORMATION *versus* REACTION TIME

Run	Sampling time	Cu-Zn* catalyst m*l*	Reaction temperature	L.S.V.	Reduced pressure mmHg	Compositions of products by G.L.C. (wt%)					Yield of citral plus citronellal (%)
						Terpene hydrocarbons	Citronellal	Isopulegol	Citral	Geraniol	
1	after 1 hr	35	185°C	0.7	15—16	7.0	71.3	0	21.5	0	92
2	after 5 hr	35	185°C	0.7	15—16	7.0	67.7	0	25.2	0	92
3	after 8 hr	35	185°C	0.7	15—16	7.1	63.3	0	27.6	2.0	90

* Form of the catalyst was (c).

TABLE 8. EFFECT OF CITRONELLAL ADDITION ON THE YIELD OF CITRAL USING Cu-Zn CATALYST

Run	Volume of catalyst* m*l*	Reaction temperature	Reduced pressure mmHg	L.S.V.	Molar ratio of geraniol to citronellal added	Composition of products by G.L.C. (wt%)					Geraniol conversion to citral (%)
						Terpene hydrocarbons	Citronellal	Isopulegol	Citral	Geraniol	
1	30	230°C	8	0.7	1 : 0.5**	2.0	48.5	5.9	43.4	0.2	65.3
2	30	230°C	8	0.7	1 : 1**	2.0	53.7	6.0	35.5	1.8	75.0
3	30	230°C	8	0.7	1 : 1.3**	1.2	57.5	5.2	34.9	1.2	84.0
cf	30	230°C	7	0.7	only geraniol	6.2	15.7	5.2	48.0	24.9	63.9

** The composition of these mixture used was, *e.g.*, terpene hydrocarbons : citronellal : geraniol=0.5 : 32.9 : 66.6 for Run 1, 0.5 : 32.9 : 66.6 for Run 2, and 0.8 : 59.4 : 41.8 for Run 3.
* Form of the catalyst used was of (c).

addition of citronellal than in that of cyclohexanone, indicating the transformation of citronellal into isopulegol.

Vapor-phase Dehydrogenation of Geraniol at Reduced Pressure. The fact that citral, as is shown in runs 7 and 8 in Table 3, gave various products, such as terpene hydrocarbons, citronellal and isopulegol, suggests the possibility of increasing the yield of citral by quickly removing the citral formed from the reacting zone. Therefore, the vapor phase dehydrogenation of geraniol was attempted with the Cu-Zn catalyst system at a reduced pressure and at a given L. S. V.; the results are summarized in Table 5.

a) The Effect of the Reaction Temperature at a Given L. S. V. The effect of the reaction temperature on the product distribution was examined between 175°C and 230°C and at a L. S. V. of 0.7, using a reaction tube packed with 10 m*l* of the catalyst (b), the results obtained are presented in Table 5. At the lower temperature, 175°C, citral decreased and citronellal increased markedly, reaching a yield of 48.4% after 7 m*l* of geraniol had been passed through in 1 hr, with the raising of the reaction temperature, the amount of citral increased, while that of citronellal, in turn, gradually decreased. In addition, an appreciably decreased conversion of geraniol was found in this system in comparison with that in dehydrogenation under an atmospheric pressure.

b) The Effect of L. S. V. The product distribution when 30 m*l* of the Cu-Zn catalyst (b) was used was examined at the most favorable reaction temperature, 230°C, with various contact times, the results obtained are summarized in Table 6. In this system, it will be noted that in comparison with the systems previously studied, there was an appreciably improved yield of citral (50%), a smaller amount of by-products, and no citronellol. In this case, the geraniol conversion *versus* the contact time shows a linear relation, as is shown in Fig. 2. This indicates, by extrapolation, that the complete conversion of geraniol would be approximately 60% under the present conditions.

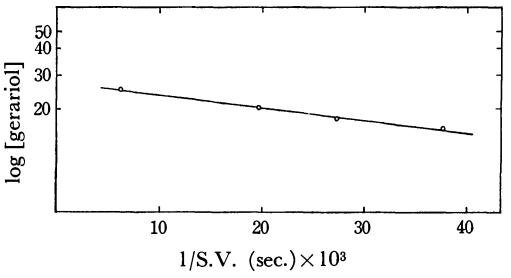

Fig. 2. Linear relationship between logarithm of geraniol molar concentration and contact time at 230°C in catalytic dehydrogenation using Cu-Zn catalyst.

c) The Effect of the Addition of Citronellal. In the results of the detailed observation of the product distribution shown in Table 7, it will be noted that the relation of the amounts of citral and citronellal is inverse, in that one increases as the other decreases, suggesting the possibility of these existing an equilibrium relation between citral, citronellal, and geraniol in this reacting zone, or of their changing the catalytic activity, controlling the equilibrium between them.

On the basis of the above reasoning, for the purpose of increasing the yield of citral, the present authors conducted the dehydrogenation at a reduced pressure by using mixtures of geraniol and citronellal in various ratios as the starting material.

As may be seen in the results shown in Table 8, the expected increased conversion of geraniol into citral was observed, while a maximum yield of citral of 84.0% was obtained.

The Preparation of Citronellal. It has already been demonstrated that the yield of citronellal was greatly affected by both the contact time and the reaction temperature. Therefore, in order to increase the yield of citronellal, the dehydrogenation of geraniol was carried out with a longer reaction tube and at a lower reaction temperature; the reaction temperature was 185°C, the reduced pressure 15 to 16 mmHg, and a reaction tube 28 mm in dia., 400 mm long, and packed with 35 m*l* of the catalyst (c) over a distance of 70 mm, was used. The results obtained are shown in Table 7. There was an excellent yield of citronellal (70%), but no formation of either isopulegol or citronellol.

A Proposal for the Catalyzed Dehydrogenation of Geraniol. On the basis of the dehydrogenation products already revealed, the following reaction process may be considered. Citronellal is formed by the hydrogenation of citral, not with hydrogen adsorbed on the catalyst, but with hydrogen participating in the dehydrogenation of geraniol. Such an example has been shown by Constable[11] in the catalyzed dehydrogenation of allyl alcohol,[12] where propionaldehyde, not acrolein, is formed as a result of hydrogen migration from the alcohol to the carbon-carbon double bond of the possibly-made acrolein.

Regarding citral, judging from its increased yield upon the addition of citronellal, there is the possibility of an equilibrium relation between citral, citronellal, and geraniol in the reacting zone, or a poisoning of the catalyst, thereby resulting in a selectivity in the making of citral.

11) F. H. Constable, *Roy. Soc. Proc.*, **109**, 254 (1926).
12) D. E. Weston and H. Adkins, *J. Am. Chem. Soc.*, **50**, 1930 (1928).

NOTES

Asymmetric Hydrogenation with Modified Raney Nickel.*1 X. Effect of the β-Substituent of α-Amino Acid as a Modifying Reagent

Yoshiharu IZUMI, Kazuyoshi MATSUNAGA, Susumu TATSUMI and Masami IMAIDA

Division of Organic Chemistry, Institute for Protein Research, Osaka University, Kita-ku, Osaka

(Received August 7, 1967)

The asymmetric activities of Raney nickel catalysts modified with optically active α-amino acids in the hydrogenation of methyl acetoacetate have previously been reported on by the present authors.[1]

From the relation between the asymmetric activities of catalysts and the structures of the modifying reagents upon modification with α-amino acids at 0°C and at their isoelectric points, it was concluded that a catalyst modified with an α-amino acid, such as L-valine or L-isoleucine, which is replaced at the β-position by a methyl group shows a higher asymmetric activity than a catalyst modified with an α-amino acid which does not have a β-alkyl substituent.

The present paper will report on the asymmetric activities of catalysts modified with L-3-ethylnorvaline,*2 its acetyl derivative, and L-alloisoleucine. The specific rotation of the materials used in the present paper are as follows:

TABLE 1. OPTICAL ROTATIONS OF MODIFYING REAGENTS

Modifying reagent	Optical rotation, $[\alpha]_D^{20}$
L-3-Ethylnorvaline	+38° (*c* 1, 6 N HCl)
N-Acetyl-L-3-ethylnorvaline	+17° (*c* 2, EtOH)

The asymmetric activity of the catalyst was studied in the hydrogenation of methyl acetoacetate to methyl 3-hydroxybutyrate, as has been described in previous papers.[2,3] In Fig. 1 the asymmetric activity of the catalyst modified with L-3-ethylnorvaline at the isoelectric point is shown as a function of the modifying temperature.

In Fig. 2 the asymmetric activities of the catalyst modified with *N*-acetyl-L-3-ethylnorvaline at 0°C and 100°C are shown. In comparison with L-3-ethylnorvaline, a decrease in the asymmetric activity of the catalyst was also found, as was also

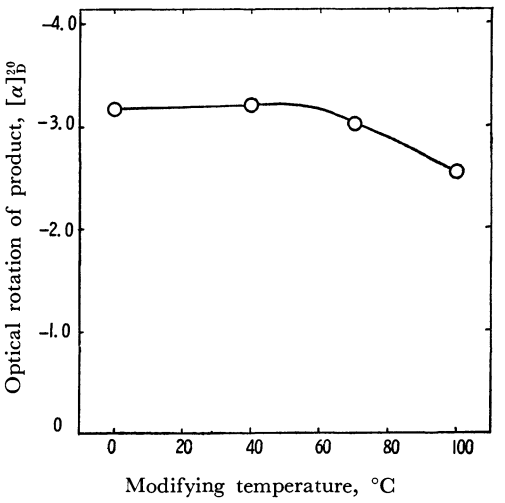

Fig. 1. Effect of modifying temperature modified with L-3-ethylnorvaline at the isoelectric point.

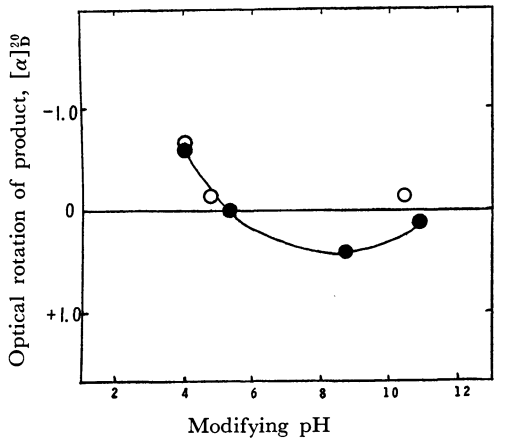

Fig. 2. Effect of modifying pH on the modifications at 0°C and 100°C with *N*-acetyl-L-3-ethylnorvaline.
● modified at 0°C, ○ modified at 100°C

*1 This work was supported by a grant from the Japanese Ministry of Education.

1) Y. Izumi, M. Imaida, H. Fukawa and S. Akabori, This Bulletin, **36**, 21 (1963).

*2 Details of the preparation of this material will be reported in this Bulletin in the near future.

2) Y. Izumi, M. Imaida, H. Fukawa and S. Akabori, *ibid.*, **36**, 155 (1963).

3) Y. Izumi, S. Tatsumi and M. Imaida, *ibid.*, **39**, 2223 (1966).

observed in the catalyst modified with the acetyl derivative of L-glutamic acid. On modification at 0°C, an inversion of the direction of asymmetric activity was observed at pH 5.0.

The asymmetric activities of catalysts modified with L-valine and L-aminobutyric acid at 0°C and at the isoelectric points, which were presented in the previous paper,[2] and those with L-3-ethylnorvaline and L-alloisoleucine in the present work are compared in Fig. 3. It may be seen from the figure that alloisoleucine gave a higher asymmetric a ctivity to the catalyst than did isoleucine, the diastereomer of alloisoleucine. As the threo configuration is more effective for the asymmetric activity of the catalyst than the erythro form, the (R)-configuration of the β-carbon in an L-α-amino acid increases the activity of the catalyst. The asymmetric activity of a catalyst modified with alloisoleucine is less than that of one modified with 3-ethylnorvaline, and the asymmetric activity caused by valine is intermediate between the asymmetric activities caused by *threo* and *erythro*-isoleucine.

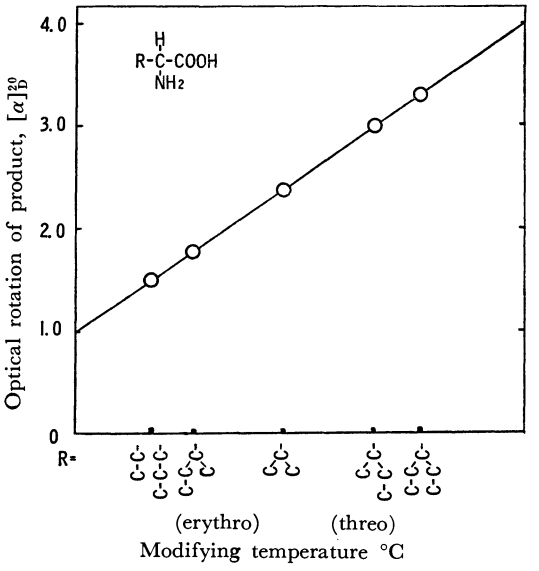

Fig. 3. Comparison of symmetric activities modified at 0°C and the isoelectric point.

As the catalysts modified with aminobutyric acid and with norvaline had the same asymmetric activity, the δ-carbon of *n*-alkyl amino acid (I) is not effective in increasing the asymmetric activity. Unlike as with *n*-alkyl amino acids, a catalyst modified with 3-ethylnorvaline has a higher asymmetric activity than one modified with valine. These facts show that the δ'-carbon of the β-side chain of β-alkyl amino acids (II) is effective in increasing the asymmetric activity.

$$\overset{\delta}{CH_3}-\overset{\gamma}{CH_2}-\overset{\beta}{CH_2}-\overset{\alpha}{CH}-COOH \quad (I)$$
$$\qquad\qquad\qquad\qquad\quad |$$
$$\qquad\qquad\qquad\qquad NH_2$$

$$\begin{matrix}\overset{\delta}{CH_3}-\overset{\gamma}{CH_2} \\ \overset{\delta'}{CH_3}-\overset{\gamma'}{CH_2}\end{matrix}\!\!>\overset{\beta}{CH}-\overset{\alpha}{CH}-COOH \quad (II)$$
$$\qquad\qquad\qquad\qquad\quad |$$
$$\qquad\qquad\qquad\qquad NH_2$$

The asymmetric activity caused by *threo*-isoleucine greatly differs from that caused by *erythro*-isoleucine. This shows that the relative conformations of the β-carbon to the α-carbon in the two isoleucines are different when they are adsorbed on the catalyst. Let us name the adsorbed conformations of an β-alkyl amino acid similar to those of the *threo*- and *erythro*-isoleucines threo- and erythro-type conformations, respectively. Valine and 3-ethylnorvaline allow at least these two types of adsorbed conformations on the catalyst, even though valine and 3-ethylnorvaline have the β-carbon, which is replaced symmetrically. Consequently, as a result of the difference between the stabilities of threo- and erythro-type conformations formed by valine or 3-ethylnorvaline, the threo- and erythro-types of the asymmetric centers may be supposed to exist in different proportions. According to the disproportion in the existent ratios of the two asymmetric centers, the observed asymmetric activity of the catalyst caused by valine or 3-ethylnorvaline can hardly be expected to show the arithmetical mean of each asymmetric activity of the two types of centers.

Because of the above reason, it is difficult to discuss the exact role of β-alkyl-substituents in the asymmetric activity of β-alkyl amino acids. A study of the asymmetric activity of a catalyst modified with 3-methylnorvaline, which may give further information on this point, will, however, be reported in this Bulletin in the near future.

The authors would like to express their thanks to M. Sc. Tadashi Tanabe for his help. This research was supported by Kawaken Fine Chemicals Co., Ltd., Tokyo.

The Reaction of Nitrosobenzene with Benzenesulfonylhydrazide in the Presence of a Base

Suketaka Ito

Department of Industrial Chemistry, Faculty of Engineering, Shinshu University, Wakasato, Nagano

(Received December 29, 1967)

The action of benzenediazonium salt upon *p*-toluenesulfonamide in the presence of an excess of sodium hydroxide,[1] and the reaction of benzenesulfonyl azide with phenylmagnesium bromide, followed by the hydrolysis[2] or pyrolysis[3] of the product, lead to the formation of phenyl azide.

These reactions involve the formation of the salt of 1-*p*-toluenesulfonyl- or 1-benzenesulfonyl-3-phenyltriazene and the elimination of the salt of arenesulfinic acid from the triazene salt.

$$C_6H_5N_2Cl + C_7H_7SO_2NH_2 \xrightarrow[NaOH]{}$$

$$C_6H_5\text{-}N{=}N\text{-}N(Na)\text{-}SO_2C_7H_7 \longrightarrow$$

$$C_6H_5N_3 + C_7H_7SO_2Na$$

$$C_6H_5MgBr + C_6H_5SO_2N_3 \longrightarrow$$

$$C_6H_5\text{-}N{=}N\text{-}N(MgBr)\text{-}SO_2C_6H_5 \longrightarrow$$

$$C_6H_5N_3 + C_6H_6SO_2MgBr$$

Accordingly, one can expect to obtain phenyl azide from the disubstituted triazene or its salt, prepared in a different reaction sequence. Since the triazene may be regarded as the condensation product of nitrosobenzene with arenesulfonylhydrazide, it is conceivable that the triazene can be prepared by the condensation of these compounds. However, the nitroso compounds do not give triazenes by reaction with hydrazines,[4,5] although the condensation reactions of aromatic nitroso compounds with such compounds as aniline,[6] hydroxylamine,[7] *N*-phenylhydroxylamine,[8] and benzyl cyanide[9] are similar to those of carbonyl compounds. In the present study, the reaction of nitrosobenzene with benzenesulfonylhydrazide was attempted for the purpose of obtaining phenyl azide.

Results and Discussion

When a mixture of nitrosobenzene and benzenesulfonylhydrazide was refluxed in absolute ethanol for thirty minutes, and then for one more hour with sodium ethoxide, azoxybenzene was obtained; the additional formation of a trace amount (0.5%) of phenyl azide was confirmed by infrared spectroscopy. The addition of a small amount of sulfuric acid in the first run of the reaction did not promote the yield of phenyl azide.

When powdered nitrosobenzene was added to an aqueous solution of equimolar amounts of benzenesulfonylhydrazide and potassium or sodium hydroxide at 45—50°C with vigorous stirring, there separated a yellowish-brown oil, and nitrogen evolved. The yield of phenyl azide increased as much as 1.4%. Along with unaltered benzenesulfonylhydrazide (24%), azoxybenzene (45%) and benzenesulfinic acid (47%) were also obtained.

The results can be outlined by the following scheme:

$$C_6H_5SO_2NHNH_2$$

$$\downarrow\uparrow OH^-$$

$$C_6H_5SO_2N^-NH_2 \rightleftarrows C_6H_5SO_2NHN^-H$$

$$\downarrow 2C_6H_5NO \qquad \downarrow C_6H_5NO$$

$$C_6H_5SO_2^- + C_6H_5N{=}NC_6H_5 \quad C_6H_5SO_2^- + C_6H_5N_3$$

$$\downarrow O$$

$$+ N_2$$

When benzenesulfonylhydrazide was treated in an aqueous alkaline solution at 60°C for an hour, no remarkable reaction occurred and no benzenesulfinic acid was obtained.[10] Furthermore, the amount of benzenesulfinic acid obtained in the reaction of benzenesulfonylhydrazide with nitrosobenzene was, as has been shown above, almost equimolar to that of azoxybenzene. Phenyl azide did not react with nitrosobenzene at 70°C, even

1) P. K. Dutt, H. R. Whitehead and A. Wormall, *J. Chem. Soc.*, **119**, 2088 (1921); *Chem. Abstr.*, **16**, 915 (1922).
2) The private communication of P. A. Smith and L. Bruner to J. H. Boyer; See: J. H. Boyer and F. C. Canter, *Chem. Revs.*, **54**, 17 (1954).
3) S. Ito, This Bulletin, **39**, 635 (1966).
4) See: Beilsteins "Handbuch der Organischen Chemie," Hw. Bd. V, p. 231—232 (1922).
5) H. Minato and T. Fujisawa, This Bulletin, **39**, 1054 (1966).
6) E. Bamberger, *Ber.*, **26**, 483 (1893); Beilsteins "Handbuch der Organischen Chemie," Hw. Bd. V, p. 231 (1922).
7) E. Bamberger, *ibid.*, **28**, 1218 (1895); *ibid.*,
8) E. Bamberger, *ibid.*, **30**, 2278 (1897); *ibid.*
9) F. Sachs, *ibid.*, **34**, 494 (1901); *ibid.*, Hw. IX, p. 442 (1926).
10) It has been reported that benzenesulfonylhydrazide decomposes by heating with water, alcohol or alkali for a long time.[11]

in the presence of alkali. Therefore, it can be concluded that the following reactions did not occur to any significant extent:

$$C_6H_5SO_2NHNH_2 \xrightarrow[OH^-]{} C_6H_5SO_2^- + H\text{-}N{=}N\text{-}H$$

$$C_6H_5NO + H\text{-}N{=}N\text{-}H \longrightarrow C_6H_5NHOH + N_2$$

$$C_6H_5N_3 + C_6H_5NO \longrightarrow C_6H_5N{=}NC_6H_5 \quad (\downarrow O)$$

The reaction in the presence of sodium ethoxide was also carried out in ethanol or *N*,*N*-dimethylformamide, but phenyl azide was thus obtained in lower yields than in water.

In conclusion, by benzenesulfonylhydrazide, nitrosobenzene is mainly subjected to reduction to *N*-phenylhydroxylamine, which then easily condenses with nitrosobenzene to give azoxybenzene.

Experimental

The reaction in an aqueous alkaline medium was described alone. The melting points are uncorrected.

Materials. Benzenesulfonylhydrazide was prepared by the action of benzenesulfonyl chloride (1 mol) upon an aqueous solution of hydrazine hydrate (1 mol) and sodium hydroxide (1 mol); yield: 76%, and recrystallized from ethanol, mp 104.5—105.5°C (lit.[11] mp 104—106°C).

The Reaction of Nitrosobenzene with Benzenesulfonylhydrazide in aqueous Potassium Hydroxide Solution. Into a vigorously-stirred solution of 17.2 g (0.1 mol) of benzenesulfonylhydrazide and 6.5 g (*ca.* 0.1 mol) of potassium hydroxide in 150 m*l* of water, there were added, over a period of 30 min, 10.7 g (0.1 mol) of powdered nitrosobenzene at 45—50°C. The reaction mixture was kept at this temperature for an additional 30 min with stirring. During the reaction, a yellowish-brown oil separated, the aqueous solution turned light brown, and nitrogen evolved.

The reaction mixture was then cooled, extracted with ether, and separated to an ether layer (A) and an aqueous layer (B). By removing the solvent from the ether solution (A), which was then washed with water and dried over anhydrous sodium sulfate, a brown liquid (A′) (9.4 g) was obtained. This liquid became solid on cooling. The infrared spectrum of the brown residue showed the absorption of azoxybenzene, accompanied with a small amount of phenyl azide. By using the absorption of the azido group at 2170 cm^{-1}, the yield of phenyl azide was determined to be 1.4%, calculated from nitrosobenzene.

The ether extract (A′) (9.3 g) was then chromatographed on 30 g of silica gel and eluted with *n*-hexane and *n*-hexane - ether; phenyl azide was concentrated in the first 20-m*l* fraction of the elution. After the solvent had been removed from the fraction, the yellow residue was fractionally distilled *in vacuo* (5 mmHg). Pure pale yellow phenyl azide was collected in a trap at −70°C (131 mg, n_D^{23}: 1.5587); its infrared spectrum was identical with that of an authentic sample. Found: N, 34.90%. Calcd for $C_6H_5N_3$: N, 35.27%.

By the reaction of dimethyl acetylenedicarboxylate with the phenyl azide, the 1-phenyl-1,2,3-triazole-4,5-dicarboxylic acid dimethyl ester, mp 127.5—128.5°C (lit.[12] mp 127—128°C), was obtained. (Found: C, 55.10; H, 4.63; N, 16.02%.)

The chromatographic treatment of the ether extract (A′) also gave 9.0 g (45%, calculated from nitrosobenzene) of yellow crystals of azoxybenzene, which melted at 35.5—36.5°C (lit.[13] mp 35.5—36.5°C) after recrystallization from methanol. (Found: C, 72.60; H, 5.43; N, 14.42%). Its infrared spectrum was identical with that of an authentic sample.

The water layer (B), when combined with washings of the ether extract of the reaction mixture, was acidified with concentrated hydrochloric acid and fully extracted with ether. From the acidic aqueous layer, by neutralization, 4.1 g (24%) of unaltered benzenesulfonylhydrazide were recovered. The ether layer was extracted with a solution of sodium hydroxide and water; the alkaline solution was then acidified with hydrochloric acid and saturated with sodium chloride. The resulting precipitate was filtered and dried to give 6.7 g (47%, calculated from benzenesulfonylhydrazide) of benzenesulfinic acid, the infrared spectrum of which was identical with that of an authentic sample.

By the treatment of the sodium salt of the sulfinic acid with benzyl chloride in ethanol, phenyl benzyl sulfone was obtained; it melted at 147.0—148.0°C (lit.[14] mp 148°C) after recrystallization from ethanol. (Found: C, 67.09; H, 5.29%.) No depression of the melting point was observed on admixture with an authentic sample.

11) T. Curtius, *J. Prakt. Chem.*, [2], **58**, 166 (1898); Beilsteins "Handbuch der Organischen Chemie," Hw. Bd. XI, p. 52 (1938).

12) A. Michael, *J. Prakt. Chem.*, [2], **48**, 94 (1893); Beilsteins "Handbuch der Organischen Chemie," Hw. Bd. XXVI, p. 298 (1937).

13) H. E. Bigelow and A. Palmer, "Organic Syntheses," Coll. Vol. II, p. 57 (1943).

14) E. Knoevenagel, *Ber.*, **21**, 1349 (1888); Beilsteins "Handbuch der Organischen Chemie," Hw. Bd. VI, p. 455 (1923).

Preparation of Polyamines by the Michael Reaction

Kentaro YODA and Takao TODA

Katata Research Institute, Toyobo Co., Ltd., Honkatata-cho, Otsu

(Received January 22, 1968)

It is well known concerning the Michael reaction that amines containing an active hydrogen add to activated double bonds.[1-3] A few attempts have been made to prepare polyamines by the Michael reaction.[4,5]

In this paper the Michael reaction was used in the preparation of polyamines from piperazine and several divinyl compounds.

Polyamine from Piperazine and Divinyl Sulfone. A typical run of the preparative method of the polyamine is shown below.

To a solution of 9.370 g (0.108 mol) of anhydrous piperazine in 60 m*l* of absolute methanol was added dropwise a mixture of 12.84 g (0.108 mol) of divinyl sulfone and 20 m*l* of absolute methanol with vigorous stirring at room temperature. The exothermic reaction took place quite rapidly. The reaction mixture was stirred for 30 min. Then the separated white solid was filtered off and washed with methanol. The yield of dried material, melting at 232—234°C, amounted to 21 g (99.0% of the theoretical amount).

Found: C, 46.45; H, 8.10; N, 13.75; S, 15.56%. Calcd for $(C_8H_{16}N_2O_2S)_n$: C, 47.03; H, 7.48; N, 13.72; S, 15.67%.

The product was soluble in sulfuric acid, glacial acetic acid, and formic acid. However, it was insoluble in *n*-hexane, benzene, methanol, ethanol, ether, chloroform, tetrahydrofuran, dioxane, dimethylformamide, dimethyl sulfoxide, dimethyl sulfate, and methyl formate. It should be noted that the product is swollen with water. The product had an intrinsic viscosity of 0.36 in sulfuric acid and one of 0.30 in glacial acetic acid at 30°C.

As the electron density of the double bonds in divinyl sulfone is decreased by the electron-withdrawing character of the oxygen atom, divinyl sulfone acts as a strong electron-acceptor in the Michael reaction. The addition reaction of piperazine to divinyl sulfone proceeded rapidly at a low temperature and formed a polymeric substance in a high yield. The results of elementary analysis and the infrared spectrum (Fig. 1) showed the polymer to have the following polyamine structure:

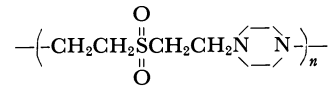

The influences of the solvents and the feed ratio of piperazine to divinyl sulfone on the yield and the molecular weight of polyamine were examined; the results are listed in Table 1. The polymer with the highest molecular weight was attained when the two reactants used were equimolar in amount. The polymerization method in which divinyl sulfone was slowly added to a solution of piperazine seemed to give a higher molecular weight and higher yield than when the two reactants were added at the same time.

No polymeric addition product was obtained by the reaction of *trans*-2,5-dimethylpiperazine with divinyl sulfone. The failure of this reaction may be due to the steric effect of the methyl group which would prevent, more or less, the attack of the nitrogen atom on the β-carbon of divinyl sulfone.

Polyamine from *p*-Phenylene Diacrylate and Piperazine. To a mixture of 10 m*l* of methanol, 40 m*l* of chloroform and 1.291 g (0.015 mol) of piperazine was added a solution of 3.273 g (0.015 mol) of *p*-phenylene diacrylate in 40 m*l* of chloroform with vigorous stirring over a period of 30 min. The temperature was maintained at 10°C during the addition of *p*-phenylene diacrylate. After the addition, the reaction mixture was refluxed for 60 min under a nitrogen atmosphere. Then the solvents were distilled off under reduced pressure. After the residual liquid has been poured into a large amount of ether, a white solid was filtered. After drying, 1.5 g of white powder was obtained, mp 180—182°C.

Found: C, 61.76; H, 6.91; N, 8.06%. Calcd for $(C_{16}H_{20}N_2O_4)_n$: C, 63.14; H, 6.22; N, 7.88%.

This polymer was readily soluble in chloroform dimethylformamide, dimethyl sulfoxide, and acetic acid. The intrinsic viscosity of this polymer was 0.11 in glacial acetic acid at 30°C. The infrared spectrum of this polymer, as shown in Fig. 2, indicates the following polyester-amine structure:

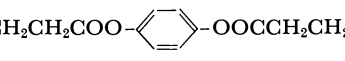

An attempt to obtain a polymeric substance from *p*-phenylene dimethacrylate and piperazine failed. It is expected that, in this reaction, the inductive effect of the methyl group is not significant, while

1) C. B. Pollard, J. P. Bain and D. E. Adelson, *J. Am. Chem. Soc.*, **57**, 199 (1953).
2) V. E. Stewart and C. B. Pollard, *ibid.*, **58**, 1980 (1936).
3) A. A. R. Sayigh, H. Ulrich and M. Green, *J. Org. Chem.*, **29**, 2042 (1964).
4) G. E. Hulse, U. S. Pat. 275993 (1956).
5) Farbwerke Hoechst A. G., Belgian Pat. 612398 (1962).

Table 1. Polyamine from piperazine and divinyl sulfone

Reactant		Solvent, m*l*		Reaction			Polymer				
PZ mol	DVS mol	PZ	DVS	Process	Time min	Temp. °C	Yield %	N%	S%	Mp, °C	η_{sp}/C*
0.0300	0.0300	MeOH 40 $CHCl_3$ 30	$CHCl_3$ 20	A	30 30	10 35	80.3	12.26	15.70	232—234	0.32
0.1080	0.1080	MeOH 60	MeOH 20	A	30 30	25 25	99.0	13.75	15.56	232—234	0.38
0.0300	0.0240	MeOH 50 $CHCl_3$ 10	$CHCl_3$ 10	A	30 30	10 35	85.7	13.55	14.49	229—232	0.19
0.0300	0.0294	MeOH 50 $CHCl_3$ 10	$CHCl_3$ 10	A	30 30	10 35	70.0	13.00	15.75	233—235	0.28
0.0300	0.0306	MeOH 50 $CHCl_3$ 10	$CHCl_3$ 10	A	30 30	10 35	68.5	12.89	15.36	232—234	0.35
0.0300	0.0360	MeOH 50 $CHCl_3$ 10	$CHCl_3$ 10	A	30 30	10 35	68.5	12.62	15.76	232—234	0.14
0.0300	0.0300	MeOH 100	MeOH 100	B	30 30	25 70	73.4	12.13	15.87	213—215	0.19
0.0300	0.0300	EtOH 100	EtOH 100	B	30 30	25 70	70.1	12.20	15.74	215—216	0.17
0.0200	0.0200	MeOH 20 DMF 30	DMF 50	A	30 30	20 150	—	—	—	—	—

PZ: Piperazine; DVS: Divinyl sulfone; DMF: Dimethylformamide.
Process A: The solution of DVS was added slowly to the solution of PZ for 30 min and the mixture was stirred for another 30 min at a given temperature.
Process B: The two reactants were mixed at the same time and the mixture was maintained at room temperature for 30 min.
* C=0.5 g/100 m*l* of acetic acid (30°C).

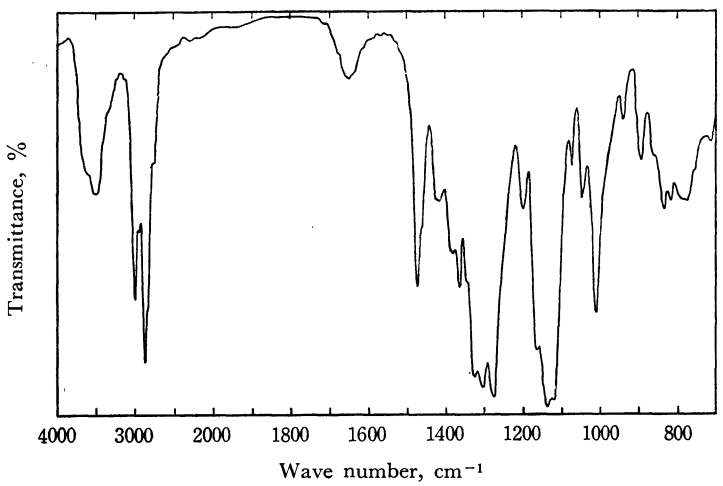

Fig. 1. Infrared spectrum of the polymer from piperazine and divinyl sulfone.

the steric hindrance of the methyl group can not be disregarded. That is, in the Michael reaction the rate-determining step[6,7] is the attack of the nitrogen atom on the β-carbon of the vinyl group, and not only the stability of the ambient anion formed, but also the steric effects of reactants play an important role.

6) Y. Ogata, M. Okano, Y. Furuya and I. Tabushi, *J. Am. Chem. Soc.*, **78**, 5426 (1956).
7) E. S. Gould, "Mechanism and Structure in Organic Chemistry," Henry Holt and Company, Inc., New York (1959), p. 392.

Experimental

Materials. Anhydrous piperazine, *trans*-2,5-dimethylpiperazine, and divinyl sulfone may be obtained from commercial sources. Anhydrous piperazine and *trans*-2,5-dimethyl piperazine were purified by the azeotropic distillation of water with benzene. Divinyl sulfone was purified by distillation under reduced pressure. Most of the solvents were dried and subjected to a simple distillation. Chloroform was freed of any alcohol stabilizer by washing it with a 5% sodium bicarbonate solution and water successively. It was

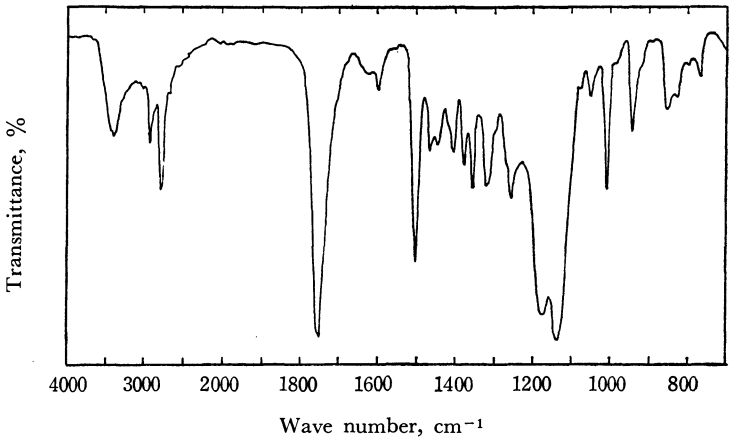

Fig. 2. Infrared spectrum of the polymer from piperazine and *p*-phenylene diacrylate.

dried over calcium chloride and then distilled. *p*-Phenylene dimethacrylate was prepared by the following method. To 23.12 g (0.12 mol) of hydroquinone in a 300 m*l*, four-necked flask, 16.8 g (0.42 mol) of sodium hydroxide in 200 m*l* of water was added with stirring under a nitrogen atmosphere. Then 43.85 g (0.42 mol) of methacrylyl chloride were added, drop by drop, over a 30-min period at 30°C. The reaction mixture was extracted with 400 m*l* of ether, and the extract was washed three times with 150 m*l* of a 5% sodium bicarbonate solution. The ether solution was then dried over 50 g of anhydrous sodium sulfate overnight, and the ether was removed. Eighteen grams of white needles were obtained by two recrystallizations from ether, mp 88°C.

Found: C, 68.17; H, 5.78%. Calcd for $C_{14}H_{14}O_4$: C, 68.28; H, 5.78%.

IR (KBr disk): 3420, 2940, 2910, 2830, 1734, 1635, 1504, 1445, 1395, 1373, 1320, 1295, 1185, 1145, 1123, 1013, 934, 885, 807 cm.$^{-1}$

p-Phenylene diacrylate was prepared from 23.12 g (0.21 mol) of hydroquinone and 37.01 g (0.42 mol) of acrylyl chloride in the presence of 16.8 g (0.42 mol) of sodium hydroxide according to a method similar to that used in the case of *p*-phenylene dimethacrylate. Seven grams of white needles were obtained after two recrystallizations from a mixture of ether and petroleum ether (1 : 1), mp 84—85°C.

Found: C, 65.64; H, 4.80%. Calcd for $C_{12}H_{10}O_4$: C, 66.04; H, 4.62%.

IR (KBr disk): 3419, 3090, 3040, 1740, 1723, 1630, 1500, 1400, 1290, 1250, 1150, 1008, 980, 908, 793, 770 cm.$^{-1}$

Synthesis of α,β-Unsaturated Carboxylic Hydrazides

Rokuro HARADA and Hisao KONDO

Basic Research Laboratories, Toyo Rayon Company, Ltd., Tebiro, Kamakura

(Received January 24, 1968)

Carboxylic hydrazides are usually prepared by the reaction of carboxylic esters with hydrazine hydrate.[1] However, when this general method is applied to the synthesis of α,β-unsaturated carboxylic hydrazides, the main product is not simple carboxylic hydrazide, but pyrazolidone (III) resulting from the Michael addition.[2]

$$RCH{=}CR'COOR'' + NH_2NH_2 \rightarrow$$

(I)

$$[NH_2NHCHR\cdot CHR'COOR''] \rightarrow$$

(II)

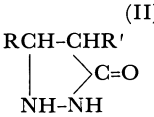

(III)

Therefore, pyrazolidones obtained by this method have often been believed to be carboxylic hydrazides. Godtfredsen[3] has, however, shown

1) R. B. Wagner and H. D. Zook, "Synthetic Organic Chemistry," John Wiley & Sons, New York (1953), p. 569.

2) C. Gansser, *Helv. Chim. Acta*, **36**, 1423 (1963); F. H. Stodla, *J. Org. Chem.*, **13**, 757 (1948); T. Lieser, *Chem. Ber.*, **84**, 4 (1951); P. Ruggli, *Helv. Chim. Acta*, **24**, 899 (1941).

3) W. Q. Godtfredsen and S. Vangedal, *Acta Chem. Scand.*, **9**, 1498 (1955).

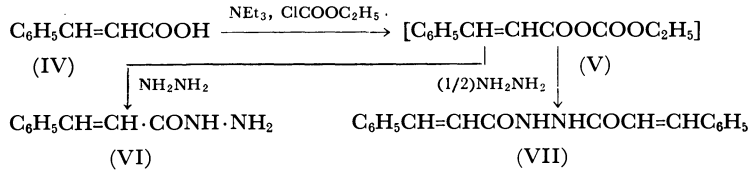

that the cinnamohydrazide synthesized by Muckermann[4] was not the hydrazide, but in fact 5-phenyl-3-pyrazolidone, he synthesized real cinnamohydrazide (VI) by the reaction of cinnamic ethoxyformic anhydride (V) with hydrazine hydrate.

Several papers have appeared reporting the synthesis of acrylo-,[5] methacrylo-[6] and crotonohydrazide[4] by the reaction of the corresponding esters with hydrazine hydrate. The structures of these hydrazides have seemed doubtful, however, so we attempted the synthesis of real hydrazides.

To accelerate the attack of hydrazine on the carbonyl carbon instead of on the α,β-double bond, the activated esters, which are usually used for the synthesis of peptides, seemed to be useful. We wish to report on the synthesis of α,β-unsaturated carboxylic hydrazides (X) by the reaction of activated esters (IX) with hydrazine hydrate.

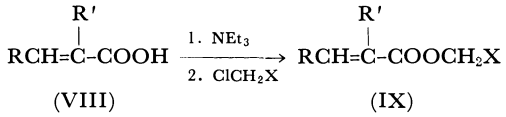

a: X=CN
b: X=OMe
c: X=COOMe
d: X=$C_6H_5NO_2$-(*p*)

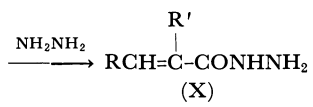

Table 1.* The reaction of hydrazine hydrate with methacrylate

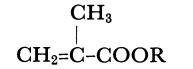

R	Yield of product (%)	
	Methacrylohydrazide	4-Methyl-3-pyrazolidone
$-CH_2CN$	83	0
$-CH_2OCH_3$	33	0
$-CH_2COOC_2H_5$	7	0
$-CH_2C_6H_4NO_2$-(*p*)	0	35

* The solvent was chloroform.

The reaction of hydrazine hydrate with several activated esters (IX) of methacrylic acid have been examined; the results are shown in Table 1.

Of these activated esters, cyanomethyl methacrylate gave the best results. The reaction was influenced by the solvents; when chloroform or methylene chloride was used as the solvent, methacrylohydrazide was obtained in 83% or 69% yield, respectively. In ethanol, however, 17% *N,N'*-dimethacroyl hydrazine, 28% 4-methyl-3-pyrazolidone, and no hydrazide were obtained.

In chloroform, cyanomethyl cinnamate gave 82% hydrazide, but under the same reaction conditions cyanomethyl acrylate and crotonate gave no hydrazides, but only 11% and 27% pyrazolidones, respectively.

For the sake of comparison with the activated ester methods, the mixed acid anhydride methods have been tried; in the case of methacrylic ethoxyformic anhydride, 72% hydrazide and 11% *N,N'*-dimethacroyl hydrazine were formed.

The methacrylohydrazide obtained above has a mp of 86—88°C and ν_{max}^{KBr} 3325, 3200, 1663, 1612, 1550, 890 cm^{-1}, and it is different from Shvaika's methacrylohydrazide (bp 140°C/11 mmHg,[6] ν_{max} 3300, 1670 cm^{-1}).

Several attempts to isolate acrylohydrazide prepared by the mixed acid anhydride method were unsuccessful because of its high polymerizability. The fairly-pure acrylohydrazide (yield 30%) isolated by silica-gel column chromatography was a viscous oil (ν_{max} 3250, 1660, 1610, 1545, 990, 910 cm^{-1}) and gave acrylic benzylidenehydrazide by the reaction with benzaldehyde.

The crotonohydrazide synthesized above has a mp of 87—89°C and ν_{max}^{KBr} 3300, 1664, 1615, 1550, 895 cm^{-1}, it is different from Muckerman's crotonohydrazide (bp 120°C/4 mmHg).[4]

The acrylo-, methacrylo-, and crotonohydrazide obtained above absorbed one mole of hydrogen and gave propiono-, isobutyro-, and *n*-butylohydrazide, respectively.

Experimental

Activated Esters of Methacrylic Acid. *a) Cyanomethyl Ester.* The ester was prepared according to the general procedure of Schwyzer.[7] Triethylammonium methacrylate (14.3 g) was reacted with chloroacetonitrile (6.8 g) in ethyl acetate. Yield, 73.2%; bp 48—49°C/2 mmHg.

4) E. Muckermann, *J. Pract. Chem.*, (2) **83**, 513 (1911); *Ber.*, **42**, 3449 (1909).
5) C. S. Rondestvedt, *J. Am. Chem. Soc.*, **77**, 6532 (1955).
6) O. P. Shvaika and Yu. I. Makarenks, *Zh. Obshch. Khim.*, **33**, 1233 (1963).
7) R. Schwyzer and B. Iselin, *Helv. Chim. Acta*, **38**, 69 (1955).

Found: C, 57.34; H, 5.87; N, 11.14%. Calcd for $C_6H_7O_2N$: C, 57.59; H, 5.64; N, 11.20%.

b) Ethoxycarbonylmethyl Ester. The ester was prepared from methacrylic acid, triethylamine, and ethyl chloroacetate according to the general method.[7] Yield, 59%; bp 67—68°C/0.8 mmHg.

Found: C, 55.67; H, 6.39%. Calcd for $C_9H_{12}O_4$: C, 55.80; H, 7.03%.

c) Methoxymethyl Ester. The ester was prepared from the acid, triethylamine, and chloromethyl methyl ether.[7] Yield, 62%; bp 70—71°C/40 mmHg.

Found: C, 55.65; H, 7.63%. Calcd for $C_6H_{10}O_3$: C, 55.40; H, 7.69%.

d) p-Nitrobenzyl Ester. The ester was prepared from the acid, triethylamine, and *p*-nitrobenzyl chloride.[8] Yield, 55%; mp. 82—84°C.

Found: C, 59.69; H, 4.97; N, 6.22%. Calcd for $C_{11}H_{11}O_4N$: C, 59.71; H, 5.01; N, 6.33%.

Methacrylohydrazide. *a) A Typical Activated-ester Method.* To a solution cyanomethyl methacrylate (3.75 g) in chloroform (100 cc), 80% hydrazine hydrate (3.0 g) was added. The solution was stirred for 2 hr at room temperature and then refluxed for 1 hr. After drying, the solvent was removed. The crystallization of the residue from ethanol-ether (1 : 1) gave colorless needles. Yield, 83%; mp 86—88°C.

Found: C, 47.85; H, 8.01; N, 27.95%. Calcd for $C_4H_8ON_2$: C, 47.98; H, 8.05; N, 27.98%.

Methacrylic benzylidenehydrazide was prepared according to the general method; mp 155—156°C, ν_{max}^{KBr} 3200, 1660, 1620, 1600, 1555 cm^{-1}.

Found: C, 69.86; H, 6.45; N, 14.82%. Calcd for $C_{11}H_{12}ON_2$: C, 70.18; H, 6.43; N, 14.88%.

Methacrylohydrazide in ethanol absorbed 1 mol of hydrogen at room temperature with a Raney nickel catalyst and afforded crystals (mp 103—104°C), just like the authentic isobutyrohydrazide.

When the reaction was carried out in ethanol, *N,N'*-dimethacroylhydrazine (yield, 17%; mp 136—137°C, ν_{max}^{KBr} 3250, 1665, 1615, 1560, 890 cm^{-1}, Found: C, 57.05; H, 7.61; N, 16.71%. Calcd for $C_6H_8O_2N_2$: C, 57.13; H, 7.19; N, 16.17%.) and 4-methyl-3-pyrazolidone (yield, 28%; 115°C/4 mmHg, ν_{max} 3300, 1670 cm^{-1}) were obtained after the reaction products had been purified by sillica-gel column chromatography.

b) Mixed Acid Anhydride Method. The hydrazide was synthesized according to the general procedure of Godtfredsen.[3] The mixed acid anhydride prepared from potassium methacrylate (13.8 g), pyridine (0.2 g), and ethyl chloroformate (12.0 g) in chloroform (100 cc) was added rapidly to a stirred, ice-cooled suspension of 80% hydrazine hydrate (10.0 g) in chloroform (100 cc). After standing at 0°C overnight, the solution was filtered. The filtrate was washed with a saturated sodium bicarbonate solution, and then dried. The solvent was removed, and the residue recrystallized from benzene. Yield, 72%; mp 86—88°C, which was identical with that of the product of Method a).

8) B. Iselin and R. Schwyzer, *ibid.*, **40**, 373 (1957).

Acrylohydrazide. *a) Mixed Acid Anhydride Method.* The mixed acid anhydride prepared from potassium acrylate (20.0 g), pyridine (0.5 g), and ethyl chloroformate (22.6 g) in methylene chloride (200 cc) was added to a stirred, ice-cooled suspension of 80% hydrazine hydrate (18.0 g) in methylene chloride (150 cc). After stirring for 30 min at 0°C, potassium chloride was filtered off. The filtrate was kept at 0°C overnight, and dried, and then the solvent was removed. The oily residue was purified by silica-gel column chromatography. From the chloroform-methanol (5%) eluted fractions, a colorless, viscous oil was obtained. Yield, 30%; ν_{max}^{KBr} 3250, 1670, 1620, 1550, 980 cm^{-1}.

Acrylic benzylidenehydrazide was prepared by the general method: Yield, 78%; mp 131—132°C.

Found: C, 68.68; H, 5.90; N, 16.27%. Calcd for $C_{10}H_{10}ON_2$: C, 68.95; H, 5.79; N, 16.08%.

Acrylohydrazide in ethanol absorbed 1 mol of hydrogen at room temperature with a Raney nickel catalyst; the product (mp 38—40°C) was identical with the authentic propionohydrazide.

b) Activated-ester Method. Cyanomethyl acrylate was prepared according to the general method. Yield, 71%; bp 66—68°C/6.5 mmHg.

Found: C, 54.22; H, 4.59; N, 12.55%. Calcd for $C_5H_5O_2N$: C, 54.05; H, 4.54; N, 12.61%.

80% Hydrazine hydrate (4.5 g) was added to a solution of the cyanomethyl ester (3.3 g) in chloroform (100 cc), and the solution was stirred for 2 hr at room temperature. After drying, the solvent was removed *in vacuo*.

The residue was purified by silica-gel chromatography. From the chloroform-methanol (5%) eluted fractions, an oily product (0.24 g, yield, 9.3%) was obtained, its IR spectrum (ν_{max}) 3300, 1670 cm^{-1}) was identical with that of the 3-pyrazolidone derivative.

Crotonohydrazide. Crotonohydrazide was prepared according to the general procedure of Godtfredsen.[3] Yield, 48%; mp 86—89°C, ν_{max}^{KBr} 3300, 1665, 1620, 1530, 960 cm^{-1}.

Found: C, 48.07; H, 8.02; N, 27.90%. Calcd for $C_4H_8ON_2$: C, 47.98; H, 8.05; N, 27.98%. The crotonic benzylidenehydrazide was prepared by the general method. Yield, 58%; mp 165—166°C.

Found: C, 69.91; H, 6.41; N, 14.83%. Calcd for $C_{11}H_{12}ON_2$: C, 70.18; H, 6.43; N, 14.88%.

Crotonohydrazide in ethanol absorbed 1 mol of hydrogen at room temperature in the presence of a Raney nickel catalyst. The product (mp 41—43°C) was identical with the authentic butyrohydrazide.

Cinnamohydrazide. Cyanomethyl cinnamate was prepared by the same procedure as cyanomethyl methacrylate. Yield, 79.0%; mp 62—63°C.

Found: C, 70.47; H, 4.86; N, 7.57%. Calcd for $C_{11}H_9O_2N$: C, 70.58; H, 4.85; N, 7.48%.

The reaction of cyanomethyl cinnamate with 80% hydrazine hydrate gave 82% of cinnamohydrazide, mp 116—117°C, which was identical with Godtfredsen's cinnamohydrazide (mp 117—117.5°C).[3]

Azirines. IV. The Photolysis of β-Azidovinyl Ketones*[1]

Shimao SATO

Kyorin Chemical Laboratory, Kyorin Pharmaceutical Co., Ltd., Ukima, Kita-ku, Tokyo

(Received February 15, 1968)

Although the pyrolysis[1] and photolysis[2-4] of vinyl azides as a method of preparing azirine have already reported on, there has been no report with regard to the photolysis of azidovinyl ketones. Therefore, we have been trying to obtain the functional derivatives of azirine by means of the photolysis of azidovinyl ketones. During the course of our work, Maiorana[5] reported the photolysis of azidovinyl phenyl ketone. Since, however, we tried the photolysis under slightly different conditions from his, we want here to report our results with this compound and with a cyclic azidovinyl ketone which has not hitherto been reported.

First, β-azidovinyl phenyl ketone[6] (I) was chosen as the azidovinyl ketone. The photolysis of I in benzene gave, with the evolution of nitrogen, benzoylacetonitrile (IV) in a 20% yield instead of 3-benzoylazirine (V). When the residual solution was treated with sodium methoxide, another crop of IV was obtained in a 17% yield. The formation of the second crop of IV may most reasonably be explained in terms of the alkaline hydrolysis of 5-phenylisoxazole (VI). The ready ring cleavage of isoxazoles unsubstituted at the 3-position with sodium methoxide has been known.[7] The results thus show that the nitrene II formed by the photolysis of I does not add to the double bond, but rather attacks the carbonyl group to give the VI or rearranges to the IV by the migration of a hydrogen atom, as is shown in the chart.

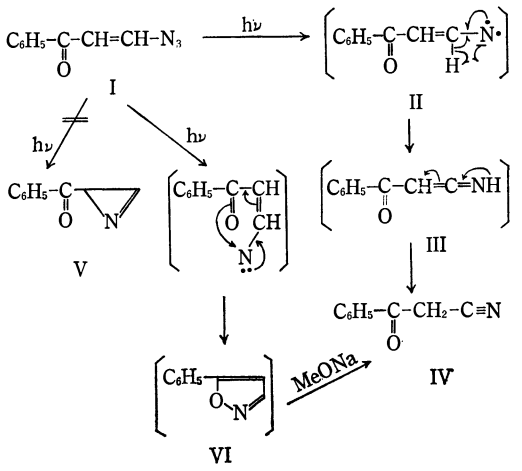

It is known[6] that β-azidovinyl ketones are decomposed on contact with acids to give substituted isoxazoles and nitriles, presumably through a vinyl nitrene intermediate.

When the photolysis of I was carried out in aqueous tetrahydrofuran instead of benzene in order to detect the III, Compound IV was obtained in a 27% yield instead of the desired benzoylacetamide. However, the v.p.c. analysis of the residual oil showed the presence of three other components (A, B and C). Component A was identified as methyl benzoate by a comparison of their v.p.c. retention times and infrared absorption spectra. The mechanism of the formation of this compound is not clear. The structure of Component B has not yet been elucidated, but it may be presumed to be a carbonyl compound because its IR spectrum exhibits a band at 1690 cm^{-1}. Component C was solidified on cooling, mp 31—33°C; the infrared spectrum of this compound has no characteric absorption bands except for that of phenyl group. These spectral data and the melting point suggest that it may be presumed to be a 5-phenyloxazole or its isomer.

Next, we attempted the irradiation of 5,5-dimethyl-3-azido-2-cyclohexene-1-one, prepared by the reaction of 5,5-dimethyl-3-chloro-2-cyclohexene-1-one and sodium azide, as a cyclic azidovinyl ketone, in benzene, but no nitrogen evolved. When this photolysis was carried out in aqueous tetrahydrofuran, the evolution of nitrogen was observed and colorless plates with a composition of $C_8H_{13}NO_2$ were obtained. This product was assigned as 6,6-dimethylhexahydroazepine-2,4-dione (XI) on the basis of the spectral data described below. The infrared spectrum of this compound exhibits bands at 3090 and 3200 cm^{-1} for the cyclic lactam NH group, 1710 cm^{-1} for the carbonyl group, and 1670 cm^{-1} for the amido-carbonyl group. The NMR spectrum shows a singlet at

*1 Part III. S. Sato, This Bulletin, **41**, 1440 (1968).

1) G. Smolinsky, *J. Org. Chem.*, **27**, 3557 (1962).
2) L. Horner, A. Christman and A. Gross, *Chem. Ber.*, **96**, 399 (1963).
3) A. Hassner and F. W. Fowler, *Tetrahedron Letters*, **1967**, 1545.
4) F. W. Fowler, A. Hassner and L. A. Levy, *J. Am. Chem. Soc.*, **89**, 2077 (1967).
5) Maiorana, *Ann. Chim.*, (Rome) **56**, 1531 (1966); *Chem. Abstr.*, **67**, 32420 (1967).
6) A. N. Nesmeyanov and M. I. Rybinskaya, *Izv. Akad. Nauk. SSSR, Otd. Khim. Nauk.*, 816 (1962); *Chem. Abstr.*, **58**, 3408 (1963).
7) L. Claisen and R. Sock, *Ber.*, **24**, 130 (1891).

τ 9.1 (6H) for the *gem*-dimethyl group, a singlet at τ 7.6 (2H) for the methylene on the 5-position of the ring, a multiplet at τ 6.8—6.9 (2H) for the methylene on the 7-position of the ring, a singlet at τ 6.6 (2H) for the methylene on the 3-position of the ring, and a multiplet at τ 2.0 (1H for the hydrogen on the nitrogen.

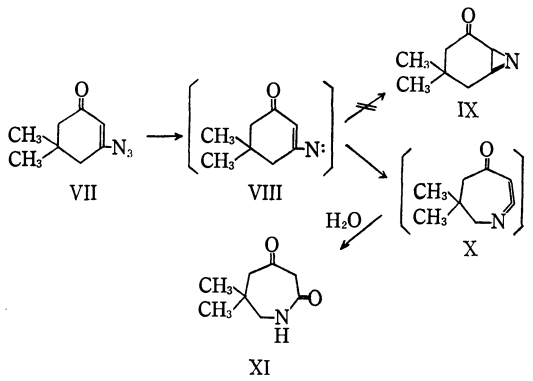

These results show that the migration of the methylene group to the nitrene occurs, giving a cyclic seven-membered keteneimine X, in preference to the intramolecular addition of the nitrene, giving condensed azirine IX.

Experimental

All the melting points were determined on a micro hot stage and are not corrected. The infrared spectra were taken on KBr tablets or neat liquid films.

Photolysis of β-azidovinyl Phenyl Ketone. a) A solution of 3.4 g (0.02 mol) of β-azidovinyl phenyl ketone[6] in 100 m*l* of dry benzene was irradiated through a Pyrex filter with a high-pressure mercury lamp under a nitrogen atmosphere for 20 hr, until nitrogen evolution ceased. The solution was then concentrated, and the residual oil was dissolved in ether and extracted with 10% sodium hydroxide, after which the extract was acidified with 10% hydrochloric acid. The solid which separated out was collected and recrystallized from water to give benzoylacetonitrile as colorless needles, mp 76—78°C (lit. 80.5°C).[8] (Found: C, 73.96; H, 4.88; N, 9.80%.) IR: 2200 (C≡N) and 1690 cm^{-1} (C=O). To the residual ethereal solution, a solution of excess sodium methoxide in 10 m*l* of methanol was added with cooling and stirring. The mixture was then stirred for one hour, after which 20 m*l* of water was added; the resulting mixture was washed with ether, and then the aqueous layer was acidified with 10% hydrochloric acid to give 0.3 g of colorless needles melting at 76—78°C. The melting point of this substance was undepressed on admixture with the benzoylacetonitrile obtained previously.

b) A solution of 2.2 g of I in 100 m*l* of tetrahydrofuran and 15 m*l* of water was irradiated through a Pyrex filter with a high-pressure mercury lamp under a nitrogen atmosphere for 16 hr, until nitrogen evolution ceased. When the solution was then treated by the method described above, 0.8 g of benzoylacetonitrile was obtained. The v.p.c. analysis of the residual oil showed the presence of three components; one of them was identified as methyl benzoate by a comparison of the retention times and the IR spectrum.

5,5-Dimethyl-3-azido-2-cyclohexene-1-one (VII). To a solution of 10 g (0.063 mol) of 5,5-dimethyl-3-chloro-2-cyclohexene-1-one[9] in 40 m*l* of methanol, a solution of 4.5 g (0.069 mol) of sodium azide in 70 m*l* of methanol and 5 m*l* of water was added with cooling and stirring. The mixture was then stirred for two hours at room temperature. To the reaction mixture, 100 m*l* of water was added, and the resulting mixture was extracted with ether; the extract was then washed thoroughly with water and dried over sodium sulfate. The solvent was removed by distillation; the IR spectrum of this residual oil exhibits a band at 2100 cm^{-1} for the azido group, 150 m*l* of tetrahydrofuran was added to the residue and the resulting solution was used for the photolysis without purification.

Photolysis of VII. To a solution of VII in THF, 30 m*l* of water was added. The mixture was irradiated with a high-pressure mercury lamp for 18 hr, until nitrogen evolution ceased. The solution was then concentrated by distillation under reduced pressure. The residual aqueous layer was washed with ether to remove any unreacted material, and then concentrated on a rotary evaporator. The solid which separated out was collected and recrystallized from *n*-pentane-ethanol to give 1 g of colorless plates, mp 148—149°C. Found: C, 61.91; H, 8.39; N, 8.92%. Mol wt, 142.8. Calcd for $C_8H_{13}NO_2$: C, 61.91; H, 8.44; N, 9.30%. Mol wt, 155.1.

The author wishes to express his deep gratitude to Professor M. Ohta and Dr. H. Kato, Tokyo Institute of Technology, for their advice and guidance on this study. Thanks are also due to Dr. S. Ogihara, President of Kyorin Pharmaceutical Co., Ltd., and Dr. T. Irikura, Director of Kyorin Chemical Laboratory, for their permission to publish this work.

8) A. Obregia, *Ann.*, **266**, 326 (1891).

9) A. W. Crossley and H. Lesueur, *J. Chem. Soc.*, **83**, 110 (1903).

The Stereochemistry of Tetralin-1-ols

Sekio MITSUI

Department of Applied Science, Faculty of Engineering, Tohoku University, Sendai

and Akira KASAHARA and Kaoru HANAYA

Department of Chemistry, Faculty of Science, Yamagata University, Koshirakawa-cho, Yamagata

(Received February 15, 1968)

Clark-Lewis *et al.*[1] and other authors[2] have studied the NMR spectra of the 4α- and 4β-hydroxyflavans and their relative configurations as deduced from the coupling constants. Inoue *et al.*[3] and Anjaneyulu *et al.*[4] have carried out similar investigations on isoflavanols.

Tetralin-1-ols are considered to have configurations similar to those of the corresponding hydroxyflavans. One of the present authors, Hanaya, obtained 3-phenyl-1-tetralol (Ia, Ib),[5] 3-methyl-1-tetralol (IIa, IIb),[5] 2-phenyl-1-tetralol (IIIa, IIIb)[6] and 2-methyl-1-tetralol (IVa, IVb)[7] by the reduction of the corresponding α-tetralones, as is show in Table 1; he tentatively assigned a *trans* configuration to Ia, IIa, IIIb, and IVb and a *cis* configuration to Ib, IIb, IIIa, and IVa,[5-7] on the basis of the mechanism of the reduction and their IR spectra.

TABLE 1

Compound		mp or bp
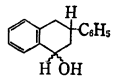	Ia	mp 100—101.5°C
	Ib	mp 96—98°C
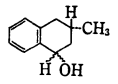	IIa	mp 96.5—98°C
	IIb	mp 113—115°C
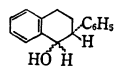	IIIa	mp 66—68°C
	IIIb	mp 80—81°C
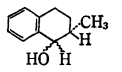	IVa	bp 109—113°C/7 mmHg
	IVb	mp 69—70°C

In order to confirm these assignments and to decide whether or not a relationship similar to those found in the case of the hydroxyflavans exists between the coupling constants and the configurations of the tetralin-1-ols, we investigated the NMR spectra of the tetralin-1-ols.

Already, Argabright *et al.*[8] have reported that IIb exhibits a triplet with $J_{1\cdot2}=3.2$ cps in the NMR spectrum and that the hydroxyl group must be axial, while IVb exhibits a doublet with $J_{1\cdot2}=7$ cps and both the hydroxyl and methyl groups must be of the equatorial conformation.

The experimental results are summarized in Table 2.

The hydroxyl group exists in the α-position to the phenyl or methyl group, and if it is assumed that the phenyl or methyl group is in the equatorial conformation on a half-chair ring, the Karplus relationship[9] predicts that $J_{1\cdot2}$ will be significantly smaller for 1,2-*cis* than for 1,2-*trans* isomers. In the NMR spectra of III, IV, and their acetates the $J_{1\cdot2}$ values of IIIb and IVb are larger than those of IIIa and IVa, respectively. Therefore, these results indicate that in IIIb and IVb the phenyl or methyl group is *trans* to the hydroxyl group, and in IIIa and IVa, *cis*. These findings are consistent with the assignment proposed in preceding papers.[6,7] On the other hand, when the hydroxyl group exists in the β-position to the phenyl or methyl group, the assignment based on the examination of the NMR spectra is contrary to the assignment made before.[5] In the NMR spectra of I, II, and their acetates, the signal of the 1H protons of Ib and IIb appears as a triplet, while the signal of the 1H protons of Ia and IIa appears as a double doublet. Consideration of the Karplus relationship[9] suggests that the 1H protons of Ib and IIb exist in a quasi-equatorial conformation, while the 1H protons of Ia and IIa exist in a quasi-axial conformation on a half-chair

1) J. W. Clark-Lewis, T. M. Spotswood and L. R. Williams, *Proc. Chem. Soc.*, 20 (1963); J. W. Clark-Lewis, T. M. Spotswood and L. R. Williams, *Aust. J. Chem.*, **16**, 107 (1963).

2) C. P. Lillya, D. Kehoe, E. M. Philbin, M. A. Vickars and T. S. Wheeler, *Chem. Ind.*, **1963**, 84; C. P. Lillya, S. E. Derwes and D. G. Roux, *ibid.*, **1963**, 783; H, G. Krishnamurty, T. R. Seshadri and D. G. Roux, *Tetrahedron Letters*, **1965**, 3689; B. G. Bolger, A. Hirwe, K. G. Marathe, E. M. Philbin, M. A. Vickars and C. P. Lillya, *Tetrahedron*, **22**, 621 (1966).

3) S. Yamaguchi, S. Ito, A. Nakamura and N. Inoue, This Bulletin, **38**, 2187 (1965).

4) A. S. R. Anjaneyulu, M. G. Rao, L. R. Row and C. S. Krishna, *Tetrahedron Letters*, **1966**, 3199.

5) K. Hanaya, *Nippon Kagaku Zasshi (J. Chem. Soc. Japan, Pure Chem. Sect.)*, **87**, 995 (1966).

6) K. Hanaya, *ibid.*, **87**, 745 (1966).

7) K. Hanaya, *ibid.*, **87**, 991 (1966).

8) D. A. Argabright, H. D. Rider and M. W. Hanna, *Tetrahedron*, **21**, 1931 (1965).

9) M. Karplus, C. F. Conroy, "Advances in Organic Chemistry," Vol. 2, Interscience, New York (1960), pp. 308—311.

TABLE 2. NMR SPECTRA OF TETRALIN-1-OLS AND THEIR ACETATES

Compound	Position of peaks (ppm)	No. of protons	Assignment	Remark
Ia	5.21	1	H	Double doublet $J_{1\cdot2}$=6.0 ; 11.0 cps
Acetate of Ia	1.90	3	$CH_3\cdot CO\cdot O$	Singlet
	5.98	1	H	Double doublet $J_{1\cdot2}$=6.5 ; 11.0 cps
Ib	5.13	1	H	Triplet, $J_{1\cdot2}$=3.0 cps
Acetate of Ib	1.82	3	$CH_3\cdot CO\cdot O$	Singlet
	5.93	1	H	Triplet, $J_{1\cdot2}$=3.5 cps
IIa	1.05	3	CH_3	Doublet, J=6.0 cps
	4.64	1	H	Double doublet $J_{1\cdot2}$=6.0 ; 11.0 cps
Acetate of IIa	1.04	3	CH_3	Doublet, J=6.0 cps
	2.07	3	$CH_3\cdot CO\cdot O$	Singlet
	6.0	1	H	Double doublet $J_{1\cdot2}$=6.0 ; 10.5 cps
IIb	1.07	3	CH_3	Doublet, J=6.0 cps
	4.63	1	H	Triplet, $J_{1\cdot2}$=3.0 cps
Acetate of IIb	1.06	3	CH_3	Doublet, J=5.6 cps
	1.98	3	$CH_3\cdot CO\cdot O$	Singlet
	6.01	1	H	Triplet, $J_{1\cdot2}$=3.0 cps
Acetate of IIIa	1.65	3	$CH_3\cdot CO\cdot O$	Singlet
	6.08	1	H	Doublet, $J_{1\cdot2}$=3.5 cps
Acetate of IIIb	1.83	3	$CH_3\cdot CO\cdot O$	Singlet
	6.18	1	H	Doublet, $J_{1\cdot2}$=8.0 cps
IVa	1.12	3	CH_3	Doublet, J=6.0 cps
	4.51	1	H	Doublet, $J_{1\cdot2}$=3.0 cps
Acetate of IVa	1.00	3	CH_3	Doublet, J=6.0 cps
	1.95	3	$CH_3\cdot CO\cdot O$	Singlet
	5.92	1	H	Doublet, $J_{1\cdot2}$=3.0 cps
IVb	1.08	3	CH_3	Doublet, J=6.0 cps
	4.25	1	H	Doublet, $J_{1\cdot2}$=6.0 cps
Acetate of IVb	1.02	3	CH_3	Doublet, J=6.2 cps
	2.08	3	$CH_3\cdot CO\cdot O$	Singlet
	5.75	1	H	Doublet, $J_{1\cdot2}$=6.5 cps

ring. The conformations of the phenyl or methyl group in the 3-position of I and II are assumed to be equatorial, as usual. Therefore, these results indicate that Ib and IIb have a *trans* relation between the phenyl or methyl group and the hydroxyl group, and that Ia and IIa have a *cis* relation.

From the above findings, the relationship between the 1,2-coupling constants and the configurations which was observed with tetralin-1-ols is similar to that seen in the case of the hydroxyflavans. Therefore, it may be concluded that the configuration of the tetralin-1-ols can be assigned on the basis of the coupling constant of the 1- and 2-protons. When the hydroxyl group exists in the β-position to the phenyl or methyl group, as has been mentioned before, the assignment based on the examination of the NMR spectra is contrary to that made on the basis of the mechanism of the reduction. This problem will be discussed in more detail later.

Experimental

Samples. The tetralin-1-ols were prepared according to the method previously reported.[5-7] The acetates of the tetralin-1-ols were prepared by the acetylation of the corresponding tetralin-1-ols with acetic anhydride and pyridine at room temperature overnight. The crystal products were purified by recrystallization, while the oily products were checked by a study of their IR spectra and VPC.

The acetate of Ia, mp 74.5—76.5°C.

Found: C, 80.88; H, 6.91%. Calcd for $C_{18}H_{18}O_2$: C, 81.17; H, 6.81%.

The acetate of IIIa, mp 102—103°C.

Found: C, 81.49; H, 6.56%. Calcd for $C_{18}H_{18}O_2$: C, 81.17; H, 6.81%.
The acetate of IIIb, mp 112—113°C.

Found: C, 80.87; H, 7.15%. Calcd for $C_{18}H_{18}O_2$: C, 81.17; H, 6.81%.

NMR Measurements. The NMR spectra were measured at 60 MHz on a Varian A-60 spectrometer. The sample was dissolved in $CDCl_3$, containing TMS as the internal reference.

The authors wish to express their gratitude to Dr. Hiizu Iwamura, The University of Tokyo, and Dr. Yasuhisa Senda, Tohoku University, for their useful advice.

A Kinetic Study of the Hydrogenation of Mesityl Oxide over Unpoisoned and Poisoned Raney Nickel Catalysts. Temperature Variation of the Reaction Order

Sanae KISHIDA and Shiichiro TERANISHI

Department of Chemical Engineering, Faculty of Engineering Science, Osaka University, Machikaneyama, Toyonaka, Osaka

(Received February 17, 1968)

The kinetics of the liquid-phase hydrogenation of acetone in *n*-hexane over a Raney nickel catalyst, and of various ketones in cyclohexane over a nickel boride catalyst, have been successfully interpreted by a simplified Langmuir-type rate equation,[1]

$$v = kaC_R/(1+aC_R)^2, \quad (1)$$

where C_R represents the concentration of the reactant to be hydrogenated and where a has the form:

$$a = a_0 \exp(-\delta\Delta G/\boldsymbol{RT}), \quad (2)$$

where $\delta\Delta G$ is the difference between the free energies of the adsorption of the reactant and hydrogen and where a_0 is a constant which is independent of the temperature.

The rate equation has been derived on the following assumptions:

i) Hydrogen and the reactant adsorb reversibly and compete for the same surface sites, whence the ratio of the fractional surface coverage of the reactant(ϑ_R) to that of hydrogen(ϑ_H) is given by[2]:

$$\vartheta_R/\vartheta_H = aC_R \quad (3)$$

The liquid-phase concentration of hydrogen is considered to be independent of the temperature and is included in the a_0 constant.

ii) The surface of the catalyst is fully covered by the adsorbed species of the reactant and hydrogen during the reaction:

$$\vartheta_R + \vartheta_H = 1 \quad (4)$$

iii) The rate-determining step is the surface reaction:

$$v = k\vartheta_R \cdot \vartheta_H \quad (5)$$

where k is the rate constant of the surface reaction.

In this paper the rates of the liquid-phase hydrogenation of the carbon-carbon double bond of mesityl oxide have been measured over a wide range of temperature, and the kinetics of the reaction have been interpreted by Eq. (1).

The rate over the catalyst poisoned by potassium iodide has also been measured, and the kinetics over unpoisoned and poisoned catalysts have been compared. It has been found that the thermodynamic parameter in the rate equation, a, as well as the rate constant decreases as a result of the poisoning.

Experimental

The preparation of the catalyst, the apparatus, and the procedure for the rate measurements were as previously reported.[1]

To poison the catalyst by KI, the sample prepared was added to 10 cc of a KI solution, the concentration of which was 1.07 mol/*l*, and stirred for 10 min. The sample was then washed with water by decantation until no trace of KI was detected. The amount of KI adsorbed on the catalyst by such a treatment was found to be 0.169 mmol/g-Ni.

The analysis by gas chromatography certified that the product of the initial state of the reaction was only isobutyl methyl ketone, the further hydrogenation of which did not proceed until mesityl oxide had been completely hydrogenated. The reaction in this paper is, therefore, concerned with the hydrogenation of the C=C of mesityl oxide.

Results and Discussion

The rate of the hydrogenation of mesityl oxide was found to decrease with an increase in the concentration. The results of the rate measurement

1) S. Kishida, S. Kajimoto and S. Teranishi, *Shokubai (Catalyst)*, **9**, 58 (1967); Y. Murakami, S. Kishida, T. Imanaka and S. Teranishi, *ibid.*, **9**, 61 (1967).

2) G. C. Bond, "Catalysis by Metals," Academic Press, London and New York (1962), p. 124.

at −10°C, −35°C, −50°C, and −78°C are shown in Fig. 1. The peak of the rate expected from

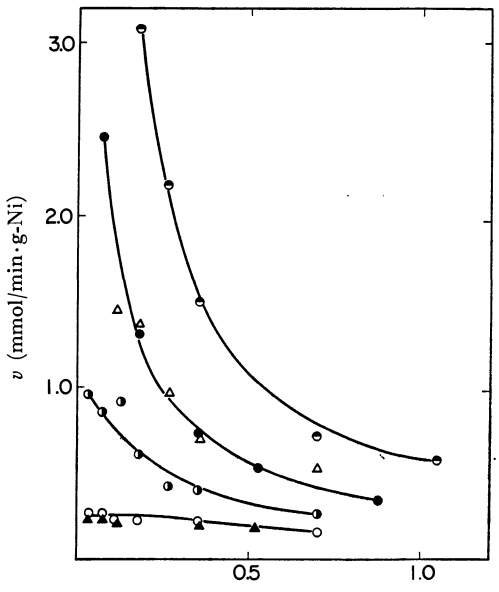

Fig. 1. Hydrogenation of mesityl oxide in *n*-hexane.
i) on unpoisoned Raney nickel catalyst
◓, −10°C; ●, −35°C; ◑, −50°C; ○, −78°C
ii) on poisoned catalyst
△, −10°C; ▲, −35°C

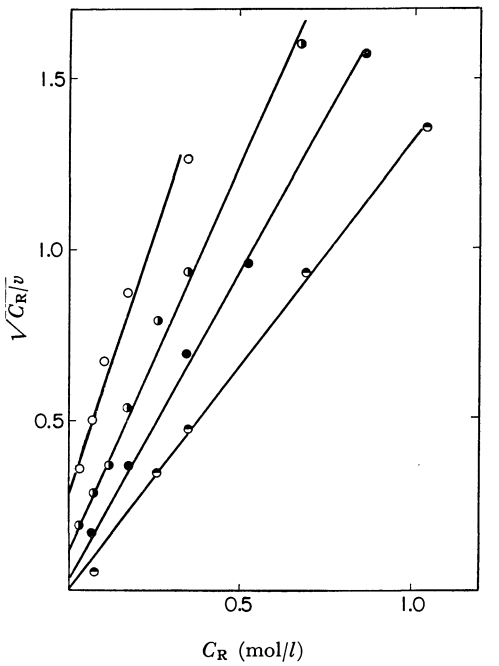

Fig. 2. $\sqrt{C_R/v}$-C_R plots for unpoisoned catalyst.
◓, −10°C; ●, −35°C; ◑, −50°C; ○, −78°C.

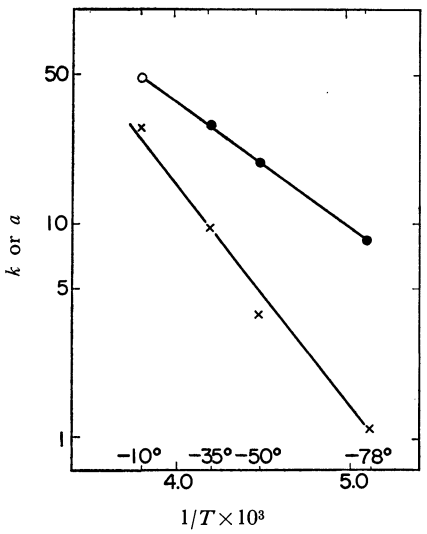

Fig. 3. Arrhenius plot (×) and log a - $1/T$ plot (●) for unpoisoned catalyst.

Eq. (1) could not be observed, indicating that a is so large that the peak exists in a lower concentration range than the experimental one.

Since Eq. (1) can be rearranged as:

$$\sqrt{C_R/v} = \sqrt{1/a\cdot k} + \sqrt{a/k}\cdot C_R \qquad (6)$$

the plot of $\sqrt{C_R/v}$ *vs.* C_R gives a straight line. Figure 2 shows the plots, from which the rate constant and the adsorption parameter, a, can be evaluated at each temperature. However, k and a at −10°C can not be evaluated from the plot, since the plot at −10°C passes through the point of origin. It is obvious from Eq. (6) that the intersect (or the slope) of the plot becomes near zero when a is too large (or too small), and that, in these cases, it is not possible to determine k and a separately. Therefore, a at −10°C was determined by extrapolating the plot of log a *vs.* $1/T$ (see the open circle in Fig. 3), and k at −10°C was then evaluated from the slope of the plot of $\sqrt{C_R/v}$ *vs.* C_R.

The rate constants and the adsorption parameters are listed in Table 1. The a increases as the reaction temperature rises, indicating that $\delta\Delta G$ is positive and that the adsorption of hydrogen is stronger than that of mesityl oxide.

The reaction orders with respect to mesityl oxide at each temperature, as evaluated from the plot of log v *vs.* log C_R, are also listed in Table 1. The order with respect to mesityl oxide becomes lower as the reaction temperature rises.

Since Eq. (1) predicts that the reaction order with respect to the reactant is −1 when $a\cdot C_R \gg 1$ and 1 when $a\cdot C_R \ll 1$, the reaction order determined over the limited concentration range becomes higher as the a value decreases. Therefore, the temperature variation of the reaction order depends

TABLE 1. TEMPERATURE VARIATIONS OF k, a AND REACTION ORDER OF HYDROGENATION OF MESITYL OXIDE

Temperature (°C)	k (mmol/min·g-Ni)	a (l/mol)	Order of reaction
−78	1.11	8.53	−0.15
−50	3.81	19.7	−0.60
−35	9.60	29.0	−0.75
−10	(27.9)	(48.0)	−1.0
Temperature coefficient (kcal/mol)	4.35	2.63	

on that of a. When $\delta\Delta G$ is positive (or negative), the reaction order becomes higher (or lower) with a decrease in the temperature.

It can, therefore, be said that the temperature variation of the reaction order with respect to the A, for example, of a heterogeneous catalytic reaction between A and B, tells us whether the adsorption of A or that of B is stronger.

The rate data measured over the poisoned catalyst at −10°C and −35°C are shown by, respectively, the open and filled triangles in Fig. 1. It was observed that k and a become smaller by the poisoning. This indicates that the adsorption of mesityl oxide is more inhibited by the poisoning than that of hydrogen.

It has been reported by the present authors that, for the liquid-phase hydrogenation of isobutyl methyl ketone and mesityl oxide over a Raney nickel catalyst,[3] the fractional surface coverage of hydrogen in course of the reaction (ϑ_H) is increased by the poisoning. This phenomenon has been interpreted as evidence that the adsorption strength of the reactant is decreased more than that of hydrogen by the poisoning.

Since ϑ_H is given by Eq. (7):

$$\vartheta_H = 1/(1+a\cdot C_R) \tag{7}$$

the ϑ_H measured at the same concentration of the reactant increases with a decrease in the a.

The poisoning effect on kinetics has scarcely been considered in the literature.[4] This phenomenon appears important, however, and has to be taken into account in discussing the mechanism of the poisoning.

3) S. Kishida, Y. Tanaka and S. Teranishi, *Nippon Kagaku Zasshi (J. Chem. Soc. Japan, Pure Chem. Sect.)*, **89**, 271 (1968).

4) I. Matsuzaki, T. Nakajima and A. Tada, *J. Res. Inet. Catalysis, Hokkaido Univ.*, **13**, 187 (1966); I. Matsuzaki, A. Tada and T. Nakajima, *Shokubai (Catalyst)*, **8**, 5 (1966).

Cyclization of Citronellal to Isopulegol by Cu-Cr and Cu-Cr-Mn Catalysts

Kunio KOGAMI and Ju KUMANOTANI

The Engineering Research Institute, Faculty of Engineering, The University of Tokyo, Yayoi, Tokyo

(Received February 23, 1968)

Isopulegol is usually prepared by heating[1] citronellal with or without silica gel,[2] active carbon,[3] or boric acid.[4]

In their studies of the catalytic dehydrogenation of geraniol, the present authors found that Cu-Cr-Mn also catalyzes the cyclization of citronellal to isopulegol. In this paper, the results of the catalysis of Raney Nickel, Ni-diatomaceous earth, Cu-Cr, and Cu-Cr-Mn, and the effect of the hydrogen treatment of the catalysts on the cyclization, will be presented. Cu-Cr and Cu-Cr-Mn, without any hydrogen treatment, were found to be good catalysts for this reaction.

Experimental

Materials. Citronellal was prepared from citronellal oil (made in Formosa) by the known method.[5] The catalysts used here were supplied by the Nikki Chem. Co., Ltd. Raney Nickel was pretreated with alkali. Cu-Cr N202, Cu-Cr-Mn N203, and Nickel-diatomaceous earth N111, treated or untreated, were used.

The Procedure of the Cyclization of Citronellal. In the case of a catalyst pretreated with hydrogen, a 0.5 g portion of it placed at the bottom of a 300 m*l* flask equipped with an air-tight stirrer, a reflux condenser, a gas outlet tube with a rubber stopper, and a

1) V. Grignard and J. Doeuvre, *Compt. rend.*, **190**, 1164 (1930).
2) H. B. Glass, U. S. Pat. 2117414 (1936).
3) S. Kimura, *Mem. Coll. Sci. Kyoto. Imp. Univ.*, **10**, 330 (1935).
4) S. Katsura, O. Okuda and A. Komatsu, Japanese Pat. 8875 (1957).
5) A. Lewinson, *Perfumery and Essential Oil Record*, **14**, 360 (1923).

two-necked glass tube with a thermometer, and then a glass inlet-tube reaching to the bottom of the flask was fitted on. The flask was immersed in an oil bath at 150—170°C. The hydrogen was passed through the catalyst at a rate of 200 ml/min for 1.5 hr, and then it was replaced by nitrogen at the same flow rate for 0.5 hr. Then citronellal (50 g, 0.23 m) was put into the flask, and the flask was kept at 160—200(±1)°C with stirring under a nitrogen flow. In a case without a catalyst or with a catalyst not treated with hydrogen, citronellal was put into a flask which had previously been filled with nitrogen, and the flask was kept at 205°C by means of an oil bath and allowed to react much as has been described above for 5 to 7 hr under a nitrogen atmosphere.

When the reaction was complete, the reacting mixture was cooled to room temperature, and 150 ml of ether was added to it. After the catalyst had been removed by filtration, the ethereal solution was washed with an aqueous solution of sodium carbonate, and then with water, and dehydrated over sodium sulfate. After evaporation, an oily product was obtained.

Determination of the Composition of the Product by Gas Chromatography. Each sample (0.05 ml) was taken by a mycrosyringe from the reactor through the rubber stopper and analyzed by a gas chromatograph, Kotaki GU-21, under the following conditions: column temperature, 150°C; split temperature 250°C; carrier gas, helium; inlet pressure, 0.8 kg/cm^2; flow rate, 26 ml/min; sensitivity, 8 mV; chart speed, 0.5 cm/min. The column was of stainless steel and was 3 mm in diameter and 3 m long, packed with Diabase A, 80—60 mesh, coated by an acetone solution of Hyprose SP 80. The accuracy of the analysis was estimated to be ±1% (the product obtained at 200°C for 5 to 7 hr was analyzed for the fraction; bp 72—110°C/4 mmHg).

The standard materials used for the analysis were: (1) citronellal (the same as the starting material); (2) citronellol (from the ABRAC Co., Ltd.; bp 100°C/6 mmHg, n_D^{30} 1.4639, d_{30}^{30} 0.8572); (3) isopulegol (from Tokyo Kasei, Inc.); a mixture of 20% neo-isopulegol; 75% isopulegol; and 5% iso-isopulegol (by gas chromatographic analysis; bp 74—78°C/6 mmHg, n_D^{30} 1.4679), and (4) pulegone (from Tokyo Kasei, Inc.; bp 98°C 6 mmHg, n_D^{30} 1.4880, d_{30}^{30} 0.9731, $[\alpha]_D^{25}$ +20°).

Separation of Isopulegol. The cyclization product (154 g) which was obtained under the conditions (Run 4) shown in Table 1 was treated with 400 ml of a 35% sodium hydrogen sulfite solution at 40°C for 3 hr. The reaction mixture was then cooled to room temperature and extracted with 300 ml of benzene. The benzene layer was washed with an aqueous sodium carbonate solution and with water, and then dried over sodium sulfate. Upon the removal of the benzene, the oily product was distilled *in vacuo* to give a fraction of bp 72—90°C/4 mmHg (124 g), together with the residue (9.2 g); the former was found to be a mixture of 1.8% pulegone and 98.2% isopulegol isomers (20.2% neo-iso, 70% iso, and 8.0% iso-isopulegol); while the latter exhibited no peak in its gas chromatogram. From the aqueous sodium hydrogen sulfite solution, 12 g of citronellal used recovered.

Results and Discussion

The results obtained at 200°C are given in Table 1. Table 1 shows that, among the catalysts used here, Raney Nickel and Ni-diatomaceous earth were ineffective. The Cu-Cr and Cu-Cr-Mn catalysts, without hydrogen treatment, gave higher cyclization yields. The latter catalyst (Run 4) was most useful; the yield with it was 80% of the theoretical value. Using the Cu-Cr-Mn catalyst, further studies were then undertaken at 160°C, 180°C, and 200(±1)°C. Figure 1 and Table 2 show some of these results. In Table 2, the results obtained without a catalyst are also given. From these results, the rate of reaction was found to be first order with respect to the concentration of citronellal (see Table 2). The activation energies for the catalytic and non-catalytic reactions were

Table 1. Catalyzed and thermal cyclization of citronellal

Run	Catalyst: Amount (wt% of citronellal)	Catalyst: Treatment with H_2	Reaction temperature °C	Reaction time hr	Conversion of citronellal into each product (% theor.): Citronellal	Unknown	Neo-isopulegol	Iso pulegole	Iso-isopulegol	Pulegone	Citronellal	Distillation residue	Cyclization* yield, %
1	Cu-Cr 0.5	+	200	5	12.5	1.8	15.3	48.9	6.2	3.7	3.6	4.4	74
2	Cu-Cr-Mn 0.5	+	200	6	9.0	4.7	14.2	49.4	6.5	4.3	3.9	4.0	74
3	Cu-Cr 1.0	−	200	6	11.7	0	16.6	52.7	6.3	2.7	0	5.9	78
4	Cu-Cr-Mn 1.0	−	200	7	9.3	0	16.3	56.0	6.3	1.4	0	5.9	80
5	Ni-Diatomaceous earth 0.5	+	200—205	5	16.7	0	14.1	46.0	5.7	2.8	2.6	8.5	69
6	Raney Ni 0.5		200—205	6	7.1	1.2	13.5	50.8	5.5	4.3	5.6	7.9	72
7	None		200	6	13.5	2.6	17.8	48.3	4.8	0	0	9.6	71

* Cyclization yield; a combined yield (%) of isopulegol isomers and pulegone.

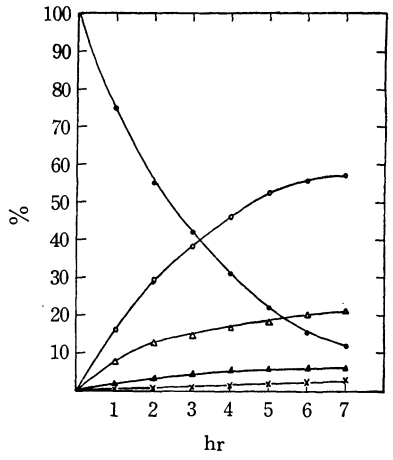

Fig. 1. The composition of reacting mixture *vs.* reaction time, using Cu-Cr-Mn catalyst (1 wt%) without H_2 pretreatment; reaction temperature 200°C; ● citronellal, ○ isopulegol, △ neo-isopulegol, ▲ iso-isopulegol, × pulegone.

estimated to be 17.2 kcal/mol and 20.4 kcal/mol, respectively.

Table 2. Rate constant K and activation energy E

Reaction temperature °C	K*, $sec^{-1} \times 10^5$	
	Cu-Cr-Mn (1% by weight) without H_2 treatment	Thermal reaction without catalyst
200	10.3	8.14
180	4.01	3.41
160	1.37	1.19
Activation energy obtained from Arhenius plots E	17.2 kcal/mol	20.4 kcal/mol

* $K = 1/t \cdot \log(100/(100-X))$
X: Weight percent of remaining citronellal

It has become obvious that the Cu-Cr and Cu-Cr-Mn catalysts without hydrogen treatment have a catalytic activity for the cyclization. The reaction process with the Cu-Cr-Mn catalyst without hydrogen treatment may proceed according to the thermal isomerization mechanism already proposed by Ohloff.[6]

6) G. Ohloff, *Tetrahedron Letters*, **1960**, No. 11, 11—14 (1960).

Oxidation of Dihydrothiophenes with Iodosobenzene*[1]

Takao TAKAYA, Satoru HIJIKATA and Eiji IMOTO

Department of Applied Chemistry, School of Engineering, University of Osaka Prefecture, Sakai-shi, Osaka

(Received February 26, 1968)

In a previous paper,[1] we have reported that the oxidation of 3,4-disubstituted 2,5- and 4,5-dihydrothiophenes with 30% hydrogen peroxide in acetic acid or with perbenzoic acid in chloroform gives the following results: 1) when both of the two substituents attached to the 3- and 4- positions are electron-withdrawing, oxidation with 30% hydrogen peroxide in acetic acid tends to produce the corresponding thiophene derivatives; 2) when one of two substituents is electron-withdrawing and the other is electron-releasing, the oxidation tends to produce the corresponding sulfone derivatives, and 3) the oxidation of 2,5- and 4,5-dihydrothiophenes with perbenzoic acid in chloroform produces mainly the corresponding sulfone derivatives.

In this paper, we will report that the oxidation of 3,4-disubstituted 2,5- and 4,5-dihydrothiophenes with iodosobenzene in dioxane gives the corresponding thiophene derivatives (III) without any dependence on the nature of the substituent, as is shown in Table 1. This finding is in contrast with that concerning the oxidation with 30% hydrogen peroxide in acetic acid or with perbenzoic acid in chloroform.

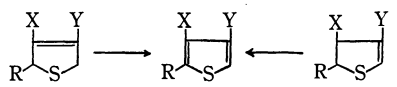

I II III

A probable mechanism for the formation of the thiophene, III, is as follows: the 3,4-disubstituted dihydrothiophenes, I or II, are oxidized by iodosobenzene[2] to the corresponding sulfoxide derivatives, which are then dehydrated to the thiophene derivatives, III.

*1 Studies of the Syntheses of Heterocyclic Compounds. Part IX.

1) Part VIII: T. Takaya, S. Kosaka, Y. Otsuji and E. Imoto, This Bulletin, **41**, 2086 (1968).

2) a) A. H. Ford-Moore (*J. Chem. Soc.*, **1949**, 2126) has reported that iodosobenzene is a reagent for the oxidation of sulfides to sulfoxides without further oxidation to sulfones. b) For the method of preparation, see H. J. Lucas, E. R. Kennedy and M. W. Formo, "Organic Syntheses," Coll. Vol. III, p. 483 (1955).

TABLE 1. OXIDATION PRODUCTS OF DIHYDROTHIOPHENES WITH IODOSOBENZENE

III

Starting materials	Substituents X	Y	R	Products	Yields (%)
Ia_1	CO_2H	CO_2H	H	$IIIa_1$	89
Ia_2	CO_2H	CO_2H	CH_3	$IIIa_2$	80
Ib_1	$CO_2C_2H_5$	CN	H	$IIIb_1$	81
Ib_2	$CO_2C_2H_5$	CN	CH_3	$IIIb_2$	81
Id_1	$CO_2C_2H_5$	$NHCONH_2$	H	$IIId_1$	61
Id_2	$CO_2C_2H_5$	$NHCONH_2$	CH_3	$IIId_2$	53
Ie_1	$CO_2C_2H_5$	$NHCO_2C_2H_5$	H	$IIIe_1$	72
Ie_2	$CO_2C_2H_5$	$NHCO_2C_2H_5$	CH_3	$IIIe_2$	73
If_1	$CO_2C_2H_5$	OCH_3	H	$IIIf_1$	54
IIa_1	CO_2H	CO_2H	H	$IIIa_1$	94
IIa_2	CO_2H	CO_2H	CH_3	$IIIa_2$	76

TABLE 2. PHYSICAL PROPERTIES AND ANALYTICAL DATA FOR THE THIOPHENES III

Compound	Mp (Bp, °C/mmHg)*1	Recryst. Solvent	Formula		Analysis C	H	N
$IIId_1$	171—172	Ethyl acetate	$C_8H_{10}O_3N_2S$	Found	44.95	4.67	12.76
				Calcd	44.86	4.71	13.08
$IIId_2$	185—186	Ethyl acetate	$C_9H_{12}O_3N_2S$	Found	47.32	5.55	12.01
				Calcd	47.37	5.30	12.28
$IIIe_1$	34—35 (114—115/0.1)	*n*-Hexane	$C_{10}H_{13}O_4NS$	Found	49.61	5.34	5.82
				Calcd	49.38	5.39	5.76
$IIIe_2$	78—79	Methanol-water	$C_{11}H_{15}O_4NS$	Found	51.21	5.78	5.37
				Calcd	51.36	5.88	5.45
$IIIf_1$	(73—75/0.2)		$C_8H_{10}O_3S$	Found	51.80	5.37	
				Calcd	51.61	5.41	
IV*2	141—143	Benzene	$C_6H_2O_3S$	Found	46.53	1.60	
				Calcd	46.77	1.31	
V	108—110	Benzene	$C_7H_6O_4S$	Found	44.96	3.30	
				Calcd	45.17	3.25	

*1 All melting and boiling points are uncorrected.
*2 Mp 145—146.[5]

The other interesting fact is that the reaction of 3,4-dimethoxycarbonyl-2,5- and 4,5-dihydrothiophene (Ic_1 and IIc_1) with iodosobenzene afforded thiophene-3,4-dicarboxylic acid anhydride (IV) and 3-carboxy-4-methoxycarbonylthiophene (V) as by-products in addition to the main product, 3,4-dicarbomethoxythiophene ($IIIc_1$). When Ic_1 was treated in dry toluene with iodosobenzene using a 1 : 1 ratio, two products, $IIIc_1$ and V, were isolated, in 81 and 14% yields respectively. The similar treatment of IIc_1 gave $IIIc_1$ (73%) and V (11%). When a 1 : 2 ratio of Ic_1 or IIc_1 to iodosobenzene was used in dry dioxane; a mixture of $IIIc_1$ and IV was obtained, along with a trace of V. The approximate ratio[3] of the mixture of $IIIc_1$ and IV was in a range from 8 : 2 to 9 : 1. Neither IV nor V was obtained in

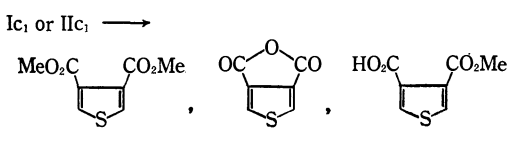

$IIIc_1$ IV V

3) The approximate molar ratio of the two derivatives in the mixture was estimated by comparing the infrared spectra of the reaction mixture with those of a mixture of the authentic samples, $IIIc_1$ and IV, the relative concentrations of $IIIc_1$ and IV being varied correspondingly.

the reaction of $IIIc_1$ with iodosobenzene.

All the starting materials, 3,4-disubstituted 2,5- or 4,5-dihydrothiophenes, I or II, and the authentic samples, $IIIa_1$, $IIIa_2$, $IIIb_1$, $IIIb_2$ and $IIIc_1$, were prepared according to the methods described in the previous paper.[1]

Experimental

A General Procedure for the Oxidation of I and II by Iodosobenzene. A mixture of the 3,4-disubstituted dihydrothiophene, I or II (10 mmol), and iodosobenzene (11 mmol) in dry dioxane (30 m*l*) was refluxed for 12 hr in a stream of nitrogen gas. After the solvent and iodobenzene had then been removed *in vacuo*, the residue was distilled under reduced pressure or recrystallized from an appropriate solvent to give the corresponding thiophene, III, whose properties were identical in every respect with those of the authentic sample.

Reaction of 3,4-Dimethoxycarbonyl-2,5- and 4,5-dihydrothiophene, Ic_1 and IIc_1. *In Toluene.* A solution of 1.01 g (5 mmol) of IIc_1 and 1.21 g (5.5 mmol) of iodosobenzene in 20 m*l* of dry toluene was gently refluxed for 6 hr in a stream of nitrogen gas. After the solvent and iodobenzene had then been carefully removed *in vacuo*, the residue was distilled to give 0.81 g (81%) of $IIIc_1$, bp 125—127°C/3 mmHg. After the distillation of the $IIIc_1$, the residue was sublimed under a pressure of 0.2 mmHg at the bath temperature of 120°C to give 0.31 g (14%) of V, mp 105—109°C.

In a similar manner, 0.73 g (73%) of $IIIc_1$ and 0.10 g (11%) of V were obtained from 1.01 g of Ic_1 and 1.21 g of iodosobenzene.

In Dioxane. A solution of 3.06 g (15 mmol) of IIc_1 and 6.6 g (30 mmol) of iodosobenzene in dry dioxane (60 m*l*) was refluxed for 12 hr in a nitrogen stream. After the evaporation of the solvent and iodobenzene, the residue was distilled at 80—100°C/0.2 mmHg to give a mixture (2.22 g) of $IIIc_1$ and IV. A trace of V was obtained by the sublimation of the residue remaining after the distillation of the above mixture.

In a similar manner, a mixture (2.0 g) of $IIIc_1$ and IV was obtained, along with a trace of V, from 3.02 g of Ic_1 and 6.6 g of iodosobenzene.

Preparation of the Authentic Samples of the Oxidation Products, $IIId_1$, $IIId_2$, $IIIe_1$, $IIIe_2$ and $IIIf_1$. The following procedure is representative of those used for the preparation of 3-ethoxycarbonyl-4-ureidothiophene ($IIId_1$) and 2-methyl-3-ethoxycarbonyl-4-ureidothiophene ($IIId_2$). A mixture of 3-ethoxycarbonyl-4-ureido-2,5-dihydrothiophene (Id_1, 10 mmol) and chloranil (11 mmol) was refluxed for 12 hr in dry toluene (20 m*l*). The reaction mixture was then cooled, washed with a dilute sodium hydroxide solution and with water, and then evaporated to dryness *in vacuo*. Several recrystallizations from ethyl acetate gave the pure product. The yields of $IIId_1$ and $IIId_2$ were 40 and 35%, respectively.

The following procedure is representative of those used for the preparation of 3-ethoxycarbonyl-4-ethoxycarbonylaminothiophene ($IIIe_1$), 2-methyl-3-ethoxycarbonyl-4-ethoxycarbonylaminothiophene ($IIIe_2$), and 3-ethoxycarbonyl-4-methoxythiophene ($IIIf_1$). A mixture of 3-ethoxycarbonyl-4-ethoxycarbonylamino-2,5-dihydrothiophene (Ie_1, 10 mmol) and chloranil (11 mmol) in dry toluene (20 m*l*) was refluxed for 6 hr. After the evaporation of the solvent *in vacuo*, the residue was diluted with chloroform (5 m*l*). The chloroform solution was chromatographed on alumina (20 g) using a mixture of chloroform and petroleum ether[4] (5 : 1) as an eluent. After the evaporation of the solvent, the residue was distilled *in vacuo* to give the product. The yields of $IIIe_1$, $IIIe_2$, and $IIIf_1$ were 80, 65 and 40% respectively.

Thiophene-3,4-dicarboxylic Acid Anhydride IV. The anhydride IV was prepared in a 67% yield by refluxing thiophene-3,4-dicarboxylic acid ($IIIa_1$)[1] with acetyl chloride for 4 hr according to the method of Sice.[5]

3-Carboxy-4-methoxycarbonylthiophene V. A solution of 1.0 g of IV in 10 m*l* of absolute methanol was refluxed for 1 hr. After the solvent had then been removed *in vacuo*, the residue was recrystallized to give 0.84 g (70%) of V.

The physical properties and analytical data for $IIId_1$, $IIId_2$, $IIIe_1$, $IIIe_2$, $IIIf_1$, IV and V are summarized in Table 2.

4) Bp 40—60°C.
5) J. Sice, *J. Org. Chem.*, **19**, 70 (1954).

Absorption Spectra of Cation Radicals Derived from *p*-Phenylenediamine and Its *N*-Methyl Derivatives

Yôichi IIDA and Yoshio MATSUNAGA

Department of Chemistry, Faculty of Science, Hokkaido University, Sapporo

(Received March 9, 1968)

The cation radical salts made by the one-electron oxidation of aromatic diamines have been the subject of interest for many years. Naturally, considerable attention has been paid to their magnetic properties. In connection with our spectroscopic study of the solid salts, we examined the absorption spectra of the cation radicals derived from *p*-phenylenediamine and all the *N*-methyl derivatives in a dilute ethanol solution. The spectra of the same cations were examined by Michaelis *et al.* nearly thirty years ago.[1] Unlike us, however, they oxidized the diamines in a methanol+dilute aqueous solution of acetic acid with bromine and examined the spectra without isolating the salts. Their measurements were very qualitative and covered only the α band. Therefore, we wish to present here a brief summary of our measurements.

The following solid salts were prepared by the methods given in the references[2-4]: *p*-phenylenediamine bromide (I), *N*-methyl-*p*-phenylenediamine bromide (II), *N,N*-dimethyl-*p*-phenylenediamine bromide (III), *N,N'*-dimethyl-*p*-phenylenediamine perchlorate (IV), *N,N,N'*-trimethyl-*p*-phenylenediamine iodide (V), and *N,N,N',N'*-tetramethyl-*p*-phenylenediamine perchlorate (VI).

The measurements were performed at room temperature, using a Beckman DK-2A spectrophotometer, on ethanolic solutions at concentrations of the order of 10^{-5} mol/*l*.

All the spectra bear a close resemblance to each other and show the general features shown schematically in Fig. 1. The positions and molar extinction coefficients (ε) of the three electronic absorption bands, designated as α, β and γ, are summarized in Table 1.

The structures of the α bands are regarded as vibrational.[5] The α band shows a remarkable red-shift upon the introduction of the methyl group (about 1 kK per group), while the other two bands are nearly independent of the number of the substituent.

The agreement between our positions and those reported by Michaelis *et al.*[1] is fair. Accurate measurements of the molar extinction coefficients are much hampered by the instability of the salts. Moreover, in the case of the *p*-phenylenediamine cation the presence of a small amount of the dimeric

TABLE 1. ABSORPTION SPECTRAL DATA FOR THE CATION RADICALS DERIVED FROM *p*-PHENYLENEDIAMINE AND ITS *N*-METHYL DERIVATIVES

Substituent	Color*	α band		β band	γ band	
		$\tilde{\nu}$ (kK)	ε (l/mol·cm)	$\tilde{\nu}$ (kK)	$\tilde{\nu}$ (kK)	ε (l/mol·cm)
None (I)	Yellow	20.4 21.1	(>4950) (>5120)	~27.6	30.5 doublet	(>13500)
N-Methyl (II)	Pink	19.1 20.4	— —	26.7—27.0	31.0	—
N,N-Dimethyl (III)	Red	18.0 19.4	9100 8960	~26.7	30.7	18800
N,N'-Dimethyl (IV)	Red	18.1 19.6	(7930) (7660)	~26.7	30.8	(15150)
N,N,N'-Trimethyl (V)	Violet	17.2 18.6	— —	~26.7	30.9	—
N,N,N',N'-Tetramethyl (VI)	Blue	16.4 17.8	11100 11100	~26.7	30.6	18800

* In dilute ethanolic solution at room temperature.

1) L. Michaelis, M. P. Schubert and S. Granick, *J. Am. Chem. Soc.*, **61**, 1981 (1939).
2) L. Michaelis and S. Granick, *ibid.*, **65**, 1747 (1943).
3) J. Piccard, *Ann.*, **381**, 351 (1911).
4) G. K. Hughes and N. S. Hush, *J. Proc. Roy. Soc. N. S. W.*, **81**, 48 (1947).
5) A. C. Albrecht and W. T. Simpson, *J. Am. Chem. Soc.*, **77**, 4454 (1955).

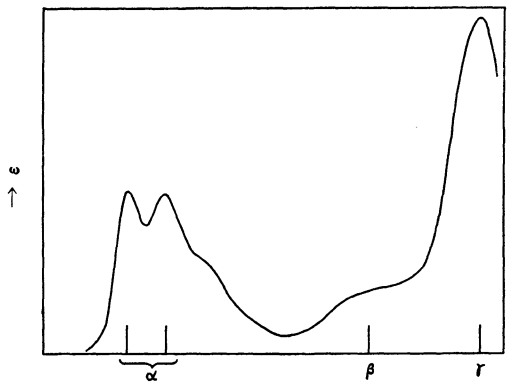

Wave number (kK)

Fig. 1. General feature of the spectra of the cation radicals derived from *p*-phenylenediamine and its *N*-methyl derivatives.

form, indicated by a peak around 16.4 kK, hinders the estimation.[6] The values in parentheses must, therefore, be considered no more than rough estimates.

A simple molecular orbital consideration of the *p*-phenylenediamine cation shows that the odd electron is in the orbital of the b_{3g} symmetry. The transitions associated with the α, β, and γ bands are $^2B_{3g}\rightarrow{}^2B_{1u}$, $^2B_{3g}\rightarrow{}^2A_u$ and $^2B_{3g}\rightarrow{}^2B_{1u}$, respectively. Thus, from symmetry considerations the transition moments in the α and γ bands appear to be along the long axis of the molecular ion, and that in the β band, along the short axis. It is gratifying to see that this prediction agrees well with the results obtained by Albrecht and Simpson, by means of polarized photo-oxidation in a rigid medium, for the *N,N,N',N'*-tetramethyl-*p*-phenylenediamine cation.[5]

6) K. Uemura, S. Nakayama, Y. Seo, K. Suzuki and Y. Ooshika, This Bulletin, **39**, 1348 (1966).

Excess Volumes of Binary Solutions Containing Some Diketones

Koichiro NAKANISHI,*1 Hidekazu TOUHARA,*1 Kohei SATO and Makoto NAGAO

Department of Industrial Chemistry, Shinshu University, Wakasato, Nagano

(Received March 22, 1968)

As part of thermodynamic studies on binary solutions containing diketones, the excess volumes of the following four systems have been measured at 25.00°C. They are acetylacetone(2,4-pentanedione)-acetone, acetylacetone-isopropanol, acetonylacetone(2,5-hexanedione)-acetone, and acetonylacetone-isopropanol. Acetylacetone is one of those molecules which exhibit keto-enol tautomerism. It is frequently used as a substrate of metal complex in coordination chemistry. The purpose of this study is to examine a combined effect of size difference in polar molecules and keto-enol equilibrium on the thermodynamic excess functions, in this particular case, on the excess volume.

Experimental

All the sample liquids were purified by distillation under nitrogen atmosphere and/or at reduced pressure. The final purified liquids obtained from the middle fraction gave no peaks due to impurities on gas chromatogram. The density measurements were done by the pycnometry described in our previous report.[1]

Results and Discussion

The densities of the four systems studied are shown in Table 1. The excess volumes which were calculated from the density data are also given in the same table and are plotted as a function of mole fraction in Fig. 1. The excess volumes of acetone-isopropanol system, calculated from the density data given by Parks and Chaffee,[2] are also included. The solid lines in Fig. 1 are based on the values calculated by the following equation,

$$\Delta V^E = x_1(1-x_1)\sum_{n=0}^{2} A_n(1-2x_1)^n \qquad (1)$$

where the constants A_n's were estimated by the method of least-squares. The data for acetonylacetone-acetone system show fairly large scatter owing to a high relative volatility and viscous nature of one component. The results for other systems are satisfactory.

The results shown in Fig. 1 may be summarized as follows:

*1 Present address: Department of Industrial Chemistry, Kyoto University, Kyoto.

1) K. Nakanishi, N. Kato and M. Maruyama, *J. Phys. Chem.*, **71**, 817 (1967).

2) G. S. Parks and C. S. Chaffee, *ibid.*, **31**, 439 (1927).

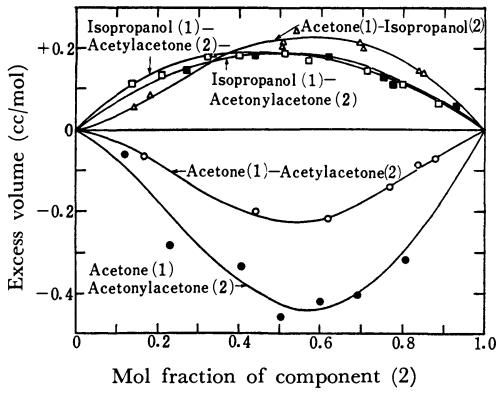

Fig. 1. Excess volumes at 25.00°C.

1) In binary systems containing isopropanol, the excess volumes are positive and their values coincide almost completely with each other.

2) Since the molar volume ratio of acetone, acetylacetone and acetonylacetone is 1.00 : 1.40 : 1.60, the first two can be regarded approximately as dimers of acetone molecule. The excess volumes of the systems containing acetone and diketones are negative and their absolute value increases with the molar volume difference.

Owing to the lack of adequate theory for such polar and associated solutions, quantitative evaluation of the present data is difficult. However, it is interesting to compare them with the results for mixtures of nonpolar molecules. For mixtures of nonpolar molecules, it is found by Brønsted and Koefoed[3] that the absolute value of the excess volume changes regularly with the size difference (principle of congruence). According to the available experimental evidences,[4-6] the magnitude of the excess volume is proportional to the size difference. On the other hand, the sign of the excess volume is dependent of the shape of molecules. For example, negative excess volume is observed for mixtures of molecules of similar shape such as *n*-alkane-*n*-alkane,[4] and an opposite result is obtained for mixtures of molecules of different shape (*e. g.*, cyclohexane-*n*-alkanes[5] or *trans*-decalin-*n*-alkane[6]).

Table 1. Density and excess volume at 25.00°C

Mole fraction of 1st component x_1	Density d (g/cc)	Excess volume ΔV^E (cc/mol)
Acetone (1)—Acetylacetone (2)		
0.0	0.96942	
0.1686	0.94710	−0.0649
0.4407	0.90527	−0.2001
0.6179	0.87303	−0.2198
0.6715	0.86233	−0.2109
0.7712	0.84076	−0.1405
0.8359	0.82585	−0.0875
0.8796	0.81559	−0.0719
1.0	0.78392	
Isopropanol (1)—Acetylacetone (2)		
0.1386	0.94810	+0.1148
0.2105	0.93679	+0.1372
0.3264	0.91752	+0.1839
0.3996	0.90500	+0.1834
0.5116	0.88477	+0.1865
0.5722	0.87344	+0.1703
0.7092	0.84611	+0.1467
0.7991	0.82706	+0.1123
0.8827	0.80850	+0.0626
1.0	0.78056	
Acetone (1)—Acetonylacetone (2)		
0.0	0.96758	
0.1201	0.95361	−0.0629
0.2310	0.94092	−0.2856
0.4049	0.90567	−0.3396
0.5025	0.90062	−0.4612
0.5989	0.88274	−0.4202
0.6623	0.86991	−0.3782
0.6891	0.86471	−0.4074
0.8071	0.83780	−0.3210
Isopropanol (1)—Acetonylacetone (2)		
0.2677	0.91413	+0.1502
0.4356	0.88785	+0.1838
0.6174	0.85673	+0.1826
0.7528	0.83181	+0.1291
0.7750	0.82753	+0.1130
0.9306	0.79566	+0.0613

The present data conform with such rules. We expected that there should be some unnegligible effect of the presence of keto-enol equilibrium on the excess function behavior. As far as the present data are concerned, no such effect was found.

The authors thanks to A. Furukoshi and O. Touyama for their assist in experimental work.

3) J. N. Brønsted and J. Koefoed, *Kgl. Danske. Videnskab. Selskab., Mat. Fys. Medd.*, **22**, 1 (1946).
4) J. D. Gômez-Ibánẽz and T.-C. Liu, *J. Phys. Chem.*, **65**, 2148 (1961).
5) J. D. Gómez-Ibánẽz and T.-C. Liu, *ibid.*, **67**, 1388 (1963).
6) J. D. Gômez-Ibánez and T. C. Wang, *ibid.*, **70**, 391 (1966).

Synthetic Studies Starting from β-Cyanopropionaldehyde. VI.*1 The Synthesis of α-Cyanomethylacrolein

Sadayoshi SATSUMABAYASHI and Shinichi MOTOKI

Department of Chemistry, Faculty of Science, Science University of Tokyo, Shinjuku-ku, Tokyo

(Received March 22, 1968)

As a part of synthetic studies starting from β-cyanopropionaldehyde (β-CPA) (I), the synthesis of a new vinyl compound, α-cyanomethylacrolein (VI) containing an aldehyde group and a nitrile group, will be presented in this paper. Two synthetic methods illustrated in Fig. 1 have been used.

The reaction of the diethyl acetal of β-CPA (II) with acetyl chloride caused an exchange of ethoxy group for chlorine leading to obtain α-ethoxy-γ-cyanopropyl chloride (III). This reaction was carried out at room temperature, but the reaction was difficult to control and a large amount of tar was formed above 60°C. Treatment of this chloride (III) in dry diethyl ether with an excess of anhydrous pyridine gave ethyl γ-cyanopropenyl ether (IV), which was also obtained by heating II with phthalic anhydride with loss of ethyl alcohol from II. As the boiling point of this product was not so different from that of II, several times of fractional distillation were required. When dibutyl acetal was used in place of II, the corresponding butyl derivative was obtained. A reaction of IV with diethyl formal in the presence of boron trifluoride etherate as a catalyst was carried out, and the reaction mixture obtained was directly hydrolyzed with hydrochloric acid to give α-cyanomethylacrolein (VI). In these successive reactions, V was regarded as an intermediate,[1] but it was not really isolated.

Some examples of the reaction of acetals with vinyl ethers were reported by Hoaglin,[1] but formaldehyde acetal was not used for this reaction. As stated above, however, it was found that formaldehyde diethyl acetal undergoes the same reaction with vinyl ether as diethyl acetal of other aldehydes containing more than two carbon atoms does.

The IR spectrum of the product (VI) showed the characteristic absorptions of unconjugated nitrile at 2250 cm^{-1}, of α,β-unsaturated aldehyde at 1693 cm^{-1} and of the carbon-carbon double bond at 1640 cm^{-1}. Moreover, the structure of VI was confirmed by the NMR spectrum, as illustrated in Fig. 2.

On the other hand, the labile hydrogen at the α-position of the aldehyde group of β-CPA was readily removed by condensation with both formaldehyde and an amine as in the Mannich reaction. When morpholine or piperidine was used as the amine component, a Mannich base was obtained and subsequent thermal decomposition of the base gave VI. When dimethylamine was used, however, no Mannich base was obtained.

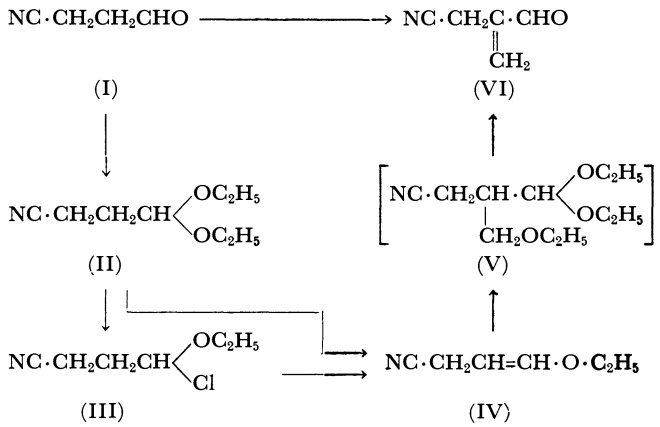

Fig. 1.

*1 Part V: S. Motoki, S. Satsumabayashi and F. Minemura, *J. Org. Chem.* **33**, 3667 (1968).

1) R. I. Hoaglin and D. H. Hirsh, *J. Am. Chem. Soc.*, **71**, 3468 (1949).

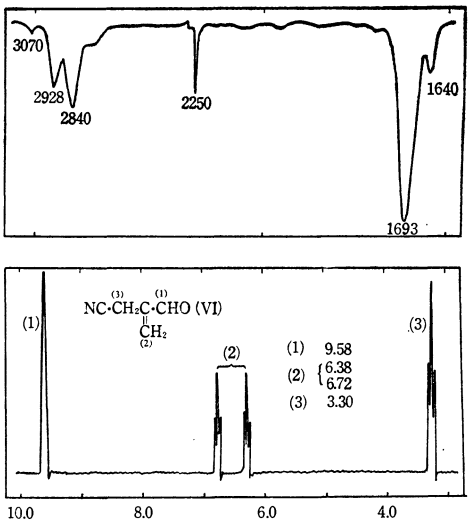

Fig. 2. The IR and NMR spectra of VI.
A Varian A-60 NMR spectrometer was employed using tetramethylsilane as an internal standard.

Experimental

α-Ethoxy-γ-cyanopropyl Chloride (III). To 31.4 g (0.2 mol) of β-CPA diethyl acetal, 23.6 g (0.3 mol) of acetyl chloride was added slowly at about 20°C, and the mixture was stirred for 5 hr at room temperature. By fractional distillation, 23.0 g of III was obtained, bp 68—70°C/3 mmHg, yield 78.0%. Found: C, 48.65; H, 7.07; N, 9.73%. Calcd for $C_6H_{10}ONCl$: C, 48.82; H, 6.83; N, 9.49%.

Ethyl γ-Cyanopropenyl Ether (IV). Under an anhydrous condition, 29.5 g (0.2 mol) of III was added slowly to 39.5 g (0.5 mol) of pyridine at room temperature. After the solution was stirred for 6 hr, the reaction mixture was extracted with ether, washed with water and dried. Distillation of the extract gave 9.4 g of IV, bp 60—61°C/4 mmHg, yield 42.3%. Found: C, 64.92; H, 8.33; N, 12.74%. Calcd for C_6H_9ON: C, 64.84; H, 8.16; N, 12.60%.

A mixture of 157 g (1 mol) of II and 177.6 g (1.2 mol) of phthalic anhydride was heated at 150°C for 8 hr, and filtered. The filtrate was then distilled and the fraction boiling at 55—75°C/4 mmHg was collected. When this fraction was redistilled two more times, 31.4 g of IV was obtained, bp 60—62°C/4 mmHg, yield 28.5%. Found: C, 64.55; H, 8.11; N, 12.89%. Calcd for C_6H_9ON: C, 64.84; H, 8.16; N, 12.60%.

Similarly, 26.8 g of *n*-butyl γ-cyanopropenyl ether was obtained from 106.5 g (0.5 mol) of β-CPA dibutyl acetal, bp 83—85°C/4 mmHg, yield 38.5%. Found: C, 68.81; H, 9.60; N, 10.14%. Calcd for $C_8H_{13}ON$: C, 69.03; H, 9.41; N, 10.06%.

α-Cyanomethylacrolein (VI) from IV. A mixture of 22.2 g (0.2 mol) of IV and 31.2 g (0.3 mol) of diethyl formal was stirred. To this mixture was added 1.0 g of boron trifluoride etherate in 10 m*l* of diethyl ether, with the internal temperature kept at about 20°C. After 10 hours' stirring, the catalyst was neutralized with good agitation by 4 g of anhydrous sodium carbonate during a period of 4 hr. The reaction mixture thus obtained was refluxed with 100 m*l* of 5% hydrochloric acid for 8 hr. The product was extracted with ether, washed with water and dried. Distillation gave 3.5 g of VI, bp 96—98°C/20 mmHg, yield 18.4%. Found: C, 63.02; H, 5.25; N, 14.61%. Calcd for C_5H_5ON: C, 63.15; H, 5.30; N, 14.73%.

α-Cyanomethylacrolein (VI) from I. Into a solution of 41.5 g (0.5 mol) of β-CPA (I) dissolved in 50 m*l* of water, a solution of 61.8 g (0.5 mol) of morpholine hydrochloride and 50 g of 37% formaline was added over a two-hours' period, the temperature being maintained at about 65°C. After another 8 hours' stirring, the solution was neutralized with potassium carbonate, extracted with chloroform and the extract was dried. Dry hydrogen chloride was run into the extract, then the yellowish white Mannich base was precipitated as its hydrochloride. This crude Mannich base was placed in a Claisen flask and heated gently for half an hour using an oil bath, the temperature of which was maintained at about 150°C. At the end of this period, the system was placed under a reduced pressure of about 20 mmHg. The fraction which boiled at 70—110°C/20 mmHg was collected, washed with water, extracted with ether and the extract was dried. After redistillation, 7.5 g of VI was obtained, bp 96—97°C/21 mmHg, yield 15.8% based on I. Found: C, 62.96; H, 5.47; N, 14.75%. Calcd for C_5H_5ON: C, 63.15; H, 5.30; N, 14.73%.

Mannich reaction was also carried out with piperidine instead of morpholine. Yield 18.0%.

The authors wish to thank Professor Yojiro Tsuzuki for his helfpul advice and encouragement.

Preparation and Photolysis of 1-*t*-Butyl-3-benzoylazetidine

Teng-Yueh CHEN[1]

Laboratory of Organic Chemistry, Tokyo Institute of Technology, Ookayama, Meguro-ku, Tokyo

(Received April 16, 1968)

A photo-induced ring expansion of 1-*t*-butyl-2-phenyl-3-benzoylazetidine to 1-*t*-butyl-2,4-diphenylpyrrole has recently been reported by Padwa *et al.*[3] Since this is the first example of the conversion of an azetidinyl ketone into the corresponding substituted pyrrole, further study was carried out with 1-*t*-butyl-3-benzoylazetidine (II), which had been synthesized by the reaction of 1-*t*-butyl-3-cyanoazetidine (I)[3] with phenylmagnesium bromide.

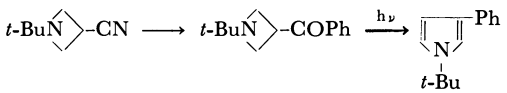

I II III

The infrared spectrum of the azetidinyl ketone II shows a carbonyl band at 1680 cm^{-1} and is quite consistent with the proposed structure. The formations of 2,4-dinitrophenylhydrazone and the picrate of the azetidinyl ketone II and their analytical data all support the assigned structure.

A dilute solution of II in ethanol was irradiated through a Pyrex filter with a high-pressure mercury lamp to give the corresponding 1-*t*-butyl-3-phenylpyrrole (III). The structure of III was determined by comparing the IR and NMR spectra with those data obtained by Padwa *et al.*[2] The infrared spectrum of the distilled product exhibits some small peaks between 3080—3030 cm^{-1} and sharp peaks at 1605, 1555, 1500, 750, and 693 cm^{-1} for the characteristic absorptions of phenyl and the pyrrole ring. The strong absorptions of the tertiary butyl group appear at 1245 and 1225 cm^{-1}. The NMR spectrum of the product exhibits a sharp singlet at τ 8.54 (9H) for the *t*-butyl group, and three signals of doublet of doublet at 3.77 (1H), 3.40 (1H), and 3.12 (1H) for the three protons at the 4, 5, and 2-positions of the pyrrole ring. The phenyl group on the pyrrole ring appears between 2.6 and 3.06 (5H) as a multiplet.

Isomerization was not observed when an alcoholic solution of II was warmed in the presence of boron trifluoride etherate or when the ketone II was heated at 254°C or at 340°C.

Experimental[4]

1-*t*-Butyl-3-benzoylazetidine (II). A solution of 5.4 g (0.039 mol) of I in 7 m*l* of absolute ether was stirred into a cooled solution of phenylmagnesium bromide prepared from 2.5 g (0.12 mol) of magnesium and 21 g (0.13 mol) of bromobenzene in 80 m*l* of absolute ether. After the completion of the addition, the reaction mixture was stirred for another four hours and then set aside overnight at room temperature. The reaction mixture was decomposed with about 100 m*l* of ice water and extracted four times with a total of 200 m*l* of ether. After drying over magnesium sulfate, the ether was removed and the residue was distilled to give 3.5 g (40% yield) of a colorless liquid; bp 140—144°C/ 3 mmHg, n_D^{25} 1.5062. IR: 3060, 1600, 1580, 700 cm^{-1} (C_6H_5), 1680 cm^{-1} (CO), 1240 and 1225 cm^{-1} (*t*-Bu).

Found: C, 77.72; H, 8.75; N, 6.11%. Calcd for $C_{14}H_{19}NO$: C, 77.38; H, 8.81; N, 6.45%.

2,4-Dinitrophenylhydrazone of II: mp 88—89.5°C.

Found: C, 60.89; H, 5.90; N, 17.36%. Calcd for $C_{20}H_{23}N_5O_4$: C, 60.44; H, 5.83; N, 17.62%.

Picrate of II: mp 157.5—159.5°C.

Found: C, 54.11; H, 4.96; N, 12.64%. Calcd for $C_{20}H_{22}N_4O_8$: C, 53.81; H, 4.97; N, 12.55%.

Photolysis of II. A solution of 0.5 g of II in 100 m*l* of 99% ethanol was irradiated through a Pyrex filter with a 100 W high-pressure type mercury lamp under a nitrogen atmosphere for seventeen hours. After the removal of the ethanol under reduced pressure, the residue was distilled *in vacuo* to give 0.1 g of a colorless liquid; bp 120—124°C/1 mmHg. The product was positive to a pine-splinter test (red color).

Found: C, 83.93; H, 8.76; N, 6.83%. Calcd for $C_{14}H_{17}N$: C, 84.37; H, 8.60; N, 7.03%.

The author is indebted to Professor Masaki Ohta and Dr. Hiroshi Kato for their discussions and to Miss Mizuko Yoshida for the measurement of the NMR spectra.

1) Present address: National Tsing Hua University, Taiwan, The Republic of China.

2) A Padwa, R. Gruber and L. Hamilton, *J. Am. Chem. Soc.*, **89**, 3077 (1967).

3) Part III, T. Chen, T. Sanjiki, H. Kato and M. Ohta, This Bulletin, **40**, 2401 (1967).

4) The general conditions for the measurements of the physical constants and spectra were the same as those described in Part I; T. Chen, H. Kato and M. Ohta, This Bulletin, **40**, 1964 (1967).

SHORT COMMUNICATIONS

Die Absolutkonfiguration des Melleins

Hisao ARAKAWA

Science Education Institute of Osaka Prefecture, Karitacho, Sumiyoshiku, Osaka

(Eingegangen am 10. Juli, 1968)

Aus der Kulturlösung von *Aspergillus melleus*[1] wurde ein Dihydroisocumarin-Derivat, Mellein (I) isoliert, das optisch aktiv ist und mit Ochracin aus der Kulturlösung von *Aspergillus ochraceus* identisch ist.[2] Die Struktur wurde synthetisch sichergestellt.[3] Die Absolutkonfiguration wurde nun mit Hilfe des Circulardichroismus bestimmt.

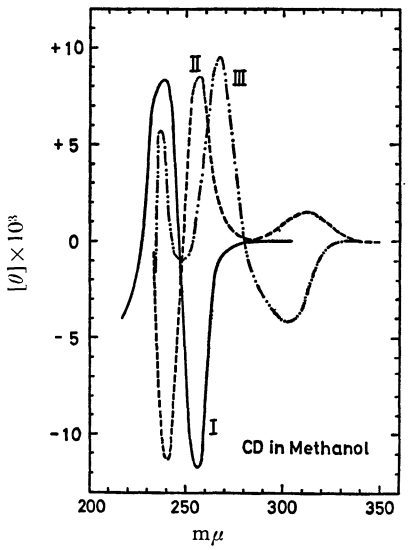

Neuerdings hat der Verfasser die Absolutkonfiguration von anderen Dihydroisocumarin-Derivaten, Phyllodulcin (II)[4] und Agrimonolid (III),[5] bestimmt und diese Verbindungen zeigten in beiden Fällen einen positiven CD um 257—268 mμ (in Methanol), der mit der K-Bande des konjugierten Enlactons zusammenhängt.[5]

Mellein (I) und Phyllodulcin(II) enthalten einen Salizylsäure-Rest als Chromophor, aber einerseits zeigte II einen positiven CD bei 257 mμ, anderseits zeigte I einen negativen CD bei 257 mμ (in Methanol).

Danach, unter der Annahme, daß große Substituent am Dihydroisocumarin äquatoriale Konformation einnimt, muss Mellein (I) das (3R)-konfigurierte Dihydroisocumarin-Derivat sein. Diese ist ähnlich der Beziehung zwischen dem CD um 260 mμ und der Absolutkonfiguration der Parasorbinsäure (IV).[6]

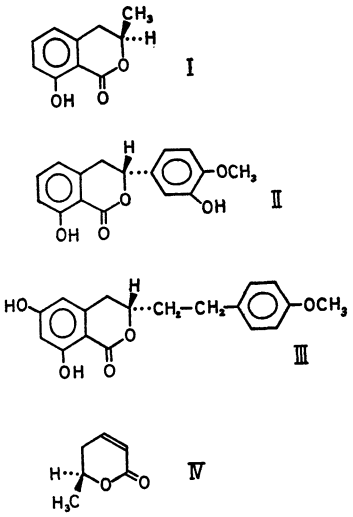

1) H. Nishikawa, *J. Agr. Chem. Soc. Japan*, **9**, 772, 1059 (1933).
2) T. Yabuta und Y. Sumiki, *ibid.*, **9**, 1264 (1933); **10**, 703 (1934).
3) M. Matsui, K. Mori und S. Arasaki, *Agr. Biol. Chem.*, **28**, 896 (1964).
4) H. Arakawa, Dieses Bulletin, **33**, 200 (1960); H. Arakawa und M. Nakazaki, *Chem. Ind.*, **1959**, 671.
5) H. Arakawa, N. Torimoto und Y. Masui, *Tetrahedron Letters*, **1968**, (38), 4115.
6) G. Snatzke, *Angew. Chem.* Internat. Edit. **7**, 14 (1968).

Separation of Cr(III)-Hexacyanoferrate(II)-Complexes by Sephadex Column Chromatography*1

Yoshio MATSUMOTO, Michiko SHIRAI and Hiroko SAITO

Department of Chemistry, Faculty of Hygienic Science, Kitasato University, Minato-ku, Tokyo

(Received May 18, 1968)

The color reaction between chromium(III) ions and potassium hexacyanoferrate(II) has attracted the attention of the several investigators.[1-6] However, reaction products have not been isolated because of their great solubility in water. The chemical compositions of the products remain undetermined after a variety of electroanalytical and spectrophotometric investigations were carried out applying a continuous variation method.[4-6]

In the present work, employing a chromatographic method using Sephadex columns, at least three complex compounds differing with each other in color, chemical composition and molecular size were separated from the reaction mixture. The mixture obtained by reacting potassium hexacyanoferrate(II) with Cr(III) ions (chrome alum) in a molar ratio of 5 : 1 for one hour in an aqueous solution at 47°C, when applied to a Sephadex G-25 column, gave a bluish-green fraction eluting first and a reddish-brown one eluting second, the unreacted hexacyanoferrate(II) and sulfate ions remaining behind in the column. After repeating chromatography a further three times, the second fraction appeared to be pure, not only in paper electrophoresis but in further subjection to chromatography with Sephadex of a smaller pore size. The first fraction, giving two components in paper electrophoresis, was definitely separated when further applied to Sephadex G-75 or G-100 columns, into two fractions, blue and green. Each proved to be a definite constituent in paper electrophoresis and in any further application to a Sephadex column of larger pore size. The three substances separated all consisted of K, Cr, Fe and CN. The reddish-brown and green substances permeated a cellophane film, while the blue substance did not, being confirmed of high molecular size.

The reddish-brown substance was the main product in which more than 90% of the reacted Cr(III) ions were contained, and was the smallest of the three substances in molecular size. It proved on electrophoretic and polarographic examination[3] to include a negatively charged complex ion containing Cr, Fe and CN. The reddish-brown solution described above was evaporated to dryness *in vacuo* in a rotary evaporator at 30°C, and the composition of the resulting solid film was determined by elementary analysis to have the empirical formula $K_5CrFe_2(CN)_{12}\cdot 7H_2O$.

Found: K, 24.2; Cr, 6.5; Fe, 13.8; C, 17.6; N, 20.7; H_2O, 15.1%. Calcd for $K_5CrFe_2(CN)_{12}\cdot 7H_2O$: K. 24.5; Cr, 6.5; Fe, 14.0; C, 18.1; N, 21.1; H_2O, 15.7%.

The same three components separated from reaction mixtures as long as the molar ratio of the reactants, potassium hexacyanoferrate(II) to Cr(III) ions, remaining not below 2.5. The elution diagram in Fig. 1 illustrates the chromatographic separation of the reddish-brown complex on a Sephadex G-25 column from the reaction mixture resulting at a reactant ratio of 2.5.

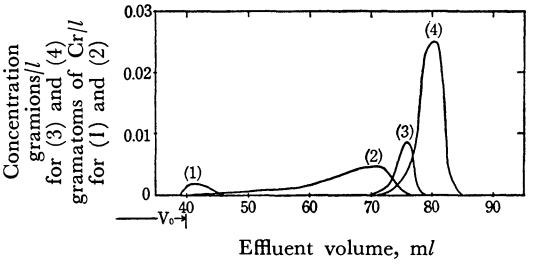

Fig. 1. Separation of the reaction mixture resulting from the mixture containing the reactants in the molar concentrations of 0.076 for $KCr(SO_4)_2$ and 0.19 for $K_4Fe(CN)_6$.
Sephadex G-25, fine (particle size 20—80 microns)
Column dimensions: dia. 2 cm, length 27 cm
Sample volume: 0.8 ml Eluant: Water
Elution velocity: 98 ml/hr Temp: 26°C
(1) Bluish green (In this curve the concentration was exaggerated for distinctness.)
(2) Reddish brown
(3) Hexacyanoferrate(II) ion
(4) Sulfate ion

Details on the products at varying reactant ratios, as well as the results of a structural study, will be presented later.

*1 This work was partly presented at the 16th and 17th Symposia on Co-ordination Chemistry (1966 and 1967), and at the 19th and 20th Annual Meetings of the Chemical Society of Japan (1966 and 1967).

1) Y. Matsumoto and M. Shirai, *Bunseki Kagaku (Japan Analyst)*, **12**, 608 (1963).
2) Y. Matsumoto and M. Shirai, This Bulletin **39**, 55 (1966).
3) Y. Matsumoto and M. Shirai, Proceeding of the 15th Symposium on Co-ordination Compounds (1965).
4) W. U. Malik, *J. Sci. Ind. Res.*, **18B**, 463 (1959).
5) W. U. Malik, *ibid.*, **20B**, 213 (1961).
6) W. U. Malik and J. Singh, This Bulletin, **39**, 2541 (1966).

Photooxidation of Some 1,5-Benzodiazepines

Teijiro YONEZAWA, Masakatsu MATSUMOTO and Hiroshi KATO

Department of Hydrocarbon Chemistry, Kyoto University, Kyoto

(Received June 10, 1968)

It has been reported that 1,5-benzodiazepines (I) are oxidized to 3-acylquinoxalines (II) with monopersulfuric acid or with peracetic acid, but do not give 3,6-diaza-4,5-benzotropones (III). Syntheses of the ketones (III) have been attempted by several workers, but no attempts have been successful.[1,2]

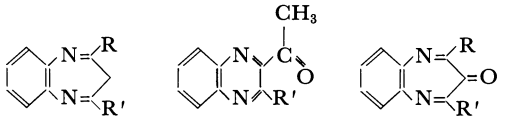

(I) (II) (III)

a: R, R'=CH_3 a: R'=CH_3 a: R, R'=CH_3
b: R=CH_3, R'=C_6H_5 b: R'=C_6H_5 b: R=CH_3, R'=C_6H_5
c: R, R'=C_6H_5 c: R, R'=C_6H_5

This communication will report that 3,6-diaza-4,5-benzotropones (III) can be prepared by the photooxidation of 1,5-benzodiazepines (I) in a non-aqueous medium.

The compound (I-c) in a 4% benzene solution was irradiated with a low-pressure mercury arc under an oxygen atmosphere for 20 hr. After this irradiation, the reaction mixture was chromatographed on silica gel in benzene. Thus a ketone (IV) and an amide (V) were obtained in yields of 1.4% and 2.0%, respectively.

The ketone (IV) consisted of pale yellow needles melting at 120—121°C. The infrared spectrum in KBr showed the absorption of the carbonyl group at 1680 cm^{-1}. The NMR spectrum in $CDCl_3$ simply showed two multiplets centered at τ= 2.0 and 2.6. The ultraviolet spectrum in ethanol showed λ_{max} at 264 mμ (ε=19200), 297 (11300), and 333 (8910). The mass spectrum[3] showed a parent peak at *m/e* 310 and a fragment peak at *m/e* 282 which was probably produced through the elimination of the carbonyl group of the parent ion. On the basis of these results, the ketone (IV) was identified as 2,7-diphenyl-3,6-diaza-4,5-benzotropone (III-c). This compound was very unstable and easily formed 2,3-diphenylquinoxaline by decarbonylation in warm concentrated sulfuric acid or in warm acetic acid.[4]

The amide (V) consisted of colorless needles which melted at 301°C; it was identified as dibenzoyl-*o*-phenylenediamine. The infrared spectrum in KBr showed $\nu_{C=O}$ at 1649 cm^{-1}.

In the case of the photooxidation of 2,4-dimethyl-1,5-benzodiazepine(I-a) in benzene, the corresponding benzotropone (III-a) was not obtained; the ring contraction products, 2-acetyl-3-methylquinoxaline (II-a) and 2-hydroxy-3-methylquinoxaline (VI), were obtained in yields of 29% and 4%, respectively.

2-acetyl-3-methylquinoxaline (II-a) consisted of colorless needles which melted at 87°C after crystallization from aqueous ethanol. The infrared spectrum showed $\nu_{C=O}$ 1668 cm^{-1} in KBr.

As in the oxidation of (I-a) with peracids, in the photooxidation of (I-a) the quinoxaline (II-a) might be produced through the 6-oxo intermediate (III-a). We presumed that the quinoxaline (II-a) might be produced *via* either Scheme I or II;

In Scheme I, as has been described in the work of Barltrop *et al.*,[1] the 6-oxo intermediate (III-a) is hydrolyzed in the first step.

In Scheme II, the benzotropone (III-a) formed under the action of ultraviolet light is subjected to the second photochemical reaction.

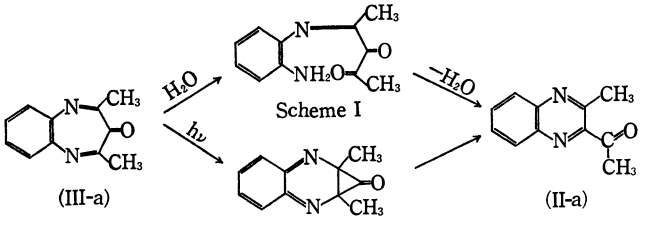

(III-a) Scheme I (II-a)

Scheme II

1) J. A. Barltrop, C. G. Richards, D. M. Russell, and G. Ryback, *J. Chem. Soc.*, **1959**, 1132.

2) W. Paterson and G. R. Proctor, *ibid.*, **1965**, 485.

3) Thanks are due to Professor Y. Takegami and Dr. T. Ueno for the mass spectrum.

4) The mechanism of the decarbonylation reaction may be considered to be as follows, with reference to the decomposition of diphenyltriketone suggested. J. D. Roberts, D. R. Smith and C. C. Lee, *J. Am. Chem. Soc.*, **73**, 618 (1951):

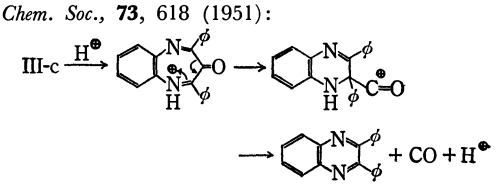

Hydrogen-Deuterium Exchange in the Methyl Group of Diammine-bis-(acetylacetone)ethylenediimine-cobalt(III) Chloride in Deuterium Oxide Solution

Hayami YONEDA* and Yukiyoshi MORIMOTO**

* *Department of Chemistry, Wakayama University, Masagocho, Wakayama*

** *Research Laboratories, Fujisawa, Pharmaceutical Company, Kashimacho, Higashiyodogawa-ku, Osaka*

(Received June 18, 1968)

We have reported several papers on the study of the proton magnetic resonance spectra of a series of cobalt(III) complexes.[1] In this communication we should like to report hydrogen-deuterium exchange found in the study of the proton magnetic resonance spectra of diammine-bis(acetylacetone)-ethylenediimine-cobalt(III) chloride $[Co(NH_3)_2$-acac-en$]Cl$[2] dissolved in deuterium oxide, where

acac-en=

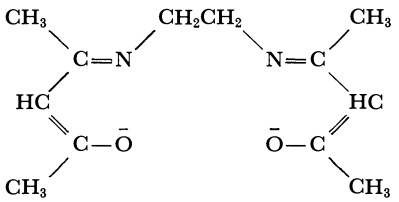

Figure 1 shows the spectra of the complex. Curve (a) represents the spectrum of the complex dissolved in neutral deuterium oxide. Putting aside a large peak due to HOD (the second peak from the left-hand side), the spectrum consists of four peaks, whose assignments can be made by considering their relative intensities. The small peak on the extreme left (I) is assigned to the CH proton, the peak in the middle (II) to the CH_2CH_2 protons, and the two peaks of equal intensities on the right (III, III') to the two kinds of CH_3 protons. Addition of a few drops of concentrated NaOD solution caused a slight downfield shift of all four peaks and, at the same time, a time-dependency of intensity of peaks I and III as shown in curves (b), (c), and (d). The CH peak on the extreme left decreased its intensity markedly after standing one hour and disappeared completely after 72 hr. This fact indicates that the hydrogen atom of the CH had been replaced by deuterium. This exchange can be expected, since several electrophilic substitution reactions of the CH of the acetylacetonato complexes have been reported.[3] In addition to this, the inspection of curve (d) reveals another exchange. Here one of the two CH_3 peaks (III) is markedly smaller than the other (III'). Since the two CH_3 signals should have an equal intensity, this inequality can be interpreted as a result of the deuterium exchange in one of the two CH_3 groups. To ascertain this interpretation, the solution was kept at 100°C for 10 min to accelerate the exchange. As shown in curve (e), one of the two CH_3 peaks disappeared almost completely. Thus the above interpretation proved to be valid. The latter exchange is very interesting, because it provides an example where the CH_3 protons also can be activated by chelation.

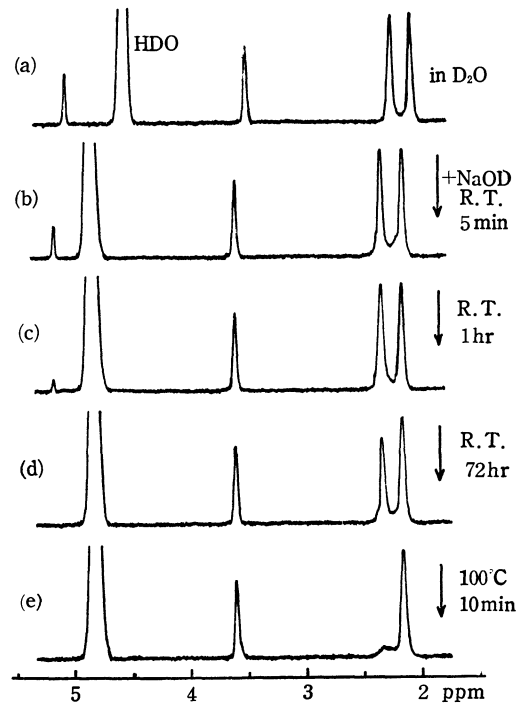

Fig. 1. The PMR spectra of $[Co\ acacen(NH_3)_2]Cl$ in D_2O, recorded by Varian A-60 spectrometer. Tetramethylsilane was used as an external standard.

We are now working on complexes of other metal ions to see the effect of the central metal ion on the exchange. The details of the investigation will be reported elswhere.

1) H. Yoneda and Y. Morimoto, This Bulletin, **39**, 2180 (1966); **40**, 1737 (1967); **41**, 255 (1968); *Inorg. Chim. Acta*, **1**, 413 (1967).

2) The complex was prepared according to the report by J. D. Main Smith, *J. Chem. Soc.*, **1925**, 2030. The complex was reported to be stable in acidic and basic solutions at ordinary temperatures.

3) J. P. Collman, R. A. Mose, H. Maltz and C. C. Heindel, *J. Am. Chem. Soc.*, **83**, 531 (1961); *J. Org. Chem.*, **28**, 1449 (1963); *Inorg. Chem.*, **2**, 576 (1963).

Raman Effect in Ferroelectric Sodium Nitrite Crystal

Masamichi TSUBOI,* Minoru TERADA** and Teruo KAJIURA***

* *Faculty of Pharmaceutical Sciences, The University of Tokyo, Hongo, Bunkyo-ku, Tokyo*

** *Mitsubishi Atomic Power Industries, Inc., Omiya, Saitama*

*** *Japan Electron Optics Laboratory, Company, Nakagami, Akishima, Tokyo*

(Received June 24, 1968)

The Raman effect in sodium nitrite ($NaNO_2$) crystal has been observed by the use of the continuous helium-neon and ionized argon lasers as sources.[1] Several single crystals in the ferroelectric phase C_{2v}^{20}-*Im*2*m* of $NaNO_2$ were obtained through the kindness of Dr. S. Hirotsu and Mr. K. Suzuki, Tokyo Institute of Technology. The instruments used were a Perkin-Elmer Model LR-1 Laser-Excited Raman Spectrometer and a Spex 1400II Spectrometer.

In the first four columns of Table 1, a part of the result of our experiment is given. Here, the orientations of the crystal, directions of the incident and scattered beams, and the directions of the electric vectors of the incident and scattered beams were fixed so that all of the nine Raman-active fundamental frequencies (*i. e.* $3A_1+1A_2+2B_1+3B_2$) should be observed and that, for A_1, B_1, and B_2-type vibrations, frequencies of the pure transverse vibrations should be observed. In the fifth and sixth columns of Table 1, resonance frequencies are given, which were derived from the result of a recent measurement of the infrared reflectivity as the parameters characterizing the dielectric dispersion of this crystal.[2] On the basis of these data, all of the fundamental frequencies of the expected nine optically-active (in-phase), transverse vibrations have now been fixed. The translatory vibrations along the b and a axes are considered to cause only very small polarizability oscillation in the crystal in comparison with the rotatory vibrations of the NO_2^- ion. Therefore, it is probable that the Raman scatterings corresponding to these vibrations are not detected in our present experimental set up. This was taken into account in the assignments which are given in the last column of Table 1.

Besides what are given in the second column of Table 1, various orientations of the incident and scattered beams have been examined, and in many cases appreciably different frequencies from what are given in the third column of Table 1 have been observed. In the c(bc)a (instead of a(bc)b) orientation, for example, the B_2 frequencies are observed at 158, 172, and 1307 cm^{-1} (instead of 158, 191, and 1230 cm^{-1}). From such frequencies, we can obtain an information of the polarization forces[3] besides the elastic forces in the crystal.

TABLE 1. OPTICALLY-ACTIVE (TRANSVERSE) VIBRATIONS IN THE $NaNO_2$ CRYSTAL WITH THE C_{2v}^{20} SYMMETRY

Symmetry type of the vibration	Raman effect[a]			Resonance frequency[c]		Assignment
	Directions of the beams and their polarizations[b]	Frequency cm^{-1}	Intensity	Frequency cm^{-1}	Intensity	
A_1	a′(cc)b′	—	—	194	strong	Transl. along b
		830	medium	826	weak	NO_2^- scissor.
		1323	strong	1323	weak	NO_2^- sym. str.
A_2	a(ca)b	117	strong	—	—	Rot. around b
B_1	b(ab)c	—	—	149	strong	Transl. along a
		223	weak	223	weak	Rot. around c
B_2	a(bc)b	158	strong	157	strong	Rot. around a
		191	medium	188	strong	Transl. along c
		1230	medium	1235	strong	NO_2^- antisym. str.

a) Present experiment.

b) These directions are expressed by four symbols two inside a parenthesis and two out. The four mean, from left to right, the propagation direction of the incident light, the polarization direction of the incident light, polarization direction of the scattered light, and propagation direction of scattered light. a: 45° with a in the ab plane. b′: 45° with b in the ab plane.

c) Derived from the infrared reflectivity (Ref. 2).

1) In 1959, André Tramer (*Compt. rend.*, **248**, 3546) observed Raman effect of this crystal by the use of mercury lamp as source. What he observed are mostly in accord with our results, but their assignments were not yet complete.

2) J. D. Axe, *Phys. Rev.*, **167**, 573 (1968).

3) M. Tsuboi and A. Wada, *J. Chem. Phys.*, **48**, 2615 (1968).

Enhancement of Hydrogen Adsorption on an Acetone-covered Nickel Catalyst

Yutaka KUBOKAWA, Hisashi MIYATA and Mitsuhiko MINOBE

Department of Applied Chemistry, University of Osaka Prefecture, Sakai, Osaka

(Received July 20, 1968)

In order to obtain information on the nature of the adsorption complex during the hydrogenation of acetone on metal catalysts, the interaction of hydrogen with acetone adsorbed on a silica-supported nickel catalyst (15 wt % Ni) was investigated. On the catalyst which had already adsorbed acetone it was found that the amount of hydrogen adsorbed was increased markedly compared to the adsorption on the cleaned catalyst. Such an enhanced adsorption of hydrogen was an activated process, its rate being increased with increasing temperature. The activation energy of adsorption was determined as 10—13 kcal/mol in the temperature range 0—20°C. Adsorption equilibrium was almost attained after several hours at 20°C. The increase in the amount of hydrogen adsorbed at equilibrium q_{H_2} was proportional to the amount of acetone previously adsorbed q_A as seen in Fig. 1. The ratio of q_{H_2} to q_A was 0.83 at 20°C.[1] After the adsorption of hydrogen, the hydrogen remaining in the gas phase was removed by Töpler pump at 0°C. The temperature of the catalyst was raised up in stages, the desorbed gas being collected. It was found that by evacuation at 0°C 25 per cent of the hydrogen adsorbed was removed while after evacuation at 50°C only 20 per cent of the hydrogen adsorbed remained on the surface. On the other hand, the amounts of acetone and isopropyl alcohol appearing in the gas phase during such experiments were very small even at 50°C.[2] Such behavior suggests that hydrogen is held relatively weakly on the acetone-covered nickel surface.

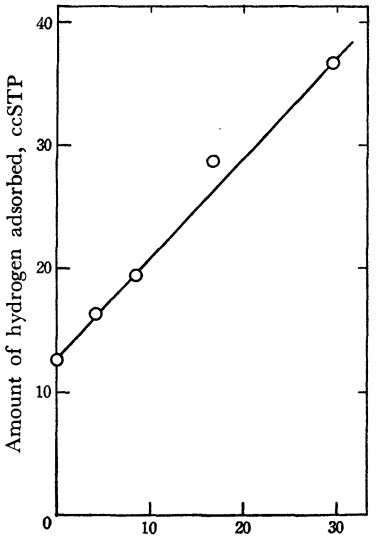

Fig. 1. Adsorption of hydrogen on the acetone-covered surface.
The amount of catalyst and the equilibrium pressure were 6.67 g and 20 mmHg, respectively.

The infrared spectra of the adsorbed layer were investigated by means of an apparatus similar to that used by Peri.[3] When hydrogen was admitted to the acetone-covered surface, no new bands due to hydrogen adsorption were detected, and in addition, little or no change in the band at 1706 cm^{-1} due to the C=O stretching vibration, was observed. The spectra obtained were completely different from those with the surface which had adsorbed isopropyl alcohol.

The results described above suggest the formation of an acetone-hydrogen complex on the nickel catalyst when hydrogen is adsorbed at room temperature in the presence of acetone. In the temperature range above 80°C at which formation of isopropyl alcohol takes place considerably, the situation may be somewhat different. It seems necessary, however, to take into consideration the formation of such an acetone-hydrogen complex when we work out the mechanism of the hydrogenation of acetone.

1) Such an increase in the hydrogen adsorption caused by the preadsorbed acetone was also found for a non-supported nickel catalyst.

2) The desorbed products were analyzed gas chromatographically by using a 2 m polyethylene glycol column at 65°C.

3) J. B. Peri, *Discussions Faraday Soc.*, **41**, 121 (1966).

Reduction Process of Silver(I) Oxide By Ethylene in the Presence of Oxygen

Toshiro YAMASHINA and Masahiro SEO

Faculty of Engineering, Hokkaido University, Sapporo

(Received July 26, 1968)

It has been postulated by several workers[1-3] that the some particular species of surface oxygen on silver catalyst may be reactive for the partial oxidation of ethylene. In order to reveal the property of the species, it is of interest to study the reaction process of silver oxide with ethylene. In the present report, the reaction velocity was found to be considerably accerelated by the presence of oxygen in ethylene, an optimum pressure of oxygen being found to give the maximum velocity.

The CP grade Ag_2O powder was used as the sample of silver oxide in the experiment. Gravimetric analysis by hydrogen reduction showed that the sample contains the nonstoichiometric excess oxygen of 7.8%, *i. e.*, $Ag_2O_{1.078}$. The reaction gases were prepared by redistillating the cylinder grade ethylene (99.8%) and oxygen (99.9%) at liquid nitrogen temperature. The reaction velocities were measured in all glass, closed system (1800 m*l*) of a Gulbransen type microbalance with a sensitivity of 6.34×10^{-7} g/div. (1 div.=0.01 mm).

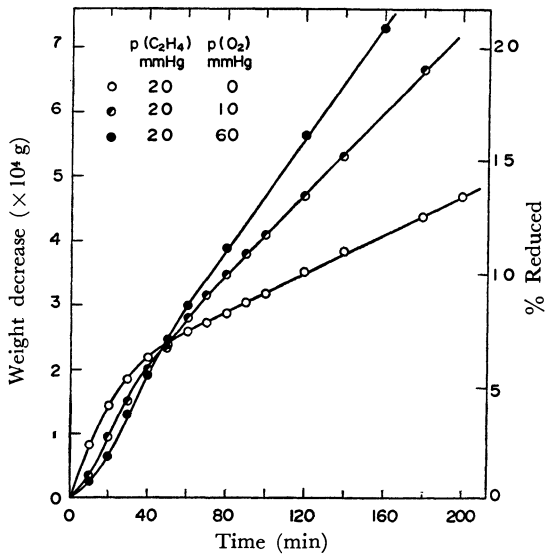

Fig. 1. Typical reaction curves of silver(I) oxide with ethylene and oxygen (170°C).

The reaction experiments were performed in duplicate and were found to be quite reproducible. Figure 1 shows typical results for the reaction of silver oxide (100 mg) with ethylene of 20 mmHg at 170°C in the presence of oxygen. The progress of the reaction with the time was followed by a complicated form in the initial 50 min. It was found that after about 8% reduction of silver oxide sample, the reaction became to proceed linearly with time in any case. The reaction rate constants are shown in Fig. 2 as a function of the oxygen

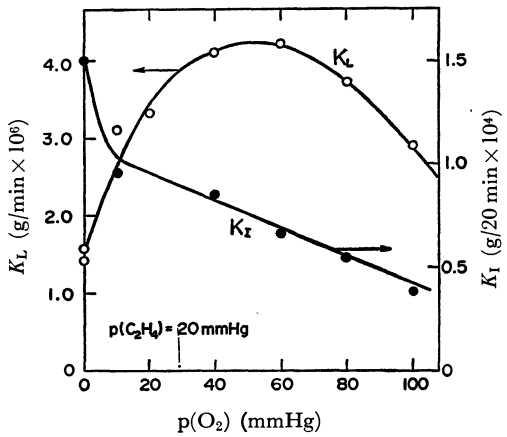

Fig. 2. Reaction velocities as a function of oxygen pressure under a constant pressure of ethylene (170°C).

pressure, where K_I is the reduced amount with the reaction during initial 20 min while K_L is the reaction velocity estimated from the slope of the linear part subsequent to the initial process of 50 min. It is noted that K_I and K_L values changed in much different ways with the oyxgen pressure, K_I being decreased with the pressure while in the curve for K_L the maximum reaction rate being observed in about 50 mmHg of oxygen pressure. No changes in weight of the silver oxide sample were found in pure oxygen (50 mmHg) at 170°C. It is of particular interest that the reaction of silver oxide with ethylene could be accelerated by the coexisting oxygen in the certain partial pressure. It would appear that a coupled reaction of oxidation-reduction on the surface occurred to accelerate the reaction of silver oxide with ethylene.

1) G. H. Twigg, *Trans. Faraday Soc.*, **42**, 284 (1946).
2) L. Ya. Margolis, *Bull. Acad. Sci. USSR, Div. Chem. Sci.*, 1134 (1958).
3) S. Kagawa, E. Tokunaga, K. Kono and T. Seiyama, *Shokubai (Catalyst)*, **9**, (No. 4) 10 (1967).

Major Source of Intensity in the $n\pi^*$ Transition of Aromatic Carbonyls

Martin Vala, Jr.,*[1] and Jiro TANAKA

Department of Chemistry, Nagoya University, Chikusa-ku, Nagoya

(Received July 26, 1968)

The problem of the major source of intensity in the nominally orbitally forbidden, spin allowed $n\pi^*$ transitions in aromatic carbonyl compounds has been investigated by several authors.[1-3] However, no conclusive evidence has been presented in support of either of the two most probable mechanisms: (1) Herzberg-Teller vibronic coupling and (2) delocalization of the carbonyl n and/or π^* orbitals onto the substituents.

We report here the main conclusions of our investigation on the polarized absorption spectrum of the spin-allowed $n\pi^*$ transition in single crystals of 4,4'-dichlorobenzophenone (DCBP) at room and liquid helium temperatures. Details of this work and further work on the singlet-triplet absorption and emission will be reported later.

Our major findings are discussed below. (1) The $n\pi^*$ transition is exclusively polarized in the carbonyl plane and parallel to the carbonyl axis. From this finding we may immediately reject vibronic coupling *via* non-totally symmetric b-type modes and magnetic dipole allowed transitions as possible source of intensity since a perpendicular-to-CO polarization is expected for these mechanisms. It is not possible to eliminate vibronic coupling *via* totally symmetric (a) vibrational modes, as they will have parallel-to-CO polarization. Indeed, there is evidence that several weaker vibronic bands observed in the structure-rich $n\pi^*$ band are gaining intensity in this manner. (2) The 0-0 transition is observed as a very sharp band ($\simeq 2$ cm^{-1} wide) at 26552 cm^{-1}. A careful study of thick crystals (up to 2.5 mm) at room and liquid helium temperatures failed to reveal any absorption to the red of this band which could be assigned to a singlet-singlet transition. The 0-0 transition is followed by a long ($\simeq 10$ member) progression of broad vibronic bands of 38 cm^{-1} spacing. These observations are strongly indicative of the intrinsic allowed electronic character of the $n\pi^*$ transition. (3) The appearance of a large number of sharp vibronic origins upon which are built 38 cm^{-1} progressions of varying length is a prominent feature of the 4.2°K spectrum. We interpret these progressions as due to the totally symmetric in-phase torsional oscillations of the phenyl rings about their long axes. The fact that such oscillations can be observed in the $n\pi^*$ transition is direct experimental proof of the delocalization of the carbonyl n and/or π^* orbitals onto the phenyl rings.

We may write the wave function for the perturbed carbonyl n and π^* orbitals as:

$$\Psi_n{}^{\dagger} = \phi_n + \lambda_\pi{}'\phi_\pi{}'$$

$$\Psi_\pi{}^{*\dagger} = \phi_\pi{}^* + \lambda_\pi{}^{*\prime}\phi_\pi{}^{*\prime}$$

where ϕ_n and $\phi_\pi{}^*$ are the unperturbed carbonyl orbitals and $\phi_\pi{}'$ and $\phi_\pi{}^{*\prime}$ are the substituent pi orbitals. $\lambda_\pi{}'$ and $\lambda_\pi{}^{*\prime}$ are the first order mixing coefficients, for example:

$$\lambda_\pi{}' = \frac{\langle \phi_n | V | \phi_\pi{}' \rangle}{\varepsilon_n - \varepsilon_\pi{}'}$$

Here ε_n and $\varepsilon_\pi{}'$ are the respective orbital energies. Now writing the transition moment integral to first order, we find:

$$\langle \Psi_n{}^{\dagger} | \vec{R} | \Psi_\pi{}^{*\dagger} \rangle =$$

$$\lambda_\pi{}^{*\prime} \langle \phi_n | \vec{R} | \phi_\pi{}^{*\prime} \rangle + \lambda_\pi{}' \langle \phi_\pi{}' | \vec{R} | \phi_\pi{}^* \rangle$$

Thus the $n\pi^*$ transition gains electronic allowed character from intramolecular CT transitions in so far as the perturbation coefficients are non-zero, *i. e.*, as long as there is finite overlap of the carbonyl orbitals with the phenyl orbitals. The intensity of the $n\pi^*$ transition is directly dependent on the magnitude of this mixing. Since the mixing is a first order effect, it will be inversely proportional to the energy separation between the $n\pi^*$ and intramolecular CT transition.

To further test this explanation we have determined the $n\pi^*$ intensities of three different compounds in this class, whose $n\pi^*$ and intramolecular CT transition energy separations are dissimilar. From these energy differences, we predict the $n\pi^*$ intensity to decrease in the order 4,4'-dimethoxybenzophenone > DCBP > benzophenone.[3] Observation gave $f=0.006$, 0.004 and 0.0024, respectively, as predicted. This result leads to the overall conclusion of our work that the $n\pi^*$ transition in symmetric aromatic carbonyl compounds is formally electronically allowed and gains the major component of its intensity by mixing with the intramolecular CT transition.

---

*1 National Science Foundation US-Japan Cooperative Science Program Fellow, 1966—1967. Present address: University of Florida, Department of Chemistry, Gainesville, Florida, 32601.

1) R. Shimada and L. Goodman, *J. Chem. Phys.*, **43**, 2027 (1965).

2) W. D. Chandler and L. Goodman, *ibid.*, **45**, 4088 (1966).

3) D. S. McClure and P. L. Hanst, *ibid.*, **23**, 1772 (1955).

Spectroscopic Investigation of Foreign Gas Effect upon CO_2 Laser Frequencies

Isao SUZUKI* and Shigeko SUZUKI**

* *Department of Chemistry, Faculty of Science, The University of Tokyo, Hongo, Tokyo*

** *Department of Pure and Applied Sciences, College of General Education, The University of Tokyo, Komaba, Meguro-ku, Tokyo*

(Received August 6, 1968)

Under CW (continuous wave) operating conditions in a CO_2 laser, the laser action normally occurs on a few P-branch transitions of the 10.6 μ band of CO_2. Wood and Schwarz[1] observed that introduction of sulfur hexachloride gas to a cell placed within the cavity causes the laser oscillations to shift to a few R-branch transitions. We have found that similar phenomena occur in a wide variety of organic and inorganic gases as well as in SF_6. Not only were the frequencies of the laser transitions dependent upon the foreign gases employed, but they were found very sensitive to the pressures of given gases. With some foreign gases of appropriate pressures within the cavity we have also observed the CW laser oscillations in a few P-branch lines of the 9.6 μ band: a Fermi resonance partner of the 10.6 μ band.

The experimental setup is similar to that reported by Wood and Schwarz[1] and will be described in detail elsewhere.[2] The gases were introduced to a 10 cm cell with KCl windows which was placed inside the cavity. The spectroscopic studies were made with a Perkin-Elmer 112G grating spectrophotometer with a KBr foreprism.[3] Part of our results is shown in Table 1 and in Fig. 1.

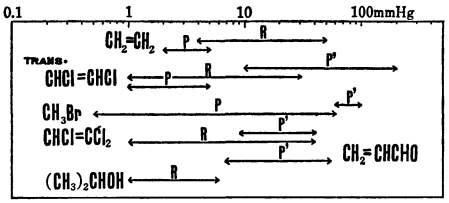

Fig. 1. Dependence of laser frequencies on the vapour pressures of foreign gases. (P' refers to the P-branch of the 9.6 μ band.)

In most cases, our results can be interpreted simply from the absorbances of given gases in this region. A good example is sulfur hexafluoride shown in Table 1. This molecule absorbs strongly in the P-branch region of the 10.6 μ band, much less strongly in the R-branch region, and it has practically no absorption in the P-branch region of the 9.6 μ band. This explains rather remarkable changes in its oscillation frequencies with the gas pressures. This interpretation seems to hold for the most gases observed. Similar results were also obtained when some liquids were introduced in a liquid cell inside the cavity. However, ammonia and methyl bromide seem to be exceptions. In the case of NH_3 gas (85 mmHg), the usually strong P(20) line was completely missing from the emmis on spectrum, whereas no strong absorption seems to be present at the corresponding frequency. Even when the pressure of NH_3 was reduced to 7 mmHg, the P(20) line was the weakest among the transitions in the P-branch region. This result may be related to a near coincidence of the laser line with one of vibration-rotation transitions of NH_3. The 2sQ(4,2) line which Garing *et al.* reported at 944.14 cm^{-1} is most likely to coincide with the P(20) line at 944.18 cm^{-1}. This band is very weak in intensity, however, a close matching in frequency may suppress the laser oscillation of the particular line involved. It may also be the case with methyl bromide.

TABLE 1. THE EFFECT OF FOREIGN GASES ON THE OSCILLATION OF CO_2 LASER
(in approximate order of intensisties)

(a) NH_3 Pressure (mmHg)	10.6 μ band P-branch	10.6 μ band R-branch	(b) SF_6 Pressure (mmHg)	10.6 μ band P-branch	10.6 μ band R-branch	9.6 μ band P-branch
170		20, 22	13			20, 22, 24, 18, 16
50	22, 18	20, 22, 18	5.3		16, 18, 14	
20	22, 18, 24, 16		0.5		18, 20, 16	
7	22, 18, 20		0.0_3	20, 18, 22	18	
3	20, 22, 18					

1) O. R. Wood and S. E. Schwarz, *Appl. Phys. Letters*, **11**, 88 (1967).
2) I. Suzuki and S. Suzuki, to be published.
3) S. Mizushima *et al.*, A Report on the Perkin-Elmer Grating Spectrophotometer Model 112G, The Perkin-Elmer Corp., 1959.
4) J. S. Garing, H. H. Nielsen and K. N. Rao, *J. Mol. Spectry.*, **3**, 496 (1959).

Chromatographic Behavior of Magnesium and Ethylenediaminetetraacetate Ions, and Their Complex on Sephadex G-15 Column

Norimasa YOZA, Takayuki OGATA, Yôichiro UENO and Shigeru OHASHI

Department of Chemistry, Faculty of Science, Kyushu University, Hakozaki, Fukuoka

(Received August 8, 1968)

Several investigations concerning the chromatographic behavior of inorganic species on columns of Sephadex[1,2] (cross-linked dextran) and Bio-Gel[3] (cross-linked polyacrylamide) have recently been reported. From the fact that in general the chemical species on the Sephadex column were eluted in the order of decreasing molecular weight (or molecular size) the principle of this method has been explained in terms of molecular sieving effect[4] in the gel phase. The elution volume, V_e, of individual species in column operation is characterized by the equation

$$V_e = V_0 + K_d V_i \qquad (1)$$

where V_0 represents the void volume, V_i the internal volume and K_d a fraction of internal volume available for the solute.

In column operation of the equilibrium system such as Mg+EDTA⇌Mg-EDTA, where magnesium and ethylenediaminetetraacetate (EDTA) ions interact rapidly to form magnesium ethylenediaminetetraacetate complex, it is required to characterize the behavior of metal complex in addition to that of metal and ligand ions. The present paper describes briefly the behavior of magnesium and EDTA ions, and their complex eluted on a Sephadex G-15 column ($1.5\phi \times 56.5$ cm) at room temperature with 0.1 M sodium chloride solution as an eluent. Sample solutions for three chemical species were prepared by dissolving magnesium chloride, disodium ethylenediaminetetraacetate and disodium magnesium ethylenediamintetraacetate in 0.1 M sodium chloride solution, respectively.

The observed elution volumes and K_d values (calculated by Eq. (1)) of four species are shown in Table 1, together with those of Blue Dextran (molecular weight=2000000) and tritiated water which were used as standard materials of K_d=0 and 1, respectively. Both magnesium and EDTA ions gave symmetrical elution curves when 0.01 M sample solutions were individually eluted. However, the peak skewing became more remarkable with increase of the sample concentration, which might be ascribed to the nonlinear isotherm. It resembles type III of Brunauer *et al.*[5] but is in contrast with adsorption behavior of calcium ion on cation exchanger.[6]

TABLE 1. ELUTION VOLUMES AND K_d VALUES ON SEPHADEX G-15 COLUMN
(Flow rate: 20—30 ml/hr, Volume of fraction: 1.02 ml)

Chemical species	V_e, ml	K_d
Blue Dextran	35.7	0.00
EDTA ion	45.9	0.22
Magnesium-EDTA complex	50.0	0.31
Magnesium ion	64.3	0.62
Sodium ion	70.4	0.76
Tritiated water	81.6	1.00

The sample composed of equimolar concentrations (0.05 M) of magnesium and EDTA ions gave a more complicated elution profile because of the partial dissociation of magnesium-EDTA complex into two reactants which migrated on the Sephadex column with different velocities. However, a sharp, well-defined elution peak of magnesium-EDTA complex was obtained by differential analysis (complexiometric titration) of three components. The complex showed an elution position of molecular size slightly smaller than free EDTA ion. Graphic representation of their behavior will be presented in the near future.

1) S. Ohashi, N. Yoza and Y. Ueno, *J. Chromatog.*, **24**, 300 (1966).
2) P. A. Neddermeyer and L. B. Rogers, *Anal. Chem.*, **40**, 755 (1968).
3) D. Saunders and R. L. Pecsok, *ibid.*, **40**, 44 (1968).
4) R. L. Pecsok and D. Saunders, *Sep Sci.*, **1**, 613 (1966).
5) S. Brunauer, L. S. Deming, W. E. Deming and E. Teller, *J. Am. Chem. Soc.*, **62**, 1723 (1940).
6) Y. Ya. Pronin, S. K. Musaev, K. V. Chmutov and E. S. Krasyuk, *Russ. J. Phys. Chem.*, **41**, 1097 (1967).

Phosphorescence of Crystalline Pyrazine: Emission due to Crystal Defects

Tohru AZUMI, Yasuko NAKANO and Mitsuo ITO

The Institute for Solid State Physics, The University of Tokyo, Roppongi, Minato-ku, Tokyo

(Received August 13, 1968)

Phosphorescence of crystalline pyrazine at 4°K is considerably more complex when compared with the solution spectrum. The onset of the phosphorescence spectrum of a vacuum sublimed pyrazine crystal, which is shown in Fig. 1a, consists of several dozen bands. In this communication we present experimental evidences which reveal that all of these bands are due to pyrazine at some crystalline defects; this observation is in contrast to the interpretation given recently by Moomaw and El-Sayed.[1] The present paper also aims to point out the importance of the sample preparation in the measurements of crystal emission.

Of the bands shown in Fig. 1a we focus our attention to the highest energy weak band, labeled A, and to the relatively intense and sharp bands, B,C···, and G. All of these bands constitute progressions of 606, 759, 953, 1012 and 1254 cm^{-1}. In view of the agreement of these values with the observed Raman frequencies[2] it is certain that all of the above-mentioned bands are due to pyrazine, and not to some chemical impurities.

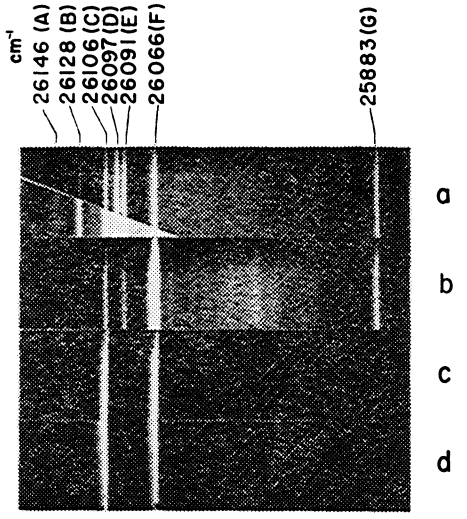

Fig. 1. Phosphorescence spectrum of crystalline pyrazine at 4°K. Spectrum for vacuum sublimed sample, shown in a), changes by successive continuation of zone-melting as shown in b), c) and d).

The vacuum sublimed sample, for which the phosphorescence shown in Fig. 1a is obtained, is subject to zone-melting. Phosphorescence spectra observed at various stages of zone-melting are shown in Fig. 1b, c and d. As is clear from Fig. 1 in the earlier stage of zone-melting bands B and D are weakened. By further continuation of zone-melting bands E and G also are weakened, and finally, only bands C and F remain intense. These observations lead us to conclude that those bands which disappear by the zone-melting process, which is nothing but a repetition of slow crystallization, are due to pyrazine at some crystal defects. The nature of the remaining bands C and F, which are 40 and 80 cm^{-1} apart, respectively, from the highest-energy band A, remains unsolved. However, since no ground state phonons of these frequencies exist, we believe that these bands are also due to crystal defects, which are very difficult to remove.

Moomaw and El-Sayed[1] interpreted the bands shown in Fig. 1a to be due to the coupling with the ground state phonon. They state that bands E and F are[3] due to two strongly coupled phonons of 57 and 86 cm^{-1}. Disagreeing with these authors, we emphasize, in the first place, that the former band is to disappear by zone-melting process, and secondly, that for the latter band the energy separation of 80 cm^{-1} (which is accurate to within 1 cm^{-1}) from band A is greatly different from the observed Raman frequency of 86 cm^{-1} (which is accurate to within 2 cm^{-1}) at 4°K and can, is no way, be correlated with the phonon.[4]

In further support of the above conclusion, phosphorescence lifetimes are obtained for bands E and F, separately, and the results are 19 and 22 msec, respectively. Such different decay behavior alone can unambiguously verify the fact that the emitting states are different for these bands.

1) W. R. Moomaw and M. A. El-Sayed, *J. Chem. Phys.*, **47**, 2193 (1967); **48**, 2502 (1968).
2) M. Ito and T. Shigeoka, *ibid.*, **44**, 1001 (1966).

3) Wave numbers given by Moomaw and El-Sayed[1] are different from ours by about 10 cm^{-1}. This difference is probaly caused by the two factors: a) These authors *apparently* did not convert to the wave numbers *in vacuo*. b) The errors of the wave numbers given by these authors[1] amount to 3 cm^{-1}.

4) It is probably the large wave number errors (as much as 3 cm^{-1}) inherent to the work of Moomaw and El-Sayed[1] which have led these authors to the interpretation different from ours.

Synthesis of Pyrrole Nucleosides by Photodehydrogenation of a Δ^3-Pyrroline Derivative

Masajiro KAWANA and Sakae EMOTO

Rikagaku Kenkyusyo (The Institute of Physical and Chemical Reseach), Yamato-machi, Kita-Adachi-gun, Saitama

(Received August 6, 1968)

Although extensive studies of the synthesis of the nucleosides of heterocycles have been carried out by many workers, simple pyrrole nucleosides have been neglected. Plisov[1] reported that when a mixture of glucose and pyrrole was heated, a probable product (mp 190°C) formed by the condensation of the two was obtained after crystallization from pyridine. However, its structure was unsubstantiated by experimental details or physical data.

We wish to report the synthesis of pyrrole nucleosides by means of a novel photochemical dehydrogenation of a Δ^3-pyrroline derivative. D-Glucose was heated with Δ^3-pyrroline[2] (2 mol eq.) without solvents at 80—85°C to produce 1-(D-glucosy)-Δ^3-pyrroline (I) in a 74% yield, the structure being tentatively identified; mp 130—135°C (decomp.), $[\alpha]_D^{20}$ −28.8°(4 min) → +13.0° (46 hr, constant, *c* 0.40, H_2O). 60-Mc NMR (in D_2O); τ 4.23 2H), singlet, olefinic protons). Found: C, 51.78; H, 7.14; N, 6.09%. Calcd for $C_{10}H_{17}O_5N$: C, 51.94; H, 7.41; N, 6.06%.

On acetylation with acetic anhydride in pyridine, I gave 1-(2',3',4',6'-tetra-*O*-acetyl-β-D-glucopyranosyl)-Δ^3-pyrroline (II) in a 73% yield; mp 121—122°C, $[\alpha]_D^{25}$ −23.7° (*c* 0.49, degassed $CHCl_3$). Found: C, 54.10; H, 6.05; N, 3.51%. Calcd for $C_{18}H_{25}O_9N$: C, 54.13; H, 6.31; N, 3.51%. The site of the glycosidic linkage of the pyrroline ring and the pyranose structure were confirmed by, respectively, the IR spectrum of II and the degradation of II with aqueous formic acid to the known 2,3,4,6-tetra-*O*-acetyl-D-glucose. The NMR spectrum (in $CDCl_3$) was consistent with the structure of II. The methylene and olefinic protons of the pyrroline ring appeared as a singlet at τ 6.22 and 4.32 respectively. The anomeric proton was observed as a doublet centered at τ *ca.* 5.7 (J=*ca.* 8 cps), thus indicating the β configuration.

After a solution of II in benzene containing benzophenone as a sensitizer[3] had been irradiated[4] externally in a Pyrex vessel under bubbling O_2 at 20°C for 1 hr, the TLC analysis of the reaction mixture showed the presence of one main product as well as of several minor by-products. The evaporation of the benzene gave, after recrystallization from ethanol, 1-(2',3',4',6'-tetra-*O*-acetyl-β-D-glucopyranosyl)pyrrole (III) in a 85% yield; mp 178—178.5°C, $[\alpha]_D^{22}$ −10.9° (*c* 0.67, $CHCl_3$). UV; λ_{max}^{EtOH} 211 mμ (ε 8150). Found: C, 54.53; H, 5.73; N, 3.52%. Calcd for $C_{18}H_{23}O_9N$: C, 54.40; H, 5.83; N, 3.53%. A reagent useful for dehydrogenation, 2,3-dichloro-5,6-dicyano-1,4-benzoquinone, was also effective in obtaining III from II in the dark.

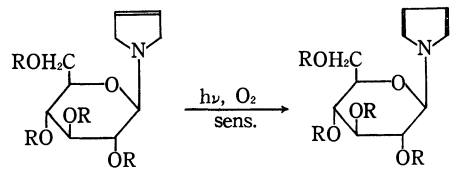

I: R=H
II; R=$COCH_3$
III: R=$COCH_3$
IV: R=H

The NMR spectrum (in $CDCl_3$) of III showed two characteristic triplets, centered at τ 3.83 and 3.21, indicative of the presence of the pyrrole ring. The position of the 2'-acetyl signal (τ 8.15) was at a higher field than the other acetyl signals (τ 7.99—7.93), as has been observed in the case of acetylated nucleosides.[5]

The deacetylation of III with sodium methoxide in methanol afforded 1-(β-D-glucopyranosyl)pyrrole (IV) (76% yield) as a hygroscopic glassy mass after chromatography on a silica-gel column (ethyl acetate-ethanol, 4 : 1); mp *ca.* 80°C, $[\alpha]_D^{25}$ +10.3° (*c* 0.74, H_2O). UV; $\lambda_{max}^{H_2O}$ 210 mμ (ε 6950). Found: C, 52.15; H, 6.38; N, 6.09%. Calcd for $C_{10}H_{15}O_5N$: C, 52.39; H, 6.60; N, 6.11%. Its purity was ascertained by GLC and TLC analyses. The NMR spectrum (in D_2O) exhibited two characteristic triplets centered at τ 3.74 and 3.01 for the protons of the pyrrole ring, and a doublet centered at τ 4.86 (J=8.4 cps) for the anomeric proton. Therefore, the β configurations of III and IV were assigned. Further investigations are in progress.

1) A. K. Plisov, *Ukrainskii Khem. Zhur.*, **3**, 477 (1928); *Chem. Abstr.*, **23**, 3224 (1929).
2) L. H. Andrews and S. M. McElvain, *J. Am. Chem. Soc.*, **51**, 887 (1929).
3) D. C. Neckers, "Mechanistic Organic Photochemistry," Reinhold Publishing Co., New York (1967), p. 163.
4) Super-high-pressure mercury lamp (100 W), Matsuda SHL-100UV-1.
5) R. J. Cushley, K. A. Watanabe and J. J. Fox, *J. Am. Chem. Soc.*, **89**, 394 (1967).

BULLETIN OF THE CHEMICAL SOCIETY OF JAPAN VOL. 41 2553—2557 (1968)

Solvent and Temperature Effects on the Proton hfs in the ESR Spectra of the Organic Radical

Shigeyuki AONO and Masahiko SUHARA

Department of Chemistry, Faculty of Science Kanazawa University, Maru-no-uchi, Kanazawa

(Received January 25, 1968)

A theoretical investigation is made into the solvent and temperature effects on the proton hfs in the ESR spectra of such organic radicals as:

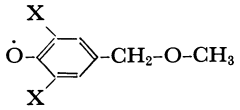

where X stands for the CH_3 group, in several solvents. Both effects are explained on the assumption that a molecular complex is formed between radical and solvent, so that the charge-transfer occurs from radical to solvent: The solvent effect is caused by the fact that, in various solvent molecules, slight changes take place in their lowest vacant levels, which are occupied by the electron transferred from the radical; on the other hand, the temperature effect is explained by the thermal motion of the molecules, which changes the probabilities of the radical being in the solvated state and in the free state.

Recently, experimental observations were made by Deguchi[1] of the proton hfs in the ESR spectra of such phenoxyl radicals as:

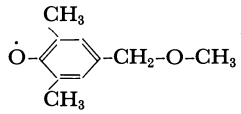

under various conditions. The results are shown in Table 1.

TABLE 1. THE METHYLENE PROTON HFS CONSTANTS

a) at room temperature and in various solvents

Solvent	Coupling const. (gauss)
n-Hexane	11.68
Benzene	12.00
Toluene	12.25
o-, *m*-, *p*-Xylene	12.50
Mesitylene	12.70

b) in tetrahydrofuran at two different temperatures

Temperature (°C)	Coupling const. (gauss)
−54	12.88
9	12.29

These results indicate, in short, that the proton hfs constants increase with an increase in the number of methyl substituents in solvent molecules, and with a decrease in the temperature. However, no such behavior of the coupling constants was not observed in another type of radical:

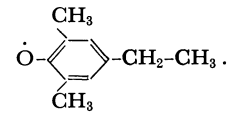

Therefore, we can presume that these phenomena are responsible for the existence of the lone-pair electrons in the oxygen of the methoxy group. Further it should be pointed out that the solvents used here are known to be non-polar.

Mechanism

First of all, we assume that a sort of molecular complex between radical and solvent is formed. It then seems reasonable to assume that the charge-transfer from the oxygen lone-pair of the methoxy group in the radical to the lowest vacant level of the solvent molecule is a characteristic property responsible for the change in the proton hfs constants in the radical, since radicals which have no lone pair never behave thus. On the above assumptions, our theoretical procedures are as follows: The charge-transfer brings about a change in the coulomb term of oxygen by the amount of α'_O, which in turn alters the odd-electron density at the methylene proton by q'_M. Using the standard perturbation procedure, we then obtain:

$$q'_M = 2\alpha'_O c_{iO} c_{iM} \sum_{j \neq i} c_{jO} c_{jM}/(\varepsilon_i - \varepsilon_j), \qquad (1)$$

where ε_j is the orbital energy of the jth level, and where the ith level represents, especially, the level

1) Y. Deguchi, private communication.

for the odd electron, to the zeroth approximation. c_{jO} and c_{jM} are the LCAO coefficients of the jth orbital at the positions of the oxygen atom and the methylene H_2 group respectively. Here it must be noted that the H_2 or H_3 in the methylene or methyl group respectively gives a pseudo-π orbital constructed of 1s atomic orbitals. The radical in question is a π-radical, so that the odd electron occupies, to a good approximation, the highest occupied level of the mother molecule. In the perturbation calculation shown by Eq. (1), the main contributions should be those from the levels closest to the previous one. It follows from a simple investigation that the ith level is nearly the zero level, having a little of the bonding character due to the deeper coulomb terms of the oxygen in both the methoxy and phenoxy groups; the closest two levels, which are refered to the jth and j'th levels, corresponding to those occupied and vacant respectively, may be expected to show, roughly, the pairing property. Taking into account the facts that the contribution from the jth level exceeds than that from the j'th, and also that the oxygen atom of the methoxy group and the methylene H_2 belong to the same class (in the sense of classification to put star or unstar in the alternant hydrocarbon), the coefficient of α'_O in Eq. (1) must be positive. Therefore, we rewrite Eq. (1) as:

$$q'_M = C_1\alpha'_O, \quad C_1 > 0. \tag{2}$$

It can be seen that the sign of C_1 depends upon the position of the proton under consideration.

Since the value of the proton hfs is proportional to the odd-electron density at that position, a change in the latter produces one in the former with the same proportionality constants:

$$a'_M = C_2q'_M, \quad C_2 > 0. \tag{3}$$

Next, let us discuss α'_O in relation to solvent molecules. It is assumed that the radical in question combines to some extent with the solvent molecule. There being several ways in which the molecular complex may originate, the charge transfer from radical to solvent will be picked up as a property responsible for the above-mentioned phenomena.

The ground-state wave function of this complex, to the zeroth approximation, is written as non-bonding, $\Psi_0(R, S)$, where R and S represent radical and solvent respectively. In the higher approximation, the dative structure denoted by $\Psi_1(R^+, S^-)$ will mix with $\Psi_0(R, S)$ to make a more accurate ground state[2]:

$$\Psi = \Psi_0(R, S) + \lambda\Psi_1(R^+, S^-). \tag{4}$$

Here the mixing parameter, λ, is determined by the perturbation method to be:

$$\lambda = H_{01}/\Delta E_{01}, \tag{5}$$

where, using the electronic Hamiltonian H,

$$\left.\begin{aligned} E_{01} &= H_{00} - H_{11} - e^2/r\sigma, \\ H_{ij} &= (\Psi_i|H|\Psi_j). \end{aligned}\right\} \tag{6}$$

In the above, r is the distance between the radical and the solvent, and σ the dielectric constant of the solvent.

As a result, the charge density at the oxygen atom of the methoxy group is reduced by the factor of the normalization factor of Eq. (4), namely $(1+\lambda^2)^{-1}$. Then we have:

$$q'_O \propto (1 + \lambda^2)^{-1} - 1 = -\lambda^2. \tag{7}$$

On the other hand, the charge density is related with the coulomb term by such a formula as:

$$\alpha = \alpha_1 - \alpha_2q'_O, \tag{8}$$

where α_1 and α_2 are constants. Hence:

$$\alpha'_O \propto -q_O'. \tag{9}$$

By combining Eqs. (2), (3), (7) and (9), we obtain:

$$a'_M \propto \lambda^2. \tag{10}$$

That is to say, the formation of the charge-transfer complex results in an increase in the proton hfs coupling constant of the methylene group in the radical.

As to the ring proton at the meta position, since the carbon atom next to the proton belongs to a different class, the sign of C_1 in Eq. (2) must be reversed. However, in the relation:

$$a_H = Qq \tag{11}$$

which relates the ring proton hfs constant, a_H, with the odd electron density on the neighboring carbon atom, the sign of the proportionality constant, Q, is negative, so that we also have the solvent effect, which increases the meta proton hfs constants in the radical. This is consistent with Deguchi's observation.[1]

Solvent Effect Depending on the Number of Substituent Groups

Since, in Eq. (5), the resonance integral in the charge-transfer process refers essentially to the interaction between the carbon and oxygen 2p atomic orbitals, in, respectively, the solvent and the radical, its value is nearly independent on the solvent species, but the denominator, ΔE_{01} is dependent on it. ΔE_{01} can be approximately rewritten, by using the oxygen lone-pair level, ε_0, and the lowest vacant level of the solvent molecule, $\varepsilon_1(n)$, as:

$$\Delta E_{01} = \varepsilon_0 - \varepsilon_1(n) - e^2/r\sigma, \tag{12}$$

where n represents the number of methyl substituents in the solvent molecule. We denote $\varepsilon_1(n)$ as a function of n:

2) R. S. Mulliken, *J. Am. Chem. Soc.*, **74**, 811 (1952).

$$\varepsilon_1(n) = \varepsilon_1(0) - \nu_n\delta, \quad \delta > 0, \tag{13}$$

in which δ is a small positive quantity: ν_n, the function of n, depending on the relative positions of the substituents, and $\varepsilon_1(0)$, the value for benzene. The last term in Eq. (13) arises from the very small perturbation due to the methyl substitution. Then:

$$\begin{aligned} \Delta E_{01} &= \varepsilon_0 - \varepsilon_1(0) - e^2/r\sigma + \nu_n\delta\,, \\ &= \Delta E_{01}(0)(1 - \nu_n\delta'), \end{aligned} \tag{14}$$

with:

$$\left.\begin{aligned} \Delta E_{01}(0) &= \varepsilon_0 - \varepsilon_1(0) - e^2/r\sigma\,, \\ \delta' &= -\delta/\Delta E_{01}(0) > 0\,. \end{aligned}\right\} \tag{15}$$

Considering that $|\nu_n\delta'| \ll 1$, we obtain:

$$\lambda^2 \propto \Delta E_{01}{}^{-2} \cong (1+2\nu_n\delta')/(\Delta E_{01}(0))^2\,. \tag{16}$$

Now we can define:

$$\Delta a(n) = (a'_{\mathrm{M}}(n) - a'_{\mathrm{M}}(0))/a'_{\mathrm{M}}(0)\,, \tag{17}$$

where $a'_{\mathrm{M}}(n)$ or $a'_{\mathrm{M}}(0)$ is the deviation of the proton hfs constant at the methylene group, when benzene or the n methyl-substituted benzene, respectively, is used as the solvent, from that with no solvent effect. Using Eqs. (9), (16) and (17), we get finally:

$$\Delta a(n) = 2\nu_n\delta'. \tag{18}$$

Thus, we conclude that, since ν_n should be positive, the proton hfs constants under consideration increase with an increase in the n value. In order to get a rough estimation, neglecting the position factors of the substituents, and by putting:

$$\nu_n \cong n, \qquad \delta' \cong 0.1 \tag{19}$$

say, $\Delta E_{01}(0)=1$, $\delta=-0.1$ in units of β, the resonance integral of benzene, we have $\Delta a(3)$ to be nearly 0.6. It should be noted that r is nearly 4 Å in usual molecular complexes, while σ is larger than 2 in the solvents under consideration. As to the empirical value, $a'(0)$, we might estimate it from Table 1a as:

$$a'(0) = a(\text{benzene}) - a(n\text{-hexane}) = 0.3 \text{ gauss}.$$

However, taking into account the fact that $a(n$-hexane) has some solvent effect, we have to use a little smaller value for the coupling constant in the bare state. If we take $a(\text{bare})=11.0$ gauss instead of $a(n\text{-hexane})=11.7$ gauss, we can obtain:

$$\Delta a(3) = (12.7 - 12.0)/(12.0 - 11.0) = 0.7$$

in accordance with the calculated value.

Temperature Effect

In discussing the temperature effect or the hfs constants of the solvated radical, it seems that two points are important; first, the equilibrium between the radical-solvent pair and the radical in the free (or loosely-combined) state,[3,4] second, the structural factor in the radical-solvent pair.[5] For the system under consideration, the first seems more important.

Let Ψ_{A} denote the solvated radical which corresponds to the ground state in the higher approximation, as has been discussed in the preceding section, of the radical-solvent pair formed by some sort of intermolecular forces, including the charge-transfer force, and let Ψ_{B} denote the radical in the free state, which was previously written as $\Psi_0(\mathrm{R}, \mathrm{A})$. Assuming the rapid exchange between two states, the value of the hfs coupling constant is observed as:

$$\bar{a} = a_{\mathrm{A}}P_{\mathrm{A}} + a_{\mathrm{B}}P_{\mathrm{B}}\,, \tag{20}$$

where, for example, a_{A} and P_{A} are values of the coupling constant and the existing probability respectively of A state.

As has been shown in the preceding treatment,

$$a_{\mathrm{A}} = a_{\mathrm{B}} + a' \tag{22}$$

with a small positive quantity, a'. Then, considering that P_{A} and P_{B} are temperature-dependent, if we define such a quantity that:

$$\Delta a(T) = (a(T) - a(T_0))/a(T_0),$$

we can easily derive:

$$\Delta a(T) = (a'/a_{\mathrm{B}})(P_{\mathrm{B}}(T_0) - P_{\mathrm{B}}(T)), \tag{23}$$

where we have used the $a_{\mathrm{B}} \gg a'$ relation. Then, further, using $\Delta T = T - T_0$, we can rewrite Eq. (23) as:

$$\begin{aligned} \Delta a(T) &= (a'/a_{\mathrm{B}})\Delta T(P_{\mathrm{B}}(T_0) - P_{\mathrm{B}}(T))/\Delta T \\ &= -(a'/a_{\mathrm{B}})\Delta T\left(\frac{\partial P_{\mathrm{B}}}{\partial T}\right)_{T=T_0}. \end{aligned} \tag{24}$$

Therefore, if we can show that $(\partial P_{\mathrm{B}}/\partial T)_{T=T_0}$ has a positive value, it may be concluded that the hfs coupling constant tends to decrease with an increase in the temperature.

Now let us consider the perturbation causing the transition from the A state to the B state. It originates in the colliding motions of solvents against the radical; the perturbing Hamiltonian is written as:

$$V(t) = Vf(t), \tag{25}$$

where $f(t)$ is the time-dependent factor, which may reasonably be assumed to have a random property with an average value of zero, fluctuating many times in the time interval, t_0(actually the reciprocal of the hfs frequency).

Describing the wave function of the system under consideration as:

3) A. H. Reddoch, *J. Chem. Phys.*, **43**, 225 (1965).
4) A. Crowly, N. Hirota and R. Kreilick, *ibid.*, **46**, 4815 (1967).
5) S. Aono and K. Oohashi, *Prog. Theoret. Phys.*, **30**, 162 (1963); **32**, 1 (1964).

$$\Psi = C_A(t)\Psi_A e^{-i\omega_A t} + C_B(t)\Psi_B e^{-i\omega_B t} \quad (26)$$

with standard notations, we can obtain:

$$C_B(t) = -\frac{i}{\hbar} V_{BA} \int_0^t f(t') e^{-i\omega_{AB} t} \, dt', \quad (27)$$

$$\omega_{AB} = \omega_A - \omega_B, \quad (27a)$$

$$V_{BA} = (\Psi_B | V | \Psi_A). \quad (27b)$$

Here it should be noted that, since we have derived Eq. (27) under the initial conditions, $C_A(0)=1$ and $C_B(0)=0$, the existing probability of the B state is replaced by the transition probability from A to B. Therefore, we have:

$$P_B(t_0) = \frac{1}{\hbar^2} |V_{BA}|^2 \int_0^{t_0} dt \int_{-t_0}^{t_0-t} d\tau \times f(t+\tau) f(t) e^{-i\omega_{AB}\tau}. \quad (28)$$

As in the case in the treatment of the NMR relaxation problem, the integral (28) is a random function, but the statistical average value of the expression:

$$G(\tau) = \overline{f(t+\tau) f(t)}$$

for a fixed τ generally has a definite value, independent of the time t. $G(\tau)$ is generally a rapidly decreasing function of τ, and when t_0 is large, the second integral in Eq. (28) (taking the statistical average) becomes almost independent of t_0, while integration with respect to t_0 gives a factor of t_0 in the answer:

$$P_B(t_0) = t_0 P_B, \quad (30)$$

in which P_B, the transition probability from A to B per unit of time, is:

$$P_B = \frac{1}{\hbar^2} |\overline{V}_{BA}|^2 \int_{-\infty}^{\infty} G(\tau) e^{i\omega_{BA}\tau} \, d\tau. \quad (31)$$

Now, we assume that $G(\tau)$ decays exponentially with a characteristic correlation time τ_c:

$$G(\tau) = e^{-|\tau|/\tau_c}. \quad (32)$$

The transition probability per unit time then becomes:

$$P_B = \frac{1}{\hbar^2} |\overline{V}_{BA}|^2 \frac{2\tau_c}{1+\omega_{BA}^2 \tau_c^2}. \quad (33)$$

At this stage, we need to consider τ_c and ω_{BA} a little more deeply. Colliding motions of solvents against the radical will cause the translational and rotational motions of the radical, and their characteristic correlation times are known to be orders of 10^{-11} sec and 10^{-8} sec respectively, while the value of ω_{BA} may be estimated as the order of the activation energies for the corresponding motions, having values of a few kcal. Therefore, as we have the relation:

$$\omega_{AB}^2 \tau_c^2 \gg 1$$

in our case, P_B in Eq. (33) is approximately:

$$P_B = \frac{1}{\hbar^2} \frac{|\overline{V}_{BA}|^2}{\omega_{AB}^2} \frac{2}{\tau_c}. \quad (34)$$

Since τ_c(rotational) $\ll \tau_c$(translational), it is obvious that the effect of the rotational motion predominates in our case.

According to Debye,[6] the rotational correlation time is:

$$\tau_c = \frac{4\pi\eta a^3}{3kT}, \quad (35)$$

where k is the Boltzman constant, and where the assumption is made that the molecules are spheres with the a radius. η, the viscosity of the liquid, is also temperature-dependent; it is given, by the use of the Eyring transition state theory,[7] as:

$$\eta = nh \, e^{\Delta G^{\neq}/RT}, \quad (36)$$

where n is the number of molecules per unit of volume and $\Delta G^{\neq}$, the Gibbs free energy of the transition state.

Using the relation:

$$\Delta G^{\neq} = -\Delta S^{\neq} T + \Delta H^{\neq} \quad (37)$$

and substituting Eqs. (35) and (36) into Eq. (34), we obtain:

$$P_B = \frac{|\overline{V}_{BA}|^2}{(E_A - E_B)^2} \frac{3kT}{2\pi nha^3} e^{\Delta S^{\neq}/R} e^{-\Delta H^{\neq}/RT}. \quad (38)$$

Inserting this into Eq. (24), we can obtain the temperature dependence of the hfs coupling constant in terms of macroscopic quantities. We may expect that these values, $\Delta S^{\neq}$ and $\Delta H^{\neq}$, negative in sign, will be several tens of eu and a few kcal respectively. As to the temperature-dependent factors, the exponential term should exceed the linear one, so that the value of the coupling constant will decrease with an increase in the temperature. However, it seems almost impossible to estimate it numerically because of the difficulty of determining the parameters, $\Delta S^{\neq}$, $\Delta H^{\neq}$, and so on.

Conclusion

We have presented some considerations concerning the solvent and temperature effects on the proton hfs coupling constants in the ESR spectra of the phenoxy radicals, on the assumption that the charge-transfer takes place from the oxygen lone pair of the radical to the vacant levels of the solvent. The increase in the values of the hfs constants with an increase in the number of the methyl substituents in the solvents is interpreted in terms of the lowering of the lowest vacant level of the solvent

6) P. Debye, "Polar Molecules," Dover Publications, New York (1945), Chapter V.
7) J. O. Hirschfelder and C. F. Curtis, "Molecular Theory of Gases and Liquids," Wiley, New York (1945), p. 627.

due to the methyl substitution. In this case, we have used the rough proportionality which holds between the extent of the lowering in level and the number of methyl substituents.

On the other hand, the temperature effect has been explained by the use of an idea similar to those of Reddoch and Crowly *et al.* in some details. Using the time-dependent perturbation theory, we have obtained the hfs constant in terms of the rotational correlation time, or the liquid viscosity constant, from which the temperature-dependent factor arises. However, it was almost impossible for us to make a quantitative estimate because some parameters were difficult to determine.

BULLETIN OF THE CHEMICAL SOCIETY OF JAPAN VOL. 41 2557—2562 (1968)

Decomposition of Formic Acid over Metal Phthalocyanines

Sadao TANAKA, Takaharu ONISHI and Kenzi TAMARU

Department of Chemistry, The University of Tokyo, Hongo, Bunkyo-ku, Tokyo

(Received March 21, 1968)

The decomposition of formic acid was studied over two sorts of metal phthalocyanines: Mg- and Fe-phthalocyanines. The rates of the decomposition reactions over Mg-Phc and Fe-Phc were proportional to the pressure of formic acid, and the decomposition proceeded to dehydrogenation as well as to dehydration over these phthalocyanines. The isotope distribution in the hydrogen (H_2, HD, and D_2) produced by the decomposition of HCOOD leads to the conclusion that the hydrogen molecule is mainly formed between the hydrogen atom bonded to the carbon atom and that bonded to the oxygen atom in the formic acid molecule. Formic acid was adsorbed to a considerable extent over Mg-Phc in the temperature range between 70°C and 220°C. The amount of formic acid adsorbed obeyed the Langmuir adsorption isotherm, and the infrared spectra demonstrated the presence of the formate ion $HCOO^-$ on the Mg-Phc. It was also confirmed that Mg-Phc was hydrogenated during the course of the decomposition. The adsorption during the catalytic reaction was also measured. These measurements revealed that the overall rate of the reaction is proportional to the amount of formic acid adsorbed. The mechanism of formic acid decomposition was discussed on the basis of these results.

Catalysis by organometallic compounds in the liquid phase is a topic of great interest in the field of chemistry, and the reactivity of such compounds is in many cases correlated with their electronic properties. In heterogeneous catalysis over metals or metal oxides, the complexity of surface properties, such as the heterogeneity of the surface, frequently brings ambiguity into the elucidation of the reaction mechanism. However, the catalysis by molecular crystals of organometallic compounds proceeds over each of the surface molecules independent of the others, and may be treated as catalysis over each of the surface molecules, as with homogeneous catalysis.

The metal phthalocyanine is a biologically-notable substance as it is similar to heme and chlorophyll in its structure. Over this compound the decomposition of formic acid was studied.[1-3] The reaction is known for its selectivity, as it proceeds to different reaction products, dehydrogenation and dehydration. The selective catalysis over the phthalocyanine molecular crystal is, accordingly, a subject of considerable interest.

The importance of adsorption measurements during the course of the reaction has already been emphasized by one of the present authors.[4] The adsorption on the catalyst surface and the behaviour of the chemisorbed species in its working state is directly associated with the elucidation of the mechanism of the surface catalysis.

In this report, by means of adsorption measurements during the course of the decomposition over the phthalocyanines of magnesium and iron, as well as by means of infrared technique and hydrogen isotope distribution, the mechanism of the catalytic decomposition of formic acid will be studied.

1) H. Rosswarm and A. Doiwa, *Naturwissenschaften*, **52**, 159 (1965).
2) W. Hanke, *ibid.*, **52**, 475 (1965).
3) W. Hanke, *Z. Anorg. Allgem. Chem.*, **343**, 121 (1966).
4) K. Tamaru, *Adv. Catalysis* (Academic Press), **15**, 65 (1964).

Experimental

Mg-Phc and Fe-Phc were synthesized according to the Linstead procedures.[5] A magnesium metal film, or iron powder (either 99.9% pure), was boiled with phthalonitrile for 30 hr; the phthalocyanines thus prepared were then carefully purified by washing them with benzene, alcohol, acetone, and water, and by recrystallization in quinoline and by repeated sublimation. The visible and infrared spectra of these phthalocyanines were in reasonable agreement with those reported previously by Linstead[6] and Sidorov[7]. The formic acid was purified by distillation at room temperature, after the removal of the water with anhydrous boric acid. The phthalocyanines of magnesium and iron were evacuated at 250°C and 290°C respectively for 10 hr prior to their use.

The apparatus employed was a closed circulating system with an electromagentic circulating pump. The amount of gases adsorbed on the catalyst surface was calculated from the amount of the reactant introduced into the reaction system and that of the circulating gases. The reactant and products were analyzed by means of gas chromatography: the formic acid, water, and carbon dioxide were analyzed by a dioctyl sebacate (D.O.S.) separatory column, while the carbon monoxide and hydrogen were measured by a silica column at 90°C, employing helium as the carrier gas. The isotopic abundance in hydrogen, H_2, HD, and D_2, was determined by gas chromatography.[8] The infrared cell used in this study was similar to that described previously.[9]

Results and Discussion

I. Adsorption of Formic Acid over Mg-Phc. The adsorption of formic acid over Mg-Phc was studied by a volumetric method at 70, 100, and 130°C, where the decomposition of formic acid scarcely takes place. Due allowance was made for the adsorption of formic acid by the apparatus. The total surface area of the Mg-Phc evaporated film employed was 13.6 m^2. The adsorption was reversible, and, as shown in Fig. 1, it is approximated by the Langmuir adsorption isotherm; the rate of adsorption was proportional to the formic acid pressure throughout the coverage. The heat of adsorption was estimated from the Clapeyron-Clausius equation to be about 5.5 kcal/mol. The adsorption equilibrium constant was also calculated to be $K=e^{-8.85}e^{5.5\times10^3/RT}$ $mmHg^{-1}$, while the saturated amount of adsorption was 10 m*l* (stp) of monomer formic acid. The number of Mg-Phc molecules in the surface

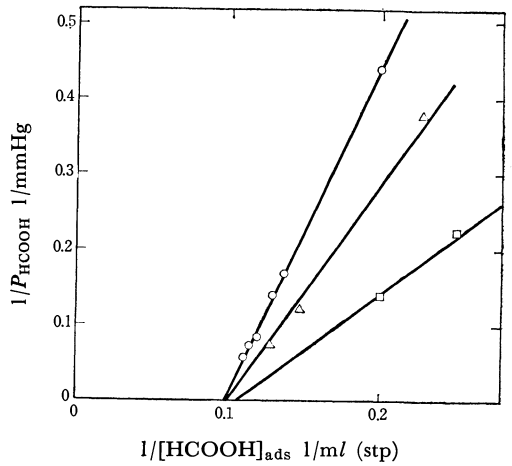

Fig. 1. Dependence of the amount of formic acid adsorbed upon the pressure of formic acid over Mg-Phc.

was estimated to be approximately 3.1×10^{11}, asuming that a (001) plane is exposed on the surface, this value corresponds to nearly one-ninth the number of formic acid molecules having saturated adsorption.

When water was first adsorbed on Mg-Phc at room temperature, and subsequently formic acid was introduced into the adsorption system, all the preadsorbed water was desorbed, being replaced by the formic acid molecules; this demonstrates that formic acid was adsorbed on the sites where water was adsorbed.

II. Decomposition of Formic Acid. Formic acid was decomposed over Mg-Phc at 200°C. Some typical results are given in Fig. 2, where the amounts of formic acid (m*l*, stp as monomer)

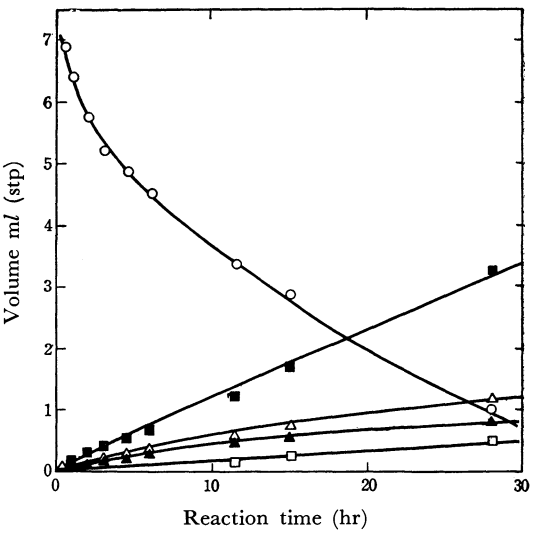

Fig. 2. Decomposition of formic acid over Mg-Phc at 220°C.
○: HCOOH, ■: CO_2, □: H_2, △: H_2O, ▲: CO

5) R. P. Linstead and A. R. Lowe, *J. Chem. Soc.*, **1934**, 1022.
6) P. A. Barrett, R. P. Linstead, F. G. Rundall and G. A. P. Tuey, *ibid.*, **1940**, 1079.
7) A. N. Sidorov and I. P. Kotlyar, *Optics and Spectroscopy*, **11**, 93 (1961).
8) S. Ohkoshi, Y. Fujita and T. Kwan, This Bulletin, **31**, 771 (1958).
9) Y. Noto, K. Fukuda, T. Onishi and K. Tamaru, *Trans. Faraday Soc.*, **63**, 2300 (1967).

and of the reaction products (m*l*, stp) are plotted against the reaction time (hr). Trace amounts of HCHO, CH_3OH, and $HCOOCH_3$ were also detected.*1 It should be noted here that the amount of hydrogen produced was much less than that of carbon dioxide.

The results obtained over Fe-Phc, where the total surface area is 1.6 m^2, are shown in Fig. 3. In this case as much hydrogen as carbon dioxide

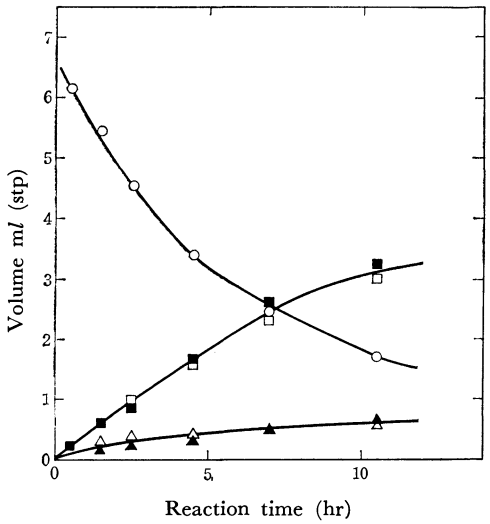

Fig. 3. Decomposition of formic acid over Fe-Phc at 232°C.
○: HCOOH, ■: CO_2, □: H_2, △: H_2O, ▲: CO

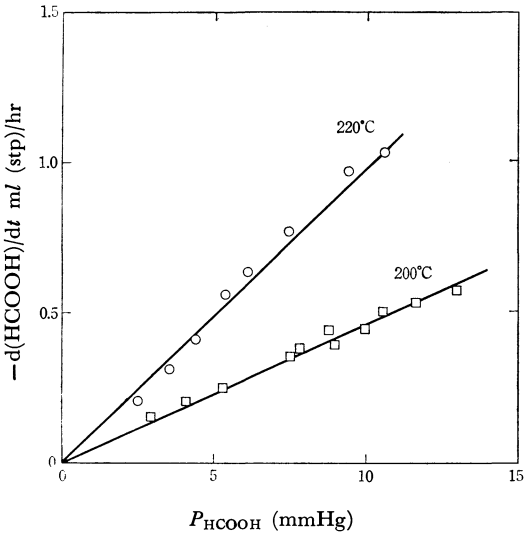

Fig. 4. Dependence of the rate of the decomposition of formic acid upon the partial pressure of formic acid over Mg-Phc.

*1 CH_3OH and $HCOOCH_3$ were clearly found by infrared spectra when formic acid was decomposed at 150°C.

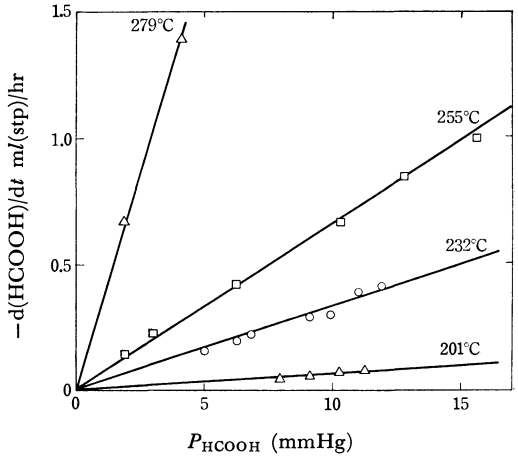

Fig. 5. Dependence of the rate of the decomposition of formic acid upon the partial pressure of formic acid over Fe-Phc.

was evolved unlike the case of Mg-Phc. The ratios of dehydration to dehydrogenation were 1 : 5 at 200°C and 1 : 3 at 279°C.

The rates of formic acid decomposition over Mg-Phc and Fe-Phc were proportional to the pressure of formic acid, as is shown in Figs. 4 and 5. The temperature dependence of the decomposition rate gave the activation energies for the decomposition as 17 kcal/mol for Mg-Phc and 26.1 kcal/mol for Fe-Phc. The frequency factors were calculated to be $5.5\times10^2(m)^{-2}(sec)^{-1}$ for Mg-Phc and $1.1\times10^7(m)^{-2}(sec)^{-1}$ for Fe-Phc.

The adsorption during the decomposition on Mg-Phc was estimated from Fig. 2; it is given in Fig. 6. The composition of the adsorbate was approximately equal to that of formic acid in the first stage of the reaction; later it had a composition richer in hydrogen. The amount of formic acid in the first stage of the reaction was in conformity with the amount estimated by the extrapolation of the adsorption equilibrium up to the

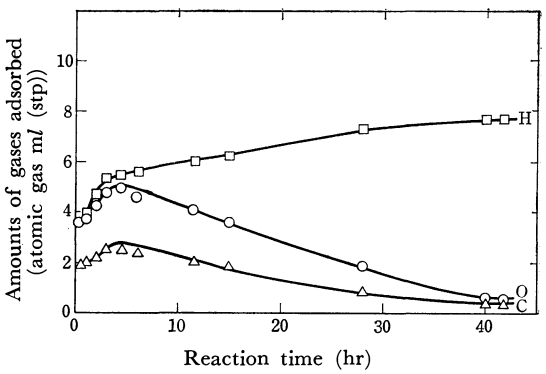

Fig. 6. The adsorption during the course of the decomposition of formic acid over Mg-Phc at 220°C.

reaction temperature. Water, hydrogen, carbon monoxide, and carbon dioxide were separately introduced over the phthalocyanine; it was confirmed that these gases were not adsorbed in the temperature range studied. These results suggest that Mg-Phc is hydrogenated during the course of the formic acid decomposition.

From the results given in Fig. 6, the amount of formic acid adsorbed was plotted against the rate of the decomposition; this plot is given in Fig. 7, where a linear relation was obtained under similar reaction conditions. The adsorption over Fe-Phc, the total surface area of which was 17 m^2, was much less than that over Mg-Phc, and Fe-Phc was not hydrogenated during the course of the decomposition.

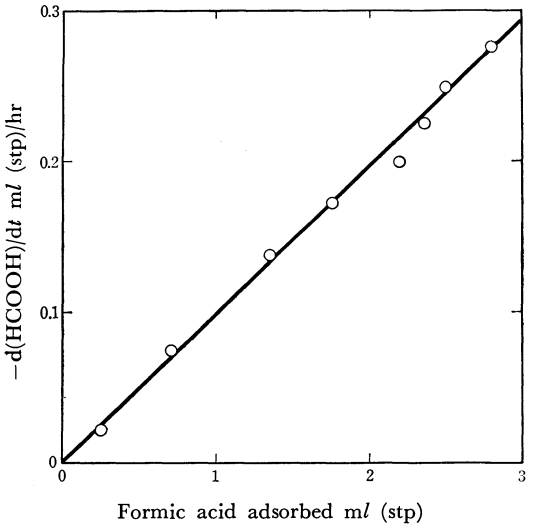

Fig. 7. Dependence of the rate of the decomposition of formic acid upon the amount of formic acid adsorbed over Mg-Phc at 220°C.

When the monodeuterated formic acid, HCOOD, was introduced onto the hydrogenated Mg-Phc, which had previously been evacuated for 10 hr at 250°C, an exchange reaction took place between the deuterium in the HCOOD and the hydrogen in the hydrogenated Mg-Phc, and exchange equilibrium being reached at 100°C. Then the ambient HCOOD was replaced by HCOOH; HCOOD was consequently formed. Accordingly, during the reaction, the isotopic mixing takes place between the hydrogen in water, that in the OH group of formic acid, and that added to the phthalocyanine. The hydrogen in a fresh Mg-Phc, or Fe-Phc, on the other hand, did not participate in the exchange reaction, and no hydrogen exchange with HCOOD could be detected.

When HCOOD was decomposed over a fresh Mg-Phc at 220°C, the ratio of hydrogen to deuterium in the hydrogen gas produced was the same as in the case of HCOOD, though a part of the hydrogen was fixed by the phthalocyanine. The isotopic abundance in the hydrogen produced is given in Table 1.

TABLE 1

Catalyst		Observed %	Equilibrium value %
Mg-Phc*	H_2	13	32
	HD	84	46
	D_2	3	22
Fe-Phc**	H_2	18	29
	HD	79	48
	D_2	3	23

* The D content in HCOOD was 90%.
** The D content in HCOOD was 95%.

Hydrogen was mostly HD, while D_2 corresponded to 13.6% of the equilibrium value of the isotopic exchange.

When HCOOD was similarly decomposed over Fe-Phc at 250°C, a considerable amount of HD was produced and the D_2 corresponded to 12.9% of the exchange equilibrium. It may, accordingly, be concluded that the majority of the hydrogen was produced between the hydrogen bonded to carbon and that bonded to oxygen. The H_2-D_2 exchange reaction did not proceed over Mg-Phc or Fe-Phc under the conditions of formic acid decomposition.

Formic acid was repeatedly introduced over Mg-Phc in order to continue the decomposition for more than 20 days at 220°C. The colour of the Mg-Phc film thereupon changed from violet to blue. When formic acid was decomposed over the catalyst thus treated, the amount of hydrogen produced was the same as that of carbon dioxide; this seemingly suggests the saturation of the hydrogenation. The selectivity or the ratio of CO_2 to CO in the reaction products was not changed.

The infrared spectra, in the region from 4000 to 700 cm^{-1}, of the evaporated Mg-Phc film on a NaCl plate are shown in Fig. 8(a). The spectra were those of the α-form of Mg-Phc. When the Mg-Phc was evacuated for two hours at 200°C, its infrared spectra were changed to the β-form, as is shown in Fig. 8(b). The spectra changed markedly when the β-form of Mg-Phc was treated with 2 cmHg formic acid for a few hours at 100°C, as is shown in Fig. 8(c). The change in the spectra was almost the same as that when CH_3COOH was adsorbed on the α-form of Mg-Phc at room temperature.[10] Most of the change may be interpreted as being due to the α-β transformation. In addition to this change, the spectra of the formate ion, such as 1610 and 1375 cm^{-1}, were observed; this indicates that formic acid was adsorbed on the Mg-Phc, dissociating to a formate ion and a proton. When

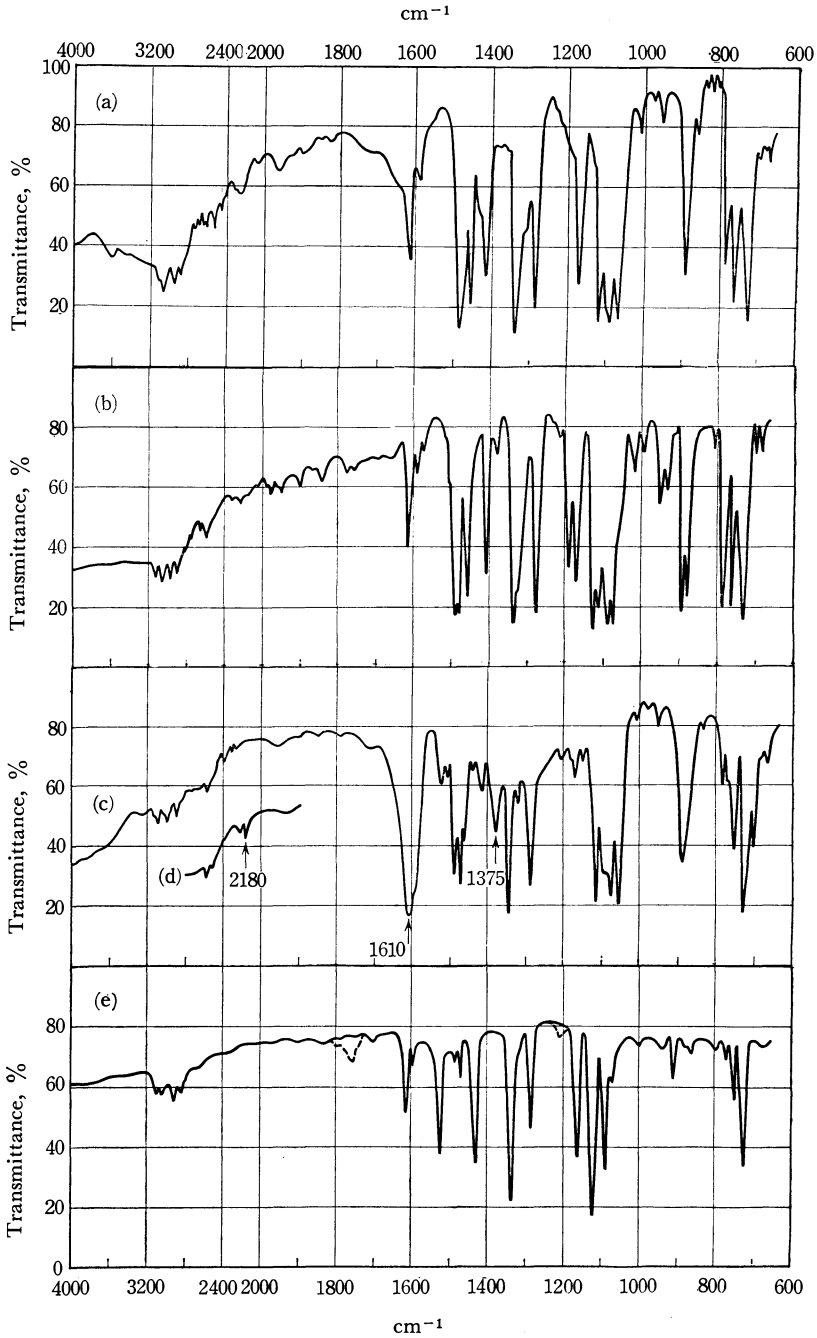

Fig. 8. (a) Infrared spectra of evaporated Mg-Phc film.
(b) Infrared spectra of the Mg-Phc film treated at 200°C.
(c) Infrared spectra of the Mg-Phc where formic acid is adsorbed at 70°C.
(d) Infrared spectra of adsorbed DCOOD on Mg-Phc during the course of the decomposition at 150°C.
(e) Infrared spectra of Fe-Phc (——) and after the exposure to HCOOH vapour at room temperature (- - -).

the Mg-Phc which adsorbed formic acid was evacuated for two hours at 200°C, the spectra of the formate ion disappeared and the structure of the phthalocyanine returned to the β-form.

The infrared spectra were also studied during the decomposition of DCOOD over Mg-Phc for ten hours at 150°C, as is shown in Fig. 8(d); a new weak band at about 2180 cm^{-1} was observed,

a band which became stronger with the progress of the decomposition. The band at 2180 cm^{-1} is close to that of the ND^+ stretching vibration, which appears when DCl is adsorbed on Mg-Phc, deuterium being added to the peripheral nitrogen of Mg-Phc.[10] This band did not disappear upon evacuation. After evacuation, HCOOH was introduced into the reaction system and the band at 2180 cm^{-1} rapidly disappeared.

When Fe-Phc which had been evacuated for two hours at 220°C was exposed to formic acid for a few hours in the temperature range between room temperature and 100°C, neither any formate ions nor any changes in its crystal structure were detected, except for the weak peaks resulting from physically adsorbed formic acid.

From these results, it was concluded that the hydrogenation takes place at the nitrogen of Mg-Phc and that the hydrogen thus fixed can exchange with the proton in the formic acid molecules. Formic acid is adsorbed over Mg-Phc, dissociating to a formate ion and a proton, as is demonstrated in the infrared spectra. The adsorption quickly reaches an adsorption equilibrium, and the amount of formic acid adsorbed in the first stage of the reaction is in conformity with the amount calculated from the adsorption equilibrium.

The linear relation between the adsorption and the overall rate of the decomposition excludes the possibility of the mechanism of the reaction taking place between the adsorbed species and the acid molecule in the ambient gas. It indicates that the reaction intermediate for the decomposition over Mg-Phc is the adsorbed species, or the surface formate ion, and that the reaction takes place *via* the unimolecular decomposition of the formate ion in a manner similar as that over zinc oxide.[11]

The amount of hydrogen evolved was much less than that of carbon dioxide in the initial stage of the decomposition, and Mg-Phc is hydrogenated during the course of the decomposition. The hydrogen thus added to Mg-Phc takes part in the exchange reaction with the hydrogen of the OH group in the formic acid and water molecules. Accordingly, when HCOOD was decomposed over Mg-Phc the hydrogenation of Mg-Phc proceeds to the extent of the reaction; this results in the quick mixing of hydrogen isotopes in the hydrogen bonded to oxygen in the acid and water. The hydrogen-isotope mixing should not be marked in the initial stage of the reaction, where the extent of hydrogenation, and also the amount of water produced, are little. As the rate of hydrogen evolution was much slower than that of carbon dioxide, it took some time to collect enough hydrogen sample for the isotopic analysis; this delay inevitably results in some isotopic mixing. If we take this mixing into consideration, the results given in Table 1 indicate that dehydrogenation overwhelmingly takes place, forming hydrogen from the hydrogen in OH and from that of the CH in the formic acid molecule, as follows, in a manner similar to that with ZnO:[11]

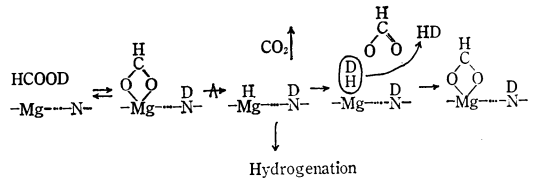

The selectivity of the decomposition, on the other hand, was independent of the extent of hydrogenation; this suggests that different reaction intermediates can be excluded for the dehydrogenation and dehydration for instance, the hydrogen in the phthalocyanine molecule added from the acid molecule. As the dehydration also proceeds in proportion to the amount of adsorption, the following mechanism may be considered for the dehydration:

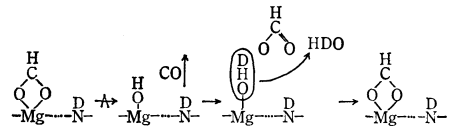

It has been reported that some organic polymer catalysts are also hydrogenated.[12] For example, polycyanoacetylene was hydrogenated during the course of the dehydrogenation of alcohol or cyclohexene, as follows:

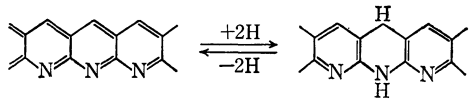

The uptake of hydrogen by the organic polymers is interesting in connection with the behaviour of Mg-Phc.

10) A. N. Sidorov and A. N. Terenin, *Optics and Spectroscopy*, **11**, 175 (1961).

11) Y. Noto, K. Fukuda, T. Onishi and K. Tamaru, *Trans. Faraday Soc.*, **63**, 3081 (1967).

12) J. Manassen and J. Wallch, *J. Am. Chem. Soc.*, **87**, 2671 (1965).

BULLETIN OF THE CHEMICAL SOCIETY OF JAPAN VOL. 41 2563—2570 (1968)

Sensitization of Photoconductivity. Poly-*N*-vinylcarbazole with the Copolymerized Dye Molecule

Kenichi OKAMOTO, Yo HASEGAWA,*1 Shigekazu KUSABAYASHI and Hiroshi MIKAWA

Department of Chemical Technology, Faculty of Engineering, Osaka University, Yamadakami, Suita, Osaka

(Received March 25, 1968)

The sensitization of the photoconductivity of PVCz by dyes was investigated by the measurement of the characteristics of the decay of the surface charge put on the polymer films. MG was selected as a dye and the following three systems were measured and the degree of the sensitization was compared; *i. e.*, PVCz-MG, copolymer of VCz and VMG and PVCz-PVMG systems. The sensitization was observed in the wavelength region from 300 to 1200 mμ. Sensitization in the visible region was larger than in the ultraviolet. The copolymer system was inferior to the PVCz-MG system, probably because of the large loss of the carriers by the recombination and trapping in the bulk. There was the optimum concentration of the dye content, probably because of the disturbing effect of the dye molecule for the migration of the carriers. To make sure this point, the inhomogeneous films with the dye only on the surface were investigated. The results were explained by the difference in the distiribution of the centers of carrier generation and those of recombination and trapping of the carriers in the bulk.

Poly-*N*-vinylcarbazole (PVCz) film is photoconductive and useful as an organic photoconductive material for electrophotography. However its sensitivity is small and limited only in the ultraviolet region. It is, therefore, necessary to improve the senstivity. There are two kinds of method which have been much studied. One is the formation of charge transfer complexes,[1-4] and the other is the addition of dyes.[2,3]

There are many reports about the sensitization with dyes, but there are none about the sensitization by the copolymerization with dye monomers. It has been reported that the absorption spectrum of polyvinylmalachitegreen (PVMG) shows a new peak at 590 mμ in methanol solution beside the absorption bands of the malacitegreen (MG).[5] This peak seems to be due to the associated MG structures caused by the large interaction between neighboring MG groups.[6] If we introduce MG dye molecules directly into the PVCz molecular chain by chemical bond, we may expect results different from the case where MG dye is simply mixed, because the interaction between carbazole groups and MG groups will be different in both cases.

From this view point *N*-vinylcarbazole(CVz)-4''-vinylmalachitegreen(VMG) copolymer was synthesized, and the characteristics of the surface potential decay of its film were investigated and compared with that of the PVCz film mixed with MG (PVCz-MG system). The characteristics of the surface potential decay of the PVCz film mixed with PVMG (PVCz-PVMG), were investigated also.

Experimental

(a) Materials.

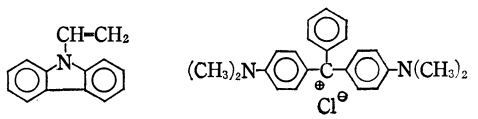

(VCz) (MG)

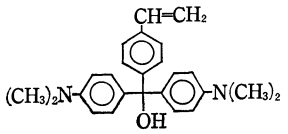

(VMG carbinol)

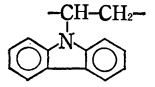

PVCz: -A-A-A-A-A-

(express as A)

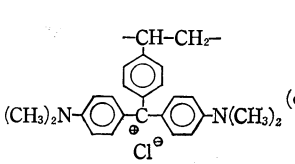

VCz-VMG copolymer: -A-A-A-B-A-

(express as B)

PVMG: -B-B-B-B-B-

*1 Present address: Research Laboratory, Wireless Divission, Matsushita Electric Industrial Co. Ltd., Kadoma, Osaka.

1) S. Oka, T. Mori, S. Kusabayashi, A. Taniguchi, Y. Yamamoto, M. Ishiguro and H. Mikawa, *Electrophotography*, **5**, (No. 3), 77 (1964).
2) H. Högel, Japanese Pat. 261664.
3) Y. Hayashi, M. Kuroda and A. Inami, This Bulletin, **39**, 1660 (1966).
4) M. Lardon, E. L. Döller and J. W. Weigl, *Molecular Crystals*, **2**, 241 (1967).
5) D. Braun, *Makromol. Chem.*, **33**, 181 (1959).
6) To be published.

PVCz: Purified VCz was polymerized by azobisisobutylonitrile in benzene and the polymer obtained was used after being purified by repeated reprecipitation ($\overline{M}_v=110000$).

MG: Commercial MG was purified by the L. Lewis's method.[7]

PVMG: PVMG was prepared from VMG carbinol.[8]

VCz-VMG Copolymer: The copolymer was obtained from VCz and VMG carbinol.[6] The dye mentioned above was used as HCl salts. In changing the dye carbinols into HCl salts, all attention was payed in order to prevent the formation of their dications by excess HCl, chlorine content being confirmed by potentiometric analyses.

(b) Preparation of the Films for the Measurement. In the case of the PVCz-MG and PVCz-PVMG systems, the methanol solution of MG or PVMG was added to the benzene solution of PVCz with stirring (benzene : methanol=20 : 1 by volume), 0.2 m*l* of 5 wt% solution thus prepared was dropped on a copper plate (22 mm in diameter) and the solvent was evaporated slowly.

In the case of the VCz-VMG system, 5 wt% benzene solution of the copolymer was treated likewise. The films were used for the measurement, after being dried for more than 20 hr under 1 mmHg vacuum. These films were estimated to be 20 μ thick.

(c) Measurement of the Decay of Surface Potential. A 500 W xenon lamp was used for the light source. Its energy distribution is shown in Fig. 1. This is different from the usual energy distribution of the xenon lamp, for the relative light intensity is expressed by the number of photons and the slit width of the monochrometer is fixed at 2 mm in the whole wavelength region. Figure 2 is the schematic representation of the experimental arrangement. The films were charged positive or negative by corona discharge. The initial surface potential of the films as observed by our arrangement was about 100 V.

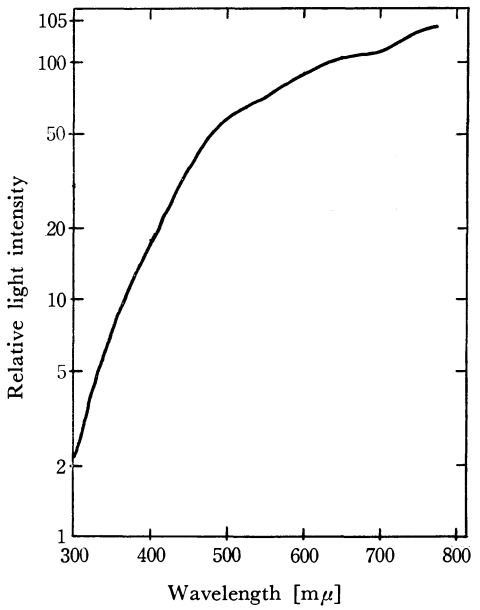

Fig. 1. Energy distribution of the light of xenon lamp measured by a thermopile using a monochrometer (slit width: 2 mm).

Results

(a) Absorption Spectra of the Films. The absorption spectra of PVCz, MG, PVMG, VCz-VMG copolymer and PVCz-MG mixture*2 (99.7 : 0.3 mol%) are shown in Fig. 3. The absorption spectrum of the film of PVCz-MG mixture is similar to that of the MG solution rather than to the MG solid film. In the film of PVCz-MG mixture, the splitting reported in MG solid[9] was not observed and only a slight red-shift of the first absorption peak was observed with somewhat broadening of the peak in comparison with that of the MG solution.

(b) Experimental Equation of the Surface Potential Decay. An example of the decay of surface potential is shown in Fig. 4(a). A linear relation was found between the logarithm of surface potential V and the root of time t as shown

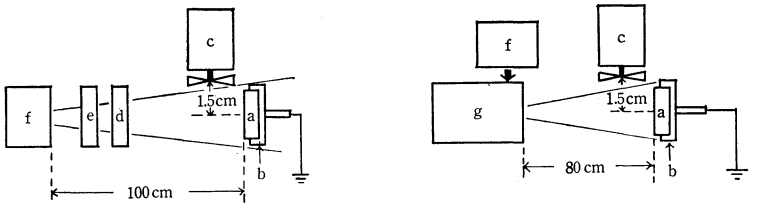

Fig. 2. Schematic arrangement of the measurement of the photo-decay of surface charge.
a) Copper plate with photoconductive films charged positive or negative. b) Supporter for a copper plate. c) Probe of the rotating sector type fieldmeter. The signal is amplified and fed to a recoder. d) Toshiba's filter UV39 (390 mμ<), if necessary. e) Water filter (2 cm thick). f) 500 W xenon lamp. g) Monochrometer.

7) L. Lewis, T. Magel and D. Lipkin, *J. Am. Chem. Soc.*, **64**, 1774 (1942).
8) G. Manecke and G. Kosmehl, *Chem. Ber.*, **93**, 1899 (1960).

*2 The concentration of dye is expressed in this paper by the amount of the dye structure unit to the carbazole unit.
9) J. W. Weigl, *J. Chem. Phys.*, **24**, 364 (1956).

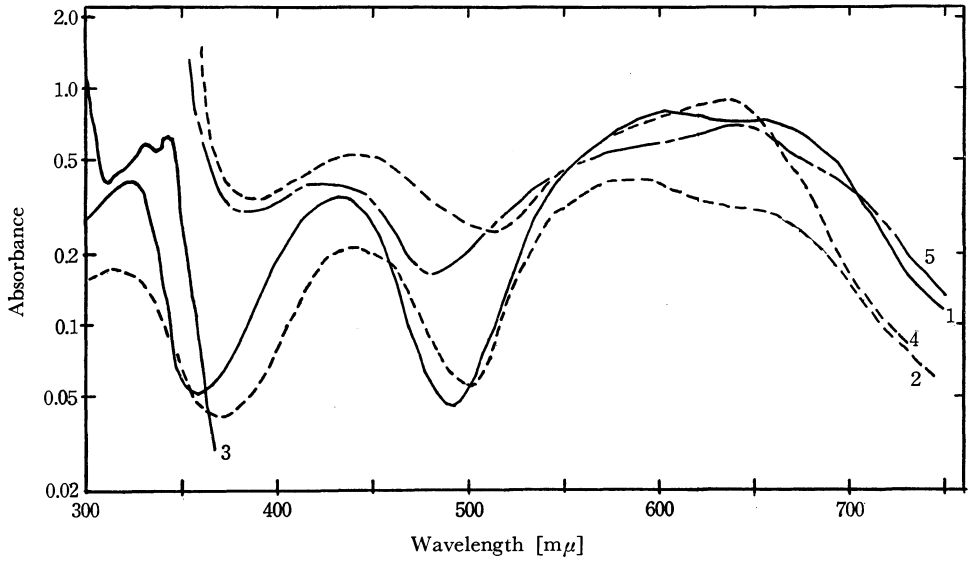

Fig. 3. The absorption spectra of solid films.
1 MG, 2 PVMG, 3 PVCz, 4 VCz-VMG copolymer (0.15 mol%),
5 PVCz-MG (0.3 mol%)

in Fig. 4(b). The results can be described as $V=V_0\exp(-\alpha t^{1/2})$, which equation had been used for ZnO by Inoue[10] and for several organic materials by us.[1,11] We shall use the value of α as the decay constant in the present paper.

(c) Effect of the Dye Content on Dark Decay Constant α_d. As shown in Fig. 5, α_d increases a little with the dye content (especially in the VCz-VMG copolymer system). The sign

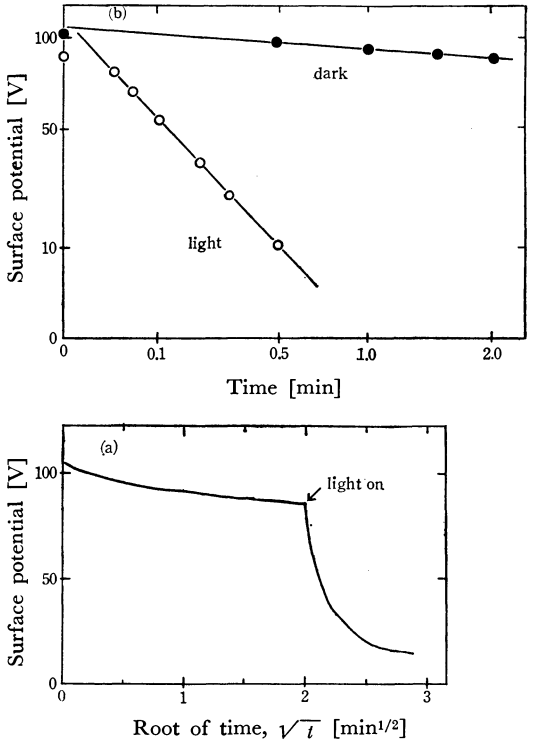

Fig. 4. Decay curves of surface potential.

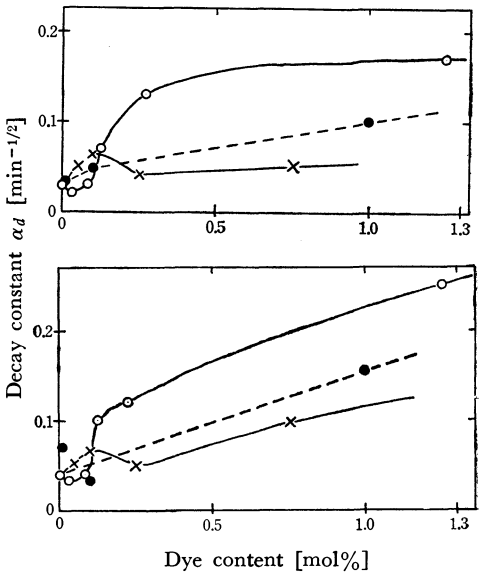

Fig. 5. Dark decay constant *versus* dye content.
—○— VCz-VMG copolymer
--●-- PVCz-MG
—×— PVCz-PVMG

10) E. Inoue, H. Kokado, T. Yamaguchi, S. Nagashima and K. Takahashi, *Electrophotography*, **1**, (No. 2), 27 (1959).

11) S. Oka, T. Mori, S. Kusabayashi, A. Taniguchi, Y. Yamamoto, M. Ishiguro and H. Mikawa, *ibid.*, **5**, (No. 2), 52 (1963).

of the charge put on the film causes no difference in the α_d value.

(d) Effect of the Dye Content on the Light Decay Constant $\alpha_{1,v}$ and $\alpha_{1,t}$. $\alpha_{1,v}$ is defined as the decay constant observed under the illumination with visible light covering from 390 to 1200 mμ and $\alpha_{1,t}$ as that under illumination with the total light from the ultraviolet to 1200 mμ. Preliminary experiment with the PVCz-MG system showed that $\alpha_{1,v}$ reached a maximum at the MG concentration of about 0.1 mol% and decreased considerably at higher concentrations. Decay constants were, therefore, measured with the films containing about 0.1 mol% of the dye.

Figure 6 shows the relation between $\alpha_{1,v}$ or $\alpha_{1,t}$ and the dye content. In every system, the light decay constants have maximum values at the dye content of 0.1 mol% and these values are in the following order; *i.e.*, PVCz-MG system>VCz-VMG copolymer system$\gg$ PVCz-PVMG system. The value of $\alpha_{1,t}$ is much larger as a film is charged positive than as it is charged negative. These values denoted respectively as $\alpha^+{}_{1,t}$ and $\alpha^-{}_{1,t}$. There is no large difference in $\alpha_{1,v}$ between a film charged positive ($\alpha^+{}_{1,v}$) and a one charged negative ($\alpha^-{}_{1,v}$). However in PVCz-MG system and PVCz-PVMG copolymer system $\alpha^-{}_{1,v}$ is a little larger than $\alpha^+{}_{1,v}$, and in VCz-VMG copolymer system $\alpha^+{}_{1,v}$ is a little larger than $\alpha^-{}_{1,v}$.

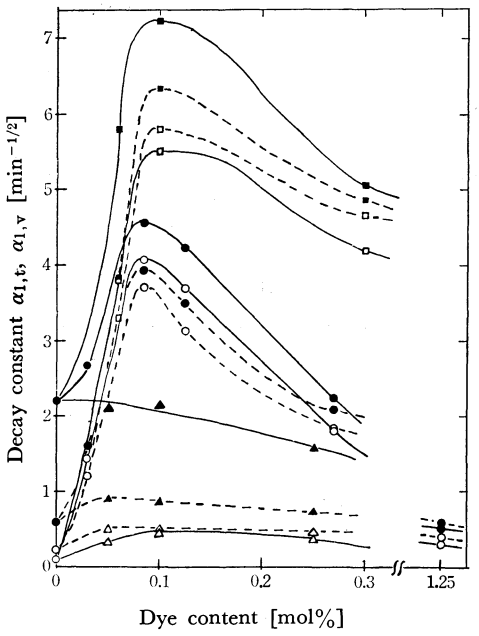

Fig. 6. Decay constant *versus* dye content.

$\alpha_{1,t}$	$\alpha_{1,v}$	Systems
—■—	—□—	PVCz-MG
—●—	—○—	VCz-VMG copolymer
—▲—	—△—	PVCz-PVMG

Solid lines show α values when charged positive and dotted lines show α values when charged negative.

The value, $\alpha_{1,UV}$, which is defined as $\alpha_{1,t}-\alpha_{1,v}$, is a measure of the effect of the UV light under the illumination with the total light. Figure 7 shows the effect of the dye content on $\alpha_{1,UV}$. The $\alpha^-{}_{1,UV}$ value ($\alpha_{1,UV}$ for the films charged negative) decreases

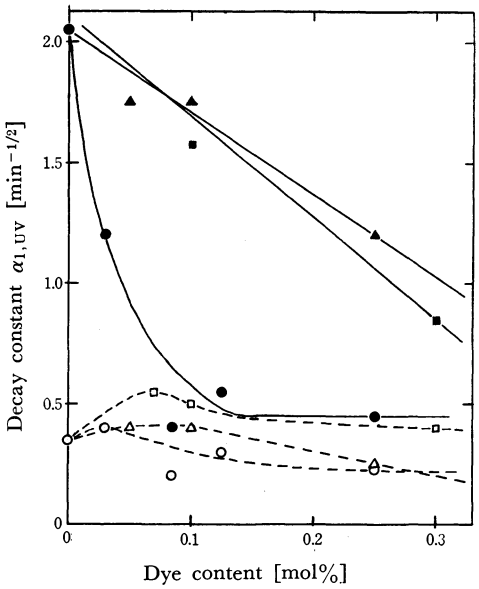

Fig. 7. Decay constant *versus* dye content.
—○— VCz-VMG copolymer
—□— PVCz-MG
—△— PVCz-PVMG
Solid lines show α value when charged positive and dotted lines show α values charged negative.

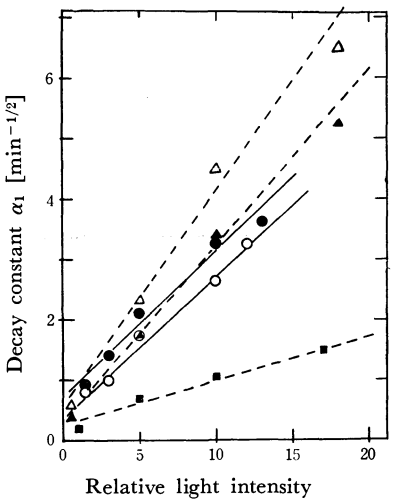

Fig. 8. Decay constant *versus* light intensity.

Charged	λ	System
—○— (−)	625 mμ	VCz-VMG copolymer
—●— (+)	625 mμ	VCz-VMG copolymer
--△-- (−)	625 mμ	PVCz-MG
--▲-- (+)	625 mμ	PVCz-MG
--■-- (+)	435 mμ	PVCz-MG

with the increasing dye content after having reached a maximum, but $\alpha^{+}_{1,UV}$ decreases uniformly with the increasing dye content. It must be noted that in VCz-VMG copolymer system the amount of decrease is much larger than in the other systems.

(e) Spectral Response of the Decay Constant. The linear relation between the decay constant under the illumination with a monochromatic light, $\alpha_{1,m}$ and the relative light intensity is shown in Fig. 8. Figure 9 shows the spectral response of the decay constant normalized for the relative light intensity shown in Fig. 1, photon number of 365 mμ light being defined as a unity. In every system the sensitization by the dyes is positive at every wavelength measured and its degree is in the following order; *i.e.*, PVCz-MG system > VCz-VMG copolymer system ≫ PVCz-PVMG system. This order is the same with one

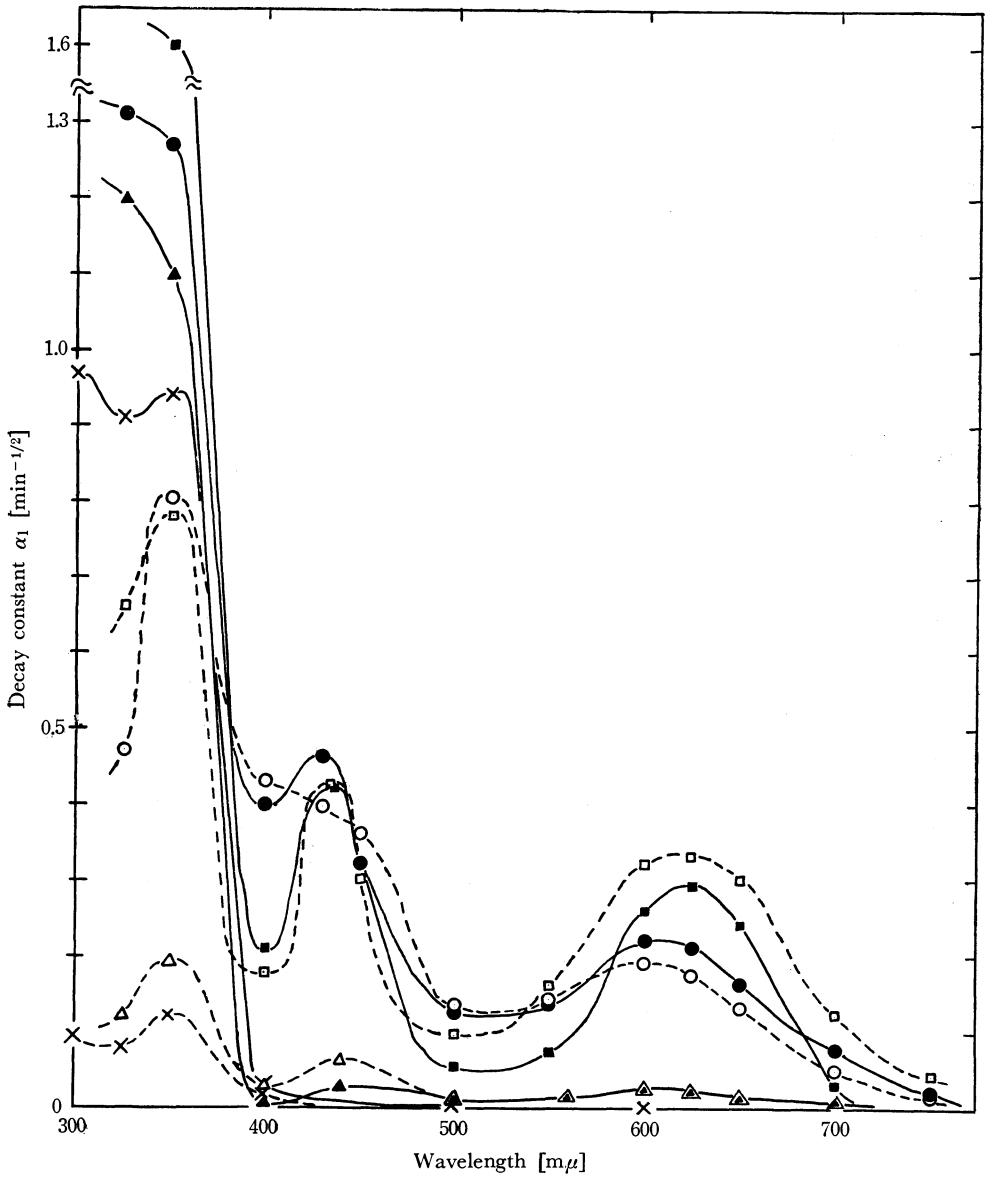

Fig. 9. Spectral response of decay constants normalized for the light intensity at 365 mμ.

Charged: Positive	Charged: Negative	System
—×—	--×--	PVCz
—●—	--○--	VCz-VMG copolymer (0.085 mol%)
—■—	--□--	PVCz-MG (0.1 mol%)
—▲—	--△--	PVCz-PVMG (0.1 mol%)

for $\alpha_{1,v}$ mentioned above.

The spectral response of $\alpha_{1,m}$ is in agreement with the absorption spectra of the films, although in VCz-VMG copolymer system the considerable sensitization is found even in the weakly absorbed region (400 mμ) in comparison with PVCz-MG system. There is no difference in $\alpha_{1,m}$ between the films charged positive and negative in the visible light region. In the ultraviolet region, however, $\alpha_{1,m}$ of the former is considerably larger than the latter. The degree of sensitization in the ultraviolet region is about one and a half-fold when charged positive and about seven-fold when charged negative.

Discussion

(a) The Effect of HCl Addition on the Decay Constant. MG reacts with excess HCl to give its dication and the photoconductivity of this dication has been reported to be smaller than that of MG.[12] In preparing HCl salts of MG, PVMG and VCz-VMG copolymer, therefore, strictly controlled amount of HCl was used in order to avoid any formation of the dication structure.

The effect of HCl on the decay constants when added to PVCz and PVCz-MG (0.1 mol%) systems is shown in Fig. 10. By the addition of HCl the PVCz-MG system was desensitized, probably because of the formation of the dication structure. The PVCz system was, however, sensitized especially in the case of the positively charged film illuminated with total light.

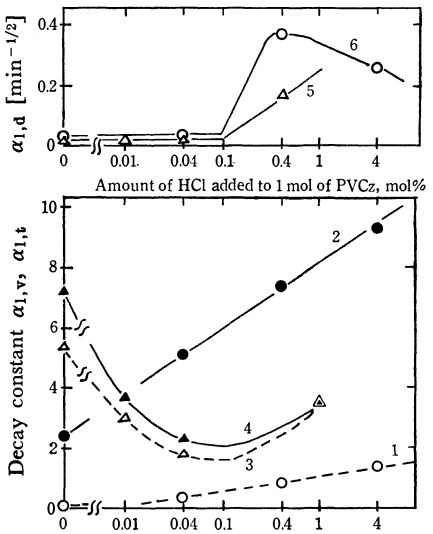

Fig. 10. Effect of HCl on decay constant (when charged positive).
1 $\alpha_{1,v}$ of PVCz, 2 $\alpha_{1,t}$ of PVCz,
3 $\alpha_{1,v}$ of PVCz-MG (0.1 mol%),
4 $\alpha_{1,t}$ of PVCz-MG (0.1 mol%),
5 α_d of PVCz,
6 α_d of PVCz-MG (0.1 mol%)

α_d of both films increased with the increasing amount of HCl. Thus HCl gives a large effect on the decay constants.

As one and a half-fold excess of HCl was used to get the HCl salt of the copolymer, the dication structure might be formed and this dication structure might have made the light decay constant of the copolymer smaller than that of PVCz-MG film. In order to confirm this point the effect of the amount of HCl on α was investigated which was added to obtain the HCl salt of the copolymer. As the amount of HCl (up to two fold excess) had no effect on α, the HCl salt of the copolymer used in this experiment seems not to contain the dication structure and the α_1 value of the copolymer seems to be small in itself.

(b) A Simple Model Explaining the Surface Potential Decay Constant under Light Illumination. The surface potential of the amorphous selenium charged positive by the corona discharge has been investigated as a function of the illumination time and explained by a model based on trapping and recombination of carriers.[13] The experimental results in this paper can also be explained by assuming an appropriate location of generation, trapping and recombination of carriers.

(i) In the case of the illumination with strongly absorbed light, the light creates electrons and holes near the illuminated surface. A part of them disappears by recombination and the rest moves in the electric field causing the surface potential decay. The carriers trapped in the bulk contribute also to the surface potential decay according to their positions.

All investigated systems when illuminated with only UV light and the PVCz system when illuminated with total light belong to the case (i). The values of $\alpha_{1,m}$ in the UV region and of $\alpha_{1,t}$ in the PVCz system are much larger when charged positive. This suggests that the hole carrier is more mobile than the electron carrier in these systems. PVCz film has been reported to be p-type.[1,3]

(ii) In the case of the illumination with weakly absorbed light, the light is absorbed uniformly in the bulk creating electron and hole carriers and the carriers move to the oppositely charged surfaces, a part of them being lost by trapping and recombination. As the situation is nearly equal both for positive and negative polarity, $\alpha^+_{1,v}$ and $\alpha^-_{1,v}$ are almost equal. The PVCz-MG, VCz-VMG copolymer and PVCz-PVMG systems containing less than 0.3 mol% of dye structures belong to the case (ii) when illuminated with visible light. As

12) R. C. Nelson, *J. Chem. Phys.*, **19**, 798 (1951).

13) H. Tung Li and P. J. Regensberger, *J. Appl. Phys.*, **34**, 1730 (1963).

expected, $\alpha^{+}_{1,v} \approx \alpha^{-}_{1,v}$ in these systems.

(iii) In the case of the simultaneous illumination with strongly and weakly absorbed light, the phenomena (i) and (ii) take place simultaneously. The PVCz-MG, VCz-VMG copolymer and PVCz-PVMG systems containing less than 0.3 mol% of dye structural unit belong to the case (iii)when illuminated with total light.

The results of Fig. 7 suggest as follows. The $\alpha_{1,UV}$ value may be thought to be the measure of the surface potential decay by the carriers which are created near the illuminated surface and move through the bulk to the oppositely charged surface. If no dye is contained, the loss of the carriers in the bulk may be small.

If dyes are contained, however, the carriers are generated also in the bulk by the light absorbed by dyes. The dyes may act as the trapping centers for the carriers and a part of the carriers generated near the surface by UV light will be lost by the recombination and by the trapping in the bulk. For this reason $\alpha_{1,UV}$ seems to decrease with the increasing amount of dyes. As the decrease of $\alpha^{+}_{1,UV}$ is larger than that of $\alpha^{-}_{1,UV}$, the hole carriers will be lost much more than the electron carriers while passing through the bulk containing the dye. It should be noted that this loss of carriers in the VCz-VMG copolymer system may apparently be much larger than that in the other systems.

(c) Comparison of the Surface Potential Decay Constants of Homogeneous Films with That of the Inhomogeneous Films. Probably because of the two reasons there will be the most effective concentration of dyes for the sensitization of PVCz. One is a change in the state of the aggregation of the dye structures causing the change in the efficiency of carrier generation[14,15] and another is the disturbance of the carrier migration through the bulk. The following experiment was done to confirm the latter effect.

Inhomogeneous films (about 24 μ thick) were made from PVCz film (about 20 μ thick) by coating the surface with 0.04 m*l* of the 5 wt% benzene solution of PVCz-MG or VCz-VMG copolymer. These inhomogeneous films consist of the surface layer (about 4 μ thick) containing dyes and the base film of PVCz (about 20 μ thick). Decay constants of the inhomogeneous films thus prepared were compared with those of the homogeneous films (about 24 μ thick). In the case of the inhomogeneous films the decay curves deviated considerably from $V=V_0\exp(-\alpha t^{1/2})$. The experimental results were, however, expressed by this equation, and the parameter α thus obtained was compared with the α values of the homogeneous films. The results are shown in Table 1. The following four important differences were evident.

(i) $\alpha^{+}_{1,v} > \alpha^{-}_{1,v}$ In homogeneous films $\alpha^{+}_{1,v}$ is nearly equal to $\alpha^{-}_{1,v}$, on the other hand, in inhomogeneous films $\alpha^{+}_{1,v}$ is much larger than $\alpha^{-}_{1,v}$. As the surface potential decay in inhomogeneous films belongs to the case of (b-i) mentioned above, this result is explainable.

(ii) $\alpha^{h+}_{1,UV} < \alpha^{ih+}_{1,UV}$ There is no difference in $\alpha^{-}_{1,UV}$ between homogeneous and inhomogeneous films, but $\alpha^{+}_{1,UV}$ of the latter ($\alpha^{ih+}_{1,UV}$) is much larger than $\alpha^{+}_{1,UV}$ of the former ($\alpha^{h+}_{1,UV}$). As in inhomogeneous films the base PVCz film does not contain the dye and carriers are not created in the bulk, the carriers created near the illuminated surface will not be lost much by the recombination and trapping in the bulk. $\alpha^{ih+}_{1,UV}$ may be, therefore, larger than $\alpha^{h+}_{1,UV}$.

On the other hand in negative polarity, both for inhomogeneous and homogeneous films the values of $\alpha^{ih-}_{1,UV}$ and $\alpha^{h-}_{1,UV}$ are nearly equal to each other, probably because the loss of electrons by the existence of the dyes in the bulk, as stated above, is much smaller than that of holes, and

Table 1. Comparison of α values of homogeneous films with those of inhomogeneous films

Systems	Dye content	$\alpha^{+}_{1,v}$	$\alpha^{-}_{1,v}$	$\alpha^{+}_{1,t}$	$\alpha^{-}_{1,t}$	$\alpha^{+}_{1,UV}$	$\alpha^{-}_{1,UV}$
PVCz-MG	mol%			$min^{-1/2}$			
homogeneous	0.1	3.7	4.3	4.2	4.7	0.5	0.4
	0.3	1.8	1.9	2.2	2.2	0.4	0.4
inhomogeneous	0.1	6.6	4.3	9.2	4.9	2.6	0.6
	0.3	5.6	4.8	7.0	5.4	1.4	0.6
VCz-VMG copolymer							
homogeneous	0.087	3.7	3.2	4.2	3.3	0.5	0.1
	0.127	3.8	3.8	3.8	3.9	0	0.1
	0.27	2.6	2.1	2.7	2.3	0.1	0.2
inhomogeneous	0.087	3.5	1.5	5.0	1.6	1.5	0.1
	0.127	3.1	1.4	4.8	1.3	1.7	0
	0.27	3.7	1.3	4.5	1.4	0.8	0.1

14) R. C. Nelson, *J. Opt. Soc. Am.*, **1958**, 948 .

15) R. C. Nelson, *J. Phys. Chem.*, **71**, 2517 (1967).

consequently, for electrons, the influence of the difference of the bulk constituents in homogeneous and inhomogeneous films may effectively be very small.

(iii) In homogeneous films $\alpha^{h+}{}_{l,v}$ decreases much with the increasing dye concentrations both in PVCz-MG films and in VCz-VMG copolymer films. In inhomogeneous films, however, $\alpha^{ih+}{}_{l,v}$ changes little with increasing dye concentrations. $\alpha^{ih+}{}_{l,v}$ is therefore much larger than $\alpha^{h+}{}_{l,v}$.

In carrier generation, the homogeneous films must be superior to the inhomogeneous films, as the increase of the total carrier is expected with the increasing volume where the dye molecules exist. The fact that in positive polarity $\alpha^{ih+}{}_{l,v}$ is larger than $\alpha^{h+}{}_{l,v}$ must, therefore, be understood by assuming the dual effect of the dye molecules, the generation of carriers and the disturbance for carrier migration. The latter effect must be predominant in this case.

In the case of the VCz-VMG copolymer system $\alpha^{-}{}_{l,v}$ of the homogeneous films is larger than that of the inhomogeneous films, probably because the carrier generation effect may be superior to the disturbance effect. In the case of the PVCz-MG system, however, the former is smaller than the latter, probably because the carrier generation effect may be inferior to the disturbance effect.

These results, (ii) and (iii), support that the hole carrier is lost much more than the electron carrier while passing through the bulk by the existing dye molecules and the loss is especially much in the VCz-VMG copolymer films.

(iv) α_d of inhomogeneous films is considerably smaller than that of homogeneous films in both VCz-VMG copolymer and PVCz-MG systems.

(d) The Degree of Sensitization. The degree of sensitization is in the following order; *i. e.*, PVCz-MG system > VCz-VMG copolymer system $\gg$ PVCz-PVMG system.

From this result it will be supposed that the efficiency of the carrier generation of PVMG is inferior to that of MG and the copolymer. The dyes in the aggregated states have been reported to have poor efficiency of sensitization, which fact has been explained on the electron transfer mechanism.[14,15]

If so, the small degree of sensitization of PVMG as observed in the present investigations will be due to easy aggregation of the dye structures in the polymer chain.

In sensitizing PVCz the copolymer is inferior to the PVCz-MG system because of the loss of mobile carriers by the recombination and trapping in the bulk.

BULLETIN OF THE CHEMICAL SOCIETY OF JAPAN VOL. 41 2570—2574 (1968)

Unperturbed Dimension of Poly(butylene oxide)

Masahiro MATSUSHIMA, the late Masaaki FUKATSU and Michio KURATA

Institute for Chemical Research, Kyoto University, Uji, Kyoto

(Received April 5, 1968)

Viscosity and light scattering measurements of poly(butylene oxide) were carried out in various solvents, including a theta solvent, isopropanol. The intrinsic viscosity *vs.* molecular weight relationships obtained in the range of molecular weight from 2.1×10^5 to 2.3×10^6 were:

$$[\eta]=3.39\times10^{-5}M_w^{0.84} \text{ in benzene at } 30°C,$$

$$[\eta]=4.08\times10^{-5}M_w^{0.79} \text{ in methyl ethyl ketone at } 30°C,$$

$$[\eta]=8.65\times10^{-4}M_w^{0.50} \text{ in isopropanol at } 29.8°C.$$

The ratio σ between the end-to-end distance of the polymer chain in the unperturbed state and that in the freely rotating state was estimated to be 1.66.

As the second part of a series of papers on the dilute solution properties of polyoxides,[1] we here report the results of light scattering and viscosity measurements performed on poly(butylene oxide).

Experimental

Polymer Sample. Poly(butylene oxide) was a gift from Dr. Yutaka Matsui of the Takeda Chemical Industries, Ltd., which was polymerized in *n*-hexane at 60°C using a zinc diethyl complex catalyst with butylene glycol.[2] The polymer was dissolved in acetone to make an original solution for the fractionation. The

1) Part I of this series: M. Kurata, H. Utiyama and K. Kamada, *Makromol. Chem.*, **88**, 281 (1965).

2) Y. Matsui, N. Hashimoto, T. Saegusa and J. Furukawa, *Kogyo Kagaku Zasshi (J. Chem. Soc. Japan, Ind. Chem. Sect.)*, **69**, 1375 (1966).

concentration was 0.8 g/dl. To the solution, methanol was added at 34°C until the solution became turbid. Then, the solution was cleared at an elevated temperature, cooled again and stood at 34°C at which phase separation was proceeded. After removal of the solution phase by siphoning, the precipitate was dissolved in benzene, and dried, and dissolved again in benzene with a small amount (about one hundredth of polymer weight) of antioxidant, *p*-benzylamino phenol. This solution was freeze-dried, and stored in a freezer at about −20°C. The removed solution phase was subjected to the next cycle of the fractionation. The procedures described above were repeatedly applied until the original polymer was separated into 20 fractions. Nine of these fractions were put in light scattering and viscosity measurements.

Solvents. Benzene, methyl ethyl ketone and isopropanol were used as solvents. These solvents were put in physical measurements after dried with drying agents and fractionally distilled. The drying agents used were sodium metal for benzene, active anhydrous calcium sulfate for methyl ethyl ketone and anhydrous copper sulfate for isopropanol, respectively.

Theta Temperature. The theta temperature was found to be 29.8°C in isopropanol by light scattering measurements. Figure 1 shows the apparent second virial coefficient for the whole polymer plotted against the temperature. In the figure, an arbitrary scale is used for the ordinate, since the refractive index increment was not determined in this solvent.

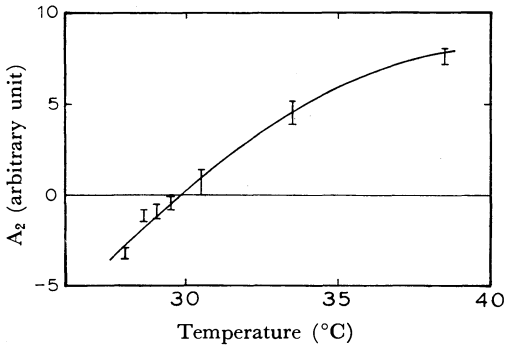

Fig. 1. Determination of the theta temperature.

Intrinsic Viscosity. Viscosity measurements were made in three solvents, *i. e.*, benzene at 30.0°C, methyl ethyl ketone at 30.0°C and isopropanol at 29.8°C, using dilution viscometers of the Ubbelohde type. Corrections for kinetic energy and shear rate were both immaterial. The intrinsic viscosities $[\eta]$ and the Huggins constants k' were determined by extrapolating the plots of η_{sp}/c *vs.* c, and of $(\ln \eta_{rel})/c$ *vs.* c to zero concentration in such a manner that both plots gave the same ordinate intercept. In such a case that the η_{sp}/c *vs.* c plot displayed a marked curvature, the plot of η_{sp}/c *vs.* η_{sp} was used for the extrapolation.

Refractive Index Increments. Measurements were made in a differential refractometer of the Debye type (Shimadzu Seisakusho, Ltd., Kyoto) which was calibrated against aqueous potassium chloride. Five solutions with different concentrations were prepared by dilution from two initial solutions whose concentrations were determined by weighing the dried amount of polymers recovered from a known volume of the solutions. The refractive index increment obtained for the light of 436 mμ wavelength was 0.0863 ml/g in methyl ethyl ketone at 30°C.

Light Scattering. Measurements were made on nine fractions of the polymer in methyl ethyl ketone at 30°C by using a light scattering photometer of the Brice type (Shimadzu Seisakusho, Ltd., Kyoto). The calibration of the photometer was made against pure benzene using the Rayleigh ratio determined by Carr and Zimm. The test solutions were cleaned by spinning for 1.5 hr at 22000 rpm in a preparative centrifuge (type 55P, Hitachi Ltd., Tokyo). Vertically polarized light of 436 mμ wavelength was used as the incident beam, and the vertical component of the scattered light was measured at various scattering angles between 30° and 140°. The weight average molecular weight M_w, the second virial coefficient A_2 and the z-average value of the mean-square statistical radius $\langle S^2 \rangle_z$ were determined by the standard method.

Results and Discussion

Intrinsic Viscosity *vs.* Molecular Weight Relationships. The results of the light scattering and viscosity measurements are summarized in Table 1. These data of the intrinsic viscosities

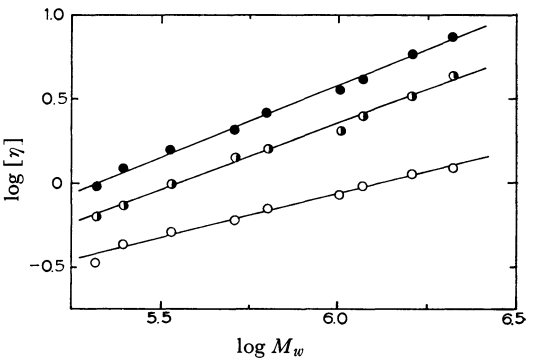

Fig. 2. Intrinsic viscosity *vs.* molecular weight relationships for poly(butylene oxide). White circles, in isopropanol at 29.8°C; half-filled circles, in methyl ethyl ketone at 30.0°C; black circles, in benzene at 30.0°C.

are plotted in Fig. 2 against the molecular weight using the double logarithmic scale. The following relationships are obtained between these two quantities in the range of molecular weight from 2.1×10^5 to 2.3×10^6:

$$[\eta] = 3.39 \times 10^{-5} M_w^{0.84}$$

(in benzene at 30.0°C),

$$[\eta] = 4.08 \times 10^{-5} M_w^{0.79}$$

(in methyl ethyl ketone at 30.0°C),

$$[\eta] = 8.65 \times 10^{-4} M_w^{0.50}$$

(in isopropanol at 29.8°C).

As expected, the intrinsic viscosity in the theta solvent was proportional to the square-root of

TABLE 1. MOLECULAR WEIGHTS AND INTRINSIC VISCOSITIES OF POLY(BUTYLENE OXIDE)

Fraction No.	$M_w \times 10^{-5}$	Benzene (30°)		MEK (30°C)		Isopropanol (29.8°)	
		$[\eta]$[a)]	k'	$[\eta]$[a)]	k'	$[\eta]$[a)]	k'
2	21.0	7.21	0.29	4.27	0.32	1.24	0.55
3	16.1	5.79	0.32	3.24	0.44	1.14	0.57
5	11.8	4.14	0.33	2.47	0.41	0.955	0.48
7	10.2	3.56	0.32	2.10	0.40	0.851	0.56
9	6.34	2.60	0.31	1.60	0.43	0.704	0.51
10	5.16	2.05	0.32	1.41	0.36	0.596	0.51
11	3.43	1.58	0.32	0.985	0.41	0.509	0.41
14	2.50	1.23	0.33	0.724	0.39	0.429	0.42
15	2.09	0.953	0.33	0.623	0.48	0.334	0.54

a) expressed in dl/g.

TABLE 2. UNPERTURBED DIMENSIONS OF POLY(EPOXIDES)

Polymer	Temp. (°C)	$(\langle L^2\rangle_0/M)^{1/2}$ (Å)	σ	Reference
Poly(ethylene oxide)	35	0.790	1.46	5), 7)
Poly(propylene oxide)	39.5	0.735	1.56	6), 7)
	38	0.792	1.68	unpublished
Poly(butylene oxide)	30	0.700	1.66	this work
Poly(styrene oxide)	25	0.640	1.95	8)

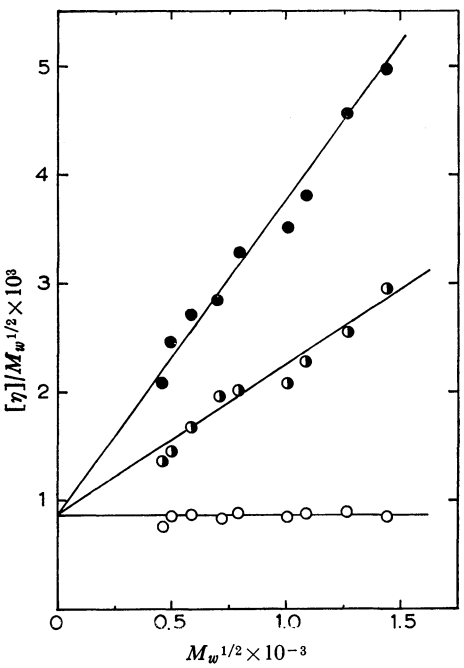

Fig. 3. Plots of $[\eta]/M_w^{1/2}$ *vs.* $M_w^{1/2}$ on poly(butylene oxide) in three solvents. The same marks as those in Fig. 2 are used.

the molecular weight. On the other hand, the intrinsic viscosity in benzene was proportional to as high the power of the molecular weight as 0.84, indicating benzene was an extremely good solvent.

Unperturbed Dimension. The viscosity data given in Table 1 are replotted in Fig. 3 according to the Kurata-Stockmayer-Fixman theory:[3,4]

$$[\eta]/M^{1/2} = K + 0.51\,\Phi_0\,BM^{1/2} \quad (4)$$

$$K = \Phi_0(\langle L^2\rangle_0/M)^{3/2} \quad (5)$$

Here $\langle L^2\rangle_0$ is the mean-square end-to-end distance of the unperturbed chain, B is a parameter representing the thermodynamic interaction between polymer segments, and Φ_0 is the Flory universal constant. As shown in Fig. 3, we can determine three straight lines with a common ordinate intercept, showing that the value of K, and hence the unperturbed dimension of the chain, is essentially independent of the solvents. It has recently been pointed out by various investigators that the $[\eta]/M^{1/2}$ *vs.* $M^{1/2}$ plots for the good solvent systems often display downwards curvature in the region of high molecular weights. Such a tendency, however, was not observed in the present systems.

The unperturbed dimension $(\langle L^2\rangle_0/M)^{1/2}$ is determined to be 0.700×10^{-8} (cm·mol$^{1/2}$·g$^{-1/2}$), assuming that $\Phi_0 = 2.5\times 10^{21}$. The conformational parameter σ which is defined as the ratio of the end-to-end distance of the unperturbed chain to that of the freely-rotating chain is then evaluated as 1.66×0.05.

3) M. Kurata and W. H. Stockmayer, *Fortschr. Hochpolymeren-Forsch.*, **3**, 196 (1963).
4) W. H. Stockmayer and M. Fixman, *J. Polymer Sci.*, **C1**, 137 (1963).

TABLE 3. STATISTICAL RADII AND THE SECOND VIRIAL COEFFICIENTS OF POLY(BUTYLENE OXIDE) IN METHYL ETHYL KETONE AT 30°C

Fraction No.	$M_w \times 10^{-5}$	From $[Kc/R(\theta)]^{1/2}$ plot				From $Kc/R(\theta)$ plot		
		$\langle S^2\rangle_z^{1/2}$ a)	$\Phi \times 10^{-21}$ b)	$A_2 \times 10^4$ c)	$A_2M_w/[\eta]$	$\langle S^2\rangle_z^{1/2}$ a)	$A_2 \times 10^4$ c)	$A_2M_w/[\eta]$
2	21.0	645	2.27	2.3	113	790	3.0	148
3	16.1	540	2.24	2.4	119	640	3.2	160
7	10.2	400	2.27	2.3	110	460	3.2	155
9	6.34	310	2.32	2.2	87	320	4.0	158
10	5.16	285	2.13	1.7	63	300	4.1	150
11	3.43	245	1.68	1.8	56	260	3.8	133

a) expressed in Å unit. b) $\Phi=[\eta]M_w/6^{3/2}\langle S^2\rangle_z^{3/2}$. c) expressed in mol·ml·g^{-2}.

The unperturbed dimensions of various poly(epoxide) chains given in literature are listed in Table 2. The data show that the side group of poly(butylene oxide) gives rise to an enlarging effect on the unperturbed chain dimension to the same degree as that of the methyl group in poly(propylene oxide).[5-7] The effect is clearly smaller than that of the phenyl group in poly(styrene oxide).[8] The similar trend can be found within the group of vinyl polymers, in which polypropylene and polybutene show approximately the same value of σ, 1.6—1.8, while polystyrene a relatively high value, 2.3.[3,7]

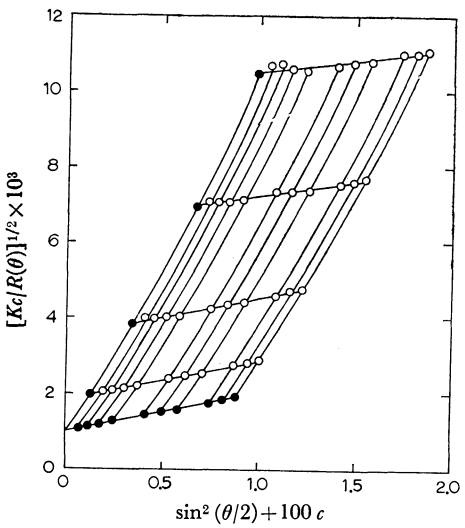

Fig. 4. Plots of $Kc/R(\theta)$ *vs.* $\sin^2(\theta/2)+100\,c$ for the sample, fraction 7. The polymer concentrations c are 0.00991, 0.00671, 0.00345 and 0.00128 g/ml from top to bottom. The scattered angles θ are 30, 40, 50, 60, 80, 90, 100, 120, 130 and 140° from left to right. Black circles represent the values of $Kc/R(\theta)$ extrapolated to $\theta=0$ or $c=0$.

Mean-square Statistical Radius and the Second Virial Coefficient. The z-average value of the mean-square statistical radius $\langle S^2\rangle_z$ can be estimated from the angular dependence of the scattered light intensity using the plots either of $Kc/R(\theta)$ or of $[Kc/R(\theta)]^{1/2}$ *vs.* $\sin^2(\theta/2)$. Here K is an optical constant, $R(\theta)$ is the reduced intensity of scattered light at the scattering angle θ, and c is the polymer concentration. The former ordinate $Kc/R(\theta)$ is known to be appropriate to ordinary polymer samples, especially to the samples with the most probable distribution of the molecular weight, while the latter ordinate $[Kc/R(\theta)]^{1/2}$ to the monodisperse polymers.[9] Since the present

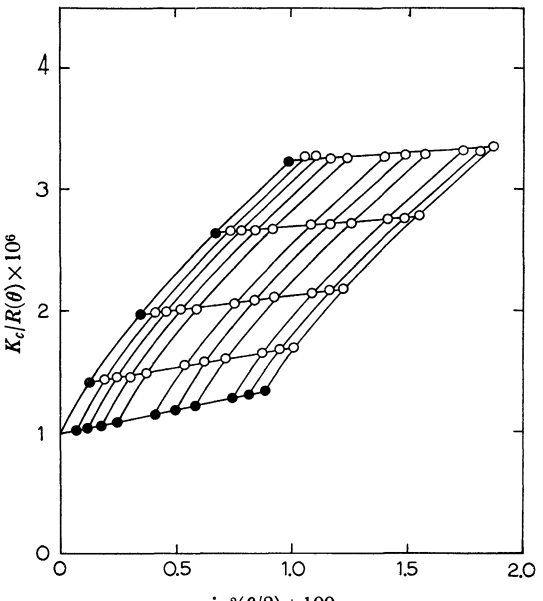

Fig. 5. Plots of $[Kc/R(\theta)]^{1/2}$ *vs.* $\sin^2(\theta/2)+100c$ for the sample, fraction 7. The polymer concentrations and scattering angles are the same as those in Fig. 4.

5) F. E. Bailey, Jr., and R. W. Callard, *J. Appl. Polymer Sci.*, **1**, 56 (1959).
6) J. Moacanin, *ibid.*, **1**, 272 (1959).
7) See also, M. Kurata, M. Iwama and K. Kamada, Table IV-D in "Polymer Handbook," ed. by J. Brandrup and E. H. Immergut, Interscience Pub., New York (1966).
8) G. Allen, C. Booth, S. J. Hurst, M. N. Jones and C. Price, *Polymer*, **8**, 391 (1967).
9) G. C. Berry, *J. Chem. Phys.*, **44**, 4550 (1966).

polymer samples are intermediate in the nature between the two above, we tried the two plots and obtained the results given in Table 3. For illustration, the two plots for fraction 7 are shown in Figs. 4 and 5. These plots lead to the same value of molecular weight, but to rather different values of $\langle S^2 \rangle_z$. As is seen from the table, the $\langle S^2 \rangle_z$ values obtained by the $[Kc/R(\theta)]^{1/2}$ plot lead to values of Φ close to the widely accepted value, $2.1—2.2 \times 10^{21}$, while those by the $Kc/R(\theta)$ plot to lower values of Φ.

As for the concentration dependence of the scattered light intensity, the plot of $Kc/R(\theta)$ *vs.* c gave correlation curves with curvature less than the plot of $[Kc/R(\theta)]^{1/2}$ *vs.* c does. The second virial coefficients A_2 evaluated from the ordinary $Kc/R(\theta)$ plot were found to be larger by a factor about 1.5, on the average, than those evaluated from the $[Kc/R(\theta)]^{1/2}$ plot. Because of the uncertainties involved in the estimates of $\langle S^2 \rangle_z$ and A_2, we here avoid further discussions on these quantities.

This work was supported in part by a grant from the Takeda Chemical Industries, Ltd. Kind help of Dr. Yutaka Matsui of this industries in supply of the original polymer samples is gratefully acknowledged.

BULLETIN OF THE CHEMICAL SOCIETY OF JAPAN VOL. 41 2574—2577 (1967)

Kinetics of Oxidation of Pinacol by Peroxydisulphate Catalysed by Silver Ions

G. D. MENGHANI and G. V. BAKORE[1]*

Department of Chemistry, University of Jodhpur, Jodhpur, India

(Received December 20, 1967)

The kinetics of the reaction between peroxydisulphate and piancol catalysed by silver ions (Ag^+) has been studied. The rate of peroxydisulphate disappearance was found to be dependent (i) on $[S_2O_8^{2-}]$ (ii) on (Ag^+). The rate is independent of the concentration of pinacol. Effects of $[H^+]$, temperature on the rate were studied. ΔE, Pz, ΔS, ΔF, *etc.* were evaluated. Mechanism of oxidation of pinacol based on the formation of reactive $[Ag^{2+}]$ is postulated.

Kinetic studies on oxidation of a variety of substrates, both organic and inorganic by peroxydisulphate were reviewed recently by House[1)] and Wilmarth and Haim.[2)] The reactions involving peroxydisulphate ion are generally slow at ordinary temperature and the oxidation does not proceed at a convenient rate at room temperature unless a catalyst is present. The most thoroughly investigated catalyst is silver(I) ion, although cupric ion (Cu^{2+}) has also been studied.

A review of literature on the oxidation by peroxydisulphate shows that oxidation of diols by peroxydisulphate has not received any attention. This investigation, has therefore been undertaken. The present work summarizes the results obtained in the oxidation of pinacol by peroxydisulphate, catalysed by silver(I) ions.

Experimental

Material. Pinacol (B. D. H. A. R.) and potassium peroxydisulphate E. Merck were used. All other chemicals were chemically pure.

Kinetic Method. Reactions were carried out in bottles at constant temperature (±0.03°C). Reaction mixture containing the requisite quantities of diol, Ag^+ was prepared in reaction vessel. The reaction mixture and peroxydisulphate solution were thermostated for about 20 min to attain experimental temperature (48.5°C). A known volume of peroxydisulphate solution was then transferred to the reaction mixture and aliquots were removed and analysed from time to time. The rate at which peroxydisulphate was consumed was estimated by the method of BARTLETT and COTMAN.[3)]

Results

The rate at which the peroxydisulphate was consumed follows first order rate laws. The first order rate constants at different peroxydisulphate concentrations are summarised in Table 1.

*1 Present address: University Professor and Head, Department of Chemistry, M.B. College, University of Udaipur, India.

1) D. A. House, *Chem. Revs.*, **62**, 185 (1962).

2) W. K. Wilmarth and A. Haim, "Mechanisms of Oxidation by Peroxydisulphate Ion," in "Peroxide, Reaction Mechanisms," J. O. Edwards, ed., John Wiley, New York (1961), p. 175—225.

3) P. D. Bartlett and J. D. Cotman, *J. Am. Chem. Soc.*, **71**, 1419 (1949).

Table 1. Variation of rate constant with concentration of peroxydisulphate

$[Pinacol]=4.90\times10^{-2}$ M Temp. 48.5°C
$[Ag^+]=5.30\times10^{-4}$ M

$[S_2O_8^{2-}]\times10^3$ mol/l	$k_1\times10^3$ sec^{-1}
0.98	1.81
1.96	1.70
2.94	1.34
3.92	1.18
4.90	1.08

The first order rate constants are expected to be independent of initial concentration of peroxydisulphate, however, results show a small decrease with increase in concentration of the oxidant. This decrease may be ascribed to specific inhibitory effect of potassium ions, as reported in the oxidation of oxalate[4] also.

Table 2. Variation of rate constant with concentration of pinacol

$[S_2O_8^{2-}]=1.96\times10^{-3}$ M Temp. 48.5°C
$[Ag^+]=5.30\times10^{-4}$ M

Pinacol$\times10^2$ mol/l	$k_1\times10^4$ sec^{-1}
0.981	15.3
1.96	15.1
2.94	15.2
3.92	16.0
4.90	15.1

The results show that the rate is independent of the concentration of pinacol.

The results show that rate of oxidation is proportional to the first power of the concentration of silver(I) ions. The effect of H^+ ion concentration on the rate of oxidation was studied by adding sulphuric acid, at the same time adjusting the concentration of sulphate to a constant value by adding potassium sulphate. It is found that when the sulphate ion concentration is kept constant, addition of small quantities of acid decreases the rate constant appreciably, but further addition of acid does not produce any change in the rate of oxidation. The effect of ionic strength on the rate of reaction has been summarised in Table 5. The effect of ionic strength was studied by adding potassium sulphate and potassium nitrate. It is observed that change in ionic strength produced by either K_2SO_4 or KNO_3 has more or less the same effect on rate.

Table 3. Variation of rate constant with concentration of silver(I) ions

$[Pinacol]=4.90\times10^{-2}$ M Temp. 48.°C
$[S_2O_8^{2-}]=4.90\times10^{-3}$ M

$[Ag^+]\times10^4$ mol/l	$k_1\times10^4$ sec^{-1}	$k_1/[Ag^+]$
2.65	7.21	2.71
5.30	15.5	2.92
7.95	22.0	2.76
10.6	29.7	2.81
13.25	36.9	2.79
15.9	46.1	2.89

Table 4. Effect of H^+ ions concentration on the rate of reaction keeping concentration of sulphate ion constant

$[Pinacol]=4.90\times10^{-2}$ M $[Ag^+]=5.3\times10^{-4}$ M
$[S_2O_8^{2-}]=4.90\times10^{-3}$ M $[SO_4^{2-}]=0.245$ M
Temp. 48.5°C

$[H^+]\times10^2$ mol/l	$k_1\times10^4$ sec^{-1}
0.0	15.67
4.90	3.07
9.81	2.82
14.7	3.13
18.7	3.99

As shown in Fig. 1 a plot of log$K$ against $\sqrt{\mu}$ in case of K_2SO_4 and KNO_3 gives a straight line with

Table 5. Effect of ionic strength on rate of reaction

$[Pinacol]=4.90\times10^{-2}$ M Temp. 48.5°C
$[Ag^+]=5.23\times10^{-4}$ M $[S_2O_8^{2-}]=4.90\times10^{-3}$ M

$\sqrt{\mu}$, M	K_2SO_4		KNO_3	
	$k_1\times10^4$ sec^{-1}	K, l mol^{-1} sec^{-1}	$k_1\times10^4$ sec^{-1}	K, l mol^{-1} sec^{-1}
0.0	17.7	3.38	17.7	3.38
0.336	—	—	10.1	1.93
0.358	8.2	1.56	—	—
0.402	6.56	1.25	7.39	1.41
0.459	5.91	1.13	7.56	1.45
0.561	5.05	0.97	—	—
0.562	—	—	5.54	1.06
0.632	4.45	0.85	4.30	0.82
0.675	4.04	0.77	4.94	0.94
0.777	3.05	0.58	3.57	0.68

4) Y. K. Gupta and S. Ghosh, *J. Inorg. and Nuclear Chem.*, **1**, 178 (1959).

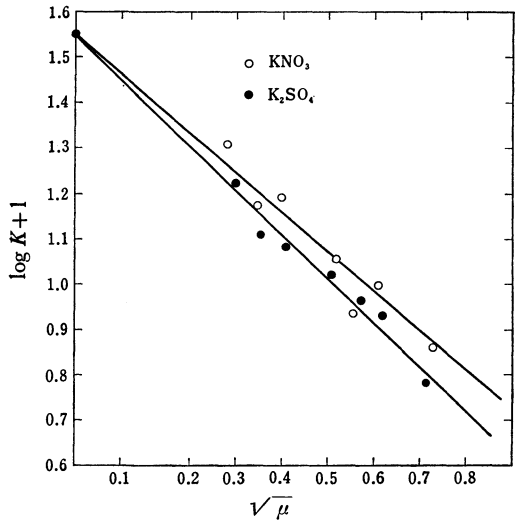

Fig. 1. Effect of addition of K_2SO_4 and KNO_3 on rate of oxidation of pinacol. *cf.* Table 5.

TABLE 6. EFFECT OF TEMPERATURE
$[Pinacol]=4.90\times10^{-2}$ M $[Ag^+]=5.30\times10^{-4}$ M
$[S_2O_8^{2-}]=4.90\times10^{-3}$ M

Temp. °C	$k_1\times10^4$ sec^{-1}	K, l mol^{-1} sec^{-1}
28.5	5.42	1.03
40.0	10.6	2.0
48.5	15.6	2.96
54.0	24.6	4.46

TABLE 7

Specific rate constant at 48.5°C	2.96
Frequency factor, l mol^{-1} sec^{-1}	8.28×10^7
ΔE, kcal/mol	10.87
ΔS, e. u.	−23.1
ΔF, kcals	18.3

slope equal to 0.97 and 0.82 respectively. The reaction was studied at 28.5, 40.0, 48.5 and 54.0°C. The specific rate constant (K) was obtained by dividing the first order rate constant by the concentration of silver ions. A plot of $\log k_1$ against inverse of absolute temperature gives a straight line. This show that Arrhenius equation is valid. The energy of activation was estimated from the slope of the straight line obtained by plotting $\log k_1$ against the inverse of T. The energy of activation comes out to be 10.87 kcal mol^{-1}. The frequency factor and entropy of activation, free energy of activation were estimated from data in Table 6 and have been summarised in Table 7.

Discussion

The reaction between pinacol and peroxydisulphate in absence of silver(I) ions is extremely slow. The rate of (Ag^+) ions catalysed reaction is proportional to the concentration of (Ag^+) ions and of peroxydisulphate but independent of the concentration of pinacol. Since the uncatalysed reaction between peroxydisulphate and pinacol is extremely slow, it therefore suggests that peroxydisulphate or sulphate radical ions do not react with pinacol. However, to explain the increased rate of disapprearance of peroxydisulphate on addition of substrate, it is necessary to postulate that reactive silver species and pinacol react to produce a radical. The radical so produced from the substrate further induces peroxydisulphate decomposition.

Gupta and Ghosh[4] have proposed a mechanism involving an equilibrium which is followed by a termolecular rate determining step:

$$S_2O_8^{2-} \rightleftharpoons 2SO_4^- \text{ (rapid)} \quad (1)$$

$$2SO_4^- + Ag^+ \rightarrow 2SO_4^{2-} + Ag^{3+} \text{ (slow)} \quad (2)$$

The break down of peroxydisulphate into sulphate free radicals appears to be irreversible, as it seems likely that sulphate free radicals would exchange electrons with sulphate ions at a rate comparable with their recombination to perxoydisulphate. However no exchange has been observed under the conditions of the kinetic experiments.[5-8] Thus postulation of termolecular rate determining step introduces difficulties and consequently any proposed mechanism of decomposition involving equilibrium between peroxydisulphate and sulphate ion radicals—step (i) is probably incorrect.

Alternatively catalytic effects of silver ions may be explained by considering the following initial steps:

$$Ag^+ + S_2O_8^{2-} \rightarrow Ag^{2+} + SO_4^- + SO_4^{2-} \quad (3)$$

$$Ag^+ + SO_4^- \rightarrow Ag^{2+} + SO_4^{2-} \quad (4)$$

The nature of the silver intermediate in the oxidations by peroxydisulphate is uncertain. Both Ag^{2+} and Ag^{3+} ions have been postulated as intermediates.[4,9-13] The postulation of Ag^{2+} and SO_4^- as the reactive species accords with the observations of Subbaraman and Santappa,[14] Higgenison and Marshall[15] that one electron transfer is more likely in oxidation-reduction system between a transition

5) K. J. Maccalium and R. L. Enger, *Can. J. Chem.*, **32**, 692 (1954).
6) F. C. Riescbos and A. W. H. Aten, *J. Am. Chem., Soc.*, **74**, 2440 (1952).
7) M. S. Tsao and W. K. Wilmorth, *J. Phys. Chem.*, **63**, 346 (1959).
8) K. B. Wiberg, *J. Am. Chem. Soc.*, **81**, 252 (1959).
9) R. G. Bacon, R. Grime and D. J. Munro, *J. Chem. Soc.*, **1954**, 2275.
10) C. E. Bawn and D. Margerison, *Trans. Faraday Soc.*, **51**, 925 (1955).
11) P. C. Carman, *ibid.*, **30**, 566 (1934).
12) S. Fromacus, *Acta Chem. Soc.*, **10**, 1606 (1956).
13) S. Fromacus and C. O. Ostman, *ibid.*, **10**, 320 (1956).
14) L. R. Subbaraman and M. Santappa, *Z. phys. Chem. Neue Folge I and II*, **48**, 3/4 (1966).
15) W. C. Higgenison and J. W. Marshall, *J. Chem. Soc.*, **1957**, 447.

metal ion and an ion derived from a non transition element. In view of the above consideration we are led to suggest the following mechanism:

$$Ag^+ + S_2O_8^{2-} \xrightarrow{k_3} Ag^{2+} + SO_4^- + SO_4^{2-} \quad (3)$$

$$Ag^+ + SO_4^- \xrightarrow{k_4} Ag^{2+} + SO_4^{2-} \quad (4)$$

$$Ag^{2+} + \begin{matrix}(CH_3)_2COH\\ |\\ (CH_3)_2COH\end{matrix} \xrightarrow{k_5} CH_3COCH_3 + Ag^+ + H^+ + (CH_3)_2\dot{C}OH \quad (5)$$

$$(CH_3)_2\dot{C}OH + S_2O_8^{2-} \xrightarrow{k_6} (CH_3)_2CO + H^+ + SO_4^{2-} + SO_4^- \quad (6)$$

$$(CH_3)_2\dot{C}OH + SO_4^- \xrightarrow{k_7} (CH_3)_2CO + H^+ + SO_4^{2-} \quad (7)$$

Application of steady state condition gives:

$$\frac{d[Ag^{2+}]}{dt} = k_3[Ag^+][S_2O_8^{2-}] + k_4[Ag^+][SO_4^-] - k_5[Ag^{2+}][(CH_3)_2COHCOH(CH_3)_2] = 0 \quad (I)$$

$$\frac{d[(CH_3)_2\dot{C}OH]}{dt} = k_5[Ag^{2+}]\left[\begin{matrix}(CH_3)_2COH\\ |\\ (CH_3)_2COH\end{matrix}\right] - k_6[(CH_3)_2\dot{C}OH][S_2O_8^{2-}] - k_7[(CH_3)_2\dot{C}OH][SO_4^-] = 0 \quad (II)$$

$$\frac{d[SO_4^-]}{dt} = k_3[Ag^+][S_2O_8^{2-}] + k_6[(CH_3)_2\dot{C}OH][S_2O_8^{2-}] - k_4[Ag^+][SO_4^-] - k_7[(CH_3)_2\dot{C}OH][SO_4^-] = 0 \quad (III)$$

From I, II and III following relationship follows:

$$[k_3[Ag^+] - k_6[(CH_3)_2\dot{C}OH]][S_2O_8^{2-}] = [k_7[(CH_3)_2\dot{C}OH] - k_4[Ag^+]][SO_4^-]$$

$$[k_3[Ag^+] + k_6[(CH_3)_2\dot{C}OH]][S_2O_8^{2-}] = [k_7[(CH_3)_2\dot{C}OH] + k_4[Ag^+]][SO_4^-]$$

and

$$[(CH_3)_2\dot{C}OH] = \left\{\frac{k_3k_4}{k_6k_7}\right\}^{1/2}[Ag^+]$$

The rate at which peroxydisulphate disproportionates is given by:

$$\frac{-d[S_2O_8^{2-}]}{dt} = k_3[Ag^+][S_2O_8^{2-}] + k_6[(CH_3)_2\dot{C}OH][S_2O_8^{2-}] = \left[k_3 + k_6\left\{\frac{k_3k_4}{k_6k_7}\right\}^{1/2}\right][Ag^+][S_2O_8^{2-}] = K[Ag^+][S_2O_8^{2-}]$$

Where $K = \left[k_3 + k_6\left\{\frac{k_3k_4}{k_6k_7}\right\}^{1/2}\right]$

This mechanism leads to correct rate laws and explains the dependence of rate constant on the first power of silver(I) ion concentration. The product of the oxidation of pinacol as confirmed by its usual tests has been found to be Acetone.

BULLETIN OF THE CHEMICAL SOCIETY OF JAPAN VOL. 41 2578—2586 (1968)

Formation and Decay of the Transient Species in Radiation Chemistry. Radiolysis of Alkyl Halide Systems

Hisashi UEDA

Department of Chemistry, The Ohio State University, Columbus, Ohio 43210, U.S.A., and Tokyo Kogyo Shikenjo, Mita, Meguro-ku, Tokyo

(Received April 15, 1968)

Biphenyl and *trans*-stilbene were irradiated by a pulse of 300 mA × 0.5 μsec in two types of solvents, alkyl halides and methyltetrahydrofuran. The spectra obtained by *n*-butylchloride, 1,1-dichloroethane, 1,2-dichloroethane, 1,1,2-trichloroethane, and 1,1,2,2-tetrachloroethane were concluded to be those of the cations, while the spectra obtained by CCl_4, 1,1,1-trichloroethane, and pentachloroethane were concluded to be due to something other than the cations. The spectra of *o*-terphenyl in 1,1,2-trichloroethane and in 2-methyltetrahydrofuran were different, the reason for this was discussed. The decay curves of the optical densities due to both the cations and the anions all exhibited first-order rates. The decay of the cation of the aromatic solute was concluded to consist of two processes, the transportation of the charged species and the neutralization of the ion pair thus formed. The rate-determining step is the neutralization process, the activation energies of which are 2.17 and 3.62 kcal/mol for *trans*-stilbene and biphenyl respectively. The transportation of the charged species was concluded to be not by the movements of the anion and the cation across the solution, but by the electron-trap- and hole-conductions, such as have been observed in semiconductors.

Shida and Hamill[1] established the existence of the cations of aromatic compounds in the frozen-glass or polycrystalline matrices of alkyl halides. Unfortunately, however, the absorption spectra of the cation and the anion of an aromatic hydrocarbon are, in most cases, very similar to each other. It is, therefore, rather difficult to establish the exstence of either one of these ions with complete definiteness. In spite of such difficulties, however, it seems fairly reasonable to accept the conclusions of Shida and Hamill. It is for this reason that the present work was planned with the hope of establishing the formation and the decay of the radiation-chemical transient species in a solution of an aromatic hydrocarbon in an alkyl halide solvent in the liquid phase.

The present author[2] has studied the effects of additives on the radiolysis of 1,2-dichloroethane. In that study it was shown that those additives with larger reaction-rate constants with hydrated electrons than that of 1,2-dichloroethane decreased the *G*-values of ethylene and HCl, while those additives with smaller rate constants increased the *G*-values of ethylene and HCl, except in the cases of such additives as NH_3. It was also found that there is a parallel relation between the decrease in the *G*-value of ethylene and the increase in the rate constant with hydrated electrons. These facts suggested the existence of both positively- and negatively-charged species as the precursors of the radiolysis products, and also revealed the very quick and efficient charge transfer from the originally-formed solvent cation to the solute molecule.

Arai and Dorfman[3] studied the decay rate and the kinetics of an anion of aromatic hydrocarbon formed in isopropyl alcohol and found that the decay rate curve obeys a first-order reaction rate. This does not agree with a collision-initiated charge neutralization model, which predicts a second-order reaction. They interpreted this phenomenon as possibily resulting from an unknown impurity which still existed in the solution despite the greatest possible efforts at purification. The present author, therefore, also desired to see if such impurity effects are found with alkyl halide solvents.

The rigid-glass method is undoubtedly one of the best ways to take the spectrum of a radiation-chemical transient species, provided that the nature of the species formed is well known. Though in some instances a "fast detection" is equivalent to a "detection after freezing," there are several advantages to the pulse radiolysis method compared to the rigid matrix method. 1) It is possible to ascertain the kinetics of the formation and the decay of the transient species. 2) The successive transformations of the transient species, if any,

1) T. Shida and W. H. Hamill, *J. Chem. Phys.*, **44**, 2375 (1966).
2) H. Ueda, *J. Phys. Chem.*, **71**, 3084 (1967).
3) S. Arai and L. M. Dorfman, *J. Chem. Phys.*, **41**, 2190 (1964).

can be traced. 3) More varied types of compounds can be employed as solvents (matrix). 4) The effects of added impurities, which crystallize out if the solution is solidified by cooling, can easily be observed. Because of these considerations, it is important to study again, this time by pulse radiolysis techniques, the kind of system which has already been investigated by the rigid matrix method.

Experimental

The details of the experimental procedures of pulse radiolysis have appeared in many places[4,5] and so will not be particularly described here. Two or three different types of solvents were used after they had been purified. The alkyl halides were shaken with concentrated sulfuric acid and then distilled three times in a vacuum. The ethers, 2,2-dimethoxypropane, 2,5-dimethoxytetrahydrofuran, and 2-methyltetrahydrofuran (abbreviated as MTHF) were treated with sodium, distilled in a vacuum, distilled over a sodium mirror, and then distilled into the cell under a vacuum. The solute hydrocarbons, special reagent grade, were recrystallized twice from alcohol. The polaroid pictures (105 mm×82 mm for 100 mm×60 mm graticule) were enlarged to twice their original dimensions and used for the reaction-rate and absorption-rate analyses.

Results

In Figs. 1—7, Table 1 and Table 2 the results obtained with *trans*-stilbene as the solute are shown. In Fig. 1, the intensity of light absorption by the transient species is plotted as a function of the solute concentration. It may be seen in the figure that the intensity of light absorption is saturated if the solute concentration exceeds 10^{-2} mol/*l*. The effects of the solvents on the intensity of absorption

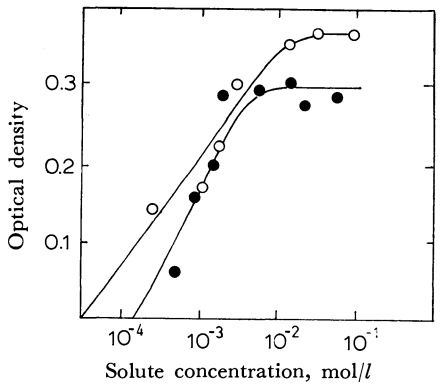

Fig. 1. The dependence of the optical densities of the solute cations on the concentration of *trans*-stilbene in *n*-butylchloride (●) and in 1,1-dichloroethane (○).

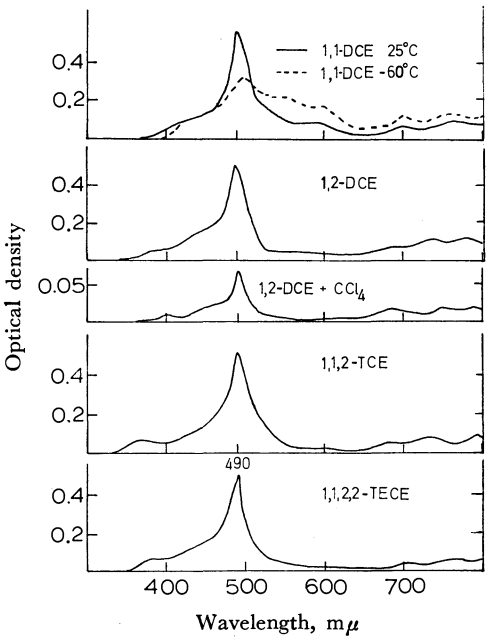

Fig. 2.

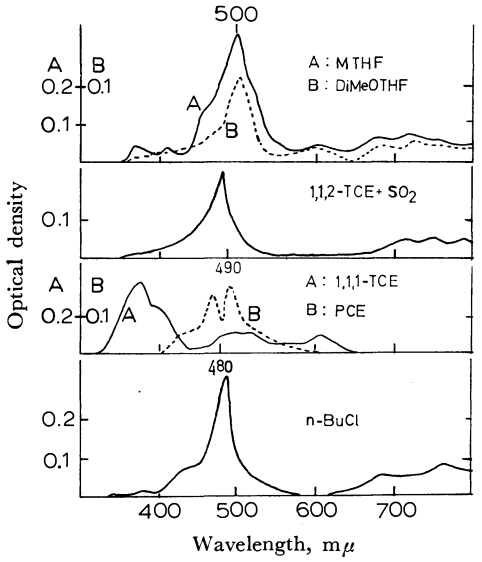

Fig. 3.

Fig. 2 and Fig. 3. The absorption spectra of the transient species of *trans*-stilbene in various solvents. About the abbreviations of the names of the solvents, see text. In the spectrum, third from top of Fig. 2, the ratio of 1,2-DCE and CCl_4 is 15 m*l*: 5 m*l*. In Fig. 3, top spectrum, DiMeOTHF signifies 2,5-dimethoxytetrahydrofuran. A similar, but far weaker, absorption spectrum was observed with 2,2-dimethoxy propane as solvent.

4) M. Ebert, J. P. Keene, A. J. Swallow and J. H. Baxendale, Ed.; "Proceedings of the International Symposium on Pulse Radiolysis at Manchester April 1965," Academic Press, New York (1965).

5) L. M. Dorfman and M. S. Macheson, "Pulse Radiolysis," American Chemical Society, Washington, D. C., to be published.

TABLE 1. TRANSIENT SPECIES OF *trans*-STILBENE IN VARIOUS SOLVENTS

Solvent	Additive	Observed wavelength	Optical density[a]	O.D./E.D.[b]	k_1[c]
n-Butylchloride	none	490 mμ	0.236	8.0×10^{-25}	2.03×10^{5} [d]
1,1-Dichloroethane	none	490 mμ	0.673	18.8	2.24
1,2-Dichloroethane	none	490 mμ	0.567	14.9	1.57
1,1,2-Trichloroethane	none	490 mμ	0.701	16.3	1.61
1,1,2,2-Tetrachloroethane	none	490 mμ	0.750	17.1	1.38
1,1,2,2-Tetrachloroethane	Hydroquinone 4.51×10^{-3} mol/*l*	490 mμ	0.160	3.64	1.42
1,1,2-Trichloroethane	β-Naphthol 1.53×10^{-3} mol/*l*	490 mμ	0.630	14.7	1.63
1,1,2-Trichloroethane	SO_2[e]	490 mμ	0.220	5.11	1.49
1,1,2-Trichloroethane	N_2O [f]	490 mμ	0.376	8.75	0.79
1,1,2-Trichloroethane	CCl_3CCl_3 1.91×10^{-1} mol/*l*	490 mμ	0.493	11.5	0.67
1,1,2-Trichloroethane	NH_3 [g]	490 mμ	0.000	0	—
1,1,2,2-Tetrachloroethane	MTHF, 8 mol%	490 mμ	0.066	1.54	
2-Methyltetrahydrofuran	none	500 mμ	0.390		1.83
2,5-Dimethoxytetrahydrofuran	none	500 mμ	0.130		1.85

a) At 0.5 μsec after pulse (300 mA × 500 *n*sec).
b) Optical density/Electron density.
c) First-order decay rate constant.
d) sec^{-1}.
e) 2.00 mmol in 70 m*l* cell and 17.2 m*l* solution.
f) 3.85 mmol in 70 m*l* cell and 17.2 m*l* solution.
g) 3.54 mmol in 70 m*l* cell and 17.2 m*l* solution.

TABLE 2. EFFECT OF MIXED SOLVENTS ON THE FORMATION OF THE TRANSIENT SPECIES OF *trans*-STILBENE

Mol% of *n*-butylchloride	0	22	45	70	100
Mol% of 1,1-dichloroethane	100	78	55	30	0
Optical densities at 0.5 μsec after pulse and at 490 mμ	0.351	0.339	0.328	0.316	0.251

TABLE 3. TRANSIENT SPECIES OF BIPHENYL IN VARIOUS SOLVENTS

Solvent	Additive	Observed wavelength	Optical density[a]	O.D./E.D.[b]	k_1[c]
n-Butylchloride	none	690 mμ	0.051	1.67×10^{-25}	1.57×10^{5} [d]
1,1-Dichloroethane	none	690 mμ	0.070	1.92	2.40
1,2-Dichloroethane	none	690 mμ	0.152	4.00	1.72
1,1,2-Trichloroethane	none	690 mμ	0.140	3.20	1.81
1,1,2-Trichloroethane	NH_3[e]	690 mμ	0.000	0.00	
1,1,2-Trichloroethane	N_2O[f]	690 mμ	0.157	3.6	1.78
1,1,2,2-Tetrachloroethane	none	690 mμ	0.178	4.05	1.58
Carbon tetrachloride	none	680 mμ	0.027	0.6	
1,1,1-Trichloroethane	none	685 mμ	0.015	0.4	
Pentachloroethane	none	650 mμ	0.017	0.3	
Methyltetrahydrofuran	none	625 mμ	0.080		

a) At 0.5 μsec after pulse.
b) Optical density/electron density.
c) First order decay rate constant.
d) sec^{-1}.
e) 3.43 mmol in 70 m*l* cell and 19.9 m*l* solution.
f) 3.66 mmol in 70 m*l* cell and 17.8 m*l* solution.

by the transient species were studied using solutions containing the solute at higher concentrations than this saturating concentration. The results are shown in Table 1. A similar procedure was taken when determining the values in Table 3.

Figures 2 and 3 show the absorption spectra of the transient species of *trans*-stilbene in various solvents. The spectra shown are not the entire absorption corresponding to all the species existing in the system at the time of measurements, but are the differences between the two spectra at 1 and 9 μsec after pulse: (Spectrum at $t=1.0$)—(Spectrum at $t=9.0$ μsec). In Fig. 4 the absorption spectra of the transient species of *trans*-stilbene

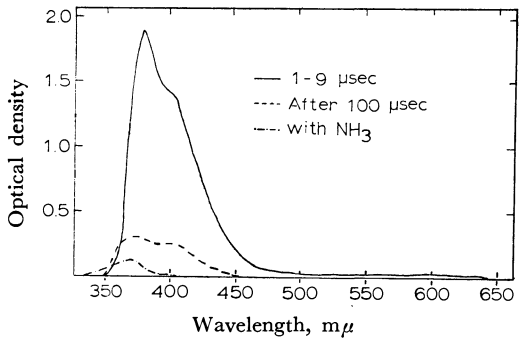

Fig. 4. The absorption spectra of the transient species of *trans*-stilbene in CCl_4. "1—9 μsec," means the difference of the spectra: (absorption at $t=1$ μsec)—(absorption at $t=9$ μsec). "After 100 μsec" means the entire absorption still left at $t=100$ μsec.

in carbon tetrachloride are shown.

It will be seen in Figs. 2, 3, 4, 8, and 9 that there are two types of alkyl halides. The one type consists of *n*-butylchloride (BuCl), 1,1-dichloroethane (11DCE), 1,2-dichloroethane (12DCE), 1,1,2-trichloroethane (112TCE), and 1,1,2,2-tetrachloroethane (TECE). These are called DCE type solvents in this report. The other group consists of 1,1,1-trichloroethane (111TCE), Pentachloroethane (PCE), and carbon tetrachloride. These are called CCl_4-type solvents in this report. The DCE-type solvents give almost identical absorption spectra, which are also quite similar to those reported by Shida and Hamill,[1] when biphenyl and *trans*-stilbene are the solutes, while the CCl_4-type solvents give spectra which are completely different from those observed with the DCE-type solvents.

Figure 5 shows the decay-rate curves of the transient species of *trans*-stilbene in 11DCE at

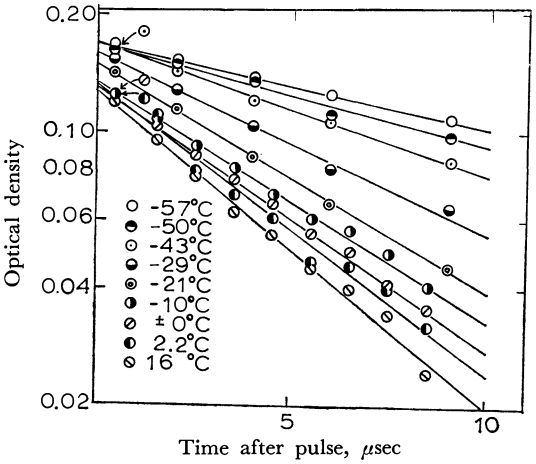

Fig. 5. The decay rate curves of the cations of *trans*-stilbene formed in 1,1-DCE at various temperatures.

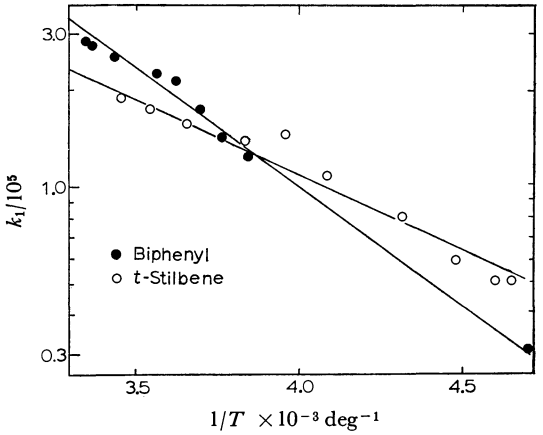

Fig. 6. Arrhenius plots of the 1st order rate constants k_1s in the temperature range between −60°C and +10°C.

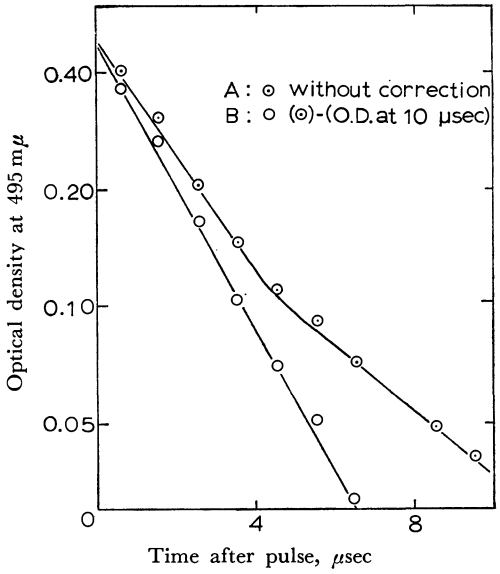

Fig. 7. The decay rate of the anion of *trans*-stilbene in methyltetrahydrofuran.

various temperatures between −60°C and +20°C. The intensity of absorption was observed at 490 mμ. The Arrhenius plots of the rate constants are shown in Fig. 6. The activation energy for the first-order rate constant, k_1, was 1.27 kcal/mol.

In Fig. 7 the decay rate of the transient species in MTHF observed at 495 mμ is shown. The A curve indicates that the absorption curve does not obey the first order decay. However, the absorption spectra showed a clear change in shape after 10 μsec. This means that the species existing during an initial 1—9 μsec, and the species existing after 10 sec, are somehow different. In view of this fact, the optical densities until 9 μsec were corrected by subtracting the value at 10 μsec. The corrected optical densities fall along the straight

line B, which indicates a first-order decay. Such is also true with most of the transient species of *trans*-stilbene in various solvents at 25°C. In other words, all the decay-rate curves, after correction, obey the first-order rate and are identified by the initial optical density at $t=0$, and the rate constant, k_1. Table 1, therefore, shows the initial optical density, at $t=0.5$ μsec, and the k_1.

Though it seems to be beyond question that the effects of the DCE-group solvents on the formation of the transient species are all the same in quality, the present author tested this point by mixing many pairs of the solvents in the group. For example, the results obtained by mixing BuCl and 11DCE are shown in Table 2. However, the effects of 12DCE and CCl_4 are not added to each other when these two solvents are mixed and used. As is shown in Fig. 2, the optical density of the transient species which is qualitatively the same as that obtained by 12DCE is greatly reduced by adding CCl_4. Also, MTHF and TECE have opposite effects. The mixing of 0.08 mol of MTHF with 0.92 mol of TECE reduced the optical density of the transient species of *trans*-stilbene at 490 mμ from the 0.750 of pure TECE to 0.066, as is shown in Table 1.

Figures 8 and 9 show the absorption spectra by the transient species formed from biphenyl in various solvents. In Fig. 10 the decay curves of the transient species of biphenyl in 11DCE at various temperatures between −60°C and 20°C are shown. The intensity of absorption was measured at 370 mμ. The results show first-order rate curves, and the temperature dependence

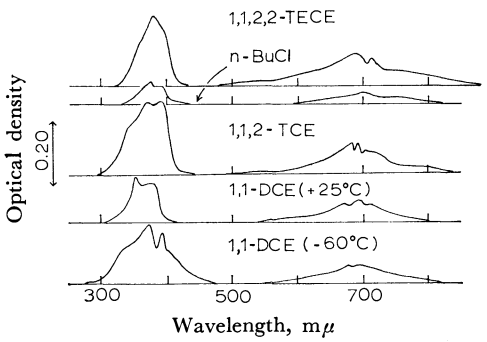

Fig. 8.

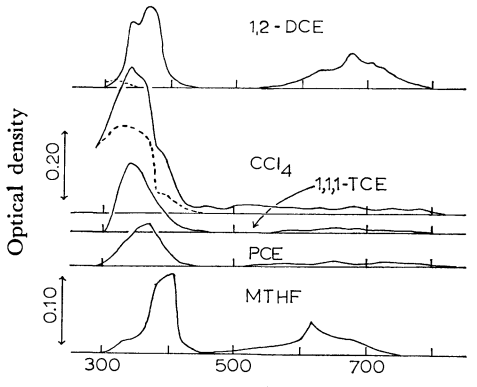

Fig. 9.

Fig. 8 and Fig. 9. The absorption spectra of the transient species of biphenyl in various solvents. In the spectra marked as CCl_4 and 1,2-DCE the dotted lines indicate the spectra after 100 μsec. All the others are the differences as are used in the caption for Fig. 4.

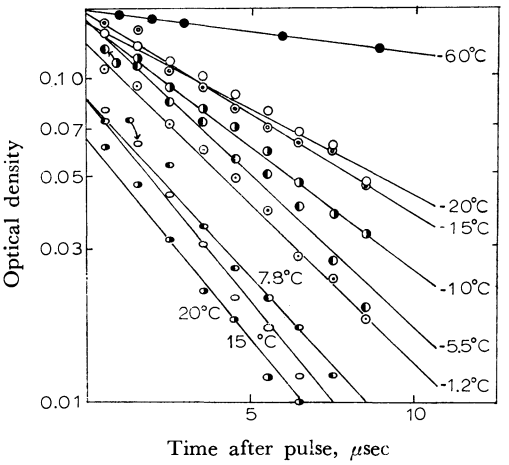

Fig. 10. The decay rate curves of the cation of biphenyl formed in 1,1-DCE at various temperature.

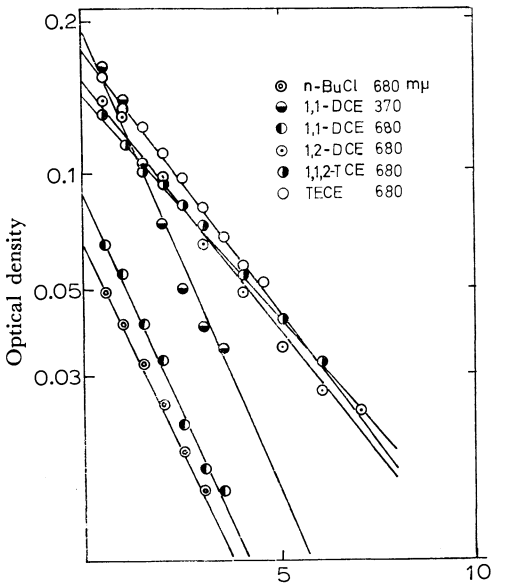

Fig. 11. The decay rates of the cation of biphenyl formed in various solvents. The wavelengths shown are those at which optical density measurements were made.

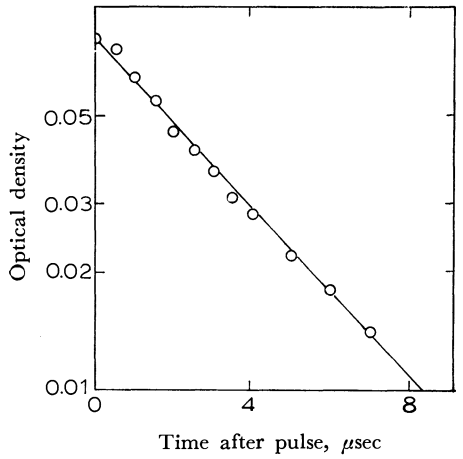

Fig. 12. The decay rate of the anion of biphenyl in MTHF.

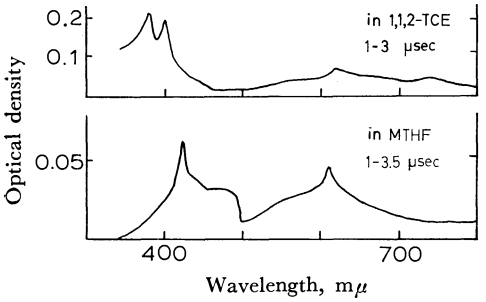

Fig. 13. The absorption spectra of the transient species of *o*-terphenyl formed by pulse radiolysis of *o*-terphenyl in MTHF and 1,1,2-trichloroethane. The upper spectrum is the difference: (absorption at $t=1.0$ μsec)−(absorption at $t=3.0$ μsec), and the lower spectrum is the difference between 1.0 and 3.5 μsec, respectively.

of the rate constant, shown in Fig. 6, gives 3.62 kcal/mol as the activation energy. Figure 11 shows the various decay rates of the transient species of biphenyl in several alkyl halide solvents. Figure 12 shows the decay rate of the transient species of biphenyl in MTHF. The absorption was measured at 625 mμ. The formation and the decay of the radiation-chemical transient species of biphenyl in various solvents are summarized in Table 3.

Though *trans*-stilbene and many other aromatic hydrocarbons give almost identical spectra[6] in both types of solvents, *i.e.*, alkyl halides and aliphatic ethers, biphenyl gives different spectra, as shown in Fig. 8 and Fig. 9. For a reason to be discussed later, *o*-terphenyl was also expected to give two different spectra in the two types of solvents. Figure 13, therefore, shows the absorption spectra of the transient species of *o*-terphenyl in 112TCE and in MTHF.

6) L. M. Dorfman and H. Ueda, unpublished results.

Discussion

The light absorption of positive and negative ions of aromatic hydrocarbons have already been studied. Hoijtink[7] studied the negative ions formed with metallic sodium in tetrahydrofuran and the positive ions formed in concentrated sulfuric acid. In most cases the spectra of the cation and the anion were similar to each other. A simple Hückel MO calculation does not predict any difference in the values of the differences in energy levels corresponding to the light absorption by a cation and by an anion.[8] The rigid matrix method used by Shida and Hamill[1,9] also gave many spectra of the unstable species trapped in the matrices of MTHF and alkyl halides (mostly CCl_4 and *s*-butyl chloride) at 77°K. In these cases, however, it is not possible to conclude strightforwardly the pure existence of either a cation or an anion.

There are many possible ways to detect an ion of an aromatic compound in the liquid phase by using some of its physical properties. One of them is the visible-light absorption method, and another is the ESR method. The transient species to be predicted for a system subjected to an ionizing radiation are not limited to only one. For example, the aromatic compound C_nH_m would form $C_nH_m^+$, $C_nH_m^-$, $C_nH_{m-1}\cdot$, $C_nH_{m+1}\cdot$ and so on, generally speaking, there is no reason to deny the existence of any one of them. If this system is investigated in the liquid phase by the use of the ESR method, the difference in the number of protons of the paramagentic species may be found rather easily. Thus the difference between $C_nH_m^+$ or $C_nH_m^-$ and $C_nH_{m-1}\cdot$ or $C_nH_{m+1}\cdot$ will be clear. In addition, some modified or improved MO calculations can predict some difference in the spin density distributions between $C_nH_m^+$ and $C_nH_m^-$, a difference which is to be observed as the difference in the spacings of the lines in the ESR spectrum. At any rate, the information obtained by the ESR method in the liquid phase is normally more useful than that obtained by light absorption specetroscopy. Therefore, if it be possible to apply ESR method to the liquid-phase pulse radiolysis studies, it would be quite powerful.

In the case of the rigid glass method, the ESR method is less powerful than the absorption spectroscopy because of the averaging out of the anisotropy of the resonance lines. Therefore, the results of this method cannot be precisely compared in detail with any MO calculations.

7) G. J. Hoijtink and W. P. Weijland, *Rec. Trav. Chim.*, **76**, 836 (1957); W. Ij. Aaldberg, E. L. Mackor and W. P. Weijland, *J. Chem. Soc.*, **1959**, 3049, 3055.

8) For example, A. Streitwieser, Jr., "Molecular Orbital Theory for Organic Chemists," John Wiley & Sons, Inc., New York (1961).

9) T. Shida and W. H. Hamill, *J. Chem. Phys.*, **44**, 4372 (1966).

It has already been established that the negative ion of biphenyl is formed by the action of alkali metal in pure tetrahydrofuran or similar solvents. According to Hoijtink,[7] the absorption maximum appears at 625 mμ. Absorption maximum at the same wavelength was also obtained by the pulse radiolysis of biphenyl in ethanol.[3] The present results show that the absorption maximum of 625 mμ is observed only from the solution of biphenyl in MTHF. In the DCE-type solvents, the maximum is 690 mμ. These facts suggest that the species formed in MTHF is the same as that formed in ethanol and that, therefore, it is the anion. However, they do not necessarily indicate that the species formed in 12DCE is the cation. Nevertheless, the effects of gases on the formation of the transient species, Table 3, indicate that only NH_3 affects the formation. The decay kinetics, in all cases, are simple first-order rates, showing that only one short-lived species exists. Such a short-lived species, the origin of which is effectively cancelled by NH_3, must be a species with a positive charge. The only question left is whether or not it is a protonated biphenyl. However, the elimination and transfer of a proton from a DCE-type solvent at these velocities must be doubted.

The absorption spectra for the cation and the anion of *trans*-stilbene have not yet been established. The only available information is that reported by Shida and Hamill.[1] They obtained an absorption spectrum by the use of a rigid glass of *trans*-stilbene in *s*-butylchloride, they ascribed it to the cation. The present pulse-radiolysis results show that there is no considerable difference between the spectrum in MTHF and that in an alkyl halide of the DCE type. The only difference, as may be seen in Fig. 3, is the position of the absorption maximum, which is at 500 mμ for MTHF and 2,5-dimethoxy tetrahydrofuran and at 490 mμ for the alkyl halides of the DCE type. As in the case of biphenyl, it is not easy to decide on the nature of the transient species of *trans*-stilbene formed in each type of solvent. However, the first-order rate curve suggests that there can be only one species which gives the spectrum. The results from the effects of gases, Table 1, show that the transient species formed in DCE type alkyl halides are not much affected by any added N_2O or SO_2, but completely disappear if NH_3 is added. This, it seems, is strong evidence for the formation of the cation in these solvents. Therefore, the species giving rise a spectrum with the peak absorption at 490 mμ can be concluded to be the cation. The mixing of two solvents such as 11DCE and BuCl shows that the effects of the two solvents are added in the mixed solvent. On the other hand, a mixture of 8 mol% of MTHF and 92 mol% of TECE decreased the optical density at 490 mμ to only 9% of that observed with pure TECE. The latter fact indicates that MTHF scavenges the species formed in TECE. Therefore, the electronic nature of the transient species formed in MTHF seems to be exactly the reverse of that formed in TECE. Hence, it is highly probable that the species with the absorption maximum at 500 mμ is the anion.

In the studies of the effect of additives on the radiolysis of 1,2-dichloroethane,[2] it was shown that the *G*-value of ethylene goes down if those additives with larger rate constants with hydrated electrons are added. It was, therefore, concluded that ethylene is formed through a negative ion of 12-DCE. On the other hand, MTHF and tetrahydrofuran, which have smaller affinities with hydrated electrons, increase the *G*-value of ethylene from 2.1 to 3.6 and 5.2 respectively. The explanation of this was that the holes formed in pure 12DCE are normally neutralized by the negative ions. If MTHF or tetrahydrofuran exists, a hole is neutralized by this compound before a negative ion comes into contact with it. The result is an increase in the number of the negative ions which spontaneously disintegrate into ethylene and Cl_2. The conclusion of the product analysis method, therefore, agrees very well with the present pulse-radiolysis results.

The difference between the spectra of the cation and the anion of biphenyl seems to be due to a steric electronic interaction between the *o*-positions in two different benzene rings. If so, a stronger steric effect should be observed in the cation and the anion of *o*-terphenyl. The two spectra from the solutions of *o*-terphenyl in 112TCE and in MTHF are different, as shown in Fig. 13. Therefore, the above explanation may be worth consideration. The electronic charge is conducted through the systems under investigation very well in spite of the insulating nature of both the aromatic solutes and the solvents used, all of which contain only covalent bonds. The concentration dependence of the optical density, Fig. 1, shows that the optical density will be zero at a solute concentration of 10^{-4} mol/*l*. This concentration is equivalent to a cubic lattice model with a unit dimension of 255 Å, one in which all the lattice points are occupied by a *trans*-stilbene molecule while the space inside the lattice is filled with solvent molecules. Therefore, if a cation (hole) of the solvent molecule is formed, at least one of the solute molecules is within less than 220 Å from this hole. The positive charge must travel this distance in order to be transferred to the solute molecule.

A covalently-bonded insulator becomes a semiconductor if some excess electric charge is injected into the lattices. The present system during and immediately after pulsed irradiation seems to be such a semiconductor. This does not mean, however, that a measurable macroscopic

conductivity is observed with an aid of some external circuit connected to the cell. The hole travels only 220 Å before it is captured by the anion. If a solute molecule with a lower ionization potential exists within this range from the hole of the solvent molecule, the hole will migrate to the solute molecule.

Such a semiconduction process also explains the charge transfer within a rigid glass matrix. Unless there is such a conduction, it will be difficult to trap the holes and electrons formed in the matrix molecules completely with less than 10^{-1} mol/l of the solute molecules.

The electricity in the present systems is carried in two ways, by an electron and by a hole. The total conductivity is the sum of the two conductivities, σ_h and σ_e. These quantities are functions of the ionization potential, the electron affinity, the temperature, and so on. In the case of MTHF, the σ_h is small due to the low ionization potential. As a result, the conductivity by the electron traps, σ_e, is dominant, and a negative ion is formed far more easily than a positive ion. The slowly-travelling holes, therefore, are mostly caught by the solvated electrons before they meet a solute molecue. In the case of 12DCE, the σ_h is larger as a result of the high ionization potential. Therefore, only the cation of the solute molecule is formed. In some media in which the σ_h and σ_e are comparable, the simultaneous formation of both the ionic species can be expected. Such is the case with 3-methyl pentane.

To ignore the minor conductivity, however, is not possible, especially more than 1 μsec after a pulse. The ionic species of the solute molecule formed begin to meet the counter electric charge, which is conducted by the minor conductivity. This is observed as the decay of the solute ions. Another piece of experimental evidence to support such a conductivity theory is, then, the kinetics of the decay of the optical densities resulting from the ionic species of the solute.

By analogy with the recombinations of free radicals in the gas-phase photolysis, it has been generally believed that a cation or an anion disappear by the recombination process and that the charge carriers are individual ions. In the present theory, the movements of each molecule are ignored; rather the entire solution is handled as one continuous system. The rate-determining step in the collision-recombination theory is the movement of each molecule, while in the present theory the activation energy for the neutralization of the hole and the trapped electron (or the electron itself) determines the rate. The transportation of a hole or an electron trap is not considered to be rate-determining. It will be helpful to use an ion-pair model to interpret this theory. By, say 0.5 μsec after a pulse, each electron trap has already moved and occupied one of the lattice points which are close to or next to the site which is occupied by a solute cation. By 10 μsec after a pulse all the ion pairs have recombined by going over the activated state. This activation energy is supplied thermally by the surrounding lattices. This theory, therefore, predicts a first-order decay rate of the solute cation. Actually the rate is first-order. Arai and Dorfman[3] suggested the first-order decay rates of the solute anions in isopropyl alcohol with some unknown impurities. It may not have been correct, and the evidence may more properly be interpreted by the present theory.

Though in Shida and Hamill's experiments CCl_4 was a good matrix for observing a cation, in the present study it has been found that CCl_4 gives something else. The fact that a cation is not formed in CCl_4 has already been postulated.[10] The effect of NH_3 on the CCl_4 - *trans*-stilbene system has indicated that the transient species, whose spectrum is entirely different from that of the cation, is also effectively quenched by NH_3. This result can be explained as follows. The initial radiation-chemical product of CCl_4 will be an e^- and a cation, CCl_4^+. CCl_4^+ is, however, extremely unstable. Before a solute cation is formed by a hole conduction started from CCl_4^+, it decomposes to CCl_3 and Cl^+. As Cl^+ is quite different in shape from the matrix molecules, the hole conduction from it to a CCl_4 molecule is rather difficult, and Cl^+ is a stable hole. The transient species observed will have been formed through a direct molecule-to-molecule reaction of Cl^+ and the solute. If NH_3 exists, Cl^+ will react with NH_3 leaving almost nothing to be detected in the visible region. For the cases of other CCl_4-type solvents, namely, 111TCE and PCE, the instability of CCl_3-CH_3^+ and $CCl_3CCl_2H^+$ will explain the odd transient species formed.

CCl_4, CCl_3CH_3 and, CCl_3CCl_2H all have a CCl_3 group, and none of them gives a cation of an aromatic compound in the liquid phase. However, it seems that $CHCl_3$[11] gives a solute cation. Therefore, it is possible to say that a -CCl_3 group without a hydrogen atom connected to it makes the original cation very unstable. In a frozen solid, all the Cl atoms are rigidly fixed by the surounding lattice, as a result, the lifetime of CCl_4^+ is long enough to allow a charge transfer by the hole conduction. If CCl_4 is added to 12DCE, the hole conduction through 12DCE lattice points is greatly disturbed by the presence of CCl_4 molecules. One possible reason is that the conducting holes are not in their ground state (the shallowest holes), but that some deeper holes are contributing to the conduction. Therefore, if the hole arrives at a site of the lattice which is occupied by a CCl_4 molecule, which may have a higher ionization

10) R. E. Bühler and T. Gäumann, p. 279, Ref. 4.
11) S. Arai, private communication.

potential than 12DCE, such an "excited" hole will become a "ground-state" hole of CCl_4 and no longer contribute to the conduction. This impurity effect can also serve to explain the effects of added N_2O and CCl_3CCl_3 on the formation and decay of the cation of *trans*-stilbene in 112TCE, shown in Table 1. As N_2O has a large rate constant with hydrated electrons, it is expected that it will fix negatively-charged species and, as a result, the life of the cation will become longer. This actually happens. However, N_2O also reduces the formation of the solute cation. This indicates that the hole conduction is also reduced by the presence of the N_2O molecule in the system. N_2O^+ as well as N_2O^- is, probably formed, and the charge transfer from a N_2O^+ to a 112TCE molecule is, like that from a N_2O^- to a 112TCE molecule, not easy. This is what the postulate in the previous work of the present author has meant[2]: all electron scavengers would undoubtedly behave both as electron scavengers and as hole scavengers, but after the overall competetion with the solvent molecules, they will behave as electron scavengers. In the case of CCl_3CCl_3, the formation of the cation is not distrubed much, but the decay rate is considerably lower.

The generally-accepted idea of the dissociative attachement process in the gas phase can be doubted in the liquid phase. If the negative charge (or an electron) is permanently trapped in the form of Cl^-, no semiconductivity by the negative charge, σ_e, can be expected. As a result, the decay curve must obey a second-order rate because of the collision-initiated nature of the neutralization. Therefore, the formation of a negative ion, $(RCl)^-$, is more suitable as an explanation of the formation of the cations in these solvents in either the solid or the liquid phase.

The author is greatly indebted to Mr. E. G. Wendell for his technical assistance in this work. He also wishes to thank Dr. L. M. Dorfman for his interest. The helpful opinions of Dr. S. Arai are also appreciated.

BULLETIN OF THE CHEMICAL SOCIETY OF JAPAN VOL. 41 2586—2591 (1968)

Calorimetric Study of the Glassy State. III.*1 Novel Type Calorimeter for Study of Glassy State and Heat Capacity of Glassy Methanol*2

Masayasu SUGISAKI, Hiroshi SUGA and Syûzô SEKI

Department of Chemistry, Faculty of Science, Osaka University, Toyonaka, Osaka

(Received April 16, 1968)

An adiabatic Nernst-Type calorimeter with a cell for condensing a sample vapor as an amorphous state was constructed. By making use of this calorimeter, the heat capacities of the glassy, supercooled liquid, and crystalline states of methanol were measured from 20°K to 120°K. It was found that the state of methanol deposited on the chilled substrate at about 95°K from its vapor state shows a glass transition phenomenon at about 103°K accompanied with the sudden increase of heat capacity, ΔC_P, amounting to 26 J/(mol°K). The drastic crystallization with the exothermic effect coming to 1.54 kJ/mol was observed near 105°K. The residual entropy for the glassy methanol was found to be 7.07 J/(mol°K). Based on these results it seems very plausible to propose that any non-crystalline solid deposited on the chilled substrate from the vapor state will show the glass transition phenomenon.

Usually, a glassy state is considered as a non-crystalline solid which can be obtained by supercooling a liquid sample without any crystallization phenomenon. When the supercooled liquid goes further into a glassy state, a glass transition phenomenon is necessarily found out at a definite temperature characteristic of the sample.

Nowadays, we are able to obtain the non-crystalline solids by using other various kinds of method[1] including the method of the supercooling of liquid. These methods are, *e. g.*, shock wave

*1 Our papers on isopentane (This Bulletin, **41**, 593 (1968)) and on cyclohexanol (*ibid.*, **41**, 1073 (1968)) may be denoted as 1st and 2nd papers of our series of investigation on the glassy state hereafter.

*2 Read before The Third Japanese Calorimetry Conference held at Osaka in 1967. Part of this paper was reported as the short communication in this Bulletin (**40**, 2984 (1967)).

1) D. R. Secrist and J. D. Mackenzie, "Modern Aspect of the Vitreous State," Vol. 3, ed. by J. D. Mackenzie, Butterworths Scientific Publication, Ltd., London (1964), chapter 6.

treatment, neutron bombardment, vapor condensation, solution method (hydrolysis and anodization), and dehydration of hydrated crystal, *etc.* These non-crystalline solids prepared by these different methods have common features that they exhibit a crystallization phenomenon on heating.

Are they also plausible to be called as a glass? In order to reply this question, it seems to be most decisive to find out their glass transition phenomena, because the glass transition phenomenon is of characterisitc to the glassy state.

Up to the present time, there has been reported no successful and quantitative work which confirms the glass transition phenomena for such non-crystalline solids prepared by the above cited uncommon methods.

In order to find out the glass transition phenomenon of the non-crystalline state prepared by the vapor condensation method, we have constructed a novel type of calorimeter which involves the sample cell for condensing the sample vapor. By making use of this calorimeter, the heat capacities of the glassy, supercooled liquid, and crystalline states of methanol were measured successfully.

Experimental

Apparatus. The calorimeter consists of a filling tube made of monel and soft copper, a copper cell with a platinum resistance thermometer, inner and outer adiabatic shields, a copper block as thermal station, and a vacuum jacket and others. The filling tube, two adiabatic shields and the copper block are all wound closely with constantan heaters.

The total view of the constructed calorimeter and the sketch of the sample cell are given in Figs. 1 and 2. As is shown in Fig. 2, a part of the filling tube enters into the sample cell. During the procedure of sampling, this part of the filling tube is warmed by the heat conduction from the upper part of the filling tube which is wound closely with the constantan heater. The part of the filling tube inside the cell can be kept at about 15°C, when the temperature of the wall of the sample cell is adjusted to be about 80°K and the outer part of the filling tube is warmed around 30°C under high vacuum condition of about 10^{-6} mmHg inside the cell. In this case the heat conduction between the filling tube and the sample cell occurs spontaneously through the outer short stainless steel tubing put on the top of the cell. The amount of this heat conduction is estimated as 1.3 (J/s), when the above cited temperature difference is maintained. Therefore the effect of the thermal switch is necessitated whose power of the heat exchange is at least larger than 1.3 (J/s). For this purpose the conduction gas method by using helium gas is sufficiently adequate when the apparatus is operated above the boiling point of liquid nitrogen.

In order to carry out the heat capacity measurement under a good adiabatic condition, the adequate combination of monel and copper metals for the filling tube outside the cell is designed for preventing the heat leak through this tube.

Measurements of temperature are made with the platinum resistance thermometer calibrated in terms of International Temperature Scale between 90°K and 500°K and the provisional scale of the National Bureau of Standards between 11°K and 90°K. Measurement of heat capacity is made in quite a same fashion as that reported by Suga and Seki.[2)]

It is found that a heat capacity of the empty cell is about 8.5 (J/degK) at room temperature, and that the attainment of the thermal equilibrium after the finish of energy input takes about 25 min at all temperature region between 13 and 330°K, and that the values of heat capacity deviate from the smoothed curve within 0.1% in the temperature region between 13 and 330°K.

Next, the procedures for condensing the vapor of a sample into the calorimeter as an amorphous state will be described. Firstly the vacuum jacket is immersed into the liquid nitrogen, and helium gas at about one atmospheric pressure is then introduced as a conduction gas into the vacuum jacket, the filling tube and the copper block being simultaneously warmed up at the desired temperature with the constantan heaters wound around them. Their temperatures are registered by the seven chromel P-constantan thermocouples, one of which is attached on the copper block, all the

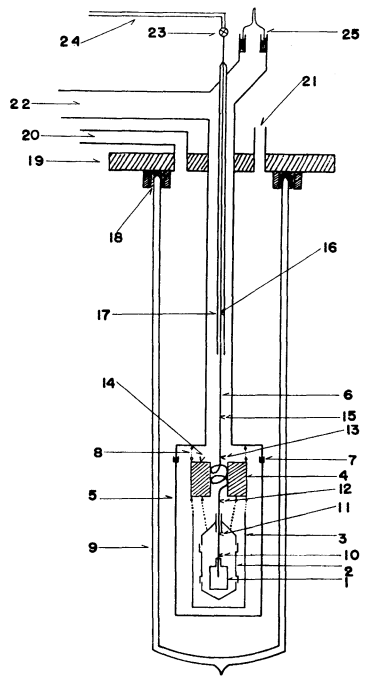

Fig. 1. Description of the type-2 calorimeter.

1) sample container, 2) inner shield, 3) outer shield, 4) copper block, 5) vacuum jacket, 6) filling tube, 7) wood alloy joint, 8) nylon thread, 9) glass dewar, 10)—16) thermocouples, 17) sheath of the filling tube, 18) picein joint, 19) brass plate for supporting the apparatus, 20) outlet tube, 21) tube for introducing liquid hydrogen or nitrogen, 22) to vacuum pumps, 23) needle valve for sampling, 24) glass tube for introducing the vapor of sample, 25) picein joint for taking out of lead wires.

2) H. Suga and S. Seki, This Bulletin, **38**, 1000 (1965).

TABLE 1. EXPERIMENTAL DATA OF METHANOL

Number of sample	Rate of condensation (g/hr)	Total amount of sample (g)	Heat of crystallization (kJ/mol)	ΔC_p at T_g (J/mol°K)	Amorphous part of sample (%)
1	0.101	1.214	1.54 ±0.05	26	100
2	0.366	1.645	0.57	10	37.4

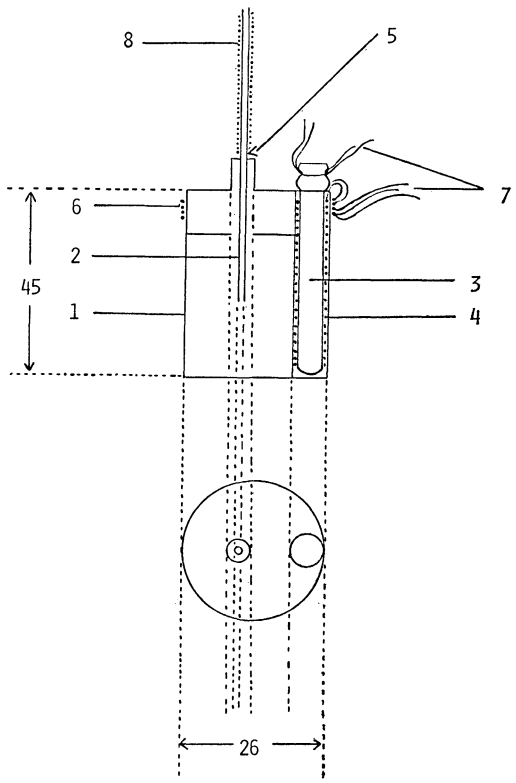

Fig. 2. Description of the sample container.
1) wall of the cell (made of copper), 2) filling tube, 3) platinum resistance thermometer, 4) constantan heater for energy-input, 5) thermocouple, 6) and 7) lead wires, 8) heater for sampling.

others being attached on the filling tube (see Fig. 1). The temperature of the sample cell is watched by recording the resistance of the platinum thermometer on the "Speedomax" recorder (Type G, Leeds & Northrup Co.). Under such an operation of the heaters, only the wall of the sample cell is chilled down to sufficiently low temperature, because the heat exchange between the filling tube and the sample cell is pressed down. The temperature difference between them can be easily regulated at any desired values up to about 200°C by changing the level height of liquid nitrogen or by changing the amount of electric current through the heater wound on the filling tube. When the temperature distribution of the calorimeter becomes to be steady, the vapor of the sample is slowly condensed into the calorimeter by opening the needle valve situated at the upper part of the calorimeter (see Fig. 1). The rate of condensation must be regulated to be very slow, since the surface of the amorphous sample produced in the cell may be warmed up above a crystallization temperature with the accumulation of the heat of condensation if the rate of condensation is pretty high. Usually the preparation of the vitreous sample needs about 10—20 hr and a total amount of condensed vitreous substance is of about 1—2 g. After the sampling is over, the heaters of the filling tube and of the copper block are switched off, and the total parts of the calorimeter are chilled down to 80°K, then helium gas (20 mmHg at 80°K) being introduced in the calorimeter cell in order to facilitate the attainment of the thermal equilibrium. Finally the conduction gas in the vacuum jacket is evacuated down to 10^{-6} mmHg for the realization of the adiabatic condition. With this adiabatic calorimeter measurements of the heat capacities can be carried out from 13°K to 330°K.

When the measurement is over, the calorimeter cell is heated up and the sample in the cell is gathered into the glass tube out of the calorimeter and its total amount is determined by measuring its weight.

Purification of Methanol. The commercial extra pure methanol (Wako Chemical Industries, Ltd.) was dried by magnesium metal (Lund and Bjerrum method). This product was distilled twice in high vacuum (10^{-6} mmHg) and the final product was degassed very carefully by repeating melting and freezing of the sample under high vacuum (10^{-6} mmHg). This final product was then introduced into the calorimeter in high vacuum (10^{-6} mmHg) as an amorphous state.

Preparation of Glassy Methanol. For this material, the outer jacket of the calorimeter was removed so that the temperature of the sample cell may be kept as low as possible. During the vitrification process, the temperature of the sample cell was kept between 94 and 97°K, and the filling tube around 220°K. Two kinds of rate of condensation were adopted as given in the second column of Table 1.

Heat Treatment adopted for the Heat Capacity Measurement. For the sample (1) heat capacities of glassy state were measured from 94°K to just above the glass transition temperature, and this sample was again chilled down slowly to 80°K as soon as the sample reached just above the glass transition temperature, and heat capacities were measured again from 80°K to 104°K. When the temperature of the sample reached about 105°K, a drastic crystallization took place and the temperature of the sample rises spontaneously due to the exothermic effect. For the sample (2) the measurements were made for the glassy state from 20°K to 104°K. After the crystallization, the crystalline sample was chilled down to 20°K and the measurements were made from 20 to 120°K.

Experimental Results

Results of Heat Capacity Measurement. *(a) Heat Capacity of the Crystalline State.* The numerical data for the sample (2) are given in

Table 2A, and are represented by hollow circles in Fig. 3. In this figure the smoothed curve above 120°K is drawn on the basis of Kelley's data.[3] It is found that our present data below 120°K agree with his data within the experimental error of 1.3% in the temperature region of liquid hydrogen, and 0.5% in the temperature region of liquid nitrogen.

TABLE 2A. HEAT CAPACITY OF METHANOL(CRYSTAL) IN J/(mol °K)

T (°K)	C_P	T(°K)	C_P	T (°K)	C_P
21.61	6.019	51.28	23.94	84.40	38.24
23.97	7.402	55.26	25.75	88.47	40.07
26.66	9.311	58.74	28.25	92.46	41.49
29.73	11.30	62.46	29.98	96.30	42.33
32.93	13.29	65.91	31.69	100.25	43.21
36.25	15.57	69.68	32.82	104.29	44.51
39.83	17.59	73.73	34.44	108.22	45.76
43.51	19.87	77.56	36.39	112.04	46.83
47.24	21.84	79.92	36.64		

TABLE 2B. HEAT CAPACITY OF METHANOL (GLASS AND SUPERCOOLED LIQUID) IN J/(mol °K)

T (°K)	C_P	T (°K)	C_P
sample (1)		60.19	29.06
series 1		63.38	30.54
96.30	44.30	66.65	31.97
97.96	45.96	70.05	33.31
99.58	49.77	series 3	
101.13	83.56	21.92	7.046
series 2		24.73	8.665
82.88	39.54	27.86	10.79
85.80	40.82	31.36	13.23
88.64	41.85	34.81	15.99
91.42	42.23	38.50	17.98
93.63	43.18	42.28	20.12
95.34	43.75	46.32	22.66
97.02	45.09	series 4	
98.74	47.21	72.26	34.56
100.39	57.28	76.22	35.96
101.97	76.84	80.86	37.71
102.96	71.62	85.50	39.54
103.87	68.92	89.27	41.04
105.16	67.70	92.02	41.80
sample (2)		93.79	42.45
series 1		95.54	43.09
23.64	8.074	97.25	43.97
26.64	10.03	98.94	44.88
30.03	12.33	100.58	48.64
series 2		102.14	58.56
49.39	24.21	103.54	53.43
51.85	25.42	104.82	54.04
54.38	26.40	106.22	53.61
57.14	27.58		

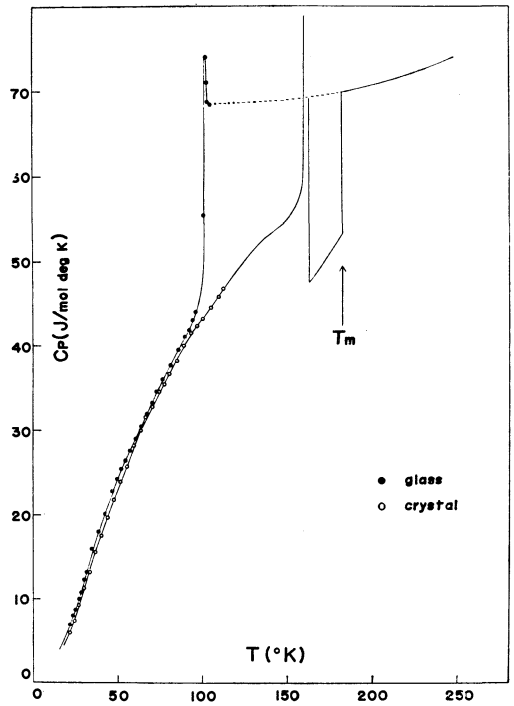

Fig. 3. Heat capacity curve of methanol.

The filled circles represent glassy and supercooled liquid states, and the hollow circles a crystalline state.

(b) Heat Capacities of the Glassy and Supercooled Liquid States. The results of the samples (1) and (2) are given in Table 2B and illustrated by the filled circles in Fig. 3. In this figure, the values for the sample (1) are plotted around the glass transition point and those for the sample (2) are plotted below 80°K (see Table 2A). As is seen in this figure it is found that the state of aggregation of methanol obtained by the present method of vapor condensation shows a glass transition phenomenon at about 103°K. On further heating, we found a drastic crystallization phenomenon at about 105°K just above this glass transition point. The dotted line represents the assumed heat capacity curve for the supercooled liquid which is obtained by an extrapolation of those of the normal liquid. The jump height of heat capacity (ΔC_P) at the glass transition point (T_g) and the total amount of exothermic effect accompanying the crystallization are given in Table 1. By comparing the heat of crystallization with the magnitude of ΔC_P at T_g for both samples, it is easily concluded that the sample (1) is in almost complete glassy state while the sample (2) is in partial glassy state. In Table 1 the amorphous part of the samples are also estimated by comparing the heat of crystallization with each other by assuming that the sample (1) is composed of 100 per cent amorphous material.

Thermodynamic Properties and Residual Entropy. The values of heat capacity, entropy, and also the enthalpy and Gibbs energy functions of methanol at selected temperatures are listed for the glassy and supercooled liquid states in Table 3.

TABLE 3. THERMODYNAMIC PROPERTIES OF METHANOL (GLASSY AND SUPERCOOLED LIQUID STATES) IN J/(mol°K)

T (°K)	$C°_P$	$S°-S°_0(gl)$*	$(H°-H°_0(gl))/T$	$-(G°-G°_0(gl))/T$
5	(0.310)	(0.082)	(0.070)	(0.012)
10	(1.700)	(0.619)	(0.447)	(0.172)
15	(4.350)	(1.796)	(1.297)	(0.499)
20	7.250	3.444	2.421	1.023
30	13.75	7.572	5.081	2.491
40	19.96	12.40	8.043	4.357
50	25.30	17.44	10.97	6.466
60	30.02	22.48	13.76	8.720
70	34.42	27.44	16.40	11.04
80	38.59	32.31	18.91	13.40
90	42.40	37.07	21.31	15.76
103	Glass transition point			
110	68.10	48.65	28.04	20.61
120	68.39	54.59	31.38	23.21
130	68.70	60.05	34.24	25.81
140	68.98	65.16	36.71	28.45
150	69.20	69.90	38.87	31.03
160	69.41	74.39	39.78	34.61
175.22	70.00	80.70	43.27	37.43

$H°_0(gl)-H°_0(c)$**$=1538$ J/mol.

The values in parentheses are extrapolated by means of the Debye function.

*: (gl) indicates glassy state.

**: (c) indicates crystalline state.

The residual entropy, $S°_0$, which amounts to 7.07J/(mol°K), was also determined by using the results of heat capacity measurement. We could not measure unfortunately the heat of capacity 100 per cent glassy sample of methanol below 80°K, so the heat capacities of the glassy methanol below 80°K were calculated on the assumption that the additivity of the heat capacities of crystalline and glassy states holds as follows,

$$C_P(obs) = \alpha C_P(gl) + (1-\alpha)C_P(cryst),$$

here $C_P(obs)$ is the actually measured heat capacity of the sample, $C_P(gl)$ the heat capacity of completely glassy sample, $C_P(cryst)$ that of the crystalline sample and α the mole fraction of the glassy part of the sample. In the case of sample (2) α was estimated as 0.374, so the heat capacity of the glassy state below 80°K was calculated by using the values of the sample (2).

In passing, the entropy of the crystalline state is based on the Kelley's data.[3]

3) K. K. Kelley, *J. Am. Chem. Soc.*, **58**, 1144 (1936).

Discussion

Design of the Calorimeter. In the past, there has been known no successful work on the precise measurement of heat capacities for an amorphous material deposited directly onto the wall of a calorimeter cell from its vapor state.[4] This fact is due to some difficulties for constructing the calorimeter which fulfills the following few rather severe requirements.

(a) The calorimeter must be equipped with the filling tube, through which vapor of a sample passes, kept at a sufficiently higher temperature above the melting point of the sample, and with the calorimeter cell into which the vapor of the sample is condensed as an amorphous state, kept at a sufficiently lower temperature far below a glass transition temperature of the amorphous sample. For instance, the temperature of the filling tube should be higher about 100—200°C than that of the calorimeter cell if the glass transition point of the sample used situates around 100°K. (b) In order to hold the above cited steady distribution of large temperature difference in the calorimeter, a thermal switch is required whose power of heat exchange is sufficiently large enough. (c) It seems very difficult to obtain a considerable amount of a condensed amorphous substance, so a good adiabatic conditioning of the calorimeter is needed in order to perform precise measurements.

In order to satisfy the condition (a), all previous workers[4] have adopted the method of construction that a sample cell is directly immersed into the liquid nitrogen. This method is, however, inadequate to satisfy the condition (c), because a contamination during the sampling obstructs a realization of an adiabatic conditioning by high vacuum. By taking into consideration the above cited three conditions we have constructed the calorimeter with following devices.

(a) In order to maintain the steady temperature difference between the sample cell and the filling tube, the heat conduction between them is sufficiently reduced by joining them through a thin stainless tube (3 mm in diameter, 0.15 mm in thickness and 10 mm in length). (b) For simplicity of the handling of the apparatus, a conduction gas method was chosen as the thermal switch. If we adopt a mechanical thermal switch which has a comparable efficiency of heat exchange with that of the conduction gas thermal switch, the apparatus becomes to be very complicated. This complication necessarily causes an increase of heat capacity of the sample cell itself, so the mechanical switch is inadequate for the precise measurement.

4) J. A. Pryde and G. O. Jones, *Nature*, **170**, 685 (1952); H. J. de Nordwall and L. A. K. Staveley, *Trans. Faraday Soc.*, **52**, 1061 (1956); R. H. Beaumont, H. Chihara and J. A. Morrison, *J. Chem. Phys.*, **34**, 1456 (1961).

(c) In order to realize a good adiabatic condition, it seems preferable to design the calorimeter equipped with two adiabatic jackets; the structure satisfies the conditions that the convection current of the conduction gas is facilitated, and that a heat leak due to radiation is completely precluded.

Glass Transition Phenomenon of Methanol. Van Thiel and Pimentel[5] observed that methanol deposited on the chilled substrate between 4.2 and 120°K gives an infrared absorption spectrum resembling that of the normal liquid methanol, and that once this deposited state was heated up above 120°K, the spectrum disappeared and changes to that characteristic of the crystalline state. Based on the above observation, they have conjectured that this deposited state of methanol might be a glass. However, their conclusion seems too hasty, because a glass transition phenomenon, which necessarily accompanies the glassy state, has not been discovered yet. Therefore, our present finding of the glass transition phenomenon certifies for the first time that the methanol condensed onto the chilled substrate below 105°K exists as a glassy state. Moreover, it is to be noted that the vitreous methanol of the sample (1) is composed of about 100 per cent amorphous material judging from the heat of crystallization as well as the jump height of heat capacity, ΔC_P, at T_g.

In general, it seems very difficult to obtain the completely vitreous state by the method of vapor condensation. In fact there has been no quantitative work of obtaining completely vitreous material by this method. In the case of our calorimetry, the temperatures of several parts of the apparatus can be regulated accurately and finely and also the rate of condensation can be controlled very precisely during the vitrification process, so that it is rather easy to obtain a completely vitreous material, when the suitable condition for the adjustment of temperature distribution is established. The fact that the sample (2) contains the appreciable crystalline part seems to be due to the warming up of the surface of the sample above the crystallization point by the high rate of condensation.

Judging from the results of our experiment on methanol it seems very plausible to propose that any non-crystalline solid deposited on the chilled substrate from the vapor state will show the glass transition phenomenon.

The authors would like to express their sincere thanks to the Toyo Rayon Co., Ltd. who defraid a part of the financial support for the present investigation.

5) G. C. Pimentel and A. L. McClellan, "The Hydrogen Bond," W. H. Freeman and Company, San Francisco and London (1960), p. 103.

BULLETIN OF THE CHEMICAL SOCIETY OF JAPAN VOL. 41 2591—2599 (1968)

Calorimetric Study of the Glassy State. IV. Heat Capacities of Glassy Water and Cubic Ice

Masayasu SUGISAKI, Hiroshi SUGA and Syûzô SEKI

Department of Chemistry, Faculty of Science, Osaka University, Toyonaka, Osaka

(Received April 16, 1968)

By making use of the vapor-condensation type calorimeter, the heat capacity measurements of amorphous, cubic and hexagonal ices were made between 20°K and 250°K. The glass transition phenomenon was found near 135°K with the sudden change of the heat capacity amounting to 35 J/(mol°K). The drastic crystallization with the exothermic effect which amounts to 1.64 kJ/mol was then followed at this temperature. The transformation of the cubic crystal to the hexagonal one was confirmed to occur in the temperature region from 160 to 210°K and to proceed in two steps with the activation energies of 21.3 and 44.7 kJ/mol, respectively. The amount of the exothermic effect accompanying this transformation was found to be about 160 J/mol.

In the previous paper,[1] we have reported the construction of the novel type of calorimeter for studying a glassy state and the experimental data on the glassy state of methanol. In the present paper we should like to report our results of investigation on water.

1) M. Sugisaki, H. Suga and S. Seki, This Bulletin, **41**, 2586 (1968).

Since the work by Burton and Oliver[2] in 1935, it has been reported by many workers[2-12] that so-called amorphous state of water may be obtained when the water vapor is condensed onto the chilled substrate below about 140°K. In 1952 Pryde and Jones[4] have first tried to find out the glass transition phenomenon of the amorphous state deposited on a chilled substrate, and several such trials have been followed by many other workers. They are, for example, Ghormley (1956),[5] de Nordwall and Staveley (1956),[6] and McMillan and Los (1965).[12] Nevertheless, there had been no successful work before the study with a differential thermal analysis method by McMillan and Los who have found an endothermic effect at 139°K just below a crystallization temperature for an amorphous ice. Furthermore, many other workers have reported by use of the X-ray or electron diffraction methods that the amorphous ice crystallizes into a cubic form when it is heated up to about 140°K, and that the cubic ice transforms into the hexagonal one very sluggishly and irreversibly around 200°K.[7-11,13] McMillan and Los have also found that this transformation is accompanied with the exothermic effect. Although there have been thus accumulated considerable number of data on the glassy state of this material, it may be said that there is no quantitative and conclusive evidence about the presence of the glassy state of water.

In the present investigation, we have tried to perform the quantitative heat-capacity measurements of the amorphous, cubic and hexagonal ices, and further to obtain some thermodynamical data of the glass transition phenomenon of the amorphous ice, of its crystallization effect and further of the phase transformation of the cubic form to the hexagonal one.

Experimental

Apparatus. An adiabatic Nernst-type calorimeter with a cell for condensing a sample vapor as an amorphous state was used. The detailed structure of the calorimeter and of the experimental procedures were already reported in the previous paper.[1]

Purification of Water. The water treated by ion-exchange resin was distilled under atmospheric pressure, and then this product was distilled twice in high vacuum (10^{-6} mmHg). After the final product was degassed very carefully by repeating melting and freezing of the sample under high vacuum (10^{-6} mmHg), the sample was condensed into the calorimeter in high vacuum (10^{-6} mmHg) as an amorphous state at about 120°K.

Preparation of the Vitreous Water. Four kinds of sample of water were vitrified by condensing their vapor into the calorimeter cell in quite a same fashion as reported in the previous paper.[1] During the vitrification, the temperature of the sample cell was kept first between 103°K and 106°K [sample (1)] and between 120 and 123°K in the other three cases of sample [(2), (3) and (4)]. The filling tube was kept around 300°K in each case for all samples. The rate of condensation and the total amount of the sample used for the measurements are given in Table 1.

Experimental Results

Heat Treatment Adopted for the Heat-capacity Measurement. *Sample (1).* The measurements of heat capacities of the glassy state were made in the region between 118 and 136°K covering the glass transition temperature, through which some exothermic effect was always traced above 115°K. The drastic crystallization was observed at about 135°K which is just above the glass transition point.

TABLE 1. VITRIFICATION CONDITION AND SOME EXPERIMENTAL DATA ON GLASSY WATER

Number of sample	Rate of condensation (g/hr)	Total amount of sample (g)	Heat of crystallization (kJ/mol)	ΔC_P at T_g (J/mol°K)	Amorphous part of sample (%)
1	0.032	0.6054	1.64	35	100 (assumed)
2*	0.033	0.5897	1.46	29	89.0
3**	0.024	0.6959	1.06 ±0.05	19	64.6
4***	0.030	0.7745	0.85	11	49.0

* Annealed at 128°K for 4 hr.
** Annealed at 128°K for 16 hr.
*** Annealed at 128°K for 13 hr.

2) E. F. Burton and W. F. Oliver, *Proc. Roy. Soc.*, **A153**, 166 (1935).
3) L. Staronka, *Roczniki Chem.*, **19**, 201 (1939).
4) J. A. Pryde and G. O. Jones, *Nature*, **170**, 685 (1952).
5) J. A. Ghormley, *J. Chem. Phys.*, **25**, 599 (1956).
6) H. J. de Nordwall and L. A. K. Staveley, *Trans. Faraday Soc.*, **52**, 1061 (1956).
7) M. Blackman and N. D. Linsgarten, *Proc. Roy. Soc.*, **A239**, 93 (1957); N. D. Linsgarten and M. Blackman, *Nature*, **178**, 39 (1956).
8) F. V. Shallcross and G. B. Carpenter, *J. Chem. Phys.*, **26**, 782 (1957).
9) J. G. Dowell and A. P. Linfret, *Nature*, **188**, 1144 (1960).
10) K. Shimaoka, *J. Phys. Soc. Japan*, **15**, 106 (1960).
11) R. H. Beaumont, H. Chihara and J. A. Morrison, *J. Chem. Phys.*, **34**, 1456 (1961).
12) J. A. McMillan and S. C. Los, *Nature*, **206**, 806 (1965).
13) H. Konig, Nachr. Akad. Wiss. Göttingen, No. 1, 1 (1942); *Z. Krist.*, **105**, 279 (1943).

Sample (2). The measurements for the glassy state were made in the region from 118 to 136°K including the glass transition temperature. In this case the exothermic effect was observed above 123°K. The drastic crystallization was observed at about 135°K. After the crystallization was over this sample was chilled down to 110°K and measurements were carried out again from 180 to 237°K. The appreciable exothermic effect accompanying the phase transition was observed between 180 and 210°K. After the previous series of measurement was completed, this sample was chilled down once more to 180°K and the measurements were made from 180 to 225°K for the hexagonal phase.

Sample (3). Prior to the measurement of the glassy state, the sample was annealed at 128°K for 12 hr. The measurements of the glassy state were made from 20 to 135°K. After the crystallization was performed, this sample was chilled down to 20°K, and the measurements were made again from 20 to 240°K, an appreciable exothermic effect being also observed between 160 and 210°K during this series of measurement. This sample was again chilled down to 60°K and the measurements were carried out from 60 to 240°K.

Sample (4). After the measurement on the glassy state between 60 and 125°K was over, the sample was annealed at 128°K for 12 hr, and then for this annealed sample the measurements were made between 120 and 135°K in which the drastic crystallization was observed at about 135°K.

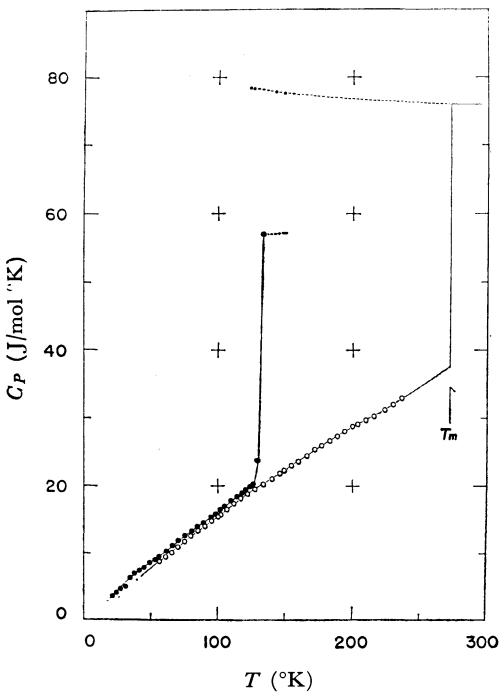

Fig. 1. Heat capacity curve of water.
● Amorphous ○ Hexagonal ice

After the completion of this crystallization, the sample was chilled down to 60°K and the measurements were repeated from 60 to 240°K.

Determination of a Number of Mole of the Sample. A total amount of the sample, which was condensed into the calorimeter cell for the heat-capacity measurement, was determined first by measuring the weight of the sample collected into the glass tube equipped outside the calorimeter. However, the heat capacities of the hexagonal ice calculated based on this value of the number of mole were smaller than those of Giauque's data[14] by 10%. This seems to be due to the fact that some amount of water were condensed in the filling tube situated out of the sample

Table 2. Heat capacity of water (hexagonal ice) in J/(mol °K)

T (°K)	C_P	T (°K)	C_P
Sample (3)		Sample (4)	
56.02	9.058	59.29	9.473
61.13	9.761	63.46	10.13
65.69	10.49	68.05	10.50
70.28	11.30	72.68	11.27
75.20	12.05	77.25	12.37
80.01	12.73	82.30	12.77
85.00	13.98	87.60	14.50
89.70	14.64	92.72	14.62
95.15	15.28	97.58	14.95
99.90	15.98	97.79	14.97
102.10	15.83	102.55	15.55
107.22	16.53	107.36	16.44
112.17	17.41	112.24	17.45
117.20	18.22	116.98	17.99
122.32	18.77	121.57	19.02
127.95	19.52	126.06	19.32
134.04	20.28	130.67	19.74
140.00	20.98	135.42	20.58
145.81	21.87	140.06	21.47
149.26	22.18	144.67	21.45
154.93	23.04	136.89	20.86
160.48	23.61	141.56	21.21
165.93	24.39	146.15	21.94
171.54	25.35	150.66	22.20
177.27	25.95	155.09	22.36
182.97	26.63	159.67	23.48
188.58	27.31	165.44	23.81
194.10	28.11	170.73	24.93
199.53	29.54	175.37	25.71
203.78	29.02	181.01	26.29
210.18	30.46	186.57	26.88
216.49	30.59	192.04	28.07
		197.44	28.82
		202.77	29.45
		208.03	30.20
		213.09	30.85

14) W. F. Giauque and J. W. Stout, *J. Am. Chem. Soc.*, **58**, 1144 (1936).

cell, because the sample in the filling tube does not take part in the heat-capacity measurement, so the number of mole of the sample in the cell was over-estimated than the true value. In this respect, the number of mole of the sample was determined by fitting our values of hexagonal ice to those of Giauque's data between 100 and 140°K.

The accuracy of our calorimeter was checked already in the case of methanol, and so this method of determination may be reasonable and satisfactory for the present purpose. So that, in place of the value determined by direct measurement of the weight of the sample collected into the glass tube, the number of mole based on the Giauque's data was adopted in the following.

Table 3. Heat capacity of water (glass and supercooled liquid) in J/(mol°K)

T (°K)	C_P	T (°K)	C_P
		76.05	12.68
Sample (1)		80.80	13.30
118.82	19.42	85.27	14.47
120.21	19.63	89.74	14.86
122.23	20.17	94.23	15.28
124.21	20.64	98.57	15.75
126.17	21.12	102.75	16.50
128.11	21.45	104.94	16.97
130.01	21.89	109.77	17.67
131.88	23.37	114.46	18.35
133.58	57.30	118.20	18.90
135.86	46.47	121.01	19.39
		123.79	19.94
Sample (2)		126.56	20.72
118.05	19.20	129.34	23.74
119.90	19.72	131.97	32.36
121.81	20.21	134.67	38.47
123.72	20.49		
125.61	20.83	Sample (4)	
127.48	21.38	79.98	13.71
129.35	21.78	84.23	14.29
131.23	25.44	88.51	14.78
133.19	35.42	92.93	15.27
135.50	50.04	97.50	15.88
		101.91	16.63
Sample (3)		106.49	17.19
21.75	3.644	111.25	18.17
24.73	3.957	115.88	19.09
27.75	4.061	120.38	19.88
31.10	4.685		
34.53	6.378	Series after annealing	
38.10	7.002	at 128°K for 12 hr	
41.70	7.393	119.95	19.30
45.40	7.653	122.16	19.93
49.33	8.590	124.35	20.33
53.56	9.032	126.52	21.17
57.83	9.501	128.69	22.31
58.04	9.527	130.90	24.49
62.22	10.26	132.73	28.14
66.59	11.24	134.18	31.51
71.24	11.92		

Results of Heat-capacity Measurement. *Hexagonal Ice.* The results for the samples (3)

Table 4. Heat capacity of water (cubic ice) in J/(mol°K)

T (°K)	C_P	T (°K)	C_P
		170.40	24.18
Sample (2)		176.11	25.25
182.56	24.73	181.79	26.32
187.11	25.71	187.47	26.94
191.64	25.80	193.15	25.25
196.19	24.05	198.82	26.60
200.59	27.40	204.24	29.13
204.87	29.25	210.08	30.12
209.08	30.04	216.36	30.85
213.26	30.07	222.55	31.81
217.39	30.44		
221.48	31.19	Sample (4)	
		60.14	9.496
Sample (3)		64.62	10.41
21.62	1.275	69.14	11.02
24.08	3.019	73.72	12.12
26.64	3.462	78.21	12.35
29.79	4.139	82.68	13.15
33.45	5.076	87.47	13.94
37.24	5.805	92.56	14.34
41.00	6.716	97.44	14.95
44.83	7.106	97.72	14.95
48.82	8.069	102.76	15.58
53.10	8.434	107.77	16.51
57.63	8.980	112.61	17.47
58.98	9.397	117.32	18.22
63.25	10.26	121.90	18.85
67.54	11.04	126.10	19.48
72.10	11.66	126.62	19.74
76.86	12.21	130.92	20.02
81.57	13.38	131.43	20.00
86.02	14.03	135.64	20.84
90.51	14.58	136.17	20.98
95.08	15.16	140.26	21.40
99.49	15.54	144.82	22.29
103.75	16.16	149.30	22.62
108.11	17.02	153.72	22.97
109.94	17.36	156.21	23.53
114.64	18.27	162.22	23.32
119.20	19.13	168.17	24.04
123.69	19.65	174.03	24.40
128.33	20.20	179.82	25.03
133.07	20.85	185.51	26.10
137.70	21.55	191.14	26.80
142.28	22.18	196.77	25.57
146.77	22.65	202.24	28.91
151.18	23.48	208.07	29.77
155.79	23.64	214.34	30.83
159.67	23.01	220.52	31.34
164.57	23.69		

and (4) are given in Table 2 and are represented by the hollow circles in Fig. 1. The deviation of the values around the smoothed curve is within 3% in the vicinity of the boiling point of liquid nitrogen and within 1% around 200°K.

Glass and Supercooled Liquid. The results for the samples (1), (2), (3) and (4) are all given in Table 3. The temperature-dependence of the heat capacity in the vicinity of the glass transition point is drawn for each case of the samples in Fig. 2. Amongst the filled circles given in Fig. 1 the values on the sample (1) are plotted around T_g and those of the sample (3) for the temperature region below 80°K. As is seen in these figures the amorphous solid of water obtained by the method of vapor condensation was found to show a glass transition phenomenon at about 135°K. On further heating the drastic crystallization was found to occur just above the glass transition point. The jump of heat capacity at the glass transition point and the total amount of the exothermic effect accompanying the crystallization are given in Table 1.

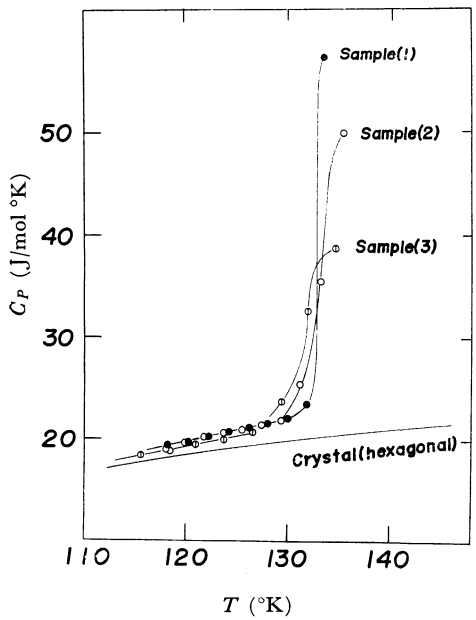

Fig. 2. Heat capacity curve of water near the glass transition temperature.

Cubic Ice. The results for the samples (2), (3) and (4) are given in Table 4, and are illustrated in Figs. 3 and 4 in comparison with those of the hexagonal ice. The total exothermic effect was observed in the temperature region from 160 to 210°K, and in particular we can recognize the remarkably anomalous region of heat capacities between 190 and 210°K. The corresponding enthalpy amount of this exothermic effect was estimated between 160 and 210°K for each sample as is given in Table 5.

Table 5. Total amount of exothermic effect accompanying irreversible transformation of the cubic ice to the hexagonal one

Number of sample	$-\Delta H$ (J/mol)	
2	158.9	±15
3	164.4	
4	159.5	

Discussion

Realization of Glassy State. From the results of our heat-capacity measurement, it is quite clear that the amorphous water condensed

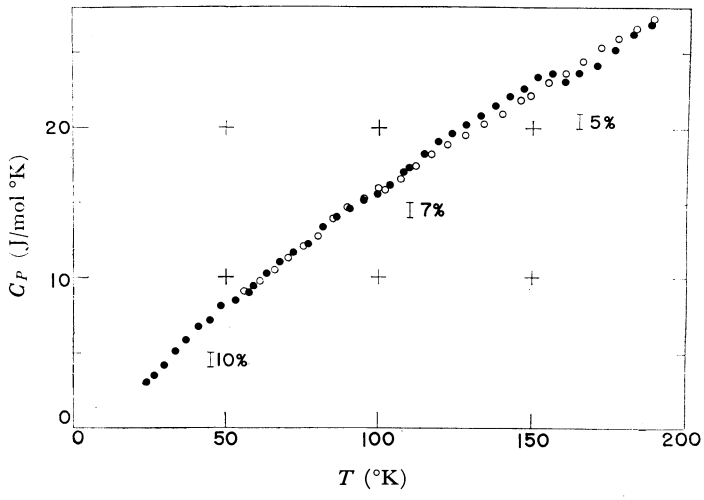

Fig. 3. Heat capacity of ice. The filled circle represents the cubic ice and the hollow circle the hexagonal one.

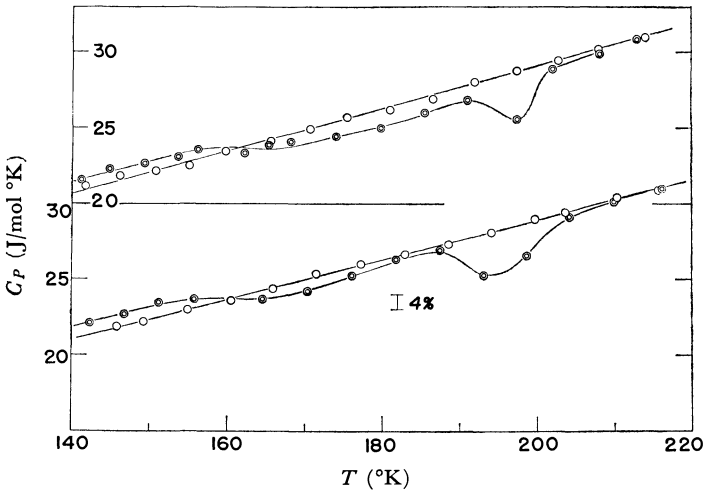

Fig. 4. Heat capacity of ice near the transformation temperature. The lower figure is results for the sample (3) and the upper for the sample (4).
◎ Cubic ○ Hexagonal

from the vapor onto the substrate chilled below 135°K shows a glass transition phenomenon. This fact shows that the condensed amorphous water exists in the glassy state below 135°K. This new finding of the glass transition phenomenon gives a definite resolution to the question whether the non-crystalline solid obtained by the vapor-condensation method is really a glass or not.

It is to be noted that the jump height of heat capacity at the glass transition point, and the heat of crystallization have different four values from sample to sample (see Table 1). This fact suggests that each of samples contains a few amount of a crystalline part. This crystalline part of the sample is considered to appear during the process of annealing. This is evidenced by the fact that the exothermic effect was observed even after the annealing at 128°K for 16 hr, and that the heat of crystallization gets smaller as the time of duration for annealing is longer (see Table 1), and further that the heat capacity curves of two series do not agree with each other in the case of the sample (4), as is shown in Fig. 5, where one series of measurements is made prior to annealing and the other after annealing at 128°K for 13 hr.

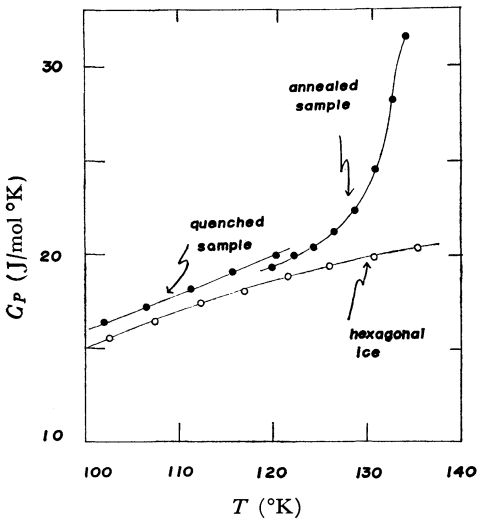

Fig. 5. Heat capacity of the glassy state of water.

In the case of sample (1), the jump height of heat capacity ΔC_P at T_g is of the highest value among all samples (see Table 1 and Fig. 2). The heat capacity just above T_g of this sample is, however, appreciably smaller than that of the supercooled liquid at the same temperature assumed by the extrapolation of the heat capacity of the liquid above the melting point. This fact is, at the first glance, considered to be due to the existence of crystalline part in the vitreous sample. This interpretation seems, however, to be inadequate because of some thermodynamical contradiction as will be described below. If C_P values of the supercooled liquid are assumed to be extended like a dotted line in Fig. 1, the corresponding enthalpy curve of the supercooled liquid comes out to be drawn in Fig. 6. At first sight of this figure it is shortly understood that the curve of the supercooled liquid intersects that of the crystal far above 135°K($=T_g$). This circumstance is evidently incompatible with the fact that the crystallization is necessarily accompanied by the exothermic effect. Consequently, it turns out to be inappropriate to assume that the C_P values of the supercooled liquid is equal to those obtained with extrapolating the C_P values of the liquid above the melting point.

Now, water has been known as a typical anomalous liquid. For example, its C_V values are

much higher than those of other normal liquids composed of triatomic molecules. In order to interpret the remarkably abnormal physical properties, Eucken[15] has proposed that water is an equilibrating mixture of several kinds of associated species (*e. g.*, H_2O, $(H_2O)_2$, $(H_2O)_4$ and $(H_2O)_8$), and that the anomalous large value of heat capacity is caused by the dissociation of the associated species with the rise of temperature. Recently, Wada[16] has calculated the heat capacity of water reduced to a normal liquid assuming the existence of two states in water such as icy and packed states. According to his calculation, the C_P value of water reduced to the normal liquid is smaller than that of crystal at 0°C. Although his result does not directly stand for our present results, the hypothetical C_P value of water consisting of exclusively monomer molecules might be smaller than the observed one. Based on this consideration, it seems to be supported that the vitreous water obtained in the present work (in particular sample (1)), may be nearly 100 per cent amorphous state.

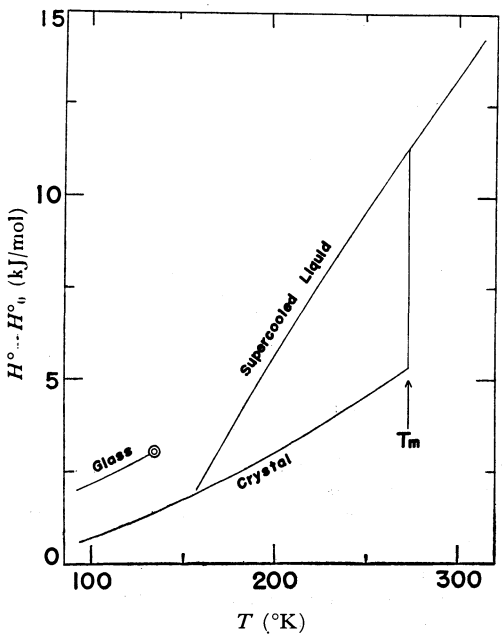

Fig. 6. Enthalpy relation of various states of water.

Appearance of the Cubic Ice and Its Transformation into the Hexagonal Ice. During past many years, a great deal of investigations[7-11,13] have been reported concerning the appearance of the cubic ice and its transformation to the hexagonal ice. As the results of these studies it is now well known that the cubic form of ice can be obtained either as a product of crystallization of amorphous ice or as a kind of high pressure form. In this section, we should like to concern only with the cubic ice prepared by the former method.

Up to the present, the existence of sluggish and irreversible transformation of the cubic ice to the hexagonal one has been observed by several workers. There has been, however, no quantitative experiment on the sample at the thermodynamically equilibrium state, so there remains still a confusion about the temperature interval of the appearance of the cubic ice, and also a more important problem whether the cubic ice is more stable than the hexagonal ice or not in the lower temperature region.

According to our present heat capacity measurements, the cubic ice transforms sluggishly and irreversibly into the hexagonal ice with an appreciable exothermic effect between 160 and 210°K. The average total amount of the exothermic enthalpy change, 160 J/mol, is close to the value, 150 J/mol, previously reported by McMillan and Los. This agreement seems, however, to be fortuitous, because their experiment was of dynamical nature and their results were based on the Ghormley's value (1.26 kJ/mol)[5] for the heat of crystallization which does not agree with our present data (1.64 kJ/mol).

As is well known, the hexagonal ice has a center of symmetry in the direction vertical to *c*-axis and a mirror of symmetry in the direction parallel to this axis with regard to the conformation of oxygen atoms in the lattice. On the other hand the cubic ice has the center of symmetry in these two directions, *i. e.*, a diamond structure.

The enthalpy change of the transformation amounting to about 160 J/mol, which is obtained in the present experiment, is considered to be due to the difference of the lattice energy between these two structures. Such an exothermic phenomenon seems to be concordant with the result calculated by Bjerrum[17] *i. e.*, the hexagonal ice is more stable than the cubic ice with regard to its lattice energy.

Now, the kinetics of this transformation has been studied by several previous workers who have interpreted this phenomenon in terms of the activation energy.[12,18] McMillan and Los have reported that this irreversible transformation may be characterized by the activation energy of about 7.4 kcal/mol, which is calculated based on the X-ray data by Dowell and Rinfret.[9] On the other hand Nozik and Kaplan,[18] by use of the Mössbauer resonance method for the ice doped with ferrous ion, have reported that the transformation occurs at least in two stages with a certain intermediate

15) A. Eucken, Nachricht. Akad. Wiss. Göttingen, Math. Physik Klasse S. 38 (1946).
16) G. Wada, This Bulletin, **34**, 955 (1961).
17) N. Bjerrum, *Kgl Danskab. Selskab. Math-fys. Medd*, **27**, 1 (1951); *Science*, **115**, 385 (1952).
18) A. J. Nozik and M. Kaplan, *Chem. Phys. Letters*, **1**, 391 (1967).

state, and that the activation energy for the process of the cubic-to-intermediate comes to about 29 kcal/mol.

We have also estimated the activation energy for this irreversible phenomenon from the results of heat-capacity measurement. When the cubic ice transforms into the hexagonal one with the exothermic effect, the temperature of the sample rises spontaneously if an adiabatic condition is well maintained. Concerning this phenomenon, the following equations were assumed to hold,

$$\dot{T} = (\Delta H/C_P)\cdot\dot{x} = 1/\tau(\Delta H/C_P)\cdot x,$$
$$\dot{x} = (1/\tau)\cdot x \qquad \tau \propto \exp(E/RT)$$

here $\dot{T}$ is the time-derivative of the temperature of the sample, C_P the heat capacity of the sample including the sample-container, ΔH enthalpy change accompanying the cubic-hexagonal phase transition, $\dot{x}$ the time-derivative of the mole number of the cubic ice, τ the relaxation time characteristic of this phenomenon, x the mole number of the cubic ice, E the activation energy for this rate process. The values of $\dot{T}$, C_P, ΔH, and x are all obtained as a function of the temperature from the results of heat capacity measurement, so τ is easily calculated for all temperatures. The obtained relation between $\log \tau$ and $1/T$ is drawn in Fig. 7. From this figure we see that this rate process may be separated into two processes, one of which is characterized with the activation energy of about 5 kcal/mol, the other with the activation energy of about 11 kcal/mol. The fact that this phenomenon occurs in two stages in our study is quite concordant with the results by Nozik and Kaplan, but the values of the activation energy are different from each other. Taking into consideration the difference that our experiments are based on the pure ice, whereas Nozik and Kaplan's works are based on the frozen solution, it is not quite clear to what extent such a comparison is plausible.

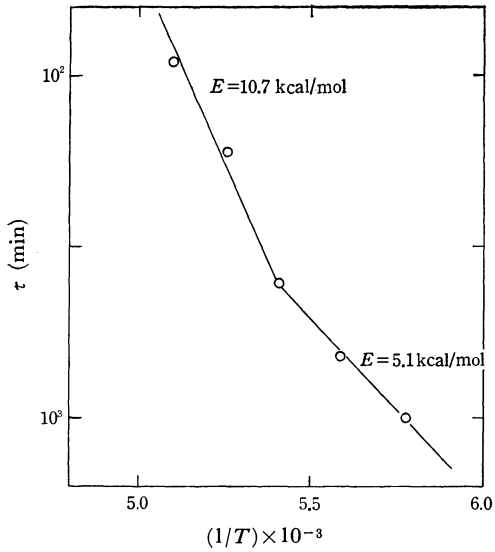

Fig. 7. Relaxation time characteristic of the irreversible transformation of cubic to hexagonal ice.

It is to be noted here that the activation energy of about 11 kcal/mol concerning the higher-temperature process is concordant with the result of Dowell and Rinfret. As their experiment was carried out with the X-ray analysis method, it may be possible that they have observed mainly the higher-temperature process for which the rate of transformation is pretty high.

Definition of the Glassy State. As to the difinition of the glassy state, no unequivocal conclusion has been given hitherto, so there has been still a few confusions concerning the usage of the term "glassy state."[19] This seems to be due to the fact that the past definitions of the glassy state are almost concerned with the chemical composition of the glass or with the methods of obtaining the glassy state.

Commonly, a glassy state has been considered to be equivalent to a non-crystalline or amorphous solid obtained by supercooling the liquid. However, the non-crystalline solid can be obtained also by using other rather uncommon methods, such as vapor condensation, neutron bombardment, and others. Such a non-crystalline solid has been observed to crystallize on heating. For this kind of solid, the glass transition phenomenon has not ever been verified. As far as the glass transition phenomena are not observed, we may feel a certain hesitation to call this non-crystalline solid as a glass. However, our previous finding of the glass transition phenomena of methanol[1] and the same result for water prepared by the vapor condensation method in the present study afford the conclusion that the non-crystalline solids of these materials prepared by this uncommon method must be called as a glass. On the basis of our new observation we may propose a more general properties of the glassy state as follows: (a) The glassy state must be distinguished from other states only by the fact that the thermodynamically equilibrium state is never attained. (b) The glassy state must show the glass transition phenomenon which characterizes the boundary between

19) D. R. Secrist and J. D. Mackenzie, "Modern Aspect of the Vitreous State," Vol. 3, ed. by J. D. Mackenzie, Butterworths Scientific Publication, Ltd., London (1964), Chapter 6.

Note added in proof: Quite recently J. A. Ghormley [*J. Chem. Phys.*, **48**, 503 (1968)] has re-investigated the glass transition phenomenon of water by use of the method of thermal analysis and suspected the observation of T_g by J. A. McMillan and S. C. Los cited in this text. I. Yannas has pointed out also the elusive nature of the glass transition point of water and estimated the glass transition point of water to be 127±4°K indirectly by the extrapolation of T_g for glycerol with the increase of water content [*Science*, **160**, 298 (1968)].

the glassy and the supercooled liquid states. (c) The glassy state is established irrespective of either the method of preparation or the chemical composition of the material.

The authors would like to express their sincere thanks to the Toyo Rayon Co., Ltd. who defraid a part of the financial support for the present investigation.

BULLETIN OF THE CHEMICAL SOCIETY OF JAPAN VOL. 41 2599—2603 (1968)

The Fluorescence Spectrum of Benzene in Solution at 77°K

Yoshio MURAKAMI and Yoshiya KANDA

Department of Chemistry, Faculty of Science, Kyushu University, Hakozaki, Fukuoka, Japan

(Received April 25, 1968)

The fluorescence spectrum of benzene in methylcyclohexane at 77°K has been analyzed in detail. The forbidden 0–0 band appeared weakly, and all the bands were interpreted as allowed bands except for the 0–992 band. The fluorescence spectrum has also been studied in carbon tetrachloride; the anomalous vibrational structure has been found in solutions as dilute as 10^{-3} M, irrespective of the cooling procedure. The correlation with the absorption and with the phosphorescence spectrum of benzene reported previously has been discussed.

Ivanova and Sveshnikov[1] studied the fluorescence spectrum of benzene in an alcoholic solution at 77°K and gave a tentative vibrational analysis. The 0–0 band was not observed, and the 992-cm^{-1} progression appeared from bands separated by 606 and 1178 cm^{-1} from the assumed position of the 0-0 band. The $606+n\times992$ series was much stronger in intensity than the $1178+n\times992$ cm^{-1} series. Wolf[2] also gave a simple analysis of the fluorescence spectrum of crystalline benzene at 77°K. The forbidden 0–0 band appeared weakly, while the $606+n\times992$ series appeared strongly. The 992-cm^{-1} progression was also seen to start from the 0–0 band with quite a strong intensity. The crystal spectrum at 77, 20.4, and 4.2°K has also been reported on by Shpak, Solov'ev, and Sheremet[3] and by Vatulev, Sheremet, and Shpak.[4]

We studied the fluorescence spectrum of benzene in solutions in ethanol, cyclohexane, and methylcyclohexane and of the crystal at 77°K in order to check if all the analyses previously reported were correct.

We also studied the fluorescence spectrum in carbon tetrachloride at 77°K. In previous papers[5] we have found anomalous vibrational structures in the phosphorescence spectrum of benzene in carbon tetrachloride and in the absorption spectrum in a rapidly-cooled carbon tetrachloride solution. Here we experimented in order to check if any anomalous feature was also present in the fluorescence spectrum.

Experimental

Benzene was purified according to a method previously described.[5] In the course of study toluene was found to be an impurity in benzene, since it emitted a characteristic fluorescence spectrum overlapping the benzene spectrum. The toluene in the benzene was therefore removed through oxidation with a potassium permanganate solution acidified with sulfuric acid. This operation was repeated several times before the ordinary purification operation of benzene.

Ethanol, cyclohexane, methylcyclohexane, and carbon tetrachloride were purified by methods previously described.[6] A super-high vapor pressure mercury arc lamp of the ORC 1 kW type, CHM-621, was used as the light source, and Hg 2537 Å was introduced into the cell through a filter system.[7] A RIKEN medium quartz spectrograph corresponding to a Hilger E2 was used throughout the work. The optical setup was exactly the same as that described previously except for a phosphoroscope.[5] Here it was unnecessary. The surface of a frozen sample was oblique to the incident light. The concentration was fixed at 10^{-3} M for all the solutions. The slit-width was 50 μ, and Eastman Kodak plates 103a-0 were used. Exposure

1) T. V. Ivanova and B. Ya. Sveshnikov, *Opt. Spectry.*, **11**, 332 (1961).
2) H. C. Wolf, "Solid State Physics," Vol. IX, ed. by F. Seitz and D. Turnbull, Academic Press, New York and London (1959), p. 1.
3) M. T. Shpak, A. V. Solov'ev and N. I. Sheremet, *Opt. Spectry.*, **13**, 393 (1962).
4) V. N. Vatulev, N. I. Sheremet and M. T. Shpak, *ibid.*, **15**, 315 (1964).
5) Y. Kanda and R. Shimada, *Spectrochim. Acta*, **17**, 7 (1961); Y. Kanda, Y. Gondo and R. Shimada, *ibid.*, **17**, 424 (1961).
6) Y. Kanda and R. Shimada, *ibid.*, **15**, 211 (1959); Y. Kanda, R. Shimada and Y. Sakai, *ibid.*, **17**, 1 (1961).
7) C. L. Braga and M. D. Lumb, *J. Sci. Instrum.*, **43**, 341 (1966).

times ranged from 2 to 15 h. The accuracy of measurement was about $\pm 3\ cm^{-1}$ for sharp bands and about $\pm 20\ cm^{-1}$ for broader bands.

Results and Discussion

The fluorescence spectrum of benzene in solutions in ethanol, methylcyclohexane, cyclohexane, carbon tetrachloride and in the crystal was studied at 77°K; some of the tracing curves are shown in Figs. 1 and 2. The spectrum in ethanol appears broad in comparison with that in methylcyclohexane; the vibrational analysis has been made with the latter at the beginning. The results are given in Table 1. A band at $37820\ cm^{-1}$ is ascribed to the 0–0 band of the spectrum, a band which is forbidden by symmetry but which is allowed weakly by solvent perturbation. The $992\text{-}cm^{-1}$ progressions appear, perturbed by vibrations of $606(e_{2g})$, $405\times 2(e_{2u}\times e_{2u})$, $405+671$ $(e_{2u}\times a_{2u})$, $1178(e_{2g})$, $405\times 2+606(e_{2u}\times e_{2u}\times e_{2g})$, $849\times 2(e_{1g}\times e_{1g})$, $970\times 2(e_{2u}\times e_{2u})$ or $606+1326$ $(e_{2g}\times a_{2g})$, and $606+703\times 2(e_{2g}\times b_{2g}\times b_{2g})$, and $606+849\times 2(e_{2g}\times e_{1g}\times e_{1g})$. Therefore, all the bands in the progressions are allowed except for two bands, those at 37820 (0–0) and $36830\ cm^{-1}$ (0–992). The spectrum in ethanol looks smoothed out of that in methylcyclohexane. The progression assigned to $1178+n\times 992$ by Ivanova and Sveshnikov must be interpreted as the overlap of the $405\times 2+n\times 992$, $405+671+n\times 992$, $1178+n\times 992$, $970\times 2+n\times 992$ *etc.*, series. They did not find the 0–0 band of the fluorescence spectrum and assumed an unobserved position at $37780\ cm^{-1}$ as the band origin. That the differences between the observed and calculated values are greater for the $1178+n\times 992$ series than those for the $606+n\times 992$ series means that their assignment, $1178+n\times 992$, was not complete enough.

The fluorescence spectrum of benzene in cyclohexane was analyzed in the same way as that in methylcyclohexane. Cyclohexane undergoes a phase transition at −87°C, and the spectrum of a rapidly frozen sample contains bands from the high- and low-temperature phases. By the use of a careful annealing technique, the low-temperature-phase spectrum (the 0–0 band at 37705 cm^{-1}) was separated from the high-temperature one (the 0–0 band at $37790\ cm^{-1}$). Only the low-temperature spectrum is shown in Fig. 1.

The fluorescence spectrum of crystalline benzene was analyzed in comparison with the solution spectra. A weak band at $37713\ cm^{-1}$ looked like the band origin of the spectrum. However, reabsorption must be taken into account, and an unobserved position at $37814\ cm^{-1}$ was assumed here to be the 0–0 band of the spectrum. This really corresponds to the band at $37811\ cm^{-1}$, one of the components of the 0–0 band of the absorption spectrum of the benzene crystal at 90°K suggested by Bronde, Medvedev, and Prikhot'ko.[8] The spectrum photographed at 77°K

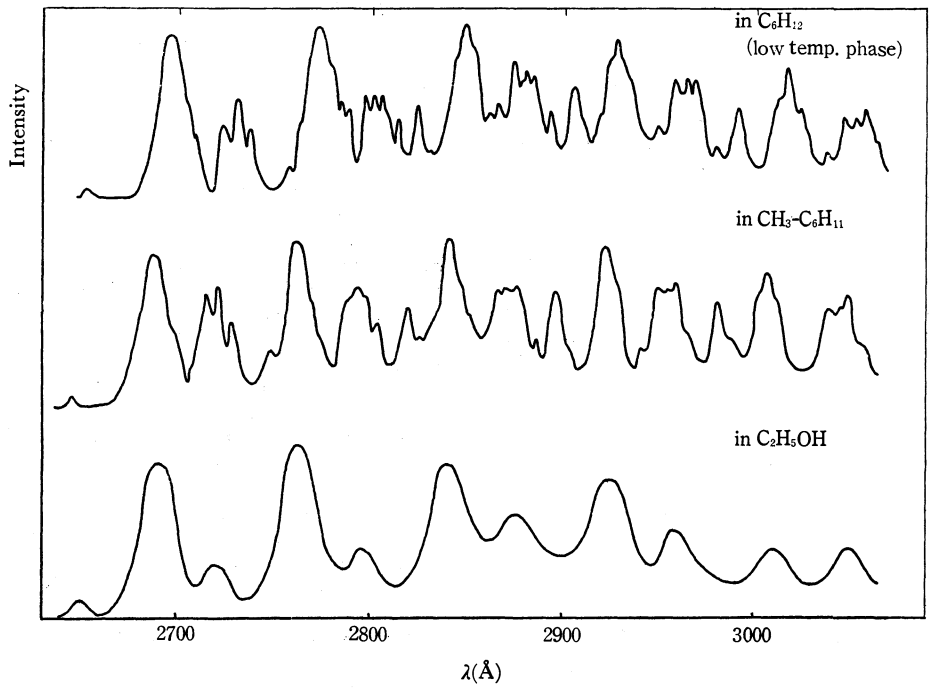

Fig. 1. Fluorescence spectra of benzene in various matrices at 77°K.

8) V. L. Broude, V. S. Medvedev and A. F. Prikhot'ko, *Zhur. Exptl. Teoret. Fiz.*, **21**, 665 (1951).

TABLE 1. FLUORESCENCE SPECTRUM OF BENZENE IN ETHANOL AND METHYLCYCLOHEXANE MATRICES AT 77°K

in Ethanol			in Methylcyclohexane			Assignment
$\tilde{\nu}$ (cm^{-1})	Rel. int.	$\Delta\tilde{\nu}$ (cm^{-1})	$\tilde{\nu}$ (cm^{-1})	Rel. int.	$\Delta\tilde{\nu}$ (cm^{-1})	
37735	1	0	37820	4	0	0, 0
37145	9	590	37210	10	610	0−606 (e_{2g})
			37030	5	790	0−405 (e_{2u})×2
36745	3	990	36830	6	990	0−992 (a_{1g})
			36745	6	1075	0−405(e_{2u})−671(a_{2u})
			36645	3	1175	0−1178(e_{2g})
			36410	2	1410	0−405(e_{2u})×2−606(e_{2g})
36180	10	1555	36215	10	1605	0−606−992
			36135	8	1685	0−849(e_{1g})×2
			36025	6	1795	0−405×2−992 0−606(e_{2g})−1178(e_{2g})
			35885	7	1935	0−970(e_{2u})×2 0−606(e_{2g})−1326(a_{2g})
35745	4	1990	35810	7	2010	0−606(e_{2g})−703(b_{2g})×2
			35745	7	2075	0−405−671−992
			35660	5	2160	0−1178−992
			35520	6	2300	0−606(e_{2g})−849(e_{1g})×2
			35420	4	2400	0−405×2−606−992
35170	9	2565	35225	10	2595	0−606−992×2
			35145	8	2675	0−849×2−992
			35025	6	2795	0−405×2−992×2
			34885	8	2935	0−970×2−992
34760	6	2975	34820	8	3000	0−606−703×2−992
			34765	8	3055	0−405−671−992×2 0−3047(e_{2g})
			34670	6	3150	0−1178−992×2
			34525	7	3295	0−606−849×2−992
			34425	5	3395	0−405×2−606−992×2
34175	8	3560	34240	10	3580	0−606−992×3
			34165	8	3655	0−849×2−992×2
			34010	6	3810	0−405×2−992×3
			33900	8	3920	0−970×2−992×2
33790	5	3945	33830	7	3990	0−606−703×2−992×2
			33785	8	4035	0−405−671−992×3
			33685	5	4135	0−1178−992×3
			33535	6	4285	0−606−849×2−992×2
			33455	4	4365	0−405×2−606−992×3
			33300	7	4520	
33195	4	4540	33250	8	4570	0−606−992×4
			33180	6	4640	0−849×2−992×3
			32915	6	4905	0−970×2−992×3
32785	4	4950	32830	6	4990	0−606−702×2−992×3
			32800	6	5020	0−405−671−992×4
			32705	2	5115	0−1178−992×4
			32550	2	5270	0−606−849×2−992×3
			32470	1	5350	0−405×2−606−992×4
32220	2	5515	32300	3	5520	
			32260	4	5560	0−606−992×5
			32195	1	5625	0−849×2−992×4
31795	2	5940				

in this experiment is essentially the same as that reported by Shpak, Solov'ev, and Shermet[3] and will not be reproduced here. It is to be discussed elsewhere.[9] However, we would like to propose here a suggestion concerning the interpretation of the 0–0 band of the fluorescence spectrum of the benzene crystal they studied.

If we use the data in Fig. 2 in Ref. 3 and add the vibrational frequencies of 607 and 990 cm^{-1} to 37221 and 36838 cm^{-1} respectively, we obtain 37828 cm^{-1} for both cases. This must be the band origin; it corresponds to one of the 0–0 bands of the absorption spectrum. The band at 37775 cm^{-1} may be a band from a trap or a remainder band due to reabsorption. The same interpretation can be applied to the spectra at 20.4 and 4.2°K in Fig. 1 in the paper by Vatulev, Sheremet, and Shpak.[4]

No bands corresponding to the III series in Figs. 1 and 2 of Ref. 8 were found in our spectrum. They were not in Fig. 1 in Ref. 10 either and so must be ascribed to an impurity.

The fluorescence spectrum of benzene was also studied in carbon tetrachloride. In previous papers[5] we have reported an anomalous vibrational structure in the phosphorescence spectrum of benzene in carbon tetrachloride and have examined the absorption spectrum of benzene in carbon tetrachloride with rapidly- and slowly-cooled samples. The spectrum of a rapidly-cooled solution has a strong and broad 0–0 band, while that of a slowly-cooled solution gives weak and split 0–0 bands. No difference was found between the phosphorescence spectra of rapidly- and slowly-cooled samples; this phenomenon may tentatively be ascribed to the mixing of the rapidly-cooled phase in the slowly-cooled phase. The phosphorescence spectrum of weak intensity of the slowly-cooled sample might have been overshadowed by the phosphorescence spectrum of strong intensity of the rapidly-cooled sample. In the absorption experiment, the concentration was as high as 10 mol% since a thin-layer sample had to be used. For the phosphorescence spectrum the concentration was of the order of 10^{-3} M and the volume was about 2 *ml*. These incoincidences in concentrations and in the sample mounting may sometimes be crucial for the interpretation of the spectrum. Therefore, it is necessary to study the fluorescence spectrum at various concentrations. Concentrations were chosen according to a phase diagram of the CCl_4-Benzene System. While a phase diagram designed by Kapustinskii and Drakin[10] was used in the previous papers,[5] a new diagram recently suggested by

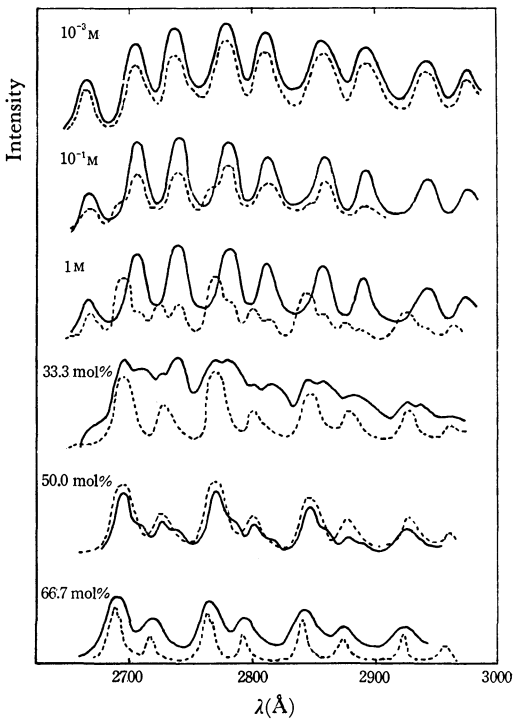

Fig. 2. Fluorescence spectra of benzene in carbon tetrachloride at 77°K.
——: Rapid cooling ·····: Slow cooling

Ott, Goates and Gudge[11] has been used in this work. Samples were mounted as thin layers between quartz plates at 77°K. The results are shown in Fig. 2.

It is interesting to see that there is no difference between the fluorescence spectra of the rapidly- and slowly-cooled solutions at 10^{-3} M; this is in agreement with the results in the phosphorescence spectrum. In one of our previous papers[5] we assumed the mixing of the rapidly-cooled phase in the slowly-cooled phase, but this interpretation proves untenable. At such a low concentration both samples have the same phase and give an anomalous vibrational structure due to a strong environmental effect. At concentrations such as 33.3 and 50.0 mol%, the fluorescence spectrum of the slowly-cooled samples gives a weak 0–0 band (hereafter we will call this the H-spectrum), unlike the spectrum at concentrations as low as 10^{-3} M, which has a strong 0–0 band (hereafter we will call this the L-spectrum). A question arose whether the H-spectrum of the slowly-cooled samples of 33.3 and 50.0 mol% solutions could be the spectrum of the benzene crystal crystallized out of the solution during the cooling processes. However, this is not the case, since the wavelength of each band was different from that of the benzene crystal.

9) A. Nakahara, M. Koyanagi, Y. Murakami, T. Edamura and Y. Kanda, to be published.
10) A. F. Kapustinskii and S. I. Drakin, *Bull. acad. sci. U.S.S.R. classe sci. chim.*, 475 (1947); *Chem. Abstr.*, **42**, 1902 (1948).
11) J. B. Ott, J. R. Goates and A. H. Gudge, *J. Phys. Chem.*, **66**, 1387 (1962).

The spectra of the slowly-cooled samples at 10^{-3} and 1 M (the latter corresponding to about 10 mol%) and that of the rapidly-cooled samples at 33.3 and 50.0 mol% show an overlapping of the L- and H-spectra. The species giving the H-spectrum is considered to be C_6H_6-$2CCl_4$ on the basis of the finding that the H-spectrum appears in the slowly-cooled samples over the wide range from 10^{-1} M to 50.0 mol% (of benzene) and the results of the study of the molecular complex of carbon tetrachloride with benzene from the far infrared spectrum by Chantry, Gebbie, and Mirza.[12]

12) G. W. Chantry, H. A. Gebbie and H. N. Mirza, *Spectrochim. Acta*, **23A**, 2749 (1967).

The spectrum of the slowly-cooled sample at much higher concentrations, such as 66.7 mol%, is the same as the spectrum of the benzene crystal, and the spectrum of the rapidly-cooled sample is an overlapping of the H-spectrum and the spectrum of the benzene crystal. These results show that benzene was crystallized out of the solution during the cooling process; the presence of the C_6H_6-CCl_4 complex, which is indicated by the freezing-point method, is not clearly shown in the fluorescence spectrum.

The authors wish to express their hearty thanks to Assistant Professor Ryoichi Shimada and Dr. Motohiko Koyanagi for their kind support and helpful discussions.

BULLETIN OF THE CHEMICAL SOCIETY OF JAPAN VOL. 41 2603—2608 (1968)

Quenching of the Scintillation from a γ-Irradiated Cyclohexane Solution Containing *p*-Terphenyl by Electron Scavengers, Positive Ion Interceptors and Some Hydrocarbons

Tsunenari SAITO, Koji TAKAHASHI and Shin SATO

Department of Applied Physics, Tokyo Institute of Technology, Ookayama, Meguro-ku, Tokyo

(Received May 1, 1968)

The luminescence from a cyclohexane solution containing *p*-terphenyl irradiated with ^{60}Co γ-rays has been quenched by various compounds. The quenching efficiencies were found to be in the following order; sulfur hexafluoride$\sim$carbon tetrachloride$>$nitrous oxide$>$ethanol$>$ammonia$>$carbon dioxide. These compounds are known in radiation chemistry as electron scavengers or as positive-ion interceptors. Cyclopropane and ethylene have also shown an appreciable quenching ability, but *n*-butane has shown scarecely any. These results have been explained by assuming that ionic reactions are responsible for the luminescence from a cyclohexane-*p*-terphenyl scintillator.

The mechanism of energy transfer occurring in a liquid organic scintillator has been a concern of many investigators.[1,2] The type of energy transfer seems to depend upon many factors, such as the kind of solvent molecule and the mode of excitation.

In an earlier short communication,[1] we have suggested the possibility that emission from a cyclohexane solution of *p*-terphenyl irradiated by γ-rays of ^{60}Co results from the ionic reactions occurring in the system. Such an ionic process had already been suggested by Kropp and Burton[3] as a possible mechanism, but the insight had not been pursued because the excitation-energy-transfer process was thought to be more plausible at that time.

In this paper, we intend to enlarge our remarks in the short communication[1] and to show more evidence for the participation of an ionic process in the formation of the scintillating state of *p*-terphenyl in cyclohexane.

Experimental

Research-grade cyclohexane purchased from the Wako Chemical Co. was passed through a 1 m column packed with silica gel and distilled twice at 80.8°C prior to use. Scintillation-grade *p*-terphenyl was purchased from the Nakarai Chemical Co. and used as supplied. The other compounds used as quenchers were all of a research grade and were used after usual purifications, such as bulb-to-bulb distillation.

1) T. Yoshida and S. Sato, This Bulletin, **40**, 2216 (1967).
2) "Luminescence of Organic and Inorganic Materials," ed. by H. P. Kallmann and G. M. Spruch, John Wiley & Sons, New York (1962).
3) J. L. Kropp and M. Burton, *J. Chem. Phys.*, **37**, 1742 (1962).

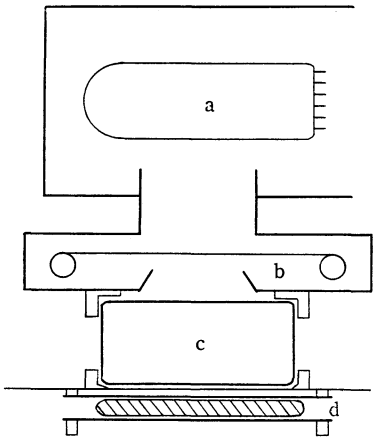

Fig. 1. Arrangement for measuring luminescence.
a, Photomultiplier b, Photographic shutter
c, Scintillator solution d, γ-Rays source
(1 m Ci-^{60}Co).

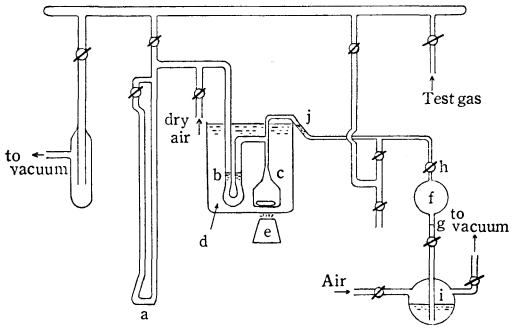

Fig. 2. Apparatus for measuring solubility.
a, Mercury manometer. b, Mercury-filled U-tube, which balances the pressures of both sides. c, A flask of known volume (82 m*l*). d, Water bath. e, Magnetic stirrer. f, A glass flask (Volume is calibrated from the mark g to the stopcock h.). i, Mercury leveling bulb (Mercury goes up to the mark j when introducing a gas.).

A schematic diagram of the apparatus for the measurement of scintillation is shown in Fig. 1. Cyclohexane containing a constant amount of *p*-terphenyl was degassed by repeated freeze-pump-thaw cycles. At least five cycles were needed to obtain a constant emission intensity. Quencher gases were introduced with the aid of a liquid nitrogen trap after the pressure had been measured in a calibrated volume.

Since the solubilities of most gases in cyclohexane are not known, a separate apparatus was constructed for this measurement. A schematic diagram of it is shown in Fig. 2. The method is almost the same as that proposed by Loprest.[4] The apparatus for the preparation of scintillator solutions was constructed so as to be mercury free to avoid the possibility of the participation of dissolved mercury in the scintillation.

4) F. J. Loprest, *J. Phys. Chem.*, **61**, 1128 (1957).

Results

Figure 3 shows the Ostwald absorption coefficients of five quencher gases (NH_3, N_2O, C_2H_4, CO_2, and SF_6) in cyclohexane as a function of the temperature. The other quenchers used (C_2H_5OH, CCl_4, cyclo-C_3H_6, and n-C_4H_{10}) were assumed to be completely soluble in cyclohexane. The values with nitrous oxide, carbon dioxide, sulfur hexafluoride, and ethylene were in good agreement with those previously measured.[5,6]

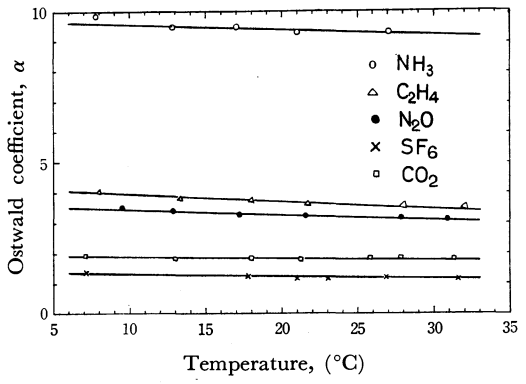

Fig. 3. Ostwald coefficients of quencher gases in cyclohexane as a function of temperature. (at 200 Torr)

In Fig. 4 the reciprocal of the emission intensity is plotted against the reciprocal of the concentration of *p*-terphenyl in cyclohexane. Such a linear relationship as has previously been reported by

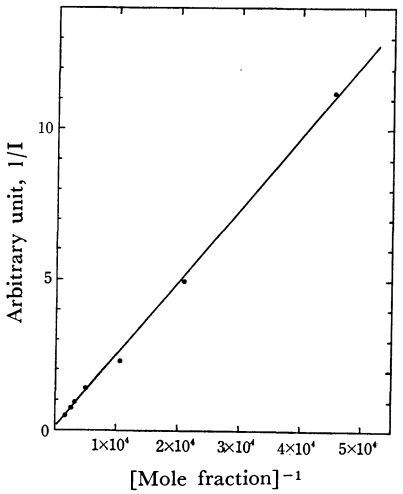

Fig. 4. Dependence of emission intensity on the concentration of *p*-terphenyl in cyclohexane.

5) S. Sato, T. Terao, M. Kono and S. Shida, This Bulletin, **40**, 1818 (1967).
6) K. Kikuchi, S. Sato and S. Shida, *Nippon Kagaku Zasshi (J. Chem. Soc. Japan, Pure Chem. Sect.)*, **84**, 561 (1963).

many investigators[7,8] is obtained. The slope/intercept ratio has been calculated to be 1.6×10^{-2} mol l^{-1}, a value which agrees reasonably well with the 1.3×10^{-2} mol l^{-1} reported by Burton *et al.*[7] Here, the emission from the quartz vessel and pure solvent has been substracted from the total emission. In the case of a 5.7×10^{-3} mol l^{-1} *p*-terphenyl solution, the emission from the vessel was 8.5%, and that from pure solvent was 6.9%, of the total emission.

In Figs. 5, 7, and 8, the relative emission intensities are plotted as a function of the mole fraction of the quenchers. The quencher gases in Fig. 5 are known in radiation chemistry as electron scavengers. An abnormal curve has been obtained with carbon tetrachloride; *i. e.*, the intensities of the emission from cyclohexane solutions containing high concentrations of carbon tetrachloride were lower than that from pure cyclohexane. The

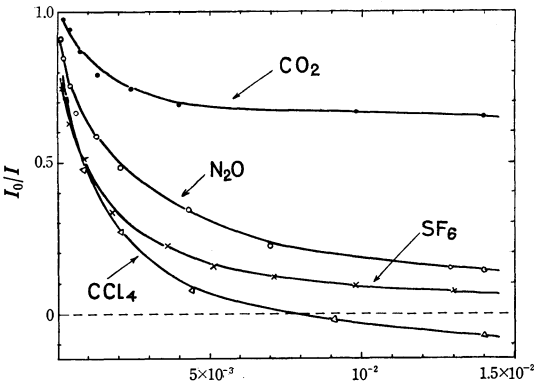

Fig. 5. Relative emission intensity from a 5.7×10^{-3} mol l^{-1} *p*-terphenyl solution as a function of the concentrations of electron scavengers.

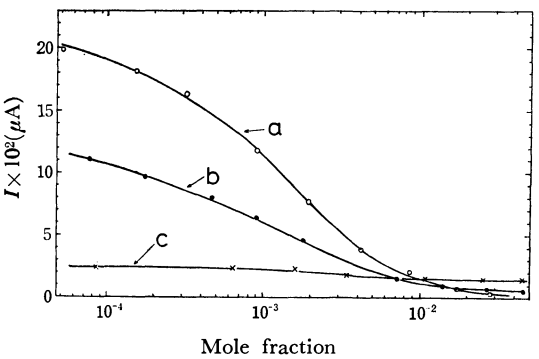

Fig. 6. Quenching by carbon tetrachloride.
a, 5.7×10^{-3} mol l^{-1} *p*-terphenyl. b, 1.9×10^{-3} mol l^{-1} *p*-terphenyl. c, Pure cyclohexane.

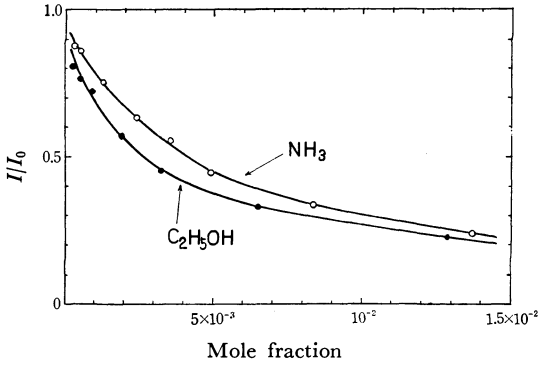

Fig. 7. Relative emission intensity from a 5.7×10^{-3} mol l^{-1} *p*-terphenyl solution as a function of the concentrations of positive ion interceptors.

details are shown in Fig. 6, where the observed currents from the photomultiplier are plotted as a function of the concentration of carbon tetrachloride. Sulfur hexafluoride, which is as effective in quenching as carbon tetrachloride at low concentrations, did not have such an effect. In Fig. 7, the data with ammonia and ethanol are plotted. Their effects are obviously much weaker than strong electron scavengers, such as sulfur hexafluoride, carbon tetrachloride, and nitrous oxide. Figure 8 compares the quenching efficiencies of aliphatic hydrocarbons with those of electron scavengers. Since hydrocarbons were not effective in quenching, a low concentration of *p*-terphenyl was used. The quenching efficiencies of the hydrocarbons used are in the following order; cyclopropane, ethylene, and *n*-butane.

By using the amplification factor of the photomultiplier and the geometry of the apparatus, the *G*-value of the luminescence has been estimated roughly. The values obtained range from 0.01 to 0.1 with a solution containing 5.7×10^{-3} mol·l^{-1} *p*-terphenyl.

Discussion

Dependence on the Concentration of *p*-Terphenyl. If the excitation-energy-transfer is operative as the mechanism of energy transfer occurring in the present system, a linear relationship between $1/I_0$ and $1/N_s$ can easily be obtained by the steady-state treatment, as Lipsky and Burton have already done.[9] Here, I_0 denotes the emission intensity, and N_s, the concentration of *p*-terphenyl. However, this linear relationship does not necessarily mean that the excitation-energy-transfer is the real mechanism. As has been stated in the earlier communication,[1] *p*-terphenyl molecules are known to capture electrons

7) M. Burton, P. J. Berry and S. Lipsky, *J. chim. phys.*, **52**, 48 (1955).
8) M. Burton, M. A. Dillon, C. R. Mullin and R. Rein, *J. Chem. Phys.*, **41**, 2236 (1964).
9) S. Lipsky and M. Burton, *J. Chem. Phys.* **31**, 1221 (1959).

in cyclohexane[10] and the negative ions formed may become precursors of excited *p*-terphenyl molecules. The reaction scheme is:

$$C \text{ -}\!\!\wwvy\!\!\rightarrow C^+ + e \quad (1)$$

$$e + T \longrightarrow T^- \quad (2)$$

$$C^+ + T^- \longrightarrow C + {}^1T^* \text{ (or } {}^3T^*) \quad (3)$$

$${}^1T^* \longrightarrow T + h\nu \quad (4)$$

Here, C and T denote cyclohexane and *p*-terphenyl molecules respectively. $^1T^*$ and $^3T^*$ denote excited singlet and triplet states of *p*-terphenyl. The former is responsible for the luminescence from the solution, while the latter may be deactivated without radiation to the ground state.[11]

For discussing the kinetics of the reactions occurring in a γ-irradiated solution, the steady-state treatment is not adequate, because the charged species produced are believed not to be distributed homogeneously in the solution.[12] A tentative treatment for such a system has recently been developed by Freeman[13] and this laboratory.[5,12] Using the formulation already described[12] with a little modification of the distribution function of the charged species, a linear relationship between $1/I_0$ and $1/N_s$ can be derived; the procedure is shown in the Appendix. In this treatment, the k ratio, which is the slope/intercept ratio of the linear relationship in Fig. 4, has the following relation:

$$k = \alpha/(zn^0_-)$$

while

$$r_{av} = \alpha^{-1/3}\Gamma(4/3)$$

Here, n^0_- is the number of jumps which a "solvated" electron[5] makes when diffusing a unit distance. z is the coordination number, and r_{av} is the average initial distance between an electron and its parent ion. By substituting the observed value, 1.6×10^{-2} mol l^{-1} for k, we can obtain 70 Å for r_{av}. This value is in good agreement with the value, 50—60 Å, estimated previously from the data of an experiment using a different approach.[12]

The Effects of Electron Scavengers. In the previous communication[1] we have reported the effects of sulfur hexafluoride, nitrous oxide, and carbon dioxide. The reinvestigated data of these compounds agree well with the previous data. The quenching efficiencies are in the following order: sulfur hexafluoride, carbon tetrachloride, nitrous oxide, and carbon dioxide. This order seems to correspond to the order of the efficiency of electron scavenging in the gas phase.[14,15]

On the other hand, we have shown that the $G(H_2)$ from cyclohexane is suppressed by the addition of sulfur hexafluoride, nitrous oxide, or carbon dioxide, and that the concentration dependence of the effect is almost constant with any of the three electron scavengers.[5] This discrepancy may be explained as follows. In the scintillator system, we have *p*-terphenyl together with a quencher. Since the *p*-terphenyl molecule is known to capture an electron in cyclohexane,[10] a competition for electrons will occur between the two reactions, (2) and (5):

$$S + e \rightarrow S^- \quad (5)$$

Here, S denotes an electron scavenger. In such a system, electron-transfer reactions must occur when the electron affinities of T and S are different.

$$T^- + S \rightleftharpoons T + S^- \quad (6)$$

If sulfur hexafluoride and carbon tetrachloride, which have high electron affinities, undergo a forward reaction, and carbon dioxide, which has a low electron affinity, does the reverse, the order of efficiencies shown in Fig. 5 can be explained.

If this reasoning is correct, the present experiment provides a method of determining the order of the electron affinities of some compounds. However, as will be seen below, complications airse.

At high concentrations of carbon tetrachloride, the luminescence from a cyclohexane solution of *p*-terphenyl was weaker than that from pure cyclohexane (Fig. 6). Since the origin of the luminescence from pure cyclohexane is difficult to explain,*1 the mechanism of the quenching observed is far beyond our speculation. Obviously, further experiments using different approaches are needed on this problem.

Recently, Holroyd has shown that nitrous oxide in a cyclohexane solution is decomposed by light irradiation at 1470 Å and has concluded that the excitation-energy transfer occurs from an excited cyclohexane molecule to nitrous oxide.[16] According to his estimation, the *G*-value of excited cyclohexane molecules in the γ-radiolysis of cyclohexane is 1.2, if the *G*-value of charge separation is assumed to be 3. In the present system, therefore, the process suggested by Holroyd may play a part in the reaction, especially at high concentrations of quenchers. However, since we are concerned with a qualitative correlation between the quenching of the scintillation and the electron or positive-ion scavenging of quenchers, we neglect the energy-transfer process for the sake of simplicity.

The Effects of Positive-ion Interceptors. Ammonia and ethanol are known to behave as

10) S. Arai and L. M. Dorfman, *ibid.*, **41**, 2190 (1964).
11) F. B. Harrison and G. T. Reynolds, *Phys. Rev.*, **79**, 732 (1950).
12) S. Sato, This Bulletin, **41**, 304 (1968).
13) G. R. Freeman, *J. Chem. Phys.*, **46**, 2822 (1967).
14) W. J. Holtslander and G. R. Freeman, *Can. J. Chem.*, **45**, 1649 (1967).
15) J. M. Warman, *J. Phys. Chem.*, **71**, 4066 (1967).
*1 The possibility that impurities in cyclohexane play a role in the scintillation of pure cyclohexane cannot be excluded.
16) R. A. Holroyd, *ibid.*, **72**, 759 (1968).

proton scavengers in the radiation-induced reaction of hydrocarbons.[17,18] The reaction in cyclohexane may be described as follows:

$$RH + C_6H_{12}^+ \rightarrow RH_2^+ + C_6H_{11} \quad (7)$$

Here, RH denotes ammonia or ethanol. In the present case, the reaction which interferes with the formation of excited *p*-terphenyl molecules may be as follows:

$$RH_2^+ + T^- \rightarrow RH + HT \quad (8)$$

The radicals produced (HT) would not luminescence. The fact that ethanol is more effective than ammonia in quenching (Fig. 7) is consistent with the order of their efficiencies as proton scavengers.[18]

The Effects of Ethylene, Cyclopropane, and *n*-Butane. Recently, Stephenson *et al.* have shown that some diolefins can quench the fluorescence from excited aromatic compounds in *n*-hexane.[19] Therefore, ethylene could behave as a quencher as has been observed in the present experiment (Fig. 8). However, the concentration of dienes used in the above experiment is much higher than ours. Moreover, as is shown in Fig. 8,

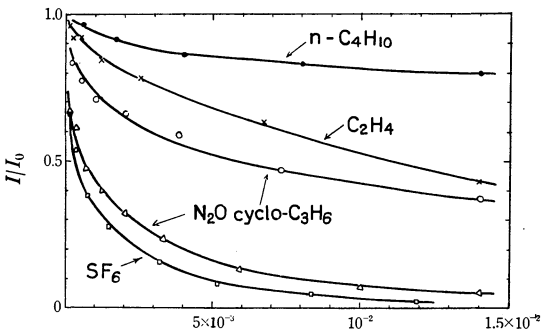

Fig. 8. Relative emission intensity from a 1.9×10^{-3} mol l^{-1} *p*-terphenyl solution as a function of the concentrations of some hydrocarbons and electron scavengers.

cyclohexane has been shown to quench the luminescence as much as ethylene. Cyclopropane is a paraffin and is not expected to quench an excited *p*-terphenyl molecule efficiently. On the other hand, *n*-butane is found to be much less effective even in quenching.

Ausloos *et al.*[20] have recently uncovered a series of ion-molecule reactions occurring in the liquid phase:

$$C_6H_{12}^+ + RH \rightarrow C_6H_{11}^+ + RH_2 \quad (9)$$

$$\searrow C_6H_{10}^+ + RH_3 \quad (10)$$

Here, RH represents cyclopropane or ethylene. If these reactions occur in the present system, quenchings observed with cyclopropane and ethylene may be explained by a combination of the reactions (9) and (10) and the reaction (11):

$$C_6H_{11}^+ + T^- \rightarrow C_6H_{10} + HT \quad (11)$$

Reaction (11) interferes with the formation of excited *p*-terphenyl. In the case of *n*-butane, reactions such as (9) and (10) have not been reported. Probably, they would not occur efficiently.

Alternative Ionic Reactions to Form the Excited *p*-Terphenyl. So far, we have addopted *p*-terphenyl negative ions as the precursors of excited *p*-terphenyl molecules. However, since *p*-terphenyl has an ionization potential lower than cyclohexane, alternative ionic processes can be constructed for the formation of the excited *p*-terphenyl. One of these reaction schema is:

$$C \rightsquigarrow C^+ + e \quad (1)$$

$$C^+ + T \rightarrow C + T^+ \quad (12)$$

$$T^+ + e \rightarrow {}^1T^* \text{ (or } {}^3T^*) \quad (13)$$

However, if this mechanism is the only process producing the excited *p*-terphenyl, the difference in quenching efficiency of the four electron scavengers cannot easily be explained. Therefore, reactions (12) and (13), should they occur, should be taken into account, along with the series of reactions from (1) to (4). In that case, the reaction (14) should probably be included also:

$$T^+ + T^- \rightarrow {}^1T^* \text{ (or } {}^3T^*) + T \quad (14)$$

The data obtained in the present paper cannot make a possible decisive choice of a reaction scheme, but they do show that ionic processes seem to play an important role in the scintillation from a cyclohexane solution of *p*-terphenyl.

The authors are grateful to Professor S. Shida for his valuable suggestions.

Appendix

Electrons ejected into a cyclohexane solution by γ-ray irradiation drift toward the parent positive ions by means of the Coulombic interaction. On the way, a part of electrons will be scavenged by *p*-terphenyl. If the reaction is diffusion-controlled, the fraction (f_T) of electrons scavenged by *p*-terphenyl may be expressed as follows:[12]

$$f_T = 1 - \frac{1}{N}\int_0^\infty \phi(r)(1-N_s)^{zn}\mathrm{d}r$$

$$= 1 - \frac{1}{N}\int_0^\infty \phi(r)\exp(\beta r^3)\mathrm{d}r$$

where N_s is the mole fraction of *p*-terphenyl, z is

17) F. Williams, *J. Am. Chem. Soc.*, **86**, 3954 (1964).
18) J. W. Buchanan and F. Williams, *J. Chem. Phys.*, **44**, 4377 (1966).
19) L. M. Stephenson, D. G. Whitten and G. S. Hammond, "The Chemistry of Ionization and Excitation," ed. by G. R. A. Johnson and G. Scholes, Taylor & Francis Ltd., London (1967), p. 35.
20) P. Ausloos, A. A. Scala and S. G. Lias, *J. Am. Chem. Soc.*, **89**, 3677 (1967).

the coordination number, and n_- is the number of jumps which an electron makes in diffusion to the parent ion ($n_- = n_-{}^0 r^3$).

$$\beta = \left(\frac{2z}{\sigma^2 r_c}\right)\left(\frac{D_-}{D_+ + D_-}\right)\log(1 - N_s)$$
$$\simeq -\left(\frac{2z}{\sigma^2 r_c}\right)\left(\frac{D_-}{D_+ + D_-}\right)N_s$$

The symbols used here have been discussed in a previous paper;[12] σ is the diameter of the cyclohexane molecule, r_c is defined by the $r_c = e^2/\varepsilon \boldsymbol{k} T$ relation, and D_- and D_+ are the diffusion coefficients of an electron and the parent positive ion in cyclohexane. $\phi(r)$ is the distribution function for ion pairs, for which we used the $r^2\exp(-\alpha r^2)$ function in the previous paper.[12] With this function, the integration shown above cannot easily be carried out. Here, a modified function, $r^2\exp(-\alpha r^3)$,*2 is tentatively introduced for $\phi(r)$, so that the integration can easily be performed. The relation obtained is as follows:

$$f_T = \beta/(\beta - \alpha)$$

According to the preceding discussion, I_o is proportional to f_T:

$$1/I_o \propto 1/f_T = 1 - \alpha/\beta = 1 + k/N_s$$
$$k = \left(\frac{\sigma^2 r_c}{2z}\right)\left(\frac{D_+ + D_-}{D_-}\right)\alpha$$

Obviously, a linear relationship between $1/I_o$ and $1/N_s$ is obtained.

*2 The distribution expressed by this function corresponds to that between $r^2\exp(-\alpha r^2)$ and the function calculated by Freeman.[13]

BULLETIN OF THE CHEMICAL SOCIETY OF JAPAN VOL. 41 2608—2611 (1968)

The Ultraviolet Absorption Spectrum of Quinazoline Vapor Due to the n–π^* Transition

Yoshinori HASEGAWA,*1 Yoshito AMAKO and Hiroshi AZUMI

Department of Chemistry, Faculty of Science, Tohoku University, Katahiracho, Sendai

(Received May 2, 1968)

The ultraviolet absorption spectrum of quinazoline vapor due to the n–π^* transition was photographed and analysed. The lowest n–π^* transition has its origin at 27581 cm^{-1}, and consists of two strong and prominent progressions, 515 and 784 cm^{-1}. The vibrational analysis of the strong bands is reported on.

The visible and ultraviolet absorption spectra of azanaphthalenes in solutions have been reported on by Hirt *et al.*,[1] Mason,[2,3] Favini *et al.*,[4] Müller and Dörr,[5] and Wait and Grogan.[6] In general, the weak bands at the longest wavelength in their spectral measurements have been assigned to the n–π^* transitions, on the basis of their blue shift in polar solvents, while the much stronger bands at the shorter wavelength have been assigned to the lowest π–π^* transitions, similar to the 3200 Å system of naphthalene.

The n–π^* and the lowest π–π^* absorption spectra of cinnoline(1,2-diazanaphthalene) vapor have been reported on by Wait and Grogan.[6] It has been found that the n–π^* transition of cinnoline has its origin at 22711 cm^{-1}, and that the vibronic structure of the n–π^* transition consists primarily of a strong prominent progression of 516.0 cm^{-1}, upon which singly-excited vibrations are superimposed, while the lowest π–π^* transition has its origin at 31542 cm^{-1}.

The n–π^* absorption spectrum of quinoxaline-(1,4-diazanaphthalene) vapor has been observed by Ito and Shiratsuchi[7] and by the present authors[8] independently. They all observed that the n–π^* absorption bands of quinoxaline consists of two band systems, one sharp and one broad band system. The broad bands have their origin at 26017 cm^{-1}, and the 525 cm^{-1} progression with the origin is very prominent. On the other hand, the sharp bands have strong false origins at 27496 and 27670 cm^{-1}, and also the 525 cm^{-1} progressions are very prominent.*2

*1 Present address: College of General Education, Tohoku University, Kawauchi, Sendai.

1) R. C. Hirt, F. T. King and J. C. Cavagnol, *J. Chem. Phys.*, **25**, 574 (1956).

2) S. F. Mason, *Chem. Soc. (London), Spec. Publ.*, **3**, 139 (1955).

3) S. F. Mason, *J. Chem. Soc. (London)*, **1962**, 493.

4) G. Favini, S. Carro, V. Pierpaoli, S. Polezzo and M. Simonetta, *Nuovo Chimento*, **8**, 60 (1958).

5) R. W. Müller and F. Dörr, *Z. Elektrochem.*, **63**, 1150 (1959).

6) S. C. Wait, Jr., and F. M. Grogan, *J. Mol. Spectry.*, **24**, 383 (1967).

7) M. Ito and Y. Shiratsuchi, Private communcication.

8) Y. Hasegawa, Y. Amako and H. Azumi, The lecture at the 21st Annual Meeting of the Chemical Society of Japan, 1968.

*2 Further work on quinoxaline is now in progress by Ito and Shiratsuchi and by the present authors.

The present authors have previously assigned the broad band system to the allowed $n-\pi^*$ transition and the sharp band system to the "forbidden"[9,10] bands in the allowed $n-\pi^*$ transition.

The electronic absorption spectra of the other azanaphthalenes in the vapor phase have never been reported on. The present investigation is concerned with the $n-\pi^*$ absorption spectrum of quinazoline(1,3-diazanapthalene) vapor.

Experimental

The vapor spectrum of quinazoline was photographed with a Shimadzu Littrow quartz spectrograph with a dispersion of 8.9 Å/mm at 3700 Å, and with a Shimadzu GE-100 grating spectrograph (Ebert type) with a dispersion of 2.7 Å/mm in the third order. The bands were measured on microphotometer tracings of the plates. The wavelength calibration was made by an iron arc. The wavelengthes of the bands were converted into frequencies *in vacuo*. The frequencies are estimated to be accurate about $\pm 2\ cm^{-1}$ for the strong bands, and to about $\pm 5\ cm^{-1}$ for the weak and broad bands. The light source was a 500 W Xenon arc lamp. A Toshiba UV-D2 filter was used to eliminate all the radiation in the higher orders and lower orders. The absorption cell with quartz windows was helically wound with Nichrome wire over an asbestos sheet and covered with an asbestos sheet. The light-pass length of the absorption cell was 60 cm. The cell temperature could be regulated between room temperature and 250°C. The solution spectrum of quinazoline was obtained using a Cary automatic recording spectrometer, Model 14.

The quinazoline used in this study was prepared by following the method described by Riedel[11] and by Bogert and McColm[12]; it was recrystallized repeatedly, and finally sublimated before the experiment. The *n*-hexane was purified according to the procedure described by Morgan and Lowry.[13]

Results and Discussion

The ultraviolet absorption spectra of quinazoline have been reported on in solutions of heptane, ethanol, and an acidic solvent by Müller and Dörr,[5] and in a solution of cyclohexane by Mason.[3] The 3650 Å band system has been assigned to the $n-\pi^*$ transition, and the 3100 Å band system, to the lowest $\pi-\pi^*$ transition. The results of the present investigation in *n*-hexane are shown in Fig. 1, which corresponds well to that in heptane reported by Müller and Dörr.

The $n-\pi^*$ absorption spectrum of quinazoline vapor under a low dispersion consists of a number of band groups. Each of the strong band groups under a moderate dispersion consists of a principal band and of associated $15\ cm^{-1}$ sequence bands, which appear with up to two or three members.

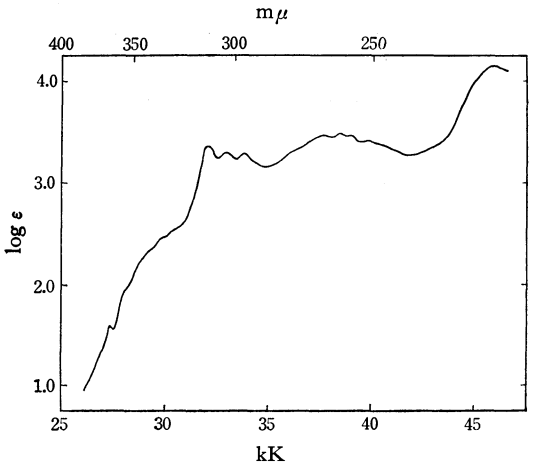

Fig. 1. The ultraviolet absorption spectrum of quinazoline in *n*-hexane.

The $n-\pi^*$ absorption spectrum of quinoxaline vapor has been observed by Ito and Shiratsuchi and by the present authors, as has been stated above. The spectrum consists of two systems, one sharp and one broad, as is shown in the Plate. The $n-\pi^*$ absorption spectrum of quinazoline vapor, however, does not show such two band systems.

The vibronic structure shown in Fig. 2 consists of three progressions with their origins*3 at 27581 cm^{-1}; the members are separated by 515, 784, and 879 cm^{-1} respectively. On their progressions are superimposed a number of singly-, doubly- or triply-excited vibrations. The band at 27581 cm^{-1}, which is the first member of their progressions, was assigned to the 0–0 band. The frequecies and assignments of the principal bands are shown in Table 1. No bands could be observed below 27494 cm^{-1}, and so the frequencies corresponding to the ground state vibrations could not be obtained.

The quinazoline molecule has two nitrogen atoms in the "meta" position of the naphthalene-like ring, and belongs to the C_s point group in the ground state. Because of the interaction between the respective nonbonding orbitals of these nitrogen atoms,[14-16] two allowed $n-\pi^*$ transitions of the $^1A' \rightarrow {}^1A''$ type may be expected to appear. However, no suggestion with respect to the "$n-\pi^*$

*3 With moderate dispersion the origin shows several broad structures, probably due to its sequence bands. Unfortunately, under the conditions used, they do not have intensities sufficient for definite assignments to be made. Therefore, the apparenly strongest peak on the microphotometer tracing was taken as the 0-0 band, which might be one of the sequences of the true origin.

9) A. C. Albrecht, *J. Chem. Phys.*, **33**, 156 (1960).
10) A. C. Albrecht, *ibid.*, **33**, 169 (1960).
11) J. D. Riedel, *Chem. Zentr.*, **1906** II, 1372.
12) M. T. Bogert and E. M. McColm, *J. Am. Chem. Soc.*, **49**, 2650 (1927).
13) S. O. Morgan and H. H. Lowry, *J. Phys. Chem.*, **34**, 2385 (1930).
14) S. F. Mason, *J. Chem. Soc. (London)*, **1959**, 1240.
15) L. Goodman, *J. Mol. Spectry.*, **6**, 109 (1961).
16) K. K. Innes, J. P. Byrne and I. G. Ross, *ibid.*, **22**, 125 (1967).

TABLE. 1. FREQUENCIES AND ASSIGNMENTS OF PRINCIPAL BANDS

Wave numbers (cm^{-1})	Intensities	Differences (from 0-0)	Assignments (cm^{-1})	Differences (from cald. value)
27494	w	−87	0−87	0
27581	s	0	origin	0
27632*	vw	51	(0+51)	0
27834	vw	253		
27883*	vw	302		
27941*	vw	360	(0+360)	0
27976	w	395	(0+395)	0
28007	w	426	0+515−87	−2
28096	s	515	0+515	0
28147	w	566	(0+51+515)	0
28213	w	632	0+632	0
28365	vs	784	0+784	0
28460	s	879	0+879	0
28501*	vw	920	(0+395+515)	+10
28522*	vw	941	0+2×515−87	−2
28613	s	1032	0+2×515	+2
28668*	vw	1087	(0+51+2×515)	+6
28727	vw	1146	(0+632+515)	−1
			or (0+360+784)	+2
28753	vw	1172	(0+395+784)	−7
28787*	vw	1206	(0+784+515−87)	−6
28869	vs	1288	0+784+515	−11
28933	w	1352	(0+51+515+784)	+2
28974	s	1393	0+879+515	−1
29025	w	1444	(0+1444)	0
29153	s	1572	0+2×784	+4
29242	vs	1661	0+879+784	−2
29346*	m	1765	0+2×879	+7
29382*	s	1801	0+784+2×515	−13
29446	vw	1865	(0+51+2×515+784)	0
29493	m	1912	0+879+2×515	+3
29649	vs	2068	0+2×784+515	−15
29751	vs	2170	0+879+784+515	−8
29804*	vw	2223	(0+1444+784)	−5
29860*	w	2279	0+2×879+515	+6
29897*	w	2316	0+784+3×515	−13
30028	s	2447	0+879+2×784	0
30154*	s	2573	0+2×784+2×515	−25
30267	s	2686	0+879+784+2×515	−7
30529	s	2948	0+879+2×784+515	−14

a) Symbol * denotes that the corresponding frequencies are accurate to about 5 cm^{-1}.
b) Usual abbreviation for intensities is taken as; v=very, w=weak, m=moderate and s=strong.
c) The assignments shown by parenthesis are less certain.

splitting" could be obtained under the experimental conditions used; further studies under better conditions will be necessary.

The totally symmetric vibrational intervals, 515 and 784 cm^{-1}, are very prominent. Superimposed on 0-0, 0+879 cm^{-1} and other bands, the 515 and 784 cm^{-1} progressions appear with up to two or three members. According to Wait and Grogan,[6] the interval, 516.0 cm^{-1}, in the n-π^* transition of cinnoline is very prominent. The interval, 525cm^{-1}, in the n-π^* transition of quinoxaline is also very prominent, as has been mentioned above. This normal mode of quinazoline with the 515 cm^{-1} frequency probably corresponds to the same type of mode of cinnoline and quinoxaline with frequencies of 516.0 and 525 cm^{-1} respectively.

In the case of azines,[15,16] the ring breathing vibrations of ~900 cm^{-1} dominate the progressions

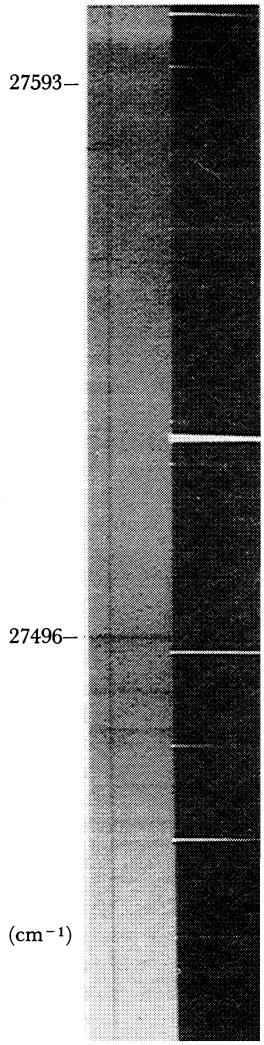

Plate. The two different band systems in the $n-\pi^*$ absorption spectrum of quinoxaline vapor.
(a) the broad band at 27593 cm^{-1}
(b) the sharp band at 27496 cm^{-1}

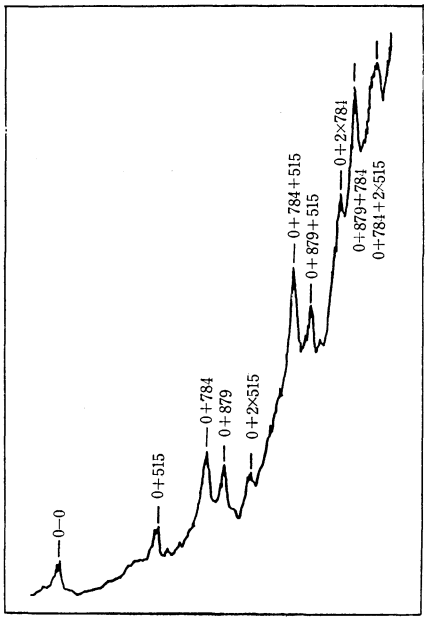

Fig. 2. The microphotometer tracing of the $n-\pi^*$ absorption spectrum of quinazoline vapor (cm^{-1}).

in the $\pi-\pi^*$ transitions, while the ring angle bending modes, notably the ν_{6a} of $\sim$600 cm^{-1}, are prominent in the $n-\pi^*$ transitions. These normal modes of the $n-\pi^*$ states of these three diazanaphthalenes with $\sim$520 cm^{-1} are probably ring angle bending modes, or ring deformation modes. The other prominent frequency, 784 cm^{-1}, will be a skeletal stretching mode.

At the present time no further detailed attempts to assign these and other frequencies have been carried out for lack of experimental data.

The authors wish to express their sincere thanks to Misses M. Nyugaku and Y. Kato for their assistance in this work.

BULLETIN OF THE CHEMICAL SOCIETY OF JAPAN VOL. 41 2612—2615 (1968)

The Analysis of the Solubility of Hydrocarbons in Water

Kōzō SHINODA and Masamichi FUJIHIRA

Department of Chemistry, Yokohama National University, Ookamachi, Minamiku, Yokohama

(Received May 2, 1968)

Enthalpy and entropy of solution of non-polar solutes in water diverge strikingly from the normal behavior established for regular solutions. This abnormality has been considered mostly due to the iceberg formation around solute molecules in water. The abnormal solubility and enthalpy and entropy of solution of non-polar solutes in water have been explained coherently by the extension of the regular solution theory, taking into account the iceberg formation of water molecules. Unlike currently accepted views on the hydrophobic bonding, it is concluded that the enthalpy of mixing (interchange) of non-polar solute with water is large, but the enthalpy decrease due to the iceberg formation of water largely cancels the enthalpy increase of mixing (interchange). Thus, the apparent enthalpy of solution is small or negative at low temperature. It is concluded that 1) the small solubility of non-polar solutes in water is not an entropy effect, and 2) the solubility of non-polar solutes is promoted by the iceberg formation of water molecules.

Frank and Evans[1] analyzed the entropy of solution of non-polar molecules in water which diverges strikingly from the normal behavior established for regular solutions. The small or negative enthalpy of solution and large negative unitary entropy of solution lead them to the idea that the water forms frozen patches or microscopic icebergs around such solute molecules, the extent of the iceberg increasing with the size of the solute molecule. (More ordered structure formation around the solute molecule may express the phenomenon better than iceberg formation.)

In the present paper, the apparently abnormal solubility and enthalpy and entropy of solution of hydrocarbons in water due to the iceberg formation of water molecules will be explained coherently by the extension of the regular solution theory.[2]

The Enthalpy and Entropy of Solution in Regular Solutions. It is necessary to explain the dissolution in regular solutions in order to understand the dissolution of hydrocarbons in water. The enthalpy and entropy of solution of solute (2nd component) in liquid state in solvent (1st component) in regular solutions is[2];

$$\Delta\bar{S}_2 = -R\ln X_2$$

liquid(2 nd component) → solute, (1)

$$\Delta\bar{H}_2 = V_2\phi_1^2B'$$

liquid(2 nd component) → solute, (2)

where X_2 is the solubility of 2nd component in mole fraction unit, V_2 the molar volume, ϕ_1 the volume fraction of solvent, B' the experimental constant. In the case when the 1st component is sparingly soluble in 2nd component, the 2nd component in pure liquid state and in solute state are in an equilibrium, so that the Gibbs free energy is equal, $\Delta\bar{G}_2=0$, and we obtain,

$$V_2\phi_1^2B' = -RT\ln X_2 . \quad (3)$$

If the 2nd component is a pure solid which does not form solid solution with solvent, the enthalpy and entropy of solution is expressed as follows,

$$\Delta\bar{H}_2 = V_2\phi_1^2B' + \Delta H_2^f$$

solid(2nd component) → solute, (4)

$$\Delta\bar{S}_2 = -R\ln X_2 + \Delta S_2^f$$

solid(2nd component) → solute, (5)

where ΔH_2^f and ΔS_2^f are the enthalpy and entropy of fusion of solid at the temperature of solution. The solid (2nd component) melts at this temperature and mixes with solvent in the process of dissolution. Additional term due to the melting is incidental to the solution of solid in liquid.[3,4] As the 2nd component in solid state and in solute state are in equilibrium, the partial molal Gibbs free energy of solution is zero.

$$\Delta\bar{G}_2 = 0, \qquad \Delta\bar{H}_2 = T\Delta\bar{S}_2 . \quad (6)$$

If we express the vapor pressure of solid by p_2^s and that of supercooled liquid by p_2^l, the Gibbs free energy change of fusion is expressed as,

1) H. S. Frank and M. W. Evans, *J. Chem. Phys.*, **13**, 507 (1945).
2) J. H. Hildebrand and R. L. Scott "Regular Solutions," Prentice Hall, Inc., Englewood Cliffs, New Jersey (1962).
3) J. H. Hildebrand, *J. Phys. Chem.*, **64**, 370 (1960).
4) K. Shinoda and J. H. Hildebrand, *ibid.*, **62**, 292 (1958).

$$\Delta G_2^f = \Delta H_2^f - T\Delta S_2^f = RT\ln(p_2^l/p_2^s) . \quad (7)$$

Combining Eqs. (4), (5) and (6), we obtain

$$T\Delta S_2^f - \Delta H_2^f = RT\ln X_2 + V_2\phi_1^2 B' . \quad (8)$$

Substituting Eq. (7) into (8), we obtain

$$RT\ln(p_2^s/p_2^l) = RT\ln a_2 = RT\ln X_2 + V_2\phi_1^2 B' . \quad (9)$$

The enthalpy of solution and the temperature dependence of solubility is related as follows,

$$-R\left(\frac{\partial \ln a_2}{\partial \ln X_2}\right)_T\left(\frac{\partial \ln X_2}{\partial 1/T}\right)_{sat} = \Delta\bar{H}_2 = T\Delta\bar{S}_2 , \quad (10)$$

where $(\partial \ln a_2/\partial \ln X_2)_T \approx 1$ in dilute solution.

It is clear from Eqs. (10) and (4) that the temperature dependence of the logarithm of solubility is proportional to the enthalpy of solution and increases discontinuously by the amount ΔH_2^f below the melting point of solute. However, the enthalpy and entropy of fusion cancel each other, so that the solubility is scarcely affected by the increased enthalpy of solution slightly below the melting point.

The Enthalpy and Entropy of Solution of Non-polar Solutes in Water. In the process of solution of non-polar solutes in water the iceberg formation[1] and hydrogen bond breaking occurs around the hydrocarbon chains. In dilute solution of this system, the amount of water which forms icebergs and the hydrogen bond breaking increases proportionally to the number of moles of solute, but does not increases with the amount of added solvent. Thus, the iceberg formation of water and the hydrogen bond breaking affect the partial molal quantity of solute, but they little affect that of solvent in dilute solution. This statement is clear from the general partial molal equation for a binary system,

$$n_1 d\bar{Y}_1 + n_2 d\bar{Y}_2 = 0,$$

where Y is any extensive property of the solution. According to the equation, $d\bar{Y}_1$ is negligibly small in dilute solution, because n_2/n_1 is very small (about 10^{-3} at the present system). If n mol of water form icebergs and n' units of hydrogen bonds are destroyed per mole of solute, the enthalpy and entropy of solution of non-polar solutes in water is expressed as fcllows,

$$\Delta\bar{H}_2 = V_2\phi_1^2 B' - n\Delta\bar{H}_i^f + n'\Delta\bar{H}_h$$

non-polar liquid $\rightarrow$ solute in H_2O, (11)

$$\Delta\bar{S}_2 = -R\ln X_2 - n\Delta\bar{S}_i^f + n'\Delta\bar{S}_h$$

non-polar liquid $\rightarrow$ solute in H_2O, (12)

where $-n\Delta\bar{H}_i^f$ $(-n\Delta\bar{S}_i^f)$ is the partial molal enthalpy(entropy) change of 2nd component due to the iceberg formation of n moles of the surrounding water and $n'\Delta\bar{H}_h$ $(n'\Delta\bar{S}_h)$ is the partial molal enthalpy(entropy) change due to the hydrogen bond breaking. As the effect of iceberg formation seems predominant in aqueous solution, only the iceberg formation may be taken into account as an abnormality in the present paper. The iceberg formation proceeds with the temperature decrease and n increases with the temperature depression. On the other hand, the solubility and the enthalpy of solution approach to the regular values at higher temperature.

Analysis of the Temperature Dependence of the Solubility of Alkanes in Water. The solubility of alkanes (C_1—C_4) at 1 atm as a function of temperature has been published.[5-7] In order to gain an insight into the dissolution phenomena, the solubility of alkanes at 1 atm pressure was recalculated to that of hypothetical liquid alkanes. The recalculation has been performed as follows. The fugacity of liquid alkanes divided by the critical pressure of respective alkanes, f°/p_c, at various temperature was obtained from the empirical diagram drawn by Prausnitz based on the principle of corresponding state.[8] The solubility at 1 atm multiplied f° is the solubility of hypothetical liquid alkanes. The recalculated solubility was plotted in Fig. 1.

As the iceberg formation decreases with the temperature rise, n in Eqs. (11) and (12) decreases

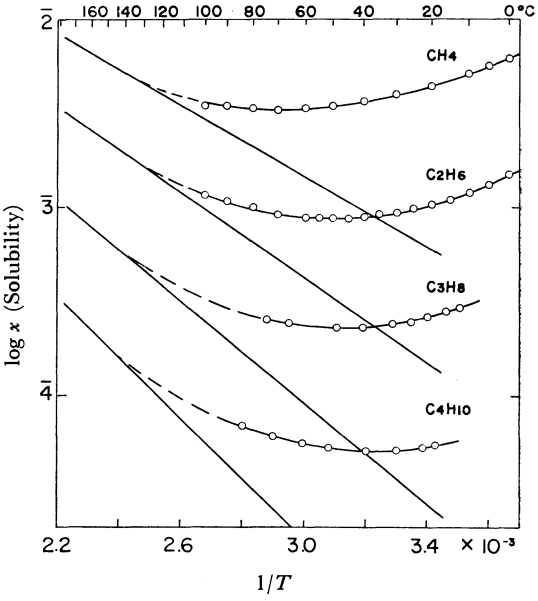

Fig. 1. The solubility of hypothetical liquid alkanes in water as a function of temperature. Calculated from the data at 1 atm (Refs. 5, 6 and 7).

5) W. F. Claussen and M. F. Polglase, *J. Am. Chem. Soc.*, **74**, 4817 (1952).
6) T. J. Morrison and F. Billet, *J. Chem. Soc.*, **1952**, 3819.
7) L. W. Winkler, *Ber.*, **36**, 1408 (1901).
8) J. M. Prausnitz, *J. Phys. Chem.*, **66**, 640 (1962).

Table 1. The analysis of the enthalpy and entropy of solution of liquid hydrocarbons in water at 25°C

Enthalpy of solution $=\Delta\bar{H}_2=-\boldsymbol{R}\left(\frac{\partial \ln X_2}{\partial\, 1/T}\right)_{\text{sat}}$; Entropy of solution $=\Delta\bar{H}_2/T$

Enthalpy of mixing $=V_2\phi_1^2B'$ (estimated); Entropy of mixing $=-\boldsymbol{R}\ln X_2$

Enthalpy of iceberg formation $=-n\Delta\bar{H}_i^f$; Entropy of iceberg formation $=-n\Delta\bar{S}_i^f$

Solute	$\Delta\bar{H}_2=V_2\phi_1^2B'-n\Delta\bar{H}_i^f$ (cal/mol)	$\Delta\bar{S}_2=-\boldsymbol{R}\ln X_2-n\Delta\bar{S}_i^f$ (cal/deg/mol)	$\Delta\bar{H}_i^f/\Delta\bar{S}_i^f$ (°K)
CH_4	$-1900=4300-6200$	$-6.4=10.8-17.2$	360
C_2H_6	$-2000=5100-7100$	$-6.7=13.7-20.4$	348
C_3H_8	$-1880=6100-7980$	$-6.3=16.5-22.8$	350
C_4H_{10}	$-820=7200-8020$	$-2.7=19.6-22.3$	359
C_6H_6	$+580=5100-4520$	$+1.9=15.4-13.5$	335
$CH_3C_6H_5$	$+640=6050-5410$	$+2.2=17.9-15.7$	345
$C_2H_5C_6H_5$	$+390=7000-6610$	$+1.4=20.4-19.0$	348

and the slope of $-\partial \ln X_2/\partial(1/T)$ increases with the temperature rise as shown in Fig. 1. The change of the slope with temperature, $-[\partial^2 \ln X_2/\partial(1/T)^2]$, decreases with temperature and is almost zero at 120—160°C at which the iceberg formation seems mostly disappear. We can evaluate the solubility at this temperature by extrapolation and then calculate the enthalpy of solution by the aid of Eqs. (2), (3) and (10). The straight lines in Fig. 1 express the hypothetical solubility of alkanes in water assuming no iceberg formation. The temperature dependence of solubility, $-(\partial \ln X_2/\partial 1/T)$, decreases with the temperature depression as shown in Fig. 1 and the solubility increases relatively with the iceberg formation of water. Similar relation is observed for aromatic hydrocarbons[9,10] and the analysis of the data is listed in Table 1.

The straight line and the experimental solubility curve approaches asymptotic at high temperature. This is an important finding, because the entropy of solution of hydrocarbon from the pure liquid state to the solute state in water is then given by,

$$\Delta\bar{S}_2 = -\boldsymbol{R}\ln X_2 = \bar{S}_2 - S_2^\circ. \tag{13}$$

As the partial molal entropy of hydrocarbon (2nd component) in aqueous solution, $\bar{S}_2$, and the hypothetical standard entropy of hydrocarbon in which the mole fraction is formally taken as unity, $\bar{S}_2^\circ$, are related as,

$$\bar{S}_2 = \bar{S}_2^\circ - \boldsymbol{R}\ln X_2, \tag{14}$$

the fact implies the assertion that the hypothetical standard entropy of the 2nd component as a solute is equal to the standard entropy of that component as a pure liquid,

$$\bar{S}_2^\circ = S_2^\circ. \tag{15}$$

This relation holds in regular liquid-liquid mixtures regardless the difference between δ_1 and δ_2, as can be derived from Eq. (1) or (13),

$$\bar{S}_2^\circ = \bar{S}_2 + \boldsymbol{R}\ln X_2 = \bar{S}_2 - (\bar{S}_2 - S_2^\circ) = S_2^\circ. \tag{16}$$

Namely, the enthalpy of mixing in regular solutions is purely energetic and the cratic entropy compensates the enthalpy change to give $\Delta G_2=0$. If the dissolution involves phase change such as the melting of solute, both the enthalpy and entropy changes with the process of melting as shown in Eqs. (4) and (5). In this case both changes largely cancel each other and the cratic entropy to compensate the difference, $\Delta H_2^f - T\Delta S_2^f$, is small. It is evident from Eq. (5) that

$$\bar{S}_2^\circ - S_2^\circ = \Delta S_2^f \quad (\text{solid} \rightarrow \text{solute}). \tag{17}$$

The iceberg formation resembles to the phase change. Both enthalpy and entropy are lost due to the process as expressed in Eqs. (11) and (12). Standard entropy of solute decreases due to the iceberg formation of water, but this abnormality diminishes gradually with the temperature rise. The hydrogen bond breaking on the other hand, increases the enthalpy and entropy of solute. These two abnormalities decrease with the temperature and cancel each other at 120—160°C. Because, the experimental entropy of solution at this temperature is equal to $-\boldsymbol{R}\ln X_2$ (*cf.* Eq. (12)). As the effect of iceberg formation is so large at lower temperature that $n'\Delta\bar{S}_h$ and $-n\Delta\bar{S}_i^f$ (at 120°C) were neglected from the following discussion.

Estimation of Respective Factors to the Enthalpy and Entropy of Solution of Hydrocarbons in Water at 25°C (First Approximation). The enthalpy and entropy of solution of liquid hydrocarbons in water at 25°C are calculated from the temperature dependence of the solubility

9) R. L. Bohon and W. F. Claussen, *J. Am. Chem. Soc.*, **73**, 1571 (1951).
10) D. M. Alexander, *J. Phys. Chem.*, **63**, 1021 (1959).

and shown in Table 1. The enthalpy of solution assuming regular behavior is obtained from the slope of straight lines in Fig. 1, then the enthalpy change of iceberg formation, $n\Delta\bar{H}_i^f$, is readily obtained by the aid of Eq. (11). The entropy of mixing is calculated from the solubility,[11] and $n\Delta\bar{S}_i^f$ is obtained by the aid of Eq. (12) assuming $-n\Delta\bar{S}_i^f$ (at 120°C)$+n'\Delta\bar{S}_h$ (25°C) is small. All these values are summarized in Table 1.

The enthalpy of mixing is approximately proportional to the molal volumes of respective alkanes, and the ratio of $\Delta\bar{H}_i^f/\Delta\bar{S}_i^f$ (mean freezing point of iceberg formation) is nearly constant, 350°K, for all hydrocarbons examined. As the iceberg formation proceeds at above room temperature, this is a reasonable value as a first approximation. These relations support the consistency of the present theory. Unlike currently accepted views,[12,13] it is evident from Fig. 1 and Table 1 that the enthalpy of mixing is a large positive value as would be expected on the basis of the intermolecular forces. Small negative enthalpy of solution, $\Delta\bar{H}_2$, is resulted from a large positive enthalpy of mixing and a large negative enthalpy of iceberg formation.

Introducing the relation $\Delta\bar{H}_2=T\Delta\bar{S}_2$ in Eqs. (11) and (12), (and neglecting $n'\Delta\bar{H}_h-n'T\Delta\bar{S}_h$ as a first approximation,) we obtain,

$$n\Delta\bar{H}_i^f - nT\Delta\bar{S}_i^f = \boldsymbol{R}T\ln X_2 + V_2\phi_1{}^2B' . \quad (18)$$

The left hand side of Eq. (18) corresponds to the free energy term of 2nd component, $\boldsymbol{R}T\ln a_2$. Unlike the process of solid (2nd component) in liquid, the relative activity is larger than 1 in the process of mixing liquid in liquid accompanied with iceberg formation. Equation (18) is useful to understand that the small solubility of hydrocarbons in water is mainly resulted from the large positive enthalpy of mixing and the enthalpy decrease of the iceberg formation is largely cancelled[1,14] by the accompanying entropy decrease (about 83% cancelled) at 25°C, and that the solubility increases as much as $\exp(n\Delta\bar{H}_i^f-n\Delta\bar{S}_i^f)/\boldsymbol{R}T$ times due to the iceberg formation.

11) K. Shinoda and J. H. Hildebrand, *J. Phys. Chem.*, **61**, 789 (1957).
12) W. Kauzmann, *Advances in Protein Chem.*, **14**, 1 (1959).
13) G. Nemethy and H. A. Scheraga, *J. Chem. Phys.*, **36**, 3401 (1962).
14) H. S. Frank, *Federation Proc. Suppl.*, **24**, 1 (1965).

BULLETIN OF THE CHEMICAL SOCIETY OF JAPAN VOL. 41 2615—2619 (1968)

Diffuse Reflection Spectra of Some Würster Salts

Yôichi IIDA and Yoshio MATSUNAGA

Department of Chemistry, Faculty of Science, Hokkaido University, Sapporo

(Received May 6, 1968)

Nine Würster salts derived from *p*-phenylenediamine, benzidine, and their *N*-methyl derivatives were examined for diffuse reflection spectra and classified into three groups, namely, those showing a strong charge-transfer band similar to that in the solution's dimer spectrum, those showing a strong α-band characteristic of the monomer and a relatively weak charge-transfer band, and, finally, those showing a spectrum which bears no resemblance to either the monomer or dimer spectrum. The mode of intermolecular interaction in these cation-radical salts was speculated upon on the basis of the spectra and the magnetic susceptibilities.

Prior to about 1960 the chief emphasis in studies of solid ion-radical salts was on measuring the magnetic susceptibilities of Würster salts, cation-radical salts obtained by the one-electron oxidation of aromatic diamines.[1-4] However, since the appearance of a series of TCNQ anion-radical salts, which are more stable and easily obtainable in the form of single crystals, studies of the electron spin resonance and the electrical conductivity have been among the most fruitful of pursuits.[5-8] The application of these physical methods has

1) L. Michaelis and S. Granick, *J. Am. Chem. Soc.*, **65**, 1747 (1943).
2) G. K. Hughes and N. S. Hush, *J. Proc. Roy. Soc. N. S. W.*, **81**, 48 (1947).
3) W. Duffy, Jr., *J. Chem. Phys.*, **36**, 490 (1962).
4) K. Okumura, *J. Phys. Soc. Japan*, **18**, 69 (1963).
5) D. B. Chesnut and W. D. Phillips, *J. Chem. Phys.*, **35**, 1002 (1961).
6) D. D. Thomas, H. Keller and H. M. McConnell, *ibid.*, **39**, 2321 (1963).
7) W. J. Siemons, P. E. Bierstedt and R. G. Kepler, *ibid.*, **39**, 3523 (1963).
8) R. G. Kepler, *ibid.*, **39**, 3528 (1963).

thus far revealed that intermolecular interactions in such solids are often more-than-by-pairs. The electronic spectrum, which has been traditionally the most popular tool for elucidating the electronic structures of molecules and solids, should be able to produce some information concerning the interactions in solid ion-radical salts. It is the purpose of this paper, the first of our attempts along this line, to report the results of our electronic spectrum measurements of nine solid Würster salts and to make a tentative classification of the salts on the basis of their optical and magnetic properties.

The cation-radicals in solution have been known to be in monomer-dimer equilibria.[9] For example, the cation radical derived from *p*-phenylenediamine shows a visible spectrum comprising the α, β, and γ-bands, a doublet at 20.4 and 21.1, a broad shoulder at 27.6, and a strong band at 30.5 kK, when the concentration is low.[10] If the solution is more concentrated or cooled, a new broad band appears at 16.4 kK. This band has been ascribed to the charge-transfer absorption in the dimer by Hausser and Murrell.[11] According to their theory, the cation-radicals in a dimer are stacked face-to-face and the spin exchange interaction leads to a singlet ground state and an excited triplet state. Then, we must take into consideration the fact that intermolecular charge-transfer may make a significant contribution to stabilizing the ground singlet state of the dimer. The low-energy absorption characteristic of the dimer arises from a transition from the thus-stabilized ground state to an excited singlet state expressed by an antisymmetric combination of the wave-functions for charge-transfer structures, $R\text{-}R^{+}{}^{+}$.

Both the present cation-radicals and TCNQ anion-radicals are platelike, and, to the best of our knowledge, they are stacked in the solid salts flat upon one another to form parallel chains.[6,12-15] Any individual radical may interact most strongly with one or two other radicals. In the former case, the interaction is predominantly pair-by-pair; therefore, we may speculate that the solid-state spectrum will be close to the solution's dimer spectrum. If the singlet-triplet excitation energy, to which both the spin exchange and charge-transfer interactions contribute, is rather small, the triplet state may become thermally accessible and paramagnetism may be observed. Secondly, when a radical interacts equally strongly with two neighbors, the following two extreme cases may be conceived. With a weak interaction, the solid-state spectrum may bear some resemblance to the monomer spectrum and paramagnetism of close to 100% free radicals may be exhibited. If any charge-transfer absorption is observable, the paramagnetism may decrease accordingly. On the other hand, if the more-than-by-pairs interaction is strong enough, the salt may be considered to be a linear antiferromagnet. Here again, the charge-transfer interaction may contribute to the stabilization of the state where spins are antiparallel. Therefore, the spectrum may have no similarity to either the monomer or dimer spectrum and the susceptibility may be low or even negative. These speculations clearly represent oversimplified cases; however, we have found that they are well followed in the Würster salts.

Experimental

Materials. The following Würster salts were prepared according to the methods of Michaelis and Granick[1] and of Hughes and Hush[2]; *p*-phenylenediamine bromide,[1] *N,N*-dimethyl-*p*-phenylenediamine (Würster's red) bromide,[1] Würster's red ferrocyanide,[2] *N,N,N',N'*-tetramethyl-*p*-phenylenediamine (Würster's blue) perchlorate,[1] Würster's blue ferrocyanide,[2] Würster's blue iodide prepared in aqueous methanol (high-susceptibility form),[2] Würster's blue iodide prepared in methanol - ether (low-susceptibility form),[2] benzidine bromide,[2] and *N,N,N',N'*-tetramethylbenzidine bromide.[2] They were assumed to exhibit the magnetic behavior reported in the references.

Measurements. The solid bromide was diluted with potassium bromide in a ratio of about 1 : 200 by grinding it to obtain a reasonable reflectance. The spectra were recorded as the difference in reflectance between the mixture and pure potassium bromide in the range from 4.0 to 30.8 kK by a Beckman DK-2A spectroreflectometer, and were then plotted using the Kubelka-Munk function $f(R)=(1-R)^2/2R$, where R is the reflectance. To avoid anion-exchange between the salt and the diluent, the iodide was ground with potassium iodide, and the perchlorate and ferrocyanide, with naphthalene. (With the last diluent, the measurements are reliable only in the range from 10 to 25 kK because of absorption due to the hydrocarbon.)

Results and Discussion

***p*-Phenylenediamine Bromide (Fig. 1, Curve a).** The low-energy band in the solid-state spectrum is found at 12.7 kK, which is much lower than the 16.4 kK value for the charge-transfer band in the dimer spectrum and also the 20.4 and 21.1 kK values for the α-band in the monomer spectrum. Although no information is available on the crystal structure, we suppose that the intermolecular interaction in this salt is

9) K. Uemura, S. Nakayama, Y. Seo, K. Suzuki and Y. Ooshika, This Bulletin, **39**, 1348 (1966).
10) Y. Iida and Y. Matsunaga, *ibid.*, **41**, 2535 (1968).
11) K. H. Hausser and J. N. Murrell, *J. Chem. Phys.*, **27**, 500 (1957).
12) C. J. Fritchie, Jr., and P. Arthur, Jr., *Acta Cryst.*, **21**, 139 (1966).
13) C. J. Fritchie, Jr. *ibid.*, **20**, 892 (1966).
14) J. Tanaka, T. Sakabe, M. Mizuno and C. Tanaka, Paper presented at the 19th Annual Meeting of the Chemical Society of Japan, Tokyo, April, 1966.
15) M. Mizuno, T. Sakabe and J. Tanaka, Paper presented at the Symposium on Molecular Structure, Osaka, October, 1966.

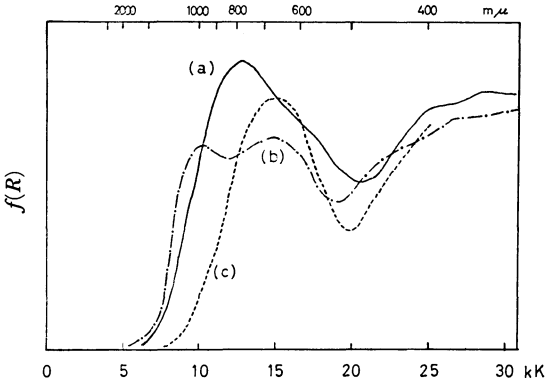

Fig. 1. Diffuse reflection spectra of *p*-phenylenediamine bromide (curve a), Würster's red bromide (curve b) and Würster's red ferrocyanide (curve c).

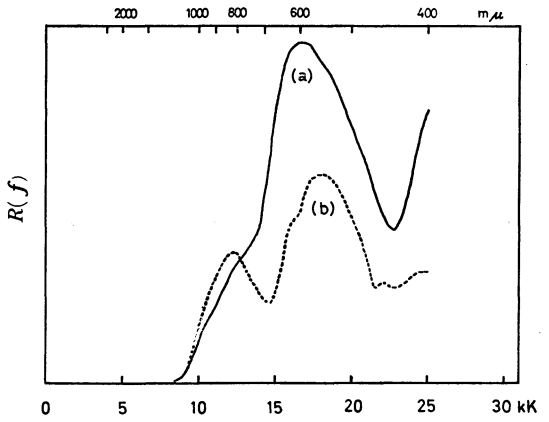

Fig. 2. Diffuse reflection spectra of Würster's blue perchlorate (curve a) and ferrocyanide (curve b).

strong and more-than-by-pairs. The magnetic susceptibility reported by Michaelis and Granick is $-(109\pm10)\times10^{-6}$ emu/mol, which is in agreement with the estimated diamagnetic term, $-(98\pm16)\times10^{-6}$.[1]

Würster's Red Bromide (Fig. 1, Curve b). The solid-state spectrum has absorptions at 10.4 and 14.8 kK. The charge-transfer band in the dimer is located at 14.7 kK, and the α-band in the monomer, at 18.0 and 19.4 kK.[10,16] Again, the spectrum is different from either the dimer or monomer spectrum and extends to the lower-energy region. The crystal structure has been examined by Tanaka *et al.*[14] The cation-radicals are equally spaced in a linear chain at the remarkably short distance of 3.135 Å. These pieces of evidence indicate that the intermolecular interaction here is more-than-by-pairs and is strong. The salt is diamagnetic, the reported values being -102×10^{-6} by Michaelis and Granick[1] and -130×10^{-6} emu/mol by Hughes and Hush.[2] This is in accordance with our conclusion. Tanaka *et al.* have reported that the low-energy absorption is polarized out of the molecular plane, presumably in the direction to connect the centers of neighboring molecules.[14]

Würster's Red Ferrocyanide (Fig. 1, Curve c). Unlike the dark-green bromide, this salt shows only one broad absorption in the low-energy region, at 14.8 kK. This energy is in good agreement with the 14.7 kK value for the charge-transfer band in the solution's dimer spectrum.[16] According to the measurements by Hughes and Hush, this salt is paramagnetic; $+1098\times10^{-6}$ emu/mol at 293°K.[2] A cation-radical in this salt appears to interact predominantly with one neighbor, but merely weakly.

Würster's Blue Perchlorate (Fig. 2, Curve a). The crystal is known to be orthorhombic and to be built up from linear chains of equivalent cation-radicals at room temperature. A phase change into the monoclinic form occurs at 186°K, and the radicals pair up to form dimers. The singlet-triplet energy separation in the latter phase has been estimated as 0.246 kK.[6] Thus, the salt at room temperature has been considered to be a normal paramagnet. In accordance with this view, the strong band at 16.7 kK in the solid-state spectrum corresponds well with the α-band in the monomer spectrum, 16.4 and 17.8 kK.[10] However, the presence of a shoulder around 12 kK must be noted. This is the place where the charge-transfer band appears in the solution's dimer spectrum[16] and also in the solid-state spectrum at low temperatures.[17] The paramagnetic susceptibility above the transition temperature has been reported to be consistent with a Curie-Weiss law; however, the observed paramagnetism is often short of the expected 100% free radical value. For example, Duffy has found it to be 94% and Okumura, as low as 81%.[3,4] It is difficult to see how these deviations from 100% free radicals are related with the weak charge-transfer absorption in the solid-state spectrum. At any rate, both the optical and magnetic pieces of evidence clearly indicate that the interaction in Würster's blue perchlorate is weak at room temperature.

Würster's Blue Ferrocyanide (Fig. 2, Curve b). Although the main bands, located at 16.4 and 18.2 kK, again correspond well with the α-band in the monomer spectrum, the charge-transfer band at 12.3 kK is clearly recorded. The susceptibility reported by Hughes and Hush is as high as $+1031\times10^{-6}$ emu/mol at 291°K,

16) K. Suzuki, Y. Ooshika, Y. Seo, K. Uemura and S. Nakayama, Paper presented at the Symposium on Molecular Structure, Nagoya, October, 1965.

17) T. Sakata and S. Nagakura, *Technical Report of ISSP*, Ser. A, No. 244, March, (1967), published by the Institute for Solid State Physics, the University of Tokyo.

which is only a little bit lower than the $+1114\times10^{-6}$ emu/mol value for the perchlorate.[2] As is indicated by the strong charge-transfer absorption and lower susceptibility, the cation-radicals in the ferrocyanide must interact with each other slightly more strongly than those in the perchlorate; otherwise, the situations in these two substances seem to be very much alike.

Würster's Blue Iodide (Fig. 3, Curves a and b). Judging from the spectrum and the susceptibility (as high as $+1004\times10^{-6}$ emu/mol at 289°K),[2] the high-susceptibility form is similar to the perchlorate and ferrocyanide discussed above. The charge-transfer band at 11.4 kK and the band at 25.8 kK are very much intensified in the low-susceptibility form, for which a value of $+51\times10^{-6}$ emu/mol at 289°K has been found by Hughes and Hush.[2] On the other hand, the α-band at 16.4 kK and the γ-band at 30.6 kK almost disappear. This feature is the one expected for the dimer spectrum.[16] Therefore, it is likely that the cation-radicals pair up strongly in the low-susceptibility form. However, the possibility that the sample for the high-susceptibility form is contaminated with a small amount of the low-susceptibility form, or *vice versa*, can not be excluded.

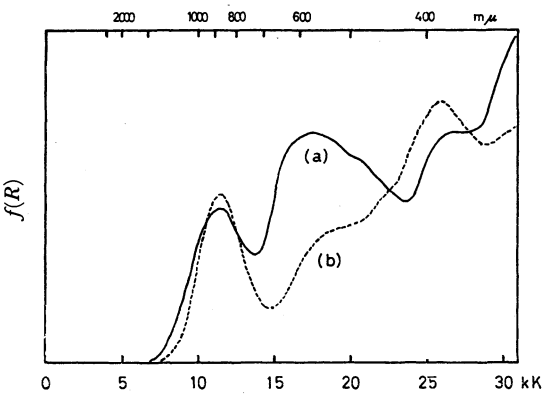

Fig. 3. Diffuse reflection spectrum of Würster's blue iodide, high-susceptibility form (curve a) and low-susceptibility form (curve b).

Mizuno *et al.* have studied the crystal structure of a dark-green Würster's blue bromide recrystallized from methanol.[15] The perpendicular separation between the molecular planes has been found to be as great as 3.515 Å. It is interesting to note that the spectrum reported by them is similar to that of the high-susceptibility form of the iodide.

Benzidine Bromide (Fig. 4, Curve a). The monomer spectrum comprises bands at 11.6 and 13.1, and shoulder at 14.3, and a strong band with some vibrational structures around 21.6 kK, while at low temperatures these absorptions are diminished and new bands appear at 12.4, 16.4, and 27.8 kK.[18] They have been assigned to the dimer. Unfortunately, the lower-energy region, in which we are most interested, could not be examined because of absorption due to the solvent. Consequently, there are not enough data for comparison and we cannot choose between a pair-by-pair and a more-than-by-pairs charge-transfer interaction as the cause of the absorption at 6.7 kK in the solid-state spectrum. The salt is known to be diamagnetic (-123×10^{-6} emu/mol);[2] therefore, the interaction is certainly strong.

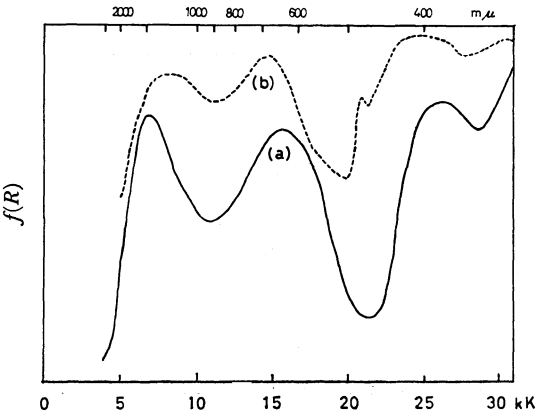

Fig. 4. Diffuse reflection spectra of benzidine bromide (curve a) and *N,N,N',N'*-tetramethylbenzidine bromide (curve b).

***N,N,N',N'*-Tetramethylbenzidine Bromide (Fig. 4, Curve b).** The solution study by Takemoto *et al.*, although valuable as an example of monomer-dimer equilibrium, does not provide us with a complete dimer spectrum for comparison.[19] The solid-state spectrum is very much like that of the afore-mentioned benzidine bromide except for the shift of the low-energy absorption to 8.0 kK. The salt has a susceptibility of -173×10^{-6} emu/mol.[2]

General Remarks. Summarizing the above-mentioned results, we may note that the Würster salts can tentatively be classified into the following three groups:

(I) The paramagnetic Würster's red ferrocyanide and the low-susceptibility form of Würster's blue iodide are in this group. The solid-state spectrum has a strong low-energy absorption near the place where the charge-transfer band is located in the solution's dimer spectrum. The intermolecular interaction seems to be predominantly pair-by-pair. A possible candidate for this group is the monoclinic form of Würster's blue perchlorate provided that the measurements are made well

18) H. Matsusaka and K. Suzuki, Paper presented at the 19th Annual Meeting of the Chemical Society of Japan, Tokyo, April, 1966.
19) K. Takemoto, H. Matsusaka, S. Nakayama, K. Suzuki and Y. Ooshika, This Bulletin, **41**, 764 (1968).

below the transition temperature. The diamagnetic benzidine and tetramethylbenzidine bromides may be classified into this group or the third group.

(II) The group is represented by Würster's blue perchlorate, ferrocyanide, and iodide (the high-susceptibility form). All of them are highly paramagnetic, containing over 80% free radicals. In addition to a strong absorption corresponding to the α-band in the monomer spectrum, a relatively weak low-energy absorption, almost corresponding to the charge-transfer band in the dimer spectrum, is observed in the solid-state spectrum. The intermolecular interaction is supposed to be perfectly symmetric, but so weak that the absorption process is confined to a region no wider than a single pair.

(III) The *p*-phenylenediamine and Würster's red bromides belong to this group; both are diamagnetic. The solid-state spectrum bears no resemblance to either the monomer or dimer spectrum and extends to a lower-energy region. A strong, more-than-by-pairs interaction is expected to cause such behavior.

Now we have to say a few words why we took only the extremes into consideration for the more-than-by-pairs interaction. The intermediate case may be observed only when the temperature of the measurement is comparable with the interaction. This condition may be fulfilled by Würster's blue perchlorate near the transition temperature. However, carrying out the measurements at room temperature, we can scarcely ever meet with such an intermediate case.

Discussing paramagnetic excitons in solid free radicals, McConnell and Lynden-Bell have speculated that, as linear chains of $S=1/2$ atoms or molecules are unstable with respect to distortions that produce an alternation in the distances between the interacting units, one individual radical can interact equally strongly with two others only at temperatures large compared to the exchange interaction.[20] The Würster salts in the second group apparently fit this speculation; however, we must remark that the very presence of a third group violates their speculation.

The mode of interaction depends naturally on the stacking of the cation-radicals, which is in turn affected not only by the size and shape of the cation itself, but also by those of the counter ion. Understandably, methyl substitution on the cation and a counter ion as bulky as ferrocyanide are unfavorable factors for a strong intermolecular interaction.

The authors wish to express their thanks to Mr. Nobuhiko Miyajima for his technical assistance throughout the course of this work.

20) H. M. McConnell and R. Lynden-Bell, *J. Chem. Phys.*, **36**, 2393 (1962).

BULLETIN OF THE CHEMICAL SOCIETY OF JAPAN VOL. 41 2619—2623 (1968)

β-Diketonates of a Few Lanthanide Elements

M. HASAN, K. KUMAR, S. DUBEY and S. N. MISRA*[1]

Chemical Laboratories, University of Jodhpur, Jodhpur, India

(Received September 11, 1967)

The reactions of isopropoxide of praseodymium and neodymium with benzoylacetone, dibenzoylmethane have been studied and the derivatives of the type $M(O\text{-}iPr)_2(lig.)$, $M(O\text{-}iPr)(lig.)_2$ and $M(lig.)_3$ (where lig.=benzoylacetone or dibenzoylmethane) have been isolated. The isopropoxide-diketonates on treatment with tertiary butanol interchange their isopropoxide group with tertiary butoxide group. Anhydrous acetylacetonates of lanthanum, praseodymium, neodymium and samarium have been prepared from the reactions of the alcoholic solution of the chlorides with alcoholic solution of ammonium acetylacetonates. The molecular weights of these β-diketonates and alkoxides β-diketonates have been measured ebullioscopically in boiling benzene.

In recent years there has been considerable interest in the preparation and properties of metal acetylacetonate derivatives. An extensive study of literature reveals that an appreciable amount

of work has been done on the acetylacetonates of lanthanide elements.[1-9]

In almost all the methods, the reactions were carried out in an aqueous medium (hydrated organic solvents were also employed), by taking hydrated metal chloride and the mono- and trihydrated acetylacetonates were isolated.

Recently the anhydrous acetylacetonates and alkoxide acetylacetonates of praseodymium and neodymium[10] have been synthesised from the reactions of their isopropoxides with acetylacetone in different stoichiometric ratios in benzene: The raction mechanism appears most probably of S_N2 type:

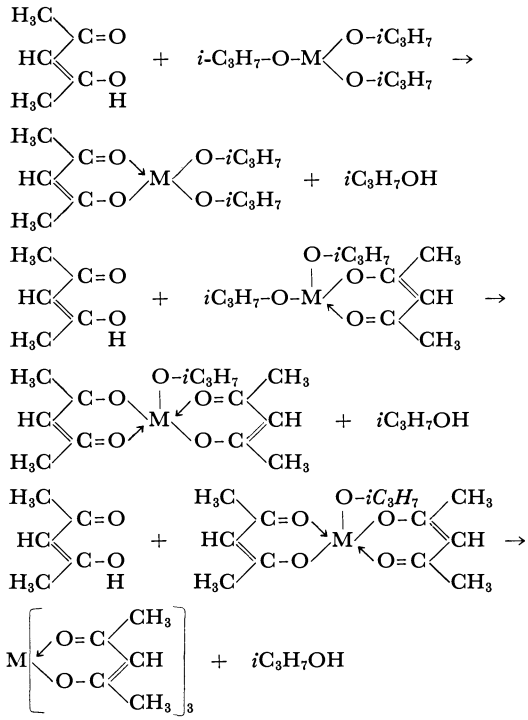

In view of the above, it was considered of interest to study the reactions of praseodymium and neodymium isopropoxides with benzoylacetone and dibenzoylmethane in benzene.

All these derivatives are coloured microcrystalline solids, soluble in benzene and ethanol from which the pure samples could be crystallised.

The alkoxide β-diketonates interchange their isopropoxide group with tertiary butoxide group, when refluxed with tertiary butanol in benzene, isopropanol produced in the reaction was fractionated out azeotropically with benzene:

$$M(O\text{-}iC_3H_7)_2L + 2tC_4H_9OH = M(\text{-}O\text{-}tC_4H_9)_2L + 2iC_3H_7OH$$

$$M(O\text{-}iC_3H_7)L_2 + tC_4H_9OH = M(\text{-}O\text{-}tC_4H_9)L_2 + iC_3H_7OH$$

The synthesis of anhydrous acetylacetonates of lanthanum, praseodymium, neodymium and samarium has been followed by another route. Ammonium acetylacetonate (prepared by passing a controlled slow current of ammonia through the solution of acetylacetone in benzene when a crystalline solid separated out; it was filtered) was dissolved in ethanol and this solution was added to the alcoholic solution of metal chloride, when a white precipitate of ammonium chloride separated out leaving clear liquor. The product was obtained after evaporating off the solvent under reduced pressure. The product was recrystallized from refluxing benzene and thus could be obtained in a high grade of purity.

The molecular weight determination of the di-isopropoxide monoligand derivative showed that the molecule is a trimer and thus can be represented-most probably by the following structure:

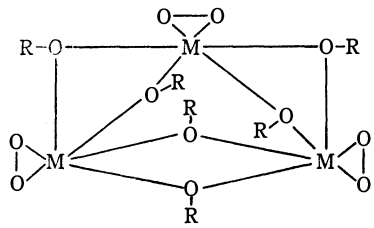

Where we have three metal octahedra with two edges in common. In this structure the coordination number of the metal appears to be six.

The mono alkoxide diligand derivative has been found to be dimeric and thus can be represented by the following structure:

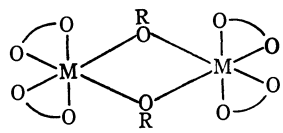

Where two metal octahedra are bridged through alkoxide oxygen bridges.

The triligand derivative has been found to be dimeric and thus the following structure appear to be a probable one:

---

*1 Present address: University of Washington, Seattle, U.S.A.

1) G. Janstch and E. Meyer, *Ber.*, **53B**, 1577 (1920).
2) S. Freed, S. I. Weissman and F. E. Fortess, *J. Am. Chem. Soc.*, **63**, 1079 (1941).
3) J. K. Marsh, *J. Chem. Soc.*, **1947**, 1084.
4) J. G. Stites, C. N. Mc. Carty and L. L. Quill, *J. Am. Chem. Soc.*, **70**, 3140 (1949).
5) T. Moeller and W. F. Ulrich, *J. Inorg. Nucl. Chem.*, **2**, 164 (1956).
6) N. K. Dutt and P. Bandyopadhyay, *Science and Culture*, **23**, 105 (1957); **23**, 690 (1957); **23**, 365 (1957); **24**, 38 (1958); **27**, 403 (1961).
7) J. F. Steinbach and J. H. Burne, *J. Am. Chem. Soc.*, **80**, 183 (1958).
8) T. Moeller, E. Gulyas and R. H. Marshall, *J. Inorg. Nucl. Chem.*, **9**, 82 (1959).
9) G. W. Pope, J. F. Steinabach and W. F. Wagner, *ibid.*, **20**, 304 (1961).
10) S. N. Misra, T. N. Misra and R. C. Mehrotra, *Indian J. Chem.*, **3**, 525 (1965).

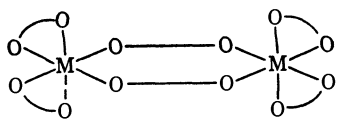

Where two metal octahedra are bridged through oxygen atoms of ligand molecule. The probability of following structure, however, could not be ruled out:

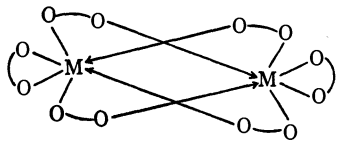

Where the oxygen atoms of ligands are donating electrons to empty d_π orbital of the metal.

Experimental

Glass apparatus with interchangeable joints was used. Anhydrous lanthanum, praseodymium, neodymium and samarium chlorides were prepared as described in earlier publications.[11] Pure lanthanum, praseodymium and neodymium isopropoxides were prepared by sodium alkoxide method already reported[12]; solvents dried as described in earlier communication.[11]

Molecular Weights. The molecular weights of these derivatives were determined ebullioscopically by semi-micro gallenkemp ebulliometer using thermistor sensing in refluxing benzene. The experimental

TABLE 1. REACTIONS OF ISOPROPOXIDES OF NEODYMIUM AND PRASEODYMIUM WITH BENZOYLACETONE AND DIBENZOYLMETHANE IN DIFFERENT RATIO

Reaction mixture in g.	Molar ratio	Formula, yield (g) and nature of the product	Analysis % Found		Analysis % Calculated	
			Metal	Isopropoxy	Metal	Isopropoxy
Praseodymium isopropoxide 1.132 Benzoylacetone 0.561 Benzene 86.0	1 : 1	Pr $(O\text{-}iC_3H_7)_2(O_2C_{10}H_9)$ Green crystalline solid 1.48	33.29	28.08	33.53	28.11
Neodymium isopropoxide 1.137 Benzoylacetone 0.563 Benzene 83.00	1 : 1	$Nd(O\text{-}iC_3H_7)_2(O_2C_{10}H_9)$ Pink microcrystalline solid 1.50	34.00	27.68	34.05	27.089
Praseodymium isopropoxide 1.087 Benzoylacetone 1.091 Benzene 78.00	1 : 2	$Pr(O\text{-}iC_3H_7)(O_2C_{10}H_9)_2$ Green crystalline solid 1.78	26.88	11.29	26.97	11.31
Neodymium isopropoxide 1.113 Benzoylacetone 1.119 Benzene 79.00	1 : 2	$Nd(O\text{-}iC_3H_7)(O_2C_{10}H_9)_2$ Pink microcrystalline solid 1.84	27.38	11.20	27.44	11.24
Praseodymium isopropoxide 1.321 Benzoylacetone 1.893 Benzene 76.00	1 : 3	$Pr(O_2C_{10}H_9)_3$ Green crystalline solid 2.50	22.42	—	22.54	—
Neodymium isopropoxide 1.001 Benzoylacetone 1.50 Benzene 75.00	1 : 3	$Nd(O_2C_{10}H_9)_3$ Pink microcrystalline solid 2.00	22.88	—	22.98	—
Praseodymium isopropoxide 1.002 Dibenzoylmethane 0.704 Benzene 76.00	1 : 1	$Pr(O\text{-}iC_3H_7)_2(O_2C_{15}H_{11})$ green crystalline solid 1.50	29.10	24.38	29.33	24.49
Neodymium isopropoxide 1.163 Dibenzoylmethane 0.811 Benzene 78.00	1 : 1	$Nd(O\text{-}iC_3H_7)_2(O_2C_{15}H_{11})$ Pink crystalline solid 1.65	29.60	23.96	29.70	24.03
Praseodymium isopropoxide 1.012 Dibenzoylmethane 1.401 Benzene 78.00	1 : 2	$Pr(O\text{-}iC_3H_7)(O_2C_{15}H_{11})_2$ Green crystalline solid 2.61	21.63	9.10	21.79	9.12
Neodymium isopropoxide 1.003 Dibenzoylmethane 1.387 Benzene 81.00	1 : 2	$Nd(O\text{-}iC_3H_7)(O_2C_{15}H_{11})_2$ Pink crystalline solid 2.00	22.06	9.00	22.16	9.07
Praseodymium isopropoxide 1.112 Dibenzoylmethane 2.368 Benzene 80.00	1 : 3	$Pr(O_2C_{15}H_{11})_3$ green crystalline solid 2.80	17.29	—	17.36	—
Neodymium isopropoxide 0.879 Dibenzoylmethane 1.85 Benzene 83.0	1 : 3	$Nd(O_2C_{15}H_{11})_3$ pink crystalline solid	17.52	—	17.72	—

11) S. N. Misra, T. N. Misra and R. C. Mehrotra, *J. Inorg. Nucl. Chem.*, **27**, 105 (1965); *J. Indian Chem. Soc.*, **42**, 351 (1965).

12) S. N. Misra, T. N. Misra, R. N. Kapoor and R. C. Mehrotra, *Chem. & Ind.*, **1963**, 120.

Table 2. Alcohol-interchange with *t*-butanol

Compound taken in g	*t*-Butanol in g	Formula, nature and yield (g) of the product	Analysis of the metal		Isopropanol in azeotrope	
			Found %	Calcd %	Found (g)	Calcd (g)
$Pr(O\text{-}iC_3H_7)_2(O_2C_{10}H_9)$ 1.05	5.7	$Pr(O\text{-}tC_4H_9)_2(O_2C_{10}H_9)$ green crystalline solid, sparingly soluble in benzene but dissloves in refluxing ethanol. (1.09)	31.50	31.65	0.28	0.30
$Nd(O\text{-}iC_3H_7)_2(O_2C_{10}H_9)$ 1.00	6.3	$Nd(O\text{-}tC_4H_9)_2(O_2C_{10}H_9)_2$ Pink microcrystalline solid, sparingly soluble in benzene but dissolves in refluxing ethanol (1.03).	31.87	31.39	0.29	0.30
$Pr(O\text{-}iC_3H_7)(O_2C_{10}H_9)_2$ 1.30	5.9	$Pr(O\text{-}tC_4H_9)(O_2C_{10}H_9)_2$ Green solid, sparingly soluble in benzene but dissolves in refluxing ethanol (1.31).	26.28	26.28	0.15	0.15
$Nd(O\text{-}iC_3H_7)(O_2C_{10}H_9)_2$ 1.06	6.7	$Nd(O\text{-}tC_4H_9)(O_2C_{10}H_9)_2$ Pink solid, sparingly soluble in benzene but dissolves in refluxing ethanol (1.07).	26.58	26.72	0.13	0.14
$Pr(O\text{-}iC_3H_7)_2(O_2C_{15}H_{11})$ 0.98	6.8	$Pr(O\text{-}tC_4H_9)_2(O_2C_{15}H_{11})$ Green solid, sparingly soluble in benzene but dissolves in ethanol (0.98).	27.50	27.61	0.23	0.24
$Nd(O\text{-}iC_3H_7)_2(O_2C_{15}H_{11})$ 1.12	7.5	$Nd(O\text{-}tC_4H_9)_2(O_2C_{15}H_{11})$ Pink solid, sparingly soluble in benzene but dissolves in ethanol (1.14).	27.98	28.08	0.27	0.28
$Pr(O\text{-}iC_3H_7)(O_2C_{15}H_{11})_2$ 1.63	5.0	$Pr(O\text{-}tC_4H_9)(O_2C_{15}H_{11})_2$ Green solid, sparingly soluble in benzene but dissolves in refluxing ethanol (1.65).	21.20	21.33	0.14	0.15
$Nd(O\text{-}iC_3H_7)(O_2C_{15}H_{11})_2$ 1.78	4.7	$Nd(O\text{-}tC_4H_9)(O_2C_{15}CH_{11})_2$ Pink solid, sparingly soluble in benzene but dissolves in refluxing ethanol (1.81).	21.58	21.73	0.15	0.16

technique was the same as described in our earlier communication.[13]

Analytical Methods. Praseodymium was estimated as oxinate while lanthanum, neodymium and samarium were estimated by precipitating them as oxalate followed by the ignition to corresponding oxide. The isopropanol content of benzene-isopropanol azeotrope was determined by an oxidimetric method.[14]

Reaction between Praseodymium Isopropoxide and Benzoylacetone (Molar Ratio 1 : 3) in Benzene. The mixture of praseodymium isopropoxide (1.32 g) benzoylacetone (2.01 g) and benzene (84 g) was shaken thoroughly when a clear green solution was obtained. The reaction mixture was refluxed and the liberated isopropanol was fractionated out azeotropically with benzene. The product was obtained after distilling off excess solvent under reduced pressure.

13) S. N. Misra, T. N. Misra and R. C. Mehrotra, *J. Inorg. Nucl. Chem.*, **25**, 195 (1963); **25**, 201 (1963).
14) D. C. Bradley and W. Wardlaw, *J. Chem. Soc.*, **1950**, 3450.

Reaction of Praseodymium Di-isopropoxide Mono-benzoylacetonate with *t*-Butanol in Benzene. Praseodymium di-isopropoxide monobenzoylacetonate (1.43 g) benzene (83 g) and tertiary butanol (2.43 g) were refluxed under the column. After the removal of binary azeotrope (benzene - isopropanol), excess solvent was distilled out under reduced pressure and at the room temperature leaving a green micro-crystalline solid (Yield 1.56 g).

For brevity the reaction of isopropoxides of praseodymium and neodymium with benzoylacetone and dibenzoylmethane are summarised in Table 1, and those from the reaction between above derivatives and tertiary-butanol and summarised in Table 2.

Anhydrous Acetylacetonates of Lanthanum, Praseodymium Neodymium and Samarium. *a) Preparation of Ammonium Acetylacetonate.* Acetylacetone (18.3 g) was dissolved in benzene (150 g) and a current of anhydrous ammonia was slowly passed through the solution. The reaction was exothermic and a white crystalline solid separated out from the solvent. The completion of the reaction was indicated by cooling of

TABLE 3.

Reaction mixture in g		Nature of the product	Analysis % Metal Found	Analysis % Metal Calcd
Lanthanum chloride	2.47	$La(O_2C_5H_7)_3$, light yellow crystalline solid, soluble in refluxing ethanol but sparingly soluble in benzene.	31.90	31.84
in ethanol	57.00			
Amm. acetylacetonate	3.41			
Acetylacetone	10.0			
in ethanol	150.0			
Praseodymium chloride	2.03	$Pr(O_2C_5H_7)_3$ Green crystalline solid, soluble in refluxing ethanol but sparingly soluble in benzene.	32.0	32.15
in ethanol	54.0			
Amm. acetylacetonate	2.80			
Acetylacetone in	10.0			
ethanol	100.0			
Neodymium chloride	2.18	$Nd(O_2C_5H_7)_3$ Pink crystalline solid, soluble in refluxing ethanol but sparingly soluble in benzene.	32.48	32.67
in ethanol	60.0			
Amm. acetylacetonate	3.14			
Acetylacetonate in	10.0			
ethanol	153.0			
Samarium chloride	2.00	$Sm(O_2C_5H_7)_3$	33.36	33.59
in ethanol	60.0			
Amm. acetylacetonate	2.70	Yellow crystalline solid, soluble in refluxing ethanol but insoluble in benzene.		
acetylacetone	10.0			
in ethanol	190.0			

the reaction mixture. It was filtered, washed thoroughly with benzene and dried under reduced pressure (Yield 19.0 g).

b) Preparation of Lanthanum Triacetylacetonate. Lanthanum chloride (2.47 g) was dissolved in ethanol (87 g) when a clear solution was obtained. Ammonium acetylacetonate (3.41 g) taken in ethanol (89 g) containing 10.0 g of acetylacetone, was added to alcoholic lanthanum chloride solution when a white solid separated out. Excess acetylacetone most probably checks the alcoholysis of the product. On evaporating off the excess solvent a faint yellow crystalline solid sparingly soluble in benzene but soluble in refluxing ethanol and benzene was obtained (Yield 4.09 g).

The preparation of the anhydrous acetylacetonates of lanthanum, praseodymium, neodymium and samarium is summarised in Table 3.

The authors wish to express their deep gratitude to Professor R. C. Mehrotra for his valuable suggestions. They are also thankful to Professor R. C. Kapoor, Head of the Department of Chemistry, University of Jodhpur, Jodhpur, and Professor A. B. Sen, Head of the Department of Chemistry, University of Lucknow, Lucknow, for providing research facilities and encouragement throughout the work. They thankfully acknowledge the helpful criticism of Drs. C. S. Pande and R. C. Agarwal of Chemistry Department, Lucknow University, Lucknow. One of us (K. K.) is grateful to the Ministry of Education, Government of India for providing research scholarship.

BULLETIN OF THE CHEMICAL SOCIETY OF JAPAN VOL. 41 2624—2627 (1968)

Synthesis of Copper(II) Complexes with Maleic Acid[1]*

Kazuo GORA, Eishin KYUNO and Ryokichi TSUCHIYA

Department of Chemistry, Faculty of Science, Kanazawa University, Kanazawa

(Received July 12, 1967)

Three copper(II) complexes with maleic acid, [Cu mal(H_2O)] (I) (mal=$C_2H_2(COO)_2$), [Cu(Hmal)$_2$(H_2O)$_4$] (II) and [Cu_2(Hmal)$_4$]·H_2mal·4EtOH (III) (EtOH=C_2H_5OH), were synthesized. Compound I was prepared from an aqueous solution of copper(II) sulfate pentahydrate and sodium hydrogenmaleate at room temperature as fine blue crystals. Compound II was prepared by adding little by little copper(II) hydroxide or copper(II) hydroxycarbonate to an aqueous solution of maleic acid at a temperature below 0°C in an ice-salt bath, obtaining light-blue powdered crystals. Compound III was prepared by heating a mixed alcoholic solution of maleic acid anhydride, copper(II) sulfate pentahydrate and sodium carbonate anhydride (3 : 1 : 1) in a flask with a reflux condenser for two hours. Fine bluish-green crystals were obtained. By using copper(II) hydroxide instead of copper(II) sulfate in the above preparation, a better yield can be obtained. The effective magnetic moments of I and II were 2.00 B. M. (20°C) and 1.97 B. M. (20°C), respectively, which are relatively close to the spin-only value of the divalent copper ion. On the other hand, the magnetic moment of III was subnormal, being 1.12 B. M. (18°C). The reflection spectrum of III gave a shoulder near 370 mμ, which is specific to green copper complexes. The product (IV) obtained by the thermal decomposition of I at 220°C and the product (V) obtained from II at 160°C, which are presumed to have the chemical formula [Cu-mal(H_2O)$_{0.1}$] and [Cu(Hmal)(mal)$_{1/2}$], respectively, gave normal magnetic moments, 1.91 and 1.89 B. M. (20°C). However, product (VI), obtained by expelling the alcohol from III had a magnetic moment of 1.31 B. M. (17°C). Different from the corresponding copper(II) phthalate complexes, no green copper complexes having subnormal magnetic moments could be obtained through dehydration of the blue maleate complex I or the light-blue complex II having normal magnetic moments.

Maleate anions coordinate to metal ions as seven-membered chelate ligands in the same way as succinate and phthalate anions. The fact that the copper(II) succinate complex has a subnormal effective magnetic moment, 1.40 B. M., has already been reported by Kubo *et al.*[1]

The copper(II) complexes with phthalic acid have been prepared and discussed for dimer or monomer structures with respect to two copper atoms in an earlier paper.[2] It was found by the authors that, in an aqueous solution at low temperature below 79°C, monomer phthalate complexes were produced preferably, whereas the dimer began to crystallize at temperatures above 79°C. On the basis of these results, it is assumed that the tendency of hydration of copper(II) ion in an aqueous solution would decrease steadily as the temperature is elevated. Instead of the use of an aqueous medium, some suitable organic solvents have been known to be effective for the preparation of several complexes having subnormal magnetic moments.[3,4]

Although the properties of the copper(II) complexes with maleic acid are partly known,[5] further investigation has not progressed. The present study is an attempt to prepare new copper(II) complexes with maleic acid in different media and to discuss their properties.

In the case of copper(II) phthalate complexes, a green complex having a dimer structure with respect to two copper atoms was obtained by the thermal decomposition of the blue and light-blue complexes. This was ascertained through reflection spectra and X-ray diffraction measurements carried out in an earlier paper.[2]

Despite great interest in the color and structural changes which take place in the thermal decomposition process of copper(II) phthalate complexes as above, such a study has rarely been made for other copper(II) complexes. A further purpose of this study is to find whether or not green copper maleate complex can be obtained through thermal

*1 Read at the 20th Annual Meeting of the Chemical Society of Japan, Tokyo, April, 1967.

1) O. Asai, M. Kishita and M. Kubo, *J. Phys. Chem.*, **63**, 96 (1959).

2) I. Shimizu, R. Tsuchiya and E. Kyuno, This Bulletin, **40**, 1162 (1967).

3) M. Bobtelsky and I. Bargadda, *Bull. Soc. Chim. France*, **1953**, 276, 687.

4) C. V. Souvray, *Compt. rend.*, **233**, 164 (1951).

5) S. U. Pickering, *J. Chem. Soc.*, **101**, 174 (1911).

decomposition of the blue or light-blue complex in the similar way as in the thermal preparation of the corresponding green copper(II) phthalate complexes described in an earlier paper.[2]

Experimental

Syntheses. *Maleatoaquocopper(II)*, [Cu mal(H_2O)] (I). A solution of copper(II) sulfate pentahydrate (25 g; 0.1mol) in 100m*l* of water was mixed with a solution containing maleic acid (20g; 0.2mol) and sodium carbonate (11g; 0.1mol) in 2000m*l* of water. On allowing the mixed solution to stand for a while at room temperature, fine blue crystals precipitated out. After filtration, the precipitate was washed with a small amount of water, ethanol and ether in that order and then dried in a silicagel desiccator. The results of chemical and thermal analyses were: Found: Cu, 32.54; C, 24.58; H, 1.96%. Calcd for $[Cu(C_4H_2O_4)(H_2O)]$: Cu, 32.48; C, 24.56; H, 2.06%.

Bis(hydrogenmaleato)tetraaquocopper(II), $[Cu(Hmal)_2 \cdot (H_2O)_4]$ (II). When copper(II) hydroxycarbonate (12 g; 0.05mol) or copper(II) hydroxide (9.8g; 0.1mol) was added little by little to 300m*l* of an ice-cold aqueous solution containing maleic acid (20g; 0.2mol), a light-blue powder was obtained. It was washed several times with a mixture of ethanol and water (1 : 2), ethanol and ether and then air-dried. Found: Cu, 17.63; C, 26.96; H, 3.93%. Calcd for $[Cu(C_4H_3O_4)_2(H_2O)_4]$: Cu, 17.37; C, 26.28; H, 3.86%.

Tetra(hydrogenmaleato)dicopper(II) Maleate Tetraalcoholate $[Cu_2(Hmal)_4] \cdot H_2mal \cdot 4EtOH$ (III). By refluxing a mixed solution of maleic acid anhydride (30g; 0.3mol), copper(II) sulfate pentahydrate (25g; 0.1mol) and sodium carbonate (11g; 0.1mol) in alcohol (300m*l*) for two hours, a green solutuon was obtained. On allowing the solution to stand for a while at room temperature, green powdered crystals precipitated out. Through recystallization with a saturated ethanol solution, fine green crystals were obtained with a good yield. They were washed with a mixture of ethanol and water (1 : 2), ethanol and ether in a similar way as described above and air-dried. Found: Cu, 14.46; C, 38.28; H, 4.77%. Calcd for $[Cu_2(C_4H_3O_4)_4] \cdot (C_4H_4O_4) \cdot 4C_2H_5OH$: Cu, 14.31; C, 37.88; H, 4.54%.

Thermal Decomposition Product (IV) from I. When complex I was heated to 220°C, a violet compound was obtained. It was thought to have the formula [Cu mal$(H_2O)_{0.1}$] after thermogravimetric (TG) analysis.

Thermal Decomposition Product (V) from II. Complex II was also heated at 160°C in the similar way as described above. The resulting blue powder was assigned to $[Cu(Hmal)(mal)_{1/2}]$ on the basis of its TG analysis. This formula was also confirmed through elementary analysis: Found: Cu, 27.17; C, 31.16; H, 1.69%. Calcd for $[Cu(C_4H_3O_4)(C_4H_2O_4)_{1/2}]$: Cu, 26.96; C, 30.58; H, 1.71%.

Thermal Decomposition Product (VI) from III. Complex III was heated at 100°C in the same way. After TG analysis, the resulting compound was thought to corresponding to $[Cu_2(Hmal)_4] \cdot H_2mal$. It was also confirmed by an analysis of the copper content. Found: Cu, 17.95%. Calcd for $[Cu_2(C_4H_3O_4)_4] \cdot (C_4H_4O_4)$: Cu, 18.07%.

Measurements. Thermal analysis was carried out with a Shimadzu Thermano Balance. Magnetic susceptibilities were measured by the Gouy method using powdered sample at room temperature. The measurements of visible and UV absorption spctra were carried out in an ethanol solution with a Hitachi EPU-2A Spectrophotometer; reflection spectra of finely powdered solid samples were obtained with the same spectrophotometer equipped with a standard Hitachi reflection attachment. With a Nippon-Bunko DS-301 IR Spectrometer, the IR spectra of these complexes were measured in a Nujol or HCB mull state and in a KBr disk. The X-ray diffraction patterns were obtained with a Rigaku-Denki Geiger-flex X-ray Analyzer.

Results and Discussion

Conditions for the Formation of These Copper(II) Maleate Complexes. Complex I was obtained at room temperature, but complex II was prepared at a lower temperature in an ice-salt bath. However, II was sometimes contaminated with a small amount of I even at the low temperature when copper(II) salt was added in relatively larger amounts at a time. The use of copper(II) hydroxide instead of copper(II) hydroxycarbonate, in general, led to rather good yields.

Complex III could not be obtained in a medium consisting of ethanol and water (1 : 1), but was obtained only refluxing an alcoholic solution of the materials required for preparation. On the other hand, I was formed preferably in aqueous media at approximately 100°C and III was transformed to I in the presence of water. These results suggest that the existence of water obstructs the formation of III.

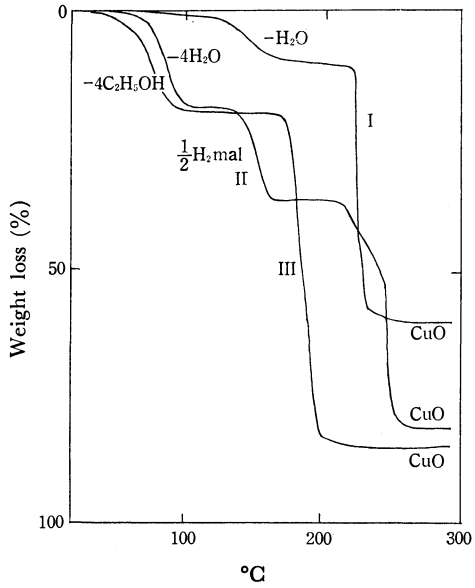

Fig. 1. TG curves for copper(II) maleate complexes.
I $[Cu\ mal(H_2O)]$
II $[Cu(Hmal)_2(H_2O)_4]$
III $[Cu_2(Hmal)_4] \cdot (H_2mal) \cdot 4EtOH$

Thermal Decomposition. Figure 1 shows the TG curves for complexes I, II and III. The thermal decomposition processes in these complexes are expressed as follows:

$$\mathrm{I} \xrightarrow{220^\circ\mathrm{C}} [\mathrm{Cu\ mal}(\mathrm{H_2O})_{0.1}] \xrightarrow{235^\circ\mathrm{C}} \text{decompose}$$

$$\mathrm{II} \xrightarrow{100^\circ\mathrm{C}} [\mathrm{Cu(Hmal)_2}] \xrightarrow{160^\circ\mathrm{C}} [\mathrm{Cu(Hmal)(ma)_{1/2}}] \xrightarrow{260^\circ\mathrm{C}} \text{decompose}$$

$$\mathrm{III} \xrightarrow{100^\circ\mathrm{C}} [\mathrm{Cu_2(Hmal)_4}]\cdot\mathrm{H_2mal} \xrightarrow{200^\circ\mathrm{C}} \text{decompose}$$

The complexes I and II have already been prepared by Pickering,[5] who, however, found the composition of the complex to be $[\mathrm{Cu(Hmal)_2}]\cdot 8\mathrm{H_2O}$, which loses four hydrated water molecules upon heating at 100°C and then loses the remaining four water molecules at 170°C, differing from complex II obtained by the present authors.

Although transformation from complex III to I in the presence of water easily took place as described above, the reverse reaction *via* thermal decomposition was not achieved, apart from the case of the corresponding phthalate complexes.[2]

Magnetic Susceptibility. The effective magnetic moments of these complexes evaluated from magnetic susceptibility measurements are given in Table 1. It is seen in the table that complexes I and II and their thermal decomposition products have normal magnetic moments of a spin-only value for divalent copper ion, exhibiting no specific interactions between two copper atoms, whereas both complex III and its thermal decomposition product possess a subnormal magnetic moment, probably due to a strong interaction between Cu(II)-Cu(II) atoms in a molecule.

Table 1. Magnetic moments, μ_{eff}, of copper(II) maleate complexes

Complex	μ_{eff} B.M. (°C)
I	2.00 (20)
II	1.97 (20)
III	1.12 (18)
IV	1.91 (20)
V	1.89 (20)
VI	1.31 (17)

IR Spectra. The wave numbers of the band assigned to C=O stretching and of the specific absorption band concerning the maleate ion in IR spectra are listed in Table 2. In complexes II and III and their thermal decomposition products both free and coordinated carboxyl groups are found to coexist from the appearance of two strong bands in the regions 1720—1700 and 1660—1620 cm^{-1} assigned to both groups, respectively, whereas in complex I and its thermal decomposition product only one broad band is found in the range of 1660—1620 cm^{-1}, showing that all carboxyl groups are coordinated to the central metal ion in the molecule.

Table 2. IR spectra of copper(II) maleate complexes (cm^{-1})

$\nu_{(COOH)}$ and $\nu_{(COOM)}$ are stretching vibration of free and coordinated COO group; δ, specific absorption band of maleate

Complex	$\nu_{(COOH)}$	$\nu_{(COOM)}$	$\delta_{(mal)}$
I	—	1665, 1620	854, 838
II	1700	1660	835
III	1715	1660—1620	863, 838, 822
IV	—	1660—1620	851, 832
V	1720	1650—1615	835, 825, 810
VI	1720	1650—1615	835, 825, 810

The fact that all the complexes show a specific band assigned to the maleate anion in the region 860—810 cm^{-1} confirms that the complex molecules hold maleate coordinated, not fumarate, in themselves.

Reflection Spectra. The reflection spectra of the complexes, I, II, III and IV are shown in Fig. 2. The absorption bands of I and II are found near $14.5\times10^3\ cm^{-1}$, whereas IV gives a new, relatively strong band near $17.0\times10^3\ cm^{-1}$ instead of the depression of the former band at $14.5\times10^3\ cm^{-1}$. This suggests that the new band can be assigned to the ligand field produced by maleate anion only coordinated to copper as a result of the liberation of coordinated water.

On the other hand, in complex III, there are two bands near 14.7 (d–d transition band) and at $27.0\times10^3\ cm^{-1}$, the latter band appearing at almost the same position as that observed in the

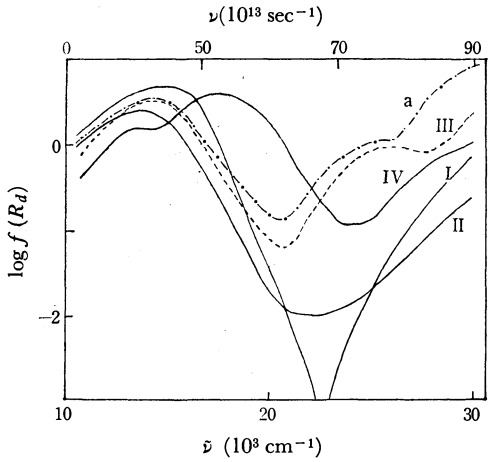

Fig. 2. Reflection spectra of copper(II) maleate complexes.
I $[\mathrm{Cu\ mal}(\mathrm{H_2O})]$
II $[\mathrm{Cu(Hmal)_2}(\mathrm{H_2O})_4]$
III $[\mathrm{Cu_2(Hmal)_4}]\cdot\mathrm{H_2mal}\cdot 4\mathrm{EtOH}$
IV $[\mathrm{Cu\ mal}(\mathrm{H_2O})_{0.1}]$
a, $[\mathrm{Cu_2ph_2}]$ (for reference)

green copper(II) phthalate complex as already described in an earlier paper,[2] which is also shown by (a) in Fig. 2 for reference.

X-Ray Powder Pattern Measurement. Complexes I, II and III give essentially different X-ray powder patterns showing that their structures are different. In the copper(II) phthalate complexes, the interesting fact that the green complex, which has a subnormal magnetic moment, is also produced by the thermal decomposition of the blue or lightblue complex was verified from X-ray powder diffraction patterns in an earlier paper.[2] However, in the copper(II) maleate complexes, such a phenomenon has never been observed. Information on crystal structure was found only for I, which is a hexagonal system with the axial parameters $a=8.10$ Å and $c=10.59$ Å, and of chemical units $Z=4$ with a density $\rho=2.16$.

BULLETIN OF THE CHEMICAL SOCIETY OF JAPAN VOL. 41 2627—2631 (1968)

The Separation of the Cerium-group Rare Earth Elements by Ion Exchange using a Citrate-acetate Mixed Solution as Eluting Agent*[1]

Muraji SHIBATA,*[2] Isao TANABE, Kinnosuke OKUDA and Kazuo KADOTA

Takaoka Factory, Azuma Kako Company, Noo-machi, Takaoka, Toyama

(Received August 3, 1967)

The separation of rare earth elements by ion exchange was studied. The new eluting agent consists of an aqueous solution of diammonium hydrogencitrate and an aqueous ammonia-acetic acid mixture; the two solutions were mixed in definite ratios. Using a column of Dowex 50 W resin, the separation of Sm, Nd, Pr, Ce and La was successfully achieved. As practical samples, mixed chlorides obtained from monazite concentrates were used. Both the purities and the yields of the recovered rare earths were greater than 99%. This eluting agent was applied to the separation of yttrium-group rare earths such as Dy, Er, Yb and Y, but the attempt was not successful.

During the past twenty years, a great number of papers have been published on the separation of rare earths by ion-exchangers. In the earlier papers, citric acid solution buffered with ammonia was widely used as eluting agent. Initially, 5% citrate at pH 2.5—3.0 was used, but this concentration was found costly in large scale operations.[1,2] Subsequently, 0.5% citrate at pH 3.9 was applied to pilot plant scale separations of the cerium-group rare earths.[3] Systematic studies on the effects of such variables as temperature, pH, size of resin particles and flow rate were also made with the same concentration of eluting agent.[4] Furthermore, certain workers used 0.1% citrate at pH 5.0—8.0 and found that the eluting agent was useful for macro separations of the cerium-group in kilogram quantities.[5] Shiokawa *et al.*[6-9] used 0.1% citric acid at pH 6.0 to separate cerium-group rare earths. Their experiments indicated yields of La, Pr, Nd and Sm at 96.2, 70.3, 90.0 and 77.2%, respectively.

A number of complexing agents beside citrate have also been used for analytical purposes. These are lactate, glycolate, malate, α-hydroxyisobutylate, *etc.* For commercial separation, aminopolycarboxylates such as ethylenediaminetetraacetate and nitrilotriacetate have now been used in conjunction with Cu(II)- or Zn(II)-resin retaining beds. Detailed reviews of such developments of ion exchange methods are described in a book edited by Spedding and Danne.[10]

*1 Presented at the 16th Annual Meeting of the Chemical Society of Japan, Tokyo, April, 1963.

*2 Department of Chemistry, Faculty of Science, Kanazawa University, Marunouchi, Kanazawa City.

1) F. H. Spedding, A. F. Voigt, E. M. Gladrow and N. R. Sleight, *J. Am. Chem. Soc.*, **69**, 2777 (1947).

2) F. H. Spedding, A. F. Voigt, E. M. Gladrow, J. E. Powell, J. M. Wright, T. A. Butler and P. Figard, *ibid.*, **69**, 2786 (1947).

3) F. H. Spedding, E. I. Fulmer, T. A. Butler, E. M. Gladrow, M. Gobush, P. E. Porter, J. E. Powell and J. M. Wright, *ibid.*, **69**, 2813 (1947).

4) F. H. Spedding, E. I. Fulmer, T. A. Butler and J. E. Powell, *ibid.*, **72**, 2349 (1950).

5) F. H. Spedding, E. I. Fulmer, J. E. Powell and T. A. Butler, *ibid.*, **72**, 2354 (1950).

6) J. Shiokawa, T. Inoko, M. Tanifuji and T. Ishino, *Denki Kagaku*, **32** 817 (1964).

7) J. Shiokawa, T. Doi, R. Shimano and T. Ishino, *ibid.*, **32**, 823 (1964).

8) J. Shiokawa, Y. Murakami and T. Ishino, *ibid.*, **32**, 897 (1964).

9) J. Shiokawa, T. Yonebayashi and T. Ishino, *ibid.*, **33**, 342 (1965).

10) F. H. Spedding and A. H. Danne, "The Rare Earths," John Wiley & Sons, New York (1961), pp. 55—73.

The present paper deals with a new eluting agent. The eluting agent consists of a mixed system of citrate and acetate solutions. The minor component, acetate, greatly affects the rapid and sharp separation of the cerium-group elements (La, Ce, Pr, Nd and Sm). Successful separations on an analytical scale were provided with practical samples from monazite concentrates.

Experimental

The Eluting Agent. Two hundred grams of citric acid monohydrate and 50 g of diammonium hydrogencitrate were dissolved in water and diluted to 4000 m*l*. Hereafter, this solution is called the "A" solution for convenience. On the other hand, aqueous ammonia (40 m*l* of 28% ammonia diluted to 160 m*l*) was mixed with aqueous acetic acid (100 m*l* of glacial acetic acid diluted to 300 m*l*). This solution is called the "B" solution. Both the "A" and "B" solutions were mixed in definite ratios and used as eluting agents.

The Samples. Stocks of rare earths of 99% or higher purity were available for La, Pr, Nd and Sm as oxides. These were weighed in amounts to produce 10 mg per m*l* of solution. The calculated amount of nitric acid necessary to dissolve the oxide and to produce a final excess of 0.1 M acid was added, and each stock solution was brought to a definite volume with water. For cerium stock solution, cerium(III) nitrate hexahydrate was used. These solutions were used individually or as mixtures for determining optimum conditions for the separation of cerium-group rare earths.

For practical separation of the cerium-group, concentrates from monazite sand were obtained from our company. The concentrates were mixed chloride hydrates of the cerium-group rare earths. Furthermore, mixed oxides prepared from the mixed chlorides were also available for analytical separation. Further details of these separations will be described for each experimental result.

Some of yttrium-group rare earths were used: Stock solutions of Dy, Er and Yb were made from their oxides and that of Y, from the nitrate.

General Procedure. A few preliminary experiments comparing Dowex 50 W X8 resin with Amberlite IR-120 indicated the former to be superior. Therefore, unless otherwise noted, the Dowex resin of 100—200 mesh was used. Prior to elution, the column was washed with the "B" solution and then regenerated to hydrogen-form with 2 N hydrochloric acid. After removing excess acid with water, a sample solution was introduced into the column, the column was again rinsed with water and then eluted with a mixture of the "A" and "B" solutions. Other conditions, such as column dimensions, resin-bed length, flow rate and composition of rare earths are given in each experimental result.

The rare earths were recovered from the eluate as oxalates by adding 5% oxalic acid. The oxalates were ignited to oxides for weighing. Fractions which seemed to be contaminated with adjacent elements were spectrophotometrically analyzed according to the method described by Spedding *et al.*[4] Sm was measured at 401 mμ, Nd at 740 mμ and Pr at 444 mμ. The values for the molar extinction coefficients of Sm, Nd and Pr at the above wavelengths were 3.09, 6.53 and 10.07, respectively. For portions which seemed to be recovered in pure states, characteristic absorption spectra were taken by means of a recording spectrophotometer over the visible range (350—700 mμ).

Results and Discussion

Optimum Composition of the Eluting Agent. In the beginning of the present work, it was found that the "B" solutions show much greater effects on the elution of the rare earth ions than the "A" solutions. When "A" solution was applied alone to a column ($\phi = 1.6$ cm, 10 g the Amberlite resin) which was charged with *ca.* 10 mg of Sm, the elution of Sm ranged from 300 to 700 m*l* of the eluate. In the case of "B" solution, the corresponding elution completed within 50 m*l* of the eluate. This fact suggested that mixing solutions "A" and "B" would be favorable. Then, a few experiments on the elution of Sm-Nd mixtures were made in order to find a suitable composition for the mixed solution. The results indicated that a solution consisting of one volume of "B" and forty volumes of "A" is effective. From this, a set of experiments was made to determine the optimum composition of the eluting agent for the separation of Sm, Nd and Pr. The parts of "A" to be mixed with one part of "B" were varied, maintaining other conditions constant. The results are shown in Figs. 1—3. It is clear from these figures that the best separation of Sm, Pr and Nd was achieved with an eluting agent having a 50 : 1 ("A" : "B") ratio by volume.

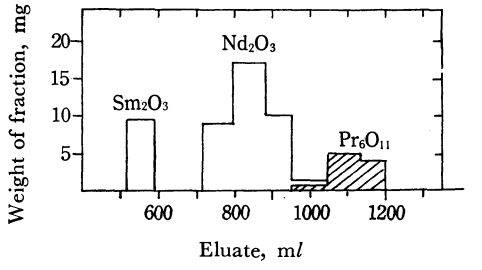

Fig. 1. Elution of Sm, Nd and Pr mixture with 40 : 1 eluting agent.
Weight of sample: Sm_2O_3 10 mg, Nd_2O_3 40 mg, Pr_6O_{11} 10 mg; column diameter 1.6 cm; resin height 19.3 cm (20 g); 1 fraction of eluate 20 m*l*.

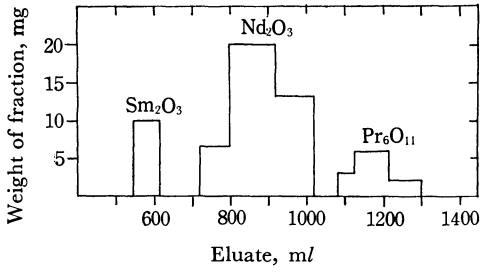

Fig. 2. Elution of Sm, Nd and Pr mixture with 45 : 1 eluting agent.
All the other conditions are the same as in Fig. 1.

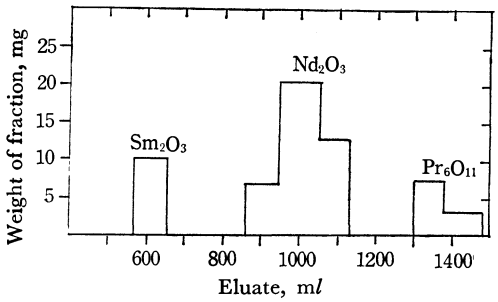

Fig. 3. Elution of Sm, Nd and Pr mixture with 50 : 1 eluting agent.
All the other conditions are the same as in Fig. 1.

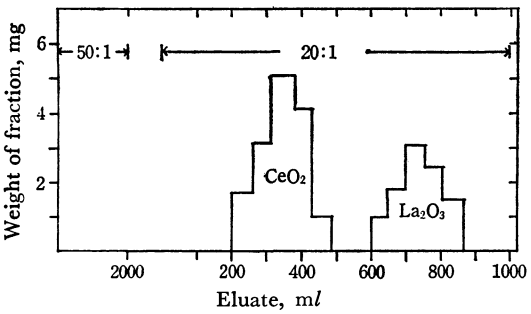

Fig. 4. Elution of Ce and La with 20 : 1 eluting agent.
Weight of sample: CeO_2 20 mg, La_2O_3 20 mg; The other conditions are the same as in Fig. 1.

Similar experiments were made with a mixture of Ce and La. When eluting agent consisting of a 50 : 1 ratio was applied, neither species of Ce nor La appeared in the eluate even when the eluate was 2000 ml. With decreasing the "A" component, each breakthrough volume of both elements was more and more reduced, and complete separation was obtained by using 20 : 1 eluting agent (Fig. 4).

The Elution of Mixed Chlorides of the Cerium-group Rare Earths. Conditions for this separation, based on the above results using Dowex 50W X8 (100—200 mesh), are;

Diameter of column: 2.2 cm
Height of bed: About 22.5 cm
Sample: Two kinds of $LnCl_3 \cdot nH_2O$ (Ln represents rare earths) were available and denoted as sample A and sample B for convenience; two grams of each sample was dissolved in 50 ml of 1 N HCl.
Flow rate: 0.7 cm/min.

The column in hydrogen-form was loaded with sample and washed with water (500 ml). Elution was started with 50:1 eluting agent. With progress in the elution process, movements of colored Nd and Pr bands were clearly observed visually. When the pale greenish band of Pr disappeared from the column, the eluting agent was changed to a 20 : 1 mixture for the elution of Ce and finally to 5 : 1 for the effective removal of La. Typical elution curves are shown in Figs. 5 and 6 and approximate compositions obtained by weighing as oxides are given in Table 1.

Table 1. Elution results of mixed chlorides

	Sample A		Sample B	
	Ln_2O_3 recovered mg	Composition as oxides %	Ln_2O_3 recovered mg	Composition as oxide %
Sm	42.6	6.1	67.0	7.6
Nd	135.1	19.3	184.3	20.8
Pr	42.4*	5.8	40.4*	4.6
Ce	327.4**	44.5	404.7**	45.6
La	170.5	24.3	189.3	21.4

* as Pr_6O_{11} ** as CeO_2

As is shown in Fig. 5, complete separation of Sm, Nd, Pr, Ce and La is obtained for sample A, while a little overlapping of the Nd fraction with Pr is observed in Fig. 6 for sample B. This somewhat poorer separation arises from the higher content of Nd in sample B as compared with that in sample A.

Our elution method was developed for larger scale separation; the sample A absorbed corresponded to 10 g of $LnCl_3 \cdot nH_2O$. The resin was 50—100 mesh in size, and its 540 ml was put into a column 3.0 cm in diameter; the flow rate was 1.5 cm/min, and the results are shown in Fig. 7.

Analyses of Rare Earth Oxides. Samples "C" and "D" were obtained from our company in the form of mixed chlorides after removing almost all the Ce from the other rare earths; these mixed chloride hydrates were first converted to mixed oxides and the oxides were treated with dilute nitric acid to remove the remaining cerium as an insoluble residue. The other rare earths in the solution were precipitated as oxalates and converted to oxides by ignition. The experimental conditions employed were: sample, about 1 g; column, 2.0×50 cm; Dowex 50W X8 (100—200 mesh), 40 g; bed length, about 22 cm; flow rate, 1.0 cm/min.

Elution was started with 50 : 1 eluting agent for Sm. Then the eluting agent was changed to 30 : 1 solution for the effective elution of Nd, where contamination of the Nd fraction with Pr was not observed. The elutions of Pr and Ce were carried out with 20 : 1 and 10 : 1 solutions in turn. Finally, 5 : 1 eluting agent was used for La. The eluates were collected for each fraction and tested for the presence of rare earth species by adding oxalic acid to the fractions placed at intervals of five fractions. The portions containing each species were brought together and evaporated to

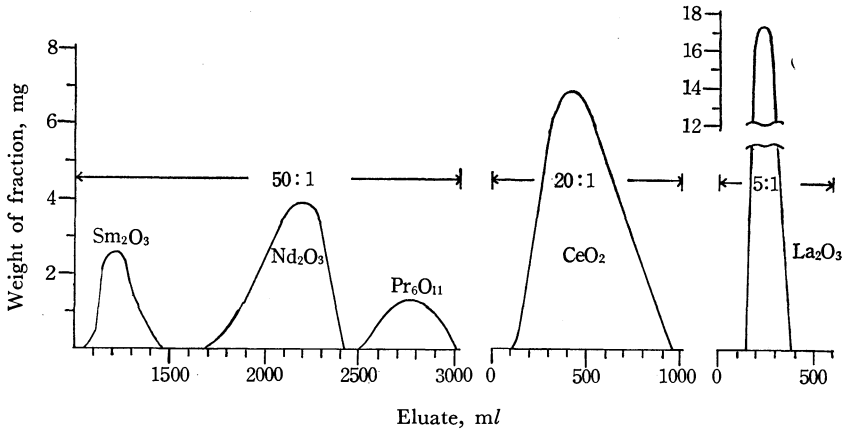

Fig. 5. Elution of the sample "A" in 2 g scale.
One fraction of eluate. 50 ml

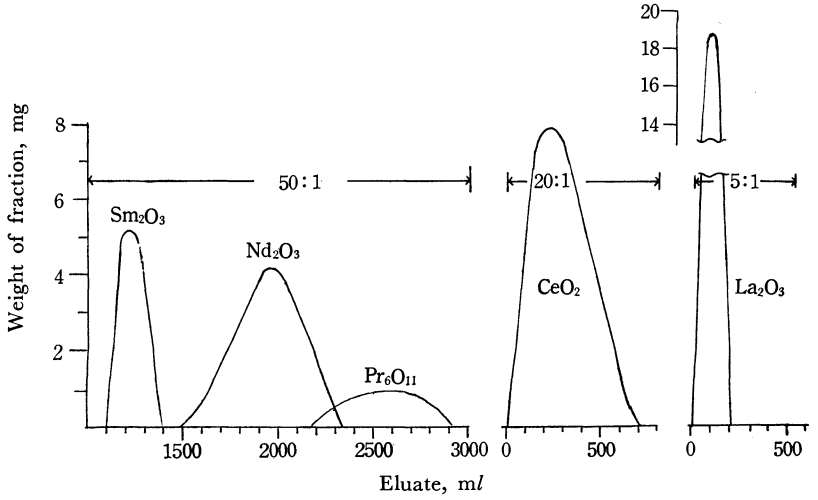

Fig. 6. Elution of the sample "B" in 2 g scale.
One fraction of eluate, 50 ml

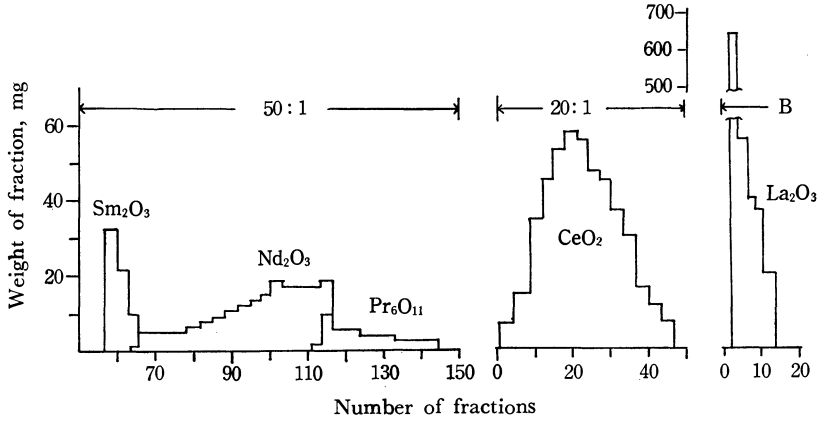

Fig. 7. Elution of the sample "A" in 10 g scale.
One fraction of eluate, 120 ml

a suitable volume. A large excess of oxalic acid was added to the concentrated solution and its pH adjusted to about 1.5 with ammonia. After heating for about 20 min, the whole was allowed to stand overnight. The precipitated oxalate was converted to oxide at 900°C. Typical results are given in Table 2.

TABLE 2. ELUTION RESULTS FOR MIXED OXIDES

Sample	C		D	
Sample taken, mg	1054.0		828.8	
	Recovered mg	Recovered %	Recovered mg	Recovered %
Sm_2O_3	129.1	12.25	74.0	8.93
Nd_2O_3	373.0	35.39	291.6	35.18
Pr_6O_{11}	98.3	9.33	81.1	9.79
CeO_2	0*	0	6.2	0.75
La_2O_3	450.6	42.75	371.6	44.84
Total	1051.0	99.72	824.5	99.48

* Qualitative test for its presence was also negative.

Behavior of the Yttrium-group Rare Earths. The utility of the new eluting agent for the cerium-group directed our attention to the separation of the yttrium-group rare earths, and some experiments were carried out in order to investigate the possibility. The individual elutions of Dy, Er, Yb and Y with 50 : 1 eluting agent are presented for comparison (Fig. 8). It is seen from the results that these elements show similar behavior. When 70 : 1 eluting agent was used, the nature of the elution was slightly improved, but it was still hopeless to separate these elements.

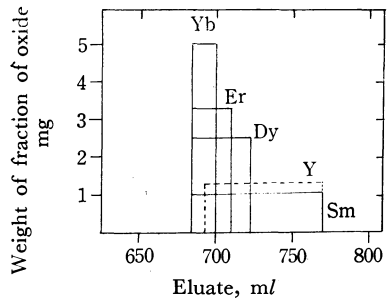

Fig. 8. Individual elution for the yttrium-group rare earths.
Weight of each sample, 10 mg as oxide; column diameter, 1.8 cm; bed height, 18 cm; flow rate 1.0 cm/min; eluting agent, 50 : 1; 1 fraction of eluate, 20 ml

On the Eluting Agent. A distinctive feature of our eluting agent is that the solution contains acetate anions in addition to citrate anions. Both anions may be responsible for the separation of the rare earths in the manner of complex formation. Tompkins and Mayer[11] mentioned that three H_2Cit^- ions are predominantly complexed with a rare earth ion under the condition of 0.25 M (5%) citrate at a pH lower than 3.2. In our eluting agent, the citrate concentration is about 6% and the pH values are 2.9 in 50 : 1 and 3.0 in 30 : 1 eluting agents. Therefore, formation of such complex species as $R(H_2Cit)_3$ should be considered in the elution process. On the other hand, the effect of the "B" component on the separation also suggests the formation of acetate-complex species. Kolat and Powell[12] reported the first two formation constants of acetate anions with rare earths. According to their data, a regular increase in stability is observed in the La-Sm region, while a decrease appears for the heavier elements. This decrease in stability reflects the failure to separate the yittrium-group rare earths.

Summary

A mixed system consisting of citric acid - ammonium citrate and acetic acid - ammonia was found to be a new eluting agent for the separation of La, Ce, Pr, Nd and Sm. The essential feature of this eluting agent is that the solution contains acetate anions in addition to citrate anions, and the former greatly affects the separation. As examples of separation, mixed chlorides obtained from monazite concentrates were eluted on an analytical scale. Mixed oxide samples were also analyzed successfully by this elution method.

Application of this eluting agent to heavier rare earths (yttrium-group) was unsuccessful.

11) E. R. Tompkins and S. W. Mayer, *J. Am. Chem. Soc.*, **69**, 2859 (1947).
12) R. S. Kolat and J. E. Powell, *Inorg. Chem.*, **1**, 293 (1962).

BULLETIN OF THE CHEMICAL SOCIETY OF JAPAN VOL. 41 2632—2636 (1968)

The Chelate Formation of *o*-Substituted Phenylazochromotropic Acids with Alkaline Earth Metals*[1]

Susumu NAKASHIMA,*[2] Haruo MIYATA and Kyoji TÔEI

Department of Chemistry, Faculty of Science, Okayama University, Tsushima, Okayama

(Received April 24, 1968)

The acid dissociation constants of phenyl, *o*-, *m*-, and *p*-sulfophenyl-, *o*-carboxyphenyl-, *o*-phenol- and *o*-arsonophenylazochromotropic acid and the formation constants of their 1 : 1 metal chelates with alkaline earth metals have been measured by potentiometric titration. The measurements have been carried out at 25°C and $\mu=0.10$ (KNO_3). The influence of these substituents on the acid dissociation constants of the reagents, and on the chelate formation constants was discussed. The dissociation constants of the naphtholic protons of the *o*-substituted reagents increase as follows: *o*-OH <*o*-$AsO(OH)_2$ <*o*-COOH <*o*-SO_3Na <*o*-H. The metal chelate stabilities of *o*-phenol-, phenyl- and *o*-arsonophenylazochromotropic acids decrease as follows: Mg> Ca> Sr> Ba, while for chelates of *o*-carboxyphenyl- and *o*-sulfophenylazochromotorpic acids the order is Mg> Ca> Sr≈Ba. The sulfonic group in *o*-sulfophenylazochromotropic acid, in spite of its remarkable electron-withdrawing effect, depress the acid dissociation, and form more stable barium chelate than phenyl-, *m*- and *p*-sulfophenylazochromotropic acid do. The plot of the formation constants, log *K*, against the sum of the dissociation constants, pK_A ($=pk_{a_1}+pk_{a_2}+pk_{a_3}$), was approximately linear.

A variety of azo dyestuffs have found a wide application in analytical chemistry, especially many azo derivatives of chromotropic acid are well known as colorimetric reagents and as metal indicators in chelatometry.[1] In the authors' laboratory numerous azo compounds showing a high sensitivity for metal ions were synthesized, and the acid dissociation constants of these reagents and the formation constants of thorium chelates were measured spectrophotometrically.[2] The present authors have extended the studies to alkaline earth metal chelates with seven substituted phenylazochromotropic acids, namely phenyl-, *o*-, *m*-, and *p*-sulfophenyl-, *o*-carboxyphenyl-, *o*-phenol- and *o*-arsonophenylazochromotropic acid, and investigated the effect of substituents on the dissociation constants and the chelate formation constants by means of potentiometric titration method.

Experimental

Reagents. Phenylazochromotropic acid [2-(phenylazo)-1,8-dihydroxynaphthalene-3,6-disulfonic acid disodium salt], *o*-sulfophenylazochromotropic acid [2-(2-sulfophenylazo)-1, 8-dihydroxynaphthalene - 3, 6 - disulfonic acid trisodium salt], *m*-sulfophenylazochromotropic acid ([2-(3-sulfophenylazo)-1,8-dihydroxynaphthalene-3,6-disulfonic acid trisodium salt], *p*-sulfophenylazochromotropic acid [2-(4-sulfophenylazo)-1,8-dihydroxynaphthalene-3,6-disulfonic acid trisodium salt], *o*-carboxyphenylazochromotropic acid [2-(2-carboxyphenylazo)-1,8-dihydroxynaphthalene-3,6-disulfonic acid disodium salt], *o*-phenylazochromotropic acid [Acid Chrome Blue K, 2-(2-hydroxyphenylazo)-1,8-dihydroxynaphthalene-3,6-disulfonic acid disodium salt] and *o*-arsonophenylazochromotropic acid [Neo-Thorin, Arsenazo, 2-(2-arsonophenylazo)-1,8-dihydroxynaphthalene-3,6-disulfonic acid disodium salt] were synthesized by the coupling reaction of chromotropic acid with diazobenzene, *o*-diazobenzenesulfonic acid, *m*-diazobenzenesulfonic acid, *p*-diazobenzenesulfonic acid, *o*-diazobenzoic acid, *o*-diazophenol and *o*-diazophenylarsonic acid, respectively. These reagents are all fine crystals. They were dried at 60°C *in vacuo*, and cooled in a phosphorus pentoxide desiccator. The

TABLE 1. ANALYSIS OF SODIUM CONTENT IN THE REAGENTS BY THE FLAME ANALYSIS

Substituent X	Calcd	Found
o-H	9.8%	9.7%
o-SO_3Na	12.1	12.3
o-COOH	9.0	8.8
o-OH	9.5	10.6
o-$AsO(OH)_2$	7.8	7.6
m-SO_3Na	12.1	12.7
p-SO_3Na	12.1	12.9

*1 Most part of this paper was presented at the 17th Annual Meeting of Coordination Chemistry, Hiroshima, December, 1967.

*2 Present address: The Ohara Institute for Agricultural Biology, Okayama University, Kurashiki, Okayama.

1) J. S. Fritz, R. T. Oliver and D. J. Pietrzyk, *Anal. Chem.*, **30**, 1111 (1958); S. Shibata and T. Matsumae, This Bulletin, **31**, 377 (1958), *etc.*

2) H. Miyata, This Bulletin, **40**, 1875 (1967); H. Miyata, *ibid.*, **40**, 2815 (1967), *etc.*

analytical data of sodium content by the flame analysis are given in Table 1.

The stock solutions of these reagents were standardized by potentiometric titration with standard 0.10 M potassium hydroxide.

Analytical grade $Mg(NO_3)_2 \cdot 6H_2O$, $Ca(NO_3)_2 \cdot 4H_2O$, $Sr(NO_3)_2$ and $Ba(NO_3)_2$ are used to make stock solutions and the solutions are standardized by chelatometric titration.

Potentiometric Titration. The apparatus for potentiometric titration is presented in Fig. 1. The hydrogen ion concentration was measured by using a Metrohm pH meter E 388 [Metrohm A. G., Herisau, Switzerland] with a combined glass electrode. The pH meter was calibrated with an acetate buffer and with potassium hydroxide. Ten milliliters of solution were titrated by addition of 0.10 M potassium hydroxide from a calibrated 0.50 ml Agla micrometer syringe. All measurements were made at 25.0±0.1°C, and the ionic strength was maintained at 0.10 M with potassium nitrate. Solutions under titration were kept in a nitrogen atmosphere.

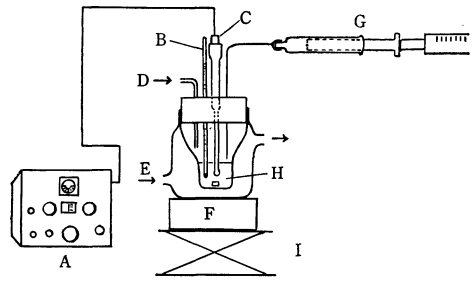

Fig. 1. Micro-titration apparatus.
A : "Metrohm" pH meter E-388
B : Thermometer
C : "Metrohm" combined glass electrode
D : N_2 gas
E : 25°C water
F : Magnetic stirrer
G : "Agla" micrometer syringe
total volume 0.5 ml
H : volume 10 ml
I : Laboratory jack

Calculations of Acid Dissociation Constants and Chelate Formation Constants. The dissociation constants, k_{a_1}, k_{a_2} and k_{a_3} and the formation constant, K, were evaluated by similar equations to those described elsewhere.[3]

k_{a_1}, k_{a_2}, k_{a_3} and K are expressed as follows:

$$k_{a_1} = \frac{[H][HL]}{[H_2L]}, \quad k_{a_2} = \frac{[H][H_2L]}{[H_3L]},$$

$$k_{a_3} = \frac{[H][H_3L]}{[H_4L]}, \quad K = \frac{[MHL]}{[M][HL]}$$

where the ionic charge was neglected for the sake of convenience.

The formation constant of o-arsonophenylazochromotropic acid chelate was calculated by the following equations:

$$K = \frac{T_L - F}{[L^{5-}]\{F + T_M - T_L\}}$$

where

$$[L^{5-}] = \frac{3T_L - T_{OH} - [H^+] + [OH^-]}{\frac{[H^+]}{k_{a_1}} + \frac{2[H^+]^2}{k_{a_1}k_{a_2}} + \frac{3[H^+]^3}{k_{a_1}k_{a_2}k_{a_3}}}$$

$$F = [L^{5-}]\left\{1 + \frac{[H^+]}{k_{a_1}} + \frac{[H^+]^2}{k_{a_1}k_{a_2}} + \frac{[H^+]^3}{k_{a_1}k_{a_2}k_{a_3}}\right\}$$

where T_L, T_M and T_{OH} represent the total concentration of ligand, metal ion species and alkali added, respectively. These equations can be simplified for the calculations of the other chelate formation constants.

These constants were calculated by an NEAC-2203 computer (the Nippon Electric Co., Ltd) in the Electronic Computer Center of Okayama University.

Results and Discussion

Titration Curves. The potentiometric titration curves for o-substituted phenylazochromotropic acids with or without equivalent amounts of

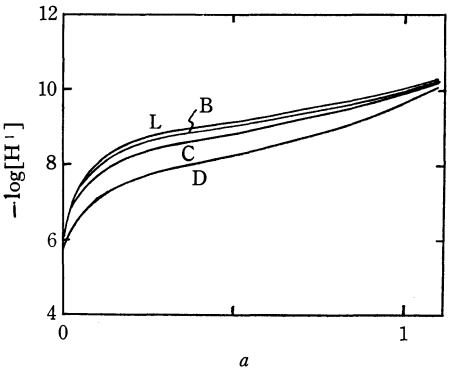

Fig. 2. Titration of phenylazochromotropic acid chelate system at 25°C, μ=0.10.
L, ligand only; B, Sr; C, Ca; D, Mg
[Ligand]=[Metal ion]=2.24×10^{-3} M
a=moles of base added per mole of ligand

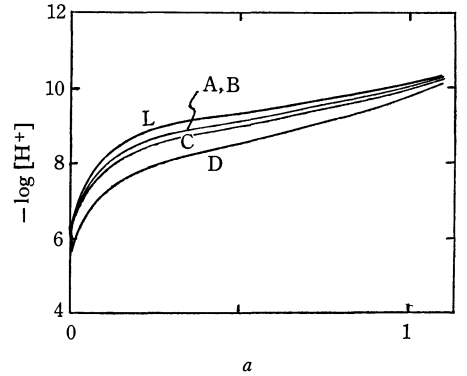

Fig. 3. Titration of o-sulfophenylazochromotropic acid chelate system at 25°C, μ=0.10.
L, ligand only; A, Ba; B, Sr; C, Ca; D, Mg
[Ligand]=[Metal ion]=2.20×10^{-3} M

3) S. Nakashima, H. Miyata and K. Tôei, This Bulletin, **40**, 870 (1967).

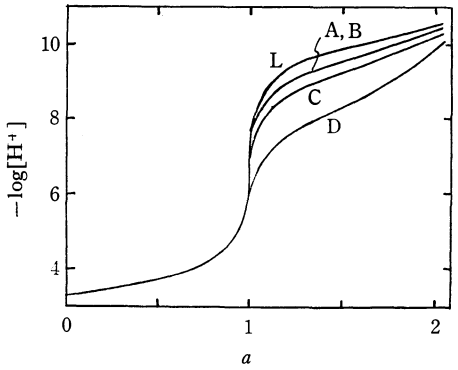

Fig. 4. Titration of *o*-carboxyphenylazochromotropic acid chelate system at 25°C, $\mu=0.10$.
L, ligand only; A, Ba; B, Sr; C, Ca; D, Mg
[Ligand]=[Metal ion]=2.39×10^{-3} M

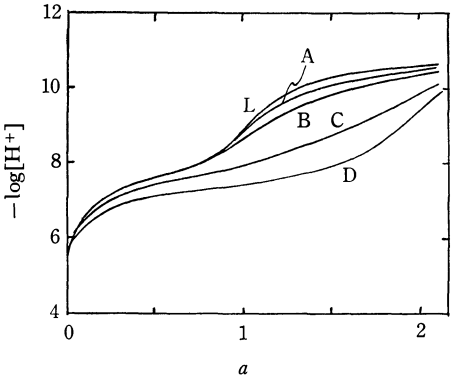

Fig. 5. Titration of *o*-phenolazochromotropic acid chelate system at 25°C, $\mu=0.10$.
L, ligand only; A, Ba; B, Sr; C, Ca; D, Mg
[Ligand]=[Metal ion]=1.56×10^{-3} M

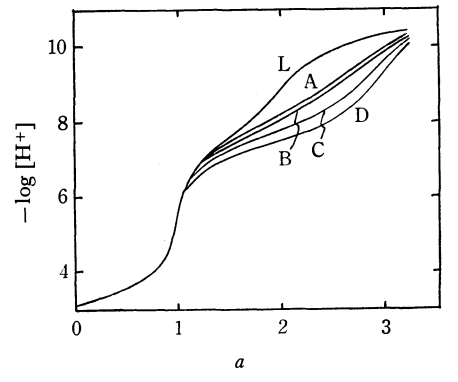

Fig. 6. Titration of *o*-arsonophenylazochromotropic acid chelate system at 25°C, $\mu=0.10$.
L, ligand only; A, Ba; B, Sr; C, Ca; D, Mg
[Ligand]=[Metal ion]=1.09×10^{-3} M

alkaline earth metal ions are illustrated in Figs. 2—6. The clear inflections at $a=1$ in the titration curves of the ligands in Figs. 4 and 5 show the dissociation of carboxyl and hydroxyl protons of the reagents, respectively, and similarly the inflections at $a=1$ and $a=2$ in Fig. 6 correspond to the dissociation of two arsonic protons. No inflection is observed at all on the neutralization of the naptholic protons of the above three reagents. Modification of the titration curves in the presence of metals is due to the chelate formation giving rise to free protons.

Acid Dissociation Constants. Substituted phenylazochromotropic acid is shown in the following structure:

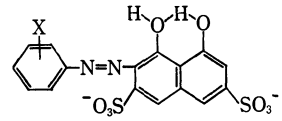

X: *o*-H, *o*-SO_3^-, *o*-COOH, *o*-OH, *o*-$AsO(OH)_2$, *m*-SO_3^-, *p*-SO_3^-

The acid dissociation constants of the above seven derivatives are calculated from the titration curves and summarized in Table 2. As the pk_{a_3} value of *o*-arsonophenylazochromotropic acid is low, it is determined by titrating the reagent solution of 2.06×10^{-3} M. The constants obtained by this apparatus are in good agreement within experimental error with previous results[3] for the dissociation constants of *o*-phenolazochromotropic acid and the formation constants of its magnesium and calcium chelates.

In Table 2, the pk_{a_1} value corresponds to the dissociation of one of the naphtholic hydroxyl groups; the other naptholic hydroxyl group is not dissociated under ordinary experimental conditions, owing to a strong hydrogen bridge between two oxygen atoms of chromotropic acid as shown in the above structure. These ligands may be considered to be monobasic acids for phenyl-, *o*-, *m*-, and *p*-sulfophenylazochromotropic acids, dibasic acids for *o*-carboxyphenyl- and *o*-phenolazochromotropic acids and tribasic acid for *o*-arsonophenylazochromotropic acid.

The pk_a's of benzoic acid, phenol and phenylarsonic acid are 4.17,[4] 9.98[5] and 8.25 and 3.39 (obtained from potentiometric titration) respectively, whereas those of the corresponding azochromotropic acids are smaller. On the other hand, the pk_a's of the naphtholic hydroxyl groups in the azo compounds are much larger than that of chromotropic acid (5.44).[6] This implies that the formation of the intramolecular hydrogen bonding between the naphtholic hydroxyl group and the azo nitrogen atom adjacent to the phenyl group forms a stable six-membered ring.

4) I. M. Kolthoff and W. Bosch, *J. Phys. Chem.*, **36**, 1695 (1932).
5) F. G. Bordwell and G. D. Cooper, *J. Am. Chem. Soc.*, **74**, 1058 (1952).
6) M. Sakaguchi, A. Mizote, H. Miyata and K. Tôei, This Bulletin, **36**, 885 (1963).

TABLE 2. ACID DISSOCIATION CONSTANTS OF SUBSTITUTED PHENYLAZOCHROMOTROPIC ACIDS AND FORMATION CONSTANTS OF THEIR CHELATES

(t=25°C, μ=0.10; KNO_3)

Substituent X	Acid dissociation constant			Formation constant, log K			
	pk_{a_1}	pk_{a_2}	pk_{a_3}	Mg	Ca	Sr	Ba
o-H	9.15			3.64	2.70	1.78	1.06
o-SO_3Na	9.35			3.58	2.91	2.58	2.66
o-COOH	9.94	3.71		4.55	3.40	2.81	2.81
o-OH	10.60	7.60		6.15	5.01	3.49	2.73
o-$AsO(OH)_2$	9.98	7.57	2.97	5.58	5.09	4.41	4.15
m-SO_3Na	8.85						1.44
p-SO_3Na	8.90						1.58

where $k_{a_1}=\frac{[H][HL]}{[H_2L]}$, $k_{a_2}=\frac{[H][H_2L]}{[H_3L]}$, $k_{a_3}=\frac{[H][H_3L]}{[H_4L]}$

Owing to the formation and the stabilization of the ring, the dissociation of the substituents in *o*-COOH, *o*-OH and *o*-$AsO(OH)_2$ compounds is easier than those of the corresponding phenyl compounds, meanwhile the dissociation of naphtholic hydroxyl groups is much more difficult than chromotropic acid.

Electron-withdrawing sulfonic group enhances the ligand acidity and thus the pk_a values of *m*- and *p*-sulfophenylazochromotropic acids are lower than that of phenylazochromotropic acid. However, the contribution of the sulfonic group in *o*-sulfophenylazochromotropic acid leads to the depression of the dissociation of the naphtholic proton as seen in Table 2.

This suggests that the sulfonic group in the ortho position for the azo group forms a hydrogen bond with the naphtholic proton in aqueous solution as the following structure shows:

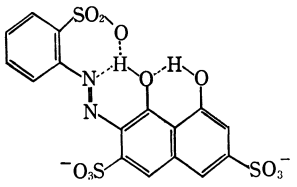

Formation Constants. The formation constants of the 1 : 1 chelates of substituted phenylazochromotropic acids with alkaline earth metals are also tabulated in Table 2. The formation constant, log K, is plotted *versus* the sum of the disscoiation constants, pK_A ($=pk_{a_1}+pk_{a_2}+pk_{a_3}$), in Fig. 7. An approximately linear correlation between pK_A and log K is obtained for the chelates of a series of alkaline earth metals.

It is of interest that the log K values are nearly proportional to the pK_A values in spite of the complicated chelate structures and the differences of the numbers of the chelate ring formed. In barium chelates, however, a considerable deviation from the linearity is observed in comparison

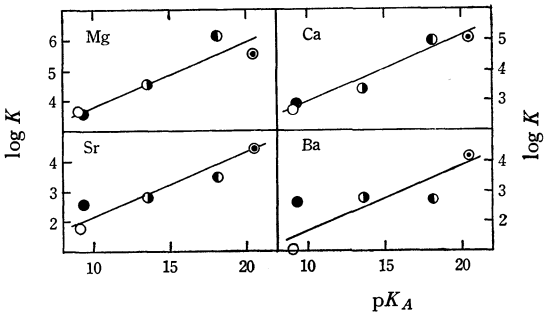

Fig. 7. Relation between pK_A of *o*-substituted phenylazochromotropic acids and log K of their metal chelates.

$pK_A = pk_{a_1} + pk_{a_2} + pk_{a_3}$

○ -H, ● $-SO_3^-$, ◑ -COOH, ◐ -OH, ⊙ $-AsO(OH)_2$

with the other metal chelate systems.

It should be noted that the formation constants of *o*-sulfophenylazochromotropic acid chelates are larger than those of phenylazochromotropic acid chelates except the magnesium chelate. It seems that the sulfonic group takes part in the chelate coordination. Particularly, its stability for barium chelate is much higher than that for *m*-, *p*-sulfophenyl- and phenylazochromotropic acid chelates. This result suggests that the sulfonic group at the ortho position has a strong coordination ability to barium ion. The order of decreasing stability of the metal chelates of phenyl-, *o*-phenol- and *o*-arsonophenylazochromotropic acid, magnesium> calcium> strontium> barium, agrees with the orders already reported for a large number of other ligands. However, in *o*-carboxyphenylazochromotropic acid chelate, the orders of decreasing stability is magnesium> calcium> strontium= barium and furthermore in *o*-sulfophenylazochromotropic acid it is magnesium> calcium> barium> strontium.

The relation of the formation constants, log K, of the chelates of *o*-substituted phenylazochromotropic acids to the reciprocal of the effective

radii, $1/r$, for alkaline earth metal ions, which were calculated by Latimer,[7] is given in Fig. 8. Latimer suggests that these effective radii give a good estimate of ionic size in solution. Figure 8 shows two different trends on the chelates of the ligands investigated. The one is a straight line shown by a solid line on which lie chelates of phenyl-, *o*-phenol- and *o*-arsonophenylazochromotropic acid, but the log K values of the calcium chelates show a larger deviation from that line. The other includes *o*-sulfophenyl- and *o*-carboxyphenylazochromotropic acid, for which another linear relationship is observed from strontium to magnesium as shown by a dotted line, but the log K values of the barium chelates are equal to or larger than that of the strontium chelates.

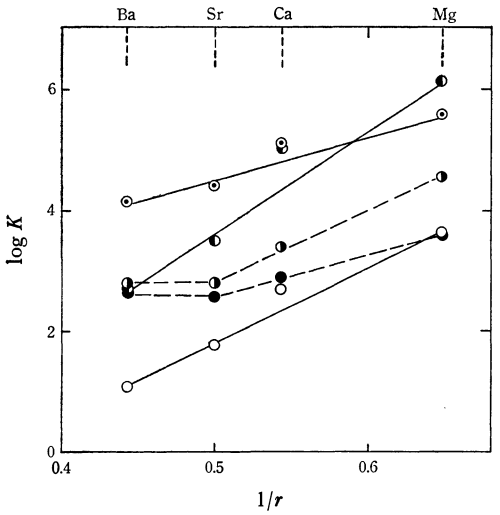

Fig. 8. Correlation of log K for *o*-substituted phenylazochromotropic acid chelates against $1/r$ of metal ions.
○ -H, ● $-SO_3^-$, ◑ -COOH, ◐ -OH, ⊙ $-AsO(OH)_2$

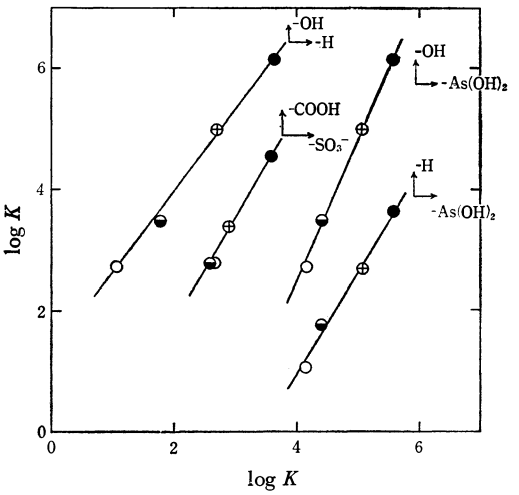

Fig. 9. Relation between log K's for pairs of ligands.
●: Mg, ⊕: Ca, ◒: Sr, ○: Ba

The plot of the log K value of one reagent against that of another reagent is given in Fig. 9. A good linear relationship is obtained among phenyl-, *o*-phenol- and *o*-arsonophenylazochromotropic acid chelate systems and between *o*-carboxyphenyl- and *o*-sulfophenylazochromotropic acid chelate systems.

7) W. M. Latimer, *J. Chem. Phys.*, **23**, 90 (1955).

BULLETIN OF THE CHEMICAL SOCIETY OF JAPAN VOL. 41 2637—2640 (1968)

Mass Spectrometry of Organometallics. I. Titanium Cyclopentadienyl Complexes*[1]

Yoshinobu TAKEGAMI, Toru UENO, Toshimitsu SUZUKI and Yuichi FUCHIZAKI

Department of Hydrocarbon Chemistry, Faculty of Engineering, Kyoto University, Sakyo-ku, Kyoto

(Received April 23, 1968)

The possibility of mass spectral analysis of less volatile and air sensitive organometallic compunds has been studied with an electron-impact, Muttauch-type mass spectrograph. Several organotitanium compounds, $(C_5H_5)_2Ti$, $(C_5H_5)_2Ti$-methylacetylene complex, $(C_5H_5)_2Ti$-allylchloride and $(C_5H_5)_2TiCl_2$-$AlEt_2Cl$ complex, have been subjected to mass spectral analysis, and the parent ion has been detected for each compound. The $(C_5H_5)_2Ti$-methylacetylene complex gave a parent ion of $(C_5H_5)_2Ti(C_3H_4)_2^+$; NMR and IR suggested the structure as a five-membered cyclic diene complex of $(C_5H_5)_2Ti$. The $(C_5H_5)_2Ti$-allylchloride gave a parent ion of $(C_5H_5)_2Ti(C_3H_5)^+$ which proves the existence of allyl complex of $(C_5H_5)_2Ti$. The $(C_5H_5)_2TiCl_2$-$AlEt_2Cl$ complex gave a parent ion of $(C_5H_5)_2TiCl_2AlEtCl^+$ which is in agreement with the composition reported in the literature.

There has been considerable interest in mass spectra of organometallics of transition metals in recent years. It has been felt that the mass spectral study should shed direct light on the composition of the organometallic catalysts. Although a variety of the organo transition metal compounds have been subjected to mass spectral analysis, these compounds, in most cases, are either stable to air and moisture or sufficiently volatile to use the conventional reservior inlet system. Relatively few studies on the mass spectral analysis of organometallic compounds which are less volatile and sensitive to air and moisture have been reported in the literature. The work described in this report resulted from our interest in learning whether less volatile, air sensitive organotitanium compounds would be detected by a mass spectrograph.

Experimental

The mass spectra were determined with a Japan Electron Optics Lab. double-focusing mass spectrograph (JMS-01SG). Since the compounds were not sufficiently volatile to use the conventional reservior inlet system, samples were introduced directly into the ion source from a glass tube. In the cases of the compounds which were sensitive to air and moistrue, all operations were carried out under argon or nitrogen atmosphere and samples were introduced as dilute solutions. The solvents were removed in the pre-evacuation chamber of the direct sample inlet system. Ions were formed by the electron bombardment with 75 V electrons and were accelerated at 6000 V. Ions were detected by the Ilford Q2 photographic plate. Perfluorokerosene was used as an internal reference.

Bis(cyclopentadienyl)titaniumdichloride was obtained from Arapahoe Chem. Co. and used without further purification. Bis(cyclopentadienyl)titanium was prepared by the reduction of bis(cyclopentadienyl)titaniumdichloride with sodium amalgam according to the direction of Shikata.[1)]

A 10 m*l* portion of benzene solution (0.075 mol/*l*) of bis(cyclopentadienyl)titanium was stirred under methylacetylene atmosphere at 50°C for 2 hr. The solution turned immediately from green to reddish one. The excess methylacetylene was removed under reduced pressure and the complex was subjected to IR, NMR and mass spectral analysis.

Bis(cyclopentadienyl)titanium solution was also treated with allylchloride in the molar ratio of 1 : 2; the color of the solution turned from green to red. The reaction mixture was subjected to mass spectral analysis.

Bis(cyclopentadienyl)titanium dichloride-diethylaluminumchloride complex was obtained by the reaction of these two reagents at 50°C in the Al/Ti ratio of 4. The solvent (*n*-heptane) was removed under reduced pressure (4 mmHg) at 20°C and the complex was subjected to mass spectral analysis.

Results and Discussion

Bis(cyclopentadienyl)titaniumdichloride. Inasmuch as the usual organotitanium compounds are very sensitive to air and moisture, initial experiments were carried out with the air stable bis(cyclopentadienyl)titaniumdichloride to see the possibility of accurate mass determination. As may be seen in Table 1, nine lines were observed at *m/e* 246—254, the region of which corresponds to the molecular ion of bis(cyclopentadienyl)-titaniumdichloride. Since titanium, chlorine and carbon atoms have five, two and two appreciable isotopes respectively, forty masses might be written in combination with these isotopes. It is impossible, however, to distinguish the masses which

*1 This report was presented at the 21st Annual Meeting of the Chemical Society of Japan, Osaka, April, 1968.

1) K. Shikata, K. Nishino and K. Azuma, *Kogyo Kagaku Zasshi, (J. Chem. Soc. Japan, Ind. Chem. Sect.)*, **68**, 490 (1965).

TABLE 1. MOLECULAR IONS OF $(C_5H_5)_2TiCl_2$

m/e	Found		Calculated				
	RI*	Mass	Mass	Isotope assign. Ti,	Cl,	Cl	RA**
246	m	245.966	245.969	(46,	35,	35)	10.9
247	m	246.965	246.968	(47,	35,	35)	10.2
248	vs	247.965	247.964	(48,	35,	35)	100
249	m	248.968	248.965	(47,	35,	37)	6.8
			248.964	(49,	35,	35)	7.5
250	s	249.961	249.961	(48,	35,	37)	66.6
			249.961	(50,	35,	35)	7.5
251	m	250.966	250.961	(49,	35,	37)	5.0
252	m	251.965	251.958	(48,	37,	37)	11.1
253	w	252.965	252.958	(49,	37,	37)	0.8
254	w	253.950	253.955	(50,	37,	37)	0.8

* RI: relative intensity, judged by the degree of blackening of the photographic plate.
** RA: relative abundance, calculated from the natural abundance of isotopes.

belong to the same *m/e* value, *e.g.* $^{48}Ti^{35}Cl_2C_{10}H_{10}$ (247.964 m. u.), $^{47}Ti^{35}Cl_2{}^{13}CC_9H_{10}$ (247.971 m.u.), $^{46}Ti^{35}Cl^{37}ClC_{10}H_{10}$ (247.966 m.u.), *etc.* Among these, only the principal masses with their assignments for isotopes are listed in Table 1. From the agreement between the experimental data and the calculated ones, the nine lines can be reasonably assigned to the molecular ion of bis(cyclopentadienyl)titaniumdichloride. The limit of error in determining of these masses can be drawn within 0.009 m.u. In the present work, ions were detected only by the photographic plate and no attempt was made to achieve quantitative fragmentation patterns (pattern coefficients); the object instead was to determine accurate masses of the parent ions.

Bis(cyclopentadienyl)titanium and Its Complexes. The mass spectra of cyclopentadienyl complexes of several transition metals have been reported.[2] The mass spectral data on bis(cyclopentadienyl)titanium, however, has not been reported, whereas it has been well known that bis(cyclopentadienyl)titanium can be prepared by sodium amalgam reduction of bis(cyclopentadienyl)-titaniumdichloride[1] or by the decomposition of bis(cyclopentadienyl)dimethyltitanium with hydrogen.[3] Difficulty in introducing the bis(cyclopentadienyl)titanium into a mass spectrograph because of its sensitivity to air and moisture appears to be responsible, in part, for the paucity of data on bis(cyclopentadienyl)titanium. Then, in this work, a dilute solution of bis(cyclopentadienyl)titanium was handled under nitrogen atmosphere. Solvent was removed in the pre-evacuation chamber of the direct sample inlet system and the bis(cyclopentadienyl)titanium was introduced directly into the ion source. Table 2 represents the mass spectrum of bis(cyclopentadienyl)titanium thus analyzed. The molecular ion was detected concerning to five isotopes of titanium. Various

TABLE 2. MASS SPECTRUM OF $(C_5H_5)_2Ti$

Ion	$(Mass)_{found}$	IR	$(Mass)_{calcd}$	
$Ti(C_5H_5)_2^+$	176.027	s	176.031	(^{46}Ti)
	177.032	s	177.030	(^{47}Ti)
	178.024	vs	178.026	(^{48}Ti)
	179.028	s	179.026	(^{49}Ti)
	180.028	s	180.023	(^{50}Ti)
$TiC_9H_8^+$	164.002	vw	164.011	
$TiC_8H_8^+$	152.001	m	152.011	
$TiC_7H_8^+$	140.000	vw	140.011	
$TiC_6H_6^+$	126.001	w	125.995	
$TiC_6H_5^+$	124.991	w	124.987	
$TiC_5H_5^+$	112.985	vs	112.987	
$TiC_5H_4^+$	111.991	s	111.980	
$TiC_4H_3^+$	98.962	w	98.971	
$TiC_3H_3^+$	86.965	m	86.971	
$TiC_3H_2^+$	85.958	m	85.964	
$TiC_2H_2^+$	73.956	w	73.964	
TiC_2H^+	72.955	m	72.956	
$(C_5H_5)_4Ti_2O^+$	372.041	w	372.047	
$(C_5H_5)_2TiOH^+$	195.035	m	195.029	
$(C_5H_5)_2TiO^+$	194.027	vw	194.021	
$C_5H_5TiOH^+$	129.991	s	129.989	
$C_5H_5TiO^+$	128.985	s	128.981	

2) a) L. Friedman, A. P. Irsa and G. Wilkinson, *J. Am. Chem. Soc.*, **77**, 3689 (1955). b) J. Müller and L. D'Or, *J. Organometal. Chem.*, **10**, 313 (1967). c) A. F. Reid, J. S. Shannon, J. M. Swan and P. C. Wailes, *Austral. J. Chem.*, **18**, 173 (1965). d) M. I. Bruce, *Inorg. Nucl. Chem. Letters*, **3**, 157 (1967). e) A. N. Nesmeyanov, V. A. Duboritskii, O. V. Nogina and V. N. Bochkarev, *Dokl. Akad. Nauk SSSR*, **165**, 125 (1965). f) E. Schmacher and R. Taubenest, *Helv. Chim. Acta*, **49**, 1447 (1966). g) R. E. Winters and R. W. Kiser, *J. Phys. Chem.*, **69**, 3198 (1965). h) R. G. Denning and R. A. D. Wentworth, *J. Am. Chem. Soc.*, **88**, 4619 (1966). i) R. B. King, *ibid.*, **88**, 2075 (1966).
3) K. Clauss and H. Bestian, *Ann.*, **654**, 8 (1962).

fragment ions were also detected. The assignments of these ions are somewhat uncertain, however, by the fact that the isotope lines which belong to the same *m/e*, *e. g.* $^{48}TiC_6H_6^+$ and $^{49}TiC_6H_5^+$, *etc.* could not be distinguished, since the spectrum was determined at resolution of 12000. The assignment was done by the qualitative relative intensities. Under these conditions, the accuracy of determination somewhat diminished because of broadening of the lines; a probable limit of error can be taken as 0.012 m.u.

Ions which could be taken as support for the existence of bis(cyclopentadienyl)titanium dimer have never been detected; bis(cyclopentadienyl)-titanium appears to vaporize as a monomer. On the other hand, several oxygen-containing ions which might come from the reaction of bis(cyclopentadienyl)titanium with air and moisture were detected at *m/e* of 129, 130, 194, 195 and 372. From these ions, it appears to be reasonable to conclude that oxygen-containing compounds such as $(C_5H_5)_2$-TiO, $(C_5H_5)_2TiOH$ and $(C_5H_5)_4Ti_2O$ existed in the sample; it is noteworthy that oxygen-containing bis(cyclopentadienyl)titanium dimer exists in the vapor phase.

When the benzene solution of bis(cyclopentadienyl)titanium was treated with methylacetylene at 50°C, the color of the solution turned green to reddish. Mass spectral analysis of this solution gave a line at 258.092 m.u., which can be assigned to $(C_5H_5)_2Ti(C_3H_4)_2^+$ (258.089 m.u.). Infrared spectra of bis(cyclopentadienyl)titanium and its methylacetylene complex are shown in Fig. 1. The complex exhibited absorption bands at 1580 and 1410 cm^{-1} which are characteristic of a conjugated diene system, and did not exhibit any absorption bands at 2100—2260 cm^{-1} which corresponds to a carbon-carbon triple bond. It can, therefore, be concluded that the two molecules of methylacetylene bond to bis(cyclopentadienyl)-titanium as a conjugated diene. The 60 Mc NMR spectrum of the complex exhibited rather broad signals at δ(benzene)=335 cps and δ(benzene)=354 cps.

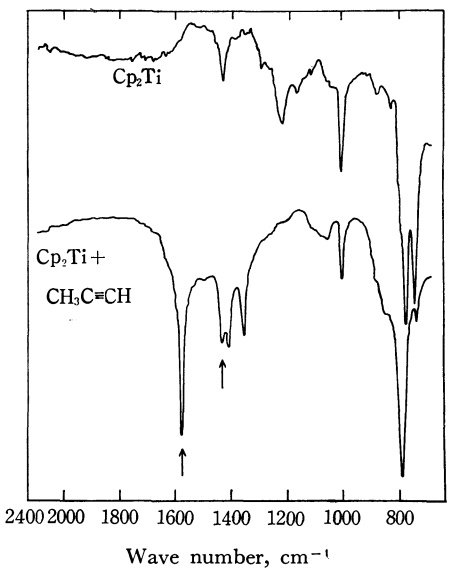

Fig. 1. Infrared spectra of $(C_5H_5)_2Ti$ and $(C_5H_5)_2Ti$-methylacetylene complex.

Vol'pin and his co-workers[4] studied the complex of bis(cyclopentadienyl)titanium with phenylacetylene and assumed the structures of I and II. Sonogashira and Hagihara[5] also investigated this complex by means of NMR, IR and electronic absorption spectra and supported the structure I.

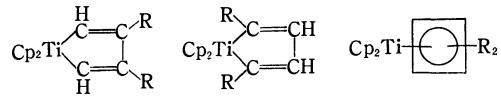

Ia Ib II

The present work supports the structure I and NMR (60 Mc) signals at δ(benzene)=335 cps and δ(benzene)=354 cps can be assigned to the methyl groups of Ia and Ib. The fact that $C_6H_8^+$ which is expected from structure II was not detected in the mass spectrum may support the structure I rather than the structure II.

In connection with the cyclic diene complex, a reaction mixture of bis(cyclopentadienyl)titanium with allylchloride was subjected to mass spectral analysis to see the possibility of the formation of allyl complex of bis(cyclopentadienyl)titanium. The results are presented in Table 3. As may be seen in Table 3, the predominant product of the reaction was bis(cyclopentadienyl)titaniumdichloride. A line was, however, observed at 219.062 m.u. which can be taken as a support of the formation of allyl complex of bis(cyclopentadienyl)titanium. Besides the titanium-containing ions, $C_6H_{10}^+$ was also observed.

Table 3. Mass spectral analysis of $(C_5H_5)_2Ti$-allylchloride

m/e	RI	Ion	$(Mass)_{found}$	$(Mass)_{calcd}$
219	w	$(C_5H_5)_2TiC_3H_5^+$	219.062	219.065
248	vs	$(C_5H_5)_2TiCl_2^+$	247.962	247.964
82	m	$C_6H_{10}^+$	82.081	82.078

Bis(cyclopentadienyl)titaniumdichloride-diethylaluminumchloride Complex. While the complex of bis(cyclopentadienyl)titaniumdichloride with diethylaluminumchloride was investigated in

4) M. E. Vol'pin, V. A. Dubovitskii, O. V. Nogina and D. N. Kursanov, *Dokl. Akad. Nauk SSSR*, **151**, 1100 (1963).

5) K. Sonogashira and N. Hagihara, This Bulletin, **39**, 1178 (1966).

TABLE 4. MASS SPECTRAL ANALYSIS OF $(C_5H_5)_2TiCl_2$-$AlEt_2Cl$

Ion	Found		Calculated				
	Mass	RI	Mass	Isotope assign.			
				Ti,	Cl,	Cl,	C
$(C_5H_5)_2TiCl_2AlClEt^+$	338.950	m	338.953	(48,	35,	35,	12)
	339.953	vw	339.956	(48,	35,	35,	13)
	340.950	m	340.950	(48,	35,	37,	12)
	341.954	vw	341.954	(48,	35,	37,	13)
$(C_5H_5)_2TiCl_2AlCl^+$	307.915	vw	307.919	(46,	35,	35,	12)
	308.915	vw	308.918	(47,	35,	35,	12)
	309.910	s	309.916	(46,	35,	37,	12)
			309.914	(48,	35,	35,	12)
	310.906	w	310.915	(47,	35,	37,	12)
			310.917	(48,	35,	35,	13)
			310.915	(49,	35,	35,	12)
	311.906	s	311.913	(46,	37,	37,	12)
			311.911	(48,	35,	37,	12)
	312.905	w	312.912	(47,	37,	37,	12)
			312.914	(48,	35,	37,	13)
			312.911	(49,	35,	37,	12)
	313.908	m	313.908	(48,	37,	37,	12)
			313.908	(50,	35,	37,	12)
$(C_5H_5)_2TiCl_2AlEt^+$	303.981	w	303.985	(48,	35,	35,	12)
$(C_5H_5)_2TiEt^+$	207.070	w	207.065	(48,	—,	—,	12)
$TiEt^+$	96.981	w	96.987	(48,	—,	—,	12)

detail by Natta and Mazzanti,[6] the mass spectral data on this complex has never been reported. Then, the mass spectral analysis was carried out in the same manner as described for bis(cyclopentadienyl)titanium. The lines observed in the highest mass region was *m/e* 339—342, which are shown in Fig. 2. These ions can be assigned to $(C_5H_5)_2TiCl_2$-$AlEtCl^+$ and its isotopic ions, as may be seen in the first four entries of Table 4. Besides $(C_5H_5)_2TiCl_2$-$AlEtCl^+$, a weak line was observed at 333.019m.u.

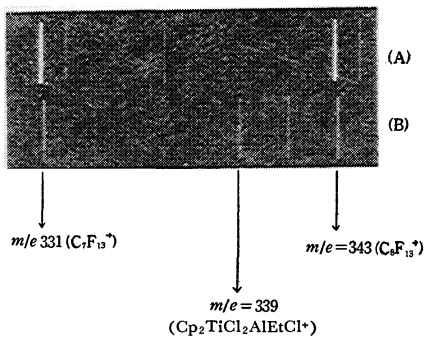

Fig. 2. Partial spectrum of $(C_5H_5)_2TiCl_2AlEtCl^+$.
(A) Perfluorokerosene
(B) Perfluorokerosene + complex

6) G. Natta and G. Mazzanti, *Tetrahedron*, **8**, 86 (1960).

which corresponds to $(C_5H_5)_2TiCl_2AlEt_2^+$. This is not, however, conclusive in establishing proof for the existence of the complex in the form of $(C_5H_5)_2TiCl_2AlEt_2$, because diethylaluminumchloride unfortunately gives a line at 333.021 m.u.*2 Although it is not clear whether the line at 333.019 m.u. is due to the existence of $(C_5H_5)_2TiCl_2AlEt_2^+$ or whether the diethyaluminumchloride also plays a part, it is more likely that the complex is predominantly in the form of $(C_5H_5)_2TiCl_2AlEtCl$, because the line at *m/e* 339 is much more intense than that at *m/e* 333 as may be seen in Fig. 2. This composition of the complex agrees with that reported by Natta and Mazzanti.[6] Fragment ions of the complex are also included in Table 4. The only observable fragment ions are $(C_5H_5)_2$-$TiCl_2AlCl^+$ and $(C_5H_5)_2TiCl_2AlEt^+$, which correspond to (P-Et) and (P-Cl), respectively.*3 Absence of other fragment ions which contain both titanium and aluminum appears to suggest the weakness of chlorine-bridged titanium-aluminum cluster.

*2 Diethylaluminumchloride gives a variety of oxygen-containing ions at *m/e* 150—400; Preprints for the 21st Annual Meeting of the Chemical Society of Japan (Osaka, 1968), III, p. 1959.

*3 $(C_5H_5)_2TiEt^+$ and $TiEt^+$ would not be the fragment ions of the complex but come from an ethyltitanium compound produced presumably by the exchange reaction between $(C_5H_5)_2TiCl_2$ and $AlEt_2Cl$.

BULLETIN OF THE CHEMICAL SOCIETY OF JAPAN VOL. 41 2641—2645 (1968)

Synthesis of Sulfosodalite, an Ultramarine-Relating Phase

Goro YAMAGUCHI and Yasushi KUBO*1

Department of Industrial Chemistry, Faculty of Engineering, The University of Tokyo, Hongo, Tokyo

(Received April 25, 1968)

A sulfur-containing sodalite-type aluminosilicate, $6NaAlSiO_4 \cdot Na_2S$ (designated sulfosodalite in this paper), was synthesized in the system $NaAlSiO_4$-Na_2S at temperatures 850 to 950°C in an H_2 or N_2 atmosphere. All of the sulfur in this substance was contained as sulfide ion S^{2-}, and its equilibrium content in a unit cell increases with temperature from 1.5 S at 850°C to 1.8 S at 950°C. This substance was only pale colored, yellowish or pinkish, but the partial substitution of Si for Al produced a deep vermilion red color.

By heating the system $NaAlSiO_4$-Na_2S in an H_2 or N_2 atmosphere at temperatures 850 to 950°C, a sulfur-containing aluminosilicate phase of sodalite-type was obtained. This phase was found to contain sulfur only in the form of monosulfidic sulfur ion S^{2-}, and thus gave an X-ray diffraction pattern closely resembling that of sodalite, $6NaAlSiO_4 \cdot 2NaCl$. Differing from ultramarine, which contains disulfidic sulfur ion,[1] this substance is only very lightly colored, yellowish or pinkish.

Kirk has already synthesized a sodalite solid-solution of the composition $6NaAlSiO_4 \cdot xNaCl \cdot yNa_2S$ in his study of the luminescence of sodalite.[2,3] The phase synthesized in the present study corresponds to the Na_2S-end member, and thus the name of sulfosodalite may be given. The essential difference between this substance and sodalite, however, is that its composition is not constant as with sodalite but varies considerably with synthetic conditions; also this phase contains usually more than eight Na ions. The synthetic conditions and the composition will be reported in this papaer.

Experimental

Starting Materials. The starting material $NaAlSiO_4$ was prepared by heating a mixture of kaolinite and Na_2CO_3 at about 700°C. The actual composition of this material was $Na_{0.98}Al_{0.98}Si_{1.02}O_4$ because of the composition of the kaolinite employed as raw material. To examine the effect of substitution of Si for Al, SiO_2 (Merck's silica gel for chromatographic use, ignition loss 3.68%) was added to the kaolinite - Na_2CO_3 mixture and the same heat-treatment made. The starting materials $Na_uAl_uSi_{2-u}O_4$ (u=0.90, 0.80 and 0.66) were thus prepared.

The starting mixtures $NaAlSiO_4 + aNa_2S$ (a=0.50, 0.75, 1.00, 1.25 and 1.50) and $Na_uAl_uSi_{2-u}O_4 +$ Na_2S were made with sufficient caution against the oxidation of Na_2S.

Details on these raw materials and on the mixing method are described in another paper.[1]

Apparatus. A silica glass tube set perpendicularly in a cylindrical electric furnace was used as the heating apparatus. H_2 or N_2 gas, which was purified by passage through active copper and water absorbent, was passed through this pipe. The starting mixture, which was put in a silica crucible, was hung from a molybdenum wire into the heating zone kept at the predetermined temperatures between 850 and 950°C. After heating for 1 hr, the crucible was removed rapidly to a cool zone for quenching.

Method of Analysis. *a) Treatment of the Synthesized Specimen.* The synthesized specimen was fully washed with water until no alkali was detected by phenolphthalein indicator, and was dried at 110°C. Then carbon disulfide extraction was carried out to completely remove any free sulfur which condensed on the specimen.

b) Chemical Analysis. The specimen was decomposed by dilute sulfuric acid and the analyses of SiO_2, Al_2O_3, Fe_2O_3, CaO, MgO and alkalis were carried out following the usual procedure of silicate analysis. Fe_2O_3 was determined colorimetrically using sulfosalicylic acid. CaO+MgO, the total content of which was about 1%, was removed on the way and was not determined. The alkalis were determined as residual sulfates where the ratio of K_2SO_4/Na_2SO_4 was determined to be less than 0.005 by flame photometry. The alkali content can also be determined indirectly by the charge balance to the ionic sulfur content. Since the former residual sulfate method always gave a lower result, the latter more reliable method was actually adopted.

Total sulfur content was determined through $BaSO_4$ precipitation. In this case, the specimen was decomposed by a Br_2+HCl solution.

For the analysis of ionic sulfur, the specimen was suspended in a solution of $AgNO_3$ and decomposed with dilute sulfuric acid. To decompose the specimen completely, warming in a hot-water bath was necessary. After the Ag_2S precipitate formed was filtered off, the residual $AgNO_3$ was back-titrated with a KCNS solution.

c) Determination of the Sodalite-type Phase Content. Usually the complete formation of the sodalite-type phase

*1 Present address: Institute of Industrial Science, The University of Tokyo, Roppongi, Tokyo.

1) G. Yamaguchi and Y. Kubo, This Bulletin, **41**, 2645 (1968).
2) R. D. Kirk, *J. Electrochem. Soc.*, **101**, 461 (1954).
3) R. D. Kirk, *Am. Mineral.*, **40**, 22 (1955).

TABLE 1. DETERMINATION OF THE COMPOSITION OF SODALITE-TYPE PHASE

Sample	Phase content, %	SiO_2	Al_2O_3	Fe_2O_3	Ionic S	Non-ionic S	Na
		37.6	30.4	0.4	4.88	0.26	19.5
H-F	Neph. 6	2.6	2.1		—	—	1.0
	Sod. 94	35.0	28.7		4.88	0.26	18.5

was not achieved and unreacted nepheline phase coexisted in the specimen. Quantitative analyses of both phases were made by powder X-ray diffraction. As internal standard, 1 part (by weight) of MgO powder was added to 2 parts of the specimen. The diffraction intensity of the peak (20·2) of nepheline at $2\theta=29°38'$ (Cu$K\alpha$), I_N, that of the peak (211) of the sodalite-type phase at $2\theta=$about 24°, I_S, and that of the peak (220) of magnesia at $2\theta=62°18.5'$, I_{MgO}, was measured using a diffractometer. A calibration curve between the nepheline content in the mixture and the value I_N/I_{MgO} was made. Another calibration curve between the sodalite-type phase content and the value I_S/I_{MgO} was also made. Strictly speaking, however, the diffraction intensity of the sodalite-type phase may vary in every specimen differeing in composition. Therefore, the calibration was made using the former calibration curve for the nepheline content as far as possible. Thus the sodalite-type phase content was determined from 100(%)−Nepheline(%). In the specimens where SiO_2 was added, an amorphous phase coexisted in addition to nepheline. In this case, calibration had to be made based on the latter calibration curve.

d) Determination of the Composition of Sodalite-type Phase. Components present due to unreacted nepheline were calculated using the nepheline content determined from X-ray diffraction analysis. Then, these values were subtracted from those obtained from the total chemical analysis and the rest was considered to be in the sodalite-type phase. Impurities such as Fe_2O_3, CaO and MgO were neglected.

e) An Example. An Example of this analytical procedure is given for one of the specimens. The results obtained from the total chemical analysis are given in the first line of Table 1. From an X-ray diffraction analysis, the coexisting nepheline and sodalite-type phase components of this specimen were determined as 6% and 94%, respectively. The components due to coexisting nepheline, as given in the second line, were subtracted from values obtained from the total chemical analysis given in the first line, and components in the sodalite-type phase were obtained as given in the third line. The chemical formula for a unit cell of the sodalite-type phase is calculated from this result as $Na_{8.43}Al_{5.89}Si_{6.11}O_{24}\cdot 1.60\,S^{2-}\cdot 0.08\,S$ (the Na ion content required from charge balance with the S^{2-} ion content is 9.08.).

Results and Discussion

Product Composition. The molar compositions which were determined, based on an analysis of total components are shown in Table 2 for several specimens. The values for a unit cell of sodalite-type structure are given. The analytical data for all specimens which were synthesized under conditions given in columns 2 to 4 of Table 3, are shown in columns 5 to 8 of the same table; Al number in the product, sodalite-type phase content and total and ionic sulfur contents are given.

Now, the average valences of sulfur ions (defined as 2×Ionic S/Total S) were calculated as given in column 9 of Table 3, and were also plotted in Fig. 1.

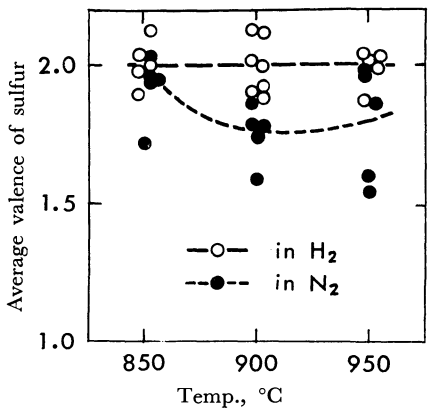

Fig. 1. Average valence of sulfur for specimens synthesized in H_2 and N_2 atmospheres.

As seen in Fig. 1, the average valence of sulfur ions for specimens synthesized in an H_2 atmosphere is equal to 2 within an error of ±5%, while that for specimens synthesized in an N_2 atmosphere ranges from 1.8 to 2. Thus, the former specimens which completely form sulfide may be expressed by the formula $6NaAlSiO_4\cdot xNa_2S$, while the latter, containing some polysulfidic ions, may be expressed by the formula $6NaAlSiO_4\cdot xNa_2S\cdot yS$. When variation in the Si/Al ratio or Al number is taken into consideration, the general formula is given by $6Na_uAl_uSi_{2-u}O_4\cdot xNa_2S\cdot yS$ for a unit cell of a sodalite-type structure.

Based on the general formula, the numbers of ionic sulfurs and non-ionic sulfurs per unit cell (x and y, respectively) were calculated using analytical data on the Al number in the product, u_P, and the total and ionic sulfur contents given in Table 3. The results are shown in columns 10 and 11 of the same table, respectively. When comparison is made between the values (x and y) of Tables 2 and 3, those of Table 2, which were calculated based on an analysis of total components, are in good agreement with those of Table 3, which were calculated based on only the total and ionic sulfur contents according to the general formula. This justifies the general formula, and

TABLE 2. MOLAR COMPOSITION OF SULFOSODALITE FOR A UNIT CELL

Sample	SiO_2	$AlO_{1.5}$	$NaO_{1.5}$	Ionic S	Non-ionic S	Na^+	Total Na
H-C	6.23	5.77	5.77	1.47	0.01	2.94	8.71
H-F	6.11	5.89	5.89	1.60	0.08	3.20	9.08
H-M	6.21	5.79	5.79	1.49	0	2.97	8.76
H-N	6.52	5.48	5.48	1.32	0	2.64	8.12
H-O	7.5	4.5	4.5	0.85	0.15	1.7	6.2
H-T	5.96	6.04	6.04	1.65	0.08	3.30	9.34
N-E	6.1	5.9	5.9	1.8	0.2	3.5	9.4
N-I	6.1	5.9	5.9	1.8	0.1	3.6	9.5
N-J	6.2	5.8	5.8	1.7	0.3	3.4	9.2
N-M	6.1	5.9	5.9	1.7	0.1	3.4	9.3
N-N	6.5	5.5	5.5	1.3	0.3	3.7	9.2
N-O	7.4	4.6	4.6	0.9	0.2	1.9	6.5

the values x and y can be used as characteristic values of the specimen.

Relationships between Synthetic Conditions and Product Composition. Figure 2 shows the variation in the number of ionic sulfurs (or total sulfurs) per unit cell (x), with the amount of Na_2S mixed in the reaction system (a) for specimens synthesized in an H_2 atmosphere at 900°C. The value x increases with increase in a for a less than 1.0, and reaches a constant value for a greater than 1.0. This indicates that the system has not reached equilibrium in a reaction time of 1 hr, until the amount of Na_2S mixed in the reaction system, a, was increased to greater than 1.0 which corresponds to about three times the Na_2S content of the product phase. A similar tendency was observed in specimens synthesized at other temperatures.

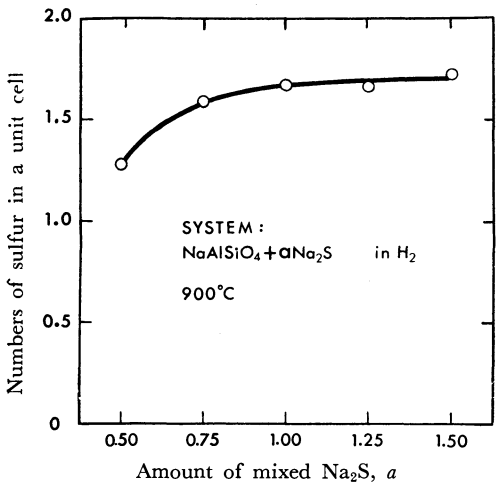

Fig. 2. Variation of sulfur content expressed by numbers in a unit cell with the amount of Na_2S mixed in the reaction system.

Figure 3 shows the change in the value x for a equal to 1.0 with reaction temperature. The value x increases with temperature; the higher the temperature, the more sulfur ions are pressed into

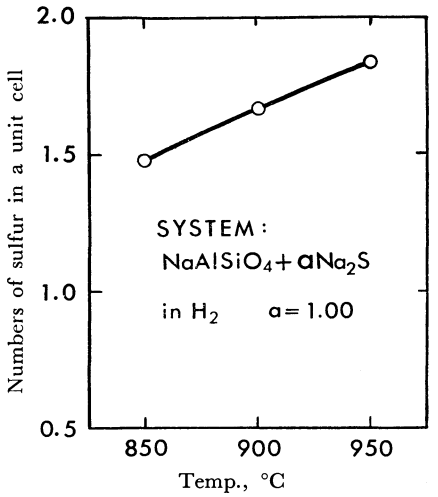

Fig. 3. Variation of sulfur content expressed by numbers in a unit cell with reaction temperature.

the sodalite-type structure. This means that the increase in chemical potential of the Na_2S component with temperature is larger in the Na_2S phase than in the sodalite-type phase.

For specimens synthesized in an N_2 atmosphere, the composition is similar to that of specimens synthesized in an H_2 atmosphere, but the data do not show a constant tendency. Some oxidation of sulfur ion has occurred, giving rise to a small amount of non-ionic sulfur. This may be due to an error caused by residual O_2 in the N_2 gas stream.

Effect of Si Substitution for Al. It must be noted that in this experiment only a small portion of the added SiO_2 has been taken up in the product phase. As shown in columns 4 and 5 of Table 3, the Al number in the reaction system (u_R) and that in the product (u_P) differ considerably; 0.90 *vs.* 0.97, 0.80 *vs.* 0.92 and 0.66 *vs.* 0.76, respectively. Thus, the substitution of Si for Al has taken place only to a small extent compared with the amount of SiO_2 added to the reaction system. This may

TABLE 3. SYNTHETIC CONDITIONS AND ANALYTICAL DATA OF SULFOSODALITE SPECIMENS SYNTHESIZED FROM $Na_uAl_uSi_{2-u}O_4+aNa_2S$ SYSTEMS

1) In H_2 atmosphere

$6Na_uAl_uSi_{2-u}O_4 \cdot xNa_2S \cdot yS$											
(1) Sample	(2) Temp. °C	(3) a	(4) u_R	(5) u_P	(6) S. C.	(7) Total S	(8) Ionic S	(9) A. V.	(10) Na_2S x	(11) S y	(12) Total S, $x+y$
H-A	850	0.50	0.98	0.98	66	3.6	3.4	1.9	1.0	0	1.0
H-B	850	0.75	0.98	0.98	70	4.2	4.2	2.0	1.2	0	1.2
H-C	850	1.00	0.98	0.98	96	4.9	4.9	2.0	1.5	0	1.5
H-D	900	0.50	0.98	0.98	68	4.3	4.6	2.1	1.3	0	1.3
H-E	900	0.75	0.98	0.98	88	5.2	5.3	2.0	1.6	0	1.6
H-F	900	1.00	0.98	0.98	94	5.5	5.2	1.9	1.7	0	1.7
H-S	900	1.25	0.98	0.98	81	5.5	5.2	1.9	1.7	0	1.7
H-T	900	1.50	0.98	0.98	98	5.6	5.4	1.9	1.7	0	1.7
H-G	950	0.50	0.98	0.98	80	4.9	4.9	2.0	1.5	0	1.5
H-H	950	0.75	0.98	0.98	83	4.9	5.0	2.0	1.5	0	1.5
H-I	950	1.00	0.98	0.98	88	5.9	5.6	1.9	1.8	0	1.8
H-J	850	1.00	0.90	0.97	93	4.9	4.9	2.0	1.5	0	1.5
H-K	850	1.00	0.80	0.92	81	4.5	4.8	2.2	1.3	0	1.3
H-L	850	1.00	0.66	0.76	96	3.4	3.0	1.8	0.95	0	0.95
H-M	900	1.00	0.90	0.97	91	5.0	5.0	2.0	1.5	0	1.5
H-N	900	1.00	0.80	0.92	92	4.4	4.7	2.1	1.3	0	1.3
H-O	900	1.00	0.66	0.76	82	3.5	2.9	1.7	0.97	0	0.97
H-P	950	1.00	0.90	0.97	68	5.9	6.0	2.0	1.8	0	1.8
H-Q	950	1.00	0.80	0.92	78	5.5	5.0	1.8	1.7	0	1.7
H-R	950	1.00	0.66	0.76	41	4.7	4.6	2.0	1.4	0	1.4

2) In N_2 atmosphere

$6Na_uAl_uSi_{2-u}O_4 \cdot xNa_2S \cdot yS$											
(1) Sample	(2) Temp. °C	(3) a	(4) u_R	(5) u_P	(6) S. C.	(7) Total S	(8) Ionic S	(9) A. V.	(10) Na_2S x	(11) S y	(12) Total S $x+y$
N-A	850	0.50	0.98	0.98	66	4.4	4.3	2.0	1.3	0.0	1.3
N-B	850	0.75	0.98	0.98	62	5.2	5.0	1.9	1.5	0.1	1.6
N-C	850	1.00	0.98	0.98	55	4.3	4.2	2.0	1.3	0.0	1.3
N-D	900	0.50	0.98	0.98	68	4.6	4.1	1.8	1.2	0.1	1.4
N-E	900	0.75	0.98	0.98	81	6.3	5.6	1.8	1.7	0.2	1.9
N-F	900	1.00	0.98	0.98	83	5.4	5.0	1.9	1.5	0.1	1.6
N-G	950	0.50	0.98	0.98	70	4.1	4.0	2.0	1.2	0.0	1.2
N-H	950	0.75	0.98	0.98	81	6.0	5.9	2.0	1.8	0.0	1.9
N-I	950	1.00	0.98	0.98	84	6.2	5.8	1.9	1.8	0.1	1.9
N-J	850	1.00	0.90	0.97	86	6.5	5.6	1.7	1.7	0.3	2.0
N-K	850	1.00	0.80	0.92	86	5.5	5.6	2.0	1.7	0	1.7
N-L	850	1.00	0.66	0.76	58	4.8	4.4	1.8	1.3	0.1	1.4
N-M	900	1.00	0.90	0.97	84	6.2	5.8	1.9	1.8	0.1	1.9
N-N	900	1.00	0.80	0.92	85	5.7	4.5	1.6	1.4	0.3	1.7
N-O	900	1.00	0.66	0.76	55	4.2	3.6	1.7	1.0	0.2	1.2
N-P	950	1.00	0.90	0.97	100	6.0	4.6	1.5	1.4	0.4	1.8
N-Q	950	1.00	0.80	0.92	92	5.3	4.2	1.6	1.2	0.3	1.5
N-R	950	1.00	5.66	0.76	58	3.9	3.0	1.5	0.8	0.3	1.1

(3) a: Amount of Na_2S mixed in the reaction system.
(4) u_R: Al number in the reaction system.
(5) u_P: Al number in the product.
(6) S. C.: Sulfosodalite content determined by X-ray diffraction.
(7) Total S and (8) Ionic S: Total and Ionic sulfur contents corrected by sulfosodalite content.
(9) A. V.: Average valence of sulfur defined by Ionic S/Total S.
(11) For the specimens in H_2 atmosphere y is taken as 0 according to Fig. 1.

be due to the method of preparation of the starting material, and more well-prepared starting material would result in a more complete substitution of Si for Al.

With increase in the Si substitution for Al, an amorphous phase as a coexisting phase in the specimen increased. This increases the error in the determination of the sodalite-type phase content by X-ray diffraction, since the detarmination is based on only the diffraction peak of the sodalite-type phase. Therefore, a detailed discussion can not be made only these data. As a general tendency, the sulfur content increased or did not change up to an Si fraction, Si/(Si+Al), of 0.52 (u_P of 0.97), and decreased with further increase in the Si fraction. However, it is not clear whether equilibrium had been reached in this system.

It is a noteworthy fact that, as the Si fraction increases, specimens synthesized in both H_2 and N_2 atmospheres turned vermilion red. This color faded gradually upon washing with water for a long time.

Crystal Structure. As regards the ionic valence of the anion which is contained in the sodalite-type aluminosilicic framework, the present substance is similar to noselite which contains SO_4^{2-} ion. Since the number of anions per unit cell of noselite ($Na_8Al_6Si_6O_{24}SO_4$) is half that of sodalite ($Na_8Al_6Si_6O_{24}Cl_2$), the crystal structures are not completely homo-structural.[4] In the X-ray diffraction pattern of noselite, diffractions with $h+k+l=$odd appeare, while in that of sodalite the diffractions vanish due to the extinction rule.

The present substance usually contains more than one but less than two S^{2-} ions per unit cell, and the diffraction pattern is identical with that of sodalite. It is noteworthy that the same characteristics of the diffraction pattern are maintained even in specimens which contain almost one or less than one S^{2-} ion per unit cell, though a noselite-like structure is expected in this case. This means that the anion vacancy distributes at random on the anion sites in the structure. The ionic radius of S^{2-} ion being smaller than that of SO_4^{2-} may account for the difference in the structure. Based on the characteristics of its diffraction pattern, the present substance may be named sulfosodalite.

It is a well-known fact that ultramarine abounds in varieties which have various sulfur contents and various colors. Sulfosodalite may perhaps be a phase corresponding to an end-member of a variety of ultramarine.

4) Y. Kubo and G. Yamaguchi, *J. Mineral. Soc. Japan*, **8**, 235 (1967).

BULLETIN OF THE CHEMICAL SOCIETY OF JAPAN VOL. 41 2645—2650 (1968)

Ultramarines Synthesized under Controlled Sulfur Vapor Pressures

Goro YAMAGUCHI and Yasushi KUBO*1

Department of Industrial Chemistry, Faculty of Engineering, University of Tokyo, Hongo, Tokyo

(Received April 25, 1968)

Ultramarine was synthesized in the systems $NaAlSiO_4$-Na_2S and $NaAlSiO_4 \cdot aNa_2O$-Carbon under a sulfur vapor pressure controlled between 0 and 1 atm. The average valence of sulfur contained in ultramarine changed from 2.0 to 1.0 with increase in sulfur vapor pressure. This was due to the formation of a sulfide containing monosufidic sulfur ion at 0 atm and of a polysulfide containing disulfidic ion at elevated sulfur vapor pressures. Sigmoidal characteristics were observed in the relationships between the sulfur content of ultramarine and the sulfur vapor pressure.

It is well known that ultramarine, a blue sodium aluminosilicate containing sulfur, is a non-stoichiometric compound with its composition varying to a large extent in ionic and non-ionic sulfur contents and in sodium content, as well as in alumina-silica ratio. The various chemical and physical properties of ultramarine as revealed by previous investigators[1-3] are related to its non-stoichiometric characteristics. However, the most fundamental problem, by what factor and in what range the composition of ultramarine is varied, has not yet been elucidated. The greatest reason for this is that the composition of ultramarine is so complicated that the preparation of well-characterized specimens under well-controlled conditions is

*1 Present address: Institute of Industrial Science, The University of Tokyo, Roppongi, Tokyo.

1) F. M. Jaeger, *Trans. Faraday Soc.*, **25**, 320 (1929).
2) J. Hoffmann, *Z. anorg. u. allgem. Chem.*, **183**, 37 (1929).
3) K. Leschewski, *Angew. Chem.*, **48**, 533 (1935).

TABLE 1. CHEMICAL COMPOSITION OF ZETTLITZ KAOLINITE (%)

Ig-loss	SiO_2	Al_2O_3	Fe_2O_3	CaO	MgO	Total
14.05	45.13	37.17	0.55	0.83	0.49	98.22

quite difficult. The circumstances may be common to almost all sulfide minerals, the study of which has progressed much less.

It may help to understand this situation to overlook the manufacturing process of ultramarine. In principle, the manufacture of ultramarine consists of heating a mixture of kaolin or alumino-silicic gel, sulfur or sodium sulfate and carbonaceous reducing agents to about 800°C in the absence of air. A yellow-green mass containing pale-colored ultramarine is thereby obtained, and successive reheating in air causes a deepening of the blue color; finally a dark blue product is obtained. Soluble sodium salts are then leached out, leaving blue ultramarine. It must be stressed here that, though a product excellent for practical use can be thus obtained, the meaning of these processes is not always understood. The system and the reactions are too complicated to permit a scientific approach.

In this study, an attempt was made to reduce the complicated synthetic conditions of ultramarine to its essential factors. Thus, synthesis was carried out by controlling the components necessary to produce ultramarine, $NaAlSiO_4$ and Na_2S, the sulfur vapor pressure and temperature. The relationships between the product composition and the synthetic conditions thus simplified, were investigated.

Experimental

Reaction Systems and Raw Materials. In order to strictly control reaction conditions in the production of ultramarine, as simple a reaction as possible is desired. The choice of reaction system, however, is conditioned by the reaction rate; too low a reaction rate makes synthesis practically impossible.

Through preliminary experiments, the following systems were found adoptable. In these systems, the ultramarine phase was formed in tolerable or high yields at the indicated temperatures in the reaction time of 1 hr.

(1) $NaAlSiO_4$ - Na_2S - S_2 (in an S_2+N_2 atmosphere) 950°C

(2) $NaAlSiO_4 \cdot a Na_2O$ ($a \geqq 0.5$) - C(carbon) - S_2 (in an S_2+N_2 atmosphere) 850°C

The oxides $NaAlSiO_4$ and $NaAlSiO_4 \cdot a Na_2O$ ($a=0.50$ and 0.75) were prepared by heating a mixture of Zettlitz kaolinite (chemical composition given in Table 1) and Na_2CO_3 reagent (E. P. grade) at about 700°C. The actual composition of these oxides were $Na_{0.98}Al_{0.98}Si_{1.02}O_4$ and so on, because of the composition of the original kaolinite. These oxides are composed mainly of high-carnegieite (L) phase,[4] and are favorable for use as starting material in respect to homogeneity and activity. As other raw materials, Na_2S reagent (E. P. grade), charcoal for carbon and sulfur reagent (G. R. grade) were used.

The mixtures $NaAlSiO_4+a Na_2S$ ($a=0.50$, 0.75 and 1.00) and $NaAlSiO_4 \cdot a Na_2O + aC$ ($a=0.50$ and 0.75) were prepared by mixing these raw materials with a motor-driven mortar. For the former mixture containing Na_2S, the mixing was done in liquid hexane to prevent Na_2S from being oxidized, and the mixture was heated at 550°C in an H_2 gas stream for 1 hr prior to use in order to reduce completely the partially oxidized Na_2S.

Apparatus. The vapor pressure of sulfur was controlled by making use of the temperature dependence of the vapor liquid equilibrium of sulfur. The main apparatus is shown in Fig. 1. This apparatus made of transparent silica glass, consists of two regions; the sulfur reservoir (lower part of the apparatus)and the reactor (upper part of the apparatus). Two electric furnaces were used to heat the two regions separately. The temperatures at the surface of the liquid sulfur and at the sample holder were detected with a three-forked Pt-PtRh

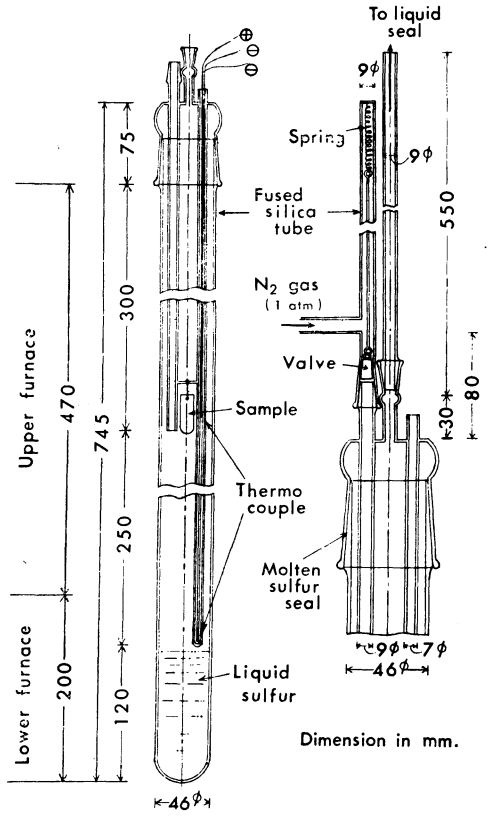

Fig. 1. Apparatus for synthesis under controlled sulfur vapor pressure.

4) Y. Kubo, G. Yamaguchi and K. Kasahara, *Mineral. J.*, **5**, 213 (1967).

thermocouple and were kept by a temperature controller at predetermined values between 380 and 440°C for the sulfur reservoir and between 850 and 950°C for the reactor.

At about 200mm above the ground glass joints, the temperature was held above the melting point of sulfur. Therefore, the condensation of sulfur took place in the perpendicular long thin tube connected to a gas outlet sealed with liquid paraffine. The condensed sulfur was melted away with a hand burner from time to time. The ground glass joints were sealed by molten sulfur.

The apparatus was also connected to an N_2 gas tank of a constant pressure of 1 atm through a valve, in order to remove the contained air before the experiment, as well as to prevent outside air from leaking in during a temporary fall in the inner gas pressure in such an instance as during the cooling process of the sample.

The temperature of the sulfur reservoir could be controlled by a derivative control within ±3°C, which corresponds to a variation in the sulfur vapor pressure of ±0.02 atm around 0.25 atm, and of ±0.04 atm around 0.75 atm. For data on the equilibrium vapor pressure of sulfur, those given by West[5] were used. Except for visual observation at the head of the apparatus, the actual sulfur vapor pressure at the sample holder was not measured. Therefore, agreement between this pressure and that at the surface of the liquid sulfur was not verified. However, since the temperature above the sulfur reservoir was so distributed as to increase towards the sample holder, the stagnation of the sulfur vapor in the lower part of the apparatus could not have occurred.

Experimental Procedures. The starting mixture was put in the sample holder and heated at temperatures of 850 to 950°C for 1 hr. Rapid cooling was carried out by opening the upper electric furnace. The specimen thus obtained was fully washed with water until no alkali was detected by phenolphthalein indicator, and was then dried at 110°C. The free sulfur condensed on the specimen was removed completely by carbon disulfide extraction.

Determination of product composition was made on the specimen by chemical and X-ray diffraction analyses. The methods were described in detail in a previous paper.[6]

Results and Discussion

Product Composition. Analytical data for the specimens which were synthesized under conditions given in columns 2 and 3 of Table 2, are given in columns 4 to 7 of the same table.

Figure 2 shows the variation in the average was valence of sulfur (in column 7) with sulfur vapor pressure, P_{S_2}. As can be seen in the figure, the average valence is 2.0 at no sulfur vapor pressure, and decreases toward 1.0 as the sulfur vapor pressure is increased. This indicates the change from sulfide to polysulfide, and the chemical composition can be expressed conventionally by the formula $6NaAlSiO_4 \cdot xNa_2S \cdot yS$ per unit cell. Based on this formula, the numbers of ionic sulfur, non-ionic sulfur and total sulfur per unit cell, x, y and $x+y$, respectively, were calculated in columns 8 to 10 of Table 2.

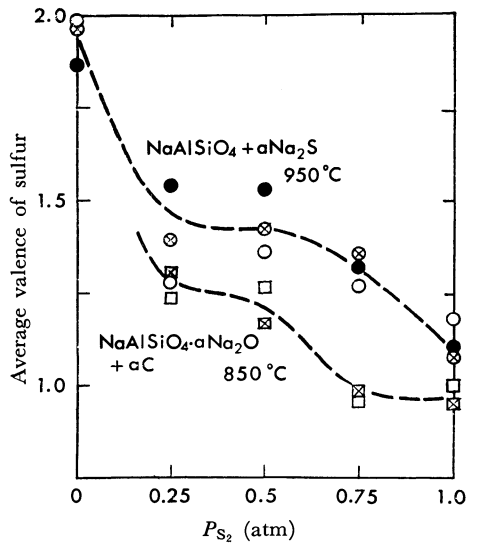

Fig. 2. Variation of average valence of sulfur with sulfur vapor pressure in atmosphere.

Relationships between Synthetic Condition and Product Composition. These values, x, y and $x+y$, change not only with sulfur vapor pressure, P_{S_2}, but also with the amount of Na_2S mixed in the reaction system, a. Changes with the former factor, P_{S_2}, are shown in Figs. 3 and 4; Fig. 3 for the system $NaAlSiO_4+aNa_2S$ at 950°C and Fig. 4 for the system $NaAlSiO_4 \cdot aNa_2O+aC$ at

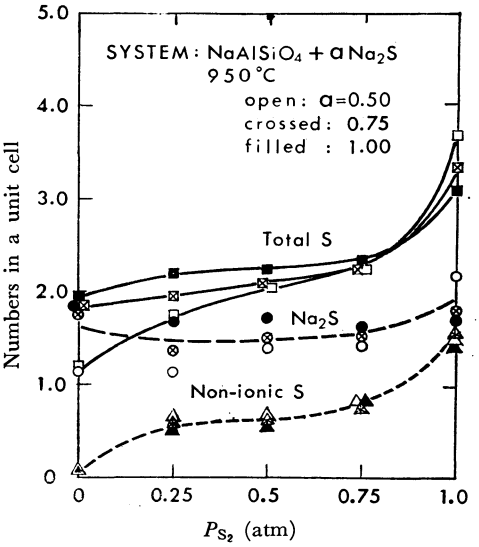

Fig. 3. Variation of numbers of total S, Na_2S, and non-ionic S in a unit cell with sulfur vapor pressure, for specimens synthesized in the system $NaAlSiO_4+aNa_2S$ in (S_2, N_2) atmosphere at 950°C.

5) J. R. West, *Ind. Eng. Chem.*, **42**, 713 (1950).
6) G. Yamaguchi and Y. Kudo, This Bulletin, **41**, 2641 (1968).

TABLE 2. SYNTHETIC CONDITIONS AND ANALYTICAL DATA OF ULTRAMARINE SPECIMENS SYNTHESIZED IN (S_2, N_2) ATMOSPHERE

1) From $Na_{0.98}Al_{0.98}Si_{1.02}O_4+aNa_2S$ systems at 950°C

	$6Na_{0.98}Al_{0.98}Si_{1.02}O_4$ $xNa_2S\cdot yS$								
(1) Sample	(2) P_{S_2} atm	(3) a	(4) U. C.	(5) Total S	(6) Ionic S	(7) A. V.	(8) Na_2S x	(9) S y	(10) Total S $x+y$
A*1	0	0.50	70	4.1	4.0	2.0	1.2	0.0	1.2
B*2	0	0.75	81	6.0	5.9	2.0	1.8	0.0	1.9
C*3	0	1.00	84	6.2	5.8	1.9	1.8	0.1	1.9
D	0.25	0.50	92	5.9	3.8	1.3	1.1	0.6	1.8
E	0.25	0.75	100	6.5	4.5	1.4	1.4	0.6	2.0
F	0.25	1.00	100	7.0	5.4	1.5	1.7	0.5	2.2
G	0.50	0.50	95	6.7	4.6	1.4	1.4	0.7	2.1
H	0.50	0.75	100	6.8	4.9	1.4	1.5	0.6	2.1
I	0.50	1.00	94	7.2	5.5	1.5	1.7	0.5	2.2
J	0.75	0.50	97	7.3	4.7	1.3	1.4	0.8	2.3
K	0.75	0.75	100	7.3	4.9	1.4	1.5	0.7	2.3
L	0.75	1.00	94	7.6	5.1	1.3	1.6	0.8	2.4
M	1.00	0.50	85	11.0	6.5	1.2	2.2	1.5	3.7
N	1.00	0.75	90	10.4	5.5	1.1	1.8	1.6	3.4
O	1.00	1.00	97	10.0	4.9	0.98	1.6	1.6	3.2

2) From $Na_{0.98}Al_{0.98}Si_{1.02}O_4\cdot aNa_2O+aC$ systems at 850°C

	$6Na_{0.98}Al_{0.98}Si_{1.02}O_4\cdot xNa_2S\cdot yS$								
(1) Sample	(2) P_{S_2} atm	(3) a	(4) U. C.	(5) Total S	(6) Ionic S	(7) A. V.	(8) Na_2S x	(9) S y	(10) Total S $x+y$
P*4	0	0.50	66	4.4	4.3	2.0	1.3	0.0	1.3
Q*5	0	0.75	62	5.2	5.0	1.9	1.5	0.1	1.6
R	0.25	0.50	51	9.7	6.0	1.2	1.9	1.2	3.1
S	0.25	0.75	43	9.1	5.9	1.3	1.9	1.0	3.0
T	0.50	0.50	64	9.4	6.0	1.3	1.9	1.1	3.0
U	0.50	0.75	54	9.3	5.4	1.2	1.7	1.2	3.0
V	0.75	0.50	84	12.8	6.1	0.96	2.0	2.2	4.2
W	0.75	0.75	70	11.4	5.6	0.99	1.9	1.9	3.8
X	1.00	0.50	79	13.7	6.8	1.0	2.3	2.4	4.7
Y	1.00	0.75	76	12.8	6.1	0.95	2.1	2.3	4.3

1*—*5: These data are of sulfosodalite in N_2 atmosphere.[6]

(3) a: Amount of Na_2S mixed in the reaction system.

(4) U. C.: Ultramarine content determined by X-ray diffraction.

(5) Total S, and (6) Ionic S: Total and ionic sulfur contents corrected by ultramarine content.

(7) A. V.: Average valence of sulfur defined by 2 Ionic S/Total S.

850°C, respectively. Sigmoidal changes are characteristic of these curves.

Changes with the latter factor, a, are shown in Figs. 5, 6 and 7 for the system $NaAlSiO_4+aNa_2S$ at 950°C. The amount of Na_2S taken up in the product phase correspodns to a value of a of about 0.3. The fact that the product composition expressed by these values varies with the amount of excess Na_2S in the reaction system, indicates that the system has not yet attained equilibrium in a reaction time of 1 hr in the range of a less than 1.0. An increased amount of Na_2S in the reaction system would result in the approach of these values to constant values at equilibrium, as was observed in the sulfosodalite synthesis of the previous paper.[6] However, the tendency of the values at equilibrium can be seen by extrapolating the curves of Figs. 5 to 7; the value x which changes greatly with a, appears to decrease with P_{S_2} at the larger value of a, while the other values, y and $x+y$, increase. The sigmoidal characteristics at equilibrium are strongly seen in Figs. 6 and 7. It is reasonable to conclude that the plateau in the sigmoidal curve corresponds to a stable composition.

Sulfur Ion Species. Now, the sulfur ion species which exist in these specimens and which give the above sulfur composition expressed

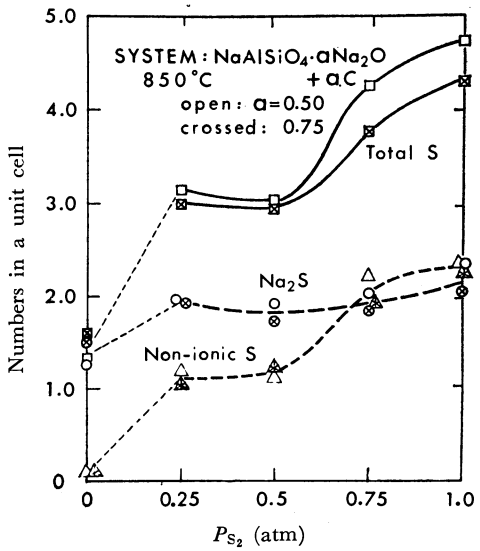

Fig. 4. Variation of numbers of total S, Na_2S, and non-ionic S in a unit cell with sulfur vapor pressure, for specimens synthesized in the system $NaAlSiO_4 \cdot aNa_2O + aC$ in (S_2, N_2) atmosphere at 850°C.

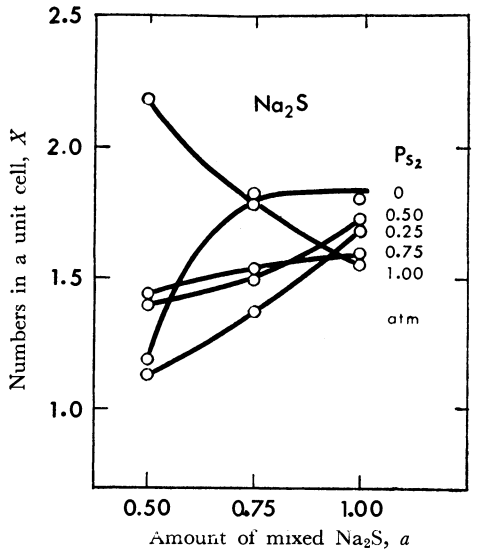

Fig. 5. Variation of numbers of Na_2S in a unit cell with the amount of Na_2S mixed in the reaction system.

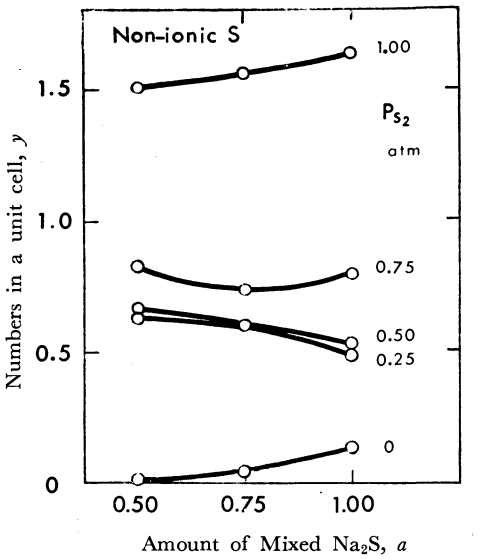

Fig. 6. Variation of numbers of non-ionic S in a unit cell with the amount of Na_2S mixed in the reaction system.

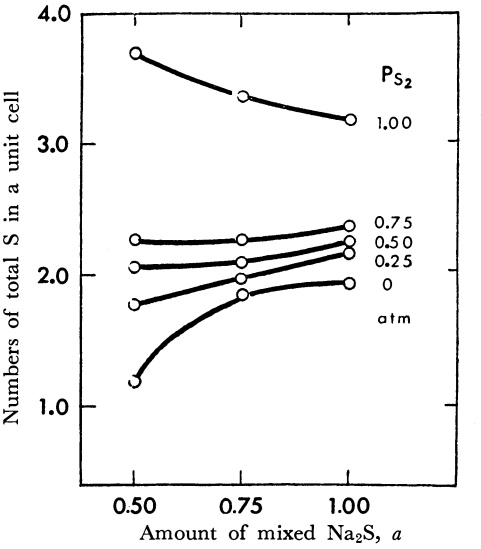

Fig. 7. Variation of numbers of total S in a unit cell with the amount of Na_2S mixed in the reaction system.

conventionally by the numbers of ionic and non-ionic sulfurs (x and y, respectively) should be considered. Here, a criterion is supposed that both the negative charges and the sulfur atoms should distribute as equally as possible on both anion sites (position notation, 2a) in the unit cell of a sodalite-type structure. This supposition is quite reasonable, since it makes anion vacancies as few as possible, as well as to make structural distortion caused by the coexistence of anions with largely different sizes as small as possible. The result of this criterion is that S^{2-} and S_2^{2-} ions coexist in most of the specimens synthesized here. In the results, this model is the same as that supposed by Podschus, Hofmann and Leschewski in their X-ray structure analysis of ultramerine.[7] Thus, the ionic constitutuion at the above-mentioned plateau is given by about $1.2S^{2-}$ $0.6S_2^{2-}$ 0.2 vacancies per unit cell.

7) E. Podshus, U. Hofmann and K. Leschewski, *Z. anorg. u. allgem. Chem.*, **228**, 305 (1936).

Some specimens, however, such as M, V, X and Y, which have either ionic sulfurs or non-ionic sulfurs, or both, more than 2 per unit cell, can not be explained by this model of ionic constitution. The formation of other sulfur ion species must be considered for these specimens. A more detailed discussion on this problem can not be made at present.

Color. In the specimen under no sulfur vapor pressure (namely sulfosodalite), the color is a very pale yellowish or pinkish. With increase in the sulfur vapor pressure, the specimens become more and more blue. This blue is particularly deep in specimens such as N, O, V, W, X and Y, the average valence of sulfur of which is near to or less than 1.0. The color, however, is much more pale than the usual ultramarine deep blue used as pigment. The heat treatment of these specimens in a SO_2 atmosphere at around 350 to 450°C caused a deepening of the blue color, with a great lowering of the average valence of sulfur. Therefore, the specimen in the present experiment is ultramarine of the leuco-form with sulfurs of a high reduction degree.

BULLETIN OF THE CHEMICAL SOCIETY OF JAPAN VOL. 41 2650—2656 (1968)

Studies of the Behavior of Trivalent Uranium in an Aqueous Solution. II. Absorption Spectra and Ion Exchange Behavior in Various Acid Solutions

Akiko SATÔ and Shin SUZUKI

The Research Institute for Iron, Steel and Other Metals, Tohoku University, Katahira-cho, Sendai

(Received April 26, 1968)

The absorption spectra of trivalent uranium in hydrochloric, sulfuric and perchloric acid solutions were investigated. It was found that there is a possibility of the formation of a chloro-complex from the fact that a large change in absorption spectra was observed at high concentrations of chloride ion. On the basis of the above facts, the behavior of trivalent uranium in those media toward ion exchange resin was studied. It was considered that an anionic complex of trivalent uranium begins to form at concentrations of hydrochloric acid above 7 N, which shows good agreement with results obtained on trivalent ions of plutonium, americium and curium, which are similar actinide elements. However, it was not possible to confirm the existence of a soluble carbonate complex of trivalent uranium, as in the case of trivalent plutonium or americium.

In 1927, Someya[1] first obtained trivalent uranium ion in a hydrochloric acid solution by treating hexavalent uranium with liquid zinc amalgam. Since then, few papers have been reported on its chemical behavior in aqueous solution except for absorption spectra in hydrochloric and perchloric acid solutions[2,3] That is, it was thought that studies on the aqueous chemistry of trivalent uranium would be difficult because trivalent uranium is very unstable and oxidizes rapidly in aqueous solution. One of the authors[4] studied the reduction of hexavalent uranium to the trivalent state and found that reduction with liquid zinc amalgam in hydrochloric, sulfuric and perchloric acid solutions is simple in operation, and gives a high yield within a short period of time and with good reproducibility; almost complete reduction is possible, particularly in 0.5 N hydrochloric acid solution. Next, the stability of trivalent uranium in these acidic solutions was investigated; it was found that trivalent uranium is fairly stable in all hydrochloric, sulfuric and perchloric acid solutions at low acid concentrations in the absence of atmospheric oxygen, but that it becomes unstable as the acid concentration increases. These observations are contrary to the previously-accepted view.[5-10] On the basis of

1) K. Someya, *Z. Anorg. Allgem. Chem.*, **161**, 46 (1927).
2) C. K. Jörgensen, *Acta Chem. Scand.*, **10**, 1503 (1956).
3) D. C. Stewart, ANL-4812 (1952).
4) A. Satô, This Bulletin, **40**, 2107 (1967).
5) R. J. Meyer and E. Pietsch, "Gmelins Handbuch der Anorganischen Chemie," 8th Edition, System No. 55, Verlag Chemie, G.m.b.H., Berlin (1936).
6) J. J. Katz and E. Rabinowitz, "The Chemistry of Uranium," National Nuclear Energy Series, Division VIII, Volume 5, McGraw-Hill Book Co., Inc., New York (1951).
7) G. T. Seaborg, "The Actinide Series" in "Comprehensive Inorganic Chemistry," Vol. 1, ed. by M. C. Sneed, J. L. Maynard and R. C. Brasted, D. Van Nostrand Company, Inc., New York (1953), Chap. 3, p. 161.
8) H. R. Hoekstra and J. J. Katz, "The Chemistry of Uranium" in "The Actinide Elements," National Nuclear Energy Series, Division IV, Vol. 14A, ed. by G. T. Seaborg and J. J. Katz, McGraw-Hill Book Co., Inc., New York (1957), Chap. 6, p. 130.
9) J. J. Katz and G. T. Seaborg, "The Chemistry of the Actinide Elments," John Wiley & Sons, Inc., New York (1957), Chap. 5, p. 94.

the above facts, the authors plan to conduct a detailed study of the aqueous chemistry of trivalent uranium.

In this paper, the absorption spectra and ion exchange behavior of trivalent uranium in hydrochloric, sulfuric and perchloric acid solutions were investigated, and the possibility of the existence of a chloro-complex of trivalent uranium in aqueous solutions was discussed through a comparison with results obtained on trivalent ions of plutonium, americium and curium, which are similar actinide elements.

Experimental

Reagents. *Uranium-237 and Various Acid Solutions of Hexavalent Uranium.* The uranium-237 isotope used as a tracer was prepared by the method reported by Ishimori *et al.*[11] Natural uranium dioxide was irradiated for about 2 hr with 20 MeV bremsstrahlung from the linear electron accelerator of the Japan Atomic Energy Research Institute. After irradiation, uranium, containing uranium-237 isotope produced by $(\gamma \cdot n)$ reaction, was separated from the fission products by the TBP-toluene extraction method from a nitric acid solution. The organic substance in the nitric acid solution of the purified uranium was decomposed completely by repeated heating to dryness with nitric acid. The radioactive decay curve of uranium-237 in the purified uranium obtained indicated half lives of 6.5 days for γ-activity and 6.7 days for β-activity, which agreed very well with priviously reported values.[11-15] Energy measurements on the γ-rays of uranium-237 were also carried out, and sharp peaks were found at energies of 59, 163, 210, 265 and 325 keV, which were assigned to γ-rays emitted by uranium-237 in reasonable agreement with the established decay scheme.[12,13] From these observations, uranium-237 thus prepared was thought adequate for use as a tracer. The uranyl nitrate solution thus obtained was heated almost to dryness several times with hydrochloric, sulfuric or perchloric acid in order to convert the salt into each form completely. The residue was then dissolved in an appropriate quantity of hydrochloric, sulfuric or perchloric acid solution in order to prepare acid solutions of various concentrations. The concentration of uranium was determined by first reducing the hexavalent uranium to the tetravalent state in the air with liquid zinc amalgam, then by titrating the tetravalent uranium with a standard solution of 0.01 N potassium dichromate, using sodium diphenylamine sulfonate as an indicator.[16]

Ion Exchange Resins. Dowex-50X8 (100—200 mesh) and Dowex-1X4 (50—100 mesh) were used for the cation and anion exchange experiments, respectively. Before use, they were conditioned sufficiently in the usual manner, converted to the desired forms (Dowex-50 to the hydrogen form; Dowex-1 to the chloride, sulfate or perchlorate form), washed with distilled water and then dried in air.

The liquid zinc amalgam was prepared by a method reported previously.[4] All other chemicals used were of the highest-purity grade.

Apparatus. For the reduction of hexavalent uranium to the trivalent state with liquid zinc amalgam, the reduction apparatus was that described in a foregoing report.[4] A Hitachi EPS-3 recording spectrophotometer and a 1 cm quartz cell with a glass stopper were used in measuring the absorption spectrum. The γ-radioactivity was measured with a Kobe-Kogyo well-type scintillation counter and a $1\frac{3}{4}''$ ida. $\times 2''$ NaI(Tl) well-type detector coupled to a Kobe-Kogyo 100 channel pulse-height analyzer, Model AN-100.

Procedures. A plastic globe-box was used throughout and all experiments were carried out in an argon, nitrogen or carbon dioxide atmosphere in order to prevent the oxidation of trivalent uranium at room temperature, which was 20—25°C.

Trivalent Uranium Solution. An acid solution of hexavalent uranium was reduced to the trivalent state by the liquid-zinc-amalgam method described in a previous paper.[4]

Absorption Spectrum. After reduction of the hexavalent uranium to the trivalent state, the uranium solution was put into the spectrophotometer cell and stopperd in an inert gas atmosphere. The absorption spectrum of 400—1400 mμ was immediately measured with reference to an acid solution of the same concentration as the sample.

Ion Exchange. The apparent distribution coeffcient was determined by equilibrating 500 mg of air-dried ion exchange resin with 25 m*l* of a 10^{-5} M trivalent uranium solution under the desired conditions with shaking. An aliquot of the supernatant liquid was taken for the measurement of γ-radioactivity. The radioactivity in the resin after equilibration was estimated from the difference between the total activity and the final activity present in the solutions.

The apparent distribution coefficient was calculated by means of the usual relationship.

$$K_{d'} = \frac{\left(\frac{\text{Radioactivity of } U^{3+} \text{ in resin}}{\text{Amount of resin (g)}}\right)}{\left(\frac{\text{Radioactivity of } U^{3+} \text{ in solution}}{\text{Volume of solution (m}l\text{)}}\right)}$$

However, the reduction of the hexavalent uranium to the trivalent state does not proceed completely, depending on the acid and its concentration, as described in a previous paper,[4] and although slowly, the trivalent uranium in the solution which has once been reduced is oxidized to the tetravalent state. Therefore, tetravalent uranium is also contained in the sample solution. Consequently, it is necessary to correct for this. The results, given in Tables 1 and 3 mentioned later, indicate that the apparent distribution coefficient

10) J. E. Grindler, "The Radiochemistry of Uranium," NAS-NS 3050, U. S. Atomic Energy Commission (1962).
11) E. Akatsu, T. Kuroyanagi and T. Ishimori, *Radiochimica Acta,* **2**, 1 (1963).
12) I. F. Wagner, Jr., M. S. Freedman, D. W. Engekemeir and J. R. Huizenga, *Phys. Rev.,* **89**, 502 (1953).
13) J. O. Rasmussen, F. L. Canavan and J. M. Hollander, *ibid.,* **107**, 141 (1957).
14) A. C. Wahl and G. T. Seaborg, *ibid.,* **73**, 940 (1948).
15) Y. Nishina, T. Yasaki, H. Ezoe, K. Kimura and M. Ikawa, *ibid.,* **57**, 1182 (1940).
16) T. Nakazono, *Nippon Kagaku Kwaishi (J. Chem. Soc. Japan),* **42**, 761 (1921).

is almost constant, even when the time of standing or the amount of resin present is varied. Therefore, it is thought that cation or anion exchange resin has no effect on the re-oxidation rate of trivalent uranium in our experiments. On the other hand, it was found from our latest study to be published in the near future, that tetravalent uranium is completely extracted with 0.1 M DBP (di-*n*-buthyl phosphate)-benzene solution from a hydrochloric acid solution in an acid concentration range above 0.35 N. However, trivalent uranium can not be extracted at all under the same condition as above. Therefore, the re-oxidation rate of trivalent uranium in hydrochloric acid solutions at acid concentrations above 0.35 N can be determined by the DBP-benzene extraction method. It was also found that the concentration of uranium in the range of 10^{-3}—10^{-5} M has no effect on the re-oxidation rate of trivalent uranium as long as all atmospheric oxygen is excluded.

On the basis of the above facts, it is thought that the percentage of reduction of hexavalent uranium to the trivalent state and the quantity of trivalent uranium present after a fixed time can be calculated by knowing the kind of acid used and its concentration in the sample solution and using the results reported in the previous paper.[4] Corrections to the radioactivity in the solution can be made on the basis of these values. Namely, the radioactivity corrected through calculating the quantity of tetravalent uranium actually present in solution is the radioactivity of trivalent uranium actually present in the solution. Next, the radioactivity of trivalent uranium adsorbed in the resin should also be corrected by obtaining the apparent distribution coefficient of tetravalent uranium under the same conditions and by calculating the cocentration of tetravalent uranium in the solution by the same method as above. That is, the radioactivity corresponding to tetravalent uranium adsorbed in the resin is deducted from the apparent radioactivity of trivalent uranium adsorbed in the resin. The value thus obtained is taken as the actual radioactivity of trivalent uranium adsorbed in the resin.

Results

The Absorption Spectra of Trivalent Uranium. The absorption spectra of trivalent uranium obtained in perchloric and sulfuric acid solutions at 400—1400 mμ are shown in Fig. 1. Even when the concentration of perchloric acid is changed in the range 0.01—6 N and the concentration of sulfuric acid in the range of 0.01—10 N, there is no change in both absorption spectra and they remain completely the same. The absorption spectra are about the same as those reported by Jörgensen[2] and Stewart[3], as the positions of the main peaks are at 455, 526, 619, 639, 740, 890, 910, 980, 1075 and 1230 mμ. The 4 peaks at 526, 890, 910 and 1230 mμ are particularly characteristic, as they are strong, and when the relation between their heights and the concentration of trivalent uranium was obtained, it was found that Beer's law is obeyed. The molar extinction coefficients, E_m, at 526, 890, 910 and 1230 mμ under the above conditions were 171, 222, 226 and 175, respectively. For reference, the absorption spectra of tetravalent uranium under the same conditions are also shown in Fig. 1. Since trivalent uranium becomes unstable as the acid concentration of perchloric or sulfuric acid increases, the experiment was not carried out with higher acid concentrations than those mentioned above.

In a hydrochloric acid solution, the absorption spectra of trivalent uranium, when the concentration is in the range 0.001—6 N, are nearly the same as those in sulfuric acid and perchloric acid solutions, as shown in Fig. 2. However, the positions of peaks at 740, 890 and 980 mμ have shifted 5 mμ to 745, 895 and 985 mμ, respectively. Furthermore, these spectra show marked changes as the hydrochloric acid concentration increases; the peak at 526 mμ shows a sudden increase in height as the acid concentration increases and at the same time, becomes broad and is shifted to 532 mμ at 11 N, and to 548 mμ at 12 N, *i. e.*, to longer wavelengths. On the other hand, the peak at 619 mμ is shifted to 618 mμ at 11 N and to 615 mμ at 12 N, to shorter wavelengths. The peak at 639 mμ does not change up to 11 N hydrochloric acid, but shows a large shift up to 654 mμ at 12 N. In order to study this phenomenon, the hydrochloric acid concentration was maintained below

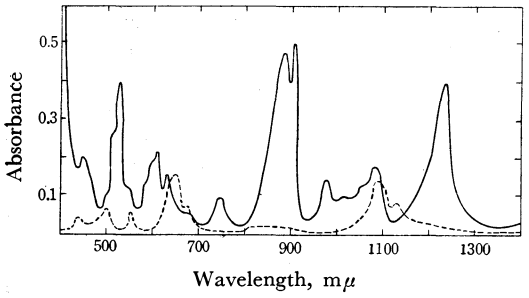

Fig. 1. Absorption spectra of tri- and tetravalent uranium in sulfuric and perchloric acid solutions.
——: U^{3+} – – –: U^{4+}
Concentration of U: 2×10^{-3} M

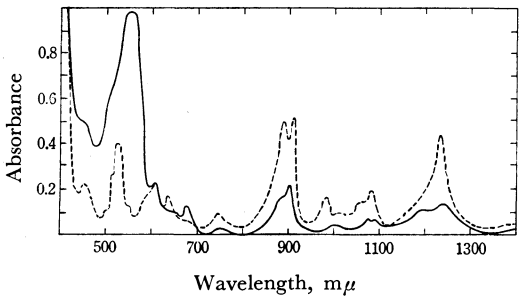

Fig. 2. Absorption spectra of trivalent uranium in hydrochloric acid solution.
——: 12 N – – –: below 6 N
Concentration of U: 2×10^{-3} M

6 N and the chloride ion concentration increased gradually by adding chloride salts such as lithium chloride, by which a marked change was observed in the absorption spectra similar to that indicated above. It is inferred from the above fact that trivalent uranium forms a chloro-complex in solutions of very high chloride ion concentration. Furthermore, the rate of decrease of the absorption peak at 526 mμ was obtained as a fuction of time and the stability of trivalent uranium in the various acidic solutions was also obtained, by which similar results to those reported in the previous paper[4] were obtained.

Finally, in order to study the formation of a soluble carbonate complex of trivalent uranium, an experiment was carried out by adding potassium or ammonium carbonate to a trivalent uranium solution to a concentration of several % or several tens of %, and also by changing the pH. However, a dark violet, insoluble precipitate was formed under all conditions and it was not possible to confirm the presence of a soluble carbonate complex even from the absorption spectra of the supernatant liquid.

The Ion Exchange Behavior of Trivalent Uranium. *Rate of Exchange.* To evaluate the time of standing necessary for batch experiments, the rate of exchange was investigated by almost the same method as in the K_d determination. The experimental accuracy becomes poor with increase in the time of standing, because the reoxidation of trivalent uranium occurs gradually, even in the absence of atmospheric oxygen; this must be avoided as much as possible. Therefore, the change in the apparent distribution coefficient was measured for anion exchange resin in a concentrated hydrochloric acid solution which is assumed to be adsorbed most. As shown in Table 1, it was found that equilibrium is reached after approximately 45 min. An almost similar result was obtained in the experiment using cation exchange resin. From the above investigation, a standing period of 1 hr is recommended for this batch equilibrium experment.

Table 1. Rate of exchange

Time, min	Distribution coefficint*	
	Dowex-1**	Dowex-50***
10	3.0	270
20	4.5	380
30	5.9	400
45	6.6	460
60	6.8	490
90	6.7	480
120	6.9	480
180	6.8	500
300	6.4	500

* Each of the value is the mean of five experiments.
** U, 1.05×10^{-5} M; HCl, 12 N
*** U, 1.30×10^{-5} M; HCl, 0.1 N

Amount of Resin. As the trivalent uranium prepared by reduction with liquid zinc amalgam, a considerable quantity of zinc dissolves, particularly in the case of hydrochloric acid solution. As Table 2 shows, the zinc concentration in the solution after reduction is 1×10^{-2} M in a 0.5 N hydrochloric acid solution and 9×10^{-1} M in a 12 N hydrochloric acid solution. It has been known that zinc ion is adsorbed on an anion exchange resin in a hydrochloric acid solution.[17] Therefore, in order to find out whether it affects the apparent distribution coefficient of trivalent uranium or not, an experiment was carried out to investigate whether the apparent distribution coefficient changes with the quantity of resin using anion exchange resin in a similar manner to that mentioned above. As seen from Table 3, the apparent distribution coefficient is almost constant in the range 0.1—5 g of resin, and there is no effect due to the liquid zinc amalgam used in the reduction. A similar experiment was carried out using cation

Table 2. Concentration of zinc in hydrochloric acid solution after the reduction with liquid zinc amalgam

Concn. of acid N	Concn. of zinc* M
0.5	1.1×10^{-2}
2.0	1.2×10^{-2}
6.0	3.7×10^{-2}
10.0	2.1×10^{-1}
12.0	8.6×10^{-1}

* Each of the value is the mean of three experiments.

Table 3. Effect of amount of resin on the distribution coefficient of trivalent uranium

Amount of resin g	Distribution coefficient*	
	Dowex-1**	Dowex-50***
0.10	6.6	490
0.25	6.1	460
0.50	6.8	480
1.00	6.4	490
2.00	6.5	500
3.00	6.5	470
5.00	6.7	500

* Each of the value is the mean of five experiments.
** U, 1.05×10^{-5} M; HCl, 12 N
*** U, 1.05×10^{-5} M; HCl, 0.1 N

17) K. A. Kraus and F. Nelson, P/837, Proc. Intern. Conf. Peaceful Uses Atomic Energy, Geneva, 1955, **7**, 113 (1956).

exchange resin and it was found that, as in the case of the anion exchange resin, there is no effect. From the above results, 0.5 g of the resin is recommended for use in this experiment.

Apparent Distribution Coefficient. The apparent distribution coefficient of trivalent uranium was determined for cation and anion exchange resins at various concentrations of hydrochloric, sulfuric and perchloric acids, using 0.5 g of the resin and 1 hr of standing. However, experiments above 6 N in the case of sulfuric acid solution and above 2 N in the case of perchloric acid solution were not carried out, because trivalent uranium becomes unstable as the acid concentration increases. The apparent distribution coefficient of tetravalent uranium under exactly the same conditions is also determined for reference.

Table 4. Distribution coefficient of tri- and tetravalent uranium in hydrochloric acid solution

Concn. of HCl N	Distribution coefficient*			
	Dowex-1		Dowex-50	
	U^{3+}	U^{4+}	U^{3+}	U^{4+}
0.01	0	0	510	3650
0.05	0	0	490	2120
0.1	0	0	480	1680
0.5	0	0	380	155
1	0	0	320	75
2	0	2.5	270	56
4	0	17	33	19
6	0	19	12	6.6
7	1.5	21	9.5	5.7
8	2.9	23	5.9	4.6
9	4.6	25	4.2	4.0
10	5.0	24	3.7	3.4
11	6.0	21	4.0	3.5
12	6.7	25	4.1	3.9

* Each of the value is the mean of six experiments.

As is clear from Table 4, in a hydrochloric acid solution trivalent uranium is adsorbed on the cation exchange resin to a considerable extent, and the apparent distribution coefficient increases with decrease in the concentration of hydrochloric acid, reaching a maximum at about 0.1 N; in the range 0.1 N to 0.01 N, the apparent distribution coefficient shows an approximately constant value of 500. In the case of tetravalent uranium, the apparent distribution coefficient increases with decrease in the concentration of hydrochloric acid, similar to trivalent uranium. However, the value is larger by nearly one order of magnitude than in the case of trivalent uranium, especially in the low acidity range. Also, the apparent distribution coefficient for the anion exchange resin is low for both trivalent and tetravalent uranium in low concentrations of hydrochloric acid, but increases gradually with increase in the concentration of hydrochloric acid. At any rate, their values are small and that for trivalent uranium is smallest.

In the case of sulfuric and perchloric acid solutions, as shown in Tables 5 and 6, trivalent uranium is not entirely adsorbed on the anion exchange resin in the range of acid concentration of the experiment. In contrast to this, a larger value than that for tetravalent uranium was obtained in the case of cation exchange resin. A very large value of the apparent distribution coefficient was indicated, particularly in a low acid solution, as it became about 7000 even at 0.1 N and is almost completely adsorbed on the cation exchange resin.

Table 5. Distribution coefficient of tri- and tetravalent uranium in sulfuric acid solution

Concn. of H_2SO_4 N	Distribution coefficient*			
	Dowex-1		Dowex-50	
	U^{3+}	U^{4+}	U^{3+}	U^{4+}
0.1	0	421	6600	340
0.5	0	57	320	40
1	0	18	12	18
2	0	5.2	2.9	2.2
4	0	2.0	0	1.7
6	0	1.3	0	1.4

* Each of the value is the mean of six experiments.

Table 6. Distribution coefficient of tri- and tefravalent uranium in perchloric acid solution

Concn. of $HClO_4$ N	Distribution coefficient*			
	Dowex-1		Dowex-50	
	U^{3+}	U^{4+}	U^{3+}	U^{4+}
0.1	0	0	7000	721
0.5	0	0	4400	59
1	0	0	2000	30
2	0	0	880	13

* Each of the value is the mean of six experiments.

Discussion

On the basis of the above experimental results, complex formation of trivalent uranium in sulfuric, perchloric and hydrochloric acid solutions was compared with that of trivalent plutonium, americium or curium ion, which are relatively stable in aqueous solution, from among the same

actinide elements. That is, as prevoiously described[18] for trivalent plutonium, both cationic and anionic complexes are formed in sulfate solutions, negatively charged complexes exist predominantly in concentrated sulfuric acid solutions and trivalent plutonium has a greater tendency to form sulfate complexes than trivalent americium; however, even in solutions where sulfate complexes are definitely known to exist, for example, in a 16 M sulfuric acid solution, changes in the absorption spectra of these solutions are very slight. According to experiments in sulfuric acid solutions, there is no formation of an anionic complex of trivalent uranium, at least at acid concentrations below 6 N, because the absorption spectra show almost no change and trivalent uranium ion is not adsorbed on the anion exchange resin over the entire range of acidity used.

Also, an investigation of complex formation by trivalent plutonium and americium in 1—5 M perchloric acid solution showed no appreciable changes in absorption spectra, and hardly any noticeable changes in absorption spectra of trivalent plutonium were observed at higher concentrations of perchloric acid.[19] Results concerning absorption spectra and the ion exchange behavior of trivalent uranium in a perchloric acid solution hitherto obtained indicate the absence of anionic complex formation at acid concentrations below 2 N, similar to the above results for a sulfuric acid solution.

In the literature, there are quite definite examples of the existence of chloride complexes of trivalent plutonium.[20-22] Changes in the absorption spectra of trivalent plutonium in hydrochloric acid solutions at acid concentrations right up to 4.4 M indicate the formation of complexes of trivalent plutonium with chloride ions.[20] In an ion exchange investigation, Diamond, Street and Seaborg[21] found that at high hydrochloric acid concentrations trivalent transuranium elements form complexes with chloride ions to a greater extent than lanthanides. Quantitative data on the composition and stability of complex chloride ions of Me^{3+} (where Me^{3+} is Pu^{3+}, Am^{3+} and Cm^{3+}) were obtained by Ward and Welch[22] through the ion exchange method. They established the formation of complex ions $MeCl^{2+}$, and at hydrochloric acid concentrations above 1 M, also complexes $MeCl_2^{+}$. Apparently, complex ions of the type $MeCl_3^{0}$ are also formed in more concentrated hydrochloric acid solutions, *i. e.*, in solutions with a large excess of chloride ions. In 12.6 M hydrochloric acid solution complex anions are formed, whose relative stabilities go as $Pu \gg Am > Cm$.

From the results of our study on absorption spectra and ion exchange behavior, it is thought that an anionic chloride complex of trivalent uranium begins to form at hydrochloric acid concentrations above 7 N, showing good agreement with results obtained on trivalent states of plutonium, americium and curium. However, in the case of trivalent plutonium, the stability of anionic chloride complexes increased rapidly at 12.6 N. On the other hand, from results obtained by the present authors, a sudden change occurred in the absorption spectra when the concentration of hydrochloric acid became greater than 10 N in the case of trivalent uranium, and similar to the case of trivalent plutonium, it can be expected that the stability of an anionic complex of trivalent uranium will increase suddenly above 10 N. However, according to results from the ion exchange experiment, a large change in the apparent distribution coefficient for anion exchange resin in high concentrations of hydrochloric acid solutions in the case of trivalent americium or curium was not indicated, contrary to expectation.

In general, the tendency of ions of a given element to form complexes increases with decrease in ionic radius and increase in charge, *i. e.*, with increase in the ionic potential,

$$\varphi = \frac{Z}{r},$$

where Z is the ionic charge and r the ionic radius. In accordance with this, it is to be expected that the ion U^{4+} will have a greater tendency to form complexes with acid anions than the ion U^{3+}. The results of investigating complex formation by uranium in tri- and tetravalence forms are in agreement with this. Also, by analogy with the lanthanides and from the known behavior of the transuranium elements, the relative strengths of the multichloride complex ions of trivalent plutonium, americium and curium should decrease in that order. In dilute hydrochloric acid solutions, the order of the relative strengths of the multichloride complex ions of trivalent uranium, plutonium, americium and curium was found to be identical, while in the case of concentrated hydrochloric acid solutions, the order of uranium and plutonium was reversed.

18) A. D. Gel'man, A. I. Moskvin, L. M. Zaitsev and M. P. Mefod'eva, "Complex Compounds of Transuranium Elements," translated from the Russian by C. T. Turton and T. I. Turton, Consultants Bureau Enterprises, Inc., New York (1962), Chap. 2, p. 32.

19) A. D. Gel'man, A. I. Moskvin, L. M. Zaitsev and M. P. Mefod'eva, *ibid.*, Chap. 2, p. 31; Chap. 4, p. 154.

20) J. C. Hindman and D. P. Ames, National Nuclear Energy Series, Plutonium Project Record, Vol. 14B, "The Transuranium Elements," McGraw-Hill Book Co., Inc., New York (1949), Paper No. 4.2: J. C. Hindman, *ibid.*, Paper No. 4.4.

21) R. M. Diamond, K. Street, Jr., and G. T. Seaborg, *J. Am. Chem. Soc.*, **76**, 1461 (1954).

22) M. Ward and G. A. Welch, *J. Inorg. Nucl. Chem.*, **2**, 395 (1956).

Finally, it was reported with respect to the formation of carbonate complexes that carbonate ions form soluble anionic complexes in 40% potassium carbonate solution in the case of actinide elements such as trivalent plutonium and americium. That is, it was reported that the absorption spectra of carbonate complexes of trivalent plutonium showing absorption maxima at wavelengths of 565, 600, 835 and 920 mμ were observed,[23] and the formation of anionic complexes confirmed by the study of the electromigration in carbonate solutions.[24,25] It is expected that there is a possibility of the formation of a soluble carbonate complex in the case of trivalent uranium, similar to the case of plutonium and americium, and consequently, this was studied from various points of view. However, in the case of trivalent uranium, a precipitate with a low solubility which is believed to be an insoluble carbonate always formed, and it was not possible to confirm the presence of a soluble carbonate complex from the absorption spectra of the supernatant liquid.

This work was partly supported by a grant-in-aid from the Ministry of Education.

23) G. E. Moore and L. B. Werner, Report CL-P-314 (1944).

24) G. N. Yakovlev and V. N. Kosyakov, Paper P/676, Proc. Intern. Conf. Peaceful Uses Atomic Energy, Geneva, 1955, **7**, 363 (1956).

25) L. B. Werner and I. Perlman, *J. Am. Chem. Soc.*, **73**, 495 (1951).

BULLETIN OF THE CHEMICAL SOCIETY OF JAPAN VOL. 41 2656—2660 (1968)

Studies on Adduct Formation of β-Diketone Chelates with Heterocyclic Bases

Tsunenobu SHIGEMATSU, Masayuki TABUSHI, Masakazu MATSUI and Megumu MUNAKATA

Institute for Chemical Research, Kyoto University, Uji, Kyoto

(Received April 27, 1968)

Stability constants of the 1 : 1-adducts with heterocyclic Lewis bases on copper chelates of six β-diketones and two ethylesters of β-ketoacids ($Cu(ligand)_2 \cdot base$) were determined by spectrophotometric measurements in visible region and the effects of β-diketone substituents, Lewis bases and organic solvents on the stability constants were studied. Terminal alkyl groups of β-diketones hardly hindered the adduct formation, because the adducts of β-diketone chelates except acetylacetone chelate had similar stability constants. Solvent effect was due to the formation of the solvates of the chelates or the solvation of N-base with solvent. This is related to the abnormal position of chloroform in the order of the adduct stability compared with oxygen-containing solvents. Infrared spectra indicate that the metal-oxygen bonding, as well as the basicity of Lewis bases is considered as an essential factor in the adduct formation of metal β-diketone chelates.

As already stated by many investigators, the adduct-formation of metal β-diketonates plays an important role in the synergistic enhancement of the solvent extraction, and therefore the adduct-forming reaction and the structure of the adducts have the interest for analytical and coordination chemists. Recently, many adducts of transition metal acetylacetone (AA) chelates were prepared and their properties studied. Nakamoto and his coworkers[1] suggested from the infrared spectra that adduct-forming Lewis bases coordinated directly to the central metal atom in the adduct of metal acetylacetonates such as $Ni(AA)_2$, $VO(AA)_2$ and $UO_2(AA)_2$. Adducts of copper(II) β-diketonates have been extensively investigated. The behavior of Lewis base, chelate ligand and solvent on the adduct-formation were studied by Graddon and Watton[2] using nitrogen-containing heterocyclic bases (N-bases), and by Rao and Li[3] using some organo-phosphorus compounds. They mentioned that (i) the base effect reflected partly donor power of the base and partly steric effect; (ii) the ligand effect related to the transfer of negative charge from the ligand to metal ion, and consequently to the residual positive charge on the metal

1) K. Nakamoto, Y. Morimo and A. E. Martell, *J. Am. Chem. Soc.*, **83**, 4533 (1961).

2) D. P. Graddon and E. C. Watton, *J. Inorg. Nucl. Chem.*, **21**, 49 (1961).

3) G. N. Rao and N. C. Li, *ibid.*, **28**, 2931 (1966).

atom; and (iii) the solvent effect was attributed to change in the solvation energy.

The present research was carried out in order to ascertain and to discuss Graddon's conclusion. Copper chelates were prepared by using six β-diketones and two methylesters of β-ketoacids; the stability constant of the 1 : 1-adducts with several N-bases (Cu^{II}(chelate ligand)$_2$N-base) was determined by means of spectrophotometric measurements, and various factors affecting the stability of the adduct were investigated. Especially, the solvent effect seemed to result from the change in the thermodynamic concentration of the Lewis base and from the solvation which took place between some oxygen-containing solvents and β-diketone chelates with CF_3 terminal group. Furthermore, the chelates were prepared, and the problem on metal ligand bonding, which had not been clarified, was discussed from the results of infrared absorption.

Experimental

Apparatus. A Hitachi Perkin-Elemer 139 UV-VIS spectrophotometer and a Shimadzu automatic recording spectrophotometer, model IV-50, were used for the visible spectrophotometeric measurements. Infrared spectra were obtained by the KBr disk method with a Perkin-Elmer, Model 521 infrared spectrophotometer.

Materials. Acetylacetone (AA), ethylacetyl acetate (EAA), ethylbenzoyl acetate (EBA), trifluoroacetylacetone (TAA) and benzoyltrifluoroacetone (BFA) were obtained from the Dojindo Co. Ltd., Research Laboratories or from Tokyo Kasei Kogyo Co., Ltd. Dipropionylmethane (DPrM), diisobutyrylmethane (DIBM) and pivaloylacetone (PvA) were prepared by the acylation of methylketones with the ethyl esters of carboxylic acids in the presence of sodium amide or sodium methoxide. These β-diketones were precipitated as copper chelates, and recrystallized from benzene. The analytical data are listed below (calculated values are shown in parentheses):

$Cu(DPrM)_2$	C: 52.88 (52.69)	H: 6.92 (7.05)
$Cu(PvA)_2$	C: 55.80 (56.70)	H: 7.69 (7.52)
$Cu(DIBM)_2$	C: 57.37 (57.80)	H: 8.27 (8.03)

Preparation of Metal Chelates. Copper chelates were prepared in the following manner: To 50 m*l* of 0.5 M copper(II) chloride solution, 20 m*l* of 2.5 M β-diketone methanol solution and 25 m*l* of 2 M sodium acetate solution were successively added under continuous stirring. After heated for a short while on a hot plate, the mixture was allowed to stand in a refrigerator for several hours. The crystalline solid was filtered off on a Buchner funnel, washed with water and dried in a desiccator. After recrystallized from benzene, the crystalline chelate was dried overnight at 60°C in an evacuated vessel. The results of elementary analysis of the chelates are shown in Table 1.

Table 1. Analysis of metal compounds

Complex	Analysis (%) C	H
$Cu(AA)_2$	45.74(45.78)	5.38(5.35)
$Cu(EAA)_2$	44.54(44.72)	5.44(5.59)
$Cu(EBA)_2$	58.67(59.26)	4.89(4.93)
$Cu(TAA)_2$	32.39(32.43)	2.21(2.16)
$Cu(BFA)_2$	48.54(48.57)	2.39(2.43)

Calculated values are in parentheses.

Results and Discussion

It has been reported that copper β-diketonates react with one mole of N-base to form 1 : 1-adducts in solution. The fact is supported by the fact that a distinct isosbestic point is observed in Fig. 1. Since the visible band shifts to longer wavelength

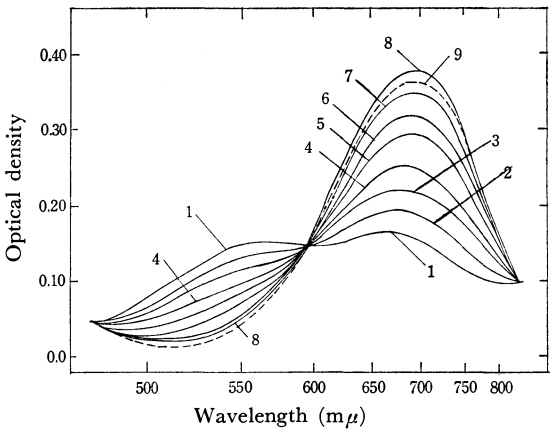

Fig. 1. Absorption spectra of 0.0025 M $Cu(TAA)_2$ and pyridine in benzene.
Pyridine concentration
1: 0; 2: 0.001 M; 3: 0.002 M; 4: 0.003 M; 5: 0.005 M; 6: 0.007 M; 7: 0.01 M; 8: 0.03 M; 9: 0.1 M.

by coordination of the N-base (see Fig. 1), the stability constant of the adducts can be determined spectrophotometrically by the following equation[2];

$$K = \frac{[E_\infty - E_0][E - E_0]}{B_0[E_\infty - E] - C_0[E - E_0]} \times \frac{1}{E_\infty - E}$$

where E is the absorbance measured at a definite wavelength, such as that is indicated in Table 2,

Table 2. Maximum wavelength (mμ) of pyridine adducts of copper(II) β-diketonates

Adduct	Solvent Benzene	Acetone	Chloroform
$Cu(AA)_2$·Py*	660	660	660
$Cu(EAA)_2$·Py	710	710	710
$Cu(EBA)_2$·Py	714	714	720
$Cu(TAA)_2$·Py	690	695	702
$Cu(BFA)_2$·Py	706	710	710

* Py: Pyridine

and E_0 the absorbance obtained in the absence of the N-base, at the same wavelength. The value of E_∞ is that found, by trial and error, to give the most reproducible value of the stability constant, K. B_0 and C_0 are total concentrations of the base and the copper chelate, respectively.

Effect of Alkyl Group of β-Diketones. It was expected that the adduct formation would be influenced by the steric effect of the terminal groups of chelate ligands.[4] The stability constants of the adducts involving AA, DPrM, DIBM and PvA as β-diketone were measured: Each copper chelate of these β-diketones except that of AA seems to have stabilities of the same magnitude. The results presented in Table 3 indicate that the terminal alkyl group scarcely affects the adduct formation. It must be noted that the steric hindrance does appear not in the chelate ligand but in the adduct forming base, as described below.

Effect of N-Base. Tables 3 and 4 show that for each copper chelate and in each solvent, the stability constants of the adducts increased in the following order:

2-methylpyridine < pyridine < 4-methylpyridine,
2-methylpiperidine < piperidine < 4-methylpiperidine

The former order was already observed by Graddon and Watton in the copper(II) β-diketone chelates,[2] and they stated that the higher stability of the 4-methyl pyridine adducts reflected the increased donor property of nitrogen atom due to substitution, and the unexpected low stability of the 2-methyl pyridine adducts was probably caused by the steric interference. The latter order supports this concept. Namely, the ability to form adducts is enhanced by the increasing basicity of the base, but weakened by the steric hindrance.

Table 3. Effect of terminal groups of β-diketones on stability constants of adducts of copper(II) β-diketonates

Base	R R′	AA CH_3 CH_3	DPrM C_2H_5 C_2H_5	PvA CH_3 $C(CH_3)_3$	DIBM $HC(CH_3)_2$ $HC(CH_3)_2$
Pyridine		9.2	6.9	6.8	5.8
γ-Picoline		14.0	11.8	11.7	11.8
α-Picoline		2.5	2.6	3.0	3.5
Pyperidine		41	48	44	57
γ-Pipecoline		52.0	—	—	—
α-Pipecoline		13.0	—	—	—

Solvent: Benzene

Table 4. Effect of heterocyclic base on stability constant of adducts

Cu-chelate	Lutidine	α-Picoline	Pyridine	γ-Picoline
$Cu(AA)_2$	—	2.5	9.2	14
$Cu(TAA)_2$	1.8×10^2	2.7×10^2	1.0×10^3	1.6×10^3

Solvent: Benzene

Effect of Organic Solvents. The effect of the solvent is shown in Table 5, which indicates that the order of the adduct stability partly depends on the presence of CF_3 terminal group of the chelate ligand. The general orders of increasing stability for $Cu(EBA)_2$ are

chloroform < butyl acetate < acetone < MIBK < benzene < cyclohexane.

While for $Cu(TAA)_2$ and $Cu(BFA)_2$ acetone < butyl acetate < MIBK < chloroform < benzene < cyclohexane.

Toluene and monochlorobenzene situate in the same position as of benzene. The stabilities of the $Cu(AA)_2$ adducts were obtained only in chloroform, acetone and benzene, because of their low solubility in the other organic solvents, and the order is quite the same with that reported by Graddon and Watton. They measured the stability of the pyridine adducts of $Cu(AA)_2$. $Cu(EAA)_2$ and Cu(benzoylacetone)$_2$ in chloroform, acetone and benzene, and stated that the increasing order of the adduct stabilities, chloroform < acetone < benzene, did not agree with the order of the dipole moments, the dielectric constants or the splitting energy of ligand-field of the solvents, but it agreed with the decreasing order in the interaction between the solvents and the copper chelates or in the solvation energy of N-bases. However, it was thought to be difficult to distinguish these two effects, although they showed some evidence in favor of the latter.

In the two kinds of order found in this experiment, the solvation to the chelates may be discriminated from that of N-bases. The relative position of chloroform to MIBK, butyl acetate and acetone may bring a solution of this interesting problem. Clarke *et al.*[5] reported that the bonding energies of chloroform solvates of tervalent metal acetylacetonates were rather small, ranging from 2 to 6 kcal/mol, which lay in the region of hydrogen bonding or dipole-dipole interaction, and with copper(II)-, zinc(II)- and cadmium(II) acetylacetonates, even such weak solvates were not produced. Graddon and Watton pointed out that considerable heat was evolved on dissolving N-bases in chloroform. Such circumstances may lead to the conclusion that the large solvation energy of the N-bases loweres the stability of the adducts of Cu-$(EAA)_2$, Cu $(EBA)_2$ and $Cu(AA)_2$ in chloroform. In other words, the thermodynamic concentration of the bases decreases by the interaction with chloroform through the hydrogen bonding.

On the contrary, for the adducts of $Cu(TAA)_2$

4) G. A. Gutter and G. S. Hammond, *J. Am. Chem. Soc.*, **81**, 4686 (1959).

5) F. R. Clarke, J. F. Steinbach and W. F. Wagner, *J. Inorg. Nucl. Chem.*, **26**, 1311 (1964).

TABLE 5. EFFECT OF ORGANIC SOLVENTS ON STABILITY CONSTANTS OF ADDUCTS

Solvent	$Cu(BFA)_2$	$Cu(TAA)_2$	$Cu(EBA)_2$	$Cu(EAA)_2$	$Cu(AA)_2$
Benzene	9.8×10^2	1.0×10^3	129	31.0	9.2
Chloroform	354	320	14.5	4.8	2.0
Acetone	99.5	54.3	47.3	21.1	4.4
Methyl isobutylketone	142	113	75.4	35.5	—
Cyclohexanone	—	71.6	72.2	43.3	—
n-Butyl acetate	105	101	35.2	13.8	—
Cyclohexane	—	5.0×10^3	164	—	—
Monochlorobenzene	1.0×10^3	8.6×10^2	88.5	25.9	—
Toluene	8.5×10^2	8.5×10^2	101	34.4	—
Nitrobenzene	468	250	69.4	17.8	—

Base: Pyridine

and $Cu(BFA)_2$, the stability in chloroform is comparatively large: At least, the adducts in this solvent are more stable than those in MIBK, butyl acetate and acetone. The phenomena may be now explained by the solvation to the copper chelates. The electron-withdrawing CF_3 group in the chelating ligands decreases the electron density around the central copper atom, but at the same time, it enhances the ability to form the solvates with some oxygen-containing solvents. Consequently, the adduct formation with N-base is weakened owing to the competition reaction with the solvents. This fact must be an important reason for the phenomena that in MIBK, butyl acetate and acetone, the adducts containing CF_3 group in the chelate ligands show lower stabilities than that in chloroform.

Effect of Metal to Ligand Bonding. Table 5 shows that irrespective of the solvents used, the stability of the adducts increases in the order:

$$Cu(AA)_2 < Cu(EAA)_2 < Cu(EBA)_2 < Cu(TAA)_2 \simeq Cu(BFA)_2$$

Graddon and Watton concluded that this was the decreasing order of effect of ligand field and the increasing order of the residual positive charge on the copper atom; but they did not carry out systematic studies. In the present work, the infrared absorptions attributed to the M–O (metal to ligand bonding), C=O and C=C stretching, were obtained to ascertain their conclusion. The spectra of the copper chelates were measured as KBr disks, and the results were summarized in Table 6. The bands for these chelates were assigned on the basis of the data of metal(II) β-diketone chelates, which had been presented by Nakamoto *et al.*[6]

It is important to examine the relationship between the stability constant of the adduct and the M–O or the C=O stretching frequencies and it will be expected that decrease in the M–O frequency reflects the increase in the stability constant of the adduct. Table 6 indicates that the order of both

TABLE 6. M–O, C=O AND C=C FREQUENCIES OF COPPER(II) β-DIKETONE CHELATES(cm^{-1})

Complex	$\nu_{C=O}$	$\nu_{C=C}$	ν_{M-O}
$Cu(AA)_2$	1575	1550 1526	455
$Cu(EAA)_2$	1595	1555 1530	452
$Cu(EBA)_2$	1595	1565 1545	460
$Cu(TAA)_2$	1604	1590	445
$Cu(BFA)_2$	1602	1590	443

the C=C and the C=O stretching frequencies is

$$Cu(BFA)_2 \simeq Cu(TAA)_2 > Cu(EBA)_2 \simeq Cu(EAA)_2 > Cu(AA)_2,$$

but the order of the M–O stretching frequency is

$$Cu(BFA)_2 \simeq Cu(TAA)_2 < Cu(EAA)_2 < Cu(AA)_2 < Cu(EBA)_2.$$

The M–O stretching frequency, except that of $Cu(EBA)_2$, is just in the reversed order to that of the C=C and C=O frequency, and decreased M–O frequency is closely concerned with the higher stability constants of the adducts as presented in Table 5. The M–O stretching frequency of $Cu(EBA)_2$ is abnormally high. The metal-oxygen bonding is weakened by the resonance between carbonyl group and lone pair electrons of ester oxygen in ketoesters such as EAA and EBA. In fact, effect of ligand field of EAA and EBA are lower than that of acetylacetone.[2] From the phenomena, the low M–O frequency must be anticipated for $Cu(EAA)_2$ and $Cu(EBA)_2$, and actually, the frequency of $Cu(EAA)_2$ is somewhat lower that of $Cu(AA)_2$. However, as described above, the M–O band of $Cu(EBA)_2$ shows higher frequency contrary to expection, and this is contradictory also to the fact that the higher C=O and C=C frequency results in the lower M–O one.[7] Then, it seems reasonable to consider that the M–O band of Cu

6) a) K. Nakamoto and A. E. Martell, *J. Chem. Phys.*, **32**, 588 (1960). b) G. T. Behnke and K. Nakamoto, *Inorg. Chem.*, **6**, 433 (1967).

7) K. Nakamoto, P. J. McCarthy, A. Ruby and A. E. Martell, *J. Am. Chem. Soc.*, **83**, 1066 (1961).

$(EBA)_2$ is not the pure metal-oxygen mode, but the M–O streching band couples with other band and subsequently, it shifts to higher frequency. It can be concluded, therefore that the chelates showing lower M–O stretching frequencies form the more stable adducts with N-base.

The results of this investigation led to the conclusion that (i) metal-oxygen (ligand) bonding—the localization of electron in the chelate ring and (ii) the basicity of Lewis bases are considered as the essential factors in the adduct formation of metal β-diketone chelates.

Furthermore, the stability constant of the adducts was influenced by (iii) steric factors of Lewis base and (iv) solvent effect due to the formation of the solvates of the chelates or the solvation of N-base.

BULLETIN OF THE CHEMICAL SOCIETY OF JAPAN VOL. 41 2660—2662 (1968)

A Study on the Yield of (γ, α) Reactions with 20 MeV Bremsstrahlung

Yoshinaga OKA, Toyoaki KATO, Koichi NOMURA, Tatsuya SAITO and Hui-Tuh TSAI

Department of Chemistry, Faculty of Science, Tohoku University, Katahira-cho, Sendai

(Received May 2, 1968)

The yields of the (γ, α) reactions on 7 elements up to an atomic number of 49, irradiated with 20 MeV bremsstrahlung, have been obtained through gamma-ray spectrometric measurements of the resultant activities. The yield values, as measured in absolute disintegration rates at the end of irradiation per mole per roentgen, have been plotted against atomic number of the target nuclides. The yield curve shows a maximum in the region of copper and zinc, and drops rapidly with increasing atomic number. The shape of this yield curve is similar to that for the photoalpha yield as a function of atomic number. It can be seen that the yield levels off in the region of silver and indium. A mechanism such as the direct photoelectric effect is thought to be responsible for this behavior. The yield of the (γ, α) reaction of an element amounts to only a small fraction, at most a few tenths of a per cent, of the total photonuclear yield.

When bremsstrahlung photons with energies in the giant resonance region are attenuated by various target elements, the main nuclear events are the emission of one neutron or one proton. In previous work,[1-4] the yield of the (γ, n) and (γ, p) reactions have been determined with 20 MeV bremsstrahlung as a function of target nuclear charge, and the applicabilities of these reaction products to activation analyses have also been discussed from the data thus obtained. Since the binding energy of alpha-particles is rather low, it is expected that the (γ, α) processes, apart from (γ, n) and (γ, p) processes, can occur in the energy region of 20 MeV bremsstrahlung. Especially for medium weight nuclei, the resultant activities due to (γ, α) processes are expected to be an appreciable fraction of the total resultant activity, because of the relatively low Coulomb barriers. Greenberg *et al.*[5] reported on the yields of alpha-particles emitted from 9 elements up to an atomic number of 58 in the energy region of 23 MeV bremsstrahlung. Some additional details have been clarified by several workers,[6-9] but not studied sufficiently.

In this report, the yields of (γ, α) reactions produced by irradiation of several medium weight nuclei with 20 MeV bremsstrahlung have been given through gamma-ray spectrometric measurements of the resultant activities.

Experimental

Samples and Irradiation. Samples of the target materials with high chemical purity, either in the form of the element or some simple compound, were irradiated for 1 hr with bremsstrahlung gamma-rays of 20 MeV maximum energy produced by the linear electron accelerator of the Japan Atomic Energy Research Institute. Each sample had a weight of 100 mg and was contained in a small quartz tube having an internal diameter of

1) Y. Oka, T. Kato, K. Nomura and T. Saito, This Bulletin, **40**, 575 (1967).
2) Y. Oka, T. Kato, K. Nomura, T. Saito and H-T. Tsai, *ibid.*, **41**, 380 (1968).
3) Y. Oka, T. Kato, K. Nomura and T. Saito, *J. Nucl. Sci. Technol.*, **4**, 346 (1967).
4) Y. Oka, T. Kato and I. Nagai, *ibid.*, **4**, 300 (1967).
5) L. H. Greenberg, J. G. V. Taylor and R. N. H. Haslam, *Phys. Rev.*, **95**, 1540 (1954).
6) P. Erdös, P. Scherrer and P. Stoll, *Helv. Phys. Acta*, **30**, 639 (1957).
7) F. Heinrich, H. Wäffler and M. Walter, *ibid.*, **29**, 3 (1956).
8) J. H. Carver, *Proc. Phys. Soc.*, **77**, 417 (1961).
9) L. Meneghetti and S. Vitale, *Nucl. Phys.*, **61**, 316 (1965).

4 mm. The experimental method involving bremsstrahlung flux monitoring and details on irradiation are essentially described in detail in previous papers.[1-4]

Chemical Separation. For the vanadium target, gamma-ray spectrometric measurements of the scandium activities were performed non-destructively after cooling. The other seven targets were processed radiochemically by the following procedures. In each case, the final precipitate was packed in a small glass tube having an internal diamter of 4 mm to determine the chemical yield and for gamma-ray counting.

Cobalt from Copper. After the addition of cobalt carrier (20.0 mg), the copper target was dissolved in nitric acid and evaporated nearly to dryness. The residue was dissolved in 6 N hydrochloric acid and subjected to anion exchange separation. Cobalt was eluted from a Dowexl X8 column with 6 N hydrochloric acid, and precipitated from this eluate by the addition of an aqueous solution of α-nitroso-β-naphthol. The precipitate was centrifuged and ignited to obtain cobalt(II) oxide. Almost complete recovery was attained.

Copper from Gallium. A gallium(II) oxide target was brought into solution by adding nitric acid along with copper carrier (67.3 mg). After evaporating nearly to dryness, the residue was made 3.5 N in hydrochloric acid, and precipitated from this solution by the addition of aqueous ammonium sulfide. After separation with a centrifuge, the sulfide was ignited to obtain copper(II) oxide. The chemical yield was 88.8%.

Zinc from Germanium. An irradiated germanium dioxide target was transferred to a 50 m*l* distilling flask, and brought into solution by adding 7 N hydrochloric acid along with gallium (269 mg) and Zinc (27.0 mg) carriers. Almost all germanium activity was removed by distillation. From the resultant solution, gallium was extracted with isopropyl ether. The aqueous layer was neutralized by the addition of a dilute aqueous sodium hydroxide solution, and the zinc hydroxide precipitate was separated by centrifugation. The precipitate was ignited to obtain zinc(II) oxide. The chemical yield was 12.9%.

Arsenic from Bromine. To the aqueous solution of an irradiated lithium bromide target arsenic(III) and arsenic(V) carriers (total 30.2 mg) were added. Arsenic was precipitated from this solution in the form of the elemental powder by reduction with tin(II) chloride in concentrated hydrochloric acid on warming. After separation by centrifugation, the precipitate was washed repeatedly with water, and dried in a vacuum. The chemical yield was 72.5%.

Rhodium from Silver. An irradiated silver target was dissolved in nitric acid with the addition of rhodium(III) and rhodium(IV) carriers (total 72.9 mg). An aqueous solution of sodium chloride was added to this solution to precipitate silver chloride. The filtrate was further purified by repeated silver chloride scavenging. Finally, metallic rhodium was precipitated by reduction with the addition of zinc dust. The precipitate was washed with dilute nitric acid and with water, and subsequently dried in a vacuum. The chemical yield was 20.4%.

Silver from Indium. After the addition of silver carrier (35.9 mg), an irradiated indium target was dissolved in nitric acid. Silver chloride was precipitated from this solution by the addition of dilute hydrochloric acid. The precipitate was purified by repeated reprecipitations involving dissolution with aqueous ammonia and precipitation with dilute hydrochloric acid. Finally, the silver chloride was washed with water and dried at 110°C. The chemical yield was 80.5%.

Yield Determination. Yield has been defined as the production rate of a given radioactive nuclide per mole of target nuclide per roentagen. The initial rates of the various activities produced were determined from their photopeak areas from decay curve analyses of the counting rates, and the corresponding saturation rates computed. After correcting for chemical yields, counting efficiencies, branching ratios and internal conversion electrons, the data has been expressed in the form of yields. The decay schemes used were those listed in the Nuclear Data Sheets.[10] A table of internal conversion coefficients[11] was also used.

Measurement of radioactivity was carried out with a 3″ dia.×3″ NaI(Tl) detector coupled to a TMC 400-channel pulse-height analyzer.

Results

Table 1 lists the characteristics and experimental results obtained from 7 gamma-ray emitting products for (γ, α) reactions of the elements studied. The threshold energies for these reactions were

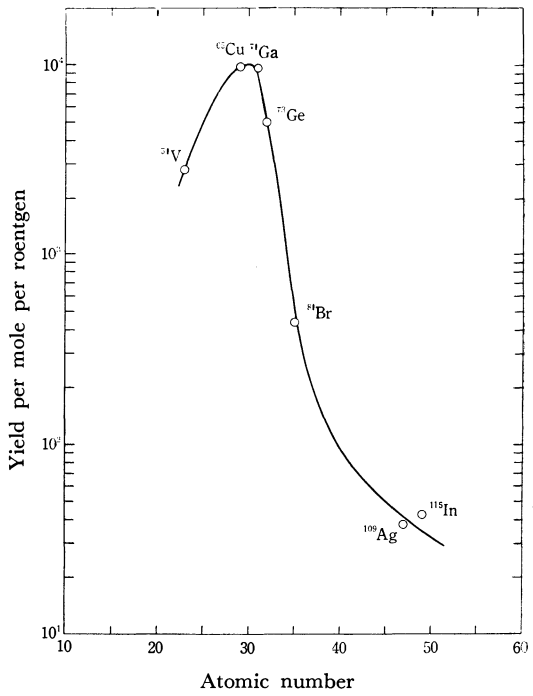

Fig. 1. The yield curve for (γ, α) reaction with 20 MeV bremsstrahlung.

10) Nuclear Data Sheets, Natl. Academy of Science-Natl. Research Council, Washington, D. C. (1961).

11) M. E. Rose, "Internal Conversion Coefficient," North-Holland Publ. Co., Amsterdam (1958).

TABLE 1. SUMMARY OF DATA ON (γ, α) REACTIONS WITH 20 MeV BREMSSTRAHLUNG

Nuclide		E_{th}	Observed gamma-ray			Results obtained	
Parent (Natural abundance, %)	Product (Half-life)	$(-Q$, MeV)	Energy (MeV)	Branching ratio (%)	Type of multipole transition	μCi/mg[a]	Yield ($mol^{-1} \cdot R^{-1}$)
^{51}V(99.75)	^{47}Sc(3.4 d)	10.27	0.160	100	$M1+E2$	1.99×10^{-3}	2.8×10^{3}
^{65}Cu(30.9)	^{61}Co(99 min)	6.75	0.068	99	$M1+E2$	7.23×10^{-3}	9.7×10^{3}
^{71}Ga(39.6)	^{67}Cu(61 hr)	5.15	0.184	41	$M1$	2.70×10^{-3}	9.6×10^{3}
^{73}Ge(7.67)	^{69m}Zn(14 hr)	5.89	0.435	100	$M4$	1.11×10^{-2}	5.0×10^{3}
^{81}Br(49.48)	^{77}As(39 hr)	6.46	0.246	2.81	$M1+E2$	1.97×10^{-4}	4.3×10^{2}
^{109}Ag(48.65)	^{105}Rh(36 hr)	3.28	0.319+0.306	24.8	$M1+E2$	8.29×10^{-4}	3.7×10^{1}
^{115}In(95.77)	^{111}Ag(7.6 d)	3.78	0.340	6	$M1+E2$	5.70×10^{-5}	4.3×10^{1}

a) The value corrected at the end of 1 hr irradiation (9.4×10^{6} R/min).

calculated on the basis of the mass differences.[12] The yield value, shown in the last column of Table 1, are expressed as the disintegration rate at the end of irradiation per mole of target nuclide per roentgen. This can be taken as the number of (γ, α) processes which occurred during irradiation. The yield values were also plotted against atomic number of the parent nuclides in Fig. 1 in which the symbol noted near each plot indicates the parent nuclide. The yield curve exhibits a maximum in the region of copper and zinc, and drops rapidly with increasing atomic number. It is seen that the yield levels off in the region of silver and indium.

Discussion

The shape of the yield curve, shown in Fig. 1, is very similar to that of the curve for the photo-alpha yield as a function of atomic number with 23 MeV bremsstrahlung presented by Greenberg *et al.*[5] The curve is also similar to that for the (γ, p) reaction yield reported previously.[2] The (γ, α) reaction yield is lower by a factor varying from 20 to 10^3 in the region of $Z<50$. The absorption cross-section for gamma-rays increases with increasing atomic number, and the potential barrier also increases. From the relative effects of these factors, the yield curve shows an initial rise and then, through a maximum point, drops rapidly with increasing atomic number. For silver and indium targets, however, the yields are much higher than those expected from the rapid drop untill the bromine target. The presence of direct effects in the photoproduction of alpha-particles from heavier elements has been suggested by several workers.[8,9] Erdös *et al.*[6] reported that the photoalpha yield curve levels off at a roughly constant value for elements with atomic number greater than 50. Furthermore, disagreement between the calculated evaporative spectra of emitted photoalpha particles and the experimental ones was pointed out by Meneghetti *et al.*[9] An excess of energetic alpha-pariticles, especially in indium and gold irradiated with 35 MeV bremsstrahlung gamma-rays, has been attributed to direct effects. The leveling-off behavior of the yield curve in the region of silver and indium obtained in this experiment suggests that a mechanism such as the direct photoelectric effect becomes more important for heavier elements.

Experimental results show that the (γ,α) reaction yield of an element amounts to only a small fraction of the total photonuclear yield. The relative yields of the (γ, α) reaction to those of the (γ, p) and (γ, n) reactions in the region of copper and zinc have been determined as

$$Y_{(\gamma,\alpha)} : Y_{(\gamma,p)} : Y_{(\gamma,n)} = 1 : 20 : 500$$

In the region of silver and indium, the relative yields are

$$Y_{(\gamma,\alpha)} : Y_{(\gamma,p)} : Y_{(\gamma,n)} = 1 : 10^3 : 3\times10^5$$

Since the yield of a photonuclear reaction is a strong function of the maximum bremsstrahlung energy, the relative probability of producing each activity as the result of photonuclear processes with various energies is to be investigated in detail through further experiments.

12) Nuclidic mass values used were those listed in G. Friedlander, J. W. Kennedy and J. M. Miller, "Nuclear and Radiochemistry," 2nd Ed., John Wiley & Sons, New York (1964), p. 533.

BULLETIN OF THE CHEMICAL SOCIETY OF JAPAN VOL. 41 2663—2668 (1968)

Free Radical Reactions in Organic Electrode Processes. V*1 Anodic Cyanation of Some Monosubstituted Benzenes*2

Tosaku SUSUKI,*3 Kikuhiko KOYAMA, Akira OMORI and Shigeru TSUTSUMI

Department of Chemical Technology, Faculty of Engineering, Osaka University, Miyakojima-ku, Osaka

(Received December 28, 1967)

The anodic reaction between cyanide ions and monosubstituted benzenes in methanol has been investigated. An examination of the products has indicated that the reaction proceeded by means of the formation of nucleus-cyanated products. The solvent perhaps also participates concurrently in this anodic reaction leading to the formation of methoxylated compounds. The results offer a striking contrast in isomer distribution between these two substitutions. The substituents on the benzene rings had a pronounced effect on the yield of the cyano compounds. The reactivity of the aromatic compounds toward the anodic cyanation decreased in the following order:

anisole ≫ toluene > ethylbenzene > cumene ≫ benzene ≫ methyl benzoate.

These results have been interpreted as resulting from the generation of an aromatic ion radical at an anode by the loss of a π-electron from each molecule.

In a previous paper,[1] we have demonstrated that the anodic reaction of sodium cyanide with some aromatic hydrocarbons, leading to the formation of cyano compounds, could be carried out in methanol by using a platinum anode. The anodic cyanation occurred only on the aromatic nuclei. The situation in this substitution closely resembles that of the electrophilic aromatic substitutions, even though napthalene and anthracene are reactive at the same position in their respective molecules toward both homolytic and electrophilic substitutions.

Two possible intermediates, *i.e.*, an electrophilic cyano radical or an aromatic cation radical, were conceivable for this anodic aromatic cyanation, but at that time we had not found conclusive evidence for making any particular choice between these two species.

In the present work, monosubstituted benzenes were chosen as the organic substrates, and the effect of substituents on the yield and on the variety of the products formed in the electrochemical reaction was investigated in order to elucidate the mode of the anodic cyanation.

Results and Discussion

All the electrolyses were conducted between a platinum anode and a mercury-pool cathode in an undivided cell under essentially similar conditions.

In the experiment with anisole added, a mixture (3 g) of *o*- and *p*-anisnitriles was obtained. From the gas chromatographic analysis, an isomer distribution of 40% *ortho* and 60% *para* was obtained. The *meta* isomer was not detected. The fractional crystallization of the mixture from ethanol led to the isolation of the *p*-isomer. The saponification of the mother liquor with alcoholic potassium hydroxide afforded *o*-anisic acid. These isolated compounds were identified by a mixed melting-point test, elemental analyses, and a study of the infrared spectra.

When toluene was added as an organic substrate, the anodic reaction proceeded by means of the formation of tolunitirles (0.78 g), methoxytoluenes, and an isonitrile. A sharp infrared absorption band at 2180 cm^{-1} and the foul odor of the crude product suggested the formation of an isonitrile. Gas chromatography indicated that the isomer distribution for tolunitriles consisted of 27% *ortho*, 5.4% *meta*, and 67.5% *para*. It yielded no indication of the formation of benzyl cyanide. Among these products, *o*- and *p*-tolunitriles could be separated by chromatography; they were identified, after treatment with alcoholic potassium hydroxide, as *o*-toluamide and *p*-toluic acid respectively.

*1 Part IV: K. Koyama, T. Susuki and S. Tsutsumi, *Tetrahedron*, **23**, 2675 (1967).

*2 Presented partly at the 17th Annual Meeting of the Chemical Society of Japan, Tokyo, April, 1964, and the 18th Annual Meeting of the Chemical Society of Japan, Osaka, April, 1965.

*3 Present address: Basic Reseach Laboratories Toyo Rayon Co., Ltd., Kamakura, Japan.

1) a) K. Koyama, T. Susuki and S. Tsutsumi, *Tetrahedron*, **23**, 2675 (1967). b) K. Koyama, T. Susuki and S. Tsutsumi, *Tetrahedron Letters*, **1965**, 627.

Table 1. Isomer distribution in the product obtained from the anode reaction of cyanide ion with ethylbenzene

	Isomer distribution			
	Methoxyethylbenzene		Cyanoethylbenzene	
	Retention time* min	%	Retention time* min	%
α-	4.3	80.3	—	—
o-	6.3	3.3	13.5	33
m-	7.4	8.4	21.2	10
p-	8.1	8.0	24.3	57

* Conditions: 3 m-column of 25% polyethyleneglycol 6000 on Shimalite; carrier gas, He, 46 ml/min; column-temp.. 180°C.

A detailed study of isomer distributions, including those of methoxylated products, was made by experiments with ethylbenzene added. The results obtained are summarized in Table 1.

As is indicated in Table 1, it is quite evident that there is a marked difference in isomer distribution between methoxyethylbenzenes and cyanated products. Side-chain methoxylation took place in preference to nuclear methoxylation, while hydrogen atoms on the aromatic ring preferred to undergo substitution with the cyano group. This product analysis was performed by gas chromatography. Several other unidentified peaks were observed on the gas chromatogram; some of them might be assignable to those of isonitriles. The precipitation of silver cyanide in an aqueous silver nitrate solution, through which evolved gases were passed, may provide evidence for the formation of hydrogen cyanide.

The anodic reaction of cyanide ions in the presence of cumene gave considerable amounts of a product arising from the side-chain substitution of cumene with the methoxy group, but it failed to give any side-chain cyanation product. The isomer distribution of the nucleus-cyanated products consisted of 35.6% *ortho*, 13.8% *meta*, and 50.6% *para*. *p*-Cumic acid was isolated from the saponification products obtained by treatment with alcoholic potassium hydroxide.

The anodic reaction of cyanide ions with benzene in methanol afforded a small amount of benzonitrile, together with anisole, but it failed to yield any cyano product when benzene was replaced with methyl benzoate.

The results obtained from the present work are summarized in Table 2.

The substituent on the aromatic ring had a pronounced effect on the yield of aromatic cyano products. The order of the reactivity of the aromatic compounds toward this anodic aromatic cyanation decreases as follows:

Table 2. Current yields of nitrile formation

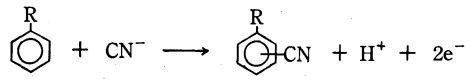

Substituent R	Half-wave oxidation potential* $E_{1/2}$(ox), V	Current yield (Y), %	Current yield for		
			Ortho	Meta	Para
$-OCH_3$	1.76[a]	12.1	4.9	—	7.2
$-CH_3$	1.98[b]	1.38	0.4	0.08	0.9
$-C_2H_5$		1.16	0.4	0.12	0.68
$-CH(CH_3)_2$		1.16	0.42	0.16	0.58
$-H$	2.30[b]	0.1			
$-CO_2CH_3$		—	—	—	—

* *vs.* SCE.

a) A. Zwig, W. G. Hodgson and W. H. Jura, *J. Am. Chem. Soc.*, **86**, 4124 (1964).
b) E. S. Pysh and N. C. Yang, *ibid.*, **85**, 2124 (1963).

anisole ≫ toluene > ethylbenzene > cumene > benzene ≫ methyl benzoate.

This order is in good agreement with that of the ability of the substituents to supply electrons to the ring. The results indicate that the substitution reaction took place at electron-rich sites in the ring. In addition, the isomer distributions in the cyano products are in striking contrast to those in the methoxylated compounds obtained together with nitriles.

In order to elucidate the mode of the anodic aromatic cyanation, a graphical plot of the logarithms of current yield against the half-wave polarographic oxidation potential is represented in Fig. 1.

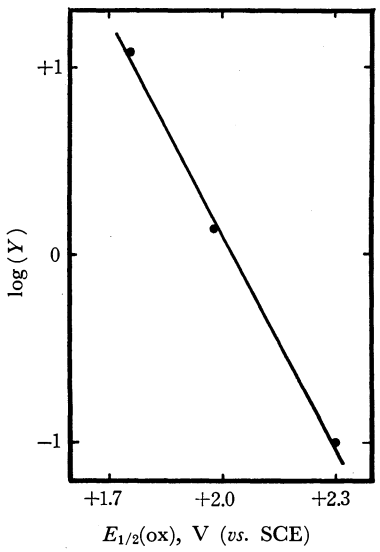

Fig. 1. Correlation of log (Y) and $E_{1/2}$(ox) for the anodic aromatic cyanation.

If cyano radicals are formed at the anode, then diffuse into the bulk solution, and finally attack the aromatic substrates, the current yield would not be expected to be related to the half-wave polarographic oxidation potential. Therefore, the good linear correlation with the half-wave oxidation potential suggests that the electrochemical behavior of the aromatic compounds at the anode plays an important part in the formation of the nitriles.

The reaction has a high sensitivity to substituent influence. The substituent-effect seems larger than that expected for homolytic reactions, even if electrochemically-generated cyano radicals behave as strong electron acceptors. This suggestion is derived from plotting the relative current yield as a function of the σ-constant (Fig. 2), even though competition experiments should be used in the evaluation of the relative current yields.[2]

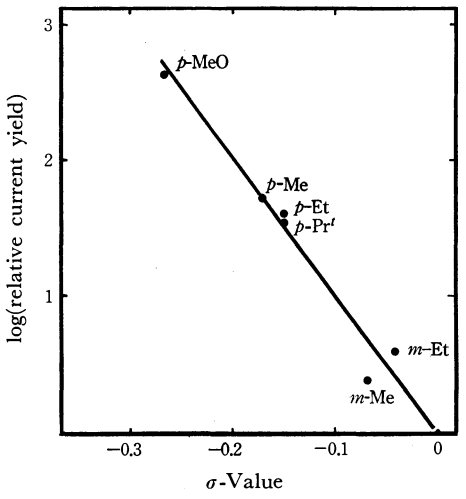

Fig. 2. Correlation of log (relative current yield) and τ for the anodic aromatic cyanation.

From the considerations described above, we would like to suggest that such good linear correlations are not to be interpreted as resulting from the attack of an electrophilic cyano radical on the aromatic substrate, but as resulting from the direct reflection of the electrochemical behavior of the aromatic compounds at the anode. The aromatic ion radical generated on the anode surface reacts immediately, or through the formation of as aryl or benzyl cation by the loss of a proton and an electron, with either cyanide ion or the radical, resulting in the formation of an aromatic cyano compound. However, if the two anodic substitution reactions, *i. e.*, cyanation and methoxylation, occurs concurrently in this reaction system, and if they proceed *via* a common intermediate, the difference in the isomer distribution between these two substitutions will have to be ascribed to the differences in the electrochemical and chemical behavior of cyanide and methoxide anions.

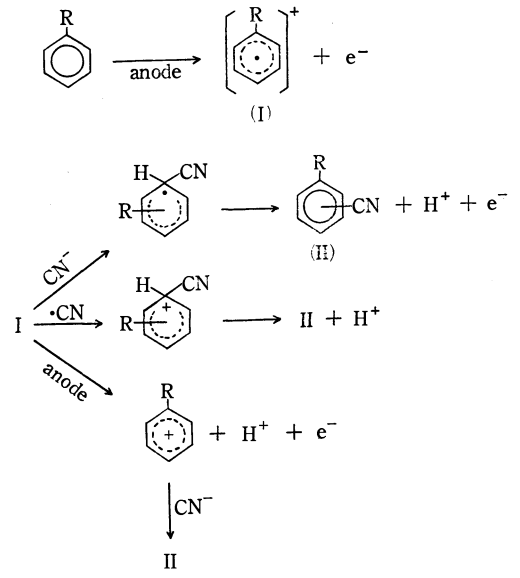

Experimental

All the melting points and boiling points are uncorrected. The infrared spectra were obtained with a Shimadzu infrared spectrophotometer IR-27C. Gas chromatograms were obtained with a Shimadzu gas chromatograph GC-2A, and a Toyo gas chromatograph GC-S-7.

Materials. Commercially-available methanol (special grade) was dried over calcium hydride and then distilled (bp 64.5°C). Anisole was obtained commercially, washed with aqueous sodium hydroxide, then with water, dried over anhydrous magnesium sulfate, and distilled from sodium; bp 154°C, n_D^{15} 1.5196. Benzene, toluene, ethylbenzene, and cumene were treated with sulfuric acid in a usual manner, and were distilled from sodium through a helices-packed column. The fractions collected had bp's of 80, 111, 135—136, and 151—153°C respectively. Methyl benzoate was obtained commercially, and then distilled; bp 78.5°C/11 mmHg.

Electrolysis of Methanol Solution of Sodium Cyanide in the Presence of Anisole. A solution of sodium cyanide (8.6 g) and anisole (36 g, 0.33 mol) in methanol (200 m*l*, 160 g) was electrolyzed between a platinum anode (2.5×6.0 cm²) and a mercury-pool cathode (surface area: *ca.* 50 cm²), at 0—5°C with an applied potential of 6 V, at a current of 0.5 A for 20 hr while a slow stream of nitrogen was passed through the solution. The electrodes were spaced *ca.* 1.3 cm apart. At the end of the electrolysis, the current passed through amounted to 9.92 A-hr. Additional sodium cyanide was introduced, portion by portion, as the electrolysis proceeded, until finally 14.9 g of the cyanide had been added by the time the current was stopped. After a

2) E. S. Gould, "Mechanism and Structure in Organic Chemistry," Henry Holt and Co., Inc., New York (1960), pp. 220—230, 434.

usual work-up of the electrolyzed solution, the residue (18 g) was distilled to yield the following fractions: (A), wt 9.7 g, bp 47—49°C at 15 mmHg; (B), 4.1 g, bp 50—125°C at 15 mmHg.

The former fraction was found by gas chromatography to consist of unreacted anisole. The infrared spectrum of the latter fraction exhibited a characteristic absorption band at 2240 cm^{-1}. The cyano products present in fraction B were determined by gas chromatography, and found to be *o*- and *p*-anisnitriles. The yields of *o*- and *p*-anisnitriles were 1.2 and 1.8 g respectively. The gas chromatography was carried out by using a 3 m column packed with 20% polyester DA on fire brick C-22, and hydrogen carrier gas, at a column temperature of 175°C. The retention times of *o*- and *p*-anisnitriles were 24.2 and 22.5 min respectively. The *m*-isomer, whose retention time would be 14.6 min under the conditions employed, could not be detected. The re-distillation of fraction B under reduced pressure gave 2.0 g of an oily distillate; bp 100—128°C at 12 mmHg. The distillate was partially crystallized on cooling, and then separated on a filter.

The solid melted at 59—60°C after recrystallization from ethanol; it was identified as *p*-anisnitrile by a mixed melting point measurement and by a comparison of its infrared spectrum with that of an authentic sample. (Found: C, 72.00; H, 5.48%. Calcd for C_6H_7NO: C, 72.16; H, 5.30%.)

The filtrate was saponified with alcoholic potassium hydroxide to give, after recrystallization from aqueous ethanol, a small amount of *o*-anisic acid, mp 94—96.5°C; mixed mp with authentic *o*-anisic acid, 99—100°C. (Found: C, 63.84; H, 5.82%. Calcd for $C_8H_8O_3$: C, 63.15; H, 5.30%.)

No further attempt was made to investigate other products, *e.g.*, the methoxylated compounds.

Electrolysis of Methanol Solution of Sodium Cyanide in the Presence of Toluene. A solution of sodium cyanide (12.2 g) and toluene (46.1 g, 0.5 mol) in methanol (300 m*l*, 240 g) was electrolyzed between a platinum foil anode (6.0×5.0 cm^2) and a mercury-pool cathode (*ca.* 50 cm^2) at 0—5°C with an applied potential of 7 V and at a current of *ca.* 1 A for 24 hr. By the end of the electrolysis, the additionally-used sodium cyanide amounted to 22.1 g and the current passed through, to 26.8 A-hr.

The solvent and the bulk of the toluene were removed from the electrolyzed solution and collected in a trap immersed in a dry ice-acetone bath. The gas chromatography of the low-boiling fraction indicated that it contained 39 g of unreacted toluene. The residue emitted a foul odor, and gave an infrared spectrum displaying an absorption band at 2180 cm^{-1}. However, treatment with diluted hydrochloric acid destroyed the odor and gave an infrared absorption band at 3300—3500 cm^{-1}, while the band at 2180 cm^{-1} disappeared. The residue was extracted with ether, and an ether-insoluble solid was removed by filtration. The solid separated on a filter was found to be unchanged sodium cyanide. The filtrate was distilled under reduced pressure to yield, after the removal of the solvent, the following fractions: (A), wt 3.1 g, bp 63—75°C at 13 mmHg; (B), 3.9 g, bp 76—110°C at 13 mmHg; (C), 2.8 g, bp 70—120°C at 0.6 mmHg; (D), 4 g of higher-boiling residue.

The infrared spectroscopic examination of these fractions revealed the presence of some cyano compounds (2240—2260 cm^{-1}), together with methoxylated compounds (1095—1110 and 1250 cm^{-1}) and isonitriles (2180 cm^{-1}). The gas chromatography was carried out by using two columns. The conditions employed and the retention times of the three isomeric tolunitriles identified are listed in Table 3.

TABLE 3. GAS-CHROMATOGRAPHIC ANALYSIS OF ISOMERIC TOLUNITRILES

	P. E. G. 6000, 3 m Column temp., 163°C H_2, min	Polyester DA, 3 m 175°C H_2, min
o-Tolunitrile	8.7	22
m-Tolunitrile	10.4	25.8
p-Tolunitrile	11.4	28.8

The quantitative determination of these three isomers was accomplished by an internal standard method; it indicated that they amounted to 0.221 g (*ortho*), 0.044 g (*meta*), and 0.515 g (*para*), respectively.

Fraction B was chromatographed over alumina. Elution with benzene gave two fractions. The first-eluted oil was heated under reflux with 10% potassium hydroxide in ethanol to yield trace amounts of a white solid, mp 137—140°C. After recrystallization from water, the solid melted at 139—140°C, and it failed to depress the melting point of authentic *o*-toluamide. Moreover, the infrared spectrum was identical with that of an authentic sample. (Found: C, 70.63; H, 6.35%. Calcd for C_6H_9NO: C, 71.09; H, 6.71%.)

The hydrolysis of the second fraction with alcoholic potassium hydroxide gave *p*-toluic acid, mp 178—179°C, undepressed by admixture with an authentic sample. The infrared spectrum was in good agreement with that of an authentic sample. (Found: C, 70.98; H, 5.86%. Calcd for $C_8H_8O_2$: C, 70.57; H, 5.92%.)

Electrolysis of Methanol Solution of Sodium Cyanide in the Presence of Ethylbenzene. A solution of sodium cyanide (14.2 g) and ethylbenzene (0.5 mol) in methanol (300 m*l*) was electrolyzed at a temperature of 0.5°C with an applied potential of 6—7 V and at a current of 1 A under a slow stream of nitrogen. The nitrogen, accompanied by the gases evolved, was washed with a 1 N acidic silver nitrate solution, and then with a 2 N aqueous sodium hydroxide solution. Additional sodium cyanide (25.8 g) was introduced, portion by portion, into the solution during the electrolysis. The electrolysis was continued until 1.016 faraday had been passed through the solution. As the reaction proceeded, a white precipitate was formed in the silver nitrate solution when portions of it were placed in a washing bottle. After the electrolysis has stopped, the alkaline solution was acidified with diluted nitric acid and silver nitrate was added, thus yielding trace quantitites of silver cyanide.

The electrolyzed solution was worked up in a manner similar to that used for toluene. Distillation gave the following fractions: (A), wt 3.4 g, bp 60—62°C at 14 mmHg; (B), 2.0 g, bp 80—85°C at 14 mmHg; (C), 8.9 g of a residue.

The compounds in each fraction were examined by gas chromatographic and infrared analyses. The infrared spectra of fractions A and B exhibited characteristic absorption bands at 1100—1120, 1250 (C-O-C),

and 2260 (-C≡N) cm^{-1}. The infrared analysis also indicated the presence of some cyano products in the residue. The gas chromatographic analysis was accomplished by using a 3 m column of 25% polyethyleneglycol 6000 on Shimalite, the carrier gas was He (flow rate: 46 ml/min) and the column-temperature, 180°C.

The product distributions in all the fractions are summarized in Table 4.

Table 4. Product distribution in the electrolysis of methanol solution of sodium cyanide in the presence of ethylbenzene

	Weight (g) in		
	Fraction A	Fraction B	Residue
α-Methoxyethylbenzene	2.708	0.086	—
o-Methoxyethylbenzene	0.078	0.036	—
m-Methoxyethylbenzene	0.095	0.199	—
p-Methoxyethylbenzene	0.073	0.205	—
o-Cyanoethylbenzene	0.044	0.18	0.043
m-Cyanoethylbenzene	0.013	0.043	0.022
p-Cyanoethylbenzene	0.037	0.175	0.243

Authentic cyanoethylbenzenes were prepared by the Sandmeyer reaction of aminoethylbenzenes. The infrared spectrum of authentic o-cyanoethylbenzene exhibited characteristic absorption bands at 760 and 2260 cm^{-1}, while p-cyanoethylbenzene showed them at 840 and 2260 cm^{-1}. These two samples were further characterized by gas chromatography. The aminoethylbenzenes used in the Sandmeyer reaction were synthesized by the high-pressure catalytic hydrogenation of a nitroethylbenzene or by the action of zinc on a nitrobenzene in hydrochloric acid. These had bp's of 100—101°C at 17 mmHg (*ortho*) and 57°C at 2 mmHg (*para*). α-Phenylpropionitrile was prepared from hydratripic aldehyde *via* the oxime according to the procedure of Newman and Closson.[3] The nitrile was distilled at 113—116°C at 18 mmHg.

α-Methoxyethylbenzene bp 56—57°C at 9 mmHg, was prepared from methylphenylcarbinol, n-buthyllithium, and dimethyl sulfate. The infrared spectrum showed absorption bands at 700, 750, and 1110 cm^{-1}, and the gas chromatogram displayed a single peak. Ring-methoxylated ethylbenzenes were prepared from the corresponding ethylphenols by methylation with dimethyl sulfate.

Electrolysis of Methanol Solution of Sodium Cyanide in the Presence of Cumene. A solution of sodium cyanide (15.3 g) and cumene (0.5 mol) in methanol was electrolyzed under conditions similar to those described for toluene. By the end of the electrolysis, 1.033 faraday had been passed through the solution. The total of sodium cyanide used was 40 g. After the electrolyzed solution had been sorked up in a manner similar to that used with toluene, the following fractions were obtained by vacuum-distillation: (A), wt 4.3 g, bp 40—44°C at 8 mmHg; (B), 3.4 g of residue. The infrared spectrum of fraction A exhibited absorption bands at 1100 and 2260 cm^{-1}. The gas chromatography was carried out by using a 3 m column packed with 25% Polyethyleneglycol 6000 on Shimalite; He was the carrier gas (40 ml/min), and the column temperature, 180°C. No evidence for the presence of α-cyanocumene in any fraction could be obtained from the gas chromatographic analysis. The product distributions in all the fractions are given in Table 5.

Table 5. Product distribution in the electrolysis of methanol solution of sodium cyanide in the presence of cumene

	Retention time min	Product (g) in	
		Fraction A	Residue
α-Methoxycumene	6.3	0.09	0.12
o-Cyanocumene	18.8	—	0.31
m-Cyanocumene	24.3	—	0.12
p-Cyanocumene	28.4	—	0.44

A portion (2.2 g) of the residue was chromatographed over silica gel. The fractions eluted with benzene were examined by thin-layer chromatography, and were combined on the basis of their thin-layer chromatographic behavior. The combined oil (0.4 g) was saponified in an autoclave with 10% alcoholic potassium hydroxide at 140°C for 14 hr; it gave, after recrystallization from benzene, a small amount (less than 0.1 g) of p-cumic acid, mp 116—118°C, undepressed by admixture with an authentic sample. (Found: C, 73.35; H, 7.18%. Calcd for $C_{10}H_{12}O_3$: C, 73.14; H, 7.37%.)

Authentic o- and p-cyanocumenes were synthesized by a route similar to that used for the preparation of cyanoethylbenzenes, but the Sandmeyer reaction was carried out using the method given in "Organic Syntheses"[4] for the preparation of o- and p-tolunitriles. α-Cyanocumene was prepared according to the directions of Hauser *et al.*[5,6] These samples were characterized by gas chromatography and infrared analysis. The method used for the preparation of α-methoxycumene, bp 65—68°C at 8 mmHg, was virtually identical with that described for α-methoxyethylbenzene. The other isomeric methoxycumenes were also prepared by the action of dimethyl sulfate on the corresponding sodium phenolates.

Electrolysis of Methanol Solution of Sodium Cyanide in the Presence of Benzene. A solution of sodium cyanide (15.5 g) and benzene in methanol was electrolyzed until 1.0 faraday had been passed through the solution. Additional sodium cyanide (29.2 g) was then added. A usual work-up of the electrolyzed solution left an oil (0.15 g), bp 30—120°C at 10 mmHg. The infrared spectrum of the oil showed characteristic absorption bands at 700, 760, 1250, and 2250 cm^{-1}. Gas chromatography (columns: 20% Polyester DA on fire brick C-22, 3 m, 25% Apiezon L on Shimalite, 3 m; carrier gas, H_2, 0.5 kg/cm^2; column temperature, 170°C) indicated the presence of benzonitriles with retention times of 5.6 and 2.2 min

3) M. S. Newman and R. D. Closson, *J. Am. Chem. Soc.*, **66**, 1553 (1944).

4) H. T. Clarke and R. R. Read, "Organic Syntheses," Coll. Vol. I, 2nd Ed., 514 (1956).

5) A. Brodhang and C. R. Hauser, *J. Am. Chem. Soc.*, **77**, 3024 (1955).

6) C. R. Hauser and W. R. Brasen, *ibid.*, **78**, 494 (1956).

under these two sets of conditions respectively. Moreover, it gave a peak with the same retention time as that of anisole on the gas chromatogram. The yield of the nitrile was 0.05 g. The treatment of the oil with an alcoholic potassium hydroxide solution under reflux for 24 hr afforded, after purification by sublimation, a trace amount of benzoic acid; mp 121—122°C, undepressed by admixture with an authentic sample. The infrared spectrum of this derivative was identical in all respects with that of an authentic sample.

Electrolysis of Methanol Solution of Sodium Cyanide in the Presence of Methyl Benzoate. The electrolysis was conducted in a manner similar to that used in the experiment with benzene until 1.0 faraday had been passed through the solution. The total amount sodium cyanide used was 39.4 g. After a usua work-up, the following fractions were obtained; (A), wt 3.0 g, bp 44—47°C at 0.8 mmHg; (B), 18.6 g, bp 47—50°C at 0.8 mmHg; (C), 1.6 g, bp 50—90°C at 0.8 mmHg; (D), 5 g of a residue.

The gas chromatographic and infrared analyses of these fractions indicated the absence of any cyano product. Each fraction gave a negative Lassigne sodium decomposition test for nitrogen,[7] and unreacted methyl benzoate was recovered from all of the fractions except the higher-boiling residue.

7) R. L. Shriner and R. C. Fuson, "The Systematic Identification of Organic Compounds," 3rd Ed., John Wiley and Sons, Inc., New York (1948), p. 52.

BULLETIN OF THE CHEMICAL SOCIETY OF JAPAN VOL. 41 2668—2671 (1968)

Free Radical Reactions in Organic Electrode Processes. VII.*1 Anodic Reaction of Benzoic Acid with Aromatic Hydrocarbons*2

Kikuhiko KOYAMA, Tatsuyoshi EBARA and Shigeru TSUTSUMI

Department of Chemical Technology, Faculty of Engineering, Osaka University, Suita, Osaka

(Received December 28, 1967)

The anodic reaction of benzoic acid in acetonitrile containing tiethylamine was carried out in the presence of toluene, ethylbenzene, cumene, and tetralin. The amounts of carbon dioxide evolved during the electrolyses were smaller than those expected to be produced through the spontaneous decomposition of the benzoyloxy radical. An examination of nongaseous products indicated that the anodic reaction proceeds by means of the formation of the benzoyloxylates and phenylates of the aromatic hydrocarbons present. The occurrence of the nuclear benzoyloxylation, to a relatively great extent, suggested that the aromatic hydrocarbons were oxidized at the anode.

In a previous paper from this laboratory, it has been shown that the anodic reaction of some aromatic carboxylic acids in the presence of anisole resulted in the formation of *o*- and *p*-methoxyphenyl esters of the corresponding acids in fairly good yields, together with traces of the Kolbe dimer and of carbon dioxide.[1] The results were interpreted as being due to a simultaneous oxidation of anisole at the anode, leading to the formation of its cation radical.

As has been pointed out by Zweig *et al.*,[2] the aromatic compounds with electron-rich molecular π-orbitals, such as methoxybenzenes, easily lose an electron and so form their cation radicals.

$$ArH \xrightarrow{-e^-} ArH\cdot^+$$

$$ArH \xrightarrow{-2e^-} ArH^{2+} \xrightarrow{+ArH} 2ArH\cdot^+$$

In fact, recent studies of the polarographic oxidation of aromatic compounds have indicated that the half-wave polarographic oxidation potential of aromatic hydrocarbons decreases with an increase in the number of electron-releasing substituents on the benzene ring, or with an increase in the number of fused rings in a series of polynuclear aromatic hydrocarbons.[3,4]

On the other hand, recent studies concerning the

*1 Part VI: T. Okubo and S. Tsutsumi, *Technol. Repts. Osaka Univ.*, **13**, 495 (1963).

*2 Presented at the 18th Annual Meeting of the Chemical Society of Japan, Osaka, April, 1965.

1) K. Koyama, K. Yoshida and S. Tsutsumi, This Bulletin, **39**, 519 (1966).

2) A. Zweig, W. G. Hodgson and W. H. Jura, *J. Am. Chem. Soc.*, **86**, 4124 (1964).

3) E. S. Pysh and N. C. Yang, *ibid.*, **85**, 2124 (1963).

4) W. C. Neikam and M. M. Desmond, *ibid.*, **86**, 4811 (1964).

5) M. Leung, J. Herz and H. W. Salzberg, *J. Org. Chem.*, **30**, 310 (1965).

6) H. W. Salzberg and M. Leung, *ibid.*, **30**, 2873 (1965).

7) S. D. Ross, M. Finkelstein and R. C. Petersen, *J. Am. Chem. Soc.*, **86**, 4139 (1964).

8) L. Eberson and K. Nyberg, *ibid.*, **88**, 1686 (1966).

9) L. Eberson and K. Nyberg, *Tetrahedron Letters*, **1966**, 2389.

10) L. Eberson, *J. Am. Chem. Soc.*, **89**, 4669 (1967).

anodic substitution reactions[1,5-10] have indicated that the organic substrates participate in the electrochemical process, generating the cationic intermediates (either the cation radical or the dication), which then react with anions to give the substitution products.

$$ArH \xrightarrow{-e^-} ArH\cdot^+ \xrightarrow{+Y^-} ArHY\cdot \longrightarrow ArY + H^+ + e^-$$

or

$$ArH \xrightarrow{-2e^-} ArH^{2+} \xrightarrow{+Y^-} ArY + H^+$$

The present investigation was undertaken to see if such a mechanism could also be operative in the anodic reaction of benzoic acid with aromatic hydrocarbons with relatively high polarographic oxidation potentials.

Results and Discussion

The electrolyses were carried out in acetonitrile containing triethylamine in the presence of toluene, ethylbenzene, cumene, and tetralin at a temperature of 18—25°C, at a current of 0.08—0.11 A, and with a relatively high applied potential (40—65 V), until a calculated amount of current (2.6—3.0 A-hr) had been passed through the solution.

The gaseous products were then collected, and analyzed by means of a column packed with silica gel. The non-gaseous products, after having been worked up in the usual ways, were separated into unchanged benzoic acid and benzene-soluble and benzene-insoluble materials. The chromatographic separation of the benzene-soluble products yielded a mixture of phenylated and benzoyloxylated aromatic compounds; the mixture was then saponified with alcoholic potassium hydroxide. The products obtained after the saponification were analyzed by vapor-phase chromatography. On the basis of the structure of those characterized phenols and hydrocarbons, the products formed during the electrolysis were determined. In all cases, considerable amounts of benzene-insoluble polymeric residues were produced. Their IR spectra suggested that they had an ester function, but they could not be completely hydrolysed. The results are summarized in Table 1.

The percentage yields given for the non-gaseous products are based on the amounts of benzoic acid not recovered at the end of the electrolysis; the Coulombic yields were calculated for the hydrogen and carbon dioxide evolved.

If the over-all electrode reaction of the carboxylic acids proceeds in exactly the following manner:

$$2RCOO^- \rightarrow 2CO_2 + R\text{-}R + 2e^- \quad (1)$$

$$2H^+ + 2e^- \rightarrow H_2 \quad (2)$$

the quantity should approach two moles of unrecovered carboxylic acid, two moles of carbon dioxide, and one mole of hydrogen per two faradays. However the results, apparently indicate that the addition of aromatic hydrocarbons alters the course of the reaction; the evolved hydrogen reaches 86—100% of the theoretical amount, while the amounts of carbon dioxide are very small. This diminished evolution of carbon dioxide may be

Table 1. Electrolysis of benzoic acid in the presence of aromatic compounds

Acid: Benzoic acid (0.05 mol)
Aromatic compound: 0.4 mol
Solvent: MeCN (50 m*l*) containing Et_3N (2.8 m*l*)
Electrode: 2Pt-Foils (15×20 mm; space, 10 mm apart)
Temperature: 18—28°C
Current: 0.08—0.12 A

Aromatic compound	Acid not recovered (%)	Product: Gaseous (%)[a]		Product: Nongaseous			
		H_2	CO_2	Benzene-soluble (g)	Benzene-insoluble (g)	Phenylate (%)[b]	Benzoyloxylate (%)[b]
Toluene	57	100	3.4	2.8	0.9	1	1.2
Toluene[c]	82	79	4.6	4.3	—	0.1	0.2
Ethylbenzene	75	86	7.5	3.2	0.7	4.0	0.8
Cumene	72	98	4.8	3.1	1.2	1.3	1.6
Tetralin[d]	57	90	1.8	5.2	0.6	neutral: 0.5 g phenolic: 0.3 g	

a) Coulombic yield
b) Based on the acid not recovered
c) Solvent: MeOH (50 m*l*) containing MeONa (0.02 mol)
d) 0.35 mol

interpreted as being due to the suppressed decarboxylation of an anodically-adsorbed benzoyloxy radical or as being due to the participation of other electrode reactions in which the discharge of the benzoate anion is not significantly operative. From a consideration of the quantitative relationship between hydrogen and the unrecovered acid, it may be suggested that a considerable portion of the hydrogen is not supplied from the electrolysis of benzoic acid, but is, rather supplied from the aromatic substrate present.

Two primary electrode reactions (Eqs. (3) and (4)) are possible in the Kolbe electrolysis:

$$RCOO^- \rightarrow R\cdot + CO_2 + e^- \quad (3)$$

(simultaneous bond-breaking)

$$RCOO^- \rightarrow RCOO\cdot + e^- \quad (4)$$

On the basis of the calculations of the standard potentials and rate constants for the two reactions, Eberson has suggested that, in the anodic reaction of benzoic acid, the latter reaction (Eq. (4)) is probable, and that it is followed by radical decomposition to the phenyl radical and carbon dioxide.[11] A sequent electrode reaction (Eq. (5)) can be ruled out since the ionization potential (9.2 eV)[12] of the phenyl radical is above the critical potential of 8 eV.

$$Ph\cdot \rightarrow Ph^+ + e^- \quad (5)$$

At least three active species, *i.e.*, $PhCOO^-$, $PhCOO\cdot$, and $Ph\cdot$, which can participate in the anodic substitution may be generated from benzoic acid in these systems. Of these however, only the phenyl radical can take part in the phenylation. Thus, the observed phenylation appears to proceed in a free radical manner, while the formation of biphenyl suggests the generation of phenyl radicals:

$$ArH + Ph\cdot \rightarrow Ar(H)(Ph)\cdot \rightarrow Ar\text{-}Ph + H^+ + e^-$$

The other two species, $PhCOO^-$ and $PhCOO\cdot$, can participate in the anodic benzoyloxylation. Homolytic benzoyloxylation has been observed when benzoyl peroxide decomposes in benzene,[13] chlorobenzene,[14,15] nitrobenzene,[14,16] and biphenyl.[13,16] With the mono-substituted benzenes, the extent of the benzoyloxylation is small. Even if the anodically-produced benzoyloxy radical is stabilized by adsorption of the electrode surface, it can undergo spontaneous decomposition; thus, the homolytic phenylation should still proceed as the main reaction. The yields of benzoyloxylates in this anode reaction are, however, rather larger than those expected to be produced by the homolytic processes.

Therefore, it is reasonable to assume that the majority of the benzoyloxylates arise from the reaction of the benzoate anion with a cationic intermediate generated from the aromatic substrate at the anode.

$$ArH \xrightarrow{-e^-} ArH\cdot^+ \xrightarrow{+PhCOO^-} ArOCOPh + H^+ + e^-$$

or

$$ArH \xrightarrow{-2e^-} ArH^{2+} \xrightarrow{+PhCOO^-} ArOCOPh + H^+$$

Experimental

All the melting and boiling points are uncorrected. The IR spectra were obtained with a Shimadzu IR spectrophotometer IR-27C. A Toyo GC-S-7 (gas chromatograph) apparatus was employed in the analysis of the products. The electrolyses were carried out in an undivided cylindrical cell (*ca.* 100 m*l*) fitted with a reflux condenser and a thermometer. Two platinum electrodes (15×20 mm; space, 10 mm apart) were inserted into the center of the cell through a ground-glass joint at the top. The cell was connected through the condenser to a gas-collection apparatus.

Materials. Commercially-availlable benzoic acid (mp 121°C), toluene (bp 110—111°C), ethylbenzene (bp 136°C), cumene (bp 152°C), tetralin (bp 77°C/10 mmHg), acetonitrile (bp 82°C), triethylamine (bp 90°C), and methanol were purified by the usual ways.

Electrolysis of Benzoic Acid in the Presence of Toluene. A solution of benzoic acid (6.1 g, 0.05 mol) and toluene (36.8 g, 0.4 mol) in acetonitrile (50 m*l*) containing triethylamine (2.8 m*l*) was electrolyzed at 18—24°C (current: 0.08—0.11 A, voltage: 40—65 V, total current passed: 2.73 A-hr).

The gas evolved during the electrolysis was then analyzed by using a silica gel column at 20—40°C; it was found to consist of hydrogen (1140 m*l*) and carbon dioxide (80 m*l*). The non-gaseous product was distilled under reduced pressure to recover the solvent and the bulk of the uncharged toluene (22.6 g, 0.25 mol). The residue (9.1 g) was separated into unchanged benzoic acid (2.6 g, mp and mixed mp 120—121°C) and benzene-soluble (2.8 g) and benzene-insoluble (0.9 g) portions. The benzene-insoluble solid (mp over 250°C) displayed IR bands assignable to the ester function at 1240—1280 and 1740 cm^{-1}; it was treated with alcoholic potassium hydroxide under reflux for 15 hr. However, it could not saponified completely. The saponification gave an acid (0.23 g), phenolic compounds (0.1 g) and other materials (0.44 g). These substances were not investigated further.

The benzene-soluble portion gave at least three major spots on TLC and was subjected to chromatographic separation (adsorbent: silica gel; eluent:

11) L. Eberson, *Acta Chem. Scand.*, **17**, 2004 (1963).
12) I. P. Fisher, T. F. Palmer and F. P. Lossing, *J. Am. Chem. Soc.*, **86**, 2741 (1964).
13) D. I. Davies, D. H. Hey and G. H. Williams, *J. Chem. Soc.*, **1961**, 562.
14) B. M. Lynch and K. H. Pausacker, *Australian J. Chem.*, **10**, 165 (1957).
15) B. M. Lynch and K. H. Pausacker, *ibid.*, **10**, 329 (1957).
16) M. Karelsky and K. H. Pausacker, *ibid.*, **11**, 39 (1958).

benzene). On the basis of the IR spectra and the results of TLC analysis, the collected fractions were combined after the evaporation of the eluent. The main combined residue (0.5 g) was saponified with alcoholic potassium hydroxide under reflux for 15 hr to give an acid (0.1 g) phenolic compounds (0.09 g) and a neutral portion (0.2 g). The latter two portions were analyzed by vapor-phase chromatography (column: 3-m Cu-column packed with 25% Silicone HV on a fire brick; carrier gas: He, 70 and 37 ml/min respectively; column temperature: 180 and 210°C respectively). The phenolic portion consisted of *m*- and/or *p*-cresol (30.4%), *o*-cresol (9.7%), and other materials. The neutral fraction consisted of *m*- and/or *p*-methylbiphenyl (16.5%), *o*-methylbiphenyl (2.1%), biphenyl, and at least two other unidentified substances.

Additionally, the electrolysis of benzoic acid (6.1 g, 0.05 mol) in methanol (50 ml) containing sodium methoxide (1.1 g) was examined in the presence of toluene (36.8 g, 0.4 mol) under similar conditions (19—24°C; 0.12 A, 15—16 V, 4 A-hr). The gaseous product consisted of hydrogen (1320 ml) and carbon dioxide (110 ml). The benzene-soluble residue (4.3 g) was separated after saponification into acid (1.1 g), a phenolic (0.1 g), and a neutral (0.9 g) portions. The phenolic portion consisted of *m*- and/or *p*-cresol (17.3%), *o*-cresol (8.8%), and other, unidentified substances. The neutral portion consisted of *m*- and/or *p*-methylbiphenyl (1.4%), *o*-methylbiphenyl (0.5%), biphenyl, and other materials.

Electrolysis of Benzoic Acid in the Presence of Ethylbenzene. A solution of benzoic acid (6.1 g, 0.05 mol) ethylbenzene (42.4 g, 0.4 mol) in acetonitrile (50 ml) containing triethylamine (2.8 ml) was electrolyzed at 16—28°C, at a current of 0.07—0.11 A and with an applied potential of 48—69 V, for 25 hr.

The gaseous product consisted of hydrogen (980 ml) and carbon dioxide (170 ml). The non-gaseous product was worked up in manners similar to those employed for toluene, and gave unchanged ethylbenzene (30 g, 0.23 mol), benzoic acid (1.5 g), a benzene-soluble portion (3.2 g), and a benzene-insoluble polymeric solid (0.7 g). The chromatographic separation of the benzene-soluble portion gave a hydrocarbon - benzoate mixture (0.7 g) and a dark-brownish residue. The mixture was treated with alcoholic potassium hydroxide to give benzoic acid (0.17 g), phenolic (0.19 g), and neutral (0.37 g) portions. The phenol portion was found to consist of *o*-ethylphenol (6.6%), *p*-ethylphenol (16.2%), and other materials. The vapor-phase chromatographic analysis of the neutral substances showed it to contain *o*-ethylbiphenyl (21.5%), *p*-ethylbiphenyl (49.8%), biphenyl (traces), α-phenylethanol, and at least two other substances.

Electrolysis of Benzoic Acid in the Presence of Cumene. A solution of benzoic acid (6.1 g) and cumene (48 g, 0.4 mol) in acetonitrile containing triethylamine was electrolyzed under similar conditions (17—25°C, 0.04—0.11 A, 54—60 V, 2.97 A-hr). A mixture of hydrogen (1100 ml) and carbon dioxide (120 ml) was obtained as the gaseous product. From the electrolyzed mixture, unchanged cumene (33.5 g, 0.28 mol) and residual tar (8.8 g) were obtained. The residue was spearated into benzoic acid (1.7 g), benzene-soluble (3.1 g), and insoluble (1.2 g) portions. A hydrocarbon - benzoate mixture (0.57 g) was obtained from the benzene-soluble portion. The mixture gave, after saponification, benzoic acid (0.2 g), phenol (0.1 g) and neutral (0.32 g) portions. The characterized components of the phenol portion were *o*-isopropylphenol (8.7%) and *p*-isopropylphenol (37.6%). *o*-Isopropylbiphenyl (7%), *p*-isopropylibiphenyl (19.7%), biphenyl (traces), and α-cumenol (traces) could be identified as the components of the neutral fraction.

Electrolysis of Benzoic Acid in the Presence of Tetralin. The electrolysis was carried out by using tetralin (47.8 g, 0.35 mol) under similar conditions (18—28°C, 0.08—0.11 A, 56—68 V, and 2.63 A-hr).

The gaseous product consisted of hydrogen (990 ml) and carbon dioxide (40 ml). Tetralin (14 g, 0.31 mol) and a residual oil (13.7 g) were obtained from the crude product. The residual oil gave benzoic acid (2.6 g), benzene-soluble (5.2 g), and insoluble (0.6 g) fractions. Portions (2 g) of the benzene-soluble fraction were chromatographed on silica gel and eluted with a benzene - methanol mixture to give a hydrocarbon - benzoate mixture (1.06 g) The saponification of the mixture yielded benzoic acid (0.2 g), phenolic (0.15 g) and neutral (0.3 g) parts. The VPC analysis of the neutral part failed to show the presence of 1-hydroxy-1,2,3,4-tetrahydronaphthalene.

BULLETIN OF THE CHEMICAL SOCIETY OF JAPAN VOL. 41 2672—2675 (1968)

Episulfones. IV. The Decomposition Reaction of Episulfones by Bases

Shoichi Matsumura, Toshikazu NAGAI and Niichiro TOKURA

Department of Applied Chemistry, Faculty of Engineering, Osaka University, Suita, Osaka

(Received January 25, 1968)

The present paper deals with the decomposition reaction of episulfones in the presence of several bases. The treatment of *cis*-stilbene episulfone (I) with 2 N NaOH gave *trans*-stilbene in a 92% yield, and a hydrogen-deuterium exchange experiment using NaOD showed that 66% of the methine protons of the episulfone were exchanged. On the other hand, the reaction of *n*-butyllithium yielded *cis*-stilbene predominantly, along with *trans*-1,2-diphenylvinyl sulfinate in about a 20% yield. Styrene episulfone (II) gave styrene (80%) and a trace of benzyl methyl sulfone when II was treated with alkali. Tetraphenylethylene episulfone (III) afforded tetraphenylethylene almost quantitatively. The cleavage mechanism by bases is then discussed on the basis of the above results. Ethylene episulfone (IV) is oligomerized by tertiary-amine catalysis.

We have been studying the physical and chemical behavior of episulfones (thiirane 1,1-dioxide) and have previously reported some new reactions.[1a,b] In the present paper, we wish to report on the base-catalyzed decompositions of episulfones and on their mechanisms. The reaction of episulfones with a base to give olefins has been investigated by several workers,[1c,2] but the reaction mechanism has not yet been clarified. In this paper, we will describe the decompositions of several episulfones (I—IV) with various bases and suggest the reaction mechanism.

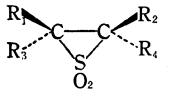

(I) $R_1=R_2=C_6H_5$ $R_3=R_4=H$
(II) $R_1=C_6H_5$ $R_2=R_3=R_4=H$
(III) $R_1=R_2=R_3=R_4=C_6H_5$
(IV) $R_1=R_2=R_3=R_4=H$
(V)[2] $R_1=R_2=CH_3$ $R_3=R_4=H$

The results of the decomposition of *cis*-stilbene episulfone (I) by various bases are summarized in Table 1.

cis-Stilbene episulfone was decomposed to *trans*-stilbene predominantly by the reaction with alkali, while the treatment of I with *n*-butyllithium afforded *cis*-stilbene predominantly. Triethylamine did not cleave the episulfone under the same conditions (0°C, 6 hr).

Recently, Neureiter[2] has proposed a mechanism in which the elimination of α-protons of V by a stronger base is followed by the epimerization to the α-sulfonyl carbanion of the *trans*-form during the process of exchange forming *trans*-olefin by a thermal process; treatment with the *t*-butoxide ion, the strong, hindered base (in *t*-BuOD), resulted in the formation of *trans*-2-butene in a 80% yield, with complete deuteration at the 2 and 3-positions (Scheme 1).

TABLE 1. DECOMPOSITION OF *cis*-STILBENE EPISULFONE (I) BY SEVERAL BASES

Base	Solvent	Temp. (°C)	*cis*-Stilbene	*trans*-Stilbene (%)
2 N NaOH	40%THF-H_2O	0	7	92
2 N LiOH	40%THF-H_2O	0	5	90
2 N KOH	40%THF-H_2O	0	2	89
n-BuLi	THF	0	70	6
$N(Et)_3$	THF	0	No Decomposition	

cis-Butene was favored when V was treated with a weaker base, suggesting that the α-hydrogens were not eliminated in this case.

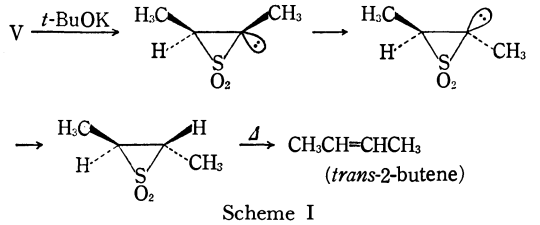

Scheme I

However, a thermal process to give the *trans*-olefin from the *trans*-episulfone can not be accepted, since the *trans*-episulfone of I or V could not be isolated, even at a low temperature. For this reason, we have tried to isolate the intermediate of the reaction in order to clarify the mechanism.

In order to trap the intermediate, we tried to treat the episulfone (I) with *n*-butyllithium at a low temperature (0°C). We chose the 1,2-diphenyl derivatives because of the ability of the phenyl group to stabilize the system by conjugation.

When I was treated with *n*-butyllithium in

1) a) S. Matsumura, T. Nagai and N. Tokura, This Bulletin, **41**, 635 (1968). b) *Idem., Tetrahedron Letters*, **1966**, 3929. c) N. Tokura, T. Nagai and S. Matsumura, *J. Org. Chem.*, **31**, 349 (1966).
2) N. P. Neureiter, *J. Am. Chem. Soc.*, **88**, 558 (1966).

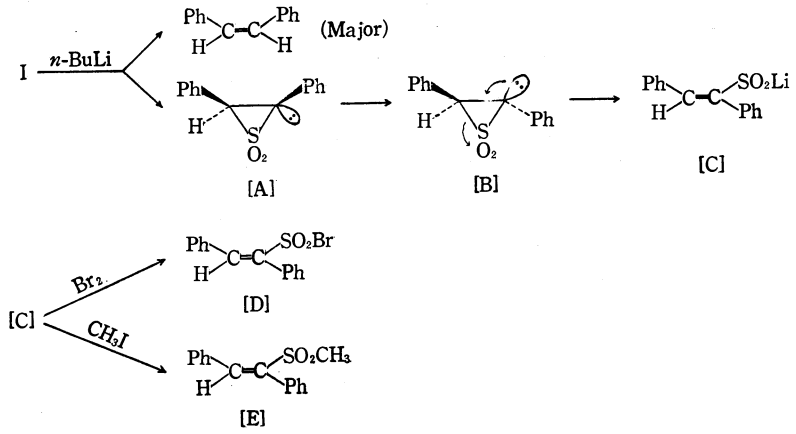

Scheme II

THF, and then with bromine or methyl iodide, *trans*-1,2-diphenylvinylsulfonyl bromide [D] and *trans*-1,2-diphenylvinyl methyl sulfone [E] were formed in 16 and 9% yields respectively, even at 0°C.[3]

These products were obviously generated through the ring-opening compound, *trans*-1,2-diphenylvinyl sulfinate [C], which was itself formed through [A], and then converted to [B]. The reactions described are outlined in Scheme II.[4]

The above-mentioned results suggest that the formation of *trans*-stilbene or *trans*-2-butene passes through Schemes II and III, if the bases which can eliminate the α-hydrogens but can not attack the sulfur atom of the episulfone, are used.[5] [C] did decompose to *trans*-stilbene when treated with acid.[6]

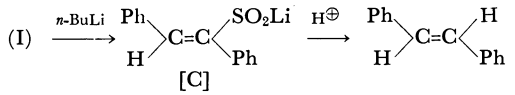

Scheme III

On the other hand, as there was a 66% hydrogen-deuterium exchange of I in the NaOD-D_2O system, the α-hydrogens are certainly eliminated prior to the formation of the [C] intermediate (Scheme III). The [C] intermediate is not unstable at 0°C, so it might be trapped by bromine or methyl iodide if the reaction followed Scheme III. However, our attempts to trap the [C] intermediate were unsuccessful. Therefore, we assumed a mechanism in which the olefinic product (*trans*-stilbene) arose as a result of a nucleophilic attack on the sulfur atom of the episulfone.[7] (Scheme IV).

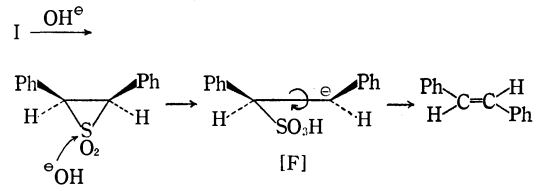

Scheme IV

The difference between *n*-BuLi and $OH^{\ominus}$ may be ascribed to the fact that *n*-BuLi is rather sterically hindered to attack the sulfur atom. (The H–D exchange reaction might be fast, and the α-sulfonyl carbanion intermediate [A], considerably stable.) Although the [F] intermediate is stable enough to rotate around the C–C single bond, the similar intermediate which arises in the case of V seems to be unstable, giving *cis*-2-butene predominantly before the rotation.

In this connection, it is interesting to note that these results demonstrate that the isomerization of α-sulfonylcarbanion in a three-membered system would also occur.[8]

As may be seen in Table 1, *cis*-stilbene was favored over the *trans*-isomer when *n*-butyllithium was used as the base. This may be interpreted in terms of the finding[1a] that the carbanion formation of I with *n*-butyllithium is slower than the thermal

3) The geometrical configurations of these two compounds, [D] and [E], were decided on the basis of a comparison of their mp's with those of an authentic specimen [E]. (M. Ōki and A. Kimura, This Bulletin, **38**, 682 (1965)).

4) Recently, L. A. Carpino and R. H. Rynbrondt (*J. Am. Chem. Soc.*, **88**, 5682 (1966) have proposed that, in vinylene sulfones, α-hydrogen is eliminated to give acetylene. However, this reaction has no relation to the stereochemical correlation.

5) Since the isomerization from [A] to [B] would be fast, [A] would not decompose to *cis*-stilbene. However, we cannot completely exclude a mechanism in which *trans*-stilbene is formed through [B], accompanied by the thermal elimination of sulfur dioxide, as has similarly been suggested by Neureiter.[2]

6) W. E. Truce and J. R. Norell, *J. Am. Chem. Soc.*, **85**, 3036 (1963).

7) A similar mechanism was recently presented by L. A. Paquette and L. S. Wittenbrook, *ibid.*, **89**, 4483 (1967).

8) E. J. Corey, H. Konig and T. H. Lowy, *Tetrahedron Letters*, **1962**, 515.

decomposition[1c] of I. *trans*-2-Butene was formed predominantly when V was treated with *t*-butoxide ion, because the carbanion formation was faster than the thermal elimination of sulfur dioxide (Scheme I).[2]

When styrene episulfone (II) was treated with alkali (2 N NaOH), styrene (80%), and a trace of the sulfinate, [G'] or [G''] (identified as benzyl methyl sulfone (0.4%)) was produced. The process of the formation of styrene may be analogous to the mechanistic route described in Scheme IV, and the benzyl sulfone may be formed according to either Scheme V or VI.[9]

Scheme V shows a C–S bond fission, and Scheme VI involves an interesting C–C bond cleavage.[1a,b] It is not yet clear which of the two schemes is correct.

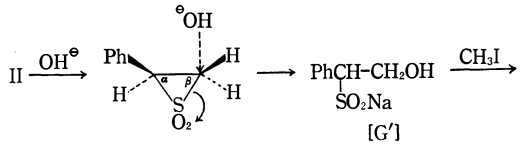

Scheme V

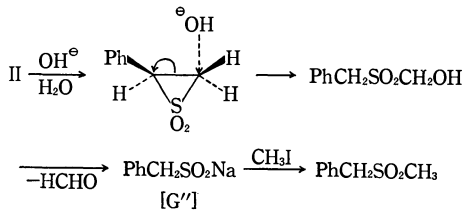

Scheme VI

The hydroxide-ion attack on the β-carbon of II essentially resembles the reaction of styrene oxide. It is interesting to compare with findings previously reported;[1a] the α-carbon of II was selectively attacked by the hydride ion ($LiBH_4$ or $LiAlH_4$) (Scheme VII). The sterically larger molecule, $OH^{\ominus}$, should attack a less hindered site.

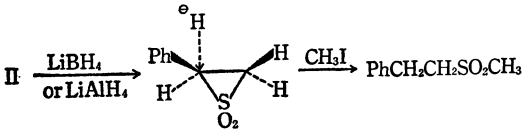

Scheme VII

Recently, Desiderate and Sass[10] reported on the crystal structure of *cis*-2-butene episulfone V and showed that the C–C bond length is, surprisingly, 1.60 Å (which is much longer than those of epoxide (1.47 Å) and episulfide (1.49 Å)). Our previous proposal[1a] concerning this abnormal bond length is thus confirmed; however, we are now studying this point in detail.

Tetraphenylethylene episulfone (III) gave tetraphenylethylene exclusively (92%) when III was treated with 2 N NaOH, probably by attacking the sulfur atom as is described in Scheme IV.

These results suggest that the sulfur atoms of episulfones are attacked by $OH^{\ominus}$, giving olefins.

Ethylene episulfone (IV) was first synthesized by Hesse *et al.*, and several reactions toward the episulfone have been reported on; for example, when IV was treated with NaOH, unidentified products were produced. We used *t*-amines, such as pyridine, triethylamine, and 2,6-lutidine, and found that an oligomerization occurs. The elemental analyses of these products are summarized in Table 2. The products were insoluble in almost all solvents except for an alkali solution, while there was an accompanying decomposition. (The oligomers did not dissolve in concentrated H_2SO_4.)

It is well known that the olefins containing strong electron-withdrawing groups are polymerized even by *t*-amines such as triethylamine. Compared with other heterocyclic three-membered rings, episulfones are easily attacked by nucleophilic reagents because of having a strong electron-withdrawing sulfone group.

The structure of the oligomers would seem to be:

$$-(-CH_2CH_2-SO_2-)_{\overline{n}}$$

However, these products were all insoluble in the solvents, and only the IR spectra and elemental analysis gave any information, however little, about the structures. Because of the insolubility, the molecular weights could not be measured, but if the terminals are *t*-amines, the degrees of polymerization can not be very high.

TABLE 2. ELEMENTAL ANALYSES, DECOMPOSITION POINTS, AND YIELDS OF THE POLYMER (25°C, Base/IV = 1/4).

Base	C	H	N	S	D.P.	Yield (%)
	27.44	4.32	2.00	23.48	270	57
$(C_2H_5)_3N$	28.54	4.98	1.29	25.92	270	21
	29.06	4.40	1.22	28.13	270	12

Experimental

Materials. The *cis*-stilbene episulfone (I), styrene episulfone (II), tetraphenylethylene episulfone (III), and ethylene episulfone (IV) were synthesized as has described in a previous paper.[1a]

9) D. C. Dittmer and M. E. Christy, *J. Am. Chem. Soc.*, **84**, 399 (1962).
10) R. Desiderate and R. L. Sass, *Acta Cryst.*, **23**, 430 (1967).

The sodium deuteroxide and deuterium oxide were obtained from Ciba Ltd.

The tetrahydrofuran was purified by refluxing it with sodium for two days, followed by distillation in the presence of lithium aluminum hydride.

All the melting points and boiling points are uncorrected. The infrared absorption spectra were determined on a Hitachi Infrared Spectrophotometer. The NMR Spectra were run on a Nihondenshi Spectrometer at 60 Mc. Tetramethylsilane was used as an internal standard, and *d*-chloroform was used as the solvent (Ciba Ltd.). Vpc analysis was carried out on a Yanagimoto Model GCS-100 Instrument.

Reaction of Episulfones with Alkali (General Procedure). A mixture of an episulfone (about 0.002 mol) and aqueous 2 N alkali (40%) in a THF-solution (50 m*l*) was stirred for 20 min at 0°C. The reaction mixture was then added to ice water (50 m*l*) and extracted twice with 50 m*l* of ether. After the combined ether layer had been dried over sodium sulfate (anhydrous), the ether was removed under reduced pressure. The products were identified as follows. The *cis*- and *trans*-stilbene were separated by fractional crystallization. (The *cis*-stilbene was identified as has been described in a previous paper,[1c] while the *trans*-form was a solid material which melted at 124°C.) The styrene was determined by Vpc. The benzyl methyl sulfone and tetraphenylethylene were identified by comparison with authentic specimens (mp 123°C and 222°C respectively).

A deuterium exchange experiment was carried out under nitrogen; the procedure was similar to that described above. The *d-trans*-stilbene was analysed by means of the NMR spectra. The ratio of the area of the peak due to phenyl protons to that area due to olefin protons was 15 : 1, showing that 70% of the olefin protons were deuterated (τ(phenyl) 2.6, (olefin 2.85)).

Reaction of *cis*-Stilbene Episulfone (I) with *n*-Butyllithium. *n*-Butyllithium (about 0.002 mol) was prepared in dry THF, and to this solution *cis*-stilbene episulfone (1.0 g; 0.004 mol) in THF (10 m*l*) was added slowly at 0°C. After the reaction mixture had then been stirred for 30 min, bromine (3.0 g) or methyl iodide (3.0 g) was added, drop by drop; the solvents were then evaporated under reduced pressure. The products were separated on the basis of their solubility; that is, *trans*-1,2-diphenylvinylsulfonyl bromide was soluble in petroleum ether, while the residue (dibromostilbene) was sparingly soluble in petroleum ether. *trans*-1,2-Diphenylvinyl methyl sulfone was also separated and recrystallized from ether-petroleum ether.

The product [D], *trans*-1,2-diphenylvinylsulfonyl bromide, was identified on the basis of the following data: mp 122—124°C, NMR (in $CDCl_3$) τ=2.88 (5H, multiplet, aromatic) 2.53 (5H, singlet, aromatic) 2.21 (1H, singlet, olefinic porton), IR ν_{max}^{KBr} 1620, 818 (tri-substituted olefin) 1350, 1148 cm^{-1} (ν_{SO_2}), UV $\lambda_{max}^{95\%EtOH}$ 287 (14700), 270 (14800), 216 mμ (ε 20300). Found: C, 51.94; H, 3.23%. Calcd for $C_{14}H_{11}BrO_2S$: C, 52.02; H, 3.43%.

trans-1,2-Diphenylvinyl methyl sulfone [E] was identified on the basis of the following data: mp 118—119°C, NMR (in $CDCl_3$) τ=7.21 (3H, singlet, CH_3), 2.84 (5H, multiplet, aromatic), 2.56 (5H, singlet, aromatic), 2.17 (1H, singelt, olefinic proton), IR ν_{max}^{KBr} 1645, 825 (tri-substituted olefin) 1308, 1315, 1132 cm^{-1} (ν_{SO_2}). UV $\lambda_{max}^{95\%EtOH}$ 267 (17400), 217 mμ (ε 23000).

Found: C, 69.81; H, 5.61%. Calcd for $C_{15}H_{14}O_2S$: C, 69.74; H, 5.46%.

Reaction of Ethylene Episulfone (IV) with *t*-Amines (General Procedure). A mixture of ethylene episulfone (0.023 mol) and *t*-amines (0.005 mol) in THF (20 m*l*) was allowed to stand for two days at room temperature. The resulting precipitates were washed three times with 95% ethanol, and then three times with water, and dried in a desiccator.

BULLETIN OF THE CHEMICAL SOCIETY OF JAPAN VOL. 41 2676—2682 (1968)

The Acylation of 2,3-Dimethyl-*bz*-hydroxybenzofurans and the Syntheses of Di- and Tri-methylfuroisoflavones*[1]

Yoshiyuki KAWASE, Mutsumu NANBU and Fumihisa MIYOSHI

Department of Chemistry, Faculty of Literature and Science, Toyama University, Gofuku, Toyama

(Received March 2, 1968)

The acylation of 2,3-dimethyl-4-hydroxybenzofuran (1) with acetic acid, phenylacetic acid, 2-methoxyphenylacetic acid or 2,4,5-trimethoxyphenylacetic acid, and polyphosphoric acid gave a mixture of the 5- and 7-acyl compounds (2a, b, c, d, and 3a, c, d respectively). Analogously, the isomeric 2,3-dimethyl-6-hydroxybenzofuran (6) gave the 5-acyl compounds (7a, b, c, d), two (7a, b) of which were also obtained by the Friedel-Crafts acylation of the methyl ether of 6 (9), followed by demethylation. On the other hand, the formation of a dimethylfuran ring on 2,4-dihydroxyphenyl ketones by the action of polyphosphoric acid on their 4-(α-acetylethoxy) derivatives (11a, b, c) also afforded mixtures of the ketones (7a, b, c) and isomeric ketones (2a, b, c). The benzofuranyl ketones (2 and 7) thus obtained were converted to the corresponding 4'',5''-dimethyl-furo[2'',3'':7,8]isoflavones (12b, c, d) and isomeric -furo[3'',2'':6,7]isoflavones (14b, c), and also their 2-methyl derivatives (13b, c, d and isomeric 15b, c), by the general method utilizing ethyl orthoformate, piperidine and pyridine, or acetic anhydride and sodium acetate. The furoisoflavones (12b, c and 13b, c) were also prepared by building up the dimethylfuran ring on 7-hydroxyisoflavones by the action of polyphosphoric acid or sulfuric acid on their 7-(α-acetylethoxy) derivatives (16b, c and 17b, c respectively). The alkaline degradation of these furoisoflavones (12 and 13) also gave the benzofuranyl ketones (2)

Previously, furo[2'',3'':7,8]isoflavones[1,2] and the 4''-methyl derivative[2a] were prepared by building up the furan ring on 7-hydroxyisoflavones, while the 5''-alkyl derivatives[3] and isomeric furo[3'',2'' : 6,7]isoflavones[4] were prepared by the dehydrogenation of the corresponding dihydrofuroisoflavones. The furoisoflavones were also prepared by the pyrone ring formation on hydroxybenzofuranyl ketones.[1-3]

In the present experiments, 2,3-dimethyl-4- and isomeric -6-hydroxy-5-benzofuranyl ketones (2 and 7), which had been prepared by the acylation of the corresponding hydroxy- or methoxybenzofurans (1 and 6 or 9), were converted to furo[2'',3'' : 7,8]isoflavones (12 and 13) and isomeric furo[3'',2'':6,7]isoflavones (14 and 15) respectively by the formation of a pyrone ring on them. Two furoisoflavones (12 and 13) were also prepared by building up the dimethylfuran ring on 7-hydroxyisoflavones; the alkaline degradation of these furoisoflavones also gave the benzofuranyl ketones (2).

Previously, 4-hydroxy- or 4-methoxy-5-benzofuranyl ketones were prepared by the interaction of benzofurancarbonyl chloride with ethyl phenylacetate[2a] or with dibenzylcadmium[5]; also, these ketones as well as the isomeric 6-hydroxy-5-benzofuranyl ketones were prepared by the alkaline degradation of furoisoflavones,[1,4] for the direct acylation of hydroxybenzofurans to give the ketones was not successful. On the other hand, the 2-substituted 6-hydroxy-[6] or 6-methoxy-5-benzofuranyl methyl ketones[7] were obtained by the acetylation of the corresponding benzofurans,

*1 A part of this work was presented at the 20th Annual Meeting of the Chemical Society of Japan, Tokyo, March, 1967.

1) T. Matsumoto, Y. Kawase, M. Nanbu and K. Fukui, This Bulletin, **31**, 688 (1958); K. Fukui and Y. Kawase, *ibid.*, **31**, 693 (1958); Y. Kawase, K. Ogawa, S. Miyoshi and K. Fukui, *ibid.*, **33**, 1240 (1960); K. Fukui, M. Nakayama and M. Hatanaka, *ibid.*, **36**, 872 (1963); K. Fukui, M. Nakayama and K. Okazaki, *Nippon Kagaku Zasshi (J. Chem. Soc. Japan, Pure Chem. Sect.)*, **85**, 446 (1964).

2) a) L. R. Row and T. R. Seshadri, *Proc. Indian Acad. Sci.*, **34A**, 187 (1951). b) K. S. Raizada, P. S. Sarin and T. R. Seshadri, *J. Sci. Ind. Research (India)*, **19B**, 76 (1960).

3) a) P. S. Sarin, J. M. Sehgal and T. R. Seshadri, *ibid.*, **16B**, 61, 206 (1957). b) S. F. Dyke, W. D. Ollis and M. Sainsburg, *J. Chem. Soc., (C)*, **1966**, 748.

4) S. K. Pavanaram, L. R. Row and T. R. Seshadri, *J. Sci. Ind. Research (India)*, **15B**, 495 (1956); S. K. Pavanaram and L. R. Row, *Current Science (India)*, **26**, 145 (1957); K. Fukui and M. Nakayama, *Experientia*, **19**, 621 (1963); *ibid.*, **20**, 668 (1964); K. Fukui, M. Nakayama, A. Tanaka and S. Sasatani, This Bulletin, **38**, 845 (1965); A. S. R. Anjaneyulu, C. S. Krishna and L. R. Row, *Tetrahedron*, **21**, 2677 (1965).

5) Y. Kawase, T. Fujimoto and K. Fukui, This Bulletin, **31**, 691 (1958).

6) J. Oda, H. Fukami and M. Nakajima, *Agr. Biol. Chem.*, **30**, 59 (1966).

7) P. K. Ramachandran, A. T. Tefteller, G. O. Paulson, T. Cheng, C. T. Lin and W. J. Horton, *J. Org. Chem.*, **28**, 398 (1963).

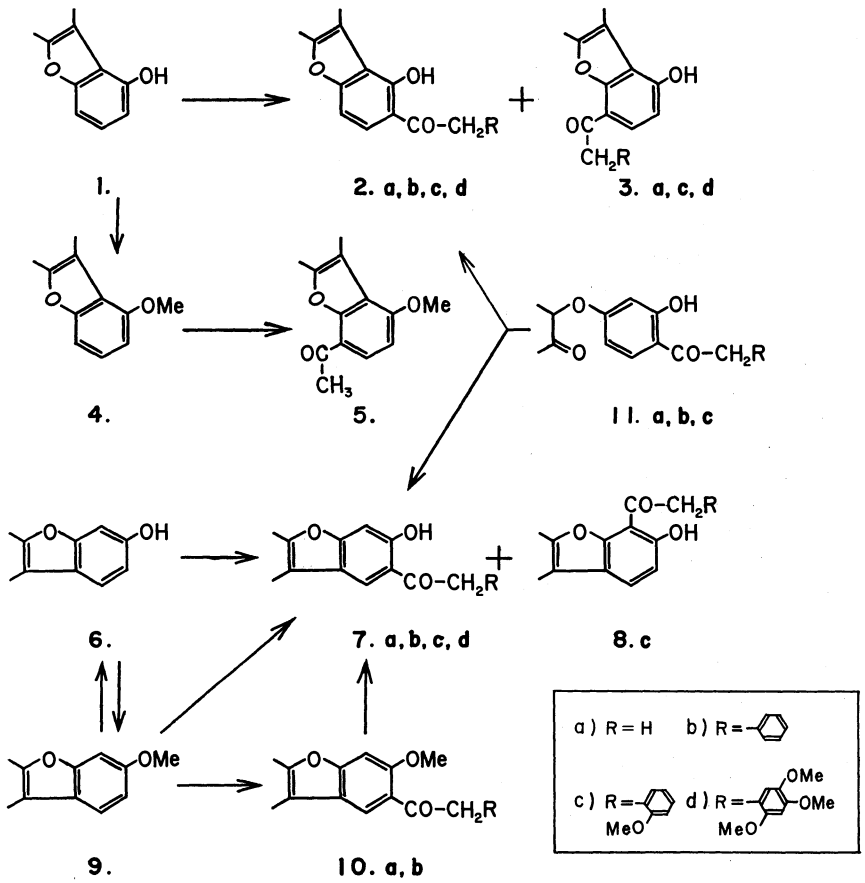

Chart 1

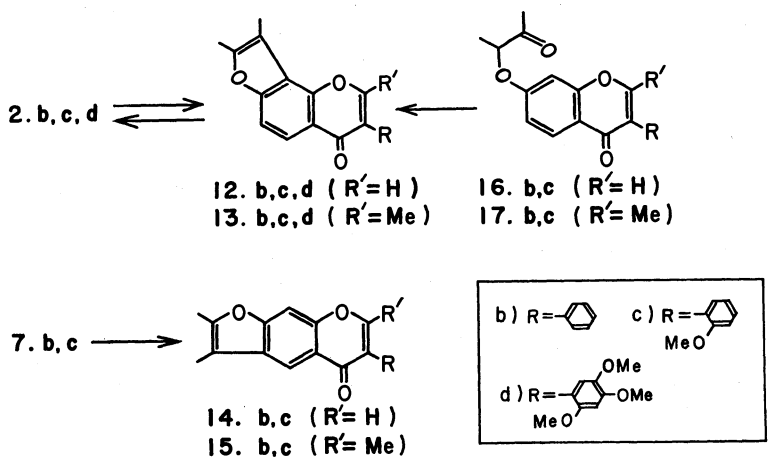

Chart 2

while the acetylation of isomeric 4-methoxy-2-methoxycarbonylbenzofuran afforded the 7-acetyl compound.[7] It has also been reported[8] that the acetylation of 2,3-dimethyl-6-methoxybenzofuran (9) by the Friedel-Crafts reaction gave the 5-acetyl compound (10a), which was then demethylated to the hydroxyketone (7a), while that of isomeric 2,3-dimethyl-4-methoxybenzofuran (4) gave the 7-acetyl compound (5).

8) R. Royer, E. Bisagni, A.-M. Laval-Jeantet and J.-P. Marquet, *Bull. Soc. Chim. France*, **1965**, 2607.

In the present experiments, 2,3-dimethyl-4-hydroxybenzofuran[8] (1) was acylated with acetic acid, phenylacetic acid, 2-methoxyphenylacetic acid or 2,4,5-trimethoxyphenylacetic acid, and polyphosphoric acid to give a mixture of the 5- and 7-acyl compounds (2a, b, c, d and 3a, c, d respectively), analogously to the case of 2,3-dihydro-4-hydroxybenzofuran.[9] The 5-acyl compounds (2) were separated from the isomers (3) by the extraction of the latter from the mixture with aqueous sodium hydroxide.

The similar acylation of isomeric 2,3-dimethyl-6-hydroxybenzofuran[8] (6) gave the 5-acyl compounds (7a, b, c, d); 7a and 7b were also prepared by the Friedel-Crafts acylation of methoxybenzofuran (9), followed by demethylation. In the case of the 2-methoxyphenylacetyl derivative (7c), a small amount of an isomeric 7-acyl compound (8c) was also obtained; the structure of this was assigned on the basis of its positive ferric chloride color reaction and the analogous formation of 7-substituted compounds in the acetylation of 6-methoxy-2-methoxycarbonylbenzofuran[7] and in the condensation of 2,3-dimethyl-6-hydroxybenzofuran with ethyl phenylmalonate.[10]

On the other hand, 2,4-dihydroxyphenyl ketones were converted to 4-(α-acetylethoxy)-2-hydroxyphenyl ketones (11a, b, c) by the action of 3-chlorobutanone-2 and potassium carbonate; the subsequent dehydro-cyclization of these ethers (11) by the action of polyphosphoric acid afforded mainly the 6-hydroxy-5-benzofuranyl ketones (7a, b, c), the dimethylfuran ring being formed towards the unhindered 5-position of the ketones, and also gave small amounts of isomeric 4-hydroxy-5-benzofuranyl ketones (2a, b, c). These experiments confirmed the structures of these ketones (2 and 7).

The *o*-hydroxybenzofuranyl ketones (2a, b, c and 7b, c) thus obtained were converted to the corresponding 4'',5''-dimethylfuro[2'',3'':7,8]-isoflavones (12b, c, d) and 4'',5''-dimethylfuro-[3'',2'':6,7]isoflavones (14b, c) by the action of ethyl orthoformate and piperidine in pyridine, and were also converted to 2,4'',5''-trimethylfuro-[2'',3'':7,8]isoflavones (13b, c, d) and 2,4'',5''-trimethylfuro[3'',2'':6,7]isoflavones (15b, c) by the action of acetic anhydride and sodium acetate.

The furo[2'',3'':7,8]isoflavones (12 and 13) were also obtained by building up the dimethylfuran ring on 7-hydroxyisoflavones. 7-Hydroxyisoflavones were converted to 7-(α-acetylethoxy) derivatives (16b, c and 17b,c) by the action of 3-chlorobutanone-2 and potassium carbonate; the subsequent dehydro-cyclization of these ethers with polyphosphoric acid or concentrated sulfuric acid afforded the furoisoflavones (12b, c and 13b, c). In this case, the dimethylfuran ring is formed towards the 8-position of isoflavones, because this position is not as hindered as the 3-position of 4-(α-acetylethoxy)-2-hydroxyphenyl ketones (11), for the one hydroxyl group of the latter is blocked by the formation of the pyrone ring in the former, and because the position is the most reactive site in such electrophilic substitutions as chloromethylation,[11] Mannich reaction,[12] Claisen rearrangement,[3a] Fries rearrengement,[2a] and formylation.[1,2a]

The alkaline degradation of the furo[2'',3'':7,8] isoflavones (12 and 13) also afforded the 4-hydroxy-5-benzofuranyl ketones (2); this method is another route for the preparation of the ketones (2).

In the infrared spectra, the di- (12b, c, d and 14b, c) and tri-methylfuroisoflavones (13,b c, d and 15b, c) exhibit an absorption at about 1655—1640 cm^{-1} (ν_{CO}), much as the furoisoflavones without dimethyl groups have an absorption at about 1650—1634 cm^{-1}.[1,4,9]

In the ultraviolet spectra, the furo[2'',3'':7,8]-isoflavones (12b, c and 13b, c) have two bands, a strong band, I, at about 247—255 mμ and a weak band, II, at about 313—320 mμ, while the isomeric furo[3'',2'':6,7]isoflavones (14b, c and 15b, c) have corresponding bands at about 248—254 mμ and at 330—338 mμ respectively. These data show that the band II of furoisoflavones with a linearly-fused furan ring is at a wavelength longer by 17—18 mμ than is that of the isomers with an angularly-fused furan ring, but the band I is at almost the same wavelength. These figures are comparable to those of furoisoflavones without dimethyl groups[1,4,9]; this proves that the introduction of dimethyl groups to the furan ring of furoisoflavones causes a bathochromical shift of 10—13 mμ in the band II and one of 2—7 mμ in the band I.

Experimental*2

The Preparation of Benzofuranyl Ketones. *a) By the Acylation of 2,3-Dimethyl-hydroxybenzofurans (1 and 6) with Carboxylic Acid and PPA.**3 A mixture of 2,3-dimethyl-4-hydroxybenzofuran[13] (1) (5 g), acetic acid (2.2 g, 1.2 mol equivalents), and PPA (n=1.5, 125 g) was heated at 90°C for 1 hr with stirring. The cooled mixture was then poured into ice water and extracted with ether. The ethereal solution was washed with

9) Y. Kawase, M. Nanbu and H. Yanagihara, This Bulletin, **41**, 1201 (1968).

10) J.-P. Lechartier, P. Demerseman, A. Cheutin and R. Royer, *Bull. Soc. Chim. France,* **1966**, 1716.

11) Y. Kawase, M. Nakayama and S. Matsutani, This Bulletin, **35**, 1367 (1962).

12) P. Da Re and L. Verlicchi, *Ann. Chim. (Rome),* **50**, 1273 (1960).

*2 All melting points are uncorrected; the IR spectra were measured in the form of KBr disks, and the UV spectra were measured in ethanol. The detailed data are summarized in the tables and figures.

*3 Polyphosphoric acid.

13) E. Bisagni and R. Royer, *Bull. Soc. Chim. France,* **1962**, 925.

Table 1. The preparation of benzofuranyl ketones

Starting compound	Reagent[a]	Procedure,[b] temp.×hr	Produced ketone (yield, %)
1	Acetic acid	A, 90°×1	2a(25)+3a(6)
1	PAA	A, 100°×1	2b(52)
1	2-Methoxy-PAA	A, 80°×1	2c(37)+3c(5)
1	2,4,5-Trimethoxy-PAA	A, 85°×0.5	2d(30)+3d(6)
6	Acetic acid	A, 100°×1	7a(28)
6	PAA	A, 100°×1	7b(20)
6	2-Methoxy-PAA	A, 80°×1	7c(10)+8c(1)
6	2,4,5-Trimethoxy-PAA	A, 80°×2	7d(20.5)
9	Acetyl chloride	B, {Room×2, Reflux×1	7a(43)
9	Phenylacetyl chloride	B, {Room×2, Reflux×10′	7b(41)
9	Phenylacetyl chloride	B, Room×2	10b(74)
10b		C, Reflux×10′	7b(56)+10b(20)
c)	Chlorobutanone	D	2a(d)+7a(9)
e)	Chlorobutanone	D	2b(d)+7b(6)
f)	Chlorobutanone	D	2c(6)+7c(d)
12b	50% KOH	E, Reflux×3	2c(75.5)
13b	50% KOH	E, Reflux×3	2b(96)
13c	50% KOH	E, Reflux×3	2c(83.5)

a) PAA: Phenylacetic acid. b) A: Polyphosphoric acid ($n=1.5$), B: Friedel-Crafts reaction in benzene, C: Aluminum chloride in benzene, D: Reflux with potassium carbonate in acetone then cyclization by polyphosphoric acid, E: In ethanol. c) 2,4-Dihydroxyphenyl methyl ketone. d) A small amount. e) 2,4-Dihydroxyphenyl benzyl ketone. f) 2,4-Dihydroxyphenyl 2-methoxybenzyl ketone.

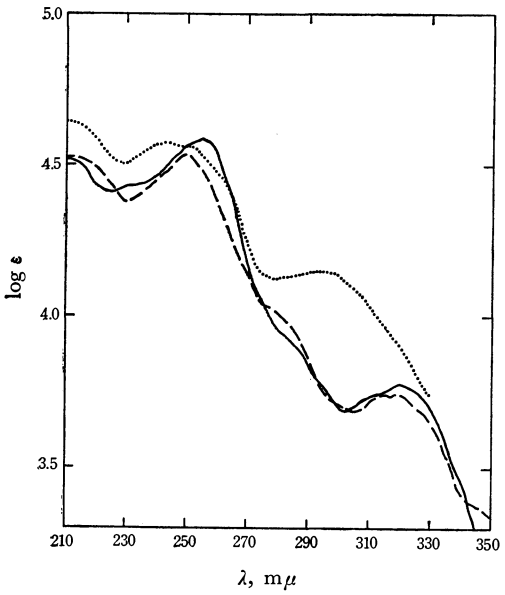

Fig. 1. The UV spectra of furoisoflavones: —— 12b, ---- 12c and ····· 12d.

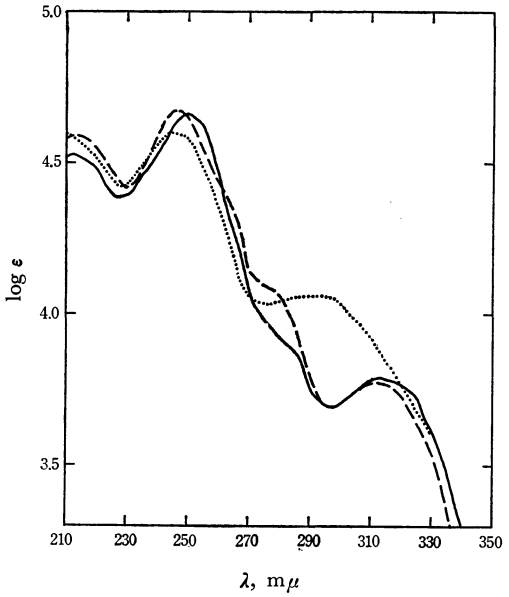

Fig. 2. The UV spectra of furoisoflavones: —— 13b, ---- 13c and ····· 13d.

aqueous sodium carbonate and then extracted with aqueous sodium hydroxide. The product obtained from the ethereal solution was recrystallized from ethanol to give 2,3-dimethyl-4-hydroxy-5-benzofuranyl methyl ketone (2a), which had a positive ferric chloride color reaction in ethanol. The alkaline solution was acidified, and the crystalline product formed was collected and recrystallized from ethanol to give the isomeric 2,3-dimethyl-4-hydroxy-7-benzofuranyl methyl ketone (3a), which had a negative ferric chloride color reaction in ethanol.

Similarly, the 2,3-dimethyl-4-hydroxy-5-benzofuranyl

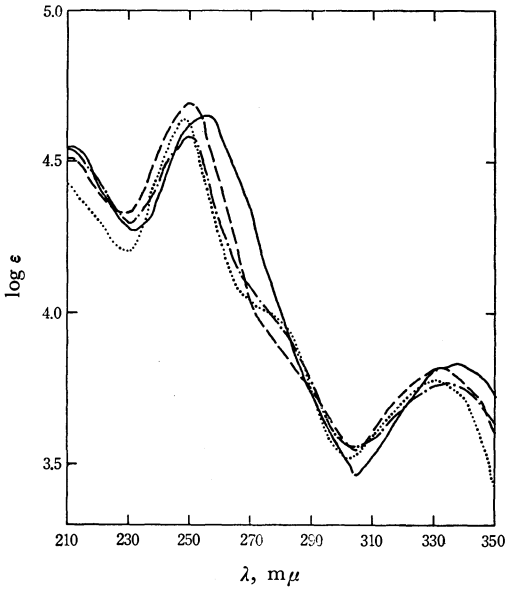

Fig. 3. The UV spectra of furoisoflavones: —— 14b, —·—· 14c, ---- 15b and ····· 15c.

benzyl ketones (2b), the 2,3-dimethyl-4-hydroxy-5-benzofuranyl 2-methoxybenzyl ketones (2c), the 2,3-dimethyl-4-hydroxy-5-benzofuranyl 2,4,5-trimethoxybenzyl ketone (2d), the isomeric 2,3-dimethyl-4-hydroxy-7-benzofuranyl 2-methoxybenzyl ketone (3c), and the 2,3-dimethyl-4-hydroxy-7-benzofuranyl 2,4,5-trimethoxybenzyl ketone (3d) were obtained by this procedure.

Further, the acylation of isomeric 2,3-dimethyl-6-hydroxybenzofuran[13] (6) by this procedure gave the 2,3-dimethyl-6-hydroxy-5-benzofuranyl methyl ketone (7a), the 2,3-dimethyl-6-hydroxy-5-benzofuranyl benzyl ketone (7b), the 2,3-dimethyl-6-hydroxy-5-benzofuranyl 2-methoxybenzyl ketone (7c), and the 2,3-dimethyl-6-hydroxy-5-benzofuranyl 2,4,5-trimethoxybenzyl ketone (7d). The ketone 7a has a mp of 121—123°C (from ethanol) (lit.[8] mp 122°C) and ν_{max}: 1650 cm^{-1} (CO). In the case of the ketone 7c, a small amount of the isomeric 2,3-dimethyl-6-hydroxy-7-benzofuranyl 2-methoxybenzyl ketone (8c) was also obtained.

b) By the Acylation of 2,3-Dimethyl-6-methoxybenzofuran (9), Followed by Demethylation. i) Methoxy-ketone 10b: Powdered anhydrous aluminum chloride (2 g) was added to a solution of 9[13] (2.6 g) and phenylacetyl chloride (2.4 g) in benzene (15 m*l*); the mixture was stirred at room temperature for 2 hr and then poured into ice water and extracted with benzene. The benzene was distilled off, and the residual product was recrystallized from ethanol to give the 2,3-dimethyl-6-methoxy-5-benzofuranyl benzyl ketone (10b), which had a negative ferric chloride color reaction in ethanol.

ii) Demethylation: Amixture of 10b (1.5 g), benzene (10 m*l*), and aluminum chloride (1 g) was refluxed for 10 min. The cooled mixture was poured into ice water and extracted with benzene. The benzene was distilled off, and the residue was recrystallized from ethanol to give the ketone 7b, which had a positive ferric chloride color reaction in ethanol. Some 10b was recovered from the mother solution.

c) By the Acylation of 9 in One Step. Aluminum chloride (3.1 g) was added to a solution of 9 (2.6 g) and phenylacetyl chloride (2.4 g) in benzene (15 m*l*); the mixture was stirred at room temperature for 2 hr and then refluxed for 10 min. The cooled mixture was treated much as has been described above to give the ketone 7b.

The ketone 7a was also prepared by this procedure.

d) By the Furan-ring Formation on 2,4-Dihydroxyphenyl Ketones through 4-(α-Acetylethoxy)-2-hydroxyphenyl Ketones (11). A mixture of the 2,4-dihydroxyphenyl methyl ketone (6.8 g), 3-chlorobutanone-2 (5.2 g), anhydrous potassium carbonate (15 g), potassium iodide (0.5 g), and acetone (60 m*l*) was refluxed for 7 hr. The cooled mixture was treated with water and extracted with ether. The ethereal layer was washed with aqueous sodium hydroxide, and then the ether was distilled off. The residual product was distilled to give the 4-(α-acetylethoxy)-2-hydroxyphenyl methyl ketone (11a); bp 148—153°C/2.5 mmHg, 5.9 g (59%). In the case of 11a, the analytical sample was recrystallized from petroleum ether.

A mixture of this crude ether 11a (1.5 g) and PPA

TABLE 2. THE PREPARATION OF 7-(α-ACETYLETHOXY)- AND FUROISOFLAVONES

Compd.	Starting compound[a]	Procedure[b] temp.×hr	Yield %
	7-(α-Acetylethoxy)isoflavones		
16b	7-Hydroxy-IF	A, (A), Reflux×5	51
16c	7-Hydroxy-2'-methoxy-IF	A, (A), (KI), Reflux×8	49
17b	7-Hydroxy-2-methyl-IF	A, (M), Reflux×5	91
17c	7-Hydroxy-2'-methoxy-2-methyl-IF	A, (M), (KI), Reflux×6	62.5
	Furoisoflavones		
12b	16b	B, 100°×1	33
12b	16b	C, 30°×1.5	43
12b	2b	D, Reflux×8	c)
12c	16c	B, 100°×2	c)
12c	2c	D, Reflux×8	19.5
12d	2d	D, Reflux×8	63
13b	17b	B, 100°×2	70
13b	17b	C, 30°×1.5	80
13c	2c	E, Reflux×12	46
13c	17c	B, 100°×2	62.5
13c	2c	E, Reflux×12	46.5
13d	2d	E, Reflux×12	75
14b	7b	D, Reflux×8	58
14c	7c	D, Reflux×8	58
15b	7b	E, Reflux×12	18.5
15c	7c	E, Reflux×12	46

a) IF: Isoflavone. b) A: Chlorobutanone and potassium carbonate in acetone (A) or methyl ethyl ketone (M) with or without the addition of potassium iodide (KI), B: Polyphosphoric acid (n=2.5), C: Concentrated sulfuric acid, D: Ethyl orthoformate, piperidine and pyridine, E: Acetic anhydride and sodium acetate. c) A small amount.

TABLE 3. THE PHYSICAL CONSTANTS AND ANALYSES OF NEW COMPOUNDS

Compd.	Mp°C (solvent)[a]	ν_{OH}^{KBr} cm^{-1}	ν_{CO}^{KBr} cm^{-1}	Formula	Found C%	Found H%	Calcd C%	Calcd H%
			Benzofuranyl Ketones					
2a	58.5—60(E)		1630	$C_{12}H_{12}O_3$	70.26	5.99	70.57	5.92
2b	116—117(E)		1635	$C_{18}H_{16}O_3$	76.53	5.78	77.12	5.75
2c	108—109.5(E)		1640	$C_{19}H_{18}O_4$	73.13	5.66	73.53	5.85
2d	152—153.5(E)		1630	$C_{21}H_{22}O_6$	67.93	5.77	68.09	5.99
3a	206—208(E)	3050	1630	$C_{12}H_{12}O_3$	70.10	5.83	70.57	5.92
3c	222—223(E)	3250	1640	$C_{19}H_{18}O_4$	73.61	5.99	73.53	5.85
3d	221—222(E)	3530 3150	1665	$C_{21}H_{22}O_6 \cdot H_2O$	65.09	6.17	64.93	6.23
7b	167—168(E)		1635	$C_{18}H_{16}O_3$	76.83	5.81	77.12	5.75
7c	122—123(E)		1645	$C_{19}H_{18}O_4$	73.86	5.96	73.53	5.85
7d	140.5—144.5(E)		1648	$C_{21}H_{22}O_6$	68.18	6.13	68.09	5.99
8c	142—145(E)		1640	$C_{19}H_{18}O_4$	73.18	5.75	73.53	5.85
10b	98—98.5(E)		1675	$C_{19}H_{18}O_3$	77.49	6.17	77.53	6.16
			Aryloxybutanones					
11a	56—57(P)		1720 1645	$C_{12}H_{14}O_4$	64.80	6.67	64.85	6.35
16b	113.5—114.5(A)		1710 1620	$C_{19}H_{16}O_4$	74.13	5.05	74.01	5.23
16c	138—138.5(A)		1710 1640	$C_{20}H_{18}O_5$	70.90	5.33	70.99	5.36
17b	114—115(A)		1700 1630	$C_{20}H_{18}O_4$	74.68	5.45	74.52	5.63
17c	121—123(A)		1715 1645	$C_{21}H_{20}O_5$	71.66	5.78	71.58	5.72
			Furoisoflavones					
12b	155—156(E)		1640[b]	$C_{19}H_{14}O_3$	78.50	4.43	78.68	4.85
12c	161—163(E)		1650[b]	$C_{20}H_{16}O_4$	74.62	5.20	74.99	5.03
12d	205—206(E)		1645	$C_{22}H_{20}O_6$	69.51	5.65	69.46	5.30
13b	164—165(E)		1640[b]	$C_{20}H_{16}O_3$	79.16	5.21	78.93	5.30
13c	182—183(E)		1640[b]	$C_{21}H_{18}O_4$	75.15	5.27	75.43	5.43
13d	209—209.5(E)		1640	$C_{23}H_{22}O_6$	70.10	5.72	70.04	5.62
14b	187.5—188.5(A)		1650	$C_{19}H_{14}O_3$	78.91	4.98	78.60	4.85
14c	197—198(A)		1655	$C_{20}H_{16}O_4$	74.73	5.17	74.99	5.03
15b	194—196(E)		1647	$C_{20}H_{16}O_3$	79.22	5.46	78.93	5.30
15c	181—182(A)		1645	$C_{21}H_{18}O_4$	75.42	5.22	75.43	5.43

a) A: Ethyl acetate, E: Ethanol, P: Petroleum ether. b) These of homologous compounds are: furo-(2'',3'':7,8)isoflavone, 1640; 2'-methoxy-, 1650; 2-methyl, 1635; 2'-methoxy-2-methyl-, 1640.

(n=1.5, 40 g) was heated at 80°C for 1 hr with stirring. The cooled mixture was poured into ice water and then extracted with ether. The ethereal layer was washed with aqueous sodium carbonate, and the ether was distilled off. The residual product was crystallized to give the ketone 7a. A small amount of the isomeric ketone 2a was also obtained from the mother solution of the crystallization of 7a.

Similarly, the ketone 7b and a small amount of isomeric 2b were also obtained by this procedure through the 4-(α-acetylethoxy)-2-hydroxyphenyl benzyl ketone (11b); bp 180—220°C/4 mmHg (yield 76%), ν_{max}: 1720 and 1620 cm^{-1} (CO). The ketone 2c and the isomeric 7c were also obtained through the 4-(α-acetylethoxy)-2-hydroxyphenyl 2-methoxybenzyl ketone (11c); bp 200—250°C/10 mmHg (yield 79%).

e) By the Alkaline Degradation of Furoisoflavones. A mixture of the furoisoflavone, 12b (1.1 g), 50% aqueous potassium hydroxide (5 g), and ethanol (60 m*l*) was refluxed for 3 hr, and then most of the ethanol was distilled off. The residue was diluted with water and acidified. The crystalline product formed was collected and recrystallized from ethanol to give the ketone 2b.

Similarly, the ketones 2b and 2c were obtained from the furoisoflavones 13b and 13c respectively.

The Preparation of Furoisoflavones. *a) By the Furan-ring Formation on 7-Hydroxyisoflavones through 7-(α-Acetylethoxy)isoflavones (16). i) The Preparation of 16*: A mixture of 7-hydroxyisoflavone (10 g), 3-chlorobutanone-2 (4.5 g), anhydrous potassium carbonate (17 g), and acetone (150 m*l*) was refluxed for 5 hr. The cooled mixture was filtered, the solvent was distilled off, and the residue was treated with water and then heated for a while on a water-bath. The precipitates

TABLE 4. THE UV SPECTRA OF FUROISOFLAVONES

Compd.	λ_{max}^{EtOH} mμ[a] (log ε)
12b[b]	214[s](4.51), 255(4.59), 320(3.78)
12c[b]	215[s](4.52), 249(4.51), 280[s](4.01), 318(3.75)
12d	213[s](4.64), 243(4.58), 252[s](4.56), 295(4.15)
13b[b]	212(4.53), 251(4.66), 285[s](3.88), 314(3.79)
13c[b]	213(4.59), 247(4.68), 280[s](4.06), 313(3.79)
13b	245(4.60), 292(4.06)
14b	213[s](4.55), 254(4.66), 338(3.83)
14c	212[s](4.54), 250(4.58), 335(3.77)
15b	212[s](4.51), 250(4.69), 332(3.82)
15c	248(4.64), 280[s](3.97), 330(3.78)

a) [s]: Shoulder. b) λ_{max} of homologous compounds are: furo(2'',3'':7,8)isoflavone, 253(4.50), 310(3.86); 2'-methoxy-, 220[s](4.31), 305(3.70); 2-methyl-, 247(4.46), 304(3.76); 2'-methoxy-2-methyl, 240(4.62), 275[s](4.02), 303(3.72).

formed on cooling were collected and recrystallized to give 7-(α-acetylethoxy)-isoflavone (16b).

ii) The Dehydro-cyclization of 16 by PPA: A mixture of 16b (1.3 g) and PPA (n=2.5, 30 g) was poured into ice water; the crystalline product thus formed was collected and recrystallized from ethanol to give 4'',5''-dimethylfuro[2'',3'':7,8]isoflavone (12b).

iii) The Dehydro-cyclization of 16 by Sulfuric Acid: The isoflavone 16b (2 g) was gradually added to concentrated sulfuric acid (20 g) at about 30°C; the mixture was allowed to stand at that temperature for 1.5 hr, and then poured into ice water. The crystalline product thus formed was recrystallized from ethanol to give 12b.

Similarly, 4'',5''-dimethyl-2'-methoxyfuro[2'',3'':7,8]isoflavone (12c), 2,4'',5''-trimethylfuro[2'',3'':7,8]isoflavone (13b), and 2'-methoxy-2,4'',5''-trimethylfuro[2'',3'':7,8]isoflavone (13c) were also prepared by this procedure through 7-(α-acetylethoxy)-2-methylisoflavone (17b) and its 2'-methoxy derivative (17c).

b) By the Action of Ethyl Orthoformate on the Benzofuranyl Ketones. A mixture of the ketone 2b (0.2 g), ethyl orthoformate (2 g), piperidine (1 drop) and pyridine (8 ml) was refluxed for 8 hr. Dilute hydrochloric acid was added to the cooled mixture, and the crystalline product formed was collected and recrystallized from ethanol to give 12b.

Similarly, 12c and 4'',5''-dimethyl-2',4',5'-trimethoxyfuro[2'',3'':7,8]isoflavone (12d) as well as the isomeric 4'',5''-dimethylfuro[3'',2'':6,7]isoflavone (14b) and 4'',5''-dimethyl-2'-methoxyfuro[3'',2'':6,7]isoflavone (14c) were also prepared by this procedure.

c) By the Action of Acetic Anhydride and Sodium Acetate on the Benzofuranyl Ketones. A mixture of the ketone 2b (0.2 g), sodium acetate (2 g), and acetic anhydride (10 ml) was refluxed for 12 hr, and then the cooled mixture was poured into ice water and left overnight. The crystalline product formed was collected and recrystallized from ethanol to give 13b.

Similarly, 13c and 2',4',5'-trimethoxy-2,4'',5''-trimethylfuro[2'',3'':7,8]isoflavone (13d), as well as the isomeric 2,4'',5''-trimethylfuro[3'',2'':6,7]isoflavone (15b) and 2'-methoxy-2,4'',5''-trimethylfuro[3'',2'':6,7]isoflavone (15c), were also prepared by this procedure.

The authors are grateful to Messrs T. Kida, T. Kishi, J. Masahashi, N. Shimizu, H. Yanagihara and H. Kawamura for their assistance, and to the Members of the Laboratory of Microanalysis, the Faculty of Pharmacology of this University, for their microanalyses. This work was supported in part by a grant from the Ministry of Education, for which the authors are also grateful.

BULLETIN OF THE CHEMICAL SOCIETY OF JAPAN VOL. 41 2683—2689 (1968)

The Syntheses of Dimethylfuro Derivatives of 4-Hydroxycoumarins and Benzofuro[1]benzopyranones*[1]

Yoshiyuki KAWASE, Mutsumu NANBU, Fumihisa MIYOSHI and Hiroshi KAWAMURA

Department of Chemistry, Faculty of Literature and Science, Toyama University, Gofuku, Toyama

(Received Mach 2, 1968)

4′,5′-Dimethyl-4-hydroxyfuro[2′,3′:7,8]coumarin (2) and its 3-phenyl, 3-(2-methoxyphenyl), and 3-(2,4,5-trimethoxyphenyl) derivatives (4, 5 and 6), and also their isomers, 4′,5′-dimethyl-4-hydroxyfuro[3′,2′:6,7]coumarins (14, 15, 16 and 17), were prepared by the action of ethyl carbonate or of ethyl chlorocarbonate on the corresponding 2,3-dimethyl-4- or isomeric 6-hydroxy-5-benzofuranyl ketones. Two furocoumarins (2 and 14) were also obtained in poor yields by the condesnation of 2,3-dimethyl-4- or 6-hydroxybenzofuran with malonic acid. The action of hydroiodic acid on the furocoumarins 5 and 6 afforded 2,3-dimethyl-5*H*-benzofuro[3,2-*c*]furo-[2,3-*h*][1]benzopyran-5-one (8) and its 7,8-dihydroxy derivative (9) respectively; 8 was also synthesized by building up the dimethylfuran ring on 3-hydroxy-6*H*-benzofuro[3,2-*c*][1]benzo-pyran-6-one, while 9 was also synthesized by the oxidative coupling of 2 with catechol. On the other hand, the action of pyridine hydrochloride on 5 caused the closure of the furan ring towards the 2-position, giving 1,2-dimethyl-6*H*-benzofuro[2,3-*b*]furo[2,3-*h*][1]benzopyran-6-one (11), which had a new pentacylic ring system; the only demethylated compound (12) was also obtained. The structure of 11 was confirmed by its IR and UV spectra and by the formation of 12 upon its alkaline hydrolysis. The action of aluminum chloride on 5 also gave 12. Analogously, isomeric 1,2-dimethyl-6*H*-benzofuro[3,2-*c*]furo[3,2-*g*][1]benzopyran-6-one (20) and its 8,9-dihydroxy compound (21) were also synthesized.

Several derivatives of benzofuran,[1)] 4-hydroxy-coumarin,[1)] furocoumarins,[1,2)] and benzofuro-coumarin[1,2)] were obtained from natural sources; some of them have biological activities. In the present experiments, some furo-derivatives of 4-hydroxycoumarins and of benzofurocoumarin are synthesized in order to test their pharmacological activities, for convenient starting compounds for the synthesis of these compounds could be obtained readily.[3)] Concerning the synthesis of these compounds, the present authors have reported previously[4)] on the synhesis of 4-hydroxyfuro[2′,3′:7,8]-coumarins and 5*H*-benzofuro[3,2-*c*]furo-[2,3-*h*][1]-benzopyran-5-one, while the synthesis of isomeric 4-hydroxyfuro[3′,2′:6,7]coumarins[5-7)] and 6*H*-benzofuro[3,2-*c*]furo[3,2-*g*][1]benzopyran-6-one derivative (erosnin)[6)] has been reported on by Fukui and Nakayama and others, and that of dimethylfuro-derivatives of 4-hydroxy-3-phenylfuro-coumarin has been reported on by Royer *et al.*[8)]

In the present experiments, 4′,5′-dimethyl-4-hydroxy-furo[2′,3′:7,8]coumarins (2—6) and isomeric -furo[3′,2′:6,7]coumarins (14—17) were synthesized from the corresponding hydroxybenzo-furanyl ketones (1 and 13); some of them (2, 5, and 6, and isomeric 14, 16, and 17) were converted to derivatives of 5*H*-benzofuro[3,2-*c*]furo-[2,3-*h*][1]benzopyran-5-one (8 and 9), 6*H*-benzo-furo[2,3-*b*]furo[2,3-*h*][1]benzopyran-6-one(11) and 6*H*-benzofuro[3,2-*c*]furo[3,2-*g*] [1] benzopyran-6-one (20 and 21), one (11) of these ring systems form-ing a new pentacyclic ring system.

4-Hydroxyfurocoumarins had been prepared previously by the action of ethyl carbonate and sodium on hydroxybenzofuranyl ketones[4-6)] and by the dehydrogenation of dihydrofurocou-marins,[5-7)] while the 4′,5′-dimethyl-3-phenyl com-pounds had been prepared by the thermal con-densation of dimethyl-hydroxybenzofurans with

*1 A part of this work was presented at the 29th Annual Meeting of the Chemical Society of Japan, Tokyo, March, 1967.

1) F. M. Dean, "Naturally-occurring Oxygen-ring Compounds," Butterworths, London (1963), pp. 135, 176.

2) A. Mustafa, "Furopyrans and Furopyrones," ed. by A. Weissberger, Interscience Publishers, London (1967), pp. 14, 243.

3) Y. Kawase, M. Nanbu and F. Miyoshi, This Bulletin, **41**, 2676 (1968).

4) Y. Kawase, M. Nanbu and H. Yanagihara, *ibid.*, **41**, 1201 (1968).

5) K. Fukui and M. Nakayama, *Nippon Kagaku Zasshi (J. Chem. Soc. Japan, Pure Chem. Sect.)*, **85**, 444 (1964).

6) K. Fukui and M. Nakayama, *Tetrahedron Letters*, **1965**, 2559.

7) A. Vialard-Goudon and N. Blanchcatte, *Compt. Rend.*, **263**, 255 (1966).

8) J.-P. Lechartier, P. Demerseman, A. Cheutin and R. Royer, *Bull. Soc. Chim. France*, **1966**, 1716.

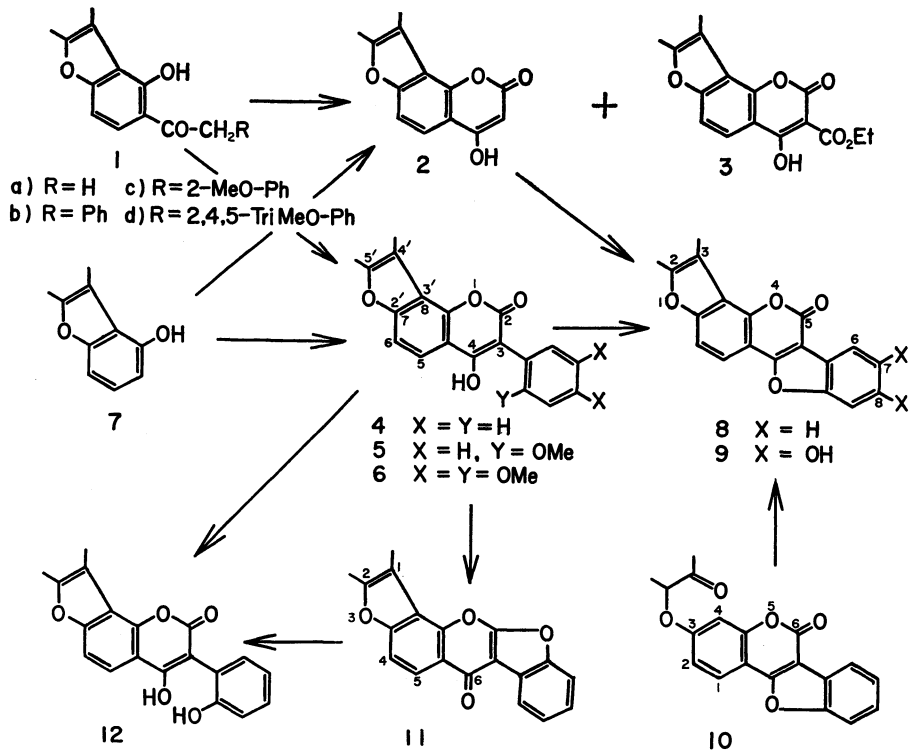

Chart 1

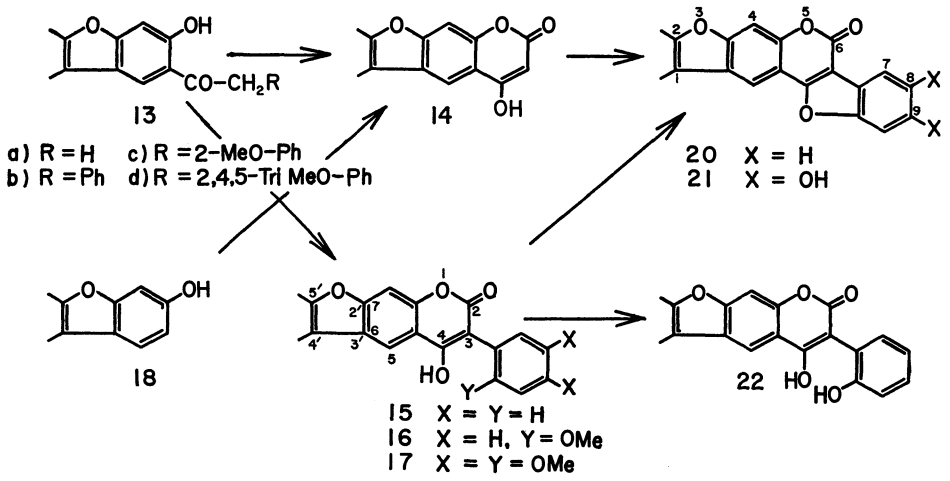

Chart 2

ethyl phenylmalonate.[8] In the present exeriments, 4',5'-dimethyl-4-hydroxyfuro[2',3':7,8]-coumarin (2) and its 3-phenyl, 3-(2-methoxyphenyl), and 3-(2,4,5-trimethoxyphenyl)derivatives (4, 5, and 6) as well as the isomeric 4',5'-dimethyl-4-hydroxyfuro[3',2': 6,7]coumarins (14, 15, 16, and 17) were synthesized in good yields from the corresponding 2,3-dimethyl-4- or -6-hydroxy-5-benzofuranyl ketones (1 or 13), the preparation of which has been reported on in a preceding paper,[3] by the action of ethyl carbonate and sodium[9] or of ethyl chlorocarbonate and potassium carbonate[10] according to the general method for the synthesis of 4-hydroxycoumarins. In the case of 2, a small

9) J. Boyd and A. Robertson, *J. Chem. Soc.*, **1948**, 174.
10) A. H. Gilbert, A. McGookin and A. Robertson, *ibid.*, **1957**, 3740.

amount of its 3-ethoxycarbonyl derivative (3) was also obtained as a by-product, much as in the case of furocoumarin without dimethyl groups;[4] its formation is probably due to the double ethoxycarbonylation of the ketone 1a, followed by cyclization. The 3-phenyl compound (4) thus obtained was identical with the furocoumarin which had been obtained by the above-mentioned thermal condensation of 2,3-dimethyl-4-hydroxybenzofuran (7) with ethyl phenylmalonate[8]; the furocoumarin 15 was an isomer of 4′,5′-dimethyl-4-hydroxy-3-phenylfuro[2′,3′:5,6]coumarin (19), which had been obtained by a similar thermal condensation from 2,3-dimethyl-6-hydroxybenzofuran (18). The condensation of hydroxybenzofurans (7 and 18) with malonic acid to obtain the corresponding 4-hydroxycoumarins directly was also attempted by the action of polyphosphoric acid[11a] or of phosphoryl chloride and zinc chloride,[11b] but such attempts resulted in the formation of furocoumarins (2 and 14) in only poor yields; this is comparable to the unfavorable results of the thermal condensation of the unsubstituted malonic ester with phenols.[12]

Then, the 4-hydroxyfurocoumarins (2, 5, 6 and isomeric 14, 16, 17) thus obtained were converted to benzofuro-furo[1]benzopyranones by procedures analogous to those reported previously. The reported procedures involve the demethyl-cyclization of 4-hydroxy-3-(2-methoxyphenyl)furocoumarins with hydroiodic acid, with pyridine hydrochloride, or with aluminum chloride,[4] or involve the oxidative coupling of 4-hydroxyfurocoumarin with catechol.[6] In the present experiments, the action of hydroiodic acid in acetic acid on the furocoumarins 5 and 6 caused demethyl-cyclization, thus giving 2,3-dimethyl-5*H*-benzofuro-[3,2-*c*]furo[2,3-*h*][1]benzopyran-5-one (8) and its 7,8-dihydroxy derivative (9) respectively. The compound 8 was also obtained by building up the furan ring on 3-hydroxy-6*H*-benzofuro[3,2-*c*]-[1]benzopyran-6-one[13,14] through the action of 3-chlorobutanone-2 and potassium carbonate to give the 3-(α-acetylethoxy) compound (10), which was then cyclized by the action of polyphosphoric acid. The compound 9 was also prepared by the oxidative coupling of the furocoumarin 2 with catechol by means of potassium ferricyanide. On the other hand, the action of pyridine hydrochloride on 5 gave 1,2-dimethyl-6*H*-benzofuro[2,3-*b*][1]-benzopyran-6-one (11), a compound with a new pentacyclic ring system, and a small amount of a merely-demethylated 3-(2-hydroxyphenyl) compound (12), which was also obtained by the action of anhydrous aluminum chloride in nitrobenzene on 5. The compound 11 has ν_{CO} at 1650 cm^{-1}, which is in the region characteristic of that of the chromone type.[3-5,14,15] The pattern of its UV spectrum, showing a strong absorption at about 250 mμ and only a weak absorption at 315 mμ, is different from that of the benzofuro[3,2-*c*][1]-benzopyranones; rather, it is comparable to that of furoisoflavones.[3-5,16] Its alkaline hydrolysis gave the hydroxyfurocoumarin 12. The structure of 11 was assigned on the basis of these observations and was confirmed by comparing it with that of lisetin,[17] a compound recently isolated from a natural source; this compound has a tetracyclic ring system, 11*H*-benzofuro[2,3-*b*][1]benzopyran-11-one, which is also included in the compound 11. The formation of 11 from 5 is probably a result of the closure of the new furan ring at the 2-hydroxy group of the 2-hydroxyisoflavone derivative, a tautomeric form[14,15] of the 4-hydroxycoumarin 12, but the attempted dehydro-cyclization of 12 by refluxing it with methanolic hydrogen chloride was unsuccessful.

Analogously, the isomeric furocoumarins (16 and 17) were converted to 1,2-dimethyl-6*H*-benzofuro[3,2-*c*]furo[3,2-*g*][1]benzopyran-6-one (20) and its 7,8-dihydroxy derivative (21) by the action of hydroiodic acid; 21 was also obtained by the oxidative coupling of 14 with catechol. The action of both aluminum chloride and pyridine hydrochloride on 16 gave the demethylated compound (22).

In the IR spectra, the furocoumarins and benzofuro-furobenzopyranones prepared have the ν_{CO} at 1740—1670 cm^{-1}, which is in the region characteristic for those of the coumarin type,[4-6,14,15,17] except that the ν_{CO} of the compounds 4, 12, 14 and 22 are at 1655—1645 cm^{-1}, which is rather in the region characteristic for those of the chromone type,[3-6,14,15,17] moreover, the wave numbers of these ν_{CO} are in general smaller by about 20 cm^{-1} than those of homologues without dimethyl groups.[4-6]

In the UV spectra, the furocoumarins and benzofuro-furobenzopyranones have two bands, the band I and the band II; the band I is in general at 235—240 mμ, while the band II of the compounds with an angularly-fused furan ring is at 320—330 mμ, which is longer by about 20—25 mμ than those of the isomers. These UV spectra are almost identical with those of the compounds without dimethyl groups.[4-6]

11) a) L. Reichel and G. Proksch, *Naturwissenschaften*, **50**, 520 (1963). The experimental conditions and the yield are not given. b) J. L. Bose, R. C. Shah and V. R. Shah, *Chem. and Ind.*, **1960**, 623; V. R. Shah, J. L. Bose and R. C. Shah, *J. Org. Chem.*, **25**, 677 (1960).
12) G. Urbain and C. Mentzer, *Bull. Soc. Chim. France*, **11**, 171 (1944).
13) T. R. Govindachari, K. Nagarajan and P. C. Parthasarathy, *Tetrahedron*, **15**, 129 (1961).
14) Y. Kawase, This Bulletin, **35**, 573 (1962).
15) Y. Kawase, *Experientia*, **14**, 345 (1958); This Bulletin, **32**, 11 (1959).
16) K. Fukui and Y. Kawase, *ibid.*, **31**, 693 (1958).
17) C. P. Falshaw, W. D. Ollis, J. A. Moore and K. Magnus, *Tetahedron*, **Supplement No. 7**, 333 (1966).

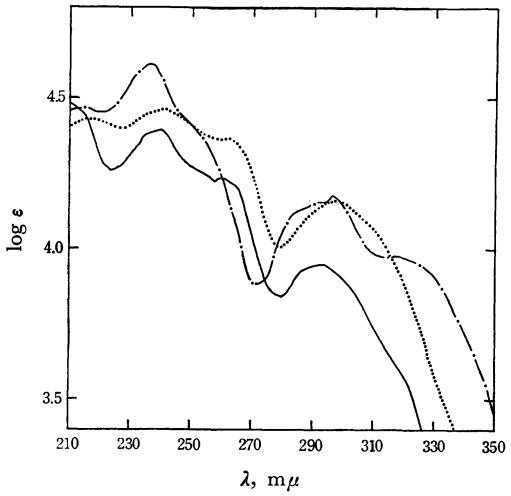

Fig. 1. The UV spectra of furocoumarins: —— 2, ···· 3 and —·—· 14.

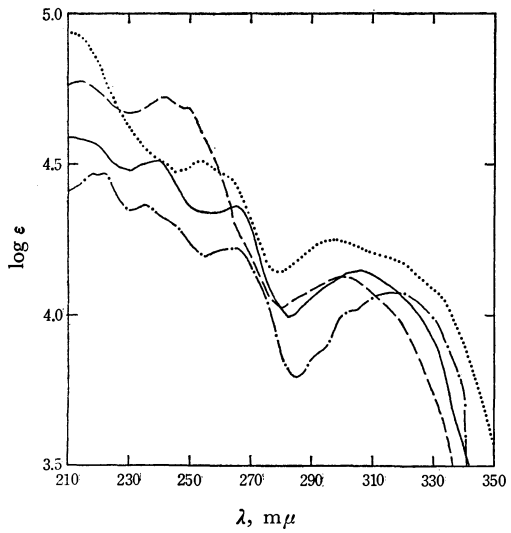

Fig. 2. The UV spectra of furocoumarins: —— 4, ---- 5, ····· 6 and —·—· 12.

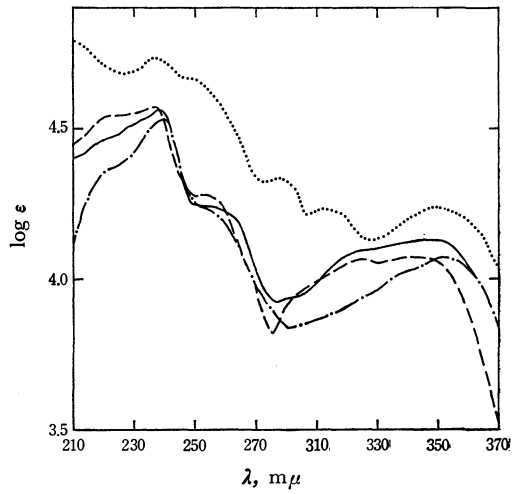

Fig. 3. The UV spectra of furocoumarins: —— 15, ---- 16, ····· 17 and —·—· 22.

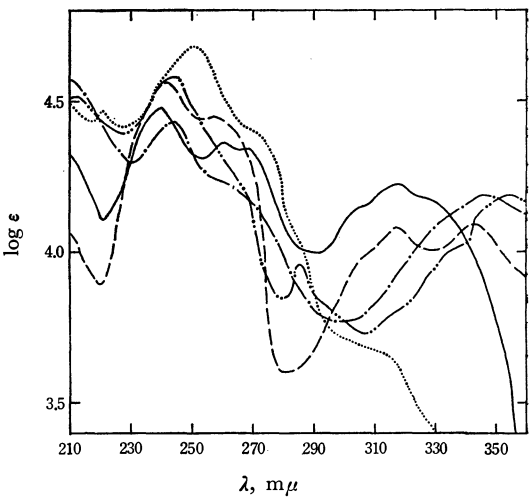

Fig. 4. The UV spectra of benzofuro-furobenzo-pyranones: —— 8, —·—· 9, ····· 11, ---- 20 and —··—·· 21.

Experimental*2

Materials. *Benzofuranyl Ketones 1a, b, c, d and Isomeric 13a, b, c, d.* These compounds were prepared by a previously-reported procedure.[3]

Hydroxybenzofurans 7 and 18. These compounds were prepared by the procedure reported by Royer *et al.*[18]

3-Hydroxy-6*H*-benzofuro[3,2-*c*][1]benzopyran-6-one was prepared, in the present experiments, by the action of ethyl chlorocarbonate and potassium carbonate[10] on the 2,4-dihydroxyphenyl 2-methoxybenzyl ketone to give hydroxycoumarin, which was then converted to the compound by demethyl-cyclization as follows:

4,7-Dihydroxy-3-(2-methoxyphenyl)coumarin. A mixture of the 2,4-dihydroxyphenyl 2-methoxybenzyl ketone[19] (10 g), ethyl chlorocarbonate (14 m*l*), acetone (100 m*l*), and anhydrous potassium carbonate (90 g) was refluxed for 3 hr. The cooled mixture was treated with water (1 *l*) and acidified, and the precipitates thus formed were collected and heated with 1 N aqueous sodium hydroxide (500 m*l*) for 1 hr. The resulting solution was acidified, and the precipitates formed were collected and recrystallized from ethanol; yield 6 g (54.5%). (See Tables 3 and 4).

3-Hydroxy-6H-benzofuro[2,3-c][1]benzopyran-6-one. A mixture of the coumarin (4 g), hydroiodic acid (d=1.7,

*2 All melting points are uncorrected; the IR spectra were measured in the form of KBr disks, while the UV spectra were measured in ethanol. The detailed data are summarized in the tables and figures.

18) E. Bisagni and R. Royer, *Bull. Soc. Chim. France*, **1962**, 925.

19) M. Nakajima, H. Fukami, K. Konishi and J. Oda, *Agr. Biol. Chem.*, **27**, 700 (1963).

Table 1. The syntheses of furocoumarins

Compd.	Starting compd.	Procedure[a]	Yield %
2	1a	A	41[b]
2	7	B	1.5
4	1b	A	72
4	1b	C	74
4	1b	D	30.5
5	1c	A	92
6	1d	A	95
12	5	E	66.5
12	5	F	6[c]
12	11	G	76
14	13a	A	72.5
14	18	B	1.5
14	18	H	d)
15	13b	A	82.5
15	13b	C	37
16	13c	A	89
17	13d	A	62
22	16	E	d)
22	16	F	26

a) A: Et_2CO_3+Na, B: Malonic acid+PPA, C: $ClCO_2Et+K_2CO_3$, D: $ClCO_2Et$+pyridine, E: $AlCl_3$, F: Pyridine-HCl, G: KOH, H: Malonic acid+$POCl_3$+$ZnCl_2$.
b) A small amount of 3 was also obtained.
c) The major product was 11.
d) A small amount.

Table 2. The syntheses of benzofuro-furobenzopyranones

Compd.	Starting compd	Procedure[a]	Yield %
8	5	A	22
8	10	B	59.5
9	2	C	49
9	6	A	35
11	5	D	22[b]
20	16	A	44.5
21	14	C	17
21	17	A	39

a) A: HI, B: PPA, C: Catechol+$K_3Fe(CN)_6$, D: Pyridine-HCl.
b) A small amount of 12 was also obtained.

100 ml), acetic acid (40 ml), and acetic anhydride (35 ml) was refluxed gently for 1 hr under a stream of nitrogen. The cooled mixture was poured into ice water containing a small amount of sodium bisulfite, and the precipitates formed were collected and recrystallized from ethanol. Mp 276—277°C (lit mp 285°C[13] or 276—277°C[14]); yield 1.6 g (45%).

The Preparation of Furocoumarins from Benzofuranyl Ketones (Table 1). *a) By the Action of Ethyl Carbonate and Sodium.* Small pieces of metallic sodium (2 g) were added to a solution of 1b (1.4 g) in ethyl carbonate (30 ml), and the mixture was heated gradually to 100°C. The mixture was heated at that temperature for 1 hr, and then methanol was added to the cooled mixture to destroy the excessive sodium. The resulting solution was diluted with water, washed with ether, and then acidified. The crystalline product formed was collected and recrystallized from ethanol to give 4',5'-dimethyl-4-hydroxy-3-phenylfuro[2',3':7,8]-coumarin (4); mp 272—273°C (lit.[8] mp 271°C) (Found: C, 74.08; H, 4.34%).

Similarly, 4',5'-dimethyl-4-hydroxyfuro[2',3':7,8]-coumarin (2) and its 3-(2-methoxyphenyl) and 3-(2,4,5-trimethoxyphenyl) derivatives (5 and 6), as well as isomeric 4',5'-dimethyl-4-hydroxyfuro[3',2':6,7]-coumarin (14) and its 3-phenyl, 3-(2-methoxyphenyl), and 3-(2,4,5-trimethoxyphenyl) derivatives (15, 16, and 17), were prepared by this procedure. In the case of 2, a small amount of ethyl 4',5'-dimethyl-4-hydroxyfuro[2',3':7,8]coumarin-3-carboxylate (3) was also obtained from the mother solution of the crystallization of 2.

b) By the Action of Ethyl Chlorocarbonate and Potassium Carbonate. A mixture of 1b (0.5 g), ethyl chlorocarbonate (0.5 g), acetone (15 ml), and anhydrous potassium carbonate (3.0 g) was refluxed for 3 hr. The cooled mixture was treated in a manner similar to that described in the case of 4,7-dihydroxy-3-(2-methoxyphenyl)-coumarin to give the furocoumarin 4.

Similarly, the furocoumarin 15 was also synthesized by this procedure.

c) By the Action of Ethyl Chlorocarbonate and Pyridine. Ethyl chlorocarbonate (0.6 g) was added gradually, with stirring and cooling, to a solution of 1b (0.6 g) in pyridine (10 ml), after which the mixture was allowed to stand overnight. The resulting mixture was poured into ice water and extracted with ether. The ether solution was washed with dilute hydrochloric acid, and the ether was distilled off. The residual product was heated with 10% aqueous sodium carbonate (40 ml) for 2 hr, and the cooled mixture was washed with ether and then acidified. The crystalline product formed was collected and recrystallized from ethanol to give 4.

The Preparation of 4-Hydroxycoumarins and 4-Hydroxyfurocumarins (2 and 14) Directly from Hydroxy-compounds (Table 1). *a) By the Action of Polyphosphoric Acid (PPA).* A mixture of the hydroxybenzofuran 7 (5 g), malonic acid (3.5 g), and PPA (n=2.5, 100 g) was heated at 100°C for 2 hr with stirring. The cooled mixture was poured into ice water and extracted with ethyl acetate. The ethyl acetate solution was extracted with 5% aqueous sodium hydroxide, and the alkaline solution was acidified. The crystalline product thus formed was collected and recrystallized from ethanol to give the hydroxyfurocoumarin 2; mp 287°C (dec.), yield 0.1 g (1.5%).

Analogously, the furocoumarin 14 was also obtained by this procedure from the hydroxybenzofuran 18, while the reaction of resorcinol or its monomethyl ether and malonic acid gave 4,7-dihydroxycoumarin[11a] or 4-hydroxy-7-methoxycoumarin, mp 264.5°C (dec.) (lit.[20] mp 265°C (dec.)) and mp 252.5°C (dec.) (from ethanol) (lit.[20] mp 256°C (dec.)) respectively, in yields of 5% and 9.5%.

b) By the Action of Phosphoryl Chloride and Zinc Chloride. A mixture of 18 (5 g), malonic acid (3.5 g), anhydrous zinc chloride (12.5 g), and phosphoryl chloride (8.5 ml) was heated at 60—70°C for 8 hr

20) A. Sonn, *Ber.*, **50**, 1292 (1917).

TABLE 3. THE MP, IR AND ANALYSIS OF NEW COMPOUNDS

Compd.	Mp °C (solvent)[a]	ν_{OH}^{KBr} cm^{-1}	ν_{CO}^{KBr} cm^{-1}	Formula	Found C%	Found H%	Calcd C%	Calcd H%
			Coumarins					
b)	265—266(A)	3120	1630	$C_{16}H_{12}O_5$	67.60	4.32	67.60	4.03
2	287(dec)(A)	3100	1690	$C_{13}H_{10}O_4$	67.67	4.49	67.82	4.38
3	188(dec)(A)	2600	1740	$C_{16}H_{14}O_6$	63.80	4.85	63.57	4.67
5	244.5—245.5(A)	2950	1670	$C_{20}H_{16}O_5$	71.40	4.78	71.42	4.80
6	245—245.5(A)	3200	1710	$C_{22}H_{20}O_7$	66.58	5.22	66.66	5.09
12	273—274(dec)(B)	3340	1655	$C_{19}H_{14}O_5$	71.01	4.54	70.80	4.38
14	288—290(A)	2550	1650	$C_{13}H_{10}O_4$	67.89	4.48	67.82	4.38
15	256—257(A)	3100	1675	$C_{19}H_{14}O_4$	74.53	4.54	74.45	4.60
16	220—221(A)	2950	1680	$C_{20}H_{16}O_5$	71.13	4.92	71.42	4.80
17	255—256(A)	3450	1705	$C_{22}H_{20}O_7$	66.54	5.08	66.66	5.09
22	267—268(dec)(A)	3000	1645	$C_{19}H_{14}O_5$	70.92	4.58	70.80	4.38
			Benzofuro-benzopyranones					
8	242—243(C)		1740	$C_{19}H_{12}O_4$	74.91	4.15	74.99	3.97
9	>360(B)	3200	1705	$C_{19}H_{12}O_6$	68.04	3.82	67.85	3.60
10	186—187.5(C)		1735	$C_{13}H_{10}O_4$	67.89	4.48	67.82	4.38
11	257.5—258.5(C)		1650	$C_{19}H_{12}O_4$	75.09	4.16	74.99	3.97
20	265.5—267(C)		1740	$C_{19}H_{12}O_4$	74.74	4.02	74.99	3.97
21	>360(B)	3270	1700	$C_{19}H_{12}O_6$	67.56	3.81	67.85	3.60

a) A: ethanol, B: acetone, C: ethyl acetate.
b) 4,7-Dihydroxy-3-(2-methoxyphenyl)coumarin.

TABLE 4. THE UV SPECTRA

Compd.	λ_{max}^{EtOH} mμ[a] (log ε)
	Coumarins
b)	286(4.02), 315(4.32)
2	215[s](4.45), 240(4.40), 260[s](4.23), 294(3.95)
3	217(4.43), 241(4.46), 263[s](4.36), 297(4.16)
4	215[s](4.59), 238(4.51), 265(4.36), 305(4.15)
5	215(4.77), 242(4.72), 250[s](4.68), 265[s](4.30), 300(4.12)
6	211(4.93), 253(4.50), 297.5(4.25), 318[s](4.18)
12	217[s](4.47), 222(4.47), 236(4.37), 262(4.22), 320(4.07)
14	212(4.47), 237(4.61), 250[s](4.41), 296(4.18), 318[s](3.98)
15	238(4.49), 255[s](4.25), 300[s](4.08), 327(4.13)
16	221[s](4.54), 237(4.58), 252[s](4.28), 305(4.07), 320(4.07)
17	235(4.71), 250[s](4.67), 294(4.25), 333(4.24)
22	220[s](4.36), 240(4.53), 255[s](4.23), 331(4.07)
	Benzofuro-benzopyranones
8	240(4.48), 261(4.36), 270(4.34), 318(4.23)
9	244(4.43), 347(4.19)
11	221(4.47), 251(4.68), 315[s](3.65)
20	241(4.56), 258(4.45), 318(4.08), 343(4.09)
21	213[s](4.52), 244(4.58), 286(3.96), 353(4.19)

a) s: shoulder.
b) 4,7-Dihydroxy-3-(2-methoxyphenyl)coumarin.

with stirring. The cooled mixture was poured into ice water, and the precipitates formed were collected and dissolved in aqueous sodium carbonate and then filtered. The filtrate was acidified and extracted with ethyl acetate. The ethyl acetate was distilled off, and the residue was recrystallized from ethanol to give the furocoumarin 14.

The Formation of 3-(2-Hydroxyphenyl)coumarins (12 and 22) (Table 1). *a) By the Action of Aluminum Chloride on Methoxyphenylcoumarins (5 and 16).* Anhydrous aluminum chloride (1.1 g) was added to a solution of 5 (0.5 g) in nitrobenzene (30 m*l*), and the mixture was heated on a water bath for 2 hr. The cooled mixture was poured into ice water containing hydrochloric acid, and then the nitrobenzene was removed by steam-distillation. The residual product was recrystallized from acetone to give 4',5'-dimethyl-4-hydroxy-3-(2-hydroxyphenyl)furo[2',3':7,8]coumarin (12).

Analogously, 4',5'-dimethyl-4-hydroxy-3-(2-hydroxyphenyl)furo[3',2':6,7]coumarin (22) was obtained from 16 by this procedure.

b) By the Action of Pyridine Hydrochloride on 5 and 16. A mixture of 16 (0.4 g) and anhydrous pyridine hydrochloride (2 g) was refluxed for 30 min, after which the cooled mixture was treated with dilute hydrochloric acid. The precipitates formed were collected and recrystallized from ethyl acetate and then from ethanol to give the hydroxycoumarin 22.

In the case of 5, a small amount of the hydroxycoumarin 12 was obtained from the mother solution of the crystallization of the major product (11), the preparation of which will be described bellow.

c) By the Alkaline Hydrolysis of 11. A mixture of 11 (64 mg), 10% aqueous potassium hydroxide (10 m*l*), and methanol (20 m*l*) was refluxed for 2 hr. The cooled mixture was acidified with dilute hydrochloric acid, and the precipitates formed were collected and recrystallized from ethyl acetate to give the hydroxycoumarin 12.

The Preparation of Benzofuro-furo[1]benzopyranones (Table 2). *a) By the Action of Hydroiodic Acid on the Methoxyphenyl-furocoumarins.* A mixture of 5 (0.5 g), hydroiodic acid (d=1.7, 11m*l*), acetic acid (4.5 m*l*), and acetic anhydride (5 m*l*) was refluxed gently for 45 min under a stream of nitrogen. The cooled mixture was treated much as has been described in the case of 3-hydroxybenzofuro-benzopyranone; this gave 2,3-dimethyl-5*H*-benzofuro[3,2-*c*]furo[2,3-*h*]-[1]benzopyran-5-one (8).

Similarly, the 7,8-dihydroxy derivative of 8 (9), 1,2-dimethyl-6*H*-benzofuro[3,2-*c*]furo[3,2-*g*][1]benzopyran-6-one (20), and its 8,9-dihydroxy derivative (21) were also obtained by this procedure.

b) By the Action of Pyridine Hydrochloride on the Furocoumarin 5. A mixture of 5 (0.4 g) and anhydrous pyridine hydrochloride (2 g) was refluxed for 20 min, after which the cooled mixture was treated much as has been described in the case of hydroxycoumarins. The crude product was recrystallized from ethyl acetate to give 1,2-dimethyl-6*H*-benzofuro[2,3-*b*]furo[2,3-*g*][1]-benzopyran-6-one (11); the hydroxycoumarin 12 was also obtained from the mother solution by the method described before.

c) By the Oxidative Coupling of 2 or 14 with Catechol. A solution of potassium ferricyanide (1.2 g) and sodium acetate (1 g) in water (10 m*l*) was added to a solution of 2 (0.3 g) and catechol (0.12 g) in a mixture of acetone (30 m*l*) and water (4.5 m*l*), after which the mixture was allowed to stand at room temperature for 2 hr. The resulting mixture was filtered from the inorganic precipitates formed, the filtrate was treated with formic acid (46%, 3 m*l*), and then the acetone was removed *in vacuo*. The precipitates formed were collected and recrystallized from acetone to give the compound 9.

d) By Building Up the Furan Ring on 3-Hydroxybenzofurobenzopyranone. i) 3-(α-Acetylethoxy)-6H-benzofuro[3,2-c][1]benzopyran-6-one (10): A mixture of 3-hydroxy-6*H*-benzofuro[3,2-*c*][1]benzopyran-6-one (1.3 g), 3-chlorobutanone-2 (0.6 g), the methyl ethyl ketone (50 m*l*), and anhydrous potassium carbonate (2.5 g) was refluxed for 10 hr. The cooled mixture was filtered, the solvent was distilled off, and the residual product was recrystallized from ethyl acetate to give the compound 10; yield 1.2 g (74%).

ii) The Ring Closure of 10: A mixture of 10 (0.5 g) and PPA (n=2.5, 20 g) was heated on a water bath for 2 hr. The cooled mixture was poured into ice water, and the precipitates formed were collected and crystallized from ethyl acetate to give the compound 8 in an impure form; mp 210—230°C, 0.4 g. A part of it (0.1 g) was purified through chromatography, using alumina and benzene as a solvent; the product obtained from the elute was recrystallized from ethyl acetate to give the pure 8.

The authors are grateful to the members of the Laboratory of Microanalysis, Faculty of Pharmacology of this University, for their microanalyses. This work was supported in part by a grant from the Ministry of Education, for which the authors are also grateful

BULLETIN OF THE CHEMICAL SOCIETY OF JAPAN VOL. 41 2690—2695 (1968)

The Isokinetic Temperature of the Acylation of *l*-Menthol

Fuminori AKIYAMA and Niichiro TOKURA

Department of Applied Chemistry, Faculty of Engineering, Osaka University, Suita, Osaka

(Received March 23, 1968)

The acylations of *l*-menthol with *p*-substituted benzoyl- and substituted acetyl chlorides were carried out, and it was found that the electron-releasing substituents accelerate the reaction rate in chloroform even though the reaction is completely of the S_N2 type. This result is interpreted in relation to the low isokinetic temperature, the reaction itself being carried out above that temperature. Such a phenomenon is discussed in terms of the configurational and the solvent effects on the entropy of activation.

The mechanism of the solvolysis of the acyl halides has been studied comprehensively. The substituent effect of such a reaction has been discussed by Hudson *et al.*[1] in relation to the mechanism of the solvolysis of the substituted benzoylchloride. In S_N1 solvolysis the acyl chloride which has an electron-releasing substituent reacts faster than the acyl chloride which has an electron-attracting substituent. However, the reverse trend has been observed in S_N2 solvolysis, where an electron-releasing substituent retards the reaction rate. These trends are quite generally accepted for nucleophilic substitutions.[2]

The present authors have studied the acylation of *l*-menthol and observed a reverse substituent effect in the reaction despite the S_N2-character of this acylation. An abnormal change in the substituent effect is often explained as the result of a shift of the reaction mechanism from S_N1 to S_N2 or from S_N2 to S_N1.[2] However, an alternative explanation, which may be reasonable in view of the present results, in that the reaction is carried out above the isokinetic temperature.[3]

Such a phenomenon is usually accompanied with a low isokinetic temperature of the acylation. The configurational and the solvent effects are discussed with regard to the cause of the anomaly.

Experimental

Solvents. The solvents—chloroform, benzene, liquid sulfur dioxide, tetrahydrofuan and acetonitrile—were purified by the methods described in earlier papers.[4,5]

Materials. Extra-pure-grade *l*-menthol was used without further purification. *p*-Substituted benzoyl chlorides were obtained by the chlorination of the corresponding *p*-substituted benzoic acids with thionyl chloride. Propionyl, monochloroacetyl, dichloroacetyl, and trichloroacetyl chlorides were commercial materials and were used after distillation.

The Identification of the Esters. The reaction mixture after the acylation was concentrated *in vacuo*, and the residual oil was fractionated. *l*-Menthyl monochloroacetate: bp 116°C/5 mmHg. Found: C, 61.89; H, 9.25%. Calcd for $C_{12}ClH_{21}O_2$: C, 61.92; H, 9.09%. *l*-Menthyl dichloroacetate: bp 128°C/5 mmHg. Found: C, 53.68; H, 7.64%. Calcd for $C_{12}Cl_2H_{20}O_2$: C, 53.94; G, 7.54%. *l*-Menthyl trichloroacetate: bp 113°C/3 mmHg. Found: C, 47.59; H, 6.50%. Calcd for $C_{12}Cl_3H_{19}O_2$: C, 47.78; H, 6.35%. *l*-Menthyl benzoate: bp 151°C/4 mmHg. Found: C, 77.73; H, 9.27%. Calcd for $C_{17}H_{24}O_2$: C, 78.41; H, 9.29%. *l*-Menthyl *p*-methylbenzoate: bp 170°C/2 mmHg. Found: C, 79.00: H, 9.93%. Calcd for $C_{18}H_{26}O_2$: C, 78.78; H, 9.55%. *l*-Menthyl *p*-chlorobenzoate: bp 187°C/3 mmHg. Found: C, 69.41; H, 7.71%. Calcd for $C_{17}ClH_{23}O_2$: C, 69.25; H, 7.86%.

Kinetic Procedure. The polarimetric procedure was used for the measurement of the reaction rate. A graphic representation of the apparatus and the details of the kinetic procedure have been given in earlier papers.[3,4] Equimolar concentrations of *l*-menthol and acyl chloride were used. The second-order reaction rate constant was given by the slope of the linear plot of:

$$\frac{1}{\alpha_\infty - \alpha} \text{ vs. the time } t,$$

since:

$$\frac{1}{\alpha_\infty - \alpha} - \frac{1}{\alpha_\infty - \alpha_0} = \frac{kt}{l\{[R]^\circ_E - [R]^\circ_A\}} \quad (1)$$

where $[R]^\circ_A$ and $[R]^\circ_E$ are the specific optical rotations of *l*-menthol and of the ester, rotations which were measured beforehand and which are listed in Table 1, where l, α, α_0, and α_∞ are the length of the cell, dm, and the rotations of the solutions at time t, zero, and infinity, respectively. The second-order plots of typical runs are shown in Fig. 1.

1) D. A. Brown and R. F. Hudson, *J. Chem. Soc.*, **1953**, 883.
2) C. K. Ingold, "Structure and Mechanism in Organic Chemistry," Cornell University Press, Ithaca, New York (1953), pp. 307—417.
3) J. E. Leffler and E. Grunwald, "Rates and Equilibria of Organic Reactions," John Wiley and Sons, New York (1963), p. 325.
4) N. Tokura and F. Akiyama, This Bulletin, **37**, 1723 (1964).
5) F. Akiyama and N. Tokura, *ibid.*, **39**, 131 (1966).

TABLE 1. THE SPECIFIC ROTATIONS OF *l*-MENTHOL AND *l*-MENTHYL ESTERS IN THE VARIOUS SOLVENTS

Substance		Solvent			
		Chloroform	Benzene	Liquid sulfur dioxide	Tetra-hydrofuran
l-Menthol	[α]*	45.0	47.6	53.5	45.8
	[R]	7.0	7.4	8.4	7.2
l-Menthyl Propionate	[α]	84.2	82.2	79.0	78.1
	[R]	17.9	17.4	16.8	16.6
l-Menthyl Monochloroacetate	[α]	82.0	74.2	88.7	76.6
	[R]	19.1	17.3	20.6	17.8
l-Menthyl Dichloroacetate	[α]	67.6	65.2	76.7	63.8
	[R]	18.0	17.4	20.5	17.0
l-Menthyl Trichloroacetate	[α]			72.1	61.7
	[R]			21.7	18.6
l-Menthyl Benzoate	[α]	87.2			
	[R]	22.7			
l-Menthyl *p*-Methoxy benzoate	[α]	78.8			
	[R]	22.9			
l-Menthyl *p*-Methyl benzoate	[α]	83.7			
	[R]	23.0			
l-Menthyl *p*-Chlorobenzoate	[α]	76.7			
	[R]	22.6			

* [α]: degree $dm^{-1} cc\ g^{-1}$
[R]: degree $dm^{-1} mol^{-1} l$

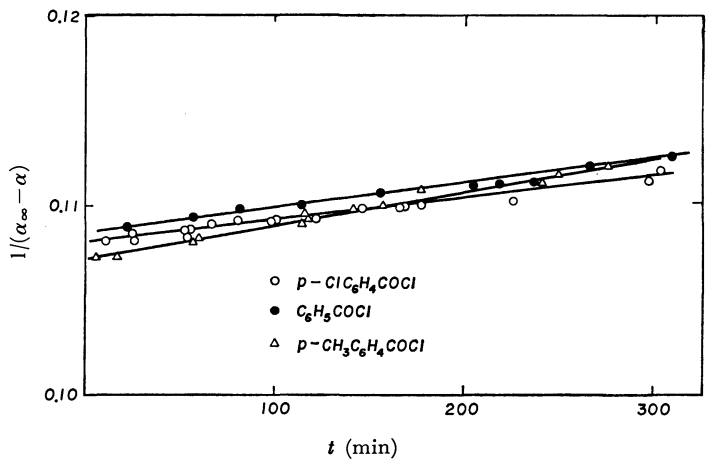

Fig. 1. The second-order rate plots of the reaction of *l*-menthol with *p*-substituted benzoyl chlorides in chloroform. (35°C)

Results

The reactions of *l*-menthol with *p*-substituted benzoyl chlorides were studied in chloroform at various temperatures. The same reactions in liquid sulfur dioxide and in acetonitrile were also performed with substituted benzoyl chlorides. However, the results were complicated and difficult to interpret, since in both solvents the S_N1 reaction was predominant under the same conditions. The second-order rate constants in chloroform are listed in Table 2, while the activation parameters of these reactions are listed in Table 3. An isokinetic relationship is observed in the linear plot of the activation enthalpy, $\Delta H^{\ddagger}$, *vs.* the activation entropy, $\Delta S^{\ddagger}$, as is shown in Fig. 2.

This result demonstrates the abnormal trend of the substituent effect and the extraordinarily low isokinetic temperature. The tendency of the rate constant in connection with the substituent is in the order:

$$p\text{-}CH_3O > p\text{-}CH_3 > H > p\text{-}Cl$$

which is the reverse of the ordinary order in an S_N2 reaction, whereas the activation enthalpy is characteristic of the S_N2 acylation, the values of $\Delta H^{\ddagger}$ being in the order:

Table 2. The second-order rate constants of the benzoylations of *l*-menthol with *p*-substituted benzoyl chlorides in chloroform ($l\,mol^{-1}\,sec^{-1}$)

	25°C	35°C	42°C	45°C	49°C
p-CH_3O	8.49×10^{-6}	2.34×10^{-5}		5.75×10^{-5}	
p-CH_3		9.26×10^{-6}	1.60×10^{-5}		2.57×10^{-5}
H		7.22×10^{-6}	1.09×10^{-5}		1.90×10^{-5}
p-Cl		5.93×10^{-6}	8.03×10^{-6}		1.10×10^{-5}

Table 3. The activation parameters of the benzoylation of *l*-menthol in chloroform at 35°C

Substituted benzoyl chloride	E (kcal/mol)	$\Delta H^{\neq}$ (kcal/mol)	$\Delta S^{\neq}$ (e.u.)
p-CH_3O	20.1	19.50	−15.0
p-CH_3	14.6	14.0	−34.9
H	13.7	13.1	−38.7
p-Cl	11.9	11.3	−45.1

Table 4. The second-order rate constants of the acetylations of *l*-menthol in chloroform ($l\,mol^{-1}\,sec^{-1}$)

	15°C	25°C	35°C	45°C
Propionylation	8.99×10^{-4}	1.35×10^{-3}	2.17×10^{-3}	
Monochloroacetylation		1.05×10^{-3}	1.23×10^{-3}	1.40×10^{-3}
Dichloroacetylation		1.00×10^{-3}	1.14×10^{-3}	1.20×10^{-3}

Table 5. The second-order rate constants of the acetylations of *l*-menthol in benzene ($l\,mol^{-1}\,sec^{-1}$)

	15°C	25°C	30°C	35°C	45°C
Propionylation	2.39×10^{-4}	4.40×10^{-4}	5.70×10^{-4}		
Monochloroacetylation		1.29×10^{-3}		1.43×10^{-3}	1.61×10^{-3}
Dichloroacetylation		1.39×10^{-3}		1.52×10^{-3}	1.68×10^{-3}

Table 6. The second-order rate constants of the acetylations of *l*-menthol in liquid sulfur dioxide ($l\,mol^{-1}\,sec^{-1}$)

	25°C	35°C	42°C
Monochloroacetylation	4.27×10^{-4}	6.81×10^{-4}	9.95×10^{-4}
Dichloroacetylation	5.52×10^{-4}	8.00×10^{-4}	1.06×10^{-3}
Trichloroacetylation	1.16×10^{-3}	1.63×10^{-3}	2.04×10^{-3}

Table 7. The second-order rate constants of the acetylations of *l*-menthol in tetrahydrofuran ($l\,mol^{-1}\,sec^{-1}$)

	15°C	25°C	35°C	42°C	45°C
Propionylation	3.17×10^{-5}	5.96×10^{-5}	1.06×10^{-4}		
Monochloroacetylation		9.93×10^{-4}	1.61×10^{-3}		2.87×10^{-3}
Dichloroacetylation		3.12×10^{-3}	4.48×10^{-3}		6.40×10^{-3}
Trichloroacetylation		7.76×10^{-3}	9.14×10^{-4}	1.04×10^{-2}	

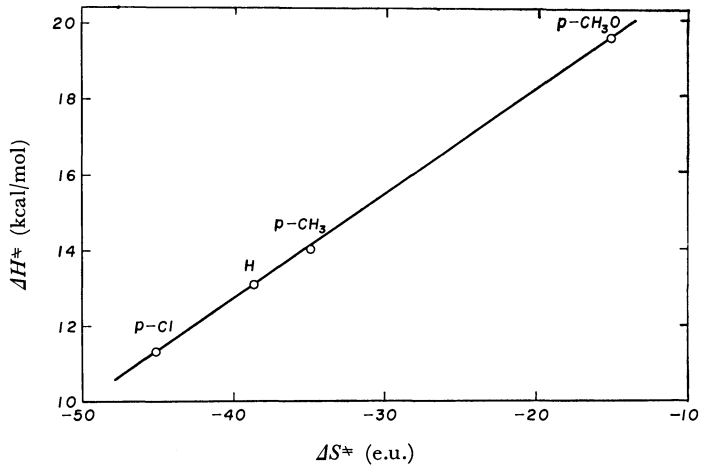

Fig. 2. The isokinetic relation of the reaction of *l*-menthol with *p*-substituted benzoyl chlorides in chloroform.

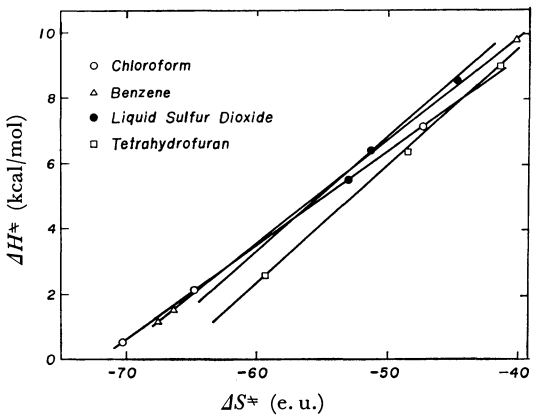

Fig. 3. The isokinetic relation of the acetylations of *l*-methanol in various solvent.

$$p\text{-}CH_3O > p\text{-}CH_3 > H > p\text{-}Cl$$

The reactions of *l*-menthol with substituted acetyl chlorides are relatively faster than with substituted benzoyl chlorides. The second-order rate constants of the acetylations of *l*-menthol in various solvents, such as chloroform benzene, liquid sulfur dioxide, and tetrahydrofuran, are listed in Tables 4, 5, 6, and 7. The isokinetic relationships obtained in these solvents are visualised in Fig. 3. From this figure the isokinetic temperatures can be estimated to be as listed in Table 9.

The trend of the activation enthalpies is also characteristic of an S_N2 reaction. However the rate in chloroform is in an anomalous order:

propionyl > monochloracetyl > dichloroacetyl

whereas in benzene, liquid sulfur dioxide, and tetrahydrofuran the order is:

trichloroacetyl > dichloroacetyl > monochloroacetyl > propionyl

Discussion

According to the absolute reaction rate theory, the reaction rate constant, k, is expressed as a function of the activation enthalpy, $\Delta H^{\neq}$, and of the activation entropy, $\Delta S^{\neq}$:[6] Since $\Delta F^{\neq} = \Delta H^{\neq} - T\Delta S^{\neq}$ (2):

$$k = \frac{kT}{h} e^{-\Delta F^{\neq}/RT} = \frac{kT}{h} e^{\Delta S^{\neq}/R} \cdot e^{-\Delta H^{\neq}/RT} \quad (3)$$

where k and h are the Boltzmann and the Planck constants respectively. Empirically, the isokinetic relation holds:[3,7]

$$\Delta H^{\neq} = \Delta H_0^{\neq} + \beta \Delta S^{\neq} \quad (4)$$

where β is an isokinetic temperature and $\Delta H^{\neq}$ is the activation enthalpy at the standard state. As a result, k is expressed as a function of β, $\Delta H^{\neq}$, and $\Delta S^{\neq}$.

From Eqs. (2) and (3), as has been derived by Leffler:[3]

$$\Delta F^{\neq} = \Delta H^{\neq} + (\beta - T)\Delta S^{\neq} = \frac{T}{\beta}\Delta H_0^{\neq} + \frac{(\beta - T)}{\beta}\Delta H^{\neq} \quad (5)$$

$$k = \frac{kT}{h} \exp -\left\{\frac{T}{\beta}\Delta H_0^{\neq} + \frac{(\beta - T)}{\beta}\Delta H^{\neq}\right\} \Big/ RT \quad (6)$$

Therefore, provided

$$\beta > T$$

then:

$$\Delta F^{\neq} \propto \Delta H^{\neq}$$

and if,

6) S. Glasstone, K. J. Laidler and H. Eyring, "The Theory of Rate Process," McGraw Hill Co., New York (1941).

7) J. E. Leffler, *J. Org. Chem.*, **20**, 1202 (1955).

$$\beta < T$$

the situation is reversed:

$$\Delta F^{\neq} \propto -\Delta H^{\neq}$$

Thus, the above discussion allows one to understand that the reaction will be accelerated (or suppressed) below the isokinetic temperature and suppressed (or accelerated) above the isokinetic temperature, as long as the isokinetic relationship is sustained.

The reaction temperatures adopted here are in the range between 15 and 49°C; actually the reactions were undertaken near the isokinetic temperatures. As may be seen in Figs. 2 and 3 and in Table 9, the isokinetic temperatures of the acylation of *l*-menthol are low, being 285° in chloroform, 315° in benzene, 344° in liquid sulfur dioxide, and 357°K in tetrahydrofuran. In general, the isokinetic temperatures of the solvolyses of substituted benzoyl chlorides are as high as 450°K[8] in ether-ethanol and over 600°K in aceton-water,[1] as Fig. 4 shows.

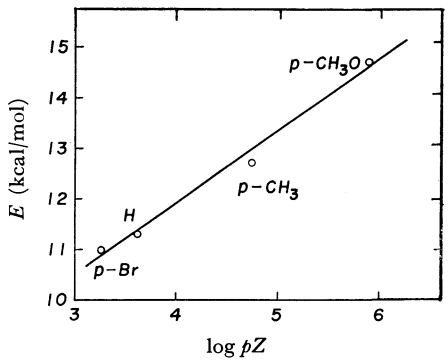

Fig. 4. The isokinetic relation of the hydrolysis of the *p*-substituted benzoylchloride in 95% acetone-5% water.[1] β=652°K

The present results indicate that the substituent effect in this reaction is contrary to the expected order in the S_N2 acylation, and that the rate decreases in the order:

$$p\text{-}CH_3O > p\text{-}CH_3 > H > p\text{-}Cl$$

Such a reversal may adequately be explained by the fact that the reaction was undertaken above isokinetic temperature, the large entropy-controlled reaction operating throughout the acylation (*vide infra*).

Such a phenomenon, encountered for the first time in acylations by the present authors, will be discussed further below.

By the definition of Eq. (3), as long as the isokinetic relation is sustained, the value of β can be rewritten as:

$$\beta \frac{\Delta\Delta H^{\neq}}{\Delta\Delta S^{\neq}} \qquad (7)$$

where $\Delta\Delta H^{\neq}$ and $\Delta\Delta S^{\neq}$ are the differentials of the activation enthalpies and entropies. As the $\Delta\Delta S^{\neq}$ becomes larger, or as the reaction becomes more entropy-controlled, the isokinetic temperature, β, will become smaller, whereas a larger value of β will be obtained when the $\Delta\Delta H^{\neq}$ becomes larger or when the reaction is enthalpy-controlled. Thus, the small value of β is attributable to the entropy-controlled reaction.

Two factors which may have a predominant influence on the low isokinetic temperature are the steric configuration of the activated complex in the reaction medium and the nature of the solvent applied.

The term $\Delta\Delta S^{\neq}$ may be divided into two parts, the change in the activation entropy of the reactant molecules, $\Delta\Delta S_R^{\neq}$, which is characteristic of the reactants, and the change in the activation entropy of the solvent molecules, $\Delta\Delta S_S^{\neq}$, which is the solvent effect. Assuming the additivity of the entropies, $\Delta\Delta S^{\neq}$ may be expressed as:

$$\Delta\Delta S^{\neq} = \Delta\Delta S_R^{\neq} + \Delta\Delta S_S^{\neq} \qquad (8)$$

The difference between the acylations of *l*-menthol and ordinary alcohols may be largely due to the difference in the transition states of the acylation, which is illustrated in Fig. 5, the value of $\Delta\Delta S_R^{\neq}$ in the acylation of *l*-menthol being much larger by steric reasons.

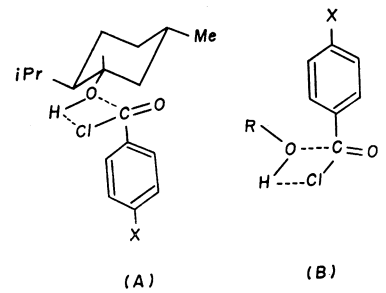

Fig. 5. The transition state of the acylation of *l*-menthol (A) and the ordinary alcohol (B).

At a lower energy state, the internal motion in the transition state of the acylation of *l*-menthol is inhibited. However, at a higher energy state the internal rotation comes into action against the steric restriction. In the acylation of ordinary alcohols, the steric inhibition to the internal motion is not as large as in the menthol. Consequently, the $\Delta\Delta S_R^{\neq}$ in the acylation of menthol may be larger than that of ordinary alcohol.

The dependency of the isokinetic temperature on the solvent is indicated in Table 9. The relative rate of the acylation of *l*-menthol with substituted acetyl chlorides at 35°C undergoes an almost complete reversal in order as the solvent is changed from chloroform to benzene, liquid sulfur dioxide, or tetrahydrofuran.

Suppose two circumstances, 1 and 2, where the

8) G. E. Branch and A. C. Nixon, *J. Am. Chem. Soc.*, **58**, 2499 (1936).

Table 8. The activation parameters of the acetylations of *l*-menthol at 35°C

Solvent	Reaction	E (kcal/mol)	$\Delta H^{\neq}$ (kcal/mol)	$\Delta S^{\neq}$ (e.u.)
Chloroform	Propionylation	7.7	7.1	−47.3
	Monochloroacetylation	2.7	2.1	−64.8
	Dichloroacetylation	1.1	0.5	−70.3
Benzene	Propionylation	10.4	9.8	−40.1
	Monochloroacetylation	2.1	1.5	−66.5
	Dichloroacetylation	2.1	1.5	−67.5
Liquid sulfur dioxide	Monochloroacetylation	9.1	8.5	−44.7
	Dichloroacetylation	7.0	6.4	−51.3
	Trichloroacetylation	6.1	5.5	−53.0
Tetrahydrofuran	Propionylation	10.6	10.0	−43.8
	Monochloroacetylation	9.6	9.0	−4.15
	Dichloroacetylation	6.9	6.3	−48.5
	Trichloroacetylation	3.2	2.6	−59.4

Table 9. The isokinetic temperature of the acetylations in various solvents

Solvent	β°K
Chloroform	285°K
Benzene	315°K
Liquid sulfur dioxide	344°K
Tetrahydrofuran	357°K

activation enthalpies and entropies are indicated as $\Delta H_1^{\neq}$, $\Delta H_2^{\neq}$, $\Delta S_1^{\neq}$ and $\Delta S_2^{\neq}$, respectively. The suffixes 1 and 2 indicate the respective cases of 1 and 2. The entropy differences, $\Delta S_1^{\neq}$ and $\Delta S_2^{\neq}$, can then be expressed as:

$$\begin{aligned}\Delta S_1^{\neq} &= \{l-(m+n)\}(S_{AB}^{\neq}-S_S) + m(S_{AB}^{\neq}-S_A) \\ &\quad + n(S_{AB}^{\neq}-S_B) \\ &= l(S_{AB}^{\neq}-S_S) - m(S_A-S_S) - n(S_B-S_S)\end{aligned} \tag{9}$$

$$\begin{aligned}\Delta S_2^{\neq} &= \{l'-(m'+n')\}(S'_{AB}{}^{\neq}-S_S) \\ &\quad + m'(S'_{AB}{}^{\neq}-S'_A) + n'(S'_{AB}{}^{\neq}S'_B) \\ &= l'(S'_{AB}{}^{\neq}-S_S) - m'(S'_A-S_S) \\ &\quad -n'(S'_B-S_S)\end{aligned} \tag{10}$$

The l, m, and n symbols are the solvation numbers of the solvents to the transition state AB$^{\neq}$, the reactants being A and B in case 1. S_A, S_B, and $S_{AB}^{\neq}$ are the entropies of the solvent molecules which solvate to A, B, and AB in case 1. All the symbols with dashes correspond to case 2. S_S is the entropy of the unsolvated solvent.[9] Since $\Delta\Delta S_R^{\neq}$ is a constant in both cases:

$$\begin{aligned}\Delta\Delta S_S^{\neq} &= \Delta S_2^{\neq} - \Delta S_1^{\neq} = l(S'_{AB}{}^{\neq}-S_{AB}^{\neq}) \\ &\quad - m(S'_A-S_A) - n(S'_B-S_B) \\ &\quad - (l-l')(S'_{AB}{}^{\neq}-S_S) - (m-m')(S'_A-S_S) \\ &\quad - (n-n')(S'_B-S_S)\end{aligned} \tag{11}$$

Equation (11) may then be rewritten as:

$$\Delta\Delta S_S^{\neq} = \Delta\Delta S_C^{\neq} + \Delta\Delta S_P^{\neq}$$

where:

$$\begin{aligned}\Delta\Delta S_C^{\neq} &= l(S'_{AB}{}^{\neq}-S_{AB}^{\neq}) - m(S'_A-S_A) \\ &\quad - n(S'_B-S_B)\end{aligned} \tag{12}$$

$$\begin{aligned}-\Delta\Delta S_P^{\neq} &= (l-l')(S'_{AB}{}^{\neq}-S^{\neq}) \\ &\quad + (m-m')(S'_A-S_S) + (n-n')(S_B'-S_S)\end{aligned} \tag{13}$$

Equation (11) indicates that $\Delta\Delta S_S^{\neq}$ consists of two components, the *solvent coordinate* and the *solvent polarity factors*, $\Delta\Delta S_C^{\neq}$ and $\Delta\Delta S_P^{\neq}$.

The $(S'_{AB}{}^{\neq}-S_{AB}^{\neq})$, (S'_A-S_A), and (S'_B-S_B) terms mean the change in the entropy of the solvent molecules with the changes in the energy state of the activated complex and the reactant molecules respectively, and may be defines as the *solvent coordinate factor*, $\Delta\Delta S_C^{\neq}$. The $(S'_{AB}{}^{\neq}-S_S)$, (S'_A-S_S), and (S'_B-S_S) terms indicate the change in the entropy of the solvent molecules with the transfer of the solvent molecules from the solvent layer to the solvation shell. These terms may be called the *solvent polarity factor*, $\Delta\Delta S_P^{\neq}$. The *solvent coordinate factor* is related to the solvent effect on the activation entropy within the solvation shell, while the *solvent polarity factor* correlates with that of the solvation of the solvent molecules.

As the non-polar solvents associate with each other more loosely than as the polar solvents in the solvent layer, the *solvent polarity factor* is larger in a non-polar solvent than in a polar solvent. Therefore, the $\Delta\Delta S^{\neq}$ value is larger in a non-polar solvent than in a polar solvent.

As a result, if the $\Delta\Delta H^{\neq}=\Delta H_2^{\neq}-\Delta H_1^{\neq}$ change is not as pronounced as the $\Delta\Delta S^{\neq}$ change, the isokinetic temperature is lower in the case of benzene and chloroform than in tetrahydrofuran and liquid sulfur dioxide.

The high isokinetic temperature in tetrahydrofuran may be due to the *solvent coordinate factor*. The change in the entropy with the change in the energy state is larger in the liquid sulfur dioxide than in tetrahydrofuran. While tetrahydrofuran is a cyclic molecule with only one solvation center, liquid sulfur dioxide has three centers, one sulfur and two oxygen atoms.

9) S_S is assumed to be constant under any circumstances.

BULLETIN OF THE CHEMICAL SOCIETY OF JAPAN VOL. 41 2696—2699 (1968)

Long-Range Spin Coupling between the Methoxyl and Ring Protons in 2-Methoxytropone Derivatives and Its Applications*[1]

Shuichi SETO, Kyozo OGURA, Hiroko TODA (SASAKI), Yusaku IKEGAMI and Tsuneo IKENOUE

Chemical Research Institute of Non-Aqueous Solutions, Tohoku University, Katahira-cho, Sendai

(Received March 26, 1968)

Bromination of 5-amino-2-methoxytropone and 2-amino-7-methoxytropone afforded 5-amino-4-bromo-2-methoxytropone and 2-amino-3,5-dibromo-7-methoxytropone, respectively, as expected from the consideration of the effect of amino group in 2-methoxytropone system. Long-range spin coupling between the methoxyl group and a neighboring ring proton was observed in 2-methoxytropone derivatives. This information was applied to elucidation of the structure of the bromination products. The comparison of their NMR spectra gave the reasonable assignment for the ring protons of 5-amino-2-methoxytropone.

Long-range spin coupling involving methoxyl groups in aromatic compounds has been reported on the derivatives of *o*-hydroxyacetophenone and salicylaldehyde by Forsén and his co-workers.[1,2] They observed that the methyl protons are coupled to a neighboring ring proton with coupling constant of 0.24—0.31 Hz in these compounds.

During the course of our study of the reaction of amino derivatives of 2-methoxytropone, long-range spin coupling was observed between the methoxyl group and a ring proton. The fact is applicable to confirm the direction of the substitution reaction.

Results and Discussion

Bromination of 5-Amino-2-methoxytropone. It is well known that the substitution in the bromination of tropolone[3-5] and 2-aminotropone[6] takes place at 3-, 5- and 7-positions of the tropone ring, and that 2-methoxytropone is subject to addition rather than substitution on its treatment with bromine.[7] Bromination of 5-amino-2-methoxytropone (I)[8] is of interest from the standpoint of the effect of the amino group on electrophilic substitution of the 2-methoxytropone system. In the NMR spectrum of I (Fig. 1), the quartet at the highest field in the ring proton region must be due to H_4 proton or H_6 proton since it has spacings 2.5, 9.0 and 2.5 Hz due to *ortho* and *meta* couplings, respectively.[9]

It seems likely that the electron density at the position 4 of I is raised by mesomeric effect of the amino group and that such an effect is not conceivable as to the position 6. Therefore, this quartet is reasonably assigned to H_4 proton, and the other signals for ring protons can be tentatively assigned as illustrated in Fig. 1. These considerations lead to an anticipation that the substitution of bromine may occur exclusively at the position 4.

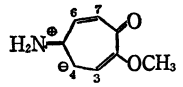

Treatment of I with bromine in methanol caused a transitory red color to appear, and then yellow crystals of a monobromo derivative (II) separated out in a high yield. The NMR spectrum of II (Fig. 2) in DMSO-d_6 shows a pair of AB type doublet (δ=6.97 and 7.13 ppm) with coupling constant of 13.9 Hz due to two adjacent ring protons and a signal with small splittings at 7.22 ppm probably due to H_3 proton. The signals corresponding to H_4 proton in I disappear in the monobromo derivative (II) and no splitting by *meta*-coupling is observed, suggesting the substitution occurred at the position 4. The splitting of the signal at 7.22 ppm was found to be due to the coupling with the methoxyl protons (J=0.5 Hz) by spin decoupling experiment; namely double irradiation at around 223 and 433 Hz sharpened the signal at 7.22 ppm and the signal for the methoxyl protons, respectively. The positional relation between methoxyl and H_3

*1 Presented in part at the 85th Annual Meeting of the Pharmaceutical Society of Japan in Tokushima, Oct. 27, 1965.

1) S. Forsén, *J. Phys. Chem.*, **67**, 1740 (1963).
2) S. Forsén, B. Akermark and T. Alm, *Acta Chem. Scand.*, **18**, 2313 (1964).
3) T. Nozoe, S. Seto, T. Mukai, K. Yamane and A. Matsukuma, *Proc. Japan Acad.*, **27**, 224 (1951).
4) J. W. Look, A. R. Gibb and R. A. Raphael, *J. Chem. Soc.*, **1951**, 2244.
5) T. Nozoe, S. Seto, Y. Kitahara, M. Kunori and Y. Nakayama, *Proc. Japan Acad.*, **26**, 38 (1950).
6) T. Nozoe, S. Seto, H. Takeda, S. Morosawa and K. Matsumoto, *Sci. Repts. Tohoku Univ., Ser. I*, **36**, 126 (1952).
7) T. Nozoe, S. Seto, T. Mukai, K. Yamane and A. Matsukuma, *Proc. Japan Acad.*, **17**, 224 (1951).
8) K. Ogura, H. Sasaki and S. Seto, This Bulletin, **38**, 306 (1965).
9) H. Sugiyama, D. Sc. Thesis, Tohoku University, 1963.

proton in II is the same as that of methoxyl derivatives of 2-hydroxyacetophenone and salicylaldehyde[2] in which a coupling between methoxyl and its adjacent ring proton is reported. Accordingly, the observation of this long-range coupling also affords a strong support for the structural elucidation of II as 5-amino-4-bromo-2-methoxytropone.

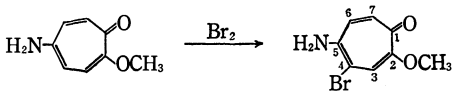

I II

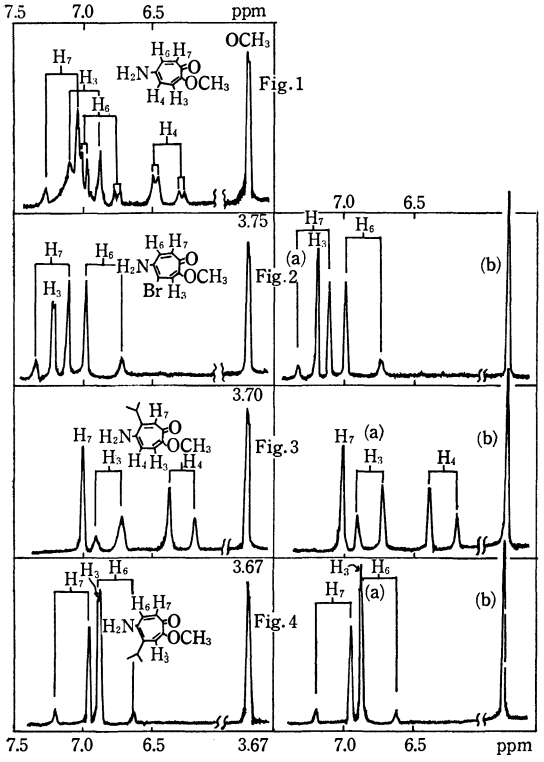

NMR Spectra
(a) OCH_3 irradiated, (b) H_3 irradiated

Fig. 1. 5-amino-2-methoxytropone (I).
Fig. 2. 5-amino-4-bromo-2-methoxytropone (II).
Fig. 3. 5-amino-6-isopropyl-2-methoxytropone (IV).
Fig. 4. 5-amino-4-isopropyl-2-methoxytropone (V).
(in DMSO-d_6)
For the sake of comparison of each spectrum, Figs. 1—4 are expressed illustratively.

Two Methyl Ethers of 5-Amino-4-isopropyltropolone. Reaction of 5-amino-4-isopropyltropolone (III)[10] with diazomethane gave two methyl ethers (IV: mp 220°C, V: mp 140°C). As shown in Fig. 3, the NMR spectrum of IV has a pair of AB type doublet (δ=6.32 and 6.82 ppm) with coupling constant of 12.0 Hz, which means an existence of two adjacent ring protons in its structure. It is noticed, moreover, that two peaks at lower fields in the pair showed further a small splitting. Spin decoupling at frequencies of 220 and 409 Hz sharpened those aromatic and methyl proton signals, respectively, indicating that the lower-field peaks in the pair of AB type doublet is assigned to a ring proton neighboring with the methoxyl group. So, the structure of IV was determined as 5-amino-6-isopropyl-2-methoxytropone. A signal at 7.00 ppm in Fig. 3 is reasonably assigned to a H_7 proton.

Isomeric methyl ether, V, is naturally assumed to be 5-amino-4-isopropyl-2-methoxytropone. The following decoupling study of its NMR spectrum supported the structure. In the spectrum shown in Fig. 4, a signal (6.84 ppm) due to an isolated ring proton appears, overlapping with a line at 6.87 ppm of a pair of doublet (δ=6.86 and 6.95 ppm, J=13.0 Hz) of two adjacent ring protons. Decoupling at frequencies of methyl protons and isolated ring-proton resonances afforded sharp and intense signals for a line at 6.84 ppm and methyl proton signal at 3.67 ppm, respectively. The phenomenon indicates that an isolated ring proton exists at a position adjacent to methoxyl group in the structure of V.

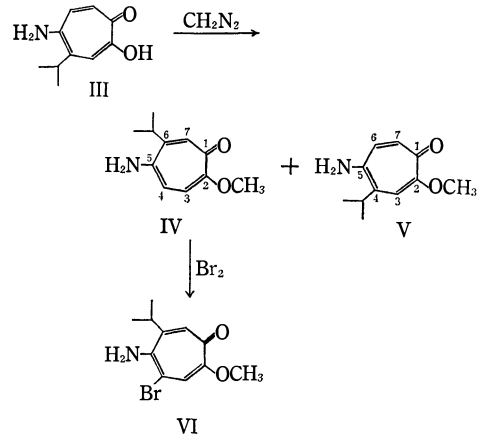

III IV V VI

Monobromo derivative (VI) of IV was obtained by its bromination, while the isomer, V, did not give any bromo derivative. Since the NMR spectrum of VI does not show any signal in the region corresponding to H_4 proton signals of IV, it is clear that the bromination of IV has occurred at 4-position similarly to the case of 5-amino-2-methoxytropone (I).

Dibromo Derivative of 2-Amino-7-methoxytropone. Reaction of 3-aminotropolone (VII) with diazomethane affords 2-amino-7-methoxytropone (VIII), together with a small amount of isomeric methyl ether (IX). The structure of VIII was confirmed by the fact that the compound (VIII) reacted with diketene giving an authentic

10) T. Nozoe, Y. Kitahara, E. Kunioka and K. Doi, *Proc. Japan Acad.*, **26**, 38 (1950).

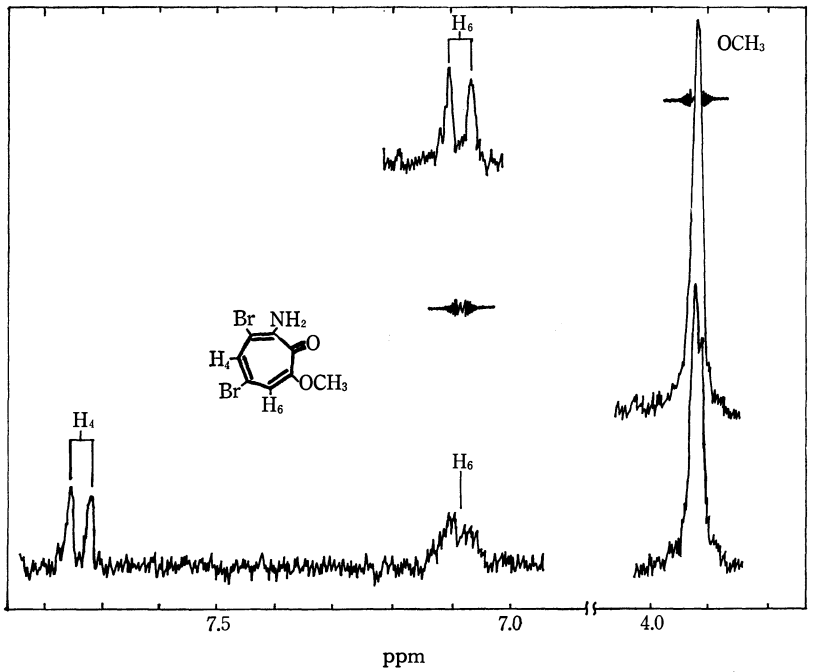

Fig. 5. NMR spectra of 2-amino-3,5-dibromo-7-methoxytropone (X) in DMSO-d_6 showing results (top two spectra) of spin decoupling experiments.

2-acetoacetamino-7-methoxytropone (XI), which had been obtained in the reaction of VII with diketene followed by methylation.[8]

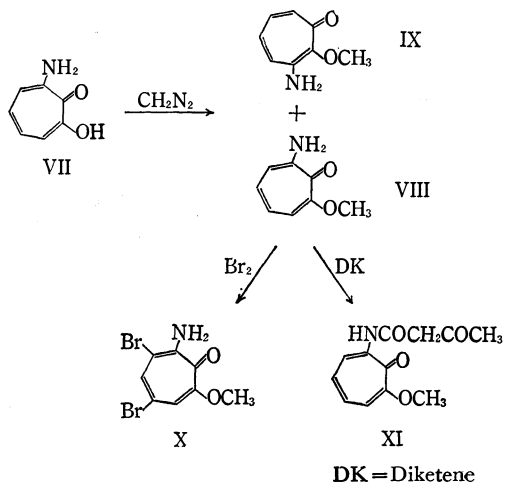

Long-range spin coupling between methoxyl and ring proton was also applied to the determination of the structure of 2-amino-3,5-dibromo-7-methoxytropone (X) which is a bromination product of VIII, as follows. Since the ultraviolet and infrared spectra of the product show the existence of tropone skeleton, the dibromo derivative of VIII should be one of the six possible isomers. Analysis of the NMR spectrum excluded the structure having two adjacent ring protons, as shown in Fig. 5. The further study by proton magnetic double resonance chose a structure of X because the double resonance spectra clearly demonstrated the existence of a splitting due to long-range coupling between methyl protons and H_6 proton, the signal of which appears at 7.10 ppm, and H_6 proton couples to H_4 proton with coupling constant of 1.9 Hz.

The formation of 3,5-dibromo derivative of VIII shows that VIII has a behavior as 2-aminotropone derivative that gives 3,5,7-tribromo-2-aminotropone derivative on bromination.

Comparison of these spectra gave a confirmation of the assignment of every signal of 5-amino-2-methoxytropone (I) as given in Fig. 1. The results obtained here suggest that the long-range coupling between methoxyl and neighboring ring protons will be widely useful for the study of structural elucidation.

Experimental*2

Bromination of 5-Amino-2-methoxytropone (I). Into a cooled solution of I (100 mg) in 1 m*l* of methanol, a solution of bromine (110 mg) in 1 m*l* of methanol was added dropwise slowly. After bromine was added, the solution was stirred for 10 min and then the crystals that separated out were collected (140 mg). When the

*2 All melting points are uncorrected. The microanalyses were carried out by Misses Noriko Matsukawa, Emiko Yoshida and Hiroko Hosokawa of this Institute, to whom the authors are indebted.

crystals were dissolved in water and the solution was neutralized with sodium carbonate, yellow crystals separated out. The recrystallization of these from ethanol gave 5-amino-4-bromo-2-methoxytropone (II); yield, 90 mg. Mp 182°C (dec.). ν_{max}^{KBr} cm^{-1}: 3290, 3160, 1632, 1615, 1550, 1488, 1450, 1240. λ_{max}^{MeOH} $m\mu$ (log ε): 242 (4.32), 354 (4.02), 390 (4.02).

Found: C, 39.18; H, 4.50; N, 5.47%. Calcd for $C_8H_8O_2NBr \cdot H_2O$: C, 38.70; H, 4.02; N, 5.60%.

Two Methyl Ethers of 5-Amino-4-isopropyltropolone (III). To a suspension of III (500 mg) in a small amount of methanol, an ethereal diazomethane was added until portions of the solution were no longer colored with ferric chloride, and then the solution was allowed to stand at room temperature overnight. Yellow needles that separated out were collected by decantation and washed with benzene - methanol. A brownish yellow oil obtained by evaporation of solvent from the supernatant was dried well and chromatographed on alumina by elution with chloroform. The first fraction gave 5-amino-6-isopropyl-2-methoxytropone (IV) as yellow crystals. The third fraction, which was obtained by elution with 1% ethanolic chloroform, gave a yellow oil that crystallized by addition of benzene. The resulting yellow needles were 5-amino-4-isopropyl-2-methoxytropone (V). The second part was chromatographed again to give IV and V.

IV: mp 224—225°C; yield, 200 mg. ν_{max}^{KBr} cm^{-1}: 3740, 3320, 3200, 1640, 1610, 1576, 1500.

Found: C, 68.32; H, 7.72; N, 7.49%. Calcd for $C_{11}H_{15}O_2N$: C, 68.37; H, 7.82; N, 7.25%.

V: mp 138—140°C; yield, 100mg. ν_{max}^{KBr} cm^{-1}: 3410, 3350, 3240, 2970, 1644, 1622, 1578, 1530, 1490.

Found: C, 68.50; H, 7.83; N, 7.10%. Calcd for $C_{11}H_{15}O_2N$: C, 68.37; H, 7.82; N, 7.25%.

Bromination of 5-Amino-6-isopropyl-2-methoxytropone (IV). Into a solution of IV (50 mg) in 1 m*l* of methanol, a solution of bromine (50 mg) in 0.5 m*l* of methanol was added dropwise on being cooled with ice-salt. After the solution was stirred for 10 min, the removal of the solvent gave a small amount of pale yellow crystals of 5-amino-4-bromo-6-isopropyl-2-methoxytropone (VI).

Two Methyl Ethers of 3-Aminotropolone (VII). A methanolic solution of VII (670 mg), to which ethereal diazomethane was added until the solution became negative to ferric chloride coloration, was held to stand overnight. After evaporation of the solvent, the resulting hygroscopic crystalline mixture was dried in a desiccator and chromatographed on alumina with chloroform. The removal of the solvent from the first eluate gave yellow crystals of 2-amino-7-methoxytropone (VIII), which were recrystallized from benzene - ether. A yellow oily mixture of VIII and IX was obtained by the elution with 5% ethanolic chloroform. Addition of a small amount of benzene to this mixture afforded yellow prisms, which were recrystallized from benzene-methanol to give 3-amino-2-methoxytropone (IX).

VIII: mp 118—119°C; yield, 160 mg. ν_{max}^{KBr} cm^{-1}: 3370, 3290, 3150, 1613, 1588, 1525. λ_{max}^{MeOH} $m\mu$(log ε): 250(4.44), 263(4.25), 273(4.14), 340(4.14), 400(3.97).

Found: C, 62.74; H, 5.98; N, 9.72%. Calcd for $C_8H_9O_2N$: C, 63.56; H, 6.00; N, 9.29%.

IX: mp 157°C; yield, 30 mg. ν_{max}^{KBr} cm^{-1}: 3370, 3300, 3170, 1630, 1578, 1512. $\lambda_{max}^{H_2O}$ $m\mu$ (log ε): 264 (4.52), 313(3.90), 323(3.83), 365(3.30).

Found: C, 63.35; H, 5.81; N, 9.10%. Calcd for $C_8H_9O_2N$: C, 63.56; H, 6.00; N, 9.29%.

Bromination of 2-Amino-7-methoxytropone (VIII). To a solution of VIII (200 mg) in 2 m*l* of methanol that was cooled with ice-water, 220 mg of bromine in methanol was added. After the mixture was allowed to stand in a refrigerator overnight, the solvent was removed off. The crystalline residue (HBr salt of X) was dissolved in water and the pH of the solution was adjusted to 4 with sodium bicarbonate, and then extracted with chloroform. The extract that had been dried over anhydrous sodium sulfate was passed through an alumina column. Yellow crystals that were obtained from the first fraction were recrystallized from methanol to give yellow prisms of 2-amino-3,5-dibromo-7-methoxytropone (X); 45 mg, mp 172°C. ν_{max}^{KBr} cm^{-1}: 3440, 3310, 1555, 1530, 1450, 1229. λ_{max}^{MeOH} $m\mu$(log ε): 266(4.26), 350(3.91), 418(3.70).

Found: C, 30.88; H, 2.73; N, 4.55%. Calcd for $C_8H_7O_2NBr_2$: C, 31.09; H, 2.27; N, 4.53%.

Spectral Measurements. Measurements of the normal NMR spectra were carried out by using a Varian A-60 NMR spectrometer. Decoupling experiments were carried out by the frequency sweep method, using a Hitachi H-60 NMR spectrometer with a decoupling unit. The saturating field intensities were 1.0—2.0 milligauss. The spectra were taken at 34°C. In the decoupling experiments coupling constants and chemical shifts were determined with an error of ± 0.1 Hz by a frequency counter in hexadeuterodimethyl sulfoxide with concentration of *ca.* 0.3 mmol per milliliter utilizing tetramethylsilane as an internal standard. The chemical shifts were given in ppm unit.

The present authors wish to express their thanks to Messrs. Yoshiharu Utsumi and Go Miyashima of Hitachi Co., Ltd., Naka Work for the measurement of NMR spectra and to Sankyo Co., Ltd., who defrayed a part of expense for the present work.

BULLETIN OF THE CHEMICAL SOCIETY OF JAPAN VOL. 41 2700—2703 (1968)

The Absolute Configuration of Pinocarvone Oxide

Jun KATSUHARA

Sun Star Dentifrice Company, Research Laboratory, Takatsuki, Osaka, Japan

(Received March 30, 1968)

The conversion of (−)-pinocarvone oxide derived from (+)-pinocarvone into (−)-(1R : 2S : 3R : 5R)-*cis*-2-hydroxypinocampheol and the conversion of (+)-pinocarvone oxide in (+)-(1R : 2R : 3R : 5R)-*trans*-2-hydroxyneoisopinocampheol and (−)-(1R : 2R : 3R : 5R)-*cis*-2-hydroxyisopinocampheol are described. With the knowledge of the absolute configurations of these glycols, it was concluded that (−)-pinocarvone oxide and (+)-pinocarvone oxide have the (1R : 2S : 5R)- and (1R : 2R : 5R)-configurations, respectively.

Although Djerassi and coworkers[1] have determined the ORD curve of a mixture of diastereomeric pinocarvone oxides, the separation of the diastereomeric pinocarvone oxides and then ORD curves have not yet been described. It seemed of interest to undertake the isolation of these epoxides and to examine the ORD and CD curves of these compounds, in order to determine the applicability of the Octant Rule to oxirane systems. We wish, at this time, to report the assignment of the absolute configuration of the pinocarvone oxides by means of unequivocal chemical transformations into diols of established configuration.

(+)-*trans*-Pinocarveol (I) was oxidized with chromic acid anhydride pyridine-complex to (+)-(1S : 5R)-pinocarvone (II) which, on the Treibs epoxidation, afforded a mixture of trans-, (III) and *cis*-pinocarvone oxide (IV) in an isomer ratio of 35.5 : 64.5 as indicated by vpc analysis. The mixed isomers were separated by means of preparative vpc followed by silica gel column chromatography, and chemically pure (−)- and (+)-pinocarvone oxides were obtained.

The diastereomeric pinocarvone oxide III gave, upon the lithium aluminum hydride reduction, (−)-2-hydroxypinocampheol (V), whose IR spectrum indicated the presence of *cis*-glycol by the absorption bands of free (3628 cm^{-1}) and bonded hydroxyl (3572 cm^{-1}; $\Delta\nu$ 56 cm^{-1}).

The (+)-diastereomer (IV) was reduced with lithium aluminum hydride to give (+)-*trans*-2-hydroxyneoisopinocampheol (VIII) and (−)-*cis*-2-hydroxyisopinocampheol (IX).

(+)-2-Hydroxypinocamphone (X) derived from (−)-α-pinene, was reduced with lithium aluminum hydride to give the diol (XI). The identity of the diol (VIII) melting at 158° with the diol XI of the same melting point was established by direct comparison of the melting points and the IR spectra. The IR spectrum of the diol XI exhibited an absorption band at 3628 cm^{-1} corresponding to a free hydroxyl group and one 3612 cm^{-1} ($\Delta\nu$ 16 cm^{-1}) of the neighboring two hydroxyl groups. The NMR spectra of XI and of monoacetate of XI also substantiated the structure.

As for the geometry of 2-hydroxypinocamphone, Schmidt[2] concluded that (−)-2-hydroxypinocamphone derived from (+)-α-pinene should be assigned the *cis*-configuration (relative to the carbon-7 bridge carrying geminal dimethyl and 10-methyl group). Accordingly, the (1R : 2R : 3R : 5R)-configuration VIII may be assigned to (+)-2-hydroxyneoisopinocampheol (XI).

The Meerwein-Ponndorf-Verley reduction of (+)-X gave a diol XII, whose IR spectrum exhibited absorption bands at 3620 cm^{-1} (free hydroxyl) and at 3552 cm^{-1} ($\Delta\nu$ 68 cm^{-1}; bonded hydroxyl), suggesting the *cis*-arrangement of the two hydroxyl groups. It was shown by tlc comparison that the diol XII was identical with the diol IX, and consequently the (1R : 2R : 3S : 5R)-*cis*-structure may be assigned to (−)-*cis*-2-hydroxyisopinocampheol (IX).

For the purpose of comparison, another diastereomeric diol VI was prepared through (−)-pinocarveyl acetate from (+)-*trans*-pinocarveol (I) as follows: Hydroxymercuration[3] of (−)-*trans*-pinocarveyl acetate yielded the corresponding hydroxy acetate VII which on alkaline hydrolysis gave the diol VI. IR spectrum of VI indicated the presence of *trans*-diol by the absorption bands of free (3625 cm^{-1}) and bonded hydroxyl (3610 cm^{-1}; $\Delta\nu$ 15 cm^{-1}). With the knowledge of absolute configuration of the starting (+)-*trans*-pinocarveol, the (1R : 2S : 3S : 5R)-configuration can be assigned for (+)-*trans*-2-hydroxyneopinocampheol (VI).

1) C. Djerassi, W. Klyne, T. Norin, G. Ohloff and E. Klein, *Tetrahedron*, **21**, 163 (1965).

2) H. Schmidt, *Chem. Ber.*, **93**, 2485 (1960).

3) H. C. Brown and W. J. Hammar, *J. Am. Chem. Soc.*, **89**, 1524 (1967).

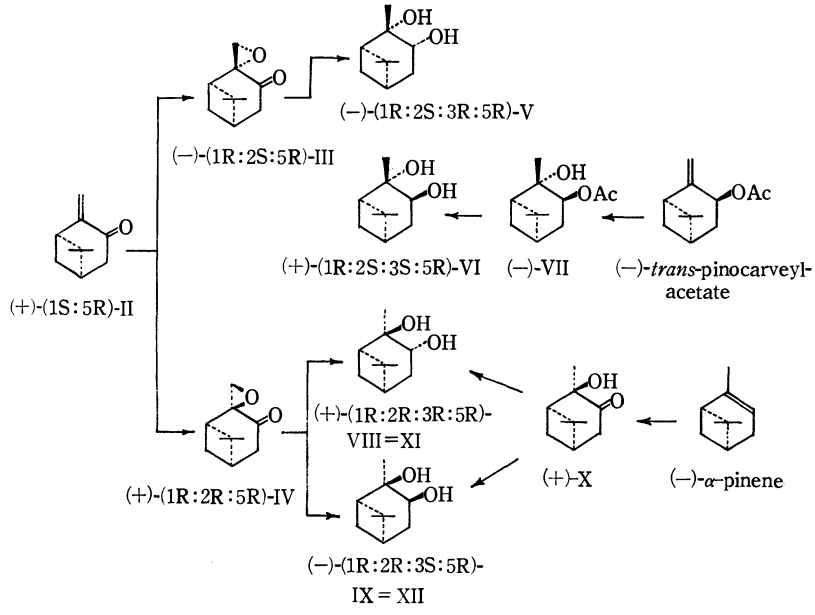

Scheme 1

The comparison of IR spectra, R_f values and physical properties proved that neither VI, VIII nor IX was identical with the diastereomeric *cis*-diol V. Since VI, VIII and IX are excluded, it may be concluded that the diol V, the product resulting from the lithium aluminum hydride reduction of (−)-epoxide III, must have the sole remaining configuration, *i. e.*, (1R : 2S : 3R : 5R).

It naturally follows that the parent (−)-pinocarvone oxide (III) from which the levorotatory diol V was derived, should have the *trans*-(1R : 2S : 5R)-configuration.

In the consequence, (+)-pinocarvone oxide (IV), the parent compound of both VIII and IX, is assigned to the *cis*-(1R : 2R : 5R)-configuration. (See Scheme 1).

The ORD and CD curves of the isomeric pinocarvone oxides whose absolute configuration is now clarified seem to permit one to speculate with some certainty on the preferred conformation of these epoxides. The red shift at 323 mμ($\Delta\nu$=20 mμ) in the CD curve of (−)-III strongly suggests the axial disposition[4] would be expected to assume the III-B conformation rather than the other possibility, III-A, as implicit in Scheme 2. In contrast, however, the isomeric (+)-epoxide IV may reasonably be expected to exist largely in the IV-A conformation with the oxirane oxygen disposed in an axial position as cogently supported by the red shift ($\Delta\nu$=20 mμ) in the observed positive Cotton curve.

If one accepts conformation III-B for (−)-III and conformation IV-A for (+)-IV, one finds,

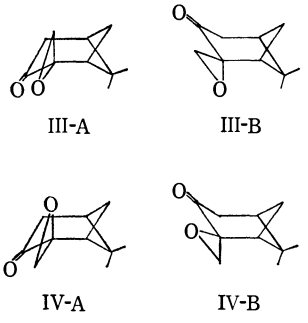

Scheme 2

with the knowledge of the absolute configurations and the experimentally determined Cotton effects, that the "reversed" Octant Rule is applicable to these oxirane systems, in agreement with the previous deduction.[1]

Experimental[5]

Preparation of Pinocarvone (II). Chromic acid anhydride (65 g) was carefully added to 1 *l* of dried pyridine at 0°. The resulting mixture was added to

4) C. Djerassi, O. Halpern, V. Halpern, O. Schindler and Ch. Tamm, *Helv. Chim. Acta*, **41**, 250 (1958).

5) Infrared spectra were recorded on a Shimadzu Model 27-G spectrophotometer. Optical rotatory dispersion and circular dichroism measurements were made on a Nippon Bunko Spectropolarimeter Model ORD/UV-5. Optical rotation measurements were recorded on a Perkin-Elmer Model 141 with 10 cm cell. Gas-liquid partition chromatography analyses were carried out using a Shimadzu 2-C gas chromatograph. A 3 mm×2.25 m column of 20% Hyporose-80 on Celite-545 served for vpc analyses. Nuclear magnetic resonance spectra were recorded with a Varian A-60 spectrometer.

30.0 g of I,[6] $[\alpha]_D^{22}$ +51.8°±1.0 (*c* 0.94, methanol), optical purity 71%, *trans*-pinocarveyl *p*-nitrobenzoate mp 91°C, in 50 m*l* of pyridine and was kept at room temperature for 18 hr. Water was then added to the mixture and was extracted with benzene - ether (1 : 1) solution. The combined benzene - ether extract was washed with 2 N hydrogen chloride solution, 3% hydrogen sodium carbonate solution and water, and dried over anhydrous sodium sulfate. After removal of solvent *in vacuo*, the crude product (26.0 g, 88% yield) was distilled to yield II[7]; bp 84—86°C/8 mmHg, (14.5 g). The IR spectrum exhibited the following characteristic absorptions (cm^{-1}): 1700s, 1680m, 1620s, 1390m, 1380m, 930s, 920s; λ_{max} 234 mμ (ε 6030) (in ethanol); $[\alpha]_D^{22}$ +48.0°±1.0 (*c* 0.84, methanol), optical purity 70%.

Preparation of Pinocarvone Oxide Mixture. A mixture of 10.0 g of pinocarvone in 65 m*l* of methanol and 22 m*l* of 30% hydrogen peroxide was cooled to −15°C, and a solution of 1.25 g of sodium hydroxide in 6 m*l* of water was added dropwise with stirring over a 15 min period. Stirring was continued for 4 hr, the temperature being maintained at 20—25°C. The reaction mixture was poured into 100 m*l* portions of ethyl ether. After the combined ether extract was washed and dried, the solvent was removed under reduced pressure and the residue was analyzed by vpc. The crude product, 8.0 g (yield 75%), consisted of 35.5%, III and 64.5%, IV.

Isolation and Properties of Pure Pinocarvone Oxides III and IV. Isolation of the pure diastereomer was effected by preparative vpc, of the fraction of distillation through a 30 cm concentric column, boiling at 98°C/5 mmHg. Further purification of the fraction on silica gel column chromatography gave III: the IR spectrum showed the following peaks (cm^{-1}): 1720s, 1390m, 1370m, 1275m, 1250m, 940w, 890m, 870m, 840m, 785m; $[\alpha]_D^{20}$ −22°±5 (*c* 0.10, dioxane); ORD mμ ([ϕ] in dioxane): 400 (−154), 340 (−789), 328sh(−369), 316sh(+478), 307(+921), 303 (+856), 300(+895), 265(−1000), 228(−3268): CD mμ ([θ] in dioxane): 333 (−668), 322.5 (−985), 313 (−788), 302 (−255); IV, IR spectra main bands (cm^{-1}): 1725s, 1385m, 1370m, 1275m, 1260m, 940m, 900m, 885m, 840m, 820m, 800m, $[\alpha]_D^{20}$ +74°±7 (*c* 0.27, dioxane): ORD mμ ([ϕ] in dioxane): 400 (+493), 340 (+2051), 332.5 (+1417), 327 (+1807), 318.5 (+390), 314 (+629), 306 (−383), 302.5 (−171), 297 (−500), 291.5 (−276), 290 (−293), 224 (+6829), 210 (−850); CD mμ ([θ] in dioxane): 336 (+967), 323 (+1781), 311 (+1628), 302 (+1018), 292 (+545), 275 (+143), 252 (+50).

Lithium Aluminum Hydride Reduction of (−)-Pinocarvone Oxide (III). The oxide III (37.0 mg) dissolved in 3 m*l* of absolute ether was added dropwise with stirring to a chilled (−10°C) slurry of 100 mg of lithium aluminum hydride in 3 m*l* of absolute ether. Upon completion of addition, the solution was stirred at 0°C for an additional hour, stirring was continued at room temperature (15—20°C) for 10 hr and finally, the reaction mixture was refluxed on water bath and cooled. Excess hydride was decomposed by addition of the ether saturated with water under cooling, and the organic layer was separated, filtered and dried. Removal of the solvent gave the diol V, $[\alpha]_D^{22}$ −17.6±1.4 (*c* 0.40, methanol), and its NMR spectrum indicated a three hydrogens singlet (τ 8.94) for methyl, a six hydrogens singlet (τ 8.78) for the geminal dimethyl, and one hydrogen AB quartet (τ_A 6.22; τ_B 6.06, J=7 Hz) for the hydrogen on the carbon bearing the hydroxyl group.

Lithium Aluminum Hydride Reduction of (+)-Pinocarvone Oxide (IV). The oxide IV (60.4 mg) was reduced with lithium aluminum hydride (100 mg) in 5 m*l* of absolute ether, in the same way as mentioned above, to give a mixture of VIII and IV, yield 54.6 mg (yield 88%). Diols VIII and IX were separated by means of silica gel column chromatography: VIII, mp 158°C, $[\alpha]_D^{22}$ −42.5°±1.0 (*c* 0.57, methanol) and oily crude (−)-IX.

Preparation of Hydroxypinocamphone (X).[2] To a solution of 28 g of (−)-α-pinene ($[\alpha]_D^{20}$ −26.8° ±1.0, *c* 0.67, methanol, optical purity 52%) in 250 m*l* of 90% acetone was added 56 g of potassium permanganate with stirring at 0—5°C for 8 hr. The manganese dioxide was filtered off, and the acetone was removed under reduced pressure to afford a crude product 20 g (58%) of (+)-X.

Reduction of Hydroxypinocamphone (X). Lithium aluminum hydride reduction of 513 mg of **X** in the same way as mentioned above gave 508 mg (98%) of XI, mp 158°, $[\alpha]_D^{22}$ −39.1° ±3.0 (*c* 0.21, methanol).

Found: C, 70.68; H, 10.67%. Calcd for $C_{10}H_{18}O_2$: C, 70.54; H, 10.66%.

The NMR spectrum of the monoacetate of XI indicated a three hydrogens singlet (τ 9.04) for methyl, a six hydrogens doublet (τ 8.75) for geminal dimethyl, a three hydrogens singlet (τ 7.87) for acetoxy and one hydrogen AB quartet (τ_A 5.02: τ_B 4.84, J=7 Hz) for the hydrogen on the carbon bearing the acetoxy group.

The Meerwein-Ponndorf-Verley reduction of 3.0 g of **X** was carried out with 10 g of aluminum isopropylate in 20 m*l* of absolute isopropanol in the usual manner.[2] There were obtained 2.9 g of the diol XII (95%).

Preparation of (+)-*trans*-2-Hydroxyneopinocampheol (VI). A mixture of 2.0 g of (+)-I and 0.4 g of anhydrous sodium acetate in 2 m*l* of acetic anhydride was heated at 140°C for 1 hr and the reaction mixture was poured into water. The reaction mixture was extracted with ether and the solvent was removed under reduced pressure to give 1.6 g (63%) of *trans*-pinocarveyl acetate, $[\alpha]_D^{22}$ −7.5°±0.7 (*c* 0.69, methanol). A mixture of 1.6 g of mercuric acetate in 10 m*l* of aqueous-tetrahydrofuran (1 : 1 by volume) was added dropwise to 0.5 g of *trans*-pinocarveyl acetate with stirring for 4 hr and then kept at room temperature for 16 hr. Then 5 m*l* of 3 M sodium hydroxide was added, followed by 6 m*l* of 0.5 M sodium borohydride in 3.0 M sodium hydroxide. The water layer was saturated with sodium chloride. The upper layer of tetrahydrofuran was separated. It contained 0.45 g (81%) of VII $[\alpha]_D^{22}$ −15.9°±0.9 (*c* 0.62, methanol).

The acetate VII (0.4 g) was refluxed in 10 m*l* of methanol with 0.2 g of potassium hydrioxide on a water bath (95°C) for 1 hr. The reaction mixture was poured

6) (+)-*trans*-Pinocarveol (I), derived from (−)-α-pinene, by means of photo-oxidation method using Rose Bengal as a photosensitizer in methanol, was supplied by Takasago Kogyo Co., Ltd. Research Laboratory.

7) J. L. Simonsen, "The Terpenes," Vol. II, The University Press, Cambridge (1957), p. 221.

into water and was extracted with ether. The solvent was removed under reduced pressure. The crude product was recrystallized from ether to yield VI (0.3 g, 95%), mp 144°C, $[\alpha]_D^{22}$ +42°±13 (*c* 0.05, methanol).

Found: C, 70.42; H, 10.97%. Calcd for $C_{10}H_{18}O_2$: C, 70.54; H, 10.66%.

The author wishes to thank Dr. T. Matsuura and Dr. T. Suga of Hiroshima University, Dr. Y. Inouye of Kyoto University, Dr. H. Minato and Dr. K. Kuriyama of Shionogi Research Laboratory, Dr. W. Herz of Florida University, Dr. M. Kobayashi, Mr. K. Hashimoto and Mr. H. Watanabe of Sun Star Research Laboratory, for many helpful discussions and suggestions during this work, and to Takasago Perfumery Co., Ltd. for their generous gifts of authentic samples.

BULLETIN OF THE CHEMICAL SOCIETY OF JAPAN VOL. 41 2703—2706 (1968)

Convenient Method for the Preparations of Carboxylic Thiolester and Acid Anhydride

Teruaki MUKAIYAMA and Harumi KATSUYAMA

Laboratory of Organic Chemistry, Tokyo Institute of Technology, Ookayama, Meguro-ku, Tokyo

(Received April 11, 1968)

The reactions of mercuric carboxylates with bivalent sulfur compounds, such as aralkyl sulfides and mercaptoles, were investigated. When mercuric acetate and aralkyl sulfides were refluxed in benzene, mercury mercaptides and aralkyl acetates were obtained. It was made clear that the reactivity of the sulfides depends on the stability of carbonium ions given by elimination of the mercapto group. Next, it was found that acetic anhydride, benzophenone and mercury phenylmercaptide were obtained in high yields by the equimolar reaction of benzophenone diphenylmercaptole with mercuric acetate. Further, the reaction was extended to the preparative method of carboxylic acid anhydrides from free acids by treating the carboxylic acids with diphenylmercury and the mercaptole. On the other hand, *S*-phenyl thioacetate, benzophenone and mercury mercaptide were produced in good yields when benzophenone diphenylmercaptole (2 mol) was treated with mercuric acetate (1 mol). Further, it was established that thiolesters were exclusively produced in good yields along with benzophenone and the mercury mercaptide by the reaction of benzophenone diphenylmercaptole or bis(*p*-chlorophenyl)mercaptole (2 mol) with free carboxylic acids (2 mol) and diphenylmercury (1 mol).

In the preceding paper,[1] it has been shown that acetic anhydride, *N,N*-dimethylbenzamide and mercury ethylmercaptide were obtained in good yields by treating *N,N*-dimethylbenzamide diethylmercaptole with mercuric acetate at room temperature. This reaction was reasoned by considering facile elimination of the mercapto group from *N,N*-dimethylbenzamide diethylmercaptole by an attack of the mercuric acetate yielding a reactive intermediate, acyloxyimmonium ion. In the present experiment, the reactions of phenyl aralkyl sulfides with mercuric acetate were tried first in order to find out the facility of elimination of phenylmercapto group from the sulfides by the attack of the mercuric salt. For example, when phenyl trityl sulfide was treated with mercuric acetate in boiling benzene for 3 hr, mercury phenylmercaptide and trityl acetate were obtained in good yields. It was found that the reaction of phenyl benzhydryl sulfide with mercuric acetate under the same conditions yields only a small amount of benzhydryl acetate and phenylmercapto mercury acetate. But, benzhydryl acetate and mercury phenylmercaptide were obtained in good yields by carrying out the reaction in the presence

Table 1. The reaction of phenyl aralkyl sulfides with mercuric acetate[a]

Aralkyl group	Catalyst	Yield, %		
		Aralkyl acetate	$(C_6H_5S)_2$-Hg	C_6H_5SHg-$OCOCH_3$
$(C_6H_5)_3C$-	—	70	90	—
$(C_6H_5)_2CH$-	—	33	—	86
$(C_6H_5)_2CH$-	$BF_3 \cdot O(C_2H_5)_2$	83	85	—
$C_6H_5CH_2$-	$BF_3 \cdot O(C_2H_5)_2$	30	—	

a) These reactions were carried out in refluxing benzene for 3 hr.

1) T. Yamaguchi and T. Mukaiyama, This Bulletin, **40**, 1952 (1967).

of a catalytic amount of boron trifluoride etherate (see Table 1).

$$C_6H_5SR + \tfrac{1}{2}(CH_3CO_2)_2Hg \rightarrow CH_3CO_2R + \tfrac{1}{2}(C_6H_5S)_2Hg$$

R: Aralkyl

These results show that the reactivity of the aralkyl sulfides decreases in the following sequence: $(C_6H_5)_3C- > (C_6H_5)_2CH- > C_6H_5CH_2-$. This order also suggests that the ease of carbon-sulfur bond fission[2] is dependent on the stability of carbonium ions formed by elimination of the mercapto group.

Next, the reactions of the mercaptoles with mercuric carboxylates were tried with the assumption that acid anhydrides, the ketone and mercury mercaptide would be produced as in the case of the reaction of mercuric acetate with *N,N*-dimethylbenzamide diethylmercaptole.

Concerning the reactions of mercaptals with heavy metal salts, Painter reported[3] that one of the ethylmercapto group of penta-*O*-acetyl diethylmercaptals of some hexoses was substituted by an acetoxy group when the mercaptals were treated with mercuric acetate. Bourne also reported[4] that the reaction of benzaldehyde dibenzylmercaptal with lead tetraacetate gave benzylidene diacetate, dibenzyl disulfide and lead acetate.

It was established that acetic anhydride, benzophenone and mercury phenylmercaptide were obtained in good yields by treating benzophenone diphenylmercaptole with mercuric acetate in boiling benzene in the presence of a catalytic amount of boron trifluoride etherate, as expected. Benzophenone diphenylmercaptole was chosen as the mercaptole with the expectation that it would readily eliminate the mercapto group, activated by two phenyl and a phenylmercapto groups attached to the same carbon.

$$(C_6H_5)_2C(SC_6H_5)_2 + (CH_3CO_2)_2Hg \rightarrow (CH_3CO)_2O + (C_6H_5)_2CO + (C_6H_5S)_2Hg$$

68% 96% 96%

Next, the reactions of carboxylic acids, diphenylmercury and the mercaptole were tried to explore a convenient method for the synthesis of acid anhydrides starting from free acids with the consideration that the mercuric carboxylates would be produced from free acids and diphenylmercury. Indeed, various acid anhydrides, benzophenone and mercury phenylmercaptide were obtained in good yields by refluxing 2 mol of free carboxylic acids, 1 mol of diphenylmercury and 1 mol of the mercaptole in anhydrous benzene for a few hours in the presence of a catalytic amount of boron trifluoride etherate. The results are listed in Table 2.

$$(C_6H_5)_2C(SC_6H_5)_2 + 2RCO_2H + (C_6H_5)_2Hg \xrightarrow{-2C_6H_6} (RCO)_2O + (C_6H_5)_2CO + (C_6H_5S)_2Hg$$

TABLE 2. THE REACTIONS OF BENZOPHENONE DIPHENYLMERCAPTOLE (1 MOL) WITH FREE CARBOXYLIC ACIDS (2 MOL) AND DIPHENYLMERCURY (1 MOL)[a]

Carboxylic acid	Yield, %		
	Acid anhydride	Benzophenone	$(C_6H_5S)_2Hg$
Acetic	67	94	85
Propionic	55	88	94
n-Butyric	63	94	80
Cinnamic	74	75	80
Benzoic[b]	51	90	87

a) These reactions were carried out in refluxing benzene for 4 hr in the presence of a catalytic amount of boron trifluoride etherate.

b) In the case of benzoic acid, 11% yield of *S*-phenyl thiobenzoate based on benzoic acid was also obtained.

On the other hand, it was found that *S*-phenyl thioacetate, benzophenone and mercury phenylmercaptide were produced in high yields by treating 2 mol of benzophenone diphenylmercaptole with 1 mol of mercuric acetate under the same conditions.

$$2(C_6H_5)_2C(SC_6H_5)_2 + (CH_3CO_2)_2Hg \rightarrow 2CH_3COSC_6H_5 + 2(C_6H_5)_2CO + (C_6H_5S)_2Hg$$

63% 92% 97%

The use of diphenylmercury extended this reaction to a preparative method of thiolesters starting from free carboxylic acids on the basis of the similar consideration as mentioned above. The reactions of benzophenone diphenylmercaptole or bis(*p*-chlorophenyl)mercaptole (2 mol) with free carboxylic acids (2 mol) and diphenylmercury (1 mol) in boiling benzene in the presence of a catalytic amount of boron trifluoride etherate gave *S*-phenyl or *S*-*p*-chlorophenyl thiocarboxylates, benzophenone and the mercury mercaptide in high yields. The results are listed in Tables 3 and 4.

$$2(C_6H_5)_2C(SC_6H_4\text{-}X\text{-}p)_2 + 2RCO_2H + (C_6H_5)_2Hg \xrightarrow[-2C_6H_6]{} 2RCOSC_6H_4\text{-}X\text{-}p + 2(C_6H_5)_2CO + (p\text{-}X\text{-}C_6H_4S)_2Hg$$

X: H or Cl

The formation of acid anhydrides or thiolesters can be explained by considering an initial formation of an intermediate (1) from mercuric carboxylates

2) D. S. Tarbell and D. P. Harnish, *J. Am. Chem. Soc.*, **74**, 1862 (1952).
3) E. P. Painter, *Can. J. Chem.*, **42**, 2018 (1964).
4) E. J. Bourne, W. M. Corbett, M. Stacey, and R. W. Stephens, *Chem. & Ind. (London)*, **1954**, 106.

Table 3. The reactions of benzophenone diphenylmercaptole (2 mol) with free carboxylic acids (2 mol) and diphenylmercury (1 mol)[a]

Carboxylic acid	Yield, %		
	S-Phenyl thiocarboxylate	Benzophenone	$(C_6H_5S)_2Hg$
Acetic	94	94	98
Propionic	84	96	97
n-Butyric	68	93	98
Benzoic	79	84	98
o-Chlorobenzoic	81	96	98
p-Toluic	79	94	95
p-Anisic	76	84	96
p-Nitrobenzoic[b]	—	36	72
Cinnamic	77	98	98

a) These reactions were carried out in refluxing benzene for 5 hr in the presence of a catalytic amount of boron trifluoride etherate.
b) In the case of *p*-nitrobenzoic acid, only 37% yield of *p*-nitrobenzoic anhydride resulted.

Table 4. The reactions of benzophenone bis(*p*-chlorophenyl)mercaptole (2 mol) with free carboxylic acids (2 mol) and diphenylmercury (1 mol)[a]

Carboxylic acid	Yield, %		
	S-*p*-Chlorophenyl thiocarboxylate	Benzophenone	$(C_6H_5S)_2Hg$
Acetic	84	88	98
n-Butyric	75	98	98
n-Stearic	60	73	92
Benzoic[b]	21	44	98
p-Anisic	79	93	98
Cinnamic	88	96	98

a) These reactions were carried out in refluxing benzene for 2 hr in the presence of a catalytic amount of boron trifluoride etherate.
b) In the case of benzoic acid, 34% yield of benzoic anhydride based on benzoic acid was obtained together with the thiolester.

and the mercaptole. When one half mole of mercuric carboxylates are used, thiolesters are exclusively produced from the intermediate (1) by an intramolecular nucleophilic displacement. On the other hand, in the presence of an additional half mole of mercuric carboxylates, the intermediate (1) further reacts with them to give the second intermediate (2), an acylal, by a nucleophilic attack of the mercapto group on the mercury atom. The second intermediate (2) then yields benzophenone and acid anhydrides by the aid of boron trifluoride.

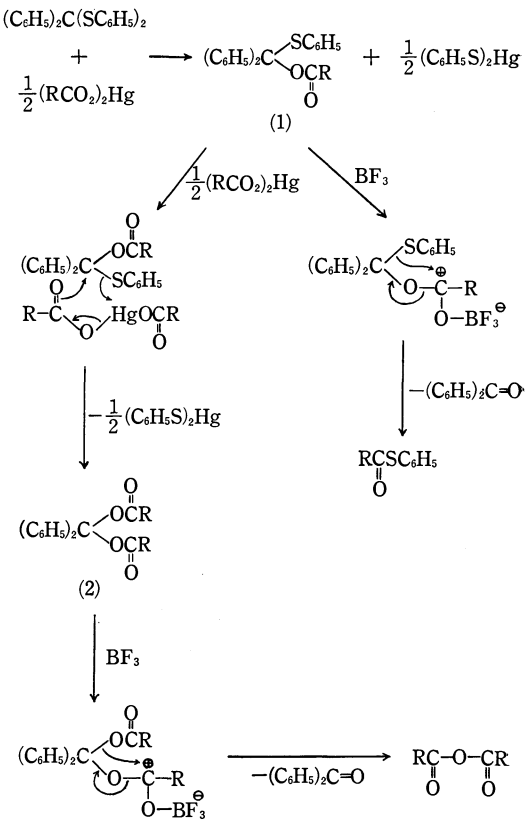

Experimental

Reaction of Phenyl Trityl Sulfide with Mercuric Acetate. A solution of phenyl trityl sulfide (3.52 g, 0.01 mol) and mercuric acetate (1.59 g, 0.005 mol) in 20 m*l* of anhydrous benzene was refluxed for 3 hr. After cooling the reaction mixture, the precipitate was filtered off to give mercury phenylmercaptide, 1.76 g (82%), mp 150°C. The filtrate was evaporated *in vacuo*. The addition of 10 m*l* of anhydrous ether-petroleum ether mixture (1 : 1 v/v) to this residue gave the precipitate containing the mercury salt, and the sulfide was recovered. It was filtered off and the filtrate was concentrated under reduced pressure. To the resulted oil a small amount of anhydrous petroleum ether was added and this mixture was heated until it became a homogeneous solution. Trityl acetate was obtained as colorless crystals from the solution, 2.10 g (70%), mp 83°C (Found: C, 82.81; H, 6.06%).

Reaction of Phenyl Benzhydryl Sulfide with Mercuric Acetate in the Presence of a Catalytic Amount of Boron Trifluoride Etherate. A solution of phenyl benzhydryl sulfide (2.76 g, 0.01 mol) and mercuric acetate (1.59 g, 0.005 mol) in 20 m*l* of benzene was refluxed for 3 hr in the presence of a catalytic amount of boron trifluoride etherate. After cooling the reaction mixture, the precipitate of mercury phenylmercaptide (1.76 g, 85%) was filtered off and the filtrate was evaporated *in vacuo*. The residue was distilled to give benzhydryl acetate, 1.95 g (86%), bp 124°C/1 mmHg (Found: C, 79.40; H, 5.96%).

Equimolar Reaction of Benzophenone Diphenylmercaptole with Mercuric Acetate. A solution of benzophenone diphenylmercaptole (7.64 g, 0.02 mol) and mercuric acetate (6.36 g, 0.02 mol) in 40 m*l* of anhydrous benzene was refluxed for 0.5 hr in the presence of a catalytic amount of boron trifluoride etherate. After cooling the reaction mixture, the precipitate was filtered off to give mercury phenylmercaptide, 8.10 g (97%). The filtrate was concentrated and distilled to give 1.39 g (68%) of acetic anhydride, bp 70—72°C/90 mmHg, and 3.32 g (92%) of benzophenone.

Reaction of Benzophenone Diphenylmercaptole (1 mol) with Cinnamic Acid (2 mol) and Diphenylmercury (1 mol). A solution of benzophenone diphenylmercaptole (3.82 g, 0.01 mol), cinnamic acid (2.96 g, 0.02 mol) and diphenylmercury (3.54 g, 0.01 mol) in 40 m*l* of anhydrous benzene was refluxed for 4 hr in the presence of a catalytic amount of boron trifluoride etherate. After the reaction mixture was cooled, the precipitate was filtered off to give mercury phenylmercaptide, 3.33 g (80%), and the filtrate was evaporated *in vacuo*. The addition of 10 m*l* of alcohol to this residue gave the precipitate of cinnamic anhydride, 2.05 g (74%), mp 136°C (Found: C, 77.92; H, 5.10%). The filtrate was evaporated *in vacuo* and the residue was distilled to give benzophenone, 1.39 g (75%) and a small amount of cinnamic acid recovered.

Reaction of Benzophenone Diphenylmercaptole (2 mol) with Mercuric Acetate (1 mol). A solution of benzophenone diphenylmercaptole (3.82 g, 0.01 mol) and mercuric acetate (1.59 g, 0.005 mol) in 20 m*l* of anhydrous benzene was refluxed for 0.5 hr in the presence of a catalytic amount of boron trifluoride etherate. After the reaction mixture was cooled, the precipitate was filtered off to give mercury phenylmercaptide, 1.92 g (92%). The filtrate was evaporated *in vacuo* and the residue was distilled to give *S*-phenyl thioacetate, 0.96 g (63%), bp 63°C/0.3 mmHg and benzophenone, 1.69 g (92%) (Found: C, 62.85; H, 5.58%).

Reaction of Benzophenone Bis(*p*-chlorophenyl)-mercaptole (2 mol) with Acetic Acid (2 mol) and Diphenylmercury (1 mol). A solution of benzophenone bis(*p*-chlorophenyl)mercaptole (3.82 g, 0.01 mol), acetic acid (0.60 g, 0.01 mol) and diphenylmercury (1.77 g, 0.005 mol) in 20 m*l* of anhydrous benzene was refluxed for 2 hr in the presence of a catalytic amount of boron trifluoride etherate. After the reaction mixture was cooled, the precipitate was filtered off to give mercury *p*-chlorophenylmercaptide, 2.07 g (98%). The filtrate was evaporated *in vacuo* and the residue was distilled to give *S*-*p*-chlorophenyl thioacetate, 0.78 g (84%), bp 142—144°C/20 mmHg, and benzophenone, 1.60 g (88%).

Found: C, 51.71; H, 3.78%. Calcd for C_8H_7OClS: C, 51.49; H, 3.78%.

Reaction of Benzophenone Diphenylmercaptole (2 mol) with *p*-Toluic Acid (2 mol) and Diphenylmercury (1 mol). A solution of benzophenone diphenylmercaptole (3.84 g, 0.01 mol), *p*-toluic acid (1.36 g, 0.01 mol) and diphenylmercury (1.77 g, 0.005 mol) in 20 m*l* of anhydrous benzene was refluxed for 5 hr in the presence of a catalytic amount of boron trifluoride etherate. After the reaction mixture was cooled, the precipitate was filtered off to give mercury phenylmercaptide, 1.98 g (95%). The filtrate was evaporated *in vacuo* and the crystalline residue was washed with 2 portions of 10 m*l* of anhydrous pentane. The crystalline product was *S*-phenyl *p*-thiotoluate, 1.80 g (79%), mp 91.5—92°C (from alcohol).

Found: C, 73.38; H, 5.31%. Calcd for $C_{14}H_{12}OS$: C, 73.67; H, 5.30%.

The pentane solution was evaporated *in vacuo* and the resulting oil was distilled to give benzophenone, 1.71 g (94%).

The authors wish to express their hearty thanks to Mr. Khoichi Wada for his help during this experiment. Grateful acknowledgment is also made to Miss Kazuko Isojima for her microanalyses.

BULLETIN OF THE CHEMICAL SOCIETY OF JAPAN VOL. 41 2707—2712 (1968)

Lactone Carboxylic Acids. VI.[1] A Synthesis of α,β-Epoxybutyrolactone *via* α-Diazolactones

Sigeru TORII, Siro ENDO, Hirotosi OKA and Yoshihiro KARIYA

Department of Industrial Chemistry, Okayama University, Okayama

and Akira TAKEDA

Department of Synthetics Chemistry, Okayama University, Okayama

(Received April 15, 1968)

Reaction of α-carboxy-β-carbethoxy-γ,γ-dimethylbutyrolactone (**3**) with equimolar amount of nitrous acid gave ethyl α-hydroxyaminoaconate (**7**). However, the nitrosation of **3** using excess nitrous acid afforded a variety of compounds such as α-diazo (**4** and **5**), α-nitro (**8**), and α-azoxybutyrolactone (**9**) derivatives. Each of the products (**4**, **5**, **8**, and **9**) could be synthesized from **7**, independently. By the action of phosphoric acid, α-diazolactones (**4** and **5**) were converted into ethyl α,β-epoxyparaconate (**6**). The nature of the product **7** was demonstrated through its conversion into ethyl α-hydroxyaconate and through its thermal decomposition to ethyl α-aminoaconate and α-isopropylidenecyanoacetic acid derivatives. A possible mechanism for the formation of **6** through **4** and **5** is described.

All of the previous reports concerning the nitrosation of α-substituted butyrolactones (**1**)[2] have only described the formation of α-hydroximinobutyrolactones (**2**) as a main product. However, we found that nitrosation of α-carboxy-β-carbethoxybutyrolactones,[3] readily prepared from α,β-dicarbethoxybutyrolacetones,[4] afforded a mixture of complex substances, some of which can be used as a potential intermediate in the synthesis of α,β-epoxyparaconic acid.

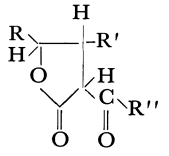

1

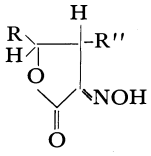

2

R=R'=H, Alkyl;
R''=CH_3, OC_2H_5, OH

In this paper, nitrosation of a model compound, α-carboxy-β-carbethoxy-γ,γ-dimethylbutyrolactone (**3**)[3] with sodium nitrite in an aqueous acetic acid, which leads ultimately to the formation of the corresponding ethyl α,β-epoxyparaconate (**6**) *via* α-diazolactones (**4** and **5**), is described.

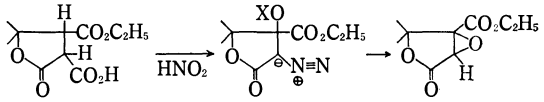

3 **4** X=Ac, **5** X=H **6**

The nitrosation of **3** with an approximately equimolar amount of sodium nitrite in an aqueous acetic acid at 0—5°C, or with a large excess of sodium nitrite at about −5°C for a short reaction period, gave mainly ethyl α-hydroxyamino-γ,γ-dimethylaconate (**7**), white crystals, mp 73°C, which showed an intense band in the 3500—3100 region, consistent with NH and OH functions, 1775, 1695 (lactone, conjugated ester C=O), and 1655 cm^{-1} due to double bond.[5] The ultraviolet spectrum of **7** had λ_{max} 224 mμ (ε 11000) and 258 mμ (ε 760) in ethanol. The NMR spectrum of **7** showed one hydroxy proton at τ 6.10, six gamma dimethyl protons at 8.44 and 8.50, three methyl protons centered at 8.73, two methylene protons centered at 5.78, and one imino proton, as a multiplet form centered at −0.90.

1) For the preceding article in this series, see A. Takeda and S. Torii, This Bulletin, **41**, 1468 (1968).

2) M. Fedorchuk and F. T. Semeniuk *J. Pharm. Sci.*, **52**, 733 (1963); *Chem. Abstr.*, **63**, 11350a (1965); A. E. Lansilotti and M. J. Weiss, *J. Org. Chem.*, **24**, 1003 (1959); W. Reppe and co-workers, *Ann.*, **596**, 164 (1955); R. Sudo, Y. Akiyama, T. Kato and M. Ohta, *Nippon Kagaku Zassi (J. Chem. Soc. Japan, Pure Chem. Sect.)*, **74**, 1009 (1953); H. R. Snyder, J. H. Andreen, G. W. Cannon and C. F. Peters, *J. Am. Chem. Soc.*, **64**, 2082 (1942); V. Feofilaktov and A. Onishchenko, *J. Gen. Chem. USSR*, **9**, 304 (1939); *Chem. Abstr.*, **34**, 378 (1940); V. Feofilaktov and A. Onishchenko, *Compt. rend. acad. sci., URSS*, **20**, 133 (1938); *Chem. Abstr.*, **33**, 1725 (1939).

3) Half-hydrolysis of the lactone diesters was carried out by treating with an equimolar amount of 1 N alcoholic sodium hydroxide solution at room temperature: A. Takeda and S. Torii, *Memoirs of School of Engineering, Okayama Univ.*, **1**, 44 (1966).

4) K. Sisido, S. Torii and M. Kawanisi, *J. Org. Chem.*, **29**, 904, 2290 (1964); E. E. Von Tamelen and S. R. Bach, *J. Am. Chem. Soc.*, **80**, 3079 (1958); G. V. Chelintsev and E. D. Osetrova, *J. Gen. Chem. USSR*, **7**, 2373 (1937); *Chem. Abstr.*, **32**, 2099 (1938); A. Haller and G. Blanc, *Compt. Rend.*, **142**, 1471 (1906).

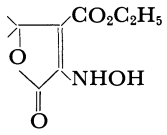

7

On the other hand, when the lactone acid **3** was allowed to react with a large excess of sodium nitrite in an aqueous acetic acid at 5—10°C for 4—5 hr, a mixture having a sharp band in the infrared at 2100 cm^{-1} was obtained together with **7**. Thin-layer chromatography (tlc) on silica gel G (E. Merck), developed by acetone - benzene mixture (1 : 8), revealed that this mixture consisted of more than four components which corresponded to R_f values: 0.70, 0.35, 0.26, and 0.16. Separation of each constituents was carried out by the extraction of the crude product with the alternate use of saturated aqueous sodium bicarbonate and saturated aqueous sodium carbonate, or by collecting each spots on silica gel plates individually. The compound corresponding to the third spot (R_f 0.26) was found to be identical with **7** by the comparison of their infrared and NMR spectral data. The top and the second constituents (R_f 0.70 and 0.35) gave total yield of 65—70% and have a sharp absorption at 2100 cm^{-1}. The elongated oval shape of the fourth spot (R_f 0.16) suggested the presence of two components.

The structure of the compound, pale yellow oil, of the top spot (R_f 0.70) is considered to be **4**, since the infrared spectrum of **4** had a sharp band at 2100 cm^{-1} due to diazo group[6] and a broad band at 1760—1750 cm^{-1}, corresponding to lactone and ester carbonyls. The NMR spectrum of **4** showed three acetoxy protons at τ 7.80 as a singlet.

5) Dr. H. Wamhoff of Bonn University suggested that from the NMR data of the compound (**7**) provided by us, there is a H-bridge from the NH-proton to the neighboring C=O group and this causes a shift of NH-proton signal to lower field down to τ −0.64 in deuterochloroform. Furthermore, he mentioned that the infrared spectrum of **7** in chloroform showed three peaks between 1600—1800 cm^{-1}: 1780 (lactone C=O), 1740 (ester C=O), and 1660 cm^{-1} (C=C), and these values are similar to those of the saturated lactones. These facts reveal that concerning the α,β-unsaturated ester group, **7** may have structures such as A or B in chloroform in contrast to the solid state in Nujol mull, which may not undergo a solvation and have a structure of C.

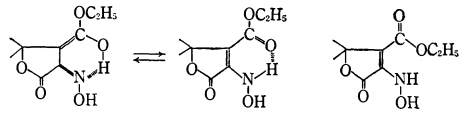

B A C

6) Diazo carbonyl compounds have a sharp infrared absorption in the 2100—2150 cm^{-1} region: G. R. Harvey, *J. Org. Chem.*, **31**, 1587 (1966); D. Hauser and H. P. Sigg, *Helv. Acta Chim.*, **50**, 1327 (1967); S. Julia, G. Cannic and G. Linstrumelle, *Compt. Rend.*, **264**, 1890 (1967).

The structure of the second component (R_f 0.35), pale yellow oil, was assigned to **5**, whose infrared spectrum showed a sharp band at 2100 cm^{-1} and a characteristic broad band at 3500—3000 cm^{-1} due to diazo and hydroxy group, respectively. It was observed that the NMR spectrum of **5** has a band at τ 5.60 due to hydroxy proton in place of a band at 7.80 due to acetoxy group of **4**. Nitrosation of **7** by treating with an excess sodium nitrite in an aqueous acetic acid at 3—7°C for 3 hr gave a major product (**5**) and a minor product (**4**) (*ca.* 5 : 1).

From the head part of the fourth constituents (R_f 0.16) was obtained the white crystals, mp 65.5—66.5°C, which exhibited sharp absorptions at 1565 and 1378 cm^{-1} due to nitro group[7] and was assigned to **8**. Its infrared spectrum exhibited two absorption bands at 1785 and 1728 cm^{-1} due to lactone and ester carbonyls. The NMR spectrum of **8** showed an AB pattern of two bands (doublet, $J_{\alpha,\beta}$ 9—10 cps) centered at τ 4.10 ($\underline{H}_\alpha$) and 5.96 ($\underline{H}_\beta$), indicating that the dihedral angle between two protons is close to 180° from the Karplus curve.[8] Confirmation of the structure of **8** was provided by an independent synthesis involving oxidation of **7** with excess sodium nitrite or nitric acid in an aqueous acetic acid at 0—2°C for about 30 min.

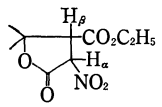

8

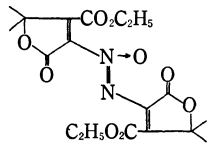

9

The last component, amorphous pale yellow solid, mp 120—123°C, was obtained from the tail part of the oval spot (R_f 0.16)on the tlc plate and purified by repeating tlc on the silica gel G plates. The infrared spectrum indicated the absence of nitro group. Its structure was assigned to **9**, which have absorptions at 1780, 1750 (lactone, ester C=O), 1635 (C=C), and strong bands at 1260 and 1300 cm^{-1}, one of which may be due to azoxy group.[9] The NMR spectrum of **9** showed no absorption except for bands in the regions of 8.9—9.3(*gem*-$C\underline{H}_3$, $C\underline{H}_3$-C-O) and 6.0—5.3 (C-$C\underline{H}_2$-O). The ultraviolet spectrum of **9** had λ_{max} 226 mμ (ε 12000) in ethanol. Considering the preparative methods of the azoxy compound such as the oxidation of hydroxyamine derivatives in neutral media[10]

7) L. J. Bellamy, "The Infrared Spectra of Complex Molecules," 2nd ed., John Wiley and Sons, Inc., New York, N. Y. (1958), p. 299; K. Nakanishi, "Infrared Absorption Spectroscopy," Nankodo, Co. Ltd., Tokyo (1960), p. 54.

8) M. Karplus, *J. Chem. Phys.*, **30**, 11 (1959).

9) J. Jander and R. N. Haszeldine, *J. Chem. Soc.*, **1954**, 919; B. W. Langley, B. Lythgoe and L. S. Rayner, *ibid.*, **1952**, 4191.

10) E. Bamberger, *Ber.*, **33**, 113 (1900).

TABLE 1. ETHYL α-SUBSTITUTED γ,γ-DIMETHYLACONATES

Compd.	Yield %	Bp °C/mmHg	Formula	Calcd, % C	Calcd, % H	Found, % C	Found, % H	Spectrum: Infrared, cm⁻¹ νC=O	Spectrum: Infrared, cm⁻¹ νC=O	Spectrum: Infrared, cm⁻¹ νC=C	Spectrum: NMR, τ α-Subst.
13	95	123/2.5	$C_{10}H_{14}O_5$	56.07	6.59	56.30	6.85	1765	1705	1645	5.75
14	85	110—112/1.5	$C_{11}H_{16}O_5$	57.89	7.07	57.99	7.37	1765	1705	1645	—
15	95	100/2.5	$C_{11}H_{14}O_6$	54.54	5.83	54.46	5.92	1780	1725	1670	7.63

and the reaction of nitroso group with hydroxyamine,[11] we attempted the oxidation of **7** with manganese dioxide in acetone for 2 days and obtained **9** in quantitative yield.

Treatment of α-diazolactone (**4** and **5**) with phosphoric acid gave the α,β-epoxybutyrolactone (**6**), bp 100°C/2 mmHg, in excellent yield (*ca.* 90%). A proof of the structure of **6** was obtained by epoxidation[12] of aconic acid (**10**),[13] followed by esterification of α,β-epoxyparaconic acid (**11**) with ethyl orthoformate.[14]

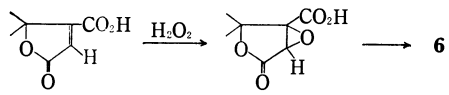

10 **11**

Several aspects of the chemical property of the *intermediates (**6** and **7**) are of particular interest.* Namely, ethyl α-hydroxyaconate (**12**)[15] was obtained readily in good yield by the treatment of **7** with concentrated hydrochloric acid at room temperature. Treatment of **6** with sodium trichloroacetate at 90—130°C also gave **12** in excellent yield along with the evolution of carbon dioxide and chloroform.[16] The structure of **12** was inferred from its spectral data[15] and microanalysis. A mechanism of the formation of **12** is given in Scheme I. The physical constants of a series of the derivatives (**12**, **13**, **14** and **15**) are shown in experimental part and Table 1.

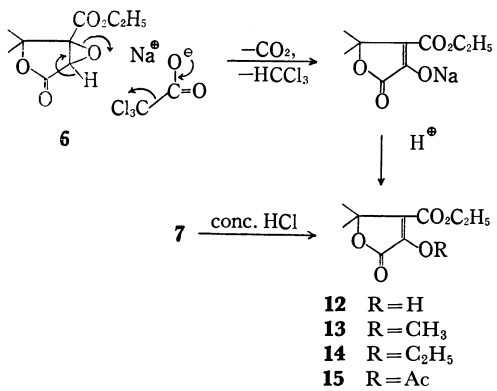

Scheme I

On the other hand, ethyl α-aminoaconate (**16**) was obtained in 15—20% yield together with isopropylidenecyanoacetic acid derivatives (**17**[17] and **18**[18]), when **7** was subjected to thermal decomposition at 140—160°C under reduced pressure. Pyrolysis of diacetate (**19**), prepared by boiling **7** with acetic anhydride, gave only **17**, indicating that normal thermal decomposition may proceed *as below, and formation of **16** may be due to a* disproportionation.

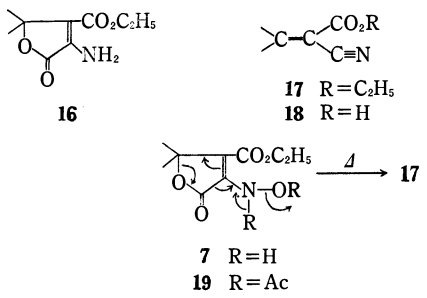

The structure of **16** was proven by its spectral data and microanalysis. Thus, mass spectrum of **16** exhibited a peak at *m/e* 199, corresponding to molecular ion. The infrared spectrum showed two bands at 3350—3450 (NH_2), two bands at 1760 and 1686 (lactone, ester C=O) and a band at 1640 cm^{-1} (C=O). The NMR spectrum showed the following absorptions: τ 4.40 (broadened, NH_2), 8.76 and 5.65 (triplet and quartet, CH_3CH_2O–), and 8.30 (singlet, 2 CH_3).

The possible mechanism of the formation of the

11) J. G. Aston and D. E. Ailman, *J. Am. Chem. Soc.*, **60**, 1930 (1938).
12) T. Oyamada and H. Baba, This Bulletin, **39**, 507 (1966).
13) R. Fittig and B. Frost, *Ann.*, **226**, 370 (1884).
14) H. Cohen and J. D. Mier, *Chem. & Ind.*, **1965**, 349.
15) G. W. Stacy, J. Wm. Cleary and M. J. Gortatowski, *J. Am. Chem. Soc.*, **79**, 1451 (1957). Recently, oxobutyrolactones, derivatives of **12**, having antiviral activity and low toxicity, have been reported: H. G. Monsimer, U. S. Pat. 3185711 (1965); *Chem. Abstr.*, **63**, 9879 (1966).
16) R. E. Buckles and C. J. Thelen, *Anal. Chem.*, **22**, 676 (1950).
17) T. Hayashi, M. Igarashi, S. Hayashi and H. Midorikawa, This Bulletin, **38**, 2063 (1965).
18) R. Carrie, R. Bougot and B. Potteau, *Compt. Rend.*, **259**, 2859 (1964); *Chem. Abstr.*, **62**, 2704 (1965).

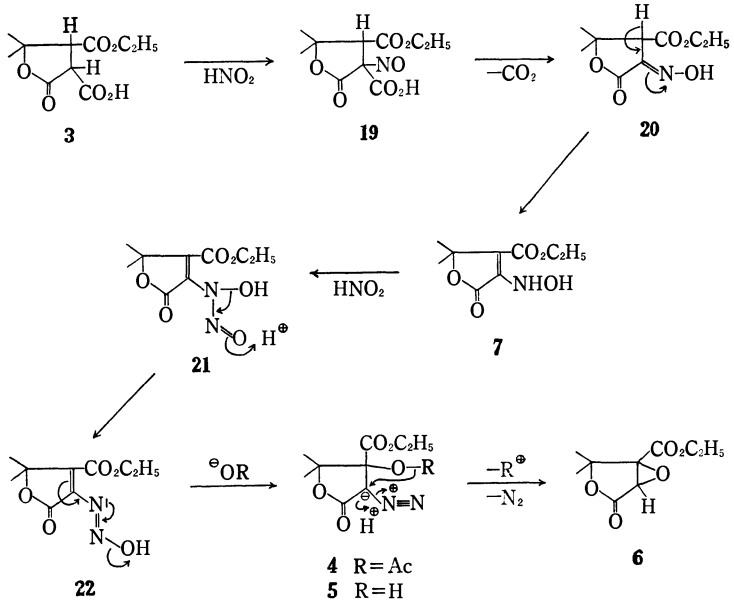

Scheme II. Mechanism of the formation of the epoxylactone.

epoxylactone (**6**) are depicted in Scheme II. The presence of the carbethoxy group at the β-position of the lactone ring would have effected a rapid transformation of the transient intermediates (**19** and **20**) to the α-hydroxyaminoaconate (**7**), which may be stabilized by forming a conjugated ring system in an acidic media. It is considered that the compound (**7**) would be the key intermediate for the present reaction, since **7** can be converted into the α-diazolactones (**4** and **5**) by the action of excess nitrous acid *via* **21** and **22**, which were affected by phosphoric acid to afford the epoxylactone (**6**), as a result of electrophilic attack of a proton to the α-carbon atom along with the elimination of a nitrogen molecule, followed by the intramolecular nucleophilic attack of the oxygen atom attached to the β-position of **4** and **5**.

Experimental[19]

Ethyl α-Hydroxyamino-γ,γ-dimethylaconate (7). To a solution of α-carboxy-β-carbethoxy-γ,γ-dimethylbutyrolactone (**3**)[3] (5 g) in glacial acetic acid (10 m*l*) sodium nitrite (1.5 g) in water (3 m*l*) was added. The reaction mixture was stirred for 30 min at 0—2°C and then diluted with water (34 m*l*) with stirring for 1 hr. The mixture was extracted with ether and the extract was washed with aqueous sodium chloride. After drying over Na_2SO_4 and concentrating by evaporation, the residue, when scrubbed, solidified and afforded 3.2 g (68.1%) of **7**, mp 71.5°C (*n*-hexane - benzene); IR (Nujol mull) 3280, 3100, 1778, 1700, 1655, 1400, 1375, 1340, 1260, 1195, 1090, 990, 910, 870, and (ethanol or chloroform) 1780—1775 (lactone C=O), 1745—1740 (ester C=O), 1660 cm^{-1} (C=C); UV max (95% EtOH) 224 mμ (ε 11000) and 258 mμ (ε 760); NMR ($CHCl_3$) τ −0.90 (m, NH), 5.77 (q, C-CH$_2$-O), 6.10 (s, OH), 8.44 (s, CH$_3$), 8.50 (s, CH$_3$), and 8.72 (t, CH$_3$-C-O).

Found: C, 50.18; H, 6.08; N, 6.47%. Calcd for $C_9H_{13}NO_5$: C, 50.23; H, 6.09; N, 6.51%.

Nitrosation of α-Carboxy-β-carbethoxy-γ,γ-dimethylbutyrolactone (3). A solution of sodium nitrite (10 g) in water (20 m*l*) was added to a solution of **3** (20 g)[3] in glacial acetic acid (36 m*l*) with stirring at 0—5°C. After the mixture had been stirred for 30 min at 10—15°C, it was diluted with water (170 m*l*), stirred for an additional 1 hr, and the organic layer was taken up in ether. The extract was washed several times with aqueous sodium chloride, once with a small portion of 5% aqueous sodium bicarbonate, twice with aqueous sodium chloride, and dried over Na_2SO_4. Removal of the solvent gave 16.0 g of slightly greenish yellow, neutral liquid (Mixture I), which showed a strong band at 2100 cm^{-1}. The tlc of the Mixture I showed four spots (R_f values: 0.70, 0.35, 0.26, and 0.16).

Separation of each components of the Mixture I was carried out as follows: the ethereal solution of the Mixture I (16.0 g) extracted several times with 5% aqueous sodium bicarbonate (2.5 *l*), washed with aqueous sodium chloride, and dried over Na_2SO_4. Evaporation of the solvent gave 4.0 g of pale greenish yellow liquid (Mixture II) which was chromatographed on thin layer

19) All melting and boiling points are uncorrected. Infrared spectra were determined on a Hitachi EPI-S$_2$ and ultraviolet spectra on a Hitachi ESP-3T spectrophotometer. Thin layer chromatography (tlc) on baked silica gel G (E. Merck) as the support with acetone-benzene (1 : 8) as the solvent and with iodine for detection purposes was employed throughout the experiments. The NMR spectra were obtained on Japan Electron Optics Laboratory spectrometer (JNM-C-60) in chloroform with TMS as internal standard. The molecular weight determinations were made on a Hitachi RMU-6E mass spectrometer using a cold injection port. Microanalyses were performed by Miss H. Nisino of our laboratory.

plate to give two spots (R_f: 0.70 and 0.16). The Mixture II (4.0 g) dissolved in ether was extracted with aqueous sodium carbonate (100 ml), washed with aqueous sodium chloride, and dried over Na_2SO_4. Removal of the ether gave slightly colored liquid (**4**) (2.5 g) which gave a spot (R_f 0.70) on silica gel plate. Analytically pure sample of **4** was obtained from the spots (R_f 0.70) on silica gel plates arranged to 0.8 mm thickness. The spectral data were as follows: IR 3000—2850, 2100, 1765—1740, 1390, 1375, 1360, 1305, 1240, 1080, 1050, 1020, 980, 930, 910, 730 cm^{-1}; UV max (95% EtOH) 217 mμ (ε 4230) and 255 mμ (ε 7050); NMR ($HCCl_3$) τ 5.27 (q, C-C$\underline{H}_2$-O), 7.84 (s, C$\underline{H}_3$COO), 8.40 (s, C$\underline{H}_3$), 8.62 (s, C$\underline{H}_3$), 8.68 (t, C$\underline{H}_3$-C-O).

Found: C, 49.26; H, 5.42; N, 9.97%. Calcd for $C_{11}H_{14}N_2O_6$: C, 48.89; H, 5.22; N, 10.37%.

The extracts with aqueous sodium carbonate were acidified with dilute sulfuric acid to pH 6.5—7 and extracted with ether. The extracts were washed with aqueous sodium chloride and dried over sodium sulfate, and the solvent was removed *in vacuo*. The remaining viscous oil (1.0 g) (Mixture III) gave an elongated elliptical spot (R_f 0.16). From the head part of the tlc spot of the Mixture III, α-nitrolactone (**8**) (0.3 g), white solid, mp 66.5°C was obtained, after repeated purification by tlc on silica gel G plates (0.8 mm thickness). The spectral data of **8** were as follows: IR (Nujol mull): 1785, 1727, 1656, 1470—1445, 1395—1390, 1375, 1315, 1300, 1265, 1245—1220, 1200, 1175, 1115, 1095, 1025, 955, 900, 860, 845, 820, 790, 765, 705 cm^{-1}; NMR ($HCCl_3$) τ 4.11 (d, $\underline{H}_\alpha$), 5.62 (q, C-C$\underline{H}_2$-O), 5.92 (d, $\underline{H}_\beta$), 8.22 (s, C$\underline{H}_3$), 8.60 (s, C$\underline{H}_3$), and 8.67 (t, C$\underline{H}_3$-C-O).

Found: C, 46.63; H, 5.84%. Calcd for $C_9H_{13}NO_6$: C, 46.75; H, 5.60%.

From the tail part of the tlc spot (R_f 0.16) of the Mixture III, azoxylactone (**9**) (0.7 g), pale yellow solid, mp 120—123°C, was obtained, after repeated purification by tlc on silica gel G plates (0.8 mm thickness). The spectral data of **9** were as follows: IR (Nujol mull): 1785, 1750, 1640, 1480, 1470, 1450, 1395, 1375, 1305—1200, 1105—1010, 960, 935—930, 900, 865, 830, 780, 740 cm^{-1}; NMR ($HCCl_3$) τ 8.9—8.2 (*gem* C$\underline{H}_3$, C$\underline{H}_3$-C-O) and 5.4—6.1 (C-C$\underline{H}_2$-O).

Found: C, 52.77; H, 5.65; N, 6.86%. Calcd for $C_{15}H_{24}N_2O_9$: C, 52.42; H, 5.86; N, 6.79%.

The alkaline extracts (2.5 *l*) from the Mixture I were neutralized with dilute sulfuric acid to pH 6.5—7 and extracted with ether. The ethereal extracts were washed with aqueous sodium chloride, dried, and concentrated. The tlc of the residual pale yellow oil (Mixture IV) (11.0 g) showed the presence of two components (R_f 0.35 and 0.26). Separation was carried out by extracting the ethereal solution of the Mixture IV with aqueous sodium carbonate. From the ether layer there was obtained 1.0 g of pale yellow, neutral oil (R_f 0.35). The analytical sample was obtained by passing the crude oil through an aluminum oxide G (E. Merck) column using acetone to remove a trace of the impurity (R_f 0.26). The spectral data of **5** were as follows: IR 3500—3000 (broad), 3000—2800, 2100, 1740—1715, 1470, 1385, 1355, 1255, 1190, 1090—1070, 1027, 905, 735 cm^{-1}; NMR ($HCCl_3$) τ 5.60 (s, O$\underline{H}$), 5.62 (q, C-C$\underline{H}_2$-O), 8.46 (s, C$\underline{H}_3$), 8.65 (s, C$\underline{H}_3$), and 8.65 (t, C$\underline{H}_3$-C-O).

Found: C, 47.61; H, 5.55; N, 11.70%. Calcd for $C_9H_{12}N_2O_5$: C, 47.37; H, 5.35; N, 12.28%.

On the other hand, the alkaline layer was neutralized with dilute sulfuric acid, washed, and dried over Na_2SO_4. Removal of the solvent gave 8.0 g of slightly colored oil (R_f 0.26), which was solidified upon standing for several days, to white crystals (**7**), mp 71.5—73°C (benzene - *n*-hexane). The structure was confirmed by comparison of the infrared spectrum with that of authentic **7**.

Ethyl α-Diazoparaconates (4 and 5). These were obtained from the α-hydroxyaminolactone (**7**) in 85—90% yield by treating with sodium nitrite (2 mol) in an aqueous acetic acid at 3—7°C for 3 hr. Separation of **4** and **5** was carried out in a manner described above. Both **4** and **5** (estimated to be 5 : 1) were identified by their R_f values of tlc and their infrared spectra, which were in good agreement with those of the reference compounds (**4** and **5**) obtained in the above experiment.

Ethyl α-Nitro-γ,γ-dimethylparaconate (8). To a solution of concentrated nitric acid (0.3 ml) and glacial acetic acid (3 ml) ethyl α-hydroxyamino-γ,γ-dimethylaconate (**7**) (200 mg) was added at 2—5°C with stirring for 20 min. The cooled mixture was poured into 50 ml of ice water. After 15 min of stirring, the precipitate was filtered, washed with water, and dried. Recrystallization from *n*-hexane - benzene (4 : 1) gave 65 mg (*ca.* 30%) of **8**, white crystal, mp 66.0—66.5°C, whose infrared spectrum was identical with that of the reference compound obtained as described in the above paragraph.

Azoxylactone (9) from Ethyl α-Hydroxyamino-γ,γ-dimethylaconate (7). A mixture of **7** (200 mg) and manganese dioxide[20] (1.0 g) in acetone (10 ml) was kept at room temperature for 2 days. The manganese dioxide was filtered off and the filtrate was concentrated under vacuum to give 150 mg of **9**, pale yellow solid, mp 118—123°C, identified by comparison with the authentic sample obtained as described in the preceding paragraph.

Ethyl α,β-Epoxy-γ,γ-dimethylparaconate (6) from α-Diazolactones (4 and 5). A mixture of **4** and **5** (5 : 1) (500 mg) was dissolved in phosphoric acid (0.5 ml) at room temperature, and immediately colorless gas was evolved. When the gas evolution was ceased, the mixture was poured into 50 ml of saturated aqueous sodium chloride with stirring, and extracted with ether. The extract was washed with water, dried over Na_2SO_4 and the solvent was stripped *in vacuo*. Upon distillation of the residual oil, there was obtained 340 mg (89.1%) of **6**, bp 100°C/2 mmHg, n_D^{20} 1.4458; IR 1780 (lactone C=O), 1740 (ester C=O), and 1250 and 865 (epoxy) cm^{-1}; NMR ($HCCl_3$) τ 5.63 (q, C-C$\underline{H}_2$-O), 5.83 (s, $\underline{H}$), 8.33 (s, C$\underline{H}_3$), 8.42 (s, C$\underline{H}_3$), and 8.67 (t, C$\underline{H}_3$-C-O).

Found: C, 54.03; H, 6.16%. Calcd for $C_9H_{12}O_5$: C, 54.00; H, 6.04%.

α,β-Epoxy-γ,γ-dimethylparaconic Acid (11). To a solution of γ,γ-dimethylaconic acid (**10**)[13] (2.4 g) in methanol (36.6 ml) and 15% hydrogen peroxide solution (20.4 ml) 16% aqueous sodium hydroxide (34.2 g) was added at 20—25°C. The mixture was kept at room temperature for overnight, then poured into water (200 ml), acidified with diluted sulfuric acid,

20) J. Attenburrow, A. F. B. Cameron, J. H. Chapman, R. M. Evans, B. A. Hems, A. B. A. Jansen and T. Walker, *J. Chem. Soc.*, **1952**, 1094.

and extracted with ether. The extracts were washed with water, dried over Na_2SO_4, and evaporated to dryness to give 1.8 g (71%) of **11**, white needles, mp 120°C (methanol-benzene); IR 1740 (lactone, carboxylic acid C=O) and 1250, 920, and 860 (epoxy) cm^{-1}.

Found: C, 48.49; H, 4.79%. Calcd for $C_7H_8O_5$: C, 48.84; H, 4.68%.

Esterification of α,β-Epoxy-γ,γ-dimethylparaconic Acid (11). A solution of α,β-epoxyparaconic acid (**11**) (300 mg) in ethyl orthoformate (2 m*l*) was refluxed for 8 hr and then distilled *in vacuo* to give **6** (250 mg), bp 100°C/2 mmHg, whose infrared spectrum was in good agreement with that of the reference compound **6** obtained as described in the preceding paragraph.

Ethyl α-Hydroxy-γ,γ-dimethylaconate (12). Method A. A solution of ethyl α-hydroxyamino-γ,γ-dimethylaconate (**7**) (2.0 g) in concentrated hydrochloric acid (20 m*l*) was kept at 25—30°C for 3 days. Then, the mixture was neutralized with 2 N aqueous sodium hydroxide to pH 4—5 and extracted with ether. The extracts were washed with saturated aqueous sodium chloride, dried over $MgSO_4$, and evaporated to dryness to give **12** (1.0 g, 55%), mp 71.0°C (lit.[15] mp 73.0—73.5°C); IR (Nujol mull) 1750 (lactone C=O), 1710 (ester C=O), and 1660 (C=C) cm^{-1}; NMR ($HCCl_3$) 2.62 (s, O<u>H</u>), 5.62 (q, C-C<u>H</u>$_2$-O), 8.38 (s, *gem* C<u>H</u>$_3$), and 8.60 (t, C<u>H</u>$_3$-C-O), 8.38 (s, *gem* C<u>H</u>$_3$), and 8.60 (t, C<u>H</u>$_3$-C-O). The microanalysis of **12** gave good result for carbon and hydrogen.

Method B. A mixture of ethyl α, β-epoxy-γ,γ-dimethylparaconate (**6**) (500 mg) and sodium trichloroacetate (500 mg) was heated to 97—135°C for 15 min, then poured into water (30 m*l*), and extracted with ether. The aqueous layer was acidified to pH 4—5 with diluted sulfuric acid and extracted with ether. This extracts were washed with saturated aqueous sodium chloride, dried over $MgSO_4$, and evaporated to dyness to afford **12** (300 mg, 60%), mp 71°C, which was identified by its infrared spectrum and by comparison with that of the authentic specimen obtained by Method A.

Preparation of the Derivatives (13, 14, and 15) of 12. The compounds (**13**, **14**, and **15**) were prepared as follows: **13** was obtained by treating **12** with diazomethane; **14** was prepared by refluxing **12** with ethyl orthoformate; **15** was prepared by refluxing **12** with acetic anhydride. The physical constants, microanalyses, and spectral data of these compounds are listed in Table 1.

Thermal Decomposition of Ethyl α-Hydroxyamino-γ,γ-dimethylaconate (7). The thermal decomposition of **7** (1.0 g) carried out at 140—160°C/25 mmHg for 3 hr and then the mixture was taken up in ether. The ether layer was extracted with aqueous sodium bicarbonate, washed with water, and dried over Na_2SO_4. After removal of the solvent, the residue was distilled to give 380 mg (53%) of ethyl isopropylidenecyanoacetate (**17**), M^+ 153 *m/e*, bp 99—100°C/8.5 mmHg (lit.[17] 116—118°C/11 mmHg), which was identical in all respects with authentic specimen (**17**).[17] Small amount of the distillate, bp 100—130°C/2 mmHg, solidified in the side tube of Claisen flask or in the receiver as colorless needles. This was recrystallized from ethanol to afford ethyl α-amino-γ,γ-dimethylaconate (**16**) as colorless needles, yield 160 mg (17%), M^+ 199 *m/e*, mp 120°C; UV max (95% EtOH) 297.5 mμ (ε 11600); IR (Nujol mull) 3450 and 3350 (NH_2), 1760 (lactone C=O), 1690 (ester C=O), 1635 (C=C), and 1583 (NH_2) cm^{-1}; NMR ($HCCl_3$) τ 4.42 (broad N<u>H</u>$_2$), 5.71 (q, C-C<u>H</u>$_2$-O), 8.40 (s, *gem* C<u>H</u>$_3$), and 8.65 (t, C<u>H</u>$_3$-C-O).

Found: C, 54.22; H, 6.63; N, 7.11%. Calcd for $C_9H_{13}NO_4$: C, 54.26; H, 6.58; N, 7.03%.

The alkaline extract was acidified with dilute sulfuric acid to pH 6.5—7 and extracted with ether. The extracts were washed with saturated aqueous sodium chloride and dried over Na_2SO_4. After removal of the solvent, there was obtained 130 mg (23%) of isopropylidenecyanoacetic acid (**18**), mp 129—130.5°C (lit.[18] 137°C). The confirmation of the structure was made based on the spectral data and from the conversion of **18** into **17** by the action of ethyl orthoformate.[14]

Ethyl α-(*N*-Acetoxy-*N*-acetyl)amino-γ,γ-dimethylaconate (19). A solution of **7** (500 mg) in acetic anhydride (3 m*l*) was refluxed for 4 hr. The solvent was removed under reduced pressure. Distillation of the residue gave 700 mg (*ca.* 95%) of **19**, bp 145°C/2.5 mmHg; IR 1805 and 1775 (lactone C=O), 1725 (ester C=O), and 1650 (C=C) cm^{-1}; NMR ($HCCl_3$) τ 5.81 (q, C-C<u>H</u>$_2$-O), 7.75 (s, C<u>H</u>$_3$-CO-O-N), 7.88 (s, C<u>H</u>$_3$CO-N), 8.37 (s, *gem* C<u>H</u>$_3$), and 8.68 (t, C<u>H</u>$_3$-C-O).

Found: C, 52.39; H, 5.97%. Calcd for $C_{13}H_{17}NO_7$: C, 52.17; H, 5.73%.

Thermal Decomposition of 19. The thermal decomposition of **19** (500 mg) was carried out at 140—160°C/ 25 mmHg for 2 hr to give exclusively a fraction boiling at 98—100°C/8.5 mmHg, whose infrared spectrum was superimposable in very fine detail with that of the authentic sample (**17**) obtained in the above paragraph.

We are indebted to Dr. Shigezo Shimokawa, Hokkaido University, for the measurement of the NMR spectra.

BULLETIN OF THE CHEMICAL SOCIETY OF JAPAN VOL. 41 2713—2718 (1968)

Photochemical Hydrolysis of Barbitals*1

Yoshio OTSUJI, Tokuyuki KURODA and Eiji IMOTO

Department of Applied Chemistry, Faculty of Engineering, University of Osaka Prefecture, Sakai-shi, Osaka

(Received April 19, 1968)

The irradiation of barbital (BA) and *N,N'*-dimethylbarbital (DMBA) in aqueous alkaline media gave diethylacetylurea and *N,N'*-dimethyldiethylmalonamide respectively. On the basis of the results of kinetic studies, the above photochemical hydrolyses of BA and DMBA were shown to be an attack of the hydroxide ion on the singlet excited states of BA monoanion and DMBA respectively. Such nucleophilic reagents as amines, mercaptide, and cyanide ions retarded the photochemical hydrolyses by quenching the excited state of the substrates.

A few examples of photochemical solvolysis reactions have hitherto been reported in the literature. Zimmerman and his co-workers[1] have observed that certain benzyl acetates and trityl ethers are readily solvolyzed upon irradiation in aqueous media. Havinga and his co-workers[2] have reported that the hydrolysis of certain aromatic phosphate and sulfate esters is accelerated by light. Recently, Barltrop and Schofield[3] have found that the substituted aromatic carbamate esters of glycine are hydrolyzed upon the irradiation of the aqueous solutions. The driving force of these photochemical solvolysis reactions has been supposed to be a decrease in electron density around the reaction center through the $\pi \rightarrow \pi^*$ excitation process of aromatic compounds.[4]

During the course of our studies of the chemistry of barbitals, we found that barbital is readily hydrolyzed to diethylacetylurea upon the irradiation of its aqueous sodium hydroxide solution with ultraviolet light. This photochemical reaction constitutes a very rare example of a photochemical solvolysis in which an aromatic ring is not involved as an entity of the excitation. This paper will describe our investigation of the photochemical reactions of barbital and its derivatives in aqueous media.

Results and Discussion

Photoproducts. When a solution of barbital (BA) in a 0.1 N aqueous sodium hydroxide was irradiated with a low-pressure mercury arc at room temperature, crystals gradually appeared on the wall of the reaction vessel. After several hour's irradiation, the collection of the deposited crystals and their recrystallization gave diethylacetylurea (**1**) in a 95% yield. The structure of the compound **1** was confirmed by a comparison of its physicochemical properties with those of an authentic sample and by elemental analysis. However, even when the solution was heated at 80°C in the dark for two periods of time the same as the light reaction period, the starting material was recovered in an almost quantitative yield. These facts clearly demonstrate that the hydrolysis of barbital is accelerated by irradiation with ultraviolet light. The urea, **1**, is supposed to be formed by the attack of the hydroxide ion on the carbonyl carbon atom at the 4 position of BA. The first intermediate produced by this reaction would be the keto acid (**2**). This keto acid **2** might be unstable under the reaction conditions and might be decomposed spontaneously to the isolable product **1**.

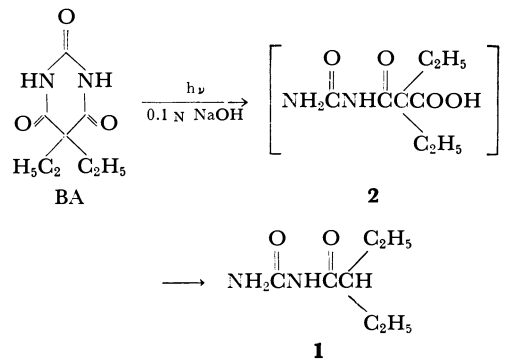

*1 This paper constitutes Part I of a series of papers entitled "Photochemistry of Heterocyclic Compounds."

1) H. E. Zimmerman and S. Somasekhara, *J. Am. Chem. Soc.*, **85**, 922 (1963); H. E. Zimmerman and V. E. Sandel, *ibid.*, **85**, 915 (1963).

2) E. O. Havinga, R. O. de Jongh and W. Dorst, *Rec. Trav. Chim.*, **75**, 378 (1956); E. O. Havinga, *Chimia*, **16**, 145 (1962); D. A. de Bie and E. O. Havinga, *Tetrahedron*, **21**, 2359 (1965).

3) J. A. Barltrop and P. Schofield, *J. Chem. Soc.*, **1965**, 4758.

4) For a list and the mechanism of such reactions, see D. C. Nechers, "Mechanistic Organic Photochemistry," Reinhold Publishing Co., New York, N. Y. (1967), pp. 253—260.

Table 1. The photoreaction products of BA in the presence of various nucleophilic reagents

Irradiated compound	Nucleophile	Product	Yield %	Irradiation time, hr
BA	0.1 N NaOH	Diethylacetylurea	95	14
	$(CH_3)_2NH$	Diethylacetylurea	35	66
		N,N-Dimethylbiuret	35	
	$C_2H_5NH_2$	Diethylacetylurea	30	66
	KCN	Diethylacetylurea	75	110
	C_2H_5SNa	Diethylacetylurea	—	90
DMBA	0.1 N NaOH	*N,N'*-Dimethyldiethylmalonamide	67	68

Since we suspected that this photochemical hydrolysis would have the nature of a nucleophilic solvolysis of BA, the photoreactions of BA were undertaken in the presence of various nucleophilic reagents. The results are summarized in Table 1.

No photochemical reaction was observed upon the irradiation of BA in water or in an aqueous hydrochloric acid, BA being recovered in both cases. The irradiation of an aqueous solution of BA in the presence of ethylamine, potassium cyanide, and sodium ethylmercaptide produced the same product, diethylacetylurea, as that obtained in the photoreaction of BA and sodium hydroxide. However, when an aqueous solution of BA in the presence of dimethylamine was irradiated, a 1 : 1 mixture of the urea **1** and *N,N*-dimethylbiuret (**3**) was obtained in a 70% yield.

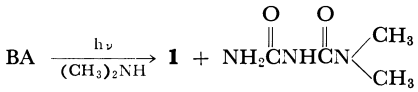

3

Unfortunately, the mechanism of the formation of the biuret, **3**, could not be elucidated in this investigation; therefore, it will not be discussed further here.

The photoreaction of *N,N'*-dimethyl barbital (DMBA) was also investigated. The irradiation of a suspension of DMBA in a 0.1 N aqueous sodium hydroxide with stirring afforded *N,N'*-dimethyl diethyl malonamide (**4**) in a 67% yield. This compound is supposed to be formed by the attack of the hydroxide ion on the carbonyl carbon at the 2 position of DMBA.

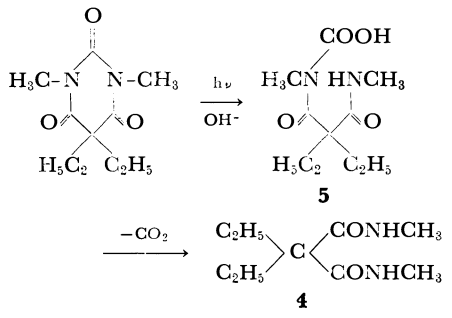

5 **4**

The hydrolysis of BA has been known to proceed with some difficulty in the dark to give **1** along with diethylacetamide (**6**) and diethylacetic acid (**7**), the relative yields of these compounds depending on the reaction conditions.[5] For this reason, the

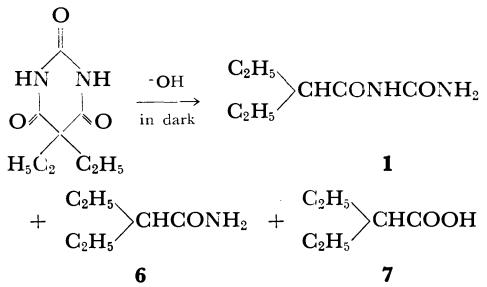

1 **6** **7**

photochemical reactions reported in this paper will provide a convenient method for the preparation of the compounds of the **1**, **6**, and **7** types.

Light-absorbing Species during the Photochemical Hydrolysis of BA and DMBA. There exist tautomeric equilibria for BA in an aqueous solution; the plausible tautomeric forms include **8**, **9** and **10**, among others:

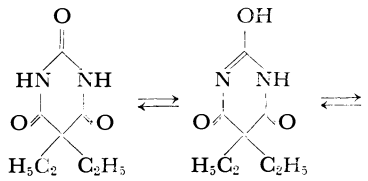

8 **9**

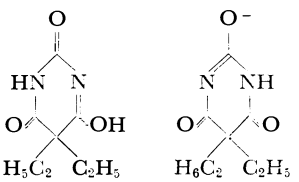

10 **11**

Sato[6] has concluded, on the basis of his molecular orbital calculations, that **9** is the most likely form in

5) a) H. Ruhkopf, *Ber.*, **73**, 938 (1940); b) E. H. Volwiler and D. L. Tabern, *J. Am. Chem. Soc.*, **58**, 1352 (1936); c) M. Freifelder, A. O. Geiszler and G. E. Stone, *J. Org. Chem.*, **26**, 203 (1961).

6) Y. Sato, *Nippon Kagaku Zassi (J. Chem. Soc. Japan, Pure Chem. Sect.)*, **78**, 924 (1957).

an aqueous solution. Furthermore, since $pK_1=7.85$ and $pK_2=12.7$ for BA,[7] BA would exist exclusively in the form of a monoanion of **9**, *i. e.*, **11** in a 0.1 N sodium hydroxide solution (pH ~11.3), in which most of the present experiments were carried out.

The spectral properties of BA were also studied in some detail. Figure 1 shows the ultraviolet spectra of $\sim 1\times10^{-4}$ M of BA in buffered aqueous solutions of various pH values. The absorbance at an absorption maximum of 240 mμ, As_{240}, decreased with a decrease in the pH values of the solutions. When As_{240} values were plotted against the concentrations of the monoanion of BA (BA^-) present in the solutions (the concentrations of BA^- were calculated from the pK_a of BA), a straight line passing through the origin was obtained, as is shown in Fig. 2. These results indicate that the only species which shows the absorption at 240 mμ is BA^-. From the data in Fig. 2, the molar extinction coefficient of BA^- was calculated to be 1.03×10^4.

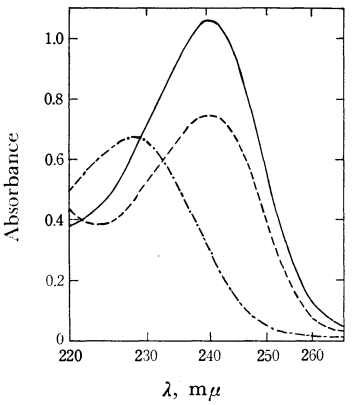

Fig. 1. Absorption spectra of BA and DMBA.
—— BA in 2×10^{-4} M NaOH
·—· DMBA in 2×10^{-4} M NaOH
---- BA in buffer solution at pH 8.27

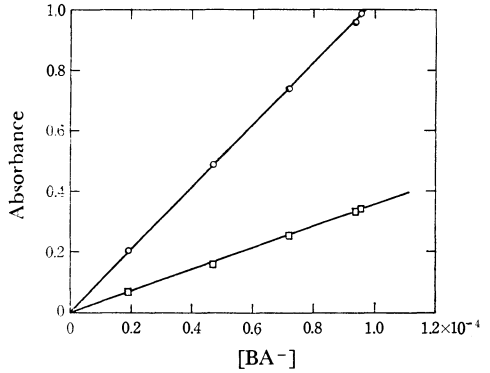

Fig. 2. Plots of absorbance *vs.* concentration of BA^-.
-○- at λ 240 mμ -□- at λ 254 mμ

The hydrolysis products of BA have no appreciable absorption at $\geq$240 mμ under the present reaction conditions, and the illuminating light used in our experiments was practically that of the wavelength at 254 mμ. Therefore, the above results also indicate that the only light-absorbing species during the photochemical hydrolysis of BA in an aqueous solution (pH>7.0) is BA^-.

The light-absorbing species of DMBA during the photochemical hydrolysis is apparently DMBA itself, since DMBA does not exhibit the tautomeric equilibria and its absorption maximum lies at 229 mμ ($\varepsilon_{229}=6.74\times10^3$); also, the hydrolysis products of DMBA has no absorption at $\geq$229 mμ under the present reaction conditions.

Kinetic Studies. In order to get some clue to the mechanism of the photochemical hydrolysis, kinetic studies of the hydrolysis of BA in the aqueous solutions were made under a variety of conditions.

If the rate of hydrolysis of BA is assumed to be proportional to the light intensity absorbed by BA^- (the only light-absorbing species present in the reaction system), then the rate of the reaction (and, hence, the rate of the disappearance of BA^-) is given by Eq. (1):

$$-\mathrm{d}[BA^-]/\mathrm{d}t = \Phi K I_{abs} \quad (1)$$

where Φ is the quantum yield for the reaction, and where K is a unit conversion factor which transforms the number of photons absorbed per second into moles per liter per photons absorbed. I_{abs} is expressed in terms of Lambert and Beer's law:

$$I_{abs} = I_0(1 - e^{-\varepsilon[BA^-]d}) \equiv I_0 A \quad (2)$$

where I_0 is the incident light intensity, ε is the molar extinction coefficient of BA^- at the wavelength band incoming from the illuminating light source, and d is the thickness of the reaction vessel through which the incident light passes. The combination of Eqs. (1) and (2), and the integration of the resulting equation, lead to:

$$[BA^-]_t + (\ln A)_t/\varepsilon d = -\Phi K I_0 t + C \quad (3)$$

where C is the integration constant.

If our assumption is correct, the plot of the values on the left side of Eq. (3) against the time should give a straight line. Thus, the relative quantum yield, Φ', defined by Eq. (4) can be calculated from the slope of the straight line:

$$\Phi' = \Phi K I_0 \quad (4)$$

In our experiments the values of $[BA^-]_t$, the concentrations of BA^- at a given time, t, were determined from the readings of As_{240} (see the previous section):

$$[BA^-]_t = (As_{240})_t/\varepsilon_{240} \quad (5)$$

The term of $(\ln A)_t/\varepsilon d$ was calculated by the use of Eq. (6):

7) Y. Sato, *ibid.*, **78**, 382 (1957).

$$(\ln A)_t/\varepsilon d = 2.303 \log (1 - e^{-\varepsilon[BA^-]_t d})/\varepsilon d \quad (6)$$

$\varepsilon = 3.55 \times 10^3$ was obtained from the data represented in Fig. 1 as the molar extinction coefficient of BA^- at 254 mμ (see the previous section and also the Experimental section). The d was measured as 3.5 cm.

The rate measurements for the hydrolysis of BA were carried out in buffered aqueous solutions of various pH values and in a 0.1 N sodium hydroxide solution. The plot of the $[BA^-]_t + (\ln A)_t/\varepsilon d$ function against the time furnished a straight line in every case. Typical data are shown in Fig. 3. The relative quantum yields, Φ', calculated from the slopes of the straight lines are summarized in Table 2. When a reciprocal of Φ' was plotted against a reciprocal of the hydroxide ion concentration, a straight line was obtained, as is shown in Fig. 4. This result demonstrates that the hydroxide ion may be involved in the rate-determining step of the reaction.

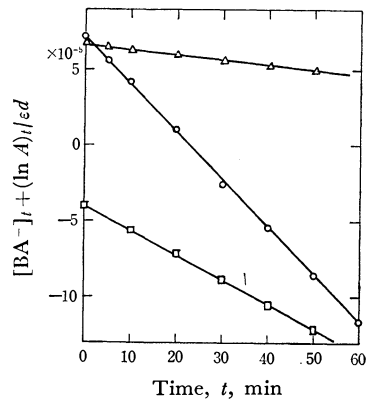

Fig. 3. Plots of Eq. (3) for BA^-.
-○- Reaction in 0.1 N NaOH
-△- Reaction in an aqueous solution containing dimethylamine
-□- Reaction in buffered solution at pH 7.70

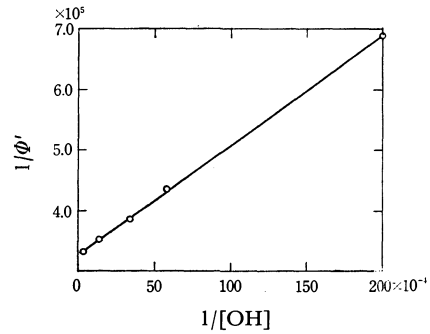

Fig. 4. Plot of $1/\Phi'$ *vs.* $1/[^-OH]$ in the photochemical hydrolysis of BA^-.

Table 2. Relative quantum yield, Φ'

I) Φ' for BA in aqueous solutions at various pH values

pH	$1/[OH^-]$	Φ'	$1/\Phi'$
7.70	200×10^4	1.47×10^{-6}	6.80×10^5
8.03	58.1×10^4	2.29×10^{-6}	4.38×10^5
8.46	34.7×10^4	2.59×10^{-6}	3.87×10^5
8.87	13.5×10^4	2.83×10^{-6}	3.53×10^5
9.50	3.16×10^4	3.01×10^{-6}	3.32×10^5

II) Φ' for the reactions of BA and DMBA with various nucleophiles

Irradiated compound	Nucleophile	Concn. mol/l	Φ'
BA	NaOH	2×10^{-4}	3.18×10^{-6}
	NaOH	2×10^{-4}	3.13×10^{-6}*
	C_2H_5SNa	3×10^{-3}	3.01×10^{-6}
	KCN	1×10^{-2}	2.79×10^{-6}
	KCN + NaOH	1×10^{-2} + 2×10^{-4}	2.85×10^{-6}
	$C_2H_5NH_2$	1×10^{-2}	0.552×10^{-6}
	$C_2H_5NH_2$ + NaOH	1×10^{-2} + 2×10^{-4}	0.552×10^{-6}
	$(CH_3)_2NH$	1×10^{-2}	0.333×10^{-6}
	$(CH_3)_2NH$ + NaOH	1×10^{-2} + 2×10^{-4}	0.333×10^{-6}
DMBA	NaOH	2×10^{-4}	0.367×10^{-6}

* This value was obtained under bubbling nitrogen.

The rates of the photochemical reactions of BA with various nucleophiles were also measured. The shapes of the spectra of BA in the presence of nucleophiles were similar to those in the buffered solutions represented in Fig. 1. Thus, the rates of the disappearance of BA^- were followed by measuring the As_{240} of BA^-, and the relative quantum yields were obtained as has been described for the reactions in the buffered solutions. A typical datum is shown in Fig. 3, while the results are summarized in Table 2. The Φ' decreased in the order of hydroxide ion $\geq$ sodium mercaptide $\geq$ potassium cyanide $>$ ethylamine $>$ dimethylamine. However, when the reactions of BA with various nucleophiles were carried out in the presence of sodium hydroxide, the relative quantum yields of the reactions remained at the same values as those in the absence of sodium hydroxide, as is shown in Table 2. This observation can be explained by noting that the excited state of BA^- may be partially quenched in a characteristic manner determined by the nature of the nucleophiles, and that the only attacking reagent in these photochemical reactions is actually the hydroxide ion, which does not practically quench the excited state of BA^- and which would have its strongest affinity for the excited state of BA^-.

A further important observation was that when the photochemical hydrolysis of BA in 0.1 N sodium hydroxide was carried out in a nitrogen stream, no change in the relative quantum yields

was observed (Table 2). This finding suggests that the photochemical hydrolysis of BA starts directly from its singlet excited state.

A kinetic study of the photochemical hydrolysis of DMBA was also made in a 0.1 N sodium hydroxide solution. The rate was measured by following the decrease in the As_{229} of DMBA. The relative quantum yield was obtained by the use of Eqs. (3) and (4). In this case ε was estimated to be 2.02×10^2 from the spectral data (ε was taken to be equal to the molar extinction coefficient of DMBA at 254 mμ under the present reaction conditions). The approximate ratio of the relative quantum yield of BA$^-$ to DMBA was 1 : 0.1 (see Table 2).

Mechanistic Pathways. The results and discussion presented earlier suggest that the pathways outlined in Chart 1 are involved in the photochemical hydrolysis reactions of BA in aqueous solutions. The symbols used in Chart 1 have the usual meanings, while Q represents any quencher participating in the reactions. The reactions probably start from the singlet excited state of BA$^-$ (BA$^-$*). The BA$^-$* reacts with hydroxide ion to give a 1 : 1 complex of the type X. The complex may be formed by the addition of the hydroxide ion to the carbonyl carbon atom at the 4 position rather than the 2 position of BA$^-$, since the accumulation of a negative charge around the carbonyl group at the 2 position prevents the addition of the hydroxide ion to that group. The complex thus formed collapses spontaneously to the hydrolyzed product, **1**, through the keto acid, **2**. The nucleophilic reagents other than hydroxide ion act as quenchers for BA$^-$* and partially prevent the formation of the complex.

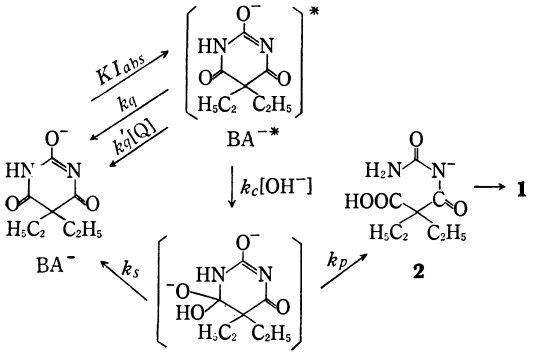

Chart 1

Making the usual steady-state assumption for BA$^-$* and the complex X, the rate equation (7) can be obtained from the above reaction scheme:

$$-\frac{d[BA^-]}{dt}=\frac{d(\mathbf{2})}{dt}=\frac{k_ck_p[^-OH]KI_{abs}}{(k_s+k_p)[k_q+k'_q[Q]+k_c[^-OH]]} \quad (7)$$

The quantum yield and the relative quantum yield defined in this investigation for the disappearance of BA$^-$ become, then, Eqs. (8) and (9) respectively:

$$\Phi=\frac{k_ck_p[^-OH]}{(k_s+k_p)[k_q+k'_q[Q]+k_c[^-OH]]} \quad (8)$$

$$\Phi'=\frac{k_ck_p[^-OH]}{(k_s+k_p)[k_q+k'_q[Q]+k_c[^-OH]]}\times KI_0 \quad (9)$$

When $[Q]\simeq0$, *i. e.*, when the photochemical hydrolysis is carried out in buffered solutions, the relation of Eq. (10) is obtained:

$$\frac{1}{\Phi'}=\frac{1}{KI_0}\frac{k_s+k_p}{k_p}+\frac{k_q(k_sk_p)}{k_ck_p[^-OH]} \quad (10)$$

Our observations are consistent with this theoretical relationship (see Fig. 4). Since at present we do not have much information about the quenching ability of the nucleophiles, no detailed discussion is given in this paper. However, amines are often known to act as effective quenchers of excited-state molecules.

In the case of DMBA, the reaction proceeds similarly except that a complex of the type of (**12**)

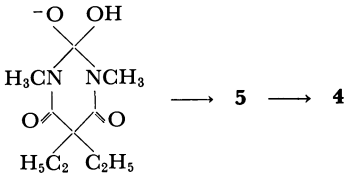

12

may be formed between the carbonyl carbon atom at the 2 position and the hydroxide ion. There is no reason for preventing the addition of the hydroxide ion to that position, because no tautomeric equilibrium exists in this compound and, hence, no accumulation of negative charge around the carbonyl group at the 2 position can be expected. The complex thus produced collapses to the expected product.

Experimental

The melting points are uncorrected. The infrared spectra were recorded with a Hitachi EPI-S2 infrared spectrometer. The ultraviolet spectra were obtained with a Hitachi recording spectrophotometer. The microanalysis were performed with a Yanagimoto MT-1 CHN Corder.

Materials. Barbital (BA) was of a Nakarai reagent grade and was purified by recrystallization from ethanol before use. *N,N'*-Dimethylbarbital (DMBA) was prepared by the method of Dox.[8] The other reagents were purchased from various companies and were purified by recrystallization or distillation.

Photochemical Hydrolysis of Barbital (BA). A solution of 500 mg of BA in 100 m*l* of 0.1 N aqueous sodium hydroxide in a quartz vessel was irradiated for 14 hr with a 15-W low-pressure mercury arc placed at

8) W. Dox, *J. Am. Chem. Soc.*, **58**, 1633 (1936).

a distance of 10 cm. During irradiation, the product deposited out on the surface of the vessel as crystals. After irradiation, the crystals thus produced were collected by filtration and recrystallized from ethanol, mp 205—206°C. The product, 400 mg (95%), was identified as diethylacetylurea by the elemental analysis and by comparison with an authentic sample prepared by the method of Volwiler and Tabern,[9] which was found to be identical in every respect.

Found: C, 53.29; H, 9.17; N, 17.81%. Calcd for $C_7H_{14}N_2O_2$: C, 53.14; H, 8.92; N, 17.71%.

An aqueous solution of BA containing ethylamine, potassium cyanide, or sodium ethylmercaptide was irradiated similarly. The product isolated was diethylacetylurea in all of the above cases.

A solution containing 1 g of BA, 5 m*l* of 40% dimethylamine, and 100 m*l* of water was also irradiated in a similar manner. After 66 hrs' irradiation, the crystals which had deposited on the surface of the vessel were collected by filtration and identified as diethylacetylurea. The filtrate was evaporated to dryness under reduced pressure; the recrystallization of the residue gave 250 mg (35%) of *N,N*-dimethylbuiret, mp 170—171°C. The structure of this compound was confirmed by the elemental analysis and by comparison with an authentic sample prepared by the method of Davis and Blanchard,[10] which was found to be identical in every respect.

Found: C, 36.89; H, 7.14; N, 32.02%. Calcd for $C_4H_9N_3O_2$: C, 36.63; H, 6.92; N, 32.05%.

Hydrolysis of Barbital in the Dark. A solution of 500 mg of BA in 30 m*l* of 0.1 N aqueous sodium hydroxide was allowed to stand at 80°C for 17 hr. The mixture was then acidified with a dilute hydrochloric acid under cooling. The precipitated crystals were collected by filtration and found to be barbital. The evaporation of the filtrate also gave barbital. The total amount of barbital recovered was 350 mg (70%).

Photochemical Hydrolysis of *N,N'*-Dimethylbarbital (DMBA). Since the solubility of DMBA in water was too small to make a homogeneous aqueous solution with a relatively high concentration, the experiment was carried out as follows. A mixture of 1.2 g of DMBA in 100 m*l* of 0.1 N aqueous sodium hydroxide in a quartz vessel, where a small amount of DMBA remained insoluble as an oil, was irradiated in a manner similar to that described above, while being stirred with a magnetic stirrer. The oil, DMBA, went into solution with irradiation. After 68 hr's irradiation, although a very small amount of the oil still remained insoluble, the reaction mixture was neutralized with a dilute hydrochloric acid, and extracted with ether and then with chloroform. Both extracts were dried over sodium sulfate. The evaporation of the ether extract gave 100 mg (8%) of the starting materials, DMBA. The evaporation of the chloroform extract under reduced pressure afforded, after recrystallization from benzene, 0.7 g (67%) of *N,N'*-dimethylmalonamide; mp 149—150°C, IR 3300, 1650, 1530 cm^{-1} (KBr).

Found: C, 58.07; H, 9.91; N, 14.80%. Calcd for $C_9H_{18}N_2O_2$: C, 58.03; H, 9.74; N, 15.04%.

A mixture of 1.1 g of DMBA in 100 m*l* of water was irradiated for 63 hr in a manner similar to that described above. When the mixture was then worked up similarly, the starting material, DMBA, was recovered in almost a quantitative yield.

Kinetic Measurements. An aqueous solution (100 m*l*, 10^{-4} M) of BA or DMBA was placed in a quartz tube of 3.5 cm in diameter and 10 cm long. The solutions were irradiated at room temperature with a 15 W low-pressure mercury arc placed 30 cm from the samples. Four-m*l* portions of the solutions were pipetted into a spectrophotometric cell at intervals. The hydrolysis rates for the samples were followed by measuring the decreases in the absorbance at 240 mμ in the case of the BA's, and at 229 mμ in the case of the DMBA's with a Hitachi Perkin-Elmer 139 UV-Vis spectrophotometer. Special care was taken to fix a relative position between the reaction vessel and the light source so that the irradiation was carried out by the light beam of a constant intensity throughout a whole series of samples for which the kinetic studies were made. For this reason, the kinetic data obtained in this investigation were always reproducible.

Since an unfiltered light beam was used for irradiation, no attempt was made to calculate the exact quantum yields for the reactions. However, it was found from the spectral examination that the light source used radiates mostly the light beam at 2537Å in the region where the absorption spectra of the samples were detected.

9) E. H. Volwiler and D. L. Tabern, *J. Am. Chem. Soc.*, **58**, 1352 (1936).

10) T. L. Davis and K. C. Blanchard, *ibid.*, **51**, 1804 (1929).

BULLETIN OF THE CHEMICAL SOCIETY OF JAPAN VOL. 41 2719—2722 (1968)

Synthesis of 3-Vinylpyrene by Wittig's Reaction, and Syntheses and Electrical Properties of Polyvinylpyrene and Its Charge Transfer Complexes

Kiyoshi TANIKAWA, Takashi ISHIZUKA, Kojiro SUZUKI, Shigekazu KUSABAYASHI and Hiroshi MIKAWA

Department of Chemical Technology, Faculty of Engineering, Osaka University, Higashinoda, Miyakojima, Osaka

(Received April 19, 1968)

Using Wittig's reaction, we synthesized 3-vinylpyrene from pyrene-3-aldehyde in 76% yield. 3-Vinylpyrene monomer was polymerized by benzoylperoxide or di-*t*-butylperoxide catalysts. Each polymer had a melting point, being observed by the method of polarizing hot stage microscopic examination. X-ray examination showed that the polymer was crystalline, although rather poor. The charge transfer complexes, containing polyvinylpyrene as an electron donor, and iodine, tetracyanoethylene or tetracyanoquinodimethane as an electron acceptor, were prepared, each having the composition of pyrene nucleus : acceptor=16 : 3, 15 : 2, 15 : 2, respectively. Electrical conductivities of the complexes at 25°C, ρ_{25}, and band gap energies, ε, were 1.3×10^{8} Ωcm, 0.80 eV; 4.5×10^{12} Ωcm, 1.32 eV; 1.1×10^{14} Ωcm, 1.34 eV, respectively. Each complex showed ohmic current-voltage characteristics in an appropriate temperature range.

Electrical properties of several vinyl polymers having large π electron systems and of their charge transfer complexes have been reported.[1,2] In order to investigate the electrical properties[3] of polyvinylpyrene (PVP), a vinyl polymer hitherto known having largest π electron systems on a polymer chain, we synthesized PVP and its charge transfer complexes.

Synthesis of 3-Vinylpyrene. 3-Vinylpyrene monomer is known and synthesized by the dehydration of 3-(1-hydroxyethyl)pyrene with Al_2O_3.[4] The product obtained by this method is, however, difficult to purify and the yield is poor. Al_2O_3 employed by us yielded ethylpyrene (isolated and identified) as a by-product, which was very difficult to be separated from 3-vinylpyrene. As reported in the present paper, we synthesized first pyrene-3-aldehyde (II) from pyrene (I) by Vilsmeier's reaction,[5] and then 3-vinylpyrene (III) by Wittig's reaction from the aldehyde.

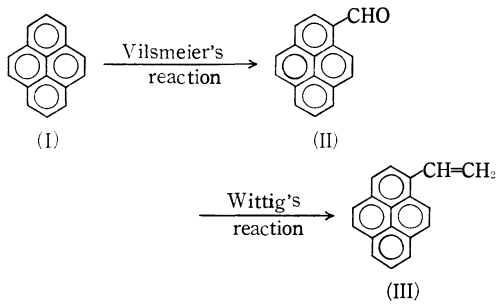

Both the yield and the quality of 3-vinylpyrene were much improved by using this synthesis method (76% and mp 88—89°C). Although methylenetriphenylphosphorane was synthesized in ether solution, the betaine intermediate obtained from pyrene and methylenetriphenylphosphorane had moderate stability and the decomposition of the betaine to 3-vinylpyrene was effected only at the boiling temperature of tetrahydrofuran (THF).

Synthesis and Properties of Polyvinylpyrene. The polymerization of 3-vinylpyrene was carried out by radical initiators, benzoylperoxide (BPO) or di-*t*-butylperoxide (DTBP), in benzene, toluene or xylene.

Although the polymerization of 3-vinylpyrene by BPO in benzene at 80°C was slow, the polymer obtained had moderate degree of polymerization ($[\eta]\sim0.1$ in THF at 25°C). By the use of DTBP catalyst in xylene at 140°C, however, the conversion was higher and the polymer began to precipitate in xylene after several hours. The polymer obtained in xylene was somewhat colored and the viscosity was lower, having lower degree

1) Y. Hayashi, M. Kuroda, T. Imura and A. Inami, *Chem. High Polymers*, **21**, 577 (1964); H. Inoue, K. Noda, T. Takiuchi and E. Imoto, *Kogyo Kagaku Zasshi (J. Chem. Soc. Japan, Ind. Chem. Sect.)*, **65**, 1286 (1962); W. Slough, *Trans. Faraday Soc.*, **58**, 2360 (1962).

2) A. Taniguchi, S. Kanda, T. Nogaito, S. Kusabayashi, H. Mikawa and K. Ito, This Bulletin, **37**, 1386 (1964).

3) T. Ishizuka, K. Tanikawa, S. Kusabayashi, K. Suzuki and H. Mikawa, the paper presented of the International Symposium on Macromolecular Chemistry, Tokyo and Kyoto, preprint VIII-189 (1966).

4) R. G. Flowers, Pittsfield, Mass., U. S. Pat. 2496867 (1950); W. E. Bechmann and M. Carmack, *J. Am. Chem. Soc.*, **63**, 2494 (1941).

5) H. Becker, M. Corell and H. Streeck, *Ann.*, **531**, 107 (1937); L. F. Fieser and J. L. Hartwell, *J. Am. Chem. Soc.*, **60**, 2555 (1938).

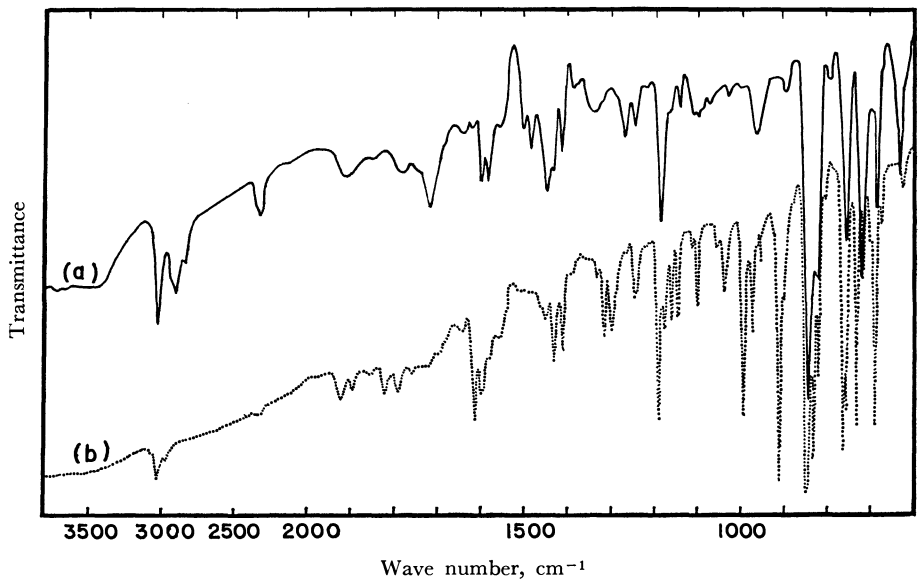

Fig. 1. Infrared spectra of (a) polyvinylpyrene and (b) 3-vinylpyrene in KBr disk.

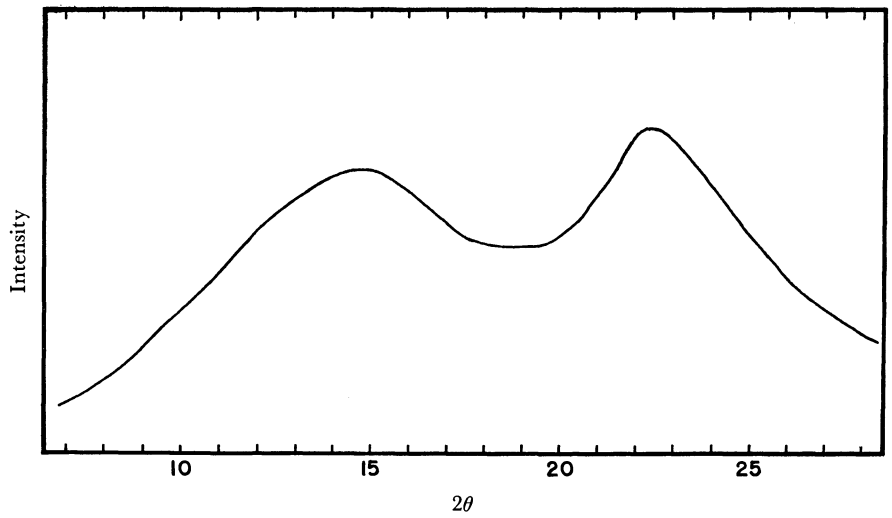

Fig. 2. X-ray diffraction pattern of polyvinylpyrene polymerized by benzoylperoxide catalyst. Rigaku Denki Co.'s X-ray diffractometer, CuK_α (Ni-filtered), 30 kV-20 mA, slit geometry 1°—1°—0.1 mm, scanning speed 1°/min, chart speed 10 mm/min, full scale 400 cps.

of polymerization.

Infrared spectrum of PVP, Fig. 1, shows the disappearance of the absorptions of the end vinyl group (910 and 990 cm^{-1}) in 3-vinylpyrene.

The partially crystalline nature of PVP has been recognized by the examinations with X-ray diffraction and polarizing hot-stage microscope. An X-ray diffraction pattern of PVP polymerized by BPO annealed at 240°C for 4 hr did not show any sharp diffraction peaks as shown in Fig. 2. This X-ray diffraction pattern shows that the polymer is poorly crystallized, if not completely in noncrystalline state.

Examinations of the PVP specimens under the polarizing hot-stage microscope showed the following facts: At room temperature, the polymer powder prepared by precipitation from its solution showed a few birefringent regions as light spots distributed in a dark visual field of crossed Nicols. When this powder is finely powdered in an agate mortar, many light spots appeared along with the considerable amount of weakly light spots. Although the latter weakly light spots may be due to an internal stress *etc.* of PVP sample, the former light spots are believed to be due to the crystalline birefringent regions in the polymer.

Table 1. Properties of charge transfer complexes

Charge transfer complexe	Donor : Acceptor	Softening range* °C	ρ Ωcm	ε eV
PVP-iodine	16 : 3	280—290	1.3×10^{8}	0.80
PVP-TCNE	15 : 2	267—280	4.5×10^{12}	1.32
PVP-TCNQ	15 : 2	230—240	1.1×10^{14}	1.34

* Softening range is observed by pressing the polymer between glass plates under microscope.

Table 2. Polymerization of polyvinylpyrene

	Condition					Product	
	Solvent ml	Monomer g	Initiator mg	Time hr	Temp. °C	Softening range, °C	Yield g
1	Benzene 25	2.3	BPO 9.7	22	80	270—295	0.53
2	Toluene 18	1.7	DTBP 11.0	21	110	230—270	0.4
3	Xylene 32	3.2	DTBP 22.0	18	140	235—250	1.0

When PVP sample is heated very slowly, the light spots disappeared completely at about 254°C (PVP polymerized by BPO in benzene), about 198°C (DTBP in toluene), and about 213°C (DTBP in xylene). These temperatures are believed to be the melting points of the polymers.

It is very interesting that PVP prepared by radical polymerization is crystalline. This may be due to the effect of very large pendant pyrene groups. It is observed that *N*-vinylcarbazole having very large carbazyl groups gives highly crystallized polymer even when polymerized by radical process. Detailed results will be published in the near future.[6]

Preparations of the Charge Transfer Complexes. The charge transfer complexes, having PVP as an electron donor, and iodine, tetracyanoethylene (TCNE) or tetracyanoquinodimethane (TCNQ) as an electron acceptor, were prepared.

The absorption spectra of the charge transfer complexes in film show charge transfer bands as shown in Fig. 3. It is known that pyrene-TCNE complex shows charge transfer bands[7] around 500 and 730 mμ in dichloromethane solution, or around 510 and 830 mμ in crystalline state, and pyrene - iodine complex has the charge transfer band[8] around 420 mμ. As shown in Fig. 3, PVP-TCNQ, PVP-TCNE and PVP-iodine complexes exhibit the absorption band due to charge-transfer excitation around 700—900 mμ. The wavelength of the charge transfer band of the PVP-TCNQ complex, 780 mμ, is much longer than that of poly(*N*-vinylcarbazol) - TCNQ complex,[2] around 620 mμ.

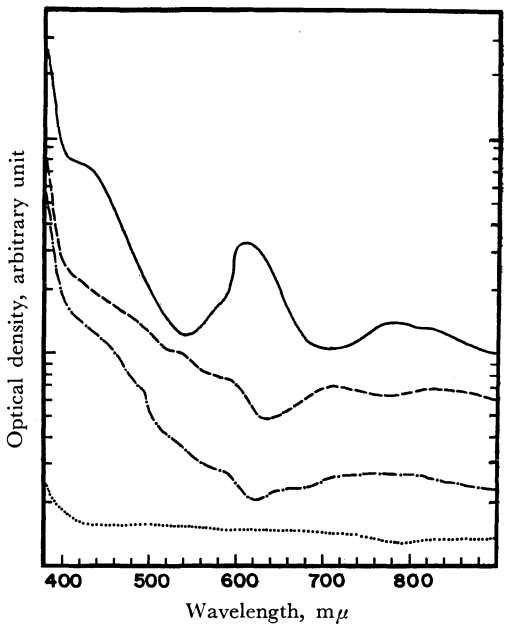

Fig. 3. Absorption spectra of the charge transfer complexes in solid film.
——, PVP-TCNQ; ----, PVP-TCNE;
·—·, PVP-iodine; ·····, PVP

From the elementary analyses of iodine and nitrogen, the compositions of the three complexes were found to be pyrene nucleus : acceptor = 16 : 3, 15 : 2, and 15 : 2, respectively (Table 1).

Electrical Properties of the Charge Transfer Complexes. A sample tablet, 12.5 mm diameter and *ca.* 1 mm thick, was made by pressing about 0.3 g of finely powdered samples of charge transfer complexes at 150—200 kg/cm^2. Silver paste was painted on both sides of the tablet, with a guard ring on one side.

6) H. Mikawa, to be published in the near future.
7) H. Kuroda, M. Kobayashi, M. Kinoshita and S. Takemoto, *J. Chem. Phys.*, **36**, 457 (1962).
8) R. Bhattachary and S. Basu, *Trans. Faraday Soc.*, **54**, 1286 (1958).

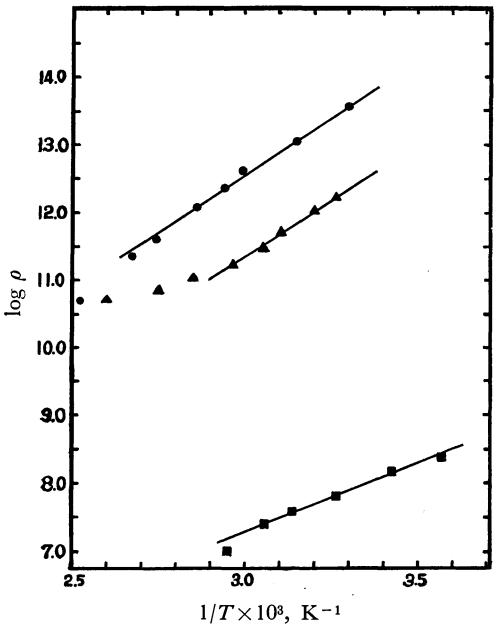

Fig. 4. The relations between resistance and temperature in charge transfer complexes.
—●—, PVP-TCNQ; —▲—, PVP-TCNE; —■—, PVP-iodine.

The electrical conductivity of the tablet thus prepared was measured by the DC method. The sample was put in a well sealed conductivity cell placed in a thermostat. The current was measured by using a Takeda Riken Vibrating Reed Electrometer.[2,9]

Electrical resistivities of these complexes are fairly low. The relation between applied voltage and current obeys Ohm's law.

Figure 4 shows the relations between resistance and temperature. In PVP-iodine complex, at about 80°C, the curve begins to deviate from an equation $\rho = \rho_0 \exp(\varepsilon/2kT)$ (ρ, specific resistance in Ω cm; ρ_0, constant; k, Boltzmann's constant; ε, energy gap of a band model in eV). The deviation may be due to the beginning of decomposition of the complex.

In PVP-TCNE complex, the curve begins to deviate from lineality at about 90°C, showing probably the beginning of decomposition in this case also. PVP-TCNQ complex is most stable to heat.

Among three polymeric charge transfer complexes, PVP-iodine complex has the best electrical conductivity and the smallest band gap energy as shown in Table 1. PVP-TCNQ complex has the best heat stability.

Experimental

Pyrene-3-aldehyde (II).[5] With stirring, 135 g of $POCl_3$ was gradually droped into a mixture of 135 g of *N*-methyl-formanilide and 100 m*l* of *o*-dichlorobenzene during 2 hr at 0—5°C. Into this reaction mixture, 100 g of powdered pyrene was added gradually. After stirring for 3 hr at 90—95°C, the reaction product was decomposed by 1000 m*l* of water containing 480 g of sodium acetate. Both *o*-dichlorobenzene and *N*-methylaniline were steam distilled, and the crude pyrene-3-aldehyde was recrystallized from ethyl alochol. Mp 125—126°C. Yield 56%.

Found: C, 88.67; H, 4.38%. Calcd for $C_{17}H_{10}O$: C, 88.40; H, 4.50%.

3-Vinylpyrene (III). From an injector, ethereal solution (*ca.* 80 m*l*) containing 0.08 mol of phenyllithium[10] was added with stirring into 28.6 g (0.08 mol) of powdered triphenylphosphonium bromide suspended in 250 m*l* of dry ether. The reaction was carried out with stirring in a dry nitrogen stream for about 23 hr at room temperature.[11] After the reaction, 100 m*l* of THF containing 16.1 g (0.07 mol) of pyrene-3-aldehyde was dropped into the reaction solution and 150 m*l* of dry THF was introduced into the solution. After stirring in a dry nitrogen stream at least for about 2 hr at room temperature, ether was removed by distillation and the refluxing of THF was continued for about 24 hr at 65—66°C. THF was distilled and the residue was extracted with benzene, washed by aq. 30% $NaHSO_3$ solution and water. Sometimes triphenylphosphinoxide crystallized out from the solution. 3-Vinylpyrene, showing yellow green fluorescence, was separated from benzene solution by adsorption chromatography (Al_2O_3), 3-vinylpyrene being most weakly adsorbed than the other components. Final recrystallization from ethyl alcohol yielded 3-vinyl pyrene, mp 88—89°C, 76%. 3-Vinylpyrene was stored in nitrogen atmosphere in the dark.

Found: C, 94.69; H, 5.30%. Calcd for $C_{13}H_{12}$: C, 94.20; H, 5.38%.

Polymerization. 3-Vinylpyrene was polymerized by BPO or DTBP in purified benzene, toluene or xylene. The polymerizations were carried out in a dry nitrogen stream under the following conditions (Table 2): The polymer was separated by precipitating with methyl alcohol. The polyvinylpyrene was purified several times by reprecipitation method. $[\eta]$ ~0.1 in THF at 25°C.

Charge Transfer Complexes. Twenty-five milliliters of chloroform containing 0.6 g of sublimed iodine was added into 10 m*l* of chloroform containing 0.5 g of PVP, and the solution was stirred for 5 hr at room temperature, set aside overnight, and poured into petroleum ether, and the very fine precipitate was separated by centrifuge, washed and dried in a desiccator. In the case of both TCNE and TCNQ, the procedures were the same. Found: PVP-iodine, iodine 17.29%; PVP-TCNE, nitrogen 2.93%; PVP-TCNQ, nitrogen 2.89%.

The authors are very much indebted to Associate Professor N. Kasai of the Faculty of Engineering, Osaka University, for his helpful advice and examination with X-ray diffraction.

9) Y. Yamamoto, S. Kanda, S. Kusabayashi, T. Nogaito, K. Ito and H. Mikawa, This Bulletin, **38**, 2015 (1965).
10) G. Wittig, *Angew. Chem.*, **53**, 242 (1940).
11) G. Wittig and G. Geissler, *Ann.*, **580**, 44 (1953).

BULLETIN OF THE CHEMICAL SOCEITY OF JAPAN VOL. 41 2723—2726 (1968)

Studies on Amino-hexoses XIV. Preparation of Partially *O*-Carboxymethylated Chitin and Its Component 3-*O*- and 6-*O*-Carboxymethyl-D-glucosamine, and the Corresponding Glucosaminitols

Tsuyoshi MIYAZAKI and Yoshio MATSUSHIMA

Department of Chemistry, Osaka University College of Science, Toyonaka

(Received April 20, 1968)

3-*O*-carboxymethyl-D-glucosamine, 6-*O*-carboxymethyl-D-glucosamine, and the corresponding glucosaminitols are prepared as reference compounds in a study of a lysozyme action on a partially-*O*-carboxymethylated chitin. The preparation of partially-*O*-carboxymethylated chitin, a substrate of hen-egg white lysozyme, is also described.

In our study of a mode of action on a partially-*O*-carboxymethylated chitin of hen-egg white lysozyme, the monomeric *O*-carboxymethylated glucosamines and the corresponding sugar alcohols were essential for characterizing the substrate and the enzymatic reaction products. In order to obtain these reference compounds, 3-*O*-carboxymethyl-D-glucosamine and the corresponding sugar alcohol were prepared *via* the synthetic route shown in Scheme 1. Because the methods we adopted in order to synthesize 6-*O*-carboxymethyl-D-glucosamine were not successful, the acid hydrolysate of the partially-*O*-carboxymethylated chitin was resolved into components by ion exchanger chromatography; a crystalline component was thus obtained which was proved analytically to be 6-*O*-carboxymethyl-D-glucosamine. The corresponding glucosaminitol was obtained by a borohydride reduction as a syrup.

Partially-*O*-carboxymethylated chitin, a substrate of the enzyme,[1] was prepared through partially-*O*-carboxymethylated chitosan,[2] different batches

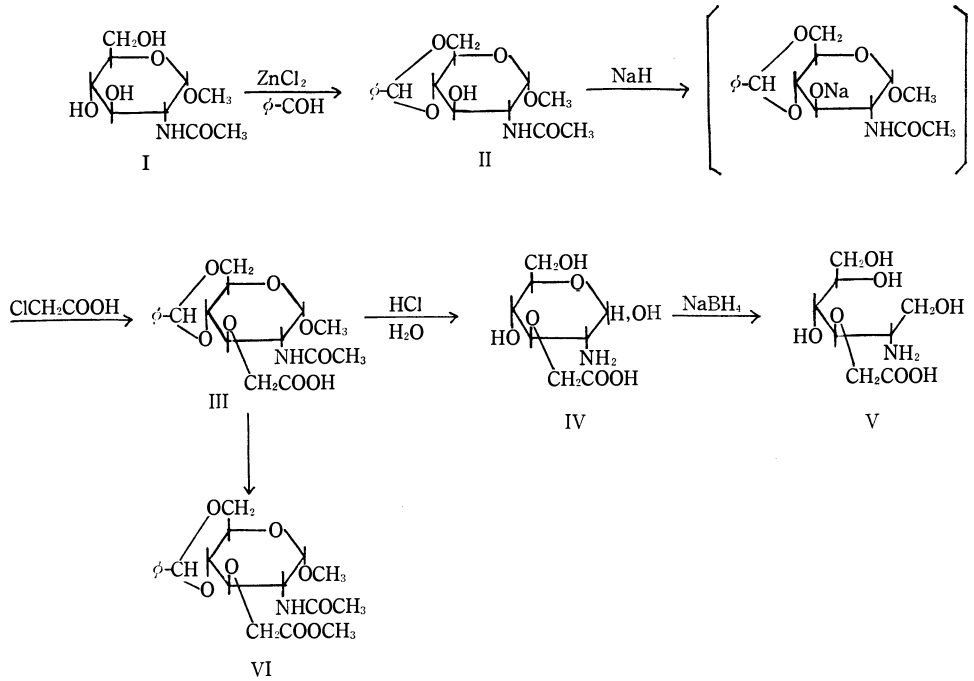

I II III IV V VI

Scheme 1

1) Y. Matsushima, S. Hara, T. Miyazaki and Y. Umemura, The 38 th Annual Meetings of the Japanese Biochemical Society, October, 1965.

2) T. Okimasu, *J. Agr. Chem. Soc. Japan*, **32** 303 (1958).

TABLE 1. COMPONENT OF PARTIALLY-*O*-CARBOXYMETHYLATED CHITIN

Component	Lot No.		
	1	2	3
Unknown-X_1	1.3%	3.6%	3.0%
Unknown-X_2	0.9%	2.5%	5.5%
3-*O*-CM-Glucosamine	2.3%	2.5%	5.5%
6-*O*-CM-Glucosamine	22.6%	33.1%	43.1%
Glucosamine	72.9%	56.9%	43.1%

For the estimation of the unknown components, color yield of the ninhydrin reaction was assumed to be the same with that of 3-*O*-CM-glucosamine.

of which had naturally varying compositions. The compositions of the specimens which we obtained are summarized in Table 1. The specimens are composed mostly of unsubstituted glucosamine, 3-*O*-, and 6-*O*-carboxymethyl-glucosamines. The enzymatic action will be described elsewhere.

Experimental

Methyl 2-Acetamido-2-deoxy-3-*O*-carboxymethyl-4,6-*O*-benzylidene-α-D-glucopyranoside (III). To a solution of 6.5 g of methyl 2-acetamido-2-deoxy-4,6-*O*-benzylidene-α-D-glucopyranoside (II,[3] mp 248—250°C) in 400 m*l* of dry dioxane, was added, at 90°C, a suspension of 2.5 g of sodium hydride in 15 m*l* of dioxane under mechanical stirring. After 30 min, 10 g of chloroacetic acid in 30 m*l* of dioxane was added, and then the stirring was continued for 3.5 hr at the same temperature. After an additional 10 g portion of sodium hydride in 50 m*l* of dioxane had been added to the reaction mixture, the heater was removed and the stirring was continued overnight. The excess sodium hydride was decomposed by the careful addition of 30 m*l* of water under ice-water cooling, after which the mixture was evaporated *in vacuo*. The residue was dissolved in 250 m*l* of warm water, and the insoluble matter was removed by filtration. The filtrate gave a colorless precipitate when the pH of the solution was adjusted to 2 by adding 6 N hydrochloric acid under ice-water cooling. The precipitate was washed thoroughly with water and recrystallized in methanol, 3.6 g of colorless crystals which melted at 215—217°C. giving $[\alpha]_D^{20}$ +69.1 (*c* 0.79, methanol).

Found: C, 56.54; H, 6.44; N, 3.54%. Calcd for $C_{18}H_{23}O_8N$: C, 56.68; H, 6.08; N, 3.67%.

An aglycon homologue of III, ethyl 2-acetamido-2-deoxy-3-*O*-carboxymethyl-4,6-*O*-benzylidene-α-D-glucopyranoside, was likewise prepared; it melted at 203—205°C. $[\alpha]_D^{20}$ +92 (*c* 0.90, methanol).

Found: C, 57.64; H, 6.35; N, 3.52%. Calcd for $C_{19}H_{25}O_8N$: C, 57.71; H, 6.37; N, 3.54%.

2-Amino-2-deoxy-3-*O*-carboxymethyl-D-glucose (IV). Three grams of III were hydrolyzed in 35 m*l* of 2.5 N hydrochloric acid at 100°C for 4 hr. The hydrolysate was then washed with ether in order to remove the benzaldehyde that had been released. After the addition of 50 m*l* of water, the pH of the solution was adjusted to 6.1 by the addition of Dowex-1 (OH^- form) resin. The filtrate from the resin was decolorized with a small amount of charcoal, and the solution was concentrated *in vacuo*. The concentrated solution (20 m*l*) gave, after standing in a refrigerator, colorless crystals which melted at 160—162°C (decomp.) after having been once recrystallized in a small amount of water. $[\alpha]_D^{20}$ +108 (*c* 1.36, water, equil.).

Found: C, 40.23; H, 6.63; N, 5.82%. Calcd for $C_8H_{15}O_7N$: C, 40.50; H, 6.37; N, 5.91%.

The physical constants agreed well with those given by Gigg and Carroll,[4] who prepared the compound *via* a different route.

2-Amino-2-deoxy-3-*O*-carboxymethyl-D-glucitol (V). To a solution of 250 mg of IV in 15 m*l* of water, was added a solution of 100 mg of sodium borohydride in 5 m*l* of water, after which the mixture was stirred overnight at room temperature. Then the pH of the mixture was adjusted to 4.5 by the addition of Amberlite IR-120 (H^+ form) resin. The filtrate from the resin was concentrated *in vacuo*. A small amount of methanol was then added to the residue, and the mixture was evaporated. This procedure was repeated six times in order to remove any boric acid. The residue was dissolved in 0.7 m*l* of water, and the subsequent addition of 7 m*l* of methanol gave 150 mg of colorless crystals which melted at 197—198°C. $[\alpha]_D^{23}$ +38 (*c* 2.0, methanol).

Found: C, 39.89; H, 7.25; N, 5.77%. Calcd for $C_8H_{17}O_7N$: C, 40.16; H, 7.16; N, 5.86%.

Methyl 2-Acetamido-2-deoxy-3-*O*-methylcarboxylate-4,6-*O*-benzylidene-α-D-glucopyranoside (VI). An ethereal solution of diazomethane was added to a solution of 300 mg of III in 100 m*l* of methanol. The addition of the reagent was stopped when a persistent yellow color remained. The mixture was then evaporated *in vacuo*, and the residue was dissolved in a small amount of methanol. After an amorphous, insoluble material had been removed, colorless crystals were obtained when the solution was cooled in a refrigerator. The specimen thus obtained (180 mg) melted at 225—226°C. $[\alpha]_D^{20}$ +77 (*c* 0.56, methanol).

Found: C, 57.84; H, 6.44; N, 3.53%. Calcd for $C_{19}H_{25}O_8N$: C, 57.71; H, 6.37; N, 3.54%.

An aglycon homologue (ethyl 2-acetamido-2-deoxy-3-*O*-methylcarboxylate-4,6-*O*-benzylidene-α-D-glucopyranoside) was likewise obtained; it melted at 174—175°C. $[\alpha]_D^{20}$ +79.4 (*c* 0.68, methanol).

Found: C, 58.54; H, 6.51; N, 3.47%. Calcd for $C_{20}H_{27}O_8N$: C, 58.67; H, 6.65; N, 3.42%.

2-Amino-2-deoxy-6-*O*-carboxymethyl-D-glucose. Two grams of *O*-carboxymethylated chitin (Lot 3 in Table 1) were hydrolyzed in a nitrogen atmosphere at 100°C for 5 hr with 200 m*l* of 4 N hydrochloric acid. The hydrolysate was then dried up *in vacuo*, and the residue was dissolved in 50 m*l* of a 0.2 M citrate buffer solution with a pH of 3.11. The solution was placed on an Amberlite IR-120 column (Na^+ form, 3×65 cm) which had been bufferized with the same buffer solution. The column was then also eluted with the same buffer solution. The elution speed was 50 m*l* per hour, and each 8.1 m*l* portion of ninhydrin-positive fraction was collected. At Fraction No. 120, the

3) Y. Matsushima and J. T. Park, *J. Org. Chem.*, **27**, 3581 (1962).

4) R. Gigg and P. Carroll, *Nature*, **191**, 495 (1961).

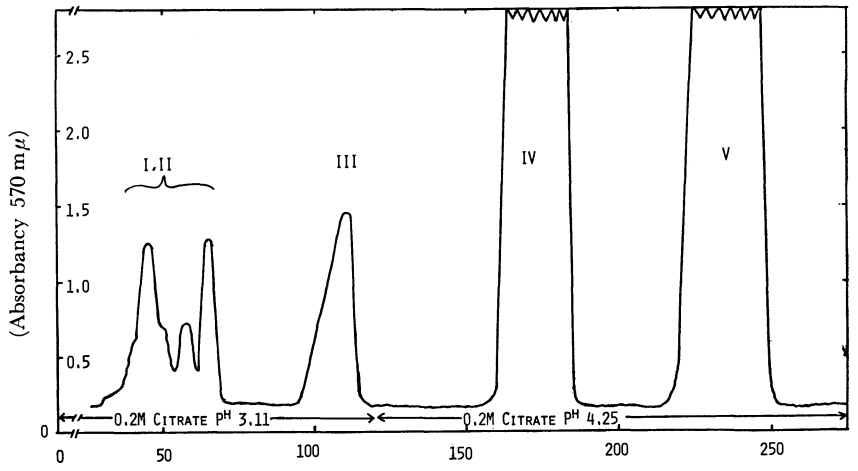

Fig. 1. Preparative chromatography of the acid hydrolyzate of partially carboxymethylated chitin (Lot 3 in Table 1). The ninhydrin-positive peaks represent unknown substances (I, II), 3-*O*-carboxymethyl-glucosamine contaminated with an unknown substance (III), 6-*O*-carboxymethyl-glucosamine (IV) and glucosamine (V).

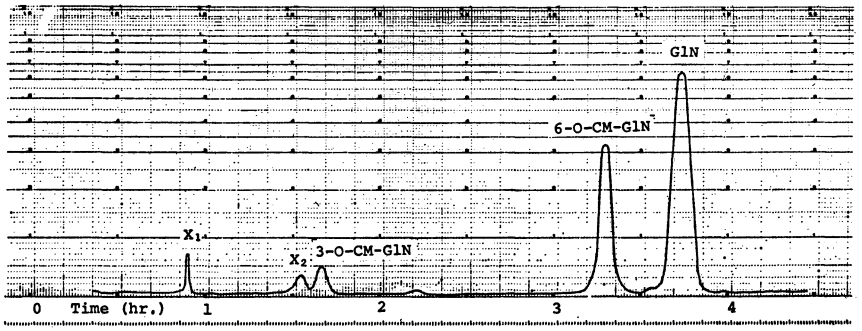

Fig. 2. Ninhydrin-positive fractions of the acid hydrolysate of partially carboxymethylated chitin. GlN: glucosamine, CM: carboxymethyl

buffer solution was changed to 0.2 M citrate with a pH of 4.25. The peak IV in Fig. 1 was evaporated *in vacuo*, and the residue was dissolved in 30 m*l* of water and placed on a column of Amberlite IR-120 (H^+ form, 2.8×12 cm). The column was then washed thoroughly with water and eluted with 0.1 N hydrochloric acid. A ninhydrin-positive fraction was obtained and evaporated *in vacuo*. The syrup thus obtained was dissolved in 50 m*l* of water, and the pH of the solution was adjusted to 6.1 by the addition of Dowex-1 (OH^- form) resin. The filtrate from the resin was decolorized with a small amount of charcoal and evaporated *in vacuo*. The remaining syrup was crystallized in 10 m*l* of ethanol. The yield of faintly yellow crystals which melted at 178—180°C (decomp.) was 430 mg. $[\alpha]_D^{18}$ +72 (*c* 1.03, water, equil.).

Found: C, 39.84; H, 6.50; N, 5.84%. Calcd for $C_8H_{15}O_7N$: C, 40.50; H, 6.37; N, 5.91%.

The position of the carboxymethyl group was determined by the periodate oxidation method. As is shown in Table 2 the specimen did not produce formaldehyde at all after the consumption of the theoretical amount of periodate. This is strong evidence of the position-6 for the carboxymethyl group. The elemental analyses agreed with its identification as a monocarboxymethylated glucosamine; its behavior was

Table 2.

	Consumption of periodate after 46 hr oxidation*	Formation of formaldehyde after 46 hr oxidation**
Glucose	6.7 mol	1.0 mol
Glucosamine	5.4	1.0
3-*O*-CM-Glucosamine	2.6	0.84
6-*O*-CM-Glucosamine	4.3	0.00

* By the method of Ikenaka.[5]

** By the method of Speck.[6] The amount of formaldehyde produced by glucose was taken as the standard.

5) T. Ikenaka, *J. Biochem.*, **54**, 328 (1963).

6) J. C. Speck, Jr., "Methods in Carbohydrate Chem.," Vol. I, Academic Press (1962), p. 441.

quite different from that of synthetic 3-*O*-carboxymethylglucosamine. All these facts indicate that the specimen is 6-*O*-carboxymethylglucosamine.

Partially-*O*-carboxymethylated Chitin. Ten grams of finely-powdered commercial chitin were soaked in 60 g of a 42% sodium hydroxide solution and then kept overnight *in vacuo*. To this mixture crushed ice was then added, portion by portion and under vigorous stirring, until the total volume reached about one liter. A solution of 300 m*l* of 4 N sodium chloroacetate was added to the paste thus obtained, after which the stirring was continued at room temperature for 24 hr. In order to *N*-acetylate the partially-released amino groups, 100 m*l* of acetic anhydride were gradually stirred in, while the pH of the solution was prevented from going below 10 by the addition of sodium hydroxide. Stirring was continued for 24 hr. The mixture was dialyzed against running water for 3 days and against deionized water for 24 hr. The insoluble material was removed in a centrifuge, and the supernatant was lyophilized. The sodium salt of partially-carboxymethylated chitin thus obtained weighed 8.5 g; it contained 14% of water and did not reveal any van Slyke nitrogen. A sample of chromatographic pattern of a specimen (Lot No. 2 in Table 1) derived by component analysis using an automatic amino-acid analyzer is shown in Fig. 2.

This investigation was supported by U. S. Public Health Service Grant AI-04586-05.

BULLETIN OF THE CHEMICAL SOCIETY OF JAPAN VOL. 41 2726—2733 (1968)

The Photochemical Reactions of Fe(III) Complexes with 1,2-Glycols. Dehydration and Dehydrogenation*1

Hiroo INOUE, Nobuyuki KOMAKINE and Eiji IMOTO

Department of Applied Chemistry, College of Engineering, The University of Osaka Prefecture, Sakai, Osaka

(Received April 20, 1968)

Ferric chloride reacts with 1,2-glycols, when irradiated with light, to afford dehydration and dehydrogenation products. The reaction course is influenced by the structure of the 1,2-glycols, the kind of ligand around the Fe(III) ion, and the solvent in the reaction system. When the number of hydrogen atoms on carbon having a hydroxyl group of 1,2-glycol increases, the yield of the dehydration product increases in comparison with that of the dehydrogenation product; the photochemical reaction of ferric chloride with ethylene glycol or pinacol gives, selectively, acetaldehyde or acetone respectively. The photochemical reaction of ferric acetate with the ethylene glycol shows a highly selective dehydrogenation, giving only formaldehyde, though it is in a good yield. Furthermore, the addition of aniline or acetic acid to the ferric chloride-ethylene glycol system results in an increase in the production of glyoxal or acetaldehyde respectively. In the photochemical reaction of ferric chloride with ethylene glycol or *cis*- and *trans*-1,2-cyclohexanediol, acetonitrile as a solvent causes the formation of the dehydrogenation products, that is, acetoxyacetaldehyde and glyoxal or 1,2-cyclohexanedione respectively.

The photochemical reaction of ethylene glycol with ferric chloride affords, selectively, the dehydration product, acetaldehyde.[1] The ferric chloride - pyridine complex, however, causes the formation of the dehydrogenation product, glyoxal and formaldehyde, from ethylene glycol.[2] The reactions are mediated by a Fe(III) ion - ethylene glycol complex in solution. The selectivity of the reaction may be interpreted in terms of the interaction of a ligand with the hydrogen of either the carbon or hydroxyl group of ethylene glycol, which is close to the ligand. Moreover, the electronic nature of the Fe(III) in a Fe(III) complex may also contribute to the selective reaction. The present paper deals with a study of the effects of the ligand of a complex, of the solvent, and of the structure of 1,2-glycols on the dehydration or dehydrogenation course. Ethylene glycol, propylene glycol, 2,3-butanediol, pinacol, and *cis*- and *trans*-1,2-cyclohexanediol as 1,2-glycols, and ferric chloride and ferric acetate as ferric salts, were used here.

Experimental

Materials. The ethylene glycol, propylene glycol, 2,3-butanediol, aniline, and acetic acid were purchased from commercial sources, while the pinacol and *cis*- and

*1 Presented at the 21th Annual Meeting of the Chemical Society of Japan, Osaka, April, 1968.

1) H. Inoue, K. Tamaki, N. Komakine and E. Imoto, This Bulletin, **39**, 1577 (1966).

2) H. Inoue, K. Tamaki, N. Komakine and E. Imoto, This Bulletin, **40**, 875 (1967).

trans-1,2-cyclohexanediol were synthesized by the methods described in the literature.[3-5] These materials were dried by the usual methods and distilled through a Vigreux column before use. Ethylene glycol: bp 76—77°C/4 mmHg, n_D^{22} 1.4321. Propylene glycol: bp 185—189°C, n_D^{32} 1.4291. 2,3-Butanediol: bp 72—73°C/5 mmHg, n_D^{31} 1.4343. Pinacol: bp 80°C/15 mmHg (lit.[3,6] bp 75°C/13 mmHg). *cis*-1,2-Cyclohexanediol: mp 97—98°C (lit.[4] mp 98°C). *trans*-1,2-Cyclohexanediol: mp 102—104°C (lit.[5] mp 101.5 103°C). The anhydrous ferric chloride and ferric acetate, and thallium oxide (Tl_2O_3) were of a commercial grade; they were dried over phosphorus pentoxide at 100°C under the reduced pressure of 10 mmHg. The acetonitrile was purified by two distillations after having been dried on calcium hydride.

General Procedure of the Photochemical Reaction. The photochemical reactions were carried out by the methods described in previous papers.[1,2] Glycols and ferric chloride or ferric acetate were transferred, under a nitrogen atmosphere, to a vycor tube. The tube was then sealed and irradiated for 20—24 hr at an equidistant place (4 cm) from a 100W mercury lamp, which irradiated waves at 2500, 3200, 3600, 4400, 5500, and 5800 Å at room temperature unless otherwise stated. The reactions of *cis*- and *trans*-1,2-cyclohexanediol with anhydrous ferric chloride or ferric acetate were carried out in an acetonitrile solvent. In the case of pinacol, chelate complexes consisting of pinacol and ferric chloride or cupric chloride were prepared, dissolved in an acetonitrile solvent, and irradiated as has been described above. The concentration of a solution of the chelate complex in acetonitrile was about 22 g/*l*. In order to isolate the reaction products, another procedure was attempted on a large scale by using a cylindrical, 300-m*l* reaction vessel.[1]

Analyses of the Products. The analyses of the products were mainly accomplished by means of gas chromatography, using Hitachi KGL-2 and Yanagimoto 5DH gas chromatographs. A column containing polyethylene glycol-6000 and -20 M and/or high-vacuum silicone grease was used in the gas chromatography analyses. Helium gas was used as the carrier gas.

Acetone, propionaldehyde, acetaldehyde, methyl ethyl ketone, 2-ethyl-4-methyl-1,3-dioxolane, 2,4-dimethyl-1,3-dioxolane, 2,2,4-trimethyl-1,3-dioxolane, 2,4,5-trimethyl-1,3-dioxolane, and 2-ethyl-2,4,5-trimethyl-1,3-dioxolane were identified by a comparison of their retention times with those of authentic materials, and by trapping the materials from the column and by then comparing the infrared spectra of the trapped materials with those of authentic materials. The amounts of these compounds were determined by means of gas chromatography, and by the paper chromatography of their 2,4-dinitrophenylhydrazones. The amounts of the oxolanes are described as those of the corresponding carbonyl compounds in Tables 1, 2, 3 and 4. 1,2-Propanedione, 1,2-cyclohexanedione, adipaldehyde, 2,3-butanedione, and glyoxal were isolated as their 2,4-dinitrophenylhydrazones, which were purified by recrystallization from ethanol or ethanol-ethyl acetate, and which were identified by comparing their infrared spectra and their melting points with those of authentic materials. The diketones were determined by measuring the weights of their 2,4-dinitrophenylhydrazones. Acetoxyacetaldehyde was isolated as the 2,4-dinitrophenylhydrazone, mp 150—151°C (lit.[7] mp 152°C), the infrared absorption spectrum of which has the absorption of the carbonyl group of the ester at 1730 cm^{-1}. Its elementary analysis indicates:

Found: C, 42.40; H, 3.44; N, 19.72%. Calcd for $C_{10}H_{10}N_4O_6$: C, 42.57; H, 3.55; N, 19.86%.

Formaldehyde and the ferrous ion were determined spectrophotometrically by using the Schiff's reagent and the 1,10-phenanthroline methods respectively.[8,9]

Analysis of Fe(III) in Fe(III) Complex. A weighed amount of the Fe(III) complex was decomposed by refluxing it in concentrated nitric acid for 3—4 hr. The solution was then diluted with distilled water, and adjusted to pH 2—3 with 1 N sodium acetate-acetic acid, after which a 2% tiron solution was added. The solution was then titrated with a 0.01 M EDTA solution by a volumetric method.

Preparations of Complexes. *Ferric Chloride-Pinacol.* Ferric chloride (7.1 g) in acetonitrile (20 g) was mixed with a solution of pinacol (10 g) in acetonitrile (2 g). The solution was heated at 70—80°C for 1—2 min, then cooled with dry ice and acetone. Pale green crystals of the complex, which decomposed above 100°C without melting, were filtered off and washed with boiling chloroform (yield, 3.8 g).

Found: C, 26.15; H, 5.26%. Calcd for $C_6H_{14}O_2$-$FeCl_3$: C, 25.70; H, 5.03%.

Ferric chloride content, 4.2×10^{-3} mol/g. Pinacol content, 3.8×10^{-3} mol/g.

The determination of the pinacol present in the complex was carried out by the following method: a portion of 0.3 g of 8-quinolinol was added to a solution of 0.1 g of the complex in 10 m*l* of acetonitrile. The mixture was then allowed to stand at 30°C for 30 min to give the precipitate of the 8-quinolinol-ferric ion complex. The pinacol thus removed was analyzed by means of gas chromatography. The infrared absorption spectrum of the complex showed absorptions at 3270, 2960, 1460, 1380, 1340, 1140, 950, 920, 880, and 690 cm^{-1}, as Fig. 1 shows.

Cupric Chloride-Pinacol. A portion of 1 g of cupric chloride was added to a solution of 2 g of pinacol in 10 g of acetonitrile. The solution was heated at 70—80°C for 1—2 min, and then cooled with a dry ice-acetone mixture. Pale green crystals of the complex, which decomposed above 100°C without melting, were filtered off and washed with boiling chloroform (yield, 1.5 g). Pinacol content, 5.7×10^{-3} mol/g. The infrared absorption spectrum of the complex showed absorptions at 3400, 3125, 3025, 2750, 2550, 2330, 1460, 1375, 1210, 1160, 1140, 1113, 947, 895, and 827 cm^{-1}.

3) R. Adams and E. W. Adams, "Organic Syntheses," Coll. Vol. I, p. 459 (1948); C. F. H. Allen, *ibid.*, Vol. 22, p. 40 (1942).
4) M. F. Clarke and L. N. Owen, *J. Chem. Soc.*, **1949**, 318.
5) A. Roebuck and H. Adkins, "Organic Syntheses," Coll. Vol. III, p. 217 (1955).
6) R. Goto and M. Araki, "Daiyuki Kagaku," Vol. 2, I, Asakura Shoten, Tokyo (1957), p. 263.
7) B. S. Gorton and J. A. Reeder, *J. Org. Chem.*, **72**, 2920 (1962).
8) A. Kubo, "Jikken Kagaku Koza," Vol. 15, II, Maruzen, Tokyo (1958), p. 278.
9) R. I. Veksler, *Zhur. Anal. Khim.*, **1**, 301 (1946); **4**, 14 (1949); **5**, 32 (1950).

Results

Photochemical Reaction of Ferric Chloride. *Eethylene Glycol.* Ethylene glycol reacts with ferric chloride under the irradiation of ultraviolet light for 24 hr to afford acetaldehyde in a 74% yield,[1] based on the amount of ferric chloride used. The addition of pyridine to the ferric chloride-ethylene glycol system, however, results in the production of glyoxal, formaldehyde, and acetaldehyde in 44, 5 and 6% yields respectively, when 60% of the Fe(III) is photo-reduced to Fe(II).[2] In this paper, aniline or acetic acid was added to a solution of ferric chloride in ethylene glycol, with the molar ratio of aniline or acetic acid to ferric chloride, of 1/2 or 1 respectively, and irradiated in an atmosphere of nitrogen at a distance of 4 cm from the light source for 24 hr at room temperature. As Table 1 shows, the addition of aniline to the reaction system gave glyoxal and acetaldehyde in 12 and 9% yields, while Fe(III) was photo-reduced to Fe(II) in a 84% yield. Thus, the product yields became considerably lower than the photo-reduction yield of Fe(III) to Fe(II). Probably, this means that aniline itself is photo-oxidized by ferric chloride. On the other hand, in the case of acetic acid, acetaldehyde was obtained as the main product in a yield which corresponded to the photo-reduction yield of Fe(III) to Fe(II). Thus, the acidic or basic ligand in the reaction system tends to contribute to the formation of the dehydration or dehydrogenation product respectively.

Propylene Glycol. When a solution of ferric chloride in propylene glycol was heated at about 100°C under a nitrogen atmosphere for 5.5 hr, no product was detected. However, the ultraviolet light irradiation of a solution of ferric chloride in propylene glycol gave mainly acetone, propionaldehyde, acetaldehyde, and formaldehyde, as is shown in Table 2. During the photo-reaction, the Fe(III) is photo-reduced to Fe(II). Acetone or propionaldehyde is produced by the elimination of the primary or the secondary hydroxyl group respectively (dehydration).

The formations of acetaldehyde and formaldehyde mean the occurrence of the oxidative cleavage of

TABLE 1. THE EFFECTS OF THE LIGANDS ADDED ON THE PHOTOCHEMICAL REACTION OF ETHYLENE GLYCOL WITH FERRIC CHLORIDE*

Ligand	Molar ratio Ligand/$FeCl_3$	Yield of product (%)**			
		CH_3CHO	CH_2O	OHCCHO	Fe(II) ion
None***	—	74	0	0	—
Pyridine***	1	6	5	44	60
Aniline	0.5	9	0	12	84
Acetic acid	1	18	0	4	22

* The amounts of ethylene glycol and ferric chloride used for the cases of none, pyridine, aniline and acetic acid were 3.56, 0.18, 0.18, 4.5×10^{-3}; 0.18, 9×10^{-3}; and 0.18, 9×10^{-3} mol, respectively. Irradiation time: 24 hr for none and 20 hr for the other cases. Irradiation method: Cylindrical vessel for none, and light irradiation at the distance of 4 cm for the other cases.

** The yields of the products were calculated by (amount of CH_3CHO)/(amount of $FeCl_3$)$\times$100 for CH_3CHO, (amount of CH_2O)/(amount of $FeCl_3$)$\times$100 for CH_2O, and 4$\times$(amount of OHCCHO)/(amount of $FeCl_3$)$\times$100 for OHCCHO.

*** H. Inoue, K. Tamaki, N. Komakine and E. Imoto, This Bulletin, **39**, 1577 (1966); *ibid.*, **40**, 875 (1967).

TABLE 2. THE PHOTOCHEMICAL AND THERMAL REACTIONS OF PROPYLENE GLYCOL WITH FERRIC CHLORIDE OR HYDROGEN PEROXIDE*

$FeCl_3$ or H_2O_2	Reaction type	Yield of product (%)**					
		CH_3COCH_3	CH_3CH_2CHO	CH_3CHO	CH_2O	CH_3COCHO	Fe(II) ion
$FeCl_3$	P***	12	23	17	1	0	64
H_2O_2	P	83	7	trace	1	8	—
$FeCl_3$	T	trace	trace	0	0	0	0
H_2O_2	T	2	10	trace	0	0	—

* The amounts of propylene glycol, ferric chloride and hydrogen peroxide were 4.04, 0.19 and 0.18 mol respectively. Irradiation time: 20 hr. Thermal reaction: temperature, 100°C and time, 5.5 hr.

** The yields of CH_3COCH_3, CH_3CH_2CHO, CH_3CHO, CH_2O and Fe(II) ion: (amount of the product)/(amount of $FeCl_3$ or H_2O_2)$\times$100, and the yield of CH_3COCHO: 2$\times$(amount of CH_3COCHO)/(amount of H_2O_2)$\times$100. The total amount of gas evolved was 4×10^{-3} and 1.5×10^{-3} mol for the photo-reactions in the case of ferric chloride and hydrogen peroxide respectively.

*** P and T are the abbreviations for the photochemical and thermal reactions.

TABLE 3. THE PHOTOCHEMICAL AND THERMAL REACTIONS OF 2,3-BUTANEDIOL WITH FERRIC CHLORIDE*

Reaction type	Yield of product (%)			
	$CH_3COCH_2CH_3$	CH_3CHO	$CH_3COCOCH_3$	Fe(II) ion
P	14	24	0	50
T	0	0	0	0

* The starting amounts of 2,3-butanediol and ferric chloride were 0.1 and 5×10^{-3} mol respectively. Irradiated time: 24 hr. Distance of irradiation: 4 cm. Thermal reaction: temperature, 100°C and time, 5.5 hr. The evolution of gas was not observed. The yield of the product was based on the starting amount of ferric chloride.

the bond between 1- and 2-carbons (dehydrogenation). The dehydration occurs twice as easily as does the dehydrogenation and, furthermore, involves twice as much elimination of the secondary hydroxyl group as of the primary hydroxyl group.

The ultraviolet-light irradiation of propylene glycol in the presence of hydrogen peroxide resulted in the formation of acetone in a 83.3% yield. This reaction is initiated by the hydroxyl radical produced by the photo-decomposition of hydrogen peroxide, followed by the abstraction of hydrogen on 2-carbon and the elimination of the primary hydroxyl group. Thus, there were remarkable differences between the photochemical behavior of ferric chloride and hydrogen peroxide in relation to propylene glycol. Probably, this is because the excited ferric chloride reacts with propylene glycol through a complex between them. Furthermore, the fact that the secondary hydroxyl group is more easily eliminated than the primary hydroxyl group supports the interpretation of the elimination mechanism by means of ferric chloride, as will be discussed later.

2,3-*Butanediol.* When a solution of ferric chloride in 2,3-butanediol was heated at about 100°C under a nitrogen atmosphere for 5.5 hr, no product was confirmed. However, the ultraviolet-light irradiation of the solution involving ferric chloride in 2,3-butanediol gave acetaldehyde, methyl ethyl ketone, and Fe(II) in 24, 14 and 50% yields respectively, as is shown in Table 3. That is, the yields of acetaldehyde and methyl ethyl ketone, based on the amount of Fe(III) converted to Fe(II), were 48 and 28% respectively. This would mean that the carbon-carbon bond cleavage occurs in a ratio similar to the elimination of the hydroxyl group.

Pinacol. A complex consisting of ferric chloride and pinacol was isolated as a pale green plate by mixing a solution of ferric chloride in acetonitrile with that of pinacol in acetonitrile. The combination of the elementary analyses of carbon and hydrogen, and the quantitative analyses of Fe(III) and pinacol in the crystals, showed that the molar ratio of the ferric chloride to the pinacol present in the complex is nearly 1, as is shown in Table 4. Furthermore, the infrared absorption spectrum of the crystals had absorptions characteristic of pinacol and ferric chloride.

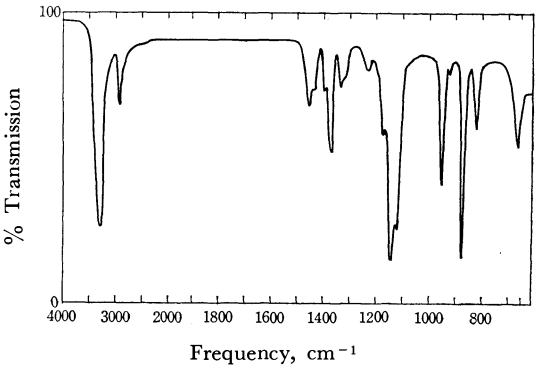

Fig. 1. Infrared spectrum of ferric chloride-pinacol complex (KBr disk).

The ferric chloride - pinacol complex dissolved in acetonitrile was irradiated with ultraviolet light for 24 hr at room temperature. As Table 4 shows, acetone was obtained as the sole product in a nearly 100% yield, based on the amount of ferric chloride in the complex as a starting material. The theoretical amount of the unreacted pinacol was recovered. When water instead of acetonitrile was used as the solvent, pinacol did not react with ferric chloride under the ultraviolet-light irradiation. This must be due to the decomposition of the ferric chloride - pinacol complex by the coordination of water.

On the other hand, when a solution of the complex in acetonitrile or water was refluxed under a nitrogen atmosphere for 6 hr, no product was detected, and pinacol was recovered in an almost 100% yield.

Although the production of pinacolone by pinacol rearrangement was predicted in the photochemical reaction of pinacol with ferric chloride, no pinacolone was detected at all. Pinacol also formed a complex with cupric chloride; the photochemical reaction of the complex gave acetone in a lower yield than in the case of the ferric chloride - pinacol complex, as is shown in Table 4. The photochemical reactions of binary metal salts, such as ferric chloride-cupric chloride and ferric chloride-thallium oxide, with pinacol gave unfavorable results, as Table 4 also shows. Thus, pinacol is photo-oxidized by ferric chloride in acetonitrile

Table 4. The photochemical reaction of pinacol-Fe(II) or Cu(II) ion complex*

Complex pinacol-metal salt	Amount (g)	Component: Metal salt (mol×10³)	Component: Pinacol (mol×10³)	Metal salt added (mol×10³)	Solvent	Reaction type	Yield of CH_3COCH_3 (%)	Recovery % pinacol
$FeCl_3$	0.22	0.7	0.8	0	CH_3CN	P	100	55
$FeCl_3$	0.33	1.4	1.3	0	H_2O	P	0	100
$FeCl_3$	0.50	1.4	2.7	0	CH_3CN	T	0	90
$FeCl_3$	0.12	0.5	0.4	0	H_2O	T	0	100
$CuCl_2$	0.42	1.0	2.4	0	CH_3CN	P	40	83
$FeCl_3$	0.12	0.5	0.5	$CuCl_2$ (0.3)	CH_3CN	P	100	48
$FeCl_3$	0.13	0.5	0.5	Tl_2O_3 (0.3)	CH_3CN	P	114	37

* Irradiated time: 24 hr. Distance of irradiation: 4 cm. Thermal reaction: temperature, 100—110°C and time, 6 hr. The yield of acetone was based on the starting amount of ferric chloride or cupric chloride, and the recovery yield of pinacol was based on that of pinacol.

Table 5. Dehydration and dehydrogenation products in the photochemical reaction of *cis*- and *trans*-1,2-cyclohexanediol with ferric chloride or ferric acetate*

1,2-Diol	Fe(III) salt	Yield of product (%):	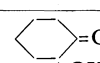 or 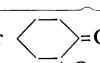	$OHC(CH_2)_4CHO$	Fe(II) ion
cis-	$FeCl_3$	trace	4—8	0	38
trans-	$FeCl_3$	trace	4—8	0	50
cis-	$Fe(OCOCH_3)_3$	trace	0	2	—
trans-	$Fe(OCOCH_3)_3$	trace	0	1	—

* The starting amounts of 1,2-cyclohexanediol, ferric chloride and ferric acetate all were 5×10^{-3} mol. Acetonitrile was used as a solvent. Irradiation time: 48 hr for ferric chloride and 24 hr for ferric acetate. Distance of irradiation: 4 cm. The yield of the product was based on the starting amount of ferric chloride or ferric acetate.

Table 6. The photochemical and thermal reactions of ethylene glycol with ferric acetate*

Ethylene glycol (mol)	$Fe(OCOCH_3)_3$ (mol×10³)	Reaction type	Yield of product (%): CH_3CHO	CH_2O	OHCCHO	Recovery %
0.33	7.8	P	0	12	0	97
0.33	16.1	T	0	0	9	—
0.32	3.2	P	0	13	0	—

* Irradiated time: 24 hr. Distance of irradiation: 4 cm. Thermal reaction: temperature, 100—110°C and time, 5—6.5 hr. No gas was evolved and the other products were not detected from the measurement of gas chromatography. The yield of the product and the recovery yield of ethylene glycol were based on the starting amount of ferric acetate and ethylene glycol respectively.

Table 7. The effect of acetonitrile on the photochemical reaction of ferric chloride with ethylene glycol

Ethylene glycol (mol)	$FeCl_3$ (mol)	CH_3CN (g)	Yield of product (%): CH_3CHO	CH_2O	OHCCHO	CH_3COOCH_2CHO	Fe(II) ion	Recovery %
3.56	0.18	0	74	0	0	0	—	81
0.11	0.11	158	0	0	1	8	50	80

* Irradiated time: 24 hr in the absence of acetonitrile and 48 hr in the presence of acetonitrile. Reaction method: cylindrical vessel. The yield of the product was based on the starting amount of ferric chloride.

to afford, selectively, acetone in a good yield. This seems to be characteristic of the photochemical action of ferric chloride.

cis- and trans-1,2-cyclohexanediol. As Table 5 shows, the photochemical reaction of ferric chloride with *cis-* and *trans-*1,2-cyclohexanediol in acetonitrile afforded, selectively, a dehydrogenation product, 1,2-cyclohexanedione or 2-hydroxycyclohexanone, in a low yield of about 10%, when Fe(III) was reduced to Fe(II) in about a 40% yield. Although we attempted to recover *cis-* or *trans-*1,2-cyclohexanediol from the reaction mixture, it was difficult to recover it completely because of the formation of a complex between *cis-* or *trans-*1,2-cyclohexanediol and ferric chloride. By means of the ligand-exchange of the complex by 8-quinolinol, about 45—50% of *cis-* or *trans-*1,2-cyclohexanediol was, however, recovered. Thus, the yield of the product was low because of the photochemical reaction of ferric chloride with acetonitrile as a solvent; no remarkable differences were observed in the cases of *cis-* and *trans-*1,2-cyclohexanediol. The coordination of acetonitrile to Fe(III) may affect the selectivity and the yield in the formation of the dehydrogenation product.

Photochemical Reaction of Ethylene Glycol with Ferric Acetate. The photochemical reaction of ethylene glycol with ferric acetate was carried out under conditions similar to those used with ferric chloride. As Table 6 shows, formaldehyde was obtained as the sole product. During the photochemical reaction, white crystals appeared on the wall of the reaction vessel. In the photochemical reaction of 0.17 mol of ethylene glycol and 0.008 mol of ferric acetate, 0.16 g of the crystals was collected by filtration after the reaction. The crystals rapidly turned from white to brown upon exposure to air. The infrared absorption spectrum of the crystals, measured by a KBr disk, shows absorptions at 3400, 2950, 2870, 1555—1530, 1450—1430, 1350, 1055, 1030, 893, and 660 cm^{-1}, absorptions characteristic of those of ferric or ferrous acetate and ethylene glycol. The iron content of the complex was 4.8×10^{-3} mol/g; this corresponded to the amount of ferric acetate required for the formation of formaldehyde. The crystals are probably a complex between ferrous acetate and ethylene glycol.

The next phenomenon concerns the photochemical reaction of a complex consisting of ethylene glycol and ferric acetate (Fe(III) ion content; 1.58×10^{-2} mol/3.8 g) in acetonitrile. The complex was prepared as follows. When a solution of 3.8 g of ferric acetate in 20.1 g of ethylene glycol was allowed to stand at room temperature for a day, there were precipitated 2.4 g of a pale prism, decomposing gradually above 100°C. After this had been filtered and then washed with acetonitrile. it was dried on calcium chloride under the reduced pressure of 10 mmHg at room temperature. The dispersion of the crystals in a solution of 8-quinolinol in acetonitrile removed the ethylene glycol from the crystals. Thus, it was confirmed that no organic compounds other than ethylene glycol and acetate anion were present in the crystals. Furthermore, the infrared absorption spectrum of the crystals, as measured by the use of a KBr disk, had absorptions at 3300—3100, 2950, 2870, 1580—1560, 1455—1420, 1390, 1300, 1245, 1230, 1070, 1040, 910, 895, and 660 cm^{-1}, absorptions characteristic of ferric acetate and ethylene glycol, as Fig. 2 shows. The absorption of the complex at 1560—1580 cm^{-1} was shifted toward a wave number shorter by about 30 cm^{-1} than that of ferric acetate. The determination of the Fe(III) present in the crystals showed the amount to be 4.1×10^{-3} mol/g. These results indicate that the crystals are a complex consisting of ferric acetate and ethylene glycol, with a molar ratio of 6.

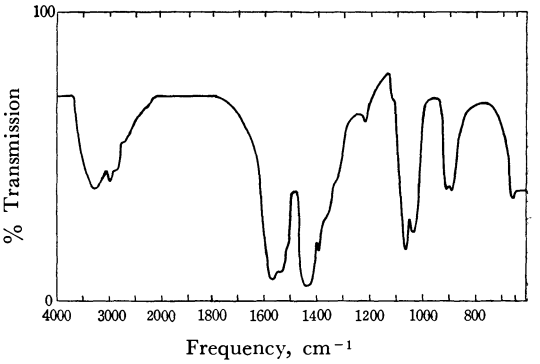

Fig. 2. Infrared spectrum of ferricacetate-ethylene glycol complex (KBr disk).

A dispersed solution of 0.1 g of the ferric acetate-ethylene glycol complex in 10.0 g of acetonitrile was irradiated in an atmosphere of nitrogen at a distance of 4 cm from the light source for 24 hr at room temperature. Formaldehyde was obtained as the sole product in a 100% yield.

It has thus been confirmed that the photochemical reaction of ferric acetate with ethylene glycol shows a highly selective oxidative cleavage of a carbon-carbon bond to formaldehyde. Furthermore, the photochemical action of ferric acetate on *cis-* and *trans-*1,2-cyclohexanediol was also similar to that for ethylene glycol; that is, it resulted in the production of adipaldehyde, as is shown in Table 5.

On the other hand, the thermal reaction of ferric acetate with ethylene glycol afforded only a dehydrogenation product, glyoxal. Thus, there was a remarkable difference between the photochemical and thermal reactions of ferric acetate with ethylene glycol.

Solvent Effect of Acetonitrile. As Table 7 shows, the photochemical reaction of ferric chloride with ethylene glycol in acetonitrile afforded glyoxal and acetoxyacetaldehyde in 1 and 8% yields respectively, while Fe(III) was photo-reduced

to Fe(II) in a 50% yield. About 80% of the ethylene glycol was recovered. Acetaldehyde and formaldehyde, which are the products of the photochemical reactions of ethylene glycol with ferric chloride and ferric acetate respectively, were not detected at all. Furthermore, when the solution of a mixture of ferric chloride and ethylene glycol in acetonitrile was allowed to stand at room temperature without any light irradiation, no acetoxyacetaldehyde was obtained. A reaction (1) involving the formation of hydroxyethyl esters by thermal interaction between nitriles and ethylene glycol has already been reported.[10] In the photochemical reaction

$$RCN + HOCH_2CH_2OH \xrightarrow[\text{reflux}]{} RCOO(CH_2)_2OH \qquad (1)$$

described above, acetoxyacetaldehyde would be produced *via* the following process, that is, by the addition to one hydroxyl group of ethylene glycol to a nitrile group of acetonitrile coordinated to ferric chloride, and by the oxidation of the other hydroxyl group of ethylene glycol by the excited ferric chloride, as is indicated in Eq. (2):

$$CH_3CN + HOCH_2CH_2OH \xrightarrow[FeCl_3]{h\nu} CH_3C(=NH)-OCH_2CHO \xrightarrow{H_2O} CH_3COOCH_2CHO \qquad (2)$$

Discussion

Ferric salts form a complex with 1,2-glycols in the reaction system. The ferric chloride - pinacol and ferric acetate - ethylene glycol complexes were isolated as crystals. The excitation of the Fe(III) of the complex with light resulted in the competition of the dehydration and the dehydrogenation of the 1,2-glycols coordinated with the Fe(III). When the number of hydrogen on carbon with a hydroxyl group increased, the dehydration increased in comparison with the dehydrogenation: the yield of the dehydration product became lower in the order of ethylene glycol> propylene glycol> 2,3-butanediol> pinacol, while that of the dehydrogenation showed the reverse order. Furthermore, in the case of propylene glycol, the secondary hydroxyl group was eliminated more readily than the primary hydroxyl group. In addition, no rearrangement product was obtained in any case. On the other hand, the irradiation of a complex consisting of ferric acetate and ethylene glycol in acetonitrile gave, selectively, the dehydrogenation product, and addition of pyridine or acetonitrile to the ferric chloride - ethylene glycol system resulted in an increase in the formation of the dehydrogenation product. Thus, there were significant effects of the ligand, the solvent, and the structure of 1,2-glycol on the selectivity for the dehydration and the dehydrogenation.

The mechanisms for the two reactions may be explained reasonably by considering the interaction of the ligand or the base with hydrogen of either the carbon or hydroxyl group of 1,2-glycol. That is, for a dehydration mechanism, we assume a mechanism involving the intramolecular abstraction of hydrogen radical or proton by a chlorine radical or anion, followed by the simultaneous elimination of the hydroxyl radical or anion by the excited Fe(III), as is shown in Eq. (3). For the occurrence of the dehydration, the existence

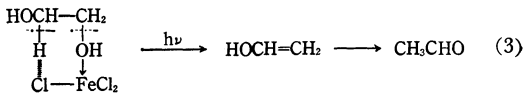

(3)

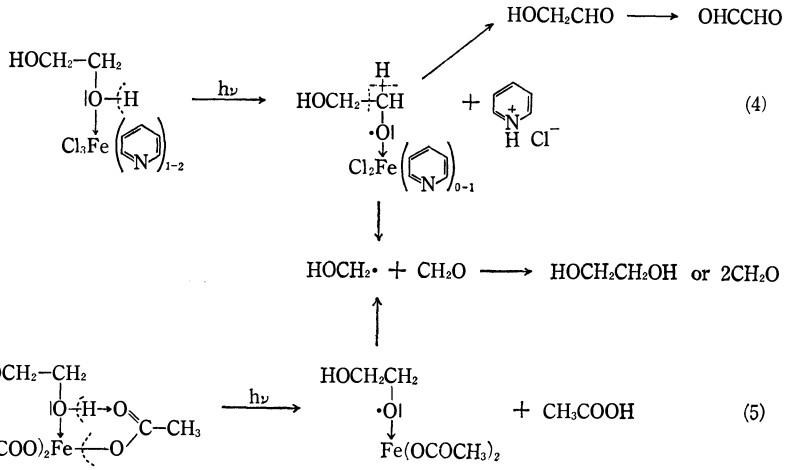

(4) (5)

10) B. Robinson, *J. Chem. Soc.*, **1963**, 2417.

of hydrogen on the carbon with a hydroxyl group and an exact stereochemical arrangement of the 1,2-glycol and ferric chloride in the complex are required.

The dehydrogenation by ferric acetate or the ferric chloride - pyridine system resembles Criegee's oxidation of glycols by lead tetraacetate.[11] Furthermore, it has been proposed that the excitation of Fe(III) complexes with OH^-, Br^-, I^-, NCS^- or $C_2O_4^{2-}$ as the ligand results in the transfer of an electron from the ligand to the Fe(III).[12] In a previous paper,[2] we have assumed the interaction of pyridine with the hydrogen of the hydroxyl group of glycol and the transfer of an electron from the oxygen of glycol or the glycol anion to the Fe(III), as is indicated in Eq. (4). The dehydrogenation by ferric acetate may also involve a mechanism similar to that of the case of pyridine, that is, the intramolecular interaction of acetate anion with the hydroxyl group and the oxidation of glycol or the glycol anion by the excited ferric acetate, thus producing formaldehyde *via* the cleavage of a carbon-carbon bond.

11) R. Criegee, E. Höger, C. Huber, P. Kruck, F. Marktscheffel and H. Schellenberger, *Ann.*, **599**, 81 (1956).

12) N. Uri, *Chem. Revs.*, **50**, 375 (1952); E. Rabinowitch, *Rev. Modern Phys.*, **14**, 112 (1942); C. A. Parker, *Trans. Faraday Soc.*, **50**, 1213 (1954); C. A. Parker and C. G. Hatchard, *J. Phys. Chem.*, **63**, 22 (1959).

BULLETIN OF THE CHEMICAL SOCIETY OF JAPAN VOL. 41 2733—2735 (1968)

Synthetic Studies of Sesamol Derivatives. X.*1 Synthesis of Dehydroneotenone

Kenji FUKUI and Mitsuru NAKAYAMA

Department of Chemistry, Faculty of Science, Hiroshima University, Higashi Sendamachi, Hiroshima

(Received April 27, 1968)

The synthesis of dehydroneotenone has been carried out using 6-hydroxy-5-(2-methoxy-4,5-methylenedioxyphenylacetyl)-2,3-dihydrobenzo[*b*]furan as an intermediate and by subjecting it to cyclization with ethyl orthoformate, followed by dehydrogenation.

Dehydroneotenone (Erosone),[1] a colorless substance, $C_{19}H_{12}O_6$, is the first naturally-occurring furanoisoflavone (I) which has been isolated, along with pachyrrhizin (II)[2], from *Pachyrrhizus erosus* (Yam bean),[3] as well as from *Neorautanenia edulis*[4] and *N. amboensis*.[4] On the other hand, I has been derived[5] from neotenone (III), a naturally-occurring furanoisoflavanone, by dehydrogenation with manganese dioxide. The present paper will describe the total synthesis of I according to a modification of a procedure reported earlier.[6]

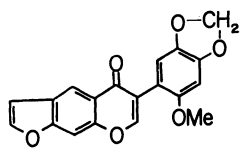

I

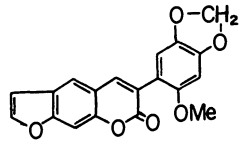

II

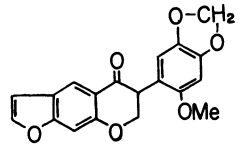

III

By a modified Hoesch reaction, 6-hydroxy-2,3-dihydrobenzo[*b*]furan (IV)[7] was condensed with 2-methoxy-4,5-methylenedioxyphenylacetonitrile

*1 This has previously been reported in a preliminary form: K. Fukui and M. Nakayama, *Experientia*, **20**, 668 (1964). Part IX: K. Fukui, M. Nakayama and T. Matsui, *Nippon Kagaku Zasshi (J. Chem. Soc. Japan, Pure Chem. Sect.)*, **87**, 1359 (1966).

1) W. D. Ollis, "Symposium on Photochemistry," ed. by H. R. Arthur, Hong Kong Univ. Press, Hong Kong (1964), p. 145.

2) E. Simonitsch, M. Frei and H. Schmid, *Monatsh. Chem.*, **88**, 541 (1957).

3) L. B. Norton and R. Hansberry, *J. Am. Chem. Soc.*, **67**, 1609 (1945).

4) C. v. d. M. Brink, J. J. Dekker, E. C. Hanekom, D. H. Meiring and G. J. H. Rall, *J. S. African Chem. Inst.*, **18**, 21 (1965); *Chem. Abstr.*, **63**, 14834 (1965).

5) L. Crombie and D. A. Whiting, *Tetrahedron Letters*, **1962**, 801; *J. Chem. Soc.*, **1963**, 1569.

6) a) K. Fukui and M. Nakayama, *Experientia*, **19**, 621 (1963); This Bulletin, **41**, 1385 (1968); b) K. Fukui and M. Nakayama, *Nippon Kagaku Zasshi (J. Chem. Soc. Japan, Pure Chem. Sect.)*, **85**, 444 (1964); c) K. Fukui, M. Nakayama, A. Tanaka and S. Sasatani, This Bulletin, **38**, 845 (1965).

7) J. S. H. Davies, P. A. McCrea, W. L. Norris and R. Ramage, *J. Chem. Soc.*, **1950**, 3206.

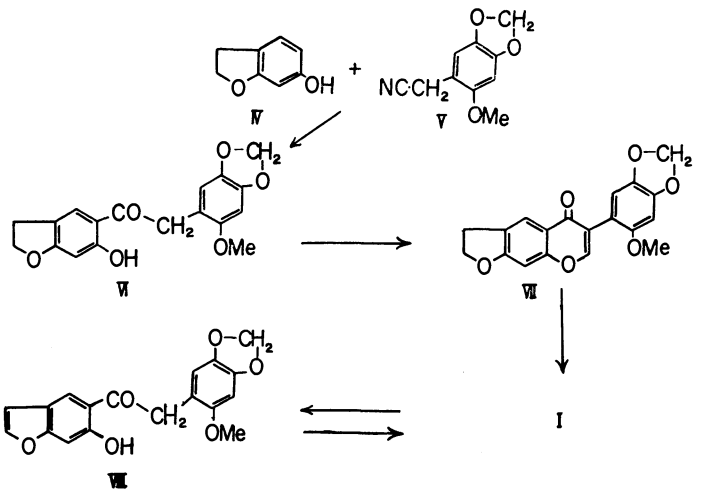

(V)[8] to give 6-hydroxy-5-(2-methoxy-4, 5-methylenedioxyphenylacetyl)-2, 3-dihydrobenzo[*b*]furan (VI). The subsequent treatment of the dihydrobenzofuran VI with ethyl orthoformate - pyridine - piperidine gave dihydrodehydroneotenone (VII). The dehydrogenation of the dihydro-compound VII with either *N*-bromosuccinimide[4,9] or 10% palladium-charcoal gave the isoflavone I. On alkaline hydrolysis, I gave 6-hydroxy-5-(2-methoxy-4,5-methylenedioxyphenylacetyl)benzo[*b*]furan (VIII).[5,9]

The partial synthesis of III had already been carried out from the isoflavone I.[5] Moreover, the racemate of (−)-neodulin (IX),[10] a naturally-occurring pterocarpan, had already been derived from the same isoflavone I *via* the corresponding isoflavanol-4.[4] Thus, the total syntheses of III and (±)-IX have been now accomplished.

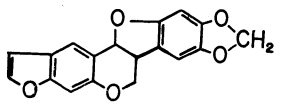

IX

The ultraviolet spectra of the isoflavone I and its dihydro-compound VII are shown in Fig. 1. There are two absorption bands, at *ca.* 230—250 mμ (band I) and at *ca.* 300—310 mμ (band II). Band I is due to furano- and dihydrofurano-benzenoid. The dehydrogenation of the dihydrofuranobenzenoid showed a marked hyperchromic effect. Many samples of this same phenomenon have been reported in previous reports.[2,6,11]

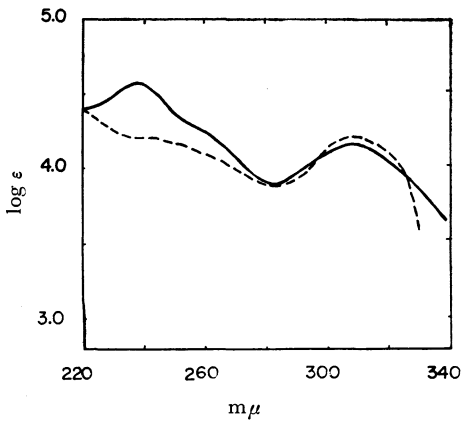

Fig. 1. UV spectra of I (——) and VII (- - -) in ethanol.

Experimental*2

6-Hydroxy-5-(2-methoxy-4,5-methylenedioxyphenylacetyl)-2,3-dihydrobenzo[*b*]furan (VI). To a mixture of 6-hydroxy-2,3-dihydrobenzo[*b*]furan (IV)[7] (4.0 g), 2-methoxy-4, 5-methylenedioxyphenylacetonitrile (V)[8a] (4.0 g), and fused zinc chloride (9.0 g) in dry chloroform (200 m*l*), anhydrous aluminum chloride (7.0 g) was added. Dry hydrogen chloride was passed through this mixture for 30 min at 0°C, and then dry ether (150 m*l*) was added. The resulting mixture was completely saturated with dry hydrogen chloride and then allowed to stand for 4 days in a

8) a) K. Fukui and M. Nakayama, *Nippon Kagaku Zasshi (J. Chem. Soc. Japan, Pure Chem. Sect.)*, **84**, 606 (1963); b) H. Suginome, *Tetrahedron Letters*, **1960** 16; This Bulletin, **39**, 1525 (1966); c) C. A. Anirudhan and W. B. Whalley, *J. Chem. Soc.*, **1963**, 6049.

9) K. Fukui and M. Nakayama, *Experientia*, **20**, 668 (1964).

10) B. L. van Durren, *J. Org. Chem.*, **26**, 5014 (1961).

11) a) K. Fukui, M. Nakayama and K. Okazaki, *Nippon Kagaku Zasshi (J. Chem. Soc. Japan, Pure Chem. Sect.)*, **87**, 1096 (1966); b) D. K. Chatterjee, R. M. Chatterje and K. Sen, *J. Org. Chem.*, **29**, 2467 (1964).

*2 All melting points are uncorrected; the infrared spectra were measured in Nujol, while the ultraviolet spectra were measured in an ethanol solution.

refrigerator. An ether solution was decanted from the ketimine hydrochloride, which had separated. The residue was washed with dry ether and then hydrolyzed with water (350 m*l*) on a steam bath for 1 hr. The precipitates were collected and recrystallized from ethanol to give VI as colorless needles, mp 153—154°C, which gave a brown ferric chloride reaction in ethanol; yield, 2.1 g (31%). IR: 1650 (C=O), 1038, 931 (O-CH_2-O) cm^{-1}. UV: λ_{max} mμ (log ε); 239 (4.21), 284 (4.14), 330 (3.70).

Found: C, 65.67; H, 4.95%. Calcd for $C_{18}H_{16}O_6$: C, 65.85; H, 4.91%.

Dihydrodehydroneotenone(4'',5''-dihydrofurano-(3'',2'':6,7)-2'-methoxy-4',5'-methylenedioxyisoflavone) (VII). To a solution of VI (1.0 g) and ethyl orthoformate (6 m*l*) in pyridine (25 m*l*), piperidine (1 m*l*) was added. The solution was then refluxed for 24 hr. The resulting solution was cooled and acidified with dilute hydrochloric acid. The resulting precipitates were collected, washed with water, and recrystallized from ethanol to give VII as colorless needles, mp 247—248°C; yield, 1.1 g (82%) (lit.[4] mp 255°C (correct.)). IR: 1644 (γ-pyrone), 1040, 919 (O-CH_2-O) cm^{-1}. UV: λ_{max} mμ (log ε); 241_i (4.22),*3 251_i (4.19), 310 (4.23).

Found: C, 67.38; H, 4.47%. Calcd for $C_{19}H_{14}O_6$: C, 67.45; H, 4.17%.

Dehydroneotenone (I). A mixture of VII (500 mg), 10% palladium-charcoal (400 mg), and diphenyl ether (20 m*l*) was refluxed for 10 hr. The catalyst was then filtered off, and the solvent removed by steam distillation. The resulting precipitates were collected and recrystallized from ethanol to give I as colorless needles, mp 234—235°C; yield, 220 mg (44%) (lit. mp 242°C (correct.),[3] 239.5—240.5°C (correct.),[4] 240—241°C[5]). This was identical with an authentic sample (mp 234—235°C) obtained from VII by the *N*-bromosuccinimide method.[9] IR: 1644 (γ-pyrone), 1626, 1589, 1544, 1508 (aromatic), 1040, 942 (O-CH_2-O) cm^{-1} (lit.[5] 1658, 1629, 1592, 1549, 1506 cm^{-1} (chloroform solution)). UV: λ_{max} mμ (log ε); 238 (4.59), 309 (4.20) (lit.[5] 239 (4.61), 308 (4.10)).

Found: C, 68.00; H, 3.84%. Calcd for $C_{19}H_{12}O_6$: C, 67.85; H, 3.60%.

The authors are grateful to Professor Tetsuo Mitsui, Kyoto University, for his microanalyses.

*3 i=Inflection point.

BULLETIN OF THE CHEMICAL SOCIETY OF JAPAN VOL. 41 2735—2742 (1968)

Sur la Structure des Dimères du *N*-Phényl Acétone-D-glycéraldimine

Masuo FUNABASHI et Juji YOSHIMURA

Laboratoire de Chimie des Substances Naturelles, Faculté des Sciences, Institut Téchnologique de Tokio Ookayama, Meguro-ku, Tokio

(Reçu le 30 Avril 1968)

N-phényl acétone-D-glycéraldimine dimérise facilement en présence d'un soupçon de l'acide acétique et donne deux dimères, dont la structure y comprise la configuration absolue partielle a été etablie par l'analyse spectrométrique et la décomposition chimique comme étant un 4-anilino-2-(2',2'-diméthyl-1',3'-dioxolanne-4'-yl)-1,2,3,4-tétrahydroquinoléine-3-spiro-4''-(2'',2''-diméthyl-1'',3'')dioxolanne. Lorsqu'on hydrolyse ces dimères partiellement avec l'acide acétique aqueux à 70%, on peut isoler 1,2,3,4,5,6-héxahydro-4-hydroxy-1,5-méthano-2,6-benzoxazocine-11-spiro-4'-(2',2'-dimethyl-1',3')dioxolanne avec un rendement d'environ 40% et en même temps l'aniline est detaché. Néanmoins, le dérivé *N*-acétyle d'un dimère n'a pas détaché l'aniline à la même condition d'hydrolyse.

En conséquence des recherches sur la synthèse asymétrique entre le *N*-phényl acétone-D-glycéraldimine (I) et les réactifs organométalliques, on a déjà rapporté[1] que le composé d'addition du type de threo se produisait supérieurement dans le cas du phénylllithium et par contre le composé d'addition d'érythro prédominait dans le cas du bromure de phénylmagnesium.

A cette occasion on a aperçu que I perdait graduellement le pouvoir rotatoire et les aiguilles se précipitaient peu à peu pendant quelques semaines. On pensait momentanément que ce phénomène doit à l'isomérisation de l'aldimine (I) en l'énamine (II) en présence d'un soupçon de l'acide:

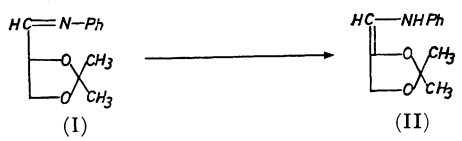

(I) (II)

1) J. Yoshimura, Y. Ohgo et T. Sato, *J. Am. Chem. Soc.*, **86**, 3858 (1964).

2) M. Funabashi, H. Ando et J. Yoshimura, *Tetrahedron Letters*, No. 1, 115 (1968).

Cependant ces aiguilles ont été confirmées d'être un dimère (III) de I selon le mesurage du poids moléculaire. On a aussi pu isoler un autre dimère (IV, les cristaux cubiques) de dedans du filtrat de III et le rendement total de ces deux dimères est au plus 30% et le rapport de III et IV est environ 2 : 1.

Dans une communication précédente,[2] on a decrit l'isolement de ces deux dimères à l'aide de la chromatographie de colonne et la cristallisation fractionnée et on y a proposé erronément une structure du type de 3-anilino-1,2,3,4-tetrahydroquinoléine (A) seulement en analysant le spectre infra-rouge et de résonance magnétique nuclaire.

Après un certain temps on a trouvé que la structure raisonable de III était le type de 4-anilino-1,2,3,4-tétrahydroquinoléine (B), en conduisant III au dérivé cétonique plus caractéristique.

Ce rapport se concerne en la vérification que ces deux dimères sont dérivés du 4-anilino-1,2,3,4-tétrahydroquinoléine et en détermination de la configuration absolue partielle de III. On voudrait ici rapporter en détail les résultats d'analyse spectrométrique et la transformation III en un dérivé cétonique.

Résultats et Discussion

Le spectre de masse de III et IV montre, outre un pic moléculaire à *m/e* 410, quelques pics caractéristiques; un pic à *m/e* 395 (M−15), un pic à *m/e* 317 correspondant au départ de $[PhNH_2]^+$, un pic à *m/e* 309 (M−101), et un pic à *m/e* 101 du à l'oxonium-cation du 2,2-diméthyl-1,3-dioxolanne.

Le spectre infra-rouge de III, auquel il y a une grande ressemblance entre III et IV, montre les bandes caractéristiques suivantes: 3410 (NH), 2985, 2935 (CH_3), 1610, 1580, 1500 (phényl), 1485 (CH_3), 1385, 1385, 1217, 1180 cm^{-1} (CMe_2), 750 et 690 cm^{-1} (le benzène monosubstitué et ortho-disubstitué). Le spectre IR du dérivé monoacétyle (V) de III montre aussi une bande amine à 3440 cm^{-1}.

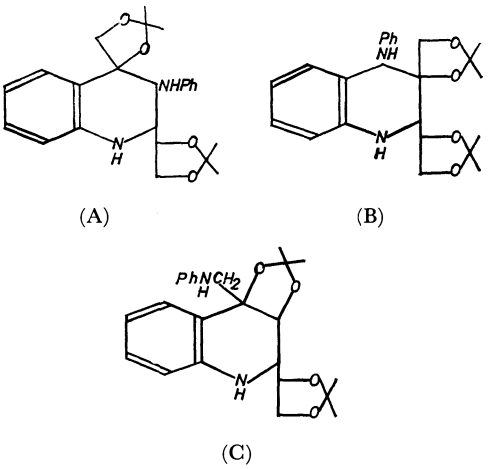

(A) (B)

(C)

Les trois structures cycliques suivantes parmi huit celles-là possibles en théorie sont en accord avec les résultats du spectre IR et de masse.

Le spectre RMN du dérivé deutérié en N de III (Fig. 1) montre les quatre pics à τ 8.46—8.67 dûs aux groupements méthyles géminés sur les cycles de dioxolanne et un multiplet à τ 2.85—3.33 attribuable au phényl correspondant à neuf protons. Les autres sept protons (sauf les duex NH) sont remarqués à τ 5.0—6.5. Il est clair que le doublet (J=2.5 cps) à τ 6.32 doit être dû au proton (He) en C-2 dans le cycle du 1,2,3,4-tétrahydroquinoléine, parce que l'irradiation de ce proton a transformé le sextet d'un proton (Ha) à τ 5.42 en un triplet et l'irradiation inverse a transformé le doublet en

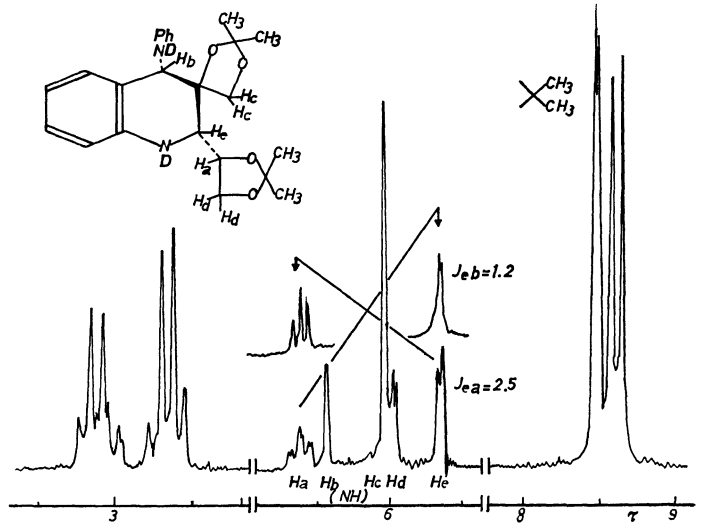

Fig. 1. Spectre RMN du composé deutérié de III et spin-spin découplage (100 Mc, $CDCl_3$).

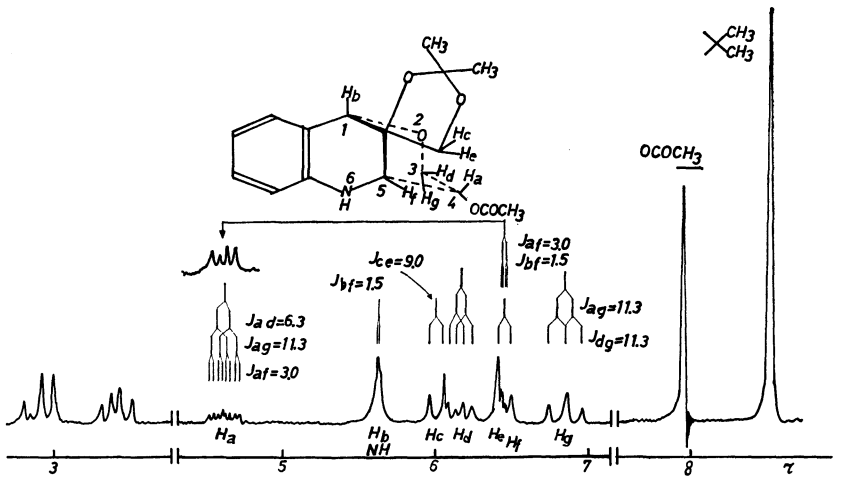

Fig. 2. Spectre RMN du composé IIIb et spin-spin découplage (100 Mc, $CDCl_3$).

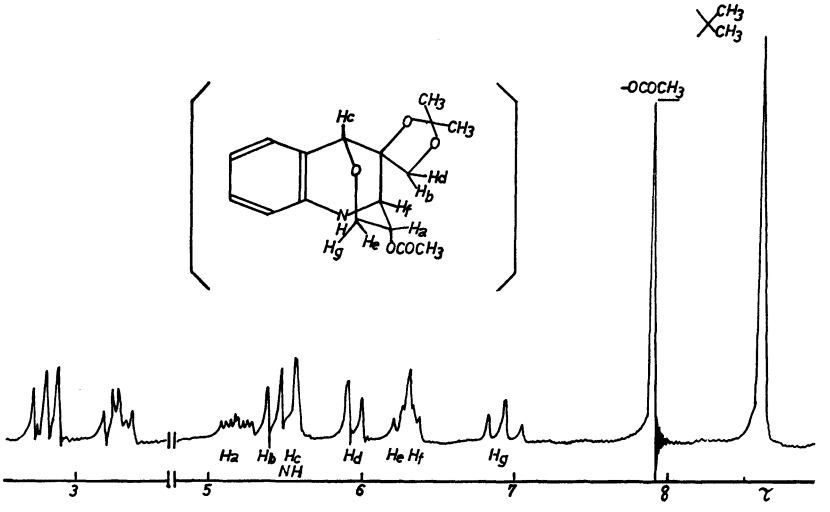

Fig. 3. Spectre RMN du composé IVb (100 Mc, $CDCl_3$).

autre doublet étroit (J=1.2 cps). Le sextet correspond au proton (Ha) de méthine dans le cycle dioxolanne lié au C-2, couplé tant avec le proton (He) à C-2 que avec les deux protons (Hd) du groupement méthylène. Le singulet à τ 5.95 attribuable aux protons d'autre méthylène se superpose avec une partie de Hd.

Comme ces interprétations du spectre RMN peuvent être appliqués à n'importe quelle structure de A, B et C, il est impossible de distinguer ces trois structures seulement par l'analyse du spectre RMN.

C'est pourquoi on a essayé de conduire III et IV au composé plus simple et plus caractéristique. Quand on d'abord hydrolyse III partiellement avec l'acide acétique aqueux à 70%, on obtient des cristaux aiguilles (IIIa) et en même temps l'aniline se détache. Dans le cas de IV, on aussi obtient les aiguillles purifiées par la chromatographie de colonne avec un rendement d'environ 40%. IIIa et IVa correspond à $C_{15}H_{19}O_4N$ selon l'analyse élémentaire et le spectre de masse montre un pic moléculaire à m/e 277 et un pic déshydraté à m/e 259 (M−18). Le spectre IR de IIIa montre les bandes caractéristiques: 3460 (OH), 3400 (NH), 1610, 1500 (phényl), 1380, 1370 (CMe_2) et 760 cm^{-1} (le benzène ortho-disubstitué), mais une bande attribuable au benzène monosubstitué à 690 cm^{-1} est disparue, ce qui est compatible avec le phénomène du détachement de l'aniline au cours de l'hydrolyse.

L'acétylation de IIIa et IVa avec l'anhydride acétique en présence de la pyridine donne les dérivés monoacétylés (IIIb et IVb), dont le spectre IR montre une bande d'éster à 1735 cm^{-1}. Le spectre RMN de IIIb, qui est donné dans la Fig. 2,

montre un singulet dû au groupement isopropylidène à τ 8.50, un singulet dû au groupement acétyle à τ 7.98 et ensuite un multiplet attribuable au groupement phényle à τ vers 3.0. Le rapport de l'intensité intégrale de ces trois groupement est environ 6 : 3 : 4.

Le spectre RMN de IVb donné dans la Fig. 3 a une ressemblance frappante avec celui-là de IIIb sauf quelques différences du déplacement chimique.

Le résultat du spectre RMN decrit ci-dessus indique qu'il n'y a qu'un seul hydroxyle dans la structure IIIa et IVa et qu'une nouvelle réaction de cyclisation intramoléculaire doit se produire au cours de l'hydrolyse partielle.

La plus possible structure parmi 18 celles-là conduites à partir de A, B et C est l'un ou l'autre des deux structures (A-1, B-1) suivantes qui sont en accord avec les donnés spectrométriques.

Dans le cas de la structure C, le détachement de l'aniline est impossible au point de vue structurale et même si l'aniline se détachait de C au cours de l'hydrolyse, le produit ne pourrait pas montre un singulet dû au grou ement iso ropylidène, mais un doublet selon le rapport de Foster et coll.[3]

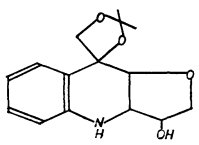

(A-1)

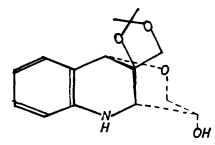

(B-1)

Citons le spectre RMN de IIIb (Fig. 2) encore une fois et distribuons les hydrogènes dans la région de τ 4.55 à τ 6.87 aux positions propres de la structure B-1, qui posséde le cycle 1,5-méthano-2,6-benzoxazocine. Le spectre montre un octet à τ 4.55 attribuable à l'hydrogène (Ha) en C-4 couplé avec trois hydrogènes (Hd, Hg, Hf) en C-3 et C-5, un doublet ($J_{b,f}$=1.5 cps) à τ 5.60 dû à l'hydrogène (Hb) en C-1 se superposant à l'hydrogène de NH, un doublet ($J_{c,e}$=9.0 cps) dû à l'un (Hc) des hydrogènes géminés dans le cycle dioxolanne à τ 5.95, un quadruplet ($J_{a,d}$ =6.3, $J_{d,g}$=11.3 cps) à τ 6.12 attribuable à l'hydrogène (Hd) en C-2 couplé avec les deux hydrogènes en C-3 et C-4, un quadruplet ($J_{a,f}$ =3.0, $J_{b,f}$=1.5 cps) dû à l'hydrogène (Hf) de C-5 à τ 6.46, un doublet ($J_{c,e}$=9.0 cps) dû à l'autre (He) de *gém*-hydrogènes à τ 6.46 et un triplet à τ 6.87 ($J_{d,g}=J_{a,g}$=11.5 cps) dû à l'hydrogène (Hg) en C-3.

Quoiqu'on peut aussi attribuer ces hydrogènes respectivement aux positions propres de A-1 ayant le squelette furano [3,2-*b*] quinoléine, il reste encore une partie un peu irrationale; c'est à dire que la constante de couplage J=1.5 cps est trop petite pour les hydrogènes vicinaux entre C-2 et C-3, parce qu'on sait[4] que celle-là entre les deux hydrogènes vicinaux à la tête de pont du cycle de cinq atomes fondu en cis au cycle de six atomes est en général 4—5 cps.

Dans le cas de la structure B-1, cette petite constante de couplage correspond au couplage à longue distance entre H-1 et H-5 attribuable au règle de W-lettre et par conséquent tous les deux substituants à C-1 et C-5 doivent être axuels. Il en résulte que la structure B-1 plûtot que A-1 est conforme à l'estimation du spectre RMN. Néanmoins, il est nésessaire de conduire IIIa au composé plus simple et plus caractéristique pour distinguer B-1 de A-1 complètement. Ainsi, IIIa est d'abord conduit au dérivé diméthylé en N, O avec l'iodure de méthyle et l'hydrure de sodium, et ensuite hydrolysé avec l'acide acétique aqueux à 70% et enfin transformé en le dérivé cétonique (IIIc) par l'oxidation avec l'acide périodique.

Si la structure A-1 était raisonable, IIIc correspondrait à A-2 et par contre si la structure B-1 était juste, IIIc s'accorderait avec B-2 comme déssiné ci-dessous.

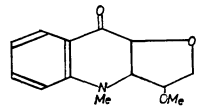

(A-2)

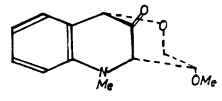

(B-2)

Le discernement B-2 de A-2 est beaucoup facilité tant par le spectre IR que par le spectre UV, parce que le spectre IR du dérivé cétonique conjugué montra une bande carbonyle conjugée[5] dans la région vers 1660 cm^{-1} et son spectre UV montra un effet bathochrome en conséquence de la conjugaison.

En vérité, le spectre IR de IIIc montre une bande carbonyle non-conjuguée[6] à 1740 cm^{-1} et le spectre UV montre deux maxima d'absorption à 258 et 313 mμ. Par conséquent, la structure A-2 correspondante au dérivé cétonique conjugué peut être rejetée aisement.

Par ailleurs, le dispersion rotatoire optique de IIIc indique l'effect Cotton négatif vers 260 mμ (Fig. 4), ce qui permet de supposer la configuration absolue de IIIc comme déssinée au-dessus d'après le règle d'octant. La configuration absolue de IIIa et III peut être aussi donnée comme déssinée plus haut sauf la partie du carbone de spiro. La configuration absolue de IV et IVa est en cours d'investigation.

D'autre part, le dérivé monoacétylé (V), qui est préparé à partir de III avec le chlorure d'acétyle et de la pyridine, montre un comportement

3) N. Baggett, K. W. Buck, A. B. Foster, R. Jefferris, B. H. Rees et J. M. Webber, *J. Chem. Soc.*, **1965**, 3382.

4) L. D. Hall, "Advances in Carbohydrate Chemistry," Vol. 19, ed, by M. L. Wolfrom and R. S. Tipson, Academic Press, New York and London (1964), p. 79.

5) J. T. Braunholz et F. G. Mann, *J. Chem. Soc.*, **1957**, 4166.

6) T. D. Perrine, *J. Org. Chem.*, **22**, 1487 (1957).

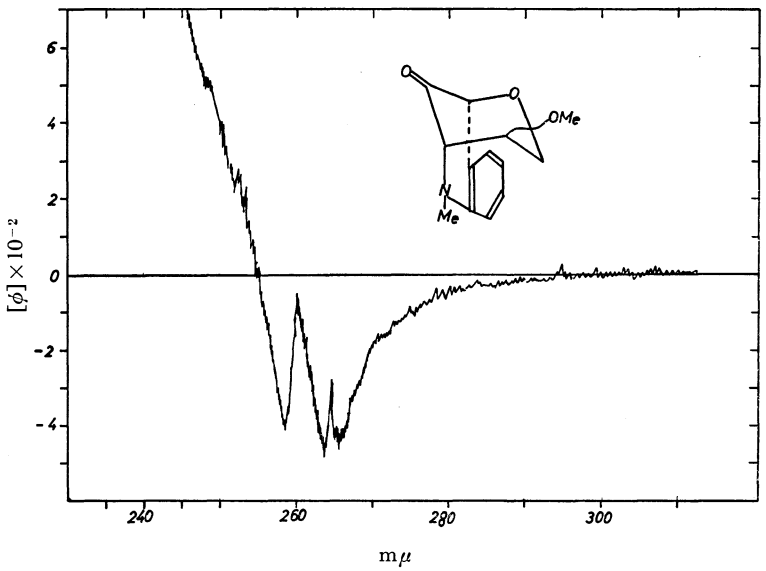

Fig. 4. Spectre DRO du composé IIIc dans le méthanol.

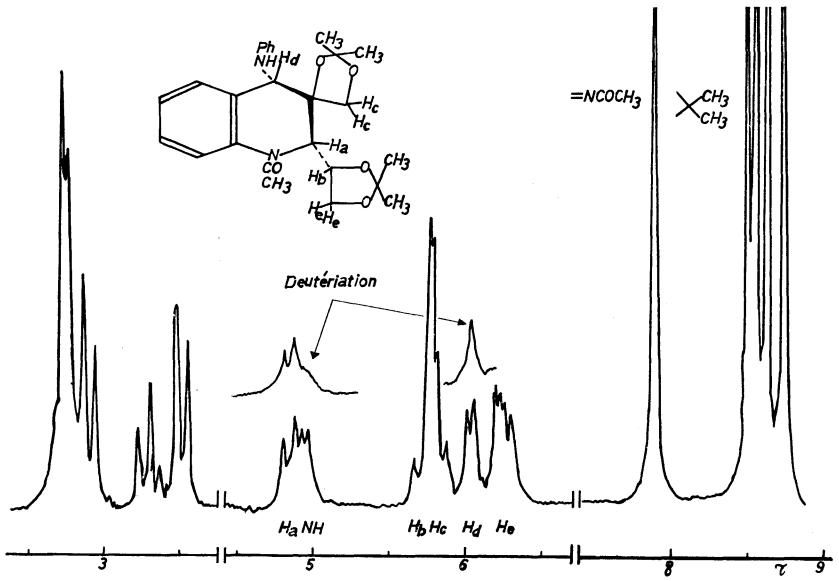

Fig. 5. Spectre RMN du composé V (100 Mc, $CDCl_3$).

différent de III contre l'hydrolyse. Le spectre RMN de V est indiqué dans la Figure 5. Le doublet ($J=7.0$ cps) est attribuable à l'hydrogène en C-2 et la distribution des autres protons est indiquée dans cette figure. Cette grandeur de la constante de couplage ($J=7.0$ cps) indique que le groupement acétyle n'est pas au nitrogène du groupement anilino en C-4, mais au nitrogène dans le cycle 1,2,3,4-tétrahydroquinoléine.

Quand on hydrolyse V à la même condition que III, on ne peut pas obtenir un composé correspondant au dérivé *N*-acétylé de IIIa, mais un composé suivant (Va) qui conserve le groupement anilino.

On ne peut pas s'empêcher de penser que la difficulté de détachement de l'aniline doive à l'éléctronégativité du groupement acétyle. Le spectre RMN (Fig. 6) de Vb (le dérivé acétylé de Va) montre trois pics vers τ 8.0 dû au groupement *O*-acétyle et un pic à τ 7.90 dû au groupement *N*-acétyle et le rapport de l'intensité intégrale de celui-là à celui-ci est 3 : 1, ce qui indique la présence de trois groupements *O*-acétyles. Un singulet d'intensité 1 à τ 6.68 est attribuable au groupement hydroxyle tértiaire, qui est disparu par deutériation. Les autres protons peuvent être distribués comme déssinés dans la figure.

Le dérivé monoacétylé (V) resiste à l'alkali à

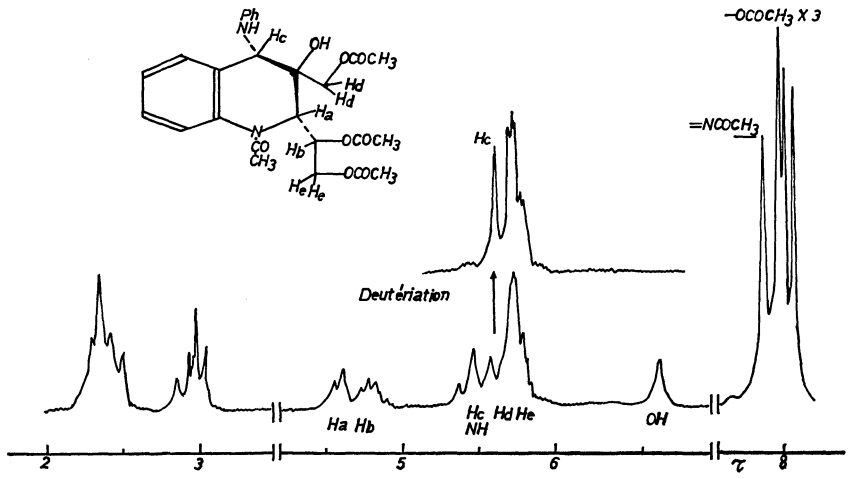

Fig. 6. Spectre RMN du composé Vb (100 Mc, $CDCl_3$).

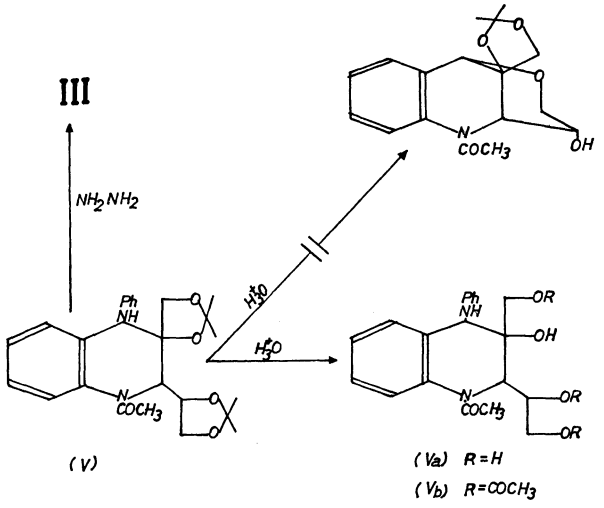

la différence de l'amide tértiaire ordinaire: quand on chauffe V au reflux dans du méthanol contenant de méthylate de sodium, on complètement retire V, qui peut être transformé en III seulement en chauffant V dans du hydrazine anhydre.

Sur méchanisme de réaction de cette dimérisation, on réfléchit maintenant comme suite; c'est à dire que I premièrement dimérise au composé additionné aldolique (I') et ensuite il se cyclise en III et IV en présence d'un soupçon de l'acide.

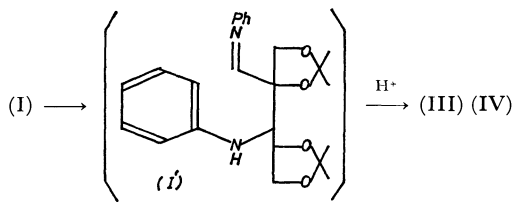

Partie Expérimentale

Les points de fusion non corrigés ont été déterminés en tube capillaire dans le bain de l'acide sulfurique. Les spectres de masse ont été pris sur Hitachi RMU-6. Les spectres IR ont été pris sur Hitachi EPI-G2 et les spectres UV et DRO ont été pris sur Hitachi EPS-3T et Nihon Bunko ORD/UV-5 respectivement en solution dans le méthanol. Les spectres RMN ont été pris sur JNM-4H-100 en solution dans le deutériochloroforme avec le tétraméthylsilane comme réference interne.

L'isolation de 4-Anilino-2-(2',2'-diméthyl-1',3'-dioxolanne-4'-yl)-1,2,3,4-tétrahydroquinoléine-3-spiro-4''-(2'',2''-diméthyl-1'',3'') dioxolanne (III et IV). A une solution de l'acétone-D-glycéraldehyde (18 g, 0.14 mol) et l'aniline (13 g, 0.14 mol) dans le benzène (20 m*l*) on ajoute l'acide acétique (1 m*l*) et laisse reposer le mélange de réaction pendant 24 h à une température ambiante. De l'eau formée et l'acide

acétique sont eliminés sur le carbonate de potassium anhydre. En chassant le solvant sous vide on obtient le sirop rouge-brun, qui est redissout dans une petite quantité du benzène (environ deux fois le volume du sirop). Les aiguilles (III) se précipitent graduellement, mais quelque fois les cristaux cubiques (IV) se précipitent avant III. En général, on sépare les deux dimères par la chromatographie de colonne du gel de silice (WAKOGEL C-100) en utilisant le mélange ligroin - benzène comme l'agent d'élution. III est un peu plus vite élué que IV. La valeur R_f de III et IV est respectivement 0.91 et 0.85 (benzène : méthanol=3 : 1) sur le couche mince du gel de silice (WAKOGEL-B-O). Le rendement total de ces dimères est au plus de 30% de la théorie et le rapport de III à IV est environ 2 : 1, III cristallise dans l'éther ou le benzène en longues aiguilles soyeuses: F=161—162°C, $[\alpha]_D^{29}=-42.0°$ (*c* 1.0, $CHCl_3$).

Analyse $C_{24}H_{30}O_4N_2$: Calc. %: C, 70.22; H, 7.55; N, 6.82. Tr.%: C, 70.18; H, 7.49; N, 6.98.

IV cristallise dans l'éthanol en cristaux cubiques; F=199—200°C, $[\alpha]_D^{28}=+2.2°$ (*c* 1.2, $CHCl_3$).

Analyse $C_{24}H_{30}O_4N_2$: Tr.%: C, 70.40; H, 7.55; N, 7.00.

1-Acétyl-4-anilino-2-(2',2'-diméthyl-1',3'-dioxolanne-4'-yl)-1,2,3,4-tétrahydroquinoléine-3-spiro-4''-(2'',2''-diméthyl-1'',3'') dioxolanne (V). A une solution du dimère III (0.5 g) dans le solvant mélangé de la pyridine (0.5 m*l*) et du chlorure de méthylène (10 m*l*), on ajoute goute à goute le chlorure d'acéthyle (0.35 m*l*) en maintenant la température au-dessous de 5°C. Après qu'on laisse reposer pendant 5 h, on la lave avec de l'eau du bicarbonate de sodium et séché sur le sulfate de sodium anhydre et puis évaporé sous vide en pourde, qui est dissout dans l'éther, décoloré avec charbon actif et laisse reposer à la température ambiante. Les cristaux cubiques (0.33 g) précipitent graduellement. F=173°C, $[\alpha]_D^{29}=-152°$ (*c* 1.0, $CHCl_3$).

Analyse $C_{26}H_{32}O_5N_2$ (452): Calc.%: C, 69.00; H, 7.13; N, 6.19, Tr.%: C, 69.03; H, 7.16; N, 6.39.

Hydrolyse de III — Preparation de 1,2,3,4,5,6-Héxahydro-4-hydroxy-1,5-méthano-2,6-benzoxazocine-11-spiro-4'-(2',2'-diméthyl-1',3') dioxolanne (IIIa). On chauffe la suspension de III (2 g) dans l'acide acétique aqueux à 70% (20 m*l*) à 100°C pendant 5—10 mn. Après refroidissement avec de l'eau courante, on verse peu à peu la solution réactionnelle sur de l'eau (300 m*l*) du bicarbonate de sodium (20 g) et on filtre le précipitate. Le filtrate est éxtrait au chlorure de méthyléne (30 m*l*×5) et l'éxtrait est lavé avec une petite quantité de l'eau, séché sur le sulfate de soude anhydre et enfin évaporé sous vide. On obtient ainsi les cristaux aiguilles crus (0.42 g), qui sont lavés à l'éther et recristallisés dans l'acétone - méthanol (10 : 1). F=279—280°C (dec.), $[\alpha]_D^{29}=+13.2°$ (*c* 1.0, méthanol).

Analyse $C_{15}H_{19}O_4N$ (277); Calc. %: C, 65.28; H, 7.12; N, 5.15. Tr.%: C, 64.96; H, 6.91; N, 5.05.

Acétylation de IIIa—Préparation de 1,2,3,4,5,6-Héxahydro-4-acétoxy-1,5-méthano-2,6-benzoxazocine-11-spiro-4'-(2',2'-diméthyl-1',3') dioxolanne (IIIb). A une solution de IIIa (100 mg) dans la pyridine (2 m*l*) on ajoute l'anhydre acétique (2 m*l*) et laisse reposer à une température ambiante pendant 24 h. La solution réactionelle est puis versée sur de l'eau glacée et éxtraite au chlorure de méthylène. L'éxtrait est puis lavé avec de l'eau, séché sur sulfate de soude anhydre et évaporé sous vide en un résidu cristallisable, qui est recristallisé dans l'acétone ou l'acétate d'éthyle. On obtient les cristaux plats (85 mg, 81%). F=215—216°C, $[\alpha]_D^{28}=+105°$ (*c* 1.0, méthanol).

Analyse $C_{17}H_{21}O_5N$ (319): Calc. %: C, 63.93; H, 6.63; N, 4.39. Tr.%: C, 63.93; H, 6.82; N, 4.76.

Hydrolyse de IV. *Procédé a.* On hydrolyse IV à la même condition que III et le traitement est aussi même. IVa, qui est plus soluble que IIIa dans les solvants organiques, a difficulté à se cristalliser.

Procédé b. On suspend IV (298 mg) dans l'acide acétique aqueux à 70% et le dissout en chauffant à 100°C pendant 5 mn. On filtre une matière insoluble et on évapore le filtrate sous vide en un sirop brun, qui est purifié par la chromatographie de colonne du gel de silice. De la partie éluée au solvant mélangé (benzène et acétone=10 : 1) on obtient les blanches aiguilles (75 mg, 37%). F=183—185°C, $[\alpha]_D^{19}=+15.0°$ (*c* 0.27, méthanol).

Analyse $C_{15}H_{19}O_4N$ (277): Calc.%: C, 64.96; H, 6.91; N. 5.05. Tr.%: C, 64.37; H, 7.69; N, 4.81.

Acétylation de IVa. IVa est acétylé à la même condition que IIIa. A partir de IVa (62 mg) on obtient les cristaux (IVb) (48 mg, 69%), qui sont recristallisés dans l'acétone. F=192°C, $[\alpha]_D^{16.5}=+17.0°$ (*c* 0.45, méthanol).

Analyse $C_{17}H_{21}O_5N$ (319): Calc.%: C, 63.93; H, 6.63; N, 4.39. Tr.%: C, 63.53; H, 7.06; N, 4.42.

Transformation de IIIa au Dérivé Cétonique (IIIc). A une solution de IIIa (277 mg) dans le diméthylsulfoxide (10 m*l*) on ajoute peu à peu l'hydrure de sodium (150 mg) et on chauffe la solution à 60—70°C pendant 5 mn. Après refroidissement jusqu'à la température ambiante, on ajoute l'iodure de méthyle (0.5 m*l*×3) et on chauffe à 60°C pendant 5 mn. La solution réactionnelle est puis versée sur de l'eau glacée, éxtraite au chlorure de méthylène, lavée à l'eau, séchée sur Na_2SO_4 et enfin évaporée sous vide en sirop. Ce sirop (environ 300 mg) est puis chauffé à 100°C avec l'acide acétique (2 m*l*) aqueux à 70% pendant 30 mn. Après évaporation du solvant sous vide, on obtient les cristaux fondants à 147—150°C.

Analyse $C_{14}H_{19}O_4N\ H_2O$: Calc.%: C, 59.35; H, 7.47; N, 4.94. Tr.%: C, 59.25; H, 7.47; N, 5.08.

Finallement dans le mélange de l'eau distillée (5 m*l*) et du méthanol (5 m*l*), on dissout ces cristaux-là et le périodate de sodium (108 mg) et puis on laisse reposer à une température ambiante pendant une nuit. Après d'élimination du solvant par distillation, le résidu obtenu est rempli sur une colonne du gel de silice (WAKOGEL C-100, 10 g) et élué au benzène ou benzène - acétone (10 : 1). On obtient un sirop (IIIc; 70 mg) par évaporation du solvant. $[\alpha]_D^{19}=107°$ (*c* 0.52, méthanol), UV λ_{max}^{MeOH} 258 mμ (log ε, 4.16), 313 mμ (log ε, 3.60).

Analyse $C_{13}H_{15}O_3N$ (233): Calc.%: C, 66.93; H, 6.48; N, 6.01. Tr.%: C, 66.24; H, 6.53; N, 5.49.

Hydrolyse de V — Préparation de 1-Acétyl-4-anilino-2-(1',2'-dihydroxy) éthyl-3-hydroxy-3-hydroxyméthyl-1,2,3,4-tétrahydroquinoléine (Va). Après qu'on chauffe à 100°C la suspension de V (0.8 g) dans l'acide acétique aqueux à 70% pendant 13 mn, on élimine le solvant sous vide. Le sirop obtenu est purifié par la chromatographie de colonne du gel de silice en utilisant benzène et acétone comme l'éluant successivement. La partie éluée au benzène - acétone

(1 : 1) est évaporée sous vide. Le poudre amorphe (0.5 g) est obtenu. $[\alpha]_D^{22} = -90.5°$ (*c* 0.61, éthanol).

Analyse $C_{20}H_{24}O_5N_2$: Calc.%: C, 64.52; H, 6.50; N, 7.52. Tr.%: C, 64.32; H, 6.54: N, 6.60.

Acétylation de Va — Préparation de 3-Acétoxyméthyl-1-acétyl-4-anilino-2-(1',2'-diacétoxy) éthyl-3-hydroxy-1,2,3,4-tétrahydroquinoléine (Vb). — A une solution du poudre amorphe (0.5 g) obtenu ci-dessus dans la pyridine (10 m*l*), on ajoute l'anhydride acétique (10 m*l*) et on laisse reposer pendant une nuit. La solution réactionnelle est puis versée sur l'eau glacée, éxtraite au chlorure de méthylène, lavée à la solution de $NaHCO_3$, séchée sur Na_2SO_4 et enfin évaporée sous vide. Le poudre amorphe obtenu est dissout dans l'acétone, décoloré avec le charbon actif et reconcentré sous vide. On obtient 0.45 g de produit (poudre amorphe). $[\alpha]_D^{20} = -4.8°$ (*c* 1.1, méthanol).

Analyse $C_{26}H_{30}O_8N_2$: Calcd.%: C, 60.45; H, 6.24; N, 5.42. Tr.%: C, 61.24; H, 5.86; N, 5.29.

Transformation de V en III par l'Hydrazine Anhydre. On met le dérivé monoacétyle (V) (73 mg) et l'hydrazine anhydre à 98% (1 m*l*) dans le tube scellé qui a 1 cm de diamètre et 10 cm de longueur, et on chauffe à 100—120°C pendant 20 hr. Par refroidissement précipitent les aiguilles (51 mg, 77%), qui sont filtrées et lavées à l'éther. Ce produit n'a pas montré l'abaissement du point de fusion à l'examen mixte avec le dimère III.

BULLETIN OF THE CHEMICAL SOCIETY OF JAPAN VOL. 41 2742—2745 (1968)

New Syntheses of Vinyl Sulfides and Unsaturated Nitriles *via* Quaternary Phosphonium Salts

Takanobu KUMAMOTO, Kazuo HOSOI and Teruaki MUKAIYAMA

Laboratory of Organic Chemistry, Tokyo Institute of Technology, Ookayama, Meguro-ku, Tokyo

(Received May 1, 1968)

New methods for the syntheses of vinyl sulfides and unsaturated nitriles *via* quaternary phosphonium salts have been established. The reaction of isopropylidenetriphenylphosphorane with *S*-ethyl thiobenzoate or substituted *S*-ethyl thiobenzoates afforded vinyl sulfides and triphenylphosphine oxide in good yields. Further, it was found that the reaction of α-benzoylalkylphosphonium salts with sodium ethylmercaptide or potassium cyanide gave olefins, such as vinyl sulfides or unsaturated nitriles, and triphenylphosphine oxide in good yields, respectively.

The reaction of alkylidenephosphoranes with *S*-ethyl thiocarboxylate affords acylalkylidenephosphoranes in high yields. A removal of ethylmercaptan from an intitially formed phosphonium ethyl mercaptides shifts the equilibrium to the side of the phosphoranes.[1]

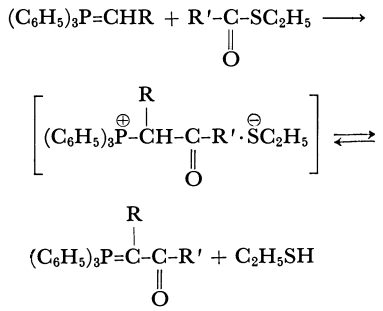

It was found by the present experiment that the reaction of thiolester with alkylidenephosphoranes having no hydrogen atom on the methylene carbon resulted in the formation of the Wittig type reaction products, vinyl sulfides and triphenylphosphine oxide. Thus, 1-ethylthio-2-methyl-1-phenylpropene and triphenylphosphine oxide were obtained in 72% and 40% yields, respectively, when isopropylidenetriphenylphosphorane was allowed to react with *S*-ethyl thiobenzoate in boiling tetrahydrofuran.

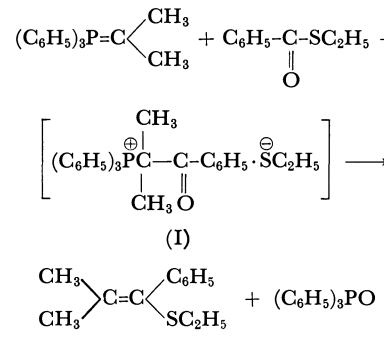

Similarly, isopropylidenetriphenylphosphorane reacted with *S*-methyl thiobenzoate and substituted *S*-ethyl thiobenzoates, such as *S*-ethyl *p*-chlorothiobenzoate and *S*-ethyl *p*-methoxythiobenzoate,

1) a) H. J. Bestmann and B. Arnason, *Chem. Ber.*, **95**, 1513 (1962). b) H. J. Bestmann and B. Arnason, *Tetrahedron Letters*, **1961**, 455.

TABLE 1. THE REACTION OF ISOPROPYLIDENETRIPHENYLPHOSPHORANE WITH THIOLESTER

Thiolester	Vinyl sulfide Yield (%)	Bp °C/mmHg	Anal. Found C(%)	Anal. (Calcd) H(%)	$(C_6H_5)_3PO$ (%)
$C_6H_5COSC_2H_5$	72	134—136/28	75.16 (74.97	8.58 8.39)	40
$C_6H_5COSCH_3$	73	118/16	73.87 (74.13	7.89 7.92)	45
p-$ClC_6H_4COSC_2H_5$	83	147/15	63.75 (63.72	6.95 6.67)	52
p-$CH_3OC_6H_4COSC_2H_5$	70	154/16	70.35 (70.24	8.13 8.16)	52

to give corresponding vinyl sulfides and triphenylphosphine oxide in good yields (see Table 1).

The above mentioned reactions are considered to proceed through an initial formation of phosphonium mercaptide (I). An intramolecular nucleophilic attack of the ethylmercapto anion on carbonyl carbon of (I) yields the vinyl sulfide and triphenylphosphine oxide probably through a betain structure (II) as shown in path B of the following scheme.

On the contrary, vinyl sulfide was not obtained when isopropylidenetriphenylphosphorane and *S*-phenyl thiobenzoate were refluxed in tetrahydrofuran. Instead, only phosphonium phenylmercaptide resulted. The phosphonium salt decomposed to yield 2-methyl-1-phenyl-1-phenylthiopropene (14%), triphenylphosphine oxide (10%), α-phenylthioisobutyrophenone (28%) and triphenylphospine (36%) when it was refluxed in toluene.

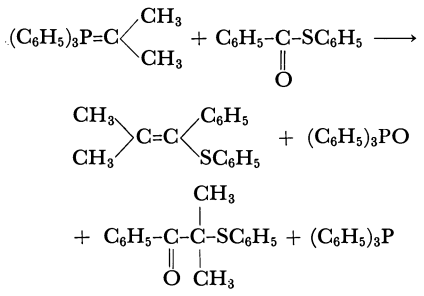

The formation of α-phenylthioisobutyrophenone and triphenylphosphine can be explained by assuming a nucleophilic attack of phenylmercapto anion on the α-carbon of the phosphonium salt (III) (Path A). It is noteworthy that, in the case of the *S*-phenyl thiocarboxylate, the nucleophilic attack of reference anion, phenylmercapto anion, occurs competitively on α-carbon and on carbonyl carbon to afford the above mentioned four products.

In the case of the reaction of isopropylidenetriphenylphosphorane with *S*-ethyl thiobutyrate in tetrahydrofuran, triphenylisopropylphosphonium iodide (99%) and *S*-ethyl α-butyrylthiobutyrate

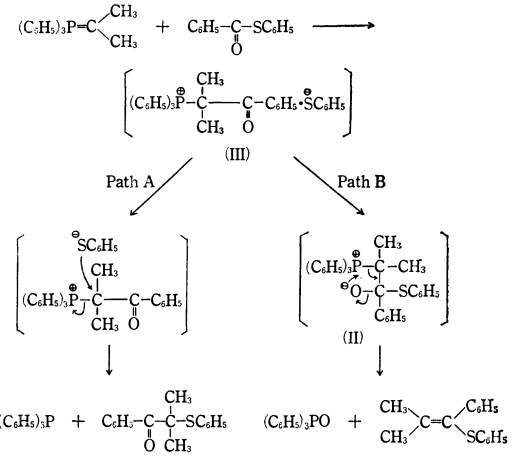

(77%) were obtained. This result shows that ester condensation reaction of *S*-ethyl thiobutyrate preferentially takes place to afford α-butyrylthiobutyrate by the influence of isopropylidenetriphenylphosphorane, a strong basic substance. The formation of triphenylisopropylphosphonium iodide can be explained by assuming the anion exchange reaction of phosphonium salt (IV) with lithium iodide.

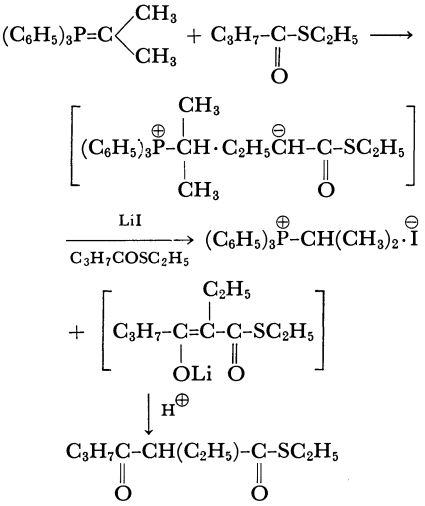

TABLE 2. THE REACTION OF α-BENZOYLALKYLPHOSPHONIUM SALT WITH SODIUM ETHYL MERCAPTIDE

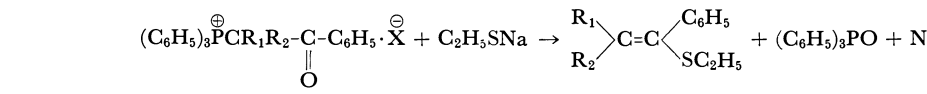

R_1	R_2	Vinyl sulfide Yield (%)	Bp (mp) °C/mmHg	Anal. Found C(%)	Anal. (Calcd) H(%)	$(C_6H_5)_3PO$ (%)
CH_3	CH_3	52	130/20	—	—	67
	H	45	150—155/7	77.87 (77.55	8.67 8.68)	47
CH_3	C_6H_5	83	113—115/1 (54)	79.78 (80.28	7.32 7.13)	82

TABLE 3. THE REACTION OF α-BENZOYLALKYLPHOSPHONIUM SALT WITH POTASSIUM CYANIDE

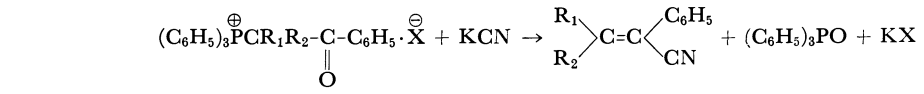

R_1	R_2	Unsaturated nitrile Yield (%)	Bp (mp) °C/mmHg	Anal. Found C(%)	Anal. (Calcd) H(%)	N(%)	$(C_6H_5)_3PO$ (%)
CH_3	CH_3	54	124—125/3	83.51 (84.04	7.06 7.05	8.86 8.91)	52
	H	72	116—117/1	85.33 (85.23	7.37 7.66	6.93 7.10)	82
CH_3	C_6H_5	75	(81)	87.47 (87.64	5.73 5.98	6.63 6.39)	82

Next, the isolation of the key intermediate (I) of the above mentioned reactions forming vinyl sulfide from sodium ethylmercaptide and triphenyl-α-benzoylisopropylphosphonium iodide was attempt. When sodium ethylmercaptide and triphenyl-α-benzoylisopropylphosphonium iodide, formed from isopropylidenetriphenylphosphorane and benzoyl chloride,[2] were refluxed in tetrahydrofuran for 6 hr, 1-ethylthio-2-methyl-1-phenylpropene (52%) and triphenylphosphine oxide (67%) were obtained as expected.

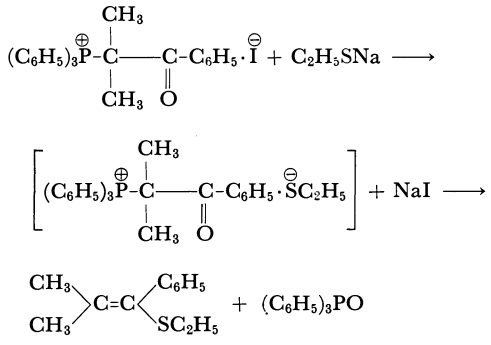

2) H. J. Bestmann and T. Denzel, *Tetrahedron Letters*, **1966**, 3591.

Similarly, the reaction of triphenyl-α-benzoylcyclohexylphosphonium bromide or triphenyl-1-benzoyl-1-phenylethylphosphonium bromide with sodium ethylmercaptide resulted in the formation of corresponding α-ethylthiobenzylidenecyclohexane or 1,2-diphenyl-1-ethylthiopropene and triphenylphosphine oxide in good yields (see Table 2). It is of interest to note that α-ethylthiobenzylidenecyclohexane could not be obtained directly from *S*-ethyl thiobenzoate and cyclohexylidenetriphenylphosphorane because the phosphonium salt, the key intermediate, could not be obtained even when they were refluxed in tetrahydrofuran.

In addition, it was found that the reaction of triphenyl-α-benzoylalkylphosphonium salt with sodium phenylmercaptide or potassium thiocyanate did not afford the expected olefins, such as vinyl sulfides or vinyl thiocyanates.

Finally, this reaction was successfully extended to the synthesis of unsaturated nitriles by reacting triphenyl-α-benzoylalkylphosphonium salts with potassium cyanide. When triphenyl-α-benzoylisopropylphosphonium iodide was allowed to react with potassium cyanide in tetrahydrofuran - water mixed solvent at room temperature, α-phenyl-β-methylcrotonitrile (54%) and triphenylphosphine oxide (52%) were obtained.

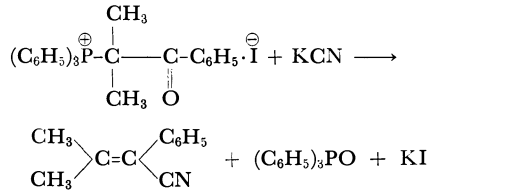

In a similar manner, cyclohexylidenephenylacetonitrile or α,β-diphenylcrotonitrile was obtained by the reaction of triphenyl-α-benzoylcyclohexylphosphonium bromide or triphenyl-1-benzoyl-1-phenylethylphosphonium bromide with potassium cyanide in good yields (see Table 3).

Further study on this type of the synthesis of unsaturated compound is now in progress.

Experimental

Reaction of Isopropylidenetriphenylphosphorane with *S*-Ethyl Thiobenzoate. *S*-Ethyl thiobenzoate (1.33 g, 0.008 mol) was added to the solution of isopropylidenetriphenylphosphorane, prepared from triphenylisopropylphosphonium iodide (4.32 g, 0.01 mol) and *n*-butyl lithium (0.01 mol) in tetrahydrofuran (20 m*l*) under nitrogen. The dark red color disappeared soon and a phosphonium salt precipitated. The reaction mixture was further refluxed for 4 hr under stirring. After resulted precipitate was filtered, the filtrate was evaporated under reduced pressure. The distillation *in vacuo* gave 1-ethylthio-2-methyl-1-phenylpropene (1.14 g, 74%), bp 133—135°C/25 mmHg. The precipitate and the residue of the distillation were collected and refluxed in a mixture of aqueous solution of 5% sodium hydroxide (10 m*l*) and benzene (10 m*l*) for 30 min. After precipitated triphenylisopropylphosphonium iodide was filtered, the benzene layer was separated. The removal of benzene gave white crystals. They were recrystallized from carbon tetrachloride, triphenylphosphine oxide was obtained, 1.20 g (40%), mp 154—156°C.

Reaction of Isopropylidenetriphenylphosphorane with *S*-Phenyl Thiobenzoate. A mixture of isopropylidenetriphenylphosphorane (0.02 mol) and *S*-phenyl thiobenzoate (4.28 g, 0.02 mol) was refluxed in toluene for 5 hr. After resulting precipitate was filtered, the filtrate was evaporated under reduced pressure. The residue was chromatographed on silica gel with petroleum ether, benzene and ether. α-Phenylthioisobutyrophenone, 1.00 g (25%) and triphenylphosphine oxide, 0.43 g (10%), mp 155—156°C, along with a mixture of triphenylphosphine and 2-methyl-1-phenyl-1-phenylthiopropene (V) were obtained from the elutate with benzene, ether and petroleum ether, respectively. α-Phenylthioisobutyrophenone was identified by the formation of its 2,4-dinitrophenylhydrazone, mp 155—156°C.

Found: C, 60.19; H, 4.73; N, 12.88%. Calcd for $C_{22}H_{20}N_4O_4S$: C, 60.54; H, 4.62; N, 12.84%. The mixture of triphenylphosphine and V was treated with an excess amount of methyl iodide to give triphenylmethylphosphonium iodide, 2.02 g. From the yield of phonium iodide, the yield of triphenylphosphine was estimated, 31%. The residue was distilled *in vacuo* to give V, 0.53 g (14%), bp 118—120°C/3 mmHg.

Reaction of Isopropylidenetriphenylphosphorane with *S*-Ethyl Thiobutyrate. A mixture of isopropylidenetriphenylphosphorane (0.01 mol) and *S*-ethyl thiobutyrate (1.32 g, 0.01 mol) in tetrahydrofruan (20 m*l*) was refluxed for 5 hr. A resulting white precipitate was filtered and recrystallized from the mixture of alcohol and ether giving triphenylisopropylphosphonium iodide, 4.18 g (99%), mp 195°C. The filtrate was evaporated *in vacuo* to give a white precipitate. After the neutralization with hydrochloric acid, an oily product was obtained. Distillation under reduced pressure gave *S*-ethyl α-butyrylthiobutyrate, 0.79 g (77%), bp 126—128°C/15 mmHg.

Preparation of Triphenyl-α-benzoylisopropylphosphonium Iodide. Benzoyl chloride (14.10 g, 0.10 mol) was added dropwise to the solution of isopropylidenetriphenylphosphorane, prepared from triphenylisopropylphosphonium iodide (43.20 g, 0.10 mol) and *n*-butyl lithium (0.10 mol) in tetrahydrofuran (200 m*l*) under nitrogen. The reaction mixture was refluxed for 5 hr under stirring. The resulting precipitate was filtered and was recrystallized from a mixture of alcohol and ether to give triphenyl-α-benzoylisopropylphosphonium iodide, 47 g (88%), mp 213—215°C.

Found: C, 62.13; H, 4.99%. Calcd for $C_{28}H_{26}IOP$: C, 62.69; H, 4.85%.

Reaction of Triphenyl-α-benzoylphosphonium Iodide with Sodium Ethylmercaptide. A mixture of triphenyl-α-benzoylisopropylphosphonium iodide (5.36 g, 0.01 mol) and sodium ethyl mercaptide (0.84 g, 0.01 mol) was refluxed in tetrahydrofuran for 5 hr under stirring. After removal of the solvent under reduced pressure, a small amount of ether was added to the residue. The precipitated crystals were filtered and the filtrate was distilled *in vacuo* to give 1-ethylthio-2-methyl-1-phenylpropene, 1.00 g (52%), bp 115—123°C/18 mmHg. The precipitate and the residue of the distillation were collected and were treated with aqueous 5% sodium hydroxide to give triphenylphosphine oxide, 2.06 g (74%), mp 153—154°C.

Reaction of Triphenyl-α-benzoylisopropylphosphonium Iodide with Potassium Cyanide. A mixture of triphenyl-α-benzoylisopropylphosphonium iodide (5.36 g, 0.01 mol) and potassium cyanide (0.66 g, 0.011 mol) in 10 m*l* of water and 10 m*l* of tetrahydrofuran was stirred at room temperature for 2 hr. The reaction mixture was extracted with 50 m*l* of ether. After the extract was evaporated under reduced pressure the residue was distilled *in vacuo* to give α-phenyl-β-methylcrotonitrile, 0.85 g (54%), bp 123—124°C/8 mmHg. The residue of the distillation was collected and was recrystallized from carbon tetrachloride to give triphenylphosphine oxide, 1.45 g (52%), mp 155—156°C.

BULLETIN OF THE CHEMICAL SOCIETY OF JAPAN VOL. 41 2746—2747 (1968)

A Convenient Method for the Preparation of Acid Anhydrides from Metallic Carboxylates

Tsujiaki HATA, Kiyohiko TAJIMA and Teruaki MUKAIYAMA

Laboratory of Organic Chemistry, Tokyo Institute of Technology, Ookayama, Meguro-ku, Tokyo

(Received May 2, 1968)

A convenient method for the preparation of carboxylic anhydrides by use of one mole of *N,N'*-dicyclohexylthiourea and two moles of silver or mercurous carboxylate has been established. According to this method, several carboxylic anhydrides were obtained in high yields under mild conditions even by microscale experiments.

In previous papers,[1,2] it has been reported that carboxylic anhydrides were prepared from the corresponding mercuric carboxylates by treatment with the addition compound of dibenzoylethylene and triphenylphosphine, or by treatments with *S*-ethylthioamidium iodide.

In the present study, a general preparative method of acid anhydrides was investigated with the expectation that acid anhydride would be formed by the reaction of *N,N'*-dicyclohexylthiourea with silver carboxylates through an intermediate, imidoyl acylate. Indeed, when one mole of *N,N'*-dicyclohexylthiourea was added to a suspension of two moles of finely pulverized silver benzoate in anhydrous acetone at room temperature, benzoic anhydride was obtained in 93% yield along with *N,N'*-dicyclohexylurea and silver sulfide.

$$2\,RCOOAg + C_6H_{11}NHCSNHC_6H_{11} \xrightarrow{\text{Room temp.}} (RCO)_2O + C_6H_{11}NHCONHC_6H_{11} + Ag_2S$$

R: C_6H_5

In a similar manner, acetic, propionic, phthalic and succinic anhydrides were obtained from the corresponding silver carboxylates. These data are recorded in Table 1.

TABLE 1. ACID ANHYDRIDES FROM SILVER CARBOXYLATES

Silver salt (0.04 mol)	Yield of acid anhydride, %	Solvent	m*l*
Acetate	68.0	Acetone	13
Propionate	88.4	Acetone	20
Benzoate	93.0	Acetone	10
Phthalate	86.9	Acetonitrile	30
Succinate	90.0	Chloroform	30

The reaction is considered to proceed through an intermediate (IV), produced from a silver carboxylate and *N,N'*-dicyclohexylthiourea. The IV in turn reacts with another silver carboxylate to form silver sulfide and the imidoyl acylate (V), which further reacts with carboxylic acid to give an acid anhydride and *N,N'*-dicyclohexylurea.

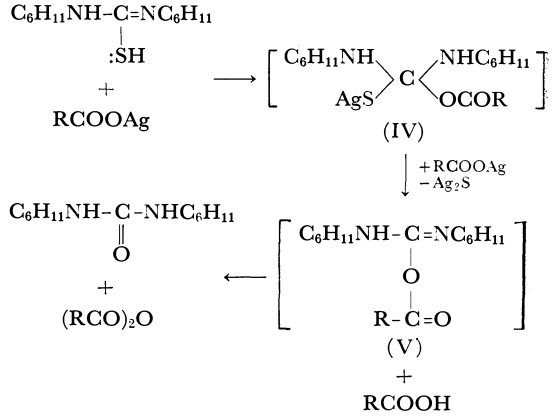

In addition, it was found that mercuric acetate also reacts with *N,N'*-dicyclohexylthiourea to give acetic anhydride, *N,N'*-dicyclohexylurea and mercuric sulfide along with a considerable amount of *N*-acetyl-*N,N'*-dicyclohexylurea (VI), a rearrangement product of imidoyl acylate (Va).

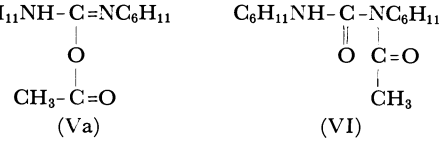

Some mercuric carboxylate, such as mercuric benzoate, contains one mole of water of crystallization, which cannot be removed by the ordinary procedure. Since water reacts with imidoyl benzoate faster than with carboxylate ion, mercuric carboxylates containing water of crystallization cannot be used in this reaction. Next, since anhydrous mercurous carboxylates are easily prepared from sodium carboxylates and mercurous nitrate,

1) I. Kuwajima and T. Mukaiyama, *J. Org. Chem.*, **29**, 1385 (1964).
2) T. Yamaguchi, K. Inomata and T. Mukaiyama, This Bulletin, **41**, 673 (1968).

the reactions of the carboxylates with *N,N'*-dicyclohexylthiourea were tried in order to avoid the above-mentioned trouble. When two moles of mercurous benzoate were allowed to react with one mole of *N,N'*-dicyclohexylthiourea, benzoic anhydride was obtained in a quantitative yield along with mercuric sulfide, metallic mercury and *N,N'*-dicyclohexylurea.

$$(RCOO)_2Hg_2 + C_6H_{11}NHCSNHC_6H_{11} \xrightarrow{\text{Room temp.}} (RCO)_2O + C_6H_{11}NHCONHC_6H_{11} + HgS + Hg$$

R: C_6H_5

Similarly, acetic, propionic, phthalic and succinic anhydrides were obtained in high yields from the corresponding mercurous carboxylates. The results are listed in Table 2.

Table 2. Acid anhydrides from mercurous carboxylates

Mercurous salt (0.04 mol)	Yield of acid anhydride, %	Solvent	m*l*
Acetate	69.0	Acetone	15
Propionate	99.2	Acetone	10
Benzoate	98.0	Acetone	30
Phthalate	81.1	Acetonitrile	25
Succinate	95.0	Chloroform	40

The reaction proceeds through an intermediate (VII), which loses mercuric sulfide to form the imidoyl acylate (V), a compound similar to that described in the case of silver carboxylate.

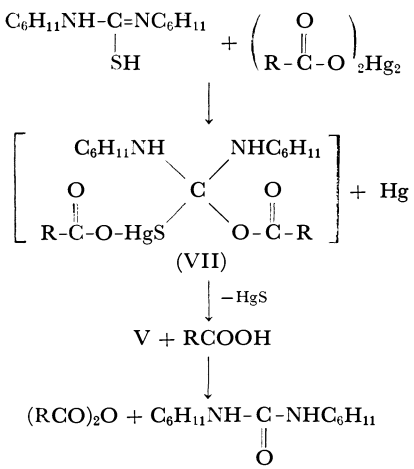

Further, it was found that one of the intermediates (IV), an 1 : 1 adduct, was successfully isolated in a quantitative yield as greenish white precipitates by treating mercurous phthalate (1 mmol) with *N,N'*-dicyclohexylthiourea (1 mmol) in a mixed solvent of anhydrous benzene (4 m*l*) and petroleum ether (1 m*l*). The adduct instantly reacted with ethanol at room temperature to give monoethyl ester of phthalic acid along with *N,N'*-dicyclohexylurea, metallic mercury and mercuric sulfide.

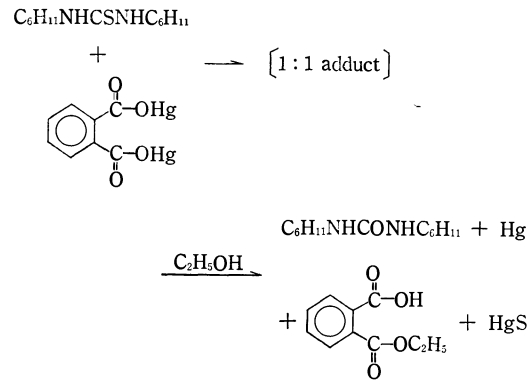

In conclusion, it is noted that mercurous carboxylates react with *N,N'*-dicyclohexylthiourea more easily than mercuric carboxylates and, in each reaction, the yield of acid anhydride markedly depend on the nature and the amount of solvent used as shown in Tables 1 and 2, probably due to the solubility of the intermediate complex (IV).

Experimental

Materials. *N,N'*-Dicyclohexylthiourea,[3] silver carboxylates[4] and mercurous carboxylates[5] were prepared by known procedures. They were ground and dried over P_2O_5 in vacuum desiccator before use.

The Preparation of Propionic Anhydride by the Reaction of *N,N'*-Dicyclohexylthiourea and Silver Propionate. *N,N'*-Dicyclohexylthiourea (4.8 g, 0.02 mol) was added to a suspension of silver propionate (7.24 g, 0.04 mol) in 20 m*l* of dry acetone and was continuously stirred about 15 hr at room temperature. During 2 hr, the suspension changed gradually from white to black. Then the black precipitates were filtered and washed with dry acetone. The filtrate and the washings were combined and evaporated. Propionic anhydride, 2.30 g (88.4%), bp 165—169°C, was obtained by distillation. After distillation, remaining oil solidified at room temperature. Recrystallization from benzene - petroleum ether gave *N*-propionyl-*N,N*-dicyclohexylurea, (0.6 g, 10.7%), mp 127—129°C. The black precipitate was throughly washed with ethanol. After evaporation of ethanol, *N,N'*-dicyclohexylurea, 4.17 g (93%), mp 218°C, was obtained.

Similarly, acetic, benzoic, succinic and phthalic anhydrides were obtained from the corresponding silver or mercurous carboxylates. The reaction conditions and the yields are summarized in Tables 1 and 2. According to this preparative method, except in the cases of acetic and propionic anhydrides, practically pure carboxylic anhydrides were separated by simply removing the black precipitate.

3) A. Skita and H. Rolfes, *Ber.*, **53**, 1247 (1920).
4) R. A. Zingaro, *J. Am. Chem. Soc.*, **71**, 575 (1949).
5) G. Brauer, "Handbuch der Präparativen Anorganischen Chemie," Ferdinand Enke Verlag, Stuttgart (1954).

BULLETIN OF THE CHEMICAL SOCIETY OF JAPAN VOL. 41 2748—2753 (1968)

Selective Chemical Cleavage of Asparagine Peptides[1)]

Tetsuo SHIBA, Akio KODA,*1 Shoichi KUSUMOTO[2]* and Takeo KANEKO

Department of Chemistry, Faculty of Science, Osaka University, Toyonaka, Osaka

(Received May 2, 1968)

Asparagine peptide was selectively cleaved by the Hofmann rearrangement followed by an alkaline treatment at the peptide linkage in which an amino group of the asparagine residue participated. Upon reaction of *N*-benzyloxycarbonyl-L-alanyl-L-asparagine with one equivalent of bromine and three equivalents of aqueous sodium hydroxide solution at 60°C, 1-(*N*-benzyloxycarbonyl-L-alanyl)-2-oxo-imidazolidine-5-carboxylic acid was obtained in quantitative yield. When this was treated with an aqueous methanolic sodium hydroxide solution at room temperature, a cleavage reaction occurred to give *N*-benzyloxycarbonyl-L-alanine and 2-oxo-imidazolidine-5-carboxylic acid. Under the same condition of the rearrangement, *N*-benzyloxycarbonyl-L-asparaginyl-L-phenylalanine was converted to 1-benzyloxycarbonyl-2-oxo-imidazolidine-5-carbonylphenylalanine. Since glutamine peptide could not give the corresponding ring compound, this cleavage reaction was found to be specific to asparagine peptide.

For the elucidation of the primary structure of protein, a number of chemical cleavage reactions specific to the particular amino acid residues have been presented as a supplementary method to the enzymic reactions which did not cover all usual amino acids in a sense of selective cleavage.[2)] Nevertheless, neither chemical nor enzymic reaction of asparagine peptide has been known so far. In our previous papers,[3-5)] chemical cleavage reactions of serine and threonine peptides were demonstrated. These reactions were based on formation of oxazolidone derivatives, by action of phosgene, which facilitated the removal of acyl group attached to the ring nitrogen atom by alkaline hydrolysis. It is expected that a similar cleavage reaction would occur readily too in the case of imidazolidone peptide where the ring O atom in oxazolidone peptide is replaced with NH group as shown in Fig. 1. Although α,β-diaminopropionic acid which will give the imidazolidone ring by reaction with phosgene, is not a constituent of natural protein, asparagine derivative can also be converted to the imidazolidone derivative *via* the Hofmann rearrangement reaction. In this respect, *N*-benzyloxycarbonyl-L-asparagine was actually converted to 1-benzyloxycarbonyl-2-oxo-imidazolidine-5-carboxylic acid by treatment with sodium hypochlorite at 60°C according to Schneider.[6)] When *N*-acetylasparagine was treated with bromine and barium hydroxide at 90°C by Karrer and Schlosser,[7)] 2-oxo-imidazolidine-5-carboxylic acid was obtained through the Hofmann rearrangement followed by cyclization to the imidazolidone ring and then elimination of acetyl group. Concerning oxidative reaction of peptide with sodium hypobromite, Goldschmidt *et al.*[8-12)] and Carpenter *et al.*[13)] had demonstrated chemical changes of *N*-terminal amino acid residue either to nitrile or to α-ketoacyl group for the purpose of the sequential analysis of peptide from *N*-terminal end. The other use of this rearrangement reaction had been investigated by Kovács *et al.*[14-16)] in order to distinguish α- and ω-acid amide group in aspartic or glutamic acid residue in peptide chain.

*1 Present address: Central Research Laboratory, Yamanouchi Pharmaceutical Co., Ltd., Azusawa, Itabashi-ku, Tokyo.

*2 Present address: Institute of Organic Chemistry, Faculty of Science, Osaka City University, Nishiogimachi, Kita-ku, Osaka.

1) This work was reported in a preliminary form at the 4th Symposium on Peptide Chemistry, Osaka, November, 1965, and also presented at the 20th Annual Meeting of the Chemical Society of Japan, Tokyo, April, 1967.

2) B. Witkop, "Advances in Protein Chemistry," Vol. 16, Academic Press, New York, N.Y. (1961), p. 221.

3) T. Kaneko and T. Inui, This Bulletin, **36**, 1541 (1963).

4) T. Kaneko, I. Takeuchi and T. Inui, *ibid.*, **41**, 974 (1968).

5) T. Kaneko, S. Kusumoto, T. Inui and T. Shiba, *ibid.*, **41**, 2155 (1968).

6) F. Schneider, *Ann.*, **529**, 1 (1937).

7) P. Karrer and A. Schlosser, *Helv. Chim. Acta*, **6**, 411 (1923).

8) S. Goldschmidt, *Z. Physiol. Chem.*, **165**, 149 (1927).

9) S. Goldschmidt and C. Steigerwald, *Ber.*, **58**, 1346 (1925).

10) S. Goldschmidt and K. Strauss, *Ann.*, **471**, 1 (1929).

11) S. Goldschmidt and K. Strauss, *Ber.*, **63**, 1218 (1930).

12) S. Goldschmidt, E. Wiberg, F. Nagel and K. Martin, *Ann.*, **456**, 1 (1927).

13) W. H. McGregor and F. H. Carpenter, *Biochemistry*, **1**, 53 (1962).

14) V. Bruckner, J. Kovács and H. Nagy, *J. Chem. Soc.*, **1953**, 148.

15) V. Bruckner, J. Kovács and K. Kovács, *ibid.*, **1953**, 1512.

16) J. Kovács, I. Kandal, M. Kandal and V. Bruckner, *Experientia*, **11**, 96 (1955).

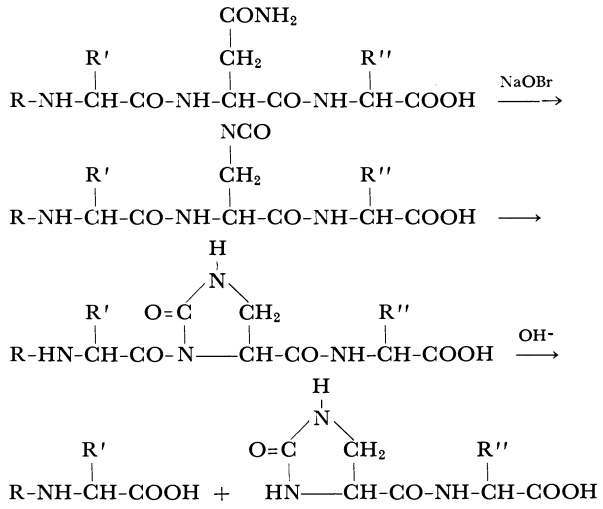

Fig. 1.

However, no attempts have been made to apply the Hofmann reaction to the selective cleavage of asparagine peptide according to a scheme outlined in Fig. 1. Asparagine peptides used in this reaction were prepared either by the mixed anhydride method or by the *p*-nitrophenyl ester method.

As a preliminary experiment *N*-benzyloxycarbonyl-L-alanyl-L-asparagine (I) was treated with one equivalent of bromine and five equivalents of aqueous sodium hydroxide at different temperatures as mentioned in Table 1. Theoretically, four equivalents of alkali are necessary to convert an acid amide to an amine in the usual Hofmann reaction, and one more equivalent should be added to neutralize the carboxyl group of I. From the reaction mixture, *N*-benzyloxycarbonylalanine (III) was obtained in crystalline state as one of the cleavage products. Although another product, *e. g.*, 2-oxo-imidazolidine-5-carboxylic acid (IV) could not be isolated, acid hydrolysis of a residue obtained by evaporation of the mother liquor gave α,β-diaminopropionic acid hydrochloride (V). Among a couple of the reaction conditions, the reaction at 60°C seemed to be most profitable in view of the yields of the products, III and V, as shown in Table 1. Although the results of the preliminary experiments suggest and strongly support the mechanism shown in Fig. 2, a route of the cleavage *via* imidazolidone peptide (II) could not be necessarily ascertained, since α,β-diaminopropionic acid would be possibly formed by the Hofmann reaction followed by the simple alkaline hydrolysis of asparagine residue without formation of imidazolidone ring.

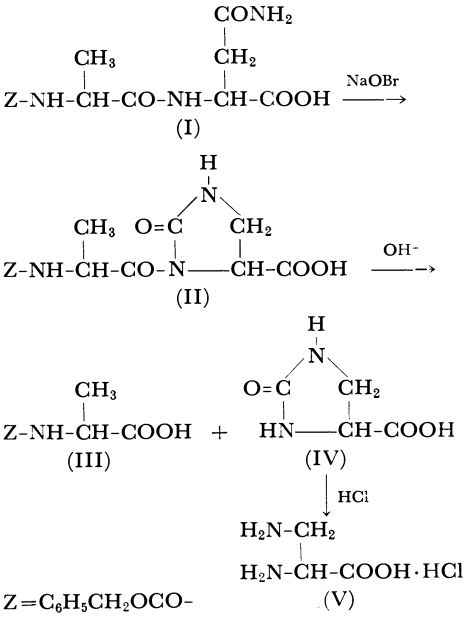

Fig. 2.

Table 1. Effects of temperature to reaction of *N*-benzyloxycarbonyl-L-alanyl-L-asparagine with sodium hypobromite in alkaline medium

Reaction Temp. (°C)	Yield of III (%)	Yield of V (%)
40	39	—
60	53	55
80	44	29

In order to prove the reaction mechanism, an isolation of the intermediate(II) was next attempted. A general mechanism of the Hofmann rearrangement by which a primary acid amide is converted to an amine is shown in Fig. 3. However, in the case of the reaction of *N*-benzyloxycarbonylalanyl-asparagine (I), the isocyanate, as soon as formed on step 4, will attack the nitrogen atom of the amino group of the original asparagine residue because of the electron-withdrawing effect of the

carbon atom of the isocyanate group. As far as the formation of the isocyanate is concerned, only two equivalents of alkali are enough. Therefore, one equivalent of bromine and totally three equivalents of 1 N sodium hydroxide, that is, two for the formation of isocyanate and one for the neutralization of the carboxyl group, were used for the reaction of I. Thus, 1-(*N*-benzyloxycarbonyl-L-alanyl)-2-oxo-imidazolidine-5-carboxylic acid (II) was obtained in a quantitative yield as expected. This compound showed an absorption of the ring carbonyl group at 1760 cm^{-1} in its infrared spectrum.

$$Br_2 + 2NaOH \rightarrow NaOBr + NaBr \quad (1)$$

$$RCONH_2 + NaOBr \rightarrow RCONHBr + NaOH \quad (2)$$

$$RCONHBr + OH^- \rightarrow RCONBr^- + H_2O \quad (3)$$

$$RCONBr^- \rightarrow RNCO + Br^- \quad (4)$$

$$RNCO + OH^- \rightarrow RNHCOO^- \quad (5)$$

$$RNHCOO^- + OH^- \rightarrow RNH_2 + CO_3^{--} \quad (6)$$

Fig. 3.

The compound II was then treated with two equivalents of an aqueous methanolic sodium hydroxide solution at room temperature, giving III and IV in yields of 50 and 10% respectively. From the result of this stepwise reaction, it is now certified that the cleavage reaction takes place through the imidazolidone intermediate without splitting of the peptide linkages by simple alkaline hydrolysis.

When the asparagine residue is located at a position other than carboxyl terminal end, there is another possibility of ring formation; that is, the isocyanate group will link with the nitrogen atom of an amino acid residue adjacent to asparagine residue at its carboxyl side to form a hydrouracil ring instead of an imidazolidone ring. In order to check this possibility, *N*-benzyloxycarbonyl-L-asparaginyl-L-phenylalanine (VII) was treated under the same reaction condition, and 1-benzyloxycarbonyl-2-oxo-imidazolidine-5-carbonylphenylalanine (VIII) was obtained as a single product. This compound showed an infrared absorption at 1790 cm^{-1} which was characteristic of the ring carbonyl absorption of the imidazolidone as compared with authentic 1-benzyloxycarbonyl-2-oxo-imidazolidine-5-carboxylic acid. Furthermore, the removal of benzyloxycarbonyl group from VIII by catalytic hydrogenation gave a ninhydrin-negative product (IX). These facts indicated that the isocyanate group was not linked with the amino group of the phenylalanine residue, but certainly with that of the asparagine residue.

At the stage of the present investigation, a solubility of longer asparagine peptide in an aqueous alkaline solution gave some restriction for an applicability of this method. For instance, in the reaction of *N*-benzyloxycarbonyl-L-alanyl-L-asparaginyl-L-phenylalanine (XI) with one equivalent of bromine and three equivalents of aqueous 1N sodium hydroxide solution, a large amount of unreacted tripeptide was recovered and no 1-(*N*-benzyloxycarbonylalanyl)-2-oxo-imidazolidine-5-carbonylphenylalanine was obtained. The original tripeptide XI was almost insoluble in this reaction medium. When five equivalents of alkali were used, *N*-benzyloxycarbonylalanine was found in the reaction mixture by a thin-layer chromatography, but could not be isolated as crystals. However, a possibility of non-selective cleavage of the peptide bond by simple alkaline hydrolysis could not be excluded in this case, since ninhydrinpositive spots of amino acids were also found on a thin-layer chromatogram of the reaction mixture.

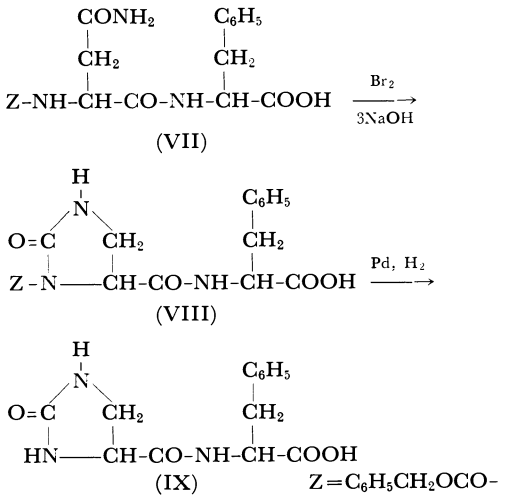

Fig. 4.

It must be investigated whether or not a glutamine residue will react in a similar way under the same condition as that of the cleavage reaction of asparagine peptide. In the Hofmann reaction of *N*-benzyloxycarbonyl-L-glutamine (XIIa), compound XIIIa was obtained as a reaction product. The removal of benzyloxycarbonyl group from XIIIa by catalytic hydrogenation yielded a free amino compound (XIV), which was then hydrolyzed by 6 N hydrochloric acid, giving three amino acids, *e.g.*, α,β-diaminobutyric acid, glutamic acid and glutamine. On the basis of this fact together with the results of the elementary analysis of XIIIa and of the observed molecular weight of dimethyl ester of XIIIa, the structure of this compound XIIIa was assigned as shown in Fig. 5. This may be formed by the intermolecular condensation of the isocyanate derivative with an intact glutamine molecule.

N-Benzyloxycarbonyl-L-alanyl-L-glutamine (XII b) gave also a corresponding product (XIIIb) under the same condition of the Hofmann reaction as mentioned in Fig. 5. This product did not afford *N*-benzyloxycarbonylalanine by treatment

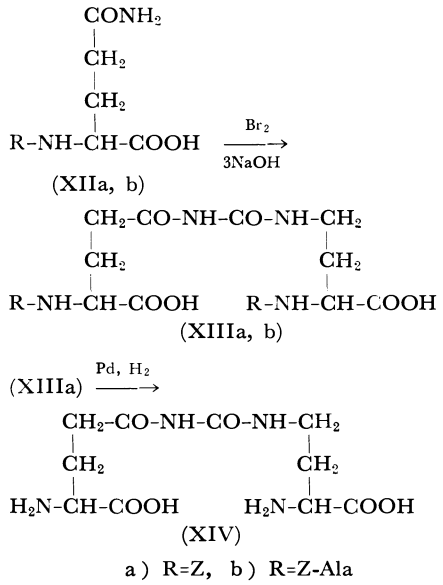

Fig. 5.

with aqueous sodium hydroxide in methanol at room temperature as expected from the structure.

From the results obtained above, it is now concluded that the isocyanate group formed as an intermediate in the Hofmann reaction could be very easily cyclized, giving a five-membered imidazolidone ring, but not a six-membered 2-hydroxytetrahydropyrimidine ring. Therefore, this selective cleavage reaction proceeded specifically only for asparagine peptide whereas glutamine peptide did not react similarly. For application of this reaction to the selective cleavage of asparagine residue in natural peptide or protein, however, the reaction condition should be somehow improved for solubility of the molecule and for prevention of the non-selective alkaline hydrolysis.

Experimental

All melting points are uncorrected. The infrared absorption spectra were obtained in Nujol mull with Nihon Bunko IR-S spectrophotometer. Thin-layer chromatography was carried out on silica gel G.

***N*-Benzyloxycarbonyl-L-alanyl-L-asparagine (I).** To a mixed solution of 13.4 g (0.060 mol) of *N*-benzyloxycarbonyl-L-alanine and 6.0 g (0.060 mol) of triethylamine in 150 m*l* of tetrahydrofuran, there was added 7.1 g (0.066 mol) of ethyl chloroformate at −2°C with stirring. After the reaction mixture had been stirred at −5°C for 20 min, a solution of 9.9 g (0.066 mol) of L-asparagine monohydrate in 66 m*l* of 1N sodium hydroxide solution was added. Stirring was continued at this temperature for 1 hr, and then at room temperature for additional 3 hr. Insoluble crystals of unreacted asparagine were filtered off; wt 2.9 g. The filtrate was acidified to pH 2 with 6 N hydrochloric acid, and an oily substance was obtained. It was extracted with totally 250 m*l* of ethyl acetate. After the extract had been allowed to stand in a refrigerator overnight, crystals formed were filtered; wt 5.5 g, mp 179—180°C (decomp.). Concentration of the mother liquor gave 3.2 g of the same crystals; total yield, 48%. Combined crystals were recrystallized from 94% ethanol to yield 8.3 g of pure crystals; mp 186—187°C (decomp.), $[\alpha]_D^{17}$ +18.7° (*c* 2.09, dimethylformamide).

Found: C, 53.20; H, 5.70; N, 12.29%. Calcd for $C_{15}H_{19}O_6N_3$: C, 53.40; H, 5.68; N, 12.46%.

***N*-Benzyloxycarbonyl-L-asparaginyl-L-phenylalanine *t*-Butyl Ester (VI).** To a solution of 5.16 g (0.020 mol) of *t*-butyl L-phenylalaninate hydrochloride[17,18] in 40 m*l* of dimethylformamide, there was added 2.02 g (0.022 mol) of triethylamine on ice-cooling. After stirring for 30 min, triethylamine hydrochloride formed was filtered off. To the filtrate, a solution of 7.74 g (0.020 mol) of *p*-nitrophenyl *N*-benzyloxycarbonyl-L-asparaginate in 40 m*l* of dimethylformamide was added and the reaction mixture was allowed to stand at room temperature. Crystals formed on addition of water were filtered off after allowing to stand overnight in a refrigerator; yield, 8.29 g (88%), mp 151—152°C. Recrystallization from ethyl acetate gave 7.60 g (81%) of pure crystals; mp 152.0—152.5°C.

Found: C, 64.16; H, 6.92; N, 8.99%. Calcd for $C_{25}H_{31}O_6N_3$: C, 63.94; H, 6.66; N, 8.95%.

***N*-Benzyloxycarbonyl-L-asparaginyl-L-phenylalanine (VII).** To 4.7 g of VI, 25 m*l* of trifluoroacetic acid was added, and the reaction mixture was stirred at room temperature for 1 hr. Crystals formed on addition of 70 m*l* of ether were filtered, washed with ether and then dried *in vacuo* over phosphrus pentoxide; yield, 3.9 g (94%), mp 202.5°C (decomp). Recrystallization from dimethylformamide - water gave needles; mp 210.5°C (decomp.).

Found: C, 60.98; H, 5.67; N, 10.28%. Calcd for $C_{21}H_{23}O_6N_3$: C, 61.01; H, 5.61; N, 10.16%.

***N*-Benzyloxycarbonyl-L-alanyl-L-asparaginyl-L-phenylalanine *t*-Butyl Ester (X).** Through a mixed solution of 14.0 g (0.031 mol) of VI and 3 m*l* of acetic acid in 400 m*l* of methanol, hydrogen gas was passed in the presence of 2 g of 10% palladium on charcoal with stirring for 6 hr. After removal of the catalyst by filtration, the filtrate was evaporated *in vacuo*. To a solution of the residue in 50 m*l* of dimethylformamide, there were added 3 g of triethylamine and a solution of 10.4 g (0.031 mol) of *p*-nitrophenyl *N*-benzyloxycarbonyl-L-alaninate[19] in 50 m*l* of dimethylformamide. The reaction mixture was stirred at room temperature for 24 hr. After addition of water, it was allowed to stand in a refrigerator overnight. Crystals formed were filtered and dried *in vacuo* at 70°C for 3 hr. Recrystallization from dimethylformamide - water gave 14.7 g (91%) of X; mp 164—165°C. Repeated recrystallization from the same solvent raised the melting point to 174—175°C (sintered at 164°C).

Found: C, 62.27; H, 6.80; N, 10.34%. Calcd for $C_{23}H_{36}O_7N_4$: C, 62.20; H, 6.71; N, 10.36%.

***N*-Benzyloxycarbonyl-L-alanyl-L-asparaginyl-L-phenylalanine (XI).** A mixture of 5.4 g (0.010 mol) of X and 30 m*l* of trifluoroacetic acid was stirred at room temperature for 1 hr, and then 100 m*l* of anhydrous

17) R. W. Roeske, *Chem. Ind.*, **1959**, 1121.
18) G. W. Anderson and F. M. Callahan, *J. Am. Chem. Soc.*, **82**, 3359 (1960).
19) M. Bodanszky and V. du Vigneaud, *ibid.*, **81**, 5688 (1959).

ether was added. A gelatinous precipitate formed was filtered after cooling and washed with ether. It was reprecipitated from dimethylformamide - water, and then dried *in vacuo* over phosphorus pentoxide; yield, 4.7 g (94%), mp 196°C (decomp.). Elementary analysis was carried out after drying *in vacuo* at 90°C for 3 hr.

Found: C, 57.32; H, 5.95; N, 11.13%. Calcd for $C_{24}H_{28}O_7N_4 \cdot H_2O$: C, 57.36; H, 6.02; N, 11.15%.

***N*-Benzyloxycarbonyl-L-alanyl-L-glutamine (XIIb).** A mixed solution of 6.7 g (0.030 mol) of *N*-benzyloxycarbonyl-L-alanine and 3.0 g (0.030 mol) of triethylamine in 75 m*l* of dioxane, there was added 3.6 g (0.033 mol) of ethyl chloroformate at −5°C for 5 min with stirring. After the stirring had been continued at this temperature for 20 min, a solution of 4.8 g (0.033 mol) of L-glutamine in 33 m*l* of aqueous 1 N sodium hydroxide was added. The reaction mixture was stirred at −5°C for 40 min and then at room temperature for 2.5 hr. A small amount of undissolved glutamine was removed by filtration. The filtrate was acidified to pH 1 with 6 N hydrochloric acid, and extracted with ethyl acetate. Crystals formed in the extract were filtered and recrystallized from water to yield 7.1 g (67%) of needles; mp 167.5—168.5°C. Recrystallization from water raised the melting point to 169.0—171.5°C.

Found: C, 54.49; H, 6.18; N, 11.99%. Calcd for $C_{16}H_{21}O_6N_3$: C, 54.69; H, 6.02; N, 11.96%.

The Hofmann Reaction of *N*-Benzyloxycarbonyl-L-asparagine. To a solution of 3.3 g of sodium hydroxide in 70 m*l* of water, 4.4 g of bromine was added dropwise with stirring at 0—5°C. To the solution, 6.7 g (0.025 mol) of *N*-benzyloxycarbonyl-L-asparagine was added, and stirred at 50°C for 1 hr.[20] After addition of sodium thiosulfate on cooling, the reaction mixture was washed with ether, and then acidified to pH 2 with 6 N hydrochloric acid to give an oily material which was crystallized after allowing to stand in a refrigerator overnight. It was filtered and recrystallized from water to yield 4.3 g (65%) of 1-benzyloxycarbonyl-2-oxo-imidazolidine-5-carboxylic acid; mp 164—168°C (decomp.). Recrystallization from methanol - ether raised the melting point to 190°C (decomp.), lit.,[6] mp 194°C.

Found: C, 54.24; H, 4.58; N, 10.64%. Calcd for $C_{12}H_{12}O_5N_2$: C, 54.54; H, 4.58; N, 10.60%.

This compound gave crystalline *N,N'*-dicyclohexylammonium salt; mp 200°C (decomp.).

Found: C, 64.19; H, 7.92; N, 9.22%. Calcd for $C_{12}H_{12}O_5N_2 \cdot C_{12}H_{23}N$: C, 64.69; H, 7.92; N, 9.43%.

2-Oxo-imidazolidine-5-carboxylic Acid (IV). Through a mixed solution of 1.32 g (5.0 mmol) of 1-benzyloxycarbonyl-2-oxo-imidazolidine-5-carboxylic acid and a few drops of acetic acid in 50 m*l* of methanol, hydrogen gas was passed in the presence of 100 mg of 10% palladium on charcoal for 8 hr. After evaporation of the solvent, a residue obtained was crystallized from methanol - ether; mp 179.5°C (decomp.), lit.,[6] 190—191°C (decomp.), lit.,[7] 184°C (decomp.).

Found: C, 37.14; H, 5.00; N, 21.48%. Calcd for $C_4H_6O_3N_2$: C, 36.93; H, 4.65; N, 21.53%.

This carboxylic acid gave long needles of *N,N'*-dicyclohexylammonium salt; mp 214°C (decomp.) (sintered at 203°C).

Found: C, 61.81; H, 9.46; N, 13.48%. Calcd for $C_4H_6O_3N_2 \cdot C_{12}H_{23}N$: C, 61.71; H, 9.39; N, 13.49%.

Cleavage Reaction of *N*-Benzyloxycarbonyl-L-alanyl-L-asparagine (I). a) A mixture of 3.4 g (10 mmol) of I and a solution of 1.8 g (11 mmol) of bromine in 50 m*l* of aqueous 1 N sodium hydroxide was stirred at 78—80°C for 1 hr. After cooling, it was acidified to pH 2—3 with 6 N hydrochloric acid. Crystals of *N*-benzyloxycarbonyl-L-alanine (III) formed were filtered; wt 0.85 g, mp 77.5—81.0°C. The filtrate was extracted with 45 m*l* of chloroform. To a concentrated extract, petroleum ether was added to give needles of a second crop of III; wt 0.58 g, mp 81.5—84.0°C, total crude yield, 64%. Recrystallization of combined product from chloroform - petroleum ether gave 0.99 g (44%) of pure crystals; mp 84—85°C, $[\alpha]_D^{17}$ −14.6° (*c* 2.2, acetic acid). Lit.,[21] mp 84°C, $[\alpha]_D^{17}$ −14.3° (acetic acid), lit.,[22] mp 87°C (corrected), $[\alpha]_D^{27}$ −13.9° (*c* 2.0, acetic acid).

The aqueous layer from the chloroform extraction was evaporated *in vacuo* to dryness. A residue was triturated with 100 m*l* of anhydrous ethanol to remove insoluble inorganic salts. The solution was evaporated *in vacuo* to a residue which was then dissolved in 15 m*l* of water. The aqueous solution was passed through Dowex 50 (H form) column, and an effluent was evaporated *in vacuo* to give an oil. This oily material was heated with 6 N hydrochloric acid under reflux for 2 hr. Residue obtained by evaporation *in vacuo* was crystallized from 99% ethanol to yield 0.41 g (29%) of L-α,β-diaminopropionic acid monohydrochloride; mp 230—231°C (decomp.). It was recrystallized from water; mp 238—239°C (decomp.), $[\alpha]_D^{16}$ +21.2° (*c* 5.61, 1 N hydrochloric acid). Lit.,[23] mp 245°C (decomp.) (corrected), $[\alpha]_D^{20}$ +25.09° (1 N hydrochloric acid), lit.,[7] $[\alpha]_D^{20}$ +25.0° (1 N hydrochloric acid.).

Reactions at different temperatures shown in Table 1 were carried out by the similar procedure to that mentioned above.

b) To a solution of 2.4 g (0.060 mol) of sodium hydroxide in 60 m*l* of water, 3.2 g of bromine was added dropwise on ice-cooling. To the sodium hypobromite solution prepared above, 6.7 g (0.020 mol) of I was added. The reaction mixture was stirred at 60°C for 1 hr. After cooling and addition of 40 m*l* of water, the reaction mixture was acidified to pH 2 with 6 N hydrochloric acid. An oily material formed was extracted with totally 750 m*l* of ethyl acetate three times. The combined extracts were washed with water, and dried with sodium sulfate. Evaporation of the solvent *in vacuo* gave a solid of crude 1-(*N*-benzyloxycarbonylalanyl)-2-oxo-imidazolidine-5-carboxylic acid (II), which was then dried *in vacuo* over calcium chloride; yield 6.5 g (95%), mp 66°C (decomp.). This compound gave a crystalline dicyclohexylammonium salt

20) In our experiment, crystalline 1-benzyloxycarbonyl-2-oxo-imidazolidine-5-carboxylic acid was obtained only when three equivalents of sodium hydroxide and one equivalent of bromine were used, although Schneider carried out the same reaction using much excess amount of sodium hydroxide and bromine.[6]

21) M. Bergmann and L. Zervas, *Ber.*, **65**, 1192 (1932).

22) M. Hunt and V. du Vigneaud, *J. Biol. Chem.*, **124**, 669 (1938).

23) E. Fischer and W. A. Jacobs, *Ber.*, **40**, 1057 (1907).

from anhydrous ether solution; mp 212.5°C (decomp.), ν_{max} 1760 cm^{-1} (ring CO).

Found: C, 62.41; H, 7.94; N, 10.82%. Calcd for $C_{27}H_{40}O_6N_4$: C, 62.77; H, 7.80; N, 10.85%.

To a solution of 0.84 g (2.5 mmol) of II obtained above in 10 m*l* of methanol, there was added 5 m*l* of aqueous 1 N sodium hydroxide solution. The reaction mixture was stirred at room temperature for 2 hr. After acidification to pH 3 with 1 N hydrochloric acid, methanol was removed by evaporation *in vacuo*. Aqueous solution was extracted with chloroform three times. To the dried extract, petroleum ether was added to yield 0.28 g (50%) of needles of *N*-benzyloxycarbonyl-L-alanine (III). Its infrared spectrum and melting point were identical with those of the authentic sample respectively.

The aqueous layer from the chloroform extraction was evaporated *in vacuo*. The residue obtained was dried over phosphorus pentoxide, and dissolved in anhydrous methanol. To the solution, dicyclohexylamine and then anhydrous ether were added giving crystals of dicyclohexylammonium salt. They were filtered and dried. A solution of this salt in a mixture of methanol and water was treated with Dowex 50 (H form) by stirring for 30 min. After removal of the resin by filtration, the solvent was evaporated *in vacuo*. A residue obtained was crystallized from methanol - ether; yield, 30 mg (10%). Its infrared spectrum and melting point were identical with those of 2-oxo-imidazolidine-5-carboxylic acid (IV) respectively.

The Hofmann Reaction of *N*-Benzyloxycarbonyl-L-asparaginyl-L-phenylalanine (VII). To sodium hypobromite solution prepared from 23.3 m*l* of 1 N sodium hydroxide and 0.42 m*l* of bromine, there was added 3.1 g (7.5 mmol) of VII. The reaction mixture was stirred at 60°C for 1 hr. After cooling, crystals formed were filtered and dried *in vacuo* over phosphorus pentoxide; yield 3.1 g (100%), mp 179—181°C (decomp.). Recrystallization from methanol - ether gave pure crystals of 1-benzyloxycarbonyl-2-oxo-imidazolidine-5-carbonylphenylalanine (VIII) containing one mole of methanol as crystallization solvent; mp 191°C (decomp.), ν_{max} 1790 cm^{-1} (ring CO).

Found: C, 59.66; H, 5.79; N, 9.15%. Calcd for $C_{21}H_{21}O_6N_3 \cdot CH_3OH$: C, 59.58; H, 5.68; N, 9.48%.

When 23.645 mg of the crystals was heated at 80°C *in vacuo*, a constant weight of 22.067 mg was obtained after 15.5 hr. The loss in weight corresponds to 92.3% of the theoretical amount of one mole of methanol as crystallization solvent.

Through a solution of 0.75 g (1.8 mmol) of VIII in a mixture of 20 m*l* of methanol, 5 m*l* of acetic acid and 5 m*l* of water, hydrogen gas was passed for 6 hr in the presence of 100 mg of 10% palladium on charcoal. After removal of the catalyst by filtration, the solvent was evaporated *in vacuo*. A residue obtained was dried *in vacuo* over phosphorus pentoxide; yield, 0.40 g (78%). Recrystallization from water gave needles of 2-oxo-imidazolidine-5-carbonylphenylalanine (IX); mp 195°C (decomp.) (sintered at 100°C). This compound gave no ninhydrin reaction.

Found: C, 53.37; H, 5.81; N, 14.16%. Calcd for $C_{13}H_{15}O_4N_3 \cdot H_2O$: C, 52.87; H, 5.80; N, 14.23%.

The Hofmann Reaction of *N*-Benzyloxycarbonyl-L-glutamine (XIIa). To a solution of 4.0 g of bromine in 100 m*l* of 0.75 N sodium hydroxide, there was added 7.0 g (0.025 mol) of *N*-benzyloxycarbonyl-L-glutamine. The reaction mixture was stirred at 60°C for 1 hr. After cooling and addition of sodium thiosulfate, the reaction mixture was acidified to pH 2 with 6 N hydrochloric acid. Crystals formed were filtered off and dried *in vacuo* over phosphorus pentoxide; wt 5.6 g. It was recrystallized from methanol - water, and then from ethanol - water to yield needles of XIIIa; mp 181.5°C (decomp.).

Found: C, 55.96; H, 5.54; N, 9.96%. Calcd for $C_{26}H_{30}O_{10}N_4$: C, 55.91; H, 5.41; N, 10.03%.

This compound gave pure crystals of bis-dicyclohexylammonium salt, mp 192°C (decomp.).

Found: C, 65.11; H, 8.32; N, 9.09%. Calcd for $C_{26}H_{30}O_{10}N_4 \cdot 2C_{12}H_{23}N$: C, 65.19; H, 8.32; N, 9.12%.

The compound IIIa was converted to its dimethyl ester by diazomethane in the usual manner; mp 160—162°C (decomp.), mol wt: Found: 545 (by the Rast method using camphor). Calcd for $C_{28}H_{34}O_{10}N_4$: 586.

Hydrogenation of IIIa by the usual procedure using 10% palladium on charcoal gave compound XIV. It was recrystallized from water; mp 226—227°C (decomp.), R_f, 0.13 on a thin-layer chromatogram (*n*-butanol - acetic acid - water, 4 : 1 : 2).

Found: C, 41.25; H, 6.47; N, 18.87%. Calcd for $C_{10}H_{18}O_6N_4$: C, 41.37; H, 6.25; N, 19.30%.

Compound XIV was then hydrolyzed by refluxing with 6 N hydrochloric acid for 3 hr. The reaction product gave three spots of α,γ-diaminobutyric acid, glutamic acid and glutamine by ninhydrin coloration on a thin-layer chromatogram and a paper chromatogram. Thin-layer chramotography (*n*-butanol - acetic acid - water, 4 : 1 : 2): R_f, 0.16 (α,γ-diaminobutyric acid), 0.22 (glutamine), 0.30 (glutamic acid). Paper chromatography (phenol - water, 4 : 1): R_f, 0.18 (α,γ-diaminobutyric acid), 0.33 (glutamic acid), 0.59 (glutamine).

The Hofmann Reaction of *N*-Benzyloxycarbonyl-L-alanyl-L-glutamine (XIIb). To a mixture of 15 m*l* of 1N sodium hydroxide and 0.80 g of bromine, there was added 1.76 g of XIIb. The reaction mixture was stirred at 60°C for 1 hr. By a procedure similar to that in the reaction of XIIa, 1.49 g of the product XIIIb was obtained. It was recrystallized from methanol - ether - petroleum ether to yield needles; mp 192.5°C (decomp.).

Found: C, 54.29; H, 5.82; N, 11.78%. Calcd for $C_{32}H_{40}O_{12}N_6 \cdot CH_3OH$: C, 54.09; H, 6.05; N, 11.47%.

Even when this product was treated with 1 N sodium hydroxide in methanol at room temperature for 2 hr, the starting material was recovered without formation of *N*-benzyloxycarbonylalanine (III).

The authors are grateful to the Central Research Laboratories of Ajinomoto Co., Inc. for donation of the amino acids.

BULLETIN OF THE CHEMICAL SOCIETY OF JAPAN VOL. 41 2754—2757 (1968)

Studies on the Substrate Specificity of Egg White Lysozyme. II. Mode of the Enzymatic Action on Partially-*O*-carboxymethylated Chitin

Tsuyoshi MIYAZAKI and Yoshio MATSUSHIMA

Department of Chemistry, Osaka University, College of Science, Toyonaka

(Received May 9, 1968)

Partially-*O*-carboxymethylated chitin was found to be a soluble substrate of hen egg white lysozyme. The products of the lysozyme action were analyzed by gel filtration and by ion-exchange chromatography. The reducing ends of the saccharides produced by the enzyme were the *N*-acetyl-glucosamine residue or the 3-*O*-carboxymethyl-*N*-acetyl-glucosamine residue. 6-*O*-Carboxymethyl-*N*-acetyl-glucosamine never appeared as a reducing end. The *O*-substituted disaccharide detected in the reaction products was 6'-*O*-carboxymethyl-di-*N*-acetyl-chitobiose. The results of the reducing-end analyses and the finding that none of the monomers were formed except for the unsubstituted *N*-acetyl-glucosamine, while an *O*-substituted dimer was formed as is mentioned above, are in conformity with the conformation of the enzyme-substrate complex proposed by Blake *et al.* as a result of their X-ray crystallographic investigations.

An elaborate model of a three-dimensional structure of an ES-complex formed between chitin oligosaccharide and hen egg white lysozyme [EC 3.2.1.17.] was presented by Blake *at al.*[1] as a result of thier X-ray crystallographic investigations. When partially-*O*-carboxymethylated chitin is used instead of a natural substrate chitin, it is expected that the fairly bulky *O*-substitutent groups will not permit the substrate molecules to bind freely with the enzyme protein. The enzyme must avoid the steric hindrance exerted by the *O*-substituent groups on the substrate and select some suitable portions of the substrate in order to make an ES-complex. If this is the case, the orientation of the *O*-substituent groups in the enzymatic reaction products will afford information on the conformation of the binding site of the enzyme protein.

Partially-*O*-carboxymethylated chitin was reported by Hultin[2] to be a soluble substrate of chitinase. The present authors prepared the substance by the *N*-acetylation of the *O*-carboxymethylated chitosan reported by Okimasu.[3] This substance was found to be a substrate of hen egg white lysozyme[4] by the release of reducing power when it was incubated with the enzyme. Among the low-molecular-weight compounds produced by the enzyme, there were *N*-acetylglucosamine (I), di-*N*-acetylchitobiose (II), tri-*N*-acetylchitotriose (III), and 6'-*O*-carboxymethyl-di-*N*-acetylchitobiose (IV). None of the *O*-substituted monosaccharides were produced by the enzyme, and the reducing-end residues of the product saccharides were either unsubstituted or 3-*O*-substituted. These findings can be well interpreted when we take into account the conformation of the *O*-substituted groups of the substrate in the ES-complex.

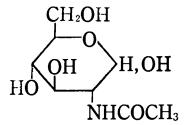

(I)

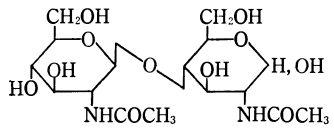

(II)

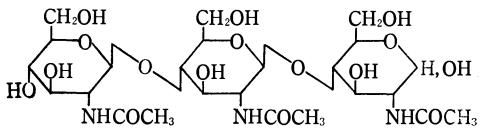

(III)

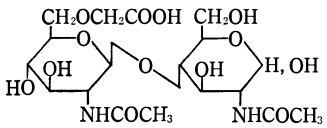

(IV)

1) C. C. F. Blake, L. N. Johnson, G. A. Mair, A. C. T. North, D. C. Phillips and V. R. Sarma, *Proc. Roy. Soc.*, **167**, **B** 378. (1967).
2) E. Hultin, *Acta Chem. Scand.*, **9**, 192 (1955).
3) T. Okimasu, *J. Agr. Chem. Soc. Japan*, **32**, 303 (1958).
4) Y. Matsushima, S. Hara, T. Miyazaki and Y. Umemura, The 38th Annual Meetings of the Japanese Biochemical Society, October (1965).

Our results offer chemical evidence for the conformation of the active sites in the Phillips model[1] of the ES-complex of hen egg white lysozyme.

Experimental

The enzyme specimen used was a thrice recrystallized one purchased from Sigma Chemicals.

Abbreviations will be used for glucosamine: GlN, *N*-acetylglucosamine: GlNAc, glucosaminitol: GlNOH, carboxymethyl: CM.

The Enzymatic Action on Partially-*O*-carboxymethylated Chitin. An example of the time course of the enzymatic reaction is shown in Fig. 1. The pH-activity curve is shown in Fig. 2. The molar composition of the substrate is: 56.7% GlNAc, 3.2%

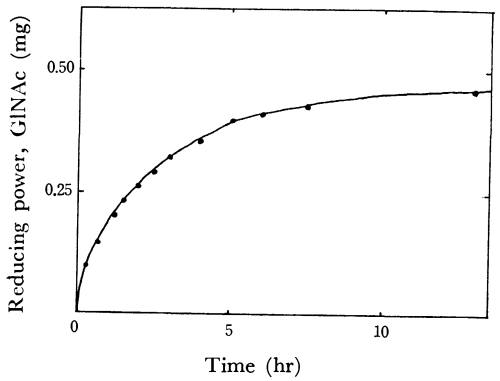

Fig. 1. Incubation mixture: Five mg of the substrate in 1 m*l* of water, 0.5 m*l* of 0.4 M acetate buffer (pH 5.6) and 0.1 mg of the enzyme in 0.5 m*l* of water. Incubation temperature: 37°C. Reducing power measurement: Somogyi-Nelson method.[5]

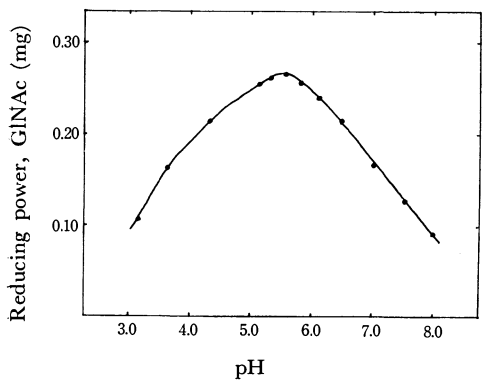

Fig. 2. Incubation mixture: Five mg of the substrate in 1 m*l* of water, 0.5 m*l* of 0.4 M acetate buffer (pH 3.3—5.8) or phosphate buffer (pH 6.0—8.0) and 0.1 mg of the enzyme in 0.5 m*l* of water. Incubation temperature: 37°C. Incubation time: 2 hr. Reducing power measurement: Somogyi-Nelson method.

5) "Methods in Carbohydrate Chem.," Vol. 1, Academic Press, New York and London (1962), p. 368.

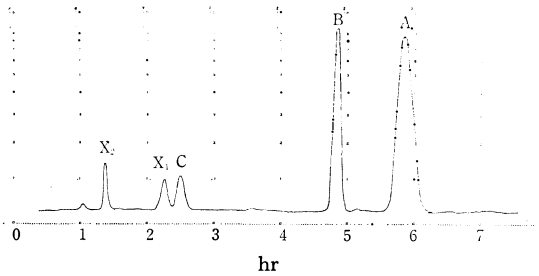

Fig. 3a. The composition of the substrate. The specimen was hydrolyzed in 4 N hydrochloric acid at 105°C for 4 hr. The hydrolysate was evaporated *in vacuo*, and 1 mg of the dried residue was placed on a column of Hitachi Autoanalyzer KLA-3. Elution was performed with 0.2 M citrate buffer (pH 3.11—4.25). The peaks shown are: GlN(A), 6-*O*-CM-GlN(B), 3-*O*-CM-GlN(C) and unknown substances (X_1, X_2). The peaks were identified by using standard specimens.[6]

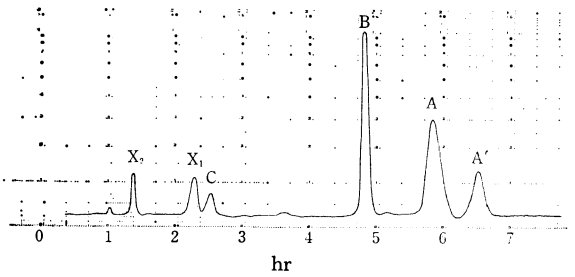

Fig. 3b. The composition of the enzymatic reaction products which was reduced with borohydride before hydrolysis. The peaks shown are: GlNOH(A'), GlN(A), 6-*O*-CM-GlN(B), 3-*O*-CM-GlN(C) and unknown substances (X_1, X_2). The peak of 3-*O*-CM-GlNOH was not recognizable due to a low ninhydrin color yield of the compound, and due to its close vicinity to the peak X_1. The retention time for the peak of 6-*O*-CM-GlNOH, which did not appear, is 4.58 hr.

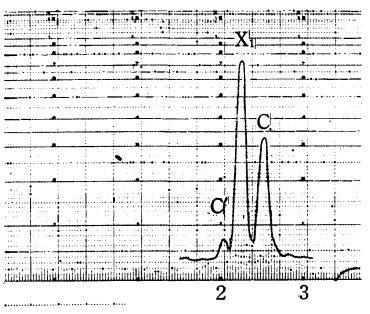

Fig. 3c. The pattern of the early region of Fig. 3b magnified by charging ten times amount (10 mg) of the specimen. The peaks shown are: 3-*O*-CM-GlN(C), an unknown substance (X_1) and 3-*O*-CM-GlNOH(C').

6) T. Miyazaki and Y. Matsushima, This Bulletin, in press.

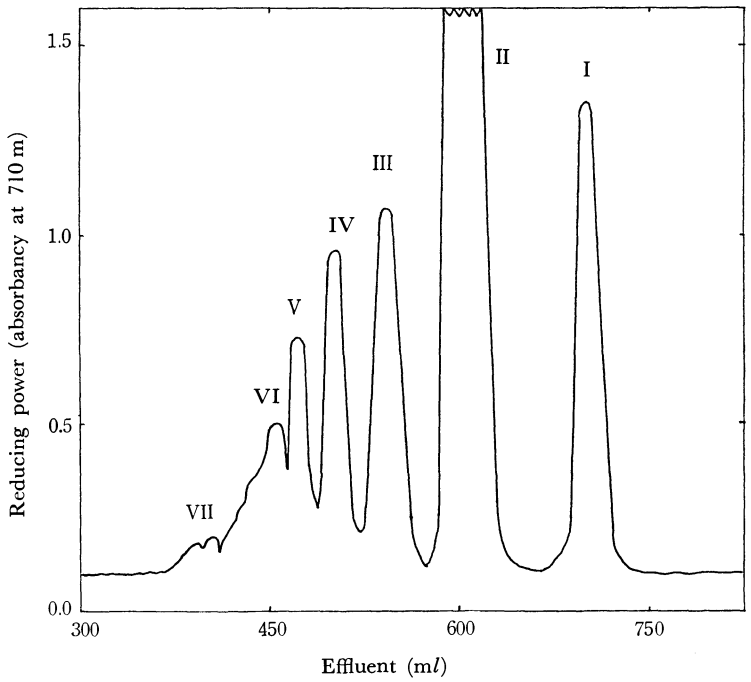

Fig. 4. The fractions of each 3 m*l* were collected. An aliquot (0.4 m*l*) was used for the reducing power measurement by Somogyi-Nelson method. Elution velocity: 4.5 m*l*/hr.

3-*O*-CM-GlNAc, 27.2% 6-*O*-CM-GlNAc, plus unknown components.

Analyses of the Reducing-end Residues Produced by the Enzyme. The whole of the enzymatic reaction mixture was reduced by sodium borohydride, and the mixture was hydrolyzed with hydrochloric acid. The acid hydrolysate contained monosaccharides and sugar alcohols, and the structure (3-*O*-, 6-*O*-, or unsubstituted) of the latter revealed what had been the reducing ends of the oligosaccharides produced by the enzyme. The chromatographic pattern of the acid hydrolysate, after the borohydride reduction, of the enzymatic reaction mixture is shown in Fig. 3(a—c) in comparison with the acid hydrolysate of the sub-substrate.

Fractionation by Dialysis and Gel Filtration of the Enzymatic Reaction Products. Three grams of the substrate were digested by 60 mg of the enzyme in a 100 m*l* of acetate buffer solution (pH 5.6) for 48 hr at 37°C. Sixty milligrams of the enzyme in 25 m*l* of water were then added to the mixture, and the incubation was continued for 24 hr more. The mixture was then dialyzed against 2000 m*l* of deionized water for 24 hr. The dialysis was repeated three times. The dialysate was then concentrated to 200 m*l* *in vacuo*, and the residual solution was passed through a column of Amberlite IR-120 (H^+ form, 3×15 cm) in order to eliminate the sodium ion of the buffer solution. The lyophilization of the solution gave 1.87 g of a mixture of saccharides. An aliquot (260 mg) of the mixture was placed on a column of Sephadex G-15 (3×160 cm) and eluted with 0.1 N acetic acid. The chromatographic pattern obtained is shown in Fig. 4.

Identification of the Fractions in Gel Filtration. *Fraction I.* On a paper chromatogram this fraction gave only one spot that corresponded to GlNAc, as is shown in Fig. 5. The identity was further confirmed by the use of an automatic amino-acid analyzer. The fraction, after it had been hydrolyzed with hydrochloric acid, gave a single peak which corresponded to GlN. After the borohydride reduction and acid hydrolysis, the fraction gave a single peak that corresponded to GlNOH. No trace of *O*-substituted saccharide was observed in this fraction. These results, when consolidated, are evidence for the fraction I being very

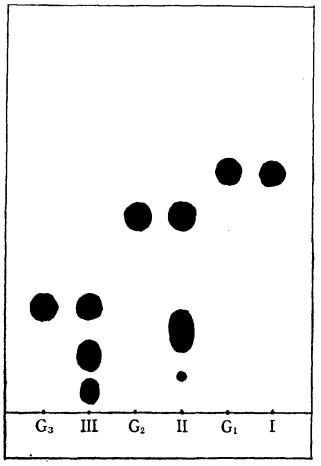

Fig. 5. Solvent system is *n*-butanol : pyridine : water = 6 : 4 : 3 (v/v). G_1: *N*-acetylglucosamine, G_2: di-*N*-acetylchitobiose, G_3: tri-*N*-acetylchitotriose.

Table 1. Molar ratio of the component sugars and sugar alcohols

	Neutral	Acidic
GlN	1.00	0.25
6-*O*-CM-GlN		1.18
GlNOH	1.00	1.00
3-*O*-CM-GlNOH		0.34

pure GlNAc. The recovery of the fraction was 0.118 g (referred to 3.0 g of the substrate).

Fraction II. This fraction was a mixture of disaccharides. As is shown in Fig. 5, the fraction contained at least three components, one of which corresponded to di-*N*-acetylchitobiose. By passing 20.2 mg of the fraction through a column of Dowex-1 (acetate form, 1.2×14 cm), it was resolved into a neutral and an acidic part. The component analyses of these two parts are shown in Table 1. The data for the neutral part demonstrate almost unequivocally the presence of di-*N*-acetylchitobiose in the enzymatic reaction products. The data for the acidic part can be interpreted as showing, along with the paper-chromatographic data, the presence of 6′-*O*-CM-di-*N*-acetylchitobiose (IV) and of 3-*O*-CM-di-*N*-acetylchitobiose, though the analytical values for the latter are not very reliable because of the low color yield in the ninhydrin reaction of 3-*O*-CM-GlNOH. The pattern in the cation-exchanger chromatography of the acidic part is shown in Fig. 6.

Fraction III. A spot corresponding to tri-*N*-acetylchitotriose is shown in Fig. 5. Further investigation of the fractions III—VII remains to be done.

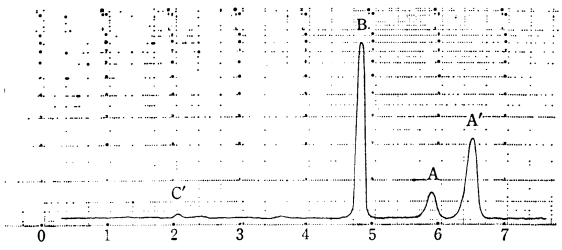

Fig. 6. The peaks are: GlNOH(A′), GlN(A), 6-*O*-CM-GlN(B) and 3-*O*-CM-GlNOH(C′).

Discussion

A three-dimensional model construction according to Blake *et al.*[7] reveals explicitly the orientation of the substituents on the substrate molecule bound to the active site (cleft) of the enzyme protein. The general features are presented in Table 2.

Table 2.

Substituent	Sub-sites A	B	C	D	E	F
3-*O*-	IN	OUT	IN	OUT	IN	OUT
6-*O*-	OUT	IN	OUT	IN	OUT	IN

The notation of the sub-sites is according to Blake *et al.*[1] "IN" means that a substituent group is directed toward inside of the "cleft", thus being ready to suffer steric hindrance, and "OUT" means contrary. Cleavage of a glycosidic bond of the substrate occurs on a residue which has been in the sub-site D. The reducing end of the saccharide chain is directed toward F.

The experimental results can be well interpreted when we take into account the general features shown in Table 2, and when the interpretation is made, as a first-order approach, only in terms of steric circumstances. The 6-*O*-substituted residue will not be able to fit into D because of its substituent group directed toward the inside of the cleft, and so this residue will not be able to be a reducing end of the various saccharides produced by the enzyme. A monosaccharide released by the enzyme must necessarily fit once into D, and once into E. Any *O*-substituted residue will suffer steric hindrance at either of these two subsites, and so can not be released as a monosaccharide. Any disaccharide to be released must fit once into C-D, and once into E-F. The disaccharides identified in the experiments meet this requirement. It seems that the C, D and E sub-sites do not have much room toward the inside of the cleft. The structure determination of the product oligosaccharides larger than disaccharide will afford information in a chemical sense about the "size" of the room of the sub-sites A, B and F. This task is now being undertaken.

This investigation was supported by U. S. Public Health Service Grant AI-04586-05. The authors are also grateful to Mr. S. Kasai for his assistance.

7) C. C. F. Blake, G. A. Mair, A. C. T. North, D. C. Phillips and V. R. Sarma, *Proc. Roy. Soc.*, **167, B**, 365 (1967).

BULLETIN OF THE CHEMICAL SOCIETY OF JAPAN VOL. 41 2758—2762 (1968)

Syntheses of 4-Alkylidene- and 4-Aralkylidene-2-chloromethyl-5-oxazolones and *N*-(Chloroacetyl)dehydroamino Acids

Hideaki KURITA, Yasuhiro CHIGIRA, Mitsuo MASAKI and Masaki OHTA

Laboratory of Organic Chemistry, Tokyo Institute of Technology, Ookayama, Meguro-ku, Tokyo

(Received May 11, 1968)

Treatment of *N*-dichloroacetyl amino acids with acetic anhydride at a temperature between 85°C and 130°C yielded 4-alkylidene- and 4-aralkylidene-2-chloromethyl-5-oxazolones, which were readily hydrolyzed to give 2-(2-chloroacetamido)-2-alkenoic acids, *i. e.*, *N*-(chloroacetyl)-dehydroamino acids.

Several synthetic methods of 2-(2-chloroacetamido)-2-alkenoic acid, *i. e.*, *N*-(chloroacetyl)dehydroamino acid have been known, since the acid can be used as one of the most convenient intermediates for dehydropeptide synthesis.[1] Greenstein and his coworkers reported the preparation of several *N*-(chloroacetyl)dehydroamino acids by treating a mixture of α-keto acids and chloroacetonitrile with dry hydrogen chloride.[2] The reaction with pyruvic acid leads to the substantially quantiative formation of 2-(2-chloroacetamido)-acrylic acid, *i. e.*, *N*-(chloroacetyl)dehydroalanine in a pure state,[2a] which can be also prepared by the condensation of pyruvic acid with chloroacetamide in 30% yield.[3] In the condensations of other α-keto acids, such as α-ketovaleric acid or α-ketocaproic acid, with chloroacetonitrile, however, the yields of the products are low and the isolation and purification are difficult.[2b,c] Bergmann and his coworkers described that *N*-(chloroacetyl)phenylserine could be dehydrated under carefully controlled conditions by the action of acetic anhydride to give 4-benzylidene-2-chloromethyl-5-oxazolone, which, upon hydrolysis with dilute alkali, afforded α-2-(chloroacetamido)-cinnamic acid, *i. e.*, *N*-(chloroacetyl)dehydrophenylalanine.[4] Sheehan and Duggins reported the formation of α-(2-chloroacetamido)cinnamic acid in the treatment of *N*-(dichloroacetyl)phenylalanine with acetic anhydride in the presence of pyridine.[5] The formation has been explained by the initial cyclization of *N*-(dichloroacetyl)phenylalanine into 4-benzylidene-2-chloromethyl-5-oxazolone, followed by a hydrolytic fission of the oxazolone ring.

This paper deals with the preparation and characterization of 4-alkylidene- and 4-aralkylidene-2-chloromethyl-5-oxazolones and those transformations into *N*-(chloroacetyl)dehydroamino acids.

The treatment of *N*-(chloroacetyl)phenylalanine or *N*-(chloroacetyl)leucine with acetic anhydride has been known to form readily 4-benzylidene- or 4-isobutylidene-2-methyl-5-oxazolone (I, R=C_6H_5 or *i*-C_3H_7; R'=H) by the elimination of one molecule each of water and hydrogen chloride.[6] On the other hand, the recent report by Steglich *et al.* showed that *N*-trichloroacetyl amino acids, upon treatment with dicyclohexylcarbodiimide or phosphorus trichloride in the presence of pyridine, gave 2-dichloromethylene-pseudo-5-oxazolones (II, X=Cl).[7]

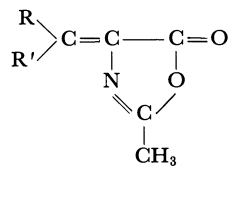

I

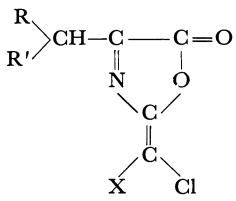

II

When *N*-dichloroacetyl-L-leucine (IIIb) was heated in acetic anhydride at 85—90°C for 1 hr, 2-chloromethyl-4-isobutylidene-5-oxazolone (IVb) was obtained in 74% yield. The structure of IVb was determined by its elemental analysis and spectral studies as well as the hydrolysis reaction. The infrared spectrum showed a strong, broad band at 1800 cm^{-1} (C=O), a strong sharp band at 1670 (C=N) and a weak band at 1615 (C=C). The

1) a) J. P. Greenstein and M. Winitz, "Chemistry of Amino Acids," Vol. 2, John Wiley and Sons, Inc., New York (1961), pp. 838—860; b) J. P. Greenstein, "Advances in Enzymology," Vol. 8, F. F. Nord, Ed., Interscience Publishers, Inc., New York (1948), p. 117.

2) a) V. E. Price and J. P. Greenstein, *J. Biol. Chem.*, **171**, 477 (1947); b) A. Meister and J. P. Greenstein, *ibid.*, **195**, 849 (1952); c) L. Levintow, S.-C. J. Fu, V. E. Price and J. P. Greenstein, *ibid.*, **184**, 633 (1950).

3) T. Wieland, G. Ohnacker and W. Ziegler, *Chem. Ber.*, **90**, 194 (1957).

4) M. Bergmann, V. Schmidt and A. Miekeley, *Z. Physiol. Chem.*, **187**, 264 (1930).

5) J. C. Scheehan and W. E. Duggins, *J. Am. Chem. Soc.*, **74**, 2475 (1950).

6) a) M. Bergmann and F. Stern, *Ann.*, **448**, 20 (1926); b) D. G. Doherty, J. E. Tiezman and M. Bergmann, *J. Biol. Chem.*, **147**, 617 (1943).

7) W. Steglich, H. Tanner and R. Hurnaus, *Chem. Ber.*, **100**, 1824 (1967).

NMR spectrum exhibited a doublet at τ 3.44, a singlet at 5.64, a multiplet centered at 6.8, and a doublet at 8.85. The peak areas were in the ratio 1.0 : 2.3 : 1.0 : 6.0 (theory 1 : 2 : 1 : 6). The peak pattern corresponds not to the pseudo-oxazolone structure II (R=*i*-C_3H_7; R'=H; X=H), but to 2-chloromethyl-4-isobutylidene-5-oxazolone structure IVb.

Analogous treatments of several *N*-dichloroacetyl amino acids (III) with actic anhydride resulted in the formation of the corresponding 4-alkylidene- and 4-aralkylidene-2-chloromethyl-5-oxazolones (IV). The yields of the oxazolones IV were affected sensitively with the reaction temperature, probably owing to the thermo-unstability of IV. After much repeated experiments under various conditions, the best yields could be obtained only at the temperature described in Experimental. Sheehan and Duggins demonstrated that the treatment of *N*-(dichloroacetyl)phenylalanine (IIId) with acetic anhydride at 100°C for seventy-five min led only to recovery of the starting material.[5] In our experiment, however, 4-benzylidene-2-chloromethyl-5-oxazolone (IVd) was obtained in 61% yield by the treatment at 130°C for 1 hr.

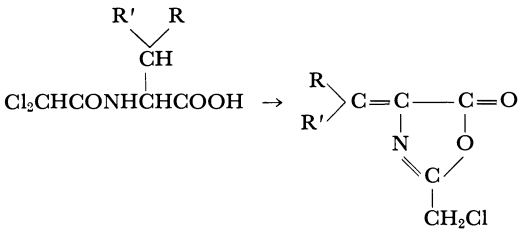

	R	R'
IIIa	CH_3	CH_3
b	*i*-C_3H_7	H
c	C_2H_5	CH_3
d	C_6H_5	H
e	*p*-HO-C_6H_4	H

IV

IVf R=*p*-AcO-C_6H_4, R'=H

4-Alkylidene-2-chloromethyl-5-oxazolones were susceptible to undergo hydrolysis. Even when left to stand at room temperature, the oily oxazolones were partially hydrolyzed by atmospheric moisture to afford the crystalline product. Treatment of 2-chloromethyl-4-isopropylidene-5-oxazolone (IVa) with water at room temperature gave 2-(2-chloroacetamido)-3-methylcrotonic acid, *i. e.*, *N*-(chloroacetyl)dehydrovaline (Va) in 80% yield.

In a similar fashion, *N*-(chloroacetyl)dehydroleucine (Vb), *N*-(chloroacetyl)dehydroisoleucine (Vc) and *N*-(chloroacetyl)dehydrophenylalanine (Vd) were prepared by the hydrolysis of the oxazolones (IVb, IVc, IVd). The acids V were characterized by elemental analyses and infrared spectra.[8] In turn, the formation of V also supported the structure of the parent oxazolone IV.

When 2-chloromethyl-4-isopropylidene-5-oxazolone (IVa) was refluxed in ethanol, the ethanolysis product, ethyl 2-(2-chloroacetamido)-3-methylcrotonate (VIa) was obtained in 17% yield. The ester VIa was also obtained in 39% yield by the esterification of the acid Va in the presence of

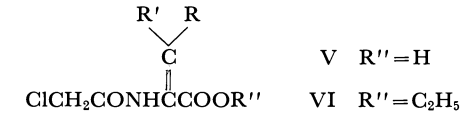

V R''=H

VI R''=C_2H_5

sulfuric acid and *p*-toluenesulfonic acid. The NMR analysis revealed that the ester has an *N*-acyl-enamine structure VIa and not the tautomeric *N*-acyl-imine structure (see Experimental).

The amination of the crude 2-(2-chloroacetamido)-2-alkenoic acids V with ammonia has been known to give *N*-(glycyl)dehydroamino acids.[2b,c] In order to study the reactivity of the chloroacetyl group, the reactions of *N*-(chloroacetyl)dehydroleucine (Vb) with several amines were carried out.

Piperidine (pK_a=11.22) reacted with Vb immediately at room temperature to afford 4-methyl-2-(2-piperidinoacetamido)-2-pentenoic acid hydrochloride. Analogously, L-leucine ethyl ester (pK_a=7.66) treated smoothly with Vb within half an hour to give 4-methyl-2-[2-(1-ethoxycarbonyl-3-methylbutylamino)acetamido] - 2 - pentenoic acid hydrochloride, while the reaction of Vb with pyridine (pK_a=5.23) occurred in acetonitrile at the refluxing temperature to yield the corresponding pyridinium chloride. The reaction with aniline (pK_a=4.6) was attempted in refluxing tetrahydrofuran or acetonitrile, but the starting materials were recovered.

N-(Chloroacetyl)dehydrophenylalanine (Vd) was again treated with acetic anhydride under the same condition as for the preparation of IVd, but this reaction gave 4-benzylidene-2-methyl-5-oxazolone in 74% yield, instead of the parent oxazolone IVb. The formation of the dechlorinated oxazolone is possibly explained by an exchange of the chloroacetyl group of Vd with acetyl group, followed by the cyclization of the resultant α-acetamidocinnamic acid.

N-Dichloroacetyl amino acids (III) were prepared by treatment of amino acids with dichloroacetyl chloride in ethyl acetate[9] or in aqueous sodium hydroxide.

Treatment of DL-valine with 1.2—1.3 equiv. of dichloroacetyl chloride in refluxing ethyl acetate afforded not only *N*-dichloroacetyl-DL-valine (IIIa), but also *N*-(chloroacetyl)dehydrovaline (Va). The formation of Va could be easily rationalized by transformation of IIIa with dichloroacetyl chloride into the oxazolone IVa, followed by hydrolysis of IVa.

8) There has been no description about the constants of *N*-chloroacetyl derivatives of dehydrovaline, dehydroleucine, and dehydroisoleucine, owing to the difficulties in the purification of the products from the reactions of α-keto acids with chloroacetonitrile.[2b,c]

9) E. Ronwin, *J. Org. Chem.*, **18**, 1546 (1953).

TABLE 1. YIELDS OF PRODUCTS IN THE REACTION OF AMINO ACIDS WITH DICHLOROACETYL CHLORIDE

Amino acid	Method[a)]	Yield of III %	Yield of V %
DL-Valine	A-1	33	12
	A-2	44	Trace
	B	32	—
L-Leucine	A-2	46	0
	B	54	—
DL-Isoleucine	A-1	48	0
	A-2	45	0
	B	69	—
DL-Phenylalanine	A-1	38	16
	A-2	48	Trace
	B	62	—
L-Tyrosine	A-1	42	Trace
	B	41	—

a) A-1 means the reaction in ethyl acetate where the amino acid and dichloroacetyl chloride were used in the mole ratio 1 : 1.2—1.3. A-2 means the reaction in ethyl acetate where the amino acid and dichloroacetyl chloride were used in the mole ratio 1 : 0.5—0.7. B means the reaction in aqueous sodium hydroxide. (See Experimental)

Analogous treatment of other amino acids with dichloroacetyl chloride in ethyl acetate led to the results summarized in Table 1.

Experimental[10)]

Dichloroacetyl chloride was prepared by using the technique of Boshard *et al.*[11)] for trichloroacetyl chloride. A mixture of dichloroacetic acid (162 m*l*, 247 g, 1.92 mol), thionyl chloride (160 m*l*, 259 g, 2.18 mol) and dimethylformamide (20 m*l*, 18.5 g, 0.25 mol) was heated at 70—85°C for 4 hr, and then distilled to give a colorless liquid (214 g, 76%), bp 104—109°C (lit.[12)] bp 105—107°C).

N-Dichloroacetyl Amino Acids (III). *A) Reaction in Ethyl Acetate.* The procedure was modified from the method of Ronwin.[9)] To a suspension of an amino acid (25 g) in ethyl acetate (300 m*l*) was added the appropriate equiv. of dichloroacetyl chloride, and the mixture was refluxed for 30 min in the case of DL-valine, L-leucine and DL-isoleucine, or for 1 hr in the case of DL-phenylalanine and L-tyrosine. After the removal of the insoluble substance, the resultant solution was concentrated and the residue was treated with a small amount of ether in the case of DL-valine, DL-isoleucine, DL-phenylalanine and L-tyrosine, or with a small amount of carbon tetrachloride in the case of L-leucine: thereby the dichloroacetyl amino acid separated as a crystalline product, which was collected and washed with the same solvent as that of the filtrate.[13)] The product was characterized by the melting point[5,9)] and the infrared spectrum, which exhibited four characteristic sharp bands at 3300—3250, 1730—1715, 1680—1660 and 1560 cm^{-1}. The yields were summarized in Table 1.

The combined filtrate and washing were concentrated to yield *N*-(chloroacetyl)dehydroamino acid in the yield shown in Table 1. The product was characterized by comparison (mp and infrared spectrum) with a sample obtained by the method described below, except *N*-(chloroacetyl)dehydrotyrosine.

B) Reaction in Aqueous Sodium Hydroxide. The procedure was modified from the method for the preparation of *N*-dichloroacetyl-DL-phenylalanine described by Sheehan and Duggins.[5)] To a solution of an amino acid (0.2 mol) in 1 N sodium hydroxide (200 m*l*) were added dropwise, with stirring, dichloroacetyl chloride (30 g) and 1 N sodium hydroxide (210 m*l*) below 0°C. After the additions had been completed, the mixture was stirred for several hr, while being allowed to warm to room temperature. The insoluble substance was removed and the filtrate was acidified to pH 1 with concentrated hydrochloric acid. The crystalline solid was collected, dissolved in ethyl acetate and dried over anhydrous sodium sulfate. Evaporation of the ethyl acetate afforded the *N*-dichloroacetyl amino acid[13)] in the yield shown in Table 1. In the case of L-tyrosine, analogous directions were followed to the procedure for the preparation of *N*-chloroacetyl-L-tyrosine described by Fisher.[14)]

4-Isopropylidene-2-chloromethyl-5-oxazolone (IVa). A suspension of *N*-dichloroacetyl-DL-valine (11.7 g) in acetic anhydride (35 m*l*) was heated at 95—105°C for 1 hr. The resultant red-brown solution was concentrated and the residual oil was distilled to give a pale yellow oil (6.9 g, 78%), bp 93—103°C/2 mmHg.[13)] A colorless fraction, bp 103.5°C/2.5 mmHg, obtained from the redistillation was submitted to analysis.[15)] IR (liquid film): 1800, 1670, 1615 cm^{-1}. NMR ($CDCl_3$): τ 5.65 (s, 2H), 7.62 (s, 3H), 7.71 (s, 3H).

Found: C, 47.50; H, 4.36; N, 7.76%. Calcd for $C_7H_8NO_2Cl$: C, 48.41; H, 4.61; N, 8.07%.

4-Isobutylidene-2-chloromethyl-5-oxazolone (IVb). In a manner analogous to the case of IVa, dichloroacetyl-L-leucine (10 g) was treated with acetic anhydride (60 m*l*) at 85—90°C for 1 hr to give a pale yellow oil (5.7 g, 74%), bp 90—102°C/3 mmHg.[13)] A colorless fraction, bp 90°C/1 mmHg, obtained from the redistillation was submitted to analysis. The spectra data were described in the text.

Found: C, 50.97; H, 5.54; N, 7.66%. Calcd for $C_8H_{10}NO_2Cl$: C, 51.20; H, 5.33; N, 7.47%.

4-*s*-Butylidene-2-chloromethyl-5-oxazolone (IVc). In a manner analogous to the case of IVa, *N*-dichloroacetyl-DL-isoleucine (17 g) was treated with acetic anhydride (30 m*l*) at 115—125°C for 1—1.5 hr to

10) All concentrations and evaporations were carried out by rotary evaporation under reduced pressure. All melting points were determined in a liquid bath, and those and boiling points are uncorrected.

11) H. H. Boshard, R. Mory and H. Zollinger, *Helv. Chim. Acta*, **42**, 1653 (1959).

12) H. C. Brown, *J. Am. Chem. Soc.*, **60**, 1326 (1938).

13) The product was sufficiently pure to be used for a next reaction without further purification.

14) E. Fisher, *Chem. Ber.*, **37**, 2494 (1904).

15) The analytical results were outside the generally accepted limits for C and H, possibly owing that the oxazolone IVa is too sensitive towards atmospheric moisture to be microanalyzed. But the formation was characterized by the spectral data and by the conversion to *N*-(chloroacetyl)dehydrovaline (Va).

give a pale yellow oil (8.9 g, 67%), bp 90—102.5°C/0.8 mmHg.[13] A colorless fraction, bp 113—115°C/3.5 mmHg, obtained from the redistillation was submitted to analysis. IR (liquid film): 1800, 1670, 1615 cm^{-1}.

Found: C, 50.83; H, 5.02; N, 7.84%. Calcd for $C_8H_{10}NO_2Cl$: C, 51.20; H, 5.33; N, 7.47%.

4-Benzylidene-2-chloromethyl-5-oxazolone (IVd). A mixture of *N*-dichloroacetyl-DL-phenylalanine (18.5 g) and acetic anhydride (80 m*l*) was heated at 130°C for 1 hr. The resultant red-brown solution was concentrated and the crystalline residue was treated with methanol (20 m*l*). The collected yellow product was washed twice with methanol (4 m*l*×2). Yield: 8.9 g (61%).[13] A part of the product was recrystallized from ethanol to give yellow plates, mp 109—110°C (lit.[4] mp 114°C). IR: 1785, 1660, 1605 cm^{-1}. NMR ($CDCl_3$): τ 2.0 and 2.7 (m, 6H), 5.65 (s, 2H).

4-(*p*-Acetoxybenzylidene)-2-chloromethyl-5-oxazolone (IVf). In a manner analogous to the case of IVd, *N*-dichloroacetyl-L-tyrosine (5.2 g) was treated with acetic anhydride (20 m*l*) at 105—115°C for 1 hr to give IVf as yellow crystals (3.9 g, 78%). Recrystallization from carbon tetrachloride afforded orange crystals, mp 123.5°C (after sintered at 110°C). IR (KBr): 1790, 1760, 1655, 1605 cm^{-1}.

Found: C, 55.57; H, 3.27; N, 4.95%. Calcd for $C_{13}H_{10}NO_4Cl$: C, 55.81; H, 3.58; N, 5.01%.

The oxazolone IVf is soluble easily in ethyl acetate and tetrahydrofuran, moderately in carbon tetrachloride and slightly in water, ether, benzene and ethanol.

2-(2-Chloroacetamido)-3-methylcrotonic Acid (*N*-(Chloroacetyl)dehydrovaline, Va). A mixture of IVa (7.7 g) and water (15 m*l*) was left to stand at room temperature overnight: thereby the oily oxazolone had been hydrolyzed to give Va as a crystalline solid. The crystals were collected (6.5 g), and the filtrate was concentrated to give additional crystals (0.3 g). Total yield was 6.8 g, 80%.[13] An analytical sample was obtained by recrystallization from acetone, as colorless needles, mp 166—166.5°C (decomp.). IR (KBr): 3250, 1690, 1670, 1640, 1530 cm^{-1}.

Found: C, 44.00; H, 5.32; N, 7.28%. Calcd for $C_7H_{10}NO_3Cl$: C, 43.86; H, 5.22; N, 7.31%.

The acid Va is soluble easily in tetrahydrofuran, ethanol and acetone, moderately in hot acetonitrile, hot ethyl acetate and hot water, and slightly in ether, carbon tetrachloride and benzene.

2-(2-Chloroacetamido)-4-methyl-2-pentenoic Acid (*N*-(Chloroacetyl)dehydroleucine, Vb). The same directions were followed as for Va. From IVb (6.2 g) and water (10 m*l*) there was obtained Vb (5.7 g, 83%). Recrystallization from water afforded colorless needles, mp 128—129°C (decomp.). IR (KBr): 3250, 1695, 1670, 1625, 1525 cm^{-1}.

Found: C, 46.34; H, 5.84; N, 6.61%. Calcd for $C_8H_{12}NO_3Cl$: C, 46.72; H, 5.84; N, 6.81%.

2-(2-Chloroacetamido)-3-methyl-2-pentenoic Acid (*N*-(Chloroacetyl)dehydroisoleucine, Vc). The same directions were followed as for Va. From IVc (5.1 g) and water (15 m*l*) there was obtained Vc (4.1 g, 73%). Recrystallization from ethyl acetate afforded colorless needles, mp 149.5—150°C (decomp.). IR (KBr): 3250, 1690, 1675, 1630, 1530 cm^{-1}.

Found: C, 46.75; H, 5.67; N, 6.82%. Calcd for $C_8H_{12}NO_3Cl$: C, 46.72; H, 5.84; N, 6.81%.

α-(2-Chloroacetamido)cinnamic Acid (*N*-(Chloroacetyl)dehydrophenylalanine, Vd). A solution of IVd (8.86 g) and water (10 m*l*) in tetrahydrofuran (120 m*l*) was refluxed for 3 hr and then left to stand at room temperature overnight. The tetrahydrofuran was evaporated and the residue was treated with ether (50 m*l*) to give an almost colorless crystalline product (8.15 g, 86%).[13] Recrystallization from isopropyl alcohol afforded colorless needles, mp 194—195°C (decomp.) (lit. mp 204.5—206°C,[5] 207°C[4]). IR (KBr): 3250, 1690, 1665, 1635, 1525 cm^{-1}. NMR (CF_3COOH): τ1.35 (s, 1NH), 2.11 (s, 1H), 2.54 (m, 5H), 5.71 (s, 2H).

α-(2-Chloroacetamido)-*p*-hydroxycinnamic Acid (*N*-(Chloroacetyl)dehydrotyrosine, Ve). This compound was obtained from the reaction of DL-tyrosine with dichloroacetyl chloride in ethyl acetate, as described above. Recrystallization from acetonitrile afforded pale yellow needles, mp 185°C (decomp.). IR (KBr): 3375, 3200, 1675 (broad), 1635, 1515 cm^{-1}.

Found: C, 51.82; H, 3.74; N, 5.75%. Calcd for $C_{11}H_{10}NO_4Cl$: C, 51.66; H, 3.91; N, 5.48%.

The acid Ve is soluble easily in tetrahydrofuran, ethanol, hot acetonitrile and hot water, and slightly in ethyl acetate and ether.

4-Methyl-2-(2-piperidinoacetamido)-2-pentenoic Acid Hydrochloride. Colorless needles (from ethyl acetate), mp 110—111°C.

Found: C, 53.72; H, 7.96; N, 9.79%. Calcd for $C_{13}H_{23}N_2O_3Cl$: C, 53.70; H, 7.92; N, 9.64%.

4-Methyl-2-[2-(1-ethoxycarbonyl-3-methylbutylamino)acetamido]-2-pentenoic Acid Hydrochloride. Colorless plates (from ethyl acetate), mp 134—135°C.

Found: C, 53.06; H, 8.09; N, 7.57%. Calcd for $C_{16}H_{29}N_2O_5Cl$: C, 52.67; H, 7.96%; N, 7.68%.

[*N*-(1-Carboxy-3-methyl-1-butenyl)carbamoylmethyl]pyridinium Chloride. Colorless crystals (from isopropyl alcohol), mp 222—223°C (decomp.).

Found: C, 55.25; H, 5.90; N, 9.55%. Calcd for $C_{13}H_{17}N_2O_3Cl$: C, 54.83; H, 5.98; N, 9.84%.

Ethyl 2-(2-Chloroacetamido)-3-methylcrotonate (VIa). *A) From IVa.* A solution of IVa (bp 89—98°C/1.5 mmHg, 6.9 g) in ethanol (20 m*l*) was refluxed for 4 hr. After evaporation of the ethanol, the residue was dissolved in ether and washed successively with a small amount of aqueous sodium bicarbonate and with water. The ethereal layer was dried over anhydrous sodium sulfate and evaporated to give the ester, which was treated with *n*-dibutyl ether and collected (1.45 g, 17%, mp 115—116°C). Recrystallization from water-methanol (11 : 9) and then from *n*-dibutyl ether gave colorless long needles, mp 118—119°C. IR (KBr): 3200, 1715, 1665, 1535 cm^{-1}. NMR ($CDCl_3$): τ 2.07 (s, 1H), 5.77 (q, 2H), 5.86 (s, 2H), 7.80 (s, 3H), 8.15 (s, 3H), 8.72 (t, 3H).

Found: C, 49.41; H, 6.24; N, 6.09%. Calcd for $C_9H_{14}NO_3Cl$: C, 49.20; H, 6.38; N, 6.38%.

B) From Va. A mixture of Va (2 g), ethanol (15 m*l*), benzene (20 m*l*), *p*-toluenesulfonic acid (0.5 g) and concentrated sulfuric acid (0.5 g) was refluxed for 5 hr. After concentration of the solution, ether and water were added to the resultant oily residue. The ethereal layer was spearated and the aqueous layer was extracted further twice with ether. The combined extracts were dried over anhydrous sodium sulfate and concentrated to give the ester (0.9 g, 39%), mp 109—

110°C. Recrystallization raised the mp to the value described in A method. The product was identical (mp and infrared spectrum) with the above sample.

Treatment of Vd with Acetic Anhydride. A suspension of Vd (1 g) in acetic anhydride (30 m*l*) was heated at 120—130°C for 1 hr. After concentration of the resultant solution, the crystalline residue was treated with ethanol (10 m*l*) and collected (0.58 g). Recrystallization from ethanol gave pale yellow needles, mp 152.5°C, which was identical in mp and infrared spectrum with authentic 4-benzylidene-2-methyl-5-oxazolone, mp 151—153°C (lit.[6a] mp 151—152°C).

BULLETIN OF THE CHEMICAL SOCIETY OF JAPAN VOL. 41 2762—2764 (1968)

Stereospecific Synthesis of 1,4-Dienes. IV.[1] The Catalytic Behavior of the Ethylenebis(diphenylphosphine) Complex of Iron(0)

Go HATA and Akihisa MIYAKE

Basic Research Laboratories, Toyo Rayon Co., Ltd., Kamakura

(Received May 16, 1968)

A zerovalent iron complex, $Fe(Ph_2P{\cdot}CH_2CH_2{\cdot}PPh_2)_2{\cdot}C_2H_4$, catalyzes addition of ethylene to butadiene to afford 1 : 1 adducts consisting of 1,*cis*-4-hexadiene, 1,3-hexadiene, 2,4-hexadiene and 1,5-hexadiene, and 2 : 1 adducts. The combination of the iron complex and a Lewis acid (triethylaluminum, diethylaluminum chloride, ethylaluminum dichloride and boron trifluoride etherate) gives 1,*cis*-4-hexadiene much more selectively. The most efficient Lewis acid component for the synthesis of 1,*cis*-4-hexadiene is diethylaluminum chloride.

There are several reports on the preparation of 1,4-dienes by addition of ethylene to 1,3-dienes using the iron-based catalysts.[2-5] The binary system consisting of iron(III) acetylacetonate and triethylaluminum[2], and the ternary system consisting of ferric chloride, ditertiaryphosphine and an organoaluminum compound[3] were reported to catalyze the reaction of ethylene with butadiene to afford 1,4-hexadiene.

In connection with investigation of the reducing property of the organoaluminum compounds in these catalyst systems, the reaction of iron(III) acetylacetonate with ethoxydiethylaluminum was carried out in the presence of ethylenebis(diphenylphosphine), and a zerovalent iron complex, $Fe(Ph_2P{\cdot}CH_2CH_2{\cdot}PPh_2)_2{\cdot}C_2H_4$, was isolated.[6] This fact suggests that one of the functions of the organoaluminum compounds in the catalyst systems is the reduction of the iron compounds to a zerovalent iron complex. It has been confirmed that this diphosphine complex catalyzed the reaction of butadiene with ethylene. This work was undertaken to study the catalytic behavior of the diphosphine complex in this reaction.

Results and Discussion

The diphosphine complex, $Fe(Ph_2P{\cdot}CH_2CH_2{\cdot}PPh_2)_2{\cdot}C_2H_4$ (hereafter the iron complex), was found to catalyze addition of ethylene to butadiene to afford 1 : 1 adducts consisting of 1,*cis*-4-hexadiene, 1,3-hexadiene, 2,4-hexadiene and 1,5-hexadiene, and 2 : 1 adducts. The 2 : 1 adducts were major products. The reaction was carried out at 85°C under ethylene pressure of 40 kg/cm^2. The result is shown in Table 1. 1,5-Hexadiene and the 2 : 1 adducts were not obtained in the iron(III) acetylacetonate-triethylaluminum catalyzed reaction.[2] The former compound was identified by comparison of its infrared spectrum and gas chromatographic retention time with those of an authentic sample. The gas chromatographic analysis of the 2 : 1 adducts using a squalane capillary column (90 m) showed that they contained four components. The molecular weights of these components were determined by mass spectroscopy to be 110 (C_8H_{14}). However, separation of these four components by preparative gas chromatography using a squalane column was unsuccessful, and hence further characterization of the adducts was not possible.

Addition of a Lewis acid to the iron complex changed remarkably the distribution of the products. The results are summarized in Tables 1

1) Part III. G. Hata and A. Miyake, This Bulletin, **41**, 2443 (1968).
2) G. Hata, *J. Am. Chem. Soc.*, **86**, 3903 (1964); G. Hata and D. Aoki *J. Org. Chem.*, **32**, 3754 (1967).
3) M. Iwamoto and S. Yuguchi, *ibid.*, **31**, 4290 (1966).
4) M. Iwamoto and S. Yuguchi, This Bulletin, **39**, 2001 (1966).
5) A. Carbonaro, A. Greco and G. Dall'Asta, *Tetrahedron Letters*, **1967**, 2037.
6) G. Hata, H. Kondo and A. Miyake, *J. Am. Chem. Soc.*, **90**, 2278 (1968).

Table 1. Reaction of butadiene with ethylene by iron complex catalyst and iron complex-$Al(C_2H_5)_3$ catalyst system

$Al(C_2H_5)_3$/Fe complex molar ratio	Products (g)					
	1,5-HD	1,4-HD	1,3-HD	2,4-HD	C_8 Dienes	Residue
0	0.5	0.9	2.5	1.7	7.0	1.1
4	2.3	2.6	1.4	1.4	9.7	0.8
8	1.4	5.0	1.8	0.6	4.2	0.8
16	0.9	7.9	1.2	0.4	2.7	1.7

HD=hexadiene

Reaction conditions: $Fe(Ph_2P\cdot CH_2CH_2\cdot PPh_2)_2\cdot C_2H_4$ 0.5 mmol, toluene 30 m*l*, ethylene, 40 kg/cm², 85°C.

Table 2. Reactions by iron complex-lewis acid catalyst system

Exp. No.	Lewis acid	(mmol)	Temp °C	Time min	Products (g) 1,4-HD	Residue
1	$(C_2H_5)_2AlCl$	(4)	30	90	2.2	0.1
2	$(C_2H_5)_2AlCl$	(8)	50	90	19.2	0.7
3	$(C_2H_5)_2AlCl$	(4)	80	5	22.6	0.5
4	$(C_2H_5)_2AlCl$	(1)	50	90	0.4	0.3
5	$C_2H_5AlCl_2$	(1)	50	45	2.3	1.0
6	$C_2H_5AlCl_2$	(4)	50	45	1.1	2.1
7	$C_2H_5AlCl_2$	(1)	80	30	20.8	0.8
8	$BF_3\cdot O(C_2H_5)_2$	(1)	80	100	1.2	0.3

Reaction conditions: $Fe(Ph_2P\cdot CH_2CH_2CH_2\cdot PPh_2)\cdot C_2H_4$ 0.5 mmol, butadiene 0.3 mol, toluene 10 m*l*, ethylene 40 kg/cm².

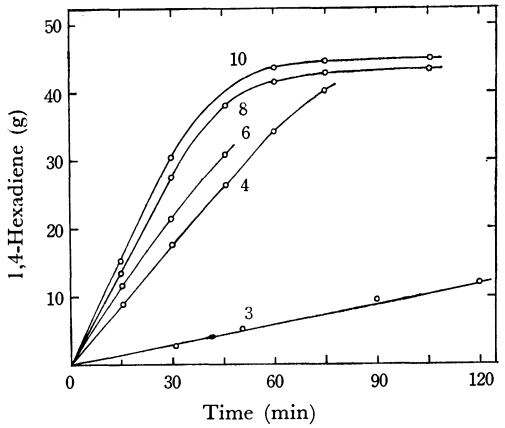

Fig. 1. Reaction of butadiene with ethylene. Reaction conditions: $Fe(Ph_2P\cdot CH_2CH_2\cdot PPh_2)_2\cdot C_2H_4$ 0.5 mmol, toluene 20 m*l*, C_4H_6 0.6 mol, C_2H_4 40 kg/cm², 50°C. The numbers in the table show molar ratios of $(C_2H_5)_2AlCl$ to the iron complex.

and 2. The combination of the iron complex and diethylaluminum chloride catalyzed the reaction of butadiene with ethylene to give 1,*cis*-4-hexadiene in high yield (95%). This reaction occurred at 30°C and proceeded very rapidly at 80°C (Table 2). The effect of the molar ratio of the catalyst components on the catalytic activity is shown in Fig. 1. At the molar ratios larger than 3, the reaction proceeded quickly. The catalyst system containing ethylaluminum dichloride and boron trifluoride etherate also afforded the 1,4-diene selectively. However, these Lewis acids were not so effective components, as compared with diethylaluminum chloride, because of decomposition of the catalyst during the reaction. The decomposition of the catalyst containing ethylaluminum dichloride occurs at the early stage of the reaction. When the reaction was conducted under the same conditions as listed in Run No. 7 of Table 2 except stirring for 20 min before introduction of ethylene (40 kg/cm²), this system showed a quite low activity and only 0.2 g of 1,4-hexadiene was obtained. Almost all of the employed butadiene was recovered. This observation indicates that the catalyst decomposed during the stirring for 20 min. In contrast to these catalyst systems, the system containing triethylaluminum as a Lewis acid component gave the same products as obtained in the reaction catalyzed by the iron complex alone. However, the distribution of the products was different and the formation of 1,*cis*-4-hexadiene increased. The molar ratio of triethylaluminum to the iron complex affected the distribution of the products as shown in Table 1. At a high molar ratio, the behavior of the catalyst resembled that of the combination of the iron complex and diethylaluminum chloride, and the major product was 1,*cis*-4-hexadiene.

The function of the Lewis acids in these catalyst systems is presumably the removal of the coordinated diphosphine from the iron complex to leave a coordination site for butadiene. The stronger Lewis acid should accomplish this removal more effectively. In fact, diethylaluminum chloride is much more effective than triethylaluminum as a catalyst component for the selective synthesis of 1,*cis*-4-hexadiene. The former aluminum compound is a stronger Lewis acid than the latter. Lewis acidity of organoaluminum compounds toward a Lewis base is correlated to the complex formation between both compounds. The easiness of the

complex formation of organoaluminum compounds with a Lewis base is in the following order: $C_2H_5AlCl_2 > (C_2H_5)_2AlCl > (C_2H_5)_3Al > (C_2H_5)_2AlOC_2H_5$.[7] Although ethylaluminum dichloride, the strongest Lewis acid, decomposes the catalyst during the reaction, this organoaluminum compound is more effective than diethylaluminum chloride at the low molar ratio (2 : 1) of the Lewis acid to the iron complex.

The catalyst system consisting of the iron complex and diethylaluminum chloride affords 1,4-hexadiene in a high selectivity as compared with the iron(III) acetylacetonate-triethylaluminum catalyst system.[2] This fact suggests the coordination of one molecule of the diphosphine in the catalyst species, which would interrupt coordination of another molecule of butadiene and suppress oligomerization of butadiene.[8]

The formation of 1,4-hexadiene occurs through transfer of a hydrogen atom of ethylene to butadiene. The mechanism of the hydrogen transfer, however, is not clear.

The mixture of iron(III) acetylacetonate, ethylenebis(diphenylphosphine) and diethylaluminum chloride showed the same catalytic activity as that of the iron complex and diethylaluminum chloride, and gave 1,*cis*-4-hexadiene in 91% yield. This fact indicates that diethylaluminum chloride in the former system acts as a reducing agent as well as a Lewis acid.

The reaction of isoprene with ethylene by the ternary system gave a mixture of 4-methyl- and 5-methyl-1,4-hexadiene in 92% yield. The ratio of the former diene to the latter was 75 : 25 (at 70°C). 1,3-Pentadiene reacted with ethylene to afford 3-methyl-1,*cis*-4-hexadiene and 1,*cis*-4-heptadiene in a ratio of 85 : 15. The preferential addition of ethylene occurs at the methyl substituted side, and this is the characteristic of the reaction by the iron(III) acetylacetonate-triethylaluminum catalyst system.[2] In the reaction catalyzed by the latter system, the above ratios were 57 : 43 and 70 : 30 at 30°C, respectively.

7) H. Lehmkuhl, *Angew. Chem.*, **75**, 1090 (1963).
8) M. Hidai, Y. Uchida and A. Misono, This Bulletin, **38**, 1243 (1965).

Experimental

Reaction of Butadiene with Ethylene. (1) A 100 m*l* autoclave was flashed with ethylene and then charged with liquid butadiene, a toluene solution of the complex, $Fe(Ph_2PCH_2CH_2PPh_2)_2 \cdot C_2H_4$, which was prepared by the method described previously,[6] and a toluene solution of the Lewis acid. The resultant solution was stirred under ethylene pressure of 40 kg/cm^2. 1,*cis*-4-Hexadiene, 1,3-hexadiene and 1,5-hexadiene were separated by preparative gas chromatography and identified by comparison of their infrared spectra and gas chromatographic retention times with those of authentic samples. 2,4-Hexadiene was characterized by gas chromatographic analysis. The C_8 hydrocarbons were separated by gas chromatography on a squalane capillary column (90 m) at 40°C into four components, which were analyzed by mass spectroscopy. All of their spectra showed parent peaks at $m/e=110$ (C_8H_{14}).

(2) A mixture of 15 m*l* of toluene, 0.3 mol of butadiene, 0.177 g (0.5 mmol) of iron(III) acetylacetonate, 0.478 g (1.2 mmol) of ethylenebis(diphenylphosphine) and 8 mmol of diethylaluminum chloride was stirred at 80°C under ethylene pressure of 40 kg/cm^2 for 30 min. The yield of 1,*cis*-4-hexadiene was 22.5 g (91%).

Reaction of Isoprene with Ethylene. A 100 m*l* autoclave was charged with 21.0 g (0.3 mol) of isoprene, 20 m*l* of xylene, 0.177 g (0.5 mmol) of iron(III) acetylacetonate, 0.478 g (1.2 mmol) of ethylenebis(diphenylphosphine) and 8 mmol of diethylaluminum chloride. The resultant mixture was stirred at 70°C under ethylene pressure of 40 kg/cm^2 for 2 hr. Gas chromatographic analysis showed that the reaction mixture contained 26.6 g (92% yield) of a mixture of 4-methyl-1,*cis*-4-hexadiene and 5-methyl-1,4-hexadiene.[2] The ratio of the products was determined by gas chromatography using a silver nitrate-benzyl cyanide column.

BULLETIN OF THE CHEMICAL SOCIETY OF JAPAN VOL. 41 2765—2769 (1968)

Studies of Aminosugars. XIX. Syntheses of O-Benzyl-α-halogeno Derivatives of 3-Acetamido-3-deoxy- and 6-Acetamido-6-deoxy-D-glucose[1]

Shinkiti KOTO, Takayuki TSUMURA, Yoshinori KATO and Sumio UMEZAWA

Department of Applied Chemistry, Faculty of Engineering, Keio University, Koganei-shi, Tokyo

(Received May, 23, 1968)

As a part of investigation of the synthesis and reaction of 1-halogeno derivatives of amino-monosaccharides, 3-acetamido-2,4,6-tri-*O*-benzyl-3-deoxy-α-D-glucopyranosyl chloride and 2,3,4-tri-*O*-benzyl-6-(*N*-benzylacetamido)-6-deoxy-α-D-glucopyranosyl chloride have been synthesized. Attempts to prepare α-glycosides from these benzyl derivatives proved to be practical, giving cyclohexyl 3-acetamido-2,4,6-tri-*O*-benzyl-3-deoxy-α-D-glucopyranoside and cyclohexyl 2,3,4-tri-*O*-benzyl-6-(*N*-benzylacetamido)-6-deoxy-α-D-glucopyranoside as main products. Removal of the masking groups gave cyclohexyl α-glucosides of 3-amino-3-deoxy-D- and 6-amino-6-deoxy-D-glucose respectively. A number of related derivatives have been described.

1-Halogeno derivatives of masked monosaccharides are important intermediates for the synthesis of glycosides. However, the corresponding derivatives of aminosugars represents a relatively unexplored territory. In the preceding papers,[2,3] the syntheses of α-acetobromo and β-acetochloro derivatives of 3-carbobenzoxyamino-3-deoxy- and 6-carbobenzoxyamino-6-deoxy-D-glucose have been developed. This paper reports the syntheses of 3-acetamido-2,4,6-tri-*O*-benzyl-3-deoxy-α-D-glucosyl chloride (IV) and 2,3,4-tri-*O*-benzyl-6-(*N*-benzylacetamido)-6-deoxy-α-D-glucopyranosyl chloride (XII). These *O*-benzyl-α-chloro derivatives have been found to be useful for preparing α-glycosides of the aminosugars, as shown here in the preparation of cyclohexyl 3-amino-3-deoxy-α-D-glucoside (VII) and cyclohexyl 6-amino-6-deoxy-α-D-glucoside (XV).

Benzylation of methyl 3-acetamido-3-deoxy-β-D-glucopyranoside[4] with benzyl bromide in the presence of barium oxide and barium hydroxide in *N,N*-dimethylformamide (DMF) gave methyl 3-acetamido-2,4,6-tri-*O*-benzyl-3-deoxy-β-D-glucopyranoside (II) in a 95% yield.

Hydrolysis of II with sulfuric acid in aqueous acetic acid followed by acetylation with acetic anhydride in pyridine gave 3-acetamido-1-*O*-acetyl-2,4,6-tri-*O*-benzyl-α- and β-D-glucopyranose

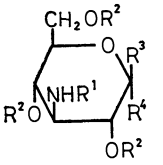

Ac = $-COCH_3$

Bzl = $-CH_2C_6H_5$

I R^1=Ac, R^2=R^4=H, R^3=OCH_3

II R^1=Ac, R^2=Bzl, R^3=OCH_3, R^4=H

IIIa R^1=Ac, R^2=Bzl, R^3=H, R^4=OAc

IIIb R^1=Ac, R^2=Bzl, R^3=OAc, R^4=H

IV R^1=Ac, R^2=Bzl, R^3=H, R^4=Cl

Va R^1=Ac, R^2=Bzl, R^3=H, R^4=OC_6H_{11}

Vb R^1=Ac, R^2=Bzl, R^3=OC_6H_{11}, R^4=H

VIa R^1=Ac, R^2=R^3=H, R^4=OC_6H_{11}

VIb R^1=Ac, R^2=R^4=H, R^3=OC_6H_{11}

VII R^1=H_2Cl, R^2=R^3=H, R^4=OC_6H_{11}

(IIIa and IIIb) which were separated by fractional crystallization from isopropanol and isopropyl ether, the ratio of α- to β-anomer being 1 : 1.

Chlorination of the α-anomer (IIIa) or β-anomer (IIIb) with dry hydrogen chloride in dioxane containing acetyl chloride gave 3-acetamido-2,4,6-tri-*O*-benzyl-3-deoxy-α-D-glucopyranosyl chloride (IV) in quantitative yield.

On the other hand, the *O*-benzyl-α-chloro derivative of 6-amino-6-deoxy-D-glucose has been synthesized by an analogous route. Methyl 6-acetamido-6-deoxy-α-D-glucopyranoside[5] (VIII) was benzylated with benzyl chloride and sodium

1) Part XXXV of "Studies on Antibiotics and Related Substances," by Sumio Umezawa. This paper was read before the 20th Annual Meeting of the Chemical Society of Japan, Tokyo, March, 1967. (See abstracts of the Meeting, III, p. 596).

2) Y. Ito, S. Koto and S. Umezawa, This Bulletin, **35**, 1618 (1962).

3) S. Umezawa, S. Koto and Y. Ito, *ibid.*, **36**, 183 (1963).

4) H. H. Baer, *J. Am. Chem. Soc.*, **83**, 1882 (1961).

5) F. Cramer, O. Otterbach and H. Springman, *Chem. Ber.*, **92**, 384 (1959).

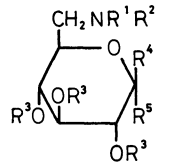

Ac = $-COCH_3$
Bzl = $-CH_2C_6H_5$

VIII $R^1=H$, $R^2=Ac$, $R^3=R^4=H$, $R^5=OCH_3$
IX $R^1=R^3=Bzl$, $R^2=Ac$, $R^4=H$, $R^5=OCH_3$
X $R^1=R^3=Bzl$, $R^2=Ac$, $R^4=OH$, $R^5=H$
XI $R^1=R^3=Bzl$, $R^2=Ac$, $R^4=OAc$, $R^5=H$
XII $R^1=R^3=Bzl$, $R^2=Ac$, $R^4=H$, $R^5=Cl$
XIIIa $R^1=R^3=Bzl$, $R^2=Ac$, $R^4=H$, $R^5=OC_6H_{11}$
XIIIb $R^1=R^3=Bzl$, $R^2=Ac$, $R^4=OC_6H_{11}$, $R^5=H$
XIVa $R^1=R^3=H$, $R^2=Ac$, $R^4=H$, $R^5=OC_6H_{11}$
XIVb $R^1=R^3=H$, $R^2=Ac$, $R^4=OC_6H_{11}$, $R^5=H$
XV $R^1=R^3=R^4=H$, $R^2=H_2Cl$, $R^5=OC_6H_{11}$

hydride to give methyl 2,3,4-tri-*O*-benzyl-6-(*N*-benzylacetamido)-6-deoxy-α-D-glucopyranoside (IX) in a 83% yield. It should be noted that the primary acetamido group of VIII is further benzylated. Hydrolysis of IX with sulfuric acid in aqueous acetic acid gave 2,3,4-tri-*O*-benzyl-6-(*N*-benzylacetamido)-6-deoxy-β-D-glucopyranose (X) in a 75% yield, which was converted to its acetate (XI). The acetate was chlorinated in like manner as described in the preparation of IV to give 2,3,4-tri-*O*-benzyl-6-(*N*-benzylacetamido)-6-deoxy-α-glucopyranosyl chloride (XII) in a 95% yield.

Infrared spectra of the above-mentioned 1-chloro derivatives (IV and XII) of two kinds of aminomonosaccharides showed absorption near 850 cm^{-1} which is characteristic of α-configuration.

Attempts to prepare α-glycosides from IV and XII proved to be practical. When shaken with a mixture of cyclohexanol, mercuric cyanide and mercuric bromide in nitromethane, IV gave cyclohexyl 3-acetamido-2,4,6-tri-*O*-benzyl-3-deoxy-α-D- and β-D-glucopyranoside (Va and Vb), the ratio of α- to β-anomer being 7 : 11. The similar glycosidation of XII gave cyclohexyl 2,3,4-tri-*O*-benzyl-6-(*N*-benzyl-acetamido)-6-deoxy-α-D- and β-D-glucopyranoside (XIIIa and XIIIb), the ratio of α- to β-anomer being about 47 : 5.

Hydrogenolysis over palladium black in methanol smoothly debenzylated Va and Vb to form cyclohexyl 3-acetamido-3-deoxy-α-D- and β-D-glucoside (VIa and VIb) respectively. Similar hydrogenolysis of XIIIa and XIIIb followed by de-*N*-benzylation with sodium in liquid ammonia gave cyclohexyl 6-acetamido-6-deoxy-α-D- and β-D-glucopyranoside (XIVa and XIVb) respectively.

Finally, treatment with hydrazine hydrate de-*N*-acetylated VIa and XIVa to form cyclohexyl 3-amino-3-deoxy-α-D-glucoside and cyclohexyl 6-amino-6-deoxy-α-D-glucoside, which were led to crystalline hydrochlorides (VII and XV) respectively.

Experimental

General Procedures. Thin layer chromatography (TLC) was performed on "Silica-Reider for TLC" (Dai-ich Pure Chemicals Co.). Paper chromatography was carried out on Toyo filter paper No. 51, using a solvent system of *n*-butanol, pyridine, water and acetic acid (6 : 4 : 3 : 1), ninhydrin in pyridine (0.3%) being sprayed on.

Methyl 3-Acetamido-2,4,6-tri-*O*-benzyl-3-deoxy-β-D-glucopyranoside (II). A mixture of methyl 3-acetamido-3-deoxy-β-D-glucopyranoside (I) (5 g), benzyl bromide (50 m*l*), powdery barium oxide (37 g) and finely crushed barium hydroxide octahydrate (17 g) in DMF (100 m*l*) was vigorously stirred at about 0°C for 4 hr and then at room temperature overnight. The reaction mixture diluted with chloroform (250 m*l*) was filtered and the filtrate was dried up under reduced pressure at 60°C to afford a yellow sirup, which was extracted with ethyl acetate (200 m*l*). Evaporation of the extract, followed by treatment with cyclohexane afforded colorless crystals of II; yield, 10.2 g (95%). Recrystallized from isopropanol; mp 163—164°C, $[\alpha]_D^{18}$ +24° (*c* 1.0, chloroform), ε_{258}^{MeOH}=544 (calcd, 558), IR spectrum (KBr): 3290, 1653 and 1576 (NHAc), 1068, 747, 737 and 695 (*O*-benzyl), 907 cm^{-1} (type 2b of pyranose ring.)

Found: C, 70.88; H, 6.63; N, 2.86%. Calcd for $C_{30}H_{35}NO_6$: C, 71.27; H, 6.98; N, 2.77%.

3-Acetamido-1-*O*-acetyl-2,4,6-tri-*O*-benzyl-α- and β-D-glucopyranose (IIIa and IIIb). A mixture of II (13 g), glacial acetic acid (240 m*l*) and 2 N sulfuric acid (63 m*l*) was heated over a boiling water bath for 2 hr. To the resulting mixture was added 2 N sulfuric acid (51 m*l*) and the mixture was further heated for 13 hr. The mixture was poured into a large amount of water to give a colorless precipitate, which was collected and washed thoroughly with water; yield 9.0 g.

The hydrolysis product (8.2 g) was acetylated with acetic anhydride (50 m*l*) and pyridine (50 m*l*) at room temperature overnight. After evaporation the residue was crystallized with isopropanol to afford IIIb; 3.8 g (43%), mp 183—184°C, $[\alpha]_D^{21}$ + 8.1° (*c* 2.6, chloroform), ε_{258}^{MeOH}=534 (calcd, 558), IR spectrum (KBr): 3310, 1659 and 1552 (NHAc), 1744 and 1237 (OAc), 1102, 743 and 697 (*O*-benzyl), 892 cm^{-1} (type 2b of pyranose ring).

Found: C, 69.95; H, 6.74; N, 2.85%. Calcd for $C_{31}H_{35}NO_7$: C, 69.78; H, 6.61; N, 2.63%.

Mother liquor was concentrated and crystallized by treatment with isopropyl ether to give 3.8 g of α-isomer (43%); mp 135—136°C, $[\alpha]_D^{21}$ +62° (*c* 2.2, chloroform), ε_{258}^{MeOH}=549 (calcd, 558), IR spectrum (KBr): 3275, 1658 and 1550 (NHAc), 1757 and 1238 (OAc), 1101, 748 and 697 (*O*-benzyl), 855 cm^{-1} (type 2a of pyranose ring).

Found: C, 69.92; H, 6.67; N, 2.27%. Calcd for $C_{31}H_{35}NO_7$: C, 69.78; H, 6.61; N, 2.63%.

3-Acetamido-2,4,6-tri-*O*-benzyl-3-deoxy-α-D-glucopyranosyl Chloride (IV). To a solution of IIIa (0.5 g) in dioxane (25 m*l*) containing dry hydrogen

chloride (4%) was added acetyl chloride (13 ml) and the mixture was kept standing at 37°C overnight in a tightly stoppered flask. After evaporation at 20°C under reduced pressure, the resulting sirup was subjected repeatedly to co-distillation with absolute toluene *in vacuo* to be freed from hydrogen chloride to give a powdery solid, which was treated with dry petroleum ether to afford the chloride IV; 0.49 g (98%), mp 143—144°C (decomp.), $[\alpha]_D^{23}$ +78° (*c* 0.7, chloroform), $\varepsilon_{258}^{AcOEt}$=530 (calcd, 558), IR spectrum (KBr): 3280, 1655 and 1550 (NHAc), 738 (C-Cl), 696 (phenyl), 856 cm^{-1} (type 2a of pyranose ring). The C=O stretching absorption of acetoxy group in IIIa completely disappeared.

Found: C, 68.01; H, 6.54; N, 2.69; Cl, 7.35%. Calcd for $C_{29}H_{32}NO_5Cl$: C, 68.30; H, 6.32; N, 2.75; Cl, 6.96%.

IIIb also gave quantitatively IV by the above-mentioned chlorination, the result being examined by TLC using a solvent system of toluene and MEK (3 : 1).

Cyclohexyl 3-Acetamido-2,4,6-tri-*O*-benzyl-3-deoxy-α- and β-D-glucopyranoside (Va and Vb). A mixture of IV (0.5 g), cyclohexanol (1.3 g), well pulverized mercuric cyanide (0.25 g) and mercuric bromide (0.35 g) in absolute nitromethane (5 ml) was shaken at 27°C for three days under anhydrous conditions. After removal of insoluble matters, the mixture was diluted with chloroform (15 ml) and washed with several 20 ml portions of 20% aqueous potassium bromide and successively twice with 20 ml portions of water. After being dried over anhydrous sodium sulfate, the solution was evaporated to dryness to give sirup, which was subjected to fractional crystallization from isopropanol. First, Va deposited and was recrystallized from isopropanol; 0.16 g (28%), mp 135—136°C, $[\alpha]_D^{28}$ +88°C (*c* 1.0, chloroform), ε_{258}^{MeOH}=539 (calcd, 558), IR spectrum (KBr): 3290, 1652 and 1567 (NHAc), 2925 and 2850 (cyclohexyl), 845 (type 2a of pyranose ring), 735 and 694 cm^{-1} (phenyl).

Found: C, 73.32; H, 7.71; N, 2.57%. Calcd for $C_{35}H_{43}NO_6$: C, 73.27; H, 7.55; N, 2.44%.

From the mother liquor β-isomer (Vb) was obtained after a few days. Recrystallized from isopropanol; yield, 0.25 g (44%), mp 179—180°C, $[\alpha]_D^{28}$ +18° (*c* 1.0, chloroform), ε_{258}^{MeOH}=541 (calcd, 558), IR spectrum (KBr): 3300, 1654 and 1568 (NHAc), 2940 2870 (cyclohexyl), 888 (type 2b of pyranose ring), 733 and 694 cm^{-1} (phenyl).

Found: C, 73.21; H, 7.69; N, 2.42%. Calcd for $C_{35}H_{43}NO_6$: C, 73.27; H, 7.55; N, 2.44%.

Cyclohexyl 3-Acetamido-3-deoxy-α-D-glucopyranoside (VIa). A sample (70 mg) of Va was hydrogenated in methanol (3 ml) containing acetic acid (0.02 ml) over palladium black (50 mg) under 3.5 atm of hydrogen pressure at room temperature. After 5 hr of hydrogenation, the catalyst was filtered off. Evaporation of the filtrate *in vacuo* gave a colorless sirup which was crystallized from acetone; yield, 36 mg (94%), mp 210—211°C, $[\alpha]_D^{23}$ +158° (*c* 1.1, methanol), IR spectrum (KBr): 2925 and 2850 (cyclohexyl), 1658 and 1563 (NHAc), 852 cm^{-1} (type 2a of pyranose ring).

Found: C, 55.64; H, 8.51; N, 4.47%. Calcd for $C_{14}H_{25}NO_6$: C, 55.44; H, 8.31; N, 4.62%.

Cyclohexyl 3-Acetamido-3-deoxy-β-D-glucopyranoside (VIb). A sample of Vb was also hydrogenated to give VIb in like manner as described above; mp 201—202°C, $[\alpha]_D^{23}$ −17°C (*c* 1.3, methanol), IR spectrum (KBr): 2930 and 2855 (cyclohexyl), 1622 and 1565 (NHAc), 888 cm^{-1} (type 2b of pyranose ring).

Found: C, 55.61; H, 8.19; N, 4.58%. Calcd for $C_{14}H_{25}NO_6$: C, 55.44; H, 8.31; N, 4.62%.

Cyclohexyl 3-Amino-3-deoxy-α-D-glucopyranoside Hydrochloride (VII). A sample (36 mg) of VIa was heated with hydrazine hydrate (1.0 ml) in a sealed tube in the boiling water for 16 hr to give a pale brown solution, which was dried up *in vacuo*. The resulting brown sirup was purified on a column of Dowex 1×2 (OH type; 10×50 mm), developing with carbon dioxide-free water. Evaporation of ninhydrin positive fractions afforded a colorless glass, 30 mg, which was took up with a small volume of water and then acidified to pH 2 with 0.1 N hydrochloric acid. After evaporation of excess acid and water, a crystalline residue remained; trituration with acetone; yield, 36 mg (72%), mp 228—230°C (decomp.), $[\alpha]_D^{23}$ +151° (*c* 0.4, water).

Found: C, 48.48; H, 8.26; N, 4.67%. Calcd for $C_{12}H_{24}NO_5Cl$: C, 48.41; H, 8.12; N, 4.71%.

On ascending paper chromatography at room temperature for 16 hr, the R_f value of VII was 0.66. When heated with 3 N hydrochloric acid at 98°C for 3 hr, VII gave 3-amino-3-deoxy-D-glucopyranose being examined by paper chromatography.

Methyl 2,3,4-Tri-*O*-benzyl-6-(*N*-benzylacetamido)-6-deoxy-α-D-glucopyranoside (IX). A mixture of methyl 6-acetamido-6-deoxy-α-D-glucopyranoside (VIII) (1.0 g, finely powdered), benzyl chloride (20 ml) and sodium hydride (1.0 g) was stirred magnetically under anhydrous conditions for 2—3 hr at 125—130°C. This reaction was exothermic and the mixture became thick and then changed into a thin slurry as the reaction reached completion. Progress of the reaction was followed by TLC and measurement of volume of the evolved hydrogen gas which showed that benzylation was virtually complete after 2 hr. The reaction mixture was passed through a thick bed of Celite and the insoluble matters were washed with a large volume of dry benzene. The combined benzene filtrate and washings were washed with water, dried over anhydrous sodium sulfate and evaporated to dryness *in vacuo* at 90°C to afford a yellow sirup, which was crystallized from *n*-hexane (50 ml); colorless needles, yield, 2.1 g (83%). This product was sufficiently pure for the next preparation as described below. Recrystallization from methanol gave an analytically pure sample; mp 81—83°C, $[\alpha]_D^{25}$ +26°C (*c* 1.0, chloroform), ε_{258}^{MeOH}=760 (calcd, 744), IR spectrum (Nujol): 1637 (NAc), 1090, 733 and 694 cm^{-1} (*O*-benzyl). No absorption appeared in the region of OH or NH stretching.

Found: C, 74.40; H, 6.77; N, 2.53%. Calcd for $C_{37}H_{41}NO_6$: C, 74.60; H. 6.94; N, 2.35%.

2,3,4-Tri-*O*-benzyl-6-(*N*-benzylacetamido)-6-deoxy-β-D-glucopyranose (X) and Its Acetate (XI). To a solution of IX (5.0 g) in glacial acetic acid (50 ml) and acetic anhydride (8 ml) was added a mixture of concentrated sulfuric acid (1.0 ml) and acetic acid (5.0 ml) at 0°C under stirring in the course of 10 min. The stirring was continued at 0°C for 1 hr under exclusion of moisture and additional 7 hr at 10—20°C. The resulting mixture was poured onto cracked pieces of ice (300 g) under stirring to separate an oily product,

which was extracted with benzene. The benzene solution was neutralized with dilute aqueous sodium bicarbonate (5%) by cautious shaking, washed with water and evaporated to give an oily product, which was not crystallizable. The product was then treated with methanolic sodium methylate (0.003%; 10 ml) at room temperature for 1 hr. After neutralization with acetic acid, the solution was evaporated to fine crystalline X; yield 3.4 g (75%). Recrystallized from methanol; mp 160—161°C, $[\alpha]_D^{18}$ +18° (*c* 1.0, chloroform), ε_{258}^{MeOH} =738 (calcd, 744), IR spectrum (Nujol): The expected absorption of OH stretching was observed at 3190 cm^{-1} and no amido II band appeared; 1624 (NAc), 734 and 696 cm^{-1} (phenyl).

Found: C, 74.51; H, 6.71; N, 2.41%. Calcd for $C_{36}H_{39}NO_6$: C, 74.35; H, 6.76; N, 2.41%.

A sample (10 g) of X was acetylated with acetic anhydride (10 ml) in pyridine (70 ml) at room temperature overnight under exclusion of moisture. The resulting mixture was evaporated to give a sirup which was crystallized with isopropanol. Recrystallized from the same solvent; mp 121—122°C, $[\alpha]_D^{25}$ +12° (*c* 1.0, chloroform), ε_{258}^{MeOH}=726 (calcd, 744), IR spectrum (Nujol): The OH stretching absorption completely disappeared; 1763 and 1240 (OAc), 1658 (NAc), 750, 735 and 701 (phenyl), 917 cm^{-1} (type 2b of pyranose ring).

Found: C, 73.49; H, 6.89; N, 2.39%. Calcd for $C_{38}H_{41}NO_7$: C, 73.17; H, 6.63; N, 2.25%.

2,3,4-Tri-*O*-benzyl-6-(*N*-benzylacetamido)-6-deoxy-α-D-glucopyranosyl Chloride (XII). A solution XI (0.6 g) in a mixture of acetyl chloride (4 ml) and dioxane (23 ml) containing dry hydrogen chloride (4%) was allowed to stand at 37°C overnight in a tightly stoppered flask. After concentration *in vacuo* at 20°C, the resulting product was repeatedly co-distilled with absolute toluene until the product became an amorphous solid. Treatment with dry petroleum ether gave a colorless powder; yield 0.55 g (95%), mp 91—92°C (decomp.), $[\alpha]_D^{23}$ +70° (*c* 1.34, chloroform), $\varepsilon_{258}^{AcOEt}$=738 (calcd, 744), IR spectrum (Nujol): The C-O stretching absorption of OAc was not observed; 1652 (NAc), 845 (broad, type 2a of pyranose ring) and 699 cm^{-1} (phenyl).

Found: C, 71.65; H, 6.24; N, 2.30; Cl 6.51%. Calcd for $C_{36}H_{38}NO_5Cl$: C, 72.06; H, 6.38; N, 2.33; Cl, 5.92%.

Cyclohexyl 2,3,4-Tri-*O*-benzyl-6-(*N*-benzylacetamido)-6-deoxy-α- and β-D-glucopyranoside (XIIIa and XIIIb). A mixture of XII (0.50 g), cyclohexanol (0.25 ml), finely powdered mercuric cyanide (0.20 g) and mercuric bromide (0.23 g) in absolute nitromethane (5 ml) was shaken at 27°C for 48 hr under anhydrous conditions. The resulting pale yellow mixture was filtered and the filtrate was diluted with a large volume of chloroform. The solution was washed with three 20 ml portions of 20% aqueous potassium bromide and successively with three 20 ml portions of water. After drying over anhydrous sodium sulfate, the solution was evaporated *in vacuo* to give an oily product. TLC using a solvent system of toluene and MEK (3 : 1) showed that the product mainly consisted of two substances of R_f values 0.70 (main) and 0.65. The product was chromatographed on a silicagel column (50g) with the same solvent system to separate into the two substances; the former with R_f value 0.70 weighed 0.32 g (47%) and the latter with R_f value 0.65 was 0.04 g (5%). The analytical sample of the main product XIIIa was prepared by chromatography on a small silica-gel column; $[\alpha]_D^{22}$ +43° (*c* 1.7, chloroform), ε_{258}^{MeOH}=765 (calcd, 744), IR spectrum (KBr): 2940 (cyclohexyl), 1650 (NAc), 850 (type 2a of pyranose ring) and 696 cm^{-1} (phenyl).

Found: C, 75.76; H, 7.60; N, 2.41%. Calcd for $C_{42}H_{49}NO_6$: C, 75.99; H, 7.44; N, 2.11%.

The minor product XIIIb crystallized from methanol; mp 143.5—144.5°C, $[\alpha]_D^{27}$ +29 (*c* 1.0, chloroform), ε_{258}^{MeOH}=738 (calcd, 744); IR spectrum (KBr): 2940 (cyclohexyl), 1650 (NAc), 912 (type 2b of pyranose ring) and 695 cm^{-1} (phenyl).

Found: C, 76.46; H, 8.06; N, 2.45%. Calcd for $C_{42}H_{49}NO_6$: C, 75.99; H, 7.44; N, 2.11%.

Cyclohexyl 6-Acetamido-6-deoxy-α-D-glucopyranoside (XIVa). A sample (0.12 g) of XIIIa was hydrogenated over palladium black (0.01 g) in methanol containing a few drops of acetic acid at room temperature under 3.5 atm of hydrogen pressure for 5 hr. After removal of the catalyst, the solution was evaporated to give a sirup, which was dissolved in liquid ammonia (30 ml) and reduced by additions of several pieces of sodium until the developed blue color maintained for 15 min. After quenching the reaction with ammonium chloride (0.2 g), excess ammonia was removed by evaporation and the residue was took up in water. The solution was successively passed through a column of Amberlite IRA-410 (OH type; 5 ml) and Amberlite IR-120 (H type; 3 ml). The deionized solution was evaporated to give a colorless crystalline residue, which was further treated with acetone; yield 0.03 g (53%), mp 113—114°C, $[\alpha]_D^{23}$ +138° (*c* 1.2, methanol), IR spectrum (KBr): 1645 and 1570 (NHAc), 2935 (cyclohexyl), and 846 cm^{-1} (type 2a of pyranose ring).

Found: C, 54.81; H, 8.27; N, 4.55%. Calcd for $C_{14}H_{25}NO_6$: C, 55.43; H, 8.31; N, 4.62%.

Cyclohexyl 6-Acetamido-6-deoxy-β-D-glucopyranoside (XIVb). A sample (20 mg) of XIIIb was hydrogenated over palladium black (5 mg) in methanol containing a few drops of acetic acid at 40—45°C for 4 hr under 3.5 atm of hydrogen pressure to de-*O*-benzylate. The catalyst was filtered off and the solution was evaporated. An oily product was dissolved in liquid ammonia (30 ml) and to the solution was added small pieces of sodium until the blue color survived for 15 min. To the solution was added an excess of ammonium chloride (0.3 g) and ammonia was removed by evaporation. The product was deionized in like manner as described in the preparation of XIVa to give a colorless crystalline residue which was crystallized from acetone; yield 4.5 mg (47%), mp 163—164°C, $[\alpha]_D^{23}$ +1.5° (*c* 0.3, methanol), IR spectrum (KBr): 2850 (cyclohexyl), 1650 and 1550 (NHAc), and 893 cm^{-1} (type 2b of pyranose ring).

Found: C, 55.12; H, 8.23; N, 4.35%. Calcd for $C_{14}H_{25}NO_6$: C, 55.43; H, 8.31; N, 4.62%.

Cyclohexyl 6-Amino-6-deoxy-α-D-glucopyranoside Hydrochloride (XV). XIVa (18 mg) was heated with hydrazine hydrate (80%; 1 ml) in a sealed tube in the boiling water for 20 hr to give a pale brown solution, which was evaporated *in vacuo* at 60°C. The resulting brown sirup was purified on a column of Dowex 1×2 (OH type; 20 ml), irrigating with distilled

water. The ninhydrin-positive fractions were evaporated *in vacuo* to give a colorless glass of XV. The free base was dissolved in a small volume of water and acidified with 0.1 N hydrochloric acid to pH 4. After evaporation of excess acid and water, a crystalline residue was obtained which was treated with acetone; yield 13 mg (75%), mp 184—185°C (decomp.), $[\alpha]_D^{23}$ +120° (*c* 0.4, water).

Found: C, 48.24; H, 7.82; N, 4.84%. Calcd for $C_{12}H_{24}NO_5Cl$: C, 48.41; H, 8.12; N, 4.71%.

On the ascending paper chromatography at room temperature for 16 hr, the R_f value of XV was 0.55. When heated with 3 N hydrochloric acid at 95—98°C for 3 hr, XV afforded 6-amino-6-deoxy-D-glucopyranose, the formation of which was examined by paper chromatography.

The authors are indebted to Mr. Saburo Nakada for his microanalysis, to Mr. Yoshito Koyama for his technical assistance.

BULLETIN OF THE CHEMICAL SOCIETY OF JAPAN VOL. 41 2769—2771 (1968)

Studies of Aminosugars. XX. The Synthesis of 6-O-(3-Amino-3-deoxy-α-D-glucopyranosyl)-2-deoxystreptamine[1]

Shinkiti KOTO, Kuniaki TATSUTA, Eiichi KITAZAWA and Sumio UMEZAWA

Department of Applied Chemistry, Faculty of Engineering, Keio University, Koganei-shi, Tokyo

(Received June 1, 1968)

6-O-(3-Amino-3-deoxy-α-D-glucopyranosyl)-2-deoxystreptamine (3AD) which is a glycoside component of kanamycin A has been synthesized. Amino and hydroxyl groups of 2-deoxystreptamine were masked with carbobenzoxy and isopropylidene groups to give racemic mono-O-isopropylidene-di-N,N'-carbobenzoxy-2-deoxystreptamine, with which 3-acetamido-2,4,6-tri-O-benzyl-3-deoxy-α-D-glucopyranosyl chloride was condensed by a modified Koenigs-Knorr reaction. Removal of all the masking groups followed by N-dinitrophenylation, acetylation and chromatography gave the product identical with an authentic specimen of the penta-O-acetyl-tri-N-(2,4-dinitrophenyl) derivative of the natural 3AD. The synthetic product was further led to 3AD identical with a natural sample.

As a part of the investigation of the synthesis of antibiotic aminoglycosides, we previously reported the syntheses of paromamine,[2] neamine,[3] 5-O-(2-amino-2-deoxy-α-D-glucopyranosyl)-deoxystreptamine,[4] 4,6-di-O-(3-amino-3-deoxy-β-D-glucopyranosyl)-deoxystreptamine,[5] 4,6-di-O-(6-amino-6-deoxy-β-D-glucopyranosyl)-deoxystreptamine,[5] diamino-dideoxy derivative of trehalose,[6] trehalosamine,[7] triamino-trideoxy derivatives of maltose,[6] sucrose[6] and raffinose[8] and hexaamino-hexadeoxy derivative of Schardinger α-dextrin.[8]

In the present paper, the synthesis of 6-O-(3-amino-3-deoxy-α-D-glucopyranosyl)-deoxystreptamine (IV: abbreviated to 3AD) is described. This is a glycoside component of kanamycin A,[9] an useful antibiotic, and was first isolated by Maeda *et al.*[10] from the hydrolyzate of the antibiotic. Synthesis of this glycoside was undertaken as an approach to the synthesis of kanamycin A which has been briefly communicated.[11]

The key intermediates for the proposed synthesis were the totally O-benzylated derivative of 3-acetamido-3-deoxy-α-D-glucopyranosyl chloride on the one hand, and the monoisopropylidene derivative of N,N'-masked 2-deoxystreptamine on the other hand. A modified Koenigs-Knorr reaction between the two intermediates formed the desired α-glycosidic linkage, though not exclusively.

The preparation of 3-acetamido-2,4,6-tri-O-benzyl-3-deoxy-α-D-glucopyranosyl chloride (I) was

1) Part XXXVI of "Studies on Antibiotics and Related Substances," by Sumio Umezawa. Presented before the 160th Meeting of the Japan Antibiotic Reasearch Association, at the Institute of Medical Science, Tokyo, March 22, 1968.

2) S. Umezawa and S. Koto, This Bulletin, **39**, 2014 (1966); *J. Antibiotics*, **A19**, 88 (1966).

3) K. Tatsuta, E. Kitazawa and S. Umezawa, This Bulletin, **40**, 2371 (1967); *J. Antibiotics*, **A20**, 53 (1967).

4) S. Umezawa, T. Tsuchiya and H. Fujita, *J. Antibiotics*, **A19**, 222 (1966).

5) S. Koto, Y. Ito and S. Umezawa, This Bulletin, **38**, 1447 (1965).

6) S. Umezawa, T. Tsuchiya and S. Nakada, *ibid.*, **40**, 395 (1967).

7) S. Umezawa, K. Tatsuta and R. Muto, *J. Antibiotics*, **A20**, 388 (1967).

8) S. Umezawa and K. Tatsuta, This Bulletin, **41**, 464 (1968).

9) H. Umezawa, M. Ueda, K. Maeda, K. Yagishita, S. Kondo, Y. Okami, R. Utahara, Y. Osato, K. Nitta and T. Takeuchi, *J. Antibiotics*, **A10**, 181 (1957).

10) K. Maeda, M. Murase, H. Mawatari and H. Umezawa, *ibid.*, **A11**, 163 (1958).

11) S. Umezawa, K. Tatsuta and S. Koto, *ibid.*, **21**, 367 (1968).

previously reported.[12] Treatment of *N,N'*-dicarbobenzoxy-2-deoxystreptamine[5] with 2,2-dimethoxypropane in the presence of *p*-toluenesulfonic acid in *N,N*-dimethylformamide at 110°C gave the monoisopropylidene derivative (II) in racemic form in a quantitative yield.

Condensation of I with II in the presence of mercuric cyanide and Drierite in an anhydrous mixture of benzene and dioxane gave a crude product, which was hydrolyzed with 80% acetic acid to remove isopropylidene group and hydrogenated over palladium black to remove benzyl groups. De-*N*-acetylation with barium hydroxide gave a crude ninhydrin-positive product. This was further dinitrophenylated with 2,4-dinitrofluorobenzene and *O*-acetylated. The resulting product showed about five spots including one main (R_f-value 0.3) and four minor spots on a silica-gel thin-layer chromatogram. The product was chromatographed on a silica-gel column and the main fraction was further separated into two fractions (R_f-values 0.30 and 0.28) of nearly equal amounts by preparative thin-layer chromatography. The substance having R_f-value 0.30 was crystallized to give 4,5-di-*O*-acetyl-6-*O*-[2,4,6-tri-*O*-acetyl-3-(2,4-dinitroanilino)-3-deoxy-α-D-glucopyranosyl]-di-*N,N'*-(2,4-dinitrophenyl)-2-deoxystreptamine (III) of mp 195—198°C (decomp.) and $[\alpha]_D$ +24° (*c* 0.9, acetone) in a 12% overall-yield from I.

On the other hand, the natural sample of 3AD was dinitrophenylated and acetylated to give penta-*O*-acetyl-tri-*N*-(2,4-dinitrophenyl) derivative, mp 194—198°C (decomp.) and $[\alpha]_D$ +22° (*c* 1.0, acetone).

The identity of the synthetic derivative III was established by direct comparison with both III and the above-mentioned derivative from natural sample.

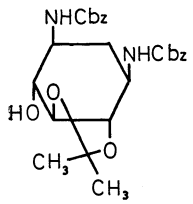

II (racemate) Cbz = $COOCH_2C_6H_5$

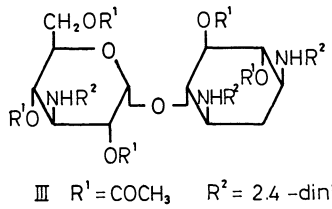

III $R^1 = COCH_3$ R^2 = 2,4-dinitrophenyl

IV $R^1 = R^2 = H$ (3AD)

V $R^1 = H$, $R^2 = COCH_3$

Hydrolysis of III with methanolic ammonia followed by treatment with Dowex 1*X*2 (OH) resin gave 3AD (IV), whose identity was established by direct comparison with both synthetic IV and natural sample.

Further, the synthetic free aminosugar (IV) was *N*-acetylated with acetic anhydride in methanol to give 6-*O*-(3-acetamido-3-deoxy-α-D-glucopyranosyl)-*N,N'*-diacetyl-2-deoxystreptamine (V), which showed $[M]_{CuAm}$ +1460, by the copper complex method[13] reported from our Laboratory. The observed value agreed with the reported value[14] of the tri-*N*-acetyl derivative of natural 3AD, indicating that IV is the 6-*O*-linked glycoside of 2-deoxystreptamine.

Experimental

General Procedure. Infrared spectra were determined in potassium bromide pellets. Thin layer chromatography (TLC) was performed by "Silica-Rider for TLC" (Dai-ichi Pure Chemicals Co.). Descending paper chromatography was carried out by Toyo filter paper No. 51, using a solvent system of *n*-butanol : pyridine : water : acetic acid = 6 : 4 : 3 : 1, with ninhydrin (0.3% in pyridine) coloration, developing at room temperature for 72 hr.

Racemic Di-*N,N'*-carbobenzoxy-mono-*O*-isopropylidene-2-deoxystreptamine (II). To a solution of 4.3 g of di-*N,N'*-carbobenzoxy-2-deoxystreptamine[5] in freshly distilled *N,N*-dimethylformamide (30 m*l*) was added *p*-toluenesulfonic acid monohydrate (0.06 g) and 2,2-dimethoxypropane (5 m*l*), and the mixture was heated at 110°C for 4 hr to result in a brown solution. After the solution was neutralized with 10 m*l* of Amberlite IRA-400 (OH type) which was washed with methanol before use, the resin was filtered off and the filtrate was evaporated to give a thick sirup, which solidified when treated with water (100 m*l*). Crude product, 4.4 g (94%), was recrystallized from ethyl acetate to give an analytically pure sample of racemic II; yield 4.0 g, 86%, mp 145—146°C; IR spectrum: 3325, 1698 1545 (NHCbz), 1067 cm^{-1} (ketal).

Found: C, 63.63; H, 6.69; N, 5.85. Calcd for $C_{25}H_{30}N_2O_7$: C, 63.82; H, 6.43; N, 5.95%.

4,5-Di-*O*-acetyl-6-*O*-[2,4,6-tri-*O*-acetyl-3-(2,4-dinitroanilino)-3-deoxy-α-D-glucopyranosyl]-di-*N,N'*-(2,4-dinitrophenyl)-2-deoxystreptamine (III). A mixture of II (1.3 g), well dried powdery mercuric cyanide (0.91 g) and Drierite (9.5 g) in a solvent mixture of benzene and dioxane (4 : 1; 40 m*l*) was heated at 110°C for 15 min with stirring and then cooled to room temperature. To this mixture was added dry 3-acetamido-2,4,6-tri-*O*-benzyl-3-deoxy-α-D-glucopyranosyl chloride[11] (1.9 g; 1.3 eq.) and stirred at 110°C for 6 hr and additional 4 hr at room temperature under anhydrous conditions. The mixture was passed through a bed of Celite. The filtrate was combined and evaporated to afford a dark-brown residue, which

12) S. Koto, T. Tsumura, Y. Kato and S. Umezawa, This Bulletin, **41**, 2765 (1968).

13) S. Umezawa, T. Tsuchiya and K. Tatsuta, *ibid.*, **39**, 1235 (1966).

14) S. Umezawa, K. Tatsuta and T. Tsuchiya, *ibid.*, **39**, 1244 (1966).

was extracted with ethyl acetate (40 ml). After removal of an insoluble matter, the solution was shaken with four 40 ml portions of 20% aqueous potassium bromide and then 20 ml portions of distilled water, dried over anhydrous sodium sulfate and evaporated to afford a sirup (2.5 g). This was dissolved in warm 80% aqueous acetic acid (25 ml) and the solution was heated at 60°C for 2 hr. Evaporation *in vacuo* gave a sirup residue. The deacetonated product was dissolved in a mixture (15 ml) of dioxane, water and concentrated hydrochloric acid (8 : 3 : 1) and hydrogenated over palladium black (0.5 g) at about 30°C for 35 hr under 3.5 atm of hydrogen pressure with occasional addition of water (total volume, 10 ml). The mixture was filtered and the solution was evaporated at below 30°C and hydrogen chloride was removed by co-distillation with *n*-butanol to give a residue (0.7 g). The ninhydrin-positive sirup was dissolved in 1 N aqueous barium hydroxide (15 ml) and heated on a boiling water bath for 2 hr. The mixture was acidified with 2 N sulfuric acid to pH 2 and filtered. The filtrate was neutralized with 2 ml of Dowex 1×2 (OH type) and evaporated *in vacuo* to afford a colorless sirup (0.5 g) of free base. The crude product was dinitrophenylated with 2,4-dinitrofluorobenzene (1.3 ml) in the presence of sodium bicarbonate (0.7 g) in 50% aqueous ethanol (10 ml) at room temperature under stirring overnight to give a yellow precipitate. To the resulting mixture was added water (10 ml) and further stirred to complete precipitation; yellow powder, 1.4 g, was obtained. The product was acetylated with acetic anhydride (11 ml) and freshly fused sodium acetate (0.5 g) by heating at 110°C for 12 hr with stirring. Evaporation of excess reagent afforded a brown residue, which was extracted with acetone and followed by evaporation of the extract *in vacuo* to give a yellow glass, 1.25 g. The product showed about five spots with R_f values 0.3 (main), 0.37, 0.45, 0.51 and 0.56 on a silica-gel thin-layer chromatogram with a solvent system of benzene and MEK (3 : 1). The product was chromatographed on a silica-gel column (200 g; 47×290 mm) using a solvent system: benzene and MEK (4 : 1), being cut into 10 g each. The main product having an R_f value 0.3 appeared in fractions of Nos. 77—101 which gave a yellow solid by evaporation *in vacuo*. This fraction was further separated into two fractions of nearly equal amount, which have R_f values 0.30 and 0.28 respectively, by preparative TLC (20×20×0.05 cm) using the above-mentioned solvent system. The substance of R_f value 0.30 was collected and recrystallized from the same solvent system to give yellow needles of III, 340 mg (12% overall-yield from II); mp 195—198°C (decomp.), $[\alpha]_D^{18}$ +24° (*c* 0.9, acetone), IR spectrum: 3340, 3100, 1625, 1595, 1340 and 745 (NHDNP), 1760, 1370 and 1225 cm^{-1} (OAc).

Found: C, 46.50; H, 4.25; N, 12.41. Calcd for $C_{40}H_{41}N_9O_{24}$: C, 46.56; H, 4.01; N, 12.22%.

The melting point of III was not depressed by admixture with the penta-*O*-acetyl-tri-*N*-(2,4-dinitrophenyl) derivative of natural 3AD described below. On TLC with a solvent system, toluene-MEK (3 : 1), the synthetic III and the above-mentioned derivative of natural 3AD showed identical mobilities and their IR spectra were superimposable.

6-*O*-(3-Amino-3-deoxy-α-D-glucopyranosyl)-2-deoxystreptamine (IV). A sample (59 mg) of III was dissolved in methanol (15 ml) saturated with dry ammonia at 0°C and the red solution was kept standing at room temperature overnight. Evaporation of the reaction mixture *in vacuo* gave a yellow residue, which was treated with Dowex 1×2 (OH type; 10 ml of wet resin) in acetone (5 ml) under stirring at room temperature overnight. The resin was filtered off and the filtrate was concentrated *in vacuo* to give a glass, 22 mg, which was chromatographed on a column of Dowex 1×2 (OH type; 2 ml) with carbon dioxide-free water. Evaporation of the middle ninhydrin positive fraction was followed by trituration with aqueous methanol-ethanol to give an analytically pure sample of III; yield 11 mg (60% from III), $[\alpha]_D^{18}$ +98°C (*c* 0.9, water).

Found: C, 44.24; H, 7.51; N, 12.69. Calcd for $C_{12}H_{25}N_3O_7$: C, 44.57; H, 7.79; N, 13.00%.

On the other hand, the natural 3AD showed $[\alpha]_D^{18}$ +98° (*c* 0.10, water). On descending paper chromatography, the R_f values of the synthetic product IV and the natural 3AD were in agreement. IR spectra of IV and natural 3AD were superimposable.

Penta-*O*-acetyl-tri-*N*-(2,4-dinitrophenyl) Derivative of Natural 6-*O*-(3-Amino-3-deoxy-α-D-glucopyranosyl)-2-deoxystreptamine. A mixture of natural 3AD (0.33 g) and sodium bicarbonate (0.4 g) in water (15 ml) was stirred for a while, and to the solution was added 2,4-dinitrofluorobenzene (0.62 g) in ethanol (7 ml). The mixture was stirred for about 6 hr at room temperature until the yellow gummy product initially formed became powdery; yield 0.74 g (90%). The crude tri-*N*-(2,4-dinitrophenyl) derivative was acetylated with acetic anhydride (10 ml) and anhydrous sodium acetate (1.0 g) by heating at 110°C for 10 hr with stirring under anhydrous conditions. Evaporation of the excess reagent gave a residue, which was extracted with acetone. Concentration of the extract gave a yellow glass which was crystallized from acetone by the gradual addition of ethanol. Two recrystallization from benzene-MEK (3 : 1) afforded a chromatographically pure product, fine neeldes, mp 194—198°C (decomp.), $[\alpha]_D^{18}$ +22° (*c* 1.0, acetone), IR spectrum: 3340, 3100, 1625, 1595, 1340 and 745 (NHDNP), 1760, 1370 and 1225 cm^{-1} (OAc).

Found: C, 46.44; H, 4.21; N, 12.36. Calcd for $C_{40}H_{41}N_9O_{24}$: C, 46.56; H, 4.01; N, 12.22%.

6-*O*-(3-Acetamido-3-deoxy-α-D-glucopyranosyl)-*N*,*N*′-diacetyl-2-deoxystreptamine (V). To a suspension of IV (20 mg) in methanol (1.2 ml) was added acetic anhydride (0.6 ml) at room temperature. The mixture became clear immediately and after 18 hr, the solution became ninhydrin-negative. The solution was evaporated to give a colorless solid, from which acetic anhydride was removed by co-distillation with ethanol and crystallized from acetone to afford the pure acetate V; yield 23 mg (80%), mp 236—239°C (decomp.), $[\alpha]_{589}^{18}$ +74° (*c* 0.91, water), $[\alpha]_{436}^{18}$ +140° (*c* 0.91, water), $[\alpha]_{436}^{8}$ +465° (*c* 0.80, CuAm), $\Delta[M]_{CuAm}$ +1460, IR spectrum: 3400, 1100—1000 (OH), 3290, 1650, 1560 and 1375 cm^{-1} (NHAc).

Found: C, 47.91; H, 6.99; N, 9.08. Calcd for $C_{18}H_{31}N_3O_{10}$: C, 48.10; H, 6.95; N, 9.35%.

The authors are indebted to Mr. Saburo Nakada for his microanalysis, to Mr. Yoshio Nishimura and Takeshi Umeda for their technical assistance.

BULLETIN OF THE CHEMICAL SOCIETY OF JAPAN VOL. 41 2772—2776 (1968)

Analogs of Oxytocin Containing Leucinamide and Glycylglycinamide in Place of Glycinamide[1]

Haruhiko Aoyagi,[2] Michio Kondo[3] and Nobuo Izumiya[4]

Laboratory of Biochemistry, Faculty of Science, Kyushu University, Hakozaki, Fukuoka

(Received June 3, 1968)

Two analogs of oxytocin, [9-leucine]-oxytocin and oxytocinoyl-glycinamide, in which the glycinamide residue at position 9 in oxytocin has been replaced by a leucinamide and glycylglycinamide, respectively, have been synthesized and tested for some of the pharmacological properties characteristic of oxytocin. The protected nona- and decapeptide intermediates were prepared by use of the azide method in a fashion of the fragment condensation. After removal of the protecting groups from the intermediates by means of either sodium in liquid ammonia or anhydrous hydrogen fluoride, the dithiols thus obtained were oxidized to the required analogs. It was found that [9-leucine]-oxytocin possessed approximately 8% oxytocic potency, and oxytocinoyl-glycinamide 0.5% potency compared with oxytocin preparation.

The synthetic approach to the study of structure-activity relationships in oxytocin hormone opens up a wide choice of structural variations.[5] Among the numerous analogs of oxytocin which have been synthesized, very few have involved modifications of the glycinamide residue in position 9; du Vigneaud *et al.* reported the properties of [9-sarcosine]-oxytocin[6] and 9-deamidooxytocin[7] in which the glycinamide residue was replaced by that of sarcosinamide and glycine, respectively. The present paper reports the syntheses and pharmacological properties of two analogs of oxytocin, [9-leucine]-oxytocin[8] and oxytocinoyl-glycinamide[8] in which leucinamide and glycylglycinamide replace the glycinamide residue, respectively. As a peptide for the comparison with these two analogs, oxytocin itself was also prepared *via* the similar reaction-sequence employed for the syntheses of the analogs.

The sequence of reaction employed for the syntheses of oxytocin and its analogs is shown in Fig. 1. For the preparation of the protected nona- and decapeptides for the syntheses of the desired peptides (XV-A, B and C), benzyloxycarbonyl-tripeptide azide which was derived from the corresponding hydrazide (XIII) was allowed to react with hexa- (XI-A and C) or heptapeptide amide (XI-B) in a manner similar to that used by Boissonnas *et al.*[9] The required hexa- or heptapeptide amide (XI-A, B or C) was itself prepared from benzyloxycarbonyl-tripeptide hydrazide (IX) and tri- or tetrapeptide amide (V-A, B or C) followed by removal of the benzyloxycarbonyl group.

The protecting groups of the nona- and decapeptide intermediates (XIV-A, B and C) were removed by treatment with sodium in liquid ammonia by the method of du Vigneaud *et al.*[10] The removal of the protecting groups of the intermediates was also performed by acidolysis with anhydrous hydrogen fluoride as was reported by Sakakibara and Shimonishi.[11] The dithiols so obtained were oxidized in neutral solution by aeration, and the hormonal activities of the products in the solutions were determined by the rat-uterine contracting and avian depressor test.

Total activities of the preparations derived from 0.06 mmol (about 80 mg) of the intermediates are shown in Table 1. The oxytocinoyl-glycinamide (XV-B) possesses a weak activity such as some 0.5% oxytocic potency compared with oxytocin preparation. The relative activities of the analogs XV-B as well as [9-leucine]-oxytocin (XV-A) toward

1) Presented in part at 17th Annual Meeting of the Chemical Society of Japan, April, 1964.

2) Present address: Department of Chemistry, Case Western Reserve University, Cleveland, Ohio, U. S. A.

3) Present address: Department of Chemistry, Saga University, Honjo, Saga.

4) To whom the inquiries should be addressed.

5) K. Hofmann, *Ann. Rev. Biochem.*, **31**, 213 (1962).

6) J. Meienhofer and V. du Vigneaud, *J. Am. Chem. Soc.*, **83**, 142 (1961). Main content of this literature was the synthesis of [Sar^9]-vasopressin, and there was a brief description that [Sar^9]-oxytocin possessed the extreme low activity.

7) B. M. Ferrier and V. du Vigneaud, *J. Med. Chem.*, **9**, 55 (1966).

8) We followed the rules naming synthetic modifications of natural peptides in *Biochemistry*, **6**, 362 (1967); *e. g.*, the semitrivial name is [9-leucine]-oxytocin and the abbreviated form is [Leu^9]-oxytocin. Oxytocinoyl-glycinamide may be alternately named as 9a-endo-glycine-oxytocin.

9) R. A. Boissonnas, St. Guttman, P.-A. Jaquenoud and J.-P. Waller, *Helv. Chim. Acta*, **38**, 1491 (1955).

10) V. du Vigneaud, C. Ressler, J. M. Swan, C. R. Roberts, P. G. Katsoyannis and S. Gordon, *J. Am. Chem. Soc.*, **75**, 4879 (1953).

11) S. Sakakibara and Y. Shimonishi, This Bulletin, **38**, 1412 (1965).

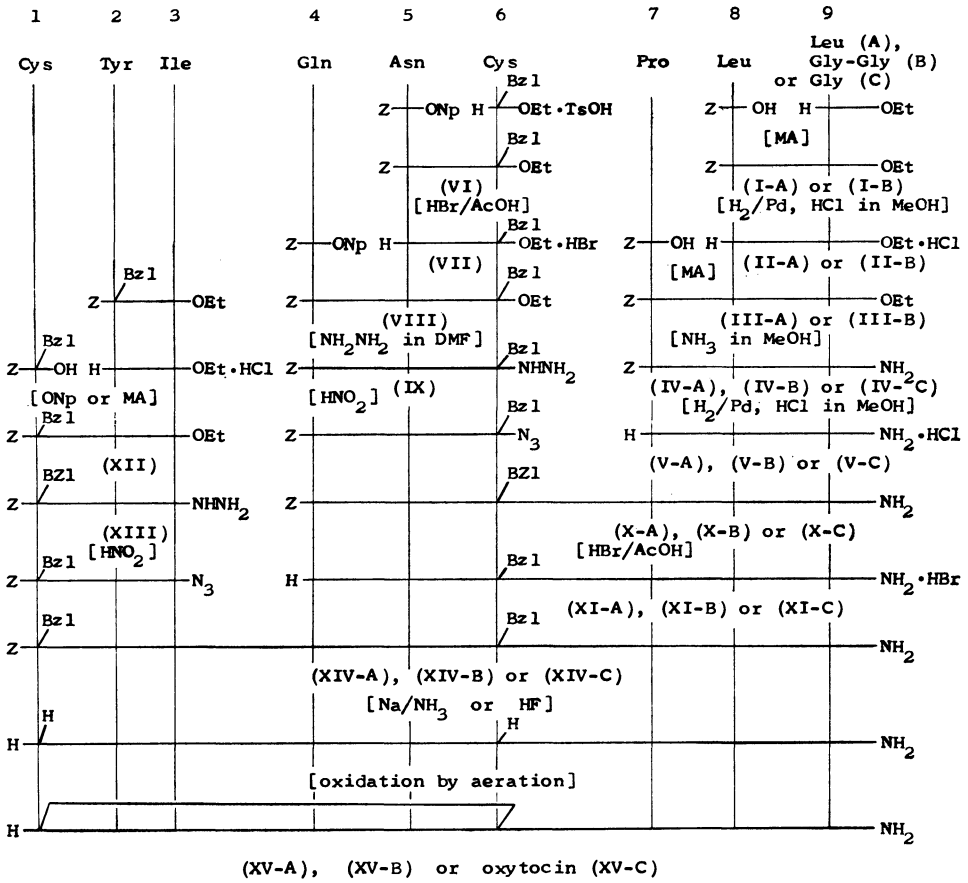

Fig. 1. Schematic diagram of syntheses of oxytocin and its analogs.
Z, benzyloxycarbonyl; Bzl, benzyl; ONp, *p*-nitrophenyl ester; [MA], mixed anhydride method; DMF, dimethylformamide.

Table 1. Total activities (units) of products derived from the protected peptides (0.06 mmol)

Compound	Oxytocic (rat)		Depressor (fowl)	
	Na/NH_3	HF	Na/NH_3	HF
	(%)			
[Leu^9]-oxytocin (XV-A)	1050(8)	225	850	190
Oxytocinoyl-Gly-NH_2 (XV-B)	63(0.5)	15	55	12
Oxytocin (XV-C)	12800(100)	2650	13100	2700

oxytocin should be considered as that of very approximation since the oxidized solution which was subjected to the biological assay might contain several by-products. It would be noteworthy that glycyl-oxytocin[12,13] carrying glycine residue to the amino group of *N*-terminal hemicystine residue showed 0.07% oxytocic potency compared with oxytocin.[13] The [9-leucine]-oxytocin preparation, however, showed appreciable biological activities; thus the replacement of the glycin residue with bulky leucine did not cause a remarkable decrease in the activities. These effects are of considerable significance to the question of the relation of structure to the biological activity of oxytocin molecule. The nature of the effects may become apparent when the role of glycine at position 9 toward the activity will be elucidated in future.

12) V. du Vigneaud, P. S. Fitt, M. Bodanszky and M. O'Connell, *Proc. Soc. Exp. Biol. (N. Y.)*, **104**, 653 (1960).
13) K. Jost, J. Rudinger and F. Sorm, *Collection Czech. Chem. Commun.*, **28**, 2021 (1963).

Experimental

All melting points are uncorrected.

Z-Leu-Leu-OEt (I-A). To a chilled solution of benzyloxycarbonyl-L-leucine (4.7 g; 20 mmol) and

triethylamine (2.8 ml) in tetrahydrofuran (40 ml), isobutyl chloroformate (2.6 ml) was added. After 15 min, a mixture of L-leucine ethyl ester hydrochloride (4.7 g; 20 mmol), triethylamine (2.8 ml) and chloroform (40 ml) was added to the solution. The reaction mixture was allowed to stand overnight and then evaporated *in vacuo*. The residual oil was dissolved in ethyl acetate, and the solution was washed successively with 4% sodium bicarbonate, 3% hydrochloric acid and water, dried over sodium sulfate and then evaporated *in vacuo*. The residual oil was solidified by the addition of petroleum ether. It was recrystallized from ethyl acetate-ether-petroleum ether; yield, 6.8 g (84%); mp 89—90°C; $[\alpha]_D^{25}$ −31.6° (*c* 1, AcOH).

Found: C, 64.92; H, 8.39; N, 7.09%. Calcd for $C_{22}H_{34}O_5N_2$: C, 65.00; H, 8.43; N, 6.89%.

H-Leu-Leu-OEt·HCl (II-A). The compound I-A (11.0 g; 27 mmol) was subjected to hydrogenolysis in the presence of palladium black and 0.76 N methanolic hydrogen chloride (37 ml). The filtrate from the catalyst was evaporated *in vacuo* leaving an oil; yield, 8.0 g (96%).

H-Leu-Gly-Gly-OEt·HCl (II-B). Z-Leu-Gly-Gly-OEt (I-B)[14] (6.7 g; 16.5 mmol) was treated as described above; yield of a hygroscopic powder, 4.2 g (92%).

Z-Pro-Leu-Leu-OEt (III-A). The mixed anhydride prepared from benzyloxycarbonyl-L-proline (3.8 g; 15 mmol) was coupled with II-A (4.7 g; 15 mmol), following the procedure used in the preparation of I-A. The crude product was recrystallized from ethanol-ether; yield, 5.6 g (73%); mp 138—139°C; $[\alpha]_D^{25}$ −88.6° (*c* 1, AcOH).

Found: C, 64.14; H, 7.96; N, 8.38%. Calcd for $C_{27}H_{41}O_6N_3$: C, 64.39; H, 8.21; N, 8.34%.

Z-Pro-Leu-Gly-Gly-OEt (III-B). The mixed anhydride prepared from benzyloxycarbonyl-L-proline (3.8 g) was coupled with II-B (4.7 g; 15.3 mmol) as has been described for the preparation of I-A. The product was recrystallized from ethyl acetate - ether - petroleum ether; yield, 4.9 g (65%); mp 133—135°C; $[\alpha]_D^{25}$ −64.8° (*c* 1, AcOH).

Found: C, 59.35; H, 7.13; N, 11.19%. Calcd for $C_{25}H_{36}O_7N_4$: C, 59.51; H, 7.19; N, 11.10%.

Z-Pro-Leu-Leu-NH_2 (IV-A). The compound III-A (6.3 g; 12.5 mmol) was dissolved in methanol (60 ml) saturated with ammonia. After it had been allowed to stand for 3 days, the solution was evaporated *in vacuo*. The remaining crystals were collected with the aid of ether. Recrystallization from ethanol-ether gave 3.9 g (66%); mp 190°C; $[\alpha]_D^{25}$ −88.5° (*c* 1, AcOH).

Found: C, 63.13; H, 7.94; N, 11.69%. Calcd for $C_{25}H_{38}O_5N_4$: C, 63.27; H, 8.07; N, 11.81%.

Z-Pro-Leu-Gly-Gly-NH_2 (IV-B). The compound III-B (5.2 g; 10.7 mmol) was converted into the amide as described above. Recrystallization from ethanol-ether gave 4.2 g (84%); mp 192—193°C; $[\alpha]_D^{25}$ −75.0° (*c* 2, AcOH).

Found: C, 57.99; H, 6.93; N, 14.75%. Calcd for $C_{23}H_{33}O_6N_5$: C, 58.09; H, 7.00; N, 14.73%.

H-Pro-Leu-Leu-NH_2·HCl (V-A). The compound IV-A (4.8 g; 10 mmol) was treated as has been described for the preparation of II-A. The product was obtained as a hygroscopic powder; yield, 3.8 g (99%).

H-Pro-Leu-Gly-Gly-NH_2·HCl (V-B). The compound IV-B (2.4 g; 5 mmol) was treated as has been described for the preparation of II-A. The product was obtained as a hygroscopic powder; yield, 1.8 g (95%).

H-Pro-Leu-Gly-NH_2·HCl (V-C). Z-Pro-Leu-Gly-NH_2 (IV-C)[15] (6.7 g; 16 mmol) was treated as described above; yield of a hygroscopic powder (V-C), 5.4 g (99%). Boissonnas *et al.* reported the synthesis of the oily hydrobromide from IV-C with hydrogen bromide-acetic acid.[9]

Z-Asn-Cys(Bzl)-OEt (VI). To a solution of *S*-benzyl-L-cysteine ethyl ester *p*-toluenesulfonate[16] (8.2 g; 20 mmol) in a mixture of dimethylformamide (20 ml) and triethylamine (4.0 ml), benzyloxycarbonyl-L-asparagine *p*-nitrophenyl ester[17] (7.7 g; 20 mmol) was added. The solution was allowed to stand at room temperature and a mass of crystals was deposited within about 1 hr. After 2 hr this mass was triturated with water (300 ml), collected by filtration, and washed successively with 4% sodium bicarbonate, 3% hydrochloric acid and water. It was recrystallized from ethanol; yield, 6.2 g (64%); mp 191°C; $[\alpha]_D^{20}$ −30.2° (*c* 2, DMF).

Found: C, 59.11; H, 6.04; N, 8.73%. Calcd for $C_{24}H_{29}O_6N_3S$: C, 59.13; H, 6.00; N, 8.62%.

H-Asn-Cys(Bzl)-OEt·HBr (VII). The compound VI (6.0 g; 12.3 mmol) was dissolved in acetic acid (40 ml) and 6.9 N hydrogen bromide - acetic acid (30 ml). After it had been allowed to stand at room temperature for 1 hr, the solution was evaporated *in vacuo*. The resulting residue was washed with ether and dried *in vacuo;* yield, 5.0 g (94%).

Z-Gln-Asn-Cys(Bzl)-OEt (VIII). To a solution of VII (5.0 g; 11.5 mmol) and triethylamine (2.5 ml) in dimethylformamide (25 ml), benzyloxycarbonyl-L-glutamine *p*-nitrophenyl ester[17] (4.6 g; 11.5 mmol) was added. After it had been allowed to stand at 30°C for 2 hr, the precipitate which formed was triturated with water (300 ml) and treated as has been described for the preparation of VI. It was recrystallized from dimethylformamide-ether; yield, 6.2 g (82%); mp 234—235°C; $[\alpha]_D^{25}$ −21.5° (*c* 2, DMF).

Found: C, 56.80; H, 6.13; N, 11.31%. Calcd for $C_{29}H_{37}O_8N_5S$: C, 56.57; H, 6.06; N, 11.38%.

Z-Gln-Asn-Cys(Bzl)-$NHNH_2$ (IX). To a solution of VIII (3.0 g; 4.8 mmol) in dimethylformamide (30 ml), hydrazine hydrate (2.5 ml) was added. After it had been allowed to stand at room temperature overnight, the mixture which contained crystals was allowed to cool for several hours. The product was then collected by filtration, and washed with water and acetone; yield, 2.7 g (95%); mp 246—248°C. Boissonnas *et al.* reported the synthesis of IX from Z-Gln-Asn-Cys(Bzl)-OMe with hydrazine in methanol by heating for 3 hr; mp 248°C.[9]

Z-Gln-Asn-Cys(Bzl)-Pro-Leu-Leu-NH_2 (X-A). To a chilled solution of IX (0.60 g; 1 mmol) in glacial acetic acid (25 ml) and 2 N hydrochloric acid (2 ml),

14) M. Bergmann, L. Zervas and J. S. Fruton, *J. Biol. Chem.*, **111**, 225 (1935).

15) M. Zaoral and J. Rudinger, *Collection Czech. Chem. Commun.*, **20**, 1183 (1955).

16) T. Kato, S. Makisumi, M. Ohno and N. Izumiya, *Nippon Kagaku Zasshi (J. Chem. Soc. Japan, Pure Chem. Sect.)*, **83**, 1151 (1962).

17) M. Bodanszky and V. du Vigneaud, *J. Am. Chem. Soc.*, **81**, 5688 (1959).

1 N sodium nitrite (1.1 ml) was added at 0°C. After 6 min, cold water (80 ml) was added to the solution. The azide which precipitated as a white mass was collected by filtration, washed with 4% sodium bicarbonate and water, and dried *in vacuo* at 0°C. The azide was added to a solution of V-A (0.40 g; 1 mmol) and triethylamine (0.14 ml) in dimethylformamide (10 ml). The mixture was stirred for 1 day at 0°C and further 1 day at room temperature, and then evaporated *in vacuo*. The precipitate which formed upon the addition of water was collected, and washed with 4% sodium bicarbonate, 3% hydrochloric acid and water. It was recrystallized from dimethylformamide - ethyl acetate - ether; yield, 0.59 g (66%); mp 220—221°C; $[\alpha]_D^{17}$ −56.9° (*c* 1, DMF).

Found: C, 58.06; H, 6.98; N, 13.76%. Calcd for $C_{44}H_{63}O_{10}N_9S$: C, 58.07; H, 6.98; N, 13.85%.

Z-Gln-Asn-Cys(Bzl)-Pro-Leu-Gly-Gly-NH_2 (X-B). The azide derived from IX (2.0 g; 3.3 mmol) was condensed with V-B (1.4 g; 3.3 mmol) as was described above. The product was recrystallized from dimethylformamide - ethyl acetate - ether; yield, 1.7 g (56%); mp 188—191°C; $[\alpha]_D^{17}$ −46.1° (*c* 1, DMF).

Found: C, 54.38; H, 6.41; N, 15.08%. Calcd for $C_{42}H_{58}O_{11}N_{10}S \cdot H_2O$: C, 54.29; H, 6.51; N, 15.08%.

Z-Gln-Asn-Cys(Bzl)-Pro-Leu-Gly-NH_2 (X-C). The azide from IX (2.46 g; 4.1 mmol) was condensed with V-C (1.32 g; 4.1 mmol) The product was recrystallized from dimethylformamide - ethyl acetate; yield, 1.68 g (48%); mp 206—208°C; $[\alpha]_D^{17}$ −53.5° (*c* 1, DMF).

Found: C, 55.59; H, 6.47; N, 14.52%. Calcd for $C_{40}H_{55}O_{10}N_9S \cdot \frac{1}{2}H_2O$: C, 55.67; H, 6.53; N, 14.61%.

Rudinger *et al.* reported the synthesis of the similar hemihydrate (mp 209—210°C),[18] and Bodanszky *et al.* reported the synthesis of the compound which has no water of crystallization (mp 233—234°C).[19]

H-Gln-Asn-Cys(Bzl)-Pro-Leu-Leu-NH_2·HBr (XI-A). The compound X-A (1.83 g; 2 mmol) was treated as has been described for the preparation of VII. The product was obtained as a hygroscopic powder; yield, 1.61 g (94%).

H - Gln - Asn-Cys(Bzl)-Pro-Leu-Gly-Gly-NH_2·HBr (XI-B). The compound X-B (0.93 g; 1 mmol) was treated as has been described for the preparation of VII. The product was obtained as a hygroscopic powder; yield, 0.85 g (96%).

H-Gln-Asn-Cys(Bzl)-Pro-Leu-Gly-NH_2·HBr (XI-C). The compound X-C (1.71 g; 2 mmol) was converted to XI-C as a hygroscopic powder; yield, 1.52 g (95%).

Z-Cys(Bzl)-Tyr-Ile-OEt (XII). *(a) ONp Method.* To a solution of H-Tyr-Ile-OEt·HCl[20] (1.9 g; 5 mmol) and triethylamine (0.7 ml) in dimethylformamide (10 ml), benzyloxycarbonyl-S-benzyl-L-cysteine *p*-nitrophenyl ester[17] (2.3 g; 5 mmol) was added at 0°C. The solution was allowed to stand overnight at room temperature. After the addition of water, the precipitate was collected by filtration and treated as has been described for the preparation of VI. It was recrystallized from ethyl acetate - ether - petroleum ether; yield, 2.5 g (80%); mp 143°C. Iselin *et al.* prepared this compound XII by the coupling of benzyloxycarbonyl-*S*-benzylcystein cyanomethyl ester and H-Try-Ile-OEt; mp 141—143°C.[21]

(b) MA Method. The product XII was also prepared from benzyloxycarbonyl-*S*-benzyl-L-cysteine and H-Tyr-Ile-OEt·HCl by the mixed anhydride method using isobutyl chloroformate; yield, 50%; mp 143°C.

Z-Cys(Bzl)-Tyr-Ile-$NHNH_2$ (XIII). The compound XII (5.2 g; 8 mmol) was converted into the hydrazide as has been described for the preparation of IX; yield, 4.0 g (80%); mp 236—238°C. Boissonnas *et al.* prepared the compound XIII from Z-Cys(Bzl)-Tyr-Ile-OMe with hydrazine in methanol; mp 238°C.[9]

Z-Cys(Bzl) - Tyr - Ile - Gln-Asn-Cys(Bzl)-Pro - Leu-Leu-NH_2 (XIV-A). The compound XIII (0.50 g; 0.8 mmol) in glacial acetic acid (40 ml) was converted to the corresponding azide with 1N hydrochloric acid (2.5 ml) and 1N sodium nitrite (0.9 ml). The azide was added to a solution of XI-A (0.69 g; 0.8 mmol) and triethylamine (0.11 ml) in dimethylformamide (8 ml). The mixture was treated in the same manner as has been described for the preparation of X-A. The crude product was recrystallized from dimethylformamide-ether; yield, 0.47 g (44%); mp 213—217°C; $[\alpha]_D^{25}$ −31.2° (*c* 1, DMF).

Found: C, 60.02; H, 6.55; N, 11.98%. Calcd for $C_{69}H_{94}O_{14}N_{12}S_2$: C, 60.07; H, 6.87; N, 12.18%.

Z-Cys(Bzl)-Tyr-Ile-Gln - Asn - Cys(Bzl) - Pro - Leu-Gly-Gly-HN_2 (XIV-B). The azide derived from XIII (0.64 g; 1 mmol) was condensed with XI-B (0.89 g; 1 mmol) as was described above. It was recrystallized from dimethylformamide-methanol-ether; yield, 0.78 g (57%); mp 225—227°C; $[\alpha]_D^{21}$ −42.0° (*c* 1, DMF).

Found: C, 58.02; H, 6.63; N, 12.85%. Calcd for $C_{67}H_{89}O_{15}N_{13}S_2$: C, 58.29; H, 6.50; N, 13.19%.

Z - Cys(Bzl) - Tyr - Ile-Gln-Asn -Cys(Bzl)-Pro-Leu-Gly-NH_2 (XIV-C). The azide from XIII (1.02 g; 1.6 mmol) was condensed with XI-C (1.26 g; 1.6 mmol) as described above; yield, 0.77 g (37%) (found: C, 58.78; H, 6.41; N, 12.55%); mp 235—237°C; $[\alpha]_D^{21}$ −45.5° (*c* 1, DMF). Lit., mp 241°C, $[\alpha]_D$ −51.5° (AcOH);[9] mp 243—245°C, $[\alpha]_D$ −43° (DMF).[22]

Removal of the Protecting Groups from XIV. *(a) Na/NH_3 Method.* Each 0.06 mmol of the protected peptide (83 mg of XIV-A, 83 mg of XIV-B or 80 mg of XIV-C) was dissolved in liquid ammonia (*ca.* 50 ml), and sodium (*ca.* 40 mg) was added until a blue color persisted for 3 min. Ammonium chloride (100 mg) was added to the solution and the ammonia was allowed to evaporate spontaneously. The residue was dissolved in water (100 ml) and the pH was adjusted to 6.5 with acetic acid, and carbon dioxide free-air was bubbled through for about 4 hr until the nitroprusside reaction for sulfhydryl groups was negative. The solution was further acidified to pH 3.5 with acetic acid, and an aliquot of the solution was subjected to the tests of the rat uterine-contracting and avian depressor activities (Table 1).[23]

18) J. Rudinger, J. Honzl and M. Zaoral, *Collection Czech. Chem. Commun.*, **21**, 202 (1956).
19) M. Bodanszky and V. du Vigneaud, *J. Am. Chem. Soc.*, **81**, 5688 (1959).
20) H. Aoyagi, K. Arakawa and N. Izumiya, This Bulletin, **41**, 433 (1968).
21) B. Iselin, M. Feurer and R. Schwyzer, *Helv. Chim. Acta*, **38**, 1508 (1955).
22) M. Bodanszky and V. du Vigneaud, *J. Am. Chem. Soc.*, **81**, 2504 (1959).
23) We wish to express our thanks to Dr. S. Matsushima of Teikoku Hormone MFG. Co., Ltd. for the biological assays.

(b) HF Method.[24] Each 0.06 mmol of XIV was treated with anhydrous hydrogen fluoride (HF) as has been described in the literature.[11] An aliquot of the oxidized solution (100 ml) was subjected to the biological assays as was described above (Table 1). Sakakibara and Shimonishi obtained oxytocin solution with 133 units (rat-uterine test) per mg of XIV-C by HF treatment, whereas we obtained oxytocin solution with 21 units per mg of XIV-C as calculated from Table 1. We cannot give a reasonable explanation for this low yield at present.

24) One (H. A.) of us carried out the experiments with HF at Sakakibara's Laboratory of Osaka University. We wish to express our thanks to Dr. S. Sakakibara and Dr. Y. Kishida of Osaka University for their courtesy.

BULLETIN OF THE CHEMICAL SOCIETY OF JAPAN VOL. 41 2776—2781 (1968)

Oxidation of Propylene over the Tin-Antimony Oxide Catalysts. II. Investigations of Physicochemical Properties of the Catalysts

Katsuhiko WAKABAYASHI,*1 Yoshio KAMIYA and Nobuto OHTA

Department of Fuel, Faculty of Engineering, The University of Tokyo, Hongo, Tokyo

(Received December 26, 1967)

The physicochemical properties of the binary system composed of Sn and Sb oxides have been investigated. The electrical conductivity increased rapidly up to 3 atom% Sb, and subsequently decreased, little by little, as the Sb oxide content in the binary system increased. The surface area also increased rapidly up to 3 atom% Sb, and in the region exceeding this content a dilution effect due to Sb oxide was observed. The behavior of the initial rate of acrolein formation as a function of the catalyst composition was fairly similar to that of the surface area. The apparent activation energies for carbon dioxide formation at first decreased, and then became nearly constant when the Sb content of the catalysts increased. On the other hand, the activation energies for acrolein formation may be considered to be always constant, independent of the catalyst composition, at about 17 kcal/mol. The activation energies for the catalyst reduction by hydrogen were 28 kcal/mol for Sn oxide, 14 for a mixture containing 25 atom% Sb, and 30 for Sb oxide. Consequently, it has been concluded from these results that it may depend on the nature of the chemisorbed oxygen which attacks propylene whether the propylene is oxidized into acrolein or into such complete combustion products as carbon dioxide.

In the studies of the binary system of Sn and Sb oxides, a former paper[1] was concerned with the effect of the catalyst compositon and the calcination conditions on the formation of acrolein, and with an investigation of the X-ray patterns of the catalysts; it was confirmed that Sb oxide was dissolved into Sn oxide and that the solid solutions thus formed were active in the production of acrolein.

The present paper will deal with the physical and catalytic properties of the binary system for the purpose of elucidating why the solid solutions composed of Sn and Sb oxides are active in acrolein formation.

Many works[2-6] have thus far been presented on various binary systems, though few have dealt with the correlation between the reaction activity and the physicochemical properties. Butler *et al.*,[6] however, observed a correlation between the conducitivity and the apparent activation energy for the decomposition of benzene over mixed catalysts of V_2O_5 containing MoO_3 or GeO_2.

From the viewpoint of controlled-valency semiconductivity, the decomposition of N_2O[7-9] and the oxidation of CO[10,11] have thus far been studied,

*1 Present address, Government Chemical Industrial Research Institute, Tokyo, Honmachi, Shibuya-ku, Tokyo.

1) K. Wakabayashi, Y. Kamiya and N. Ohta, This Bulletin, **40**, 2172 (1967).

2) C. R. Adams and T. J. Jennings, *J. Catalysis*, **2**, 63 (1963).

3) R. H. Munch and E. D. Pierron, *ibid.*, **3**, 406 (1964).

4) Ph. A. Batist, B. C. Lippens and G. C. A. Schuit, *ibid.*, **5**, 55 (1966).

5) W. M. H. Sachtler and N. H. De Boer, *Proc. 3rd Intern. Congr. Catalysis*, 252 (1965).

6) J. D. Butler and B. G. Weston, *J. Catalysis*, **2**, 8 (1963).

7) C. Wagner, *J. Chem. Phys.*, **18**, 69 (1950).

8) M. Boudart, *ibid.*, **18**, 571 (1950).

9) K. Hauffe and H. J. Engell, *Z. Elektrochem.*, **57**, 16 (1953).

10) G. Parravano, *J. Am. Chem. Soc.*, **75**, 1448 (1952).

11) G. M. Schwab and J. Block, *Z. Elektrochem.*, **58**, 756 (1954).

but the mechanism of the catalysis has not been completely elucidated.

Experimental

The apparatus, experimental procedures, and methods of catalyst preparation were the same as were employed in the previous work.[1)]

The samples used in the measurements of the surface area and of the electrical conductivity were prepared by heating the powder of SnO_2 and Sb_2O_5 at a desired ratio, the two ingredients being thoroughly admixed without any carrier.

The surface areas were measured with nitrogen by the BET method at −196°C; an area of 16.2 Å² was assumed for the nitrogen molecule. The dc resistance of a 2 g portion of the powdered sample was measured with Wheatstone's bridge. The apparatus was similar to that of Griffith *et al.*[12)] The electrodes were platinum disks 12 mm in diameter; two springs applied a constant pressure to the sample between the electrodes.

The reduction of the catalysts was carried out at the atmospheric pressure of hydrogen in the range from 400°C to 500°C by using a thermobalance.

Results

Figure 1 shows the electrical conductivity of the binary system composed of Sn and Sb oxides. The measurements were carried out in air at room temperature. The conductivity increased markedly up to 3 atom% Sb, and then decreased little by little in the region above 3 atom% Sb.

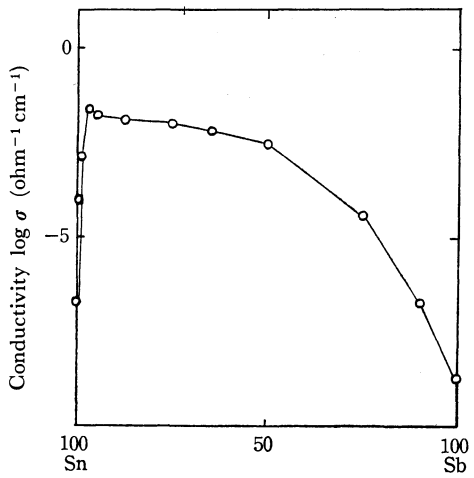

Fig. 1. The conductivity of the Sn and Sb oxide binary system.

Figure 2 shows the surface area as a function of the composition of Sn and Sb oxides. The surface area increased as markedly as may be observed in Fig. 1 up to 3 atom% Sb. However, in the region of higher Sb oxide concentrations the surface area subsequently decreased, and a dilution effect due to Sb oxide was observed.

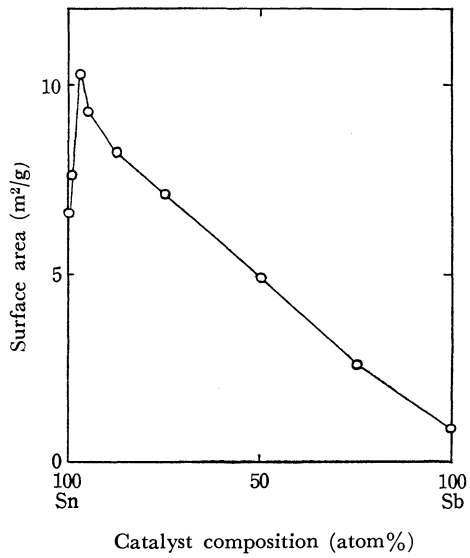

Fig. 2. The surface area of the Sn and Sb oxide binary system.

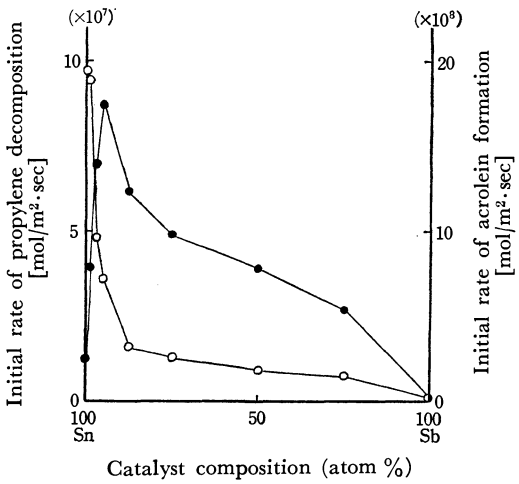

Fig. 3. Initial rate of acrolein formation and propylene decomposition.
Catalyst: calcined at 1000°C for 3 hr
Reaction temperature: 470°C
○: Propylene decomposition
●: Acrolein formation

Figure 3 shows the initial rates of acrolein formation and propylene decomposition at 470°C. A rapid increase in the initial rate of acrolein formation was caused by the addition of Sb oxide; the maximum rate was obtained at a 5 atom% Sb content. In the region of higher Sb oxide concentrations, a dilution effect seems to exist. The initial rate of propylene decomposition fell

12) P. R. Charman, R. H. Griffith and J. D. E. Marsh, *Proc. Roy. Soc.*, **224**, 419 (1954).

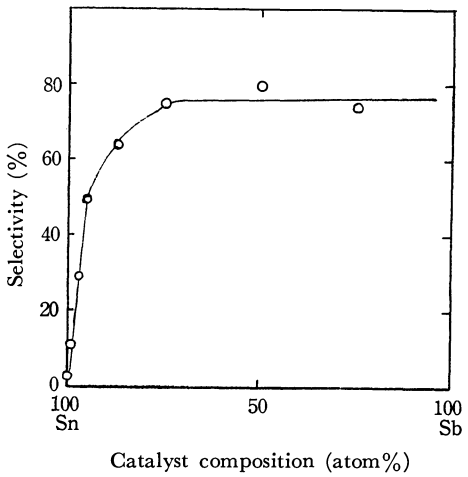

Fig. 4. Selectivity to acrolein when the consumption of propylene was about 10%.
Catalyst: calcined at 1000°C for 3 hr
Reaction temperature: 470°C

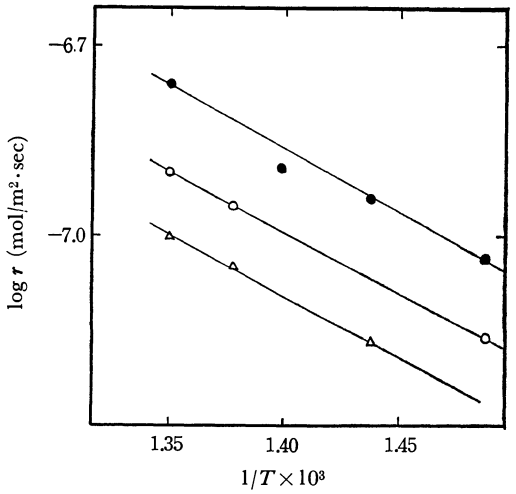

Fig. 5. Representative Arrhenius plots for acrolein formation.
Catalyst: calcined at 1000°C for 3 hr
●: Catalyst with a Sn-to-Sb atomic ratio: 95 : 5
○: Catalyst with a Sn-to-Sb atomic ratio: 7 : 1
△: Catalyst with a Sn-to-Sb atomic ratio: 7 : 1

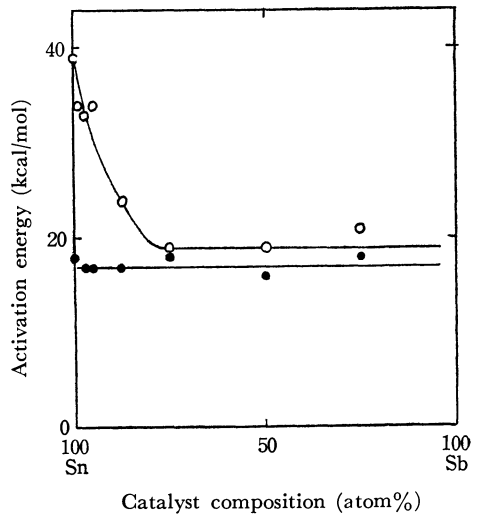

Fig. 6. Apparent activation energies for carbon dioxide formation and acrolein formation.
Catalyst: calcined at 1000°C for 3 hr
○: Carbon dioxide formation
●: Acrolein formation

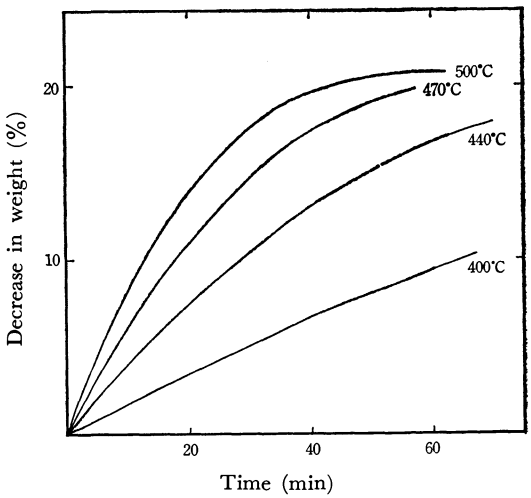

Fig. 7. Weight lost upon reduction by hydrogen.
Sample: mixture with a Sn-to-Sb atomic ratio of 3 : 1, calcined at 1000°C for 3 hr.

off rapidly as Sb oxide was added to Sn oxide. The formation of carbon dioxide was extremely depressed by the addition of Sb oxide, as is summarized in Table 1.

The selectivity to acrolein when the conversion of propylene is about 10% is shown in Fig. 4 as a function of the catalyst composition. The selectivity at first increased upon the addition of Sb oxide, and then it became almost constant in the region of Sn-to-Sb atomic ratios below 3 : 1.

The apparent activation energies for the formation of acrolein (E_{acr}) and carbon dioxide (E_{CO_2}) have been obtained from Arrhenius plots in the temperature range from 400°C to 490°C, using an initial rate, r, which is considered to be proportional to the rate constant, k. These plots of log r against $1/T$ have given a reasonably straight line for all the catalysts of various compositions. In the case of acrolein formation, representative Arrhenius plots are shown in Fig. 5. Figure 6 shows E_{acr} and E_{CO_2} as functions of the catalyst composition. E_{acr} remained constant over the entire range of compositions of the binary system. On the other hand, E_{CO_2} decreased up to 25 atom% Sb, and then became constant in the region of Sn-to-Sb atomic ratios below 3 : 1.

Table 1. Rate of reaction
Reaction temperature: 470°C

Catalyst composition (Sn/Sb)	Rate of reaction (mol/m²·sec)		
	$d(CH_2=CHCHO)/dt$ ($\times 10^8$)	$d(CO_2)/dt$ ($\times 10^8$)	$-d(C_3H_6)/dt$ ($\times 10^7$)
SnO_2	2.6	252	9.9
99/1	7.8	165	9.8
97/3	14.0	59	4.9
95/5	17.4	35	3.5
7/1	12.4	9.3	1.9
3/1	9.8	3.9	1.3
1/1	7.8	1.9	0.98
1/3	5.5	1.4	0.74

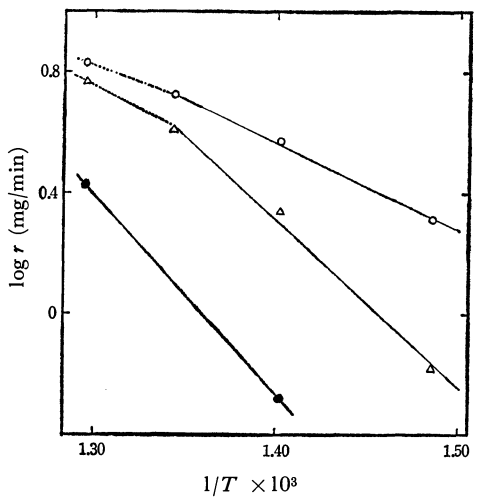

Fig. 8. Arrhenius plots for catalyst reduction by hydrogen.
○: Sample with a Sn-to-Sb atomic ratio of 3 : 1
△: SnO_2
●: Sb_2O_5
Each sample was calcined at 1000°C for 3 hr.

Figure 7 indicates the weight loss during reduction by hydrogen of a mixture with a Sn-to-Sb atomic ratio of 3 : 1. The reduction rate has been represented by the decrease in the weight of a sample between 5 and 15 min after the beginning of the reduction. Arrhenius plots for the reduction are shown in Fig. 8. The diffusion process seems to have an effect upon the reduction rate at temperatures as high as 500°C. The apparent activation energies thus obtained were 28 kcal/mol for Sn oxide, 14 for the mixture with a Sn-to-Sb atomic ratio of 3 : 1, and 30 for Sb oxide.

Discussion

As has been mentioned in the earlier paper,[1] SnO_2 and Sb_2O_5 form a substitutional solid solution. The solid solution is formed as follows:

$$(1-2\delta)SnO_2 + \delta Sb_2O_5 \rightarrow Sn_{(1-4\delta)}^{4+}Sn_{2\delta}^{3+}Sb_{2\delta}^{5+}O_2 + \frac{1}{2}\delta O_2 \quad (1)$$

or

$$Sb_2O_5 \rightarrow 2Sb_{(Sn)}^{+} + 2\ominus + 2SnO_2 + \frac{1}{2}O_2 \quad (2)$$

where $Sb_{(Sn)}^{+}$ indicates Sb^{5+} which has been substituted for Sn^{4+}. SnO_2 acts as a n-type semiconductor; accordingly Sn^{3+}, which may be called anion vacancies, or quasi-free electrons, is produced as is shown above when the lattice of SnO_2 dissolves Sb_2O_5. The Sn^{3+} content is equivalent to the amount of Sb^{5+} substituted for Sn^{4+}. The solid solutions were found, from the X-ray investigations described in the previous paper, to have a homogeneous crystal of the same structure as the original SnO_2, but the dimensions of the unit cell must be larger, as the ionic radius of Sn^{3+} is larger than that of Sn^{4+}. Hence, an expansion of the lattice by the addition of Sb_2O_5 may be expected. This has also actually been observed, as has been shown in the previous paper.

Phase Composition of Sn and Sb Oxide System. How far Sb_2O_5 is dissolved into SnO_2 is dependent upon the calcination temperature and the period. However, it is difficult to determine the solubility by measuring Δd because of the fact that the addition of Sb_2O_5 to SnO_2 does not cause much change in the d-spacings in X-ray patterns; also, it is difficult to ascertain whether Sb_2O_5 is completely dissolved into SnO_2 at a low Sb content because of the fact that the relative intensity of Sb_2O_5 in X-ray patterns is considerably smaller than that of SnO_2. It was shown by the X-ray investigations described in the previous paper that some Sb_2O_5 remains insoluble in SnO_2 in the case of a (Sn/Sb=3, 1000°C, 3 hr) mixture, and that a larger amount of Sb_2O_5 is dissolved into SnO_2 in a (Sn/Sb=3, 1100°C, 3 hr) mixture than in the (Sn/Sb=3, 1000°C, 3 hr) mixture. Here, the description of the (Sn/Sb=3, 1000°C, 3 hr) mixture means that the Sn-to-Sb atomic ratio in

the mixture is 3 : 1 and that the mixture has been calcined at 1000°C for 3 hr. Hence, it is certain that two phases consisting of Sb_2O_5 and the solid solution are present in the (Sn/Sb=3, 1000°C, 3 hr) mixture. However, it remains uncertain whether Sb_2O_5 insoluble in SnO_2 is present in the mixture with a Sn-to-Sb atomic ratio above 3 : 1 when it is calcined at 1000°C for 3 hr, as has been shown in the X-ray patterns in the previous paper.

As quasi-free electrons equivalent to the amount of Sb dissolved into SnO_2 are produced, the conductivity increases upon the addition of Sb_2O_5 to SnO_2, showing a maximum value at a 3 atom% Sb content. It is impossible, however, to determine from the conductivity measurements how far the Sb oxide is dissolved into the Sn oxide, because the conductivity is not necessarily proportional to the concentration of the foreign ion when dissolved in great quantities. Nevertheless, it may be considered, judging from the conductivity data, that the Sb oxide is almost completely dissolved up to 3 atom% Sb. The surface area also increases rapidly upon the addition of a small amount of Sb oxide; it is largest at a 3 atom% Sb content. In the region of the oxide system containing more than 3 atom% Sb, a dilution effect due to Sb oxide has been observed. Taking into consideration the conclusion of the conductivity investigations, the increase in the surface area upon the addition of a small amount of Sb oxide can be attributed to the formation of the solid solutions. As the surface area is regarded as dependent upon the dimensions of the grain size, it seems that the grain size may become small when the lattice of Sn oxide dissolves Sb oxide.

The investigation of the initial rate of acrolein formation, if based on the conclusion drawn from the conductivity and surface area data, shows that the initial rate is mainly dependent upon the amount of the solid solutions formed on the catalyst surface. A dilution effect due to the Sb oxide added seems to be present in the region above a 5 atom% Sb content. The dilution effect in the above two cases can be attributed to the Sb oxide which remains insoluble in Sn oxide. Hence, it may be concluded that the two phases composed of Sb oxide and the solid solutions are present in the system exceeding about a 5 atom% Sb content.

Why the mixtures of Sn and Sb oxides become colored upon being calcined at a high temperature may be due to the Sn^{3+} produced when the lattice of Sn oxide dissolves Sb oxide. Accordingly, the maximum solubility may be qualitatively determined from the depth of the color of the mixtures. As was mentioned in the previous paper, the mixture with a Sn-to-Sb atomic ratio of 3 : 1 is deepest in color of all the mixtures when calcined at 1000°C for 3 hr, but it is less deep than the (Sn/Sb=3, 1100°C, 3 hr) mixture. The maximum solubility of Sb oxide into Sn oxide may, therefore, be regarded as nearly 25 atom%; this value is in good agreement with the value inferred from the measurements of the apparent activation energies for the formation of carbon dioxide and of the selectivity to acrolein. Consequently, it may be concluded that Sb oxide is completely dissolved into Sn oxide up to 3 or 5 atom% Sb when calcined at 1000°C for 3 hr, and that Sb oxide as well as the solid solution is present in the system at a higher Sb content, though the maximum solubility is nearly 25 atom%.

Formation of Acrolein and Carbon Dioxide. Many mixed catalysts, for example, CuO-SeO_2,[13] Fe_2O_3-As_2O_3,[14] Bi_2O_3-MoO_3,[15] and SnO_2-Sb_2O_5,[16] recommended for the oxidation of propylene to acrolein, contain one metal oxide which is considered to produce acrolein selectively by itself, though the rate of formation is slow. The heat of the formation of this oxide from a lower oxide or metal to a higher is relatively small, as Table 2 shows. A pure molybdenum oxide catalyst, as has been reported previously,[17] scarcely oxidizes propylene at all in such a reducing atmosphere as that in this work, nor does a pure antimony oxide catalyst. This may be because these oxides are easily reduced to lower oxides or metals, whose surface is in a reducing atmosphere with a large amount of adsorbed propylene and, accordingly, almost inactive in the oxidation of propylene as a result of the poverty of active oxygen on the surface. Kominami *et*

TABLE 2. THE HEAT OF FORMATION OF THE METAL OXIDES

Metal oxide	(kcal/mol)
SnO_2	137.4
SnO	66.0
Sb_2O_5	229.6
Sb_2O_3	164.4
Fe_2O_3	195.2
FeO	64.6
As_2O_5	219.4
As_2O_3	156.6
CuO	33.0
Cu_2O	43.0
SeO_2	63.5
Bi_2O_3	137.8
MoO_3	180.4
MoO_2	142.8
V_2O_5	437
V_2O_4	361.6
V_2O_3	302

13) Distillers: Brit. Pat. 655210 (1951).
14) T. Ishikawa and T. Hayakawa, *Kogyo Kagaku Zasshi (J. Chem. Soc. Japan, Ind. Chem. Sect.)*, **67**, 1391 (1964).
15) Standard Oil: U. S. Pat. 2904580 (1959).
16) Distillers: Brit. Pat. 864666 (1961).
17) K. Wakabayashi and Y. Kamiya, This Bulletin, **40**, 401 (1967).

al.[18] have proposed the following mechanism with respect to the CuO-SeO_2 system:

$$SeO_2 \text{ (or } CuSeO_3) + C_3H_6 \rightarrow \text{acrolen} + Se \text{ (}CuSeO\text{)} \quad (3)$$

$$Se \text{ (}CuSeO\text{)} + CuO \rightarrow SeO_2 \text{ (}CuSeO_3\text{)} + Cu_2O \quad (4)$$

$$Cu_2O + O_2 \rightarrow CuO \quad (5)$$

This may mean that one oxide in the mixed catalysts is effective in the activation of oxygen, and another, in the activation of propylene. In the binary system composed of Sn and Sb oxides, antimony ions may be effective in the activated adsorption of propylene, as has been investigated with regard to Bi_2O_3-MoO_3[2,5] and Cu_2O[19]. In this discussion, however, only the chemisorption of oxygen will be taken into consideration.

Oxygen is adsorbed on a metal oxide as follows:

$$O_2 \rightleftarrows O_2^- \rightleftarrows O^- \rightleftarrows O^{2-} \quad (6)$$

At a low temperature, the oxygen adsorbed on a metal oxide is considered to be converted to O_2^- or O^-, and at a high temperature, to O^- or O^{2-}. Therefore, under these reaction conditions, it may be assumed that there may be present on the catalyst surface both O^- and O^{2-} ions. The former is an oxygen ion adsorbed on the catalyst, while the latter is an oxygen ion more strongly adsorbed, one which may be of the same nature as the lattice ion.

As is shown in Fig. 6, E_{CO_2} decreases up to about 25 atom% Sb and remains nearly constant hereafter. In the V_2O_5-MoO_3 system,[20] a vanadium-oxygen bond is weakend by the addition of MoO_3. If the SnO_2-Sb_2O_5 system is analogous, a tin-oxygen bond may become weaker as the Sb oxide is dissolved into the Sn oxide. The measurements of the activation energies for the catalyst reduction indicate that a mixture with a Sn-to-Sb atomic ratio of 3 : 1 has an activation energy smaller by 14 kcal/mol than a pure tin oxide. This finding is in fairly good agreement with the difference in E_{CO_2}. Hence, the lattice oxygen is possibly connected with the formation of carbon dioxide.

On the other hand, little change in E_{acr} was observed in spite of the change in the amount of Sb oxide added. This suggests that the formation of acrolein may be dependent upon the O^- ions, according to the report that ethylene oxide is yielded by O_2^- rather than O^- ions in the oxidation of ethylene.[21]

Thus:

Formation of carbon dioxide

$$O^{2-} \text{ (lattice oxygen)} + C_3H_6 \rightarrow \text{complete combustion products} + [O_v^{2+} \cdot 2e] \text{ (oxygen defect)} \quad (7)$$

$$\frac{1}{2}O_2 + [O_v^{2+} \cdot 2e] \rightarrow O^{2-} \text{ (lattice oxygen)} \quad (8)$$

Formation of acrolein

$$\frac{1}{2}O_2 + Sn^{3+} \rightarrow O^- + Sn^{4+} \quad (9)$$

$$O^- + C_3H_6 + Sn^{4+} \rightarrow \text{acrolein} + Sn^{3+} \quad (10)$$

where Sn^{3+} indicates an anion vacancy.

This mechanism explains very reasonably the results of the kinetic measurements and the selectivities of the catalysts as well as the dilution effects. As the amount of quasi-free electrons on the catalyst surface increases when Sb oxide is added to Sn oxide, the increase in the initial rate of acrolein formation, shown in Fig. 3, is observed. On the other hand, an active lattice oxygen ion available for carbon dioxide formation is removed from the system, leaving an anion vacancy, when Sb oxide is dissolved into Sn oxide, so the rate of carbon dioxide formation falls off. That the maximum value of the rate of acrolein formation was obtained at a 5 atom% Sb content suggests that the concentration of anion vacancies avaiable on the catalyst surface is highest at this content. It is due to the more marked decrease in the rate of carbon dioxide formation that the rate of propylene decomposition decreases upon the addition of Sb oxide to Sn oxide and that the selectivity to acrolein increases above 5 atom% Sb even though the rate of acrolein formation falls off.

The selectivity to acrolein was 32% at the contact time of 0.5 sec and 17% at 2.5 sec with a (Sn/Sb= 97/3, 1000°C, 3 hr) catalyst, though it was 74% at 7.5 sec and 68% at 25 sec with a (Sn/Sb=3, 1000°C, 3 hr) catalyst, where Sb oxide is considered to dissolve into Sn oxide almost to the maximum extent of solubility. Therefore, a lattice oxygen ion may also be related to the further oxidation of acrolein.

However, detailed information on the reaction kinetics as well as on the adsorption of oxygen and propylene is necessary before a quantitative reaction scheme can be presented.

The authors wish to express their thanks to Professor Emeritus Shingo Ando for his continued advice and encouragement in this work.

18) N. Kominami, A. Shibata and S. Minekawa, *Kogyo Kagaku Zasshi (J. Chem. Soc. Japan, Ind. Chem. Sect.)*, **65**, 1510 (1962).
19) H. H. Voge, C. D. Wagner and D. P. Stevenson, *J. Catalysis*, **2**, 58 (1963).
20) K. Tarama, S. Teranishi, S. Yoshida and N. Tamura, *Proc. 3rd Intern. Congr. Catalysis*, 282 (1965).
21) G. D. Lyubarskii, *Dokl. Akad. Nauk USSR*, **110**, 112 (1956).

BULLETIN OF THE CHEMICAL SOCIETY OF JAPAN VOL. 41 7282—2785 (1968)

Effect of Pressure on Graphitization of Carbon. V. Electron Spin Resonance in Hard Carbon Heat-Treated under High Pressure

Kan-ichi KAMIYA,* Shigemi YUGO,** Michio INAGAKI,* Hajime SAITO* and Takuro TSUZUKU**

* *Faculty of Engineering, Nagoya University, Chikusa-ku, Nagoya*
** *College of Science and Engineering, Nihon University, Kanda-Surugadai, Tokyo*

(Received May 6, 1968)

By means of the electron spin resonance (ESR), the graphitization process of a hard carbon (phenolformaldehyde resin char) under a pressure of 5 kbar was investigated in relation to the results of the X-ray diffraction analysis. In the ESR measurement, there is observed only a sharp Lorentzian line having *g*-value of about 2.003 for the products heat-treated at relatively low temperatures. On the other hand, gradual increase in the heat treatment temperature (HTT) leads to the appearance of new 15—20 G wide line having *g*-value of about 2.01, overlapping on the sharp one, and its absorption intensity tends to increase further with HTT. The appearance of the broad ESR line has been found always being accompanied by an abrupt increase of the content of graphitic component deduced from the analysis of (002) diffraction profile. From further investigation of features of these ESR lines as a function of ambient temperature, the sharp one is concluded that it originates from the so-called localized spin centers, while the broad one from the delocalized. The coexistence of these two signals suggests that the turbostratic and graphitic parts have enough extent to prevent the motional mixing of these spin centers, which has also been verified by the X-ray diffraction analysis.

The graphitization process of carbons under high pressure has recently been studied by Noda and his co-workers[1-5] through an analysis of the profiles of (001) X-ray diffraction lines. In their studies,[1,2,5] every kind of carbons examined was found to be graphitized under high pressure at relatively low temperature such as 1500°C. Furthermore, it has been deduced that the graphitization process of a hard carbon under a pressure of 5 kbar is divided into three distinctive stages[5]: In the first stage, there is observed only one component, A_H, having the so-called turbostratic structure. In the second stage, the new components G'_H and G''_H seem to coexist with A_H, and the total content of G_H' and G''_H, which will hereafter be denoted by G_H, shows a gradual increase up to 20% with the increase in heat treatment temperature (HTT). At the beginning of the third stage, *i. e.*, HTT of 1400, 1500 and 1700°C for the residence time of 60, 20 and 3 min, respectively, the content of G''_H increases so abruptly as to exceed 70%, while G'_H disappears and a small amount of A_H remains still unaltered. Therefore, the sum G_H is equal to the content of G''_H in this stage, and still increases gradually with the increase in HTT towards full graphitization. The components G''_H and A_H are concluded to have the three-dimensional graphitic and turbostratic structures, respectively, but G'_H may be of intermediate structure between the turbostratic and the graphitic.

In the present work, it has been intended to study the electron spin resonance (ESR) in the hard carbons heat-treated under high pressure, making a comparison with the results of X-ray diffraction analysis performed on the same samples.

Experimental and Results

The hard carbon sample PH-7 was prepared at 700°C from phenolformaldehyde resin which was made by a conventional method using ammonium hydroxide as catalyst. Heat treatments of this sample under a quasi-hydrostatic pressure of 5 kbar were performed at various temperatures between 1100—1800°C for residence times of 3, 20 and 60 min. The temperature of heat treatment (HTT) was evaluated from the electric input power, for which the relation between temperature and input power had preliminarily been determined by using chromel-alumel thermocouple. The accuracy of the HTT determination in this way was considered to be ±50°C

1) T. Noda and H. Kato, *Carbon*, **3**, 289 (1965).
2) T. Noda, K. Kamiya and M. Inagaki, This Bulletin, **41**, 485 (1968).
3) M. Inagaki, K. Kamiya and T. Noda, *Kogyo Kagaku Zasshi (J. Chem. Soc. Japan, Ind. Chem. Sect.)*, **71**, 652 (1968).
4) M. Inagaki, K. Kamiya and T. Noda, *ibid.*, **71**, 812 (1968).
5) K. Kamiya, M. Inagaki, M. Mizutani and T. Noda, This Bulletin, **41**, 2169 (1968).

at 1500°C. Details on the sample treatment, *e. g.*, high pressure apparatus, high pressure cell arrangement and heat treatment procedures *etc.* are the same to those reported elsewhere.[3-5]

Through the heat treatment, the sample was sintered into a cylindrical block about 6 mm in length and 4 mm in diameter. An about 2 mm long piece was cut out of the central part, where the temperature gradient was hardly observed during the treatment.[4] A half of each piece was examined with ESR in this work, and another half with the X-ray diffraction analysis previously reported.[5]

The ESR work was conducted mostly at room temperature for finely-ground samples placed in vacuum. DPPH and Mn^{+2}-doped magnesia were used as primary and secondary standards, respectively, to determine the *g*-value of signals. In Fig. 1, the change of the ESR line shape with HTT is shown for the residence time of 3 min. For HTT below 1670°C, a sharp near-symmetrical line is observed around the *g*-value of 2.003.

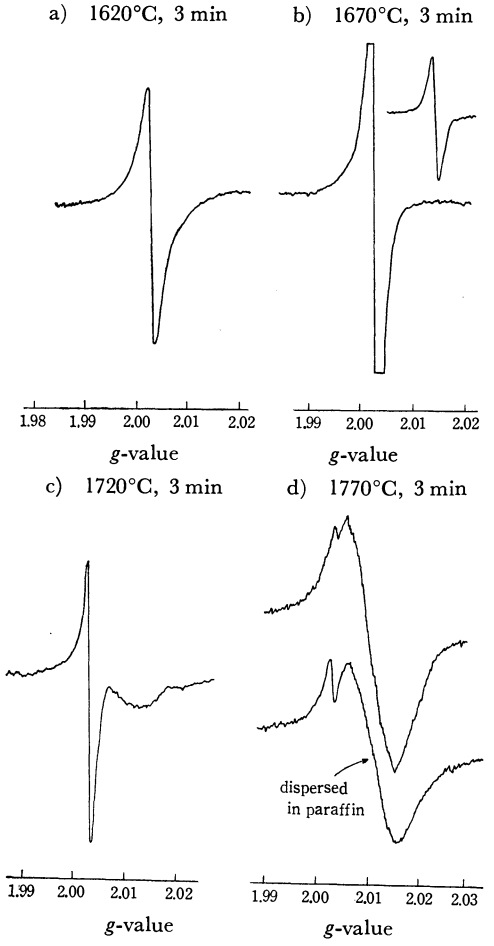

Fig. 1. Change of the line shape of ESR signal of the hard carbon, heat-treated under 5 kbar for 3 min, with HTT.

Above 1720°C, however, a new broad signal centered at $g \fallingdotseq 2.01$ turns up and develops with the increase in HTT. At 1770°C, the broad signal becomes so strong that we have to disperse the sample in solid paraffin for making clear the sharp signal (Fig. 1 d). As to the line shape and the width (w), the sharp signal is of Lorentzian type, giving $w \fallingdotseq 2$G, and the broad one considerably Dysonianized gives $w \fallingdotseq 15$ G to 20 G.

The critical temperature at which the broad signal appears is strongly dependent on the residence time; *e. g.*, about 1500°C for 20 min, and 1400°C for 60 min. It is noticeable that such critical temperatures are coincident with those at which the content of the component G_H shows an abrupt increase. As shown in Fig. 2, a beautiful correspondence between the results of ESR and X-ray analyses, where the *g*-value and the content of G_H are plotted both as functions of HTT, and the critical points are marked by arrows.

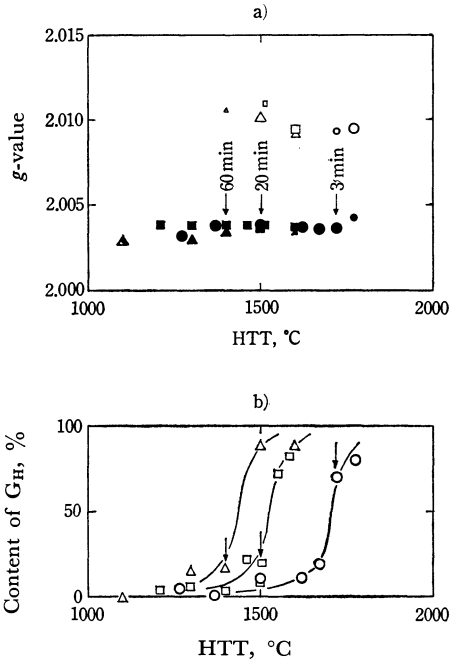

Fig. 2. a) Changes of *g*-values of ESR signals with HTT.

Localized spin	Delocalized spin	
●	○	3 min
■	□	20 min
▲	△	60 min

b) Change of content of the component G_H with HTT.[5]
○ 3 min □ 20 min △ 60 min

In order to obtain further information on the nature of the spin the absorption intensity, line width and *g*-value as functions of ambient temperature were investigated on two typical samples,

say A and B, poorly and highly graphitized, respectively. Sample A heat-treated under 5 kbar at 1370°C for 3 min does not contain the component G_H at all, while for sample B subjected to the same pressure at 1500°C for 60 min the content of G_H amounts to 89%. Ambient temperature was precisely controlled, during the ESR measurement, by suitable ventilation of cold and warm nitrogen gases into the cavity.

The experimental results for these samples are shown together in Fig. 3: Sample A exhibits only the sharp signal. Its relative intensity is found to obey the Curie law, showing an excellent linearity when plotted against $1/T$ (reciprocal temperature in $°K^{-1}$), whereas the line width ($\fallingdotseq$2G) and the g-value ($\fallingdotseq$2.003) are almost independent of temperature in the range from 140°K to 300°K. Such characters are in agreement with those of localized spin centers which have generally been found for various chars on the way of carbonization.[6] On the other hand, behaviors of the broad signal solely displayed by sample B are much different from the above; *viz.*, the line width as well as the g-value decrease with the increase of ambient temperature, while the absorption intensity shows a slightly increasing tendency. Undoubtedly, these trends are associated with the delocalized nature of spins, and hence may conform with the Pauli-McClure type paramagnetism[7] of conduction electrons in graphite which has practically been justified by Wagoner[8] (for single crystal) and further by Singer and Wagoner[9] (for polycrystal).

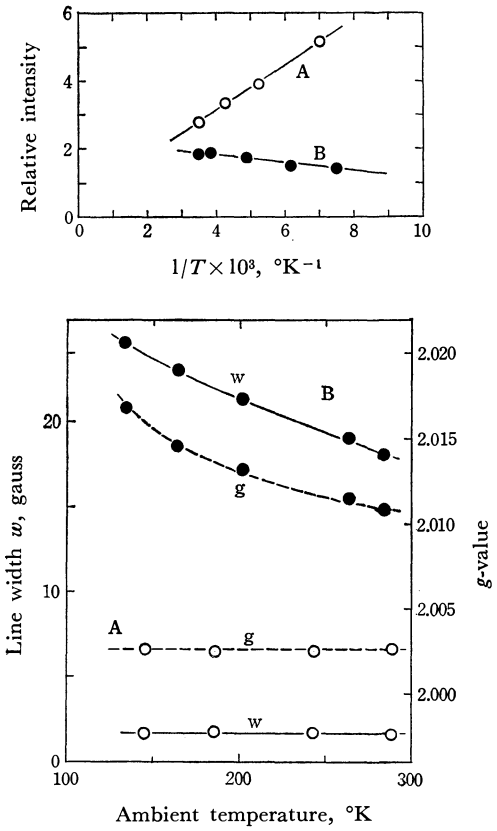

Fig. 3. Dependences of relative intensity, line width and g-value of two kinds of signals on ambient temperature (T).
○ Sample A ● Sample B

Discussion

As shown in Fig. 2, the critical points on HTT axis, at which the broad ESR signal of delocalized nature turns up, coincide with those where the abrupt increase of component G_H is observed in the X-ray analysis. On this basis, we can conclude that the conduction carriers can take part in ESR just through the agency of the three-dimensional graphitic structure. On the other hand, the free spin species giving rise to the sharp signal are mostly distributed, may be bound with some structural defects, in the turbostratic media. However, for the second-stage product in which the content of graphitic part (the component G''_H) is far below 20%, the broad signal due to conduction carriers has not yet been detected. In this sense, the ESR analysis as a tool for detecting the structural change in carbons is likely less sensitive than the well-arranged X-ray diffraction analysis.

Another fact to be remarked in this work is that for some not-fully graphitized sample, there are simultaneously observed two kinds of absorption lines which are due to the localized and delocalized spin centers, respectively. This makes a sharp contrast to the past observations[10,11]; *i. e.*, for usually-treated carbons, one can obtain an ESR line which exhibits intermediate nature between fully localized and delocalized spins as a result of the so-called motional narrowing. Therefore, in our specimens the both structures responsible for such two lines, the turbostratic and the graphitic, have enough extent to prevent such a motional mixing of these spins. This may corresponds to that in the X-ray diffraction either of the turbostratic or of the graphitic portions has enough extent to produce the coherent scattering of X-ray.

6) For instance, S. Mrozowski, "Proceedings of the Fourth Conference on Carbon," Pergamon Press, London (1960), p. 217.

7) J. McClure and Y. Yafet, "Proceedings of the Fifth Conference on Carbon," Vol. I" Pergamon Press, (1962), p. 22.
8) G. Wagoner, *Phys. Rev.*, **118**, 647 (1960).
9) L. S. Singer and G. Wagoner, "Proceedings of the Fifth Conference on Carbon," Vol. II, Pergamon Press, London (1963), p. 65.
10) K. Antonowitz, *J. Chem. Phys.*, **36**, 2046 (1962).
11) Y. Yokozawa, *ibid.*, **37**, 204 (1962).

Several years ago, Honda *et al.*[12] found double-fold ESR lines for some chars prepared in usual way from phenolformaldehyde resin and its derivatives. However, the broad component observed in their study has the same *g*-value as the sharp one. Therefore it might originate from other mechanism than that outlined in the present work. They did not mention the correspondence between the ESR and X-ray diffraction data.

The authors are indebted to Dr. T. Noda of Mie University for his encouragement and valuable discussions.

12) H. Honda, T. Toyoda, Seventh Carbon Conference, held at Cleveland, in 1965.

BULLETIN OF THE CHEMICAL SOCIETY OF JAPAN VOL. 41 2785—2788 (1968)

An Oxygen Concentration Profile of a MnO_2 Particle after Discharge Service

Kazuhide MIYAZAKI

Central Research Laboratories, Mitsui Mining & Smelting Co., Mitaka-shi, Tokyo

(Received May 6, 1968)

The behavior of oxygen in a manganese dioxide depolarizer discharged in a Leclanche-type test cell down to a cut-off voltage of 0.7 V was visually examined by means of electron probe microanalysis. The oxygen concentration profile of a typical MnO_2 particle of about 50 μ in diameter showed that the relative amount of oxygen at the surface and along the pores inside was evidently reduced due to the discharge reaction invading 5 to 10 μ towards the inner part of the particle, indicating that the discharge primarily took place in these portions and involves a process of releasing oxygen from sites at the outermost surface and along the pores. The region which contains these lower oxide portions was observed to be 20—30% of the total cross-sectional area, implying that the utility factor of MnO_2 as a depolarizer was accordingly of the order of 20—30%. It was suggested that enhancement of the use of pores or cleavages during a discharge would generally be beneficial to the service life as a depolarizer, better than merely reducing the particle size of the material.

The present paper provides results of an electron probe microanalysis of an MnO_2 specimen which was under discharging service as a depolarizer in a Leclanche-type wet cell. The purpose here is to visually examine relative concentrations of oxygen at the surface and the inner part of the MnO_2 particles during the discharge reaction.

Many years ago[1] the "polarization" of MnO_2 in a cell was explained by the formation of discharge products on the surface. In 1931, Keller[2] advanced the view that electric discharge of MnO_2 resulted in the formation of a solid solution of MnO_2 with a lower oxide of manganese and this material would degrade the electromotive force of the original MnO_2. Since then, many basic investigations have been carried out concerning the discharge mechanism of MnO_2 in terms of the primary discharge products of the MnO_2 electrode.[3] Changes in the X-ray diffraction pattern of MnO_2 during discharge were examined, as a means of revealing the reduction stages of the depolarizer in a cell, by various investigators including Matsuno,[4] McMurdie[5] and Copeland and Griffith.[6] These reports describe the formation of lower oxides and hydroxides of manganese as possible products in the discharge of MnO_2.

In recent years, a newly developed technique of electron probe microanalysis has been increasingly used in such fields as metallurgy and earth sciences in determining the nature of very small volumes of polished thin sections of alloys or mineral mounts. The principle is that the X-rays generated by the impact of the electron beam are characteristic of the elements present, and their intensity is an approximately linear function of concentration.[7]

1) E. Divers, *Chem. News*, **46**, 259 (1882).
2) A. Keller, *Z. Elektrochem.*, **37**, 342 (1931).
3) *E. g.*, W. C. Vosburgh, *J. Electrochem. Soc.*, **106**, 839 (1959); A. B. Scott, *ibid.*, **107**, 941 (1960); H. Bode, A. Schmier and D. Berndt, *Z. Elektrochem.*, **66**, 586 (1962); K. Sasaki, "Denchi Handbook," Denki-Shoin, Tokyo (1964), p. 265.
4) S. Matsuno, *Denki Kagaku*, **12**, 2 (1944).
5) H. F. McMurdie, *Trans. Electrochem. Soc.*, **86**, 313 (1944).
6) L. C. Copeland and F. S. Griffith, *ibid.*, **89**, 495 (1946).
7) J. Zussman, "Physical Methods in Determinative Mineralogy," Academic Press, London and New York (1967), p. 215.

If the MnO_2 during discharge produces a lower oxide or oxides of manganese by releasing the oxygen from MnO_2, a change in the relative concentration of oxygen at the reduced portions of the material may no doubt be visually observable, at least qualitatively, by differentiating the characteristic OK_α rays coming from the cross-sectional area of a thin section of MnO_2.

The present work has been performed in an attempt to observe the coexisting phases of reduced oxygen concentrations more directly by means of the electron probe microanalytical technique, to visualize how and where the reduction of the individual MnO_2 particles will proceed as the discharge takes place.

Experimental

Material. Electrolytically synthesized manganese dioxide was commercially available with an approximately 200 mesh fineness. This material was of a typical γ-type MnO_2 containing more than 91—93% MnO_2, and is currently used as a standard source of battery-grade manganese dioxide.

Procedures. (a) Discharging cell: A 5 g quantity of MnO_2 material was incorporated into a Leclanche-type test cell. The test cell was constructed by a method similar to that described in "Japanese Industrial Standards",[8] where 20 m*l* of a mixed solution of $NH_4Cl + ZnCl_2$ with a pH of 5.4 is provided as an electrolyte. A discharge with this type of wet cell was conveniently employed for the present purpose because of the ease of separating the MnO_2 after discharge from the cathode mix of the MnO_2 and acetylene black, rather than the paste-type cathode mix of a commercial dry battery. The cell construction used is shown in Fig. 1. A continuous discharge was performed on a fixed resistance of 10 Ω from an initial voltage of 1.6 V down to a cut-off voltage of 0.7 V.

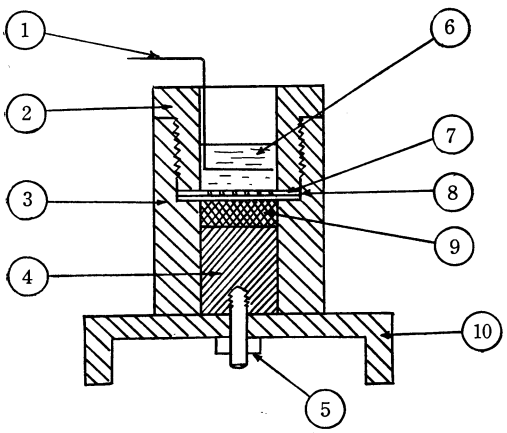

Fig. 1. Construction of the discharge cell used. (1): Zinc anode, (2): Anode bobbin, (3): Cathode bobbin, (4): Carbon rod, (5): Cathode terminal, (6): $NH_4Cl+ZnCl_2$ electrolyte, (7): perforated plate, (8): filter paper, (9): MnO_2 + acetylene black, (10): Bottom plate. (JIS K-1467 (1965))

8) JIS K-1467 (1965).

(b) Electron probe microanalysis: The cathode mix after discharge was washed and air dried. The dried sample was mixed with a polyester resin and set into a shape having a well-polished surface, and was put in an electron probe microanalyzer. This instrument was operated under the following set of conditions: accelerating voltage, 10 kV; average electron beam intensity, 0.04 μA; characteristic X-ray, OK_α; and magnification, 750. A concentration profile of the characteristic OK_α rays, integrated as well as discriminated, was taken by scanning the cross-sectional area of the MnO_2 in parallel with recording the absorbed electron image, focussing on a typical particle about 50 μ in diameter.

Results and Discussion

Figs. 2(a), 2(b) and 2(c) are a series of electron probe microanalyses for the cross-sectional area of a typical MnO_2 particle discharged down to a cut-off voltage of about 0.7 V, where Fig. 2(a) is the absorbed electron image of the profile with a magnification of 750. Figure 2(b) is a discriminated scanning of OK_α with the same magnification, which appears as an ensemble of small light spots across the same cross-sectional area as in Fig. 2(a). It is interesting to note that some darker portions cover the surface of the discharging particle and occurs along cleavages, or pores, near the surfaces of the body in Fig. 2(a), and in a corresponding manner in Fig. 2(b), the discriminated OK_α spots from the oxygen are less distributed at the border area between the cross-section and the background and around the pores in that area, reflecting a reduction in oxygen concentration in these portions. Especially the pores, either closed or open, of Fig. 2(a), are clearly observable as black voids in the upper-left areas lacking in white spots from oxygen in Fig. 2(b).

Fig. 2(c) is a photograph of the integrated intensities of the OK_α rays coming from oxygen

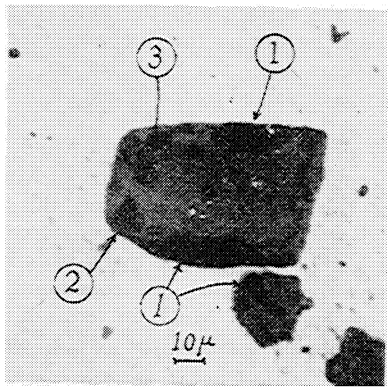

Fig. 2(a). Absorbed electron image of a profile of MnO_2 particle after discharge service. (1): discharged surfaces, (2): discharged open pore, and (3): discharged closed pore near the surface.

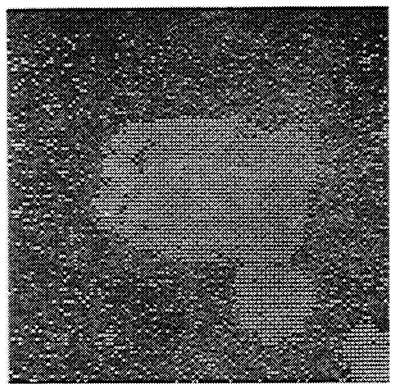

Fig. 2(b). Discriminated characteristc OK_α image scanned across the same profile of Fig. 2(a), showing that the corresponding discharged portions are less distributed with white spots which reflect the relative intensities of the characteristic OK_α rays coming from the oxygen of the cross sectional area. (Background: polyester resin of mounting piece)

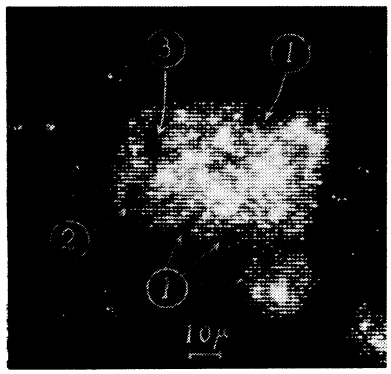

Fig. 2(c). Integrated characteristic OK_α image scanned across the same profile of Fig. 2(a), representing a well-defined light and shade of relative concentrations of oxygen of the profile. (1): discharged surfaces, (2): discharged open pore, and (3): discharged closed pore near the surface.

atoms of the same particle showing a more well-defined light and shade in the concentration profile. From a comparison of Fig. 2(c) with Fig. 2(b), it is clearly seen that the outermost surface of the particle and the vicinity around the pores are observed to contain a lesser amount of oxygen due to the reduction of MnO_2 in those portions, while the inner part of the particle is brighter, showing that the bulk still contains oxygen in the unused MnO_2.

It is noted that the parallel use of Figs. 2(a), 2(b) and 2(c) have provided a visual observation, in a sense, of the result that the discharge took place primarily at the surface and the pores, as previous workers pointed out the importance of the surface characteristics of MnO_2 including the surface area[9,10] and the pore distribution.[11,12] Furthermore, the present example with a 50 μ-particle suggests that the extension of the pores or cleavages in the MnO_2 body is seen to be roughly of the order of 10 μ. The initial pore openings have not been detected here, because the magnitude of a pore diameter is too small, previously calculated to be less than 400 Å by Cahoon[12] and predominantly 180 Å by Kozawa.[11] However, the results of Figs. 2(a), 2(b) and 2(c) show that the region containing a lower oxide of manganese, which was initiated along the micropores as well as at the surface, has invaded about 5 to 10 μ toward the inner part of the MnO_2 particle before decaying to the cut-off voltage of 0.7 V, and these invaded regions became detectable by the microanalytical method.

It also follows from an examination of the pictures that if the utility factor of the MnO_2 particle as depolarizer may be represented as a ratio of the total cross-sectional area of the particle to the darker area of reduced oxygen concentration emerging in the profile, the percentage will be 20—30% in this particular case of discharge down to a cut-off voltage of 0.7 V, which potential is well below that of the terminating voltage employed in most cases[13] when specifying the service life of a cell. This is an important observation as it shows the possibility of revealing changes in the solid phase during discharge in a cell system, provding useful data for industrial applications as well as for basic investigations of MnO_2 depolarizer, suggesting for instance that a treatment of the material to enhance a better use of the functions of cleavages or pores will be more beneficial to the service life as depolarizer than merely reducing the particle size alone.

Summary

Visual observation has been carried out with an oxygen concentration profile of an MnO_2 particle after discharge service down to 0.7 V in a Leclanche-type wet cell, by surveying the relative intensities of OK_α rays by means of an electron probe microanalytical technique. The roles of the pores inside the particle as well as the surface on the discharge process has been established by visually observing that the relative oxygen concentration of these portions becomes less after discharge. A covering of the MnO_2 by these lower oxide portions

9) M. Fukuda, T. Hirai and H. Manabe, *Denki Kagaku*, **27**, 204 (1959).
10) A. Kozawa and R. A. Powers, *Electrochem. Tech.*, **5**, No. 11—12, 535 (1967).
11) A. Kozawa, *J. Electrochem. Soc.*, **106**, 552 (1959).
12) N. C. Cahoon and M. P. Korver, *ibid.*, **109**, 1 (1962).
13) *E. g.*, G. W. Vinal, "Primary Batteries," John Wiley & Sons, Inc., New York (1961), p. 111; JIS C-8501 (1963); W. J. Hamer, *Electrochem. Tech.*, **5**, No. 11—12, 493 (1967).

is observed in a ratio of 20—30% of the total cross-sectional area. It is indicated that the discharge reaction of an MnO_2 particle involves a process of releasing oxygen from the sites of the outermost surface and along the pores.

The possibility is suggested for the use of the microanalytical examination as a powerful tool in interpreting how and where the discharge reaction proceeds across the cross-sectional area of the MnO_2 particle and in pursuing better performance for the material as a depolarizer in a cell.

The author wishes to thank Mr. H. Nakamura and Mr. S. Nakada for their cooperation in the electron probe microanalytical procedures which brought this work into being.

NOTES

Effects of Substituents of the Chain-transfer Reactivities of Nuclear-substituted Acetophenones toward the Polymethyl Methacrylate Radical

Tadahiro YAMAMOTO,*1 Masaru HASEGAWA and Takayuki OTSU

Department of Applied Chemistry, Faculty of Engineering, Osaka City University, Sugimotocho, Sumiyoshi-ku, Osaka

(Received March 27, 1968)

In previous papers,[1-5] the effects of substituents on the reactivities of substituted cumenes toward polymer radicals have been reported. The observed reactivities were not correlated with the ordinary Hammett equation, but they showed a good correlation with the Hammett equation[6] modified to include the resonance term:

$$\log (k/k_0) = \rho\sigma + \gamma E_R \qquad (1)$$

where $\rho\sigma$ is the polar term and γE_R is the resonance term. The ρ and γ show the degree of polar and resonance contributions of the substituents to the reactivities respectively.

This paper will describe the substituent effects on the chain-transfer reactivities of nuclear-substituted acetophenones toward the polymethyl methacrylate (PMMA) radical. Since the acetophenone has a carbonyl group between the benzene ring and the reacting methyl group, the nuclear-substituent effects on the reactivities of its derivatives toward a radical may be different from those observed in the abstraction of a benzylic hydrogen, as has been reported in previous papers.[1-5]

Experimental

A series of nuclear-substituted acetophenones (see Table 1), but not acetophenone itself, were synthesized. By using the method described in a previous paper,[1] the polymerizations of the methyl methacrylate in each acetophenone derivative were carried out at 60°C in the presence of 2,2'-azobisisobutyronitrile (3.32×10^{-3} mol/l) as an initiator. The polymerizations were performed below 5% conversion.

The number-average degree of the polymerization ($\overline{P}_n$) of the polymers was calculated from their intrinsic viscosities, [η], determined in benzene, according to the following equation[7]:

$$\log \overline{P}_n = 3.420 + 1.13 \log [\eta]$$

The chain-transfer constants (C) of acetophenones were determined by means of Mayo plots[8] between $1/\overline{P}_n$ and the concentrations of the acetophenones.

Results and Discussion

The C values obtained are listed in Table 1, in which the E_R and σ values are the resonance[6] and the Hammett substituent constants[9], respectively.

As may be seen in Table 1, all of the C values for the substituted acetophenones were larger than that (C_0) for the unsubstituted compound. Figure 1 shows the plots using the ordinary Hammett equation and using Eq. (1).

*1 Present address: Himeji Institute of Technology, Idei, Himeji.

1) T. Yamamoto, This Bulletin, **40**, 642 (1967).
2) T. Yamamoto and T. Otsu, *ibid.*, **40**, 2449 (1967).
3) T. Yamamoto, T. Otsu and M. Imoto, *Kogyo Kagaku Zasshi (J. Chem. Soc. Japan, Ind. Chem. Sect.)*, **69**, 990 (1966).
4) T. Yamamoto and T. Otsu, *J. Polymer Sci. A-1*, **6**, 49 (1968).
5) T. Yamamoto, T. Otsu and M. Imoto, *International Symposium on Macromolecular Chemistry (Tokyo, Kyoto), Preprint*, **1**, 16 (1966).
6) T. Otsu and T. Yamamoto, *Yuki Gosei Kagaku Kyokaisi (J. Soc. Org. Synth. Chem. Japan)*, **23**, 643 (1965); *Chem. and Ind.*, **19**, 787 (1967).
7) B. Baysal and A. V. Tobolsky, *J. Polymer Sci.*, **9**, 171 (1952).
8) F. R. Mayo, *J. Am. Chem. Soc.*, **65**, 2324 (1943).
9) D. H. McDaniel and H. C. Brown, *J. Org. Chem.*, **23**, 420 (1958).

Table 1. Chain-transfer constants (C) of nuclear substituted acetophenones in the polymerization of methyl methacrylate at 60°C

Substituent	σ	E_R	$C\times10^4$
p-CH_3O	−0.268	0.11	1.16
p-t-C_4H_9	−0.197	0.03	0.64
H	0.000	0.00	0.57
p-Cl	0.227	0.10	0.90
p-Br	0.232	0.12	1.15
m-Cl	0.373	0.08	0.83
p-CH_3CO	0.502	0.24	2.86 (1.43)*
p-CN	0.660	0.24	2.18

* This value indicates the value per CH_3CO group.

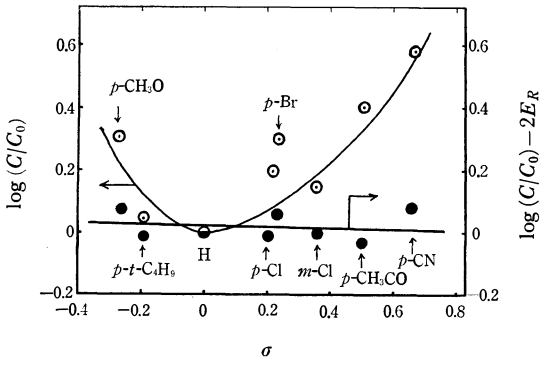

Fig. 1. Application of the Hammett equation and Eq. (1).

As is shown in Fig. 1, the ordinary Hammett plots for this reaction series failed to give a linear relationship. However, when the γ value in Eq. (1) was assumed to be 2.0, the plots with Eq. (1) gave linear relationship. From the slope of this line, the ρ value was obtained as nearly zero.

Table 2. Application of Eq. (1) to the chain-transfer reactions toward the PMMA radical at 60°C

Substrate	ρ	γ	Lit.
Cumenes	0.03	0.9	4)
Toluenes	0.01	0.6	10)
Dibenzoyl disulfides	0.07	0.75	11)
Diphenyl disulfides	0.01	0.75	12)
Phenylacetylenes	0.0	1.7	13)
Acetophenones	−0.01	2.0	This work

Table 2 summarizes the reaction constants obtained from the application of Eq. (1) to the chain-transfer reactions of various substrates toward the PMMA radical.

As can be seen from Table 2, the ρ values in these reactions are very small or are negligible in comparison with the γ values. This finding strongly demonstrates that the polar substitutent effect on the chain-transfer reactivities of these substrates toward the PMMA radical is rather small. On the other hand, the γ value in the present reaction series is much larger than those in the other reaction series. Therefore, it may be considered that the effects of substituents in the acetophenones on the chain-transfer reactivities toward the PMMA radical depend on the contributions of their resonance factors.

10) T. Yamamoto and T. Otsu, Presented at the 17 th Symposium on Organic Reaction Mechanism, Tokyo, October, 1966.
11) K. Tsuda and T. Otsu, This Bulletin, **39**, 2206 (1966).
12) T. Otsu, Y. Kinoshita and M. Imoto, *Makromol. Chem.*, **73**, 225 (1964).
13) H. Higashiura, Presented at the 14 th Annual Meeting of High Polymer Science, Tokyo, May, 1965.

Synthesis of Perylene

Satoshi IWASHIMA and Junji AOKI

Tokyo Yushi Ind. Co., Iidabashi, Tokyo,

and Department of Chemistry, Faculty of Science, Toho University, Narashino, Chiba

(Received April 1, 1968)

Perylene, $C_{20}H_{12}$(I), is of interest in the field of organic and physical chemistry. It is possible to synthesize larger polycyclic aromatic compounds from this hydrocarbon; also, perylene forms molecular compounds with various kinds of electron donors and acceptors, all of which are typical organic semiconductors.

In 1910, perylene was first prepared by heating 1,1'-dinaphthyl or naphthalene with aluminum chloride.[1] However, the yield was extremely poor. Therefore, many studies concerning the synthesis of perylene and its derivatives have been carried out by a number of workers, as is described in Schemes A, B, and C.

1) R. Scholl and R. Weitzenböck, *Mh. Chem.*, **43**, 2202 (1910).

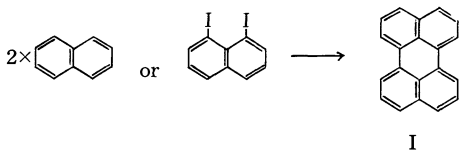

I

Scheme A

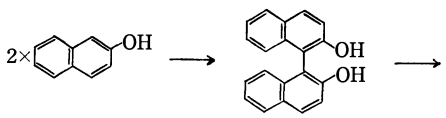

II

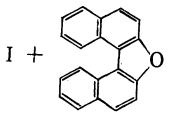

III

Scheme B

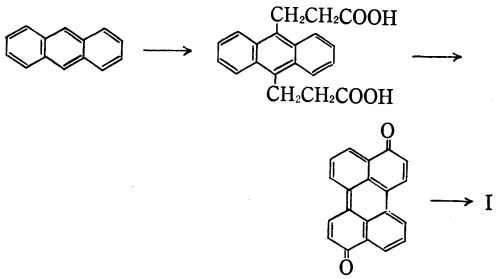

Scheme C

Of these methods, the A and C methods are very difficult to perform, and they yield only small percentages. The B method, in which the zinc-dust distillation is applied to β-dinaphthol (II), is a little easier to perform than the other two, but its yield is also low (3—7%) and purification is very difficult.

In this note, we will describe a method of preparing perylene which gives a good yield and a high purity. At first, we tried to improve the yields of perylene in the previous Schemes, A, B, and C, but we were unsuccessful. Secondly, we found that perylene is produced by the reduction of β-dinaphthylene oxide. This fact is interesting, but the yield is still low.

It has, however, also been found that perylene can readily be prepared by heating perylene tetracarboxylic acid anhydride (VI) with soda-lime in a vacuum. We denote this as Scheme D. This method gives a good yield of 80%, for the crude product has a high purity and purification can be readily carried out.

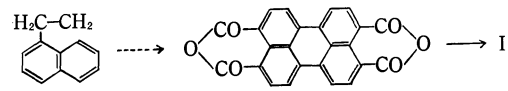

V VI

Scheme D

In addition, it has been reported that the decarboxylation of VI can also be carried out by heating it with 12% potassium hydroxide under pressure.[2] This method may also be considered a good method of preparing perylene, for it gives a considerable yield.

Experimental

The melting points are uncorrected.

Zinc-dust Fusion of β-Dinaphthylene Oxide (III). A mixture of 24 g of III, 16 g of zinc dust, 100 g of zinc chloride, and 20 g of sodium chloride was fused at 260°C for 20 min. After cooling, the mixture was dissolved in diluted hydrochloric acid. The insoluble part was collected, washed with water, and then dried. Fine, brownish-colored crystallites (2.0 g), extracted by hot xylene from this crude product, were sublimed *in vacuo* (10^{-3} Torr) and then recrystallized from xylene as yellow plates. The melting point of the crystal was 268—269°C (Ref. 1, 264—265°C). Yield, 1.5 g (6.6% of the theoretical amount).

Reduction of III by Martin's Method.[3] A mixture of 50 g of III, 125 g of zinc dust, 160 g of sodium hydroxide, 500 m*l* of xylene, and 2000 m*l* of water was refluxed for 20 hr. After the reaction mixture had cooled, the precipitate, containing zinc dust, was collected; this was then purified by a procedure similar to that described above. Yield, 3.6 g (7.7%) of fine, golden yellow plates; mp, 268—269°C.

Decarboxylation of Perylene Tetracarboxylic Anhydride (VI). A mixture of 1.00 g of VI[4] and 6 g of soda-lime was heated at 350°C for 1 hr; then, under a reducing pressure of 10^{-2} Torr, the temperature was raised to 440°C and kept there for 7hr. By the latter process, 0.60 g of fine, yellow crystals was obtained as a sublimate. This product was recrystallized from toluene, giving golden yellow plates. Yield, 0.51 g (80%); mp, 269.5°C (uncorr.), 280.3°C (corr.).

The authors wish to express their thanks to Professor Hiroo Inokuchi of the Institute for Solid State Physics, The University of Tokyo, for his kind advice.

2) N. Goto and Y. Koga, Presented at the 20th Annual Meeting of the Chemical Society of Japan, Tokyo, April 1, 1967; see also *D.R.P.* 486491 (1926).
3) E. L. Martin, *J. Am. Chem. Soc.*, **58**, 1441 (1936).
4) This material was prepared from acenaphthene (V) by the method reported by T. Maki *et al.* (*Kogyo Kwagaku Zasshi (J. Chem. Soc. Japan, Ind. Chem. Sect.)*, **54**, 480, 544 (1951)).

The Mössbauer Effect in Fe_3Sn_2

Sumio ICHIBA, Hiroshi SAKAI and Hisao NEGITA

Department of Chemistry, Faculty of Science, Hiroshima University, Hiroshima

(Received April 1, 1968)

In iron-tin alloys, the following intermetallic compounds have been reported to exist[1]: Fe_3Sn, Fe_2Sn, Fe_3Sn_2, FeSn and $FeSn_2$. Studies of the Mössbauer effect in these compounds, except for Fe_3Sn_2, have been performed by a number of workers,[2-6] because both constituents involve suitable nuclei.

Fe_3Sn_2 was shown to have a monoclinic structure with 40 atoms per unit cell and $a=13.5$Å, $b=5.34$Å, $c=9.20$Å, $\beta=103°$.[1] The Mössbauer parameters of both ^{57}Fe and ^{119}Sn nuclei in Fe_3Sn_2 are reported in this note.

Experimental

The alloy Fe_3Sn_2 was prepared by means of a sintering method. The powders of iron and tin were mixed in the stoichiometric proportion, pressed into a pellet, sealed in an evacuated quartz tube which was then heated at 800°C for a week and subsequently quenched in water. The phases which existed in the sample were identified as Fe_3Sn, Fe_3Sn_2 and β-Sn by X-ray diffractometry.

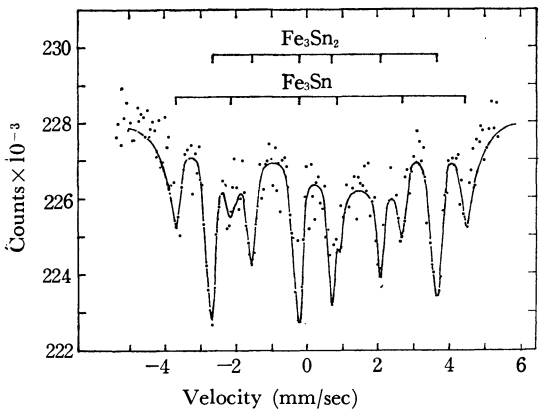

Fig. 1. Mössbauer absorption spectrum of ^{57}Fe in Fe_3Sn_2 at 24°C. The scale of the abscissa was taken toward ^{57}Fe in pure iron.

The ^{57}Fe Mössbauer spectrum of the sample at room temperature (source: ^{57}Co on Pd) is shown in Fig. 1. The spectrum shows the superimposed spectra of Fe_3Sn and Fe_3Sn_2. Table 1 gives the values of the relative velocity v of the source at which the maximum γ-ray absorption is observed for Fe_3Sn_2.

TABLE 1. THE RELATIVE VELOCITIES AND CORRESPONDING HYPERFINE COMPONENTS OF THE ABSORPTION LINE OBTAINED WITH THE SOURCE OF ^{57}Fe IN Pd AND Fe_3Sn_2 ABSORBER

hfs component	Transition	v, mm/sec
1	$+\frac{1}{2} \rightarrow +\frac{3}{2}$	-2.67 ± 0.03
2	$+\frac{1}{2} \rightarrow +\frac{1}{2}$	-1.55 ± 0.03
3	$+\frac{1}{2} \rightarrow -\frac{1}{2}$	-0.27 ± 0.03
4	$-\frac{1}{2} \rightarrow +\frac{1}{2}$	-0.69 ± 0.03
5	$-\frac{1}{2} \rightarrow -\frac{1}{2}$	2.08 ± 0.03
6	$-\frac{1}{2} \rightarrow -\frac{3}{2}$	3.63 ± 0.03

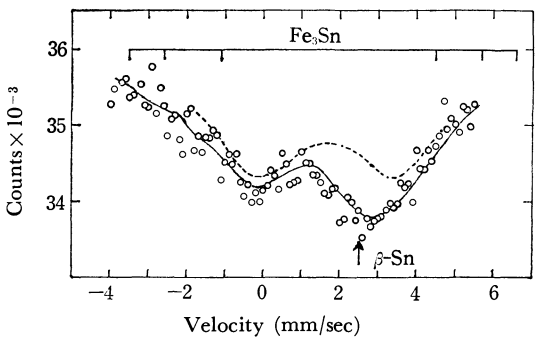

Fig. 2. Mössbauer absorption spectrum of ^{119}Sn in Fe_3Sn_2 at 24°C.

From the data in Table 1 the Mössbauer parameters of ^{57}Fe in Fe_3Sn_2 can be estimated as follows: isomer shift, $\delta=0.37\pm0.01$ mm/sec (relative to pure iron); quadrupole splitting, $2\varepsilon=0.21\pm0.02$ mm/sec; internal magnetic field, $H_i=196\pm3$ kOe; magnetic splitting of the ground level, $\alpha=2.30\pm0.03$ mm/sec; and magnetic splitting of the excited level, $\beta=1.33\pm0.03$ mm/sec. The ratio $\alpha/\beta=1.72\pm0.04$ is in good agreement with the value reported by Nikolaev *et al.*[4] for $FeSn_2$ and also with that by Kistner and Sunyar[7] for Fe_2O_3.

1) M. Hansen, "Constitution of Binary Alloys," McGraw-Hill Book Co., New York, N. Y. (1958).
2) C. Djega-Mariadassou, P. Lecocq, G. Trumpy, J. Täff and P. Cstergaard, *Nuovo Cimento*, **46B**, 35 (1966).
3) H. Yamamoto, *J. Phys. Soc. Japan*, **21**, 1058 (1966).
4) V. I. Nikolaev, Yu. I. Shcherbina and S. S. Yakimov, *Soviet Phys. JETP*, **18**, 878 (1964).
5) G. Fabri, E. Germagnoli, M. Musci and G. C. Locati, *Nuovo Cimento*, **40B**, 178 (1965).
6) O. C. Kistner, A. W. Sunyar and J. B. Swan, *Phys. Rev.*, **123**, 179 (1961).
7) O. C. Kistner and A. W. Sunyar, *Phys. Rev. Letters*, **4**, 412 (1960).

Figure 2 shows the ^{119}Sn Mössbauer spectrum of the sample at room temperature for 23.8 keV γ-ray against the $^{119m}SnO_2$ source. This spectrum also shows the superimposed spectra of Fe_3Sn, β-Sn and Fe_3Sn_2. The two peaks in the center of the spectrum are thought to be due mainly to β-Sn and Fe_3Sn_2, because the absorption peaks of Fe_3Sn are situated far from the center. Then, the ^{119}Sn Mössbauer spectrum of Fe_3Sn_2 can be obtained by subtracting the β-Sn absorption from the peak. The resulting spectrum is shown by the dotted line in Fig. 2. In this case, the spectrum cannot be resolved into its hyperfine structure. However, the value of the internal magnetic field can be estimated to be about 38 kOe by using together values for the magnetic moment of -1.0411 ± 0.002 nm for the ground state and $+0.672\pm0.025$ nm for the first excited state of ^{119}Sn obtained by Kistner.[6] The isomer shift δ is found to be about 1.7 mm/sec.

The authors are indebted to Dr. Yutaka Maeda of the Research Reactor Institute of Kyoto University for the measurement of the Mössbauer spectra of ^{57}Fe.

Zone-Refining of Phenanthrene and Studies on the Purity*[1]

Shoichi MATSUMOTO

Central Research Laboratory, Tokyo Shibaura Electric Co., Ltd., Komukai, Kawasaki, Kanagawa

(Received April 9, 1968)

There is no available organic solid from commercial products which is in a state of such purity as is enough for the investigation of semiconductive properties. Thus, the purification of a specimen becomes a matter of special importance in the field of organic semiconductors; there have recently begun to appear many papers handling specimens of the utmost purity obtained by zone-refining.[1-5]

This paper deals with the practice of zone-refining of phenanthrene, which was adopted as the specimen of the experiments in the preceding papers,[6,7] and also studies on the purity of the purified specimen.

Experimental

The starting material was phenanthrene of a chemical purpose-grade obtained from Eastman Kodak Co. This material is henceforward denoted as phenanthrene C.

Phenanthrene C was at first recrystallized from an ethanol solution; phenanthrene R stands for the product after the four times recrystallization.

The zone-refining was carried out by using a modified zone-melting apparatus of the type designed by Herington, Handley and Cook.[8,9] The essential features of our apparatus are given in Fig. 1: the cycle of a slow and fast pass of the heater carriage can be continued automatically in our apparatus.

Phenanthrene R was loaded into a Telex-glass tube with an inner diameter of 10 mm, and the tube was sealed under a vacuum after it had been evacuated at 10^{-5} mmHg for eight hours. Then, the phenanthrene in the tube was automatically subjected to a number of zone-passes by the apparatus described above. The-

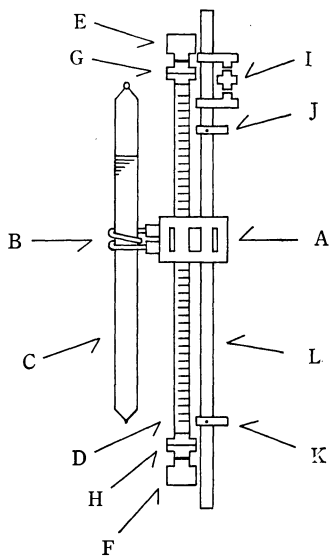

Fig. 1. Automatic zone-melting apparatus.
A: Heater carriage, B: Wire wound heater, C: Zone-tube, D: Drive shaft, E: Slow motor, F: Fast motor, G and H: Solenoid clutch, I: Micro switch, J and K: Limit switch, L: Control rod.

*1 Presented at the Symposium on Molecular Structure, Sapporo, October, 1967.

1) R. G. Kepler, *Phys. Rev.*, **119**, 1226 (1960).
2) N. Parkyns and A. R. Ubbelohde, *J. Chem. Soc.*, **1960**, 4188.
3) G. P. Brown and S. Aftergut, *J. Chem. Phys.*, **38**, (1963).
4) I. Nakada, K. Ariga and A. Ichimiya, *J. Phys. Soc. Japan*, **19**, 1587 (1964).
5) P. A. Andrews, A. F. Armington and B. Rubin, *Appl. Phys. Letters*, **7**, 86 (1965).
6) S. Matsumoto and T. Fukuda, This Bulletin, **40**, 743 (1967).
7) S. Matsumoto, *ibid.*, **40**, 2749 (1967).
8) E. F. G. Herington, R. Handley and A. J. Cook, *Chem. Ind.*, **1956**, 292.
9) P. Heneage and W. W. Taylor, U. S. Pat. 2990257 (1961).

molten zone about 5 mm long was controlled to move slowly downward at a speed of 20 mm per hour.

The zone-rod of the phenanthrene after being subjected to 130 zone-passes (denoted as phenanthrene Z), with a total length of 130 mm in a Telex-glass tube, was cut into eight sections with a length of about 15 mm, and the phenanthrene of each section was denoted as phenanthrene Z-0, phenanthrene Z-1, ···, and phenanthrene Z-7 from the bottom of the zone-tube.

Results and Discussion

Purification and Electronic Spectra. All electronic spectra were measured in cyclohexane of a spectro-grade with a Cary Model-14 recording spectrophotometer, using 1 cm quartz cells. The variation of the electronic spectrum of phenanthrene Z observed according to distance along the zone-rod is shown in Fig. 2, where the spectra of phenanthrene Z-0, Z-3, Z-5, and Z-7 are represented, and they are accompanied with the spectrum of anthracene of a zone-grade (Tokyo Kasei Co.).

The electronic spectrum of phenanthrene Z near the bottom of the zone-tube, *e.g.*, phenanthrene Z-0, agrees with the spectrum of phenanthrene reported in the literatures,[10,11] while as for the spectrum of the phenanthrene Z in the distance far from the bottom of the tube, *e.g.*, phenanthrene Z-5 and Z-7, there appear four absorptions at 376, 371, 356, and 352 mμ which are not assigned to the spectrum of phenanthrene. These four absorptions become more intensified according to an increase in distance from the bottom of the zone-tube.

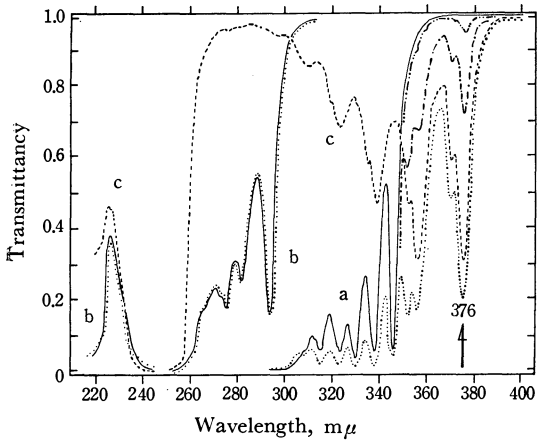

Fig. 2. Variation of the electronic spectrum of phenanthrene Z according to distance along the zone-rod (—— Z-0, —··— Z-3, —·— Z-5, ····· Z-7) and the spectrum of anthracene of a zone-grade purity (----). Symbols a, b for 5.05×10^{-3}, 5.05×10^{-5} mol/l phenanthrene solutions; symbol c for 4.24×10^{-5} mol/l anthracene solution.

Here, it was investigated from which compound among the probable impurities of acenaphthene, anthracene, carbazole, and fluorene, these four absorptions were originated. As a result, these absorptions in question were proved to correspond to the para-bands of anthracene,[11] and further it seemed very improbable spectroscopically that the above-mentioned impurities other than anthracene were present.*2 Therefore, anthracene may be a main impurity in the phenanthrene R.

Purification and Infrared Spectra. The variation of the infrared spectrum of phenanthrene Z according to distance along the zone-rod was investigated further to confirm the preceding results. The representative spectra of phenanthrene Z-0, Z-3, Z-5, and Z-7 are shown in Fig. 3, together with the spectrum of the zone-grade anthracene; it is observed that the absorption to be assigned to the very intensitive absorption at 882 cm^{-1} which is characteristic of anthracene and belongs to out of plane CH-bending vibrations of

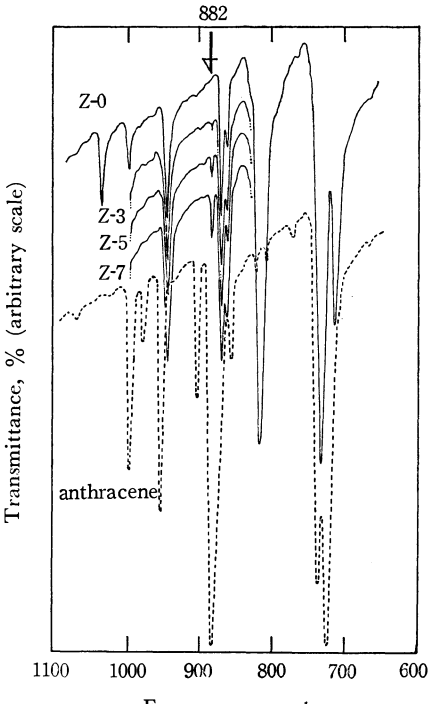

Fig. 3. Variation of the infrared spectrum of phenanthrene Z according to distance along the zone-rod and the spectrum of anthracene of a zone-grade purity.

10) E. Clar, *Spectrochim. Acta*, **4**, 116 (1950).
11) R. A. Friedel and M. Orchin, "Ultraviolet Spectra of Aromatic Compounds," "John Wiley & Sons, Inc., New York (1951).

*2 The relative intensity of the absorption at 352 mμ among the four absorptions seems to be rather stronger, compared with the corresponding one in the parabands of anthracene, but at the present time a reasonable explanation for it is not available.

it,[12] appaers at the same wave number in the spectrum of phenanthrene Z in the distance far from the bottom of the zone-tube, *e. g.*, phenanthrene Z-5 and phenanthrene Z-7.

The intensity of this absorption at 882 cm^{-1} increases with an increase in distance from the bottom of the zone-tube, while the spectrum of each phenanthrene Z is practically identical with each other except at 882 cm^{-1}. All absorptions other than that at the wave number in question in the spectrum of each phenanthrene Z shown in Fig. 3 coincide with those in the spectrum of phenanthrene reported in the literatures. These observations in the infrared spectroscopy are consistent with the result derived from the electronic spectroscopy, that anthracene is a main impurity in the phenanthrene R.*3

The infrared spectra were measured in the region 4000—650 cm^{-1} with a Jasco DS-402 G infrared spectrophotometer, and a potassium bromide disk method was employed.

Concentration-Distribution of Anthracene in the Zone-Rod. The quantity of anthracene as an impurity in each phenanthrene Z was spectroscopically evaluated by employing the absorption at 376 mμ after Beer's law was confirmed to be valid at this wavelength for the cyclohexane solution of phenanthrene containing a minute quantity of anthracene.

Figure 4 shows the resultant concentration-distribution of anthracene in phenanthrene Z; the concentration in moles of anthracene per one mole of phenanthrene (denoted as M) is plotted as the ordinate, and the distance measured from the bottom of the zone-tube is plotted as the abscissa, together with the corresponding position of the section of each phenanthrene Z. As to the concentration of anthracene in phenanthrene Z-0, 7×10^{-6} M was graphically estimated. The result reveals that anthracene travelled in the direction opposite to the direction of zone-travel and aggregated towards the top of the zone-tube.

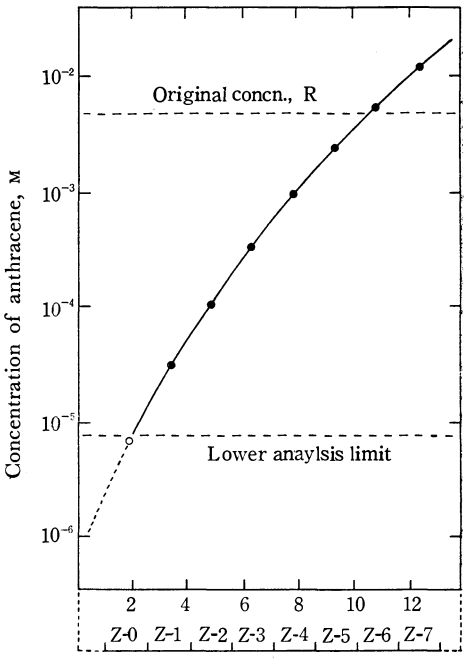

Fig. 4. Concentration-distribution of anthracene in the zone-rod of phenanthrene Z.

As for phenanthrene C and phenanthrene R, the concentration of anthracene was also analyzed spectroscopically; it was evaluated as 1.1×10^{-2} M and 5.6×10^{-3} M, respectively.

The extremely low concentration of anthracene observed at near the bottom of the zone-tube, 10^{-6}—10^{-5} M, indicates the effectiveness of the zone-melting with a sufficient number of zone-passes for the purification of phenanthrene containing anthracene which has been proved to be difficult by the conventional methods of purification.

12) M. Randic, *J. Chem. Phys.*, **33**, 710 (1960).

*3 It should be kept in mind that there is the possible presence of some impurities which could not be spectroscopically detected.

The Formation of Salicylonitrile *via* the Thermal Decomposition of Bis(salicylaldimine)copper

Akira MISONO and Seiichiro KODA

Department of Industrial Chemistry, Faculty of Engineering, The University of Tokyo, Hongo, Bunkyo-ku, Tokyo

(Received April 10, 1968)

It is well known that the bis(salicylaldimine)-copper is a stable chelate. But the thermal properties of this chelate have not been fully studied. The authors have investigated on the preparation of nitriles from aldehydes and ammonia,[1] the reaction catalysed by a copper cation, for example, and also on the thermal properties of copper halide complexes of ketimines.[2] In due course, the bis(salicylaldimine)copper is expected to yield salicylonitrile through the thermal decomposition. Wendlandt *et al.*[3] investigated on the thermal decomposition of this chelate and reported that this chelate decomposed at high temperatures with evolving water, carbon monoxide, carbon dioxide and nitrogen. But they did not studied the fate of the ligand fully. Then, the present authors tried to detect salicylonitrile among the decomposition products.

The differential thermal analysis and thermogravimetric analysis were carried out and the results are shown in the Fig. 1. At about 215—240°C, the decomposition reaction proceeded, as was reported previously by Wendlandt.[3]

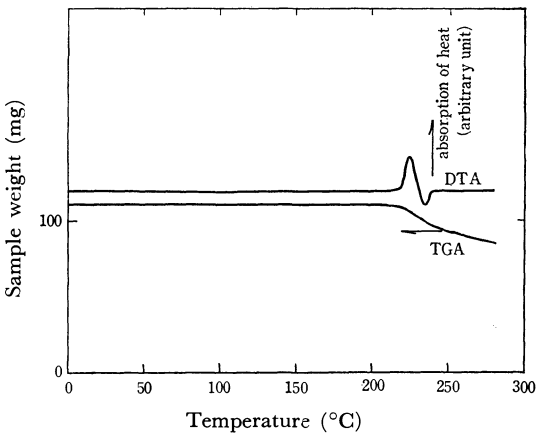

Fig. 1. The differential thermal analysis (DTA) and the thermogravimetric analysis (TGA). Heating rate: 2.5°C/min under a dynamic nitrogen atmosphere the reference: α-alumina.

The chelate was set at the bottom of an ample under reduced pressure at 220°C; the volatile decomposition products were trapped on the water-cooled wall of the upper part of the ample. From the trapped material, a considerable amount of salicylonitrile (nearly the half of the total amount of the ligand contained) was obtained after suitable treatments. Among the trapped material, some resinous products were also found. The unvolatile part was dark purple in color after the decomposition reaction, which contained metallic copper.

The thermal decomposition may proceed through the internal oxidation-reduction, in which the central cation is reduced to its metallic form and the coordinated ligands lose their some hydrogen atoms by oxidation and yield the nitrile as the main product. Some residual products may contain the further reaction products of the nitrile. It has been made clear that the coordinated imino group could be dehydrogenated to the cyano group by the action of the central cation.

Experimental

The bis(salicylaldimine)copper(II) was synthesized according to Tyson and Adams.[4] (Found: C, 55.66; H, 4.05; N, 9.39%)

The chelate, 2.98 g (9.8 mmol) in weight, was set in the bottom of an ample, the upper part of which was cooled with water. The lower part of the ample was heated at about 220°C for 3 hr under reduced pressure (about 1 mmHg). The yellow material trapped on the water-cooled wall was dissolved into acetone (yield, 1.78 g). The infrared spectrum of this material showed a strong absorption signal at about 2220 cm^{-1} assigned as the C≡N stretching (other main signals at about 3400—3000 (broad), 1605, 1460, 1310, 1280, 1240, 1160, 1030, 860, 850, 755 cm^{-1}: KBr disc method), but was not fully identical with that of a pure salicylonitrile. Salicylonitrile as the product was isolated according to the following procedure. The ether solution of the trapped material was treated with aqueous sodium hydroxide, and then the aqueous part was separated and acidified by hydrochloric acid. The aqueous solution thus obtained was again extracted with ether, and from the ethereal part, a yellow solid was obtained after evaporating the solvent. Its infrared spectrum was almost identical with that of a pure salicylonitrile (main signals at about 3290, 2220, 1605, 1505, 1460, 1360, 1310, 1275, 1240, 1160, 1100, 850, 750,

1) A. Misono, T. Osa and S. Koda, This Bulletin, **40**, 912 (1967); *ibid.*, 2875 (1967).
2) *Ibid.*, **41**, 373 (1968).
3) W. W. Wendlandt, S. I. Ali and C. H. Sternbridge, *Anal. Chim. Acta*, **30**, 84 (1964).
4) G. N. Tyson and S. C. Adams, *J. Am. Chem. Soc.*, **62**, 1228 (1940).

735 cm^{-1}: KBr disc method). Gross yield, 0.98 g (8.2 mmol) Recry. from toluene after the treatment with activated carbon. Mp 95.7—96.5°C (the mixture with an authentic salicylonitrile showed the identical melting point), lit.[5] 96°C.

Found: C, 70.68; H, 4.16; N, 11.95; O, 14.35%. Calcd for C_7H_5NO: C, 70.58; H, 4.23; N, 11.80; O, 13.34%.

5) M. Tanaka, *Nippon Kagaku Zasshi (J. Chem. Soc. Japan, Pure Chem. Sect.)*, **78**, 1385 (1957).

In the X-ray diffraction pattern (Rigaku-Denki Co., Ltd., Geigerflex D-8C) of the unvolatile part (yield, about 1 g), strong signals were observed at about 43.5, 50.5, 74.0 and 90.0° of 2θ, which coincide with the signals of metallic copper. No other remarkable signals were observed.

The thermal analyses (TGA, DTA) were carried out with Rigaku-Denki Co., Ltd., differential thermal and thermogravimetric analyser. The decomposition was observed in a dynamic nitrogen atmosphere, at a heating rate of 2.5°C/min. Sample weight, 111 mg.

Short-range Dating of Fresh Nuclear Debris by the Activity Ratio of Iodine-133 to Iodine-131

Takeshi SOTOBAYASHI, Toshio SUZUKI and Seitaro KOYAMA

Department of Chemistry, Faculty of Science, University of Niigata, Niigata

(Received April 10, 1968)

In order to investigate the radiochemical composition at time-zero of short-lived radionuclides in fallout particles and its time variation shortly after a nuclear test explosion, it is necessary to determine as accurately as possible the age of the fallout particles. Fresh nuclear debris particles usually consist mainly of short-lived nuclides, such as ^{97}Zr, ^{99}Mo, ^{143}Ce, ^{132}Te-^{132}I, ^{133}I and ^{239}Np. Recently we proposed a simple method for the short-range dating of fresh nuclear debris;[1] this method was successfully carried out by the determination of the activity ratio of ^{97}Zr to ^{95}Zr at a given time 2—7 days after a nuclear explosion.

Results and Discussion

According to the radiochemical composition of short-lived fission products present in hot fallout particles, the particles can be grouped roughly into two classes. The first is enriched with refractory nuclides, such as ^{97}Zr, ^{99}Mo, and ^{144}Ce, and depleted in volatilely-behaving ones, such as ^{132}Te-^{132}I and ^{133}I. The second shows the reverse trend regarding the enrichment of these nuclides; that is, refractory nuclides are depleted and volatile ones, enriched. In many cases these two different types of particles were not found at the same time among hot particles or in rain samples resulting from a given nuclear test explosion, but one of the two types was detected shortly after a nuclear detonation. The first type of particles was recently found among the fallout particles derived from the May 9, 1966, Chinese nuclear test explosion[2] and the second, in the particles (Fig. 1) and rain samples from the December 28, 1966, Chinese nuclear test. Figure 1 shows three γ-ray spectra of a hot particle collected on December 30, 1966; the spectra, A, B, and C, were measured 9, 28 and 37 days after the explosion, respectively. From these spectra it is obvious that this particle consisted mainly of ^{103}Ru, ^{132}Te-^{132}I, ^{133}I, and ^{239}Np, and that it contained no detectable amounts of ^{95}Zr-^{95}Nb or, hence, of ^{97}Zr-^{97}Nb.

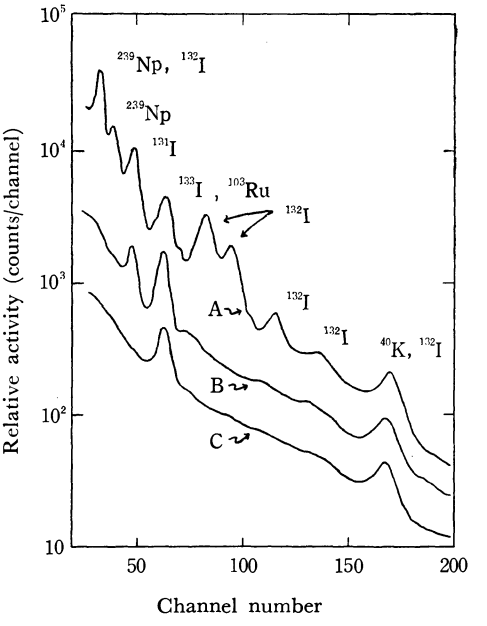

Fig. 1. Gamma-ray spectra of a fallout particle from the December 28, 1966, Chinese nuclear explosion. The spectra A, B and C were measure on January 6, 25 and March 3, 1967 respectively.

1) T. Sotobayashi, T. Suzuki and S. Koyama, *Nature*, **215**, 728 (1967).
2) T. Sotobayashi, T. Suzuki and S. Koyama, This Bulletin, **40**, 1555 (1967).

The $^{97}Zr/^{95}Zr$ dating method is not suitable for the radioiodine-rich particle shown in Fig. 1 because of the very great trouble needed to collect a number of fallout particles large enough for the activity ratio to be determined with sufficient accuracy. In the present work, therefore, we have especially examined two isotopes, ^{133}I and ^{131}I, present in large quantities in the particles in question. The ^{133}I and ^{131}I isotopes decay, with 20.8-h and 8.05-d half-lives, to ^{133}Xe and ^{131}Xe, respectively. Thus, we can expect the $^{133}I/^{131}I$ activity ratio to provide a radioactive clock very sensitive to small differences in time. The two mass chains, 133 and 131, are relatively complex compared with those for 97 and 95:

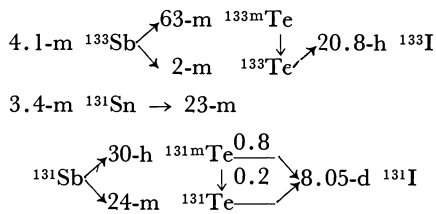

At the earlier stages of the formation processes of fallout particles, it seems that the two nuclides, ^{133}I and ^{131}I, still remain in the forms of ^{133}Sb and ^{131}Sn, respectively; this is on the assumption that the time taken for fission products to condense and to form a fallout particle is 40 sec or less after an explosion.[3] The melting points of antimony and tin are 630 and 230°C, respectively, and the solidification temperature of the carrier material (silicate soil) of fallout particles can reasonably be considered to be ~1700°C.[4] Taking these points into consideration, we will show here that the requirements for a successful dating are fulfilled by the ^{133}I and ^{131}I fission fragments extracted from the particles or rain samples resulting from the December 28, 1966, explosion.

Highly-radioactive fallout particles and rain-water samples were collected at Niigata between December 30, 1966, and January 2, 1967. One particle and 3 rain samples were submitted to preliminary treatment for chemical separation. The sample solutions thus obtained (1 M HNO_3) were then analyzed by the HNO_2-CCl_4 extraction method. The activities of the purified radioiodines in the form of silver iodide were measured using a $1\frac{3}{4}$ in $\times$ 1 in NaI(Tl) scintillation detector with a 200-channel pulse-height analyzer, and were determined by measuring the areas of the photopeaks at 0.36 and 0.53 MeV.

Figure 2 shows the activity ratios of ^{133}I to ^{131}I as a function of the time 2—10 days after the explosion. The solid line in this figure was drawn

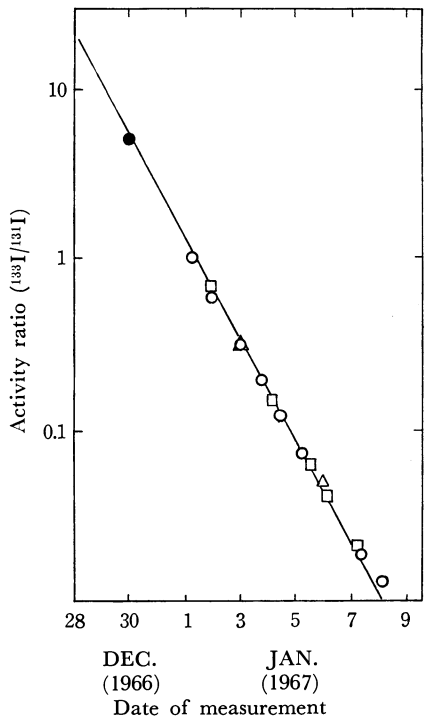

Fig. 2. Activity ratios of ^{133}I to ^{131}I as a function of time 2-10 days after the explosion.
●, a particle sample collected on Dec. 30, 1966
○, a rain sample collected on Dec. 31, 1966
□, a rain sample collected on Jan. 1, 1967
△, a rain sample collected on Jan. 2, 1967

against the time on the assumption that the cumulative fission yields of ^{133}I and ^{131}I are 6.9 and 3.1, respectively.[5] Further, the Chinese nuclear bomb was estimated to have been blasted at 14 : 30 h on December 28, 1966 (Japanese time), by the $^{97}Zr/^{95}Zr$ method.[1] We regarded this estimated time of explosion as the time-zero of the nuclear fission event because the exact time of the explosion was not announced by the Chinese agency responsible. It can clearly be seen in Fig. 2 that most of the measured ratios lie nearly along the assumed line. This finding suggests that, in spite of some differences in the physical and nuclear properties of each first member for the two mass chains, 133 and 131, no significant fractionation occurred between ^{133}I and ^{131}I during the formation of fallout particles. As a result, the dating method by the activity ratio $^{133}I/^{131}I$ is well suited for the short-range dating of fresh nuclear debris of the second type.

In conclusion, when any kind of fresh nuclear debris is found shortly after a nuclear explosion, either of the two dating methods will enable us to determine readily the age of this fresh nuclear debris with sufficient accuracy.

3) R. S. Clark, K. Yoshikawa, M. N. Rao, B. D. Palmer, M. Thein and P. K. Kuroda, *J. Geophys. Res.*, **72**, 1793 (1967).
4) S. H. Cassidy and G. R. Crocker, USNRDL-TR-67-70, 8 (1967).
5) S. Katcoff, *Nucleonics*, **16**, 78 (1958).

The Intramolecular Hemiacetal Structure of Benzoyl-(2-hydroxybenzoyl)methyl Bromide*1

Heitaro OBARA and Jun-ichi ONODERA

Department of Applied Chemistry, Faculty of Engineering, Yamagata University, Yonezawa

(Received April 12, 1968)

During the course of their studies of the properties of benzoyl(2-hydroxybenzoyl)methyl bromide (II), which was afforded from benzoyl(2-hydroxybenzoyl)methane (I) by bromination in a chloroform solution in the presence of potassium carbonate, the present authors found that a ring-chain tautomerism exists between II and its cyclic hemiacetal structure (III). II was prepared by Hlavka,[1] in 1965, from I by bromination with *N*-bromosuccinimide in a chloroform solution for the purpose of its photolysis, and it has been reported that this bromide converts easily into 3-benzoylcoumaranone (IV)[2] and 3-bromoflavone (V)[3] with a base or an acid respectively.

However, no investigation has been made concerning its cyclic hemiacetal structure. In order to ascertain this tautomerism, the NMR, IR and UV spectra of this bromide and its homologue will be discussed in the present paper.

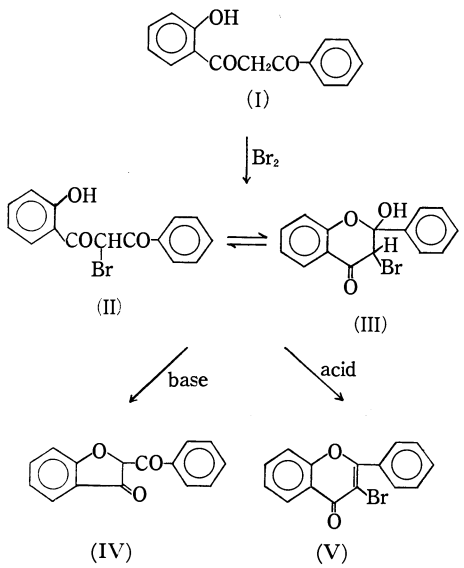

Results and Discussion

The NMR spectrum of this bromide in $CDCl_3$ exhibits four groups of signals (a, b, c, and d) in addition to the aromatic proton groups (6.65 ppm—8.20 ppm), as is shown Fig. 1. From the fact that the a and d bands disappear after the D_2O exchange, the a peak on the lowfield side of these bands was attributed to the hydrogen bonding phenolic OH proton in II, while the d peak was attributed to the hemiacetal OH proton in III. The c band was assigned by comparing it with the signal due to the -COCHBrCO- proton in dibenzoyl methyl bromide,*2 and the b band was assigned to the -COCHBr- proton in the hemiacetal (III).

From the relative peak areas of a, b, c, and d, the molar ratio of the tautomer II and III in this case was found to be approximately 3 : 11.

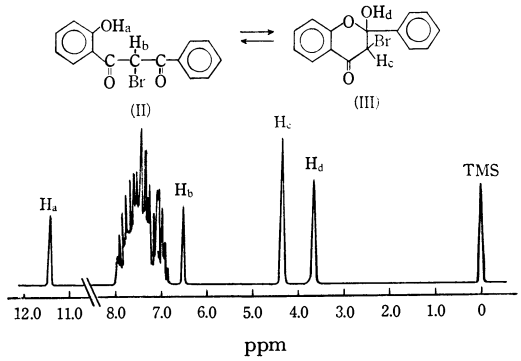

Fig. 1

The IR spectrum of this bromide in a chloroform solution gave an interesting result in the 1600 cm^{-1}—1700 cm^{-1} region. It showed a strong carbonyl absorption band at 1678 cm^{-1} immediately after it had been dissolved in chloroform; however, this absorption band decreased slowly with the lapse of time, and a new absorption band appeared at 1634 cm^{-1} and then remained unchanged for at least 4 hr (Fig. 2). It is considered that this new band is a characteristic absorption band due to the intramolecular chelated carbonyl group in the structure II which is observed in aromatic *o*-hydroxyketones.[4]

*1 Presented at the Tohoku Local Meeting of the Chemical Society of Japan, Hirosaki, October, 1967.

1) J. J. Hlavka, *Chem. Ind.*, **1965**, 1500.

2) T. A. Geissman and Ardy Armen, *J. Am. Chem. Soc.*, **77**, 1623 (1955).

3) Hrishikesh Krishna Pendse, *Rasâyanam.*, **2**, 121 (1956); *Chem. Abstr.*, **51**, 5063 (1957).

*2 This bromide was prepared by the bromination of dibenzoylmethane, mp 92—93°C.

4) L. J. Bellamy, "The Infra-red Spectra of Complex Molecules," John Wiley & Sons, Inc., New York (1958), p. 143.

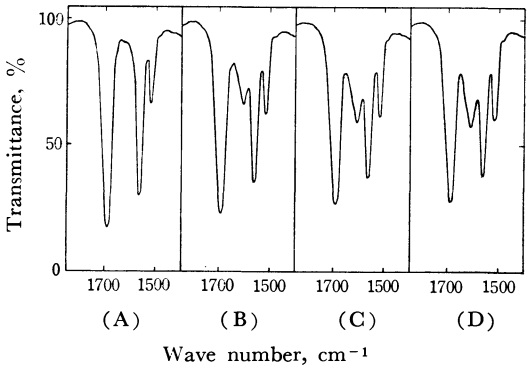

Fig. 2. The variation of the IR spectra of (II) with time in $CHCl_3$.
A: Immediately after dissolving. B: After 10 min. C: After 30 min. D: After 4 hr.

From the results of these IR spectra measurements, it is expected that this bromide has the structureIII before dissolving, and that it reaches equilibrium between II and III in a solution. It seems to be a very valuable result that the variation in such ring-chain tautomerism between II and III was observed in the IR spectrum measurements. On the other hand, the IR spectrum of this bromide in a KBr disk is similar to those of flavanone (VI) and 3-hydroxyflavanone (VII), and there is no chelated carbonyl absorption band near 1634 cm^{-1}, which would be expected if the structure of this bromide were II (Fig. 3).

From these observations, the cyclic hemiacetal structure III rather than II must be given for this bromide in the crystalline state. Accordingly, it is presumed that the strong peak of this bromide shown at 3270 cm^{-1} in Fig. 3 is not a phenolic OH peak but a hemiacetal OH-stretching peak.

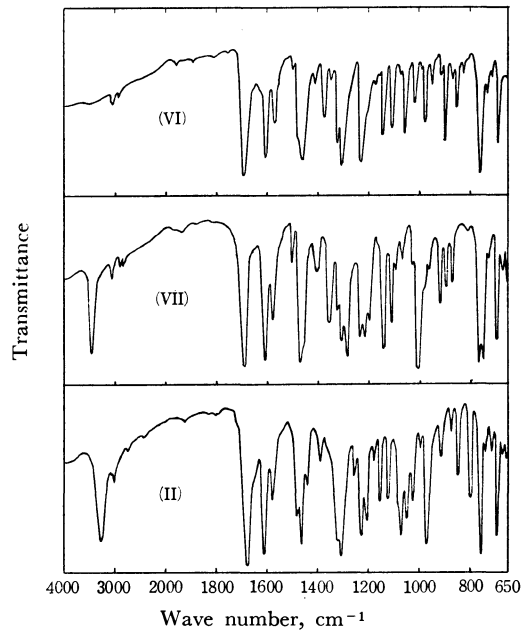

Fig. 3. The IR spectra of flavanone (VI), 3-hydroxyflavanone (VII) and benzoyl(2-hydroxybenzoyl)methyl bromide (II) in KBr disks.

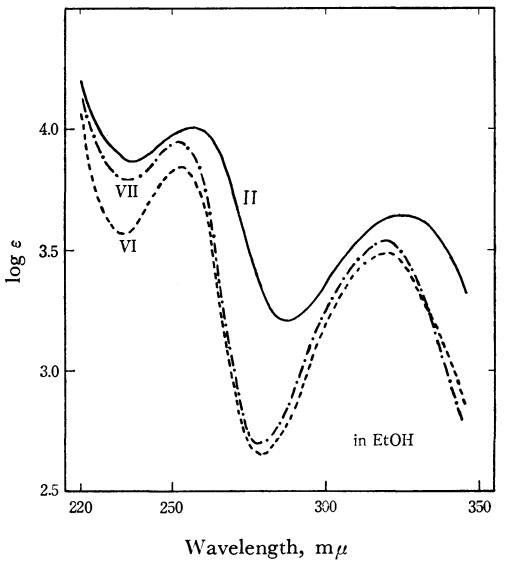

Fig. 4. The UV spectra of benzoyl(2-hydroxybenzoyl)methyl bromide (II); flavanone (VI) and 3-hydroxyflavanone (VII).

The UV spectrum of this bromide exhibits its absorption maxima at 257 mμ and 324 mμ in ethanol; the similarity of the absorption curve with those of flavanone (VI) and 3-hydroxyflavanone (VII) was observed.

Finally, the existence of ring-chain tautomerism in II and III was ascertained by the chemical

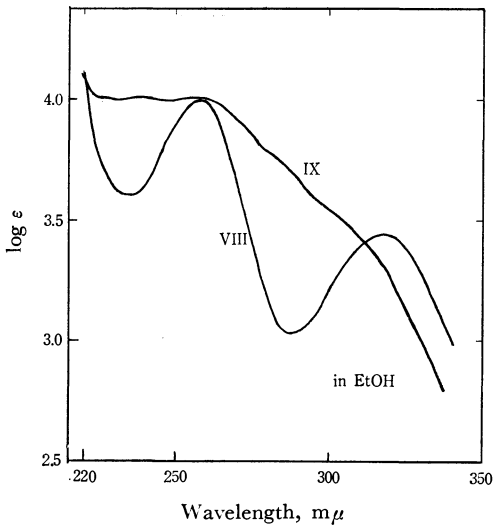

Fig. 5. The UV spectra of benzoyl(2-acetoxybenzoyl)methyl bromide (IX) and 2-acetoxy-3-bromoflavanone (VIII).

method. Two acetates were obtained from this bromide by acetylation with acetic anhydride in pyridine; one was crystalline (mp 151—152°C), and the other was a viscous oil, while both were analyzed as acetates of II or III.

The UV spectrum of the crystal acetate exhibits its absorption maxima at 257 mμ and 318 mμ, and its absorption curve is similar to those of flavanones (VI and VII); however, the oily acetate is not. (Fig. 5). The IR spectra of both acetates showed the same CO bands due to the acetyl groups at 1766 cm^{-1} and 1767 cm^{-1}, but two different CO bands were observed in the 1670 cm^{-1}—1700 cm^{-1} region (Fig. 6).

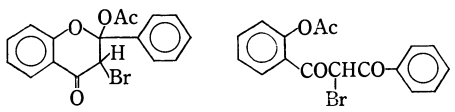

(VIII) (IX)

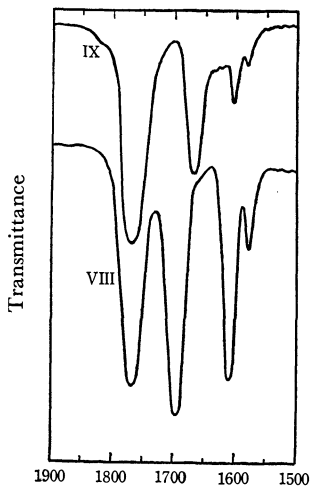

Fig. 6. The IR spectra of benzoyl(2-acetoxybenzoyl)methyl bromide (IX) and 2-acetoxy-3-bromoflavanone (VIII) in $CHCl_3$.

In these experiments, the ring-chain tautomerism between II and III was confirmed by NMR, IR and UV spectra measurements, and by the formation of two isomeric acetates; furthermore, it was proved that this bromide exists as the cyclic hemiacetal structure (III) *i. e.*, 2-hydroxy-3-bromoflavanone in the crystalline state.

Experimental

Benzoyl(2-hydroxybenzoyl)methyl Bromide (II). A solution of 1.0 g of bromine in 8 m*l* of chloroform was stirred into a mixture of 1.40 g of benzoyl(2-hydroxybenzoyl)methane (I) and 2.5 g of anhydrous potassium carbonate in 60 m*l* of chloroform at 0°C. After the addition was completed, the reaction mixture was filtered, and the filtrate was evaporated *in vacuo*. Ligroin was added to the oily residue, which was then allowed to stand overnight in an ice box. By the recrystallization of the resulting pale yellow solid from chloroform-ligroin, 1.29 g of II were afforded as colorless needles. Mp 141°C. Reported mp 145—146°C[1] IR (KBr), 3270 cm^{-1} (ν OH), 1678 cm^{-1} (ν CO). UV λ_{max}^{EtOH} mμ (log ε), 257 (4.01), 324 (3.65).

Found: C, 56.63; H, 3.70%. Calcd for $C_{15}H_{11}O_3Br$: C, 56.45; H, 3.47%.

Formation of 2-Benzoylcoumaranone (IV) and 3-Bromoflavone (V). a) II was converted to yellow crystals by heating it with pyridine at 75°C for 5 min. Recrystallization from methanol gave IV as yellow needles melting at 79—81°C. Reported mp 79—80°C.[2] IR (KBr), 1616 cm^{-1} (ν CO). UV λ_{max}^{EtOH} mμ (log ε), 241(4.05) 258(4.02) 348(4.21). b) To a solution of II in acetic acid, a drop of concentrated sulfuric acid was added, and the mixture was heated for 10 min at 100°C. It was then poured into water. The recrystallization of the resulting crystals from ethanol gave V as colorless needles melting at 124—125°C. Reported mp 126.5°C.[3] IR (KBr), 1660 cm^{-1} (ν CO). UV λ_{max}^{EtOH} mμ (log ε) 249 (4.27) 309 (4.09).

Acetylation of Benzoyl(2-hydroxybenzoyl)-methyl Bromide (II). To a solution of 500 mg of II in 5 m*l* of acetic anhydride, 2 drops of pyridine were added, after which the mixture was allowed to stand at room temperature for 2 days. The resulting yellow solution was poured into cold water, and the oily product was extracted with ether. The ether layer was washed with a dilute sodium hydrogencarbonate solution and water, and was dried over anhydrous sodium sulfate. The ether was removed by distillation, and the residue was chromatographed on a column of silica gel. Elution with ether-petroleum ether (2 : 1) gave 10 mg of 2-acetoxy-3-bromoflavanone (VIII) as colorless prisms. Mp 151—152°C. IR ($CHCl_3$), 1695, 1767 cm^{-1}. UV λ_{max}^{EtOH} mμ (log ε) 257 (4.01) 318 (3.45).

Found: C, 56.62; H, 3.68%. Calcd for $C_{17}H_{13}O_4Br$: C, 56.53; H, 3.63%.

Continuing elution with the same eluents yielded 23 mg of white crystals, which were identified as 3-bromoflavone (V) by means of their IR spectra, their melting points, and a mixed melting point determination with an authentic sample (mp 124—125°C). Using the same procedure from the last eluents 234 mg of benzoyl-(2-acetoxybenzoyl)methyl bromide (IX) were afforded as viscous oil. IR ($CHCl_3$) 1672, 1766 cm^{-1} (ν CO). UV λ_{max}^{EtOH} mμ (log ε) 237 (4.04) 257 (4.03).

Found: C, 56.63; H, 3.91%. Calcd for $C_{17}H_{13}O_4Br$: C, 56.53; H, 3.63%.

The authors wish to express their thanks to Professor Tetsunosuke Nishi for his encouragement and to Professor Ichiro Murata for the NMR spectra. They are also grateful to Mr. Hajime Baba for supplying the flavanones and to Miss Chiyo Itô for her technical assistance.

The Reactions of 4-Thiazone Imine Hydrochlorides with Amines[1]

Shigeru SATO and Masaki OHTA

Laboratory of Organic Chemistry, Tokyo Institute of Technology, Ookayama, Meguro-ku, Tokyo

(Received April 24, 1968)

In the preceding paper of this series,[2] it was reported that mesoionic compounds with an exocyclic imino group such as thiazone imine and sydone imine are stable only in the forms of salts or of *N*-acyl derivatives and do not exist in the form of free bases.

The treatment of 2-phenyl-3-*p*-chlorophenyl-4-thiazone imine hydrochloride (I) with sodium bicarbonate afforded cyanomethyl *N*-(*p*-chlorophenyl)benzthioimidate (II), which could then be converted back into I by treating it with hydrogen chloride, while the treatment of 2,3-diphenylthiazone imine hydrochloride (III) with sodium bicarbonate gave only tarry substances, from which neither the expected cyanomethyl *N*-phenylbenzthioimidate (IV) nor the free base of the corresponding thiazone imine hydrochloride could be obtained. It seems that the nucleophilic attack of a base upon thiazone imine hydrochloride might not be simple; therefore we investigated the behavior of thiazone imine hydrochloride towards the nucleophilic attack of amines.

Results and Discussion

The treatment of III with triethylamine, pyridine, and sodium alkoxide afforded tarry substances in all cases. When the solution of III in aniline was allowed to stand overnight, and was then neutralized with hydrochloric acid, colorless needles (V) were separated out; the results of an elemental analysis of them were consistent with the formula resulting from the removal of hydrogen chloride from III. In the infrared spectrum of V a band at 3300 cm^{-1}, which may be due to an NH stretching vibration, and a band at 1540 cm^{-1}, due to an N=C stretching vibration, appeared. V showed characteristic absorptions at 275 mμ, (ε=36000) and 362 mμ, (ε=4800) in its ultraviolet spectrum, absorptions suggestive of an aromatic heterocyclic system. These spectral analyses suggest that Compound V may be 2-phenyl-4-anilinothiazole. In addition, in the NMR spectrum V had an absorption at 3.85 τ. On the basis that the proton of the 5-position of 2,4-dimethylthiazole exhibits a singlet at 3.34τ,[3] this absorption was attributed to the proton of the 5-position of the above structure for V. Very few 4-aminothiazole derivatives have been found in the literature,[4] and no 4-anilinothiazole derivatives have been known. Although the structure of V was not confirmed by an independent sythesis, it may possibly be supported by the elemental and spectral analyses.

The consideration that the formation of V might proceed through the intermediate IV led us to examine the reaction of IV with aniline. When IV was treated with aniline under the same reaction conditions as in the case of the reaction of III with aniline, V was obtained in a good yield. In order to investigate the role of aniline, other bases were used in the reaction with IV. The treatment of IV with *o*-toluidine also gave V; this fact showed that the anilino group of the 4-position of V was not derived from the aniline used as the solvent, but was rather derived by the rearrangement of IV. When dimethylaniline was used instead of aniline, the starting material was recovered. This fact suggests, further, that aniline participates in the rearrangement by forming an adduct with IV.

As a consequence, the mechanism of the formation of V may be formulated in the way pictured in Scheme I.

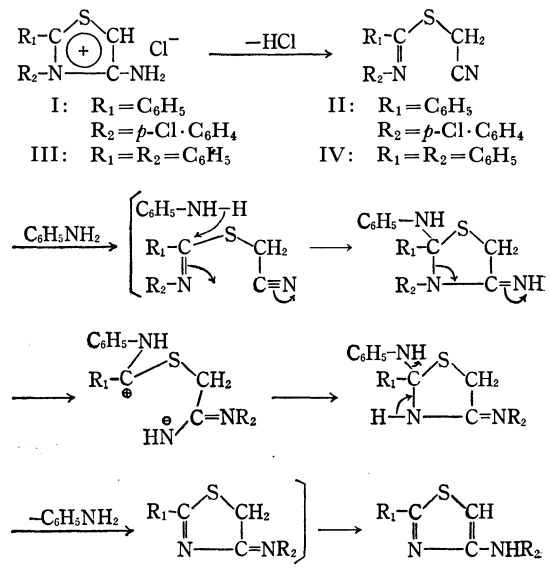

Scheme I

1) Studies on Mesoionic Compounds. XXXI.
2) M. Ohta, K. Yoshida and S. Sato, This Bulletin, **39**, 1269 (1966).
3) "NMR Spectra Catalog," Varian Associates, Palo Alto, Calif.
4) E. C. Taylor, J. A. Anderson and G. A. Berchtold, *J. Am. Chem. Soc.*, **77**, 5444 (1955).

A rearrangement analogous to this was observed in that of *N*-acetyl-sydnone imine hydrochloride into a 5-hydroxytriazole derivative.[5] When 2-*p*-methoxyphenyl-3-phenyl-thiazone imine hydrochloride was treated with aniline, 2-*p*-methoxyphenyl-4-anilinothiazole was obtained, but in the case of II, the corresponding thiazole was not obtained by the treatment of II with aniline. When 2-phenyl-3-benzyl-thiazone imine hydrochloride was treated with aniline, V was obtained. The isolation of this unexpected product may be explained on the assumption that there was an exchange of the benzylamino group of the first-formed 2-phenyl-4-benzylaminothiazole with aniline.

When IV was treated with benzylamine, two substances were obtained; one was *N*-phenyl-*N'*-benzyl-benzamidine, but the structure of the other

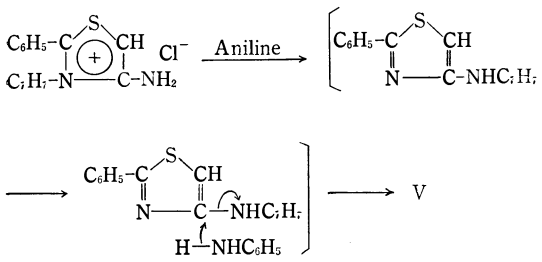

Scheme II

was not clear. When IV was allowed to stand in liquid ammonia, thiobenzanilide was isolated.

V formed the hydrochloride and picrate; the former was so unstable that it was converted into polymeric substances within one or two days. When an ethanolic solution of V was boiled with hydrochloric acid, a tarry substance was formed, from which nothing was obtained in a pure state, but when it was boiled with sodium hydroxide for eight hours, V was almost quantitatively recovered unchanged. V was acetylated with acetyl chloride to form 2-phenyl-4-anilino-*N*-acetyl-thiazole. Attempts to form the quaternary salt with benzyl chloride and the *N*-nitroso derivative were not successful. By the treatment of 2-phenylsydnone imine hydrochloride with aniline, an analogous rearrangement product was not obtained, in contrast with the case of thiazone imine hydrochloride, but *N*-nitroso-*N*-phenyl-glycinonitrile was obtained.

Experimental[6]

The Reaction of 2,3-Diphenyl-thiazone Imine Hydrochloride(III) with Aniline. A solution of 1 g of III in 10 m*l* of aniline was allowed to stand overnight at room temperature, and then it was neutralized with 10% hydrochloric acid under ice cooling. The precipitates were collected and recrystallized from ethanol to give colorless needles; mp 102—102.5°C. Yield, 0.4 g. UV: λ_{max}^{EtOH} 275 mμ (ε=36300), 362 mμ (ε=4800). IR: 3200, 1600, 1530 cm^{-1}. Found: C, 71.14; H, 4.59; N, 11.08%. Calcd for $C_{15}H_{12}N_2S$: C, 71.42; H, 4.76; N, 11.11%.

The treatment of 2-*p*-methoxyphenyl-3-phenyl-thiazone imine hydrochloride with aniline gave the corresponding thiazole under the same experimental conditions as have been described. Mp 120—121°C. The yield was 70%. Found: N, 10.23%. Calcd for $C_{16}H_{14}N_2OS$: N, 9.93%.

The Reaction of Cyanomethyl *N*-Phenylbenzthioimidate (IV) with Amines. *With Aniline.* A solution of 1 g of IV in 10 m*l* of aniline was allowed to stand overnight at room temperature, and then it was neutralized with 10% hydrochloric acid under ice cooling. After collection by filtration, the precipitates were recrystallized from ethanol to give colorless needles; mp 102—103°C. No depression of the melting point was observed on admixture with V. The yield was 0.7 g.

With o-Toluidine. The treatment of IV with *o*-toluidine instead of aniline under the above experimental conditions afforded V. The yield was 15%.

With Dimethylaniline. A solution of 1 g of IV in 10 m*l* of dimethylaniline was allowed to stand for a week, and then it was neutralized with 10% hydrochloric acid under ice cooling. The precipitates which separated out were collected and recrystallized from methanol to give colorless needles; mp 65—67°C. No depression of the melting point was observed on admixture with the starting material.

With Liquid Ammonia. A solution of 1 g of IV in liquid ammonia was allowed to stand for four days at room temperature. After the removal of the ammonia, the residue was collected and recrystallized from ethanol to give yellow prisms; mp 96—97°C.

No depression of the melting point was observed on admixture with thiobenzanilide.

With Benzylamine. A solution of 1 g of IV in 10 m*l* of benzylamine was allowed to stand overnight and was then neutralized with 10% hydrochloric acid under ice cooling. From the precipitates which separated out, *N*-phenyl-*N'*-benzyl-benzamidine was isolated by fractional recrystallization from ethanol.

The Reaction of 2-Phenyl-3-benzyl-thiazone Imine Hydrochloride with Aniline. A solution of 1 g of 2-phenyl-3-benzyl-thiazone imine hydrochloride in 10 m*l* of aniline was allowed to stand overnight, and was then neutralized with 10% hydrochloric acid under ice cooling. The precipitates were collected and recrystallized from ethanol to give colorless needles; mp 102—103°C. No depression of the melting point was observed on admixture with V.

The Acetylation of 2-Phenyl-4-anilinothiazole (V). In 20 m*l* of acetyl chloride 0.2 g of V was dissolved, and then the solution was refluxed for one hour. After the removal of the excess acetyl chloride, ether was added to the oily residue. The precipitates were collected and recrystallized from ethanol to give colorless prisms; mp 107—109°C. The yield was 0.2 g. Found: C, 69.51; H, 4.90; N, 10.06%. Calcd for $C_{17}H_{14}N_2OS$: C, 69.39; H, 4.76; N, 9.52%.

5) H. U. Daeniker and J. Druey, *Helv. Chim. Acta*, **45**, 2426 (1962).

6) All melting points were determined on a micro hot stage, and are not corrected.

Spectrophotometric Determination of the Stability Constants of Mixed Ligand Complexes of Mercury(II)-Ethylenediaminetetraacetate with Thiocyanate and Bromide

Toshiaki NOMURA

Department of Chemistry, Faculty of Science, Shinshu University, Asahi, Matsumoto

(Received April 25, 1968)

Mercury(II) reacts with ethylenediaminetetraacetate (EDTA or H_2Y^{2-}) to form mercury(II)-ethylenediaminetetraacetate (Hg-EDTA or HgY^{2-}). Thiocyanate,[1] cyanide,[2] iodide and bromide[3] (X^-) react with Hg-EDTA to form a mixed ligand complex $[HgY(X)]^{3-}$. The degrees of the dissociation (α) of the mixed ligand complexes were determined by measuring its absorption. Then, the apparent stability constants of the thiocyanato or bromo mixed ligand complexes of these ions could be calculated by the molar ratio method.[4]

The $[HgY(X)]^{3-}$ mixed ligand complex dissociated to HgY^{2-} and X^-:

$$\underset{C(1-\alpha)}{[HgY(X)]^{3-}} \rightleftharpoons \underset{\alpha C}{HgY^{2-}} + \underset{\alpha C}{X^-} \qquad (1)$$

where C is the molar concentration of the mixed ligand complex assumed to have no dissociation and α, the degree of dissociation for the mixed ligand complex. The apparent stability constant (K) for this reaction may be expressed by:

$$K = \frac{[[HgY(X)]^{3-}]}{[HgY^{2-}][X^-]} = \frac{1-\alpha}{\alpha^2 C} \qquad (2)$$

The degree of dissociation is given by:

$$\alpha = \frac{E_{max} - E_s}{E_{max}} \qquad (3)$$

where E_{max} is the assumed absorbance of the mixed ligand complex, to which all HgY^{2-} should be reacted with X^-, and where E_s is the measured absorbance of the mixed ligand complex, at the equivalent point C. However, HgY^{2-} and X^- had appreciable absorptions in the ultraviolet region. Therefore, if the absorbances of HgY^{2-} and X^- at the equivalent point are given as E_R and E_T respectively, the measured absorbance (E_s') is the sum of the absorbances of the mixed ligand complex (E_s), E_R and E_T:

$$E_s' = E_s + E_R + E_T$$
$$E_s = E_s' - E_R - E_T \qquad (4)$$

Since E_R and E_T are the α times of the absorbances of HgY^{2-} and X^- at the concentration of C (abbreviated as E_r and E_t respectively), Eq. (4) is given as follows:

$$E_s = E_s' - \alpha(E_r + E_t) \qquad (5)$$

When we substitute Eq. (5) into Eq. (3), the expression for the degree of dissociation becomes:

$$\alpha = \frac{E_{max} - E_s'}{E_{max} - E_r - E_t} \qquad (6)$$

Experimental

Reagents. All the analytical-grade reagents employed in this experiment were used without any further purification.

The stock Hg-EDTA solution of 1×10^{-2} M was prepared by dissolving 6.07 g of Doctite Hg-EDTA and diluting it to a volume of exactly 1 *l* with water. The working solution was prepared by diluting this stock solution with water.

The exact concentrations of stock solutions of thiocyanate and bromide prepared by dissolving potassium salts in water were standardized according to Volhard's method. The working thiocyanate solution of 5×10^{-4} M (F=0.977) and bromide solution of 1×10^{-3} M (F=0.998) were prepared by diluting this stock solution with water.

The pH and ionic strength were adjusted to the desired values with 0.1 M potassium perchlorate, 0.1 M disodium hydrogen phosphate, and 0.2 M sodium dihydrogen phosphate solutions.

Apparatus. The absorption measurements were made with a Hitachi Perkin Elmer 139-type spectrophotometer with 10.0 mm quartz cells. A Hitachi-Horiba M-4-type pH meter was used to measure the pH.

Procedure. According to the molar ratio method, the solutions containing 5 m*l* of 5×10^{-4} M (thiocyanate) or 1×10^{-3} M (bromide) Hg-EDTA solutions were adjusted to pH 6.1 and an ionic strength, μ of 0.10; a thiocyanate or bromide solution and then water were added to make the volume exactly 50 m*l*. After these solutions had stood for a few minutes, these absorbances were measured at a fixed wavelength against water.

Results and Discussion

Thiocyanato Mixed Ligand Complex. The thiocyanate ion reacts with Hg-EDTA to form a $[HgY(SCN)]^{3-}$ complex at pH 3—8.3, and the mixed ligand complex has a considerable absorption at 235 mμ.[1] Therefore, the molar ratio method for the thiocyanato mixed ligand complex

1) S. Komatsu and T. Nomura, *Nippon Kagaku Zasshi (J. Chem. Soc. Japan, Pure Chem. Sect.)*, **87**, 841 (1966).
2) S. Komatsu and T. Nomura, *ibid.*, **87**, 845 (1966).
3) S. Komatsu and T. Nomura, *ibid.*, **88**, 63 (1967).
4) A. E. Harvey and D. L. Manning, *J. Am. Chem. Soc.*, **72**, 4488 (1950).

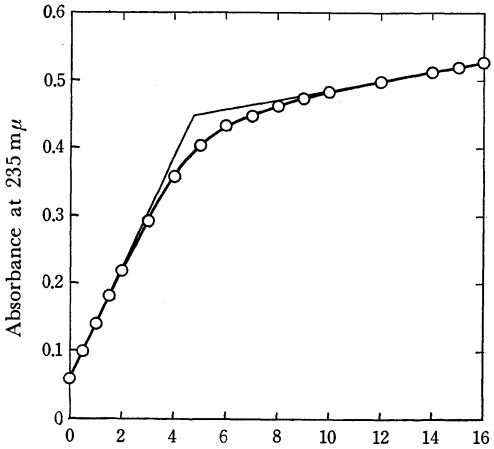

5×10^{-4} M Thiocyanate solution (F=0.977), m*l*

Fig. 1. The apparent stability constant of thiocyanato mixed ligand complex (molar ratio method) 5 m*l* of 5×10^{-4} M Hg-EDTA solution. pH 6.1, μ=0.10

was performed at pH 6.1 and 235 mμ using the previous procedure. The results for this method are shown in Fig. 1. In this figure E_{max}=0.448, E_s'=0.394, E_r=0.059, and E_t=0.033; therefore, the degree of the dissociation of this mixed ligand complex was calculated as α=0.152 using Eq. (6). Further, C, which could be determined as the section point of this method, was 4.64×10^{-5} mol. By putting these results into Eq. (2), the apparent stability constant of the complex was calculated as $K_{SCN}=7.9\times10^5$, or $\log K_{SCN}$=5.9.

Bromo Mixed Ligand Complex. Similarly, the bromide ion also reacts with Hg-EDTA to form the $[HgY(Br)]^{3-}$ complex at pH 3.5—7.7; this complex has a considerable absorption at 250 mμ.[3] Therefore, the molar ratio method was

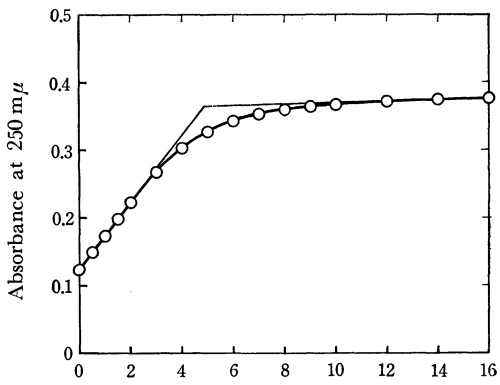

1×10^{-3} M Bromide solution (F=0.998), m*l*

Fig. 2. The apparent stability constant of bromo mixed ligand complex (molar ratio method). 5 m*l* of 1×10^{-3} M Hg-EDTA solution. pH 6.1, μ=0.10

performed at pH 6.1 and 250 mμ. The results are shown in Fig. 2. The degree of the dissociation of the bromo mixed ligand complex was calculated as was that for the thiocyanate ion. Here, E_{max}=0.366, E_s'=0.326, E_r=0.124, E_t=0.006, and C=9.82×10^{-5} mol. Using these values, the following values were obtained: α=0.169, and $K_{Br}=3.0\times10^5$ or $\log K_{Br}$=5.5.

The apparent stability constants of cyano and iodo mixed ligand complexes can not, however, be calculated with this method, because these mixed ligand complexes dissociate to mercury(II) salts and EDTA by means of the reaction between the complexes and the excess cyanide or iodide ions.[2,3]

The author wishes to thank Professor S. Komatsu for many helpful discussions and suggestions during this work.

Synthetic Studies of the Flavone Derivatives. VIII.*1 The Synthesis of 5,7,4′-Trihydroxy-3,8,3′-trimethoxyflavone*2

Kenji FUKUI, Takashi MATSUMOTO, Mitsuru NAKAYAMA and Tokunaru HORIE*3

Department of Chemistry, Faculty of Science, Hiroshima University, Higashi-sendamachi, Hiroshima

(Received May 6, 1968)

Recently, two new pigments were isolated from the leaves and terminal branches of *Cyanostegia angustifolia* Turcz. by Ghisalberti *et al.*[1] On the basis of spectral and chemical studies, they established the structures of these pigments to be 5,7,4′-trihydroxy-3,8,3′-trimethoxyflavone (I) and 5,7,4′-trihydroxy-3,8-dimethoxyflavone (II).

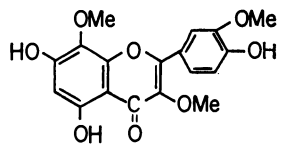

I

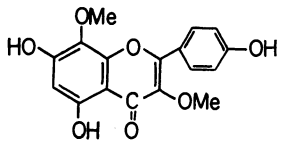

II

The present paper will deal with two different syntheses of I and will confirm the proposed structure.

According to Allan-Robinson's flavone synthesis, the condensation of 2,4-dihydroxy-3,6,ω-trimethoxyacetophenone (III)[2] with *O*-benzoylvanillic anhydride, followed by treatment with alcoholic potassium hydroxide, afforded 7,4′-dihydroxy-3,5,8,3′-tetramethoxyflavone (IV), which was then converted to the dibenzyl ether (V) with benzyl chloride. The oxidative demethylation[3] of V with nitric acid gave 7,4′-dibenzyloxy-3,3′-dimethoxyflavone-5,8-quinone (VI) as an intermediate; this was easily reduced to the corresponding 5,8-dihydroxy compound (VII). The partial methylation of VII with diazomethane gave 7,4′-dibenzyloxy-5-hydroxy-3,8,3′-trimethoxyflavone (VIII), which was then debenzylated to I by catalytic hydrogenolysis over palladium-charcoal.

An alternative synthesis of I was carried out as follows. In a previous paper,[4] 2,4,6-trihydroxy-3,ω-dimethoxyacetophenone (IX) was reacted with *O*-benzylvanillic anhydride to give 4′-benzyloxy-5,7-dihydroxy-3,6,3′-trimethoxyflavone (X). Investigating this reaction further, we found that 4′-benzyloxy-5,7-dihydroxy-3,8,3′-trimethoxyflavone (XI), an isomer of X, was produced as a by-product. Each product could be successfully separated by fractional recrystallization from

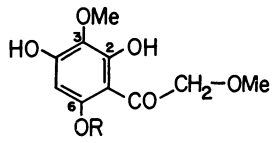

III R=Me
IX R=H

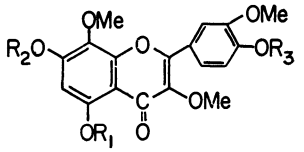

IV R_1=Me, R_2=R_3=H
V R_1=Me, R_2=R_3=$C_6H_5CH_2$
VIII R_1=H, R_2=R_3=$C_6H_5CH_2$
XI R_1=R_2=H, R_3=$C_6H_5CH_2$

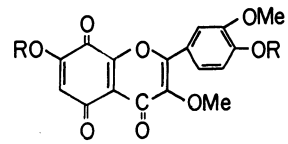

VI R=$C_6H_5CH_2$

*1 Part VII: K. Fukui, T. Matsumoto, S. Nakamura, M. Nakayama and T. Horie, This Bulletin, **41**, 1413 (1968).

*2 A part of this work has been briefly communicated: *Experimentia*, **24**, 417 (1968).

*3 Department of Applied Chemistry, Faculty of Engineering, University of Tokushima, Tokushima.

1) E. L. Ghisalberti, P. R. Jefferies and C. I. Stacey, *Australian J. Chem.*, **20**, 1049 (1967).

2) V. D. N. Sastri and T. R. Seshadri, *Proc. Indian Acad. Sci.*, **24A**, 238 (1946).

3) M. Krishnamurit, T. R. Seshadri and P. R. Shankaran, *Tetrahedron*, **22**, 941 (1966), and the references cited therein.

4) K. Fukui, T. Matsumoto, S. Nakamura, M. Nakayama and T. Horie, *Experientia*, **24**, 108 (1968); This Bulletin, **41**, 1413 (1968).

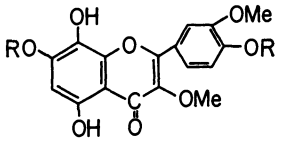

VII R=$C_6H_5CH_2$

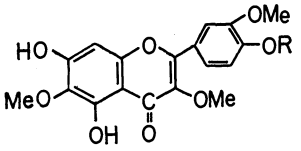

X R=$C_6H_5CH_2$

aqueous alcohol. This suggests that the ring-closure of the ketone IX proceeds in two directions, that is, toward the 2- and 6-hydroxyl group positions with respect to the ketonic group, and that it eventually affords X and XI. The benzyl protective group for the phenolic hydroxyl of XI was eliminated by catalytic hydrogenolysis over palladium-charcoal to yield I, which was identical with the sample described above. The physical properties of synthetic I were in good accordance with those of the natural pigment. Synthetic I was also characterized as triacetate and triethyl ether.

Experimental*4

7,4'-Dihydroxy-3,5,8,3'-tetramethoxyflavone (IV). A mixture of III (2.4 g), *O*-benzoylvanillic anhydride (14.0 g), and potassium *O*-benzoylvanillate (9.0 g) was ground together and heated at 180°C under a vacuum for 5 hr. The reaction mixture was then powdered, refluxed with a solution of aqueous potassium hydroxide (40%: 50 g) and ethanol (170 m*l*) for 20 min, and evaporated under a vacuum to dryness. The residue was dissolved in water, and the alkaline solution, after the removal of a small amount of an insoluble material, was acidified with dilute hydrochloric acid. The precipitate was collected, washed successively with aqueous sodium bicarbonate and water, and then recrystallized from aqueous ethanol to give yellow needles of IV, mp 250—252°C, which gave a green ferric chloride reaction in ethanol; yield, 1.0 g.

Found: C, 61.05; H, 4.73%. Calcd for $C_{19}H_{18}O_8$: C, 60.96; H, 4.85%. UV: λ_{max}^{EtOH} mμ (log ε); 253.5 (4.30), 271.5 (4.30), 353 (4.30).

The Diacetate. Hot acetic anhydride - pyridine method; mp 158—160°C (pale yellow needles from aqueous methanol).

Found: C, 60.03; H, 4.80%. Calcd for $C_{23}H_{22}O_{10}$: C, 60.26; H, 4.84%.

7,4'-Dibenzyloxy-3,5,8,3'-tetramethoxyflavone (V). A mixture of IV (1.2 g), benzyl chloride (980 mg), anhydrous potassium carbonate (2.3 g), and dimethylformamide (2.0 m*l*) was heated at 160—165°C in an oil bath for 1 hr. The reaction mixture was then diluted with water (*ca.* 30 m*l*), and the precipitate was collected, washed with water, and then recrystallized from ethanol to give pale yellow microneedles of V, mp 161—163°C; yield, 1.6 g.

Found: C, 71.47; H, 5.49%. Calcd for $C_{33}H_{30}O_8$: C, 71.47; H, 5.45%. UV: λ_{max}^{EtOH} mμ (log ε); 253.5 (4.38), 272.5 (4.36), 354 (4.32).

7,4'-Dibenzyloxy-5,8-dihydroxy-3,3'-dimethoxyflavone (VII). A suspension of V (1.0 g) in nitric acid (45%: 25 m*l*) was stirred vigorously at 40°C in a water bath for 20 min. After the mixture had cooled, the precipitate was collected, washed with water, and then recrystallized once from acetone to give crude 7,4'-dibenzyloxy-3,3'-dimethoxyflavone-5,8-quinone (VI), mp 194—196°C, as brown microneedles; yield, 0.3 g.

When a solution of crude VI (0.3 g) in hot acetic acid (10 m*l*) was treated with sodium sulfite heptahydrate (1.5 g), the solution turned from deep red to bright yellow.

The reaction mixture was heated on a steam bath for 1 min and then diluted with water. After the mixture had cooled, the yellow precipitate was collected, washed with water, and then recrystallized from ethyl acetate to give yellow microneedles of VII, mp 198—200°C, which gave a green ferric chloride reaction in ethanol; yield, 220 mg.

Found: C, 70.89; H, 5.01%. Calcd for $C_{31}H_{26}O_8$: C, 70.71; H, 4.98%.

7,4'-Dibenzyloxy-5-hydroxy-3,8,3'-trimethoxyflavone (VIII). VII (140 mg) in acetone (30 m*l*) was treated with an excess of diazomethane in ether. After standing at room temperature for 3 hr, the mixture was evaporated under a vacuum to dryness. The residue was recrystallized from an acetone-ethanol mixture to give yellow microneedles of VIII, mp 172—173°C, which gave a green ferric chloride reaction in ethanol; yield, 120 mg.

Found: C, 71.07; H, 5.20%. Calcd for $C_{32}H_{28}O_8$: C, 71.10; H, 5.22%.

4'-Benzyloxy-5,7-dihydroxy-3,8,3'-trimethoxyflavone (XI). The reaction of the ketone (IX) (3.0 g) with *O*-benzylvanillic anhydride (27.0 g) was carried out in a manner previously reported.[4] The crude product was dissolved in hot aqueous ethanol, after which the solution was allowed to stand overnight at room temperature. The precipitate gave 4'-benzyloxy-5,7-dihydroxy-3,6,3'-trimethoxyflavone (X)[4], mp 180—181.5°C; yield, 1.2 g (20%). The solvent of the mother liquor was removed by evaporation to afford a yellowish residue, which was washed with hot acetone and then recrystallized from methyl ethyl ketone to give 4'-benzyloxy-5,7-dihydroxy-3,8,3'-trimethoxyflavone (XI), mp 206—208°C (golden yellow prisms), which gave a green ferric chloride reaction in ethanol; yield, 0.55 g (9%).

Found: C, 66.91; H, 4.70%. Calcd for $C_{25}H_{22}O_8$: C, 66.66; H, 4.92%. UV: λ_{max}^{EtOH} mμ (log ε); 257 (4.23), 276 (4.29); 340 (4.18).

5,7,4'-Trihydroxy-3,8,3'-trimethoxyflavone (I). *a) From VIII.* A solution of VIII (60 mg) in ethyl acetate (20 m*l*) was submitted to catalytic hydrogenolysis at room temperature in the presence of Pd-C (10%: 100 mg). After the catalyst had been filtered, the

*4 All melting points are uncorrected.

filtrate was evaporated under a vacuum; the residue was then recrystallized from methanol to give yellow plates of I, mp 217—219°C, (lit.[1] mp 215—217°C), which gave a green ferric chloride reaction in ethanol; yield, 25 mg.

Found: C, 59.87; H, 4.56%. Calcd for $C_{18}H_{16}O_8$: C, 60.00; H, 4.48%. UV: λ_{max}^{EtOH} mμ (log ε); 260 (4.23), 276.5 (4.29), 340^{sh} (4.17), 365 (4.21).

b) From XI. By a reaction similar to that described above, XI (284 mg), Pd-C (10%: 300 mg), and ethyl acetate (100 m*l*) gave I (mp 213.5—215°C), which was identical with a sample derived by the above described method a); yield, 185 mg.

The Triacetate. Mp 140—141°C, after resolidifying 147—148.5°C (colorless needles from methanol) (lit.[1] mp 146—147°C).

Found: C, 59.25; H, 4.63%. Calcd for $C_{24}H_{22}O_{11}$: C, 59.26; H, 4.56%.

The Triethyl Ether. Mp 104.5—105.5°C (colorless needles from aqueous ethanol) (lit.[1] mp 110—111°C).

Found: C, 62.34; H, 6.49%. Calcd for $C_{24}H_{28}O_8 \cdot H_2O$: C, 62.49; H, 6.22%. Drying at 100°C/0.1 mmHg for 3 hr, mp 121—121.5°C (104.5°C sinter).

Found: C, 64.59; H, 6.18%. Calcd for $C_{24}H_{28}O_8$: C, 64.85; H, 6.35%.

The authors are grateful to Professor P. R. Jefferies, the University of Western Australia, for his gift of the natural pigment. This work was supported by a grant-in-aid from Ministry of Education.

The Studies of 5-Aminosalicylaldehyde Derivatives. III.[1] The Preparation of 5-Aminosalicylaldehyde Hydrazones by Reduction of 5-(*p*-Sulfophenylazo)salicylaldehyde Hydrazone

Mitsunori TANAKA

The Faculty of Education, Kagawa University, Takamatsu, Kagawa

(Received May 9, 1968)

In a previous paper,[1] it was reported that the reduction of the sodium salt of 5-(*p*-sulfophenylazo)-salicylaldehyde (Formula I) with sodium hydrosulfite gave only a resinous product. This fact can be interpreted as follows. Even if the aminosalicylaldehyde is formed in the course of the reduction of I, the formyl and amino groups in aminosalicylaldehyde are so reactive that aminosalicylaldehyde may undergo spontaneous condensation polymerisation. Therefore, in order to obtain the monomeric compound, either the formyl or amino group must be protected from the polymerisation. The purpose of the present investigation is to prepare 5-aminosalicylaldehyde derivatives with the free amino group, which may be formed by the reductive cleavage of the azo linkage in the derivatives of I. According to Weil *et al.*,[2] Oddo *et al.*,[3] and Tanaka,[1] 5-aminosalicylaldehyde phenylhydrazone is one of only a few derivatives

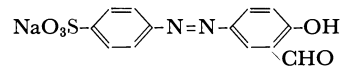

I

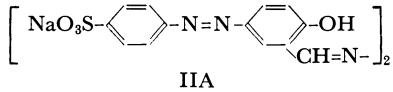

IIA

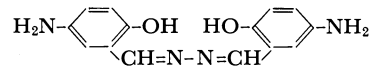

IIB

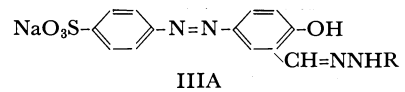

IIIA

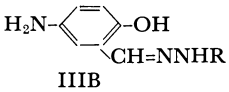

IIIB

R: a $-CH_3$ b $-C_6H_5$
c $-C_6H_4CH_3$(o) d $-C_6H_4CH_3$(m)
e $-C_6H_4CH_3$(p) f $-C_6H_4Cl$(p)
g $-COCH_3$ h $-COC_2H_5$
i $-COC_6H_5$ j $-COC_6H_4OH$(o)
k $-COC_6H_4OH$(m) l $-COC_6H_4OH$(p)
m $-COC_6H_4NH_2$(o) n $-COC_6H_4NH_2$(p)
o $-COC_5H_4N$(2) p $-COC_5H_4N$(3)
q $-COC_5H_4N$(4) r $-CONH_2$
s $-CSNH_2$

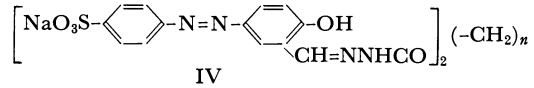

IV

n: 0, 1, 2 and 4

that are stable in spite of the presence of a free amino group. On the basis of this fact, I was converted to various kinds of hydrazones in order to block the formyl group.

The reaction of hydrazine with the sodium salt of I gave the sodium salt of 5-(*p*-sulfophenylazo)-salicylaldehyde azine (Formula IIA). In the similar way, methyl-, phenyl-, and tolyl-hydrazines

1) Part II: M. Tanaka, This Bulletin, **40**, 1724 (1967).
2) H. Weil, M. Traun and Marcel, *Chem. Ber.*, **55**, 2664 (1958).
3) G. Oddo and A. Giacalone, *Gazz. Chim. Ital.*, **58**, 290 (1928).

Table 1. Hydrone derivative of sodium salt of

Hydrazone	Appearance	Formula
IIA	Yellowish powder	$C_{26}H_{18}O_8N_6S_2Na_2 \cdot 1.5H_2O$
IIIA, a	Yellowish plates	$C_{14}H_{13}O_4N_4SNa$
IIIA, b	Yellowish powder	$C_{19}H_{15}O_4N_4SNa$
IIIA, c	Reddish orange plates	$C_{20}H_{17}O_4N_4SNa \cdot 2H_2O$
IIIA, d	Orange plates	$C_{20}H_{17}O_4N_4SNa \cdot 2.5H_2O$
IIIA, e	Orange yellow plates	$C_{20}H_{17}O_4N_4SNa \cdot 4H_2O$
IIIA, f	Brown red needles	$C_{19}H_{14}O_4N_4SClNa$
IIIA, g	Orange yellow needles	$C_{15}H_{13}O_5N_4SNa \cdot 3H_2O$
IIIA, h	Yellowish needles	$C_{16}H_{15}O_5N_4SNa \cdot 3H_2O$
IIIA, i	Orange yellow needles	$C_{20}H_{15}O_5N_4SNa \cdot 6H_2O$
IIIA, j	Orange yellow needles	$C_{20}H_{15}O_6N_4SNa \cdot 3H_2O$
IIIA, k	Orange yellow needles	$C_{20}H_{15}O_6N_4SNa \cdot 5.5H_2O$
IIIA, l	Orange needles	$C_{20}H_{15}O_6N_4SNa \cdot 2H_2O$
IIIA, m	Orange needles	$C_{20}H_{16}O_5N_5SNa \cdot 3.5H_2O$
IIIA, n	Orange needles	$C_{20}H_{16}O_5N_5SNa \cdot 2.5H_2O$
IIIA, o	Orange plates	$C_{19}H_{14}O_5N_5SNa \cdot 3H_2O$
IIIA, p	Orange yellow plates	$C_{19}H_{14}O_5N_5SNa \cdot 3H_2O$
IIIA, q	Yellowish plates	$C_{19}H_{14}O_5N_5SNa \cdot 3H_2O$
IIIA, r	Yellowish plates	$C_{14}H_{12}O_5N_5SNa \cdot H_2O$
IIIA, s	Yellowish needles	$C_{14}H_{12}O_4N_5S_2Na \cdot H_2O$
IV, 0	Yellowish plates	$C_{28}H_{20}O_{10}N_8S_2Na_2 \cdot 2H_2O$
IV, 1	Yellowish plates	$C_{29}H_{22}O_{10}N_8S_2Na_2 \cdot 2H_2O$
IV, 2	Yellowish plates	$C_{30}H_{24}O_{10}N_8S_2Na_2 \cdot 2H_2O$
IV, 4	Yellowish plates	$C_{32}H_{28}O_{10}N_8S_2Na_2 \cdot 2.5H_2O$

Table 2. Hydrazone derivative of

Hydrazone	Appearance	Recryst. solvent	Mp, °C	Formula
IIB	Yellowish powder	Dimethyl formamide	over 300	$C_{14}H_{14}O_2N_4$
IIIB, b	Yellowish powder	Benzene	165	$C_{13}H_{13}ON_3$
IIIB, i	Yellowish powder	Benzene	167	$C_{14}H_{13}O_2N_3 \cdot H_2O$
IIIB, j	Yellowish powder	Methyl cellosolve	226	$C_{14}H_{13}O_3N_3$
IIIB, k	Yellowish powder	Methyl cellosolve	206	$C_{14}H_{13}O_3N_3$
IIIB, l	Yellowish powder	Methyl cellosolve	244—246	$C_{14}H_{13}O_3N_3 \cdot H_2O$
IIIB, o	Yellowish powder	Benzene	186	$C_{13}H_{12}O_2N_4$
IIIB, p	Yellowish powder	Benzene	220	$C_{13}H_{12}O_2N_4 \cdot H_2O$
IIIB, q	Yellowish powder	Benzene	over 300	$C_{13}H_{12}O_2N_4 \cdot H_2O$
IIIB. r	Pale yellow powder	Water-ethanol	over 300	$C_8H_{10}O_2N_4$
IIIB, s	White yellow powder	Water-ethanol	over 300	$C_8H_{10}ON_4S$

invariably yielded the corresponding hydrazones (Formula IIIA, a—f). The reaction product of I with acid hydrazide differed depending on the solvent used and on the chemical nature of the acid hydrazide. Acetyl-, propionyl-, oxalyl-, malonyl-, succinyl-, or adipoyl-hydrazine and I gave the expected hydrazone (Formula IIIA, g and h. Formula IV, n: 0, 1, 2 and 4) in alcohol or in a pyridine-water mixed solvent. However, in an aqueous solution these hydrazine derivatives all gave the same compound, IIA. This fact was confirmed by the elementary analysis and by a study of the infrared spectrum. Oxalyl-, benzoyl-, hydroxybenzoyl-, aminobenzoyl-, or pyridyl-carbonyl-hydrazine, -semicarbazide, or -thiosemicarbazide and I yielded the expected hydrazones (Formula IV. n : 0. Formula IIIA. i—s) in any solvent (water, alcohol, or a pyridine-water

5-(*p*-SULFOPHENYLAZO)SALICYLALDEHYDE (Formula IIA and IIIA)

Analysis, %							
Found				Calcd			
C	H	N	Na	C	H	N	Na
46.02	3.28	12.51	6.36	45.95	3.11	12.37	6.77
47.74	3.60	15.70	6.31	47.19	3.68	15.72	6.45
54.58	3.72	13.47	5.63	54.51	3.61	13.39	5.49
51.11	4.30	12.08	6.56	51.28	4.52	11.96	6.84
50.38	4.77	11.74	4.45	50.31	4.64	11.73	4.82
47.94	5.10	11.20	4.64	47.61	4.99	11.11	4.56
50.67	3.22	12.28	5.01	50.39	3.12	12.37	5.08
41.84	4.28	13.24	5.30	41.86	4.45	13.02	5.34
42.53	4.73	12.52	5.14	42.48	4.68	12.38	5.08
43.37	4.79	10.17	4.13	43.32	4.91	10.10	4.15
46.47	4.24	10.92	4.50	46.51	4.10	10.85	4.45
42.62	4.79	9.78	4.01	42.78	4.67	9.98	4.06
47.78	4.09	11.12	4.46	48.19	3.84	11.24	4.61
45.48	4.35	13.10	4.05	45.80	4.42	13.35	4.38
47.64	4.36	13.98	4.82	47.43	4.18	13.83	4.54
45.34	4.18	13.76	4.65	45.51	4.02	13.97	4.58
45.25	4.03	13.87	4.21	45.51	4.02	13.97	4.58
45.68	4.24	14.17	4.34	45.51	4.02	13.97	4.58
41.89	3.31	17.07	5.37	41.66	3.50	17.36	5.26
38.50	3.73	15.89	5.10	38.44	3.69	16.01	5.26
43.53	3.38	14.69	5.36	43.47	3.13	14.48	5.94
44.06	3.52	14.01	5.48	44.16	3.32	14.21	5.83
44.89	3.50	13.92	5.62	44.89	3.52	13.96	5.73
45.86	4.09	13.24	5.35	45.77	3.96	13.34	5.48

5-AMINOSALICYLALDEHYDE (Formula IIB and IIIB)

Analysis, %							
Found				Calcd			
C	H	N	H_2O	C	H	N	H_2O
62.44	5.36	20.73		62.21	5.22	20.73	
68.04	5.86	18.65		68.70	5.77	18.49	
61.90	5.66	15.35	6.32	61.53	5.53	15.38	6.59
61.56	4.85	15.03		61.98	4.83	15.49	
61.69	5.03	15.42		61.98	4.83	15.49	
58.17	5.24	14.37	6.58	58.12	5.23	14.53	6.23
60.84	5.14	21.57		60.93	4.72	21.87	
57.03	5.12	20.13	6.23	56.93	5.15	20.43	6.57
57.13	5.15	20.24	6.88	56.93	5.15	20.43	6.57
49.30	5.28	28.96		49.48	5.19	28.85	
45.78	4.63	26.88		45.70	4.79	26.66	

mixture). The experimental results are listed in Table 1.

The marked difference in the hydrazone formation in an aqueous solution between acylated hydrazine and oxalyl- or aroyl-hydrazine or semicarbazides, appears to be due to the difference between stabilities in the face of the hydrolysis of the acid hydrazides.

These hydrazones and azine were used for the preparation of 5-aminosalicylaldehyde derivatives with a free amino group. In the case of the stable 5-(*p*-sulfophenylazo)salicylaldehyde hydrazones, the reductive cleavage of the azo linkage was accomplished in an aqueous solution without any change in the hydrazone group, and the corresponding 5-aminosalicylaldehyde hydrazones (Formula IIIB, b, i—l and o—s) were obtained. The less stable 5-(*p*-sulfophenylazo)salicylaldehyde

hydrazones derived from acylated hydrazines underwent drastic change in the hydrazone moiety during the reduction; they gave 5-aminosalicylaldehyde azine, which was also obtained by reducing bis [5-(*p*-sulfophenylazo)salicylaldehyde] azine (Formula IIB). These results, confirmed by the results of the elementary analyses and by the infrared spectra, are tabulated in Table 2.

Thus, the above-mentioned experimental results show that the less stable hydrazones are reduced at the hydrazone moiety, whereas the stable hydrazones are reduced to 5-aminosalicylaldehyde hydrazone without any change in the hydrazone moiety.

Experimental

Sodium Salt of 5-(*p*-Sulfophenylazo)salicylaldehyde (I). This salt was prepared by Tummely's method.[4] (Found: C, 42.65; H, 3.52; N, 7.83; Na, 5.98%.)

Sodium Salt of Bis[5-(*p*-sulfophenylazo)salicylaldehyde]azine (IIA). To a hot stirred, solution of 3.64 g of I in 150 m*l* of water, there was added, drop by drop 0.628 g of hydrazine hydrate (80%) in 50 m*l* of water. The precipitate was collected by filtration, washed with water, and recrystallized from a pyridine-water mixture. The yield was almost quantitative.

Sodium Salt of 5-(*p*-Sulfophenylazo)salicylaldehyde methylhydrazone (IIIA, a). To a hot stirred, solution of 3.64 g of I in 150 m*l* of water, there was added 0.46 g of methylhydrazine in 150 m*l* of methanol. The precipitate was treated in a manner similar to that described above.

Sodium Salt of 5-(*p*-Sulfophenylazo)salicylaldehyde Arylhydrazone (IIIA, b, c, d, e and f). A mixture of 0.01 mol arylhydrazine hydrochloride and 0.01 mol of sodium acetate monohydrate (or 0.005 mol of sodium carbonate) in 50 m*l* of ethanol was added to a hot solution of 0.01 mol of the I in 150 m*l* of water. The precipitate was then collected and recrystallized from a pyridine-water mixture.

Sodium Salt of Aliphatic Monocarboxylic Acid Hydrazone and Aliphatic Dicarboxylic Acid Dihydrazone of 5-(*p*-Sulfophenylazo)salicylaldehyde (IIIA, g and h. IV. *n*: 0, 1, 2 and 4). To a hot solution of 0.01 mol of the I in 100 m*l* of a pyridine-water mixture, there was added a solution monohydrazide (0.01 mol) or dihydrazide (0.005 mol) in water or ethyl alcohol. The precipitate was collected and recrystallized from a pyridine-water mixture.

Sodium Salt of Aroylhydrazone, Semicarbazone and Thiosemicarbazone of 5-(*p*-Sulfophenylazo)-salicylaldehyde (IIIA, i—s). To a hot solution of 0.01 mol of the I in 150 m*l* of water, there was added a solution of aroylhydrazine, semicarbazide, or thiosemicarbazide in ethyl alcohol. The precipitate was then treated in a manner similar to that described above.

Bis(5-aminosalicylaldehyde)azine (IIB). To a solution of 4.40 g of IIA and 1.60 g of sodium hydroxide in 300 m*l* of water, 8.40 g of sodium hydrosulfite were added at 60—70°C. The precipitate was then collected by filtration and washed with water. The products were recrystallized from dimethylformamide and washed with ethyl alcohol.

Aryl-, Aroyl-, Pyridylcarbonyl-, Carbamoyl- and Thiocarbamoyl-hydrazones of 5-Aminosalicylaldehyde (IIIB. b and i—s). To a solution of 0.01 mol of IIIA (b and i—s) and 1.60 g of sodium hydroxide in 200 m*l* of water, 4.20 g of sodium hydrosulfite were added at 60—70°C. The precipitate was treated in a manner similar to that described above. The hydrazones, together with the solvents for crystallization, are listed in Table 2.

The author wishes to express his thanks to President Dr. Tokuichi Tsumaki of the Kyushu Institute of Technology and to Professor Dr. Tamotsu Yoshino and Professor Dr. Masaru Yamaguchi of Kyushu University for their exceedingly kind direction of this work.

4) E. Tummely, *Ann.*, **251**, 180 (1889).

The Preparation of Some Triorganosiloxy Derivatives of Bis-cyclopentadienyltitanium Dichloride

Toshio TAKIGUCHI and Hideo SUZUKI

Department of Synthetic Chemistry, Kiryu College of Technology, Gunma University, Tenjin-cho, Kiryu

(Received May 13, 1968)

Very little researches have been made on the organosiloxytitanium compounds with cyclopentadienyl groups attached to the titanium atom. The preparation of triphenylsiloxy-bis-cyclopentadienyltitanium chloride[1] and bis-triphenylsiloxy-bis-cyclopentadienyltitanium[1] from the reaction of bis-cyclopentadienyltitanium dichloride with sodium triphenylsilanolate are the only examples reported in the literature.

We wish to report on the preparation of some triorganosiloxy derivatives of bis-cyclopentadienyltitanium dichloride from the reaction of bis-cyclopentadienyltitanium dichloride with the corresponding triorganosilanols in the presence of triethylamine as a hydrogen chloride acceptor

1) J. G. Noltes and G. J. M. Van der Kerk, *Rec. Trav. Chim.*, **81**, 39 (1962).

according to the following schemes:

$$Cp_2TiCl_2 + R_3SiOH + Et_3N \rightarrow R_3SiOTi(Cl)Cp_2 + Et_3N\text{-}HCl \text{ and}$$

$$Cp_2TiCl_2 + 2R_3SiOH + 2Et_3N \rightarrow (R_3SiO)_2TiCp_2 + 2Et_3N\text{-}HCl$$

Most of the products obtained were colored crystalline substances. They are bis-triphenylsiloxy-bis-cyclopentadienyltitanium, bis-diphenylmethylsiloxy-bis-cyclopentadienyltitanium, diphenylmethylsiloxy-bis-cyclopentadienyltitanium chloride, bis - dimethylphenylsiloxy - bis - cyclopentadienyltitanium, dimethylphenylsiloxy-bis-cyclopentadienyltitanium chloride and diphenylbutylsiloxy-bis-cyclopentadienyltitanium chloride, the last five being new compounds. All products were well-defined and characterized by their IR spectra. As for crystalline substances, the X-ray powder patterns were also determined for their rapid identification.

Experimental

Triorganochlorosilanes. Triphenylchlorosilane (mp 98—99°C) was isolated from the high boiling residue[2] of the direct synthesis of phenylchlorosilanes. Diphenylmethylchlorosilane (bp 128—130°C/3 mmHg), dimethylphenylchlorosilane (bp 55—56°C/5 mmHg), diphenylbutylchlorosilane (bp 153—155°C/4 mmHg) were prepared by a Grignard route.[3]

Triorganosilanols. Triphenylsilanol (mp 150—151°C), diphenylmethylsilanol (bp 132—133°C/1.5 mmHg), dimethylphenylsilanol (bp 73.5—74.5°C/5 mmHg) and diphenylbutylsilanol (bp 157—158°C/1.5 mmHg) were prepared by the method[4] reported previously.

Bis-cyclopentadienyltitanium Dichloride. The reaction of cyclopentadienylsodium with titanium tetrachloride in tetrahydrofuran gave bis-cyclopentadienyltitanium dichloride, mp 288—290°C (lit.[5] mp 289—291°C), as bright-red acicular crystals with a yield of 33—35%.

The Preparation of Bis-diphenylmethylsiloxy-bis-cyclopentadienyltitanium and Diphenylmethylsiloxy-bis-cyclopentadienyltitanium Chloride. Typical procedures will be described in detail, using the preparations of mono- and di-diphenylmethylsiloxy derivatives of bis-cyclopentadienyltitanium dichloride as examples. A mixture of bis-cyclopentadienyltitanium dichloride (5 g, 0.02 mol), diphenylmethylsilanol (10.1 g, 0.047 mol) and triethylamine (5 g, 0.05 mol) gave a deep red solution when dissolved in 250 m*l* of tetrahydrofuran. The red solution gradually turned yellowish when refluxed with gentle stirring, and triethylamine hydrochloride precipitates. After it was refluxed for 25 hr, the hydrochloride was filtered off and the filtrate was concentrated under reduced pressure, leaving a brown viscous liquid from which a brown semi-solid separated on addition of cold *n*-hexane.

Extraction of the brown mass with hot *n*-hexane for 30 hr gave a deep yellow solution from which, on cooling in an ice-bath, 1 g (11.7%) of diphenylmethylsiloxy-bis-cyclopentadienyltitanium chloride was obtained as red acicular crystals melting at 160—161.5°C. After filtration of the red crystals, the yellow filtrate was evaporated, giving 5 g (41.3%) of pale yellow platelets.

The extraction residue was a brown solid which proved to be a mixture of unreacted bis-cyclopentadienyltitanium dichloride and its cleavage products.

Further purification of the platelets was effected by recrystallization from *n*-hexane, giving pure bis-diphenylmethylsiloxy-bis-cyclopentadienyltitanium melting at 113.5—114.5°C.

$Ph_2MeSiOTi(Cl)Cp_2$: Found: Si, 6.49; Ti, 11.29; C, 65.00; H, 5.43; Cl, 8.35% (determined by combustion method); mol wt (determined ebullioscopically in benzene), 424. Calcd for $C_{23}H_{23}OSiTiCl$: Si, 6.58; Ti, 11.22; C, 64.71; H, 5.43; Cl, 8.31%; mol wt, 426.9.

$(Ph_2MeSiO)_2TiCp_2$: Found: Si, 9.15; Ti, 8.16; C, 71.85; H, 5.90%; mol wt, 616. Calcd for $C_{36}H_{36}O_2Si_2Ti$; Si, 9.29; Ti, 7.92; C, 71.50; H, 6.00%; mol wt, 604.8.

All of the attempts to modify above procedure, using dioxane, toluene and xylene as reaction media and using pyridine, aniline, *N,N*-dimethylaniline as hydrogenchloride acceptors, proved to be less satisfactory than the combination of tetrahydrofuran and triethylamine because of the complexity of the procedure and the lower yield of the aimed products.

The reaction of bis-cyclopentadienyltitanium dichloride with equimolar diphenylmethylsilanol gave diphenylmethylsiloxy-bis-cyclopentadienyltitanium chloride with reproducible yields of 60—65%, and bis-diphenylmethylsiloxy-bis-cyclopentadienyltitanium was obtained in the yield of less than 5%.

Other Triorganosiloxy Derivatives. Bis-triphenylsiloxy-bis-cyclopentadienyltitanium, white platelets melting at 199—200°C (lit.[1] mp 208—210°C); bis-phenyldimethylsiloxy-bis-cyclopentadienyltitanium, a deep red low melting solid; phenyldimethylsiloxy-bis-cyclopentadienyltitanium chloride, a carmine red solid melting at 56°C; diphenylbutylsiloxy-bis-cyclopentadienyltitanium chloride, an orange yellow crystalline mass melting at 97—99°C. These were all obtained by procedures similar to those used for diphenylmethylsiloxy derivatives.

$(Ph_3SiO)_2TiCp_2$: Found: Si, 7.86; Ti, 6.45; C, 76.3; H, 5.58%; mol wt, 739. Calcd for $C_{46}H_{40}O_2Si_2Ti$: Si, 7.71; Ti, 6.57; C, 75.80; H, 5.53%; mol wt, 728.9.

$Ph_2BuSiOTi(Cl)Cp_2$: Found: Si, 5.76; Ti, 10.09; C, 66.80; H, 6.37; Cl, 7.73%; mol wt, 457. Calcd for $C_{26}H_{29}OSiTiCl$; Si, 5.99; Ti, 10.21; C, 66.59; H, 6.23; Cl, 7.56%; mol wt, 469.0.

$(Me_2PhSiO)_2TiCp_2$: Found: Si, 11.81; Ti, 10.05; C, 65.60; H, 6.75%; mol wt, 461. Calcd for $C_{26}H_{32}O_2Si_2Ti$: Si, 11.69; Ti 9.97; C, 64.98; H, 6.71%; mol wt, 480.6.

$Me_2PhSiOTi(Cl)Cp_2$: Found: Si, 7.81; Ti, 13.30; C, 59.25; H, 5.79; Cl, 9.90% mol wt, 355. Calcd for: $C_{18}H_{21}OSiTiCl$: Si, 7.70; Ti, 13.13; C, 59.26; H, 5.80; Cl, 9.72%; mol wt, 364.8.

2) T. Takiguchi and M. Abe, *Kogyo Kagaku Zasshi (J. Chem. Soc. Japan, Ind. Chem. Sect.)*, **68**, 679 (1965).
3) T. Takiguchi and M. Abe, *ibid.*, **66**, 625 (1963).
4) T. Takiguchi, *J. Am. Chem. Soc.*, **81**, 2359 (1959).
5) G. Wilkinson and J. M. Birmingham, *ibid.*, **76**, 4281 (1954).

All products thus obtained were readily soluble in tetrahydrofuran, toluene, benzene, chloroform and acetone, partly soluble in boiling *n*-hexane and sparingly soluble in cyclohexane, ether and carbon tetrachloride.

IR Absorption Spectra and X-Ray Powder Patterns. As for the IR absorption spectra, the absorption bands due to the Ti-O-Si bonding were observed at 915 cm^{-1} with $(R_3SiO)_2$ $TiCp_2$ type derivatives and at 950 cm^{-1} with $R_3SiOTi(Cl)Cp_2$ type derivatives as a sharp and strong peak in agreement with the previous descriptions[1].

The X-ray powder diffraction was observed for crystalline products by using the Cu$K\alpha$ radiation filtered by Ni as follows.

$(Ph_3SiO)_2TiCp_2$:

d,kX:	2.99	3.48	3.59	3.74	4.08	4.64	4.87	5.13	5.28
	5.95	6.50	6.70	7.55	9.86	13.15			
I/I_0:	0.23	0.18	0.21	0.25	0.35	0.65	0.90	1.00	0.20
	0.24	0.20	0.26	0.44	0.55	0.25			

$Ph_2BuSiOTi(Cl)Cp_2$:

d,kX:	4.00	4.54	4.64	4.89	5.29	5.80	7.25	7.38	8.30
	9.79								
I/I_0:	0.55	0.58	0.47	0.54	0.54	0.71	0.56	1.00	0.71
	0.40								

$(Ph_2MeSiO)_2TiCp_2$:

d,kX:	4.15	4.61	4.76	5.50	6.11	6.92	10.07
I/I_0:	0.37	0.32	0.20	1.00	0.23	0.22	0.34

$Ph_2MeSiOTi(Cl)Cp_2$:

d,kX:	3.89	4.00	4.57	5.04	5.19	5.46	5.78	6.01	6.90
	7.89	9.40	12.06						
I/I_0:	0.39	0.52	1.00	0.24	0.48	0.33	0.41	0.38	0.29
	0.73	0.23	0.32						

The authors are grateful to the Shin-etsu Chem. Ind. Co. for the supply of chlorosilanes, to the Hitachi Chem. Works Co. for the supply of dicyclopentadiene and to Dr. S. Nakatani of the National Institute of Science and Technology, Tokyo, for his kind co-operation in the elementary analyses of the products reported herein.

The Catalytic Activity of Sulfate in the Decomposition of Formic Acid

Ken-ichi TANAKA and Atsumu OZAKI

Research Laboratory of Resources Utilization, Tokyo Institute of Technology, Ookayama, Meguro-ku, Tokyo

(Received June 4, 1968)

In our previous papers[1] it has been shown that the acidity of the aquo-ion given by the hydrolysis equilibrium constant (pK_a) can be formulated with a generalized electronegativity of the metal ion (X_i) as follows;

$$pK_a = 20\left(1-\frac{X_i}{14}\right)$$

$$X_i = (1+2Z)X_0$$

where X_0 is the electronegativity of the neutral atom ($Z=0$) given by Pauling and where Z is the charge of the ion. This parameter can be successfully applied to solid surfaces; the acid-base properties of the hydrated oxide surface designated by Zero Point of Charge are expressed by the following equation;

$$\text{Zero Point of Charge} = 16.8(1-22/X_i)$$

and the catalytic activity of sulfate in the hydration reaction of propylene and the polymerization of acetaldehyde increase with the acidity parameter, X_i.

It is known that the decomposition of formic acid involves two reactions, dehydration and dehydrogenation, and that the dehydration reaction is commonly promoted by acid. In this experiment, the decomposition of formic acid has been adopted as a test reaction in order to demonstrate a general trend of the catalytic activity of the sulfate.

Experimental

The apparatus employed for this experiment was a flow system with nitrogen as the carrier gas.

The carrier gas was passed through the formic acid evaporator at a constant flow rate of 41 cc/min. The temperature of the evaporator was kept at 22±1°C and the room temperature was about 30—32°C. The carrier gas containing formic acid was allowed to flow through the reactor at the selected temperature. The concentration of formic acid in the carrier gas was determined by the concentration of carbon monoxide in the effluent gas when the formic acid was completely decomposed.

TABLE 1. DETAILS OF THE CATALYST USED

Sulfate	Molecular weight	Amounts doped on 10 g SiO_2 (g)
$ZnSO_4 \cdot 7H_2O$	287.56	0.288
$NiSO_4 \cdot 6H_2O$	262.87	0.263
$MnSO_4 \cdot 4H_2O$	223.07	0.223
$MgSO_4 \cdot 7H_2O$	246.50	0.246
$Fe_2(SO_4)_3 \cdot 9H_2O$	562.04	0.281
$Cr_2(SO_4)_3 \cdot 5H_2O$	482.30	0.241
$Al_2(SO_4)_3 \cdot 16—18H_2O$	630.5—666.5	0.333
$CuSO_4 \cdot 5H_2O$	249.7	0.250

1) K. Tanaka and A. Ozaki, This Bulletin, **40**, 1723 (1967); *J. Catalysis*, **8**, 1 (1967).

The catalyst was prepared as follows: a reagent-grade sulfate of about a 10^{-3} g-cation was supported on 10 g of silica gel (30—50 mesh Wako-gel-G was used) and dried at 100°C. Each experiment was carried out with 3.5 g of a catalyst. The details of the catalysts used are given in Table 1.

The reaction over these catalysts was completely the dehydration; therefore, the reaction was followed by the analysis of the carbon monoxide in the effluent gas by means of gas chromatography.

Results and Discussion

The reaction rate was calculated from the ratio of carbon monoxide to nitrogen in the effluent gas and from the flow rate of the carrier gas, nitrogen.

Figure 1 shows the rate of reaction at various

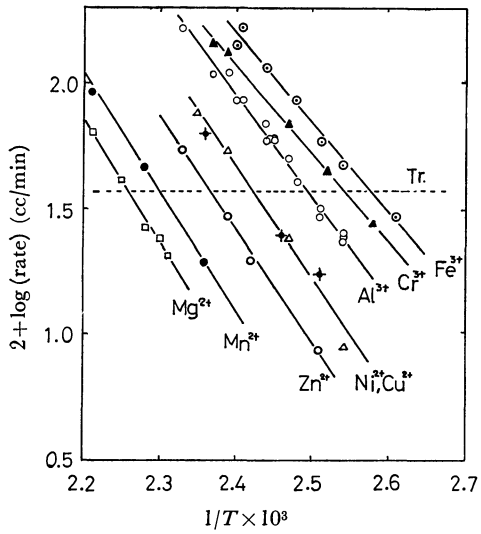

Fig. 1. Reaction rates at various temperatures.

temperatures. From this figure, the relative catalytic activities of the sulfates are in the following sequence:

$$Fe^{3+} > Cr^{3+} > Al^{3+} > Cu^{2+} \simeq Ni^{2+} > Zn^{2+} > Mn^{2+} > Mg^{2+}.$$

This sequence is very similar to that observed in the hydration of propylene.[2]

The catalytic activity of each sulfate, characterized by the temperature at which the concentration of carbon monoxide in the carrier gas reached 1% (approximately an 11% conversion to the formic

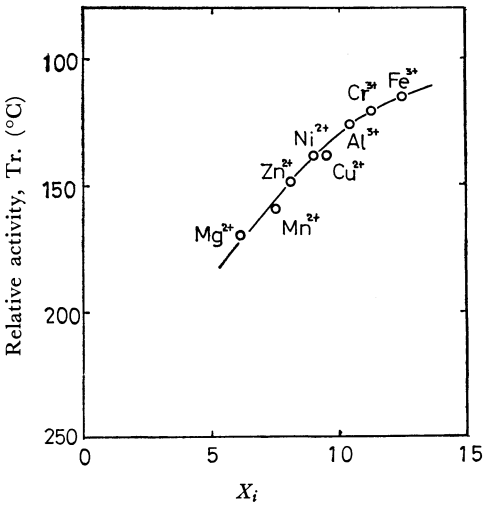

Fig. 2. Relative catalytic activity of sulfates. X_i denotes the electronegativity of metal ion.

acid introduced), is plotted against the acidity parameter of the metal ion (X_i) in Fig. 2.

From this figure, it is obvious that the sulfate containing an acidic metal ion has a high catalytic activity and that the activity sequence is determined by the parameter, X_i.

On the other hand, it has been recognized that the surface acidity of sulfate is strongly affected by the temperature at which the sulfate is dehydrated. Tanabe *et al.*[3] ascribed this phenomena to a specific structure of the sulfate which appeared in the dehydration of sulfate.

In our experiment, however, the surface of the sulfates during the dehydration of formic acid was hydrated with the water produced, so the specific structure such as appearing in the rather rigorous dehydration of sulfate seemingly disappeared from the surface during the reaction. Accordingly, it may be concluded that the dehydration of formic acid is promoted by the acidity of the hydrated cation on the sulfate surface.

The parameter, X_i, is thus seemingly valuable for predicting the acidity and the catalytic activity of the hydrated surfaces.

One of authors is grateful to the Matsunaga Science Foundation for a grant in support of this work.

2) Y. Ogino, *J. Catalysis*, **8**, 64 (1967).

3) T. Takeshita, R. Ohnishi, T. Matui and K. Tanabe, *J. Phys. Chem.*, **69**, 4077 (1965).

SHORT COMMUNICATIONS

X-Ray Diffraction Studies on Some Co(III) Complexes

Luigi CAMPANELLA

Institute of Analytical Chemistry, University of Rome, Italian National Researches Council, Rome, Italy

(Received April 27, 1968)

In connection with studies conducted at this Institute on the polarographic behavior of some Co(III) complexes,[1] structural studies on these compounds were undertaken. In this paper the results obtained for *cis*- and *trans*-$[Co\ en_2Cl_2]ClO_4$ and *cis*- and *trans*-$[Co\ en_2(C_6H_{11}COO)_2]ClO_4$ are reported. All the salts were characterised by the X-ray powder patterns taken in a Debye-Scherrer camera of diameter 114,8 mm with monochromatized Cu$K\alpha_1$ and Fe$K\alpha_1$ radiations. The salts were prepared as described by Linhard and Stirn[2] and by Carunchio, Illuminati and Maspero.[3]

Ito's[4] and Hesse-Lipson's[5,6] methods were successful in indexing powder patterns. The use of an IBM computer was helpful in applying the above said methods. X-ray powder studies so far performed lead to the following conclusions:

a) *cis*-$[Co\ en_2Cl_2]ClO_4$: the unit cell is monoclinic with dimensions $a=(7.032\pm0.001)$Å $b=(8.772\pm0.002)$Å $c=(8.000\pm0.002)$Å and $\beta=(107°2'\pm1')$. The measured density is 1.25 g/cm^3; the cell content is 1 formula unit, giving a calculated density of 1.22 g/cm^3.

b) *trans*-$[Co\ en_2Cl_2]ClO_4$: the unit cell is monoclinic with dimensions $a=(6.253\pm0.001)$Å $b=(8.065\pm0.002)$Å $c=(7.587\pm0.001)$Å and $\beta=(100°23'\pm1')$. The measured density is 1.54 g/cm^3; the cell content is 1 formula unit, giving a calculated density of 1.55 g/cm^3.

c) *cis*-$[Co\ en_2(C_6H_{11}COO)_2]ClO_4$: the unit cell is orthorhombic with dimensions $a=(8.696\pm0.002)$ Å $b=(15.625\pm0.006)$Å and $c=(10.870\pm0.003)$Å. The measured density is 1.18 g/cm^3. For 2 formula units in the unit cell the calculated density is 1.20 g/cm^3.

d) *trans*-$[Co\ en_2(C_6H_{11}COO)_2]ClO_4$: the unit cell is orthorhombic with dimensions $a=(7.407\pm0.001)$Å $b=(16.667\pm0.007)$Å and $c=(10.753\pm0.003)$Å. The measured density is 1.35 g/cm^3. For 2 formula units in the unit cell the calculated density is 1.33 g/cm^3.

Financial assistance was given by the Italian National Researches Council.

1) V. Carunchio and L. Campanella, *Ann. Chim.*, **57**, 1372 (1967).
2) V. M. Linhard and G. Stirn, *Z. anorg. u allgem. chem.*, **268**, 105 (1952).
3) V. Carunchio, G. Illuminati and F. Maspero, *J. Inorg. Nuclear Chem.*, **28**, 2693 (1966).
4) T. Ito, "X-Ray Studies on Polymorphism," Maruzen Co., Ltd., Tokyo (1950), pp. 187—228.
5) R. Hesse, *Acta Cryst.*, **1**, 200 (1948).
6) H. Lipson, *ibid.*, **2**, 43 (1949).

A Tertiary Phosphine-catalyzed Reaction of Acrylic Compounds with Aldehydes

Ken-ichi MORITA, Zennosuke SUZUKI and Hiromitsu HIROSE

The Basic Research Laboratories, Toyo Rayon Company, Ltd., Kamakura

(Received August 14, 1968)

We report here a novel reaction which gives new vinyl monomers. Reaction of acrylonitrile or methyl acrylate with various aldehydes in the presence of tricyclohexylphosphine as a catalyst furnished vinyl compounds 1 to 12 in 70 to 90% yields.[1,2] A typical example is as follows: reaction of 34.4 g (0.4 mol) of methyl acrylate, 26.4 g (0.6 mol) of acetaldehyde and 0.7 g (2.5 mmol) of tricyclohexylphosphine in 12 m*l* of dioxane in an atmosphere of nitrogen at 120—130°C for 2 hr afforded compound 9 in a yield of 85% based on converted methyl acrylate (conversion 23%).

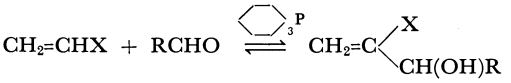

1, X=CN; R=CH_3. 2, CN; CH_2CH_3. 3, CN; $(CH_2)_2CH_3$. 4, CN; $CH(CH_3)_2$. 5, CN; $(CH_2)_6 \cdot CH_3$. 6, CN; C_6H_5. 7, CN; *p*-Cl-C_6H_4. 8, CN; *p*-CH_3-C_6H_4. 9, CO_2CH_3; CH_3. 10, CO_2CH_3, CH_2CH_3. 11, CO_2CH_3; $(CH_2)_2CH_3$. 12, CO_2CH_3; C_6H_5.

Structures for compounds 1 to 12 were assigned on the basis of their elemental analyses, the NMR spectra, the infrared spectra (nitrile band at 2229 cm^{-1} and double bond band at 1623 cm^{-1} for compounds 1 to 8; ester band between 1917 and 1722 cm^{-1} and double bond band between 1631 and 1635 cm^{-1} for compounds 9 to 12), and the ultraviolet absorption spectra (maximum between 202.5 and 206.5 mμ in methanol).

The structures of compound 1 and 9 were further confirmed by conversion of them into 1,4-dicyano-4-vinyl-1-cyclohexene,[4] and 1,4-dicarbomethoxy-4-vinyl-1-cyclohexene,[4] respectively, by treatment with boiling acetic anhydride and pyridine. 2-Cyano-1,3-butadiene and 2-carbomethoxy-1,3-butadiene dimerize readily under these conditions.

The possible mechanisms[5] of the reaction are depicted below.

mechanism I

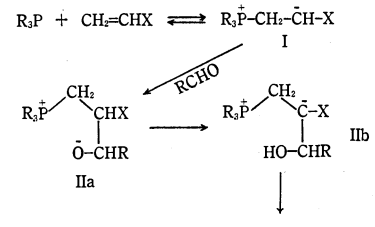

mechanism II

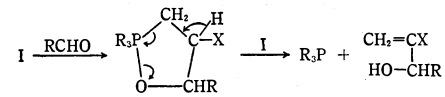

1) The novel reaction can be called Carbinol. Addition.

2) It has been reported[3] that the reaction of acrylonitrile and triphenylphosphine with benzaldehyde in the presence of alcohol at 140—175°C afforded *trans*-4-phenyl-3-butenenitrile and triphenylphosphine oxide.

3) R. Oda, T. Kawabata and S. Tanimoto, *Tetrahedron Letters*, **1964**, 1653.

4) C. S. Marvel and N. O. Brace, *J. Am. Chem. Soc.*, **71**, 37 (1949).

5) It is conceivable that if triphenylphosphine is used for the reaction the zwitterion I (R=phenyl) can isomerize to an ylid (III) by a proton transfer which then undergoes irreversible reaction with aldehydes to produce triphenylphosphine oxide and an olefin as Oda[3] reported. The absence of the interconversion I $\rightleftarrows$ III when R is alkyl is supported by the absence of 1,4-dicyanobutene in the product when acrylonitrile is dimerized in the presence of catalytic quantities of trialkylphosphines such as tri-*n*-butylphosphine or tricyclohexylphosphine.[6]

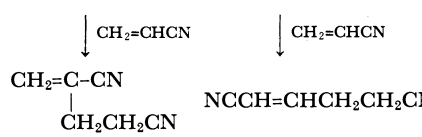

6) *Cf.* M. M. Baizer and J. D. Anderson *J. Org. Chem.*, **30**, 1357 (1965); P. Charardes, C. Grard, P. Lafont and M. Thiers (to Rhnoe-Poulene), French Pat. 1226081 (1964).

Synthesis of an Analogue of Desamino-lysine-vasopressin Containing No Disulfide Bond

Shumpei SAKAKIBARA and Satoe HASE

Peptide Center, Institute for Protein Research, Osaka University, Kita-ku, Osaka

(Received August 19, 1968)

Jošt and Rudinger synthesized two analogues of desamino-oxytocin which have no disulfide bond, and they demonstrated for the first time that the disulfide bond in oxytocin is important as a structural element but is not necessary for biological activity.[1] The present communication will report the synthesis of an analogue of desamino-lysine-vasopressin which has an ethylene linkage in place of the disulfide bond.

The following new compounds were synthesized as starting materials by conventional methods:*1 Z-Lys(Pht)-ONp, mp 99—100°C, $[\alpha]_D^{22}$ −16.0° (*c* 4, DMF); bis-[Z-Asu(OBu^t)-OH] piperazine salt which was derived from Z-Asu-OH,[2] mp 130—131°C, $[\alpha]_D^{28}$ −2.7° (*c* 2, AcOH); Z-Asn-OSu, mp 129—130°C, $[\alpha]_D^{24}$ −27.5° (*c* 2, DMF); Aoc-Phe-OSu, 130—131°C, $[\alpha]_D^{18}$ −52.0° (*c* 2, DMF); Aoc-Tyr(Bu^t)-OSu, mp 112—113°C, $[\alpha]_D^{23}$ −43.4° (*c* 2, DMF).

The synthesis of the protected peptide was started from glycine amide by the step-by-step elongation method using the respective acylamino acid active esters. Carbobenzoxy (Z) groups were removed by catalytic hydrogenation. *t*-Amyloxycarbonyl (Aoc) groups were removed by treatment with trifluoroacetic acid. Thus, the following intermediates were synthesized: Z-Lys(Pht)-Gly-NH_2, mp 215—217°C, $[\alpha]_D^{22}$ −2.2° (*c* 2.1, DMF); Z-Pro-Lys(Pht)-Gly-NH_2, mp 173—175°C, $[\alpha]_D^{22}$ −36.4° (*c* 2.1, DMF); Z-Asu(OBu^t)-Pro-Lys(Pht)-Gly-NH_2, mp 112—115°C, $[\alpha]_D^{18}$ −37.5° (*c* 2, DMF); Z-Asn-Asu-(OBu^t)-Pro-Lys(Pht)-Gly-NH_2, mp 188—190°C, $[\alpha]_D^{19}$ −38.0° (*c* 2, DMF); Z-Gln-Asn-Asu-(OBu^t)-Pro-Lys(Pht)-Gly-NH_2, mp 189—191°C, $[\alpha]_D^{19}$ −36.9° (*c* 1.6, DMF); Aoc-Phe-Gln-Asn-Asu(OBu^t)-Pro-Lys(Pht)-Gly-NH_2, mp 188—190°C (decomp.), $[\alpha]_D^{22}$ −35.4° (*c* 1.5, DMF); Aoc-Tyr(Bu^t)-Phe-Gln-Asn-Asu-Pro-Lys(Pht)-Gly-NH_2 (I), mp 224—226°C (decomp.), $[\alpha]_D^{25}$ −41.9° (*c* 1, AcOH). Found: C, 59.08; H, 6.75; N, 12.76%. Calcd for $C_{66}H_{90}O_{17}N_{12}\cdot H_2O$: C, 59.09; H, 6.91; N, 12.53%. The product, I, was converted to the *p*-nitrophenyl ester at the *ω*-position of the Asu-residue with *p*-nitrophenyl trifluoroacetate;[3] mp 217—220°C (decomp.), $[\alpha]_D^{25}$ −29.2° (*c* 1, DMF). The Aoc and *t*-butyl ether groups were removed with trifluoroacetic acid, and the product was treated in pyridine at 50°C (1 mmol/*l*). Then, the phthalyl group was removed with hydrazine acetate in DMF. The final product was purified by column chromatography on CM-Sephadex C-25, and lyophilized; yield 22% (calcd from I). $[\alpha]_D^{27}$ −80° (*c* 0.44, 1 N AcOH). Found: C, 54.30; H, 6.85; N, 15.89%. Calcd for $C_{48}H_{68}O_{12}N_{12}\cdot 3H_2O$: C, 54.43; H, 7. 04; N, 15.87%. Amino acid analysis: $Tyr_{0.98}$, $Phe_{1.05}$, $Glu_{0.96}$, $Asp_{1.00}$, $Asu_{1.00}$, $Pro_{1.06}$, $Lys_{1.03}$, $Gly_{0.97}$. These analytical data support the following structure for this material:

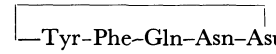

—Tyr-Phe-Gln-Asn-Asu-Pro-Lys-Gly-$NH_2\cdot 3H_2O$ (II)

Paper chromatography showed that this material was homogeneous: R_f 0.33 (*n*-BuOH : AcOH : H_2O=4 : 1 : 1), R_f 0.57 (Pyridine : AcOH : H_2O= 50 : 35 : 15).

The material II showed distinct pressor and antidiuretic activities, as is shown in Table 1.

TABLE I. BIOLOGICAL ACTIVITY OF COMPOUND II

Compound	Pressor (Rat)	Antidiuretic (Rat)
II	10.4 U/mg	7.8 U/mg
Desamino-Lys-vasopressin[a]	126	301

a) R. D. Kimbrough, Jr., W. D. Cash, L. A. Branda, W. Y. Chan and V. du Vigneaud, *J. Biol. Chem.*, **238**, 1411 (1963).

Thus, it was shown that the disulfide bond in vasopressin was replaceable by a stable ethylene bridge without any essential loss of biological activity.

1) K. Jošt and J. Rudinger, *Coll. Czech. Chem. Commun.*, **32** 1229 (1967).

*1 The tentatively proposed rules by the IUPAC-IBC were followed in the use of abbreviations: *J. Biol. Chem.*, **241**, 2491 (1966). DMF=dimethylformamide. Asu=*α*-aminosuberic acid. -OSu=*N*-hydroxysuccinimide ester. The amino acids used were in the L-form.

2) S. Hase, R. Kiyoi and S. Sakakibara, This Bulletin, **41**, 1266 (1968).

3) S. Sakakibara and N. Inukai, *ibid.*, **38**, 1979 (1965).

Ligand Field Activation Energy for Ligand Substitution in Octahedral Complexes

Hideo YAMATERA

Department of Chemistry, Nagoya University, Chikusa-ku, Nagoya

(Received August 23, 1968)

Crystal field theory has been successful in interpreting the relative rate of ligand substitution of transition-metal octahedral complexes, especially the relative inertness of the d^3, d^8 and low-spin d^6 complexes.[1] However, there has been disagreement between the crystal field prediction and observation in a few cases.

(1) In the series Mn^{2+}, Fe^{2+} and Co^{2+}, the observed rate of water exchange was $Mn^{2+} > Fe^{2+} > Co^{2+}$ (the activation energy remains nearly unchanged).[2] However, the crystal field activation energy (CFAE) was predicted to become more negative in going along the above series.

(2) Low-spin d^5 complexes, *e. g.*, $[Fe(CN)_6]^{3-}$, are known to be the most inert next to d^6 complexes, and are much more inert than predicted.[3]

In the present communication, the ligand field activation energy (LFAE) is predicted on the basis of molecular orbital theory. The calculation is based on second-order perturbation theory, like that previously reported in connection with the interpretation of the splitting of absorption bands of cobalt(III) complexes.[4] This approach is essentially equivalent to "the angular overlap model" proposed by Schäffer and Jørgensen.[5] Using the latter model, Yatsimirski *et al.*[6] calculated σ- and π-antibonding effects. The present calculation also led to similar results, which were then used to obtain LFAE.

For high-spin d^3, d^5 and d^8 and low-spin d^6 complexes, the present calculation of LFAE gives exactly the same values as the conventional CFAE values, irrespective of the relative contributions of the σ- and π-interactions. This is the case for each model of the transition state: the tetragonal pyramid (C_{4v}), the trigonal bipyramid (D_{3h}) and the pentagonal bipyramid (D_{5h}) models. For other complexes, however, the present LFAE differs appreciably from the conventional CFAE. The results for the C_{4v} model are given in Fig. 1.

Unlike CFAE, LFAE increases in the order $d^5 \leq d^6 \leq d^7 < d^8$ for high-spin and $d^3 \leq d^4 < d^5 < d^6$ for low-spin complexes. This explains the above observations (1) and (2) (crystal field calculations can also explain these observations, if $\rho_2(r)$ is assumed approximately equal to $\rho_4(r)$ instead of $2\rho_4(r)$ as in the conventional calculation).[7]

Additional spin-pairing may occur, in some transition states. Quantitative calculations showed that this is possibly the case for pentagonal bipyramidal transition states of some low-spin d^4 complexes. This gives a molecular orbital version of Adamson's mechanism[8] that $[Mn(CN)_6]^{3-}$—CN^- exchange should proceed through hepta-coordinated, spin-paired $[Mn(CN)_6H_2O]^{3-}$.

Full theoretical results, including those for other models, and detailed discussions on particular cases will be given elsewhere.

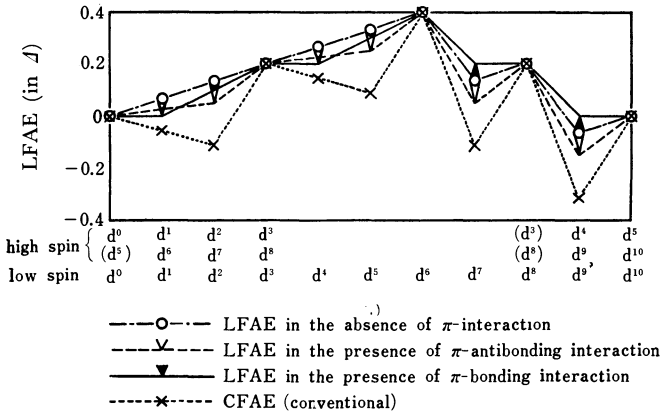

Fig. 1. LFAE and CFAE for the tetragonal pyramid (C_{4v}) model.

1) *E. g.*, F. Basolo and R. G. Pearson, "Mechanisms of Inorganic Reactions," John Wiley and Sons, Inc., New York (1967), p. 145.
2) T. J. Swift and R. E. Connick, *J. Chem. Phys.*, **37**, 307 (1962).
3) A. C. MacDiarmid and N. F. Hall, *J. Am. Chem. Soc.*, **76**, 4222 (1954).
4) H. Yamatera, This Bulletin, **31**, 95 (1958).
5) C. E. Schäffer and C. K. Jørgensen, *Mol. Phys.*, **9**, 401 (1965).
6) K. B. Yatsimirski, T. V. Mal'kova and L. I. Budarin, "Proceedings 10 th I.C.C.C.," Chem. Soc. Japan, Tokyo (1967), p. 290.
7) S. T. Spees, Jr., J. R. Perumareddi and A. W. Adamson, *J. Phys. Chem.*, **72**, 1822 (1968).
8) A. W. Adamson, J. P. Welker and W. B. Wright, *J. Am. Chem. Soc.*, **73**, 4786 (1951).

Mechanism of Ammonia Synthesis over Molybdenum Nitride

Ken-ichi AIKA and Atsumu OZAKI

Research Laboratory of Resources Utilization, Tokyo Institute of Technology, Ookayama, Meguro-ku, Tokyo

(Received August 23, 1968)

The mechanism of ammonia synthesis has been studied extensively with iron catalysts by many workers, but less frequently with other catalysts of different elements. It has been accepted for the iron catalyst that the elementary step of dissociation of nitrogen molecule determines the rate of the reaction.[1] This might be different for the other catalysts. It has been suggested, for those metals which are known to form stable nitrides, that the step of hydrogenation of the dissociated nitrogen determines the rate of the reaction, the step of the dissociation being fast enough.[2] In accordance with this suggestion, Kemball *et al.*[3] have concluded that the rate of ammonia synthesis over molybdenum nitride is determined by the hydrogenation of adsorbed nitrogen. Since the ready formation of nitride is known with molybdenum, this conclusion appears to be reasonable. However if this conclusion is true, a normal isotope effect by deuterium is expected for the rate of ammonia synthesis over the molybdenum nitride, although a reverse isotope effect was observed for the iron catalyst.[4] Thus the deuterium isotope effect in ammonia synthesis over molybdenum nitride was investigated. The catalyst was prepared by reducing molybdenum trioxide (5.09 g) with flowing hydrogen at 492°C followed by nitriding with nitrogen at 502°C. The catalyst thus obtained was identified by X-ray analysis to be Mo_2N. The synthesis runs were carried out in a closed circulating system with a liquid nitrogen trap. The reaction rate was measured by the decrease in total pressure.

It was found that the rate depended on the flow rate and that deuterium reacted faster than hydrogen. A kinetic equation which fits the rate data at 330°C irrespective of the isotopic species of hydrogen is obtained

$$r = 2.5\times10^{-3}\,P/(1+Ky\sqrt{P})^2,\ (l_{NH_3}/\mathrm{hr})$$

where P is the total pressure, y the concentration of ammonia in the effluent gas from the reactor and K a constant, the value of which is different for hydrogen and deuterium, that is, $K_H=1900$, $K_D=600$.

This result is similar to that on the iron catalyst,[4] and a similar interpretation can be applied, that is, the constant K can be interpreted as the equilibrium constant of a dissociative adsorption of ammonia.

$$NH_3 \rightarrow N(a) + 1.5H_2$$

The value of the ratio K_H/K_D ($=1900/600=3.2$) is close to the theoretical one (3.82) which is given as the inverse ratio of the equilibrium constants of ammonia synthesis with hydrogen and deuterium. Thus the rate determining step of the synthesis over molybdenum nitride seems to be the dissociation of nitrogen molecule as was the case for the iron catalyst.

The last conclusion was further examined by the isotopic exchange in nitrogen during the synthesis reaction. The initial isotopic composition of the reactant nitrogen was as follows.

$^{30}N_2$, 28.9%; $^{29}N_2$, 26.6%; $^{28}N_2$, 44.5%

Seventeen samplings were made during 122 hr of the synthesis over the molybdenum nitride at 330°C by which 72.6 m*l* (N.T.P.) of the reactant gas was consumed. During this synthesis the concentration of $^{29}N_2$ remained at 26.6±0.2%. This result clearly shows the absence of isotopic mixing in nitrogen during the synthesis and confirms the non-equilibration of nitrogen dissociation during the synthesis reaction.

It may be concluded that the rate of the ammonia synthesis over molybdenum nitride is not determined by the step of hydrogenation of adsorbed nitrogen atom, but by that of dissociation of nitrogen. The rate equation obtained, the isotope effect observed and the non-equilibration of nitrogen dissociation during the synthesis can be understood only from this view.

1) K. Tanaka, *J. Res. Inst. Catalysis Hokkaido Univ.*, **13**, 119 (1965).
2) W. G. Frankenburg, "Catalysis," Vol III, ed, by P. H. Emmett, Reinhold, N. Y. (1955), p. 190.
3) M. R. Hill, G. Kemball and M. W. Roberts, *Trans. Faraday Soc.*, **63**, 3570 (1967).
4) A. Ozaki, M. Boudart and H. S. Taylor, *Proc. Roy. Soc.*, **A258**, 47 (1960).

Photolysis of Tropone in the Vapor Phase[1]

Toshio MUKAI and Toshiya SATO

Department of Chemistry, Faculty of Science, Tohoku University, Sendai

and Makoto TAKAHASI and Hitoshi MIKUNI

Department of Pure and Applied Sciences, College of General Education, The University of Tokyo, Komaba, Meguro-ku, Tokyo

(Received September 4, 1968)

In solution, most tropone derivatives (I), upon irradiation, afford their valence isomer, II[2]. On the other hand, the thermolysis of the troponoids gives benzenoids in a very good yield.[3] The kinetic study of the thermoylsis has suggested that the decarbonylation proceeds *via* norcaradienones.[3] The good contrast between the photochemical behavior and the thermal behavior of the troponoid can be supported by the molecular orbital symmetry theory.[4] The disrotatory process of the lowest vacant molecular orbital can lead to II while the highest occupied molecular orbital leads to III. However, the photoreaction of tropone (I, R=H) is an exceptional case: dimers[5] and benzene[2] were obtained instead of II (R=H). Although the yield was very poor, the photochemical formation of benzene may be assumed to arise from the use of III as an intermediate.[2] However, this assumption is contrary to the molecular orbital symmetry theory described above.

We have studied the photolysis of tropone *in the vapor phase* in order to clarify the mechanism for the decarbonylation of tropone. The photolysis was carried out in a Pyrex vessel (170 ml) at 100±5°, under completely degassed conditions, by external irradiation using Toshiba H 400-P

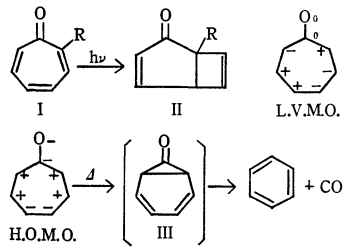

lamp.[6] The results obtained are shown in the table, although all of them are only preliminary.

The yield of the decarbonylation (runs 1 and 2) increased to about 30% compared with the photolysis in solution, where the yield was 1%. In addition, when an inert gas such as carbon dioxide was added to the reaction system, a decrease in the yield for the decarbonylation was observed (run 3).

These facts suggest that the excited molecule of tropone converts isoenergetically to the vibrationally-excited molecule, which then gives benzene and carbon monoxide through the intermediate III. Although the photo-excited state of tropone cannot be assigned on the basis of the results of the present experiment, it seems unlikely that the triplet state is involved, considering that the estimated triplet energy of tropone (42—53 kcal/mol)[5d] is rather less than the activation energy of the thermal decarbonyl process of tropone (54.1 kcal/mol).[3] The interpretation of the quenching effect of oxygen (run 4) is left for future investigation.

TABLE 1

Run	Tropone μ mol (mmHg)	Gas added (mmHg)	Irr. time hr	CO (μ mol)	Benzene (μ mol)
1	32.1(4.30)	—	1.0	12.2	10.0
2	26.0(3.53)	—	0.5	7.96	5.1
3	41.5(5.63)	CO_2(15)	0.5	0.42	not detect
4	38.5(5.22)	O_2(21)	0.5	0.27	not detect

1) Organic Photochemistry. IX.

2) O. L. Chapman, "Advances in Photochemistry," Vol. I, ed. by W. A. Noyes, Jr., G. S. Hammoed, and J. N. Pitts, Jr., Interscience Publishers. New York, N. Y. (1963), p. 326.

3) T. Mukai, T. Nakazawa and T. Shishido, *Tetrahedron Letters*, **1967**, 2465.

4) a) R. B. Woodward and R. Hoffmann, *J. Am. Chem. Soc.*, **87**, 395 (1965). b) R. Hoffmann and R. B. Woodward, *ibid.*, **87**, 2046 (1965).

5) a) Mukai, T. Tezuka and Y. Akasaki, *J. Am. Chem. Soc.*, **88**, 5025 (1966). b) T. Tezuka, Y. Akasaki and T. Mukai, *Terahedron Letters*, **1967**, 1397, 5003. c) A. S. Kende, *J. Am. Chem. Soc.*, **88**, 5026 (1966). d) A. S. Kende and J. E. Lancaster, *J. Am. Chem. Soc.*, **89**, 5283 (1967).

6) Control reaction indicated that, under the same condition, heating of tropone underwent no decarbonylation.

New Catalytic Synthesis of Ketones by the Oxidation of Olefins

Yoshihiko MORO-OKA, Shyoji TAN, Yusaku TAKITA and Atsumu OZAKI

Research Laboratory of Resources Utilization, Tokyo Institute of Technology, Ookayama, Meguro-ku, Tokyo

(Received September 4, 1968)

It is well known that α-olefins are oxidized to ketones by a palladium chloride catalyst with copper chloride in the presence of hydrogen chloride and water.[1] However, in the heterogeneous oxidation of olefins, allylic oxidation has been mainly reported to occur and no catalyst effective in forming ketones has yet been found. In this communication we wish to report a new catalytic synthesis of ketones by the gas-phase oxidation of olefins in the presence of steam.

The catalyst used in the present synthesis is composed of tin- or cobalt oxide combined with molybdenum trioxide. The atomic ratio of the tin or the cobalt to the molybdenum in the catalyst is usually larger than unity. Sn-90/Mo-10 and Co-90/Mo-10 catalysts were used in this experiment. The catalyst was prepared by the thermal decomposition of a mixture of tin- or cobalt hydroxide and an aqueous solution of ammonium molybdate. It was molded into cylindrical tablets and was fired in air at 550°C for 5 hr before the run. The reactions were carried out in a flow system at an atmospheric pressure. The reaction products were separated by gas chromatography and were identified by mass spectrometry. Typical experimental results are tabulated in Table 1.

Propylene, *n*-butenes, and 1-pentene were converted to acetone, methyl ethyl ketone, and methyl propyl ketone (including diethyl ketone), respectively. When the reactions were carried out at higher temperatures, the per-pass conversion of olefins increased, whereas the selectivity to ketones was decreased by the side reactions forming acetaldehyde, acetic acid, and carbon dioxide.

Ethylene did not react under the same conditions and gave only carbon dioxide at higher temperatures. Isobutene, which has no corresponding ketone, was converted mainly to tertiary butanol and diisobutene under the same conditions, and to α-methylacrolein and carbon dioxide at higher temperatures. On both the tin and cobalt catalysts, primary and secondary alcohols were easily oxidized to the corresponding aldehydes and ketones respectively. These results suggest that ketones, were formed *via* the hydration of olefins to form alcoholic intermediates followed by oxydehydrogenation. Since it has been established that acid catalysts are effective for the hydration of olefins, and since tin-molybdenum and cobalt-molybdenum heteropolyacids are known, it seems that the heteropolyacid is responsible for the first step of the reaction.

Some binary oxides, such as Cr_2O_3-MoO_3, Fe_2O_3-MoO_3, and CuO-MoO_3, were also effective in forming acetone from propylene, however, the selectivities to acetone were far lower than in the cases of SnO_2-MoO_3 and Co_3O_4-MoO_3.

TABLE 1. REACTIONS OF OLEFINS OVER SnO_2-MoO_3 AND Co_3O_4-MoO_3 CATALYSTS

Olefin	Ketone	Catalyst	Reaction temp. (°C)	Conversion of olefin (%)	Selectivity to ketone* (%)
CH_2=$CHCH_3$	CH_3COCH_3	Sn-Mo	135	9.0	85.3
		Co-Mo	210	4.0	75.3
CH_2=CHC_2H_5	$CH_3COC_2H_5$	Sn-Mo	135	4.8	85.3
		Co-Mo	240	2.2	60.8
CH_3CH=$CHCH_3$	$CH_3COC_2H_5$	Sn-Mo	155	9.2	58.8
(trans)		Co-Mo	233	2.5	26.7
CH_2=CHC_3H_7	$CH_3COC_3H_7$**	Sn-Mo	158	8.0	65.4

Experimental condition.
Catalyst, 16—20 g. GHSV, 400—450.
Reactant gas composition, Olefin 20 vol%, O_2 30%, H_2O 30%, N_2 20%.
* Values exclusive of isomerization.
** Including diethyl ketone.

1) J. Smidt, W. Hafner, R. Jira, J. Sedlmeier, R. Sieber, R. Ruttinger and H. Kojer, *Angew. Chem.*, **71**, 176 (1959); **74**, 93 (1962).

Effect of Laser Irradiation on Infrared Spectrum of Ammonia

Isao SUZUKI* and Shigeko SUZUKI**

* *Department of Chemistry, Faculty of Science, The University of Tokyo, Hongo, Bunkyo-ku, Tokyo*

** *Department of Pure and Applied Sciences, College of General Education, The University of Tokyo, Komaba, Meguro-ku, Tokyo*

(Received September 10, 1968)

Although a few observations have been reported on the laser-induced fluorescence of vibration-rotation transitions,[1-3] they have been limited to the region where laser frequencies locate, and hardly have they been extended to the region of pure rotational transitions. In this communication, we report on the observation of emission spectrum of ammonia as well as the change in the absorption spectrum in the far-infrared by irradiation of a CO_2 laser. Similar measurements have also been made for the ν_2 band in the 10 μ region, with which the laser frequencies coincide.

The CO_2 laser used consists of a 1.5 m discharge tube with two internal mirrors; one is a concave mirror of radius 3.5 m and the other is a flat germanium plate from which the laser beam is taken out. A leakage transformer (15 kV) was used for ac-excitation. The laser output is distributed among a few vibration-rotation transitions of the 10.6 μ band, of which the P(20) line at 944.25 cm^{-1} is the strongest.

For spectroscopic measurements a cross-cell similar to that described by Ronn[1] was used. The emission perpendicular to the incident laser beam was observed. With this cell we also made absorption measurements with or without laser irradiation. In Fig. 1, we show the emission spectrum of NH_3 (150 mmHg) obtained in the 340—200 cm^{-1} region with a Hitachi EPI-L spectrophotometer, along with the absorption spectra of NH_3 at the same pressure with and without the laser irradiation. The emission is strongest at about 275 cm^{-1} ($J=13\rightarrow14$), where the difference between the normal and irradiated absorption spectra is largest.

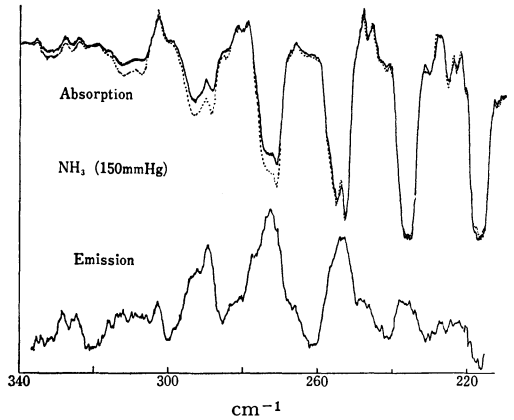

Fig. 1. Infrared spectra of ammonia (150 mmHg) in the 340—200 cm^{-1} region: laser-induced emission (below), and absorption spectra (above). Dotted line indicates the irradiated spectrum.

In the 10 μ region we have also observed rather strong emission. As reported by Ronn,[1] the spectrum is quite complex, probably due to the coincidence of the laser lines with "hot transition" $\nu_2^s\rightarrow2\nu_2^a$ of NH_3. The change in the absorption spectrum is also complex; however, a few remarks can be made: (1) Remarkable change in intensity was observed for the R(12)-R(16) lines of $0^s\rightarrow1^a$ band, and their intensities increased up to twice. (2) The Q-lines with $J=\sim10$ at about 950 cm^{-1} also exhibited intensity increase under the same conditions, whereas the changes were not appreciable for the corresponding P-lines. (3) Every absorption band associated with $1^s\rightarrow2^a$ transitions increases its intensity when irradiated. (4) Some fundamental lines with low J showed intensity decrease.

The above results may be interpreted as follows: since the CO_2 laser serves as a pumping source, the molecules absorb the light of characteristic frequencies and are exicted to the corresponding vibration-rotation levels. The collison relaxation time, however, is sufficiently short to allow the redistributions of the molecules among all the vibration-rotation levels. We may say that a dynamical equilibrium is established, in which the populations of the upper vibrational levels as well as the rotational temperature of each vibration level are higher than those in the thermal equilibrium. Thus, the CO_2 laser irradiation affects not only the vibration rotation transitions around the laser frequencies but also the other vibration-rotation transitions. The observed pure rotational emission and the intensity change in the absorption spectrum can also be explained on the same basis.

1) A. M. Ronn, *J. Chem. Phys.*, **48**, 511 (1968).
2) M. C. Borde, A. Henry, and M. C. Henry, *Compt. Rend.*, **B262**, 1389 (1966); **B267**, 19 (1967).
3) M. H. Bunnet, *ibid.*, **B264**, 1721 (1967).

No Scrambling in the Decomposition of Labeled Benzoyl Peroxide

Michio KOBAYASHI, Hiroshi MINATO and Yoshikuni OGI

Department of Chemistry, Tokyo Metropolitan University, Fukazawa, Setagaya, Tokyo

(Received September 11, 1968)

Taylor and Martin[1] showed that *ca.* 38% of all radical pairs formed in the decomposition of acetyl peroxide recombined in the solvent cage to give acetyl peroxide with scrambling of label. We have investigated a similar reaction with benzoyl peroxide labeled with oxygen-18 in the carbonyl oxygen. We wish to report on a rather surprising finding that the scrambling of the label does not occur during the decomposition of the labeled benzoyl peroxide.

The labeled benzoyl peroxide was prepared from the labeled benzoyl chloride and sodium peroxide. A solution of 120 m*l* of benzene containing 8.00 g of the benzoyl peroxide was refluxed at 78°C for 340 min (a half life of the peroxide). The carbon dioxide evolved was collected in a liquid nitrogen trap. The reaction mixture upon 50% decomposition was cooled and separated into benzoyl peroxide, benzoic acid and an ester fraction, from which phenyl benzoate was isolated by elution chromatography.

These products were converted into carbon dioxide which were assayed for oxygen-18 by mass spectrometry. Several methods were investigated in order to separate the carbonyl oxygen and the peroxidic oxygen in the benzoyl peroxide, and the best method found was converting it into benzhydrazide by the reaction with hydrazine. The hydrazide obtained from the starting peroxide contained all the oxygen-18 that was present in the peroxide. It is interesting to note that hydrazine attacks the carbonyl carbon of benzoyl peroxide, whereas dimethylaniline attacks the peroxidic oxygen.[2] The results are shown in Table 1.

TABLE 1. SPECIFICITY OF ^{18}O-LABELING

Sample	% ^{18}O-excess	% ^{18}O Calcd
Starting BPO	0.696	0.673
Its hydrazide	1.345	(1.345)
Recovered BPO	0.708	0.673
Its hydrazide	1.314	1.345
PhCOOH	0.682	0.673
PhCOOPh	0.628	0.673
CO_2	0.669	0.673

The hydrazide produced from the peroxide recovered after 50% decomposition contained all the oxygen-18 that was present in the starting peroxide (within the experimental error). This finding clearly shows that the scrambling of the label does not occur in the decomposition of the ^{18}O-labeled benzoyl peroxide in contrast to the case of acetyl peroxide.[1] It is difficult to determine the reason for the difference of the behavior of these two peroxides, but following explanation seems to be possible. There are two limiting conformations, I and II, for peroxides. Conformation I is favorable for the scrambling upon decomposition. Because of the resonance with the benzene ring, the carbonyl oxygen of benzoyl peroxide is negatively charged to a greater extent than that of acetyl peroxide. Due to the repulsion of the greater charge on the oxygen, the conformations of the decomposing benzoyl peroxide probably do not contain Conformation I. The majority of the peroxide will be decomposing from the conformations similar to Conformation II.

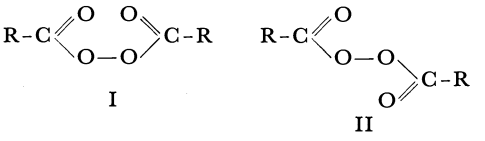

I II

In order for the radicals produced from Conformation II to scramble, the carboxyl group must rotate. The bond between the methyl carbon and the carboxyl carbon is not restricted, whereas the bond between the benzene ring and the carboxyl carbon is somewhat restricted because of the resonance. The rotation of the benzoyloxy radical as a whole is also expected to be more difficult than the acetoxy radical which is much smaller. However, further investigation is necessary for the clarification of these points.

1) J. W. Taylor and J. C. Martin, *J. Am. Chem. Soc.*, **88**, 3650 (1966).

2) C. Walling, " Free Radicals in Solution," John Wiley, New York (1957), p. 590—595.

BULLETIN OF THE CHEMICAL SOCIETY OF JAPAN VOL. 41 2823—2828 (1968)

Effect of Surface Active-Agents and Some Molecules on the Electrical Properties of Lipid Membranes

Masao HASHIMOTO

Department of Physics, Faculty of Science, Tokyo Metropolitan University, Setagaya-ku, Tokyo

(Received February 9, 1968)

The electric and mechanical properties of lipid membranes between two electrolyte solutions were observed. The electric resistance was 10^7—10^8 $\Omega \cdot cm^2$; the capacity, 0.2—1 $\mu F/cm^2$, and the surface tension, 2.2—4.9 dyn/cm. The electric conductivity increased with an increase in the surface area of the lipid membranes. Furthermore, the electric resistance and the capacity decreased when an ionic surface-active agent was adsorbed to the lipid membranes. The effect may be caused by the structural change of the lipid membranes due to both the electric and the hydrophobic interactions between the ionic surface-active agent and the lipid membranes.

It has been pointed out experimentally by Overton[1] and Collander[2] that the permeability coefficient of a substance through the membrane of a plant cell is proportional to its oil/water partition coefficient, and that the membrane shows a comparatively high permeability to lipid-soluble substances. On the basis of such experiments, they suggested that lipids might be involved in the membrane structure. On the other hand, the physico-chemical nature of the lipid monolayer has been investigated by many authors, beginning with Gorter and Grendel.[3]

From the fact[4-6] that the surface tension of the urchin egg is larger than that of the lipid monolayer in the range of physiological pH values, Danielli and Davson[7] proposed the lipid bilayer coated with protein as the fundamental element of the biological membranes. Their proposal has been supported by the electron-microscopic observations,[8,9] the X-ray diffraction pattern,[10-12] and so on.

In investigating biological membranes, studies of lipid bilayers will be more useful than those of the monolyaer.

Several years ago, Mueller *et al.*[13-17] and Thompson *et al.*[18-22] succeeded in forming lipid bilayers between two electrolyte solutions, and reported on some physico-chemical properties, *i. e.*, the electric conductivity, the electric capacity, the surface tension, *etc.*, of such systems.

The present author has been especially interested in the work of Mueller *et al.* They found that the electric resistance of a lipid bilayer adsorbing some water-soluble substances is much lower than that of the original, bare lipid bilayer, and showed that the resistance of biological membranes is of an order similar to that of the coated lipid bilayers. Because of the lack of detailed information of the adsorbed molecules, however, we can not really explain the mechanism of such a reduction of the electric resistance.

It is the purpose of this paper to investigate

1) L. F. R. Picken, "The Organisation of Cells and Other Organisms," Oxford University Press, Oxford (1960), p. 910.
2) R. Collander, *Trans. Farad. Soc.*, **33**, 985 (1937).
3) E. Gorter and F. Grendel, *J. Exp. Med.*, **41**, 439 (1925).
4) E. N. Harvey, *J. Franklin Inst.*, **214**, 1 (1932).
5) K. S. Cole, *J. Cell Comp. Physiol.*, **11**, 1 (1932).
6) N. K. Adam, "The Physics and Chemistry of Surfaces," Oxford University Press, Oxford (1941).
7) J. F. Danielli and H. Davson, "Permeability of Natural Membrane," Cambridge University Press, Cambridge (1943) p. 204.
8) B. B. Geren, *Expt. Cell. Res.*, **7**, 558 (1954).
9) J. D. Robertson, *J. Biophys. Biochem. Cytol.*, **1**, 271 (1955).
10) F. O. Schmitt, R. S. Bear and K. J. Palmer, *J. Cell Comp. Physiol.*, **18**, 31 (1941).
11) J. B. Finean, *Biochim. Biophys. Acta*, **12**, 371 (1953).
12) A. Engström and J. B. Finean, "Biological Ultrastructure," Acad. Press, New York, N. Y. (1958), p. 223.
13) P. Mueller, D. O. Rudin, H. Ti Tien and W. C. Wescott, *Circulation*, **26**, 1167 (1962).
14) P. Mueller, D. O. Rudin, H. Ti Tien and W. C. Wescott, *Nature*, **194**, 979 (1962).
15) P. Mueller, D. O. Rudin, H. Ti Tien and W. C. Wescott, *J. Phys. Chem.*, **67**, 534 (1963).
16) P. Mueller and D. O. Rudin, *J. Theoret. Biol.*, **4**, 268 (1963).
17) P. Mueller, D. O. Rudin, H. Ti Tien and W. C. Wescott, "Recent Progress in Surface Science," Vol. 1, Academic Press Inc., New York, N. Y. (1964), p. 379.
18) T. E. Thompson, "Cellular Membranes in Development," ed. by M. Locke, Academic Press Inc., New York, N. Y. (1964). p. 83.
19) C. Huang, L. Wheeldon and T. E. Thompson, *J. Mol. Biol.*, **8**, 148 (1964).
20) C. Huang and T. E. Thompson, *ibid.*, **13**, 183 (1965).
21) C. Huang and T. E. Thompson, *ibid.*, **15**, 539 (1966).
22) C. Huang and T. E. Thompson, *ibid.*, **16**, 576 (1966).

the effect of the well-defined adsorbed materials on the physico-chemical nature of the lipid bilayers. The author used some surface-active agents, proteins, and polypeptides as the adsorbed materials, and observed such properties as the electric conductivity, the electric capacity, the surface tension, and the relationship between the surface area and the electric conductivity.

Experimental

Apparatus. The block diagrams of the apparatus are given in Figs. 1a and 1b. In Fig. 1a, the glass tube (A) is held vertically, and the end is bent horizontally. The diameter (E) at the end of the tube was 2 mm.

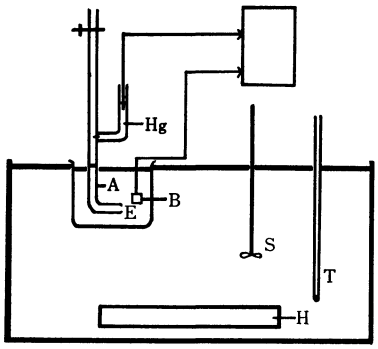

Fig. 1a. The main apparatus used to measure the electrical properties of the membrane.

Both beaker and tube were filled with an electrolyte solution. B, S, T, and H were the platinized platinum plate, stirrer, thermister, and heater respectively. The beaker was immersed in the water both, and the temperature of the electrolyte solution was kept constant within a range of error of ± 0.2°C.

Figure 1b shows the details of the neighborhood of the membrane.

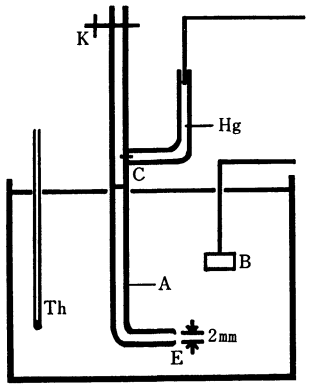

Fig. 1b. The enlargement figure near the membrane.

Th, C, and K are the thermometer, the platinized line, and the glass cock respectively. The membrane was formed by drawing the solution of the lipid with a small brush across the hole at the end of the tube. The surface of the membrane could be seen through a magnifying glass.

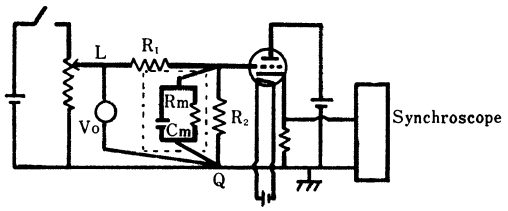

Fig. 2. Outline of the electric circuit.

The outline of the circuit is given in Fig. 2. The equivalent circuit for the membrane is enclosed with a dotted line. It is assumed that the membrane can be represented by an equivalent circuit in which the electric resistance, R_m, and the electric capacity, C_m, are connected in parallel.

A square-wave current was applied across the membrane. The potential difference across the membrane was measured with a synchroscope (Tektro 531 or Iwasaki Synchro Junior 5022). Since the measured potential difference contained the potential difference of the electrolyte solution, the latter was corrected. The resistances, R_1 and R_2, were adjusted to keep the potential difference between L and Q constant. On the basis of the assumption given above, the values of R_m and C_m can be obtained by:

$$V_m = V_0 \frac{\left(\frac{1}{R_m} + \frac{1}{R_2}\right)^{-1}}{\left(\frac{1}{R_m} + \frac{1}{R_2}\right)^{-1} + R_1}$$

$$V = V_m \cdot [1 - \exp(-t/C_m R)]$$

$$R = \left(\frac{1}{R_1} + \frac{1}{R_2} + \frac{1}{R_m}\right)^{-1}$$

where

V_m = Potential difference across the membrane in equilibrium
V = Potential difference across the membrane at time t
V_0 = Potential difference between L and Q measured by a voltage-ampere meter
$C_m R$ = Time constant

Materials. The lipid was extracted from ox brain in the same way as was done by Mueller *et al.* and was preserved in a refrigerator as a chloroform-methanol solution, kept from exposure to light and air.

The experiments were carried out for the *n*-decane solution as well as the chloroform-methanol solution. In the former case, after the evaporation of the solvent of the chloroform-methanol solution, the lipid was again dissolved in *n*-decane.

The salts used for the electrolyte solution were as follows: 1) NaCl, KCl, LiCl, *etc.*, 2) $MgCl_2$ and $CaCl_2$, 3) tetra-methylammonium chloride (TMA) and tetrabutylammonium chloride (TBA). Each of them was dissolved in a 1/500 M phosphoric acid buffer solution (pH 3.5, 7.0, and 10.0, mainly 7.0) after having been boiled in order to remove any oxygen.

Sodium dodecyl sulfate, sodium laurate, dodecyl trimethyl-ammonium chloride, and dodecyl trimethyl-ammonium bromide were used as ionic surface-active agents, while polyoxyethylene sorbitan mono-palmitate

Table 1. The CMC value of ionic agents used in our experiment

Compound	CMC value in water, mM	Temp. °C	CMC value in 0.1 M NaCl soln., mM[1]	Temp. °C
Dodecyl trimethylammonium chloride	16—20	30	2.7—3.3	36
Dodecyl trimethylammonium bromide	15—17	25	2.6—2.9	36
Sodium dodecyl sulfate	8—11	35	1.39	36
Sodium laurate	23—26	25	10—11	36

(I) and polyoxethylene sorbitan mono-oleate (II) were used as non-ionic surface-active agents. All these materials were originally commercial products. In order to purify them further, the ionic agents were recrystallized from ethanol.

The values of the critical micelle concentration (CMC) of these detergents were determined from the measurements of the surface tension by using the drop method.[23,24] These values are shown in Table 1.

One criterion of the ionic detergent purity employed in this work was the agreement of the observed CMC values with those reported in the literature.[25-28] Another criterion was that the curve relating the surface tension with the ionic detergent concentration did not show a minimum. The non-ionic agents were used without purification.

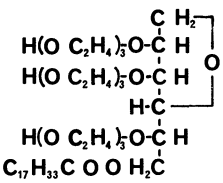

(I)

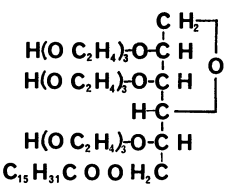

(II)

Polyglutamic acid (PGA) and the lysine-glutamic acid copolymer (L-G copolymer, lysine fraction 6 wt%) were offered by Akiyoshi Wada, while the histone was offered by Koichi Iwai.

Results

Electric Resistance and Electric Capacity of the Membrane. The values of the electric resistance of the lipid membrane at pH 7.0 and 36.0±0.2°C are shown in Table 2. The lipid membrane was formed from the chloroform-methanol solution.

The resistance decreased with an increase in the concentration of the electrolyte solution. Hanai *et al.*[29] reported a similar tendency in the lecithin bilayer. The electric resistance of the membrane in TMA and TBA solutions was larger than that in other electrolyte solutions. The electric capacity was nearly the same for all sorts of electrolyte solutions, the values ranging from 0.2 to 1.0 μF/cm^2.

Table 2. Effect of the concentration of the salt on the electric resistance at 36.0°C and pH 7.0

Salt	Concentration of salt, M	Resistance of the membrane $10^7\ \Omega\cdot cm^2$
NaCl	2.5	2.0
	1.0	2.4
	0.1	3.2
	0.01	3.8
KCl	1.0	1.0
	0.1	8.5
	0.01	15
LiCl	1.0	2.5
	0.1	5.7
	0.01	12
LiF	0.01	4.9
$CaCl_2$	0.1	8.5
	0.01	14
$MgCl_2$	1.0	2.4
	0.1	3.3
	0.01	5.1
TMA	0.1	12
TBA	0.1	18

On the other hand, the pH dependence of the electric resistance and of the capacity of the membrane was very small in each of these electrolyte solutions. For example, the electric resistance in the NaCl solution was $4.1\times10^7\ \Omega\cdot cm^2$ at pH 3.5, $3.2\times10^7\ \Omega\cdot cm^2$ at pH 7.0, and $5.0\times10^7\ \Omega\cdot cm^2$ at pH 10.0.

The membrane broke down upon the application of the electric voltage, 200—250mV.

The Effect of Surface-active Agents. When a cationic active agent, dodecyl trimethylammonium chloride, was added to the electrolyte solution, the resistance of the membrane decreased at the concentration of 0.5m M as is shown in Fig. 3. This concentration is about 1/6 the CMC value.

When the concentration of the surface-active agent was increased to about 2.5m M (about 9/10

23) W. D. Harkins and F. E. Brown, *J. Am. Chem. Soc.*, **38**, 288 (1916).
24) W. D. Harkins and F. E. Brown, *ibid.*, **41**, 499 (1919).
25) J. N. Phillips, *Trans. Faraday Soc.*, **51**, 561 (1955).
26) R. C. Merrill and R. Getty, *J. Phys. and Colloid Chem.*, **52**, 774 (1948).
27) I. M. Kolthoff and W. Stricks, *ibid.*, **53**, 424 (1949).
28) "Kagaku Binran Kiso-hen II" ed. by The Chem. Soc. Japan, Maruzen Co., Ltd., Tokyo (1966), p. 707. (in Japanese)
29) T. Hanai, D. A. Haydon and J. Taylor, *J. Gen. Physiol.*, **48**, Part 2, 59 (1965).

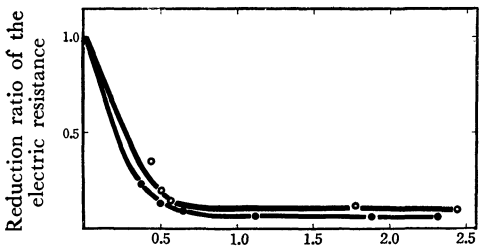

Fig. 3. Effect of the concentration of dodecyl trimethylammonium chloride and dodecyl trimethylammonium bromide on the electric resistance of the lipid membrane.
○ Dodecyl trimethylammonium chloride
● Dodecyl trimethylammonium bromide

the CMC value), the membrane broke down upon the application of an electric impulse. A further increase in the concentration of the detergent did not allow the membrane to be reformed.

As for dodecyl trimethylammonium bromide, the resistance of the membrane decreased at the concentration of 0.4 mM and the membrane broke down at the concentration of 2.3 mM The anionic agents, sodium dodecyl sulfate and sodium laurate, also reduced the resistance of the membrane (Figs. 4 and 5).

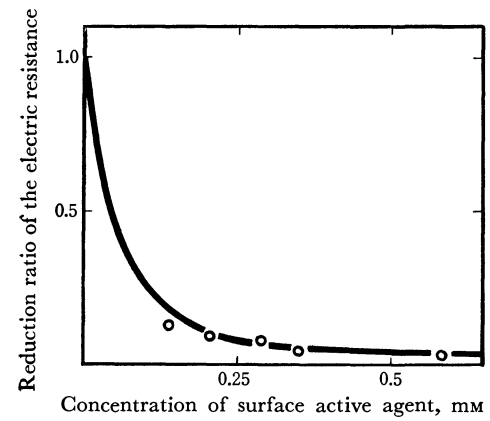

Fig. 4. Effect of the concentration of sodium dodecyl sulfate on the electric resistance of the lipid membrane.

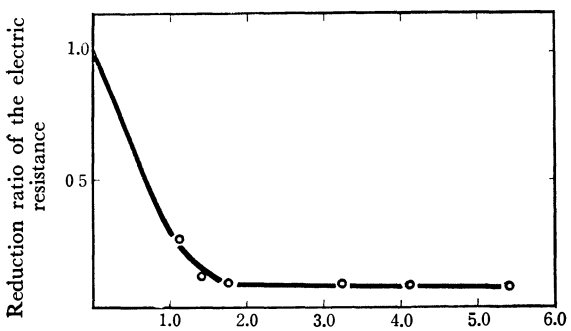

Fig. 5. Effect of the concentration of sodium laurate on the electric resistance of the lipid.

In the concentration range shown in Figs. 3, 4 and 5, the capacities ranged from 0.2 to 0.3μF/cm^2.

On the other hand, the non-ionic agents, polyoxyethylene sorbitan mono-palmitate and polyoxyethylene sorbitan mono-oleate, did not affect either the electric resistance or the capacity of the membrane.

Some Properties of the Membrane. As is well known, PGA is in a helical conformation at pH 4.5 and in a random coil at pH 10.0. In the present experiment, each solution of PGA, at pH 4.5, 7.0 and 10.0 was added to the electrolyte solution on both sides of the membrane.

In order to investigate the ionic effect of the copolymer on the resistance of the lipid membrane, on the other hand, we added the L-G copolymer to the electrolyte solution at pH 3.0, 7.0 and 10.0. In each case, however, no effect was found. Furthermore, the addition of neither histone nor aspartic acid had any effect, either.

In order to measure the surface tension of the membrane, a hydrostatic pressure difference was applied across the membrane in order to observe the radius of the curvature of the curved membrane. The surface tension can then be obtained from the following equation:

$$\gamma = \frac{1}{4} p \cdot r \text{ (dyn/cm)}$$

where p=hydrostatic pressure difference and r= radius of curvature.

The surface tension of the membrane in a NaCl solution was 2.2—4.9 dyn/cm at pH 7.0 and 36.0°C. Hanai *et al.*[30] measured the surface tension of a lecithin membrane formed from an *n*-decane solution by using the same method; they obtained the value of *ca.* 1 dyn/cm. They also reported[29-31]

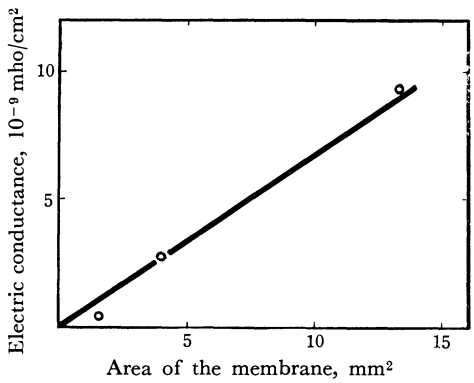

Fig. 6. The relation of the conductivity and the area of the bulged membrane.

30) T. Hanai, *Hyomen*, **4**, 643 (1966). (in Japanese)
31) T. Hanai, D. A. Haydon and J. Taylor, *J. Theoret. Biol.*, **9**, 433 (1965).

that the conductance of the lecithin membrane was nearly proportional to the surface area of the membrane and that the conductance per unit area 1.3×10^{-9} mho/cm in a 0.1 M NaCl solution. We also measured the conductance of the lipid membrane in relation to the surface area. The results are shown in Fig. 6.

The effect of the temperature on the membrane resistance was investigated in the 7—45°C temperature range. The membrane was stable only in the 20—40°C temperature range. The resistance was nearly independent of the temperature within the limits of the experimental error. This finding is not in agreement with that of Thompson.[18] He showed that the resistance changed discontinuously with the temperature. In our experiment described above, a chloroform-methanol mixture was used as the lipid solvent.

In order to investigate the effect of the solvent on the resistance of the membrane, we used *n*-decane as another solvent. The resistance of such a lipid membrane was much larger than that of the lipid membrane formed from a chloroform-methanol solution and was somewhat different from that obtained by Hanai *et al.*[30]

Discussion

As a lipid bilayer is rather simpler than a biological membrane in the sense that it does not contain protein, it is more important to investigate how the lipid bilayer adsorbs substances such as proteins and surface-active agents. Mueller *et al.* have for instance, reported that the resistance of the bilayer decreased when it adsorbed unidentified water-soluble substances extracted from egg white.

We observed that the resistance of the membrane decreased upon the addition of ionic surface-active agents to the electrolyte solution. The resistance did not change upon the addition of non-ionic agents, however.

We interpret the decrease in the electric resistance of the membrane as follows. Since the electric conductivity is due to the ionic current through the membrane, it is reasonable to surmise that the decrease in the electric resistance was caused by the increase in the ionic permeability due to the formation of several kinds of channels for ions with a structural change in the lipid membrane.

It may be considered that the added ionic agents adsorb on the membrane due to the interaction of the ionic agents with ionic sites in the outer region of the phospholipid membrane. Besides, hydrocarbon chains of the ionic agents may interact with the inner region of the lipid membrane. On the other hand, non-ionic agents will interact only with hydrocarbon chains of the lipid membrane.

Our experimental results suggest that the structural change of the membrane may be caused by both electrostatic and hydrophobic interactions of ionic surface-active agents with the membrane, and that the electrostatic interaction is necessary for the change in the membrane structure. That is, no structural change can be effected without ionic interaction in the outer region of the membrane. However, hydrophobic interaction may not be neglected.

The C number of the hydrocarbon chain of the surface active agents in our experiment was 11 or 12; in this case, hydrophobic interaction is plausible. No decrease in the membrane resistance was observed on the addition of substances with a few carbon atoms, for example, tetramethylammonium chloride, tetrabutylammonium chloride, aspartic acid, and caprylic acid. The structural change in the membrane may require the cooperation of electrostatic and hydrophobic interactions.

We shall now discuss the relation between the decrease in the resistance and the CMC values of the ionic agents. The resistance of the membrane decreased abruptly at a concentration of about 1/6 and at 1/10 the CMC value for cationic and anionic agents respectively. The lipid membrane may be sensitive to the solubilizing power of ionic detergents adsorbed due to electrostatic and hydrophobic interactions; the structural change in the membrane may be the consequence.

The CMC value of each ionic detergent may affect the critical concentration at which the abrupt decrease in the membrane resistance occurs. The difference between the decrease in the membrane resistance for cationic and anionic agents may correspond to the difference between the number of cationic and of anionic agents adsorbing on the membrane. As it is considered that the positive ions in the outer region of the

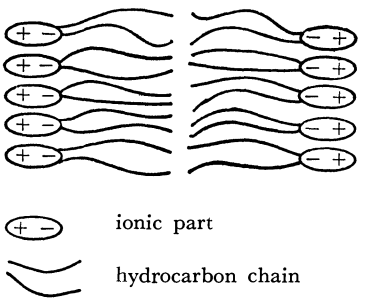

Fig. 7a. Lipid bilayer model.

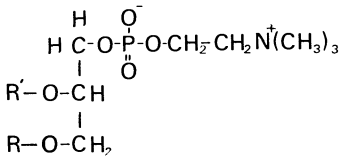

R, R′: Hydrocarbon chain (16 to 22 carbons long)

Fig. 7b. Structural formula of phospholipid.

membrane are nearer to the bulk solution than are the negative ions, the anionic agents will adsorb on the membrane easier than will cationic agents. The details of the lipid bilayer membrane are shown in Figs. 7a and 7b. The proportionality of the conductivity to the surface area of the membrane was not very good, though the conductivity did increase with the increase in the surface area.

In our experiment, the surface tension of the lipid bilayer was larger than that of the biological membrane. This is because the lipid bilayer is not coated with protein.[32-33]

The author wishes to express his deep gratitude to Professor Akiyoshi Wada of the University of Tokyo for his valuable advice and support throughout the course of this work, to Mr. Masaiku Hara for his experimental assistance, and to Professor Koichi Iwai supplying the histone.

Thanks are also due to Professors Syoten Oka and Misazo Yamamoto of Tokyo Metropolitan University for their helfpul suggestions.

32) J. F. Danielli and E. N. Harvey, *J. Cell. Comp. Physiol.*, **5**, 483 (1934).
33) J. F. Danielli, *Cold Spring Harbor Symposia*, **6**, 190 (1938).

BULLETIN OF THE CHEMICAL SOCIETY OF JAPAN VOL. 41 2828—2832 (1968)

The Structure of an Electrical Double Layer around a Surfactant Micelle

Fumikatsu Tokiwa and Kenji Ohki

Research Laboratories Kao Soap Company, Minato-Yakushubata, Wakayama-shi

(Received February 13, 1968)

Electrophoretic measurements have been made of the micelles of dimethyldodecylamine oxide (DDAO) and *N*-dodecyl-β-aminopropionic acid (DAPA), while changing the pH values of the solutions in the presence of 0.10 M sodium chloride. A picture of the structure of the electrical double layer around the micelle at different pH's was then constructed, according to Stern's theory, by a combination of the zeta potential, ζ, calculated from the electrophoretic mobility and the surface potential, ψ_0, obtained previously from the potentiometric titration. With the micelle of DDAO, the thickness of the immobile part of the double layer depends slightly on the pH of the solution and is estimated to be about 5 Å. With the micelle of DAPA, the estimated thickness of the immobile part seems rather high, especially on the alkaline side of the solution. The ζ/ψ_0 ratio for the micelles of DDAO and DAPA depends on the pH of the solution; in the case of DDAO the value of ζ/ψ_0 increases with a decrease in the surface potential.

The structure of an electrical double layer around a charged surfactant micelle is governed in general by the potential at the surface of the micelle, ψ_0, and the distribution of counter-ions and co-ions in the locality of the charged surface. The thickness of the immobile part of the double layer, the distance from the surface of the micelle to the plane of shear, is related in particular to the zeta potential of the micelle, the potential at the plane of shear, ζ. Several studies have been reported of the ζ-potentials of micelles of ionic surfactants,[1-4] but there has been a lack of studies of the thickness of the immobile layer of micelles.[5]

In the present paper, the ζ-potentials of the micelles of the surfactants, whose surface-charge density depends on the pH of the solution, have been discussed in connection with the surface potentials of the micelles previously evaluated from potentiometric data[6,7] in order to obtain knowledge of the thickness of the immobile layer. Stern's theory[8] is used to construct a picture of the structure of the electrical double layer around the micelle. The surfactants studied are a nonionic-cationic surfactant, dimethyldodecylamine oxide (abbreviated as DDAO), and an amphoteric surfactant, *N*-dodecyl-β-aminopropionic acid (abbreviated as DAPA). The surface-charge densities of the micelles depend on the pH of the solutions. With DDAO, the nonionic and cationic forms related by the equilibrium[6]:

1) D. Stigter and K. J. Mysels, *J. Phys. Chem.*, **59**, 45 (1955).
2) T. Nakagawa and H. Inoue, *Nippon Kagaku Zassi (J. Chem. Soc. Japan, Pure Chem. Sect.)*, **78**, 636 (1957).
3) H. W. Hoyer and A. Greenfield, *J. Phys. Chem.*, **61**, 735 (1957).
4) F. Tokiwa and K. Ohki, *Kolloid-Z. Z. Polymere*, **223**, 38 (1968).
5) D. Stigter, *J. Colloid Interface Sci.*, **23**, 379 (1967).
6) F. Tokiwa and K. Ohki, *J. Phys. Chem.*, **70**, 3437 (1966).
7) F. Tokiwa and K. Ohki, *ibid.*, **71**, 1824 (1967).
8) H. R. Kruyt, "Colloid Science," Elsevier Publishing Co., New York (1952).

$$C_{12}H_{25}N(CH_3)_2O \overset{H^+}{\rightleftharpoons} C_{12}H_{25}N^+(CH_3)_2OH$$

With DAPA, the anionic and cationic forms are related by the equilibrium[7]:

$$\begin{array}{ccccc} CH_2CH_2COO^- & & CH_2CH_2COO^- & & \\ | & \overset{H^+}{\rightleftharpoons} & | & \overset{H^+}{\rightleftharpoons} & \\ R\text{-}N\text{-}H & & R\text{-}N^+\text{-}H_2 & & \\ CH_2CH_2COOH & & & & \\ | & & & & \\ R\text{-}N^+\text{-}H_2 & & (R=C_{12}H_{25}) & & \end{array}$$

Experimental

Materials. The dimethyldodecylamine oxide (DDAO) was prepared by the H_2O_2 oxidation of highly-pure dimethyldodecylamine by the method described in a previous paper.[6] The sample was purified by repeated extraction with petroleum ether and by subsequent recrystallization from a mixture of acetone and benzene. The *N*-dodecyl-β-aminopropionic acid (DAPA) was the same as that used elsewhere.[7] The sodium chloride, hydrochloric acid, and sodium hydroxide were of an analytical reagent grade. The water used in this experiment was distilled and subsequently passed through an ion-exchange column.

Electrophoresis. The electrophoretic measurements were carried out in a Tiselius-type cell using a Hitachi Model HTB-2A Tiselius apparatus equipped with a Schlieren optical system. The concentrations of the surfactant in both the upper and lower layers of the cell were taken to be higher than the critical micelle concentration (CMC) in order to avoid the dissociation of the micelle into the monomers at a boundary.[2,4] The concentration of the supporting electrolyte, sodium chloride, was 0.10 M. The pH of solutions was adjusted with hydrochloric acid or sodium hydroxide, and the pH values of all the solutions were rechecked after measurements.

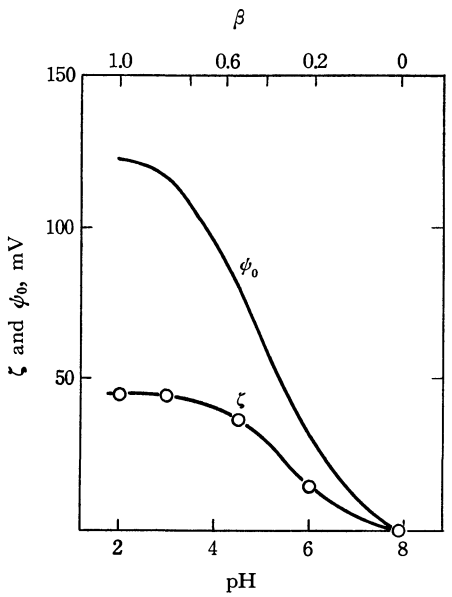

Fig. 1. The values of ζ and ψ_0 for the micelle of DDAO in the presence of 0.10 M NaCl plotted against pH.

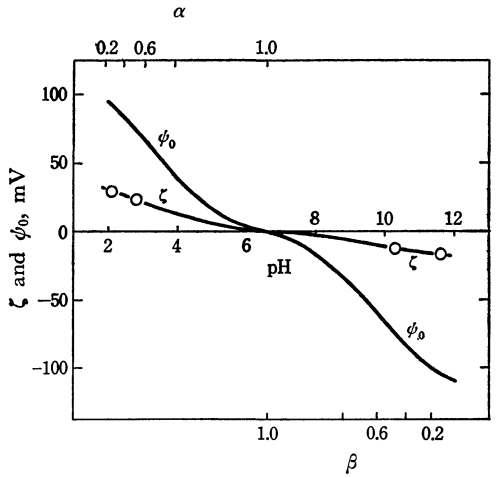

Fig. 2. The values of ζ and ψ_0 for the micelle of DAPA in the presence of 0.10 M NaCl plotted against pH.

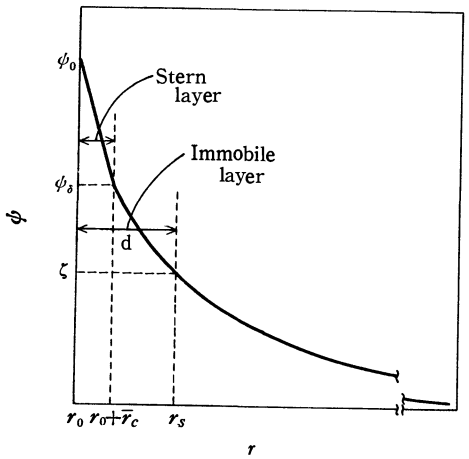

Fig. 3. Schematic representation of the structure of the double layer for the micelle of DDAO at pH 3.0: $\psi_0=117$ mV, $\psi_\delta=73.5$ mV, $\zeta=44.4$ mV, $r_0=29.1$ Å, $\bar{r}_c=1.8$ Å, and $d=5.1$ Å.

Results

In all the systems examined, only one moving boundary was obtained in each of the ascending and descending patterns. The electrophoretic mobility of the micelle, u_M, was calculated from the velocities of the ascending and descending boundaries by applying Dole's theory to the present system.[9,10] The value of u_M was calculated by the equation[2,4]:

$$u_M = X - \frac{Y - X}{(T_M{}^\eta/T_M{}^\alpha) - 1} \qquad (1)$$

9) V. P. Dole, *J. Am. Chem. Soc.*, **67**, 1119 (1945).
10) L. G. Longsworth, "Electrophoresis," ed. by M. Bier, Academic Press, New York (1959), p. 91.

Table 1. Electrical properties for the micelle of DDAO in the presence of 0.10 M NaCl

pH	β	$r_0\times10^8$ cm	n	$u_M\times10^4$ cm²/V·sec	ζ mV	ψ_0 mV	ψ_δ mV	ζ/ψ_0	$d\times10^8$ cm
2.0	1.00	29.5	134	2.55	44.7	122	74.1	0.366	5.2
3.0	0.91	29.1	129	2.54	44.4	117	73.5	0.380	5.1
4.5	0.55	25.4	85.9	2.06	36.3	81.9	59.1	0.443	5.0
6.0	0.21	22.2	67.0	0.81	14.4	30.9	22.2	0.466	4.7
7.9	0.0	22.1	66.5	0	0	0	0	—	—

Table 2. Electrical properties for the micelle of DAPA in the presence of 0.10 M NaCl

pH	α and β	$u_M\times10^4$, cm²/V·sec	ζ mV	ψ_0 mV	ψ_δ mV	ζ/ψ_0	$d\times10^8$ cm
2.1	$\alpha=0.27$ ($\beta=1.00$)	1.67	29.5	93.0	56.1	0.317	6.0
2.8	$\alpha=0.54$ ($\beta=1.00$)	1.30	22.9	71.4	48.0	0.321	6.9
10.3	$\beta=0.48$ ($\alpha=1.00$)	−0.71	−12.5	−75.0	−44.2	0.167	11.4
11.6	$\beta=0.01$ ($\alpha=1.00$)	−0.93	−16.4	−105	−46.5	0.157	9.2

Assuming $r_0=25$Å and $n=100$.

The details of Eq. (1) and its derivation are described in the Appendix. Tables 1 and 2 give the values of u_M for DDAO and DAPA respectively, calculated in terms of Eq. (1).

On several simplifying assumptions,[1,5,11] the relation between ζ and u_M may be written in the form[12]:

$$\zeta = 6\pi\eta u_M/D\cdot f(\kappa r_0) \qquad (2)$$

where $f(\kappa r_0)$ is Henry's function;[14] r_0, the radius of the micelle; κ, the inverse Debye radius, and η and D, the viscosity and the dielectric constant of the medium respetively. The ζ-potentials of the micelles of DDAO and DAPA as calculated by Eq. (1) are plotted in Figs. 1 and 2 respectively, together with the surface potentials of the micelles, ψ_0,[6,7] as a function of the pH of the solutions. In calculating Eq. (2), the r_0 values for DDAO were estimated from the potentiometric data reported previously,[15] and the value for DAPA was assumed to be 25 Å.

Discussion

A schematic representation of the structure of a double layer around a micellar particle according to Stern's model is given in Fig. 3 as a simple illustration. The surface potential, ψ_0, is divided into one potential, ψ_δ, over the diffuse part of the double layer and another, $\psi_0-\psi_\delta$, over the molecular condenser, as is shown in Fig. 3, where ψ_δ is a potential at the surface of the Stern layer.[8]

For the Stern layer, the equation for a spherical condenser may be used to obtain the value of ψ_δ from ψ_0. If one assumes that the Stern layer is the adsorbed monolayer of counter-ions,[16,17] and that, hence, the thickness of the layer is equal to the radius of the counter-ions, $\bar{r}_c$, the value of ψ_δ may be estimated by the equation:

$$\psi_\delta = \psi_0 - \frac{Q}{D}\left(\frac{1}{r_0} - \frac{1}{r_0+\bar{r}_c}\right) \qquad (3)$$

where Q is the net charge of the micelle, which is given by $\varepsilon n\beta$ for DDAO and by $\varepsilon n(\beta-\alpha)$ for DAPA, where ε is the elementary charge; n, the number of molecules per micelle; α, the degree of ionization of the carboxyl group, and β, the degree of the protonation of the nitrogen atom. The counter-ion for DDAO is Cl^-, and that for DAPA is Cl^- on the acid side and Na^+ on the alkaline side. A reasonable value of $\bar{r}_c$ is 1.84 Å for Cl^- and 2.17 Å for Na^+.[18] The ψ_δ values for the DDAO micelle at different pH's, as calculated by Eq. (3), are given in Table 1, together with the values of ψ_0, r_0 and n which have previously been obtained from potentiometric titration data in previous works.[6,15] Table 2 also gives the rough ψ_δ values for the DAPA micelle estimated by assuming that $n=100$.

11) D. J. Shaw, "Introduction to Colloid and Surface Chemistry," Butterworth & Co., London (1966).
12) Recently Wiersema *et al.*[13] have reported a more strict method of calculating the ζ-potential of a spherical colloidal particle by using an electronic computer. In the present case, however, the difference between the values obtained from Eq. (2) and their calculated values is not significant since the ζ-potentials are relatively low.
13) P. H. Wiersema, A. L. Loeb and J. Th. G. Overbeek, *J. Colloid Interface Sci.*, **22**, 78 (1966).
14) D. C. Henry, *Proc. Roy. Soc.*, **A133**, 106 (1931).
15) F. Tokiwa and K. Ohki, *J. Colloid Interface Sci.*, **24**, 219 (1967).
16) M. Nagasawa and A. Holtzer, *J. Am. Chem. Soc.*, **86**, 531 (1964); M. Nagasawa, T. Murase and K. Kondo, *J. Phys. Chem.*, **69**, 4005 (1955).
17) J. T. Davies and E. K. Rideal, "Interfacial Phenomena," Academic Press, New York, N. Y. (1961), p. 85.
18) C. B. Monk, "Electrolytic Dissociation," Academic Press, New York, N. Y. (1961), p. 271.

For the diffuse layer, a potential, ϕ, at a certain distance from the center of a particle, r, may be calculated by Gouy-Chapman's equation for a spherical double layer. With $1/m$ valent electrolyte, Gouy-Chapman's equation is written in the form[19]:

$$r^{-2}\frac{d}{dr}\left(r^2\frac{d\phi}{dr}\right)=\frac{4\pi\varepsilon n_0}{D}\left[\exp\left(\frac{\varepsilon\phi}{kT}\right)-\exp\left(-\frac{\varepsilon\phi}{kT}\right)\right] \quad (4)$$

where n_0 is the concentration (number/cm^3) of positive or negative ions in the bulk of the solution. For the sake of convenience, by introducing a dimensionless "reduced potential" y $(=\varepsilon\phi/kT)$ and a "reduced distance" $q(=\kappa r)$ into Eq. (4), we obtain[19]:

$$q^{-2}\frac{d}{dq}\left(q^2\frac{dy}{dq}\right)=\frac{1}{2}(e^y-e^{-y}) \quad (5)$$

The solutions of Eq. (5) under different boundary conditions, y_0 and q_0, and using an electronic computer have been given by Loeb *et al.*[19] and are tabulated in Ref. 19. In the present case, y_0 and q_0 are written:

$$y_0=\varepsilon\psi_\delta/kT, \quad \text{and} \quad q_0=\kappa(r_0+\bar{r}_c)$$

Thus, we can construct ϕ *vs.* r curves, an example of which for the micelle of DDAO is given in Fig. 3.

The thickness of the immobile part of the double layer, $d(=r_s-r_0)$, may be obtained from the ζ-potential and the ϕ *vs.* r curve. The d values for the DDAO micelle at different pH's are given in Table 1; about 5 Å, they depend slightly on the pH of the solution. The thickness obtained here is comparable to that obtained by Stigter for the micelle of sodium dodecyl sulfate (4—5 Å) from the viscosity and the diffusion data.[5] It is of interest to calculate the ratio of ζ to ϕ_0 from the present data. The ζ/ϕ_0 ratio has been discussed by Davies and Rideal.[20] According to their calculation, the tendency is for ζ/ϕ_0 to increase as the surface potential is lowered. The results obtained here agree in tendency with their calculations.

Table 2 gives the rough values of the thickness of the immobile layer for the DAPA micelle. The thickness is roughly 6—7 Å on the acid side and 9—11 Å on the alkaline side, thicker than that for DDAO. The ζ/ϕ_0 ratios for DAPA are lower than those for DDAO, especially on the alkaline side. The reason for this is not clear; however, the results probably have some relation with the configuration of charged groups[21] at the surface of the micelle. The charged groups would be located relatively inside the surface of the micell.

The authors wish to express their thanks to Dr. H. Kita, Director of the Research Laboratories, for his encouragement and for permission to publish this paper.

Appendix

An initially sharp boundary between two solutions containing n ion species will generally split, upon the passage of an electric current, into $n-1$ separate boundaries, each moving at a different rate. According to Dole,[9,10] the following polynomials can be derived for each moving boundary:

$$\sum_j\frac{T_j^\alpha}{u_j-X_k}=0, \qquad \sum_j\frac{T_j^\eta}{u_j-Y_k}=0 \quad (A1)$$

$$k=1,2,3,\cdots,n-1$$

where:

$$X_1=V^{\alpha\beta}{}_\sigma{}^\beta \qquad Y_1=V^{\alpha\beta}{}_\sigma{}^\alpha$$
$$X_2=V^{\beta\gamma}{}_\sigma{}^\gamma \qquad Y_2=V^{\beta\gamma}{}_\sigma{}^\beta$$
$$\cdots\cdots \qquad \cdots\cdots$$
$$X_{n-1}=V^{\zeta\eta}{}_\sigma{}^\eta \qquad Y_{n-1}=V^{\zeta\eta}{}_\sigma{}^\zeta$$

Here T_j and u_j are the transference number and the mobility of j ion species respectively, σ is the specific conductance of the solution, and V is the boundary velocity. The superscripts α, β,$\cdots$, η refer to the α, β,$\cdots$,η phases, and $\alpha\beta$, $\beta\gamma$,$\cdots$, $\zeta\eta$ refer to $\alpha\beta$,$\beta\gamma$,$\cdots$, $\zeta\eta$ boundaries, respectively. Since the total of each transference number must be unity, *i.e.*, $\sum_j T_j^\alpha=1$, and $\sum_j T_j^\eta=1$, the solutions of Eq. (A1) become:

$$T_j^\alpha=\frac{(u_j-X_1)(u_j-X_2)\cdots(u_j-X_{n-1})}{(u_j-u_1)(u_j-u_2)\cdots(u_j-u_n)} \quad (A2)$$

$$T_j^\eta=\frac{(u_j-Y_1)(u_j-Y_2)\cdots(u_j-Y_{n-1})}{(u_j-u_1)(u_j-u_2)\cdots(u_j-u_n)} \quad (A3)$$

The denominators of Eqs. (A2) and (A3) are identical and may be eliminated to give:

$$\frac{T_j^\alpha}{T_j^\eta}=\frac{(u_j-X_1)(u_j-X_2)\cdots(u_j-X_{n-1})}{(u_j-Y_1)(u_j-Y_2)\cdots(u_j-Y_{n-1})} \quad (A4)$$

In the present system, the ionic species are surfactant monomer (m) and micelle (M) ions, and positive and negative electrolyte ions (Na^+ and Cl^-). However, since the concentrations of m ions can be assumed to be equal in the initial two phases, we can expect two boundaries to appear, one of which is stationary; in fact, we have experimentally obtained only one moving boundary. Thus, the experession of Eq. (A4) for micelles is simplified to:

$$T_M^\alpha/T_M^\eta=(u_M-X)/(u_M-Y) \quad (A5)$$

or:

$$u_M=X-\frac{Y-X}{(T_M^\eta/T_M^\alpha)-1} \quad (A6)$$

The X and Y in Eq. (A6) are written in the following forms when an apparatus of the Tiselius type is used.

19) A. L. Loeb, P. H. Wiersema and J. Th. G. Overbeek, "The Electrical Double Layer Around a Spherical Colloid Particle," M. I. T. Press, Cambridge, Massachusetts (1961).

20) J. T. Davies and E. K. Rideal, "Interfacial Phenomena," Academic Press, New York (1961), p. 140.

21) K. Durham, Proc. 3rd Intern. Congr. Surface Activity, Cologne, 1960, B/1/3, p. 130.

$$X = V_d\sigma^\eta, \quad \text{and} \quad Y = V_a\sigma^\alpha$$

where V_d and V_a are the velocities of the descending and ascending boundaries respectively. The $T_M{}^\eta/T_M{}^\alpha$ ratio is given by:

$$T_M{}^\eta/T_M{}^\alpha = (C_M{}^\eta/\sigma^\eta)/(C_M{}^\alpha/\sigma^\alpha)$$

where $C_M{}^\alpha$ and $C_M{}^\eta$ are the concentrations of M ions in the upper and lower layers in the cell respectively; they are given by:

$$C_M{}^\alpha = (C - \text{CMC})_\alpha, \text{ and } C_M{}^\eta = (C - \text{CMC})_\eta$$

The values of $C_M{}^\alpha$ and $C_M{}^\eta$ are known, and V_a, V_d, σ^α, and σ^η are all determinable. The u_M values given in Tables 1 and 2 are thus obtained from Eq. (A6).

BULLETIN OF THE CHEMICAL SOCIETY OF JAPAN VOL. 41 2832—2834 (1968)

Rate of Electron Exchange between Cuprous and Cupric Ions in Concentrated HCl by Electron Spin Resonance*1

R. Allan STEWART*2 and L. W. REEVES

Department of Chemistry, University of British Columbia, Vancouver, British Columbia

and Shizuo FUJIWARA

Department of Chemistry, The University of Tokyo, Hongo, Tokyo

(Received March 5, 1968)

Contrary to previous reports, the linewidth of the electron spin resonance spectrum of cupric ion as measured in gauss between points of maximum slope is a sensitive function of ionic strength, chloride ion concentration and cuprous ion concentration. Assuming that electron spin relaxation rates do not change greatly on the addition of cuprous ion, it is possible to derive an electron exchange rate for the reaction:

$$Cu^+ + Cu^{2+} \longleftrightarrow Cu^{2+} + Cu^+$$

of $k = 1.53 \times 10^9$ *l*/mol/sec. This value is in good agreement with a previous determination of the same rate constant by McConnell and Weaver using the ^{63}Cu nuclear magnetic resonance (0.5×10^8). The results for the linewidth changes can be rationalized in all cases by assuming that bridge chloride ions between two cupric ions or one cupric and one cuprous ion change drastically in concentration as such factors as ionic strength or chloride ion concentration changes. The *g* value of the electron (free) decreases as chloride ion is added, indicating delocalization of the unpaired electron onto chloride ligands.

While nuclear magnetic resonance (NMR) studies of chemical exchange are widespread, little attention has been paid to the study of electron exchange processes by electron spin resonance (ESR). A recent authoritative review of the subject of exchange studies by magnetic resonance lists only 8 studies[1] carried out by ESR. These 8 investigations are comprised solely of investigations of electron transfer between radical ions and parent molecule. The ESR spectra of these species are composed of many hyperfine transitions, but some attempt has been made to compute lineshapes at various exchange rates, and to compare them with experimental curves.[2] Part of the reason for the absence of more activity in this field is the shortage of suitable systems and the complexity of the ones avaiable. A system which has been studied by an NMR method[3] is the cuprous-cupric electron exchange in aqueous solutions of the chloride. Although this system is complicated, it has the attraction that a single broad ESR line is observed, and the exchange process can be clearly demonstrated to dominate changes in linewidth. The study of linewidths of Cu^{2+} ions in aqueous solutions has already been investigated to some extent.[4]

Solutions of cupric chloride do not obey Beer's law[5,6] due to the formation of chloride complexes.

*1 Presented in part at a seminar on coordination chemistry held at the Institute of Solid State Physics of Tokyo University in 1967, by R.A.S.

*2 Research carried out while a Research Fellow of the Ministry of Education of Japan at the Department of Chemistry, Faculty of Science, University of Tokyo (1964—66).

1) "Advances in Magnetic Resonance," ed. by J. S. Waugh, Vol. 1 (1965), p. 33.

2) J. E. Harriman and A. M. Maki, *J. Chem. Phys.*, **39**, 778 (1963).

3) H. M. McConnell and H. E. Weaver, *ibid.*, **25**, 307 (1956).

4) S. Fujiwara and H. Hayashi, *ibid.*, **43**, 23 (1965).

5) W. V. Bhagwat, *J. Indian Chem. Soc.*, **17**, 52 (1940).

6) T. Moeller, *J. Phys. Chem.*, **48**, 111 (1944).

McConnell and Davidson,[7] by optical methods, established the presence of chlorine bridged complexes containing more than one copper ion, *e. g.*, $Cu_2Cl_5^-$, in aqueous solution. The bridge chloride ion promotes electron exchange between the two copper ions, giving rise to an intense coloration. It is probable that these bridge chloride ions are also responsible, in view of the anomalous spectral coloration, for the electron exchange process $Cu^+ \leftrightarrow Cu^{2+}$ in solutions of mixed oxidation states.

The present study is an attempt to compare directly the same exchange rate obtained by both NMR and ESR methods, and to study related processes which influence the ESR linewidth.

Experimental

Solutions were prepared by standard volumetric methods. The exclusion of air from sample tubes prevented the oxidation of cuprous ion to cupric ion. Samples were measured immediately after preparation of the solutions, but in any case, remained stable in closed tubes for periods in excess of one month. The solubility of $CuCl_2$ decreases in solutions of high HCl concentration, so that measurements were limited to more dilute regions. The cuprous ion is more stable in highly acid solutions. The ESR linewidth varies from 50 to 400 gauss as cupric and chloride ion concentrations are changed. This is in contradiction to a statement of Kozyrev,[8] and the published results of Al'tschuler and Kozyrev,[9] who observed no change from the value of 140 gauss. A JES-118 ESR spectrometer operating in the X-band at room temperature, manufactured by the Japan Electron Optics Company, was used for measurement, and DPPH was the external reference material.

Results and Discussion

It has been pointed out[1,2] that the electron exchange problem in magnetic resonance can be considered as a simple modulation of the electron Larmor frequency by the various nuclear spin states responsible for hyperfine interaction. In this sense, the analogy with the influence of chemical exchange on nuclear magnetic resonance in the interruption of scalar coupling to other nuclei is almost complete. The problem of the natural relaxation processes in electron spin resonance is a complicated one, but it is sufficient that it be considered as a separate relaxation rate process, which is additive to any electron site exchange. This latter effect can be attacked by the time tested methods of chemical kinetics. Precautions must be taken that other relaxation mechanisms do not change greatly over the range of concentrations investigated.

In the present case, the single broad ESR line observed in solution has been interpreted as originating from incomplete averaging of the hyperfine coupling to ^{63}Cu and ^{65}Cu nuclei by relaxation mechanisms which have been previously discussed.[4,10] The gyromagnetic ratios of the two copper isotopes are almost the same, and the spin quantum numbers are identical.

At constant $CuCl_2$ concentration in concentrated HCl, the ESR linewidth (maximum slope to maximum slope in gauss) was measured for a series of solutions of increasing CuCl concentrations. The results are plotted in Fig. 1 for a great excess of chloride ion (concentrated HCl).

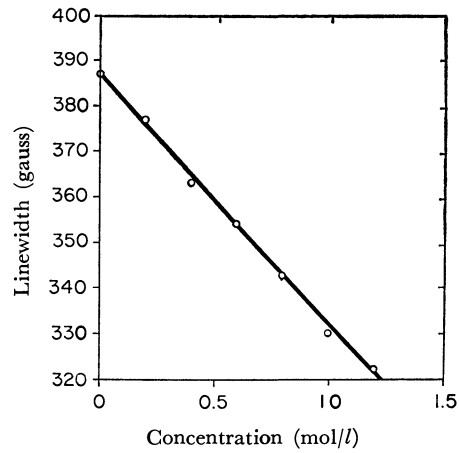

Fig. 1. Linewidth of 1 molar $CuCl_2$ in excess HCl as a function of added CuCl.

The concentration of cupric chloride was maintained at 1 molar. There was a sharp and linear decrease in linewidth of 55 gauss/mol/*l*, indicating that an exchange process, first order in Cu^+ ion is taking place, which results in exchange narrowing. An electron exchange rate can be obtained[1] by converting to appropriate frequency units. A value for the electron exchange rate constant $k = 1.53 \times 10^8$ *l*/mol/sec was obtained for the process

$$Cu^{2+} + Cu^+ \underset{k}{\longleftrightarrow} Cu^+ + Cu^{2+}. \qquad (1)$$

This ESR value is quite close to the value $k = 0.5 \times 10^8$ *l*/mol/sec obtained from ^{63}Cu NMR studies by McConnell and Weaver.[3] The linewidth of the cupric ion resonance is very sensitive to chloride ion concentration in excess of 5 molar, and independent of concentration below this. The results of this study are plotted graphically in Fig. 2 for 1 molar cupric ion (chloride ion added by way of HCl). The pH was found to have little effect on the width or *g* value of the resonance line. The large increase in linewidth in Fig. 2 of the cupric ion resonance is interpreted as being due to

7) H. M. McConnell and N. Davidson, *J. Am. Chem. Soc.*, **72**, 3168 (1950).
8) B. Kozyrev, *Discussions Faraday Soc.*, No. **19**, 137 (1955).
9) S. Al'tschuler and B. Kozyrev, "Electron Paramagnetic Resonance," Academic Press, London (1964).
10) D. Kivelson, *J. Chem. Phys.*, **33**, 1094 (1960).

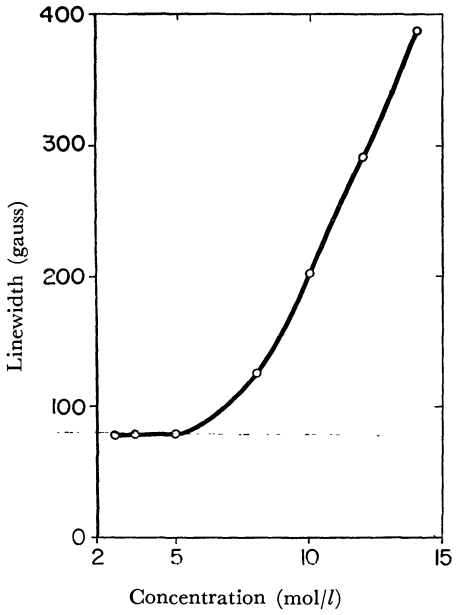

Fig. 2. Linewidth of 1 molar $CuCl_2$ *versus* Cl^- ion (HCl) concentration.

a change in the average species present in solution as Cl^- ion is added.[7] As copper ion becomes more highly complexed by Cl^- ion, the symmetry of the complexes present in solution changes, resulting in a change in the basic ESR relaxation mechanism for copper ion, that of spin-orbit coupling.

In excess HCl, the linewidth of the cupric ion resonance as a function of cupric ion concentration is plotted in Fig. 3, curve (a). The excess chloride was limited to approximately 10 molar by solubility considerations for cupric ion in more concentrated solutions. The linewidth passes through a minimum at approximately 0.55 molar cupric ion. These results are understandable in terms of the two electron exchange mechanism

$$Cu^{2+} + Cu^{2+} \longleftrightarrow Cu^{2+} + Cu^{2+} \qquad (2)$$

if the maximum concentration of bridge chloride ions occurs near that of the minimum linewidth. The rate of electron exchange represented by Eq. (2) is most rapid at this point. Simultaneous electron exchange occurs between two cupric ions, thereby affecting the linewidth of the electron resonance. The rate of this exchange is expected to be slower than that for the process represented by Eq. (1), where only one electron changes site. It is also interesting to note that in Fig. 3, curve (b), where 1 molar cuprous chloride is added to the solutions of curve (a), that the linewidths are always considerably reduced (by 15 to 25 gauss), and the minimum linewidth is displaced by 0.2 mol/*l* to higher cupric ion concentrations. This displacement is thought due to the effect of ionic strength. The ionic strength was kept constant

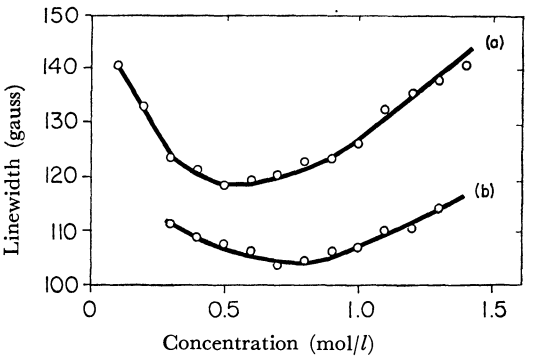

Fig. 3. Curve (a). Linewidth of Cu^{2+} ion resonance *versus* $CuCl_2$ concentration.
Curve (b). Curve (a) with 1 molar CuCl added.

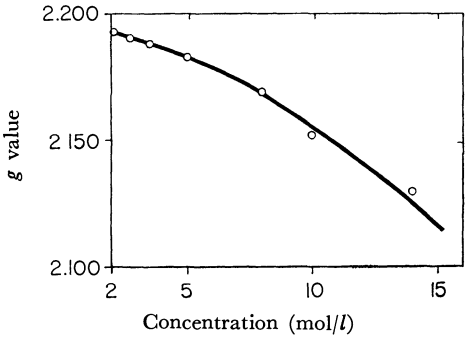

Fig. 4. *g* Value of Cu^{2+} ion resonance *versus* Cl^- ion (HCl) concentration.

in various copper solutions previously investigated[4] through the addition of zinc nitrate (chosen because of its similar ionic properties to copper). The linewidth was found to behave in a similar but more simple fashion with change in other linewidth-influencing factors (such as cupric and chloride ion concentrations) at constant ionic strength.

The *g* value measurements for the cupric ion as a function of concentration are also of some interest. These are plotted as a function of chloride ion (HCl) concentration for a 1 molar cupric ion concentration in Fig. 4. There is a large monotonic decrease in the *g* value of the unpaired electron as the chloride ion concentration increases. This is illustration of the increasing coordination of cupric ion by chloride ion, and the delocalization of electron spin density onto the ligand chloride ions. Stability constants of the various cupric and cuprous chloride complexes are very imperfectly known,[11] but the stable complex in very concentrated chloride solutions is known[5,6] to be $CuCl_4^{2-}$. The hydrated cupric ion has a much more localized unpaired electron spin and the *g* value is higher.

11) "Stability Constants," The Chemical Society, London, Special Publication No. 17, ed. by L. G. Sillén.

BULLETIN OF THE CHEMICAL SOCIETY OF JAPAN VOL. 41 2835—2839 (1968)

ESR Studies of Copper(II) Complexes of Ethylenediamine and Its Analogues

Hiroshi YOKOI and Taro ISOBE

The Chemical Research Institute of Non-Aqueous Solutions, Tohoku University, Katahira-cho, Sendai

(Received March 6, 1968)

The ESR spectra of the copper(II) complexes of ethylenediamine, 1,2-diaminopropane, *meso*-2,3-diaminobutane, 1,3-diaminopropane, and ammonia were measured in methanolic and aqueous solutions at room temperature and in frozen solutions at the temperature of liquid nitrogen. The covalency of the bonding of the copper atom to the ligand atoms in these complexes was evaluated from the g values, the copper hyperfine constants, and the nitrogen super-hyperfine constants. Even in the case of amino groups which were coordinating groups, the π bonding seemed to be as important in determining the properties of the complexes as the σ bonding.

ESR has been proved effective for investigating the bonding in copper(II) complexes.[1-6] However, ESR studies of the copper(II) chelate complexes of ethylenediamine and its analogues have not been carried out in full detail. In these complexes the central copper atom is coordinated to the amino groups, one of best known kinds of coordinating groups; the investigation of the bonding character of copper-amino group bonds is very important in coordination chemistry. The purpose of this work is to obtain the magnetic parameters, neamely, the g values, the copper hyperfine constants, and the nitrogen super-hyperfine constants of the copper(II) complexes of ethylenediamine, 1,2-diaminopropane, *meso*-2,3-diaminobutane, 1,3-diaminopropane, and ammonia in solutions at room temperature and at the temperature of liquid nitrogen, and to discuss the covalency of the bonding of the copper atom to amino groups as evaluated from these magnetic parameters.

Experimental

The copper(II) complexes employed in this study were [I] $[Cu(en)_2](ClO_4)_2$, [II] $[Cu(pn)_2](ClO_4)_2$, [III] $[Cu(m\text{-}bn)_2](ClO_4)_2$, [IV] $[Cu(tn)_2](ClO_4)_2$, and [V] $[Cu(am)_4](ClO_4)_2$, where en, pn, m-bn, tn, and am are ethylenediamine, 1,2-diaminopropane, *meso*-2,3-diaminobutane, 1,3-diaminopropane, and ammonia respectively. All the amines were commercially

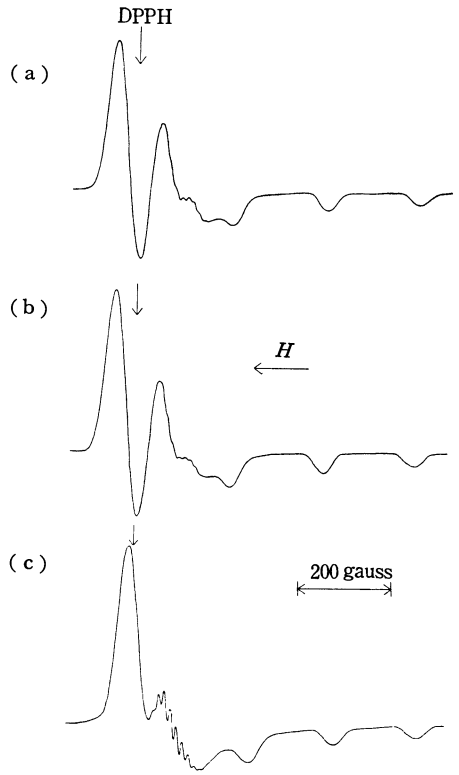

Fig. 1. ESR spectra (first derivative, X-band) at 77°K.
(a) $[Cu(en)_2](ClO_4)_2$ in 50% water - 50% methanol
(b) $[Cu(m\text{-}bn)_2](ClO_4)_2$ in 50% water - 50% methanol
(c) $[Cu(am)_4](ClO_4)_2$ in methanol

1) K. W. H. Stevens, *Proc. Roy. Soc. (London)*, **A219**, 542 (1953); J. Owen, *ibid.*, **A227**, 183 (1955).
2) A. H. Maki and B. R. McGarvey, *J. Chem. Phys.*, **29**, 31, 35 (1958).
3) D. Kivelson and R. Neiman, *ibid.*, **35**, 149 (1961).
4) E. M. Robert and W. S. Koski, *J. Am. Chem. Soc.*, **82**, 3006 (1960); F. R. Gersman and J. D. Swalen, *J. Chem. Phys.*, **36**, 3221 (1962); S. J. T. Owen, K. J. Standley and A. Walker, *ibid.*, **40**, 183 (1964); B. G. Malmstom and T. Vanngard *J. Mol. Biol.*, **2**, 118 (1960).
5) A. K. Wiersma and J. J. Windle, *J. Phys. Chem.*, **68**, 2316 (1964); W. Schneider and A. v. Zelewsky, *Helv. Chim. Acta*, **48**, 1529 (1965).
6) S. E. Harrison and J. M. Assour, *J. Chem. Phys.*, **40**, 365 (1964); S. E. Harrison and J. M. Assour, "Paramagnetic Resonance," ed. by W. Low, Academic Press, New York (1963), p. 861; H, A. Kuska, F. M. D'itri and A. I. Popov, *Inorg. Chem.*, **5**, 1272 (1966).

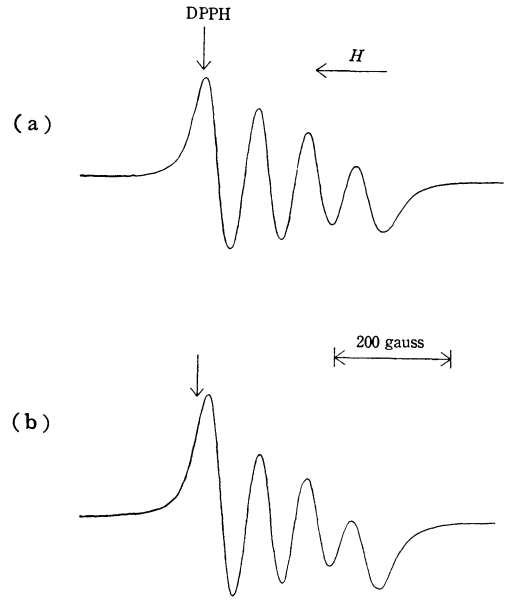

Fig. 2. ESR spectra (X-band) at room temperature in 50% water - 50% methanol.
(a) $[Cu(en)_2](ClO_4)_2$
(b) $[Cu(tn)_2](ClO_4)_2$

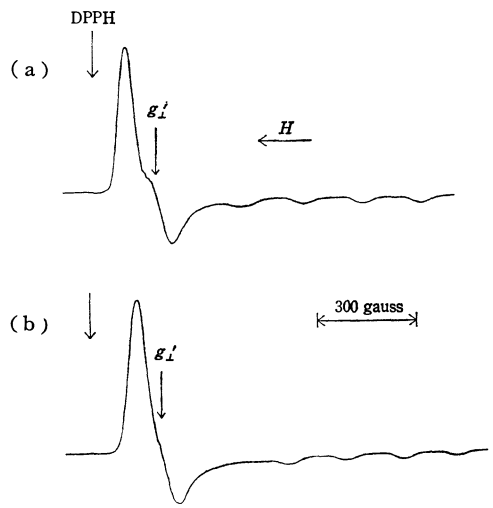

Fig. 3. ESR spectra (first derivative, K-band) on frozen solutions.
(a) $[Cu(pn)_2](ClO_4)_2$ in 50% water - 50% methanol
(b) $[Cu(am)_4](ClO_4)_2$ in methanol

available except for m-bn, which was prepared and purified according to the method of literature.[7] The solvents were methanol and a 50% water - 50% methanol mixture (per cent in volume). The ESR spectra of the complexes were measured in solutions at room temperature and on frozen solutions at the temperature of liquid nitrogen with a Hitachi X-band and K-band

7) F. Basolo, Y. T. Chen and R. K. Murmann, *J. Am. Chem. Soc.*, **75**, 1478 (1953).

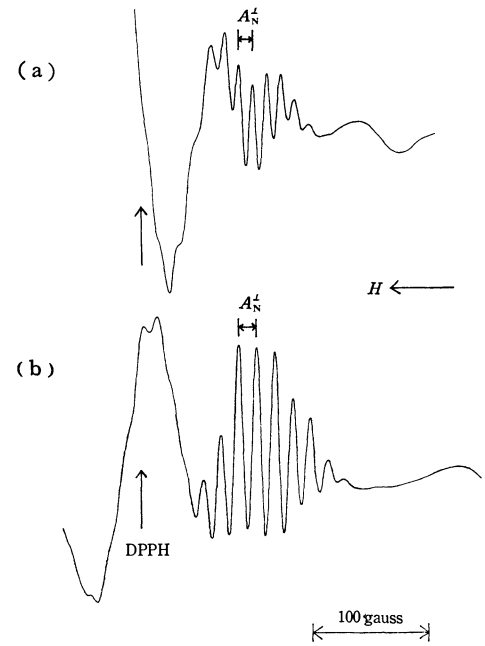

Fig. 4. The high field part of ESR spectra (second derivative, X-band) at 77°K.
(a) $[Cu(pn)_2](ClO_4)_2$ in 50% water-50% methanol
(b) $[Cu(am)_4](ClO_4)_2$ in methanol

ESR spectrometer, model MES-4001, equipped with a 100 kc/s field modulation unit. Furthermore, the second derivative ESR spectra were obtained using 100 kc/s-40 c/s field modulations in order clearly to resolve the nitrogen super-hyperfine structure. The field was calibrated with an NMR probe and then with a benzene solution of vanadyl acetylacetonate or with Mn(II) ions in MgO powder. Some of the ESR spectra observed are shown in Figs. 1—4. The optical absorption spectra of the complexes in solutions were measured with a Cary model 14 spectrometer.

Results and Discussion

Magnetic Parameters. As may be seen in Fig. 1, the copper(II) complexes employed in this work show broad ESR absorption lines. This is due to the poor resolution of the nitrogen super-hyperfine strcture, which is, however, observed on $g_\perp$ components in the high-field part of the spectra of Fig. 1. Figure 4 exibits the second derivative of the super-hyperfine lines, from which the super-hyperfine constants can be obtained with considerable accuracy. The problem of determining the magnetic parameters from the ESR spectra of polycrystalline samples or rigid glass solutions has been studied extensively by several authors.[8]

8) R. H. Sands, *Phys. Rev.*, **99**, 1222 (1955); R. Neiman and D. Kivelson, *J. Chem. Phys.*, **35**, 156 (1961); T. Vanngard and R. Aasa, Proc. 1st. Intern. Congr. "Paramagnetic Resonance," Jerusalem, 1962, Academic Press, New York (1963), p. 509.

Table 1. Magnetic parameters

Copper(II) complex		Solvent[a]	$g_{//}$	$g_\perp$[b]	$g'_\perp$[c]	$A_{//}$ $\times 10^4$ cm^{-1}	$A_\perp$[b] $\times 10^4$ cm^{-1}	g_0[d]	A_0[d] $\times 10^4$ cm^{-1}	$A_N^\perp$ $\times 10^4$ cm^{-1}
[I]	Ethylenediamine	M	2.209			207				
		MH	2.206	2.050	2.052	209	25	2.102	86	10.5
[II]	1,2-Diaminopropane	M	2.209			206				
		MH	2.208	2.050	2.051	210	26	2.103	87	10.7
[III]	*meso*-2,3-Diaminobutane	M	2.203			204				
		MH	2.203	2.050	2.050	205	27	2.101	86	11.3
[IV]	1,3-Diaminopropane	M	2.219			202				
		MH	2.222	2.052	2.052	201	21	2.109	81	12.6
[V]	Ammonia	M	2.242	2.056	2.055	199	17	2.118	77	12.7

a) M: methanol, MH: 50% water-50% methanol (volume %).
b) $g_\perp$ was calculated using the following equation, $g_0=1/3\ (g_{//}+2g_\perp)$. $A_\perp$ was also calculated in the same way.
c) $g'_\perp$ was directly obtained from the ESR spectrum measured at K-band.
d) Measured at room temperature.

However, it is difficult to analyze completely such ESR spectra as are shown in Fig. 1. The ESR measurements of the copper(II) complexes of ethylenediamine and ammonia in single crystals have revealed that the complexes have axial symmetry (two distinct g values).[9,10] It is now desirable to ascertain whether or not the complexes under discussion have axial symmetry in solutions. Since ESR measurements at both the K-band and X-band are often used to distinguish between two lines of different g values, the ESR spectra were measured at the K-band in this study; some of the ESR spectra are shown in Fig. 3. This figure indicates that, in solutions, axial symmetry is approximately maintained; approximate $g_\perp$ values can be obtained directly from the ESR spectra shown in this figure.

The spin Hamiltonian is expressed as follows:

$$\begin{aligned} H = {} & \beta_0[g_{//}H_zS_z + g_\perp(H_xS_x + H_yS_y)] \\ & + A_{//}S_zI_z + A_\perp(S_xI_x + S_yI_y) \\ & + A_N^{//}S_zI_z^N + A_N^\perp(S_xI_x^N + S_yI_y^N) \end{aligned} \quad (1)$$

The experimental data are listed in Table 1. It is interesting to see in this table that $g_\perp \doteqdot g'_\perp$; therefore, $A_\perp$ was also calculated using the values of $A_{//}$ and A_0 in the same way as in calculating $g_\perp$.

Chemical Bonding. The experimentally determined quantities, $g_{//}$, $g_\perp$, $A_{//}$, $A_\perp$, and $A_N^\perp$ can be used to estimate the character of the chemical bonding of the copper atom to ligand nitrogen atoms by means of the molecular orbital theory. In the complexes of amines, the σ orbitals of ligand nitrogen atoms are the lone-pair electron orbitals formed by sp^3 hydridization. Therefore, these nitrogen atoms do not have pure π orbitals such as the oxygen atoms of acetylacetonate anion have. However, in this study the complexes of amines have been treated on the assumption that amino groups have a kind of π orbital; we used the same procedure as did Maki and McGarvey,[2] and Kivelson and Neiman[3] in treating Cu(II) bisacetylacetonate. The notation of Maki and McGarvey for a square planar complex will be used here. The following antibonding molecular orbitals, in the order of increasing energy, can be formed for the "hole" configuration:

$$\left.\begin{aligned} \Psi_{b_{1g}} &= \alpha d_{x^2-y^2} - \alpha'(-\sigma_x^{(1)} \\ &\quad + \sigma_y^{(2)} + \sigma_x^{(3)} - \sigma_y^{(4)})/2 \\ \Psi_{b_{2g}} &= \beta_1 d_{xy} - \beta_1'\phi_L(xy) \\ \Psi_{a_{1g}} &= \alpha_1 d_{z^2} - \alpha_1'(\sigma_x^{(1)} \\ &\quad + \sigma_y^{(2)} - \sigma_x^{(3)} - \sigma_y^{(4)})/2 \\ \Psi_{e_g} &= \begin{cases} \beta d_{xz} - \beta'\phi_L(xz) \\ \beta d_{yz} - \beta'\phi_L(yz) \end{cases} \end{aligned}\right\} \quad (2)$$

where $\sigma^{(i)}=np^{(i)}\mp(1-n^2)^{1/2}s^{(i)}$, in which $0\leq n\leq 1$, and where $\varphi_L(xy)$, $\varphi_L(xz)$, and $\phi_L(yz)$ are pseudo-π orbitals of amino groups which have been assumed to interact with the d_{xy}, d_{xz} and d_{yz} of copper orbitals respectively. $\Psi_{b_{2g}}$ and Ψ_{e_g} represent the in-plane π bonding and the out-of-plane π bonding respectively. The normalization of the $\Psi_{b_{1g}}$ orbital yields:

$$\alpha^2 + \alpha'^2 - 2\alpha\alpha' S = 1 \quad (3)$$

where S is the overlap integral between the $d_{x^2-y^2}$ of the copper atom and the σ orbitals of ligand nitrogen atoms.

The second-order perturbation calculation results in the following approximate expressions for the spin Hamiltonian parameters in Eq. (1):

9) H. Abe and K. Ono *J. Phys. Soc. Japan*, **11**, 947 (1956).
10) E. H. Carlson and R. D. Spence, *J. Chem. Phys.*, **24**, 471 (1956).

$$\left.\begin{aligned} g_{//} &= 2.002 - \frac{8\lambda}{\Delta E_{xy}}\alpha^2\beta_1^2(1-f_1) \\ g_{\perp} &= 2.002 - \frac{2\lambda}{\Delta E_{xz}}\alpha^2\beta^2(1-f_2) \\ A_{//} &= P\left[-\alpha^2\left(\frac{4}{7}+\kappa_0\right)+(g_{//}-2)+\frac{3}{7}(g_{\perp}-2)+f_3\right] \\ A_{\perp} &= P\left[\alpha^2\left(\frac{2}{7}-\kappa_0\right)+\frac{11}{14}(g_{\perp}-2)+f_4\right] \end{aligned}\right\} \quad (4)$$

Furthermore, $A_N^{\perp}$ is expressible in the form:[2,6]

$$A_N^{\perp} = \left(\frac{\alpha'}{2}\right)^2(2\beta_0\beta_N\gamma_N)\left[\frac{8\pi}{3}(1-n^2)\rho_{2s}(0)+\frac{2}{5}n^2\langle r^{-3}\rangle_{2p}\right] \quad (5)$$

where $P=2\gamma\beta_0\beta_N\langle d_{x^2-y^2}|r^{-3}|d_{x^2-y^2}\rangle$, where κ_0 is the Fermi contact term, where $\Delta E_{xy}=E_{xy}-E_{x^2-y^2}$ and $\Delta E_{xz}=E_{xz}-E_{x^2-y^2}$, where $\rho_{2s}(0)$ is the value of the ligand 2*s* function at the nitrogen nucleus, where r is the radius of the 2*p* ligand orbital, and where f_1, f_2, f_3 and f_4 are small and almost constant values for a variety of copper(II) complexes (f_1, $f_2 \leqq 0.04$, $f_3 \leqq 0.33$, and $f_4 \leqq 0.005$).

Next, the values of ΔE_{xy} and ΔE_{xz} must be determined in order to calculate β_1 and β. The visible absorption spectrum of a square planar copper(II) complex generally consists of three component absorption bands, corresponding to ΔE_{xy}, ΔE_{xz} and ΔE_{z^2}, where $\Delta E_{z^2}=E_{z^2}-E_{x^2-y^2}$. However, the visible absorption spectra of the copper(II) complexes employed in this study show in solutions only a single broad band, the position of the peak of which is tabulated in Table 2, so that it is not easy to determine accurately the values of ΔE_{xy} and ΔE_{xz} for the complexes. The absorption spectral data of the single crystal of bis(ethylenediamine)copper(II) complex are not sufficient to determine the energy values.[11]

The circular dichroism measurements of various metal complexes have been used to estimate the structure of their electronic absorption spectra.[12] 1,2-Diaminopropane contains an optically-active asymmetric carbon. Recently Gillard observed the circular dichroism of $[Cu(-pn)_2]^{2+}$ in an aqueous solution, and showed two bands corresponding to 657 mμ and 510 mμ.[13] The two bands are thought to be due to components of $^2T_2 \leftarrow {}^2E$ from the symmetry arguments of the magnetic dipole transition. Therefore, it may reasonably be considered that the ΔE_{xy} and ΔE_{xz} of $[Cu(pn)_2](ClO_4)_2$ in an aqueous solution correspond approximately to 657 mμ and 510 mμ respectively. The energy values of the ΔE_{xy} and ΔE_{xz} of the other copper(II) complexes under discussion could be estimated roughly on the assumption that there is the same relationship in energy values among ΔE_{xy}, ΔE_{xz} and the maximum absorption peak for these complexes as with the copper(II) complexes of 1,2-diaminopropane. The estimate ligand field energy values of ΔE_{xy} and ΔE_{xz} are listed in Table 2.

Table 2. Ligand field energies

Copper(II) complex	λ_{max}* (mμ)	log ε	Estimated ligand field energies (cm^{-1})	
			ΔE_{xy}	ΔE_{xz}
[I]	547	1.80	15200	19600
[II]	547	1.84	15200	19600
[III]	546	1.85	15200	19600
[IV]	568	2.02	14600	18900
[V]	598	1.70	13900	17900

* Solvents were MH for [I]—[IV] and M for [V]. The description of MH and M is in the footnote of Table 1.

The values of the bonding parameters, namely, α, β_1, β, and κ_0 were calculated using Eq. (4), where $P=0.036\ cm^{-1}$; they are listed in Table 3. Furthermore, the values of α were also calculated from the nitrogen super-hyperfine constants using Eq. (5), where $n=\sqrt{3}/2$ for sp^3 hybrid ligand orbitals, $\rho_{2s}(0)=33.4\times10^{24}\ cm^{-3}$, $\langle r^{-3}\rangle_{2p}=21.1\times10^{24}\ cm^{-3}$, and $S=0.08$.

There are several points of interest in the results shown in Table 3. Values of β_1^2 and β^2 which are indicated to be considerably smaller than unity, namely, $\beta_1^2=0.6$ and $\beta_2=0.7$, are found for all the copper(II) complexes in this work. This implies that remarkably covalent π bonding is

Table 3. Bonding parameters[a]

Copper(II) complex	From Eq. (4)				From Eq. (5)[b]	
	α^2	β_1^2	β^2	κ_0	α'^2	α^2
[I]	0.83	0.58	0.72	0.42	0.29	0.79
[II]	0.84	0.58	0.70	0.42	0.30	0.78
[III]	0.82	0.58	0.72	0.43	0.31	0.77
[IV]	0.84	0.60	0.70	0.41	0.35	0.73
[V]	0.87	0.59	0.68	0.39	0.35	0.73

a) Calculated from the experimental data measured in solvent MH for [I]—[IV] and solvent M for [V]. The description of M and MH is in the footnote of Table 1.

b) $n^2=3/4$ (sp^3 hybrid) was assumed in Eq. (5).

11) S. Yamada and R. Tsuchida, This Bulletin, **29**, 289 (1956).

12) A. J. McCaffery and S. F. Mason, *Mol. Phys.*, **6**, 359 (1963); B. E. Douglas, R. A. Haines and J. B. Brushmiller, *Inorg. Chem.*, **2**, 1194 (1963); T. Yasui, J. Hidaka and Y. Shimura, *J. Am. Chem. Soc.*, **87**, 2762 (1965).

13) R. D. Gillard, *J. Inorg. Nucl. Chem.*, **26**, 1455 (1964).

found in the copper-amino group bonds of the complexes. This finding, to which little attention has yet been paid, is considered to be reliable from the point of ESR. Rajan also suggested the existence of π bonding in $[Cu(en)_2](NO_3)_2$, on reasoning a simple basis.[14] It has generally been believed that the metal-ligand bonding in the metal complexes of amines is almost equivalent to σ bonding, where the ligand orbitals concerned with the bonding are the lone-pair electron orbitals of amines formed by sp^3 hybridization. The values of α^2 in Table 3 indicate that the σ bonding in the copper(II) complexes of amines is also covalent, but the degree of the covalency of the bonding is not very different from that reported for many common copper(II) complexes.[2-6] Accordingly, it is characteristic of the copper(II) complexes of amines that such covalent π bonding as that indicated in Table 3 is present. Now, a very important but difficult problem is that of considering what orbitals of amino groups are used as π orbitals, which are expressed, for convenience, in Eq. (2) as $\varphi_L(xy)$,φ_L (xz), and $\varphi_L(yz)$. One of most probable answers to the problem is that amino groups fulfil such a function of hyperconjugation as does the methyl group of toluene molecule. The fact that the convalent π bonding is present in the metal complexes of amines has much meaning for coordination chemistry and biochemistry, because it suggests that charge transfer, which is thought to be initial step of reactions, may occur easily between the metal atom and ligand molecules through amino groups.

The values of κ_0 in Table 3 are about 0.42 for [I]—[IV], but 0.39 for [V]. The former value is equal to the one reported for some copper(II) complexes,[2,3] and the value of κ_0 has been assumed to be essentially constant for all copper(II) complexes.[15] However, we must bear our mind in cases which the κ_0 value in some copper(II) complexes like [V] in Table 3 deviates from 0.42.[16]

Another point of interest is the values of α^2 calculated from the nitrogen super-hyperfine constants using Eqs. (5) and (3). The super-hyperfine constants listed in Table 1 are almost equal in magnitude to those reported for many nitrogen-bonded copper(II) complexes whose nitrogen valence orbitals are clearly known to be sp^2 hybridized orbitals;[2,3,5,6] therefore, the nitrogen super-hyperfine constants listed in Table 1 seem to be rather too large considering that the nitrogen valence orbitals of amines are nearly sp^3 hybridized orbitals. In Table 3 the values of α^2 calculated from Eq. (5) are compared with those calculated from Eq. (4). The agreement for [I]—[III] in Table 3 is comparatively good considering the various assumptions involved in Eqs. (4) and (5). However, the former is much smaller than the latter for [IV] and [V] in Table 3. This implies that there are slight differences in the characters of copper-amino group bonds between the first three complexes and the last two complexes in Table 3. [IV] in the table is more similar to [V] in chemical and physical properties, for instance, in stability constants,[17] optical absorption spectra and magnetic parameters, than to the first three complexes. This seems to be because the amino groups of 1,3-diaminopropane can be bonded to the copper atom with the same bonding nature as ammonia because of the structural flexibility of the trimethylene group in 1,3-diaminopropane. Since the values of α^2 calculated from Eq. (5) are alway smaller than those calculated from Eq. (4), it seems that the nitrogen orbitals of the copper(II) complexes of amines are not pure sp^3 hybridized orbitals, but, rather, orbitals with a greater degree of s-character. However, further studies of these problems are desirable in order to make the nature of chemical bonding in the complexes clearer.

14) R. Rajan, *J. Chem. Phys.*, **37**, 1901 (1962).
15) A. Abragam and M. H. L. Pryce, *Proc. Roy. Soc.*, **A206**, 164 (1951); A. Abrgam, J. Horowitz and M. H. L. Pryce, *ibid.*, **A230**, 169 (1955).
16) B. R. McGarvey, *J. Phys. Chem.*, **71**, 51 (1967); H. A. Kuska and M. T. Rogers, *J. Chem. Phys.*, **43**, 1744 (1965); H. Yokoi and T. Isobe, This Bulletin, **39**, 2054 (1966).
17) L. G. Sillen and A. E. Martell, "Stability Constants of Metal-ion Complexes" (Special Publication No. 7), The Chemical Society, Burlington House, London (1964).

BULLETIN OF THE CHEMICAL SOCIETY OF JAPAN VOL. 41 2840—2845 (1968)

Spectroscopic Studies of Catalysis by Vanadium Pentoxide

Kimio TARAMA, Satohiro YOSHIDA, Shingo ISHIDA and Hideo KAKIOKA

Faculty of Engineering, Kyoto University, Sakyo-ku, Kyoto

(Received March 18, 1968)

The role of the V=O bond in V_2O_5 in the adsorption of several gases was studied by measuring the electron spin resonance (ESR) and the infrared (IR) spectra. The ESR spectra of V_2O_5 supported on γ-Al_2O_3 were similar to those of $VOSO_4$ on γ-Al_2O_3. When such electron-donating gases as CO, SO_2 and C_2H_4 were adsorbed on this V_2O_5 - γ-Al_2O_3, the signal intensity of ESR increased and the splitting of the h.f.s. became clear. Upon treatment with an electron-accepting gas such as O_2, a reverse change was observed. In the case of V_2O_5 supported on SiO_2, similar ESR spectra were observed by the adsorption of CO after a mild reduction. The IR spectra of V_2O_5 have a sharp absorption peak at 1023 cm^{-1} due to the stretching vibration of the $(V=O)^{3+}$ bond; this peak became broader by adsorption of such gases as CO and SO_2. Simultaneously, the center of the peak shifted to the red region and a weak hump appeared at 980—990 cm^{-1}, probably due to $(V=O)^{2+}$. These results of the ESR and IR measurements reveal that these electron-donating gases are adsorbed on the $(V=O)^{3+}$ bonds on the surface of V_2O_5, and that the increase in electron densities in the adsorption sites results from adsorption of these gases. Furthermore, the role of this $(V=O)^{3+}$ bond in oxidation reaction was also discussed.

Vanadium pentoxide is a well-known oxidation catalyst. There are fairly many works attempting to elucidate the catalytic action of this catalyst by kinetical studies or by studies of its physico-chemical properties.

The present authors[1] themselves previously reported a study of some physico-chemical properties of V_2O_5 and emphasized the importance of the role of the V=O bond, at the 3rd International Congress on Catalysis.

In the present work, the role of this V=O bond in the adsorption of several gases was studied by measuring the electron spin resonance (ESR) and the infrared (IR) spectra.

Recently, van Reijen and Cossee[2] studied the state of V^{4+} ions in V_2O_5 supported on SiO_2 and Al_2O_3 by the ESR method and reported the existence of $(VO_4)^{4-}$ or $(VO)^{2+}$. Ioffe *et al.*[3] studied the change in the IR spectra of V_2O_5 by doping of MoO_3, CoO_2 or P_2O_5 and by treatment with a mixture of benzene and O_2. But these papers were not very helpful for our purpose of elucidating the role of the V=O bond in the gas adsorption.

The present authors' results reveal that the $(V=O)^{3+}$ bond on the surface of V_2O_5 plays an important role as the adsorption site for the electron-donating gas and also as a reaction site for the oxidation reaction.

1) K. Tarama, S. Teranishi, S. Yoshida and N. Tamura, Proc. 3rd Int. Cong. Catalysis, Amsterdam (1965), p. 282.
2) L. van Reijen and P. Cossee, *Discussions Faraday Soc.*, **41**, 277 (1966).
3) B. E. Zaitsev, S. I. Ezhkova and I. I. Ioffe, *Kinetika i Kataliz*, **7**, 755 (1966).

Experimental

Apparatus and Procedures. The ESR absorption measurements were made on a JES-3BSX-type, X-band spectrometer manufactured by the Japan Electron Optics Co. The cavity input power was 10 mW, and the modulation width was 10 gauss. DPPH was used as the standard for the measurement of the intensity of the ESR signal.

The samples for ESR measurement were evacuated for 3 hr at 350°C and 10^{-6} Torr in a glass reactor which had a quartz tube for ESR measurement as a side arm and which was joined to a vacuum line. After various treatments, the samples were moved to the side tube and the ESR absorptions were measured at room temperature.

The infrared absorption measurements were carried out with an IR-S-type spectrometer manufactured by the Japan Spectroscopic Co. The samples dispersed on a NaCl disk were placed in the center of a specially devised *in situ* cell and the IR absorptions were measured under various atmospheres and temperatures.

The adsorbed amounts of gases were measured by the usual volumetric method.

The catalytic activities for CO oxidation with air were determined by a flow method described previously[1] at 350°C. The gas flow rate was 7.5 cc (NTP)/min for 500 mg of the catalyst, and the ratio of CO to air was kept at 1 : 4.

Materials. Several kinds of V_2O_5 catalysts were used. The unsupported V_2O_5-powders used mainly for the IR measurements were prepared from commercial extra-pure-grade V_2O_5 by grinding it to powder. This sample contained about 0.7 atom% of V^{4+}.

The V_2O_5-samples supported on γ-Al_2O_3 and SiO_2 were prepared by impregnation with an aqueous solution of extra-pure NH_4VO_3, followed by drying at 100°C and calcination at 450°C for 6 hr in a dry-air stream.

The γ-Al_2O_3 was a commercial product of the highest purity from the Sumitomo Chemical Ind. Co. The SiO_2 was prepared from ethyl silicate which had been carefully purified by distillation.

The surface areas of these samples are given in Table 1.

Table 1. The B.E.T. surface areas of the supported catalysts

V_2O_5 Content (wt%)	Surface area (m^2/g)
1 (on γ-Al_2O_3)	170
3 (on γ-Al_2O_3)	180
5 (on γ-Al_2O_3)	180
20 (on γ-Al_2O_3)	170
5 (on SiO_2)	280

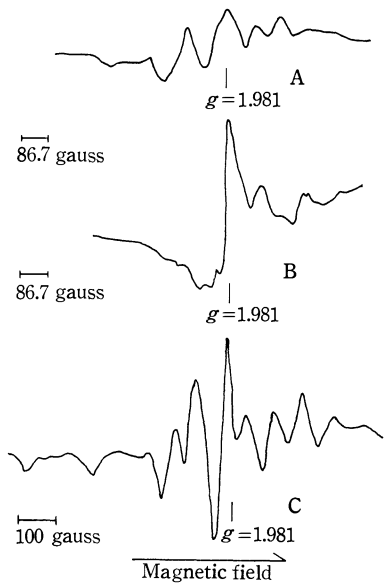

Fig. 1. ESR spectra of V_2O_5 - γ-Al_2O_3 after evacuation for 3 hr at 350°C.
A: V_2O_5(5%) - γ-Al_2O_3
B: V_2O_5(50%) - γ-Al_2O_3
C: $VOSO_4$(0.6%) - γ-Al_2O_3

Results

ESR Spectra of V_2O_5 Dispersed on γ-Al_2O_3. Figures 1-A and B show the ESR absorption spectra of the samples of 5 wt% and 50 wt% V_2O_5 respectively supported on γ-Al_2O_3. These spectra, with the h.f.s., were similar to that of $VOSO_4$ (0.6 wt%) on γ-Al_2O_3 (Fig. 1-C). The average h.f.s. coupling constants are 100 and 85 gauss for 5% V_2O_5-γ-Al_2O_3 and $VOSO_4$-γ-Al_2O_3 respectively. These spectra with h.f.s. were identified as those of $(V{=}O)^{2+}$.

When CO, SO_2 or C_2H_4 was adsorbed on this 5% V_2O_5 - γ-Al_2O_3 at room temperature and at 150°C, the signal intensities of the ESR spectra increased, as is shown in Table 2; the splitting of the h.f.s. also became clear, as Figs. 2-A, B and C show. The adsorbed amounts of CO, SO_2, and C_2H_4 (at room temperature, 200 Torr) were 0.5, 18 and 6 cc/g-cat respectively. The evacuation of gas at room temperature caused a decrease in the signal intensity, but this change was partially irreversible.

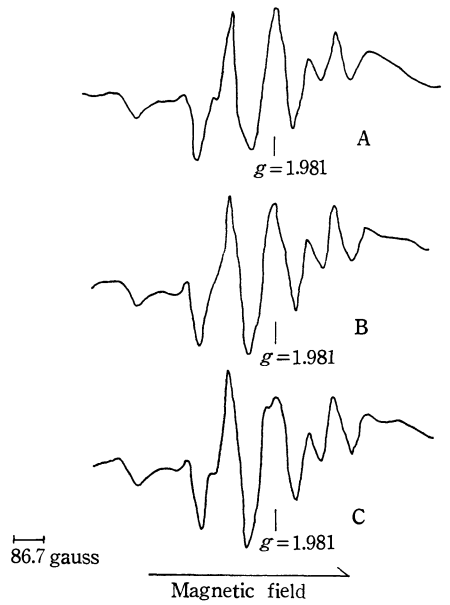

Fig. 2. ESR spectra of V_2O_5(5%) - γ-Al_2O_3.
A: SO_2 was adsorbed for 40 hr at 160 Torr and room temp.
B: C_2H_4 was adsorbed for 150 hr at 260 Torr and room temp.
C: CO was adsorbed for 150 hr at 226 Torr and room temp.

In the case of O_2 adsorption (200 Torr, 150°C, 1 hr), the relative signal intensity decreased to half of that of the starting sample. (The amount of O_2 adsorbed was 0.03 cc/g-cat.)

When O_2 (150 Torr) was introduced at room temperature after the adsorption of CO at 150°C, the relative signal intensity changed from 1.4 to 0.9, as is shown in Table 2 (VC-5, 6).

ESR Spectra of V_2O_5 Supported on SiO_2. In the case of V_2O_5 (5 wt%) supported on SiO_2, no signal of ESR absorption could be observed even after evacuation at 350°C. However, the ESR signal appeared after further reduction with CO at 350°C, as is shown in Fig. 3-A; furthermore, the h.f.s. with a characteristic feature of $(VO)^{2+}$ was observed in the ESR spectrum (Fig. 3-B) of this V_2O_5-SiO_2, which adsorbed CO at room temperature. van Reijen and Cossee[2] have reported

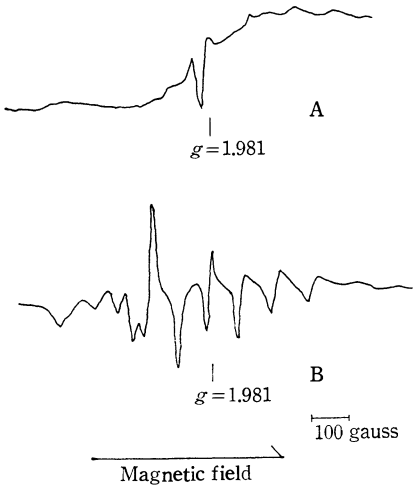

Fig. 3. ESR spectra of V_2O_5(5%)-SiO_2.
A: The sample reduced by CO at 350°C.
B: CO was adsorbed at room temp. on the reduced sample.

a similar ESR spectrum of V_2O_5-SiO_2, one which was evacuated at 500°C and which was subsequently treated with H_2O at 20°C.

When C_2H_4 was adsorbed at room temperature and 150 Torr, a weak signal similar to that in Fig. 1-A appeared.

Infrared Absorption of V_2O_5 Adsorbing Some Gases. V_2O_5 gives infrared spectra composed of a sharp absorption at 1023 cm^{-1} and a broad one at 830 cm^{-1}. This sharp absorption band at 1023 cm^{-1} is assignable to the stretching vibration mode of the $(V=O)^{3+}$ bond by comparison with that of $VOCl_3$.[4,5] It has been reported that this sharp absorption shifts to a longer-wavelength region upon treatment with cyclohexane[4] or after the catalyst has been used for benzene oxidation.[3]

The changes in the absorption spectra by the adsorption of several gases were studied under mild conditions. Figures 4 and 5 show the changes in the spectra by the adsorption of SO_2 and CO respectively.

By the adsorption of SO_2, the absorption band due to the $(V=O)^{3+}$ bond became broader and the center of the absorption peak shifted from 1023 cm^{-1} to 1005 cm,$^{-1}$ and, furthermore, a weak shoulder appeared at 980—990 cm^{-1} as is shown in curves A, B and C of Fig. 4. Almost all these changes in the IR spectra remained even after evacuation for 2 hr at 110°C, but when O_2 was introduced into the cell at 75°C, the center of the absorption band returned from 1005 cm^{-1} to 1013 cm^{-1}, as is shown in curve D of Fig. 4. On the other hand, the broad absorption band at

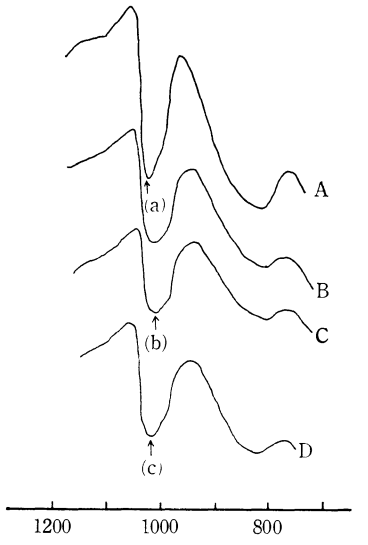

Fig. 4. IR spectra of V_2O_5 treated by SO_2 and O_2.
A: V_2O_5 untreated.
B: V_2O_5 treated by SO_2 at 226 Torr and 24°C for 16 hr.
C: V_2O_5 treated by SO_2 at 226 Torr and 50°C for 3 hr after B.
D: V_2O_5 treated by O_2 at 342 Torr and 75°C after evacuation of SO_2.
(a) 1023 cm^{-1}, (b) 1005 cm^{-1}, (c) 1013 cm^{-1}

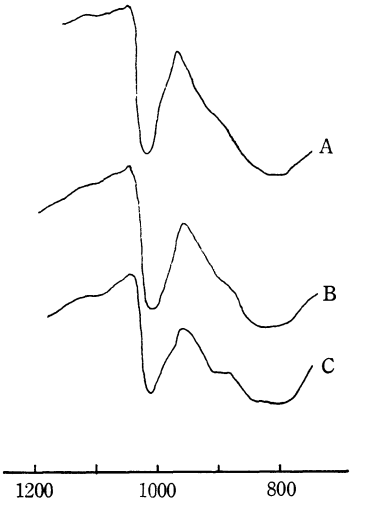

Fig. 5. IR spectra of V_2O_5 treated by CO.
A: V_2O_5 untreated.
B: V_2O_5 treated by CO at 157 Torr and 100°C for 1 hr.
C: V_2O_5 treated by CO at 157 Torr and 140°C for 3 hr after B.

830 cm^{-1} was almost unchanged by this treatment. When a V_2O_5 sample, freshly prepared, was

4) K. Tarama, S. Teranishi and S. Yoshida, *Shokubai*, **6**, 299 (1964).
5) L. Frederickson and D. Hausen, *Anal. Chem.*, **35**, 818 (1963).

TABLE 2. THE CHANGES OF ESR SIGNAL INTENSITIES BY TREATMENT WITH SOME GASES

Sample	Condition of treatment with gases				Relative intensity
	Gas	Pressure	Temperature	Duration	
V-O	evacuation for 3 hr at 350°C*				1.0
VC-1	CO	3.9 Torr	room temp.	84 hr	1.3
VC-2	CO	98 Torr	room temp.	55 hr	1.5
VC-3	CO	226 Torr	room temp.	84 hr	2.0
VC-4	VC-3 evacuated for 8 hr at room temp.				1.8
VC-5	CO	17 Torr	150°C	17 hr	1.4
VC-6	VC-5 treated with O_2 (150 Torr) at room temp.				0.9
VC-7	VC-6 kept for 3 hr at 150°C				0.8
VC-8	CO	110 Torr	150°C	17 hr	1.9
VC-9	VC-8 evacuated for 3 hr at room temp.				1.6
VS-1	SO_2	15.2 Torr	room temp.	7 hr	1.2
VS-2	SO_2	163 Torr	room temp.	7 hr	1.6
VS-3	SO_2	300 Torr	room temp.	14 hr	1.4
VS-4	VS-3 evacuated for 8 hr at room temp.				1.2
VE-1	C_2H_4	28.2 Torr	room temp.	192 hr	1.8
VE-2	VE-1 evacuated for 15 hr at room temp.				1.6
VE-3	C_2H_4	260 Torr	room temp.	168 hr	2.1
VE-4	VE-3 evacuated for 15 hr at room temp.				1.6

* The starting samples are V_2O_5(5 wt%) - γ-Alumina evacuated for 3 hr at 350°C in all cases and signal intensity of this sample is adopted as standard.

treated by O_2 at 100°C, no change in the spectra could be observed.

The change induced by the adsorption of CO was the same as that in the case of SO_2, but effect was smaller and a new peak, at 910 cm^{-1}, appeared at 140°C, as is shown in Fig. 5. This peak probably belongs to the absorption band of V_2O_4.[5] Therefore, the appearance of this peak suggests that V_2O_5 was partially reduced to V_2O_4 by CO-treatment at 140°C. In the case of C_2H_4, no change in the IR spectra could be observed upon the treatment at 25°C, but a partial reduction of V_2O_5 to V_2O_4 was observed at 80°C, as in the case of CO.

These results indicate that the reducing power of these gases increases in the order of SO_2, CO and C_2H_4 under these experimental conditions.

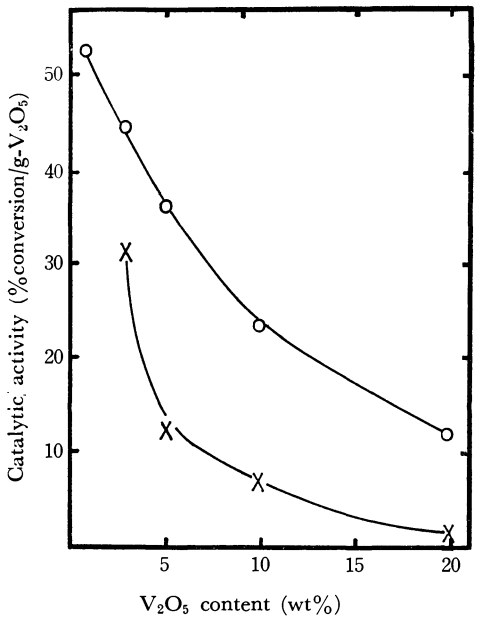

Fig. 6. Catalytic activity for CO-oxidation of supported V_2O_5.
○ and × marks stand for the catalysts supported on γ-Al_2O_3 and SiO_2 respectively.

Oxidation of CO with Air. Because a linear relation between the conversion (α, %) of CO to CO_2 and the contact time was observed up to 30% conversion, the values of α at the same contact time were adopted as the measure of the activity.

The activities of V_2O_5 on γ-Al_2O_3 of various concentrations and V_2O_5 on SiO_2 are shown in Fig. 6. The relative activities per gram of V_2O_5 in the catalysts decreased with the increase in the concentration of V_2O_5. This indicates that the number of effective sites of V_2O_5 is increased by dispersion on carriers.

TABLE 3. REDUCTION OF CATALYST BY CO AT 350°C FOR 1 HR (P_{CO}: 150 Torr)

Catalyst	Produced CO_2 cc(NTP)/g-cat.	Reduction % (V^{4+}/V^{5+} initial)
V_2O_5(5%) on γ-Al_2O_3	4.1	65
V_2O_5(5%) on SiO_2	0.55	9

TABLE 4. THE ADSORPTION SITE ON THE METAL OXIDE OR SULFIDE OF SEMICONDUCTOR

Adsorbent (catalyst)	Adsorbate (gas)	Adsorption site in surface (example)
n-Type semiconductor (example, V_2O_5)	Electron donor	Metal ion at normal lattice point (V^{5+})
	Electron acceptor	Metal ion adjacent to defect of anion (V^{4+})
p-Type semiconductor (example, NiO)	Electron donor	Metal ion adjacent to excess anion (Ni^{3+})
	Electron acceptor	Metal ion at normal lattice point (Ni^{2+})

V_2O_5 - γ-Al_2O_3 catalysts are more active than the V_2O_5-SiO_2 catalyst. These activities are closely correlated with the reducibilities of these catalysts by CO at 350°C, as is shown in Table 3.

Discussion

The State of Vanadium Ions in V_2O_5 Dispersed on Carriers. The unsupported V_2O_5 powder gave a broad single ESR signal, and the line width (ΔH_{msl}) of this absorption signal became larger at a low temperature (ΔH_{msl}; 90 gauss at room temperature and 180 gauss at the temperature of liquid nitrogen), as has previously been reported.[1,6] In the case of V_2O_5 dispersed on γ-Al_2O_3, however, the h.f.s. of the ESR spectrum due to $(V{=}O)^{2+}$ was observed. The appearance of this h.f.s. by the dispersion of V_2O_5 on a carrier seems to result from the decrease in the delocalizability of the electron associated to $(V{=}O)^{2+}$. Therefore, it is clear that V(IV) ions in V_2O_5 on γ-Al_2O_3 are stabilized in the form of $(V{=}O)^{2+}$. However, $(V{=}O)^{2+}$ seems not to be in the isolated state, but to be stabilized as $(V{=}O)^{2+}$ in the thin layer of the micro crystal of V_2O_5 on γ-Al_2O_3 for the following reasons: a) Even the sample of V_2O_5 (50 wt%) on γ-Al_2O_3 gave ESR spectra with fairly well resolved h.f.s. (Fig. 1-B). In this sample, it is quite difficult to believe that $(V{=}O)^{2+}$ ions are isolated on the surfaces of carriers. b) The observed ESR signal for V_2O_5 (5 wt%) on γ-Al_2O_3 is similar to that of $VOSO_4$ in γ-Al_2O_3, but there is some difference in resolutions and in coupling constants between the h.f.s.'s of the two samples. Of course, the resolution of the spectrum depends on the concentration of the paramagentic species. Though the concentration of V(IV) ions is about 1% of the total vanadium in V_2O_5 (5%) on γ-Al_2O_3, and is thus so small that the interaction between paramagnetic species is negligible, the resolution of h.f.s. is not clear.

In the case of V_2O_5 on SiO_2, the state of V(IV) is not clear, either, no signal could be observed as has been reported above; the amount of V(IV) ions in this sample may be too small to be detected by the ESR method.

On the other hand, V(V) ions (the diamagnetic species) can not be detected by ESR measurement, and so their state in V_2O_5 is presumed indirectly from the change in the ESR signal and in the IR specta with gas adsorption or reduction.

The Adsorption Sites on V_2O_5. When electron-donating gases, such as CO, SO_2 and C_2H_4, were adsorbed on V_2O_5 supported on γ-Al_2O_3, the signal intensity of the ESR spectra increased and the splitting of the h.f.s. became clear. Even in the case of the sample supported on SiO_2, which gave no ESR signal after evacuation at 350°C, a weak signal with a h.f.s. identified as $(V{=}O)^{2+}$ appeared by the adsorption of these gases.

The growth of this signal intensity indicates an increase in $(V{=}O)^{2+}$. Therefore, it seems sure that these electron-donating gases are adsorbed on $(V{=}O)^{3+}$ bonds on the surface of a V_2O_5 crystal, and that an electron is transferred from adsorbed gas to an adsorption site, thus leading to the formation of $(V{=}O)^{2+}$.

On the other hand, the signal intensity became weak by O_2 adsorption. As O_2 is an electron-accepting gas, this shows that oxygen is adsorbed on $(V{=}O)^{2+}$ and that this adsorption site is converted to $(V{=}O)^{3+}$ by electron transfer.

The above model for gas adsorption is supported by the IR measurements, too. By the adsorption of CO or SO_2, the IR absorption band due to $(V{=}O)^{3+}$ bond broadened, the center of the peak shifted to the red region, and a weak hump, probably due to the $(V{=}O)^{2+}$ bond,[5] appeared at 980—990 cm^{-1}.

These changes in the IR spectra reflect the increase in the electron density in the V-ion of the $(V{=}O)^{3+}$ bond. The effect of the treatment with O_2 on the IR spectrum was the reverse of that with CO or SO_2.

From the results of these ESR and IR measuremenets, it can be concluded that the adsorption sites on V_2O_5 are $(V{=}O)^{3+}$ for such electron-donating gases as CO, SO_2 and C_2H_4 and $(V{=}O)^{2+}$ for such electron-accepting gases as O_2.

This conclusion is very probable in the light of the general rule previously proposed by one of authors[7] for the adsorption site on the metal oxide or sulfide of a semiconductor, as is shown in Table 4.

6) K. Tarama, S. Teranishi, S. Yoshida, N. Tamura and S. Ishida, *Kogyo Kagaku Zasshi (J. Chem. Soc. Japan, Ind. Chem. Sect.)*, **68**, 1499 (1965).

7) K. Tarama, *Kogyo Kagaku Zasshi (J. Chem. Soc. Japan, Ind. Chem. Sect.)*, **63**, 675 (1960); *Ryusan*, **12**, 161 (1959).

The Role of the V=O Bond in Oxidation Reaction. It is generally accepted that the catalysis by V_2O_5 for oxidation reaction is effected by the oxidation-reduction mechanism in which the lattice oxygen of the catalyst is taken away by gas and the catalyst is reoxidized by O_2.

This mechanism seems also to be supported by the finding that the activity of the catalyst in CO-oxidation is closely correlated with its reducibility by CO.

The present authors have presented a hypothesis that the strength of a V=O bond is a controlling factor in the activity of the catalytic oxidation.[1] Recently, Hirota and his collaborators[8] studied the exchange of isotopic oxygen between CO_2 containing ^{18}O and V_2O_5, and showed that this oxygen exchange proceeded through a surface V=O bond of V_2O_5. This finding supports the preceding hypothesis.

Therefore, it can be concluded that the V=O bond on the surface of V_2O_5 performs an important role as the adsorption site and also as the reaction site for the oxidation reaction.

8) Y. Kera, S. Teratani and K. Hirota, This Bulletin, **40**, 2458 (1967).

BULLETIN OF THE CHEMICAL SOCIETY OF JAPAN VOL. 41 2845—2848 (1968)

Gel Filtration of Mixtures of Surfactants on Sephadex

Fumikatsu TOKIWA, Kenji OHKI and Isao KOKUBO

Research Laboratories, Kao Soap Company, Minato-Yakushubata, Wakayama

(Received April 2, 1968)

The gel filtrations of mixtures of sodium dodecyl sulfate (SDS) and sodium tetradecyl sulfate (STS) have been studied for different mole ratios of STS/SDS with varying total concentrations. Above the critical micelle concentration (CMC) of the mixture, two retention volumes V^1_{obs} and V^2_{obs} were obtained from the elution curve, and the difference between V^1_{obs} and V^2_{obs} depends on the total concentrations of the mixture. The initial part of the effluent contains only STS, which means that the separation of STS from the mixture occurs after passing through the column. These results have been discussed by taking into consideration the equilibrium between monomers and micelles for the mixtures of the two surfactants. It is shown that the separation factor is determined by the CMC values of the two surfactants—the greater the ratio CMC_A/CMC_B ($CMC_A > CMC_B$), the greater the degree of separation.

In a previous work[1] an attempt was made to apply gel filtration on Sephadex to micellar solutions of single surfactants. The results have been successfully interpreted by taking into account the existence of both micellized and unmicellized species in solution.

In the present work, the gel filtration study has been extended to the micellar solutions of mixed surfactants. The surfactants studied were sodium dodecyl sulfate (SDS) and sodium tetradecyl sulfate (STS), which were mixed in different ratios. The data obtained were analyzed through equilibrium equations for a two component system containing both monomer and micelle phases.

Experimental

Materials. Sephadex G-50, a cross-linked dextran gel with a particle size of 20—80 microns, and Blue Dextran 2000 with a molecular weight of 2×10^6 were obtained from Pharmacia, Sweden. Sodium dodecyl sulfate (SDS) and sodium tetradecyl sulfate (STS) were the same samples as used in the previous work.[1]

Gel Filtration. Sephadex G-50 was allowed to swell in distilled water for at least 24 hr and then poured into a jacketed column, 1.3 cm in diameter $\times$35.5 cm in height, with a sintered glass plate at the bottom. The column was prepared in the same way as that previously described.[1] The void volume of the column was checked on alternated runs using Blue Dextran 2000. The gel filtrations were carried out at 32$\pm$0.1°C. Fifty milliliters sample solution (SDS-STS mixture) was applied continuously to the top of the column through a siphon connected to the sample reservoir. An automatic fraction-collector was used and fractions of approximately 1 m*l* were collected. The electrical conductivity of each fraction was measured to obtain the elution curve.

Determination of CMC. The critical micelle concentrations (CMC) of the mixtures of SDS and STS for different mixing ratios were determined at 32°C by an electrical conductivity method[2] using a Toa Dempa Model CM-IDB conductance bridge.

1) F. Tokiwa, K. Ohki and I. Kokubo, This Bulletin, **41**, 2285 (1968).

2) F. Tokiwa, ibid., **36**, 281 (1963).

Gas Chromatography. The SDS and STS present in the fractions of the effluents were hydrolyzed with hydrochloric acid to obtain dodecyl- and tetradecyl-alcohols, which were extracted with *n*-hexane. The mole fractions of dodecyl- and tetradecyl-alcohols were determined by gas chromatography with a Shimadzu Model 4APT apparatus using a Carbowax 20M column at 230°C.

Results and Discussion

Figure 1 shows typical elution curves for mixed solutions of SDS and STS, whose mixing ratio is 1 to 1 in moles, at various total concentrations, C^t. Below the CMC of the mixture, the elution curve is sigmoidal and the retention volume obtained from the curve is independent of C^t. Above the CMC, on the other hand, the elution curve consists of two sigmoidal plots with a plateau between them, as seen in Fig. 1. The curve is characterized by

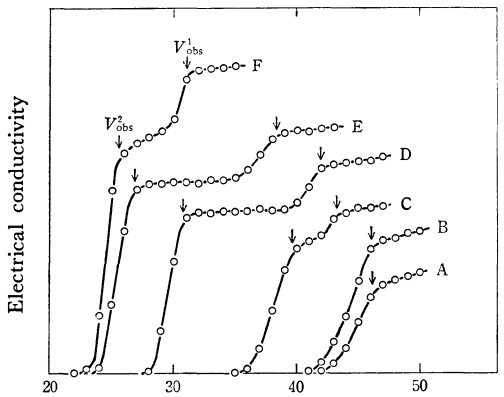

Fig. 1. Elution curves for mixed solutions of SDS and STS at a mixing ratio of 1 to 1 in mole at various total concentrations: A, 0.0020 M; B, 0.0035M; C, 0.0045M; D, 0.0075M; E, 0.011M; F, 0.02 5M. The arrows indicate the retention volumes of the mixture.

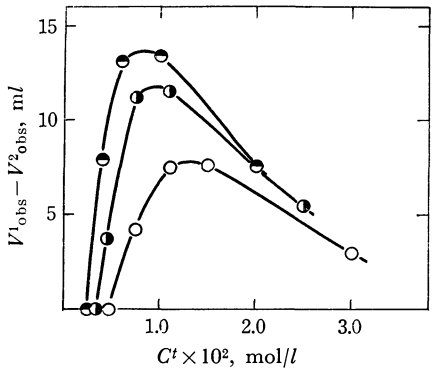

Fig. 2. The values of $(V^1_{obs}-V^2_{obs})$ plotted against C^t at different mixing ratios of STS/SDS: ○, 25/75; ◑, 50/50; ◓, 75/25.

the two retention volumes V^1_{obs} and V^2_{obs} for two shoulders of the curve. The fact that two retention volumes V^1_{obs} and V^2_{obs} are obtained may be explained as due to a continuous change in micelle composition during gel filtration, as will be described later. In Fig. 2, the values of $(V^1_{obs}-V^2_{obs})$ are plotted against C^t for different ratios of STS/SDS. The value of $(V^1_{obs}-V^2_{obs})$ at a given ratio of STS/SDS increases rapidly with C^t and then decreases through a maximum.

It is reasonable to consider that SDS and STS in aqueous solution form mixed micelles rather than the respective micelles of each surfactant. If we now consider a two component system containing both monomer and micelle phases and assume the system to be ideal, we know that for each component the chemical potentials in the two phases are identical at equilibrium. Under such a condition, the equilibrium between monomers and micelles in the mixed solution of SDS(subscript 1) and STS (subscript 2) may be expressed[3]

$$y_1 C^0_{1,2} = x_1 C_1{}^0 \tag{1}$$

and

$$y_2 C^0_{1,2} = x_2 C_2{}^0 \tag{2}$$

or

$$(1-y_1) C^0_{1,2} = (1-x_1) C_2{}^0 \tag{2'}$$

where x or y is the mole fraction of each surfactant in the micelle or monomer phase, respectively, $C^0_{1,2}$ the CMC of the mixture of the two surfactants and C^0 the CMC of the single surfactant. These equations are analogous to Raoult's equation in the form. From Eqs. (1) and (2'), the CMC value of mixed surfactants $C^0_{1,2}$ is written in the following forms as a function of x_1 or y_1.

$$C^0_{1,2} = \frac{C^0_1 - C^0_2}{C^0_1 - (C^0_1 - C^0_2) y_1} \tag{3}$$

and

$$C^0_{1,2} = (C^0_1 - C^0_2) x_1 + C^0_2 \tag{4}$$

The relation between x_1 and y_1 is written

$$y_1 = \frac{C^0_1}{C^0_1 - C^0_2 + (C^0_2/x_1)} \tag{5}$$

The curve of $C^0_{1,2}$ *vs.* x_1 or y_1 is shown in Fig. 3, where the values of CMC for SDS and STS (*i. e.*, C^0_1 and C^0_2) were taken to be 8.1×10^{-3} mol/*l* and 2.2×10^{-3} mol/*l*, respectively. At a given CMC, y_1 is always greater than x_1, that is, the fraction of SDS in the monomer phase is always greater than that in the micelle phase. In Fig. 3 the CMC values of the mixtures of SDS and STS are also shown, determined by electrical conductivity measurement for various total mole fractions of SDS, α_1. The $C^0_{1,2}$ values experimentally obtained lie on the $C^0_{1,2}$ *vs.* y_1 curve. This supports

3) F. Daniels and R. A. Alberty, "Physical Chemistry," John Wiley, New York, N. Y. (1966), p. 145.

Table 1. Mole fractions of SDS in each region of the effluent for the mixtures of SDS and STS

Mixture		Mole fraction of SDS						
STS/SDS	$C^t \times 10^3$, mol/l	Initial	I	II	III	IV	V	VI
25/75	11.0	0.75	0	0	0.55	0.66	0.76	0.80
50/50	11.0	0.50	0	0	0.38	0.49	0.54	0.52
75/25	10.0	0.25	0	0	0.19	0.23	0.28	0.30

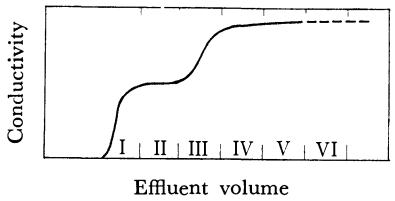

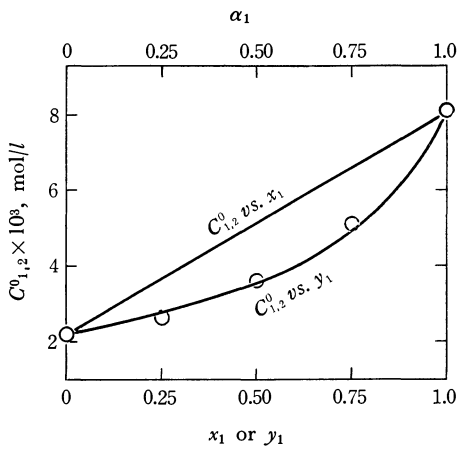

Fig. 3. The relation between $C^0_{1,2}$ and x_1 or y_1, where x_1 and y_1 are the mole fractions of SDS in the micelle and monomer phases respectively. The CMC values determined experimentally are also shown by circles as a function of the total mole fraction of SDS α_1.

the use of Eqs. (1) and (2′) for the equilibria between monomers and micelles.

With gel filtration of a surfactant solution, the micelles flow faster down through the column than the monomers, and dissociate into monomers in the frontal region of the solution since micelles can not exist without monomers. The dissociated monomers will flow more slowly, and the concentration of monomers will be increased by similarly dissociated monomers from other micelles. Then, the monomers will again associate to form new micelles when the concentration reaches the CMC. Thus, the processes of dissociation→association, and association → dissociation will be repeated; in other words, the repeated decomposition and formation of micelles occur continuously during gel filtration. With the gel filtration of a mixture of SDS and STS, the fraction of SDS in the micelle decreases with increasing number of steps of decomposition-formation of micelle and ultimately becomes zero when a long gel column is used, since the fraction of SDS in the micelle is always less than that in the monomer phase at the CMC, as shown in Fig. 3. This explains the fact that two shoulders appear in the elution curve of a mixture of SDS and STS. Table 1 shows the mole fractions of SDS, determined through gas chromatography, in the regions of I, II, III,··· of the effluent which are indicated schematically below the table. As expected from the above discussion, the frontal parts of the effluent, *i. e.*, the regions I and II, contain only STS after passing through the column. Then, the mole fraction of SDS in the effluent increases with increasing elution volume, but would finally become equal to the initial mole fraction through a maximum value.

Now, one has to explain why the difference between V^1_{obs} and V^2_{obs} becomes smaller at higher concentrations of the mixture of SDS and STS, as seen in Fig. 2. The mole fraction of SDS in the micelle phase, x_1, is defined

$$x_1 = \frac{C^M{}_1}{C^M{}_1 + C^M{}_2} = \frac{C^t{}_1 - C^m{}_1}{C^t - C^0{}_{1,2}} \tag{6}$$

that is,

$$x_1 = \frac{\alpha_1 C^t - C^0{}_{1,2} y_1}{C^t - C^0{}_{1,2}} \tag{7}$$

where superscripts m and M refer to monomer and micelle, respectively, and α_1 is the total mole fraction of SDS, *i. e.*, the sum of the mole fractions of SDS in the monomer and micelle phases. Combining Eq. (7) with Eqs. (1) and (4), we have

$$\alpha_1 = \frac{1}{n} \cdot x_1 \{(1+n) - x_1\}, \quad n = C^t/(C^0{}_1 - C^0{}_2) \tag{8}$$

The relations between x_1 and α_1 for different values of n are shown in Fig. 4. The relations between y_1 and α_1 at different values of n are similarly obtained by combination of Eq. (8) and Eq. (5), which

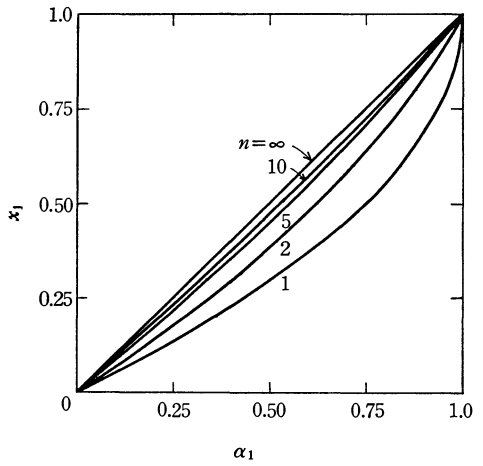

Fig. 4. Curves of x_1 *vs.* α_1 at different values of n, where n is $C^t/(C^0{}_1-C^0{}_2)$.

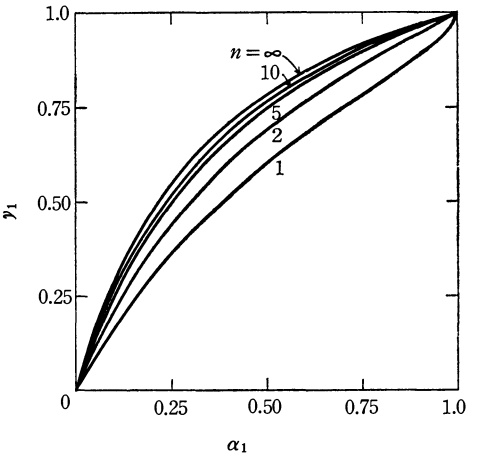

Fig. 5. Curves of y_1 *vs.* α_1 at different values of n, where n is $C^t/(C^0{}_1-C^0{}_2)$.

are also shown in Fig. 5. At very high concentrations where $n \gg 1$, *i.e.*, $C^t \gg (C^0{}_1-C^0{}_2)$, x_1 approaches α_1. This means that the change in the mole fraction of SDS by repeated micelle formation during gel filtration, which has already been described, is small at high concentrations. Thus, the difference between $V^1{}_{obs}$ and $V^2{}_{obs}$ becomes smaller at those concentrations.

The separation factor, β, is generally used as a measure of separation in partition chromatography.[4] In the present case, the β may be defined as K_{STS}/K_{SDS}, where K is the partition coefficient of the surfactant for micelle and monomer phases; that is,

$$\beta = \frac{(C^t-C^0{}_{1,2})x_2/C^0{}_{1,2}y_2}{(C^t-C^0{}_{1,2})x_1/C^0{}_{1,2}y_1} \tag{9}$$

Using Eqs. (1) and (2), Eq. (9) is rewritten

$$\beta = \frac{(C^t-C^0{}_{1,2})x_2/C^0{}_2x_2}{(C^t-C^0{}_{1,2})x_1/C^0{}_1x_1} = \frac{C^0{}_1}{C^0{}_2} \tag{10}$$

Equation (10) indicates that the separation of two surfactants is governed by the CMC values of each surfactant. The greater the ratio of CMC_A/CMC_B where $CMC_A > CMC_B$, the greater is the degree of separation of surfactant B from the mixture of surfactants A and B.

The authors express their thanks to Dr. H. Kita, Director of the Research Laboratories, for his encouragement and permission to publish this paper.

4) E. Lederer and M. Lederer, "Chromatography," Elsevier, New York, N. Y. (1954).

BULLETIN OF THE CHEMICAL SOCIETY OF JAPAN VOL. 41 2849—2852 (1968)

A Study on the Electronic Spectra of 1-(*p*-Substituted phenyl)pyrroles*[1]

Taku MATSUO, Hideto SHOSENJI and Reiji MIYAMOTO

Department of Organic Synthesis, Faculty of Engineering, Kyushu University, Hakozaki, Fukuoka

(Received April, 20, 1968)

The longest wavelength electronic absorption band of 1-(*p*-substituted phenyl)pyrrole has been found to show a regular bathochromic shift as the electronegativity of the substituent on the phenyl group increases. The substituent effect is closely related to that for the intramolecular charge-transfer bands of *p*-substituted anilines. Therefore, the longest wavelength absorption band of 1-(*p*-substituted phenyl)pyrroles have been suggested to be originated from an electron transfer from the pyrryl group to the phenyl group. Only one exception is the spectra of 1-(*N,N*-dimethyl-*p*-aminophenyl)pyrrole. In this case, the longest wavelength electronic absorption band is suggested to be due to an electron-transfer from the *N,N*-dimethylamino group to the phenyl group.

A large number of experimental studies have been reported on the electronic spectra of pyrrole derivatives.[1] The present status of the theoretical interpretation, however, is far from satisfactory except for the case of pyrrole itself.[1g,2] The situation may be improved by making a systematic study of the spectra of a series of related pyrrole derivatives. In the present paper, the nature of the longest wavelength absorption bands of 1-(*p*-substituted phenyl)pyrroles are described and the origin of the electronic transitions is discussed.

Results and Discussion

The longest wavelength electronic absorption bands of 1-(*p*-substituted phenyl)pyrroles are invariably strong and appear in the region between 250 mμ and 350 mμ. The wave numbers and the extinction coefficients for the absorption maxima are summarized in Table 1. It is clearly observed there that the absorption band shows a regular bathochromic shift, except for the case of *N,N*-dimethylamino group, as the electronegativity of the *p*-substituent increases. The trend may be taken to indicate that the absorption bands arise from intramolecular charge-transfer as has been suggested in the cases of mono-substituted benzenes.[3,4] Since pyrryl group is a very strong π-electron donor in the formation of charge-transfer complexes,[5] it is very likely that the pyrryl group in 1-phenylpyrrole donates its electrons to the phenyl group. The substituent effect on

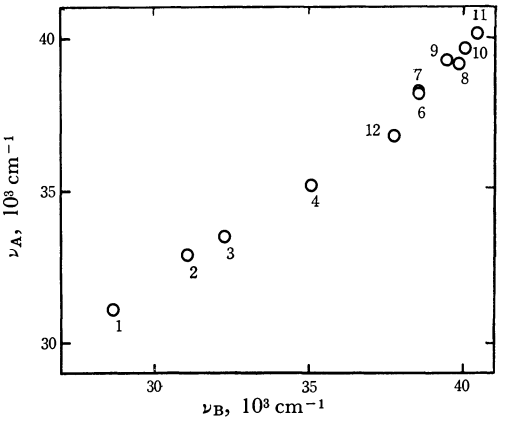

Fig. 1. Plot of the ultraviolet bands of 1-(*p*-substituted phenyl)pyrroles (ν_A) *vs.* those of *p*-substituted *N,N*-dimethylanilines (ν_B) in *n*-hexane. The numbers correspond to the numbering of the compounds listed in Tables 1 and 2.

*1 Contribution No. 154 from the Department of Organic Synthesis, Faculty of Engineering, Kyushu University.

1) a) G. Milazzo, *Gazz. Chim. Ital.*, **83**, 392 (1953). b) J. Davoll, *J. Chem. Soc.*, **1953**, 3802. c) G. Battista, B. Marinangeli and A. M. Marinangeli, *Atti accad. Nazl. Lincei, Rend. (Classe sci. fis., mat. e nat.)* **19**, 222 (1955); *Chem. Abstr.*, **50**, 11111c (1956). d) R. Andrisano, G. Pappalardo and L. Bolognari, *Gazz. Chim. Ital.*, **85**, 1430 (1955). e) L. Chierici and G. Pappalardo, *ibid.*, **88**, 453 (1958); *Chem. Abstr.*, **53**, 18000d (1959). f) A. Bertoluzza and A. M. Marinangeli, *Ann. Chim.*, **52**, 731 (1962). g) Y. Chiang, R. L. Hinman, S. Theodoropulos and E. B. Whipple, *Tetrahedron*, **23**, 745 (1967).

2) a) R. D. Brown and M. L. Heffernan, *Australian J. Chem.*, **12**, 319 (1959). b) J. P. Dahl and A. E. Hansen, *Theoret. Chim. Acta*, **1**, 199 (1963). c) N. Solony, F. W. Briss and J. B. Greenshields, *Can. J. Chem.*, **43**, 1569 (1965).

3) a) H. C. Longuet-Higgins and J. N. Murrell, *Proc. Phys. Soc.*, **A68**, 601 (1955). b) J. N. Murrell, *ibid.*, **A68**, 969 (1955).

4) a) S. Nagakura, M. Kojima and Y. Maruyama, *J. Mol. Spectry.*, **13**, 174 (1964). b) K. Kimura and S. Nagakura, *Mol. Phys.*, **9**, 117 (1965).

5) T. Matsuo and H. Shosenji, This Bulletin, **41**, 1068 (1968).

Table 1. The longest wavelength electronic absorption bands of 1-(*p*-substituted phenyl)pyrroles

No.	Compound	The *n*-hexane solution		The ethanol solution	
		ν[a]	ε[b]	ν[a]	ε[b]
1	1-*p*-Nitrophenylpyrrole	31.1	17.4	30.3	16.4
2	1-*p*-Formylphenylpyrrole	33.4	27.5	32.6	22.8
		32.3	26.3		
3	1-*p*-Acetylphenylpyrrole	34.1	25.1	33.4	24.0
		32.8[c]	19.6		
4	1-*p*-Cyanophenylpyrrole	35.2	22.0	34.8	22.8
5	1-*p*-Carbomethoxyphenylpyrrole	35.0	23.3	34.5	22.2
6	1-*p*-Bromophenylpyrrole	38.2	18.7	38.1	18.2
7	1-*p*-Chlorophenylpyrrole	38.3	17.9	38.4	17.2
8	1-Phenylpyrrole	39.2	13.5	39.4	13.2
9	1-*p*-Tolylpyrrole	39.3	14.7	39.3	14.5
10	1-*p*-Anisylpyrrole	39.7	15.7	39.8	15.1
		34.1[c,d]	2.0	34.1[c,d]	1.9
11	1-*p*-Hydroxyphenylpyrrole	40.2	e)	40.0	26.9
		33.9[c,d]	e)	33.8[c,d]	3.3
12	1-(*N,N*-Dimethyl-*p*-amino-phenyl)pyrrole	36.8	21.0	36.6	18.6
		31.1[c,d]	2.0	31.2[c,d]	2.1

a) The values are given in units of 10^3 cm^{-1}, and the uncertainty is within 100 cm^{-1} unless otherwise specified.
b) The values are given in units of 10^3 $l/mol \cdot cm$, and the uncertainty is within 100 $l/mol \cdot cm$.
c) The position of a shoulder (± 200 cm^{-1}).
d) The absorption band may be mainly due to the locally excited B_{2u} configuration of the phenyl group.
e) No reliable value has been obtained because the solubility of the sample is extremely low.

the charge-transfer band of *N,N*-dimethylaniline*2 was also investigated for the comparison (Table 2). In Fig. 1, the positions of absorption maxima of the 1-phenylpyrrole analogues are plotted against those of the corresponding *N,N*-dimethylanilines. A very close resemblance is observed between the substituent effects in the two series. Analogously to the case of aniline, the absorption spectra of the 1-phenylpyrrole analogues are suggested then to be related to the charge-transter conffgurations of the following type:

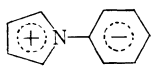

In agreement with this suggestion, the absorption band shows both hypsochromic shift and hypochromic effect when the conjugation between the pyrryl and phenyl groups is hindered by the presence of methyl group at either the 2- or the 2′-position*3 (Table 3, Fig. 2). Similar observation was reported also by several investigators.[1b,1g]

When an electronegative group is attached to the *p*-position of the phenyl group, the energy of the charge-transfer configuration should be lowered.

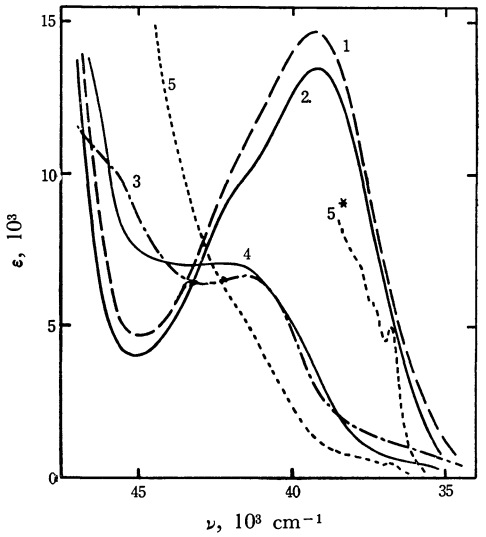

Fig. 2. The ultraviolet spectra of 1-phenylpyrrole and its methyl-substituted analogues in *n*-hexane. The numbers correspond to the numbering of the compounds listed in Table 3. * The real molecular extinction coefficient is one tenth of the value shown in this figure.

*2 The charge-transfer nature of this band has been well established by Nagakura and his associates.[4b]

*3 If one uses Braude and Sondheimers' relationship (Eq. (1))[7] to estimate the angle of twist, θ, between the two groups;

$$\varepsilon/\varepsilon_0 = \cos^2\theta \qquad (1)$$

he gets 50° for 1-(*o*-tolyl)pyrrole. On the basis of a three dimensional molecular model with appropriate van der Waals radii, θ for the same compound is estimated to be approximately 60°.

Table 2. The longest wavelength intramolecular charge-transfer bands of *p*-substituted *N,N*-dimethylanilines[a]

No.[b]	Compound	ν[c]	ε[d]
1	*N,N*-Dimethyl-*p*-nitroaniline[e]	28.7	
2	*N,N*-Dimethyl-*p*-amino-benzaldehyde	31.4	29.9
		30.8	29.6
3	*N,N*-Dimethyl-*p*-amino-acetophenone	32.8[f]	24.1
		31.8	27.5
4	*N,N*-Dimethyl-*p*-cyanoaniline	35.6	29.0
		34.6[f]	23.5
6	*N,N*-Dimethyl-*p*-bromoaniline	38.6	19.5
7	*N,N*-Dimethyl-*p*-chloroaniline	38.6	19.6
8	*N,N*-Dimethylaniline	39.9	15.1
9	*N,N*-Dimethyl-*p*-toluidine	39.5	15.2
10	*N,N*-Dimethyl-*p*-anisidine	40.1	13.3
11	*N,N*-Dimethyl-*p*-aminophenol[g]	40.5	11.0
12	*N,N,N',N'*-Tetramethyl-*p*-phenylenediamine	37.8	16.4

a) Solvent: *n*-hexane.
b) The numbering of the compounds is made so that the substituent on the para position of the phenyl group in this table is the same to that of the corresponding number in Table 1.
c) The values are given in units of 10^3 cm^{-1}, and the uncertainty is within 100 cm^{-1} unless otherwise specified.
d) The values are given in units of 10^3 *l*/mol·cm, and the uncertainty is within 100 *l*/mol·cm.
e) K. Semba, This Bulletin, **34**, 722 (1961).
f) The position of a shoulder ($\pm$200 cm^{-1}).
g) A. Mangini and R. Passerini, *J. Chem. Soc.*, **1956**, 4954.

Table 3. The ultraviolet absorption bands of methyl substituted 1-phenylpyrroles[a]

No.	Compound	ν[b]	ε[c]
1	1-*p*-Tolylpyrrole	42.2$\pm$0.2[d]	9.80$\pm$0.03
		39.3$\pm$0.1	14.7 $\pm$0.1
2	1-Phenylpyrrole	42.2$\pm$0.2[d]	9.00$\pm$0.03
		39.2$\pm$0.1	13.5 $\pm$0.1
3	1-Phenyl-2,5-dimethylpyrrole	45.7$\pm$0.2[d]	10.1 $\pm$0.1
		41.4$\pm$0.1	6.66$\pm$0.02
4	1-*o*-Tolylpyrrole	41.2$\pm$0.2[d]	6.70$\pm$0.02
5	1-(2',6'-Xylyl)pyrrole	41.3$\pm$0.2[d]	4.80$\pm$0.02

a) Solvent: *n*-hexane.
b) The values are given in units of 10^3 cm^{-1}.
c) The values are given in units of 10^3 *l*/mol·cm.
d) The position of a shoulder.

The experimental facts are certainly in accordance with this expectation. The only one exception is *N,N*-dimethylamino group. In order to investigate the reason for the bathochromic effect of this group, the spectra were measured in acidic medium. Since the spectra of 1-(*N,N*-dimethyl-*p*-aminophenyl)pyrrole in acidic medium is very close to that of 1-phenylpyrrole in the neutral solution (Fig. 3), the former compound is concluded to be protonated on its *N,N*-dimethylamino group. This conclusion is in agreement with the fact that the basicity of pyrrole (pK_a, -4.4)[1g] is much lower than that of *N,N*-dimethylaniline (pK_a, 5.10).[6] In other words, *N,N*-dimethylamino group is more basic than pyrryl group. Therefore it is very important to take into account the contribution of the charge-transfer configurations where an electron is transferred from the *N,N*-dimethylamino group to the phenyl group. Such electronic configurations are of minor importance in the cases of other substituents in Table 1. Thus the nature of the longest wavelength absorption band of 1-(*N,N*-dimethyl-*p*-aminophenyl)pyrrole may be suggested to be different from those of the other 1-(*p*-substituted phenyl)pyrroles.

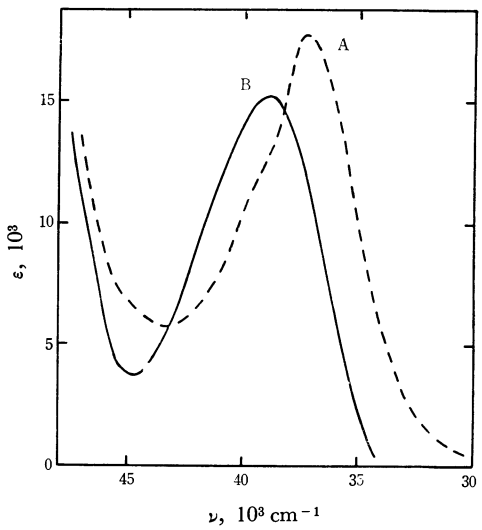

Fig. 3. The ultraviolet spectra of 1-(*N,N*-dimethyl-*p*-aminophenyl)pyrrole in 10% (vol/vol) ethanol-water solution; A, the neutral solution; B, the 10^{-2} N hydrochloric acid solution.

In order to understand the nature of electronic transitions of complex molecules, it is very useful to utilize the method of composite molecules.[3,4] In the present case, the constituent molecules are pyrrole (A) and substituted benzene (B). The presence of an electronegative group in the phenyl group will increase the electron affinity of B. Then the energy of local excitation in either A or B will be above that of the charge-transfer state (A^+B^-) where an electron is transferred from A to B. The situations is entirely different, if the substituent is *N,N*-dimethylamino group which is a highly electron-donating group. Since the electron affinity of B is considerably reduced, in this case, the energy of the charge-transfer state (A^+B^-)

6) N. F. Hall, *J. Am. Chem. Soc.*, **52**, 5115 (1930).

will be raised appreciably. The energy of the lowest excited state in B (*i. e.*, *N,N*-dimethylaniline), on the other hand, is known to be much less than that of unsubstituted benzene.[4b] Then it is quite likely that the local excitation in B may require less energy than an electron-transfer from A to B. If this is the case, the longest wavelength electronic absorption band of 1-(*N,N*-dimethyl-*p*-aminophenyl)pyrrole is considered to be due to an electron transfer from the *N,N*-dimethylamino group (rather than from the pyrryl group) to the phenyl group. The experimental facts are certainly in accordance with this view point. In order to testify the proposed explanation, a quantum mechanical calculation is being carried out to estimate the relative importance of various electronic configurations.

It may be adequate to mention here also that a weak absorption band corresponding to the B_{2u} state of benzene seems to be hidden under the longest wavelength absorption bands discussed above. The band appears only slightly at the tail of the absorption edge of 1-(2′,6′-xylyl)pyrrole (Fig. 2).

Experimental

Chemicals. The preparations of the materials other than described below have been reported elsewhere.[5] The following compounds were prepared according to the literatures as given in the parentheses: 1-*p*-nitrophenylpyrrole (Ref. 8, mp 180.2—181.2°C), 1-*p*-formylphenylpyrrole (Ref. 9,*4 mp 94.5—95.5°C. Found: C, 77.31; H, 5.16; N, 8.12%. Calcd for $C_{11}H_9NO$: C, 77.17; H, 5.29; N, 8.18%), 1-*p*-cyanophenylpyrrole (Ref. 9,*4 mp 104.5—105.5°C. Found: C, 78.58; H, 4.81; N, 16.50%. Calcd for $C_{11}H_8N_2$: C, 78.55; H, 4.80; N, 16.65%), 1-*p*-carbomethoxyphenylpyrrole (Ref. 9,*4 mp 127.7—128.7°C. Found: C, 71.58; H, 5.60; N, 7.17%. Calcd for $C_{12}H_{11}NO_2$: C, 71.68; H, 5.47; N, 6.96%), *N,N*-dimethyl-*p*-aminobenzaldehyde (Ref. 10, mp 74.0—75.0°C) and *N,N*-dimethyl-*p*-aminobenzonitrile (Ref. 11, mp 76.5—77.5°C). The prepared samples were identified by the nuclear magnetic resonance spectra and infrared spectra.

n-Hexane and ethanol were supplied by commercial sources as reagent grade chemicals. They were repeatedly purified by usual methods until they proved to be pure from spectroscopic points of view.

Spectroscopic Measurements. Spectra were measured at 17—19°C by a Baush & Lomb Spectronic Model 505 or Hitachi Model EPS-2 Recording Spectrophotometer. The concentration of the solutions were between 10^{-4} and 10^{-5} mol/*l*.

*4 These compounds were synthesized by modifying the method for the preparations of similar compounds described in the references.

7) E. A. Braude and F. Sondheimer, *J. Chem. Soc.*, **1955**, 3754.
8) J. Dhont and J. P. Wibant, *Rec. Trav. Chim.*, **62**, 177 (1943).
9) R. A. Jones, *Australian J. Chem.*, **19**, 289 (1966).
10) H. H. Bosshard and Hch. Zollinger, *Helv. Chim. Acta*, **42**, 1659 (1959).
11) T. van Es, *J. Chem. Soc.*, **1965**, 1564.

BULLETIN OF THE CHEMICAL SOCIETY OF JAPAN VOL. 41 2852—2854 (1968)

Diffuse Reflection Spectra of Some Dinitrobiphenyl Complexes

Kunihiro ABE, Yoshio MATSUNAGA and Gunzi SAITO

Department of Chemistry, Faculty of Science, Hokkaido University, Sapporo

(Received May 6, 1968)

The 4,4'-dinitrobiphenyl complexes with benzidine and tetramethylbenzidine, in which the long axes of the component molecules are known to be perpendicular to each other, were examined for the diffuse reflection spectra. The deep coloration in these complexes was found to be due to the appearance of broad, weak charge-transfer absorptions.

A common feature in the crystal structures of electron donor-acceptor complexes is a plane-to-plane stacking of the molecules.[1] As the structure of a particular complex is a compromise between those molecular orientations most favorable to donor-acceptor interaction and those which give the most efficient molecular packing, the maximum overlap between π-orbitals of the component molecules is not always attained. 4,4'-Dinitrobiphenyl has been known to form complexes with biphenyl and its 4- and 4,4'-derivatives with a structure in which dinitrobiphenyl molecules form a stack with the planar molecules overlying each other, while the other component molecules are in the tubular cavities resulting from the parallel packing of the stacks.[2] The composition is determined by the number of dinitrobiphenyl

1) S. C. Wallwork, *J. Chem. Soc.*, **1961**, 491.

2) W. S. Rapson, D. H. Saunder and E. T. Stewart, *ibid.*, **1946**, 1110.

molecules in a stack that can be accommodated at right angles to each donor molecule. Thus, the structure of these molecular complexes is exclusively determined by geometrical considerations. Nevertheless, the complexes with benzidine and its tetramethyl derivative are much more deeply colored than the component compounds. This is known to be a general feature in electron donor-acceptor complexes. Therefore, it seemed very interesting to find out whether or not the deep coloration in these dinitrobiphenyl complexes, which are supposed to be in crystal structures unfavorable to π-π interaction, is due to the appearance of new low-energy electronic absorptions, charge-transfer absorptions.

Experimental

The complexes with biphenyl, 4,4'-dihydroxybiphenyl, 4,4'-dimethoxybiphenyl, benzidine, and *N,N,N',N'*-tetramethylbenzidine were prepared as has been described by Rapson *et al.*[2] The pulverized sample was diluted with sodium chloride, mostly in a ratio of 1 : 100 by weight, by grinding it in order to obtain a reasonable reflectance. The spectra were recorded as the difference in reflectance between the mixture and pure sodium chloride by a Beckman DK-2A spectroreflectometer and then plotted using the Kubelka-Munk function, $f(R)=(1-R)^2/2R$, where R is the reflectance. The complexes of dimethoxybiphenyl, benzidine, tetramethylbenzidine, and *N,N,N',N'*-tetramethyl-*p*-phenylenediamine with various acceptors were examined in a chloroform solution for the charge-transfer absorptions using a Beckman DK-2A spectrophotometer.

Results and Discussion

The compositions of the red benzidine and dark red tetramethylbenzidine complexes are known to be 1 : 4. Tetramethylbenzidine also forms a steel-gray colored complex with a composition of 1 : 1. Their diffuse reflection spectra are presented in Fig. 1, along with the spectrum of dinitrobiphenyl. The absorptions of the other component compounds appear at wave numbers larger than that of dinitrobiphenyl. All these complexes are found to show new low-energy absorptions. Although the appearance of the tetramethylbenzidine 1 : 1 complex is quite different from that of the 1 : 4 complex, their spectra are very much alike. The difference in color arises from a small shift in the low-energy absorption. As these absorptions are weak and broad, and overlap with the strong dinitrobiphenyl absorption, there is some uncertainty in the location of their maxima. The following values may, however, be obtained as rather rough estimates: about 18.5 kK for the tetramethylbenzidine 1 : 1 complex, about 21 kK for the 1 : 4 complex, and about 22.5 kK for the benzidine complex. The complexes with biphenyl, 4,4'-dihydroxybiphenyl, and 4,4'-dimethoxybiphenyl have compositions of 1 : 3, 1 : 3 and 2 : 7 respectively. They have approximately the same colors with dinitrobiphenyl. The only difference observed in the spectra is little tails extending from the small-wave number side of the dinitrobiphenyl absorption.

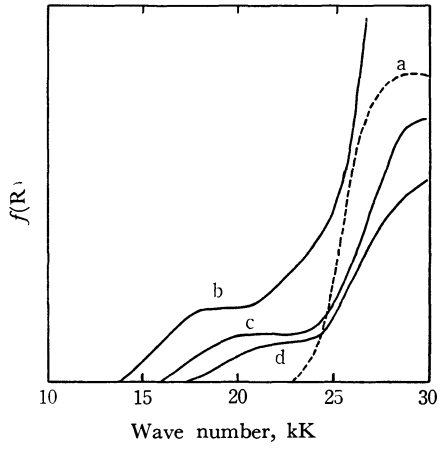

Fig. 1. Diffuse reflection spectra of dinitrobiphenyl (a), the tetramethylbenzidine 1 : 1 (b) and 1 : 4 (c) complexes and the benzidine 1 : 4 complex (d).

Nothing is known of the structure of the tetramethylbenzidine 1 : 1 complex. However, because of its simple composition, the molecules in this complex are presumably in a plane-to-plane stacking. Therefore, the low-energy absorption appearing in this particular complex may be considered to be a charge-transfer absorption arising from electron donor-acceptor interaction between tetramethylbenzidine and dinitrobiphenyl. If so, the weak absorption in the 1 : 4 complex may be of the same nature because of the close similarity in location and shape. As benzidine has a higher ionization potential than its tetramethyl derivative, the charge-transfer absorption in the benzidine complex may be expected to appear at a larger wave number than that of the tetramethylbenzidine complex. This is in accordance with observations. Thus qualitative considerations lead to the tentative conclusion that charge-transfer absorptions are the cause of the deep colors in the dinitrobiphenyl complexes with benzidine and its tetramethyl derivative.

Now we wish to proceed in a more quantitative way. Foster has proposed the empirical relationships that the energies of charge-transfer absorption in a set of complexes of a donor (acceptor) with a series of acceptors (donors) are proportional to those in complexes of the same series of acceptors (donors) with a second donor (acceptor).[3] Such a correlation has been established in a number of

3) R. Foster, *Tetrahedron*, **10**, 96 (1960).

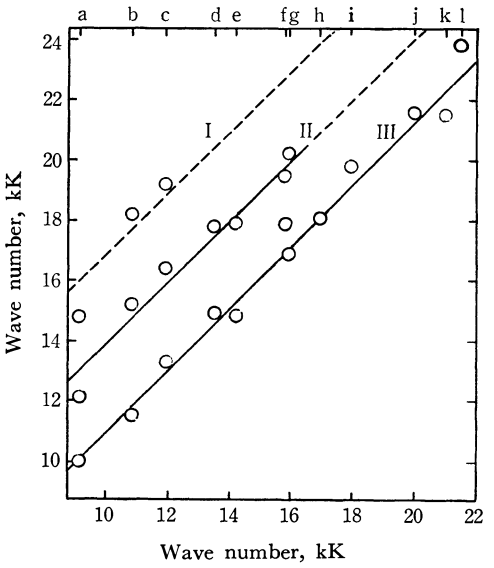

Fig. 2. Plots of wave numbers of maxima of the charge-transfer absorptions in complexes of tetramethyl-*p*-phenylenediamine with the acceptors: tetracyanoethylene (a); *p*-chloranil (b); 2,5-dichloro-*p*-benzoquinone (c); dichloro-*p*-xyloquinone (d); chloro-*p*-benzoquinone (e); *p*-benzoquinone (f); *s*-trinitrobenzene (g); *p*-dinitrobenzene (h); trinitrotoluene (i); *m*-dinitrobenzene (j); dinitrobiphenyl (k); 2,4-dinitrotoluene (l); against wave numbers of the charge-transfer absorptions in the corresponding complexes with the donors: dimethoxybiphenyl (I); benzidine (II); tetramethylbenzidine (III).

the cases by Foster himself and also by Beukers and Szent-Györgyi, and has often been considered as evidence for charge-transfer absorption.[3-5] In Fig. 2 the wave numbers of the absorption maxima in dimethoxybiphenyl, benzidine, and tetramethylbenzidine complexes with each of several acceptors are plotted against those in the corresponding tetramethyl-*p*-phenylenediamine complexes. A large part of the data for the tetramethyl-*p*-phenylenediamine and tetramethylbenzidine complexes was taken from the work by Foster and Thomson.[6] With dinitrobiphenyl as an acceptor (k), the maximum of the low-energy absorption could be located only in the complex of tetramethylbenzidine, the strongest donor among the biphenyl derivatives examined, at about 21.5 kK. This value fits fairly well into the linear relationship shown in Fig. 2, and must be considered to be consistent with the maxima observed in the solid 1 : 1 and 1 : 4 complexes. The appearance of charge-transfer bands in solid complexes at energies a few kK lower than those in a solution is quite common. Furthermore, an examination of Fig. 2 indicates that the charge-transfer interaction between benzidine and dinitrobiphenyl gives an absorption with a maximum around 25 kK. Again, this estimation is in fair agreement with the low-energy absorption in the solid-state spectrum, 22.5 kK. As for the remaining complexes the available data are not enough to enable us to prepare plots like those for benzidine and its tetramethyl derivative. However, if they show charge-transfer absorptions, the maximum in the dimethoxybiphenyl complex may be expected around 28 kK and those in the other two, higher. In accordance with the experimental results, the observation of such absorptions is hardly possible because of the strong absorptions due to the component compounds lying in the same region. Consequently, the thesis that the low-energy absorptions appearing in the solid dinitrobiphenyl complexes arise from charge-transfer interaction, where dinitrobiphenyl acts as an electron acceptor, receives strong support from these considerations.

4) R. Beukers and A. Szent-Györgyi, *Rec. Trav. Chim.*, **81**, 255 (1962).
5) R. Foster and P. Hanson, *Trans. Faraday Soc.*, **60**, 2189 (1964).
6) R. Foster and T. J. Thomson, *ibid.*, **59**, 1059 (1963).

BULLETIN OF THE CHEMICAL SOCIETY OF JAPAN VOL. 41 2855—2858 (1968)

Polarized Absorption Spectra of Single Crystals of Ion Radical Salts. I. Molecular Compounds of 7,7,8,8-Tetracyano-*p*-quinodimethane with *N*,*N*,*N*′,*N*′-Tetramethyl-*p*-phenylenediamine and *N*,*N*-Dimethyl-*p*-phenylenediamine

Haruo KURODA, Shoji HIROMA and Hideo AKAMATU

Department of Chemistry, Faculty of Science, The University of Tokyo, Hongo, Tokyo

(Received May 6, 1968)

Polarized absorption spectra in the 10—40 kK region were observed on single crystals of the molecular compounds of tetracyano-*p*-quinodimethane (TCNQ) with tetramethyl-*p*-phenylenediamine (TMPD) and with dimethyl-*p*-phenylenediamine (DMPD). These molecular compounds possess an ionic structure in the ground state. A strong, broad absorption band appears in the near-infrared region of the crystal spectra with a polarization parallel to the crystal axis along which the component ions are alternately stacked making their molecular planes parallel to each other. The absorption maximum of this band is located at 7.7 kK in TMPD·TCNQ and at 8.5 kK in DMPD·TCNQ. These bands are assigned as a one associated with the charge transfer from $TCNQ^-$ ion to the positive ion of the donor. Other absorption bands found in the spectra can be assigned as local excitation bands associated with the intramolecular transitions of the component ions. However, they are found to be considerably broadened and appreciably shifted to higher energy as compared with the solution spectrum of each component ion.

There is a class of solid molecular compounds which possess an ionic structure in the ground state. Such molecular compounds can be formed by the interaction between a strong π-electron donor and a strong π-electron acceptor. The crystal of the 1 : 1 molecular compound involving *N*,*N*,*N*′,*N*′-tetramethyl-*p*-phenylenediamine (TMPD) as the donor and 7,7,8,8,-tetracyano-*p*-quinodimethane (TCNQ) as the acceptor has been suggested to possess a ground state consisting of TMPD monopositive ion and TCNQ mononegative ion.[1,2] This solid molecular compound exhibits a marked electron spin resonance absorption, which has been ascribed to the triplet state arising from the interaction between the radical ions of TMPD and TCNQ.[2] The presence of the visible absorption bands corresponding to the component ions has been reported by Foster and Thomson[1] in the absorption spectrum observed for a Nujol mull of the solid molecular compound. However, no observation has been made on the absorption spectrum of its single crystal, which should provide much informations concerning its electronic structure. In the present investigation, we have studied the polarized absorption spectra of the single crystals of this molecular compound as well as those of the solid molecular compound of *N*,*N*-dimethyl-*p*-phenylenediamine (DMPD) with TCNQ.

Experimental

The polarized absorption spectra in the 10—40 kK region were measured on very small single crystals by using a microspectrophotometer. The details of the apparatus and the experimental procedures were described in a preceding paper.[3]

The solid molecular compound, TMPD·TCNQ, was prepared by mixing an acetonitrile solution of Würster's blue perchlorate (TMPD·ClO_4) and a methanol solution of Li·TCNQ. The black powder of TMPD·TCNQ precipitated as the solution containing equivalent amounts of TMPD·ClO_4 and Li·TCNQ was concentrated by evaporation of the solvent. The solid thus obtained was recrystallized from an acetonitrile solution. The mole ratio of TMPD to TCNQ was confirmed to be 1 : 1 by the elementary analysis. The DMPD·TCNQ was prepared by mixing a chloroform solution of TCNQ with a chloroform solution of an equimolar amount of DMPD.

Minute crystals freshly prepared from an acetonitrile solution were used for the measurement of spectra. The crystals were found to be frequently twinned, so that the selection was needed to find a single crystal which was not twinned, by examinnig by the polarizing microscope. The absorption spectra of the crystalline powders were also observed by the use of liquid paraffin mulls.

1) R. Foster and T. J. Thomson, *Trans. Faraday Soc.*, **59**, 296 (1963).

2) M. Kinoshita and H. Akamatu, *Nature*, **207**, 291 (1965).

3) H. Kuroda, T. Kunii, S. Hiroma and H. Akamatu, *J. Mol. Spectry.*, **22**, 61 (1967).

Results and Discussion

The polarized absorption spectra observed of a single crystal of TMPD·TCNQ are shown in Fig. 1. According to the crystal structure analysis by Hanson,[4] the crystal is monoclinic with the lattice constants, $a=9.88$ Å, $b=12.71$ Å, $c=7.72$ Å and $\beta=97.34°$, and belongs to the space group $C2/m$. The unit cell contains two molecules of each component. The donor and acceptor molecules are alternately stacked along the c-axis. The absorption spectra shown in Fig. 1, were obtained for a very thin single crystal of a few microns in width, elongated along the c-axis, the developed face of which was assigned to (010) plane. The projection of the crystal structure onto the (010) plane along the b-axis is reproduced schematically in Fig. 2.

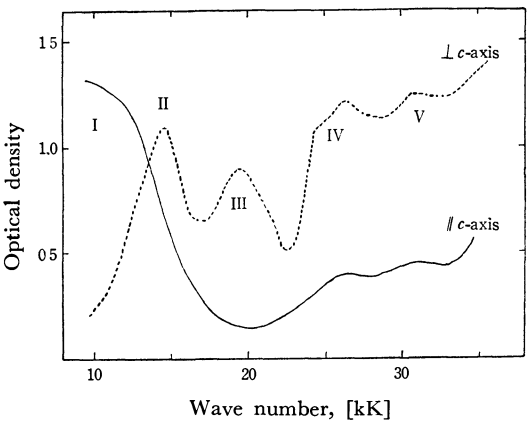

Fig. 1. Polarized absorption spectra of a single crystal of TMPD·TCNQ.

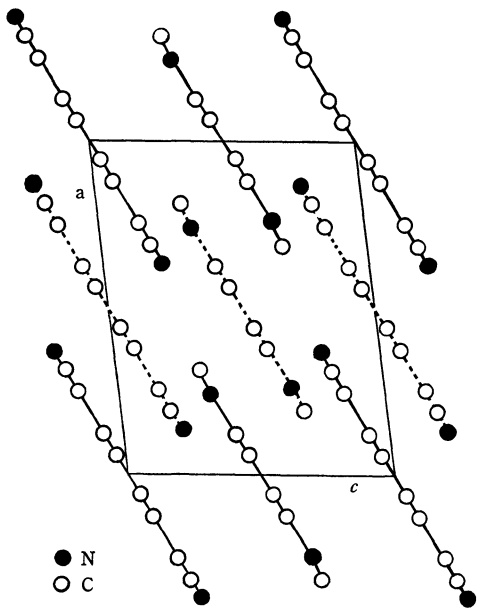

Fig. 2. Crystal structure of TMPD·TCNQ: The short axes of the component ions are parallel to the b-axis; the layer of molecules shown with broken line is $b/2$ above that of the molecules shown with solid line.

Evidently there is a strong band in the near-infrared region, which seems to be exclusively polarized in the c-axis direction. Unfortunately, our microspectrophotometer could not be applied to the region below 9 kK. Thus the absorption in the low energy region was examined by observing the absorption spectrum of the powder sample. The result is shown in Fig. 3, in which one absorption band with a maximum located at about 7.7 kK is found in the near-infrared region. This must correspond to the low energy band found in the $\|c$ spectrum of the single crystal. The intensities of the absorption bands associated with the long-axis polarized transitions of the component ions should be higher in the $\perp c$ spectrum than in the $\|c$ spectrum, since the oriented-gas model predicts the intensity ratio $I_{\perp c}/I_{\|c}$ of 2.5 as shown in Table 1, and the short-axis polarized transitions of the component ions should not appear in the $\|c$ spectrum, nor in the $\perp c$ spectrum. Thus we can assign the 7.7 kK band, which we shall denote as "Band I," to the one associated with the charge-transfer between $TMPD^+$ and $TCNQ^-$ ions stacked on each other. Probably it is associated with a transfer of an electron from a $TCNQ^-$ ion to a $TMPD^+$ ion. A similar charge-transfer band has been found in several other molecular compounds having an ionic structure.[5,6]

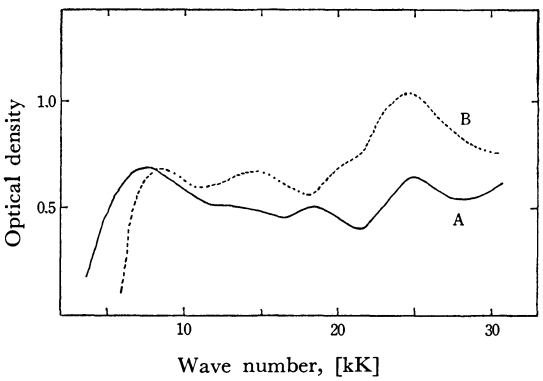

Fig. 3. Absorption spectra of liquid paraffin mulls of the crystalline powders of TMPD·TCNQ (A) and DMPD·TCNQ (B).

In the $\perp c$ spectrum, there are four absorption bands, which are denoted respectively II, III, IV and V in Fig. 1. All these bands are stronger in the $\perp c$ spectrum than in the $\|c$ spectrum.

4) A. W. Hanson, *Acta Cryst.*, **19**, 610 (1965).
5) T. Amano, H. Kuroda and H. Akamatu, This Bulletin, **41**, 83 (1968).
6) B. G. Anex and E. B. Hill, Jr., *J. Am. Chem. Soc.*, **88**, 3648 (1966).

TABLE 1.

	Bands in the crystal spectra		Assignment	Transitions of component ions		Calculated oscillator strength in crystal spectra*		
	$\tilde{\nu}$ [kK]	polarization ratio ($I_{\perp c}/I_{\parallel c}$)		$\tilde{\nu}$ [kK]	$f_{soln.}$	$f_{\perp c}$	$f_{\parallel c}$	$f_{\perp c}/f_{\parallel c}$
I	7.7	~0	CT-Band					
II	14.7	—	$TCNQ^-$ ($B_{3u}\leftarrow B_{2g}$)	12.0	0.31	0.66	0.26	2.5
III	19.6	~6	$TMPD^+$ ($B_{3u}\leftarrow B_{2g}$)	18.0	0.25	0.54	0.21	
IV	26.3	2.9	$TCNQ^-$ ($B_{3u}\leftarrow B_{2g}$)	23.0	0.44	0.92	0.36	
V	31.0	2.8	$TMPD^+$ ($B_{3u}\leftarrow B_{2g}$)	30.9	0.44	0.92	0.36	

* Oriented-gas values.

In effect, no absorption maximum corresponding to Band II and Band III can not be found in the $\parallel c$ spectrum. These four bands seem to be mainly associated with the intramolecular transitions of the component ions. The absorption spectra of $TMPD^+$ and $TCNQ^-$ ions in solution are shown in Fig. 4. The open-shell SCF-LCAO-MO calculations have been carried out recently by Lowitz[7] on the electronic transitions of $TCNQ^-$ ion. According to his result, the first strong absorption band located at about 12 kK is due to π–π^* transition polarized along the long-axis of the molecule and the next band is composed of a strong, long-axis polarized transition and a weak, short-axis polarized transition. The polarizations of the transition in $TMPD^+$ ion have been experimentally studied by Albrecht and Simpson,[8] who have concluded that the 18 kK and 30.9 kK transitions are of the long-axis polarization, while the weak 26.2 kK transition is of the short-axis polarization. These are in agreement with theoretical predictions.[9,10]

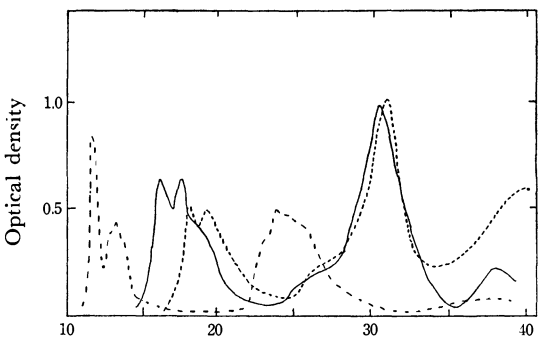

Fig. 4. Absorption spectra of the component ions in acetonitrile: —— $TMPD^+$, - - - $DMPD^+$, —·— $TCNQ^-$.

The probable assignements of the observed bands and the oriented-gas values of the oscillator strength of each intramolecular transition are summarized in Table 1. The observed polarization ratio well agrees with the oriented-gas value in the cases of Band IV and Band V. There seems to be some deviation between the observed and calculated polarization ratios in the cases of Band II and Band III, especially in the last one. From the experiment by Albrecht and Simpson[8] as well as from the reported crystal spectra of the ionic compound formed between TMPD and chloranil,[5,6] there can be no doubt that the 18 kK and 30.9 kK transitions in $TMPD^+$ ion are same as regards the polarization. Thus the difference between their polarization ratios must be associated in someway with the interactions of ions in the crystal lattice. It should be also noticed that the bands II, III and IV in the crystal spectra are shifted to higher energy by about 2 kK compared with the corresponding bands in the solution spectra, and, at the same time, all bands are considerably broadened. A similar effect can be generally found in the crystal spectra of a molecular compound which is composed of positive ions of donor and negative ions of acceptor, when there exists a relatively strong charge-transfer interaction between the component ions.[5]

The polarized absorption spectra of the DMPD·TCNQ are shown in Fig. 5. The crystal structure has not been determined for this molecular compound. The spectra were observed, on a thin single crystal elongated along one direction, for the two polarizations of light parallel and perpendicular to the elongated axis, which we shall denote here as the "*l-axis*" of the crystal.

The observed spectra are quite similar to the

7) D. A. Lowitz, *J. Chem. Phys.*, **46**, 4698 (1967).
8) A. C. Albrecht and W. T. Simpson, *J. Am. Chem. Soc.*, **77**, 4458 (1955).
9) M. Geoppert-Mayer and K. J. McCallum, *Rev. Mod. Phys.*, **14**, 248 (1942).
10) H. J. Monkhorst and J. Kommandeur, *J. Chem. Phys.*, **47**, 391 (1967). They assigned the 13 and 31 kK band to the transitions, polarized along the "*x-axis*", which corresponds to the short-axis according to the notation of molecular axes given in their paper. However, they have recently informed us that this notation is incorrect, and the "*x-axis*" is the long-axis of molecule.

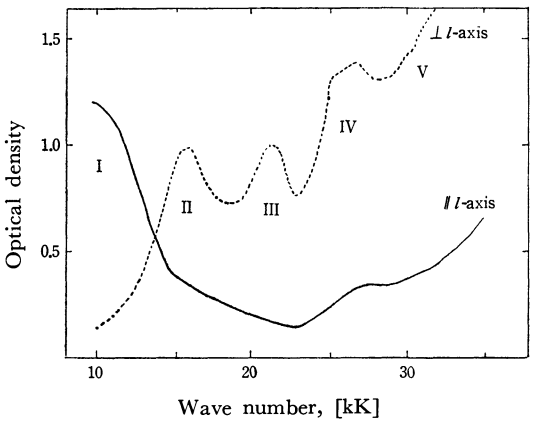

Fig. 5. Polarized absorption spectra of a single crystal of DMPD·TCNQ.

spectra of TMPD·TCNQ: namely, the first absorption band in the near-infrared region is exclusively polarized in the *l-axis* derection while the bands in the 12—35 kK region are stronger in the $\perp l$ spectrum than in the $\parallel l$ spectrum. The absorption maximum of the first band is located at about 8.5 kK according to the absorption spectrum of the liquid paraffin mull of the powder already shown in Fig. 3. We shall assign this low energy band to the charge-transfer from a $TCNQ^-$ ion to the neighboring $DMPD^+$ ion. We can assign the other bands in Fig. 5 to the bands mainly associated with the intramolecular transitions of the component ions: Bands, II and IV, are due to the long-axis polarized transitions of $TCNQ^-$ ions, and Bands, III and V to the long-axis polarized transitions of $DMPD^+$ ion. Band III of DMPD·TCNQ is located at a wave number higher by 1.7 kK than the corresponding band of TMPD·TCNQ. This difference is nearly equal to the difference between the enrgy of the lowest transition of $TMPD^+$ ion and that of $DMPD^+$ ion.

The similarity found between the polarized spectra of TMPD·TCNQ and those of DMPD·TCNQ seems to suggest the resemblance between their crystal structures. Thus we may consider that, in the crystal of DMPD·TCNQ, the ions of the two components are alternately stacked on each other along one crystal axis making their long molecular axes parallel to each other as in the crystal of TMPD·TCNQ.

Finally it should be noted that the intensity of the charge-transfer band is considerably strong in the crystal spectrum of TMPD·TCNQ as well as in that of DMPD·TCNQ. Although we have not carried out the absolute measurement of the intensity of absorption, the fact that the charge-transfer band is observed in the crystal spectra of these molecular compounds with an intensity comparable to or higher than the absorption bands associated with strong intramolecular transitions of the component ions, evidently indicates that the intensity of the charge-transfer band is fairly strong. This phenomenon seems to suggest the presence of a strong charge-transfer interaction between the neighboring ions in the crystal lattice.

BULLETIN OF THE CHEMICAL SOCIETY OF JAPAN VOL. 41 2858—2860 (1968)

Relative Determination of Soret Coefficients of Alkaline Earth Chlorides

Toshio IKEDA, Hidefusa OHE and Saburo KAWAMURA

Department of Chemistry, Faculty of Science, Shizuoka University, Oiwa, Shizuoka

(Received May 7, 1968)

The Soret coefficients of aqueous solution of alkaline earth chlorides were determined indirectly using combined thermocells. "Combined thermocell" refers to a cell system of a back to back combination of two thermocells made of common electrodes and different electrolytes without liquid junction. The values are -2.79 for $MgCl_2$, -3.43 for $CaCl_2$, -4.09 for $SrCl_2$, and -4.73 for $BaCl_2$, respectively (in the unit of 10^{-3} deg^{-1}) at 0.005 M and 25°C. These agree with reported values found by the direct method.

General Scheme

The Soret coefficients of a series of the alkaline earth chlorides, MCl_2, solution were determined by using combined thermocells of the following system:

$$\underset{T}{\text{Hg-HgCl}},\ \text{LiCl}(m),\ \underset{T+\Delta T}{\text{HgCl-Hg-HgCl}}$$
$$\text{MCl}_2\left(\frac{1}{2}m\right),\ \underset{T}{\text{HgCl-Hg}} \qquad (1)$$

where the concentrations of chloride ion are taken common in both left and right halves of the cell. Lithium chloride was taken as a standard reference because it shows a very slight Soret effect. The initial thermoelectric powers, ε_0^{LiCl} and $\varepsilon_0^{MCl_2}$ for the left and right halves of (1) are expressed respectively as follows:[1]

$$F\varepsilon_0^{LiCl} = S_{Hg} - S_{HgCl} + 2RTt_{Li^+}^{LiCl}B^{LiCl}\sigma^{LiCl} + \overline{\overline{S}}_{Cl^-}^{LiCl} - \overline{\overline{S}}_{el}$$

$$F\varepsilon_0^{MCl_2} = S_{Hg} - S_{HgCl} + \frac{3}{2}RTt_{M^{2+}}^{MCl_2}B^{MCl_2}\sigma^{MCl_2} + \overline{\overline{S}}_{Cl^-}^{MCl_2} - \overline{\overline{S}}_{el}$$

where σ's are the Soret coefficients, t's the ionic transport numbers for ions indicated by the subscripts. Superscripts, LiCl or MCl_2, indicate the solution phases, and so forth. B's are defined by

$$B^{LiCl} = (1 + \mathrm{d}\ln\gamma_{\pm}^{LiCl}/\mathrm{d}\ln m)_{T,P}$$

$$B^{MCl_2} = (1 + \mathrm{d}\ln\gamma_{\pm}^{MCl_2}/\mathrm{d}\ln m)_{T,P}$$

where $\gamma_{\pm}$'s are the mean activity coefficients in the molality scale. $\overline{\overline{S}}_{el}$ is the transported entropy of electrons in the metallic phase, and $\overline{\overline{S}}_{Cl^-}$'s represent the transported entropies of the chloride ions. F, R and T have their usual significances. The temperature coefficient of the resultant thermoelectromotive force, E, of (1) at the initial state, or the initial thermoelectric power, $(\mathrm{d}E/\mathrm{d}T)_0$, of (1) is given by the relation, $(\mathrm{d}E/\mathrm{d}T)_0 = \varepsilon_0^{MCl_2} - \varepsilon_0^{LiCl}$. Then we have

$$\sigma^{MCl_2} = \frac{4t_{Li^+}^{LiCl}B^{LiCl}}{3t_{M^{2+}}^{MCl_2}B^{MCl_2}}\sigma^{LiCl} + \frac{2F(\mathrm{d}E/\mathrm{d}T)_0}{3RTt_{M^{2+}}^{MCl_2}B^{MCl_2}} - \frac{2(\overline{\overline{S}}_{Cl^-}^{MCl_2} - \overline{\overline{S}}_{Cl^-}^{LiCl})}{3RTt_{M^{2+}}^{MCl_2}B^{MCl_2}} \quad (2)$$

Experimental Results and Discussion

All aqueous solutions were prepared from Wakô Guaranteed Reagent grade chemicals (99.8% purity) for a concentration of 0.01 M with respect to the chloride ion. Accuracy of the concentration was within ±0.4%. Experimental equipments are entirely the same as those reported in the previous paper.[2] The measurements were begun after allowing cells to stand at a medium temperature near 25°C for more than 10 days, because, in the early stage, usually during several days after the set up of cell, the stability of electrode system was not sufficient to get reproducible results in measuring such a minute change in emf as the case the present work. Emf of the cell (1) was measured by using a precision Yokogawa potentiometer (New type P-7 for low voltage use) by the aid of Yokogawa sensitive galvanometer, and was accurate within ±0.1 μV. The range of ΔT was about 10° around a mean temperature 25°C, while the temperature on the terminal electrodes was kept constant at 25°C. Measurements were repeated for every possible combination of four or five well-conditioned MCl_2 thermocells with four or five well-conditioned reference LiCl thermocells. Some of the typical results are represented in Fig. 1. The values of $(\mathrm{d}E/\mathrm{d}T)_0$, the initial thermoelectric power of the combined thermocells of type (1), were determined at 25°C with the least squares method, and are listed in Table 1. The data are reproducible, mostly within ±1% of fluctuation.

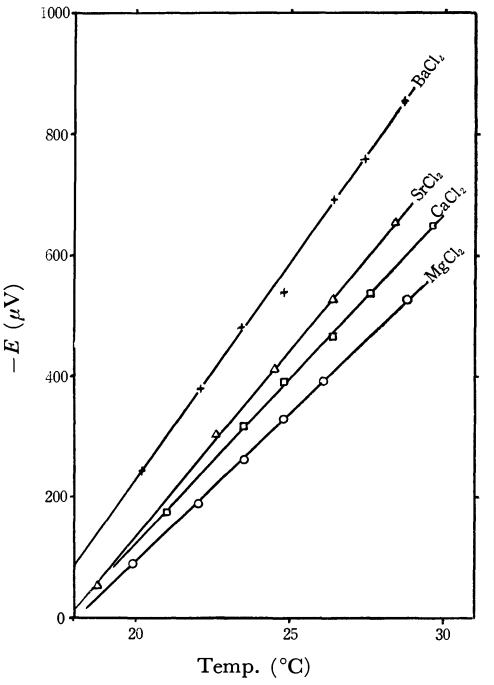

Fig. 1. Emf plots of combined thermocells of the type (1) against the temperature, $(T+\Delta T)$, around the mean temperature 25°C, where the temperature on two terminal electrodes was kept at 25°C constantly. The concentration of solutions was adjusted to 0.01 M with respect to the chloride ions.

According to Snowdon and Turner,[3] the Soret coefficient of LiCl is $0.02\times10^{-3}\,\mathrm{deg}^{-1}$ at 25.3°C and 0.01 M. This value was adjusted to the 25°C

1) *E. g.*, H. J. V. Tyrrell, "Diffusion and Heat Flow in Liquid, "Butterworths and Co., Ltd., London (1961); T. Ikeda, *Report Liberal Arts Sci. Fac. Shizuoka Univ.*, **2**, 153 (1959).

2) T. Ikeda, This Bulletin, **38**, 407 (1965); T. Ikeda and H. Kimura, *J. Phys. Chem.*, **69**, 41 (1965); T. Ikeda and M. Matsumoto, *ibid.*, **69**, 3755 (1965).

3) P. N. Snowdon and J. C. R. Turner, *Trans. Faraday Soc.*, **56**, 1409 (1960).

TABLE 1. SORET COEFFICIENTS OF ALKALINE EARTH METAL CHLORIDES AT 25°C AND 0.005 M
(The σ-value in parentheses is adopted as the standard for the relative determination of σ^{MCl_2}.)

Chloride	m	t_+[a]	B[b]	$(dE/dT)_0$ $\mu V/deg$	$-\sigma \times 10^3\ deg^{-1}$	
					This work	Literature value
LiCl	0.01006	0.3289	0.969	—	(−0.01)	−0.01[c]
$MgCl_2$	0.00501	0.394	0.917	−38.8±0.4	2.79	2.80[d]
$CaCl_2$	0.00501	0.4264	0.905	−51.0±0.3	3.43	3.17[d]
$SrCl_2$	0.00502	0.424	0.923	−61.6±0.6	4.09	3.99[e]
$BaCl_2$	0.00502	0.439	0.898	−71.2±0.5	4.73	4.65[e]

a) E. Conway, "Electrochemical Data," Elsevier Publishing Co., Amsterdam (1952).
b) Graphical determination from Landolt-Börnstein, "Physikalische Chemische Tabellen," Erg. II (1931) and III (1936).
c) Adjusted to the value for 0.01 M at 25°C (Ref. 3).
d) The value for 0.0050 M at 25.1°C (Ref. 4).
e) The value for 0.0051 M at 24.9±0.1°C (Ref. 4).

value, $0.01 \times 10^{-3}\ deg^{-1}$, and was used as the standard in the present calculation. B-Values were determined graphically at a concentration $m=$ 0.01 M in the case of LiCl and at 0.005 M in the case of MCl_2, respectively, at 25°C. These values and the present data on $(dE/dT)_0$ were used to get the relative values of the Soret coefficients, σ^{MCl_2}, at 25°C and 0.005 M by the aid of (2). In this treatment $\bar{\bar{S}}^{MCl_2}_{Cl^-} = \bar{\bar{S}}^{LiCl}_{Cl^-}$ was assumed. The results agree very well with those obtained by the direct method by Payton and Turner,[4] except calcium chloride. According to the theory of Helfand and Kirkwood,[5] $\bar{\bar{S}}_{Cl^-}$'s should differ from solution to solution involving different cation species, particularly of high ionic valency, however, the present studies indicate that the difference between $\bar{\bar{S}}_{Cl^-}$'s is practically negligible. This fact seems to indicate that our combined thermocell method is applicable extensively to determine the Soret coefficients of bivalent metal chlorides in water at low concentration by assuming $\bar{\bar{S}}^{MCl_2}_{Cl^-} = \bar{\bar{S}}^{LiCl}_{Cl^-}$.

4) A. D. Payton and J. C. R. Turner, *ibid.*, **58**, 55 (1962).

5) E. Helfand and J. G. Kirkwood, *J. Chem. Phys.*, **32**, 857 (1960)

BULLETIN OF THE CHEMICAL SOCIETY OF JAPAN VOL. 41 2861—2866 (1968)

Radiolysis of Methylcyclohexane. I. Effects of Temperature and Electron Scavengers on Hydrogen Formation

Toyoaki KIMURA, Tetsuo MIYAZAKI, Kenji FUEKI and Zen-ichiro KURI

Department of Synthetic Chemistry, Faculty of Engineering, Nagoya University, Chikusa-ku, Nagoya

(Received May 15, 1968)

The effects of temperature and electron scavengers on the hydrogen yield in the radiolysis of methylcyclohexane have been investigated by conventional kinetic techniques. The G value for hydrogen formation from pure methylcyclohexane varied from 4.9 to 4.4 in the range from room temperature to liquid nitrogen temperature. In the iodobenzene-methylcyclohexane system, the decrease in hydrogen yield was equal to the yield of benzene produced within experimental error. It is concluded that the benzene is formed through H atom abstraction from the solvent molecules by phenyl radicals which are formed by dissociative electron attachment to iodobenzene and that the benzene yield indicates the scavenged electron yield. Furthermore, a kinetic treatment for electron scavenging in the glassy state was presented. In the N_2O-methylcyclohexane system, it was found that the ratio of the nitrogen yield, $G(N_2)$, to the decrease in hydrogen yield, $\Delta G(H_2)$, is 2 in the temperature range from room temperature to -140°C, 1 at -160°C, and increases from 1 to 4 with increasing N_2O concentration at -196°C, respectively.

The mechanism of radiolysis at -196°C has been investigated mainly by physical methods such as ESR and optical absorption measurements but rarely by chemical methods which involve product analysis. Since it is difficult to apply information obtained by physical methods at -196°C directly to the mechanism of radiolysis at room temperature, it seems useful to get information by chemical methods at -196°C. If both physical and chemical methods are applied to the same system, it can be expected that deeper understanding of the radiolysis mechanism will be obtained. For this purpose we have made a study of the radiolysis of methylcyclohexane at room temperature, -196°C, and several temperatures between room temperature and -196°C. Hitherto, the radiolysis of methylcyclohexane has been studied in the liquid[1-3] and gas phases,[4,5] but not in the glassy state at -196°C.

We studied the effects of temperature on the hydrogen yield in γ-irradiated pure methylcyclohexane, N_2O-methylcyclohexane, and iodobenzene-methylcyclohexane systems. It is well known that organic halides scavenge an electron to yield a halogen anion and a radical.[6,7]

$$RX + e^- \rightarrow R\cdot + X^- \qquad (1)$$

In the case of iodobenzene, the phenyl radical was not detected by ESR[8] in γ-irradiated organic glass at -196°C. This fact indicates that the phenyl radical in hydrocarbon glass abstracts an H atom from the solvent molecule even at -196 °C.[8] Nitrous oxide has extensively been used as an electron scavenger in irradiated gaseous,[5,9-12] liquid,[13-17] and solid[18] hydrocarbons. In this work, an attempt is made to estimate the scavenged electron yield in liquid and glassy methylcyclohexane using iodobenzene and nitrous oxide as electron scavengers and the mechanism of electron scavenging in the glassy state as well as the liquid state is considered.

Experimental

Materials. Tokyo-Kagaku-Seiki standard pure 99.9 % methylcyclohexane was used partly as received and

1) G. R. Freeman, *J. Chem. Phys.*, **36**, 1534 (1962).
2) G. R. Freeman, *ibid.*, **36**, 1542 (1962).
3) J. F. Merklin and S. Lipsky, *J. Phys. Chem.*, **68**, 3297 (1964).
4) W. J. Holtslander and G. R. Freeman, *Can. J. Chem.*, **45**, 1649 (1967).
5) W. J. Holtslander and G. R. Freeman, *ibid.*, **45**, 1661 (1967).
6) R. F. C. Claridge and J. E. Willard, *J. Am. Chem. Soc.*, **87**, 4992 (1965).
7) D. W. Skelly, R. G. Hayes and W. H. Hamill, *J. Chem. Phys.*, **43**, 2795 (1965).
8) S. Noda, K. Fueki and Z. Kuri, unpublished results.
9) G. R. A. Johnson and J. M. Warman, *Nature*, **203**, 73 (1964).
10) G. R. A. Johnson and J. M. Warman, *Trans. Faraday Soc.*, **61**, 512 (1965).
11) J. M. Warman, *J. Phys. Chem.*, **71**, 4066 (1967).
12) J. M. Warman, *ibid.*, **72**, 52 (1968).
13) G. Scholes and M. Simic, *Nature*, **202**, 895 (1964).
14) W. V. Sherman, *J. Chem. Soc., (A)*, **5**, 599 (1966).
15) S. Sato, R. Yugeta, K. Shinsaka and T. Terao, This Bulletin, **39**, 156 (1966).
16) N. H. Sagert and A. S. Blair, *Can. J. Chem.*, **45**, 1351 (1967).
17) R. A. Holroyd, *J. Phys. Chem.*, **72**, 759 (1968).
18) N. H. Sagert, *Can. J. Chem.*, **46**, 89 (1968).

partly after purification. Being passed through a silica gel column, methylcyclohexane was dried over calcium hydride *in vacuo* until bubbles of hydrogen gas could not be seen. Then the methylcyclohexane was transferred by vacuum distillation to a glass tube coated with a sodium mirror to remove water, passed through soda-lime which had been thoroughly dried and degassed in order to remove carbon dioxide, transferred to another glass tube with a break-seal by vacuum distillation and sealed off. The difference between the results obtained with methylcyclohexane with and without purification was negligible.

Tokyo-Kasei extra pure iodobenzene was passed through a silica gel column, and distilled *in vacuo*. The middle fraction was used. Takachiho-Shoji Co. pure reagent N_2O (99.9%) was used as received.

Sample Preparation. Amounts of methylcyclohexane and iodobenzene were measured volumetrically. Usually 1 m*l* of methylcyclohexane was used. Solutions in irradiation glass cells (equipped with a break-seal and usually 2 m*l*) were degassed by the freeze-pump-thaw technique until bubbles were hardly observed and then sealed off. Nitrous oxide was introduced into a bulb of known volume to the desired pressure and then condensed into the irradiation cell.

Irradiation. A 3000 Ci ^{60}Co source was used for irradiation. The doses used are shown in Table 1.

TABLE 1. DOSES AT VARIOUS IRRADIATION TEMPERATURES

Irradiation temperature	Dose
Room temperature	3.06×10^{20} eV/g
Dry ice - ethanol temperature	3.19×10^{20} eV/g
−123°C	7.99×10^{19} eV/g
−140°C	7.99×10^{19} eV/g
−160°C	2.86×10^{19} eV/g
−196°C	2.75×10^{20} eV/g

The dose rate was determined by Fricke dosimetry with nitrogen saturated ($G(Fe^{3+})=8.07$). Irradiations were performed at room temperature (20°C), dry ice-ethanol temperature, and liquid nitrogen temperature. In addition, the experiments were performed at −123, −140, and −160°C. To keep the sample at −123 and −140°C slushy ethanol and ethanol - *n*-propanol mixture, chilled by mixing with liquid nitrogen, were used respectively. The experiments at −160°C were performed by blowing nitrogen vapor from liquid nitrogen against the samples. Blowing was controlled automatically to keept the temperature within ±2.5°C. These temperatures were measured with a chromel-alumel thermocouple during irradiation to be −123±2.5, −140±5, and −160±2.5°C, respectively.

Analysis. Gaseous products not condensable at liquid nitrogen temperature were collected by a Toepler pump and determined the volume by a gas burette. Then the gas was circulated about 20 cycles through a cupric oxide furnace heated at 220—260°C and a liquid nitrogen trap to convert hydrogen into water. The residual gas was recollected and determined the volume again. Benzene was analyzed by a Hitachi-K53 gas chromatograph with FID using a column of *n*-hexatriacontane (4 mm×2 m).

Results

Pure Methylcyclohexane. The *G* value of hydrogen from pure methylcyclohexane depended little upon the irradiation temperature and amounted to 4.9 at room temperature and 4.4 at −196°C. The *G* value at room temperature agrees with Freeman's value.[1] There are no previous data on the *G* value at −196°C.

Iodobenzene - Methylcyclohexane System. The *G* values for hydrogen and benzene produced from mixtures of methylcyclohexane and iodobenzene irradiated at room temperature and −196°C are shown in Figs. 1 and 2, respectively. At both temperatures, $G(H_2)$ decreased with

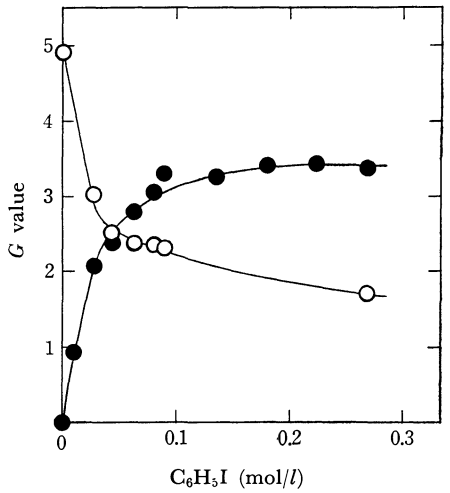

Fig. 1. Yields of hydrogen and benzene from the iodobenzene-methylcyclohexane system irradiated at room temperature.
○, $G(H_2)$; ●, $G(C_6H_6)$

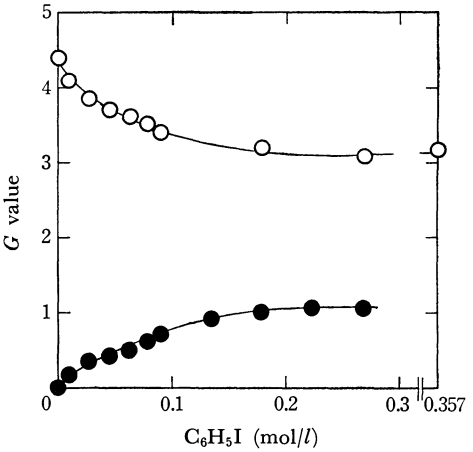

Fig. 2. Yields of hydrogen and benzene from the iodobenzene-methylcyclohexane system irradiated at −196°C.
○, $G(H_2)$; ●, $G(C_6H_6)$

increasing iodobenzene concentration more effectively than in N_2O-methylcyclohexane systems which will be described later on. This seems to indicate that iodobenzene scavenges electrons more effectively than N_2O both in the liquid and glassy states. On the other hand, $G(C_6H_6)$ increases with increasing iodobenzene concentration. Further it should be noted that the decrease in hydrogen yield is equal to the increase in benzene yield at any iodobenzene concentration within experimental error. This result indicates that one molecule of benzene is produced by quenching one precursor of hydrogen.

N_2O-Methylcyclohexane System. The yields of hydrogen and nitrogen produced from mixtures of methylcyclohexane and N_2O irradiated at room temperature, dry ice - ethanol temperature and -196°C are shown in Figs. 3, 4 and 5, respectively. The G values of hydrogen and nitrogen from pure methylcyclohexane and methylcyclohexane containing 0.3 M of N_2O irradiated at various temperatures are shown in Fig. 6. The hydrogen yield from methylcyclohexane containing 0.3 M of N_2O was nearly constant in the range from room temperature to -140°C, changed from 2.5 to 3.8 (G unit) at a temperature between -140 to -160°C, and remained constant in the temperature range from -160 to -196°C. These results seem to indicate that the efficiency of electron scavenging in these systems changes significantly at a temperature between -140 to -160°C.

In the range from room temperature to -140°C, the following relationship holds between the nitrogen yield and the decrease in hydrogen yield at any N_2O concentration,

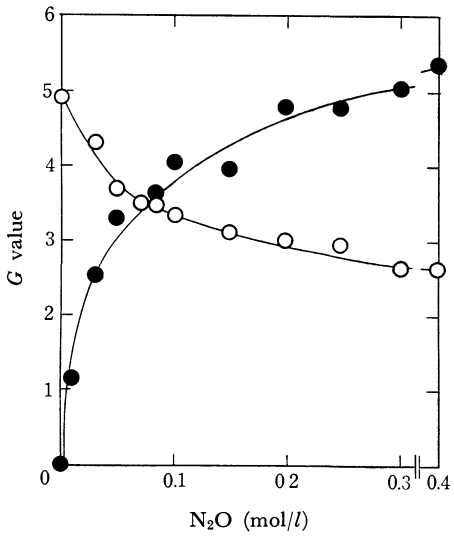

Fig. 3. Yields of hydrogen and nitrogen from the N_2O-methylcyclohexane system irradiated at room temperature.
○, $G(H_2)$; ●, $G(N_2)$

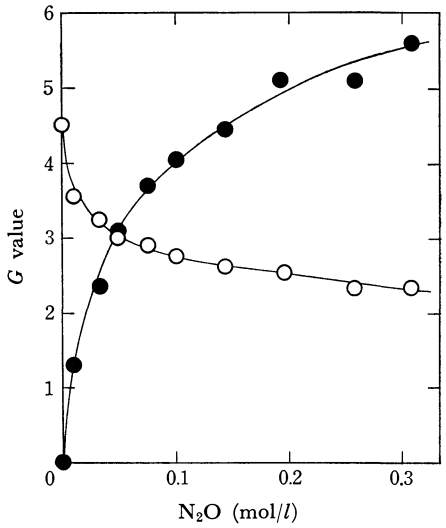

Fig. 4. Yields of hydrogen and nitrogen from the N_2O-methylcyclohexane system irradiated at dry ice-ethanol temperature.
○, $G(H_2)$; ●, $G(N_2)$

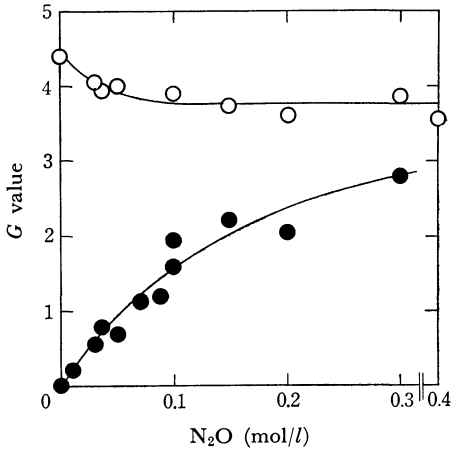

Fig. 5. Yields of hydrogen and nitrogen from the N_2O-methylcyclohexane system irradiated at -196°C.
○, $G(H_2)$; ●, $G(N_2)$

$$G(N_2) = 2\Delta G(H_2) \quad (2)$$

Such a relationship has been reported by other workers for the radiolysis of cyclohexane at room temperature.[15,16] However, at -196°C the ratio of the nitrogen yield to the decrease in hydrogen yield increased from 1 to about 4 with increasing N_2O concentration.

$$G(N_2)/\Delta G(H_2) = 1\text{—}4 \quad (3)$$

The mechanism of nitrogen formation from the mixtures of methylcyclohexane and N_2O in the range from room temperature to -140°C differs apparently from that at -196°C. Furthermore, at -160°C the ratio, $G(N_2)/\Delta G(H_2)$, was 1 at N_2O concentration of 0.3 M.

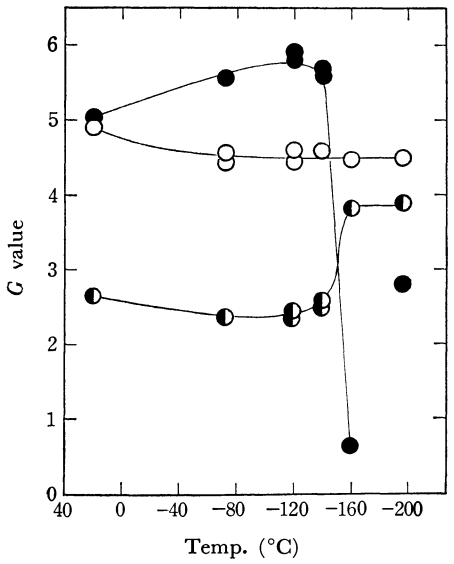

Fig. 6. Yields of hydrogen and nitrogen at various temperature.
○, $G(H_2)$ from pure methylcyclohexane; ◐, $G(H_2)$ from methylcyclohexane containing 0.3 M N_2O; ●, $G(N_2)$ from methylcyclohexane containing 0.3 M N_2O.

Discussion

Iodobenzene - Methylcyclohexane System. As is shown in Figs. 1 and 2, the hydrogen yield decreases and the benzene yield increases with increasing iodobenzene concentration. Therefore it is considered that iodobenzene scavenges electrons to produce I^- and the phenyl radical, the latter of which immediately abstracts a hydrogen atom from the solvent molecule (methylcyclohexane) to form benzene.[8,19]

$$MCH \rightsquigarrow MCH^+ + e^- \quad (4)$$

$$MCH^+ + e^- \rightarrow H_2 + \text{residue} \quad (5)$$

$$C_6H_5I + e^- \rightarrow C_6H_5\cdot + I^- \quad (6)$$

$$C_6H_5\cdot + MCH \rightarrow C_6H_6 + MCH\cdot \quad (7)$$

Hydrogen atom abstraction from hydrocarbons by phenyl radicals was previously reported by Bennet *et al.*[19] Our experimental results also support the mechanism described above. If benzene is produced by Reactions (6) and (7), the decrease in hydrogen yield must be equal to the yield of electrons scavenged by iodobenzene and consequently equal to the benzene yield.

$$\Delta G(H_2) = G(C_6H_6) \quad (8)$$

It was found that this relationship holds both in the liquid and glassy states (Figs. 1 and 2). Thus it is concluded that the benzene yield corresponds to the scavenged electron yield. The limiting G value of benzene formation in methylcyclohexane glass at −196°C is about 1.1 which is in good agreement with $G(CH_3\cdot)$ in 3MP and MCH glasses containing CH_3I reported by Shirom and Willard.[20] It should be noted that iodobenzene may be used to measure the scavenged electron yield by the yield of benzene produced.

We now consider the kinetics of electron scavenging. Recently a kinetic treatment of electron scavenging in liquids has been presented by Freeman.[21] In the present treatment the probability of electron scavenging by solute in liquid methylcyclohexane is quoted from that calculated by Freeman. We have calculated the probability of electron scavenging in the glassy state at −196°C by extending Freeman's treatment. In these calculations the following assumptions are made: (i) In the glassy state at −196°C, the mobility of positive ions and the diffusion constant of scavenger (iodobenzene) are negligibly small compared with those of electrons, *i. e.*,

$$u_+ \ll u_- \quad \text{and} \quad D_s \ll D_- \quad (9)$$

where u_+ and u_- are the mobility of positive ion and electron respectively, and D_s and D_- are the diffusion constant of iodobenzene and an electron, respectively. In other words, electrons in the glassy state are treated as "quasifree" electrons,*1 while electrons in the liquid state are treated as "solvated" electrons. (ii) The following equation is used:

$$u/D = \boldsymbol{k}T/e \quad (10)$$

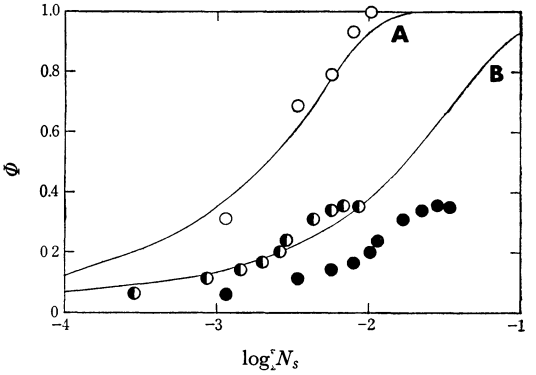

Fig. 7. Probability of electron scavenging in methylcyclohexane.
N_s, mole fraction of iodobenzene; A, calculated curve at room temperature; B, calculated curve at −196°C; ○, observed probability, $G(e^-)_s/G(e^-)_0$, at room temperature, $G(e^-)_0=3$; ●, observed probability at −196°C; ◐, observed probability, assuming aggregation, at −196°C.

19) J. E. Bennett, B. Mile and A. Thomas, *Proc. Roy. Soc.*, **293**, 246 (1966).

20) M. Shirom and J. E. Willard, *J. Chem. Phys.*, **47**, 286 (1967).

21) G. R. Freeman, *ibid.*, **46**, 2822 (1967).

*1 The term quasifree electrons was used as those neither trapped nor solvated in rigid matrices.

where k is Boltzmann constant, T is the absolute temperature, and e is the charge on an electron. (iii) In the glassy state at −196°C, the initial separation distances between positive ions and electrons may be reduced to 70% of those in the liquid state at room temperature, since the density of the medium at −196°C is 1.4 times that at room temperature.

The calculated curve for the probability of electron scavenging in methylcyclohexane at room temperature (quoted from Freeman's results) and that at −196°C calculated here are shown in Fig. 7. The experimental values are also plotted in Fig. 7. In the liquid state at room temperature, the probabilities of electron scavenging obtained by the experiments are in good agreement with the calculated ones, but those in the glassy state at −196°C are a little lower than the calculated results. The reason for this may be explained by assuming aggregation of iodobenzene molecules in nonpolar solvents. Aggregation of organic halides in hydrocarbon glasses has also been suggested by Willard *et al.*[22] and Hamill *et al.*[23] If iodobenzene molecules aggregate in methylcyclohexane glass, the effective concentration of iodobenzene would be lower than the apparent concentration. Assuming the effective concentration to be a quarter of the apparent concentration, the probabilities of electron scavenging were recalculated and plotted in Fig. 7. As is shown in Fig. 7, if it is assumed that three or four iodobenzene molecules aggregate, the probability of electron scavenging obtained by the experiments is in fairly good agreement with the calculated curve. Since the encounter efficiency, f_-, at −196°C is expected to be smaller than 1, the calculated curve probably shows the maximum probability of electron scavenging. Thus it is concluded that electrons in rigid matrices at −196°C may be treated as "quasifree" electrons, while electrons in the liquid state can be treated as "solvated" electrons.[21]

N_2O-Methylcyclohexane System. Nitrous oxide scavenges electrons ejected from γ-irradiated methylcyclohexane to give N_2 and O^- and therefore causes the decrease in hydrogen yield.

$$N_2O + e^- \rightarrow N_2 + O^- \qquad (11)$$

The ratio of the nitrogen yield to the decrease in hydrogen yield indicates that nitrogen is not formed only by single electron attachment process (Reaction (11)) except at −160°C. The other mechanisms of nitrogen formation than the single electron attachment have been proposed by some workers; (i) O atom abstraction from N_2O molecule by O^-,[9] (ii) chain reactions initiated by H atom abstraction from solvent molecules by O^-,[5] (iii) energy transfer from excited solvent molecules to nitrous oxide molecules.[17] However, at −196°C, it is difficult to explain the nitrogen formation by Mechanism (i) or (ii) because $G(N_2)/\Delta G(H_2)$ reaches 4. This ratio will be 2 according to Mechanism (i) and possibly 4 if the chain reactions by (ii) would more easily occur at −196°C than room temperature. The energy transfer (iii) cannot explain the experimental curve shown in Fig. 6. As a possible mechanism at −196°C the following reaction is considered:

$$O^- + N_2O \rightarrow O + N_2O^- \qquad (12)$$

$$N_2O^- \rightarrow N_2 + O^- \qquad (11')$$

The reaction (12) was observed by Paulson in mass spectrometric study.[24] It would be necessary for Reactions (12) and (11') to proceed that nitrous oxide molecules aggregate at −196°C. Such aggregation may be possible because liquid nitrogen temperature is below the glass transition temperature of methylcyclohexane.[25] As is shown in Fig. 8, the increase of $G(N_2)/\Delta G(H_2)$ from 1 to 4 with increasing N_2O concentration seems to indicate this aggregation. However, it is also uncertain if the above reactions occur at −196°C, because Reaction (12) is endothermic in the gas phase.[24] Thus the mechanism for formation of nitrogen from mixtures of nitrous oxide and methylcyclohexane (as well as other hydrocarbons) is not clear at present and remains to be resolved in future.

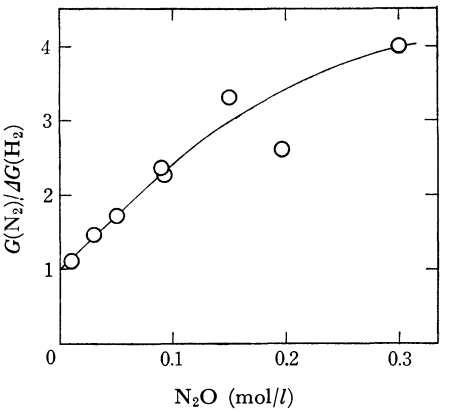

Fig. 8. The ratio of $G(N_2)/\Delta G(H_2)$ *vs.* N_2O concentration.

Mechanism of Hydrogen Formation. The mechanism of hydrogen formation may be written as follows:

22) R. F. C. Claridge and J. E. Willard, *J. Am. Chem. Soc.*, **89**, 510 (1967).
23) E. P. Bertin and W. H. Hamill, *ibid.*, **86**, 1301 (1964).
24) J. F. Paulson, "Ion-Molecule Reactions in the Gase Phase," ed. by F. Gould, American Chemical Society Publications, Washington, D. C. (1966).
25) M. R. Carpenter, D. B. Davies and A. J. Matheson, *J. Chem. Phys.*, **46**, 2451 (1967).

$$C_7H_{14} \xrightarrow{\sim\sim} \begin{cases} C_7H_{14}^* & (13) \\ C_7H_{14}^+ + e^- & (14) \end{cases}$$

$$C_7H_{14}^* \rightarrow H(\text{hot}),\ H(\text{thermal}),\ \text{and/or}\ H_2 \quad (15)$$

$$C_7H_{14}^+ + e^- \rightarrow \begin{cases} H_2 + C_7H_{12} & (16) \\ H(\text{hot}) + C_7H_{13}\cdot & (17) \\ H(\text{thermal}) + C_7H_{13}\cdot & (18) \end{cases}$$

At room temperature both hot and thermal hydrogen atoms can abstract an H atom from the solvent molecule to yield a hydrogen molecule and a solvent radical.

$$H(\text{hot}) + C_7H_{14} \rightarrow H_2 + C_7H_{13}\cdot \quad (19)$$

$$H(\text{thermal}) + C_7H_{14} \rightarrow H_2 + C_7H_{13}\cdot \quad (20)$$

Since thermal H atoms cannot abstract H atoms from solvent molecules at −196°C, they must combine one another or with the solvent radicals. The hydrogen yield from pure methylcyclohexane irradiated at −196°C decreases by 0.5 G unit in comparison with that at room temperature (Fig. 6). If the decrease in hydrogen yield is due to thermal H atoms, the yield of thermal H atoms may be estimated to be lower than 1.0 (G unit).

As has been described already, one molecule of benzene is formed by scavenging an electron and decreasing one hydrogen molecule at −196°C as well as room temperature. Therefore one molecule of hydrogen is formed by neutralization of a positive ion and an electron. A large fraction of hydrogen formed by neutralization will be hot, since its G value is expected to be 4 from W value and that of thermal H atoms is estimated to be about 1.0. Consequently the two solvent radicals produced by Reactions (17) and (19) seem to be very close to each other in the solid state. Then it will be suggested that the amount of trapped radicals does not increase after neutralization, since recombination or disproportionation of these two radicals may immediately occur even at −196°C. Further study on this point is being planned.

BULLETIN OF THE CHEMICAL SOCIETY OF JAPAN VOL. 41 2866—2871 (1968)

The Structure of Meisenheimer Complex as Determined by X-ray Crystal Analysis

Hideo UEDA,*1 Noriyoshi SAKABE and Jiro TANAKA*2

Department of Chemistry, Faculty of Science, Nagoya University, Chikusa, Nagoya

and Akio FURUSAKI

Faculty of Science, Kwansei Gakuin University, Nishinomiya, Hyogo

(Received May 16, 1968)

The structure of the Meisenheimer complex has been determined by the X-ray method. The complex is characterized by a symmetrical structure, in which the two methoxyl groups are nearly equivalent to each other. The results showed a peculiar shape of the reaction intermediate, the substituted carbon atom is transformed into a tetrahedral shape, while the planarity of the whole molecule is kept with an increased conjugation between the nitro group and the ring system.

The Meisenheimer complex, a reaction intermediate in a nucleophilic substitution reaction, has been widely investigated from both chemical and structural points of view. The structural formula (I) proposed as an explanation of the chemical behavior has been discussed by many people[1-5]; recent nuclear magnetic resonance results[6,7] indicate that the two methoxyl groups are equivalent in solution.

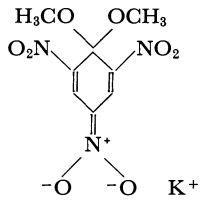

(I)

*1 Present address: Ube Industries Ltd., Ube, Yamaguchi

*2 To whom any correspondence should be mailed.

1) J. Meisenheimer, *Ann.*, **323**, 205 (1902).
2) L. K. Dyall, *J. Chem. Soc.*, **1960**, 5160.
3) S. Nagakura, *Terahedron*, **19**, Suppl. **2**, 361 (1963).
4) R. Foster and R. K. Mackie, *J. Chem. Soc.*, **1963**, 3796.
5) M. R. Crampton and V. Gold, *ibid.*, **1964**, 4293.
6) M. R. Crampton and V. Gold, *Chem. Commun.*, **1965**, 256.
7) K. L. Servis, *J. Am. Chem. Soc.*, **89**, 1507 (1967).

The crystal of the complex was first isolated by Meisenheimer,[1] while preliminary structure reports have been presented by us[8] and by Destro, Gramaccioli and Simonetta[9] independently. The present paper will describe the full details of the structure of the 1,1'-dimethoxy-2,4,6-trinitrobenzene potassium dihydrate, $(K^+[C_6H_2(NO_2)_3(OCH_3)_2]^- \cdot 2H_2O)$.

Experimental

The material was obtained from the reaction of picryl chloride and potassium methoxide. It was recrystallized from an acetonitrile solution. The crystal includes two molecules of water, which has been confirmed by the elemental analysis (Found: C, 27.36; H, 3.91; N, 11.96%. Calcd for $C_8H_8O_8N_3K \cdot 2H_2O$: C, 27.50; H, 3.45; N, 12.00%.). The unit-cell dimensions and space group were determined by the oscillation and by Weissenberg photographs. The three-dimensional intensity data were collected using Cu$K\alpha$ radiation with a Weissenberg camera by the multiple-film technique for layer lines 0—5 about the b axis and for layer lines 0—5 about the c axis. The intensities were measured visually, and 1897 independent data were obtained. The scaling of the intensity data, including corrections for different films, corrections for Lorentz and polarization factors, and Wilson's statistical-data analysis, were performed on the HITAC 5020 computer at the Computation center of the University of Tokyo. No corrections were made for either absorption or extinction, since the crystal used was sufficiently small in size for these effects to be neglected.

Crystal Data. $K^+[C_6H_2(NO_2)_3(OCH_3)_2]^- \cdot 2H_2O$ MW 348, Triclinic, $P\bar{1}$ $a=9.36\pm0.02$, $b=10.84\pm0.02$, $c=7.40\pm0.02$ Å, $\alpha=87°40'$, $\beta=106°43'$, $\gamma=102°45'\pm 20'$, $Z=2$.

The crystal density, determined by the floatation method in a carbon tetrachloride and methylene iodide mixture, was 1.64 g·cm^{-3}, while the calculated value was 1.65 g·cm^{-3}. No systematic absent spectra have been found.

Structure Analysis. A three-dimensional Patterson synthesis was made using the observed structure factors. The position of the potassium atom was easily found after ascertaining the highest peak. By the aid of the image-seeking method on the Patterson map, we were able to find the location of the benzene ring. At this stage the trial coordinates for all the atoms except the two water molecules were determined, and a least squares refinement with isotropic temperature factors was initiated. After several refinements the R-factor was 26%, at this stage the Fourier synthesis was done, and the locations of two water molecules were established. Including the water molecules, the least-squares refinement was then repeated, the R-factor was 0.16. Using the anisotropic temperature factors for all the atoms the final R-factor was found to be 0.130. The atomic coordinates determined are listed in Table 1, together with the anisotropic temperature factors. The calculated and observed structure factors for all 1897 reflections are kept at the Chemical Society of Japan*[3].

Table 1. Atomic coordinates and anisotropic temperature factors

Atom	x/a	y/b	z/c	B_{11}	B_{22}	B_{33}	B_{12}	B_{23}	B_{31}
K- 1	0.1358	0.0567	0.2982	0.0067	0.0030	0.0041	0.0036	0.0007	0.0007
O- 1	0.3150	0.8754	0.3605	0.0039	0.0021	0.0074	−0.0001	0.0011	0.0032
O- 2	0.0966	0.7902	0.4134	0.0041	0.0020	0.0089	0.0017	−0.0030	0.0045
O- 3	0.0544	0.8668	0.0412	0.0110	0.0030	0.0102	0.0069	−0.0051	−0.0066
O- 4	0.0551	0.7243	0.8522	0.0123	0.0075	0.0015	0.0054	0.0029	0.0003
O- 5	0.3574	0.8078	0.7375	0.0090	0.0051	0.0095	0.0034	−0.0046	−0.0060
O- 6	0.3869	0.6182	0.8123	0.0175	0.0056	0.0038	0.0105	0.0063	0.0005
O- 7	0.2412	0.3600	0.0586	0.0133	0.0056	0.0085	0.0068	−0.0092	−0.0026
O- 8	0.3231	0.3164	0.3551	0.0127	0.0026	0.0099	0.0069	−0.0015	0.0021
O- 9	0.8317	0.9903	0.3224	0.0080	0.0050	0.0094	0.0033	−0.0023	0.0044
O-10	0.3248	0.1296	0.0209	0.0097	0.0047	0.0130	0.0027	−0.0095	0.0002
N- 1	0.3478	0.6980	0.6950	0.0063	0.0037	0.0037	0.0019	−0.0011	−0.0002
N- 2	0.0880	0.7663	0.0110	0.0067	0.0048	0.0019	0.0042	−0.0009	−0.0016
N- 3	0.2771	0.3907	0.2277	0.0056	0.0033	0.0119	0.0001	−0.0057	0.0009
C- 1	0.2169	0.7546	0.3590	0.0035	0.0027	0.0053	0.0012	−0.0021	0.0039
C- 2	0.1654	0.6968	0.1676	0.0056	0.0024	0.0055	0.0040	0.0011	0.0047
C- 3	0.1895	0.5840	0.1265	0.0048	0.0026	0.0090	0.0026	−0.0028	0.0047
C- 4	0.2571	0.5085	0.2687	0.0056	0.0023	0.0115	−0.0001	−0.0041	−0.0025
C- 5	0.3052	0.5469	0.4578	0.0045	0.0031	0.0103	0.0017	−0.0010	0.0029
C- 6	0.2876	0.6628	0.4978	0.0045	0.0029	0.0061	−0.0011	−0.0007	0.0016
C- 7	0.4545	0.8732	0.3137	0.0060	0.0059	0.0212	0.0008	0.0019	0.0148
C- 8	0.9678	0.6889	0.4118	0.0006	0.0059	0.0195	−0.0080	−0.0064	0.0065

8) H. Ueda, N. Sakabe, J. Tanaka and A. Furusaki, *Nature*, **215**, 956 (1967).

9) R. Destro, C. M. Gramaccioli and M. Simonetta, *Nature*, **215**, 389 (1967).

*3 The complete data of the F_o-F_c table are kept as Document No. 6803 at the office of the Bulletin of the Chemical Society of Japan. A copy may be secured by citing the document number and by remitting, in advance, ¥600 for photoprints. Pay by check or money order, payable to Chemical Society of Japan.

Results and Discussion

The bond distances and angles in the Meisenheimer complex are shown in Figs. 1 and 2. The standard deviations for atomic positions are tabulated in Table 2, the maximum standard deviation for ring carbon atoms is 0.013 Å, while that for substituent methoxyl groups is 0.016 Å. The standard deviation for the bond length in the benzene ring is 0.017 Å, while the values for the substituents are 0.019 Å.

The most important result concerning the structure is that the two methoxyl groups are perfectly equivalent, this confirms the earlier chemical and spectroscopic evidence concerning the symmetrical structure. The lengths of C(1)-O(1) and C(1)-O(2) bonds are 1.42 Å, normal for saturated compound. The C(7), O(1), C(1), O(2) and C(8) atoms are almost on a plane, which can be represented by the equation $0.4951\,X+0.8618\,Y-0.1106\,Z-1.2544=0$ in which the X, Y, and Z coordinates, in Å units, refer to the orthogonal axes a′, b and c′. The orthogonal axes were b, the crystal axis, a′, the projected a axis (a sin γ), and third axis, c′, perpendicular to a′ and b. The deviations from this plane are shown in Table 3. This plane makes an angle of 87°49′ with the

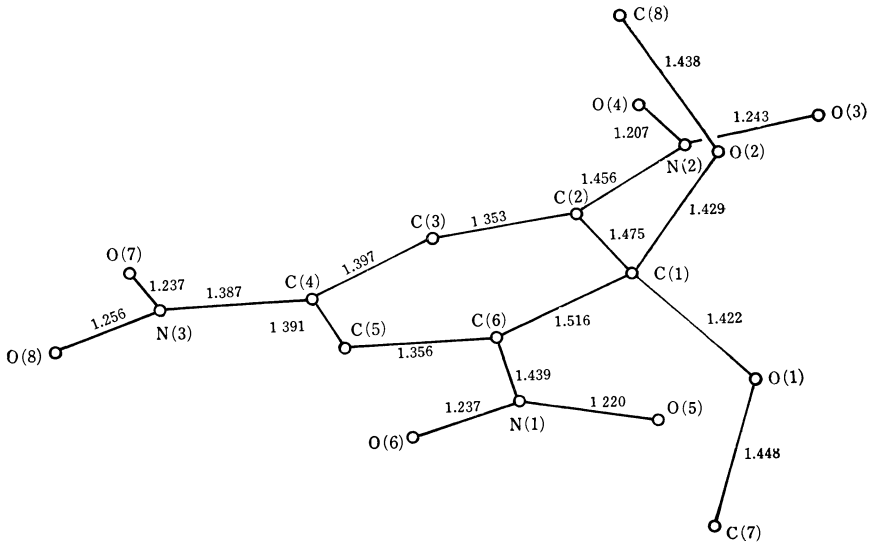

Fig. 1. The bond lengths in Meisenheimer complex.

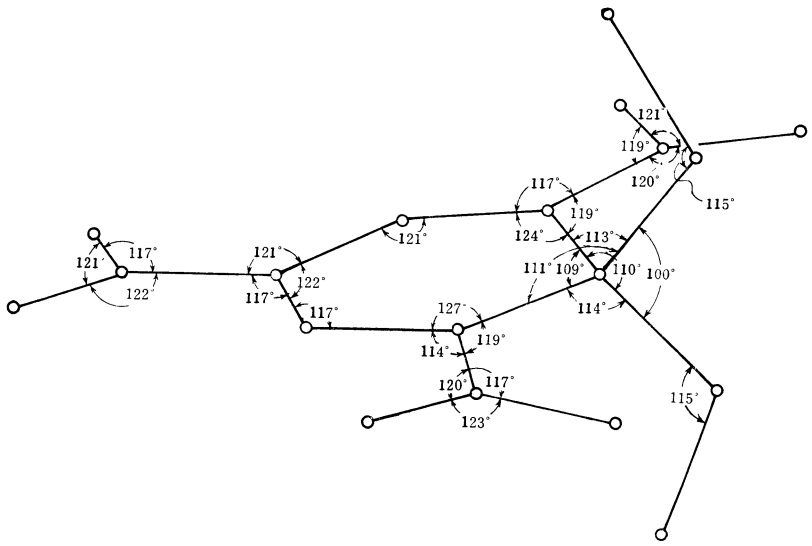

Fig. 2. The bond angles in Meisenheimer complex.

Table 2. Standard deviation of atomic positions (in Å)

Atom	σ(x)	σ(y)	σ(z)
K- 1	0.0026	0.0024	0.0025
O- 1	0.0071	0.0069	0.0077
O- 2	0.0072	0.0070	0.0078
O- 3	0.0093	0.0079	0.0088
O- 4	0.0097	0.0093	0.0081
O- 5	0.0090	0.0087	0.0089
O- 6	0.0108	0.0089	0.0086
O- 7	0.0101	0.0090	0.0089
O- 8	0.0096	0.0079	0.0087
O- 9	0.0086	0.0086	0.0087
O-10	0.0093	0.0087	0.0093
N- 1	0.0095	0.0092	0.0092
N- 2	0.0096	0.0096	0.0090
N- 3	0.0097	0.0095	0.0105
C- 1	0.0099	0.0101	0.0107
C- 2	0.0107	0.0101	0.0110
C- 3	0.0107	0.0105	0.0116
C- 4	0.0115	0.0107	0.0126
C- 5	0.0109	0.0108	0.0120
C- 6	0.0105	0.0105	0.0112
C- 7	0.0127	0.0135	0.0155
C- 8	0.0101	0.0125	0.0141

Table 3. The deviation of atoms from the two methoxyl group plane

C-7	−0.009 (Å)
O-1	−0.007
C-1	0.007
O-2	0.039
C-8	−0.032

benzene-ring plane; this implies that the methoxyl group plane bisects the benzene ring. It also means that the C(1) carbon atom is nearly tetrahedral and is coplanar with the rest of the benzene ring. This conformation is recognized to be the least-hindered structure from the steric repulsion of the nitro group. The substituted benzene ring keeps its planarity; the plane can be represented by the equation $0.8250X-0.3683Y+0.4287Z-2.6464=0$. The deviations from this plane for the ring and nitrogen atoms are tabulated in Table 4. The maximum deviation for ring atoms is 0.03 Å at C(2). The bond angles around the C(1) atom are interesting; the C(2)-C(1)-C(6) angle is 108.8° a nearly exact tetrahedral angle, while the O(1)-C(1)-O(2) angle is 100.1°, appreciably smaller than the tetrahedral. The strain produced by this distrotion is significant; it may be explained in terms of the steric repulsion between the methyl groups and the benzene ring, since the C(2)-C(8) and C(6)-C(8) distances are 2.95 Å, both smaller than the sum of the van der Waals radii of two carbon atoms. The bond lengths of C(2)-C(3) and C(5)-C(6) are shorter than those of C(3)-C(4) and C(4)-C(5); this means that the double bonds are localized, as in the structural formula (I) rather than delocalized, as in the structure (II). Of the three nitro groups, the one at the para-position and that at the C(2) ortho-position are tilted 6°30′ and 5°30′ to the benzene ring respectively; the third one, at the C(6) ortho-position, is twisted as much as 11°19′. The crystal structure of 2,4,6-trinitrophenetole, a related parent compound of the nucleophilic substitution reaction, was recently analyzed by Gramaccioli, Destro and Simonetta[10]; it was found that the nitro group at the para position is tilted 3°, the one at the ortho-position is twisted 33°, and the third, at the other ortho-position, is rotated 62°.

Table 4. The deviation of ring atoms from the benzene ring plane

C-1	0.022(Å)
C-2	−0.030
C-3	0.013
C-4	0.011
C-5	−0.020
C-6	0.004
N-1	0.064
N-2	−0.075
N-3	−0.002

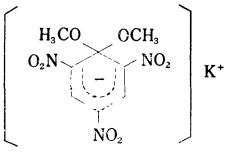

(II)

In the present complex three nitro groups are much plainer with the benzene ring than with the trinitrophenetole; this means that the conjugation between the nitro groups and the benzene ring is increased, presumably because an excess electronic charge delocalizes between the nitro groups and the benzene ring. This explanation is also supported by the recent theoretical calculations of Hosoya, Hosoya and Nagakura[11] on this ion. Although the bond lengths of C(1)-C(2) and C(1)-C(6) are slightly different, the present results are not accurate enough for exact discussion. However, these bond lengths are somewhat shorter than the usual single bond length of 1.54 Å; this may be attributed to the hyperconjugation effect of the pseudo π-orbital, composed of two C-O bonds. If we assume that the shortening of the C(1)-C(2)

10) C. M. Gramaccioli, R. Destro and M. Simonetta, *Chem. Commun.*, **1967**, 331.
11) H. Hosoya, S. Hosoya and S. Nagakura, Preprints for the 21st Annual Meeting of the Chemical Society of Japan (Osaka, 1968).

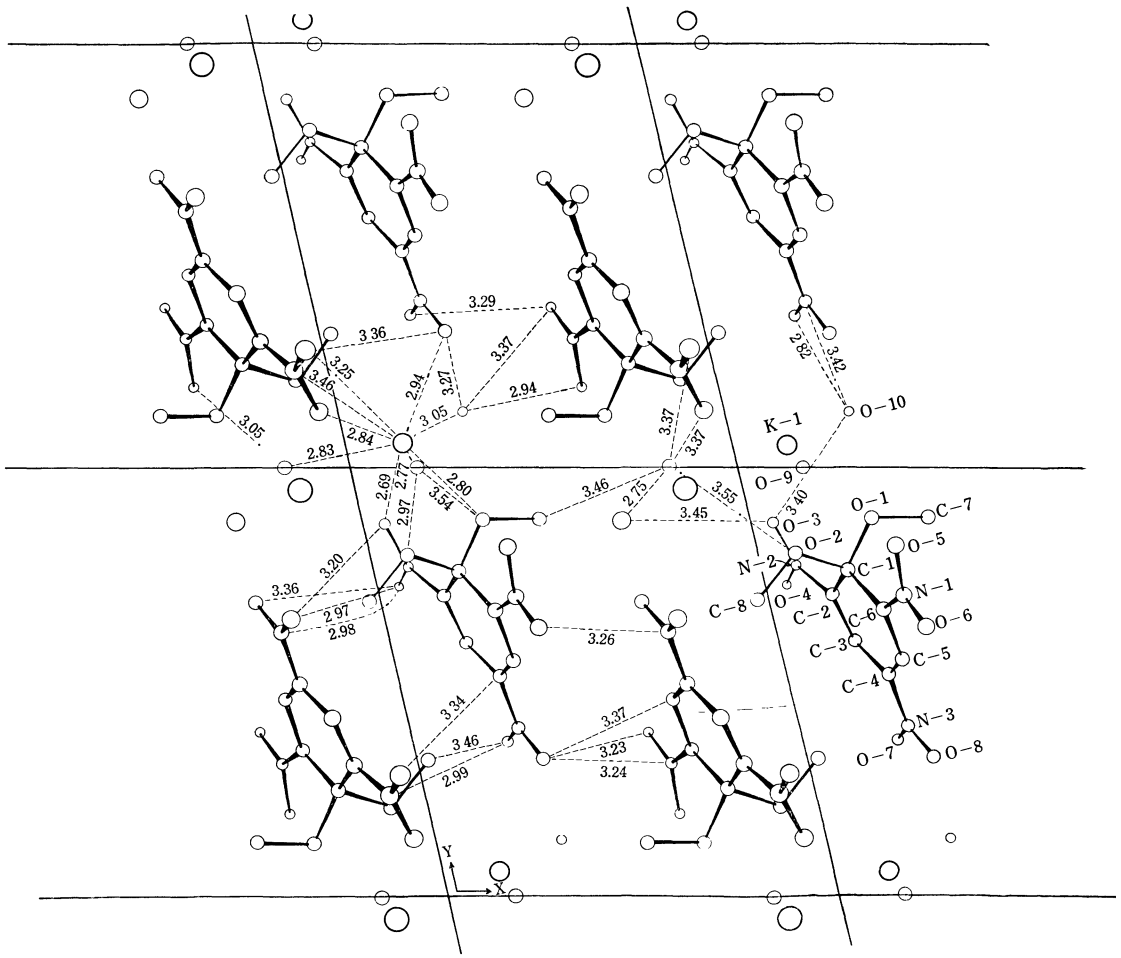

Fig. 3. Interatomic distances between the complex, potassium ion (large and heavy medium circles) and crystalline water (light medium circle and small circles).

or C(1)-C(6) bonds is correlated to the hyperconjugation, it is found that the shorter these bond lengths, the smaller the twisting of the nitro groups at the ortho-positions.

The comparison of the three C-N bond lengths indicates that the shortest one is at the para-position; this is in accord with the structure (I). The distances, C(2)-N(2) and C(6)-N(1), are slightly different from each other, and they are in order on the reverse of that suggested by the magnitude of the conjugation effect. The asymmetry of the Meisenheimer complex with regard to the two ortho nitro groups is unthinkable in a solution. In a crystal, however, the location of the potassium ion is not symmetrical to the three nitro groups. The close distances between the potassium ion and the complex are at two oxygen atoms, (O(3) and 0(8)), of the nitro groups and O(1) and O(2) of the methoxyl groups, as is shown in Fig. 3. The potassium ion in a crystal will attract a negative charge on the neighboring oxygen atoms; as a result, the N-O bond will be lengthened and the nitro group will be more coplanar with the benzene ring. The nitro group at the C(6) ortho position has not potassium ion in the neighborhood; this can explain the largest twisting of this nitro group.

Finally, we should comment on the structure of this complex ion in connection with the mechanism of the nucleophilic substitution reaction. Since Wheland[12] calculated the resonance energy of the activated complex of the substitution reaction, there have been many studies concerning the structure of the reaction intermediate. Two structural formulae, I and II have been proposed, but the structure has not yet been determined accurately. In the present study the complex ion is found to have a quinoid structure of I, and the substituted carbon atom takes a nearly tetrahedral form.

The unusual stability of the reaction intermediate can be explained as resulting from the fact that;

12) G. W. Wheland, *J. Am. Chem. Soc.*, **64**, 900 (1942).

(1) the unsaturated five-membered system is stable in the case of the anion; (2) the possibility of hyperconjugation at the tetrahedral carbon atom, and (3) the coplanarity of nitro groups with the benzene ring, which increases the degree of the delocalization of π-electrons.

One of the author (J. T.) wishes to express his thanks to Professor Saburo Nagakura and Dr. Toshio Sakurai for their kind advice in the early stage of experimentation.

BULLETIN OF THE CHEMICAL SOCIETY OF JAPAN VOL. 41 2871—2876 (1968)

Radiolysis of Hydrogen Cyanide in an Aqueous System.[1] II. Effects of Additives and Reaction Mechanism

Hajime OGURA

Department of Chemistry, Faculty of Science, Tokyo Metropolitan University, Setagaya-ku, Tokyo

(Received May 21, 1968)

The ^{60}Co γ-irradiation of dilute aqueous solutions of hydrogen cyanide (6 mM) in the absence of oxygen yielded mainly ammonia with $G=1.9$, formaldehyde with $G=1.1$, and carbon dioxide with $G=0.8$, while $G(-HCN)=5.8$ molecules per 100 eV. Polymeric hydrogen cyanide was also observed with the $G(-HCN(polymer))\simeq 4$, which showed an intense broad absorption band in the UV region upon γ-irradiation. The following material balances were observed with the main products:

$$G(-HCN) \simeq G(NH_3) + G(-HCN(polymer)) \simeq G(CO_2) + G(HCHO) + G(-HCN(polymer))$$

The results can be interpreted in terms of a mechanism involving HCN^-, H_2CN, and $H(OH)CN$ radicals. The ratio of the rate constants for the reactions of e^-_{aq} and H atoms with hydrogen cyanide to those with several scavengers have been determined as $k(e^-_{aq}+HCN)/k(e^-_{aq}+NO_3^-)=0.019$ and $k(H+HCN)/k(H+2\text{-propanol})=1.4$, all at 17°C.

In our previous papers,[1,2] studies have been made of the radiolysis of aqueous solution of hydrogen cyanide with the purpose of elucidating the nature of the reaction, the radiolytic yields of hydrogen cyanide, and the products of the radiolysis, including the HCN tetramer.

The work reported here was undertaken in order to obtain additional information about radiolytic products and a general mechanism of the radiolysis by using several scavengers.

Experimental

The general procedures have already been described,[1] but a review will be given of what was introduced in the present experiment.

Samples. A 5-m*l* portion of an air-free solution, prepared by the conventional vacuum technique with freezing-thawing recycles, was sealed in a 20 m*l* cylindrical glass cell. Nitrous oxide purified by distillation was taken in a calibrated volume until a definite pressure and temperature had been reached and then transfered to the irradiation vessel by using liquid nitrogen. The concentration of the gas in the solution was calculated from the solubility data.[3]

Irradiation. Gamma irradiation was carried out with a ^{60}Co source at a dose rate of 1.68×10^{18} eV·ml^{-1}hr^{-1} based on Fricke dosimetry, taking $G(Fe^{3+})=15.5$.

Analysis. The nitrite ion was determined spectrophotometrically at 520 mμ by using sulfanilic acid and α-naphthylamine.[4] The formaldehyde was determined by means of chromotropic acid when the solution was irradiated in an acidic medium (H_2SO_4 pH=2). However, in the neutral and basic solutions, this method could not be used because of the formation of cyanohydrin[5] from the cyanide ion and formaldehyde produced by γ-irradiation even at low concentrations. Since it has been confirmed that cyanohydrin can also be determined by the use of an acetylacetone reagent which has been generally used for the determination of

1) Preliminary report: H. Ogura, *J. Rad. Res. (Tokyo)*, **8**, 93 (1967); Presented in part at the 8th and 10th Symposia on Radiation Chemistry, Tokyo, Nov. 12, 1965, and Hiroshima, Oct. 26, 1967, respectively.

2) H. Ogura and M. Kondo, This Bulletin, **40**, 2448 (1967).

3) Intern. Critical Tables, **3**, (1933), p. 254.

4) F. D. Snell and C. T. Snell, "Colorimetric Method of Analysis," Vol II, 3rd ed., D. Van Norstrand, New York (1958), p. 803.

5) N. V. Sidgwick, "The Organic Chemistry of Nitrogen," Oxford (1937), new ed. (revised by T. W. J. Taylor and W. Baker), p. 309.

formaldehyde in a neutral medium,[6] the concentration of formaldehyde in the presence of hydrogen cyanide in a neutral medium was estimated as follows. A mixture of the irradiated solution and the acetylacetone reagent in equal volumes was kept at 58°C for 90 min; the resulting yellow coloration was determined spectrophotometrically at 412 mμ. The validity of this method under the present experimental conditions, with 6 mM HCN, was established well. The formic acid was determined as was formaldehyde after being reduced by metallic magnesium and hydrochloric acid.[7] The hydrogen peroxide was determined by the ceric sulfate method.

Results and Discussion

Yields of Products. Figure 1 presents typical results of the radiolysis of an air-free 6 mM HCN solution at a natural pH. The initial yields of products expressed as G (molecules per 100 eV) are summarized in Table 1. By improving the analytical procedure, it became possible to observe

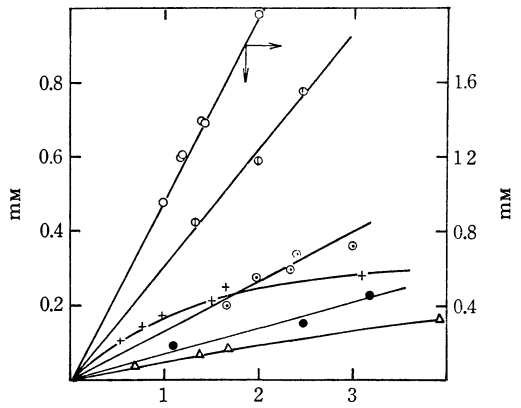

Fig. 1. Radiolysis of 6 mM HCN in air-free system.
○: HCN consumed ⊕: NH_3 produced
+: HCHO produced ⊙: CO_2 produced
●: H_2 produced △: H_2O_2 produced
Dose rate: 1.68×10^{18} eV ml^{-1} hr^{-1}

TABLE 1. PRODUCT YIELDS IN THE RADIOLYSIS OF 6 mM HCN

Product	Yield (G-value)
Ammonia	1.9
Formaldehyde*	1.1
Carbon dioxide	0.8
Formic acid	0.1
Nitrogen	<0.1
Hydrogen	0.42
Hydrogen peroxide	0.3
Polymeric product	$4\simeq G(-HCN)$

* Presented as cyanohydrin

6) T. Nash, *Biochem. J.*, **55**, 416 (1955).
7) Ref. 4, p. 303.

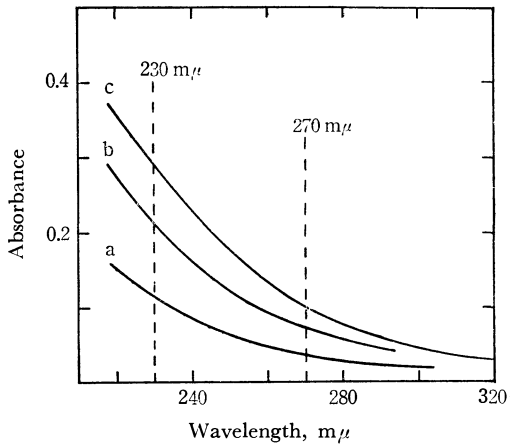

Fig. 2. UV absorption spectra of γ-irradiated 6 mM HCN in air-free system.
Dose rate: 1.68×10^{18} eV ml^{-1} hr^{-1}
a: 4 hr b: 8 hr c: 11 hr

formaldehyde as one of major products in addition to those previously observed.[1] Besides the radiolysis products of a low molecular weight listed in Table 1, a polymeric form of hydrogen cyanide was also observed. It has been known that when a small amount of base is added to aqueous solutions of hydrogen cyanide, there appears a very strong broad absorption extending into the UV region; this formation is due to the formation of polymeric hydrogen cyanide.[8,9] In irradiated aqueous solutions of hydrogen cyanide, an absorption of nearly the same type as that chemically prepared was observed in Fig. 2, indicating the polymerization of hydrogen cyanide by γ-irradiation.*1

Figure 3 presents the increase in the absorbance at 230 mμ and 270 mμ against the absorbed dose. The wavelength at which the absorbance was measured was chosen for the sake of convenience in experimentation. The absorbance is seen to increase linearly with the dose, and, from the slope of the line, one can obtain the increase in absorbance per unit dose (−log T/dose), an increase which corresponds to the radiolytic yield of polymeric hydrogen cyanide. One can indicate

8) S. Fujise, N. Nagai and T. Numata, *Kogyo Kagaku Zasshi (J. Chem. Soc. Japan, Ind. Chem. Sect.)*, **64**, 1889 (1961).
9) J. Kato, I. Hayashi, I. Noda, R. Yuwanaga and T. Yoshida, *ibid.*, **65**, 92 (1962).
*1 According to Kondo[10] and Hummel *et al.*,[14] in either pure or aqueous solutions of hydrogen cyanide at high concentrations, radiolysis with ^{60}Co γ-rays yields a massive, dark brown solid formulated as $(HCN)_n$ and quite similar in its chemical property to the azulmic acid produced from an alkaline solution of hydrogen cyanide.
10) A. Matsumoto, T. Masuda, C. Nakazato, H. Ogura and M. Kondo, presented at the 15th Annual Meeting of Chemical Society of Japan, Kyoto, April, 1962.

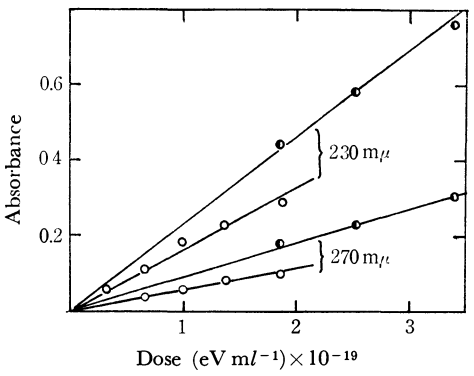

Fig. 3. Increase in absorbance at 230 mμ and 270 mμ with dose in γ-irradiated HCN solutions.
○: 6 mM HCN ◐: 23 mM HCN

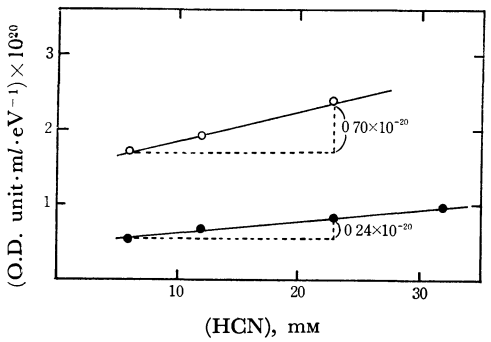

Fig. 4. Dependence of absorbance per unit dose on HCN concentration.
○: at 230 mμ ●: at 270 mμ

as examples of the calculation from Fig. 3, as written, 1.70×10^{-20} (O.D. unit ml eV^{-1}) at 230 mμ and 0.56×10^{-20} (O.D. unit ml eV^{-1}) at 270 mμ with a 6 mM HCN solution.

In Figure 4, the absorbance per unit dose is plotted against the initial concentration of hydrogen cyanide. The increase in this value with the concentration, ranging from 6 mM to 23 mM, is found to be $\Delta(-\log T/\text{dose})=0.70\times10^{-20}$ (O.D. unit ml eV^{-1}) at 230 mμ and 0.24×10^{-20} (O.D. unit ml eV^{-1}) at 270 mμ respectively. In an air-free system, G(-HCN) was determined previously to be 5.8 at 6 mM HCN and 7.5 at 23 mM HCN respectively. Assuming that this increase in the yield, ΔG(-HCN)=1.7, with the concentration is to be attributed to the increasing formation of a polymeric form of hydrogen cyanide*2 which results in an increase in the optical absorption per unit dose, $\Delta(-\log T/\text{dose})$, one can find that the radiolytic yield of hydrogen cyanide leading to the polymeric form is about G(-HCN(polymer))≃ 4 at 6 mM HCN. The difference between the total 100 eV yield of radiolysed hydrogen cyanide and the 100 eV yield of radiolysed hydrogen cyanide leading to the polymeric form is found to be 1.8. This value may correspond to the yields of the major products which give no absorption in the UV region. These products are demonstrated to be ammonia, carbon dioxide, and formaldehyde, the 100 eV yields of which are listed in Table 1. It seems that the following material balances can be established with the major products:

$$G(-\text{HCN}) \simeq G(\text{NH}_3) + G(-\text{HCN(polymer)})$$
$$\simeq G(\text{HCHO}) + G(\text{CO}_2) + G(-\text{HCN(polymer)})$$

Effect of Nitrate Ions. In a previous study,[1] it was shown that dissolved oxygen effectively reduced the radiolytic yields of hydrogen cyanide. This finding indicates the contribution of hydrated electrons to the radiolysis of hydrogen cyanide because of their high reactivity towards oxygen. To confirm this explanation, the nitrate ion, which is known as an effective scavenger[11] for the hydrated electrons, was introduced. Figure 5 illustrates the

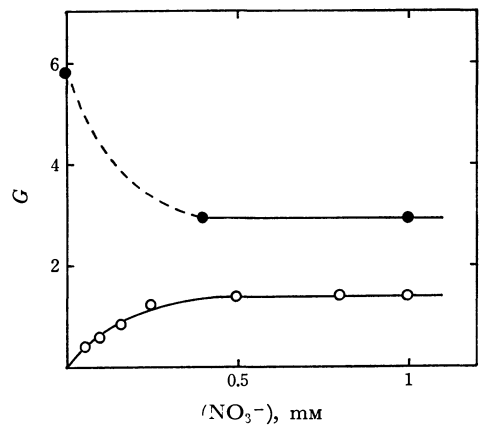

Fig. 5. Effect of nitrate ion on the radiolysis of 6 mM HCN in air-free system.
●: $G(-\text{HCN})$ ○: $G(\text{NO}_2^-)$

effect of these nitrate ions on the radiolysis of an air-free 6 mM HCN solution. The concentration of hydrogen cyanide was chosen at 6 mM, where an almost steady radiolytic yield, G(-HCN) =5.8, was observed;[1] this value is also in close agreement with the total radical yield of water. Nitrate ions are seen to reduced G(-HCN) with an increase in the concentration, leading to a steady value at 0.3 mM. Since the decrease in $G(-\text{HCN})$ at its steady value is found to be 2.9, close to the yield of hydrated electrons, $G_{e^-_{aq}}$, the effect of nitrate ions can readily be explained in terms of the scavenging action of the hydrated

*2 Unlike the increase in the total radiolytic yield of hydrogen cyanide from 6 mM up to 23 mM HCN, the observed increases in the yields of low-molecular products listed in Table 1 are almost negligible in the same concentration region.

11) H. A. Mahlman, *J. Phys. Chem.*, **67**, 1466 (1963).

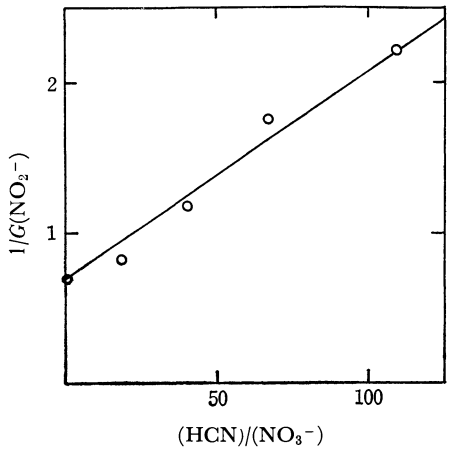

Fig. 6. Competition for hydrated electron between HCN and nitrate ion plotted according to Eq. (I).

electrons. Figure 5 also shows the yield of nitrite ions, $G(NO_2^-)$, which increases with the concentration of nitrate ions, tending to a steady value of 1.4, nearly a half of the $G_{e^-_{aq}}$ value in water radiolysis. These findings may result from the competitive reactions between hydrogen cyanide and nitrate ions for hydrated electrons:

$$e^-_{aq} + HCN \xrightarrow{k_1} P \qquad (1)$$

$$e^-_{aq} + NO_3^- \xrightarrow{k_2} NO_2 + 2OH^- \qquad (2)$$

followed by:

$$2NO_2 + H_2O \rightarrow NO_2^- + NO_3^- + 2H^+ \qquad (3)$$

$G(NO_2^-)$ can thus be expressed as:

$$\frac{1}{G(NO_2^-)} = \frac{2}{G_{e^-_{aq}}}\left\{1 + \frac{k_1(HCN)}{k_2(NO_3^-)}\right\} \qquad (I)$$

The plots of $1/G(NO_2^-)$ *vs.* $(HCN)/(NO_3^-)$ are presented in Fig. 6. The linear plots indicate the adequacy of the proposed mechanism given above. From the slope of the line, k_1/k_2 is obtained as 0.019. Taking the well-established rate constant of k_2 as 1.1×10^{10} M^{-1} sec^{-1},[12] the rate constant for the reaction (1) is found to be 2×10^8 M^{-1} sec^{-1}. As to what becomes of P, only two processes can be postulated. The one is an electron attachment of HCN

$$e^-_{aq} + HCN \rightarrow HCN^- \qquad (1a)$$

The presence of an anionic form of hydrogen cyanide is evidenced by the ESR spectra found in alkaline halide matrices at 77°K by Root *et al.*[13] Hummel *et al.*[14] also indicated its presence as an initiator of the radiation-induced polymerization of pure hydrogen cyanide. The other is possibly a dissociative electron capture process:

$$e^-_{aq} + HCN \rightarrow H + CN^- \qquad (1b)$$

Since the dissociation energy of H-CN is 114.9 kcal/mol,[15] and since the electron affinity of CN is 74 kcal/mol,[16] the reaction (1b) is not likely from a thermochemical point of view.

Effect of Nitrous Oxide. The effect of nitrous oxide[17] on the radiolysis of hydrogen cyanide and the formation of a gaseous product are presented in Fig. 7. The concentrations of nitrous oxide and hydrogen cyanide are about 16 mM and 5.8 mM respectively. It may be seen that nitrous oxide does not affect G(-HCN) and that $G(N_2)$ is very close to $G_{e^-_{aq}}$. Since $G(N_2)$ is quite negligible (<0.1) in the absence of nitrous oxide, as is shown in Fig. 7, the nitrogen observed in this experiment can be taken as almost entirely arising from the reaction (4):

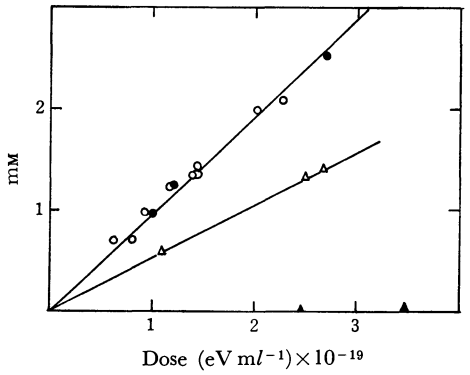

Fig. 7. Effect of nitrous oxide on the radiolysis of 6 mM HCN.
○: HCN consumed, △: N_2 produced in the presence of 16 mM N_2O, ●: HCN consumed, ▲: N_2 produced in the absence of N_2O

$$e^-_{aq} + N_2O \rightarrow N_2 + OH + OH^- \qquad (4)$$

If one assumes that the reactivity of OH radicals towards hydrogen cyanide is nearly equal to that of hydrated electrons, the above finding can be explained well.

As for the reaction of OH radicals with hydrogen cyanide, two reactions, (5a) and (5b), can possibly be expected:

$$OH + HCN \rightarrow H(OH)CN \qquad (5a)$$

$$\searrow H_2O + CN \qquad (5b)$$

The fate of the intermediate in the reaction (5a)

12) J. K. Thomas, S. Gordon and E. J. Hart, *J. Phys. Chem.*, **68**, 1524 (1964).
13) K. D. J. Root, M. C. R. Symons and B. C. Weatherly, *Mol. Phys.*, **11**, 161 (1966).
14) D. Hummel and O. Jassen, *Z. Physik. Chem.*, **31**, 111 (1962).
15) C. A. McDowell and J. W. Warren, *Trans. Faraday Soc.*, **48**, 1084 (1952).
16) J. T. Herren and V. H. Dibeler, *J. Am. Chem. Soc.*, **82**, 1555 (1960).
17) F. S. Dainton and D. B. Peterson, *Proc. Roy. Soc., (London)*, **A267**, 443 (1962).

will be described later. The dehydrogenation reaction (5b) is found not to be important on a thermochemical basis. If this occurred, most CN radicals would be expected to react with water, thus regenerating hydrogen cyanide.[18] On this basis, the reaction (5b) can be excluded.

Yield of Hydrogen. The radiolytic yield of hydrogen, $G(H_2)$, is found to be 0.42, which is independent of the concentration of hydrogen cyanide as well as of that of hydrogen ions, as is illustrated in Fig. 8; it is equal to G_{H_2}, the molecular yield of hydrogen from water.[19] One must, therefore, conclude that hydrogen is not formed from

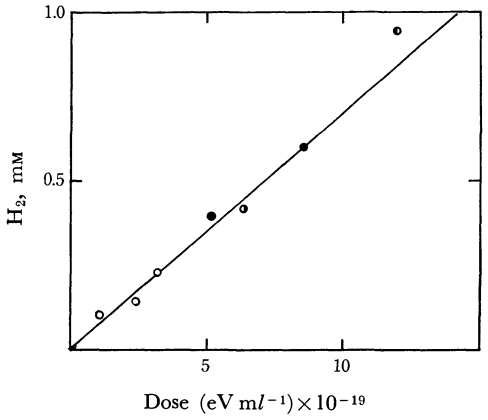

Fig. 8. Formation of hydrogen in γ-irradiated HCN solutions.
6 mM HCN; ◐: pH=1, ◑: pH=2, ○: pH=5.5
30 mM HCN; ●: pH=5.1

the abstraction of hydrogen atom from the HCN molecule:

$$H + HCN \rightarrow H_2 + CN \qquad (6a)$$

As to the fate of the H atom produced primarily from water, an addition to hydrogen cyanide may occur, in which case the adduct will be the methyleneimino radical, H_2CN, according to the reaction (6b):

$$H + HCN \rightarrow H_2CN \qquad (6b)$$

This intermediate has been identified by Cochran *et al.*[19] by means of ESR studies at a low temperature.

Scholes *et al.*[21] have been demontrated a general method of investigating the reactivity of H atoms towards some compound which are not dehydrogenated. This includes the use of 2-propanol and nitrous oxide as scavengers of H atoms and hydrated electrons respectively, and was used in studying the reactivity of H atoms towards hydrogen cyanide in an aqueous solution. In a deaerated N_2O (16 mM)+2-propanol (5—20 mM)+HCN (6 mM) system, the following three processes are involved:

$$e^-_{aq} + N_2O \rightarrow N_2 + OH + OH^- \qquad (4)$$

$$H + HCN \rightarrow H_2CN \qquad (6b)$$

$$H + (CH_3)_2CHOH \rightarrow H_2 + (CH_3)_2COH \qquad (7)$$

In the absence of hydrogen cyanide, the yield of hydrogen, $G(H_2)$, should be equal to $G_H+G_{H_2}$, where G_H denotes the yield of H atoms. In the presence of hydrogen cyanide, $G(H_2)$ is decreased by the simple competition between the reactions (6b) and (7); therefore, the following equation is derived:

$$\frac{1}{G(H_2)-G_{H_2}} = \frac{1}{G_H}\left\{1 + \frac{k_{6b}(HCN)}{k_7(CH_3)_2CHOH}\right\} \qquad (II)$$

where k_{6b} and k_7 represent the rate constants of H atoms with hydrogen cyanide and 2-propanol respectively. The plot of the observed value of $1/[G(H_2)—G_{H_2}]$ against (HCN)/(2-propanol) shown in Fig. 9, indicates the linear relation between the two quantities. From the slope of the line, k_{6b}/k_7 is found to be 1.4; hence, $k_{6b}=3\times 10^7$ M^{-1} sec^{-1}, taking $k_7=2.3\times 10^7$ M^{-1} sec^{-1}.[22]

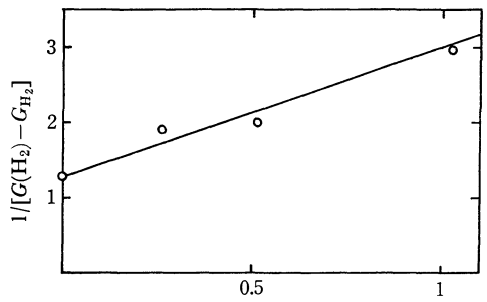

Fig. 9. Competition for H atom between HCN and 2-propanol plotted according to Eq. (II).

Reaction Mechanism. According to the findings described above and the observed yields of products, the following reaction sheme for the present study is proposed:

$$H_2O \text{ -WW-} e^-_{aq}, H, OH, H_2, H_2O_2, H^+_{aq} \qquad (0)$$

As the reactions of the reactive species produced in reaction (0) with hydrogen cyanide, the (1a), (5a), and (6b) reaction have previously been indicated. In addition to these, the reaction (8) can be proposed:

18) R. P. Mitra, D. V. S. Jain, A. K. Bannerjee and K. V. Raghavachari, *Nature*, **200**, 163 (1963).
19) A. O. Allen, "The Radiation Chemistry of Water and Aqueous Solutions," D. Van Norstrand, New York (1961), p. 47.
20) E. L. Cochran, F. J. Adrian and V. A. Bowers, *J. Chem. Phys.*, **36**, 1938 (1962).
21) G. Scholes and M. Simic, *J. Phys. Chem.*, **68**, 1738 (1964).
22) E. Hayon and M. Moreau, *J. Chim. Phys.*, **62**, 301 (1965).

$$HCN^- + H^+ \rightarrow H_2CN \quad (8)$$

Since $G(-HCN)$ is in close agreement with the total radical yield, $G_{e^-_{aq}}+G_H+G_{OH}$, this finding elucidates the fact that reaction intermediates such as HCN^-, H_2CN, and H(OH)CN will not react further with HCN at low concentrations of hydrogen cyanide (6 mM). The fates of these intermediates are supposed to be as follows:

$$H_2CN + H(OH)CN \rightarrow (HCN)_2 + H_2O \quad (9)$$
$$\searrow H_2CNH + HCNO \quad (10)$$

Methyleneimine and cyanic acid are readily hydrolysed to yield ammonia, formaldehyde, and carbon dioxide:

$$H_2CNH + H_2O \rightarrow HCHO + NH_3 \quad (11)$$

$$HCNO + H_2O \rightarrow CO_2 + NH_3 \quad (12)$$

The expected mole ratio of the products, such as $NH_3 : HCHO : CO_2 = 2 : 1 : 1$ from the reactions (11) and (12), is almost equal to that shown in Table 1. The HCN dimer is usually considered to be iminocyanomethane, NH=CH–CN. Serre *et al.*[23] and Matthews *et al.*[24] have pointed out that the HCN dimer would be more stable by 20 kcal/mol in the form of amino cyanomethylene, NH_2–$\dot{C}$=C=$\dot{N}$ (biradical), than in iminocyanomethane. Though neither isomeric form has been isolated, the HCN dimer is likely to grow into a more stable polymeric form, which is considered to be responsible for the broad absorption observed in the UV region. There was observed an increase in the UV absorption with the increase in the HCN concentration resulting from the polymeric products introduced by γ-irradiation, but it was effectively eliminated by the presence of acid or dissolved oxygen, which are effective scavengers of hydrated electrons. These results can most likely be explained in terms of the contribution of the anionic form of HCN as an initiator of the polymerization. as has been indicated by Hummel *et al.*:[14]

$$HCN^- + n HCN \rightarrow \text{polymeric products} \quad (13)$$

The presence of formic acid as a minor product may suggest that formamide is formed by:

$$H(OH)CN + H \searrow$$
$$H_2CN + OH \nearrow H_2NCOH \xrightarrow{H_2O}$$
$$HCOOH + NH_3 \quad (14)$$

Formamide is usually considered to be an intermediate yielding formic acid and ammonia in the course of the hydrolysis of hydrogen cyanide in aqueous solutions.

As is illustrated in Table 1, the observed yield of hydrogen peroxide is fairly low compared with its molecular yield in water;[19] however, its behavior is not clear in detail.

Although more work needs to be done to establish the detail of the system, the mechanism described above appears to be a plausible explanation of the present observation.

The author wishes to express his thanks to Professor M. Kondo of Tokyo Metropolitan University for his interest throughout this work. The author is indebted to Mr. K. Kurita for his assistances in this experimental work.

23) J. Serre and F. Schneider, *ibid.*, **61**, 1655 (1964).
24) C. N. Matthews and R. E. Moser, *Proc. Natl. Acad. Sci.*, **56**, 1087 (1966).

BULLETIN OF THE CHEMICAL SOCIETY OF JAPAN VOL. 41 2877—2881 (1968)

γ-Radiolysis of a Binary Mixture of Methanol and Water. The Formation of Formaldehyde in the Radiolysis of Liquid Methanol

Hiroshi SEKI, Reiko NAGAI and Masashi IMAMURA

The Institute of Physical and Chemical Research, Yamato-machi, Saitama

(Received May 23, 1968)

The γ radiolysis of a binary mixture of methanol and water over a wide concentration range has been investigated. The observed yields of products are expressed as a linear function of the electron fraction of methanol in the mixture. The yields of molecular hydrogen were also determined. Analyzing the results on reasonable assumptions, one could obtain for neutral water, $G^{w}_{e_S^-}=2.3$—2.5 and $G^{w}_{OH}\geq 2.6$. It was concluded that, in the radiolysis of methanol, formaldehyde may be produced through the decomposition of CH_2OH radicals in the spur region, not by the disproportionation of these radicals.

Liquid methanol and water have been long-term subjects of the most extensive study in radiation chemistry, with plenty of information being accumulated, especially for water.[1,2] The radiolysis of liquid methanol is more complicated than that of water and there remain some unsolved problems.

This work was initiated with the hope of obtaining more detailed information about reactions involving the initial species produced in irradiated methanol using precise data on aqueous systems. Although methanol is frequently used as a radical scavenger in the radiolysis of water, few studies on binary mixtures over a wide concentration range have been reported so far.[3,4]

We obtained some interesting results not only on the radiolysis mechanism of methanol but also on that of water, which will be presented in this paper.

Experimental

Extra-pure grade methanol supplied by the Wako Pure Chemical Co. was purified and dried as described previously.[5] Reagent grade anhydrous ferric chloride was used (as a scavenger) without further purification. Water was triply distilled according to Allen's description.[1]

A definite amount of purified water was pipetted into an irradiation ampoule and degassed thoroughly on a vacuum line before adding degassed methanol by distillation. Methanol-water mixtures containing ferric chloride were prepared beforehand and degassed in a small refluxing apparatus.

Irradiation ampoules were made of hard or Pyrex glass and were cleaned carefully as described previously.[5] Irradiation was carried out at room temperature with ^{60}Co γ rays at a dose rate in the vicinity of 1.5×10^{17} eV/ml·min based on a ferrous sulfate dosimeter taking $G(Fe(III))=15.5$. The dose rate was corrected for the electron density of each mixture.

The radiolysis products, hydrogen, carbon monoxide, methane, ethylene glycol and formaldehyde, were determined by methods previously used.[5] Hydrogen peroxide was determined by the Ghormely method.[6]

Results

Yields of Products. In Fig. 1 the observed yields of the main products, hydrogen, ethylene glycol and formaldehyde, were plotted as a function of the electron fraction of methanol, x, in the mixture. $G(H_2)$, $G(C_2H_6O_2)$ and $G(CH_2O)$ all appear to decrease linearly with increasing concentration of water, the yields for pure methanol being determined as 4.92, 2.95 and 2.15, respectively. (The symbol, G, is the yield as expressed by the number of molecules produced per 100eV of absorbed energy.) It should be noted that the extrapolated $G(CH_2O)$ to $x=0$ is not zero but 0.60. No hydrogen peroxide was detected for all mixtures investigated. Several separate experiments definitely indicated that no hydrogen peroxide was present even immediately after irradiation.[7] The yields of carbon monoxide and methane also show a linear dependence, the extrapolated G values to $x=0$ being zero (not shown in Fig. 1).

The observed yields can be expressed by such

1) A. O. Allen, "The Radiation Chemistry of Water and Aqueous Solutions," D. van Nostrand, New York (1961).
2) A. O. Allen, *Radiat. Res., Suppl.* **4**, 54 (1964).
3) W. R. McDonell, *J. Chem. Phys.*, **23**, 208 (1955).
4) Z. Schweiner, I. Janocský and J. Bednář, *Coll. Czech. Chem. Commun.*, **31**, 43 (1966).
5) H. Seki and M. Imamura, *J. Phys. Chem.*, **71**, 870 (1967).
6) C. J. Hochanadel, *ibid.*, **56**, 587 (1952).
7) This series of experiments was carried out by Miss R. Maki.

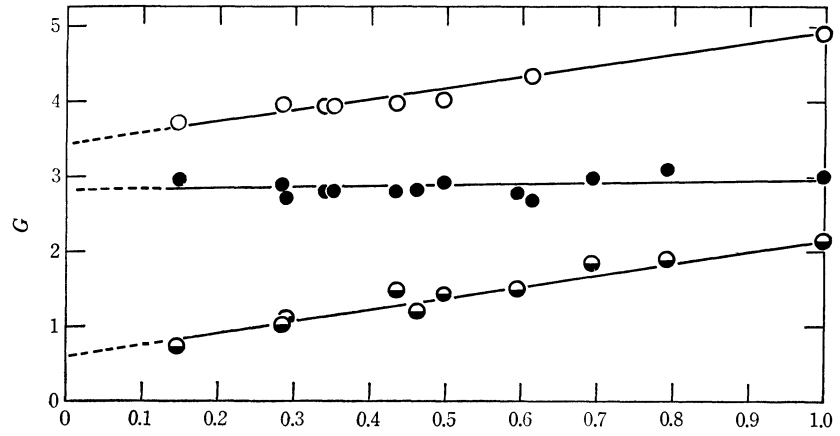

Fig. 1. Yields of hydrogen (○), ethylene glycol (●) and formaldehyde (◒) in methanol-water mixtures irradiated with γ rays.

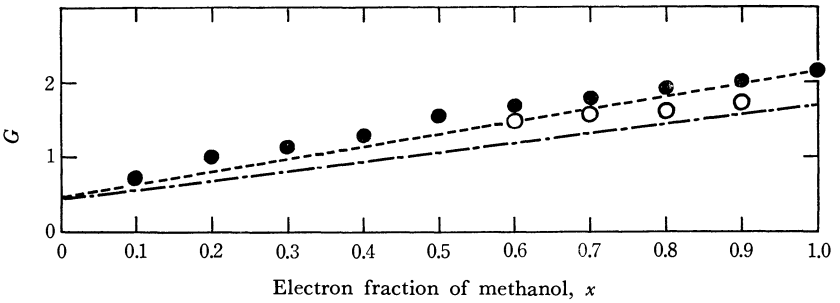

Fig. 2. Yields of the total gas (●) and hydrogen (○) in methanol-water mixtures containing 5×10^{-2} M $FeCl_3$.
----: the line connecting $G^{w}_{H_2}$ and $G_{H_2}+G_{CO}+G_{CH_4}$
·—·: the line connecting $G^{w}_{H_2}$ and G_{H_2}

linear functions of x as

$$G(H_2) = 1.52x + 3.40 \quad \text{(A)}$$

$$G(C_2H_6O_2) = 0.15x + 2.80 \quad \text{(B)}$$

$$G(CH_2O) = 1.55x + 0.60 \quad \text{(C)}$$

Yields of Molecular Hydrogen. The yield of molecular (unscavengeable) hydrogen, G_{H_2}, from γ-irradiated liquid methanol has been determined as 1.6,[8] 1.8[9] and 1.9.[10] We also determined G_{H_2} to be 1.7, using ferric chloride as a scavenger, in good agreement with published data. The yields of molecular methane and carbon monoxide were determined at the same time. Their sum is about 0.3, in agreement with the result of Choi and Lichtin.[10]

The yield of total gas as well as that of hydrogen was also determined for methanol-water mixtures containing 5×10^{-2}M of ferric chloride. The yields are plotted in Fig. 2 as a function of x. Although the plots are not linear, the extrapolated values are very close to the yield of molecular hydrogen from water, $G^{w}_{H_2}$,[11] at $x=0$, and close to the total yield of the molecular gases from methanol, $G_{H_2}+G_{CO}+G_{CH}$, and G_{H_2} at $x=1$. These results apparently indicate that the formation of molecular hydrogen from methanol or water is not prevented at all by the presence of water or methanol, respectively.

Discussion

As early as 1955, McDonell reported the γ radiolysis of methanol-water mixtures, in which only the yields of ethylene glycol and formaldehyde were determined.[3] The variations in yields are similar to the present ones, but there are some differences.

8) J. H. Baxendale and F. W. Mellows, *J. Am. Chem. Soc.*, **83**, 4720 (1961).
9) G. E. Adams and J. H. Baxendale, *ibid.*, **80**, 4125 (1958).
10) S. U. Choi and N. N. Lichtin, *ibid.*, **86**, 3948 (1964).
11) $G^{w}_{H_2}=0.4$ in Ref. 2 and 0.4—0.45 in Proc. 5th Informal Conf. Radiation Chemistry of Water (Univ. Notre Dame 1966), p. 27.

The variation in $G(C_2H_6O_2)$ is linear from 100% methanol ($G=2.9$) down to 30%, the linear portion of the curve to 100% water being extended $G=2.5$. The variation in $G(CH_2O)$ is also linear over the entire range. However, the yield for pure methanol is $G=1.3$ and the extrapolated yield to 100% water is zero.

Recently Schweiner *et al.* observed non-linear variation in $G(H_2)$ for methanol-water mixtures.[4] They assumed that the probability of localization of part of the absorbed energy, leading to hydrogen formation from methanol is higher for a methanol molecule than for a water molecule. No such a deviation from linearity is observed for $G(H_2)$ as well as for other yields in the present study (Fig. 1). The slight deviation observed for G_{H_2} (Fig. 2) might be due, at least in part, to some effect of the relatively high concentration of ferric chloride used, no further discussion being given here.

Equations (A), (B) and (C) could be analyzed on the reasonable assumptions described below.

Hydrogen Yield. Hydrogen is formed by three processes: molecular, ionic and radical processes. Molecular hydrogen is formed separately from methanol and water, the yields of which are represented as G_{H_2} and $G^w_{H_2}$, respectively. As mentioned in Results (Fig. 2). G_{H_2} and $G^w_{H_2}$ are not affected by the presence of water and methanol, respectively. The independent of $G^w_{H_2}$ of the presence of methanol is also supported by results from the radiolysis of aqueous solutions of CD_3OH (0.01—1.0 M).[12] Similar results were obtained in the radiolysis of 2-propanol solutions in D_2O containing nitrous oxide, in which $G(D_2)$ was found constant (0.33) over the concentration range 0.01—1.0 M 2-propanol.[13]

Irradiation of methanol and water produces both solvated electrons and hydrogen atoms. The solvated electrons which arise from methanol and water are assumed to form hydrogen atoms through Reactions (1)—(3).

$$e^-_{solv} + CH_3OH_2^+ \rightarrow H\cdot + CH_3OH \quad (1)$$

$$e^-_{solv} + CH_3OH \rightarrow H\cdot + CH_3O^- \quad (2)$$

$$e^-_{solv} + H_3O^+ \rightarrow H\cdot + H_2O \quad (3)$$

Protonated methanol, $CH_3OH_2^+$, is assumed to form through an ion-molecule reaction similar to that in the gas phase.

$$CH_3OH^+ + CH_3OH \rightarrow CH_3OH_2^+ + CH_3O\cdot, CH_2OH\cdot \quad (4)$$

The hydrogen atoms produced directly both from methanol and water, and indirectly through Reactions (1)—(3) abstract hydrogen atoms from methanol to form hydrogen.

$$CH_3OH + H\cdot \rightarrow H_2 + CH_2OH\cdot \quad (5)$$

Reactions (1) and (2) have been assumed to take place by Baxendale and Mellows,[8] the former being commonly accepted as the principal reaction of the solvated electron in liquid methanol. Reaction (2) has sometimes also been assumed to be the principal reaction.[14] Although the rate constant of Reaction (2) is less than 10^4 M^{-1} sec^{-1},[15] this reaction may become more or less important in the high concentration range of methanol studied.

These assumptions lead to the expression for the yield of hydrogen from the mixtures

$$\begin{aligned} G(H)_2 &= x(G_{H_2} + G_{e^-_s} + G_H) \\ &\quad + (1-x)(G^w_{H_2} + G^w_{e^-_s} + G^w_H) \\ &= x(G_{H_2} + G_{e^-_s} + G_H - G^w_{H_2} - G^w_{e^-_s} - G^w_H) \\ &\quad + (G^w_{H_2} + G^w_{e^-_s} + G^w_H) \end{aligned} \quad (a)$$

Here, the primary yields with superscript w refer to water, those without w to methanol.

Comparison of Eq. (a) with Eq. (A) gives the relations

$$G_{H_2} + G_{e^-_s} + G_H = 4.92 \quad (i)$$

$$G^w_{H_2} + G^w_{e^-_s} + G^w_H = 3.40 \quad (ii)$$

The yield of molecular hydrogen from neutral water seems well-established at 0.4—0.45.[11] The primary yield of hydrogen atoms from neutral water has also been established at 0.55—0.65.[2,16,17] From Eq. (ii), therefore, the yield of hydrated electrons, $G^w_{e^-_s}$, is claculated to be 2.3—2.5.

The yield of hydrated electrons has repeatedly been reported. Czapski and Allen[18] reported 2.85, Allan and Beck[19] 2.80 and Sawai[20] 2.77. Lower values have also been reported: 2.65 by Rabani and Stein,[21] 2.6 by Hochanadel and Casey,[22] 2.45 by Head and Walker,[17] 2.3 by Scholes and Simic,[23] Hayon[24] and Seddon and Allen.[25] A recent study of Russell and Freeman

12) R. Nagai and M. Imamura, to be published.
13) F. S. Dainton, A. R. Gibbs and D. Smithies, *Trans. Faraday Soc.*, **62**, 3170 (1966).
14) J. Teplý and A. Habersbergerová, *Coll. Czech. Chem. Commun.*, **32**, 1350 (1966). For ethanol, J. J. J. Myron and G. R. Freeman, *Can. J. Chem.*, **43**, 1484 (1965); J. W. Fletcher and G. R. Freeman, *ibid.*, **45**, 635 (1967).
15) M. Anbar and P. Neta, *Intern. J. Appl. Radiation Isotopes*, **18**, 493 (1967).
16) E. Hayon, *J. Phys. Chem.*, **68**, 1242 (1964).
17) D. A. Head and D. C. Walker, *Nature*, **207**, 517 (1965); *Can. J. Chem.*, **45**, 2051 (1967).
18) G. Czapski and A. O. Allen, *J. Phys. Chem.*, **66**, 262 (1962).
19) J. T. Allan and C. M. Beck, *J. Am. Chem. Soc.*, **86**, 1483 (1964).
20) T. Sawai, This Bulletin, **39**, 955 (1966).
21) J. Rabani and G. Stein, *J. Chem. Phys.*, **37**, 1865 (1966).
22) C. J. Hochanadel and R. Casey, *Radiation Res.*, **25**, 198 (1965).
23) G. Scholes and M. Simic, *Nature*, **199**, 276 (1962).
24) E. Hayon, *Trans. Faraday Soc.*, **61**, 123 (1965).
25) W. A. Seddon and A. O. Allen, *J. Phys. Chem.*, **71**, 1914 (1967).

gave a "free ion" yield $G^{w}_{e^-_s}=2.7$ according to their model.[26] The current value of 2.3—2.5 for the yield of the hydrated electron is in agreement with those of the lower group. In the present study, however, a plausible reaction which lowers the yield can be taken into account,

$$e^-_{solv} + H_2O_2 \rightarrow OH\cdot + OH^- \qquad (6)$$

which might also be responsible for the absence of hydrogen peroxide in the system. Reaction (6) produces OH radicals, which consecutively give CH_2OH radicals through reaction with methanol. However, as will be discussed in a latter section, the majority of CH_2OH radicals do not give formaldehyde but ethylene glycol in the bulk. The excess yield of formaldehyde observed upon extrapolation of the plot of $G(CH_2O)$ to $x=0$ (Fig. 1) is not accounted for by Reaction (6). Thus the possibility of Reaction (6) may be excluded. The excess yield of formaldehyde will be explained in a latter section.

Equation (i) indicates that the total yield of hydrogen from pure methanol is 4.92, which is the experimental value and is less than the "true" value of 5.40 deduced from the methanol-nitrous oxide system.[5] The discrepacny between these two values has been discussed previously;[5] a few experiments show that the values of $G(H_2)+G(N_2)$ obtained from methanol-waterm ixtures containing nitrous oxide fall on the line connecting $G=5.4$ ($x=1$) and 3.4 ($x=0$).

Ethylene Glycol Yield. Ethylene glycol is produced, except for a minor portion by a molecular process, by a combination reaction of CH_2OH radicals

$$2CH_2OH\cdot \rightarrow C_2H_6O_2 \qquad (7)$$

Hydroxymethyl radicals are produced through the reaction of methanol with all radicals, R·, produced in the solution (H· (including H· produced by Reactions (1)—(3)), OH·, CH_3·, CH_3O· and CH_2OH·)

$$CH_3OH + R\cdot \rightarrow CH_2OH\cdot + RH \qquad (8)$$

It is sometimes assumed that some CH_2OH radicals give rise to the formation of formaldehyde through the disproportionation reaction

$$2CH_2OH\cdot \rightarrow CH_2O + CH_3OH \qquad (9)$$

On the basis of the assumptions made above, the yield of ethylene glycol in the present system can be expressed as

$$G(C_2H_6O_2) = x\left(G_{C_2H\ o_2} + \frac{\alpha}{2}G_R\right) + (1-x)\frac{\alpha}{2}(G^{w}_{e^-_s} + G^{w}_{H} + G^{w}_{OH})$$

$$= x\left[G_{C_2H_6O_2} + \frac{\alpha}{2}G_R - \frac{\alpha}{2}(G^{w}_{e^-_s} + G^{w}_{H} + G^{w}_{OH})\right] + \frac{\alpha}{2}\left(G^{w}_{e^-_s} + G^{w}_{H} + G^{w}_{OH}\right) \qquad (b)$$

The molecular yield of ethylene glycol from pure methanol, $G_{C_2H_6O_2}$, has been determined as 0.09[27]—0.1.[10] The factor, α, represents the fraction of CH_2OH radicals which produce ethylene glycol

$$\alpha = k_7/(k_7 + k_9)$$

The superscript w refers to water, as before.

Comparing Eq. (b) with Eq. (B), one obtains the relations

$$\alpha(G^{w}_{e^-_s} + G^{w}_{H} + G^{w}_{OH}) = 5.60 \qquad (iii)$$

$$\alpha G_R = 5.72 \qquad (iv)$$

In the preceding section, we came to the conclusion that $G^{w}_{e^-_s}=2.3-2.5$ depending upon the values of $G^{w}_{H_2}$ and G^{w}_{H}. It is easily found, however, that, from Eqs. (ii) and (iii),

$$G^{w}_{OH} \geq 2.6$$

because α should not exceed unity.

On the other hand, the total yield of radicals from methanol has been determined experimentally as 6.2,[10] which is in agreement with other results.[8] If the value of 6.2 is used for G_R in Eq. (iv), α is calculated to be 0.92. The rate-constant ratio of disproportionation to combination of CH_2OH radicals, k_9/k_7, is then 0.087.[28] Applying $\alpha=0.92$ to Eq. (iii), one obtains $G^{w}_{OH}=3.0$, which is higher than the value quoted by Allen ($G=2.2$).[2]

Daniels and Wigg[29] reported $G^{w}_{OH}=2.53\pm0.10$ for NO_3^- solution, and similar and higher values have also been reported by Hochanadel and Casey[22] (2.59 for $CO+H_2$ solution), by Seddon and Sutton[30] (2.9 for NO solution) and by Sawai[20] (3.0 for 2-propanol+NO_3^- solution). Although it is not possible to give a satisfactory account for the discrepancy at present, it should be emphasized that α is close to unity, *i. e.*, the contribution of the disproportionation reaction of CH_2OH radicals to the formation of formaldehyde is rather small.

Formaldehyde Yield. As described in Results, no hydrogen peroxide was detected in

26) J. C. Russell and G. R. Freeman, *J. Chem. Phys.*, **48**, 90 (1968).

27) M. Imamura and H. Seki, *Sci. Papers Inst. Phys. Chem. Res.*, **59**, 146 (1965).

28) No such a rate-constant ratio seems to have been reported for the CH_2OH radical, the results for several alkyl radicals being published. *Cf.*, J. A. Kerr and A. F. Trotman-Dickenson, "Progress in Reaction Kinetics," Vol. 1, ed. by G. Porter, Pergamon Press, Oxford (1961), p. 105; J. O. Terry and J. H. Futrell, *Can. J. Chem.*, **45**, 2327 (1967), and the papers cited therein. It is to be noted that k_9/k_7 has been assumed to be $\approx$0.2 for CH_2OH radicals in the aqueous medium. (P. Kelly and M. Smith, *J. Chem. Soc.*, **1961**, 1487).

29) M. Daniels and E. E. Wigg, *Science*, **153**, 1533 (1966); *J. Phys. Chem.*, **71**, 1024 (1967).

30) W. A. Seddon and H. C. Sutton, *Trans. Faraday Soc.*, **59**, 2323 (1963).

the present system. Similar results have been found for the deaerated neutral ethanol solution,[31] which was ascribed to the efficient secondary decomposition of hydrogen peroxide. In the present study, the extrapolated value of $G(CH_2O)$ to $x=0$ is 0.60 (Fig. 1), which is very close to the value for $G^{w}_{H_2O_2}$.[2] We therefore assume that this excess yield of formaldehyde results from the reaction of the CH_2OH radical with hydrogen peroxide produced molecularly from water.

$$CH_2OH\cdot + H_2O_2 \rightarrow CH_2O + H_2O + OH\cdot \quad (10)$$

A similar reaction has been suggested for C_2H_4OH radicals.[25] The occurrence of Reaction (10) does not reduce $G(C_2H_6O_2)$ because OH radicals will regenerate CH_2OH radicals.

An alternative explanation for the absence of hydrogen peroxide might be given by assuming reaction occurs between the precursor of molecular hydrogen peroxide and methanol. It does not seem that the precursor of molecular hydrogen peroxide in the radiolysis of water has been well-defined, some species other than OH radicals being proposed.[32,33] Such a reaction being assumed to occur, the possibility of OH radical being the precursor of molecular hydrogen peroxide can be excluded also from the fact that an excess yield of aldehyde is close to the value corresponding to $G^{w}_{H_2O}$. If OH radical is the precursor of molecular hydrogen peroxide, scavenging the radical with methanol in the spur region would give rise to the formation of a CH_2OH radical, most of which forms ethylene glycol as discussed in the preceding section. No further discussion on the nature of the precursor is given here.

Several reaction mechanisms for the formation of formaldehyde in the radiolysis of methanol have been discussed. Of possible mechanisms, the disproportionation reaction of CH_2OH radicals (Reaction (9)) has been ruled out as mentioned above. The disproportionation reaction of CH_3O radicals has also been proposed, especially to explain the increasing yield of formaldehyde in the radiolysis of liquid methanol by high LET (linear energy transfer) radiations[34,35]

$$2CH_3O\cdot \rightarrow CH_2O + CH_3OH \quad (11)$$

In fact, the isotopic composition of hydrogen produced by γ radiolysis of CH_3OD shows that $HD > H_2$,[36] indicating the primary yield of the CH_3O radical is greater than that of the CH_2OH radical. If Reaction (11) is responsible for the increasing yield of formaldehyde in the dense ionization tracks of the high LET radiations, the isotopic composition of the hydrogen produced in such systems should also show a tendency similar to that observed for γ radiolysis. This is not the case, but it was found that $H_2 > HD$ for radiolysis with recoiled α, ^{7}Li-particles.[36] Therefore, the second possibility as represented by Reaction (11) may be unimportant.

The remaining possibilities are molecular detachment[37,38]

$$CH_3OH \rightarrow CH_2O + H_2 \quad (12)$$

and thermal decomposition of CH_2OH radicals[37]

$$CH_2OH\cdot \rightarrow CH_2O + H\cdot \quad (13)$$

Both reactions have been proposed for the photolysis of methanol vapor. Phibbs and Darwent found that the activation energy of Reaction (13) is 29 kcal/mol, and pointed out that the reaction is increasingly important above 400°C.[37]

It may be reasonable, from the above discussions, to assume that in the radiolysis of liquid methanol, formaldehyde may be produced molecularly (in the spur region) by Reaction (13) and/or Reaction (12). The increasing yield of formaldehyde in radiolysis with high LET radiations may therefore be explained by assuming thermal spikes in these radiation tracks, which will promote Reaction (13) to produce formaldehyde in a higher yield. Similar processes have also been proposed by McDonell and Gordon.[39]

Now, the observed yield of formaldehyde can be expressed as

$$\begin{aligned} G(CH_2O) &= xG_{CH_2O} + (1-x)G^{w}_{X} \\ &= x(G_{CH_2O} - G^{w}_{X}) + G^{w}_{X} \end{aligned} \quad (c)$$

Here, G^{w}_{X} corresponds to $G^{w}_{H_2O_2}$, as mentioned above. From Eq. (C) and Eq. (c), the molecular yield of formaldehyde from pure methanol is 2.15.

31) G. G. Jayson, G. Scholes and J. Weiss, *J. Chem. Soc.*, **1957**, 1358.
32) M. Anbar and I. Pecht, *J. Chem. Phys.*, **44**, 3635 (1966).
33) G. Hughes and C. Willis, *Discussions Faraday Soc.*, **36**, 223 (1963).
34) L. M. Theard and M. Burton, *J. Phys. Chem.*, **67**, 59 (1963).
35) M. Imamura, S. U. Choi and N. N. Lichtin, *J. Am. Chem. Soc.*, **85**, 3565 (1963).
36) H. Seki and M. Imamura, *J. Chem. Phys.*, **48**, 1866 (1968).
37) M. K. Phibbs and B. deB. Darwent, *ibid.*, **18**, 495 (1950).
38) R. P. Porter and W. A. Noyes, Jr., *J. Am. Chem. Soc.*, **81**, 2307 (1959); R. F. Pottie, A. G. Harrison and F. P. Lossing, *Can. J. Chem.*, **39**, 102 (1961).
39) W. R. McDonell and S. Gordon, *J. Chem. Phys.*, **23**, 208 (1955).

BULLETIN OF THE CHEMICAL SOCIETY OF JAPAN VOL. 41 2882—2886 (1968)

ESR and Optical Studies of the Reaction Intermediates Produced from Phenyl Halides by Dissociative Electron Attachment in γ-Irradiated Organic Glasses at 77°K

Syozi NODA, Kenji FUEKI and Zen-ichiro KURI

Department of Synthetic Chemistry, Faculty of Engineering, Nagoya University, Chikusa-ku, Nagoya

(Received May 29, 1968)

ESR and optical studies have been made of dissociative electron attachment by phenyl halides and reaction intermediates produced in γ-irradiated glassy solid matrices at 77°K. Dissociative electron attachment by phenyl halides is an efficient process and the ratio of cross sections $C_6H_5I/C_6H_5Br/C_6H_5Cl$ for this process in MTHF glass is 1.5/1.0/1.0. The phenyl radical produced abstracts a hydrogen atom from solvents (MTHF, 3MP) at 77°K and is stable in aqueous alkali-metal hydroxide glass. A part of 3MP radicals in a γ-irradiated solution of phenyl bromide in 3MP at 77°K disappear by a first-order process for which $k=4.3\times10^{-2}$ min^{-1}. γ-Irradiated 3MP glasses containing phenyl halides exhibit the optical absorption spectra having characteristic absorption bands in the visible and UV region which are assigned to solute cations and hydrogen-adducts respectively.

Dissociative electron attachment by organic halides ($RX+e^-\rightarrow R+X^-$) has been shown by ESR[1,2] and optical[3] measurements to be an efficient process in glassy solid matrices whenever the electron affinity of X exceeds the bond dissociation energy of R-X. Consequently, low concentrations of organic halides may serve as electron scavengers in radiolytic systems. It is also expected that dissociative electron attachment could selectively yield the radical R from organic halides RX. Most of the previous studies are concerned with alkyl halides as solutes.

In the present work, a study was made of dissociative electron attachment by phenyl halides in γ-irradiated organic glasses and reaction intermediates produced in these systems at 77°K. ESR and optical absorption techniques were applied to detect the reaction intermediates.

Experimental

Materials. MTHF was purified by passing through an activated alumina column. 3MP and *n*-butyl chloride were purified by passing through a silica-gel column. Solvents were dried with calcium hydride. Commercially available purest phenyl halides were used with purification by vacuum distillation.

Sample Preparation. Phenyl halide was stored in vacuum and was distilled from the storage bulb, pipetted into an ESR tube or an optical absorption cell containing a known amount of solvent, then returned to the vacuum line and degassed by conventional vacuum techniques before sealing the tube or the cell.

Irradiations, ESR and Optical Measurements. Samples were prepared, γ-irradiated and measured in quartz ESR tubes (i. d. 5 mm) or optical absorption cells (1 cm × 1 cm), sealed in vacuum and immersed in liquid nitrogen prior to irradiation and subsequent measurements. They were examined using a JES-3BX ESR spectrometer and a Hitachi-Perkin-Elmer-139 UV-VS spectrophotometer. Doses were 2.3×10^5 rad and 8.0×10^4 rad for ESR and optical experiments, respectively. Photobleaching of γ-irradiated samples was performed with visible light from a tungsten lamp and using glass filters as needed.

Results

Phenyl Halides in MTHF. γ-Irradiated MTHF glasses containing phenyl halides displayed the ESR spectrum of trapped electron superimposed on that of MTHF radical, the intensity of their signals depending on solute concentration. Figure 1 shows the dependence of trapped electron or MTHF radical concentration on the concentration of phenyl iodide. It can be seen from Fig. 1 that the concentration of trapped electrons decreases and that of MTHF radicals increases with increasing phenyl iodide concentration. The concentration of MTHF radicals approaches to a limiting value of twice that of the radicals in pure MTHF at *ca.* 2 mol% solute concentration, while the concentration of trapped electrons is nearly zero at the same solution concentration.

A γ-irradiated MTHF glass containing 1.0 mol% phenyl iodide did not exhibit any absorption bands in the wavelength region $\lambda > 300$ mμ in

1) D. W. Skelly, R. G. Hayes and W. H. Hamill, *J. Chem. Phys.*, **43**, 2795 (1965).
2) R. F. C. Claridge and J. E. Willard, *J. Am. Chem. Soc.*, **87**, 4992 (1965).
3) J. B. Gallivan and W. H. Hamill, *J. Chem. Phys.*, **44**. 1279 (1966).

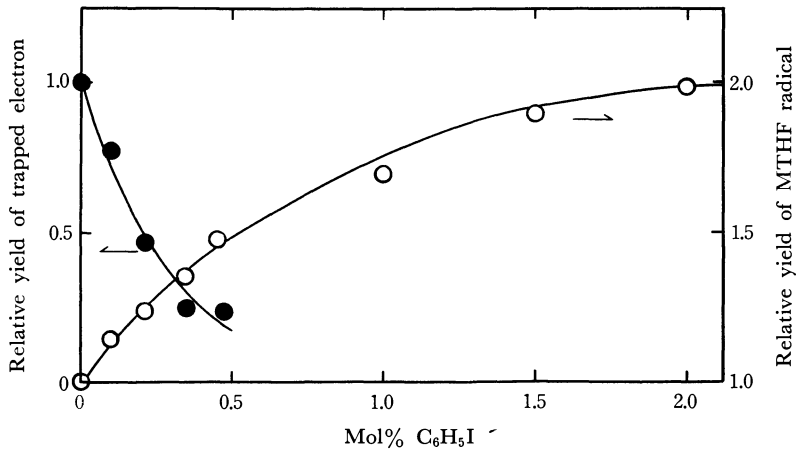

Fig. 1. Dependence of the yields of trapped electron and MTHF radical on phenyl iodide concentration in γ-irradiated solutions of phenyl iodide in MTHF at 77°K.

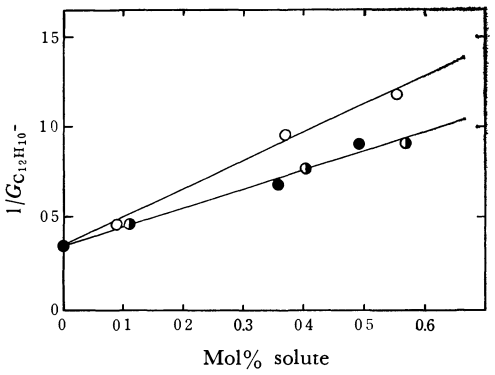

Fig. 2. $1/G_{C_{12}H_{10}^-}$ *vs.* mol% phenyl halides in γ-irradiated MTHF solutions containing 0.15 mol% biphenyl at 77°K.
○, C_6H_5I; ◑, C_6H_5Br; ●, C_6H_5Cl

the optical absorption spectrum. Figure 2 shows a plot of $1/G_{C_{12}H_{10}^-}$ *vs.* the concentration of phenyl halides (iodide, bromide, and chloride) in MTHF solutions containing 0.15 mol% biphenyl. $G_{C_{12}H_{10}^-}$ is the *G*-value for biphenyl anions formed. There are linear relationships between these quantities for all the solutes. Optical measurements were made for determination of the yield of biphenyl anion, in which the extinction coefficient for biphenyl anion was taken to be 3.7×10^4 $l\,mol^{-1}\cdot cm^{-1}$ at 410 mμ.[4] As shown in Fig. 2, straight lines drawn through the experimental points can be extrapolated to the same point on the ordinate.

Phenyl Halides in 3MP. The ESR spectrum of γ-irradiated 3MP glass containing 0.2 mol% phenyl iodide was similar in shape to that of pure 3MP glass, indicating only the solvent radical (Fig. 3). However, the amount of solvent radicals produced in 3MP containing phenyl iodide was larger than that in pure 3MP under the same irradiation condition.

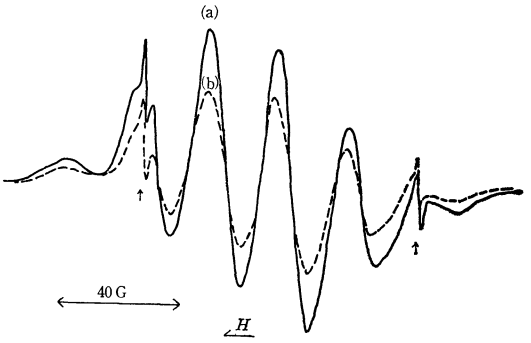

Fig. 3. ESR spectra of γ-irradiated 3MP solutions with and without phenyl iodide at 77°K. (a) 3MP containing 0.2 mol% phenyl iodide; (b) pure 3MP. Arrows indicate the signal of Mn.

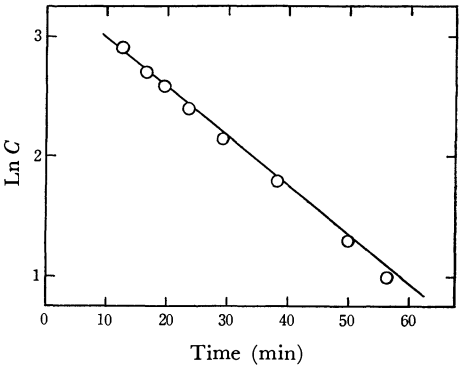

Fig. 4. First-order plot for the decay of 3MP radical in a γ-irradiated solution of 0.2 mol% phenyl bromide in 3MP at 77°K. *C*, concentration of 3MP radical in arbitrary unit.

4) M. R. Ronayne, J. P. Guarino and W. H. Hamill, *J. Am. Chem. Soc.*, **84**, 4230 (1962).

In γ-irradiated 3MP glasses containing phenyl halides, a part of solvent radicals disappeared much rapidly than those in pure 3MP glass. A first-order plot for the decay of such 3MP radicals at 77°K is shown in Fig. 4. The decay rate for these radicals is obtained to be $k=4.3\times10^{-2}$ min^{-1}. After the rapidly decaying 3MP radicals had disappeared, residual 3MP radicals disappeared very slowly as those in pure 3MP.

3MP glasses containing phenyl iodide or bromide, after γ-irradiation, exhibited the optical absorption spectra as shown in Fig. 5 or 6. In a 3MP glass containing 0.2 mol% phenyl iodide, the absorption bands having $\lambda_{max}=300$, 560 and 710 mμ were observed in the spectrum obtained 0.5 hr after termination of the γ-irradiation. Although the 300 mμ band did not change with time, the 710 mμ band decreased in intensity and new absorption bands having $\lambda_{max}=410$ and 520 mμ appeared in the spectrum obtained 2 hr after termination of the γ-irradiation. In a 3MP glass containing 0.2 mol% phenyl bromide, the absorption bands having $\lambda_{max}=290$ and 620 mμ and a shoulder at 330 mμ were observed in the spectrum obtained 0.5 hr after termination of the γ-irradiation. The 620 mμ band decreased in intensity and the 330 mμ band increased in the spectrum obtained 1.5 hr after termination of the γ-irradiation, while the 290 mμ band did not change with time. In a 3MP glass containing phenyl chloride, the absorption band having $\lambda_{max}=580$ mμ was observed and other bands were too broad for their maxima to be discernible in the spectrum.

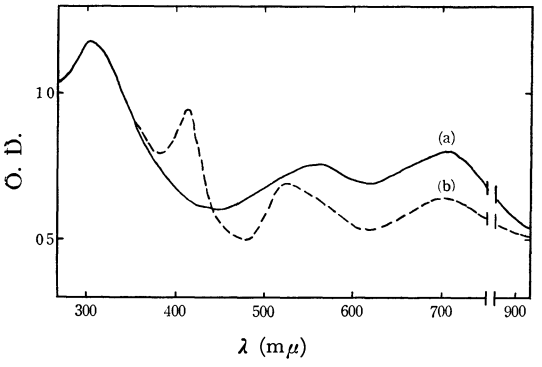

Fig. 5. Absorption spectra of a γ-irradiated solution of 0.2 mol% phenyl iodide in 3MP at 77°K. (a) 0.5 hr, (b) 2 hr after termination of the γ-irradiation.

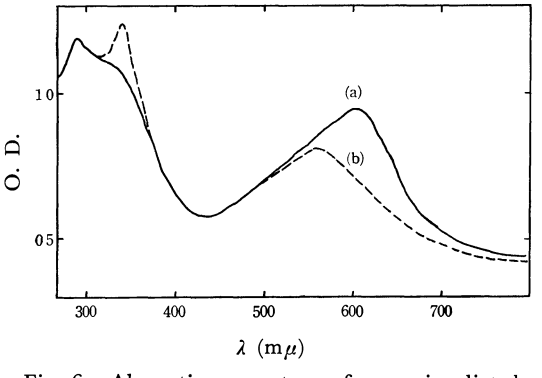

Fig. 6. Absorption spectra of a γ-irradiated solution of 0.2 mol% phenyl bromide in 3MP at 77°K. (a) 0.5 hr, (b) 1.5 hr after termination of the γ-irradiation.

Phenyl Halides in *n*-BuCl. It was found by ESR measurements that the yield of solvent radicals produced in γ-irradiated *n*-BuCl glass containing 1.0 mol% phenyl iodide was nearly equal to that in pure *n*-BuCl glass under the same irradiation condition.

γ-Irradiated *n*-BuCl glasses containing 0.5 mol% phenyl iodide or bromide displayed the optical absorption spectra having an absorption band with $\lambda_{max}=710$ or 620 mμ, respectively, in addition to the bands attributable to the intermediates from *n*-BuCl.

Phenyl Halides in Aqueous Alkali-metal Hydroxide Glass. γ-Irradiated glassy aqueous solutions of 10 mol% NaOH containing a saturated concentration of phenyl iodide exhibited a narrow

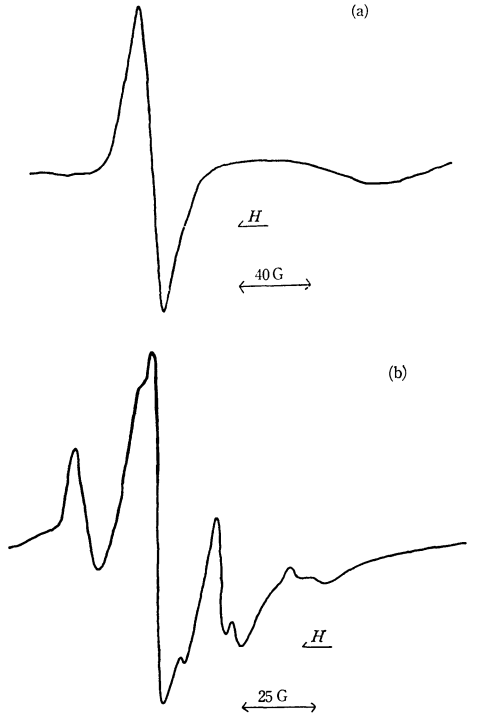

Fig. 7. ESR spectra of a γ-irradiated 10 mol% NaOH aqueous solution containing a saturated concentration of phenyl iodide at 77°K. (a) before photobleaching, (b) after photobleaching with visible light. The spectrum (b) was obtained using a 50 times greater sensitivity than the spectrum (a).

ESR singlet at $g=2.001$ and a broad singlet in the lower magnetic field (Fig. 7(a)). Photobleaching of the same sample as the preceding with visible light yielded the spectrum with the hyperfine structure as shown in Fig. 7(b).

Discussion

It is well known that trapped electrons are produced in γ-irradiated MTHF glass at 77°K.[4,5] The results that the yield of trapped electrons decreases in the presence of phenyl halides indicate that phenyl halides compete with the solvent for capturing electrons. Electrons are captured almost completely by phenyl iodide at *ca.* 2 mol% concentration in MTHF. On the other hand, the yield of MTHF radicals increases with phenyl iodide concentration, approaching to a limiting value of twice that of the radicals in pure MTHF. It is generally accepted that the MTHF radical is formed by the ion-molecule reaction $C_5H_{10}O^+ + C_5H_{10}O \rightarrow C_5H_{10}OH^+ + C_5H_9O$ in γ-irradiated pure MTHF.[6,7] The increase in the yield of MTHF radicals observed in MTHF solutions containing phenyl iodide is interpreted in terms of H-abstraction by phenyl radicals from the solvent. When electrons are captured completely by phenyl halides, the yield of phenyl radicals formed should be equal to that of MTHF cations. Therefore, at sufficiently high concentrations of phenyl iodide, the yield of MTHF radicals reaches twice that in pure MTHF.

The relative cross section for electron attachment is obtained by making use of competitive reactions for electrons between a reference solute and other solutes in MTHF. A simple kinetic treatment leads to the relation[8]:

$$\frac{1}{G_{Y^-}} = \frac{1}{G^\circ_{Y^-}} + \frac{1}{G^\circ_{Y^-}} \frac{\sigma_X[X]}{\sigma_Y[Y]} \qquad (1)$$

where Y is a reference solute of known anion spectrum, X any second solute, and σ_Y and σ_X are the respective electron attachment cross sections. G_{Y^-} and $G^\circ_{Y^-}$ are the G-values for formation of anion Y^- in solutions with and without the second solute respectively. A plot of $1/G_{Y^-}$ *vs.* $[X]$ with a fixed concentration of Y yields the relative cross section σ_X/σ_Y and extrapolation of this plot to $[X]=0$ gives $G^\circ_{Y^-}$ in Eq. (1). In the present study, in which biphenyl is used as the reference solute, $G^\circ_{Y^-}$ is obtained as 2.9 which is in agreement with the literature value.[4] The ratio of cross sections $C_6H_5I/C_6H_5Br/C_6H_5Cl$ for dissociative electron attachment in MTHF is 1.5/1.0/1.0.

The increase in the yield of 3MP radicals observed in 3MP glasses containing phenyl halides is also interpreted in terms of H-abstraction by phenyl radicals from the solvent.*1 Such an interpretation is supported by the fact that the yield of benzene formed is equal to the decrease in hydrogen yield in the radiolysis of methylcyclohexane glass at 77°K.[9]

A part of 3MP radicals produced in a 3MP solution containing phenyl bromide at 77°K disappear rapidly by a first order process unitl the concentration of 3MP radicals in this solution becomes equal to that produced in pure 3MP under the same irradiation condition, and the residual 3MP radicals disappear very slowly as those in pure 3 MP. The 3MP radicals which disappear rapidly may combine with some intermediates formed in close proximity to those 3MP radicals. Aggregation of phenyl halides in 3MP glass may be responsible for this phenomenon, because such a rapid decay of solvent radicals as that in 3MP glass is not observed in MTHF glass. Aggregation of alkyl iodides in 3MP glass at 77°K has previously been suggested by Claridge and Willard[10] and Mittal and Hamill.[11] The detailed mechanism for the rapid decay of 3MP radicals has not yet been established.

The narrow ESR singlet and the broad singlet observed in a γ-irradiated aqueous alkali-metal hydroxide glass containing phenyl iodide are apparently the same as those in an aqueous alkali-metal hydroxide glass without the solute. These singlets are attributed to trapped electrons and the O^- radical ions respectively.[12-18] The ESR spectrum obtained after photobleaching of the tra ed electron si nal is identified with that of the phenyl radical.[19] The low yield of phenyl radicals observed is probably due to the low solubility of phenyl iodide in aqueous solution at 77°K.

5) D. R. Smith and J. J. Pieroni, *Can. J. Chem.*, **43**, 876 (1965).
6) F. S. Dainton and G. A. Salmon, *Proc. Roy. Soc.*, **A285**, 319 (1965).
7) T. Shida and W. H. Hamill, *J. Chem. Phys.*, **44**, 4372 (1966).
8) J. P. Guarino, M. R. Ronayne and W. H. Hamill, *Radiation Res.*, **17**, 379 (1962).

*1 H-abstraction by phenyl radicals from alkanes at 77°K has previously been shown by Bennett *et al.* (Ref. 19).
9) T. Kimura, T. Miyazaki, K. Fueki and Z. Kuri, unpublished results.
10) R. F. C. Claridge and J. E. Willard, *J. Am. Chem. Soc.*, **89**, 510 (1967).
11) J. P. Mittal and W. H. Hamill, *ibid.*, **89**, 5749 (1967).
12) D. Schulte-Frohlinde and K. Eiben, *Z. Naturforsch.*, **17a**, 445 (1962); *ibid.*, **18a**, 199 (1963).
13) M. J. Blandamer, L. Shields and M. C. R. Symons, *Nature*, **200**, 902 (1963); *J. Chem. Soc.*, **1964**, 4352.
14) T. Henriksen, *Radiation Res.*, **23**, 63 (1964).
15) P. N. Moorthy and J. J. Weiss, *Phil. Mag.*, **10**, 659 (1964).
16) P. B. Ayscough, R. G. Collins and F. S. Dainton, *Nature*, **205**, 965 (1965).
17) L. Kevan, *J. Am. Chem. Soc.*, **87**, 1481 (1965).
18) J. Zimbrick and L. Kevan, *J. Chem. Phys.*, **47**, 2364 (1967).
19) J. E. Bennett, B. Mile and A. Thomas, *Proc. Roy. Soc.*, **293**, 346 (1966).

It is understandable in view of the difference in bond dissociation energy between C-H and O-H that the phenyl radical can abstract an H-atom from the solvents in MTHF and 3MP glasses, but not in aqueous alkali-metal hydroxide glass at 77°K.

The 300 or 290 mμ band in the optical absorption spectrum of γ-irradiated 3MP glass containing phenyl iodide or bromide is attributed to H-atom addition to the benzene ring.[20] The 710, 620 and 580 mμ bands observed in 3MP containing phenyl iodide, bromide and chloride are attributed to the respective halide cations, because the same absorption bands are observed in *n*-BuCl glass, in which positive holes migrate to the solutes and electrons are trapped in the matrix.[7] Recently, Baker *et al.* have measured various ionization potentials of phenyl halides by photoelectron spectroscopy.[21] According to their results, the difference in energy between the lowest and second ionization energy bands is $\sim$2 eV, which is in general agreement with the transition energies of the cation bands observed in the present study. The lowest ionization energy bands are attributed to the removal of an electron from the orbitals corresponding to the highest occupied π orbitals in benzene and the second ionization energy bands to the removal of an electron from halogen lone pairs. Thus the observed cation bands are attributed to the $n\rightarrow\pi$ transition of an electron in the phenyl halide cations. The assignment of the 560 mμ band observed in γ-irradiated phenyl iodide in 3MP glass is not established at present.

Since the 410 and 520 mμ bands observed in γ-irradiated 3MP glass containing phenyl iodide increase in intensity with time after termination of the γ-irradiation, these bands must be attributed to secondary intermediates produced by the reaction between primary intermediates. These bands are tentatively assigned to a complex, $C_6H_5I\cdot I$, which may be produced by ion recombination between $C_6H_5I^+$ and I^-. Such an assignment is consistent with the result that the cation band decreases in intensity with time. The 390 and 480 mμ bands produced by γ-irradiation of alkyl iodides (RI) in alkane matrices at 77°K have previously been assigned to $RI\cdot I$.[11] However, the possibility of I_2^- [10] for the 410 mμ band cannot be excluded at present. The 330 mμ band observed in 3MP containing phenyl bromide may be attributed to $C_6H_5Br\cdot Br$, although the possibility of Br_2^- cannot be excluded. Further study is required to establish the assignment of the secondary reaction intermediates.

20) B. Chutny, *Nature*, **213**, 593 (1967).
21) A. D. Baker, D. P. May and D. W. Turner, *J. Chem. Soc., (B)*, **1968**, 22.

BULLETIN OF THE CHEMICAL SOCIETY OF JAPAN VOL. 41 2886—2894 (1968)

On the Isomerization of Dimers of Perchloro-(3,4-dimethylenecyclobutene) as Revealed by X-ray Methods

Akio FURUSAKI

Faculty of Science, Kwansei Gakuin University, Nishinomiya

(Received June 6, 1968)

The isomerization of several dimers of perchloro-(3,4-dimethylenecyclobutene) (I) has recently been reported by Fujino *et al.* Of these dimers, one (II) is transformed to other isomers (IIIa) and (IIIb) by means of pyrolysis at *ca.* 200°C. When heated to *ca.* 250°C, IIIa and IIIb are further converted into a fourth isomer (IV). The present X-ray study has revealed that II corresponds to perchloro-(3,4,7,8-tetramethylene-tricyclo[4.2.0.$0^{2,5}$]octane), as supposed from the chemical evidence, and IV, to perchloro-(4,8-dimethylene-tricyclo[3.3.2.$0^{1,5}$]deca-2,6-diene). It has been further established, from the results of the X-ray analysis of the dichloride of IIIa with the help of the chemical information, that IIIa and IIIb have the same two-dimensional chemical structure, perchloro-(3,4,7,8-tetramethylene-cycloocta-1,5-diene), rather than perchloro-(2,3,7,8-tetramethylene-bicyclo[4.2.0]octa-4-ene) which was speculated by Fujino *et al.*, and that IIIa and IIIb are different from each other in the conformation of the cyclooctadiene ring. These structures for II, IIIa, IIIb, and IV give a reasonable explanation of the mechanism of the successive isomerization reactions mentioned above.

It has been reported by Fujino *et al.* that the pyrolysis of perchloro-(3,4-dimethylenecyclobutene) (I) affords, depending on the heating temperature applied, at least four different isomeric

compounds, $C_{12}Cl_{12}$.[1] Of these isomers, one (II), mp 166°C, is obtained from I in a 30% yield by means of pyrolysis at *ca.* 160°C, as is shown in Fig. 1. When heated to *ca.* 200°C, either as it is

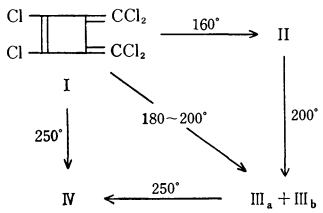

Fig. 1. The relationship among the four isomers of the formula $C_{12}Cl_{12}$.

or in the medium of nitrobenzene, II is further transformed to a mixture of other isomers, (IIIa) and (IIIb), in which IIIa with a mp of 215°C dominates IIIb, mp 262°C. These two isomers show very similar IR absorption spectra in spite of fairly different chemical behavior. With the exception of its melting point, which is close, IIIb is different from II in all respects. Lastly, the application of pyrolysis at *ca.* 250°C to III results in a low-yield formation of the fourth isomer (IV), mp 273°C. III and IV are also derived directly from I through pyrolysis at 180—200°C and 250°C respectively. The yields are, however, much lower than those in the step-by-step conversion, since the direct transformation is always accompanied by the production of perchlorobenzene (ordinarily the major product), perchlorofulvene, perchloro-4-methylenecyclopent-1-ene, and an uncharacterized glassy material with the composition of $(CCl)_x$, which is the major product, particularly in higher-temperature pyrolyses in a solution.

Of the four isomers produced in the course of the pyrolytic transformation described above, II has been supposed, on the basis of the chemical analysis, to be perchloro-(3,4,7,8-tetramethylene-tricyclo[4.2.0.0^{2,5}]octane) (V).[1] Further, it has been tentatively proposed, on the basis of the chemical and IR data, that the two-dimensional chemical structure of IIIa and that of IIIb are both perchloro-(2,3,7,8-tetramethylene-bicyclo-[4.2.0]octa-4-ene) (VI).[1] On the other hand, the structure determination of IV by means of the chemical analysis did not seem feasible because of the poor yield of the compound in the pyrolytic reaction.

It is the purpose of the present study to confirm, or to determine by means of X-ray analysis, the molecular structures of II, III, and IV, and to elucidate the mechanism of the successive isomerization reactions. Of these substances, the molecular structures of II[2] and IV[3] have already been determined by such methods and found to correspond to V and VII respectively. Since, unfortunately, the sample supplied as IIIb was not such, but the dichloride of IIIa, the X-ray analysis has been carried out with this compound. However, the structure determination of the dichloride has enabled us to conclude unequivocally the structures of IIIa and IIIb.

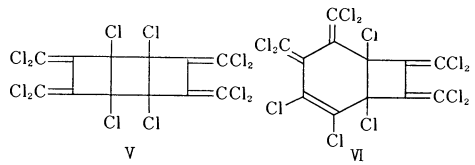

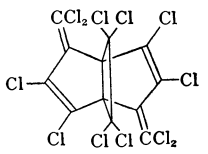

VII

All the samples used in the present experiment were kindly supplied by Professor Akira Fujino, Research Institute for Atomic Energy, Osaka City University. The calculations necessary for the present study were carried out on a Bendix G-20 computer at the C. Itoh Electronic Computing Service Co., Ltd., and on a HITAC 5020 computer at the University of Tokyo, using programs devised at this laboratory.

Structure Determination of th Dichloride of IIIa

Experimental. The crystals of the dichloride of the isomer IIIa were colorless and in the shape of thick rhombic plates. The samples used were cut out from thse crystals into adequate rod-shapes with a razor. The crystal data have been derived from Weissenberg photographs around the *a* and *b* axes, taken with Cu$K\alpha$ radiation; the results are summarized in Table 1. From the systematic absences, the space group was found to be either

Table 1. Crystal data of the dichloride of IIIa

Monoclinic	
	$a=17.16\pm0.04$ Å
	$b=9.31\pm0.03$
	$c=13.73\pm0.04$
	$\beta=91.8°\pm0.3°$
Space group	$C2/c$
Z	4
ρ_{calcd}	1.94 g/cm^3

1) K. Mano, K. Kusuda, A. Fujino and T. Sakan, *Tetrahedron Letters*, **1966**, 489.

2) A. Furusaki, This Bulletin, **40**, 758 (1967).

3) A. Furusaki, *ibid.*, **40**, 2518 (1967).

$C2/c$ or Cc. As a final result of the present analysis, the former has been concluded to be the corresponding group.

In order to collect three-dimensional intensity data, equi-inclination Weissenberg photographs were taken with Ni-filtered Cu$K\alpha$ radiation for the zeroth to the twelfth layer around the a axis and for the zeroth to the sixth layer around the b axis. The intensities were measured visually using a calibrated scale. Due to the rule of absences corresponding to $C2/c$, the intensities of (hkl) reflections with h and k even and those with h and k odd cannot be compared directly with each other only using the intensity data from the a and b axes. Therefore, the (hkk) photographs were taken around the [011] axis in order to obtain an approximate intensity ratio between two such types of reflections. This intensity ratio was then revalued by a comparison of the observed and calculated structure factors in the course of analysis. Thus, the structure factors of 1683 reflections were uniquely derived; they were then converted into an absolute scale by Wilson's method. Though the samples used were not very small, no correction was applied with regard to the absorption effect.

Structure Determination. The crystal structure was successfully elucidated by using the same method as was applied to the structure determination of IV.[3] The three vectors used for the minimum function method were (3/60, 11/30, 7/60), (33/60, 12/30, 37/60), and (30/60, 23/30, 30/60). The minimum function diagram thus obtained contained twenty-four significant peaks per quarter of the unit cell. As it was believed at this stage that the compound presently being studied had the molecular formula $C_{12}Cl_{12}$, the twelve peaks were chosen as the chlorine atoms out of the twenty-four peaks solely on condition of satisfying the Patterson map. The arrangement of these twelve peaks showed the presence of two-fold rotation axes. Therefore, the space group was concluded to be $C2/c$, as has already been mentioned.

The coordinates of the chlorine atoms were refined by the use of the diagonal-matrix least-squares method. However, five cycles of the refinement lowered the R factor from its initial value of 0.46 by only 0.05. In order to ascertain the correctness of the structure obtained from the minimum function, a three-dimensional electron density distribution was calculated using Sim's method.[4] From the electron density diagram, the positions of the six independent chlorine atoms already obtained were found to be essentially correct. Besides, the diagram revealed not only the positions of the six independent carbon atoms, but also the presence of an additional chlorine atom per asymmetric unit. Consequently, the molecular formula of the compound presently being studied might not be $C_{12}Cl_{12}$, but $C_{12}Cl_{14}$. This was also supported by the fact that, for the $C_{12}Cl_{12}$ formula, the calculated density is 1.73 g/cm^3; this value seems too small compared with those of II and IV, 2.07 and 2.17 g/cm^3 respectively, the crystal structures of which have already been determined.

The atomic parameters of the seven chlorine and six carbon atoms were refined by the use of the diagonal-matrix least-squares method with individual isotropic temperature factors using 1319 data around the b axis. After five cycles, the R factor dropped only to 0.207. This large value may be due to the weakness of the reflection intensities recorded on the Weissenberg photographs, or it may be attributed to the absorption effect, since the samples used were not small enough, as has been mentioned already. The electron density distribution, calculated at this stage using all the observed data, is given in Fig. 2. Further, the atomic coordinates were refined by the block-diagonal-matrix least-squares method assuming anisotropic thermal motions of all the atoms using 827 data around the b axis except for very weak reflections. After three cycles of the refinement, R was lowered to 0.100. The final atomic parameters thus obtained are listed in Table 2.

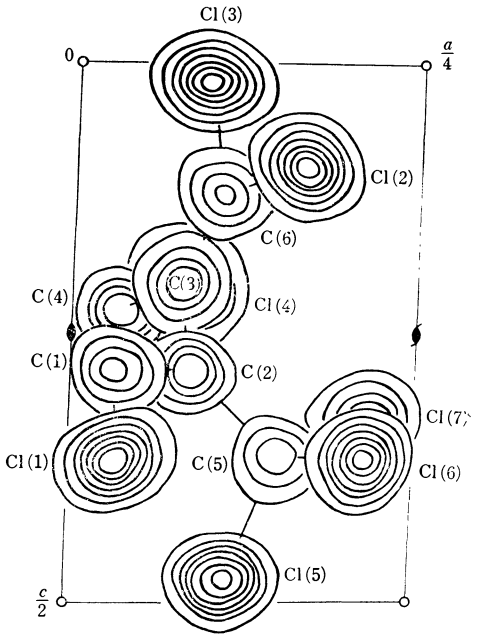

Fig. 2. The electron density distribution of the dichloride of IIIa.
A composite diagram of the (010) sections taken as through the atomic centers. Contours are at intervals of 2 e/Å^3 for carbon atoms and 4 e/Å^3 for chlorine atoms, beginning at 2 e/A^3.

4) G. A. Sim, *Acta Cryst.*, **12**, 813 (1959).

TABLE 2.

(a) The final atomic coordinates

Atom	x/a	y/b	z/c	Atom	x/a	y/b	z/c
Cl(1)	0.4676	−0.0553	0.1329	C(1)	0.4644	0.0821	0.2130
Cl(2)	0.3343	0.1296	0.4031	C(2)	0.4140	0.1861	0.2144
Cl(3)	0.4046	0.3834	0.4806	C(3)	0.4206	0.3043	0.2962
Cl(4)	0.4189	0.5938	0.2943	C(4)	0.4625	0.4332	0.2684
Cl(5)	0.3852	0.2339	0.0206	C(5)	0.3460	0.2042	0.1329
Cl(6)	0.2862	0.0486	0.1322	C(6)	0.3911	0.2752	0.3764
Cl(7)	0.2856	0.3508	0.1658				

(b) The anisotropic temperature factors in form of $\exp(-B_{11}h^2-B_{22}k^2-B_{33}l^2-B_{12}hk-B_{23}kl-B_{31}lh)$

Atom	B_{11}	B_{22}	B_{33}	B_{12}	B_{23}	B_{31}
Cl(1)	0.00313	0.00673	0.00472	0.00266	−0.00671	−0.00186
Cl(2)	0.00425	0.00948	0.00450	−0.00706	0.00042	0.00261
Cl(3)	0.00446	0.01045	0.00357	−0.00023	−0.00512	0.00101
Cl(4)	0.00344	0.00229	0.00746	0.00168	−0.00203	0.00363
Cl(5)	0.00396	0.01124	0.00307	−0.00097	0.00422	−0.00082
Cl(6)	0.00229	0.01263	0.00552	−0.00527	0.00070	−0.00157
Cl(7)	0.00436	0.01519	0.00825	0.01197	−0.01118	−0.00657
C(1)	0.00140	0.00473	0.00257	0.00047	−0.00183	0.00026
C(2)	0.00166	0.00534	0.00285	−0.00187	0.00014	0.00073
C(3)	0.00215	0.00330	0.00442	−0.00162	−0.00294	0.00121
C(4)	0.00206	0.00375	0.00366	−0.00089	−0.00309	0.00012
C(5)	0.00299	0.01413	0.00545	−0.00184	−0.01025	0.00160
C(6)	0.00237	0.00820	0.00382	0.00098	−0.00035	0.00529

Description of the Structure of the Dichloride of IIIa

The molecular framework thus obtained and the bond lengths and angles calculated with the final atomic coordinates are shown in Figs. 3 and 4 respectively. The standard deviations of the coordinates are 0.008 Å for chlorine atoms and 0.021 Å for carbon atoms; therefore, those of the distances between mutually-independent atoms are

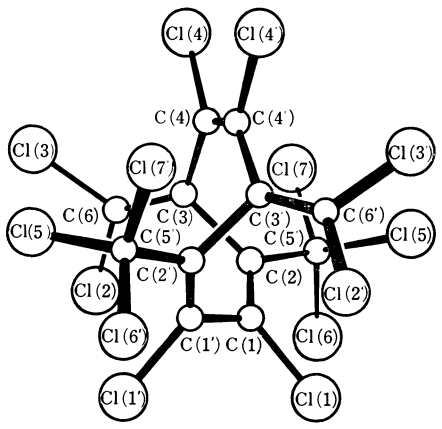

Fig. 3. The molecular framework of the dichloride of IIIa.

0.022 Å for C–Cl and 0.030 Å for C–C. Judging from the present results, it may be concluded that the dichloride of the isomer IIIa corresponds to perchloro-(1,4-dimethyl-5,8-dimethylene-cycloocta-1,3,6-triene).

The molecule has a symmetry of C_2, the diad of which coincides with a crystallographic one and runs parallel to the mean plane of the cyclooctatriene ring. The ring has a somewhat distorted tub-form compared with that of cyclooctatetraene.

The mean plane through the six atoms, Cl(1), C(1), C(2), C(3), C(5), and C(1'), is determined by means of the least-squares method as the following equation:

$$0.5904X + 0.5489Y - 0.5916Z - 3.374 = 0 \quad (1)$$

where X, Y, and Z are the rectangular coordinates in Å unit, where $X = x + z\cos\beta$, $Y = y$, and $Z = z\sin\beta$. As is shown in Fig. 5, four of the six atoms, Cl(1), C(1), C(2), and C(3), are nearly coplanar, but the C(5)–C(2)–C(1)–C(1') segment is somewhat concave toward the center of the molecule. Such a deviation from planarity may be due to the close approaches between Cl(1) and the trichloromethyl group (Cl(5), Cl(6), Cl(7), or C(5)) and between Cl(1) and Cl(1'); Cl(1) is located at distances of 3.19 Å from C(5), 3.26 Å from Cl(6), 3.39 Å from Cl(5), and 3.37 Å from Cl(1'). As is shown in Fig. 6, the trichloromethyl group takes such a conformation around the C(2)–C(5) bond that one

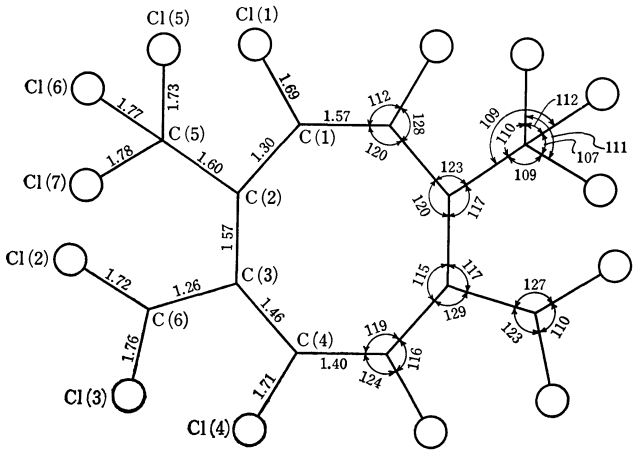

Fig. 4. The bond lengths (Å) and angles (°) of the dichloride of IIIa.

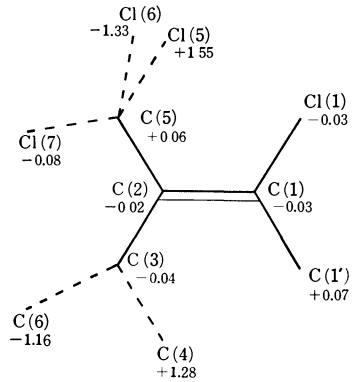

Fig. 5. The deviations of the atoms from the mean plane (1).

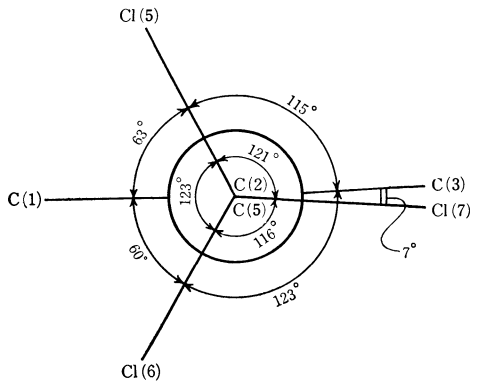

Fig. 6. The conformation of the trichloromethyl group around the bond C(2)-C(5).

of the three planes of the trichloromethyl group, through Cl(7), C(2), and C(5), is approximately coplanar with the plane (1) given above, Cl(7) being most remote from Cl(1). The adjacent endo-cyclic double bonds, C(1)-C(2) and C(1')-C(2'), deviate by 62° from the virtual cis-conformation around C(1)-C(1'). Since, besides, the bond distance C(1)-C(1') is about 1.57 Å, the conjugation between these two double bonds seems to be very weak.

The best plane, determined to run through Cl(2), Cl(3), C(2), C(3), C(4) and C(6), is described by the equation:

$$0.8305\,X-0.4715\,Y+0.2966\,Z-5.772=0$$

Figure 7 shows the deviations of the atoms from this plane. The double bond C(3)-C(6) is shown to be twisted to a considerable degree. Since, of these six atoms, two sets, Cl(2), Cl(3), C(3), and C(6), and C(2), C(3), C(4), and C(6), are almost coplanar, the angle of twisting around C(3)-C(6) is represented by the angle between the mean planes of these two sets of atoms; the twisting angle is estimated at about 8°. The sense of this twisting is just such that the chlorine atoms, Cl(3) and Cl(4), separate from each other, giving rise to an interatomic distance still with a value of 3.24 Å.

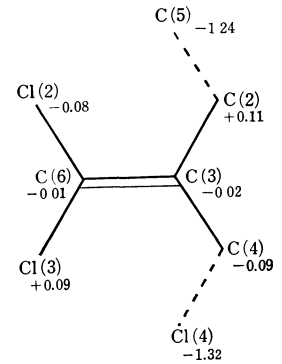

Fig. 7. The deviations of the atoms from the mean plane,
$0.8305X - 0.4715Y + 0.2966Z - 5.772 = 0$.

Since the double bond C(3)-C(6) makes an azimuthal angle of about 96° with C(1)-C(2), these two double bonds seem hardly to be conjugated at all. This idea is supported by the fact that the bond, C(2)-C(3), between the two double bonds is about 1.57 Å long. As a result of the large azimuthal angle (about 81°) of the bonds, C(2)-C(5) and C(3)-C(6), around C(2)-C(3), the trichloromethyl group and the dichloromethylene group adjoining to it are sufficiently apart from each other; the nearest approach between their chlorine atoms occurs between Cl(2) and Cl(7), when the distance is 3.92 Å.

The six atoms, Cl(4), C(3), C(4), Cl(4') C(3'), and C(4') (the double bond of which is C(4)-C(4')), are nearly coplanar in spite of the close approach between Cl(4) and Cl(4') at a distance of 3.07 Å, their mean plane being described by the equation:

$$0.4020X + 0.9156Z - 6.546 = 0$$

The deviations of the atoms from this plane are shown in Fig. 8. The double bond C(4)-C(4') makes an azimuthal angle of about 125° with C(3)-C(6) and C(3')-C(3'). These three double bonds are closest to planarity among all the pairs

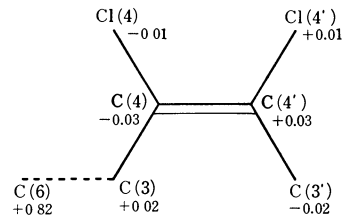

Fig. 8. The deviations of the atoms from the mean plane.
$0.4020X + 0.9156Z - 6.546 = 0.$

of double bonds adjacent to each central single bond. The length of the C(3)-C(4) bond is 1.46 Å, and that of C(4)-C(4'), 1.40 Å. Thus, it may be concluded that the three double bonds are conjugated with one another to a certain extent.

The projection of the crystal sturcture along the *a* and *b* axes are shown in Figs. 9 and 10 respectively, where all the intermolecular distances smaller than 4.0 Å are also given. It is of interest to note that the center of a molecule is located at $x=1/2$, $y\approx 1/4$, and $z=1/4$; therefore, those of the three remaining molecules in the unit cell are situated at approximately (0, 3/4, 1/4), (0, 1/4, 3/4),

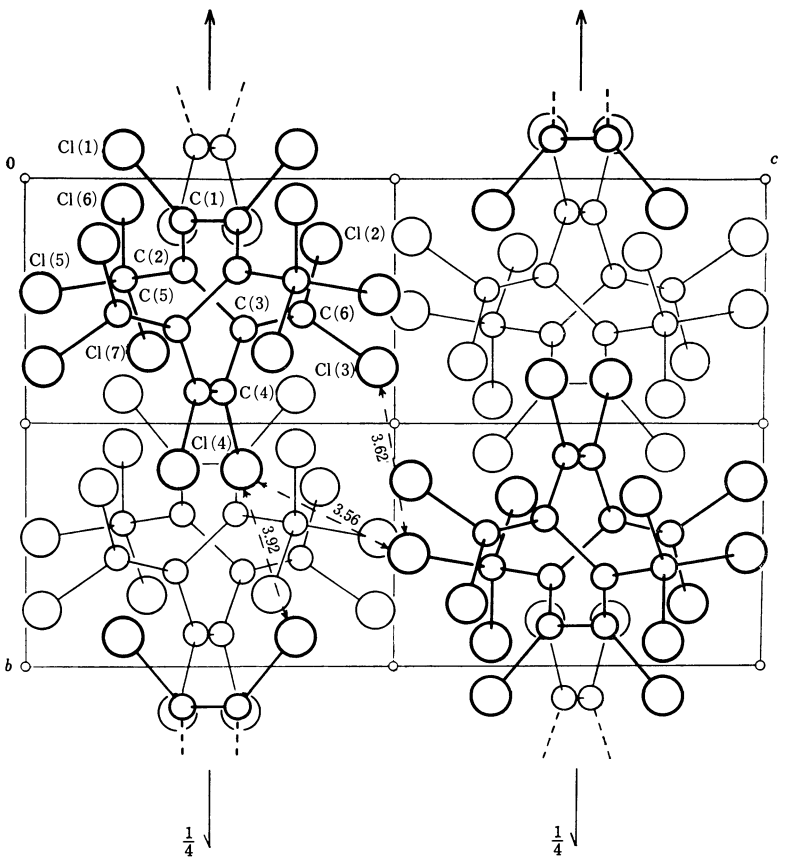

Fig. 9. The crystal structure of the dichloride of IIIa viewed along the *a* axis.

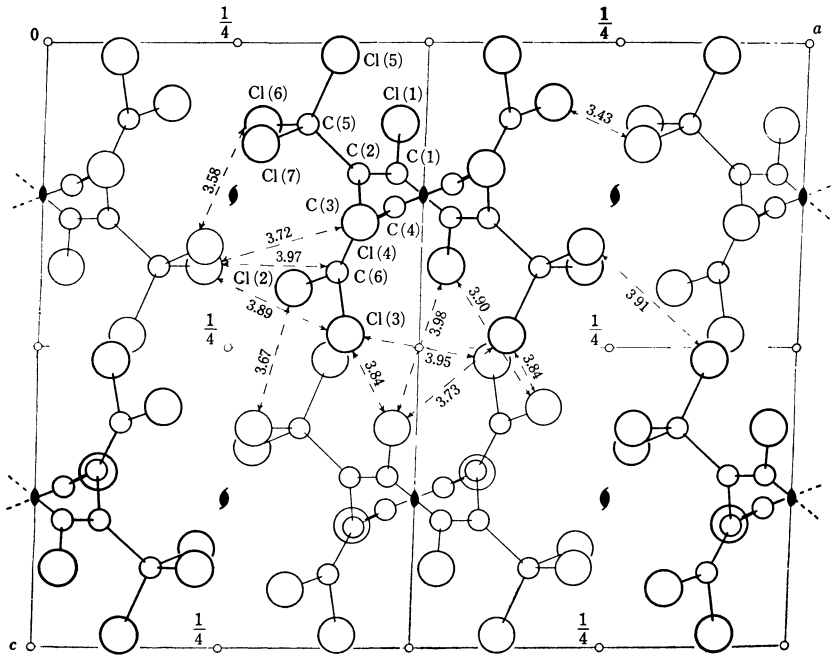

Fig. 10. The crystal structure of the dichloride of IIIa viewed along the *b* axis.

and (1/2, 3/4, 3/4); these four sets of coordinates correspond to those of lattice points in the face-centered cubic lattice. If adjacent molecules with intermolecular contacts of less than 4.0 Å are taken as nearest neighbors, each molecule is found to have twelve nearest neighbors. The central molecule at the height of $y \approx 1/4$ has two neighbors at the same height, four at the $y \approx -1/4$ height, four at $y=3/4$, and two just above and below. Due to the deviation of the molecular form from an ideal sphere, the three principal axes, *a*, *b*, and *c*, are not equal in length, but are in the ratio 1.84 : 1.00 : 1.47, the β angle deviating from a right angle by 1.8°.

As in II and IV, in the present crystal also close intermolecular Cl···Cl contacts are found: 3.43, 3.56, and 3.58 Å. Of these three close contacts, the former two occur between the chlorine atoms, one of the chloroethylene type and the other of the chloromethane type. The last one is that between the chlorine atoms, both of the chloromethane type. The difference between this observed distance and twice the standard van der Waals radius, 3.60 Å, may not be significant considering the accuracy of the present determination. Thus, the closer approaches found in the present crystal may be looked upon as due to the chlorine atoms of the chloroethylene type.

Discussion

All the molecular sturctures of II, IV, and the dichloride of IIIa have now been elucidated by means of X-ray analysis. Judging from the facts that IIIa reacts with liquid chlorine to form its dichloride, while the dichloride loses two chlorine atoms in the presence of Raney nickel to form IIIa, IIIa should have a structure closely similar to that of its dichloride. Thus, it may be concluded that the two-dimensional chemical structure of IIIa is perchloro-(3,4,7,8-tetramethylene-cycloocta-1,5-diene) (VIII) rather than perchloro-(2,3,7,8-tetramethylene - bicyclo[4.2.0]octa - 4 - ene) (VI), which, as has already been mentioned, was proposed from the chemical analysis. For the former, the formation of the dichloride can be simply explained through the 1,6-addition of chlorine to IIIa, as is shown in Fig. 11, whereas, for the latter, any explanation has to assume a complicated structural change.

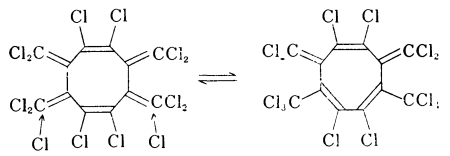

Fig. 11. The 1,6-addition of Cl_2 to IIIa.

As for the structure VIII, the conceivable molecular forms can be divided into two groups. Of these two, the one (VIIIa) with a twisted ring has a symmetry of D_2, but this molecular form can be easily changed into another with a lower symmetry C_2 by a conformational change around the single

bonds. On the other hand, the other group (VIIIb) has a symmetry of C_{2h}, and the cyclooctadiene ring takes the very rigid frame of a chair-like form.

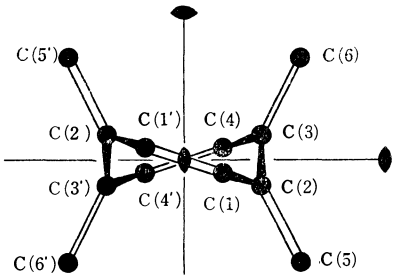

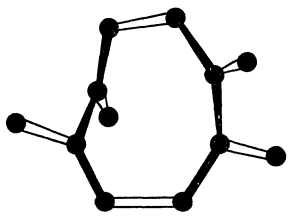

VIIIa

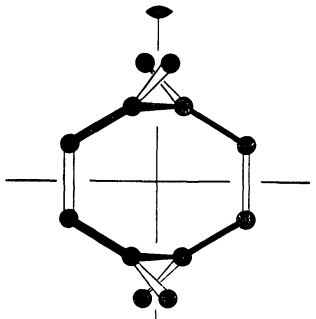

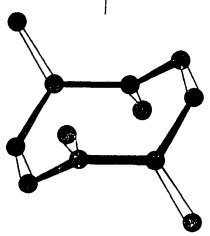

VIIIb

The molecular structure VIIIa makes possible a lucid explanation of the isomerization reaction of III into IV. In VIIIa, the two exo-cyclic double bonds, C(2)–C(5) and C(3)'–C(6'), or C(3)–C(6) and C(2')–C(5'), which are to form a four-membered ring, stand out to the same side of the mean plane of the ring: moreover, because of the ring's flexibility, these bonds can approach each other without much bond distortion. Thus, the addition reaction of such two double bonds results in the formation of a four-membered ring, giving rise to IV,

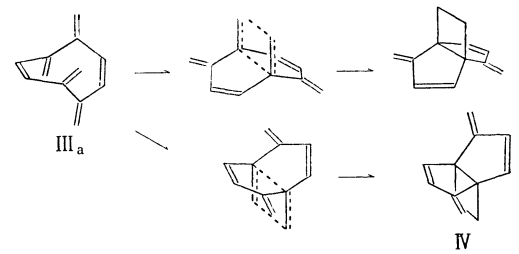

Fig. 12. The process of the isomerization of IIIa into IV.

as is shown in Fig. 12. On the other side, neither VI nor VIIIb can give so adequate an explanation of the isomerization of III as VIIIa can. Thus, it is reasonable to consider that VIIIa is the molecular structure of either IIIa or IIIb.

From the similarity of the IR data, it has been proposed by Fujino *et al.* that two isomers, IIIa and IIIb, have the same two-dimensional chemical structure. According to them, it seems that either the molecular structure of IIIa corresponds to VIIIa and IIIb to VIIIb, or *vice versa*. The former possibility seems to be more probable judging from the following points. In the first place, the fact that IIIb resists the oxydization of nitric acid and the addition of chlorine, while IIIa does not, seems to favor the present conclusion that IIIb has an inflexible and rigid structure, VIIIb, while IIIa has a labile and deformable structure, VIIIa, which is more likely to be attacked by reagents. Further, the change in the π-bond location seems to be effected by the attack of chlorine more smoothly in VIIIa than in VIIIb, because the part which is concerned with the 1,6-addition of chlorine is closer to planarity in the

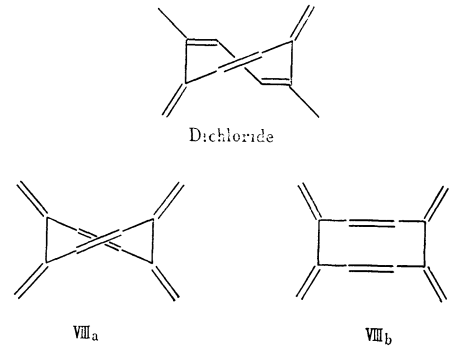

Fig. 13. The conformational resemblance of VIIIa to the dichloride.

former. The unchanged part of the 1,6-addition product found in the present analysis is more similar in conformation to the corresponding part of VIIIa than to that of VIIIb, as is shown in Fig. 13. Therefore, it may be concluded that the molecular structure of IIIa, the precursor of the 1,6-addition

product, corresponds to VIIIa rather than to VIIIb.

The transformation of IIIa into IV has already been explained. Thus, the only remaining problem is to elucidate how II is transformed into IIIa and IIIb. As has been mentioned above, the molecular structure of II has been found to be perchloro-(3,4,7,8-tetramethylene-tricyclo-[4.2.0.0^{2,5}]octane) (V) by the X-ray method. The three adjoining four-membered rings take a chair-like form, and the two pairs of alternating double bonds are both nearly planar. Thus, the whole molecule has a symmetry of C_{2h}. It seems reasonable to suppose that the transformation of II begins with the cleavage of the two single bonds which partition the eight-membered ring into three four-membered rings. As this cleavage proceeds, two dichloromethylene groups in the same conjugated system come to be unable to keep their planarity because these groups move on toward each other due to the relaxation of the considerable bond distortions in the three adjoining four-membered rings. Thus, two exo-cyclic double bonds, C(2)-C(5) and C(3)-C(6), or C(2')-C(5') and C(3')-C(6'), are rotated around the single bond, C(2)-C(3) or C(2')-C(3'), so as to avoid close approaches between the dichloromethylene groups. In this case, there are two different ways conceivable as to how the two pairs of the adjoining double bonds deviate from their planar conformation. One is that out of the molecular symmetry, C_{2h}, of II, a center of symmetry is preserved, as is shown in Fig. 14; the other is that a two-fold rotation symmetry is kept, as is shown in Fig. 15. Of course, such rotations around the single bonds, C(2)-C(3) and C(2')-C(3'), are accompanied by a change in the

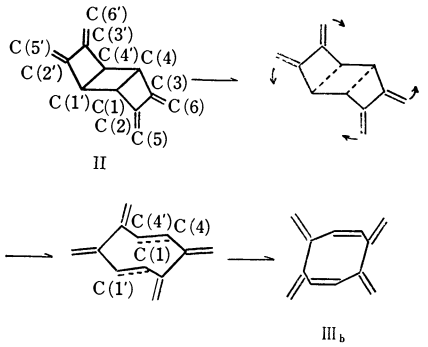

Fig. 14. The process of the isomerization of II into IIIb.

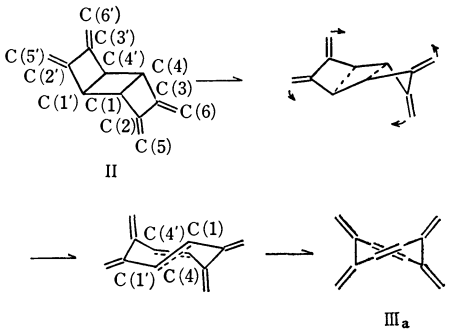

Fig. 15. The process of the isomerization of II into IIIa.

conformation around the bonds, C(1)-C(1') and C(4)-C(4'). Then new π-bonds begin to be formed, as the conformation around the latter bonds becomes favorable for the overlapping of the 2pπ-orbitals of these two pairs of atoms. Thus, one may assume two possible processes of the isomerization reaction; in the former, the isomer IIIb, with a molecular symmetry of C_{2h}, is formed, while in the latter the other isomer, IIIa, with C_2 or D_2 is formed.

After all, the problems regarding the mechanism of the successive isomerization reactions posed in the introduction to the present paper may be looked upon as solved through the series of X-ray structure analyses made on the compounds II, the dichloride of IIIa, and IV.

Tables of the observed and calculated structure factors are preserved by the Chemical Society of Japan.*1

The author is very grateful to Professor Akira Fujino and his co-workers, Research Institute for Atomic Energy, Osaka City University, for providing him with the samples and for their valuable discussions. The author also wishes to acknowledge with deep gratitude his debt to Professor Isamu Nitta and the late Professor Yujiro Tomiie for their kind guidance and helpful discussions during this work. Thanks are also due to the staff of the C. Itoh Electronic Computing Service Co., Ltd., for allowing the use of the Bendix G-20 computer.

*1 The complete data of the F_o-F_c table are kept as Document No. 6804 at the office of the Bulletin of the Chemical Society of Japan. A copy may be secured by citing the document number and by remitting, in advance, ¥300 for photoprints. Pay by check or money order, payable to: Chemical Society of Japan.

BULLETIN OF THE CHEMICAL SOCIETY OF JAPAN VOL. 41 2895—2899 (1968)

Phase Changes in the ZrO_2-TiO_2 System

Tetsuo NOGUCHI and Masao MIZUNO

Government Industrial Research Institute, Nagoya, Hirate-machi, Kita-ku, Nagoya

(Received March 28, 1968)

The liquidus curve in the ZrO_2-TiO_2 system previously reported by the present authors was again examined with a heliostat-type solar furnace in order to determine the peritectic point in the ZrO_2-rich side region. Quenched specimens from the melt of the ZrO_2-rich side region were analysed by the X-ray technique. The cooling curves from the melt suggested the existence of a new phase stable at higher temperatures, and a tentative phase diagram at high temperatures is presented.

The phase diagram in the ZrO_2-TiO_2 system has been studied by many investigators. Since the liquidus curve in the system was first published by von Wartenberg[1] in 1931, Sowman and Andrew[2] have demonstrated the results of high-temperature X-ray diffractometry on the ZrO_2-TiO_2 system, while Coughanour *et al.*[3] and later Brown and Duwez[4] proposed the phase diagrams which have been generally accepted up to the present. Recently, however, the subliquidus phase in the diagram was revised by Cocco and Torriano.[5]

Phase changes in the ZrO_2-TiO_2 system were also studied with a heliostat-type solar furnace; the results of the freezing point measurement and of the X-ray analysis of quenched specimens from the melt have been reported by the present authors previously.[6] The subliquidus phase study in the system and the freezing-point data on the specimens between 2.5 and 20 mol% TiO_2 compositions will be supplemented in the present work, and a revised diagram at higher temperatures will be presented.

Apparatus and Materials

In the freezing-point measurements undertaken to obtain additional data, a heliostat-type solar furnace equipped with a brightness pyrometer was used, and the specular reflection method[7,8] reported previously was used. The accuracy of the pyrometer was within $\pm 20°$ at 3000°K and $\pm 15°$ at 2000°K, including the reading error for oscillograms.

ZrO_2 99.8% pure (including about 1.8% HfO_2) from the Yokozawa Chemicals Co., Tokyo, and TiO_2 99.7% pure from the Kanto Chemicals Co., Tokyo, both used in the previous work, were carefully mixed in an agate mortar and then heated in an electric resistance furnace at 1500°C for 3 hr. After two grinding and heating cycles, the specimen was pressed into a $6 \times 6 \times 30$ mm bar under 4000 kg/cm^2 pressure without any lubricant or binder for the freezing-point measurements. No repeated fusion was made for the sample preparation in order to avoid any deviation from the stoichiometry of the composition at higher temperatures and also any contamination by impurities resulting from the grinding process and pressing.

X-Ray diffraction measurements of the quenched specimen were made using a diffractometer on a Shimadzu diffraction unit GX-3 and by nickel-filtered Cu$K\alpha$ radiation. High-temperature X-ray diffraction data were obtained with a Shimadzu HX-II model, the hot stage of which consists of a platinum-rhodium-wound heating element encased in an alumina refractory sleeve. Temperature measurements were made with platinum *versus* platinum-10% rhodium thermocouple.

Results and Discussions

Freezing-point Measurements. On the basis of the results of Cocco and Torriano, who claimed to have found a solid solution boundary between tetragonal zirconia and the two phase region (tetragonal zirconia plus $ZrTiO_4$) of 15mol% TiO_2 at elevated temperatures, the former anomaly in the liquidus curve reported by the authors was again examined in the compositions containing between 2.5 and 17.5 mol% TiO_2.

1) H. von Wartenberg and W. Gurr, *Z. anorg. Chem.*, **196**, 374 (1931).
2) H. G. Sowman and A. I. Andrew, *J. Am. Ceram. Soc.*, **34**, 298 (1951).
3) L. W. Coughanour *et al.*, *J. Res. Natl. Bur. Standards.*, **52**, 37 (1954).
4) F. H. Brown and P. Duwez, *J. Am. Ceram. Soc.*, **37**, 129 (1954).
5) A. Cocco and G. Torriano, *Annali di Chimica.*, **55**, 153 (1965).
6) T. Noguchi and M. Mizuno, *Solar Energy.*, **11**, 7 (1967).
7) T. Noguchi and T. Kozuka, *ibid.*, **10**, 125 (1966).
8) T. Noguchi and M. Mizuno, This Bulletin, **41**, 1583 (1968).

The seven specimens, in 2.5 mol% TiO_2 increments, were fused by means of the solar furnace, and their freezing temperatures were obtained from the cooling curves and spectral emissivity measurements. The cooling curves for each specimen were measured, using a dual-beam cathode ray oscilloscope, at several points across the sun's image under various heating temperatures after the thermal equilibrium had been attained. The thermal equilibrium was attained wihtin several seconds[9] from the attenuater opening. The measurements were repeated on different parts of the specimen surface more than thirty times in order to confirm the homogeneity of the composition in the specimen; the data agreed within the limits of error of the pyrometer reading. The cooling curves for each composition are shown schematically in Fig 1. The spectral reflectivity was also measured in order to obtain the spectral emissivity at 0.65μ near and at the respective freezing-point.

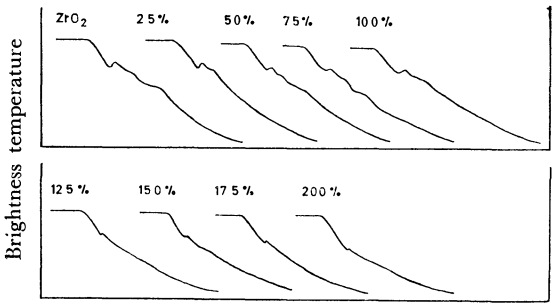

Fig. 1. Schematic cooling curves of the compositions containing TiO_2 up to 20 mol percent.

Table 1. Freezing point data of the compositions containing TiO_2 up to 20 mol percent

TiO_2 content (mol%)	Freezing point (±20°C)	Spectral emissivity at 0.65 μ	Temperature of* exothermic peaks in solid state (°C)	
0**	2706	0.81	—	—
2.5	2701	0.83	2487	—
5.0	2655	0.87	2498	2338
7.5	2618	0.84	2484	2332
10.0**	2580	0.95	2468	—
12.5	2495	0.94	—	—
15.0	2395	0.92	—	—
17.5	2343	0.96	—	—
20.0**	2316	0.92	—	—

* These values were calculated from their brightness temperatures and the emissivity data at the respective freezing point.

** Quoted from the previous work by the authors.

The average values of the freezing temperature for each composition are listed in Table 1, along with the spectral emissivity data. The results show that the anomaly in the liquidus curve is shifted from 20 mol% to 17.5 mol% TiO_2.

Chemical Analysis of Quenched Specimens. In order to examine the stoichiometry of the composition in specimens fused with the solar furnace in air, chemical analysis was made on specimens containing 10, 20, 30, 50 and 70 mol% TiO_2. The specimens were kept about 100°C higher than the respective melting temperatures for 3 min.*1 Because of the difficulty in separating TiO_2 from ZrO_2, the ZrO_2 content in the specimen was determined by the following method.

A weighed specimen of about 50 mg in a platinum crucible was fused with the addition of ten times as much sodium pyrosulfate and then dissolved with nitric acid into a sample solution. After the addition of an excess amount of an EDTA standard solution (0.009594 M), a 10% solution of ammonium tartarate was added; the pH of the sample solution was then adjusted to between 1—2 with nitric acid or ammonia water. The sample solution was heated for five minutes and then back-titrated with a bismuth nitrate standard solution (0.017669M) using the XO indicator. The end point was shown by the color change from yellow to red purple; the results are shown in Table 2.

The ZrO_2 content was determined by the spectrochemical analysis to contain about 1.8% HfO_2, which was calculated as ZrO_2. Therefore, a correction was made in examining the stoichiometry,

Table 2. Results of chemical analysis on quenched specimens from the melt

Sample	ZrO_2 content % (theoretical)	ZrO_2 content % (determined)	Corrected values		Deviation from theoretical value
			wt%	mol%	mol%
ZT-2	93.28	92.01	93.2	89.9	−0.1
ZT-3	86.05	85.00	86.1	80.1	+0.1
ZT-4	78.25	77.31	78.3	70.1	+0.1
ZT-6	60.66	59.52	60.3	49.6	−0.4
ZT-8	39.79	39.53	40.0	30.2	+0.2

9) T. Noguchi and T. Kozuka, *Solar Energy.*, **10**, 203 (1966).

*1 Several seconds were necessary for the fusion of a specimen with the solar furnace, and several additional seconds were required to attain the thermal equilibrium. Therefore, the time for the cooling curve measurements was about 10 sec.

and the deviation from the theoretical values was found to be less than 0.4 mol%. The titanium content in the fused TiO_2 specimen was determined by the gravimetric method. The composition was found to be $TiO_{1,997}$ and to agree with the results of Bauer and Littke.[10]

X-Ray Diffraction Data

X-Ray diffraction measurements were made on quenched specimens from the melt and on those heated at 1700°C for 6 hr in an electric-resistance furnace. The molten specimens were prepared with the solar furnace by heating them to about 100°C higher than the respective melting points for 20 sec before quenching. The diffraction data are listed in Table 3, along with the data on the ZrO_2-TiO_2 system obtained in a previous paper.

The single phase of the $ZrTiO_4$ compound was observed on the specimen (1:1) heated at 1700°C, while the quenched specimen from the melt showed three components, $ZrTiO_4$, monoclinic ZrO_2, and tetragonal TiO_2 as an incongruently melting material. The lattice parameters of the $ZrTiO_4$ solid solution with compositions containing 35 to 60 mol% TiO_2 were obtained using the diffraction lines from (032), (014) and (400) with the scanning speed of 2θ 1/8° min for the specimens fired at 1700 °C. Both a and c axes contracted from 41 mol% composition, and the unit cell volume increased from a 50 mol to a 53 mol% composition. Moreover, the boundaries of the $ZrTiO_4$ solid solution for ZrO_2 and TiO_2 sides at 1700°C were located at 41 mol% and 53 mol% TiO_2 respectively, as is shown in Fig. 2.

Table 3. X-ray diffraction data on the quenched specimens in ZrO_2-TiO_2 system

Compositions (mol%)		Results of X-ray diffraction					
		1700°C			Solar furnace melt		
ZrO_2	TiO_2						
97.5	2.5	M			M		
95.0	5.0	M			M		
92.5	7.5	M			M		
90.0	10.0	M			M		
87.5	12.5	M			M		
85.0	15.0	M			M	ZT	
82.5	17.5	M	ZT		M	ZT	
80.0	20.0	M	ZT		M	ZT	
75.0	25.0	M	ZT				
70.0	30.0	M	ZT		M	ZT	*
65.0	35.0	M	ZT				
62.0	38.0	M	ZT				
60.0	40.0	M	ZT		M	ZT	R*
59.0	41.0	M	ZT				
56.0	44.0		ZT				
55.0	45.0		ZT		M	ZT	R*
53.0	47.0		ZT				
50.0	50.0		ZT		M	ZT	R*
49.0	51.0		ZT				
47.0	53.0		ZT				
45.0	55.0		ZT		M	ZT	R*
40.0	60.0		ZT	R		ZT	R*
30.0	70.0		ZT	R		ZT	R*
20.0	80.0		ZT	R		ZT	R*
10.0	90.0			R			R*

* Quoted from the previous work by the authors.
Note: M: monoclinic ZrO_2 solid solution,
ZT: $ZrTiO_4$ s. s. R: TiO_2 s. s.

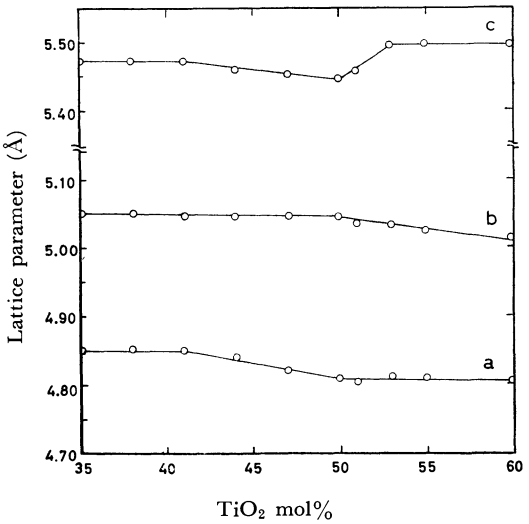

Fig. 2. Lattice parameters of $ZrTiO_4$ solid solutions.

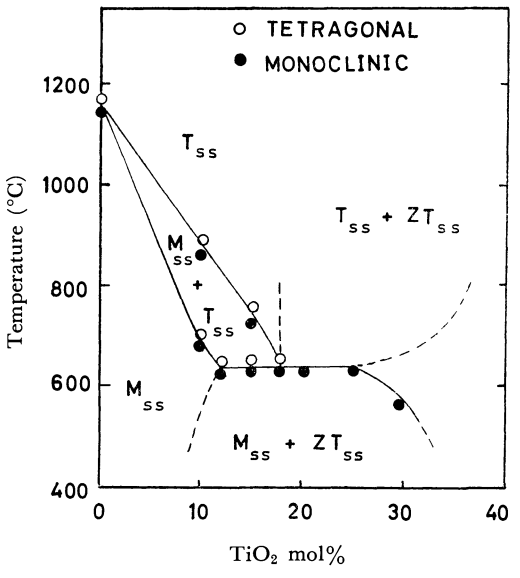

Fig. 3. High temperature X-ray diffraction data in ZrO_2 rich side region.

10) G. Bauer and W. Littke, *J. Inorg. Nucl. Chem.*, **16**, 67 (1960).

The specimens containing up to 30 mol% of TiO_2 were fired at 1700°C for 3 hr and then examined by high-temperature X-ray diffractometry in order to determine the solid solution boundaries at lower temperatures. The diffraction data were obtained from 2θ 27° through 33° and by the heating and cooling rates of 2°C/min. The average values obtained by five heating and cooling cycles are shown in Fig. 3; the data agreed with Cocco's results, which differ from those of Duwez, who estimated the solid solution boundary on the basis of the thermal expansion measurement. However, the boundary between tetragonal and monoclinic ZrO_2 solid solutions in the present work seems to be about 140°C higher than that obtained by Cocco. Moreover, this boundary was not straight with the increase in the TiO_2 content, the transformation temperature decreasing, as was claimed by Duwez.

The lattice parameters of the monoclinic solid solution in the specimens quenched from the melt and at 1700°C are shown in Fig. 4. The quenching rate from the melt was about 2300°C/sec. The data were obtained with the diffraction lines from (111), (11$\bar{1}$), (011), and (002).

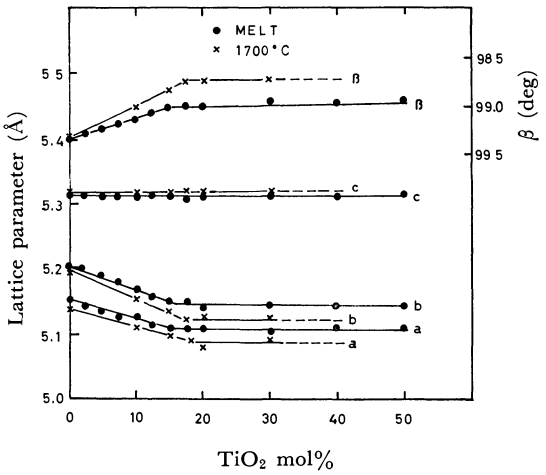

Fig. 4. Lattice parameters of monoclinic ZrO_2 solid solution.

While the solubility limit of TiO_2 in a $ZrTiO_4$ solid solution in the specimens quenched from the melt was previously found at 80 mol% TiO_2, the quenched specimen from 1700°C showed a solid solution boundary at 83.5 mol% TiO_2.

Phase Diagram

Tentative additions to the phase diagram in the ZrO_2-TiO_2 system were made to the revised diagram by Cocco and Torriano, using the liquidus curve in the system shown in Fig. 5.

Pure zirconia has shown the exothermic peaks[7] at 2494° and 2325°C respectively, while the latter

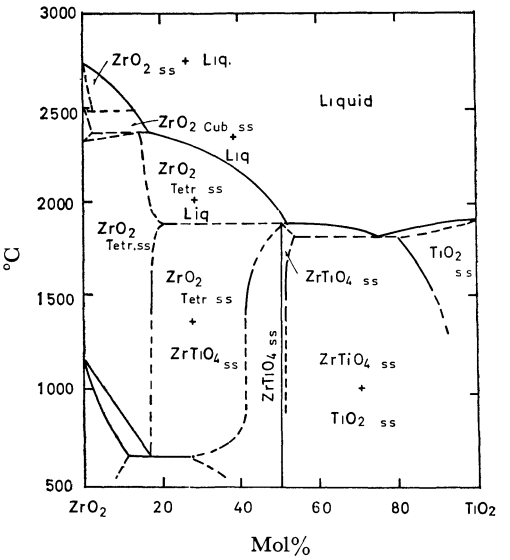

Fig. 5. Tentative phase diagram of ZrO_2-TiO_2 system at high temperature.

was estimated to be the transformation from a cubic to a tetragonal modification of ZrO_2. The very weak exothermic peaks which appeared in the cooling curves of the compositions containing 2.5, 5, 7.5 and 10 mol% TiO_2 in the solid state*2 were observed at temperatures slightly lower than 2500 °C. Although the high accuracy in the temperature measurement upon a transformation in the solid state can not usually be expected by such a dynamic method, the ZrO_2 modification in this region was not frozen by the quenching rate in the present work and was considered to show a diffusionless phase change.[11] Therefore, the accuracy of these values were estimated to be close to that obtained in the freezing-point measurements. A complete interpretation of these phenomena was not possible in the present work; however, a transformation from a stable form at above 2500°C to a cubic form might be suggested on the basis of the experimental evidence in establishing the phase relation on the ZrO_2-rich side region at very high temperatures. The existence of a very narrow two-phase region was assumed without actual experimental proof below 2500°C in order to satisfy the phase rule. The highly speculative hypothesis developed by Sense[12] that ZrO_2 may have the monoclinic crystal structure and be quenchable might not be acceptable in the present work, though the crystal structure of zirconia above 2500°C is not yet known. The lattice parameters of zirconia specimens of both the green and those quenched

*2 The freezing point was confirmed by visual observation through the ocular lens of the brightness pyrometer and with both oscillograms and data from the automatic voltage-recording meter.

11) G. M. Wolten, *J. Am. Ceram. Soc.*, **46**, 418 (1963).
12) K. A. Sense, *ibid.*, **44**, 465 (1961).

from the melt showed no remarkable difference within the limits of accuracy of the measurements. An electron micrograph of the quenched zirconia from the melt showed a crack on the thermally-etched surface as in the previous paper.

The second exothermic peaks appearing in the solid state were slightly higher than the transition point from the cubic to the tetragonal form of ZrO_2; the temperatures of these points, almost identical to the freezing temperature of the 17.5 mol% TiO_2 composition, accounted for the solidus line.

The solid solution boundary between tetragonal ZrO_2 and the two-phase region of tetragonal ZrO_2 plus $ZrTiO_4$ under the solidus line was located at 15 mol% TiO_2, while that at 1700°C was located at 17.5 mol% TiO_2 (*cf.* Fig. 4).

The other parts of the diagram were based on the following experimental results:

1) The solid solution boundaries between tetragonal and monoclinic forms of zirconia, and other two-phase regions at lower temperatures, as is shown in Fig. 3.

2) The solid solution boundaries of $ZrTiO_4$ for both ZrO_2 and TiO_2 sides.

3) The solid solution field of TiO_2.

Conclusions

The anomaly in the liquidus curve in the ZrO_2-TiO_2 system has been found at 17.5 mol% TiO_2. A tentative phase diagram for the ZrO_2-TiO_2 system at higher temperatures has been presented, and the existence of a new high-temperature modification of ZrO_2 above 2500°C has been suggested. Further, the phases of ZrO_2 at very high temperatures should be examined by a dynamic method such as high temperature X-ray diffractometry with imaging furnaces.

The authors wish to express their appreciation to Dr. Hiroshi Hayashi for his cooperation in the chemical analysis of the specimens and to Drs. Hiroshi Okuda and Toshiyasu Horibe for their valuable suggestions regarding the experimental results.

BULLETIN OF THE CHEMICAL SOCIETY OF JAPAN VOL. 41 2899—2903 (1968)

Alkali Fusion - Gas Chromatography of Alkyl Sulfates

Terumichi NAKAGAWA, Koichiro MIYAJIMA and Toyozo UNO

Faculty of Pharmaceutical Sciences, Kyoto University, Sakyo-ku, Kyoto

(Received April 1, 1968)

The alkali fusion of alkyl sulfates was investigated by pyrolyzing a mixture of alkyl sulfates and alkali metal hydroxide between 200—500°C. The pyrolyzates were isolated and identified to be 1-olefins, internal olefins, alcohols, and dialkyl ethers by gas chromatography and IR spectroscopy. The mechanism of this reaction was proposed from these results and an attempt was carried out to estimate the alkyl chain carbon number distribution of the commercially available sodium alkyl sulfates.

The analysis of the lipophylic groups of alkyl sulfates has been carried out by means of acid hydrolysis followed by gas chromatographic identification of the resulting alkyl alcohols.

Knight and Hous[1] reported the decomposition of alkyl sulfates in hot phosphoric acid to result the corresponding olefins, which was comfirmed by several other workers.[2,3] Lew[4] described that the pyrolysis of alkyl sulfates with P_2O_5 gave a mixture of 1-olefin and internal olefin isomers with the same carbon numbers as the alkyl group of the original sulfate, but gave neither alcohols nor dialkyl ethers. The direct pyrolysis of alkyl sulfates without any reagent also yielded the corresponding olefins,[4,5] and alcohols.[5] Moreover, Nishi[6] presented a simple identification method of anionic surfactants by alkali fusion. He reported that the alkyl sulfates were decomposed only to alcohols, but he did not give any detailed discussion. The present paper deals with the mechanism of alkali fusion of alkyl sulfates as compared with that of alkyl sulfonates, which has been reported in the previous paper.[7]

1) J. D. Knight and R. Hous, *J. Am. Oil Chem. Soc.*, **36**, 195 (1959).
2) E. A. Setzkorn and A. B. Carel, *ibid.*, **40**, 57 (1963).
3) S. Nishi, *Bunseki Kagaku (Japan Analyst)*, **14**, 912 (1965).
4) H. L. Lew, *J. Am. Oil Chem. Soc.*, **44**, 359 (1967).
5) T. H. Liddicoet and L. H. Smithson, *ibid.*, **42**, 1097 (1965).
6) S. Nishi, *Bunseki Kagaku (Japan Analyst)*, **14**, 914 (1965).
7) T. Nakagawa, K. Miyajima and T. Uno, *J. Gas Chromatog.*, **6**, 292 (1968).

Experimental

Preparation of Sodium *n*-Alkyl Sulfates. One tenth mole of *n*-alkyl alcohol (alkyl carbon numbers: 5, 6, 7, 8, 9, 10, 12, 14 and 16) was placed in a 500 m*l* flask fitted with a mechanical stirrer, a dropping funnel, a thermometer, and a reflux condenser, from the top of which HCl gas was removed. The flask was cooled in an ice bath at 0—5°C and 0.1 mol of chlorosulfonic acid was added dropwise with a thorough agitation. After addition, stirring was continued for two hours at room temperature, then the reaction mixture was allowed to stand overnight, neutralized with sodium hydroxide solution, and evaporated to almost dryness. Alkyl sulfate was extracted from the dried residue with absolute ethyl alcohol for 6 hr by using a Soxhlet extractor to remove the inorganic impurity, *i. e.*, NaCl. After removing ethyl alcohol from the extract, the crude sulfate which still contained a minor amount of unchanged original alcohol was recrystallized twice from absolute ethyl alcohol, rinsed by acetone and dried in the desiccator. The raw materials, *n*-alkyl alcohols, had been purified by distillation and checked cautiously by gas chromatography. The IR spectra of the sulfates, obtained above, did not indicate contamination with the original alcohols.

Preparation of Di-*n*-alkyl Ethers. Di-*n*-alkyl ethers were prepared by Williamson's reaction. One tenth gram atom of sodium metal was dissolved in 0.2 mol of *n*-alkyl alcohol at 100°C with stirring. Then 0.1 mol of *n*-alkyl bromide with the same carbon numbers as the alcohol was added dropwise into the solution. The stirring was continued at 100°C until the pH of the reaction mixture became nearly neutral. After reaction, 100 m*l* of ethyl ether was poured into the reaction mixture and sodium bromide was removed by extracting the ethereal layer with 50 m*l* of water. The ethereal layer was dried over anhydrous sodium sulfate and the ether was removed. The residue was distilled under reduced pressure. Purity of these dialkyl ethers was checked by gas chromatography. The boiling points and the results of elemental analysis are listed in Table 1.

Other Reagents. Reagent grade LiOH, NaOH, KOH, RbOH, CsOH, were used. *cis*-*n*-2-Octene (K & K Laboratories Inc.), and *trans*-*n*-3-octene, *trans*-*n*-4-octene (Aldrich Chemical Co., Inc.), and other olefins (Tokyo Kasei Kogyo Co., Ltd.) were used without further purification. All the olefins were pure enough to use for the standard of gas chromatography.

Pyrolysis Apparatus. A Shimadzu Pyrolyzer Model PYR-1A was used. The apparatus was equipped with 170 mm length and 6 mm i. d. quartz pipe which was heated externally by nichrome wire. Its temperature was measured by thermocouple and heating was controlled by a voltage regulator. The pyrolyzer and the gas chromatography were connected in series. The alkali fusion was carried out in a platinum boat in the quartz pipe in an atomosphere of nitrogen.

Gas Chromatographic Conditions.

Apparatus: Shimadzu Gas Chromatograph Model GC-1C

Packing: 20 wt% Apiezon L, 20 wt% squalane, 10 wt% DEGS and 20 wt% PEG 20 M coated on 60/80 mesh Chromosorb W pretreated with HCl and DMCS-methanol.

Column: Stainless steel U tube, 3 mm i. d.

Carrier gas: Nitrogen

Detector: FID

The column temperature, column length, and nitrogen flow rate were appropriately adjusted in each case.

Isolation of the Pyrolyzates. Two grams of a sodium *n*-alkyl sulfate prepared was ground quickly and mixed uniformly with 10 g of alkali metal hydroxide in a mortar and put in a stainless steel reactor, which

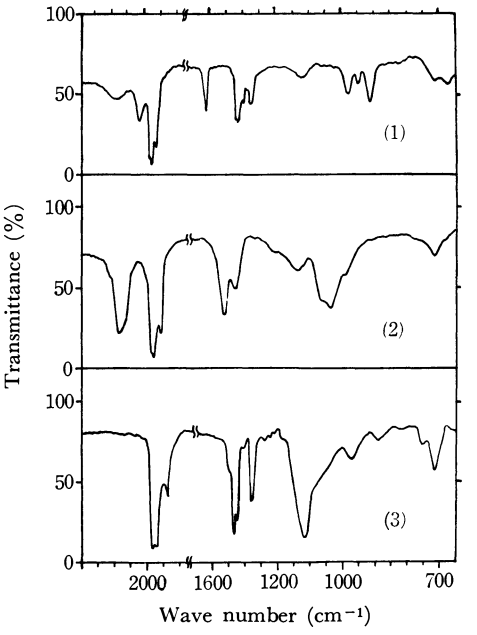

Fig. 1. Infrared spectra of alkali fusion products of sodium *n*-octyl sulfate.
(1) A mixture of *n*-1-octene and internal octene isomers
(2) *n*-Octyl alcohol
(3) Di-*n*-octyl ether

TABLE 1. BOILING POINTS AND RESULTS OF ELEMENTAL ANALYSIS OF DI-*n*-ALKYL ETHERS

Compound	Boiling point	Elemental analysis			
		Calcd		Found	
		C	H	C	H
$(n\text{-}C_6H_{13})_2O$	73—75°C/2 mmHg	77.35	14.01	77.59	14.20
$(n\text{-}C_8H_{17})_2O$	113—114°C/1 mmHg	79.26	14.14	79.55	14.00
$(n\text{-}C_{10}H_{21})_2O$	156—158°C/1.7 mmHg	80.46	14.18	80.75	14.46
$(n\text{-}C_{12}H_{25})_2O$	194—195°C/1 mmHg	81.28	14.21	81.55	14.49

was heated at 400°C for one hour. After reaction, the products were cooled and extracted with ethyl ether, and the extract was filtered, dried, and condensed carefully. Distillation of the residue gave *n*-alkyl alcohol, di-*n*-alkyl ether and a mixture of 1-olefin and internal olefin isomers with the same number of carbon atoms as the alkyl group of the original sulfates. Pentenes and hexenes were, however, so volatile that they could not be isolated. The products were identified employing authentic samples by gas chromatography and IR spectroscopy. The IR spectra of *n*-octyl alcohol, di-*n*-octyl ether, and a mixture of *n*-1-octene and internal octenes, which were the alkali fusion products of sodium *n*-octyl sulfate, and the corresponding gas chromatograms are shown in Figs. 1 and 2, respectively. Discussion on the identification of the alkali fusion products is given below.

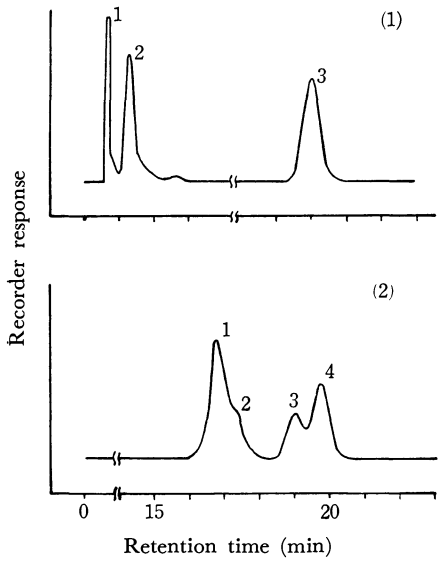

Fig. 2. Gas chromatogram of alkali fusion products of sodium *n*-octyl sulfate.
(1) 1. Overlapping peak of *n*-octene isomers
2. *n*-Octyl alcohol
3. Di-*n*-octyl ether
(2) 1. *n*-1-Octene
2. *n*-4-Octene
3. *n*-3-Octene
4. *n*-2-Octene

Results and Discussion

Identification of Alkali Fusion Products. The identification of the alkali fusion products of alkyl sulfates to be *n*-1-olefins, a mixture of internal olefins, higher alcohols, and dialkyl ethers are based on a comparison of their retention times and IR spectra with those of authentic samples.

The absorption bands of IR spectrum (Fig. 1 (1)) at 990 cm^{-1} and at 910 cm^{-1} indicate the formation of monosubstituted ethylene group and the bands at 965 cm^{-1} and 680 cm^{-1} suggest the existence of *trans*- and *cis*-disubstituted ethylene group, respectively.

On the other hand, the formation of 2,2-disubstituted and trisubstituted ethylene group is ruled out because of the absence of the absorption bands near 890 cm^{-1} and between 800 cm^{-1} and 840 cm^{-1}, respectively. According to these observations, it is concluded that the olefinic compounds obtained from the alkali fusion reaction of sodium *n*-octyl sulfate are *n*-1-octene and a mixture of *trans* and *cis* internal octene isomers, and that the branching of the alkyl group does not take place during the reaction. The IR spectra of alkali fusion products of sodium *n*-octyl sulfate shown in Figs. 1(2) and 1(3) agreed with those of authentic *n*-octyl alcohol and di-*n*-octyl ether, respectively.

Figure 2 shows the gas chromatograms of alkali fusion products of sodium *n*-octyl sulfate. The peak 1 in Fig. 2(1) is the overlapping peak of *n*-1-octene and internal octene isomers that can not be separated under the conditions (20 wt% Apiezon L, 75 cm, 220°C, 40m*l*). Peak 2 and peak 3 are assigned to *n*-octyl alcohol and di-*n*-octyl ether by comparing the retention times with those of authentic samples. Further separation of the olefinic products was carried out under the conditions (20 wt% squalane, 3 m, 100°C, 30 m*l*). In Fig. 2(2), the peak assignments to *n*-1-octene, *n*-2-octene, *n*-3-octene, and *n*-4-octene are based on a comparison of their retention times with those of standard *n*-1-octene, *cis*-*n*-2-octene, *trans*-*n*-3-octene, and *trans*-*n*-4-octene, respectively. The peak 1 is identified to be *n*-1-octene. Because a mixture of *trans*- and *cis*-*n*-2-octene gave only a single peak whose retention time agreed with that of standard *cis*-*n*-2-octene, it is assumed to be impossible to separate the mixture of *trans*- and *cis*-octene isomers from each other under the above conditions. Thus the peaks 2, peak 3, and peak 4 may be identified to be a mixture of *trans*- and *cis*-*n*-4-octenes, *n*-3-octenes, and *n*-2-octenes, respectively.

Reaction Mechanism. The mechanism of acid hydrolysis of an alkyl sulfate is represented as follows:[8]

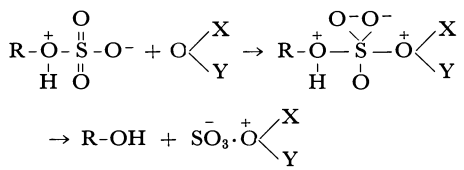

On the other hand, although alkyl sulfates are stable in the alkaline medium,[9] they are hydrolyzed to the corresponding alcohols in the fused alkali metal hydroxide. The mechanism of this reaction may be considered to be

8) V. A. Motsavage and H. B. Kostenbauder, *J. Colloid Sci.*, **18**, 603 (1960).
9) R. Aoki and E. Iwayama, *J. Pharm. Soc. Japan*, **80**, 1749 (1960).

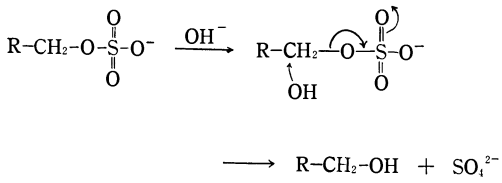

In order to elucidate the mechanism of formation of dialkyl ether, *n*-alkyl alcohol was heated with an excess amount of KOH at 400°C in a sealed glass tube. In the reaction products obtained, an appreciable amount of di-*n*-alkyl ether and a mixture of *n*-1-olefin and internal olefin isomers were detected by gas chromatography and IR spectroscopy. From these facts the mechanism of formation of di-*n*-alkyl ether and olefins may be considered to be the dehydration of one molecule of water from two molecules of *n*-alkyl alcohol, and one molecule of water from one molecule of *n*-alkyl alcohol, respectively. The formation route of internal olefins from 1-olefin was discussed in the previous paper.[7]

Effect of Alkali Metal Hydroxide and Reaction Temperature. The variation of the reaction temperature between 200°C and 500°C did not affect the kinds of the reaction products obtained. The pyrolysis without any reagent also gave the same products, but the temperature at which the reaction occured was higher than that of the pyrolysis with alkali metal hydroxide.

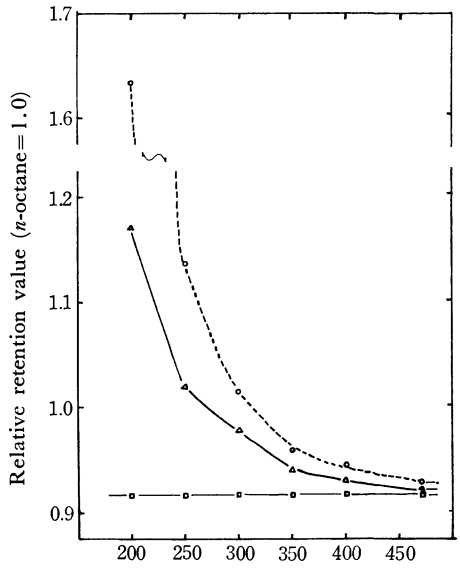

Fig. 3. Relation between alkali fusion temperature and relative retention value of *n*-1-octene from sodium *n*-octyl sulfate.

○···○ with KOH
□—□ standard *n*-1-octene
△—△ without KOH

The relation between the reaction temperature and the relative retention value against *n*-octane (the internal standard) of *n*-octenes produced by alkali fusion of sodium *n*-octyl sulfate with KOH is shown in Fig. 3. Such relation suggests that the addition of KOH accelerates the reaction. These effects, however, are not so remarkable as in the case of alkyl sulfonates.

Practical Application

The present method was applied to determine the alkyl chain carbon number distribution of the commercially available sodium alkyl sulfates (SDS). Three to five milligrams of a mixture of the same amount of SDS and KOH was put in a platinum boat in the pyrolyzer which had been heated at 400°C and the volatile reaction products were swept into a column by the continuous nitrogen stream which flowed in series from the pyrolyzer to gas chromatograph. The chromatogram of the sample B in Table 2 obtained by this method is shown in Fig. 4 (1). The chromatographic conditions were 20 wt% PEG 20M, 1.5 m, 120—240°C, temperature programming rate 10°C/min, 40 m*l*.

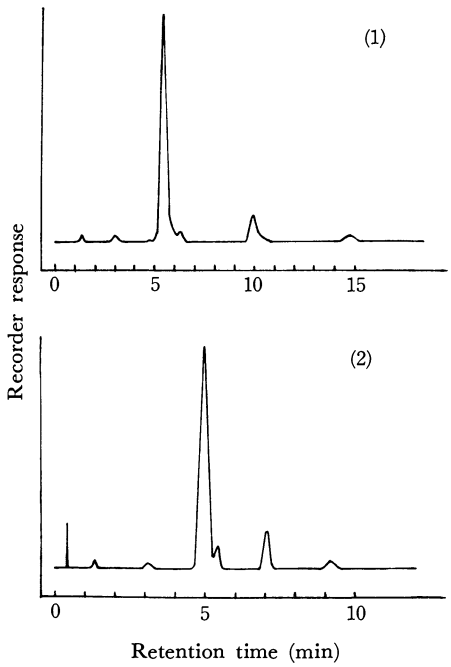

Fig. 4. Gas chromatogram of SDS.

(1) Olefinic products of alkali fusion of SDS
(2) Acetates from the same SDS

Under these conditions, the peaks of the alcohols did not interfere the separation of the olefinic products by which the alkyl carbon number distribution of the SDS was determined. On the other hand, the alcohols obtained by the acid

TABLE 2. ALKYL CARBON NUMBER DISTRIBUTION OF SDS

		Based on acetate* from SDS		Alkali fusion of SDS	
		A	B	A	B
Alkyl chain carbon number distribution, wt%	C_8	2.78	1.78	2.79	1.14
	C_{10}	2.54	1.82	2.28	1.85
	C_{12}	59.25	82.59	58.49	83.59
	C_{14}	23.83	11.48	25.79	10.56
	C_{16}	8.52	2.32	7.57	2.82
	C_{18}	3.08	trace	3.08	trace
Average molecular weight		299.76	291.00	299.85	291.37
Average alkyl chain carbon number		12.84	12.21	12.85	12.24

* Acetate from acetylation of alcohol obtained by acid hydrolysis of SDS was analyzed in Shimadzu Gas Chromatograph Model GC-1C with 75 cm × 3 mm, 10 wt% DEGS on Chromosorb W (AW, HMDS); column temp., 150—210°C, temp. programming rate, 10°C/min, nitrogen, 40 ml/min.

hydrolysis of the same SDS were acetylated by acetic anhydride in pyridine and the alkyl carbon number distribution was measured by the peaks of the acetates (Fig. 4 (2)) in order to confirm the reliability of this method. The distribution values are listed in Table 2 together with the average molecular weight and the average alkyl carbon number calculated from them. The agreement between these two methods is satisfactory. The qualitative and quantitative analysis of the lipophylic groups of *n*-alkyl sulfates can be successfully carried out by this method rapidly and briefly.

BULLETIN OF THE CHEMICAL SOCIETY OF JAPAN VOL. 41 2903—2908 (1968)

Polarography of Lead-Arginine Hydrochloride Complexes

Tsai-Teh LAI and Mon-Chao CHEN

Chemical Engineering Department, Cheng Kung University, Tainan, Taiwan, China

(Received April 11, 1968)

The complexation of lead ion with arginine hydrochloride has been studied polarographically at 30°C. Four kinds of complex species, $PbCl^+$, $Pb(H_2Arg)Cl^{2+}$, $Pb(H_2Arg)(OH)^{2+}$ and $Pb(H_2Arg)_2(OH)^{3+}$ (where H_2Arg denotes the arginine univalent cation) were confirmed in various pH range, respectively. The logarithmic dissociation constant of $Pb(H_2Arg)_2(OH)^{3+}$ was found to be 10.33 ± 0.03 at ionic strength 0.9.

The complexes of arginine with copper and zinc have been studied by polarographic and other methods and the metal-ligand ratios have been shown to be 1 : 1 and 1 : 2.[1-3] The effect of amino acid structure on the stability of the complexes formed with metals of Hg, Be, Zn and Cd has been reported by Perkins.[4,5] The stability constant of calcium-arginine chelate was determined by pH titration method.[6] The effect of temperature on the dissociation constants of arginine and its different metal complexes was investigated by Pelletier.[7]

This paper presents the results of the polarographic behavior of lead-arginine hydrochloride system.

Experimental

Apparatus. All polarograms were recorded manually using a Sargent Model XII Polarograph, equipped with a Leeds and Northrup Student Potentiometer. A modified H-cell, containing an external saturated calomel reference electrode (SCE) and a potassium chloride - agar plug was used. All experiments were carried out at 30 ± 0.1°C.

1) N. C. Li and E. Doody, *J. Am. Chem. Soc.*, **74**, 4184 (1952).
2) N. C. Li and E. Doody, *ibid.*, **76**, 221 (1954).
3) A. Taurins, *Can. J. Res.*, **28B**, 762 (1950).
4) D. J. Perkins, *Biochem. J.*, **51**, 487 (1952).
5) D. J. Perkins, *ibid.*, **55**, 649 (1953).
6) M. Hardel, *Z. Physiol. Chem.*, **346**, 224 (1966).
7) S. Pelletier, *Compt. Rend.*, **248**, 2567 (1959).

The mercury flow rate and the dropping time of the capillary used were 2.067 mg/sec and 3.56 sec respectively at an applied potential −0.5 V *vs.* SCE with the mercury column height 73.2 cm, measured in a solution which contained 1.0 mM lead nitrate, 0.4 M arginine hydrochloride, 0.5 M sodium nitrate, and 0.003% Triton X-100 at pH 6.85.

Chemicals. The stock solution of 0.01 M lead nitrate was prepared and analyzed as described previously.[8] The arginine hydrochloride (Aldrich Chemical Co.) was research grade and the solutions were freshly prepared before use. Triton X-100 was used as a maximum suppressor. Sodium nitrate was used as supporting electrolyte with which the ionic strength of the polarographic solutions were adjusted to 0.9. The pH values of the polarographic solutions were adjusted with nitric acid or sodium hydroxide and no buffer was used.

Results and Discussion

The polarographic characteristics of the lead-arginine hydrochloride complex were studied with the solutions which contained 1.0 mM lead nitrate and varying concentration of arginine hydrochloride from 0.1 M to 0.6 M over the pH range 0.80—9.05. At higher pH value precipitation occurred when the arginine hydrochloride concentration was lower than 0.2 M.

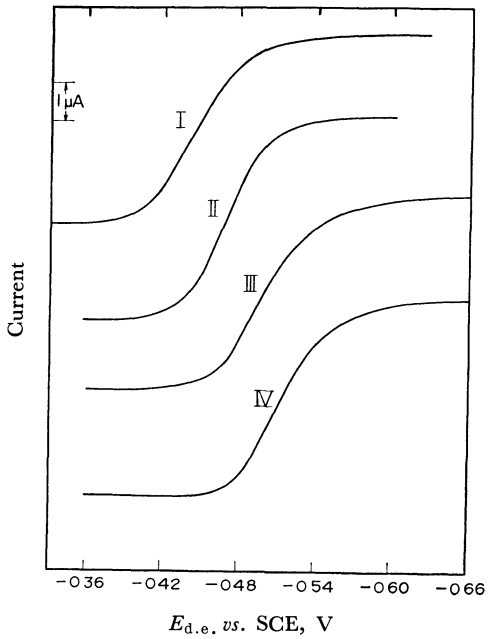

Fig. 1. Polarograms at various conditions.
1.0 mM $Pb(NO_3)_2$, $NaNO_3$ at μ 0.9, $[Cl^-]=C_{Arg}$
I 0.006% Triton X-100, C_{Arg} 0 M, pH 2.68
II 0.003% Triton X-100, C_{Arg} 0.2 M, pH 7.92
III 0.003% Triton X-100, C_{Arg} 0.2 M, pH 8.62
IV 0.003% Triton X-100, C_{Arg} 0.2 M, pH 9.05

8) T. T. Lai and C. C. Hsieh, *J. Electrochem. Soc.*, **112**, 218 (1965).

As shown in Table 1 a reversible two-electron reduction was held at pH lower than 8.30 for the ligand concentrations between 0.1 M to 0.4 M and

TABLE 1. EVIDENCE FOR THE REVERSIBILITY (1.0 mM $Pb(NO_3)_2$, 0.003% Triton X-100 and $NaNO_3$ at μ 0.9)

C_{Arg} (M)	pH	$-E_{1/2}$ *vs.* SCE (V)	$-\Delta E_{d.e.}/\Delta\log\frac{i}{i_d-i}$
0.1	0.91	0.406	0.030
	1.42	0.408	0.031
	2.62	0.410	0.031
	3.20	0.411	0.031
	4.00	0.412	0.030
	4.95	0.411	0.032
	6.18	0.423	0.029
	6.99	0.430	0.032
	7.47	0.442	0.030
	8.00	0.461	0.031
0.2	0.80	0.408	0.031
	1.45	0.408	0.030
	2.73	0.414	0.029
	4.18	0.415	0.032
	5.00	0.416	0.031
	6.05	0.427	0.028
	7.58	0.450	0.030
	8.00	0.476	0.031
0.4	0.95	0.417	0.029
	2.45	0.426	0.031
	4.50	0.427	0.028
	5.30	0.429	0.031
	6.55	0.442	0.029
	7.23	0.460	0.032
	8.30	0.502	0.030
0.6	1.30	0.423	0.029
	3.10	0.432	0.031
	4.71	0.433	0.030
	6.05	0.443	0.030
	7.78	0.488	0.028
	8.80	0.528	0.030
	8.95	0.531	0.030
	9.05	0.536	0.029

TABLE 2. QUASI-REVERSIBLE CHARACTER ABOVE pH 8.30 (1.0 mM $Pb(NO_3)_2$, 0.003% Triton X-100 and $NaNO_3$ at μ 0.9)

C_{Arg} (M)	pH	$-E_{1/2}$ *vs.* SCE (V)	$-\Delta E_{d.e.}/\Delta\log\frac{i}{i_d-i}$
0.1	8.05	0.464	0.031
	8.30	0.471	0.039
0.2	8.20	0.483	0.030
	8.45	0.490	0.039
	9.05	0.513	0.038
0.4	8.00	0.491	0.029
	8.80	0.518	0.038
	9.05	0.528	0.039

at pH lower than 9.05 for the ligand concentration 0.6 M.

At pH>8.30 and ligand concentrations between 0.1 M and 0.4 M the electrode process was regarded as a quasi-reversible reduction as can be evidenced from the slopes of $\log i/(i_d-i)$ *vs.* $E_{d.e.}$, 0.038—0.039 (Table 2), and the asymmetrical waves (Fig. 1). The distortion of the polarograms was attributed to the adsorption effect of the maximum suppressor.[9,10] In confirm this assertion solutions containing higher concentration of maximum suppressor were polarographed. As can be observed from the curve 1 in Fig. 1, the addition of 0.006% Triton X-100, was enough to cause the wave become asymmetric when the polarographic solution contained no chelating agent.

The temperature coefficient of the half-wave potential was -0.2 mV/°C at pH<8.30 and in the conditions of the asymmetrical waves it was -0.7 mV/°C, which is still in the limiting value for a reversible reduction.

The constant value of $i_d/\sqrt{h}$, 0.766±0.014, for h=71.6—32.2 cm and ligand concentration 0.1 M at pH 6.18, revealed that the limiting current was entirely diffusion-controlled.

The temperature coefficient of the diffusion current was 1.4%/°C in the whole pH range investigated in this work. This also proves the diffusion-controlled system.

Effect of pH on Half-wave Potential and Diffusion Current. The dependences of half-wave potential and diffusion current on the pH value are shown in Figs. 2 and 3 respectively. In the two figures the curves all break into four sections at the same pH values. This fact reveals the existence of four kinds of complex species at each section of pH<2.0, pH 2.0—5.0, pH 5.0—7.0 and pH 7.0—9.1.

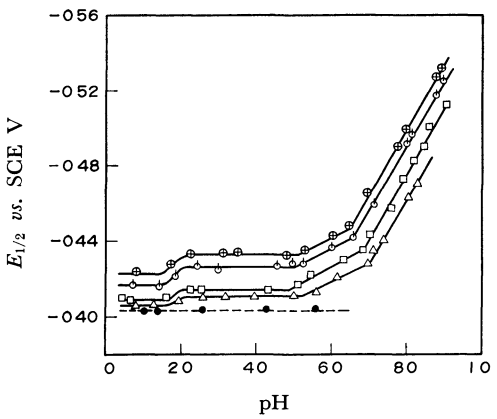

Fig. 2. Variation of half-wave potential with pH.
1.0 mM $Pb(NO_3)_2$, 0.003% Triton X-100, $NaNO_3$ at μ 0.9 $[Cl^-]=C_{Arg}$

	C_{Arg} (M)
●	0
△	0.1
□	0.2
◇	0.4
⊕	0.6

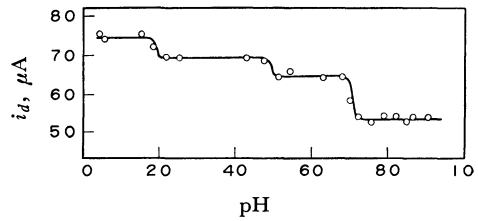

Fig. 3. Effect of pH on the diffusion current.
1.0 mM $Pb(NO_3)_2$, 0.003% Triton X-100, $NaNO_3$ at μ 0.9 $[Cl^-]=C_{Arg}=0.2$ M

The horizontal lines at pH<2.0 for varying concentrations of complexing agent in Fig. 2 were ascribed to the formation of the lead chloro complex rather than the lead-arginine complex, as can be confirmed by the half-wave potential data of the lead-sodium chloride system in Table 3.

In the pH range 2.0—5.0, the half-wave potentials shifted a little to negative side, and the diffusion current decreased (Fig. 3). These changes indicate the participation of arginine ligand to the lead-chloro complex.

In the pH range 5.0—7.0 in Fig. 2, the slope of the curve is 0.010 V. This minute slope demonstrates the partial substitution of the chloride ligand in the lead complex with the hydroxyl ligand and the releasing of the hydroxyl ion in the cathodic reduction. The higher the ligand concentration, the greater the shifting of the breaking point to lower pH value. This fact indicates that the higher arginine concentration is in favor of the substitution of the chloride ligand with the hydroxyl ligand.

When the pH value is greater than 7.0, the $E_{1/2}$ *vs.* pH curves show a third inflection with a slope of 0.034 V, showing that one hydroxyl ion was involved in the reduction.

It is obvious from Fig. 3, that each change in complex species resulted in a separate diffusion current drop.

Effect of Ligand Concentration on Half-wave Potential. To determine the metal-ligand ratio of the lead-arginine hydrochloride complexes, the half-wave potentials were plotted against the logarithm of the concentration of arginine hydrochloride (Fig. 4).

As shown in Fig. 4, lead does not form complexes with arginine hydrochloride below pH 5.0 when the ligand concentration is lower than 0.22 M. At pH<2.0 and C_{Arg}>0.22 M, the reciprocal slope is 0.030 V. In referring to the Fig. 2 and Table 3, the formation of the complex species, $PbCl^+$, was

9) J. Koryta, *Coll. Czech. Chem. Commun.*, **18**, 206 (1953).
10) J. Weber, J. Koutecky and J. Koryta, *Z. Electrochem.*, **63**, 583 (1959).

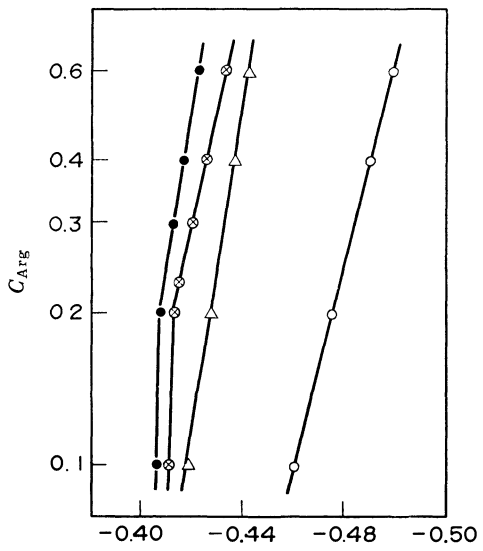

Fig. 4. Plots of C_{Arg} *vs.* $E_{1/2}$ ($[Cl^-]=C_{Arg}$).
1.0 mM $Pb(NO_3)_2$, 0.003% Triton X-100, $NaNO_3$ at μ 0.9
● pH 1.08; ⊗ pH 3.00; △ pH 6.05; ○ pH 8.00

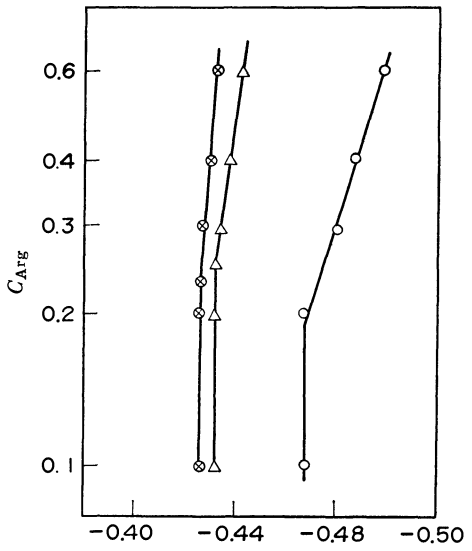

Fig. 5. Plots of log C_{Arg} *vs.* $E_{1/2}$ ($[Cl^-]=0.60$ M).
1.0 mM $Pb(NO_3)_2$, 0.003% Triton X-100, $NaNO_3$ at μ 0.9
⊗ pH 3.00; △ pH 6.05; ○ pH 8.00

proved. When $C_{Arg}>0.22$ M, the reciprocal slopes of the other curves in Fig. 4 are 0.044 V, 0.030 V, and 0.050 V; those values show the ligand numbers to be 1.5, 1.0 and 1.7 for the pH ranges 2.0—5.0, 5.0—7.0 and 7.0—9.1 respectively.

TABLE 3. POLAROGRAPHIC CHARACTERISTICS OF Pb-NaCl SYSTEM AT LOW pH REGION (1.0 mM $Pb(NO_3)_2$, 0.003% Triton X-100 and $NaNO_3$ at μ 0.9)

NaCl (M)	pH	$-E_{1/2}$ *vs.* SCE (V)	i_d (μA)	$-\Delta E_{d.e}/\Delta\log\frac{i}{i_d-i}$
0.1	0.78	0.407	7.75	0.030
	3.08	0.406	7.54	0.031
0.2	0.69	0.409	7.85	0.031
	1.40	0.408	7.65	0.030
	3.00	0.409	7.65	0.030
0.4	1.34	0.417	7.60	0.032
	2.71	0.417	7.70	0.031
	2.58	0.417	7.80	0.029
	3.50	0.417	7.70	0.030
0.6	2.55	0.423	7.60	0.031
	3.81	0.423	7.70	0.029

The competition between arginine and chloride ion for electron pair donation to the lead ion was demonstrated in Fig. 5, in which the polarographic solutions contained sodium chloride besides arginine hydrochloride to maintain the chloride ion concentration at 0.60 M.

It is evident from Fig. 5, when $C_{Arg}<0.22$ M and $[Cl^-]=0.60$ M, the chloride ion predominate arginine in the competition for electron pair donation in the pH range 2.0—9.1. Even under the condition, $C_{Arg}>0.22$ M at pH<5.0, the arginine ligand predominates scarcely the chloride ligand, and the arginine coordinates with lead ion rather weakly, as can be confirmed from the minute reciprocal slope 0.016 V in Fig. 5. When $C_{Arg}>0.22$ M, the reciprocal solopes are 0.030 V and 0.052 V for the pH ranges 5.0—7.0 and 7.0—9.1, respectively, indicating the formation of 1 : 1 and 1 : 2 lead-arginine complexes in these pH ranges.

Complex Species and Dissociation Constant. The pK_1 and pK_2 values of arginine are 2.17 and 9.04[11] and the isoelectric point is 10.76,[12] so that the predominant ligand species in the pH region studied in this work must be arginine univalent cation (H_2Arg^+) rather than the dipolar molecule (HArg).

If a complex $Pb(H_2Arg)_m(OH)_nCl_r^{2+m-n-r}$ was formed in the solution, the cathodic reduction at the dropping mercury electrode must be

$$Pb(H_2Arg)_m(OH)_nCl_r^{2+m-n-r} + 2e + Hg = Pb(Hg) + mH_2Arg^+ + nOH^- + rCl^- \quad (1)$$

The shift of the half-wave potential by complexation and reduction in Eq. (1) must obey:

11) E. H. Rodd, "Chemistry of Carbon Compounds," Vol. 1, Elsevier Publishing Co. (1951), p. 1341.
12) L. F. Fieser and M. Fieser, "Introduction to Organic Chemistry," D. C. Heath and Co., Boston (1957), p. 301.

Table 4. Ligand number and complex species

pH range	Ligand concn. $C_{Arg}=[Cl^-]$	Total ligand No. $(m+r)$	Arginine ligand No. (m)	Cl^- ligand No. (r)	OH^- ligand No. (n)	Complex species
0.8—2.0	0—0.22	0	0	0	0	Pb^{2+}
	0.22—0.6	1.0	0	1.0	0	$PbCl^+$
2.0—5.0	0—0.22	0	0	0	0	Pb^{2+}
	0.22—0.6	1.5	0.5	1.0	0	$Pb(H_2Arg)Cl^{2+}$
5.0—7.0	0.22—0.6	1.0	1.0	0	0.3	$Pb(H_2Arg)(OH)^{2+}$
7.0—9.1	0.22—0.6	1.7	1.7	0	1.1	$Pb(H_2Arg)_2(OH)^{3+}$

$$(E_{1/2})_c = (E_{1/2})_s + 0.030\log K_c - 0.030\log(D_c/D_s) - 0.030m\log[H_2Arg^+] - 0.030n\log[OH^-] - 0.030r\log[Cl^-] \quad (2)$$

where $K_c = \dfrac{[H_2Arg^+]^m[OH^-]^n[Cl^-]^r[Pb^{2+}]}{[Pb(H_2Arg)_m(OH)_nCl_r^{2+m-n-r}]}$

D_c and D_s are diffusion coefficients of complex and simple lead ion, respectively.

For $pK_1 < pH < pK_2$

$$C_{Arg} \simeq [H_2Arg^+] = [Cl^-]$$

and $$-\log[OH^-] = 14 - pH$$

where C_{Arg} is the nominal concentration of arginine hydrochloride solution, then, the values of m, n and r can be determined as follows:

$$m + r = -\Delta(E_{1/2})_c/0.030(\Delta\log C_{Arg})$$

(when pH keeps constant)

$$m = -\Delta(E_{1/2})_c/0.030(\Delta\log C_{Arg})$$

(when both pH and $[Cl^-]$ keeps constant)

$$n = -\Delta(E_{1/2})_c/0.030(\Delta pH)$$

(when C_{Arg} keeps constant)

and $r = (m + r) - m$

Results based on the foregoing polarographic data and discussion were summarized in Table 4. Thus, the predominant complex species formed in various pH range were proved to be $PbCl^+$, $Pb(H_2Arg)Cl^{2+}$, $Pb(H_2Arg)(OH)^{2+}$ and $Pb(H_2Arg)_2(OH)^{3+}$ for pH <2.0, pH 2.0—5.0, pH 5.0—7.0 and pH 7.0—9.1, respectively. These change in complex species and the increment in the size for each complex may cause the stepwise decrease in diffusion current. This reduction was in good agreement with the results in Fig. 3 and was supported by Fig. 2.

Although from the data in Figs. 2, 4 and 5 the assignment of other formula $Pb(H_2Arg)(Harg)^{3+}$ in pH 7.0—9.1 is possible, the calculated dissociation constant ($pK_c=4.87\pm0.03$) (Table 5) shows that it is much less stable than $Pb(H_2Arg)_2(OH)^{3+}$ ($pK_c=10.33+0.03$) (Table 6), so that the latter formula was adopted as a predominant species.

In these complex species mentioned above only the complex species $Pb(H_2Arg)_2(OH)^{3+}$ in pH 7.0—9.1 can be regarded as a steady form and the others are in transition.

Table 5. Dissociation constants of $Pb(H_2Arg)(HArg)^{3+}$

pH	C_{Arg}	$(E_{1/2})_s-(E_{1/2})_c$	$(i_d)_c/(i_d)_s$	pK_c
7.0	0.1	0.026	0.79	4.87
	0.2	0.040	0.73	4.84
	0.4	0.056	0.72	4.87
	0.6	0.065	0.71	4.88
8.0	0.1	0.057	0.73	4.87
	0.2	0.072	0.71	4.87
	0.4	0.087	0.67	4.87
	0.6	0.096	0.64	4.88
				ave. 4.87 ± 0.03

Table 6. Dissociation constant of $Pb(H_2Arg)_2(OH)^{3+}$

pH	C_{Arg}	$(E_{1/2})_s-(E_{1/2})_c$	$(i_d)_c/(i_d)_s$	pK_c
7.0	0.1	0.026	0.79	10.33
	0.2	0.040	0.73	10.30
	0.4	0.056	0.72	10.34
	0.6	0.065	0.71	10.35
8.0	0.1	0.057	0.73	10.33
	0.2	0.072	0.71	10.33
	0.4	0.087	0.67	10.33
	0.6	0.096	0.64	10.34
				ave. 10.33 ± 0.03

When a complex species $Pb(H_2Arg)_m(OH)_n^{2+m-n}$ is reduced reversibly, the half-wave potential obeys the Eq. (2) except losing the last term, $-0.030\,r\log[Cl^-]$.

In pH range, $pK_1 \ll pH < pK_2$

$$[H_2Arg^+] = \frac{C_{Arg}\cdot[H^+]}{[H^+]+K_2}$$

and $$D_c/D_s = (i_d)_c/(i_d)_s$$

then, $$pK_c = \frac{(E_{1/2})_s-(E_{1/2})_c}{0.030} - \frac{1}{2}\log(i_d)_c/(i_d)_s - m\log C_{Arg} + (m-n)pH + m\log([H^+]+K_2) + 14n$$

It has been shown above that at pH 7.0—9.1, $m=1.7$ (Fig. 4) and $n=1.1$ (Fig. 2). Then, the dissociation constant of the comlpex $Pb(H_2Arg)_2(OH)^{3+}$ was calculated to be $pK_c=10.33+0.03$ (Table 6).

The authors thank the National Council of Science which supported the work described.

BULLETIN OF THE CHEMICAL SOCIETY OF JAPAN VOL. 41 2908—2913 (1968)

The Thermal Decomposition of Hexamminenickel(II) Complexes

Nobuyuki TANAKA, Masahiro KAGAWA and Minoru KAMADA*1

Department of Chemistry, Faculty of Science, Tohoku University, Sendai

(Received May 9, 1968)

From the thermogravimetric analysis, hexamminenickel(II) complexes were confirmed to decompose in two or three steps through lower ammine intermediates $NiX_m \cdot nNH_3$: $n=2$, 1 and $m=2$ for X=Cl; $n=2$ and $m=2$ for X=I, Br; $n=4$ and $m=2$ for $X=NO_3$ and $n=2$, 1/2 and $m=1$ for $X=SO_4$. The diffuse reflectance spectra of these intermediates have been measured in a range between 5000 to 27000 cm^{-1}, and they suggested that these intermediates may be polymers in which nickel ions were octahedrally coordinated with ammonia molecules and bridging halogen atoms. The infrared absorption spectra of these intermediates obtained in a range between 5000 and 60 cm^{-1} are also reported.

There have been several papers on the relative thermal stability, the stoichiometry of the decomposition process and other thermal properties of hexamminenickel(II) complexes.[1-4] In addition, the kinetics of the decomposition process and the structures of the intermediates have been reported recently.[5-10] Nevertheless, the effects of the heating rate on the processes and the structures of the intermediates in the thermal decomposition of hexamminenickel(II) complexes do not seem to be satisfactorily clear yet.

In the present study, the decomposition processes of various salts of hexamminenickel(II) have been reexamined by the methods of thermogravimetric analysis under the condition of smaller heating rates and by the chemical analysis of the intermediates. The structures of the intermediates have also been investigated by the measurements of the diffuse reflectance spectra and the infrared absorption spectra.

Experimental

Preparation of Complexes. Chloride, bromide, iodide, sulfate and nitrate of hexamminenickel(II) were precipitated from the strongly ammoniacal solution of nickel sulfate with appropriate ammonium salts. Only the sulfate was precipitated with ethanol because of its greater solubility in water. These compounds were recrystallized from concentrated ammonia, washed with ethanol and ether, and dried in air. They were identified by the measurements of their infrared absorption spectra.

Apparatus and Procedure. Thermogravimetric curves were recorded with a recording thermobalance, Shimadzu Thermano Balance RT-2, with 400 mg of sample at about 3°C/min of heating rate in nitrogen atmosphere of the flow rate of about 300 ml/min.

Hitachi infrared spectrometers EPI-2G and FIS-1 were used for the measurement of the infrared absorption spectra in the regions from 5000 to 400 cm^{-1} and from 500 to 60 cm^{-1}, respectively. Nujol mull method was adopted; in potassium bromide disk an absorption band due to ammonium ions was observed at 1400 cm^{-1}, which were considered to be formed by the reaction between ammonia of a complex or an intermediate and a trace of water contained in potassium bromide.

The diffuse reflectance spectra were recorded for magnesium oxide as a reference with a standard integrating sphere attached to a Hitachi spectrophotometer Type EPU-2 and a recording EPS-3T.

*1 Present address: Department of Chemistry, College of General Education, Tohoku University, Kawauchi, Sendai.

1) W. Biltz and B. Fetkenheuer, *Z. Anorg. Chem.*, **83**, 163 (1913); **89**, 134 (1914).
2) F. Ephraim and F. Muller, *Ber.*, **54**, 973 (1921).
3) T. D. George and W. W. Wendlandt, *J. Inorg. Nucl. Chem.*, **25**, 395 (1963).
4) M. Viltange, *Mikrochim. Acta*, **1965** (4), 609.
5) T. Flora, *Acta Chim. Acad. Sci. Hung.*, **48**(3), 225 (1966).
6) I. G. Murgulescu, E. Segal and D. Fătu, *Rev. Roumaine Chim.*, **11**(3), 291 (1966).
7) I. G. Murgulescu and E. Segal, *Acad. Rep. Polulare Romine, Studii Cercetari Chim.*, **10**, No. 1, 39 (1962).
8) I. G. Murgulescu and E. Segal, *Rev. Roumaine Chim.*, **11**(1), 13 (1966).
9) S. M. Nelson and T. M. Shepherd, *J. Chem. Soc.*, **1965**, 3276.
10) R. J. H. Clark and C. S. Williams, *J. Chem. Soc.*, (*A*), **1966**, 1425.

The chemical analysis was carried out as follows: Nickel and sulfate contents were determined by the gravimetric method by precipitating nickel ions with dimethylglyoxime and sulfate ions with barium chloride. The determination of halogens was followed by Fajans' method after removing nickel ions with a cation exchanger Dowex-50W-X8 in Na-form. Ammonia was analyzed in the following way. After a sample was dissolved into a known amount of excess standard hydrochloric acid, the unreacted acid was determined by the back titration with a standard sodium hydroxide solution. The mixed indicator, *i. e.*, the alcoholic solution of bromocresol green and methyl red, was used to detect the end-point (pH 5.5). Its color is gray or colorless at the end-point, pink in an acid and green in an alkaline region. It was found from the preliminary experiments carried out with synthetic samples that the color of nickel ions did not interfere with the detection of the end-point and the result was not affected by the amount of ammonium ions present in the solution. After removing nickel ions by using a cation exchanger in the potassium form, the nitrate content was determined with spectrophotometric method using absorption band at 200 mμ which is due to the charge transfer between a nitrate ion and a water molecule.

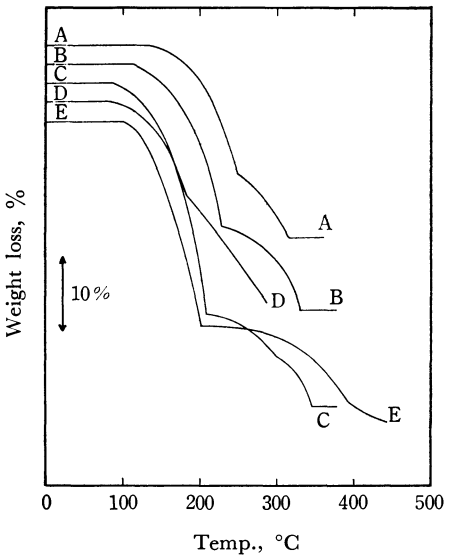

Fig. 1. Thermogravimetric curves of (A) $[Ni(NH_3)_6]I_2$, (B) $[Ni(NH_3)_6]Br_2$, (C) $[Ni(NH_3)_6]Cl_2$, (D) $[Ni(NH_3)_6](NO_3)_2$ and (E) $[Ni(NH_3)_6]SO_4$.

Results and Discussion

Thermogravimetric and Chemical Analyses. Figure 1 shows the thermogravimetric curves of hexamminenickel(II) complexes. The values of weight loss determined by the measurement of the thermogravimetric curves were well agreed with the calculated values, when the weight loss was assumed to be due to only the loss of ammonia. The analytical data of the intermediates are given in Table 1.

Hexamminenickel(II) chloride decomposed in three steps. On the thermogravimetric curves, the first one corresponding to the reaction

$$[Ni(NH_3)_6]Cl_2 \rightarrow NiCl_2 \cdot 2NH_3 + 4NH_3$$

proceeded in a temperature range from 85 to 211°C, the second one corresponding to the reaction

$$NiCl_2 \cdot 2NH_3 \rightarrow NiCl_2 \cdot NH_3 + NH_3,$$

from 211 to 303°C and the third one corresponding to the reaction

$$NiCl_2 \cdot NH_3 \rightarrow NiCl_2 + NH_3,$$

from 303 to 350°C. Since a small amount of NH_4Cl was formed above 300°C, the results of chemical analyses of $NiCl_2 \cdot NH_3$ and $NiCl_2$ somewhat deviated from the calculated values. However, the diffuse reflectance spectra and the infrared absorption spectra of these two intermediates

Table 1. Analytical data of intermediates

	Ni, %		NH_3, %		Anion, %	
	Found	Calcd	Found	Calcd	Found	Calcd
$[Ni(NH_3)_6]Cl_2$	25.4	25.3	43.8	44.1	30.6	30.6
$NiCl_2 \cdot 2NH_3$	35.6	35.9	20.6	20.8	43.4	43.3
$[Ni(NH_3)_6]Br_2$	18.3	18.3	32.0	31.9	49.9	49.8
$NiBr_2 \cdot 2NH_3$	23.0	23.2	13.4	13.5	63.2	63.3
$NiBr_2$	26.4	26.9			71.3	73.1
$[Ni(NH_3)_6]I_2$	14.0	14.2	24.5	24.6	61.1	61.2
$NiI_2 \cdot 2NH_3$	16.6	16.9	9.8	9.8	72.6	73.2
NiI_2	18.3	18.8			80.1	81.2
$[Ni(NH_3)_6]SO_4$	22.0	22.8	37.4	39.8	36.1	37.4
$NiSO_4 \cdot 2NH_3$	30.5	31.1	17.6	18.0	51.2	50.9
$NiSO_4 \cdot \frac{1}{2}NH_3$	35.4	36.0	5.0	5.2	58.6	58.8
$NiSO_4$	36.5	37.9			59.7	62.1
$[Ni(NH_3)_6](NO_3)_2$	20.5	20.6	35.9	35.9	43.9	43.5
$Ni(NO_3)_2 \cdot 4NH_3$	23.4	23.4	27.1	27.2	48.2	45.4

indicated that the greater parts of these intermediates were $NiCl_2 \cdot NH_3$ and $NiCl_2$, respectively.

The formation of $NiCl_2 \cdot NH_3$ is considered to depend greatly on the experimental condition, especially on the heating rate. For example, according to George and Wendlandt,[3] $NiCl_2 \cdot NH_3$ was not found in the process of decomposition at the larger heating rate, 7°C/min.

Hexamminenickel(II) iodide and bromide decomposed to NiX_2 (X=Br, I), obviously in two steps through $NiX_2 \cdot 2NH_3$. The first step,

$$[Ni(NH_3)_6]X_2 \rightarrow NiX_2 \cdot 2NH_3 + 4NH_3$$

proceeded at 109 to 231°C for X=Br and at 131 to 252°C for X=I. The second step,

$$NiX_2 \cdot 2NH_3 \rightarrow NiX_2 + 2NH_3$$

took place at 231 to 335°C for X=Br and at 252 to 318°C for X=I. Although the formation of $NiBr_2 \cdot NH_3$ had been reported,[1,5] it was not observed in this experiment.

Hexamminenickel(II) sulfate also decomposed to anhydrous $NiSO_4$ in three steps through $NiSO_4 \cdot 2NH_3$ and $NiSO_4 \cdot \frac{1}{2}NH_3$. The reaction,

$$[Ni(NH_3)_6]SO_4 \rightarrow NiSO_4 \cdot 2NH_3 + 4NH_3$$

proceeded at 100 to 205°C, the reaction,

$$NiSO_4 \cdot 2NH_3 \rightarrow NiSO_4 \cdot \tfrac{1}{2}NH_3 + \tfrac{3}{2}NH_3$$

at 205 to 397°C, and the reaction,

$$NiSO_4 \cdot \tfrac{1}{2}NH_3 \rightarrow NiSO_4 + \tfrac{1}{2}NH_3$$

at 397 to 455°C. $NiSO_4 \cdot \frac{1}{2}NH_3$ was not found at the heating rate 7°C/min,[3] whereas it was found at the heating rate 5°C/min.[4]

Hexamminenickel(II) nitrate was changed to $Ni(NO_3)_2 \cdot 4NH_3$ in a temperature range from 78 to 181°C by the reaction,

$$[Ni(NH_3)_6](NO_3)_2 \rightarrow Ni(NO_3)_2 \cdot 4NH_3 + 2NH_3 \cdot$$

Upon further heating, it decomposed violently leaving a black residue. The ratio of ammonia to nickel contents in this intermediate was confirmed to be exactly 4 : 1 by the chemical analysis. George and Wendlandt,[3] and Viltange[4] have reported that the intermediate which was formed at the first step had ammonia less than 4 mol. This disagreement is considered mainly due to the difference in heating rate. The smaller heating rate employed in this experiment may be the main cause of the formation of the tetrammine intermediate, similarly to the fact that $NiCl_2 \cdot \frac{1}{2}NH_3$ has been demonstrated by Murgulescu *et al.*[6] at the smaller heating rate, 2°C/min.

The thermal stability or the decomposition temperature of hexamminenickel(II) complexes at which a complex begins to decompose increased in order of the nitrate<the chloride<the sulfate<the bormide<the idodide. Especially, the order of the halides is the same as the increasing order of the size of halide ions, *i. e.*, $Cl^- < Br^- < I^-$. This may indicate a possibility that the dissociation of ammonia of hexamminenickel(II) complexes occurs after an outer-sphere ion enters into the coordination sphere (S_N2 mechanism), because, if the bond breaking between ammonia and nickel takes place before the bond formation between nickel and outer-sphere ion, the decomposition temperature is expected to be independent of the kind of outer-sphere ion.

Diffuse Reflectance Spectra. The wave numbers of the band maxima of diffuse reflectance spectra of hexamminenickel(II) complex and the intermediates are given in Table 2. The measurement of NiI_2 was not successful.

The diffuse reflectance spectra of nickel(II) chloride and nickel(II) bromide have been analyzed in the field of octahedral symmetry,[11] and these halides are reported to have a polymeric structure similar to cadmium chloride.[11] The reflectance spectra of $NiCl_2 \cdot 2NH_3$, $NiBr_2 \cdot 2NH_3$ and $NiI_2 \cdot 2NH_3$ obtained in the region above 10000 cm^{-1} have also been reported.[9,10] These compounds

TABLE 2. WAVE NUMBERS OF BAND MAXIMA OF DIFFUSE REFLECTANCE SPECTRA (in 10^3 cm^{-1})

Complex	Assignment*					
	$^3T_{2g}$ (F)		$^3T_{1g}$ (F)			$^3T_{1g}$ (P)
$[Ni(NH_3)_6]Cl_2$	—		17.9			
$NiCl_2 \cdot 2NH_3$	7.7		14.3	19.8 w	23.0 sh	24.9
$NiCl_2 \cdot NH_3$	—	12.5 sh	13.3			22.7
$NiCl_2$	—	12.2 sh	13.0	9.0 sh		22.2
$[Ni(NH_3)_6]Br_2$	11.1		17.9			
$NiBr_2 \cdot 2NH_3$	7.3		13.9	18.9 w	22.2 sh	24.1
$NiBr_2$	7.0		11.9	16.5 w	18.2 sh	20.7
$[Ni(NH_3)_6]I_2$	11.1		17.9			
$NiI_2 \cdot 2NH_3$	7.3		13.9			23.3

* Assignment is for O_h symmetry. sh means shoulder; w means weak. — not measured.

11) A. Ludi and W. Feitknecht, *Helv. Chim. Acta*, **46**(3), 2226 (1963).

are considered to have polymeric pseudo-octahedral symmetry; the absorption band, $^3A_{2g} \rightarrow {}^3T_{2g}$ (F), was confirmed in this experiment. Their configurational structure is assumed to be not similar to $CdCl_2$ but similar to $NiCl_2 \cdot 2py$ (py= pyridine). In $NiX_2 \cdot 2NH_3$ (X=halogens), each nickel ion is considered to be surrounded by four bridging halogens arranged in a square planar configuration and two ammonia molecules located in trans position. Some spin-forbidden bands were observed because the symmetry of their ligand field was lower than the octahedral one.

It may be concluded from these results that the nickel ion keeps the coordination number 6 in whole thermal decomposition process when ammonia molecules are replaced stepwise by halogen ions. The fact that ammonia molecules and halogens are coordinated to a nickel ion is important for the band assignment of the infrared absorption spectra of these intermediates.

Although a nickel(II) ion of monoammine compound, $NiCl_2 \cdot NH_3$, is considered to be also six-coordinated because its spectrum has a great resemblance to that of $NiCl_2$ or $NiCl_2 \cdot 2NH_3$, its configurational structure has not been known yet.

Nelson and Shepherd[9] were successful in explaining the well-known fact that $NiX_2 \cdot 4py$ could be prepared whereas $NiX_2 \cdot 4NH_3$ has not been found yet. According to their discussion, in the case of $NiX_2 \cdot 4py$, the excess negative charge on nickel caused by the electron transfer from coordinated halogen could be reduced with the presence of a π-electron acceptor capacity of coordinated pyridine molecule; the "electroneutrality principle" holds. This seems to be the most probable cause of the stabilization of $NiX_2 \cdot 4py$. This consideration explains the instability of $NiX_2 \cdot 4NH_3$, because an NH_3 molecule does not have such a π-electron acceptor capacity and, consequently, if the compound were formed, negative charges must be localized on nikel. Since bridging halogens have a smaller capacity of electron transfer, $NiX_2 \cdot 2NH_3$ may exist in stable form though it has four halogens coordinated to nickel ion. The discussion cited above may be one of the important examples in which the process of the thermal decomposition is attempted to be explained from the considerations of the electronic structure.

Infrared Absorption Spectra. Figure 2 shows the infrared absorption spectra of the chloride, and Table 3 gives the wave numbers and the assignment of the absorption bands of the hexamminenickel(II) halides and their thermal decomposition products.

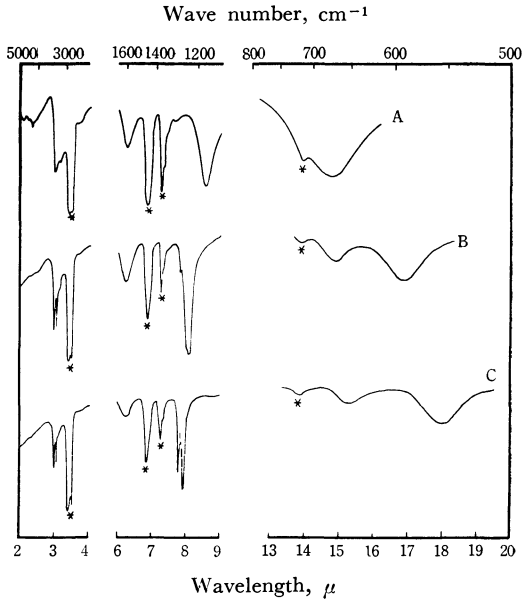

Fig. 2. The infrared absorption spectra of (A) $[Ni(NH_3)_6]Cl_2$, (B) $NiCl_2 \cdot 2NH_3$ and (C) $NiCl_2 \cdot NH_3$ in the range from 5000 cm^{-1} to 500 cm^{-1}. Optical density scale displaced arbitrarily.
* Indicates the Nujol band.

Table 3. The wave numbers of the main infrared absorption bands of $[Ni(NH_3)_6]X_2$ and the related compounds

	ν(NH)	$\delta_{deg}(NH_3)$	$\delta_s(NH_3)$	$\rho_r(NH_3)$	ν(NiN)	ν(NNiN)	Lattice
$[Ni(NH_3)_6]Cl_2$	3344 s	1607m	1176 s	683.2sb	334 s	220 s	120 s
$[Ni(NH_3)_6]Br_2$	3344 s	1607m	1187 s	673.1sb	327 s	216 s	95 s
$[Ni(NH_3)_6]I_2$	3322 s	1597m	1203 s	655.2sb	321 s	214 s	85 s

	ν(NH)		$\delta_{deg}(NH_3)$	$\delta_s(NH_3)$	$\rho_r(NH_3)$		ν(NiN)	ν(NiX)		
$NiCl_2 \cdot 2NH_3$	3344 s	3268 s	1607m	1243 s	674.0w	590.3m	435 s	216sb	189 s *	150 s *
$NiBr_2 \cdot 2NH_3$	3344 s	3268 s	1610m	1249 s	674.0w	603.1m	—	191 s	156 s *	135 s *
$NiI_2 \cdot 2NH_3$	3322 s	3236 s	1597m	1243 s	—	618.4m	—	178 s	130 s	116 s *
$NiCl_2 \cdot NH_3$	3344 s	3268 s	1604m	1287 s 1264 s		555.6m	—	250sb	206sb*	130w*
$NiCl_2$								292m	235sb*	193m*
$NiBr_2$								229 s	163 s *	140 s *
NiI_2								183 s	161 s *	118 s *

s, strong; m, medium; w, weak; sb, strong and broad.
— not observed. * not assigned.

TABLE 4. THE WAVE NUMBERS OF THE INFRARED ABSORPTION BANDS OF $[Ni(NH_3)_6]SO_4$ AND $[Ni(NH_3)_6](NO_3)_2$ AND THE RELATED COMPOUNDS (cm^{-1})

	ν(NH)		$\delta_{deg}(NH_3)$	$\delta_s(NH_3)$	$\rho_r(NH_3)$	SO_4^{2-}				
$[Ni(NH_3)_6]SO_4$	3344 s	3185 m	1636 m	1219 mb	683.7 sb	1082 sb	971.0 w	610.5 sb		
$NiSO_4 \cdot 2NH_3$	3378 s	3356 s	1617 m	1226 m	590.4* s	1202 m	1116 s	1062 s	984.3 m	719.4 m
						669.2 m	509.4 m	590.4* s		
						NO_3^-				
$[Ni(NH_3)_6](NO_3)_2$	3356 s	3268 m	1620 m	1196 s	653.5** sb	1349 s	831.9 m	653.5** sb		
$Ni(NO_3)_2 \cdot 4NH_3$	3378 s	3300 m	1620 m	1207 s	645.6*** sb	1404 s	1323 s	1047 m	814.3 m	645.6*** sb

*, **, and ***, may overlap each other, respectively.

The assignment of the absorption bands of hexamminenickel(II) halides has been reported previously.[4,12] It is interesting to know how the absorption bands due to ammonia are affected by the structure change which occurs when the monomeric structure in the hexammine complex is changed to the polymeric one bridged with halogen ions in the lower ammine intermediates.

In the case of the diamminenickel(II) chloride, for example, the ν(NH) split into two peaks, whereas $\delta_{deg}(NH_3)$ neither split nor shifted, compared with those of hexamminenickel(II) chloride. The $\delta_s(NH_3)$, being affected by the structure change, shifted to higher wave numbers. Ammonia is considered to coordinate to nickel ion from the diffuse reflectance spectra, which suggests that the absorption band due to the $\rho_r(NH_3)$ must appear. A weak absorption band, however, was observed in the usual rocking region, while a strong absorption band appeared at 590.3 cm^{-1} and a new band at 435 cm^{-1}. This phenomenon has been recently reported on various kinds of diammine complexes by Clark and Williams,[10] who assigned the former two bands to $\rho_r(NH_3)$ and the latter to the ν(NiN). Although $\delta_s(NH_3)$, $\rho_r(NH_3)$ and ν(NiN) are generally expected from their modes of vibration to shift to the same direction, the experimental results did not agree with this expectation. However, since ammonia and halogen must be coordinated to nickel ion, this assignment is considered as reasonable. Especially, the $\rho_r(NH_3)$ of the diammine complexes shifted to higher wave numbers in order of the iodide > the bromide > the chloride, which was the reverse of the order in the hexammine compounds. This change may be explained by considering that the effect of outer-sphere ions[12] disappears as the halogen ion is coordinated to nickel. The ν(NiN) of the diammine complexes was observed at higher wave numbers by 100 cm^{-1} than that of hexamminenickel(II). The reason why, in the case of the diammine complexes, the $\delta_s(NH_3)$ and ν(NiN) shift to higher wave numbers in the opposite direction of the $\rho_r(NH_3)$ has not been understood yet. The strong absorption band observed at 216 cm^{-1} may be assigned to ν(NiCl). However, other absorption bands observed at 189 cm^{-1} and 150 cm^{-1} were not assigned yet. The same was also observed with the bromides and the iodides.

Nickel chloride, bromide and iodide gave the same type of absorption bands. The absorption bands at 292 cm^{-1} for nickl chloride, at 229 cm^{-1} for nickel bromide and at 183 cm^{-1} for nickel iodide may be assigned to ν(NiCl), ν(NiBr) and ν(NiI), respectively. Other absorption bands were not assigned.

As to monoamminenickel(II) chloride, $NiCl_2 \cdot NH_3$, the $\delta_s(NH_3)$ split and shifted to higher wave numbers than that of diamminenickel(II), whereas the $\rho_r(NH_3)$ shifted to lower wave numbers, 555.6 cm^{-1}. It is interesting that the $\rho_r(NH_3)$ was observed in a region of such lower wave numbers.

The infrared absorption spectra of $[Ni(NH_3)_6]SO_4$ and its diammine intermediate are given in Table 4. In the diammine compound, the ν(NH), the $\delta_{deg}(NH_3)$ and the $\delta_s(NH_3)$ due to ammonia showed the same behavior as the diamminenickel(II) chloride. The SO_4^{2-} absorption band may be explained with C_{2v} symmetry, though it is not clear whether the SO_4^{2-} ion behaves as a simple bidentate or a bridging bidentate. As for the hemiammine compound, it was difficult to deduce whether the SO_4^{2-} ion is coordinated to a nickel(II) ion or not, because the band at 1130 cm^{-1} did not split and that at 977 cm^{-1} was strong; the former is characteristic of a free SO_4^{2-} ion and the latter is characteristic of a coordinated one. These may be attributed to the distortion of the SO_4^{2-} ion which was caused by heating.

12) J. Fujita, K. Nakamoto and M. Kobayashi, *J. Am. Chem. Soc.*, **78**, 3295 (1956).

The wave numbers of the absorption bands of hexamminenickel(II) nitrate and its intermediate are also given in Table 4. The measurement was made by both nujol and HCB mull methods. The NO_3^- ion was considered to be coordinated to nickel ion in the tetrammine compound from its spectral change from a D_{3h} symmetry in the hexammine complex to a C_{2v} symmetry in the dinitratotetrammine complex. The structure of the tetramminenickel(II) nitrate may be monomeric because the shift of the $\rho_r(NH_3)$ to lower wave numbers was not observed.

The measurement of infrared absorption spectra was carried out by Mr. Mitsuo Sato and the members of the late Professor Kinumaki's Labolatory at the Chemical Research Institute of Non-aqueous Solutions, Tohoku University. The authors wish to thank the Ministry of Education for the financial support granted for this research.

BULLETIN OF THE CHEMICAL SOCIETY OF JAPAN VOL. 41 2913—2918 (1968)

Polarography of Halides in Dimethylformamide. I. Bromide Ion and Its Mercuric Compounds

Yoshihisa MATSUI, Ryuji KAWAKADO and Yoshio DATE

Department of Agricultural Chemistry, Faculty of Agriculture, Shimane University, Nishikawazu-cho, Matsue

(Received May 14, 1968)

The complex formation between tetraethylammonium bromide (TEB) and mercuric bromide in dimethylformamide was observed conductometrically, and a complex, tetraethylammonium tribromomercurate (TETM), was isolated. Voltammetric studies of TEB, TETM, and mercuric bromide were made, using the dropping mercury electrode in dimethylformamide containing 0.1 M tetraethylammonium perchlorate. It was found that TEB gives two reversible anodic waves, of which the more negative one is due to the oxidation of mercury to TETM, and the more positive, to the oxidation of mercury to mercuric bromide. The electrode reaction mechanism was also investigated by means of large-scale electrolysis with a controlled potential.

At the dropping mercury electrode the halide ion gives a reversible anodic wave due to the oxidation of mercury to halogenated mercury species. For example, it is well known that the halide ion in water depolarizes the dropping mercury electrode upon the formation of insoluble mercurous halide.[1]

However, the polarographic behavior of halide ions in dimethylformamide (DMF) has been shown to differ from that in water.[2,3] Given and Peover[2] observed that the iodide ion in DMF gives two anodic waves, of which the more negative may be attributed to the oxidation of mercury to the tetraiodomercurate ion on the basis of the analysis of the wave. The more positive wave was suggested to arise from the oxidation of mercury to the triiodomercurate ion, but it was not proved experimentally. They also reported that the chloride ion in DMF showed virtually the same polarographic behavior as the iodide ion except for some departures of the more negative wave from that to be expected on the basis of the equation of the wave, probably as a result of the partial dissociation of the tetrachloromercurate ion to the trichloromercurate ion and the chloride ion. The behavior of the bromide ion in DMF was studied by Breant and Kiet,[3] who reported the formation of the tetrabromomercurate ion by the oxidation of mercury. However, the behavior of these halide ions on the electrode surface has still remained obscure, especially the electrode reaction mechanism at the potential of the more positive wave.

In the present paper, the polarographic behavior of the bromide ion and its mercuric compounds in DMF will be examined in detail in order to make clearer the mechanism of the electrooxidation of mercury; we will use the methods of d. c. polarography, large-scale electrolysis with a controlled potential, and conductometry.

Experimental

Materials. DMF obtained commercially was purified by the method of Wawzonek *et al.*[4] (bp 51.0—52.3°C/18 mmHg). Tetraethylammonium perchlorate

1) I. M. Kolthoff and C. S. Miller, *J. Am. Chem. Soc.*, **63**, 1405 (1941).
2) P. H. Given and M. E. Peover, *J. Chem. Soc.*, **1959**, 1602.
3) M. Breant and N. V. Kiet, *Compt. Rend.*, **262**, 955 (1966).
4) S. Wawzonek, E. W. Blaha, R. Berkey and M. E. Runner, *J. Electrochem. Soc.*, **102**, 235 (1955).

(TEP) was prepared from tetraethylammonium hydroxide and perchloric acid according to the directions of Geske and Maki.[5] The crude product was recrystallized twice from water and dried in a vacuum oven at 65°C. The 0.10 M solution of TEP in DMF showed virtually no polarographic wave within the range from +0.4 to −2.7 V *vs.* SCE. Tetraethylammonium bromide (TEB) was prepared according to the directions of Fleischer and Nachod.[6]

Found: Br, 37.77%. Calcd for $C_8H_{20}NBr$: Br, 38.02%.

Mercuric bromide obtained commercially was purified by recrystallizing it from ethanol-water. A reagent-grade sample of mercurous bromide was used without further purification.

Tetraethylammonium Tribromomercurate (TETM). This was prepared by a method similar to that described by Cruse, Goertz, and Petermöller.[7] Mercuric bromide (3.60 g) and TEB (2.10 g) were added to 30 m*l* of DMF and stirred until they were in solution. The solution was then poured into 150 m*l* of water; the precipitate was collected by filtration, washed with water, and recrystallized from DMF-ethanol. There was thus obtained 2.2 g (39%) of TETM, which had the following characteristics: mp 138.0—139.5°C (lit.[7] mp 124°C), IR (KBr disk): 1456 and 1402 cm^{-1} (δ C-H), 1183 and 1030 cm^{-1} (ν C-N).

Found: C, 16.83; N, 2.63%. Calcd for $C_8H_{20}NHgBr_3$: C, 16.84; N, 2.46%.

Conductivity Measurements. A Yanagimoto conductivity outfit (model MY-7) was used for these measurements. A conductivity cell was fitted with circular, blacked platinum electrodes separated by 10 mm. The cell constant was 0.4455. All the measurements were made at 25±0.1°C.

Polarographic Measurements. Anhydrous DMF was used as a solvent, with 0.10 M TEP as the supporting electrolyte. An H-type cell was used for the polarography. The current-potential curves were recorded with a Shimadzu polarograph, model RP-50. The bridged saturated calomel electrode proposed by Takaoka[8] was used throughout as a reference electrode. All the potentials were corrected for the bridge potentials measured in the way described in the literature. The potential drifting during one polarographic measurement was less than ±5 mV. All the potentials were corrected automatically for the IR-drop across the electrolysis cell with a Shimadzu automatic potential corrector, model AIC-50. The dropping mercury electrode had the following characteristics in a 0.10 M solution of TEP in DMF (open circuit): m=1.165 mg/sec and t=5.6 sec for h=66.0 cm. All the measurements were made at 25±0.1°C.

Large-Scale Electrolysis with Controlled Potential. Electrolysis was carried out in a cell similar in construction to that used by Fujinaga *et al.*[9] The mercury pool and the platinum electrode used had areas of approximately 75 and 60 cm^2 respectively. The bridged saturated calomel electrode mentioned above was used as a reference electrode. The potential of the mercury pool was controlled with an improved Yanagimoto VE-3 controlled potential electrolyser.

A solution of 300 m*l* of DMF with 6.89 g of TEP, and 3.60 g of mercuric bromide or 1.26 g of TEB was degassed for 2 hr with pure nitrogen, and then electrolyzed at a controlled potential with stirring and with cooling in an ice bath (3—5°C). The quantity of electricity required for the electrolysis was estimated graphically from the current-time curve. After the electrolysis, the electrolyte was concentrated by vacuum distillation to about 20 m*l*. The products were isolated by fractional crystallization from water. All the products were identified by their melting points, IR spectra, elementary analyses, and/or polarograms.

Results and Discussion

Solubility Relations. TEB and mercuric bromide are easily soluble in DMF, while mercurous bromide is insoluble. If a concentrated solution of mercuric bromide in DMF is shaken with mercury, mercurous bromide precipitates at once, but if the solution is dilute enough (below 0.025 M at 25°C), no precipitation occurs. If a trace amount of mercurous bromide is shaken with DMF, it dissolves with the separation of mercury. These observations indicate that the equilibrium between mercuric and mercurous bromide (Eq. (1)) is established rapidly, and that the solubility of mercuric bromide in the presence of mercury is about 0.025 M at 25°C.

$$HgBr_2 + Hg \rightleftharpoons Hg_2Br_2 \qquad (1)$$

Accordingly, when a dilute solution of mercuric bromide (below 0.005 M) is polarographically studied in DMF, it is not necessary to consider the reaction between mercuric bromide and mercury.

There is no separation of mercurous bromide when a concentrated solution of mercuric bromide in DMF is shaken with mercury in the presence of TEB. This suggests that the complex formation between mercuric bromide and TEB occurs in solution, as has been reported by Cruse et al. in the case of acetonitrile.[7]

Conductometric Measurements. If the complex formation between mercuric bromide and TEB occurs in DMF and if the value of the conductivity of the complex is different from those of the constituents, the mole-ratio between the constituents can be determined by the method of conductometric titration. The results of conductometric titration are given in Fig. 1. The addition of mercuric bromide to the solution of TEB in DMF lowered the specific conductivity, which reached the minimum value when the concentration of mercuric bromide added became equal to that of TEB. This obviously suggests that complex formation occurs in solution and that

5) D. H. Geske and A. H. Maki, *J. Am. Chem. Soc.*, **82**, 2671 (1960).
6) K. D. Fleischer and F. C. Nachod, *Anal. Chem.*, **33**, 208 (1961).
7) K. Cruse, E. P. Goertz and H. Petermöller, *Z. Elektrochem.*, **55**, 405 (1951).
8) K. Takaoka, *Rev. of Polarography*, **14**, 63 (1966).
9) T. Fujinaga, K. Takaoka, T. Nomura and K. Yoshikawa, *Nippon Kagaku Zasshi (J. Chem. Soc. Japan, Pure Chem. Sect.)*, **89**, 185 (1968).

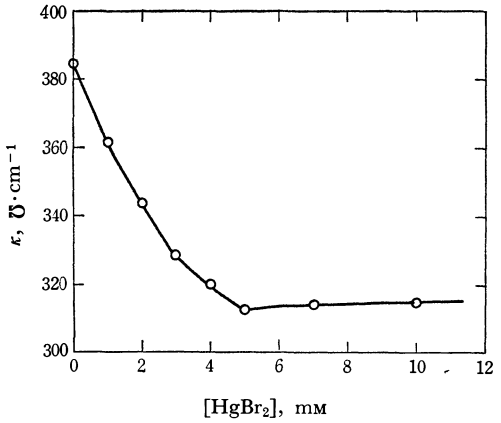

Fig. 1. Effect of $HgBr_2$ on specific conductance of 5 mM TEB in DMF at 25°C.

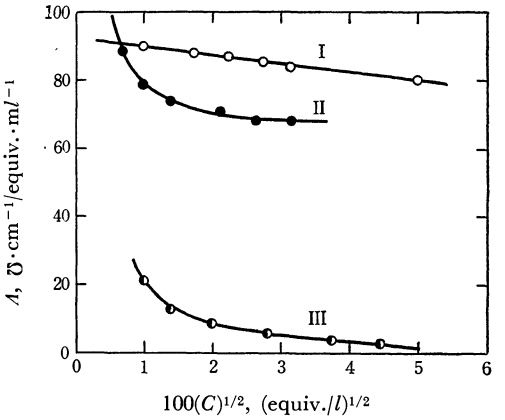

Fig. 2. Equivalent conductivities of TEB (I), TETM (II), and $HgBr_2$ (III) *vs.* square root of concentration in DMF at 25°C.

the mole-ratio between the constituents is equal to one. The equivalent conductivity of the mixture of mercuric bromide and TEB with the mole ratio of 1 : 1 is plotted in Fig. 2, together with those of the constituents.

The complex, TETM, was isolated as has been described in the Experimental section. The polarographic and conductometric behavior of this complex in DMF coincided with those of the mixture of the constituents with the mole ratio of 1 : 1. Irrespective of the presence or absence of mercury, TETM is easily soluble in DMF (about 50% by weight), while it is insoluble in water.

Polarographic Measurements. Using anhydrous DMF as a solvent with 0.10 M TEP as a supporting electrolyte, the polarographic behavior of TEB, TETM, and mercuric bromide was investigated (Fig. 3). TEB gives two anodic waves and no maximum over the potential range of +0.4——2.7 V *vs.* SCE in the concentrations studied. TETM gives two waves, anodic and cathodic; on the latter a maximum appears at concentrations above 0.25 mM. Mercuric bromide gives two cathodic waves, on the more negative wave of which a maximum arises in the concentrations above 0.50 mM. Since both of these maxima arise at a more negative potential of the more negative waves, they do not prevent us from estimating the half-wave potentials and the limiting currents of the more negative waves.

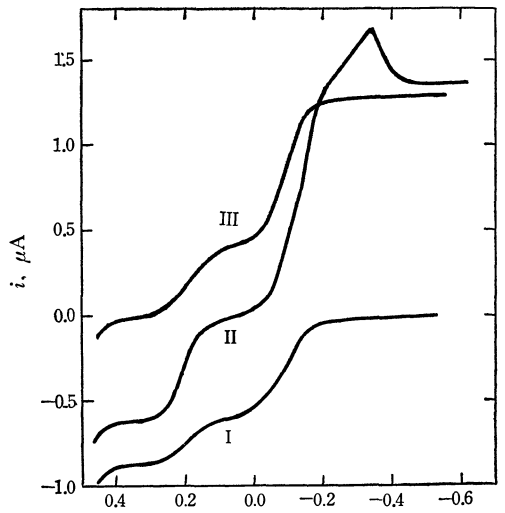

Fig. 3. Polarograms of the 0.25 mM solutions of TEB (I), TETM (II), and $HgBr_2$ (III) in DMF containing 0.10 M TEP at 25°C.

Table 1. Polarographic behavior of TEB, TETM, and mercuric bromide in DMF containing 0.10 M TEP at 25±0.1°C

Depolarizers	Concn. (mM)	$E_{1/2}$ (V *vs.* SCE) more pos.	$E_{1/2}$ (V *vs.* SCE) more neg.	I_d more pos.	I_d more neg.
TEB	0.10	+0.199	−0.092	0.80	2.02
	0.25	+0.205	−0.103	0.70	1.58
	0.50	+0.221	−0.114	0.74	1.52
	1.00	+0.234	−0.136	0.74	1.49
	2.50	+0.247	−0.159	0.69	1.55
	5.00	+0.264	−0.184	0.67	1.49
TETM	0.10	+0.191	−0.122	1.56	3.45
	0.25	+0.210	−0.137	1.61	3.66
	0.50	+0.219	−0.154	1.73	3.66
	1.00	+0.231	−0.170	1.95	3.54
	2.50	+0.247	−0.196	1.91	3.38
$HgBr_2$	0.10	+0.142	−0.073	1.10	2.33
	0.25	+0.171	−0.094	1.14	2.33
	0.50	+0.217	−0.121	1.27	2.36
	1.00	+0.225	−0.146	1.31	2.35
	2.50	+0.229	*	1.29	*
	5.00	+0.245	*	1.28	*

* Impossible to measure owing to the maxima.

Table 2. Relation between i_d of 0.50 mM TEB and the effective pressure ($h_{corr.}$) on the dropping mercury electrode

$h_{corr.}$ (cm)	i_d (μA)		$i_d/(h_{corr.})^{1/2}$	
	more pos.	more neg.	more pos.	more neg.
84.3	0.60	1.24	0.065	0.135
74.3	0.55	1.12	0.064	0.130
64.3	0.52	1.05	0.065	0.131
54.4	0.47	0.97	0.064	0.131
44.4	0.42	0.85	0.064	0.129
38.4	0.40	0.78	0.065	0.126

The half-wave potentials ($E_{1/2}$) and the diffusion current constants (I_d) in various concentrations of these depolarizers are given in Table 1. All the I_d's were effectively constant over the concentration range studied. The limiting currents for 0.50 mM TEB were found to be proportional to the square root of the effective pressure of the mercury applied to the dropping mercury electrode (Table 2). Similar results were obtained for both TETM and mercuric bromide, indicating that the limiting currents of all these waves are diffusion-controlled.

The ratios of the I_d's of the more positive waves to those of the more negative waves caused by these depolarizers were approximately 1 : 2, suggesting that the ratios of the numbers of electrons transferred at the more positive wave to those transferred at the more negative wave may be 1 : 2. Assuming that the overall electroreduction of three molecules of mercuric bromide is due to the reversible transfer of six electrons from the dropping mercury electrode, yielding mercury and bromide ions, it follows that two electrons should be assigned to the more positive reduction process and four electrons to the more negative reduction process. A similar deduction may be made with regard to the electrooxidation of mercury in the presence of bromide ions. Thus, the mechanism of the electrode reactions may be given by:

$$3HgBr_2 + 2e \rightleftarrows Hg + 2HgBr_3^- \quad (2)$$

$$2HgBr_3^- + 4e \rightleftarrows 2Hg + 6Br^- \quad (3)$$

This mechanism can make clear the polarographic characteristics of TETM. Namely, it indicates that the more positive wave should be anodic, the more negative wave, cathodic, and the ratio between the I_d's, 1 : 2.

This hypothetical mechanism was substantiated by analyzing the waves of complex mercury ions studied by Kolthoff and Miller.[1] By applying their method to this mechanism, the potential of the dropping mercury electrode is given for the more positive wave by:

$$E_p = C_p + (\boldsymbol{RT}/2\boldsymbol{F}) \ln ([HgBr_2]_0^3/[HgBr_3^-]_0^2) \quad (4)$$

and for the more negative wave by:

$$E_n = C_n + (\boldsymbol{RT}/2\boldsymbol{F}) \ln ([HgBr_3^-]_0/[Br^-]_0^3) \quad (5)$$

where the subscript zero denotes the concentration at the surface of the dropping mercury electrode, and where C_p and C_n are constant. It can easily be shown that the equations of the waves of bromide ion are:

$$E_p = C_p' + (\boldsymbol{RT}/2\boldsymbol{F}) \ln [i^3/(i_d - i)^2] \quad (6)$$

$$E_n = C_n' + (\boldsymbol{RT}/2\boldsymbol{F}) \ln [i/(i_d - i)^3] \quad (7)$$

These equations show that the half-wave potentials should change with i_d or with the concentrations of bromide ion according to:

$$E_{p,1/2} = C_p'' + (\boldsymbol{RT}/2\boldsymbol{F}) \ln [Br^-] \quad (8)$$

$$E_{n,1/2} = C_n'' - (\boldsymbol{RT}/\boldsymbol{F}) \ln [Br^-] \quad (9)$$

The results of the analyses of the waves are given in Fig. 4. The plotting of $\log[i^3/(i_d-i)^2]$ against the potential for the more positive wave gave a fairly good straight line, with a slope equal to 0.032 V (calculated for Eq. (6); 0.030 V), indicating that Eq. (2) is valid. The plot of $\log [i/(i_d-i)^3]$ against the potential for the more

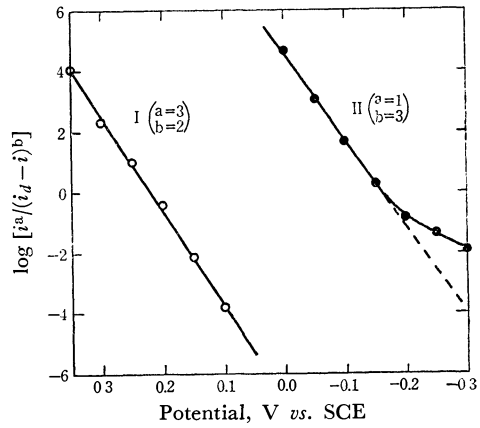

Fig. 4. Analyses of the waves of 0.50 mM TEB.
Slope: (I), 0.032; (II), 0.034

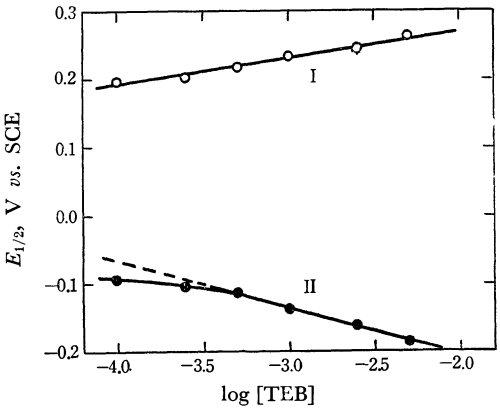

Fig. 5. Effect of concentration of TEB on its half-wave potential.
Slope: (I), 0.035; (II), −0.062

Table 3. Large-scale electrolysis of mercuric bromide and TEB with controlled potential in DMF containing 0.10 M TEP at 4±1°C

Depolarizers	E[a] (V *vs.* SCE)	Time (min)	i (μA) Start	i (μA) Finish	n[b] (F) Obsd	n[b] (F) Calcd[c]	Products (%)
$HgBr_2$[d]	+0.11	165	90	1.0	0.66	0.67	TETM (26)
$HgBr_2$[d]	−0.55	120	430	2.0	2.12	2.00	TEB (41)
TEB[e]	−0.04	395	185	2.0	1.01	0.67	TETM (40)
TEB[e]	+0.36	240	315	80.0	2.45	1.00	$HgBr_2$ (27)

a) Set potential for electrolysis.
b) Quantity of electricity used per one mole of depolarizer.
c) Calculated for Eq. (2) and/or (3).
d) Electroreduction with Hg cathode and Pt anode.
e) Electrooxidation with Hg anode and Pt cathode.

negative wave was also linear, with a slope equal to 0.034 V, over the greater part of the potential range, but it became curved at the more negative potentials (above −0.2 V *vs.* SCE), indicating a behavior different, probably due to the adsorption of bromide ions on the surface of the dropping mercury electrode, as has been shown by Biegler in an aqueous solution.[10]

The relation between the half-wave potentials and the concentrations of the bromide ion is plotted in Fig. 5. A straight line relation was obtained for the more positive wave with a slope equal to 0.035 V (calculated for Eq. (8); 0.030 V) and one for the more negative wave with a slope equal to −0.062 V (calculated for Eq. (9); −0.059 V), though the plot for the latter became somewhat curved at low concentrations. Similar studies were carried out concerning TETM and mercuric bromide; all the results agreed well with the equations derived from the mechanism postulated above.

Large-Scale Electrolysis with a Controlled Potential. In order to make sure of the electrode reaction mechanism, a large-scale electrolysis of mercuric bromide and TEB was carried out with a controlled potential in DMF. The results are given in Table 3.

The electroreduction of mercuric bromide with the Hg cathode at the potential of the plateau of the more positive wave yielded TETM (26%); the quantity of electricity transferred per mole of the depolarizer (n) was 0.66 F (calculated for Eq. (2); 0.67 F), indicating that Eq. (2) is valid. TEB was obtained (41%) by the electroreduction of mercuric bromide at the potential of the plateau of the more negative wave, and the value of n was equal to 2.12 F (calculated for Eq. (2) and (3); 2.00 F), indicating that Eq. (3) is also valid. The polarograms of the catholytes after electrolysis, in both cases, agreed closely with those of the products.

The electrooxidation of TEB with the Hg anode at the potential of the plateau of the more negative wave yielded TETM (40%), as expected, whereas the value of n (1.01 F) was much greater than that expected on the basis of Eq. (3) (0.67 F). The polarogram of the anolyte showed that there was considerable increase in the anoidc wave as well as in the wave of TETM, caused probably by the formation of oxidizable species at the cathode, but the details have not been studied. The electrooxidation of TEB at the potential of the plateau of the more positive wave yielded mercuric bromide (27%), as expected, while the value of n (2.45 F) was also much greater than that expected on the basis of Eqs. (2) and (3) (1.00 F).

The Mechanism of the Anodic Dissolution of Mercury in the Presence of the Bromide Ion in DMF. On the basis of the observations presented above, it is reasonable to conclude that the two anodic waves given by the bromide ions in DMF are due to oxidation of mercury to tribromomercurate ions (Eq. (3)) and to mercuric bromide (Eq. (2)). On the other hand, it has already been reported by Given and Peover[2] that halide ions in DMF depolarize the dropping mercury electrode, mainly forming tetrahalogenomercurate ions (HgX_4^{2-}). However, they also observed that the ratios between the I_d's of the two waves of these depolarizers are approximately 1 : 2, indicating the formation of trihalogenomercurate ions. We have also observed, by means of conductometric titration, that complex formation occurs between mercuric iodide and tetraethylammonium iodide in the mole ratio of 1 : 1. Accordingly, it may be necessary to reinvestigate the polarographic behavior of halide ions other than the bromide ion.

The mechanism proposed in the present paper is similar to that at such inert electrodes as platinum[11,12] and graphite[13] in DMF or acetonitrile, where halide ions also give two anodic

10) T. Biegler, *J. Electroanal. Chem.*, **6**, 365 (1963).

11) I. M. Kolthoff and J. F. Coetzee, *J. Am. Chem. Soc.*, **79**, 1852 (1957).
12) M. Breant and C. Sinicki, *Compt. Rend.*, **260**, 5016 (1965).
13) D. Dryhurst and P. J. Elving, *J. Electroanal. Chem.*, **12**, 416 (1966).

waves, one of which corresponds to that of the oxidation of halide ions (X^-) to trihalide ions (X_3^-), and the other, to that of trihalide ions to halogen molecules (X_2). Considering that both trihalide ions and halogen molecules react rapidly with mercury, it might be possible to divide the anodic dissolution processes of mercury into the oxidation stpes of halide ions and the reaction steps between the oxidized species and mercury as follows:

$$\begin{array}{ccccc} 6X^- & \rightleftharpoons & 2X_3^- + 4e & \rightleftharpoons & 3X_2 + 6e \\ & & \downarrow{\scriptstyle 2Hg} & & \downarrow{\scriptstyle 3Hg} \\ & & 3HgX_3^- & & 3HgX_2 \end{array} \qquad (10)$$

With this mechanism, however, it is difficult to explain that the anodic waves are reversible, because the reactions between mecury and trihalide ions and between mercury and halogen molecules are both certainly irreversible. According to this mechanism, it is also difficult to explain the polarographic behavior of TETM and mercuric bromide, indicating that this mechanism is implausible.

The polarographic behavior of the bromide ion in DMF is obviously different from that in water. This difference can be related to the difference in the stability of the mercury species in these solvents. It is well known that mercuric halides in water react with mercury even in a very dilute solution, forming insoluble mercurous halides.[14] On the other hand, we have observed that mercuric bromide in DMF remains inert to mercury even in a comparatively concentrated solution, as has been described above. TETM is reported to possess great stability in acetonitrile, but less stability in water.[7] We have also observed that it is very stable in DMF. Thus, in an aqueous solution the bromide ion depolarizes the dropping mercury electrode, thus forming mercurous bromide, which is the most stable species in water. In DMF, however, mercurous bromide is less stable than either the tribromomercurate ion or mercuric bromide, so the bromide ion gives two anodic waves in DMF which correspond to the formation of the latter.

14) I. M. Kolthoff and C. S. Miller, *J. Am. Chem. Soc.*, **63**, 2732 (1941).

BULLETIN OF THE CHEMICAL SOCIETY OF JAPAN VOL. 41 2918—2921 (1968)

Preparation and Properties of Metal Complexes in Non-aqueous Solutions. I. Preparation of the *trans*-Dicyano-bis(ethylenediamine)cobalt(III) Complex by the Use of Dimethylsulfoxide as Solvent[1]

Masayuki MUTO, Tetsuo BABA[2] and Hayami YONEDA

Department of Chemistry, Wakayama University, Masagocho, Wakayama

(Received May 14, 1968)

An isomeric form of the hitherto known *cis*-$[Co(CN)_2\ en_2]^+$ was prepared from *cis*- or *trans*-$[CoCl_2\ en_2]^+$ and potassium cyanide in dimethylsulfoxide solution. The new complex was characterized by UV, IR and NMR spectra, and its trans configuration was established.

Two peculiarities may be noticed about the preparation of $[Co(CN)_2en_2]^+$. One is the fact that only the cis form is known. The other is the way of its preparation. Usually, diacido-bis-ethylenediamine complexes, $[CoX_2en_2]^+$ can be prepared from *trans*-$[CoCl_2en_2]^+$ by substitution of X for Cl. However, the cyano mixed complex is obtained only via *trans*-$[Co(S_2O_3)_2en_2]^-$. When the dichloro complex is treated with potassium cyanide in an aqueous solution, disproportionation occurs to produce $[Co\ en_3]^{3+}$ and $[Co(CN)_6]^{3-}$. This fact indicates that the incoming cyano groups expel the other kind of ligands from the coordination sphere. On the other hand, it is generally known that cobalt(III) ammines were quite labile in an alkaline solution. In the preparation of the cyano mixed complex, the reaction mixture is fairly alkaline due to hydrolysis of the added cyanide. This alkalinity of the solution might make

1) Presented at the 17th Symposium of Coordination Chemistry held at the Hiroshima University, Hiroshima, December 11, 1967.

2) On leave from the Minoshima High School, Arita-shi, Wakayama.

3) H. Yoneda, This Bulletin, **31**, 74 (1958).

the complex labile and lead it to disproportionation.

In our previous report[3] on the decomposition of cobalt(III) ammines, the proton dissociation mechanism was proposed. In that mechanism, it was assumed that, in the decomposition process, proton dissociation from the coordinated NH_3 takes place first, and that then the NH_2^- thus produced came out of the coordination sphere. A similar proton dissociation may be considered in the present case. Therefore, it was felt necessary to work under conditions where proton dissociation can not occur. To fulfill these conditions, we tried to use dimethylsulfoxide as a solvent and succeeded in obtaining the cyano diamine mixed complex which proved to be isomeric to the hitherto known *cis*-$[Co(CN)_2en_2]^+$ complex, directly from the dichloro complex.[4,5]

Experimental

Method of Preparation. One gram (0.016 mol) of powdered potassium cyanide was dissolved in 150 m*l* of dimethylsulfoxide heated at 60°C. To this solution was added in small portions 1.5 g (0.05 mol) of *trans*-$[CoCl_2en_2]NO_3$ under constant stirring. The added complex reacted gradually with the cyanide and, after a while, yellow precipitate of greenish tint was formed. At about 60°C, the reaction was complete in 15—20 min. When *cis*-$[CoCl_2en_2]Cl$ was used as a starting material, the reaction proceeded much more smoothly to form an orange yellow precipitate in one or two minutes. (Both reactions gave the same final product). The greenish tint probably originated from unreacted green *trans*-$[CoCl_2en_2]NO_3$. The precipitate thus formed was filtered and washed with warm dimethylsulfoxide and then with acetone. Through this procedure the precipitate became light yellow. This product was supposed to be $[Co(CN)_2en_2]Cl$ with some contamination. This was not soluble in dimethylsulfoxide nor in ethanol. In water it was too much soluble to obtain good crystals. Therefore, purification was attempted by converting it to the perchlorate salt. The crude product was dissolved in a small volume of water and, after filtration, was added with the saturated solution of sodium perchlorate. An orange yellow crystalline powder came out. This was washed with small amount of water and ethanol, and dried in air.

Found: C, 21.79; H, 5.06; N, 24.88%. Calcd for $[Co(CN)_2en_2]ClO_4$: C, 21.80; H, 4.88; N, 25.42%.

Spectral Measurements. The UV spectra were measured with a Shimadzu QR 50 spectrophotometer. The IR spectra were recorded with a Hitachi EPI S2 spectrophotometer equipped with NaCl optics. The KBr disc method was adopted in the IR measurement. The NMR spectra were run on a Varian A60 NMR spectrometer. Deuterium oxide was used as solven., and the sodium salt of trimethylsilylpropane sulfonic acid was used as an internal reference.

Results and Disucssion

The Ligand Field Absorption Bands. The UV absorption curve of the new $[Co(CN)_2en_2]ClO_4$ is shown in Fig. 1 with that of the known *cis*-$[Co(CN)_2en_2]ClO_4$. The absorption data are summarized in Table 1. The main difference

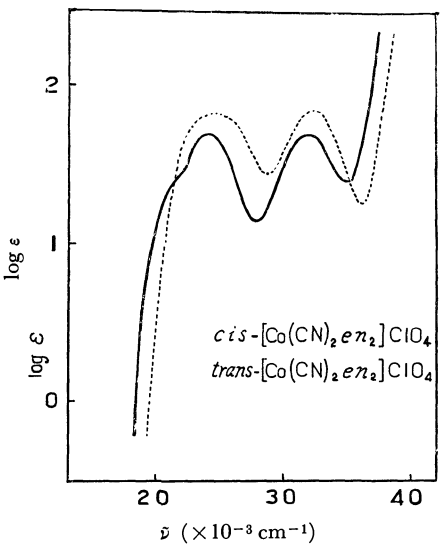

Fig. 1. UV Absorption spectra of *cis*-$[Co(CN)_2en_2]\cdot ClO_4$ and its new isomer (aqueous solution).
····· *cis*-$[Co(CN)_2en_2]ClO_4$
—— new isomer

Table 1. The absorption data of *cis*-$[Co(CN)_2en_2]ClO_4$ and its new isomer

	1st Band		2nd Band	
	$\tilde{\nu}_{max}$ (cm^{-1})	$\log \varepsilon_{max}$	$\tilde{\nu}_{max}$ (cm^{-1})	$\log \varepsilon_{max}$
cis form	24.6	1.82	32.4	1.83
new isomer	19.3(shoulder)		32.0	1.68
	24.0	1.69		

between the absorption curves of both isomers appears in their first absorption bands: While the first band of the cis isomer shows no clear split, that of the new one seems to split into two components. A similar kind of difference is observed in the first bands of *cis*- and *trans*-$[CoCl_2en_2]^+$ too.[6] In this case also, the cis isomer has no

4) Two works concerning the preparation of $[Co(CN)_2en_2]^+$ in an aqueous solution were reported at the 21st Annual Meeting of the Chemical Society of Japan (April, 1968): K. Kuroda prepared *cis*-$[Co(CN)_2en_2]^+$ by treating $[CoCO_3en_2]^+$ with CN^- in an aqueous solution. M. Shibata *et al.* prepared *cis* and *trans*-$[Co(CN_2)en_2]^+$ from $[Co\ en_3]^{3+}$ and CN^- in an aqueous solution.

5) Previously we reported the preparation of *cis*-$[Co(CN)_2en_2]Cl$ by the use of dimethylsulfoxide as solvent. H. Yoneda, T. Baba and M. Muto. This Bulletin, **40**, 1736 (1967). However, no attempts were successful to reproduce the result. The interconversion between the cis and trans forms is now being studied.

6) M. Linhard and M. Weigel, *Z. anorg. Chem.*, **271**, 101 (1952).

split band, and the trans isomer has a markedly split first band. Therefore, if we assume the trans configuration for the new $[Co(CN)_2en_2]^+$, the present situation can reasonably be understood. However, this can not be a decisive proof for the trans configuration, because we know that the first band of *trans*-$[CoCl(CN)en_2]^+$ shows no split, while that of the cis isomer split markedly into two components.[7] In addition, there are several possible structures which are isomeric to the known *cis*-$[Co(CN)_2en_2]^+$.

Corey and Bailar[8] classified two possible conformations of the ethylenediamine molecules in $[Co\ en_3]^{3+}$ into the "lel" and "ob" forms. The "lel" form represents the conformation in which the C-C axis is nearly parallel to the threefold axis of $[Co\ en_3]^{3+}$, and the "ob" form to the conformation in which the C-C axis is almost perpendicular to the threefold axis of the complex (In the actual $[Co\ en_3]^{3+}$, all three ethylenediamine molecules take the "lel" form). Such kinds of conformation can be considered in the *cis* bisethylenediamine complex too. In this case, there are three possible combinations of two ethylenediamine molecules, lel-lel, lel-ob and ob-ob form. The active chloride[9] of *cis*-$[(Co(CN)_2en_2]^+$ proved to have an ob-ob conformation, while the racemic chloride[10] of *cis*-$[CoCl_2en_2]^+$ a lel-ob conformation. Thus our new complex can be considered to have the following several possible structures.

1) The two cyano groups are linked to the metal ion with the nitrogen atom.[11]

2) The two ethylenediamine molecules take a lel-lel or lel-ob conformation.

3) The two cyano groups are coordinated to the metal ion in trans positions.

IR Spectra. In order to obtain informations concerning the structure of the new complex, the IR spectra of the new and the *cis*-$[Co(CN)_2en_2]^+$ were measured.[12] For comparison, the spectra of *cis*- and *trans*-$[CoCl_2en_2]^+$ were also measured. The results are shown in Fig. 2. Usually CN^- is linked to the metal ion with the C atom. In the case of *cis*-$[Co(CN)_2en_2]^+$, this was confirmed by

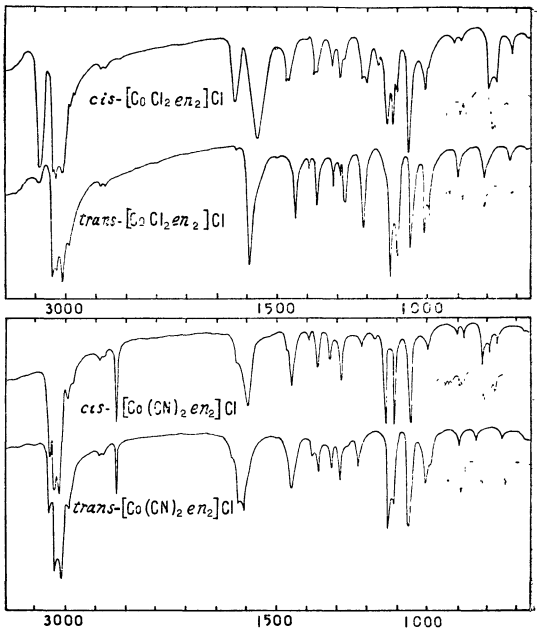

Wave number (cm^{-1})

Fig. 2. IR absorption spectra of diacido-bis-ethylenediamine cobalt(III) complexes.
—— chlorides ····· perchlorates

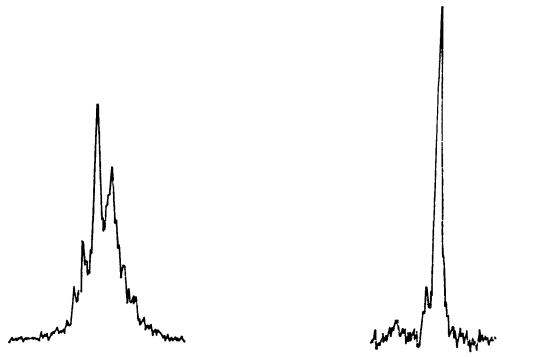

cis-$[Co(CN)_2en_2]ClO_4$ *trans*-$[Co(CN)_2en_2]ClO_4$

Fig. 3. NMR spectra of *cis*-$[Co(CN)_2en_2]ClO_4$ and its new isomer (D_2O solution).

X-ray analysis.[9] If CN^- were linked to the metal ion through the N atom in the new complex, the CN bond nature in the new isomer should be different from that of the *cis* isomer. While in the C coordination, CN^- should have a triple bond character ($Co^{3+}\leftarrow{}^-C{\equiv}N$), in the N coordination it should have a triple bond character ($Co^{3+}\leftarrow{}^-N{=}C$). Therefore, the absorption band due to the CN stretching in the new isomer should appear in longer wavelength region than that in the cis

7) K. Ohkawa, J. Hidaka and Y. Shimura, This Bulletin, **39**, 1715 (1966).
8) E. J. Corey and J. C. Bailar, Jr., *J. Am. Chem. Soc.*, **81**, 2620 (1959).
9) K. Matsumoto, Y. Kushi, S. Ooi and H. Kuroya, This Bulletin, **40**, 2988 (1967).
10) K. Matsumoto, S. Ooi and H. Kuroya, *Nippon Kagaku Zasshi (J. Chem. Soc. Japan, Pure Chem. Sect)*, **89**, 167 (1968).
11) K. Kuroda and P. S. Gentile, Proceedings of 10th ICCC, p. 280 (1967).
12) The pure chloride of the new $[Co(CN)_2en_2]^+$ for IR measurement was obtained as follows. The crude chloride was dissolved in a small volume of water, and, after filtration, ethanol was added in small portions until a slight turbidity appeared. The solution was filtered and the filtrate was evaporated to dryness under reduced pressure without heating. The dried residue was dissolved in water, and the procedure was repeated.
13) Baldwin also reported that the spectrum pattern in these regions is more complicated in the *cis*-$[CoX_2en_2]^+$ than in the trans isomer. M. E. Baldwin, *J. Chem. Soc.*, **1960**, 4369.

isomer. However, this is not the case. The CN stretching absorption band appears just at the same wave number (2130 cm^{-1}). Therefore, the N coordination can not be considered. If the new complex had the lel-ob conformation, the spectrum pattern of the new complex should be similar to that of *cis*-$[CoCl_2en_2]^+$. This is not the case. The IR spectra of the new $[Co(CN)_2\ en_2]^+$ and the *cis*-$[CoCl_2en_2]^+$ are fairly different in appearance. Rather, the spectrum pattern of the new complex shows a similarity to that of *trans*-$[CoCl_2en_2]^+$, especially in the CH_2 twisting and NH_2 rocking regions (see Fig. 2, 900—700 cm^{-1}). On the other hand, *cis*-$[CoCl_2en_2]^+$ and *cis*-$[Co(CN)_2en_2]$ show quite a unique splitting of bands in the CH_2 twisting and the NH_2 rocking region.[13] This fact makes a marked contrast to the trans isomer. This situation holds not only in the chlorides but also in the perchlorates. These findings seem to support the trans configuration of the new isomer, although they can not exclude the possibility of the lel-lel conformation.

NMR Spectra. To obtain the decisive conclusion concerning the structure of the new complex, the NMR spectra of the new and the known *cis*-$[Co(CN)_2en_2]^+$ dissolved in deuterium oxide were recorded. Figure 3 shows the CH_2 signals of both isomers (The NH_2 signals disappeared soon after dissolution due to deuteration). As expected, the CH_2 signal of the cis isomer shows a complicated pattern. On the contrary, the new isomer shows a sharp singlet which corresponds to the single species of the CH_2 protons. Thus the trans configuration of the new isomer was established.

The authors wish to thank the Ministry of Education of Japan for the financial support granted for this study.

BULLETIN OF THE CHEMICAL SOCIETY OF JAPAN VOL. 41 2921—2927 (1968)

The Selective Reduction of Aromatic Compounds by Electrolysis. I. Reduction of Naphthalene by Electrolysis[1)]

Akira MISONO, Tetsuo OSA and Takamichi YAMAGISHI

Department of Industrial Chemistry, Faculty of Engineering, University of Tokyo, Hongo, Tokyo

(Received May 15, 1967)

The direct electro-reduction of naphthalene was investigated in various solvents, mainly in an acetonitrile-water solution using supporting electrolytes containing tetraethylammonium and tetra-*n*-butylammonium cations. The main reduction product was 1,4-dihydronaphthalene, though small amounts of 1,2-dihydronaphthalene and tetralin were also detected. Under optimum conditions, the selectivity and the current efficiency of the formation of 1,4-dihydronaphthalene were 98% and 86.4% respectively. It was found that the water concentration and the solvent had a significant influence on the reduction products and the current efficiency. 1,4-Dihydronaphthalene is mainly formed through the step-by-step addition of two electrons and protons. In addition, 1,4-dihydronaphthalene may be formed by the protonation of the dianion formed by the disproportionation of the anion radical. Further, it was proposed that the formation of the tetraethylammonium radical might partly occur by means of the electron transfer from the anion radical of naphthalene to the tetraethylammonium cation, besides the direct electron transfer to the cation from the electrode.

The reduction of aromatic hydrocarbons by an alkali metal in liquid ammonia or in low-molecular-weight amine, especially in a mixture of liquid ammonia and alcohol (Birch reduction), has been studied by many investigators and a mechanism for the reduction has been proposed.[2)] In the electrolytic reduction, many polarographic studies of condensed aromatic hydrocarbons in aprotic solvents in the presence or in the absence of a proton-donor have been reported,[3)] but the reduction products and the effect of reaction conditions have scarcely been investigated at all. In regard to the macro-scale electro-reduction of naphthalene, which

1) A preliminary announcement of this work appeared in this Bulletin, **40**, 427 (1967).

2) W. Hückel and H. Bretshneider, *Ann.*, **540**, 157 (1937); A. J. Birch, *Quart. Rev.*, 69 (1950); A. J. Birch and D. Naspuri, *Tetrahedron*, **6**, 148 (1959); A. P. Krapcho and A. A. Bothner-By, *J. Am. Chem. Soc.*, **81**, 3658 (1959), *etc.*

3) P. H. Given, *J. Chem. Soc.*, **1958**, 2684; L. H. Klemm and A. J. Kohlik, *J. Org. Chem.*, **28**, 2044 (1963); I. Bergman, *Trans. Faraday Soc.*, **50**, 829 (1954); S. Wawzonek and E. W. Blaha, *J. Electrochem. Soc.*, **102**, 235 (1955); K. S. V. Santhanam and A. J. Bard, *J. Am. Chem. Soc.*, **88**, 2669 (1966), *etc.*

indicates the most negative value in the polarographic half-wave potential among all polycondensed unsubstituted aromatic hydrocarbons, only a few studies have been reported.[4,5] In the reduction of naphthalene by an alkali metal in liquid ammonia or amine, a considerable isomerization of unconjugated products to conjugated compounds occurs, whereas there hardly exists such possibility in the electro-reduction.

The present paper will deal with the macro-scale electro-reduction of naphthalene in organic solvents, such as acetonitrile, *N,N*-dimethylformamide (DMF), 1,4-dioxane (DIOX), tetrahydrofuran (THF), 1,2-dimethoxyethane (DME), or diglyme (DGL), in the presence of a proton-donor; the investigation was undertaken in order to clarify the reaction mechanism of the above reaction, to obtain 1,4-dihydro-product selectively, and also to examine the influence of the reaction conditions on the reaction products.

Experimental

Reaction Apparatus. Two different types of cells, H-type and cylindrical cells, with a glass-fritted disk of medium porosity (No. 3 and 4) and of different radii (from 5 to 12 mm) in order to separate the catholyte and anolyte were used. Mercury and platinum were used as the cathode and the anode respectively.

Materials. Naphthalene was purified by recrystallization from methanol - water (mp 79.9—80.0°C). Acetonitrile was purified by distillation from phosphorus pentoxide[6] (bp 81.4°C). DMF was distilled *in vacuo* from calcium oxide (bp 64—65°C/25 mmHg). DIOX and THF were distilled from sodium wire after having been treated with potassium hydroxide[7] (bp 66°C and 101—102°C respectively). DME and DGL were prepared by a variation of the directions in the literature[8] and were purified by distillation from sodium wire[7] (bp 82.5—83.0°C and 162.5—163.0°C respectively). Tetraethylammonium *p*-toluenesulfonate (McKee's salt) was prepared and purified according to the literature.[9] Tetra-*n*-butylammonium bromide was purified by recrystallization from acetone.

Procedure. The base electrolyte was prepared by dissolving a supporting electrolyte in a 100 m*l* solution of a solvent and a proton-donor. This base electrolyte was named, for the sake of convenience, solution A. The catholyte consisted of a substrate to be reduced and 70 m*l* of solution A, while the anolyte was a 30 m*l* portion of solution A. The reaction cell was cooled by a water bath in order to maintain the temperature near room temperature during electrolysis. The cathode potential was set up and controlled by using the saturated calomel electrode (SCE) as a reference electrode and a controlled potential electrolyzer from the Yanagimoto Co., Ltd. (type VE-3). Electrolysis was carried out for about 8 hr with a constant stirring of the catholyte by the use of a magnetic stirrer. The current passed through was measured by a copper coulometer. The variations in the reaction conditions were as follows: water concentration, 0—30 vol%; concentration of the supporting electrolyte, 3—30 g/100 m*l* CH_3CN-H_2O; naphthalene concentration, 6—14 g/100m*l* solution A; cathode potential, from −2.3V to −2.4V *vs.* SCE; current density, 0.05—0.40 A/dm^2; reaction temperature, 2—50°C. The cathode area was about 50 cm^2 in all the experiments.

Identification and Analysis of the Reduction Products. The reduction products were 1,4-dihydronaphthalene (1,4-DHN), 1,2-dihydronaphthalene (1,2-DHN), and tetralin. No further reduction products of naphthalene could be identified.

After the reaction, water was added to the reaction mixture, and the oily upper layer was separated. The oily products were distilled *in vacuo* after having been dried with anhydrous sodium carbonate. The fraction boiling at 71.8—72.6°C/5 mmHg (uncorrected) gave a white crystal (I) (mp 24.8°C) by recrystallization from methanol - water. The reduction products in a THF solution were similarly treated and fractionated to give a fraction boiling at 93.0—93.2°C/19 mmHg. This fraction contained I, another compound, II, which was supposed to be a dihydro-product, and small amounts of naphthalene and tetralin. From the NMR and IR spectra of I, I was identified as 1,4-DHN. By comparing the NMR and IR spectra of the fraction containing II with those of 1,2-DHN prepared from 1,4-DHN by isomerization with sodium isopropoxide in DMF, II was identified as 1,2-DHN. The retention time of II accorded with that of 1,2-DHN in gas chromatography. In NMR spectra, I had absorptions at τ=6.65, 4.11, and 2.94 (intensity ratio 4 : 2 : 4), whereas II had them at τ=7.75, 7.30, 4.15, 3.67, and 3.09 (intensity ratio 2 : 2 : 1 : 1 : 4). In the 1700—1400 cm^{-1} region of the IR spectra, I had absorptions at 1665, 1597, 1590, 1500, 1455, and 1425 cm^{-1}, while II had them at 1600, 1490, 1480, 1450, 1431, and 1420 cm^{-1}. Tetralin was confirmed by the retention time in the gas chromatogram.

The quantitative analysis of the reduction products was performed by the gas chromatographic method (Column, Carbowax 1500 (10%) on Diasolid M (60—80 mesh) 2 m; Column temperature, 180°C; Carrier gas, H_2, 30 cc/min; Detector, Thermal conductivity cell. The calibration of 1,2-DHN was performed with a hydrogen-flame ionizing detector, assuming that the relative molar sensitivities of 1,2- and 1,4-DHN were equal when the hydrogen-flame ionizing detector was used.

The NMR spectra were measured with a JES model LAB-2160 spectrometer (60 Mc), and the IR spectra, with a Hitachi Infrared Spectrophotometer, Model EPI-S2.

Results

Effect of the Reaction Conditions. The electrolytic reduction was mainly carried out in

4) S. Wawzonek and D. Wearring, *J. Am. Chem. Soc.*, **81**, 2067 (1959).
5) V. V. Levchenko and K. V. Meleshko, *Zhur. Obshchei Khim.*, **20**, 831 (1950).
6) P. Walden, *Z. physik. Chem.*, **144A**, 269 (1929).
7) "Zikken Kagaku Koza," Vol. 2, Maruzen, Tokyo (1956), p. 82.
8) J. V. Capinjola, *J. Am. Chem. Soc.*, **67**, 1615 (1945).
9) M. M. Baizer, *J. Electrochem. Soc.*, **111**, 215 (1964).

a medium of acetonitrile-water containing McKee's salt as a supporting electrolyte. In the examination of the reaction conditions, the current efficiencies for the formation of dihydro- and tetrahydro-products were defined as follows:

$$\eta_{DH} = \frac{\text{Amount of the dihydro-product (mole)} \times 2}{\text{Current passage (Faraday)}} \times 100\ (\%)$$

$$\eta_{TH} = \frac{\text{Amount of the tetrahydro-product (mole)} \times 4}{\text{Current passage (Faraday)}} \times 100\ (\%)$$

In the above equations, the 2 and 4 factors correspond to the numbers of electrons required for the formation of dihydro- and tetrahydro-products respectively.

Effect of the Water Concentration. In the electro-reduction of naphthalene, the concentration of a proton-donor was supposed to be an important factor affecting the reduction products and the current efficiency. The effect of the addition of water as a proton-donor to a solution of tetraethylammonium *p*-toluenesulfonate in acetonitrile was investigated. As is indicated in Fig. 1, the current efficiency was very dependent on the water concentration. As the water concentration increased, the current efficiency for 1,4-DHN ($\eta_{1,4DH}$) also increased, reaching a maximum value of 74.8% at a 25% water concentration; on the other hand, the current efficiency for 1,2-DHN ($\eta_{1,2DH}$) decreased with an increase in the addition of water and became almost zero when the water concentration reached 20%. η_{TH} was nearly constant and small except in very low water concentrations. In the electrolysis without water, the catholyte turned dark green and tetralin was formed preferentially, but upon the addition of 5% water no coloration was observed. This color may be due to the anion radical of naphthalene solvated by acetonitrile.

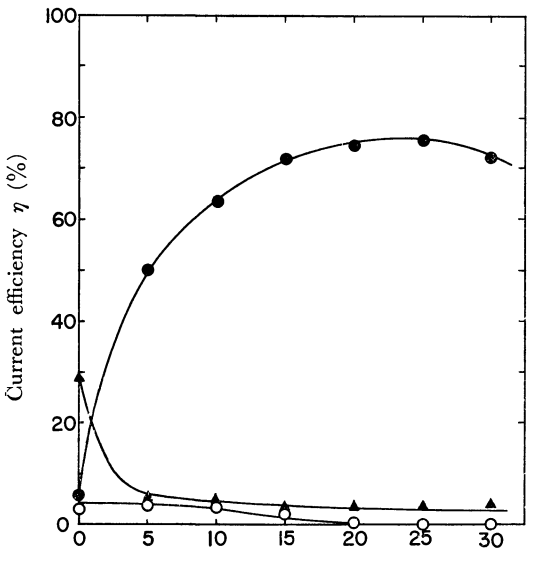

Fig. 1. Effect of the water concentration.
Cathode potential: −2.4 V *vs.* SCE;
McKee's salt concentration: 30 g/100 m*l* CH_3CN-H_2O
Naphthalene Concentration: 14.29 g/100 m*l* solution A
Current density: about 0.35 A/dm²
—●— $\eta_{1.4DH}$ —○— $\eta_{1.2DH}$ —▲— η_{TH}

Effect of the McKee's Salt Concentration. This effect was examined in a 25% water-acetonitrile solution. $\eta_{1,4DH}$ increased with an increase in the McKee's salt concentration in the low concentration range, but it decreased inversely in the high concentration range. Under the reaction conditions examined, 1,2-DHN was not detected, while η_{TH} remained constant and low (Fig. 2).

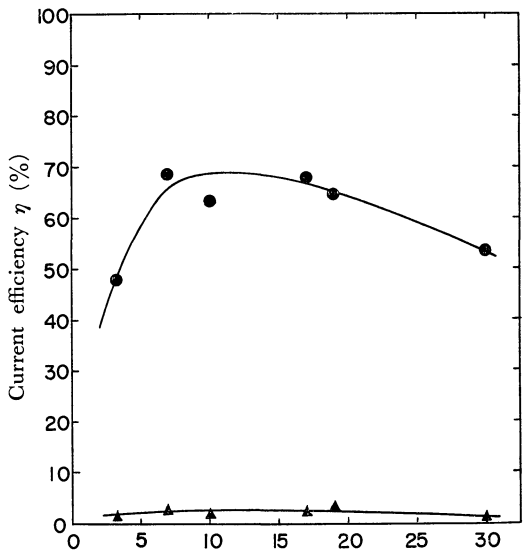

Fig. 2. Effect of the McKee's salt concentration.
Cathode potential: −2.4 V *vs.* SCE;
Water concentration: 25 vol%;
Naphthalene concentration: 11.43 g/100 m*l* solution A;
Current density: about 0.3 A/dm².
—●— $\eta_{1.4DH}$ —▲— η_{TH}

Effect of the Naphthalene Concentration. The effect of the naphthalene concentration is shown in Fig. 3. $\eta_{1,4DH}$ reached the maximum value of 83% at an optimum naphthalene concentration, but it did not vary much under the conditions examined. η_{TH} remained low and nearly constant. 1,2-DHN was not observed.

Temperature Effect. The reaction temperature was changed over the range from 2 to 50°C. Within this temperature range, $\eta_{1,4DH}$ increased as the reaction temperature rose (Table 1).

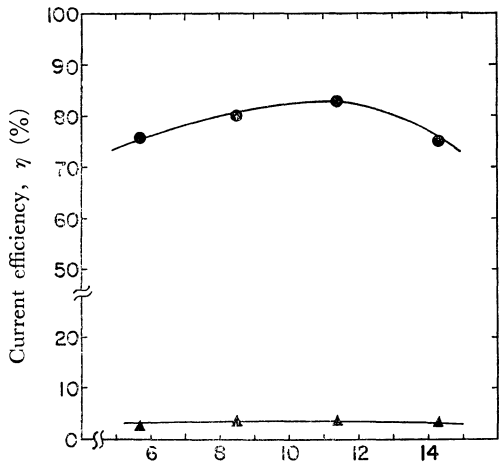

Fig. 3. Effect of the naphthalene concentration.
Cathode potential: −2.4 V *vs.* SCE;
Water concentration: 25 vol%;
Current density: about 0.3 A/dm².
—●— $\eta_{1.4DH}$ —▲— η_{TH}

Table 1. Temperature effect in the reduction of naphthalene

Temperature (°C)	Reaction time (min)	Current passage (Faraday)	Current density (A/dm²)	$\eta_{1.4DH}$ (%)
2	540	0.0082	0.049	21.4
11	480	0.0119	0.081	37.3
13	460	0.0110	0.078	40.7
30	500	0.0150	0.097	44.2
53	440	0.0266	0.195	55.0

Cathode potential: −2.4 V *vs.* SCE;
Naphthalene concentration: 8.57 g/100 ml solution A;
McKee's salt concentration: 20 g/100 ml acetonitrile-water;
Water concentration: 20 vol%.

As is shown in Table 1, $\eta_{1,4DH}$ at 30°C was about 1.1 times larger than that at 10°C (both were of approximately same current densities.).

Electrolysis in Various Solvents. The electrolytic reduction of naphthalene was investigated in the following solvents: acetonitrile, DIOX, THF, DME, and DGL. In these experiments, tetra-*n*-butylammonium bromide was used as the supporting electrolyte in place of tetraethylammonium *p*-toluenesulfonate. In an acetonitrile-water medium, $\eta_{1,2DH}$ was low, though it was larger than in an acetonitrile-water-tetraethylammonium *p*-toluenesulfonate system. However, reduction in other solvents (ethers) gave fairly large values of $\eta_{1,2DH}$. η_{TH} was low in all solvents. The ratio of $\eta_{1,2DH}+1/2\eta_{TH}$ to $\eta_{1,4DH}$ was in the following order:

$$DGL > DME \approx THF > DIOX > Acetonitrile$$

This order seems to be independent of the dielectric constant of the solvents (Table 2).

Effect of Proton-donors. In the electrolysis, water, methanol, ethanol, phenol, and *p*-hydroxybenzoic acid were used as the proton-donors. The effects of the proton-donors are shown in Table 3. Water, methanol, and ethanol all served as effective proton-donors, though the current efficiency ($\eta_{DH}+\eta_{TH}$) using methanol was a little higher than that using water or ethanol. This result partly depends on the difference in the current density. In the reduction using phenol or *p*-hydroxybenzoic acid as the proton-donor, the main reaction was hydrogen evolution and no formation of dihydro- or tetrahydro-products was observed.

Effect of the Current Density. As shown in Table 3, a large difference was observed in the current efficiencies when methanol was used as the proton-donor. This difference was supposed to be caused mainly by the difference in the current densities. Therefore, we examined the effect of

Table 2. Solvent effect in the reduction of naphthalene using $(C_4H_9)_4NBr$ as a supporting electrolyte

Solvent	CH_3CN	DIOX[a]	THF	DME[b]	DGL[c]
Naphthalene (g/100 ml)	11.66	11.66	11.66	11.66	11.66
Reaction time (min)	180	240	180	180	180
Current passage (Faraday)	0.0083	0.0096	0.0201	0.0272	0.0199
$\eta_{1.4DH}$ (%)	27.9	43.0	43.6	49.5	38.8
$\eta_{1.2DH}$ (%)	7.4	22.9	26.8	30.3	34.8
η_{TH} (%)	—	—	6.1	4.5	2.9
$\frac{\eta_{1.2DH}+\frac{1}{2}\eta_{TH}}{\eta_{1.4DH}}$	0.27	0.53	0.68	0.66	0.94
Dielectric constant	37.5 (20°C)	2.209 (25°C)	7.39 (25°C)		7 (20°C)

Cathode potential: −2.4 V *vs.* SCE; Reaction temperature: 20—24°C
Water concentration: 12.5 vol%; $(C_4H_9)_4NBr$ concentration: 15 g/100 ml solution A.
a) Dioxane. b) 1,2-Dimethoxyethane. c) Diglyme.

TABLE 3. EFFECT OF THE PROTON-DONOR IN THE REDUCTION OF NAPHTHALENE

Proton-donor	Concentration (mol/l)	A/dm²	$\eta_{DH}+\eta_{TH}$ (%)	pK_a
Phenol[a)]	6.22	0.10	0	9.9
p-Hydroxybenzoic acid[b)]	3.22	0.22	0	13.8
Water[b)]	3.22	0.37	66	14
Water[a)]	6.22	0.21	68	
Methanol[b)]	3.22	0.40	71	16
Methanol[a)]	6.22	0.10	47	
Ethanol[b)]	3.22	0.28	58	18
Acetonitrile[a)]		0.12	38	25
Water[c)]	13.99	0.14	52	

a) Cathode potential: −2.4 V *vs.* SCE; Naphthalene concentration: 8.57 g/100 m*l* solution A; McKee's salt concentration: 20 g/100 m*l* acetonitrile-water.
b) Cathode potential: −2.3 V *vs.* SCE; Naphthalene concentration: 11.43 g/100 m*l* Solution A; McKee's salt concentration: 22.2 g/100 m*l* acetonitrile-water.
c) *N,N*-Dimethylformamide was used as a solvent instead of acetonitrile, other conditions were the same as a).

TABLE 4. EFFECT OF CURRENT DENSITY

Current density (A/dm²)	Reaction time (min)	Current passage (Faraday)	$\eta_{1,4DH}$ (%)	η_{TH} (%)
0.08	420	0.0110	46.1	2.3
0.13	300	0.0118	49.2	1.0
0.17	480	0.0258	74.2	3.5
0.68	180	0.0380	86.2	2.3
0.78	200	0.0483	86.4	2.8

Cathode potential: −2.3 V *vs.* SCE; Naphthalene concentration: 11.43 g/100 m*l* solution A; McKee's salt concentration: 30 g/100 m*l* acetonitrile-water; Water concentration: 20 vol%.

the current density by altering the porosity and radius of the glass-fritted disk*1 (Table 4). It was observed that $\eta_{1,4DH}$ increased with an increase in the current density, while η_{TH} did not vary much. Therefore, the ratio of $\eta_{1,4DH}$ to η_{TH} increased with an increase in the current density.

Discussion

Among the reaction factors examined, the water concentration and the solvent showed the most considerable influence on the reduction of naphthalene.

The measurement of the polarogram of naphthalene has shown that the first reduction wave involves only one one-electron addition, while the next one-electron addition occurs at a more negative potential in an aprotic system.[10] In the presence of a proton-donor, the anion radical is immediately protonated to become a monohydro radical. As the reduction potential of this monohydro radical is more positive than that of the original molecule,[11] the one-electron addition that follows occurs easily, without any change in the reduction potential, and a two-electrons transfer wave is observed. Therefore, in a reduction with an unsufficient amount of a proton-donor, the current efficiency of 1,4-DHN will be low. The tendency shown in Fig. 1 was consistent with this prediction, though the behavior of η_{TH} was in contrast with that of $\eta_{1,4DH}$. In the presence of a large amount of water, the solubility of naphthalene lowered and a considerable evolution of hydrogen occurred; thus $\eta_{1,4DH}$ had a maximum value under optimum conditions when the addition of water increased.

As has been mentioned previously, during the reduction of naphthalene in the medium of anhydrous acetonitrile, the catholyte turned dark green and the overall current efficiency was low. A considerable amount of the anion radical may take the following possible courses prior to protonation in the absence of water, for acetonitrile is not such an effective proton-donor as water, ethanol, or methanol:

1. Dimerization of anion radicals.
2. Electron transfer to a tetraethylammonium cation.
3. Electron exchange with an electrode.

If the dimerization of the anion radicals occurs, 1,4,1',4'-tetrahydro-1,1'-binaphthalene will be formed. The naphthalene consumed was, however, almost entirely converted to the monomeric reduction products and no dimeric products could be detected. Therefore, the dimerization of the anion radicals is regarded as negligible.

*1 The current density was changed fairly much by this means, but the cathode potential could not be maintained at the set potential for long (for a few hours in the extreme case) after the reaction started in electolyses with low current densities.

10) P. H. Given and M. E. Peover, *J. Chem. Soc.*, **1960**, 385.

11) G. J. Hoijtink, J. van Schooten, E. de Boer and W. Ij. Aalbersberg, *Rec. Trav. Chim.*, **73**, 355 (1954).

If the electron transfer to a tetraethylammonium cation takes place, the tetraethylammonium radical will be formed. This radical, being unstable, decomposes into triethylamine and ethyl radical.[12] The gas-chromatographic analysis of the gaseous products of the electrolysis of naphthalene in anhydrous acetonitrile containing tetraethylammonium *p*-toluenesulfonate indicated that the gaseous products contained a considerable amount of C_2H_4 and a small amount of C_2H_6 (the ratio of C_2H_4 to C_2H_6 was about 30 : 1, and the current efficiency for $C_2H_4+C_2H_6$, about 30%). The tetraethylammonium radical is also formed by the direct electron transfer to the tetraethylammonium cation from the electrode.[13] The polarographic analysis of naphthalene in anhydrous acetonitrile-tetraethylammonium *p*-toluenesulfonate showed that naphthalene was reduced at about 0.25 V more anodic potential than the cation of the supporting salt. Accordingly, the following process may be included in the reaction scheme besides the direct electron transfer to the tetraethylammonium cation:

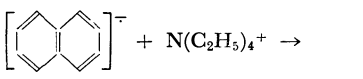

$$+ \cdot N(C_2H_5)_4$$

$$\cdot N(C_2H_5)_4 \rightarrow N(C_2H_5)_3 + \cdot C_2H_5$$

In Table 2, the ratios of $\eta_{1,2DH}+\frac{1}{2}\eta_{TH}$ to $\eta_{1,4DH}$ for the solvent used increase in the following order:

DGL > DME ≈ THF > DIOX > Acetonitrile

The order of the ethers was consistent with the basicity of the ethers as Lewis bases. The above order may be supposed to represent the solvation effect on the anion radical or the monohydro radical of naphthalene by the solvents used. The anion radical of naphthalene may be tentatively shown as below:

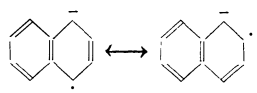

As the basicity of the solvent increases, the electronic configuration of the naphthalene anion radical solvated will be changed and the electron density of the 2 position may increase. A similar change will occur with the monohydro radical of naphthalene. Therefore, the formation of 1,2-DHN will increase as the basicity of the solvent increases in the cases of ether solvents.

In Fig. 1, the behavior of η_{TH} is remarkable. η_{TH} has a value of 29.3% when the water concentration is 0%. This predominant formation of tetralin in anhydrous acetonitrile can be similarly ascribed to the change in the electronic configuration of the naphthalene radical, brought about by the solvation by acetonitrile. This change results in the preferential formation of 1,2-DHN, which is then easily reduced to tetralin as the polarographic half-wave potential of 1,2-DHN is nearly the same as that of naphthalene (though it is slightly more negative than that of naphthalene).[14] The addition of water will change the solvation by acetonitrile and will cause 1,4-DHN to be preferentially formed.

The solvation state cannot be simply interpreted by the apparent physical properties of the solvent, such as its basicity as a Lewis base, its dielectric constant, and so on. We intend, therefore, to clarify the solvent effect by utilizing the ESR technique.

The effect of the concentration of McKee's salt can be interpreted as the coexistence of the stabilization of the naphthalene anion radical by the tetraethylammonium cation and the electron transfer to the cation from the anion radical. At a low concentration of McKee's salt, the stabilization effect is predominant, but with an increase in the concentration the electron transfer may increase. Furthermore, the approach of the water molecule may be hindered by the bulky tetraethylammonium cation.

The rise of the reaction temperature seems to accelerate the protonation of the anion radical by water and relatively suppress the side reactions of the anion radical within the temperature range examined.

As may be seen in Table 3, the values of $\eta_{DH}+\eta_{TH}$ were not very different when water or methanol was used as a proton-donor with fairly high current densities over about 0.3 A/dm^2. The dissociation constants of water and methanol are, however, different. In the case of ethanol, $\eta_{DH}+\eta_{TH}$ had a fairly large value (52%). Furthermore, in the medium of acetonitrile without water, the sum of the current efficiencies was about 38%, not much less than what we had expected from the dissociation constant of acetonitrile if the protonation was mainly the addition of a free proton to the anion radical or to the monoanion. In the reduction using phenol or *p*-hydroxybenzoic acid as a proton-donor, 1,4-DHN was not formed and the evolution of hydrogen occurred predominantly. Therefore, the protonation of the naphthalene anion radical and monoanion occurred mainly by the abstraction of the proton from the proton-donor, as has been proposed on the basis of the results of

12) H. H. Schlubach, *Ber.*, **53B**, 1689 (1920).
13) M. Finkelstein, R. C. Petersen and S. D. Ross, *J. Am. Chem. Soc.*, **81**, 2361 (1959); S. D. Ross, M. Finkelstein and R. C. Petersen, *ibid.*, **82**, 1582 (1960); M. Finkelstein, *J. Org. Chem.*, **27**, 4076 (1962).
14) S. Wawzonek and H. A. Laitinen, *J. Am. Chem. Soc.*, **64**, 2365 (1942).

the polarographic studies,[10,15] though a part of the protonation may occur by the addition of a free proton to the anion. The fact that phenol or *p*-hydroxybenzoic acid did not serve as the proton-donor indicates that the hydrogen atom scarcely contributed at all to the reduction of naphthalene.

It is obvious that the reaction proceeds in accordance with the following reaction scheme:

$$R + e \rightleftarrows R^{\cdot-}$$
$$R^{\cdot-} + HX \rightarrow \cdot RH + X^-$$
$$\cdot RH + e \rightarrow RH^-$$
$$RH^- + HX \rightarrow RH_2 + X^-$$

15) S. Wawzonek and J. W. Fan, *ibid.*, **68**, 2541 (1946).

where HX is the proton-donor. Further, as shown in Table 4, a tendency for $\eta_{1,4DH}$ to increase with an increase in the current density was observed. Therefore, it may be supposed that this equilibrium may exist:

$$2R^{\cdot-} \rightleftarrows R^{2-} + R$$

The increase in the current density may result in an increase in R^{2-}, thus suppressing the side reactions of $R^{\cdot-}$ (as the proton affinity of a dianion is larger than that of an anion radical) and increasing the current efficiency for 1,4-DHN formation. As has been described before, the naphthalene consumed was exclusively converted to the monomeric hydrogenated products, and the proportion of the dimerization of anion radicals was small.

BULLETIN OF THE CHEMICAL SOCIETY OF JAPAN VOL. 41 2927—2931 (1968)

Syntheses and Structures of Acetylformoin and Related Compounds. VI. Substituent Effects

Yo MIYAGI, Sadao KIMURA and Ryozo GOTO

Department of Chemistry, Faculty of Science, Kyoto University, Sakyo-ku, Kyoto

(Received October 19, 1967)

In the presence of cyanide ions, an α-ketoaldehyde dimerizes to give an acylformoin. The tautomerism of this compound was studied. It was found that the tautomerism between I and II is affected by the solvents and by the substituents. In proton-accepting solvents (EtOH, THF), I predominates. In ethanol-free chloroform, II is dominant for almost all substituents. In ethanol-containing chloroform, some acylformoins exist as I, while the others exist as II. The former case is observed when R=*t*-Bu and *p*-X-C_6H_4 (X=H, *t*-Bu, Cl, and Br); the latter case, when R=Me, *i*-Pr, and *p*-Me-C_6H_4. In the former case, ethanol reacts slowly with I to give an *O*-ethyl derivative (III). When R=2,4,6-Me_3-C_6H_2, II predominates in all states. When R=*p*-Cl-C_6H_4 and *p*-Br-C_6H_4, I and II were isolated as crylstals. The solvent effects are interpreted in terms of the hydrogen-bonding interactions of I with basic and hydroxylic solvents.

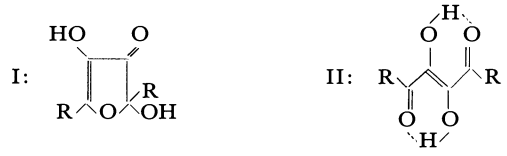

By a self-condensation similar to the benzoin condensation, an α-ketoaldehyde (an alkyl- or aryl-glyoxal) gives an acylformoin (Eq. (1)). Although five tautomers are possible for such compounds, only two tautomers, 2,5-dialkyl (or diaryl)-2,4-dihydroxyfuranone-3 (I) and *trans*-1,2-diacyl (or diaroyl)-1,2-dihydroxyethylene (II), have been found to exist for various acylformoins.[1] I and II have quite different spectral properties; these properties are summarized in Table 1. This paper will be concerned with the tautomerism of some homologues of benzoylformoins. Some detailed studies of chloroform solutions of acylformaoins will also be reported. Table 2 summarizes the spectral results.

1) a) R. Goto, Y. Miyagi and H. Inokawa, This Bulletin, **36**, 147 (1963). b) Y. Miyagi and R. Goto, *ibid.*, **36**, 650. c) Y. Miyagi and R. Goto, *ibid.*, **36**, 921. d) Y. Miyagi, *ibid.*, **37**, 12 (1964). e) S. Kimura, Y. Miyagi and R. Goto, *ibid.*, **39**, 1333 (1966). f) The references in a—e.

TABLE 1. SPECTRAL CHARACTERISTICS

Tautomer	State	IR absorption bands (cm^{-1}) ν_{OH}	$\nu_{C=O}$	$\nu_{C=C}$	UV absorption bands R in Eq. (1)	λ_{max}(mμ)
I	Solid state	Two bands 3600—3200	1695	1620	Aliphatic	305—310
I	Solution	One bond (distinct but broad) 3500—3200	1705	1625	Aryl	355—360(C_2H_5OH) 370($CHCl_3$-C_2H_5OH)*
II	Solid state	broad and weak	1620	—	Aliphatic	355—360
II	Solution	broad and weak	1630	—	Aryl	390—410

* Eisters stated[6] that the ultraviolet absorption in chloroform containing ethanol shows up at 355 mμ. In our measurements, however, it arises at 370 mμ.

TABLE 2. SPECTRAL RESULTS

Formoin	R in Eq.(1)	ν_{max}, cm^{-1} Solid state (Nujol)	ν_{max}, cm^{-1} Solution in THF	λ_{max}, mμ (ε_{max}) C_2H_5OH	$CHCl_3$-C_2H_5OH*	$CHCl_3$* (C_2H_5OH free)	CCl_4*
p-Bromobenzoyl-	*p*-Br-C_6H_4	red cryst. 1580	3240	358(17700)	370	410	415
		yellow cryst. 3180, 3440	1700	350(14800)			
		yellow cryst. 1690	1625	238(14800)		300	305
		yellow cryst. 1605, 1585	1580				
p-Chlorobenzoyl-	*p*-Cl-C_6H_4	red cryst. 1549	3200	360(15000)	373	410	420
		yellow cryst. 3500, 3200	1710				
		yellow cryst. 1700	1630	247(14000)		300	300
		yellow cryst. 1617, 1595	1600				
p-Anisoyl-	*p*-MeO-C_6H_4	1590	3260				415
			1703	355(19000)			
			1623	225(17200)	—	—	320
			1608				
Mesitoyl-	2,4,6-Me_3-C_6H_2	1615	1620	380(13300)	383	383	383

* Intensities of absorption bands were not determined because of low solubility or technique of vacuum sealed cell (see: experimental parts).

$$2RCOCHO \xrightarrow{CN^-} RCOCH(OH)COCOR \quad (1)$$

I 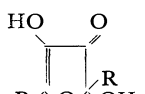

II 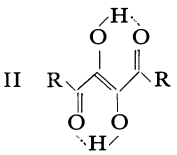

p-Chloro- and p-Bromo-benzoylformoin. *p*-Chloro- and *p*-bromo-benzoylformoins (R=*p*-Cl-C_6H_4 and *p*-Br-C_6H_4 respectively, in Eq. (1)), were first reported by Karrer and his co-workers.[2] They carried out the condensation in an aqueous alcoholic solution containing potassium cyanide and obtained red crystals by recrystallizing the reaction products from hot benzene in both cases. Following their method, the present authors found that the addition of water to a reaction solution precipitates yellow crystals, which can then be recrystallized from ethanol. When a hot benzene solution of yellow crystals is allowed to stand, at first red crystals and then yellow crystals precipitate. After a prolonged heating of the benzene solution, only the red crystals precipitate. The red crystals of both acylformoins do not change their color on heating and melt sharply at their melting points. On the other hand, the yellow crystals of both acylformoins gradually turn red on heating and melt at a temperatures slightly lower than the melting point of the corresponding red crystals. Thus, the melting points proper to the yellow crystals can not be observed. The yellow crystals have IR spectral characteristics of I, while the red crystals have those of II, in both cases.

p-Anisoylformoin and Mesitoylformoin. The syntheses of *p*-anisoylformoin[3] and mesitoylformoin[4] (R=*p*-MeO-C_6H_4 and 2,4,6-Me_3-C_6H_2 in Eq. (1) respectively) have been reported in the literature. In these cases, the present authors could not isolate the two tautomers as crystals. Both acylformoins are red crystals and show IR

2) P. Karrer and C. Musante, *Helv. Chim. Acta*, **18**, 1140 (1935).

3) P. Karrer and A. v. Segesser, *ibid.*, **18**, 273 (1935).

4) A. R. Gray and R. C. Fuson, *J. Am. Chem. Soc.*, **56**, 1367 (1934).

spectra characteristic of II.

Tautomers in Tetrahydrofuran and Ethanol. Solutions of the three acylformoins other than mesitoylformoin in tetrahydrofuran or ethanol show the IR and UV spectra characteristic of I. It has been reported that I arises also in these solutions of other acylformoins, and it has been suggested that proton-accepting solvents might stabilize I by a solvation such as that depicted in Fig. 1, so that I can be predominant in these solvents.[1d]

Unlike the others, however, mesitoylformoin does not show any tautomerism and exists as II in chloroform and also in tetrahydrofuran.

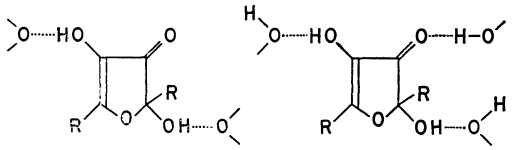

(A) (B)

Fig. 1. Solvation by ethers (A) and alcohols (B).

Tautomers in Chloroform. Since benzoyl-, *t*-butylbenzoyl-, and neopentoyl-formoins are easily oxidized in chloroform, the UV spectra of the solutions were measured in vacuum-sealed cells. Solutions of these acylformoins in ethanol-containing chloroform[5] show the UV spectra characteristic of I.

However, Eistert isolated an *O*-ethyl derivative (III, $R=C_6H_5$) by refluxing an ethanol-chloroform solution of benzoylformoin.[6] III ($R=C_6H_5$) shows the same UV spectra as that of II ($R=C_6H_5$).

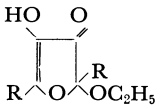

III

He suggested that benzoylformoin reacts with ethanol to give III ($R=C_6H_5$) in ethanol-containing chloroform. The spectrum observed in our experiments could, therefore, be due to III and not to I.

The following facts suggest, however, that the absorption of the ethanol-containing chloroform solution is not always caused by III. In a vacuum-sealed cell, a solution of neopentoylformoin in ethanol-containing chloroform shows an absorption at 310 mμ characteristic of I or III. After the solution has stood overnight, the intensity of this absorption does not change. When the cell is then opened to the atmosphere, the intensity decreases gradually, as has been reported previously[1d] (Fig. 2). However, when the cell is opened immediately after sealing, the 310 mμ band decreases rapidly and disappears after two hours. Since I may be more easily oxidized than III, these facts suggest the predominance of I immediately after dissolution and the subsequent predominance of III after the solution has been allowed to stand overnight. This means that I reacts slowly with ethanol to give III.[7]

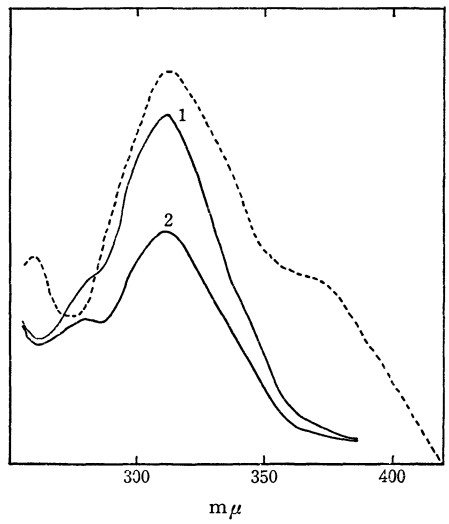

Fig. 2. Ultraviolet spectra of neopentoylformoin in vacuum-sealed cells: ——1, in ethanol-containing chloroform, ——2, 2 hr after breaking seal of a cell after standing overnight an ethanol-containing chloroform solution; ---- in ethanol-free chloroform.

The spectrum of neopentoylformoin in ethanol-free chloroform[8] (Fig. 2) shows its main absorption at 311 mμ, with a shoulder at about 370 mμ, indicating a mixture of I (the major component) and II (the minor component). It may be concluded that, in the case of neopentoylformoin, I predominates even in this solvent where stabilization by solvation by ethanol is absent. An ethanol-containing chloroform solution of acetylformoin shows an absorption band characteristic of II at 355 mμ; this band gradually decreases in an open cell. When measured in a vacuum-sealed cell, however, the spectrum did not change on standing. This means that acetylformoin does not react with ethanol in chloroform, since, if this were the case, an absorption would arise at about 310 mμ on standing.

5) As the ethanol-containing chloroform, we used spectro-grad chloroform (Dotite) containing ethanol as a stabilizer (the ethanol content was about 0.5%).

6) B. Eistert, private communication. We are indebted to him for informing us of his observations prior to publication.

7) There is a possibility that this etherification is catalyzed by a trace amount of hydrogen chloride present as an impurity.

8) Ethanol-free chloroform was prepared by shaking spectro-grade chloroform with sulfuric acid, washing it with water, drying, and distilling.

As has been briefly mentioned in a previous paper[1e], *p*-*t*-butylbenzoylformoin behaves interestingly. In a vacuum-sealed cell, the λ_{max} value of its ethanol-containing chloroform solution is 371 mμ. However, an ethanol-free chloroform solution shows an absorption at about 380 mμ immediately after dissolution; this absorption maximum shifts to 405 mμ in about five minutes (Fig. 3). These facts mean that this acylformoin exists as I immediately after dissolution, but is rapidly converted to II in this solvent. The fact that I exists in ethanol-containing chloroform, while II exists in ethanol-free chloroform, can be explained in terms of the solvation of I by ethanol, as is shown in Fig. 1.

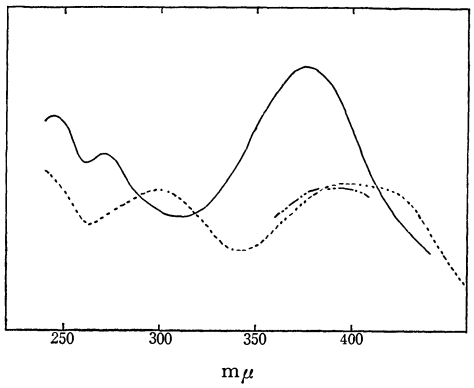

Fig. 3. UV spectra of *p*-*t*-butylbenzoylformoin in vacuum-sealed cells: ——— immediately after dissolving in ethanol-free chloroform; ---- about five minutes after dissolving in ethanol-free chloroform; —— in ethanol-containing chloroform.

p-Toluylformoin shows an absorption at 380 mμ, with a should around 410 mμ in ethanol-containing chloroform (Fig. 4). On the other hand, in ethanol-free chloroform the only absorption maximum is at 405 mμ. Thus, II seems to exist in ethanol-free chloroform and an equilibrium

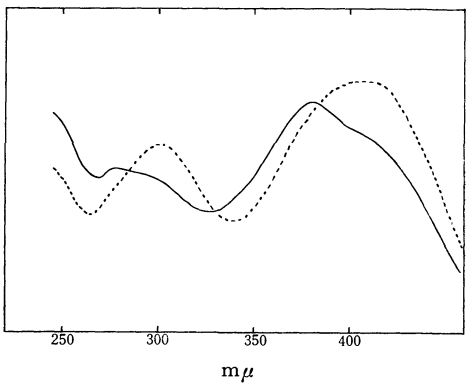

Fig. 4. UV spectra of *p*-toluylformoin in vacuum-sealed cells: —— in ethanol-containing chloroform; ---- in ethanol-free chloroform.

mixture of I (the major component) and II (the minor component) in ethanol-containing chloroform.

p-Chloro- and *p*-bromo-benzoylformoins are not easily oxidized in chloroform. Their UV sepctra can be measured in open cells. These acylformoins show absorption bands at 370 mμ in ethanol-containing chloroform and at 410 mμ in ethanol-free chloroform and in carbon tetrachloride.

p-Anisoylformoin shows an absorption at 410 mμ in carbon tetrachloride, but a broad band around 350—400 mμ in chloroform. Nothing conclusive has been obtained regarding the latter solution.

Discussion

The tautomeric behavior of the acylformoin is summarized in Table 3.

In tetrahydrofuran and ethanol, all the acylformoins studied except mesitoylformoin exist as I, presumably solvated as depicted in Fig. 1. Although some acylformoins are easily oxidized

Table 3. Tautomers of acylformoins

Formoin	Ref.	R in Eq. (1)	Solid state	Solution in		
				THF, C_2H_5OH	$CHCl_3$-C_2H_5OH	$CHCl_3, CCl_4$
Acetyl-	1a	Me	II	I	II	II
Isobutyryl-	1c	Me_2CH-	I	I	II	II
Neopentoyl-	1b	Me_3C-	I	I	I	I+II (I>II)
p-*t*-Butylbenzoyl	1e	*p*-Me_3C-C_6H_4	I	I	I	II
Benzoyl-	1a,d	C_6H_5	I	I	I	II
p-Chlorobenzoyl-	2	*p*-Cl-C_6H_4	I,II	I	I	II
p-Bromobenzoyl-	2	*p*-Br-C_6H_4	I,II	I	I	II
p-Anisoyl-	3	*p*-Me O-C_6H_4	II	I	I	II
p-Toluyl-	1e	*p*-Me-C_6H_4	I	I	I+II (I>II)	II
Mesitoyl-	4	2,4,6-Me_3-C_6H_2	II	II	II	II

in chloroform, they are rather stable to oxidation in these solvents.

In most cases, I predominates in ethanol-containing chloroform, while II is dominant in ethanol-free chloroform or carbon tetrachloride. Since I is solvated by ethanol in the former solvent, it may be considered that II is more stable than I in the absence of solvation by ethanol. However, as for neopentoylformoin, I is more stable than II, even in the absence of ethanol and its accompanying solvation.

It may be feasible to consider that the stability of II is affected by the substituent, R. For acetyl-, isobutyryl- and *p*-toluyl-formoins, II may be considered to be more stable than for the other acylformoins. For the first two, II exists as a sole component, even in ethanol-containing chloroform. For the third, II is observed as one component of an equilibrium mixture. Consequently, for the above three acylformoins II is present in ethanol-containing chloroform, while other acylformoins exist as I in this solvent. In the case of neopentoylformoin, in which the R is *t*-butyl, II is unstable, as has been mentioned above.

Mesitoylformoin exists as II in all states.

In the case of *p*-chloro- and *p*-bromo-benzoylformoins, the stability of II presumably becomes comparable with that of I and the isolation of both tautomers is possible.

From the above considerations, it may be suggested that hyperconjugation is effective in stabilizing II. However, nothing confirmative has yet been obtained.

Experimental

Acylformoins. The following four acylformoins were prepared in the same way. A solution of sodium cyanide (0.2 g) in 20 m*l* of 50% aqueous ethanol was added to a solution of a glyoxal hydrate (5 g) in 50 m*l* of ethanol. After standing for 3 hr in an ice-cold bath, the solution was poured into cold water. The precipitated crystals were collected by filtration.

p-Bromobenzoylformoin. Yellow crystals, recrystallized from ethanol; on heating began to turn red at around 80°C and melted at 178—184°C. Red crystals, recrystallized from benzene; mp 195°C.

p-Chlorobenzoylformoin. Yellow crystals, recrystallized from ethanol; on heating, began to tunr red at around 145°C and melted at 181—182°C. Red crystals, recrystallized from benzene; mp 181—182°C.

p-Anisoylformoin. Red crystals, recrystallized from ethanol; mp 145—146°C (lit.,[3] 151°C).

Mesitoylformoin. Red crystals, recrystallized from ethanol; mp 188—189°C.

Technique of Vacuum-sealed Cell; explained in experimental part of Reference 1d; the absorption intensities in Figs. 2—4 are arbitrary.

BULLETIN OF THE CHEMICAL SOCIETY OF JAPAN VOL. 41 2931—2935 (1968)

Metal-Containing Initiator Systems. III.*[1] Polymerization of Styrene by Some Activated Metals in the Presence of Organic Halides

Takayuki OTSU and Masami YAMAGUCHI

Department of Applied Chemistry, Faculty of Engineering, Osaka City University, Sugimotocho, Sumiyoshi-ku, Osaka

(Received December 27, 1967)

The polymerization of styrene with systems of various metals and organic halides was investigated at 60°C. It was found that the metals which could be used as hydrogenation catalysts were effective as initiators and that the organic halides with a weak carbon-halogen bond showed a high initiating activity for styrene polymerization. From the kinetic studies of the polymerization of styrene by reduced nickel and chloroform, the rate of polymerization was shown to be proportional to the monomer concentration and to the square-root concentration of both nickel and chloroform in the lower concentration range of chloroform. Some radical inhibitors were also found to inhibit this polymerization. These results indicated that this initiator system could induce the radical polymerization. The apparent overall activation energy for the polymerization by this system was estimated as 11 kcal/mol. The resulting polystyrene was found to be a relatively-low-molecular-weight atactic polymer.

In previous papers,[1,2] it has been reported that some activated metals can serve as radical initiators of vinyl monomers in the presence of some organic

*1 Parts I and II of this series are Refs. 1 and 2 respectively.

1) T. Otsu, M. Yamaguchi, Y. Takemura, Y. Kusuki and S. Aoki, *J. Polymer Sci.*, **B**, **5**, 697 (1967).
2) T. Otsu, S. Aoki, M. Nishimura, M. Yamaguchi and Y. Kusuki, *ibid.*, **B**, **5**, 835 (1967).

halides. Recently, similar investigations have been published independently by Olivé and Olivé[3] and by Iwatsuki *et al.*[4]

The present paper will describe our detailed findings on the polymerization of styrene by systems of various metals and organic halides at 60°C, and on our kinetic studies of the polymerization by a system of reduced nickel and chloroform.

Experimental

Materials. Raney metals were prepared from their commercial aluminum alloys according to the Adkins W-5 method,[5] followed by successive washings with water, methanol, and benzene.

The Urushibara metals were obtained by adding zinc dust to a metal chloride aqueous solution by the method of Taira[6]; they were used after having been washed with water, methanol, and benzene.

The reduced nickel used was a commercially-obtainable stabilized hydrogenation catalyst (Nikki Chemical Co.) composed of a 50% Ni atom on kieselguhr. Before use, this catalyst was activated by heating it at about 200°C in a stream of hydrogen for an hour. The other hydrogenation catalyst, formate nickel (Nikko Rikagaku Co.), prepared by the thermal decomposition of nickel formate, was a commercial product (50% Ni atom on kieselguhr). The commercial metal powders were also used without further purification.

The organic halides used in this study were purified by distillation or recrystallization. The styrene was purified by the ordinary method and distilled under reduced pressure before use. The other reagents were purified by ordinary methods.

Polymerization Procedure. Into a hard glass tube containing a given amount of the metal, the required amounts of organic halide and monomer were placed. After degassing the contents of this tube by a successive freezing and thawing technique, the tube was sealed off under a vacuum.

Polymerizations were carried out in the dark with shaking in a thermostat maintained at 60°C. After polymerization, the contents of the tube were poured into a large amount of methanol containing concentrated hydrochloric acid in order to precipitate the polymer and dissolve the residual metal initiator. The resulting polymer was then purified by reprecipitating it two or three times using a system of benzene and methanol. The conversion was calculated from the weight of the dried polymer thus obtained.

Analysis of the Polymers. The number-average molecular weight ($\overline{M}_n$) of the polymers was calculated from their intrinsic viscosities, [η], determined in benzene at 30°C according to the following equation[7]:

$$[\eta] = 1.74\times10^{-4}\,\overline{M}_n^{0.71}$$

3) G. Henrici-Olivé and S. Olivé, *Makromol. Chem.*, **88**, 117 (1965).
4) S. Iwatsuki, H. Kasahara and Y. Yamashita, *ibid.*, **104**, 254 (1967).
5) H. Adkins and H. R. Billica, *J. Am. Chem. Soc.*, **70**, 695 (1948).
6) S. Taira, This Bulletin, **34**, 261 (1961).
7) R. Gregg and F. R. Mayo, *J. Am. Chem. Soc.*, **70**, 2373 (1948).

Results and Discussion

Effect of Metals. The effects of various kinds of metals on the polymerization of styrene in the presence of carbon tetrachloride at 60°C in benzene were investigated. The results are shown in Table 1.

Table 1. Polymerization of styrene with the systems of some metals and carbon tetrachloride at 60°C for 18 hr
[M]=4.14 mol/l, [CCl_4]=0.49 mol/l
[Metal]=0.81 g-atom/l in benzene

Metal	Polymer yield, %	Metal	Polymer yield, %
Raney Ni	68.3	Raney Cu	60.7
Urushibara Ni	78.6	Urushibara Cu	70.7
Formate Ni	17.7	Commercial Cu	1.8
Reduced Ni	90.2	Raney Fe	51.2
Commercial Ni	0.5	Urushibara Fe	46.1
Raney Co	76.8	Commercial Fe	1.9
Urushibara Co	76.2	Commercial Zn	0.3
Commercial Co	1.1	None	0.5

As can be seen from Table 1, the systems of Raney and Urushibara metals with carbon tetrachloride were effective as initiators of the styrene polymerization. However, the systems consisting of commericial metal powders were completely inactive with regard to initiation, indicating it is necessary that the metals have a fresh surface.

No definite relationship between the initiating activities and the kinds of metals can be observed from Table 1, because the polymerization system was heterogeneous. However, it might be considered that both the oxidation potential of the metals, as was suggested by Olivé *et al.*,[3] and their preparation and activation methods, which determined their surface area and purity, were the controlling factors in the initiating activity of these systems.

The resulting polymers were soluble in methyl ethyl ketone at room temperature, indicating that no isotactic polystyrene was obtained and that these systems could not induce the stereospecific polymerization of styrene.

Effect of Organic Halides. Table 2 shows the results of the polymerization of styrene with reduced nickel in the presence of various kinds of organic halides at 60°C.

In Table 2 the initiating activity can be seen to increase as the substitution by halogen atom increases and also as the labile halogen atom is involved. These results suggest that the effectiveness of organic halides in initiation increases with a decrease in the bond-dissociation energy of the carbon-halogen bonds involved in organic halides. The reactivity of the initiating radical

Table 2. Effect of organic halides on the polymerization of styrene at 60°C for 8 hr
[M]=4.14 mol/*l*, [Halide]=0.2 mol/*l*
[Ni]=0.4 g-atom/*l* in benzene

Organic halide	Polymer yield, %	Degree of polymerization
CH_2Cl_2	6.9	2300
$CHCl_3$	21.7	160
CCl_4	26.5	80
$CHBr_3$	48.6	50
CHI_3	36.0	20
C_2H_5Br	16.8	500
n-C_4H_9Cl	1.4	—
t-C_4H_9Cl	7.7	1500
C_6H_5Cl	1.0	—
$C_6H_5CH_2Cl$	46.8	120
CH_2=$CHCH_2Cl$	11.3	700
None	0.6	—

produced from organic halides toward the styrene monomer might also be important.

In Table 2 the degree of polymerization of the resulting polymers can also be observed to decrease in proportion to the increase in the initiating activity of the systems. Since the chain-transfer reactivity of these organic halides has been known to be correlated also with the bond-dissociation energy of their carbon-halogen bonds, such a change in the degree of polymerization might be expected from the reactivities of organic halides in both the initiation and the chain-transfer reaction.

Kinetic Studies of the Polymerization by the System of Reduced Nickel and Chloroform. Figure 1 shows the relationship between the conversion and the polymerization time at 30, 45, 60, and 80°C. In this figure, straight-line relationships can be observed between them at every temperature.

The rates of polymerization (R_p), which were determined from the slopes of the straight lines in Fig. 1, are plotted against the reciprocal polymerization temperatures in Fig. 2. From the slope of the resulting straight line, the apparent activation energy for the overall polymerization by this initiator system was calculated to be 11.1 kcal/mol. Accordingly, the activation energy for initiation was obtained as 9.2 kcal/mol by using the reported rate constants[8] for propagation and termination. This value is quite small compared with that of benzoyl peroxide (29.6 kcal/mol).[9]

Figure 3 shows the relationship between the rate of polymerization and the concentration of reduced nickel at constant concentrations of both

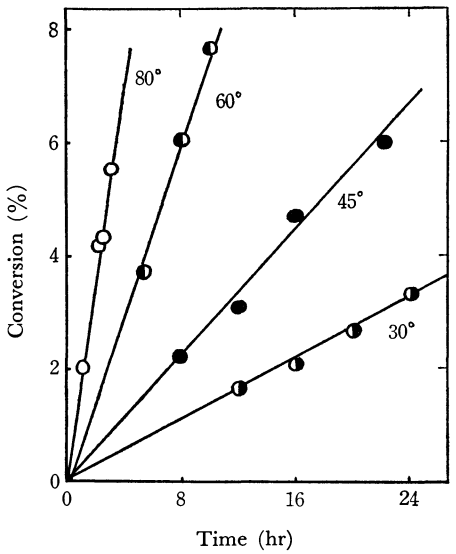

Fig. 1. Time-conversion relations on the polymerization of styrene by the system of reduced nickel and chloroform at 30—80°C: [Ni]=2.5 $\times 10^{-2}$ g-atom/*l*, [$CHCl_3$]=2.5$\times 10^{-2}$ mol/*l*, [M] =4.35 mol/*l* in benzene.

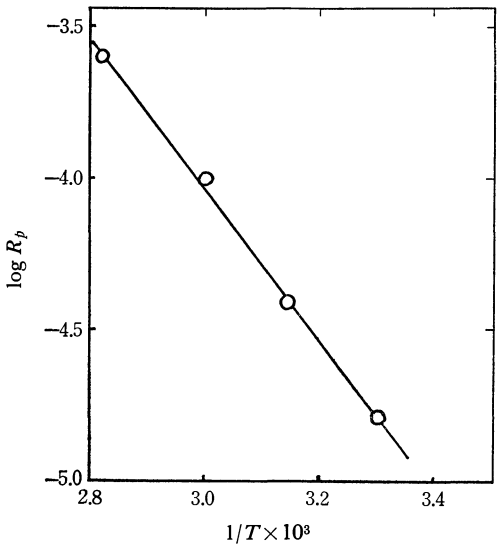

Fig. 2. Arrehnius plot between R_p and $1/T$.

the styrene monomer and chloroform. From this figure, the rate can be seen to be proportional to the square-root concentration of reduced nickel, indicating that the radical polymerization occurred.

The relationship between the rate of polymerization and the concentration of chloroform is shown in Fig. 4, from which the square-root dependence of the concentration of chloroform on the rate was observed only in the concentration range lower than 5×10^{-3} mol/*l*. In the concentration range above this, the rate was constant independently of the concentration of chloroform. This result

8) A. V. Tobolsky and B. Baysal, *J. Polymer Sci.*, **11**, 471 (1953).
9) C. E. H. Bawn and S. F. Mellish, *Trans. Faraday Soc.*, **47**, 1216 (1951).

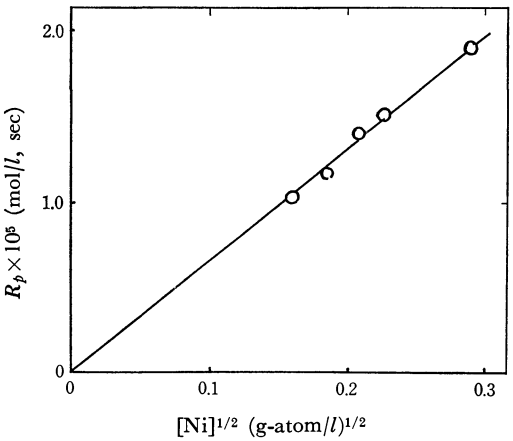

Fig. 3. Relationship between R_p and the concentration of reduced nickel: $[CHCl_3]=2.5\times10^{-2}$ mol/l, $[M]=4.35$ mol/l in benzene at 60°C.

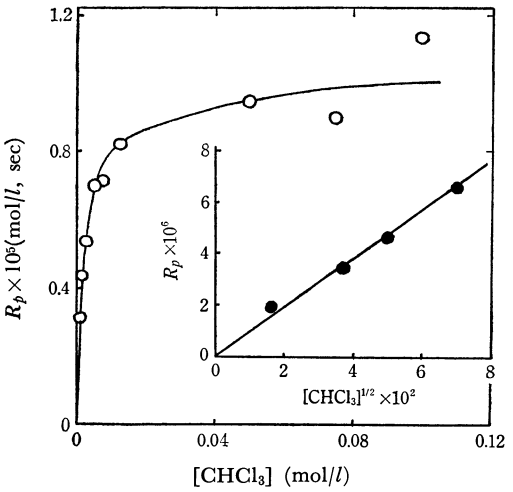

Fig. 4. Relationship between R_p and the concentration of chloroform: $[Ni]=2.5\times10^{-2}$ g-atom/l, $[M]=4.35$ mol/l in benzene at 60°C.

suggests that the initiating radical is produced *via* a complex formation between reduced nickel and chloroform, as was pointed out by Olivé and Olivé[3] and by Iwatsuki *et al.*[4]

Figure 5 shows the plot of the polymerization rate against the concentration of the styrene monomer. It was clear that the rate was directly proportional to the monomer concentration. This result also indicates that the monomer did not participate in intiating radical production.

Effect of Radical Inhibitor. The effect of some radical inhibitors on the polymerization by a system of reduced nickel and carbon tetrachloride was also investigated. The results are shown in Table 3.

In Table 3, *p*-benzoquinone, diphenylpicrylhydrazyl (DPPH), and oxygen can be seen to inhibit this polymerization. Accordingly, it is

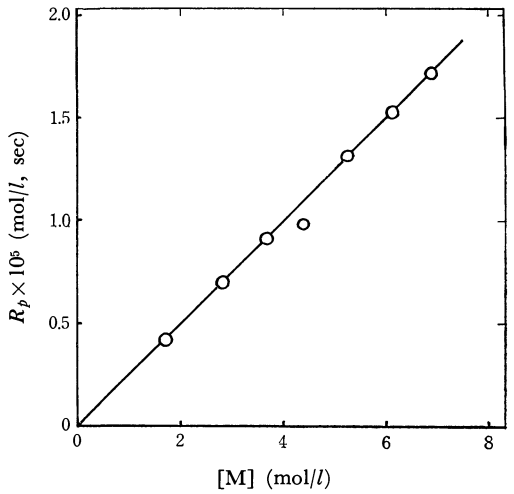

Fig. 5. Relationship between R_p and monomer concentration: $[Ni]=2.5\times10^{-2}$ g-am/l, $[CHCl_3]=2.5\times10^{-2}$ mol/l in benzene at 60°C.

Table 3. Effect of radical inhibitor on the polymerization of styrene with the system of reduced nickel and carbon tetrachloride

$[M]=4.14$ mol/l, $[CCl_4]=0.2$ mol/l
$[Ni]=0.4$ g-atom/l in benzene, at 60°C, for 10 hr

Inhibitor (g)	Polymer yield (%)
None	20.2
Air	6.5
Hydroquinone (0.05)	16.7
p-Benzoquinone (0.05)	4.0
DPPH (0.05)	0.4

obvious that this initiator system induced the radical polymerization of styrene. However, the hydroquinone does not act as a radical inhibitor.

Mechanism of Styrene Polymerization by These Systems. From the results of the polymerization kinetics and of the radical inhibitor, it is clear that the polymerization of styrene by these systems proceeds via a radical mechanism. This conclusion is also supported by the results of copolymerization with methyl methacrylate by a system of reduced nickel and carbon tetrachloride at 60°C.[10]

As was pointed out Olivé and Olivé[3] and by Iwatsuki *et al.*,[4] the initiation by these systems may be considered to occur in the following way: a complex between the metal (Me) and the organic halide (RX) is formed, and then a one-electron transfer from the metal to the carbon-halogen bond in the halide to give the initiating radical occurs:

$$R\text{-}X + Me \rightleftarrows [complex] \rightarrow R\cdot + Me^+ + X^-$$

This mechanism is also confirmed by the fact

10) T. Otsu and M. Yamaguchi, *J. Polymer Sci.*, **A1**, **6**, 3075 (1968).

that hexachloroethane and nickel chloride were found in a reaction mixture of reduced nickel and carbon tetrachloride.[10]

If the step of the one-electron transfer is rate-determining, the ease of the initiating radical production may be dependent on both the oxidation potential of the metal and the bond-dissociation energy of the carbon-halogen bond in the halide. However, no definite correlation was obtained between the initiator activity and the kind of metal, as may be seen in Table 1. This result is understandable if it is assumed that the surface area and the purity of the metal are more significant than its oxidation potential in the formation of the complex with the halide rather.

The probable structure of the complex in the transition state may be written as follows:

$$\underset{\text{I}}{[R:X\ Me} \rightarrow \underset{\text{II}}{R\cdot X^{-}:Me^{+}]}$$

in which the I structure is the structure near the reactant system and the II structure is that after the one-electron transfer has occurred. The importance of a similar transition-state structure has been discussed by Kochi *et al.*[11] for the reduction of alkyl halides with the chromium(II) ion.

From Table 2, the degrees of polymerization of some polystyrenes can be seen to be lower than that to be expected from the chain-transfer constant and the concentration of the organic halides used. In connection with this observation, we found recently that the systems of reduced nickel and methylchlorosilanes could induce the cationic polymerization of styrene.[12] This point will be clarified in a later paper.

11) J. Kochi and D. Davis, *J. Am. Chem. Soc.*, **85**, 5264 (1964).
12) T. Otsu, S. Aoki, M. Nishimura, M. Yamaguchi and Y. Kusuki, *J. Polymers Sci.*, **A1**, in press.

BULLETIN OF THE CHEMICAL SOCEITY OF JAPAN VOL. 41 2935—2941 (1968)

Tropylation of Azulene, 1-Oxaazulan-2-one, and Their Derivatives, and Electrophilic Reactions of the Tropylazulene Derivatives*[1]

Tetsuo NOZOE, Takashi TODA, Toyonobu ASAO and Akira YAMANOUCHI*[2]

Department of Chemistry, Faculty of Science, Tohoku University, Katahira-cho, Sendai

(Received January 29, 1968)

The tropylation of azulene, oxaazulan-2-one, and their derivatives was investigated, and various 1 and/or 3-tropylazulenes and 3-tropyloxaazulan-2-ones were obtained. The NMR, UV, and visible spectra of these tropylazulenes were then discussed. Some electrophilic reactions, such as azo-coupling and the acid treatment of four kinds of tropylazulenes, were studied, and it was found that exchanges of the tropyl group and the attacking electrophilies occurred.

The tropylium ion, one of the most stable carbonium ions, is known to react with various bases (anionoid reagents) resulting in the tropylation of nucleophiles, and in hydride abstraction in some cases.[1,2] The reaction can also be carried out conveniently using tropyl ethers,[2] sometimes with the addition of catalytic amounts of the tropylium ion or acids, in place of tropylium salts because of the facile ionization of the former to the latter under these conditions. In our laboratory, a continuous effeort has been made to tropylate various phenols[3,4] and tropolone[5] with these reagents, as well as to abstract the hydride ion from the tropylated products by means of the tropylium ion or other oxidizing reagents.[3,4]

Since sodium salts of cyclopentadiene[1,6] and indene[6] are also known to undergo tropylation by

*1 Presented at the 15th Annual Meeting of the Chemical Society of Japan, Kyoto, April, 1962, and at the Local Meeting of the Tohoku District of the Society, Koriyama, October, 1963.

*2 Present Address: Kureha Chemical Co., Shinjuku-ku, Tokyo.

1) W. von E. Doering and H. Krauch, *Angew. Chem.*, **68**, 661 (1956); W. von E. Doering, "Theoretical Organic Chemistry" (The Kekule Symposium), Butterworth, London (1959), p. 35; T. Nozoe, "Progress in Organic Chemistry," Ed. by J. W. Cook, Vol. 5, Butterworth, London (1961), p. 132; D. M. G. Ll'oyd, "Carbocyclic Non-Benzenoid Aromatic Compounds," Elsevier (1966), pp. 98—114.

2) M. E. Vol'pin, I. S. Akhrem and D. N. Kursanov, *Izvest. Acad. Nauk USSR, Otdel, Khim. Nauk,* **1957**, 1501.

3) T. Nozoe, S. Ito, and T. Tezuka, *Chem. & Ind.*, **1960**, 1088.

4) T. Nozoe and K. Kitahara, *ibid.*, **1962**, 1192, K. Takahashi, This Bulletin, **40**, 1462 (1967); T. Nozoe and K. Takahashi, *ibid.*, **40**, 1473, 1480 (1967).

5) T Nozoe, T. Tezuka and Y. Mukai, *ibid.*, **36**, 1470 (1963).

the tropylium ion, the 1 and 3 positions of azulene, being of the highest electron density in the ring system and having properties similar to those of these carbanions,[7a] may have sufficient anionic property to undergo tropylation. This anticipation led us to investigate the reaction of tropyl ethers with azulene (I) as well as 1-oxaazulan-2-one (II), the 3-position of which was also expected to be capable of electrophilic substitution.[7b] However, apart from our studies, Hafner *et al.*[8] and Anderson and Replogle[9] have reported the synthesis of some tropylazulenes by the reaction of of azulenes with tropylium perchlorate or tropylium fluoroborate.

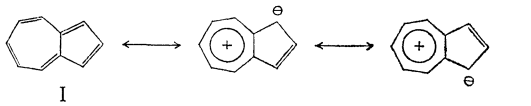

I

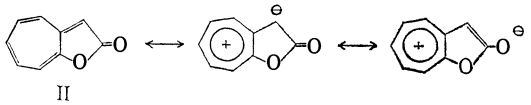

II

The intermediate of the electrophilic substitution reactions of azulenes may be represented as Formula A; it gives a final procuct such as B.[7b]

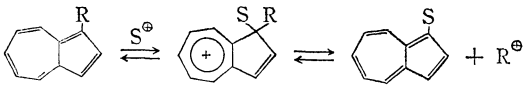

A B

It is a well-known phenomenon that when azulenes are dissolved in concentrated acids, the color of the azulenes disappears,[7a,10] while when R and S are hydrogen atoms, it has actually been proved by NMR[11] and UV[12] spectral techniques that azulenes exist in Formula A. When R is a group or atom can be eliminated easily, R will be replaced by other reagents, S. In fact, when R is acetyl, carboxyl, or sulfonyl, those groups are replaced by arylazo or halogens.[13,14] Since the tropyl groups readily forms the tropylium ion, the 1-tropylazulenes obtained above may be expected to cause an exchange reaction with other electrophilic reagents.

No reaction took place in benzene or cyclohexane between azulene and tropyl ethyl ether or ditropyl ether, even when the mixture was heated. However, the addition of a catalytic amount of tropylium bromide or mineral acids to the above mixture caused a smooth reaction, one which gave 1,3-ditropylazulene (III). In a similar manner, 5-isopropylazulene and 2-acetamidoazulene yielded the corresponding 1,3-ditropyl derivatives, (IV) and (V) respectively. Although it was difficult to control the reaction at the stage of monotropylation in the above reactions, this was achieved with 2-chloroazulene (VI); 2-chloro-1-tropylazulene (VIII) and 2-chloro-1,3-ditropylazulene (VII) were obtained using a half-molar equivalent of the reagent.

1-Methylazulene and guaiazulene (IX) which are substituted at the 1-position, gave monotropyl derivatives, (X) and (XI) respectively; diethyl azulene-1,3-dicarboxylate did not undergo tropylation, even when the reaction mixture was heated. Hence, it may be considered that the tropyl groups in the tropylazulenes are located at the 1 and/or 3-positions of azulene nuclei; this is clear from the studies of their NMR spectra and visible absorption spectra, which will be described later.

A formyl or ethoxycarbonyl group at the C 1-position diminishes the reactivity of azulene to tropylation; however, 1-formylazulene, ethyl azulene-1-carboxylate (XII), and their 2-chloro derivatives gave, in the reaction with ditropyl ether in the presence of tropylium bromide or hydrochloric acid, the corresponding monotropyl derivatives (XIII-XVI) in high yields at an elevated temperature. Ethyl 2-aminoazulene-1-carboxylate also gave the 3-tropyl derivative (XVII). XV was also obtained by the formylation of 2-chloro-1-tropylazulene (VIII) by Vilsmeyer's method.

1-Tropylazulene (XVIII) was obtained from ethyl 1-tropyl-azulene-3-carboxylate (XIV) by alkaline hydrolysis and subsequent decarboxylation. The heating of the oxime of XV with acetic anhydride furnished 2-chloro-1-cyano-3-tropylazulene (XIX).

It has been known[15] that the thermal isomerization of double bonds in a tropyl group occurs readily. Therefore, the tropyl group in XVIII or XIX obtained through thermal process might undergo isomerization.*3

6) H. Prinzbach, *Angew, Chem.*, **73**, 167 (1961); H. Prinzbach and D. Seip, *ibid.*, **73**, 169 (1961); H. Prinzbach and W. Rosswog, *ibid.*, **73**, 543 (1961).

7) a) T. Nozoe and T. Asao, "Dai-Yuki Kagaku" (Comprehensive Organic Chemistry), Vol. 13, Asakura Shoten, Tokyo (1960), p. 439, and the references cited therein; b) T. Nozoe and K. Kikuchi, *ibid.*, p. 455.

8) K. Hafner, A. Stephan and C. Bernhard, *Ann.*, **650**, 42 (1961).

9) A. G. Anderson, Jr., and L. L. Replogle, *J. Org. Chem.*, **28**, 262 (1963).

10) A. E. Sherndal, *J. Am. Chem. Soc.*, **37**, 167, 1537 (1915).

11) W. G. Schneider, J. H. Bernstein and J. A. Pople, *J. Am. Chem. Soc.*, **80**, 3497 (1958); H. W. Frey, *J. Chem. Phys.*, **25**, 600 (1956).

12) Pl. Plattner, E. Heilbronner and S. Weber, *Helv. Chim. Acta*, **35**, 1036 (1952).

13) A. G. Anderson, J. A. Nelson and J. J. Tazuma, *J. Am. Chem. Soc.*, **75**, 4980 (1953).

14) W. Treibs and W. Schroth, *Ann.*, **586**, 202 (1954).

15) A. P. ter Borg. H. Kloosterzield and N. van Meurs, *Proc. Chem. Soc.*, **1962**, 359; *Rec. trav. chim.*, **82**, 717 (1963); A. P. ter Borg and H. Kloosterziel, *ibid.*, **82**, 741 (1963); T. Nozoe and K. Takahashi, This Bulletin, **38**, 665 (1965).

*3 Anderson *et al.*[9] reported that 1-tropylazulene has a mp of 60.5°C, however, the substance obtained in this experiment did not crystallize, perhaps because of the contamination of the thermal isomerization products.

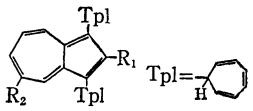

III $R_1=R_2=H$
IV $R_1=H$, $R_2=$isopro.
V $R_1=NHCOCH_3$, $R_2=H$
VII $R_1=Cl$, $R_2=H$

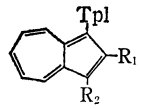

VIII $R_1=Cl$, $R_2=H$
X $R_1=H$, $R_2=CH_3$
XIII $R_1=H$, $R_2=CHO$
XIV $R_1=H$, $R_2=COOC_2H_5$
XV $R_1=Cl$, $R_2=CHO$
XVI $R_1=Cl$, $R_2=COOC_2H_5$
XVII $R_1=NH_2$, $R_2=COOC_2H_5$
XVIII $R_1=R_2=H$
XIX $R_1=Cl$, $R_2=CN$

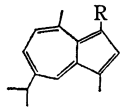

IX R=H
XI R=Tpl
XXIV $R=N=N-C_6H_4(CH_3)p$
XXVI $R=COC_6H_5$

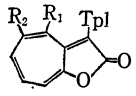

XX $R_1=R_2=H$
XXI $R_1=CH_3$, $R_2=H$
XXII $R_1=H$, $R_2=$isopro.

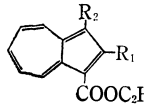

XXV $R_1=NH_2$, $R_2=N=N-C_6H_4(CH_3)p$
XXVIII $R_1=H$, $R_2=COC_6H_5$
XXIX $R_1=NH_2$, $R_2=NO$

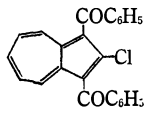

XXVII

Fig. 1

Since it has been found[16] that diethyl 2-amino- or 2-hydroxy-azulene-1,3-dicarboxylate was brominated on its 6-position, the tropylation of diethyl 2-amino or 2-hydroxyazulene-1,3-dicarboxylate was attempted. However, even at an elevated temperature, the azulenes failed to undergo tropylation, and the starting azulenes were recovered.

As in the case of azulene, the tropylation of 1-oxaazulan-2-one (II) with tropyl ethyl ether in the presence of tropylium bromide or hydrochloric acid yielded the 3-tropyl derivative (XX). In a similar manner, the 4-methyl and 5-isopropyl derivatives of II gave the corresponding 3-tropyl derivatives, (XXI) and (XXII).

In order to determine the position of the extra hydrogen in the tropyl group attached to azulene, the NMR spectra were studied. The peaks due to the extra hydrogen (C_7-H) in the tropyl group appear as a triplet at τ 6.68 (J=5.3 cps) in III, 6.42 (J=5.3 cps) in VII, and 7.38 (J=5.4 cps) in XX, and the peaks due to olefinic protons of the 1- and 6-positions in the tropyl group appear as a double doublet (d, d) at τ 4.46 (J=5.3 and 9.0 cps) in III, 4.48 (J=5.3 and 9.4 cps) in VII, and 4.59 (J=5.4 and 9.6 cps) in XX. The ratio of the areas of above two kinds of proton signals is about 1 : 2, showing clearly that the bonds are formed between the 7-position of tropilidene and the azulene nuclei.

The facts that the signal of the C_2-H of the azulene nucleus of III appears at τ 1.90 as a singlet, and that no signals of C_1-H and C_3-H are observed in the spectra of III and VII, clearly show tropyl groups are located at the and 3-positions of azulenes. The large down-field shifts of the C_7-H of the tropyl groups in these compounds compared with that of tropilidene[17] (7.806 τ) may be ascribed to the paramagnetic deshielding effects of the azulene or oxaazulanone nucleus.

The absorption maxima in the visible spectra of tropylazulenes are recorded in Table 1. From this table, it is clear that the introduction of one tropyl group causes a bathochromic shift of 16—24 mμ in the maxima of the highest intensity, this effect being almost equal to that of alkyl groups.[7a,18]

In order to clarify the electronic and steric effects of the electrophilic substitution reactions of substituted tropylazulenes, 2-chloro-1-tropylazulene (VIII), 3-tropylguaiazulene (XI), ethyl 3-tropylazulene-1-carboxylate (XVII) were submitted to electrophilic substitution reactions.

The treatment of XI and XVII with *p*-toluenediazonium chloride (XXIII) under mild conditions readily afforded the corresponding azo compounds, 3-(*p*-tolylazo)guaiazulene (XXIV) and ethyl 2-amino-3-(*p*-tolylazo)azulene-1-carboxylate

16) T. Nozoe, S. Seto and S. Matsumura, This Bullethin, **35**, 1990 (1962); T. Nozoe, T. Asao and M. Oda, to be published.

17) G. Fraenkel, R. E. Carter, A. McLachlan and J. H. Richard, *J. Am. Chem., Soc.* **82**, 5846 (1960).

18) Cf. E. Heilbronner, "Non-Benzenoid Aromatic Compounds," ed. by D. Ginsburg, Interscience, New York (1959), p. 171.

Table 1. Visible spectra of tropylazulenes

Compounds*	λ_{max}: mμ (ε)	λ'_{max}**	$\Delta\lambda$***
III	742(130), 674(333), 640s(341), 618(391), 590s(326), 570s(280)	580	19
IV	730s(133), 656(320), 628(362), 575s(292)	590	19
V	704s(138), 634(350), 594(393), 550s(289)	540	27
VII	690(136), 630(346), 584(392), 545s(282)	552	16
VIII	674(119), 662(128), 615(323), 605(321), 567(368), 530s(265)	552	15
X	730(139), 684(282), 663(311), 628(354), 610(340), 588s(297)	608	20
XI	750s(106), 677s(229), 624(369), 600s(347), 575s(303)	603	21
XIII	670(108), 607(299), 560(368), 525s(300)	542	18
XIV	673(105), 648s(142), 612(324), 588(348), 565(392)	544	21
XV	620s(144), 566(351), 534(398)		
XVI	624s(180), 575(423), 540(464)	521	19
XVIII	720(101), 650(244), 604(286), 560s(226)	580	24
XIX	655s(153), 596(377), 558(427)		

* Solvent: cyclohexane except V (benzene).
** Maxima having the highest intensity of the corresponding compounds without tropyl group.
*** $\Delta\lambda=(\lambda_{max}$ of the highest intensity$-\lambda'_{max})$/number of tropyl group in a molecule.

Table 2. The results of the acid treatment of tropylazulene derivatives

Tropylazulene / Condition	VIII	XI	XIV	XVII
Conc. H_2SO_4	VI and VIII	IX (74%)	Recovery (94%)	Recovery (61%)
Dil. H_2SO_4	VI and VIII	IX (90%)	Recovery (100%)	Recovery (90%)

(XXV).[19] However, VIII and XIV were recovered when treated under the same reaction conditions. Also, ethyl azulene-1-carboxylate was recovered by the same treatment. Although the azo-coupling reaction of VIII was carried out at an elevated temperature, 80% of the starting material was recovered, plus a small amount of a black resinous substance, which has so far not been identified.

The Friedel-Crafts reaction of XI with an equimole of benzoyl chloride afforded 32% of guaizulene and 23% of 3-benzoylguaiazulene (XXVI).[20] The yield of XXVI from guaiazulene (IX) under the same reaction conditions was also not good, 16%. The treatment of XVII under the same reaction conditions resulted in an entire recovery of the starting material. This may be explained as follows: the formation of the complex of the 2-amino-group of XVII with aluminum chloride decreases the electron density of the azulene nucleus, and, at the same time the bulkiness of the complex causes serious steric hindrance. On the other hand, the reaction of VIII and XIV with 2 equimoles of benzoyl chloride afforded 1,3-dibenzoyl-2-chloro-azulene (XXVII), together with a small amount of the recovered starting substances, and ethyl 3-benzoylazulene-1-carboxylate (XXVIII), respectively. Although the C-3 position of VIII is not substituted, 3-benzoyl-2-chloro-1-tropylazulene could not be isolated even when an equimole of benzoyl chloride was used. It was also found that the reaction of 2-chloroazulene and one mole of benzoyl chloride resulted in the formation of XXVII and the recovery of 2-chloroazulene.

It is expected that the reaction of tropylazulene with acids regenerates azulenes and the tropylium ion. The results of the treatment of tropylazulenes with concentrated and diluted sulfuric acid are shown in Table 2.

Although a small amount of VI was separated from the reaction mixture of VIII and acid, the complete separation of VI and VIII was unsuccessful. The mixture was identified with a mixture of authentic samples of VI and VIII by means of their IR spectra. However, the exact ratio of VI and VIII was not clear.

The recovery of XIV can be explained as follows: the protonation of XIV took place not only at C-3, as has been shown before, to form a D intermediate, but also at the carbonyl group to form a C intermediate. In fact, the NMR spectrum of XIV shows at τ 8.3 and the methylene quartet at τ 5.6 in carbon tetrachloride, but the signal is changed to a complex multipet in a trifluoroacetic acid solution. It can resonably be understood that XIV is protonated to form and equilibrium mixture of substances such as C, D, and XIV in the acidic solution, and presumably the equilibrium

19) T. Nozoe, T. Asao and M. Kobayashi, to be published.
20) W. Treibs, *Chem. Ber.*, **90**, 761 (1957); D. H. Reid, W. H. Stafford and W. L. Stafford, *J. Chem. Soc.*, **1958**, 1118.

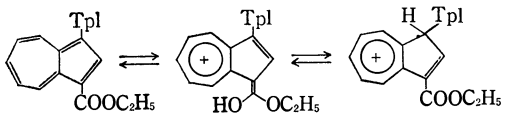

XIV C D

tends to the C form; because XIV was recovered quantitatively. An analogous phenomenon was observed when 1-nitroazulene was dissolved in strong acid and protonation was favorable at the oxygen atoms of the nitro group, but not at the C-3 position.[21] In the case of XVII, the protonation takes place not only at the carbonyl group, but also at the amino group, this makes protonation at C-3 harder and no proton-tropylium cation exchange reaction occurs. In the case of VIII, E- and F-type intermediates may form, 2-chloroazulene should be obtained from the E-type intermediate. Therefore, the prolonged treatment of VIII with acid would give VI in a good yield.

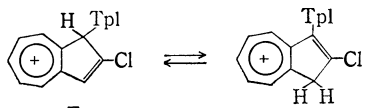

E F

However, because of the unstability of the tropyl group in relation to acid, the prolonged treatment of VIII increases the amount of intractable resinous products and does not give any clear-cut results.

The treatment of XVII with isoamyl nitrite and sulfuric acid afforded brown micro needles (XXIX) which were identical with ethyl 2-amino-3-nitrosoazulene-1-carboxylate.[22] As has been mentioned above, XVII did not eliminate the tropylium cation to form ethyl 2-aminoazulene-1-carboxylate upon acid treatment. Therefore, the nitrosation of XVII must happen by the direct exchange reaction of the tropylium cation and the nitrosonium ion. It is interesting and noteworthy that even though the C-1 and C-3 positions of azulene nuclei of XVII are substituted, the diazotization of amino group does not take place and an exchange reaction occurs.

Experimental*4

General Procedure for the Tropylation of Azulenes and 1-Oxaazulanones. To a stirred solution of azulenes (or 1-oxaazulanones) in cyclohexane (or benzene), ditropyl ether (or tropyl ethyl ether) and a catalytic amount of tropylium bromide (or concentrated hydrochloric acid) were added at room temperature. After the solution has been stirred at room temperature for 2 hr—one day, it was washed with water and dried over anhydrous sodium sulfate, and the products purified by passing them through an alumina column and then recrystallizing them.

1,3-Ditropylazulene (III). The reaction of azulene and 2 molar equivalents of tropyl ether afforded III as blue needles (62%), mp 137—138°C (from cyclohexane).

Found: C, 93.23; H, 6.46%. Calcd for $C_{24}H_{20}$: C, 93.46; H, 6.54%.

1,3-Ditropyl-5-isopropylazulene (IV). The reaction of 5-isopropylazulene and 2-molar equivalents of tropyl ether gave IV as a blue oil (90%). IV did not give a trinitrobenzene complex and changed to a dark yellow substance upon standing in air.

Found: C, 92.30; H, 7.79%. Calcd for $C_{27}H_{26}$: C, 92.52; H, 7.48%.

2-Acetamido-1,3-ditropylazulene (V). The reaction of 2-acetamidoazulene and 2 molar equivalents of tropyl ether gave V as blue crystals (45%), mp 206.5—207°C (from benzene-cyclohexane).

Found: C, 85.58; H, 6.65; N, 3.42%. Calcd for $C_{26}H_{23}ON$:C, 85.45; H, 6.34; N, 3.83%.

2-Chloro-1,3-ditropylazulene (VII). The reaction of 2-chloroazulene and 2-molar equivalents of tropyl ether afforded VII as blue needles (85%), mp 164—165°C (from cyclohexane).

Found: C, 83.79; H, 6.01%. Calcd for $C_{24}H_{19}Cl$: C, 84.08; H, 5.59%.

2-Chloro-1-tropylazulene (VIII). The reaction of 2-chloroazulen with one molar equivalent of tropyl ether afforded VII (27%) and VIII (62%) as violet needles, mp 87—88°C (from petroleum ether), besides the recovered 2-chloroazulene.

Found: C, 80.60; H, 5.56%. Calcd for $C_{17}H_{13}Cl$: C, 80.60; H, 5.17%.

1-Methyl-3-tropylazulene (X). X was obtained from 1-methylazulene as a blue oil (75%).

Trinitrobenzene complex: mp 155.5—156°C.

Found: C, 64.98; H, 4.19; N, 9.07%. Calcd for $C_{21}H_{19}O_6N_3$: C, 64.71; H, 4.30; N, 9.43%.

3-Tropylguaiazulene (XI). XI was obtained from guaiazulene as blue crystals (86%), mp 74—75°C.

Found: C, 91.56; H, 8.50%. Calcd for $C_{22}H_{24}$: C, 91.61; H, 8.39%.

Trinitrobenzene complex: black needles, mp 96—97°C.

Found: C, 67.12; H, 5.24; N, 8.23%. Calcd for $C_{28}H_{27}O_6N_3$: C, 67.05; H, 5.43; N, 8.38%.

1-Formyl-3-tropylazulene (XIII). XIII was obtained from 1-formylazulene as a reddish-violet oil.

Trinitrobenzene complex: brown needles, mp 108—109°C.

Found: C, 63.02; H, 3.92; N, 8.60%. Calcd for $C_{24}H_{17}O_6N_3$: C, 62.74; H, 3.73; N, 9.15%.

Ethyl 3-Tropylazulene-1-carboxylate (XIV). XIV was obtained from ethyl azulene-1-carboxylate as a reddish-violet oil (98%).

Trinitrobenzene complex: brown needles, mp 80°C.

Found: C, 61.97; H. 4.18; N, 8.11%. Calcd for $C_{26}H_{21}O_8N_3$: C, 62.02; H, 4.20; N, 8.35%.

2-Chloro-1-formyl-3-tropylazulene (XV). a) A solution of 65 mg of VIII, 3 m*l* of dimethylformamide, and 50 mg of phosphoryl chloride was allowed to stand overnight. Water (30 m*l*) was then added, and the mixture was neutralized with sodium hydrogen carbonate and extracted with benzene. The extract was

21) D. Menche and E. Heilbronner, *Helv. Chim. Acta*, **45**, 1965 (1962).
22) T. Nozoe, P. W. Yang, H. Ogawa and T. Toda, This Bulletin, **41**, 2095 (1968).
*4 All melting points are uncorrected.

dried and passed through an alumina column. VIII (52 mg) was recovered from the first eluate, and 14 mg of XV, from the next eluate. Recrystallization from benzene-petrolum ether afforded XV as reddish-violet needles, mp 192.5—193.5°C.

Found: C, 77.13; H, 4.91%. Calcd for $C_{18}H_{13}OCl$: C, 77.01; H, 4.67%. b) The tropylation of 2-chloro-1-formylazulene afforded XV (68%), mp 191—192°C, which showed no depression of melting point on admixture with the sample obtained by Procedure a).

Ethyl 2-Chloro-3-tropylazulene-1-carboxylate (XVI). The tropylation of ethyl 2-chloroazulene-1-carboxylate afforded XVI as reddish-violet crystals (quantitative yield), mp 115°C.

Found: C, 74.30; H, 5.23%. Calcd for $C_{20}H_{17}O_2Cl$: C, 73.95; H, 5.28%.

Ethyl 2-Amino-3-tropylazulene-2-carboxylate (XVII). The tropylation of ethyl 2-aminoazulene-1-carboxylate afforded XVII as a reddish-brown oil (quantitative yield).

Picrate, mp 133—134°C.

Found: C, 58.45; H, 3.89; N, 10.03%. Calcd for $C_{26}H_{22}O_9N_4$: C, 58.42; H, 4.15; N, 10.43%.

1-Tropylazulene (XVIII). A solution of 390 mg of XIV and 230 mg of potassium hydroxide in 20 m*l* of ethanol and 6 m*l* of water was refluxed for 4.5 hr. After the ethanol had then been removed, the solution was acidified with hydrochloric acid. A reddish-violet precipitate was collected, dried, and heated in a sublimation apparatus under reduced pressure to give a blue oil. This oil was purified by chromatography to afford 1-tropylazulene as a greenish-blue oil.

Found: C, 93.30; H, 6.39%. Calcd for $C_{17}H_{14}$: C, 93.53; H, 6.47%.

Trinitrobenzene complex: mp 97.5°C.

Found: C, 64.50; H, 4.02; N, 9.83%. Calcd for $C_{23}H_{17}O_6N_3$: C, 64.03; H, 3.97; N, 9.74%.

2-Chloro-1-cyano-3-tropylazulene (XIX). A solution of 130 mg of XV, 200 mg of hydroxylamine hydrochloride, and 2 m*l* of a 0.5 N sodium hydroxide solution in 3 m*l* of ethanol was refluxed for 20 min. The ethanol was removed, water was added and then extracted with chloroform, and the extract was evaporated to leave a green solid. When a solution of the solid in 2 m*l* of acetic anhydride was refluxed for 30 min, 20 mg of reddish-violet crystals (XIX) were obtained, mp 155°C.

Found: C, 64.57; H, 3.80; N, 5.35%. Calcd for $C_{14}H_{10}O_2NCl$: C, 64.77; H, 3.88; N, 5.40%.

3-Tropyl-1-oxaazulan-2-one (XX). The tropylation of 1-oxaazulan-2-one afforded XX (85%), as yellowish-orange plates, mp 108-110°C (from ethanol).

Found: C, 81.65; H, 5.48%. Calcd for $C_{16}H_{12}O_2$: C, 81.34; H, 5.12%.

4-Methyl-3-tropyl-1-oxaazulan-2-one (XXI). The tropylation of 4-methyl-1-oxaazulan-2-one gave XXI (80%), as orange prisms, mp 170—171°C (from acetone).

Found: C, 81.44; H, 5.63%. Calcd for $C_{17}H_{14}O_2$: C, 81.58; H, 5.64%.

5-Isopropyl-3-tropyl-1-oxaazulan-3-one (XXII). The tropylation of 5-isopropyl-1-oxaazulan-2-one gave XXII (73%), as orange needles, mp 87—89°C (from ethanol).

Found: C, 82.08; H, 6.74%. Calcd for $C_{19}H_{18}O_2$: C, 81.98; H, 6.52%.

3-(*p*-Tolylazo)guaiazulene (XXIV). a) Into a solution of 100 mg of IX in 1 m*l* of pyridine cooled in an ice bath, aqueous *p*-toluidine diazonium chloride (XXIII) prepared from 54 mg of *p*-toluidine, 50 mg of sodium nitrite, 0.5 m*l* of 6 N hydrochloric acid, and 0.3 m*l* of water, was stirred, drop by drop. The solution turned from blue to a brownish yellow. After the solution had been stirred for one hour at room temperature, 2 m*l* of water were added and then extracted with chloroform. The combined chloroform layers were dried over sodium sulfate, filtered off, and concentrated to give a dark green, crystalline substance. Recrystallization from ethanol afforded 144 mg of XXIV, mp 138°C.

Found: C, 83.46; H, 7.50; N, 8.45%. Calcd for $C_{22}H_{24}N_2$: C, 83.50; H, 7.64; N, 8.85%.

b) To a solution of 100 mg of XI in 1 m*l* of pyridine cooled in an ice bath, a solution of XXIII prepared from 75 mg of *p*-toluidine was added, drop by drop. The reaction was carried out for 4 hr at room temperature, and then the results were treated as above to give 50 mg of XXIV, mp 136°C, which was identical with the XXIV obtained above.

Ethyl 2-Amino-3-(*p*-tolylazo)azulene-1-carboxylate (XXV). From 100 mg of XVII in 1 m*l* of pyridine and XXIII prepared from 53 mg of *p*-toluidine, 160 mg of an oily substance was obtained. The oil was chromatographed on alumina; the cyclohexane eluate afforded 107 mg of reddish-brown micro-needles whose melting point was 119.5°C after having been recrystallized from ethanol and which was identical with authentic XXV.[15]

Azo-coupling Reaction of VIII. Into a solution of 100 mg of VIII in 1.5 m*l* of pyridine in an ice bath, aqueous XXIII (from 43 mg of *p*-toluidine) was stirred. A precipitate formed immediately, but the reaction was continued for 2 hr. The precipitate was then filtered off and dried in a desiccator. The mother layer was extracted with chloroform, and the combined extracts were washed with water, dried over sodium sulfate, and concentrated to give a residue. The residue and the precipitate were dissolved in petroleum ether and chromatographed on alumina to give 86 mg of recovered VIII.

Ethyl 3-Benzoylazulene-1-carboxylate (XXVIII). a) To 30 m*l* of dry carbon disulfide, 200 mg of XIV, 195 mg of benzoyl chloride, and 183 mg of anhydrous aluminum chloride were added, and the resulting solution was refluxed for 15 hr. The organic layer was separated, washed with water and N sodium hydroxide, dried over sodium sulfate, and then concentrated to give a residue. The residue was dissolved in petroleum chromatographed on alumina. The petroleum ether eluate afforded 125 mg of XIV while the benzene-petroleum ether eluate gave 70 mg of a dark red residue, which in turn afforded 64 mg of dark red prisms of XXVIII, mp 107°C, after recrystallization from ethanol.

Found: C, 79.26; H, 5.39%. Calcd for $C_{20}H_{16}O_3$: C, 78.93; H, 5.30%.

b) A solution of 200 mg of ethyl azulene-1-carboxylate, 282 mg of benzoyl chloride, and 266 mg of aluminum chloride in 30 m*l* of carbon disulfide was heated to reflux for 13 hr and then worked up as above to give 170 mg of XXVII, mp 108°C, after recrystallization from ethanol.

3-Benzoylguaiazulene (XXVI). A solution of 400 mg of XI, 215 mg of aluminum chloride, and 202 mg of benzoyl chloride in 20 m*l* of carbon disulfide was heated to reflux for 14 hr. After the reaction had been

completed, the mixture was worked up as above and chromatographed on alumina. The first benzene effluent afforded 87 mg of a blue oil which was identical with guaiazulene (31.6%), while the second effluent gave 41 mg of a dark green semisolid which in turn afforded 10 mg of XXVI, mp 119°C, after recrystallization from ethanol and which was identical with the 3-benzoylguaiazulene prepared by the reported method.[20]

2-Chloro-1,3-dibenzoylazulene (XXVII). a) solution of 150 mg of VIII, 168 mg of benzoyl chloride, and 160 mg of aluminum chloride in 25 m*l* of carbon disulfide was refluxed for 14 hr, and then worked up in the usual manner. The first petroleum ether effluent gave 22 mg of VI, while the second gave 124 mg of a dark red oil. The latter was rechromatographed, and the benzene effluent gave 25 mg of red prisms of XXVII, mp 179—180°C; recrystallization from benzene raised its melting point to 185°C.

Found: C, 77.85; H, 4.28%. Calcd for $C_{24}H_{15}O_2Cl$: C, 77.73; H, 4.35%.

b) A solution of 200 mg of VI, 260 mg of benzoyl chloride, and 245 mg of aluminum chloride in 30 m*l* of carbon disulfide was refluxed for 13 hr; a subsequent work-up in the usual manner afforded 32 mg of VI and 143 mg of XXVII.

Ethyl 2-Amino-3-nitrosoazulene-1-carboxylate (XXIX). a) To a solution of 450 mg of XVII in 20 m*l* of ethanol in an ice bath, 1 m*l* of concentrated sulfuric acid was added, and then 342 mg of isoamyl nitrite were added. After the mixture had been allowed to stand overnight at room temperature, the precipitate thus formed was filtered off, washed with aqueous sodium hydrogen carbonate and water, and dried in a desiccator. Recrystallization from chloroform afforded 190 mg of dark brown scales of XXIX, mp 174—174.5°C.

Found: C, 63.61; H, 4.73; N, 11.25%. Calcd for $C_{13}H_{12}O_3N_2$: C, 63.92; H, 4.95; N, 11.47%.

b) A solution of 300 mg of XVII in 12 m*l* of ethanol cooled in an ice bath was saturated with dry hydrogen chloride, and then 230 mg of isoamyl nitrite were added, drop by drop. After 4 hr, the solution was poured into 50 m*l* of water, and the separated water layer was neutralized with sodium hydrogen carbonate to form a precipitate. The precipitate was washed with water, dried in a desiccator, and recrystallized from chloroform to afford 90 mg of XXIX, mp 174°C.

The Exchange Reactions of the Tropyl Group with the Proton on the Tropylazulenes. *i) 3-Tropylguaiazulene.* a) A solution of XI in 4 m*l* of concentrated sulfuric acid was allowed to stand at room temperature for 1 hr; then it was poured into 20 m*l* of ice water and extracted with benzene. The combined extract was washed with aqueous sodium hydrogen carbonate and water, dried over sodium sulfate, and chromatographed on alumina to afford 50 mg of a blue oil. The IR, UV, and visible spectra of the oil were identical with those of guaiazulene.

b) To a solution of 100 mg of XI in 4 m*l* of dioxane, 2 m*l* of 1 N sulfuric acid were added, after which the mixture was heated on a water bath for 30 min. After cooling, the solution was neutralized with aqueous sodium hydrogen carbonate, and extracted with benzene. The combined extracts were washed with water, dried over sodium sulfate, and chromatographed on alumina to give 60 mg of IX.

ii) Ethyl 2-Amino-3-tropylazulene-1-carboxylate. a) A solution of 100 mg of XVII in 5 m*l* of concentrated sulfuric acid was treated as above; the ethyl acetate effluent yielded 61 mg of the starting material.

b) To a solution of 100 mg of XVII in 4 m*l* of dioxane, 2 m*l* of 1 N sulfuric acid were added, after which the mixture was heated on a water bath for 2 hr. A subsequent work-up in the usual method gave 92 mg of the unchanged, recovered substance.

iii) Ethyl 3-Tropylazulene-1-carboxylate. a) To a solution of 100 mg of XIV in 4 m*l* of dioxane, 1 m*l* of dioxane, 1 m*l* of concentrated sulfuric acid was added, after which the solution was allowed to stand for 1 hr at room temperature. The reaction mixture was then worked up in the usual manner: the benzene effluent of the chromatography of the crude substance gave 94 mg of the starting substance.

b) A mixture of 100 mg of XIV, 4 m*l* of dioxane, and 2 m*l* of 1 N sulfuric acid was heated on a water bath for 2 hr; then it was worked up as above to give 100 mg of the recovered starting substance.

iv) 2-Chloro-1-tropylazulene. a) To a solution of VIII in 3 m*l* of dioxane, 1 m*l* of concentrated sulfuric acid was added, after which the solution was allowed to stand at room temperature for 30 min and then worked up as above. The petroleum ether effluent of the chromatography afforded 76 mg of a blue oil substance whose IR spectrum showed that the oil was a mixture of VIII and 2-chloroazulene.

b) A mixture of 100 mg of VIII, 4 m*l* of dioxane, and 2 m*l* of 1 N sulfuric acid was heated on a water bath for 2 hr, and then worked up as above. The first petroleum ether effluent gave 10 mg of 2-chloroazulene, mp 91°C, while the second effluent afforded 70 mg of a blue oil which was a mixture of VI and VIII.

The authors wish to express their gratitude to the Sankyo Co. for its donation of a research fund which covered a part of the expenses for this work. The infrared and ultraviolet spectrophotometers used in this study were purchased with a Grant-in-aid for Fundamental and Technical Research from the Toyo Rayon Co., Ltd., to which the authors are also grateful.

BULLETIN OF THE CHEMICAL SOCIETY OF JAPAN VOL. 41 2942—2948 (1968)

3,4-Benzotropolone and Related Compounds. V.[1] Bromo- and Hydroxy-2,3-benzotropones

Seiji EBINE, Masamatsu HOSHINO and Kazuko TAKAHASHI*1

Department of Chemistry, Faculty of Science and Engineering, Saitama University, Urawa, Saitama-ken

(Received February 8, 1968)

Isomeric 5,7- and 4,7-dibromo-2,3-benzotropones were prepared, not *via* 2,3-benzotropone, but by the bromination and subsequent dehydrobromination of 2,3-benzocycloheptenone. The tropone structure of these compounds was based on spectral data and hydrogenation to 2,3-benzocycloheptenone. The dibromo-2,3-benzotropones, when treated with hydroxylamine, underwent cine-reaction to 5- and 4-bromo-6-hydroxylamino-2,3-benzotropone oximes, which were then hydrolyzed and debrominated to the same 6-hydroxy-2,3-benzotropone. 5,7,5'-Tribromo-2,3-benzotropone was obtained by the drastic bromination, followed by the dehydrobromination, of 2,3-benzocycloheptenone. The position of a hydroxyl group in 6-hydroxy-2,3-benzotropone was confirmed by oxidation to *o*-carboxycinnamic acid, while that of the 5'-bromo substituent in 5,7,5'-tribromo-2,3-benzotropone was confirmed by hydrogenation to 5'-bromo-2,3-benzocycloheptenone.

It has previously been found that the treatment of 2-cycloheptenone[2] or cycloheptanone[3] with bromine brings about bromination, followed by spontaneous dehydrobromination, to afford 2,4,7-tribromotropone. According to this reaction, an attempt was made to prepare a bromo-substituted benzotropone by treating 2,3-benzocycloheptenone (I) with bromine. The reaction of I with excess bromine, however, did not give a brominated benzotropone, but instead produced two isomeric tetrabromo-2,3-benzocycloheptenones (IIa, mp 142°C and IIb, mp 146.5°C). The application of less bromine to I gave tribromo-2,3-benzocycloheptenone, and the reaction of I with bromine in the presence of sodium acetate produced dibromoacetoxy-2,3-benzocycloheptenone.*2

The dehydrobromination of IIa was then attempted. IIa remained unchanged when heated with sodium acetate in an ethanolic or acetic acid solution, and resinified when treated with diethylamine or potassium hydroxide in an ethanolic solution at room temperature. IIa was effectively dehydrobrominated when its pyridine solution was allowed to stand at room temperature for a week it yielded two isomeric dibromo-2,3-benzotropones (IIIa and IIIb), with a predominance of the former. Under the same conditions, IIb produced only IIIa. The tropone structure of IIIa and IIIb is assumed on the basis of the catalytic reduction to 2,3-benzotropone (in a low yield) and I (in a fair yield), the ultraviolet absorption spectra having peaks in the 220—270 and 300—350 mμ

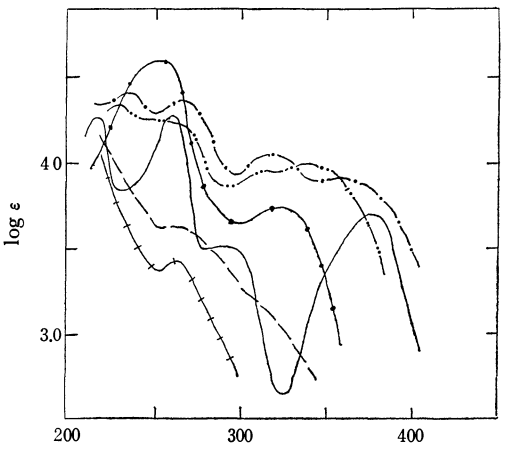

Fig. 1. Ultraviolet absorption spectra of isomeric tetrabromo-2,3-benzocycloheptenones (IIa, — — and IIb, +—+), isomeric dibromo-2,3-benzotropones (5,7-dibromo-, IIIa, —·— and 4,7-dibromo-, IIIb, —··—), uncharacterized compound (VII, ——) and 6-hydroxy-2,3-benzotropone (VIII, —•—•—) in methanol.

1) Part IV, This Bulletin, S. Ebine, **38**, 2029 (1965).

*1 Present address: Department of Chemistry, Faculty of Science, Tohoku University, Sendai.

2) H. J. Dauben and H. J. Ringold, *J. Am. Chem. Soc.*, **73**, 876 (1951).

3) T. Nozoe, Y. Kitahara, T. Ando and S. Masamune, *Proc. Japan Acad.*, **27**, 415 (1951); T. Nozoe, Y. Kitahara, T. Ando, S. Masamune and H. Abe, *Sci. Repts. Tohoku Univ., Ser. I*, **36**, 166 (1952).

*2 These brominated benzocycloheptenones, when oxidized with permanganate, gave phthalic acid, indicating that they possess all the bromo substituents in the cycloheptenone ring.

regions (Fig. 1), and the infrared absorption spectra having carbonyl bands at frequencies below 1650 cm^{-1} (Experimental), characteristics which are in accord with the spectral features of troponoid compounds.[4] IIIa and IIIb, like other troponoid compounds, dissolve in concentrated sulfuric acid and precipitate unchanged upon dilution with water. IIIa was not affected when heated with sodium acetate in a methanolic or an acetic acid solution at 120°C for 10 hr, with cupric acetate in a pyridine solution at 110°C for 12 hr, and with concentrated hydrochloric acid in an acetic acid solution at 150°C for 50 hr. It has been found that the out-of-plane deformation vibration of troponoid CH in halogenated benzotropolones is correlated with the position of the halogen substituents,[5] but the infrared absorption spectra of IIIa and IIIb made possible no definite conclusion regarding the position of substituents. IIIa showed an infrared absorption band at 898 cm^{-1}, hardly suggesting the presence of isolated hydrogen atoms.

In order to elucidate the position of the bromo substituents, IIIa and IIIb were subjected to Diels-Alder reaction with maleic anhydride, and the NMR spectra of the adducts were examined. The spectrum of the IIIb - maleic anhydride adduct contained AB-type absorption bands at 7.05 and 6.30 ppm (J=9.5 cps) ascribable to adjacent two ethylenic hydrogens, indicating that the adduct carries the bromo substituents at the positions given in Formula XVIIIb. It follows, therefore, that IIIb is the 4,7-dibromo compound. The spectrum of the IIIa - maleic anhydride adduct contained a doublet at 6.61 ppm with a long-range coupling constant (J=1.8 cps) ascribable to an ethylenic hydrogen which couples with a distant hydrogen, suggesting that the adduct carries the bromo substituents as given in formula XVIIIa or XVIIIa'. Accordingly, IIIa is either the 5,7- or 4,6-dibromo compound. As will be described below, IIIa and IIIb gave isomeric bromo-hydroxy-benzotropones (VIa and VIb, respectively) when treated with hydroxylamine and then with sulfuric acid, and these two isomers gave the same hydroxy-benzotropone (VIII) upon debromination. This fact leads to the conclusion that IIIa is the 5,7-dibromo compound. The position of bromo substituents was further proved to be 5,7- in IIIa and 4,7- in IIIb from an NMR spectral study of IIIa, IIIb, and related compounds, the details of which will be published elsewhere.[6] IIIa is presumably identical with Buchanan's dibromo-2,3-benzotropone obtained by the bromination of 2,3-benzotropone or 2,3-benzo-2,4-cycloheptadienone.[7]

IIIa was allowed to react with methanolic potassium hydroxide at room temperature to yield 5-bromo-6-methoxy-2,3-benzotropone (V), 5-bromo-6-hydroxy-2,3-benzotropone (VIa), and an uncharacterized compound (VII),*3 along with a considerable amount of tar. The ultraviolet absorption spectrum of V (Fig. 1) is essentially superimposable upon that of isomeric 7-bromo-3,4-benzotropolone methyl ether.[8]

IIIa and IIIb were treated with hydroxylamine in a pyridine solution to give 5-bromo-6-hydroxylamino-2,3-benzotropone oxime (Xa) and the corresponding 4-bromo isomer (Xb), which were then hydrolyzed with sulfuric acid to 5-bromo-6-hydroxy-2,3-benzotropone (VIa) and the corresponding 4-bromo isomer (VIb) respectively. These, in turn, were debrominated with hydrogen over a palladium-charcoal catalyst to the same 5-hydroxy-2,3-benzotropone (VIII). VIII was also produced from Xa or Xb *via* 6-hydroxylamino-2,3-benzotropone oxime (XI). VIII is soluble in dilute alkali or in concentrated sulfuric acid, and can be precipitated unchanged upon the neutralization of its alkaline solution or on the dilution of its concentrated sulfuric acid solution with water. VIII gives no ferric chloride coloration. The tropone structure of VIII is based on its ultraviolet absorption spectrum, which shows two peaks at 255 and 335 mμ (Fig. 1), and its infrared absorption spectrum, which shows a carbonyl band below 1650 cm^{-1}.[4] The position of a hydroxyl group of VIII was confirmed by oxidation with alkaline hydrogen peroxide to *o*-carboxycinnamic acid (XII), and by hydrogenation with excess hydrogen over a platinum oxide catalyst to 4,5-benzocycloheptene-1,3-diol (IX), followed by oxidation with potassium permanganate to *o*-carboxyhydrocinnamic acid (XIII).

4) For a reference on the ultraviolet spectra of troponoid compounds, see M. Tsuboi, This Bulletin, **25**, 369 (1952). For references on the infrared spectra of troponoid compounds, see S. Kinumaki, K. Aida and Y. Ikegami, *Sci. Repts. Res. Inst. Tohoku Univ.*, **A-8**, 263 (1956), and E. Kloster-Jensen, N. Tarkoy, A. Eschenmoser and E. Heilbronner, *Helv. Chim. Acta*, **39**, 780 (1956).

5) S. Ebine, This Bulletin, **35**, 119 (1962).

6) S. Ebine and M. Hoshino, This Bulletin, to be published.

7) G. L. Buchanan and D. R. Lockhart, *J. Chem. Soc.*, **1959**, 3586.

*3 The uncharacterized compound (VII) dissolves in alkali, shows a weak silver-mirror reaction, and produces a monoacetate. Its ultraviolet absorption spectrum (Fig. 1) deviates from those of general troponoid compounds and rather resembles those of hydroxynaphthaldehydes (N. C. Melchior, *J. Am. Chem. Soc.*, **71**, 3647 (1949).). The infrared absorption band at 1670 cm^{-1} (KBr) corresponds to carbonyl bands of hydroxynaphthaldehydes (I. M. Hunsberger, *ibid.*, **72**, 5626 (1950).). From these facts and by analogy with the transformation of 2-bromo-7-chlorotropone with alkali to 3-chlorosalicylaldehyde (T. Nozoe, S. Seto and S. Matsumura, *Proc. Japan Acad.*, **28**, 483 (1952); S. Seto, *Sci. Repts. Tohoku Univ., Ser. I*, **37**, 377 (1953).), VII is assumed to be hydroxy-methoxy-naphthaldehyde; however, it was not further investigated because we lacked a sample.

8) S. Ebine, This Bulletin, **35**, 115 (1962).

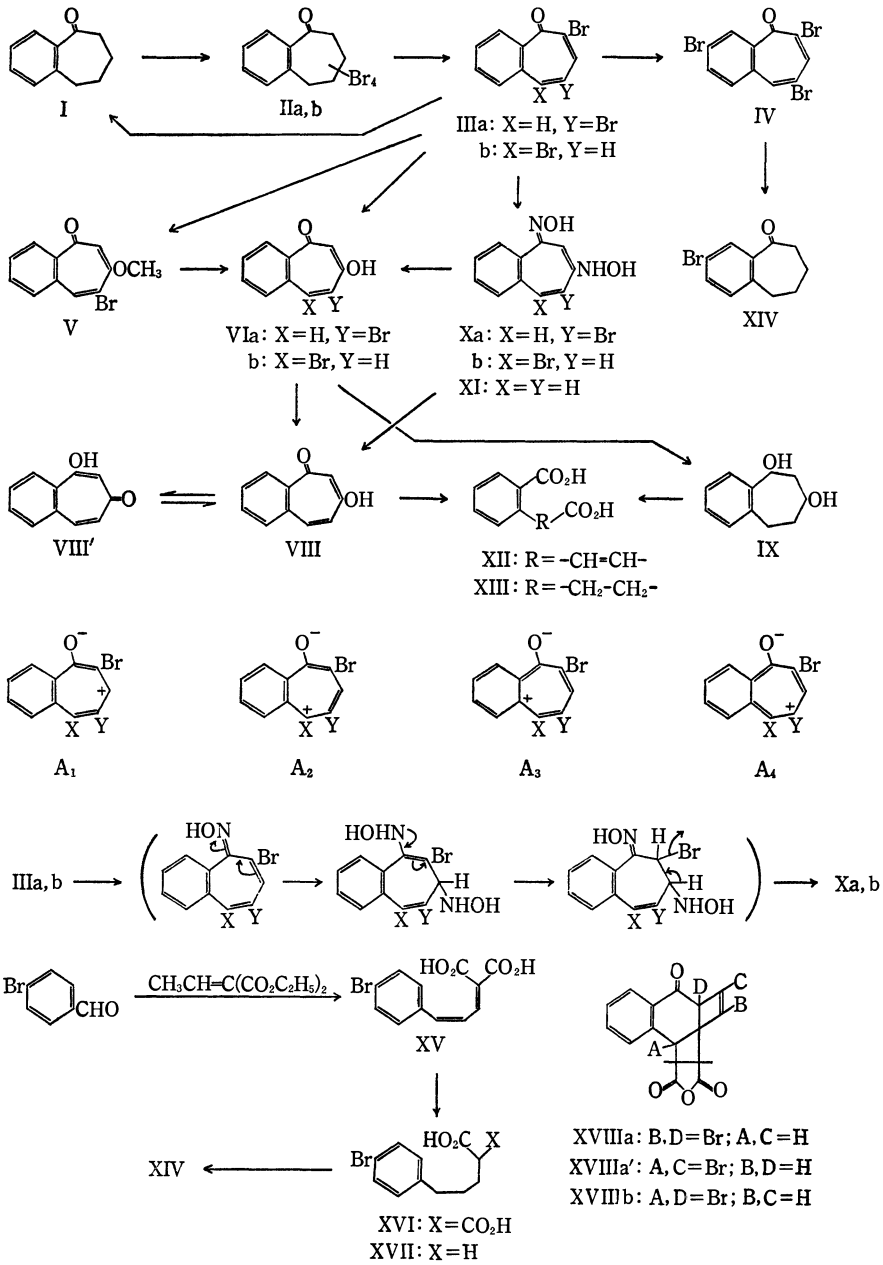

VIII is a novel isomer of previously-reported 4-hydroxy-2,3-benzotropone,[9] 3,4-benzotropolone,[10] and 4,5-benzotropolone.[11] VIII is capable of existing as a tautomeric mixture with 3-hydroxy-4,5-benzotropone (VIII'), but this compound gives a single methyl ether, acetate, and 2,4-dinitrophenylhydrazone. Although it is not clear which form predominates in the tautomeric mixture, the VIII formula is tentatively employed in this paper. VI and X would also hold under the same circumstances as VIII.

The halogenated troponoids tend to undergo abnormal "cine-reaction" on being treated with basic reagents.[12] The formation of V, VI and

9) G. L. Buchanan, *J. Chem. Soc.*, **1954**, 1060. G. L. Buchanan and J. K. Sutherland, *ibid.*, **1956**, 2620.

10) J. W. Cook and A. R. Somerville, *Nature*, **163**, 410 (1949). J. W. Cook, A. R. M. Gibb, A. R. Raphael and A. R. Somerville, *J. Chem. Soc.*, **1952**, 603.

11) H. Fernholz, E. Hartwig and J. C. Salfeld, *Ann.*, **576**, 131 (1952).

12) T. Nozoe and Y. Kitahara, *Proc. Japan Acad.*, **30**, 204 (1954). T. Nozoe, S. Seto and T. Sato, *ibid.*, **32**, 473 (1956).

X from III falls in the same category. The reason why III brings about such a type of reaction is as follows: the resonance structure of III is much contributed to by the A_1 and A_2 formulas, but little by the A_3 and A_4 formulas, because the condensed benzene ring of the former is aromatic, while that of latter is quinonoid[5,8,13]; moreover, a substitution reaction at the 4-position encounters a slight steric hindrance caused by the *peri* position of the benzene ring.[5] The mechanism of the formation of X from III is illustrated in the chart.

5,7,5'-Tribromo-2,3-benzotropone (IV) was prepared by the further bromination of IIIa, or by the bromination of I under drastic conditions and by subsequent treatment with pyridine. The position of the 5'-bromo substituent was determined by its oxidation to 4-bromophthalic acid and by its hydrogenation to 5'-bromo-2,3-benzocycloheptenone (XIV), which was identified by a synthesis consisting of the successive reactions shown in the chart: the condensation of *p*-bromobenzaldehyde with diethyl ethylidenemalonate to *p*-bromocinnamylidenemalonic acid, hydrogenation, followed by decarboxylation to δ-(*p*-bromophenyl-)valeric acid, and ring-closure with polyphosphoric acid to XIV.

It is noteworthy that, upon being treated with anionoid reagents, a 7-bromo substituent of 2,3-benzotropone derivatives undergoes an abnormal "cine substitution" exclusively.

Experimental*4

Bromination of 2,3-Benzocycloheptenone (I). *Dibromo-acetoxy-2,3-benzocycloheptenone.* A solution of 4 g of bromine in an equal amount of acetic acid was added to a solution of 1 g of 2,3-benzocycloheptenone (I) in 20 m*l* of acetic acid containing 6.6 g of sodium acetate, and the mixture was heated on a water bath for 5 hr. The evaporation of the acetic acid, and the crystallization of the residue from petroleum ether gave 470 mg (20%) of colorless needles; mp 104—105°C, infrared spectrum (Nujol): 1748 cm^{-1} for an acetyl carbonyl and 1720 cm^{-1} for a cycloheptenone carbonyl.

Found: C, 41.63; H, 3.42%. Calcd for $C_{13}H_{12}O_3Br_2$: C, 41.51; H, 3.22%.

Tribromo-2,3-benzocycloheptenone. A solution of 1 g of I and 4.0 g of bromine in 6 m*l* of acetic acid was heated on a water bath for 15 hr. The subsequent recrystallization of the product from dilute ethanol afforded 0.57 g (23%) of a colorless crystalline powder; mp 133—134°C.

Found: C, 33.45; H, 2.30%. Calcd for $C_{11}H_9OBr_3$: C, 33.28; H, 2.29%.

Isomeric Tetrabromo-2,3-benzocycloheptenones (IIa and IIb). A solution of 10 g of I and 40 g of bromine in 50 m*l* of acetic acid was heated on a water bath for 7 hr. To this there was again added 40 g of bromine, and heating was continued for a further 7 hr. The fractional recrystallization of the product from ethanol gave 12.6 g (43%) of IIa and 0.8 g (2.8%) of IIb.

IIa, colorless granular crystals, mp 141.5—142°C, infrared spectrum (Nujol): 1712 cm^{-1} for carbonyl, ultraviolet spectrum (MeOH): 265 mμ (log ε 3.65).

Found: C, 27.82; H, 2.03%. Calcd for $C_{11}H_8OBr_4$: C, 27.76; H, 1.70%.

IIb, colorless plates, mp 145.5—146.5°C, infrared spectrum ($CHCl_3$): 1717 cm^{-1} for carbonyl, ultraviolet spectrum (MeOH): 263 mμ (log ε 3.47).

Found: C, 27.79; H, 1.75%. Calcd for $C_{11}H_8OBr_4$: C, 27.76; H, 1.70%.

The admixture of IIa and IIb showed a depression in the melting point to *ca.* 112°C. Crude IIa and IIb produce severe vesication on the skin, but purified samples are harmless and can be handled safely.

Oxidation of IIa and IIb. IIa or IIb (0.5 g) dissolved in 180 m*l* of acetone was oxidized with 5 g of potassium permanganate by heating it under reflux for 2 hr; this afforded phthalic acid in 60—65% yields; mp and mixed mp 192—194°C. (It was further identified by conversion to phthalanil; mp and mixed mp 201—202°C.)

Isomeric 5,7-Dibromo-2,3-benzotropone (IIIa) and 4,7-Dibromo-2,3-benzotropone (IIIb). A solution of 8 g of IIa in 24 m*l* of pyridine was set aside at room temperature for a week. The crystalline product which thus separated was filtered and recrystallized from ethanol (100 m*l*) to yield 3.30 g (63%) of IIa as pale yellow fibrous needles; mp 165°C, infrared spectrum, (KBr) in carbonyl region: 1620, 1595, 1535 cm^{-1}, ultraviolet spectrum (MeOH): mμ (log ε), 242 (4.37), 277 (4.33), 325 (4.03), 370 (3.87).

Found: C, 41.97; H, 1.78%. Calcd for $C_{11}H_6OBr_2$: C, 42.07; H, 1.93%.

After the IIIa had been removed, the pyridine filtrate was diluted with water (50 m*l*) to give a precipitate of a second product. Recrystallization from petroleum ether gave 1.00 g (19%) of IIIb as pale yellow fibrous needles melting at 65.5°C; infrared spectrum (KBr) in carbonyl region: 1627, 1607, 1592, 1561, 1532 cm^{-1}, ultraviolet spectrum (MeOH): mμ (log ε), 235 (4.33), 270 (4.22), 320 (3.97), 340 (3.95).

Found: C, 42.29; H, 2.17%. Calcd for $C_{11}H_6OBr_2$: C, 42.07; H, 1.93%.

Hydrogenation of IIIa. a) A solution of 500 mg of IIIa in 250 m*l* of acetic acid was hydrogenated in the presence of 250 mg of 5% palladium-on-charcoal and 500 mg of anhydrous sodium acetate at an ordinary temperature and pressure. The uptake of hydrogen amounted to 4 mol equiv. After a usual work-up, crude I was obtained in good yield and identified by conversion to its 2,4-dinitrophenylhydrazone; red crystals, mp 204—205°C, undepressed on admixture with an authentic specimen of 2,3-benzocycloheptenone 2,4-dinitrophenylhydrazone. (Found: C, 59.74; H, 4.48; N, 16.53%. Calcd for $C_{17}H_{16}O_4N_4$: C, 59.99; H, 4.74; N, 16.46%).

b) A solution of 500 mg of IIIa in 100 m*l* of ethanol was hydrogenated as above until 2 mol equivalent of hydrogen had been taken up. The oily product was treated with 2,4-dinitrophenylhydrazine, giving 75 mg of 2,3-benzotropone 2,4-dinitrophenylhydrazone, mp 227—228°C. (Found: C, 61.07; H, 3.51; N, 16.06%. Calcd for $C_{17}H_{12}O_4N_4$: C, 60.71; H, 3.61; N, 16.66%).

13) S. Ebine, This Bulletin, **34**, 887 (1961).

*4 Thanks are due to the Department of Chemistry, Faculty of Science, Tohoku University, for the microanalyses.

Reaction of IIIa with Methanolic Potassium Hydroxide. A solution of 3.2 g of IIIa and 8 g of potassium hydroxide in 800 m*l* of methanol was allowed to stand at room temperature for 24 hr. The solution was acidified with 2 N hydrochloric acid and then concentrated to a semi-solid mass. The fractional recrystallization of the product from ethanol afforded 205 mg (6.4% recovery) of an unchanged material (IIIa), 360 mg (13%) of 5-bromo-6-methoxy-2,3-benzotropone (V), 50 mg (2.0%) of 5-bromo-6-hydroxy-2,3-benzotropone (VIa), and 50 mg of an uncharacterized product (VII).

5-Bromo-6-methoxy-2,3-benzotropone (V), colorless prisms, mp 140.5°C, infrared spectrum (KBr) in carbonyl region: 1617, 1578, 1565 cm^{-1}, ultraviolet spectrum (MeOH): mμ (log ε), 260 (4.58), 337 (3.76). V was also obtained in an excellent yield by the methylation of VIa with diazomethane.

Found: C, 54.43; H, 3.55%. Calcd for $C_{12}H_9O_2Br$: C, 54.36; H, 3.42%.

5-Bromo-6-hydroxy-2,3-benzotropone (VIa), described below.

An Uncharacterized Compound (VII), assumed to be hydroxy-methoxy-naphthaldehyde, pale yellow needles, mp 186°C, infrared spectrum (KBr) above 1500 cm^{-1}: 3447, 1670, 1621, 1601 cm^{-1}, ultraviolet spectrum (MeOH): mμ (log ε), 220 (4.32), 265 (4.26), 290 (3.52), 380 (3.64).

Found: C, 70.70; H, 4.74%. Calcd for $C_{12}H_{10}O_3$: C, 71.28; H, 4.99%.

Acetate of VII, colorless needles, mp 60—61°C.

Found: C, 68.78; H, 4.98%. Calcd for $C_{14}H_{12}O_4$: C, 68.84; H, 4.95%.

Isomeric 5-Bromo-6-hydroxylamino-2,3-benzotropone Oxime (Xa) and 4-Bromo-6-hydroxylamino-2,3-benzotropone Oxime (Xb). A solution of 5 g of IIIa (or IIIb) and 3.5 g of hydroxylamine hydrochloride in 160 m*l* of pyridine was allowed to stand at room temperature for 24 hr. The pyridine was then distilled below 30°C under reduced pressure, and the residue was recrystallized from ethanol; this yielded 2.40 g (71%) of Xa (or 2.47 g, 73%, of Xb).

Xa, colorless needles, mp 228°C (dec.).

Found: C, 46.92; H, 3.30; N, 9.66%. Calcd for $C_{11}H_9O_2N_2Br$: C, 47.00; H, 3.23; N, 9.97%.

Diacetate, colorless needles, mp 148—149°C.

Found: C, 49.61; H, 3.33; N, 7.49%. Calcd for $C_{15}H_{13}O_4N_2Br$: C, 49.82; H, 3.59; N, 7.67%.

Xb, colorless needles, mp 185—186°C (dec.).

Found: C, 47.16; H, 3.18; N, 9.59%. Calcd for $C_{11}H_9O_2N_2Br$: C, 47.00; H, 3.23; N, 9.97%.

Isomeric 5-Bromo-6-hydroxy-2,3-benzotropone (VIa) and 4-Bromo-6-hydroxy-2,3-benzotropone (VIb). a) Xa or Xb (2 g) dissolved in 75 m*l* of 80% sulfuric acid was heated at 160—165°C for 2.5 hr. After dilution with 1 *l* of water, the solution was extracted with ethyl acetate and the extract was shaken with 1 N sodium hydroxide. The acidification of the alkaline layer gave a crude product, which was then recrystallized from dilute ethanol or acetic acid to yield 1.52 g (85%) of VIa or 1.61 g (90%) of VIb.

VIa, pale yellow needles, mp 234°C (dec.).

Found: C, 52.67; H, 2.97%. Calcd for $C_{11}H_7O_2Br$: C, 52.61; H, 2.81%.

Acetate of VIa, colorless scales, mp 164.5°C.

Found: C, 53.00; H, 3.06%. Calcd for $C_{13}H_9O_3Br$: C, 53.27; H, 3.10%.

Methyl ether of VIa, described above as V.

VIb, pale yellow needles, mp 201—202°C (dec.).

Found: C, 52.59; H, 3.04%. Calcd for $C_{11}H_7O_2Br$: C, 52.61; H, 2.81%.

b) V (500 mg) was heated with 100 m*l* of concentrated hydrochloric acid on a water bath for 3.5 hr, this afforded VIa in a quantitative yield. The action of methanolic potassium hydroxide on IIIa also gave VIa, as has been described above.

Oxidation of VIa and VIb. VIa or VIb (350 mg) dissolved in 50 m*l* of 0.5 N sodium hydroxide was oxidized with 4 m*l* of 35% hydrogen peroxide in the same way as will be described below for the oxidation of VIII; this afforded phthalic acid in 40—45% yields.

6-Hydroxylamino-2,3-benzotropone Oxime (XI). a) The catalytic debromination of Xa or Xb (1 g) in ethanolic solution, using 5% palladium-on-charcoal (400 mg) and anhydrous sodium acetate (400 mg), was allowed to proceed until the hydrogen uptake amounted to 1 mol equivalent. The product was then recrystallized from ethanol, giving XI (590 mg, 82%), colorless needles, mp 205°C (dec.).

Found: C, 65.19; H, 4.72; N, 13.33%. Calcd for $C_{11}H_{10}O_2N_2$: C, 65.53; H, 4.98; N, 13.86%.

b) XI (130 mg, 74%) was also obtained by the reaction of VIII (150 mg) with hydroxylamine hydrochloride (150 mg) in a pyridine solution at 100°C for 2 hr in the same way as has been described for the formation of Xa and Xb.

6-Hydroxy-2,3-benzotropone (VIII). A solution of 1 g of VIa or VIb in 100 m*l* of ethanol, containing 200 mg of 5% palladium-on-charcoal and 660 mg of anhydrous sodium acetate, was shaken under a hydrogen atmosphere and at an ordinary temperature and pressure until 1 mol equivalent of hydrogen had been taken up. The product was recrystallized from ethanol to yield 540 mg (79%) of VIII, pale yellow needles, mp 208.5°C (dec.), infrared spectrum (KBr) above 1500 cm^{-1}: 3400, 3040, 2640, 2550, 1640, 1582, 1557, 1535 cm^{-1}, ultraviolet spectrum (MeOH): mμ (log ε), 255 (4.57), 335 (3.72).

VIII (70 mg, 21%) was also obtained by the hydrolysis of XI (400 mg) with 80% sulfuric acid (30 m*l*) at 160—165°C.

Found: C, 76.50; H, 4.46%. Calcd for $C_{11}H_8O_2$: C, 76.73; H, 4.68%.

Methyl Ether, colorless needles, mp 73—74°C.

Found: C, 77.71; H, 5.09%. Calcd for $C_{12}H_{10}O_2$: C, 77.40; H, 5.41%.

Acetate, colorless needles, mp 97—98°C.

Found: C, 72.72; H, 4.78%. Calcd for $C_{13}H_{10}O_3$: C, 72.89; H, 4.71%.

VIII reacted with 2,4-dinitrophenylhydrazine to give 6-(2,4-dinitrophenylhydrazino-)2,3-benzotropone 2,4-dinitrophenylhydrazone, reddish-brown granular crystals, mp 273—275°C.

Found: C, 51.70; H, 2.81; N, 20.94%. Calcd for $C_{23}H_{16}O_8N_8$: C, 51.88; H, 3.03; N, 21.05%.

VIII reacted with hydroxylamine in pyridine at 100°C to give XI, mp and mixed mp 205°C.

Oxidation of VIII. To a solution of 200 mg of VIII in 20 m*l* of 0.5 N sodium hydroxide, 10 m*l* of 35% hydrogen peroxide were added; the resulting solution

14) F. Ramirez and A. F. Kirby, *J. Am. Chem. Soc.*, **75**, 6226 (1953).

was allowed to stand at room temperature (25°C) for 10 days. The product that separated on acidification was recrystallized from ethanol to give 130 mg (58%) of *o*-carboxycinnamic acid, mp 196—197°C (Found: C, 62.61; H, 4.19%. Calcd for $C_{10}H_8O_4$: C, 62.50; H, 4.20%). The mp was not depressed on admixture with an authentic sample,[15] and the infrared spectra of the two samples were superimposable in all respects.

4,5-Benzocycloheptene-1,3-diol] (IX). VIa (1 g), dissolved in 100 m*l* of ethanol, was hydrogenated over 200 mg of platinum oxide and 660 mg of anhydrous sodium acetate until the hydrogen uptake ceased. The semisolid product was then dissolved in benzene and chromatographed on silica gel, yielding 600 mg (85%) of colorless needles of IX, mp 98.5°C.

Found: C, 73.94; H, 7.73%. Calcd for $C_{11}H_{14}O_2$: C, 74.13; H, 7.92%.

Oxidation of IX. To a solution of 570 mg of IX in 50 m*l* of acetone, 990 mg of powdered potassium permanganate were added in small portions over a period of an hour, after which the reaction mixture was heated at 30°C for 5 hr. After the manganese dioxide had been removed by filtration, the filtrate was acidified, evaporated, and extracted with ether. The extract was evaporated to a syrup, which was then allowed to crystallize in an ice-chest. The recrystallization of the product from benzene gave 75 mg (12%) of *o*-carboxyhydrocinnamic acid, colorless needles, mp 165°C[16] (Found: C, 61.84; H, 4.98%. Calcd for $C_{10}H_{10}O_4$: C, 61.85; H, 5.19%).

5,7,5'-Tribromo-2,3-benzotropone (IV). a) Bromine (25 g) was dropped into 5 g of 2,3-benzocycloheptenone (I) under ice-cooling; the resulting solution was allowed to stand at room temperature for 2 days and was then heated on a water bath for 15 hr. After the evaporation of the excess bromine, a dark brown, syrupy residue was dissolved in 10 m*l* of pyridine and set aside overnight to give a crystalline mass. The recrystallization of the product from acetic acid gave 2.7 g (24%) of IV, yellow needles, mp 205°C, and 1.0 g (11%) of IIIa.

Found: C, 33.89; H, 1.40%. Calcd for $C_{11}H_5OBr_3$: C, 33.62; H, 1.28%.

b) A solution of 300 mg of 5,7-dibromo-2,3-benzotropone (IIIa) in 1.5 g of bromine was refluxed for 3 hr. The excess bromine was evaporated, and the residual solid was crystallized from acetic acid to give 110 mg (29%) of IV, mp 205°C, (Found: C, 33.77; H, 1.38%).

Hydrogenation to 5'-Bromo-3,2-benzocycloheptenone (XIV). A solution of 400 mg of IV in 350 m*l* of acetic acid was shaken with hydrogen in the presence of 200 mg of 5% palladium-on-charcoal and 330 mg of fused sodium acetate at an ordinary temperature and pressure. After 4 mol equivalents (97 m*l*) of hydrogen had been taken up, the catalyst and the solvent were removed, the residue was extracted with ether, and the extract was evaporated. The crude XIV thus obtained was identified by converting it to its 2,4-dinitrophenylhydrazone, yellowish-orange needles, mp 243°C, (Found: C, 48.35; H, 3.45; N, 13.06%. Calcd for $C_{17}H_{15}N_4O_4Br$: C, 48.70; H, 3.61; N, 13.37%.), not depressed on admixture with a synthetic sample to be described below.

Oxidation to 4-Bromophthalic Acid. To a boiling solution of 500 mg of IV in 100 m*l* of acetone was added, portion by portion, 7.0 g of potassium permanganate; the solution was then refluxed for 3 hr. The excess potassium permanganate was decomposed by the addition of a little methanol, and the manganese dioxide that precipitated was collected and washed with 1 N potassium hydroxide. The acetone filtrate and alkaline washings were combined, acidified with hydrochloric acid, concentrated to a small volume, and extracted with ether. The ether extract was evaporated and the residual 4-bromophthalic acid was sublimed to give 245 mg (85%) of 4-bromophthalic anhydride, colorless granular crystals, mp and mixed mp 108—109.5°C.[17]

5,5'-Dibromo-6-hydroxylamino-2,3-benzotropone Oxime. A solution of 1 g of 5,7,5'-tribromo-2,3-benzotropone (IV) and 0.4 g of hydroxylamine hydrochloride in 80 m*l* of pyridine was treated in the same way as in the case of Xa. The product was recrystallized from ethanol to give 0.6 g (67%) of colorless crystals, mp 225°C.

Found: C, 37.01; H, 2.30; N, 7.39%. Calcd for $C_{11}H_8O_2N_2Br_2$: C, 36.69; H, 2.24; N, 7.68%.

5,5'-Dibromo-6-hydroxy-2,3-benzotropone. A solution of 500 mg of the above 5,5'-dibromo-6-hydroxylamino-2,3-benzotropone oxime in 22 m*l* of 66% sulfuric acid was heated at 160°C for 2 hr and then treated as has been described for VIa, b. The recrystallization of the product from ethanol gave 350 mg (76%) of pale yellow prisms melting at 243°C (dec.).

Found: C, 40.10; H, 1.57%. Calcd for $C_{11}H_6O_2Br_2$: C, 40.03; H, 1.83%.

Acetate: colorless needles (recrystallized from ethanol), mp 193—193.5°C.

Found: C, 41.93; H, 1.87%. Calcd for $C_{13}H_8O_3Br_2$: C, 41.97; H, 2.17%.

Synthesis of 5'-Bromo-3,2-benzocycloheptenone (XIV). The synthesis was carried out according to the reported method for the preparation of 2,3-benzocycloheptenone derivatives.[18]

p-Bromocinnamylidenemalonic Acid (XV). To a solution of 34.6 g of diethyl ethylidenemalonate and 11.3 g of *p*-bromobenzaldehyde in 113 m*l* of absolute ethanol, there was added, in small portions, 24.5 g of powdered potassium hydroxide; the resulting solution was allowed to stand at room temperature (18°C) for 2 days. The solution was then acidified with dilute hydrochloric acid, and the precipitate that separated was recrystallized from dilute acetone to yield 11.73 g (65%) of XV, yellow prisms, mp 199°C.

Found: C, 48.31; H, 3.37%. Calcd for $C_{12}H_9O_4Br$: C, 48.51; H, 3.02%.

δ-(p-Bromophenyl-)valeric Acid (XVII). A solution of 12 g of XV in 1200 m*l* of methanol was hydrogenated in the presence of 400 mg of platinum oxide. The hydrogenation was stopped after the uptake of 2 mol equivalents of hydrogen, the catalyst and the solvent were removed, and the residual γ-(*p*-bromophenyl)-propylmalonic acid (XVI) was decarboxylated by

15) J. Boesekin, *Rec. Trav. Chim.*, **30**, 146 (1911).
16) F. Strauss and A. Rohrbadher, *Ber.*, **54**, 66 (1921).
17) F. F. Blicke and F. D. Smith, *J. Am. Chem. Soc.*, **51**, 1871 (1929).
18) P. D. Gardner, W. J. Horton, G. Thompson and R. R. Twelves, *ibid.*, **74**, 5527 (1952).

heating it at 145—150°C under 10 mmHg. The recrystallization of the product from benzene - petroleum ether (1 : 1) gave 3.5 g (34%, based on XV) of XVII, colorless granular crystals, mp 91—92°C, along with a considerable amount of δ-phenylvaleric acid.

Found: C, 51.47; H, 4.91%. Calcd for $C_{11}H_{13}O_2Br$: C, 51.38; H, 5.10%.

5'-Bromo-2,3-benzocycloheptenone (XIV). XVII (3 g) was added, portion by portion, to hot (90°C) and stirred polyphosphoric acid prepared from 107 g of phosphoric acid and 95 g of phosphorus pentoxide. After heating at 100°C for 5 hr, the solution was poured onto crushed ice and extracted with ether. The extract was washed with dilute alkali. The acidification of the alkaline washings gave 2.0 g (66.7% recovery) of unreacted XVII, and the evaporation of the ether extract gave 0.8 g (28.6%) of crude XIV. 2,4-Dinitrophenylhydrazone of XIV: yellowish orange needles (from acetic acid), mp 243°C.

Found: C, 48.40; H, 3.51; N, 13.11%. Calcd for $C_{17}H_{15}N_4O_4Br$: C, 48.70; H, 3.61; N, 13.37%.

Diels-Alder Reaction of IIIa and IIIb. *Adduct of IIIa with Maleic Anhydride.* A mixture of 500 mg of IIIa and 500 mg of maleic anhydride was heated at 165°C for 30 min. After cooling, ether was added to the reaction mixture and an insoluble product was collected by filtration. The product was recrystallized from ether to give 400 mg (68%) of XVIIIa, colorless granular crystals, mp 216—217°C. The NMR spectrum in deuteriochloroform: 8.33—7.37 ppm (4H, multiplet, aromatic hydrogens), 6.61 ppm (doublet, J=1.8 cps, an ethylenic hydrogen), 4.40 ppm (multiplet, a benzylic hydrogen), 3.97 ppm (1H, a doublet, J=9 cps, of doublets, J=2.5 cps) and 3.70 ppm (1H, doublet, J=9 cps) (the latter two bands are attributable to two α-hydrogens of maleic anhydride part).

Found: C, 43.78; H, 2.33%. Calcd for $C_{15}H_8O_4Br_2$: C, 43.72; H, 1.96%.

Adduct of IIIb with Maleic Anhydride (XVIIIb). This was obtained in a similar manner by heating a mixture of 500 mg of IIIb and 500 mg of maleic anhydride at 165°C for 5 hr. Colorless needles, mp 255—256°C (dec.). Yield, 320 mg (55%). The NMR spectrum in acetonitrile; 8.20—7.25 ppm (4H, multiplet, aromatic hydrogens), 7.05 and 6.30 ppm (2H, AB-type doublets, J=9.5 cps, adjacent two ethylenic hydrogens), 4.65 and 4.20 ppm (2H, AB-type doublets, J=10.8 cps, adjacent two α-hydrogens of the maleic anhydride part).

Found: C, 44.22; H, 2.27%. Calcd for $C_{15}H_8O_4Br_2$: C, 43.72; H, 1.96%.

The present work has been supported in part by a Grant for Scientific Research from the Ministry of Education.

BULLETIN OF THE CHEMICAL SOCIETY OF JAPAN VOL. 41 2949—2953 (1968)

3,4-Benzotropolone and Related Compounds. VI.[1] Brominated 6-Hydroxy-2,3-benzotropone (or Brominated 3-Hyroxy-4,5-benzotropone). Formation and Reaction

Masamatsu HOSHINO and Seiji EBINE

Department of Chemistry, Faculty of Science and Engineering, Saitama University, Urawa, Saitama-ken

(Received March 7, 1968)

6-Hydroxy-2,3-benzotropone (or 3-hydroxy-4,5-benzotropone) (I) was brominated under various conditions, and the bromination products were subjected to debromination, substitution, and some other reactions. I reacted with a molar equivalent of bromine at 25°C to give 7-bromo-6-hydroxy-2,3-benzotropone (II), and with two molar equivalents of bromine at 25°C to give an adduct of II with bromine (V), which, on heating, was dehydrobrominated to 5,7-dibromo-6-hydroxy-2,3-benzotropone (IV). On the other hand, I reacted with bromine at 100°C to give 5-bromo-6-hydroxy-2,3-benzotropone (III), IV, and 2,2,7-tribromo-4,5-benzocyclohepta-4,6-diene-1,3-dione (VI), depending on the amount of bromine employed. All these bromination products could be debrominated with ease with hydrogen in the presence of catalyst to yield I. When II was heated with hydrobromic acid, the 7-bromo substituent was in part eliminated to give I and migrated in part to give III. When IV and 4,7-dibromo-6-hydroxy-2,3-benzotropone (X) were heated with hydrobromic acid, the 7-bromo substituents were eliminated and the 4- or 5-bromo substituent remained unreacted, producing III and 4-bromo-6-hydroxy-2,3-benzotropone (IX) respectively. When II and IV were heated with hydrochloric acid, the 7-bromo substituents were not eliminated but, rather, substituted with chlorine atoms to give 7-chloro-6-hydroxy-2,3-benzotropone (VII) and 5-bromo-7-chloro-6-hydroxy-2,3-benzotropone (VIII) respectively. These facts suggest that I and its bromo derivative sometimes behave as unsaturated β-diketones (I').

In a previous paper[1] the present authors reported the formation of 6-hydroxy-2,3-benzotropone (I). Attention has now been directed toward the chemical properties of I and toward comparing those properties with those of three well-known isomers, 3,4-benzotropolone,[2,3] 4,5-benzotropolone,[4] and 4-hydroxy-2,3-benzotropone.[5] The present paper will deal with the formation and reaction of bromo derivatives of I. I is tautomeric with 4,5-benzocyclohepta-4,6-diene-1,3-dione (I') and with 3-hydroxy-4,5-benzotropone (I''). In this paper the (I) formula is tentatively employed as representative of these tautomers because it is at present unknown which of these is predominant.

An acetic acid solution of I was brominated under various conditions. The reaction of I with a molar equivalent of bromine at 25°C gave 7-bromo-6-hydroxy-2,3-benzotropone (II), the position of the bromo substitutent of which was established by its oxidation with alkaline hydrogen peroxide to *o*-carboxycinnamic acid, and by a study of its NMR absorption spectrum which contained AB-type double doublets at 7.55 and 6.98 ppm, doublets ascribable to two hydrogen atoms at the 4 and 5 positions. The same reaction of I with bromine, but at 100°C instead of 25°C, gave 5-bromo-6-hydroxy-2,3-benzotropone (III), which was identified by a mixed-melting-point determination and by a comparison of its infrared spectrum with that of a sample obtained previously[1] by another method. On being heated at 100°C with a molar equivalent of bromine, both II and III produced dibromo-2,3-benzotropone (IV). This fact indicates that the dibromo substituents of IV are situated at the 5- and 7-positions. IV was oxidized to phthalic acid under the same conditions as in the oxidation of II to *o*-carboxycinnamic acid. II, III, and IV were debrominated with ease to I when treated with hydrogen in the presence of a palladium-charcoal catalyst. These bromo derivatives exhibit two peaks in the 265—285 mμ and 355—365 mμ ranges in the ultraviolet absorption spectra (Fig. 1) and a carbonyl band below 1650 cm^{-1} in the infrared spectra (see

1) Part V: S. Ebine, M. Hoshino and K. Takahashi; This Bulletin, **41**, 2942 (1968).
2) J. W. Cook and A. R. Sommerville, *Nature*, **163**, 410 (1949); J. W. Cook, A. R. Gibb, R. A. Raphael and A. R. Sommerville, *J. Chem. Soc.*, **1952**, 603.
3) S. Ebine, This Bulletin, **35**, 114, 117, 122 (1962); **38**, 2029 (1965).
4) H. Fernholz, E. Hartwig and J. G. Salfeld, *Ann.*, **576**, 137 (1952).
5) G. L. Buchanan, *J. Chem. Soc.*, **1954**, 1060; G. L. Buchanan and J. K. Sutherland, *ibid.*, **1956**, 2620.

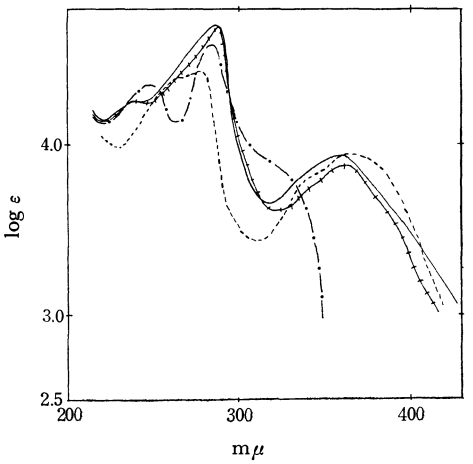

Fig. 1. Ultraviolet absorption spectra of 7-bromo-6-hydroxy-2,3-benzotropone (II, ----), 5,7-dibromo-6-hydroxy-2,3-benzotropone (IV, —+), 7-chloro-6-hydroxy-2,3-benzotropone (VII, —·) and 5-bromo-7-chloro-6-hydroxy-2,3-benzotropone (VIII, ——).

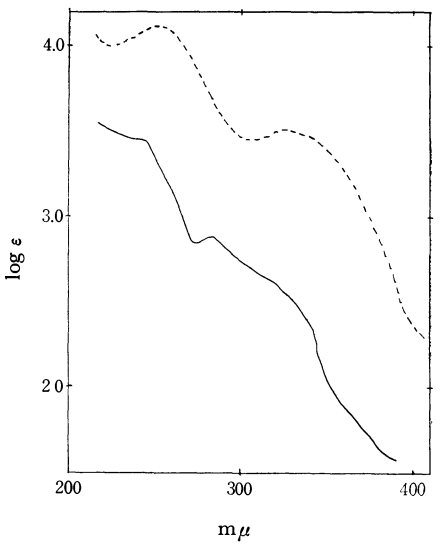

Fig. 2. Ultraviolet absorption spectra of adduct of II with Bromine (V, ----), and 2,2,7-tribromo-4,5-benzocyclohepta-4,6-diene-1,3-dione (VI, ——).

Experimental section), in agreement with the spectral features of troponoids.[6] It has been reported that the methylation of 3-bromotropolone gives two isomeric methyl ethers, 3-bromo-2-methoxy- and 7-bromo-2-methoxy-tropones.[7] However, II, III, and IV gave a single methyl ether and acetate, suggesting that one form predominates in their tautomerism. IV was further brominated at 100°C to 2,2,7-tribromo-4,5-benzocyclohepta-4,6-diene-1,3-dione (VI), which had carbonyl bands at 1710 and 1692 cm^{-1} in the infrared absorption spectrum. VI was also produced directly from I, II, and III when they were heated at 100°C with excess bromine. VI was debrominated to IV when its methanolic solution was left to stand with alkali and to I when treated with hydrogen in the presence of a palladium-charcoal catalyst. II reacted with bromine at 20°C to give an adduct (V), which was debrominated with ease to IV when its ethanolic or acetic acid solution was heated. I, with two molar equivalents of bromine at 20°C, gave the same adduct. Under the same conditions, III did not add bromine, but gave IV. V and VI showed ultraviolet absorption spectra entirely different from those of troponoids, as is shown in Fig. 2. From the above results, it is evident that the bromination of I proceeds in the sequence of II and V at 20°C, and in that of III, IV, and VI at 100°C.

When II was heated at 100°C with hydrobromic acid in an acetic acid solution, its 7-bromo substituent migrated in part to the 5-position, giving III, and was in part eliminated, giving I. II reacted with hydrochloric acid in a similar way to give 7-chloro-6-hydroxy-2,3-benzotropone (VII) and I. However, III remained unreacted when heated with hydrobromic or hydrochloric acid. IV as well as VI reacted with hydrobromic acid to give III, and with hydrochloric acid to give 5-bromo-7-chloro-6-hydroxy-2,3-benzotropone (VIII). To make sure of the positions of the substituents, VII and VIII were oxidized with alkaline hydrogen peroxide to give *o*-carboxycinnamic acid and phthalic acid respectively, and VIII was treated with one molar equivalent of hydrogen in the presence of a palladium-charcoal catalyst to give III and VII. Both VII and VIII were dehalogenated to I with the calculated amount of hydrogen in the presence of the catalyst. The formation of free bromine was verified during the reaction of II, IV, and VI with hydrobromic acid. These debromination reactions, therefore, may be illustrated as in the scheme. The bromo migration may consist of two reactions: the debromination of II with hydrobromic acid to I, with the liberation of bromine, and the subsequent bromination of I to give III. It has been described above that the bromination of I at 100°C takes place at the 5-position to give III. In a similar manner, 4-bromo-6-hydroxy-2,3-benzotropone (IX), reported on in the preceding paper,[1] was brominated to 4,7-dibromo-6-hydroxy-2,3-benzotropone (X), while the latter was debrominated to the former when heated with hydrobromic acid.

6) M. Tsuboi, This Bulletin, **25**, 369 (1952); S. Kinumaki, K. Aida and Y. Ikegami, *Sci. Rept. Res. Inst. Tohoku Univ.*, **A-8**, 263 (1956); E. Kloster-Jensen, N. Tarkoy, A. Eschenmoser and E. Heilbronner, *Helv. Chim. Acta*, **39**, 780 (1956).

7) T. Nozoe, Y. Kitahara and S. Masamune, *Proc. Japan Acad.*, **27**, 649 (1951); T. Sato, *Nippon Kagaku Zasshi (J. Chem. Soc. Japan, Pure Chem. Sect.)*, **80**, 1340 (1959).

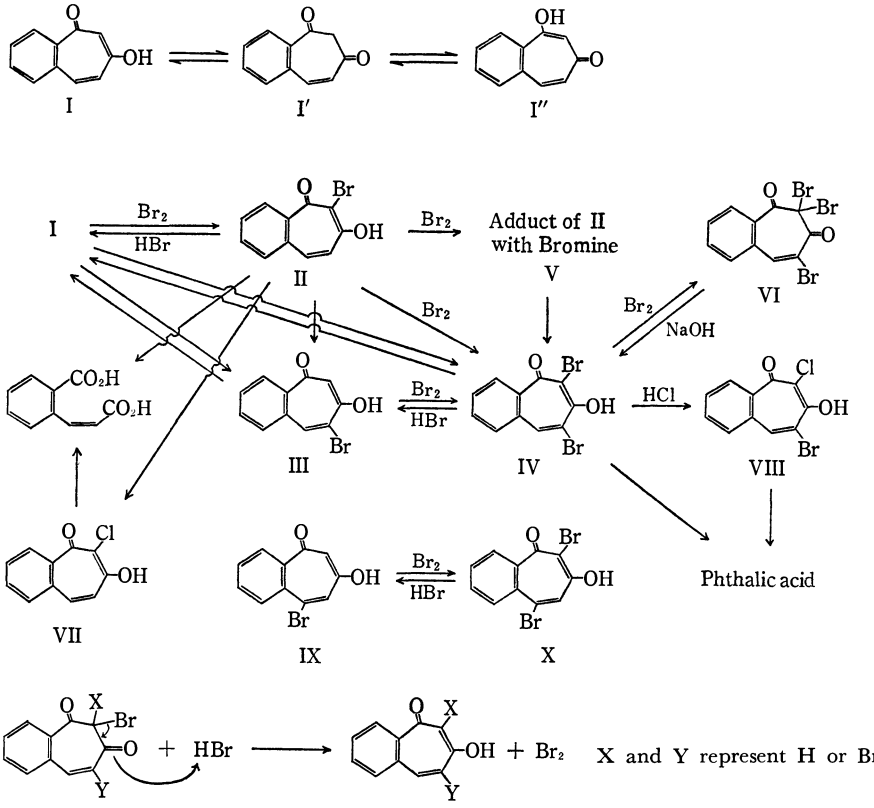

From the above results it has become evident that, although I and its bromo derivatives exhibit ultraviolet and infrared spectra characteristic of troponoids, they sometimes behave like unsaturated β-diketones represented by the (I') formula; for example, the bromination of I, III, and IX takes place at the 7-position (or the 2-position as a β-diketone) to give II, IV, and X respectively, IV is further brominated to VI, and II adds bromine to give V. Furthermore, it has proved that the 7-bromo substituents of brominated 6-hydroxy-2,3-benzotropones is especially reactive; for example, upon heating with hydrobromic acid, the 7-bromo substituents of II, IV, and X were eliminated to give I, III, and IX respectively, while simultaneously the substituent of II migrated in part to give III. No such type of reaction has ever been described in connection with the bromo derivatives of isomeric 3,4-benzotropolone, 4,5-benzotropolone, and 4-hydroxy-2,3-benzotropone. It is of peculiar interest to compare the enhanced reactivity of the 7-bromo substituent described above with the reported[8] inertness of 7-chloro-2,3-benzotropone.

Experimental

7-Bromo-6-hydroxy-2,3-benzotropone (II). To a solution of 300 mg (1.74 mmol) of I in 30 m*l* of acetic acid, there was dropped, at 15°C, a solution of 280 mg (1.75 mmol) of bromine in 1 m*l* of acetic acid. After the mixture had stood for an hour at room temperature (17°C), the acetic acid was removed below 25°C under reduced pressure and the crystalline residue was fractionally recrystallized from ethanol to give 215 mg (55%) of II (pale yellow granular crystals melting at 173—173.5°C (dec.); also, 30 mg of unreacted I were recovered. The same bromination in the presence of 215 mg of anhydrous sodium acetate gave 421 mg (96%) of II. Ultraviolet spectrum (methanol): mμ (log ε), 269 (4.40), 365 (3.93), infrared spectrum (KBr) in the region above 1500 cm^{-1}: 3026, 1645, 1569, 1511 cm^{-1}.

Found: C, 52.92; H, 2.87%. Calcd for $C_{11}H_7O_2Br$: C, 52.61; H, 2.81%.

The NMR spectrum in deuterated dimethyl sulfoxide (d_6-DMSO): 8.47—7.85 ppm (4H, multiplet, aromatic hydrogens), 7.55 and 6.98 ppm (2H, AB-type doublets, J=12.8 cps, two hydrogens at the 4 and 5 positions).

5-Bromo-6-hydroxy-2,3-benzotropone (III). Bromine (110 mg, 0.69 mmol), diluted with 1 m*l* of acetic acid, was dropped into a warm solution of 100 mg (0.58 mmol) of I in 5 m*l* of acetic acid, and the resulting solution was heated at 100°C for 3 hr. When the mixture stood overnight at room temperature, a crystalline product separated out; this product was collected by filtration. The filtrate was concentrated to give a further crop of the product. The combined products (90 mg, 62%) were recrystallized from ethanol to give pale yellow needles of III melting at 234°C (dec.),

8) W. E. Parham, D. A. Bolon and E. E. Schweizer, *J. Am. Chem. Soc.*, **83**, 603 (1961).

ultraviolet spectrum (methanol): 275 mμ, (log ε 4.64), infrared spectrum (KBr) in the region above 1500 cm^{-1}: 3050, 2970, 2730, 2580, 1615, 1584, 1552, 1512 cm^{-1}.

Found: C, 52.38; H, 2.88%. Calcd for $C_{11}H_7O_2Br$: C, 52.61; H, 2.81%.

Adduct of II with Bromine (V). *a) From I.* To a solution of 300 mg (1.74 mmol) of I in 45 m*l* of acetic acid, there was added, drop by drop at 20°C, a solution of 560 mg (3.5 mmol) of bromine in 5 m*l* of acetic acid. After it has stood at this same temperature for 2.5 hr, the reaction mixture was concentrated below 25°C under diminished pressure; the product which separated was collected and recrystallized from benzene or dilute ethanol to give 460 mg (64%) of V in the form of colorless, granular crystals with a double melting point of 135—136°C and 179—180°C (dec.).

b) From II. A solution of 100 mg (0.63 mmol) of bromine in 1 m*l* of acetic acid was added to a solution of 150 mg (0.60 mmol) of II in 14 m*l* of acetic acid, and the resulting solution was worked up as above to give 105 mg (43%) of III.

The above two samples showed the same ultraviolet and infrared spectra. Ultraviolet spectrum (methanol): 330—336 mμ (log ε 3.82), infrared spectrum (KBr): 3340, 1635, 1617, 1595, 1552, 1540, 1525 cm^{-1}.

Found: C, 32.50; H, 1.77%. Calcd for $C_{11}H_7O_2Br_3$: C, 32.15; H, 1.72%.

5,7-Dibromo-6-hydroxy-2,3-benzotropone (IV). *a) From I.* A solution of 100 mg (0.58 mmol) of I and 200 mg (1.25 mmol) of bromine in 6 m*l* of acetic acid was heated at 100°C for 3 hr and then worked up in the same way as has been described for the bromination of I to III; this gave 180 mg (94%) of pale yellow needles of IV melting at 181—182°C (dec.).

b) From II. A similar work-up of a solution of 150 mg (0.60 mmol) of II and 100 mg (0.63 mmol) of bromine in 14 m*l* of acetic acid gave 170 mg (86%) of IV.

c) From III. III (1 g, 3.98 mmol) and 770 mg (4.82 mmol) of bromine, dissolved in 100 m*l* of acetic acid, were heated at 100°C for 3 hr to give 1.2 g (91%) of IV. The same reaction, but at 20°C, gave an 80% yield of IV.

d) From V. A solution of 100 mg of V in 3.5 m*l* of acetic acid was heated at 100°C for 2.5 hr. A crystalline product which separated on cooling was filtered, and the filtrate was concentrated to give an additional crop of the product. The recrystallization of the combined products from ethanol afforded 68 mg (84%) of IV. When dissolved in 1 N sodium hydroxide and allowed to stand for 1.5 hr at room temperature, V decomposed to produce IV in a fair yield.

e) From VI. A solution of 100 mg of VI in 3 m*l* of methanol containing 0.15 m*l* of 2 N sodium hydroxide was allowed to stand for 3 hr, and then the precipitate which had separated on acidification was collected and recrystallized. Yield, 30 mg (37%).

The identities of the samples obtained above have been confirmed by mixed-melting-point determinations and by infrared-spectrum comparisons. Ultraviolet spectrum (methanol): mμ (log ε), 285 (4.71), 355 (3.82), infrared spectrum (KBr) in the region above 1500 cm^{-1}: 3330, 1593, 1568, 1513 cm^{-1}.

Found: C, 40.30; H, 1.81%. Calcd for $C_{11}H_6O_2Br_2$: C, 40.03; H, 1.83%.

Acetate of IV, colorless granular crystals (recrystallized from methanol), mp 172—173°C.

Found: C, 41.90; H, 2.27%. Calcd for $C_{13}H_8O_3Br_2$: C, 41.97; H, 2.17%.

Methyl ether of IV, colorless needles (recrystallized from methanol), mp 160—161°C.

Found: C, 42.22; H, 2.21%. Calcd for $C_{12}H_8O_2Br_2$: C, 41.89; H, 2.34%.

2,2,7-Tribromo-4,5-benzocyclohepta-4,6-diene-1,3-dione (VI). *a) From IV.* A mixture of 100 mg (0.30 mmol) of IV and 2 g (12.5 mmol) of bromine was refluxed for 4 hr, the excess bromine was distilled, and then the residue was recrystallized from ethanol to afford 90 mg (73%) of yellow needles of VI melting at 132—133°C.

b) From I and III. A similar treatment of 100 mg (0.58 mmol) of I with 2 g (12.5 mmol) of bromine gave 50 mg (21%) of VI and 20 mg (10%) of IV, while the treatment of 100 mg (0.40 mmol) of III with 2 g (12.5 mmol) of bromine gave 110 mg (68%) of VI. Ultraviolet spectrum (methanol): 288 mμ, (log ε 3.77), infrared spectrum (KBr) in the region above 1500 cm^{-1}: 1710, 1692, 1591, 1569 cm^{-1}.

Found: C, 32.32; H, 1.64%. Calcd for $C_{11}H_5O_2Br_3$: C, 32.31; H, 1.23%.

Debromination of II, IV, and VI to I. The reaction was carried out in the same way as has already been described for the debromination of III to I. A solution of 300 mg (0.91 mmol) of IV in 100 m*l* of ethanol was shaken with hydrogen in the presence of 100 mg of 5% palladium chloride-charcoal and 100 mg of anhydrous sodium acetate. After 43.6 m*l* (1.84 mmol) of hydrogen had been taken up at 16°C, the catalyst was filtered, the filtrate was evaporated, and the residue was recrystallized from ethanol, giving 130 mg (83%) of I, mp and mixed mp 208.5°C (dec.). A similar treatment of II and VI with hydrogen gave I in 80% and 48% yields respectively.

Reaction of II with Hydrobromic or Hydrochloric Acid. a) II (200 mg), dissolved in 25 m*l* of acetic acid and 15 m*l* of 47% hydrobromic acid, was heated under reflux for 2.5 hr. The solution gave a positive patassium iodide - starch paper test, indicating the presence of free bromine. The solution was then concentrated, and the product was fractionally recrystallized from ethanol to give 58 mg (29%) of III and 5 mg (4%) of I.

b) The heating of 120 mg of II, dissolved in a mixture of 15 m*l* of acetic acid and 12 m*l* of 6 N hydrochloric acid for 2 hr, and the recrystallization of the product from dilute ethanol gave 70 mg (71%) of 7-chloro-6-hydroxy-2,3-benzotropone (VII) as pale yellow needles melting at 172—173°C (dec.), along with 10 mg (12%) of I. VII, ultraviolet spectrum (methanol): mμ (log ε), 245 (4.34), 283 (4.60), infrared spectrum (KBr) in the region above 1500 cm^{-1}: 3006, 1646, 1570, 1518, 1507 cm^{-1}.

Found: C, 63.77; H, 3.53%. Calcd for $C_{11}H_7O_2Cl$: C, 63.94; H, 3.41%.

Reaction of IV with Hydrochloric or Hydrobromic Acid. The reaction was carried out in the same way as above. The reaction of 200 mg of IV with 20 m*l* of 47% hydrobromic acid in 15 m*l* of acetic acid gave 130 mg (85%) of III, mp and mixed mp 243°C (dec.), while the reaction of 300 mg of IV with 15 m*l* of 6 N hydrochloric acid in 30 m*l* of acetic acid gave

5-bromo-7-chloro-6-hydroxy-2,3-benzotropone (VIII) as yellow needles (from ethanol), mp 213—214°C (dec.), yield 215 mg (83%). VIII, ultraviolet spectrum (methanol): mμ (log ε), 287 (4.73), 357 (3.93), infrared spectrum (KBr) in the region above 1500 cm^{-1}: 3306, 1590, 1566, 1514 cm^{-1}.

Found: C, 46.22; H, 2.25%. Calcd for $C_{11}H_6O_2ClBr$: C, 46.27; H, 2.12%.

During the former reaction a considerable amount of bromine was liberated; it was identified by a potassium iodide - starch paper test.

Acetate of VIII, colorless, granular crystals, mp 183—184°C.

Found: C, 48.03; H, 2.57%. Calcd for $C_{13}H_8O_3ClBr$: C, 47.66; H, 2.46%.

Reaction of VI with Hydrobromic or Hydrochloric Acid. A similar treatment of VI (400 mg) with 47% hydrobromic acid (30 m*l*) in acetic acid (50 m*l*) gave III (173 mg, 71%), while that of VI (400 mg) with 6 N hydrochloric acid (30 m*l*) in acetic acid (50 m*l*) gave VIII (100 mg, 36%).

Dehalogenation of VIII. The dehalogenation was carried out in the same manner as has been described for the debromination of II, IV, and VI. a) A solution of 300 mg of VIII in 100 m*l* of ethanol was treated with hydrogen in the presence of 150 mg of 5% palladium chloride - charcoal and 130 mg of anhydrous sodium acetate. The reaction was stopped when a molar equivalent of hydrogen had been taken up. The recrystallization of the product from ethanol gave 81 mg (31%) of III and 101 mg (47%) of VII. b) When stopped after the uptake of two molar equivalents of hydrogen, the same reaction, using 300 mg of VIII, 150 mg of 5% palladium chloride-charcoal, 260 mg of anhydrous sodium acetate, and 100 m*l* of ethanol, produced 121 mg (67%) of I. The products obtained in a) and b) were identified by a mixed-melting-point determination and by a comparison of the infrared spectra.

Oxidation of II, IV, VII and VIII. A 200-mg sample was dissolved in 20 m*l* of 0.5 N sodium hydroxide, and to this 5 m*l* of 35% hydrogen peroxide were added. After standing at 50°C for 5 hr, the solution was acidified by dilute hydrochloric acid to precipitate unreacted material (30—50% recovery), which was removed by filtration. The filtrate was extracted with ether, and the extract was evaporated to give the product. The oxidation of II and VII gave *o*-carboxycinnamic acid (mp and mixed mp 185—186°C) in 47 and 33% yields respectively, while that of IV and VIII gave phthalic acid, mp and mixed mp 200°C, in 40 and 35% yields respectively.

Bromination of 4-Bromo-6-hydroxy-2,3-benzotropone (IX) to 4,7-Dibromo-6-hydroxy-2,3-benzotropone (X) and Debromination of X to IX. These reactions were carried out exactly as has been described above for the bromination of III and for the reaction of IV with hydrobromic acid. The reaction of IX (400 mg) and bromine (300 mg) in acetic acid at 100°C for 1 hr gave X (410 mg, 78%) as pale yellow prisms (from dilute ethanol) melting at 156—157°C. X, ultraviolet spectrum (methanol): mμ (log ε), 265 (4.39), 349 (3.79), infrared spectrum (KBr) in the region above 1500 cm^{-1}: 3186, 1616, 1599, 1581, 1555, 1543, 1528 cm^{-1}.

Found: C, 39.99; H, 2.05%. Calcd for $C_{11}H_6O_2Br_2$: C, 40.03; H, 1.83%.

The reaction of X (150 mg) and 47% hydrobromic acid (20 m*l*) in acetic acid (15 m*l*) at 100°C for 2 hr produced IX (60 mg, 53%).

Part of the expenses of this work has been defrayed by a Scientific Research Grant from the Ministry of Education.

BULLETIN OF THE CHEMICAL SOCIETY OF JAPAN VOL. 41 2954—2959 (1968)

1,3-Dipolar Cycloaddition Reaction of Thiophenecarbonitrile *N*-Oxides with Various Dipolarophiles

Yoshio IWAKURA, Keikichi UNO, Shinsaku SHIRAISHI and Tatsuhiko HONGU

Department of Synthetic Chemistry, Faculty of Engineering, The University of Tokyo, Bunkyo-ku, Tokyo

(Received February 29, 1968)

Thiophene-2-carbonitrile *N*-oxide (I) and 5-chlorothiophene-2-carbonitrile *N*-oxide (II) were synthesized by the chlorination of corresponding aldoxime with nitrosyl chloride. These compounds gave Δ^2-isoxazolines and isoxazoles through 1,3-dipolar cycloaddition reaction with compounds having double or triple bond as dipolarophiles. In the cycloaddition reaction, II was less reactive than I. This would be explained by stability of II owing to electron-withdrawing ability of chlorine atom at 5-position in the thiophene ring. Furoxans, the dimers of the nitrile *N*-oxide, were formed from these 1,3-dipoles in the absence of dipolarophile.

Many kinds of aromatic and aliphatic carbonitrile *N*-oxides and their reactions have been known.[1-7] We have also reported the 1,3-dipolar cycloaddition reaction as an elementary reaction of polymer formation.[8] However, neither synthesis of thiophenecarbonitrile *N*-oxides nor 1,3-dipolar cycloaddition reaction with them have ever been reported up to date. In the present study, synthesis of thiophene- and 5-chlorothiophene-2-carbonitrile *N*-oxides and their reactions with dipolarophile have been studied. Although thiophene-2-carbonitrile *N*-oxide and 5-chlorothiophene-2-carbonitrile *N*-oxide themselves could not be isolated, thiophene- and 5-chlorothiophene-2-carbohydroxamoyl chlorides reacted with dipolarophiles in the presence of triethylamine to give the products which would be expected from the corresponding carbonitrile *N*-oxides and dipolarophiles. The details will be described below.

Results and Discussion

I. Synthesis of Thiophene- and 5-Chlorothiophene-2-carbohydroxamoyl Chlorides. For a synthesis of hydroxamoyl chloride, the reaction of aldoxime with chlorine has generally been utilized.[5-8]

$$\mathrm{R\text{-}CH{=}NOH + Cl_2 \rightarrow R\text{-}\overset{\displaystyle Cl}{\overset{|}{C}}{=}NOH + HCl}$$

When thiophenecarboxaldoxime was subjected to such a chlorination procedure, the product obtained was not hydroxamoyl chloride but 5-chlorothiophene-2-carboxaldoxime resulted through chlorination of thiophene nuclei. The product was identical with the one prepared from 5-chlorothiophene-2-carboxaldehyde and hydroxylamine.

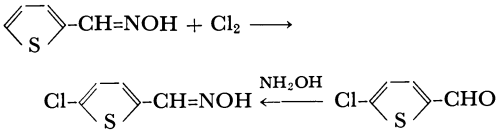

Accordingly, this reaction is inadequate to the preparation of thiophenecarbohydroxamoyl chloride.

The reaction of aldoxime with nitrosyl chloride has been reported by Rheinbolt[9] as an another method of preparing hydroxamoyl chloride.

When the cooled ether solution of nitrosyl chloride was added to the cooled ether solution of thiophene-2-carboxaldoxime, precipitates were formed immediately and then disappeared slowly with evolution of gas on standing the reaction mixture at a low temperature. After the precipitates were dissolved completely and the evolution of gas stopped, hydroxamoyl chloride was obtained from the reaction mixture. If the precipitate was kept in chloroform-benzene at room temperature for a long period, thiophene-2-carbonamide was obtained. On contact with air, the precipitate decomposed slowly to give thiophene-2-carboxaldehyde and thiophene-2-carbonitrile. The results of the reaction of thiophenecarboxaldoxime with nitrosyl chloride are summarized in Table 1.

1) R. Huisgen, R. Grashey and J. Sauer, "The Chemistry of Alkenes," Interscience Publishers, New York, N. Y. (1964), p. 806. R. Huisgen, *Angew. Chem.*, **75**, 604 (1963); R. Huisgen, *ibid.*, **75**, 742 (1963).
2) C. Grudmann, *Angew. Chem.*, **75**, 450 (1963).
3) H. Wieland, *Ber.*, **40**, 418 (1907); H. Wieland, L. Semper and E. Gmelin, *Ann.*, **367**, 61 (1909).
4) G. S. Skinner, *J. Am. Chem. Soc.*, **46**, 734 (1924).
5) O. Piloty and H. Steinkock, *Ber.*, **35**, 3114 (1902).
6) A. Werner, *ibid.*, **27**, 2846 (1894).
7) R. H. Wiley and B. J. Wakefield, *J. Org. Chem.*, **25**, 546 (1960).
8) Y. Iwakura, M. Akiyama and K. Nagakubo, This Bulletin, **37**, 767 (1964).
9) H. Rheinbolt, *Ann.*, **451**, 161 (1927).

Table 1. Reaction products between nitrosyl chloride and thiophene-2-carboxaldoxime

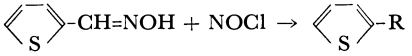

React. temp. (°C)	Reaction time (hr)		Yield (%) of 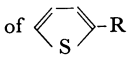				
	Stir	Stand	R=-$CONH_2$	-CN	-CHO	-CH=NOH·HCl	-C(Cl)=NOH
0— 5	1.5	0	trace		53.4[b]	15.0	0[a]
−5— 0	3.0	0	0		23.0[b]	54.5	19.3
−10—−5	21.5	28	0	0	30.0	23.3	42.1
−15—−10	25.0	30	0	0	5.5	22.3	65.2

a) Starting material of aldoxime was recovered.
b) Combined yield of nitrile and aldehyde. They could not be separated because of their similar boiling points (nitrile; 196°C, aldehyde; 198°C).

Table 2. Results of reaction of thiophene- and 5-chlorothiophene-2-cabohydroxamoyl chlorides with amine

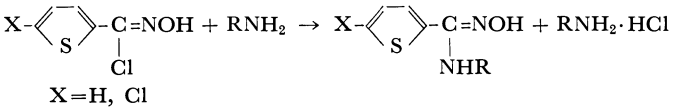

X=H, Cl

RNH_2	Product 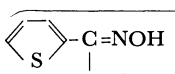					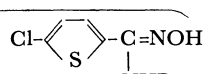				
	Mp (°C)	Yield (%)	Anal. (Calcd), % C	H	N	Mp (°C)	Yield (%)	Anal. (Calcd), % C	H	N
Aniline	90—93	74.5	60.75 (60.54	5.36 4.61	13.65 12.84)	132—134	70	52.21 (52.08	3.58 3.59	10.89 11.09)
p-Toluidine	170 (d)	67.0	62.18 (62.06	5.38 5.21	12.02 12.06)					
Triethylamine*	112—114 (d)	96.5	48.46 (48.01	2.41 2.42	10.99 11.20)	157—159 (d)	100	38.52 (37.46	1.76 1.26	8.58 8.78)

* In these cases, the products were furoxans, and their physical and analytical data are listed.

Table 3. 1,3-Dipolar cycloaddition products (1)

Dipolarophile	Product	Recrystallization solvent	Mp (°C)	Yield (%)	Anal. (Calcd), % C	H	N
$CH_2=CHCOOCH_3$	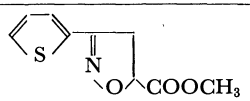		(Oil)[a]	80.7[c]			
$CH_2=C(CH_3)COOCH_3$	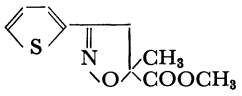		(Oil)[a]	81.0[c]			
$CH_2=CHCONH_2$	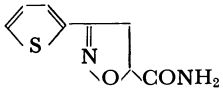	Benzene	160—162	59.0	49.22 (48.98	4.16 4.11	14.32 14.28)
$CH_2=C(CH_3)CONH_2$	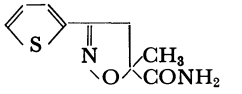	Benzene	160	56.7	50.71 (51.42	5.13 4.80	13.36 13.33)
$CH_2=CHCH_2OH$	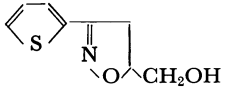	Ligroin	97—98	54.5	52.63 (52.46	4.63 4.95	7.42 7.65)
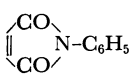	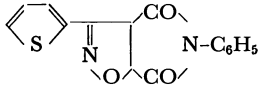	Benzene + Ligroin	170—171	86.5	60.18 (60.40	3.45 3.38	8.97 9.36)
$HC\equiv CCOOCH_3$	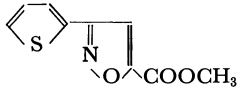	Ligroin	100—101	54.0	51.98 (51.68	3.22 3.37	6.64 6.70)
$CH_3OCOC\equiv CCOOCH_3$	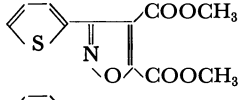	Ligroin	55—56	42.0	49.77 (49.44	3.05 3.40	5.13 5.24)
$HC\equiv C-C_6H_5$	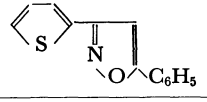	Ligroin	106—107[b]	43.0	69.06 (68.72	3.76 3.99	6.08 6.17)

a) Identified as the corresponding amides derived by treating them with aqueous ammonia solution.
b) Furoxan as a by-product was formed. c) Raw yield.

Table 4. 1,3-Dipolar cycloaddition products (2)

Dipolarophile	Products	Recrystallization solvent	Mp (°C)	Yield (%)	Anal. (Calcd), % C	H	N
$CH_2=CHCOOCH_3$	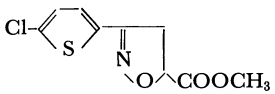	Ligroin	102—103	40.3[a]	44.39 (44.01	3.66 3.28	5.65 5.70)
$CH_2=C(CH_3)CONH_2$	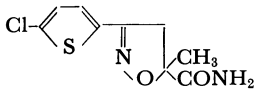	Benzene	182—183	45.0[a]	44.62 (44.18	4.10 3.71	11.43 11.45)
$CH_3OCOC\equiv CCOOCH_3$	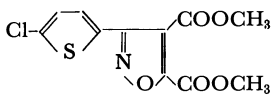	Ligroin	81	23.7[a]	43.95 (43.80	2.96 2.67	4.50 4.65)
$HC\equiv CCOOCH_3$	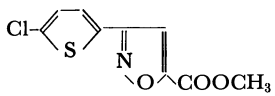	Ligroin	141—142	29.7[a]	44.69 (44.37	2.79 2.48	5.65 5.75)

a) Furoxan as a by-product was formed.

II. Reaction of Thiophene- and 5-Chlorothiophene-2-carbohydroxamoyl Chlorides.

II-1. Reaction with Amines. The amidoxime derivatives were obtained by the reaction of hydroxamoyl chloride with aniline or *p*-toluidine.

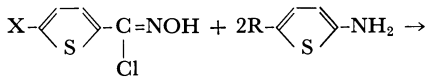

X=H (III) R=H, CH_3
X=Cl (IV) R=H

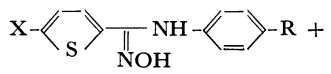

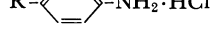

the presence of chlorine on 5-position in thiophene ring gave profound effect on the reaction of thiophenecarbohydroxamoyl chloride with amines. Thiophene-2-carbohydroxamoyl chloride reacted explosively with amines in the absence of solvent, but 5-chlorothiophene-2-carbohydroxamoyl chloride did not react unless it was heated. The influence of chlorine on 5-position to the reactivity was also observed in an aldoxime. When 5-chlorothiophene-2-carboxaldoxime was heated in an aqueous alkaline solution, it rearranged readily to 5-chlorothiophene-2-carbonamide, but thiophene-2-carboxaldoxime gave only alkali salt, and could be was recovered by treating the salt with acid.

Thiophenecarbohydroxamoyl chlorides gave furoxan in a quantitative yield in the presence of triethylamine.

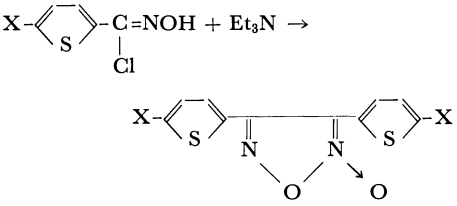

The furoxan derived from 5-chlorothiophenecarbohydroxamoyl chloride was hardly soluble in usual organic solvents and was decomposed slowly above 100°C, whereas the furoxan derived from thiophenecarbohydroxamoyl chloride was more stable. Results are summarized in Table 2.

II-2. 1,3-Cycloaddition Reaction. When hydroxamoyl chloride was treated with triethylamine in the presence of alkenes or alkynes, it reacted with them preferentially. For example, 3-(2-thienyl)-4,6-dioxo-3a,4,5,6a-tetrahydro-6*H*-pyrrolo-[3,4-d]-isoxazole was obtained from thiophene-2-carbohydroxamoyl chloride and *N*-phenylmaleimide. It would be reasonable to consider that thiophenecarbohydroxamoyl chloride reacts with double bond or triple bond through nitrile *N*-oxide as an intermediate.

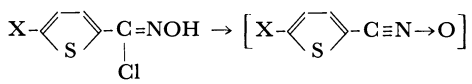

X=H (III) X=H (I)
X=Cl (IV) X=Cl (II)

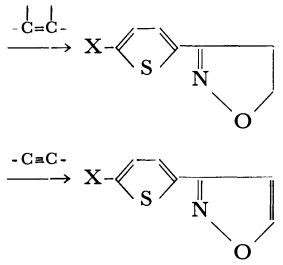

Results of 1,3-cycloaddition reaction are shown in Tables 3 and 4.

Allyl alcohol was less reactive upon hydroxamoyl chloride than maleimide. Such a result would be interpreted by following consideration accepted generally. 1,3-Dipolar cycloaddition reaction was enhanced by electron-withdrawing group in dipolarophile.[1] Further, a difference in the reactivity was observed between thiophene and 5-chlorothiophene derivative. Furoxan was obtained as a by-product in every reaction of 5-chlorothiophene derivative. Therefore, the reactivity of 5-chlorothiophenecarbohydroxamoyl chloride seems to be reduced by chlorine atom at 5-position. This might be explained by resonance effect of chlorine substituent.

Experimental

5-Chlorothiophene-2-carboxaldehyde. 5-Chlorothiophene-2-carboxaldehyde was prepared by Vilsmeier reaction[10] from 2-chlorothiophene, bp 105—107°C/19 mmHg (lit.[11] 100—105°C/18 mmHg).

Thiophene-2-carboxaldoximes. The oxime was prepared by treating 1 mol of thiophenecarboxaldehyde with 1.1 mol of hydroxylamine hydrochloride and 1.1 mol of sodium hydroxide in aqueous ethanol solution. Thiophene-2-carboxaldoxime was recrystallized from benzene, mp 136°C (lit.[12] 135—136°C). 5-Chlorothiophene-2-carboxaldoxime; mp 140°C (from EtOH) (lit.[11] 140°C).

Thiophenecarbohydroxamoyl chlorides. A solution of 19.7 g (0.155 mol) of the thiophene-2-carboxaldoxime in 250 m*l* of anhydrous ether was cooled below −10°C. Into the stirred solution was added a solution of 35 g (0.54 mol) of nitrosyl chloride in 180 m*l* of anhydrous ether in 30 min under dry nitrogen atmosphere. After the reaction mixture was allowed to stand at a temperature below −10°C for 5 hr, another 200 m*l* of anhydrous ether was added. Stirring and introducing nitrogen gas were continued until the evolution of hydrogen chloride stopped. It took about

10) "Org. Syntheses," Coll. Vol. IV, p. 915 (1963).
11) P. Fournari and J. P. Chane, *Bull. Soc. Chim. France*, **1963**, 479; *Chem. Abstr.*, **59**, 1570 (1963).
12) P. Grunanger and P. V. Finzi, *Gazz. Chim. Ital.*, **89**, 1771 (1959); *Chem. Abstr.*, **55**, 4480 (1961).

evolution of hydrogen chloride stopped. It took about 25 hr.

After filtration of oxime hydrochloride, the solvent was removed under reduced pressure without heating, and light brown solid and small amount of oil were obtained. The solid was recrystallized from ligroin to give colorless crystals of thiophene-2-carbohydroxamoyl chloride (III), 11 g (44%), mp 102°C.

Found: C, 37.54; H, 2.81; N, 8.49%. Calcd for C_5H_4ClNOS: C, 37.17; H, 2.50; N, 8.67%.

The oily product was identified as thiophene-2-carboxaldehyde by IR.

In a similar way 5-chlorothiophene-2-carbohydroxamoyl chloride (IV) was prepared, mp 127—128°C (ligroin).

Found: C, 30.48; H, 1.75; N, 7.12%. Calcd for $C_5H_3Cl_2NOS$: C, 30.64; H, 1.54; N, 7.15%.

5-Chlorothiophene-2-carboxaldehyde was also detected by IR.

5-Chlorothiophene-2-carbonamide. In 20 m*l* of 0.1 N aqueous sodium hydroxide solution was dissolved 0.1 g of 5-chlorothiophene-2-carboxaldoxime, refluxed for 30 min and was allowed to stand overnight. The reaction mixture was evaporated under reduced pressure to give a solid mass. Extraction and recrystallization of this solid with benzene gave white needles, 5-chlorothiophene-2-carbonamide, mp 178°C (lit.[13] 179°C, 181°C). IR(KBr): -NH(3400, 3200 cm^{-1}), amide I (1685 cm^{-1}) and amide II (1600 cm^{-1}).

Reaction of III and IV with Aniline and *p*-Toluidine. To a solution of 0.5 g of III in 20 m*l* of anhydrous THF, 0.56 g of aniline (0.006 mol) was added dropwise, and white needles formed within a few minutes. The reaction mixture was refluxed for 2 hr and allowed to stand overnight. The needles deposited were filtered and the filtrate was evaporated *in vacuo* to give a solid mass, which was recrystallized from benzene - *n*-hexane to yield crystals, mp 90—93°C. The reaction of III with *p*-toluidine and of IV with aniline were conducted similarly.

Reaction of III and IV with Triethylamine. To a mixture of 20 m*l* of anhydrous THF and 0.5 g (0.003 mol) of III was added 0.4 g (0.004 mol; 30 mol% excess) of triethylamine at room temperature with stirring. The reaction mixture was allowed to stand for 2 days. The precipitate was filtered off and washed with anhydrous THF. Combined THF solution was evaporated *in vacuo* to afford white mass. Recrystallization from THF - benzene gave white powder of 2,2'-dithienylfuroxan, mp 112—114°C (dec.). This furoxan was soluble in THF, but hardly soluble in benzene, toluene, carbon tetrachloride, chloroform, methanol, ethanol, and water. The reaction of IV with triethylamine was conducted by the similar procedure as described above.

Reaction of III and IV with Various Dipolarophiles (1,3-Dipolar Cycloaddition Reaction). All of the reaction were conducted in anhydrous THF using triethylamine as a hydrogen chloride acceptor. In each reaction, 30 mol% excess amount of a dipolarophile was used. A typical example of the reaction is as follows. To a mixture of 10 m*l* of anhydrous THF, 0.5 g (0.003 mol) of III and 0.7 g (0.004 mol) of *N*-phenylmaleimide was added dropwise 0.5 g (0.0031 mol) of triethylamine at −5°C with stirring. Triethylamine hydrochloride formed immediately. The reaction mixture was allowed to stand overnight at room temperature. The triethylamine hydrochloride was filtered and washed with a large amount of anhydrous THF. The solid product was obtained by removing the solvent from the filtrate. Recrystallization three times from benzene gave 0.8 g (87%) of colorless needles, mp 170—171°C.

13) R. Graft, *Ann.*, **661**, 141 (1963); G. Kuhnhanss, *J. Prakt. Chem.*, **3**, 137 (1956).

BULLETIN OF THE CHEMICAL SOCIETY OF JAPAN VOL. 41 2960—2963 (1968)

Studies on Heteroaromaticity. XXI.[1] 1,3-Dipolar Cycloaddition of *N*-Phenyl-*C*-(6-uracilyl)nitrone

Tadashi SASAKI and Moriyasu ANDO

Institute of Applied Organic Chemistry, Faculty of Engineering, Nagoya University, Chikusa-ku, Nagoya

(Received March 1, 1968)

N-Phenyl-*C*-(6-uracilyl)nitrone (II) was prepared in 80% yield from orotaldehyde (I) and phenylhydroxylamine. II underwent 1,3-dipolar cycloaddition reactions with several ethylenic and acetylenic compounds to afford the corresponding isoxazolidines (IIIa—f) and isoxazolines (IVg—i). Similar reactions of II with phenyl isocyanate, carbon disulfide and with enamine were carried out successfully. The structural elucidation of these products was done on the basis of their NMR spectra.

The 1,3-dipolar cycloaddition reactions of nitrones with olefins are known to supply a general synthetic method of isoxazolidines.[2] Many papers have been published on this line, but little has been documented on the nitrones of nitrogen heteroaromatic systems except on ring nitrogen *N*-oxide.[3] A recent publication of the most convenient preparative method for orotaldehyde (I) among hitherto reported ones[4] opened a new synthetic route for preparing new chemical species involving an uracil moiety. This paper is concerned with the 1,3-dipolar cycloaddition of *N*-phenyl-*C*-(6-uracilyl)nitrone (II), a nitrone readily prepared from orotaldehyde (I).

Results and Discussion

Orotaldehyde (I) was treated with phenylhydroxylamine in ethanol according to the general procedure for preparing nitrones[5] to give a nitrone II in 80% yield; II was stable in the air but reactive enough to undergo the 1,3-dipolar cycloaddition reactions with several ethylenic and acetylenic compounds to afford the corresponding isoxazolidines (IIIa—f) and isoxazolines (IVg—i) respectively, as shown in Tables 1 and 2.

As is obvious from Table 1, the 1,3-dipolar cycloaddition of II to α,β-unsaturated carbonyl compounds such as b, c and f, aryl-conjugated alkenes such as d and e, and non-conjugated alkene such as a proceeded similarly with high yields, but it was necessary for a to be heated for a longer time than when b was used. In each case, the reaction time was seemingly parallel to the reactivity of the used dipolarophile. In fact, the reaction with maleic anhydride, which is regarded as one of the strongest dipolarophiles,[6] resulted in the formation of intractable tars even on cooling, and the reaction with *trans*-stilbene, which is a weak dipolarophile, resulted in recovering the starting materials even on heating the reaction mixture for 1 day. With acetylenic compounds, the reactions were carried out in dioxane instead of dimethylformamide (DMF) for avoiding the reaction of DMF with such acetylenic compounds.[7] As illustrated in Table 2, the yields were generally lower than those with ethylenic compounds, presumably because of their lower reactivity as dipolarophiles and higher tendency to the thermal polymerization. In fact, the thermal polymerization was clearly observed in the reactions of II with dimethyl acetylenedicarboxylate, propargyl bromide, ethyl phenylpropiolate and chlorocyanoacetylene,[8] all resulted in the thermal polymerization of used alkynes and in recovering II, except those with propargyl alcohol (g), cyanoacetylene (h)[9] and phenylacetylene (i), which afforded the corresponding isoxazolines (IVg—i) as indicated in Table 2.

Conversion of II to III is clearly observed in the

1) Part XX of this series: T. Sasaki and T. Yoshioka, this Bulletin, **42**, 258 (1969).
2) R. Huisgen, R. Grashey and J. Sauer, "Cycloaddition Reactions of Alkenes" in 'The Chemistry of Alkenes', S. Patai, Ed., Interscience Publishers, New York, N. Y. (1964), p. 861.
3) R. Grashey, R. Huisgen and H. Leitmann, *Tetrahedron Letters*, **1960**, 9; W. E. Noland and D. A. Jones, *Chem. & Ind.*, **1962**, 363; H. Seidl and R. Huisgen, *Tetrahedron Letters*, **1963**, 2022.
4) K-Y. Zee-Cheng and C. C. Cheng, *J. Heterocyclic Chem.*, **4**, 163 (1967).
5) L. I. Smith, *Chem. Revs.*, **23**, 193 (1938).
6) H. Seidl, Ph. D. Thesis, University of Munich, 1963. Ref. 2, p. 865.
7) E. Winterfeldt, *Angew. Chem.*, **79**, 389 (1967).
8) E. Kloster-Jensen, *Acta Chem. Scand.*, **18**, 1629 (1964).
9) C. H. Moureu and J. Ch. Bongrand, *Compt. Rend.*, **151**, 946 (1920); *Arch. Chim.*, (9), **14**, 53 (1920); S. Murahashi, T. Takizawa, S. Kurioka and S. Maikawa, *Nippon Kagaku Zasshi (J. Chem. Soc. Japan, Pure Chem. Sect.)*, **77**, 1689 (1956); L. J. Krebaum, *J. Org. Chem.*, **31**, 4103 (1966).

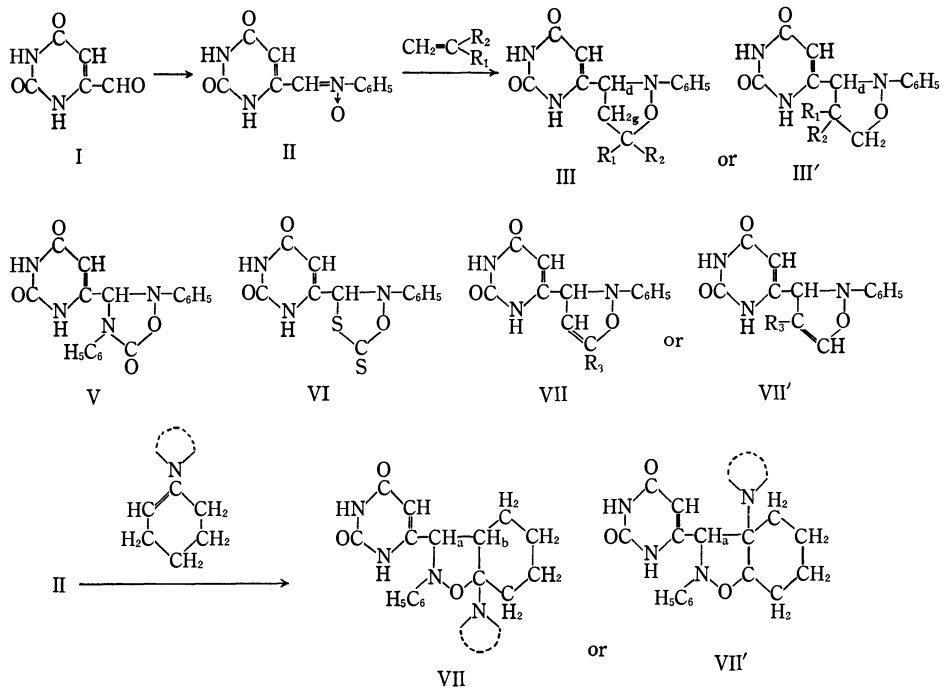

TABLE 1. ISOXAZOLIDINES (III)

	Dipolarophile $CH_2=CR_1R_2$ R_1	R_2	Reaction time hr	Yield %	Product (mp,*1 °C)	Microanalyses Found (Calcd) C	H	N	MeOH UV λ_{max} mμ (log ε)
a	H	CH_2OH	12	100	IIIa (206—209)	58.32 (58.12	5.27 5.23	14.32 14.53)	237(3.18) 260(3.06)
b	H	$COOCH_3$	5	100	IIIb (204—209)	56.49 (56.78	4.86 4.77	12.98 13.24)	236(3.11) 254(3.09)
c	H	$CONH_2$	7	100	IIIc (190—196)	55.43 (55.63	4.44 4.67	18.36 18.54)	236(3.12) 258(3.06)
d	H	C_6H_5	9	100	IIId (206—210)	68.07 (68.05	4.97 5.11	12.31 12.53)	238(3.26) 258(3.11)
e	H	C_5H_4N	8	100	IIIe (210—214)	64.44 (64.28	4.55 4.79	16.57 16.66)	234(3.18) 256(3.12)
f	CH_3	$COOCH_3$	5	86	IIIf (200—204)	57.63 (58.00	4.93 5.17	12.57 12.68)	244(3.18)

*1 decomp.

TABLE 2. ISOXAZOLINES (IV)

	Dipolarophile $HC\equiv CR_3$ R_3	Reaction time hr	Yield %	Product (mp, °C)	Microanalyses Found (Calcd) C	H	N	MeOH UV λ_{max} mμ (log ε)
g	CH_2OH	24	62	IVg (188—189)	55.63 (55.81	4.08 4.35	18.67 18.60)	241 (3.98)
h	CN	24	48	IVh (181—183)	59.61 (59.57	3.43 3.57	20.01 20.19)	241 (3.92)
i	C_6H_5	48	61	IVc (192—194)	68.47 (68.46	4.48 4.45	12.44 12.61)	242 (4.14)

comparison of their ultraviolet and infrared spectra; in the ultraviolet spectra as indicated in Fig. 1 and Table 1, which IIIa—e show the similar patterns of absorptions except IIIf, all indicating hypsochromic shifts compared with that of II. This suggests interruption of the conjugation between the pyrimidine ring and a substituent at the 6-position in II by the conversion. In the infrared spectra, disappearance of a $\nu_{N\to O}$ absorption[10] after the conversion also supports the occurrence of the 1,3-dipolar cycloaddition. In the ultraviolet spectral comparison of III and IV, slightly bathochromic shifts of IV indicate the increase in unsaturation of IV, but other general patterns resemble each other as shown in Tables 1 and 2.

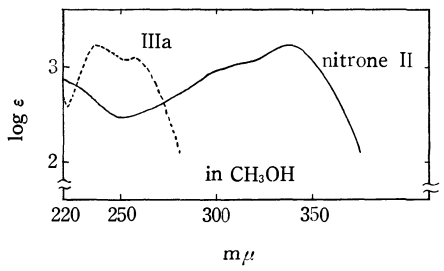

Fig. 1. UV absorption spectra of II and IIIa.

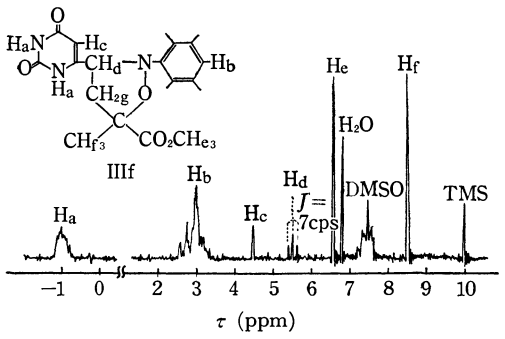

Fig. 2. NMR spectrum of IIIf (DMSO-d_6).

For III, there are two possible structures, III and III', depending on two different directions of addition. In the NMR spectrum in DMSO-d_6, a signal due to H_d was observed at 5.37τ as a triplet, (J=7.0 cps), as shown in Fig. 2, and consequently IIIf was concluded to be a correct structure.*1 Similarly, appearance of a H_d signal at 5.25 τ as a quartet supports IIId structure. The fact that no reaction had occurred between II and ethyl cinnamate even on heating for a longer time may be explained by the steric hindrance of a

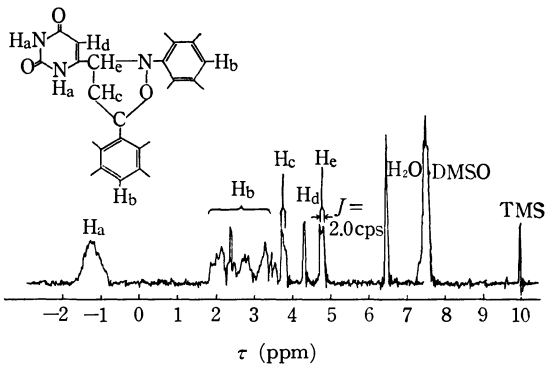

Fig. 3. NMR spectrum of IVi.

bulky phenyl group attached to the vinyl carbon of the cinnamate.

The structural elucidation of IV was carried out on the basis of their NMR spectra. For example, IVi was confirmed to be a 5-substituted isoxazoline from its NMR spectrum as shown in Fig. 3.

For further investigation of the reactivity of this nitrone, II was treated with heterocumulenes like phenyl isocyanate, carbon disulfide, phenyl isothiocyanate, benzoyl isocyanate and benzoyl isothiocyanate, and with enamines. Among these dipolarophiles, the first two and the last one were successfully subjected to the 1,3-dipolar cycloaddition; in the reaction with phenyl isocyanate, a catalytic amount of triethylamine was added to the reaction mixture, since without triethylamine, no reaction had occurred. In the reaction with carbon disulfide, the yield of the product was below 10%. A recent publication of the formation of isoxazolidines by the reactions of enamines with diphenylnitrone[11] prompted us to report our results. The reaction of II with 1-morpholino-1-cyclohexene was carried out in a sealed tube under nitrogen, because the same reaction in the air resulted in the formation of intractable tars.

For the reaction product of II with the enamine, there are two possible structures, VII and VII', assumable, depending on two directions of addition. Appearance of a signal due to H_a at 4.56 τ in the NMR spectrum in DMSO-d_6 indicates that VII is preferable to VII'. The coupling constant J_{ab} was 3.8 cps, which is different from the value reported by Nomura and his coworkers.[11]

Experimental

All the melting points are uncorrected. Infrared spectra were determined on a Nippon Bunko IR-S type spectrometer and electronic spectra were obtained with a Nippon Bunko optical rotary dispersion recorder,

10) L. G. Bellamy, "The Infrared Spectra of Complex Molecules," 2nd Ed., John Wiley and Sons, Inc., New York, N. Y. (1958), pp. 115, 305.

*1 For IIIf, a signal due to H_d should be a triplet or a quartet by the presence of vicinal protons. H_g, on the contrary, for IIIf', it should be a singlet because of the absence of a vicinal proton.

11) Y. Nomura, F. Furusaki and Y. Takeuchi, This Bulletin, **40**, 1740 (1967).

12) W. Schulze and Wullitzer, *J. prakt. Chem.*, **33**, 50 (1966).

Model ORD/UV-5. NMR spectra were determined on a Varian A-60 spectrometer, with tetramethylsilane as an internal standard and the peak positions are expressed by τ-values.

***N*-Phenyl-*C*-(6-uracilyl)nitrone (II).** Orotaldehyde (I)[4] (1 g) was suspended in 30 m*l* of ethanol and 0.8 g of phenylhydroxylamine was added to this suspension. The reaction mixture was refluxed for 2 hr until the suspension of I went into solution. After cooling, the precipitates were filtered and recrystallized from ethanol to give II as yellow needles, mp 280—285°C. IR (KBr) cm^{-1}: 1060 ($\nu_{N\to O}$). NMR (DMSO-d_6)τ: −1.20 (2H, broad, NH), 1.49 (1H, singlet, –CH–N–), 2.0—2.5 (5H, multiplet, phenyl protons), 3.35 (1H, singlet, 5-C–H).

Found: C, 57.39; H, 3.63; N, 17.98%. Calcd for $C_{11}H_9O_3N_3$: C, 57.14; H, 3.92; N, 18.18%.

All attempts for preparing II from 6-methyluracil by the reported procedures[12] were unsuccessful.

2-Phenyl-3-(6-uracily)-5-hydroxymethylisoxazolidine (IIIa). To a suspension of 0.2 g of II in 20 m*l* of dry DMF was added 0.5 m*l* of allyl alcohol with stirring. The mixture was heated at 85°C for 12 hr with occasional stirring until the suspension went into solution. After cooling, excess allyl alcohol and DMF were removed under reduced pressure to afford 0.23 g of IIIa as colorless crystals. The mps, yields, elemental analyses and ultraviolet spectra of the reaction products with several ethylenic compounds are summarized in Table 1.

2-Phenyl-3-(6-uracilyl)-5-hydroxymethylisoxazoline (IVg). To a suspension of 0.2 g of II in 20 m*l* of dry dioxane was added 0.5 m*l* of propargyl alcohol. The mixture was fused in a glass tube and heated at 100°C for 1 hr until a clear solution was obtained. After removing an excess amount of propargyl alcohol and dioxane under reduced pressure, the oily residue was dissolved in methanol and a crystalline material precipitated upon addition of ether was recrystallized from tetrahydrofuran to yield IVg as colorless crystals. The yields, mps, elemental analyses and ultraviolet spectral data of the reaction products with several acetylenic compounds are summarized in Table 2.

2-Phenyl-3-(6-uracilyl)-4-phenyl-1,2,4-oxadiazole-5-one (V). Three drops of triethylamine was added to a suspension of 0.3 g of II in 15 m*l* of dioxane and 0.12 m*l* of phenyl isocyanate. The mixture was fused in a glass tube and heated at 85°C for 2 days until a clear solution was obtained. After removing the distillable parts from the reaction mixture under reduced pressure on a water bath, the residue was extracted with 1 m*l* of ethyl acetate - acetone (1 : 1). Solvents were removed from the extract and the residue was recrystallized from benzene-ethyl acetate to afford 0.28 g (62%) of a 1 : 1 adduct (V) as pale yellow crystals, mp 254°C. IR (KBr): 1825 cm^{-1} (ν_{CO}). UV λ_{max}^{MeOH} mμ (log ε): 366 (3.00), 256 (3.84), 222 (4.18).

Found: C, 61.31; H, 3.79; N, 16.00%. Calcd for $C_{18}H_{14}O_4N_4$: C, 61.71; H, 4.03; N, 15.99%.

4-(6-Uracilyl)-5-phenyl-1,3,5-oxathiazole-2-thione (VI). To a suspension of 0.3 g of II in a mixture of 2 m*l* of carbon disulfide and 15 m*l* of dry dioxane was added 3 drops of triethylamine. The mixture was fused in a glass tube filled up with nitrogen and heated at 85°C for 3 days. Work-up as above afforded a 1 : 1 adduct (VI) in 10% yield. Mp 218°C after recrystallization from ethyl acetate. IR (KBr): 1300 cm^{-1} (ν_{CS}). UV λ_{max}^{MeOH} mμ (log ε): 308 (3.75, shoulder), 253 (3.88, shoulder), 253 (3.88, shoulder).

Found: C, 46.16; H, 3.42; N, 12.99%. Calcd for $C_{12}H_9O_3N_3S_2$: C, 46.89; H, 2.95; N, 13.67%.

Reaction of II with 1-Morpholino-1-cyclohexene. A mixture of 0.3 g of II and 0.5 g of 1-morpholino-1-cyclohexene was added to 15 m*l* of dioxane. The resulting mixture was fused in a glass tube filled up with nitrogen and heated at 85°C for 3 days. After removing the distillable parts from the reaction mixture under reduced pressure on a water bath, the residue was dissolved in 5 m*l* of benzene. Upon addition of ether, 0.36 g (72%) of a 1 : 1 adduct (VII) precipitated as brown crystals, mp 203°C. UV λ_{max}^{MeOH} mμ (log ε): 265 (4.09, shoulder), 245 (4.26). NMR (DMSO-d_6)τ: 2.49—3.24 (multiplet, phenyl protons), 4.17 (singlet, 5-C–H), 4.56 (doublet, J=3.8 cps, 3-C–H), 7.0—7.7 (multiplet, morpholine ring protons), 8.0—9.0 (multiplet, cyclohexane ring protons).

Found: C, 63.70; H, 6.90; N, 13.82%. Calcd for $C_{21}H_{26}O_4N_4$: C, 63.30; H, 6.58; N, 14.06%.

The authors are much indebted to Mr. Akiho Ishihara for elemental analyses and to be Dainippon Pharmaceutical Co. for the NMR measurement.

BULLETIN OF THE CHEMICAL SOCIETY OF JAPAN VOL. 41 2964—2969 (1968)

Studies of Heteroaromaticity. XXIV. 1,3-Dipolar Cycloaddition of *C*-(5-Nitro-2-furyl)-*N*-phenylnitrone[1]

Tadashi SASAKI, Toshiyuki YOSHIOKA and Iwao IZURE

Institute of Applied Organic Chemistry, Faculty of Engineering, Nagoya University, Chikusa-ku, Nagoya

(Received April 15, 1968)

C-(5-Nitro-2-furyl)-*N*-phenylnitrone (I) was prepared from 5-nitro-2-furfural and phenylhydroxylamine in an 80% yield. The 1,3-dipolar cycloaddition reactions of I with various olefins were carried out, and the corresponding 5-substituted isoxazolidine derivatives were obtained. The structual elucidation of these products was made on the basis of the nmr spectral data. Several observations support the theory that these reactions proceed *via* a concerted one-step process.

In a previous paper[2] we reported the 1,3-dipolar cycloaddition reactions of a nitrone derived from orotaldehyde. This paper will deal with its preparation and with its 1,3-dipolar cycloaddition reactions with several olefins of a nitrone containing a nitrofuran ring as a heaterocyclic side chain. Furthermore, the structural elucidation of the products will be discussed, mainly on the basis of the nmr spectral data.

Results and Discussion

C-(5-Nitro-2-furyl)-*N*-phenylnitrone (I) was prepared from 5-nitro-2-furfural and phenylhydroxylamine in an 80% yield by the usual procedure.[3] All attempts to synthesize I by the thermal isomerization of the corresponding oxaziridine derivative (III), which might be produced as an intermediate in the direct peracetic acid-oxidation of *N*-(5-nitro-2-furfurylidene)aniline (II), were unsuccessful, though this is regarded as a general procedure for preparing nitrones,[4] and from the tar-like products, 5-nitro-2-furanilide (IV) was isolated as a crystalline product in a 20% yield. Various alkyloxaziranes are known to be converted to amides under pyrolytic conditions through such a concerted rearrangement mechanism as:[5]

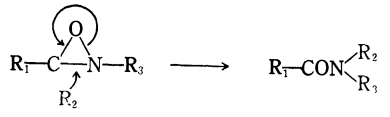

This amide (IV) is, therefore, assumed to be produced *via* the oxazirane (III) by a mechanism similar to that are described above; in fact, IV could not be isolated from the reaction of I with acetic anhydride when heated as low as 80°C.

The nitrone structure of I was confirmed by the elemental analysis and by the presence in the infrared spectrum of a 1096 cm^{-1} absorption due to $\nu_{N\rightarrow O}$. A bathochromic shift of the ultraviolet absorption maximum of I compared with that of II (*cf.* Fig. 1) indicates some contribution to a conjugation of an azomethine linkage with a nitrofuran ring by the formation of N→O bonding.

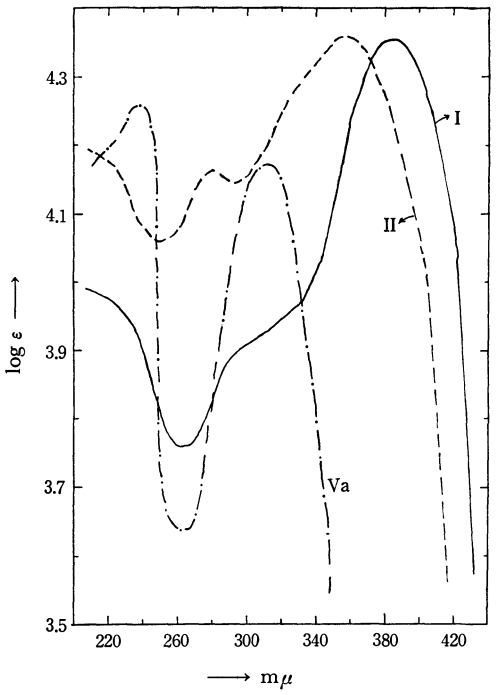

Fig. 1. UV comparison of I, II and Va (in EtOH).

1) Part XXIII of this series: T. Sasaki and T. Yoshioka, This Bulletin, submitted.
2) Part XXI of this series: T. Sasaki and A. Ando, This Bulletin, **41**, 2960 (1968).
3) L. I. Smith, *Chem. Revs.*, **23**, 193 (1938).
4) M. F. Hawthorne and R. D. Strahm, *J. Org. Chem.*, **22**, 1263 (1957).
5) W. D. Emmons, "Oxaziranes" in 'Heterocyclic Compounds,' A. Weissberger, ed., InterscincePu blishers, New York, N. Y. (1964), p. 635.

I was sensitive to the light and gradually decomposed to a black tar; therefore, it must be stored in a dark and cool place.

The 1,3-dipolar cycloaddition of I was carried out both in ethanol and in toluene at each refluxing temperature by using several olefins. The results are summarized in Table 1.

As is obvious from this table, the yields of Va, for instance, were 41% after 5 hrs' refluxing in ethanol and 98% after 2 hrs' refluxing in toluene,

Table 1. 1,3-Cycloaddition with olefins

Olefin	Reaction temp.,* °C	Reaction time, hr	Yield %	Product (mp, °C)	UV λ_{max}^{EtOH} mμ ($\varepsilon \times 10^{-4}$)	Microanalyses Found (Calcd) C	H	N
Styrene	E	5	41**	Va	314(1.2)	68.31	4.39	8.52
	T	2	98	(118)	236(1.5)	(68.85	4.80	8.33)
4-Vinylpyridine	E	30	26**	Vb	311(1.0)	64.05	4.10	11.85
	T	6	88	(107)	232(1.3)	(64.09	4.48	12.46)
Isoprene***	90	24	31	Vc	313(1.6)			9.07
				(80)	233(1.9)			(9.33)
Allyl alcohol	E	72	16**	Vd	311(1.5)	57.70	4.57	9.30
	T	3.5	95	(100)	231(1.6)	(57.93	4.86	9.65)
Allyl bromide	T	2	66	Ve	313(2.0)	47.82	2.96	7.74
				(126)	233(2.1)	(47.61	3.71	7.93)
Acryl amide	T	4	77	Vf	311(1.8)	55.40	4.09	13.28
				(124)	230(1.9)	(55.44	4.32	13.86)
trans-Stilbene	T	12	7	Vg	311(2.3)	73.37	4.57	6.88
		48	10	(125)	237(3.1)	(72.80)	4.89	6.79)
Dicyclopentadiene	E	48	16**	Vh+Vh'				
	T	4	47	Vh	313(1.7)	69.37	5.37	7.54
				(184)	231(2.2)			
			19	Vh'	312(1.8)	69.41	5.41	7.46
				(133)	241(1.2)	(69.21	5.53	7.69)
Cyclooctadiene	T	9.5	61	Vi	312(1.4)	67.22	5.53	8.06
				(115)	229(2.5)	(67.04	5.92	8.23)
Methallyl chloride	T	12	44	Vj	313(1.9)	55.80	4.44	8.71
				(109)	238(2.0)	(55.82	4.67	8.67)

* E: refluxing in ethanol T: refluxing in toluene.
** accompanied with the recovered I.
*** in a sealed tube.

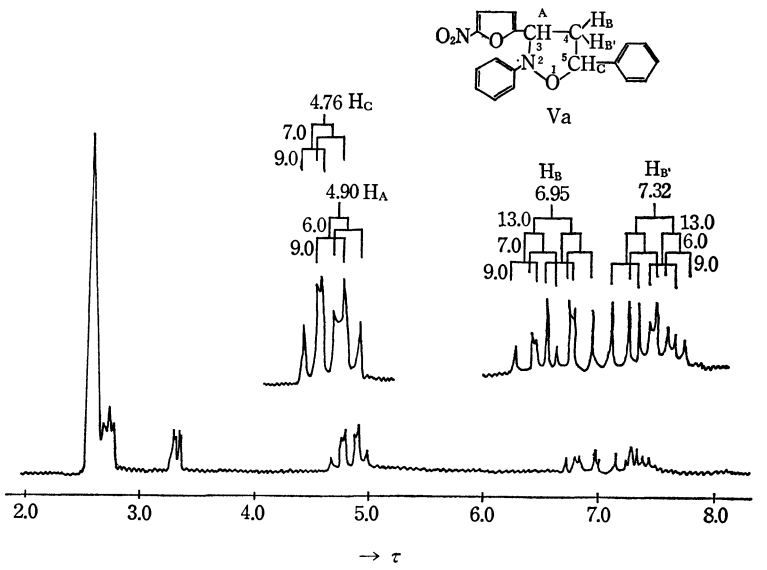

Fig. 2. NMR spectrum of Va (in $CDCl_3$ by τ-values).

indicating these reactions proceeded by the general principle of the larger temperature dependence rather than the polarity dependence of the solvent used.[6] This trend can be observed in other cases in Table 1. It can be concluded that the yields of the 1,3-dipolar cycloaddition products are much more influenced by the reaction temperature and by the steric factor of the dipolarophilic olefins than by the polarity of the solvent and by the electronic character of the olefins. All these features seem to support the theory that the 1,3-dipolar cycloaddition of I proceeds *via* the concerted one-step mechanism suggested by Huisgen.[8]

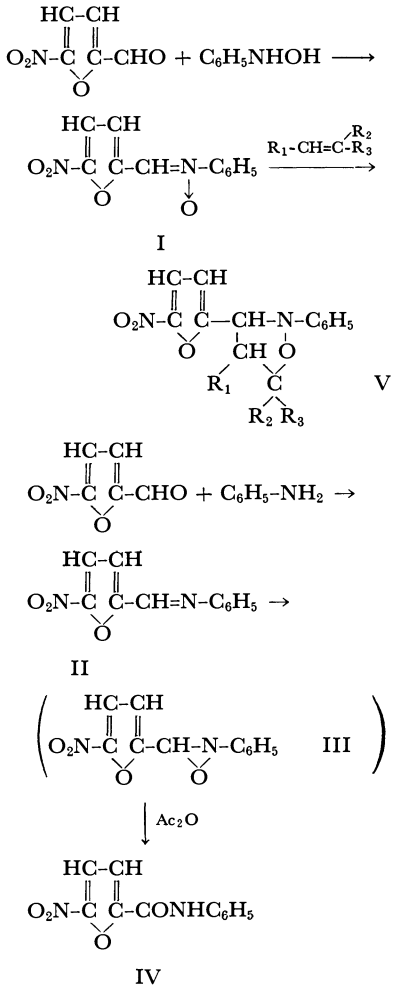

The occurrence of the cycloaddition of I at the N→O linkage is established by the disappearance of an N→O absorption in the infrared spectrum of Va; it is further supported by a hypsochromic shift of Va compared with that of I in their ultraviolet spectra, as is indicated in Fig. 1. For Va, there are two possible structures, Va and Va', depending on which of two different directions of addition holds. Figure 2 shows the nmr spectrum of Va, in which the signals at 2.5—3.5 τ (12 H) are readily assignable to benzene and nitrofuran ring protons, while those at 4.90 τ (1 H, quartet) and at 4.76 τ (1 H, quartet) should be assigned to two methine protons at the C-3 and C-5 respectively of an isoxazolidine ring.[7] These results support a 5-substituted structure for Va rather than the corresponding 4-substituted structure Va'.

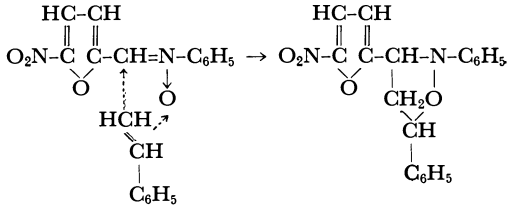

Va: 5-substituted structure

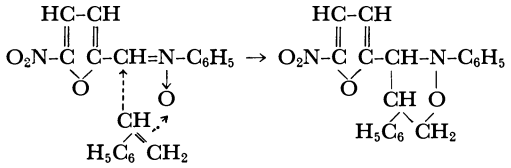

Va': 4-substituted structure

The nmr spectra of other products, which are summarized in Table 2, were similarly considered; all the products seem to have 5-substituted structures.

In the reaction with dicyclopentadiene, two products, Vh and Vh', with the same elemental analyses and only slightly different ultraviolet spectra, but with different nmr spectra could be isolated. (*Cf.* Tables 1 and 2). Alder and Stein[9] have distinguished *endo-* and *exo*-dicyclopentadiene by their chemical conversion to their adducts with phenyl azide and Bruson and others[10] have repotred that *endo*-dicyclopentadiene reacts under acidic conditions with proton donors to give products possessing the *exo*-configuration. At the same time, the possibility of the *endo-* and *exo*-attack of I on dicyclopentadiene should be considered, since a similar type of attack has been observed in the 1,3-dipolar cycloaddition of diphenylnitrilimine to

6) R. Huisgen, R. Grashey and Sauer, "Cycloaddition Reactions of Alkenes" in 'The Chemistry of Alkenes,' S. Patai, ed., Interscience Publishers, New York, N. Y. (1964), p. 865.

7) 5.27τ for C-3-H and 4.85 for C-5-H of 3-(6-uracilyl)-2,5-diphenylisoxazolidine.[2] 5.01τ for C-3-H and 4.55 for C-5-H of 3-(2-benzimidazolyl)-2,5-diphenylisoxazolidine. T. Sasaki and T. Ohishi, This Bulletin, **41**, 3012 (1968).

8) R. Huisgen, L. Feiler and G. Binsch, *Angew. Chem. Intern. Ed. Engl.*, **3**, 753 (1964).

9) K. Alder and G. Stein, *Liebigs Ann.*, **504**, 216 (1933).

10) H. A. Bruson and T. W. Riener, *J. Am. Chem. Soc.*, **67**, 723, 1178 (1945); P. D. Bartlett and A. Schneider, *ibid.*, **68**, 6 (1946); F. Bergman and H. Japhe, *ibid.*, **69**, 1826 (1947).

TABLE 2. NMR OF ISOXAZOLIDINES (τ)

	C-3-H	C-4-H	C-5-H	Solvent	Remark
Va	4.90(q)	7.10(m)	4.76(q)	$CDCl_3$	*Cf.* Fig. 1
Vb	4.89(q)	6.85(q) 7.36(q)	4.72(q)	$CDCl_3$	
Vc	5.00(m)	7.36(m)		$CDCl_3$	4.92(d) (J=8.0 cps) 5.32(t) (J=8.0 cps) } for $-CH=CH_2$
Ve	4.48(q)	7.17(q) 7.40(q)	5.40(m)	$CDCl_3$	
Vf	4.71(q)	7.00(m)	5.30(q)	DMSO-d_6	
Vg	4.88(q)	5.99(q)	4.73(d)	$CDCl_3$	
Vh	4.95(q)	7.10(m)	5.70(m)	$CDCl_3$	
Vh'	5.59(q)	7.40(m)	6.00(m)	$CDCl_3$	
Vj	5.04(q)	6.98(q) (J=13 and 8 cps) 7.53(q) (J=5 and 13 cps)		$CDCl_3$	

d: doublet, q: quartet, m: multiplet (τ-values are given by that of its center)

norbornene.[11] As is shown in Table 2, the shift of a C-3-H signal for Vh' to a higher magnetic field than that for Vh, which is located in the normal region of 4.95 τ, may be explained by postulating for Vh' the structure of an adduct produced by the *endo*-attack of I on *endo*-dicyclopentadiene,[12] in which the anisotropy effect of a neighboring ethylenic linkage of the cyclopropene ring caused a shift of C-3-H to a higher magnetic field.

The conversion of the 1,3-dipolar cycloaddition reaction of I with isoprene was as high as 95% after their purification by column chromatography; it was found on TLC[13] to be a mixture of two products, which were separated by fractional crystallization to Vc as a high-melting-point fraction and Vc' as a low one. The presence of a vinyl absorption in the infrared spectrum of Vc at 990 and 910 cm^{-1} [14] and that of a terminal methylene in Vc' at 890 cm^{-1} [14] suggest that their structures are as follows:

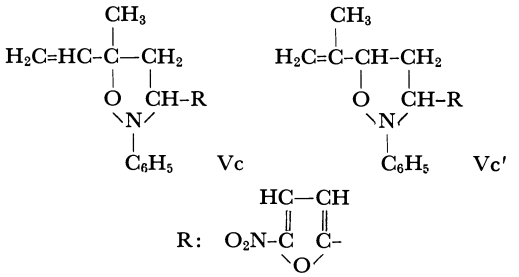

The validity of Vc structure was further confirmed by the nmr spectrum, as is illustrated in Table 2.

So far the 1,3-dipolar cycloaddition of nitrones has been reported mainly with olefins,[15] and only a few times with acetylenic compounds.[2] I was treated with phenylacetylene, propargyl bromide, and propargyl alcohol, but instead of the expected isoxazolines, an anil, II, and amide, IV, were isolated, as is shown in Table 3: the main product was a black polymer with a mp of over 300°C.

Similarly, the reactions of I with heterocumulenes such as carbon disulfide, dicyclohexylcarbodiimide, and phenyl isocyanate gave only II as an isolated crystalline product; the main product was a black polymer, as is indicated in Table 3. It is noteworthy that in the latter reactions, no amide (IV) formation could be observed. The similar treatment of I in the absence of any dipolarophile resulted only in the formation of black tars. The

11) R. Huisgen, H. Knupfer, R. Sustman, G. Wallbillich and V. Weberdorfer, *Chem. Ber.*, **100**, 1580 (1967).

12) The commerical dicyclopentadiene is known to possess the *endo*-configuration mainly. Therefore, two possible structures can most reasonably assigned to the products depending on the *endo*- and *exo*-attack of I on *endo*-dicyclopentadiene. About their absolute configuration, a more detailed investigation is necessary.

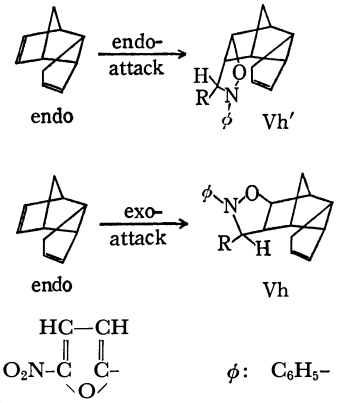

13) Thin layer chromatograghy on silica-gel, using chloroform as the eluent.

14) K. Nakanishi, "Sekigaisen Kyushu Spectrum," Nankodo, Tokyo (1960). p. 30.

15) N. A. Le Bel and J. J. Whang, *J. Am. Chem. Soc.*, **81**, 6334 (1959); N. A. Le Bel, C. M. J. Slusarczuk and L. A. Spurlock, *ibid.*, **84**, 4360 (1962); C. W. Brown, K. Marsden, M. A. T. Rogers, C. M. B. Raylor and R. Wright, *Proc. Chem. Soc. (London)*, 254 (1960); R. Grashey, R. Huisgen and H. Leitermann, *Tetrahedron Letters*, **12**, 9 (1960).

TABLE 3. 1,3-CYCLOADDITION WITH ACETYLENES AND HETEROCUMULENES

	Reaction temp., °C	Reaction time, hr	Anil	Amide	Polymer*
Acetylene					
C_6H_5-C≡CH	90	20	13	39	39
Br-CH_2-C≡CH	120	4	3	3	50
OH-CH_2-C≡CH	120	6	3	3	90
Heterocumulene					Recovered I
CS_2	120	12	61	—	27
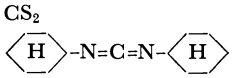	120	22	18	—	77
C_6H_5-N=C=O	120	13	33	—	57

* resin-like, deep-colored substance of mp >300°C

mechanism of the formation of II and IV from I in the above reactions is uncertain at present. However, I was treated with deoxygenator like triphenylphosphine to afford II, as expected.

Similarly, *C*-2-(5-nitro-2-furyl)vinyl-*N*-phenylnitrone (VI) was prepared from β-(5-nitro-2-furyl)acrolein[19] and phenylhydroxylamine; VI was very stable and did not react at all with triphenylphosphine under refluxing in toluene; furthermore, all attempts at the intermolecular cyclization of VI were unsuccessful.

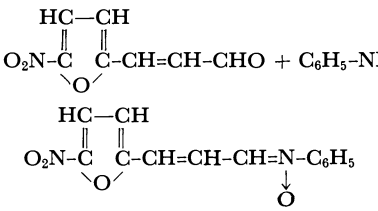

VI

Experimental

All the melting points were determined on a Yanagimoto micromelting-point apparatus and are uncorrected. The microanalyses were carried out on a Yanagimoto C. H. N. Corder, Model MT-1. The infrared spectra were recorded on a JASCO Model IR-S infrared spectrometer, while the nmr spectra were obtained with a Hitachi high resolution NMR spectrometer, Model H-6031, at 60 Mc, and the chemical shifts are reported in τ-values relative to tetramethylsilane as the internal standard. The ultraviolet spectra were measured with a JASCO Model ORD/UV-5 optical rotatry dispersion recorder.

***C*-(5-Nitro-2-furyl)-*N*-phenylnitrone (I).** A solution of 2.8 g (20 mmol) of 5-nitro-2-furfural and 2.2 g (20 mmol) of phenylhydroxylamine in 50 m*l* of ethanol was refluxed at 80°C for 5 min. After cooling, the precipitated yellow crystals were collected and recrystallized from ethanol to give 3.8 g (80%) of I as yellow crystals, mp 184°C (decomp). IR (KBr) cm^{-1}: 1603 ($\nu_{C=N}$), 1096 ($\nu_{N\to O}$).

Found: C, 57.19; H, 3.49; N, 12.18%. Calcd for $C_{11}H_8O_4N_2$: C, 56.90; H, 3.47; N, 12.07%.

Attempts at Synthesizing I. *N*-(5-Nitro-2-furfurylidene)aniline,[16] (II) (0.5 g (2.3 mmol)) was dissolved in 15 m*l* of dichloromethane, and to this solution there was added a solution of peracetic acid, prepared from 0.5 m*l* of 60% hydrogen peroxide and 2.5 g of acetic acid. After the addition of a catalytic amount of 98% sulfuric acid, the reaction mixture was kept standing at room temperature for 12 hr. The mixture was then poured into 250 m*l* of water and extracted with chloroform. The chloroform layer was washed with 5% aqueous ammonia, and then with 10% sulfuric acid, and dried over magnesium sulfate. The removal of the chloroform at room temperature under reduced pressure afforded an oil, whichw as purified by chromatography (silica-gel, chloroform). Yellow needles with a mp of 177°C were separateed from the second fraction, which was characterized as 5-nitro-2-furanilide (II) by a comparison of its IR spectrum with a specimen prepared by a known method.[17]

1,3-Dipolar Cycloaddition of I with Styrene. A mixture of 0.5 g (2 mmol) of I, 1 m*l* of styrene, and 30 m*l* of toluene was refluxed for 2 hr after the addition of five drops of triethylamine as a catalyst. After the distillable parts had been removed under reduced pressure, the residue was dissolved in chloroform and purified on a silica-gel column. Va was obtained as yellow crystals from the first fraction. Similarly, Vb—j were obtained; their yields, UV spectra, and microanalyses are summarized in Table 1.

Reaction of I with Triphenylphosphine. A solution of 0.4 g (1.2 mmol) of I and 0.45 g (1.2 mmol) of triphenylphosphine in 16 m*l* of dry benzene was heated at 90°C in a sealed tube for 2 hr. After the solvent had then been removed under reduced pressure, the residue was purified on a silica-gel column, using chloroform as the eluent. From the first fraction there was obtained a small amount of an oil, which was discarded. 0.15 g (40%) of yellow crystals (mp 124—128°C) was obtained from the second fraction; this substance was identified as II by a comparison of its IR spectrum with that of a specimen[16] and by a mixed-melting-point determination. From the third fraction, 40 mg (10%) of I were recovered, while from the fourth fraction, 0.25 g (60%) of triphenylphosphine oxide, mp 156°C,[18] was obtained.

16) T. Takahashi, H. Saikachi, S. Yoshina and C. Mizuno, *Yakugaku Zasshi (J. Pharm. Soc. Japan)*, **69**, 284 (1949).
17) L. Marquis, *Ann. Chim.*, **4**, 196 (1905).
18) Mp 155°C; V. K. Kucherov, *Zhur. Obshchei Khim.*, **19**, 126 (1949).

Reaction of I with Acetic Anhydride. I (0.4 g (1.7 mmol)) was dissolved in 10 m*l* of acetic anhydride, and the reaction mixture was heated at 140°C for 8 hr.*1 After the excess amount of acetic anhydride had been removed under reduced pressure, water was added to the residue. The resulting precipitates were collected and recrystallized from ethanol to give 0.3 g (75%) of IV, which was confirmed by a comparison of its IR spectrum with a specimen.[16]

***C*-2-(5-Nitro-2-furyl)vinyl-*N*-phenylnitrone (VI).** A solution of 0.34 g (2 mmol) of β-(5-nitro-2-furyl) acrolein[19] and 0.31 g (2 mmol) of phenylhydroxylamine in 10 m*l* of ethanol was refluxed for half an hour; the resulting crystals were collected after cooling and recrystallized from dimethylformamide-ethanol to give 0.42 g (75%) of VI as red crystals, mp 195°C (decomp). IR (KBr): 1070 cm^{-1} ($\nu_{N\rightarrow O}$). UV λ_{max}^{EtOH}: 406 mμ (ε 26000).

Found: C, 60.81; H, 3.96; N, 10.98%. Calcd for $C_{13}H_{10}O_4N_3$: C, 60.46; H, 3.90; N, 10.85%.

*1 As has been described before, I did not react at all with acetic anhydride when heated at 80°C.

19) H. Saikachi and H. Ogawa, *J. Am. Chem. Soc.*, **81**, 3642 (1958).

BULLETIN OF THE CHEMICAL SOCIETY OF JAPAN VOL. 41 2969—2974 (1968)

The Reaction Products of the Hydroformylation of Acrolein Acetals and Acetates*1

Itsutoshi MAEDA and Ryonosuke YOSHIDA

Central Research Laboratories, Ajinomoto Co., Inc., Kawasaki

(Received March 4, 1968)

The hydroformylation reactions of acrolein acetals and acetates were carried out in order to discuss the side reactions and any subsequent reactions. Acrolein cyclic acetals reacted with carbon monoxide and hydrogen in the presence of a dicobalt octacarbonyl catalyst to give *n*- and iso-aldehydes in a 2 : 1 ratio; they gave no further reaction products. Acrolein diethylacetal underwent hydroformylation using a rhodium catalyst to give *n*- and iso-aldehydes in a 1 : 2 ratio. In the presence of a cobalt catalyst, however, various products were obtained. As a result of the acidity of cobalt hydrocarbonyl and a high reaction temperature, *n*-aldehyde, first formed in benzene, underwent change to 2,5-diethoxytetrahydrofuran and 1,1,4-triethoxybutane. In ethanol, *n*- and iso-aldehydes gave the corresponding acetals. In the hydroformylation of acrolein acetate, only *n*-aldehyde was obtained. Iso-aldehyde seemed to be converted into 2-methyl-3-acetoxyacrolein by deacetylation. In ethanol, besides *n*-acetal, iso-acetal and propionaldehyde acetate, 2,5-diethoxytetrahydrofuran and 2-methyl-3-ethoxyacrolein were recognized. The former seemed to be formed from *n*-aldehyde by ring closure and ethanolysis. The latter seemed to be formed by the ethanolysis of 2-methyl-3-acetoxyacrolein. In ethyl orthoformate, no side reaction was observed and the yield of the main product, 1,1-diacetoxy-4,4-diethoxybutane, amounted to 80%.

Customarily hydroformylation is carried out using a cobalt carbonyl as the catalyst. The cobalt carbonyl shows an acidity under the reaction conditions.

In this case the aldehydes formed first undergo subsequent reactions to give various reaction products. It has been reported[1] that acrolein diethylacetal absorbed 50—70% of the amount of hydrogen and carbon monoxide required for complete hydroformylation, but no aldehyde could be isolated from the reaction mixture. The present investigation of the hydroformylation of acrolein acetals and acrolein acetates was undertaken in order to confirm the by-products and propose a scheme for the subsequent reaction.

Results and Discussion

The Hydroformylation of Acrolein Cyclic Acetals. The treatment of acrolein cyclic acetals with hydrogen and carbon monoxide at 110°C and 200 atm in the presence of a cobalt carbonyl catalyst gave the usual hydroformylation products, *n*- and iso-aldehydes, in a 2 : 1 ratio. The results are summarized in Table 1. The hydroformylation products of acrolein cyclic acetals did not

*1 Presented in part at the 19th Annual Meeting of the Chemical Society of Japan, Yokohama, March, 1966.

1) H. Adkins and G. Krsek, *J. Am. Chem. Soc.*, **71**, 3051 (1949).

TABLE 1. THE HYDROFORMYLATION PRODUCTS OF ACROLEIN CYCLIC ACETALS

Acrolein cyclic acetal	Yield (%)	Bp °C/mmHg	Product Elementary analysis Found (%)	Calcd (%)	G. C.* *n* : *i*	NMR *n* : *i*
2-Vinyl-4,4,6-trimethyl-1,3-dioxane	54.6	74—76/3	C 64.35 H 9.87	64.49 9.74	2.18 : 1	2.34 : 1
2-Vinyl-4-methyl-1,3-dioxane	57.0	61—64/3	C 60.61 H 9.11	60.74 8.92	2.01 : 1	2.00 : 1
2-Vinyl-1,3-dioxane	53.8	82/5	C 57.93 H 8.52	58.31 8.39	—	2.25 : 1

* The ratios of normal aldehyde(*n*) and isomeric aldehyde(*i*) were measured by gas chromatographic (G. C.) and NMR analyses.

TABLE 2. THE HYDROFORMYLATION PRODUCTS OF ACROLEIN DIETHYLACETAL

	Reaction temperature	130°C				150°C			
	Solvent	Benzene		Ethanol		Benzene		Ethanol	
	Reaction time (hr)	1	2	1	2	1	2	1	2
Reaction products (mol%)	Acrolein acetal	62	35	62	28	1	1	0	0
	Propionaldehyde acetal	0	7	—	—	19	8	—	—
	2,5-Diethoxytetrahydrofuran	1	3	5	4	8	5	7	4
	1,1-Diethoxy-2-formylpropane	3	4	1	2	0	0	0	0
	1,1,4-Triethoxybutane	0	0	1	2	14	10	10	12
	1,1-Diethoxy-3-formylpropane	11	16	2	2	T	2	1	1
	1,1,3,3-Tetraethoxy-2-methylpropane	0	0	T	1	2	2	T	T
	1,1,4,4-Tetraethoxybutane	0	0	2	7	0	0	4	2
	X_1	0	0	T	+	+	+	+	++
	X_2	0	0	T	T	+	+	+	+
	X_3	0	0	+	+	0	+	++	+

Mol% of X_1, X_2 and X_3 were calculated by calibration curves of 2,5-diethoxytetrahydrofuran, 1,1,4-trithoxybutane and 1,1,4,4-tetraethoxybutane respectively.
+; 1—5 mol%, ++; 5—10 mol%, +++; 10—mol%, T; trace

TABLE 3. THE SUBSEQUENT REACTION OF THE HYDROFORMYLATION PRODUCTS OF ACROLEIN DIETHYLACETAL

Starting material		2,5-Diethoxy-tetrahydrofuran	2,5-Diethoxy-tetrahydrofuran	1,1,4,4-Tetra-ethoxybutane	1,1,4,4-Tetra-ethoxybutane	1,1-Diethoxy-3-formylpropane
Reaction condition	Solvent	Ethanol	Ethanol	Ethanol	Benzene	Ethanol
	Temp. (°C)	150	130	150	150	150
	Time (hrs.)	2	2	2	2	2
Reaction products (mol%)	2,5-Diethoxytetra-hydrofuran	20	3	0	0	T
	1,1,4-Triethoxybutane	8	16	26	7	19
	1,1-Diethoxy-3-formyl-propane	2	1	1	2	2
	1,1,4,4-Tetraethoxy-butane	36	3	3	3	2
	X_1	+	T	+	+	+
	X_2	++	+	++	+	+
	X_3	0	+++	++	++	++

Measurements were similar to Table 2.

undergo any further, subsequent reaction because of their stability.

The Hydroformylation of Acrolein Diethylacetal. With a rhodium carbonyl catalyst, the hydroformylation of acrolein diethylacetal resulted in a mixture of aldehydes, *n*- and iso-aldehydes, in a 1 : 2 ratio. On the other hand, with a cobalt carbonyl catalyst various products were obtained.

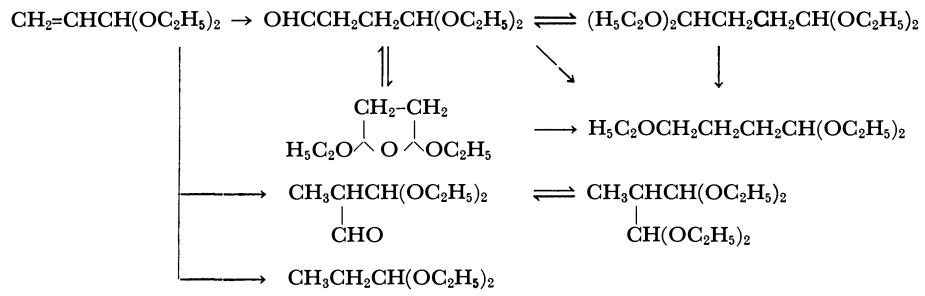

Scheme I

Gas-chromatographic analysis showed 11 peaks. Eight of them were identified by mixed chromatography with authentic samples and by preparative chromatography. The results of gas chromatographs for various products obtained from acrolein diethylacetal by reactions at 130°C and 150°C with a cobalt carbonyl catalyst are given in Table 2. The yields of the products were calculated on the basis of the area of each peak in a gas chromatograph after a usual calibration using authentic samples.

In order to evolve a scheme consistent with all these observations, the present authors considered the possibility that 1,1-diethoxy-3-formylpropane and 1,1-diethoxy-2-formylpropane underwent subsequent reactions. To test this hypothesis, 1,1-diethoxy-3-formylpropane, 1,1,4,4-tetraethoxybutane, and 2,4-diethoxy-tetrahydrofuran were synthesized and then treated under the hydroformylation reaction conditions respectively. They were thus converted into several compounds, which were listed in Table 3.

These compounds were almost identical with the hydroformylation products of acrolein diethylacetal.

On the basis of these data, it seemed reasonable to assume that the hydroformylation products of acrolein diethylacetal were formed according to the scheme shown below (scheme I).

The Hydroformylation of Acrolein Acetates. It has previously been reported by Adkins[1] that acrolein acetate (1,1-diacetoxypropene) was converted to *n*-aldehyde (1,1-diacetoxy-3-formylpropane) alone by hydroformylation in benzene using a cobalt carbonyl catalyst. The present authors carried out the hydroformylation of acrolein acetate with a rhodium carbonyl catalyst in benzene. As the products, 2-methyl-3-acetoxyacrolein and acetic acid were obtained; iso-aldehyde with a branched chain structure could not be obtained. The NMR-spectrum analysis of the mixture of 2-methyl-3-acetoxyacrolein and acetic acid is shown in Table 4.

TABLE 4. NMR SPECTRUM OF THE MIXTURE OF 2-METHYL-3-ACETOXYACROLEIN AND ACETIC ACID

(TMS)	No. of H	Assignment
1.76	3.0	Methyl
2.04	1.5	Methyl of acetic acid
2.32	3.0	Methyl of ester
8.06	1.0	CH
8.54	0.5	H of acetic acid
9.50	1.0	H of aldehyde

The evidence thus obtained suggests that the isoaldehyde formed by the hydroformylation decomposed to 2-methyl-3-acetoxyacrolein and acetic acid.

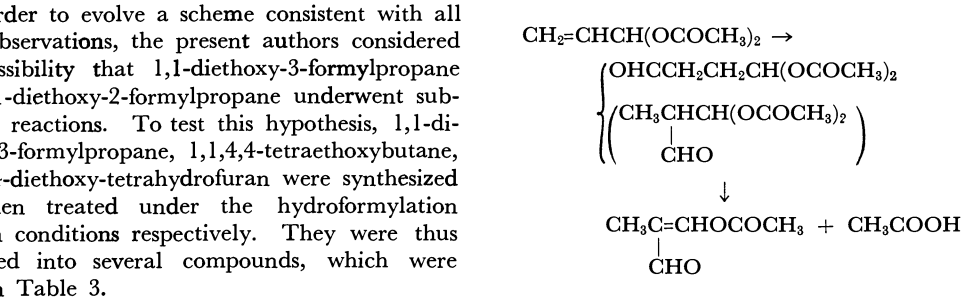

In alcohol the yield of the *n*-aldehyde acetal did not exceed 50%.

The hydroformylations of various kinds of acrolein acetates were carried out in an alcohol solution with cobalt catalysts. The results are listed in Table 5. According to the reaction of acrolein acetates, the yields of the major products, 1,1-diacyloxy-4,4-dialkoxybutane, were 30—50%; the side reaction products were identified by gas-chromatographic and NMR spectra analyses. The results are given in Table 6.

On the basis of these data, it seemed reasonable to assume that the hydroformylation products of acrolein acetate formed first were *n*-aldehyde (1,1-diacetoxy-3-formylpropane, about 60%), iso-aldehyde (1,1-diacetoxy-2-formylpropane, about 5—10%), and propionaldehyde acetate (1,1-diacetoxypropane, about 5%). Then these aldehydes were converted to their acetals, and a part of the *n*-aldehyde was converted to 2,5-diethoxytetrahydrofuran (10%)[2] by the acidity of the cobalt catalyst, while the iso-aldehyde was decomposed to 2-methyl-3-acetoxyacrolein and acetic acid.

2) W. R. Privette, H. W. Schulz and D. M. Yound, U. S. Pat. 2920081 (1960).

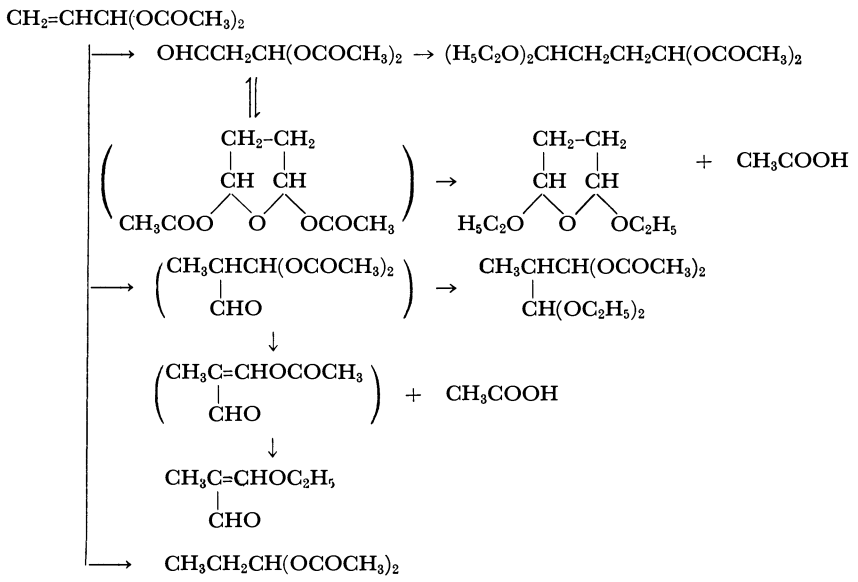

Scheme II

TABLE 5. THE HYDROFORMYLATION OF ACROLEIN ACETATES

$CH_2=CHCH(OCOR)_2 \xrightarrow{R'OH} (R'O)_2CHCH_2CH_2CH(OCOR)_2$

R	R'	Yield %	Concn. of $Co_2(CO)_8$ g/*l*	Bp °C/mmHg			Elementary analysis Calcd %	Found %
CH_3	CH_3	44.6	4	119—120/5	$C_{10}H_{18}O_6$	C	51.27	51.60
						H	7.75	7.75
	C_2H_5	37.0	2	125—128/4	$C_{12}H_{22}O_6$	C	54.95	55.08
						H	8.45	8.53
	i-C_3H_7	34.8	3	130—132/3	$C_{14}H_{26}O_6$	C	57.91	57.53
						H	9.03	9.08
	C_4H_9	41.6	3	160—163/3	$C_{16}H_{30}O_6$	C	60.35	60.94
						H	9.50	9.79
C_2H_5	CH_3	36.2	3	128—130/3	$C_{12}H_{22}O_6$	C	54.95	55.01
						H	8.45	8.38
	C_2H_5	40.0	3	137—139/3	$C_{14}H_{26}O_6$	C	57.91	57.50
						H	9.03	9.00
	C_4H_9	46.3	3	160/1	$C_{18}H_{34}O_6$	C	62.40	62.38
						H	9.89	9.76
C_3H_7	CH_3	40.3	3	142—143/1	$C_{14}H_{26}O_6$	C	57.91	57.71
						H	9.03	8.97
	C_2H_5	49.3	3	153—156/3	$C_{16}H_{30}O_6$	C	60.35	60.81
						H	9.50	9.52

TABLE 6. THE HYDROFORMYLATION PRODUCTS OF 1,1-DIACETOXYPROPENE

Reaction product	Yield %
1,1-Diacetoxy-3-formylpropane	2.0
1,1-Diacetoxy-4,4-diethoxybutane	45.5
2,5-Diethoxytetrahydrofuran	10.3
1,1-Diacetoxy-2-methyl-3,3-diethoxy-propane	0.8
2-Methyl-3-ethoxyacrolein	5—10
1,1-Diacetoxypropane	4.9

The overall reaction scheme may be illustrated as follows (Scheme II).

To prevent these side reactions and to promote the formation of 1,1-diacetoxy-4,4-diethoxybutane (I), the hydroformylation was carried out in the presence of ethyl orthoformate instead of ethanol. In these cases the formation of 1,1-diacetoxy-3-formylpropane, 2,5-diethoxytetrahydrofuran, 2-methyl-3-ethoxyacrolein and acetic acid were not seen, while 1,1-diacetoxy-2-methyl-2,3-diethoxy-propane (II) and 1,1-diacetoxypropane were found as by-products. The presence of ethyl orthoformate

was useful for the formation of I and II and reduced the formation of acetic acid. When ethyl orthoformate was used in excess to acrolein acetate, as shown in Table 7, the yield of main product, 1,1-diacetoxy-4,4-diethoxybutane, amounted to 80%.

Table 7. The yield of the hydroformylation products of 1,1-diacetoxypropene in the presence of ethyl orthoformate

Reaction temp.	110°C		130°C	
E. O/A. A*	I %	II %	I %	II %
0	37.7	1.6	36.5	—
0.5	55.4	3.0	56.9	1.3
1.0	68.6	5.4	69.7	2.0
1.0		—	74.2	2.9
1.2	75.0	6.3	76.0	2.7
1.4		—	78.6	3.0
1.5		—	80.0	3.9

* Mol ratio of ethyl orthoformate and acrolein acetate.

Experimental*2

Materials. These acrolein cyclic acetals (2-vinyl-4, 4,6-trimethyl-1,3-dioxane, 2-vinyl-4-methyl-1,3-dioxane and 2-vinyl-1,3-dioxane) were prepared from acrolein and glycols according to the directions of Fischer and Smith.[3] The acrolein diethylacetal was prepared according to the procedures described in a previous paper.[4] These acrolein acetates (1,1-diacetoxypropene, 1,1-dipropoxypropene, and 1,1-dibutyroxypropene) were prepared from acrolein and acid anhydrides.[5] All of the above materials were shown by gas chromatographic analysis to have no impurity affecting the results.

Reaction Procedures. *(1) The Hydroformylation of Acrolein Cyclic Acetals.* Acrolein acetal (0.1 mol) and 9 m*l* of a dicobalt octacarbonyl solution in benzene (containing 17.8 g/*l* as cobalt) were put into an autoclave with a 100 m*l* capacity and equipped with a magnetic stirrer. Benzene was added until it filled half of the vessel. Hydrogen and carbon monoxide mixture (1 : 1) were then introduced to 200 kg/cm^2, using a compressor, after the air in the alutoclave had been replaced with their gases. The autoclave was kept at 110°C by electrical heating for about one hour, and then after the gauge pressure ceased to decline, it was chilled. The gas mixture was purged, and the carbonyl catalyst was decomposed by triphenylphosphine. The filtrate of the reaction mixture was distilled under reduced pressure. The analyses of the ratio of *n*- and iso-aldehydes were carried out on the reaction mixture by gas chromatography and NMR spectra.

(2) The Hydroformylation of Acrolein Diethylacetal. (a) With a rhodium carbonyl catalyst in benzene. Acrolein diethylacetal (39.0 g, 0.3 mol), rhodium oxide (129.6 mg, 0.5 g/*l* as Rh) and benzene (104 m*l*) were charged in a 300 m*l*, stainless-steel pressure reactor. The mixture was then treated in a manner similar to that used in the experiment described for (1) except that the reaction was carried out at 110°C for 30 min. After the solvent had been removed under reduced pressure, the mixture (29.9 g), consisting of 1,1-diethoxy-2-formylpropane (I) and 1,1-diethoxy-3-formylpropane (II), was distilled at 61—64°C/5 mmHg. Found: C, 60.00; H, 10.17%. Calcd for $C_8H_{16}O_3$: C, 59.98; H, 10.07%. The ratio of I and II was determined to be 1.82 : 1 by using the integral of the NMR spectra ($CHCl_3$); CHO, 0.40 τ. I and II were separated by preparative gas chromatography. I; n_D^{25} 1.4178, II; n_D^{25} 1.4167.

(b) With a cobalt carbonyl catalyst in benzene or ethanol. The method used here was virtually identical with that described for (a), but acrolein diethylacetal (13.0 g, 0.1 mol) and dicobalt octacarbonyl (4 g/*l* as cobalt) in benzene (or ethanol) were charged in a 100 m*l* autoclave. The benzene (or ethanol) was added until it filled half of the vessel. The reaction was carried out at 130°C (or 150°C) for one hour (or two hours).

(3) The Hydroformylation of Acrolein Acetates. (a) With a rhodium carbonyl catalyst in benzene or ethanol. Rhodium oxide (260 mg, 1 g/*l* as Rh), 1,1-diacetoxypropene (47.4 g, 0.3 mol), and 105.6 m*l* of benzene (or ethanol) were put into a 300 m*l*, stainless-steel autoclave. The reaction was similar to that described for (1), but the reaction temperature was kept at 100°C. The reaction mixture was filtered and diluted with benzene (or ethanol) to 200 m*l*, then the aldehydes were distilled

Table 8. The hydroformylation products of 1,1-diacetoxypropene with cobalt carbonyl in ethanol

Fraction of the distillate	Weight	Substance	Weight calcd by gas chro. anal.
I 26—62°C/5 mmHg	11.3 g	Acetic acid	
		2,5-Diethoxytetrahydrofuran	6.4 g } 6.6 g
II 62—95°C/5 mmHg	7.4 g	2,5-Diethoxytetrahydrofuran	0.2 g }
		2-Methyl-3-ethoxyacrolein	
		Propionaldehyde acetate	2.4 g } 3.5 g
III 95—123°C/5 mmHg	2.8 g	Propionaldehyde acetate	1.1 g }
IV 123—131°C/5 mmHg	49.9 g	1,1-Diacetoxy-4,4-diethoxybutane	47.7 g

*2 All boiling points are uncorrected.

3) R. F. Fischer and C. W. Smith, *J. Org. Chem.*, **25**, 319 (1960).
4) J. A. Van Allen, *Organic Syntheses*, **32**, 5 (1952).
5) C. W. Smith, U. S. Pat. 2483852 (1949).

and analysis of the reaction products will be described in analytical procedures.

(b) With a cobalt carbonyl catalyst in ehtanol. A dicobalt octacarbonyl solution in ethanol (2—4 g/*l* as cobalt) and 1,1-diacyloxypropene (0.1 mol) were put into a 100 m*l* autoclave. The reaction was carried out according to the procedure described for (1), except that the reactor was kept at 110°C for 15 min after the gauge pressure ceased to decline. The contents of the autoclave were then filtered and diluted with ethanol to 100 m*l*. The distillation and analysis of aldehyde acetals and other reaction products will be described below.

(c) With a cobalt carbonyl catalyst in ethyl orthoformate. The method used here was identical with that described for (b), but ethyl orthoformate was added (0.5, 1, 1.1, 1.2, 1.4 and 1.5 mol per mol of 1,1-diacetoxypropene).

Analytical Procedures. *(1) The Hydroformylation of Acrolein Acetals.* (a) Authentic-sample preparation. The 2,5-diethoxy-tetrahydrofuran was prepared by the bromination of furan and its reduction.[6] (Found: C, 60.05; H, 10.24%). By the Grignard reaction of acetylene and ethyl orthoformate,[7] 1,1,4,4-tetraethoxybutyne-2 was prepared; it was then reduced to 1,1,4,4-tetraethoxybutane.[8] (Found: C, 61.51; H, 11.00%). Propionaldehyde diethylacetal was prepared using the technique for acrolein acetal. 1,1-Diethoxy-2-formylpropane and 1,1-diethoxy-3-formylpropane were separated by preparative gas chromatography (the column packed with 10% Carbowax 20M coated on Diasolid M at 100°C) from their mixture prepared by the hydroformylation of acrolein diethylacetal with a rhodium carbonyl catalyst. From 1,1-diethoxy-2-formylpropane and ethyl orthoformate, 1,1,3,3-tetraethoxy-2-methylpropane was prepared. Found: C, 61.44; H, 11.19%. Calcd for $C_{12}H_{26}O_4$: C, 61.50; H, 11.18%. By preparative gas chromatography, 1,1,4-triethoxybutane was separated from the hydroformylation solution of acrolein diethylacetal with a cobalt carbonyl catalyst. The structure of 1,1,4-triethoxybutane was established by its IR and NMR spectra. Found: C, 63.08; H, 11.23%. Calcd for $C_{10}H_{22}O_3$: C, 63.01; H, 11.58%. n_D^{25} 1.4124.

(b) Gas chromatography was carried out with 5% carbowax 6000 on Diasolid M (4 mmϕ×3 m; column temperature, 95°C; flow rate of He, 80 m*l*/min; internal standard, acetophenone). The individual peaks were identified by a comparison of their retention times with those of authentic samples. The low-boiling substances, propionaldehyde diethylacetal and acrolein diethylacetal, were analyzed with 20% β,β'-oxydipropionitrile on chromosorb W (4 mmϕ×2 m; column temperature, 70°C; flow rate of He, 80 m*l*/min; internal standard, *n*-butanol).

(2) The Hydroformylation of Acrolein Acetates. The separation and identification of reaction products were performed by distillation and by gas chromatographic and NMR spectra analyses. The gas chromatography was carried out with 5% polyethylene glycol 4000 on chromosorb T (4 mmϕ×2 m; column temperature, 150°C; flow rate of He, 75 m*l*/min; internal standard, diethyl adipate).

(a) With a rhodium carbonyl catalyst in benzene. After the benzene had been removed, the reaction mixture was distilled under reduced pressure. By fractionating low-boiling fractions collected from several runs (bp 33—61°C/5 mmHg), the following compounds were isolated and identified. Gas chromatography showed two kinds of compounds; their NMR spectra showed that they were acetic acid and 2-methyl-3-acetoxyacrolein, is shown in Table 4. The next boiling fractions (bp 61—113°C/5 mmHg) were mixtures of acetic acid, 2-methyl-3-acetoxyacrolein and 1,1-diacetoxy-3-formylpropane. The only high-boiling fraction (bp 113—114°C/5 mmHg) was 1,1-diacetoxy-3-formylpropane. In gas chromatographic analysis, 1,1-diacetoxy-2-formylpropane was not found.

(b) With a rhodium carbonyl catalyst in ethanol. Five compounds were found in the distillate by gas-chromatographic analysis. In the fractions of the distillate, the following compounds were identified: Bp 54—117°C/7 mmHg, a mixture of acetic acid, 2-methyl-2-acetoxyacrolein, an unknown substance, 1,1-diacetoxy-2-formylpropane, and 1,1-diacetoxy-3- formylpropane; bp 118—124°C/7 mmHg, a mixture of 1,1-diacetoxy-2-formylpropane and 1,1-diacetoxy-3- formylpropane. Found: C, 50.67; H, 6.54%. Calcd for $C_8H_{12}O_5$: C, 51.06; H, 6.43%.

(c) With a cobalt carbonyl catalyst in ethanol. After the hydroformylation of 1,1-diacetoxypropene (0.4 mol), the reaction mixture was distilled. In the fractions of the distillate, the compounds as shown in Table 8 were identified and quantified by gas-chromatographic and NMR spectra analyses.

(d) With a cobalt carbonyl catalyst in ethyl orthoformate. After the hydroformylation of 1,1-diacetoxypropene (0.1 mol), the 1,1-diacetoxy-4,4-diethoxybutane and 1,1-diacetoxy-2-methyl-3,3-diethoxypropane were analyzed by gas chromatography. Gas chromatography was carried out with 5% carbowax 20 M on chromosorb T (4 mmϕ×2 m; column temperature, 165°C; flow rate of He, 75 m*l*/min; internal standard, dimethyl terephthalate).

The authors wish to thank Mr. Masahiko Takesada and Dr. Hachiro Wakamatsu for many helpful discussions and suggestions during this work.

6) J. Fakstorp, D. Raleigh and L. E. Schniepp, *J. Am. Chem. Soc.*, **72**, 869 (1950).
7) K. Henkel, *Ber.*, **76B**, 812 (1943).
8) A. Wohol and U. B. Mylo, *Ber.*, **45**, 839 (1912).

BULLETIN OF THE CHEMICAL SOCIETY OF JAPAN VOL. 41 2975—2978 (1968)

A Synthesis of DL-Tryptophan from Acrolein*[1]

Itsutoshi MAEDA and Ryonosuke YOSHIDA

Central Research Laboratories, Ajinomoto Co., Inc., Kawasaki

(Received March 4, 1968)

DL-Tryptophan hydrantoin was obtained from phenylhydrazone of β-(hydanto-5-yl)-propionaldehyde acetal (5-(γ,γ-dialkoxypropyl)hydantoin) by Fischer's indole synthesis. β-(Hydanto-5-yl)propionaldehyde acetal was prepared by Bucherer's reaction from 1,1-diacetoxy-4,4-dialkoxybutane obtained by the hydroformylation of acrolein acetate. Attempts to crystallize β-(hydanto-5-yl)-propionaldehyde acetal from Bucherer's reaction solution were unsuccessful, but 5-alkoxy-1,3-dioxoperhydropyrro[1,2-*c*]imidazole was obtained by treating the solution with ion exchange resins in alcohol. It could be also converted to tryptophan hydantoin.

Tryptophan, an essential amino acid for human and animals, has been prepared by various synthetic routes since the first successful synthesis, by Ellinger, in 1907. The method using acrolein as the starting material was employed by Warner and Moe[1] and developed by Chibata and Yamada.[2] Namely, DL-tryptophan was obtained by the hydrolysis and decarboxylation of the indole derivative prepared from phenylhydrazone of γ-acetamido-γ,γ-dicarbethoxybutyraldehyde by Fischer's indole synthesis. The aldehyde was obtained by a Michael-type condensation between acrolein and ethyl acetamidomalonate. Of the hitherto reported methods, the synthetic route employed by Komachiya *et al.*[3] appears to be one of the most suitable routes for industrial synthesis. Tryptophan was obtained by the hydrolysis of β-(hydanto-5-ylmethyl)indole prepared from phenylhydrazone of β-(hydanto-5-yl)propionaldehyde by Fischer's indole synthesis. The aldehyde was formed by the catalytic hydrogenation of the 5-(β-cyanoethyl)-hydantoin obtained by Bucherer's reaction of β-cyanopropionaldehyde in aqueous acetic acid in the presence of a Raney nickel catalyst poisoned with lead. Considering these facts, it seemed possible to prepare DL-tryptophan from the 1,1-diacetoxy-4,4-dialkoxybutane obtained by the hydroformylation of acrolein acetate described in a previous paper.[4] The object of this paper is to describe this method.

The acetals of 4,4-diacyloxybutyraldehyde have two reactive groups. The diacetoxy group may be converted to the hydantoin group by Bucherer's reaction, while the acetal group may remain unchanged under these conditions, thus the acetals of 4,4-diacyloxybutyraldehyde can be converted to 5-(γ,γ-dialkoxypropyl)hydantoin. Therefore, the phenylhydrazone of this hydantoin derivative can be employed advantageously in the synthesis of DL-tryptophan.

Results and Discussion

In a previous paper,[4] it was reported that 1,1-diacetoxy-4,4-dialkoxybutane (I) was obtained by the hydroformylation of acrolein acetate. In the usual manner, 5-(γ,γ-dialkoxypropyl)hydantoin (II) was obtained from I by Bucherer's reaction. The reaction mixture in Bucherer's reaction was dried up, and attempts to crystallize II from the resultant syrup were unsuccessful. The alcohol solution of the syrup was then added to cation exchange resins and the mixture boiled for several hours. When the reaction solution was dried up, the residual oil crystallized spontaneously to colorless needles upon cooling. It has been shown by elementary analysis that this substance was not in agreement with II, but it was identified with the structure lost by one mole of alcohol from the formula of II. The infrared spectra of the substance showed that there was evidently a hydantoin ring, while the NMR spectra showed that one of the two NH functional groups of hydantoin ring has no hydrogen atom. Either the 1- or 3-position of hydantoin appeared to be substituted. Stucky[5] has shown that hydantoin in an aqueous or alcoholic alkaline solution underwent amido-imidol tautomerism involving the hydrogen of the 3-position; therefore, substitution in the 3-position was easily detected by the change in the ultraviolet absorption

*1 Presented in part at the 19th Annual Meeting of the Chemical Society of Japan, Yokohama, March, 1966.

1) D. T. Warner and O. A. Moe, *J. Am. Chem. Soc.*, **70**, 2763 (1948).

2) I. Chibata and S. Yamada, *Bull. Agr. Chem. Soc. Japan*, **21**, 58 (1957).

3) Y. Komachiya, K. Suzuki, T. Yamada, H. Miyayashiki and S. Sakurai, *Nippon Kagaku Zasshi (J. Chem. Soc. Japan, Pure Chem. Sect.)*, **86**, 856 (1965).

4) I. Maeda and R. Yoshida, This Bulletin, **41**, 2969 (1968).

5) R. E. Stucky, *J. Chem. Soc.*, **1947**, 331.

spectra. The substance not substituted in the 3-position of hydantoin indicates the absorption at wavelengths from 2000 to 2300 Å, while the 3-substituted substance does not show the absorption. The UV spectrum of the substance obtained from II is shown in Fig. 1.

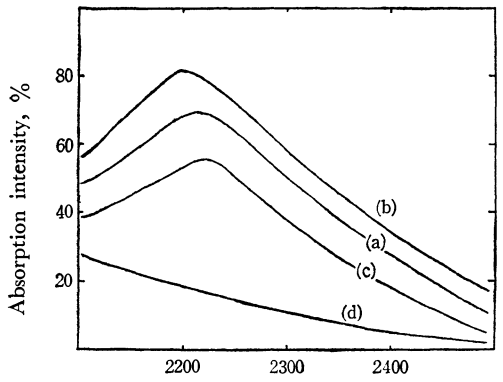

Fig. 1. The UV spectrum in 0.01 N aqueous sodium hydroxide solution.
(a) III λ_{max} 2205 Å $\varepsilon_{max}=9060$
(b) Tryptophan hydantoin λ_{max} 2195 Å $\varepsilon_{max}=38650$
(c) 5-Methylhydantoin λ_{max} 2210 Å $\varepsilon_{max}=6375$
(d) 3-Cyanoethylhydantoin

It seemed likely that this substance was a hydantoin derivative which was substaituted not in the 3-position, but in the 1-position. In view of the above facts, the most reasonable structure of this substance was 5-alkoxy-1,3-dioxoperhydropyrro[1,2-*c*]imidazole (III). III could also be obtained by another route. Namely, 5-(β-cyanoethyl)-hydantoin was reduced to 5-(β-formylethyl)hydantoin according to the directions of Komachiya *et al.*[3]; this latter substance could be isolated as a crystalline semicarbazone derivative from the reaction mixture. When treated with ion exchange resins in alcohol as has been described above, this semicarbazone was converted to III. Similarly, the semicarbazone of 5-(γ-formylpropyl)-hydantoin obtained from 5-(γ-cyanopropyl) hydantoin was converted to 5-alkoxy-1,3-dioxoperhydropyrido[1,2-*c*]imidazole (VIII).

The phenylhydrazone of III was unstable to heat and light. It was converted to tryptophan hydantoin using the technique of Fischer's indole synthesis. This reaction could also be carried out without the isolation of the unstable phenylhydrazone. The procedure was simple, and satisfactory results were obtained. Instead of crystalline III, the syrup obtained from I by Bucherer's reaction could be employed for the Fischer's indole synthesis. Although the yield based on the starting material was low, the procedure has the advantage of simplicity. The results of these experiments are summarized in Scheme I.

Experimental*2

5-Alkoxy-1,3-dioxoperhydropyrro[1,2-*c*]imidazole (III) from β-(Hydanto-5-yl)propionaldehyde Semicarbazone (VI). *(1) 5-Ethoxy-1,3-dioxoperhydropyrro[1,2-c]imidazole (IIIa).* A mixture of 21.3 g

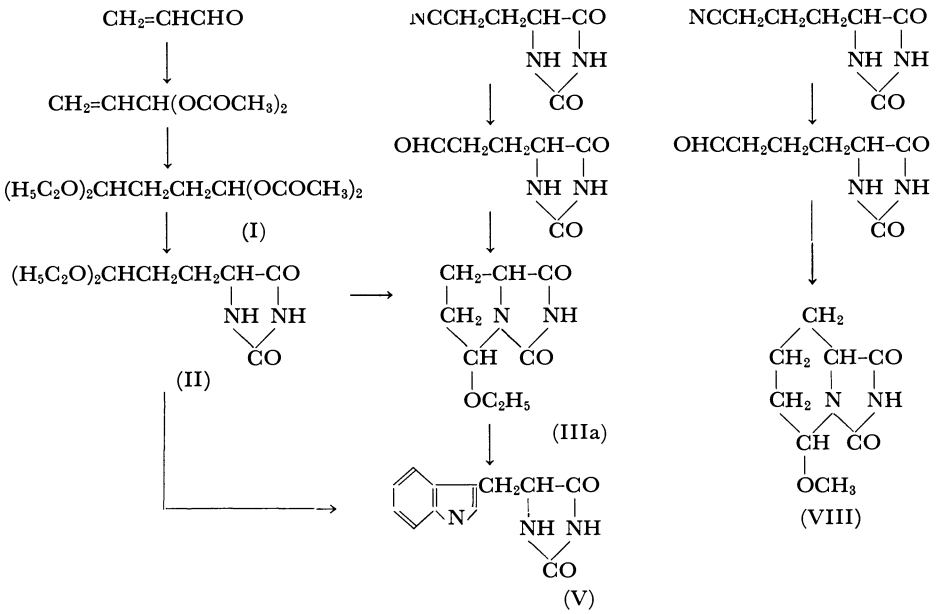

Scheme I

*2 All melting points are uncorrected.

(0.1 mol) of β-(hydanto-5-yl)propionaldehyde semicarbazone (VI)[8] and 250 ml of dried cation exchange (H^+) resins (Diaion SK #1) in 400 ml of ethanol was heated with stirring for 3 hr at from 50 to 60°C. The resins were then filtered off and washed with ethanol. The removal of the ethanol by evaporation from the filtrate yielded 13.4 g (72.5%) of crude crystals; mp 102—104°C. Recrystallization from ethanol gave white needles; mp 119—120°C.

Found: C, 52.20; H, 6.63; N, 15.18%. Calcd for $C_8H_{12}O_3N_2$: C, 52.16; H, 6.57; N, 15.21%. Mol wt (Rast), 185.9, Calcd 184.2. The 2,4-dinitrophenylhydrazone prepared by the usual procedure decomposed at 216.5—217.5°C.

Found: C, 42.53; H, 3.75; N, 24.01%. Calcd for $C_{12}H_{12}O_6N_6$: C, 42.86; H, 3.60; N, 24.99%.

(2) 5-Methoxy-1,3-dioxoperhydropyrro[1,2-c]imidazole (IIIb). The method was identical with that described for (1), except that the ethanol was replaced with 500 ml of methanol. The crude product obtained weighed 13.8 g (81%). It was recrystallized from methanol to afford white crystals; mp 118—119°C.

Found: C, 49.42; H, 6.26; N, 16.42%. Calcd for $C_7H_{10}O_3N_2$: C, 49.40; H, 5.92; N, 16.46%.

γ-(Hydanto-5-yl)butyraldehyde Semicarbazone (VII) from 5-(γ-Cyanopropyl)hydantoin. To a mixture of 40 ml of water and 10 ml of methanol was added 4.2 g (0.025 mol) of 5-(γ-cyanopropyl)hydantoin, which had been obtained by Bucherer's reaction of γ-cyanobutyraldehyde. After the hydantoin had dissolved upon slight warming, these were added to the solution at room temperature 7.45 ml of glacial acetic acid, 0.058 g of lead acetate, and 1.05 g of Raney nickel which had been treated with sodium hydroxide in the usual manner. The reaction was run at room temperature under a hydrogen atmosphere in a shaking vessel. The hydrogen uptake was almost complete in about two hours. After the removal of the catalyst, 2.8 g (0.025 mol) of semicarbazide hydrochloride was added to the reaction mixture and it was stirred for half a day. The semicarbazone which crystallized when the mixture stood in an ice box overnight was filtered, washed with water, dried, and weighed; 3.7 g (65.8%), mp 198.5—199.5°C.

Found: C, 42.23; H, 6.20; N, 29.96%. Calcd for $C_8H_{13}O_3N_5$: C, 42.29; H, 5.77; N, 30.82%.

5-Methoxy-1,3-dioxoperhydropyrido[1,2-c]-imidazole (VIII) from γ-(Hydanto-5-yl)butyraldehyde Semicarbazone (VII). A mixture of 2.8 g (0.012 mol) of VII and 200 ml of dried cation exchange (H^+) resins in 300 ml of methanol was heated at from 50°C to 60°C for 3 hr with stirring. The resins were then filtered off and washed with methanol. After the methanol had been removed under reduced pressure, 1.8 g (79.2%) of a crude, powder-like product were obtained. Recrystallization from methanol gave white needles (mp 156—158°C).

Found: C, 52.46; H, 6.74; N, 15.05%. Calcd for $C_8H_{12}O_3N_2$: C, 52.16; H, 6.57; N, 15.21%. Mol wt (Rast), 183.4, Calcd 184.2. The NMR spectrum of this substance was measured in a $CDCl_3$ solution, with tetramethylsilane as the standard; these measurement showed that the ratio of the NH functional group to the CH functional group was 1 : 1. The UV spectrum indicated a maximum absorption at 2275 Å (ε_{max} = 6,840).

β-(Hydanto-5-yl)propionaldehydediethylacetal (II) from 1,1-diacetoxy-4,4-diethoxybutane (I). Into a mixture of 14.3 g (0.125 mol) of ammonium carbonate and 73.6 ml (0.11 mol as CN^- ion) of ammonium cyanide in an ammonia solution (1.5 mol per l as CN^- ion and 11 mol per l as NH_4^+ ion), 26.2 g (0.1 mol) of I were stirred at room temperature. The mixture was heated with stirring at from 50°C to 60°C for 3 hr, and then at from 60°C to 70°C for an additional hr. After the mixture had been dried up *in vacuo*, attempts to crystallize the resultant syrup were unsuccessful. The 2,4-dinitrophenylhydrazone was prepared by the usual procedure, which yielded red needles (74.5%). It decomposed at 217—218°C.

Found: C, 42.89; H, 3.87; N, 25.01%. Calcd for $C_{12}H_{12}O_6N_6$: C, 42.86; H, 3.60; N, 24.99%.

5-Ethoxy-1,3-dioxoperhydropyrro[1,2-c]imidazole (III) from II. By treating 0.05 mol of I by the method described above, II was obtained in a syrupy state. The syrup was added to 50 ml of cation exchange (H^+) resins in ethanol. The mixture was then heated at from 60°C to 70°C with stirring for 4 hr. After the resins had been removed and the ethanol evaporated, a white, crystalline substance was separated, dried, and weighed; 7.2 g (78.5% based on I, mp 116—117°C). Recrystallization from ethanol gave white needles; mp 119—120°C.

Found: C, 52.20; H, 6.66; N, 15.20%. Calcd for $C_6H_{12}O_3N_2$: C, 52.16; H, 6.57; N, 15.21%.

β-(Hydanto-5-yl)propionaldehyde Phenylhydrazone (IV). *(1) From 5-Ethoxy-1,3-dioxoperhydropyrro-[1,2-c]imidazole (IIIa).* A solution of 9.2 g (0.05 mol) of IIIa in 50 ml of water was refluxed for 1.5 hr. The solution was then cooled and added to a solution of 7.2 g (0.05 mol) of phenylhydrazine hydrochloride in 50 ml of water. The product which crystallized from the reaction mixture upon standing overnight in an ice box was filtered, washed, dried *in vacuo* at room temperature in a dark desiccator, and weighed; 10.5 g (82%).

Found: C, 58.16; H, 5.89; N, 22.23%. Calcd for $C_{12}H_{14}O_2N_4$: C, 58.52; H, 5.73; N, 22.75%.

(2) From II. The syrup of II was obtained by treating 0.025 mol of I by the method described above. Ethanol was added to the syrup, and it was evaporated again to remove the ammonia. A mixture of the syrup and diluted hydrochloric acid was refluxed for 1.5 hr. After cooling, the reaction mixture was poured into a solution of 3.6 g of phenylhydrazine hydrochloride in 40 ml of water; the crystals obtained on standing overnight in an ice box were filtered, washed, dried and weighed; 2.2 g (34.1% based on I). The infrared spectrum of the crystals was identical with that of the product described in the case of (1).

Tryptophan Hydantoin (V) from II. This method is a modification of the directions of Komachiya *et al.*[8] A syrup of II was afforded by treating 0.1 mol of I as above. To the syrup these were then added 2.5 ml of conc. hydrochloric acid, after which the mixture was diluted to 200 ml with water. A mixture of 1.25 ml of conc. hydrochloric acid and 13.9 g (0.096 mol) of phenylhydrazine hydrochloride was diluted to 200 ml with water. In a 1 l, four-necked, round-bottomed flask equipped with a reflux condenser, a sealed stirrer, a dropping funnel, and a thermometer, the solution of phenylhydrazine was placed. To the boiled solution in the flask, the solution of II was added, drop by drop,

through the dropping funnel. After the addition, the mixture was refluxed while being stirred for 30 min. The flask was chilled to 80°C and then cooled with water to 20°C. After being allowed to stand at 20°C for 30 min, the crystals were filtered, washed, and dried. The yield was 10.3 g (45% based on I); mp 215°C.

Found: C, 63.03; H, 5.16; N, 18.37%. Calcd for $C_{12}H_{11}O_2N_3$: C, 62.87; H, 4.84; N, 18.33%.

In this case, a deposit of polymer was observed on the bottom of the flask. When the volume of conc. hydrochloric acid added to the syrup of II was increased to 7.5 m*l*, the yield of V was 14.2 g (62.1%), mp 212—213°C.

Found: C, 62.91; H, 5.25; N, 18.45%.

Tryptophan Hydantoin (V) from III. The reaction of 13.6 g (0.08 mol) of III in 200 m*l* of 0.1 N hydrochloric acid with 14.5 g (0.1 mol) of phenylhydrazine hydrochloride in 200 m*l* of 0.1 N hydrochloric acid was carried out in a manner similar to that used in the experiment described above. The first crop of crystals of tryptophan hydantoin (melting at 212—213°C) weighed 15.8 g (86.2%).

Found: C, 62.48; H, 5.36; N, 18.7%.

The second crop (1.3 g, melting at 207—208°C) was obtained by allowing the mother liquor to stand at room temperature. The total yield of tryptophan hydantoin was 93.2% based on III.

Our thanks are due to Dr. Yoshioki Komachiya for helpful discussions and technical advice.

BULLETIN OF THE CHEMICAL SOCIETY OF JAPAN VOL. 41 2978—2984 (1968)

The Electrophilic Substitution Reactions of 2-Aminotropone and Its *N*-Alkyl Derivatives[1]

Tetsuo Nozoe, Shoji Ryu[2] and Takashi Toda

Department of Chemistry, Faculty of Science, Tohoku University, Katahira-cho, Sendai

(Received March 15, 1968)

The electrophilic substitution reactions of 2-aminotropone (I), 2-methylaminotropone (II), and 2-dimethylaminotropone (III) were investigated. The structure of the products was proved by hydrolysis to lead to known tropolone derivatives. By the nitrosation of II, *N*-nitroso-2-methylaminotropone was obtained in a good yield; this compound is a new type of active troponoid compound. The substitution reactions of III gave tropolone derivatives, accompanied by the hydrolysis of the dimethylamino group. The mechanism of the hydrolysis is then discussed.

The relation of tropolone and 2-aminotropone (I) corresponds to the relation of phenol and aniline, and to investigate the chemical properties of I is both important and interesting. Althougth the reactivities of tropolones have been investigated in detail,[3] the chemical properties of I have been known for only a few examples of such cationoid substitution reactions as bromination and the azo-coupling reaction[4] and of reactions with active methylene compounds to synthesize 1-azaazulan-2-one and its derivatives.[5] No report has appeared about the chemical properties of 2-methylaminotropone (II)[4] and 2-dimethylaminotropone (III),[4] even though these compounds are an important family of I, corresponding to *N*-methylaniline and *N*-dimethylaniline. From this point of view, the electrophilic substitution reactions of 2-aminotropone and its *N*-alkyl derivatives, II and III, were undertaken. The authors wish to report here the results obtained.

Halogenations of 2-Aminotropone, 2-Methylaminotropone, 2-Dimethylaminotropone, and the Copper Complex of 2-Aminotropone. The bromination of I in acetic acid or chloroform was investigated in detail.[4] It was proved that substitution took place in the following order; at C-7 first, then at C-5, and finally at the C-3 position of I.[4] The halogenations of I, II, and III under a variety of conditions were then reinvestigated by comparison with the results previously obtained. The results of the reinvestigation

1) Presented at the 19th Annual Meeting of the Chemical Society of Japan, Yokohama, April, 1966.

2) Present address: Zenyaku Kogyo KK, Oizumi-machi, Nerima-ku, Tokyo.

3) a) P. L. Pauson, *Chem. Revs.*, **55**, 19 (1955). b) T. Nozoe, K. Takase and H. Matsumura, "Dai Yuki Kagaku" (Comprehensive Organic Chemistry), Vol. 13, ed. by M. Kotake, Asakura Shoten, Tokyo (1960).

4) T. Nozoe, S. Seto, M. Takeda, S. Morosawa and K. Matsumoto, *Sci. Repts. Tohoku Univ. Ser. I*, **36**, 126 (1952).

5) T. Nozoe, S. Seto, S. Matsumura and T. Terasawa, *Chem. & Ind.*, **1954**, 1356; T. Nozoe, S. Seto and S. Nozoe, *Proc. Japan Acad.*, **32**, 472 (1956); S. Seto and S. Nozoe, *ibid.*, **32**, 765 (1956); N. Soma and G. Sunagawa, *Yakugaku Zasshi*, **82**, 418 (1962); N. Soma, *ibid.*, **82**, 892, 898 (1962); H. Toda, *ibid.*, **87**, 1351 (1967); S. Matsumura, This Bulletin, **34**, 1362 (1961); K. Ogura, H. Sasaki and S. Seto, *ibid.*, **38**, 306 (1964); T. Toda, S. Seto and T. Nozoe, *ibid.*, **41**, 2102 (1968).

TABLE. 1. THE RESULTS OF HALOGENATION OF I, II AND III

Condition	Product % (recovery %) I	II	III
$Cl_2/CHCl_3$	V 31.5% (66.5%)		
$Br_2/AcOH$	VI 22%* (mixtures)**	VIII 28% (59%)	
$3Br_2/AcOH$	VI 83%*	VIII 80%	
$PPB/CHCl_3$***	VI 30% (55%)	VIII 27% (59%)	
$2PPB/CHCl_3$***	VI 55% (27%)	VIII 55% (mixtures)**	
$Br_2/MeOH$		IX 37% (44%)	XI 22%, XII 10% (67%)
$3Br_2/MeOH$		IX 85%	XII 92%
$I_2/MeOH \cdot H_2O$	VII 25% (66%)	X 94%	XIII 85%

* The results of lit. 4.
** Mixtures of starting substance, mono- and di-bromo derivatives.
*** Pyridine perbromide.

are shown in Table 1, which shows that the halogenation of these compounds occurs at the C-7 position first, and then at the C-5 and C-3 positions. The reactivities of I and II are almost the same. On the other hand, III shows different properties and the hydrolysis of the dimethylamino group occurs during halogenation, giving tropolone derivatives.

The bromination of the copper complex (IV)[4] of I was also investigated by comparison with the properties of the copper complex of tropolone.[6] In chloroform, IV with equimolar bromine gave

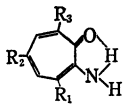

I: $R_1=R_2=R_3=H$
V: $R_1=R_2=R_3=Cl$
VI: $R_1=R_2=R_3=Br$
VII: $R_1=R_2=H$, $R_3=I$

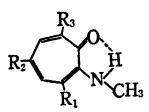

II: $R_1=R_2=R_3=H$
VIII: $R_1=R_2=R_3=Br$
IX: $R_1=H$, $R_2=R_3=Br$
X: $R_1=R_2=H$, $R_3=I$

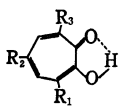

XI: $R_1=R_3=Br$, $R_2=H$
XII: $R_1=R_2=R_3=Br$
XIII: $R_1=I$, $R_2=R_3=H$

Fig. 1. The structures of the halogenation products of I, II and III.

6) T. Toda, H. Kubota and T. Nozoe, *Nippon Kagaku Zasshi (J. Chem. Soc. Japan, Pure Chem. Sect.)*, **88**, 1234 (1967).

5,7-dibromo-2-aminotropone[4] in a 50% yield; the rest of the starting substance was recovered. This result is parallel with the properties[6] of the copper complex of tropolone.

3,5,7-Trichloro-2-aminotropone (V), 7-iodo-2-aminotropone (VII), 3,5,7-tribromo-2-methylaminotropone (VIII), 5,7-dibromo-2-methylaminotropone (IX), and 7-iodo-2-methylaminotropone (X) are new compounds. The hydrolyses of these compounds gave known tropolone derivatives: 3,5,7-trichlorotropolone[7] from V, 3-iodotropolone (XIII)[8] from VII and X, 3,5,7-tribromotropolone (XII)[9] from VIII, and 3,5-dibromotropolone[9a] from IX. Thus, the structures of these compounds are proved. VII and X were also obtained from the methyl ether of XIII by treating it with ammonia and monomethylamine respectively.

Nitration, Azo-coupling Reaction and Sulfonation of 2-Methylaminotropone. As has been shown above, in properties I and II are very similar to each other. Because it is easy to handle, the nitration, azo-coupling reaction, and sulfonation of II were undertaken.

The nitration of II with an equimole of nitric acid in acetic acid afforded 5-nitro-2-methylaminotropone (XIV) in an 85% yield. Generally,

7) T. Nozoe, S. Seto, K. Yamane and A. Yoshikoshi, *Proc. Japan Acad.*, **27**, 224 (1951); W. von E. Doering and L. H. Knox, *J. Am. Chem. Soc.*, **74**, 5683 (1952).
8) Y. Kitahara and T. Arai, *Proc. Japan Acad.*, **27**, 423 (1951).
9) a) T. Nozoe, S. Seto, Y. Kitahara, M. Kunori and Y. Yamanaka, *ibid.*, **26**, (7) 38 (1950). b) J. W. Cook, A. R. Gibb, R. A. Raphael and A. R. Sommervill, *J. Chem. Soc.*, **1951**, 503.

nitrotropolones give nitro-2-aminotropone derivatives when treated with amines.[3b,10] By the application of this method, the treatment of 5-nitrotropolone[10b,11] with methylamine afforded XIV. Thus, the structure of XIV is proved. In the same manner, the reaction of II with excess nitric acid gave a yellow, crystalline substance (XV) in a 60% yield besides 35% of XIV. XV was obtained when 3,5-dinitrotropolone[10b] was treated with methylamine; hence, XV is 5,7-dinitro-2-methylaminotropone. The treatment of XV with alcoholic alkali gave 2,4-dinitrobenzoic acid in a good yield, just as with nitrotropolones.[3b,10]

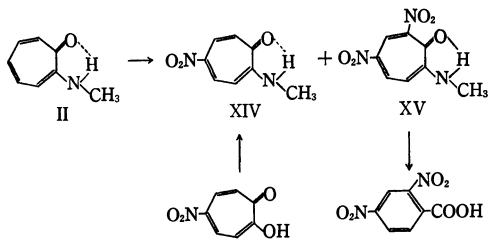

On the other hand, the treatment of I and III with excess nitric acid under the same reaction conditions as above resulted in the recovery of the starting substances.

The azo-coupling reaction of 2-aminotropones has been known to give 5-arylazo derivatives.[4,12] The treatment of II with phenyldiazonium salt and *p*-nitrophenyldiazonium salt gave the corresponding 5-phenylazo-2-methylaminotropone (XVI) and 5-(*p*-nitrophenyl)azo-2-methylaminotropone (XVII) in 45% and 95% yields respectively. XVI and XVII were also obtained from the corresponding methyl ethers[13] of 5-arylazotropolones by treatment with methylamine.

The reaction of 1.5 mol of sulfamic acid at 150—160°C gave a high-melting-point substance (XVIII) in a 50% yield, while II was also recovered (40%). The elemental analysis of XVIII is agreeable with the sulfonic acid derivative of II, and the hydrolysis of XVIII formed tropolone-5-sulfonic acid.[14] Hence, XVIII is 2-methylaminotropone-5-sulfonic acid. The nitration of XVIII with excess nitric acid resulted in XV in a 70% yield; there was also an exchange of the sulfonic acid group with the nitro group. The same type of exchange reaction was observed when tropolone-5-sulfonic acid was treated with nitric acid.[10b] On the other hand, the bromination of XVIII in an aqueous solution gave 3,7-dibromotropolone-5-sulfonic acid (XIX) in a 65% yield, while the 2-methylamino group was hydrolyzed.

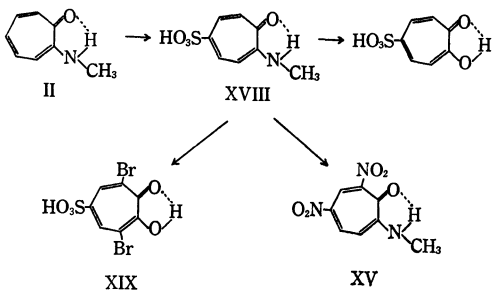

Nitrosation of 2-Methylaminotropone. Although 2-aminotropone gave an unidentified powder when treated with nitrous acid,[4] it is expected that 2-methyaminotropone, as a secondary amine, would form an *N*-nitroso derivative. When II was treated with nitrous acid, white needles (XX) and yellow scales (XXI) were obtained in 80% and 10% yields respectively. The elemental analyses of them agree with those of the nitroso derivatives of II. The IR spectrum of XX does not show any NH stretching vibrations, while that of XXI possesses a broad NH stretching band at 3250 cm^{-1} (KBr pellet). Therefore, XX is assumed to be the *N*-nitroso derivative of II, and XXI, the 5-nitroso compound of II. It is known that 5-nitrosotropolones[11a,15] give 5-nitroso-2-aminotropones when treated with ammonia.[16] Since the treatment of 5-nitrosotropolone with methylamine afforded XXI, the structure of XXI is established to be 5-nitroso-2-methylaminotropone. On the other hand, the reaction of XX with alcoholic potassium hydroxide gave benzoic acid; hence, the structure of XX is 2-*N*-nitroso-2-methylaminotropone, as has been predicted. This is the first *N*-nitroso-2-methylaminotropone derivative obtained. XX is a new type

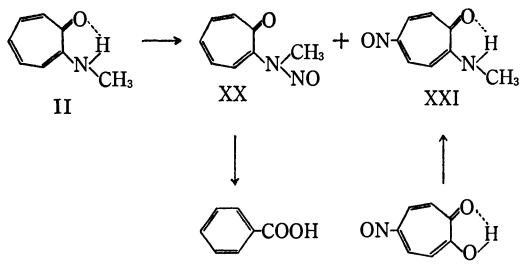

10) a) T. Nozoe, *Sci. Repts. Tohoku Univ., Ser. I*, **34**, 199 (1950). b) T. Nozoe, Y, Kitahara, K. Doi and T. Arai, *Bull. Chem. Res. Inst. Non-Aqueous Soln., Tohoku Univ.*, **7**, 13 (1957).

11) a) W. von E. Doering and L. H. Knox, *J. Am. Chem. Seoc.*, **73**, 828 (1951). b) T. Nozoe, Y. Kitahara, E. Kunioka and T. Ando, *Proc. Japan Acad.*, **27**, 190, 231 (1951). c) J. W. Cook, J. D. London and D. K. V. Steel, *J. Chem. Soc.*, **1954**, 530.

12) P. Akroyd, R. D. Howorth and J. D. Hobson, *ibid.*, **1951**, 3427.

13) Unpublished result of experiments made in the authors' laboratory.

14) T. Nozoe, S. Seto, T. Ikemi and T. Arai, *Proc. Japan Acad.*, **27**, 24 (1951).

15) T. Nozoe, S. Seto, S. Ebine and S. Ito, *J. Am. Chem. Soc.*, **73**, 1875 (1951).

16) T. Nozoe, M. Sato and T. Matsuda, *Sci. Repts Tohoku Univ., Ser. I*, **37**, 407 (1953).

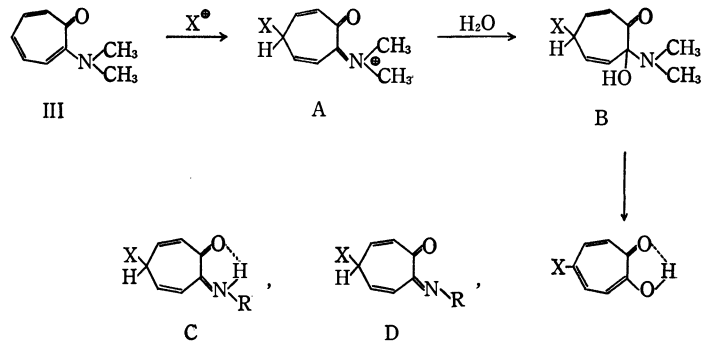

of active troponoid compound[17] and has interesting properties.

Azo-coupling Reaction, Nitrosation and Sulfonation of 2-Dimethylaminotropone. Substitution reactions do not occur when tropolone methyl ethers are treated with cationoid reagents, but addition reactions do take place.[18] However, the halogenation of III shows that the substitution reactions occur with the hydrolysis of the dimethylamino group, as has been mentioned before. Therefore, the reactions of III with cationoid reagents other than halogens were undertaken.

Although the nitration of III resulted in the recovery of the starting substance, as has been mentioned before, the nitrosation of III in ordinary ways gave 5-nitrosotropolone[11a,15] in a 95% yield. Also, 5-(*p*-nitrophenyl)azotropolone[19] was obtained quantitatively when III was treated with *p*-nitrophenyl diazonium salt. The reaction of III with 1.5 mol of sulfamic acid afforded tropolone-5-sulfonic acid[14] in a 35% yield; there was also a 50% recovery of III.

The electrophilic substitution reactions of III always resulted in the hydrolysis of the 2-dimethylamino group, thus forming tropolone derivatives as in the case of halogenations. It is possible that III is hydrolized to form tropolone first, and that then the attack of a cationoid reagent takes place. However, the treatment of III under the same conditions as in the substitution reactions, but without reagents, resulted in the recovery of III unchanged. Moreover, in the case of nitration, III was recovered quantitatively even if reagents were present. It is also known that if a reaction is carried out under anhydrous conditions, III and its derivatives give substituted derivatives of III without any hydrolysis of the 2-dimethylamino group.[20] Therefore, the mechanism of the reactions can be explained as follows: the nucleophilic attack of water on the C-2 position of the intermediate A to give tropolone derivatives *via* a B-type intermediate, because the steric interference of the dimethylamino group of A makes it difficult for A to keep the dimethylamino group in the same plane of the seven-membered ring.

On the other hand, II can form a C-type intermediate which possesses a hydrogen bond that contributes to the stability of C; the hydrogen is even able to leave to form D and other types of intermediates under some conditions. These entities do not have serious steric interference like that of A. This is the reason why only III gives hydrolized products during the electrophilic substitution reactions.

It is very interesting that, unlike tropolone methyl ethers,[18] not addition reactions but substitution reactions take place in the case of electrophilic reactions of III.

By cationoid substitution reactions under acidic conditions as in nitration, I and III were recovered unchanged, but only II afforded substitution products. This relation is parallel with the order of basicity of primary-, secondary-, and tertiary-amines.

Experimental[21]

3,5,7-Trichloro-2-aminotropone (V). To a solution of 0.60 g of I in 5 m*l* of chloroform cooled in an ice bath, 0.35 g of chlorine in 5 m*l* of chloroform was added drop by drop, and then the mixture was allowed to stand overnight at room temperature. The precipitate formed was separated by filtration; then the chloroform layer was washed with aqueous sodium bicarbonate and water and dried over sodium sulfate, and the chloroform was removed. The residue was recrystallized from benzene-methanol to give 0.35 g of V; yellow needles, mp 183—185°C.

Found: C, 37.85; H, 2.00; N, 6.62%. Calcd for $C_7H_3ONCl_3$: C, 37.45; H, 1.79; N, 6.24%.

The former precipitate was treated with aqueous sodium bicarbonate and extracted with chloroform. The chloroform layer was washed with water and dried

17) Recording the definition of active troponoid compounds, see Ref. 3b, p. 179.

18) M. Yasunami, D. Sc. thesis of Tohoku University, Feb., 1966.

19) T. Nozoe, S. Ito, S. Suzuki and K. Hiraga, *Proc. Japan Acad.*, **32**, 344 (1956).

20) T. Toda, Y. Miura and T. Mukai, *Nippon Kagaku Zasshi (J. Chem. Soc. Japan, Pure Chem. Sect.)*, **89**, 804 (1968).

21) All melting points are uncorrected.

over sodium sulfate; the chloroform was then removed under reduced pressure to give 0.40 g of I.

Hydrolysis of V; 3,5,7-Trichlorotropolone. A mixture of 0.10 g of V and 5 m*l* of 1.6 N potassium hydroxide was heated on a water bath for 4 hr. The V was then gradually dissolved, whereupon ammonia gas evolved. The solution was acidified with N hydrochloric acid and extracted with chloroform. The chloroform layer was washed with water and dried over sodium sulfate, and then the chloroform was removed under reduced pressure to give 70 mg of pale yellow needles, the melting point of which failed to show any depression on admixture with authentic 3,5,7-trichlorotropolone.[7]

Bromination of 2-Aminotropone Copper Complex (IV). To a solution of 1.21 g of IV in 100 m*l* of chloroform, 1.09 g of sodium acetate was added, and then 30 m*l* of chloroform containing 1.28 g of bromine was added, drop by drop. A dark green precipitate was formed immediately, and then the mixture was allowed to stand overnight. The precipitate formed was separated by filtration and recrystailized from chloroform to give greenish scales of the complex of VI, mp 253—255°C. The complex was dissolved in 100 m*l* of methanol containing a few drops of 1 N hydrochloric acid, and the mixture was treated with hydrogen sulfide. The solvent was removed, and the residue obtained was recrystallized from cyclohexane - acetone to give 1.00 g of yellow needles, mp 203—205°C, which was undepressed on admixture with an authentic sample of 5,7-dibromo-2-aminotropone.[4]

The chloroform layer was treated as above to give 0.38 g of recovered I.

Bromination of I with Pyridine Perbromide (PPB); 3,5,7-Tribromo-2-aminotropone (VI). *a) With 1 mol of PPB.* A solution of 0.37 g of I in 5 m*l* of chloroform cooled in an ice bath was treated with 0.72 g of PPB prepared by McElvain's method.[22] The precipitate thus formed was recrystallized from ethanol to give 0.32 g of yellow needles, mp 196—198°C, which were found to be identical with the 3,5,7-tribromo-2-aminotropolone[4] by a comparison of their mixed mp and IR spectra.

The chloroform layer was neutralized and concentrated to give 0.20 g of recovered I.

b) With 2 mol of PPB. From 0.37 g of I and 1.44 g of PPB, 0.60 g of VI and 0.10 g of recovered I were obtained.

Bromination of II by PPB; 3,5,7-Tribromo-2-*N*-methylaminotropone (VIII). *a) With 1 mol of PPB.* From 0.34 g of II and 0.60 g of PPB, 0.25 g of yellow needles of VIII was obtained; mp 197—199°C after recrystallization from cyclohexane - acetone.

Found: C, 26.26; H, 2.09; N, 4.03%. Calcd for $C_8H_6ONBr_3$: C, 25.84; H, 1.63; N, 3.78%.

From the chloroform layer, 0.20 g of II was recovered.

b) With 2 mol of PPB. From 0.34 g of II and 1.20 g of PPB, 0.51 g of VIII and 0.20 g of a mixture of mono- and dibromo-derivatives of II were obtained.

Bromination of II in Acid. *a) With 1 mol of Bromine.* Into a solution of 0.34 g of II in 5 m*l* of acetic acid cooled in an ice bath, 0.40 g of bromine in 2 m*l* of acetic acid was stirred, drop by drop: then the mixture was allowed to stand overnight at room temperature. The yellow precipitate thus formed was separated by filtration and washed with aqueous sodium bicarbonate and water. Recrystallization from cyclohexane - acetone gave 0.26 g of yellow needles of VIII. The acetic acid layer was diluted with water, and extracted with chloroform, and the chloroform layer was washed with water, and dried over sodium sulfate. After the chloroform had then been removed, the residue was recrystallized from cyclohexane to give 0.20 g of recovered II, mp 75—76°C.

b) With 3 mol of Bromine. From 0.34 g of II, 3 equivalent moles of sodium acetate, and 1.2 g of bromine, 0.82 g of VIII was obtained under the same reaction conditions.

Hydrolysis of VIII; 3,5,7-Tribromotropolone. A solution of 100 mg of VIII in 4 m*l* of 1.6 N methanolic potassium hydroxide was refluxed on a water bath for 4 hr. After cooling, the solution was acidified with 1 N hydrochloric acid and extracted with benzene. The benzene layer was washed with water, dried over sodium sulfate, and concentrated. The residue thus obtained was recrystallized from cyclohexane - benzene to give 60 mg of pale yellow needles, mp 125—127°C, which failed to show any depression upon admixture with 3,5,7-tribromotropolone.

Bromination of II in Methanol: 5,7-Dibromo-2-methylaminotropone (IX). *a) With 1 mol of Bromine.* Into a solution of 0.34 g of II in 5 m*l* of methanol cooled in an ice bath, 0.40 g of bromine in 10 m*l* of methanol was stirred drop by drop, and then the mixture was allowed to stand at room temperature overnight. The precipitate thus formed was separated by filtration, washed with aqueous sodium bicarbonate and water, and dried in a desiccator. Recrystallization from cyclohexane - acetone afforded 0.20 g of yellow needles of IX, mp 204—205°C.

Found: C, 32.77; H. 2.36; N, 4.73%. Calcd for $C_8H_7ONBr_2$: C, 32.80; H, 2.41; N, 4.75%.

From the methanol layer, 0.15 g of II was recovered.

b) With 3 mol of Bromine. From 0.34 g of II and 1.2 g of bromine, 0.62 g of IX was obtained.

Bromination of III in Methanol. *a) With 1 mol of Bromine.* A methanol solution (5 m*l*) of 0.15 g of III was cooled in an ice bath, and then into this solution 0.16 g of bromine in 1 m*l* of methanol was stirred, drop by drop. The color of the bromine disappeared gradually. The solution was allowed to stand at room temperature for 1 hr and then the methanol was removed under reduced pressure. The addition of water caused the precipitation of a crystalline substance, 62 mg, the melting point of which was 156—158°C after recrystallization from methanol. This substance was found to be identical with 3,5-dibromotropolone by a comparison of their IR spectra and by a mixed-melting-point determination.

To the filtrated mother layer, 5 m*l* of 1 N sodium hydroxide was added, and then the mixture was extracted with chloroform. From the water layer, 37 mg of pale yellow crystals were obtained, mp 126—127°C, which were found to be identical with 3,5,7-tribromotropolone by comparison of thir IR spectra and by a mixed-melting-point determination.

From the chloroform layer 0.10 g of a yellow oil was obtained; this oil was found to be identical with be original substance by a comparison of their IR spectra.

22) S. M. McElvain and L. R. Morris, *J. Am. Chem. Soc.*, **73**, 206 (1951).

and the mixed mp of the picrate, mp 155°C.

b) With 3 mol of Bromine. From 0.15 g of III and 3 equivalent moles of bromine, 0.38 g of 3,5,7-tribromotropolone was obtained by the treatment described above.

7-Iodo-2-aminotropone (VII). I (0.60 g) and potassium carbonate (1.5 g) were dissolved in 6 m*l* of water and methanol (1 : 1) cooled in an ice bath, and into this, a solution of 1.4 g of iodine and 1.0 g of potassium iodide in 10 m*l* of cold water was stirred, drop by drop. The mixture was then allowed to stand at room temperature overnight. The mixture was slightly acidified by the addition of 1 N hydrochloric acid; the precipitate thus formed was then recrystallized from cyclohexane to give 0.28 g of pale green needles of VII, mp 202—203°C.

Found: C, 35.72; H, 2.50; N, 5.76%. Calcd for C_7H_6ONI: C, 35.45; H, 2.55; N, 5.92%.

The mother layer was extracted with chloroform, after which the chloroform layer was treated as before to give 0.35 g of recovered I.

7-Iodo-2-methylaminotropone (X). From 0.67 g of II, 1.5 g of potassium carbonate, and a solution of 1.4 g of iodine and 1.0 g of potassium iodide, 1.22 g of X, mp 179—180°C, was obtained by the treatment described above.

Found: C, 36.35; H, 3.46; N, 5.03%. Calcd for C_8H_8ONI: C, 36.81; H, 3.09; N, 5.37%.

Hydrolysis of VII and X; 3-Iodo-tropolone (XIII). A solution of 0.10 g of VII in 5 m*l* of 1.6 N methanolic potassium hydroxide was heated under reflux for 4 hr; then it was concentrated, and water was added. The water layer was neutralized with 1 N hydrochloric acid and extracted with benzene. After the benzene had been removed, the residue was sublimated under reduced pressure. The recrystallization of the sublimated from cyclohexane - benzene afforded 60 mg of a pale yellow, crystalline substance, mp 101—102°C, which was identical with authentic 3-iodotropolone. By the same procedure, 0.10 g of X gave 70 mg of XIII.

Iodination of III. A solution of 0.75 g of III and 1.5 g of potassium carbonate in 4 m*l* of methanol and water (1 : 4), and a solution of 1.4 g of iodine and 1.0 g of potassium iodide in 10 m*l* of water were treated in the same way as I and II. After recrystallization from cyclohexane, 1.02 g of XIII were obtained.

Nitration of II. *a) With 1 mol of Nitric Acid, 5-Nitro-2-methylaminotropone (XIV).* A solution of 0.40 g of II in 3 m*l* of acetic acid was cooled in an ice bath, and into this, 0.33 g of 60% nitric acid in 2 m*l* of acetic acid was added stirred, drop by drop. The reaction mixture was then poured into crushed ice, and the prepipitate thus formed was separated by filtration and dried in a desiccator overnight. Recrystallization from cyclohexane - benzene afforded 0.45 g of green-yellow, micro needles of XIV, mp 214—216°C.

Found: C, 54.85; H, 4.32; N, 15.30%. Calcd for $C_8H_9O_3N_2$: C, 55.33; H, 4.48; N, 15.55%.

b) With Excess Nitric Acid. XIV and 5,7-Dinitro-2-methylaminotropone (XV). From 0.40 g of II and 1.0 m*l* of 60% nitric acid, 0.70 g of a crude substance was obtained by the same treatment as above. Recrystallization from ethanol gave 0.19 g of pale green needles, mp 214—216°C, which were identical with XIV. Ethanol-layer condensation afforded 0.41 g of a residue the recrystallization of which from cyclohexane-benzene gave orange-yellow needles of XV, mp 195—196°C.

Found: C, 43.04; H, 3.39; N, 18.26%. Calcd for $C_8H_7O_5N_3$: C, 42.70; H, 3.14; N, 18.64%.

Treatment of Nitrotropolones with Monomethylamine. *a) XIV.* A solution of 0.20 g of 5-nitrotropolone in 20 m*l* of benzene cooled in an ice bath, was saturated with dry monomethylamine, then the mixture was allowed to stand overnight. After the benzene and monomethylamine had been removed under reduced pressure, the residue was recrystallized from cyclohexane - benzene to give 0.16 g of yellow needles, mp 210—213°C, which did not show any depression on admixture with XIV.

b) XV. 3,5-Dinitrotropolone (0.20 g) was treated as above to give 0.14 g of XV.

Nitration of I. Nitric acid (60%, 1 m*l*) was stirred into a solution of 0.60 g of I in 2 m*l* of acetic acid cooled in an ice bath, and then the mixture was allowed to stand overnight. The reaction mixture was poured into crushed ice, the precipitate thus formed was separated by filtration, dried in a desiccator, and recrystallized from cyclohexane to give 0.55 g of the starting material.

Nitration of III. III (0.45 g) was treated with 1 m*l* of 60% nitric acid as above. An oily substance was obtained; this was found to be identical with III by a comparison of their IR spectra. This oil afforded 0.75 g of the picrate of III, mp 143—145°C.

5-Phenylazo-2-methylaminotropone (XVI). a) Into a solution of 0.135 g of II in 0.4 m*l* of 4 N of hydrochloric acid cooled in an ice bath, a phenyldiazonium chloride solution, prepared from 0.10 g of aniline in the ordinary way, was stirred. After 2 hr, the pH of the solution was adjusted to about 7.5 with aqueous sodium bicarbonate and extracted with benzene. The benzene layer was washed with water, dried over sodium salfate and chromatographed on alumina. From the cyclohexane-benzene elution part, 0.10 g of red needles of XVI was obtained; mp 145—146°C from the same mixed solvent.

Found: C, 70.65; H, 5.34; N, 17.26%. Calcd for $C_{14}H_{13}ON_3$: C, 70.27; H, 5.48; N, 17.56%.

From the benzene-acetone elution part, 40 mg of II were recovered.

b) 5-Phenylazotropolone methyl ether (0.20 g) was treated with excess methylamine in a sealed tube at room temperature for 4 days. After the methylamine had then been removed, the residue was recrystallized from cyclohexane-benzene to give 0.20 g of red needles of XVI, mp 140—141°C.

5-(*p*-Nitrophenylazo)-2-methylaminotropone (XVII). a) From 0.28 g of II and 1.5 equimoles of *p*-nitroaniline, 0.54 g of dark red scales of XVII, mp 254—256°C from cyclohexane - benzene was obtained by the same treatment as above.

Found: C, 59.87; H, 4.70; N, 20.52%. Calcd for $C_{14}H_{12}O_3N_4$: C, 59.15; H, 4.26; N, 19.71%.

b) 5-*p*-(Nitrophenylazo)tropolone methyl ether (50 mg) was treated with excess methylamine as above; 40 mg of XVII, mp 214—216°C from cyclohexane-benzene were thus obtained. The azo compounds obtained by the a and b method were found to be identical with each other by a comparison of their IR spectra and by a mixed-melting-point determination.

Azo-coupling Reaction of 2-Dimethylaminotropone (III); 5-(*p*-Nitrophenylazo)tropolone. *p*-Nitrophenyl diazonium chloride prepared from 0.60 g

of *p*-nitroaniline was added, drop by drop, to a solution of 0.45 g of III in 5 m*l* of dioxane, and then the mixture was allowed to stand for 2 hr while being stirred. The reaction mixture was neutralized with aqueous sodium bicarbonate.

The precipitate thus formed was separated by filtration, dried in a desiccator, and recrystallized from benzene to give 0.78 g of orange scales, mp 233—235°C, which were found to be identical with 5-(*p*-nitrophenylazo)tropolone by a comparison of their IR spectra and by a mixed-melting-point determination.

Sulfonation of II; 2-Methylaminotropone-5-sulfonic acid (XVIII). A well-ground mixture of 2.70 g of II and 2.90 g of sulfamic acid was heated in fusion at 160°C for 6 hr under a nitrogen atmosphere. After the reaction, the reaction mixture was extracted with chloroform and hot water. The concentration of the chloroform afforded 1.07 g of recovered II. The water layer was concentrated under reduced pressure to give pale yellow needles which, when recrystallized from methanol, afforded 2.01 g of pale yellow needles of XVIII, mp>350°C. This was treated with an equimole of benzylthiourea in diluted methanol; the recrystallization of the benzylthioronium salt thus obtained afforded pale yellow needles, mp 172—174°C.

Found: C, 50.37; H, 4.81; N, 10.77%. Calcd for $C_{16}H_{19}O_4N_3S_2$: C, 50.31; H, 5.02; N, 11.01%.

Sulfonation of III; Tropolone-5-sulfonic Acid. III (0.40 g) and sulfamic acid (0.39 g) were treated at 180°C for 10 hr in the way described above. From the chloroform extract, 0.51 g of III was recovered as its picrate, mp 145°C. The water layer showed a positive ferric chloride test and the addition of *p*-toluidine afforded colorless needles, mp 236—238°C. The melting point did not show any depression on admixture with *p*-toluidinium salt of tropolone-5-sulfonic acid, and their IR spectra were identical.

Hydrolysis of XVIII. On a water bath, 0.10 g of XVIII was heated for reflux in 2 m*l* of 1.6 N ethanolic potassium hydroxide for 4 hr. The pH of the solution was then adjusted about 3 with 1 N hydrochloric acid and 0.10 g of *p*-toluidine was added. The needles thus formed, mp 237—239°C, were identical with the *p*-toluidinium salt of tropolone-5-sulfonic acid.

Nitration of XVIII; 5,7-Dinitro-2-methylaminotropone (XV). Into a solution of 0.20 g of XVIII in 20 m*l* of acetic acid cooled in an ice bath, 1.0 m*l* of 60% nitric acid was stirred. After it had been allowed to stand for a couple of hours, the reaction mixmixture was poured onto ice; the precipitate thus formed was then separated by filtration and dried in a desiccator. Recrystallization from cyclohexane - benzene gave 0.15 g of orange yellow scales, mp 197—199°C, which were identical with 5,7-dinitro-2-methylaminotropone.

Bromination of XVII; 3,5-Dibromotropolone-5-sulfonic Acid (XIX). XVIII (0.20 g) was dissolved in 10 m of water and methanol (1 : 1), and then the mixture was cooled in an ice bath. Into this, 0.60 g of bromine was stirred, drop by drop, and then the reaction was continued for 30 min. The concentration of the solution caused the precipitation of a crystalline substance, the recrystallization of which from ethanol afforded 0.22 g of white rhombo prisms, mp 217—220°C.

Found: C, 23.50; H, 1.52%. Calcd for $C_7H_4O_5SBr_2$: C, 23.35; H, 1.12%.

Nitrosation of II; 2*N*-Nitrosomethylaminotropone (XX) and 5-Nitroso-2-methylaminotropone (XXI). Into a cold solution of 0.68 g of II in 5 m*l* of 10% hydrochloric acid, 0.43 g of sodium nitrite dissolved in 10 m*l* of water was stirred; the mixture was then allowed to stand for a couple of hours. The reaction mixture was then poured onto crushed ice, and the precipitate thus formed was separated by filtration and dried in a desiccator. Recrystallization form cyclohexane afforded 0.70 g of white needles of XX, mp 98—99°C.

Found: C, 58.74; H, 4.78; N, 16.78%. Calcd for $C_8H_8O_2N_2$: C, 58.53; H, 4.91; N, 17.07%.

The water layer was neutralized with aqueous sodium bicarbonate and extracted with benzene. The benzene layer was dried over sodium sulfate, and then filtered off, and the residue was recrystallized from cyclohexane - benzene to give 80 mg of brown-yellow scales of XXI, mp 128—130°C.

Found: C, 58.98; H, 5.18; N, 16.84%. Calcd for $C_8H_8O_2N_2$: C, 58.53; H, 4.91; N, 17.07%.

5-Nitrosotropolone (0.30 g) was dissolved in 20 m*l* of benzene, and the mixture was cooled in an ice bath. This was then saturated with dry methylamine. The precipitate thus formed was then separated by filtration and recrystallized from cyclohexane - benzene to give 0.15 g of brown-yellow scales, mp 123—125°C, which were identical with the XXI obtained above.

Rearrangement of XX. XX (0.16 g) was refluxed in 3 m*l* of 1.6 N ethanolic potassium hydroxide for 4 hr. After cooling, the solution was acidified with N hydrochloric acid and extracted with ether. The ether layer was washed with water and dried over sodium sulfate, and the ether was removed. White needles, mp 120—121°C, were obtained; the melting point did not show any depression on admixture with benzoic acid.

BULLETIN OF THE CHEMICAL SOCIETY OF JAPAN VOL. 41 2985—2989 (1968)

Electrolytic Reduction of Naphthalene in Various Alcohol-Hexamethylphosphoramide Systems

Teruzo ASAHARA, Manabu SENŌ and Hideaki KANEKO

The Institute of Industrial Science, The University of Tokyo, Roppongi, Minatoku, Tokyo

(Received April 26, 1968)

The electrolytic reduction of naphthalene was carried out in various alcohol-hexamethylphosphoramide (HMPA) systems in the presence of lithium chloride. The reduction of naphthalene proceeds effectively at relatively low cathode potentials in the presence of HMPA; the composition of the products varies with the changes in the reduction potential, the kind of alcohols, and the concentration of HMPA. The dark blue color is observed at the cathode during the electrolysis in HMPA solutions in either the presence or the absence of ethanol. It is suggested that the color reflects the generation of solvated electrons, and that reduction of naphthalene is caused not through a direct electron-transfer from the cathode, but through a reaction with solvated electrons as the reductive agent.

In this series of investigations, the reduction of various organic compounds by solvated electrons will be discussed. It has been considered that the solvated electrons are generated especially in polar solvents by high-energy radiation and exist in amine or ether solutions of alkali metals, especially in a dilute metal-ammonia solutions.[1] Extensive investigations have been carried out into their properties and reactions with various compounds in metal-ammonia solutions; however, there have been few investigations of reactions in other systems.[2,3] The existence and the properties of solvated electrons have been suggested and examined by the methods of electric conductivities, absorption spectra, and electron-spin resonances, but a complete understanding has not yet been obtained. Recently, Sternberg *et al.* reported a series of investigations of the electrolytic reduction of aromatic compounds in the ethylenediamine-lithium chloride systems and suggested that the reduction was caused by an indirect electron-transfer mechanism.[4,5] In these systems, it might be considered that the solvated electrons act as a reductive agent. In the present paper, the electrolytic selective reduction of naphthalene in mixed solvent systems of various alcohols and hexamethylphosphoramide in the presence of lithium chloride will be reported. The generation of solvated electrons has been suggested in this system.[6]

Experimental

Reagents. The hexamethylphosphoramide (HMPA, Japan Oil Seal Co.) was purified by reflux over calcium hydride and by subsequent distillation under reduced pressures. The alcohols (methanol, ethanol, 1-propanol, and 2-propanol) were purified by reflux over calcium oxide and by distillation. Lithium chloride of a reagent grade was used without further purification, while the naphthalene was purified by recrystallization and sublimation.

Apparatus and Procedure. The electrolysis vessel used is an H-cell with a total capacity of 40 m*l*. It is separated by a filter paper, Toyo Roshi No. 2, into two compartments. A platinum anode and cathode were used through the present experiments. The area of each electrode is 3 cm^2. The electrode potential was measured against an Ag wire used as a reference electrode. The electrolysis vessel was set in a water bath maintained at nearly constant temperatures, 18—20°C. All electrolyses were carried out at constant voltages or constant currents by a manually-controlled device.

The concentrations of naphthalene and lithium chloride are 0.2 and 0.5 M respectively, except when otherwise stated; the total volume of the reaction mixture is 20 m*l*, and the HMPA content varies from 0 to 50 vol%. The reduction products were analyzed by gas chromatography (column, polyethylene glycol 6000, 2.5 m; column temperature, 150°C; helium flow rate, 40 m*l*/min) and by mass-spectrometry. The identification was made through a comparison of the retention time with those of the authentic samples, while the yield was estimated by the measurement of the peak heights.

Results

Ethanol-HMPA System. The results for the electrolysis of naphthalene in a mixed ethanol-HMPA system containing lithium chloride are

1) "Solvated Electron," Adv. Chem. Ser., 50 (1965).
2) M. C. R. Symons, *Quart. Rev. (London)*, **13**, 99 (1959).
3) M. J. Sienko and G. Lepoutre, eds., "Metal-Ammonia Solutions," Benjamin, New York (1964).
4) H. W. Sternberg, R. E. Markby and I. Wender, *J. Electrochem. Soc.*, **110**, 452 (1963).
5) H. W. Sternberg, R. E. Markby and I. Wender, *ibid.*, **113**, 1060 (1066).
6) H. W. Strernberg, R. E. Markby and I. Wender, *J. Am. Chem. Soc.*, **89**, 186 (1967).

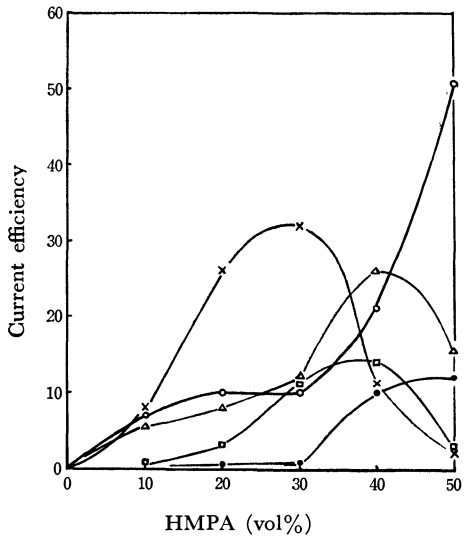

Fig. 1. Ethanol-HMPA system at −3.10 V *vs.* Ag wire.
○—○ Dihydronaphthalene ●—● Tetralin
△—△ Hexaline □—□ Octalin
×—× Decalin

given in Fig. 1. The concentrations of naphthalene and lithium chloride were 0.4 and 0.5M, respectively, and the cathode potential was maintained at nearly −3.10 V *vs.* Ag wire. This potential is more negative by about 1 volt than the reduction potential of naphthalene. As is shown in Fig. 1, no reduction products were detected in the absence of HMPA. When HMPA is added, the reduction of naphthalene occurs effectively, and the total current efficiency for the production of hydronaphthalenes increases with an increase in the HMPA content. The selectivity of reduction depends remarkably on the HMPA content. The current efficiencies for dihydronaphthalenes and tetralin increase monotonously with an increase in the content of HMPA, ranging from 0 to 50 vol%; on the other hand, the maximum current efficiencies of hexalin, octalin, and decalin are found at 40, 35, and 30 vol% of HMPA, respectively.

The electrolytic reduction at various reduction potentials was carried out under similar conditions.

Table 1. Electrolytic reduction of naphthalene in ethanol-HMPA system at −1.70±0.05 V *vs.* Ag wire

HMPA (vol%) Product (mole ratio, %)	40	30	20	10
1,2-Dihydronaphthalene	12	—	34	33
1,4-Dihydronaphthalene	88	100	66	67
Curr. eff. (%)	61.3	50.4	44.0	25.2

Table 1 shows the results of electrolytic reduction at −1.7±0.05 V *vs.* Ag wire. The reduction products are 1,2- and 1,4-dihydronaphthalene, with the latter the main product. The electrolyses carried out at −2.0±0.05 V and −2.5±0.05 V *vs.* Ag wire also afford only 1,2- and 1,4-dihydronaphthalene.

Methanol-HMPA System. In order to get some insights into the effect of alcohols on the reduction of naphthalene, the electrolytic reduction was carried out in the methanol-HMPA system under conditions similar to those in the ethanol-HMPA system. The results are shown in Tables 2 and 3.

Table 2. Electrolytic reduction of naphthalene in methanol-HMPA system at −1.20—−1.30 V *vs.* Ag wire

HMPA (vol%) Product (mole ratio, %)	40	30	20	10
1,4-Dihydronaphthalene	100	100	88	64
Tetralin	—	—	12	36
Curr. eff. (%)	8.2	15.3	16.1	26.2

Table 3. Electrolytic reduction of naphthalene in methanol-HMPA system at −1.70—−1.75 V *vs.* Ag wire

HMPA (vol%) Product (mole ratio, %)	50	40	30	20	10
1,4-Dihydronaphthalene	88	90	83	82	82
Tetralin	6	10	16	18	18
Hexalin	6	—	1	—	—
Curr. eff. (%)	85.3	38.8	40.8	27.1	20.1

In the absence of HMPA, the reduction of naphthalene does not occur. When HMPA is added, the main products are dihydronaphthalenes and tetralin, but the yield of tetralin decreases with an increase in the HMPA content. The selective reduction into dihydronaphthalenes becomes almost complete at higher HMPA contents, especially when the electrode potential is low. The total current efficiency increases with an increase in the content of HMPA, except for the case of a lower electrode potential (−1.20—−1.30 V *vs.* Ag wire). Table 4 shows the effect of the cathode potential in the range from −1.20 to −1.75 V *vs.* Ag wire at the HMPA content of 30 vol%. The increase in reduction potentials results in an increase in the total current efficiency, but a decrease in the selectivity for the formation of dihydronaphthalenes.

It must be noticed that the electrolytic reduction of naphthalene takes place steadily at the cathode potential of −1.20—−1.30 V *vs.* Ag wire. The polarographic half-wave potential of naphthalene

Table 4. Effect of cathode potentials on reduction of naphthalene in methanol-HMPA system (HMPA content 30 vol%)

Cathode potential V *vs.* Ag wire	Product (mole ratio, %)			Curr. eff. (%)
	1,4-Dihydro-naphthalene	Tetralin	Hexalin	
−1.25±0.05	100	—	—	15.3
−1.52±0.03	82	18	—	35.3
−1.72±0.03	83	16	1	40.8

Table 5. Electrolytic reduction of naphthalene in 2-propanol-HMPA system under constant current 20 mA (Total electricity 190 coul.)

HMPA (vol%) Porduct (mole ratio, %)	30	20	10	0
1,2-Dihydronaphthalene	90	84	63	70
1,4-Dihydronaphthalene	3	5	15	15
Tetralin	7	8	11	10
Hexaln	—	3	11	5
Curr. eff. (%)	100	92	92	50
Cathode potential (V *vs.* Ag wire)	3.5—4.2	6.4—7.0	10—20	40—60*

* This value is very irreproducible.

Table 6. Electrolytic reduction of naphthalene in 2-propanol-HMPA system under constant current 20 mA (Total electricity 190 coul.)

HMPA (vol%) Product (mole ratio, %)	30	20	10	0
Dihydronaphthalene	2	—	—	100
Tetralin	5	5	—	—
Hexalin	9	10	12	—
Octalin	4	—	—	—
Decalin	80	85	88	—
Curr. eff. (%)	100	100	100	10
Cathode potential (V *vs.* Ag wire)	4.9—5.5	6.0—10	6.0—7.8	50—60*

* This value is very irreproducible.

has been reported to be −1.98 V *vs.* SCE in an ethylene glycol monomethyl ether solution using 0.1 M tetrabutylammonium iodide as a supporting electrolyte,[7] and −2.53 V *vs.* SCE in a 75% dioxane solution.[8] Even if the reduction potential in the macro-electrolysis differs somewhat from that in micro-electrolysis, this finding shows that the electrolytic reduction of naphthalene does occur in a system containing HMPA at lower cathode potentials than the half-wave potential, which is required for the direct electron-transfer from the cathode to naphthalene molecules. This fact may be interpreted on the assumption of some indirect electron-transfer machamism, which is probably closely connected with the existence of HMPA, as will be discussed in detail later.

Propanol-HMPA System. In order to examine the effect of alcohols further investigations were carried out by using 2-propanol and 1-propanol. The electrolysis was done under a constant current of 20 mA, because these systems are very resistive and a sufficiently high current is not obtained when a similar cathode potential as employed in the methanol and ethanol system is used. The results in the 2-propanol-HMPA system are shown in Table 5, where the cathode potentials are also given. Upon an increase in the HMPA content, the cathode potential decreases remarkably. In the absence of HMPA, the cathode potential is irreproducible but very high, and naphthalene is reduced electrolytically into hydronaphthalenes; this is in contrast to the case of a pure methanol or ethanol system, where a high-electrode potential sufficiency for direct electron-transfer is not retained.

7) E. M. Elofson, *Anal. Chem.*, **21**, 916 (1949).
8) G. J. Hojitink and J. V. Schooten, *Rec. Trav. Chim.*, **71**, 1089 (1952).

The results of electrolyses in the mixed solvents of 1-propanol-HMPA are shown in Table 6. In the absence of HMPA, the cathode potential is very high and naphthalene is reduced into dihydronaphthalenes electrolytically, but the current efficiency is very low. Upon an increase in the HMPA content, the cathode potential necessary for the passage of a constant current, 20 mA, decreases, but the total current efficiency for the reduction of naphthalene is nearly quantitative and the main product is decalin.

Effect of the Addition of Water. In order to examine the effect of the addition of water as a proton donor, the electrolysis of naphthalene in the ethanol-HMPA-water system (volume ratio, 10 : 10 : 4) was carried out. The conditions of electrolysis were as follows: the concentration of naphthalene and LiCl are 0.32 M and 0.4 M, respectively, and the cathode potential is 3.0 V *vs.* Ag wire. During the electrolysis the evolution of gas is violent at the cathode, probably because of the electrolytic decomposition of water, but naphthalene is not reduced on the passage of 4.68×10^2 coulomb.

Current-Voltage Relation. In Fig. 2 the current-voltage relationships in systems of water, methanol, ethanol, 1-propanol, 2-propanol, and respective alcohol-HMPA mixed solvents containing 0.5 M lithium chloride are shown. The cell temperature was maintained at 18—20°C in a water bath.

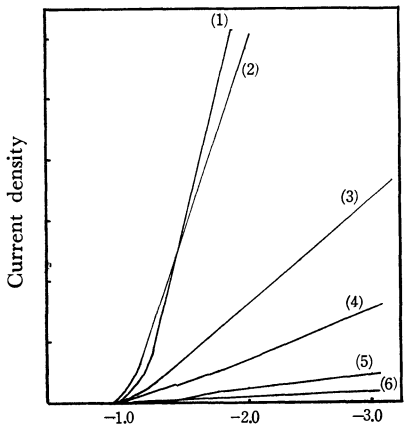

Fig. 2. Current-voltage relation.
(1) H_2O, (2) Methanol, (3) Methanol+HMPA (vol. ratio 1 : 1), (4) Ethanol, (5) 1-Propanol, (6) 2-Propanol; containing 0.5 M lithium chloride in all cases.

In these systems the addition of naphthalene (0.5 M) has little effect on the current-voltage curve. The decomposition voltages are nearly the same, about −1.0 V *vs.* Ag wire, in all these systems. In the methanol system, the current density is very high compared to that in the other alcohol systems. The current density at the same electrode potential decreases in the order: $H_2O \sim$ methanol > ethanol > 1-propanol > 2-propanol, an order which agrees with the order of the decreasing dielectric constant or acidity. In the methanol system, the addition of HMPA depresses the current density by about half compared to the case of its absence; on the contrary, the addition of HMPA has little effect on the current density in the other alcohol systems.

Discussion

As has been described in the preceding section, the reduction of naphthalene does not take place in the absence of HMPA if the cathode potential is not extremely high, while naphthalene is effectively reduced even at cathode potentials lower than the polarographic half-wave potential if HMPA is added. These results suggest that the reduction of naphthalene is not caused through a direct electron-transfer mechanism in the present systems. The reduction mechanism is characteristic of an alcohol-HMPA system containing lithium chloride, as has been suggested by Sternberg *et al.*[6] They observed a dark blue color at the cathode during the electrolysis of lithium chroride in an HMPA-ethanol system, and suggested the generation of solvated electrons. These observations were confirmed in the present investigation, as will be described below.

When the electrolysis of lithium chloride in a pure HMPA system was carried out in an open H-cell with a diaphragm, the generation of dark blue globules was observed at the cathode after the evolution of gases. The globules disappear during the diffusion into the bulk solution and the liquid surface. When the electrolysis was carried out in a vacuum system, dark blue globules generate at the cathode, diffuse into the bulk, and disperse thoroughly in the cathode compartment. The coloration remains for several hours after the electrolysis.

When the vacuum electrolysis is carried out in the HMPA-ethanol system (volume ratio 1 : 1), a dark blue color is observed at the cathode surface, but it disappears during diffusion into the bulk. When naphthalene is added to this system, only a faint color is observed.

This coloration is the same as that observed in the system where alkali metals are dissolved in HMPA and shows a strong absorption band around 650 mμ. This absorption band is the same as that ascribed to the solvated electrons.[9] Moreover, it may be pointed out that the decomposition potentials in various HMPA-alcohol systems

9) M. Ottolenghi, K. Bar-Eli, H. Linschitz and T. R. Tuttle, *J. Chem. Phys.*, **40**, 3729 (1964).

are nearly all the same, around -1.0 V *vs.* Ag wire. At the electrode potentials over this value, naphthalene is reduced effectively. This value is lower than that ascribed to the reduction of naphthalene.

These results show that the reduction of naphthalene proceeds according to a mechanism similar to that proposed by Krapcho *et al.*[10] for the reduction of aromatic hydrocarbons by alkali metals in liquid ammonia and by Sternberg *et al.*[4] for the electrolytic reduction of the benzene ring in ethylenediamine saturated with lithium chloride. The general reaction scheme is as follows:

$$\mathrm{Li^+ + e \rightarrow (Li\cdots e)_{solv}}$$
$$\mathrm{(Li\cdots e)_{solv} + R \rightarrow Li^+ + R^{\mp}}$$
$$\begin{cases} \mathrm{R^{\mp} + DH \rightarrow RH + D^{\mp}} \\ \mathrm{R^{\mp} + (Li\cdots e)_{solv} \rightarrow R^{2-} + Li^+} \\ \mathrm{R^{2-} + 2DH \rightarrow RH_2 + 2D^-} \end{cases}$$

where R is an unsaturated compound to be reduced, DH is a proton donor, and $\mathrm{(Li\cdots e)_{solv}}$ is the solvated lithium and electron.

It is proposed that naphthalene is reduced into dihydronaphthalene according to the following scheme:

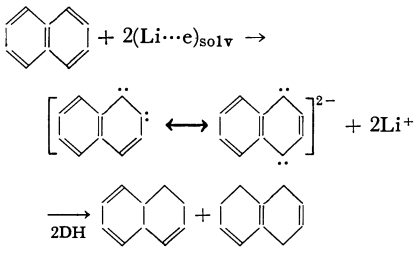

It may be supposed from the polarographic results of the one-step two-electron reduction that the two-electron transfer occurs successively from solvated lithium to naphthalene in the first step of reduction. In the present systems, alcohols probably act as proton donors.

The selectivity of the reaction is affected by various factors: the kind of alcohols, the alcohol content, and the reduction potentials. In the ethanol-HMPA system, the hydrogenation proceeds more intensively with an increase in the ethanol content, as is shown in Fig. 1. This is reasonable when ethanol is considered to act as a proton donor. Dihydronaphthalenes are the main product when the HMPA content is high. In the methanol-HMPA and the 2-propanol-HMPA systems, the main products are dihydronaphthalene and tetralin; the yield of the former increases with an increase in the HMPA content.

It may be considered that the hydrogenation proceeds more extensively with an increasing acidity of alcohols and that, on the other hand, more strongly acidic alcohols react more intensively with solvated lithium and electrons, resulting in the hydrogen evolution. This is the reason why water does not act as a proton donor for the reduction of naphthalene and why extensively hydrogenated products are obtained only in a system consisting of ethanol, a moderately strong proton donor.

The increase in reduction potentials extensively encourages the hydrogenation as shown in Table 4 in the methanol-HMPA system. This result can also be understood in view of the fact that the solvated electrons increase in quantity with an increase in the potential.

In the 1-propanol-HMPA system, the main product is decalin. This result can not be interpreted from the standpoint described above; it is now being investigated further.

A detailed discussion of the selectivity of this reaction system will be reported in the near future, together with the results of the polarographic examination and of the reduction of benzene in similar systems.

10) A. P. Krapcho and A. A. Bothner-By, *J. Am. Chem. Soc.*, **81**, 3658 (1959).

BULLETIN OF THE CHEMICAL SOCIETY OF JAPAN VOL. 41 2990—2994 (1968)

Studies of the Organic Reactions of Metal Carbonyls. XIV.*1 The Reaction of Potassium Iron Carbonylates with Isoprene

Yoshinobu TAKEGAMI, Yoshihisa WATANABE, Isao KANAYA, Takeaki MITSUDO, Toshiharu OKAJIMA, Yoshihiko MORISHITA and Hiromitsu MASADA

Department of Hydrocarbon Chemistry, Faculty of Engineering, Kyoto University, Sakyo-ku, Kyoto

(Received May 8, 1968)

The reaction between potassium iron carbonylates ($KHFe(CO)_4$, $K_2Fe(CO)_4$ and $K_2Fe_2(CO)_8$) and isoprene has been studied. Isoprene is reduced at room temperature to give three olefins (3-methyl-1-butene (I), 2-methyl-1-butene (II), and 2-methyl-2-butene (III)). The reaction conditions (solvents, atmospheres, additives such as water) have a great effect on the yield and distribution of the olefins. Under carbon monoxide in the presence of water, the reduction is highly promoted, giving 2 mol/mol-$Fe(CO)_4^{2-}$ of the olefins. The percentage of II is almost constant (about 15%) in any case, but the percentages of I and III, very dependent on the conditions, change in the 3—40 and 50—80% ranges respectively. The reaction is suggested to proceed *via* some kinds of σ- and π-allyl iron carbonyl complexes. Under carbon monoxide the carbonylation of isoprene also occurs.

Previous work in this laboratory has shown that potassium iron carbonylates ($KHFe(CO)_4$, $K_2Fe(CO)_4$ and $K_2Fe_2(CO)_8$) react with styrene oxide under carbon monoxide to give styrene and carbon dioxide.[1] Several workers have also shown that $H_2Fe(CO)_4$ and $KHFe(CO)_4$ have a large activity in the reduction of organic compounds, such as acetone, nitrobenzene, quinone, and acetylene.[2]

The present study will deal with the reaction of the iron carbonylate, mainly $KHFe(CO)_4$, with isoprene. The results obtained indicate that isoprene is reduced to give three different monoolefins, and that the yield and distribution of the olefins are remarkably affected by the reaction conditions.

Experimental

The Preparation of Potassium Iron Carbonylates, $KHFe(CO)_4$, $K_2Fe(CO)_4$. The alcoholic solutions of these salts were prepared according to the method described in a previous paper.[1] An 80 m*l* portion of 0.14 M $KHFe(CO)_4$ or $K_2Fe(CO)_4$ solution was used in each run.

When $KHFe(CO)_4$ is prepared, an equivalent mole of water is formed:[3]

$$Fe(CO)_5 + 3KOH \xrightarrow{\text{in alcohol}} KHFe(CO)_4 + K_2CO_3 + H_2O$$

Therefore, when a dry solution of $KHFe(CO)_4$ was required, the solvent of $KHFe(CO)_4$ solution was once distilled under a vacuum, and then 80 m*l* of a new dry solvent was added.

Materials. The isoprene, iron pentacarbonyl, methyl ethyl ketone, tetrahydrofuran, isopropyl ether, and other compounds employed in this study were all commercial products.

Reaction Procedures. Under Atmospheric Pressure. To the solution of the potassium iron carbonylate described above, 5 m*l* (50 mmol) of isoprene and 0.4 m*l* of cyclopentane, as an internal standard for analysis, were added. The mixture was then agitated for a certain reaction time at 30°C under an atmosphere of carbon monoxide, nitrogen, or hydrogen. After a certain reaction time, a 0.5 m*l* sample of the solution was removed and then diluted with 1.5 m*l* of cyclohexane. This cyclohexane solution was immediately submitted to analysis.

Under Hydrogen Pressure. An autoclave (100 m*l*) equipped with a magnetic stirrer was used. 1.5 m*l* of $Fe(CO)_5$, 33 m*l* of a 1 N KOH solution in ethyl alcohol, and 5 m*l* of isoprene were placed into the autoclave at −80°C. After the air in the autoclave had been replaced with nitrogen, hydrogen were introduced at 60 kg/cm^2. The autoclave was then kept at a certain temperature for 5 hr.

Analysis of the Products. The reaction products (three different olefins) were identified by gas chromatography using a PEG-Golay column. Further, the monoolefins produced were confirmed by being converted to isopentane; after hydrogenation with Raney

*1 Part XIII: This Bulletin, **41**, 158 (1968). Presented in part at the Annual Meeting of the Chemical Society of Japan, Osaka, April, 1968.

1) Y. Takegami, Y. Watanabe, T. Mitsudo, I. Kanaya and H. Masada, This Bulletin, **41**, 158 (1968).

2) Ger. Patent 441, 179 (1925); H. W. Sternberg, R. A. Friedel, R. Markby and I. Wender, *J. Am. Chem. Soc.*, **78**, 3621 (1956); H. W. Sternberg, R. Markby and I. Wender, *ibid.*, **78**, 5704 (1956); H. W. Sternberg, R. Marbky and I. Wender, *ibid.*, **79**, 6116 (1957).

3) P. Krumholz and H. M. A. Stettiner, *ibid.*, **71**, 3035 (1949).

nickel, the peaks of the monoolefins in a gas chromatogram vanished and a new peak of isope ntaneappeared.

Results

The Reaction of $KHFe(CO)_4$ and $K_2Fe(CO)_4$ with Isoprene in Ethyl Alcohol. The results of the reactions are summarized in Table 1 and

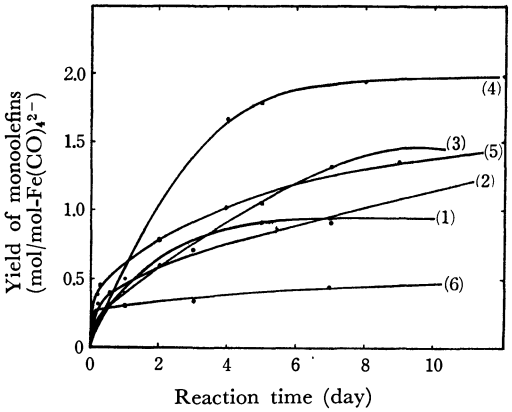

Fig. 1. Yield of monoolefins *vs.* time plots for the reaction of $KHFe(CO)_4$ with isoprene (in EtOH, at 30°C, 1 atm).
Number: (Exp. No. in Table 1)
(H_2O content mol/mol-Fe(CO)$_4^{2-}$, atmosphere)
(1) (0, N_2) (2) (1, N_2)
(3) (10, N_2) (4) (1, CO)
(5) (1, H_2) (6) $K_2Fe(CO)_4$ (0, N_2)

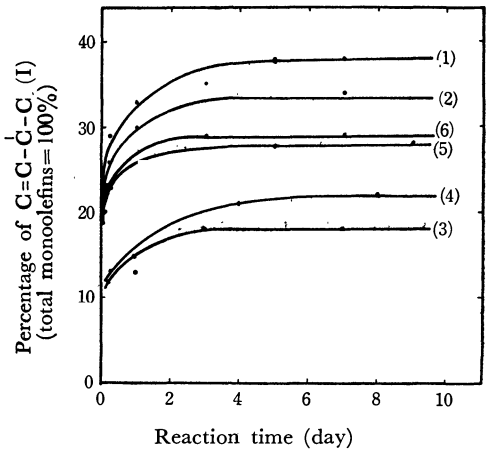

Fig. 2. Percentage of (I) *vs.* time plots for the reaction of $KHFe(CO)_4$ with isoprene (in EtOH, at 30°C 1 atm).
Number: (Exp. No. in Table 1)
(H_2O content mol/mol-Fe(CO)$_4^{2-}$, atmosphere)
(1) (0, N_2) (2) (1, N_2)
(3) (10, N_2) (4) (1, CO)
(5) (1, H_2) (6) $K_2Fe(CO)_4$ (0, N_2)

in Figs. 1 and 2. All of the reactions were carried out in ethyl alcohol at 30°C.

As Table 1 shows, isoprene reacts with $KHFe(CO)_4$ and $K_2Fe(CO)_4$, while the reaction solution gradually turns from light brown to deep ruby red. As the reaction products, 3-methyl-1-

Table 1. The reaction of $KHFe(CO)_4$ with isoprene

Exp. No.	Reaction conditions*1			Yield of*2 monoolefins	Distribution of monoolefins (%)		
	Atmosphere	Time (hr)	H_2O*2 content		C-C-C=C (I)	C=C-C-C (II)	C-C=C-C (III)
1	N_2	2	0	0.15	20	13	67
		5	0	0.32	29	13	58
		7(d)	0	0.95	38	11	51
2	N_2	2	1	0.15	19	14	57
		5	1	0.30	26	13	61
		14(d)	1	1.40	32	16	52
3	N_2	4	10	0.21	12	20	68
		7(d)	10	1.32	18	16	66
4	CO	2	1	0.11	14	13	73
		7	1	0.29	13	13	74
		12(d)	1	1.96	21	13	66
5	H_2	6	1	0.46	23	14	63
		18(d)	1	1.84	28	18	54
6*3	N_2	4	0	0.28	23	15	63
		3(d)	0	0.33	29	15	56
		7(d)	0	0.46	29	17	54

*1 In EtOH, at 30°C *2 mol/mol-Fe(CO)$_4^{2-}$ *3 $K_2Fe(CO)_4$ *4 (d): day

butene (I), 2-methyl-1-butene (II), and 2-methyl-2-butene (III) are obtained. Isopentane is not obtained, indicating that $KHFe(CO)_4$ is not active in the reduction of monoolefins under the conditions employed. As Figs. 1 and 2 show, the yield and distribution of the monoolefins obtained are remarkably affected by the reaction conditions.

The Yield of Monoolefins. In dry ethyl alcohol under nitrogen, the yield of the monoolefins is 1.0 mol/mol-$Fe(CO)_4^{2-}$ at its maximum (Exp. 1).

When there is 1 or 10 mol*2 of water present in the system (Exps. 2 and 3), the yield increases to about 1.5 mol. Under carbon monoxide, the reduction is highly promoted and the maximum yield of the olefins amounts to 2.0 mol (Exp. 4). Under hydrogen the maximum yield is also 2 mol (Exp. 5). In dry ethyl alcohol, $K_2Fe(CO)_4$ also reduces isoprene, but more slowly, and the maximum yield of the olefins is less than 0.5 mol (Exp. 6).

The Distribution of the Olefins. As Fig. 2 shows, the amount of water and the atmosphere have a great effect on the distribution of the olefins (I and III). The percentage of the olefin II, however, is almost constant (about 15%) in any case. In dry ethyl alcohol under nitrogen, the percentage of I increases with an increase of the reaction time, finally amounting to 40% (Exp. 1). In the presence of 1 or 10 mol of water, the percentage of I decreases to about 32 or 18%, respectively (Exps. 2 and 3). Under carbon monoxide or hydrogen, the percentage of I also decreases to about 21 or 28%, respectively (compare Exps. 4 and 5 with Exp. 2). In the case of $K_2Fe(CO)_4$,

TABLE 2. THE REACTION OF $KHFe(CO)_4$ WITH ISOPRENE

Exp. No.	Reaction conditions*				Yield of** mono-olefins	Distribution of monoolefins (%)		
	Atmosphere	Solvent	Time (hr)	H_2O** content		C-C-C=C (I)	C=C-C-C (II)	C-C=C-C (III)
7	N_2	*iso*-PrOH	4	0	0.14	~0	14	86
			4(d)***	0	0.51	11	18	71
			12(d)	0	0.62	13	17	70
8	N_2	*iso*-PrOH	5	1	0.38	2	14	84
			8(d)	1	1.05	6	17	77
9	CO	*iso*-PrOH	5	1	0.35	3	10	87
			10(d)	1	0.35	3	10	87
10	N_2	*n*-PrOH	5	1	0.34	22	17	61
			9(d)	1	1.18	23	18	59
11	N_2	*n*-PrOH	5	10	0.45	3	14	83
			9(d)	10	1.41	6	16	78
12	CO	*n*-PrOH	5	1	0.26	4	11	85
			5(d)	1	1.06	3	10	87

* at 30°C ** mol/mol-$Fe(CO)_4^{2-}$ *** (d): day

TABLE 3. THE REACTION OF $KHFe(CO)_4$ WITH ISOPRENE

Exp. No.	Reaction conditions*		Yield of** monoolefins	Distribution of monoolefins (%)		
	Solvent	Time (day)		C-C-C=C (I)	C=C-C-C (II)	C-C=C-C (III)
13	Methyl ethyl ketone	4 (hr)	0.14	9	9	82
		18	0.50	11	12	77
14	Tetrahydrofuran	11	0.21	9	8	83
15	Isopropyl ether	8	0.16	14	24	72

* N_2: 1 atm, H_2O content 0, at 30°C. ** mol/mol-$Fe(CO)_4^{2-}$

*2 Mol means mole per mole of $Fe(CO)_4^{2-}$ in the further description.

even in dry ethyl alcohol under nitrogen, the percentage of I is less than 30% (Exp. 6).

Carbonylated Products. Under carbon monoxide, more than 1 mol of the gas is absorbed for about 20 hr (Exp. 4). The infrared spectrum of the reaction mixture has strong bands at 2005, 1982, and 1971 cm^{-1} characteristic of some iron carbonyls, and one at 1700 cm^{-1}. The band at 1700 cm^{-1} seems to be attributable to some acyliron carbonyl complex.

The reaction mixture treated with an iodine and hydrogen chloride solution in alcohol shows a band at 1735 characteristic of an ester and one at 1720 cm^{-1}.

On the basis of these facts, it may reasonably be concluded that isoprene is carbonylated to give some acyliron carbonyl complex, which seems to be converted to a corresponding ester by the treatment with iodine. The yield of the ester is about 0.1 mol. The structures of the complex and the ester, however, are not yet clear in this study.

The Reaction of $KHFe(CO)_4$ with Isoprene in Other Solvents. The solvent effects on this reaction were examined; the results are summarized in Tables 2 and 3. In *n*- and isopropyl alcohol, the monoolefins are also produced (Table 2). The water added and atmosphere have effects on the yield and distribution of the olefins (I and III) similar to those in ethyl alcohol; the presence of a water and carbon monoxide atmosphere promotes the reduction, but is less favorable for the production of I. The distribution of the olefins (I and III) depends remarkably on the kind of alcohols. The percentage of I is greatest in ethyl alcohol, followed by *n*-propyl alcohol and isopropyl alcohol in that order; in isopropyl alcohol even in a dry system, the percentage of I is only 13% (Exp. 7 *cf.* Exp. 1). As Table 3 shows, in methyl ethyl ketone, tetrahydrofuran, and isopropyl ether the reduction occurs much more slowly and the maximum yield of the olefins is less than 0.5 mol.

The Reaction of Isoprene under Hydrogen Pressure. The results are summarized in Table 4. Under 60 kg/cm^2 of hydrogen at 35°C, the reduction occurs more rapidly to give 2.5 mol of the olefins (compare Exp. 16 with Exp. 5). Even at 100°C, the yield of the olefins is 2.5 mol at most (Exp. 17), indicating that the iron carbonylate ($KHFe(CO)_4$) does not catalyze the hydrogenation of isoprene under the conditions used and that the carbonylate acts as a reducing reagent in the

Table 4. The reaction of $KHFe(CO)_4$ with isoprene

Exp. No.	Reaction conditions*		Yield of monoolefins	Distribution of monoolefins (%)		
	Temperature °C	Time (hr)		C-C(-C)-C=C (I)	C=C-C-C (II)	C-C(-C)=C-C (III)
16**	35	5	2.59	10	23	61
17**	100	5	2.51	15	24	61
18***	100	5	2.42	26	17	57

* In EtOH, H_2: 60 kg/cm^2, H_2O content 1 mol/mol-$Fe(CO)_4^{2-}$
** $KHFe(CO)_4$ (11 mmol): isoprene=1 : 4.5 (in mole ratio)
*** $KHFe(CO)_4$ (4 mmol): isoprene=1 : 13.5 (in mole ratio)
**** mol/mol-$Fe(CO)_4^{2-}$

Table 5. The reaction of $K_2Fe_2(CO)_8$ with isoprene

Exp. No.	Reaction conditions*			Yield of** monoolefins	Distribution of monoolefins (%)		
	Atmosphere	H_2O** content	Time (day)		C-C(-C)-C=C (I)	C=C-C-C (II)	C-C(-C)=C-C (III)
19	N_2	0	5	0.32	31	11	58
		0	14	0.53	31	14	55
20	N_2	1	5	0.86	3	17	80
		1	14	0.69	3	16	82
21	CO	1	5	1.06	4	13	83
		1	14	1.37	3	10	88

* EtOH solution, at 30°C
** mol/mol-g atm Fe, which exists as iron carbonylate.

reaction. This explanation is consistent with the fact that the amount of olefins decreases proportionally with a decrease in the amount of the carbonylate used (Exp. 18).

The Reaction of $K_2Fe_2(CO)_8$ with Isoprene. The results are summarized in Table 5. All of the reactions were carried out in ethyl alcohol at 30°C.

As Table 5 shows, $K_2Fe_2(CO)_8$ also reacts with isoprene. In dry ethyl alcohol under nitrogen, the reduction occurs slowly to give about 0.5 mol of the olefins, and the percentage of I amounts to 31% (Exp. 19). When 1 mol of water is present, the yield increases to about 0.9 mol, but the percentage of I decreases to only 3% (Exp. 20). Under a carbon monoxide atmosphere the reduction is promoted to give more than 1 mol of the olefins (Exp. 21).

Discussion

Recently we have found that allyl halide reacts rapidly with $K_2Fe(CO)_4$ in ethyl alcohol, accompanied by an evolution of carbon monoxide and propylene.*3 This reaction is considered to proceed *via* the σ- and π-allyl iron carbonyl complexes.

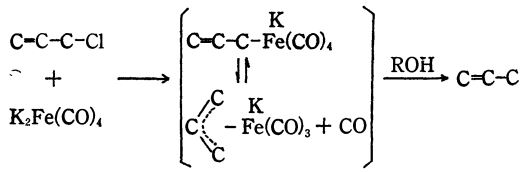

These complex may be unstable in an alcoholic solution, giving propylene in a good yield.

In the light of this reaction, the reaction of isoprene with $KHFe(CO)_4$ is considered to follow the following reaction scheme.

At first the four isomeric σ- allyl iron carbonylates are possible; then from these the two π- allyl iron carbonylates may be derived. In protic solvents these complexes decompose to give three different olefins and $K_2Fe_2(CO)_8$.

In aprotic solvents such as methyl ethyl ketone, $KHFe(CO)_4$ seems to give less than 0.5 mol of the olefins and $K_2Fe_2(CO)_8$. In these reactions $KHFe(CO)_4$ seems to be the only hydrogen source.

The formation of $K_2Fe_2(CO)_8$ may be supported by the fact that the reaction mixture turns from

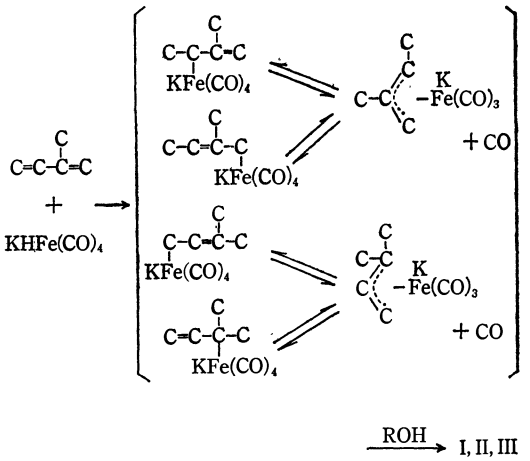

light brown to deep ruby red. In the presence of water and under carbon monoxide, the $K_2Fe_2(CO)_8$ thus formed has been proposed to give new iron hydride complexes:[4]

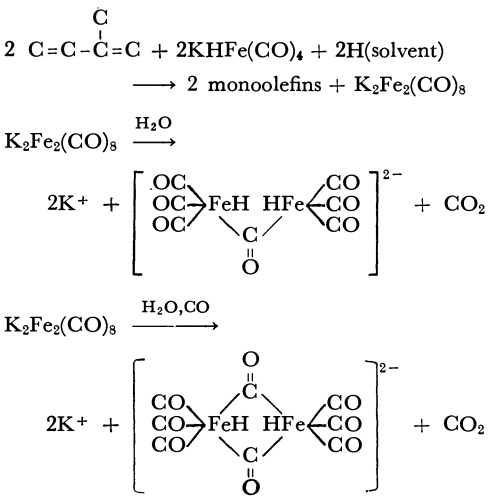

Thus, the promoting effect of water and carbon monoxide on the reduction may be attributed to the formation of the new hydrides, which react further with isoprene.

A detailed mechanism, especially concerning the effect of water, solvents, and carbon monoxide on the distribution of the olefins, is not yet clear.

This work was supported in part by the Kawakami Foundation, to which our thanks are due.

*3 A more detailed study will be presented later.

4) H. W. Sternberg, and I. Wender, Advances in Catalysis IX p. 601 (1957).

BULLETI NOF THE CHEMICAL SOCIETY OF JAPAN VOL. 41 2995—3001 (1968)

Copolymerization of Vinyl Chloride with Ethylene by the $VO(OEt)_3$-Alkylaluminum Catalyst Systems

Akira MISONO*, Yasuzo UCHIDA*, Kunikazu YAMADA** and Tadashi SAEKI*

* *Department of Industrial Chemistry, Faculty of Engineering, The University of Tokyo, Hongo, Tokyo*
** *Research Laboratory, Sekisui Chemical Co., Shimamoto-cho, Mishima-gun, Osaka*

(Received May 14, 1968)

The copolymerization of vinyl chloride with ethylene was carried out in *n*-heptane by using the catalyst systems consisting of $VO(OEt)_3$ and $AlEt_3$, $AlEt_2Cl$, or $AlEtCl_2$ at 50°C. It was found that each of the above catalyst systems produces a random copolymer at Al/V molar ratios below 1.5; however, polyethylene is mainly obtained above the ratio of 1.5. With the $VO(OEt)_3$/$AlEt_3$ catalyst system, its good catalyst activity being in contrast with the inactivity of the $Ti(O\text{-}n\text{-}Bu)_4$/$AlEt_3$ catalyst system, the maximum catalyst activity was observed at the Al/V molar ratio of 0.5. The copolymerization rate decreased with an increase in the ethylene fraction in the monomer mixture, reaching a minimum value at a 80 mol% ethylene feed; however, the rate increased above this feed ratio with a further increase in the ethylene feed. The contamination of a copolymer with polyethylene which has been observed in the copolymerization by the $Ti(O\text{-}n\text{-}Bu)_4$/$AlEt_2Cl$ or $AlEtCl_2$ catalyst system was not observed in the present case. The monomer reactivity ratios for the copolymerization by the $VO(OEt)_3$/$AlEt_3$ catalyst system were found to be r_1(vinyl chloride)=2.48 and r_2(ethylene)=0.02. The reaction between $VO(OEt)_3$ and $AlEt_3$ was investigated by means of infrared spectroscopy and gasometry, and it was found that the average valency states of the V of the catalyst system is higher than four at the Al/V molar ratio range where a random copolymer is exclusively obtained.

The copolymerization of vinyl chloride with ethylene has been drawing attention from the fundamental as well as from the industrial point of view. In previous papers[1-4] the present authors have already reported the copolymerization of vinyl chloride with ethylene by the trialkylboron/peroxide as well as by the $Ti(O\text{-}n\text{-}Bu)_4$/alkylaluminum catalyst systems. The copolymerization by Ziegler-Natta catalysts seems especially interesting in view of the expectation that ethylene is more susceptible to coordination polymerization than to free-radical polymerization; a copolymer richer in ethylene than that obtained from radical copolymerization could be obtained.

The present authors have found that the catalyst systems consisting of alkyl orthovanadate and alkylaluminum can copolymerize vinyl chloride with ethylene; it seems interesting to compare these results with the copolymerization results obtained by using the $Ti(O\text{-}n\text{-}Bu)_4$/alkylaluminum catalyst systems. In this paper, the authors wish to report the general features of the copolymerization of vinyl chloride with ethylene by the $VO(OEt)_3$/alkylaluminum catalyst systems, and also discuss briefly the reaction of the catalyst component in order to elucidate the nature of the active site-formation reaction.

Experimental

Materials. Vinyl chloride supplied by the Chisso Co. was purified by passing it through a column containing calcium chloride and then one containing phosphorous pentoxide. Ethylene supplied by the Nihon Petrochemical Co. was used without further purification. Each alkylaluminum was purified by distillation under reduced pressure and was stored as a normal solution in *n*-heptane. Ethyl orthovanadate was prepared from vanadium pentoxide and absolute ethanol according to the method of Prandtl *et al.*,[5] and was stored much like an alkylaluminum, bp 80°C/5 mmHg. The solvent was purified by shaking it with concentrated sulfuric acid and by distillation over sodium wire.

Polymerization. The reaction vessel was a 100 m*l* stainless-steel autoclave equipped with an electromagnetic agitating device. The catalyst system was

1) A. Misono, Y. Uchida and K. Yamada, This Bulletin, **39**, 2458 (1966).
2) A. Misono, Y. Uchida and K. Yamada, Preprints for the International Symposium on Macromolecular Chemistry (Tokyo and Kyoto, 1966), Vol. I, p. 132.
3) A. Misono, Y. Uchida and K. Yamada, *J. Polymer Sci.*, **B5**, 401 (1967).
4) A. Misono, Y. Uchida and K. Yamada, This Bulletin, **40**, 2366 (1967).
5) W. Prandtl and L. Hess, *Z. Anorg. Allgem. Chem.*, **82**, 103 (1913).

prepared by mixing $VO(OEt)_3$ and an alkylaluminum as a *n*-heptane solution in *n*-heptane at room temperature in the absence of the monomers under a pure nitrogen atmosphere; it was then aged for about one hour prior to use in the polymerization. After the autoclave had been cooled below −40°C, the inner nitrogen was evacuated. Vinyl chloride and then ethylene were introduced into the autoclave according to the method described in a previous paper.[1] Then the autoclave was set in an electric heater and maintained at 50°C for three hours. The resultant products were treated and purified as has been reported in a previous paper.[4] The composition of the product was calculated from the results of elemental C and Cl analyses. The reduced specific viscosity of the polymer was measured in a 0.5 g/100 m*l* cyclohexanone solution at 30.0°C. The infrared spectrum of the polymer was measured with a Hitachi model EPI-S2 infrared spectrometer (KBr disk method). The NMR spectrum of the polymer was measured with a Nihon Denshi model C-60 high-resolution NMR spectrometer at 60 Mc and 110°C in a 10 wt/vol% monochlorobenzene solution, using tetramethylsilane as the internal standard.

Gasometric Measurements. The reaction of $VO(OEt)_3$ and $AlEt_3$ was carried out in an apparatus fitted with a side arm. A *n*-heptane solution of $AlEt_3$, stored in the side arm of the Schlenk apparatus, was added to a *n*-heptane solution of $VO(OEt)_3$ placed in the bottom of the apparatus. During the operation, the catalyst solution was kept at 20°C with stirring under a pure nitrogen atmosphere. The gaseous products were analyzed by means of gas chromatography using a column packed with silica gel at 70°C.

Results and Discussion

The Influence of the Structure of Alkylaluminum. Table 1 summarizes the results of the copolymerization of vinyl chloride with ethylene by the $VO(OEt)_3/AlEt_mCl_{3-m}$ catalyst systems at various Al/V molar ratios. Figure 1 shows the infrared spectra of the copolymerization products obtained by some of the catalyst systems shown in Table 1. As has been reported in a previous paper,[6] a random copolymer of vinyl chloride with ethylene shows a characteristic absorption at 745 cm^{-1}, an absorption which has been assigned to the methylene rocking mode of a boundary structure in the copolymer chain as follows:

$$-CHCl-CH_2-CH_2-CH_2-CHCl-$$

On the basis of the arguments presented in a previous paper,[4] it follows, from the results shown

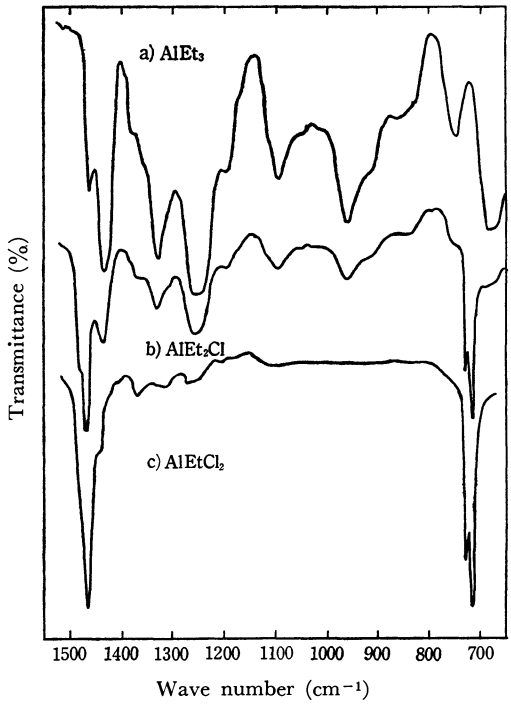

Fig. 1. Infrared spectra of copolymerization products.
a) Al/V=1.5, VCl mol%=82.3
b) Al/V=3.0, VCl mol%=14.1
c) Al/V=5.0, VCl mol%=1.0

Table 1. Copolymerization results by the $VO(OEt)_3/AlEt_mCl_{3-m}$ catalyst systems

Alkylaluminum	Al/V molar ratio	Yield(%)	VCl mol% in product	Main product	η_{sp}/c (dl/g)
$AlEt_3$	1.5	11.3	82.3	Copolymer	0.346
$AlEt_3$	3.0	3.2	6.4	PE	—
$AlEt_3$	5.0	0.3	18.3	PE+Copolymer	—
$AlEt_2Cl$	1.5	5.8	86.6	Copolymer	0.367
$AlEt_2Cl$	3.0	13.1	14.1	PE+Copolymer	—
$AlEt_2Cl$	5.0	25.2	2.5	PE	—
$AlEtCl_2$	1.5	2.6	82.5	Copolymer	0.283
$AlEtCl_2$	3.0	18.2	2.5	PE	—
$AlEtCl_2$	5.0	15.4	1.0	PE	—

Experimental conditions: vinyl chloride, 0.3 mol; ethylene, 0.2 mol; $VO(OEt)_3$, 2.0 mmol; solvent, *n*-heptane; volume of catalyst solution, 50 m*l*; polymerization temperature, 50°C; polymerization time, 3 hr.

6) A. Misono, Y. Uchida and K. Yamada, This Bulletin, **40**, 2696 (1967).

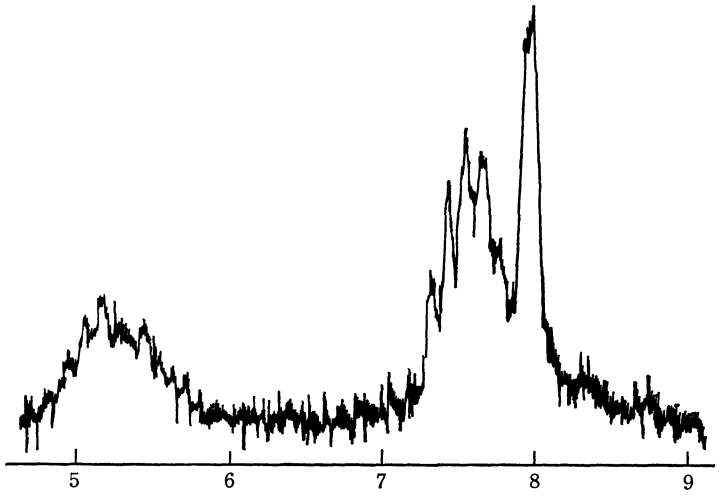

Fig. 2. NMR spectrum of a copolymer (VCl mol% = 82.3)

in Table 1 and Fig. 1, that the catalyst systems consisting of $VO(OEt)_3$ and each alkylaluminum produce random copolymers at the Al/V molar ratio of 1.5. Figure 2 shows the NMR spectrum of the copolymerization product obtained by the $VO(OEt)_3/AlEt_3$ catalyst system at the Al/V molar ratio of 1.5. The resonance peak observed at 8.35 τ has been assigned to the protons of a methylene group having a methine and a methylene group in the nearest neighbors in the copolymer chain presented above,[7] also indicating that the product consists of a random copolymer.

At the Al/V molar ratio of 3 and 5, the resultant products are composed mainly of polyethylene. However, a considerable amount of vinyl chloride was found in the products obtained by the $VO(OEt)_3/AlEt_2Cl$ catalyst system at the Al/V molar ratio of 3. The results of successive solvent extractions using tetrahydrofuran and monochlorobenzene indicate that the products consist of a random copolymer (26.0wt%) and polyethylene (74.0wt%).

The Influence of the Al/V Molar Ratio. With the $VO(OEt)_3/AlEt_2Cl$ or $AlEtCl_2$ catalyst system, the copolymer yield increases remarkably with an increase in the Al/V molar ratio at higher molar ratio, where polyethylene is the main product. These tendencies are analogous to what has been observed in the copolymerization by the $Ti(O\text{-}n\text{-}Bu)_4/AlEt_2Cl$ or $AlEtCl_2$ catalyst system. On the other hand, the copolymer yield decreases with an increase in the Al/V molar ratio when the $VO(OEt)_3/AlEt_3$ catalyst system is adopted. At Al/V molar ratio below 1.5 in the copolymerization by this catalyst system, the products consists exclusively of random copolymers with essentially the same compositions as that obtained at the ratio of 1.5.

In the copolymerization by the $VO(OEt)_3/AlEt_3$ catalyst system, the copolymer yield increases with an increase in Al/V molar ratio, reaching the maximum at the ratio of 0.5, and then it decreases continuously at ratios higher than this, as is shown in Fig. 3. It is interesting to note that $AlEt_3$, in combination with $VO(OEt)_3$, shows such a good catalyst activity in the copolymerization of vinyl chloride with ethylene in spite of the fact it is inactive in the copolymerization when combined with $Ti(O\text{-}n\text{-}Bu)_4$.

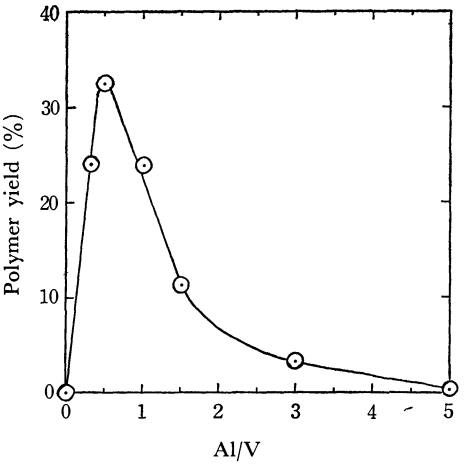

Fig. 3. Influence of the Al/V molar ratio.
Experimental conditions: vinyl chloride, 0.3 mol; ethylene, 0.2 mol; $VO(OEt)_3$, 2.0 mmol; $AlEt_3$, varied; solvent, *n*-heptane; volume of catalyst solution, 50 m*l*; polymerization temperature, 50°C; polymerization time, 3 hr.

7) A. Misono, Y. Uchida and K. Yamada, Preprints for the 21st Annual Meeting of Chemical Society of Japan (Osaka, 1968), No. 17313.

The Influence of the Monomer Feed Ratio. The copolymerization products obtained by using the $VO(OEt)_3/AlEt_3$ catalyst system at Al/V molar ratios lower than 1.5 at various monomer feed ratios consist exclusively of random copolymers, and there occurs no such contamination of the copolymer with polyethylene as has been observed in the copolymerization by the $Ti(O\text{-}n\text{-}Bu)_4$/alkylaluminum catalyst systems at higher ethylene feed ratios.[4] Therefore, it may be considered that only one kind of active site producing random copolymers exclusively operates in the copolymerization by the $VO(OEt)_3/AlEt_3$ catalyst system at relatively low Al/V molar ratios. The rate of copolymerization and the reduced specific viscosity of the copolymer decrease with an increase in the ethylene feed ratio, reaching a minimum value at 80 mol% ethylene feed ratio, as is shown in Fig. 4. The facts that the copolymerization rate again increases above this ethylene feed ratio, and that ethylene homopolymerizes in the presence of the catalyst systems active in the vinyl chloride-ethylene copolymerization, are in contrast with what has been observed in the copolymerization by the $Ti(O\text{-}n\text{-}Bu)_4$/alkylaluminum catalyst systems.

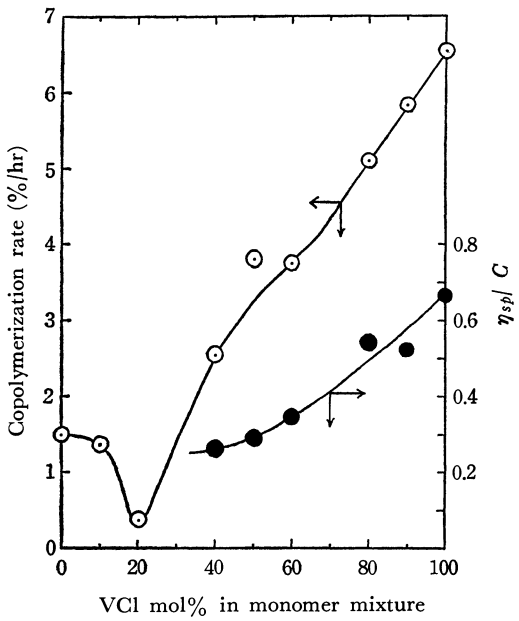

Fig. 4. Influence of monomer feed ratio. Experimental conditions: vinyl chloride + ethylene, 0.5 mol; $VO(OEt)_3$, 2.0 mmol; Al/V, 1.5; volume of catalyst solution, 50 ml; polymerization temperature, 50°C; polymerization time, 3 hr.

The Copolymer Composition. The copolymer composition curve for the copolymerization by the $VO(OEt)_3/AlEt_3$ catalyst system is shown in Fig. 5. The compositions of the copolymers obtained by the $VO(OEt)_3/AlEt_2Cl$ or $AlEtCl_2$ were 86.6 and 85.5 mol% vinyl chloride respectively; these values are comparable to that of 82.3 mol% vinyl chloride obtained for the $VO(OEt)_3/AlEt_3$ catalyst system. Using the Fineman-Ross plot shown in Fig. 6, the monomer reactivity ratios were determined; in Table 2 they are compared with those found in the copolymerization by the $Ti(O\text{-}n\text{-}Bu)_4$/alkylaluminum as well as those obtained by the use of the trialkylboron/peroxide catalyst systems. The monomer reactivity ratios found in the copolymerization catalyzed by the $VO(OEt)_3/AlEt_3$ catalyst system are of values

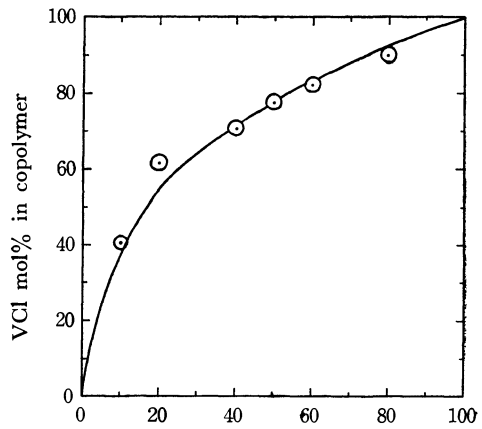

Fig. 5. Copolymer composition curve obtained by the $VO(OEt)_3$-$AlEt_3$ catalyst system at the Al/V molar ratio of 1.5.

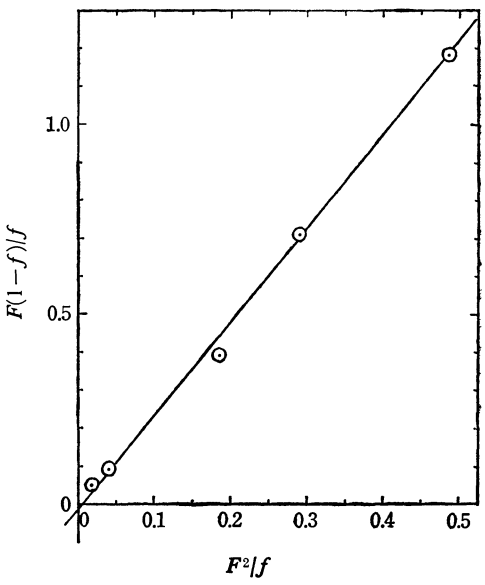

Fig. 6. Determination of r_1 and r_2 by Fineman-Ross method.

intermediate between those found for the $Ti(O-n-Bu)_4$/alkylaluminum-catalyzed and the trialkylboron-catalyzed copolymerizations. The copolymerization catalyzed by the alkyl orthovanadate catalyst system seems to be of a more radical nature than that catalyzed with the alkyl titanate catalyst systems, judging from the monomer reactivity ratios. The copolymerization by the $VO(OEt)_3/AlEt_3$ catalyst system was completely inhibited upon the addition of diphenylpycrylhydrazyl in an amount equimolar to $VO(OEt)_3$. However, it seems unclear whether or not this fact directly supports a radical polymerization mechanism for a reason presented in a previous paper.[4]

Table 2. Comparison of monomer reactivity ratios

Catalyst	r_1 (vinyl chloride)	r_2 (ethylene)	Ref.
$B(n-Bu)_3/t$-BHP	3.39	0.03	1
$Ti(O-n-Bu)_4/AlEt_2Cl$	2.03	0.20	4
$Ti(O-n-Bu)_4/AlEtCl_2$/THF	2.70	0.45	3
$VO(OEt)_3/AlEt_3$	2.48	0.02	this work

t-BHP: *t*-butyl hydroperoxide, THF: tetrahydrofuran

Observation of the Catalyst System. $VO(OEt)_3$ reacts with $AlEt_3$, with gas evolution, to form a colored solution in *n*-heptane; this indicates the occurence of a chemical reaction between the two components. At Al/V molar ratios higher than unity, the dark brown color of the catalyst solution grows deeper as the molar ratio increases. At Al/V molar ratios lower than unity, however, the brown color of the catalyst solution observed soon after it is prepared gradually fades and a green color appears; the solution is essentially green when it has been aged for about one hour. Each color change suggests the presence of a new chemical species and illustrates the complexity of the catalyst-forming reaction. In order to obtained further information concerning the active site-forming reaction, the $VO(OEt)_3/AlEt_3$ catalyst system was investigated by means of infrared spectroscopy and gasometry.

Figure 7 shows the infrared spectra of both the catalyst components, together with that of diethylaluminum ethoxide, each sample having been prepared as a *n*-heptane solution. Sekiguchi *et al.*[8] have studied the infrared spectrum of alkyl orthovanadates in their crude phase. They have considered the strong absorption at 970 cm^{-1} of $VO(O-i-Pr)_3$, which shifted to a somewhat lower

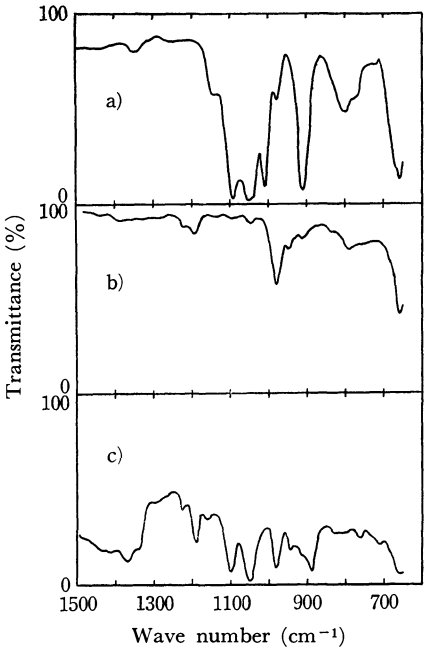

Fig. 7. Infrared spectra of catalyst components.
a) $VO(OEt)_3$ in *n*-heptane, 40 mmol/*l*
b) $AlEt_3$ in *n*-heptane, 40 mmol/*l*
c) $AlEt_2(OEt)$ in *n*-heptane, *ca.* 100 mmol/*l*.

frequency in the case of $VO(OEt)_3$, to be due to the V–O–C structure in the orthovanadates. No such a strong absorption is observed in the spectrum of $VO(OEt)_3$ There are no other available data concerning the infrared spectra of $VO(OEt)_3$ and other alkyl orthovanadates; hence, not even tentative assignments of the absorptions observed in the spectrum under consideration have yet been made.

Figure 8 shows the infrared spectra of the catalyst solutions in *n*-heptane at various Al/V molar ratios, the concentration of $VO(OEt)_3$ in each solution being adjusted to 40 mmol/*l*. It is obvious from the spectra shown in Figs. 7 and 8 that, in addition to the absorptions of both $VO(OEt)_3$ and $AlEt_3$, some new absorptions appear in the spectrum of the catalyst solution. For example, a strong and sharp band appears at 890 cm^{-1}. However, it is not clear whether this band arises from the V–O–C structure, which would shift to a lower frequency on complex-formation with $AlEt_3$, or from the Al–O–C structure, which would be formed in the ligand exchange reaction between $VO(OEt)_3$ and $AlEt_3$. A weak absorption at 1155 cm^{-1}, which is not observed in the spectrum of each component, slightly shifts to 1160 cm^{-1} as the Al/V molar ratio of the catalyst system increases. The original strong bands of $VO(OEt)_3$ at 1010, 910, and 800 cm^{-1} quickly disappear as the Al/V molar ratio increases from 0.25 to 1.0, whereas those at 1090 and 1050 cm^{-1} keep their original intensities

8) S. Sekiguchi and A. Kurihara, *Kogyo Kagaku Zasshi (J. Chem. Soc. Japan, Ind. Chem. Sect.)*, **69**, 2002 (1966).

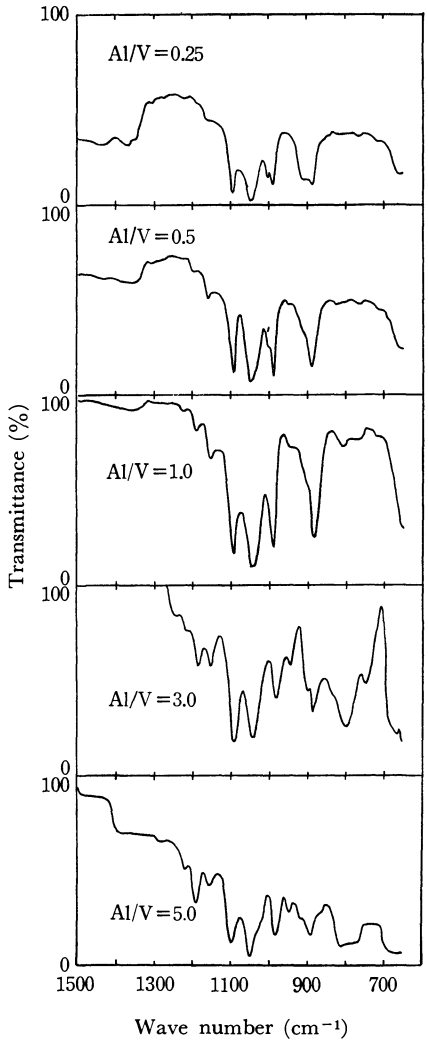

Fig. 8. Infrared spectra of catalyst solutions.

almost independent of the Al/V molar ratio. The absorption at 1090 cm^{-1}, however, shifts to 1100 cm^{-1} as the Al/V molar ratio increases. Other absorptions are observed in the spectrum of the catalyst solution which may be due to $AlEt_3$ present in the solution absorptions at 1225 (weak), 1190(weak), 985(strong), and 800(weak when Al/V<1.0, but strong when Al/V>3.0) cm^{-1}.

It is obvious that the spectrum of the catalyst solution becomes similar to that of $AlEt_2(OEt)$ as the Al/V molar ratio increases, and that the spectrum at the ratio of 5 is essentially identical with that of $AlEt_2(OEt)$ over the frequency range from 850 to 1300 cm^{-1}. The absorptions at 1160, 1100, and 890 cm^{-1} in the spectrum of $AlEt_2$-(OEt) may be related to the Al–O–C structure in the catalyst solution, judging from the results of a comparison of it with the spectrum of $AlEt_3$. Such absorptions are also observed in the spectrum of the catalyst solution, as has been mentioned previously. In the spectrum of $Al(O\text{-}n\text{-}Bu)_3$ the Al–O–C stretching mode appears at 1080 cm^{-1}. Therefore, one or both of the strong absorptions at 1050 and 1090 cm^{-1}, and the resulting overlapping of the absorptions arising from the two different chemical species, make it impossible to measure quantitatively the concentration of the Al–O–C structure in the catalyst system.

From the results mentioned above, it is, at any rate, obvious that the catalyst system is not a mere mixture of the two components, but that some ligand exchange reaction proceeds, leading to the formation of the Al–O–Et and the V–Et structure in the catalyst system:

$$VO(OEt)_3 + AlEt_3 \rightarrow EtVO(OEt)_2 + AlEt_2(OEt)$$

followed by the reductive dealkylation of the unstable organovanadium compound:

$$EtVO(OEt)_2 \rightarrow VO(OEt)_2 + Et\cdot$$

At higher Al/V molar ratios, ligand exchange and reductive dealkylation may be considered to proceed successively.

Figure 9 shows the amount of gaseous products liberated from the catalyst solution plotted *versus* the reaction time for the reaction of $VO(OEt)_3$ with $AlEt_3$ at 20°C. The gaseous products from the reactions of these two components at the Al/V molar ratio of 1.0 were analyzed after a reaction period of 72 hr; they were found to be composed of ethane and ethylene (1.00 : 0.64), only a small amount of C_4 fractions, and a considerable amount of an unidentified product the peak of which in the gas chromatogram appeared behind the position of that of *n*-heptane. Assuming the unidentified product to be a C_9 fraction resulting from the

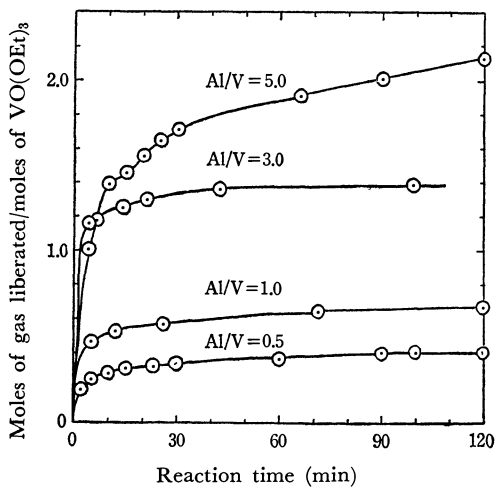

Fig. 9. Reaction of $VO(OEt)_3$ with $AlEt_3$. Experimental conditions: $VO(OEt)_3$, 1.0 mmol, 0.5 mmol for Al/V=3.0); solvent, *n*-heptane; volume of catalyst solution, 10 m*l*; reaction temperature, 20°C.

reaction of the ethyl radical with the solvent, its amount could be estimated to be about 20 mol%.

As the reduction of one mole of each organovanadium compound by one valency state leads to the liberation of one mole of gaseous products, it is possible to estimate the average valency state of vanadium in the catalyst system from the results shown in Fig. 9. Figure 10 shows the average valency state of vanadium after the reaction period of one hour plotted against the Al/V molar ratio of the catalyst system. It is obvious that, at the lower Al/V molar ratios, where random copolymers are obtained, the vanadium in the catalyst system is in the valency states higher than four; however, the valency state of vanadium is lower than four at the higher Al/V molar ratios, where polyethylene is mainly obtained in the copolymerization of vinyl chloride with ethylene. This is analogous to what has been considered to hold in the copolymerization of vinyl chloride with ethylene by the $Ti(O\text{-}n\text{-}Bu)_4/AlEtCl_2$ catalyst system[3,9]; the active site producing a random copolymer in this catalyst system may be a titanium complex in a higher valency state, probably a tetravalent one.

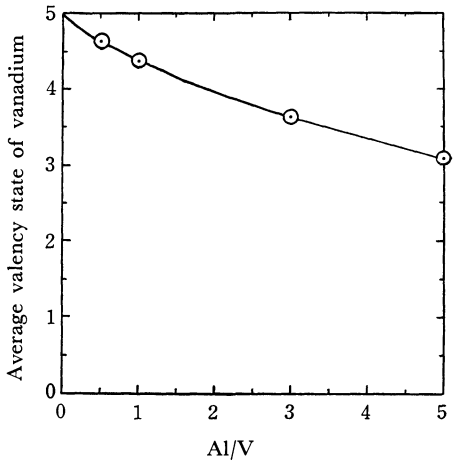

Fig. 10. Average valency state of vanadium *vs.* Al/V molar ratio.

At this stage of invesigation, it can tentatively be considered that the active site in the copolymerization of vinyl chloride with ethylene by the $VO(OEt)_3$/alkylaluminum catalyst systems is an unstable carbon-vanadium bond resulting from the ligand exchange reaction between the two components, as has usually been assumed in polymerizations by Ziegler-Natta catalysts.[10]

9) N. Yamazaki, K. Sasaki and S. Kambara, *Kogyo Kagaku Zasshi (J. Chem. Soc. Japan, Ind. Chem. Sect.)*, **68**, 881 (1965).

10) P. Cossee, *J. Catalysis*, **3**, 80 (1964).

BULLETIN OF THE CHEMICAL SOCIETY OF JAPAN VOL. 41 3001—3007 (1968)

The Reductive Coupling Reactions of Benzyl Chloride by Copper(I) Complexes*1

Keisuke WADA and Harukichi HASHIMOTO

Department of Synthetic Chemistry, The University of Tokyo, Hongo, Bunkyo-ku, Tokyo

(Received May 21, 1968)

The reactions between benzyl chloride and cuprous chloride were studied. It was found that good yields of bibenzyl were obtained by the addition of ethylenediamine, diethylenetriamine, triethylenetetramine, acetylacetone and EDTA. Nothing of bibenzyl was observed in the cases of ethanolamine, pyridine, dipyridyl, phenanthroline and triphenylphosphine. These facts, together with the spectral studies of copper complexes can reasonably be explained by the formation of reactive species of the type $Cu^{I}(en)_nCl$. The course of the reaction was discussed on the basis of the substituent and medium effects. Radical but not free type mechanisms which include the transient organocopper species were considered. Some additional comments were also made.

It may safely be pointed out that in many of the copper-catalyzed organic reactions the redox ligand transfer processes key roles. In other words, the reaction of organic substrate XY and cuprous complex $Cu^{I}Z$, for example, can be delineated in the following way. (M=Cu).

$$XY + M^{(n-1)+}Z \rightarrow X\cdot + M^{n+}YZ \quad (1)$$

$$X\cdot + M^{(n-1)+}Z \rightarrow XM^{(n-1)+}Z \quad (2)$$

$$X\cdot + X\cdot \rightarrow XX \quad (3)$$

*1 Oxidation-Reduction Reactions by Transition Metal Complexes. III.

$$X\cdot + M^{n+}YZ \rightarrow XZ + M^{(n-1)+}Y$$
$$\text{or } XY + M^{(n-1)+}Z \quad (4)$$
$$X\cdot + SH \rightarrow XH + S\cdot \quad (5)$$
$$S\cdot + M^{n+}YZ \rightarrow SZ + M^{(n-1)+}Y$$
$$\text{or } SY + M^{(n-1)+}Z \quad (4')$$
$$X\cdot + C{=}C \rightarrow X{-}C{-}C\cdot \quad (6)$$
$$X{-}C{-}C\cdot + M^{n+}YZ \rightarrow X{-}C{-}C{-}Z + M^{(n-1)+}Y$$
$$\text{or } X{-}C{-}C{-}Y + M^{(n-1)+}Z \quad (4'')$$

The well-known copper-catalyzed peroxide reactions are typical of these processes.[1,2] Similar argument may possibly be made to the Sandmeyer-Meerwein reactions,[3] to the copper-catalyzed halogen transfer reactions[4-13] and, to some extent, to the copper-catalyzed halogen exchange reactions of aryl halides.[14-16]

The reaction (4) is commonly called "ligand transfer oxidation." This process, though not sufficiently, is relatively well studied and some discussion was already made by us in the previous studies of this series.[17] Little is known, however, about the reaction (1) which we tentatively named "ligand transfer reduction." Much is to be learned about the nature of the interaction of low valent copper complexes with organic structures in somewhat simplified reaction environments.

In this paper, the reactions of cuprous complexes and organic halides will be discussed.

Experimental

Materials. Cuprous perchlorate $CuClO_4 \cdot CH_3CN$ was prepared according to the method of Kubota and Johnston.[18] Cuprous chloride, bromide, iodide and cyanide were commercial reagent grade and purified as usual manner. Authentic samples of dichloro-bis-ethylene-diamine copper(II) and dichloro-monoethylenediamine copper(II) were prepared by the method of Olszewski and Martin.[19]

Benzyl chloride and benzyl bromide were reagent grade and distilled twice. Benzyl iodide was prepared according to the method of Coleman and Hanser.[20] *p*-Methoxybenzyl chloride was synthesized from *p*-methoxybenzyl alcohol.[21] *p*-Methylbenzyl chloride, *p*-chlorobenzyl chloride and *p*-nitrobenzyl chloride were commercially first grade. All of these benzyl chlorides were checked by NMR spectra.

Reagent grade ethanolamine, ethylenediamine, diethylenetriamine, triethylenetetramine, pyridine, bipyridyl, phenanthroline, EDTA, triphenylphosphine and acetylacetone were used. Some of these were recrystallized or distilled if necessary. Sodium acetylacetonate was prepared from acetylacetone and sodium metal.

Acetonitrile was purified by the method of O'Donnell *et al.*[22] Dimethyl sulfoxide and Dimethylformamide were purified according to the method of Gutmann *et al.*[23] and Thomas *et al.*[24]

Typical Reaction Procedure. Benzyl chloride (0.633 g, 0.500×10^{-2} mol) and cuprous chloride (0.990 g, 1.00×10^{-2} mol) were dissolved in 40 m*l* of acetonitrile in a four-necked, 100 m*l*, round-bottomed flask equipped with a 30 cm Dimroth condenser, a nitrogen inlet, a thermometer, a dropping funnel and a magnetic stirrer. The solution was then swept with oxygen-free nitrogen and heated with stirring to the refluxing temperature. At that time, a solution of ethylenediamine (0.601 g, 1.00×10^{-2} mol) in 10 m*l* of acetonitrile was added through the dropping funnel. The reaction was continued for an hour under nitrogen stream.

Product Analyses. Two types of the standard methods were employed for the product analysis. In the first method the reaction mixture was treated with water, extracted with heptane, dried on sodium sulfate, concentrated to *ca.* 5 m*l* volume and analyzed by g.l.c. In the second, the solvent was removed by distillation from the reaction mixture. In this procedure the temperature of oil bath was maintained at 90°C. The remaining solid was treated with benzene and filtered. The filtrate was again concentrated to *ca.* 5 m*l* and analyzed by g.l.c. employing a 2 m silicone DC 550 column at 80 and 160°C. Bromobenzene and *p*-nitrotoluene were used as markers. The qualitative analyses by NMR and IR spectra were also made in some cases. The analytical values of the products but toluene did not markedly differ from one another

1) J. K. Kochi, *Tetrahedron*, **18**, 483 (1962).
2) G. Sosnovsky and S. O. Lawesson, *Angew. Chem. Intern. Edit.*, **3**, 245 (1964).
3) J. K. Kochi, *J. Am. Chem. Soc.*, **79**, 2942 (1957).
4) M. Asscher and D. Vofsi, *J. Chem. Soc.*, **1961**, 2261.
5) M. Asscher and D. Vofsi, *Chem. Ind.*, **1964**, 209.
6) M. Asscher and D. Vofsi, *J. Chem. Soc.*, **1963**, 1887.
7) M. Asscher and D. Vofsi, *ibid.*, **1963**, 3921.
8) S. Murai and S. Tsutsumi, *J. Org. Chem.*, **31** 3000 (1966).
9) S. Murai and S. Tsutsumi and N. Sonoda, *ibid.*, **29**, 2104 (1964).
10) D. J. Burton and L. J. Kohoe, *Tetrahedron Letters*, **1966**, 5163.
11) R. R. Lavine, T. R. Iwamoto and J. Kleinberg, *J. Am. Chem. Soc.*, **88**, 4304 (1966).
12) I. V. Nelson, R. T. Iwamoto and J. Kleinberg, *ibid.*, **86**, 364 (1964).
13) Y. Amano and T. Uno, *Nippon Kagaku Zasshi (J. Chem. Soc. Japan, Pure Chem. Sect.)*, **86**, 1105 (1965).
14) C. E. Castro, E. J. Gaugham and D. C. Owsley, *J. Org. Chem.*, **31**, 4071 (1966).
15) R. G. R. Bacon and H. A. O. Hill, *Quart. Rev.*, **19**, 95 (1965).
16) T. Cohen and A. H. Lewin, *J. Am. Chem. Soc.*, **88**, 4521 (1966).
17) K. Wada, J. Yamashita and H. Hashimoto, This Bulletin, **40**, 2410 (1967).
18) M. Kubota and D. L. Johnston, *J. Inorg. Nucl. Chem.*, **29**, 769 (1967).
19) J. Olszewski and D. F. Martin, *ibid.*, **26**, 1577 (1964).
20) G. H. Coleman and C. R. Hauser, *J. Am. Chem. Soc.*, **50**, 1193 (1928).
21) R. Grice and L. N. Owen, *J. Chem. Soc.*, **1963**, 1947.
22) J. F. O'Donnell, J. T. Ayres and C. K. Mann, *Anal. Chem.*, **37**, 1161 (1965).
23) V. Gutmann and G. Schober, *Z. Anal. Chem.*, **171**, 339 (1959).
24) A. Thomas and E. Rochow, *J. Am. Chem. Soc.*, **79**, 1843 (1957).

Table 1. The chemical shifts of benzylic methylene protons in benzene

Benzyl halide	τ, ppm	Y-$C_6H_4CH_2CH_2C_6H_4$-Z		τ ppm
$C_6H_5CH_2Cl$	5.85	Y=CH_3O	Z=CH_3O	—
$C_6H_5CH_2Br$	6.00	CH_3O	CH_3	—
$C_6H_5CH_2I$	6.12	CH_3	CH_3	7.20
CH_3O-$C_6H_4CH_2Cl$	5.76	CH_3	H	7.20
CH_3-$C_6H_4CH_2Cl$	5.90	H	H	7.20
Cl-$C_6H_4CH_2Cl$	6.13	H	Cl	7.30
NO_2-$C_6H_4CH_2Cl$	6.19	Cl	Cl	7.55
		CH_3	NO_2	7.40
$C_6H_5CH_2C_6H_5$	6.27	NO_2	NO_2	7.65

Table 2. Effects of ethylenediamine concentration

$C_6H_5CH_2Cl$: 0.500×10^{-2} mol 81.6°C
CH_3CN: 50 m*l*, 60.0 min

$CuClO_4\cdot4CH_3CN$ $\times10^{-2}$ mol	en $\times10^{-2}$ mol	$C_6H_5CH_2CH_2C_6H_5$ $\times10^{-3}$ mol	$C_6H_5CH_3$ $\times10^{-3}$ mol
1.00	0.000	0.000	0.000
0.500	0.500	0.088	0.020
0.500	1.00	1.61	0.000
1.00	0.500	0.170	0.024
1.00	1.00	0.565	0.019
1.00	2.00	2.02	0.000
1.00	4.00	1.56	0.021
1.00	4.00	1.52	0.014
1.50	1.50	0.713	0.000
1.50	3.00	2.03	0.000

in these two methods. Hence, almost all analyses were conducted according to the latter. The violet crystals remaining in the filter were dried *in vacuo* for several days and checked by elemental analyses, powdered X-ray diffraction patterns, electronic, vibrational and paramagnetic resonance spectra.

In the cases of competitive reactions of *p*-substituted benzyl chlorides, quantitative analyses were undertaken by nuclear magnetic resonance spectra. The chemical shifts used to identify the materials were tabulated in Table 1. Diphenylmethane was used as marker.

Results and Discussion

The Effect of Ethylenediamine. The results of reactions in acetonitrile are summarized in Tables 2, 3, 4 and 5. It should be noted that complexing of the cuprous ion with ligands such as ethylenediamine greatly enhance its ability to reduce benzyl chloride to toluene and bibenzyl. It was also found that even the less reactive iodobenzene is successfully reduced by these cuprous complexes. These results are somewhat interesting since only the reactive substrates such as organic peroxides and polyhalohydrocarbons have shown to be sensitive to the normal cuprous ion at moderately low temperature.[1-13]

The yield of bibenzyl increases monotonously with cuprous ion concentration. In contrast, a small but definite retarding effect is observed when a large excess of ethylenediamine exists in the system. This may possibly be due to the

Table 3. Effects of ligands

$C_6H_5CH_2Cl$: 0.500×10^{-2} mol
$CuClO_4\cdot4CH_3CN$: 1.00×10^{-2} mol, 81.6°C
CH_3CN: 50 m*l*, 60.0 min

Ligand (amine) $\times10^{-2}$ mol		$C_6H_5CH_2CH_2C_6H_5$ $\times10^{-3}$ mol	$C_6H_5CH_3$ $\times10^{-3}$ mol
ethanolamine			
	1.00	0.000	0.065
	2.00	0.000	0.016
en	1.00	0.565	0.019
dien	1.00	1.58	0.016
trien	1.00	1.47	0.015
	0.500	1.27	0.020
py	2.00	0.000	0.009
phen	1.00	0.000	0.060
dipy	1.00	0.000	0.065
EDTA	1.00	0.000	0.012
	1.00[a]	0.401	0.064
Hacac	1.00	0.066	0.040
Naacac	1.00	0.061	0.026
TPP	2.00	0.000	0.000

a) CH_3CN 25 m*l* H_2O 25 m*l*

TABLE 4. THE REACTIONS OF BENZYL HALIDES
$C_6H_5CH_2X$: 2.50×10^{-2} mol CH_3CN: 50 ml
$ClC_6H_4CH_2Cl$: 2.50×10^{-2} mol, 81.6°C
en: 1.00×10^{-2} mol, 60.0 min
CuCl: 0.500×10^{-2} mol ($\times10^{-3}$ mol)

X	Substituted bibenzyl			Relative reactivity[a]
	H-H	H-Cl	Cl-Cl	
Cl	0.380	0.722	0.708	1.00
Br	1.88	0.351	0.249	7.66
I				b)

a) Calcd from substituted bibenzyls.
b) Considerably reactive and side-reactions with ethylenediamine can not be neglected.

TABLE 5. THE REACTIONS WITH CUPROUS HALIDES
$C_6H_5CH_2Cl$: 0.500×10^{-2} mol, 81.6°C
en: 1.00×10^{-2} mol, 60.0 min
CuX: 1.00×10^{-2} mol
CH_3CN: 50 ml ($\times10^{-2}$ mol.)

Cuprous salt	$C_6H_5CH_2CH_2C_6H_5$	$C_6H_5CH_3$
$CuClO_4$	0.565	0.019
CuCl	1.32	0.032
CuBr	1.30	0.023
CuI	1.38	0.037
CuCN[a]	trace	0.000

a) heterogeneous

inaccessibility of benzyl chloride to the coordinative site of copper ion by the intervention of ethylenediamine which occupy the coordination sphere preferentially. This view of the reaction is supported by the results of supplementary experiments C and D in Table 6. To some extent, the retarding effect is also ascribed to the side-reaction of benzyl chloride with ethylenediamine. The NMR studies of the reaction products, however, have shown that the effect is not interpreted by the latter mechanism only.

Furthermore, the experiments C and D in Table 6 support the idea that the intrinsic reagent in the system is cuprous complexes of the type $Cu^I(en)_nCl$. Though the details of the complexes are not yet clear, the species is found to be sensitive to the molecular oxygen and oxidized easily to the stable copper(II) state. This is cofirmed by the reaction E in Table 6. The yield of bibenzyl is considerably decreased by the preliminary contact with oxygen. The marked difference between the reactions B and E may be understood if we assume that the rates of the reactions between the complexes and benzyl chloride are faster than that of air oxidation.

As is seen in Table 3, in addition to ethylenediamine, several other ligands such as diethylenetriamine, triethylenetetramine, EDTA and acetylacetone are effectively used to promote the reaction. Monoethanolamine, however, and pyridine, dipyridyl, *o*-phenanthroline and triphenylphosphine are ineffective. These facts remind us of the change in the oxidation-reduction potential of copper(II)-copper(I) couple by complexing. The data of the potentials from references are listed in Table 7. There seems to be a certain relationship between the ligand effect and the potentials.[25-30] Thus, we conclude with some hesitation that the accelerating effects of the ligands exist in the formation of the reactive copper(I) complexes.

Studies of Copper(I) and Copper(II) Complexes. From the discussion given above the general feature of the reaction is profiled as follows.

$$Cu^ICl + n(en) \rightarrow Cu^I(en)_nCl \quad (7)$$

$$2C_6H_5CH_2Cl + 2Cu^I(en)_nCl \rightarrow (C_6H_5CH_2)_2 + 2Cu^{II}(en)_nCl_2 \quad (8)$$

As is shown in Fig. 1, a remarkable spectral change is observed when ethylenediamine is added to the solution of cuprous chloride in acetonitrile, assuring the formation of cuprous complexes. Further

TABLE 6. SUPPLEMENTARY REACTIONS
CuCl: 0.500×10^{-2} mol, 81.6°C CH_3CN: 50 ml, 60.0 min
($\times10^{-2}$ mol)

			CuCl : en : halide	$C_6H_5CH_2CH_2C_6H_5$
A	CuCl, $C_6H_5CH_2Cl$ followed by en	(N_2)	1 : 2 : 1	0.125
B		(air)	1 : 2 : 1	0.105
C	CuCl, en followed by $C_6H_5CH_2Cl$	(N_2)	1 : 2 : 1	0.138
D		(N_2)	1 : 3 : 1	0.0751
E	CuCl, en, air followed by $C_6H_5CH_2Cl$	(air)	1 : 2 : 1	0.0783

25) E. Frieden, S. Osaki and H. Kobayashi, *J. Gen. Physiol.*, **49**, 213 (1965).
26) W. Latimer, "The Oxidation States of the Elements and Their Potential in Aqueous Solution," Prentice-Hall, New York (1952).
27) E. Ochiai, *Tetrahedron*, **20**, 1831 (1964).
28) J. K. Kochi and P. E. Mocadlo, *J. Am. Chem. Soc.*, **88**, 4094 (1966).
29) M. Singleton and J. K. Kochi, *ibid.*, **89**, 6547 (1967).
30) D. Copper and R. A. Plane, *Inorg. Chem.*, **5**, 2211 (1966).

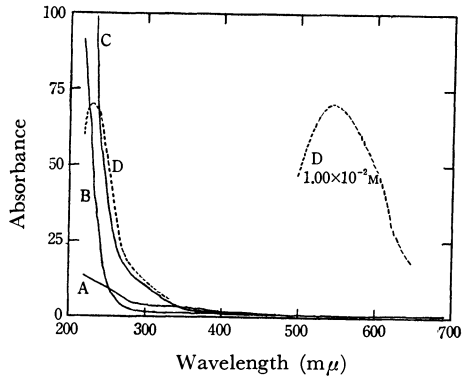

Fig. 1. Electronic spectra of copper complexes in nitrogen atmosphere.
A en 1.00×10^{-4} M
B CuCl 1.00×10^{-4} M
C CuCl 1.00×10^{-4} M, en 2.00×10^{-4} M 10 min after mixing
D CuCl 1.00×10^{-4} M en 2.00×10^{-4} M benzyl chloride 1.00×10^{-4} M 60 min after mixing

change is also observed if an amount of benzyl chloride is introduced to this solution. This last spectrum, together with the studies about isolated cupric complexes from typical runs, strongly suggests the production of cupric complexes of the type $Cu^{II}(en)_nCl_2$. These are illustrated in Table 8. It has been shown that the complexes produced are $Cu^{II}(en)Cl_2$ and $Cu^{II}(en)_2Cl_2$ in the reactions of ratios halide: Cu^{I} : en = 1 : 2 : 2 and 1 : 2 : 4, respectively.

The Mechanisms of the Reaction. As in the case of ligand transfer oxidation, the reverse process is explainable by the following scheme.

$$C_6H_5CH_2Cl + Cu^{I}Cl \rightarrow C_6H_5CH_2Cl\cdot Cu^{I}Cl \quad (9)$$

$$C_6H_5CH_2Cl\cdot Cu^{I}Cl \rightarrow [C_6H_5CH_2\overset{\circ}{\underset{\circ}{}}Cl\circ Cu^{II}Cl \longleftrightarrow \text{(J)}$$

$$C_6H_5CH_2^{-}\overset{\circ}{\underset{\circ}{}}Cl + Cu^{II}Cl \longleftrightarrow \text{(K)}$$

$$C_6H_5CH_2^{+}\circ Cl^{-}\overset{\circ}{\underset{\circ}{}}Cu^{II}Cl] \rightarrow \text{(L)}$$

$$C_6H_5CH_2^{\circ}\cdot ClCu^{II}Cl \quad (10)^{31}$$

Table 7. The oxidation potentials of copper(I)-copper(II) couple

Copper complex	E°	E° (pH=7.0)
en (dien, trien)		0.37
Acetylacetone		
EDTA		
Ethanolamine		
Perchlorate	−0.15	0.17
Chloride	−0.54	
Pyridine	Ref. 27	
Diquinolyl (dipy, phen)		−0.77
Triphenylphosphine	Ref. 30	

Table 8. Physical properties of copper complexes

	Electronic spectra[a] max (ε)	mμ	Far infrared spectra[b] cm^{-1}			
A-1[d]	680 (30)	232 (3000)	623	525	473	
$Cu(en)Cl_2$	680 (32)	231 (3200)	623	525	473	
A-2[e]	550 (63)	231 (6450)	643	523	474	450
$Cu(en)_2Cl_2$	550 (65)	232 (6500)	643	523	474	450

a) 1.00×10^{-2} M for visible spectra solvent: H_2O
4.00×10^{-5} M for ultraviolet spectra temp: 20—22°C
b) The spectra of KBr pellet

	ESR spectra[c] g	g	Elementary analysis Cu	Cl	C	H	N
A-1	2.049	2.339	32.58	36.82	12.54	4.34	14.08
$Cu(en)Cl_2$	2.049	2.339	32.66	36.45	12.34	4.14	14.40
A-2	2.040	2.236	24.87	28.02	18.69	6.42	21.85
$Cu(en)_2Cl_2$	2.040	2.236	24.96	27.80	18.80	6.31	22.01

c) The spectra in powder state
d) CuCl : en : benzyl chloride = 2 : 2 : 1
e) CuCl : en : benzyl chloride = 2 : 4 : 1

31) Some comments may be need for the Eq. (10). The equation somewhat differs from a generally accepted Russell's mechanism for the hydrogen abstraction reaction by organic radical of Eq. (19).[32]
32) G. A. Russell and H. C. Brown, *J. Am. Chem. Soc.*, **77**, 4578 (1955).

TABLE 9. THE COMPETITIVE REACTIONS

$YC_6H_4CH_2Cl$: 0.500×10^{-2} mol; en: 1.00×10^{-2} mol; CH_3CN: 50 ml;
$ClC_6H_4CH_2Cl$: 0.500×10^{-2} mol; CuCl: 0.500×10^{-2} mol, 81.6°C, 60.0 min

Y	Recovered $YC_6H_4CH_2Cl$		Substituted bibenzyl			Relative reactivity	
	Y or	a) Y=Cl b) Y=CH_3	Y-Y Y-Y	Y-Cl Y-CH_3	Cl-Cl CH_3-CH_3	R_1	R_2
CH_3O	(b)	0.611	1.84	0.327	0.848	not determined	
CH_3	(a)	1.43	1.29	0.402	0.802	0.782	0.992	0.967
H	(a)	1.38	1.27	0.370	0.694	0.674	1.000	1.000
Cl							1.03	1.43
NO_2	(b)	1.07	2.81	0.677	0.752	0.201	1.74	2.05

R_1: relative conversion ($\times10^{-3}$ mol)
R_2: calcd from produced bibenzyls

TABLE 10. THE EFFECT OF SOLVENT

$C_6H_5CH_2Cl$: 0.500×10^{-2} mol, 81.6°C; en: 1.00×10^{-2} mol, 60.0 min; $CuClO_4\cdot4CH_3CN$: 1.00×10^{-2} mol

Solvent	ml	$C_6H_5CH_2CH_2C_6H_5$ $\times10^{-3}$ mol	$C_6H_5CH_3$ $\times10^{-3}$ mol
CH_3CN	50	0.565	0.019
CH_3CN-DMSO	(25—25)	0.000	0.000
-DMF	(25—25)	0.255	0.006
-HOAc	(25—25)	0.000	0.015
-HOAc	(45— 5)	0.125	0.020
-H_2O	(25—25)	0.033	0.015
-H_2O	(45— 5)	0.455	0.010
-$(CH_3)_2CHOH$	(25—25)	0.323	0.017
-$(CH_3)_2CHOH$	(45— 5)	0.627	0.009
DMSO	50	0.000	0.000
DMF	50	0.000	0.000

TABLE 11. THE EFFECTS OF ADDITIVE

CuCl: 0.00×10^{-2} mol, 81.6°C; $ClC_6H_4CH_2Cl$: 0.500×10^{-2} mol, 60.0 min; en: 1.00×10^{-2} mol

Solvent	Additive	$ClC_6H_4CH_2CH_2C_6H_4Cl$ ($\times10^{-3}$ mol)	$ClC_6H_4CH_3$ ($\times10^{-3}$ mol)
CH_3CN 50 ml		1.53	0.020
CH_3CN 25 ml	$(CH_3)_2CHOH$ 25 ml	0.852	0.005
CH_3CN 50 ml	HOC_6H_4OH 0.500×10^{-2} mol.	1.35	0.014

This scheme certainly reflects the close similarity to the chlorine atom abstraction reactions by organic radicals. The contribution of step (9) is fairly plausible since our recent work have revealed that a stable cuprous complex $Cu^ICl(C_6H_5CH_2I)$-$(TPP)_2$ is quantitatively obtained in the reaction of cuprous chloride, benzyl iodide and triphenylphosphine in acetonitrile.[33]

Concerning the reaction step (10), the substituent effect on benzyl chloride was examined. The results are in Table 9. Though the effect observed is very feasible, its electrophilic character may probably refer to the contribution of the structure (K).[31] The extraordinary large effect of nitro group, reminiscent of its effect in Ullmann coupling reaction,[34] can be ascribed to the considerable resonance term. *p*-Methoxybenzyl chloride is so unstable that certain side reactions must be present in its competitive reaction, and hence the datum is that for only reference.

Although the radical feature of the reaction is backed up by the formation of coupling product and the data in Table 3, there remains some uncertainty. To assure this, several additional experiments were achieved. Tables 10 and 11 illustrate the effects of solvents and hydrogen donors. No appreciable change, however, is observed in the yield of toluene despite rather large

33) K. Wada and H. Hashimoto, to be published.

34) P. E. Fanta, *Chem. Revs.*, **64**, 613 (1964).

changes in environment. Therefore, the existence of benzyl radical in its free state is hardly accepted. Hence, it appears plausible to presume the mechanisms depicted below.

$$2C_6H_5CH_2\cdot ClCu^{II}Cl \rightarrow (C_6H_5CH_2)_2 + 2Cu^{II}Cl_2 \quad (11)$$

$$C_6H_5CH_2\cdot ClCu^{II}Cl + C_6H_5CH_2Cl + Cu^{I}Cl \rightarrow (C_6H_5CH_2)_2 + 2Cu^{II}Cl_2 \quad (12)$$

$$C_6H_5CH_2\cdot ClCu^{II}Cl + Cu^{I}Cl \rightarrow C_6H_5CH_2\cdot Cu^{I}Cl + Cu^{II}Cl_2 \quad (13)$$

$$C_6H_5CH_2\cdot Cu^{I}Cl + C_6H_5CH_2Cl \rightarrow (C_6H_5CH_2)_2 + Cu^{II}Cl_2 \quad (14)$$

$$2C_6H_5CH_2\cdot Cu^{I}Cl \rightarrow (C_6H_5CH_2)_2 + 2Cu^{I}Cl \quad (15)$$

At the present stage, however, we are not able to decide which of these processes prevails.

Finally, some comments must be made about the reactions of chromous species. Recent works by several groups of laboratories have shown that the relatively longlived organochromium species are effectively formed in the reactions of alkyl halides and chromous ion.[35-39] The hydrolysis and dimerization reactions of these species were also studied and various mechanisms have been discussed for these reactions. For example, Kochi and his coworkers have suggested the following scheme.[29,30,35-38]

$$C_6H_5CH_2Br + Cr^{II}_{aq} \rightarrow C_6H_5CH_2\cdot + Cr^{III}Br_{aq} \quad (16)$$

$$C_6H_5CH_2\cdot + Cr^{II}_{aq} \rightarrow C_6H_5CH_2\cdot Cr^{II}_{aq} \quad (17)$$

$$C_6H_5CH_2Cr^{II}_{aq} + C_6H_5CH_2Br \rightarrow (C_6H_5CH_2)_2 + Cr^{III}Br_{aq} \quad (18)$$

In contrast to our results mentioned above, free benzyl radical is included in their scheme.

Further works must be necessary for the discussion of this discrepancy.

$$R\cdot + S\text{-}T \rightarrow [R\cdot S:T \longleftrightarrow R^-:S\cdot{}^+T \longleftrightarrow R:S\cdot T] \rightarrow R\text{-}S + \cdot T \quad (19)$$

The mechanism (19), however we think, is erroneous or not sufficient for its unreasonably estimated resonance terms.

Here, we are rather inclined to suggest a more reasonable reformation. The Eq. (20) is a schematical description of transition state in our idea.

$$\underset{(O)}{R\cdot S:T} \longleftrightarrow \underset{(P)}{R^-:S^+\cdot} \longleftrightarrow \underset{(Q)}{R^+S^-\!\!:\!\!\cdot T} \quad (20)$$

The structure (O) represents the system in which one electron stays in the half-occupied orbital of group R and two electron in the S–T bonding orbital. The structure (P) is a picture of a charge transfer from S–T bonding orbital to originally half-occupied orbital of group R. A charge transfer from half-occupied orbital to S–T antibonding orbital is drawn out by the structure (Q). It may be considered that the position of group S and the charge distribution in the transition state and hence the degree of the contribution of (O), (P) and (Q) are changed variously from reaction to reaction.

In most of the organic reactions, the contribution of the structure (P) prevails. In the reactions of copper complexes, however, the larger contribution may be expected from the structure (Q).

In the case of ligand transfer oxidation of phenyl radical,[17] the groups R, S and T, correspond to phenyl group, chlorine atom and cupric ion, respectively. In this system the structure (P) needs the unstable $(3d)^8$ configuration of copper moiety. In the ligand transfer reduction of benzyl chloride, cuprous ion, chlorine atom and benzyl group are expressed by R, S and T respectively. In this case, the structure (P) demands the configuration of $(3d)^{10}$ (4s) character. This configuration is also rather difficult to be achieved at the condition employed. Thus, it may be concluded that the substituent effects in both of the reactions are well explained by the contribution of relatively favourable structure (Q).

It may safely be pointed out also that the nucleophilic character of attacking radical which is overlooked by Russell's mechanism can successfully be introduced by this consideration.

The comments mentioned above is not at all a qualitative one. Thus, a more elaborated refinement must be made for the discussion of the detail aspects of the group transfer reactions.

35) J. K. Kochi and F. F. Rust, *J. Am. Chem. Soc.*, **83**, 2017 (1961).
36) J. K. Kochi and D. D. Davis, *ibid.*, **83**, 5264 (1961).
37) J. K. Kochi and D. B. Buchman, *ibid.*, **87**, 853 (1965).
38) J. K. Kochi and P. E. Moradlo, *J. Org. Chem.*, **30**, 1134 (1965).
39) H. H. Zeiss and R. P. A. Sneedern, *Angew. Chem. intern. Edit.*, **6**, 435 (1967).

NOTES

Synthesis of 5 : 6-Benzphenanthridines

V. KESAVAN, V. C. DEVANATHAN and N. ARUMUGAM

Department of Chemistry, Madurai University, Madurai-2, South India

(Received January 11, 1968)

5:6-Benzphenanthridine (A) is one of the six benzphenanthridines possible depending upon the manner of fusion of a benzene ring to the phenanthridine nucleus.

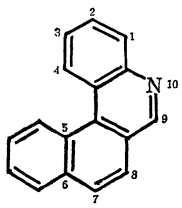

A

The synthesis of this benzphenanthridine nucleus has not received much attention. Mills and Schofield[1] reported the syntheses of a few 5 : 6-benzphenanthridines by cyclisation of 1-*O*-acylaminophenylnaphthalenes. But the handicap in this method, according to the above authors was the low yields of 1-(*o*-nitroaryl)naphthalenes from the Ullmann reaction of the relevant halo compounds. Brown and co-workers[2] recorded the synthesis of *N*-methyl-5:6-benzphenanthridone from 1-amino-*N*-methyl-2-naphthalide and the difficulty in this approach is stated to be the preparation of 1-amino-2-naphthoic acid. Keene and Schofield[3] had employed Schmidt reaction of benzofluorenone which resulted in the difficultly separable mixture of 3:4- and 5:6-benzphenanthridones. We report here the syntheses of a few 5:6-benzphenanthridines through the well known Bruckner method.[4]

Addition of dinitrogen trioxide to 1-(α-naphthyl)-cyclohexene yields according to the conditions 1-(α-naphthyl)-2-nitrocyclohexene and an alkali soluble compound (X), mp 210°C. This behaviour of 1-(α-naphthyl)-cyclohexene is similar to 1-phenyl- or 1-substituted phenylcyclohexenes.[5,6] The reduction of 1-(α-naphthyl)-2-nitrocyclohexene by lithium aluminum hydride gave the *cis*-2-(α-naphthyl)-cyclohexylamine (B) in good yields. The amino group in this amine is shown to be axial on the basis of the IR spectrum and comparison with the trans isomer.[7]

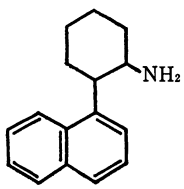

B

The formyl, acetyl and the benzoyl derivatives of this amine when cyclised with 4:5 phosphorus pentoxide-phosphoric acid mixture yielded the corresponding *cis*-1,2,3,4,4a,10b-hexahydro-5:6-benzphenanthridines (C).

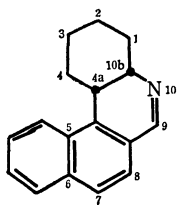

C

The above hexahydrobenzphenanthridines on dehydrogenation over palladised charcoal in decalin yielded the fully aromatised 5:6-benzphenanthridines.

The 1-(4-methyl-1-naphthyl)-cyclohex-1-ene, 1-(4-methoxy-1-naphthyl)-cyclohex-1-ene and 1-(9'-phenanthryl)-cyclohexene when carried through a

1) B. Mills and K. Schofield, *J. Chem. Soc.*, **1956**, 4213.
2) D. N. Brown, D. H. Hey and C. W. Rees, *ibid.*, **1961**, 3873.
3) B. R. T. Keene and K. Schofield, *ibid.*, **1958**, 2609.
4) V. Bruckner, *Ann. Chem.*, **518**, 227 (1935); G. Bruckner Jr., G. V. Fodor, L. Bence and E. Borcsok, *Ber.* **76**, 466 (1943).
5) T. R. Govindachari, K. Nagarajan, B. R. Pai and N. Arumugam, *J. Chem. Soc.*, **1956**, 4280.
6) T. R. Govindachari, K. Nagarajan and V. N. Sundararajan, *Tetrahedron*, **15**, 60 (1961).
7) V. Kesavan and N. Arumugam, Paper accepted for publication, *Indian. J. Chem.*

TABLE 1. 1-SUBSTITUTED 2-NITROCYCLOHEXENES

Substituent at position 1	Mp (°C)	Molecular formula	Analysis % Calcd	Analysis % Found
(4-Methyl-1-naphthyl)-	90—91 (ether)	$C_{17}H_{17}NO_2$	C, 76.4 H, 6.4	C, 76.2 H, 6.2
(9'-Phenanthryl)-	146 (acetone)	$C_{20}H_{17}NO_2$	C, 79.2 H, 5.6	C, 79.2 H, 5.6
(4-Methoxy-1-naphthyl)-	Oil	—	—	—

TABLE 2. 2-SUBSTITUTED 3-NITROCYCLOHEX-2-EN-1-ONE OXIMES*

Substituent at position 2	Mp (°C)	Molecular formula	Analysis % Calcd	Analysis % Found
(4-Methyl-1-naphthyl)-	242 (decomp.) (ethanol)	$C_{17}H_{16}N_2O_3$	C, 68.9 H, 5.4	C, 68.6 H, 5.4
(4-Methoxy-1-naphthyl)-	234 (decomp.)	$C_{17}H_{16}N_2O_4$	C, 65.4 H, 5.1	C, 65.4 H, 5.3

* Bruckner addition to 1-(9'-phenanthryl)-cyclohexene did not yield analogous compound.

TABLE 3. ACYL DERIVATIVES OF *cis*-2-SUBSTITUTED CYCLOHEXYLAMINES

Substituent at position 2	Acyl group	Mp (°C)	Molecular formula	Analysis % Calcd	Analysis % Found	IR peak ν_{max} (KBr)
(4-Methyl-1-naphthyl)-	Acetyl	186 (benzene)	$C_{13}H_{23}NO$	C, 81.1 H, 8.2	C, 81.0 H, 8.3	3340 cm^{-1} 3060 cm^{-1}
	Benzoyl	138 (dil. ethanol)	$C_{24}H_{25}NO$	C, 83.8 H, 7.3	C, 83.5 H, 7.5	
(4-Methoxy-1-naphthyl)-	Acetyl	184 (benzene)	$C_{19}H_{23}NO_2$	C, 76.8 H, 7.8	C, 76.8 H, 7.9	3340 cm^{-1} 3060 cm^{-1}
(9'-Phenanthryl)-	Acetyl	237—238 (benzene)	$C_{22}H_{23}NO$	C, 83.3 H, 7.25	C, 83.0 H, 7.4	3340 cm^{-1} 3060 cm^{-1}
	Benzoyl	200 (alcohol)	$C_{27}H_{25}NO$	C, 85.6 H, 6.6	C, 85.5 H, 6.8	

similar series of reactions yielded (i) *cis*-7,9-dimethyl-1,2,3,4,4a,10b-hexahydro-5:6-benzphenanthridine, (ii) *cis*-7-methyl-9-phenyl-1,2,3,4,4*a*,10*b*-hexahydro-5:6-benzphenanthridine, (iii) *cis*-9-methyl-7-methoxy-1,2,3,4,4a,10b-hexahydro-5:6-benzphenanthridine, (iv) *cis*-9-methyl-1,2,3,4,4a,10b-hexahydro-5:6,7:8-dibenzphenanthridine and (v) *cis*-9-phenyl-1,2,3,4,4a,10b-hexahydro-5:6,7:8-dibenzphenanthridine. Compounds (i) and (iv) were aromatised to 7,9-dimethyl-5:6-benzphenanthridine and 9-methyl-5:6,7:8-dibenzphenanthridine. The ultraviolet spectra of 9-methyl- and 7,9-dimethyl-5:6-benzphenanthridines are recorded (Fig. 1).

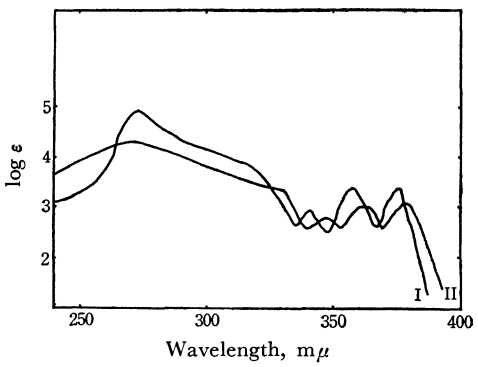

Fig. 1. Ultraviolet spectra of
i: 9-methyl-5:6-benzphenanthridine,
ii: 7,9-dimethyl-5:6-benzphenanthridine.

The compound (X), mp 210°C, mentioned earlier is regarded as 3-nitro-2-(α-naphthyl)-cyclohex-2-en-1-one oxime on the basis of the IR spectrum, and in analogy with the work of Govindachari *et al.*[6] This compound on hydrolysis gives a ketone which can be reconverted to the original compound (X) through hydroxylamine hydrochloride. It is inferred that the similar alkali soluble compcunds obtained from the addition of dinitrogen trioxide to 1-(4-methyl-1-naphthyl)-cyclohex-1-ene and 1-(4-methoxy-1-naphthyl)-cyclohex-1-ene possess structures similar to the compound (X).

TABLE 4. *cis*-1,2,3,4,4a,10b-HEXAHYDRO-5:6-BENZPHENANTHRIDINES

Substituent	Yield %	Mp (°C)	Molecular formula	Analysis % Calcd	Analysis % Found	Mp of picrate (°C)	Molecular formula	Analysis % Calcd	Analysis % Found
9-Methyl-	75	oil	—	—	—	223 (decomp.) (ethanol)	$C_{24}H_{22}N_4O_7$	C, 60.25 H, 4.6	C, 60.2 H, 4.4
9-Phenyl-	82	150—151 (ethanol)	$C_{23}H_{21}N$	C, 88.8 H, 6.7	C, 88.7 H, 7.0	234 (decomp.) (ethanol)	$C_{29}H_{24}N_4O_7$	C, 64.3 H, 4.6	C, 64.7 H, 4.4
7,9-Dimethyl-	63	oil	—	—	—	234 (decomp.) (ethanol)	$C_{25}H_{24}N_4O_7$	C, 61.0 H, 4.9	C, 61.3 H, 5.1
7-Methyl- } 9-Phenyl- }	64	165—166 (ethanol)	$C_{24}H_{23}N$	C, 88.6 H, 7.1	C, 88.2 H, 6.8	—	—	—	—
7-Methoxy-9-phenyl**	20	oil	—	—	—	214 (decomp.) (ethanol)	$C_{25}H_{24}N_4O_8$	C, 59.0 H, 4.7	C, 59.2 H, 4.6
9-Methyl-7:8-benz-	83	108—110 (ethanol)	$C_{22}H_{21}N$	C, 88.3 H, 7.0	C, 88.2 H, 7.0	222 (decomp.) (ethanol)	$C_{28}H_{24}N_4O_7$	C, 63.5 H, 4.5	C, 63.5 H, 4.3
9-Phenyl-7:8-benz-	61	171 (ethanol)	$C_{27}H_{23}N$	C, 89.75 H, 6.5	C, 89.5 H, 6.5	—	—	—	—

** Cyclisation by the described procedure failed. Adding the acetyl derivative (1 g) in phosphorus oxychloride (5 m*l*) to a stirred mixture of phosphorus pentoxide (5 g) and phosphoric acid (5 m*l*) and heating to 100°C gave the cyclised product.

TABLE 5. 5:6-BENZPHENANTHRIDINES

Substituent	Mp (°C)	Molecular formula	Analysis % Calcd	Analysis % Found	UV spectrum λ_{max} mμ	UV spectrum log ε	Mp of picrate (°C)	Molecular formula	Analysis % Calcd	Analysis % Found
9-Methyl-	95—96 (benzene-pet. ether)	$C_{18}H_{13}N$	C, 88.9 H, 5.3	C, 88.9 H, 5.3	273 341 357 375	4.63 3.02 3.39 3.39	216 (decomp.) (ethanol)	$C_{24}H_{16}N_4O_7$	C, 61.0 H, 3.4	C, 61.2 H, 3.2
7,9-Dimethyl-	129—130 (ethanol)	$C_{19}H_{15}N$	C, 88.7 H, 5.8	C, 88.3 H, 6.0	273 348 361 380	4.3 2.8 3.0 3.1	243 (decomp.) (ethanol)	$C_{25}H_{18}N_4O_7$	C, 61.8 H, 4.0	C, 62.0 H, 4.0
9-Methyl-7 : 8-benz-	143—144 (ethanol)	$C_{22}H_{15}N$	C, 90.1 H, 5.1	C, 89.7 H, 5.3	262 325 348 380	4.4 3.6 3.5 3.0	—	—	—	—

Experimental

All melting points are uncorrected. Ultraviolet spectra were taken in Hilger and Watts model 700. Infrared spectra were recorded in Perkin-Elmer model 421. Detailed experimental procedures are presented only for one representative sequence of reactions. All other sequences were conducted in a similar manner using appropriate quantities of reactants. The relevant data are given in tables.

1-(α-Naphthyl)-2-nitrocyclohexene. A mixture of saturated solution of sodium nitrite (50 m*l*) and 1-(α-naphthyl)-cyclohexene (3 g) in ether (50 m*l*) was cooled in ice water and treated with 4 N sulfuric acid in drops till the green colour changed to yellow. The ether layer was immediately separated, washed with water and dried. The combined ether extracts from ten such experiments were treated with sodium (10 g) in methanol (100 m*l*) with vigorous shaking, diluted with water and the basic aqueous layer was separated. The ether layer was washed with 10% sodium hydroxide till free from alkali soluble material, washed with water, dried (sodium sulfate) and evaporated to yield 1-(α-naphthyl)-2-nitrocyclohexene (20 g), mp 95°C (from ether). ν_{max} (KBr) 1640 (-C=C-), 1550 and 1350 cm^{-1} ($-NO_2$).

The alkaline extracts were cooled and acidified with concentrated hydrochloric acid to give 3-nitro-2-(α-naphthyl)-cyclohex-2-en-1-one oxime (8 g) mp 210°C (from ethanol).

Found: C, 67.8; H, 5.2%. Calcd for $C_{16}H_{14}N_2O_3$: C, 68.08; H, 5.0%.

ν_{max} (KBr) 3247 (-OH), 1640 (-C=N) and 1515 and 1337 cm^{-1} ($-NO_2$).

A suspension of the above oxime (3 g) in 4 N sulfuric acid (50 m*l*) and dioxane (30 m*l*) was refluxed for three hours. The mixture was poured onto ice, extracted with ether, dried (sodium sulfate) and evaporated to yield 3-nitro-2-(α-naphthyl)-cyclohex-2-en-1-one (1.5 g), mp 130—131°C (from methanol). This ketone (1 g) and hydroxylamine hydrochloride (1 g) in alcohol (5 m*l*) and pyridine (5 m*l*) refluxed for three hours gave the oxime, mp 210°C (from ethanol). Mixed mp with the 3-nitro-2-(α-naphthyl)-cyclohex-2-en-1-one oxime showed no depression.

***cis*-2-(α-Naphthyl)-cyclohexylamine.** To a stirred solution of lithium aluminum hydride (2 g) in ether was added gradually a solution of 1-(α-naphthyl)-2-nitrocyclohexene (5 g). The mixture was left at 30°C for twenty four hours, then decomposed with water. The ether layer was decanted and extracted repeatedly with 2 N hydrochloric acid. The combined acid extracts were cooled, made alkaline and extracted with ether. The extract on evaporation left *cis*-2-(α-naphthyl)-cyclohexylamine as an oil (3.5 g).

Formyl derivative, mp 160—162°C (from ethanol).

Found: C, 80.4; H, 7.5%. Calcd for $C_{17}H_{19}NO$: C, 80.61; H, 7.5%.

Acetyl derivative, mp 186°C (from benzene - light petroleum).

Found: C, 81.1; H, 7.6%. Calcd for $C_{18}H_{21}NO$: C, 80.9; H, 7.9%.

Benzoyl derivative, mp 165—166°C (from dilute ethanol).

Found: C, 83.9; H, 7.1%. Calcd for $C_{23}H_{23}NO$: C, 83.9; H, 7.0%.

ν_{max} (KBr) 3340 and 3060 cm^{-1} (NH association band for axial -NH).[8]

***cis*-1,2,3,4,4a,10b-Hexahydro-5:6-benzphenanthridine.** A mixture of *cis*-1-formamido-2-(α-naphthyl)-cyclohexane (1 g) and 4:5 phosphorus pentoxide-phosphoric acid (20 g) was heated on an oil bath for two hours at 160°C. The mixture was cooled, decomposed with ice, the aqueous layer made alkaline and extracted with ether. The base in the etheral layer after purification by one more passage through acid gave *cis*-1,2,3,4,4a,10b-hexahydro-5:6-benzphenanthridine as an oil (0.6 g). The picrate prepared in the usual manner was crystallised from alcohol as yellow needles. Mp 239°C (decomp.).

Found: C, 59.8; H, 4.5%. Calcd for $C_{23}H_{20}N_4O_7$: C, 59.5; H, 4.3%.

5:6-Benzphenanthridine. *cis*-1,2,3,4,4a,10b-Hexahydro-5:6-benzphenanthridine (1 g) was dehydrogenated over 30% palladised charcoal (0.5 g) in refluxing decalin (25 m*l*) during eight hours, in a current of nitrogen. The 5:6-benzphenanthridine crystallising from acetone had mp 108°C.

Found: C, 89.2, H, 5.0%. Calcd for $C_{17}H_{11}N$: C, 89.1; H, 4.9%.

λ_{max} 272, 341 and 376 mμ. (log ε 4.5, 3.0 and 3.2 respectively).

The picrate was crystallised from alcohol as yellow needles, mp 253°C (decomp).

Found: C, 60.2; H, 2.9%. Calcd for $C_{23}H_{14}N_4O_7$: C, 60.3; H, 3.1%.

Summary

Syntheses of 5:6-benzphenanthridine, 9-methyl- and 7,9-dimethyl-5:6-benzphenanthridine, 9-methyl-5:6,7:8-dibenzphenanthridine, *cis*-9-phenyl-, *cis*-7-methyl-9-phenyl- and *cis*-7-methoxy-9-phenyl-1,2,3,4,4a,10b-hexahydro-5:6-benz-phenanthridine and *cis*-9-phenyl-1,2,3,4,4a,10b-hexahydro-5:6,7:8-dibenzphenanthridine are reported.

We thank R. Balasubramanian, Department of Chemistry, University of Madras, and CIBA Research Centre, Bombay, for analyses and IR spectra. Our thanks are also due to Government of India and U. G. C. for a scholarship and a Fellowship to V. K. and V. C. D. respectively.

8) Z. Yoshida, *Tetrahedron Letters*, **1965**, 2757.

Studies on Heteroaromaticity. XXV.[1] 1,3-Dipolar Cycloaddition of *C*-(2-Benzimidazolyl)-*N*-phenylnitrone

Tadashi SASAKI and Toshio OHISHI

Institute of Applied Organic Chemistry, Faculty of Engineering, Nagoya University, Chikusa-ku, Nagoya

(Received April 2, 1968)

In continuation from the previous papers concerning the heterocyclic nitrones involving nitrofuran-[1] and pyrimidine-ring,[2] this paper deals with a nitrone having a benzimidazole ring and its 1,3-dipolar cycloaddition reactivity with dipolarophilic olefins such as styrene and methyl acrylate. *C*-(2-Benzimidazolyl)-*N*-phenylnitrone (I) was readily prepared from benzimidazole-2-carboxaldehyde[3] and phenylhydroxylamine in a 55% yield by the routine procedure.[4] I was relatively stable and could be stored in a brown desiccator but readily decomposed to colored tars in the light.

As typical examples of its 1,3-dipolar cycloaddition reactions, styrene and methyl acrylate were treated in dioxane with I affording the corresponding adducts, II and III, in 40 and 50% yields, respectively. Each structure of both compounds, II and III, was determined by the NMR spectrum. Figure 1 shows the NMR spectrum of

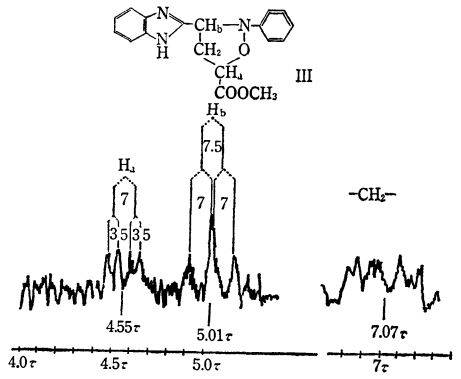

Fig. 1. NMR spectrum of III (DMSO-d_6).

III as an example. The existence of two quartets around 4.55 and 5.01 τ for two methine protons of an isoxazolidine ring in the NMR spectrum supports structure III, which is 5- instead of 4-carbomethoxy structure.[1] Similarly, II is concluded to have 5-phenylisoxazolidine ring. Such a constant direction of the addtion irrespective of the electronic character of a substituent of the olefin demonstrates that this reaction proceeds in the manner similar to that in the case of *C*-(5-nitro-2-furyl)-*N*-phenylnitrone,[1] both followed by the general principle suggested by Huisgen.[5]

Experimental[6]

Preparation of *C*-(2-Benzimidazolyl)-*N*-phenylnitrone (I). A solution of 6 g (41 mmol) of benzimidazole-2-carboxaldehyde[3] and 8 g (40 mmol) of phenylhydroxylamine[7] in 400 m*l* of ethanol was refluxed for two days. The precipitates were collected after cooling, washed with acetone and recrystallized from ethanol to give 5.3 g (55%) of I as yellow needles, mp 245—248°C (decomp). IR (KBr) cm^{-1}: 1565, 1580 ($\nu_{C=N}$), 1065 ($\nu_{N\to O}$). UV λ_{max}^{EtOH} mμ (log ε): 355 (4.45).

Found: C, 71.21; H, 4.56; N, 17.90%. Calcd for $C_{14}H_{11}ON_3$: C, 70.87; H, 4.67; N, 17.71%.

Reaction of I with Styrene. A solution of 0.3 g (1.3 mmol) of I and 0.2 g (1.9 mmol) of styrene in 30 m*l* of dioxane was heated at 90°C on a water bath for 27 hr. After dioxane was removed under reduced pressure, the residual oil was dissolved in a small amount of chloroform and made turbid by addition of petroleum ether. A separated oil solidified gradually in an ice box. The separated crystals were collected and recrystallized from chloroform-ether to give 0.11 g (40%) of II as colorless powders, mp 178—180°C. In the infrared spectrum, a $\nu_{N\to O}$ absorption disappeared and a new one appeared at 1620 cm^{-1} due to $\nu_{C=N}$. UV λ_{max}^{EtOH} mμ (log ε): 238 (4.27), 274 (4.01), 280 (4.02).

Found: C, 77.35; H, 5.38; N, 11.84%. Calcd for $C_{22}H_{19}ON_3$: C, 77.39; H, 5.61; N, 12.31%.

Reaction of I with Methyl Acrylate. A solution of 0.3 g (1.3 mmol) of I and 0.2 g (2.3 mmol) of methyl acrylate in 26 m*l* of dioxane was heated at 90°C on a water bath for 25 hr. Work-up as above afforded 0.17 g (50%) of III as colorless crystals, mp 172—174°C. IR (KBr) cm^{-1}: 1740 (ν_{CO}), 1620 ($\nu_{C=N}$), UV λ_{max}^{EtOH} mμ (log ε): 238 (3.60), 275 (3.57), 280 (2.57).

Found: C, 66.71; H, 5.08; N, 12.73%. Calcd for $C_{18}H_{17}O_3N_3$: C, 66.86; H, 5.30; N, 13.00%.

1) Part XXIV of this series: T. Sasaki, T. Yoshioka and I. Izure, This Bulletin, **41**, 2964 (1968).
2) As Part XXI of this series: T. Sasaki and M. Ando, This Bulletin, **41**, 2960 (1968).
3) H. R. Hensel, *Chem. Ber.*, **98**, 1325 (1965).
4) L. I. Smith, *Chem. Revs.*, **23**, 193 (1938).
5) R. Huisgen, L. Feiler and G. Binsch, Angew. *Chem. Intern. E. Engl.*, **3**, 753 (1964); J. C. Martin, V. W. Goodlett and R. D. Burpitt, *J. Org. Chem.*, **30**, 4309 (1965).
6) All the melting points were not corrected. Infrared spectra were determined on a Nippon-Bunko, Model IR-S spectrometer and electronic spectra were obtained with a Nippon-Bunko optical rotatry dispersion recorder, Model ORD/UV-5. NMR spectra were determined on a Varian A-60 spectrometer, with tetramethylsilane as an internal standard and the peak positions are expressed by τ-values.
7) O. Kamm, "Org. Synth.," Coll. Vol. 1, p. 445 (1956).

Studies of the Alkaline Earth Complexes in Various Solutions. IV. Solvent Extraction Study of Radium(II) Complexes with Some Aminocarboxylic Acids in Perchlorate Media

Tatsuya SEKINE, Yoshimitsu KAWASHIMA, Takaaki UNNAI and Mitsuo SAKAIRI

Department of Chemistry, Science University of Tokyo, Kagurazaka, Shinjuku-ku, Tokyo

(Received April 11, 1968)

Few investigations have been conducted on complex formation of radium(II) in aqueous solutions. This may be due to the fact that only tracer studies are possible in practice because of the high level radioacitivity of radium isotopes.

In the present paper, the complex formation of radium(II) with six very common aminocarboxylic acids has been studied by a liquid-liquid distribution method. Radium(II) was extracted with a mixture of thenoyltrifluoroacetone (TTA) and tributylphosphate (TBP) in carbon tetrachloride. Stability constants were determined by a graphic method from the distribution data.

Experimental

Radium-228 was imported from Radiochemical Center, Amersham, England. It was purified by a solvent extraction cycle which was reported previously.[1] The organic phases were always carbon tetrachloride containing 0.1 M TTA and 0.1 M TBP. The aqueous phase was sodium perchlorate media at ionic strength 0.1 M. No special buffer was added to the aqueous phase, but the hydrogen ion concentration was adjusted by the substitution of 0.1 M sodium hydroxide for 0.1 M sodium perchlorate. This hydroxide carried an equivalent amount of TTA from the organic phase into the aqueous phase and this dissociated TTA anion, together with a small amount of undissociated TTA,*1 buffered the aqueous phase. The addition of a complex forming ligand was made by way of various amounts of disodium salt solution of the aminocarboxylic acid. The aqueous and organic phases were placed in stoppered glass tubes (volume 20 m*l*) and agitated mechanically for one hour. The initial volume of the two phases was 5.0 m*l*. The two phases were then centrifuged and a 2 m*l* portion was pipetted from each phase and the samples thus separated let stand for 3 days. The γ-radioactivity of the samples in which radium-228 (half-life 6.7 yr.) was in transient radioactive equilibrium with γ-radioactive actinium-228 (half-life 6.13 hr) was measured with a well-type (NaI) scintillation counter. A small portion was also taken from the aqueous phase and the hydrogen ion concentration measured potentiometrically using an aqueous solution containing 0.0100 M perchloric acid and 0.09 M sodium perchlorate as the standard of $-\log[H^+]=2.00$.

TABLE 1. DISSOCIATION CONSTANTS OF THE AMINOCARBOXYLIC ACIDS AND THE STABILITY CONSTANTS OF THE ALKALINE EARTH METAL COMPLEXES WITH THESE LIGANDS IN 0.1 M SODIUM PERCHLORATE MEDIA AT 25°C

$K = [RaL^{2-l}]/[Ra^{2+}][L^{l-}]$

Ligand*	pK_a**					log K***				
	1	2	3	4	5	Mg	Ca	Sr	Ba	Ra
CyDTA	2.51	3.60	6.20	11.78	—	10.3	12.5	10.0	8.0	8.3
DTPA	1.94	2.87	4.37	8.69	10.56	9.3	10.6	9.7	8.8	8.5
EDTA	2.07	2.75	6.24	10.34	—	8.7	10.7	8.6	7.8	7.5
EGTA	2.08	2.73	8.93	9.54	—	5.2	11.0	8.5	8.4	7.7
HEDTA	2.72	5.41	9.81	—	—	5.2	8.0	6.8	6.2	5.6

* CyDTA Cyclohexane-1,2-diamine-*N,N,N',N'*-tetraacetic acid
DTPA Diethylenetriamine-*N,N,N',N'',N''*-pentaacetic acid
EDTA Ethylenediamine-*N,N,N',N'*-tetraacetic acid
EGTA 2,2'-Ethylenedioxyl bis[ethyliminodi(acetic acid)]
HEDTA *N'*-(2-Hydroxylethyl)ethylenediamine-*N,N,N'*-triacetic acid
NTA Nitrilotriacetic acid

** The acid dissociation constants were taken from Ref. 5.

*** Stability constants for radium(II) complexes are obtained from the present work. Other constants were taken from Ref. 5.

*1 The distribution constant of TTA between carbon tetrachloride containing 0.1 N TBP and 0.1 N sodium perchlorate is 27,[2] and the acid dissociation constant of TTA in this aqueous phase is 8×10^{-7}.[3]

1) T. Sekine, Y. Koike and M. Sakairi, *J. Nucl. Technolog.*, **4**, 308 (1967).
2) Y. Hasegawa and T. Sekine, unpublished data.
3) J. Stary, "The Solvent Extraction of Metal Chelates," Pergamon Press, Oxford (1964).

Results

The distribution ratio of radium(II) was calculated as follows:

$$D = \frac{[\mathrm{Ra(II)}]_{\mathrm{org,total}}}{[\mathrm{Ra(II)}]_{\mathrm{total}}} = \frac{\gamma\text{-count-rate per ml org. phase}}{\gamma\text{-count-rate per ml aq. phase}}$$

Figure 1 gives the $\log D$ *vs.* $-\log[\mathrm{H^+}]$ plot when the aqueous phase was 0.1 M sodium perchlorate

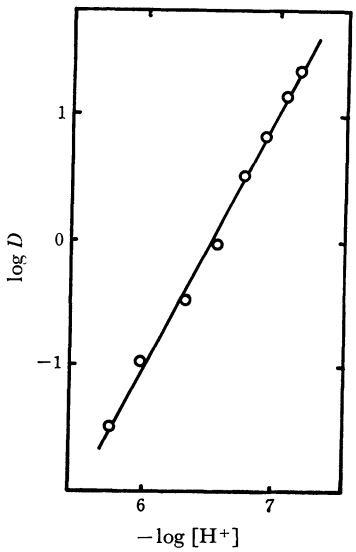

Fig. 1. $-\log[\mathrm{H^+}]$ dependence of radium(II) extraction from 0.1 M $NaClO_4$ at 25°C.
Organic phase: carbon tetrachloride containing 0.1 M TTA and 0.1 M TBP.
The solid line is $\log D = -2\log[\mathrm{H^+}] - 12.94$

containing no ligand. The following extraction constant was obtained from these data;

$$K_{ex_0} = D_0[\mathrm{H^+}]^2[\mathrm{HA}]_{\mathrm{org}}^{-2} = 10^{-10.92} \quad ([\mathrm{TBP}]_{\mathrm{org}} = 0.1\ \mathrm{M}) \qquad (1)$$

here D_0 denotes $[\mathrm{RaA_2}]_{\mathrm{org}}/[\mathrm{Ra^{2+}}]$ and HA denotes TTA.

The stability constant of the first complex is defined as;

$$K = [\mathrm{RaL^{2-}}^{l}]/[\mathrm{Ra^{2+}}][\mathrm{L}^{l-}] \qquad (2)$$

When the aqueous phase contains only the first metal complex, the following equation may be written;

$$D = [\mathrm{RaA_2}]_{\mathrm{org}}/([\mathrm{Ra^{2+}}] + [\mathrm{RaL^{2-}}^{l}]) \qquad (3)$$

From Eqs. (2) and (3), the following extraction constant may be obtained;

$$K_{ex} = D[\mathrm{H^+}]^2[\mathrm{HA}]_{\mathrm{org}}^{-2} = \frac{D_0[\mathrm{H^+}]^2[\mathrm{HA}]_{\mathrm{org}}^{-2}}{1 + K[\mathrm{L}^{l-}]} \qquad (4)$$

Then from Eqs. (1) and (4), the following equation is obtained;

$$K_{ex}/K_{ex_0} = (1 + K[\mathrm{L}^{l-}])^{-1} \qquad (5)$$

Further details on the statistical treatment have already been given in Paper I of this series.[4]

The ligand concentration was calculated using

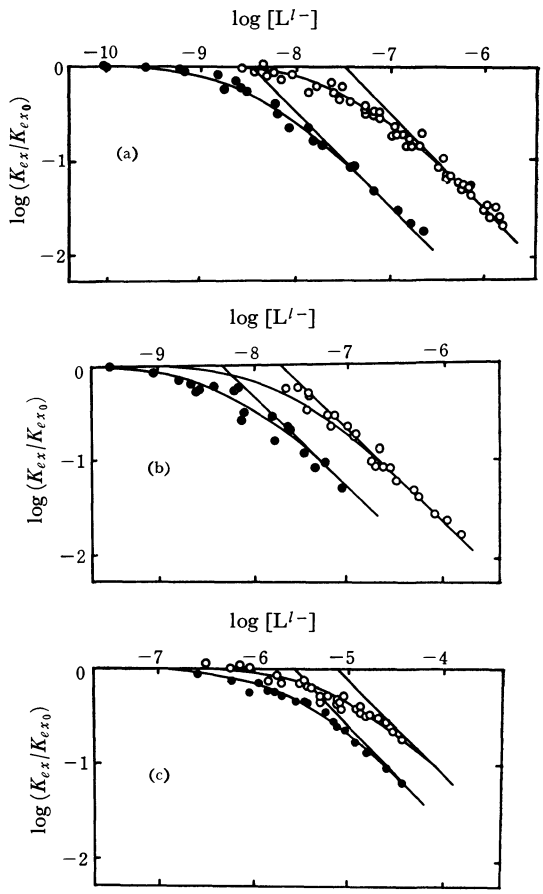

Fig. 2. $\log(K_{ex}/K_{ex_0})$ *vs.* $\log[\mathrm{L}^{l-}]$ plot.
Organic phase: carbon tetrachloride containing 0.1 M TTA and 0.1 M TBP.
Aqueous phase: 0.1 M $Na(ClO_4)$
The ligand and the curves drawn in the figures are as follows:

(a) Open circles:
EDTA, $Y = -\log(1 + 10^{7.5}[\mathrm{L^{4-}}])$
Closed circles:
DTPA, $Y = -\log(1 + 10^{8.5}[\mathrm{L^{5-}}])$

(b) Open circles:
EGTA, $Y = -\log(1 + 10^{7.7}[\mathrm{L^{4-}}])$
Closed circles:
CyDTA, $Y = -\log(1 + 10^{8.3}[\mathrm{L^{4-}}])$

(c) Open circles:
NTA, $Y = -\log(1 + 10^{5.1}[\mathrm{L^{3-}}])$
Closed circles:
HEDTA, $Y = -\log(1 + 10^{5.6}[\mathrm{L^{3-}}])$

4) T. Sekine, M. Sakairi and Y. Hasegawa, This Bulletin, **39**, 2141 (1966).

the acid dissociation constants[5] given in Table 1. These acid dissociation constants previously reported were calculated from pH measurements. On the other hand, in the present work, the stoichiometric hydrogen ion concentration was always measured and thus the activity coefficient of hydrogen ion, 0.86,[6] was used to convert $-\log[H^+]$ into pH.

Figures 2a to 2c show the log (K_{ex}/K_{ex0}) *vs.* $\log[L^{l-}]$ plot. The stability constants were determined by a curve-fitting method.[4] Data analysis was carried out assuming no formation of complexes containing protons. This assumption seems reasonable because no remarkable deviation of the points, which might be caused by the formation of such complexes, is observed in the figures containing experimental data obtained at various different hydrogen ion concentrations ($6<-\log[H^+]<7$).

The present measurement for the EDTA complex ($\log K=7.5$) is very close to a previous measurement ($\log K=7.4$).[7] No data seems to have been reported on radium(II) complexes with other ligands.

Part of this work was carried out at the Laboratory of Nuclear Chemistry, the Institute of Physical and Chemical Research. The authors are grateful to Professor Nobufusa Saito, Head of the laboratory.

5) A. Ringbom, "Complexation in Analytical Chemistry", John Wiley and Sons Inc., New York (1963).

6) B. E. Conway, "Electro Chemical Data," page 102, Elsevier (1952).

7) F. Nelson, R. A. Day and K. A. Kraus, *J. Inorg. Nucl. Chem.*, **15**, 140 (1960).

Oxygen-18 Tracer Study on the Reduction of Arylsulfonyl Chloride with Zinc

Norio KUNIEDA, Kazuo SAKAI and Shigeru OAE

Department of Applied Chemistry, Faculty of Engineering, Osaka City University, Sumiyoshiku. Osaka

(Received April 12, 1968)

Optically active, ^{18}O-labeled sulfoxides are very convenient for studying the nature of substitution reactions on the trivalent sulfur atom, while ^{18}O-labeled arylsulfinic acids are essential starting materials for the preparation of optically active and ^{18}O-labeled sulfoxides.[1] Meanwhile sulfonyl chlorides are known to be reduced by treating with metallic zinc to the corresponding sulfinic acids.[2] In this note, we wish to report a tracer study on this reduction and a convenient procedure for the preparation of the arylsulfinic acid-^{18}O. ^{18}O-Labeled arylsulfonyl chloride can be prepared readily by treating aryl mercaptan with chlorine in a media containing $H_2{}^{18}O$. If there is no oxygen exchange between the reactants and water during the reduction of the ^{18}O-labeled sulfonyl chlorides, this zinc reduction of sulfonyl chlorides will be definitely simpler and better than the conventional procedure in which the ^{18}O-labeled sulfinic acids are usually obtained by the hydrolysis of the corresponding unlabeled sulfinyl chlorides with ^{18}O-enriched water,[3] thereby the sulfinic acids obtained contain only a half the concentration of ^{18}O of that of ^{18}O-enriched water used. An ^{18}O-labeled arylsulfonyl chloride was treated with zinc dust in hot water, and the sodium arylsulfinate was obtained by the successive treatments with sodium hydroxide and sodium carbonate according to the method described by Whitmore and Hamilton.[2] Sodium arylsulfinate thus obtained was converted to the corresponding sulfinic acid by neutralization and also to sulfinyl chloride by the treatment with thionyl chloride, respectively. The results of ^{18}O-analyses of these products are listed in Table 1. As shown in Table 1, the ^{18}O-concentrations of all the products obtained were found to be identical to that of the arylsulfonyl chloride started.

Table 1. Results of ^{18}O-analyses

R	(Atom%-^{18}O)			
	RSO_2Cl	RSO_2Na	RSO_2H	$RSOCl$
C_6H_5	1.14	1.14	1.15	1.13
p-CH_3-C_6H_4	1.59	1.50	1.52	—
p-Br-C_6H_4	1.43	1.39	1.40	—

Natural CO_2; 0.206 atm%-^{18}O

$$2\ ArSO_2Cl + 2\ Zn \rightarrow (ArSO_2)_2Zn + ZnCl$$

$$+ INa_2CO_3 \xrightarrow{(NaOH)} 2\ ArSO_2Na + ZnCO_3$$

1) K. K. Andersen, *Tetrahedron Letters*, **1962**, 93; H. Phillips, *J. Chem. Soc.*, **1925**, 2575.
2) F. C. Whitmore and F. H. Hamilton, "Organic Syntheses," Coll. Vol. I, p. 492 (1956).
3) M. Kobayashi, M. Terao and A. Yamamoto, This Bulletin, **39**, 802 (1966).

This reduction has been known to proceed stoichiometrically according to the following manner.

At first the chlorine atom of the sulfonyl chloride is considered to be replaced by zinc to form a complex (I), the intermediary product, by the same fashion as in the preparation of zinc dialkyls from alkyl halides and metallic zinc.[4] This complex (I) would be stabilized by the coordination of several water molecules around zinc atom of (I). When the complex (I) is decomposed by the treatment with alkali, sodium arylsulfinate is formed. In fact, Haszeldine and Kidd have successfully isolated zinc trifluoromethanesulfinate, $(CF_3SO_2)_2Zn\cdot 4H_2O$, as an intermediate in this zinc reduction.[5,6] The complex (I) would assume either one of the following form, A or B, however, in view of the fact that the oxygen atom of the sulfinate ion is more basic than the sulfur atom, the form B seems to be more plausible.[7]

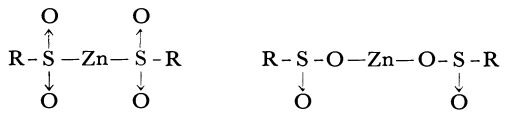

A B

Since there was no oxygen exchange in the next step, *i. e.*, the reaction between the complex (I) and alkali hydroxide, the process involving the ligand exchange with hydroxide ion is the only conceivable path for the formation of sodium aryl sulfinate.

4) E. G. Rochow, D. H. Hurd and R. L. Lewis, "The Chemistry of Organometallic Compounds," John Wiley & Son, New York, N. Y. (1967), p. 100.
5) R. N. Haszeldine and J. M. Kidd, *J. Chem. Soc.*, **1955**, 2901.
6) The structure of the product of dimethylzinc and sulfur dioxide has been also proposed to be $(CH_3SO\cdot O)_2\cdot Zn$ based on IR spectra; N. A. D Carey and H C. Clark, *Can. J. Chem.*, **46**, 649 (1968).
7) We do not intend to specify the bonding of this complex which would assume either ionic or covalent bonding. Presumably, however, Zn-O bond of I is near covalent. See also the related observation that *p*-tolylsulfinyl copper complex has O-Cu bond with considerable covalent character; D. A. Langs and C. R. Hare, *Chem. Commun.* (London), **1967**, 853.

Experimental

^{18}O-Labeled Arylsulfonyl Chloride. A mixture of aryl mercaptan (0.1 mol) and ^{18}O-enriched water (0.22 mol, 1.60 atom%-^{18}O) was cooled in an ice bath, and chlorine gas was passed till the color of the mixture became pale yellow. Then the mixture was poured into ice water and extracted with chloroform. The extract was washed with 10% aqueous sodium carbonate, 10% aqueous sodium thiosulfate and water succesively. The ^{18}O-labeled arylsulfonyl chloride was distilled or recrystallized from n-hexane several times. RSO_2Cl; [R, mp or bp(°C)(lit.), yield(%), atom%-^{18}O]. C_6H_5, 77—78/2 mmHg (147/45 mmHg),[8] 90, 1.14. *p*-CH_3-C_6H_4, 69(69),[9] 93, 1.53, 1.59. *p*-Br-C_6H_4, 73—74 (74—75),[10] 91, 1.43.

The Reduction of Arylsulfonyl Chloride with Zinc was carried out following the procedure described by Whitmore and Hamilton,[2] using ^{18}O-labeled arylsulfonyl chloride (0.06 mol). The sodium arylsulfinate dihydrate was obtained in a good yield, 75—90%. The dihydrate was dehydrated *in vacuo* for 5 hr at 120—130°C for the mass analysis.

^{18}O-Labeled Arylsulfinic Acid was prepared by the careful neutralization of the ^{18}O-labeled sodium arylsulfinate with hydrochloric acid. It was recrystallized from *n*-hexane - ether. RSO_2H; [R, mp(°C)(lit)]. C_6H_5, 83(83).[11] *p*-CH_3-C_6H_4, 85(85).[12] *p*-Br-C_6H_4, 113 (114).[11]

^{18}O-Labeled Benzenesulfinyl Chloride was prepared from anhydrous sodium benzenesulfinate(1.8 g) and thionyl chloride (4.0 g),[13] bp 81—82°C/2 mmHg (lit[14] 96—98°C/4 mmHg), yield 1.1 g.

The Mass-spectrometric Analysis was carried out in the form of carbon dioxide gas and the atom%-^{18}O was calculated from the mass peak heights 44 and 46.

8) R. Adams and C. S. Marvel, "Organic Syntheses," Coll. Vol. I, p. 84 (1941).
9) F. E. Ray and L. M. Soffer, *J. Org. Chem.*, **15**, 1039 (1950).
10) A. J. Prinsen and H. Cerfontain, *Rec. Trav. Chem.*, **84**, 24 (1965).
11) E. Knoevenagel, *Ber.*, **41**, 3315 (1908).
12) J. L. Kice and K. W. Bowers, *J. Am. Chem. Soc.*, **84**, 605 (1962).
13) F. Kurzer, "Organic Syntheses," Coll. Vol. IV, p. 937 (1963).
14) E. S. Leuchenko, N. Ya. Derkach and A. V. Kirsonov, *Zh. Obshch. Khim.*, **31**, 1971 (1962).

The Base-induced Pyrolysis of Tosylhydrazones of Mesityl Oxide and Dypnone*1

Tadashi SATO and Sotaro WATANABE

Department of Applied Chemistry, School of Science and Engineering, Waseda University, Shinjuku-ku, Tokyo

(Received May 13, 1968)

Closs, Closs, and Böll[1] carried out the base-induced pyrolysis of tosylhydrazones of α,β-unsaturated aldehydes and ketones and found that the decomposition gave mainly cyclopropenes when the β-carbon atom was replaced by two alkyl groups, while it gave mainly pyrazoles when the β-carbon atom was monosubstituted or not replaced by an alkyl group. They proposed that this difference arose bacause the steric hindrance and inductive effect resulting from increasing methyl substitution at the β-position retarded the rate of cyclization of the diazo intermediates and accelerated the rate of nitrogen elimination of the diazo intermediates.

As an extension of the study concerned with the effect of substituents on the reaction routes, the base-induced pyrolysis of tosylhydrazones of mesityl oxide (I) and dypnone (V) was compared under several conditions.

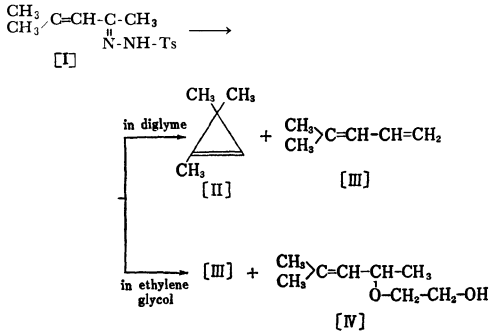

Chart 1

Mesityl oxide tosylhydrazone (I) has been known[1] to give 1,3,3-trimethylcyclopropene (II) as the major product, and 4-methylpenta-1,3-diene (III) as the minor product, when added to a suspension of sodium methoxide in an aprotic solvent (diglyme) at 160°C. The pyrolysis of I with sodium alkoxides in a protic solvent (ethylene glycol) was carried out; 4-methylpenta-1,3-diene (III) and β-hydroxyethyl ether IV were obtained in ratios of 5 : 1, indicating that under these conditions nitrogen elimination was predominant.

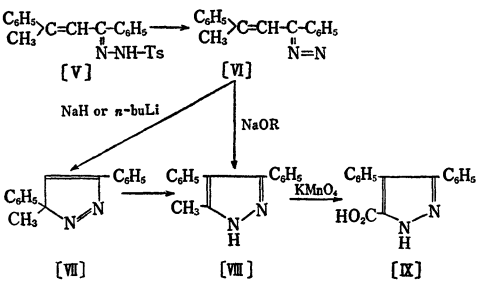

Chart 2

When dypnone tosylhydrazone (V) was added to a solution or suspension of sodium methoxide in a protic solvent (ethylene glycol) or in an aprotic solvent (diglyme), a red color developed which was attributable to the diazo intermediate VI. The red color disappeared when the solution was heated, and 5-methyl-3,4-diphenylpyrazole (VIII) was obtained quantitatively. Obviously phenyl migration occurred during the VI—VIII reaction; this migration seemed to be effected by the action of the proton from ethylene glycol or from methanol, which was formed *in situ* from the tosylhydrazone and sodium methoxide in diglyme. In support of this, the pyrolysis of V with *n*-butyllithium or sodium hydride in refluxing *n*-hexane afforded 3-methyl-3,5-diphenyl-3*H*-pyrazole (VII) in an excellent yield, and VII was rearranged into VIII when refluxed in ethanol.

The structure of VIII was established by its oxidation to the known 3,4-diphenylpyrazole-5-carboxylic acid (IX).[2] This pyrazolecarboxylic acid was identical with the authentic sample prepared according to the method reported by Borsche and Hahn.[3]

Shapiro and Heath[4] and Kaufman, Cook, and Shechter[5] have reported olefin synthesis by treating tosylhydrazones with *n*-butyllithium. It should be noted that the reactions of both sodium alkoxides and *n*-butyllithium with tosylhydrazone of dypnone afforded the cyclization products

*1 Part V of a series on the pyrolysis of organic compounds. Part IV: T. Sato, *Tetrahedron Letters*, **1968**, 835.

1) G. L. Closs, L. E. Closs, and W. A. Böll, *J. Am. Chem. Soc.*, **85**, 3796 (1963).
2) W. E. Parham and W. R. Hasek, *J. Am. Chem. Soc.*, **76**, 799 (1954).
3) W. Borsche and H. Hahn, *Ann.*, **537**, 236 (1939).
4) R. H. Shapiro and M. J. Heath, *J. Am. Chem. Soc.*, **89**, 5734 (1967).
5) G. Kaufman, F. Cook, and H. Shechter, *ibid.*, **89**, 5737 (1967).

(VII and VIII) of the diazo intermediate VI, without any accompanying nitrogen elimination. It was concluded that, unlike the case of tosylhydrazone of mesityl oxide, the diazo intermediate VI formed by the decomposition of tosylhydrazone of dypnone was so stabilized by aromatic groups that no reaction accompanying the nitrogen elimination could be observed, even though the cyclization leading to the 3*H*-pyrazole or pyrazole might be considered to be unfavorable because of the two bulky groups on the β-carbon atom.

Experimental

The NMR spectra were measured on a Hitachi R-20 spectrometer in a deuterochloroform solution. The chemical shifts are described in ppm downfield from an internal tetramethylsilane reference.

Pyrolysis of Mesityl Oxide Tosylhydrazone (I). A suspension of mesityl oxide tosylhydrazone (20 g, 0.075 mol) in ethylene glycol (50 m*l*) was added, over a period of 30 to 60 min, to a solution of sodium ethylene glycolate (0.15 mol) in ethylene glycol (100 m*l*) heated to 160—190°C. The volatile matter which distilled during the addition separated into two layers. The lower layer was found by gas chromatographic analysis to be composed mainly of ethylene glycol. The upper layer (0.8—1 g) was fractionated into two components in the ratio of 5 : 1 by preparative gas chromatography on a Silicone SE 30 column at 120°C. The major component was shown to be 4-methylpenta-1,3-diene (III) from its IR and NMR spectra.[1]

NMR: δ 1.8 (m, 6H), δ 4.8 (m, 2H), δ 6.0—6.5 (m, 2H). IR: 1650, 1605, 885, 874 cm^{-1}.

The minor component was shown to be β-hydroxyethyl ether (IV) from its IR and NMR spectra.

NMR: δ 1.15 (d, 3H), for $C\underline{H}_3$-CH-, δ 1.70 (d, 6H) for $(C\underline{H}_3)_2C$=, δ 2.80 (s, 1H) for -O<u>H</u>, δ 3.2—3.7 (m, 4H) for -$C\underline{H}_2$-$C\underline{H}_2$-, δ 3.8—4.4 (m, 1H) for -C<u>H</u>-CH_3, δ 4.6—5.6 (m, 1H) for -C<u>H</u>=. IR: 3600—3200 cm^{-1} for O-H, 1670 cm^{-1} for C=C, 1105 cm^{-1} for -O-, 1050 cm^{-1} for C-OH.

Dypnone Tosylhydrazone (V). A mixture of dypnone (1 g, 0.0045 mol), tosylhydrazide (0.84 g, 0.0045 mol), and concentrated hydrochloric acid (0.1 m*l*) in methanol (10 m*l*) was refluxed for 30 min. The solution was then cooled to room temperature, and the product was allowed to crystallize, filtered, and recrystallized from methanol, mp 149—150°C. Yield: 84%.

Found: C, 70.51; H, 5.99; N, 7.22%. Calcd for $C_{23}H_{22}N_2SO_2$: C, 70.77; H, 5.65; N, 7.18%.

Pyrolysis of Dypnone Tosylhydrazone (V). *a) With Sodium Methoxide in Ethylene Glycol or Diglyme.* Dypnone tosylhydrazone (1 g, 0.0025 mol) was added all at once to a solution or suspension of sodium methoxide (0.0050 mol) in ethylene glycol or diglyme (25 m*l*) heated to 160—190°C, and then the solution was refluxed for 1 hr. After the solvent had been evaporated *in vacuo*, water was added and the reaction product was extracted with ether. The ether extract was dried over anhydrous sodium sulfate, and the ether was evaporated. The product was recrystallized from benzene - *n*-hexane to give white needles of 5-methyl-3,4-diphenylpyrazole (VIII) in a 92% yield; mp 179—180°C, lit.[2] mp 185—186°C, (IR: 3400—2400 cm^{-1} for N-H, Found: C, 82.01; H, 6.15; N, 12.01%).

N-Acetyl derivative; mp 66°C.

Found: C, 78.13; H, 5.79; N, 9.94%. Calcd for $C_{18}H_{16}N_2O$: C, 78.26; H, 5.79; N, 10.15%.

b) With n-Butyllithium or Sodium Hydride in n-Hexane. Dypnone tosylhydrazone (1 g, 0.0025 mol) was added all at once to a solution or suspension of *n*-butyllithium (0.0050 mol) or sodium hydride (0.0050 mol) in *n*-hexane (15 m*l*). When the solution was heated to a boiling point, a red color indicating the formation of a diazo intermediate developed; the solution was then refluxed for 2—5 hr, during which period the red color disappeared. The solution, after being washed with water, was left to stand overnight. The crystals were filtered and recrystallized from *n*-hexane. White needles of 3-methyl-3,5-diphenyl-3*H*-pyrazole(VII) melting at 83—84°C were obtained in a yield of 90—92%.

Found: C, 81.82; H, 6.15; N, 12.17%. Calcd for $C_{16}H_{14}N_2$: C, 82.05; H, 5.99; N, 11.96%.

Oxidation of 5-Methyl-3,4-diphenylpyrazole (VIII) to 3,4-Diphenylpyrazole-5-carboxylic Acid (IX). 5-Methyl-3,4-diphenylpyrazole (0.37 g, 0.016 mol) was oxidized with potassium permanganate (0.50 g, 0.038 mol) in a mixture of water (5 m*l*) and *t*-butyl alcohol (6 m*l*) according to the method reported by Parham and Hasek[2]. A crude acid (0.07 g) melting at 254—255°C was obtained; it was identical with an authentic sample of 5-methyl-3,4-diphenylpyrazole, mp 261°C[3] (IR spectra and mixed mp).

Conversion of 3-Methyl-3,5-diphenyl-3*H*-pyrazole (VII) to 5-Methyl-3,4-diphenylpyrazole (VIII). A solution of 3-methyl-3,5-diphenyl-3*H*-pyrazole (0.5 g) in ethanol (15 m*l*) was refluxed for 1 hr. The solvent was then evaporated, and the product was recrystallized to give a 95—100% yield of 5-methyl-3,4-diphenylpyrazole.

The authors are indebted to the Asahi Glass Foundation for its financial support.

Force Constants and Mean Amplitudes of Glyoxal

Tsutomu FUKUYAMA, Kozo KUCHITSU and Yonezo MORINO

Department of Chemistry, Faculty of Science, The University of Tokyo, Hongo, Bunkyo-ku, Tokyo

(Received May 22, 1968)

In a recent investigation of the gas-phase structures of butadiene, acrolein and glyoxal,[1] a least-squares analysis was carried out on the electron diffraction intensities and rotational constants as joint observables. The method is based on the conversion of electron-diffraction r_a distances into r_α^0 distances, and that of ground-state rotational constants into average rotational constants. For the conversions, one must know the quadratic force field. The force constants for butadiene were determined by Abe and Shimanouchi,[2] but no data were available on the force fields for glyoxal and acrolein except for the out-of-plane force constants for glyoxal reported by Brand.[3] Thus, a set of force constants have been estimated for the latter molecules from the reported vibrational frequencies of normal and certain deuterated species, at least with sufficient accuracy for calculating small correction terms ($r_\alpha^0-r_a$, A_z-A_0, *etc.*).

Observed Vibrational Frequencies. Glyoxal is a molecule with C_{2h} symmetry and has twelve fundamental frequencies: $5A_g+4B_u+2A_u+B_g$. In accordance with the rule of mutual exclusion, the B_u and A_u species are infrared active and the A_g and B_g species Raman active. Because of the experimental difficulty, the Raman spectra of glyoxal have never been observed successfully. Harris assigned all infrared-active fundamentals and some combination frequencies, from which he estimated the frequencies of the Raman active fundamentals.[4] The present note on the force constants for glyoxal is mainly based on the frequencies reported by him. The fundamental frequencies of $C_2D_2O_2$ reported by Brand and Minkoff[5] were also taken into account, in addition to the frequencies of the normal species by Harris.

In-plane Vibrations. A modified Urey-Bradley force field was assumed for the description of the in-plane vibrations: The potential

TABLE 1. UREY-BRADLEY FORCE CONSTANTS FOR GLYOXAL (in mdyn/Å)

	K		H	F		f
C-H	3.90	HCC	0.200	0.200	CO, CO	−0.890
C-C	3.25	CCO	0.375	0.410	CCO, CCO	0.225
C=O	10.60	HCO	0.357	0.610		

TABLE 2. OBSERVED AND CALCULATED FREQUENCIES OF GLYOXAL (in cm^{-1})

			$C_2H_2O_2$		$C_2D_2O_2$	
			Obsd	Calcd	Obsd	Calcd
A_g	ν_1	C-H str	2844	2840	—	2132
	ν_2	C=O str	1745	1761	1722	1709
	ν_3	C-H bend	1338	1341	—	1129
	ν_4	C-C str	1060	1063	—	915
	ν_5	C-C=O bend	550	542	537	531
B_u	ν_9	C-H str	2836	2840	2141	2116
	ν_{10}	C=O str	1730	1732	1712	1713
	ν_{11}	C-H bend	1312	1310	1008	1006
	ν_{12}	C-C=O bend	341	346	—	320
A_u	ν_6	C-H wag	802	802	630[a]	630
	ν_7	C-C torsion	128	128	117	117
B_g	ν_8	C-H wag	1048	1048	911	911

a) Evaluated by the product rule.

1) K. Kuchitsu, T. Fukuyama and Y. Morino, *J. Mol. Structure*, **1**, 463 (1968).
2) K. Abe and T. Shimanouchi, to be published.
3) J. C. D. Brand, *Trans. Faraday Soc.*, **50**, 431 (1954).
4) R. K. Harris, *Spectrochim. Acta*, **20**, 1129 (1964).
5) J. C. D. Brand and G. J. Minkoff, *J. Chem. Soc.*, **1954**, 2970.

energy was expressed in terms of the three sets of force constants (force constants for the bond stretching K, for the valence angle deformation H and for the non-bonded interaction F) and two interaction constants f. The latter constants were introduced between the two coordinates corresponding to the C=O stretching and between the two C–C=O bending coordinates. An apparent difference between the bond-stretching force constant for C–H and that for C–D was taken into account through the relation $K_{C-D}/K_{C-H}=1.026$.[6]

The force constants transferred from formaldehyde, acetaldehyde and acetone[7] were used as initial values, and then adjusted by trial-and-error calculations. In the final stage, a least-squares fit was made by taking K_{C-C}, H_{HCO}, H_{CCO}, f(CO, CO), and f(CCO, CCO) as variable parameters. The result is shown in Table 1 and the frequencies calculated using those force constants are compared with the observed values in Table 2.

The two interaction constants f(CO, CO) and f(CCO, CCO) were essential for reproducing the symmetric and antisymmetric frequencies of the C=O stretching and the CCO bending vibrations. The situation is essentially the same as that for butadiene, as indicated in Table 11 of Ref. 2, where the corresponding force constants, f_{dd} and f_{gg}, are relatively large negative and positive elements, respectively.

Out-of-plane Vibrations. Glyoxal has three out-of-plane vibrations: two in the A_u species and one in the B_g species. The number of elements in the F_s matrix are therefore three and one for respective symmetry blocks. The use of the frequencies of $C_2H_2O_2$ and $C_2D_2O_2$ made it possible to determine the F_s matrices uniquely. The result is shown in Table 3 in an internal coordinate system (F_R matrix). Brand determined the out-of-plane force constants by assuming that $(GF)_{76}$ was zero.[3] The F_R elements for each isotopic species (also given in Table 3) calculated by his method with the molecular geometry determined recently[1] are close to the present estimates.

TABLE 3. F_R MATRIX FOR OUT-OF-PLANE VIBRATIONS OF GLYOXAL[a] (in mdyn Å)

CH wag	F_k		
C-C torsion	f	F_m	
CH wag	f_{kk}	f	F_k

	Present work	Brand[b]	
		Normal species	Deuterated species
F_k	0.480	0.507	0.497
F_m	0.0515	0.0478	0.0491
f_{kk}	−0.049	−0.022	−0.033
f	0.0048	−0.022	−0.017

a) See Ref. 2 for notations.
b) Ref. 3.

TABLE 4. MEAN AMPLITUDES FOR GLYOXAL (in Å)

	Calcd	Obsd[a]
C—C	0.0485	$0.054_6 \pm 0.004_1$
C=O	0.0380	$0.037_1 \pm 0.003_0$
C—H	0.0799	0.057 ± 0.010
C···O	0.0635	$0.059_9 \pm 0.003_7$
O···O	0.0589	$0.060_2 \pm 0.004_0$

a) Ref. 1.

Mean Amplitudes. Mean square amplitudes for several atom pairs of glyoxal were calculated from the derived force constants. The results shown in Table 4 account for the observed values reasonably except for the C–H amplitudes. The small discrepancy in the C–H amplitude may be ascribed to a systematic error included in the diffraction experiment.

The authors are indebted to Mr. Koichi Abe for his helpful information and discussion.

6) T. Shimanouchi and I. Suzuki, *J. Chem. Phys.*, **42**, 296 (1965).
7) P. Cossee and J. H. Schachtschneider, *ibid.*, **44**, 97 (1966).

Force Constants and Mean Amplitudes of Acrolein

Tsutomu FUKUYAMA, Kozo KUCHITSU and Yonezo MORINO

Department of Chemistry, Faculty of Science, The University of Tokyo, Hongo, Bunkyo-ku, Tokyo

(Received May 22, 1968)

As mentioned in the preceding note for glyoxal,[1] the force constants were estimated for acrolein in order to obtain the correction terms necessary for correlating the structural data observed by electron diffraction and spectroscopy.

Observed Vibrational Frequencies. Acrolein is a planar molecule (C_s symmetry) with eighteen fundamental frequencies: 13A'+5A''. All but one of them were assigned by Brand and Williamson[2] on the basis of the observation of near-ultraviolet spectra. They assigned most of the fundamental frequencies of CH_2=CHCDO as well. On the other hand, Harris observed infrared and Raman spectra and assigned the fundamentals of the normal species.[3] His assignment differs from that of Brand in that the schematic descriptions of the 1158 cm^{-1} (ν_{10}) and 912 cm^{-1} (ν_{11}) modes are interchanged. We accepted the assignment of Harris since it is consistent with a

TABLE 1. UREY-BRADLEY FORCE CONSTANTS FOR ACROLEIN[a] (in mdyn/Å)

	K		H	F
C-H_1	4.64	$H_1C_2H_3$	0.262	0.21
C-H_4	4.46	$H_1C_2C_5$	0.190	0.52
C-H_7	3.78	$C_2C_5C_6$	0.325	0.35
C=C	7.14	$C_2C_5H_4$	0.186	0.52
C-C	3.46	$H_4C_5C_6$	0.259	0.27
C=O	10.30	$H_7C_6O_8$	0.375	0.61
		$C_5C_6O_8$	0.500	0.46
		$H_7C_6C_5$	0.200	0.20

p(CH, CH)	f(CC, CO)	f(CCC, CCO)
−0.157	−0.681	0.209

a) Numbering of atoms: 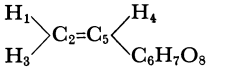

TABLE 2. OBSERVED AND CALCULATED FREQUENCIES OF ACROLEIN (in cm^{-1})

			CH_2=CHCHO		CH_2=CHCDO	
			Obsd	Calcd	Obsd	Calcd
A'	ν_1	CH_2 str	3103	3103	3101	3103
	ν_2	CH_2 str	3000	3009	2988	3009
	ν_3	CH str	3000	2991	—	2991
	ν_4	formyl CH str	2800	2801	2060	2098
	ν_5	C=O str	1724	1728	1709	1695
	ν_6	C=C str	1625	1619	1621	1618
	ν_7	CH_2 scis	1420	1413	1403	1413
	ν_8	HCO bend	1360	1360	—	1033
	ν_9	CH bend	1275	1270	1275	1275
	ν_{10}	C-C str	1158	1147	1153[a]	1169
	ν_{11}	CH_2 rock	912	915	877[a]	871
	ν_{12}	C-C=O bend	564	566	562	563
	ν_{13}	C-C=C bend	327	324	—	313
A''	ν_{14}	CH_2 twist	993	1002	993	997
	ν_{15}	formyl CH wag	980[b]	990	846	866
	ν_{16}	CH_2 wag	959	955	959	962
	ν_{17}	CH wag	593	592	556	557
	ν_{18}	torsion	157	157	151	149

a) The assignments are interchanged in the original report by Brand.[2] See text.
b) Evaluated by the product rule.

1) T. Fukuyama, K. Kuchitsu and Y. Morino, This Bulletin, **42**, 3019 (1968).

2) J. C. D. Brand and D. G. Williamson, *Discussions Faraday Soc.*, **35**, 184 (1963).

3) R. K. Harris, *Spectrochim. Acta*, **20**, 1129 (1964).

recent assignment of the fundamentals of butadiene reported by Abe and Shimanouchi.[4]

In-plane Vibrations. The potential energy was expressed in terms of K, H, F and three additional force constants. One interaction constant was introduced between the two C–H stretching coordinates of the methylene group. The other constants were introduced between the C=C and the C=O stretching coordinates and between the CCC and the CCO bending coordinates. Initial values of the force constants were taken from those for butadiene and glyoxal. After several trials, they were adjusted by a least-squares method with K_{C-C}, H_{HCH} and f(CCC, CCO) as variable parameters. The result is shown in Table 1, and the calculated frequencies are compared with observed values in Table 2.

The force constants for the vinyl group, including p(CH, CH), are close to the corresponding constants for butadiene, except for the C=C stretching force constant $K_{C=C}$ (7.1 mdyn/Å), which is larger than that for butadiene (6.6 mdyn/Å).[4] The force constants for the aldehyde group are roughly equal to those for glyoxal. A systematic decrease in the C–C stretching force constant observed for butadiene (3.82 mdyn/Å), acrolein (3.46 mdyn/Å) and glyoxal (3.25 mdyn/Å) correspond to a systematic increase in the bond distance r_g(C–C) (1.465, 1.480, and 1.526 Å, respectively)[5] and a systematic decrease in the π-bond order (0.224, 0.200, and 0.132).

Out-of-plane Vibrations. Abe and Shimanouchi introduced an F_a matrix of nearly general form in the analysis of the out-of-plane vibrations of butadiene.[4] For acrolein the F_R matrix, which is here equivalent to F_a, was set up in an analogous manner. Initial values of the elements were transferred from butadiene and glyoxal and then adjusted by trial and error. The final matrix is shown in Table 3. In order to facilitate comparison, notations for the elements are taken from Table 10 of Ref. 4. Effective two-fold torsional barriers around the central C–C bonds are found to be 8.1, 6.3 and 3.7 kcal/mol, respectively, for butadiene, acrolein and glyoxal. They are in essential agreement with the pure torsional transitions observed by Fateley *et al.* in the far infrared;[6] according to their one-dimensional analysis, V_1 and V_3 being ignored, their V_2 values are 7.0, 5.3 and 3.4 kcal/mol, respectively. It is interesting to note that a roughly linear relation exists between the torsional barriers and the lengths of the C–C bonds.

Table 3. F_R matrix for out-of-plane vibrations of acrolein (in mdyn Å)

CH_2 wag	F_j			
CH wag	F_{jk}	F_k		
CH_2 twist	0	F_{kl}	F_l	
C-C torsion	0	0	0	F_m
CH formyl wag	f_{jk}	f_{kk}	f_k	F_k'

F_j	0.327	F_{jk}	−0.054	f_{jk}	0.023
F_k	0.380	F_k	0.034	f_{kk}	−0.018
F_l	0.512	F_k'	0.524	f_{kl}	−0.047
F_m	0.0877				

Table 4. Mean amplitudes for acrolein[a] (in Å)

	Calcd	Obsd[b]
C-C	0.0486	$0.042_2 \pm 0.003_2$
C=C	0.0414	$0.047_7 \pm 0.003_3$
C=O	0.0396	$0.036_0 \pm 0.004_5$
C-H_1	0.0774	0.070 ±0.006
C_2-C_6	0.0704	0.075 ±0.09
C_2-O_8	0.0653	0.065 ±0.06
C_5-O_8	0.0579	$0.049_4 \pm 0.003_7$

a) For the numbering of atoms, see footnote of Table 1.
b) Ref. 5.

Mean Amplitudes. Mean square amplitudes for some of the atom pairs of acrolein are calculated from the force constants and compared with the observed values in Table 4. The agreement is as good as that for glyoxal.

4) K. Abe and T. Shimanouchi, to be published.
5) K. Kuchitsu, T. Fukuyama and Y. Morino, *J. Mol. Structure*, **1**, 463 (1968).
6) W. G. Fateley, R. K. Harris, F. A. Miller and R. E. Witkowski, *Spectrochim. Acta*, **21**, 231 (1965).

A Comment on the Structure of Glassy Carbon

Tokiti NODA,* Michio INAGAKI** and Shigehiko YAMADA***

* *Mie University, Tsu, Mie-Ken*
** *Faculty of Engineering, Nagoya University, Chikusa-ku, Nagoya*
*** *Nagoya Plant, Tokai Electrode Mfg. Co., Showa-ku, Nagoya*
Department of Applied Chemistry, Aichi Institute of Technology, Chikusa-ku, Nagoya

(Received June 4, 1968)

Glassy carbon is an apparently isotropic, continuous and non-porous material, showing conchoidal surface of fracture. It has a similar spectral dependence of reflectance to that of graphite.[1] Its electrical resistivity is of the same order as that of regular carbon materials and its thermal conductivity is relatively high compared with that of common ceramic materials.[2] The changes in Hall coefficient and magnetoresistance of glassy carbon with heat treatment temperature (HTT) resemble those of very hard carbon.[3] Its high strength, high Young's modulus, high hardness and also high impermeability to gases[2] suggest that glassy carbon must have a unique structure different from those of regular carbons.

The first proposal concerning the structure of glassy carbon was made with the aid of radial distribution function by two of the present authors.[4] Two other models of the structure of glassy carbon have been proposed since then.[5,6] Noda and Inagaki[4] proposed the contribution of tetrahedral bond together with trigonal bond as the principal bonds to the construction of glassy carbon. The extension of region consisting of only trigonally-bound carbon atoms or only tetrahedrally-bound carbon atoms can not be known by the radial distribution analysis. From the observation that the X-ray diffraction pattern of glassy carbon is very similar to that of turbostratic carbons,[4] it was deduced for the structure of glassy carbon that trigonal carbon atoms make small domains of two-dimensional graphite-like arrangement and that these domains are linked by tetrahedral bonds, while tetrahedral carbon atoms themselves make no domain of regular arrangement.

Furukawa[5] composed a model of three-dimensional irregular network configuration which contains all kinds of C-C bonds, *i. e.*, tetrahedral, planar double, linear triple and also conjugated C-C bonds. This model has no repetition of hexagonal rings of trigonal carbon atoms more than three. Insofar as glassy carbon heat-treated at such a low temperature as 800°C is concerned, the above two models are similar to each other, because the model of Noda and Inagaki consists of a large amount of tetrahedral carbon atoms and a number of small domains of trigonal carbon atoms, and Furukawa's model mainly consists of carbon atoms bound by tetrahedral and planar double bonds. According to Noda and Inagaki,[4] the content of trigonal carbon atoms increases and so the content of tetrahedral carbon atoms decreases with rise of HTT, and the X-ray diffraction band of (00*l*) becomes narrower with rise of HTT. These changes may be attributed to the increase in the size of the domains of trigonal carbon atoms. Takahashi and Westrum[7] measured the specific heat of glassy carbon, which was heat-treated at 3000°C, by adiabatic calorimetry from 6 to 350°K and found its T^2-dependence. This result suggests that glassy carbon mainly consists of two-dimensional layer lattice. Furukawa's model is not in harmony with this suggestion.

Kakinoki[6] proposed a model which consists of two kinds of domains, which are respectively composed of tetrahedral and trigonal carbon atoms and linked to neighboring domains by oxygen bridges. In his model, the oxygen bridges are responsible for the low density of glassy carbon and for the fact that the carbon is hardly graphitized at temperatures as high as 3000°C.[2,4] The oxygen content of glassy carbon directly determined by chemical analysis[8] was found to be about 1.2 per cent for 900°C-treated and about 0.3 per cent for 1200°C-treated glassy carbons, and 0.1—0.2 per cent for glassy carbon heat-treated at 1300—3000°C, respectively, the last value was determined by activation analysis.[9] The porosity of glassy carbon changes with HTT. Glassy carbon heat-treated at 600—700°C has the maximum apparent porosity (10—11%) and absorbs moisture of about 10 per cent by weight.[10] The oxygen

1) E. A. Taft and H. R. Philipp, *Phys. Rev.*, **138A**, 197 (1965).
2) S. Yamada and H. Sato, *Nature*, **193**, 261 (1962); *Carbon*, **2**, 253 (1964).
3) T. Yamaguchi, *Carbon*, **1**, 47 (1963).
4) T. Noda and M. Inagaki, This Bulletin, **37**, 1534 (1964).
5) K. Furukawa, *Nihon Kessho Gekkai Shi*, **6**, 101 (1964).
6) J. Kakinoki, *Acta Cryst.*, **18**, 578 (1965).
7) Y. Takahashi and E. F. Westrum, Jr., presented at the First Japanese Calorimetry Conference, Osaka, Nov., 1965.
8) K. Imaeda, private communication.
9) I. Fujii, mentioned in Ref. No 5.
10) H. Sato and S. Yamada, presented at Symposium on Carbon, Tokyo, July, 1964.

content as high as about 5—6 per cent, which was mentioned by one of the present authors (S. Y.) at an informal meeting of the Symposium on Carbon in Tokyo (1964) and was used by Kakinoki for construction of his model, was found later by Yamada to be mainly due to the moisture absorbed in glassy carbon. Fitzer, Schäfer and Yamada also obtained similar results on moisture absorption[11] and oxygen content[12] in the cases of glass-like carbons obtained from phenolic and furan resins. Therefore, Kakinoki's model seems to be inappropriate, because it has been derived from the presumption that glassy carbon contains several per cent of oxygen.

Ergun and Tiensuu[13] pointed out that X-ray diffraction study is not sufficient to ascertain the presence of diamond-like structures in amorphous carbons, but other properties of carbons such as hardness, density, electronic properties, graphitizability, *etc.*, must be considered. From the above discussions and also by considering the properties of glassy carbon,[2,3] the structural model of Noda and Inagaki, *viz.*, trigonal carbon atoms make small domains of two-dimensional graphite-like arrangement and these domains are linked by tetrahedral bonds, may be considered to be the most probable for the structure of glassy carbon. The possibility, that some kinds of bonds other than the tetrahedral one contribute to the linking of graphite-like layers, may not be ruled out.

Small graphite-like layers linked by C–C bonds three-dimensionally without any ordering make a continuous and low-density glassy carbon body which is isotropic and homogeneous in the long range ordering. In low-temperature-treated glassy carbons, the size of graphite-like layers is small and the percentage of linking carbon atoms is relatively high, but the size of layers increases and the percentage of linking carbon atoms decreases with rise of HTT. Insofar as to the structure that graphite-like layers are linked by so-called criss-cross linkages, glassy carbon is basically similar to regular carbons. The characteristics of glassy carbon, such as high strength, high hardness, impermeability, *etc.*, are mostly due to the high content of carbon atoms linking graphite-like layers successively in the three-dimensional way without any ordering. The high content of linking carbon atoms is also the main reason for non-graphitizability of glassy carbon.

11) E. Fitzer, W. Schäfer and S. Yamada, presented at the Eighth Conference on Carbon, Buffalo, June, 1967.
12) E. Fitzer, W. Schäfer and S. Yamada, unpublished.
13) S. Ergun and V. H. Tiensuu, *Acta Cryst.*, **12**, 1050 (1959).

SHORT COMMUNICATIONS

Photolysis of Sugar Tosylate. A New Procedure for the De-*O*-tosylation

Shonosuke ZEN, Seiko TASHIMA and Shinkichi KOTŌ

College of Pharmaceutical Sciences, Kitasato University, Shirokane-sankocho, Shiba, Minato-ku, Tokyo

(Received October 1, 1968)

The authors wish here to report a new method for the photolytic de-*O*-tosylation of sugar tosylate.[1]

Sugar tosylates are extensively used as important intermediates in the synthesis of carbohydrate derivatives. De-*O*-tosylations have usually been performed by catalytic hydrogenolysis,[1] but the application of this reaction is somewhat limited by the fact that a side reaction of a considerable extent might occur simultaneously.

Very recently it has been found in our laboratory that a tosyl group of sugar derivatives can be readily removed by a photolysis without any side reaction.

When a sugar tosylate in methanol is irradiated by UV in the presence of an equimolecular amount of sodium methoxide at room temperature, a parent sugar derivative is regenerated in an excellent yield. Without any UV irradiation, the de-*O*-tosylation does not occur under the same reaction conditions. A typical method is as follows: a methanolic solution (250 ml) of methyl 6-*O*-tosyl-α-D-glucopyranoside[2] (1.0 g) containing sodium methoxide was irradiated with a 100-W high-pressure mercury lamp in a water-cooled quartz immersion well (*Ushio Denki Co.*) at 25—27°C for 5 hr, with a gentle bubbling-in of nitrogen. The progress of the reaction was examined by thin-layer chromatography (TLC). The irradiated mixture was filtered and evaporated *in vacuo* to afford a brown syrup, which was then purified by silica-gel column chromatography. Methyl α-D-glucopyranoside was recovered in a 90% yield; it was identified with an authentic sample by a mixed-melting-point determination and by a comparison of their infrared spectra.

Without any UV irradiation, the starting material was recovered quantitatively under the same conditions. By cutting off wavelengths under 3100 A in an UV irradiation with a Pyrex tube,*1 the reaction was also retarded completely.

A similar procedure for 1,2:3,4-di-*O*-isopropylidene-6-*O*-tosyl-α-D-galactopyranose,[3] which has a primary tosyloxy group, gave quantitatively the syrupy 1,2 : 3,4-di-*O*-isopropylidene-α-D-galactopyranose, which could be identified with an authentic specimen[3] by a comparison of their IR spectra and by TLC, and which could also be converted into the tosylate again. This tosylate was identified with the starting material by a comparison of their melting point and IR spectra.

The method described above has been successfully applied to a secondary tosyloxy group: from methyl 3-*O*-tosyl-β-D-glucopyranoside, which had been prepared by the selective de-*O*-acetylation of methyl 2,4,6-tri-*O*-acetyl-3-*O*-tosyl-β-D-glucopyranoside,[4] methyl α-D-glucopyranoside was obtained in a 80% yield, while from 1,2 : 5,6-di-*O*-isopropylidene-3-*O*-tosyl-α-D-glucopyranose[5] 1,2 : 5,6-di-*O*-isopropylidene-α-D-glucopyranose was regenerated in a quantitative yield.

The details of this work will be reported later.

1) R. S. Tipson, *Advances in Carbohydrate Chem.*, **8**, 107 (1953).
2) F. Cramer, H. Otterbach and H. Springmann, *Ber.*, **92**, 384 (1959).

*1 This tube (Corning 774) may be used for experiments at wavelengths longer than 3100A.
3) K. Freudenberg and R. M. Hixon, *ibid.*, **56**, 2119 (1923).
4) S. Peat and L. F. Wiggins, *J. Chem. Soc.*, **1938**, 1088.
5) K. Freudenberg and O. Ivers, *Ber.*, **55**, 929 (1922).

Reaction of Bromine Activated by Bromine-82m Isomeric Transition in Liquid and Solid Benzene*[1]

Chiro SHINOMIYA and Toshiaki KISHIKAWA

Department of Industrial Chemistry, Faculty of Engineering, Kumamoto University, Kurokami-cho, Kumamoto

(Received May 31, 1968)

The discovery of the ^{82m}Br(I.T.)^{82}Br nuclear reaction[1,2] has made it possible to study isomeric transition-induced reactions free from any possible influence of the gamma-radiation from a reactor. The chemical effects of the subjecting transformation in liquid organic media have been investigated by Iyer and Willard[3] and by Stamouli and Katsanos.[4] To determine whether a similar chemical effect occurs (1) in the solid state, we mixed neutron-irradiated molecular bromine with benzene, and allowed it to stand at the temperature of dry ice for 60 min, by which time almost all the ^{82m}Br had decayed to ^{82}Br. The inorganic radiobromine was then separated by means of extraction.

A separate run was performed (2) in the liquid state. After mixing irradiated bromine with benzene at room temperature, the inorganic radiobromine in a portion of the mixture was separated by extraction at different time intervals. To analyze the rate of growth of the organic yield in the run (2), $OY^{\infty}_{obs}-OY^{\Delta t}_{obs}$ were plotted against Δt, where OY^{∞}_{obs} represents the ^{82}Br organic yield reached in the system (1) or system (2) after all the ^{82m}Br had decayed to the ^{82}Br ground state, and where $OY^{\Delta t}_{obs}$ represents it at any time before the ^{82m}Br has completely decayed. The plot gave a straight line. The half-time of the reaction so obtained was 6.27 min.

Correcting for the contributions of the activities of the ground-state ^{82}Br produced directly from radiative neutron capture and for those of the activities decayed from ^{82m}Br before mixing, one can obtain the net organic yields (OY^{∞}_{net}).

TABLE 1. ORGANIC YIELD OF ^{82}Br PRODUCED IN SOLID AND LIQUID BENZENE AS A RESULT OF THE DECAY OF ^{82m}Br(Br_2) BY ISOMERIC TRANSITION

Phase	Mole fraction of $Br_2\cdot10^3$	Total organic yield, OY^{∞}_{net} %	Ref.
Solid	4.23	113.1±15.6	
Liquid	4.23	34.0± 3.1	
Liquid	8.11	26.1± 0.6	4a

Bromine-82m decays by a highly converted transition[2] of 46 keV (internal conversion coefficient $\alpha_k=268$). This means that a large fraction of the ^{82}Br is produced with a positive charge. If the observed increases in the ^{82}Br organic yield result from chemical excitation by the isomeric transition, the rate of growth should depend only on the decay of ^{82m}Br (the half-lives in Refs. 1—3 are 6.05, 6.20, and 6.20 min, respectively). The closed value of the rate data may be attributed to the ^{82m}Br-decay-depending reaction. Because it is well known that aromatic bromination with molecular bromine proceeds quite gently in a nonpolar organic medium unless an electrophilic reagent such as ferric bromide is added. Stamouli *et al.*[4a] have reported the organic yield value of 26.1% where the bromine concentration was 8.11×10^{-3} mol fraction. Though the value in the present work is a little higher, it may be considered to be reasonable[4a] if the difference in the bromine concentration is taken into consideration.

In the solid system at the temperature of dry ice, a valid amount of activities in the system was found only in the benzene layer. Bromine forms a 1 : 1 molecular compound with benzene[5] (mp −14.0°C). Though the phase diagram of the system has not yet been completed, no evidence of the bromine clumping which is formed in certain hydrocarbon systems[6,7] is found in the present system. Electron capture during partial neutralization from the immediate environment (*i. e.*, a molecular compound or molecular compound-benzene) will cause further excitation and damage within a highly-localized region. The high solid-state organic yield must be the result of recombination reactions with damaged organic fragments or benzene. A more detailed report will be published later.

The investigation was performed at the Research Reactor Institute, Kyoto University.

*1 Presented in part at the 21st Annual Meeting of the Chemical Society of Japan, Suita, April, 1968.

1) O. U. Anders, *Phys. Rev.*, **138**, B1 (1965).
2) J. F. Emery, *J. Inorg. Nucl. Chem.*, **27**, 903 (1965).
3) R. M. Iyer and J. E. Willard, *J. Am. Chem. Soc.*, **87**, 2494 (1965).
4) a) M. I. Stamouli and N. A. Katsanos, *Z. phys. Chem. Neue Folge*, **47**, 306 (1965); b) *Radiochim. Acta*, **7**, 126, 177 (1967).
5) O. Hassel and K. O. Strømme, *Acta Chem. Scand.*, **12**, 1146 (1958).
6) J. A. Merrigan and E. P. Rack, *J. Phys. Chem.*, **69**, 2795; 2806 (1965).
7) R. M. A. Hane and J. E. Willard, *ibid.*, **68**, 2582 (1964).

A Convenient Synthesis of Benzo[*b*]-1-azaazulene Derivatives

Kahei TAKASE, Toyonobu ASAO and Naonori HIRATA

Department of Chemistry, Faculty of Science, Tohoku University, Katahira-cho, Sendai

(Received July 1, 1968)

It has been reported that the hydride abstraction of *p*-tropylphenol, followed by the base treatment, furnished a deep-colored dye named *p*-benzoquinonetropide (Ia).[1] The hydride abstraction of *p*-tropylanilines also afforded immonium ions (Ib).[1b,2]

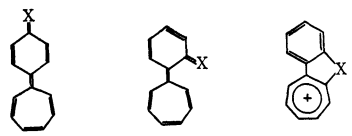

Ia X=O
Ib X=$\overset{+}{N}R_2$

IIa X=O
IIb X=NH

IIIa X=O
IIIb X=NH

On the other hand, the similar treatment of *o*-tropylphenol did not yield *o*-benzoquinonetropide (IIa), but the tricyclic tropylium cation (IIIa).[1d,3] These results led us to investigate the hydride abstraction of *o*-tropylanilines to see if the reaction would give either *o*-benzoquinonetropidimine (IIb) or the tricyclic compound (IIIb). The results will be reported in this communication.

The tropylation of *p*-toluidine (IV) with ethoxytropilidene in ethanol in the presence of hydrochloric acid afforded oily 2-(7-tropyl)-*p*-toluidine (V).*1

The distillation of V under reduced pressure easily triggered the thermal isomerization of the tropyl group[4] to give mainly 2-(3-tropyl)-*p*-toluidine (VI), bp 143°C/1.8 mmHg; *N*-acetyl derivative, mp 113—114°C. The treatment of VI with 2.3 molar equivalents of triphenylmethyl perchlorate in methylene chloride yielded a tropylium perchlorate (VII), mp 260°C (decomp.), in a 62.6% yield. The use of a smaller amount of the reagent in the above reaction diminished the yield of the compound VII. The basification of VII with sodium hydrogencarbonate yielded violet crystals (VIII), mp 120—120.5°C, in a quantitative yield; these crystals were readily reversed to VII with perchloric acid.

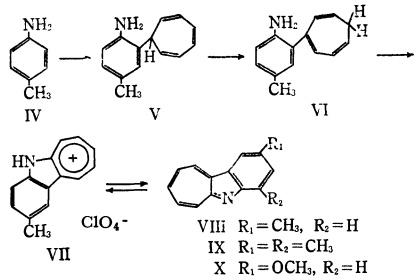

IV V VI

VII ClO_4^-

VIII $R_1=CH_3$, $R_2=H$
IX $R_1=R_2=CH_3$
X $R_1=OCH_3$, $R_2=H$

The spectroscopic properties of the compound (VIII) as well as the results of the elemental analyses support the idea that the compound is not a *o*-benzoquinonetropidimine derivative, but 2-methylbenzo[*b*]-1-azaazulene: UV (Table 1); similar to that of benzo[*b*]-1-azaazulene, NMR (in $CDCl_3$); methyl protons at 2.58 ppm and aromatic protons (8H) between 7.5—8.7 ppm, mass spectrum; parent ion peak (base peak) at 193.

Although benzo[*b*]-1-azaazulenes have already been synthesized by several methods, the present method is the simplest and most convenient.

2,4-Dimethylbenzo[*b*]-1-azaazulene (IX), deep violet crystals, mp 100—101°C, and 2-methoxybenzo[*b*]-1-azaazulene (X), deep violet plates, mp 132.5—133°C, were synthesized by a similar method starting from 2,4-dimethylaniline and *p*-anisidine respectively. The ultraviolet and visible absorption maxima of these azaazulenes are shown in Table 1.

TABLE 1. ABSORPTION MAXIMA OF THREE BENZO[*b*]-1-AZAAZULENES

Compound	λ_{max}^{MeOH} mμ (log ε)
VIII	230^{sh}(4.50), 290^{sh}(4.57), 313(4.70), 360^{sh}(4.10), 490(2.64)
IX	238(4.27), 291.5(4.39), 318.5(4.48), 360^{sh}(3.76), 520(2.60)
X	228(4.40), 314(4.65), 324(4.64), 363(3.89), 550(2.66)

1) a) R. van Helden, A. P. ter Borg and A. F. Bickel, *Rec. Trav. Chim.*, **81**, 599 (1962); b) C. Jutz and F. Voithenleitner, *Chem. Ber.*, **97**, 29 (1964); c) T. Nozoe, Japanese Pat. 17674 (1964); see *Chem. Abstr.*, **62**, 5234 (1965); d) P. Bladon, P. L. Pauson, G. R. Proctor and W. J. Rodger, *J. Chem. Soc., (C)*, 926 (1966); e) T. Nozoe and K. Takahashi, This Bulletin, **40**, 1473 (1967); f) J. J. Looker, *J. Org. Chem.*, **32**, 2941 (1967).

2) J. J. Looker, *J. Org. Chem.*, **30**, 4180 (1965).

3) T. Nozoe and K. Takahashi, This Bulletin, **40**, 1480 (1967).

*1 All the compounds were characterized by their IR and NMR spectra.

4) A. P. ter Borg, H. Kloosterziel and N. van Meurs, *Rec. Trav. Chim.*, **82**, 717 (1963); A. P. ter Borg and H. Kloosterziel, *ibid.*, **82**, 741 (1963); T. Nozoe, T. Tezuka and T. Mukai, This Bulletin, **36** 1471 (1963); T. Nozoe and K. Takahashi, *ibid.*, **38**, 665 (1965).

The Formation of Peptide Bonds at the Coordination Sites around Copper(II)

Tadayoshi HIGASHIYAMA, Hideo UEDA and Akitsugu NAKAHARA

Institute of Chemistry, College of General Education, Osaka University, Toyonaka, Osaka

(Received August 30, 1968)

In a previous paper[1] we reported the metal ion promoted hydrolysis of some oligopeptides. The structure of the intermediate complexes postulated then has recently led us to undertake the formation reaction of peptide bonds, without being confined to the cleavage reaction of them. This was because of the successful experiments of Buckingham[2] and Collman[3]; they reported that treatment of β_2-[Co(trien)Cl(glyOEt)]$(ClO_4)_2$ with glycine ethyl ester in nonaqueous solution results in the rapid condensation of two glycinester residues and the formation of the β_2-[Co(trien)glyglyOEt] ion.

Now we have also succeeded in finding out another type of formation reaction of peptide bonds by using copper(II) complex of the Schiff base derived from salicylaldehyde and glycinamide. The outline of the reactions can be represented by the schemes (1) and (2):

$$\text{Cu(Salal=Glyam)}^{*1} + \text{GlyOEt} \xrightarrow[\text{5 min, in DMFA}]{\text{KOH, 25°C}} \text{Cu(Salal=Glyglyam}^{*1}\text{)}, \quad (1)$$

$$\text{Cu(Salal=Glyam)} + \alpha\text{-AlaOEt} \xrightarrow[\text{5 min, in DMFA}]{\text{KOH, 25°C}} \text{Cu(Salal=}\alpha\text{-Alaglyam)}. \quad (2)$$

The isolation of resulting chelates shown in the schemes (1) and (2) has been carried out by using a Sephadex column and the techniques of vacuum condensation. The confirmation of peptide bond formation has been attained on the basis of three experimental results. Firstly, the infrared spectrum of the resulting chelate in the scheme (1) has shown good agreement with that of the standard samples, whose structure was already established as the copper(II) chelate of the Schiff base derived from salicylaldehyde and glycylglycinamide.[4] Secondly, the results of amino acid analyses*2 of the reaction products have clearly shown the presence of glycylglycine or its amide in the solution for the scheme (1), and α-alanylglycine or its amide in the solution for the scheme (2), respectively. Thirdly, the one- and two-dimensional paperchromatographic tests have unambiguously shown that the reaction product for the schemes (1) or (2) is not the complex with glycylglycine or α-alanylglycine but that with glycylglycinamide or α-alanylglycinamide, respectively.

Comparison between the reactions of Buckingham or Collman and of the present authors is of interest. In the reaction of Buckingham or Collman, the condensation reaction occurs between the terminal carbethoxy group of the glycinester in coordination and the amino group of free glycinester. On the other hand, in the present authors' reaction, condensation occurs between the imino-nitrogen of the glycinamide moiety in coordination and the carbethoxy group of free glycinester. Accordingly, the reaction of glycine residue in coordination with free α-alanine is expected to give glycyl-α-alanine in the Buckingham-Collman reaction, and reversely α-alanylglycine in the present authors' reaction, as has already been described. The present reaction can be interpreted to proceed as depicted in Fig. 1, though it still awaits further pursuit.

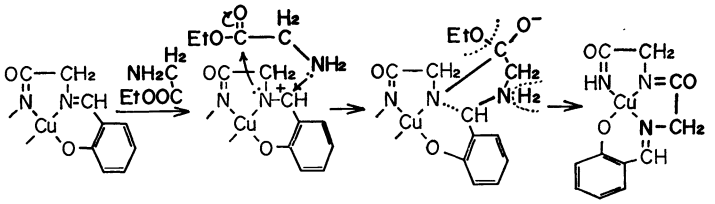

Fig. 1. A possible mechanism of the peptide formation reaction.

1) A. Nakahara, K. Hamada, Y. Nakao and T. Higashiyama, *Coordin. Chem. Rev.*, **3**, 207 (1968).
2) D. A. Buckingham, L. G. Marzilli and A. M. Sargeson, *J. Am. Chem. Soc.*, **89**, 2772 (1967).
3) J. P. Collman and E. Kimura, *ibid.*, **89**, 6096 (1967).
4) K. Hamada, H. Ueda, Y. Nakao and A. Nakahara, This Bulletin, in press.

*1 The notation "Salal=Glyam" or "Salal=Glyglyam" denotes the Schiff base derived from salicylaldehyde and glycinamide or glycylglycinamide, respectively.

*2 The sample solutions for the paperchromatography and amino acid analysis were free from copper(II) by treating with hydrogen sulfide.

Electronic Spectra of Copper(II) Acetylacetonates and Their Activity as Initiators of the Polymerization of Styrene

Kaku UEHARA, Makoto TANAKA and Niro MURATA

Department of Applied Chemistry, College of Engineering, University of Osaka Prefecture, Sakai-shi, Osaka

(Received September 2, 1968)

In a preceding communication,[1] we reported that copper(II) chelates A showed a high activity as initiators of the radical polymerization of styrene and methyl methacrylate. The polymerization proceeds *via* the reduction of Cu(II), and the ligand is incorporated into the polymer chain.

As is shown in Table 1, the order of the activity in initiation of the polymerization of styrene is as follows:

$$A>B>C>D>E>F>G$$

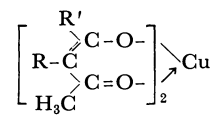

A_1: R=

A_2: R=$CH_3CH=CH-$

A_3: R=$CH_3CH_2CH=CH-$

C_1: R=$CH_3CH_2CH_2-$

C_2: R=$CH_3CH_2CH_2CH_2-$

D_1: R=$CH_2=CHCH_2-$

D_2: R= 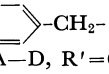

B_1: R=

B_2: R=

E: R′=$(CH_3)_3C-$

F: R′=CH_3-

G: R′=CF_3-

(A—D, R′=CH_3; E—G, R=H)

TABLE 1. RATE OF BULK POLYMERIZATION OF STYRENE INITIATED BY COPPER(II) CHELATES AT 80°C AND THE ULTRAVIOLET ABSORPTION BAND(III) OF THE CHELATES IN CHLOROFORM

Cu(II)	Chelate (mol/l)[a]	Rate of Polymerization (wt%/hr)	λ_{max} (mμ)	ε_{max}
A_1	0.0137	11.90	312	20300
A_2	0.0135	6.20	312	23400
A_3	0.0137	8.70	312	24500
B_1	0.0135	3.30	312	25600
B_2	0.0139	2.70	312	25700
C_1	0.0068	1.30	312	27100
C_2	0.0068	1.40	312	27100
D_1	0.0068	1.00	309	30300
D_2	0.0068	1.05	309	28600
E	0.0068	0.80	299	22900
F	0.0068	0.60	297	25100
G	0.0068	0.30	300	22100
None	—	0.60	—	—

a) Concentration of chelate added in the polymerization.

Figure 1 presents the visible spectra of these chelates in chloroform. The marked color changes from G to A upon the substitution of the hydrogen of F, $Cu(acac)_2$, are associated with the ultraviolet tail of the first allowed electronic absorption band (Band III in terms of the notation of a recent paper[2]; it occurs at ~300 mμ). Table 1 lists the wave lengths and intensities observed for Band III in chloroform.

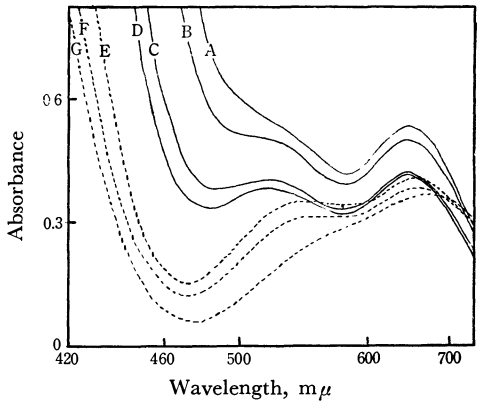

Fig. 1. Visible spectra of copper(II) chelates in chloroform.
[Cu(II) chelate]=0.01 mol/l

It is observed that the Band III of the chelate A is most remarkably broadened and that the tail extends considerably into the visible region of the spectrum. The order of the magnitude of the broadening of Band III upon substitution and the extending of the ultraviolet tail into the visible region seem to be as follows:

$$A>B>C>D>E(>F)>G$$

This order is essentially the same as the order of the activity in the polymerization. A similar broadening is also observed in the visible spectra of the chelate F with a rise in the temperature, this compound being known as a thermochromic substance.[3,4]

1) K. Uehara, T. Matsumura, T. Nishi, F. Tamura and N. Murata, *Kogyo Kagaku Zasshi (J. Chem. Soc. Japan, Ind. Chem. Sect.)*, **69**, 591, 2027 (1966).
2) J. P. Fackler, F. A. Cotton and D. W. Barnum, *Inorg. Chem.*, **2**, 97 (1963).
3) R. D. Gillard and G. Wilkinson, *J. Chem. Soc.*, **1963**, 5885.
4) K. Sone, K. Mizutani and T. Sakai, Proceeding of the X. ICCC, Tokyo-Nikko (1967), p. 138.

A Base Induced Oxidation-Reduction Reaction of Bis(salicylaldimine)copper(II)

Akira MISONO and Seiichiro KODA

Department of Industrial Chemistry, Faculty of Engineering, The University of Tokyo, Hongo, Bunkyo-ku, Tokyo

(Received September 5, 1968)

It seems interesting to determine what kind of effects an external base has on the internal oxidation-reduction reactions of complexes. We studied this in connection with our study of the role of an existing base in an oxidation reaction by a metal ion. We investigated the oxidation reactions of imines,[1] and so, naturally, have been interested in the internal oxidation-reduction reaction of bis(salicylaldimine)copper(II). This complex decomposes through an internal oxidation-reduction reaction at a higher temperature (for thermal-induced oxidation-reduction reactions, *cf.* Ref. 2); at the same time, the central copper(II) ion is reduced to metallic copper and some of the ligands are oxidized to the corresponding nitrile.[3] At room temperature, however, this complex is very stable in the solid state and also in a pyridine solution. Oxygen oxidizes this complex in a pyridine solution at relatively high temperatures, thus yielding coordinated salicylonitrile, according to Shinra *et al.*[4]

The present authors found that this complex decomposed easily in a pyridine solution when treated with a strong base such as sodium amide, sodium hydroxide, and sodium methoxide.

When this complex and a base was stirred in pyridine under a nitrogen atmosphere at room temperature, the color of the mixture changed from green to a final yellow-brown in several steps. After the resulting mixture had been treated by adequate methods, copper(I) oxide, salicylonitrile, and salicylaldehyde were found. These products and their relative amounts (the starting complex: Cu_2O : salicylonitrile $\fallingdotseq$ 2 : 1 : 1) suggest the following stoichiometric reaction:

$$2\ Cu(HN{=}CH\text{-}C_6H_4\text{-}O)_2 + 4\ NaOH \xrightarrow[\text{after-treatments}]{\text{reaction and}} Cu_2O + 3H_2O + \text{salicylonitrile}$$

+ other products such as salicylaldehyde (products obtained through no electron transfer)

When the copper complex was not stirred with a strong base in pyridine, no salicylonitrile was detected.

The existing base may abstract the imine hydrogen of the complex dissolved in pyridine, and then an oxidation-reduction reaction may occur between the deprotonated ligand and the central ion. The deprotonated ligand may be more easily oxidized than the undeprotonated one. This supposition may also be supported by the fact that a similar mechanism has been suggested for other oxidation reactions by the copper(II) ion.[5]

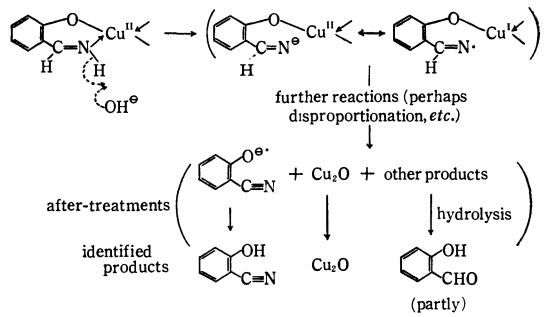

This reaction should also be compared to the deprotonation reaction of cobalt(III) complexes with amines by an amide ion in liquid ammonia, which is followed by no internal electron transfer from the deprotonated ligand to the central ion.[6] The redox potential of the central ion of the resulting complex after the deprotonation reaction may mainly decide whether a successive electron transfer reaction proceeds or not.

The reaction mechanism is now being examined in detail.

1) A. Misono, T. Osa and S. Koda, This Bulletin, **41**, 735 (1968).
2) N. Tanaka and M. Nanjo, "Muki Hanno Kiko," Kagaku-zokan **32**, ed. by N. Tanaka, K. Tamaru and S. Kawaguchi, Kagakudojin, Kyoto (1967), p. 211.
3) A. Misono and S. Koda, This Bulletin, **41**, 2795 (1968).
4) T. Matsushita, T. Okuyama, I. Masuda and K. Shinra, *Sakuenkagaku toronkai*, **17**, 11. 1. 9. (1967).
5) K. B. Wiberg and W. G. Nigh, *J. Am. Chem. Soc.*, **87**, 3849 (1965).
6) G. W. Watt and J. F. Knifton, *Inorg. Chem.* **7**, 1159 (1968). G. W. Watt and D. G. Upchurch, *J. Am. Chem. Soc.*, **90**, 914 (1968). G. W. Watt, P. W. Alexander and B. S. Manhas, *ibid.*, **89**, 6483 (1967).

Formation and Pyrolysis of Bis(chloroalkyl)tellurium Dichloride

Masao OGAWA

Central Research Laboratory of Showa Denko K. K., Tamagawa, Ota-ku, Tokyo

(Received September 17, 1968)

The present work was undertaken in connection with the tellurium-catalyzed allylic chlorination of olefins.[1] Little is known as to the reaction of tellurium tetrachloride(I) with olefins.[2,3]

The treatment of I with excess cyclohexene at 5°C afforded bis(2-chlorocyclohexyl)tellurium dichloride(II) in a 80% yield (based on I) as colorless needles (from acetic acid); mp 134—135.5°C (decomp). Found: C, 33.4; H, 4.9; Cl, 33.1%. Calcd for $C_{12}H_{20}TeCl_4$: C, 33.2; H, 4.6; Cl, 32.8%. Previously De Moura Campos and Petragnani[3] had reported the formation of 2-chlorocyclohexyltellurium trichloride(III), mp 113°C(decomp). III was obtained when I was allowed to react with an equivalent amount of cyclohexene in carbon tetrachloride. Thus, whether a 1/1 or a 1/2 adduct is formed depends on the reaction conditions.

The pyrolysis of II (at 150°C, under 1 mmHg pressure) gave, besides hydrogen chloride and inorganic telluride, cyclohexene (41%), chlorocyclohexane(33%), benzene (11% based on II), and a small amount of 3-chlorocyclohexene. The formation of chlorocyclohexane shows that tellurium-catalyzed hydrogen transfer occurs between the alkyl groups of II.

Butene-1 was bubbled into an acetonitrile solution of I at room temperature. After evaporating acetonitrile *in vacuo*, the mixture of the isomer of bis(chloro-*n*-butyl)tellurium dichloride(IV) was obtained in a quantitative yield as a faint yellow viscous oil. Found: Te, 33.2%; mol wt (cryoscopic in benzene), 385. Calcd for $C_8H_{16}TeCl_4$: Te, 33.4%; mol wt, 382.

(IVa)

(IVb)

The IR spectrum did not show the presence of a double bond. The NMR spectrum of IV in deuteriochloroform showed bands at 6.3 ppm from benzene as the internal standard (a pair of triplets; for methyl, relative area 3), 5.5 ppm (a multiplet; for methylene; relative area 2), and 2.5—3.7 ppm (multiplets; for chloromethyl and methine protons; relative area 3). If methyl protons of IVa absorbed at a higher field than those of IVa, the ratio of formation, IVa/IVb, was estimated to be about 0.6.

IV was pyrolyzed at 150°C, under 1 mmHg pressure, and the products except inorganic compounds were analyzed by gas chromatography. The liquid contained 1-chloro-2-butene (V, 52%), 2-chlorobutane (VI, 21%), 3-chloro-1-butene (14%), and 1,2-dichlorobutane (VII, 13%). The gaseous products were 1-butene (88%), *cis*- and *trans*-2-butenes (3%), butadiene (4%), and an unidentified compound (5%). The absence of vinylic chloride suggests that the preliminary formation of the carbonium cation at α-carbon is not probable as a mechanism of the pyrolysis. By postulating that chlorine is more preferentially attacked than hydrogen when both chlorine and hydrogen are bonded to the same carbon atom, most of the products can be explained by β-Cl elimination, β-Cl transfer, β-H elimination, or β-H transfer, as is shown in the following equations, respectively.

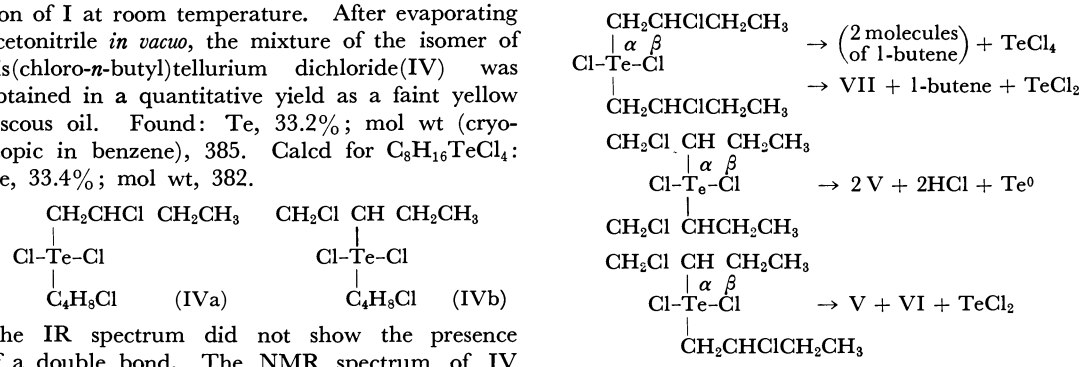

However, the formation of 3-chloro-1-butene and 2-butene, which were produced in minor amounts, cannot be accounted for by the above schemes, and a sort of allyl or π-allyl intermediate should be considered for their formation in the course of pyrolysis. The results with other olefins will be reported elsewhere.

1) Höchst A. G., German Pat. 1224301.
2) C. H. Fischer and A. Eisner, *J. Org. Chem.*, **6**, 169 (1941).
3) M. De Moura Campos and N. Petragnani, *Tetrahedron Letters*, No. 6, 11 (1959); *Tetrahedron*, **18**, 521 (1962).

Bromination of 2-Oxo-5β-steroids

Yasuo SATOH, Akira HORIUCHI, Tadaaki MATSUKURA and Akira HAGITANI

Department of Chemistry, College of Science, St. Paul's University (Rikkyo Daigaku), Nishi-Ikebukuro, Toshima-ku, Tokyo

(Received September 20, 1968)

In the bromination of any given keto-steriod, Corey has proposed a means of predicting the configuration of bromine in the product.[1] The bromination of keto-5α-steroids which possess a carbonyl group on each position in ring A has been thoroughly investigated,[2] and the configuration of the brominated product in every case was in agreement with Corey's prediction. In the case of the bromination of keto-5β-steroids, however, only that of the 3-oxo derivative has been reported.[3]

The authors wish to report on the bromination of 2-oxo-5β-steroids and on the relation between these products and Corey's prediction.

5β-Chlestan-2-one[4] (4.24 g) was dissolved in acetic acid (100 ml) and a few drops of 49% hydrogen bromide were added, followed by addition of bromine (1.75 g) in acetic acid (10 ml) with stirring for 25 min at 18°C. The reaction mixture was cooled and then the crystals formed were collected. The crystals were dissolved in ether and the ethereal solution was washed, dried and evaporated. Crystallization of the residue from methanol-ether gave needles (3.82 g), mp 128—130°C. IR (KBr disk): 1714 ($\nu_{C=O}$) and 668 cm^{-1} (ν_{C-Br}). NMR (in $CDCl_3$) τ: 4.32 (singlet, one proton). ORD (*c* 0.52, Di) at 26°C: $[\alpha]_{589}$ +9.6°, $[\alpha]_{400}$ +421°, $[\alpha]_{336}$ +2187° (peak), $[\alpha]_{314}$ 0°, $[\alpha]_{288}$ −2369° (trough). Found: C, 69.78; H, 9.80%. Calcd for $C_{27}H_{45}OBr$: C, 69.65; 9.74%.

The bromination of methyl 2-oxocholanate (834 mg)*1,5 was carried out using the technique as described above. The reaction mixture was taken up in ether and the ether extracts were washed, dried and evaporated. On chromatography of the residue on silica gel (50 g), elution with benzene gave an oily product (650 mg). The crystallization of this product from methanol afforded needles (81 mg), mp 138—140°C. IR (KBr disk): 1735, 1710 ($\nu_{C=O}$), 1171 (ν_{C-O-C}) and 673 cm^{-1} (ν_{C-Br}). NMR (in $CDCl_3$) τ: 5.66 (singlet, one proton) and 6.35 (singlet, three protons). ORD (*c* 0.62, Di) at 25°C: $[\alpha]_{589}$ +67.7°, $[\alpha]_{400}$ +271°, $[\alpha]_{335}$ +1394° (peak), $[\alpha]_{313}$ 0°, $[\alpha]_{289}$ −1468° (trough). Found: C, 63.33; H, 8.00%. Calcd for $C_{25}H_{39}O_3Br$: C, 64.24; H, 8.41%. An oily product from the mother liquor was identical with the above crystals in IR- and NMR-spectra.

These compounds are 1β-bromo-2-oxo-5β-steroids, not 1α- or 3-bromo isomers. This has been confirmed by signs of the Cotton effect, Δ[A]- (+233 for 5β-cholestan-2-one and +164 for methyl 2-oxocholanate) and $\Delta\lambda_1$-values (+20 and +18 mμ, respectively) in ORD, by the shifts of C=O stretching bands (+4 and +2 cm^{-1}, respectively) in the IR spectra and by the patterns of the NMR spectra.

In connection with the above investigation, we carried out the enol acetylation of 5β-chloestan-2-one according to directions of Djerassi *et al.* described for the 5α-series.[2] The reaction product was chromatographed in petroleum ether on silica gel. Elution with benzene gave 5β-cholest-1-en-2-ol acetate, mp 103—105°C, $[\alpha]_D^{26}$ +52.0° (*c* 0.997, in $CHCl_3$), from ethanol. IR (KBr disk): 1750 ($\nu_{C=O}$), 1687 ($\nu_{C=C}$) and 1215 cm^{-1} (ν_{C-O-C}). NMR (in $CDCl_3$) τ: 4.66 (singlet, one proton) and 7.93 (singlet, three protons). It has been found, moreover, that bromination of this enol acetate with bromine in acetic acid gave the same product as described above for 5β-cholestan-2-one.

From these results, we may conclude that the enolization of the 2-oxo-5β-steroids occurs in the direction of C_1, not C_3, and that the bromination of these ketones forms the 1β-bromo-2-oxo derivatives. The configuration of these bromoketones is consistent with Corey's prediction for the 2-oxo-5β-steroids.[1]

Further details will be published later.

1) E. J. Corey, *J. Am. Chem. Soc.*, **75**, 2301 (1953); **76**, 175 (1954).
2) C. Djerassi, "Steroid Reactions," Holden-Day, Inc., San Francisco (1963), p. 179.
3) A. Butenandt and A. Wolff, *Ber.*, **68**, 2091 (1935); L. F. Fieser and R. Ettorre, *J. Am. Chem. Soc.*, **75**, 1700 (1953); C. W. Shoppee, A. B. Devine, and R. E. Lack, *J. Chem. Soc.*, **1965**, 6458.
4) M. Tomoeda and T. Koga, *Tetrahedron Letters*, **1965**, 3231.
*1 ORD (*c* 0.59, Di) at 26°C: $[\alpha]_{317}$ −273° (trough), $[\alpha]_{307}$ −166° (shoulder), $[\alpha]_{275}$ +509° (peak).
5) This compound, not yet given in literature, will be reported at the Sendai Meeting of the Chemical Society of Japan, October, 1968.

A Method of Preparing Dicyano Cobalt(III) Complexes with a *Trans*-Configuration

Nobufumi MAKI, Setsuro ITO and Shukichi SAKURABA

Department of Chemistry, Faculty of Engineering, Shizuoka University, Johoku, Hamamatsu

(Received September 30, 1968)

Recently, Konya *et al.*[1] reported the preparation of cyano-ammine and amine cobalt(III) complexes in a water solution, while Yoneda *et al.*[2] independently described the synthesis of the dicyanobis(ethylenediamine)cobalt(III) complex in dimethyl sulfoxide (DMSO).

In the present communication, the step-by-step substitution method *via* the monocyanomonochloro complex of the $[Co(CN)ClN_4]$-type has been attempted in DMSO and found to be suitable for replacing a chloro-ligand with a CN^- ion without disrupting the complex. This method has been used in the preparation of *trans*-$[Co(CN_2)(NH_3)_4]NO_3 \cdot H_2O$ and *trans*-$[Co(CN)_2en(NH_3)_2]Cl \cdot H_2O$ (a new compound). The direct substitution in DMSO *via* the dichloro complex was not adequate for obtaining dicyano-ammine complexes, since the substitution was always accompanied by a disproportionation.

Preparation of *trans*-$[Co(CN)_2(NH_3)_4]NO_3 \cdot H_2O$. The dimethyl sulfoxide (500 m*l*) in which 3.00 g of KCN had been completely dissolved at 60°C was transferred into a three-necked flask equipped with a reflux condenser and a mechanical stirrer. To this solution were added 11.7 g of *trans*-$[Co(CN)Cl(NH_3)_4]NO_3$.[3] The suspension was heated on a water bath at 70—85°C for three hours. After the solution had been allowed to stand overnight, orange-yellow crystals separated from the solution, they were then filtered and washed with acetone. The crude complex was recrystallized from hot water. The yield was 53.4% of theory. Found: Co, 22.51; C, 9.08; N, 37.72; H, 5.60%. Calcd for $[Co(CN)_2(NH_3)_4]NO_3 \cdot H_2O$: Co, 22.74; C, 9.27; N, 37.84; H, 5.45%.

Preparation of *trans*-$[Co(CN)_2en(NH_3)_2]Cl \cdot H_2O$. The complex was prepared according to the following reaction steps: *trans*-$[Co(CN)(SO_3)(NH_3)_4] \cdot 2H_2O$[4] $\xrightarrow{en}$ *cis*-$[Co(CN)(SO_3)en(NH_3)_2]$ $\xrightarrow{HCl}$ *cis*-$[Co(CN)Clen(NH_3)_2]Cl$ $\xrightarrow[\text{in DMSO}]{KCN}$ *trans*-$[Co(CN)_2en(NH_3)_2]Cl \cdot H_2O$. (1) The water solution (100 m*l*) containing 30 g of *trans*-$[Co(CN)(SO_3)(NH_3)_4] \cdot 2H_2O$[4] was treated with ethylenediamine (8.6 g) at 80°C for two hours. The starting complex was once dissolved completely in a solution, evolving ammonia; then again deeper-colored brown crystals deposited from the solution. This reaction mixture was further heated for four hours, filtered, and washed with hot water, ethanol, and ether. The product of *cis*-$[Co(CN)(SO_3)en(NH_3)_2]$ (12 g) was used for the next reaction without further purification, since it is insoluble in water. (2) Thirty grams of *cis*-$[Co(CN)(SO_3)\ en(NH_3)_2]$ were treated with 300 m*l* of concentrated HCl at 80—85°C for five hours. Red crystals of *cis*-$[Co(CN)Clen(NH_3)_2]Cl$ were obtained by adding 200 m*l* of ethanol to the solution under ice cooling. (3) Analogously to the case of the dicyanotetra-ammine complex, 6 g of *cis*-$[Co(CN)Clen(NH_3)_2]Cl$ were continuously stirred in small portions into 300 m*l* of dimethyl sulfoxide containing 2.3 g of KCN, and then the mixture was heated at 80°C for an hour. The yellow solution soon became muddy as the reaction proceeded, it was filtered and washed with acetone. The crude product was recrystallized from hot water below 60°C.

Found: Co, 22.63;C, 18.50; N, 32.61; H, 6.39%. Calcd for $[Co(CN)_2en(NH_3)_2]Cl \cdot H_2O$: Co, 22.79; C, 18.58; N, 32.49; H, 6.24%.

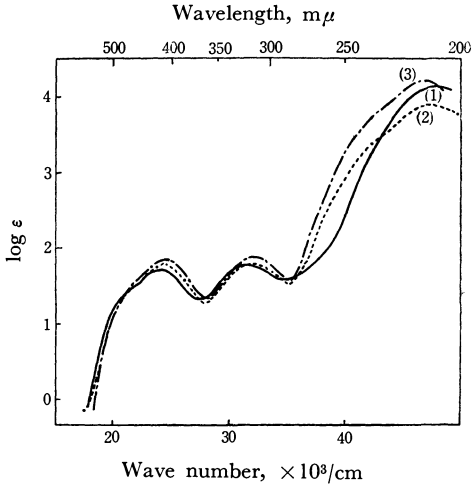

Fig. 1. The absorption spectra of the dicyanocobalt(III) complexes: (1) —— *trans*-$[Co(CN)_2(NH_3)_4]NO_3 \cdot H_2O$; (2) ····· *trans*-$[Co(CN)_2en(NH_3)_2]Cl \cdot H_2O$; (3) — — — *trans*-$[Co(CN)_2en_2]NO_3$.

1) K. Konya, H. Nishikawa and M. Shibata, *Inorg. Chem.*, **7**, 1165 (1968).
2) H. Yoneda, T. Baba and M. Muto, This Bulletin, **40**, 1736 (1967).
3) K. Ohkawa, J. Hidaka and Y. Shimura, *ibid.*, **40**, 2830 (1967).
4) H. Siebert, *Z. Anorg. Allgem. Chem.*, **327**, 63 (1964).

The Reaction of Copper(II) Acetylacetonates with 2,2-Diphenyl-1-picrylhydrazyl in Benzene

Kaku UEHARA, Makoto TANAKA and Niro MURATA

Department of Applied Chemistry, College of Engineering, University of Osaka Prefecture, Sakai-shi, Osaka

(Received October 2, 1968)

Sutcliffe and Walkley[1] have pointed out that the redox reaction of metal acetate with 2,2-diphenyl-1-picrylhydrazyl (DPPH) in anhydrous acetic acid gives first-order kinetics for each reactant and that the rate is reduced by the addition of benzene.

This communication relates to a novel reaction of DPPH with metal complexes. Copper(II) acetylacetonates were allowed to react with DPPH in benzene at various temperatures. It was observed that as the reaction proceeded the absorption of DPPH at 525 mμ disappeared and that the reaction was accelerated by the presence of air. Furthermore, the rate was enormously enhanced in a frozen solution. In the experiments to be described below, the reaction mixture was degassed by a modified method because the conventional freeze-thaw cycle was unsuitable for this study.

The rate of the reaction varied remarkably with the structure of the ligand. As is shown in Table 1, the order of the reactivity of the copper(II) chelates was as follows:

$$A > B \gg C > D \gg E \gg F(\text{no reaction})$$

The order is essentially the same as that of the activity in the radical polymerization of styrene and the degree of extension of the ultraviolet tail of the copper(II) chelates[2] into the visible region.

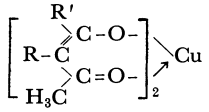

A_1: R = $CH_3CH_2CH{=}CH-$
A_2: R = $CH_3CH{=}CH-$
A_3: R =
B_1: R =
B_2: R =
C_1: R = $CH_3CH_2CH_2CH_2-$
C_2: R = $CH_3CH_2CH_2-$
D_1: R = $CH_2{=}CHCH_2-$
D_2: R =
E: R' = CH_3
F: R' = CF_3
(A—D, R' = CH_3; E and F, R = H))

Table 1. Rate data of the reaction of DPPH with Cu(II) chelates in benzene

Cu(II)	Chelate (mol/l) $\times 10^4$	DPPH (mol/l) $\times 10^4$	Temperature (°C)	Rate (mol/l sec) $\times 10^9$
A_1	0.5	0.6	25	2.5
A_2	0.5	0.6	25	3.8
A_3	0.5	0.6	25	1.6
B_1	0.5	0.6	25	1.3
B_2	0.5	0.6	25	0.5
C_1	0.5	0.6	25	0.0
C_2	0.5	0.6	25	0.0
D_1	0.5	0.6	25	0.0
D_2	0.5	0.6	25	0.0
E	0.5	0.6	25	0.0
F	0.5	0.6	25	0.0
B_2	0.5	0.6	50	4.4
C_1	0.5	0.6	50	0.0
C_1	10.0	0.6	70	2.6
C_2	10.0	0.6	70	2.3
D_1	10.0	0.6	70	1.1
D_2	10.0	0.6	70	1.3
E	10.0	0.6	70	0.2
F	10.0	0.6	70	0.0
None	—	0.6	70	0.0
A_1	1.4	1.4	10	5.4
A_1	1.4	1.4	3[a]	19.5

a Frozen benzene solution.

In a frozen benzene solution (3°C), the rate of the reaction was enormously enhanced. A similar acceleration of rate was also observed in frozen *p*-dioxane and *p*-xylene.

The kinetic studies of this reaction were carried out with Cu(II) chelate A_1 in the range from 10 to 30°C. 0.6-order kinetics for DPPH and first-order kinetics for the Cu(II) chelate were observed. The activation energy of the reaction in the liquid benzene was 7.5 kcal/mol. The rate was reduced by the addition of 2,2-diphenyl-1-picrylhydrazine (DPPH-H), but increased by the addition of pyridine.

$Mn(acac)_3$, which is an effective initiator of the radical polymerization,[3] also reacts with DPPH in benzene and shows an enhanced rate in a frozen solution.

1) L. H. Sutcliffe and J. Walkley, *Nature*, **178**, 999 (1956).
2) K. Uehara, M. Tanaka and N. Murata, This Bulletin, **41**, 3029 (1968).
3) C. H. Bamford and D. J. Lind, *Proc. Roy. Soc.*, **302**A, 145, (1968).